Volume 119 Supplement 1 April 2016 ISSN 0167-8140

ELSEVIER

Radiotherapy & Oncology

Journal of the European SocieTy for Radiotherapy and Oncology

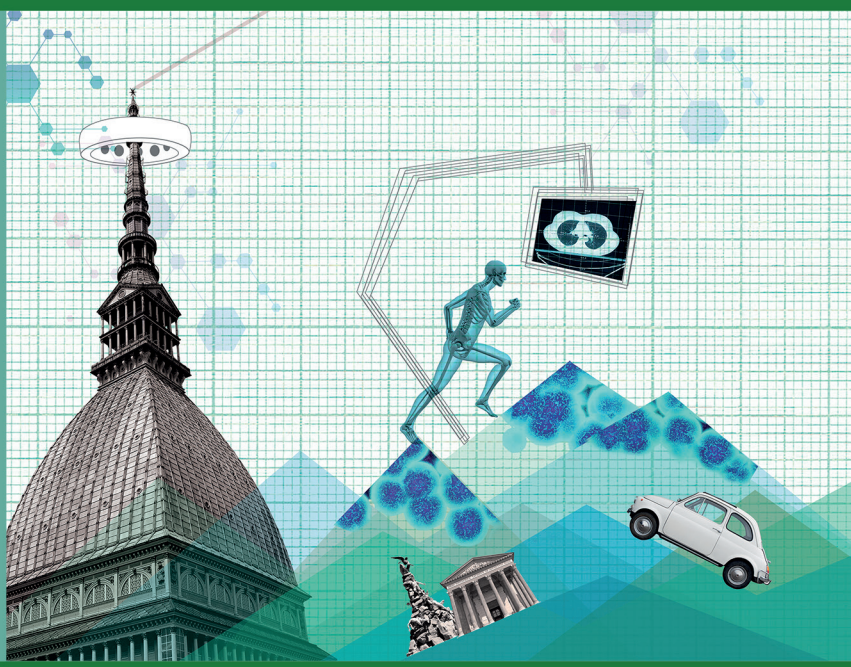

ESTRO 35

29 April - 3 May 2016
Turin, Italy

ESTRO
European SocieTy for
RADIOTHERAPY
& ONCOLOGY

Radiotherapy &Oncology

Journal of the European SocieTy for Radiotherapy and Oncology

INFORMATION FOR AUTHORS

ARTICLES should deal with original research or reviews of topics defined in the aims of the journal. Radiotherapy and Oncology publishes original material only. It is therefore understood that the content of the paper has not previously been published in the same or a similar form and that it is not under consideration for publication elsewhere. The act of submitting a manuscript to the journal carries with it the right to publish that paper.

Radiotherapy and Oncology uses an online manuscript submission and peer review process.
Papers and correspondence should be submitted online at **http://www.ees.elsevier.com/ro** and the instructions on the site should be closely followed. Authors may submit manuscripts and track their progress to final decision. Reviewers can download manuscripts and submit their reports to the Editors electronically.

The full contact details for the Editorial Office are shown below:

Professor Jens Overgaard, M.D., Radiotherapy and Oncology Secretariat, Department of Experimental Clinical Oncology, Aarhus University Hospital, Nörrebrogade 44, Building 5, DK-8000 Aarhus C, Denmark (Tel.: +45 78 46 26 29; Fax: +45 86 19 71 09; E-mail: ro@oncology.dk)

TYPES OF PAPERS

1. *Full length original papers (max. 3000 words)*
Describe original scientific work in the field of radiation oncology or related areas. The content of the paper should be sufficient to reach valid conclusions. Full papers should include a structured abstract and be divided into sections (Introduction; Materials and Methods; Results; Discussion; References; Tables; Figures) and should not normally exceed 6 printed pages, including references and a maximum of 6 tables/figures. Additional material can be submitted as supplementary files.

2. *Short communications and Technical notes (max. 2000 words)*
Provide a brief but complete account of a particular piece of work, e.g. Phase I or II study, and should in total be no longer than 4 printed pages, normally including a maximum of 2 figures or tables. A summary of not more than 50 words should be included (not a structured abstract), but the manuscript can have fewer subheadings (e.g. short introduction; materials and methods; results and discussion). Authors are advised to see a recent issue of the journal for size and lay-out.

3. *Review articles*
Rigorous critical assessment of clinical and/or laboratory research in a field of interest to the journal and its subscribers. Reviews are normally solicited by the editors, and it is suggested that authors wishing to contribute a review article contact the editor-in-chief.

4. *Editorials and commentaries*
Editorials and commentaries relate to articles in the journal or to issues of relevance for the readership. This type of communication is normally solicited by the editors.

5. *Letters to the Editor*
On topics of current interest or comment upon material previously or simultaneously published in the journal. They should be limited to 500 words and may include 1 table or figure.

6. *Announcements*
The inclusion of announcements, etc. is at the discretion of the Editors and the Publisher and subject to space availability. Request for inclusion of meeting announcement should be send to the ESTRO secretariat (see address in journal).

Author inquiries
For inquiries relating to the submission of articles (including electronic submission where available) please visit this journal's homepage at http://www.elsevier.com/locate/radonc. For detailed instructions on the preparation of electronic artwork, please visit http://www.elsevier.com/artworkinstructions. Contact details for questions arising after acceptance of an article, especially those relating to proofs, will be provided by the publisher. You can track accepted articles at http://www.elsevier.com/trackarticle. You can also check our Author FAQs at http://www.elsevier.com/authorFAQ and/or contact Customer Support via http://support.elsevier.com

Language services. Authors who require information about language editing and copyediting services pre- and post-submission please visit http://webshop.elsevier.com/languageediting or our customer support site at http://support.elsevier.com.

A full and complete Guide for Authors is availabe online at http://www.thegreenjournal.com

Printed by Henry Ling Ltd., Dorchester, United Kingdom

International Standard Serial Number 0167-8140

Orders, claims, and journal inquiries: please contact the Elsevier Customer Service Department nearest you:

St. Louis: Elsevier Customer Service Department, 3251 Riverport Lane, Maryland Heights, MO 63043, USA; phone: (800) 6542452 [toll free within the USA]; (+1) (314) 4478871 [outside the USA]; fax: (+1) (314) 4478029; e-mail: JournalsCustomerService-usa@elsevier.com
Oxford: Elsevier Customer Service Department, The Boulevard, Langford Lane, Kidlington, Oxford OX5 1GB, UK; phone: (+44) (1865) 843434; fax: (+44) (1865) 843970; e-mail: JournalsCustomerServiceEMEA@elsevier.com
Tokyo: Elsevier Customer Service Department, 4F Higashi-Azabu, 1-Chome Bldg, 1-9-15 Higashi-Azabu, Minato-ku, Tokyo 106-0044, Japan; phone: (+81) (3) 5561 5037; fax: (+81) (3) 5561 5047; e-mail: JournalsCustomerServiceJapan@elsevier.com
Singapore: Elsevier Customer Service Department, 3 Killiney Road, #08-01 Winsland House I, Singapore 239519; phone: (+65) 63490222; fax: (+65) 67331510; e-mail: JournalsCustomerServiceAPAC@elsevier.com

Funding Body Agreements and Policies

Elsevier has established agreements and developed policies to allow authors whose articles appear in journals published by Elsevier, to comply with potential manuscript archiving requirements as specified as conditions of their grant awards. To learn more about existing agreements and policies please visit http://www.elsevier.com/fundingbodies

Radiotherapy &Oncology

Journal of the European SocieTy for
Radiotherapy and Oncology

Volume 119 Supplement 1 (2016)

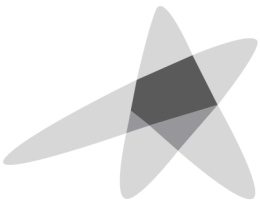

Radiotherapy & Oncology is available online:
For ESTRO members: http://www.thegreenjournal.com
For institutional libraries: http://www.sciencedirect.com

Amsterdam • Boston • London • New York • Oxford • Paris • Philadelphia • San Diego • St. Louis

ESTRO 35 content

Saturday 30 April 2016

Teaching Lecture

Technology assessment (Abs. 1)

CRISPR/CAS technology: from cells to mice to stem cell therapy (Abs. 2)

Partial Breast Irradiation: who, when and how? (Abs. 3)

New tools to reduce toxicity in pelvic radiation (Abs. 4)

Role of brachytherapy in the management of paediatric tumors (Abs. 5)

Challenges in MR guided radiotherapy (Abs. 6)

Patient specific quality assurance in proton therapy (Abs. 7)

Balancing toxicity and disease control in the evolution of radiotherapy technology (Abs. 8)

Symposium

Selection of patients for proton therapy (Abs. 9-11)

Mitigating normal tissue toxicity (Abs. 12-14)

Regional nodal irradiation for breast cancer (Abs. 15-17)

Assessment and management of rectal morbidity (Abs. 18-20)

Towards user oriented QA procedures for treatment verification (Abs. 21-23)

Robust and accurate functional MRI for radiotherapy (Abs. 24-26)

Joint Symposium

ESTRO-IAEA: Joint ESTRO-IAEA efforts on dosimetry, QA and audit for advanced treatment techniques (Abs. 27-29)

Symposium

Strategies for treatment planning (Abs. 30-32)

Poster Viewing

1: Brachytherapy (Abs. 33-40)

Symposium

Protons or heavy ions? (Abs. 41-43)

Proffered Papers

Radiobiology 1: Radiation effects on normal tisssues and the microenviroment (Abs. 44-48)

Clinical 1: Breast (Abs. 49-54)

Clinical 2: Adverse effects in radiotherapy (Abs. 55-60)

Brachytherapy 1: Prostate (Abs. 61-66)

Physics 1: Images and analyses (Abs. 67-72)

Physics 2: Basic dosimetry (Abs. 73-78)

RTT 1: Novelties in treatment planning (Abs. 79-84)

Poster Viewing

2: Clinical: Health economics, urology and brain (Abs. 85-91)

Presidential Symposium

Presidential (Abs. 92)

Award Lecture

E. Van der Schueren Award (Abs. 93)

Symposium with Proffered Papers

Hot topics in SABR: time for randomised clinical trials? (Abs. 94-97)

Symposium

Tumour targeting - considering normal tissue biology (Abs. 98-101)

Debate

This house believes that progress in the treatment of locally advanced NSCLC will come from: (Abs. 102-103)

Symposium

Active surveillance for low risk prostate cancer: to treat or not to treat? (Abs. 104-106)

Achieving excellence in image guided brachytherapy (Abs. 107-109)

Imaging markers for response prediction and assessment (Abs. 110-112)

Debate

There are many existing IGRT options for highly accurate dose delivery. Is there a need for large-scale in-room MR-guidance? (Abs. 113-114)

Symposium

Additional tools for contouring (Abs. 115-117)

Poster Viewing

3: Clinical: Gastrointenstinal and gynaecology (Abs. 118-125)

Joint Symposium

ESTRO-ESR: MR-PET (Abs. 126-128)

Proffered Papers

Radiobiology 2: Interplay between cancer stem cells ,hypoxia and the radiation response (Abs. 129-134)

Clinical 3: Lung (Abs. 135-140)

Clinical 4: Late breaking abstracts (Abs. 141-146)

Brachytherapy 2: EYE GI (Abs. 147-152)

Physics 3: Anatomical CT and MR imaging for treatment preparation (Abs. 153-158)

Physics 4: Inter-fraction motion management I (Abs. 159-164)

RTT 2: Improving quality for breast cancer treatments (Abs. 165-170)

Poster Viewing

4: Physics: Treatment planning: applications III (Abs. 171-176)

Honorary Members Lecture

Honorary Members (Abs. 177-179)

Sunday 1 May 2016

Teaching Lecture

Trade off between standardisation and individualisation (Abs. 180)

DNA repair and response for beginners (Abs. 181)

Anal cancer: current guidelines and remaining questions (Abs. 182)

Radiotherapy and immune-therapy, biological basis and potential for future clinical trials (Abs. 183)

Underestimated importance of Intraluminal brachytherapy: bronchus, oesophageal, anorectal and hepatobiliary duct cancer (Abs. 184)

Big data in radiotherapy: technology, challenges and opportunities (Abs. 185)

The role of dosimetry audit in safety, quality and best practice for external beam and brachytherapy (Abs. 186-187)

General introduction to head and neck radiotherapy (Abs. 188)

e-Learning for Professionals in Radiation Oncology: What, Why and How? (Abs. 189)

Symposium with Proffered Papers

Quality beyond accuracy: are we failing to see the forest for the trees? (Abs. 190-193)

Symposium

Targeting DNA repair / DDR pre-clinical evidence (Abs. 194-196)

New approaches in rectal cancer (Abs. 197-199)

Changing paradigm in the management of kidney cancer (Abs. 200-202)

Modern techniques for old indications (Abs. 203-205)

Quantitative imaging to individualise radiotherapy (Abs. 206-208)

Proffered Papers

Physics 5: Intra-fraction motion management I (Abs. 209-215)

Symposium

Head and neck: reduction of margins and side effects (Abs. 216-218)

The future of Radiation Oncology publishing: views through the Red and Green telescopes (Abs. 219-221)

Poster Viewing

5: RTT (Abs. 222-230)

Symposium

QA in clinical trials: processes, impact and future perspectives (Abs. 231-233)

Proffered Papers

Radiobiology 3: Novel targeting approaches in combination with radiation (Abs. 234-238)

Clinical 5: Upper and lower GI (Abs. 239-244)

Clinical 6: Hadron therapy (Abs. 245-250)

Brachytherapy 3: Detectors and dose verification (Abs. 251-256)

Physics 6: Radiobiological modelling (Abs. 257-262)

Physics 7: Treatment planning: optimization algorithms (Abs. 263-268)

RTT 3: Ensuring quality in head and neck treatment (Abs. 269-274)

Poster Viewing

6: Clinical: Lung, palliation, sarcoma, haematology (Abs. 275-281)

Proffered Papers

Donal Hollywood Award (Abs. 282)

Highlights of Proffered Papers (Abs. 283-286)

Symposium

Planning ahead: how to finish your residency / PhD project with a job offer (Abs. 287-290)

Symposium with Proffered Papers

Standardisation in clinical practice (Abs. 291-295)

Symposium

DNA repair inhibition and radiotherapy: moving towards clinic (Abs. 296-298)

Radiotherapy of prostate cancer: technical challenges (Abs. 299-301)

Debate

This house believes that SBRT should become the standard of care for T1 and small T2 NSCLC tumours (Abs. 302-303)

Is brachytherapy the best for partial breast irradiation? (Abs. 304-307)

Symposium

New challenges in modelling dose-volume effects (Abs. 308-310)

Automated treatment plan generation in the clinical routine (Abs. 311-313)

Elderly and radiation therapy (Abs. 314-316)

A Joint session of Young Radiation Oncologists National Societies & YROG (Abs. 317-321)

Poster Viewing

7: Physics: Intra-fraction motion management II (Abs. 322-329)

Symposium with Proffered Papers

Uncovering the gap between optimal and actual utilisation of radiotherapy in Europe (Abs. 330-334)

Debate

Maximising tumour control: crank up the volume or turn off the switches? (Abs. 335-338)

Proffered Papers

Clinical 7: Urology (Abs. 339-344)

Clinical 8: Adult and paediatric CNS malignancies (Abs. 345-350)

Brachytherapy 4: Gynae-Breast (Abs. 351-356)

Physics 8: Dose measurement and dose calculation I (Abs. 357-362)

Physics 9: Adaptive RT for inter-fraction motion management (Abs. 363-368)

RTT 4: How to increase the knowledge for patients and staff (Abs. 369-374)

Poster Viewing

8: Physics: Inter-fraction motion management II (Abs. 375-379)

Award Lecture

Academic award: Jack Fowler University of Wisconsin Award (Abs. 380)

Company Award Lectures (Abs. 381-382)

Monday 2 May 2016

Teaching Lecture

How to bring QUANTEC into the 21st century? (Abs. 383)

Shared decision making (Abs. 384)

The study of therapy resistance in genetically engineered mouse models for BRCA1-mutated breast cancer (Abs. 385)

SBRT/SABR for oligometastatic disease (Abs. 386)

Advanced treatment strategies for head and neck cancer (Abs. 387)

Dose to water vs. dose to tissue in advanced treatment planning: myths, realities and concerns (Abs. 388)

Nanodosimetry: from radiation physics to radiation biology (Abs. 389)

Brachytherapy for the pelvic region: status and perspective for the future (Abs. 390-391)

Symposium with Proffered Papers

Adaptive radiotherapy for coping with anatomical variations: hope or hype? (Abs. 392-395)

Time is not on our side: cardiovascular toxicity after radiotherapy (Abs. 396-400)

Symposium

Emerging biomarkers (Abs. 401-404)

SBRT for oligometastatic disease (Abs. 405-407)

Head and neck: state-of-the-art and directions for future research (Abs. 408-410)

SBRT in lung - choices and their impact on related uncertainties (Abs. 411-413)

Proffered Papers

Physics 10: Functional Imaging I (Abs. 414-420)

Symposium

Adaptive treatments in the pelvic region (Abs. 421-423)

Poster Viewing

9: Radiobiology (Abs. 424-432)

Symposium

Modern ART based on functional / biological imaging (Abs. 433-435)

Secondary cancer after radiotherapy: from cancer registries to clinical implications (Abs. 436-438)

Proffered Papers

Radiobiology 4: Molecular biomarkers for patient selection (Abs. 439-443)

Clinical 9: SBRT and oligometastatic disease (Abs. 444-448)

Clinical 10: Head and neck (Abs. 449-454)

Physics 11: Dose measurement and dose calculation II (Abs. 455-460)

Physics 12: Treatment planning: applications I (Abs. 461-466)

RTT 5: Optimizing treatment planning and delivery in the pelvic region (Abs. 467-472)

Poster Viewing

10: Physics: Functional Imaging II (Abs. 473-478)

Proffered Papers

Selected randomised trials (Abs. 479-481)

Award Lecture

Breur Award Lecture (Abs. 482)

Joint Symposium

ESTRO-ASTRO: In room adaptive imaging with a focus on MRI (Abs. 483-486)

Symposium

Communication with patients (Abs. 487-490)

Imaging biology (Abs. 491-493)

Debate

This house believes that centralised large radiotherapy units will provide the best academia and the best treatment quality (Abs. 494-495)

Joint Symposium

ESTRO-ILROG: Modern radiotherapy in lymphoma (Abs. 496-498)

ESTRO-PTCOG: ART in particle therapy (Abs. 499-503)

Symposium

Small animal irradiation (Abs. 504-506)

Focus on the pelvic region (Abs. 507-509)

Poster Viewing

11: Clinical: Breast, head and neck (Abs. 510-519)

Symposium

Dose painting: those pending issues (Abs. 520-522)

ACROP (Abs. 523-525)

Proffered Papers

Radiobiology 5: Imaging and molecular biomarkers in radiation

oncology (Abs. 526-530)

Clinical 11: Health Economics and patient reported outcomes (Abs. 531-536)

Clinical 12: Rare tumours (Abs. 537-542)

Physics 13: New Technology and QA (Abs. 543-548)

Physics 14: Treatment planning: applications II (Abs. 549-554)

RTT 6: Advanced radiation techniques in prostate cancer (Abs. 555-560)

Poster Viewing

12: Physics: Dose measurement and dose calculation III (Abs. 561-566)

General Assembly

General Assembly

Tuesday 3 May 2016

Teaching Lecture

The new 'Rs' in radiation biology (Abs. 567)

Texture analysis of medical images in radiotherapy (Abs. 568)

Biology of high-energy proton and heavy ion particle therapy versus photon therapy: recent developments (Abs. 569)

Neuroendocrine tumours – personalised diagnosis and treatment using radiolabelled peptides (Abs. 570)

Radiotherapy for paediatric brain tumours (Abs. 571)

Role and validation of deformable image registration in clinical practice (Abs. 572)

VMAT QA: To do and not to do, those are the questions (Abs. 573)

Optimising workflow in a radiotherapy department - an introduction to lean thinking (Abs. 574)

Symposium

New concepts of tumour radioresistance (Abs. 575-577)

Symposium with Proffered Papers

Towards Personalised Radiation Oncology (PRO) (Abs. 578-582)

Symposium

The tumour in 3D: the role of tumour microenvironment (Abs. 583-586)

WBRT for brain metastases- the end of an era? (Abs. 587-589)

Radiotherapy "autovaccination" with systemic immune modulators for modern immunotherapy (Abs. 590-592)

Joint Symposium

ESTRO-AAPM-EFOMP: Functional / biological imaging and radiotherapy physicists: new requests/challenges and the need for better and more specific training (Abs. 593-595)

Symposium

The future of QA lies in automation (Abs. 596-599)

Management and optimisation of the daily workflow (Abs. 600-602)

Combining radiotherapy with molecular targeted agents: learning from successes and failures (Abs. 603-605)

Symposium with Proffered Papers

Radiomics - the future of radiotherapy? (Abs. 606-609)

Symposium

Radiobiology of proton / carbon / heavy ions (Abs. 610-612)

New insights in treating vertebral metastases (Abs. 613-615)

IMRT, the new standard in treatment of gynaecological, lung and breast cancers? (Abs. 616-618)

Symposium with Proffered Papers

Plan of the day (PotD): current status (Abs. 619-621)

Debate

We don't need better dose calculation, it's doing more bad than good (Abs. 622-623)

Are we precisely inaccurate in our adaption? (Abs. 624-625)

Moving away from 2 Gray: are we ready for a paradigm shift? (Abs. 626-629)

Posters

Clinical track: Head and neck (Abs. 630-640)

Clinical track: CNS (Abs. 641-661)

Clinical track: Haematology (Abs. 662-671)

Clinical track: Breast (Abs. 672-677)

Clinical track: Lung (Abs. 678-695)

Clinical track: Upper GI (oesophagus, stomach, pancreas, liver) (Abs. 696-714)

Clinical track: Lower GI (colon, rectum, anus) (Abs. 715-722)

Clinical track: Gynaecological (endometrium, cervix, vagina, vulva) (Abs. 723-735)

Clinical track: Prostate (Abs. 736-758)

Clinical track: Urology-non-prostate (Abs. 759-760)

Clinical track: Skin cancer / malignant melanoma (Abs. 761-763)

Clinical track: Sarcoma (Abs. 764-768)

Clinical track: Paediatric tumours (Abs. 769-771)

Clinical track: Palliation (Abs. 772-779)

Clinical track: Elderly (Abs. 780-782)

Clinical track: Health services research / health economics (Abs. 783-789)

Clinical track: Other (Abs. 790-791)

Physics track: Basic dosimetry and phantom and detector development (Abs. 792-801)

Physics track: Dose measurement and dose calculation (Abs. 802-832)

Physics track: Radiation protection, secondary tumour induction and low dose (incl. imaging) (Abs. 833-836)

Physics track: Treatment plan optimisation: algorithms (Abs. 837-841)

Physics track: Treatment planning: applications (Abs. 842-869)

Physics track: (Radio)biological modelling (Abs. 870-877)

Physics track: Intra-fraction motion management (Abs. 878-893)

Physics track: Inter-fraction motion management (excl. adaptive radiotherapy) (Abs. 894-904)

Physics track: Adaptive radiotherapy for inter-fraction motion management (Abs. 905-911)

Physics track: CT Imaging for treatment preparation (Abs. 912-918)

Physics track: (Quantitative) functional and biological imaging (Abs. 919-931)

Physics track: Images and analyses (Abs. 932-938)

Physics track: Implementation of new technology, techniques, clinical protocols or trials (including QA & audit) (Abs. 939-951)

Physics track: Professional and educational issues (Abs. 952)

Brachytherapy track: Breast (Abs. 953-955)

Brachytherapy track: Gynaecology (Abs. 956-963)

Brachytherapy track: Head and neck (Abs. 964-965)

Brachytherapy track: Physics (Abs. 966-973)

Brachytherapy track: Prostate (Abs. 974-979)

Radiobiology track: Molecular targeted agents and radiotherapy (Abs. 980-985)

Radiobiology track: Tumour biology and microenvironment (Abs. 986-989)

Radiobiology track: Normal tissue effects: pathogenesis and treatment (Abs. 990-992)

Radiobiology track: Biomarkers and biological imaging (Abs. 993-994)

Radiobiology track: Cellular radiation response (Abs. 995-998)

Radiobiology track: Radiobiology of protons and heavy ions (Abs. 999-1000)

RTT track: Strategies for treatment planning (Abs. 1001-1009)

RTT track: Head and neck reduction of margins and side effect (Abs. 1010)

RTT track: Elderly and radiation therapy (Abs. 1011)

RTT track: Adaptive treatments in the pelvic region (Abs. 1012-1014)

RTT track: Other topics for RTTs (Abs. 1015-1022)

RTT track: Position verification (Abs. 1023-1026)

Electronic Posters

Clinical track: Head and neck (Abs. 1027-1110)

Clinical track: CNS (Abs. 1111-1137)

Clinical track: Haematology (Abs. 1138-1143)

Clinical track: Breast (Abs. 1144-1199)

Clinical track: Lung (Abs. 1200-1255)

Clinical track: Upper GI (oesophagus, stomach, pancreas, liver) (Abs. 1256-1279)

Clinical track: Lower GI (colon, rectum, anus) (Abs. 1280-1310)

Clinical track: Gynaecological (endometrium, cervix, vagina, vulva) (Abs. 1311-1332)

Clinical track: Prostate (Abs. 1333-1385)

Clinical track: Urology-non-prostate (Abs. 1386-1390)

Clinical track: Skin cancer / malignant melanoma (Abs. 1391-1397)

Clinical track: Sarcoma (Abs. 1398-1410)

Clinical track: Paediatric tumours (Abs. 1411-1421)

Clinical track: Palliation (Abs. 1422-1440)

Clinical track: Elderly (Abs. 1441-1449)

Clinical track: Health services research / health economics (Abs. 1450-1459)

Clinical track: Communication (Abs. 1460-1462)

Clinical track: Other (Abs. 1463-1481)

Physics track: Basic dosimetry and phantom and detector development (Abs. 1482-1517)

Physics track: Dose measurement and dose calculation (Abs. 1518-1604)

Physics track: Radiation protection, secondary tumour induction and low dose (incl. imaging) (Abs. 1605-1624)

Physics track: Treatment plan optimisation: algorithms (Abs. 1625-1644)

Physics track: Treatment planning: applications (Abs. 1645-1711)

Physics track: (Radio)biological modelling (Abs. 1712-1728)

Physics track: Intra-fraction motion management (Abs. 1729-1774)

Physics track: Inter-fraction motion management (excl. adaptive radiotherapy) (Abs. 1775-1804)

Physics track: Adaptive radiotherapy for inter-fraction motion management (Abs. 1805-1825)

Physics track: CT Imaging for treatment preparation (Abs. 1826-1849)

Physics track: (Quantitative) functional and biological imaging (Abs. 1850-1885)

Physics track: Images and analyses (Abs. 1886-1910)

Physics track: Implementation of new technology, techniques, clinical protocols or trials (including QA & audit) (Abs. 1911-1952)

Physics track: Professional and educational issues (Abs. 1953-1956)

Brachytherapy track: Breast (Abs. 1957-1959)

Brachytherapy track: Gynaecology (Abs. 1960-1981)

Brachytherapy track: Head and neck (Abs. 1982-1984)

Brachytherapy track: Physics (Abs. 1985-1998)

Brachytherapy track: Prostate (Abs. 1999-2013)

Brachytherapy track: Anorectal (Abs. 2014)

Brachytherapy track: Miscellaneous (Abs. 2015-2022)

Radiobiology track: Molecular targeted agents and radiotherapy (Abs. 2023-2036)

Radiobiology track: Tumour biology and microenvironment (Abs. 2037-2040)

Radiobiology track: Normal tissue effects: pathogenesis and treatment (Abs. 2041-2046)

Radiobiology track: Biomarkers and biological imaging (Abs. 2047-2061)

Radiobiology track: Cellular radiation response (Abs. 2062-2070)

Radiobiology track: Radiobiology of protons and heavy ions (Abs. 2071-2073)

RTT track: Strategies for treatment planning (Abs. 2074-2087)

RTT track: Additional tools for contouring (Abs. 2088-2089)

RTT track: Head and neck reduction of margins and side effect (Abs. 2090-2092)

RTT track: Adaptive treatments in the pelvic region (Abs. 2093-2100)

RTT track: Other topics for RTTs (Abs. 2101-2108)

RTT track: Position verification (Abs. 2109-2119)

ABSTRACTS

Teaching Lecture: Technology assessment

SP-0001
Technology assessment
D. Verellen[1]
[1]*Universitair Ziekenhuis Brussel, Radiotherapy, Brussels, Belgium*

Radiation therapy is a highly technology driven discipline, and as treatments become more complex and automated, safe implementation and quality assurance become less intuitive. Moreover, the discipline seems to face a dichotomous situation in that on one hand there is a tendency towards truly individualized treatments adapted to patient specific characteristics, short or long term variations in anatomy and delivered dose, that require flexible interventions and optimizations. These individualized treatments call for dedicated QA/QC programs. On the other hand the automatization in delineation and treatment planning in combination with the need to optimize workflows, drive development towards template driven, almost "app-like" solutions. The latter, seems to facilitate workflows and QA/QC procedures in that a strong standardization reduces the need for detailed verification. In fact, commercial solutions are being offered as "plug-and-play" with limited user interaction and QA/QC, almost ignoring the department's responsibilities towards patient safety and quality. Mix the previous with rapid succession of upgrades and updates, and it becomes clear that the assessment and QA of technology (still) requires constant attention and vigilance. Special care should be given to the workflow and how the individual components are integrated and mutually influence each other in this constantly evolving and increasingly complex situation. The presentation will also focus on the discussion between "one shoe fits all" solutions versus the need for dedicated technology. Are these decisions driven by clinical relevance or a "me-too" argumentation? Finally, some comments will be given comparing mono-vendor and multi-vendor situations.

Teaching Lecture: CRISPR/CAS technology: from cells to mice to stem cell therapy

SP-0002
CRISPR/Cas9 technology: from cells to mice to stem cell therapy
H. Te Riele[1], T. Harmsen[1], H. Van de Vrugt[1], J. Riepsaame[1]
[1]*Netherlands Cancer Institute/Antoni van Leeuwenhoek Hospital, Division of Biological Stress Response, Amsterdam, The Netherlands*

Protocols to efficiently generate small genomic sequence alterations in a targeted fashion are of great value to fundamental and clinical applications. We are particularly interested in developing protocols to correct the genetic defects underlying bone marrow failure in Fanconi anemia patients.
The most promising protocols for targeted correction or deletion of small mutations in terms of efficiency and facility make use of site-specific nucleases designed to generate a DNA double-strand break (DSB) in the genomic DNA closely located to the site to be modified. The *Streptococcus pyogenes* derived RNA-guided nuclease Cas9 combines strong and site-specific endonuclease activity with unprecedented design simplicity. By exploiting the endogenous error-free homology-directed repair (HDR) pathway that makes use of sequence homology, repair of the DSB can be accompanied by the introduction of specific base-pair alterations. When a double- or single-stranded DNA template is offered, the HDR reaction copies subtle sequence alterations present in the template sequence effectuating their introduction into the genomic DNA. For introduction of small alterations, short chemically synthesized single-stranded DNA oligonucleotides comprising 80-120 nucleotides are highly effective. We have optimized the protocol for single base-pair substitution in the genome of mouse embryonic stem (ES) cells by oligonucleotide-templated HDR of a CRISPR/Cas9-generated break, achieving precise introduction of a planned modification in 50% of the recovered cells. Furthermore, we studied the influence of the cell's DNA mismatch repair system on the efficiency of gene modification.
Fanconi anemia (FA) is a recessive heritable disorder characterized by skeletal abnormalities, progressive anemia and cancer predisposition. The disease is caused by bi-allelic defects in any of 17 genes, designated *FANCA*, *B*, *C*, etc. When a matching donor is available, bone marrow failure can often be treated by hematopoietic stem cell transplantation. Also, bone marrow transplantation from a non-matching donor can be offered, however, this is often associated with severe complications. An alternative strategy to re-establish a functional hematopoietic system may be the functional correction of the FA defect in the patient's own cells. Ideally, the defect is restored in the patient's own hematopoietic stem cells (HSC), which can subsequently be used to reconstitute the entire hematopoietic system. For FA patients with insufficient bone marrow cellularity, the FA defect may first be corrected in patient-derived primary fibroblasts. The corrected fibroblasts subsequently need to be reprogrammed into HSCs, most likely requiring the generation of induced pluripotent stem cells (iPSCs). As a first step towards this approach, we demonstrated that CRISPR/Cas9 genome editing can effectively be exploited to repair a deleterious mutation in *Fancf* and restore the FA pathway in cultured mouse ES cells and fibroblasts.
The next step is to use this protocol to correct the *Fancf* mutation in mouse-derived hematopoietic stem cells (HSC) and iPSCs. Gene-edited HSCs will subsequently be transplanted into lethally-irradiated recipient mice to determine their potential to drive long-term hematopoiesis. These preclinical studies are aimed to pave the way for the clinical development of CRISPR/Cas9-mediated gene correction protocols to restore FA gene defects and relieve bone marrow failure in Fanconi anemia patients.

Teaching Lecture: Partial Breast Irradiation: who, when and how?

SP-0003
Partial Breast Irradiation: who, when and how?
C. Coles[1]
[1]*Addenbrooke's Hospital, Oncology Centre University of Cambridge, Cambridge, United Kingdom*

This lecture will explore the rationale for partial breast irradiation and then discuss the results from randomised trials to date. These will include intra-operative radiotherapy, brachytherapy and external beam radiotherapy. There is considerable heterogeneity between these techniques in terms of target volume, dose and fractionation and possible consequences from these differences will be considered. Appropriate patient selection for partial breast irradiation and treatment outside clinical trials will also be discussed.

Teaching Lecture: New tools to reduce toxicity in pelvic radiation

SP-0004
New tools to reduce toxicity in pelvic radiation
I. Joye[1,2], K. Haustermans[1,2]
[1]*KU Leuven - University of Leuven, Department of Oncology, Leuven, Belgium*
[2]*University Hospitals Leuven, Department of Radiation Oncology, Leuven, Belgium*

Radiotherapy plays an important role in the treatment of pelvic tumors. The advances in patients' prognosis come at the expense of radiation-induced late toxicity. Progressive cell depletion and inflammation are the leading mechanisms of acute toxicity which is observed during or shortly after treatment. The pathogenetic pathways of late toxicity, developing 90 days or later after the onset of radiotherapy, are more complex and involve processes such as vascular sclerosis and fibrosis. Since many patients have become long-term survivors, awareness and recognition of radiation-related toxicity has gained in importance and increased efforts are made for its prevention and management.
Technical innovations contribute to a reduction in radiotherapy-associated toxicity. The steep dose gradients of highly-conformal radiotherapy techniques allow for an accurate dose delivery with optimal sparing of the normal tissues. Several studies have demonstrated the dosimetrical benefit of intensity-modulated radiotherapy (IMRT) and volumetric modulated arc radiotherapy (VMAT) compared to conventional radiotherapy techniques. It has been shown that the dosimetrical benefit of IMRT translated into a clinically significant reduction in lower gastrointestinal toxicity compared with three-field conventional radiotherapy. In the near future MRI-linacs and proton therapy are likely to broaden the therapeutic window further. Prone positioning on a bellyboard reduces small bowel toxicity by pushing away the small bowel loops from the high dose region. Image-guided radiotherapy allows for an accurate definition, localization and monitoring of tumor position, size and shape before and during treatment and may help to reduce set-up margins.
Small randomized controlled trials have shown that the administration of several agents might have a beneficial effect for the prevention of acute (e.g. intrarectal amifostine, oral sulfasalazine and balsalazide) and/or late-onset radiation-induced toxicity (intrarectal beclomethasone and oral probiotics). Once severe toxicity develops, total replacement of the diet with elemental formula may be appropriate. Probiotics influence the bacterial microflora and seem promising in reducing the incidence and severity of radiation-induced diarrhea. Currently there is insufficient evidence for cytoprotective and anti-inflammatory drugs in the management of radiation-induced toxicity. Future challenges lie in the prediction of treatment-related toxicity, which might be a promising step towards an individualized risk-adapted treatment.

Teaching Lecture: Role of brachytherapy in the management of paediatric tumors

SP-0005
Role of brachytherapy in the management of paediatric tumours

C. Haie-Meder[1], H. Martelli[2], C. Chargari[3], I. Dumas[4], V. Minard-Colin[5]
[1]*Institut Gustave Roussy, Brachytherapy Service- Radiation Onocolgy Department, Villejuif, France*
[2]*CHU Bicêtre-Paris XI, Department of Pediatric Surgery, Le Kremlin-Bicêtre, France*
[3]*Gustave Roussy, Brachytherapy Service-Radiation Oncology Department, Villejuif, France*
[4]*Gustave Roussy, Physics Department, Villejuif, France*
[5]*Gustave Roussy, Pediatric Department, Villejuif, France*

As the cure rates for childhood cancers continue to improve with better local control and outcome, the incidence and management of long-term consequences are a constant challenge. Conservative treatments include a combination of chemotherapy, radiotherapy and surgery that may lead to 5 year-survival rates > 90%. The use of brachytherapy, whenever feasible, is an attractive alternative when ionizing radiation is needed for the treatment of paediatric cancers, especially rhabdomyosarcomas (RMS). In genital RMS, brachytherapy represents an alternative to radical surgery: hysterectomy or colpectomy in girls and cysto-prostatectomy in boys. When brachytherapy is properly applied, the probability of late complications remains low with a high cure-rate. At Gustave Roussy Hospital, since decades, brachytherapy –when possible– has been proposed as an alternative to external irradiation or radical surgery. So far, more than 150 children have been treated with brachytherapy, in the context of multidisciplinary approach, including chemotherapy +/- conservative surgery. The most frequent tumour sites were vagina/uterine cervix, bladder/prostate and nasolabial fold, the most common histopathological type being RMS. In a series of 39 girls treated between 1971 and 2005, interstitial brachytherapy was used for vulval tumors, and endocavitary brachytherapy was used in vaginal tumours with individually tailored moulded vaginal applicators. Among them, 20 patients were treated before 1990, where the initial tumoral extension was included in the brachytherapy volume, while after 1990, only residual disease after initial chemotherapy was treated. The usual prescribed dose was 60-65 Gy delivered in one to three brachytherapy applications, taking into account the doses to organs at risk. With a median follow of 8.4 years, local recurrence was reported in 2 patients (5.1%) in the first year following the treatment, regional relapse in 1 patient (2.6%) and distant recurrences in 7 patients (17.9%). Among the 20 patients treated before 1990, 15 presented long-term sequelae, (vaginal or urethral sclerosis or stenosis) with three requiring surgical treatment. By contrast, among the 19 patients treated after 1990, four patients had vaginal or urethral stenosis, none of them requiring surgery. A recent long-term toxicity analysis confirmed the increase of the total number of G3-4 late effects in patients treated before 1990. From 1991 to 2007, 26 boys with bladder/prostate RMS were treated with brachytherapy as a perioperative procedure. All of them underwent a conservative surgical procedure, with bladder-neck and urethra preservation. Brachytherapy was systematically performed after tumor resection, consisting of two loops encompassing the prostate and the bladder-neck area. A total dose of 60 Gy was delivered with low dose rate. With a median follow-up of 4 years (10 months-14.5 years), only one patient locally relapsed out of the brachytherapy treated area. Among 11 boys older than 6 years, 9 (82%) were normally continent, two had diurnal dribbling treated by bladder education. Recently, sexual and urinary functions, assessed with a quality of life (QoL) questionnaire, were studied in a cohort of 22 long-term survivors. The results showed that the great majority of long terms surviving males (76%) considered themselves as having normal QoL. Between 1971 and 2005, 16 children with RMS of the nasolabial fold were treated with brachytherapy. Ten presented embryonal RMS and six alveolar RMS. In 12 cases, brachytherapy was combined with local excision. The doses ranged from 50 to 70 Gy, depending on chemotherapy response, and surgical margins. With a median follow-up of 4.4 years (1.7–33), 10 patients relapsed: 4 local, 6 regional, and 2 metastatic failures were reported. In this particular context, brachytherapy provided an acceptable local control rate, but with a poor regional control. The ballistic interest of BT has been clearly demonstrated in paediatric RMS, with a very high dose gradient, sparing normal tissue and very high tumor dose. In our experience low dose-rate brachytherapy was used and recently had to move to pulsed dose-rate brachytherapy. Such conservative approach, minimizing late sequelae without detrimental effect on local control, should be offered whenever possible. This treatment is a clear demonstration of the multidisciplinary team approach, including surgeons, pediatricians and radiation oncologists.

Teaching Lecture: Challenges in MR guided radiotherapy

SP-0006
Challenges in MR guided radiotherapy

J. Jonsson[1]
[1]*Umeå University - Norrlands Universitetssjukhus, Department of Radiation Sciences, Umeå, Sweden*

Radiotherapy has relied on computed tomography (CT) for both target definition and treatment planning during the last decades. However, the increasing accuracy in radiation

delivery, through highly conformal techniques such as intensity modulated radiotherapy (IMRT) and image guided radiotherapy (IGRT), has highlighted deficiencies in target delineations based on CT. Several studies have shown large variability in target definitions based on CT, for multiple treatment sites. To address this issue, magnetic resonance imaging (MRI) has made its way into the clinical routine at modern radiotherapy departments over the last years. This, however, has presented several new problems that need to be solved.

The traditional method of including MR information in the radiotherapy process is as a complement to the CT. To accomplish this in an integrated and accurate fashion, the images must be placed in a common coordinate system through image registration. This process in itself introduces new uncertainties into the treatment chain, which must be quantified and minimized. Another method of using MR information is to base the entire treatment on MR and exclude the CT altogether. This alleviates uncertainties that stem from the image registration process, but introduces another set of problems. To perform accurate dose calculations, heterogeneity corrections based on CT data have been the clinical standard for many years. MR data does not provide information that can be used for such corrections; however, much research effort has been invested in creating valid photon attenuation maps from MR data over the last years.

Whatever method employed, MR for radiotherapy purposes also imposes practical issues that need to be addressed. The patient needs to be positioned in the same way that will be employed during the radiotherapy itself. This includes a flat table top and immobilization devices such as cast masks and tilted boards, which may not be MR compatible. For example, many radiotherapy fixation devices can contain metal parts such as nuts and bolts, which cannot be used in the MR. Plastic replacements must be used instead. Also, the standard MR coils will often not accommodate the immobilized patient, which forces MR adopters to acquire special coils or coil holders for flexible coils to be able to scan the patient in the radiotherapy treatment position.

MR images do not have the same geometric integrity as CT, which is an issue in the radiotherapy setting. The image distortions can come from the machine itself or from the patient that is in the machine. Machine specific distortions are caused by inhomogeneity in the main magnetic field or gradient non-linearity. Patient specific distortions are mostly caused by susceptibility effects. The machine specific distortions can be measured, modelled and corrected for to a certain extent, while patient specific distortions often needs to be handled by choosing imaging parameters wisely.

In the end, the images acquired from the MR scanner must be of sufficient quality to allow physicians to base the radiotherapy treatment on them. MR for radiotherapy has a different set of demands on the images than their diagnostic counterparts, for example slice thickness and gap, as well as other parameters. Also, the vast variety of MR contrasts may be an initial obstacle for radiotherapy oncologists. Many studies have shown differences in target definitions based on CT and MR images, and the effects of these changes in target volumes have not yet been studied in clinical trials.

Teaching Lecture: Patient specific quality assurance in proton therapy

SP-0007
Patient specific quality assurance in proton therapy

R. Amos[1]
[1]*University College London Hospitals NHS Foundation Trust, Department of Radiotherapy Physics, London, United Kingdom*

Interest in proton therapy continues to grow worldwide, yet access to proton therapy facilities remains relatively low compared to those offering conventional radiotherapy. As a consequence, pressure exists to maximize patient throughput in each facility. Most facilities operate 24 hours per day, 7 days per week to meet the demands of the clinical load and to complete machine maintenance, routine quality assurance, and patient specific quality assurance. With the advent of advanced delivery techniques such as pencil beam scanning, the complexity of patient specific quality assurance is increasing. However, there is a need to improve efficiency of these tests whilst maintaining accuracy.

This presentation will summarize contemporary patient specific quality assurance practice for both passive scattering and pencil beam scanning proton therapy, and describe off-line tests that potentially enable improved efficiency.

Teaching Lecture: Balancing toxicity and disease control in the evolution of radiotherapy technology

SP-0008
Balancing toxicity and disease control in the evolution of radiotherapy technology

B. O'Sullivan[1], S. Huang[2]
[1]*Princess Margaret Cancer Centre, Toronto, Canada*
[2]*Princess Margaret Cancer Centre/University of Toronto, Radiation Oncology, Toronto, Canada*

Radiotherapy (RT) is an effective option for treatment of many cancers. It offers organ and functional preservation and enhances surgical outcomes when administered pre-operatively or post-operatively, and for some diseases, such as nasopharyngeal cancer, it is often the only curative option. Disease control is generally of paramount importance to most patients during the urgent point of decision-making following diagnosis. However toxicity will almost certainly emerge as being just as relevant in the aftermath of treatment and in the subsequent follow-up period. In essence, when a patient dies of toxicity or treatment-related complications, it is just as tragic as dying of disease. The long-term result of RTOG 9111 and 9501 suggest that treatment -related deaths are blunting originally observed difference in cancer-related outcome. The recent RTOG 0617 trial was designed to test whether a higher RT dose (74 Gy vs 60 Gy) +/- cetuximab could confer a survival benefit but showed an unexpected therapeutic “disadvantage” with higher RT dose attributable to significant acute and late toxicities. These findings highlight the importance of balancing toxicity and disease control to optimize therapeutic gain. Several strategies have been employed to mitigate toxicities, such as respecting the biology of radiation injury by altered dose fractionation (typically using smaller than conventional fractions), or optimising radiotherapy technical delivery to reduce dose to vulnerable anatomy. Implementing novel RT technologies need to be closely monitored to prove clinical benefit. Historical lessons have shown that putative benefits may not always transfer to real clinical advantages since many unforeseen factors may modify potential anticipated gains. While modern RT technologies, such as IMRT-IGRT, adaptive, and IMPT provide opportunities to reduce RT late toxicity by providing more conformal dose distribution to spatially avoid normal tissue, the steps to achieve this are complex. One needs to appreciate many diverse factors. These include radiobiology of normal tissue (dose/constraints), optimal imaging quality and registration, systematic quality control involving “target” delineation to delivery, and knowledge of a variety of inherent pitfalls in the process(e.g. poor delineation, dose dumping, erratic planning, tumor or normal tissue deformation, and set up uncertainties that may emerge throughout the treatment course). For example, beam path toxicities have been reported due to “dose dumping” from parotid-sparing IMRT in head and neck cancer. Increased local failure has been observed when delivering tight margin carotid-sparing partial organ irradiation for T2 glottic cancer using vertebrae rather than laryngeal soft tissue as the image guidance surrogate. Adaptive radiotherapy appears to be feasible in some situations but the therapeutic advantages are yet to be proven and may be tedious and inefficient under the current technical configurations of many departments. Also, while intensity-modulated proton therapy (IMPT) is an attractive emerging approach that is probably able to spare normal tissue, indications and clinical benefit

are also largely unproven at this time. The path to implementing these approaches will require rigorous attention to the radiotherapy planning and delivery elements, and careful systematic and prospective documentation of tumor and normal tissue outcomes. Even if randomised trials are deemed unsuited to the setting, protocol based approaches in registered phase I/II trials are appropriate to enhance standards and should probably include audit and quality assurance processes, as well as realistic stopping rules to address unexpected or aberrant outcomes.

Symposium: Selection of patients for proton therapy

SP-0009
Patient selection for proton therapy: a clinicians view

A. Mahajan[1]
[1]*MD Anderson Cancer Center, Proton Therapy Center, Houston, USA*

Proton therapy is a radiation modality that has become increasingly available world wide over the past decade. It is an attractive radiotherapy intervention because of the charged particles dose deposition profile of characterized by the Bragg peak. By using proton therapy strategically, there is the possibility to deliver effective radiation dose to the target while reducing radiation to the surrounding non-target structures. The goals of any radiotherapy approach is to improve tumor control and/or reduce side effects and proton therapy offers an opportunity to achieve either one or both of these goals.Despite the promise of proton therapy, one must consider its associated risks and benefits, and as with any other radiation approach, to maximize the benefit to the patient. In general concepts that are useful in selecting and predicting a the benefit of proton therapy in individual patients include the following:
1) Proton therapy has the same risk of injury within the target area and high dose as other radiation therapies. For infiltrative tumors that require irradiation of a margin of normal tissue (example rhabdomyosarcoma) or those that have normal cells embedded within the tumor (example low grade glioma), the tissues receiving the high dose of radiotherapy will have similar risks of injury as non-proton approaches; therefore, one would not expect a lower risk of injury in the high dose area.
2) Since proton therapy is typically associated with a lower risk of late effectsPatient who has a very low chance of surviving a long time due to the natural history of the disease, may not benefit from proton therapy, example widely metastatic cancer.
3) Patients, for example children, who can derive benefit from normal tissue radiation dose reduction are usually good candidates
4) Patients who require high doses of radiation to achieve tumor control, but would otherwise be limited due to normal tissue tolerance, for example patients with skull base chordoma or primary or secondary liver.
5) Tumor geometry and surrounding anatomy must be evaluated to estimate the potential benefit of proton therapy. For example, a 2 year old patient requiring flank radiation for Wilms tumor may have not benefit with proton therapy, whereas an 18 year old with a paravertebral Ewing's sarcoma may have significant advantage with proton therapy.
6) Patient set up, tissue uncertainties, external devices or implanted need to be evaluated to minimize the risk of uncertainties and disruption in the proton dosimetry.
7) Proton therapy may be a good option for re-irradiation in selected patients.In summary, proton therapy can be an excellent option to provide better local control and/or reduced toxicities in selected patients.

SP-0010
Selection of patients for proton therapy: a physicists view

M. Hoogeman[1], T. Arts[1], S. Van de Water[1], S. Van der Voort[1], Z. Perko[2], D. Lathouwers[2], S. Breedveld[1], B. Heijmen[1]
[1]*Erasmus Medical Center Rotterdam, Erasmus MC Cancer Center, Rotterdam, The Netherlands*
[2]*Delft University of Technology, Radiation Science and Technology, Delft, The Netherlands*

Intensity Modulated Proton therapy (IMPT) is a highly promising approach for radiation treatment of cancer patients due to its increased potential to reduce side effects and improve quality of life compared to contemporary radiation therapy techniques, such as IMRT. However, IMPT is associated with high costs and hence limited availability. Ideally, patient selection for IMPT should be based on the highest expected complication reduction compared to IMRT.
For a given patient, it is possible to predict the risk of side effects for proton and photon therapy by applying Normal Tissue Complication Probabilities (NTCP) models to optimized dose distributions. Only patients with clinically relevant reductions in NTCP exceeding minimum pre-defined thresholds will then qualify for proton therapy. While this approach should guarantee effective use of proton therapy, there are several concerns that will be discussed in this presentation:
1. The generation of a radiotherapy treatment plan is a complex procedure and its quality is highly dependent on the planner skills. To enable unbiased comparisons between IMPT and IMRT for each patient, automation of the treatment planning process is imperative.
2. IMPT is highly susceptible to inaccuracies in patient setup, anatomic changes, and to uncertainties in the calculation of the proton range. In IMRT, uncertainties in dose delivery are accounted for in the CTV-to-PTV margin. In IMPT, however, the PTV concept is not applicable. Alternatively, robust treatment planning can be used to take into account patient setup and range uncertainties. However, it is currently unknown which robustness settings need to be used to achieve an adequate target coverage for given population-based distributions of setup and range errors.
3. Image-guidance technology improves the accuracy of radiation therapy delivery, however its impact and current state-of-the-art may vary for proton and photon radiotherapy due to the physical differences between protons and photons and for historical reasons. The applied image-guidance technology will have an impact on the magnitude of NTCP reduction and hence on the selection of patients qualifying for proton therapy.

SP-0011
Future selection practice for proton therapy: selection of patients based on treatment planning comparison and NTCP-modelling

H. Langendijk[1]
[1]*University Medical Center Groningen, Department of Radiation Oncology, Groningen, The Netherlands*

The last decade, many new radiation delivery techniques have been clinically introduced without being subjected to randomized controlled trials. Many of these new techniques have been introduced in order to reduce the dose to the healthy tissues and subsequently to prevent radiation-induced side effects. Due to its superior beam properties, radiotherapy with protons compared to photons enables similar dose administration to the target volume with substantially lower dose to the normal tissue. In the Netherlands, we applied a 4-step model-based approach to select patients for proton therapy and to validate the benefit of protons compared to photons with regard to reducing the risk on radiation-induced side effects.
Step 1 consists of the development and validation of multivariable Normal Tissue Complication Probability (NTCP) models. NTCP models describe the relationship between radiation dose distribution parameters and the probability of a given side effect (NTCP-value). One of the output parameters of this step are the most relevant Dose Volume Histogram (DVH) parameters that can be used to optimize radiation treatment.
Step 2 includes in silico planning comparative studies. In this phase protons are compared with photons with regard to their ability to reduce the most relevant DVH-parameters resulting from step 1 (ΔDose).
Step 3: Integration step 1 and 2. By integrating the results of the individual in silico planning comparison into the validated

NTCP-models, the differences in dose can be translated into a difference in NTCP-value in each individual patient (ΔNTCP). In the Netherlands, a national consensus has been reached regarding the threshold for (ΔNTCP
Finally, the potential benefits of protons can be clinically validated in step 4, based on external validation of the NTCP-models when patients are treated with protons. The model-based approach is an evidence-based methods for selection and validation of new radiation technologies.

Symposium: Mitigating normal tissue toxicity

SP-0012

The use of ACE inhibitors to attenuate thoracic irradiation-induced cardiopulmonary toxicity.

S.J. Van der Veen[1]
[1]*University Medical Center Groningen UMCG and University of Groningen RUG, Cell Biology and Radiation Oncology, Groningen, The Netherlands*

Synopsis:

In thoracic irradiation, the maximum radiation dose is restricted by the risk of radiation-induced cardiopulmonary damage and dysfunction limiting tumor control. Unfortunately, current clinical practice does not include preventative measures to attenuate radiation-induced lung or cardiac toxicity. Inhibition of the renin-angiotensin system (RAS) seems to be an alluring strategy for attenuating radiation-induced cardiopulmonary dysfunction.
Interestingly, angiotensin-converting enzyme inhibitors (ACEi) have been shown to reduce the risk of radiation-induced respiratory dysfunction in preclinical (1) and clinical studies (2). More recently a study in rats showed that ACEi reduces respiratory dysfunction indirectly by reducing acute heart damage (3).
So far, the mechanisms of the protective effect of ACEi on radiation-induced toxicity are not clear. Apart from their hypotensive action, ACEi are known to have other properties such as an anti-inflammatory action. Further, it has been suggested that the sulfhydryl group in the molecular structure of captopril confers in a free radical scavenger activity. All these effects can account in part for its radioprotection. Besides, it might act as an antioxidant to reduce inflammatory reactive oxygen species and thus mitigate radiation-induced toxicity.
To conclude, ACE inhibitors have been shown to mitigate radiation-induced cardio-/pulmonary toxicity in (pre)clinical models. However, the mechanisms of action are not clear. As such the use of ACE inhibitors should be further evaluated as a strategy to reduce cardiopulmonary complications induced by radiotherapy to the thoracic area.

1. Ghosh SN, Zhang R, Fish BL, et al. Renin-angiotensin system suppression mitigates experimental radiation pneumonitis. *Int J Radiat Oncol Biol Phys* 2009;75:1528-36.
2. Kharofa J, Cohen EP, Tomic R, et al. Decreased risk of radiation pneumonitis with incidental concurrent use of angiotensin-converting enzyme inhibitors and thoracic radiation therapy. *Int J Radiat Oncol Biol Phys* 2012;84:238-43.
3. van der Veen SJ, Ghobadi G, de Boer RA, et al. ACE inhibition attenuates radiation-induced cardiopulmonary damage. *Radiother Oncol* 2015;114:96-103.

SP-0013

Radiation-induced musculosqueletic late damages: possible clinical cure or simple mitigation?

S. Delanian[1]
[1]*Hôpital Saint-Louis- APHP, Oncologie-Radiothérapie, Paris, France*

RI musculo-squeletic sequelae combine opposite tissular aspects of fibrosis and atrophy in an heterogeneous patchwork comprising concomitant active cellular and sclerotic matricial areas. Tissue remodeling follow early, subacute, chronic inflammatory changes, then fibrosis and necrosis, that provides signaling pathways through growth factors and their receptors.
In medicine, clinical cure of a chronic disease is never binary or surgical, if exists, because of the pathologic underground network well-established in the tissues.
Cure for radiation-induced (RI) late damages should be approach by a strategy using a hierarchical control of accurate protagonists. During last decades, each therapeutic intervention has illustrated successively one of the facets of this fibrotic process:
- In seventies, STEROIDS, then non anti-inflammatory drugs, showed able to stop acute RIF progression and are always required today as the first treatment in all sequelae, while anti-collagenic drugs were too toxic.
- In eighties, vascular approach revealed antithrombotic help in some acute aspects (HEPARIN), and interesting role of PENTOXIFYLLINE (speed healing) or HBO.
- In nineties, successful clinical use of superoxide dismutase (SOD) allowed to bring to light reactive oxygen species (ROS)
- fibroblasts and their related anti-oxidant strategy, then PENTOXIFYLLINE-VITAMIN E (PE) combination. The fibrotic clinical regression was slow but measurable, followed by convincing "preclinical" studies (histological reversion, in vitro modulation): first cases of fibrotic clinical cure [1,2].
- Then anticytokines (TGFβ, CTGF, …).
- After 2000, adding clodronate, in a PENTOCLO combination, allowed speeder and durable clinical RI responses, highlighting its anti-macrophagic effect on bone necrosis : first cases of osteoradionecrosis clinical cure [3]. However, therapeutic range of these drugs is tight, related to bisphosphonate absence of specificity and the bivalent macrophagic action (M1/M2 populations).
Clinical cure is a difficult art: it should take in account all these several facets. In the future, controlled trials and preclinical studies are necessary to identify best antifibrotic agents (phenotypic revesion of deficient cells), and organ specific targeted drugs and/or stem cell therapy (compensate tissular depletion after cell death), to obtain regular clinical cure if any.

REF [1] Delanian et al. Kinetics of response to long-term treatment combining pentoxifylline - tocopherol in patients with superficial radiation-induced fibrosis. J Clin Oncol 2005, 23, 8570. [2] Lefaix et al. Striking regression of subcutaneous fibrosis induced by high doses of gamma-rays using a combination of pentoxifylline and tocopherol: an experimental study. IJROBP 1999, 43, 839. [3] Delanian et al. Complete restoration of refractory mandibular osteoradionecrosis by prolonged treatment with a pentoxifylline-tocopherol-clodronate combination (PENTOCLO): phase II trial. IJROBP 2011, 80: 832.

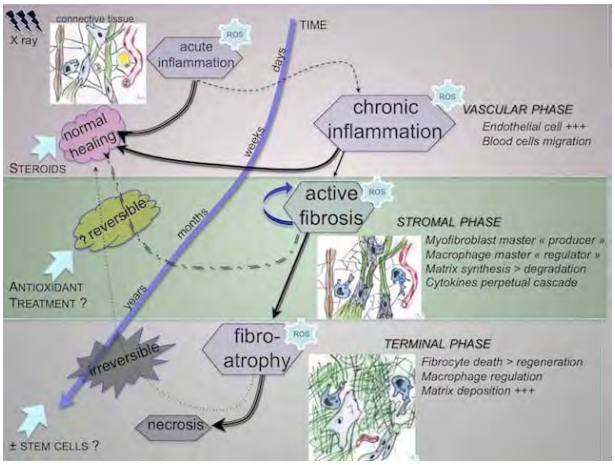

Normal 0 21 false false false FR JA X-NONE

SP-0014

Radiation-induced lung fibrosis is associated with M2 interstitial and hybrid alveolar macrophages

L. Meziani[1], M. Mondini[1], B. Petit[2], M.C. Vozenin[2], E. Deutsch[1]
[1]*Institut Gustave Roussy, INSERM U1030, Villejuif, France*
[2]*Centre Hospitalier Universitaire Vaudois, Radio-Oncologie/Radiothérapie, Lausanne, Switzerland*

Radiation-induced fibrosis is a delayed complication of radiotherapy often associated with chronic inflammatory process and macrophage infiltration. Nowadays, macrophages are suggested to be important cellular contributors to fibrogenic process, but their implication in the context of RIF is not well known.
To investigate the role of macrophages in RIF we have used a classical experimental model of lung fibrosis developed in C57Bl/6 mice after 16Gy thorax-IR. We then profiled both alveolar macrophages (AM) and interstitial macrophages (IM) during the various steps of the fibrogenic process.
We confirmed the fact that total lung irradiation at 16Gy (IR) induces an interstitial fibrosis associated with delayed recruitment of pulmonary macrophages. We found a transient depletion of AM associated with cytokine secretion during the acute post-IR phase (15 days), followed by an active repopulation and an enhanced number of AM during the late post-IR phase (20 weeks). Interestingly, AM were mostly recruited from the bone marrow and exhibit a hybrid polarization (M1/M2) associated with up-regulation of Th1 and Th2 cytokines. The number of M2-polarized IM significantly increased during the late time points after irradiation and a down-regulation of Th1 cytokine was measured in tissue lysate. These results suggest a differential contribution of hybrid AM *vs*M2-IM to fibrogenesis. Interestingly, in contrast to activated hybrid AM, activated M2-IM were able to induce fibroblast activation *in vitro* mediated by an enhanced TGF-ß1 expression suggesting a profibrotic role of M2-IM. Specific depletion of hybrid AM using intranasal administration of clodrosome increased radiation-induced fibrosis score and enhanced M2-IM infiltration suggesting a protective role of hybrid AM.
These present study shows a dual and opposite contribution of alevolar *versus* intertitial macrophages in radiation-induced fibrosis and identify M2-IM as a potential therapeutic target to treat radiation-induced fibrosis.

Symposium: Regional nodal irradiation for breast cancer

SP-0015

The axilla- less surgery, more radiotherapy?

M.I. Algara López[1]
[1]*Hospital de la Esperança, Radiation Oncology, Barcelona, Spain*

Irradiation of lymph node areas in breast cancer patients, especially in early stages of the disease is a controversial topic. The recommendation to irradiate lymph nodes is clearly indicated in patients with more than three involved nodes. In these cases, after standard lymphadenectomy, the volumes to irradiate include supraclavicular fossa and axillary level III nodes. Until a few years ago, irradiation of axillary levels I and II, are reserved for cases of very large axillary involvement, or in patients whom lymphadenectomy was insufficient (less than 10 lymph nodes resected). However, when only 1 to 3 nodes are involved, there is no unanimity on the radiotherapy recommendations, despite several studies having show clearly a disease free survival improvement in irradiated patients. The Canadian trial NCIC-CTG MA20, including high risk patients, most of them with 1 to 3 involved nodes, showed that local irradiation with regional lymph node irradiation improved disease-free survival, both loco-regional and distant disease control. The EORTC trial also demonstrates the same findings: regional irradiation in breast cancer patients improve even the overall survival. Therefore the current trend, described in international guidelines, lymph node irradiation is recommended for all patients regardless of the number of positive nodes. Nevertheless, the therapeutic value of axillary lymphadenectomy has been questioned for a long time. The ACOSOG Z0011 study results have caused clinical practice changes since many axillary dissections are being avoided. Even several clinical practice guidelines, including prestigious ones such as those of National Comprehensive Cancer Network, don't recommend lymphadenectomy. The ACOSOG Z0011 does not exactly describe the irradiated nodal volumes exactly. Therefore, the nodal volumes to include in the irradiation treatment of early stages of breast cancer remains under discussion, especially without axillary lymphadenectomy despite involvement of sentinel lymph nodes. In most cases, breast irradiation with tangent fields implies certain "incidental" of axillary level I, and also in some cases the level II. For this reason, some groups have decided to avoid intentional irradiation of these axillary areas, while others advocate to irradiate them intentionally, without clear evidence to do that. The AMAROS trial demonstrated that lymph node radiotherapy obtains the same results as axillary dissection in node-positive patients without primary systemic treatment, with less morbidity. Therefore, it is possible to replace the surgery with radiation. The current situation is that some groups decide to irradiate lymph node in cases with positive sentinel node without lymphadenectomy and other groups in these cases do not treat the lymph node, and accept that some incidental irradiation will arrive by tangential fields. But, we do not know which patients, with positive nodes, do not require lymph node irradiation. It is possible that in patients with low axillary involvement intentional irradiation would not be necessary. In order to demonstrate this hypothesis, we have started the OPTYMAL trial (www.clinicaltrials.gov /ct2/show/NCT02335957?term=osna&rank=7) to investigate the non-inferiority of incidental versus intentional irradiation of axillary nodes in patients with axillary involvement of 250-15000 copies/uL with One Step Nucleic Acid Amplification method (OSNA). We decided to use this method to unify the pathological reports. This international multicenter trial must help us to elucidate the necessity of node area irradiation by combining with reliable information about the tumor load involvement in axillary nodes.

SP-0016

The internal mammary chain - should we treat it in every node-positive patient?

P. Poortmans[1]
[1]*Radboud UMC, Department of Radiation Oncology, Nijmegen, The Netherlands*

Locoregional radiation therapy (RT) improves locoregional control and survival for patients treated with breast conserving therapy and for patients after mastectomy with risk factors including involved axillary lymph nodes. In the past, however, this treatment could be linked to an increased risk for late cardiovascular morbidity and mortality as a result of cardiac exposure to radiation. This was especially the case for the treatment of the internal mammary lymph node target volume, for which this was abandoned by many

radiation oncology centers worldwide. We now know that these side effects can most often be attributed to the use of outdated RT techniques. As treatment techniques started to improve, enabling to limit the dose to the organs at risk, prospective trials were initiated to evaluate the contribution of lymph node treatment to overall outcome for early stage breast cancer patients. The results of several studies were presented over the last couple of years. They demonstrate that an increased disease-free survival rate following a decrease of the risk of distant metastases can be obtained in patients with risk factors, including those with involvement of the axillary lymph nodes and those with a centrally or medially located primary tumour. Moreover, a trend towards an improved overall and (statistically significant for some of the studies) breast cancer specific survival was demonstrated. No increase was seen in the other causes of death and, at a median follow-up of around 10 years, no significant or clinical relevant increased toxicity was found, apart from a slight increase in the risk for pulmonary toxicity. The concept of "any recurrences", introduced by the EBCTCG in 2011, as important endpoint of the evaluation of the effect of all types of treatments (including locoregional ones such as surgery and RT) fits much better to the interpretation of the recently presented results. In this era of earlier diagnosis and more widespread use of adjuvant systemic treatments leading to a 10-year overall survival exceeding 80%, clinically detectable locoregional recurrences as a separate endpoint might indeed be considered as less relevant. Firstly, the patient will be affected heavily by any type of recurrence and secondly because of the complex interaction between the efficacy of systemic treatments with the influence of loco-regional treatments on overall survival. By merely focusing on locoregional control, we risk to neglect that once distant metastases are found no further efforts are undertaken to detect locoregional recurrences. By eliminating microscopically non-detectable cancer cells in the lymph nodes with RT, the risk of secondary metastasizing of those cells and thereby ultimately the overall risk of recurrence of the breast cancer will be reduced. This is in line with the findings of the EORTC trial in which a trend was seen towards more benefit for patients who where treated with both hormonal treatment and chemotherapy and less benefit for the small group of patients with 10 or more involved axillary lymph nodes: patients with a better prognosis (lower risk factors and/or better systemic therapy) experience more benefit from locoregional treatments. With modern RT techniques, the benefits of optimizing locoregional control will likely not be counterbalanced by side effects including late cardiovascular mortality. Moreover, the new ESTRO guidelines for target volume delineation clearly reduce the size of the target volumes while simultaneously considering the regional lymph nodes even more than before as a whole. We also expect that the real benefit of loco-regional RT used to be diluted in the past (including the recently presented trials) by suboptimal dose coverage of the target volumes. Therefore, we expect that with contemporary RT techniques and appropriate target volume delineation, not only a significant reduction of the dose to the organs at risk but also a much better coverage of especially the internal mammary lymph nodes is achievable, which is likely to result in a further improvement of the benefit of locoregional RT for patients with early stage breast cancer that have a risk for bearing microscopical tumor deposits in the regional lymph nodes.

SP-0017

Technical approaches to regional lymph node irradiation for breast cancer

A. Kirby[1]

[1]*The Institute of Cancer Research and The Royal Marsden NHS Foundation Trust, Radiation Oncology, London, United Kingdom*

The quality of radiotherapeutic approaches to treating locoregional lymph nodes in breast cancer is improving. This talk will review the latest evidence pertaining to each aspect of the planning and treatment pathway in order to inform best practice. Recently published atlases capable of improving consistency in outlining target and non-target volumes will be reviewed. Using data relating outcomes to dosimetry, we will then review the evidence base for target and non-target tissue dose constraints and objectives. Different radiotherapeutic approaches including breath-hold, volumetric-modulated arc therapy, and proton beam therapy will be compared in terms of dosimetry and resource implications. Potential efficiency savings in the treatment pathway will also be discussed together with a review of the possible impact of bluer-sky technologies.

Symposium: Assessment and management of rectal morbidity

SP-0018

Towards a scoring system built on six distinct radiation-induced illnesses producing late gastrointestinal effects

G. Steineck[1], R. Jörnsten[2], V. Skokic[1], U. Wilderäng[1], G. Dunberger[1]

[1]*Göteborg University, Department of Oncology- Institute of Clinical Sciences, Göteborg, Sweden*

[2]*Göteborg University, Chalmer's Technical Institute, Göteborg, Sweden*

As shown in randomized studies, radiotherapy has a critical role when we cure prostate cancer by using multimodal treatment strategies. We frequently use radiotherapy to cure gynecological cancer. Both Intensity-Modulated Radiation Therapy and Volumetric Modulated Arc Therapy have the potential to drastically increase the ratio between possibilities for cure and risk of late effects. Still, crude measurements of patient-reported outcomes, as well as factors that may modify the how radiation cause late effects, compromise these possibilities. We lack details to provide parameters from dose-volume modelling to utilize the full potential of these new technologies. Concerning bowel health, current scoring systems of radiation-induced late gastrointestinal must be refined. Important socially invalidating symptoms are not scored. An example is unexpected defecation into clothing – not sensing the need to go to the toilet and a sudden defecation into clothing as if one were already on the toilet. We documented this symptom among 11 percent of gynecological-cancer survivors. Another example is frequent and uncontrolled noisy flatulence. Traditional scoring systems have scales that do not distinguish or clearly depict person-incidence (events per individual per time unit), intensity and duration. But, probably most important, as we learn that decreased bowel health depends on several different types of radiation-induced illness, we understand that grouping symptoms from different illnesses together in a score compromises our ability to acquire knowledge for prevention or relief. We cannot disentangle these different radiation-induced illnesses when symptoms from several illnesses are grouped together in the data sets we retrieve. Clearly, new strategies are needed. In my talk, I will propose a scoring system based on the data indicating that the at least 28 radiotherapy-induced atomized late gastrointestinal symptoms derive from six distinct illnesses, that is, six sets of risk organs or mechanisms. We have data from around 1500 survivors supporting this position. As we accumulate data for each of these six illnesses, we can define parameters in dose-volume models built on patient-reported outcomes much better than we previously could. Possibly we can also learn how, by employing probiotics or dietary changes, we can influence the interplay between the gut flora and stem-cell renewal to counteract inflammatory processes that probably are important for several of the six illnesses. Moreover, the knowledge may stimulate development of mouse models in which we can test, for example, how different bacterial species influence radiation-induced inflammation in the rectal wall. In the talk, I will give preliminary results from the establishment of such a model. A simplified nomenclature could label the six illnesses as involving processes resulting in leakage-related symptoms, urgency-related symptoms, constipation-related symptoms, symptoms

related to excessive mucus production, symptoms related excessive gas production gas and symptoms related excessive blood production. A modern scoring system should have two or more atomized symptoms related to each of the six illnesses and appropriate response scales for frequency, intensity and duration.

SP-0019
Measuring anorectal toxicity and function
D. Vordermark[1]
[1]*Martin Luther University Halle-Wittenberg, Radiation Oncology, Halle / Saale, Germany*

Anorectal toxicity is a relevant side effect of pelvic radiotherapy for rectal, anal, gynaecologic and prostate cancer. Toxicity can be scored objectively by the physician according to established systems such as the CTCAE classification. In recent years, patient-reported outcomes (PROs) have received increasing attention when evaluating acute toxicity as well as late effects of cancer treatment. These include information directly obtained from the patient on symptoms and impairment as well as on quality of life. This presentation will focus on validated instruments to measure PROs related to anorectal function, including quality-of-life questionnaires and organ modules, e. g. those developed by the EORTC Quality of Life Group, and symptom questionnaires e. g. to measure continence. Objective measurements to quantify anorectal function such as sphincter manometry and endoscopic scores will be reviewed. The relationship between PROs and objective function assessment with physician-rated toxicity will be addressed. The outcomes for the above endpoints in major trials of pelvic radiotherapy will be presented, with a focus on rectal cancer and the effects of treatment concepts including short-course radiotherapy and long-course chemoradiation. Finally, dose-volume constraints in pelvic radiotherapy treatment planning and potential effects of highly conformal techniques such as IMRT or VMAT on anorectal symptoms, function and quality of life will be examined.

SP-0020
Rectal spacers to minimise morbidity in radiotherapy for prostate cancer
M. Pinkawa[1]
Uniklink RWTH Aachen, Radiation Oncology, Aachen, Germany

Radiotherapy is a well recognozed curative treatment option for localized prostate cancer. Optimal tumor control rates can only be achieved with high local doses, associated with a considerable risk of rectal toxicity - regarded as dose-limiting toxicity. Apart from already widely adapted technical advances, as intensity-modulated radiation therapy and image-guided radiotherapy techniques, the application of spacers placed between the prostate and anterior rectal wall has been increasingly used in the last years.
Biodegradable spacers, including hydrogel, hyaluronic acid, collagen or an implantable balloon can create the desired effect. They can be injected or inserted in a short procedure under transrectal ultrasound guidance via a transperineal approach. A distance of about 1.0-1.5cm is usually achieved between the prostate and rectum, excluding the rectal wall from the high isodoses. Several studies have shown well tolerated injection procedures and treatments. Apart from considerable reduction of rectal dose compared to radiotherapy without a spacer, clinical toxiciyt results are favourable. A prospective randomized trial demonstrated a reduction of rectal toxicity after hydrogel injection in men undergoing prostate image-guided intensity-modulated radiation therapy. The results are encouraging for continuing evaluation in dose escalation, hypofractionation, stereotactic radiotherapy or re-irradiation trials in the future.

Symposium: Towards user oriented QA procedures for treatment verification

SP-0021
How to ensure the quality in brachytherapy treatment planning systems?
F.A. Siebert[1]
[1]*University Hospital S-H Campus Kiel, Academic Physics, Kiel, Germany*

Treatment planning systems (TPSs) are of high importance in modern brachytherapy. The users rely on the output of these special software; wrong calculations may result in severe patient harm. Thus it is necessary to systematically check these software programs.
Many checks in TPSs are identical for high-dose-rate brachytherapy with afterloaders and low-dose-rate brachytherapy with seeds. But some differences exist, e.g. as checking of afterloader parameters.
After the installation of the software the acceptance test is to be carried out. This test protocol is typically provided by the vendor and should be passed before further checking. In a second step the commissioning is carried out. In this procedure all clinical relevant data and properties of the TPS must be tested and reported. Examples for items to check are:
- Afterloader characteristics (number of channels, min./max. channel lengths, max. allowed dwell time, …)
- Source characteristics (nuclide, decay, …)
- TG-43 consensus dataFor Model-based dose calculation algorithms, commissioning following TG-186 report
- Applicator checks

To ensure the consistency and data integrity of the TPS periodical tests should be performed after the commissioning. Important points are to validate the integrity of base parameters of the TG-43 data and the recalculation of patient treatment plans.
Most TPSs offer inverse planning algorithms. The algorithm itself is often not fully transparent by the user, thus comparison with manual calculations is not practical. Nevertheless, the consistency of such planning technique can be checked by recalculation of a test plan using a constant parameter set. In addition to the tests above end-to-end tests can be performed to check the whole treatment chain, including imaging, TPS, afterloader, and data transfer.

SP-0022
Imaging
T.P. Hellebust[1]
[1]*Oslo University Hospital, Dep. of Medical Physics, Oslo, Norway*

In the past decade 3D image guided brachytherapy has been introduced into clinical practice worldwide. This enables conformation of the dose distribution to the target volume and avoidance of high dose to organs at risk (OAR) using CT, MR, and/or ultrasound (US) imaging. In such modern techniques sectional images give the relationship of the shape and the position of the applicator(s)/sources in relation to the anatomy of the patients. This means that the quality assurance (QA) programs also should include specific topics related to image quality additional to traditional procedures checking the source strengths and dose calculation issues. QA for image quality is well established in the area diagnostic and many of these procedures can be used also for brachytherapy. However, the procedures should be modified in order to reflect the conditions of use in brachytherapy compared to a diagnostic session.
To optimise the image quality in diagnostic procedures dedicated phantom is often used. Various image quality parameters are tested by evaluation for example slice thickness, spatial resolution, uniformity and noise. In contrast to diagnostic imaging, the ability to reconstruct several points or a geometric structure with high accuracy is crucial in brachytherapy. Therefore, a procedure to check the geometric accuracy have to be included in a QA program.

A phantom with known geometry should be used, either including markers with known relative coordinates or test objects with known shapes and volumes. The design of the phantom will be depend of the modality to be tested.
For ultrasound imaging the AAPM Task Group 128 includes a list with 8 elements of a phantom that allow for all the recommended tests [1]. It is referred to a commercial phantom that include nylon monofilaments in a N-shaped pattern and spherical and non-spherical volume in order to test key imaging parameters such as depth of penetration, axial and lateral resolution, distance, area and volume measurements and geometric consistency.
Roué et al used a commercial PMMA phantom with 25 stainless steel markers with known relative position to check the geometric accuracy of CT and conventional x-ray imaging [2]. A phantom including several inserts with different density can be used to check the volume reconstruction accuracy for CT. Several commercial phantoms are available.
It is well known that geometrical distortions can frequently occur in MR images. The magnitude of the distortions should be investigated by using phantoms with markers or tubes filled with for example Cu2+-doped water solution. Additional, the influence of an applicator should also be investigated since for example the presence of a titanium applicator may produce geometric distortion in a high field MR machine.
The slice thickness will also influence the ability to reconstruct the geometry correctly. With too large distance between the slices the partial volume effect will influence the accuracy of the volume reconstruction [3]. On the other hand, de Brabandere et al showed that too small distance between the slices decreased the accuracy of seed detection in a dedicated phantom with agarose gel and 60 iodine seeds with known position using MR imaging [4].
References
1. Pfeiffer D et al. AAPM Task Group 128: Quality assurance tests for prostate brachytherapy ultrasound. Med Phys 2008;35:5471-5489.
2. Roué A et al. The EQUAL-ESTRO audit on geometric reconstruction techniques in brachytherapy. Radiother Oncol 2006;78:78-83.
3. Kirisits C et al. Accuracy of volume and DVH parameters determined with different brachytherapy treatment planning systems. Radiother Oncol 2007;84:290-297.
4.De Brabandere M et al. Accuracy of seed reconstruction in prostate postplanning studied with a CT- and MRI-compatible phantom. Radiother Oncol 2006;79:190-197.

SP-0023
Dose verification
K. Tanderup[1]
[1]*Aarhus University Hospital, Department of Oncology, Aarhus C, Denmark*

Any radiotherapy delivery is associated with uncertainties and with risk of misadministration/error. Misadministration/error refers to treatment incidents/accidents which can be prevented, while uncertainties can only be controlled to a certain degree and the residual variation must be accounted for through tolerances and treatment margins. Patient safety through prevention of radiation dose misadministration is highly prioritised and several authorities and societies worldwide are focusing on radiation safety and medical events. In 2004, the International Commission of Radiation Protection (ICRP) reported an analysis of 500 radiation events in BT. This investigation and others have shown that a significant share of radiation events are caused by human errors related to the manual procedures of BT. Verification in radiation therapy means the whole process of proof that planned dose is delivered to the patient within a specific level of accuracy. During the last two decades enormous developments and technological innovations in the field of external beam radiotherapy (EBRT) treatment verification have taken place. These developments have focussed on imaging technologies for 2D and 3D (and very actually also 4D) localization and anatomy reconstruction under treatment delivery conditions. Striking innovations have been imaging technologies such as flat panel detectors, cone beam CT (CBCT), and most recently MRI, which is integrated with the linear accelerators. The combination of 3D-imaging techniques and dose measurements enables the estimation of the daily 3D-dose delivery in the patient anatomy. In contrast, on-board or real-time treatment verification of BT is currently not performed, simply because adequate tools are not available. There is currently a striking unbalance between the availability of treatment verification technology for EBRT and BT, and consequently a different level of safety. Adding even further to this unbalance, BT is related with higher risk of major dose misadministration than EBRT, since BT involves: 1) more manual procedures (e.g. assembly and implantation of applicators, catheter reconstruction, and guide tube connection), 2) mechanical equipment with a higher susceptibility to malfunction (e.g. source cable drive and applicators), 3) more frequent application of hypo-fractionation schedules, and finally 4) steeper dose gradients. New methodologies for treatment verification are highly warranted. Dose and source geometry are closely linked entities in brachytherapy. Dose calculation with TG43 is the current standard of dose calculation in brachytherapy, and has excellent accuracy in most clinical scenarios. TG43 is based on geometry. Given a direct correspondence between brachytherapy source geometry and dose, a geometric verification is nearly equivalent to a dosimetric verification. There are only few error scenarios where source geometry would be correct, but not dosimetry – e.g. source mis-calibration. Therefore several novel “on-board” treatment verification tools are focused on verification of geometry: EM tracking of catheters, flat panel monitoring of source progression, fluoroscopy, and real-time in vivo dosimetry. Given the source geometry is correct, the next important step is to secure that the relation between sources and anatomy is correct. This last step is typically explored with imaging. Combinations between different verification tools may be the way to proceed to reach a higher level of treatment verification in brachytherapy which address geometry, patient anatomy and consequent dose delivery to the patient. The presentation will outline current developments in “on-board” treatment verification tools. The table below shows the current status of treatment verification in EBRT and BT, and indicates visions that can bring brachytherapy treatment verification forward.

Symposium: Robust and accurate functional MRI for radiotherapy

SP-0024
Needs and technical requirements for functional MRI in radiotherapy
U.A. Van der Heide[1]
[1]*The Netherlands Cancer Institute, Department of Radiation Oncology, Amsterdam, The Netherlands*

Anatomical imaging with T1 and T2-weighted MRI is increasingly used in combination with CT for precise delineation of tumors and normal structures. MRI also offers functional techniques, such as diffusion-weighted MRI (DWI) and dynamic contrast-enhanced MRI (DCE-MRI). These can be applied in radiotherapy for tissue classification, monitoring of treatment response as well as for dose painting. In the diagnostic setting, these sequences are often part of routine scanning protocols. However, as for anatomical MRI sequences, there are some specific issues that need to be considered when applying these techniques in radiotherapy. For image registration with the planning CT, patients need to be scanned in treatment position. If the functional images are used for target delineation, their geometrical fidelity needs to be verified. In particular diffusion-weighted MRI is prone to geometrical distortions. Methods to reduce these distortions will be discussed. The spatial resolution of functional imaging tends to be lower than that of anatomical imaging. Although acquisition with small imaging voxels is feasible, this doesn’t mean that the functional quantity (apparent diffusion coefficient for DWI and tracer kinetics parameters for DCE-MRI) can be reliably determined in a

single voxel. Test-retest measurements are a method to determine the smallest volume for which a reliable measurement can be obtained. A key asset of functional imaging is the capacity to measure physical quantities in tissue rather than contrast. In particular for longitudinal studies, monitoring treatment response, or in multi-center studies, this is critical. For radiotherapy dose painting it is necessary to know which threshold should be used to define a subvolume of the target for dose escalation. In the presentation, various quantitative methods and their reliability will be discussed.

SP-0025

Variation in DCE-MRI methodology and its implications for radiotherapy

A. Garpebring[1]
[1]*Umeå University, Department of Radiation Sciences, Umeå, Sweden*

Dynamic contrast-enhanced magnetic resonance imaging (DCE-MRI) is a technique based on rapid acquisition of a series of images depicting the uptake of a contrast agent (CA) in tissue. Through mathematical modeling of the CA's influence on the MR signal and the distribution of CA in the tissue, physiological parameters can be obtained on a voxel by voxel level.
These parameters, which for instance reflect flow, vessel integrity, cell and vessel density, are highly relevant in cancer treatments such as radiotherapy (RT). Several studies have shown that pretreatment parameter values as well as changes during RT can be correlated with outcome. However, drawing firm conclusions on the practical value of DCE-MRI in RT is currently difficult.
The reason for this difficulty has its roots in the complexity of performing a DCE-MRI study. Obtaining accurate quantitative parameter values reflecting primarily the physiology of a tumor requires advanced imaging as well as complicated post processing. Unfortunately, even though state of the art acquisition and analysis is performed it is likely that influences from the precise acquisition settings and the analysis tools remain in the final result. Hence it is crucial that all variations during a study is minimized to maximize the sensitivity.
Not only is it of great importance to reduce the variability within a study, ideally this should also be the case between studies. But here we have a significant issue. There are a large number of unavoidable trade-offs in DCE-MRI. For instance between spatial and temporal resolution and between accuracy, complexity and robustness of the analysis. Usually each group performing a study make their own decision on where to compromise and what parameters to evaluate. Although this may be optimal in each study it is problematic when drawing conclusions on the overall value of DCE-MRI in RT.
Of this reason several authors are calling for standardization of DCE-MRI acquisition and analysis. One organization that has responded to this call is the Quantitative Imaging Biomarkers Alliance (QIBA) which has published guidelines for standardizing DCE-MRI. In a comparison of methodology in studies employing DCE-MRI in RT the results are mixed. Overall, the technical quality of studies, measured as compliance with QIBA guidelines, is improving with time. However, the spread is also increasing. Hopefully, in the future more people will adhere to the attempts to standardize DCE-MRI and thus enable more homogenous data which can be used for better answering how DCE-MRI can be employed to improve RT.

SP-0026

Importance of b-value selection and geometrical accuracy in DW-MRI for radiotherapy

M. Lambrecht[1]
[1]*University Hospital Gasthuisberg, Department of Radiotherapy and Oncology, Leuven, Belgium*

Over the last decade, Diffusion Weighted MRI(DWI) has emerged as a promising imaging technique in the field of radiation oncology.
The ability of DWI to assess a tissue's microstructure makes it potentially very valuable in tumor characterization, delineation, detection of pathological lymph nodes, response prediction and response evaluation.
However, acquisition, analysis and interpretation of the images is far from straightforward. The imaging technique is prone to distortions interfering with the accurate geometrical localisation and quantification of the tissue of interest.
Furthermore quantification is heavily influenced by the choice of machine parameters, making reproducibility an important issue.
Overcoming these problems is of the utmost importance to move DWI out of the realm of research and into daily practice.
In this talk we will identify the important parameters influencing acquisition and quantification of DWI, with emphasis on the choice of b-values and geometrical accuracy. We will discuss the implications when using DWI for extracranial radiotherapy. Finally we will look into possible solutions and provide a framework to ensure maximal exploitation of the imaging technique for the future.

Joint Symposium: ESTRO-IAEA: Joint ESTRO-IAEA efforts on dosimetry, QA and audit for advanced treatment techniques

SP-0027

New IAEA-AAPM Code of Practice for dosimetry of small photon fields used in external beam radiotherapy

H. Palmans[1,2]
[1]*National Physical Laboratory, Acoustics and Ionising Radiation, Teddington, United Kingdom*
[2]*EBG MedAustron GmbH, Medical Physics, Wiener Neustadt, Austria*

Increased use of small photon fields in stereotactic and intensity modulated radiotherapy has raised the need for standardizing the dosimetry of such fields using procedures consistent with those for conventional radiotherapy. While many problems of small field dosimetry have been raised in the past, e.g. in Report 103 of the Institute of Physics and Engineering in Medicine, a vast amount of literature has addressed most of those and solutions have been proposed for specific situations. What has hampered the development of a Code of Practice until recently was the availability of data but in the last few years a considerable number of publications have provided new data and insights that have enhanced our understanding of small field dosimetry.
An international working group, established by the International Atomic Energy Agency (IAEA) in collaboration with the American Association of Physicists in Medicine (AAPM), has finalised a Code of Practice for the dosimetry of small static photon fields. The Code of Practice consists of six chapters and two appendices. The first chapter provides an introduction to situate the distinct role of this Code of Practice as compared to previous recommendations for reference dosimetry in external beam radiotherapy. The second chapter provides a brief discussion of the physics of small photon fields with emphasis on those aspects that are relevant to understanding the concepts of the Code of Practice. Particular issues that are addressed are the definition of field size, the field size dependent response of detectors, volume averaging, fluence perturbation corrections, reference conditions and beam quality in non-conventional reference fields. The third chapter introduces all details of the formalism used, which is based on the IAEA-AAPM formalism published by Alfonso et al. (Med Phys 35:5179-5186, 2008) and is extended to clarify its application to flattening-filter-free beams (FFF beams). The fourth chapter provides a comprehensive overview of suitable dosimeters for reference dosimetry in the conventional 10 cm x 10 cm reference fields, for reference dosimetry in machine-specific reference fields at machines that cannot establish a conventional 10 cm x 10 cm reference field and for the determination of field output factors in small fields. The fifth chapter gives practical recommendations for implementing reference dosimetry in both conventional 10 cm x 10 cm

reference fields and machine-specific reference fields. The sixth chapter provides the practical recommendations for the determination of field output factors in small photon fields.
Comprehensive data on beam quality correction factors for ionization chamber types recommended for reference dosimetry are provided in chapter five and a detailed discussion on how they have been derived from the literature as well as a discussion of their uncertainties is given in the first Appendix. For beams with flattening filter (WFF beams) these data are consistent with the ones given in IAEA TRS-398 and the update to AAPM TG-51. For FFF beams additional corrections are taken into account for the difference in water to air stopping power ratios between FFF and WFF beams and for volume averaging due to the non-uniform lateral beam profiles. Comprehensive data on small field correction factors are given in chapter six for a wide range of recommended small field detectors. The second Appendix discusses in detail how these data have been compiled from the literature including both Monte Carlo calculated and experimental data and also provides a thorough evaluation of the uncertainties of those data.
The Code of Practice has been reviewed by referees selected by the AAPM and by the IAEA and is currently submitted for publication by the IAEA. This presentation is given on behalf of the IAEA-AAPM Working Group on small and non-standard field dosimetry.

SP-0028

Which dosimetric uncertainties in small fields are clinically acceptable for IMRT/VMAT?

D. Georg[1,2], W. Lechner[1]
[1]*Medizinische Universität Wien Medical University of Vienna, Department of Radiation Oncology, Vienna, Austria*
[2]*Christian Doppler Lab for Medical Radiation Rsearch, Department of Radiation Oncology, Vienna, Austria*

During the last years small field dosimetry (re-)gained importance. Several working groups highlighted its relevance in the context of high precision radiotherapy techniques. Non-conventional linear accelerators that do not support standard reference geometry and the upcoming unflattened photon beams had an impact on upcoming recommendations in this context as well. However, recent audits revealed large uncertainties in small field dosimetry with deviations up to 10% for 2 x 2 cm2 fields, which motivated the present contribution. Clinically used beam models of two TPS (Monaco, ELEKTA and iPlan, BrainLAB) were modified to mimic the large uncertainties in small field output factors. Next IMRT and VMAT treatment plans for prostate and head and neck cancer cases as well as treatment plans for stereotactic brain lesions were generated and calculated with correct and incorrect beam models, respectively. Finally, treatment plans were delivered with an ELEKTA Versa HD linac. Dose calculations were compared with measurements performed with EBT films and a detector array. Effects of uncertainties in small field output factors were less pronounced for IMRT and VMAT plans compared to stereotactic techniques delivered with static fields or dynamic arcs. TPS specific sequencing of IMRT and VMAT had an impact on the final results. The gamma evaluation performed with detector arrays was not able to dissolve uncertainties in small field dosimetry due to the rather large detector. On the other hand single detector signal was sensitive to such uncertainties. Upcoming treatment techniques like dose painting will use small fields more extensively and motivates highest accuracy in small field dosimetry. Published reference data and guidelines including detector correction factors contribute to eliminate gross uncertainties (>5%) in small field dosimetry.

SP-0029

IAEA external audits for advanced radiotherapy - lessons learnt and their relevance for industrialised countries

J. Izewska[1]
[1]*IAEA - International Atomic Energy Agency, Dosimetry and Medical Radiation Physics Section, Vienna, Austria*

The postal dose audit programme for radiotherapy dosimetry operated jointly by the International Atomic Energy Agency (IAEA) and the World Health Organization (WHO) has been in existence for over 45 years. To-date the calibration of over 11300 radiotherapy beams in 2200 hospitals in 132 countries has been audited. Several hospitals have improved their dosimetry practices over the years, and the percentage of acceptable results is > 95% at present. The IAEA records suggest that regular participation in audits is associated with higher quality dosimetry than the first participation. It confirms that the dosimetry audit is useful to enhance confidence in radiotherapy dosimetry for both medical physicists and clinicians who need assurance that their patients receive safe and high quality radiation treatment, which is not possible without accurate dosimetry. However, with the increasing complexity of radiotherapy treatments, basic dosimetry audits are no longer sufficient and more complex audit programmes testing different dosimetry parameters and treatment delivery techniques are required.
The first IAEA 'end-to-end' audit methodology was developed for 3D conformal radiotherapy. It reviewed dosimetry, imaging, treatment planning and radiotherapy delivery processes following the pathway similar to that of the patient undergoing radiotherapy. The audit was implemented at national levels with the IAEA providing an anthropomorphic thorax phantom (CIRS) and expert advice. National groups conducted the audit at local hospitals through on-site visits. TPS calculated doses were compared with ion chamber measurements for a set of test cases. In Europe, the audit has been carried out in 60 hospitals in 8 countries. About 200 data sets have been collected and reviewed. Discrepancies requiring interventions were discovered in about 10% of datasets. In addition, suboptimal beam modelling in TPSs occurred in several centres. Overall, the audit contributed to better understanding of the performance of TPSs and helped to resolve discrepancies related to imaging, dosimetry and treatment planning.
Recently, a new methodology has been developed for on-site 'end-to-end' audits to review the physics aspects of head and neck IMRT treatments. It uses a dedicated anthropomorphic head and shoulders phantom (CIRS) with a set of contours representing the target volumes and organs at risk. The contours are imported and superimposed on the CT scans of the phantom. The treatment plan is developed and transferred to the treatment machine for the dose delivery. Ion chambers and radiochromic films are used for dose measurements. Comparisons are made between the TPS calculated and measured doses. The audit methodology is currently tested within an international study group.
For >20 years the IAEA has supported the development of audit methodologies for national audit groups using remote audit tools. Current projects focus on remote IMRT audits involving different audit steps, e.g. small beam dosimetry relevant for IMRT. One study compared TPS calculated beam outputs to the published reference data sets. The results showed good agreement (within 1%) between the TPS output and the reference data for field sizes ≥ 4×4 cm2 and dose overestimation by TPSs by 2-3% for field sizes ≤ 3×3 cm2. Auditing methodology was also developed to verify the TPS modelling of small MLC shaped beam profiles using radiochromic film measurements for 2×5 cm2 and a 2×2 cm2 fields. Relative differences between the profiles at 20%, 50% and 80% dose levels were evaluated. Only 64% beam profiles were within 3 mm agreement between the TPS calculated and film measured doses. This highlights some limitations in TPS modelling of small beam profiles in the direction of MLC leave movements. Such differences can affect patient treatments, especially for stereotactic radiotherapy and IMRT. Another study evaluated MLC performance using picket fence tests and confirmed that most MLCs performed as expected. A comparison of gamma analysis techniques was also conducted through a multicentre analysis of a film irradiated with a complex field arrangement. Differences in gamma agreement occurred that were attributed to the differences in film scanning parameters and gamma calculation algorithms. A newest study on remote 'end-to-end' IMRT audit is on-going. Overall, the results of these studies demonstrate challenges in TPS commissioning for

small fields and challenges in multicentre comparison of gamma analysis for complex dose distributions.
Overall, the IAEA supports developments of various audit tools for radiotherapy with the audit scope corresponding to the evolving complexity of radiotherapy technology, in order to verify radiotherapy physics practices and improve the quality of treatments delivered to cancer patients in participating countries.

Symposium: Strategies for treatment planning

SP-0030
Comparisons of treatment planning with photons and protons
M. Enmark[1], I. Kristensen[1], C. Vallhagen Dahlgren[2]
[1]*Skåne University Hospital, Department of Radiation Physics, Lund, Sweden*
[2]*Skandionkliniken, Uppsala, Sweden*

This presentation will focus on the main differences between the radiotherapy treatment planning with photons and protons. An important issue in all treatment planning is the dosimetric uncertainties and margins to account for these. Compared to photons, protons have additional sources of uncertainties that should be analysed and understood. Insufficient quantification of margins can have more serious consequences in proton therapy than is the case for photons.
The main advantage of proton beams is the finite range and sharp distal dose fall off in depth, an advantage that often is a contradiction in the sense that the range uncertainty limits the use of this advantage. A second advantage is the ability to, with every single field, give the target volume a higher dose than the surrounding tissue. The sources of range uncertainties are caused by the patient variations in anatomy and the uncertainties in the conversion of CT numbers to tissues with the correct proton interaction properties. The handling of range uncertainties play a critical role in proton planning and has an impact on the entire treatment planning process that differs from photons.
The generic PTV margin recipes used in photon planning, are not adequate in proton planning. Primarily, this is used to account for lateral beam uncertainties. In proton planning, two margins have to be considered, the lateral and the margin in depth i.e. range uncertainty. In principle, these two margins arises from different physical processes. According to ICRU 78 [1] the PTVs are recommended to be used in proton planning for dose reporting purposes. Additional volumes with beam specific margins, have to be used to account for uncertainties in range. Paganetti has suggested margin recipes that is widely used in proton planning [2].
Consequently, the range uncertainty also has an influence on the selection of beam and their entry angles. In this phase of the treatment planning process, proton planning emphasizes other considerations than photons. Robust planning has the potential of mitigate the impact of range uncertainties, aiming for a robust beam path i.e. heterogeneous geometry along the beam path. Likewise, the robustness should be considered during the optimization as well as during the treatment plan evaluation and the comparison with a photon treatment plan to choose the best treatment plan.
The contents of this presentation are based on experiences from the start-up of the first Scandinavian Proton Centre, Skandionkliniken, where the first patients were treated in late august 2015. Nearly four years before that, in January 2012, we started the Proton School in order to prepare for the clinical start and to train a group of medical physicists, dosimetrists and radiation oncologists in proton planning [3,4]. Thinking protons instead of photons has been the greatest challenge for the group as a whole. *How do we achieve the best plan?* This includes selecting robust beam angles and thinking about what the protons interact with on its way to the target volume. Discussions about target volumes has been frequent, as the use of them. Delineation is a major issue, not only for CTV/PTV but for other structures the protons might interact with in its beam path, as well as optimisation structures to provide the best treatment plan.

References

1. ICRU Vol 7 No 2 (2007) Report 78, PRESCRIBING, RECORDING, AND REPORTING PROTON-BEAM THERAPY
2. Paganetti, H. (2012) "Range uncertainties in proton therapy and the role of Monte Carlo simulations." Phys Med Biol; 57
3. Kristensen I, Vallhagen Dahlgren C, Nyström H. (2013) "Treatment planning training for a large group in geographically spread centres", ESTRO 2013, abstract PO-0896
4. Vallhagen Dahlgren C, Kristensen I, Nyström H, Nyström P W, Bäck A, Granlund U, Josefsson D, Medin J. (2013), "Proton treatment planning for beginners - to build up the competence and skills in a multi-centre environment", PTCOG 2013, abstract P304

SP-0031
When to re-plan: a practical perspective
B. Bak[1]
[1]*Greater Poland Cancer Centre, Department of Radiotherapy, Poznan, Poland*

Anatomical changes are important issue during radiotherapy because they could potentially lead to inadequate dose distribution to target and organs at risk (OAR). Radiation induced complications have a significant adverse impact on health-related quality of life. To minimize the risk adaptive radiotherapy (ART) has become state of art of modern radiotherapy. In clinical practice ART is expressed mostly by Image-Guided Radiation Therapy (IGRT) and re-planning, the last is very individualized but should be more unified. Clear guidelines are therefore needed to determine the timing of re-planning, and an increasing amount of information needs to be acquainted, transferred and stored.
There are several indications that anatomic changes are more pronounced in the first half of treatment, and therefore repeated imaging and replanning should be performed in this first time period.The parotid gland was the most studied OAR and showed the largest volume changes during radiotherapy (26% average volume decrease). The average number of radiation fractions delivered between baseline and re-planning CT scans was 15 (±5) fractions which equals 21 (±8) days. It is also well established in the Head and neck (H&N) area that, because of i.e. weight loss and/or tumor shrinkage especially in more advanced stages of cancer (T3/T4, large N+), re-planning improves relapse–free survival and significantly alleviated the late effects. In many dosimetric studies without replanning during treatment, the doses to normal structures were significantly increased and doses to target volume significantly decreased. According to literature replanning frequency increases also with smaller PTV margins.
To answer the question „When to re-plan?" we need to know which sites would most benefit. In regard to literature studies it seems that re-plan would be the most beneficial for tumors of the biggest volume or the nearest proximity of the OAR's. Still it does not explain „when" should we perform it. Despite of the great amount of reports and analysis further research are needed.

SP-0032
Fully automated treatment planning: benefits and potential pitfalls
E. Damen[1], R. De Graaf[1], R. Glorie[1], J. Knegjens[1], C. Van Vliet-Vroegindeweij[1]
[1]*Netherlands Cancer Institute Antoni van Leeuwenhoek Hospital, Radiotherapy Department, Amsterdam, The Netherlands*

Purpose/Objective: Labor-intensive procedures, such as adaptive radiotherapy, result in an increased workload in the treatment planning department, which can be reduced by introducing fully automated treatment planning. The benefits of automated planning are many: reduction of workload, increased workflow efficiency, and reduction of plan variability. However, a potential pitfall could be loss of

knowledge and skills among RTTs, leading to less ability to design, judge or adapt treatment plans. The purpose of this work is to show the capabilities of automatic planning and discuss its consequence for a radiation-oncology department.

Material and Methods: At the NKI a project was started to develop single-click treatment planning for techniques based on a class solution. Technically this was accomplished by separating medical planning protocol definition from actual control of the treatment planning system (Pinnacle3, version 9.10, Philips Medical Systems). After target delineation, a single mouse-click initiates the following actions: Pinnacle patient record generation, auto-segmentation of organs at risk (OARs), beam setup, optimization of the dose distribution, and creation of PDF documentation. The plan is then ready for inspection by RTT and physician. This procedure is currently implemented into our clinic for prostate, breast and vertebral metastases. Currently, knowledge and skills among RTTs is primarily maintained by the requirement to perform a certain number of treatment plans per year for a given tumor site. In addition, all treatment plans are checked by a second RTT, and feedback is given on deviations from protocol and/or possibilities to improve the plan. Finally, special cases are discussed with all RTTs on a monthly basis.

Results: A fully automated treatment plan requires 20 minutes for prostate and breast, and 7 minutes for vertebral metastases. Up to now, 185 patients have received a fully automated treatment planning procedure. In about 15% of the cases, the automatically produced plan required manual adjustment, either because of errors in auto-segmentation of OARs, or due to a sub-optimal dose distribution. In general, RTT hands-on time reduced with up to 2 hours per plan, while maintaining plan quality.
To prevent loss of knowledge and skills among RTTs, 10% of the requested plans for a tumor site are randomly assigned for manual treatment planning. In addition, planning challenges are organized in which a number of RTTs makes a treatment plan for the same patient. The results are discussed with all RTTs.

Conclusion: Complete automation of the treatment planning process is feasible for selected tumor sites and results in considerable reduction of hands-on time. By designing new QA methods, loss of skills and knowledge among RTTs can be prevented, thus ensuring that RTTs remain capable of manually designing and/or adapting treatment plans.

Poster Viewing : 1: Brachytherapy

PV-0033
Assessing dose contribution to pelvic lymph nodes in intracavitary brachytherapy for cervical cancer

G.W.Y. Chua[1], D.B.H. Tan[1], G.H. Tay[1], Y.W. Foo[1]
[1]*National Cancer Centre - Singapore, Department of Radiation Oncology, Singapore, Singapore*

Purpose or Objective: In definitive radiotherapy for cervical cancer, a HDR brachytherapy boost is most commonly used after external beam radiation (EBRT). While brachytherapy doses are chosen such that a cumulative EqD2 of 80 to 90Gy is delivered to the primary tumour after a 45 to 50.4Gy EBRT dose, there is less certainty regarding the brachytherapy dose contribution to pelvic lymph nodes. This poses a challenge as to how high a preceding EBRT dose should be prescribed to gross nodal disease, in order to achieve a cumulative tumoricidal effect.
While the use of MRI guided 3-dimensional brachytherapy is increasing, the point-based Manchester system remains the most widely utilized technique. The objective of this study is to determine the brachytherapy dose contribution to individual pelvic lymph node regions, using CT planning with the Manchester system.

Material and Methods: CT planning datasets from 40 patients who had undergone intracavitary HDR brachytherapy for stage III or IVA cervical cancer were retrieved. All patients received prior 3D conformal EBRT to a dose of 50.4Gy in 28 fractions, followed by four fractions of CT-based brachytherapy, prescribing to Manchester point A. Half of the patients (n=20) received a brachytherapy dose of 5Gy per fraction, while the other half received 6Gy. Decision on brachytherapy dose was dependent on the ability to meet D2cc constraints for the adjacent organs-at-risk.
Following international consensus guidelines, the right and left external iliac, internal iliac and obturator groups of lymph nodes were separately contoured on the CT dataset (see Figure 1). Applying the initial brachytherapy plan on the Oncentra TPS, mean doses to each nodal group according to laterality (i.e. left and right) were calculated for each patient, and both results combined to obtain the average mean dose to the entire nodal group. All individual patient results were then averaged across the respective study groups (5 and 6 Gy groups) and corresponding EqD2s calculated.

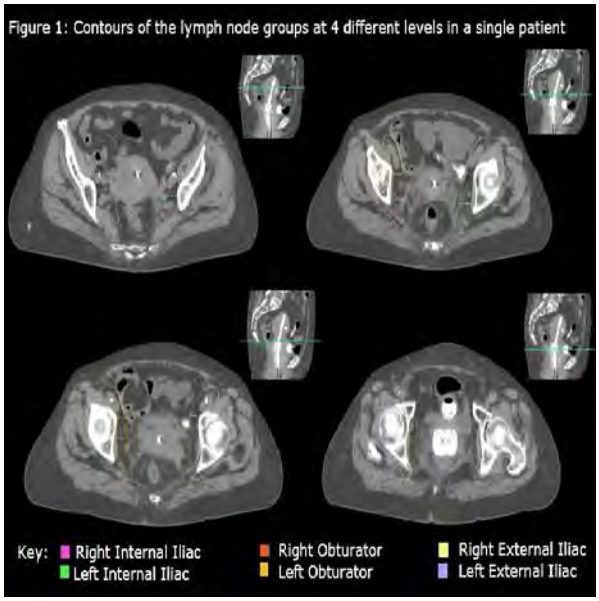

Results: A summary of results is shown in Table 1.
For patients who received a per fraction brachytherapy dose of 5 Gy, average mean absolute dose to the external iliac, internal iliac, and obturator nodal groups was 0.80 Gy, 1.12 Gy and 1.34 Gy respectively. The corresponding EQD2s were 0.72 Gy, 1.05 Gy, and 1.28 Gy respectively.
For patients who received a per fraction brachytherapy dose of 6 Gy, average mean absolute dose to the external iliac, internal iliac, and obturator nodal groups was 1.16 Gy, 1.56 Gy and 1.80 Gy respectively. The corresponding EQD2s were 1.08 Gy, 1.50 Gy and 1.79 Gy respectively.

Table 1: Summary of the per fraction average mean absolute doses and corresponding EqD2 (highlighted in grey) to each lymph node region, classified according to patients who received 5Gy or 6Gy prescribed dose.

Per fraction brachytherapy dose contribution	Average mean doses (Gy)	
	5 Gy/ fraction (n=20)	6 Gy/ fraction (n=20)
EXTERNAL ILIAC		
Absolute dose	0.793	1.156
Corresponding EqD2	0.717	1.083
INTERNAL ILIAC		
Absolute dose	1.124	1.546
Corresponding EqD2	1.048	1.497
OBTURATOR		
Absolute dose	1.343	1.803
Corresponding EqD2	1.276	1.787

Conclusion: Our study demonstrates that the pelvic lymph nodes receive a significant dose contribution from brachytherapy in cervical cancer, when employing the Manchester prescription system. This must be taken into account during external beam radiotherapy planning, and adequate external beam boost doses calculated to achieve cumulative tumoricidal doses to pelvic nodal disease.

PV-0034

HDR BT alone in endometrial cancer: up-date of Piedmont experience in 18 years (71 patients)

S. Gribaudo[1], U. Monetti[1], E. Madon[2], V. Richetto[2], M. Tessa[3], F. Moretto[3], A. Ruggieri[3], S. Cosma[4], S. Danese[4], A. Urgesi[1]
[1]*A.O.U. "Città della Salute e della Scienza di Torino" P.O. Sant Anna, Radiotherapy, Torino, Italy*
[2]*A.O.U. "Città della Salute e della Scienza di Torino" P.O. Sant Anna, Physics, Torino, Italy*
[3]*A.S.L. AT P.O. Cardinal Massaia, Radiotherapy, Asti, Italy*
[4]*A.O.U. "Città della Salute e della Scienza di Torino" P.O. Sant Anna, Gynecology 4, Torino, Italy*

Purpose or Objective: Endometrial cancer is the mainly gynaecologic malignancy, 80-85% in stage I at diagnosis. The standard primary treatment remains TAH&BSO, with appropriate surgical staging. The epidemiology of this disease favours elderly, obese women with multiple medical problems (hypertension, diabetes, cardiovascular diseases, coagulation disorders, respiratory disorders) that render some of them medically inoperable. RT alone is the only efficient option for these women. BT is the main component in this cohort of patients (pts).

Material and Methods: September 1997-September 2015: 90 pts RT alone, 71 BT HDR alone. Median age 79 years (range 57-93). Staging: clinical examination, TVUS, MR or CT scan and fractionated curettage. Stage Ia 32 pts, Stage Ib 36 pts, Stage II 3 pts. OS, DSS, LC and late side effects were analysed retrospectively. Follow-up > 10 years (mean 57 months). BT HDR with Rotte **"Y"** applicator, plus VBT in stage II. Dose prescription at **''uterine points''** that are two points located 1 cm over the middle of a line drawn between the tips of the two ends of the **"Y"** applicator and at series of points placed laterally to the tandem according to the pre-treatment imaging data. We treat the entire length of the uterus to ensure coverage of the fund. To maintain the bladder and rectal maximum point doses below 100% of the prescribed dose we optimize with TPS. Until 2002 BT was performed 4-5 times, weekly, mean dose 29.3 Gy (range 18-35 Gy); from 2003 (42 pts) we deliver 30 Gy in five frs, 6 Gy each b.i.d. schedule, 6 hours interval between frs.

Results: 5 years OS, DSS and LC: 52.1%, 85.9%, and 91.2%. **Stage Ia: 56.3%, 87.5%, and 90.6%; Stage Ib: 50%, 86.1%, and 94.4%; Stage II:** 33.3%, 66.7%, and 66.7%. DSS was not affected by tumour grade or age. One patient had a PD, 6 (10.6%) developed recurrence after a median of 13 months (3 with distant metastases), 2 (3.5%) a lymph node recurrence with distant metastases. One patient have a GE grade III late side effect (1.8%) at 5 years, not related with rectal dose.

Conclusion: HDR BT with **"Y"** applicator is a very effective treatment modality with good LC rates and suitable DSS for pts who are not fit for surgery. This technique has proven to have a low risk of acute complications and long-term side effects. Longer follow-up will be required to document the incidence of late effects using the b.i.d. schedule. In the short term, it seems that this approach is a feasible way to limit the number of procedural complications and length of hospital stay and bed rest.

PV-0035

Electronic brachytherapy for basal cell carcinoma: two prospective pilot trials with different doses

O. Pons[1], R. Ballester-Sánchez[2], C. Candela-Juan[3], F.J. Celada-Álvarez[4], C. Barker[5], R. Chicas-Sett[4], J. Burgos-Burgos[4], D. Farga-Albiol[4], M.J. Pérez-Calatayud[4], A. Tormo-Micó[4], J. Pérez-Calatayud[6], R. Botella-Estrada[7]
[1]*Hospital Universitario y Politecnico La Fe, Radiotherapy, Valencia, Spain*
[2]*La Fe University and Polytechnic Hospital, Dermatology Department-, Valencia, Spain*
[3]*La Fe University and Polytecnic Hospital, Radiotherapy Physics Section- Oncology Department, Valencia, Spain*
[4]*La Fe University and Polytechnic Hospital, Radiation Oncology Department, Valencia, Spain*
[5]*Memorial Sloan Kettering Cancer Center, Department of Radiation Oncology, New York, USA*
[6]*La Fe University and Polytecnic Hospital, Radiotherapy Physics Section- Radiation Oncology Department, Valencia, Spain*
[7]*La Fe University and Polytechnic Hospital-, Dermatology Department, Valencia, Spain*

Purpose or Objective: Basal cell carcinoma (BCC) is a very common cancer in the Caucasian population. Treatment aims to eradicate the tumor with the lowest possible functional and aesthetic impact. Electronic brachytherapy (EBT) is a treatment technique currently emerging. This study aims to show the outcomes of two consecutive prospective pilot clinical trials using different radiation doses of EBT with Esteya® EB system for the treatment of superficial and nodular basal cell carcinoma.

Material and Methods: Two prospective, single-center, non-randomized, pilot studies were conducted. Twenty patients were treated in each study with different doses. The first group (1) was treated with 36.6 Gy in 6 fractions of 6.1 Gy and the second group (2) with 42 Gy in 6 fractions of 7 Gy. In one case the 6.1 Gy/fraction resulting from the theorical RBE calculation was used, and in the second arm (7 Gy/fraction) the same dose as the Valencia applicator study was used. Cure rate, acute toxicity and late toxicity related to cosmesis were analyzed in the two treatment groups.

Results: In group 1, a complete response in 90% of cases was observed at the 1 year follow-up, whereas in group 2 the complete response was 95%. Tumor persistence or recurrence was suspected clinically and dermoscopically in two patients in the first group at 3 and 6 months respectively and in one patient in the second group at 1 year follow-up. The differences with reference to acute toxicity and the cosmetic results between the two treatment groups were not statistically significant.

Conclusion: Our initial experience with Esteya® EB system to treat superficial and nodular BCC shows that a dose of 36.6 Gy and 42 Gy delivered in 6 fraction of 7 Gy achieves a 90% and 95% clinical cure rate at 1 year respectively. Both groups had a tolerable toxicity and a very good cosmesis.

PV-0036

Dosimetric evaluation of 3D printed applicators for High Dose Rate brachytherapy

A. Vavassori[1], R. Ricotti[1], A. Bazani[2], F. Pansini[2], R. Spoto[1,3], D. Ciardo[1], V. Sammarco[1,4], F. Cattani[2], R. Orecchia[1,3], B.A. Jereczek-Fossa[1,3]
[1]*European Institute of Oncology, Department of Radiation Oncology, Milan, Italy*
[2]*European Institute of Oncology, Unit of Medical Physics, Milan, Italy*
[3]*University of Milan, Department of Oncology and Hemato-oncology, Milan, Italy*
[4]*University of Milan, Tecniche di Radiologia Medica per Immagini e Radioterapia, Milan, Italy*

Purpose or Objective: Feasibility and dosimetric study of 3D-printed cylindrical and skin mould applicators for High Dose Rate brachytherapy (HDR-BRT) using acrylonitrile butadiene styrene (ABS).

Material and Methods: Three cylindrical applicators (1 as reference and 2 as test) with a single 2.5 mm catheter channel and a 1 mm radial slit for radiochromic film support were 3D printed (HP3DX100, Hamlet, Dublin, IE) using ABS plastic. The reference had the radiochromic slit in contact

with the catheter channel and was printed with 20% infill percentage. The test configurations had the radiochromic slit at 6.3 mm distance from the center of the catheter channel and were printed with 20% (Test 1) and 40% (Test 2) infill percentage. Physical quality of ABS plastic were evaluated by analyzing the depth dose profiles measured by Gafchromic EBT3 films (International Specialty Products, Wayne, NJ) when the 192Ir source passing through the catheter channel delivered 2 Gy at 10 mm distance from the axis of the channel (Fig.1a).
Four skin mould applicators with 4 parallel catheter channels of 2.5 mm diameters, 5 mm distance between the axis of the channel and the surface, and 10 mm distance between consecutive channel axes were 3D-printed. Two geometrical shapes were compared to the commercial Freiburg Flap applicator (Nucletron, Stockholm, SE, Fig. 1b): a group of 16 semi-spheres reproducing the actual Freiburg geometry printed at 10% infill percentage (Fig.1c) and a parallelepiped applicator with 10%, 20% and 40% infill printing percentage (Fig.1d). A prescription dose of 2 Gy to the surface at 5 mm distance from the channels axes was delivered using an 192Ir source. Surface dose distributions were measured with Gafchromic EBT3 films for both the 3D-printed skin mould applicators and the commercial Freiburg Flap applicator considered as reference. The gamma index method with dose difference (DD) criteria of 3%, distance-to-agreement criteria (DTA) of 3 mm and 10% dose threshold was evaluated.

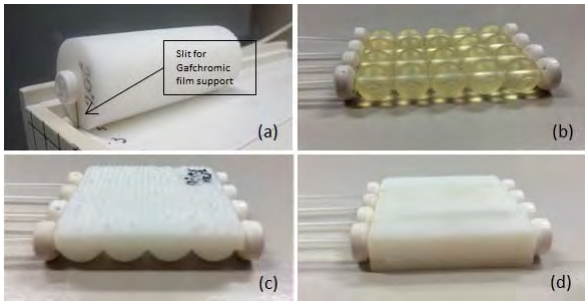

Results: The radiation attenuation profiles were comparable in all the cylindrical configurations. Dose attenuation were not sensitive to the density of the material (Tab.1a). When comparing 3D-printed skin mould applicators with commercial Freiburg Flap in terms of gamma index analysis, a high pass rates >90% was obtained. Therefore, the isodose overlay and linear dose profiles of film measured using 3D printed applicator and commercial Freiburg were in close agreement (Tab.1b).

(a) Cylindrical Applicator		Profile dose distribution			
		Source distance			
		10 [mm]	15 [mm]	20 [mm]	25 [mm]
Measured Dose [Gy]	Reference configuration	2.0	1.4	1.0	0.8
	Test configuration ABS 20%	1.9	1.2	0.9	0.7
	Test configuration ABS 40%	1.9	1.2	0.9	0.7

(b) Skin mould applicators	Gamma analysis – passing rate –			
	3D printed Freiburg Flap ABS 10%	Parallelepiped ABS 10%	Parallelepiped ABS 20%	Parallelepiped ABS 40%
Commercial Freiburg Flap	97.74%	98.57%	98.03%	91.66%

Conclusion: ABS3D-printed applicators are a reliable solution for patient-specific HDR-BRT of superficial lesions. Further assessment of 3D printing techniques and materials are required for clinical development.

PV-0037

Application of brachytherapy for residual nasopharyngeal carcinoma after external beam radiotherapy

G. Cheng[1], H. Zhao[1], M. He[1], J. Wang[1], Z. Zhao[1]
[1]*China-Japan Union Hospital of Jilin University, Department of Radiation Oncology, Changchun, China*

Purpose or Objective: Local residual disease occurs in 7-13 % after primary treatment for nasopharyngeal carcinoma (NPC). To prevent tumor progression and/or distant metastasis, treatment is indicated. This studies focus on the application of 3D-CT based and endoscopical guided brachytherapy for the treatment of residual lesion in nasopharyngeal cavity of NPC after the radical external beam radiotherapy and to assess the safety and clinical outcome of this technical.

Material and Methods: 26 patients with stage T1-T2b NPC who suffered from locally residual lesion in nasopharyngeal cavity (All the tumors were less than 1 cm below the nasopharyngeal epithelium) after standard radical radiotherapy (70-74 Gy) ± platinum-based chemotherapy were further administrated by the 3D-CT based and endoscopical guided brachytherapy using the Foshan applicator or the standard nasopharyngeal applicator according the tumor location. The prescribed salvage dose of brachytherapy was 3.5 Gy/fraction, twice- daily with an interval of 6 h to a total dose of 7-14 Gy (one week apart) depending on the total dose of external beam radiotherapy. The total dose ranged from 81.8-85.6 Gy when transformed to EQD2 models, and the Pstem D1%< 60 Gy was restricted in planning. The primary endpoint was 1-, 3-year overall survival and secondary endpoints were: local control, distant metastasis and grade 3-4 adverse events.

Results: The whole brachytherapy procedure was well tolerated under local anesthesia. 24 patients (92.3%) get complete response (CR) as confirmed by enhanced CT/MRI after 1-3 month after the brachytherapy. With a median follow-up time of 40 months, no serious complications or late sequelae occurred. The 1-, and 3-year overall survival, locoregional free survival, and distant-metastasis free survival rates were 96.2%, 80.8%, 92.3% and 84.6%, respectively. And the patients with early-T stage at initial diagnosis had 100% local control rate.

Conclusion: Brachytherapy is of benefit to improve the local control of primary lesion of NPC with residual nasopharyngeal cavity involvement. It is a safe and effective approach for patients with poor tumor regression at the end of external beam radiotherapy for boosting the local irradiation dose.

PV-0038

Multivariable model development for mortality after total salvage Iodine-125 prostate brachytherapy

M. Peters[1], J.R.N. Van der Voort van Zyp[1], M.A. Moerland[1], C.J. Hoekstra[2], S. Van de Pol[2], H. Westendorp[2], M. Maenhout[1], R. Kattevilder[2], H.M. Verkooijen[3], P.S.N. Van Rossum[1], H.U. Ahmed[4], T. Shah[4], M. Emberton[4], M. Van Vulpen[1]
[1]*UMC Utrecht, Radiation Oncology Department, Utrecht, The Netherlands*
[2]*Radiotherapiegroep, Radiation oncology Department, Deventer, The Netherlands*
[3]*UMC Utrecht, Imaging Division, Utrecht, The Netherlands*
[4]*University College London, Division of Surgery and Interventional Science, London, United Kingdom*

Purpose or Objective: Total salvage Iodine-125 brachytherapy (TS I-125-BT) is a potentially curative treatment strategy for localized prostate cancer (PCa) recurrences after radiotherapy. Prognostic factors influencing PCa-specific and overall mortality (PCaSM & OM) are not known. The objective was therefore to develop a multivariable, internally validated prognostic model for survival after TS I-125-BT.

Material and Methods: Retrospectively, sixty-two TS I-125-BT patients were analyzed. These patients were treated from 1993-2010 in the Netherlands. Multivariable Cox-regression was used to assess the influence of pre-salvage characteristics on PCaSM and OM. Missing data was handled by using multiple imputation (20 imputed sets). Internal validation was done using 500 bootstrap resamples of every imputed set. Discriminatory ability was quantified with the C-statistic. Calibration plots were created to visually assess the

goodness-of-fit of the final model. Optimism-corrected survival proportions were calculated. All analyses were performed according to the TRIPOD statement.

Results: 28 (45%) patients died from PCa after mean (±SD) 82 (±36) months. Median total follow-up was 78 months (range 5-139). In total, 36 patients (58%) patients died after mean 84 (±40) months. PSA doubling time (PSADT) remained as a predictive factor for both PCaSM and OM: corrected hazard ratio's (HR's) 0.92 (95%-CI: 0.86-0.98, p=0.02) and 0.94 (95%-CI: 0.90-0.99, p=0.01), respectively. The adjusted C-statistics were 0.71 and 0.69, respectively. Predictive ability (calibration) was good up to 96 months follow-up. Over 80% of patients can survive 8 years if PSADT>24 months (PCaSM) and >33 months (OM) (Figure 1).

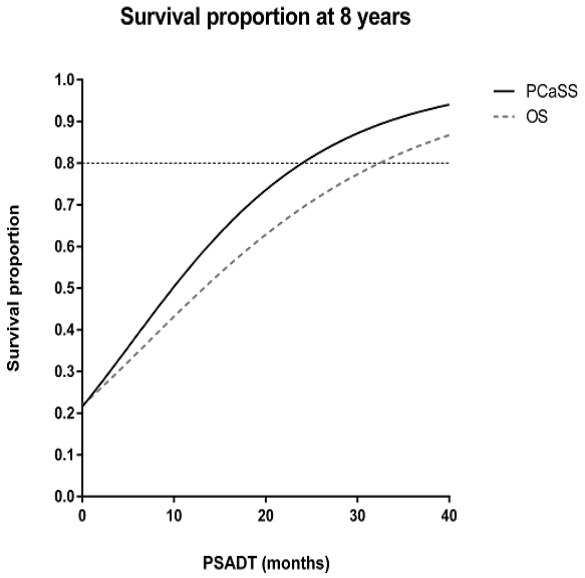

Figure 1: Prostate cancer specific survival (PCaSS) and overall survival (OS) as a function of PSADT.

Conclusion: A PSADT >24 months and >33 months can result in a high probability (>80%) of prostate cancer specific and overall survival 8 years after TS I-125 BT. Larger series and external validation are necessary.

PV-0039

Urinary incontinence rates in salvage high-dose-rate brachytherapy prostate cancer patients

P. Wojcieszek[1], M. Szlag[1], A. Cholewka[1], B. Białas[1], S. Kellas-Sleczka[1], M. Fijałkowski[1], A. Andrejczuk[1]

[1]Maria Sklodowska-Curie Memorial Cancer Center and Institute of Oncology III Dept, Brachytherapy Department, Gliwice, Poland

Purpose or Objective: Locally recurrent prostate cancer reirradiation may lead to urethral stricture and increase of urinary symptoms including urinary retention. Such patients may undergo urethretomy or transurethral resection of the prostate (TURP), which may cause urinary incontinence. Our purpose was to evaluate risk of urinary incontinence after salvage high-dose-rate brachytherapy (HDR BT) with or without urological intervention.

Material and Methods: We included in the analysis all salvage HDR BT patients with at least 6 months of follow-up. Urinary retention, urological interventions and urinary incontinence rates were assessed. 5-year adverse event-free survivals were calculated.

Results: One hundred and two men were enrolled in this retrospective analysis. Median age was 71 years (57-81). Median follow-up was 37 months (6-76). Twenty-three men (23%) underwent urological intervention after salvage HDR BT. Fourteen of them suffered from urinary retention, 9 men were treated due to refractory obstructive urinary symptoms. TURP or urethretomy was performed 15 and 12 times, respectively. Four patients underwent combination of both. Twelve patients suffered from urinary incontinence with no intervention, twenty men developed it after urological intervention. Five patients needed suprapubic catheter. 5-year urological intervention-free survival was 65%. 5-year urinary incontinence-free survival (UIFS) was 69%. Any urological intervention was linked with higher urinary incontinence probability (4-year UIFS 88% vs 5%, p-0.0000; HR-14.05; 95% CI 13.25-14.85).

Conclusion: There is high probability of urinary incontinence in salvage HDR BT prostate cancer patients after urological intervention (TURP/urethrotomy). Therefore patients suffering from refractory obstructive urinary symptoms without urinary retention should be carefully evaluated and counseled before any urological management.

PV-0040

MRI guided focal primary and (secondary) salvage HDR-BT in prostate cancer patients seems safe

M. Maenhout[1], M.A. Moerland[1], K.M. Van Vliet-van den Ende[1], R.I. Schokker[1], M. Borot de Battisti[1], M. Peters[1], M. Van Vulpen[1], J.R.N. Van der Voort van Zyp[1]

[1]UMC Utrecht, Department of Radiation Oncology, Utrecht, The Netherlands

Purpose or Objective: To evaluate the technical feasibility and safety of focal MRI guided HDR brachytherapy as a primary, salvage or secondary salvage treatment in 37 patient with a localized (recurrent) prostate cancer.

Material and Methods: From May 2013 until October 2015, 37 patients were treated with focal MRI guided HDR brachytherapy. 26 patients received MRI guided primary focal HDR brachytherapy, 8 patients salvage treatment and 3 patient secondary salvage treatment. The prescribed dose to the PTV was 19 Gy, with strict limitations to the organs at risk. Patients with a (recurrent) PA proven prostate cancer were included in this evaluation. Before treatment, a diagnostic multiparametric MR was performed to define the tumor region. In patients with recurrent disease, a choline PET scan or PSMA scan was performed to exclude patients with early distant metastasis. The treatment was performed through MR guidance, in a combined MR/HDR facility (Figure 1).

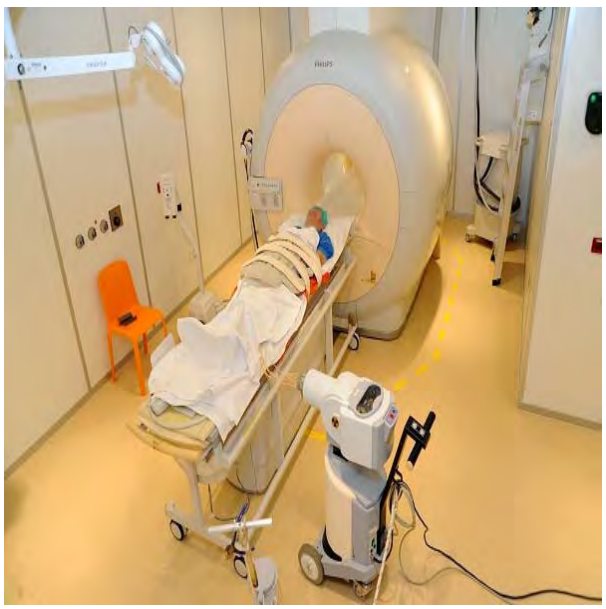

After ultrasound guided insertion of the catheters, an MRI of the prostate was performed for the reconstruction of the inserted catheters. Consequently, a per-operative treatment plan was performed prior to dose delivery. Toxicity was measured using the CTCAE version 4.

Results: For all patients, the treatment was tolerated well. In some patients, a lower dose to the PTV was given in order to protect the organs at risk. This was especially the case in patients that received a second salvage treatment. No patients developed a new grade 3 (or more) toxicity. One patient developed an acute urinary retention after primary focal HDR brachytherapy. Other grade 2 toxicity was uncommon in patients that received HDR brachytherapy as a primary treatment. In patients with a salvage treatment, grade 2 toxicity such as urinary infections and incontinence occurred in 3 of 8 patients. The 3 patients that received a second salvage treatment had not developed severe toxicity. However, follow up of these patients is very short (1-6 months).

Conclusion: Focal HDR brachytherapy as focal, salvage and secondary salvage treatment seems clinically feasible and safe. It could be a promising treatment modality to reduce severe side effect in patients with primary prostate cancer. Furthermore, it could postpone hormonal treatment in patients with recurrent or secondary recurrent prostate cancer.

Symposium: Protons or heavy ions?

SP-0041
Physical advantages of particles: protons vs. heavy ions, what is certain what is not?

O. Jäkel[1,2]
[1]*German Cancer Research Center, Medical Phyiscs in Radiation Oncology, Heidelberg, Germany*
[2]*Heidelberg Ion Beam Therapy Center, Medical Physics, Heidelberg, Germany*

In this contribution the physical properties of protons and other Ions will be outlined and the differences between different ions will be highlighted. The relevance of these properties with respect to radiotherapy will be discussed. In detail the physical properties to be discussed are the depth dose distribution, lateral scattering and energy loss straggling. These quantities will mainly affect the dose conformation potential of the various ion beams through the distal and lateral penumbra and the dose in the entrance region. The most important difference here arises through the multiple small angle scattering of particles which is strongly depend on the mass of the Ions: for heavier Ions, the lateral penumbra will be significantly smaller than for protons.
Another very important physical paramter is the stopping power of the particles, as this quantity will influence the radiobiological properties of the differnt ions. The stopping power describes the energy loss of a particle per pathlength and be accuaretly calculated using the Bethe formalism. More important for the radiobiological effects is the linear energy transfer (LET), which is often used synomyously to stopping power. LET describes the eneryg transferred into a narrow region around the primary ion track and can also be calculated using the Bethe formalism. While the LET of a pure beam of ions with a fixed energy is well defined, the LET of a mixed radiation field is more complex. The reason for that is, that in a mixed radiation field, LET has to be averaged over the different Ions contributing. This is often done by using the so-called "dose averaged LET", where the LET of each particle is weighted according to the dose it is contributing. Another way of defining an average LET is by averaging over the fluence (or alternatively over the track length). Both average LET definitions are being used for various biological applications and will be presented. When discussing the relative biological effectiveness (RBE) of ion beams, one has to be aware of this difference.
Finally the nuclear fragmentation of ions may lead to strong differences in the spectrum, or mixture of ions of different kind at different points in depth. The relevance of these nuclear fargments becomes clear, when comparing the dose just behind the Bragg peak of a primary carbon ion beam (which is completely due to light fragments) and a proton beam (which is completely due to protons). An overview of the characteristics of the fragmentation spectra of Ions will therefore also be given.

SP-0042
Radiobiological benefits of protons and heavy ions - advantages and disadvantages

C.P. Karger[1]
[1]*German Cancer Research Center DKFZ, Department of Medical Physics, Heidelberg, Germany*

Both, carbon ions and protons show an inverted depth dose profile (Bragg-peak) and allow for highly conformal irradiations of tumors in the neighborhood of radiosensitive normal tissues. Heavier ions such as carbon ions additionally show an increased linear energy transfer (LET) towards the distal edge of the Bragg-peak leading to an increased relative biological effectiveness (RBE) with respect to photon irradiations [1]. While the RBE for clinical proton beams is currently fixed to 1.1, the RBE of carbon ion varies significantly within the treatment field and has to be calculated by RBE-models. The RBE-models, however, introduce additional uncertainties, which have to be considered in treatment planning and especially in clinical dose prescription.
As protons and carbon ions exhibit almost comparable geometrical accuracy, the clinical question whether protons or carbon will be more beneficial for the patient mainly addresses the independent role of the high-LET effect in radiotherapy. The answer to this question is related to the following subquestions: (i) How accurate is the applied RBE-model? (ii) Is a fixed proton RBE of 1.1 accurate enough for all field configurations? (iii) Which tumor types are best suited for heavy ions? (iv) Can high-LET irradiations overcome radioresistance of hypoxic tumors?
While questions (i) and (ii) refer to normal tissue reactions, (iii) and (iv) address the impact of tumor-specific resistance factors on the radiation response. An additional benefit of heavy ions will strongly depend on the differential response between tumor and normal tissue. Although the final prove or disprove of advantages has to be provided by prospectively randomized clinical trials, ongoing preclinical experiments can help to study the subquestions (i)-(iv) separately, i.e. to benchmark RBE-models (e.g. LEM I vs IV), to select suitable tumor entities, to setup clinical trials and to generally improve the understanding of normal and tumor tissue response after high- vs. low-LET irradiation.
The presentation will give an introduction on the concepts describing the response to high-LET irradiations and will give an overview on the available in vivo data with focus on the current answers to the above questions.
References
[1] Suit H, DeLaney T, Goldberg S et al. Proton vs carbon ion beams in the definitive radiation treatment of cancer patients. Radiother Oncol 2010;95:3-22.

SP-0043
How strong is the current clinical evidence for protons and heavy ions ?

P. Fossati[1,2]
[1]*Fondazione CNAO Centro Nazionale Adroterapia Oncologica, Clinical Department, Pavia, Italy*
[2]*European Institute of Oncology, Radiotherapy Division, Milano, Italy*

Particle therapy has been available in hospital setting since 1991. About 100.000 Patients have been treated worldwide with protontherapy and more than 10.000 patients have been treated with carbon ion radiotherapy. After almost 15 years in which this modality was available only in few centres in the last ten years the number of new particle facilities has steeply increased in the US and in Asia and more recently several facilities have been planned in Europe. Protontherapy has traditionally been used because of its strong preclinical rationale based on its favourable physical properties that allow a substantial reduction in integral dose and exposure of non-target tissues. Carbon ion radiotherapy has mainly been used for its radiobiological property that may offer an advantage in the treatment of macroscopic tumours made of

an heterogeneous cell population with a radio-resistant compartment. Evidence to support the use of particle therapy evolved in the past 25 years from level III (preclinical rationale) to level II (prospective non randomized trials). A hot debate has been on-going in the scientific community about the need of prospective RCT testing head to head particles versus modern X-ray radiotherapy. Those against the need of RCT argued that dose distribution was such a strong surrogate endpoint that RCT were not needed and that dose distribution had always guided the evolution of radiotherapy without the need of RCT. Those in favour argued that the only relevant endpoints were clinical outcome and measurable toxicity and that dose distributions of protontherapy despite its unquestionable advantage in terms of integral dose may be in some case less favourable than advanced x-ray dose distribution because of lateral scattering and shallower dose gradients in the high dose region. Historically only a single RCT of particle versus photons has been conducted, namely the UCSF-LBNL trial comparing helium ions radiotherapy versus Iodine-125 plaque brachytherapy for choroidal and ciliary body melanoma . Long terms result of the trial a showed a clear advantage of charged particles over brachytherapy in terms of local control. However this result did not definitively solve the issue as helium is no longer used in clinical practice and extrapolation of this trial to protontherapy is maybe not straightforward; moreover the trial was criticized because of a supposed suboptimal technique in the brachytherapy arm. With the increased availability of proton facilities the amount of non-randomized evidence is rapidly increasing and several prospective non-randomized trial are being conducted. At present particle therapy has found its way in several guidelines. As an example in the last version of ESMO guidelines for bone sarcoma particle therapy is considered the first option for chordoma both in the post operative setting and for inoperable disease. In this framework also RCT are at present being conducted. A prospective phase II RCT in stage II-IIB NSCLC patients (NCT00915005) randomized to either photons or protons adaptive IGRT with two levels of dose (66 Gy [RBE] + vs. 74 Gy [RBE]) with primary endpoints local control and toxicity G≥3 has completed its accrual. Two other trials are testing protontherapy vs photons X-Ray in locally advanced NSCLC (RTOG 1308) or in centrally located stage I NSCLC (NCT01511081) and are expected to complete accrual in 2020 and 2016. Another prospective phase III RCT ongoing at MGH testing IMRT vs protontherapy for prostate cancer (NCT01617161) is expected to complete accrual in 2016 A prospective phase II/III RCT for stage III and IV oropharyngeal SCC (NCT01893307) is comparing 70 Gy [RBE] delivered with either IMRT or intensity modulated protontherapy. And is expected to complete accrual by 2023 Another trial is testing protons vs photons in GBM (NCT01854554) and should complete accrual by 2017. A RCT is recruiting patient with oesophageal cancer to test chemo radiation with photons vs. chemo radiation with protons (NCT01512589) and should be completed within 2018. Other RCT are ongoing comparing protons versus carbon ions in sacral chordoma (ISAC trial NCT01811394) in skull base chordoma (NCT01182779) and in skull base chondrosarcoma (NCT01182753). RCT are recruiting patient to test protontherapy vs RF ablation in HCC (NCT01963429) or protontherapy + sorafenib vs. sorafenib alone in HCC (NCT01141478). A RCT of particle therapy vs surgery for sacral chordoma (SACRO) is in its final design stage in Europe. Another phase III RCT of carbon ion radiotherapy versus photons or protons radiotherapy for head and neck soft tissue sarcoma and adenoid cystic carcinoma (PHRC ETOILE-ULICE) is going to start recruitment in the next year. In conclusion the present day clinical evidence for particle therapy is of level II (with the only exception of eye melanoma). A large effort to produce level I evidence is ongoing worldwide.

Proffered Papers: Radiobiology 1: Radiation effects on normal tisssues and the microenviroment

OC-0044

Fingolimod mitigates radiation-induced cognitive deficits by restoring dentate gyrus neurogenesis

A. Stessin[1], M. Banu[2], V. Blaho[3], S. Ryu[1]
[1]*Stony Brook University Hospital, Department of Radiation Oncology, Stony Brook, USA*
[2]*Columbia University, Department of Neurological Surgery, New York, USA*
[3]*Weill Cornell Medical College, Department of Pharmacology, New York, USA*

Purpose or Objective: This study evaluates FTY720/Fingolimod as a potential mitigator of radiation-induced neurocognitive dysfunction.

Material and Methods: The effects of radiation and FTY720 on neural progenitor cells (NPCs) and brain tumor stem cells (BTSCs) were tested *in vitro*. To study radiation-induced neurocognitive deficits, 6 week-old C57/Bl/6J mice received 0 or 7 Gy cranial irradiation and were treated with intraperitoneal FTY720 or vehicle for seven weeks. Fear conditioning and the Morris water maze were then employed to test learning and memory. Immunohistochemical staining for NPCs and mature neurons was used to assess changes in neurogenesis. To test effects on tumor growth, mice harboring BTSC xenografts were treated with intraperitoneal FTY720 or vehicle for six weeks.

Results: In NPCs, FTY720 induced ERK1/2 phosphorylation in the presence of radiation. In glioma cells, ERK1/2 phosphorylation was detected at baseline, and FTY720 did not elicit any further increase. Correspondingly, FTY720 increased the viability of NSCs but not glioma cells after radiation. Inhibiting S1P1/MAPK signaling in NPCs abolished the protective effects of FTY720. In irradiated mice, learning deficits were manifested by significantly longer latency times compared to non-irradiated controls ($p = 0.001$). The deficits were fully restored by FTY720. In irradiated brains, FTY720 maintained a viable NPC pool and restored the cytoarchitecture of the DG granular cell layer. In mice harboring BTSC xenografts FTY720 delayed tumor growth and improved survival ($p=0.012$).

Conclusion: FTY720 mitigates radiation-induced learning dysfunction by partially restoring DG neurogenesis. Furthermore, FTY720 appears to delay tumor growth and improve survival in a xenograft glioma mouse model.

OC-0045

Dual pathway inhibition attenuates radiation-induced pulmonary inflammation and fibrosis

N.H. Nicolay[1,2], M. Dadrich[2,3], R. Lopez Perez[2], U. Wirkner[2], P. Peschke[2], J. Debus[1,2], P.E. Huber[1,2]
[1]*Heidelberg University Hospital, Radiation Oncology, Heidelberg, Germany*
[2]*German Cancer Research Center, Radiation Oncology, Heidelberg, Germany*
[3]*Frankfurt University Hospital, Radiology, Heidelberg, Germany*

Purpose or Objective: Radiation therapy is a mainstay for lung cancer therapy, but the effective dose is commonly limited by the onset of radiation-induced lung damage. Single pathway inhibitors against transforming growth factor ß (TGFß), platelet-derived growth factor (PDGF) and others have been shown in experimental models to attenuate radiation-induced pulmonary injury. However, the effects of multiple pathway inhibition regarding the development of these diseases remain unknown.

Material and Methods: C57BL/6 mice were treated with a single dose of up to 20 Gy photons to their thoraxt o induce radiation induced lung toxicity. After Irradiation , small molecule kinase inhibitors against PDGF, VEGF and TGFß

receptors were administered orally either as single agents or in combination approaches. Survival and treatment-related side effects were followed up for more than 6 months. Lung density and septal fibroses were measured at various time points by HR-CT and MRI, and the molecular changes of irradiated lung tissue were analyzed using immunohistochemistry and gene expression analyses.

Results: Treatment with individual inhibitors attenuated radiation-induced pulmonary inflammation, and reduced radiological and histological signs of pulmonary injury and fibrosis. Multi-pathway inhibition resulted in a significant additional attenuation of radiation-induced pulmonary damage and increased overall survival of treated mice compared to single-agent inhibition. Irradiation induced gene expression changes in lung tissue of downstream genes in particular for PDGF and TGFß pathways; kinase inhibitors altered the expression of downstream proteins suggesting significant crosstalk between pathways during the development of radiation-induced lung injury. The expression of osteopontin as an established biomarker for pulmonary fibrosis was significantly upregulated by irradiation both on mRNA and protein levels; multi pathway inhibition completely normalized its overexpression when administered after radiation therapy.

Conclusion: Multi-pathway signaling inhibition for PDGF, VEGF and TGFß was shown to be an effective treatment for radiation-induced pulmonary damage and correlated well with reduced immune cell influx and expression of the pulmonary fibrosis biomarker osteopontin. Microarray-based gene expression analysis suggested extensive crosstalk between pathways upon thoracic Irradiation, warranting a combined Treatment approach. Multi-pathway inhibition suggests a novel treatment approach for the therapy of fibrotic lung diseases.

OC-0046

Radiation induced carcinogenesis of cells with stem cell potential from breast and thyroid gland

M. Zwar[1], N. Hosper[2], K. Manda[1], D. Buttler[1], U. Giesen[3], R. Nolte[3], R. Coppes[2], G. Hildebrandt[1]

[1]Radiol. Univ. Klinik Rostock, Department of Radiotherapy and Radiation Oncology, Rostock, Germany

[2]University Medical Center Groningen, Departments of Cell Biology and Radiation Oncology, Groningen, The Netherlands

[3]Physikalisch-Technische Bundesanstalt, PTB, Braunschweig, Germany

Purpose or Objective: During treatment of cancer patients using proton therapy, neutrons are generated as unwanted by-products. This out-of-field neutron exposure may affect the whole body of the patients and has been suggested to lead to enhanced formation of secondary cancer, especially in young patients. In recent years, indications for the involvement of stem cells in carcinogenesis have been increasing. Due to their long life span, stem cells may have an increased propensity to accumulate genetic damage relative to differentiated cells. Against this background, the intention of this study is to estimate the risks from neutrons compared to photons. Therefore, the investigation of damage induction on healthy adult stem cells from breast and thyroid tissue as an evidence of relative carcinogenic effectiveness following low and intermediate doses from neutrons compared to photons is performed.

Material and Methods: Human breast cells with stem cell potential as well as murine thyroid stem cells are exposed to x-rays or neutrons (monoenergetic 0.56 MeV and 1.2 MeV neutron fields, neutron field with a broad energy distribution and a mean energy of 5 MeV) at various dose rates. In order to detect early indicators of carcinogenic modifications various *in vitro* analyses are utilised. By means of xenograft mouse models, tumour transformation for both cell types is analysed *in vivo*.

Results: Previous results for cells originated from breast tissue show significant differences in survival, DNA repair and in the expression of stem cell marker MUC-1 and genes commonly associated with cancer following neutron exposure. The influence of radiation quality on the ability for self-renewal could be demonstrated by the use of a spheres formation assay. By analysing residual double strand breaks via the γH2AX assay, an effect on DNA repair could be observed, particularly after irradiation with neutrons with a low energy of 0.56 MeV. Furthermore the expression of the proteins p53, p27 and RB1 is modified considerably due to neutron irradiation. Similarly, exposure of thyrosphere derived cells showed differences in stem cell survival and remaining γH2AX foci after 24 hours. Long term passaging revealed changes in growth speed, stem cell marker expression and cancer associates genes changed in individual samples.

Conclusion: Summing up, the study of stem cell behaviour may be a valuable tool in the investigation of carcinogenesis induced by ionizing radiation. The evaluation of the Relative Biological Effectiveness (RBE) of different types and energies of radiation may have a strong impact on our knowledge about the role of stem cells in carcinogenesis and will provide great benefit on the understanding of long-term risks of secondary cancers following low-dose exposure to neutrons during proton therapy.

This work is financially supported from the 7th Framework Programme of European Commission (EURATOM) under contract FP7- 295970 (ANDANTE).

OC-0047

PD-L1/PD-L2 gene expression differs in tumor vs. lung tissue in non-small cell lung cancer patients

K. Reynders[1,2], E. Wauters[3,4], J. Vansteenkiste[4], H. Decaluwé[5], P. De Leyn[5], K. Nackaerts[4], S. Peeters[2], C. Dooms[4], W. Janssens[6], D. Lambrechts[3], D. De Ruysscher[2]

[1]KU Leuven, Experimental Radiation Oncology, Leuven, Belgium

[2]University Hospitals Gasthuisberg, Radiation Oncology, Leuven, Belgium

[3]KU Leuven, Laboratory of Translational Genetics Vesalius Research Center, Leuven, Belgium

[4]University Hospitals Gasthuisberg, Respiratory Oncology Pneumology, Leuven, Belgium

[5]University Hospitals Gasthuisberg, Thoracic Surgery, Leuven, Belgium

[6]University Hospitals Gasthuisberg, Pneumology, Leuven, Belgium

Purpose or Objective: Targeted therapies like immune checkpoint inhibitors are rapidly turning out to be important assets in the treatment of non-small scell lung cancer (NSCLC). The expression of these genes in both tumor and the surrounding non-malignant lung tissue might play an important role in determining their therapeutic window. This project aims to identify different expression patterns of these target genes. We therefore performed transcriptome analysis and investigated correlations with histology, gender, age, CRP level and smoking status in primary resected NSCLC and the surrounding non-malignant lung of the same patient. Additionally, differentially methylated gene sites were checked for impact on gene regulation.

Material and Methods: Tissue of primary tumor as well as distant lung tissue was collected from 25 untreated, primary resected NSCLC patients. Illumina HiSeq 2000 was used to determine the differential gene expression between different conditions for 14 different target genes. DeSeq was chosen as the definitive method for statistical analysis. Differential methylation status was analyzed on an Infinium HumanMethylation 450K BeadChip. Differential gene expression and methylation status of the 14 chosen target genes were compared for 11 different conditions; results with P-values <0.05 after Benjamini-Hochberg correction were considered significant. For each differentially expressed gene, the locations of differentially methylated sites were checked in the UCSC Genome Browser. Histone markers H3K4Me1, H3K4Me3 and H3K27Ac as well as presence of CpG

islands were used to identify methylated regulatory elements.

Results: Nineteen men and 6 women, with a median age of 69 years, were included. Ten were current smokers, 14 ex-smokers (stopped more than 4 weeks before surgery) and 1 non-smoker. Fourteen patients had adenocarcinoma, eleven patients had squamous cell carcinoma. When compared to distant lung tissue, gene expression of PD-L2, HGF, VEGFR2 and VEGFR3 were downregulated in tumor tissue. PD-L1 expression was also downregulated in tumor tissue, but only in active smokers. For PD-L2, HFG, VEGFR2 and VEGFR3, methylation data shows a clear hypermethylation pattern in the promoter and enhancer regions of tumor tissue, which is conform the results of the transcriptome sequencing. Qualitative results of the expression and methylation data are depicted in figure 1.

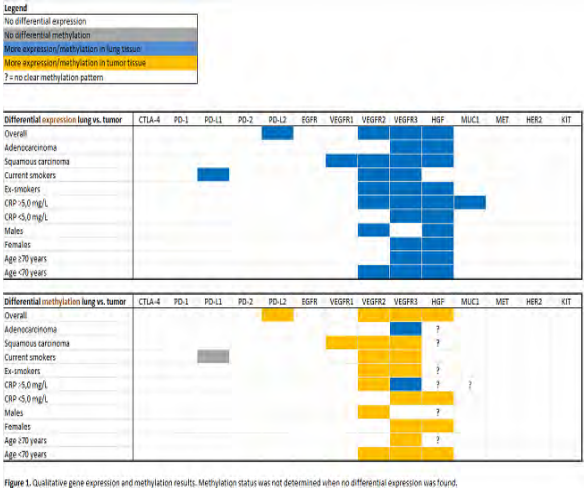

Figure 1. Qualitative gene expression and methylation results. Methylation status was not determined when no differential expression was found.

Conclusion: Our results show a lower expression of PD-L1 in tumors of active smokers. PD-L2, VEGFR2 and VEGFR3 and HGF have a lower expression in tumors overall. Methylation data confirms these findings. The therapeutic ratio with targeted treatment might be narrow as a result of this higher expression in distant lung tissue and in the case of immune checkpoint inhibitors, increase the chance of pneumonitis.

OC-0048

Tumor microenvironment response and bone marrow cell migration after pulsed radiotherapy

J.L. Kane[1], S.A. Krueger[1], A. Hanna[1], T.R. Raffel[2], G.D. Wilson[1], G.J. Madlambayan[2], B. Marples[1]
[1]*Beaumont Health, Radiation Oncology, Royal Oak MI, USA*
[2]*Oakland University, Biology, Rochester, USA*

Purpose or Objective: Recent studies have shown that alterations in the pattern of radiation delivery, such as pulsed radiotherapy (PRT), can produce significant changes to the tumor microenvironment. Given the positive effects of PRT on maintaining tumor vasculature, we hypothesized that PRT treatment would allow tumor microenvironments to remain more oxygenated and result in better overall tumor killing compared with SRT. We further postulated that this effect would be associated with decreased tumor hypoxia, leading to lower vascular endothelial growth factor (VEGF) and stromal derived factor-1 alpha (SDF-1α) production and subsequently lower recruitment of bone marrow derived cells (BMDCs) in PRT-irradiated tumors.

Material and Methods: Subcutaneous Lewis lung carcinoma (LLC) tumors were established in C57BL/6 mice. Tumors were allowed to grow to 100-200mm3 before irradiation with a 160 kVp Faxitron cabinet (HVL: 0.77 mm Cu) using a dose rate of 0.69 Gy/min. SRT or PRT was given to 20 Gy at 2 Gy/day using a 5 day-on, 2 day-off schedule to mimic clinical delivery. Tumors were harvested 2-3 days post treatment. Radiation-induced changes in the tumor microenvironment were examined using flow cytometry and antibody-specific histopathology. Normal tissue effects were determined using non-invasive 18F-FDG PET/CT and MR imaging after naïve animals were given whole-lung irradiation to 40 Gy using the same 2 Gy/day regimens.

Results: PRT was more effective than SRT at reducing tumor growth rate (0.24±0.02mm3/day and 0.67±0.06mm3/day respectively; p<0.0001). Histopathology analysis showed a significant reduction in the levels of Ki-67 (13±8%), hypoxia (8±1%), VEGF (3.5±1%) and SDF-1α (4.2±1.5%) as well as a concomitant decrease in CD45+ BMDC migration (7.8±2.2%) after PRT when compared to SRT. Higher vessel density was also observed in PRT irradiated tumors. No short-term differences were observed in normal lung tissue after PRT or SRT although all irradiated animals demonstrated higher levels of inflammation than controls.

Conclusion: Using a rapidly proliferating LLC allograft model, we have found evidence for improved tumor killing with PRT relative to SRT due to vascular maintenance. PRT irradiated tumors exhibited slower growth rate and reduced hypoxia coincident with loss of supportive mechanisms utilized by tumors in low oxygen microenvironments, such as angiogenesis and recruitment of BMDCs. This study demonstrates the efficacy of PRT and highlights the importance of microenvironment responses during tumor radiotherapy. We conclude that PRT represents an improved treatment strategy that may result in better overall patient outcomes with little alteration in normal tissue toxicity.

Proffered Papers: Clinical 1: Breast

OC-0049

Trends in the use of postoperative radiotherapy following mastectomy: a population-based study

S. Corradini[1], J. Engel[2], C. Belka[1], M. Niyazi[1]
[1]*University of Munich, Radiation Oncology, Munich, Germany*
[2]*University of Munich, Munich Cancer Registry MCR of the Munich Tumour Center TZM at the Department of Medical Informatics- Biometry and Epidemiology IBE, Munich, Germany*

Purpose or Objective: The objective of this population-based study was to provide an overview on trends and changing patterns in the adoption of postmastectomy radiotherapy (PMRT) over a 25-year period, and to validate the effectiveness of postoperative radiotherapy. Focused attention was given to disparities and barriers related to the use of postoperative radiotherapy in nodal positive disease and elderly patients.

Material and Methods: The study included epidemiological data of 16,675 patients diagnosed with invasive breast cancer from 1988 to 2012, within the catchment area of the Munich Cancer Registry. Use of PMRT, local recurrence free survival (LRFS), cumulative incidence (CI) of time to local recurrence, relative survival and conditional overall survival (cOS), were analysed for different time periods (1988-1997 and 1998-2012). Factors predicting the use of postoperative radiotherapy were analysed using multivariate logistic regression.

Results: Use of PMRT was associated with significant improvements in local control, with a 10-year LRFS of 88.9% with PMRT vs. 84.1% following mastectomy alone (p<0.001). After adjusting for age, tumour characteristics and other therapies, the Cox-regression analysis for LRFS identified PMRT as an independent predictor for improved local control (hazard ratio [HR]: 2.145; 95% CI: 1.787-2.574, p<0.001). Patients with 1-3 involved lymph nodes had a 10-year CI of time to local recurrence of 13.7% following mastectomy alone, compared to 6.5% following PMRT (p= 0.001). Comparable findings were obtained for the subgroup of patients presenting with 4 po sitive lymph nodes – presenting with 17.8% 10-year CI of time to local recurrence in the mastectomy only group, compared to 8.2% in the PMRT group (p<0.001). All effects were smaller or extinct in elderly patients aged ≥ 70 years. On multivariate analysis for cOS, no

advantage for PMRT was detected (HR: 1.084; 95% CI:0.986-1.191, p=0.095). Variables favouring the use of postoperative radiotherapy on multivariate logistic regression analysis included young age (p<0.001), large tumour size (pT3/4) (p<0.001), positive resection margin (p<0.001), and positive nodal status (p<0.001). High-risk patients with≥ 4 positive lymph nodes who underwent mastectomy in 1998-2012 had a significant increased likelihood of receiving PMRT (OR 6.245) as compared to patients treated in the early period of analysis, from 1988-1997 (OR 2.837).

Conclusion: The present study was useful in providing a window on the adoption of PMRT in a large population-based cohort, and to determine trends over time, as well as to characterize and quantify the outcome in clinical practice. A significant shift in indications for PMRT was registered, especially for high-risk patients with≥ 4 positive lymph nodes. Moreover, the present findings track a substantial variation and apparent underuse of PMRT within the vulnerable population of elderly patients aged ≥ 80 years.

OC-0050

Variations in use of hypofractionation for early, node-negative breast cancer in NSW 2007-2012

G. Delaney[1], S. Gandhidasan[2], F. Terlich[3], D. Baker[3], R. Walton[3], D. Currow[3]
[1]*Liverpool Hospital, Area Cancer Services, Liverpool, Australia*
[2]*Peter MacCallum Cancer Institute, Radiation Oncology, Melbourne, Australia*
[3]*Cancer Institute NSW, Ministry of Health, Sydney, Australia*

Purpose or Objective: Phase III randomised controlled trials and subsequent evidence-based treatment guidelines suggest that breast hypofractionation has low toxicity and similar cancer outcomes compared to patients undergoing standard fractionation. However, uptake of hypofractionation has not been universal. The aim of this study was to investigate the uptake of hypofractionation regimens in all public radiation oncology facilities in NSW.

Material and Methods: Data from the NSW Clinical Cancer Registry were extracted, cleaned and verified. The inclusion criteria included those patients that are node negative breast cancer (TNM stage I or IIA), year of diagnosis between 2007 to 2012, year of treatment between 2008 and 2012 and received external beam radiotherapy in a public radiotherapy facility. Data extracted included dose and fractionation type, patient age at first fraction, distance from treatment facility, year of diagnosis, year of treatment, laterality of treatment and department of treatment. In this analysis, standard fractionation was defined as dose per fraction of between 1.8 – 2.4 Gy per fraction and hypofractionation as above 2.4 Gy per fraction. Univariate and multivariate analyses were performed to assess which factors predict for hypofractionation use.

Results: Of the 6066 early breast cancer patients fulfilling the study criteria, 3947 patients (65%) had standard fractionation and 2119 patients (35%) received hypofractionation in 14 public radiotherapy centres in NSW. There was a wide spread of fractionation used across departments ranging from 6% to 92%. Hypofractionation use exceeded 50% in only 4 departments. Statistically significant factors to predict for hypofractionation use were increasing patient age, right sided breast cancer, further distance from home to the treating facility, more recent treatment, facility and clinician treating.

Conclusion: While hypofractionation has become more common across NSW, there remains a substantial proportion of patients for whom hypofractionation would be considered appropriate who are not receiving hypofractionation. This has also been found to be the case in US studies, although we believe we are the first to identify laterality as an indicator. Understanding factors that may predict standard fractionation use might assist in developing strategies to address the issue. Hypofractionation for early breast cancer being adopted more widely would lead to greater patient convenience, better resource efficiencies in radiation oncology departments and perhaps even increase the use of post-lumpectomy radiotherapy, as some patients might currently forego radiotherapy due to the perceived inconvenience of standardly fractionated radiotherapy.

OC-0051

Variability in lymph node delineation for breast cancer radiotherapy: an AIRO multicenter study

D. Ciardo[1], R. Ricotti[1], B.A. Jereczek-Fossa[1,2], A.I.R.O. Breast Cancer Working Group[3]
[1]*European Institute of Oncology, Department of Radiation Oncology, Milan, Italy*
[2]*University of Milan, Department of Oncology and Hemato-Oncology, Milan, Italy*
[3]*Associazione Italiana di Radioterapia Oncologica, AIRO, Milan, Italy*

Purpose or Objective: To investigate inter-operator and inter-center variability in lymph node (LN) volume delineations in breast cancer (BC) nodal irradiation.

Material and Methods: The study was conducted by the Italian Society of Radiation Oncologists (AIRO) - Breast Cancer Working Group. For each center, 3 radiation oncologists (ROs) with different expertise were involved: 1 junior (J), 1 senior (S) not dedicated to BC, and 1 senior (E) expert in BC. The CT series of 3 patients at different levels of complexity were selected: 1 with simple anatomy (P1), 1 obese (P2) and 1 with impaired arm mobility (P3). ROs were asked to contour axillary nodes, as follows: I level (L1), II level (L2) and III level, the latter was further divided into infra (L3) and supraclavicular (L4) nodes on CT images by applying guidelines on breast contouring released by AIRO. The inter-category and the inter-center variability were investigated, by evaluating the variability in volume size, structure overlap (measured as Dice similarity coefficient, DSC), and average Hausdorff distance (AHD) between contours.

Results: Thirty-nine ROs from 14 centres participated and 468 contours were obtained. Firstly, the analysis was focused on volume size. By comparing the operators, E-ROs contoured slightly larger volumes than S-ROs and J-ROs, with no statistically significant differences. Conversely, statistically significant differences were found in volume size when stratifying for patients (larger volumes were obtained for P2) and for LN levels (in order of size: L1, L4, L2, L3 – L1 being the largest and L3 the smallest). Secondly, descriptive and statistical intra-group analysis showed that all the 3 principal factors (different expertise, LN level and patient) contributed to inter-operator variability. When analysing DSC, poor agreement was found among ROs stratified for expertise (Fig. 1a) and the differences between S-ROs and the other groups were statistically significant. Considering the LN levels (Fig. 1b), the highest concordance was found in the contouring of L1 and L4 levels and the lowest for L3 (p<0.05). Moreover, inter-operator consistency dramatically decreased as patient complexity increased (Fig. 1c). Consistent results were found in the analysis of AHD. Finally, considering the inter-center variability, statistically significant differences were found in 38.5% of comparisons when considering intra-center median DSC (Fig. 1d) and in 33% of comparisons when considering intra-center median AHD.

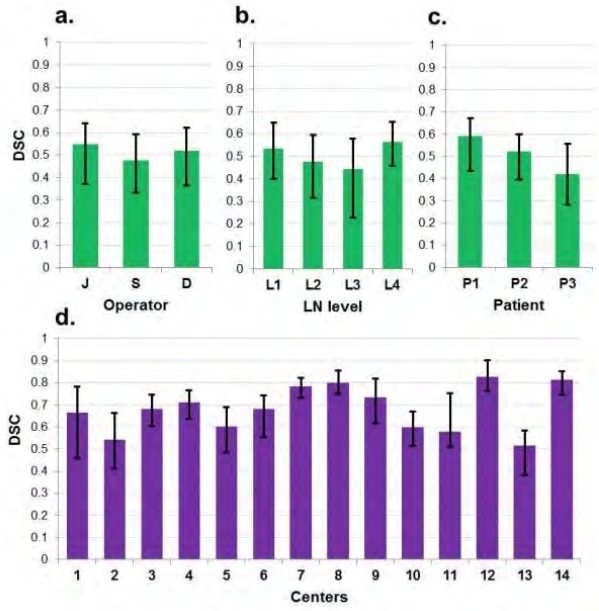

		L1		L2		L3		L4	
		mean	st.dev.	mean	st.dev.	mean	st.dev.	mean	st.dev.
J	P1	62.8	15.7	20.1	4.7	9.1	3.1	30.3	8.7
	P2	89.6	34.8	31.4	12.3	17.0	6.5	37.7	9.8
	P3	39.3	16.6	24.0	9.5	12.2	6.6	22.2	10.3
S	P1	65.1	28.4	18.0	3.0	12.4	5.6	35.3	16.8
	P2	87.1	49.1	30.7	12.2	21.8	8.2	42.9	21.7
	P3	41.4	22.8	26.4	11.6	16.1	10.5	23.8	12.6
E	P1	70.4	35.8	17.7	5.3	11.5	7.0	32.4	6.8
	P2	116.2	67.3	32.6	10.6	22.5	11.5	39.0	9.0
	P3	48.6	21.2	22.2	5.8	16.3	12.6	23.0	7.7

Conclusion: Guidelines for regional LN did not significantly improve the consistency of contouring among ROs. The J-ROs were the most accurate in contouring according to AIRO guidelines and showed the highest level of homogeneity, while the S-ROs followed the guidelines to a lesser extent, probably because of higher self-confidence.

OC-0052

Long-term age dependent failure pattern after BCT vs. mastectomy in low-risk breast cancer patients

T. Laurberg[1], C. Lyngholm[1], J. Alsner[1], P. Chritiansen[2], J. Overgaard[1]

[1]*Aarhus University Hospital, Department of Experimental Clinical Oncology, Aarhus, Denmark*

[2]*Aarhus University Hospital, Department of Surgery P- Breast and Endocrine Section, Aarhus, Denmark*

THIS ABSTRACT FORMS PART OF THE MEDIA PROGRAMME AND WILL BE AVAILABLE ON THE DAY OF ITS PRESENTATION TO THE CONFERENCE

OC-0053

Re- irradiation for locally recurrent breast cancer

E. Bräutigam[1], C. Track[1], M. Geier[1], H. Geinitz[1]

[1]*Krankenhaus der Barmherzigen Schwestern - Linz, Radiation Oncology, Linz, Austria*

Purpose or Objective: To report an analysis of treatment outcomes and toxicity of a cohort of patients re- irradiated after a second breast conserving surgery or no further surgery.

Material and Methods: Between 11/05 and 10/15, 32 women were re- irradiated with 50- 60 Gy for locally recurrent breast cancer. The first RT course included postoperative radiotherapy with a total dose of 50 Gy in 25 or 50,4Gy in 28 fractions followed by a boost dose to the tumor bed according to risk factors in 81.3%. In 18.7% supraclavicular nodes were treated with 50Gy.The median age at first diagnosis was 53.3 years (range 36- 69.7). 78.1% of the women were postmenopausal. 81.25% of the tumors were pathologically classified as T1, 12.5% as T2 and 6.25% as ductal carcinomas in situ. Axillary lymph node involvement was seen in 34.3%. Most of the tumors were estrogen positive (68.75%) and progesterone positive (65.6%). A systemic therapy was given in 81.25% of the patients. After second breast conserving therapy or no surgery re- RT was given to the involved quadrant using external- beam ports (electrons or photons) with doses of 50-60Gy in 2Gy per fraction. The median age at local relapse was 65.8 years. A second breast conserving therapy was performed in 90.7% of the women, 9.3% had no surgery and were re-irradiated to a dose of 60Gy. A systemic therapy was given in 84.3%.Survival and local control were calculated by the Kaplan-Meier actuarial method.

Results: A total of 32 patients were retrospectively analyzed. The median follow up of survivors was 181 months from first diagnosis and 33 month from second RT. At the time of analysis 4 patients had died. The median time between first and second RT was 9.9 years (range 1.8- 20.3). Fifteen years after first diagnosis 86% of the patients were still alive. Four women died, 3 on cancer. After second RT only one acute G2 toxicity of the skin was reported (desquamation).Late toxicity was scored using the LENT- SOMA Score Criteria. Lymphedema (G1) of the ipsilateral arm was observed in 3.1%, 3.1% reported on intermittent pain in the breast and 9.3% presented with an asymptomatic breast edema. The highest rate of late toxicity was G2 fibrosis in 18.7%.No G3 or G4 toxicity was observed.

Conclusion: Carefully planned re-RT of the involved breast quadrant is a safe alternative therapy for those women who did not gave their consent to the recommended mastectomy. No second local relapse was detected after re-RT. Acute side effects were low. In 18.7% of the women fibrosis G2 was detected.

OC-0054

Reirradiation+hyperthermia for recurrent breast cancer-en-cuirasse in previously irradiated area

S. Oldenborg[1], J. Crezee[1], Y. Kusumanto[1], R.M. Van Os[1], S.B. Oei[2], J.L.M. Venselaar[2], P.J. Zum Vörde Sive Vörding[1], C.R.N. Rasch[1], G. Van Tienhoven[1]

[1]*Academic Medical Center, Radiation Oncology, Amsterdam, The Netherlands*

[2]*Institute Verbeeten, Radiation Oncology, Tilburg, The Netherlands*

Purpose or Objective: Cancer en cuirasse is a severe locoregional manifestation of breast cancer, usually occurring after a number of treatment failures. Treatment options are limited. One hundred and sixty-nine patients were treated with re-irradiation and hyperthermia (reRT+HT) from 1982 till 2006. Response and toxicity rates as well as the locoregional progression free interval were determined to assess the palliative value of this treatment.

Material and Methods: All patients had received extensive previous treatments, including surgery, irradiation (median dose 50Gy with or without boost) and systemic treatments.. Seventy-five percent of patients had 1-7 previous locoregional recurrence episodes; 68% were treated with systemic therapies and 27% underwent salvage surgery.
At start of re-RT+HT the tumor area comprised > 3/4 ipsilateral chest wall in 54% of patients. Fifty-two percent had areas of ulcerating tumor. Distant metastases were present in 45% of patients. reRT consisted typically of 8x4Gy, twice a week or 12x3Gy, four times a week. Superficial hyperthermia was applied once or twice a week using 434MHz Contact Flexible Microstrip Applicators (CMFA), heating the tumor area to 41-43°C for one hour.

Results: The treatment was well tolerated; 154 patients completed treatment, only 15 patients did not, due to

disease progression in 12, toxicity in 2 and refusal in 1 patient. Overall clinical response rate was 72% (30% CR; 42% PR), while only 6% showed PD. Median follow-up time was 7 months. The 1-year progression-free-interval was 24% with a 1-year survival rate of 36%. Acute ≥ grade 3 toxicity occ urred in 33% of patients and consisted mostly of ulceration and dermatitis. The occurrence of radiation ulcera was significantly related to the presence of ulcerating tumor before the start of the reRT-HT (P=0.004, HR = 4.4).

Conclusion: The combination of re-irradiation and hyperthermia is well tolerated and results in high response rates despite extensive disease and resistance to previous treatments. ReRT+HT is a worthwhile palliative treatment option for this patient group who suffer from extensive locoregional tumor growth and have a very poor prognosis.

Proffered Papers: Clinical 2: Adverse effects in radiotherapy

OC-0055

Pseudo-progression after stereotactic radiotherapy of brain metastases is serious radiation toxicity

R. Wiggenraad[1], M. Mast[1], J.H. Franssen[2], A. Verbeek- de Kanter[1], H. Struikmans[1]
[1]*Radiotherapy Centre West, Radiotherapy, The Hague, The Netherlands*
[2]*Haga Hospital, Radiotherapy, The Hague, The Netherlands*

Purpose or Objective: Stereotactic radiotherapy (SRT) of brain metastases results in regression of most treated metastases, but subsequent lesion growth may occur and is caused by either tumor progression or pseudo-progression, which is probably a radiation effect on surrounding normal brain tissue. It is unknown if active treatment is indicated in symptomatic patients, or if it is better to wait for spontaneous recovery. The purpose of this study is to describe the clinical course of brain metastasis patients developing pseudo-progression after SRT to improve clinical decision-making.

Material and Methods: Follow-up MRI scans of all patients who received SRT of brain metastases from 2009 through 2012 were reviewed for post SRT lesion growth. Depending on the volume of the metastasis, the patients had received one fraction of 21Gy, 18Gy, or 15Gy, or three fractions of 8Gy or 8.5Gy. The GTV-PTV margin was 2mm. Pseudo-progression was considered to be the cause of this lesion growth if a histological diagnosis of necrosis had become available, if the lesion had shown subsequent regression or if two neuro-radiologists agreed upon this diagnosis based on a review of the follow-up perfusion MRI scans. The clinical course of the patients with these pseudo-progressive lesions was retrospectively studied.

Results: In a total of 237 treated patients we identified 37 patients with 50 pseudo-progressive lesions. The median follow-up of all patients still alive was 40.7 months. The main clinical symptoms that were attributed to this lesion growth were neurologic deficits, headache and seizures in 19 (51%), 3 (8%) and 4 (11%) patients respectively (unknown in one). Ten patients (27%) had no symptoms attributed to the lesion growth and remained asymptomatic afterwards. Of the 19 patients with neurologic deficits one improved after spontaneous regression of the lesion, one improved after surgery and 17 did not improve. Two out of the four patients with seizures improved with ant-epileptic drugs (AED's), one improved after surgery and one did not improve. Only one of the three patients with headache improved with steroids. Spontaneous regression of an initially pseudo-progressive lesion was observed in 18 patients. Twelve of these 18 patients had symptomatic pseudo-progression, but only one of these 12 patients experienced neurologic improvement without treatment. In 6 patients their deaths were related to the pseudo-progressive lesion.

Conclusion: Patients with an asymptomatic pseudo-progressive lesion frequently remain asymptomatic. Patients with a symptomatic pseudo-progressive lesion only rarely recover spontaneously. Active treatment, such as surgery, should be considered for these patients. Therefore, symptomatic pseudo-progression after SRT of brain metastases needs to be considered as a serious radiation induced toxicity. Reduction of the high dose volume of normal brain tissue may prevent this toxicity.

OC-0056

FLAME: Influence of dose escalation to 95Gy for prostate cancer on urethra-related toxicity and QOL

J. Van Loon[1], M. Van Vulpen[1], F. Pos[2], K. Haustermans[3], R. Smeenk[4], L. Van den Bergh[3], S. Isebaert[3], G. McColl[4], M. Kunze-Busch[4], B. Doodeman[2], J. Noteboom[1], E. Monninkhof[5], U.A. Van der Heide[2]
[1]*UMC Utrecht, Radiation Oncology, Utrecht, The Netherlands*
[2]*The Netherlands Cancer Institute, Radiation Oncology, Amsterdam, The Netherlands*
[3]*University Hospital Leuven, Radiation Oncology, Leuven, Belgium*
[4]*University Medical Center Radboud, Radiation Oncology, Nijmegen, The Netherlands*
[5]*UMC Utrecht, Julius Center for methodology, Utrecht, The Netherlands*

Purpose or Objective: Following EBRT for prostate cancer, patients can develop aggravation of urinary symptoms mostly due to urethral dose. With dose-escalated EBRT it is suggested that genitourinary toxicity increases with increasing dose. In the experimental arm of the FLAME-trial (284 patients) a dose of 77Gy to the entire prostate gland in 35 fractions was administered, with an integrated boost up to 95Gy to the macroscopic lesions. No dose constraints for the urethra were set during the trial. The objective of this study is to evaluate urethral dose parameters, urethra-related toxicity and prostate-specific QoL scores for patients treated with and without dose-escalated EBRT.

Material and Methods: Between 2009 and 2015, 571 intermediate and high risk prostate cancer patients were enrolled in the FLAME trial, a phase 3, single blind, multi-center randomized controlled trial (NCT01168479). The control arm (287 patients) received a dose of 77Gy to the entire prostate gland in 35 fractions. The experimental arm (284 patients) received the same dose, but with an integrated boost up to 95Gy to the multi-parametric MRI-based intraprostatic lesion. For this study, the urethra was delineated retrospectively on T2 weighted MRI, using a circle shape with a diameter of 3 mm, to obtain dose parameters. These dose parameters, the Genitourinary Toxicity scores(CTCAE v3.0) and the urinary symptoms scale of the EORTC QLQ-PR25, were compared for both treatment arms. The physician in attendance scored toxicity at baseline, weekly during treatment, 4 weeks after treatment and every 6 months up to 10 years. QoL was filled out 1 week before treatment and the next questionnaires were sent to the patient every 6 months up to 10 years. Mean differences between groups at 1 year of follow-up were calculated using an independent samples t-test (dosimetry and QoL), Chi-square test or Fisher's exact test (toxicity). Statistical significance was considered P<0.01.

Results: Results after analysis of 100 patients (50 patients in each treatment arm) with a median follow-up of 22 months show for the control arm an average Dmean (mean dose to the urethra) of 77.3 ± 0.5 Gy (range 75.9-78.0 Gy), with an average Dmax (maximum dose to the urethra) of 79.6 ± 0.8 Gy (range 78.0-81.3). In the experimental arm, average Dmean was 82.0 ± 2.8 Gy (range 77.4-89.0 Gy) and average Dmax was 89.7 ± 0.6 Gy (range 80.7-97.7 Gy). For both Dmean and Dmax the difference between treatment arms was significant (p=0.000). Grade 3 GU toxicity did not occur, grade 2 GU toxicity occurred in a subset of patients, although no significant difference was found between both treatment arms for the separate GU items (table 1). Urinary symptoms-

related QOL was not significantly different across treatment arms.

Time of follow-up	1 year		Difference
Treatment group	77Gy	95Gy	P-value
Urinary frequency/urgency - ≥ grade 2 toxicity	15 (30%)	14 (28%)	0.83 (Chi-Square)
Urinary retention - ≥ grade 2 toxicity	4 (8%)	2 (4%)	0.68 (Fisher's exact)
Bladder spasms - ≥ grade 2 toxicity	0 (0%)	0 (0%)	-
Incontinence, urinary - ≥ grade 2 toxicity	3 (6%)	2 (4%)	1.0 (Fisher's exact)
Hemorrhage - ≥ grade 2 toxicity	0 (0%)	1 (2%)	1.0 (Fisher's exact)
Dysuria - ≥ grade 2 toxicity	5 (10%)	5 (10%)	1.0 (Fisher's exact)

Table 1. Incidence of GU toxicity at 1 year after radiation treatment.

Conclusion: Results showed a significant difference in urethral dose, but no significant differences in toxicity or quality of life when comparing both treatment arms of the FLAME trial.

OC-0057

Cardiotoxicity and cardiac substructure dosimetry in dose-escalated lung radiotherapy

S. Vivekanandan[1], N. Counsell[2], A. Khwanda[3], S. Rosen[3], E. Parsons[4], Y. Ngai[2], L. Farrelly[2], L. Hughes[2], M. Hawkins[1], D. Landau[5], J. Fenwcik[1]

[1]University of Oxford, Oncology, Oxford, United Kingdom
[2]University College London Clinical Trials Unit, Clinical Trials Unit, London, United Kingdom
[3]Imperial College London, Cardiology, London, United Kingdom
[4]RTTQA, Mount Vernon, London, United Kingdom
[5]Guy's and St Thomas' Hospital, Oncology, London, United Kingdom

Purpose or Objective: Radiotherapy of lung cancer delivers quite high doses of radiation to the heart. We explored associations between overall survival (OS) and radiation dose to heart and its substructures and electrocardiographic (ECG) changes.

Material and Methods: We analysed data from 79 patients in IDEAL CRT, a phase I/II trial of isotoxic radiotherapy (RT) dose escalation trial, sponsored by University College London (C13530/A10424). Mean and maximum prescribed doses were 69 and 75.6Gy calculated as 2Gy fractionation equivalents (EQD2, α/ß=10Gy). Whole heart, left ventricle (LV), right ventricle (RV), right atrium (RA), left atrium (LA) and AV node (AVN) were outlined on RT planning scans and differential dose volume histograms (DVHs) extracted, converting physical DVHs to EQD2s (α/ß=3). Patient-to-patient DVH variability was represented using a small number of Varimax-rotated principal components (PCs) explaining 95% of total variance. ECGs were analysed at baseline, 6 and 12 months (mo) after treatment, and changes in heart rate (HR) recorded, with patients dichotomised according to presence or absence of 'any ECG rhythm change' (conduction abnormalities or ischaemia). OS was modelled using Cox regression from the start of treatment. Univariate analysis (UVA) and multivariate analysis (MVA) of clinical factors included 'any rhythm ECG change' at 6 and 12 months, change in HR at 6 or 12 months, planning target volume (PTV), and prescribed dose (PD). MVA of whole heart dosimetric factors included all 7 Heart PCs, PTV, and PD. MVA of heart substructures included heart substructure PCs with p < 0.2 on UVA having similar dosimetric distributions to significant Heart PCs, PTV and PD.

Results: ECGs at baseline and 6 mo were available for 54 patients, and at baseline and 12 mo for 49 patients. At 6 mo and 12 mo, 10 and 6 patients had ischemic changes and 12 and 15 patients had conduction abnormalities (AF or sinus tachycardia). Median PTV was 403.4cm3 (Range 138.7-1262.1). Larger PTV and 'any ECG rhythm change' at 6 mo were associated with worse OS (HR = 1.005, 95% CI: 1 - 1.01 p 0.04; HR = 7.9843, 95% CI: 1.293 - 47.583 p 0.03 respectively) on MVA. Increasing values of Heart PC2, Heart PC3 and Heart PC7 (characterizing heart volume (vol) receiving 10-30Gy plus 70-80Gy, 65-75Gy and 1-5Gy respectively) were associated with worse OS (HR = 0.844, 95% CI: 0.715- 0.995 p 0.04; HR = 1.238, 95% CI: 1.051 - 1.457 p 0.01; HR = 1.725, 95% CI: 1.006 - 2.958, p 0.05 respectively) on MVA. Increasing values of LA PC4 (LA vol receiving 65-75Gy) was associated with worse OS on MVA (HR = 1.129, 95% CI: 1.033 - 1.235 p <0.01).

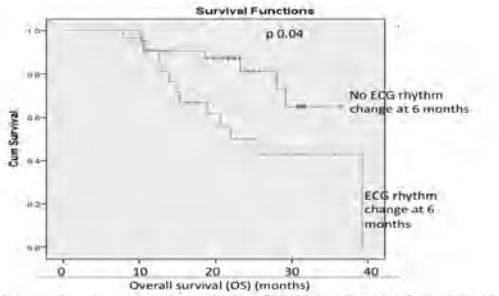

Figure shows on Cox regression patients with 'Any ECG rhythm change' at 6 months were associated with worse OS compared to those with no ECG rhythm change ay 6 months

Conclusion: We found evidence of a possible association between lower OS in IDEAL-CRT patients and high PTV, ischaemic or conduction change on ECG at 6 mo, and relatively high heart volume receiving doses <5Gy, 10-30Gy, 65-75Gy and 70-80Gy with the 65-75Gy localising to LA. Further prospective studies are required to improve understanding of cardiac irradiation in NSCLC.

OC-0058

Coronary calcifications in breast cancer patients and association with cardiovascular risk factors

S.A.M. Gernaat[1], H.J.G. Van den Bongard[1], B.D. De Vos[2], I. Isgum[3], N. Rijnberg[4], T. Leiner[5], D.E. Grobbee[6], Y. Van der Graaf[6], J.P. Pignol[7], H.M. Verkooijen[3]

[1]Universiteits Medisch Centrum Utrecht, Radiotherapy, Utrecht, The Netherlands
[2]Universiteits Medisch Centrum Utrecht, Image Sciences Institute, Utrecht, The Netherlands
[3]Universiteits Medisch Centrum Utrecht, Imaging, Utrecht, The Netherlands
[4]University of Utrecht, Radiotherapy, Utrecht, The Netherlands
[5]Universiteits Medisch Centrum Utrecht, Radiology, Utrecht, The Netherlands
[6]Universiteits Medisch Centrum Utrecht, Epidemiology, Utrecht, The Netherlands
[7]Erasmus Medical Centre, Radiation Oncology, Rotterdam, The Netherlands

Purpose or Objective: Breast cancer patients with cardiovascular risk factors are at increased risk of radiation- and chemotherapy- induced cardiovascular complications. Presence of coronary artery calcifications (CAC) is a major independent risk factor for cardiovascular disease (CVD). This study investigates the prevalence of CAC in breast cancer patients on radiotherapy (RT) planning CT scans, and its association with cardiovascular risk factors.

Material and Methods: This study was conducted within the Utrecht cohort for Multiple BReast cancer intErvention studies and Long-term evaLuAtion (UMBRELLA), and includes 561 breast cancer patients undergoing planning CT scans at the UMC Utrecht between October 2013-March 2015. CAC was automatically scored using a validated algorithm that

identifies CAC with a supervised pattern and threshold of 130 Hounsfield Units. Patients were categorized according to CAC (Agatston) scores: 0, 1-10, 11-100, 101-400, >400. Cardiovascular risk factors (diabetes, smoking status, hypercholesterolemia, hypertension, history of CVD) were collected for 36 patients with intermediate to high CVD risk (scores>100), and for a random selection of patients with fair to moderate CVD risk (1≤ scores ≤100, n=36) and low CVD risk (without CAC, i.e. scores of 0, n=36). Demographic, disease characteristics, and presence of cardiovascular risk factors were compared between groups using Chi-square analysis and Kruskal-Wallis test for categorical and continuous data respectively.

Results: Median age of the cohort was 58 years (range: 26-85). There were 427 (76%) patients without CAC, 50 (9%) with scores between 1-10, 43 (7%) with scores between 11-100, and 36 (7%) patients with scores >100. Patients with scores >100 had significantly more often diabetes than those without CAC (28% vs. 3%, p<0.001). Patients with scores >100 had more often three to four CVD risk factors compared to patients with scores between 1-100 or without CAC: 30%, 5%, 0% respectively, p=0.002. Ten (28%) patients with scores >100

did not have any other CVD risk factor

Conclusion: CAC is present in one in four breast cancer patients. In one third of patients with CAC scores >100, no other CVD risk factors were present, and these patients would not have been identified as high risk using standard CVD risk factors. Since CAC can be automatically detected without additional cost or radiation exposure in breast cancer patients undergoing RT, it represents a simple and useful way to detect those requiring additional cardio protective measures.

OC-0059

A radiation dose-response relationship for risk of heart failure in survivors of Hodgkin lymphoma

B.M.P. Aleman[1], F.A. Van Nimwegen[2], G. Ntentas[3], S.C. Darby[3], M. Schaapveld[2], M. Hauptmann[2], P.J. Lugtenburg[4], C.P.M. Janus[5], A.D.G. Krol[6], F.E. Van Leeuwen[2], D.J. Cutter[7]

[1]The Netherlands Cancer Institute, Radiation Oncology, Amsterdam, The Netherlands

[2]The Netherlands Cancer Institute, Epidemiology, Amsterdam, The Netherlands

[3]University of Oxford, Clinical Trial Service Unit- Nuffield Department of Population Health, Oxford, United Kingdom

[4]Erasmus MC Cancer Institute, Hematology, Rotterdam, The Netherlands

[5]Erasmus MC Cancer Institute, Radiation Oncology, Rotterdam, The Netherlands

[6]Leiden University Medical Center, Clinical Oncology, Leiden, The Netherlands

[7]Oxford University Hospitals NHS Trust, Oxford Cancer Center, Oxford, United Kingdom

Purpose or Objective: Cardiovascular diseases are increasingly recognized as late effects of Hodgkin lymphoma (HL) treatment. Radiation therapy is known to contribute to the risk of heart failure (HF), but a dose-response relationship has yet not been well described. The purpose of this study was to identify risk factors for HF, and to quantify effects of radiation dose to the heart, chemotherapy, and other cardiovascular risk factors.

Material and Methods: We conducted a nested case-control study in a cohort of 2,617 5-year HL survivors, treated between 1965-1995. Cases were patients who developed HF in the form of either symptomatic congestive heart failure or cardiomyopathy (Common Terminology Criteria for Adverse Events version 4.0: grade≥2) as their first clinically significant heart disease. Detailed treatment information was collected from medical records of 91 cases and 278 matched controls. Mean heart dose (MHD) was retrospectively estimated by reconstruction of individual treatments on representative computed tomography datasets. All statistical tests were two-sided.

Results: The median interval between HL and HF was 20.6 years. Fifty-seven percent of the cases had died at the end of follow-up, with a median time from HF to death of 3.6 years (interquartile range: 0.2-5.6 years). Mediastinal radiotherapy was applied through parallel-opposed fields. Average MHD for cases treated with RT was 25 Gy and for controls 22 Gy. Risk of HF increased in a non-linear way, with no increase at a MHD of 10 Gy, a 1.2-fold increased risk at a MHD of 20 Gy, and a 2.5-fold increased risk at a MHD of 30 Gy. Relatively low doses of anthracyclines (10-279 mg/m2) were associated with a 3.2-fold increased risk of developing HF (95%CI: 1.3-7.7) compared with patients who did not receive anthracyclines. High doses of anthracyclines (280-800 mg/m2) were associated with a similarly increased risk (RR: 2.8, 95%CI: 1.6-5.1). For patients who received anthracyclines in combination with mediastinal radiotherapy the risk of HF (RR: 2.90 at a MHD of 25 Gy) was slightly higher than the risk of mediastinal radiotherapy without anthracyclines (RR: 1.8 at a MHD of 25 Gy), although the difference was not statistically significant (p interaction=0.10). Classical risk factors for cardiovascular diseases did not confound or modify the association between treatment-related risk factors and HF risk.

Conclusion: Risk of HF increased non-linearly with mean heart dose in patients treated for HL. Our findings can be used to predict HF risk and may therefore be useful for patients and doctors both before treatment, during radiation treatment planning and in follow-up. Patients who received both anthracyclines and mediastinal radiation need to be followed carefully.

OC-0060

Cardiac risk prediction: Moving beyond a mean heart dose model?

M. Maraldo[1], F. Giusti[2], I. Vogelius[1], M. Lundemann[1], S. Bentzen[3], M. Van der Kaaij[4], B. Aleman[5], M. Henry-Amar[6], P. Meijnders[7], E. Moser[8], C. Fortpied[2], L. Specht[1]

[1]Rigshospitalet, Department of Clinical Oncology, Copenhagen, Denmark

[2]European Organisation of Research and Treatment of Cancer, Department of Statistics, Brussels, Belgium

[3]University of Maryland School of Medicine, Department of Biostatistics, Baltimore, USA

[4]University Medical Centre Groningen, Department of Hematology, Groningen, The Netherlands

[5]Netherlands Cancer Institute, Department of Radiation Oncology, Amsterdam, The Netherlands

[6]Centre François Baclesse, Cancéropôle Nord-Ouest Data Processing Centre, Caen, France

[7]GZA/Iridium Cancer Network, Department of Radiation Oncology, Antwerp, Belgium

[8]Champalimaud Cancer Center, Department of Radiation Oncology, Lisbon, Portugal

Purpose or Objective: Among 6039 patients with Hodgkin lymphoma enrolled in nine successive EORTC-GELA randomized trials (1964-2004), the effect of individual radiotherapy and chemotherapy doses on the risk of developing cardiac disease was investigated. We specifically analysed the added value from radiation dose-volume metrics on cardiac risk prediction as well as the impact of relapse treatment.

Material and Methods: For all patients, dose-volume metrics for the heart (mean dose, volume receiving 5 Gy (V5Gy), V10Gy, V20Gy, V30Gy, V40Gy) were retrospectively estimated by reconstructing individual treatments on representative computed tomography datasets. Cumulative doses of anthracyclines and vinca-alkaloids (mg/m2) were also obtained individually. Relapse occurring before a cardiac disease was analysed qualitatively (no, yes). Cardiac disease was reported during follow-up and through a patient-reported questionnaire (LSQ responders, 2009-2010 cross-sectional study). A multivariable Cox proportional hazards

model with backwards selection was applied to test for patient- and treatment-related factors associated with cardiac disease. The resulting model was compared to a "mean heart dose"-model in terms of prognostic discrimination ability.

Results: 599 patients developed at least one cardiac disease event (465 events obtained from the 1919 LSQ responders). Significant predictors of cardiac disease were: cumulative dose of anthracyclines (HR=1.002 per 1 mg/m2 increase in cumulative dose; 95% CI, 1.001-1.003, p=0.005); (any) treatment given for a relapse (HR=1.286; 95% CI,1.001-1.65, p=0.049) and the radiation dose-volume metrics V30Gy (HR=1.007 per 1% increase in dose; 95% CI, 1.003-1.011, p=0.001) and V40Gy (HR=1.018 per 1% increase in dose; 95% CI,1.008-1.029, p<0.001). The freedom from cardiac disease estimates with the "V30Gy, V40Gy"-model are plotted against a "mean heart dose"-model (= mean heart dose, cumulative dose of anthracyclines, any relapse treatment) in figure 1.

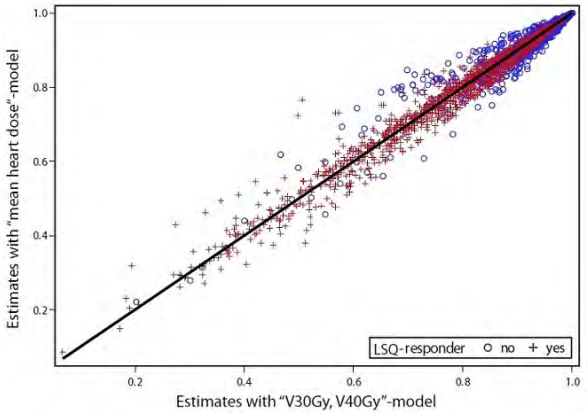

Figure 1: Freedom from cardiac disease estimates with the resulting "V30Gy, V40Gy"-model versus a "mean heart dose"-model.

Conclusion: In patients treated for Hodgkin lymphoma, the radiation dose-volume metrics V30Gy and V40 Gy, the cumulative dose of anthracyclines, and (any) treatment given for a relapse have a significant impact on the risk of subsequent cardiac disease. There seems to be no improved discrimination ability of the prognostic model when using radiation dose-volume metrics compared to the mean heart dose metric.

Proffered Papers: Brachytherapy 1: Prostate

OC-0061

Focal brachytherapy: what dose to what volume?

A. Haworth[1,2], H. Reynolds[1,2], M. DiFranco[3], Y. Sun[2], D. Wraith[4], S. Williams[2,5], B. Parameswaran[6], C. Mitchell[7], M. Ebert[8,9]

[1]*Peter MacCallum Cancer Centre, Physical Sciences, Melbourne, Australia*
[2]*University of Melbourne, Sir Peter MacCallum Department of Oncology, Melbourne, Australia*
[3]*Medical University of Vienna, Centre for Medical Physics and Biomedical Engineering, Vienna, Austria*
[4]*Queensland University of Technology, School of Public Health & Social Work, Brisbane, Australia*
[5]*Peter MacCallum Cancer Centre, Dept. Radiation Oncology, Melbourne, Australia*
[6]*Peter MacCallum Cancer Centre, Division of Radiation Oncology and Cancer Imaging, Melbourne, Australia*
[7]*Peter MacCallum Cancer Centre, Dept. Pathology, Melbourne, Australia*
[8]*University of Western Australia, Faculty of Science, Nedlands, Australia*
[9]*Sir Charles Gairdner Hospital, Dept Radiation Oncology, Nedlands, Australia*

Purpose or Objective: A novel approach to treatment planning for focal brachytherapy is described, utilizing a biologically-based inverse optimization algorithm and biological imaging to target an ablative dose at known regions of significant tumour burden and a lower, therapeutic dose to low-risk regions. We describe our methods for defining target volume and prescription dose.

Material and Methods: To demonstrate how tumour characteristics may be extracted from multi-parametric MRI (mpMRI) to inform the previously validated biological model(1), 21 patients underwent in vivo mpMRI prior to radical prostatectomy. Co-registration of histology and imaging data using rigid and deformable registration was validated by matching feature points and annotated zonal regions. Automated methods for defining tumour location, tumour cell density (TCD) and Gleason Score (GS) in histology were developed to provide high resolution ground truth data(2,3). Similarly, using ground truth histology data, machine learning methods have been developed and tested to predict tumour location in mpMRI. Further developments are underway to predict TCD, GS and hypoxia in mpMRI to build a multi-level voxel map defining tumour location and characteristics to inform the biological treatment planning model.

Results: Co-registration of the in-vivo mpMRI with histology was achieved with an overall mean estimated error of 3.3 mm (Fig 1).

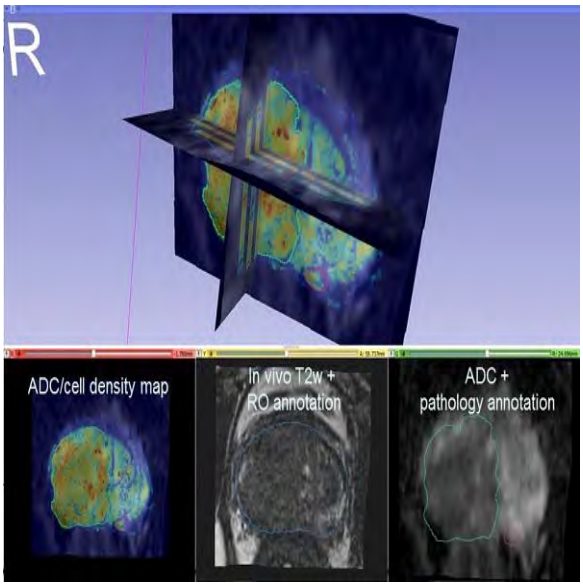

An ensemble-based supervised classification algorithm, trained on textural image features, demonstrates a highly sensitive method for automated tumour delineation in high resolution histology images(2). Colour deconvolution and the use of a radial symmetry transform provides measures of cell density, shown to highly correlate with an expert pathologist markup of tumour location(3). A Gaussian-kernel support vector machine demonstrated a tumour location predictive accuracy of >80% with potential for significant improvement using Bayesian methods to incorporate neighbourhood information. Similar statistical methods have demonstrated potential for mpMRI parameter/pharmacokinetic maps to be correlated with tumour characteristics including TCD, GS and hypoxia. Whilst imaging methods for hypoxia exist, providing reliable, high spatial resolution ground truth data remains challenging.

Conclusion: A novel approach to focal brachytherapy planning has been developed that incorporates mpMRI parameter/pharmacokinetic maps to inform a biological model and an inverse optimisation algorithm to maximise tumour control probability and minimise dose to organs at risk in prostate brachytherapy. The model can be equally applied to low and high dose rate brachytherapy, and

possibly EBRT with high precision treatment delivery techniques. 1) Haworth, A. et al. Brachytherapy. 12, 628-36, (2013). 2) DiFranco, D. et al., Proc. SPIE 9420 (2015). 3) Reynolds, H. et al.. Proc. SPIE 90410S (2014).

OC-0062

High-dose-rate HDR boost for localized prostate cancer decreases long term rectum toxicity

S. Aluwini[1], M. Hoogeman[1], J. Lebesque[2], C. Bangma[3], L. Incrocci[1], W. Heemsbergen[2]

[1]*Erasmus MC Cancer Institute, Department of Radiation Oncology, Rotterdam, The Netherlands*

[2]*Netherlands Cancer Institute, Department of Radiation Oncology, Amsterdam, The Netherlands*

[3]*Erasmus MC Cancer Institute, Department of Urology, Rotterdam, The Netherlands*

Purpose or Objective: A High-Dose-Rate Brachytherapy (HDR-BT) boost combined with external beam radiotherapy (EBRT) produced excellent long term outcome and is an alternative for escalated EBRT (>72 Gy) for low and intermediate risk prostate cancer (PC) patients. The question remains whether the use of HDR-BT results in lower complication rates for equal tumour control. The aim of this study was to compare HDR-BT/EBRT combined to EBRT-only in terms of long-term patient-reported toxicity and oncological outcome for low and intermediate risk PC patients.

Material and Methods: Between 2000 and 2007 low and intermediate risk PC patients (n=231) were treated (stage T1b-T2a, G≤7, iPSA≤17) with a HDR -BT boost (3x6 Gy) combined with EBRT (25x1.8 Gy). Patients with a maximum prostate volume of 120 cc and a PSA, T-stage, and Gleason in the same range were selected (68 Gy: n=83, 78 Gy: n=74) from the Dutch randomized dose-escalation study (1997-2003). At least 1 follow-up questionnaire had to be completed. Genitourinary (GU) and gastrointestinal (GI) toxicity symptoms were prospectively assessed using same questionnaires in the period 1-7y years post-treatment. Prevalence of long term GU and GI symptoms were calculated with intervals of 1 year and compared between treatment groups (chi-square test). Biochemical failure free survival (BFFS) using the Phoenix definition (stratified for Gleason score) was calculated and compared (log-rank test).

Results: Median follow up was 8.8y for both 68 Gy and 78 Gy patients, and 6.8y for HDR-BT/EBRT. Median age was 69y and 68y, respectively. In general, post-treatment GU complaints were comparable between groups (dysuria, nocturia, day frequency, incontinence). Rectal blood loss was significantly lower for HDR-BT compared to 78 Gy, from the first year of follow-up and onwards ($p<0.001$). Rectal discomfort (pain/cramps) was significantly lower at 3y follow-up ($p<0.01$). Rectal incontinence showed lower rates as well, but these were not significant ($p=0.08$). Differences in stool frequency ≥ 4 were small and not significant. BFFS rates at 7y were 79%, 90%, and 96% (68 Gy, 78 Gy, HDR-BT) for Gleason <7 and 43%, 75%, and 91% for Gleason 7. BFFS was significantly higher in both the HDR-BT and 78 Gy group compared to 68 Gy ($p=<0.001$ and $p=0.034$ respectively), the difference between HDR-BT and 78 Gy was not significant ($p=0.11$).

Conclusion: HDR-BT/EBRT is associated with significantly lower long-term GI toxicity compared to escalated EBRT-only (78 Gy) with a favorably comparable 7 years tumor control.

OC-0063

Real-time in-vivo dosimetry in HDR prostate brachytherapy

J. Mason[1], B. Al-Qaisieh[1], A. Henry[2], P. Bownes[1]

[1]*St James Institute of Oncology, Department of Medical Physics, Leeds, United Kingdom*

[2]*St James Institute of Oncology, Clinical Oncology, Leeds, United Kingdom*

Purpose or Objective: Implement routine in-vivo dosimetry in HDR prostate brachytherapy and develop error detection thresholds for real-time treatment monitoring.

Material and Methods: In vivo dosimetry was performed for 40 HDR prostate brachytherapy patients treated with single fractions of 15Gy (boost) or 19Gy (monotherapy). Treatments were planned using intra-operative trans-rectal ultrasound (TRUS) and for in-vivo dosimetry, an additional needle was inserted centrally in the prostate gland and dose measured using a MOSFET. MOSFET measurements were compared to predicted readings based on exported treatment planning system (TPS) data, per-needle and for total plan dose. To assess impact of needle movement between planning TRUS and treatment, TRUS images were acquired immediately after treatment for 20 patients. To assess impact of heterogeneities (for example steel needles) on the dose at the MOSFET position Monte Carlo (MC) simulations of treatment plans were performed for 10 patients. A retrospective investigation of thresholds for real-time error detection was based on per-needle and total plan uncertainty analysis. Uncertainties included MOSFET calibration/commissioning results, source calibration, TPS, relative source/ MOSFET position and MOSFET reading reproducibility.

Results: The mean measured total plan reading was 6.6% lower than predicted (range +5.1% to -15.2%). Plan reconstruction on post-treatment TRUS showed mean reduction in dose at the MOSFET position of 1.8% due to needle movement. MC simulations showed that heterogeneities caused a mean dose reduction at the MOSFET position of 1.6%. Uncertainty estimates varied between individual treatment plans, for example the uncertainty is higher if the MOSFET is close to a heavily weighted source position. Assuming a source/MOSFET position uncertainty of 1mm, total plan dose uncertainty (k=2) ranged from 10.6% to 17.0% and per needle dose uncertainty (k=2) ranged from 18.2% to 110% (mean 31.0%). Retrospectively applying these uncertainty estimates as error detection thresholds resulted in 1 out of 40 plans and 5% of needles being outside the error detection threshold. The figure shows an example for one patient of predicted versus measured reading for each needle with the k=2 uncertainty illustrated by error bars.

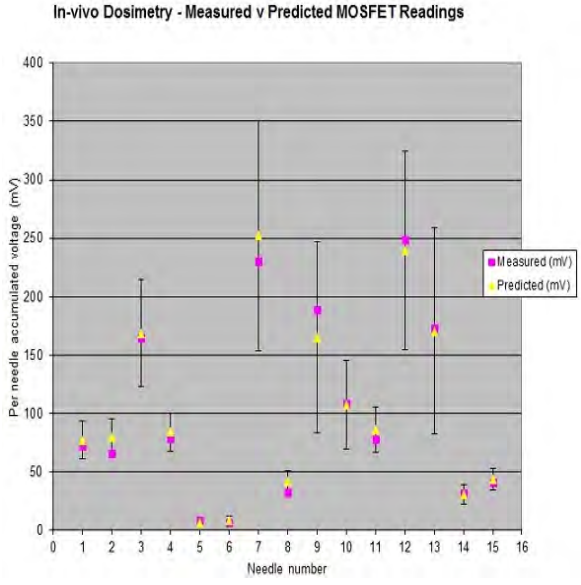

Conclusion: In vivo measurements of dose during HDR prostate brachytherapy treatment delivery show good agreement with TPS predictions within measurement uncertainties, providing reassurance in the accuracy of dose delivery. Thresholds for real-time in vivo error detection using this measurement technique should be calculated on an individual plan basis but would still be likely to generate some false errors, with the main limitation of the

measurement technique being that dose is only measured at a single point.

OC-0064

A prediction model for biochemical failure after salvage Iodine-125 prostate brachytherapy

M. Peters[1], J.R.N. Van der Voort van Zyp[1], M.A. Moerland[1], C.J. Hoekstra[2], S. Van de Pol[2], H. Westendorp[2], M. Maenhout[1], R. Kattevilder[2], H.M. Verkooijen[1], P.S.N. Van Rossum[1], H.U. Ahmed[3], T. Shah[3], M. Emberton[3], M. Van Vulpen[1]

[1]*UMC Utrecht, Radiation Oncology Department, Utrecht, The Netherlands*

[2]*Radiotherapiegroep, Radiation Oncology Department, Deventer, The Netherlands*

[3]*University College London, Division of Surgery and Interventional Science, London, United Kingdom*

Purpose or Objective: Localized recurrent prostate cancer after primary radiotherapy can be curatively treated using salvage, including Iodine-125 brachytherapy (BT). Selection of patients for salvage is hampered by a lack of knowledge on predictive factors for cancer control, particularly in salvage BT. The aim of this study was to develop and internally validate a prediction model for biochemical failure (BF) after salvage I-125-BT using the largest cohort to date in order to aid patient selection in the future.

Material and Methods: Patients with a clinically localized prostate cancer recurrence who were treated with a whole-gland salvage I-125 implantation were retrospectively analyzed. Patients were treated in two centers in the Netherlands. Multivariable Cox-regression was performed to assess the predictive value of clinically relevant tumor-, patient- and biochemical parameters on BF, which was defined according to the Phoenix-definition (PSA-nadir+2 ng/ml). Missing data was handled by multiple imputation (20 datasets). The model's discriminatory ability was assessed with Harrell's C-statistic (concordance index). Internal validation was done using bootstrap resampling (using 2000 resampled datasets). Goodness-of-fit of the final model was evaluated by visual inspection of calibration plots, after which individual survival was calculated for categories of the predictor variables from multivariable analysis. All analyses were performed using the recently published TRIPOD statement.

Results: Sixty-two whole-gland salvage I-125-BT patients were identified. After median follow-up of 25 (range 0-120) months, 43 patients developed BF. In multivariable analysis, disease-free survival interval (DFSI) after primary therapy and pre-salvage prostate-specific antigen doubling time (PSADT) were predictors of BF; corrected hazard ratio (HR) 0.99 (95% confidence interval [CI]: 0.98-0.997 [p=0.01]) and 0.94 (95%CI: 0.90-0.99 [p=0.01]), respectively. Calibration plots demonstrated accurate predictive ability up to 36 months. The adjusted C-statistic was 0.71. Of patients with a PSADT>30 months and DFSI>60 months, >70% remained free of recurrence until 3 years. With every 12 months increase in DFSI, PSADT can decrease with 3 months to obtain the same survival proportion (Figure 1).

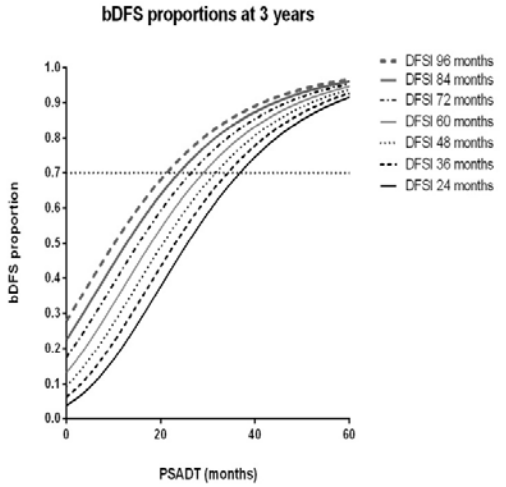

Conclusion: Salvage I-125-BT patients can be selected based on their disease free survival interval after primary therapy and the PSA-doubling time pre-salvage, ensuring sufficient biochemical control of >70% until three years.

OC-0065

Risk of second malignancies after seed prostate brachytherapy as monotherapy in a single institution

A. Fernandez Ots[1], J. Bucci[1], D. Malouf[2], L. Browne[3], Y. Chin[1]

[1]*ST George Hospital, Cancer Care Centre, Sydney, Australia*

[2]*ST George Hospital, Urology, Kogarah, Australia*

[3]*ST George Hospital, Statistics Cancer Care Centre, Sydney, Australia*

Purpose or Objective: To report the incidence of second primary cancer (SPC) after Iodine-125 brachytherapy for early prostate cancer in a single institution with an intense urological surveillance and to compare it with the cancer incidence in the Australian population

Material and Methods: This retrospective, single-institution study included 889 patients treated with Iodine-125 brachytherapy alone. All the patients had a baseline cystoscopy before the implant. Data were collected on all subsequent SPC diagnoses. SPC incidences were retrieved for all type of cancers and for cancers close to the radiation field. Interval since the implant was evaluated for potential association to the treatment. Standardized incidence ratios (SIRs) were calculated for all cancers and for bladder cancers and matched with the general population. The absolute excess risk (AER) was expressed in relation to 10000 persons-years in the study. Kaplan-Meier analysis was used to determine the actuarial second malignancy and pelvic malignancy rates and the death from SPC and from any cause

Results: Patients were followed for a median of 4.16 (0-12) years with 370 (42 %) patients having 5 years or more follow up. 62 % patients were older than 60 years. 61 patients (6.8%) subsequently developed a SPC with 12 pelvic malignancies : 8 bladder and 4 rectal cancer. The 5- and 10- year cumulative incidences are 6.9% (95% Confidence Interval 5.0-9.4) and 19% (95% CI 14-26) for any second malignancy, 1.3% (95%CI 0.6-2.7) and 3.9% (95% CI 1.9-7.8) for any pelvic malignancy and 1% (95% CI 0.4-24) and 3.2% (1.4-7.1) for bladder cancer, respectively. The SIR was significantly higher for all pelvic malignancies at 2.10 (95% CI 1.09-3.67) and for all bladder cancers at 3.33 (95% CI 1.44-6.57). In the subgroup analysis bladder SPC risk was higher than expected for patients under 60 years (SIR 6.52; 95%CI 1.3-19; AER 13) and within the first 5 years of follow up (SIR 2.9 ; 95% CI 0.97-6.95; AER 10). Rectal cancer SIR were not significant or close in any of the categories. The 5- and 10-year rates of death from SPC were 1.9 % (95% CI 1.0-3.5) and 9.1% (95% CI 5.2-16) and from any cause were 3.2% (95% CI 2-5) and 14.4% (95% CI 9.5-21.6). On multivariable analysis, older age was associated with increased SPC risk (HR 1.05, p=0.021) , all cause mortality (HR 1.13, p<0.001) and mortality due to SPC (HR 1.09, p=0.014). Smoking status was associated with all cause

mortality (HR 2.15, p=0.026) and with mortality from second malignancy (HR 2.59, p=0.045)

Conclusion: There may be an increased but small risk of second pelvic malignancy after prostate brachytherapy. A tendency towards a higher risk of bladder SPC after brachytherapy was found in the first 5 years of follow-up , probably resulting from screening bias . There was no significant increased rate of rectal cancer in any of the categories. Longer follow up is needed to draw strong conclusions.

OC-0066

Adaptive cone-beam CT planning improves progression-free survival for I-125 prostate brachytherapy

M. Peters[1], D. Smit Duijzentkunst[1], H. Westendorp[2], S. Van de Pol[2], R. Kattevilder[2], A. Schellekens[2], J. Van der Voort van Zyp[1], M. Moerland[1], M. Van Vulpen[1], C. Hoekstra[2]
[1]*University Medical Center Utrecht, Radiation Oncology, Utrecht, The Netherlands*
[2]*Radiotherapiegroep Deventer, Radiation Oncology, Deventer, The Netherlands*

Purpose or Objective: To determine the independent effect of additional intraoperative adaptive C-arm cone-beam computed tomography (CBCT) planning versus transrectal ultrasound (TRUS)-guided interactive planning alone in primary permanent I-125 brachytherapy for prostate cancer on long term biochemical disease free survival (bDFS).

Material and Methods: All patients with biopsy proven T1/T2-stage prostate cancer treated with I-125 brachytherapy were included in this cohort. Treatments were performed with TRUS-guided primary brachytherapy (+/- neoadjuvant hormonal therapy (NHT)) in a single institution in the period of November 2000 to December 2014. From October 2006 onwards, all patients received additional intraoperative adaptive CBCT planning for dosimetric evaluation and, if indicated, subsequent remedial seed placement in underdosed areas (which was performed in 15% of all patients). These procedures lasted 1-1.5 hours and were performed by a team of 2 radiation oncologists and 2 therapeutic radiographers. Pre-operative characteristics, follow-up PSA and mortality were prospectively registered. Patients were stratified into National Comprehensive Cancer Network (NCCN) risk groups. Kaplan-Meier analysis was used to estimate bDFS (primary outcome), overall survival (OS) and prostate cancer specific survival (PCSS) (secondary outcomes). Cox-proportional hazard regression was used to assess the independent predictive value of CBCT use on biochemical failure (BF) (Phoenix definition) and overall mortality (OM).

Results: 1623 patients were included. Median follow-up was 99 months (interquartile range (IQR) 70-115) for TRUS patients (n=613) and 51 months (IQR 29-70) for CBCT patients (n=1010). BF occurred 203 times and 206 patients died, of which 26 due to prostate cancer. For TRUS and CBCT patients, estimated 7-year bDFS was 87.2% vs. 93.5% (log rank: p=0.04) for low risk patients, 75.9% vs. 88.5% (p<0.001) for intermediate risk patients and 57.1 vs. 85.0% (p<0.001) for high risk patients. For TRUS and CBCT patients with low, intermediate and high risk disease, estimated 7-year OS was respectively 86.5% vs. 90.4% (p=0.11), 79.6% vs. 85.1% (p=0.30) and 66.4% vs. 84.2% (p=0.01). For TRUS and CBCT patients, 7-year PCSS was 96.0% vs. 100% (p<0.0001). After Cox regression, CBCT patients had lower rates of BF: HR 0.45 (95%-CI 0.33-0.61; p<0.0001). Corrected for age, IPSA, Gleason grade, T-stage, NHT-status and duration of NHT use, year of implantation, activity of the implant and prostate volume, CBCT showed to be an independent predictor of BF: HR 0.54 (95%-CI 0.33-0.89; p=0.02). CBCT was not an independent predictor of OM: HR 0.66 (95%-CI 0.40-1.07; p=0.09).

Conclusion: Additional intraoperative adaptive C-arm cone-beam CT planning in I-125 prostate brachytherapy leads to a significant increase in biochemical disease free survival in all NCCN risk groups.

Proffered Papers: Physics 1: Images and analyses

OC-0067

An automated patient-specific and quantitative approach for deformable image registration evaluation

R.G. Kierkels[1], C.L. Brouwer[1], R.J. Steenbakkers[1], H.P. Bijl[1], J.A. Langendijk[1], N.M. Sijtsema[1]
[1]*University of Groningen- University Medical Center Groningen, Department of Radiation Oncology, Groningen, The Netherlands*

Purpose or Objective: In adaptive radiotherapy, deformable image registration (DIR) is used for contour propagation and dose warping. Contour evaluation is visual and qualitative and only accurate in high contrast regions. Dose warping requires fully spatial and quantitative DIR evaluation measures also valid in low contrast regions. While quantitative measures such as the target registration error can be used during commissioning, such measures are not fully spatial and too user intensive in clinical practice. Therefore, we propose a fully automatic and quantitative approach to DIR quality assessment including multiple measures of numerical robustness and biological plausibility.

Material and Methods: Ten head and neck cancer patients who received weekly repeat CT (rCT) scans were included. Per patient, the first rCT was deformable registered (using B-spline DIR algorithm) to the planning CT. The ground-truth deformation error of this registration was derived using the scale invariant feature transform (SIFT), which automatically extracts and matches stable and prominent points between two images. Moreover, complementary quantitative and spatial measures of registration quality were calculated. Numerical robustness was derived from the inverse consistency error (ICE), transitivity error (TE), and distance discordance metric (DDM). For the TE calculations a third CT was used. The DDM was calculated using five CT sets per patient. Biological plausibility was based on the deformation vector field between the planning CT and rCT. Relative deformation threshold values were set based on physical tissue characteristics: 5% for bone and 50% for soft tissues. All measures were evaluated in bone and soft tissue structures and compared against the ground-truth deformation error.

Results: On average, SIFT detected 133 matching points scattered throughout the planning CT, with a mean (max) registration error of 1.6 (8.3) mm. Our combined and fully spatial DIR evaluation approach, including the ICE, TE and DDM, resulted in a mean (max) error of respectively 0.6 (2.0), 0.7 (2.7), and 0.6 (2.7) mm within the external body contour, averaged over all patients. The largest errors were detected in homogeneous regions and near air cavities. Furthermore, 87% of the bone and 2% of the soft tissue voxels were classified as unrealistic deformations. Figure 1 shows the planning CT, DDM, tissue deformation, and error volume histograms of the ICE, TE, and DDM of the body contour of one patient.

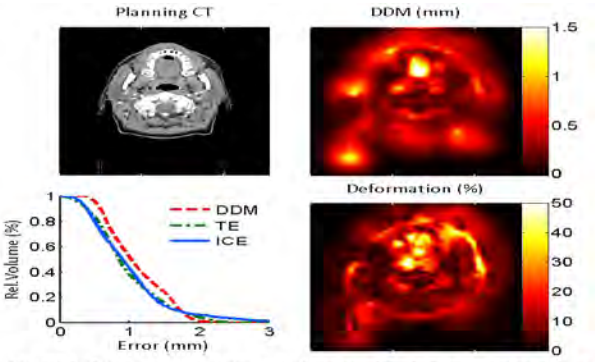

Figure 1. Axial cross section of a planning CT, distance discordance metric (DDM) and tissue deformation of a representative patient. The error volume histograms show the DDM, transitivity error (TE), and inverse consistency error (ICE) of the body contour.

Conclusion: The combination of multiple automatic DIR quality measures highlighted areas of concern within the registration. While current methods on DIR evaluation, such as visual inspection and target registration error are time-consuming, local, and qualitative, this approach provided an automated, fully spatial and quantitative tool for clinical assessment of patient-specific DIR even in image regions with limited contrast.

OC-0068

Can atlas-based auto-contouring ever be perfect?

B.W.K. Schipaanboord[1], J. Van Soest[2], D. Boukerroui[1], T. Lustberg[2], W. Van Elmpt[2], T. Kadir[1], A. Dekker[2], M.J. Gooding[1]

[1]*Medical Ltd, Science and Medical Technology, Oxford, United Kingdom*

[2]*Maastricht University Medical Centre, Department of Radiation Oncology MAASTRO- GROW School for Oncology and Developmental Biology, Maastricht, The Netherlands*

Purpose or Objective: Various approaches have been proposed to select the most similar atlases to a patient for atlas-based auto-contouring. While it is known that increasing the size of an atlas database improves the results of auto-contouring for a small number of atlases, such selection assumes the hypothesis that increasing the atlas pool size always increases the chance of finding a good match. The objective of this study is to test this hypothesis, and answer the question; "Given a large enough database of atlases, can single atlas-based auto-contouring ever be perfect?".

Material and Methods: 35 test cases were randomly selected from a dataset of 316 clinically contoured head and neck cases, and were auto-contoured treating each of the remaining cases as potential atlases to be used. Thus, results of contouring were available for approximately 11000 atlas-patient pairs. Dice Similarity Coefficient (DSC), Hausdorff distance (HD), Average Distance (AD) and Root Mean Square Distance (RMSD) were computed between the auto-contours and the clinical contours for each structure and atlas-patient pair. In order to estimate achievable performance under the assumptions of an infinite size atlas database and "perfect" atlas selection, the Extreme Value Theory statistical technique Points over Threshold, used in other domains to perform tasks such as estimating the magnitude of one-in-a-hundred-years flooding, was used to model the distribution of the best scores. Analysis was performed for the ten most commonly contoured structures within the database, with a minimum of 6800 atlas-patient pairs per structure being considered.

Results: The figure shows the distribution of observed extreme values for the left parotid DICE scores, together with the model fit.

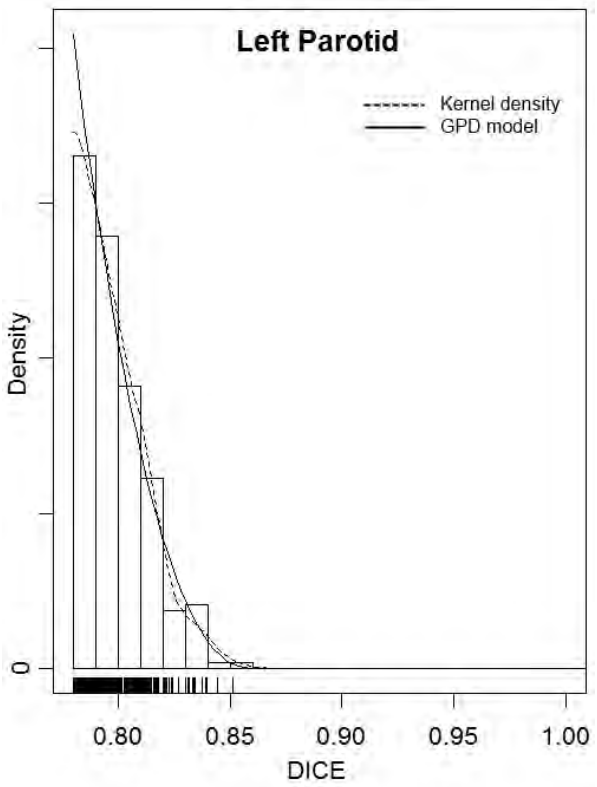

For all measures and structures, the model fit indicated a limit on the performance in the extreme. While this is expected since all measures have a limit at perfection, the performance limit in the extreme fell short of a perfect result. Variation was observed between structures, with well-defined structures performing better than more complex ones. This may indicate that the limit on performance reflects the inter-observer variation in delineation. The table shows the best observed score for the experiments performed, together with the expected achievable result predicted by the model assuming an atlas database of 5000 atlases.

Structure	DICE		HD (mm)		AD (mm)		RMSD (mm)	
	Best	Exp	Best	Exp	Best	Exp	Best	Exp
Brain	0.987	0.997	5.98	5.98	0.54	0.52	0.86	0.83
Brainstem	0.886	0.887	4.58	4.50	1.15	1.09	1.43	1.34
Cochlea L	0.909	0.935	0.48	0.47	0.19	0.17	0.22	0.21
Cochlea R	0.909	0.945	0.52	0.47	0.19	0.17	0.23	0.20
Oral Cavity	0.894	0.894	8.07	8.13	1.79	1.75	2.34	2.31
Parotid L	0.852	0.854	6.12	5.68	1.32	1.31	1.70	1.70
Parotid R	0.849	0.853	6.10	6.09	1.41	1.34	1.89	1.83
Spinal cord	0.881	0.881	2.92	3.05	0.65	0.65	0.86	0.82
Submandibular gland L	0.840	0.845	4.88	4.79	1.10	1.05	1.40	1.35
Submandibular gland R	0.841	0.842	4.16	4.04	1.02	1.03	1.34	1.34

Conclusion: Increasing the size of an atlas database within achievable ranges would be insufficient on its own for consistently perfect single atlas auto-contouring, even in the presence of a "perfect" atlas selection method. Thus, improvements in the underlying methods for pre- and post-processing, such as deformable registration or multi-atlas fusion, are necessary to improve the results of atlas-based auto-contouring. Additionally, consistent delineation within an atlas database is required to minimise the effect of inter-observer error on the achievable performance.

OC-0069

Using texture analysis to detect prostate cancer for automated outlining and adaptive radiotherapy

D. Welsh[1], D. Montgomery[1], D.B. McLaren[2], W.H. Nailon[1]

[1]*Western General Hospital, Oncology Physics, Edinburgh, United Kingdom*

[2]Western General Hospital, Clinical Oncology, Edinburgh, United Kingdom

Purpose or Objective: In radiotherapy, the prostate is one of few anatomical sites where the whole organ is targeted, even in cases of localised cancer. Improvements in outcomes may be achieved by escalating the dose to the dominant intraprostatic lesion (DIL), and thereby reducing the dose to the remainder of the gland. However, reliably identifying the DIL requires considerable clinical experience and is extremely time consuming. Automated outlining would alleviate this problem, and is also desirable for online adaptive radiotherapy. This work investigated the feasibility of automatically detecting the DIL on T2-weighted MR images using image texture analysis methods.

Material and Methods: On the diagnostic T2-weighted MR images from 14 prostate cancer patients previously treated with radiotherapy, the prostate and DIL volumes were defined by a clinician. Two separate projects were carried out using the same data, looking at 2D and 3D texture analysis, respectively. In both cases, a range of texture features were calculated on a sub-volume basis and a machine learning classification scheme was trained to classify individual pixels surrounded by each sub-volume as either healthy prostate or DIL, based on the calculated features, with the clinician defined contours as the ground truth. The classifier was tested on each patient case in turn, with the remaining 13 patients used as the training data in a leave-one out schema. Classification results were assessed in terms of receiver operator characteristic (ROC) and confusion statistics.

		Sensitivity	Specificity	aucROC
2D	Mean	0.43 ± 0.34	0.91 ± 0.09	0.82 ± 0.13
	Min	0.00	0.68	0.54
	Max	0.95	0.99	0.95
3D	Mean	0.43 ± 0.27	0.74 ± 0.12	0.60 ± 0.16
	Min	0.02	0.56	0.26
	Max	0.93	0.94	0.80

Table 1: Summary of classifier performance across the 14 patient cases.

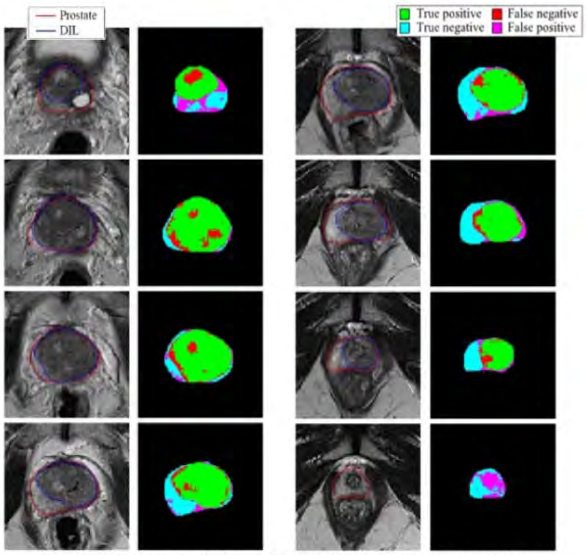

Figure 1: Illustration of classifier results for an example case, with colour map of results shown alongside corresponding MR image slice.

Results: Over the 14 patients, the best performing 2D analysis resulted in a mean area under the ROC curve (aucROC) of 0.82 ± 0.13, whilst the 3D analysis gave an aucROC of 0.60 ± 0.16. A summary of the results is shown in Table 1 and Figure 1 shows a visualisation of the (2D) classification results for an example case. There is wide variation in classifier performance from case to case - performance tended to be poorer on patients with small DILs, giving a low sensitivity but high specificity. The mean value of sensitivity is heavily affected by these low scoring cases. It is expected that the results could be improved with a larger training dataset and morphological post-processing of the detected DIL region.

Conclusion: This work shows that, in principle, texture analysis can be used to identify focal lesions on MR images, facilitating automated delineation for adaptive radiotherapy. 3D analysis does not necessarily lead to improved performance over 2D, although further optimisation of both methods may be possible.

OC-0070

Do radiomics features excel human eye in identifying an irradiated tumor? Rat tumor to patient HNSCC

K. Panth[1], S. Carvalho[1], A. Yaromina[1], R. T.H. Leijenaar[1], S. J. Van Hoof[1], N. G. Lieuwes[1], B. Rianne[1], M. Granzier-Peeters[1], F. Hoebers[1], D. Eekers[1], M. Berbee[1], L. Dubois[1], P. Lambin[1]

[1]MAASTRO clinic, Radiation Oncology, Maastricht, The Netherlands

Purpose or Objective: Radiomics hypothesizes that imaging features reflect the underlying gene expression patterns and intratumoral heterogeneities. In this study, we hypothesized that radiation treatment (RT) affects image features and that these radiation-dependent features could distinguish irradiated tumor better than human eye.

Material and Methods: Rhabdomyosarcoma R1 tumors grown on the lateral flank of WAG/Rij rats were irradiated with 12 Gy or 0 Gy (control). Computed tomography (CT) scans were acquired both before and 7 days post RT [2]. These data were used as a training dataset to select RT-related features. For validation, radiomics features were extracted from CT images of head and neck squamous cell carcinoma (HNSCC) patients before and post 10 fractions of radiation. A total of 723 features were extracted and the top 100 robust features were selected for further analysis based on inter-class correlation coefficient (ICC) values obtained from test-retest (TRT) scans. Imaging experts and radiation oncologists were consigned to identify irradiated tumors (IR) vs. non-irradiated (Non-IR) tumors blinded for patient information. Area under the curve of the receiver operating characteristics curve (AUC-ROC) was computed for each individual feature identified in the rat and HNSCC datasets as being both stable and significant for distinguishing IR and non-IR tumors.

Results: 17 significant differentially expressed features were identified between the two imaging time points after TRT feature selection. 8 out of 17 (2 shape and 6 wavelets) significantly ($p<0.05$) distinguished between pre and post RT scans. AUC-ROC curves demonstrate that out of 8 features, 2 shape and 4 wavelet features had an accuracy of 0.71 and >0.62 respectively in identifying IR tumor from the non-IR ones, whereas imaging experts could only correctly identify 56% (56 ± 5.7) of true cases in rats. 2 (shape) out of 8 features identified in rats also were found to be significantly different between pre and post RT in HNSCC patients (Fig. 1). These two features had an AUC-ROC of 0.85 in identifying a IR tumor while, radiation oncologists were able to solely identify 50% (50 ± 5.6) of true cases in HNSCC patients.

Conclusion: RT radiomics features identified in rats and HNSCC patients were able to distinguish irradiated tumors better than human eye. Thus, in future these features might be used for dosimetric measures and might help in segregating effects of RT from combination treatments that enables to understand the effect of drug or RT alone.

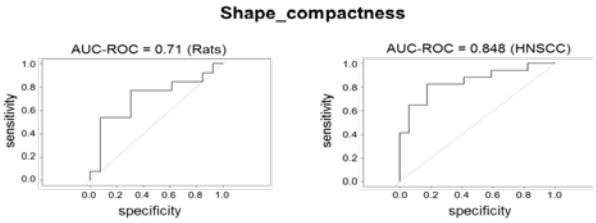

OC-0071

Analysis and reporting patterns of failure in the era of IMRT: head and neck cancer applications

A.S.R. Mohamed[1], D.I. Rosenthal[1], M.J. Awan[2], A.S. Garden[1], E. Kocak-Uzel[3], A.M. Belal[4], A.G. El-Gowily[5], J. Phan[1], B.M. Beadle[1], G.B. Gunn[1], C.D. Fuller[1]

[1]MD Anderson Cancer Center, Radiation Oncology, Houston, USA

[2]Case Western University, Radiation Oncology, Cleveland, USA

[3]Şişli Etfal Teaching and Research Hospital, Radiation Oncology, Istanbul, Turkey

[4]Alexandria University, Radiation Oncology, Alexanria, Egypt

[5]Alexandria University, radiation Oncology, Alexandria, Egypt

Purpose or Objective: To develop a methodology to standardize the analysis and reporting of the patterns of loco-regional failure after IMRT of head and neck cancer.

Material and Methods: Patients with evidence of local and/or regional failure following IMRT for head-and-neck cancer at MD Anderson cancer center were retrospectively reviewed under approved IRB protocol. Manually delineated recurrent gross disease (rGTV) on the diagnostic CT documenting recurrence (rCT) was co-registered with the original planning CT (pCT) using both deformable (DIR) and rigid (RIR) image registration software. Subsequently, mapped rGTVs were compared relative to original planning target volumes (TVs) and dose using volume overlap and centroid-based approaches. Failures were then classified into five types based on combined spatial and dosimetric criteria; A (central high dose), B (central elective dose), C (peripheral high dose), D (peripheral elective dose), and E (extraneous dose) as illustrated in figure 1.Paired-samples Wilcoxon signed rank test was used to compare analysis metrics for RIR versus DIR registration techniques.

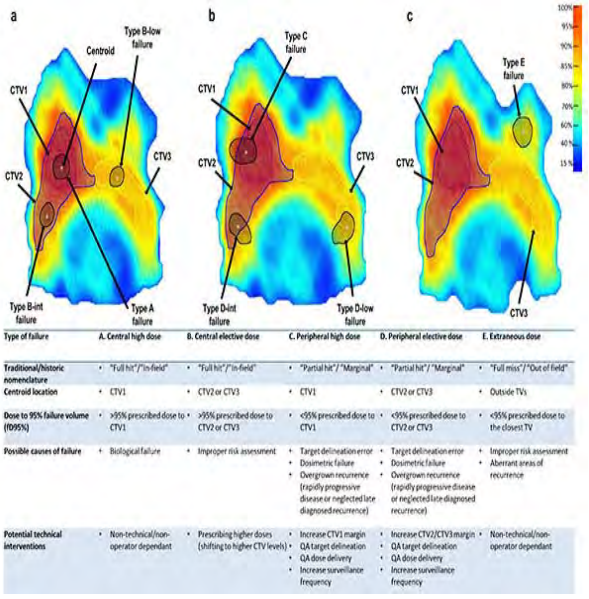

Results: A total of 21 patients were identified. Patient, disease, and treatment characteristics are summarized in table 1. The registration method independently affected the spatial location of mapped failures (n=26 lesions). Failures mapped using DIR were significantly assigned to more central TVs compared to failures mapped using RIR for both the centroid-based and the volume overlap methods. 42% of centroids mapped using RIR were located peripheral to the same centroids mapped using DIR (p= 0.0002), and 46% of the rGTVs whole volumes mapped using RIR were located at a rather peripheral TVs compared to the same rGTVs mapped using DIR (p< 0.0001). rGTVs mapped using DIR had significantly higher mean doses when compared to rGTVs mapped rigidly (mean dose 70 vs. 69 Gy, p = 0.03). According to the proposed classification 22 out of 26 failures were of type A as assessed by DIR method compared to 18 out of 26 for the RIR because of the tendencey of RIR to assign failures more peripherally.

Table 1. Patient demographics, disease, and treatment characteristics

	Total	
	n=21	(%)
Age (years)		
Median	58	
Range	30-75	
Time to Failure (months)		
Median	12	
Range	5-69	
Sex		
Male	18	(86)
Female	3	(14)
Origin		
Nasopharynx	6	(28)
Oropharynx	5	(24)
Hypopharynx	5	(24)
Unknown primary	5	(24)
T-category		
T0	5	(24)
T1	1	(5)
T2	7	(33)
T3	5	(24)
T4	3	(14)
N-category		
N0	1	(5)
N1	5	(24)
N2	12	(57)
N3	3	(14)
Treatment		
Radiation alone	4	(19)
Concurrent ChemoRadiation	9	(43)
Induction Chemotherapy + Radiation	1	(5)
Induction Chemotherapy + Concurrent ChemoRadiation	7	(33)
Radiation dose		
Mean (SD)	69.2	(1.7)
Radiation fractions		
Mean (SD)	33	(2)

Conclusion: DIR-based registration methods showed that the vast majority of failures originated in the high dose target volumes and received full prescribed doses suggesting biological rather than technology-related causes of failure. Validated DIR-based registration is recommended for accurate failure characterization and a novel typology-indicative taxonomy is recommended for failure reporting in the IMRT era.

OC-0072

Respiratory time-resolved 4D MR imaging for RT applications with acquisition times below one minute

C.M. Rank[1], T. Heußer[1], A. Wetscherek[1], A. Pfaffenberger[2], M. Kachelrieß[1]

[1]German Cancer Research Center DKFZ, Medical Physics in Radiology, Heidelberg, Germany

[2]German Cancer Research Center DKFZ, Medical Physics in Radiation Oncology, Heidelberg, Germany

Purpose or Objective: 4D MRI has been proposed to improve respiratory motion estimation in radiotherapy (RT), aiming to achieve a higher treatment accuracy in the thorax and the upper abdomen. In contrast to 4D CT, acquisition time in 4D MRI is not limited by radiation dose, such that multiple breathing cycles can be imaged routinely. However, standard MR reconstruction methods, such as gated gridding, have limitations in either temporal or spatial resolution, signal-to-noise ratio (SNR), contrast-to-noise ratio (CNR) and artifact level or demand inappropriately long acquisition times. The purpose of this study is to provide high quality 4D MR images from super short acquisitions.

Material and Methods: MR data covering the thorax and upper abdomen of three free-breathing volunteers were acquired at a 1.5 T Siemens Aera system. We applied a gradient echo sequence with radial stack-of-stars sampling and golden angle radial spacing: total acquisition time: 37 s, slice orientation: coronal, field-of-view: 400×400×192 mm^3, voxel size: 1.6×1.6×4.0 mm^3, TR/TE = 2.48/1.23 ms, 240 spokes per slice, undersampling factor: 16.8, flip angle: 12°. MR data were sorted into 20 overlapping 10% wide motion phase bins employing intrinsic MR gating. Respiratory motion compensated (MoCo) 4D MR images were generated using our

newly developed 4D joint MoCo-HDTV algorithm, which alternates between motion estimation and image reconstruction. With MoCo, each motion phase is reconstructed from 100% of the measured rawdata. In the motion estimation step, the motion vector fields (MVFs) are estimated between adjacent motion phases and regularized by cyclic constraints. Results were compared to the standard reconstruction methods 3D gridding and 4D gated gridding.

Results: 3D gridding reconstructions revealed strong blurring of structures in the lungs, in the diaphragm region and in the liver caused by respiratory motion. 4D gated gridding images were deteriorated by noise and severe streak artifacts, arising from high azimuthal undersampling. These artifacts obscured small anatomical structures. In contrast, 4D joint MoCo-HDTV reconstructions yielded appropriate image quality combining low streak artifact levels and high temporal resolution, SNR, CNR and image sharpness. Thus, the displacement between end-exhale and end-inhale of small liver structures could be determined, which was not possible using 4D gated gridding images due to their limited image quality.

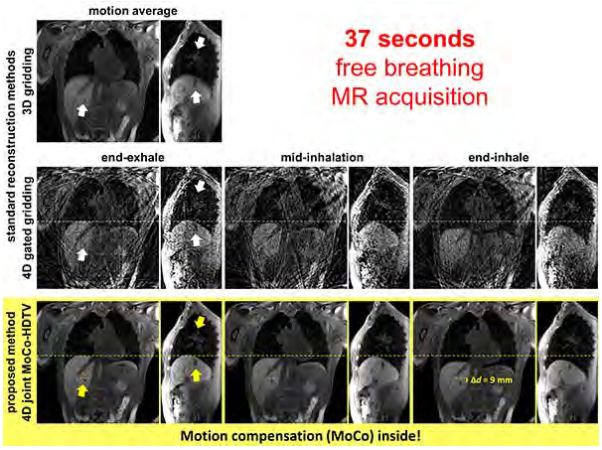

Conclusion: 4D joint MoCo-HDTV facilitates 4D respiratory time-resolved MRI and provides respiratory MVFs at acquisition times below one minute. The method is promising for reliable target delineation in radiation therapy, patient-specific margin or gating window definition, and for adaptive planning based on the provided MVFs. The short acquisition time makes it attractive also for online imaging in an MR-LINAC setting.

Proffered Papers: Physics 2: Basic dosimetry

OC-0073

Difference in using the TRS-398 code of practice and TG-51 dosimetry protocol for FFF beams

J. Lye[1], D.J. Butler[2], C.P. Oliver[2], A. Alves[1], I.W. Williams[1]
[1]*Australian Radiation Protection and Nuclear Safety Agency, Australian Clinical Dosimetry Service, Melbourne- Victoria, Australia*
[2]*Australian Radiation Protection and Nuclear Safety Agency, Radiotherapy, Melbourne- Victoria, Australia*

Purpose or Objective: The two most commonly used protocols for reference dosimetry in external beam radiotherapy are IAEA TRS-398 and AAPM TG-51. Increasingly flattening filter free (FFF) linacs are in clinical use and published theoretical analysis suggests that a difference of 0.5 % is expected between the two protocols (Xiong 2008).

Material and Methods: The Australian Clinical Dosimetry Service (ACDS) has measured FFF beam dose outputs on 11 linacs using both TRS-398 and TG-51 protocols. The response of an NE2561 chamber was modelled using DOSRZnrc. The model was used to study the difference in *kQ* in Varian and Elekta linacs when the flattening filter was removed, and when the flattening filter was replaced by a thin metal plate.

Results: Measured differences in dose output derived from TRS-398 and TG-51 protocols were less than 0.1 % for 6 MV FFF beams and less than 0.2 % for 10 MV FFF beams. Figure 1 shows the modelled response from the NE2561 for Elekta and Varian beams with the flattening filter, with the flattening filter removed, and with a thin metal plate replacing the flattening filter. The modelled FFF *kQ* as a function of TPR20,10 is 0.6 % lower than the *kQ* with flattening filter (WFF). This difference is reduced to 0.3 % when considering *kQ* as a function of %*dd*(10)x. Thus the measured difference in the TRS-398 and TG-51 protocols should be 0.3% according to the modelled results, however the average measured difference is less than 0.1 %. The commercial realisation of FFF beams includes a thin metal filter in the place of the flattening filter. When a 2-3 mm metal plate was included in the model, the difference between the FFF *kQ* and the WFF *kQ* was reduced to approximately 0.1%.

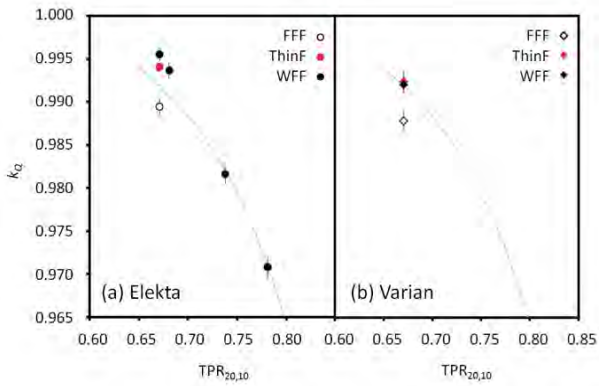

Figure 1 *kQ* of modelled NE2561 chamber with beams with the flattening filter (closed shapes), beams with the flattening filter removed (open shapes) and beams with thin replacement filter (red shapes). (a) shows the results for Elekta beams and (b) shows the results for Varian beams. The dashed grey line shows the average of kQ from TRS-398 and Muir *et al.*

Conclusion: The average difference between linac outputs measured with TRS-398 and TG-51 protocols was less than 0.2 % for 6 MV FFF and 10 MV FFF. Modelling suggests a 2-3 mm metal plate used in place of the flattening filter offers sufficient filtration for the FFF beam to produce a similar *kQ* to WFF beams.

OC-0074

A real time in vivo dosimeter integrated in the radiation protection disc for IORT breast treatment

M. Iori[1], A. Montanari[2], N. Tosi[3], E. Cagni[1], A. Botti[1], A. Ciccotelli[4], G. Felici[4]
[1]*Arcispedale S. Maria Nuova, Medical Physics Unit, Reggio Emilia, Italy*
[2]*Istituto Nazionale di Fisica Nucleare, Sezione di Bologna, Bologna, Italy*
[3]*Istituto Nazionale di Fisica Nucleare e Università, Sezione di Bologna, Bologna, Italy*
[4]*S.I.T. – Sordina IORT Technologies S.p.A., R&D Department, Aprilia, Italy*

Purpose or Objective: IORT breast carcinoma treatment clinical practice has evidenced the need of real time monitoring the dose delivery on the target. The actual discussion on the efficacy of the technique is mainly related with the effective coverage degree of the whole PTV. Furthermore the correct positioning of the radiation protection with respect to the applicator is a critical aspect that cannot presently be determined in real time. The commercially available in vivo dosimetry technologies allow either a real time measurement in one point (MOSFET type detectors) or a non real time measurement over a surface (radio chromic films). A cooperation between a clinical hospital, a research institute and an industrial company has led to the conceptual design of a new device capable of satisfying the above mentioned needs. Such device has been

patented. The new dosimeter consists in four leaf shaped plastic scintillators positioned between the two parts of the radiation protection disc, composed by a PTFE and a steel element (see figure). Therefore such device can measure in real time the dose in the four sectors, providing both the integral dose and a measurement of the field symmetry on the target.

Material and Methods: The accelerator employed is a mobile IORT dedicated electron accelerator capable of producing a 4, 6, 8 and 10 MeV electron beam, collimated by means of PMMA applicators. Measurements have been performed with a prototype based on a plastic scintillator tile placed in a PMMA phantom, with the signal processed and integrated by dedicated electronics. The plastic scintillator data has been compared with the standard dose measurements, performed by means of the PTW Roos ionization chamber and the Unidos E electrometer.
Results: The behavior of the plastic scintillator has been tested with the IORT accelerator electron beam. Several tests have been performed, comparing the reading of the system with the reading of the plane parallel ionization chamber in a PMMA phantom. On the basis of the preliminary measurements, the system fully complies with the standards requirements (see figure).

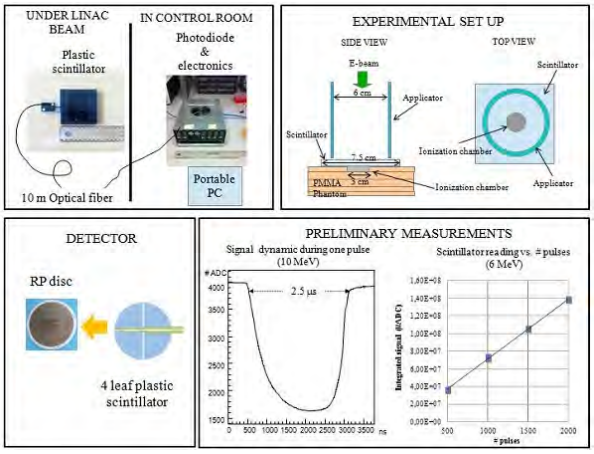

Conclusion: The above described in vivo dosimeter significantly improves the IORT clinical documentation, allowing the real time check of the dose delivery over the whole PTV. Furthermore, since the device sensitivity is high enough to produce a precise dose map with an overall delivery of less than 1 cGy, the correct positioning of the disc with respect to the PTV and the applicator can be checked before delivering the treatment, allowing the surgeon to correct it should the symmetry on the PTV be out of tolerance levels. The system will be engineered in order to meet the standards required for a temporarily implanted medical device too (biocompatibility, sterilizability, etc.) and will undergo the certification process during 2016. It is planned to organize a multicentre study for verifying in the clinical practice the efficacy and safety of the new dosimeter.

OC-0075

Impact of air around an ion chamber: solid water phantoms not suitable for dosimetry on an MR-linac

S. Hackett[1], B. Van Asselen[1], J. Wolthaus[1], J. Kok[1], S. Woodings[1], J. Lagendijk[1], B. Raaymakers[1]
[1]*UMC Utrecht, Department of Radiotherapy, Utrecht, The Netherlands*

Purpose or Objective: A protocol for reference dosimetry for the MR-linac is under development. The response of an ion chamber must be corrected for the influence of the 1.5T magnetic field as deflection of electron trajectories by the Lorentz force is greater in the air-filled chamber than the surrounding phantom. Solid water (SW) phantoms are used for dosimetry measurements on the MR-linac, but a small volume of air is present between the chamber wall and phantom insert. This study aims to determine if this air volume influences ion chamber measurements on the MR-linac. The variation of chamber response as the chambers were rotated about the longitudinal chamber axis was assessed in SW and water to distinguish between the effect of the anisotropic dose distribution in a magnetic field and any intrinsic anisotropy of the chamber response to radiation. The sensitivity of the chamber response to the distribution of air around the chamber was also investigated.

Material and Methods: Measurements were performed on an MR-linac and replicated on an energy-matched Agility linac for five chambers, comprising three different models. The response of three waterproof chambers was measured with air and with water between the chamber and insert to measure the influence of the air volume on the absolute chamber response. Angular dependence of the waterproof chambers and two NE 2571 chambers was measured in an SW phantom, both parallel and perpendicular to the magnetic field, and in water (waterproof chambers only). The influence of the distribution of air around the chambers in the SW phantom was measured by displacing the chamber in the insert using a paper shim, approximately 1 mm thick, positioned in different orientations between the chamber casing and the insert.

Results: The responses of the three waterproof chambers measured on the MR-linac increased by 0.6% to 1.3% when the air volume in the insert was filled with water. The responses of the chambers on the Agility linac changed by less than 0.3%. The angular dependence ranged from 0.9% to 2.2% in solid water on the MR-linac, but was less than 0.5% in water on the MR-linac and less than 0.3% in SW on the Agility linac. An example of the angular dependence of a chamber is shown in Figure 1.

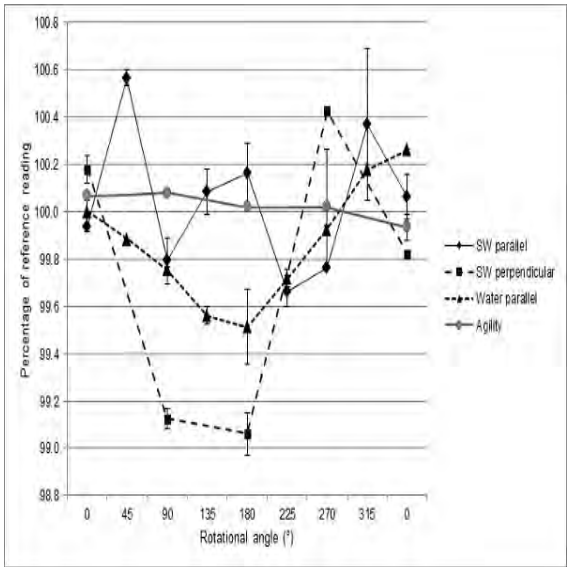

Changing the distribution of air around the chamber induced changes of the chamber response in a magnetic field of up to 1.1%, but the change in chamber response on the Agility was less than 0.3%.

Conclusion: The interaction between the magnetic field and secondary electrons in the air volume around the chamber reduces the charge collected by between 0.6 and 1.3%. The large angular dependence of ion chambers measured in SW in a magnetic field appears to arise from a change of air distribution as the chamber is moved within the insert, rather than an intrinsic isotropy of the chamber sensitivity to radiation. It is therefore recommended that reference dosimetry measurements on the MR-linac be performed only in water, rather than in SW phantoms.

OC-0076

Towards MR-Linac dosimetry: B-field effects on ion chamber measurements in a Co-60 beam

J. Agnew[1], G. Budgell[1], S. Duane[2], F. O'Grady[1], R. Young[1]
[1]*The Christie NHS Foundation Trust, CMPE, Manchester, United Kingdom*
[2]*National Physical Laboratory, Radiation Dosimetry Group, Teddington, United Kingdom*

Purpose or Objective: To quantify the effect of small air gaps at known positions on ionisation chamber (IC) measurements in the presence of a strong magnetic (B-)field, and to characterise the response of ICs over a range of B-field strengths in the absence of air gaps.

Material and Methods: The ratio of responses of four commercially available ICs was measured in a Co-60 beam with and without a 1.5T B-field ($M_{1.5T}/M_{0T}$) using a GMW electromagnet unit and a 5cm pole gap. Measurements were made in custom-built Perspex phantoms with the chamber, beam and B-field all orthogonal. The measurements were repeated with the phantoms at each cardinal angle (rotated about the long axis of the ICs). The phantoms were designed to be symmetric under rotation about this axis except for a shallow 90° section next to the sensitive volume of the ICs. The measurements were repeated with the air gap removed by introducing water to the phantom cavity. For the PTW 30013 chamber further measurements were performed after introducing a small (approximately 30 mm^3) bubble into the recess when the cavity was otherwise filled with water, which was made possible by the novel phantom design. The measurements in water were repeated with additional build-up material and in multiple phantoms at a single phantom orientation.
Measurements were also taken to characterise the ratio of responses for five ICs over a range of B-field strengths (0 – 2T in 0.25T increments).

Results: For all 4 ICs in the rotating setup, the response varied consistently with the position of the recess when the air gap was present, with the lowest value of $M_{1.5T}/M_{0T}$ obtained when the recess was upstream of the IC. The maximum peak-to-peak (PTP) variation was 8.8%, obtained for the PTW 31006 'Pinpoint' IC, and the minimum was 1.1%, obtained for the Exradin A1SL IC. This variation all but disappeared (maximum PTP variation 0.7%, seen for PTW 31010 IC) when the air gap was removed. A large (3.9%) PTP variation was observed for the PTW 30013 when an air bubble was inserted into an otherwise airless setup (0.2% variation without air gap).

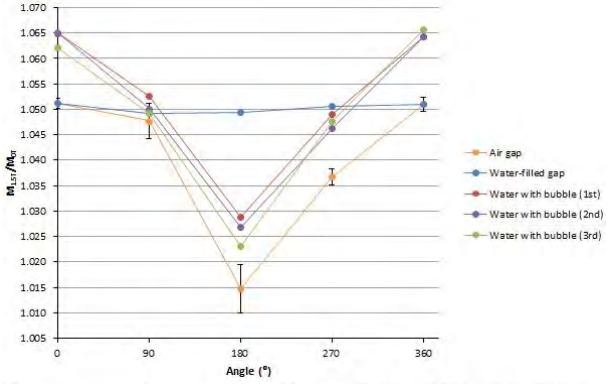

	Chamber	$(M_{1.5T}/M_{0T} - 1) \times 100$ averaged over cardinal angles (%)	PTP Variation over cardinal angles (%)
Air Gap	PTW 30013	3.9	2.9
	*PTW 30013**	*4.7*	*3.9*
	PTW 31006	-1.3	8.8
	PTW 31010	7.1	4.0
	Exradin A1SL	6.4	1.1
Without Air Gap	PTW 30013	5.0	0.2
	PTW 31006	6.3	0.2
	PTW 31010	5.1	0.7
	Exradin A1SL	8.6	0.2
** Bubble air gap*			

Conclusion: Small air gaps are responsible for large variations in IC response in the presence of a magnetic field. These variations can be eliminated by introducing water into the cavity, but even small bubbles will cause large variations in the response. Further, IC response in the presence of a 1.5T B-field is insensitive to changes in depth and scatter conditions of the phantoms investigated here. Each IC has different M/M_{0T} response across the range of B-field strength 0 – 2T.

OC-0077

Dual energy CT proton stopping power ratio calibration: Validation with animal tissues

Y. Xie[1], L. Yin[1], C. Ainsley[1], J. McDonough[1], T. Solberg[1], A. Lin[1], B.K. Teo[1]
[1]*University of Pennsylvania, Department of Radiation Oncology, Philadelphia, USA*

Purpose or Objective: One main source of uncertainty in proton therapy is the conversion of Hounsfield Unit (HU) to proton stopping power ratio (SPR). In this study, we measured and quantified the accuracy of dual energy CT (DECT) SPR prediction in comparison with single energy CT (SECT) calibration.

Material and Methods: We applied a stoichiometric calibration method for DECT to predict the SPR using CT images acquired sequentially at 80 kVp and 140 kVp. The dual energy index was derived based on the HUs of the paired spectral images and then used to calculate the effective atomic number, electron density, and SPR of the materials. The materials were irradiated with a collimated 2 mm width pristine pencil beam and the water equivalent thickness (WET) and SPRs deduced from the residual proton range measured using a multi-layer ion chamber (MLIC) device. Multiple proton energy (130 to 160 MeV) measurements were made on the tissues to achieve sub mm WET measurement accuracy. Tissue surrogates (lung, adipose, muscle and bone) with known chemical compositions were used for calibration and validated with animal tissues. The animal tissues (veal shanks) were kept in a frozen state during the CT scans and proton range measurements. The results were compared to traditional stoichiometric calibration with SECT at 120 kVp.

Results: The percentage difference of DECT predicted SPR from MLIC measurements were reduced 1) from 3.9% to 0.7% for tissue surrogates; 2) from 1.8% to <0.1% for veal bone (tibia); and 3) from 1.7% to 0.9% for veal muscle compared with SECT calibration. The systematic uncertainties from CT scans were studied by varying the effective phantom size (<1%), surrogate locations (<1%), and repeat CT scans (<0.6%). The choice of the mean ionization values of the chemical elements resulted in a 0.2~0.9% variation in calculated SPRs.

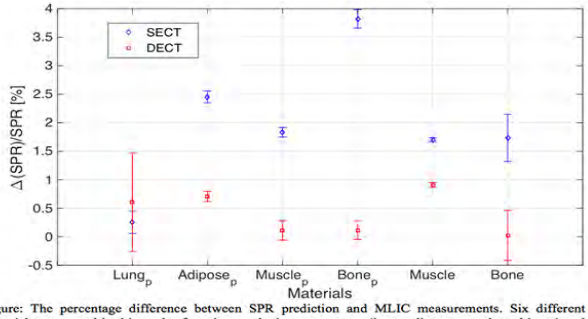

Figure: The percentage difference between SPR prediction and MLIC measurements. Six different materials were used in this study: four tissue substitute surrogates (lung, adipose, muscle and bone) and two animal tissues (veal tibia bone and muscle). The blue diamond symbols represent the predictions from SECT and red squares represent the predictions from DECT. As observed from the figure, SPRs from DECT prediction agree better with MLIC measurements.

Material	SPR		
	MLIC	DECT	SECT
Bone (phantom)	1.107	1.108	1.149
Muscle (phantom)	1.047	1.048	1.028
Adipose (phantom)	0.962	0.955	0.985
Lung (phantom)	0.511	0.514	0.509
Bone (veal)	1.742	1.742	1.773
Muscle (veal)	1.042	1.032	1.024

Table: SPRs from MLIC measurements, DECT prediction, and SECT prediction for the six materials used in this study: four tissue substitute surrogates (lung, adipose, muscle and bone) and two animal tissues (veal tibia bone and muscle).

Conclusion: Our study indicated that DECT is superior to SECT for proton SPR prediction and has the potential to reduce the range uncertainty to less than 2%. DECT may permit the use of tighter distal and proximal range uncertainty margins for treatment thereby increasing the precision of proton therapy.

OC-0078

Monte Carlo calculated beam quality correction factors for proton beams

C. Gomà[1], P. Andreo[2], J. Sempau[3]
[1]*ETH Zürich, Department of Physics, Zürich, Switzerland*
[2]*Karolinska University Hospital, Department of Medical Physics, Stockholm, Sweden*
[3]*Universitat Politècnica de Catalunya, Institut de Tècniques Energètiques, Barcelona, Spain*

Purpose or Objective: To calculate the beam quality correction factors (kQ) in monoenergetic proton beams using detailed Monte Carlo simulation of ionization chambers. To compare the results with the kQ factors tabulated in IAEA TRS-398, which assume ionization chamber perturbation correction factors (pQ) equal to unity.

Material and Methods: Two different Monte Carlo codes were used: (i) Gamos/Geant4 to generate a phase-space file just in front of the ionization chamber and (ii) PENH to simulate the transport of particles in the ionization chamber geometry (or water cavity). Seven ionization chambers (5 plane-parallel and 2 cylindrical) were studied, together with five proton beam energies (from 70 to 250 MeV). kQ calculations were performed using the electronic stopping powers resulting from the adoption of two different sets of I-values for water and graphite: (i) Iw = 75 eV and Ig = 78 eV, and (ii) Iw = 78 eV and Ig = 81 eV.

Results: The kQ factors calculated using the two different sets of I-values were found to agree within 1.5% or better. The kQ factors calculated using Iw = 75 eV and Ig = 78 eV were found to agree within 2.3% or better with the kQ factors tabulated in IAEA TRS-398; and within 1% or better with experimental values determined with water calorimetry (see figure 1). The agreement with IAEA TRS-398 values was found to be better for plane-parallel chambers than for cylindrical. For cylindrical chambers, our kQ factors showed a larger variation with the residual range than IAEA TRS-398 values (see figure 1). This is, in part, due to the fact that our kQ factors take inherently into account the dose gradient effects in unmodulated proton beams.

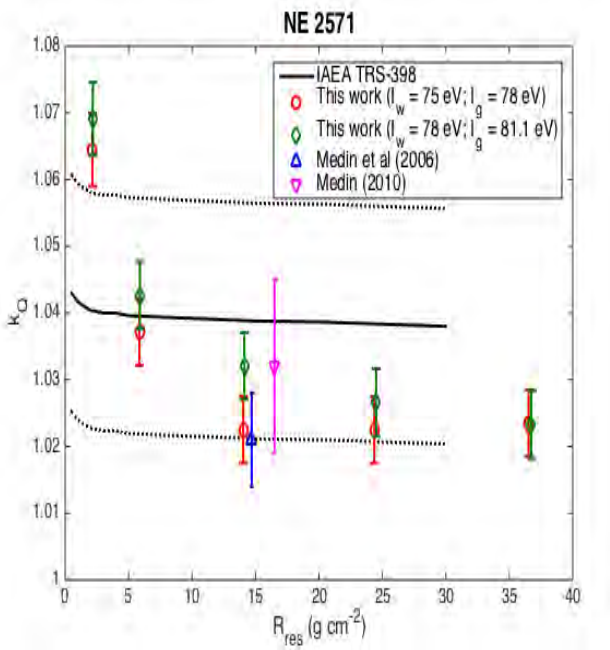

Figure 1: kQ factor of the NE 2571 cylindrical chamber, as a function of the residual range, (i) tabulated in IAEA TRS-398, (ii) calculated in this work with Monte Carlo simulation and (iii) determined with water calorimetry. The uncertainty bars correspond to one standard uncertainty in the data points. The dashed lines correspond to one standard uncertainty in the IAEA TRS-398 values.

Conclusion: The results of this work seem to indicate that ionization chamber perturbation correction factors in unmodulated proton beams could be significantly different from unity, at least for some of the ionization chamber models studied here. In general, the uncertainty of Iw and Ig seems to have a smaller effect on kQ factors than the assumption of pQ equal to unity. Finally, Monte Carlo calculated kQ factors of plane-parallel ionization chambers seem to be in better agreement with the IAEA TRS-398 values currently in use, than those of cylindrical chambers.

Proffered Papers: RTT 1: Novelties in treatment planning

OC-0079

Automated instead of manual planning for lung SBRT? A plan comparison based on dose-volume statistics

B. Vanderstraeten[1], B. Goddeeris[1], C. Derie[1], K. Vandecasteele[1], M. Van Eijkeren[1], L. Paelinck[1], C. De Wagter[1], Y. Lievens[1]
[1]*University Hospital Ghent, Radiotherapie, Ghent, Belgium*

Purpose or Objective: Automated planning (AP) aims to simplify the treatment planning process by eliminating user variability. We performed a detailed plan comparison based on clinical objectives and dose-volume histogram (DVH) parameters in a group of stereotactic body radiation therapy (SBRT) lung cancer patients.

Material and Methods: Between March 2012 and May 2015, 55 lung cancer patients were treated with SBRT at our institution. A total dose of 60 Gy in 3 fractions was prescribed to the PTV (D95). For each patient, an IMRT plan was created using in-house developed optimization software by manually tweaking a set of optimization objectives during several iterations. Final dose calculation was performed in Pinnacle 9.8 (Philips Medical Systems Inc, USA). These plans are further referred to as the manual plans (MP).
For each patient, an additional plan was created retrospectively using the Pinnacle 9.10 Auto-Planning software with a template representing the clinical objectives for the following structures: GTV, PTV, lungs minus GTV, spinal cord, esophagus, heart, aorta, trachea, main stem bronchus and chest wall. Using automatic optimization tuning

methods, an automated plan (AP) was created for each patient using the same IMRT beam directions as for the MP. No additional manual tweaking whatsoever was performed.
For all of the above-mentioned structures the following DVH parameters were included in our analysis: D99, D98, D95, D90, D50, D5, D2 (in which xx% of the PTV volume receives a dose of at least Dxx) and Dmean. For the organs at risk (OAR) V5, V10 and V20 were also included (in which Vxx is the volume receiving at least xx Gy). The acceptability of each plan was judged against our clinical objectives (result: pass, minor deviation or fail). Additionally, pairwise comparisons of the DVH parameters were performed using paired, two-sided t-tests between the MPs and APs.

Results: Three APs failed in terms of our clinical objectives (1 plan: heart D2, 2 plans: chest wall D2), while 13 plans showed a minor deviation (12 plans: lungs minus GTV V20, 1 plan: chest wall D2). None of the MPs failed our clinical objectives, but 9 also showed a minor deviation (8 plans: lungs minus GTV V20, 1 plan: PTV D99). The graph shows average values over all patients of the dose (in Gy) –volume (in %) parameters for which statistically significant ($p < 0,05$) differences were found between the MPs and APs. Top: GTV and PTV; bottom: clinical OAR objectives. All plans were normalized to PTV D95 = 60 Gy.

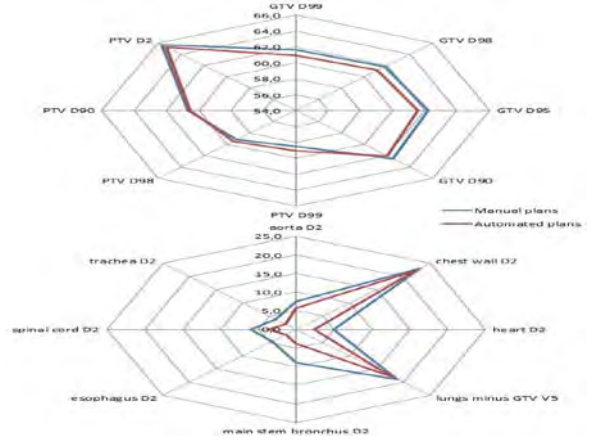

Conclusion: Without user intervention, AP resulted in plans that comply with our clinical objectives for almost all patients. Some APs may require slight additional manual tweaking. From a statistical point of view, AP delivers significantly less dose to the OARs, while preserving target coverage. In the near future, all plans will be blindly evaluated by three experienced radiation oncologists to assess the clinical significance of the observed statistical differences.

OC-0080

In-silico implementation of MRI-60Co based RT: a dosimetrical comparison with rectal cancer (SIMBAD)

E. Placidi[1], N. Dinapoli[2], L. Boldrini[2], G.C. Mattiucci[2], L. Azario[1], D. Piccari[2], S. Teodoli[1], M.A. Gambacorta[2], S. Chiesa[2], A. Piermattei[1], V. Valentini[2]
[1]*Università Cattolica del Sacro Cuore -Policlinico A. Gemelli, Institute of Physics, Rome, Italy*
[2]*Università Cattolica del Sacro Cuore -Policlinico A. Gemelli, Radiation Oncology Department- Gemelli-ART, Rome, Italy*

Purpose or Objective: The ViewRay MRI-Co60 hybrid system (MRIdian) allows MRI based targeting, autosegmentation and direct planning for numerous anatomical districts. Our department is implementing this technology and, up to date, we are comparing planning procedures to our clinical standards in order to define which districts could take advantage from the use of the MRIdian technology. Aim of this investigation was to assess the impact of the MRIdian radiation therapy system through a planning analysis for rectal cancer treatments.

Material and Methods: Ten sets of 3 plans (MRIdian, RapidArc and 5 beams sliding windows IMRT) were calculated for 10 patients affected by locally advanced rectal cancer (cT3-cT4; cN0, cN+). ROIs were contoured on Eclipse TPS. RapidArc (6-15 MV) and 5 beams (6-15 MV) sliding windows IMRT treatment plans were calculated on Eclipse according to our QA protocols. The PTV1 (CTV1+7 mm margin) was represented by tumor+1.5 cm margin craniocaudally and correspondent mesorectum, the PTV2 (CTV2 + 7 mm margin) by mesorectum in toto and pelvic nodes. The body, the bowel bag and the bladder were the OaR considered. The prescribed dose for PTV2 was 45 Gy and 55 Gy for PTV1 through simultaneous integrated boost. The PTV V95 and OaRs QUANTEC dose constraints on the DVHs and Wu's homogeneity indexes (HI) were considered for the QA of the plans. The structure sets were then uploaded on the MRIdian TPS and Co60 step and shoot IMRT plans (7 groups of 3 fields) were calculated. The DHVs and HIs were then compared to the RapidArc and IMRT plans in order to evaluate MRIdian's performances.

Results: MRIdian showed a better HI when compared to the other techniques for PTV1, while this advantage could not be appreciated for PTV2, even if a better PTV2 V100 (45 Gy) was observed. Comparable mean doses for the bladder were registered, while a higher bowel V45 was observed (even if still in the constraints limits). Low dose body V5 was higher for the MRIdian plans. The mean results and the standard deviations are summarized in the table.

Mean	MRIdian	RapidArc	IMRT
V95 PTV1 [%]	99.2	97.8	98.2
V105 PTV1 [%]	0.0	0.0	0.1
V95 PTV2 [%]	98.2	98.4	97.7
V100 PTV2 [%]	62.0	47.3	54.8
V105 PTV2 [%]	14.8	5.0	7.3
V5 Body [cc]	12809	10826	10039
V20 Body [cc]	6871	4559	5901
V45 Bowel Bag [cc]	59.4	10.6	48.7
Mean Dose Bladder [Gy]	35.4	34.0	36.5
Homogeneity Index PTV1	1.3	1.6	1.5
Homogeneity Index PTV2	6.7	3.7	4.4

Standard Deviation	MRIdian	RapidArc	IMRT
V95 PTV1 [%]	0.4	1.1	0.7
V105 PTV1 [%]	<0.1	<0.1	0.4
V95 PTV2 [%]	0.4	1.3	1.6
V100 PTV2 [%]	2.7	6.4	7.1
V105 PTV2 [%]	5.9	2.8	3.3
V5 Body [cc]	1847	1729	1487
V20 Body [cc]	567	730	1071
V45 Bowel Bag [cc]	36.0	23.3	11.6
Mean Dose Bladder [Gy]	3.3	4.5	4.9
Homogeneity Index PTV1	0.2	0.4	0.5
Homogeneity Index PTV2	0.9	1.5	2.2

Conclusion: A comparable PTV dose coverage between the 3 plans was found for rectal cancer, with a HI advantage for the PTV1 for the MRIdian plan. Differences were described for OaRs, especially for low dose areas (V5 Body). MRIdian allowed to reach dosimetrical goals comparable to RapidArc and IMRT gold standards. The evaluation of a possible reduction in PTV margin and a proper target coverage by MRI based gating will be analyzed when the system will become operative at Gemelli ART.

OC-0081

Robust photon versus robust proton therapy planning with a library of plans for cervical cancer

K. Crama[1], A. Van de Schoot[1], J. Visser[1], A. Bel[1]
[1]*Academic Medical Center, Radiotherapy, Amsterdam, The Netherlands*

Purpose or Objective: The cervix-uterus shows large day-to-day variation in position and size, mainly depending on bladder and rectum filling. Image-guided adaptive radiotherapy with a library of plans (LOP) is a strategy to mitigate these large variations, resulting in less dose to organs at risk (OAR) compared to the use of a single plan with a population-based PTV margin. A further reduction of OAR dose can be achieved using proton therapy. However, it is challenging to achieve a target coverage that is robust for range and position uncertainties. The aim of this study is to compare target coverage of robustly optimized photon and

proton therapy plans using a LOP adaptive strategy for cervical cancer.

Material and Methods: Five cervical cancer patients treated with photon therapy were retrospectively included. For each patient a full and empty bladder planning CT and weekly repeat CTs were acquired. Depending on the magnitude of cervix-uterus motion, one to three ITV sub ranges were generated by interpolation of the CTV delineations on full and empty bladder CT. Target and OARs were delineated on all repeat CTs. Robustly optimized photon (VMAT) library plans and proton (IMPT) library plans were generated with a prescribed dose of 46 Gy in 23 fractions to the ITV. For robust optimization, a position uncertainty of 0.8 cm was applied; for protons 3% range uncertainty was included as well. The plans were required to have sufficient target coverage (V95%>99%) for both the nominal scenario and twelve scenarios with different range and position errors. Both for protons and photons the actual delivered dose was simulated. Repeat CTs were registered to the full bladder planning CT using bony anatomy, the best fitting library plan was selected and the dose was recalculated. The DVH for the whole treatment was estimated by adding and scaling DVHs. The target coverage was evaluated for the total CTV as well as the CTVs of the corpus uteri, cervix, vagina and elective lymph nodes.

Results: For the total CTV, on average, the V95% for the whole treatment was 99.9% (range 97.3%-99.8%) for photons and 96.3% (93.5%-98.1%) for protons. The V95% of the corpus uteri was 95.7% (86.3%-99.9%) and 88.7% (68.4%-99.9%) for photons and protons, respectively. Figure 1 shows a repeat CT with insufficient target coverage both for photons and protons. The elective lymph nodes received sufficient dose with photons, on average, V95% was 99.1% (98.1%-99.8%). With protons this volume decreased to 96.2%(94.9%-98.8%). For the cervix and vagina no differences between the use of photons and protons were observed.

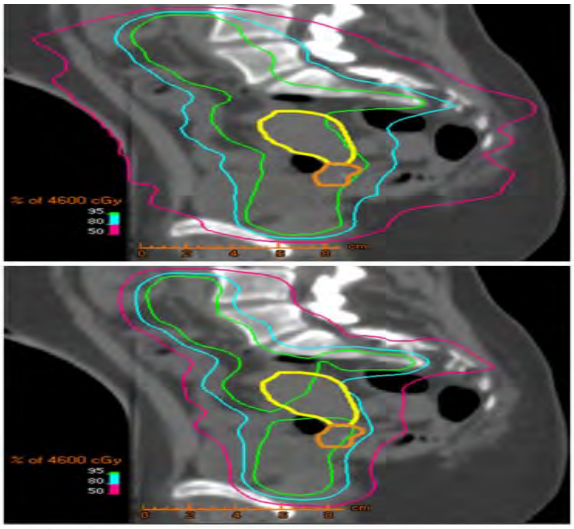

Figure 1. Example of a recalculated dose distribution in a sagittal view. The CTV of the corpus uteri is the yellow structure, the GTV the orange structure. The top view shows the photon therapy plan, the bottom view the proton therapy plan. The green line represents the 95% isodose.

Conclusion: The robustly optimized proton therapy plans did not result in an adequate target coverage for all patients for the realistic robustness parameters used. For some cases the used LOP strategy is not sufficient to cope with the large movements of the cervix-uterus for both modalities. The impact of underdosing is larger using protons than using photons.

OC-0082

alidation of MR based dose calculation of prostate cancer treatments

R.L. Christiansen[1], H.R. Jensen[1], D. Georg[2], C. Brink[1,3]

[1]*Odense University Hospital, Laboratory of Radiation Physics, Odense, Denmark*

[2]*Medical University Vienna, Department of Radiation Oncology, Vienna, Austria*

[3]*University of Southern Denmark, Institute of Clinical Research, Odense, Denmark*

Purpose or Objective: Dose calculation is currently based on the density map provided by CT. However, for delineation of the prostate gland and organs at risk T2-weighted MR imaging is the gold standard. Dose calculation based on MR information would remove the need for a CT scan and avoid the uncertainty related to registration of the images. Pseudo-CT generation from MR scans has recently become available. This study investigates the validity of dose calculation based on pseudo CT created with commercial software (MR for Calculating ATtenuation – MRCAT) compared to standard CT based dose calculation.

Material and Methods: Seven high risk prostate cancer patients were MR and CT scanned. The clinical, curatively intended treatment (78 Gy in 39 Fx) using single arc VMAT was based on the conventional CT. From the MR scan pseudo-CT were created using MRCAT (Philips, Helsinki, Finland). To eliminate dose comparison uncertainties related to patient positioning differences between CT and MR rigid CT-MR registration was performed. The VMAT plan was transferred to the pseudo-CT and dose calculation was performed using Pinnacle (V9.10). Pass rate of the Gamma index was used to evaluate the similarity of the dose distributions. The dose acceptance criterion was evaluated as a percentage of the prescribed dose applying 2 %/2 mm and 1 %/1mm criteria.

Results: MRCAT was generated for six of the seven patients. One patients' pelvic anatomy was not correctly recognized by the software model, which prohibited MRCAT reconstruction. Pass rates for both acceptance criteria are summarized in table 1. For 2%/2 mm, pass rates are high, above 97.6% for all analyzed structures. Even for the 1%/1 mm criterion, pass rates are generally above 97%. In patient 3, lower pass rates in PTV78, seminal vesicles and rectum are observed. For this patient the gamma values above one are located mainly in and around an air cavity in the rectum (see figure 1). MRCAT does not assign air density to air cavities inside the patient, leading to the observed dose differences. However, in the pelvic region it might be at least as good an approximation to treat air cavities as water due to the mobility of the rectal air during the treatment course. As seen in figure 1, gamma values above one are also present close to the surface of the patient, which is caused by differences in definition of the outer contour of the patient.

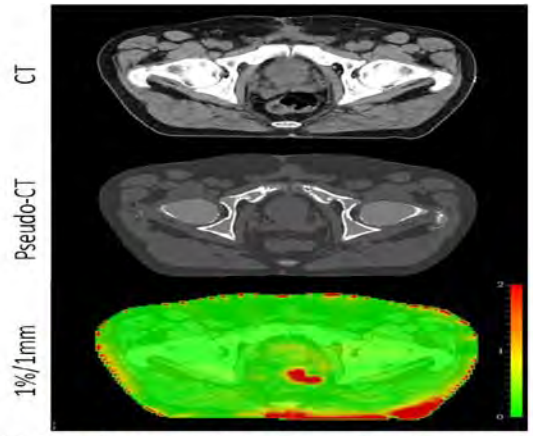

Figure 1: Corresponding slice on CT and pseudo-CT and gamma analysis of respective dose calculations.

		PTV78	Prostate	Seminal vesicles	Rectum	Small bowel	Bladder	Outer contour
2%/2mm	Patient 1	100	100	100	100	100	100	99.5
	Patient 2	100	100	100	99	99.2	100	99.2
	Patient 3	97.6	100	98.5	98.1	100	100	99.6
	Patient 4	100	100	100	100	100	100	99.7
	Patient 5	100	100	100	100	100	100	99.3
	Patient 6	100	100	100	100	99.9	100	99.6
1%/1mm	Patient 1	99.7	98.9	100	99.9	100	100	99.0
	Patient 2	100	100	100	96.6	96.9	100	98.3
	Patient 3	91.5	99.0	84.1	91.7	100	99.9	98.8
	Patient 4	100	100	100	100	100	100	99.0
	Patient 5	100	100	100	100	98.5	100	98.2
	Patient 6	100	100	100	100	97.8	100	98.9

Table 1: Pass rates are shown for selected structures. Gamma analysis for penile bulb, left and right femoral heads yielded 100 % pass rates for all patients under all criteria.

Conclusion: Overall the pseudo-CT based dose calculations are very similar to the CT based calculation for prostate cancer patients. The MRCAT software classifies internal air cavities as water density leading to dose differences compared directly to CT. In terms of the dose precision observed in this study the MRCAT is able to substitute the standard CT simulation, but a larger cohort of patients is needed to validate this finding. This will also reveal whether bone recognition capability is sufficiently versatile for standard clinical use.

OC-0083

When using gating in left tangential breast irradiation? A planning decision tool

N. Dinapoli[1], D. Piro[1], M. Bianchi[1], S. Teodoli[2], G.C. Mattiucci[1], L. Azario[2], A. Martino[1], F. Marazzi[1], G. Mantini[1], V. Valentini[1]

[1]*Università Cattolica del Sacro Cuore -Policlinico A. Gemelli, Radiation Oncology Department, Rome, Italy*

[2]*Università Cattolica del Sacro Cuore -Policlinico A. Gemelli, Physics Institute, Rome, Italy*

Purpose or Objective: The use of gating in tangential breast irradiation has shown to reduce the dose delivered to the heart, resulting in the possibility of decreasing heart toxicity in long time surviving patients. The use of gating requires to identify which patients could be addressed to this methodic by comparing planning results of gated and not-gated simulation CT based plans. However, the required double CT scan (with and without gating technology), for patients undergoing to left-breast tangential radiation treatment, can result in working overhead for RTTs executing CTs and for planners that have to produce two opponent plans for allowing final gated, or not-gated treatment decision. In this work a tool for deciding which patients could be selected for gating procedures by using only not gated CT scan is presented.

Material and Methods: Patients addressed to left-breast tangential irradiation without need to irradiate supra-clavicular nodes have been retrospectively recruited in this study. Both gated and not-gated simulation CT were available for all of them. Two series of opponent, gated and not-gated, treatment plans have been produced and analyzed using Varian™ Eclipse workstation. DVHs have been extracted from plans and have been analyzed in order to detect which dosimetrical parameters are able to predict the final outcome: mean heart dose in gated treatment plan. Maximum heart distance (MHD) has been also recorded. A multiple linear regression model has been used to predict the final outcome.

Results: 100 patients have been enrolled in this study and 200 plans on 100 gated-CT and 100 not-gated CT have been produced. 10 patients showed mean not-gated CT heart dose (MNGHD) > 5 Gy (institutional threshold for addressing the patient to gating), resulting in a 90% overhead in terms of performed gated-CTs and plans. The final model shows the possibility to predict mean heart dose in gated treatment plan with a p-value < 2.2e-16, adjusted R-squared = 0.5486, using not gated CT based planning and geometrical parameters summarized as follows:

Coefficients name:	**β value**	**P-val - Pr(>|t|)**
Intercept	0.92151	2.27e-11
V31.5 Gy Lung Basal	-4.20188	0.000299
Mean Basal CT Heart Dose	0.54065	1.29e-13
Basal MHD	-0.44137	0.000748

In order to easily predict which gated-CT mean heart dose would result if patients underwent to this scanning procedure a nomogram has been produced allowing the users to manually calculate this value without scanning the patients with gated CT (figure 1).

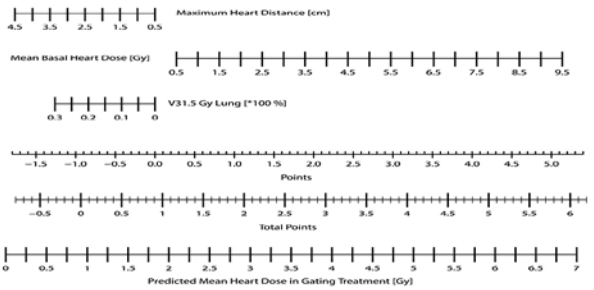

Conclusion: The use of gated treatment in left breast tangential radiotherapy can result in high quantity of unrequested CT scans and plans for patients not needing to be addressed to this kind of delivery method. Our decision tool is able to evaluate patients that will benefit from using gating technology without the need to acquire a double CT scan and producing a double treatment plan, so making the whole workflow easier and faster.

OC-0084

Hybrid RapidArc for breast with locoregional lymph node irradiation spares more normal tissue

E. Bucko[1], M. Jeulink[1], P. Meijnen[1], B. Slotman[1], W. Verbakel[1]

[1]*VU University Medical Center, Radiotherapy, Amsterdam, The Netherlands*

Purpose or Objective: The conventional radiotherapy technique for breast cancer with locoregional lymph nodes consists of half beam tangential fields for the breast, junctioning a 3-field AP-PA half beam block for the supraclavicular nodes. The AP-PA fields treat a considerable volume of healthy tissue to high doses, and the lack of slip zone makes it unsuitable for deep inspiration breathhold where some variation of breathhold is expected. Full volumetric modulated arc would lead to an unwanted low-dose spread. We therefore investigated the improvements of a novel hybrid RapidArc (hRA) technique which is now standard in our hospital.

Material and Methods: Previously contoured CT scans from 10 patients with breast tumors including lococregional lymph nodes were used for planning (Eclipse, Varian Medical Systems). Prescription was 16 fractions of 2.67 Gy. Clinically treated hRA plans consisted of 2 tangential open fields with a 2 cm cranial slip zone delivering 85% of breast dose and 3 partial RapidArc arcs of each 80°, delivering the remaining dose to the breast and slipzone and full dose to the cranial lymph nodes. A range of organs at risk (OAR) constraints (from high to low dose) were set on heart, contralateral (CL) breast, ipsilateral (IL) and CL lung, esophagus, thyroid and ring structures. PTV and OAR dosimetry of hRA plans were compared with our old conventional technique hybrid (h)-IMRT). hIMRT plans consisted of 3 APPA half fields, delivering full dose to the cranial lymph nodes, 2 tangential open half fields delivering 85% of breast dose and 2 tangential IMRT fields delivering the remaining dose to the breast and junction. Plans were normalized to deliver similar mean dose. PTV and OAR metrics were compared.

Results: Compared to hIMRT, hRA provided better PTV coverage and OAR sparing (see Table). V107% of PTV reduced from 4.9% to 1.3%. Both the volumes outside the PTV receiving 20Gy and 40Gy were reduced significantly by hRA (from 2014 to 1440cm3 and from 789 to 312 cm3). hRA spared better the esophagus and thyroid gland. Mean lung dose and IL lung receiving 20Gy reduced significantly, at the expense of a non-significant 5% increase of V5Gy to the IL lung.

Table, dosimetric data averaged over 10 patients

Metric	hRA	hIMRT	p-value
PTV volume=1222 cm^3			
PTV $V_{95\%}$ (%)	99.0	98.0	0.05
PTV $V_{107\%}$ (%)	1.3	4.9	0.001
PTV D_{mean} (%)	101.3	101.3	0.36
PTV D_{max} (%)	111.9	114.9	0.011
PTV $D_{98\%}$ (%)	96.2	95.1	0.013
PTV $D_{2\%}$ (%)	106.3	108.5	3e-4
IL-Lung D_{mean} (Gy)	12.9	14.3	0.004
IL-Lung V_{20Gy} (%)	26.0	32.2	2e-4
IL-Lung V_{5Gy} (%)	55.1	50.2	0.13
CL-Breast V_{2Gy} (%)	6.2	2.4	0.002
Esophagus V_{20Gy} (%)	2.0	9.0	0.026
Esophagus V_{30Gy} (%)	0.2	3.2	0.12
Thyroid D_{mean} (Gy)	11.7	12.3	0.39
Thyroid V_{30Gy} (%)	14.8	21.8	0.05
Body minus PTV V_{20Gy} (cm^3)	1440	2014	8e-8
Body minus PTV V_{40Gy} (cm^3)	312	789	4e-7

Conclusion: The novel hRA technique had dosimetric advantages for almost all investigated OAR. hRA spared significantly the healthy tissue around the supraclavicular lymph nodes. The 2cm slip zone in the hRA plan, which is not possible to create when using junctioning half beams, makes this technique also suitable for breathhold treatment.

Poster Viewing: 2: Clinical: Health economics, urology and brain

PV-0085

The level of innovations routinely implemented in Dutch radiotherapy centers:a cross-sectional study

M. Jacobs[1], A. Dekker[2], L. Boersma[2], F. Van Merode[3], G. Bosmans[2], L. Linden[2], P. Simons[2], S. Moorman[2], P. Lambin[2]

[1]MAASTRO clinic, Department of Radiation Oncology MAASTRO- CAPHRI School for Public Health and Primary Care- Health Services Research- Maastricht University Medical Centre + MUMC+, Maastricht, The Netherlands

[2]MAASTRO clinic, Department of Radiation Oncology MAASTRO- GROW School for Oncology and Developmental Biology- Maastricht University Medical Centre + MUMC+, Maastricht, The Netherlands

[3]MUMC+, Executive Board of Maastricht University Medical Centre + MUMC+, Maastricht, The Netherlands

Purpose or Objective: Radiotherapy centres have the complex task to simultaneously improve patient outcomes (survival and toxicity), safety, service (such as shared decision making) and efficiency. To address this multi headed challenge, centres are forced to innovate. The objective of our study is to investigate how well Dutch Radiotherapy centres have implemented innovation within the care environment. Our two research questions are: 1. What is the annual number of treatment -, technological - and organisational innovations? And 2. Are there differences between the centres?

Material and Methods: A descriptive cross-sectional study was conducted. Two investigators started with semi structured interviews in participating centres, generally with the head of physics and the head of the department. Innovations in the annual policy plans from 2011- 2013 (3 years) were classified into 3 distinct categories based on literature: new or significantly improved 1) treatment, 2) technology, or 3) organisational processes, implemented in clinical routine. Incremental improvements to existing treatments, technologies, or organisational processes were not included in the results below. Centres without annual policy plans were asked to create their own inventory, or to tick listed innovations from other centres. Finally, all participating centres received the listed innovations from other centres with the request to check if their own inventory was complete. The classification was checked independently by two senior investigators.

Results: Out of the 20 centres invited to participate in the study 15 took part in the final study, 8 of which were academic and 7 non-academic.As shown in the table below, the number of innovations in academic centres was higher but not significantly different from non-academic centres. An academic centre implemented on average 17 (range 12-27) innovations per year and a non-academic centre on average of 14 (range 10-18). Treatment innovation (e.g. breath hold mamma, IGRT) was the most frequently implemented innovation (n=102) followed by organisational innovation (e.g. starting a satellite, new Electronic Patient Record)(n=71) and technological innovation (e.g. IMRT, technological new linacs)(n=61). In each innovation category an academic centre is performing the highest number of innovations.

	AC 1	AC 2	AC 3	AC 4	AC 5	AC 6	AC 7	AC 8	sub
treatment innovation	3	7	16	4	3	8	6	11	58
technological innovation	7	8	5	0	4	5	0	6	35
organisational innovation	2	12	5	5	3	3	6	7	43
total	12	27	26	9	10	16	12	24	136

	NAC 1	NAC 2	NAC 3	NAC 4	NAC 5	NAC 6	NAC 7	sub
treatment innovation	7	11	5	6	8	1	6	44
technological innovation	4	6	3	2	2	7	2	26
organisational innovation	3	1	2	8	6	6	2	28
total	14	18	10	16	16	14	10	98

Totals	
treatment innovation	102
technological innovation	61
organisational innovation	71
	234

AC: Academic Centre
NAC: Non-Academic Centre

Conclusion: Radiotherapy centres in the Netherlands implement on average 16 innovations per year in their department; this number is not significantly different for academic or non-academic centres. These numbers confirm that radiotherapy is a very dynamic and innovative discipline. In our next study we will investigate what are the key drivers for innovation.

PV-0086 Clinical implementation of research within a radiotherapy department. A quality indicator?

M. Jacobs[1], L. Boersma[2], F. Van Merode[3], A. Dekker[2], F. Verhaegen[2], L. Linden[2], S. Moorman[2], P. Lambin[2]

[1]MAASTRO clinic, Department of Radiation Oncology MAASTRO- CAPHRI School for Public Health and Primary Care- Health Services Research- Maastricht University Medical Centre + MUMC+, Maastricht, The Netherlands

[2]MAASTRO clinic, Department of Radiation Oncology MAASTRO- GROW School for Oncology and Developmental Biology- Maastricht University Medical Centre + MUMC+, Maastricht, The Netherlands

[3]MUMC+, Executive Board of Maastricht University Medical Centre + MUMC+, Maastricht, The Netherlands

Purpose or Objective: The efficiency in the translation of scientific discoveries into clinical practices in general

healthcare is low. Previous research concluded that approximately 5 % of peer-reviewed papers concern findings which are routinely implemented. We hypothesize that implementation rates in radiotherapy will be higher, in particular in an institution which has an integrated strategy for research, valorisation and patient care, and has a data centre for clinical trials including a software development team.Our aim is to study the efficiency of research implementation in the clinic either in routine or in clinical trials in a large radiotherapy institution over a period of 4 years. The research questions are two-fold: 1) what is the percentage of published findings routinely implemented in clinical practice? And 2) what is the rate of clinical testing of laboratory and technological published findings? Furthermore, we have tried to identify the facilitators and barriers within this process.

Material and Methods: The scientific publications of researchers of our own institute were listed for the period from 2008-2011 (4 years), categorized as shown in the table below. From the literature we listed the facilitators and barriers in the implementation process. We asked clinicians of the tumour expert groups if the published study had yet been implemented into clinical practice or clinical trials, and which facilitators or barriers were applicable. This has been verified by an independent investigator. We calculated implementation rates and the frequency of mentioned facilitators and barriers. Furthermore the head of research scored whether pre-clinical and technological scientific publications had been tested in clinical trials. This was checked independently by two senior investigators.

Results: Internal researchers published 244 papers of which 79 (32%) were clinical (technological) papers. In total, 45/244 papers (18%) were routinely implemented; of the 79 clinical (technological) papers, this percentage was even higher: 33% (26/79). Overall 73/244 (30%) papers (all technical or laboratory papers) were tested in a clinical environment, mostly in the context of a research project (Table).The main facilitator was level of evidence, and the main barriers were workload and high complexity (Figure).

	Number of Publications	Implemented in clinical routine	Tested in part of (matrix/all) (Non IRB approved study)	Tested in prospective clinical trial (IRB approved)
Clinical Research	61	29		
• Radiosensitive	11	2		
• Cohort	24	9		
• Trials	26	18		
Clinical/Technical Research	10	3		
• Physics	5	0		
• ICT/Computer Science	1	0		
• Imaging	14	9		
Preclinical Research	66	0	33	8
Technical Research	47	12	43	13
• Physics	31	7	30	4
• ICT/Computer Science	6	4	2	1
• Imaging	11	1	11	8
Other Categories	53	7		
• Reviews	34	4		
• Case reports	6	0		
• Cost-benefit analysis	9	3		
• In Silico Work	4	0		
TOTAL	244	48 (19.44%)	56 (22.96%)	17 (6.52%)

* IRB Internal Review Board

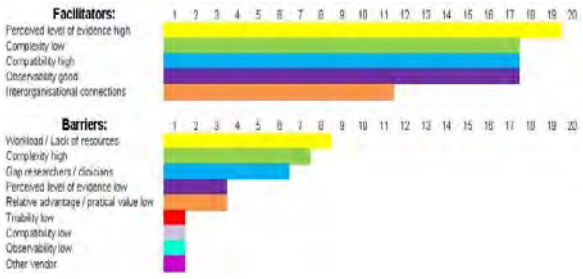

Conclusion: The efficiency in translation of published research in radiotherapy in reaching the clinic was much higher than in general healthcare. Level of evidence was an important facilitator, whereas high workload and complexity were important barriers. The next step will be to look at the time needed for implementation and to investigate implementation rate in other centres. We propose that the rate of clinical implementation of published research findings, routinely or in trials, should be a quality indicator of integrated research-patient care organisation such as a comprehensive cancer centre.

PV-0087

Non-publication of Phase-3 clinical trails in radiotherapy

J. Perez-Alija[1], P. Gallego[1]
[1]*Hospital Plató, Radioterapia y Oncología, Barcelona, Spain*

THIS ABSTRACT FORMS PART OF THE MEDIA PROGRAMME AND WILL BE AVAILABLE ON THE DAY OF ITS PRESENTATION TO THE CONFERENCE

PV-0088

Rapid changes in brain metastasis during radiosurgical planning – implications for MRI timing

A.L. Salkeld[1], W. Wang[1], N. Nahar[1], L. Gomes[2], K. Ng[2]
[1]*Crown Princess Mary Cancer Centre Westmead Hospital, Radiation Oncology, Westmead, Australia*
[2]*Westmead Hospital, Radiology, Westmead, Australia*

Purpose or Objective: The aim of this prospective study was to determine any changes in brain metastases or resection cavity volumes between the planning MRI and radiosurgical (RS) treatment and if these impacted on management or led to an alteration of the RS plan.

Material and Methods: 33 patients with 42 metastases and 12 tumour resection cavities underwent a planning MRI (MRI-1) which was fused to the planning CT. GTV (metastasis) or CTV (cavity) were contoured from the T1 and T2 post-gadolinium MRI. The GTV/CTV had a 2mm circumferential expansion creating a PTV with a plan generated. In addition, a verification MRI (MRI-2) was performed 24-48 hours prior to RS with volumes re-contoured on MRI-2 (verGTV/verPTV). The GTV/CTV and PTV volume changes between MRI-1 and MRI-2 were recorded and the original plan assessed for coverage of the verPTV. A change in plan or management based on MRI-2 was recorded.

Results: Patient and tumour characteristics are shown in Table 1. The median time between MRI-1 and MRI-2 was 7 days with 27 patients (82%) having 14 days or less and 22 patients (66%) with 7 days or less. Changes in GTV/CTV and PTV volumes between MRI-1 and MRI-2 are shown in Figure 1. 19 (58%) patients required a change in management based on changes in lesions on MRI-2 including: re-planning of RS, or a change in treatment to whole-brain radiotherapy (WBRT), surgery or best supportive care (BSC). Per lesion, 30 out of 54 lesions (56%) required re-planning based on MRI-2 including 5 (42%) cavities and 25 (60%) metastases. 2 patients had rapid progression with lepto-meningeal disease diagnosed on MRI-2 and received WBRT. 1 patient (previously received WBRT) had a rapid increase in lesion size and number, with an additional 9 lesions noted on MRI-2 and received BSC. Reasons for re-planning included: increase in volume (27 lesions) with 25 verGTV lying outside the original PTV and 2 touching the original PTV; 2 lesions with a reduction in verGTV/verPTV volumes, and 3 patients with an increase in the number of metastases or leptomeningeal disease on MRI-2.

Conclusion: This study is the first to demonstrate changes in brain metastases volume from planning MRI to RS treatment, where changes often occurred with an interval of 7 days or less. An MRI performed within 24-48 hours of RS led to re-planning or a change in management in more than 50% of patients. Therefore, even a short interval between planning MRI and RS may result in a geographical miss or over treatment, emphasising the need for efficient planning processes.

PV-0089

CyberKnife for prostate cancer patients – early results of 350 patients irradiation

L. Miszczyk[1], A. Namysl-Kaletka[1], A. Napieralska[1], G. Wozniak[1], M. Stapor-Fudzinska[2], G. Glowacki[1], K. Grabinska[1]
[1]*Maria Sklodowska-Curie Memorial Cancer Center and Institute of Oncology, Radiotherapy, Gliwice, Poland*
[2]*Maria Sklodowska-Curie Memorial Cancer Center and Institute of Oncology, Treatment Planning, Gliwice, Poland*

Purpose or Objective: The aim of this study was an evaluation of a toxicity and an early effectiveness of prostate cancer patients CyberKnife based radioablation.

Material and Methods: 350 PC patients (186 Low Risk, 164 Intermediate Risk) aged from 53 to 83 (mean 69) irradiated with CK every other day (fd 7.25Gy, TD 36.25Gy, OTT 9 days). Before the treatment start PSA varied from 0.3 to 19.5 (median 7.5) and T stage from T1c to T2c. Mean prostate dimensions were 42.6x37.2x41.1mm. FU ranged to 48 months (mean 12). Directly after the treatment, 1, 4, 8 months later and the next every 6 months, the percentage of patients with Androgen Deprivation Therapy (ADT), GI (gastro-intestinal) and GU (genito-urinary) toxicity (acute up to the 4th month and the next late) using the EORTC/RTOG scale and PSA concentration were checked.

Results: The percentage of patients without ADT increased from 42.6% to 100% 32 months later. The maximal percentage of acute G3 adverse effects was 0.5% for GI, 0.6% for GU and G2 – 1.9% for GI and 6.0% for GU. No G3 late toxicity was observed. The maximal percentage of late G2 toxicity was 0.5% for GI and 3.0% for GU. PSA median decreased from 2.2 to 0.2 ng/ml during FU. One patient relapsed (18 months after RT- next treated with salvage BT) and one developed metastasis in lymphatic node (treated next with salvage CK). The detailed results are presented in the Table.

	RT end	1 month	4 months	8 months	14 months	20 months	26 months	32 months	38 months
N of observed patients	350	214	255	212	146	91	53	22	7
No ADT [%]	42.6	64.8	72.7	78.1	85.7	84.4	96.2	100	100
GI 0 [%]	90.3	91.0	93.9	93.3	97.8	96.1	100	100	100
GI 1 [%]	9.1	6.6	4.9	6.2	2.2	3.9	-	-	-
GI 2 [%]	0.6	1.9	0.8	0.5	-	-	-	-	-
GI 3 [%]	-	0.5	0.4	-	-	-	-	-	-
GU 0 [%]	77.1	70.8	89.4	95.9	87.3	97.4	98.1	95.2	100
GU 1 [%]	16.3	25.0	8.2	3.6	9.7	2.6	1.9	4.8	-
GU 2 [%]	6.0	3.8	2.4	0.5	3.0	-	-	-	-
GU 3 [%]	0.6	0.4	-	-	-	-	-	-	-
PSA range [ng/ml]	0.008-20.4	0.003-16.3	0.002-8.2	0.0-6.4	0.002-3.5	0.04-2.2	0.0-3.3	0.02-3.8	0.003-0.6
PSA mean	3.7	1.9	1.1	0.7	0.5	0.4	0.4	0.5	0.3
PSA median	2.2	1.0	0.3	0.3	0.2	0.2	0.2	0.1	0.2

Conclusion: The results obtained permit us to form the conclusion that CK based radioablation of low and intermediate risk PC patients is an effective treatment modality enabling OTT shrinkage and giving a very low percentage of adverse effects.

PV-0090

Stereotactic body radiotherapy for localized prostate cancer: a 7-year experience

Y.W. Lin[1], K.L. Lin[2], L.C. Lin[1]
[1]*Chi Mei Medical Center, Department of Radiation Oncology, Tainan City, Taiwan*
[2]*Chi Mei Medical Center, Department of Radiation Onoclogy, Tainan City, Taiwan*

Purpose or Objective: Recent understanding of radiobiology for prostate cancer suggested hypofractionation might achieve a higher therapeutic benefit. Stereotactic body radiation therapy (SBRT) is able to delivery high dose per fraction precisely. SBRT for prostate cancer might escalate biological effective doses while without increasing toxicity. Here, we reported our 7-year experience of SBRT for localized prostate cancer.

Material and Methods: Between November 2008 and Sep 2013, a total of 135 patients with clinically localized prostate were enrolled for analysis. Patients were low-risk (19%), intermediate-risk (37%), and high-risk (44%). Low- and intermediate-risk patients were treated with SBRT alone (37.5Gy in 5 fractions). High-risk patients were treated with whole pelvic irradiation (45Gy in 25 fractions) and SBRT boost (21Gy in 3 fractions). All of intermediate- and high-risk patients received hormone therapy with different duration. The toxicities of gastrointestinal (GI) and genitourinary (GU) tracts were scored by Common Toxicity Criteria Adverse Effect (CTCAE v3.0). Biochemical failure was defined as Phoenix definition.

Results: With a median follow-up of 52 months, there were seven patients with biochemical failure (one low-risk patient; one intermediate patient; five high-risk patients). The estimated 50-month biochemical failure-free survival (BFFS) was 95.8%, 96.4% and 81.5% for low-, intermediate, and high-risk patients, respectively. In the high-risk group, there were two late biochemical failures around 60 months. In the SBRT alone group, acute Grade 3 GU and GI toxicities were seen in 2.8% and 1.4% of the low/intermediate-risk patients, respectively; the incidence rate of late Grade 3 GU and GI toxicity were 3.5% and 0%. In the whole pelvic irradiation with SBRT boost group, acute Grade 2 GU and GI toxicity occurred in 31% and 21% of the high-risk patients, respectively; there was no grade 3 or higher late toxicity of GU and only one patient experienced grade 3 GI tract. Most of acute toxicity effects in the both groups resolved within three to six months of treatment completion.

Conclusion: SBRT with or without whole pelvic irradiation for localized prostate cancer is feasible with minimal toxicity and encouraging biochemical failure-free survival but should be aware of late failure in the high-risk group. Use of whole pelvic irradiation for high-risk patients was not associated with higher GU or GI toxicity. Continued accrual and follow-up would be necessary to confirm the biochemical control rate and the toxicity profiles.

PV-0091

Early salvage RT for PSA recurrence postprostatectomy improves biochemical progression free survival

A.B. Hopper[1], A.P.S. Sandhu[1], J.P. Einck[1]
[1]*University of California San Diego, Radiation Medicine and Applied Sciences, San Diego, USA*

Purpose or Objective: The definition of biochemical recurrence following radical prostatectomy for prostate cancer remains controversial in the era of ultrasensitive PSA. The AUA definition of PSA > 0.2 ng/mL may not be valid when PSA can be detected as low as 0.01 ng/mL. Randomized trials have shown a benefit in terms of biochemical progression-free survival (bPFS) and metastasis free survival with adjuvant radiation compared to salvage but many patients enrolled as adjuvant actually had detectable PSA values. We compared patient outcomes with salvage radiotherapy based on pretreatment PSA in order to identify whether early salvage radiotherapy is more effective than treating later.

Material and Methods: We performed an institutional review board-approved retrospective analysis of patients treated at our institution with post-prostatectomy image guided radiotherapy from 2005 to 2013. Patients with positive lymph nodes, those with an undetectable PSA and those with metastatic disease were excluded from our analysis. Data were abstracted from each patient's electronic medical record including age, pathologic stage, Gleason score, margin

status, androgen deprivation therapy, treatment to the pelvis, dose and PSA values. Patients were either treated with intensity modulated radiotherapy (IMRT) or volumetric arc therapy (VMAT) using daily image guidance. The use of ADT and the treatment of nodes was at the discretion of the treating physician. Radiation dose ranged from 6200-7400 cGy. Post-salvage bRFS was defined as PSA < 0.4 ng/mL. Kaplan-Meier survival analysis was used to compare patients with a pre-RT PSA value ≤ 0.2 ng/mL to those with a value > 0.2 ng/mL. Multivariate Cox regression analysis was used to evaluate significance of covariates on bPFS.

Results: 196 patients staged N0 or Nx were treated with salvage RT after prostatectomy during the study period. Median pre-treatment PSA was 0.29 ng/mL; 117 patients had a PSA > 0.2 ng/mL and 79 ≤ 0.2 ng/mL. Median follow up time was 36 months, determined by the reverse Kaplan-Meier method. Overall comparison of the two groups showed that patients treated with a PSA < 0.2 ng/mL had significantly improved bPFS (p=0.003) and increased 36 month bPFS (76% vs 56%, p=0.0074) compared to those treated with higher PSA values (Figure 1). In multivariate analysis a pre-RT PSA > 0.2 and increasing T stage and Gleason score were all significantly associated with worsening bPFS while positive margins were significant for improved bPFS (Table 1). Other covariates including treatment of nodes and use of ADT did not significantly influence bPFS following salvage.

Figure 1: Kaplan-Meier plot of biochemical progression free survival in post-prostatectomy patients stratified by pre-treatment PSA

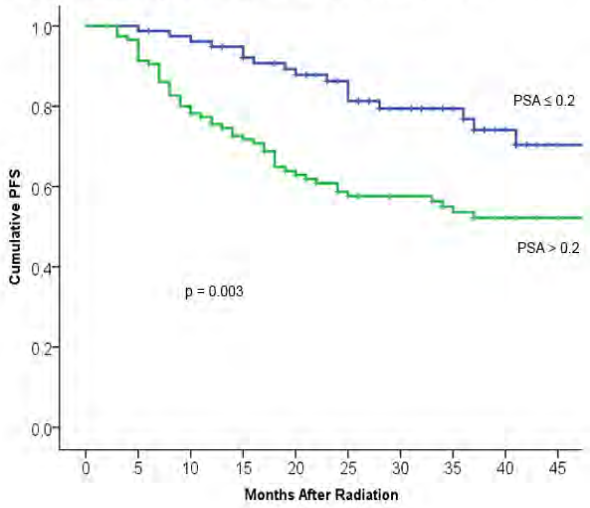

Table 1: Multivariate Cox regression analysis for predictors of PFS

Covariate	Hazard Ratio	95% CI	p-value
T stage†	1.580	1.176-2.123	0.002
Positive Margins	0.592	0.356-0.985	0.043
Gleason Score°	1.368	1.054-1.774	0.018
Neoadjuvant ADT	0.780	0.399-1.527	0.469
Whole Pelvis	0.662	0.367-1.195	0.171
Age	0.989	0.957-1.023	0.527
PSA > 0.2 ng/mL	2.358	1.350-4.119	0.003

† HR for T stage represents each increase in stage with T2a/b as the reference

° HR for GS represents each increase in GS with 6 as the reference up to 10

Conclusion: Early post-prostatectomy salvage radiation before the PSA reaches 0.2 ng/mL results in superior bPFS compared to those treated later. This strongly suggests that a new definition of post-prostatectomy progression is needed.

Presidential Symposium:

SP-0092
Patient centric approach: myth or fact?
P Poortmans[1]
[1]*UMC St Radboud, Radiation Oncology, Nijmegen, The Netherlands*

Award Lecture: E. Van der Schueren Award

SP-0093
Did I do it right? What was the result? Process and outcomes in radiotherapy
A.Barrett[1]
University of East Anglia, Radiation Oncology, Norwich, United Kingdom

I am honoured to have been invited to give this memorial lecture for which there are three main criteria: it is firstly to honour Emmanuel van der Scheuren, one of the fathers of our society. Secondly it aims to recognise scientific work within the field of radiation oncology and thirdly a contribution to education through the ESTRO programmes, in which I have been privileged to participate for the last 30 years or so.
The first ESTRO annual conference was held in London in 1982 and was memorable with the preparations being agreed between Emmanuel and Mike Peckham, my boss at the Royal Marsden Hospital at the time. I also want to acknowledge how dependent we were on many others for support, particularly among others for Lea, of whom we are thinking with gratitude especially at this time.
Scientific breakthroughs usually build on work that others have done and there are many examples from within the field of radiation oncology which I have experienced particularly in my area of research into whole-body irradiation. We work with the unchanging laws of physics but technology advances all the time and new biological understanding and new agents impact on the way in which we practice oncology.
I will discuss some of the ways in which progress in radiotherapy may occur and consider the factors which determine the impact of clinical trials, with particular reference to the START trials run by John Yarnold and his team. Consensus guidance, such as that contained in the ICRU report 50, has changed practice but there is still much evaluation work to be done in some areas. In our activity currently, process sometimes seems to take precedence over everything else, without the evaluation which would validate it.
ESTRO's contribution to education has been enormous and it has been exciting to be involved in the teaching courses and publications of ESTRO with its ever-changing and innovative approaches .It is good to note that a new era is starting for the School. Amongst all the changes in current practice the needs of individual patients must remain our priority

Symposium with Proffered Papers: Hot topics in SABR: time for randomised clinical trials?

SP-0094
Do we need randomised clinical data to justify the use of SABR for primary and oligometastatic cancer?

To be confirmed

SP-0095
Pre-clinical and clinical data on the radiobiological mechanism for the efficacy of SABR
M. Brown[1]
[1]*Stanford University School of Medicine, Department of Radiation Oncology, Stanford, USA*

Because the results obtained with stereotactic radiosurgery (SRS) and stereotactic ablative radiotherapy (SABR) have been impressive they have raised the question of whether classic radiobiological modeling are appropriate for large doses per fraction. In addition to objections to the LQ model, the possibility of additional biological effects resulting from endothelial cell damage and/or enhanced tumor immunity, have been raised to account for the success of SRS and SABR. However, the preclinical data demonstrate the following:
1) Quantitative *in vivo* endpoints, including late responding damage to the rat spinal cord, acute damage to mouse skin and early and late damage to the murine small intestine, are consistent with the LQ model over a wide range of doses per fraction, including the data for single fractions of up to 20 Gy.
2) Data on the response of tumors to high single doses are consistent with cell killing at low doses. Thus the dose to control 50% of mouse tumors (the TCD50) can be predicted from cell survival curves at low doses and the number of clonogenic cells in the tumors.
Further the clinical data show:
3) The high local control of NSCLC and of brain metastases by SABR and SRS is the result of high radiation doses leading the high BED. In other words the high curability is predicted by current radiobiological modeling.
4) Because high doses are required in SABR it is not possible to use it in all circumstances (e.g. for tumors close to critical normal structures). But because these high doses are needed because of tumor hypoxia there is a major opportunity to improve SABR by the use of hypoxic cell radiosensitizers.
Normal 0 21 false false false FR-BE X-NONE X-NONE

SP-0096
Technical developments in high precision radiotherapy: a new era for clinical SABR trials?
M. Aznar[1]
[1]*Rigshospitalet, Section for Radiotherapy Department of Oncology 3993, Copenhagen, Denmark*

The technological developments in radiotherapy have had a considerable impact on the way stereotactic radiotherapy is delivered. Increased confidence, provided for example, by the wide availability of image guidance, has permitted more and more institutions to offer SABR as a treatment option. However, some characteristics of SABR plans such as heterogeneous dose prescription, can make the comparison between different institutions and different technological approaches very challenging. In this session, we will review the impact of image guidance strategies, dose calculation algorithms, and normalization guidelines on the planned dose distribution. We will also discuss how these technological aspects should influence how we look at clinical trials of the past, and what should be taken into account when designing new multi-centre trials.

OC-0097
Radiation dose-volume effects for liver SBRT
M. Miften[1], Y. Vinogradskiy[1], V. Moiseenko[2], J. Grimm[3], E. Yorke[4], A. Jackson[4], W.A. Tomé[5], R. Ten Haken[6], N. Ohri[5], A.M. Romero[7], K.A. Goodman[1], L.B. Marks[8], B. Kavanagh[1], L.A. Dawson[9]
[1]*Univerisity of Colorado Denver, Department of Radiation Oncology, Aurora, USA*
[2]*University of California San Diego, Department of Radiation Medicine and Applied Sciences, San Deigo, USA*
[3]*Holy Redeemer, Department of Radiation Oncology, Meadowbrook, USA*
[4]*Memorial Sloan-Kettering Cancer Center, Department of Radiation Oncology, New York, USA*
[5]*Albert Einstein College of Medicine, Department of Radiation Oncology, New York, USA*
[6]*University of Michigan, Department of Radiation Oncology, Ann Arbor, USA*
[7]*Erasmus MC Cancer Institute, Department of Radiation Oncology, Rotterdam, The Netherlands*
[8]*University of North Carolina, Department of Radiation Oncology, Chapel Hill, USA*
[9]*Princess Margaret Cancer Centre, Department of Radiation Oncology, Toronto, Canada*

Purpose or Objective: SBRT is highly effective in providing local control in selected patients with hepatic malignancies. However, various dosing and fractionation schemes with a wide range of toxicity end-points have been reported in the literature. The objective of this work was to review the normal tissue dose-volume effects for liver SBRT and derive normal tissue complication probability models.

Material and Methods: A literature review by the AAPM Working Group on SBRT was performed. Twelve studies that contained both dose/volume and toxicity data from 541 patients with hepatocellular carcinoma, intrahepatic cholangiocarcinoma, and/or liver metastases were identified and analyzed. Patients received a median total dose of 40 Gy (range 18-60 Gy) in 1-6 fractions. The 3 end-points that were chosen for pooled dose-response relationships analysis were grade 3+ (G3+) liver enzyme elevation as a function of mean liver dose (MLD), G2+ GI toxicity as a function of prescription (RX) or PTV dose, and G3+ GI toxicities as a function of RX/PTV dose. The RX/PTV doses were chosen because doses to specific OARs were not available in many instances. Dose-response modeling was performed using a probit model with maximum likelihood (ML) parameter fitting. The model used the average reported toxicity rates and corresponding dose metrics reported in each included study. The average toxicity rate was then binned into binary outcomes to facilitate ML parameter fitting. Confidence intervals for dose-response curves were calculated using bootstrap method using random sampling with replacement.

Results: Increased MLD was positively correlated with G3+ enzyme toxicity; however, the probit model fitting did not produce a statistically significant dose-response fit. Possible explanations are the sparsity of data, low incidence of complications, variations in baseline liver function and cancer type, and lack of standardization of definitions used for liver enzyme abnormalities. The analysis relating G2+ GI toxicity to RX/PTV dose showed a statistically significant probit model fit. Model fitting parameters were D50 of 47.7 Gy (95% CI 43.0 - 68.8 Gy) and γ50 of 0.79 (95% CI 0.34 - 1.25). The plot relating G3+ GI toxicity to RX/PTV dose demonstrated a dose response with a statistically significant probit model fit. Model fitting parameters were D50 of 90.2 Gy (95% CI 67.2 - 516.4 Gy) and γ50 of 1.17 (95% CI 0.68 - 1.69). The large D50 value of 90.2 Gy can be attributed to the low rates of G3+ GI toxicity.

Conclusion: Our analysis shows a mean RX/PTV dose of 50 Gy in 3 to 6 fractions has resulted in G3+ GI toxicity risk of < 10%. The QUANTEC liver report recommends MLD limits of 13 Gy in 3 fractions and 18 Gy in 6 fractions for primary disease and 15 Gy in 3 fractions and 20 Gy in 6 fractions for metastases. Our analysis shows that the QUANTEC recommended MLD limits would likely result in acceptable G3+ liver enzyme toxicity risks of < 20%.

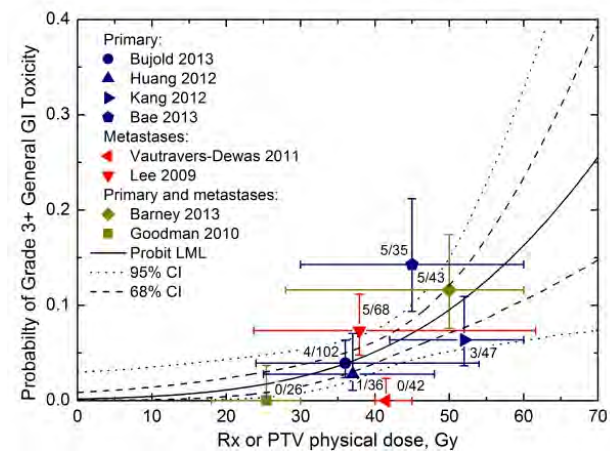

Symposium: Tumour targeting - considering normal tissue biology

SP-0098
Organoids, a disease and patient specific in vitro model system
R. Vries[1]
[1]*Hubrecht Institute, Developmental Biology and Stem Cell Research, Utrecht, The Netherlands*

The group of Hans Clevers at the Hubrecht Institute discovered a unique marker (LGR5) for epithelial stem cells of the intestine (Barker et al., Nature 2007). Since then, LGR5 has been shown to be a marker of adult stem cells of multiple other tissues such as liver, pancreas, breast, and lung (eg: Huch et al., Nature 2013; Boj et al., Cell 2014; Karthaus et al., Cell 2014). With the identification of these stem cells and the tools to isolate them, we were able to develop a culture system that allowed for the virtually unlimited, genetically and phenotypically stable expansion of the cells from several animal models including human (Sato et al., Nature 2009, 2011; Gastroenterology 2011; Gao et al., Cell 2014; Boj et al., Cell 2015; Huch et al., Cell 2015; van de Wetering et al., in press Cell). The organoids faithfully represent the in vivo cells also after prolonged expansion in vitro. Hubrecht Organoid Technology (HUB), an entity founded to implement the organoid technology of the Clevers group, in collaboration with the Hubrecht institute, has generated a large collection of patient organoids from a variety of organs and diseases. The intestinal organoids have been shown to be a very power tool for the study of Cancer, Cystic Fibrosis and Inflammatory Bowel Disease (Dekkers, Nat Med 2013; van de Wetering, Cell in press). The models represent previously unavailable in vitro models and patient specific samples for drug development, patient stratification and diagnostics. In addition, we recently showed the organoids are amendable to genetic corrections by novel and conventional biochemical techniques such as Crispr/Cas9 (Drost et al., Nature 2015; Schwank et al., Cell Stem Cell 2013). Finally, the in vitro stability of the organoid was demonstrated by the integration after transplantation of human liver cells into recipient mice. This makes the organoid a unique new platform for drug development, for precision medication for patients in the clinic, and a possible new source for cell therapy.

SP-0099
The role of ATM and p53 in normal tissue radiation response
D. Kirsch[1]
[1]*Kirsch Lab, Durham, USA*

Following ionizing radiation exposure, double strand DNA breaks activate the ataxia telangiectasia mutated (ATM) kinase, which then phosphorylates a large number of target proteins to orchestrate the DNA damage response. One of the key proteins that is activated by ionizing radiation in an ATM-dependent manner is the tumor suppressor protein p53. Our laboratory has utilized the Cre-loxP system to delete ATM, p53 or both genes in different cell types in mice. We have also employed reversible in vivo shRNA to temporarily inhibit p53 during radiation exposure. We find that the roles of ATM and p53 in normal tissue radiation response are cell type specific. In bone marrow exposed to radiation, p53 acts to kill stem and progenitor hematopoietic cells, which increases acute hematological toxicity and promotes radiation-induced lymphomas. In gastrointestinal epithelial cells, p53 prevents the radiation-induced gastrointestinal syndrome. In endothelial cells, p53 prevents radiation-induced heart disease. Although deletion of ATM in endothelial cells does not sensitize mice to radiation-induced cardiac injury, in the setting of p53 deletion, ATM further sensitizes mice to radiation-induced heart disease. Taken together, these studies define cell type specific roles for ATM and p53 in mediating normal tissue response to ionizing radiation and suggest opportunities for combining radiotherapy with inhibitors of the ATM-p53 pathway to improve the therapeutic ratio when treating cancers at specific anatomic sites.

SP-0100
Radiation sensitivity of human skin stem cells : dissecting epigenetic effects of radiation
M. Martin[1], N. Fortunel[2], P. Soularue[2]
[1]*Laboratoire de Génomique et Radiobiologie du Kérat, Evry, France*
[2]*Laboratoire de Génomique et Radiobiologie du Kérat, CEA, Evry, France*

Due to its anatomical localization and high turnover, epidermis is a major target for carcinogens, and skin carcinoma is one of the most frequent human cancers. Ionizing radiation (IR) can induce carcinoma in skin, but the respective roles of keratinocyte stem cells and their progeny in the carcinogenic process is unclear. We characterized cell intrinsic radiosensitivity of keratinocyte stem cells (KSC) to gamma rays. Primary KSC were found radioresistant to high radiation doses *(Rachidi, 2007)*, as well as to low doses. They repair rapidly all types of DNA damage *(Harfouche, 2010)*, both after ionizing radiation and UVB exposure *(Marie, submitted)*, without going to apoptosis. Activated repair was notably due to increased levels of DNA repair proteins and activation of nuclear FGF2 signaling. To evaluate the potential impact of irradiation on the epigenetic status of keratinocyte precursor cells, the Illumina 450K array was used, which measures the methylation level of 480,000 methylation sites (or CpG islands). More than 36 million of GpCs have been identified in the human genome, most of them located directly in gene sequences or in gene promoters. In the present study, analysis of the lists of the modified genes obtained by normalized graph-cut DNA-ranking allowed the definition of: 1) a specific signature of long-term alterations after 2 Gy: hundred genes presented methylation changes over 3 weeks in culture, with 18 genes exhibiting the most discriminant methylation changes at 16 and 23 days after exposure. Six genes were members of the super-family of protocadherins of the alpha type, pointing to alterations of cell-cell interactions. 2) a specific signature of long-term alterations after 10 mGy: 15 specific genes had methylation changes that were discriminant after 16 and 23 days. From their functions, it appears that the major cell responses after 10 mGy were localized at the cell membrane, for processes involved in calcium-related cell adhesion, signaling, energy status and carcinoma development. As a major function of methylation changes is to inhibit transcription, these signatures have been validated by characterizing the expression of the genes found in the signatures. In summary, high and low-dose exposures of immature keratinocytes from human epidermis result in epigenetic changes, part of them being specific to the dose. Methylation changes appear to regulate notably cell functions related to cell-cell interactions, cell adhesion and energy status.

SP-0101
A radiation systems biology view of radiation sensitivity of normal and tumour cells
K. Unger[1], A. Michna[1], J. Heß[1], I. Gimenez-Aznar[1], U. Schötz[2], A. Dietz[3], D. Klein[4], M. Gomolka[3], S. Hornhardt[3], V. Jendrossek[4], K. Lauber[2], C. Belka[2], H. Zitzelsberger[5]
[1]*Helmholtz Zentrum Muenchen - German Research Center for Environmental Health, Research Unit Radiation Cytogenetics/Clinical Cooperation Group Personalised Radiotherapy in Head and Neck Cancer, Muenchen, Germany*
[2]*University of Munich, Department of Radiation Oncology/Clinical Cooperation Group Personalised Radiotherapy in Head and Neck Cancer, Munich, Germany*
[3]*Federal Office for Radiation Protection, Department SG Radiation Protection and Health, Oberschleissheim, Germany*
[4]*Institute of Cell Biology Cancer Research, University Hospital- University of Duisburg-Essen, Essen, Germany*
[5]*Helmholtz Zentrum Muenchen - German Research Center for Environmental Health, Research Unit Radiation Cytogenetics / Clinical Cooperation Group Personalised Radiotherapy in Head and Neck Cancer, Muenchen, Germany*

Background: One of the main aims of radiotherapy alone or combined with chemo-, immuno- or biologically targeted therapy is the maximisation of tumour tissue eradication whilst preserving the surrounding normal tissue. This requires a deep understanding of the molecular mechanisms of radiation sensitivity in order to identify its key players and potential therapeutic targets. Currently, a paradigm shift is taking place from pure frequentistic association analysis to the rather holistic systems biology approach that seeks to mathematically model the system to be investigated and to allow the prediction of an altered phenotype as the function of one single or a signature of biomarkers.

Methods: In the current study cell culture models of radiation-resistant tumour cells and normal radiation-sensitive cells were investigated by multi-level (genome, transcriptome, miRNA) omics profiling over time and the resulting multi-layer radiation interactome was reconstructed. Validation of key network elements in biopsy-derived multi-omics data from radiotherapy treated HNSCC patients was performed and tested for association with clinical outcome.

Results: Molecular frameworks including signalling pathways senescence, cell cycle, immune system and PI3K/Akt have been identified and are therefore likely to drive radiation response in tumour and normal cells. Moreover, the identified networks could be used to identify molecular key players and potential targets for the simultaneous modulation of radiation sensitivity. A subset of these candidate molecules could be validated having an impact in clinical outcome of radiation therapy treated HNSCC patients.

Conclusion: Our study demonstrates that multi-level radiation systems biology allows gaining deeper insights into chief mechanisms of radiation sensitivity, thereby paving the way for targeted individualised therapy approaches in radiation oncology.

Debate: This house believes that progress in the treatment of locally advanced NSCLC will come from:

SP-0102 Radiation treatment intensification

J. Belderbos[1]
[1]*Netherlands Cancer Institute Antoni van Leeuwenhoek Hospital, Radiation Oncology, Amsterdam, The Netherlands*

A large proportion of non-small cell lung cancer (NSCLC) patients are diagnosed with locally advanced (stage III) disease. For this patient group the treatment of choice is definitive concurrent chemoradiation (CCRT). CCRT results in an improved overall survival (OS) compared to sequential chemoradiotherapy or radiotherapy alone because of improved locoregional control. However 2-year OS rates of 30-35% are still poor because many patients develop locoregional failures (about 30%) and distant metastases (about 40%)[1]. Currently locally advanced NSCLC patients selected for CCRT have FDG-PET scanning and imaging of the brain (MRI or CT scan). Despite this brain imaging with the present chemotherapy regimens used we are faced with the problem of brain metastases in about 10% of the patients within 1 year after chemoradiation.
In several chemoradiation studies it was reported that the Gross Tumor Volume is correlated with OS. This is rational since the tumor volume represents the number of clonogenic tumor cells that needs to be eradicated. To improve locoregional control the dose prescription could be escalated taking into account the individual Gross Tumor Volumes and tolerances using image guided adaptive Intensity Modulated Radiotherapy (IMRT). However there are radiation oncologists who challenge the usefulness of RT dose escalation and intensification in patients with stage III NSCLC. The outcome of a randomized phase III trial, RTOG 06171, revealed that NSCLC patients within the 74 Gy arm given in 7.5 weeks had worse local control and significantly worse overall survival as compared to the patients treated to 60 Gy arm in 6 weeks[2]. Patients in all study arms received two additional cycles of consolidation chemotherapy ± cetuximab. So the obvious question is: How do we continue?
Dose escalation with prolonged overall treatment time in NSCLC has previously been proven disappointing because of accelerated repopulation[3].In an individual patient data meta-analysis in patients with non-metastatic lung cancer, which included trials comparing modified radiotherapy with conventional radiotherapy, a significant OS benefit from accelerated or hyperfractionated radiotherapy was reported[4].
Another issue is the use of consolidation chemotherapy after concurrent chemoradiation. In the RTOG 0617 trial the increase in mortality started < 3 months after randomization during the period of consolidation paclitaxel-carboplatin chemotherapy. Generally taxanes given after RT increases toxicity and the combination of high dose to the heart and consolidation taxane-based chemotherapy might have caused toxic deaths and biased the outcome. RT dose intensification while using modern image guided adaptive IMRT and accelerated schemes is an important area of ongoing clinical research and should not be discontinued.
In Stereotactic Ablative Body Radiotherapy (SABR) much higher biologically equivalent doses are delivered compared to conventionally fractionated RT (typically EQD2 of 70-85 Gy), and has generated outstanding tumor control in early stage NSCLC. For SABR a significant dose–response relationship was observed for prescription EQD2 of 105 Gy or more (2-year LC 96%) or of less than 105 Gy (2-year LC 85%)[5]. Tumor size and overall treatment time were also important factors influencing outcome.
The tumor control probability of SBRT (small tumor volume) and conventionally fractionated chemoradiation (large tumor volume) were successfully described in a single model[6] suggesting that a dose-response relation in NSCLC does exist.
Recently there is a growing interest in genetic profiles that predict a patient's response to radiotherapy, because severe toxicity in a minority of patients limits the doses that can be safely given to the majority. Recent progress in genotyping raises the possibility of genome-wide studies. If we know the normal tissue reactions to radiotherapy by genotype we will really be able to tailor the individual radiation dose.
In conclusion: Besides the unsolved problem of the occurrence of distant metastases there is room for improvement of locoregional control in locally advanced NSCLC patients treated with chemoradiation. In the era of personalized treatment, radiotherapy dose intensification using image guided adaptive IMRT could be directed towards individual tumor volumes and tolerances. RT dose intensification while using accelerated schemes is an important area of ongoing clinical research

1. Auperin A, Le Pechoux C, Rolland E, et al. Meta-analysis of concomitant versus sequential radiochemotherapy in locally advanced non-small-cell lung cancer. *J Clin Oncol*. 2010;28:2181-90.

2. Bradley JD, Paulus R, Komaki R, et al. Standard-dose versus high-dose conformal radiotherapy with concurrent and consolidation carboplatin plus paclitaxel with or without cetuximab for patients with stage IIIA or IIIB non-small-cell lung cancer (RTOG 0617): a randomised, two-by-two factorial phase 3 study. *The Lancet Oncology* 2015; **16**(2): 187-99.

3. Machtay M, Hsu C, Komaki R, et al. Effect of overall treatment time on outcomes after concurrent chemoradiation for locally advanced non–small-cell lung carcinoma: Analysis of the Radiation Therapy Oncology Group (RTOG) experience. *International Journal of Radiation Oncology Biology Physics* 2005; **63**(3): 667-71.

4. Mauguen A,Le Péchoux C,Saunders MI, et al. Hyperfractionated or accelerated radiotherapy in lung cancer: an individual patient data meta-analysis. J Clin Oncol. 2012 Aug 1;30(22):2788-97. doi: 10.1200/JCO.2012.41.6677.

5. Kestin L,Grills I,Guckenberger M, et al. Dose-response relationship with clinical outcome for lung stereotactic body radiotherapy (SBRT) delivered via online image guidance. Radiother Oncol.2014 Mar;110(3):499-504. doi: 10.1016/j.radonc.2014.02.002. Epub 2014 Mar 11.

6. Selvaraj J, Lebesque J, Peulen H, et al. TCP modeling in a large cohort of NSCLC patients inclusive of geometric uncertainties ESTRO Forum 2015:S468 PO-0908

SP-0103
Better systemic therapy

J. Van Meerbeeck[1]
[1]*University Hospital Antwerp, Department of Thoracic Oncology-MOCA, Edegem, Belgium*

About one third of patients with non-small cell lung cancer (NSCLC) present with locoregional disease extension in either the mediastinum (T4) or the mediastinal lymph nodes (N2/3). Apart from a fraction in which resection after induction therapy is sometimes considered, selected patients with stage 3 are candidate for a so-called definitive radiochemotherapy, administered either sequentially or concomitantly. Despite staging with PET-CT scan and endosonographic mapping of mediastinal lymph nodes and notwithstanding a patient selection for this radical treatment, the outcome in stage 3 is nevertheless moderate with a median survival of 2 years [1]. Progression occurs after a median of 10 months and is due to local relapse or distant metastasis in 30 and 45% of cases, respectively. Any advance in the outcome in stage 3 NSCLC will hence depend on improvements in systemic therapy directed at distant metastasis. The past 10 years have seen important changes in the paradigm of treatment in selected patients with advanced NSCLC, in whom platinum-based doublet chemotherapy used to be the standard of care. The discovery of drugable genomic alterations has introduced precision medicine in oncology. Patients whose NSCLC harbour either an activating EGFR mutation, EML-ALK translocation or ROS1 amplification are now routinely treated with oral small molecule kinase inhibitors of the 1st, 2nd and 3rd generation instead of chemotherapy, with a significant improvement in outcome and a substantial impact on quality of life. Similar, although less pronounced effects have been observed when adding monoclonal antibodies directed at targets associated with angiogenesis or cell growth to the chemotherapy backbone. Unfortunately, the incorporation of these 'targeted' agents in current radiochemotherapy, either given concomitantly or as consolidation, was not successful with even detrimental results due to an increased toxicity and mortality. A lack of adequate patient selection based on the presence of the target biomarker may have contributed to these failures, as subgroup analyses suggest a benefit in target expressing patients. Trials are ongoing specifically addressing patients with stage 3 NSCLC and either an activating EGFR mutation or EML-ALK translocation. 2015 has seen the rapid implementation of immunotherapy in NSCLC treatment, with several monoclonal antibodies inhibiting checkpoint molecules showing superior outcome over 2nd line docetaxel. These agents will now advance in earlier stages and phase 3 trials with a consolidation strategy are ongoing. Controversial issues remain patient selection based on predictive biomarker expression, the combination of different checkpoint inhibitors and the risk of synergistic late pulmonary toxicity, when added to definitive thoracic radiotherapy. Although it is tempting to early implement promising new drugs in stage 3 treatment, caution should guide its sequencing within the radiochemotherapy backbone. Window of opportunity trials with induction treatment in biomarker selected patients will allow to explore the single agent activity and minimize the risk of additional toxicity.

1: Bradley JD et al. Lancet Oncol 2015; 16: 187–99

Symposium: Active surveillance for low risk prostate cancer: to treat or not to treat?

SP-0104

Does (very) low risk prostate cancer really exist?

F. Algaba[1]
[1]*Fundacio Puigvert, Barcelona, Spain*

Prostate cancer could be considered as insignificant or indolent (IPCa) when its presence does not bring about any risk for the life of the patient. If we start with this idea it is easy to understand that this situation is very difficult to predict since it depends on many variables of each patient, among which the life expectancy of the patient is one of the most important; therefore, it would seem to be a more theoretical question than practical, if it were not because it reflects an emerged reality by finding that up to 31% of the prostate carcinomas detected by high PSA serum levels, through study of the prostatectomy specimen, there were only small nodules of carcinoma that could have remained totally localized (latent) during the entire life of the patient, therefore they could have been treated with watchful waiting. It is clear that all of this supposition is a speculative exercise and only comes from indirect suppositions of the probable biology of a carcinoma node by its pathological characteristics. This fact explains that there are diverse definitions of IPCa in the radical prostatectomy specimens, although all coincide in requiring a small volume of tumor (< 5cc, although there is an author that accepts < 1cc), absence of aggressive Gleason patterns (no 4 or 5 patterns or Gleason score <7) and the majority also require, for a tumor to be accepted as indolent, to be a confined organ tumour with negative margins. In accordance with these criteria, the prevalence of IPCa varies between 2.3% and 31%, with an average of 18.3%. However, this uniformity of criteria is not the same at the time of determining the pre-operative model to predict IPCa, possibly because all the studies that try to correlate the extension of the prostate cancer in the biopsy with the volume in the prostatectomy specimen show that this correlation is very weak; and therefore, although all the needle biopsy criteria for defining an IPCa require the absence of an aggressive Gleason pattern (pattern 4 and 5 or Gleason score ≤ 7) would vary as regards the extension of the tumor in the cores (< 3 core with no core >50% of the surface, only one positive core < 3mm, 1% of all the cores, no core > 10% of the surface) and the inclusion between the criteria of the PSAD (PSA density). With all this variability the presumption of a possible IPCa in the radical prostatectomy specimen of the different authors has a sensitivity of 23% to 83.9% (average 53.2%) and a specificity of 61.9% to 99% (average 89.1%). Maybe it will help us to better identification of very low aggressive P.Ca patients the recent redefinition of Gleason patterns and the proposed grouping of prognostic grades. A new International Society Urogenital Pathology revision in November 2014 defined the current criteria with a precise definition of Gleason pattern 3 as small glands with variation in size and shape infiltrating amongst non neoplasic glands and Gleason pattern 4 according four different aspects as all cribriform growth (some of them previously considered as pattern 3), fused glands, ill defined glands and glomeruloid glands. But with the intention to improve the correlation with the clinical parameters a new grading system was. This new system follows the accepted the new Gleason patterns grouping them in five prognostic groups: Group 1 (Gleason 3+3), Group 2 (Gleason 3+4), Group 3 (Gleason 4+3), Group 4 (Gleason 4+4) and Group 5 (score Gleason 9 and 10). According this new arrangement an excellent correlation with the risk of biochemical recurrence we can obtain in needle biopsy and radical prostatectomy specimens.
Prostate cancer is considered insignificant (IPCa) when its presence does not bring any vital risk. IPCa in the radical prostatectomy is a small (< 5cc,), No Gleason 4 or 5, organ confined, negative margins. The average prevalence is 18.3%. The pre-operative model to predict IPCa is difficult. In the IPCa identification can help the new ISUP Gleason revision, pattern 3 small glands with variation in size and shape and Gleason pattern 4 according four different aspects as all cribriform growth, fused, ill defined and glomeruloid glands. A new system was accepted grouping them in five prognostic groups: 1 (3+3), 2 (3+4), 3 (4+3), 4 (Gs8) 5 (Gs9,10), with excellent clinical correlation .

SP-0105

The role of MRI in active surveillance

G. Villeirs[1]
[1]*Ghent University Hospital, Genitourinary Radiology, Ghent, Belgium*

T2-weighted MRI (T2w) typically shows a prostate cancer as a low signal-intensity area among the high signal-intensity normal peripheral zone tissue background. In the transition zone, prostate cancer has an equally low signal-intensity, although contrasting less well with the surrounding heterogeneous signal-intensity of glandular and stromal hypertrophy. It has been shown that the observed signal intensity inversely correlates to some extent with the aggressiveness of the cancer (lowest signal intensities in

higher grade cancers). The sensitivity of T2w imaging for prostate cancer (of any Gleason grade) is quite high (up to 85%), but with a low specificity (about 55%) due to many false positive calls. Therefore, functional imaging tools are required to improve the overall diagnostic accuracy.
Diffusion-weighted MRI (DWI) is currently the most important functional technique in addition to T2w MRI. Its mechanism is based on the inhibition of spontaneous water diffusion in tumor areas, due to both increased cellularity (more hydrophobic cell membranes inhibiting water diffusion) and destruction of fluid-rich acini and ductules. Prostate cancers can hence be detected as areas of decreased signal-intensity on apparent diffusion coefficient (ADC) maps or as increased signal-intensity on high b-value images. It is more than noteworthy that a quite robust inverse correlation exists between ADC-values and tumor aggressiveness (lowest ADC-value in higher grade cancers).
Dynamic contrast-enhanced MRI (DCE) measures the amount and characteristics of tumoral neoangiogenesis. After an intravenous bolus injection of gadolinium-containing contrast media, prostate cancers tend to enhance earlier, more rapidly and with a more pronounced de-enhancement (wash-out) than benign or normal tissue. DCE greatly helps detecting cancers in the peripheral zone, but suffers from false positive calls in the transition zone due to similar enhancement characteristics in glandular hypertrophy.
Magnetic resonance spectroscopic imaging (MRSI) is a more advanced tool that currently is mainly performed in expert centers and in clinical trials. It is based on measurement of the relative concentrations of citrate and choline, markers of benign and malignant tissue, respectively. MRSI adds specificity to T2w MRI (reduction of false-positive findings), but its main value lies in its direct correlation between the choline-to-citrate ratio and tumor aggressiveness.
mpMRI currently more and more consists of T2w MRI combined with DWI. DCE is additionally performed in all cases by some institutions, or only in doubtful cases by others. Meanwhile, it remains very important that all mpMRI studies are performed according to uniform quality and reporting standards, as pointed out by the European Society of Urogenital Radiology Guidelines and the recently revised Prostate Imaging Reporting and Data System (PI-RADS version 2). The latter consists of a diagnostic probability scale, in which PI-RADS 1 and 2 signify “clinically significant disease (highly) unlikely”, PI-RADS 3 “clinically significant disease is equivocal”, and PI-RADS 4 and 5 signify “clinically significant disease (highly) likely”. These scales are largely based on the unique ability of mpMRI to more easily detect high-grade and larger (i.e. clinically significant) tumors than small lower-grade lesions. This holds promise in the assessment of patients suspected of having prostate cancer. In patients who are candidates for active surveillance on the basis of clinical parameters, a PI-RADS 1 or 2 scale can corroborate this choice owing to a negative predictive value for excluding high-grade disease up to 98%, while in patients with a PI-RADS 4 or 5 a targeted biopsy can be performed in the suspicious area, including areas that are more difficult to reach with standard biopsy (e.g. anteriorly located tumors). PI-RADS 3, on the other hand, requires a biopsy in selected cases, taking into account clinical parameters such as PSA-density, PSA-kinetics, patient age and potential comorbidity. Hence, the performance for correctly assigning patients to active surveillance can be increased and mpMRI is currently recommended at enrolment in active surveillance by the UK National Institute for Health and Care Excellence (NICE).

SP-0106

Active surveillance: challenges and perspectives. The clinician point of view

R. Valdagni[1]
[1]*Fondazione IRCCS Istituto Nazionale dei Tumori, Milan, Italy*

Prostate cancer (PCa) is the most common male malignancy. The number of diagnoses has increased since the introduction of the PSA in the early ‘90ies. Up to 50% of the new PCa detected can be considered clinically insignificant or indolent: this relatively new concept in oncology means that these very well localized, small and non aggressive tumors (GPS=3+3), which are generally diagnosed with a biopsy following PSA rises, would not cause symptoms and/or death during one’s life. Despite this non aggressive behavior, most of these tumors are still treated with curative standard therapies (prostatectomy, external radiotherapy and brachytherapy), which, although equally effective treatment options, are burdened by potentially severe side effects.
As a matter of fact, there is no way to entirely distinguish upfront, before as well as after the biopsy, non aggressive, clinically insignificant, indolent tumors from aggressive, potentially lethal cancers that need to be treated immediately. To deal with the problem of overdiagnosis and overtreatment, active surveillance (AS) is being proposed in alternative to radical treatment to very selected men with favourable disease characteristics. AS is widely accepted in uro-oncologic communities and included in several guidelines, even if its routine application in the clinic is still suboptimal.
Understanding the natural history of clinically insignificant PCa is of primary importance to obtain reliable tools to select and follow-up AS patients. AS inclusion criteria are presently based on≤T2a at DRE, PSA/PSA density, number and percentage of positive biopy cores and GPS. Originally, the approach was more restrictive (i.e. selection of very low risk PCa patients). Nowadays, considering that feasibility and safety of these more strict protocols were assessed, more inclusive protocols are enrolling patients (e.g. including selected GPS=3+4).
One of the main issues AS is currently facing is the chance of “inadequate” diagnoses from biopsies, known to result in upgrading and upstaging at prostatectomy, especially for low-grade PCa. PSA/PSA density or the number of positive cores at diagnostic biopsy do not appear to be associated with the probability of upgrading patients initially fit for AS. This is the main reason to consider a confirmatory biopsy (time varying between 3 and 12 months) in most AS protocols, which can help identify patients ineligible for AS as a result of disease upgrading. The rate of “reclassification” at confirmatory biopsy varies between 16 and 30%, very similar to the one after prostatectomy.
Due to its great potential, MRI is increasingly used, being able to identify lesions that might be missed by standard biopsy. A positive MRI is associated to higher upgrading rates after prostatectomy and also after confirmatory biopsy. At present, in men on AS, MRI is used as an aid to detect clinically significant disease and help target suspicious lesions; however, there is still no solid evidence to endorse MRI in place of repeated biopsies.
Investigation on genetic/biomolecular/biochemical signatures is urgently needed to better classify our patients, trying to take benefit from non-invasive indicators of progression or reclassification. Research is currently focused on finding genetic signatures of both positive biopsy and adjacent normal tissue/stroma and on studying biomolecular markers possibly present in urine and blood (liquid biopsy). Recently, tests based on high expression of selected genes in biopsy specimens were found to be associated with higher risk of disease progression, but the possible true impact on AS is still to be determined.
AS follow-up plays a crucial role, since it enables to monitor the tumor behavior and potentially detect the more aggressive forms, which may benefit from treatment. In most protocols, follow up is based on clinical data (DRE, PSA and repeat biopsies), some protocols recently including mpMRI. Biomarkers (e.g. PCA3 or -2proPSA) are not routinely used in AS protocols, due to confusing results coming from the literature.
In conclusion, the results of AS programs should be primarily assessed on their ability to avoid overtreatment, while guaranteeing the same curability window of upfront radical treatments. The percentage of patients who remain treatment free is one of these measures, with current estimates being ≈40% at 20 years from diagnosis. Evaluation of oncological outcomes such as OS and CSS rates is also important, being in the Canadian AS cohort 62% and 94% at 15 yrs, respectively. Secondary objectives should include quality-of-life and comparison of AS vs radical therapies costs. The variety of inclusion criteria and follow-up

protocols makes the evaluation difficult. However, to date, the published outcomes are similar to those in patients receiving immediate curative treatment.

Symposium: Achieving excellence in image guided brachytherapy

SP-0107
Physician training in contouring
P. Petric[1]
[1]*National Center for Cancer Care & Research A member of Hamad Medical Corporation, Doha, Qatar*

In the past 2-3 decades we have witnessed major advances of radiotherapy planning. These developments were based on implementation of sectional imaging, computerized treatment planning and high precision treatment technologies in the radiotherapy process. When compared with the conventional radiography based method, modern 3-4 dimensional approaches require accurate and reproducible delineation of the target volume and organs at risk on the sectional images of various modalities, including computed tomography, magnetic resonance imaging, positron emission tomography and ultrasound. Contouring variation represents one of the most important contributors to the overall uncertainties in radiotherapy. The dosimetric and clinical benefits of modern high precision radiotherapy can be compromised by inaccurate delineation [Njeh CF. Med Phys 2008]. Assurance of consistent and accurate contouring of the regions of interest is one of the main preconditions for safe treatment delivery, optimal clinical outcome and meaningful reporting and comparison of treatments.
In addition to high quality imaging and contouring guidelines, solid knowledge of radiological anatomy is a precondition to achieve best contouring standards. While this subject is recognized as one of the key competencies in the radiation oncology core curricula and training programmes [Eriksen JG, et al. Radiother Oncol 2012, www.acgme-i.org,], there is limited published data regarding the actual impact of the teaching interventions on contouring skills and the characteristics of the learning curve [Jaswal JK, et al. IJROBP 2014, Cabrera AR, et al. J Am Coll Radiol 2011, Bekelman JE, et al. IJROBP 2009, D'Souza L, et al. BMC 2014]. Furthermore, published national surveys among radiation oncology residents and residency program directors indicate that there is room for improvement of training and evaluation of contouring competencies during residency [Jani AB, et al. Pract Rad Onc 2015, 12Jaswal JK, et al. IJROBP 2013].
Contouring training should not be viewed as a process limited to the residency and fellowship programs and core-curriculums. In a study evaluating the impact of prospective contouring rounds in a high volume academic centre, 36 % of cases required modification of contouring or written directives prior to treatment planning [Cox BW, et al. Pract Rad Onc 2015]. In a study of stereotactic body radiotherapy for lung cancer, the institutional peer-reviewers recommended major and minor changes of delineations in 23 % and 37 % of 472 contoured structures, respectively [Lo AC, et al. J Thor Onc 2014]. In view of the rapid developments of imaging and radiotherapy delivery, accompanied by constant evolution and development of new contouring recommendations, the importance of continuous education of the experienced practitioners, mentors and trainers cannot be overemphasized.
Research focusing on site-specific volumetric, topographic and qualitative aspects of contouring variation informs the educational activities in this field. The growing number of published inter-observer studies offers valuable resource to guide the training process. Limiting the learning to didactic and case-based instructions has improved knowledge scores and resident satisfaction in one study. However, this was not translated into improved contouring accuracy [D'Souza L, et al. BMC 2014]. In our experience, site-specific curriculum based on intensive sequence of didactic presentations, system-based instructions and hands-on contouring workshops represents an optimal strategy to achieve good learning results [Segedin B, et al. Submitted to Radiol Oncol 2016]. Feasibility and effectiveness of similar intensive educational interventions has been confirmed by others [Jaswal J, et al. IJROBP 2014].
These favourable early outcomes of teaching cannot be extrapolated on the long-term scale.Further evidence-based characterization of the learning curve is required to quantify the needs for continuous education and identify strategies for long term knowledge consolidation. Relative impact of the individual educational modules and qualifications of trainers on the learning outcome needs to be quantified, taking the tumour-site specific challenges into account. Development of training tools, including e-learning platforms and tools for objective assessment of contouring represent some of the main pre-requisites for future improvements in this field.

SP-0108
Physicist training in 3D dose planning
P. Bownes[1]
[1]*St James Institute of Oncology, Department of Medical Physics and Engineering, Leeds, United Kingdom*

New physicists entering in to the speciality of brachytherapy normally undertake a formal training scheme in Medical Physics. Within the specialised field of brachytherapy the depth and breadth of training received can be dependent on the training scheme undertaken, training hospital's expertise in brachytherapy, length of time dedicated to brachytherapy training and the assessment process.
This presentation will summarise the key components of knowledge and experience a physicist should be expected to receive during their brachytherapy training and cross reference this to example training schemes. Several key questions need to be addressed when reviewing the training needs for image guided brachytherapy: Is additional training still required after completion of the formal training scheme? Are they appropriately focussed on image guided brachytherapy?
It is important that any training gaps are identified and that measures are put in place to ensure that physicists have an understanding across all the components of image guided brachytherapy, have a full appreciation of the uncertainties and limitations within the brachytherapy pathway and of the systems used.
Additional training resources will likely have to be explored to complement the core training schemes. Examples of available training resources will be presented and how they can potentially help facilitate the training and professional development of brachytherapy physicists.
It is important that we ensure that opportunities for physicist training is not restricted and that physicists are allowed to develop their knowledge, understanding and skill set required for the modern image guided brachytherapy era. Training schemes need to continue to evolve and new training resources explored to complement formal training schemes and work based learning.

SP-0109
New avenues for training with e-learning
L.T. Tan[1]
[1]*Addenbrooke's Hospital - Oncology Centre University of Cambridge, Cambridge, United Kingdom*

E-learning has the potential to deliver educational content to large numbers of learners world-wide. In 2008, Cook *et al* from the Mayo Clinic conducted a meta-analysis of 201 studies of e-learning in the health professions. They found that internet-based instruction for medical professionals is associated with favorable outcomes across a wide variety of learners, learning contexts, clinical topics, and learning outcomes. Internet-based instruction appears to have a large effect compared with no intervention and appears to have an effectiveness similar to traditional methods. In a separate review in 2010, they identified that interactivity, practice exercises, repetition, and feedback improved learning outcomes.
This talk discusses the potential of e-learning for teaching competency in target volume delineation (TVD). A crucial

component of such a programme is automated assessment of contours with individualised feedback. The talk will compare conventional and novel methods for creating reference contours for TVD assessment, and conventional and novel metrics for automated assessment of TVD competency in individuals and groups of learners. The talk will also discuss the potential to investigate the impact of different instructional designs (e.g. live lectures, podcasts, annotated clinical cases, interactive demos) on TVD competency using quasi-experimental methodology.

Symposium: Imaging markers for response prediction and assessment

SP-0110

Imaging markers for response prediction: the clinical need

V. Goh[1]

[1]*Guys and St Thomas NHS Foundation Trust, Department of Radiology, London, United Kingdom*

A variety of therapeutic options are now available to cancer patients. It is recognised that significant biologic heterogeneity exists that may affect a patient's likelihood of response to particular therapies and development of resistance on therapy. To be able to predict whether a patient will respond or not respond to a specific therapy is advantageous in streamlining patient management and minimising the costs of continuing therapy that is not working as well as minimising unwanted side-effects of such therapy.
Imaging currently play an important role in routine clinical care and clinical trials in triaging patients to appropriate management and in monitoring patients on therapy. In terms of treatment assessment it is essential for imaging markers to be consistent, reproducible and validated. Standardized response assessment based on morphological change, such as RECIST 1.1 is well established in the clinical trial setting although its limitations for therapies beyond standard chemotherapy are recognised e.g. immunotherapy, and for which alternative response criteria have been proposed. Computed tomography (CT) remains that most commonly performed imaging modality due to its high spatial resolution and its cost-effectiveness, but positron emission tomography (PET) and magnetic resonance imaging (MRI) have advantages in their capability to image beyond morphology.
Measurement of glucose metabolism, cell proliferation, hypoxia, and vascularisation is now possible in clinical practice as well as quantification of their spatial variation, providing an imaging phenotype that is likely to be more beneficial than simple biomarkers e.g. size in predicting individual patient response to therapy. These imaging methods can also be integrated with genomic and pathological data allowing a comprehensive approach to address the clinical need towards individualisation of therapy in the future.

SP-0111

Response prediction in rectal cancer using PET Radiomics

R.T.H. Leijenaar[1], P. Lambin[1]

[1]*MAASTRO clinic, GROW - School for Oncology and Developmental Biology- Maastricht University Medical Centre, Department of Radiation Oncology, Maastricht, The Netherlands*

In personalized medicine, early prediction of pathologic complete response for locally advanced rectal cancer (LARC) patients is essential to tailor treatment. The standard treatment for LARC patients consists of preoperative chemoradiotherapy (CRT) followed by surgery, with a complete response being observed in 15-30% of the patients after the neo-adjuvant treatment. Overtreatment of complete responders could be avoided if an accurate prediction of pCR is available, by selecting a wait-and-see policy instead of surgery after CRT, and thereby reducing treatment related complications. Further treatment strategies based on the prediction of pCR include a radiotherapy boost after CRT for patients with good response to achieve a higher complete response rate, and additional chemotherapy after initial CRT for the worst responding patients.
In recent years, [18F] fluoro-2-deoxy-D-glucose positron emission tomography (FDG-PET) imaging has been increasingly used for decision support, treatment planning and response monitoring during radiotherapy. Radiomics (www.radiomics.org; animation: http://youtu.be/Tq980GEVP0Y) is a high throughput approach to extract and mine a large number of quantitative features from medical images, characterizing tumor image intensity, shape and texture. The core hypothesis of radiomics is that it can provide valuable diagnostic, prognostic or predictive information. FDG-PET radiomics may therefore facilitate early and accurate prediction of tumor response to treatment to identify LARC patients eligible for a wait and see or organ preserving approach, or patients who may benefit from treatment intensification.
This presentation will focus on the methodology of, and technical challenges in, the development and validation of a predictive PET radiomic model for pCR in LARC patients, illustrated with recent data.

SP-0112

MRI imaging of irradiated liver tissue for *in vivo* verification in particle therapy

C. Richter[1,2,3,4], D.G. Duda[5], A.R. Guimaraes[5,6,7], T.S. Hong[5], T.R. Bortfeld[5], J. Seco[5]

[1]*OncoRay - National Center for Radiation Research in Oncology, Faculty of Medicine and University Hospital Carl Gustav Carus- Technische Universität Dresden, Dresden, Germany*
[2]*German Cancer Research Center DKFZ and German Cancer Consortium DKTK, Partner site Dresden, Dresden, Germany*
[3]*Helmholtz-Zentrum Dresden – Rossendorf, Institute of Radiooncology, Dresden, Germany*
[4]*Faculty of Medicine and University Hospital Carl Gustav Carus- Technische Universität Dresden, Department of Radiation Oncology, Dresden, Germany*
[5]*Massachusetts General Hospital and Harvard Medical School, Department of Radiation Oncology, Boston, USA*
[6]*Massachusetts General Hospital, Department of Radiology-Division of Abdominal Imaging, Boston, USA*
[7]*Martinos Center for Biomedical Imaging, Department of Radiology, Boston, USA*

In vivo treatment verification is highly desirable, especially but not only in particle therapy where uncertainties in the particle range can compromise the physical advantage of this treatment modality. Existing measurement techniques for range measurements exploit physical effects, in particular secondary radiation that is produced by the proton beam, for example through activation of positron emitters, or prompt gamma radiation. Also biological effects caused by the irradiation can be used for *in vivo* treatment verification, if a functional imaging method is available to visualize the effect.
One prominent example for biology-driven range verification is an irradiation-induced change in contrast-enhanced MRI of the liver. A strong systematic decrease in uptake of the hepatobiliary-directed contrast agent Gd-EOB-DTPA has been shown in irradiated healthy liver tissue 6-9 weeks after irradiation [1-3] using different treatment modalities (brachytherapy, stereotactic body radiation therapy with photons and protons). The underlying mechanism seems to be based on a pro-inflammatory reaction of the irradiated liver tissue resulting in a downregulation of the Gd-EOB-DTPA uptake transporters and an upregulation of the respective excretion transporters [4].
In a prospective clinical study, carried out at Massachusetts General Hospital in Boston (USA), we investigated whether MRI of the liver can be used for *in vivo* dosimetric verification already during the course of hypo-fractionated proton therapy of liver metastases (5 fractions within 2 weeks). In contrast to the previously found late changes weeks after the end of treatment that were seen in all patients, for the early Gd-EOB-DTPA enhanced MR imaging large inter-patient variations were found. For 10 patients, strong or moderate signal changes were detected for 2 and 3 patients,

respectively. For 5 patients no dose-correlated early signal change was found at all. This qualitative scoring was consistent with a quantitative voxelwise dose to signal change correlation. The analysis of additional parameters that could potentially explain inter-patient variations (e.g. dose delivered at time of MRI scans, several timing parameters, liver function parameters and circulating biomarkers of inflammation determined from blood samples taken before and during treatment) revealed no clear correlation or trend with the strength of the signal decrease. Hence, irradiation-induced effects in the liver can be detected with Gd-EOB-DTPA enhanced MRI within a few days after proton irradiation in a subgroup of patients. As all patients possessed a signal decrease in late follow up scans, only the early dynamics of the liver response is influenced by these inter-patient variations. The reason for these large variations in early response is not yet fully understood and needs further investigation.
This presentation will cover a brief overview of biological effects used for treatment verification and will then focus on the irradiation-induced signal change in Gd-EOB-DTPA enhanced MRI of the liver. The hypothesis for the biological mechanism, the available data for late and early MRI signal changes will be presented and open questions will be discussed.

Debate: There are many existing IGRT options for highly accurate dose delivery. Is there a need for large-scale in-room MR-guidance?

SP-0113
For the motion

F. Lohr[1]
[1]*University Medical Center Mannheim, Department of Radiation Oncology, Mannheim, Germany*

The statements that will be made highlighting the strong position we are already in when using all currently available advanced image-guidance strategies are used are the following:
- If there is a necessity for on line MR-guidance, there is a general necessity for broad use of advanced image guidance strategies, particularly as successful screening programs such as those for lung cancer and potentially even pancreatic cancer are established, as this potentially leads to more localized disease being treated.
- Several such strategies are now available but are underutilized, typically for lack of funding or perceived complexity. Recent developments such as FFF-delivery and fast collimators have, however, shortened a lot of treatments and thus rendered advanced imaging strategies more feasible. Considerable expertise is needed, as it is mandatory also for MR-guidance.
- MR-guidance can be and has already been more easily applied to brachytherapy, a highly effective form of local therapy where technically applicable.
- Continuous 2D-tracking based on fiducials placed in minimally invasive procedures has entered the clinical routine for the ablation of small lesions without complex interference of OARs.
- 3D-imaging with CBCT, particularly in conjunction with breathhold strategies, still has considerable potential. Accuracies in the range of 3mm can be consistently achieved across treatment targets, in deep inspiration breathhold typically with very favorable dose distributions and straightforward dose accumulation. 4D-approaches are available, ultrafast "snapshot" volume imaging is ready to be deployed clinically.
- Ultrasound, where applicable, allows not only for positioning but for tracking in 2D and 3D.
- Surface scanning may simultaneously provide patient surveillance and gating signals during a therapy session.
- Noncoplanar treatment strategies and high-LET radiation may have further potential to improve clinical results independent of imaging strategy and are currently not possible in conjunction with in-room MR-guidance.
The statements suggesting that in-room MRI guidance will add significantly to the current armamentarium comprise the following:
- Cancer is primarily a soft tissue disease. MRI offers unparalleled soft tissue contrast imaging across a wide range of cancer types and locations. In-room MRI guidance for cancer radiotherapy combines exquisite soft tissue imaging of the cancer and surrounding healthy structures with precision radiotherapy to optimally target the cancer and spare healthy tissues, affecting quality of life, cancer outcomes and reducing the health and economic burden of managing treatment-related side effects.
- This ability to simultaneously image and target the cancer with radiotherapy is intuitive to patients and the treatment team alike. Indeed, the image quality of MRI-guidance is so high that a commercial online adaptive radiotherapy solution is only available with these systems.
- Cancer physiology is heterogeneous and changes with time. MRI is the only in-room physiological targeting system for cancer radiotherapy. An example, tumor hypoxia, is a strong negative prognostic indicator of survival across a wide range of cancer sites, and the tumor hypoxic status changes over the time period of a single treatment. The ability to selectively image and target the most aggressive and resistant parts of the cancer opens up a new window to dramatically change cancer outcomes.
- In addition to in-room MRI-guidance offering an improved treatment across a range of cancer sites, this new device also opens up the opportunity to explore the treatment of non-oncologic diseases. An example is atrial fibrillation, a disease suffered by 6 million Europeans, with many of these patients treated in an invasive, long, expensive procedure. MRI-guided radiotherapy offers a non-invasive, short and cost-effective treatment of atrial fibrillation. This treatment is enabled by using MRI to solve the challenging problem of imaging and targeting small volumes affected by both respiratory and cardiac motion, a problem too difficult for other in-room imaging systems.
- The improved outcomes and applications observed from in-room MRI-guided radiotherapy will affect patient referral patterns and policy guidelines to increase the global radiotherapy need, benefiting the radiation oncology and global communities.

SP-0114
Clinical evidence for in-room MRI guidance

P. Keall[1]
[1]*University of Sydney, Sydney- NSW, Australia*

Joint abstract submitted

Symposium: Additional tools for contouring

SP-0115
Functional and molecular imaging techniques and personalised radiotherapy

M. Niyazi[1]
[1]*Klinik und Poliklinik für Strahlentherapie und Radioonkologie, Department of Radiation Oncology, München, Germany*

Advances in radiotherapy delivery have been due to improved technique and image guidance. In contrary to the "one size fits it all" paradigm, personalized medicine trys to incorporate all available imaging information in order to optimally delineate the target volume. It will be highlighted, in how far molecular imaging such as PET has become a cornerstone for certain types of cancer and how PET information may be integrated into target delineation. Furthermore, it will be discussed in how far there is a role for a biological target volume (BTV) and how appropriate margins can be chosen; new tracers beyond FDG are discussed. The meaning of MRI and its applications as well as

available pitfalls will be presented employing an example of a brain tumor treatment.

SP-0116

General recontouring with deformal registration

X. Geets[1], E. Sterpin[2], J. Lee[2]
[1]*UCL Cliniques Univ. St.Luc - MIRO Lab - IREC, Radiation Oncology, Brussels, Belgium*
[2]*UCL - MIRO Lab - IREC, Radiation Oncology, Brussels, Belgium*

Significant patient anatomy changes may occur during the course of radiotherapy, more particularly for head and neck, pelvic and lung tumours. These modifications may degrade the plan quality over time, and hence require treatment adaptation based on the anatomy depicted from images of the treatment day.
Any comprehensive adaptive solution will necessarily require automatic tools that, first, depict patients who actually need adaptation (dose recomputation on daily image and clinical indicators of plan quality), and then assist the radiation oncologist/therapist in the labour-intensive task of target volumes and organs at risk recontouring. Ultimately, this approach should allow treatment plan re-optimization if required, without unmanageable additional workload in real-life clinical routine.
In this framework, deformable image registration allows the alignment of datasets in a non-linear way, providing a voxel-to-voxel mapping between the initial planning scan and the treatment scan. Therefore, deformation maps can be applied to propagate contours from planning CT to daily images, but also to compute dose distribution from the deformed images for dose accumulation purpose.
In this presentation, we will describe the general framework of deformable image registration, and will cover the main class-solutions for registration-based recontouring according to the tumor location and the available imaging modality, i.e. kV- or MV/CB-CT. Typical adaptive workflows based on deformable registration will be presented, as well as their advantages and potential limitations. Last, we will emphasize the essential role of the operator for accuracy and consistency check of the deformed contours, any inaccuracy in this step necessarily introducing systematic errors in the planning process.

SP-0117

Clinical appplication of atlas-based autosegmentation for contouring of multiple treatment sites

M. Ten Kley[1], J.J. Penninkhof[1], M. Stoevelaar[1], S. Quint[1], B.J.M. Heijmen[1], M. Hoogeman[1]
[1]*Erasmus Medical Center Rotterdam Daniel den Hoed Cancer Center, Department of Radiotherapy, Rotterdam, The Netherlands*

In the Erasmus MC radiotherapy department, atlas-based auto-segmentation of both clinical target volumes and organs at risk (OARs) is an important time-saving tool in daily clinical routine to assist both physicians and technicians. The accuracy of delineations has become increasingly important due to enhanced conformality of dose distributions as realized by IMRT and VMAT, and the use of reduced PTV margins in combination with image guidance. Clinical validation of atlas-based auto-segmentation for head-and-neck patients showed a reduction of hands-on time for delineation from 180 to 66 minutes, where structures were evaluated as 'minor-deviations, editable' or better (D. Teguh ; Int. J. Radiation Oncology Biol. Phys., Vol. 81, No. 4, pp. 950–957, 2011). The influence of geometric differences between autocontours and manual delineations by different observers on the dosimetric impact can differ for CTV and for OAR (Voet PW, Radiother. Oncol. 2011 Mar;98(3):373-7). We clinically implemented Admire (Elekta AB, Sweden) as part of our workflow in 2010. In this workflow, critical review and editing of the autocontours is still relevant.
For several target sites, a database was created containing fully contoured reference CT data sets (atlases). Depending on the tumor site, one or more atlases are used as an input for the generation of the patient-specific delineation (using the staple algorithm). The strategy of a single atlas can particularly be useful in case of adaptive treatments, resulting in a quick and more accurate autocontouring using the original delineated patient CT as the only atlas. An overview of the clinical implementation of Admire with regard to several tumor sites and the relation to treatment techniques such as breath-hold will be presented.

Poster Viewing: 3: Clinical: Gastrointenstinal and gynaecology

PV-0118

Prognostic impact of presurgical Ca 19-9 level in pancreatic adenocarcinoma: a pooled analysis.

G.C. Mattiucci[1], A. Arcelli[2], F. Bertini[2], F.A. Calvo[3], M. Falconi[4], A. Farioli[2], A. Guido[2], G. Frezza[5], J.M. Herman[6], R.C. Miller[7], V. Picardi[8], G. Macchia[8], W. Regine[9], M. Reni[10], N. Sharma[9], A.G. Morganti[2], V. Valentini[1]
[1]*Università Cattolica del Sacro Cuore -Policlinico A. Gemelli, Departement of radiotherapy, Rome, Italy*
[2]*University of Bologna- S. Orsola-Malpighi Hospital, Radiation Oncology Center- Department of Experimental- Diagnostic and Specialty Medicine – DIMES, Bologna, Italy*
[3]*Hospital General Universitario Gregorio Marañón-Complutense University, Department of Oncology, Madrid, Italy*
[4]*Università Politecnica delle Marche, Department of Surgery, Ancona, Italy*
[5]*Ospedale Bellaria, Radiotherapy Department, Bologna, Italy*
[6]*Johns Hopkins University School of Medicine, Department of Radiation Oncology and Molecular Radiation Sciences, Baltimore, USA*
[7]*University of Virginia, Department of Radiation Oncology, Charlottesville, USA*
[8]*Fondazione di Ricerca e Cura Giovanni Paolo II- Università Cattolica del Sacro Cuore, Radiotherapy Unit, Campobasso, Italy*
[9]*University of Maryland Medical Center, Department of Radiation Oncology, Baltimore, USA*
[10]*S. Raffaele Scientific Institute, Department of Oncology, Milan, Italy*

Purpose or Objective: Preoperative level of CA 19-9 (prCA19.9) predicts survival of patients (pts) undergoing surgery for pancreatic adenocarcinoma (PAC). Actually, there is no evidence of using prCA19.9 as a marker customizing and modulating effectiveness of adjuvant treatment or predicting pattern of failure. Therefore, the purpose of this pooled analysis was to determine whether prCA19.9 could predict overall survival (OS), local control (LC), disease metastasis free survival (DMFS) and evaluate effectiveness of adjuvant therapies in a broad population.

Material and Methods: We performed a multicenter retrospective analysis of 1122 patients (pts) who underwent surgical resection +/- adjuvant treatment [chemotherapy (aCT), radiotherapy +/- concomitant CT (RCT)] for PAC between 2000 and 2014 from 8 different institutions. Among 700 pts with prCA19.9 value we applied the Kaplan-Meier method and the log-rank test to investigate differences in OS, LC, DMFS between defined groups based on: clinical and pathological factors, 4 prCA19.9 cutoff (5, 37, 100, 353) and 5 relative prCa19.9 classes (0.0-5.0, 5.1-37.0, 37.1-100, 100.1-353.0, >353.1). We fitted Weibull regression model with shared frailty on institution to identify independent predictors of OS using data from 404 pts with complete information. We applied a backward stepwise strategy to select the covariates, forcing CRT and RT in the final model.

Results: Median follow-up (FU) was 27 months (2-225). At univariate analysis there was a strong impact of prCA19.9 classes (0.0-5.0, 5.1-37.0, 37.1-100, 100.1-353.0, >353.1) on 5-years OS (5.7% vs 37.9 vs 27.1 vs 17.4 vs 10.9, p< 0.001, Figure 1), 5-years LC (47.2% vs 63.3% vs 59.4% vs 43.4% vs 50.2%, p= 0.008), 5-years DMFS (17.0% vs 46.0% vs 39.0% vs 26.7 vs 23.4, p<0.001), respectively. Only in pts with prCA 19.9 > 353.1 U/ml aCT had positive impact on 5-year OS

(47.4% in pts treated with aCT vs 30.2% in pts not treated with aCT, p= 0.006). At multivariable model, sub-analysis of 404 pts showed (Table 1): worse OS for grading 3 tumor (HR: 1.85 95%CI 1.26-2.70, p= 0.002) tumor diameter > 30 mm (HR: 1.85, 95%CI: 1.35-2.53, p< 0.001), and better OS for pts treated with RCT doses > 50 Gy (HR: 0.38, 95%CI: 0.23-0.63, p< 0.001). Median OS worsened in pts with prCA19.9 >100 and <353 (HR: 1.77, 95%CI: 1.23-2.56, p= 0.002) and in pts with prCA19.9 ≥353.1 (HR: 1.92, 95%CI: 1.34-2.76, p<0.001).

Figure 1: Impact of prCA19.9 on OS

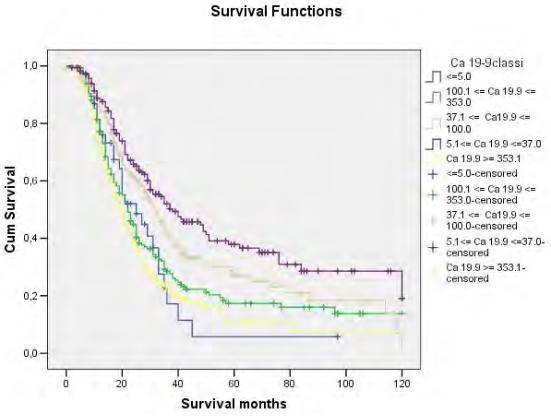

Table 1: Overall survival: estimates from Weibull proportional hazards regression models assuming shared frailty among centers. Analysis of 404 patients with complete information.

Variable	Value	Deaths	Univariate analysis HR	(95%CI)	P	Median (OS)*	Multivariate analysis* HR	(95%CI)	P	Median (OS)*
Age (years)	≤59	81	1.00	(Ref.)		24				
	60-69	116	1.32	(0.99-1.75)	0.059	24				
	≥70	82	1.67	(1.15-2.35)	0.005	21				
Gender	Female	120	1.00	(Ref.)	0.044	28	1.00	(Ref.)		24
	Male	149	1.27	(1.01-1.61)	<0.001	23	1.27	(1.00-1.62)	0.052	21
Tumor Site	Head	243	1.00	(Ref.)		24				
	Body	28	0.63	(0.42-0.93)	0.019	35				
	Tail	8	0.77	(0.37-1.58)	0.472	56				
Type of resection	DCP	235	1.00	(Ref.)		25				
	DP	31	0.59	(0.40-0.86)	0.006	38				
	TP	15	1.06	(0.78-2.38)	0.273	18				
Grading	1	42	1.00	(Ref.)		35	1.00	(Ref.)		33
	2	126	1.54	(1.07-2.28)	0.020	24	1.50	(1.00-2.23)	0.051	22
	3	109	1.78	(1.23-2.58)	0.002	22	1.85	(1.26-2.70)	0.001	19
	4	2	1.56	(0.38-6.47)	0.538	24	1.79	(0.41-7.78)	0.434	19
Margins status	R0	168	1.00	(Ref.)		28	1.00	(Ref.)		24
	R1	111	1.35	(1.05-1.74)	0.019	23	1.27	(0.95-1.65)	0.071	20
Tumor diameter (mm)	<30	135	1.00	(Ref.)		31	1.00	(Ref.)		31
	≥30	144	1.35	(1.07-1.722)	0.013	23	1.83	(1.35-2.53)	<0.001	20
pT-stage	1	3	1.00	(Ref.)		60				
	2	21	1.42	(0.69-3.46)	0.166	29				
	3	242	2.15	(1.01-4.83)	0.049	24				
	4	19	2.27	(0.64-7.98)	0.216	12				
pN-stage	N0	55	1.00	(Ref.)		57				
	N+	226	1.90	(1.40-2.57)	<0.001	22				
Adjuvant chemotherapy	No	81	1.00	(Ref.)		22	1.00	(Ref.)		23
	Yes	198	0.75	(0.59-1.01)	0.059	27	0.80	(0.60-1.08)	0.144	23
Postoperative RT +/- CCT	No	174	1.00	(Ref.)		13	1.00	(Ref.)		17
	<50 Gy	55	0.37	(0.25-0.63)	<0.001	38	0.34	(0.20-0.57)	0.053	37
	>50 Gy	70	0.28	(0.18-0.46)	<0.001	34	0.38	(0.23-0.64)	<0.001	35
CA 19-9 (U/mL)	≤5.0	19	1.93	(1.13-3.29)	0.016	23	1.72	(0.99-3.01)	0.054	23
	5.1-37.0	50	1.00	(Ref.)		38	1.00	(Ref.)		29
	37.1-100.0	49	1.21	(0.82-1.80)	0.335	31	1.12	(0.75-1.68)	0.585	27
	100.1-353.0	98	2.01	(1.49-2.87)	<0.001	21	1.79	(1.24-2.58)	0.002	19
	≥353.1	83	2.98	(1.52-5.08)	<0.001	20	1.91	(1.33-2.74)	<0.001	18

abbreviations: CI, confidence interval; CRT concurrent chemoradiation; DCP, duodeno-cefalo pancreatectomy; DP, distal pancreatectomy; OS, overall survival; PD, pancreatico-duodenectomy; Ref, reference category; RT, radiotherapy.

*Covariates to be included in multivariable models were selected with a stepwise backward elimination (p removal ≥ 0.10; p addition <0.10) based on likelihood ratio test. Adjuvant chemotherapy and postoperative RT were forced in the model.

†Median overall survivals, expressed in months, were estimated as average marginal effects from Weibull proportion hazards regression model

Conclusion: PrCA19.9 was a marker predicting OS and pattern of failure. ACT had positive impact on 5-year OS in pts with prCA19.9 > 353.1 U/ml. Our results suggest that prCA19-9 should be included in predictive models in order to customize treatments basing on prognostic factors of individual pts. Innovative treatments should be tested especially in pts with high prCA19.9 value.

PV-0119

Pattern of regional recurrence in adenocarcinoma of GEJ: implication for target delineation

J. Zhang[1], J. Jin[1], X. Wang[1]
[1]*Cancer Hospital- CAMS, Radiation Oncology, Beijing, China*

Purpose or Objective: To investigated the frequency and location of regional recurrence of locally advanced adenocarcinoma of GEJ patients after curative resection and refine the clinical target volume (CTV) delineation of radiotherapy.

Material and Methods: From 2009 to 2013, we retrospectively reviewed 1140 esophagogastric cancer patients treated in our institute. Patients who had curative resection, and were histopathologically diagnosed with locally advanced adenocarcinoma of GEJ (T3/4 or any N+) and confirmed of regional recurrence in follow-up CT images were selected into the analysis. First regional recurrence was recorded and one diagnostic radiologist with specialty of gastrointestinal tract investigated. The frequency and location of regional failure at each node station were analyzed according to Siewert types. Reference CT images was obtained from a healthy volunteer. We then delineated the epicenters of recurrence sites at the equivalent location, based on the same vessels of reference CT images compared with the recurrence CT images on Pinnacle treatment planning system. The combined contour of all recurrence sites was presented on a digitally reconstructed radiograph (DRR) image.

Results: Regional recurrence was identified in 78 patients. The majority of recurrence occurred within 2 years of follow-up (Median, 10.9 months). Of all, 35 (44.9%) patients were regional nodule failure (NF) only, 24 (38%) experienced regional NF simultaneous with distant failure, 11 (14.1%) were locoregional, and 8 (10.3%) had concurrent distant and locoreginal failure. The most common recurrent lymph nodes station were No.16 (62.8%), No. 9 (32.1%), No. 11 (24.4%), No. 8 (17.9%), No. 7 (16.7%), No. 112 (12.8%), No. 4 (12.8%) and No. 12 (10.3%), respectively. 11 patients (14.1%) had recurrence at mediastinal lymph nodes. There was significant difference of NF in No. 9 (42.2% vs 18.2%, P=0.027) between Siewert type II and III AEG, but no difference was observed in the other node stations. Different frequency and location of regional recurrence were shown by CT and digitally reconstructed radiograph (DRR) images. A three-dimensional (3D) atlas based on vessel delineation and distribution of regional recurrence was established.

Conclusion: The most prevalent nodal recurrence in patients with adenocarcinoma of GEJ after curative resection was along the abdominal aorta, celiac artery and splenic artery. Our findings suggest a modified elective lymphatic nodal target volume for IMRT contours in those patients.

PV-0120

Gastric fundus irradiation increases risk of postoperative anastomotic leakage in esophageal cancer

L. Goense[1], P.S.N. Van Rossum[1], J.P. Ruurda[2], M. Van Vulpen[3], G.J. Meijer[3], R. Van Hillegersberg[2]
[1]*UMC Utrecht, Department of Radiotherapy and Department of Surgery, Utrecht, The Netherlands*
[2]*UMC Utrecht, Department of Surgery, Utrecht, The Netherlands*
[3]*UMC Utrecht, Department of Radiotherapy, Utrecht, The Netherlands*

Purpose or Objective: Concerns have been raised regarding the toxicity of neoadjuvant chemoradiotherapy (nCRT) for esophageal cancer that could contribute to an increased risk of complications after subsequent esophagectomy such as anastomotic leakage. In this respect, radiation dose to the gastric fundus is of interest as this part of the stomach is used for the esophagogastric anastomosis after esophagectomy. The aim of this study was to determine the influence of neoadjuvant radiation dose to the gastric fundus on the risk of postoperative anastomotic leakage in patients with esophageal cancer undergoing nCRT followed by transthoracic esophagectomy.

Material and Methods: Between 2012 and 2015, 97 consecutive patients with esophageal cancer who underwent nCRT followed by transthoracic esophagectomy with cervical anastomosis were analyzed. The nCRT regimen consisted of a total radiation dose of 41.4 Gy in 23 fractions of 1.8 Gy in 5 weeks combined with weekly intravenous administration of carboplatin and paclitaxel. The gastric fundus was retrospectively contoured on the pre-treatment planning CT. Within this contour, dose-volume histogram parameters were calculated and univariable and multivariable logistic regression analyses were used to determine their influence on the risk of anastomotic leakage.

Results: In 25 patients (26%) anastomotic leakage occurred. The mean radiation dose to the gastric fundus was significantly higher in patients with versus without anastomotic leakage (median [interquartile range]: 35.6 Gy [20.2-39.9] versus 24.9 Gy [11.9-35.1], respectively; *p*=0.047, *Table 1*). A mean dose above versus below 31.4 Gy was associated with leakage rates of 43% versus 15%, respectively. Two typical examples of dose distributions in relation to the gastric fundus in patients with and without

anastomotic leakage are depicted in *Figure 1*. Adjusted for potential confounders including tumor location, clinical T-stage and radiation modality, the mean radiation dose to the gastric fundus remained significantly and independently associated with an increased risk of anastomotic leakage in multivariable analysis (adjusted odds ratio 1.05 per 1 Gy increase, 95% confidence interval: 1.003-1.10, p=0.035). Also, in patients with anastomotic leakage the minimum radiation dose, V25, V30, and V35 to the gastric fundus were significantly higher (*Table 1*).

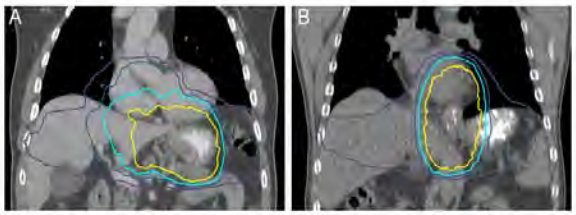

Figure 1. Examples of pre-treatment planning CT scans with dose distributions in (A) a patient who developed postoperative anastomotic leakage after receiving a mean dose to the gastric fundus of 41.2 Gy, and in (B) a patient who did not experience postoperative anastomotic leakage after receiving a mean dose to the gastric fundus of 11.8 Gy. The areas within the yellow, light blue, dark blue and purple lines received at least 40, 30, 20, and 10 Gy, respectively.

Table 1. Univariable logistic regression analysis of gastric fundus dose characteristics among patients with versus without anastomotic leakage.

Characteristic	Anastomotic leakage (n = 25)	No anastomotic leakage (n = 72)	OR (95% CI)	p value
Volume (mL)	11.1 [8.1-12.8]	11.8 [8.3-15.9]	0.92 (0.83-1.02)	0.121
Mean dose (Gy)	35.6 [20.2-39.9]	24.9 [11.9-35.1]	1.04 (1.00-1.08)	**0.047***
Minimum dose (Gy)	15.1 [11.9-26.1]	8.9 [2.8-16.9]	1.06 (1.02-1.11)	**0.006***
D50 (Gy)	39.0 [16.7-41.2]	21.8 [11.7-38.9]	1.03 (1.00-1.07)	0.054
Maximum dose (Gy)	42.5 [40.9-43.0]	41.9 [23.2-42.7]	1.02 (0.98-1.05)	0.328
V20 (%)	94.5 [27.5-100]	60.0 [2.6-93.9]	1.12 (0.99-1.27)†	0.066
V25 (%)	90.1 [22.3-99.8]	38.3 [0.0-81.3]	1.15 (1.02-1.30)†	**0.025***
V30 (%)	73.1 [17.9-96.1]	26.2 [0.0-76.5]	1.16 (1.02-1.31)†	**0.021***
V35 (%)	63.4 [13.2-93.3]	17.4 [0.0-65.2]	1.16 (1.03-1.32)†	**0.018***

Data presented as median with interquartile range (IQR) between brackets.
*Significant difference between patients with versus without anastomotic leakage (p< 0.05).
†Odds ratio per 10% increase in volume-percentage.
OR: odds ratio. CI: confidence interval.

Conclusion: Neoadjuvant radiation dose to the gastric fundus has a significant influence on the risk of postoperative anastomotic leakage in patients with esophageal cancer treated with nCRT followed by transthoracic esophagectomy and cervical anastomosis. This finding is important for clinical practice because it suggests that efforts should be made to minimize the radiation dose to the gastric fundus when planning neoadjuvant radiation treatment for esophageal cancer.

PV-0121

Falcon based Clinical Target Volume Delineation to support Inter-Society Rectal Cancer Guidelines.

M. Gambacorta[1], G. Chiloiro[1], P. Das[2], K. Haustermans[3], I. Joye[3], L. Kachnic[4], P. Maingon[5], C. Marijnen[6], S. Ngan[7], V. Valentini[1]

[1]*Università Cattolica del Sacro Cuore, Radiation Oncology Department, Rome, Italy*
[2]*University of Texas MD Anderson Cancer Center, Department of Radiation Oncology, Houston, USA*
[3]*University Hospitals Leuven, Department of Oncology, Leuven, Belgium*
[4]*Boston Medical Center, Department of Radiation Oncology, Boston- Massachusetts, USA*
[5]*Centre Georges-François Leclerc, Department of Radiation Oncology, Dijon, France*
[6]*Leiden University Medical Center, Department of Radiation Oncology, Leiden, The Netherlands*
[7]*Peter MacCallum Cancer Centre, Division of Radiation Oncology and Cancer Imaging, Melbourne, Australia*

Purpose or Objective: The delineation of clinical target volume (CTV) is a crucial step) in radiation therapy procedure. Uncertainties are related to the availability of several contouring guidelines suggesting different subvolumes and anatomical limits in rectal cancer. Furthermore, individual training creates large inter-operator variability in delineation. An international consensus among expert radiation oncologists might significantly reduce this variability. The definition of the procedures needed to produce consensus guidelines for rectal cancer through Falcon, the educational web-based multifunctional platform for delineation endorsed by ESTRO, was the primary aim of this study

Material and Methods: Seven skilled radiation oncologists, delegated from ESTRO,ASTRO, TROG,EORTC, defined the steps to produce consensus rectal cancer guidelines on elective nodal level delineation during a preliminary meeting held in August 2014. Step 1: six rectal cancer cases with different clinical stage were chosen and the related CT scans were shared and unanimously approved. Step 2: the experts firstly delineated online the selected CT scan slices following each his own approved guidelines. Step 3: Meeting on person to discuss the first delineation outcome, with also surgeon and radiologist ad hoc invited. Step 4: all the experts had to delineate online the same CT scan slices, based on the new table of boundaries. Step 5: Peer review meeting to evaluate the final outcome and to define the publication plan. the degree of agreement was evaluated through the EduCause ™STAPLE algorithm (ECSa). Step 6: preparation of the cases in Falcon to allow a free consultation after the publication of the guidelines

Results: Falcon platform allowed to succeed in any steps: selection and upload of the proper CT scans proposed among the experts leaving different countries; optimal compliant of all expert their delineation exercise; the possibility to review and share the online delineation, to support the discussion by telephone conference.Some Falcon's features were considered significant to compare concurrently all the experts' delineations, allowing to identify critical nodal boundaries as areas of disagreement. ì Furthermore the ECSa, has allowed to evaluate during the validation step the degree of agreement where the shared voxels between experts' delineations are graphically represented through an area with different levels of confidence (from 85% to 100%) for each structure set.

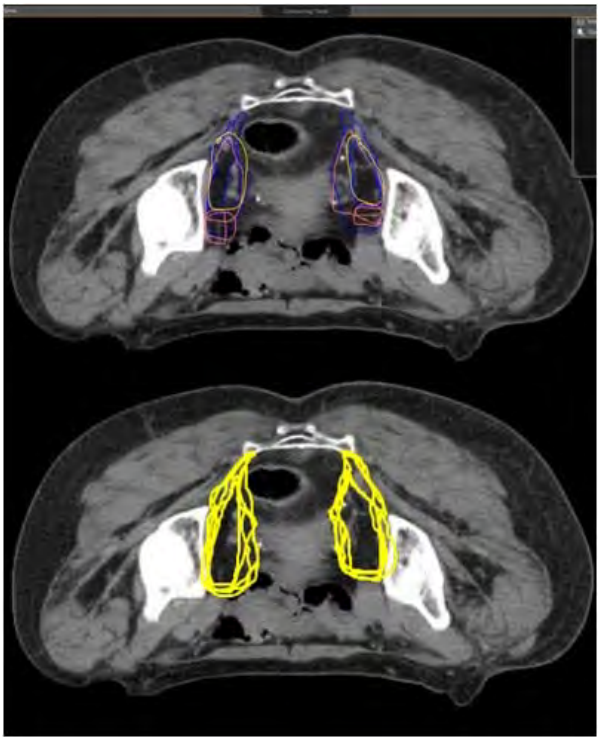

Conclusion: The ESTRO's Falcon platform of delineation showed to be a valuable tool in the definition of consensus guidelines for rectal cancer. These procedures might be reproduced to support the validation, discussion and comparison of delineations among skilled radiation oncologists to converge to consensus guidelines also for other scenarios.

PV-0122

Clinical factors as a selection tool for organ-preserving treatment strategies in rectal cancer

I. Joye[1], A. Debucquoy[2], S. Fieuws[3], A. Wolthuis[4], A. D'Hoore[4], K. Haustermans[1]

[1]*KU Leuven/University Hospitals Leuven, Department of Radiation Oncology, Leuven, Belgium*

[2]*KU Leuven, Department of Oncology, Leuven, Belgium*

[3]*KU Leuven/Hasselt University, I-Biostat, Leuven, Belgium*

[4]*University Hospitals Leuven, Department of Abdominal Surgery, Leuven, Belgium*

Purpose or Objective: The standard treatment for locally advanced rectal cancer is radio(chemo)therapy (RCT) followed by total mesorectal excision (TME) surgery. Patients who achieve a good response to RCT may be offered less invasive surgery such as local excision or even no surgery at all. Before such a policy could be safely implemented, precise selection of the eligible patients is mandatory. This study identifies the pretreatment clinical factors that are associated with pathological complete response (pCR) and ypT0-1N0 and evaluates their performance as a tool to select patient for organ-preserving treatment strategies.

Material and Methods: Patients with histologically confirmed rectal adenocarcinoma who were treated with preoperative RCT and TME between January 2000 and December 2014 were retrospectively included. Patients who received no preoperative RCT, patients treated with postoperative RCT and those treated for a local recurrence were excluded. Following pretreatment clinical characteristics were extracted from the medical files: age, gender, body mass index, ASA score, cT-stage, cN-stage, tumor distance from the anal verge, pretreatment CEA, pretreatment hemoglobin and distance from the mesorectal fascia. Univariable and multivariable binary logistic regression models were used to predict pCR and ypT0-1N0. A multivariable prediction model was obtained by combining all predictors and by applying a backward selection procedure with 0.157 as critical level for the p-value. The discriminative ability of the prediction models was evaluated by receiver operating characteristic analysis.To avoid that the same data were used to develop and to validate the model, the area under the curve (AUC) was based on a leave-one out cross-validation.

Results: A total of 620 patients were included of whom 120 patients experienced a pCR (19%) and 170 patients achieved a ypT0-1N0 response (27%). A low pretreatment CEA, a high pretreatment hemoglobin and a high cN-stage were associated with pCR in multivariable analysis (Table). A low pretreatment CEA, a low cT-stage and a high cN-stage were associated with ypT0-1N0. After cross-validation, the AUC of the pCR and ypT0-1N0 prediction model equaled 0.609 and 0.632, respectively.

Table: Multivariable logistic regression models to predict pCR and ypT0-1N0

		pCR		ypT0-1N0	
		OR (95% CI)	p-value	OR (95% CI)	p-value
Gender	Female	1.62 (0.99-2.66)	0.0557	1.15 (0.74-1.79)	0.5282
	Male	#		#	
Age at surgery		1.02 (0.99-1.04)	0.0624	1.01 (0.99-1.03)	0.3110
BMI		0.98 (0.93-1.03)	0.3626	0.97 (0.92-1.01)	0.1464
ASA			0.6832		0.7203
	ASA=2	0.98 (0.56-1.72)	0.9504	1.23 (0.74-2.05)	0.4308
	ASA=3	1.30(0.59-2.86)	0.5087	1.12 (0.54-2.35)	0.7614
	ASA=1	#		#	
cT-stage/MRF			0.1860		**0.0009**
	cT=3/MRF-	0.86 (0.44-1.66)	0.6458	0.44 (0.24-0.78)	0.0054
	cT=3/MRF+	0.53 (0.26-1.08)	0.0798	0.28 (0.15-0.52)	<0.0001
	cT=4	1.00 (0.40-2.48)	0.9966	0.47 (0.21-1.06)	0.0674
	cT=1-2	#		#	
cN-stage			**0.0453**		**0.0176**
	cN=1	3.42 (1.03-11.32)	0.0444	2.96 (1.17-7.52)	0.0226
	cN=2	4.52 (1.32-15.55)	0.0167	3.96 (1.50-10.43)	0.0054
	cN=0	#		#	
Distance to anal verge		1.00 (0.95-1.05)	0.9015	0.98 (0.94-1.03)	0.4714
Initial CEA		0.86 (0.74-1.00)	**0.0490**	0.79 (0.68-0.90)	**0.0006**
Initial Hb		1.30 (1.10-1.53)	**0.0023**	1.15 (1.00-1.32)	0.0526

Abbreviations: BMI = body mass index; CEA = carcinoembryonic antigen; Hb = hemoglobin; MRF = mesorectal fascia; OR = odds ratio; pCR = pathological complete response.

Conclusion: Despite their statistical significance, the value of pretreatment clinical variables in the prediction of pCR and ypT0-1N0 is very limited. To safely select rectal cancer patients for organ-preservation, other strategies using functional imaging or molecular markers need to be explored.

PV-0123

Gender and secondary malignancies in rectal cancer patients with and without radiation therapy

R. Warschkow[1], U. Güller[2], T. Cerny[2], B.M. Schmied[1], L. Plasswilm[3], P.M. Putora[4]

[1]*Kantonsspital St. Gallen, Department of Surgery, St. Gallen, Switzerland*

[2]*Kantonsspital St. Gallen, Department of Medical Oncology and Hematology, St. Gallen, Switzerland*

[3]*Kantonsspital St. Gallen, Department of Radiation Oncology, St. Gallen, Switzerland*

[4]*Kantonsspital St. Gallen, Radiation Oncology, St Gallen, Switzerland*

Purpose or Objective: The relationship between radiation therapy for rectal cancer and secondary malignancies is debated. The present study is the first population-based analysis using conventional multivariable analyses as well as propensity score matching to assess this relationship.

Material and Methods: Overall, 87,956 patients after resection of localized or locally advanced rectal adenocarcinoma diagnosed between 1973 and 2012 were identified in the Surveillance, Epidemiology, and End Results (SEER) registry. The occurrence of secondary malignancies diagnosed at least 1 year after diagnosis of rectal cancer was compared in patients who did and did not undergo radiation using adjusted and propensity score matched Cox regression analysis.

Results: Of 77,484 patients, 34,114 underwent radiation and 43,370 did not. Overall, radiation therapy was not associated with secondary malignancies (hazared ratio [HR] = 0.97 (95%CI: 0.92–1.02, P=0.269). In female patients (HR = 1.11, 95%CI:1.02–1.21, P=0.021) the risk for secondary malignancies was increased after radiation therapy, while a decrease of secondary maligancies was found in male patients (HR = 0.90, 95%CI:0.85–0.96, P=0.002). The risk for prostate cancer was significantly decreased (HR=0.44, 95%CI:0.38–0.51, P<0.001) whereas the risk for endometrial cancer was increased (HR=2.07, 95%CI:1.56–2.75, P<0.001). The risks for lung cancer (HR=1.20, 95%CI:1.14–1.08 P<0.001), bladder cancer (HR=1.50, 95%CI:1.27–1.76 P<0.001), and lymphoma (HR=1.29, 95%CI:1.06–1.02 P=0.032) were increased after radiation in the overall population.

Conclusion: The present analysis provides compelling evidence regarding gender-specific differences in the occurence of secondary malignancies after pelvic radiation. Indeed, radiation for rectal cancer is associated with a significantly decreased risk of prostate cancer, however, an increased risk of endometrial, lung, and bladder cancer as well as lymphoma. Patients undergoing radiation for rectal cancer must be informed regarding the potentially increased risk of secondary malignancies.

PV-0124

Does daily intake of resistant starch reduce the acute bowel symptoms in pelvic radiotherapy? RCT

B.K. Sasidharan[1], P.N. Viswanathan[1], S. Prasanna[2], B. Ramadass[3], S. Pugazhendhi[4], B.S. Ramakrishna[5]

[1]*Christian Medical College Hospital, Radiation Oncology, Vellore, India*

[2]*Christian Medical College Hospital, Biostatistics, Vellore, India*

[3]*Christian Medical College Hospital, Wellcome Research-Microbiology, Vellore, India*

[4]*Christian Medical College Hospital, Wellcome Research-Biochemistry, Vellore, India*

[5]*Christian Medical College Hospital, Gastroenterology, Vellore, India*

Purpose or Objective: The purpose of the study is to look at the benefit of administration of an oral prebiotic starch in reducing the incidence of acute radiation proctitis, a distressing symptom in patients receiving radiation therapy for cancer of the cervix.

Material and Methods: The study was conducted between 2011 and 2014 in 104 patients receiving radical chemo-radiotherapy for carcinoma cervix. Patients were randomized to two arms receiving 30 gm of resistant starch or digestible starch on a daily basis through out the course of the external radiotherapy. All patients received standard 4-field box radiation portals, 50 Gy in 25 fractions with 4 cycles of weekly concurrent Cisplatin. All of them underwent LDR brachytherapy of 30 Gy at completion of external beam radiotherapy. The study was double blinded and allocation was concealed from the investigators. The investigator recorded the radiotherapy related toxicity of the patients according to CTC V 3.0. The incidence and severity of grade 2-4 diarrhoea and proctitis were documented on a weekly basis and compared across the two randomized groups and analysed. Stool short chain fatty acid concentrations were measured at baseline at 2nd and 4th week and after 6 weeks of completion of radiotherapy in both study arm and placebo arm and reported. 2 patients progressed during therapy and were not included in analyses and two patients discontinued the intervention. A per protocol analyses was done.

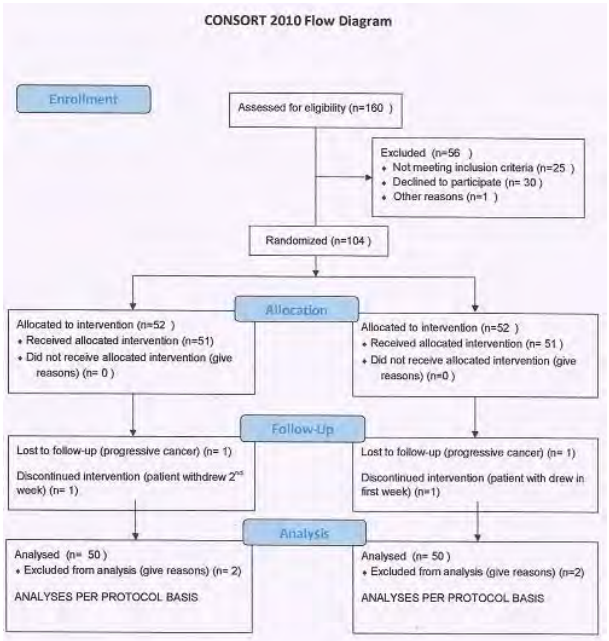

Results: At analysis there were 50 patients in each arm. The severity of clinical proctitis was found to be similar in both groups of patients with 12.2 % of patients experiencing toxicity of grade 2 and above in digestible starch group versus 14.6% in the resistant starch group. Functional proctitis was similarly graded and it was found that 16.3 % patients in digestible starch group experienced toxicity against 10.2 % patients in the amylase resistant starch group. This difference was seen at 4th week and continued in the subsequent weeks till the end of radiation. Both groups had similar reported toxicity at 6 weeks post intervention. Both groups were also found to have similar incidence of grade 2 and above diarrhea. The non-digestible starch group was found to have 8% incidence as compared to 2% in the other group at the 5th and 6th week. The short chain fatty acid concentrations were found to be not significantly different in the groups at any point.

Variables		Digestible			Non-Digestible		
		n	Mean(SD)	Median(min,max)	n	Mean(SD)	Median(min,max)
Acetate	Time 1	49	66.41(19.2)	64.07(22.4,120.3)	49	69.74(27.9)	65.99(17.2,141.6)
	Time 2	48	66.7(33.9)	60.26(23.4,181.1)	44	71.82(30.8)	70.57(23.9,158.1)
	Time 3	46	62.41(27.78)	51.68(24.3,134.3)	43	73.02(36.4)	67.72(18.2,151.7)
	Time 4	39	69.49(25.6)	64.04(25.9,129.7)	36	69.74(33.8)	59.68(17.1,169.3)
Propionate	Time 1	48	10.9(5.9)	10.29(1.5,21.2)	48	10.64(6.3)	8.64(2.4,30.5)
	Time 2	45	11.09(8.5)	8.34(0.35.9)	43	9.91(7.6)	8.73(1.2,37.2)
	Time 3	42	9.48(6.9)	6.88(0.03,28.8)	42	9.38(8.0)	7.76(0.1,40.8)
	Time 4	39	12.76(7.7)	10.72(2.3,34.3)	35	11.81(7.2)	10.76(1.5,30.1)
Butyrate	Time 1	48	19.48(13.8)	14.73(1.3,60.23)	49	16.85(11.9)	13.48(0.8,60.23)
	Time 2	47	14.99(10.6)	12.45(0.56.4)	44	14.31(7.3)	13.82(2.6,30.9)
	Time 3	45	15.79(11.2)	16.3(0.3,48.1)	43	16.5(15.5)	10.82(0.5,82.9)
	Time 4	39	18.51(13.6)	12.76(1.3,56.3)	36	19.61(15.1)	15.82(2.3,85.0)

Conclusion: The study failed to demonstrate a benefit in administration of resistant starch in excess of normal diet to patients receiving pelvic radiotherapy. This may be postulated to be due to concurrent use of chemotherapy and decrease in intestinal probiotics.

PV-0125

Chemoradiation+surgery vs chemoradiation+BRT in advanced cervical carcinoma: a case-control study

S. Cima[1], G. Macchia[2], A. Galuppi[3], M. Nuzzo[2], P. De Iaco[4], F. Deodato[2], A.M. Perrone[4], M.C. Valli[1], A. Richetti[1], A. Arcelli[3], F. Bertini[3], A. Farioli[5], S. Cammelli[3], A. Bisceglie[2], M. Pieri[3], S.G. Picchi[3], A. Zamagni[3], G. Frezza[6], A.G. Morganti[3], G. Ferrandina[7]

[1]*Oncology Institute of Southern Switzerland, Radiation Oncology Unit, Bellinzona-Lugano, Switzerland*

[2]*Fondazione di Ricerca e Cura "Giovanni Paolo II"- Catholic University of Sacred Heart, Radiotherapy Unit, Campobasso, Italy*

[3]*Radiation Oncology Center- S. Orsola-Malpighi Hospital-Universitiy of Bologna, Department of Experimental-Diagnostic and Specialty Medicine - DIMES, Bologna, Italy*

[4]*S. Orsola-Malpighi Hospital, Gynecologic Oncology Unit, Bologna, Italy*

[5]*S. Orsola-Malpighi Hospital- Universitiy of Bologna, Department of Medical and Surgical Sciences DIMEC, Bologna, Italy*

[6]*Bellaria Hospital, Radiotherapy Department, Bologna, Italy*

[7]*Policlinico Universitario "A. Gemelli"- Catholic University of Sacred Heart, Department of Gynecologic Oncology, Roma, Italy*

Purpose or Objective: To compare treatment outcomes in locally advanced cervical carcinoma (LACC) patients treated with neoadjuvant chemoradiation followed by radical surgery (surgery group: SG) versus radical chemoradiation plus brachytherapy boost (control group: CG). Results in terms of local control (LC), metastases-free survival (MFS), disease free survival (DFS) and overall survival (OS) were compared.

Material and Methods: Seventy-six patients with LACC (SG) were matched to 76 patients (CG) with respect to age, histology and stage. Matching was performed without knowledge of outcomes. Patients characteristics are summarized in Table 1. The median FU was 35 months (range: 2-107) for SG and 29 months (range: 1-125) for CG, respectively.

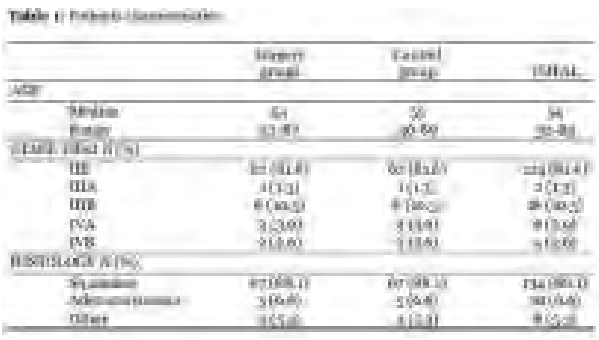

Results: At univariate analysis no significant differences between the two groups were recorded. Two-year and 5-year LC were 77.6% and 71.0% for SG and 76.1% and 70.3% for CG

(p=0.8), respectively. Two-year and 5-year MFS were 79.3% and 70.8% for SG and 78.8% and 78.8% for CG (p=0.6), respectively. Two-year and 5-year DFS were 71.9% and 61.6% for SG and 66.1% and 61.0% for CG (p=0.8), respectively. Two-year and 5-year OS were 90.9% and 84.4% for SG and 90.3% and 69.9% for CG (p=0.4), respectively.

Conclusion: The two treatment approaches achieved comparable outcomes in patients with locally advanced cervical carcinoma. Further analyses are needed to compare the toxicity profile of these two treatment strategies.

Joint Symposium: ESTRO-ESR: MR-PET

SP-0126
MR-PET for radiation oncology: the imaging perspective

K. Riklund[1]
[1]*Umeå University- Umeå University Hospital, Department of Diagnostic Radiology, Umeå, Sweden*

MR-PET is an advanced hybrid imaging method giving both structural, functional, molecular and biochemical information simultaneously or almost simultaneously. There are still challenges, not only with the attenuation correction, but also with performance of the examination and timing of the MR and PET acquisition.
It is well known that MR data contains detailed information with high tissue contrast and that PET imaging gives molecular/biochemical information with high molecular sensitivity but what is the added value? A major goal with treatment planning is to delineate the tumor volume, which can be done with both MR and PET, but since the both modalities show different characteristics of the tumor the volume might differ between them. Challenges from the imaging point of view will be discussed. The availability to PET/CT is much higher and the challenges with this method are fewer. Some comparison of the two hybrid modalities will be done. The majority of PET studies are done with the tracer fluorodexyglucose, FDG, but beyond FDG a large number of tracer are available, all giving information about different biochemical properties of the tumor. A few of these tracers will be presented and discussed.

SP-0127
MR-PET for radiation oncology: the sub-volume opportunities

D. Thorwarth[1]
[1]*University Hospital Tübingen Eberhard Karls University Tübingen, Tübingen, Germany*

Purpose: To investigate the value of combined PET/MR imaging for biologically individualized radiotherapy (RT) planning.

Methods: Hybrid PET/MR imaging offers the possibility to combine molecular information from PET with high resolution anatomical MR imaging. Consequently, a combination of the two different imaging data sets seems promising for improved automatic target volume delineation (TVD). An automatic co-segmentation algorithm has been developed in our institution which derives probabilities of tumor presence by combining PET and MR data. Finally, the PET/MR-based probability maps are segmented to generate RT target volumes. Automatically segmented target volumes were compared to manual delineations from three experienced radiation oncologists.
Furthermore, combined PET/MR imaging allows to assess PET and functional MR data at the same time. In the context of a clinical study, diffusion weighted (DW) as well as dynamic contrast enhanced (DCE) MRI were acquired in addition to anatomical images as well as FMISO and FDG PET images. Pairwise correlations of the different functional parameters were calculated in order to analyze for redundancy or complementarity respectively.

Results: Automatic co-segmentation of tumor volumes based on combined FDG PET/MR imaging in head and neck cancer revealed robust and reproducible contours. The comparison of automatic and manual target volumes showed good agreement in terms of volume overlap. Deviation of the automatic compared to the manual contours was in the same order of magnitude as inter-observer variation. Compared to PET-based TVD, additional information from high resolution MR data improves automatic segmentation.
A pairwise correlation analysis of parameters derived from FMISO PET, FDG PET, DW- and DCE-MRI on a voxel-level did only show moderate to low correlation coefficients hinting at a complementarity of the different investigated imaging methods. However, large inter-patient variations in terms of pairwise parameter correlations were observed.

Conclusion: Functional and molecular imaging with combined PET/MR has the potential to improve TVD. At the same time, PET/MR allows to assess different levels of biological information which may in the future be important to derive individualized measures of radiation sensitivity. As a consequence, PET/MR imaging opens new doors for personalized RT planning and delivery in the near future.

SP-0128
MR-PET for radiation oncology: the implementation issues

T. Nyholm[1]
[1]*Uppsala University, Immunology- Genetics and Pathology, Uppsala, Sweden*

Imaging is fundamentally important in modern radiotherapy. For several of the most common diagnoses both PET and MR provide important information in the clinical decision making at the radiotherapy department. The combination of PET and MR in integrated PET/MR scanners could be the most efficient imaging modality for these patients. PET/MR has however primarily been designed for diagnostics and adjustments are needed to enable effective use in radiotherapy. This includes for example the ability to image the patient in treatment position, the ability to account for immobilization devices in the attenuation correction, and the development of adequate quality assurance methods.

Proffered Papers: Radiobiology 2: Interplay between cancer stem cells, hypoxia and the radiation response

OC-0129
Nitroglycerin decreases the hypoxic fraction of non-small cell lung cancer lesions

B. Reymen[1], C.M.L. Zegers[1], W. Van Elmpt[1], F. Mottaghy[2], A. Windhorst[3], A. Van Baardwjik[1], S. Wanders[1], J. Van Loon[1], D. De Ruysscher[1], P. Lambin[1]
[1]*MAASTRO clinic, Radiotherapy, Maastricht, The Netherlands*
[2]*Maastricht University Medical Centre, Nuclear Medicine, Maastricht, The Netherlands*
[3]*VU University Medical Centre, Nuclear Medicine, Amsterdam, The Netherlands*

Purpose or Objective: Nitroglycerin is a nitric oxide donor being investigated because of its potential to increase tumour oxygenation. In phase II trial NCT01210378 nitroglycerin is added to radical radiotherapy in patients with NSCLC stage IB-IV. Using a dedicated hypoxia PET tracer ([18F]HX4; ref: Dubois et al, Proc Natl Acad Sci USA.2011) we investigate the effect of nitroglycerin on tumour hypoxia. Here, we report the results of the first 14 patients that completed the hypoxia scanning program.

Material and Methods: A baseline [18F]HX4 PET scan (4h p.i.) was performed to measure hypoxia in the primary tumour and nodes. At least 48 hours later, a second [18F]HX4 PET scan was taken after application of a nitroglycerin patch (Transiderm nitro 5 mg). Between the two scans, patients did not receive any treatment. The primary tumour and involved nodes were defined on the planning FDG-PET-CT scan and fused with the HX-4 scan for analysis. The tumour-to-blood ratio (TBR) of [18F]HX4 and the Hypoxic Fraction (HF; the fraction of the volume with a TBR >1.4) were calculated for

all lesions. The Wilcoxon signed rank test was used to evaluate differences between scan time points.

Results: In 14 patients, the median interval between the scans was 4.5 +/-2.1 days (range: 2-7days). Seven patients (50%) exhibited hypoxia (HX-4 TBR>1.4) in the primary tumour and 4 of 10 patients (40%) had nodal disease with an HX4 TBR>1.4 in the lymph nodes. In total 9/14 patients (64%) showed hypoxia at baseline in the primary tumour and/or the lymph nodes. The effect of nitroglycerin on HX-4 uptake in hypoxic lesions was as follows: in 8/11 volumes (72%) and in 6/9 patients (66%) nitroglycerin administration resulted in a decrease of the TBR of HX-4. Also, the median HF decreased from 12.9% to 1.2% (p=0.029), corresponding to a decrease in the median hypoxic volume of 5.4 cc to 0.5 cc (p=0.033). In the 7 non-hypoxic tumours and 6 non-hypoxic nodal volumes present at baseline, nitroglycerin caused a decrease of the TBR of HX-4 in 5, an increase in 5 and no effect in 3 lesions. None of the non-hypoxic lesions became hypoxic (TBR >1.4) after administration of nitroglycerin.

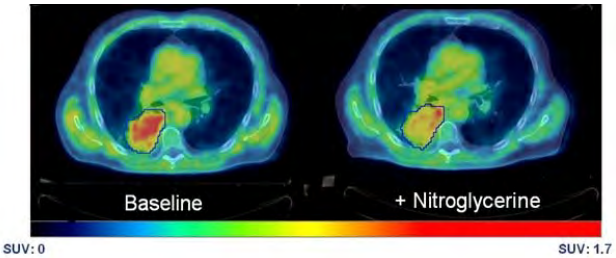

Figure 1: Example of HX-4 uptake in lung tumour before and after nitroglycerin.

Conclusion: Nitroglycerin causes a significant decrease in the hypoxic fraction and hypoxic volume of a majority of hypoxic non-small cell lung cancer tumours and metastatic lymph nodes. This promising result encourages further investigation of nitroglycerin as a sensitizing agent in a selected population. CT-based perfusion studies and lab experiments (data not shown) suggest this effect is mediated by an inhibition of mitochondrial respiration rather than a vascular effect.

OC-0130

Biomarker-based hypoxia-adapted radiochemotherapy: preclinical study in HPV+/- H&N cancer xenografts

L. Koi[1], L. Moebius[1], C. Weise[1], C. Erdmann[1], C. Valentini[1], M. Schmidt[1], M. Krause[1], M. Baumann[1]
[1]*Universtaet Klinikum Carl Gustav Carus- Onco Ray, Radiation Oncology, Dresden, Germany*

Purpose or Objective: Previous *in vivo* experiments demonstrated that hypoxia and perfusion determined during fractionated RT are associated with local tumour control (LC) in human head and neck squamous cell carcinoma (hHNSCC). In a randomized clinical trial Nimorazole improved LC and survival of patients with HNSCC treated with RT. Biomarker studies using tumour material from this trial indicate that hypoxic tumours predominantly benefit from nimorazole, supporting a predictive value for hypoxia assessment. However, this has not been prospectively evaluated for radiochemotherapy (RCTx) which represents the current standard of care in locally advanced head and neck cancer. The hypothesis of the ongoing study is that the microenvironmental parameters are also predictive for response to hypoxic cell sensitizing with nimorazole in combination with RCTx.

Material and Methods: We studied 8 different human HPV-negative and -positive HNSCC in a nude mice xenograft model. Irradiation was performed with 30 fractions (fx) in six weeks combined with weekly cisplatin (3 mg/kg i. p.). Nimorazole (0.3 mg/g i. p.) was applied before each irradiation and was started with the first fx or after 10 fx. Effect of nimorazole was quantified as LC 120/180 days after irradiation. For histological evaluation tumours were excised unirradiated or after 10 fx with and without nimorazole. Using quantitative image analysis, microenvironmental parameter such pimonidazole hypoxic volume (pHV), relative vascular area (RVA) and perfused fraction of vessels (PF) were determined.

Results: The data of the cell lines show pronounced heterogeneity in the effect of nimorazole on local tumour control after fractionated radiochemotherapy. Nimorazole significantly improved local tumour control in four of the eight tumours. In the two responder models FaDu and SAS, nimorazole was equally effective when given from start of radiochemotherapy or after 10 fx. The treatment with both, RCTx and the application of nimorazole and cisplatin were well tolerated by the animals. Furthermore, pHV was significantly reduced after 10 fx RCT with and without nimorazole in all four responder models in contrast to the non-responders.

Conclusion: Apparently, the decrease of pHV after the first fractions of RCTx has potential as a predictive biomarker for LC for combination of RCTx with nimorazole and should therefore be further evaluated in experimental FMISO analysis and also in clinical trials using hypoxic cell radiosensitisation during RCTx.

OC-0131

miR-875-5p enhances radiation response of prostate cancer cells via EGFR suppression

R. El Bezawy[1], D. Cominetti[1], P. Gandellini[1], R. Valdagni[2], N. Zaffaroni[1]
[1]*Fondazione IRCCS Istituto Nazionale dei Tumori, Department of Experimental Oncology and Molecular Medicine, Milan, Italy*
[2]*Fondazione IRCCS Istituto Nazionale dei Tumori, Department of Radiation Oncology, Milan, Italy*

Purpose or Objective: There is increasing interest in defining a functional association between miRNAs, endogenous small non-coding RNA molecules that negatively regulate gene expression, and tumor radiation response, with the aim of rationally designing miRNA-based strategies to increase patient radiosensitivity. In this study, we investigated for the first time the ability of *miR-875-5p,* a miRNA the role of which in human cancer has not been so far investigated, to enhance the radiation response of prostate cancer (PCa) cells.

Material and Methods: The search for *miR-875-5p* targets relevant to radiation response was carried out by prediction algorithms and confirmed by the luciferase assay. *miR-875-5p* reconstitution by miRNA mimics in PCa cell lines (DU145 and PC-3) was used to elucidate its biological role. Radiation response in miRNA-reconstituted and control cells was assessed by clonogenic assay, immunofluorescence-based detection of nuclear γ-H2AX foci and single-cell electrophoresis comet assay.

Results: EGFR was predicted by 6 different algorithms and confirmed by luciferase assay as a direct target of *miR-875-5p.* Given the role of EGFR in determining tumor cell resistance to ionizing radiation by promoting epithelial-to-mesenchymal transition (EMT) and enhancing DNA-dependent protein kinase activity and DNA damage repair, we assessed whether *miR-875-5p* reconstitution in PCa cells was able to counteract EGFR-mediated radio-resistance. Indeed, miRNA ectopic expression significantly increased the sensitivity of both DU145 and PC-3 cell lines to radiation, as indicated by the reduced clonogenic cell survival. Consistently, the kinetics of accumulation and repair of γ-H2AX nuclear foci showed that the resolution of foci was significantly slower in *miR-875-5p* reconstituted cells compared to control cells. In addition, when a more direct assessment of radiation-induced DNA damage and repair at the single cell level was performed by the comet assay, DNA comet tail moments were found to be significantly extended in *miR-875-5p* reconstituted cells compared to control cells, confirming the ability of the miRNA to impair DNA repair processes. Ectopic expression of *miR-875-5p* in PCa cells was also able to counteract EMT as

indicated by changes in cell morphology, marked cytoskeleton architecture rearrangements, reduced migration ability and increased mRNA and protein levels of E-cadherin and ß-catenin, the two most important molecular players in the EMT process.

Conclusion: Overall, results from this study support the clinical interest in developing a novel therapeutic approach for PCa based on *miR-875-5p* reconstitution to increase response to radiotherapy.

OC-0132

FoxO proteins and non-functional p53 determine stemness and radiosensitivity of GBM-stem cells

E. Firat[1], G. Niedermann[1]
[1]*Uniklinik Freiburg, Dept. of Radiation Oncology, Freiburg, Germany*

Purpose or Objective: Dual inhibitors of PI3K and mTOR do not efficiently radiosensitize glioblastoma multiforme stem cells (GBM-SCs). However, p53-proficient GBM-SCs are more responsive than p53-deficient GBM-SCs. Here we found that either forkhead box O (FoxO) proteins or non-functional p53 maintain stemness and survival of primary GBM-SCs after combination treatment with gamma-IR and dual PI3K/mTOR inhibitors.

Material and Methods: Patient-derived GBM-SCs were cultured under stem cell culture conditions. Western blot was used for protein expression analyses. Sphere formation served as a surrogate assay for self-renewal and cell death was assessed flow cytometrically. Lentiviral RNA-knockdowns or overexpression of p53 and FoxO proteins were employed for molecular studies. ChiP assay was used to assess binding of FoxO transcription factors to the regulatory region of the sox2 gene.
Results: p53-proficient GBM-SCs lost stem cell markers and self-renewal ability and underwent differentiation a few days after the combination treatment with γIR and a PI3K/mTOR inhibitor (PI-103 or NVP-BEZ235); expression of FoxO proteins was also lost. In contrast, stem cell markers and FoxO proteins were not lost anymore upon p53 shRNA knockdown or in p53-deficient GBM-SCs. FoxO1/3 knockdown also caused reduced sphere formation and cell survival after the combination treatment in p53-proficient but not in p53-deficient GBM-SCs. Furthermore, FoxO1 and FoxO3 were found to bind to the sox2 regulatory region in GBM-SCs, and combined FoxO1/3 deletion abolished Sox2 expression which was confirmed with a novel synthetic FoxO1 inhibitor. Finally, FoxO overexpression prevented GBM-SC differentiation upon combination treatment with gamma-IR and dual PI3K/mTOR inhibitors.

Conclusion: Our results suggest that FoxO proteins are crucial for functional stemness and survival in p53-proficient GBM-SCs and that non-functional p53 can maintain these functions instead.

OC-0133

Radioresistance of glioblastoma stem-like cells is associated with replication stress

R. Carruthers[1], S. Ahmed[2], D. Biasoli[3], K. Strathdee[4], E. Hammond[3], A. Chalmers[2]
[1]*Beatson West of Scotland Cancer Centre, Clinical Oncology, Glasgow, United Kingdom*
[2]*University of Glasgow, Institute of Cancer Sciences, Glasgow, United Kingdom*
[3]*University of Oxford, Oxford Institute of Radiation Oncology, Oxford, United Kingdom*
[4]*University of Glasgow, Institte of Cancer Sciences, Glasgow, United Kingdom*

Purpose or Objective: Tumour recurrence in glioblastoma (GBM) patients is inevitable despite multi-modality treatment with surgery, radiotherapy and chemotherapy. Tumour recurrence is thought to be driven by a small population of glioblastoma stem-like cells (GSCs) that are resistant to conventional therapies. DNA damage response (DDR) signalling has been shown to be up-regulated in GSCs and implicated in radioresistance and treatment failure. However the cause of enhanced DDR signalling in GSCs and its contribution to radiation resistance and tumour recurrence is not well understood. The objectives of this study were to investigate the underlying cause of DDR upregulation and treatment resistance in GSCs and to identify novel therapeutic targets.

Material and Methods: A panel of primary GBM cell lines cultured under conditions to enrich for or deplete the tumour stem cell population (GSC vs bulk respectively) were utilised to investigate enhanced GSC DDR under basal conditions and after ionising radiation. Confirmatory studies were performed in cells sorted for the putative GSC marker CD133. The effects of a panel of small molecule DDR inhibitors on cell survival in GSC and bulk cells were explored.

Results: GSCs exhibited higher levels of total and activated DDR targets ATR, CHK1, ATM and PARP1 under basal conditions and were radioresistant compared to paired bulk populations. Augmented DDR in GSCs has been linked to increased reactive oxygen species levels by other authors, however we were unable to demonstrate this in our GSC cultures. Instead, we show that RPA is significantly higher in replicating GSCs and confirm by DNA fibre assays that GSCs and CD133+ cells have increased numbers of stalled replication forks, fewer new origins and slower DNA replication compared to bulk or CD133- populations, suggesting that replication stress may be important to constitutive DDR activation seen in GSCs. Importantly, inhibition of ATR or CHK1 was cytotoxic to GSCs and when combined with PARP inhibition caused DNA double strand breaks and reduced neurosphere formation.

Conclusion: This study demonstrates that replication stress is a hallmark of GSCs. We implicate replication stress in GSCs as the driver of enhanced DDR and radioresistance in GSCs and therefore a cause of tumour recurrence in GBM. This suggests that replication stress is a GSC specific therapeutic target, and we are able to demonstrate the effectiveness of inhibitors of replication stress response in targeting this treatment resistant tumour subpopulation.

OC-0134

Irradiation-induced plasticity of the cancer stem cell population in prostate cancer

C. Peitzsch[1], M. Cojoc[1], L. Hein[1], M. Baumann[1,2,3], A. Dubrovska[1,3]
[1]*OncoRay - Center for Radiation Research in Oncology, Medical Faculty Carl Gustav Carus- Technische Universität Dresden, Dresden, Germany*
[2]*Medical Faculty and University Hospital Carl Gustav Carus-Technische Universität Dresden, Department of Radiation Oncology, Dresden, Germany*
[3]*German Cancer Consortium DKTK, German Cancer Research Center DKFZ, Heidelberg, Germany*

Purpose or Objective: Although prostate cancer is the most common malignancy in men, the cellular and molecular mechanisms underlying tumor progression and therapy resistance remain poorly understood. Within this study we discovered cancer stem cell (CSC)-related properties, CSC plasticity and tumor heterogeneity as a source for radiotherapy resistance. Therefore, analysis of CSC-based biomarkers might be an important predictive tool for individualized radiotherapy and treatment.

Material and Methods: Global gene expression and membrane proteomic profiling of radioresistant sublines from established prostate cancer cell lines identified novel biomarker for prostate cancer radioresistance, which were validated in NMRI nu/nu mice *in vivo*, with immunohistochemical analysis of tumor sections and in short-term *ex vivo* cultures of primary prostate cancer tissue.

Results: Within this study we found that the aldehyde dehydrogenase (ALDH) activity is a predictive marker of a

radioresistant prostate cancer progenitor population with enhanced DNA repair capacity and activation of epithelial-mesenchymal transition (EMT). The activation of the WNT/ß-catenin signaling pathway was identified as a key molecular mechanism, which link CSC-related properties to radioresistance. We found that the ß-catenin/TCF transcriptional complex is directly activating the *ALDH1A1* gene transcription, and molecular targeting of the WNT pathway with XAV939 leads to radiosensitization. Moreover, our study revealed that irradiation causes long-term up-regulation of stem cell markers and induces tumor cell reprogramming. This phenotypic plasticity is associated with genetic and epigenetic changes induced by irradiation, such as the histone H3 methylation within the promotor sequence of the *ALDH1A1* gene. The inhibition of histone methylation by DZNep triggered radiosensitization by apoptosis induction *in vitro* and *in vivo*.

Conclusion: Our findings suggest that ALDH-positive CSCs contribute to tumor radioresistance, but these radioresistant properties are dynamic in nature. Therapeutic agents inhibiting tumor cell reprogramming may have the potential to increase the effectiveness of radiotherapy. Moreover, monitoring of CSC-related biomarker before and during the course of radiotherapy may be able to predict therapy response and clinical outcome.

Proffered Papers: Clinical 3: Lung

OC-0135

Can we select stage I NSCLC patients at high risk for early death prior to SBRT treatment?

R. Klement[1], I. Grills[2], J. Belderbos[3], J.J. Sonke[3], F. Mantel[4], A. Hope[5], M. Johnson[2], M. Werner-Wasik[6], M. Guckenberger[4]
[1]*Strahlentherapie Schweinfurt, Klinik für Strahlentherapie und Radioonkologie, Schweinfurt, Germany*
[2]*William Beaumont Hospital, Department of Radiation Oncology, Royal Oak, USA*
[3]*Antoni van Leeuwenhoek Hospital, The Netherlands Cancer Institute, Amsterdam, Netherlands Antilles*
[4]*University Hospital Zurich, Department of Radiation Oncology, Zurich, Switzerland*
[5]*University of Toronto, Princess Margaret Hospital, Toronto, Canada*
[6]*Thomas Jefferson University Hospital, Department of Radiation Oncology, Philadelphia, USA*

Purpose or Objective: This study analyzed whether short-term death of patients with peripheral stage I NSCLC can be predicted reliably to select a sub-group of patients, which will not have a benefit from SBRT and which can be referred to wait and see.

Material and Methods: 802 patients with early stage NSCLC treated with SBRT in 5 institutes for whom information on overall survival within the first six months after treatment was available were included in this analysis. The probability of dying within six months after treatment was modeled by multivariate logistic regression; this interval was chosen because death of early stage NSCLC is a rare event within six months after diagnosis. Model fitting was performed using the LASSO method which simultaneously serves to select the features most closely related to the outcome. The performance of the model that would be achieved on an independent dataset was estimated using double 10-fold cross validation (CV). Because with CV the estimation of test performance depends somewhat on the splitting of the data sets, double 10-fold CV was repeated 100 times, resulting in 1000 models from which the variance in the performance measure could be obtained. The variables age, gender, ECOG status, operability, FEV1 and Charlson comorbidity index (CCI) where considered for model building.

Results: Using different variable combinations for model building resulted in different sample sizes and model performances (Table 1). Common among all models was the identification of the CCI as the most frequently selected and thus most important variable predicting six-months death, with increasing values predicting higher probability of death. Gender was consistently the second-most frequently selected variable. Regressing on the individual components of the CCI with the LASSO method showed that presence of a second solid tumor was the most important predictor, followed by various forms of heart disease (Figure 1). Replacing the CCI by these individual components in model building confirmed the strong relation between the presence of a second tumor and early death, but led to a worse model performance than with the full CCI (Table 1). Overall the accuracy of all models predicting six-months death was poor with maximum AUC=0.62.

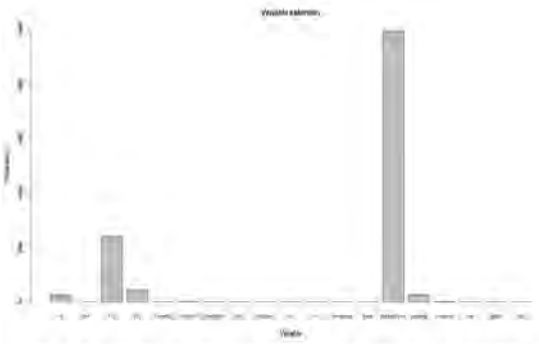

Figure 1: Results of variable selection by the LASSO method when using the individual components of the CCI for predicting death within six months after treatment. 10-fold CV was repeated 1000 times, resulting in a total of 1000 individual models. Shown is the frequency with which a variable was selected into a model.

Variables	(Age, Gender, ECOG,Operability,FEV1,CCI)	(Age, Gender,CCI)	(Age, Gender, MI, PVD, CVD, second tumor)
Sample size	655	801	801
Number of events	48	66	66
AUC	0.619±0.002	0.552±0.002	0.537±0.002
Accuracy [%]	61.0±0.1	56.5±0.2	56.1±0.1
Sensitivity [%]	66.7±1.1	57.5±1.4	57.3±1.0
Specificity [%]	55.2±1.1	55.4±1.4	54.9±0.8
Variables selected into more than 20% of models	CCI: 99.9%	CCI: 99.4% Gender: 69.1%	Secondary tumor: 99.8% PVD: 49.4% CVD: 34.7% Gender: 34.3% MI: 30.5%

Table 1: Results of the model fitting procedure applied to three sub-samples of the data. MI: Myocardial infarct; PVD: Peripheral vascular disease; CVD: Cardiovascular disease.

Conclusion: General patient characteristics together with comorbidity data, especially the history of a previous malignancy, can predict early death, however, prediction accuracy is insufficient to select patients to wait and see instead of offering SBRT as a curative treatment.

OC-0136

Primary Study Endpoint Analysis of NRG Oncology/RTOG 0813 Trial of SBRT for centrally located NSCLC

A. Bezjak[1], R. Paulus[2], L. Gaspar[3], R.D. Timmerman[4], W. Straube[5], W. Ryan[6], Y.I. Garces[7], A.T. Pu[8], A.K. Singh[9], G.M.M. Videtic[10], R.C. McGarry[11], P. Iyengar[12], J.R. Pantarotto[13], J.J. Urbanic[14], A.Y. Sun[15], M.E. Daly[16], I.S. Grills[17], D.P. Normolle[18], J. Bradley[19], H. Choy[20]
[1]*Princess Margaret Cancer Center, University of Toronto, Radiation Oncology, Toronto*
[2]*NRG Oncology Statistics and Data Management Center, Statistician, Philadelphia, USA*
[3]*University of Colorado, Radiation Oncology, Denver, USA*

[4]University of Texax Southwestern Medical Center, Radiation Oncology, Dallas, USA
[5]Washington University, Physicist, St. Louis, USA
[6]Procono Cancer Center under Thomas Jefferson University of Hospital, Radiation Oncology, East Stroudsburg, USA
[7]Mayo Clinic, Radiation Oncologist, Minnesota, USA
[8]Radiological Associates of Sacramento, Radiation Oncology, Sacramento, USA
[9]Roswell Park Cancer Institute, Radiation Onoclogy, Buffalo, USA
[10]Cleveland Clinic Foundation, Radiation Oncology, Cleveland, USA
[11]Univeristy of Kentucky, Radication Oncologist, Lexington, USA
[12]University Of Texas SouthWestern Medical Center, Radiation Oncologist, Dallas, USA
[13]Ottawa Hospital Cancer Center, Radiation Oncology, Ottawa, Canada
[14]Arizona Oncology Services Foundation, Radiation Oncology, Encinitas, USA
[15]Princess Margaret Cancer Center, Radiation Oncology, Toronto, Canada
[16]Univerity of California Davis, Radiation Oncology, Sacramento, USA
[17]Beaumont CCOP, Radiation Oncology, Royal Oak, USA
[18]University of Pittsburgh Cancer Institute, Statistician, Pittsburgh, USA
[19]Washington University, Radiation Oncology, St. Louis, USA
[20]University of Texas Southwestern Medical Center, Radiation Oncology, Dallas, USA

Purpose or Objective: NRG/RTOG 0813 is a phase I/II study designed to determine the maximal tolerated dose (MTD) and efficacy of SBRT for NSCLC with centrally located tumors. We hereby report the primary endpoint of the phase I portion of the study.

Material and Methods: Medically inoperable pts with biopsy proven, PET staged T1-2 (<5cm)N0M0 NSCLC and centrally located tumors (within or touching the zone of the proximal bronchial tree or adjacent to mediastinal or pericardial pleura) were successively accrued onto a dose-escalating 5 fraction SBRT schedule ranging from 10-12 Gy/fraction delivered over 1.5-2 weeks. Dose-limiting toxicity (DLT) was defined as any grade 3 or worse toxicity (per CTCAE v.4) occurring within first year, possibly, probably, or definitely related to treatment from a pre-specified list of cardiac, esophageal, respiratory or neurological toxicities. Any potential DLT within the initial year post-SBRT could have led to dose reduction for subsequent patients accrued, using TITE-CRM (time-to-event continual reassessment method) statistical design. MTD was defined as SBRT dose associated with a 20% probability of DLT.

Results: 120 pts were accrued Feb 2009 to Sept 2013 from 43 participating centers. Numbers (n) accrued into each cohort, n eligible for analysis (20 pts were excluded as they did not receive protocol treatment (12) or were ineligible (8)), and n evaluable for DLT analyses (11 not evaluable, 10 of whom died in the first year without a DLT) are shown in the table. Pts were elderly (median age 72), slightly more females (57%), majority had performance status 0-1 (84%). Most cancers were T1 (65%) and squamous cell (45%). Median follow up was 26.6 months. There were 5 events that met the definition of DLTs; Table details the protocol pre-specified DLTs and the worst treatment-related AEs (ie occurring at any time). MTD is 12.0 Gy/fr; Bayesian-based probability of DLT on this arm was 7.2% (95% CI 2.8 -14.4%). The grade 5 AEs occurred at a mean 13 mo postSBRT (range 5.5-14mo).

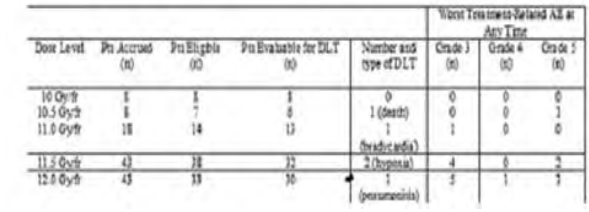

Dose Level	Pts Accrued (n)	Pts Eligible (n)	Pts Evaluable for DLT (n)	Number and type of DLT	Worst Treatment-Related AE at Any Time: Grade 3 (n)	Grade 4 (n)	Grade 5 (n)
10 Gy/fr	8	8	8	0	0	0	0
10.5 Gy/fr	8	7	6	1 (death)	0	0	1
11.0 Gy/fr	18	14	13	1 (bradycardia)	1	0	0
11.5 Gy/fr	43	38	32	2 (hypoxia)	4	0	2
12.0 Gy/fr	43	33	30	1 (pneumonitis)	5	1	1

Conclusion: The rates of toxicity pre-specified as DLT were relatively low. The highest dose level allowed by the protocol was reached, and associated with 7.2% rate of DLT. This phase I/II trial of SBRT provides data to inform patients of the potential toxicities with a 5 fraction SBRT schedule for centrally located NSCLC, but data on efficacy are still awaited.

OC-0137

Tumour size but not location determines survival and control of lung stereotactic body radiotherapy

M. Roach[1], S. Rehman[1], T. DeWees[1], J. Bradley[1], C. Robinson[1]
[1]Siteman Cancer Center, Radiation Oncology, Saint Louis, USA

Purpose or Objective: Patients with early stage non-small lung carcinoma (NSCLC) located centrally within the thorax present a therapeutic challenge with stereotactic body radiation therapy (SBRT). We compared outcomes of early stage NSCLC located in central and peripheral locations.

Material and Methods: A total of 472 patients with early stage NSCLC were identified from a prospective IRB-approved thoracic SBRT registry. Tumors were classified as central if they were within 2 cm of the proximal bronchial tree or immediately adjacent to the mediastinal or pericardial pleura. Peripheral tumors were treated to 54 Gy in 3 fractions, and central tumors to 50 or 55 Gy in 5 fractions. Patients were reviewed for overall survival (OS) calculated from completion of therapy and local failure (LF). The log-rank test and Cox regression were used to identify factors predictive of OS and LF.
Results: 127 patients had central tumors and 345 had peripheral tumors. Median follow-up was 30 months for living patients. For the entire cohort at 2 years, OS was 57% and LF was 10%. OS at 2 years was 50% for patients with central tumors and 60% for those with peripheral tumors (p=0.11). LF at 2 years was 19% for central lesions and 8% for peripheral lesions (p=0.08). On multivariate analysis, increasing tumor size (HR 1.21 per cm, 95% CI: 1.10-1.33, p<0.0001), increasing age-adjusted Charlson comorbidity score (HR 1.15 per point, 95% CI: 1.09-1.20, p<0.0001), and worse KPS (HR 10.1 per 10% loss, 95% CI: 10.1-10.2, p=0.0003), but not location predicted for worse OS. Only increasing tumor size (HR 1.37/cm, 95% CI: 1.06-1.78, p=0.02) predicted for LF on multivariate analysis.

Conclusion: The use of five SBRT fractions of 10-11 Gy for central early stage NSCLC results in similar outcomes as peripheral early stage NSCLC treated in three SBRT fractions of 18 Gy. Larger tumors result in worse outcomes suggesting the need for additional treatment strategies.

OC-0138

Apnea-like suppression of respiratory motion: first clinical evaluation

N. Peguret[1], M. Ozsahin[1], C. Beigelman[2], M. Zeverino[3], A. Durham[1], F. Duclos[1], K. Grant[4], B. Belmondo[4], J. Simons[4], O. Long[4], R. Moeckli[3], J. Prior[5], R. Meuli[2], J. Bourhis[1]
[1]Centre Hospitalier Universitaire Vaudois, Department of Radiation Oncology, Lausanne Vaud, Switzerland
[2]Centre Hospitalier Universitaire Vaudois, Department of Radiology, Lausanne Vaud, Switzerland
[3]Centre Hospitalier Universitaire Vaudois, Institute of Radiation Physics, Lausanne Vaud, Switzerland
[4]Centre Hospitalier Universitaire Vaudois, Department of Physiotherapy, Lausanne Vaud, Switzerland

[5]*Centre Hospitalier Universitaire Vaudois, Department of Nuclear Medicine, Lausanne Vaud, Switzerland*

Purpose or Objective: Pulmonary tumours are subject to respiratory motion which induces PET/MRI artefacts and imposes to use specific additional margins when treated by radiotherapy (RT). Gating techniques can solve these issues by stabilizing lung targets, and sustaining breath-holds in maximal inspiration (MI). However, these are limited by the patient's capacity to hold his breath. The purpose of this work was to implement a new non-invasive respiratory assistance using high frequency percussive ventilation (HFPV - Percussionaire®; Idaho, USA), and to report its first clinical use in maintaining breath holds long enough during chest imaging and complex RT treatments.

Material and Methods: ethical committee approval was obtained to conduct a clinical study, after evaluating its feasibility and tolerability in a cohort of volunteers. HFPV was applied in patients eligible for breast 3DRT, lung stereotactic RT, locally-advanced lung RT. Durations of breath hold obtained under HFPV for each clinical situation were reported. Dosimetric parameters in free breathing (FB), MI gating, or HFPV conditions were compared. The HFPV was also adapted and tested for thoracic MRI and PET.

Results: For volunteers, HFPV offered a mean duration time for apnea like breath hold of 10.6 minutes. Transferred in patients, this percussion assisted radiotherapy (PART) was applied with good tolerance in the first 3 patients without treatment breaks during the overall fractionated RT. All together, 50 RT fractions have been delivered under PART, and the mean duration of apnea-like breath hold necessary for "beam on" was 7.61 minutes (SD 2.3). HFPV offered a favorable dosimetric profile when compared to MI or FB for these 3 clinical RT situations (table). In addition, the HFPV markedly improved both PET and MRI image quality in detecting small pulmonary lesions (figure).

Conclusion: the HPFV allowed prolonged apnea-like breath hold that could be used both for fractionated RT and chest imaging. These preliminary results were very promising and prompt to develop larger studies to evaluate its reproducibility and potential clinical benefits both for radiotherapy and for lung PET/MRI imaging.

OC-0139

Expert knowledge vs. data-driven algorithms: Bayesian prediction models for post-radiotherapy dyspnea

T.M. Deist[1], A. Jochems[1], C. Oberije[1], B. Reymen[1], K. Vandecasteele[2], Y. Lievens[2], R. Wanders[1], K. Lindberg[3], D. De Ruysscher[4], W. Van Elmpt[1], S. Vinod[5], A. Dekker[1], P. Lambin[1]

[1]*MAASTRO Clinic, Department of Radiation Oncology MAASTRO Clinic- GROW – School for Oncology and Developmental Biology- Maastricht University Medical Centre, Maastricht, The Netherlands*

[2]*Ghent University Hospital, Department of Radiation Oncology, Ghent, Belgium*

[3]*Karolinska University Hospital, Karolinska Institutet, Stockholm, Sweden*

[4]*KU Leuven, Universitaire Ziekenhuizen Leuven, Leuven, Belgium*

[5]*University of New South Wales, South Western Sydney Clinical School, Liverpool, Australia*

Purpose or Objective: Moving away from guideline-based treatment to a more personalized approach requires accurate outcome prediction. Yet, physicians' predictions of survival and toxicity after lung radiotherapy are as good as flipping a coin (Oberije et al.,Radiother. Oncol. 2014). We hypothesize that the physicians' knowledge of complex interactions between clinical variables and treatment outcomes is a valuable resource for prediction modelling. Therefore, we created and compared expert-based and data-driven prediction models. The predicted endpoints are severe dyspnea (CTCAE dyspnea scores ≥ 2) and increases in the CTCAE dyspnea score after radiotherapy (RT). Severe dyspnea occurs in approximately 15% of all patients treated with lung radiotherapy and has a possibly severe impact on patients' quality of life.

Material and Methods: Data from 1152 lung cancer patients treated in clinical routine (2006-2015, partially incomplete data) were used. Seven experts selected causal links between 19 variables (patient, disease, treatment, and dose-related variables) and post-RT dyspnea to construct Bayesian Networks (BNs). Their individual choices, the consensus choices, and a data-driven algorithm were used to build BNs for both endpoints. 80% of the data were used for model building. Validation was performed for all models in terms of discrimination (Area under the Curve) in the remaining 20% of the data, isolated before modelling.

Results: Expert-based networks were more complex than algorithmically-constructed networks (range: 7-30 vs. 3-6 arcs) but their predictions for severe dyspnea in non-dyspneic patients were not significantly better (see 95% confidence intervals in table). Furthermore, all models besides expert model 6 were not different from chance as AUC confidence intervals include 0.5. Models predicting increases in CTCAE dyspnea scores performed better (all models' AUCs > 0.6) and different from 0.5 with 97.5% confidence. Among those, the data-driven approach performed significantly better than 3 of the 7 expert models. Consensus networks between experts did not improve the predictive performance.

	Predicting Severe Dyspnea (CTCAE dyspnea scores ≥2)			Predicting Dyspnea Score Increase			Number of Arcs
	AUC	AUC 95%CI	(AUC - $AUC_{Alg.}$) 95% CI	AUC	AUC 95%CI	(AUC - $AUC_{Alg.}$) 95% CI	
Expert 1	0.58	[0.42,0.73]	[-0.07,0.22]	0.63	[0.55,0.71]	[-0.21,-0.03]	30
Expert 2	0.61	[0.43,0.77]	[-0.14,0.32]	0.71	[0.63,0.78]	[-0.12,0.03]	9
Expert 3	0.49	[0.32,0.65]	[-0.19,0.15]	0.61	[0.53,0.69]	[-0.22,-0.07]	23
Expert 4	0.59	[0.45,0.73]	[-0.06,0.22]	0.61	[0.52,0.7]	[-0.21,-0.08]	22
Expert 5	0.65	[0.5,0.8]	[-0.05,0.32]	0.73	[0.65,0.81]	[-0.06,0.03]	20
Expert 6	0.69	[0.56,0.83]	[-0.03,0.39]	0.7	[0.62,0.78]	[-0.11,0.02]	14
Expert 7	0.57	[0.43,0.7]	[-0.08,0.2]	0.7	[0.61,0.78]	[-0.1,0.01]	7
Alg.	0.52	[0.38,0.66]	[0,0]	0.75	[0.67,0.83]	[0,0]	6 | 3

AUC and Brier scores in validation. CIs based on 1000 bootstraps.

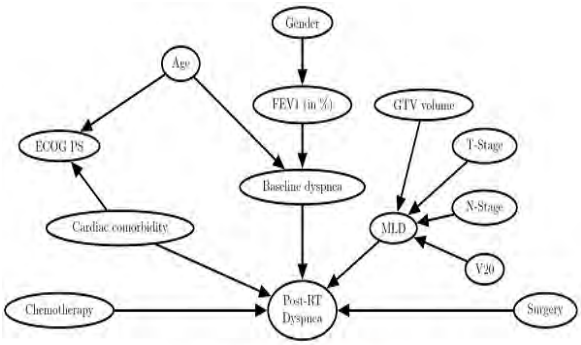

Bayesian Network constructed by expert 6.

Conclusion: The results suggest that reliable predictions of post-RT dyspnea scores ≥ 2 in non-dyspneic patients are not achievable with any of the presented models. Clinical routine appears to still miss appropriate biomarkers. In contrast, prediction modelling for post-RT increases in dyspnea is feasible with expert knowledge as well as data-driven algorithms. The comparison between expert- and data-driven modelling indicates that data-driven modelling can yield simpler models with similar performance as expert-driven modelling.

OC-0140

Management of patients with extensive-stage small-cell lung cancer: A European survey of practice

K. Haslett[1], D. De Ruysscher[2], R. Dziadziuszko[3], M. Guckenberger[4], C. Le Pechoux[5], U. Nestle[6], C. Faivre-Finn[7]

[1]*Institute of Population Health, Manchester University, Manchester, United Kingdom*

[2]*University Hospital Leuven, Radiation Oncology, Leuven, Belgium*

[3]Medical University of Gdansk, Oncology and Radiotherapy, Gdansk, Poland
[4]University Hospital Zurich, Radiation Oncology, Zurich, Switzerland
[5]Gustave Roussy, Radiation Oncology, Villejuif, France
[6]University Medical Center Freiburg, Radiation Oncology and Nuclear Medicine, Freiburg, Germany
[7]Institute of Cancer Sciences, Manchester University, Manchester, United Kingdom

Purpose or Objective: The role of thoracic radiotherapy (TRT) in extensive stage small-cell lung cancer (ES-SCLC) has been evaluated in a recent phase 3 randomised control trial. The results of the Chest Radiotherapy Extensive stage Small cell lung cancer Trial (CREST) were published in the Lancet (2015,385,36-42). This study showed that TRT did not significantly improve 1-year overall survival, which was the primary endpoint. However there was a significant improvement in 2-year overall survival, suggesting TRT should be considered for all patients with ES-SCLC who respond to chemotherapy. An additional analysis showed that in patients with a response but residual disease after chemotherapy, the difference in 1-year survival was significantly better after TRT (Lancet 2015,385,1292-3). We carried out a European survey to determine the impact of the publication on clinical practice.

Material and Methods: In May 2015 an electronic questionnaire of 34 items was composed using Select Survey software designed for running online surveys. Questions covered the use of TRT before and after the CREST study, evaluated the current practice of prophylactic cranial irradiation (PCI), including dose and fractionation, and asked whether practice was restricted based on performance status (PS) and age. The survey was distributed by email to one thoracic clinical/radiation oncologist per centre in 7 European countries. A reminder was sent to non-responders.

Results: This European-wide survey received 95 complete responses (UK n=42, Belgium n=23, Netherlands n=14, France n=8, Switzerland n=5, Germany n=2, Poland n=1). A response rate of 74% was achieved within the UK. Before the publication of the CREST study only 25% of centres were giving TRT routinely to patients who had responded to chemotherapy, compared to the current practice of 81%. Currently the preferred dose and fractionation of TRT is 30 Gy in 10 fractions in 70% of centres, however a wide variety of fractionations were used before the CREST publication. An upper limit of PS ECOG 2 is commonly applied to TRT (83 %). In the 18 centres (19%) not implementing TRT there were a wide variety of explanations with no single reason standing out. Regarding the practice of PCI in ES-SCLC, 96% of centres give PCI routinely if patients have responded to chemotherapy. Of these, 52% deliver 25Gy in 10 fractions and 44% deliver 20Gy in 5 fractions. An upper age limit was applied in 76% of all centres, the most common age limit being 75 (60 %). An upper limit for PS was applied in 88% of all centres, most commonly ECOG 2.

Conclusion: Following the publication of the CREST study there has been a dramatic increase in the use of TRT in patients with ES-SCLC who have responded to chemotherapy. The dose and fractionation schedule used in the study has widely been adopted as standard practice across Europe. There is also evidence of high consistency in European practice in the use of PCI in patients with ES-SCLC.

Proffered Papers: Clinical 4: Late breaking abstracts

OC-0141
Does an integrated boost increase acute toxicity in prone hypofractionated breast irradiation?

L. Paelinck[1], A. Gulyban[2], F. Lakosi[2], T. Vercauteren[1], W. De Gersem[1], B. Speleers[1], C. Monten[1], T. Mulliez[1], P. Berkovic[2], A. Van Greveling[1], P. Coucke[2], W. De Neve[1], L. Veldeman[1]
[1]University Hospital Ghent, Department of Radiation Oncology, Ghent, Belgium
[2]University Hospital Liège, Department of Radiation Oncology, Liège, Belgium

Purpose or Objective: To compare acute skin toxicity between prone whole-breast irradiation (WBI) with a sequential boost (SeqB) and a simultaneous integrated boost (SIB).

Materials and Methods: 167 patients were randomized between WBI with a SeqB or a SIB. 150 patients were treated at Ghent University Hospital (UZ Gent) and 17 at Liège University Hospital. All patients were treated in prone position to 40.05 Gy in 15 fractions to the whole breast. In the SeqB arm a median dose of 10 Gy in 4 fractions (negative surgical margins) or 14.88 Gy in 6 fractions (transsection) was prescribed to the PTV_boost (CTV to PTV margin of 5 mm). In the SIB arm a median dose of 46.8 or 49.95 Gy (negative and positive surgical margins, respectively) was prescribed to the CTV_boost with dose decay to 40.05 Gy in the first 2 cm around the CTV_boost. In the SeqB arm dose parameters were calculated on the summed plan (WBI + boost). For comparison, a PTV_optim was created including the PTV for WBI more than 2 cm away from the CTV_boost as illustrated in Figure 1.

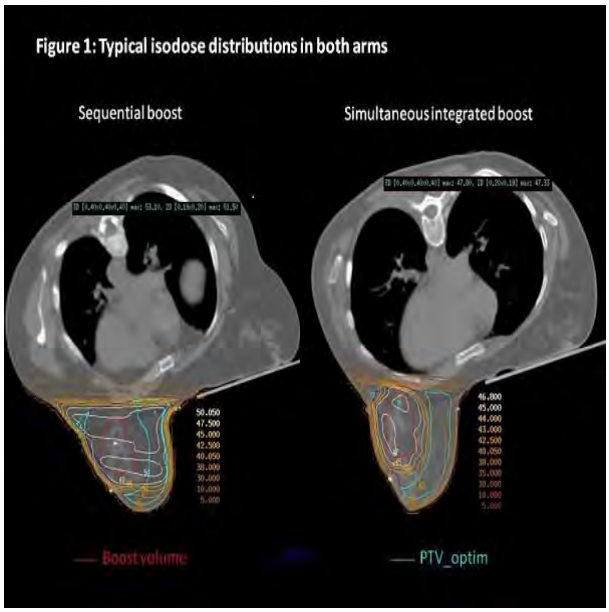

Dermatitis was scored using the Common Toxicity Criteria for Adverse Events (CTCAE). Desquamation was scored as: none, dry or moist; pruritus as absent or present.

Results: The analysis of dose parameters was done on 146 patients treated at UZ Gent. Reasons for excluding patients were electron boost (2), 3 different plans on 3 different CTs (1) and changed treatment arm due to machine breakdown (1). This latter patient was excluded from the toxicity analysis as well. Patient age was the only significantly different parameter between treatment arms (mean age 59.6 ± 11.0 vs 55.7 ± 10.4 years, p=0.0210). Dose coverage of the CTV_boost was slightly better in the control arm (D95 of 98 ± 1% vs 97 ± 2%, p<0.01). The volume of the PTV_optim and the skin receiving more than 105% of the prescription dose were significantly higher in the SeqB-arm than in the SIB-arm (27 ± 20% vs 9 ± 6% for the PTV_optim and 394 ± 216cc vs 201 ± 125cc for the skin, both p<0.01).In both arms, 6/83 patients developed moist desquamation (primary endpoint). Grade 2/3 dermatitis was significantly more frequent in the SeqB arm (38/83 vs 24/83 patients, p=0.037). In the SIB and SeqB arm, respectively, 36 and 51 patients developed pruritus (p=0.015). The incidence of edema was lower in the SIB arm (59 vs 68 patients), but not statistically significant (p=0.071).

Conclusion: Acute toxicity is not increased using a SIB in prone hypofractionated WBI. In contrast, grade 2/3 dermatitis and pruritus are significantly less frequent. With

our SIB-technique, high dose regions outside the boost region are smaller than with a SeqB.

OC-0142

Hypo- vs normofractionated radiation of early breast cancer in the randomised DBCG HYPO trial

B.V. Offersen[1], E.H. Jacobsen[2], M.H. Nielsen[3], M. Krause[4], L. Stenbygaard[5], I. Mjaaland[6], A. Schreiber[7], U.M. Kasti[8], M.B. Jensen[9], J. Overgaard[10]

[1]*Aarhus University Hospital, Dept Oncology, Aarhus C, Denmark*
[2]*Lillebaelt Hospital, Dept Oncology, Vejle, Denmark*
[3]*Odense University Hospital, Dept Oncology, Odense, Denmark*
[4]*University Clinic Carl Gustav Carus- Technical University Dresden, Clinic for Radiotherapy and Oncology, Dresden, Germany*
[5]*Aalborg University Hospital, Dept Oncology, Aalborg, Denmark*
[6]*Stavanger University Hospital, Dept Oncology, Stavanger, Norway*
[7]*Academic Teaching Hospital Dresden-Friedrichstadt, Dept Oncology, Dresden, Germany*
[8]*Kristiansand Hospital, Dept Oncology, Kristiansand, Norway*
[9]*Copenhagen University Hospital, DBCG- Rigshospitalet, Copenhagen, Denmark*
[10]*Aarhus University Hospital, Dept Experimental Clinical Oncology, Aarhus C, Denmark*

Purpose or Objective: Based on poor results using hypofractionated adjuvant radiotherapy (RT) of early breast cancer (BC) 50 Gy/25 fr. has been Danish Breast Cancer Group (DBCG) standard since 1982. Results from the UK and Canada stimulated a renewed interest in hypofractionation, and the non-inferiority DBCG HYPO trial was initiated. The hypothesis was that 40 Gy/15 fr (2.67 Gy/fr, 3 weeks) does not result in more grade 2-3 breast induration than 50 Gy/25 fr (2.0 Gy/fr, 5 weeks) 3 years post RT.

Materials and Methods: From 2009-2014 1868 patients >40 years operated with breast conservation for early pT1-2 pN0-1(mic) BC (n=1617) or DCIS (n=251) were enrolled irrespective of breast size, systemic therapy and boost, and randomized 50 Gy/25 fr vs. 40Gy/15 fr. Strata were institution, breast size (≤ 600 ml vs. > 600 ml), systemic therapy and boost. The primary endpoint was grade 2-3 induration 3 years post RT, secondary endpoints were other normal tissue responses, genetic risk profile for RT-induced fibrosis and recurrences. ClinicalTrial NCT00909818.

Results: 942 pts (50.4%) were assigned to the 50 Gy group and 926 (49.6%) to the 40 Gy group. Median age was 59 years (range 39-83). Median follow up was 3 years. The analysis was by intention to treat. Results are actuarial 3 year rates using morbidity in 1801 pts 1 yr post RT as baseline. 1086 pts (60%) had 3 year scores of morbidity and the rate of grade 2-3 induration was 12.2%±1%. Grade 2-3 induration was seen in the 50 Gy group in 119 out of 904 pts with the rate 14.2%±1.4%, and in the 40 Gy group in 97 out of 897 pts, the rate being 10.1% ±1%, representing a HR 1.27 (95% CI 0.97-1.66), p=0.08. 859 pts (48%) had small breasts with a rate of grade 2-3 induration of 9.8%±1% compared to 14.3%±1% among 942 pts with large breasts, HR 1.56, (95% CI 1.18-2.05), p=0.001. Among the 653 pts (36%) treated with chemotherapy (CT) the rate of grade 2-3 induration was 12.4%±1%, whilst in the 1148 pts with no CT the rate was 11.8%±2%, HR 0.98 (95% CI 0.74-1.30), p=0.90. In 423 pts (23%) treated with sequential boost (10-16 Gy/5-8 fr) the rate of grade 2-3 induration was 12.4%±1% compared to 12.1%±1% among 1378 pts with no boost, HR 0.93 (95% CI 0.67-1.29), p=0.65. Multivariate analysis using grade 2-3 induration at 3 yr as endpoint and including hypofractionation, breast size, chemotherapy and boost identified large breast size as the only independent risk factor. Overall the 3 yr risk of loco-regional recurrence was 0.3%±0.1%. In the 50Gy / 40 Gy group loco-regional recurrence was reported in 2 pts / 4 pts, distant failure 4 pts / 3 pts, new contralateral cancer or DCIS 2 pts / 3 pts.

Conclusion: Moderately hypofractionated whole breast irradiation in early node-negative BC or DCIS does not result in more grade 2-3 induration compared to normofractionated therapy. Large breast size is an independent risk factor for developing induration. The 3 yr loco-regional recurrence risk is very low.

OC-0143

A Bayesian randomisation trial of IMRT vs. PSPT for locally advanced non-small cell lung carcinoma

Z. Liao[1], J. Lee[2], R. Komaki[1], D. Gomez[1], M. O'Reilly[1], P. Allen[1], F. Fossella[3], J. Heymach[3], N. Choi[4], T. Delaney[4], S. Hahn[1], C. Lu[3], J. Cox[1], R. Mohan[5]

[1]*The University of Texas MD Anderson Cancer Center, Radiation Oncology, Houston- TX, USA*
[2]*The University of Texas MD Anderson Cancer Center, Biostatistics, Houston- TX, USA*
[3]*The University of Texas MD Anderson Cancer Center, Thoracic Medical Oncology, Houston- TX, USA*
[4]*Masachusetts General Hospital- Harvard University School of Medicine, Radiation Oncology, Boston, USA*
[5]*The University of Texas MD Anderson Cancer Center, Radiation Oncology Physics, Houston- TX, USA*

Purpose or Objective: We report preliminary results from a Bayescian randomized trial of IMRT vs. PSPT , both given with concurrent chemotherapy, for locally advanced (stage II-IIIB) NSCLC. The purpose of the trial was to assess and compare the incidence and time to development of treatment failure defined as (1) grade≥3 pneumonitis or (2) local failure, whichever occurred first in 12 month.

Materials and Methods: The sample size for this trial (n=150) was based on the assumption that incidence would be log-normally distributed and that IMRT would produce event rates of 30% at 6 mo and 40% at 12 mo, and PSPT would reduce the event rate by 10%. The Bayescian design was chosen so that more patients will be randomly allocated to the more effective of the two treatments. All patients must have been candidates for concurent chemoradiation, and all underwent 4D CT-based treatment planning. An IMRT and a PSPT plan were created for each patient. Patients were eligible for randomization only if both plans satisfied normal tissue constraints at the same prescription dose (74 Gy (RBE) if achievable , otherwise 66 Gy (RBE), where RBE is 1 for photons and 1.1 for protons)

Results: Total 147 patients who were randomized to IMRT (n=90) or PSPT (n=57) and treated according to randomization were included for this analysis. Demographic characteristics were well balanced between the two arms. The GTV and PTV volumes were bigger in the PSPT arm though the difference was not statisically significant. More patients in PSPT arm received higher tumor dose. Patients in PSPT arm had larger volume of the lung receiving≥30 -80 Gy (RBE) compared with IMRT patients, presumably due to the larger target volume and 3D nature of PSPT. The incidence of protocol failure at 12 month were 20.7%, 15.6%, and 24.6% in all, in IMRT, and in PSPT patients, respectively. The median failure free survival times were 67.6, 67.6, and 69. 8 months in all, in IMRT, and in PSPT patients, respectively. Total of 12 patients developed grade ≥3 or higher RP, 6 in each arm. Two of the 6 patients had grade 5 RP in IMRT arm. The incidences of grade≥3 RP were 8.7%, 7.2%, and 11.0% in all, in IMRT, and in PSPT patients, respectively.

Conclusion: Considerably fewer events occurred in the evaulable randomized patients than were expected from historical experience. No statistical differences were found between IMRT vs. PSPT in the incidence of treatment failure, grade ≥3 pneumonitis, or local failure. Future analyses will involve comparing data from CT and PET images, blood samples and symptoms and their correlations with dose distributions to clarify factors affecting outcomes and to determine how physical and biological uncertainties affect proton dose distributions. *Supported in part by NCI grants P01 CA021230 and U19 CA021239.

OC-0144

Maximum response and PCI are important prognostic factors in LD SCLC patients staged with cMRI

C. Eze[1], O. Roengvoraphoj[1], M. Niyazi[1], S. Gerum[1], G. Hildebrandt[2], R. Fietkau[3], C. Belka[1], F. Manapov[1]

[1]*Ludwig-Maximilian University Munich, Department of Radiation Oncology, Munich, Germany*

[2]*University of Rostock, Department of Radiation Oncology, Rostock, Germany*

[3]*Friedrich-Alexander University Erlangen-Nuernberg, Department of Radiation Oncology, Erlangen, Germany*

Purpose or Objective: The role of prophylactic cranial irradiation (PCI) in limited disease (LD) small-cell lung cancer (SCLC) has proven to significantly decrease the incidence of brain metastases (BMs) with only modest improvement of overall survival.

Materials and Methods: To evaluate the impact of PCI on survival we reviewed 179 LD SCLC patients treated with definitive chemoradiotherapy (CRT) in the concurrent or sequential setting. PCI was applied in the partial and complete responders exclusively provided contrast-enhanced cranial magnetic resonance imaging (cMRI) before and after primary treatment showed no signs of occult BMs. Correlation between PCI and time to progression (TTP) as well as overall survival (OS) was analysed. Kaplan-Meier analysis, uni- and multivariate Cox regression were used to describe survival within subgroups defined by treatment response and application of PCI.

Results: Concurrent and sequential chemoradiotherapy CRT was applied in 71 (40%) and 108 (60%) patients, respectively. In 58 (32%) patients metachronous BMs were detected. PCI was applied in 71 (39%) patients. 15 patients developed BMs after PCI. Median TTP and OS in responders treated with PCI were 812 and 801 compared to 355 (range: 284 - 456) ($p < 0.0001$, log-rank test) and 385 (range: 318 – 452) ($p < 0.0001$, log-rank test) days in the rest of the patient cohort. In multivariate analysis, application of PCI in treatment responders comprehensively staged with cMRI was a variable that significantly correlated with TTP (HR 2.16 CI HR 1.37-3.42, $p < 0.001$) and OS (HR 1.89 CI HR 1.37-2.63, $p < 0.0001$) after adjustment of other patient- and treatment-related factors.

Conclusion: In this LD SCLC patient cohort comprehensively staged with cMRI, achievement of maximum treatment response and application of PCI significantly affects time to progression and overall survival.

OC-0145

Preoperative radiotherapy with an integrated boost compared to chemoradiotherapy for rectal cancer.

M. De Ridder[1], A. De Paoli[2], E. Delmastro[3], F. Munoz[4], S. Vagge[5], D. Norkus[6], H. Everaert[1], G. Tabaro[2], E. Garibaldi[3], U. Ricardi[4], E. Borsatti[2], T. Gevaert[1], P. Gabriele[3], G. Boz[2], A. Sermeus[1], M.A. Mahé[7], B. Engels[1]

[1]*Universitair Ziekenhuis Brussel, Department of Radiotherapy, Brussels, Belgium*

[2]*National Cancer Institute Aviano, Department of Radiation Oncology, Aviano, Italy*

[3]*IRCC Candiolo, Department of Radiation Oncology, Candiolo, Italy*

[4]*University of Torino, Department of Oncology, Torino, Italy*

[5]*IRCCS San Martino-IST Genoa, Department of Radiation Oncology, Genoa, Italy*

[6]*National Cancer Institute, Department of Radiotherapy, Vilnius, Lithuania*

[7]*Institut de Cancérologie de l'Ouest, Department of Radiotherapy, Nantes, France*

Purpose or Objective: Preoperative chemoradiotherapy (CRT) has been established as the standard treatment for T3-4 rectal cancers. In a phase II trial, we reported limited toxicity and excellent local control using image-guided and intensity-modulated RT (IG-IMRT) with a simultaneous integrated boost (RTSIB) instead of concomitant chemotherapy. The present multicentric randomized trial compares this strategy to CRT. In addition, the neutrophil-to-lymphocyte ratio (NLR) and C-reactive protein (CRP) were examined as a prognostic immunoscore in a subset of patients.

Materials and Methods: cT3-4 rectal cancer patients were randomly assigned to receive either preoperative IG-IMRT 46Gy/23 fractions plus capecitabine 825 mg/m2 twice daily (CRT-arm) or IG- IMRT 46Gy/23 fractions with a SIB to the rectal tumor up to a total dose of 55.2 Gy (RTSIB- arm). Metabolic tumor activity reduction, by measuring the percentage of SUVmax difference (Response Index = RI) on sequential 18-fluorodeoxyglucose positron emission tomography (FDG-PET), was the primary endpoint. We assessed whether RTSIB was non-inferior to CRT with a non-inferiority margin of -10% for RI.

Results: A total of 174 patients were randomly assigned to the CRT-arm (n=89) or RTSIB- arm (n=85). A consort flow diagram is presented in Figure 1. The RI difference between RTSIB and CRT was -2.9% (95% CI, -10.1% to 4.3%). The ypCR rate was 24% with CRT compared to 14% with RTSIB (p=0.13). There was no significant difference in sphincter preservation (75% vs 68%, p=0.29). The R0 resection rate was 98% in the CRT-arm and 97% in the RTSIB-arm. Acute grade 3 toxicity was 6% and 4% in the CRT- and RTSIB-arm, respectively. A detailed analyses of early adverse events is shown in Table 1. The highest quartiles of NLR and CRP identified high-risk patients in terms of disease free and overall survival.

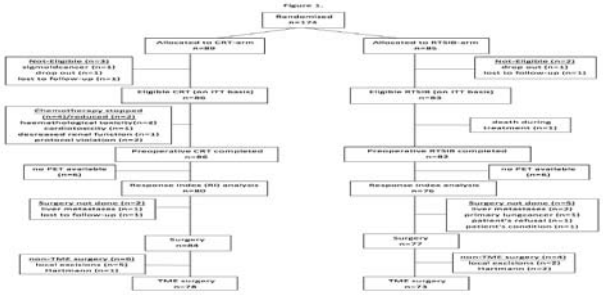

Table 1. Early Adverse Events

	CRT (n=86)		RTSIB (n=82)		p-value
Grade	2	3	2	3	
	No. of Patients (%)	No. of Patients (%)	No. of Patients (%)	No. of Patients (%)	
Gastrointestinal	36 (42)	1 (1)	35 (43)	2 (2)	.91 (.53)
Diarrhea	17 (20)	0	17 (21)	1 (1)	.88 (.30)
Enteritis (abdominal pain)	18 (21)	0	10 (12)	0	.13
Proctitis	13 (15)	1 (1)	18 (22)	1 (1)	.25 (.97)
Urinary	7 (8)	0	11 (13)	0	.27
Dysuria	4 (5)	0	10 (12)	0	.08
Urinary frequency	5 (6)	0	4 (5)	0	.79
Haematology	3 (3)	1 (1)	2 (2)	0	.69 (.33)
Anemia	0	1 (1)	1 (1)	0	.30 (.33)
Leucopenia	3 (3)	1 (1)	0	0	.09 (.33)
Thrombopenia	0	0	1 (1)	0	(.30)
Other					
Hand-foot syndrome*	0	0	0	0	
Radiation dermatitis	14 (16)	2 (2)	10 (12)	1 (1)	.45 (.59)
Vaginal mucositis	2 (2)	2 (2)	1 (1)	0	.59 (.16)
Overall toxicity score	43 (50)	5 (6)	46 (56)	3 (4)	.43 (.51)

* 5 patients (6%) in the CRT-arm experienced grade 1 hand-foot syndrome
p-value from test grade 2 (grade 3)

Conclusion: Preoperative CRT is well tolerated when IG-IMRT is used. RTSIB represents an attractive alternative to CRT for patients with a contra-indication for chemotherapy. The immunological landscape of colorectal cancer shapes novel possibilities for risk assessment.

OC-0146

The PROS-IT CNR study: comorbidities and medications at the time of diagnosis of prostate cancer

S. Magrini[1], U. Ricardi[2], F. Bertoni[3], R. Corvò[4], E. Russi[5], R. Santoni[6], W. Artibani[7], P. Bassi[8], S. Bracarda[9], G. Conti[10], M. Gacci[11], P. Graziotti[12], S. Maggi[13], V. Mirone[14], R. Montironi[15], G. Muto[16], M. Noale[13], S. Pecoraro[17], A. Porreca[18], A. Tubaro[19], V. Zagonel[20], F. Zattoni[21], G. Crepaldi[13]

[1]*Spedali Civili di Brescia, Radiation Oncology University Department, Brescia, Italy*

[2]*Turin University, Radiation Oncology, Turin, Italy*

[3]*AIRO - Italian Society for Radiation Oncology, Prostate Group of AIRO - Italian Association for Radiation Oncology, Rome, Italy*

[4]*AOU IRCCS San Martino - IST National Cancer Research Institute and University, Department of Radiation Oncology, Genua, Italy*

[5]Azienda Ospedaliera "Santa Croce", Radiation Oncology, Cuneo, Italy
[6]University "Tor Vergata", Radiation Oncology, Rome, Italy
[7]Azienda Ospedaliera Universitaria Integrata and University of Verona, Urologic Clinic- Department of Oncological and Surgical Sciences, Verona, Italy
[8]Catholic University, Department of Urology, Rome, Italy
[9]Ospedale S Donato- AUSL 8, Medical Oncology, Arezzo, Italy
[10]S Anna Hospital, Department of Urology, Como, Italy
[11]University of Florence, Department of Urology, Florence, Italy
[12]Ospedale S. Giuseppe, Urology Department, Milano, Italy
[13]CNR, Neuroscience Institute- Aging Branch, Padua, Italy
[14]University Federico II, Department of Urology, Naples, Italy
[15]Polytechnic University of the Marche Region, Section of Pathological Anatomy, Ancona, Italy
[16]Campus Bio-Medico University, Department of Urology, Rome, Italy
[17]Malzoni Center, Department of Nephrourolog, Avellino, Italy
[18]Abano Terme General Hospital, Department of Urology, Padua, Italy
[19]University of Rome La Sapienza - S Andrea Hospital, Urology, Rome, Italy
[20]Istituto Oncologico Veneto IOV – IRCCS, Medical Oncology, PaduaPadua, Italy
[21]Padua University, Urology Clinic, Padua, Italy

Purpose or Objective: PROS-IT is a national, multicenter, observational prospective cohort study on prostate cancer (PCa) coordinated by the Italian National Research Council, aiming at a comprehensive evaluation of the impact of PCa and its treatment in an unselected aging population. Present analysis evaluates the frequencies of the different comorbidities and medications in the study population at diagnosis.

Materials and Methods: 1684 patients (pts) consecutively enrolled 9/2014 to 7/2015 in 96 Institutions were submitted to a structured interview to record comorbidities and drugs assumption. The severity of comorbidities was measured with the Cumulative Illness Rating Scale (CIRS). Quality of life (QoL) was assessed by the SF-12 questionnaire (PCS = Physical and MCS = Mental Component Summary) and through the Italian UCLA P Ca Index (Function/Bother: UF,UB=Urinary , SF,SB=Sexual , BF,BB=Bowel). Differences between pts enrolled by Urology [URO] and Radiation Oncology Centers [RO] were assessed with logistic regression and/or general linear models.

Results: 996/1684 (59.1%) and 688/1684 (40.9%) pts were respectively enrolled by URO and RO Centers; CIRS data were available for 1637 pts. RO pts were older (average 71.9 yrs vs 66.4, p<0.0001), with more advanced T category (T1 cases: 38% vs 54.6%, p<0.0001). 445/1684 (27.2%) pts suffered from vascular, lymphatic or hematopoietic moderate, severe or very severe (MSVS) diseases; 304/1684 (18.6%) from heart MSVS disease; 231/1684 (14.2%) had gastro-intestinal problems; 163/1684 (10%) neurological diseases. The presence of ≥3 MSVS comorbidities had a significant negative impact on PCS, MCS, UB, BF and BB, SF if compared to 0-2 MVSV comorbidities (p<0.001).Diabetes was more frequent in RO pts than in URO ones (18.4% vs.11.4%, p=0.0082); MSVS gastrointestinal disease (18.8% vs. 7.5%), abdominal hernia (5.7% vs. 4.8%), and neurological disease (11.4% vs. 7.9%) in URO pts. 74.3% of the pts use drugs for vascular disease, 36.7% antithrombotic agents, 34.2% digestive drugs, 14.4% hypoglycemic drugs, 31.6% drugs for low urinary tract symptoms. A significant difference between URO and RO populations in the use of antithrombotic agents was evident: 32.5% URO vs. 44% RO (p=0.0377).

Conclusion: This study shows that number and severity of comorbidities had a negative impact on QoL at the time of diagnosis of PCa. Moreover, men enrolled in URO and RO Centers present a different pattern of associated diseases/medications.

Proffered Papers: Brachytherapy 2: EYE GI

OC-0147

Organ preservation in T2 T3 NX M0 rectal. French results using the new Papillon 50TM machine

J.P. Gérard[1], A. Frin[2], J. Doyen[1], N. Barbet[3], R. Coquard[4], K. Benezery[1], S. Marcié[5]
[1]Centre Antoine Lacassagne, Radiotherapy, Nice, France
[2]CHU Nice, Gastroenterology, Nice, France
[3]Centre Radiotherapie, Radiotherapy, Macon, France
[4]Centre Bayard, Radiotherapy, Lyon-Villeurbanne, France
[5]Centre Antoine Lacassagne, RadioPhysic, Nice, France

Purpose or Objective: Contact X Ray Brachytherapy (CXB) was pioneered in France for conservative treatment of rectal cancer using the Philips RT 50TM machine. Since 2009 the new Papillon 50TM was manufactured. It delivers high dose rate (20 Gy/ mn) well targeted dose (30 Gy) into the rectal tumor using an endoscopic approach. For T2 T3 CXB is always combined with external beam Radiotherapy(EBRT) or with chemoradiotherapy (CRT). Three centers have been treating patients in France with such regimen in Lyon-Villeurbanne, Mâcon and Nice.

Material and Methods: All patients presented adenocarcinoma of the distal or middle rectum. Staging used Digital examination, endoscopy, MRI and or Endorectal ultrasound. CXB dose was 90Gy in 3 fractions (Day 1- 14 -28) and EBRT delivered 50 Gy/25 fr/5 weeks usually with concurrent capecitabine (800 mg/m2 BID). After clinical complete response (cCR) either watch and Wait (W§W) or Local excision (LE) was proposed.

Results: Between 2009 and 2014, 44 patients were treated. All these patients were either high surgical risk, refusal of surgery or referred after MDT approval for such a conservative approach Results are shown in Table .

Centre	N° pts	T2	T3	cCR	Loc. Rec.	Organ Preserv	Surv. 3 years
Mâcon	14	6	8	10	3	9	75%
Nice	22	13	9	20	2	21	70%
Villeurbanne	8	6	2	8	1	7	87%
Total	44	25	19	89% (38)	13% (6)	83% (37)	77%

Conclusion: The present early results achieved with the Papillon 50 machine are at least equivalent to the previous one using Philips RT 50. CXB technique is validated in France for rectal cancer since 2008 (HAS) and recently in UK (NICE). Organ preservation using CXB in frail, elderly patients is a well admitted treatment and the ongoing OPERA trial is aiming at showing its benefit in operable patients. Gerard JP et al. Acta Oncol. 2015 Apr;54(4):545-51.

OC-0148

Evaluation of EBRT and HDRBT for inoperable rectal cancer patients: an update of the HERBERT study

E.C. Rijkmans[1], L.A. Velema[1], A. Cats[2], K.J. Neelis[1], Y.M. Van der Linden[1], R.A. Nout[1], B. Van Triest[3], J. Buijsen[4], T. Rozema[5], M. Ketelaars[1], C.A.M. Marijnen[1]
[1]Leiden University Medical Center LUMC, Department of Radiotherapy, Leiden, The Netherlands
[2]The Netherlands Cancer Institute, Department of Gastroenterology and Hepatology, Amsterdam, The Netherlands
[3]The Netherlands Cancer Institute, Department of Radiotherapy, Amsterdam, The Netherlands
[4]MAASTRO Clinic, Department of Radiotherapy, Maastricht, The Netherlands
[5]Verbeeten Institute, Department of Radiotherapy, Tilburg, The Netherlands

Purpose or Objective: TME surgery, with or without pre-operative (chemo-)radiotherapy is the standard of care in patients with resectable rectal cancer. In patients unfit for surgery, radiotherapy alone is often used with palliative intent. However, complete response can be achieved when high doses are administered. In this study we examined the feasibility of external beam radiotherapy (EBRT) followed by an endorectal brachytherapy boost in elderly patients, unfit for surgery. Primary results, presented at ESTRO 2014, are now complemented with response assessment and long-term FU at 3 years.

Material and Methods: A dose finding feasibility study was performed from 2007 to 2013 in two hospitals in inoperable rectal cancer patients. Treatment consisted of EBRT (13x3 Gy) followed by 3 weekly applications of intraluminal high dose rate brachytherapy (HDRBT)starting 6 weeks after EBRT. The starting dose level was 3x5 Gy with escalation of 1 Gy per fraction if acute toxicity was acceptable. Toxicity was acceptable if <2/6 patients or <3/9 patients exhibited dose limiting toxicity (DLT), defined as grade 3 proctitis (CTCAE v 3.0), within 6 weeks after HDRBT. Secondary endpoints were severe treatment-related late toxicity, clinical tumor response and progression free survival (PFS). Clinical tumor response was evaluated based on all available endoscopy pictures and defined as complete clinical response (CR), partial response (PR), stable disease (SD) or progression (PD).

Results: Thirty-eight patients with a mean age of 81 years, entered the study of whom 36 received HDRBT. Two patients died directly after HDRBT and 3 patients refused follow-up endoscopies, leaving 31 patients for response evaluation. At time of current analyses 13 patients were still alive, with a median FU of 30 months. Primary endpoint was reached at the 8 Gy dose-level with 3/9 patients showing a DLT. Response was observed in 25 patients (80.6%); of the 18 patients achieving a CR, 6 developed progressive disease later on. Of the 7 patients with PR, 4 showed progression, whereas this occurred in 5/6 patients with SD. Median time to progression was 6.3 months. PFS at 1,2 and 3 years was 65.6%, 46.4% and 22.1% respectively. Late treatment related grade 3/4 toxicity occurred in 13 patients, of those 9 patients also showed progressive disease. Outcomes related to doselevel are displayed in table 1.

Table 1. Outcomes

Dose level	5Gy	6Gy	7Gy	8Gy
Dose limiting toxicity	1/6	0/5	0/11	3/9
Late toxicity grade 3/4	2/6	1/5	5/13	5/9
Complete response	2/7	1/4	9/12	7/9
Progression	4/7	2/4	5/12	4/9

‡due to missing data number of patients per evaluation group could vary.

Conclusion: A combination of EBRT and HDRBT is feasible in inoperable elderly patients with acceptable acute toxicity and a promising overall response rate of 80.6%. However, given the observed toxicity, a randomized trial comparing EBRT with or without HDRBT boost is necessary. In this trial the clinical relevance of the added tumor control in light of additional toxicity from HDRBT will be evaluated in this fragile population.

OC-0149

Patterns of relapse in rectal cancer patients following pre-operative high dose rate brachytherapy

T. Vuong[1], F. Desjardins[2], V. Pelsser[3], T. Niazi[1], A. Robillard[2], M. Leventhal[3]

[1]*Jewish General Hospital, Radiation Oncology, Montreal, Canada*

[2]*Centre Hospitalier Pierre-Boucher, Radiology, Longueuil, Canada*

[3]*Jewish General Hospital, Radiology, Montreal, Canada*

Purpose or Objective: Radiation therapy is an established neoadjuvant modality for patients with advanced rectal cancer. As the quality of surgery improved with Total Mesorectal Excision surgery (TME), radiation is now being challenged, as the number of patients needed to treat remains high when facing long-term normal tissue toxicity in the pelvis. High dose rate endorectal brachytherapy is a highly targeted form of radiation based on quality imaging with magnetic resonant imaging and was introduced in our institution along with TME. Unlike external beam radiation therapy, the clinical target volume is aiming mostly at the tumor bed. We are reporting the patterns of relapse of our patients after 15 years experience.

Material and Methods: Patients with operable rectal cancer based on pelvic MRI staging, are considered at risk for local recurrence were included; for physical reasons, those with obstructive tumors and positive extramesorectal nodes were excluded. Patients received treatment with 26 Gy in 4 fractions using a remote afterloader with an endoluminal cylindrical multichannel applicator and an Iridium 192 source. The CTV is defined as the gross tumor volume observed on the diagnostic MRI with no attempt to cover the perirectal nodes. 667 patients treated from 1999-2015, most of which were T3 tumors (84%), low T2 (13%) and early T4 (3%); 36 % of the patients had positive nodes on pre-operative imaging. The local failure in our patient population is 4.7 % with a median follow up time of 65 months for 608 patients (range 6-165 months). Twenty-eight patients had pelvic recurrence, of which 25 were documented with MRI and 3 were found with CT scan. The Imaging was reviewed by two radiologists.

Results: The location of recurrence were identified as: iliac or lateral nodes in 11 patients, anastomotic in 10 patients, inguinal nodes in 3 patients, anterior compartment in 4 patients and pre-sacral space in one patient (one patient had more than 2 sites). In the patients with nodal pelvic relapses, the relapse was isolated for 3 patients and in the other 8 patients there were associated systemic relapses, and these patients were asymptomatic and did not require pelvic radiation while the former 3 patients underwent successful salvage radiation with IMRT (1) /SBRT for 2 patients. Another 9 patients with isolated pelvic relapses received pre-operative pelvic radiation with salvage surgery.

Conclusion: In patients with rectal cancer treated with pre-operative HDRBT, pelvic nodal relapse was the most common site of recurrence and was often associated with asymptomatic systemic relapse. Those patients with isolated nodal relapse are salvageable with either IMRT of SBRT. For patients with localized recurrence, pre-operative pelvic radiation was possible with salvage surgery. Pre sacral recurrence is a rare event, with a single patient observed.

OC-0150

Intraluminal brachytherapy in unresectable biliary carcinoma with malignant biliary obstruction

N. Rastogi[1], V.A. Saraswat[2], S.S. Baijal[3]

[1]*Sanjay Gandhi Postgraduate Institute of Medical Sciences, Radiotherapy, Lucknow UP, India*

[2]*Sanjay Gandhi Postgraduate Institute of Medical Sciences, Gastroenterology, Lucknow UP, India*

[3]*Medanta Medicity, Radiodiagnosis, Gurgaon, India*

Purpose or Objective: Locally advanced unresectable biliary carcinoma often present as extrahepatic malignant biliary obstruction with jaundice. The aim of treatment is to relieve jaundice and pruritus either by endoscopic biliary drainage (EBD) or percutaneous transhepatic biliary drainage (PTBD) followed by stenting. Stent is frequently blocked due to either tumour ingrowth or overgrowth. Intraluminal brachytherapy (ILBT) allows high dose to of radiation to local tumor area and delays the stent block. The purpose of this study is to assess the safety and efficacy of ILBT and impact of external beam radiotherapy(EBRT) on stent patency and survival.

Material and Methods: From 1998-2008, 172 unresectable, locally advanced biliary cancers (pancreas-12, gallbladder-140, cholangiocarcinoma-20), presenting with malignant extrahepatic biliary obstruction were prospectively treated with PTBD and stenting followed by ILBT with or without EBRT. The 110/172(64%) patients received ILBT alone (ILBT group) while 62/172(36%) received ILBT followed by EBRT(EBRT group). Endoscopic retrograde cholangio pancreaticography (ERCP) and/or percutaneous cholangiogram (PC) was done in all. Biliary drainage was done by standard ultrasound and fluoroscopy guided percutaneous transhepatic puncture. The stricture was dilated by balloon catheter over the guide wire. The biliary tract was dilated repeatedly and upsized till 12 French Malecot catheter. High dose rate brachytherapy with Ir192 source used to deliver 10 Gy/1fr at 1 cm radius from the center of source. PTBD tube was replaced by 10 mm, non sheathed self expandable metallic modified Giantruco Z stent. In EBRT group, stenting, followed by EBRT(dose of 45Gy/25fr/ 5 weeks) by conformal technique to primary tumour and stent area. All the patients were given single agent 5-Fluorouracil chemotherapy 370 mg/m2 Day1-5 at 4 weekly for 6 cycles.

Results: Palliation of jaundice and pruritus was achieved in all. The median overall survival in ILBT and EBRT group was 8 and 9 months with the stent patency 7 and 8 months and overall survival at 1 year was 21% and 23%. Gastric outlet obstruction was 29% in ILBT group and 19% in EBRT group(p=ns), while distant failure rate were 60 % & 55%. No ILBT related morbidity was observed.

Conclusion: PTBD is safe, well tolerated and effective in palliation of Jaundice. Intraluminal Brachytherapy (ILBT) appears to prolong stent patency The addition of EBRT to ILBT does not show any advantage in terms of stent patency and overall survival.

OC-0151

Radiation induced toxicity and tumour control in pts treated for uveal melanoma with ru-106 plaques

C.A. Espensen[1], L.S. Fog[2], M.C. Aznar[2], L. Specht[2], J.F. Kiilgaard[3]

[1]Rigshospitalet, Department of Radiation Therapy 3994- the Oncology Clinic, Copenhagen, Denmark

[2]Rigshospitalet, Department of Radiation Therapy 3994- the Oncology Clinic, Copenhagen, Denmark

[3]Rigshospitalet, Ophthalmology Department, Copenhagen, Denmark

Purpose or Objective: In a retrospective study of 100 consecutive patients treated with Ru-106 eye plaques for uveal melanoma from 2005 to 2008 at our clinic, we aimed to investigate the correlation between the dose to the optic nerve and optic nerve damage; the dose to the macula and macular damage; and the minimum dose to the tumour and tumour control.

Material and Methods: Pre-treatment fundus images were imported into Plaque Simulator TM and the tumour was retrospectively contoured by an ophthalmologist. The plaque position was determined from the radiation scar on post-treatment images. 3D dosimetric data was calculated. The point doses to the optic nerve and macula and minimum dose to the tumour were estimated. TCP, and damage to the optic nerve and macula, were determined from the patients' notes. The correlations between optic nerve damage, macular damage and TCP with dose, dose rate, gender, and plaque type was investigated using univariate and multivariate analyses.

Results: 16 % of the patients developed optic nerve damage. Only optic nerve dose was correlated with damage to the optic nerve (p=0,000063) in univariate analysis.
51% of the patients had macular damage. Only macular dose was correlated with damage (p=0,00049) in univariate analysis.
32 % of the patients did not achieve tumour control. TCP was correlated with minimum tumour dose and gender in univariate analysis. Patients with minimum doses > 80 Gy had 100% TCP.For 80% of the patients with tumour recurrence, the plaque did not geometrically overlap the tumour.
Dose response curves were drawn for optic nerve damage, macular damage and TCP. Such curves could not be found in the literature so no comparison was possible. Previously published values for TCP are similar to, or higher than, the one found in the present material. However, the papers citing higher values have selected patients with smaller tumours, which tend to have higher values of TCP. We emphasise that the number of patients is quite small and that a study of a large patient cohort is planned.

Conclusion: Tumour control only failed in patients who received less than the prescription dose. The use of image guided planning software (such as Plaque Simulator TM) may aid in optimizing tumour control in the future. The present analysis presents the first reported dose response curves for damage to the optic nerve and macula. This information may be useful in delivering the optimal treatments in future.

OC-0152

Novel software modules for treatment planning of 106Ru eye plaque brachytherapy

G. Heilemann[1], L. Fetty[1], I. Birlescu[1], M. Blaickner[2], N. Nesvacil[3], D. Georg[3]

[1]Medical University of Vienna, Department of Radiation Oncology, Wien, Austria

[2]Austrian Institute of Technology GmbH, Health and Environment Department Biomedical Systems, Vienna, Austria

[3]Medical University of Vienna/ Christian Doppler Laboratory for Medical Radiation Research for Radiation Oncology, Department of Radiation Oncology, Vienna, Austria

Purpose or Objective: Treatment of uveal melanoma by means of brachytherapy using 106Ru eye plaques achieves very good tumor control while keeping morbidity at an acceptable level. However, a deeper understanding of the underlying dose-response relationship is still missing not least because of the lack of appropriate software packages for 3D treatment planning and volumetric dose assessment. This motivated the in-house development of software modules to calculate the dose distributions in critical, ophthalmologic structures as well as tumor for an eye model.

Material and Methods: A resizable 3D model of an eye was created in Sidefx Houdini, consisting of lens, ciliary body and optic nerve as well as macula, retina and sclera. A dome-shaped tumor model can be added with apex height and basal diameter as adjustable parameters. The position of the tumor model can be fixed by reference to the distance between tumor and macula and tumor and optical nerve. Alternatively fundus images can be incorporated into the 3D model in order to account for the individual tumor shape. A specially designed algorithm projects the images onto the virtual eye model and converts them to volumetric data. Different types of BEBIG eye plaques (CCA, CCB and COB) can be positioned within the computer model. Corresponding dosimetric lookup tables were generated from MC simulations using MCNP6. Superposition onto the 3D eye model enables the calculation of doses and dose volume parameters for the tumor and adjacent healthy tissue. Finally, dosimetric safety margins have been obtained by performing film measurements and can be included in order to determine dosimetric uncertainties.

Results: The software modules can calculate full 3D dose distributions with a cubic dose grid of 200 µm in < 5 s (and < 1 s with GPU). The 3D eye model can be adjusted on the basis of simple geometric measures such as the measured size of the eye as well the distances between tumor, macula and optic nerve and thereby be used for individual treatment planning, i.e. the selection and positioning of the type of plaque. The registered fundus projection can be used to guide the tumor delineation. Dose-volume metrics can be generated for all structures of the individualized model which in turn can be used for assessing dose-response relationships

for the target volume and organs-at-risk. The dosimetric uncertainty assessment provides information on safety margins. Local agreement between MC and film was better than 6 % for the first 7 mm.

Conclusion: In this study we presented novel software modules for treatment planning in 106Ru eye plaque brachytherapy of uveal melanomas. It is aimed to be used in daily treatment planning as well as for performing pro- and retrospective studies to provide further information on dose-response relationships and prognostic values for treatment morbidity and local control. Future works involves the registration of pre- and/or post-application MR images as well as a quantitative evaluation on the basis of retrospective data.

Proffered Papers: Physics 3: Anatomical CT and MR imaging for treatment preparation

OC-0153

Dual energy CT and iterative metal artefact reduction for accurate tumour delineation

D. Kovacs[1], L. Rechner[1], J. Bangsgaard[1], A. Berthelsen[1], J. Costa[1], J. Friborg[1], G. Persson[1], L. Specht[1], I. Vogelius[1], M. Aznar[1]
[1]*Rigshospitalet, Oncology, Copenhagen, Denmark*

Purpose or Objective: To compare the accuracy of tumor delineation on a standard CT scan and on CT scans with two metal artifact reduction methods in an oral cavity phantom with a known tumor surrogate.

Material and Methods: A set of teeth containing an amalgam-filled removable tooth and an artificial polycaprolactone tumour was placed in water and CT scanned (Siemens Somatom Definition AS) at 120 kVp, 80 kVp, and 140 kVp. The two latter scans were used to reconstruct virtual monochromatic (VM) images. All image sets were additionally reconstructed with metal artefact reduction (MAR) software (iMAR, Siemens Healthcare). The following 4 MAR reconstructions were studied: 1) 130 keV VM 2) 70 keV VM with MAR, 3) 120 kVp with MAR, 4) 130 keV VM with MAR. A conventional 120 kVp CT was also taken and a 120 kVp image where the metal tooth was removed was used as control. 3 oncologists and 2 radiologists contoured the tumour volume on all 6 image sets while blinded to the image reconstruction type. A 7th high-quality image of only the artificial tumour was contoured to obtain the true shape of the tumour. Maximal Hausdorff distances and DICE coefficients of the 5 delineated contours compared to the true contour was were used to quantify delineation accuracy in all 6 image sets. Statistically, a Friedman-test was used for primary comparisons and a Nemenyi-test is performed for pairwise post hoc analysis.

Results: In all cases, MAR reconstructions clearly improved tumour delineation precision and accuracy (see Figure 1 and Table 1).The highest level of DICE similarity between observers was found based on 120 kVp iMAR reconstructions (DICE = 0,87 [0,86 – 0,88]), while the highest level of accuracy was found in the 130 keV iMAR reconstructions (Hausdorff max = 4,0 mm [2,9 – 8,1]). A statistical analysis comparing DICE coefficients and Hausdorff distances between modalities showed that contouring accuracy on the 120 kVp standard and 130 keV VM images were significantly degraded from the control image ($p < 0,05$ for both), whereas we found no significant differences between the control and the 70 keV VM iMAR, the 120 kVp iMAR and the 130 keV VM iMAR reconstructions. Verifying the model used for this study, a high level of precision and accuracy was observed (Hausdorff max = 2,9 mm (2,0 – 3,3) and DICE = 0,9 (0,89 – 0,92)) when no metal was present during the scan.

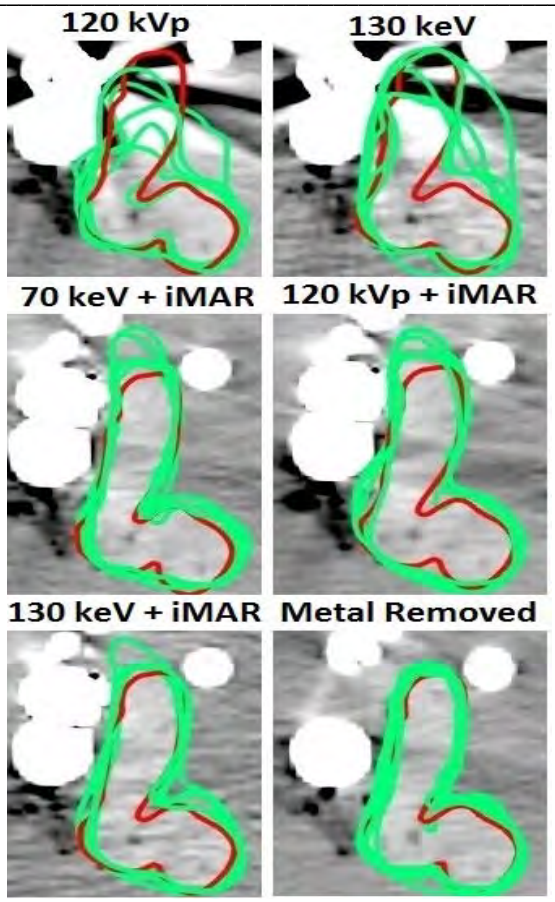

		Standard	Reconstruction Modality				Control
		120 kVp	130 keV	70 keV+iMAR	120 kVp + iMAR	130 keV + iMAR	120 kVp no metal
Haus-dorff max	Median (Range) [mm]	10,7 (6,3 – 14,5) *	9,8 (5,6 – 11,5)**	7,7 (4,1 – 9,2)	5,1 (3,9 – 8,6)	4,0 (2,9 – 8,1)	2,93 (2,0 – 3,3)
DICE	Median (Range)	0,75 (0,72 – 0,81)*	0,78 (0,75 – 0,80)*	0,84 (0,80 – 0,85)	0,87 (0,86 – 0,88)	0,88 (0,83 – 0,89)	0,9 (0,89 – 0,92)

Table 1 showing the median and range of maximal Hausdorff distances and DICE coefficients when comparing to the true contour. Statistical significance after a pairwise post-hoc Nemenyi test is shown as * (p<0.01) or ** (p<0.05)

Conclusion: MAR reconstructions resulted in a clear improvement in contouring accuracy compared to conventional CT and DECT VM images, where a significant degradation of tumour delineation accuracy was found in comparison to the control image. The highest level of similarity between observers was found in MAR reconstructions of 120 kVp, while 130 keV VM images showed potential to further improve accuracy when reconstructed with MAR software.

OC-0154

Clinical use of dual-energy CT for proton treatment planning to reduce CT-based range uncertainties

P. Wohlfahrt[1,2], C. Möhler[3,4], A. Jakobi[1], M. Baumann[1,2,3,5,6], W. Enghardt[1,2,3,5,6], M. Krause[1,2,3,5,6], S. Greilich[3,4], C. Richter[1,2,3,5,6]
[1]*OncoRay - National Center for Radiation Research in Oncology, Faculty of Medicine and University Hospital Carl Gustav Carus- Technische Universität Dresden- Helmholtz-Zentrum Dresden - Rossendorf, Dresden, Germany*
[2]*Helmholtz-Zentrum Dresden - Rossendorf, Institute of Radiooncology, Dresden, Germany*
[3]*German Cancer Research Center DKFZ, Heidelberg, Germany*
[4]*Heidelberg Institute for Radiation Oncology HIRO, National Center for Radiation Research in Oncology, Heidelberg, Germany*
[5]*Faculty of Medicine and University Hospital Carl Gustav Carus- Technische Universität Dresden, Department of Radiation Oncology, Dresden, Germany*
[6]*German Cancer Consortium DKTK, Dresden, Germany*

Purpose or Objective: To improve CT-based particle treatment planning the additional tissue information

provided by dual-energy CT (DECT) compared to single-energy CT (SECT) can be clinically used to reduce CT-based range uncertainties and to analyze intra- and interpatient tissue variations. First, a DECT scan protocol was optimized and clinically introduced. Second, in a first analysis patient DECT scans were evaluated concerning CT number variability.

Material and Methods: After an experimental analysis of several CT scan settings concerning beam hardening, image quality and planned dose distribution using tissue surrogates, head and body phantoms and real tissues, an optimized and standardized DECT protocol (voltages: 80/140 kVp, kernel: D34) is clinically applied for patients treated with protons. 45 planning and 360 control DECT scans of overall 70 patients were acquired with a single-source DECT scanner (Siemens SOMATOM Definition AS) until October 2015. Contouring and treatment planning are performed on pseudo-monoenergetic CT scans (MonoCT) derived by a weighted sum of both CT datasets. 25 patients with different tumor sites (head, head & neck, prostate, pelvis) and overall 200 DECT scans were initially investigated to evaluate intra- and interpatient tissue variabilities. Based on the frequency distribution of voxelwise 80/140kVp CT number pairs, a linear correlation of low-density, soft and bony tissues can be determined, respectively.

Results: A DECT-based MonoCT of 79 keV is found optimal for proton treatment planning. Assuming identical CT dose to a SECT scan, the MonoCT shows a signal-to-noise ratio increased by 8% and a CT number constancy raised by 23% on average and up to 69% for bones. Consequently, the current uncertainties of a heuristic conversion of CT numbers into stopping power ratios (SPR) using a look-up table are reduced.
Evaluation of patient variability revealed that 80/140kVp CT number pairs of human tissues are on average well described by linear correlations with a slope (± σ) of (1.023 ± 0.006) for low-density, (0.825 ± 0.008) for soft and (0.696 ± 0.006) for bony tissues. The slope variation between different patients, independent from tumor site and patient size, is comparable to the variability between different control DECT scans of one patient (σ of about 1-3%). However, a band of CT number pairs deviating from the mean linear correlation, e.g. caused by image noise and partial volume effects, reveals potential insuperable uncertainties of a voxel-based heuristic CT number-to-SPR conversion.

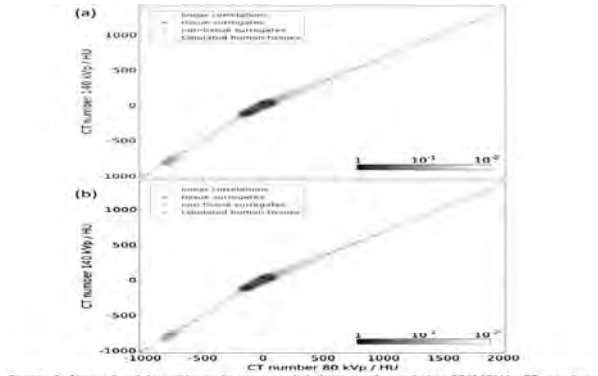

Figure 1: Normalized logarithmic frequency distribution of voxelwise 80/140kVp CT number pairs using planning DECT scans of 17 patients with different tumor sites in head and head & neck (a) as well as 12 control DECT scans of one head-and-neck patient (b). Linear correlations determined for low-density, soft and bony tissues (red line) based on the logarithmic frequency distribution describe tissue surrogates (blue dots) and tabulated human tissues (green triangles) quite well. Non-tissue surrogates differ from these relations and can thus be separated.

Conclusion: The clinical application of DECT-based MonoCT can contribute to a more precise range prediction. Further improvements are expected from a direct, non-heuristic SPR calculation, which is not yet clinically available. The further growing DECT patient database enables not only a detailed analysis of intra- and interpatient variations, but also a robustness analysis for different direct SPR prediction approaches.

OC-0155

MR-guided multi-atlas based synthetic CT for MR-only radiotherapy of head and neck cancer patients

R. Farjam[1], N. Tyagi[1], H. Veeraraghavan[1], A. Apte[1], K. Zakian[1], M. Hunt[1], J. Deasy[1]
[1]*Memorial Sloan-Kettering Cancer Center, Medical Physics, New York- NY, USA*

Purpose or Objective: To develop an image analysis approach for generation of the synthetic CT for MR-only radiotherapy of head and neck (H&N) cancer patients.

Material and Methods: Eleven sets of CT and MRI (in-phase, Philips mDixon sequence) scans were randomly selected from a pool of H&N cancer patients. A bias field correction algorithm was primarily applied to each MRI scan to eliminate the intensity variation due to B0 and B1 field inhomogeneity and tissue susceptibility effect. A landmark-based MRI standardization technique was then used to standardize the MR intensity histograms wherein each landmark, total of 4, corresponds to a different histogram extremum. Using a rigid + deformable registration, CT scan from each patient was registered to the standardized MRI to construct an atlas of CT-MRI. To improve the performance of the registration, bone intensity in the CT image was suppressed to assimilate CT and MRI scans. CT image is initially clustered into classes of air, bone and soft tissue. The cluster center of the bone class is then transformed to the air class to suppress the bone signal. To synthesize CT for a new patient, using the displacement fields achieved by registering each MRI in the atlas to the new patient MRI, all CTs from the atlas were also deformed onto the new patient. A generalized registration error (GRE) metric was then calculated as a measure of goodness of local registration between each pair of MRIs. GRE is the Euclidean distance of the mean normalized local mean, variance and entropy of the difference map between the two registered standard MRIs. The synthetic CT value at each point would be the average of GRE weighted CTs from all CT scans in the atlas. To evaluate our proposed method, the mean absolute error (MAE) between the synthetic CT and the original CT was computed over the entire CT and air and bone regions in a leave-one-out scheme. The efficiency of our proposed registration scheme was also compared with commercial software. Comparison of the dose plan between the original and synthetic CT is also ongoing.

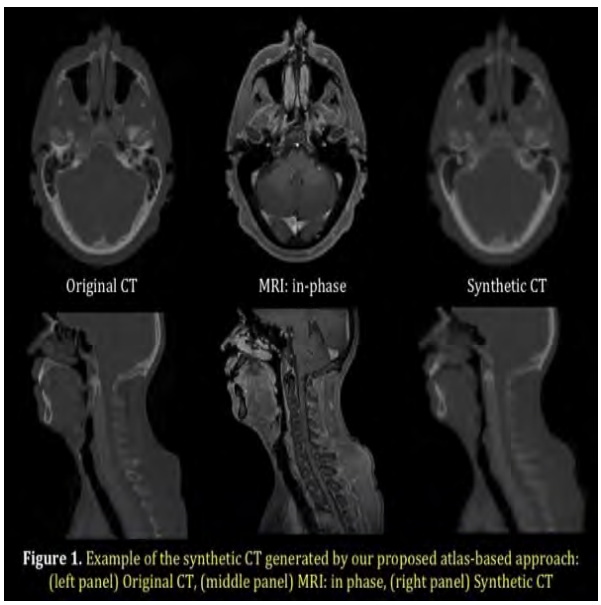

Figure 1. Example of the synthetic CT generated by our proposed atlas-based approach: (left panel) Original CT, (middle panel) MRI: in phase, (right panel) Synthetic CT

Results: MAE between the original and the synthetic CT was 67 ± 9, 114 ± 22, and 116 ± 9 HU for the entire image, air and bone regions, respectively. We found that our proposed registration strategy and GRE metric each could lower up to 30% and 15% of the MAE over the entire CT and up to 50% and 40% in the MAE of the bone regions. Our primary dose

calculation revealed highly consistent results between the original and the synthetic CT.

Table 1. Example of dose calculation for a head and neck cancer patient using original and synthetic CT generated by our proposed multi-atlas based algorithm. Numbers are in cGy.

Table 1.		PTV70	PTV66	PTD54	PTV50	Parotid		SMG		Mandible	Brachial Plexus		Larynx
						R	L	R	L		R	L	
Original CT	Min	5526	5657	2920	4026								
	Max	6585	6613	6526	5702					6300	5991	5270	5914
	Mean	6306	6352	5823	5206	1550	2386	5791	3983				
	D95	6113	6142	5482	5061								
Synthetic CT	Min	5479	5621	3114	4180								
	Max	6590	6685	6538	5689					6319	5993	5280	5933
	Mean	6307	6370	5829	5211	1597	2366	5811	4078				
	D95	6110	6144	5488	5064								

Conclusion: A multi-atlas based approach was presented in this work for generation of the synthetic CT for MR only radiotherapy of the head & neck cancer patients. While the registration scheme presented in this work enhances the performance of the atlas propagation, generalized registration error (GRE) helps to construct a better synthetic CT using a locally more similar atlas.

OC-0156

MRI only prostate radiotherapy using synthetic CT images

E. Persson[1], F. Nordström[1,2,3], C. Siversson[3,4], C. Ceberg[2]
[1]*Skåne University Hospital, Medical Radiation Physics, Lund, Sweden*
[2]*Lund University, Medical Radiation Physics, Lund, Sweden*
[3]*Spectronic Medical AB, Medical, Helsingborg, Sweden*
[4]*Lund University, Medical Radiation Physics, Malmö, Sweden*

Purpose or Objective: Introducing an MRI-only workflow into the radiotherapy clinic, requires that MR-images can be used both for treatment planning calculations and for patient positioning. The two-fold aim of this study was to evaluate the use of MR-images with respect to 1) the accuracy of treatment planning dose calculations, and 2) the reliability of fiducial marker identification for patient positioning.

Material and Methods: Synthetic CT images (sCT) were generated using the Statistical Decomposition Algorithm (SDA, MriPlanner, Spectronic Medical AB, Sweden). The algorithm uses a T2-weighted MRI for sCT generation, based on a multi-template assisted classification method. In order to exclude the effect of geometrical distortions and patient deformation owing to reposition between imaging sessions, a registered CT (rCT) was constructed by deformable registration with the MR using the Elastix toolbox.

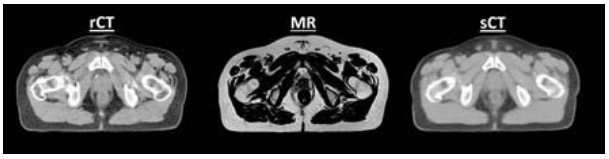

Five-field IMRT plans (both 6 and 10 MV) were created for six patients, using the Eclipse treatment planning system (Varian Medical Systems, Palo Alto, CA). Final dose calculations were made using the anisotropic analytical algorithm (AAA). The rCT was used for the initial treatment planning and the plan was recalculated on the sCT. Thus, the two treatment plans created for each patient had the same number of monitor units for each field. The resulting dose distributions from the rCT- and sCT-treatment plans were compared based on a set of dose volume histogram criteria according, and by using gamma evaluation.
The reliability of the MRI-based fiducial marker identification was evaluated by an observer study. For this part of the study, the position of gold fiducial markers were determined by six independent observers using an MRI sequence dedicated for marker identification (LAVA-flex). Each marker position, three for each patient, were compared between the observers. The observers graded (one to five, were five represents the highest level of confidence) their confidence by which the markers for each patient were identified.

Results: The mean dose differences to PTV between plans based on sCT and rCT were -0.1%±0.3% (1 s.d) (6MV) and -0.2%±0.2% (1 s.d) (10 MV). Gamma analysis showed pass rates ranging between 98% and 100% for both energies, with gamma criteria of 1%/2mm (local dose deviation). The mean standard deviation of the marker position, as determined by the observers, was 0.6 mm in all directions (x, y and z). One marker identification result was excluded due to an incorrect identification by one observer. The confidence grading ranged between 2 and 5.

Conclusion: This work demonstrates that SDA can provide sufficient dosimetric accuracy for an MRI only workflow for prostate cancer patients. However, gold fiducials cannot be identified using LAVA-flex with high enough confidence and further work is needed to develop methods for marker identification in an MRI only workflow.

OC-0157

Prostate fiducial markers detection with the use of multiparametric-MRI

C.D. Fernandes[1], C. Dinh[1], L.C. Ter Beek[2], M. Steggerda[1], M. Smolic[1], L.D. Van Buuren[1], P.J. Van Houdt[1], U.A. Van der Heide[1]
[1]*The Netherlands Cancer Institute, Department of Radiation Oncology, Amsterdam, The Netherlands*
[2]*The Netherlands Cancer Institute, Department of Radiology, Amsterdam, The Netherlands*

Purpose or Objective: Prostate cancer patients scheduled for EBRT are often implanted with fiducial markers for position verification. A precondition for an MR-only workflow is the possibility to identify them on MRI. The markers present as signal voids in most images and their apparent position depends on their shape and orientation relative to the magnetic field. Rather than acquiring a sequence for this single purpose, we propose to use a model for the automatic detection of fiducial markers combining information from the entire multiparametric (mp) MRI protocol used for target delineation.

Material and Methods: Thirty prostate cancer patients scheduled for EBRT were implanted with 2-3 gold fiducial markers (0.9x3mm). A mp-MRI (T1w, T2w, B0-mapping and mDIXON) was performed using a 3T MRI (Achieva, Philips) and a CT with a 24-slice CT scanner (Somatom-Sensation-Open, Siemens).The reference position of the markers was based on the segmented CT images. The MRI was registered to the CT and resampled to the grid of 0.9x0.9x3mm3. A logistic regression model was developed to estimate the location of the markers based on the following MRI features: signal intensity, mean, median, min, max and standard deviation values in a kernel of 3x3x3vox and a multi-scale blobness filter [1] of the prostate region. The model was cross-validated using a leave-one-out method. Performance was assessed using features from each separate imaging sequence and by combining the features from all sequences. Voxels detected as markers by the model were grouped into clusters. We defined the probability of each cluster candidate as the highest probability value of all voxels within it. Results were further post-processed by selecting the n(i) highest probability clusters, where n(i) is the number of markers implanted in patient i. Results were classified as a false positive (FP) if the distance between the reference

centroid coordinates and the detected location was larger than 2.7mm in plane and 3mm in slice direction.

Results: Table1 shows the average AUC values for the model results of all patients using a single sequence and when combined. The combined model (AUC=0.94) performs significantly better than the best imaging sequence alone (T1-THRIVE AUC=0.84). Without post-processing the model correctly identifies 80/86 markers but with a total of 98 FP. After post-processing, we reduced the FP to a total of 20 but the true positives (TP) were also reduced to 66. Figure 1 shows the model pipeline. Deviations between the reference and the correctly identified marker location are < 1mm.

Conclusion: The standard mp-MRI provides valuable information to detect fiducial markers. The combination of different sequences is more accurate than the use of a single sequence. The number of TP after processing needs to be further addressed but the overall findings support the feasibility of automatic marker detection in an MR-only workflow.

[1] Lindeberg et al, IJCV 1998

Total number of markers present in 30 patients: 86

	Average AUC	Total TP	Total FP	Average Distance (mm) x	y	z
T1-THRIVE	0.84	21	65	0.66	1.07	0.97
T2 TSE	0.69	6	80	1.15	1.95	1.31
B0 mag	0.80	29	57	0.96	1.44	0.78
mDIXON IP	0.82	12	74	0.75	1.21	1.14
Combined	0.94	66	20	0.74	0.97	0.97

Table 1 - Number of markers detected by the model when using sequences individually and when combining them together. The results presented above are obtained after post-processing. The distance was calculated between the centroid coordinates of the reference and the detected location. The distribution of AUC values over all patients is significantly different ($p<0.05$) between any of the single sequences and the combined model using a Wilcoxon signed-rank test. AUC: Area under the curve; TP: True positives; FP: False positives. The use of 'mag' in B0 mag refers to the amplitude of the signal.

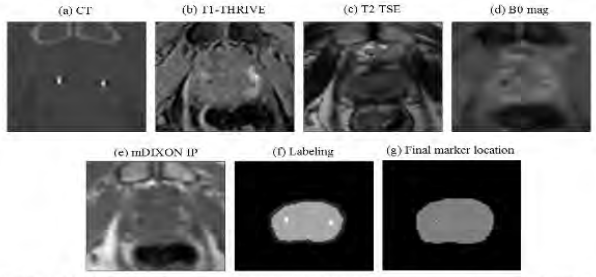

Figure 1 - Model pipeline and outcome for a representative patient. The CT image (a) is used as a reference to generate the reference position of the markers. The MRI was used for prostate delineation. The combination of prostate delineations and reference marker position is used as the labeling for our data (f). The imaging features are extracted from the MR sequences (b),(c), (d) and (e). In figure (g) one can see the final result after post-processing and reconstruction of a cylindrical structure with the dimensions of the marker based on the identified clusters' centroid coordinates.

OC-0158

Impact of breathing guidance and prospective gating on 4DCT image quality: a digital phantom study

S. Pollock[1], J. Kipritidis[1], D. Lee[1], K. Bernatowicz[2], P. Keall[1]
[1]*University of Sydney, Sydney Medical School - Central, Sydney, Australia*
[2]*Paul Scherrer Institute, Center for Proton Therapy, Villigen, Switzerland*

Purpose or Objective: Irregular breathing motion has a deleterious impact on thoracic and abdominal four-dimensional computed tomography (4DCT) image quality. Two pathways to overcome this problem are: (i) improving the regularity of breathing motion using the audiovisual biofeedback (AVB) breathing guidance system, and (ii) prospectively respiratory gating the 4DCT scan based on real-time respiratory motion. Until now, the effects of these technologies on 4DCT imaging have not been directly compared. The purpose of this study was to compare the impact of AVB and respiratory gating on thoracic 4DCT image quality and acquisition time using a deformable digital phantom driven by lung cancer patient breathing patterns

Material and Methods: We obtained simultaneous measurements of chest, abdominal, diaphragm, and tumor motion for 6 lung cancer patients with tumor motion > 5 mm. Breathing signals were acquired under two breathing conditions: (1) AVB, and (2) free breathing. For each breathing condition, we used the 4D eXtended Cardiac Torso (XCAT) to simulate 4DCT acquisitions in the cine and respiratory gated mode. For each combination of breathing condition and acquisition mode, 4DCT image quality was quantified terms of Dice similarity coefficient between reconstructed and ground truth lung and tumor volumes (DSC(lung) and DSC(tumor), respectively), in addition to an automated method of artefact detection (utilizing normalized cross coefficient (NCC)). 4DCT acquisition times were also compared for each breathing condition and acquisition mode

Results: In cine mode, AVB improved DSCl(ung) and DSC(tumor) by 0.3% ($p = 0.005$) and 0.3% ($p < 0.001$), respectively, and improved NCC by 11% ($p = 0.002$). In respiratory-gated mode, AVB did not have a significant impact on image quality. AVB increased the acquisition length of cine mode 4DCT by an average of 4 seconds, but reduced the length of respiratory gated acquisitions by 10 seconds. Respiratory gating improved image quality over cine mode irrespective of the breathing condition. Utilizing both AVB and respiratory gating together garners the greatest improvement in DSC(lung), DSC(tumor), and NCC values over conventional free breathing in cine mode by 0.9% ($p < 0.001$), 1.5% ($p = 0.25$), and 18.5% ($p < 0.001$), respectively

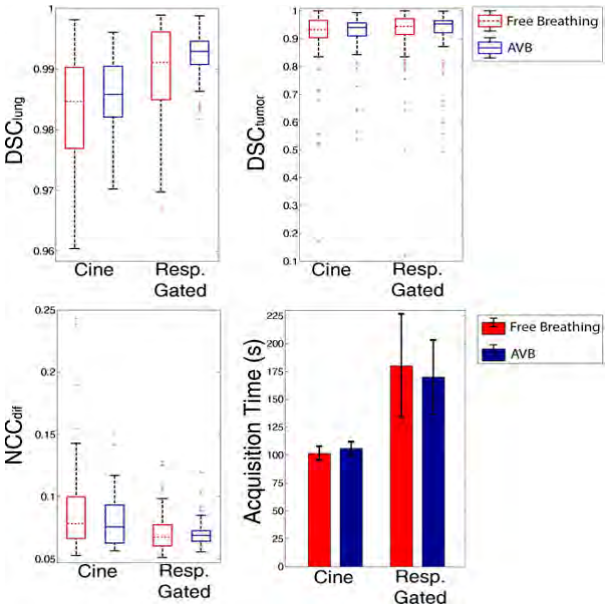

Conclusion: This was the first study to directly compare the impact of breathing guidance and respiratory gating on 4DCT acquisition. We observed that AVB significantly improves the quality of 4DCT images in cine mode over free breathing, but can also reduce the amount of time needed to acquire a respiratory gated 4DCT scan. The results presented here demonstrate that AVB and respiratory-gating can both be beneficial pathways to improve 4DCT simulation for cancer radiation therapy, but the biggest gains are achieved when using these technologies simultaneously

Proffered Papers: Physics 4: Inter-fraction motion management I

OC-0159

X-ray tube current modulation with dynamic blade collimation for CBCT guidance

D. Parsons[1], J. Robar[1]
[1]*QEII Health Sciences Centre - Dickson Building, Medical Physics, Halifax- Nova Scotia, Canada*

Purpose or Objective: The focus of this work is the development of a novel blade collimation system enabling volume-of-interest (VOI) CBCT using the kV source on a TrueBeam linear accelerator. Advantages of the system are assessed, particularly with regard to reduction and localization of dose, as well as improvement of image quality.

Material and Methods: A four-blade dynamic kV collimator was developed to track a VOI during CBCT acquisition. The system is controlled using a Raspberry Pi computer placed within the linac gantry. The current prototype is capable of tracking an arbitrary volume defined by the treatment planner for subsequent CBCT guidance. During gantry rotation, the collimator tracks the VOI with adjustment of position and dimension. CBCT image quality was investigated as a function of collimator dimension, while maintaining the same dose to the VOI, for a 20 cm diameter cylindrical water phantom with a 9 mm diameter bone insert centered on isocenter. Dose distributions for various anatomical sites were modeled using a dynamic BEAMnrc library and DOSXYZnrc. The resulting VOI dose distributions were compared to full-field distributions to quantify dose reduction and localization to the target volume. X-ray tube current modulation was investigated in combination with the VOI approach, using digitally reconstructed radiographs to estimate tube pulse width for each CBCT projection. The technique was evaluated in Developer Mode on the linear accelerator.

Results: Measurements show contrast increase by a factor of 1.3 and noise reduction by a factor of 1.7, for VOI CBCT, and thus an increase in contrast-to-noise ratio (CNR) by a factor of approximately 2.2. Depending upon the anatomical site, dose was reduced to 15%–80% of the full field value along the central axis plane and down to less than 1% along the axial planes. The use of tube current modulation allowed for specification of a desired signal-to-noise ratio within projection data. For approximately the same dose to the VOI, CNR was increased by a factor of 1.2 for tube current-modulated compared to unmodulated VOI CBCT.

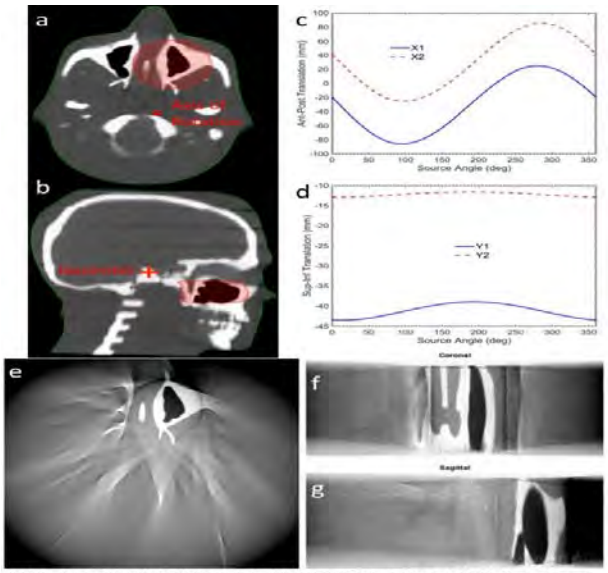

(a-b) CT volume of the ATOM head phantom in the Eclipse treatment planning system, with the volume-of-interest to be imaged in red, isocenter marked with a cross. (c) X- and (d) Y-blade translations as a function of beam central axis angle (using the Varian IEC coordinate system) calculated from the DICOM structure using MATLAB. (e-g) Reconstructed volume-of-interest.

Conclusion: The VOI CBCT approach allows imaging of a planner-defined volume, offering both image quality improvement and reduction of imaging dose for the patient.

OC-0160

Growth and oedema related shifts of brain metastasis treated with stereotactic radiosurgery

K. De Vries[1], M. Beerendonk[1], L. Dewit[1], W. Boogerd[2], D. Brandsma[2], A. Van Mourik[1], G. Borst[1]

[1]Netherlands Cancer Institute Antoni van Leeuwenhoek Hospital, Department of Radiation Oncology, Amsterdam, The Netherlands

[2]Netherlands Cancer Institute Antoni van Leeuwenhoek Hospital, Department of Neuro-oncology, Amsterdam, The Netherlands

Purpose or Objective: Stereotactic Radiosurgery (SRS) has emerged as a treatment of choice for many cancer patients with brain metastasis. Most institutes use linac-based irradiations with multiple days between imaging and irradiation and a subset of patients is treated with fractionated SRS. So far, the geometrical uncertainties induced by such time intervals have not yet been quantified. Therefore, we investigated the growth rates of different tumour entities, the effect of oedema and the use of steroids on possible tumour shifts to estimate the effect on the tumour dose.

Material and Methods: Thirty-six patients were included, equally divided over lung-, breast- and melanoma cancer patients. Patients receiving systemic cytotoxic treatment 3 months prior to the diagnostic MRI were excluded, except for breast cancer patients on hormonal therapy that started more than 6 months prior to the diagnostic MRI. All patients had undergone a diagnostic and a radiotherapy planning MRI of which the T1w+contrast sequences were registered with the planning CT scan for target definition on both scans. Consensus was reached for all delineations by two radiation oncologists. The median time between the two MRI scans was 18 days (range 6-54). For all tumour delineations, the volume, radius (assuming spherical tumours) and Centre of Mass (CoM) were calculated. Growth rates were determined from volumetric or radial increase per day between the MRI scans. CoM differences between scans served as a measure for tumour shifts that can be caused by oedema (-clearance) and/ or anisotropic growth. Oedema was scored only if an experienced radiologist diagnosed peritumoural oedema on the diagnostic MRI.

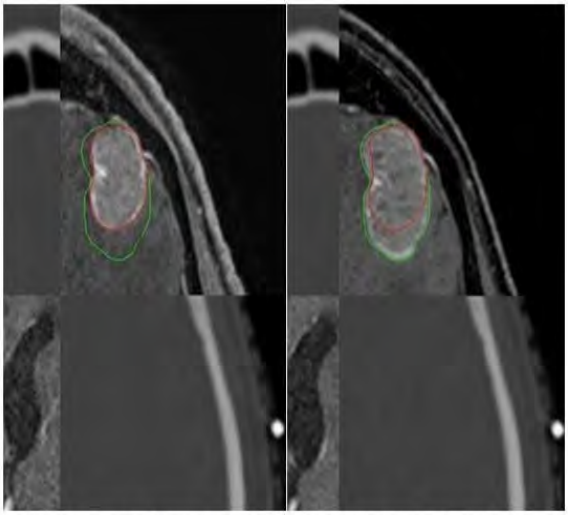

Image 1: Delineations on diagnostic (left) and plannings MRI (right), both registered on planning CT.

Results: Table 1 shows the results for tumour growth and tumour shifts. The highest growth rate in radial increase is seen in large melanoma tumours (0.07 mm/day (SD 0.02) , p=<0.01). Large heterogeneities in growth rate are seen in tumours of both small and large brain metastasis of lung cancer patients (small: mean=7%/day, SD=10%, range=0%-26%, large: mean=3 %/day, SD=6%, range=-1%-15%). In this lung group, three patients showed shrinkage; all three started steroids after diagnostic MRI. Large tumour shifts (mean=1.7 mm) and variability (SD=1.0 mm) were observed in the patient group with oedema receiving steroids (whereby the growth rate of tumours in these patients was not different).

Table 1. Growth rates and shifts of brain metastasis

	Small n=6			Large n=6		
Tumour	Volume planning MRI (cc)	Growth rate % volume/day (SD)	Growth rate mm/day (SD)	Volume planning MRI (cc)	Growth rate % volume/day (SD)	Growth rate mm/day (SD)
Melanoma (n=12)	0.21-1.29	5 (2)	0.05 (0.02)	1.32-8.41	3 (1)	0.07 (0.02)
Breast (n=12)	0.37-1.69	5 (1)	0.05 (0.01)	2.05-5.75	2 (1)	0.03 (0.04)
Lung (n=12)	0.11-1.97	7 (10)	0.04 (0.03)	2.68-8.29	3 (6)	0.03 (0.09)

Shift factors	CoM shift (mm) (SD)	p*	Growth rate (mm/day) (SD)	p*	CoM shift + growth rate (mm/day) (SD)	p*
Oedema and steroids (n=17**)	1.73 (1.02)	p<0.001	0.04 (0.04)	NS	0.15 (0.09)	p=0.002
No oedema and/or no steroids (n=18)	0.53 (0.34)		0.04 (0.02)		0.07 (0.02)	

*Unpaired parametric t-test

**1 patient was excluded because the shift was mainly caused by intratumoural bleeding

Conclusion: Within the limitations of a retrospective study, our results show that the growth and shift of brain metastasis over time can be significant and may vary over patient groups. Given the typical steep dose gradient in SRS treatments (>10%/mm), tumour growths and shifts may have a significant impact on the tumour dose. Therefore, this phenomenon must be considered if the workup and treatment of SRS for brain metastasis is encompassing multiple days.

OC-0161

Renal and diaphragmatic interfractional motion in children and adults: is there a difference?

I.W.E.M. Van Dijk[1], S.C. Huijskens[1], M.A.J. De Jong[1], J. Visser[1], R. Dávila Fajardo[1], C.R.N. Rasch[1], T. Alderliesten[1], A. Bel[1]

[1]*Academic Medical Center, Department of Radiation Therapy, Amsterdam, The Netherlands*

Purpose or Objective: One of the factors determining the size of planning target volume (PTV) margins is organ motion. Organ motion is comprehensively studied in adults and paediatric PTV margins are generally based on these data. We hypothesize that adult-based PTV margins are too large for paediatric patients because children and adults differ in body composition. Our aim was to compare renal and diaphragmatic interfractional motion in children with that in adults and to investigate the correlation with age and height.

Material and Methods: This single-centre retrospective study consisted of 35 children and 35 adults who received thoracic/abdominal irradiation between October 2009 and December 2014. The mean age of children and adults was 10.3 years (range 3.1-17.8 years) and 59.9 years (range 34.1-94.0 years) respectively. Mean height in children and adults was 140 cm (range 92-184 cm) and 175 cm (160-203 cm) respectively. According to protocol, abdominal and/or thoracic Cone Beam CT (CBCT) images were acquired for setup verification before radiation delivery. A total of 70 reference CT (refCT) scans, 350 paediatric CBCTs (mean 10; range 5-30) and 476 adult CBCTs (mean 14; range 5-27) were available for registration using Elekta XVI software. In order to assess renal and diaphragmatic motion, each CBCT was registered to its refCT in 2 steps; registration of: 1) the bony anatomy (i.e., the vertebral column), and 2) the left kidney, right kidney and diaphragm separately. For each individual, we assessed organ motion in the left-right (LR), cranio-caudal (CC), and anterior-posterior (AP) directions for the left and right kidney. Diaphragmatic motion was measured in the CC direction only as a surrogate for upper abdominal organ motion. Subsequently, for all organs the mean and standard deviation of the measurements in all directions were calculated and analysed to estimate the group systematic error (Σ) and the group random error (σ). The correlations between organ motion and age and height were investigated using a univariate regression analysis.

Results: Interfractional organ motion in children and adults was different; displacements in children were notably smaller than in adults. Consequently, the estimated group systematic (Σ) and random errors (σ) for the two groups were different (Table 1). Within each group, no correlation was found between organ motion and age or height. Overall, in the CC direction, weak correlations were found between the patient random error, and age and height (Figure 1).

Table 1. The estimated group systematic (Σ) and random error (σ) for children and adults.

	Systematic error Σ (mm)						
	Right kidney			Left kidney			Diaphragm
	LR	CC	AP	LR	CC	AP	CC
Children	1.3	3.6	1.8	1.4	3.1	4.0	3.8
Adults	1.9	6.6	3.2	2.1	6.5	2.2	9.9
	Random error σ (mm)						
	Right kidney			Left kidney			Diaphragm
	LR	CC	AP	LR	CC	AP	CC
Children	1.0	2.9	1.5	1.5	2.9	2.3	3.7
Adults	1.5	5.0	2.9	1.5	5.0	2.1	4.8

Abbreviations: *AP* anterior-posterior, *CC* cranio-caudal, *LR* left-right

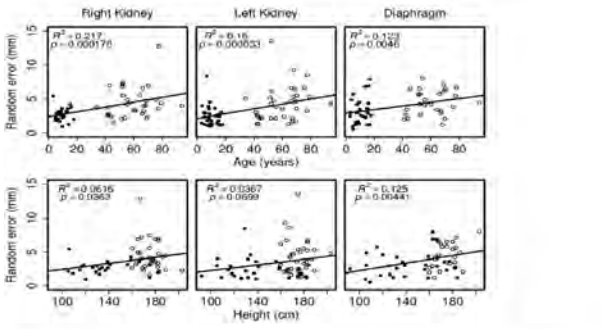

Figure 1. The correlation between the patient random error (mm), and age (years) and height (cm) in children (black dots) and adults (open circles) in the cranio-caudal direction.

Conclusion: Our results show that renal and diaphragmatic interfractional motion in children tend to be smaller than in adults, suggesting that abdominal PTV margins in children could be reduced. The difference in organ motion in the two groups could not completely be explained by age or height, indicating that further research is needed to understand the underlying mechanisms.

OC-0162

Liquid fiducial markers' performance in non small cell lung cancer during radiotherapy

J. Scherman Rydhög[1,2], S. Riisgaard Mortensen[1], K. Richter Larsen[3], P. Clementsen[4,5], R. Irming Jølck[6,7], M. Josipovic[1,2], M. Aznar[1,2], G. Persson[1], T.L. Andresen[6], L. Specht[1], P. Munck af Rosenschöld[1]

[1]*Rigshospitalet, Department of Oncology- Section of Radiotherapy, Copenhagen, Denmark*

[2]*University of Copenhagen, Niels Bohr Institute, Copenhagen, Denmark*

[3]*Bispebjerg Hospital, Department of Pulmonary Medicine, Copenhagen, Denmark*

[4]*Gentofte University Hospital, Department of Pulmonary Medicine, Copenhagen, Denmark*

[5]*Rigshospitalet, Centre for Clinical Education, Copenagen, Denmark*

[6]*DTU Nanotech, Department of Micro-and Nanotechnology, Lyngby, Denmark*

[7]*Nanovi, Nanovi Radiotherapy A/S, Lyngby, Denmark*

Purpose or Objective: We developed a new liquid fiducial marker (BioXmark®) for use in image-guided radiotherapy (IGRT). The liquid solidifies into a three dimensional (3D) structure after injection into tissue. A good level of marker's

visibility in a lung phantom using 2D and 3D x-ray imaging was previously shown. We report results and experiences from the study examining the performance (structural - and geometrical stability) of the liquid marker during radiotherapy of patients with non-small cell lung cancer (NSCLC) in free breathing (FB) or deep inspiration breath hold (DIBH).

Material and Methods: Fifteen patients had markers implanted into the primary tumour and/or involved lymph nodes. Cone-beam computed tomography (CBCT) images were acquired daily during the course of radiotherapy (66 Gy / 33 fractions). The fiducial markers were contoured automatically on all the daily acquired images, using a 400 Hounsfield Units (HU) level as threshold, in the treatment planning system Eclipse (v. 13.0), the data was retrieved and analysed using Eclipse scripting API and Matlab v2014b, respectively. The stability of the marker inside the tumour and the lymph nodes was evaluated visually. The structural stability of the marker regarding volume and radio-opacity was evaluated as physical measured volume and mean HU, analysed over time. Furthermore the positional stability of all markers was analysed by weekly measurements of the change of the distance between marker centre position and carina, as a surrogate for inter-fractional variation in position of the tumours and the lymph nodes.

Results: Two patients did not receive radiotherapy and thus 13 patients with 29 markers were analysed (9 injected into tumours and 20 injected into lymph nodes). Ten patients were treated in DIBH and three in FB. All injected markers stayed in the injected site between planning and end of treatment. The variation in global mean HU was larger for all primary tumour markers (937±227 HU, mean±SD) compared to lymph nodes markers (921±153HU). This might be because tumours have a larger anatomical change/shrinkage compared to lymph nodes, which in turn affects the liquid marker. The measured sizes of the markers showed good stability during treatment (See Figure)

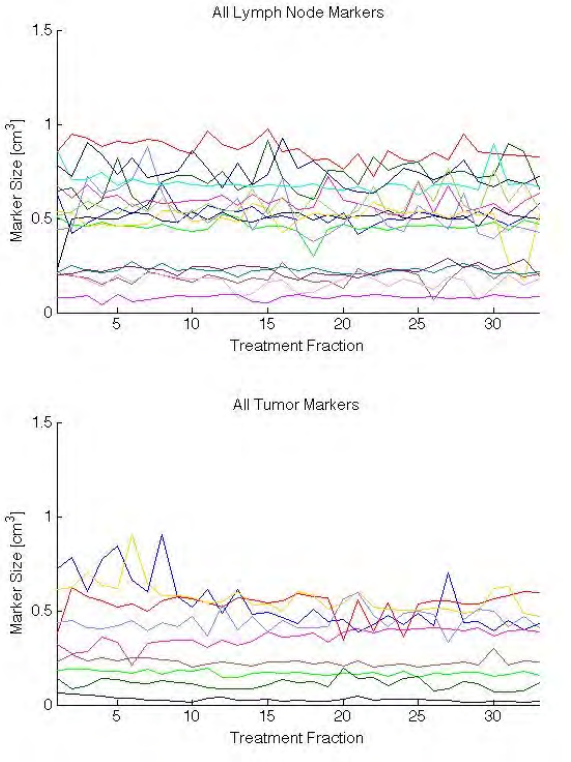

In terms of IGRT, the markers were visible on CBCT throughout the treatment; DIBH related artefacts in the markers (elongated markers due to inter-breath hold variation) were observed on a few patients. Three patients (two DIBH and one FB) showed > 5 mm inter-fraction variation in marker position relative to carina, possibly due to tumour/lymph node shrinkage or anatomical changes. They were all rescanned for treatment adaptation.

Conclusion: The liquid fiducial markers remained stable throughout the treatment course regarding position inside the target, physical volume and radio-opacity on CBCT. The BioXmark® liquid marker offers an interesting alternative to solid markers.

OC-0163

Robustness of proton RT with different beam angles towards inter-fractional motion in the pelvis

A. Andersen[1], O. Casares-Magaz[1], J. Petersen[1], J. Toftegaard[1], L. Bentzen[2], S. Thörnqvist[3], L. Muren[1]
[1]*Aarhus University Hospital, Medical Physics, Aarhus, Denmark*
[2]*Aarhus University Hospital, Radiation Oncology, Aarhus, Denmark*
[3]*Haukeland University Hospital, Medical Physics, Bergen, Norway*

Purpose or Objective: The benefit of proton therapy may be jeopardized by dose deterioration caused by water equivalent path length (WEPL) variations e.g. due to inter-fractional motion. The aim of this study was to explore patient- and population-specific patterns in the robustness towards inter-fractional motion for pelvic lymph node (LN) irradiation of prostate cancer patients using proton beams from different directions.

Material and Methods: Image data sets of 18 patients consisting of a planning computed tomography (pCT) and multiple repeat CT (rCT) scans with target volumes and organs at risk (ORs) outlined in all scans were used. Ray path WEPLs were computed by averaging over beams eye view WEPL maps at all possible beam angle configurations (for both gantry and couch in 5° angle intervals) considering left and right LNs separately. For 0° couch angle the mean and the standard deviation of the WEPL differences between all rCTs and the pCT WEPL map were extracted for the entire population. Finally, single beam spot scanning proton plans were optimized for all gantry angles (couch angle 0°) over the planning target volume (PTV) generated from the clinical target volume (CTV) using isotropic margin configurations (3 and 5 mm). The optimized fluence maps for the pCT for each beam angle were applied onto all rCTs and the dose distributions re-calculated, and dose differences were extracted.

Results: The WEPL analysis for the left and right section of the lymph nodes showed a general pattern of least variation around couch angle = 0°. Furthermore it showed three minima across the mean of the patient WEPL maps at couch angle = 0° for gantry angles of 0-25°, 125-140° and 170-180° for the left section, as well as gantry angles of 180-220° and 330-355° for the right section, which also appeared to be the angles of lowest variations among patients (Fig.1). The clustering analysis of the WEPL maps at couch angle = 0° against the angles showed for the left section of the lymph nodes that the patients split into three groups from which one group of two patients showed a clearly different pattern of lower variation in the lateral and posterior angles. The other fourteen patients were closer correlated and showed highest variation for the lateral angles (Fig.1). For the right section of the lymph nodes the patients were split into two groups of nine and seven patients, where the seven had a visibly higher variation in the posterior angles as the main difference. The dose calculation results showed similar results as for the WEPL variation, e.g. for the left LNs angles around 25-35°, 100-110° and 160-170° were consistently preferable for the bowel, bladder and rectum as well as LN dose deterioration.

Conclusion: We have found that WEPL maps show population-specific patterns and that there were consistent patterns in which angles are most robust. Similar 'robust' angles were also found in the dose/volume analysis.

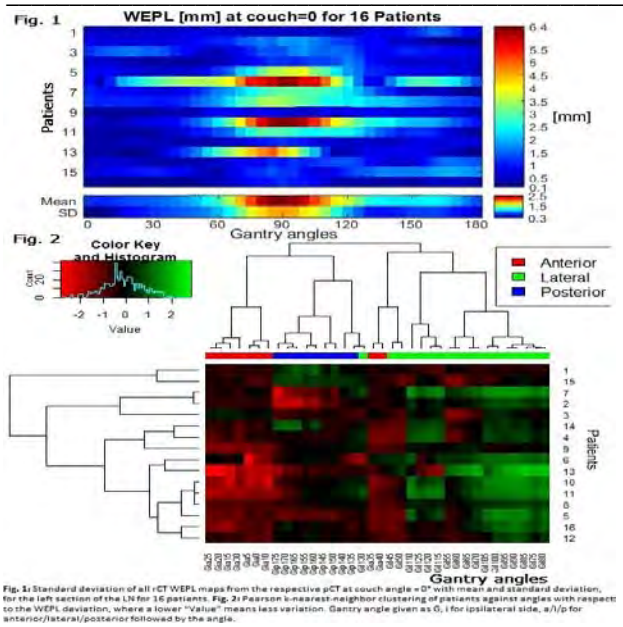

Fig. 1: Standard deviation of all rCT WEPL maps from the respective pCT at couch angle = 0° with mean and standard deviation, for the left section of the LN for 16 patients. Fig. 2: Pearson k-nearest-neighbor clustering of patients against angles with respect to the WEPL deviation, where a lower "Value" means less variation. Gantry angle given as 0, i for ipsilateral side, a/l/p for anterior/lateral/posterior followed by the angle.

OC-0164

Integrate range shifting in immobilisation for proton therapy: 3D printed materials characterisation

S. Michiels[1], N. Lammens[2], A. D'Hollander[3], K. Poels[4], W. Crijns[4], G. Defraene[1], S. Nuyts[1], K. Haustermans[1], T. Depuydt[1]

[1]KU Leuven, University of Leuven, Department of Oncology
[2]Ghent University, Department of Materials Science and Engineering, Ghent, Belgium
[3]Materialise NV, Department of BioMedical Engineering, Leuven, Belgium
[4]University Hospitals Leuven, Department of Radiation Oncology, Leuven, Belgium

Purpose or Objective: 3D printing technology is investigated for the purpose of patient immobilization during proton therapy. It potentially enables a merge of patient immobilization, bolus range shifting/compensator and other functions into one single patient-specific structure. Beside minimizing the lateral spread of the proton beam due to the removal of the air gap it also ensures the correct range shifting is present for each beam portal. Compared to a movable nozzle snout this reduces the risk of collision and treatment time, hence can increase cost-effectiveness of proton therapy. In a first step, a set of 3D printed materials is characterized, in terms of structural and radiological properties, elemental composition, directional dependence and structural changes induced by radiation damage. These data will serve as input for the design of 3D printed immobilization structure prototypes.

Material and Methods: In total 9 materials used in 4 different 3D printing production techniques were subjected to testing. Samples with a nominal dimension of 20x20x80mm were 3D printed. The actual dimensions of each printed test object were measured with a calliper. The samples were compression tested according to a standardized method (ASTM D695). The composition in terms of effective atomic number (Z_eff) and relative electron density (RED) to water was derived from dual-energy CT (DE-CT) data (80kVp,Sn140kVp), allowing estimation of the stopping power ratio (SPR) to water. Range shifting and directional dependence in 3D printed materials were investigated in a 62 MeV proton beam, using radiochromic film in a Plastic Water phantom.

Results: The data of the different experiments are compiled in Table 1. Young's moduli as low as 1 MPa and as high as 2582 MPa were seen. These experiments will be repeated after extensive radiation exposure to verify radiation hardness of the structural properties. The DE-CT decomposition yielded relative electron densities ranging from 0.62 to 1.20, and Z_eff from 6.06 up to 9.35. The calculated SPR ranged from 0.69 up to 1.21. The differences in range shifts of the obtained Bragg peaks were results of differences in SPR, and of deviations from the nominal 20 mm thickness due to printing technique geometrical tolerances. For 4 out of the 9 materials, a different orientation of the sample with respect to the beam incidence resulted in more than 5% difference in the obtained range shift. Measurements using a Bragg-peak ionization chamber will be included allowing a water equivalent thickness measurement validation of the material decomposition method with DE-CT.

Table 1: Overview of the different 3D printed materials in terms of their mechanical, radiological and range shifting capabilities.

		Dimensional measurement	ASTM D695 compression test	DE-CT derived properties (*)			62 MeV Proton beam measurements	
Material	3D-printing Production method	Thickness in orthogonal directions [mm]	Young's-modulus [MPa]	RED [#/cc]	Z_eff [-]	SPR [-]	Residual range (d90%) [mm]	Directional residual range difference [%]
ABS	Fused Deposition Modeling (FDM)	20/20.3	618	0,62	9,35	0,62	14,45	31,36
Tusk XC2700T	Stereolithography	20/20	1953	1,14	9,07	1,15	6,6	6,06
HeartPrint Flex	Polyjet digital	19,95/20	1	1,11	6,06	1,14	7,7	7,69
TangoPlus	Polyjet digital	19,8/19,8	1	1,11	6,06	1,13	7,45	2,01
VeroWhite	Polyjet digital	20,2/20	1658	1,16	5,95	1,19	5,95	4,39
PA-12	Laser sintering	20/20	/	0,99	6,50	1,00	9,2	2,79
PA-Alu filled	Laser sintering	20/20	1558	1,20	8,84	1,21	6,6	2,33
PA-Glass Fiber	Laser sintering	19,95/19,95	2582	1,22	8,03	1,21	5,6	1,82
TPU	Laser sintering	20,8/20,9	30	1,10	6,07	1,12	6,45	8,53
Plastic Water (baseline)		20/20	/	1,00	9,24	1,00	8,85	0
True water		/	/	1,00	7,41	1,00	/	/

(*) Method used from Hünemohr N. et al., "Experimental verification of ion stopping power prediction from dual energy CT data," Phys. Med. Biol. 59, 83-96 (2014)

Conclusion: 3D printed materials exhibit a wide variation in structural and radiological properties. The quantification of these characteristics can be used for optimal material selection for the design of a 3D printed immobilization structure for proton therapy with integrated range shifting.

Proffered Papers: RTT 2: Improving quality for breast cancer treatments

OC-0165

Deep inspiration breath hold – can it be detrimental to the heart?

B. Done[1], A. Michalski[1], A. Windsor[1,2]

[1]Central Coast Cancer Centre, Radiation Oncology, Gosford, Australia
[2]University of New South Wales, Faculty of Medicine, Randwick, Australia

Purpose or Objective: Deep inspiration breath hold (DIBH) is widely used internationally as a standard treatment for left sided breast cancer patients.Preliminary results from our institution suggest that there is a cohort of patients who have an increase in cardiac dose with DIBH compared to free breathing (FB). To our knowledge, there are no published studies assessing if DIBH can be a detriment in selected patients. Our primary objective was to identify patient cohorts based on the potential detriment to heart dose constraints. The secondary objective was to evaluate predictive criteria which would define the degree of benefit of DIBH.

Material and Methods: All patients who had left breast or chest wall radiotherapy and had both a FB and DIBH CT simulation scans at a single institution were selected for this study. Planning target volumes (PTV), lung, heart and left anterior descending (LAD) artery were contoured on both FB and DIBH CT data sets. Both data sets were planned using parallel opposed tangents and dynamic wedges. Plans were prescribed either 50Gy in 25 fractions or 42.4Gy in 16 fractions. DIBH plans were considered acceptable for treatment delivery where the heart dose constraints were reduced, without exceeding lung dose tolerances. Given the lack of guidelines on LAD contouring and acceptable dose constraints, LAD was contoured and doses recorded for

research purposes, but not used for clinical decision making. Doses to the PTV, lung, heart and LAD were recorded. Four patient groups were identified for comparison: those who had at least one heart parameter worse with DIBH, minimal benefit arbitrarily defined as less than 20%, moderate benefit defined as between 20%-70% and a major benefit defined as greater than 70%.

Results: Data was collected for a total of 70 patients. Overall, using DIBH, lung volume increased on average by 68% (range: 18.5% – 124.3%) while the heart volume in the treatment field was reduced by an average 69.5%. The LAD volume within the treatment field was reduced by 53%. The degree of benefit for heart and LAD doses is outlined in table 1. 10% had at least one heart parameter worse with DIBH. Where the mean heart dose was higher all other heart constraints were worse. Five patients had an increase in the heart volume and maximum heart distance in the treatment field.

Table 1: Number of patients (n) and the detriment or degree of benefit to the heart and LAD doses compared to the range of lung volume increase (%) using DIBH versus free breathing

n (% of lung volume increase)	Dose Increase	Minimal Dose Reduction (<20%)	Moderate DoseReduction(20-70%)	Maximum DoseReduction(>70%)
Heart mean	4 (18.5-86.1)	11 (27.4-98.9)	48 (24.9-124.3)	7 (54.6-108.4)
Heart max (D2%)	7 (18.5-98.9)	8 (33.2-94.4)	24 (24.9-103.3)	31 (47.9-124.3)
Heart V25Gy	4 (23.73-86.1)	5 (27.4-98.9)	16 (32.57–98)	36 (24.86-124.3)
LAD mean*	9 (27.4-98.9)	10 (23.7-103.6)	26 (33.2-103.3)	18 (24.9-124.3)
LAD max (D2%)*	10 (18.5-98.9)	20 (23.7-103.6)	17 (32.6-108.4)	16 (24.9-124.3)
LAD V20Gy*	6 (18.5-98.9)	10 (32.9-103.6)	17 (23.7-93.2)	30 (24.9-124.3)

*Only 63 patients had LAD contours completed

Conclusion: Patients where DIBH was detrimental to heart dose constraints, no clear correlation could be drawn to identify this cohort of patients. Lung volume or percentage increase did not necessarily lead to more favourable outcomes, thus could not be used as a criteria for patient selection for DIBH. We aim to establish further predictive criteria in the second phase of this study. Until such time dual planning remains essential to identify patients who should not be offered DIBH.

OC-0166

The influence of tumour location in the breast on boost modality selection.

E. Reilly[1], C. Baker[2], M. Flynn[3], H.M.O. Mayles[2], A.J. Reilly[4]
[1]*Altnagelvin Area Hospital, Radiotherapy, Londonderry, United Kingdom*
[2]*Clatterbridge Cancer Centre, Radiotherapy Physics Department, Wirral, United Kingdom*
[3]*University of Liverpool, School of Health Sciences, Liverpool, United Kingdom*
[4]*Altnagelvin Area Hospital, Radiotherapy Physics Department, Londonderry, United Kingdom*

Purpose or Objective: To establish whether photon or electron beams provide better dose coverage to tumour bed sites in different regions of the breast.

Material and Methods: 10 patient data sets were selected from a trial cohort, 2 patients each with tumour beds in one of 5 regions within the breast – Superior Lateral Quadrant (SQL), Superior Medial Quadrant (SMQ), Inferior Lateral Quadrant (ILQ), Inferior Medial Quadrant (IMQ) and the Central Quadrant. The dose to the whole breast treatment of 50Gy in 25 fractions was combined with a boost plan to the tumour bed of either photons or electrons with a dose of 16Gy in 8 fractions. Dose to the PTV, lung, heart and breast tissues outside the tumour bed were assessed by using DVHs.

Results: Tumours in the SLQ received better dose coverage by the photon boost plans. In all other areas of the breast the tumour bed coverage objectives were met with either photons or electrons.The target coverage in the combined plans was at least the same as or better than electrons with photon beams in all cases (Figure1). Electron beam coverage is dependent on surface contour regularity and tumour geometric shape, particularly if the PTV is not perpendicular to the skin surface and so requiring higher electron energies for PTV coverage at the deep margin. Lung had consistently lower doses with photon boost plans as the higher electron energies selected for target coverage in some plans increased lung dose (Figure2). The breast outside the tumour bed received lower doses with photon boosts. The heart doses were not consistently lower with either modality.

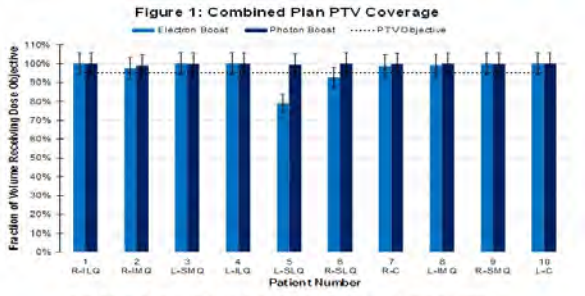

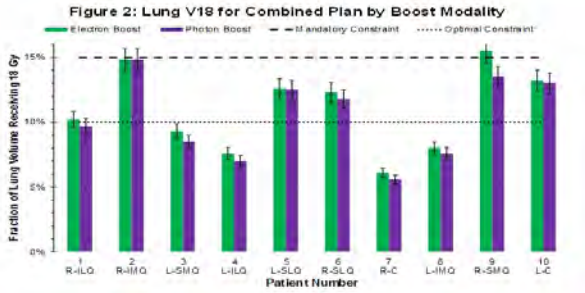

Conclusion: Electrons were a less favourable modality for SLQ tumours, but either photons or electrons could be suitable for treating tumours in other regions of the breast in terms of target coverage and organ sparing. As photon boosts provided the same as or better coverage than electrons in combined plans, it would be feasible to use photons for all boosts. However, individualised planning is necessary to account for tumour position in relation to normal anatomy, surface contour and geometrical shaping of the tumour bed to optimise PTV coverage and organ sparing. If using electrons particular attention must be paid to the use of bolus for beams planned on irregular surface contours.

OC-0167

Advanced left-side breast cancer: does VMAT allow doses of organs at risk to be reduced?

P.C. Yu[1], H.H. Nien[1], C.J. Wu[1], Y.L. Tsai[1]
[1]*Cathay General Hospital, Radiation Oncology, Taipei, Taiwan*

Purpose or Objective: This study was to quantify the reduced dose of right lung and right breast tissue by modified volumetric modulated arc therapy (MVMAT) for advanced left-side breast cancer including lymph node irradiation.

Material and Methods: For all cases, the clinical target volume (CTV) consisted of the left breast, axillary lymph nodes, internal mammary chain lymph nodes, infraclavicular lymph nodes, and supraclavicular lymph nodes. 7 patients of MVMAT and 5 patients of volumetric modulated arc therapy (VMAT) were generated with the Eclipse Version11 treatment planning system. VMAT plans were generated using a five full rotation without avoidance sector. MVMAT plans were generated using a five partial rotation with avoidance sector.Two half arcs were for supraclavicular lymph nodes. Gantry angle started at 179 degree, stopped at 335 degree, and the 60-120 degree was set to be avoidance sector.

Gantry angle started at 181 degree, stopped at 35 degree, and the 240-300 degree was set to be avoidance sector. Two half arcs were for left-side breast and axillary nodes. Gantry angle started at 153 degree, stopped at 282 degree, and the 0-90 angle was set to be avoidance sector. Gantry angle started at 282 degree, stopped at 161 degree, and the 0-90 angle was set to be avoidance sector. One quarter arc was for internal mammary node. Gantry angle started at 179 degree, stopped at 270 degree, and the 60-120 angle was set to be avoidance sector. The dose-volume-histogram were evaluated the target homogeneity and conformity and normal tissue tolerance dose.

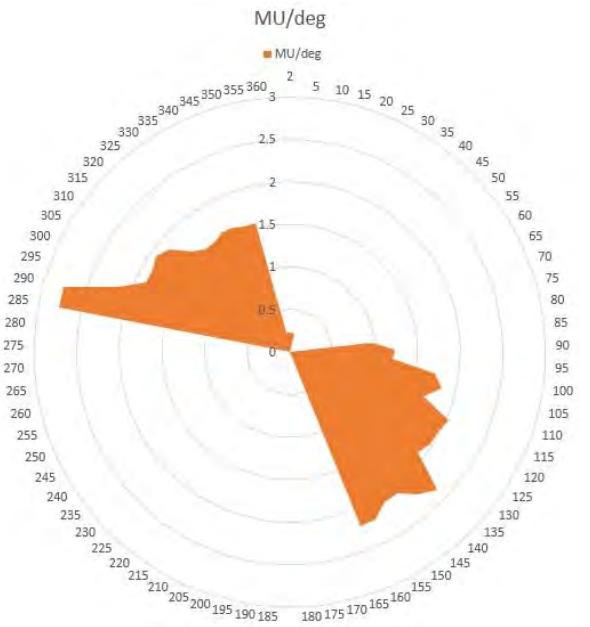

Results: MVMAT has significantly (p-value = 0.031) decreased right-side breast dose (V5Gy (%) = 39.9 ± 7.6), and has significantly (p-value = 0.005) decreased right lung dose (V5Gy (%) = 23.6 ± 7.3). Slightly less heart and left lung dose are found for MVMAT (heart V10Gy (%) = 45.7 ± 17.4, left lung V10Gy (%) = 48.6 ± 3.4) than in VMAT (heart V10Gy(%)=55.7 ± 19.9, left lung V10Gy(%)=53.4 ± 5.1). MVMAT for advanced left-side breast cancer retains target homogeneity and coverage when compared to VMAT.

		VMAT		modified VMAT		
		mean	SD	mean	SD	p value
PTV-50Gy	V47.5Gy(%)	99.0	2.0	99.4	0.7	0.605
	D2%(Gy)	54.5	0.9	55.2	0.4	0.103
PTV-CW	V47.5Gy(%)	98.9	2.3	99.6	0.5	0.536
	D2%(Gy)	54.6	0.9	55.0	0.7	0.453
PTV-nodes(IMN, SCF, ICF, AXLN)	V47.5Gy(%)	99.7	0.2	99.0	1.1	0.217
	D2%(Gy)	54.5	1.0	55.1	0.5	0.208
Heart	mean dose	14.9	5.1	12.3	3.1	0.303
	V30(%)	10.5	10.8	6.9	3.7	0.429
	V10(%)	55.7	19.9	45.7	17.4	0.393
	V5(%)	92.5	11.2	82.2	15.8	0.267
LT lung	mean dose	17.2	1.1	15.4	2.5	0.214
	V20(%)	31.1	2.0	29.1	1.0	0.096
	V10(%)	53.4	5.1	48.6	3.4	0.086
	V5(%)	85.3	5.6	80.7	7.8	0.315
RT lung	mean dose	5.9	1.5	3.7	0.7	0.007*
	V10(%)	11.7	10.3	3.1	1.5	0.136
	V5(%)	45.0	12.6	23.6	7.3	0.005*
total lung	mean dose	10.5	1.3	8.9	0.3	0.048*
	V20(%)	13.6	2.5	12.0	0.9	0.143
	V5(%)	61.8	8.7	47.8	5.2	0.006*
RT breast	mean dose	8.5	3.0	5.2	0.7	0.046*
	V10(%)	30.4	21.9	12.7	7.8	0.132
	V5(%)	62.4	17.3	39.9	7.6	0.031*

Conclusion: MVMAT is suitable for advanced left-side breast cancer treatment. It retains target homogeneity and coverage and decreases the dose of right breast and right lung.

OC-0168

A simple visual test is adequate for testing vmDIBH reproducibility in locoregional breast cancer

L.A. Den Otter[1], T.T. Nuver[1], M. Boerhof[1], H.H. Kolkman-Nijland[1], W.J. Schoevers[1], K. Muller[1], A.W.H. Minken[1]
[1]*Radiotherapiegroep, Radiotherapy, Deventer, The Netherlands*

Purpose or Objective: Voluntary moderately deep inspiration breath hold (vmDIBH) reduces the heart dose for radiotherapy of left-sided breast cancer patients. For locoregional breast cancer patients, the application of vmDIBH requires high reproducibility to assure the absence of gap or overlay between tangential breast fields and supraclavicular irradiation fields.
In this study we present a simple and fast visual method to quantify movement around the junction of the tangential and supraclavicular fields. The simple method is evaluated by testing the target volume reproducibility using two consecutive CT-scans during vmDIBH. Heart position reproducibility is assessed as well, with the resulting dosimetric consequences.

Material and Methods: For 80 consecutive breast cancer patients cranial-caudal (CC) displacement around the clavicle was quantified between five vmDIBHs. This was done in the CT room, before obtaining the planning CT scan. Intersecting CT laser lines were marked on tape and the maximum displacement was measured. This tape was positioned midclavicularly, with the horizontal laser lines on the junction line.
For 19 patients who would be irradiated locoregionally, a second CT scan was additionally acquired. The CC displacement of the left clavicle between the two breath holds was quantified by contouring the clavicle in both CT scans, and rigid registration of the two volumes in ProSoma (v.3.3.266, Medcom, Darmstadt, Germany) virtual simulation software.
The heart was delineated in both CT scans, excluding the great vessels. The two volumes were registered in ProSoma to measure CC, left-right (LR) and anterior-posterior (AP) displacements. Influence of the heart displacement on dosimetry was measured by superimposing the contoured heart volume of the second CT scan onto the treatment planning CT scan and calculating mean heart dose.

Results: Results of the tape test show a mean CC displacement of 3.3 mm (range 0.5-8.0 mm) for the midclavicular region. For the two breath hold CT scans mean CC clavicle displacement was 1.1 mm (range 0.1 - 2.8 mm). The measured CC displacements of the tape test were for all 19 locoregional patients larger than measured with CT.
Mean difference in contoured heart volume was 3.7% (range 0.5 - 11.2%). Mean heart dose differed on average 0.12 Gy (range 0.01 - 0.38 Gy), where planned mean heart dose varied between 0.59 and 3.58 Gy. Mean heart displacement was 1.7 mm (range 0-4.7 mm) CC, 1.5 mm (range 0.1-4.2 mm) AP and 1.9 mm (range 0.1-6.9 mm) LR.

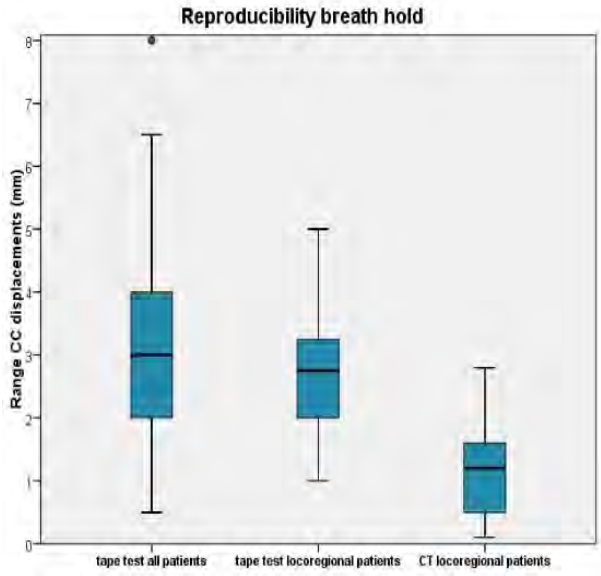

Conclusion: A simple visual test is a good surrogate for CT scans in analyzing vmDIBH reproducibility. We showed that vmDIBH is reproducible with minimal gap or overlay between

the tangential and supraclavicular fields, allowing for implementation of vmDIBH in locoregionally irradiated patients. Heart position variation is limited to 2 mm and dose variation to 0.4 Gy, between sequential breath holds for most patients.

OC-0169

Patient information through group sessions to improve knowledge regarding breast cancer radiotherapy

M.T.A. Tinggaard Axelsen[1], M.J. Jensen[1], B.H. Haislund[2], H.M.N. Melgaard Nielsen[3]
[1]*Aarhus University Hospital, Department of Oncology, Herning, Denmark*
[2]*Aarhus University Hospital, Department of Oncology-, Herning, Denmark*
[3]*Aarhus University Hospital, Department of Oncology, Aarhus, Denmark*

Purpose or Objective: To inform early breast cancer patients about postlumpectomy radiotherapy (RT) in group session, and to evaluate their knowledge regarding side-effects and precautions compared with patients informed by doctors.

Material and Methods: From April 2015 to June 2015, patients referred for RT at a single institution were informed about RT during one hour group sessions (pilot group). These were held twice a month with up to six patients and their relatives. The patients and relatives were informed about RT preparation procedures, structure of the linac and beams effect, side effects, precautions and lifestyle recommendations during and after RT, by radiation therapists, using power-point presentations. After these group sessions, the patients had a 30 min individual consultation including an examination by a doctor. The patient's knowledge regarding side-effects and precautions were evaluated using a questionnaire that they anonymously were asked to answer in connection with the following planning CT scan. The same questionnaire was filled in by patients before April 2015 (control group), thereby being able to compare knowledge of side-effects and precautions during RT among patients informed during group sessions compared with patients informed by doctors. The two groups were compared using chi-square statistics.

Results: 33 patients filled in the questionnaire after conventional information and 25 patients after group sessions. The following subjects were more often correctly answered by patients informed during group sessions: Acute toxicity (p< 0.001), sequence of acute events (p=0.16), precautions during RT (p=0.006), late toxicity (p=0.07), reasons for recommendation of non smoking (p=0.03) and use of skin care cream (0.002). The group sessions were timesaving for both the radiation therapists and the doctors and especially for left sided patients, information about respiratory gated RT resulted in reduced scheduled time for information. The patients were generally satisfied e.g.one said "I wish I was informed that way the last time I was given RT ". Participating patients were able to create personal relations to other participating patients. The radiation therapists were in general content and satisfied by the challenge of being responsible for RT information to these patients.

Conclusion: Patient's contentment and level of knowledge before initiating RT can be improved by educating and preparing the patients for RT during group sessions. These group sessions are now implemented as standard information procedure for all breast cancer patients, and it is considered to expand these sessions to other groups of cancer patients.

OC-0170

Detection of setup errors with body surface laser scanning system for whole breast irradiation

P. Jiang[1], Z. Liu[1], J. Wang[1], S. Zhou[1], J. Li[1], H. Sun[1], S. Jiang[1]
[1]*Peking University Third Hospital, Radiation Oncology department, Beijing, China*

Purpose or Objective: To investigate the clinical application of a technique for patient set-up verification in whole breast irradiation after conservative surgery based on a surface laser scanning registration system

Material and Methods: Displacements from concurrent Sentinel™ (Sentinel®, C-Rad Positioning AB, Sweden) surface imaging and Elekata Axesse accelerator cone beam CT (CBCT) registrations were compared for 10 patients with breast cancer after conservative surgery for a total of 130 set-ups. As comparison, the patient outline extracted from the planning CT system(Oncentra®, nucletron/Elekta, Sweden) was used as Sentinel™ reference (Ctref) and also was used as a reference for the CBCT method. Patients were first scanned both with surface laser scanning and CBCT, shifted to the optimal isocenter position according to CBCT verification. And then another optical scan was performed to verify the matching in relation to CBCT. Position detection by both surface scan and CBCT acquired for the first five fractions of radiotherapy and then twice weekly. The data collected by both systems were statistical analyzed by paired t-test using SPSS 13.0.

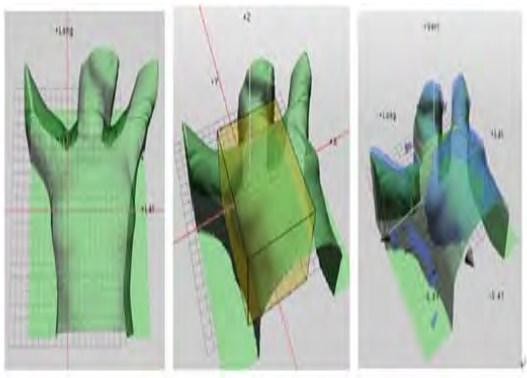

(A) extracted from the planning CT system was used as Sentinel™ reference CTref. (B) optical scan area range from the supraclavicularregion to submammary sulcus.(C) images of surface registration: green is the reference contour surface, and blue is new contour surface obtained by laser scan.

Results: The absolute translational setup errors (mean ± SD) in X (Lateral), Y (Lngitudinal), Z(Vertical) axes detected by CBCT prior radiation were 0.21±0.21cm, 0.29±0.26cm and 0.42±0.22cm respectively; rotational setup errors (mean ± SD) in Rx (Pitch), Ry (Roll), Rz (Yaw) axes were 0.83°±0.7, 1.12°±0.79 and 1.07°±0.81. The absolute translational setup errors (mean ± SD) in six directions detected by Sentinel™ prior radiation were 0.14±0.18cm, 0.15±0.14, 0.13±0.13, 0.77°±0.54, 0.76°±0.61 and 1.23°±0.95. The system accuracy was better than 1.5 mm and 1.1° when a Sentinel image was used as reference. Paired setup errors form Sentinel™ and CBCT showed no significant difference in five directions: X (t=-1.827, P=0.07), Y (t=0.125, P=0.9), Z (t=1.595, P=0.112) , Ry(t=-1.717, P=0.09) and Rz(t=2.382, P=0.6) axes, and significant difference in one direction of Rx(t=-3.409, P=0.03) axes.

Absolute set up errors of 6D directions(Mean ± SD)

	Lat(mm)	Lng(mm)	Vrt(mm)	Pitch Rx(°)	Roll Ry(°)	Yaw Rz(°)
CBCT (n=130)	0.21±0.21	0.29±0.26	0.42±0.22	0.83±0.7	1.12±0.79	1.07±0.81
Sentinel™ (n=130)	0.14±0.18	0.15±0.14	0.13±0.13	0.77±0.54	0.76±0.61	1.23±0.95

Conclusion: The Sentinel™ surface imaging device is a reproducible and consistent system able to detect misalignments with accuracy. This study shows good agreement between the surface scanner and CBCT in patient positioning. The Sentinel™ surface imaging system is a good supplement to the CBCT system for accurate set-up for fractions for whole breast irradiation after conservative surgery.

Poster Viewing : 4: Physics: Treatment planning: applications III

PV-0171

Can protons reduce bone marrow toxicity in definitive chemoradiotherapy for oesophageal tumours?

S. Warren[1], C. Hurt[2], T. Crosby[3], M. Partridge[1], M. Hawkins[1]
[1]*CRUK/MRC Oxford Institute for Radiation Oncology, Department of Oncology, Oxford, United Kingdom*
[2]*Wales Cancer Trials Unit, School of Medicine, Cardiff, United Kingdom*
[3]*Velindre Hospital, Velindre Cancer Centre, Cardiff, United Kingdom*

Purpose or Objective: Radiotherapy dose escalation using a simultaneous integrated boost (SIB) is predicted to improve local tumour control in oesophageal cancer patients (Warren IJROBP 2014), yet any increase in acute bone marrow toxicity could reduce treatment intensity, and limit any predicted improvement in patient outcome. In the SCOPE oesophageal trial, 28% of patients treated with concurrent cisplatin/capecitabine and 50 Gy in 25 fractions experienced grade ≥3 haematological toxicity (HT3+) (Crosby Lancet Oncol 2013). Proton therapy has been shown to significantly reduce haematological toxicity in lung cancer patients receiving concurrent chemotherapy (Komaki Radiother Oncol 2011); we investigate the potential of bone marrow sparing with protons compared to photons, in radiotherapy dose escalation for oesophageal tumours.

Material and Methods: 21 mid-oesophageal cancer patients with their original conformal plan (3D50) (chosen to be a representative subset of the SCOPE trial) were used to study the bone marrow dose delivered. A surrogate for bone marrow was created by outlining the thoracic vertebrae, sternum, scapulae, ribs and clavicles using the automatic thresholding tool in Eclipse (Varian). Additional plans were created retrospectively: a volumetric modulated arctherapy plan (VMAT50) with the same dose as 3D50. SIB plans with a dose prescription of 62.5 Gy to the high risk sub-region within the planning treatment volume were created using VMAT (VMAT62.5) and proton therapy plan (IMPT62.5). Bone V20 Gy and V10 Gy dose-metrics were recorded and compared across all plans using the Wilcoxon test and Holm Bonferroni correction for multiple testing. Parameters from gynaecological cancers (Bazan IJROBP 2012) were used to predict normal tissue complication probability (NTCP) of HT3+.

Results: 3D50 plans show the highest NTCP and V20 values for each patient. There is no significant difference between the VMAT50 and VMAT62.5 plans, although VMAT plans may cause a larger bone volume to be irradiated below 10 Gy than 3D50. IMPT62.5 showed significant sparing for both V10 and V20 and much reduced NTCP

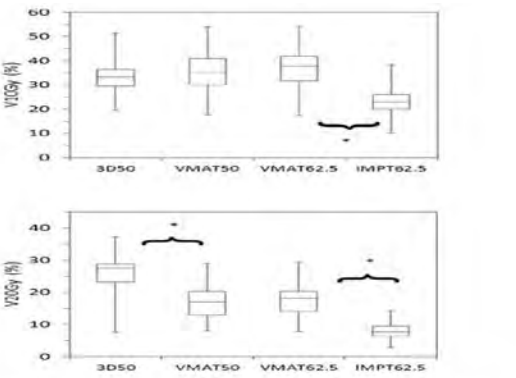

Comparing V_{10Gy} (top) and V_{20Gy} (bottom) for the four different plans. Plots show median (horizontal bar), interquartile range (box) and maximum and minimum (capped lines) values across all patients, with statistically significant differences between plans marked *.

Conclusion: Proton therapy plans show significant dose sparing for bone marrow in the 10-20 Gy dose region thought to be correlated with toxicity. These plans are predicted to reduce the risk of HT3+ by ~50% compared to photon techniques, and could therefore improve treatment efficacy of concurrent chemoradiotherapy for oesophageal cancers.

PV-0172

Selecting patients with lung cancer for proton therapy should be based on multivariable NTCP models.

M.C.A. Kramer[1], A.G.H. Niezink[1], E.W. Korevaar[1], R.G.J. Kierkels[1], H.P. Van der Laan[1], A. Van der Schaaf[1], V.C. Hamming[1], P. Kalk[1], J.A. Langendijk[1], J. Widder[1]
[1]*UMC Groningen, Radiotherapy Oncology Department, Groningen, The Netherlands*

Purpose or Objective: The aim of the study was to evaluate how the dosimetric benefit of intensity-modulated proton therapy (IMPT) translates into estimated toxicity risk reduction in patients with locally advanced non-small cell lung cancer (NSCLC). In addition, the potential to spare the heart with protons and photons was explored.

Material and Methods: Five patients with NSCLC were treated with concurrent chemoradiation, using standard lung-sparing photon volumetric-modulated arc therapy (L-VMAT) to 60 Gy in 25 fractions. Three additional treatment plans were created for each patient: heart-sparing VMAT (H-VMAT), worst-case robust heart-sparing IMPT (H-IMPT), and worst-case robust lung-sparing IMPT (L-IMPT). Doses to the organs at risk (heart, lung) were evaluated. Resulting normal tissue complication probability (NTCP) values for radiation pneumonitis were estimated using the dose-only QUANTEC model and the adjusted QUANTEC model including clinical risk factors 1.

Results: With IMPT, both H-IMPT and L-IMPT, DVH parameters including the mean lung dose (MLD), the lung volume receiving ≥20 Gy (V20L), the mean heart dose (MHD), and the volume of the heart receiving 30 Gy (V30 H) were all between 32 – 80% lower compared with L-VMAT (Tab 1). Furthermore, at these considerably lower dose levels with protons vs photons, the amount of dose redistributed to the lungs when the heart was particularly spared was still lower with protons (H-IMPT vs L-IMPT: 65% decrease MHD, 11% increase MLD), compared with photons (H-VMAT vs L-VMAT: 62% decrease MHD, 28% increase MLD). Using the dose-only QUANTEC model, comparing L-VMAT with L-IMPT, the lung-dose reductions translated into a reduction in the risk of symptomatic radiation pneumonitis between 4.5% to 9.2% (average, 5.8%). However, the QUANTEC model adjusted for a priori clinical risk factors showed a reduction of symptomatic radiation pneumonitis risk in patients without clinical risk factors by 2.5% to 5.4% (average, 3.3%) in contrast to 14.2% to 26.7% (average, 18.2%) risk reduction in patients with the highest a priori risk (Fig 1). For identical DVH reductions, and assuming a threshold risk reduction of ≥ 10% for G2-toxicity required for indicating proton therapy, an

actual indication for protons thus heavily rests on individual clinical and patient dependent a priori risk factors.

Table 1.

Dosimetric parameters for lung and heart for the different techniques and corresponding NTCP for symptomatic radiation pneumonitis (values in Gy or %).

	H-VMAT	L-VMAT (reference)	H-IMPT	L-IMPT
MeanLungDose	18.3±2.6	**14.3±1.9**	8.9±2.1	8.0±2.3
V20 Lung	34.7±4.2	**25.0±2.7**	17.0±4.0	14.8±4.4
MeanHeartDose	9.9±3.1	**15.9±2.9**	3.2±1.1	4.9±1.1
V30 Heart	10.1±5.9	**19.1±2.9**	4.3±2.0	7.1±2.1
Risk of radiation pneumonitis				
QUANTEC_dose only	17.7±4.5	**11.4±2.4**	6.2±1.7	5.6±1.6
QUANTEC_low clinical risk[1]	10. 1±1.4	**6.0±1.5**	3.0±0.9	2.6±0.9
QUANTEC_high clinical risk[1]	54.8±6.1	**41.2±6.2**	25.3±5.7	23.0±5.8

Figure 1.
Estimated NTCP value reductions (arrows) for symptomatic radiation pneumonitis for low (red line) and high (green line) a priori risk patients and patients irrespective of a priori risk factors (blue lines). Marked are the estimated risk reductions of symptomatic radiation pneumonitis for lung-sparing IMPT (grey lines) versus lung-sparing VMAT (black lines).

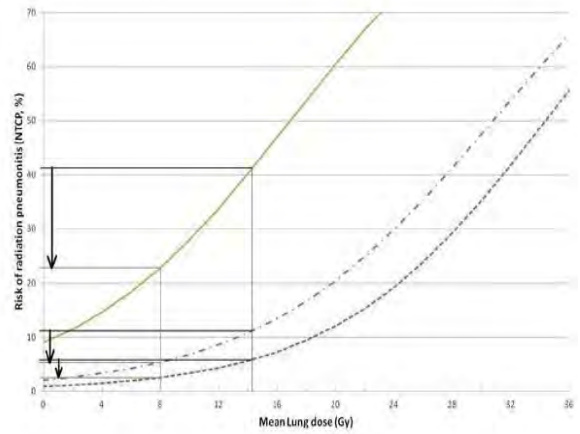

Conclusion: These results demonstrate that the potential of proton therapy to reduce the risk of radiation pneumonitis requires considerable reduction in lung dose, but translation into clinical significance is heavily driven by patient and clinical a priori risk factors. Therefore, multivariable NTCP models should play a major role in identifying patients eligible for proton therapy.

1 Appelt, Vogelius, Farr, Khalik, Bentzen. Towards individualized dose constraints: adjusting the QUANTEC radiation pneumonitis model for clinical risk factors. Acta Oncologica 2014;53:605.

PV-0173

Dosimetric assessment of three-source Co-60 and Linac-based lung SBRT for feasibility of MR-IGRT

N. Dogan[1], N. Lamichhane[1], A. Ishkanian[1]
[1]*University of Miami- Sylvester Comprehensive Cancer Center, Department of Radiation Oncology, Miami- Florida, USA*

Purpose or Objective: The purpose of this study is to provide a dosimetric assessment for the feasibility of delivering lung SBRT using an integrated three-source Co60 and Magnetic Resonance Imaging (MRI) Guided Radiation Therapy (MR-IGRT) System.

Material and Methods: Ten lung patients who were previously treated with Linac-based SBRT were included. For each patient, GTV, PTV, cord, lungs, heart, esophagus, and ribs were delineated. All Linac-based SBRT plans were generated using VMAT and consist of 2-10 6MV Rapid Arcs. Patients received prescription doses of 48 Gy/4fx to 50 Gy/5fx. The Linac-based plans were imported into the View Ray MR-IGRT system for planning. Three-source Co60 plans were generated using step-and-shoot IMRT and utilized Monte Carlo dose calculation including the magnetic field correction of 0.35T. The PTV coverage for both Linac-based three-source Co60 SBRT plans were such that 95% of the PTV received 100% the prescription dose. Finally, Linac- and three source Co60 – based plans were evaluated using dose-volume constraints for critical structures and target conformity index (CI), homogeneity index (HI) for the PTV.

Results: The differences between PTV HI for Linac- and three-source Co60 -based SBRT plans were not statistically significant, ranging from 1.05 to 1.15. Three patients with the CIs >1.2 had target volumes <20cc although the location of the target did not have much influence on meeting the criteria for the target conformity. For all patients, the critical structure doses, such as maximum cord dose (<26 Gy), dose to <15 cc of the heart (28Gy<15cc), and <5cc of the esophagus (18.8 Gy<5cc) were satisfactory with both techniques. For lung, although both the dose to <1500cc (11.6 Gy<1500cc) and <1000cc (13.6Gy<1000cc) criteria were met with both techniques, on average, the lung volumes receiving the 11.6Gy and 13.6Gy were 59.5% and 61.28% higher with three-source Co60 as compared the Linac-based SBRT plans respectively (P<0.05). As expected, low dose portion of the DVH for all critical structures generally covered much higher percentage of the critical structure volumes with three-source Co60 SBRT plans as compared to the Linac-based SBRT plans.

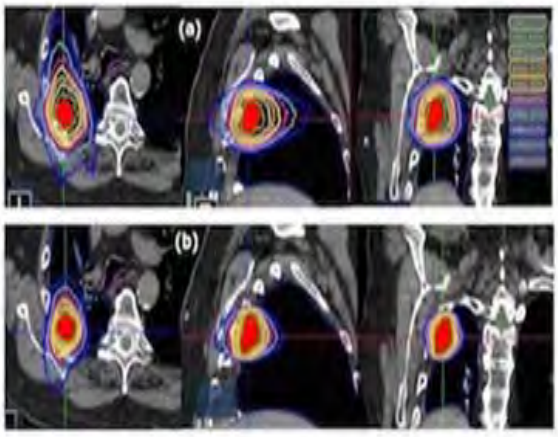

Figure 1: Dose distributions in axial, sagittal and coronal slices obtained with (a) three-source Co[60] MR-IGRT system (View Ray, Inc.) and (b) 3 Rapid Arcs (Varian Eclipse) for one of the lung SBRT cases included in this study (Prescription Dose: 50 Gy/5 fx, green isodose line).

Conclusion: Overall, a three-source Co60 integrated MR-IGRT system produced comparable dose distributions to the ones obtained with the Linac-based lung SBRT. Further studies are needed to evaluate benefits of this novel MR-IGRT system for lung SBRT, especially its ability to image and plan in real time and online adaptive treatment delivery.

PV-0174

Experimental verification of 4D Monte Carlo calculations of dose delivered to a moving anatomy

J. Cygler[1], S. Gholampourkashi[2], J. Belec[1], M. Vujicic[1], E. Heath[2]
[1]*The Ottawa Hospital Regional Cancer Centre, Medical Physics, Ottawa, Canada*
[2]*Carleton University, Physics, Ottawa, Canada*

Purpose or Objective: To experimentally validate a 4D Monte Carlo (MC) simulation method to calculate the dose

delivered by an Elekta Agility linear accelerator to a moving anatomy.

Material and Methods: A Quasar respiratory motion programmable phantom (Modus Medical) with a lung insert containing a 3 cm diameter tumour was used for dose measurements. Measurements were performed on an Elekta Agility linac with the phantom in static and moving (sinusoidal motion, 1.8 cm respiratory amplitude) states. Dose to the centre of the tumor was measured using calibrated EBT3 film and the RADPOS 4D dosimetry system. The RADPOS position tracker recorded the phantom motion with time steps of 100 ms. Static and 4DCT scans of the Quasar phantom were acquired using a helical CT scanner (Brilliance CT Big Bore). A single 6 MV 4x4 cm2 square field covering the tumour was planned on the static CT scans using the Elekta XiO V.4.7 treatment planning system. A previously validated BEAMnrc model of our Elekta Agility linac was used for all simulations. The DOSXYZnrc and defDOSXYZnrc user codes were used, respectively, for static and moving anatomy dose simulations with 500,000,000 histories to achieve a statistical uncertainty of 0.4%. The defDOSXYZnrc code was modified to sample a new geometry for each incident particle, thereby simulating the continuous phantom motion. The treatment plan was exported from XiO as DICOM format and a Python script was used to extract the data and generate input files for MC simulations. An egsphant file with 0.1250 x 0.1250 x 0.1 cm3 resolution was generated from static CT scans for all simulations. The multipass deformable image registration algorithm in Velocity (Varian Medical Systems) V.3.0.1 was used to register the CT image of the phantom in end-of-exhale state to the static CT image. For 4D simulations, deformation vectors from Velocity were input to the defDOSXYZnrc code as well as the phantom motion trace measured with RADPOS. To examine the impact of deformable registration accuracy, 4D simulations were also performed using manually generated deformation vectors that exactly modelled the rigid translation of the lung insert.

Results: Table 1 shows the calculated and measured tumor doses and their uncertainties. Calculated dose for the moving anatomy using vectors generated by Velocity was 75.9 cGy±0.4% that is 0.5% lower than the similar calculation using manually generated vectors.

Table 1. Calculated and measured tumor doses and their uncertainties

Phantom	Dose (cGy)				%Ratio					
	TPS	MC	Measured							
			Film	RADPOS	MC/TPS	Film/TPS	RADPOS/TPS	MC/Film	MC/RADPOS	Film/RADPOS
Static	80.5±0.8%	79.9±0.4%	79.2±2.3%	79.0±1.4%	-0.75%	-1.61%	-1.86%	0.88%	1.13%	0.25%
Moving (manual vectors)	-	76.3±0.4%	76.0±2.3%	77.3±1.4%	-	-	-	0.39%	-1.31%	-1.71%

Figure 1 shows the calculated and measured tumor profiles

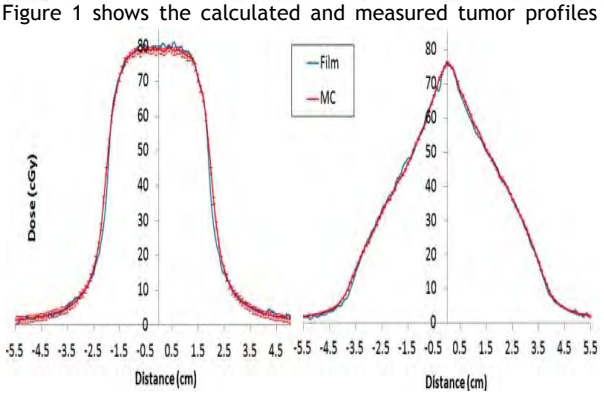

Fig1. Comparison of simulated (MC with manually generated vectors) and measured (Film) dose profiles for static (left) and moving (right) states.

.

Conclusion: The level of agreement between MC Simulation results and measurements is within 2%. This makes our 4D Monte Carlo simulations using the defDOSXYZnrc code an accurate and reliable method to calculate dose delivered to a moving anatomy.

PV-0175

Knowledge-based DVH predictions for automated individualised treatment plan quality assurance

J. Tol[1], M. Dahele[1], A. Delaney[1], B. Slotman[1], W. Verbakel[1]
[1]*VU University Medical Center, Radiotherapy, Amsterdam, The Netherlands*

Purpose or Objective: Determining whether individual treatment plans are near optimal is important for routine clinical care and clinical studies. However, plan quality assurance (QA) is difficult, time consuming and operator dependent. Furthermore, applying checklists of generic QA parameters to all patients cannot accurately gauge the quality of individual patient plans. RapidPlan (Varian Medical Systems, Palo Alto, USA), a commercial knowledge-based planning solution, could automate individualized plan QA by benchmarking the plan against predicted patient-specific organ-at-risk (OAR) doses derived from a library of plans that consists of various OAR-planning target volume (PTV) geometries and associated dose distributions. Using RapidPlan for this purpose requires that the predicted doses are achievable when RapidPlan is subsequently used to generate a plan. This was investigated for locally advanced head and neck cancer.

Material and Methods: A RapidPlan model consisting of 90 plans, generated using previously created automatically optimized plans, was used to predict achievable OAR dose-volume histograms (DVHs) for the parotid glands, submandibular glands, individual swallowing muscles and oral cavities of 20 HNC patients. Differences between the achieved and predicted DVH-lines were analyzed for all OARs. To illustrate the possible gains that individualized plan QA could realize, the RapidPlan predictions were used to evaluate achieved OAR sparing of an evaluation group (EG) of 20 manually interactively optimized plans.

Results: The Figure shows strong linear correlations (solid lines, R^2=0.94-0.99) found between the predicted and achieved mean doses for all OARs, demonstrating the accuracy of the RapidPlan DVH predictions. The dashed lines have a slope of 1 and run through the origin, meaning that for OARs on this line, the mean dose predicted by RapidPlan was exactly achieved. More detailed analysis of the predicted and achieved DVHs showed that at higher dose regions (OAR volumes <30%), the amount of achievable sparing is underestimated for OARs with mean doses <20Gy while it is progressively overestimated for OARs with higher mean doses. Using the predicted OAR DVHs identified that for 10 plans in the EG, sparing of the composite (volume weighted) salivary glands, oral cavity or composite swallowing muscles could be improved by at least 3Gy, 5Gy or 7Gy, respectively. These predicted gains were confirmed by replanning the identified patients using RapidPlan.

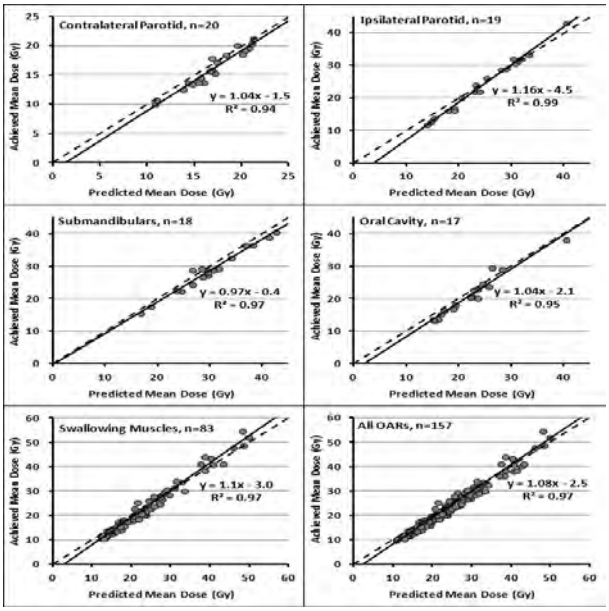

Conclusion: Strong correlations between predicted and achieved mean OAR doses indicates that RapidPlan could accurately predict achievable mean doses, showing the feasibility of using RapidPlan DVH predictions alone for automated individualized HNC plan QA. Since this QA approach does not require the creation of additional plans, these findings indicate that automated individualized plan QA is now a realistic proposition for individual centers and clinical trials.

PV-0176

Evaluation of biologically effective dose in stereotactic radiotherapy for prostate cancer

T. Viren[1], T. Lahtinen[2], J. Hopewell[3], J. Seppälä[1]
[1]*Kuopio University Hospital, Cacer Center, KYS, Finland*
[2]*Delfin Technologies Ltd, Kuopio, Finland*
[3]*University of Oxford, Green Templeton College, Oxford, United Kingdom*

Purpose or Objective: Image guided robotic stereotactic radiotherapy (SRT) is becoming increasingly commonly used in the treatment of prostate cancer. As SRT treatment may consist of 100-300 small beams, the dose-rate (DR) and thus the biologically effective dose (BED) can vary significantly within the target volume, despite the creation of a very uniform total physical dose distribution (1). However, the significance of the spatial variations in DR on BED in robotic SRT treatments remains unknown.
The aim of the present study is to measure the DR distribution, with treatment progression, in a representative robotic SRT treatment for prostate cancer and to investigate the effect of these spatial and time related variations in the measured DR on the calculated BED.

Material and Methods: A representative robotic SRT treatment plan for prostate cancer (5 x 7.25 Gy, 222 beams, treatment time 28 min) was created with the Multiplan treatment planning software (v 4.6.0., Accuray, USA). Based on this plan a quality assurance plan was calculated for a MultiCube phantom incorporating a MatriXX Detector (32 x 32 matrix of ionization chambers) spatial resolution 7.6 mm, time resolution 0.5 s (IBA Dosimetry, Germany). The DR distributions were measured in four different coronal planes (separated by 1cm) covering the volume of the target structure to create a 3D DR distribution. Then BED values, calculated using bi-exponential repair (repair half times 0.2 h and 2.5 h, α/β =1.5Gy) were calculated for each voxel based on the measured DR (BED_M), average dose-rate (measured dose divided by the overall treatment time, BED_A) and physical dose (measured dose without the repair component, BED_P) distributions.

Results: Compared to the BED_P, where no repair was allowed for, both BED_M and BED_A values, within the target volume, were significantly lower (Fig 1). Furthermore, BED_M values were found to be systematically higher than BED_A values. Significant variation was observed in BED_M values corresponding to the same BED_P value (Fig 1). This effect was not observed with BED_A values (Fig 1).

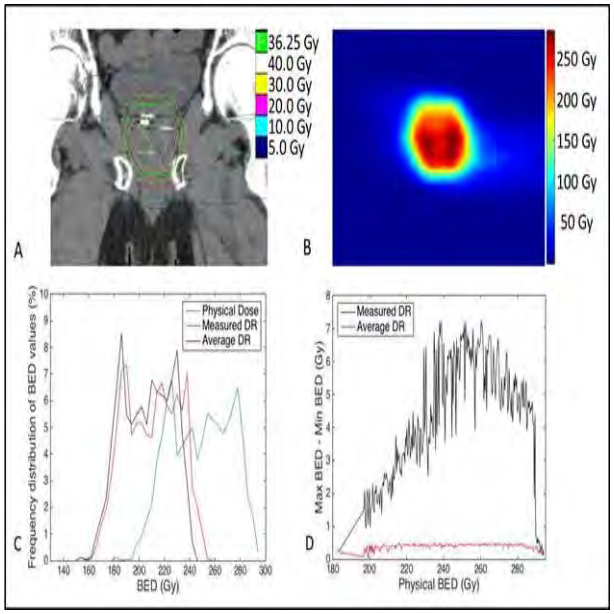

Figure 1. A: Representative SRT plan, B: corresponding BED_P values, C: Frequency distributions of BED_P, BED_M and BED_A values within the target volume, D: Range of BED_M or BED_A values corresponding uniform BED_P value.

Conclusion: The simple us of the average DR in the determination of BED does not take into account the variations in the spatial DR, and this leads to an underestimation of BED values. Furthermore, significant variations were observed in BED_M values when compared to uniform BED_P values, an observation also consistent with comparable Gamma Knife treatments (1). Thus, the actual and not the average DR should be used in the calculation of BED when the efficacy of the SRT treatments is evaluated or different treatment modalities are compared.

References

1. Millar, W.T., *et al.*, *Physica Medica: Eur. J. Med. Phys.* 31: 627-633, 2015.

Honorary Members Lectures:

SP-0177

Evidence-based education: Radiation Oncology's forgotten foundation?

S. Turner[1]
[1]*Westmead Hospital, Radiation Oncology, Sydney, Australia*

Learning Objectives

At the end of this talkyou will have a better awareness of:
1. reasons why educational 'science' may be overlooked
2. how principles of adult learning might apply to radiation oncology
3. potential benefits of applying an evidence-based approach to educationalactivities

Radiation Oncology is adiscipline with a history firmly founded on the sciences of radiobiology,radiation physics, anatomy, pathology and clinical medicine that remain asrelevant as ever to its exciting future. An evidence-based approach to practiceand progress in our field is seen as core to our identity as radiation oncologyprofessionals.
So how can it be thatthe 'science' of teaching the next generation of practitioners, as well as thecurrent one (ourselves), especially in such a rapidly changing arena, is oftenleft to chance? Why is so little focus placedon the

health education literature and scholarship in this area? And why do weaccept that random and variable acquisition of knowledge and skills, irrespectiveof the evidence for pedagogical best-practice, is good enough for our specialtyand for our patients?
This talk will dealwith possible reasons that we may be blinkered to important aspects of learningin radiation oncology. It will outline the knowledge that we *do* have to guide us, and the benefits ofworking more cooperatively in education across professions and jurisdictions.By paying attention to the 'forgotten foundation', that of high quality teachingand training, we dramatically enhance our chances of achieving the goals in quality,safety, effectiveness and leadership in cancer patient management, for which westrive.

SP-0178
The future of surgical oncology
R. Audisio[1]
[1]*University of Liverpool - St Helens Teaching Hospital, St Helens, United Kingdom*

The role of cancer surgery has been consolidated over the years but drastic changes are taking place and Surgical Oncologists need to be prepared for substantial changes. Traditionally, cancer treatment rested on tissue diagnosis: a sample of the affected area is taken, analyzed and classified according to its morphology. "Tissue diagnosis" results into "tissue-based treatment". As times are rapidly changing and we are becoming accustomed to "molecular diagnosis", leading to "genetically informed treatment plans", surgical oncologists should be up to date with newly described diagnostic and therapeutic options. Genetic counseling is also reshaping: lo prevalence (but high penetrance) genes have been associated to the risk of developing breast cancer; more interestingly, several other genetic markers (high prevalence but low penetrance) are being identified. Improved understanding of their specific role will twist the way family clinics are run. Advanced diagnostic tools are being developed and their availability will also modify the way we treat patients: digital tomosynthesis will probably reconfigure breast cancer screening; liquid biopsy is slowly but steadily being introduced into clinical practice, in view of optimizing neoadjuvant treatment as well as palliative treatment, the whole practice of follow-up and other steps of clinical practice. A multidisciplinary approach is mandatory – it is a *condition sine qua non* for the surgical oncologist to understand issues and problems from the point of view of medical and radiation oncologists radiologists and pathologists, without dismissing nurses and social workers, psycho-oncologists, geneticists, an others. Complex and inter-specialty treatment options are becoming routine (e.g. intra-operative radiotherapy). The success of new treatment plans will necessarily open new, previously unthinkable, therapeutic options. Patients' advocacy and a sympathetic approach is extremely rewarding, beside science and research. Patients are at the center of our practice and social mandate. It is therefore to keep in mind the complexity of issues affecting cancer patients, cancer survivors and their relatives in their every day's life. Education is significantly modified, with remote-learning and training labs becoming available; virtual education is becoming popular and relatively in-expensive and young generations are rather accustomed to such new educational tools. The ongoing attempt in homogenizing education with other international tween societies aims to allowing exchanges, improving knowledge and boosting cross-fertilization. The political role of cancer surgeons should be kept in mind at all times, with surgeons firmly determined to play a substantial part within the multidisciplinary oncology team.

SP-0179
Imaging in lung cancer radiotherapy: beyond the "pictures"
L. Bonomo[1]
[1]*Institute of Radiology - Catholic University, Diagnostic Imaging, Roma, Italy*

Lung cancer is still today the leading cause of death worldwide despite the availability of a variety of treatments. In particular Radiation Oncology is widely involved in lung cancer management, both as a neo or adjuvant therapy as well as a definitive one.
As the suffix "Radio-" suggests, the Radiologist and the Radiotherapist have been "step-brothers" since their origins, as co-actors in the main steps of treatment: staging / treatment planning and follow-up.
An accurate staging is essential in treatment planning in order to include macro- and micro-scopic cancer and to avoid unwanted toxicities. Lung injury is common in patients treated with Radiotherapy. The knowledge of radiological patterns of lung abnormalities after non surgical treatments is critical to accurately assess the overall effectiveness of these therapies and to differentiate normal appearances from incomplete treatments and/or local recurrences. Nowadays, a new multidisciplinary challenge for our disciplines is required: the "individualized medicine". The idea is to "design" a patient personalized therapy by identifying and integrating multimodal prognostic factors in models of treatment outcomes and also in clinical-decision support systems. Clinical imaging is particularly involved in this new field, the so-called "Radiomics" process, which offers a comprehensive and non-invasive "photograph" of patients and cancer heterogeneity.
Indeed in recent years we have witnessed a continual evolution of both Radiology and the Radiologist. Diagnostic Imaging has moved from focusing on image quality to a molecular level, from pictures to data. An important contribution has been provided by nuclear medicine, not only in identifying pathological sites, but also in outlining more active components. The "anatomical" evolution has offered the Radiotherapist the capability to better define the target and the "functional" evolution the capability to select the right one. The Radiologist, similarly, has evolved from a photographer to an interpreter and, in the future, will become a decision maker.
The aim of this lecture is to make a "journey" through the evolving role of the doctor as an "image artist" of lung cancer Radiotherapy.

References
UyBico SJ, Wu CC, Suh RD et al. Lung cancer staging essentials: the new TNM staging system and potential imaging pitfalls. Radiographics. 2010 Sep;30(5):1163-81.
Larici AR, del Ciello A, Maggi F et al. Lung abnormalities at multimodality imaging after radiation therapy for non-small cell lung cancer. Radiographics. 2011 May-Jun;31(3):771-89.
Gillies RJ, Kinahan PE, Hricak H. Radiomics: Images Are More than Pictures, They Are Data. Radiology. 2016 Feb; 278(2):563-77

Teaching Lecture: Trade off between standardisation and individualisation

SP-0180
Trade off between standardisation and individualisation
Y. Lievens[1]
[1]*University Hospital Ghent, Radiation Oncology, Ghent, Belgium*

Teaching Lecture: DNA repair and response for beginners

SP-0181
DNA repair and response for beginners
K. Borgmann[1]
[1]*University Medical Center Hamburg - Eppendorf UKE, Hamburg, Germany*

Dysregulation of the DNA damage response (DDR) is associated with a predisposition to cancer and affects responses to DNA-damaging anticancer therapies. Dysregulation of a certain DNA repair pathway may be

compensated by another, functionally overlapping DDR pathway whose activity may be increased, causing resistance to DNA-damaging radiotherapy and chemotherapy. Therefore, the DDR response makes an ideal target for therapeutic intervention by preventing or reversing therapy resistance or by using a synthetic lethality approach to specifically kill cancer cells that are dependent on a compensatory DNA repair pathway for survival in the context of cancer-associated oxidative and replicative stress. However, in the context of DNA replication several DNA repair pathways are gathered with overlapping functions, as demonstrated by the synthetic lethal interaction between the DNA double strand repair pathway homologous recombination (HR) and the base excision repair pathway (BER) as well as between checkpoint signaling (ATR/CHK1) and the Fanconi anaemia pathway. As the number of inhibitors that target components of these pathways expands the potential for using these synthetic lethal interactions increases, provided that the exploitable defects in the tumour can be identified with suitable biomarkers. These hypotheses are currently being tested in the laboratory and translated into clinical studies.

Teaching Lecture: Anal cancer: current guidelines and remaining questions

SP-0182

Anal cancer: current guidelines and remaining questions

D. Sebag-Montefiore[1]
[1]*St James Institute of Oncology, Department of Radiation Oncology, Leeds, United Kingdom*

Introduction - Anal cancer is a rare disease but its incidence is rising rapidly. The majority of tumours are squamous cell carcinoma or its histological variants. Despite its rarity phase III clinical trials have been successfully performed. The "first generation" of phase III trials tested the benefit of concurrent chemotherapy when added to radiotherapy. This led to Mitomycin C 5Fluorouracil and radiotherapy (CRT) becoming the standard of care. The shift from radical surgery with permanent stoma to non-surgical combined modality treatment was achieved through these clinical trials and recent published evidence confirms the impact on population based practice. The "second generation" of phase III did not change the standard of care. They demonstrated no benefit from the addition of neoadjuvant or maintenance chemotherapy to CRT and no improvement in outcome from the use of cisplatin based CRT. The ESMO-ESSO-ESTRO and NCCCN guidelines provide evidence based recommendations for the management of anal cancer and aspects of the guidelines will be reviewed during this teach lecture.

Staging – Whilst it is important to identify the relatively small minority of patients who present with synchronous metastatic disease, the main role of imaging is to determine the extent of disease in the pelvis prior to CRT. Although pelvic MR is not mandated in the guidelines it provides superior anatomical images of the primary tumour which is very helpful for conventional CT planning and delineation of the gross tumour volume. CT-PET is also not mandated but is shown to upstage a minority of patients from a "N0" category to "N+." Examples of this will be presented and discussed. Radiotherapy dose fractionation – there is wide variation in the prescribed radiotherapy dose to both gross tumour volume and clinical target volumes. Many centres will use higher doses of 60Gy or greater to more advanced tumours. However, to date randomized clinical trials have not demonstrated any clear benefit for dose escalation. There is also a paucity of late toxicity and patient reported outcome data to determine the impact of such an approach.

Radiotherapy technique and target volume definition - The use of IMRT has significantly increased in the treatment of anal cancer and its use is supported by the RTOG 0529 phase II trial. Although IMRT may be preferred and will reduce acute genital toxicity, careful target volume definition and delineation of organs at risk and high quality QA are required to ensure accurate treatment delivery. The AGITG contouring atlas has been very helpful to clinicians. The UK approach to introducing IMRT will be discussed.

Response assessment - Clinical and radiological assessment is required to both identify early local treatment failures and to establish whether complete response had been achieved. The European guidelines recommend assessment at 11, 18 and 26 weeks from the start of CRT. Recent published data will be reviewed. The optimal timing and imaging is the subject for further research.

Follow up - Most centres will review patients at least three monthly in the first two years, with approximately 80% of pelvic recurrences occurring during this period. The duration of follow up and the intensity of imaging varies widely.

Late toxicity - Although it is assumed that most patients will experience improved quality of life with CRT rather than radical surgery there is limited data on the impact of late radiotherapy effects on patients. New data is required particularly with the use of IMRT to understand this in more detail. An anal cancer specific module quality of life module is in development through the EORTC.

Treatment of metastatic disease - Approximately 10-20% of patients will develop metastatic disease. There is no consensus on the best first or second line chemotherapy regimens and reports of the outcomes following surgical or non surgical treatment of oligometastatic disease are sparse. The InterAAcT trial is an international randomized phase II study comparing cisplatin 5FU with Carboplatin and Paclitaxel and will be discussed

Future research - Future clinical trials will provide more information on outcome and late toxicity with the use of IMRT. The UK led PLATO trial consortium are conducting a "platform" type trial with the ACT3 ACT4 and ACT5 trials addressing specific research questions. ACT3 evaluates a selective use of reduced dose CRT for patients with T1N0 anal margin tumours; ACT 4 will compare standard versus lower dose CRT for early stage disease; ACT5 will test two IMRT SIB dose escalation CRT schedules against standard dose CRT.

Teaching Lecture: Radiotherapy and immune-therapy, biological basis and potential for future clinical trials

SP-0183

Radiotherapy and immune-therapy, biological basis and potential for future clinical trials

E. Deutsch[1]
[1]*Institut Gustave Roussy, Villejuif, France*

The immunosuppressive effects of radiation therapy have long been the only one considered. Dying cancer cell may release signals which activate the surrounding immune cells, namely through the immunological cell death process. Irradiation can also increase the diversity of tumor neo antigens which are crucial to the induction of adaptive antitumor immunity. It has recently been shown that the inhibition of immune inhibitory checkpoints synergizes with ionizing radiation in preclinical models. Hypoxia is one of the key factors influencing clinical outcome after radiotherapy responsible for reduced local control that will influence overall survival, as may the hypoxic conditions by increasing malignant progression. For decades, hypoxia was thought to act primarily on tumor cells resistance, namely the number of clonogenic cancer stem cells surviving after radiation treatment. Increased cellular turnover and hypoxia promote the production and release of large amounts of immunosupressive adenosine into the local microenvironment. Hypoxia can induce HIF-1a-dependent expression of arginase-1 and M2 polarization of macrophages. Recent data suggest that the immune contexture of tumors might be correlated with outcome after irradiation. The purpose of tumor immunotherapy is based on the principle that reversal of tolerance to immunogenic tumors would be able to activate an immune response against tumor cells. The importance of the immune component into the process of tumor response to radiation offers novel opportunities for therapeutic interventions.

Teaching Lecture: Underestimated importance of Intraluminal brachytherapy: bronchus, oesophageal, anorectal and hepatobiliary duct cancer

SP-0184

Underestimated importance of Intraluminal brachytherapy: bronchus, oesophageal, anorectal and hepatobiliary duct cancer

J. Skowronek[1]
[1]*Greater Poland Cancer Centre, Poznan, Poland*

Intraluminal brachytherapy is still an important part of brachytherapy procedures done especially in palliative patients. But large differences between countries over the world are observed. It is not clear how the future of intraluminal brachytherapy will look like. Brachytherapy is one of the most efficient methods in overcoming difficulties in breathing that is caused by endobronchial obstruction in palliative treatment of bronchus cancer. Depending on the location of the lesion in some cases brachytherapy is a treatment of choice. Because of uncontrolled local or recurrent disease, patients may have significant symptoms such as: cough, dyspnea, haemoptysis, obstructive pneumonia or atelectasis. Efforts to relieve this obstructive process are worthwhile, because patients may experience improved quality of their life. Brachytherapy plays a limited but specific role in definitive treatment with curative intent in selected cases of early endobronchial disease as well as in the postoperative treatment of small residual peribronchial disease. Various methods of palliation have been used in an attempt to improve patients' quality of life and to provide near normal, if not normal, swallowing until death occurs because of progressive esophageal cancer. Endoesophageal brachytherapy makes it possible to use high doses of radiation to the tumor itself with concurrent protection of adjoining healthy tissues due to the rapid fall in the dose with the square of the distance from the center of the dose. The above treatment also leads to a smaller proportion of late radiation complications. The aim of palliative brachytherapy is to reduce dysphagia, diminish pain and bleeding, and to improve the patient's well-being. Palliative treatment options for bile duct cancer or pancreas cancer remain limited due to the large number of patients with advanced disease at the time of diagnosis. Radical surgery is possible in less than 10-15% of these cases. Unrespectable bile duct or pancreas cancers are very difficult to treat with external beam therapy alone due to the proximity of adjacent normal organs and the high doses required to effectively irradiating these neoplasms. Although the results available in the literature are somewhat contradictory as regards the possible use of intraluminal brachytherapy in a curative setting, some evidence indicates that intraluminal brachytherapy can add something to the treatment of unresectabbe extrahepatic bile duct and pancreatic cancers if a proper subset of patients is identifled and a rational and aggressive scheme of mubtimodality treatment is designed. High rate of advanced cases affects the enrollment of brachytherapy (BT) into treatment of bile duct cancers. Indications for brachytherapy include all malignant strictures of the bile duct which can be cannulated. Intraluminal brachytherapy (ILBT) is an important component in the multimodality approach to bile duct cancers. The objective of this treatment is to deliver a high local dose of radiation to the tumor while sparing surrounding healthy tissues. The treatment can be safely adapted for right and left hepatic duct as well as for common bile duct lesions. The standard of care in rectal cancer is still surgery. For limited size rectal cancer (T1, small T2), brachytherapy alone offers an alternative to radical surgery and leads to excellent results without major morbidity. In advanced rectal cancer, a proportion of patients can achieve complete clinical response after external beam chemoradiotherapy (EBCRT) that can be demonstrated on MRI after neoadjuvant treatment. Chosen summarized indications, treatment schedules, results and complications are discussed in the following presentation.

Teaching Lecture: Big data in radiotherapy: technology, challenges and opportunities

SP-0185

Big data in radiotherapy: technology, challenges and opportunities

A. Dekker[1]
[1]*Maastricht Radiation Oncology MAASTRO GROW - School for Oncology and Development, Maastricht, The Netherlands*

Big data is a buzzword. But what is Big Data? And what can we do with Big Data in radiotherapy?
In this teaching lecture we will discuss what Big Data is and what kind of data a modern radiotherapy center produces. Innovative technology to extract, store and process these Big Data are becoming available and will be discussed.
Big Data is often seen as tremendously promising and is predicted to change health care radically, but at this point in time is mostly a challenge as we keep accumulating data without a clear path to clinical applications while privacy concerns are on the rise. Methods and examples how we go from data to making a difference in lives of cancer patients will be presented. As will the methods to do this in a way that preservers the privacy of patients.
Finally the future of Big Data is drawn and the case will be made that more data is not always the answer if we do not have a Big Machine ready to learn from these data.

Teaching Lecture: The role of dosimetry audit in safety, quality and best practice for external beam and brachytherapy

SP-0186

The role of dosimetry audit in safety, quality and best practice for external beam and brachytherapy

C. Clark[1]
[1]*National Physical Laboratory, Medical Radiation Physics, Teddington, United Kingdom*

Joint abstract submitted

SP-0187

The role of dosimetry audit in safety, quality and best practice for external beam and brachytherapy

A.L. Palmer[1], C.H. Clark[2]
[1]*Portsmouth Hospital NHS Trust, Medical Physics Department, Portsmouth Hampshire, United Kingdom*
[2]*Royal Surrey County Hospital, Department of Medical Physics, Guildford, United Kingdom*

Independent dosimetry audit is an essential component of best practice radiotherapy. However the value and concepts are not always fully understood. This lecture will review the methods and approaches of dosimetry audit and discuss its clinical importance. Examples will be given from a range of previously completed audits as well as considering what is needed in the role of audit in the implementation of new technologies.
Drawing on experience from both external beam and brachytherapy dosimetry audits worldwide, we will review the key elements of audit design, implementation and analysis, including: choice of phantoms and detectors, remote or on-site visits, efficiency and efficacy of the audit methodology, and reporting and feedback considerations.
The learning outcomes of this teaching lecture are:
· to understand why audit can improve safety, quality and best practice radiotherapy;
· to know how to choose appropriate methodology for audit and understand the outcomes;
· to appreciate the scientific, philosophical and legal reasoning for dosimetry audit.

Teaching Lecture: General introduction to head and neck radiotherapy

SP-0188
General introduction to head and neck radiotherapy
V. Gregoire[1]
[1]*UCL Cliniques Univ St Luc, Radiation Oncology, Brussels, Belgium*

Teaching Lecture: e-Learning for Professionals in Radiation Oncology: What, Why and How?

SP-0189
e-Learning for Professionals in Radiation Oncology: What, Why and How?
A. Berlanga Flores[1]
[1]*MAASTRO clinic, GROW School for Oncology and Developmental Biology- Maastricht University Medical Centre, Maastricht, The Netherlands*

Radiation Oncology is a dynamic and evolving field. Professionals need to find efficient and effective ways to stay informed of the latest developments, to collaborate and exchange knowledge with others, and to update or acquire new skills and competences.
E-Learning is an excellent way to achieve this. E-Learning is defined as the use of information and communication technologies to enable learning and performance. It has the potential to help radiation oncologists around the world to develop their competences whenever they want, at any time; allowing them to tailor their learning experiences to their goals, preferences, and needs.
This lecture will introduce the concept of e-Learning and its role for professional development in Radiation Oncology. It will present practical examples and strategies for young scientist to stay updated with recent findings and guidelines in the field, to develop their competences, and to find peers and opportunities for collaboration.

Symposium with Proffered Papers: Quality beyond accuracy: are we failing to see the forest for the trees?

SP-0190
Has higher accuracy in treatment delivery translated into noticeable improvements in clinical outcomes
N. Burnet[1]
[1]*Cambridge University Hospitals, Department of Oncology, Cambridge, United Kingdom*

We will define 'accuracy' as delivering the desired radiation dose to the target whilst minimising as much dose as possible to the surrounding normal tissues, thus embracing the classical balance which must be achieved with all radiotherapy.
The process begins with identifying the target, and therefore includes improving imaging for target volume delineation. Nevertheless, considerable uncertainties still exist especially in the personalisation of the Clinical Target Volume (CTV). Better conformation of dose to target shape has been a long term objective, beginning even in the ortho-voltage era. The biggest step, a revolutionary change, was the introduction of 3D conformal RT. IMRT represents 'ultra-conformal' treatment. Use of proton and carbon ion beams represents further steps along this path.
Improving accuracy also includes ensuring that today's highly conformal treatment plans are actually delivered to the target, without missing, and not to surrounding normal tissues. This brings us to image guidance, which appears to be vital, especially with steep dose gradient IMRT plans, but which is difficult (perhaps impossible) to test using the conventional trial paradigms.
A further concept is that the planned dose may differ from the accumulated delivered dose (DA), as the result of patient or tumour changes. Computational developments mean that individual patient DA can be estimated in a research setting using daily image guidance scans, so that clinical implementation will need to be addressed.
An additional development is the use of real time imaging *during* the exposure to monitor patient or organ movement, using X-ray or MRI approaches.
In terms of clinical outcomes, good evidence exists that better imaging improves outcomes. The introduction of 3D CRT, perhaps the most important step of all, has a strong evidence base. IMRT is also supported by strong clinical evidence. There is highly suggestive evidence that charged particle beams have a valuable role. Sadly, there is also good evidence that bad quality in plan preparation and delivery leads to worse local control and survival (TROG). Image guidance is a more challenging component of the radiotherapy chain for which to provide hard trial evidence, although it has a clear rationale.
Overall, there is a definitive evidence base that better accuracy improves outcomes for both tumour control and normal tissue sparing using current technologies. Additional opportunities are also developing, making this is a truly exciting time to be working in radiation oncology.

SP-0191
The patient: an active partner in quality and safety process in radiotherapy
S. Cucchiaro[1]
[1]*C.H.U. - Sart Tilman, Radiotherapy Department, Liège, Belgium*

Beyond the technological advances to improve radiation therapy, the patient can also actively participate in its care process and contribute to ameliorate its management. The patient is a key player in security and improvement care processes. The patient's needs and expectations can be harvested through satisfaction surveys, adverse event declarations, records of complaints and patient committee.
An important place in our Radiotherapy Department is given to harvesting and processing patient's opinions to add value for it. In order to know the views of patients on the quality of our services and help us to improve it, we have developed a survey covering 6 themes. Figure 1 shows the surveys' results of the last three years for the 6 themes, which are close or greater than the institutional goal.

Figure 1 : Patients satisfaction surveys results

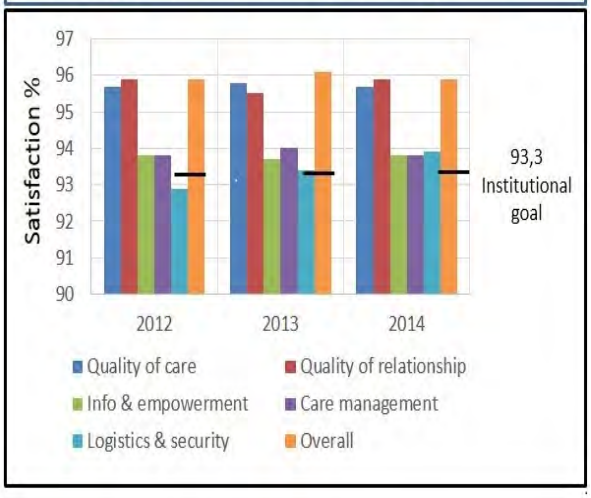

A patient committee is under construction. This committee, including former treated patients, will meet to discuss the satisfaction rates and improvement actions.
We also collect complaints and unexpected events. These are declared on adverse event reports. These reports are investigated during Experience feedback committee (EFBC).
Through these different channels the patient is actively involved in the quality processes of the Radiotherapy

Department. Thus, the patient becomes a key actor in the quality and safety of its own treatment.
In conclusions: empowerment of the patient is essential for two reasons, on one hand at the individual level by strengthening its capacity to act on health determinants and on the other hand at the organizational level with continuous improvement of the Radiotherapy Department. Our goal is to strengthen the quality and safety of treatments, adjust them to the life project of the patient and promote a participative approach focused on the patient's needs and expectations.

SP-0192
Beyond accuracy: how can medical physics help improve treatment quality?
H. Nyström[1]
[1]*The Skandion Clinic, Uppsala, Sweden*

It has often been claimed and acknowledged that Radiotherapy (RT) as a modality to combat cancer has been technology driven, or even physicist driven. Higher energies, better accuracy, computerised delivery systems, improvements in imaging are all examples of this. Together with increased knowledge of how to combine RT with e.g. systemic treatments, RT has remained one of the most important tools in cancer therapy. The continuous improvements of RT has often involved complex technology, less intuitive to its nature than earlier technologies. It has been one of the most pronounced duties of the medical physicist to ensure that the clinical introduction of such new technologies has been done with the highest possible safety standards and that any risk associated with the new technology could be brought to an absolute minimum. As a result RT, in particular advanced RT, is a very safe modality compared to almost any other hospital activities. In their quest for the highest possible level of safety, the medical physicist is often left alone with high demands, ambitions but with limited means and lack of understanding from the hospital management of the recourses needed. As a consequence the clinical introduction of new, superior treatment options are delayed, months, years and sometimes even decades, and the patients have to be content with older methods, e.g. less conformal RT. This dilemma can be boiled down to the search for the optimal balance between quality (e.g. modern high precision treatments) and safety (reliable, well proven and understood methods). The priority often tends to go towards safety rather than quality since the focus from the general public as well as regulatory authorities always favours the latter at the expense of the former. As medical physicists, however tempting it might be to focus on safety only, must take a patient oriented approach and in all considerations include the aspect of what will be the most beneficial way from a patient's perspective. Just as a high quality cannot be justified to apply is the safety issues are not properly handled, safety without quality is of limited value. In the search for the ultimate balance between quality and safety, the medical physicist is in a key position since no other profession has a better understanding of the technology, the physics and the interactions between different complex systems. A more patient-centred approach to accuracy, safety and quality can, however only result from a multidisciplinary strategy where different profession work together towards the common goal to offer the best possible treatment to all patients in need thereof.

OC-0193
Evaluation of models for plan QA using fully automated Pareto-optimal plans for prostate patients
Y. Wang[1], S. Breedveld[1], B. Heijmen[1], S.F. Petit[1]
[1]*Erasmus Medical Center Rotterdam Daniel den Hoed Cancer Center, Radiation Oncology, Rotterdam, The Netherlands*

Purpose or Objective: Current IMRT treatment planning with commercial treatment planning systems is a trial-and-error process, based on a series of subjective human decisions. So the quality of the IMRT treatment plans may not be consistent among patients, planners or institutions with different experience. Different plan quality assurance (QA) tools have been proposed recently, that could flag suboptimal plans that may benefit from an additional treatment planning effort. However, since conventional treatment planning was used to validate these models, the inherent accuracy of the existing treatment planning QA models is unknown. Therefore we fully automatically generated a dataset of Pareto-optimal prostate IMRT plans using Erasmus – iCycle, an in-house TPS for fully automated, multi-criterial plan generation. This dataset was used to assess the prediction accuracy of an overlap volume histogram (OVH) based plan QA tool.

Material and Methods: 115 prostate plans were fully automatically generated using Erasmus-iCycle. These plans were based on a fixed 'wish-list' which contains hard constraints and objectives in a predefined order of priority. An existing OVH model was modified and used to predict DVHs for these patients. First, the entire DVH of the rectum, bladder and anus of a validation cohort (N=57) were predicted, using the plans of an independent training cohort (N=58). To investigate the impact on prediction accuracy of an enlarged training cohort, the DVHs were also predicted by a leave-one-out method. The predicted rectum Dmean, V65, and V75, and Dmean of the anus and bladder were compared with the achieved values to validate the OVH QA tool.

Results: For rectum, the prediction errors (predicted-achieved) were small: -0.2±0.9 Gy (mean±1 SD) for Dmean, -1.0±1.6% for V65, and -0.4±1.1% for V75. 72% and 96% of the predicted rectum Dmean had prediction errors within 1 Gy and 2 Gy, respectively. For Dmean of anus the prediction error was only 0.1±1.6 Gy, whereas for the bladder it was much larger: and 4.8±4.1 Gy (see also Fig 1). Increasing the training cohort to 114 patients (using leave-one-out) led to minor improvement.

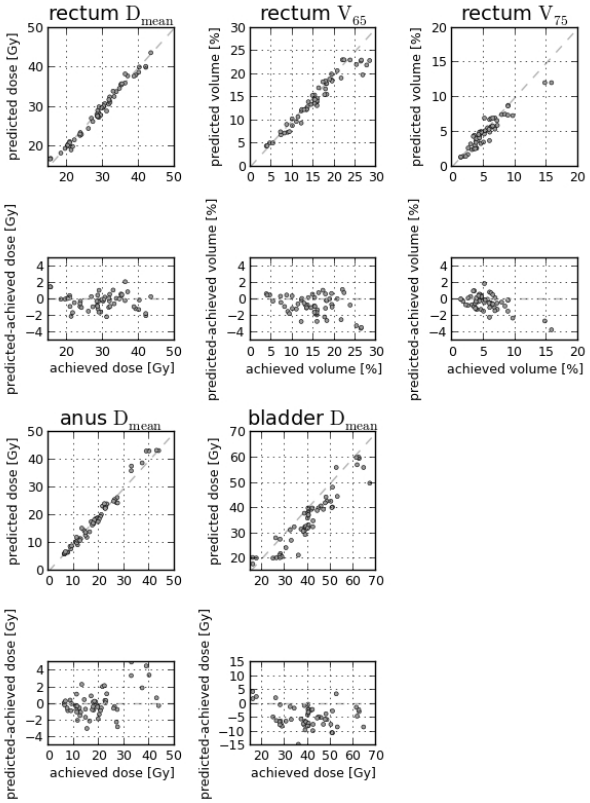

Conclusion: A dataset of consistently prioritized Pareto-optimal prostate IMRT plans was generated. This dataset can be used to validate any planning QA model and will be made publicly available at the Treatment Planning QA Section of http://www.erasmusmc.nl/radiotherapie/research/radiation oncologymedicalphysicsandimaging/research_projects. It was applied here to assess the accuracy of the OVH model. The OVH model was highly accurate in predicting rectum and anus DVHs. For the bladder large prediction errors were observed, which indicates that the OVH has difficulty in capturing the interdependence of sparing different OARs. We are currently

investigating how the OVH model should be modified to be suitable as a plan QA tool for prostate patients.

Symposium: Targeting DNA repair / DDR pre-clinical evidence

SP-0194
Tumour-specific radiosensitisation by ATR inhibitors
T. Brunner[1]
[1]*Universitätsklinik Freiburg, Department of Oncology, Freiburg, Germany*

The human ataxia telangiectasia and Rad3-related protein (ATR) kinase is activated by DNA damage and replication stress as a central transducer of a checkpoint signaling pathway. Subsequent to activation, ATR phosphorylates many substrates, including the kinase Chk1, which regulates cell-cycle progression, replication fork stability, and DNA repair. All of the three mentioned events promote cell survival during replication stress and in cells with DNA damage. It was hypothesiszed that ATR inhibitors would be therapeutically useful, with a predicted specificity for tumors sparing normal cells. Since the introduction of potent ATR inhibitors a hand full of studies in conjuction with radiotherapy has been published including our own work where we showed sensitization of pancreatic cancer in vitro and in vivo to radiotherapy in conjunction with VE-822 (=VX-970), an ATR inhibitor. The drug decreased maintenance of cell-cycle checkpoints, increased persistent DNA damage and decreased homologous recombination in irradiated cancer cells. Furthermore, we observed decreased survival of pancreatic cancer cells but not normal cells in response to XRT or gemcitabine. VE-822 markedly prolonged growth delay of pancreatic cancer xenografts after XRT and gemcitabine-based chemoradiation without augmenting normal cell or tissue toxicity. Others have shown that different tumours such as head and neck squamous cell carcinoma or promyelocytic leukaemia were also sensitized to radiation by co-treatment with an ATR inhibitor. Aditionally, human tumor cells were also sensitized to high LET radiation. The first clinical early phase trials combining ATR inhibitors with radiotherapy or chemotherapy are underway to generate important insights into the effects of ATR inhibition in humans and the potential role of inhibiting this kinase in the treatment of human malignancies.

SP-0195
Inhibition of ATR kinase activity for the treatment of lung cancer
F. Vendietti[1], B. Leibowitz[2], A. Lau[3], J. Yu[2], P. Tran[4], M. O'Connor[3], C. Bakkenist[1]
[1]*University of Pittsburgh School of Medicine, Department of Radiation Oncology, Pittsburg- PA, USA*
[2]*University of Pittsburgh School of Medicine, Department of Pathology, Pittsburg- PA, USA*
[3]*AstraZeneca, Innovative Medicines, Macclesfield, United Kingdom*
[4]*Johns Hopkins University School of Medicine, Department of Radiation Oncology, Baltimore, USA*

ATR and ATM are protein kinases activated at stalled and collapsed replication forks and DNA double-strand breaks (DSBs), respectively, where they function to maintain genome integrity by mediating cell cycle checkpoints and DNA repair. ATM has been widely studied since ataxia telangiectasia individuals who express no ATM protein are the most radiosensitive humans identified. It has therefore been postulated that ATM kinase inhibitors (ATMi's) will increase the efficacy of radiotherapy. ATR has also been widely studied, but advances have been complicated by the finding that ATR is an essential protein in mice and mammalian cells. Nevertheless, pharmacologic ATR and ATM kinase inhibitors have been identified and these sensitize cancer cells to ionizing radiation (IR) in tissue culture. ATR kinase inhibitors (ATRi's) also synergize with cisplatin to induce cell death in tissue culture. Since concurrent cisplatin and radiation is used as standard of care for locally advanced and metastatic NSCLC patients, ATR kinase inhibition may significantly improve the efficacy of first line treatment in tens of thousands of patients in the USA every year. Until recently, however, *in vivo* studies have been limited by the absence of bioavailable ATR and ATM kinase inhibitors.
Here we describe orally active and bioavailable ATR and ATM kinase inhibitors and show that, in contrast to expectations, ATRi is surprisingly well tolerated. We show that cisplatin-ATRi induces a complete response in ATM-deficient lung cancer xenografts and potentiates the effect of cisplatin in $p16^{INK4A}$-deficient lung cancer xenografts. We also show that conformal radiation-ATRi and radiation-ATMi induce profound responses in an autochthonous $Kras^{G12D}$/Twist1 mouse model of lung adenocarcinoma, and that the efficacy of radiation-ATRi for the treatment of lung cancer appears to be better than that of radiation-ATMi due to lower toxicity.

SP-0196
Realising the full potential of DNA damage response inhibition in the treatment of cancer
S. Galbraith[1]
[1]*AstraZeneca, Oncology Innovative Medicines, Cambridge, United Kingdom*

An underlying hallmark of cancers is their genomic instability, which is associated with a greater propensity to accumulate DNA damage. Historical treatment of cancer by radiotherapy and DNA-damaging chemotherapy is based on this principle, yet it is accompanied the significant risk of collateral damage to normal tissue and unwanted side effects. Targeted therapy based on inhibiting the DNA damage response (DDR) in cancers, either alone or in combination, offers the potential for a greater therapeutic window by tailoring treatment to patients with tumours lacking specific DDR functions. The recent approval of olaparib (Lynparza), the poly (ADP-ribose) polymerase (PARP) inhibitor for treating tumours harbouring BRCA1 or BRCA2 mutations, represents the first medicine based on this principle, exploiting an underlying cause of tumour formation that also represents an Achilles' heel. Different forms of DNA damage evoke responses by different repair mechanisms and signalling pathways and the choice of pathway will also be influenced by the phase of the cell cycle in which the damage occurs. DDR represents a good source of anticancer drug targets as there are at least three key aspects of DDR that are different in cancers compared with normal cells. These are a) the loss of one or more DDR capability b) the increased levels of replication stress and c) the higher levels of endogenous DNA damage in cancer cells compared to normal cells.
This talk will focus on examples of how each of these concepts is currently being exploited to treat cancer. As an example of the exploitation of the first concept, the use of PARP inhibitors to treat cancers deficient in *BRCA1* and *BRCA2* gene function, as well as other homologous recombination repair deficiencies, will be presented. The second concept - the exploitation of high levels of replication stress in cancers, will be exemplified through data presented resulting from the use of inhibitors of ATR and WEE1. As part of the discussion on how best to exploit the higher levels of endogenous DNA damage in cancers, the focus will be on the challenges associated with expanding the therapeutic window for the use of DDR inhibitors in combination with DNA damaging agents such as radiation and chemotherapy. Finally, the ambition of how best to realise the full potential of DNA damage response-based therapy will be discussed including the use of different synergistic combinations in a personalized healthcare approach.

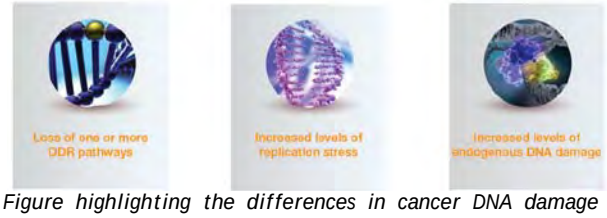

Figure highlighting the differences in cancer DNA damage response compared to normal cells that provides the

rationale for target cancer therapies based on inhibitors of DDR

Symposium: New approaches in rectal cancer

SP-0197
Consequences of bowel cancer screening programmes
M. Van Leerdam[1]
[1]*Netherlands Cancer Institute Antoni van Leeuwenhoek Hospital, Amsterdam, The Netherlands*

Colorectal cancer (CRC) is the third most common type of cancer among men and the second among women in the European region. CRC is the second most common cause of cancer related death in Europe. Several trials have shown a mortality reduction of screening by either faecal occult blood test or flexible sigmoidoscopy. Next to mortality reduction, there also is a reduction of the CRC incidence by CRC screening. Furthermore, different CRC screening modalities have been proven to be cost-effective and maybe even cost-saving. Most countries of the European Union do have a type of CRC screening, but still many countries do have opportunistic programs without an explicit policy, defined target population and without a dedicated organisation responsible for the roll out of the program. Preferable, CRC screening should be a population based program, using an up to date IT system/ data warehouse and with close monitoring and evaluation of the whole program and the outcome measures. Quality assurance is of utmost importance and can only be established in an organised program. Part of the results of the Netherlands CRC screening program will be presented as example.

SP-0198
The way forward in organ preservation strategies for rectal cancer
S. Bach[1]
[1]*Queen Elizabeth Hospital, Department of Surgery, Birmingham, United Kingdom*

Abstract not received

SP-0199
How to delineate the CTV for rectal cancer? An international consensus
V. Valentini[1]
[1]*Università Cattolica del Sacro Cuore -Policlinico A. Gemelli, Gemelli ART, Rome, Italy*

Purpose: The delineation of clinical target volume is a critical step in radiation therapy procedure. Several contouring guidelines suggest different subvolumes and anatomical limits in rectal cancer, supporting a variability in delineation that largely depends on inter-operator discordance in delineation. An international agreement among expert radiation oncologists might significantly reduce this variability, converging on a consensus rectal cancer contouring guideline through Falcon, the educational web-based multifunctional platform for delineation endorsed by ESTRO.

Material and Method: Seven skilled radiation oncologists, delegated from ESTRO, ASTRO, TROG and EORTC, defined the steps to produce consensus rectal cancer guidelines on elective nodal levels delineation. Six rectal cancer cases with different clinical stage were selected and the related CT scans were shared and uploaded on Falcon platform. The experts firstly delineated online the selected CT scan slices following each his personal guidelines. The first delineation outcome was then discussed in a face-to-face meeting with the contribution of surgeons and radiologist and a table of boundaries was compiled. All the experts had then to delineate online the same CT scan slices, considering the new table of boundaries. In a peer review meeting the final outcome was obtained and the publication plan defined.

Results: Falcon allowed a comparison of the experts' delineations, identifying critical nodal boundaries as areas of disagreement. The ontology of structure sets was defined and a new table of boundaries was generated. The major modifications to the previously published guidelines were about lateral lymph nodes (LLN) and ischiorectal fossa (IRF). One of the discussed issues was the level of the cranial and anterior border of LLN according to clinical rectal cancer stage. The delineation of the entire IRF was recommended only when there was an infiltration of the external anal sphincter or the IRF and new limits were defined (Table).

Subsite	Limits	Definition	Recommendation
Lateral lymph nodes	Anterior	When the external iliac vessels leave the pelvis, the anterior border should be limited to a virtual line at the level of the anterior wall of the ureters.	In case of: - positive nodes in the posterior lateral lymph nodes (internal iliac); - cT4; - numerous mesorectal nodes; the anterior limit is the anterior surface of obturator artery.
	Cranial	Bifurcation of common iliac artery into internal and external iliac arteries	In case of: - cT3N0; - MRF-; the cranial limit may be lowered at the level of the bifurcation of the IMA in SA and SRA (corresponding to the cranial limit of the mesorectum).
Ischiorectal fossa	Cranial	Where the inferior pudendal artery leaves the pelvis	Include both when there is an infiltration of the external anal sphincter or the ischio-rectal fossa
	Caudal	1 cm below the inferior rectal artery (which travel horizontally in the IRF)	

Conclusion: The definition of consensus guidelines for rectal cancer delineation endorsed by skilled radiation oncologists may support in reducing contouring variability. The structure sets of the six cases used will be available online as consultation atlases on the Falcon platform for individual test and a paper describing the agreed guidelines will be soon published.

Symposium: Changing paradigm in the management of kidney cancer

SP-0200
Partial nefrectomy: indication and results
P. Gontero[1]
[1]*University of Studies of Torino Molinette Hospital, Department of Surgical Sciences, Torino, Italy*

Historically, the standard treatment modality used for the vast majority of small renal masses (< 4 cm) was radical nephrectomy (RN). Partial nephrectomy (PN) was conceived to preserve renal parenchyma and function. It was pioneered in patients who would require renal replacement after RN (imperative indications). Based on the "belief" that PN is "better" than RN, utilization of PN has increased worldwide in the last few years. This has been supported by extensive literature of retrospective studies demonstrating renal functional outcomes and "overall survival" benefits of PN over RN. For T1 renal cancer (up to 7 cm lesion according to current TNM), > 95% 5 years disease specific survival rates have been reported. The probability of a positive surgical margin (PSM) on the resection bed has been shown to be below 5%. The impact of a PSM on disease recurrence remains controversial with some series suggesting no additional risk compared to a negative margin. A tumour resection technique conducted at the edge of the tumour (enucleation) has been advocated as a mean to preserve more renal parenchyma and oncologically "non-inferior" to the standard "enucleoresection" technique where a margin of up to 1 cm of healthy parenchyma is left on the resected mass. Besides, a significant reduction in the risk of developing chronic kidney disease (CKD) has been reported with PN as compared

to RN. This has also translated into a reduced risk of all cause mortality in large population series receiving PN as compared to RN, as a result of a lower rate of cardiovascular events potentially driven by CKD. Backed by these data, current guidelines (NCCN 2015, EAU 2014 and AUA 2009) make strong recommendations for PN in all T1a (up to 4 cm) and whenever feasible in T1b (4-7 cm) kidney cancers. The recommendation becomes imperative in patients with baseline CKD, bilateral tumours or tumour in a solitary kidney. Surprisingly, the only level I evidence available from a European RCT could not prove equivalence between PN and RN. While the trial did not meet accrual goals (541 out of 1300 patients required), overall survival (the primary study end point) at 9.3 years of follow up was eventually better in the RN arm in spite of a better preserved renal function in the PN arm. Notably more cardiovascular events were observed in the PN group! All these observation taken together suggest that the survival advantage of PN over RN observed in large retrospective series or metanalyses is likely the effect of unaccountable selection biases in favour of PN (healthier patients more likely to be treated with PN). The beneficial effect of PN on kidney function is out of question, yet its clinical relevancy (= reduced risk of non cancer related morbidity) is restricted to patients with baseline CKD. Up to 30% of patients with SRM have some degree of baseline CKD and hence would require a PN that must be performed with surgical skill in order to optimize both oncological efficacy (negative surgical margin) and kidney function preservation (keep ischemia time < 25 minutes or even lower). The currently available surgical techniques (open, laparoscopic and robotic assisted) have all proved effective to accomplish a PN matching the criteria for both oncological and functional efficacy.

SP-0201

Stereotactic radiotherapy for renal cell carcinoma: the hidden treasure or the forbidden kingdom

G. De Meerleer[1]
[1]*University Hospital Ghent, Department of Radiotherapy and Experimental Cancer Research, Ghent, Belgium*

Normal 0 21 false false false FR-BE X-NONE X-NONE
Renal-cellcarcinoma (RCC) is considered to be a radioresistant tumour, but this dogma iswrong and based on traditional radiation schedules. If given in a few (evensingle) fractions, but at a high fraction dose (stereotactic body radiotherapyor SBRT), RCC becomes highly radiosensitive. Both in the primary setting and intreatment of oligometastatic disease, local control rates >90% are achieved.There is an established biological rationale for the radiosensitivity ofrenal-cell carcinoma to SBRT which is based on the ceramide pathway, which isactivated only when a high dose per fraction is given. This pathway does notinvolve damage at the DNA level (nucleus) but at the level of the cellmembrane. The ultimate target of this pathway is the tumour vasculature,similar to lots of targeted drugs.
Apartfrom the direct effect of SBRT on renal-cell carcinoma, stereotactic bodyradiotherapy can also induce an abscopal effect. This effect, caused byimmunological processes and involving dendritic cells, might be enhanced whentargeted drugs and stereotactic body radiotherapy are combined. Therefore,rigorous, prospective randomized trials involving a multidisciplinaryscientific panel are needed urgently. The presence of a radiation oncologist insuch panels is vital.
Thisoral presentation will focus on:
1. Radiobiologyof SBRT in RCC (ceramide pathway).
2. Rationalefor the abscopal effect.
3. Localcontrol rates of SBRT in RCC.
4. Interactionbetween targeted drugs and SBRT.
5. Increasingvisibility if radiation oncology in this setting.
Furtherreading
1. DeMeerleer G, KhooV, EscudierB, et al. Radiotherapy for renal-cell carcinoma. Lancet Oncol 2015; 15:e170-7.
2. De Wolf K, Vermaelen K, De Meerleer G, et al. The potential of radiotherapy to enhance the efficacy of renal cellcarcinoma radiotherapy. Oncoimmunology 2015; 4: e1042198.

SP-0202

Ablative treatment for renal cancer

H. Baumert[1]
[1]*Groupe Hospitailer Paris Saint-Jospeh, Department of Uro-oncology, Paris, France*

There has been an increase in incidence of small renal masses over the last two decades. There is evidence that nephron sparing surgery offers equivalent long-term oncological results compared to radical nephrectomy. More recent evidence suggests that radical nephrectomy is associated with greater chronic renal insufficiency, which is in turn associated with increased risk of cardiovascular death, in patients with localised T1 renal mass. It is for these reasons that nephron sparing surgery is recommended, when technically feasible, for the management of renal tumour smaller than 7 cm.
Partial nephrectomy is the gold standard treatment for small renal masses, however it is associated with a significant morbidity.
Ablative treatments are alternative options that cause necrosis of the renal tumour without removing it. This can be achieved by heating tumour up to 80°C, with radiofrequency, or by freezing it below -40°C with cryosurgery. These percutaneous ablative treatments are performed under CT scan guidance or by laparoscopic approach. The percutaneous approach can be performed under local anaesthesia, which is particularly useful in fragile patients. These two minimally invasive ablative treatments allow, on average, to halve the postoperative morbidity when compared to partial nephrectomy. On the other hand, the risk of local recurrence is higher compared to partial nephrectomy.
Cancer specific survival rate on literature review is quoted around 90 to 95% for T1a (<4 cm) tumours. The 5 years overall survival or metastatic free survival, don't seem to be different from partial nephrectomy, if salvage treatments are proposed in case of local recurrence. To achieve these oncological results, appropriate patient selection along with adequate follow up is required.
According to the various urological guidelines, renal biopsy must be performed prior to these ablative treatments. When a malignant tumour is confirmed histologically, these treatments are recommended for cortical tumours, smaller than 4 cm, ideally in elderly patients or patients with multiple comorbidities who have a reasonable life expectancy. Patients with bilateral synchronous tumours, genetic diseases leading to multiple bilateral recurrences, renal insufficiency or presence of solitary kidney, are also ideal candidates for ablative treatments. Patients with shorter life expectancy, tumours in the hilum or in close proximity to the collecting system and proximal ureter are contraindications. Cryosurgery appears to treat central tumours with less morbidity compared to radiofrequency ablation. Close radiological follow up is required. Renal CT scan or MRI is usually performed at regular intervals looking for any possible enhancement of recurrent/residual tumour.
Conclusion: Partial nephrectomy remains the gold standard treatment for management of small renal tumours. Ablative treatment is a validated option associated with a favourable risk benefit balance, especially for fragile patients.

Symposium: Modern techniques for old indications

SP-0203

Robotic surgery and brachytherapy

B. Pieters[1]
[1]*Academic Medical Center, Radiation Oncology, Amsterdam, The Netherlands*

The practice of brachytherapy nowadays has been developed decennia ago. In the course of years modifications are introduced by the use of different isotopes, the development of afterloading techniques, the introduction of image-guided techniques, and many more. Robotics technologies are on a wide scale increasingly being used in the treatment of patients. Also in brachytherapy this emerging technology has been adopted and is still in development. A robot is a

reprogrammable multifunctional manipulator designed to move materials, parts, tools, or specialized devices through variable programmed motions for the performance of a variety of tasks defined by The Robotics Institute of America. Dependent on the degree of automation and autonomy different classes can be recognized. Examples where robotic systems are used in brachytherapy are e.g. in prostate and bladder implantations.
Several commercial and non-commercial systems exist to plan and place needles into the prostate. These systems can be automated for radioactive seed delivery and HDR treatments. Clinical study show robotic implantations to be feasible, although still manual corrections are done.
In bladder brachytherapy a laparoscopic robotic system is available for catheter placement without the need to open the bladder (cystotomy). As with the traditional way of implanting, the catheters can be placed parallel and equidistantly. The major advantage is reduction of treatment morbidity with this technique, although also misplacements have been observed preventing adequate brachytherapy.
Development of new technologies, such as robotic-aided brachytherapy implantations is welcomed to increase the precision and reproducibility of treatments and reduce morbidity. On the other side it should be appreciated that also for these techniques a learning curve exist. Clinical results in comparison to the traditional techniques should be awaited and carefully discussed before widespread adaptation of these new techniques.

SP-0204
New techniques in brachytherapy for head and neck
G. Kovács[1]
[1]*University of Lübeck - UKSH CL, Interdisciplinary Brachytherapy Unit, Lübeck, Germany*

Interventional radiotherapy (brachytherapy) was the first medical application in the treatment of cancer after discovering radium. User experience was growing over the time and useful rules of meaningful applicaton were developed. For many decades this experience based rules regulated the indication as well the performance of brachytherapy applications. After introducing milestone developments in the technical performance (stepping source technology and modern treatment planning software packages) as well in target definition modalities (multiparametric imaging, real-time imaging) and in quality assurance issues (medical & physical QA) biological planning and intensity modulation potential become available. Furthermore, interdisciplinary networking and education in the field lead to a higher level of cure rates with low toxicity and better Quality of Life of the patients. Economical comparison with other methods proved the necessity of involving interventional radiotherapy in to modern function preservative interdisciplinary treatments.
Head & Neck cancer represents a special need for interdisciplinary cooperation because:
1. Most of the recurrences following modern external beam radiotherapy (with or without complementary systemic treatment) are in-field recurrences. This indicates the need for higher local dose and interventional radiotherapy offers the highest possible dose in a small volume accompanied by very low radiation dose on surrounding normal tissues or organs at risk.
2. Aggressive surgery cause functional or cosmetic demages on the head & neck. The combination of surgery and perioperative interventional radiotherapy results in higher rates of function preservation or in better cosmetic results.
3. Modern multiparametric imaging techniques including hypoxia imaging has the potential to guide necessary very high dose areas to the right but very small volumes within the target.
Regarding healthcare economy issues: preliminary analyses of healthcare professionals stated the advantage of involving interventional radiotherapy in to the treatment of head & neck cancers.

SP-0205
Image guided brachytherapy in vaginal cancer
L.U. Fokdal[1], R. Nout[2]
[1]*Aarhus University Hospital, Department of Oncology, Aarhus C, Denmark*
[2]*Leiden University Medical Center, Department of Radiotherapy, Leiden, The Netherlands*

Vaginal cancer is a rare disease, accounting for only 2-3% of all gynaecological cancers. The majority (85%) of the tumours are squamous cell carcinomas and associated with a previous HPV infection.
The FIGO classification is used for clinical staging and is an important prognostic factor. Approximately 25% of patients present with FIGO stage I, limited to the vaginal wall with a 5-year survival rate of approximately 80%, compared to 20% for FIGO stage IV tumours that invade other pelvic organs or extend beyond the true pelvis (10-15% of patients). Other known prognostic factors are site, size and histologic subtype.
The treatment of vaginal cancer may include surgery in limited stage I disease, in the upper third of the vagina. However, surgery is often extensive especially if tumors extend to the lower two thirds of the vagina and it is often difficult to achieve negative margins in tumors larger than 2-3 cm. Because of these difficulties, radiotherapy is generally recommended as the standard treatment for all vaginal cancers irrespectively of the stage.
In general, radiotherapy is very similar to that for cervical cancer and includes a combination of 45-50 Gy external beam radiotherapy (EBRT) with concomitant weekly cisplatinum followed by brachytherapy boost to a total dose of 70 Gy to 80 Gy. With regard to the brachytherapy technique small residual tumors (≤5 mm thick) can be treated with intracavitary technique alone while combined intracavitary and interstitial technique should be considered for larger tumours.
Published data on the results of radiotherapy are mainly based on small retrospective studies and can be categorised in two groups. The first group includes studies where patients mainly were treated with 2-dimensional (x-ray based) radiotherapy. The second small group includes studies where patients have been treated using image guided (CT or MRI) adaptive treatment planning. Any direct comparison between the two groups of studies is difficult because of the retrospective nature of the data, limited number of patients and short follow-up. However, it seems that image guided brachytherapy is associated an increased local control rate from 75% (44-87%) for the radiograph based studies to 85% (75-94%) for the studies using an image guided approach, together with a decrease in moderate to severe treatment related morbidity. In 2005 the GEC-ESTRO GYN group successfully introduced an image guided adaptive target concept for brachytherapy in locally advanced cervical cancer. This concept takes the initial tumour extent at time of diagnosis as well as tumour regression during EBRT into account. Several studies have shown a therapeutic benefit with improvements in local control and reductions in moderate to severe morbidity using this concept.
Based on these results, a task group within GEC ESTRO GYN was formed with the aim to introduce image guided adaptive target concept in the treatment of vaginal cancer. This initiative started in the beginning of 2014 comparing the different target concepts from each of the 5 involved centres. In a next step each centre contoured 5 different cases with their own target concept in mind. During this work many similarities were found in the target concepts and between the contours of each centre. Therefore the group proceeded to investigate the differences and similarities in dose and treatment planning. In this project each centre performed treatment planning for the 5 contoured cases using both their own target contours and on a set of contours that were provided.
Importantly, radiotherapy for vaginal cancer is based on a combination of clinical findings as well as imaging. Especially for the clinical findings the precise documentation can be challenging. In order to increase the uniform reporting a clinical drawing for this documentation has been developed.

This practical tool is now at the stage that it will be evaluated clinically in each centre. By now several centres have experience with image guided adaptive brachytherapy in limited numbers of patients with vaginal cancer. To gain more knowledge from this already existing experience a retrospective database has been established with inclusion of approximately 90 patients that have been treated with CT or MRI guided brachytherapy. Although different target concepts have been used, this cohort will allow for analysis of disease control, prognostic factors and descriptive analysis of the radiotherapy related parameters in a more contemporary series. A future goal will be establishment of a prospective multicentre database with inclusion of patients treated with a common target concept.
During this presentation existing results for radiotherapy in vaginal cancer will be reviewed, followed by an overview of the work that has been performed to introduce image guided adaptive brachytherapy in primary vaginal cancer within the GEC ESTRO GYN group.

Symposium: Quantitative imaging to individualise radiotherapy

SP-0206
Tissue characterisation using quantitative radiomics

W. Van Elmpt[1]
[1]*Maastricht University Medical Centre, Department of Radiation Oncology MAASTRO, Maastricht, The Netherlands*

In this presentation the possibilities for image quantification for tissue characterization will be discussed that go beyond quantification of Hounsfield Units for CT or SUV for PET imaging. Standardization aspects of advanced imaging techniques are important for reliable and robust quantification. Besides the image acquisition, an equally important part is validation of the used image analysis techniques. Especially for textural feature calculations (e.g. radiomics) this is not a trivial task and may require some more detailed guidelines for acquisition, segmentation, analysis and reporting of results. The entire pipeline from image acquisition to analysis should be designed to allow interchangeable and robust results between e.g. institutes, software packages and imaging equipment. This presentation will illustrate the possibilities of advanced image quantification, concepts and techniques with clinical examples: Radiomics of tumours are currently investigated to predict local control, metastasis patterns or survival of patients, whereas advanced image quantification of normal tissues may allow better prediction of patients prone to toxicity.

SP-0207
Image-based radiobiological tumour control probability modelling

E. Malinen[1]
[1]*DNR - Norwegian Radium Hospital, Oslo, Norway*

Solid tumors may be heterogeneous with respect to radiosensitivity, and a homogeneous tumor dose is thus not always optimal. Thus, medical images of radiobiological relevance may be used to guide focal irradiation of tumors. Tumor control probability (TCP) modeling may be useful for optimizing dose painting treatment plans and for estimating the effect of such therapeutic strategies.
Both magnetic resonance imaging and positron emission tomography may provide voxel-by-voxel maps potentially reflecting tumor aggressiveness and radioresistance. The talk will elaborate on the biological relevance of theses imaging approaches and their pros and cons in terms of radiotherapy planning. Then, from the voxelwise mapping of tumor radiosensitivity, proposed frameworks for the tumor control probability modelling will be presented. Both data-driven and model-driven approaches are discussed. Furthermore, the potential use of TCP modelling in dose painting will be elaborated. Also, the concept of 'LET' painting in particle therapy will be highlighted.
In concluding, the current and future role of image based TCP modelling will be discussed, seen together with both advances in biologic imaging and in radiotherapy delivery and guidance techniques.

SP-0208
Validation of imaging with histology: implications for dose prescriptions

G. Ghobadi[1], J. De Jong[2], B.G. Hollman[1], B. Van Triest[1], H.G. Van der Poel[3], C. Vens[4], U.A. Van der Heide[1]
[1]*Netherlands Cancer Institute Antoni van Leeuwenhoek Hospital, Radiotherapy Department, Amsterdam, The Netherlands*
[2]*Netherlands Cancer Institute Antoni van Leeuwenhoek Hospital, Pathology Department, Amsterdam, The Netherlands*
[3]*Netherlands Cancer Institute Antoni van Leeuwenhoek Hospital, Urology Department, Amsterdam, The Netherlands*
[4]*Netherlands Cancer Institute Antoni van Leeuwenhoek Hospital, Division of Biological Stress Response, Amsterdam, The Netherlands*

In this era, image-guided radiotherapy provides the technology to modulate dose based on the variation in radiation sensitivity within cancer of the prostate. This raises the question what to irradiate and to which dose. Here, functional imaging techniques play an essential role. Multi-parametric (mp) MRI, consisting of T2-weighted, diffusion-weighted and dynamic contrast-enhanced MRI is a key element in the detection of prostate cancer, and is increasingly used for delineation of tumors inside the prostate gland. Validation with histopathology however shows that tumor detection and particularly tumor delineation is challenging. Prostate cancer is often multifocal and small lesions (<0.5cm3) are often missed. Tumor sub-volumes with low cell and microvessel density that resemble healthy tissue are also difficult to find with mp-MRI.The most aggressive parts of the tumors, containing high cell and microvessel density and a higher Gleason score, are more likely to be detected. The heterogeneity in the histopathology of prostate cancer together with the limitations of mpMRI in detecting small satellites has implications for dose prescriptions in radiotherapy. We therefore evaluated the potential impact of dose differentiation on the tumor control probability (TCP) in prostate radiotherapy using histopathological properties of prostate tumors. We defined GTV and CTV based on tumor volumes on H&E stained slices from prostatectomy specimen of 25 patients. Each patients' TCP was simulated taking into account differences in the cell numbers (N0) and Gleason Scores (GS). We further evaluated the assumption that these tumors all have the same radiosensitivity, or that radiosensitivity decreases with increasing Gleason grade. Our results demonstrate feasible dose differentiations between GTV and CTV based on the heterogeneity in the histopathology of prostate tumors and the impact on the TCP of the patient population. We will further discuss the different GTV-CTV dose differentiations considering heterogeneity only in the number of tumor cells or also in the radiosensitivity, based on Gleason grade. Further studies in carefully designed clinical trials are needed to determine the effect of heterogeneous radiosensitivity on the response of individual patients to different regimes of radiotherapy.

Proffered Papers: Physics 5: Intra-fraction motion management I

OC-0209
Real-time liver motion monitoring on conventional linac by external surrogate and sparse kV imaging

J. Bertholet[1], E. Worm[1], R. Hansen[1], M. Høyer[1], P. Poulsen[1]
[1]*Aarhus University Hospital, Departement of Oncology, Aarhus C, Denmark*

Purpose or Objective: Intrafraction motion is a challenge for accurate delivery of stereotactic body radiation therapy (SBRT) in the liver. Real-time treatment adaptation (gating,

tracking) may mitigate the detrimental effects of motion, but requires reliable target motion monitoring. On a conventional linac, monitoring can be obtained by intrafraction kilovoltage monitoring (KIM) using continuous imaging of implanted fiducials with a standard gantry-mounted x-ray imager. However, KIM adds imaging dose, is incompatible with large couch rotation, and KIM images suffer from MV scatter onto the kV imager. This study investigates the use of external monitoring combined with sparse kV imaging during beam pauses to overcome KIM limitations.

Material and Methods: Six patients with 2-3 implanted gold markers received three fraction liver SBRT on a conventional linac. A setup CBCT was acquired with simultaneous recording of the motion of an external marker block on the abdomen (Fig. A). The 3D marker motion during the CBCT was estimated at 15Hz from the 2D motion in the CBCT projections and used to establish an external correlation model (ECM) of the internal marker motion INT(t) in each direction (RL, SI, AP) as a function of the external marker block motion EXT(t): $INT(t) = A \cdot EXT(t) + B \cdot EXT(t-\tau) + C$, where A, B, C are coefficients and τ is a time constant. During treatment delivery, INT(t) was estimated from the external motion at 20Hz, while MV-scatter-free kV images were acquired every 3s during beam pauses. INT(t) was estimated from the ECM of the CBCT without any model update and with updates of the coefficient C*SI* by use of the first image of each treatment field. Post-treatment, the 3D marker positions were estimated for each intra-treatment kV image and used as ground truth to quantify the root mean square error (rmse) of the INT(t) estimations.

Results: Figs. B-C compare the estimated INT(t) with and without model updates with the ground truth positions in intra-treatment kV images at one fraction. Table 1 shows the mean rmse for all fractions. ECM updates more than halved the SI rmse. Substantial internal cranial baseline drift up to 7 mm (mean 1.4 mm) occurred between the setup CBCT and the last field without a similar drift for the external surrogate, illustrating the need for intra-treatment ECM updates.

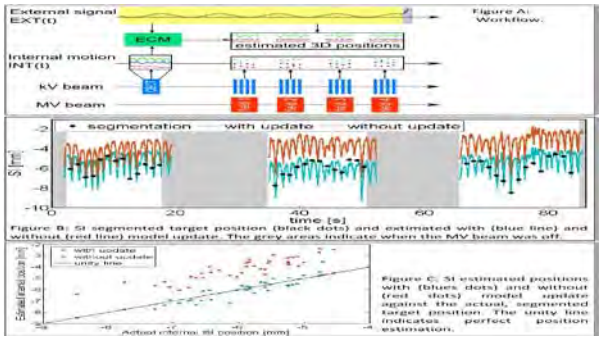

	Pre-treat	Intra-treatment kV images	
RMSE [mm]	CBCT	With update	Without update
RL	0.19	1.15	1.15
SI	0.61	1.09	2.55
AP	0.31	1.13	1.13
3D	**0.73**	**2.12**	**3.14**

Table 1 : Mean rmse of the ECM for all fractions. The first column describes the fit-performance of the ECM to motion during the CBCT. Note that model-update (second column) was only performed in the SI direction.

Conclusion: A correlation model between external surrogate motion and internal liver motion was established on a conventional linac from pre-treatment CBCT projections and used to estimate the intra-treatment target positions with and without model update. A simple update based on only one kV image per field substantially improved the localization accuracy. Real-time update of the model in all 3 motion directions is currently being developed and is expected to further improve the localization accuracy. The proposed method increases the versatility and reduces the imaging dose compared to current clinical KIM implementations.

OC-0210

Motion management for partial arc VMAT treatments using intra-fractional 2D/3D registration

H. Furtado[1], Y. Seppenwoolde[2], E. Steiner[2], M. Bsteh[3], W. Birkfellner[4], D. Georg[2]

[1]*Medical University of Vienna, Center for Medical Physics and Biomedical Engineering / Christian Doppler Laboratory for Medical Radiation Research for Radiation Oncology, Vienna, Austria*

[2]*Medical University of Vienna, Department of Radiation Oncology / Christian Doppler Laboratory for Medical Radiation Research for Radiation Oncology, Vienna, Austria*

[3]*Medical University of Vienna, Department of Radiation Oncology, Vienna, Austria*

[4]*Medical University of Vienna, Center for Medical Physics and Biomedical Engineering, Vienna, Austria*

Purpose or Objective: Rotational radiotherapy IMRT (VMAT) has shown superior delivery efficiency with similar overall treatment plan quality compared to conventional IMRT. For lung treatments intra-fractional tumor motion is a major source of uncertainty in dose application leading to the enlargement of the PTV margins and possibly to increased dose delivery to OARs. Motion management by tracking the tumor using intra-fractional kV planar images has the potential to reduce position uncertainty and reduce the PTV margins. The challenge for rotational treatments is the poor tumor visibility at certain gantry angles. In this work we investigate the feasibility of delivering VMAT treatments using only partial arcs where the tumor is well visible and therefore tracking is feasible.

Material and Methods: For our study we used the x-ray images acquired for CBCT reconstruction from five patients with NSCLC undergoing hypo-fractionated SBRT treatment (3 fractions of 13.5Gy prescribed to the 65% isodose). These x-rays are comparable to kV fluoroscopy images acquired during a VMAT treatment. For each patient the evaluation consisted of two steps: first real-time 2D/3D registration was used to track the tumor location on each of the x-rays from the CBCT acquisition. We determined the gantry angle intervals for which it was possible to track the tumor by comparing registration results with manually annotated diaphragm motion. Second, VMAT plans were created for partial arcs chosen depending on the anatomy and tumor location (U=unlimited) for a PTV based on an ITV approach (ITV plus 4mm margin) and for the limited partial arcs where the tumor tracking worked (L=limited) for a PTV based on the midventilation CTV (5mm margin). The L partial arc plans were evaluated using the U plans as benchmark.

Results: For all cases is was possible to track the tumor in two arcs of about 90 degrees, typically with imaging around anterior-posterior (AP) or posterior-anterior (PA) projections. For patient 5 it was possible to track the tumor in all projections. In terms of plan quality, a target coverage of at least 99% to the 65% isodose was aimed for and could be achieved for all the U plans and for all the L plans except for one, where the available angle range led to an unfavorable dose distribution, which would be clinically not acceptable. Therefore this patient was omitted for further data evaluation. Table 1 summarizes the tracking angles and the DVH parameters. Figure 1 shows example tracking results and obtained plans for one patient.

	Tracking angles (deg)				Used arc ranges (deg)		PTV volume (cc)		DVH parameters					
									Lung V13.4Gy (V20Gy EQD2)		Spinal cord D0.1cc (EQD2, α/β=2)		Esophagus D0.1cc (EQD2, α/β=2)	
Patient	AP		PA		U	L	U	L	U	L	U	L	U	L
1	136	25	32	155	285	185	19.7	15.4	5.08	5.94	5.70	5.50	3.00	11.30
2	160	65	20	108	NA	NA	NA	NA	NA	NA	NA	NA	NA	NA
3	141	48	52	149	160	93	27.4	23.7	5.94	7.00	3.70	20.40	5.50	9.70
4	135	51	66	127	160	84	13.2	11.4	8.40	10.00	14.90	5.70	23.30	10.90
5	180	0	0	180	245	245	33.2	32.9	17.07	16.23	2.00	2.80	12.20	8.30

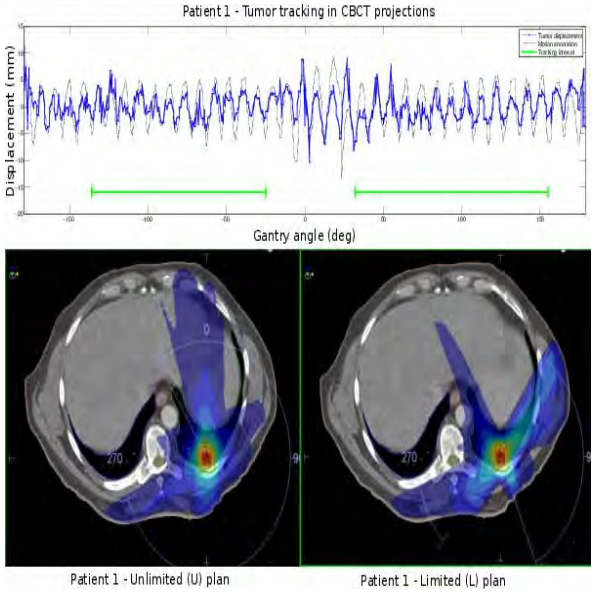

Conclusion: The results indicate the feasibility of VMAT treatments under tumor tracking for selected patients. The arcs available for planning influence the quality of treatment. The L partial arc plans had clinically acceptable quality in four patients. Treatments with reduced margins could be safely delivered by gating the treatment beam if the tumor motion exceeds the margins. Also, a great advantage is that the dose delivered to the tumor could be exactly monitored.

OC-0211

Real-time MRI-guided Radiotherapy for pancreatic cancer

S.A. Rosenberg[1], A. Wojcieszynski[1], C. Hullett[1], M. Geurts[1], S.J. Lubner[2], N.K. LoConte[2], D.A. Deming[2], D.L. Mulkerin[2], C.S. Cho[3], S.M. Weber[3], E. Winslow[3], K.A. Bradley[1], J. Bayouth[1], P.M. Harari[1], M.F. Bassetti[1]

[1]*University of Wisconsin, Department of Human Oncology, Madison, USA*

[2]*University of Wisconsin, Division of Hematology and Oncology-Department of Medicine, Madison, USA*

[3]*University of Wisconsin, Division of Surgical Oncology-Department of Surgery, Madison, USA*

Purpose or Objective: Pancreatic cancer with vascular involvement has a poor prognosis regardless of treatment. The toxicity of chemoradiation to adjacent normal organs can contribute to treatment discontinuation and adverse outcomes in some patients. We hypothesized that real-time MRI guided radiotherapy for borderline or locally advanced pancreatic carcinoma would enable safer treatment delivery with tight margins and diminished normal tissue toxicity than conventional treatment approaches.

Material and Methods: Patients with borderline or locally advanced pancreatic cancer were eligible for evaluation for MRI-guided radiotherapy. Patients underwent complete staging, including baseline CA19-9 and triple phase CT imaging. Patients underwent simulation with an inhale breath hold 3D and cine scans on a MRI Guided Treatment Planning system. Locoregional lymph node coverage was incorporated at the discretion of the Radiation Oncologist. The mean CTV to PTV expansion was 3 mm (range 2-5 mm). The primary GTV was tracked in real-time throughout treatment and the PTV or similar structure was used as a boundary for triggering treatment. A patient initiated repeated breath hold strategy was used to increase the reproducibility and duty cycle of radiotherapy.

Results: We have completed treatment for our first 5 patients with borderline or locally advanced pancreatic adenocarcinoma. The population was 4:1 Male:Female with a mean age of 61.8 years (range 52-67). All patients had an elevated CA19-9 at presentation, with a mean of 714 U/mL (range 62 – 2350 U/mL). Locoregional lymphatics were treated in 4/5 patients. The mean PTV was 222.7 cc (range 40.3-346.4 cc). The PTV was treated to 50.4 Gy at 1.8 Gy per a fraction with concurrent chemotherapy for all patients. With a median follow-up of 166 days (range 50 – 278 days), an average 66% reduction in CA19-9 1-2 months following chemoradiation was observed. The OS is 60% at time of follow up. One grade 4 toxicity was observed with duodenal ulceration during radiotherapy requiring hospitalization. The number of patients, overall survival, local control, progression free survival, and changes in CA19-9 levels will be updated at the time of presentation.

Conclusion: Real-time MRI-guided radiotherapy enables the design and delivery of highly conformal treatment for patients with borderline or locally advanced pancreatic carcinoma. A significant reduction in CA19-9 levels after treatment was observed. Real time MR imaging throughout treatment enables high precision tracking to minimize treatment margins and normal tissue dose exposure. MRI-guided radiotherapy may provide opportunities for normal organ toxicity reduction and future dose escalation strategies.

OC-0212

Liver motion tracking using optical flow cine-MRI registration

M. Seregni[1], C. Paganelli[1], P. Summers[2], M. Bellomi[2], G. Baroni[1], M. Riboldi[1]

[1]*Politecnico di Milano, Dipartimento di Elettronica-Informazione e Bioingegneria, Milano, Italy*

[2]*Istituto Europeo di Oncologia, Department of Radiology, Milano, Italy*

Purpose or Objective: Thedevelopment of radiotherapy treatment units with integrated MRI scanners isstimulating interest in fully MRI-guided treatment protocols. Cine-MRIsequences capable of acquiring 5-6 2D images per second are already available,thus providing a potential means of non-invasive, online motion monitoring withhigh soft-tissue contrast. This work investigates the feasibility of livermotion tracking using optical flow registration of Cine-MR images series.

Material and Methods: Livercine-MRI series (balanced steady-state free precession, 256x256 pixel, 1.28x1.28mm spacing, f = 3.3Hz) providing 220 images over a 70s scan were acquired in 25patients and 5 healthy volunteers after informed consent. Ground-truth livermotion consisted in the trajectories of numerous sparse features ($\mathbf{P}_{SIFT}$) extracted using apreviously tested algorithm based on the Scale Invariant Feature Transform(SIFT) [1]. For each subject, optical flow (OF) registration, as proposed in [2],was applied between the first image of the series and each subsequent frame,thus obtaining time-resolved dense motion fields [Fig. 1]. Trajectories basedon OF ($\mathbf{P}_{OF}$) were then derivedby applying these motion fields to the positions of the SIFT features detectedin the first image. To assess the accuracy of the motion fields, the 2D frame-by-framedistances ($\mathbf{D}_{SIFT-OF}$)between $\mathbf{P}_{SIFT}$ and $\mathbf{P}_{OF}$ were calculated forevery trajectory and, for each subject, their distributions were described withmedian, inter-quartile range, 5^{th} and 95^{th} percentiles.Linear correlation coefficients ($\mathbf{r}_{SIFT-OF}$) between

P_{SIFT} and P_{OF} were also calculated.Finally, the computation time required for OF registration was measured.

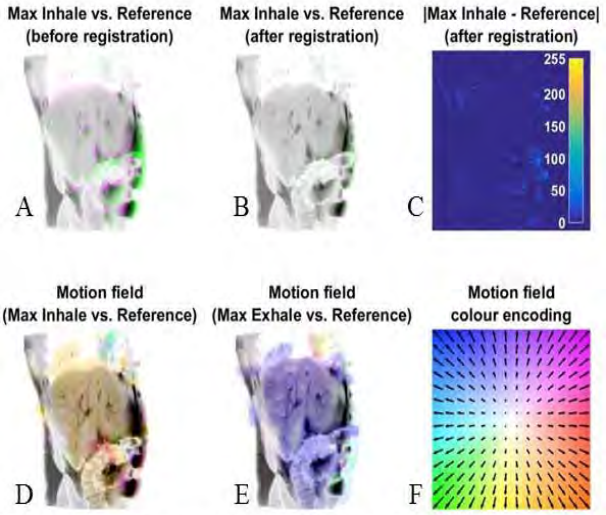

Figure 1. Panel A: overlay between reference (cine-MRI first frame) and full inhale image before optical flow registration. Panels B and C: overlay and absolute difference between reference and full inhale after registration, respectively. Panels D and E: motion field magnitude and direction at full inhale and full exhale, colour-coded as in Panel F.

Results: A total of 1345 trajectories were extracted (from5 up to 99 per subject). Table I reports the motion fields accuracy results.The median value of $D_{SIFT-OF}$ waswithin the pixel size (1.28 mm) in 27 out of 30 subjects. The median $r_{SIFT-OF}$ was 0.92 ± 0.08(mean ± SD among all subjects) with just 18/1345 trajectories reporting notstatistically significant correlations (t-test *p-value* ≥ 1%) to SIFT. The computation time for a singleregistration was 49.2 ± 2.4 ms (mean ± SD, 3.20GHz processor, 64GB RAM).

Table I. Minimum, Mean ± Standard Deviation and Maximum values among 30 subjects of the $D_{SIFT-OF}$ distributions parameters

$D_{SIFT-OF}$ [mm]	Minimum	Mean ± SD	Maximum
5th Percentile	0.21	0.26 ± 0.03	0.33
Median	0.85	1.04 ± 0.16	1.45
IQR	0.72	1.09 ± 0.29	1.89
95th Percentile	2.20	4.10 ± 1.17	8.34

Conclusion: Livermotion trajectories obtained through OF registration were comparable to thosemeasured using robust feature matching. Moreover, the OF method calculates a densemotion field that can be used to simultaneously track multiple internal structures(e.g. tumour and OAR contours) during irradiation. Finally, OF registrationappears well suited to online motion monitoring, as it is fully automated andits low computational cost allows tracking within current cine-MRI acquisition periods.

[1]Paganelli *et al* 2015 *Int J Radiat Oncol Biol Phys* 91(4)840-8
[2]Farnebäck 2003 *Image Analysis* (pp363-70) Springer Berlin Heidelberg

Acknowledgments: work supportedby AIRC, Italian Association for Cancer Research.

OC-0213

Towards on-line sub-mm and sub-second positional verification during stereotactic spine radiotherapy

C. Hazelaar[1], M. Dahele[1], B. Slotman[1], W. Verbakel[1]
[1]*VU University Medical Center, Radiation Oncology, Amsterdam, The Netherlands*

Purpose or Objective: Spine SBRT requires high positioning accuracy to avoid target miss and excessive OAR dose. However, conventional linacs do not allow high resolution spine position monitoring during irradiation. We analyzed kilo-voltage (kV) images routinely acquired by the gantry-mounted imager during spine SBRT using markerless template matching + triangulation. The aims were to determine whether this method would be suitable for sub-mm, sub-second on-line verification of spine position, and to determine spine stability.

Material and Methods: kV images, continuously acquired at 7 or 11 frames/s during FFF VMAT spine SBRT of 18 patients, comprising 89 fluoroscopy datasets (1 dataset/arc), were analyzed off-line. Four patients were immobilized in a head/neck mask, 14 had no rigid immobilization. 2D reference templates of the planning CT (1 template/°) were created in the form of filtered DRRs. The 360 templates consisted of the contoured vertebra + 2 mm. kV projection images were pre-filtered with a band-pass filter. Normalized cross correlation was used to find the 2D template position resulting in the best match between template and kV image. Multiple registrations were triangulated to determine 3D position. Average position and SD were calculated for each resulting motion trajectory. These SDs include spine stability and precision of the template matching + triangulation. To verify the accuracy and precision, mean and SD of two stationary phantom datasets with different baseline shifts were measured.

Results: Template matching + triangulation was performed within 0.1s/image. For the phantom, SDs were 0.21-0.23 mm for left-right (LR), 0.20-0.18 mm for superior-inferior (SI) and 0.24-0.23 mm for the anterior-posterior (AP) direction. The maximum difference in average detected and applied shift was 0.15 (LR), 0.37 (SI) and 0.03 (AP) mm. The table summarizes the SDs and percentages of tracked images for the clinical datasets. The template matching software performed less well for datasets in which the kV projection images contained overlying structures (e.g. clavicle, ribs, heart, diaphragm). Maximum spine position offsets were: -1.43-2.20 (LR), -3.48-0.68 (SI) and -1.14-1.52 (AP) mm. Average positional deviation was≤1 mm in all directions in 90% of the arcs. 91% of all tracked points (total combined x, y and z points=81327) deviated by <1 mm from the planned position, 97.4% by <1.5 mm, and 98.8% by <2 mm.

SD (mm)		LR	SI	AP	% Tracked
Cervical	Average	0.30	0.21	0.38	75.8
(n=16)	SD	0.07	0.04	0.10	16.1
	Min	0.21	0.14	0.24	53.8
	Max	0.42	0.28	0.63	95.6
Thoracic	Average	0.59	0.29	0.61	50.4
(n=36)	SD	0.25	0.09	0.25	18.3
	Min	0.20	0.17	0.20	31.8
	Max	1.28	0.59	1.22	93.8
Lumbar	Average	0.28	0.24	0.33	78.9
(n=37)	SD	0.07	0.05	0.12	13.1
	Min	0.16	0.15	0.19	36.8
	Max	0.43	0.37	0.77	95.3

Conclusion: Template matching + triangulation using kV images acquired during irradiation allows markerless spine position detection with sub-mm accuracy at sub-second intervals, without the need for supplementary hardware. This method is fast enough to be applied to near real-time on-line positional verification. Further technical improvements, such as increase of tracking rate, are anticipated. Although most patients were not immobilized they were stable at the sub-mm level for the majority of tracking observations.

OC-0214

Hybrid MLC and couch tracking

J. Toftegaard[1], R. Hansen[1], K. Macek[2], P.R. Poulsen[1]
[1]*Aarhus University Hospital, Department of Oncology, Aarhus C, Denmark*
[2]*Varian Medical Systems, Imaging Laboratory, Baden, Switzerland*

Purpose or Objective: MLC and couch tracking are promising techniques for intrafractional tumor motion management. However, both techniques have their limitations that result in residual dosimetric errors: MLC tracking perpendicular to the MLC leaves is limited by the finite MLC leaf width, while couch tracking has slower dynamics than the MLC and might be uncomfortable for the patient. Here, we suggest a range of potential hybrid MLC-couch tracking strategies and test the performance of each strategy with extensive tracking simulations.

Material and Methods: Three hybrid MLC-couch tracking strategies were investigated and compared with pure MLC tracking and pure couch tracking. Dividing the target motion into motion parallel and perpendicular to the MLC leaves in beam's eye view, the investigated tracking strategies were as follows (in order or increasing MLC tracking fraction). 1) Pure couch tracking; 2) Couch for all perpendicular target motion and MLC for parallel motion; 3) Couch for perpendicular motion below one leaf width and MLC for the remaining motion; 4) Same as 3) except that the couch only adapts to stable perpendicular shifts with standard deviation below 0.5mm during the last second; 5) Pure MLC tracking.
The current developer release of TrueBeam tracking system does not allow for hybrid MLC-couch tracking, but our in-house built tracking simulator allowed investigation of the hybrid strategies. The simulator was experimentally validated to mimic the TrueBeam MLC and couch tracking system. Tracking treatments with each tracking strategy were simulated for 160 lung tumor and 695 prostate trajectories. A high and a low modulated VMAT treatment (1 arc) with MLC motion in the superior-inferior direction were simulated for each trajectory.
The tracking performance of each simulated treatment was quantified as the mean MLC exposure error in beam's eye view. The MLC exposure error is the sum of under-exposed areas Au (MLC shielded areas that should ideally be exposed) and over-exposed areas Ao (MLC exposed areas that should ideally be shielded). Au+Aohas previously been shown to be a good surrogate for dosimetric errors in tracking treatments.

Results: The figure shows the cumulative distribution of mean MLC exposure errors for all trajectories and for trajectories with large motion (>3mm for prostate, >5mm for lung).The table shows the median reduction in the exposure error relative to pure MLC tracking as well as the mean 3D couch speed for all tracking strategies.

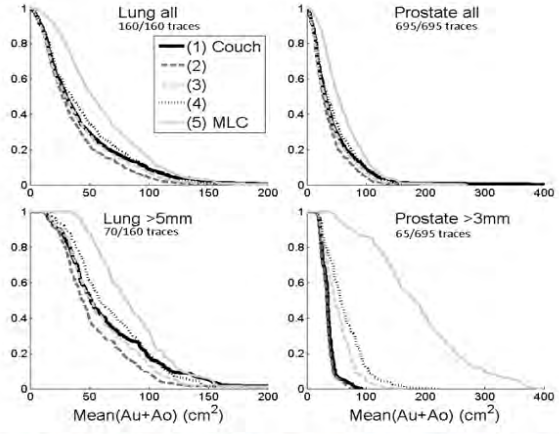

Figure 1: Cumulative plot for Mean over- and under-exposed areas for each site. Upper figure are all traces and lower are only traces with motion more than 5mm (Lung) and 3mm (Prostate). Numbers in legend refer to numbers in methods.

		Prostate		Lung	
		all	>3mm	all	>5mm
Exposure error	(1) Couch	42.31%	80.92%	42.31%	37.69%
	(2)	**48.78%**	**81.67%**	**48.78%**	**45.90%**
	(3)	42.78%	73.98%	42.78%	36.35%
	(4)	33.94%	68.57%	33.94%	29.05%
	(5) MLC	0.00%	0.00%	0.00%	0.00%
Motion	(1) Couch	0.827 mm	0.882 mm	2.52 mm	3 mm
	(2)	0.741 mm	0.86 mm	1.84 mm	2.34 mm
	(3)	0.766 mm	1.03 mm	1.84 mm	2.35 mm
	(4)	0.67 mm	0.809 mm	1.07 mm	1.17 mm
	(5) MLC	0 mm	0 mm	0 mm	0 mm

Table 1: Upper part: Median reduction in percent of mean exposure error relative to pure MLC tracking. Lower part: Average couch speed.

Conclusion: Hybrid MLC-couch tracking offers a continuum of trade-offs between tracking accuracy and couch motion. A modest degree of couch tracking (strategy 4) largely improved MLC tracking, especially for prostate motion exceeding 3mm. Couch tracking perpendicular to the MLC leaves and MLC tracking parallel to the leaves (strategy 2) gave the most accurate tracking and a large couch motion reduction compared to pure couch tracking.

OC-0215

Mapping of breathing and cardiac induced motion of lymph node targets in lung cancer patients

M.L. Schmidt[1], L. Hoffmann[2], M. Knap[1], T.R. Rasmussen[3], B.H. Folkersen[3], J. Toftegaard[1], D.S. Møller[2], P.R. Poulsen[1]
[1]*Aarhus University Hospital, Department of Oncology, Aarhus C, Denmark*
[2]*Aarhus University Hospital, Department of Medical Physics, Aarhus C, Denmark*
[3]*Aarhus University Hospital, Department of Pulmonology, Aarhus C, Denmark*

Purpose or Objective: Malignant mediastinal lymph nodes (LNs) are often included in the planning target volume for lung cancer patients (pts), but LN motion is not well investigated and this may potentially undermine the locoregional control. LNs in the mediastinum are difficult to visualize in cone-beam CT (CBCT) scans. In this study, the position of implanted fiducial markers obtained from daily CBCT projections was used to map the 3D intrafraction and interfraction motion of LN targets throughout the treatment course for ten lung cancer pts.

Material and Methods: Ten lung cancer pts with Visicoil fiducial markers implanted in LN targets by EBUS bronchoscope received intensity modulated radiotherapy (RT) treatment in 30-33 fractions. A total of 26 LN targets with Visicoils were analyzed. A pre-treatment setup CBCT scan with ~675 projections was used for daily online soft tissue match on the primary tumor (GTV-T). The Visicoil positions were segmented offline in each projection using a semi-automatic template-based algorithm. From the segmented Visicoil positions the 3D Visicoil trajectories were estimated with 11Hz sample rate by a probability-based estimation method. By frequency analysis, the 3D trajectories were separated into a cardiac and a breathing component. The motion ranges of the Visicoils were extracted in the left-right (LR), cranial-caudal (CC) and anterior-posterior (AP) direction for the total motion, as well as the separated cardiac and breathing induced motions. Also, the daily mean setup error of the Visicoils after the GTV-T soft-tissue match was extracted and used to calculate motion margins required for interfraction baseline shifts of the LN targets (using the formula $2.5\Sigma+0.7\sigma$)*.

Results: The 2-98 percentile motion ranges, for the patient group were in mean (with standard deviation) 2.1mm (0.5mm)(LR), 7.3mm (2.6mm)(CC), 3.3 mm (1.3mm)(AP). The cardiac induced mean motion ranges were 1.3mm 0.7mm)(LR), 1.3mm (0.6mm)(CC), 2.3mm (1.5mm)(AP). The figure shows the averaged waveform in the coronal plane of the cardiac and breathing motion components of each Visicoil at the first RT fraction. The waveforms were obtained by averaging over a number of breathing/cardiac cycles.

Breathing motion was largest in the CC direction and more prominent for more caudal LNs. Cardiac induced motion was often (77%) largest in the AP direction (not shown) and tended to be largest for more cranial LNs, occasionally (44 %) being the dominant motion component. The daily baseline shifts from all fractions resulted in interfraction motion margins of 4.9mm(LR), 4.7mm(CC), and 6.4mm(AP).

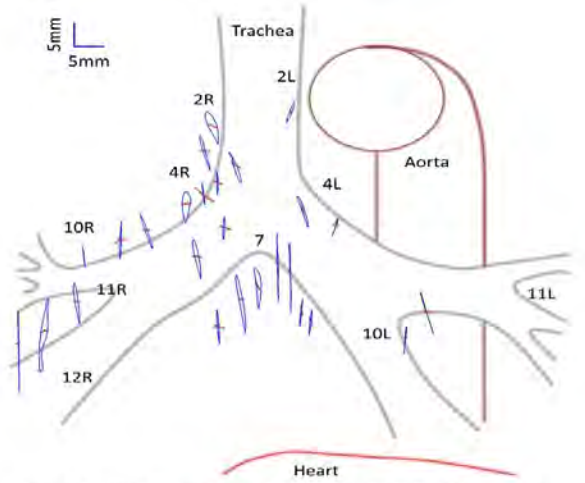

Figure 1: Bronchie-map showing the breathing (blue) and cardiac (red) component of the Visicoil lymph node motion during the first setup CBCT scan. The LN stations, trachea, aorta and heart are marked for clarity. The trajectories are displayed at the approximate Visicoil position in the planning 4DCT scan

Conclusion: The motion of Visicoils in projection images of daily CBCTs was used to map and analyze intrafraction and interfraction motion of mediastinal LNs. While the motion was governed by breathing induced motion, the most cranial LNs had substantial cardiac induced motion.

* Van Herk et al. Errors and margins in radiotherapy. 2004

Symposium: Head and neck: reduction of margins and side effects

SP-0216
Contouring of normal tissues in head and neck radiotherapy

S. Hol[1]
[1]*Dr. Bernard Verbeeten Instituut, Tilburg, The Netherlands*

In the head and neck region, there are a lot of organs at risk (OAR) to take into account when making a treatment plan. The radiation fields are often very large and can go up to the brain and down to the lungs. The OAR in this region are responsible for a lot of body functions, like walking, talking, swallowing and taste. Some of the OAR are parallel organs, so they will be able to compensate the loss of part of the organ and others are serial organs, which implies that the dose to the entire organ has to be below a threshold value in order to maintain the functionality.

In recent years most hospitals have started delineating more OAR in the head and neck region, but for some, there is no concensus on the constraints that have to be applied. Recently, consensus guidelines for head and neck OAR delineation were defined by Brouwer et al (1) To make sure that in the future we will be able to define constraints for these OAR we need a lot of data. This can only be obtained if there is consensus among institutes on delineation and reporting in the same manner.

In this presentation the different OAR will be discussed and a short summary of recently published guidelines will be provided.

(1) CT-based delineation of organs at risk in the head and neck region: DAHANCA, EORTC, GORTEC, HKNPCSG, NCIC CTG, NCRI, NRG Oncology and TROG consensus guidelines. Brouwer, C. et al. Radiother. Oncol. 2015; 117: 83–90.

SP-0217
The ESTRO perspective - a guideline for positioning of head and neck patients

M. Mast[1], M. Leech[2], M. Coffey[2], F. Moura[3], A. Ostavics[4], D. Pasini[5], A. Vaandering[6]
[1]*Haaglanden Medical Centre Location Westeinde Hospi, Den Haag, The Netherlands*
[2]*Trinity College Dublin, University of Dublin, Dublin, Ireland Republic of*
[3]*Hospital Cuf Descobertas, Radiotherapy, Lisbon, Portugal*
[4]*General Hospital Vienna AKH Wien, Radiotherapy, Vienna, Austria*
[5]*Policlinico Universitario Agostino Gemelli, Radiotherapy, Rome, Italy*
[6]*UCL Cliniques Univ. St.Luc, Radiotherapy, Brussels, Belgium*

Purpose: These guidelines have been developed to assist Radiation TherapisTs (RTTs) in positioning, immobilisation, position verification and treatment for head and neck cancer (HNC) patients presenting for radiation therapy.

Methods and materials: A critical review of the literature was undertaken by the authors, searching relevant databases including PubMed, Embase and Google Scholar. Search terms used included combinations of and Boolean operations of 'head and neck cancer', 'radiation therapy', 'radiotherapy', 'positioning', 'immobilisation', 'verification', 'cone beam CT', and 'electronic portal imaging'. Studies in English, French, Portuguese, Italian and German were included. Based on the literature review, a survey was developed to ascertain the current positioning, immobilisation and position verification methods for head and neck radiation therapy across Europe. The survey consisted of 40 questions, divided into 5 sections. The sections contained both open and closed questions on: Demographics, Patient Positioning, Immobilisation devices, CT/Simulation Practice, Position Verification as well as elements of quality assurance (QA) in relation to positioning and immobilisation. Data analysis was performed using SPSS Statistics version 20.0 (IBM SPSS Statistics for Windows. Armonk, NY: IBM Corp.). Descriptive statistics were calculated and appropriate figures and tables constructed. Cross tabulations were performed where appropriate to maximise data analysis.

Results: Results from the European-wide survey indicated that a wide variety of treatment practices and treatment verification protocols are in operation for head and neck cancer patients across Europe currently. These ranged from 3DCRT to VMAT and from daily online CBCT imaging to offline correction protocols using kV EPIs or in some cases, MV portal imaging. In terms of immobilisation, the majority of respondents use thermoplastic masks in their immobilisation of head and neck patients, with some variance in how shoulder position is maintained. The full results from this survey are available in the complete guideline document, available on the ESTRO website. Guidelines were given for: Positioning prior to thermoplastic mask constructionConstruction of thermoplastic maskThe CT procedureTreatment Verification and deliveryMatch Structures for Image Verification.

Conclusion: The preparation of this guideline document has demonstrated that although there have been substantial changes in the set up, positioning, immobilisation and verification of head and neck cancer patients over the last number of years across Europe, significant variations still exist. These variations can be attributed to differences in resource type and quality, institutional protocols as well as considerable differences in education level of radiation therapy professionals across Europe. RTTs must be aware of the potential dosimetric impact of poor positioning and immobilisation and/or position verification procedures as well as their influence on required margins for HNC radiation therapy. These guidelines have been developed to provide RTTs with guidance on positioning, immobilisation and position verification of HNC patients. The guidelines will also provide RTTs with the means to critically reflect on their own daily clinical practice with this patient group.

SP-0218

Late effects in patients treated for head and neck cancer

K. Henneberg[1], K. Jensen[1], H. Primdal[1], P.R. Olsen[1], M.W.H. Nielsen[1]

[1]*Aarhus University Hospital, Department of Radiation Oncology, Aarhus C, Denmark*

Introduction and purpose: Patients with head and neck cancer are treated with surgery, radiotherapy and chemotherapy either alone or in combination. The treatment has serious consequences for the patients, because of frequent and severe late side effects that often affects the patient's everyday life. The aim of the study was to investigate the unmet needs of the head and neck cancer survivors and to manage the late effect of the treatment. We wanted to investigate which health care efforts the patient needed in order to improve their quality of life.

Method/material: This mixed methods study included 204 patients, that were seen once during the first two years after the end of treatment. Patients were recruited from our follow up clinic and invited by letter. Patients completed three different questionnaires: EORTC QLQ C30, -H&N35 and HADS. The patients were thereafter interviewed, using focused questions dealing with 14 predefined topics and, analyzed by content analysis.

Result: In general the patients were doing well, but with large individual differences. Common side effects were dysphagia (60%) and, dry mouth (75%). The derived consequences of these side effects were – amongst others – difficulties with social interaction, speech, eating with others, fatigue, sexual problems, sleeplessness and memory problems. The frequency of side effects declined with time but some of the patients struggled years after treatment. The patients use at least three coping strategies; "avoid", "accept" and "action". In our study the patients were largely incapable of finding help to handle the late effects of the treatment. The questionnaires were not a sufficient screening tool for unmet individual needs that were commonly only identified during the interview.

Conclusion: The late effects, after treatment for head and neck cancer, have multidimensional consequences for the experienced health related quality of life. The patients need support and counseling to cope with the late effects and a specialized rehabilitation service with a multidisciplinary approach should be offered. It is important to screen and talk with head and neck patients systematically because there are large individual differences in how they deal with the long term consequences of treatment.

Symposium: The future of Radiation Oncology publishing: views through the Red and Green telescopes

SP-0219

Green Journal

J. Overgaard[1]

[1]*Aarhus University Hospital, Radiation Oncology, Aarhus C, Denmark*

Abstract not received

SP-0220

Publishing the science of radiation oncology: the perspective of the Red Journal's editor

A. Zietman[1]

[1]*Massachusetts Gen. Hosp. RT, Department of Radiation Oncology, Boston MA, USA*

Most published medical science ultimately proves to have little value as the results are founded on weak methodology and prove unrepeatable. In addition a "publish or perish" approach to academic medicine has placed pressures on investigators that weaken the ethical fabric of journal publication. This reality has become increasingly apparent in recent years, and many now feel that the traditional concepts of peer-review and static print journals are a thing of the past. This talk will address issues around the quixotic peer-review process and efforts made by the Red Journal to get around them including: double-blind review, prospective review, and editorial review of the reviewers. Three additional concepts, made possible in an electronic age, promise to upend the old order changing the way science is placed into the public arena and critiqued. These include: unselective open access publication based on methodology alone, "as-you-go" publication of original data and results in open source databases, and "crowd sourced" review. These concepts are starting to gain considerable traction in the basic science world but have yet to change the way clinical science is presented. The Red and Green Journals will have to react to this changing environment and it is likely that within 10 years the current format will have changed beyond recognition.

SP-0221

How to do a good manuscript review

L.P. Muren[1]

[1]*Aarhus University Hospital, Department for Medical Physics, Aarhus C, Denmark*

Peer review is an important basis for scientific activities and progression. Peer review is the cornerstone for evaluation of scientific work, including applications for research grants and positions as well as scientific reports and publications in scientific journals. This presentation will focus on the role of peer review of manuscripts submitted for consideration for publication in journals. Initially, the presentation will address the importance of peer review as the main method for scientific evaluation; alternatives to the conventional peer review process will also be mentioned. Subsequently the presentation will go through the major steps in reviewing a manuscript. This also includes the issues to consider when receiving the invitation from the journal. Key questions to address when evaluating the various parts of the manuscript (Introduction, Materials & methods, Results and Discussion) will be covered.

References:

1. COPE Ethical Guidelines for Peer Reviewers. http://publicationethics.org/files/u7140/Peer%20review%20guidelines.pdf

2. http://www.senseaboutscience.org/pages/peerreviewedcation.html

3. http://violentmetaphors.com/2013/12/13/how-to-become-good-at-peer-review-a-guide-for-young-scientists/

Poster Viewing : 5: RTT

PV-0222

Enhancing safety and quality of the radiotherapy process using a multidisciplinary end-to-end review

M. Albers[1], J. Stam[1], T. Janssen[1], A. Van Mourik[1], A. Van Giersbergen[1], C. Van Vliet-Vroegindeweij[1]

[1]*The Netherlands Cancer Institute, Department of Radiation Oncology, Amsterdam, The Netherlands*

Purpose or Objective: In radiotherapy (RT) extensive quality assurance (QA) protocols exist to guarantee the safety and quality of treatments. Generally, the QA consist of performance, consistency and/or stability checks of individual items such as CT acquisition, treatment planning or treatment device. Besides QA of individual items, the coherence of all items constituting the entire chain is crucial for the overall treatment quality. Therefore, in 2013, we started with the "Analysis of Process Quality" (APQ); an analysis of the RT process from CT to RT. The purpose of this retrospective analysis of the APQ results is to investigate whether the APQ improves and optimizes the RT process.

Material and Methods: The APQ is performed monthly for four randomly chosen patients for a specific tumor site. For each patient, a physicist and a radiation technologist (RTT)

review every step in the RT process. They check whether the used protocol is applicable, if the choices made in the RT process are logical and whether the workflow was correct. Afterwards, the reviews are discussed plenary by the four physicist-RTT couples and a radiation oncologist (RTO) specialized in the tumor site. In this meeting, actions to optimize the RT process are defined. For the retrospective analysis, the items on the action lists are categorized either as: protocol checks (incomplete/incorrect protocol), procedure checks (difference in interpretation of protocols) and abnormalities in human actions (misunderstanding/human error) or techniques (technical shortcoming).

Results: In three years the APQ resulted in a total of 76 actions. The results are displayed in Table 1. Examples of some typical actions include: adjusting the dose volume histogram reports in showing more relevant information, unifying the workflow around peer review of delineations, securing consistency of patient setup information.

Table 1. Percentage categories per process step

Percentage (%)	Imaging preparation	Treatment planning	Radiation treatment
Protocol	7%	14%	5%
Procedure	8%	13%	7%
Abnormality (human)	5%	8%	3%
Abnormality (technique)	5%	7%	18%

Only small abnormalities were found, which didn't influence the radiation treatment or caused any injury. In addition, the APQ turns out to be a good tool to enhance collaboration between multidisciplinary professionals like physics, RTT's and physicians.

Conclusion: From our results, it follows that the APQ detects several types of (small) abnormalities in the total RT process. It is known that large errors typically result from a combination of small abnormalities through the process chain. Therefore we believe that by finding and correcting these small abnormalities, the APQ inherently improves the quality and safety of our treatment. In discussing the quality of our treatment in this multidisciplinary setting, we increase commitment and mutual understanding. In short, the APQ is a unique and effective process audit to enhance the quality and safety of the entire RT process.

PV-0223

Accuracy of 2D angiogram to 3D MRI registration for frameless stereotactic targeting of brain AVM

I.T. Kuijper[1], O. Hertgers[1], J.P. Cuijpers[1], F.J. Lagerwaard[1]
[1]*VU University Medical Center, Radiation Oncology, Amsterdam, The Netherlands*

Purpose or Objective: Stereotactic Radiosurgery (SRS) is an established treatment option for arteriovenous malformations in the brain (bAVM). Two dimensional (2D) digital subtraction angiography (DSA) is used for accurate delineation of the AVM because of its high temporal resolution. In current practice, an invasive head frame and localizer box are used to indirectly register 2D DSA with 3D magnetic resonance angiography (MRA) datasets. The new registration method, which is commercially available, segments a vessel tree from the 3D MRA, and matches this unique vessel projection with the vessel projection in the 2D DSA images. This study aimed to measure the accuracy and feasibility of this new registration method and compare it to the traditional image localization technique.

Material and Methods: 69 image-registrations from 52 bAVM patients were analyzed. Patients with more than one AVM feeder artery had two registrations. In the traditional technique the 3D CT and 2D DSA datasets were indirectly registered using the localizer box. The CT was fused to the 3D MRA establishing a registration between DSA- and MRA-datasets. In the new technique the vessel tree segmentation from the 3D MRA was directly fused to the vessel tree from the frontal and lateral 2D DSA images of each patient (figure 1). Two observers independently performed registrations and the accuracy was compared to the traditional one. The mean rotational and translational differences and outliers were calculated for the frontal and lateral DSA images. In addition, feasibility was analyzed for different factors e.g. vertebral or carotid artery registrations, prior embolization/hemorrhage and MRA/DSA image quality.

Results: The mean difference of the new compared to the traditional registration technique was 1.1 mm and 1.3 ° for translations and rotations, and 2/69 (3%) exceeded 3 mm. The 3D vector had a mean (SD) of 1.5 ± 0.71 mm (range 0.1-4.7 mm). The mean (± 1 SD) results for 69 registrations of each DSA image are shown in figure 1. No difference >0.5 mm was seen between registrations with the DSA of either the carotid- or vertebral artery. Furthermore, no significant differences were found in patients with prior hemorrhage and/or embolization (p>0.05). The mean inter-observer disagreement between the two observers was 0.3 mm with maximum differences of 2.6 mm. Good image quality, the correct orientation of the DSA image sets together with whole brain MRA scans for optimal vessel segmentation are important criteria for accurate registration using the new method.

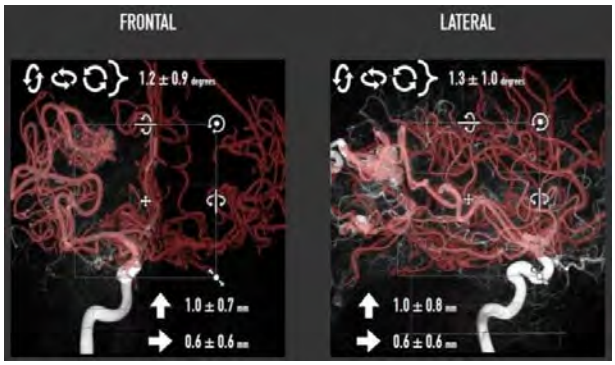

Conclusion: The new software based DSA-MRA registration using vessel tree segmentation is a feasible and accurate approach and agrees to within a mean of 1.1 mm and 1.3 ° with the traditional method using a frame and localization box. The new registration method allows the application of frameless (fractionated) radio surgery and could facilitate the import of external diagnostic DSA images for treatment planning.

PV-0224

To be greeted as a human being - A meta-synthesis of cancer patients' experiences of radiotherapy

S. Petri[1]
[1]*Copenhagen University Hospital - Rigshospitalet, Department of Oncology- Section for Radiotherapy, Copenhagen, Denmark*

Purpose or Objective: Around 35,000 Danish people are diagnosed with cancer each year, and approximately 16,000 people receive one or several radiotherapy fractions. In Denmark radiotherapy is delivered by special educated oncology nurses and radiographers, in the following referred to as radiation therapists (RTTs). Results from existing research suggest that the RTTs play an important role in relation to how the radiotherapy treatment is experienced by the patients. In addition, patients feel tied down and as slaves of the time due to the daily treatments. Furthermore the high-tech context in a radiotherapy department may seem intimidating to the patients and consequently create insecurity and uncertainty in an already vulnerable situation. However, in order to establish a culture of patient-centered care and communication in clinical practice more knowledge on how patients experience radiotherapy treatment is warranted. The purpose of the study was therefore to explore how adult cancer patients experience radiotherapy based on existing qualitative research.

Material and Methods: Based on qualitative meta-synthesis as described by Sandelowski and Barroso four research articles were systematically identified and included in the study. Only studies conducted in the Scandinavian countries were included to ensure a similar cultural context and organization of the health care system. The meta-synthesis was conducted in a hermeneutic perspective, and consisted of five phases; *search phase, appraisal phase, classification phase, analysis phase* and *synthesis phase*. The synthesis phase was complemented by the approach *imported concepts* to expand comprehension and integrate the findings.

Results: The results suggest that the experience of radiotherapy is described by the main theme: *The importance of being greeted as a human being* and six sub-themes; *The role and competence of the RTT; Continuity and relationships; Isolation; High-tech environment; Active participation* and *Knowledge and guidance*.The main theme and sub-themes are illustrated in Figure 1.

Figure 1

The results are integrated with notions on care by Kari Martinsen with reference to the Danish philosopher Loegstrup, suggesting that the RTTs must be very aware of their role in the encounter with the individual; including being responsible for building trust and protecting the continuity in the relationship. The results suggest that structural issues in the health care system, such as efficacy and task prioritization, can jeopardize the relationship and communication between the RTT and the patient.

Conclusion: The results of the study provide evidence to work more actively with ensuring continuity during the radiotherapy trajectory to provide a higher level of care and communication with the individual patient. In addition, the study introduces an increased awareness amongst RTTs regarding their specific role in the patients' experiences of a radiotherapy trajectory.

PV-0225

Investigating optimal modality for boost treatment of left breast with deep inspiration breath hold

A. Sen[1], A. Michalski[1], B. Done[1], A. Windsor[1,2]
[1]*Central Coast Cancer Centre, Radiation Oncology, Gosford, Australia*
[2]*University of New South Wales, Faculty of Medicine, Randwick, Australia*

Purpose or Objective: Deep inspiration breath hold (DIBH) for breast boost requires photons due to the limitations of the Varian RPM DIBH monitoring equipment, precluding the use of electrons. Traditionally, an electron boost was felt to be superior compared to photons due to their rapid dose fall off and resultant low dose to the heart and short treatment time. If an electron boost was deemed superior, this would need to be delivered with the patient free breathing (FB) due to aforementioned limitations. The primary aim of this study is to compare photons at DIBH to electron boost at FB with regards to plan quality and organ at risk (OAR) constraints to the heart and lungs in left sided breast patients. The secondary aim was to assess if the dosimetric detriment of the inferior modality would detract from the benefits gained in Phase 1, whole breast DIBH treatment.

Material and Methods: Twenty consecutive patients undergoing radiotherapy to the left breast with DIBH were identified. All patients underwent dual CT scans at DIBH and FB as per the standard departmental protocol. A boost treatment was retrospectively planned with electrons on the FB scan and photons on a DIBH scan to a prescription on 10Gy in 5 fractions. PTV coverage, mean and maximum, doses to the heart and left anterior descending artery (LAD) and mean doses to the lungs were compared. The results were further analysed by the location of the boost volume as defined by breast quadrants.

Results: Doses to the planning target volume (PTV) and mean heart doses were comparable between photons and electrons. Maximum heart doses reduced by 60% while maximum and mean LAD doses reduced by 54% and 51.2% respectively using photons, while mean left lung dose reduced by 43%. These reductions were seen across all four breast quadrants.
When combined with the reductions in doses seen using DIBH for Phase 1, whole breast treatment, electrons would result in an overall treatment dose increase of 11% for the heart maximum, 7.3% and 14% for LAD mean and maximum respectively and 70% for lung mean.

Conclusion: Dosimetrically photons was a superior modality when compared to electrons in phase 2 Left breast treatment maintaining benefits to the heart and lung gained through DIBH without compromising PTV coverage. The results were applicable regardless of the location of the boost volume. The increase in mean lung, maximum heart and maximum and mean LAD doses would negatively impact on the dosimetric benefit seen during DIBH for Phase 1 of left breast treatment.

PV-0226

Pattern of relapse of glioblastoma treated with Stupp protocol:could a margin reduction be proposed?

S. Pedretti[1], M. Buglione[2], P. Borghetti[1], L. Costa[1], L. Triggiani[2], L. Pegurri[1], P. Ghirardelli[2], F. Foscarini[2], S. Pandini[2], L. Spiazzi[3], G. Tesini[3], C. Uccelli[3], F. Saiani[3], S. Magrini[2]
[1]*Spedali Civili di Brescia, Radiation Oncology, Brescia, Italy*
[2]*Brescia University, Radiation Oncology, Brescia, Italy*
[3]*Spedali Civili di Brescia, Medical Physics, Brescia, Italy*

Purpose or Objective: To analyse the pattern of recurrence and acute and late toxicity of 105 patients treated with Stupp protocol in relation to both radiotherapy technique (3D, IMRT and helical IMRT) and treatment volumes; to compare in silico plans with reduced GTV-CTV margin (1 cm) with the original ones (2 cm). The CTV-PTV margin (5 mm) was maintained.

Material and Methods: Relapse was considered as in field, marginal and distant if more than 80%, 20-80% or <20% of the relapse volume was included respectively in the 95% isodose. In silico plans with reduced margin were retrospectively re-calculated using exactly the same technique, the same fields angles and, if possible, the same TPS of the original plans. Statistical analysis was performed with SPSS® software.

Results: Eighty-five patients had local recurrence: 3 were excluded because underwent follow-up MRI in other hospitals; 14 because the original treatment plans were not recoverable. The analysis was therefore executed on 68 patients. They were in field, marginal and distant respectively in 88%, 10% and 2% of the cases. This pattern of

relapse was similar (pt student= ns) when the analysis was done on the in silico plans. The margins reduction appears to avoid the inclusion in the high dose volume of about 100 cc of healthy brain (p=0.02) (Table 1). The target coverage was significantly worse in original than in the in silico plans (pt student <0.001) (Table 1), especially if the tumour was close to organs at risk (px2 <0.001). PTV coverage of original plans was significantly better with IMRT and helical-IMRT when compared with 3D ones (pAnova test=0.038). This difference was no more statistically significant with in silico planning (pAnova test= n.s.). Higher incidence of asthenia and leuko-encephalopathy was observed in patients with greater percentage of healthy brain included in the 57 Gy isodose (pAnova test=0.038 and 0.034).

Table 1:
Comparison between really delivered plans (GTV-CTV margin=2cm) and *in silico* plans (GTC-CTV margin =1cm)

		GTV-CTV 2cm	GTV-CTV 1cm	p
Pattern of recurrence	In field	60 (88%)	55 (81%)	n.s.
	Marginal	7 (10%)	10 (15%)	
	Distant	1 (2%)	3 (4%)	
Organ at risk	Brain – PTV	Median (range)	Median (range)	0.025
	percentage	80% (50%-97%)	88% (69%-98%)	
	cc	1080 cc (580-1446cc)	1175 cc (850-1547 cc)	
	Brain - isodose 95% (57 Gy)	Median (range)	Median (range)	<0.001
	percentage	75% (35%-95%)	83% (53%-98%)	
	cc	1004 cc (407-1364 cc)	1105 cc (605-1487 cc)	

Conclusion: No differences in the pattern of recurrence according to the extent of margins have been found. The incidence of asthenia and leuko-encephalopaty varies with the percentage of healthy brain included in the high dose volume. The margin reduction allows significant sparing of healthy cerebral tissue and could possibly reduce the incidence of late toxicity. Margin reduction is compatible with appropriate target coverage, thereby limiting the need for more sophisticated and costly techniques to selected cases.

PV-0227

Radiotherapy in elderly patients with lung cancer. Performance status and fractionation analysis

J.L. Monroy Anton[1], V. Sanz Ballester[2], R. Gironés Sarrió[3], C. Gaspar Martinez[4], M. Soler Tortosa[1], A. Navarro Bergada[1], M. Estornell Gualde[1]

[1]*Hospital Universitario De La Ribera, Radiation Oncology, Alzira, Spain*

[2]*Universidad Catolica De Valencia, School Of Nursing, Alzira, Spain*

[3]*Hospital Lluys Alcanyis, Medical Oncology, Xativa, Spain*

[4]*Hospital Universitario De La Ribera, Medical Oncology, Alzira, Spain*

Purpose or Objective: Elderly patients with lung cancer are often referred to treatment with radiotherapy. Tolerance to treatment and survival may be determined by their age and performance status. Different fractionation schedules in these patients can also influence the results.
Our objective was to analyze survival in patients ≥70 years, depending on age groups, Karnofsky Status (KPS) and fractionation schemes.

Material and Methods: We analyzed 70 patients, aged ≥70 years, with diagnostic of lung tumors (T1-4; N1-3), with no previous surgery treatments, referred for external radiotherapy.
Total Dose range: 20-64Gy; fractionation schedules: 1.8-2Gy (considered standard, std), >2Gy (hypofractionation/stereotactic SBRT) Karnofsky Performance Status (KPS), was the tool to evaluate functional status the first day of treatment, and analysis was performed with two KPS groups: <70 vs ≥ 70

Results: Global survival: mean 9months (m); median 8 m.
12m survival: 22patients (31,4%)
18m survival: 8pts (11,4%)
>23m survival: 4pts (5,7%)
AGE:
70-79y: mean 9m; median 8 m
≥80y: mean: 9,2m; median: 8 m
KARNOFSKY PERFORMANCE STATUS (KPS)
Survival:
KPS <70: mean: 9,2m; median: 8
KPS ≥70: mean: 9m; median: 8
FRACTIONATION SCHEDULE:
standard fx: 29 pts mean:9.2m; median: 8
hypofractionation: 34pts mean: 8m; median: 7 m
only SBRT: 7pts mean: 9.7m; median: 8.5m
fractionation survival:
≥6months: std: 20 pts (67%) hypofx: 19 (56%)
≥12m: std: 11pts (38%) hypofx: 9pts (26.4%)
≥18m: std: 5 pts (17.2%) hypofx: 2 pts (0,6%)

Conclusion: In elderly patients the most advanced age (> 80 years) does not determine differences in survival after radiotherapy treatment.
There are no differences in survival of elderly patients according to the KPS (<70 vs ≥70)
Survival is very similar regardless of the fractionation scheme used (mean 9.2 vs 8 months). However, 6, 12 and 18 months survival is greater in patients with standard fractionation We can conclude that in elderly patients, the variables age, KPS or fractionation scheme does not determine significant differences in survival.
Hypofractionation techniques or SBRT should be considered as an alternative in frail elderly patients to avoid prolonged treatment in time. The analysis of other parameters such as tumor stage or additional chemotherapy could also discriminate populations with different prognostic.

PV-0228

Size and impact of intra-fractional changes in baseline shift during lung SBRT

M. Kamphuis[1], M.A.J. De Jong[2], E.M. Dieleman[2], A. Bel[2], N. Van Wieringen[2]

[1]*Academic Medical Center, Academic Physics, Amsterdam, The Netherlands*

[2]*Academic Medical Center, Department of Radiotherapy, Amsterdam, The Netherlands*

Purpose or Objective: A baseline shift can be defined as a shift of the target volume relative to its surrounding organs at risk (OAR). The baseline shift varies from day to day and can potentially lead to an overdosage of the OARs. In our clinic, the magnitude of the baseline shift is measured at the start of treatment in patients treated for solitary lung cancer. In case an OAR moves towards the target and the baseline shift exceeds the PRV margin, treatment is prevented. Limited data is available about the intra-fractional change of the baseline shift. The aim of this study is to determine if an intra-fractional change of the baseline shift necessitates multiple measurements to ensure safe delivery of SBRT.

Material and Methods: In this study a retrospective analysis was performed using the data of 87 patients, treated for lung cancer with SBRT in the period January 2010 to February 2014. Patients were treated according to one of three protocols: 3x18Gy (n=19), 5x11Gy (n=47), or 8x7.5Gy (n=21). Treatment delivery was performed using multiple (> 9) non-coplanar conformal beams or VMAT using 2 arcs. A planning risk volume (PRV) margin of 10mm was used standard around OARs (e.g. the heart and spinal cord). Smaller PRV margins, with a minimum of 3mm, were used in case prescriptions/constraints could not be met during planning.
Conebeam-CT scans were performed at the beginning, halfway, and at the end of each treatment fraction. Grey-value registrations of Conebeam-CT scans with Planning-CT scan were performed for both the target and the patient specific most critical OAR . The difference between the registrations is the baseline shift. The number of times the vector length of the baseline shift exceeded the PRV margin

during treatment was scored. In these cases, it was investigated whether or not this would result in overdose for the OAR.
Furthermore, the change in baseline shift was calculated for the first and second half of each fraction as well as for the fraction as a whole. The average vector length and standard deviation of the change in baseline shift were determined per patient and for the population as a whole. Data were stratified according to the applied protocol.

Results: Figure 1 shows the results of change in baseline shift during treatment. Slightly larger changes in baseline shift were seen in the 3x18Gy and 5x11Gy protocol. In 11 out of 460 treatment fractions, the baseline shift exceeded the PRV margin at the end of the treatment fraction. In none of the patients this exceeding led to overdosage.

Figure 1: Intra-fractional changes in baseline shift

	Average vector (SD) Protocol 3x18Gy	Average vector (SD) Protocol 5x11Gy	Average vector (SD) Protocol 8x7.5Gy
Start – Halfway RT	0.19 cm (0.20)	0.18 cm (0.14)	0.13 cm (0.10)
Halfway RT - End	0.19 cm (0.16)	0.18 cm (0.14)	0.12 cm (0.08)
Start - End	0.27 cm (0.24)	0.24 cm (0.19)	0.18 cm (0.13)

Conclusion: Intra-fractional baseline shift can vary substantially during treatment, especially in patients treated with a 3x18Gy or 5x11Gy protocol. However, clinical impact of changes in baseline shift during treatment were not found in this study. A single assessment of the baseline shift at the start of treatment ensures a safe treatment delivery.

PV-0229

IGRT for pediatric patients: How much can we reduce the dose?

L. Johansen[1], T.H. Larsen[1], M. Aznar[1], B. Smulders[1]
[1]*Rigshospitalet- Copenhagen University Hospital, Department of Oncology - Section of Radiotherapy, Copenhagen, Denmark*

Purpose or Objective: In our institution, orthogonal kV X-rays is at present the preferred imaging method for children as imaging dose is a concern. In this study, we varied the CBCT acquisition parameters and investigated how much we can reduce dose, and still be able to perform a secure bone match in clinical practice.

Material and Methods: An Alderson phantom equivalent to an adult was CT scanned. Due to the absence of a real child size phantom only the head and neck was used. On our Varian Novalis Tx accelerator, we performed 12 full-fan 200° CBCT scans with different parameter settings. The number of projections, mA and ms were systematically decreased, while kV was constantly at 100. After each scan an automatic bone match was performed to investigate the ability to perform this kind of match, since this is our procedure in clinical practice. The image quality of the scans was visually inspected for noise and artefacts. Six of the scans were chosen for dose measurements relative to the standard preset for these types of scans. The relative dose measurements were performed using the RTI Barracuda system, consisting of a DCT10-pencil ion chamber positioned in the centre of the CTDI 16 cm diameter cylindrical phantom. The parameters from the scan comprising the largest dose reduction and with the ability to match were used for a new CBCT preset. The phantom was CBCT scanned with the old and the new preset. Additionally the phantom was four times repositioned slightly different and re-scanned. Four RTT's independently matched these CBCT scans with the original CT scan offline in order to validate the new preset.

Results: A dose reduction of up to a factor of 14 could be achieved by changing the full-fan CBCT scan parameters from 20 mA and 20 ms (standard preset) to 10 mA and 2 ms. Reducing the number of projections from 650 to 360 added no further dose reduction. The new imaging preset results in a total dose of only 0.39 mGy compared to 0.14 mGy for 2 orthogonal X-ray imaging. Table 1 shows the average match difference between the different presets. The maximum deviations are +/-0,5 mm and 0.6°. Figure 1a+b show the difference in image quality between the standard and the new preset.

Table 1 Average match difference between scans obtained with standarad preset and new.

Avg. Dev (cm)	Position 1	Position 2	Position 3	Position 4	Position 5
VRT	0.00	0.03	0.00	0.03	0.00
LNG	0.00	0.03	0.05	0.03	0.05
LAT	0.03	0.00	0.03	0.03	0.00
RTN(º)	0.03	0.18	0.03	0.63	0.03

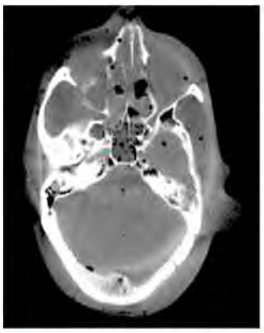

Figure 1a Scan obtained with std preset.

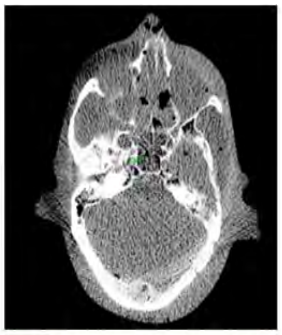

Figure 1b Scan obtained with new preset.

Conclusion: It is possible for RTT's to use low dose daily CBCT scans in paediatric radiation therapy and still perform a reliable automatic bone match.

PV-0230

Risk assessment of solid secondary malignancies in childhood Hodgkin Lymphoma after radiotherapy

G. Zanella[1,2], M. Mascarin[1], A. Drigo[3], A. Pusiol[2], E.C. Fuga[4], F.M. Giugliano[1], A. Rosolen[5], M.G. Trovò[4]
[1]*Centro di Riferimento Oncologico, Radioterapia Pediatrica, Aviano PN, Italy*
[2]*Azienda Ospedaliero Universitaria di Udine, Clinica Pediatrica, Udine, Italy*
[3]*Centro di Riferimento Oncologico, Fisica Sanitaria, Aviano PN, Italy*
[4]*Centro di Riferimento Oncologico, Radioterapia, Aviano PN, Italy*
[5]*Azienda Ospedaliera Universitaria, Clinica Pediatrica, Udine, Italy*

Purpose or Objective: This work develops risk assessments of solid secondary malignancies (SMN) after radiotherapy (RT) in survivors of childhood and adolescent Hodgkin Lymphoma (HL) patients (pts) using the Schneider's dose-response model for solid cancers induction (Theoretical Biology and Medical Modelling 2011), comparing conventional technique (3D-CRT) with IMRT delivered with Helical Tomotherapy (HT).

Material and Methods: Our cohort includes 15 pts (6 girls, 9 boys) treated with RT for HL, in age 6-25 years (median 17)

at the RT, from 2008 to 2013. The 15 pts are representative of different RT target volumes (e.g. bilateral neck, ipsilateral neck, mediastinum, mantel-field, lombo-aortic and spleen, inverted Y, inguinal field, or a combination of them). We calculated the excess absolute of risk (EAR) end the cumulative risk of "all solid" and "single organ" SMN: mouth and pharynx, parotids glands, thyroid, lung, stomach, small intestine, colon, liver, cervix, bladder, brain and spinal cord, skin, female breast, bone and soft tissue. Every HT plan has been compared with 3D-CRT plan, both for EAR, cumulative risk and target coverage.

$$EAR^{org} = \frac{1}{V_T} \sum_i V(D_i)\, \beta_{EAR}\, RED(D_i)\, \mu(agex, agea)$$

Results: The risk of SMN solids is high, for both techniques, for breast, lung, thyroid, skin and colon. Some HT treatments may lead to increased risk of SMN solid than 3D-CRT plans, depending on the patient's age at exposure, on the specific organ volume or target volume and on the dose-response of each site. All the HT plans have the best conformation to the target and the greatest homogeneity of the dose to it delivered (best conformation number and homogeneity index).

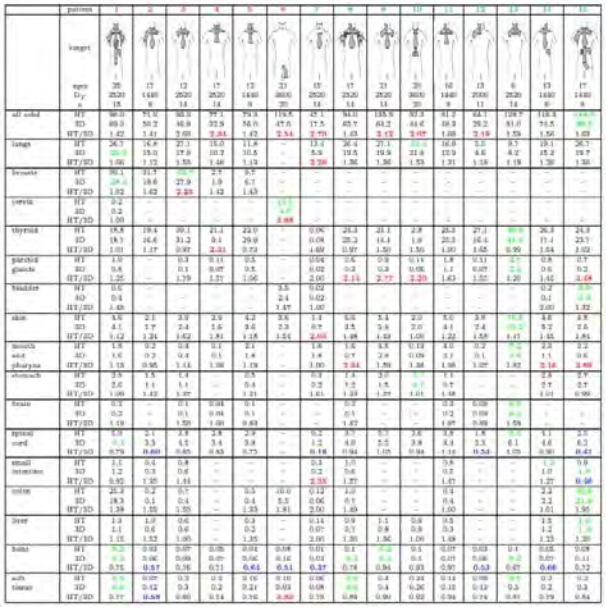

In this table: EAR (/10000 pts-year) at agea 60 in HT and 3D-CRT for all pts (1-15: pink=girl, cyan=boy); DT=target dose in cGy, agex= age at pt's radiation treatment, n= number of RT fractions.Green=max value for each line.Red= statistically significant EAR ratio with EAR HT>EAR 3D-CRT; blue= statistically significant EAR ratio with EAR 3D-CRT> EAR HT

Conclusion: Even if HT increases the target coverage in all pts, it could increase the incidence of SMN compared with 3D-CRT for long-term survivors, depending on single specific target, target volume and pts age. However, EAR estimates are affected by large uncertainties and more works should be performed to better understand the risk of SMN with modern RT techniques after a childhood cancer.

Symposium: QA in clinical trials: processes, impact and future perspectives

SP-0231
How effective is current clinical trial QA?
E. Miles[1]
[1]*Mount Vernon Hospital, Academic Physics, Northwood Middlesex, United Kingdom*

A central independent quality assurance (QA) process is acknowledged as an essential component of current radiotherapy clinical trials. QA processes are implemented both pre accrual and during accrual. The former ensures centres have the equipment, expertise and ability to comply with trial protocol requirements and that they are able to deliver treatment accurately and consistently. During accrual processes assure continued compliance and consistency of treatment delivery both within individual centres and across all recruiting centres throughout the trial. The key process areas in QA activity are:
Target volume and organ at risk outlining
Treatment planning and optimisation
Treatment delivery and verification
Dosimetry Audit
This talk will focus on the following main themes expanding on the processes involved and providing evidence and examples from individual trial QA programmes.
The implementation of clinical trial QA: Appropriate QA tasks to include questionnaires, process documents through review of example patient cases to dosimetry audit site visits, are assigned on an individual trial basis. The level of QA required will vary according to the complexity and novelty of the radiotherapy technique.
Defining standards: It is well recognised that target volume and OAR delineation and treatment planning and optimisation may be variable and open to individual interpretation. Through multi professional trial workshops, provision of delineation guidelines and setting of dose-volume constraints, consensus benchmark standards can be defined.
Assessment against a benchmark: Conformity metrics and pre-defined mandatory and optimal dose constraints can be used to review against consensus standards to highlight potential protocol variations. Historically this review has been retrospective; however increasing use of prospective evaluation with constructive feedback can allow correction of protocol variations before treatment is delivered.
Verification of treatment delivery: Dosimetry audit in the form of a postal or site visit serves to provide an independent assessment of dose delivered and directly compares individual centres. Recently, resulting from advances in image guidance, adaptive radiotherapy has been introduced in the clinical trial setting, introducing new challenges in assessment of plan selection competency and compliance.
As more advanced technology is introduced in the clinical trial setting, QA activities must continually evolve to provide a safe framework for implementation of technical radiotherapy. Increased participation in clinical trials demands a streamlined approach to QA to reduce workload, improve efficiency and facilitate opening centres for recruitment earlier. Participation in a comprehensive QA programme not only accredits the centre for recruitment but also benefits the general standard of RT delivered.

SP-0232 How does QA impact on clinical outcomes?
D.C. Weber[1]
[1]*Paul Scherrer Institute PSI- Center for Proton Therapy- ETH Domain, Radiation Oncology, Villigen PSI, Switzerland*

Radiotherapy (RT) planning and delivery for cancer management has substantially evolved over the last three decades with lately the introduction of intensity modulated RT, image-guided RT and stereotactic ablative RT to name a few techniques. The evaluation of these high precision delivery techniques in routine care and in clinical trials alike are error prone. They thus do require optimal RT quality (RTQA) assurance programs which aim at defining the range of acceptable variations and importantly developing mechanisms of action for correction and prevention of potential variations. RTQA outside a clinical trial is defined by all processes that ensure consistency of the dose prescription and the safe delivery of that prescription with regard to dose to the target and critical structures, minimization of the exposure of the RT personnel. In the framework of clinical trials assessing the efficacy of RT with or without a combined modality, RTQA is also necessary to avoid the corruption of the study-endpoint, as RT variations from study protocol decrease the therapeutic effectiveness and/or increase the likelihood of radiation-induced toxicities. Prospective trials have shown that RTQA variations have a

significant impact on the primary study end-point and could bias the analysis of the trial results[6]. A large prospective phase III (i.e. TROG 02.02) trial showed indisputably that poor radiotherapy resulted in suboptimal patient's outcomes. Moreover, the impact of poor quality radiotherapy delivery exceeded greatly the benefit of chemotherapy, thus biasing the primary end-point of this study. This large Australian trial provided a contemporary benchmark that future studies will need to exceed. Other specific consideration for RTQA in trials includes, but is not limited to, education of the accruing sites in RT-trial guidelines, promotion of consistency between centers and estimation of inter-patient and inter-institutional variations. Additionally, global cooperation is essential in the environment of common and rare cancers alike, in order to be able to create sufficiently large patient data sets within a reasonable recruitment period. This cooperation is not without issues and recently the need to have harmonized RTQA procedures has been strongly advocated by the Global Harmonisation Group. Ensuring RT compliance with protocol guidelines involves however gradually more resources-intensive procedures which are also labor intensive and are not cost-neutral. This will consequentially have a significant impact on the overall study budget. There are suggestion that QA programs are however cost-effective. This financial investment is of paramount importance, as non-adherence to protocol-specified RT requirements in prospective trials is very frequent. The European Organisation for the Research and Treatment of Cancer (EORTC) Radiation Oncology Group started to implement RTQA strategies in the 1980s, including on how to write a protocol for RT trials, defining RTQA procedures (such as benchmark case, dummy run and complex treatment dosimetry checks), assuring prospective individual case review feasibility and implementing an electronic data-exchange platform.

Keywords: Quality assurance, RTQA, prospective trial, patient's outcome, toxicity

SP-0233

What will we need for future RTQA in clinical trials?

C. Hurkmans[1]
[1]*Catharina Ziekenhuis, Eindhoven, The Netherlands*

A trial protocol with clearly established delineation guidelines and dose-volume parameters is key to all RTQA. Acceptable and unacceptable variations thereof should be defined before the trial starts as these are the standards to which all RTQA data collected will be compared. The experience so far has been addressed by the previous two speakers. Dr. Miles presented the RTQA procedures in clinical trials, differentiating between pre-accrual and during accrual tasks. Thereafter, Dr. Weber clearly showed that non adherence to protocol-specified RT requirements is associated with reduced survival, local control and potentially increased toxicity. Thus, it can be concluded that clinical trial groups have established RTQA procedures and conformance to these procedures strengthen the trial results. In this talk the remaining issues that need to be solved will be addressed. These issues can be separated in:

1. How can we further optimising the current RTQA
2. How should we include new imaging and treatment modalities in our RTQA program?

The first part of the talk will address several initiatives to further optimise current RTQA procedures. As we have learned from past RTQA experience, currently the individual case reviews (ICRs) are the most common source of variations from trial protocols. ICR variation is also the most important RTQA factor affecting trial outcome. Thus, a transition is needed from retrospective ICRs to timely, full prospective ICRs. Also, with the further advancement of tailored treatments for small subgroups of patients there is a growing need for intergroup trials to increase the accrual rates when conducting trials for such patient groups. These changes place new requirements on multiple parts in the RTQA procedure:

- Standardisation of RTQA across various trial groups. The Global Harmonisation Group initiative.
- Standardisation of protocol requirements with clear definitions of acceptable and unacceptable variations.
- Standardisation of OAR and target naming conventions.
- Automated upload of RTQA data from institutions to the RTQA review organisation, including anonymisation software, use of Dicom standards.
- Metrics and software tools to automatically evaluate image quality, delineations and treatment plans.

The second part of the talk will address the ideas of including new diagnostic, treatment and evaluation modalities and techniques in RTQA programs. Examples will be shown of RTQA trial procedures for breathing correlated 4D-CT, 4D PET-CT, MRI and CBCT currently in use or under development.

Proffered Papers: Radiobiology 3: Novel targeting approaches in combination with radiation

OC-0234

Radiotherapy and L19-IL2: perfect match for an abscopal effect with long-lasting memory

N.H. Rekers[1], A. Yaromina[1], N.G. Lieuwes[1], R. Biemans[1], W.T.V. Germeraad[2], D. Neri[3], L. Dubois[1], P. Lambin[1]
[1]*MAASTRO, Department of Radiation Oncology, Maastricht, The Netherlands*
[2]*Maastricht University Medical Centre, Department of Internal Medicine, Maastricht, The Netherlands*
[3]*Swiss Federal Institute of Technology, Department of Chemistry and Applied Biosciences, Zurich, Switzerland*

THIS ABSTRACT FORMS PART OF THE MEDIA PROGRAMME AND WILL BE AVAILABLE ON THE DAY OF ITS PRESENTATION TO THE CONFERENCE

OC-0235

Enhancing stereotactic radiation schedules using the vascular disrupting agent OXi4503

M.R. Horsman[1], T.R. Wittenborn[1]
[1]*Aarhus University Hospital, Department of Experimental Clinical Oncology, Aarhus C, Denmark*

Purpose or Objective: The novel combretastatin analogue, OXi4503, is a vascular disrupting agent (VDA) that has recently been shown to significantly enhance a stereotactic radiation treatment. This was achieved using an OXi4503 dose of 10 mg/kg combined with a stereotactic treatment of 3 x 15 Gy. The current study was undertaken to determine the OXi4503 dose dependency when using different stereotactic radiation dose schedules.

Material and Methods: A C3H mammary carcinoma grown in the right rear foot of female CDF1 mice was used in all experiments. Treatments were performed in restrained non-anaesthetised animals when tumours had reached 200 cubic mm in size. Tumours were locally irradiated (230 kV x-rays) with 3 fractions of radiation varying from 5-20 Gy (each fraction given with an interval of 2-3 days over a one week period). OXi4503 was dissolved in saline prior to each experiment; once prepared it was kept cold and protected from light. Various doses (5-25 mg/kg) were intraperitoneally injected into mice 1-hour after each irradiation treatment. Three days after the final irradiation the tumours were subjected to a clamped top-up dose which involved giving graded radiation doses with the tumour bearing leg clamped for 5 minutes before and during irradiation. The percentage of mice in each treatment group showing local tumour control 90 days after irradiating was then recorded. Following logit analysis of the clamped top-up radiation dose response curves, the TCD50 values (radiation dose to control 50% of tumours) were estimated. A Chi-squared test ($p<0.05$) was used to determine significant differences between the TCD50 values.

Results: The clamped top-up TCD50 values (with 95% confidence intervals) obtained following irradiation with 3 treatments of 10, 15 or 20 Gy were found to be 42 Gy (38-

47), 30 Gy (23-39), and 0.8 Gy (0.3-2.3), respectively. A plot of the TCD50 values against the stereotactic doses gave rise to a linear response (slope = -4.1; correlation coefficient = 0.97). OXi4503 significantly decreased the clamped radiation top-up TDC50 values and this affect appeared to be independent of both the ambient radiation dose applied with each of the 3 fractions and the VDA dose; the curve showing the TCD50 values against stereotactic radiation dose was similar to that for radiation alone (slope = -4.3; correlation coefficient = 0.94), but the radiation + OXi4503 curve was some 15 Gy lower than the radiation only curve.

Conclusion: OXi4503 is an effective agent for enhancing a stereotactic radiation treatment. But, the enhanced response appeared to be a simple additive effect independent of both the radiation dose applied with each fraction and the VDA dose used.
Supported by grants from the Danish Cancer Society and the Danish Council for Independent Research: Medical Sciences.

OC-0236

DTP-006: a novel, orally bioavailable hypoxia-activated prodrug

R. Niemans[1], A. Yaromina[1], J. Theys[1], A. Ashoorzadeh[2], R. Anderson[2], M. Bull[2], C. Guise[2], H.L. Hsu[2], M. Abbattista[2], A. Mowday[2], A.V. Patterson[2], J.B. Smaill[2], D.F. Ackerley[3], L. Dubois[1], P. Lambin[1]
[1]*Maastricht University- GROW - School for Oncology and Developmental Biology, Maastricht Radiation Oncology MAASTRO Lab, Maastricht, The Netherlands*
[2]*University of Auckland, Auckland Cancer Society Research Centre, Auckland, New Zealand*
[3]*Victoria University of Wellington, School of Biological Sciences, Wellington, New Zealand*

Purpose or Objective: Hypoxia is a common feature of solid tumors. Conventional treatments such as chemo- and radiotherapy (RT) are less effective against hypoxic tumor cells. Hypoxia-activated prodrugs (HAPs) are specifically activated in hypoxia to target hypoxic cells as well as adjacent oxygenated tumor cells via their bystander effect. DTP-006 is a newly synthesized nitroaromatic HAP with highly favorable properties: 1) activation under hypoxia, 2) high bystander effect, 3) excellent aqueous solubility, 4) murine oral bioavailability and 5) no off-mechanism activation by human aerobic reductases NQO1 and AKR1C3. Here we show the effects of DTP-006 on tumor cell viability, spheroid growth and radiation resistant tumor cells *in vivo*, and assess its pharmacokinetics and oral bioavailability in mice.

Material and Methods: The one-electron reduction potential (E1) of DTP-006 was determined by pulse and steady state radiolysis. IC50 viability ratios were assessed in 2D cell culture exposed to normoxic or anoxic ($\leq$0.02% O_2) conditions. H460 multicellular layers (MCLs) under aerobic (5% CO_2, 95% O_2) or anoxic (5% CO_2, 95% N_2) conditions were incubated with DTP-006 for 5 h after which cells were plated for clonogenic survival. H460 spheroids were incubated with DTP-006 upon confirmation of a hypoxic core. NIH-III mice bearing H460 tumors received a single i.p. dose of DTP-006 (781 mg/kg) after irradiation (10 Gy) of tumors. 18 h later tumors were excised and single cell suspensions were generated and plated for clonogenic survival. Tumor-free female NIH-III mice received a single i.v. or oral dose of DTP-006 (383 mg/kg). Terminal blood samples collected at time points via cardiocentesis were analyzed by LC/MS/MS. Plasma half-life (T1/2) and absolute oral bioavailability (Fabs) were calculated.

Results: DTP-006 has an E1 value of -351 mV, indicating strong oxygen inhibition of nitro radical formation. IC50 were lower in anoxia than normoxia by factors of 203 (MDA-MB-468), 55 (C33A), and 20 (HCT116). In a H460 MCL clonogenic assay, 100 µM DTP-006 caused 99% cell kill under anoxia but exhibited no aerobic cell kill. It caused a concentration-dependent growth delay in spheroids, where 250 µM completely halted growth. A single dose of DTP-006 caused a significant loss of clonogenicity when combined with RT in an *in vivo* excision assay (log cell kill 2.35 relative to control). T1/2 after oral administration was 0.82 h and bioavailability was 47%.

Conclusion: DTP-006 kills tumor cells only in severe hypoxic conditions *in vitro*, reduces growth of tumor cell spheroids, and sterilizes radiation resistant tumor cells *in vivo*. It has clinically relevant bioavailability after oral administration. As such, DTP-006 is a promising new HAP with potentially favorable properties for clinical use. Further studies to determine the antitumor effects of DTP-006 as a monotherapy and in combination with RT in several preclinical tumor models are ongoing.

OC-0237

Adding Notch inhibition increases efficacy of standard of care treatment in glioblastoma

S. Yahyanejad[1], H. King[2], V. Iglesias[1], P. Granton[3], L. Barbeau[1], S. Van Hoof[1], A. Groot[1], R. Habets[1], J. Prickaerts[4], A. Chalmers[5], J. Theys[1], S. Short[6], F. Verhaegen[1], M. Vooijs[1]
[1]*University of Maastricht GROW Research Institute, Department of Radiation Oncology, Maastricht, The Netherlands*
[2]*Leeds Institute of Cancer and Pathology, Department of Radiation Biology and Therapy, Leeds, United Kingdom*
[3]*London Health Sciences Center, Department of Oncology, London- Ontario, Canada*
[4]*Maastricht University, Department of Psychiatry and Neuropsychology, Maastricht, The Netherlands*
[5]*University of Glasgow Institute of Cancer Sciences, Department of Translational Radiation Biology, Glasgow, United Kingdom*
[6]*Leeds Institute of Cancer and Pathology, Department Radiation Biology and Therapy, Leeds, United Kingdom*

Purpose or Objective: Glioblastoma multiforme (GBM) is the most common malignant brain tumour in adults. The current standard of care includes surgery followed by radiotherapy (RT) and chemotherapy with temozolomide (TMZ). Treatment often fails due to the radiation and TMZ resistance of a small percentage of cells with stem cell-like behavior (CSC). The Notch signaling pathway is expressed and active in human glioblastoma and Notch inhibitors attenuate tumor growth in vivo in xenograft models. Here, we investigate the efficacy of a clinically (FDA) approved γ-secretase inhibitor (GSI) RO4929097 in tumor control in combination with standard care of treatment (TMZ+RT) in an orthotopic glioma tumour model.

Material and Methods: Treatment efficacy *in vitro* was tested in 2D cultures using proliferation and clonogenic survival assays. 3D sphere assays were used as a model for pharmacological treatment response with quantification of spheroid growth delay in the different different treatment arms. Flow cytometry was used to detect cells expressing stem cell markers. Luciferase-expressing U87 cells were intracranially injected into the brain of CD-1 mice. Tumor volume was quantified using contrast-enhanced microCT and bioluminescence imaging. Animals received TMZ (ip), RO4929097 (GSI, orally) or radiation (RT, 8Gy) alone or in combination. RT dose was calculated and prescribed using SmART-Plan software with two 5-mm parallel-opposed beams placed at the center of the tumour.

Results: GSI in combination with RT and TMZ attenuated tumour cell proliferation, clonogenic survival as well as glioma spheroid growth. The expression of glioma stem cell markers SOX2 and CD133 was blocked by single or combined treatments with Notch inhibitors *in vitro*. Using our image guided micro-CT and radiotherapy platform *in vivo*, a significant growth delay was observed in GSI-, RT- and TMZ-only treated groups compared to the control group. Standard of care treatment (RT + TMZ) or addition of GSI to either TMZ or RT irradiation resulted in a significant growth delay and prolonged survival. Strikingly, the longest tumour growth delay together with an increase in median survival was observed in mice treated with the triple combination (GSI+RT+TMZ), with 1 out of 4 mice showing tumour cure.

Conclusion: We show in an orthotopic glioblastoma mouse model that adding a clinically approved Notch inhibitor to the TMZ/RT standard of care results in a significant growth delay and increased overall survival. The observed therapeutic benefit is promising for clinical translation in order to increase survival in patients bearing glioblastoma with active Notch signaling.

OC-0238

Akt1 facilitates DNA double-strand breaks repair through a direct physical interaction with DNA-PKcs

M. Toulany[1], J. Maier[2], U. Rothbauer[2], H.P. Rodemann[1]
[1]Division of Radiobiology & Molecular Environmental Research, Department of Radiation Oncology- University of Tuebingen, Tuebingen, Germany
[2]Natural and Medical Sciences Institute at the University of Tuebingen, Reutlingen, Germany

Purpose or Objective: It is well known that PI3K/Akt pathway is hyperactivated in K-RAS mutated tumor cells and is involved in radioresistance. Exposure to ionizing radiation induces activation of DNA-dependent protein kinase catalytic subunit (DNA-PKcs) as an essential enzyme for repair of DNA double-strand breaks (DSBs) through non-homologous end joining. Radiation-induced DNA-PKcs activity is partially dependent on serine/threonine kinase Akt1. In this study, role of DNA-PKcs in Akt1-mediated DSBs repair and post-irradiation cell survival was investigated. Likewise, a direct physical interaction of Akt1 with DNA-PKcs was studied.

Material and Methods: Non-small cell lung cancer cell line A549 and colorectal cancer cell line HCT116 with point mutations in K-RAS gene were utilized. Complex formation of Akt1 with DNA-PKcs and role of Akt1 in DSBs repair were tested by immunoprecipitation and γH2AX foci assays, respectively. Localization of Akt1 to DSB site was tested by immunofluorescence staining and confocal microscopy of P-Akt (S473) and γH2AX following microbeam laser irradiation and after exposure to ionizing radiation. To determine the potential interacting domain of Akt1 with DNA-PKcs; GST, GST-Akt1 full-length, GST-Akt1-N-terminal fragment (1–150 a.a.), and GST-Akt1-C-terminal (151–480 a.a.) proteins were incubated with purified DNA-PKcs and pull-down assay was performed. In order to identify the domain of DNA-PKcs that interacts with Akt1, constructs expressing four distinct fragments of DNA-PKcs (1-426, 427-1400, 2401-3850, 3700-4128 a.a) tagged with EGFP and full length Akt1 tagged with mCherry were produced. Akt1/DNA-PKcs was studied in A549 cells, transiently transfected with the appropriate constructs.

Results: Akt1 formed a complex formation with DNA-PKcs in the nuclear fraction immediately after irradiation. Nuclear Akt1 was co-localized with γH2AX foci and found to be essential for the efficient repair of ionizing radiation-induced DSBs and post-irradiation cell survival, in a DNA-PKcs dependent manner. A direct physical interaction of DNA-PKcs to the C-terminal domain of Akt1 could be demonstrated. Additionally, Akt1 was found to make physical interaction not only with the C-terminal domain of DNA-PKcs (3700-4188 a.a.) but also with the N-terminal domain (1-426 a.a.).

Conclusion: Akt1, through a direct physical interaction with DNA-PKcs, regulates repair of ionizing radiation-induced DSBs. Thus, due to overexpression of Akt1 in tumor cells and constitutive Akt activity in K-RAS mutated tumors cells, Akt1 can be proposed as a tumor specific target for radiosensitization.

Supported by grants from the Deutsche Forschungsgemeinschaft [Ro527/5-1 and SFB-773-TP B02] and the Federal Ministry of Research and Education(BMBF grants 0258416, 03NUK006D) awarded to HPR as well as GRK 1302/2 (T11) awarded to MT.

Proffered Papers: Clinical 5: Upper and lower GI

OC-0239

Survival of clinical stage I-III rectal cancer patients: a population-based comparison

I. Joye[1], G. Silversmit[2], E. Van Eycken[2], A. Debucquoy[3], T. Vandendael[2], F. Penninckx[4], K. Haustermans[1]
[1]KU Leuven/University Hospitals Leuven, Department of Radiation Oncology, Leuven, Belgium
[2]Belgian Cancer Registry, Statistics, Brussels, Belgium
[3]KU Leuven, Department of Oncology, Leuven, Belgium
[4]KU Leuven, Department of Abdominal Surgery, Leuven, Belgium

Purpose or Objective: Total mesorectal excision is the cornerstone of rectal cancer treatment and preoperative (chemo)radiotherapy and adjuvant chemotherapy are often administered. This population-based study compares the survival in clinical stage I-III rectal cancer patients who received either preoperative radiotherapy, preoperative chemoradiotherapy or no preoperative therapy. The effect of type of radical resection and adjuvant chemotherapy on survival was also investigated.

Material and Methods: Patients diagnosed between January 2006 and December 2011 with clinical stage I-III rectal adenocarcinoma were retrieved from the national Cancer Registry database. Only first primary invasive rectal tumors were included and only patients who underwent a radical resection were retained. The observed survival was calculated from the date of surgery until the date of death or until the last known vital status. Conditional survival was defined as the survival conditional on surviving one year after surgery and was calculated in order to avoid the impact of adverse events in the postoperative course.
Multivariable Cox proportional-hazards regression models were applied to evaluate the association of preoperative treatment, type of radical resection and use of adjuvant chemotherapy with survival, adjusting for the baseline characteristics age, gender, WHO score and clinical stage.

Results: A total of 5173 eligible rectal cancer patients were identified from the national database. Preoperative treatment was as follows: none in 1354 (26.2%), radiotherapy in 797 (15.4%) and chemoradiotherapy in 3022 (58.4%) patients. Patients who received no preoperative therapy or preoperative radiotherapy and those who underwent abdominoperineal resection had a lower observed survival as compared with patients receiving preoperative chemoradiotherapy or treated with sphincter-sparing surgery respectively (Table). The patient group receiving adjuvant chemotherapy had a worse observed survival than the group receiving no adjuvant therapy. These effects were age-dependent. Multivariable analysis demonstrated similar findings for the observed survival conditional on surviving the first year after surgery.

Table: Hazard ratios of treatment-related predictors from the multivariable Cox model for observed survival and conditional survival.

	Hazard ratio	95% CI	p-value
Observed survival			
Preoperative treatment			
none vs. CRT, <65 years	1.27	0.96-1.69	0.0991
none vs. CRT, 65-74	1.04	0.78-1.37	0.8094
none vs. CRT, ≥75 years	1.77	1.46-2.14	**<0.0001**
RT vs. CRT, <65 years	1.38	1.02-1.87	**0.0281**
RT vs. CRT, 65-74 years	0.94	0.69-1.27	0.6571
RT vs. CRT, ≥75 years	1.62	1.31-2.00	**<0.0001**
none vs. RT, <65 years	0.92	0.63-1.34	0.6714
none vs. RT, 65-74 years	1.10	0.77-1.59	0.5978
none vs. RT, ≥75 years	1.09	0.90-1.33	0.8722
Type of radical resection			
APE vs. SSO, <65 years	1.97	1.59-2.44	**<0.0001**
APE vs. SSO, 65-74 years	1.47	1.18-1.82	**0.0005**
APE vs. SSO, ≥75 years	1.09	0.93-1.29	0.2974
Adjuvant chemotherapy			
yes vs. no, <65 years	2.22	1.66-2.96	**<0.0001**
yes vs. no, 65-74 years	1.48	1.17-1.88	**0.0010**
yes vs. no, ≥75 years	0.95	0.77-1.17	0.6072
Conditional survival			
Preoperative treatment			
none vs. CRT	1.33	1.12-1.57	**0.0009**
RT vs. CRT	1.33	1.17-1.57	**0.0009**
none vs. RT	1.00	0.83-1.21	0.9996
Type of radical resection			
APE vs. SSO, <65 years	1.89	1.50-2.37	**<0.0001**
APE vs. SSO, 65-74 years	1.45	1.14-1.83	**0.0021**
APE vs. SSO, ≥75 years	1.09	0.89-1.33	0.4017
Adjuvant chemotherapy			
yes vs. no, <65 years	2.61	1.87-3.64	**<0.0001**
yes vs. no, 65-74 years	1.68	1.30-2.18	**<0.0001**
yes vs. no, ≥75 years	0.88	0.69-1.11	0.2755

Abbreviations: APE = abdominoperineal rectum excision; CI = confidence interval; CRT = chemoradiotherapy; RT = radiotherapy, SSO = sphincter-saving operation.

Conclusion: In this population-based study, preoperative chemoradiotherapy, sphincter-sparing surgery and no

adjuvant chemotherapy were associated with a superior survival in clinical stage I-III rectal cancer patients.

OC-0240

Lumbarsacral bone marrow modeling of acute hematological toxicity in chemoradiation for anal cancer

P. Franco[1], F. Arcadipane[1], R. Ragona[1], M. Mistrangelo[2], P. Cassoni[3], J. Di Muzio[1], N. Rondi[1], M. Morino[2], P. Racca[4], U. Ricardi[1]

[1]*Ospedale Molinette University of Turin A.O.U. San Giovanni Battista di Torino, Department of Oncology - Radiation Oncology, Torino, Italy*

[2]*Ospedale Molinette University of Turin A.O.U. San Giovanni Battista di Torino, Digestive and Colorectal Surgical Department- Centre for Minimal Invasive Surgery- University of Turin- Turin- Italy, Torino, Italy*

[3]*Ospedale Molinette University of Turin A.O.U. San Giovanni Battista di Torino, Department of Medical Sciences - Pathology Unit, Torino, Italy*

[4]*Ospedale Molinette University of Turin A.O.U. San Giovanni Battista di Torino, Oncological Centre for Gastrointestinal Neoplasm- Medical Oncology 1- Turin- Italy, Torino, Italy*

Purpose or Objective: To model acute hematologic toxicity (HT) and dose to pelvic osseous structures in anal cancer patients treated with definitive chemo-radiation (CT-RT).

Material and Methods: 53 patients receiving CT-RT were analyzed. Pelvic bone marrow (PBM) and corresponding subsites were contoured: ilium (IBM), lower pelvis (LPBM) and lumbosacral spine (LSBM). Dose-volume histograms points and mean doses were collected. Logistic regression was performed to correlate dosimetric parameters and > G2-G3 HT as endpoint. Normal tissue complication probability (NTCP) was evaluated with the Lyman-Kutcher-Burman (LKB) model.

Results: Logistic regression showed a significant correlation between LSBM mean dose and >G2 neutropenia (β coefficient:0.109;p=0.037;95%CI:0.006-0.212) and >G3 leukopenia (β coefficient:0.122; p=0.030;95% CI:0.012-0.233) (Table 1). According to NTCP modeling, the predicted HT probability had the following parameters: *TD50*:32.6 Gy, *y50*:0.89, *m*:0.449 (>G2 neutropenia) and *TD50*:37.5 Gy, *y50*:1.15, *m*:0.347 (>G3 leukopenia) (Figure 1). For node positive patients *TD50*:30.6 Gy, *y50*:2.20, *m*:0.181 (>G2 neutropenia) and *TD50*:35.2 Gy, *y50*:2.27, *m*:0.176 (>G3 leukopenia) were found (Figure 1)

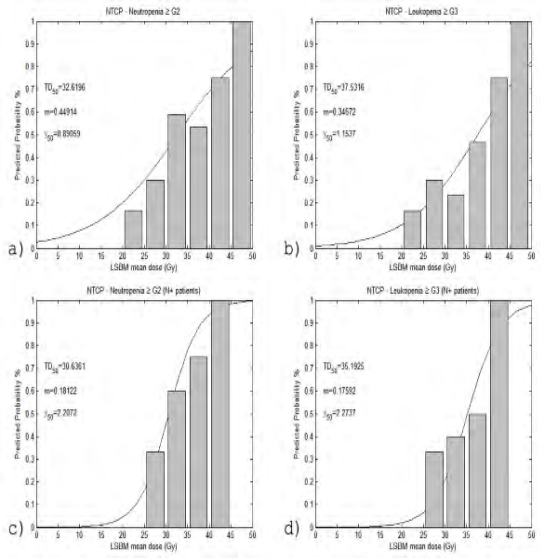

Table 1.

	> G3 neutropenia					> G2 neutropenia				
	β coeff	Std err	z value	p value	95% CI	β coeff	Std Err	z value	p value	95% CI
PBM-mean dose	-0.017	0.063	-0.28	0.781	-0.141-0.106	0.051	0.059	0.87	0.384	-0.064-0.168
IBM-mean dose	-0.041	0.055	-0.76	0.448	-0.150-0.066	0.007	0.043	0.18	0.854	-0.076-0.092
LPBM-mean dose	-0.007	0.073	-0.11	0.915	-0.151-0.135	0.071	0.070	1.01	0.312	-0.066-0.208
LSBM-mean dose	0.065	0.053	1.23	0.220	-0.490-0.536	**0.109**	**0.052**	**2.08**	**0.037**	**0.006-0.212**
	> G3 leukopenia					> G2 leukopenia				
PBM-mean dose	0.042	0.057	0.74	0.461	-0.070-0.155	0.086	0.075	1.15	0.248	-0.060-0.234
IBM-mean dose	0.017	0.043	0.40	0.688	-0.068-0.103	0.013	0.047	0.30	0.768	-0.078-0.106
LPBM-mean dose	0.001	0.069	0.03	0.979	-0.134-0.138	0.062	0.074	0.83	0.405	-0.083-0.208
LSBM-mean dose	**0.122**	**0.056**	**2.18**	**0.030**	**0.012-0.233**	0.062	0.051	1.23	0.220	-0.037-0.162

Legend–Coeff: coefficient; Std err: standard error; CI: confidence interval; PBM: pelvic bone marrow; IBM: iliac bone marrow; LPBM: lower pelvis bone marrow; LSBM: lumbo-sacral bone marrow;

.

Node positive patients had significantly higher PBM-V15 (Mean:81.1%vs86.7%;p=0.04), -V20 (Mean:72.7%vs79.9%;p=0.01) and V30 (Mean:50.2%vsMean:57.3%;p=0.03).Patients with a mean LSBM dose >32 Gy had a 1.31 (95%CI:0.75-2.35) and 1.81 (95%CI:0.81-4.0) relative risk to develop >G2 neutropenia and >G3 leukopenia. For node positive patients those risks were 1.67 (95%CI:0.76-3.64) and 2.67 (95%CI:0.71-10).To have a <5%, <10%,<20% risk to develop >G2 neutropenia and >G3 leukopenia, LSBM mean dose should be below 6 Gy, 13 Gy and 20 Gy and 14 Gy, 20 Gy and 26 Gy, respectively. For node positive patients these thresholds were below 21 Gy, 23 Gy and 26 Gy (>G2 neutropenia) and 24 Gy, 27 Gy and 30 Gy (>G3 leukopenia). On the whole cohort, within a dose range between 25 and 40 Gy, this probability rises from 30.3% to 69.1% for >G2 neutropenia and from 17.5% to 57.1% for >G3 leukopenia. For node positive patients these ranges were 16.5%-93.7% (>G2 neutropenia) and 6.7%-77.6% (>G3 leukopenia).

Conclusion: LKB modeling seems to suggest that LSBM mean dose should be kept below 32 Gy to minimize > G2-G3 HT in anal cancer patients treated with IMRT and concurrent chemotherapy. The sensitivity of LSBM and its contribution to the development of HT above 25 Gy seems higher in node positive patients.

OC-0241

MR radiomics predicting complete response in radiochemotherapy (RTCT) of rectal cancer (LARC)

N. Dinapoli[1], B. Barbaro[2], R. Gatta[1], G. Chiloiro[1], C. Casà[1], C. Masciocchi[1], A. Damiani[1], L. Boldrini[1], M.A. Gambacorta[1], M. Di Matteo[2], G.C. Mattiucci[1], M. Balducci[1], L. Bonomo[2], V. Valentini[1]

[1]*Università Cattolica del Sacro Cuore -Policlinico A. Gemelli, Radiation Oncology Department, Rome, Italy*

[2]*Università Cattolica del Sacro Cuore -Policlinico A. Gemelli, Radiology Department, Rome, Italy*

Purpose or Objective: RTCT is widely used as treatment in LARC before surgery. A challenging aspect for tailoring radiation dose prescription is prediction of cases that will show a pathological complete response (PCR) after surgery, because they have better expectation in survival outcomes. “Radiomics” refers to the extraction and analysis of large amounts of advanced quantitative imaging features with high throughput from medical images. Up today radiomics findings in LARC have been limited either to small case series and CT or PET scan imaging. Objective of this study is to find a radiomics signature able to distinguish PCR patients using pre-treatment MR.

Material and Methods: Histologically proven LARC patients were recruited retrospectively since May 2008 to December 2014. They were staged by T2 MR, high resolution (.7 x .7 x 3 mm pixel spacing on x-y-z axes) perpendicular to tumor major axis oblique scans, before RTCT start. Finally they underwent to surgery with definition of pathological response. All patients were addressed to RTCT treatment with 50.4 Gy @ 1.8 Gy/fr prescription dose on GTV+surrounding mesorectum (PTV1) and 45 Gy @ 1.8 Gy/fr on lymphatic drainage (PTV2). For radiomics analysis GTV was delineated on pre treatment MRI by a radiologist and a radiation oncologist experienced in GI. Images were processed by using a home-made software. Before analysis MR images were pre-processed using a normalization procedure and application of Laplacian of Gaussian (LoG) filter on raw data. After pre-processing, GTV volumes were analyzed extracting 1st order features (Kurtosis, Skewness and Entropy). These features were extracted by scanning all possible values of σ in LoG filter from 0.3 to 6 (step 0.01). A total number of 570 x 3 features were analyzed respect to the PCR in order to detect the most significant ones using AUC and Mann-Whitney test. Tumor clinical (cT, cN) and geometrical features (volume, surface, volume/surface ratio) were finally added for building a multivariate logistic model and predicting PCR. Model performance was evaluated by ROC analysis and internal bootstrapping for detecting calibration error (TRIPOD Ib classification).

Results: 173 patients have been enrolled in this study. 1st order features analysis shows as candidate-to-analysis ones the Skewness (σ=0.69 - SK069) and Entropy (σ=0.49 - EN049). Multivariate logistic model shows as significant covariates cT (p-val = 0.003), SK069 (p-val = 0.006) and EN049 (p-val = 0.049). AUC of model is 0.73 and bootstrap based internal calibration shows prediction mean absolute error = 0.017. The model has been summarized in a nomogram.

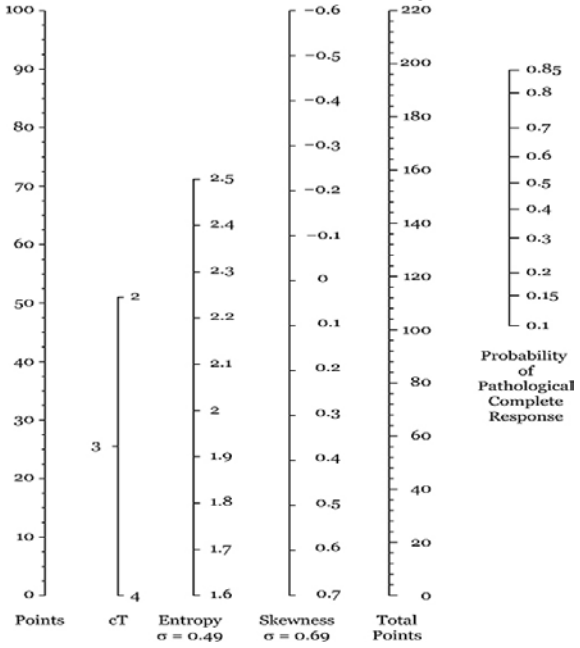

Conclusion: This is the first radiomics model able to predict PCR in LARC patients only using pre-treatment imaging. Model performance is fair but its limitation is in the availability of internal validation alone. External validation is already planned. Use of such a model could address patients to different treatment pathways according outcome expectation.

OC-0242

Follow-up time and prediction model performance in a pooled dataset of rectal cancer trials

J. Van Soest[1], E. Meldolesi[2], A. Damiani[2], N. Dinapoli[2], J.P. Gerard[3], C. Van de Velde[4], C. Rödel[5], K. Bujko[6], A. Sainato[7], R. Glynne-Jones[8], P. Lambin[1], A. Dekker[1], V. Valentini[2]

[1]*Maastricht University Medical Centre, Department of Radiation Oncology MAASTRO- GROW School for Oncology and Developmental Biology, Maastricht, The Netherlands*
[2]*Sacred Heart University, Radiotherapy Department, Rome, Italy*
[3]*Unicancer, Centre Antoine Lacassagne, Nice, France*
[4]*Leiden University Medical Centre, Department of Surgical Oncology- Endocrine and Gastrointestinal Surgery, Leiden, The Netherlands*
[5]*Goethe University Frankfurt, Department of Radiotherapy and Oncology, Frankfurt am Main, Germany*
[6]*Maria Sklodowska-Curie Memorial Cancer Centre, Department of Radiotherapy, Warsaw, Poland*
[7]*Azienda Ospedaliera Universitaria Pisana, Department of Radiotherapy, Pisa, Italy*
[8]*Mount Vernon Cancer Centre, Department of Medical Oncology, Northwood, United Kingdom*

Purpose or Objective: Predictive and prognostic models in locally advanced rectal cancer have been developed in the last years. Starting with predictions models on pathologic complete response (as intermediate endpoint), afterwards local recurrence (LR), distant metastasis (DM) and overall survival (OS) at different time points (e.g. 5 or 10 years post-treatment) finally resulting in a model for the aggregate outcome, disease free survival (DFS). The current work aimed to reproduce the prediction models for LR, DM and OS, and to investigate the time dependence of these models.

Material and Methods: The dataset characteristics are shown in Table 1. This pooled dataset merged the datasets of the ACCORD, TME, CAO/ARO/AIO '94, Polish, FFCD, Italian (Sainato) and UK (Glynne-Jones) trials. As the current pooled dataset contains different trials, we used 20% of patients (stratified on the trial) as a validation dataset. In accordance to the methods used in previous work, we trained prediction models for the outcomes LR, DM and OS on this larger dataset. Prediction model variables were selected by evaluating the univariate Kaplan Meier curves for every variable at a significance level of $p<0.05$. Afterwards, a Cox proportional hazards model and logistic regression models (in the latter situation a model for every month) were trained. Furthermore, we analyzed the covariate weights for the regression models. Finally, all the models were validated on discriminative ability using the Area under the Receiver Operating Curve (AUC).

Variable	Distribution / frequency	# missing values
Sex		0 (0%)
Male	3233 (66%)	
Female	1696 (34%)	
Age		0 (0%)
< 50	566 (11%)	
50 – 59	1272 (26%)	
60 – 69	1827 (37%)	
> 69	1264 (26%)	
Tumor distance from anal verge	6.39 (SD: 3.30)	139 (3%)
Clinical T stage		2364 (48%)
T1	2 (0%)	
T2	82 (2%)	
T3	2248 (46%)	
T4	233 (5%)	
Clinical N stage		2704 (55%)
N0	1235 (25%)	
N1	930 (19%)	
N2	60 (1%)	
Prescribed dose		1084 (22%)
< 45 Gy	1123 (23%)	
45 Gy	1830 (37%)	
> 45 Gy	1092 (22%)	
Neo-adjuvant chemotherapy		0
Yes	1385 (28%)	
No	3544 (72%)	
Adjuvant chemotherapy		93 (1%)
Yes	2287 (46%)	
No	2579 (52%)	
Surgery procedure		1302 (27%)
LAR	2141 (43%)	
APR	1486 (30%)	
Pathological T stage		190 (4%)
T0	364 (7%)	
T1	243 (5%)	
T2	1429 (29%)	
T3	2766 (52%)	
T4	128 (3%)	
Pathological N stage		300 (6%)
N0	3086 (62%)	
N1	1134 (23%)	
N2	409 (8%)	
Outcomes after 5 years		
Local Recurrence	394 (13%)	1630 (41%)
Distant Metastasis	978 (35%)	1119 (28%)
Overall Survival	1899 (63%)	951 (24%)

Results: The AUC values for the prediction models are shown in figure 1 (blue: previous model, red: current Cox PH model, black: current logistic regression models). In general, the discriminative performance of the logistic regression model is higher in comparison to the newly trained Cox proportional hazards model or the original models, for all three outcomes. The covariates which changed the most over time were adjuvant chemo (LR, DM & OS), neo-adjuvant chemo (LR & OS), prescribed radiotherapy dose (LR) and pathological N-stage (DM).

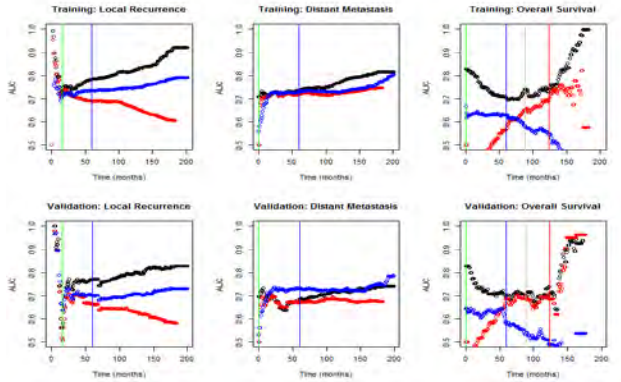

Conclusion: Based on the current results, analyzed on the current dataset, we have shown that the logistic regression model (separate model for every time point) may perform better than models trying to cover the complete follow-up period. This may be due to the optimization capabilities, when training a new model for every follow-up time point, but might be susceptible for overfitting. From a clinical perspective, this could be plausible as the influence of variables (e.g. (neo-)adjuvant chemotherapy) may vary during the follow-up period and targeted outcome and could show how clinical and/or treatment decisions have influence on the patient outcome over time. Future work also involves handling of missing values, which is a major concern when merging trial datasets.

OC-0243

Randomised trial on preoperative platin-based Radiochemotherapy in rectal cancer: 10-years analysis

M. Gambacorta[1], F. Cellini[1], M. Colangione[1], M. Lupattelli[2], V. Lancellotta[2], D. Genovesi[3], M. Cosimelli[4], V. Picardi[5], M. Osti[6], M. Portaluri[7], F. Tramacere[7], E. Maranzano[8], G. Mantello[9], V. Valentini[1]

[1]*Catholic University, Radiation Oncology - Gemelli ART, Rome, Italy*
[2]*Università degli Studi di Perugia, Dipartimento di Radioterapia, Perugia, Italy*
[3]*Università Gabriele D'annunzio, Dipartimento di Radioterapia, Chieti, Italy*
[4]*Istituto Regina Elena, Dipartimento di Chirurgia, Roma, Italy*
[5]*Centro Alta Tecnologia, Dipartimento di Radioterapia, Campobasso, Italy*
[6]*Università La Sapienza - Ospedale S. Andrea, Dipartimento di Radioterapia, Roma, Italy*
[7]*Ospedale Civile, Dipartimento di Radioterapia, Brindisi, Italy*
[8]*Ospedale Civile, Dipartimento di Radioterapia, Terni, Italy*
[9]*Azienda Ospedaliero-Universitaria Ospedali Riuniti-Università Politecnica delle Marche, Dipartimento di Radioterapia, Ancona, Italy*

Purpose or Objective: To investigate long term outcome and predictors between two schedules of platin based preoperative radiochemotherapy (RTCT)

Material and Methods: Patients with rectal adenoca, MRI based stage cT3N0-N2, were randomized into two arms:
1) PLAFUR: RT= 50.4 Gy; Concurrent chemotherapy (CT)= CDDP 60 mg m2 (days 1-29) + 5FU continuous infusion in 96 h (days 1-4 and 29-32)
2) TOMOX-RT: RT=50.4 Gy; CT= Tomudex 3 mg / m2 + oxaliplatin 130 mg / m2 (days 1, 19 and 38).
Restaging at 6-8 weeks after the end of RTCT, followed by surgery in 1-2 weeks.
Adjuvant CT was recommended in ypN1-2.
Local control (LC), metastases-free survival (MFS), disease-free survival (DFS) and overall survival (OS) were analyzed.
Predictive endpoints of clinical outcome were tested by univariate and multivariate analysis. The investigated variables were: (i) patients (age, sex), (ii) therapy (RTCT schedule, adjuvant CT, surgery type, colostomy), (iii) tumor related (cT, cN, ypT, ycN, TRG grade, site of primary T).

Results: From 2002 to 2005, 164 patients were enrolled (M: F = 104: 60); 83 were randomized to PLAFUR and 81 to TOMOX-RT. The median follow-up was 120.2 months (5.8-152.5).
The 10-years rates of the efficacy endpoints, per arm, were as follows: LC: PLAFUR= 89.2% , TOMOX-RT= 96.3% (p=0.0757); MFS: PLAFUR= 81.9% , TOMOX-RT= 81.5% (p=0.987) ; DFS: PLAFUR= 78.3% , TOMOX-RT= 77.8% (p=0.982); OS: PLAFUR =50%, TOMOX-RT= 50% (p=0.918)
TOMOX-RT showed a non-significantly higher rate of ypT0 compared to PLAFUR: 35.8% vs 24.1% (p = 0.102), respectively.
Sphincter-saving surgery procedure was applied in: PLAFUR= 87.9%, TOMOX-RT= 86.4%.
Grade 3-4 acute toxicity occurred in: 7.1% in the PLAFUR arm vs 16.4% in the TOMOX-RT arm.
Confirmed predictors of outcome were found:
- For LC: at univariate analisys= ypT; ypN, TRG Grade; at multivariate analysis= TRG Grade (p = 0.0126)
- For MFS: at univariate analisys= age ypT, ypN and TRG Grade; at multivariate analysis= TRG Grade (p = 0.0255)
- For DFS: at univariate analisys= age ypT, ypN and TRG Grade; at multivariate analysis= TRG Grade (p = 0.0224)
- For OS: at univariate analisys= age ypT, ypN and TRG Grade; at multivariate analysis= no predictor was significantly associated.

Conclusion: The TOMOX-RT schedule allowed higher non-significant local control, and comparable clinical outcome to the compared schedule. Moreover the ypT downstaging was significantly improved. Acute toxicity was comparable between arms.
The TRG Grade was a good independent variable predicting LC, MFS and DFS, but not OS.

OC-0244

Similar quality of life after short-course radiation versus chemoradiation in rectal cancer patients

A.M. Couwenberg[1], J.P.M. Burbach[1], M. Van Vulpen[1], M.P.W. Intven[1], O. Reerink[2], W.M.U. Van Grevenstein[3], M. Koopman[4], H.M. Verkooijen[5]

[1]*UMC Utrecht, Radiotherapy, Utrecht, The Netherlands*
[2]*Isala, Radiotherapy, Zwolle, The Netherlands*
[3]*UMC Utrecht, Surgery, Utrecht, The Netherlands*
[4]*UMC Utrecht, Oncology, Utrecht, The Netherlands*
[5]*UMC Utrecht, Imaging, Utrecht, The Netherlands*

Purpose or Objective: A majority of patients with rectal cancer is treated with neoadjuvant radiotherapy, with or without chemotherapy. If after chemoradiation (CRT) patients show a good clinical response, organ-preserving strategies are increasingly being offered. To increase the amount of patients with a good clinical response, it has been proposed to replace short-course radiotherapy (SCRT) by CRT. However, intensified treatment may affect patients' quality of life (QoL). This study aims to compare self-reported QoL between routinely treated rectal cancer patients receiving SCRT versus CRT before, during and after treatment.

Material and Methods: This multicenter prospective cohort study includes rectal cancer patients of all stages referred for radiotherapy between February 2013 and May 2015. QoL was assessed by EORTC-C30 and -CR29 questionnaires at baseline, 3, 6 and 12 months. For each patient, a propensity score (PS) for receiving CRT was calculated and used for restriction and adjustment. Changes in QoL over time were analyzed by mixed models between patients receiving CRT and SCRT, and additionally compared to a normative age-matched Dutch population.

Results: After PS based restriction, 191 of 208 eligible patients were included, of which 69 underwent SCRT and 122 CRT. Patients undergoing CRT were younger (62.2 vs. 68.0 year), had more mesorectal fascia invasion (66.6% vs. 27.9%),

more T4 (20.5% vs. 11.6%) and less T2 tumors (3.3% vs. 11.6%). Questionnaire return rates were 84% at baseline and 63-80% during follow-up. In both groups, 3 and 6 months QoL scores for global health, physical, emotional, social and role function were lower than at baseline and similar in both groups at all time points. At 12 months, all functional scores in both groups returned to baseline level, except for role function. No significant differences were found on symptom scales (constipation, diarrhea, pain, fatigue, nausea) between SCRT- and CRT-patients. Compared to the Dutch reference population, patients with rectal cancer still had impaired role and social function at 12 months.

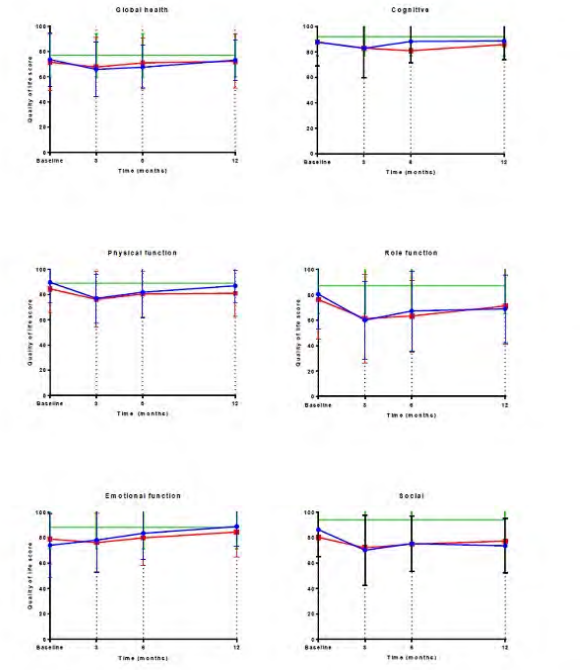

Figure 1. EORTC-C30 Quality of life function domains at baseline, 3, 6 and 12 months for patients receiving short-course radiotherapy (blue line), chemoradiation (red line) and the age-matched Dutch population (green line).

Conclusion: Over the course of neoadjuvant rectal cancer treatment, similar drops in QoL are observed for patients receiving SCRT or CRT. After 12 months, most QoL scores return to baseline levels.

Proffered Papers: Clinical 6: Hadron therapy

OC-0245

Protontherapy for uveal melanomas of temporal superior

S. Lanteri[1], C. Maschi[1], J. Herault[2], G. Angellier[2], M. Peyrichon[2], S. Baillif[1], J. Thariat[2], J. Caujolle[1]
[1]*Pasteur 2 Hospital- Eye University Clinic, Ophtalmology, Nice, France*
[2]*Centre Antoine Lacassagne, Department of Radiation Oncology, Nice, France*

Purpose or Objective: Protontherapy is a standard treatment for uveal melanomas. One area of current controversy is the use of protontherapy for uveal melanomas of temporal superior location owing to the presence of the lacrimal gland and the risk of radiation-induced dry eye syndrome (DES). Some teams have been contra-indicating such tumor locations for protontherapy and advocate brachytherapy. We investigated whether temporal superior (TS) melanomas should no longer be treated with proton therapy based on the rate of severe non manageable complications for DES.

Material and Methods: This retrospective study includes consecutive patients treated from 1999 to 2014 with protontherapy at our center. Patients received 52 Gy in four fractions and four days. Conjunctival melanomas were not excluded. Melanoma location was determined using an oriented clockwise goniometer. DES grades were defined as Group 0 : no sign of dry eye, group 1: discomfort, group 2: keratitis, group 3 (severe): corneal ulcer. Percentages of the lacrimal gland receiving 90% of the prescribed dose, 20% to 50% or ≤ 20% were assessed in the frontal and sagittal planes in Eyeplan blindly by two operators. The spss v12 statistics software was used. Kaplan Meier curves and Log rank tests were used for survival data.

Results: Of 1445 patients in the study, 14.7% and 2.0% had DES and severe DES, respectively. Two and five year DES-free survival rates were 88.9% and 83.6%, respectively. There were 7.6% melanomas of TS location. DES and severe DES correlated with TS location 13.8% vs 24.8% and 1.7% versus 5.8% in case of non-TS and TS ($p < 0.05$). 21/25 of patients with severe DES were in TS or temporal location. No patient had enucleation for DES. On MVA, diameter (hazard ratio HR:1.103, CI95:1.042-1.169, p 0.001), tumor volume (HR:0.0696, CI95:0.486-0.996, p=0.048, % of ciliary body in the 90% isodose line (HR:1.014, CI95:1.003-1.026, p=0.015), gel compensator (HR:0.717, CI95:0.535-0.960, p=0.025) and TS location (HR:2.581, CI95:1.695-3.929, p<0.001) were significantly associated with the occurrence of DES.

Conclusion: Although the incidence of DES and severe DES was increased in TS melanomas and this correlated with the dose to the lacrimal gland, their characteristics were less favorable (larger, superior involvement of ciliary body and limbus). Occurrence of severe DES in TS but also temporal locations suggests that involvement of the ciliary arteries may also be responsible for severe DES. The correlation of TS with ciliary involvement suggests that limbus cells may participate in the occurrence of DES. The role of palpebral and corneal irradiation will be further investigated. Since DES is manageable, TS location should not be considered a contraindication for protontherapy.

OC-0246

Visual outcomes of parapapillary uveal melanomas following proton beam therapy

J. Thariat[1], J. Grange[2], C. Mosci[3], L. Rosier[4], C. Maschi[5], F. Lanza[3], A. Nguyen[2], F. Jaspart[6], F. Bacin[6], M. Bonnin[6], D. Gaucher[7], W. Sauerwein[8], G. Angellier[1], M. Peyrichon[1], J. Herault[1], J. Caujolle[5]
[1]*Centre Antoine Lacassagne, Department of Radiation Oncology, Nice, France*
[2]*Eye University Clinic La Croix Rousse, Ophtalmology, Lyon, France*
[3]*National Institute for Cancer Research, Ophtalmology, Genova, Italy*
[4]*Centre D'exploration Et De Traitement De La Rétine Et De La Macula, Eye Clinic, Bordeaux, France*
[5]*Eye University Clinic Pasteur 2, Ophtalmology, Nice, France*
[6]*Eye University Clinic Gabriel Montpied, Ophtalmology, Clermont-Ferrand, France*
[7]*Eye University Clinic - Hôpital Civil, Ophtalmology, Strasbourg, France*
[8]*NCTeam, Radiation therapy, Essen, Germany*

Purpose or Objective: In parapapillary melanoma patients, radiation-induced optic complications are frequent and visual acuity is often compromised. We investigated dose effect relationships for the optic nerve with respect to visual acuity after protontherapy.

Material and Methods: of 5205 patients treated between 1991 and 2014, those treated between 1994 and 2013 (using CT-based planning) to 52 Gy in four fractions, minimal 6 month follow-up and documented initial and last visual acuity, were included. Deterioration of ≥ 0.3 logMAR between initial and last visual acuity was reported.

Results: 865 consecutive patients were included. Median follow-up was 69 months, mean age 61.7 years, tumor abutted the papilla in 64.9% and tumor to fovea distance was ≤ 3 mm in 74.2% of patients. Five-year relapse-free survival rate was 92.7%. Initially, 72.6% of patients had 20/200 visual acuity, 47.2% had ≥ 20/200 at last follow -up. A wedge filter was used in 47.8% of the patients, with a positive

impact on vision and no impact on relapse. Glaucoma, radiation-induced optic neuropathy, maculopathy were reported in 17.9%. 47.5%, and 33.6%, respectively. Patients irradiated to ≥ 80% of their papilla had better visual acuity when limiting the 50% (30 Gy) and 20% (12 Gy) isodoses to ≤ 2 mm and 6 mm of optic nerve length, respectively.

Conclusion: A personalized protontherapy plan can be used efficiently with good oncologic and functional results in parapapillary melanoma patients.

OC-0247

Carbon ion radiotherapy for adenoid cystic carcinomas invading the skull base

A. Hasegawa[1], M. Koto[1], R. Takagi[1], K. Naganawa[1], H. Ikawa[1], H. Tsuji[1], T. Kamada[1]
[1]*National Institute of Radiological Sciences, Research Center Hospital for Charged Particle Therapy, Chiba, Japan*

Purpose or Objective: To estimate the toxicity and efficacy of carbon ion radiotherapy for adenoid cystic carcinomas (ACC) invading the skull base.

Material and Methods: Between April 1997 and August 2013, a total of 193 patients with ACC of the head-and-neck were treated with carbon ion radiotherapy. All of these patients had neither regional lymph node nor distant metastasis before carbon ion radiotherapy. The prescribed tumor doses were 57.6 or 64.0 Gy (RBE) in 16 fractions over four weeks. Of the 193 patients, 78 patients with ACC invading the skull base were analyzed. There were 37 males and 41 females. The median age was 52 years (range, 23-75 years). The most common primary site was the parenasal sinus (46%), followed by the nasopharynx (13%), the nasal cavity (10%) and the hard palate (10%). The extent of surgery was biopsy alone in 52 patients (67%), partial resection in 5 patients (6%). Twenty of 78 patients (27%) had recurrence tumors after surgery. Median follow-up time was 52 months (range, 10-177.7 months). Patients were divided into two groups according to intracranial involvement; Group A was made up of 32 patients whose tumors invading the cranial fossa, Group B consisted of 46 patients whose tumors invading the intracranial region or cerebra. Acute and late morbidities were evaluated by the RTOG, the RTOG/ EORTC and the CTCAE (version 4.0).

Results: The 5-year local control and overall survival rates of all patients were 65 % and 60 %, respectively. Median survival time was 74.4 months. In total 45 patients died, the major cause of death was distant metastases (67%). The 5-year local control rates were 71% for Group A and 56% for Group B. The 5-year overall survival rates were 74% for Group A and 49% for Group B. In univariate analysis using log-rank test, there were no significant differences in local control and overall survival rates between the two groups. There was no evidence of any unexpected severe acute (grade≥4) and late (grade ≥3) reactions to the skin, the mucosa and other critical organs. In regard to brain toxicity, 5 of 32 patients (16%) in Group A and 9 of 42 patients (21%) in Group B developed grade 2 late reactions, which necessitated steroid administration temporarily. Four patients in Group B who had marginal recurrence received re-irradiation. Therefore, it was difficult to evaluate brain toxicity for these patients.

Conclusion: Our results showed acceptable brain toxicities and excellent therapeutic effectiveness for unresectable adenoid cystic carcinomas invading the skull base.

OC-0248

Proton Beam Therapy in childhood – First 2-years of practice results from the WPE

A.L. Mazhari[1], S. Schulze Schleithoff[1], F. Guntrum[2], C. Plass[2], M. Stickan-Verfürth[2], J. Lambert[1], C. Blase[3], G. Fleischhack[4], M. Christiaens[2], B. Timmermann[2]
[1]*West German Proton Therapy Center Essen, University Hospital Essen, Essen, Germany*
[2]*West German Proton Therapy Center Essen, Clinic for Particle Therapy / University Hospital Essen, Essen, Germany*
[3]*AnästhesieNetz Rhein-Ruhr ARR, West German Proton Therapy Center Essen, Bochum, Germany*
[4]*Paediatrics III, University Hospital Essen, Essen, Germany*

Purpose or Objective: Proton beam therapy (PT) has experienced increasing interest over time especially in pediatric malignancies as PT offers a chance to reduce post-treatment late effects. The West German Proton Therapy Center Essen (WPE) started treatments for pediatric tumors in June 2013. Since September 2013 all children under the age of 18 years were enrolled in the standardized prospective registry study for children ("KiProReg") at WPE. Initial findings are presented.

Material and Methods: Between September 2013 and September 2015, data on 138 children (78 males, 60 females, aged 0.9-17.9 years (median 5.7 years)) were prospectively collected in KiProReg at WPE. Diagnoses were CNS tumours (n=73), sarcomas (n=59), extracranial germ cell tumors (n=3) and others (n=3), respectively. Treatment sites were brain (n=72), head and neck including base of skull (n=38), spine (n=15), or pelvis (n=13). In 73.9% of the patients, macroscopic residual disease was present before PT. The median total dose of PT was 54.0 Gy (range 29.8-74.0 Gy). Only two patients had a mixed beam technique. Due to the very young age, sedation was necessary in 55.1% of children. Concurrent chemotherapy was applied in 54.3% of children. Side-effects were classified according to Common Terminology Criteria for Adverse Events (CTCAE) V4.0 grading system.

Results: Median follow-up (FU) since first diagnosis was 1.2 years (range 0.3-16.3 years). PT was well tolerated. No or only mild to moderate acute side-effects (grade 1 to 2) were documented in the majority of children (n=116). During PT, acute grade 3 side-effects were observed for blood/bone marrow (n=21), gastrointestinum (n=8) or as general disorders (n=3) as well as anorexia (n=1) when compared to baseline. Acute grade 4 side-effects during PT were only seen for blood/bone marrow (n=9). In 77 children, information on toxicity three months after PT is available. Only few patients presented with grade 3 or 4 toxicities, predominantly for blood/bone marrow (grade 3 n=7, grade 4 n=2). Seven of them had received chemotherapy after PT. So far, 17 patients failed due to recurrence or progression (local n=5; systemic n=12). Six of them (4.3%) have died so far, all due to disease.

Conclusion: Initial prospective data from WPE registry suggest good feasibility with only mild or moderate side-effects in the majority of children even when administering high doses at critical sites. Higher-grade side-effects primary for blood and bone marrow are obviously influenced by concurrent chemotherapy. Early local control rates achieved with PT are promising so far. However, longer FU is needed to analyze long-term outcome and late effects.

OC-0249

Five-year clinical outcomes after dose-escalated image-guided proton therapy for prostate cancer

C. Bryant[1], W. Mendenhall[1], B. Hoppe[1], R. Henderson[1], R. Nichols[1], C. Morris[1], C. Williams[1], Z. Su[1], Z. Li[1], N. Mendenhall[1]
[1]*University of Florida Proton Therapy Institute, Radiation Oncology, Jacksonville- Florida, USA*

Purpose or Objective: To report clinical outcomes for patients treated with image-guided proton therapy for localized prostate cancer.

Material and Methods: Under institutional review board approval, the medical records of 1,215 men enrolled either on a prospective protocol or an outcomes tracking study treated for localized prostate cancer with proton therapy at our institution between 2006 and 2010 were reviewed. Ninety-eight percent of patients received 78 Gy (RBE) or higher; 15% received androgen deprivation therapy (ADT). Five-year freedom from biochemical progression (FFBP),

distant metastasis-free survival, and cause-specific survival rates are reported for each risk group. Prospectively collected patient-reported quality-of-life data and high-grade toxicities are reported. A multivariate analysis was performed to identify clinical predictors of biochemical failure.

Results: The median follow-up was 5.5 years. The 5-year FFBP rates were 99%, 94%, and 74% in low-, intermediate-, and high-risk patients, respectively. Actuarial 5-year rates of late grade 3 gastrointestinal and genitourinary toxicity were 0.6% and 2.4%, respectively. Median International Prostate Symptom Scores (IPSS) before treatment and at >4 years after treatment were 7 and 7. Median changes in EPIC scores between baseline and 4+ years of follow-up were minimal in the bowel, urinary irritative/obstructive, and urinary incontinence summary domains.

Conclusion: Image-guided proton therapy provided excellent biochemical control rates for patients with localized prostate cancer. Patient-reported quality of life outcomes are favorable and actuarial rates of high-grade toxicity were low following proton therapy.

OC-0250

Hadrontherapy as re-irradiation using active beam delivery at CNAO

E. Ciurlia[1], M. Bonora[1], P. Fossati[2], V. Vitolo[1], A. Iannalfi[1], M. Fiore[1], B. Vischioni[1], A. Facoetti[3], A. Hasegawa[4], F. Valvo[1], M. Krengli[5], R. Orecchia[2]
[1]*Fondazione CNAO, Area Clinica, Pavia, Italy*
[2]*Università di Milano, Radioterapia, Milano, Italy*
[3]*Fondazione CNAO, Radiobiologia, Pavia, Italy*
[4]*NIRS, Radiotherapy, Chiba, Japan*
[5]*Università del Piemonte Orientale "Amedeo Avogadro", Radioterapia, Novara, Italy*

Purpose or Objective: Reirradiation of non resectable local recurrence, after previous full course of radiotherapy, is extremely challenging. Particle therapy may theoretically be the ideal tool for re-irradiation thanks to its complete sparing of large volumes of non target tissues already irradiated to low-medium dose with conformal X-ray based techniques. We report CNAO experience, in terms of acute toxicity and early response to hadrontherapy, in patients with head and neck, skull-base and sacral local relapse, re-irradiated with carbon ions or protons.

Material and Methods: Since February 2013 to February 2015, 70 patients (M/F = 41/29) underwent hadrontherapy in CNAO as re-irradiation. Site of disease was head and neck in 52 patients cancer, sacrum in 12 patients, skull – base in 4 patients and brain in 2 cases. The histologies were: squamous cell carcinoma (21 pts), adenoid cystic carcinoma (18 pts), chordoma (7 pts), other sarcoma (6 pts), adenocarcinoma (7 pts), meningioma (4 pts), others (7 pts). Sixty-two patients had been treated with Carbon Ions, the rest (8 pts) with protons. Average age was 59 (range 31 – 78). Previous radiotherapy doses ranged between 54 to 76 Gy (with conventional fractionation) and 20 to 28 Gy (with hypofractionation). Mean prescription dose was 61.7 Gy [RBE] (32.5 – 64), mean dose per fraction was 2.4 Gy [RBE] (2 – 4.5). Early toxicity was evaluated during, at the end and within 90 days after radiotherapy (RT). Patients were also followed up for late toxicity and radiologic response every three months after RT with magnetic resonance (MRI) and clinical evaluation.

Results: Acute toxicity was mild with no G4 event. At the end of treatment 26 pts (37%) had G0 toxicity; 27 pts (38%) had G1 toxicity; 16 pts (23%) had G2 toxicity and only 1 pts (1%) had G3 mucositis. At three months this favorable profile was maintained; FU average 9 months (range 3 – 24). Only one patient had G4 toxicity detected at 3 months (unilateral blindness due to intentional irradiation of one optic nerve beyond tolerance dose). Only 3 patients had G3 toxicity: skin fistula and osteoradionecrosis, 6 months after RT and cerebral edema (requiring medical treatment) 9 months after RT. The patient with longest FU (24 months), has late toxicity G1 (hearing impairment). At the time of analysis 11 patients had died of progressing disease (PD), 6 and 9 months progression free survival were 83% and 72% respectively.

Conclusion: Hadrontherapy as reirradiation allows good dose distribution with optimal sparing of already irradiated organs at risk. Due to mild acute toxicity hadrontherapy may be considered safe and well tollerated. Longer follow up is needed to confirm the efficacy and the late side effects.

Proffered Papers: Brachytherapy 3: Detectors and dose verification

OC-0251

Electromagnetic tracking for error detection in interstitial brachytherapy

M. Kellermeier[1], D. Elz[1,2], V. Strnad[1,2], C. Bert[1,2]
[1]*University Clinic Erlangen, Radiation Oncology, Erlangen, Germany*
[2]*Friedrich-Alexander Universität Erlangen-Nürnberg, Radiation Oncology, Erlangen, Germany*

Purpose or Objective: Catheter reconstruction errors, wrong indexer length and misidentified first dwell position are among the most common medical events related to high-dose-rate brachytherapy (HDR-BT) treatment, reported in the United States by the Nuclear Regulatory Commission. The purpose of this study is a feasibility analysis for the detection of such events based on electromagnetic tracking (EMT).

Material and Methods: In a phantom-based experiment series, swap of catheters and displacement (Δl = 0, 1, 2, 3, 4, 5 and 6 mm) of a single catheter along direction of insertion were simulated. For the detection of errors the measured implant geometry was registered to the nominal one. Then the residual distances between corresponding dwell positions were analyzed.
Within an IRB approved study the breast implants of 18 patients treated with HDR interstitial brachytherapy (HDR-iBT) were measured by EMT after implantation, after CT imaging in imaging position, and as part of each of 9 treatment fractions in treatment position. The data were used to simulate catheter reconstruction errors, wrong indexer length, and swapping of catheters. Based on determining the pairwise difference of all EMT-reconstructed dwell positions and by registering the measured implant geometry with the nominal one established during treatment planning, the feasibility of error detection by EMT was tested.

Results: Swapping of catheters can be detected in phantoms. The shift of individual catheters was detected quantitatively within the determined EMT-accuracy (95th percentile of 0.83 mm). For example, the shift of Δl = 6 mm resulted in an EMT-determined shift of 6.09 mm compared to measured values of < 0.8 mm for all catheters without an induced shift.
First analyses of the data indicate that pairwise differences result into a catheter specific “fingerprint” (see figure 1a for catheters 5-8). This fingerprint stays stable over multiple fractions (figure 1b for DICOM treatment planning, fractions 2, 4) such that, e.g., a swap as simulated in fraction 4 (fig. 1b) can easily be identified.

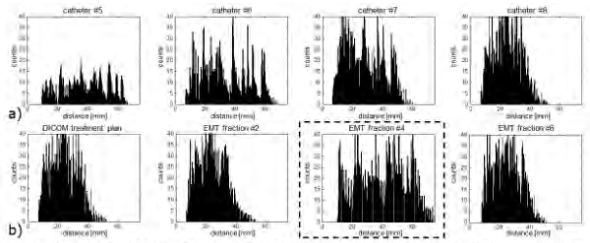

Figure 1: Histogram of pairwise dwell position distances resulting into a „fingerprint" characteristic for each catheter. a) Examples of such histograms for different catheters measured by EMT in a single fraction. b) Histogram of catheter #8 extracted from the DICOM data of the treatment plan and measured by EMT in fractions #2, #4, and #6. In fraction #4 an error was induced (swap of catheters #8 and #11) which can be identified by a change in the "fingerprint"/histogram.

Conclusion: EMT is a promising technique for error detection in interstitial brachytherapy. Further analysis of our clinical data will be conducted to determine the sensitivity and specificity of the proposed error detection methods.

OC-0252

BrachyView: A novel technique for seed localisation and real-time quality assurance

S. Alnaghy[1], M. Petasecca[1], M. Safavi-Naeini[1], J.A. Bucci[2], D.L. Cutajar[1], J. Jakubek[3], S. Pospisil[3], M.L.F. Lerch[1], A.B. Rosenfeld[1]

[1]*University of Wollongong, Centre for Medical Radiation Physics, Wollongong, Australia*

[2]*St George Hospital, St George Cancer Care Centre, Kogarah, Australia*

[3]*Institute of Experimental and Applied Physics, Czech Technical University of Prague, Prague, Czech Republic*

Purpose or Objective: In low dose rate (LDR) brachytherapy, seed misplacement/movement is common and may result in deviation from the planned dose. Current imaging standards for seed position verification are limited in either spatial resolution or ability to provide seed positioning information during treatment. BrachyView (BV) is a novel, in-body imaging system which aims to provide real-time high resolution imaging of LDR seeds within the prostate.

Material and Methods: The BV probe consists of a gamma camera with three single cone pinhole collimators in a 1 mm thick tungsten tube. Three, high resolution, pixelated detectors (Timepix) are placed directly below. Each detector comprises of 256 x 256 pixels, each 55 × 55 μm2 in area. The system is designed to reconstruct seed positions by finding the centre of mass of the seed projections on the detector plane. Back projection image reconstruction is adopted for seed localisation.

A thirty seed LDR treatment plan was devised. I-125 seeds were implanted within a CIRS tissue-equivalent ultrasound prostate gel phantom. The prostate volume was imaged with transrectal ultrasound (TRUS). The BV probe was placed in-phantom to image the seeds. A CT scan of the setup was performed. CT data were used as the true location of seed positions, as well as reference when performing the image co-registration between the BV coordinate system and TRUS coordinate system.

An in-house graphical user interface was developed to perform 3D visualisation of the prostate volume with the seeds in-situ. The BV and CT-derived source locations were compared within the prostate volume coordinate system for evaluation of the accuracy of the reconstruction method. A Dose Volume Histogram (DVH) study of the Clinical Target Volume (CTV) was performed using TG-43 calculations, using reconstructed source positions provided by BV system and CT scanner.

Results: Figure 1 (a) shows the reconstructed prostate volume using ultrasound slices. The reconstructed seed positions using BV probe and CT images are merged with the prostate volume (shown in same coordinate system). (b) shows the discrepancy between calculated seed positions using CT and BV datasets. (c) shows the DVH calculated from CT data set and BV probe.

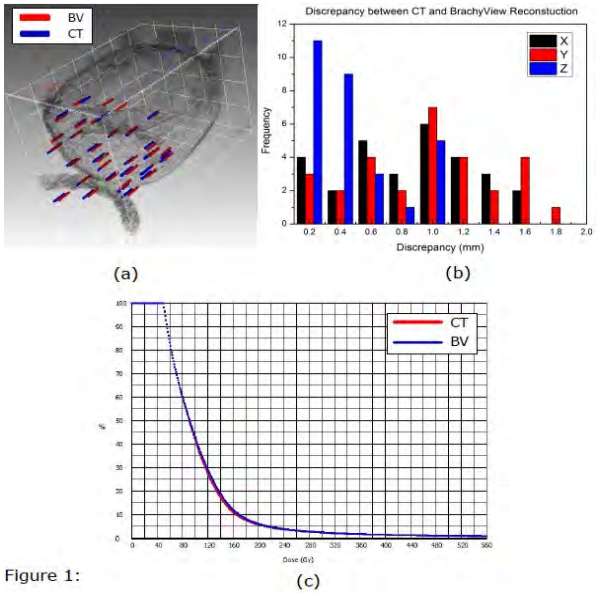

Figure 1:

Conclusion: The reconstructed seed positions measured by the BV probe demonstrate excellent agreement with seed positions calculated using CT data with a maximum discrepancy of 1.78 mm. It was observed that 75% of seed positions were reconstructed within 1 mm of their nominal location. The DVH study was performed to evaluate the effect of reconstructed seed locations on estimated dose delivered. V100 showed a discrepancy of 0.604 cm3 between CT and BV-derived 3D seed distribution. The BV technique has proven to be an effective tool for quality assurance during LDR brachytherapy, providing anatomical and seed positioning information without need for external irradiation for imaging.

OC-0253

A high sensitivity plastic scintillation detector for in vivo dosimetry of LDR brachytherapy

F. Therriault-Proulx[1], L. Beaulieu[2], S. Beddar[1]

[1]*The University of Texas MD Anderson Cancer Center, Radiation Physics, Houston, USA*

[2]*CHU de Quebec and Universite Laval, Radiation Oncology, Quebec, Canada*

Purpose or Objective: There are multiple challenges behind developing an *in vivo* dosimeter for LDR brachytherapy. The dose rates are orders of magnitudes lower than in other therapy modalities, the detectors are known to be energy-dependent, and introducing materials that are not tissue-equivalent may perturb the dose deposition. The goal of this work is to develop a high sensitivity dosimeter based on plastic scintillation detectors (PSDs) that overcomes those challenges and to validate its performance for *in vivo* dosimetry.

Material and Methods: The effect of the energy dependence of PSDs on dosimetry accuracy was studied using GEANT4 Monte Carlo (MC) simulations adapted from the ALGEBRA source code developed for brachytherapy. The photon energy distribution at different positions around a modeled I-125 source was obtained and convoluted to a typical PSD response. The effect of the different materials composing the PSD was also investigated.

To measure dose rates as low as 10 nGy/s, the selection of each single element composing a typical PSD dosimetry system was revisited. A photon-counting photomultiplier tube (PMT) was used in combination with an optical fiber designed to collect more light from the scintillator. A spectral study was performed to determine the best combination of scintillator and optical fiber to use.

Finally, doses up to a distance of 6.5 cm from a single I-125 source of 0.76U (0.6 mCi) held at the center of a water phantom were measured. The PSD was moved at different radial and longitudinal positions from the source using an in-

house computer-controlled device developed for this study and allowing for sub-mm positioning accuracy. The measurements were compared to the expected values from the updated Task-Group 43 formalism.

Results: The change in the energy distribution with position around the I-125 source was shown from MC simulations to have a limited impact on the PSD's accuracy over the clinically relevant range (<1.2%). Therefore, the energy-dependence can be neglected, as long as the PSD is calibrated using the same isotope. The effect of the different materials on the photon energy distribution was also shown to be limited (<0.1%). The different improvements made to the PSD dosimetry system are presented in Table 1. Those led to a 44 times better signal-to-noise ratio than for a typical PSD. Measurements with the PSD around a single I-125 source were shown to be in good agreement with the expected values (see Fig.1). The uncertainty was shown to be a balance between positioning uncertainty near the source and measurement uncertainty as the detector moves farther away from the source.

Improvements		Factor
Cooling PMT (reduction in dark noise)		1.6
Selection of scintillator + Shorter fiber		5.7
Using a Mylar reflector		2
NA = 0.6 vs. NA = 0.5	collected light	1.44
	increase in OPL	0.996
Scintillator length (5 mm vs 3 mm)		1.67
Total		**43.75**

Table 1. Summary of the different improvements made to the PSD dosimetry system (PMT: Photomultiplier Tube, NA: Numerical aperture, OPL: optical path length).

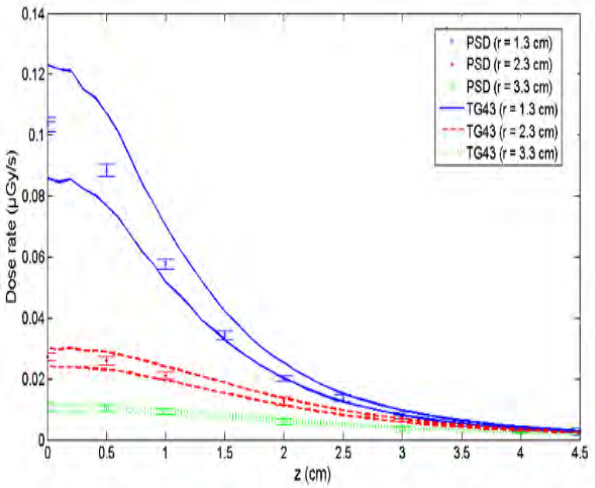

Figure 1. Measured dose-rate with the PSD as a function of position along the longitudinal axis of the source (z) for different radial distances (r) in comparison to the expected values (TG43). The TG43 values (lines) account for uncertainties in source-to-detector positioning of ±1 mm along the x- y- and z-axes.

Conclusion: This optimized PSD system was shown to be capable of accurate in-phantom dosimetry around a single LDR brachytherapy seed, which confirms the high sensitivity of the detector as a potential *in vivo* dosimeter for LDR brachytherapy applications.

OC-0254

MR compatibility of fiber optic sensing for real-time needle tracking

M. Borot de Battisti[1], B. Denise de Senneville[2,3], M. Maenhout[1], G. Hautvast[4], D. Binnekamp[4], J.J.W. Lagendijk[1], M. Van Vulpen[1], M.A. Moerland[1]

[1]*University Medical Center Utrecht, Radiotherapy, Utrecht, The Netherlands*

[2]*UMR 5251 CNRS/University of Bordeaux, Mathematics, Bordeaux, France*

[3]*University Medical Center Utrecht, Imaging Division, Utrecht, The Netherlands*

[4]*Philips Group Innovation, Biomedical Systems, Eindhoven, The Netherlands*

Purpose or Objective: The development of MR-guided HDR brachytherapy has gained an increasing interest for delivering a high tumor dose safely. However, the update rate of MR-based needle localization is inherently low and the required image interpretation is hampered by signal voids arising from blood vessels or calcifications, which limits the precision of the needle steering.
This study aims to assess the potential of fiber optic sensing for real-time needle tracking during MR-guided intervention. For this, the MR compatibility of a fiber optic tracking system and its accuracy are evaluated.

Material and Methods: *Fiber optic tracking device*: The device consists of a flexible stylet with three optic fibers embedded along its length, a broadband light source, a spectrum analyzer and a PC with Labview application. Along each fiber, Bragg gratings are evenly spaced at 20 mm intervals. To reconstruct the shape of a needle, the stylet is inserted inside the lumen of the needle. This set-up placed in the 1.5T MR-scanner provides real-time measurement of the needle profile, without adverse imaging artefacts since no ferromagnetic material is involved.
MRI-acquisition protocol: 3D MR-images were acquired with a 1.5T MR-scanner, using a 3D Spectral Presaturation with Inversion Recovery (SPIR) sequence (TR=2.9ms, TE=1.44ms, voxel size= 1.2×1.45×1mm^3, FOV=60×250×250mm^3).
Experimental evaluation: The two following experiments were conducted:

1. A needle was placed inside the MR-bore and its shape was imposed by a specially designed plastic mold with different known paths (see Fig. 1a). For path 1, 2 and 3, the shape of the needle was measured by fiber optic tracking during MR-imaging along 4 orientations (i.e 0°, 90°, 180°, 270°), by rotating the needle along its longitudinal axis.
2. Four plastic catheters were introduced in an agar phantom. The corresponding catheter shapes were measured with fiber optic sensing during simultaneous MR imaging (see Fig. 1d, phantom shifted out of scanner for photograph). The MR-based needle shape stemmed from a segmentation step followed by a polynomial fitting (order 5). A rigid registration of the obtained MR-based needle model and the fiber optic tracking was then performed.

Assessment of the fiber optic tracking: The fiber optic needle tracking accuracy was quantified by calculating the Euclidian distances between: the gold-standard shapes and fiber optic based measurements (Experiment #1); MR- and fiber optic based measurements (Experiment #2).

Results: For all tested needle shapes, the maximum absolute difference between the fiber optic based and the gold-standard values was lower than 0.9mm (Experiment #1, Fig. 1b and 1c). Over the 4 tested catheters, the maximal absolute difference between MR- and fiber optic based measurements was lower than 0.9mm (Experiment #2, Fig. 1e, 1f and 1g).

Conclusion: This study demonstrates that the employed fiber optic tracking device is able to monitor the needle bending during MR-imaging with an accuracy and update rate eligible for MR-guided intervention.

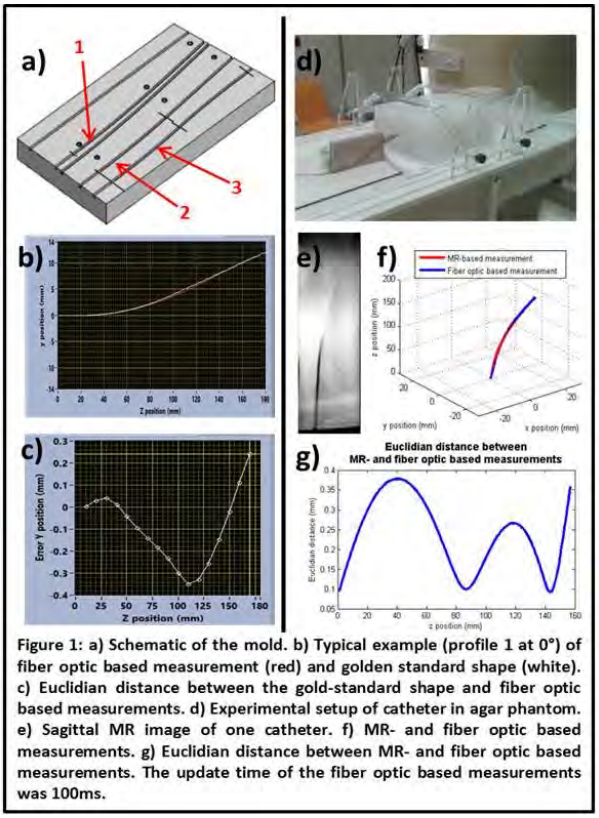

Figure 1: a) Schematic of the mold. b) Typical example (profile 1 at 0°) of fiber optic based measurement (red) and golden standard shape (white). c) Euclidian distance between the gold-standard shape and fiber optic based measurements. d) Experimental setup of catheter in agar phantom. e) Sagittal MR image of one catheter. f) MR- and fiber optic based measurements. g) Euclidian distance between MR- and fiber optic based measurements. The update time of the fiber optic based measurements was 100ms.

OC-0255

Correction function for MOSkin readings in realtime in vivo dosimetry in HDR prostate brachytherapy

G. Rossi[1], M. Carrara[2], C. Tenconi[2], A. Romanyukha[3], M. Borroni[2], G. Gambarini[4], D. Cutajar[3], M. Petasecca[3], M. Lerch[3], J. Bucci[5], A. Rosenfeld[3], E. Pignoli[2]

[1]University of Milan, Department of Physics, Milan, Italy
[2]Fondazione IRCSS Istituto Nazionale dei Tumori, Diagnostic Imaging and Radiotherapy Department, Milan, Italy
[3]University of Wollongong, Centre for Medical Radiation Physics, Wollongong, Australia
[4]National Institute of Nuclear Physics, Physics, Milan, Italy
[5]St George Hospital, Cancer Care Centre, Kogarah, Australia

Purpose or Objective: MOSkin detectors coupled to a trans-rectal ultrasound (TRUS) probe were used to perform in vivo dosimetry (IVD) on the rectal wall surface during US-based HDR prostate brachytherapy (BT). The system, called dual purpose probe (DPP), has proven to be an accurate tool to measure in vivo the integral dose, however discrepancies between planned and measured doses from each single catheter can be much higher than the overall discrepancies. In this work, three HDR prostate BT sessions were studied to find a possible distance and angle dependence correction function (CF) to be applied in real time to each single catheter, and data with and without the application of the obtained CF were compared.

Material and Methods: The DPP can be sketched as follows: four MOSkin dosimeters are firmly attached to TRUS rectal probe and are connected to a multichannel reader which provides measurements of the voltage shifts (proportional to the dose) in the MOSkin sensitive layer caused by radiation exposure. A dedicated software plots and records the measured dose with each MOSkin as a function of time, allowing the identification of the dose contribution of each single catheter in real time. Based on the treatment plan data (i.e. planned source strength, dwell times and positions) a software was implemented in the Matlab environment to compute the dose contribution to the MOSkin from each catheter based on TG-43 algorithm. The software reports also the weighted average distance of source to MOSkin for each catheter and the resulting weighted polar angles. IVD data were acquired on three patients treated between June and October 2015 and retrospectively analysed, providing 141 dose measurements for all the MOSkins. Measured and calculated contributions by each single catheter were quantified separately. Discrepancies were plotted depending on weighted average polar angles and distances between MOSkins and source, and a linearly fitting CF was calculated.

Results: A correction function CF linearly depending on the weighted average distance and polar angle of the catheter from the dosimeter was obtained (R=0.35, showing a significant correlation). The results showed an increase in sensitivity of MOSkins at higher distances (i.e., due to radiation softening) and at wider polar angles (i.e., due to increased radiation contamination by the presence of the TRUS probe). The percentage dose discrepancy between calculated and measured dose contribution from each single catheter with and without the application of obtained CF resulted in 1.3±13.1% and 1.2±7.7% (k=1), respectively (figure 1).

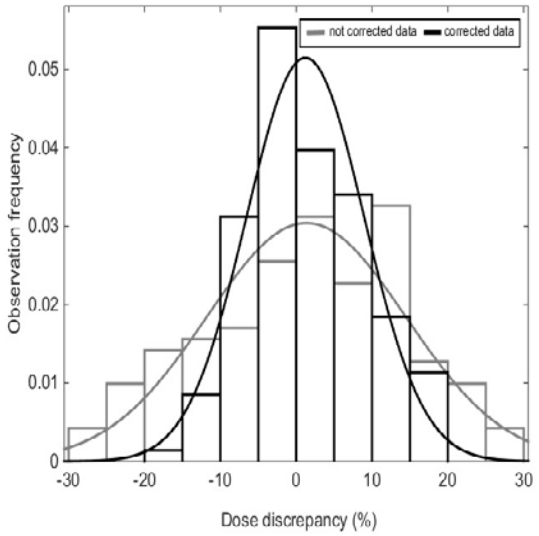

Conclusion: The use of the CF significantly reduces percentage discrepancy between planned and measured dose per single catheter. Implementation of the CF to correct MOSkin readings online is a further step towards accurate and reliable real time IVD in prostate BT performed with the DPP. Based on the real time measured dose discrepancy, the next step will be defining an action protocol to use the acquired information online.

OC-0256

Column generation-based Monte Carlo treatment planning for rotating shield brachytherapy

M.A. Renaud[1], G. Famulari[2], J. Seuntjens[3], S. A. Enger[3]

[1]McGill University, Physics, Montreal, Canada
[2]McGill University, Medical Physics, Montreal, Canada
[3]McGill University, Oncology, Montreal, Canada

Purpose or Objective: Rotating shield brachytherapy (RSBT) is an intensity modulated high dose rate (HDR) BT treatment technique, where radiation sources are surrounded by catheters containing rotating shields that direct radiation towards the tumour and away from healthy tissues. RSBT for HDR requires sources with lower energies than Ir-192, such as Gd-153 and Se-75, due to shield thickness constraints. The distinct features of shield angle, catheter material and source isotope require the development of a specific Monte Carlo (MC)-based treatment planning and optimization system.

Material and Methods: An MC based dose calculation engine for RSBT has been developed and coupled with a column-generation optimizer. At every iteration of the optimization loop, the column-generation process solves a pricing problem to determine the best dwell position and shield angle

combination to add to the treatment plan, resulting in the best possible plan with the shortest treatment time.
As a source model, the microSelectron-v2 source geometry was selected and placed inside a cylindrical platinum shield with a diameter of 1.8 mm and 3.0 mm for interstitial and intracavitary cases, respectively. An emission window coinciding with the active core of the source was created by removing half (180°) of the wall of the shield.
For an interstitial prostate case, RSBT plans were generated only using Gd-153 as a source due to the extreme limitations on shield size in interstitial catheters. For the intracavitary GYN case, both Gd-153 and Se-75 plans were generated. All RSBT plans were compared with conventional HDR BT. Only the original dwell positions used in conventional BT were sampled to create the RSBT plans.

Results: RSBT plans resulted in a considerable reduction in both rectum and bladder doses without sacrificing target coverage for the prostate case. With 95% of the PTV volume receiving over 15 Gy, only 40% of the rectum volume received more than 2 Gy for the Gd-153 RSBT case,as opposed to 85% for the unshielded Ir-192 conventional plan.

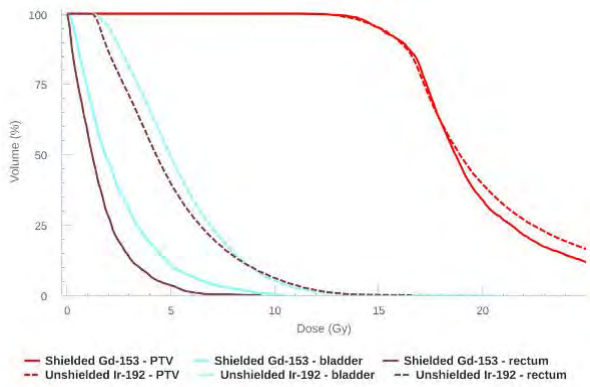

For the GYN patient, the median rectum dose was 2.4 Gy, 3.2 Gy and 3.45 Gy for Gd-153 RSBT, Se-75 RSBT and unshielded Ir-192, respectively, with an identical target coverage. The Gd-153 case was also able to reduce the dose to the bladder by 41%.

Conclusion: The development of the first MC-based TPS devoted to RSBT has been successfully accomplished. For the prostate case, a significant dosimetric improvement was achieved over conventional BT using Gd-153 with optimized shield angles. For the GYN case, the improvement was diminished by the central position of the conventional BT dwell positions within the target volume. RSBT allows the placement of dwell positions much closer to normal tissue, which will yield superior dose distributions when properly optimized. RSBT will decrease normal tissue toxicity and allow for tailoring treatments to each individual patient by treating all parts of the tumour without over-irradiation of large regions of normal tissues.

Proffered Papers: Physics 6: Radiobiological modelling

OC-0257

A Bayesian network model for acute dysphagia prediction in the clinic for NSCLC patients

A.T.C. Jochems[1], T.M. Deist[1], E. Troost[2], A. Dekker[1], C. Faivre-Finn[3], C. Oberije-Dehing[1], P. Lambin[1]
[1]*MAASTRO clinic, Radiotherapy, Maastricht, The Netherlands*
[2]*Helmholtz-Zentrum, Radiooncology, Dresden-Rossendorf, Germany*
[3]*The Christie NHS Foundation Trust & University of Manchester, Radiation Oncology, Manchester, United Kingdom*

Purpose or Objective: Acute dysphagia is a frequently observed toxicity during concurrent chemo-radiation (CRT) or high-dose radiotherapy (RT) for lung cancer. This toxicity can lead to hospitalizations, treatment interruptions and consequently reduce chances of survival. Models to predict acute dysphagia are available. However, these models were based on limited amounts of data and the performance of these models needs improvements before implementation into routine practice. Furthermore, Bayesian network models are shown to perform better than conventional modeling techniques on datasets with missing values, which is a common problem in routine clinical care. In this work, we train a Bayesian network model on a large clinical datasets, originating predominantly from routine clinical care, to accurately predict acute dysphagia in NSCLC patients during and shortly after (C)RT.

Material and Methods: Clinical data from 1250 inoperable NSCLC patients, treated with radical CRT, sequential chemo-radiation or RT alone were collected. The esophagus was delineated using the external esophageal contour from the cricoid cartilage to the GE junction. A Bayesian network model was developed to predict severe acute dysphagia (Grade 3 according to the CTCAEv3.0 or v4.0). The model utilized age, mean esophageal dose, timing of chemotherapy and N-stage to make predictions. Variable selection and structure learning was done using the PC-algorithm. The model was trained on data from 1250 patients. The model's performance was assessed internally and on an external validation set (N=218) from the United Kingdom. Model discriminative performance was expressed as the Area Under the Curve (AUC) of the Receiver Operating Characteristic (ROC). ROCs were compared using the method proposed by DeLong and colleagues. Model performance was also assessed in terms of calibration. Calibration refers to the agreement between the observed frequencies and the predicted probabilities and is expressed as the coefficient of determination (r2).

Results: One-hundred forty patients (11,2%) developed acute dysphagia (≥ Grade 3 according to the CTCAEv3.0 or v4.0). The model was first validated internally, by validating on the training cohort (N=1250, AUC = 0.77, 95% CI: 0.7325-0.8086, r2 = 0.99). Subsequently, the model was externally validated on a UK dataset (N = 218, AUC = 0.81, 95% CI: 0.74-0.88, r2 = 0.64). The ROC curves were not significantly different (p = 0.28).

Conclusion: The Bayesian network model can make accurate predictions of acute dysphagia (AUC = 0.77, 0.81 in the internal and external validation respectively), making it a powerful tool for clinical decision support.

OC-0258

Linear-quadratic modeling of acute rectum toxicity in a prostate hypo-fractionation trial

M. Witte[1], W. Heemsbergen[1], F. Pos[1], C. Vens[2], S. Aluwini[3], L. Incrocci[3]
[1]*Netherlands Cancer Institute Antoni van Leeuwenhoek Hospital, Radiation Oncology, Amsterdam, The Netherlands*
[2]*Netherlands Cancer Institute Antoni van Leeuwenhoek Hospital, Radiation Oncology- Division of Biological Stress Response, Amsterdam, The Netherlands*
[3]*Erasmus MC Cancer Institute, Radiation Oncology, Rotterdam, The Netherlands*

Purpose or Objective: In the Dutch prostate hypo-fractionation trial (19x3.4Gy versus 39x2Gy) a higher incidence of acute gastro-intestinal toxicity was observed in the experimental arm. We performed model estimations using various alpha/beta ratios to determine whether this difference can be explained according to the linear-quadratic model.

Material and Methods: Patients with localized prostate cancer were randomized between standard fractionation (SF=5x2Gy per week, N=293) and hypo-fractionation (HF=3x3.4Gy per week, N=285). Proctitis (grade 2) was defined as moderate to severe mucous or blood loss, or mild mucous or blood loss combined with at least 2 other complaints: diarrhea, incontinence, tenesmus, cramps, pain. Peak incidences over treatment weeks 4 and 6 were available

from prospectively collected patient reports. Normalized Total Dose (NTD, 2Gy equivalent) was accumulated per week for alpha/beta ratios of 3, 5, 10, and ∞ (=physical dose), and used to derive relative Dose-Surface Histograms (DSHs) of the delineated anorectum for each patient. Maximum likelihood logistic regressions were performed using a DSH point as variable. Univariate (UV) models and multivariate (MV) models with fractionation schedule as factor were constructed.

Results: Acute proctitis incidences were highest for hypo-fractionation (SF: n=67; 22.9%, HF: n=98; 34.3%, p<0.01). The 7Gy/week DSH point correlated well with proctitis, and was used for subsequent modeling. Figure 1 illustrates the models for the various alpha/beta ratios, and incidences for five (roughly) equal size patient bins. Note that the NTD correction decreases the surface areas that receive <2Gy per day, and increases surfaces receiving >2Gy. The central NTD values of the patient bins therefore lie at higher values for HF than for SF. The MV models have higher likelihood than the UV models, but likelihood for different alpha/beta ratios is similar. All MV models have odds ratios >1.5 (p<0.05) for HF versus SF, i.e. fractionation remains a factor.

Conclusion: Linear-quadratic dose correction cannot explain the observed acute rectum toxicity difference between hypo-fractionated and standard treatment in patients with prostate cancer. Subsequent modeling will concentrate on alternative mechanisms.

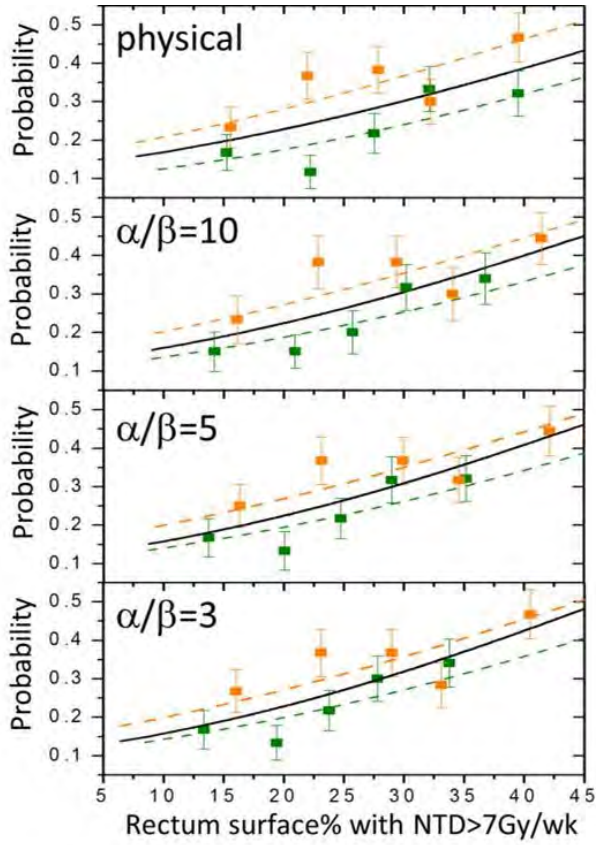

Figure 1 Acute proctitis models (UV solid, MV dashed) for standard (green) and hypo-fractionation (orange)

OC-0259

Spatial rectal dose-response for patient-reported leakage, obstruction, and urgency in prostate RT

O. Casares-Magaz[1], L.P. Muren[1], S.E. Petersen[2], V. Moiseenko[3], M. Høyer[2], J.O. Deasy[4], M. Thor[4]

[1]*Aarhus University Hospital, Department of Medical Physics, Aarhus, Denmark*

[2]*Aarhus University Hospital, Department of Oncology, Aarhus, Denmark*

[3]*University of California San Diego, Radiation- Medicine and Applied Sciences, San Diego, USA*

[4]*Memorial Sloan Kettering Cancer Center, Department of Medical Physics, New York, USA*

Purpose or Objective: To explore whether spatial dose measures explain the occurrence of rectal leakage, obstruction, and urgency after radiotherapy (RT) for localized prostate cancer.

Material and Methods: Spatial dose measures were extracted for 210 patients treated with RT in 2005-2007, and who all completed patient-reported outcomes (PROs) at a median of 3.6 years post-RT. The rectum was digitally unfolded and 2D maps were created for each patient by interpolating across 25 points for 45°-sectors of each contour. The areas and extents (lateral and longitudinal) were calculated for dose thresholds between 35 and 75 Gy in 5 Gy steps over 9 equally distributed segments over the 2D maps (Fig. 1A), and their lateral and longitudinal combinations, resulting in a total of 216 spatial dose metrics. Univariate (UVA) followed by multivariate (MVA) analysis using logistic regression with 50 times iterated 5-fold cross-validation was applied to investigate the relationship between the spatial measures and 'at least a moderate severity' of five symptoms related to defecation urgency, fecal leakage, or obstruction. The prevalence for all investigated symptoms was ³ 25%. The UVA and MVA were first conducted in 70% of the data, and the performance of the most frequent MVA model, judged by the area under the receiver-operating characteristics curve (AUC), was investigated in the complete cohort.

Results: On UVA 3-11 metrics (mean±SD: AUC=0.58±0.11) were suggested as potential predictors for the investigated symptoms (Table 1). The AUC of the final MVA models was 0.57-0.62 (Fig. 1B). Defecation urgency was explained by metrics related to high doses (>55 Gy), fecal leakage was governed by medium to high-dose extensions in the anterior part of the rectum, and obstruction by metrics related to the lower part of the rectum, as well as extents of the high dose (>75 Gy).

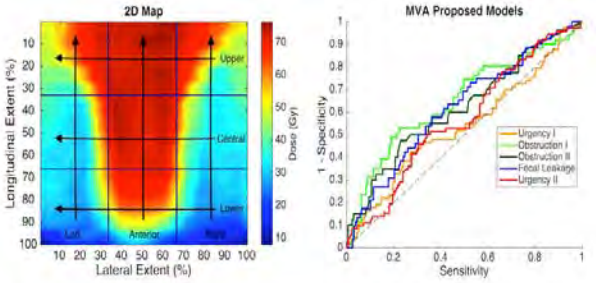

Figure 1. Left Panel: 2D map extracted from one of the patients; Right Panel: ROC plots for the five studied symptoms suggested by the final MVA models.

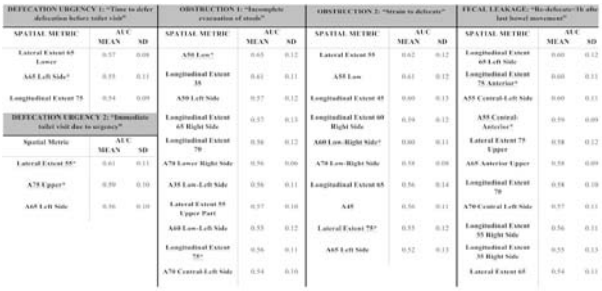

Table 1. Proposed metrics as predictors of the different studied endpoints. These metrics where extracted from the UVA performed over the 70% of the data set, and all of them were not correlated (Pearson Coefficient < 0.7). LogOdds > 0.01 and the highest AUC (> 0.54). Underlined metrics were included in the final predictor model using a MVA. "Ax" is the percentage area of the 2D map enclosed by the isoline of "X Gy" in a specific segment, the "Extent X" is the extension of the largest pixel aggregate above "X Gy" for the different segments.

Conclusion: Our analysis suggests that spatial dose metrics explain symptoms of the gastrointestinal tract such as defecation urgency, fecal leakage and obstruction, and that these symptoms present spatial-specific relationships. The robustness of these results will be explored in other available cohorts (N>500) to evaluate whether these findings, and spatial dose metrics in general should be taken into account

in the RT planning and treatment for localized prostate cancer.

OC-0260

Local dose predictors of acute urinary toxicity after RT for prostate cancer

I. Improta[1], F. Palorini[1], C. Cozzarini[2], T. Rancati[3], B. Avuzzi[4], P. Franco[5], C. Degli Espositi[6], E. DelMastro[7], G. Girelli[8], C. Iotti[9], V. Vavassori[10], R. Valdagni[4], C. Fiorino[1]

[1]*IRCCS San Raffaele Scientific Institute, Medical Physics, Milano, Italy*

[2]*IRCCS San Raffaele Scientific Institute, Radiotherapy, Milano, Italy*

[3]*Fondazione IRCCS Istituto Nazionale dei Tumori, Prostate Cancer Program, Milan, Italy*

[4]*Fondazione IRCCS Istituto Nazionale dei Tumori, Radiation Oncology 1, Milan, Italy*

[5]*Ospedale Regionale U.Parini - AUSL Valle d'Aosta, Radiotherapy, Aosta, Italy*

[6]*Ospedale Bellaria, Radiotherapy, Bologna, Italy*

[7]*IRCCS–Candiolo, Radiotherapy, Candiolo, Italy*

[8]*Ospedale ASL9, Radiotherapy, Ivrea, Italy*

[9]*Department of Oncology and Advanced Technology- ASMN Hospital IRCCS, Radiation Therapy Unit, Reggio Emilia, Italy*

[10]*Cliniche Gavazzeni-Humanitas, Radiotherapy, Bergamo, Italy*

Purpose or Objective: To investigate the relationship between patient-reported acute urinary (GU) toxicity (tox) and bladder local dose distribution in patients (pts) treated with radical RT for prostate cancer (PCa) by a pixel-wise method for analysis of bladder surface dose maps (DSMs).

Material and Methods: Analyses were performed on the final cohort of pts of a multi-centric study, consisting of 539 pts with PCa treated with conventionally (CONV: 1.8 – 2Gy/fr) or moderately hypo-fractionated RT (HYPO: 2.2-2.7 Gy/fr) in 5 fx/week. GU tox was evaluated by the International Prostate Symptoms Score (IPSS) given to the pts at the beginning and at the end of RT, comprising 7 questions relating to different symp: feeling of incomplete emptying (EMP), frequency (FRE), intermittency (INT), urgency (URG), weak stream (WST), straining (STR) and nocturia (NOC). We here considered the seven symp separately and moderate/severe tox for each item was selected as endpoint (score≥4 at RT end), including only pts who had no disturbs before RT (IPSS at basal < 4). As different fractionation schemes were allowed, DSMs of all pts were corrected into 2Gy-equivalent maps using the LQ model, converting the dose in each pixel with an α/ß equal to 10 Gy and a repair factor =0.7 Gy/day. DSMs of all pts were generated by unfolding the bladder: its contour was cut anteriorly at the points intersecting the sagittal plane passing through its centre of mass, normalised in the axial direction and aligned at the bladder base, at the posterior central point, generating a common frame for all pts. For each endpoint average DSMs of pts with/without tox were compared pixel by-pixel by two-sided t-tests, separately analyzing HYPO and CONV pts: the resulting p-value maps were used for identifying the regions better discriminating between pts with/without tox, considering a threshold of $p<0.01$.

Results: DSMs of 437/539 pts (81%) were available (185 CONV and 252 HYPO). EMP was reported by 28/358 (8%) pts, FRE by 60/361 (17%), INT by 35/366 (10%), URG by 50/357 (14%), WST by 66/341 (19%), STR by 29/377 (8%) and NOC by 63/348 (18%) pts. For HYPO pts, areas significantly correlated with GU tox were found for all endpoints (excepting WST) in the posterior region at 5-17 mm from the base of bladder, consistently with the bladder trigone, with evidence of a threshold effect around 85 Gy (2Gy equivalent). For CONV pts, only 2 endpoints (FRE and URG) showed significantly predictive areas, robustly summarized in the % surface receiving >50-70Gy at 5mm from the base and the vertical extension of 50-70Gy isodoses along the bladder central axis. In the figure, the results concerning FRE and URG are shown.

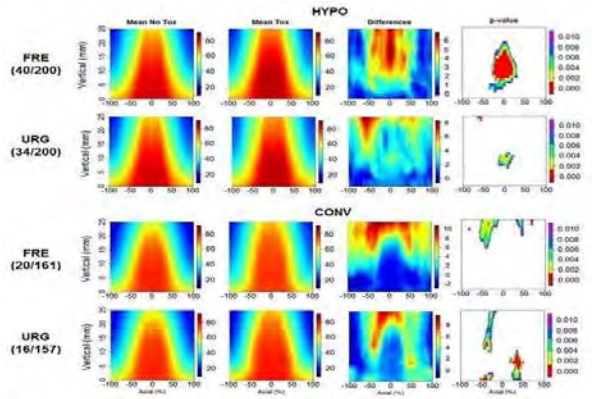

Conclusion: The method of DSMS analysis allowed to assess new local-dose descriptors that might be better correlated with tox and promises to find important applications in investigating urinary tox. The incorporation of the found local dose predictors into multi-variable models including clinical predictors is currently in progress.

OC-0261

CT Image biomarkers improve the prediction of xerostomia and sticky saliva

N.M. Sijtsema[1], L.V. Van Dijk[1], C.L. Brouwer[1], R.J. Beukinga[1], A. Van der Schaaf[1], H.G.M. Burgerhof[2], J.A. Langendijk[1], R.J.H.M. Steenbakkers[1]

[1]*University of Groningen- University Medical Center Groningen, Department of Radiation Oncology, Groningen, The Netherlands*

[2]*University of Groningen- University Medical Center Groningen, Epidemiology, Groningen, The Netherlands*

Purpose or Objective: Current models for the prediction of xerostomia and sticky saliva after radiotherapy (RT) are based on clinical and dosimetric information. Our hypothesis is that such models can be improved by the addition of patient-specific characteristics, quantified in CT image biomarkers (IBMs). The aim of this study is to improve the performance of prediction models for patient-rated moderate-to-severe xerostomia (Xer*12m*) and sticky saliva (STIC*12m*) 12 months after radiotherapy with the addition of these IBMs obtained from CT images before the start of RT.

Material and Methods: Head and neck cancer patients were primarily treated with RT alone or in combination with systemic treatment. The patient rated complications were prospectively collected (EORTC QLQ-H&N35).The potential CT IBMs represent geometric (20), CT intensity (24) and pattern characteristics (88) of the CT-image of the parotid (PG) and submandibular (SG) glands. Furthermore, Xer*baseline*, tumour, patient characteristics and mean doses to contra- and ipsi-lateral PG and SG were considered.Variables were preselected by omitting the least prognostic variable if inter-variable correlation was larger than 0.80. Lasso regularisation was used to create multivariable logistic regression models with and without IBMs to predict patient rated moderate-to-severe Xer*12m* and Stic*12m*. A repeated 10-fold cross validation was used to determine the optimal regularization term lambda. The final models were internally validated by testing the models on bootstrapped data.

Results: Of the 254 patients with follow-up information at 12 months, 100 (39%) and 62 (24%) had moderate-severe xerostomia and sticky saliva, respectively. Pre-selection of variables resulted in a selection of 26 variables for XER*12m* and 28 variables for STIC*12m*. For xerostomia, the lasso regularization selected in addition to mean contra-lateral PG dose and Xer*baseline* , the image biomarker "Short Run Emphasis" (SRE). This CT IBM quantifies the occurrence of short lengths of CT intensity repetitions and thereby indicates the homogeneity of the parotid tissue. For sticky saliva, the IBM maximum CT intensity of the submandibular gland was selected in addition to STIC*baseline* and mean dose

to SGs. The maximum intensity of the SG was related with the intra-vascular contrast in the artery or vein supplying the SG.
For the prediction of both Xer*12m* and STIC*12m*, the addition of the multivariable selected CT-IBMs improved the performance measures significantly compared to the models that were based on dose and baseline complaints only (table 1). The models were stable when internally validated.

Table 1. Model Performance of models prediction Xer_{12m} and $Stic_{12m}$ with and without CT IBMs

	Xerostomia		Sticky saliva	
	No IBM model	IBM model	No IBM model	IBM model
Log-Likelihood-ratio test (p-value)	-	0.02	-	0.006
Discrimination Slope	0.18	0.20	0.13	0.16
AUC	0.74	0.76	0.73	0.75
AUC bootstrapped	0.74	0.76	0.73	0.74

Xerostomia model : *(1) mean dose to contra lateral PG (2) $Xer_{baseline}$ (3. IBM) Short Run Emphasis (SRE)*
Sticky saliva model : *(1) $Stic_{baseline}$ (2) mean doseto SGs (3. IBM) Maximum CT intensity*

Conclusion: Prediction of XER*12m* and STIC*12m* could be improved with CT derived IBMs. The IBM associated with XER*12m*, "short run emphasis", might be a measure of non functional fatty parotid tissue. The STIC*12m* IBM, maximum intensity was related with the submandibular vascularization. Both predictive IBMs might be independent measures of radiosensitivity of the PG and SG.

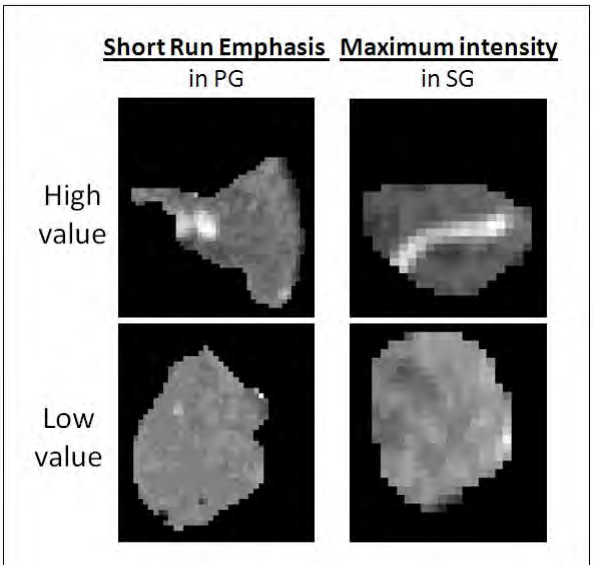

OC-0262

Comparison of machine-learning methods for predictive radiomic models in locally advanced HNSCC

S. Leger[1], A. Bandurska-Luque[1,2], K. Pilz[1,2], K. Zöphel[1,3,4], M. Baumann[1,2,4,5], E.G.C. Troost[1,2,4,5], S. Löck[1,2,4,5,6], C. Richter[1,2,4,5,6]

[1]*OncoRay - National Center for Radiation Research in Oncology, Faculty of Medicine and University Hospital Carl Gustav Carus- Technische Universität Dresden- Helmholtz-Zentrum Dresden – Rossendorf, Dresden, Germany*
[2]*Faculty of Medicine and University Hospital Carl Gustav Carus- Technische Universität Dresden, Department of Radiation Oncology, Dresden, Germany*
[3]*Faculty of Medicine and University Hospital Carl Gustav Carus- Technische Universität Dresden, Department of Nuclear Medicine, Dresden, Germany*
[4]*German Cancer Research Center DKFZ Heidelberg and German Cancer Consortium DKTK partner site Dresden, Dresden, Germany*
[5]*Helmholtz-Zentrum Dresden – Rossendorf, Institute of Radiooncology, Dresden, Germany*

Purpose or Objective: Radiomics is a new emerging field in which machine-learning algorithms are applied to analyse and mine imaging features with the goal to individualize radiation therapy. The identification of an effective and robust machine-learning method through systematic evaluations is an important step towards stable and clinically relevant radiomic biomarkers. Thus far, only few studies have addressed this question. Therefore, we investigated different machine-learning approaches to develop a radiomic signature and compared those signatures regarding to their predictive power.

Material and Methods: Two datasets of patients with UICC stage III/IV advanced head and neck squamous cell carcinoma (HNSCC) were used for training and validation (N=23 and N=20, respectively, NCT00180180, Zips et al. R&O 105: 21–28, 2012). All patients underwent FMISO- and FDG-PET/CT scans at several time points. We defined 45 radiomic-based image features, which were extracted from the gross tumour volume, delineated in CT0/FDG-PET0 and FMISO-PET0 (baseline; 0 Gy), FMISO-PET20 (end of week 2; 20 Gy) and CT40 (end of week 4; 40 Gy). Furthermore, we computed the delta features CT40/CT0 as well as FMISO-PET20/FMISO-PET0, leading to 315 image features in total. Radiomic signatures were built for the endpoints local tumour control (LC) and overall survival (OS) based on a semi-automatic approach using Cox regression models (SA) and automatic methods using random forests (RF) as well as boosted Cox regression models (CB). All models are applied to continuous survival endpoint data and were trained on the training cohort using a repeated (50 times) 2-fold cross validation. The prognostic performance was evaluated on the validation cohort using the concordance index (CI).

Results: The SA signature achieved the best prognostic performance for local tumour control (CI=0.93). Furthermore, the CB and RF signatures performed well in the validation cohort (CI=0.86 and CI=0.74, respectively). The signature for overall survival built by the RF model achieved the best performance (CI=0.91, compared to CI=0.87 by the CB model and CI=0.77 by the SA method). Figure 1 exemplarily shows Kaplan-Maier curves determined by the SA radiomic signature for both endpoints. The patients could be statistically significantly separated into a low and high risk survival group in the training (LC: p=0.015 and OS: p=0.023) and the validation cohorts (LC: p=0.003 and OS: p=0.001).

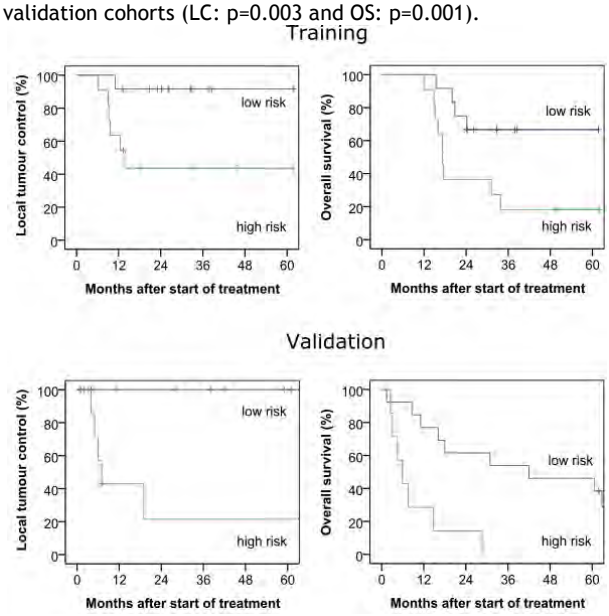

Conclusion: Our evaluation reveals that the RF and the CB model yield the highest predictive performance for both endpoints. The obtained signatures and features will be tested for stability using further delineation datasets. The comparison of machine-learning methods within the Radiomics processing chain is one important step to increase the robustness of the results and standardization of methods.

Proffered Papers: Physics 7: Treatment planning: optimisation algorithms

OC-0263

VMAT plus few optimized non-coplanar IMRT beams is equivalent to multi-beam non-coplanar liver SBRT

A.W.M. Sharfo[1], M.L.P. Dirkx[1], S. Breedveld[1], A.M. Mendez Romero[1], B.J.M. Heijmen[1]
[1]*Erasmus MC Cancer Institute, Radiation Oncology/ Radiotherapy, Rotterdam, The Netherlands*

Purpose or Objective: To compare fully non-coplanar liver SBRT with: 1) VMAT and 2) VMAT plus a few computer-optimized non-coplanar beams. Main endpoint was the highest feasible biologically effective dose (BED) to the tumor within hard OAR constraints.

Material and Methods: In our institution, liver metastases are preferentially treated with 3 fractions of 20 Gy. If not feasible for OAR constraints, the total dose of 60Gy is delivered in either 5 or 8 fractions. Assuming a tumor a/b of 10 Gy, the tumor BEDs for 3x20 Gy, 5x12 Gy, and 8x7.5 Gy are 180 Gy, 132 Gy, and 105 Gy, respectively. For fifteen patients with liver metastases we generated (i) plans with 15-25 computer-optimized non-coplanar IMRT beams (fully NC), (ii) VMAT plans, and (iii) plans combining VMAT with a few optimized non-coplanar IMRT beams (VMAT+NC). All plans were generated using our platform for fully automated multi-criterial treatment planning including beam angle optimization, based on the in-house iCycle optimizer and Monaco (Elekta AB, Stockholm, Sweden). For each patient and treatment technique we established the lowest number of feasible treatment fractions, i.e. 3, 5 or 8 to achieve highest possible tumor BED. All generated plans were clinically deliverable at our linear accelerators (Elekta AB, Stockholm, Sweden).

Results: Using 15-25 computer-optimized non-coplanar IMRT beams, 12 of the 15 patients (80%) could be treated with 3 fractions, one patient (7%) with 5 fractions, and two patients (13%) with 8 fractions. With VMAT only, achievable tumor BEDs were considerably lower for 1/3 of the patients, for 5 patients the fraction number needed to be increased to protect OARs: for 4 patients from 3 to 5 and for 1 from 5 to 8 (Table). Otherwise the healthy liver constraint (1 patient), or the constraint for the stomach (2 patients), bowel (1 patient) or oesophagus (1 patient) would be exceeded. With VMAT+NC, for all 5 patients this could be fully restored, resulting in the same low fraction numbers as for fully NC (Table). Contributions of the added NC IMRT beams to the PTV mean dose were relatively high: one patient needed a single IMRT beam with a weight of 14.8%, 1 patient needed 2 IMRT beams with a total weight of 39.9%, 2 patients required 3 IMRT beams with total weights of 45.5% and 47.7%, and 1 patient had 4 IMRT beams with a total weight of 46.1%.

Table. Number of patients planned per technique per fractionation regimen.

	3 fractions (BED = 180 Gy)	5 fractions (BED = 132 Gy)	8 fractions (BED = 105 Gy)
Fully NC	12	1	2
VMAT	8	4	3
VMAT+NC	12	1	2

Abbreviations: Fully NC = plans with 15-25 computer-optimized non-coplanar IMRT beams, VMAT = Volumetric Modulated Arc Therapy, VMAT+NC = plans combining VMAT with few optimized non-coplanar IMRT beams, BED = Biologically Effective Dose.

Conclusion: A novel approach for liver SBRT at a linear accelerator was developed. The basis of the treatment is a fast VMAT plan, supplemented with a few (1-4) computer-optimized non-coplanar IMRT beams. In terms of achievable tumor BED within the clinical OAR constraints, this approach is equivalent to time-consuming, fully non-coplanar treatment. The technique is currently also explored for other treatment sites.

OC-0264

Fast biological RBE modeling for carbon ion therapy using the repair-misrepair-fixation (RMF) model

F. Kamp[1,2,3], D. Carlson[4], J. Wilkens[1,2]
[1]*Technische Universität München- Klinikum rechts der Isar, Department of Radiation Oncology, Munich, Germany*
[2]*Technische Universität München, Physik-Department, Munich, Germany*
[3]*Klinikum der Universität München, Klinik und Poliklinik für Strahlentherapie und Radioonkologie, Munich, Germany*
[4]*Yale University School of Medicine, Department of Therapeutic Radiology, New Haven, USA*

Purpose or Objective: The physical and biological advantages of carbon ion beams over conventional x-rays have not been fully exploited in particle therapy and may result in higher levels of local tumor control and improvements in normal tissue sparing. Treatment planning must account for physical properties of the beam as well as differences in the relative biological effectiveness (RBE) of ions compared to photons. In this work, we present a fast RBE calculation approach, based on the decoupling of physical properties and the (α/β)x. The (α/β)x ratio is commonly used to describe the radiosensitivity of irradiated cells or organs. The decoupling is accomplished within the framework of the repair-misrepair-fixation (RMF) model.

Material and Methods: Carbon ion treatment planning was implemented by optimizing the RBE-weighted dose (RWD) distribution. Biological modeling was performed with the RMF and Monte Carlo Damage Simulation (MCDS) models. The RBE predictions are implemented efficiently by a decoupling approach which allows fast arbitrary changes in (α/β)x by introducing two decoupling variables c1 and c2. Dose-weighted radiosensitivity parameters of the ion field are calculated as (Fig 1). This decoupling can be used during and after the optimization.

$$\alpha_D = \alpha_X \cdot c_1 + \beta_X \cdot c_2 \text{ and } \beta_D = \beta_X \cdot c_1^2 \text{ resulting in}$$
$$RBE_{RMF}(c_1, c_2, (\alpha/\beta)_X, d) = \left(-(\alpha/\beta)_X + \sqrt{(\alpha/\beta)_X^2 + 4d(c_1(\alpha/\beta)_X + c_2 + c_1^2 d)}\right)/2d$$

Carbon ion treatment plans were optimized for several patient cases. Predicted trends in RBE are compared to published cell survival data. A comparison of the RMF model predictions with the clinically used Local Effect Model (LEM1 and 4) is performed on patient cases.

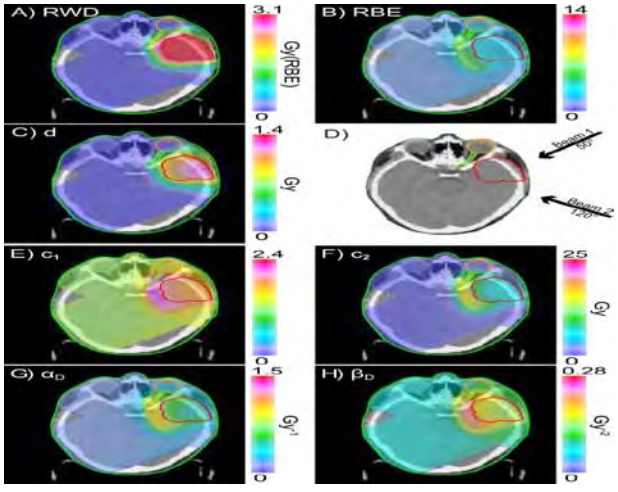

Figure 1: Axial CT slice of a treatment plan using the RMF model. The astrocytoma plan with two carbon ion fields was

optimized on 3 Gy(RBE) using a spatially constant (α/ß)x = 2 Gy (αx = 0.1 Gy^-1, ßx = 0.05 Gy^-2). The PTV is shown in red, along with 3 organs at risk: left optic nerve (green), left eye (orange) and left lens (brown). The panels show A) RWD, B) RBE, C) physical dose d and the beam geometry in D. The two decoupling variables c1 and c2 are shown in panels E and F, along with αD and ßD in panels G and H.

Results: The presented implementation of the RMF model is very fast, allowing online changes of the (α/ß)x including a voxel-wise recalculation of the RBE. For example, a change of the (α/ß)x including a complete biological modeling and a recalculation of RBE and RWD for 290000 voxels took 4 ms on a 4 CPU, 3.2 GHz workstation. Changing the (α/ß)x of a single structure, e.g. a planning target volume (PTV) of 270 cm^3 (35000 voxels), takes 1 ms in the same computational environment. The RMF model showed reasonable agreement with published data and similar trends as the LEM4.

Conclusion: The RMF model is suitable for radiobiological modeling in carbon ion therapy and was successfully validated against published cell data. The derived decoupling within the RMF model allows extremely fast changes in (α/ß)x, facilitating online adaption by the user. This provides new options for radiation oncologists, facilitating online variations of the RBE during treatment plan evaluation.

OC-0265

Efficient implementation of random errors in robust optimization for proton therapy with Monte Carlo

A.M. Barragán Montero[1], K. Souris[1], E. Sterpin[1], J.A. Lee[1]
[1]*Cliniques Universitaires Saint Luc UCL Bruxelles, Molecular Imaging Radiation Oncology MIRO, Brussels, Belgium*

Purpose or Objective: In treatment planning for proton therapy, robust optimizers typically limit their scope to systematic setup and proton range errors. Treatment execution errors (patient and organ motion or breathing) are seldom included. In analytical dose calculation methods as pencil beam algorithms, the only way to simulate motion errors is to sample random shifts from a probability distribution, which increases the computation time for each simulated shift. However, the stochastic nature of Monte Carlo methods allows random errors to be simulated in a single dose calculation.

Material and Methods: An in-house treatment planning system, based on worst-case scenario optimization, was used to create the plans. The optimizer is coupled with a super-fast Monte Carlo (MC) dose calculation engine that enables computing beamlets for optimization, as well as final dose distributions (less than one minute for final dose). Two strategies are presented to account for random errors: 1) Full robust optimization with beamlets that already include the effect of random errors and 2) Mixed robust optimization, where the nominal beamlets are involved but a correction term C modifies the prescription. Starting from C=0, the method alternates optimization of the spot weights with the nominal beamlets and updates of C, with C = Drandom – Dnominal and where Drandom results from a regular MC computation (without pre-computed beamlets) that simulates random errors. Updates of C can be triggered as often as necessary by running the MC engine with the last corrected values for the spot weights as input. MC simulates random errors by shifting randomly the starting point of each particle, according to the distribution of random errors. Such strategy assumes a sufficient number of treatment fractions. The method was applied to lung and prostate cases. For both patients the range error was set to 3%, systematic setup error to 5mm and standard deviation for random errors to 5 mm. Comparison between full robust optimization and the mixed strategy (with 3 updates of C) is presented.

Results: Target coverage was far below the clinical constraints (D95 > 95% of the prescribed dose) for plans where random errors were not simulated, especially for lung case. However, by using full robust or mixed optimization strategies, the plans achieved good target coverage (above clinical constraints) and overdose comparable to the nominal case. Doses to organs at risk were similar for the three plans in both patients.

		$CTV_{prostate}$ 74 Gy	CTV_{lung} 60 Gy
worst D_{98}	Nominal plan	67.1	38.2
	Full robust optimization	73.3	59.8
	Mixed robust optimization	70.2	56.4
worst D_5	Nominal plan	77.8	62.4
	Full robust optimization	78.9	62.6
	Mixed robust optimization	78.2	69.9

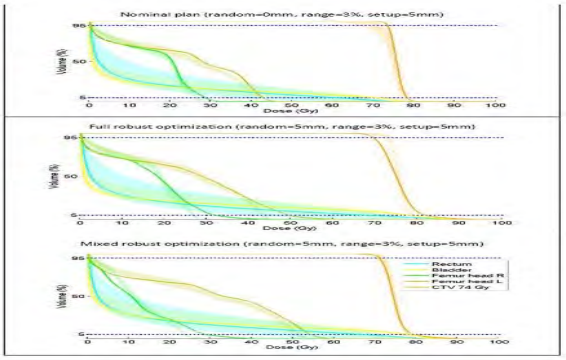

Conclusion: The proposed strategies achieved robust plans in term of target coverage without increasing the dose to the CTV nor to the organs at risk. Full robust optimization gives better results than the mixed strategy, but the latter can be useful in cases where a MC engine is not available or too computationally intensive for beamlets calculation.

OC-0266

Automated treatment plan generation for advanced stage NSCLC patients

G. Della Gala[1], M.L.P. Dirkx[1], N. Hoekstra[1], D. Fransen[1], M. Van de Pol[1], B.J.M. Heijmen[1], S.F. Petit[1]
[1]*Erasmus MC Cancer Institute, Radiation Oncology, Rotterdam, The Netherlands*

Purpose or Objective: The aim of the study was to develop a fully automated treatment planning procedure to generate VMAT plans for stage III/IV non-small cell lung cancer (NSCLC) patients, treated with curative intent, and to compare them with manually generated plans.

Material and Methods: Based on treatment plans of 7 previously treated patients, the clinical protocol, and physician's treatment goals and priorities, our in-house developed system for fully automated, multi-criterial plan generation was configured to generate VMAT plans for advanced stage NSCLC patients without human interaction. For 41 independent patients, treated between January and August 2015, automatic plan generation was then compared with manual plan generation, as performed in clinical routine. Differences in PTV coverage, dose conformality R50 (the ratio between the total volume receiving at least 50% of the prescribed dose and the PTV volume) and sparing of organs at risk were quantified, and their statistical significance was assessed using a Wilcoxon test.

Results: For 35 out of 41 patients (85%), the automatically generated VMAT plans were clinically acceptable as judged by two physicians. Compared to the manually generated plans, they considered the quality of automatically generated plans superior for at least 67% of patients, due to a combination of better PTV coverage, dose conformality and sparing of lungs, heart and oesophagus (positive values in figure). For the other acceptable plans plan quality was considered equivalent. On average, PTV coverage (V95) was improved by 1.1 % ($p<0.001$), the near-minimum dose in the PTV (D99) by 0.55 Gy ($p=0.006$) and the R50 by 12.4% ($p<0.001$). The mean lung dose was reduced by 0.86 Gy (4.6%, $p<0.001$), and the V20 of the lungs by 1.3 % ($p=0.001$). For some patients it was possible to improve PTV V95 by 3.8%, D99 by 3.3 Gy, to reduce mean lung dose by 3.0 Gy and

V20 by 6.2%. All plans fulfilled the planning constraints for the spinal cord, heart and plexus.
For the 6 automated VMAT plans that were initially not acceptable, it took a dosimetrist less than 10 minutes hands-on time to manually fine-tune the VMAT plan in our TPS to make it acceptable. In contrast, to generate a VMAT plan from scratch 3-4 hours were required.
For 5 out of 10 patients with a PTV prescription dose of less than 66 Gy in the manual plan, we were able to escalate the tumour dose using automated planning. For two patients dose escalation from 60 Gy to 66 Gy was possible, for other patients from 60.5 Gy to 66 Gy, 45 Gy to 57.75 Gy, and 55 Gy to 60.5 Gy, respectively.

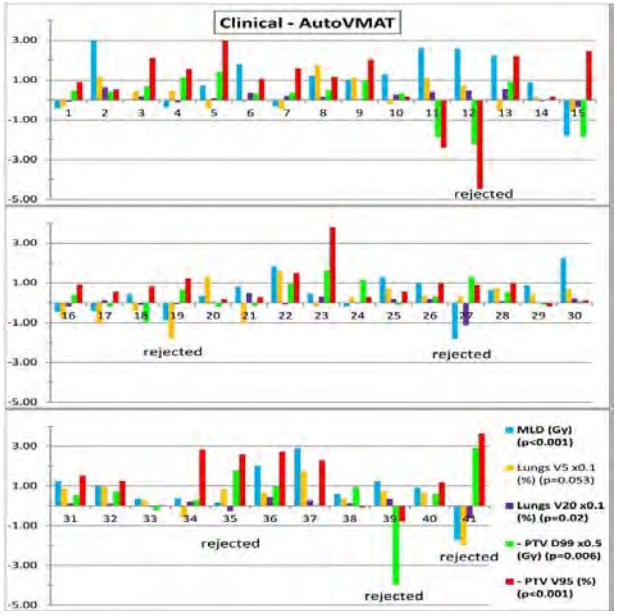

Conclusion: Using our fully automated treatment planning procedure, clinically deliverable, high quality VMAT plans for advanced stage NSCLC patients may be generated without human interaction for the far majority of patients. When manual adjustments were required, they took very little hands-on time only. With automated planning, a higher tumour dose could be achieved for a subgroup of patients. Clinical introduction has been started.

OC-0267

Fully automated planning for non-coplanar CyberKnife prostate SBRT - comparison with automatic VMAT

L. Rossi[1], S. Breedveld[1], S. Aluwini[1], B. Heijmen[1]
[1]*Erasmus MC Cancer Institute, Radiation Oncology, Rotterdam, The Netherlands*

Purpose or Objective: In stereotactic body radiation therapy, high accuracy is required to deliver high fraction doses with steep dose gradients. Non-coplanar beam setups may improve plan quality. This can be realized with a robotic CyberKnife (CK, Accuray Inc, Sunnyvale, USA). Due to its tumor tracking features, CTV-PTV margins may be reduced compared to linac treatment. In previous works we have built and validated a system for fully automated, multi-criterial VMAT plan generation (iCycle/Monaco). Recently, we have extended the system with an option for fully automated plan generation for the CK (iCycle/Multiplan). In this study we have used fully automated plan generation for un-biased comparison of non-coplanar CK with coplanar VMAT at a linac, for prostate SBRT.

Material and Methods: Our in-house iCycle system was first coupled to the Multiplan TPS that comes with the CK treatment unit. The iCycle/Multiplan and iCyle/Monaco systems were then configured for automated prostate SBRT plan generation for CK and linac-VMAT, respectively. Plans were then generated for 10 prostate SBRT patients, delivering 38 Gy in 4 fractions. Three clinically deliverable plans were automatically generated for each patient, one for CK with 3 mm PTV margin, and two for VMAT with 3 and 5 mm PTV margin, respectively.

Results: With automated planning, high quality CK and VMAT plans could be generated without user dependency and trial-and-error approach. PTV coverage was similar for the 3 approaches, with on average a V100% of 95.2, 95.4%, and 94.1% for CK, VMAT-3mm and VMAT-5mm. However, for some VMAT plans with 5mm margin, coverage > 95% was not feasible. Mean values for rectum D1cc were 26.1, 28.5, and 34.3 Gy, for rectum Dmean 6.3, 7.1, and 10.8 Gy, for bladder D1cc 37.7, 37.3, and 39.4 Gy, and for bladder Dmean 8.7, 7.5, and 9.2 Gy, for CK, VMAT-3mm and VMAT-5mm, respectively. Rectum doses were lower with CK compared to VMAT-3mm ($p = 0.015$ and $p = 0.08$ for rectum D1cc and Dmean) and highly decreased compared to VMAT-5mm ($p = 0.007$ and 0.008). Bladder sparing worsened slightly with CK compared to VMAT-3mm, but this was not statistically significant. No relevant differences were found for other OARs. With CK, the low-medium dose bath was reduced compared to VMAT: V10Gy = 1157.5, 1525.6, 1741.8 cc, V20Gy = 286.3, 325.5, 382.0 cc, for CK, VMAT-3mm and VMAT-5mm, respectively, with $p = 0.007$ and $p=0.008$ for CK comparing to VMAT 3 and 5 mm.

Conclusion: The first system for automated generation of clinically deliverable Cyberknife plans was built and used for unbiased plan comparison with VMAT at a linac. Optimized non-coplanar setups showed better rectum sparing compared to VMAT plans. This difference was especially large with the smaller CK CTV-PTV margin, possible with CyberKnife tumor tracking feature.

OC-0268

Fully automated VMAT plan generation – an international multi-institutional validation study

B. Heijmen[1], P. Voet[2], D. Fransen[1], H. Akhiat[2], P. Bonomo[3], M. Casati[3], D. Georg[4], G. Goldner[4], A. Henry[5], J. Lilley[5], F. Lohr[6], L. Marrazzo[3], M. Milder[1], S. Pallotta[3], J. Penninkhof[1], Y. Seppenwoolde[4], G. Simontacchi[3], V. Steil[6], F. Stieler[6], S. Wilson[5], R. Pellegrini[2], S. Breedveld[1]
[1]*Erasmus Medical Center Rotterdam Daniel den Hoed Cancer Center, Radiation Oncology, Rotterdam, The Netherlands*
[2]*Elekta AB, Elekta, Stockholm, Sweden*
[3]*Azienda Ospedaliero-Universitaria Careggi, Radiation Oncology, Florence, Italy*
[4]*Medical University Vienna /AKH Wien, Radiation Oncology, Vienna, Austria*
[5]*St James's Institute of Oncology- St James's Hospital, Radiation Oncology, Leeds, United Kingdom*
[6]*University Medical Center Mannheim- Heidelberg University, Radiation Oncology, Mannheim, Germany*

Purpose or Objective: Recently, iCycle/Monaco, a system for fully automated, multi-criterial plan generation, consisting of the in-house iCycle optimizer and Monaco (Elekta AB, Stockholm, Sweden) has been developed. Sofar, the system was only validated in a single institution. In this study, iCycle/Monaco was validated in 4 independent centers for prostate cancer VMAT. Hypothesis of the study was that automatically generated plans had similar or superior quality compared to plans generated by manual planning in clinical routine, using the Monaco TPS only.

Material and Methods: For each of the 4 centers, plans of 10 recently treated patients were used to configure iCycle/Monaco. For 20 independent patients, manually generated VMAT plans (MANplan) were then compared with automatically generated VMAT plans (AUTOplan). Plans were compared using dose-volume parameters and by 'blind' scoring by treating physicians. The scoring of the plans by physicians was performed in 2 sessions: A) the in total 40 anonymized plans (20 AUTO, 20 MAN) were evaluated in random order to assess clinical acceptability, B) for each of the 20 patients, the AUTOplan and MANplan were compared to select the most favorable plan. In these comparisons, plans could be scored as i) of higher quality with a clinically

relevant difference, ii) of higher quality but with a low clinical impact, or iii) of similar quality. In one participating center, plan scoring was performed independently by 2 physicians.

Results: A total of 200 separate plan evaluations and 100 plan comparisons were made in this study. In the separate plan evaluations, 100% of MANplans and 98% of AUTOplans were clinically acceptable. The 2 AUTOplans that were not clinically acceptable had too high bowel dose, which was due to the absence of patients with small bowel delineation among the patients used for configuration of iCycle/Monaco in 2 centers. For 38/100 plan comparisons, the AUTOplan was considered superior to the MANplan, with high clinical relevance. Only in 9 comparisons, the MANplan was superior with high relevance for the patient. In all other comparisons, differences were absent or of minor clinical relevance (Figure). With similar PTV coverage, dose delivery to OARs was on average lower for the AUTOplans: -14.8%, -24.6%, and -14.6% for rectum V75, V60, and Dmean (p=0.001, p<0.001, p<0.001), and -5.1% for bladder Dmean (p=0.009).

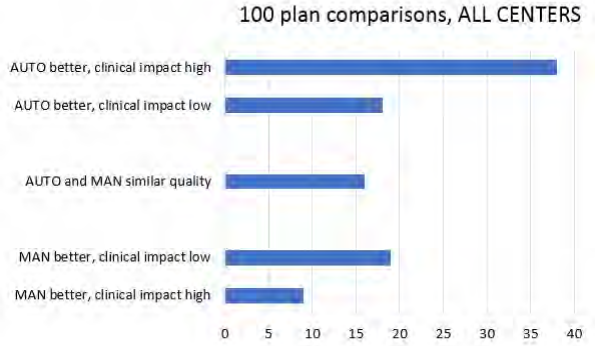

Frequency histogram showing the scores for 100 comparisons of an automatically (AUTO) and a manually (MAN) generated plan.

Conclusion: In an international, multi-institutional setting, automatic planning for prostate cancer has proven to be overall superior to manual planning. Automated planning avoids planning workload and contributes to standardized radiotherapy treatment with high plan quality.

Proffered Papers: RTT 3: Ensuring quality in head and neck treatment

OC-0269

Comparison of dosimetric parameters of two techniques with VMAT for head and neck cancers

M. Miyazaki[1], Y. Ueda[1], S. Ohira[1], K. Tsujii[1], M. Isono[1], A. Masaoka[1], T. Teshima[1]
[1]*Osaka Medical Center for Cancer and Cardiovascular Diseases, Radiation Oncology, osaka, Japan*

Purpose or Objective: Simultaneously integrated boost (SIB) used in many sites, replanning is not made. In SIB of intensity-modulated radiotherapy (IMRT), doses per fraction are often unconventional, because of equal fractions treating multiple targets. We assessed sequential SIB (SEQ-SIB) to resolve the problem. The purpose of this study is to compare dosimetric parameters of SEQ-SIB with those of SIB using deformable imaging registration (DIR) for head and neck cancer patients.

Material and Methods: Subjects were 10 cases HNC treated with IMRT at our institute in 2014. In all cases, high-risk planning target volume (PTVboost) was based on the primary tumor and clinical lymph node metastases, while PTVelective(PTVel) included bilateral cervical nodal areas. The D95 was defined as the prescribed dose. For SIB, doses were 66 and 54 Gy in 30 fractions to PTVboost and PTVel, respectively. For SEQ-SIB, they were 55 Gy to PTVboost and 50 Gy to PTVel in 25 fractions using SIB, followed by 11 Gy in 5 fractions to PTVboost.We chose to maintain the size of the original GTV when contouring the GTV on the anatomy of the second CT scan.SIB created two plans. One is 1st CT / 1st Plan and the other is SIB sum (25 fractions (deformed CT) and 5 fractions (2nd CT)) . A deformed CT (dCT) with structures was created by deforming the 1st CT to the 2nd CT. We summed up dose used in 1st Plan and 2nd Plan using a commercially software (MIM Maestro 6.3). The two types of plans were compared with respect to DVHs for other dosimetric parameters of the PTVboost, PTVel, brainstem, spinal cord and parotid gland.

Results: The mean dose for the brainstem, the spinal cord and the parotid was lower for SEQ. The D95of PTVboost and PTVel were significantly lower for SIB sum than for SIB (p<0.003, p<0.02).The D95 of PTVboost and PTVel were significantly lower for SIB sum than for SEQ-SIB (p<0.03, p<0.03). The difference between the CI of PTVboost of SIB sum and that of SEQ-SIB was not significant (p=0.03). The CI of PTVel was significantly lower for SIB sum than for SEQ-SIB (p<0.001).

Table 1. Dosimetric Parameters (means of 10 cases)

	brainstem	spinalcord	mean parotid dose		PTVboost	PTVel	PTVboost CI	PTVel CI
	max (Gy)	max (Gy)	ipsi (Gy)	contra (Gy)	D95 (Gy)	D95 (Gy)		
SIB	36.9	36.2	32.5	23.2	66	54.6	1.11	1.1
SIB sum	37.5	36.4	33.6	24.2	64.9	53.7	1.04	1.07
SEQ-SIB	34	34.2	32.4	22.4	65.7	50.8	1.08	1.19

Conclusion: SEQ-SIB is an approach for resolving the fraction size problem posed by SIB. The dosimetric parameters for OARs showed some variation between SIB and SEQ-SIB, especially for the parotid glands. SEQ-SIB is good in the point of coverage of PTV, because of replanning. The mean dose for ipsilateral and contralateral parotid was lower for SEQ-SIB, because of the lower elective dose. The availability of SEQ-SIB using replanning was suggested.

OC-0270

Development of a model to produce reference parotid dose from anatomical parameters in IMRT of NPC

W.S. Leung[1,2], V.W.C. Wu[2], F.H. Tang[2], A.C.K. Cheng[1]
[1]*Princess Margaret Hospital, Department of Oncology, Kowloon, Hong Kong SAR China*
[2]*The Hong Kong Polytechnic University, Department of Health Technology and Informatics, Hong Kong, Hong Kong SAR China*

Purpose or Objective: Dose to parotid glands in IMRT depended on the setting of constraints during inverse planning and could be varied by planners' experience. This study aimed to tackle the problem of IMRT plan variability by the development of a multiple regression model to associate parotid dose and anatomical factors. By measuring a few anatomical factors before performing inverse planning, reference parotid dose would be suggested by the model to guide planners to undergo the inverse planning optimization process.

Material and Methods: 25 NPC subjects who previously received radical IMRT (70Gy/60Gy/54Gy in 33-35 fractions) were randomly selected. Optimized IMRT plans produced by a single planner were used for data collection. Multiple regression was performed using parotid gland Dmean, and D50% as the dependent variable, and various anatomical factors as the independent variable. The anatomical factors included (1) gland size, (2) %volume with 1cm gap from PTV60, (3) volume with 1cm gap from PTV60, (4) %volume overlap with PTV60, (5) volume overlap with PTV60, (6) %volume overlap with PTV70, (7) volume overlap with PTV70 (8) max. distance from PTV60 and (9) max. distance from PTV70. Gland size was measured using the "measure volume" function. Volume with 1cm gap was measured by using "crop structure" function and cropping the parotid with 1cm gap from the PTV60. Volume overlap with PTV was measured by using the "Boolean operator" which created the overlapped

volume. Max. distance was measured by the magnitude of expanding the PTV using the "margin for structure" function until the PTV covered the whole parotid gland. Multiple regression was performed using the stepwise method which eliminated independently variables with least effect.

Results: Anatomical factors statistical significantly predicted parotid gland Dmean and D50%. For Dmean, gland size, %volume overlap with PTV60 and %volume with 1cm gap from PTV60 were included in the model. ($F(3, 46) = 44.244$, $p<0.0005$, $R2 = 0.743$). For D50%, volume overlap with PTV60, %volume with 1cm gap from PTV60 and gland size were included in the model. ($F(3, 46) = 37.709$, $p<0.0005$, $R2 = 0.711$).

Conclusion: These models explained over 70% of the dependent variables. Cross validation will be provided to support the accuracy of the model. The predicted parotid dose could be used for a guide to set dose constraints during inverse planning and as the benchmark dose during plan evaluation. Eventually the suggested model could improve the parotid sparing in the IMRT of NPC cases.

OC-0271

Positional accuracy valuation of a three dimensional printed device for head and neck immobilisation

K. Sato[1], K. Takeda[1], S. Dobashi[1], K. Kishi[2], N. Kadoya[3], K. Ito[3], M. Chiba[3], K. Jingu[3]
[1]*Tohoku University Graduate School of Medicine, Deparment of Radiotherapy- Cource of Radiological Technology- Health Sciences, Sendai, Japan*
[2]*Tohoku Pharmaceutical University Hospital, Department of Radiation Technology, Sendai, Japan*
[3]*Tohoku University School of Medicine, Department of Radiation Oncology, Sendai, Japan*

Purpose or Objective: Our aim was to investigate the feasibility of a three-dimensional (3D)-printed head-and-neck (HN) immobilization device by comparing its positional accuracy with that of the conventional thermoplastic mask.

Material and Methods: We prepared a 3D-printed immobilization device (3DID) consisting of a mask and headrest developed from the computed tomography (CT) data obtained by imaging an HN phantom. The CT data was reconstructed to generate the Digital Imaging and Communication in Medicine (DICOM) dataset. Then, the HN-phantom surface was determined by the Otsu segmentation method. After converting the DICOM dataset of the phantom surface to a Surface Tessellation Language (STL) file format, 3D modeling was performed. Next, the STL file was 3D printed using acrylonitrile–butadiene–styrene resin. For comparison of positional accuracy, the conventional immobilization device (CID) composed of a thermoplastic mask and headrest was prepared using the same HN phantom. Subsequently, the simulation CT images were acquired after fixing the HN phantom with 3DID. After positioning the HN phantom by matching surface marks, radiographs were acquired using the ExacTrac X-ray image system. Then, we quantified the positional deviations, including three translations and three rotations, between the coordinate origin in the localization images prepared from kV X-rays and the expected position on the digitally reconstructed radiograph from the simulation CT images. This process was repeated fifteen times to collect data on positional deviations. Afterwards, the same procedure was performed in the same HN phantom fixed with CID for comparison.

Results: The translational displacement (mean [standard deviation, SD]) in the vertical, lengthwise, and lateral directions was−0.28 [0.09], −0.02 [0.08], and 0.31 [0.27] [maximum, 0.81 mm (lateral direction)] for 3DID and 0.29 [0.06], 0.03 [0.14], and 0.84 [0.27] [maximum, 1.23 mm (lateral direction)] for CID, respectively. The rotational shift in the yaw, roll, and pitch directions was 0.62 [0.13], 0.08 [0.74], and −0.31 [0.08] [maximum, −0.41° (pitch direction)] for 3DID and−0.15 [0.17], 0.17 [0.67], and −0.09 [0.06] [maximum, −1.23° (roll direction)] for CID, respectively. The means of the two devices were almost similar in each direction except the vertical, lateral, and pitch directions (t-test, $p < 0.0001$), whereas the maximal deviations in the three directions were slight. The SDs were not statistically different in each direction except the lengthwise and roll directions (F-test, $p < 0.05$), although the SDs were small in the corresponding two directions for CID.

Conclusion: This study suggested that 3DID could show positional accuracy almost similar to that of CID. However, further investigation is needed for use in clinical practice.

OC-0272

A comparison of CTCAE version 3 and 4 in assessing oral mucositis in oral/oropharyngeal carcinoma

M. Hickman[1], J. Good[2], A. Hartley[2], P. Sanghera[2]
[1]*University Hospital Birmingham, Radiotherapy, Birmingham, United Kingdom*
[2]*InHANSE- University of Birmgham, Radiotherapy, Birmingham, United Kingdom*

Purpose or Objective: CTCAE version 3 is an observation based grading system for oral mucositis whereas version 4 is based on function and intervention. Although version 4 has been widely adopted in clinical trials there is limited data on its correlation with version 3 from which considerable radiobiological data has been derived. The purpose of this study was to assess the frequency of discrepancy between these two grading systems.

Material and Methods: Oral mucosal reactions of patients undergoing chemoradiation or radiation alone for oral or oropharyngeal cancer were graded by three radiation oncologists in weekly on treatment and post treatment clinics. CTCAE version 3 and 4 mucositis grading and patient factors were recorded prospectively. Differences in the rate of discrepancy were compared by time since the commencement of radiotherapy, synchronous agent and patient age.

Results: 485 measurements were recorded for 64 patients. Grading from version 3 and version 4 were equal in 270 (56 %) measurements. In the 215 (44%) measurements where version 3 and version 4 were not equal, discrepancies were seen in: Week 0-4 = 79/179 (44%); Week 5-8 = 60/163 (37%); > week 8 = 76/143 (53%) ($p=0.02$); patients receiving platinum agents = 113/316 (36%) or cetuximab= 48/70 (69%) ($p<0.01$); patients > 70 years = 26/57 (46%) or < 50 years = 21/68 (31%) ($p=0.09$).

Conclusion: Statistically significant discrepancies were seen when patients receiving platinum agents were compared with those receiving cetuximab and in those measurements performed following treatment completion. These initial results suggest that functional/interventional based grading systems should be used with care in dose escalation studies where the healing of acute mucositis may be related to subsequent late damage.

OC-0273

Including specific symptoms in clinical scoring: predictive modelling and nursing of swallowing pain

D. Nyeng Christiansen[1], K. Olling[1], L. Wee[1]
[1]*Vejle Hospital, Radiotherapy Department, Vejle, Denmark*

Purpose or Objective: Acute esophagitis (AE) is a common side-effect of radiotherapy (RT) for lung cancer. Previous predictive modelling studies focussed on clinical criteria (such as CTC) for significant AE (such as G2 or higher). Our clinic uses an integrative patient care approach where Nurse-RTTs routinely monitor symptoms and provide nursing interventions to manage side-effects. Therefore, Nurse-RTTs include with clinical scoring a note of actual symptoms mentioned by the patient during consultations, such as swallowing pain (SP). A retrospective audit of 131 patients was used to examine correlative patterns for SP, and hence to develop predictive models for SP before the start of RT. We propose that a predictive model will facilitate nurse/RTT-

led efforts to reduce the impact of SP on patient comfort, overall QoL and clinical workflow.

Material and Methods: An electronic journal audit was performed for patients commencing curative RT for lung cancer between January 2013 and March 2015. All NSCLC and SCLC patients were included, as well as various dose/fractionation, chemotherapy and medication schedules. Exported treatment plan DVHs were merged with nursing data. The highest score following weekly assessments of AE during radiotherapy was recorded, as was the appearance of SP and the time point at which it was mentioned. Predictive models of SP were developed using multivariable regression and machine learning algorithms.

Results: The most typical patient was treated for NSCLC at 60-66Gy normo-fractionated with concurrent chemotherapy. Acute esophagitis (CTC grade 1 or higher) was observed in 110/131 (84%) and patient-reported SP in 99/131 (76%). Pain medication prior to RT was marginally protective against SP but was not statistically significant in single-parameter analysis (OR 0.58, 95%CI 0.24-1.41, p=0.21). A strongly significant dose-volume response exists between SP and radiobiologically-adjusted dose to the hottest 1cc of the esophagus. Predictive models of SP with repeated cross-validation accuracy of 78-84% were developed (sensitivity 88-89%, specificity 48-75%). Trained machine learning models correctly predicted SP 76-84% of the time in an unseen validation cohort of 25 patients (sensitivity 94-100%, specificity 25-62%).

Conclusion: An integrative nursing care approach in the RT clinical workflow has been used to monitor symptoms and intervene for treatment-related pain. The risk of one particular patient-centred symptom, SP, can be sensitively predicted with nursing and treatment planning variables. A future nurse-led interventional study is planned, using predictive modelling for swallow pain, to examine the possible effects of pre-treatment pain-medication or corticosteroids on reducing dependence on additional pain medication.

OC-0274

Analysis of set-up errors in head and neck cancer treated with IMRT technique assessed by CBCT

D. Delishaj[1], S. Ursino[1], E. Lombardo[1], F. Matteucci[1], C. La Liscia[1], A. Sainato[1], F. Pasqualetti[1], B. Manfredi[1], L.R. Fatigante[1], M. Panichi[1], S. Spagnesi[1], M.G. Fabrini[1]
[1]*Azienda Ospedaliero Universitaria Pisana, Radiotherapy, Pisa, Italy*

Purpose or Objective: The aim of this study was to investigate systemic set-up errors in head and neck (H&N) cancer treated with intensity modulated radiation therapy (IMRT) by kilovoltage (kV) cone-beam computed tomography (CBCT) evaluation.

Material and Methods: Between September 2014 and August 2015, 360 CBCT in 60 patients (pts) affected by histological confirmed H&N cancer treated with IMRT technique were analyzed. The majority of patients treated 45 (75 %) were male and only 15 (25%) were female; median age was 68 years (range 44-88 years). The type of head and neck cancer treated were, oropharynx , hypopharynx, nasopharynx, larynx , tonsil, oral cavity and parotid cancer. All patients underwent planning Computerized Tomography (CT) simulation on supine position on a GE LightSpeed RT 16 CT Simulator for 2.5 mm slice thicknesses. As immobilization system we utilized a head-shoulder thermoplastic mask (Easy Frame (Candor TM)). The CT data sets were transferred to the Focal and Varian Eclipse treatment planning system through DICOM network. The target delineation was contoured by one Radiation Oncologist and according to (ICRU62) the PTVs volumes were generated by adding a 3-mm margin in all directions to the respective CTVs. The prescribed dose was 66 Gy in 30 fractions delivered to GTVs, 54-63 Gy in 30 fractions to CTVs. The IMRT plans were created on the Varian Eclipse treatment planning system using coplanar beams with 6 MV photons and the treatment was performed with DHX LINAC, VARIAN System. Pretreatment kV CBCT images were obtained at 1, 2 and 3 day of irradiations set-up corrections were made before treatment if the translational setup error was greater than 3 mm in any direction. Subsequently a weekly kV CBCT was repeated for whole duration of treatment.

Results: A total of 360 CBCT scans were acquired and analyzed. The systemic errors results 1.26 mm (SD ± 0.177) in RL direction, 1.25 mm (SD ± 0.187) in SI direction and 1.8 mm (SD ± 0.255 in AP direction. The range of deviations were 0-9 in RL directions, 0-5 mm in SI direction and 0-10 mm in AP direction. The frequencies of setup errors > 3 mm in RL direction was 3.9 %, in SI 8 % and AP directions 15.5 %, respectively. Analyzing the CBCT before set-up corrections the frequencies of set-up error > 3 mm were 17.8 %, 10.6 % and 5.6 % in AP, SI and RL respectively. After set-up errors corrections (corrections via couch shifts or patient repositioning) these rates were reduced to 13,3%, 7.2 and 2.2 % in PA, SI and RL direction, respectively.

Conclusion: The results of our study confirmed that image guidance with kV CBCT represents an effective tool for measuring set-up accuracy in the treatment of H&N cancer patients. This study suggested that kV CBCT once a week is adequate to overcome the problem of set-up errors in head and neck cancer treated with IMRT technique.

Poster Viewing: 6: Clinical: Lung, palliation, sarcoma, haematology

PV-0275

IMRT for non-small cell lung cancer: a decade of experience at the Ghent University Hospital.

P. Deseyne[1], Y. Lievens[1], W. De Gersem[1], P. Berkovic[2], M. Van Eijkeren[1], V. Surmont[3], C. Derie[1], B. Goddeeris[1], W. De Neve[1], K. Vandecasteele[1]
[1]*Ghent University Hospital, Radiation Oncology Department, Ghent, Belgium*
[2]*CHU Liège, Radiation Oncology Department, Liège, Belgium*
[3]*Ghent University Hospital, Thoracic Oncology Department, Ghent, Belgium*

Purpose or Objective: In 1998, our institute developed a class-solution for intensity-modulated radiotherapy (IMRT) for lung cancer. Clinical implementation of IMRT gradually started as of 2002. This retrospective study reports on toxicity and overall survival (OS) of non-small cell lung cancer (NSCLC) patients treated with curative intent using the described IMRT set-up.

Material and Methods: Between 2002 and 2013, a total of 434 patients with a thoracic malignancy have been treated with IMRT in the Radiation Oncology department of the Ghent University Hospital. Those with NSCLC and receiving a total dose of≥60Gy with fraction size <3Gy, a total 223, were retrospectively reviewed and formed the basis of this analysis. Clinical endpoints of OS and acute and late pulmonary and esophageal toxicity grade ≥3 were analyzed in relation to chemotherapy (concomitant vs. sequential chemoradiotherapy (CRT) vs. no chemotherapy) and use of standardized dose-volume evaluation criteria. Analysis was performed in SPSS using Kaplan-Meier curves for survival and Chi-square analysis for toxicity.

Results: Median follow-up time is 18 months (range 2-125). The table reports patient, tumor and treatment characteristics. OS was scored for all patients as date of death (N=140) or, if missing, as date of last consultation in our hospital (N=83). Acute and late toxicity data were available for 219 and 95 patients respectively. Median OS for the entire population was 25 months, 5 year OS 24%. OS was significantly better for patients treated with concomitant CRT than for those undergoing the sequential approach (median OS 30 months vs. 23; 5 years OS 32% vs. 12%) (p<0,05). Acute grade ≥3 pulmonary toxicity occurred in 7,8%

of the patients, without significant difference between concurrent and sequential CRT. Acute grade≥3 esophageal toxicity occurred in 5,5% of patients overall; and was significantly worse (p<0,01) in patients treated with concomitant CRT compared to sequential CRT: 10,4% vs. 4,3% respectively. Late grade≥3 pulmonary and esophageal toxicity was observed in 3,3% and 0% respectively; late grade 2 toxicity in 13,2% and 1,4% of the cases respectively. Although there was a trend towards reduced esophageal toxicity, the use of standardized dose-volume evaluation criteria (N=38) did not influence pulmonary (p=0.60) nor esophageal (p=0.08) toxicity significantly.

Conclusion: In spite of the low 5-year OS in patients undergoing sequential CRT, the entire NSCLC population treated with IMRT in our institution obtained OS in line with that reported in the literature. IMRT further confirms the potential for reduced toxicity as observed in other single-center experiences. Regardless of the lack of documented significant impact, we are convinced that the use of standardized dose-volume evaluation criteria has contributed to this positive outcome and is a precondition to exploit the full potential of IMRT in NSCLC.

Table: Patient, tumour and treatment characteristics (n = 223)

	Parameter	Absolute Number	Percentage (%)
Gender	Male	188	84,3
	Female	35	15,7
KPS	60	2	0,9
	70	11	4,9
	80	61	27,4
	90	108	48,4
	100	10	4,5
	Missing	31	13,9
Histology	adenocarcinoma	74	33,2
	adenosquamous	9	4,0
	"non-small cell"	42	18,8
	squamous cell carcinoma	97	43,6
	none	1	0,4
Stage	IA	1	0,4
	IB	2	0,9
	IIA	5	2,2
	IIB	10	4,5
	IIIA	114	51,2
	IIIB	88	39,5
	unknown	3	1,3
Chemotherapy	none	37	16,6
	sequential	119	53,4
	concomittant	67	30,0
Standardised dose-volume evaluation	yes	185	83,0
	no	38	17,0
	Median	Range	
Fraction Size (Gy)	2	2 – 2,7	
Total Dose (Gy)	70	60 – 80,15	
# of fractions	35	26 – 37	

PV-0276

Adaptive radiotherapy: rate of "marginal" failure after "replanning" in combined treatment of NSCLC

S. Silipigni[1], E. Molfese[1], E. Ippolito[1], M. Fiore[1], B. Floreno[1], P. Matteucci[1], A. Sicilia[1], L. Trodella[1], R. D'Angelillo[1], S. Ramella[1]

[1]*Campus Biomedico University, Radiotherapy, Rome, Italy*

Purpose or Objective: Respiratory movement and anatomical changes of the lesion during radiotherapy are the main causes of target missing and/or irradiation of healthy lung tissue. The organ motion control and the correct identification of target volume (TV) contribute to manage these issues; however, the open question is if the adaptation of TV during treatment leads to an increased incidence of recurrences in the area of target reduction. The aim of this study is to evaluate patients' pattern of failure distinguishing “marginal”, in field and out of field recurrences.

Material and Methods: In this prospective study, since 2010, locally advanced NSCLC patients treated with radiochemotherapy (RCT) underwent a weekly chest-CT simulation during therapy. In case of tumor's shrinkage, a new TV was delineated and then a new treatment plan outlined ("replanning"). At the end of treatment, patients were sent to follow-up. The patterns of failure were classified as: in field (persistence or recurrence in TV post-"replanning"), "marginal" (recurrence in the area of initial TV excluded from the post-"replanning" TV) and out of field (recurrence outside of initial TV). We also evaluated distant failure.

Results: Two hundred seventeen NSCLC patients were treated in our center. In fifty cases there was a volume reduction, so a "replanning" was outlined. Patients' characteristics were: mean age 69.6 years (range 38-92), squamous histology 56%, 32% adenocarcinoma, other 12%, stage IIIA 58% and IIIB 42%. The median total dose delivered was 65.7 Gy with standard fractionation. Median CTV at CT simulation and at "replanning" was 125.2 cc and 74.7 cc, respectively, with a median reduction of 43.1%. The "replanning" has been performed at a median dose of 45 Gy. At first follow up, 48 patients were evaluated. Response, according to RECIST criteria, was as follow: 2 complete responses (4.1%), 33 partial responses (68.8%) and 13 stable disease (27.1%). Grade 3 toxicities (CTCAE_4.0) were: acute esophageal in 4% of cases, pulmonary 6% (1 case acute and 2 chronic). With a median follow-up of 20.5 months, there have been 15 local (31%) and 22 distant (46%) failures. The observed local failures were: in field in 20.8% of cases, "marginal" in 6.1% and out of field in 4.1%. The median time to local failure, progression free survival and overall survival were 8.5, 8.3 and 30.5 months, respectively. The median onset of “marginal”, in field, out of field and distant failures was 12, 9.2, 7.1 and 7.8 months, respectively.

Conclusion: Our results show that "replanning" during RCT has an acceptable local failure rate comparable to literature data; in particular, given the low incidence of "marginal" failures combined with the low rate of acute toxicity, the strategy appears promising, bringing to a method of dose escalation aimed at reducing in field failures.

PV-0277

SBRT with concurrent chemoradiation in stage III NSCLC: first results of the phase I Hybrid trial

H. Peulen[1], J.J. Sonke[1], E. Van der Bijl[1], E. Damen[1], J. Belderbos[1]

[1]*Netherlands Cancer Institute, Radiation Oncology, Amsterdam, The Netherlands*

Purpose or Objective: To assess the feasibility and safety of combined stereotactic body radiotherapy (SBRT) of the primary tumor (PT) and concurrent chemoradiation (CCRT) in stage III NSCLC, the Hybrid study (single center phase I: NCT01933568) was initiated. Primary endpoint is the mean lung dose (MLD) associated with 15% chance on radiation pneumonitis (RP)≥ G3 and dyspnea ≥ G3. Secondary endpoints are toxicity and disease control. This is the first report of adverse events observed.

Material and Methods: Eligible patients had stage III or inoperable stage II NSCLC with a peripheral PT < 5 cm. Patient received CCRT: 24x2.75 Gy or 24x2.42 on the pathological lymph nodes (LN) with daily low dose cisplatinum 6 mg/m2 with an overall treatment time of 32 days. SBRT was delivered in 3 fractions of 14-18 Gy in the 2nd week concurrent with CCRT. If the fractionated LN treatment plan contributed to the PT dose, the total SBRT dose was corrected for accordingly. The MLD was escalated with 2 Gy increments using the Time-to-Event Continuous Reassessment Method (TITE-CRM) statistical design driven by dose limiting toxicity (RP or dyspnea≥ G3; CTCAE v4) within 12 months post treatment. The range of acceptable SBRT fraction doses allowed accruing patients in different MLD dose bins.

Results: From March 2013- October 2015 12 patients gave informed consent for the trial. One patient was excluded after the 1st week of treatment due to a baseline shift of the PT towards the mediastinum, causing unacceptable dose to the mediastinal organs at risk (OAR) if treated with SBRT. Median follow up (FU) was 8 months (range 0-26), median age was 63 years (range 61-75), 73% was male, 73% had adenocarcinoma, 18% squamous cell carcinoma, 9% large cell NOS. 73% had T1 tumors, 9% T2, 18% T3 (2 tumors), 18% N1, 73% N2 and 9% N3. Ten patients received CCRT, 1 patient radiotherapy only due to co-morbidities. No locoregional recurrences have been observed. Two patients developed distant metastases, one of which died 12 months post treatment due to leptomeningeal metastases. Median SBRT

dose was 53 Gy (range 43-54 Gy) and median LN dose was 2.75 Gy. Median MLD (α/β=3 Gy) was 11.9 Gy (range 5.2-18 Gy). In 2 patients SBRT dose was decreased: in 1 patient due to allocation in a lower MLD risk group than the treatment plan MLD, in 1 patient because of normal tissue constraints of the mediastinal OAR. During treatment 4 patient developed dysphagia G2, 2 fatigue G2, 1 thrombocytopenia G2, 1 anorexia G2 and 1 patient hemoptysis G2 . Radiation pneumonitis G2 occurred in 1 patient at 2.5 months FU with an MLD of 12.4 Gy. One patient developed chest wall pain G2 due to a rib fracture at 32 months FU. There were no G3-5 toxicities.

Conclusion: A Hybrid treatment of SBRT of the primary tumor combined with concurrent chemoradiation is feasible. This phase I trial is currently accruing and no unexpected toxicity has been observed thus far.

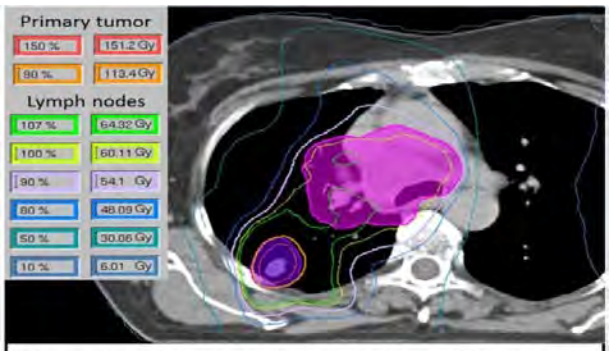

Figure 1: Axial slice with total planned biological dose ($^{\alpha}/_{\beta} = 10\ Gy$) of the hybrid treatment combining 3x18 Gy on the primary tumor (PTV, purple color wash) and 24x2.42 Gy on the lymph nodes (PTV pink color wash).

PV-0278

Volume concepts in routine radiotherapy for localized Hodgkin lymphoma: results of a national survey

R. Mazeron[1], L. Gonzague-Casabianca[2], K. Peignaux[3], V. Remouchamps[4], C. Chira[5], P. Moisan[6], J. Lazarovici[7], V. Edeline[8]

[1]*Institut Gustave Roussy, Department of Radiation Oncology, Villejuif, France*
[2]*Institut Paoli Calmette, Radiation Oncology, Marseille, France*
[3]*Centre GF Leclerc, Radiation Oncology, Dijon, France*
[4]*CHU Godinne, Radiation Oncology, Namur, Belgium*
[5]*Institut de Cancérologie de Lorraine, Radiation Oncology, Vandœuvre-lès-Nancy, France*
[6]*Institut Curie, Radiation Oncology, Saint-Cloud, France*
[7]*Gustave Roussy, Hematology, Villejuif, France*
[8]*Institut Curie, Nuclear Medicine, Saint-Cloud, France*

Purpose or Objective: Background The definition of target volumes in radiotherapy for Hodgkin lymphoma quickly evolved during the last decades, with the comings of Involved-field radiotherapy (IF), then the Involved Node (IN)1, and more recently the concept of Involved-site (IS)2. The latter two concepts are based on the observation that recurrences mainly concern the adenopathies present at diagnosis when radiotherapy is not performed and on the need to reduce the irradiated volumes to limit the radiation-induced late morbidity. If the H103 and RAPID4 trials confirmed the interest of radiotherapy in localized disease, the standard technique is still debated. The studies currently led by the LYSA illustrate this confusion since one (BREACH) made IN its standard technique, while the other (BRAPP2) requires IF-radiotherapy.
To assess routine radiotherapy practices in the treatment of localized Hodgkin lymphoma.

Material and Methods: At the initiative of multicentric and multidisciplinary working group involving radiation oncologists, hematologists, and nuclear medicine physicians, so called "PET-RT-Hodgkin", a survey focusing on the target volumes concepts (IN, IF and IS) and the use PET-CT in treatment position was sent to 35 French academic centers (university hospitals and cancer centers) through the SFRO (French Society for Radiation Oncology).

Results: Returns were obtained from 28 of the 35 centers contacted (80%). Of them, 10.7% were treating less than 5 patients per year, 28.6%, from 5 to 10, 46.4% from 10 to 20, and 14.3% more than 20. The radiation therapists in charge were 19.0 ± 9.8 years of experience, including 14.9 ± 10.1 in the treatment of Hodgkin lymphoma. 86% of practitioners said that they were comfortable with the 3 concepts of target volume. Fifteen (53.6%) stated that IN was a standard and routinely use it; 8 answered that they were applying IS (28.6%). Five responded that IF was their standard of care, off-study (17.9%). If all used PET scans to define the target volumes; 19 centers offered the opportunity to perform it in treatment position (67.9%). Three radiotherapists admitted having difficulties in accessing it (10.7%) and six reported no access at all (21.4%). In 5 centers, patients were referred after chemotherapy and therefore with no possibility to perform this examination (17.9%). While most declared having a collaboration with a nuclear medicine physician, 53.6% of the radiotherapists were interested in implementing an expert PET images review network.

Conclusion: In routine, the definition of target volumes and access to the PET-CT in treatment position remain heterogeneous. The PET-RT-Hodgkin group aims to harmonize the conditions of realization of PET and justify the means to implement

Références 1: T. Girinsky. Radioth Oncol, 2006 2: L. Specht. Int J Radiat Oncol Biol Phys, 2014. 3: JM. Raemaekers. J Clin Oncol. 2014, 4: J. Radford. N Eng J Med, 2015

PV-0279

Role of IFRT prior or after autologous stem cell rescue for refractory or relapsed Hodgkin lymphoma

M. Levis[1], C. Piva[1], A.R. Filippi[1], P. Pregno[2], P. Gavarotti[2], B. Botto[2], R. Freilone[3], G. Parvis[4], D. Gottardi[5], U. Vitolo[2], U. Ricardi[1]

[1]*Universita di Torino, Radiation Oncology, Torino, Italy*
[2]*A.O.U. Citta della Salute e della Scienza, Department of Hematology, Torino, Italy*
[3]*Ospedale Civile, Department of Hematology, Ciriè- Torino, Italy*
[4]*Ospedale San Luigi, Department of Internal Medicine and Hematology, Orbassano- Torino, Italy*
[5]*Ospedale Mauriziano, Department of Hematology, Torino, Italy*

Purpose or Objective: High-dose chemotherapy (HDCT) followed by autologous stem cell transplantation (ASCT) is the standard of care for relapsed or primary refractory Hodgkin's lymphoma (HL) after first line treatment. The role of involved-field radiotherapy (IFRT) is controversial in this setting. Aim of this retrospective study was to investigate for a possible role for IFRT by comparing patients who received IFRT (prior or after ASCT) and patients who received salvage chemotherapy (CT) alone.

Material and Methods: We enrolled 73 consecutive HL patients treated with ASCT between 2003 and 2013. Twenty-one patients (28.8%) received pre (7 patients) or post (14 patients) ASCT radiotherapy. A Cox regression analysis was performed to evaluate the prognostic role of any risk factor. OS and PFS were calculated from the first day of HDCT. Response to HDCT and ASCT were evaluated with PET scan and defined according to Cheson's criteria.

Results: Median follow up was 47 months (range 1-145) for the entire population. Population characteristics by treatment modality are summarized in Table 1.

Factors	CT-RT N = 21 (%)	CT alone N = 52 (%)	p-value
Sex			
Male	10 (47.6%)	28 (53.8%)	0.63
Female	11 (52.4%)	24 (46.2%)	
Median Age (years)	38	34.5	0.76
Stage at diagnosis			
II	10 (47.6%)	24 (46.2%)	0.42
III	4 (19.0%)	13 (25.0%)	
IV	7 (33.4%)	15 (28.8%)	
Bulky			
Yes	10 (47.6%)	18 (34.6%)	0.30
No	11 (52.4%)	34 (65.4%)	
B symptoms			
Yes	14 (66.7%)	27 (51.9%)	0.24
No	7 (33.3%)	25 (48.1%)	
PS (ECOG)			
0	13 (61.9%)	41 (78.8%)	0.14
1	8 (38.1%)	11 (21.2%)	
Extranodal involvement			
Yes	8 (38.1%)	14 (26.9%)	0.35
No	13 (61.9%)	38 (73.1%)	
Previous RT			
Yes	3 (14.3%)	24 (47.1%)	0.006
No	18 (85.7%)	27 (52.9%)	
Stage at relapse			
I-II	19 (90.5%)	31 (59.6%)	0.006
III-IV	2 (9.5%)	21 (40.4%)	
IPS at relapse			
<2	13 (61.9%)	28 (53.8%)	0.53
≥2	8 (38.1%)	24 (46.2%)	
Remission duration after rist line therapy (median time)	2.7 months	0.0 months	0.09
Response to salvage chemotherapy (PET-CT)			
CR	5 (23.8%)	31 (59.6%)	0.007
PR	7 (33.4%)	13 (25.0%)	
SD	6 (28.5%)	2 (3.9%)	
PD	3 (14.3%)	6 (11.5%)	
Median Follow up (time from relapse)	47 months	48 months	0.74

PFS and OS in the overall population were respectively 61.4% and 68.1% at 5 years. At the univariate analysis, advanced stage at relapse (HR 2.65, p = 0.026), persistent disease prior to ASCT (HR 2.53, p = 0.05) and IPS score ≥2 (HR 2.49, p = 0.04) affected OS, while advanced stage at relapse (HR 2.77, p = 0.007) and persistent disease prior to ASCT (HR 2.85, p = 0.01) were related to worse PFS. The Cox regression confirmed persistent disease prior to ASCT (HR 3.65, p = 0.013) and stage III-IV at relapse (HR 3.65, p = 0.013) as associated to an increased risk of death. OS at 3 and 5 years was slightly better in patients receiving RT (86.5% and 78.7% respectively) compared to patients treated with CT alone (76.8% and 65.9%), even without reaching statistical significance (p = 0.42). A similar faint benefit was also observed in term of PFS (p = 0.39). We then performed a subgroup analysis in patients with progressive or relapsed stage I-II disease (N = 26) who failed induction CT prior to ASCT: 14 received IFRT (pre or post ASCT) and 12 CT alone. OS rates at 3 and 5 years were higher for the IFRT group (92.3% and 79.1% respectively) compared to CT alone group (61.9% and 51.6% respectively), even if this difference was not significant at the log-rank test (p = 0.13), probably due to the small numbers (Figure 1). Similarly, PFS was higher in patients receiving IFRT (69.6% vs 50% at 3 years), again without reaching a statistical significance (p = 0.22).

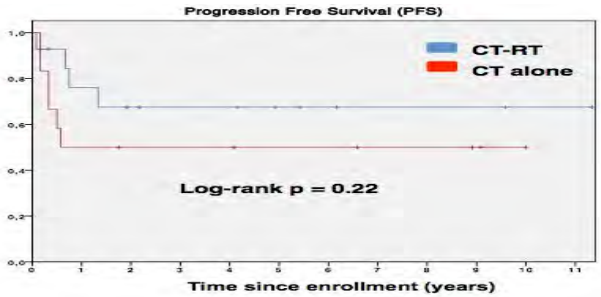

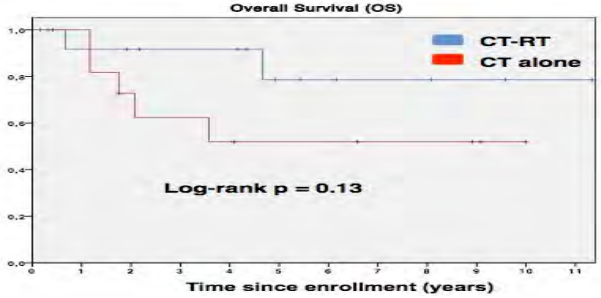

Conclusion: In our cohort, IFRT did not result to be associated to a PFS or OS benefit vs CT alone in the overall population. IFRT seemed to provide a survival benefit at 3 and 5 years compared to CT alone (92.3% vs 61.9% and 79.1% vs 51.6%) in patients with stage I-II disease at relapse and with persistent disease prior to ASCT. A larger sample size is needed to further explore the effect of IFRT in this particular setting.

PV-0280

Adjuvant radiotherapy in abdominal desmoplastic small round cell tumor: analysis of 107 patients

V. Atallah[1], C. Honoré[2], D. Orbach[3], S. Helfre[4], A. Ducassou[5], L. Thomas[1], M. Levitchi[6], A. Mervoyer[7], S. Naji[8], C. Dupin[9], G. Kantor[1], M. Sunyach[10], P. Sargos[1]

[1]*Institut Bergonié, Radiotherapy, Bordeaux Cedex, France*
[2]*Gustave Roussy Institute, Surgery, Paris, France*
[3]*Institut Curie, Pediatry, Paris, France*
[4]*Institut Curie, Radiotherapy, Paris, France*
[5]*Universitary Cancer Institute, Radiotherapy, Toulouse, France*
[6]*Alexis Vautrin Center, Radiotherapy, Nancy, France*
[7]*Institut De Cancerologie De L'ouest, Radiotherapy, Nantes, France*
[8]*Institut Paoli-Calmette, Radiotherapy, Marseille, France*
[9]*Universitary Hospital Bordeaux, Radiotherapy, Bordeaux, France*
[10]*Leon-Berard Center, Radiotherapy, Lyon, France*

Purpose or Objective: Desmoplastic small round cell tumor (DSRCT) is a rare peritoneal tumor affecting predominantly children and young adult Caucasian males with a high rate of local failure after surgery. We performed a multicentric retrospective study to identify the prognostic impact of adjuvant abdominal radiotherapy.

Material and Methods: All patients treated for primary abdominal DSRCT in 8 French centers from 1991 to 2014 were included. Patients were retrospectively staged into 3 groups: group A treated with adjuvant radiotherapy (RT) after cytoreductive surgery, group B without RT after cytoreductive surgery and group C by exclusive chemotherapy. Peritoneal progression-free survival (PPFS), progression-free survival (PFS) and overall survival (OS) were evaluated. We also performed a direct comparison between group A and B to evaluate RT after cytoreductive surgery. RT was also evaluated according to completeness of surgery: complete cytoreductive surgery (CCS) or incomplete cytoreductive surgery (ICS).

Results: Thirty-seven (35.9%), thirty-six (34.9%) and thirty (28.0%) patients were included in group A, B and C, respectively. Three-year OS was 61.2% (41.0-76.0), 37.6% (22.0-53.1), and 17.3% (6.3-32.8) for group A, B and C, respectively. OS, PPFS and PFS differed significantly between the 3 groups (p<0.001; p<0.001 and p<0.001, respectively). OS and PPFS were higher in group A (RT group) compared to group B (no RT group) (p=0.045 and p=0.006, respectively). Three-year PPFS was 23.8% (10.3-40.4) for group A and 12.51% (4.0-26.2) for group B. After CCS, RT improved PPFS (p=0.024) but differences in OS and PFS were not significant (p=0.40 and p=0.30, respectively). After ICS, RT improved OS (p=0.044). A trend of PPFS and PFS increase was observed but the difference was not statistically significant (p=0.073 and p=0.076).

Conclusion: Adjuvant radiotherapy as part of multimodal treatment seems to confer oncological benefits for patients treated for abdominal DSRCT after cytoreductive surgery and perioperative chemotherapy.This study is the largest series evaluating DSRCT treatment and the first of its kind comparing patients who received RT after cytoreductive surgery with patients who did not.

PV-0281

(ICORG 05-03): Radiotherapy in malignant spinal cord compression; The quality of life analysis

K. Lee[1], C. Small[2,3], P. Kelly[2,4], O. McArdle[1,2], J. O'Sullivan[2,5], D. Hacking[2,6], M. Pomeroy[2,3], M. Stevenson[2], J. Armstrong[1,2], M. Moriarty[1,2], M. Dunne[7], A. Clayton-Lea[2,8], I. Parker[2], C. Collins[9], P. Thirion[1,2]

[1]*St Luke's Radiation Oncology Network, Radiation Oncology, Dublin, Ireland Republic of*
[2]*All Ireland Cooperative Oncology Research Group, Radiation Oncology, Dublin, Ireland Republic of*
[3]*Galway University Hospital, Radiation Oncology, Galway, Ireland Republic of*
[4]*Cork University Hospital, Radiation Oncology, Cork, Ireland Republic of*
[5]*Belfast City Hospital, Radiation Oncology, Belfast, United Kingdom*
[6]*Whitfield Clinic, Radiation Oncology, Waterford, Ireland Republic of*
[7]*St Luke's Radiation Oncology Network, Clinical Trials, Dublin, Ireland Republic of*
[8]*St Luke's Radiation Oncology Network, Operational Services, Dublin, Ireland Republic of*
[9]*St Luke's Radiation Oncology Network, Radiology, Dublin, Ireland Republic of*

Purpose or Objective: To compare Quality of Life (QoL) outcomes in patients (pts) with Malignant Spinal Cord Compression (MSCC) not proceeding with surgical decompression and treated by External Beam Radiation Therapy (EBRT) with one of two Fractionation Schedules (FS).

Material and Methods: ICORG 05-03 was an ICH-GCP compliant prospective (1.1) randomised non-inferiority phase III trial comparing two FS: arm 1 (control): 20Gy/5 Fractions (#) vs. arm 2 (experimental): 10Gy/1#, with 80% power, 5% significant level and 0.4 non-inferiority margin. While the primary end point of this trial (previously presented (ASTRO 2014)) was change in mobility at 5 weeks (wks), the current focus is on a secondary endpoint, QoL (EORTC QLQ-C30 questionnaire).

Results: From 2006 to 2014, 5 institutions accrued 115 eligible pts (2 non-eligible pts, no treatment allocation violation). 70 pts with QoL data at 5 wks were evaluable. Baseline characteristics were balanced between arms [♀/♂: 30/40, median age: 69 (range: 30-87)]. Analysis showed a statistically significant benefit of radiotherapy (RT) for 'Pain interfered with daily activities' but not for Overall OoL. There was no statistically significant benefit between arms for either: 1. Overall QoL (mean change from pre-treatment .52 in arm 1 vs. .21 in arm 2; 95% CI: -0.84 – 1.45, p = 0.596); 2. Pain interfered with daily activities (mean change: .84 in arm 1 vs. 1.00 in arm 2; 95% CI: -0.66 – .98, p = 0.698). A non-planned exploratory regression analysis checked for independent prognostic factors for less pain at 5 wks. Multiple regression analysis revealed baseline pain as the strongest unique and statistically significant contributor to explaining less pain at 5-wks (beta = -0.63; p=0.002).
Exploratory analyses were also conducted to characterise pts dying at <5 wks,who might not benefit from RT. Primary malignancy (Chi-square test: X2 (3, n=106) = 15.6, p = 0.001, phi = 0.38) and initial mobility status (Chi-square test, X2 (2, n=106) = 11.0, p = 0.004, phi = 0.32.) were found to be associated with a life expectancy <5 wks. 67% of lung and 13% of breast cancer pts died before 5 wks, as did 49% of bed-bound and 15% of pts who could walk unaided.

Conclusion: With respect to QoL, primary RT significantly improves the pain related variables used in the trial, with 10Gy/1# FS being at least equivalent to 20Gy/5#. Baseline pain is the most significant independent prognostic factor for less pain at 5 wks. Tumour site and mobility should be considered when offering RT treatment to similar pts.

Proffered Papers: Donal Hollywood Award

OC-0282

FLAME randomised trial: 95Gy MRI-boost vs 77Gy prostate radiotherapy: toxicity and quality of life

M. Van Vulpen[1], J. Van Loon[1], F. Pos[2], K. Haustermans[3], R. Smeenk[4], L. Van den Bergh[3], S. Isebaert[3], G. McColl[4], M. Kunze-Busch[4], B. Doodeman[2], J. Noteboom[1], E. Monninkhof[5], U. Van der Heide[2]

[1]*UMC Utrecht, Radiation Oncology, Utrecht, The Netherlands*
[2]*AvL/NKI, Radiation Oncology, Amsterdam, The Netherlands*
[3]*UZ Leuven, Radiation Oncology, Leuven, Belgium*
[4]*Radboud UMC, Radiation Oncology, Nijmegen, The Netherlands*
[5]*UMC Utrecht, Julius Center for methodology, Utrecht, The Netherlands*

Purpose or Objective: The aim of this study was to compare treatment related side-effects and quality of life of an MRI-based 95Gy boost to the multi-parametric MRI visible tumor with 77Gy whole prostate external beam radiotherapy in patients with intermediate or high risk localized prostate cancer.

Material and Methods: FLAME (NCT01168479) was a phase 3, single blind, multi-center randomized controlled trial. Patients with biopsy proven intermediate and high risk prostate cancer (D'Amico risk classification) were randomly assigned and stratified per center. Analysis was done by intention to treat. The control group received a dose to the entire prostate of 77Gy in 35 fractions. The experimental arm received an additional integrated boost up to 95 Gy to the mp-MRI-visible lesions. Treatment related toxicity was measured by the Common Toxicity Criteria for adverse events version 3.0 (CTCAE). Quality of Life (QoL) was measured by SF-36, EORTC QLQ-C30 and EORTC QLQ-PR25. All items and scale scores were linearly transformed to a 0–100 scale, with higher scores reflecting either more symptoms or higher levels of functioning. Clinical relevance was considered a difference of more than 10 points between arms. Mean differences between groups were calculated using a linear mixed model with adjustment for baseline values. Statistical significance was considered P<0.01.

Results: Between 2009 and 2015 287 patients were assigned to the control group and 284 to the dose-escalated (FLAME) arm. Mean follow up was 22 months. In both arms, 84% of patients had high risk disease. Regarding GU toxicity, 134 patients (47.2%) in the FLAME arm and 147 patients (51.4%) in de control arm experienced any grade 2 or higher toxicity. Grade 3 GU toxicity occurred in 15 patients (5.3%) in the FLAME arm and 12 patients (4.2%) in the control arm. Regarding GI toxicity, 60 patients (21.1%) in the FLAME arm and 47 patients (16.4%) in the control arm experienced grade 2 or higher toxicity. Grade 3 toxicity occurred in 2 patients (0.7%) in the FLAME arm and in 5 patients (1.7%) in the control arm. None of these differences were statistically significant. For all quality of life measures no statistically significant or clinical relevant differences were observed.

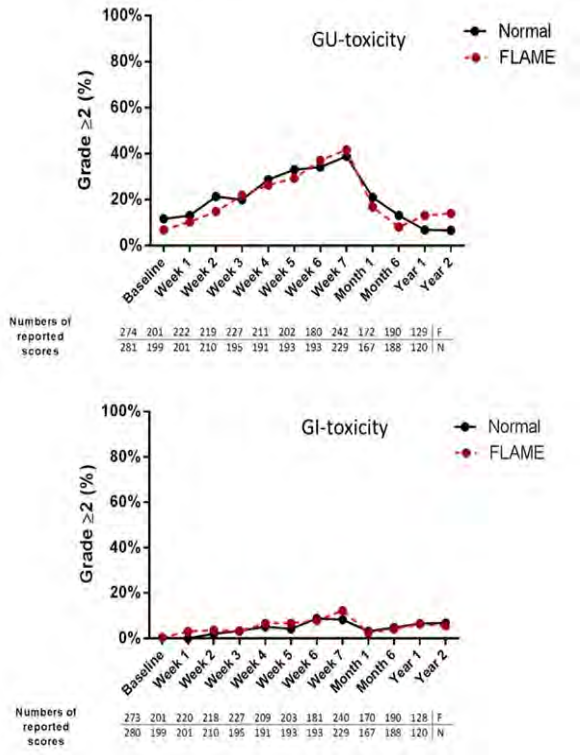

Conclusion: Up to a median follow-up of 22 months no differences in toxicity and quality of life were observed between the FLAME arm and the standard arm. Therefore, dose escalated 95Gy MRI-based lesion boost in prostate cancer external beam radiotherapy seems safe.

Proffered Papers: Highlights of Proffered Papers

OC-0283

Dose escalation with contact x-ray brachytherapy to improve organ preservation in rectal cancer

A. Sun Myint[1], F. Smith[2], K. Whitmarsh[1]
[1]*The Clatterbridge Cancer Centre - Wirral NHS Foundation Trust, Papillon Suite, Bebington- Wirral, United Kingdom*
[2]*The Royal Liverpool & Broadgreen University Hospital, Colorectal Surgery, Liverpool, United Kingdom*

Purpose or Objective: 'Watch and Wait' policy for complete clinical responders (cCR) following CRT is gaining acceptance as this avoids extirpative surgery and a stoma. However, up to 30% required major surgery for recurrences and organ preservation achieved reduced to 40% for the whole group. We report our experience with dose escalation using Contact X-ray brachytherapy [Papillon] (CXB) boost which reduce recurrences and improve the chance of organ preservation.

Material and Methods: We review 573 patients with rectal cancer treated at Clatterbridge Cancer centre from 2003 - 2012 and report on 200 patients treated radically to cure by non-surgical approach. There were 134(67%) males with median age 74 years (range 32-94). Histological diagnosis confirmed in all patients. Staging include CT in all and MRI except in 30(15%) with pace maker. Radiological stages were 21(10.5%) T1, 89(44.5%) T2, 87(43.5%) T3 and 3(1.5%) T4. EBCRT with 45 Gy /25#/35 days and capecitabine 825 mg/m 2 or 5 FU infusion 1G /m 2 X 4 days week 1+5 was given to 127 (63%)patients, except EBRT alone in unfit 57(28%) who had 25 Gy/5#/5 days. Papillon boost of 80-110 Gy in 3-4 fraction was given to 92% of patients who had EBCRT or EBRT. Papillon alone (80-110 Gy /3-4 #/ 6 weeks) was used in 16 (8%) of elderly patients with mainly cT1 cancers.

Results: Initial complete clinical response [cCR] (no residual tumor visible, palpable or on radiology) was achieved in 136(68%) and residual abnormality either clinical or radiological were seen in 64(32%). Immediate salvage surgery was carried out in 38(60%) patients with progressive residual disease who were fit. Eight (21%) had no pathological residual disease (ypT0). Surgery was withheld in further 8 (4%) out of 64 without progression of residual abnormality. Those with cCR 116(85%) maintained complete response. Sixteen (11.7%) developed local relapse after cCR. Early staged tumors respond better with less local and total relapse. At median follow up of 2.49 months following completion of treatment; complete remission was achieved in 160 (80%) patients , 12(6%) had asymptomatic static disease and 28 (14%) had progressive residual disease but not fit for salvage surgery due to age or medical co-morbidity. The main toxicity was bleeding occurring in 30% of cases and 10% needed argon beam. Organ preservation for the whole group was achieved in 158 (79%). Overall Survival (94% vs. 76%) [p=0.02] was better for responders (cCR +SD) at 2 years.

Conclusion: CXB (Papillon) boost reduced local recurrence to 11.7% after achieving cCR compared to 30-40% in those who had EBCRT alone. Organ preservation of 79% for the whole group is much higher than any 'watch and wait' studies with 40% published so far. A randomised trial OPERA has been set up to evaluate this further. Papillon has acceptable toxicity and is now recommended by NICE for patients not suitable for surgery. Papillon should be consider as a treatment option for elderly patients with early rectal cancer.

OC-0284

PD-L1 inhibition improves response of pancreatic cancer to radiotherapy

A. Azad[1], Z. D'Costa[1], S.Y. Lim[1], O. Sansom[2], W.G. McKenna[1], R. Muschel[1], E. Fokas[1]
[1]*CRUK/MRC Institute for Radiation Oncology University of Oxford, Department of Oncology, Oxford, United Kingdom*
[2]*Cancer Research UK Beatson Institute-, Glasgow- Institute of Cancer Sciences- University of Glasgow, Glasgow, United Kingdom*

Purpose or Objective: The programmed death ligand 1 (PD-L1) plays a key role in tumour progression and metastasis of pancreatic ductal adenocarcinoma (PDAC). Although recent preclinical studies have explored the radiosensitising potential of PD-1/PD-L1 inhibitors, the effect of PD-L1 blockade on the response of PDAC to radiotherapy remains unexplored.

Material and Methods: Herein, we investigated the influence of an anti-PD-L1 mAb on the tumour response to single dose and fractionated radiotherapy, and chemotherapy with gemcitabine and capecitabine.

Results: In-vitro, radiation and chemotherapy resulted in PD-L1 upregulation in both human (PSN-1) and murine (KPC-derived, Pan02) PDAC cells, although variability was observed. Exposure to conditioned media from pre-treated cells did not alter PD-L1 expression. In-vivo, PD-L1 was also upregulated in the tumour microenvironment after radiation and chemotherapy in the KPC-derived and Pan02 syngeneic mouse models. Similarly, chemotherapy induced PD-L1 upregulation in the KPC (Pdx1Cre, KRASG12D/+, P53R172H/+), a genetically-engineered mouse model of pancreatic cancer. In-vitro, PD-L1 blockade failed to radio- or chemosensitise PDAC cells. The anti-PD-L1 mAb significantly improved tumour response after irradiation in the KPC and Pan02 syngeneic mouse models. This effect was mediated by a cytotoxic T cell-dependent mechanism, whereas blockade of CD8+ cells attenuated the radiosensitising potential of anti-PD-L1. The effect of scheduling of anti-PD-L1 mAb with radiotherapy (concomitant vs sequential) was also investigated. Finally, we assessed the intratumoural and systemic expression of several immune markers (CD45+: CD8, CD4, CD19, NK1.1, CD11b Gr1, Ly6G, CXCR2, FOXP3, IFN-γ) after the different treatments.

Conclusion: Altogether, our findings support PD-L1 inhibition in combination with radiation as a promising approach in the treatment of PDAC.

OC-0285

Experimental benchmarking of a probe-format calorimeter for use as an absolute clinical dosimeter

J. Renaud[1], A. Sarfehnia[1], J. Seuntjens[1]
[1]*McGill University, Medical Physics Unit, Montreal, Canada*

Purpose or Objective: In this work, the design, fabrication, and operation of a small-scale graphite calorimeter probe (GPC) developed for use as a practical clinical dosimeter, is described. Similar in size and shape to a Farmer-type cylindrical ionization chamber, the GPC represents the first translation of calorimetry from the primary standards dosimetry laboratory to the radiotherapy clinic. Providing a measure of absolute dose, its purpose is to help meet the clinical need for accurate reference dosimetry in non-standard fields without the need for calibration.

Material and Methods: Based on a numerically-optimized design obtained in previous work, a functioning prototype capable of two independent modes of operation (constant-power & constant-temperature) was constructed in-house. In constant-power mode, the radiation-induced temperature rise, ΔT, is measured in the sensitive volume (*i.e.* the core) while the outermost portion of the device is thermally stabilized by a software-based temperature controller. In constant-temperature mode, the entire device is subject to active thermal control and the quantity of interest is the electrical power, ΔP, necessary to maintain a stable temperature while irradiated.
Absorbed dose to water measurements were performed in a water phantom, under standard conditions, using both GPC operation modes in a 6 MV photon beam and subsequently compared to dose to water measurements derived using a reference-class ionization chamber (Exradin A12). Linearity, dose rate, and field size dependence were evaluated by varying the irradiation period, the linac repetition rate, and primary collimating jaw settings, respectively.

Results: Compared to the chamber-derived dose to water of 0.765 cGy/MU, the average GPC-measured doses were 0.765 ± 0.005 (n = 25) and 0.769 ± 0.005 (n = 32) cGy/MU for the constant-power and constant-temperature modes, respectively.
The linearity of the detector response was characterized by an adjusted R^2 value of 0.9996 (n = 40), and no statistically-significant dose rate dependence for rates greater than 1.8 Gy/min was observed. For lower dose rates, an over response of 1.7 % was attributed to the resolution of the current-driven temperature controller. No field size dependence was observed down to 2 x 2 cm^2.

Table I. Estimated uncertainty budget for the GPC's constant-power and constant-temperature modes of operation in high-energy photon absolute dose to water measurements.

Quantity	Constant-power mode		Constant-temperature mode	
	Type A (%)	Type B (%)	Type A (%)	Type B (%)
Heat transfer	--	0.3	--	0.1
Reproducibility	0.6	--	0.6	--
Bridge calibration	--	0.1	--	--
Thermistor calibration	--	0.2	--	--
Electrical power	--	--	--	0.2
Specific heat capacity	--	0.8	--	--
Mass	--	--	--	0.5
Positioning	0.2	--	0.2	--
Perturbation-dose conversion	--	0.4	--	0.4
Other not considered	--	0.3	--	0.3
Quadratic summation	0.6	1.0	0.6	0.7
Combined uncertainty	1.2		1.0	

Conclusion: This work demonstrates the feasibility of using an ion chamber-sized calorimeter as a practical means of measuring absolute dose to water in the radiotherapy clinic. The potential introduction of calorimetry into the clinical setting is significant as this fundamental technique has formed the basis of absorbed dose standards in many countries for decades. Considered as the most direct means of measuring dose, a "calorimeter for the people" could play an important role in solving the major challenges of contemporary dosimetry. In particular, investigations into the use of the GPC for MR-linac dosimetry are currently underway.

OC-0286

From pixel to print: clinical implementation of 3D-printing in electron beam therapy for skin cancer

R. Canters[1], I. Lips[1], M. Van Zeeland[1], M. Kusters[1], M. Wendling[1], R. Gerritsen[2], P. Poortmans[1], C. Verhoef[1]
[1]*Radboud University Medical Center, Radiation oncology, Nijmegen, The Netherlands*
[2]*Radboud University Medical Center, Dermatology, Nijmegen, The Netherlands*

Purpose or Objective: Build-up material is commonly used in electron beam radiation therapy to overcome the skin sparing effect and to homogenise the dose distribution in case of irregular skin surfaces. Often, an individualised bolus is necessary. This process is complex and highly labour-intensive, while adaptation of the bolus is time consuming. We implemented a new clinical workflow in which the bolus is designed on the CT scan in the treatment planning system (TPS). Subsequently a cast with the bolus shape is 3D-printed and filled with silicone rubber to create the bolus itself [1].

Material and Methods: In the new workflow (figure 1), a patient-specific bolus is designed in the TPS. A 2 mm expansion is used to create a cast around the bolus. Subsequently, this cast is smoothed to remove CT scan resolution effects. After conversion to a stereolithography file, the cast is printed in polylactic acid (PLA) with a filament printer and filled with silicone rubber. After removal of the PLA cast, the bolus is ready for clinical use.
Before clinical implementation we performed a planning study with 11 patients to evaluate the difference in tumour coverage with a 3D-print bolus in comparison to the clinically delivered plan with a manually created bolus.
During clinical implementation of the 3D-print workflow, for 7 patients a second CT-scan with the 3D-print bolus in position was made to assess its geometrical accuracy and the resulting dose distribution.

Results: The planning study showed at least equal coverage of GTV and CTV: V95% of the GTV was on average 97% (3D-print) vs 84% (conventional). V85% of the CTV was on average 97% (3D-print) vs 88% (conventional).
Geometric comparison of the 3D-print bolus to the originally contoured bolus showed a high similarity (mean dice similarity coefficient of 0.87 (range 0.81 to 0.95).
Comparison of the dose distributions at the planning CT scan to dose distributions at the second CT scan with the 3D print bolus in position showed only small differences (median difference in V95% GTV and V85% CTV of 0% (interquartile range: -12% to 0%) and -1.6% (interquartile range: -3.8 to 0.5%), respectively).
Time efficiency of the 3D-print workflow is likely to increase in comparison to the conventional workflow, with one less patient visit, and up to 3 hours less mould room time.

Conclusion: The implemented workflow is feasible, patient friendly, safe, and results in high quality dose distributions. This new technique increases time efficiency and logistically aligns electron with photon external beam treatments.

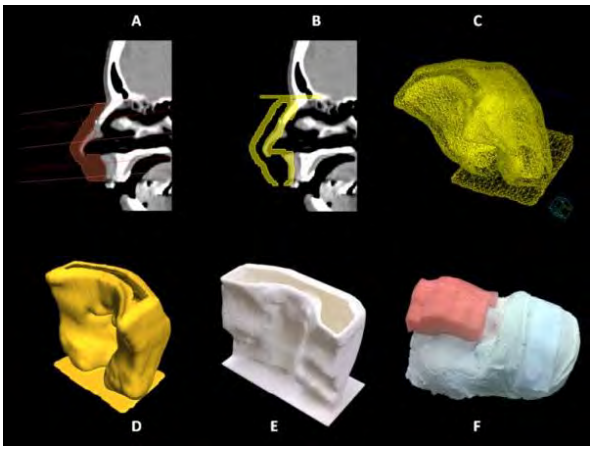

Figure 1: Illustration of the clinically implemented 3D-print workflow with designed bolus(A) and cast around the bolus(B) at the planning CT scan, smoothed cast (C), 3D model of the cast (D), printed cast (E) and silicone rubber final bolus (F).
1. Holtzer, N.A., et al., 3D printing of tissue equivalent boluses and molds for external beam radiotherapy, Estro 33. 2014: Vienna.

Symposium: Planning ahead: how to finish your residency / PhD project with a job offer

SP-0287
How to finish your residency / PhD project with a job offer as a radiation oncologist

S. Rivera[1]
[1]*Institut Gustave Roussy, Villejuif, France*

Radiation oncology is a rapidly evolving profession requiring continuous learning on the top of all routine activities. Residency is a unique period in a professional life where the main objective is to learn. Residency is full of research and educational opportunities for young radiation oncologists to gain know-how and expertise in clinical practice, patient care, fundamental, translational and/or clinical research and innovative technologies in the various aspects of our specialty. Through local, national and international programs, trainees gain valuable clinical and research experience and skills during and rapidly get the opportunity to disseminate information and update colleagues in their home institution. Playing a **proactive role in the training** will not only give access to the best training opportunities but will motivate as well supervisors in supporting trainee's career development.
In a competitive world with limited resources, building up good **curriculum vitae** with a number of **publications and presentations** is a major advantage that should be considered and kept in mind early and during the whole residency. This will not only be of value when applying for a job but will open a number of collaborations as well introducing the trainee in a virtuous circle which will tremendously facilitate future projects, recognition, satisfaction and professional pleasure.
International exchanges and mobility are of utmost importance. From personal initiatives directly contacting a department head abroad via email or at a meeting to local/national or scientific societies programs there are many opportunities to gain such an enriching experience. ESTRO for instance supports short terms (few weeks) educational visits called **mobility grants** twice a year which allow for learning a specific technique in the context of a project propose by the candidate through a motivation letter which can be an excellent way to get some connections to look for longer term mobility. Entering a **PhD** program is another excellent opportunity to access the kind of international exchange and mobility that together with the scientific production and publication resulting from it will serve a career when looking for a position in a high level academic center. Indeed, having an international professional experience and a strong scientific background will be highly considered when applying for a job offer in a university hospital or a cancer center. This will even be almost mandatory when aiming at a research/teaching position.
Mentorship can be very helpful throughout a career. Benefiting from privileged dialogue, support and guidance from a more experienced person in the field considered as a mentor can enhance the effectiveness of any talent, help avoiding painful mistakes and optimizing choices that will have a major career impact and sometimes even an impact on the balance between professional and personal life which is often a fragile point in a demanding profession. Many countries across Europe are lacking of mentorship programs but in many institutions even without a dedicated program various types of mentoring are in place. Most of more experienced people are happy to share their experience and give some advices so one should not hesitate to ask for this helpful interaction. With or without a mentor here are key questions that are essential to guide one's choices:
Who am I?
Where do I want to go?
What type of professional activity will I enjoy?
Which life will make me happy?
To conclude, the best advice would be to always wonder **how to get the most out of one's training period**. In that aspect, ESTRO offers young professionals in the field of radiation oncology a wealth of opportunities from networking, grants, educational courses, fellowships, mentorships and workshops aiming at refining skills and gaining access to the latest developments in the field that will be of value finishing your residency not only with a job offer but with the job you want.

SP-0288
How to finish your residency / PhD project with a job offer as a radiobiologist

M.C. Vozenin[1]
[1]*Centre Hospitalier Universitaire Vaudois, Department of Radiation Oncology, Lausanne Vaud, Switzerland*

PhD training/residency is a long-term and enriching experience, it requires time and commitment for scientific achievement; in addition, the future of a young scientist needs to be planed ahead. Therefore, having a clear view of your carreer's perspectives at least 18 months before your defense is the way to professional success. Early during your training discuss your career aspirations and important issues in your professional development with your mentor, he/she will be able to provide you with career information and guidance. But ultimately you will be the one to define if you are seeking for an academic career, job in the industry or other professional options. In any case your mentor will introduce you to colleagues, potential employers, and other professionals who might help to advance your career. You also need to be highly proactive and present your research and creative work as often as possible in multiple forums

including your department/university but also at professional conferences/meeting. You will need to apply for fellowships, awards, teaching opportunities and service committees in the scientific community. The aim is to create a strong network that will serve as the base for your job research and will provide you with multiple opportunities.

SP-0289
How to finish your residency / PhD project with a job offer as a physicist
D. Verellen[1]
[1]*Universitair Ziekenhuis, Radiotherapy, Brussels, Belgium*

SP-0290
How to finish your residency / PhD project with a job offer as a researcher
U. Oelfke[1]
[1]*Institute of Cancer Research, Department of Radiation Oncology, United Kingdom*

Symposium with Proffered Papers: Standardisation in clinical practice

SP-0291
Guideline-based contouring and clinical audit systems
C. Weltens[1]
[1]*University Hospital Leuven- KU Leuven, Radiotherapy-Oncology, Leuven, Belgium*

Modern radiotherapy techniques focus on the precise irradiation of the target volume while minimizing the dose to adjacent normal tissues. Technical advances at all levels of the complex radiotherapy preparation and delivery process allowed reductions of safety margins and conformation of the high dose volume to the target volume. The introduction of these technical innovations has been supported by extended quality assurance procedures. A small part of the radiotherapy preparation process however has for a long time remained unaddressed: the quality of the target delineation is still a weak link in the radiotherapy chain.Accurate, unambiguous and precise target delineation is mandatory in high conformal radiotherapy, since the treatment plan and subsequently treatment delivery are based on the delineated target volumes. Errors in target delineation will on the one hand lead to systematic errors in treatment delivery and possibly to geographical misses in clinical practice. The projected outcome will be undermined both with respect to the chances of tumor control and the risks of side effects. On the other hand, inconsistencies in target volume contouring comprise the validity of the results of clinical trials.To improve the quality of the delineations, guidelines were made for nearly all tumor sites as well as for the normal tissues. Notwithstanding these published guidelines, important inter- and intra-observer variation in target delineation have been demonstrated. Several solutions have been proposed to improve the quality of target delineation: (1) for nearly all tumor sites delineation guidelines with complementary atlases have been published, (2) the registration of CT scans in treatment position with a combination of different imaging modalities has been tested and introduced, (3) automated and semi-automated delineation software has been developed, and (4) education through hands-on workshops at radiotherapy meetings and online tutoring sessions (e.g. FALCON) is available.Studies also show that peer review can improve delineation quality. The quality of target delineation was measured in Belgium through clinical audits for rectal and breast cancer patients. We have evaluated the role of a central review platform in improving uniformity of clinical target volume delineations within a national Belgian project. All 25 Belgian radiation oncology departments were invited to participate in this QA project. CTV delineation guidelines and atlases were discussed and distributed at a national meeting. After this education of the radiation oncologists, a review process was set up. Departments were asked to delineate the clinical target volumes and to upload it to a secured server. For rectal cancer, the clinical target volume was delineated and for breast cancer, the regional nodal areas (internal mammary, level I to IV axillary and Rotter space) were contoured. A trained radiation technologist then reviewed all cases according to the guidelines and feedback was given within 24 hours. Twenty-four departments participated to the study and in total more than 2200 contours were reviewed: over 1200 rectal cancer patients and over 1000 breast cancer patients.Evaluation of the contours showed that 74 % of rectal cancer cases were modified. These high numbers indicate that the interpretation of guidelines is not always straightforward. More important however is the learning curve that was achieved. The rectal overlap and volumetric parameters significantly increased between the first ten patients per center and others. The study of the contouring of the locoregional nodal delineation in breast cancer is still ongoing and first results will be presented at presented at the ESTRO 35. For both breast and rectal cancer, some deficiencies in the description of the guidelines were demonstrated, making the interpretation ambiguous, and the guidelines will be adapted accordingly. Within a national QA project, we have shown that clinical audit of target delineation improves the quality of the contouring: the inter-observer variability and the major deviations from the guidelines are substantially reduced. Variability in anatomical contouring contributes to uncertainty in treatment planning and compromises the quality of the treatment plan and delivered treatment. The standardization of tumor and target volume contouring is therefore highly desirable and can be positively influenced by consensus guidelines, education and clinical audits.

SP-0292
Standardisation and treatment planning
B. Heijmen[1], A. Henry[2], S. Breedveld[1]
[1]*Erasmus MC Cancer Institute, Radiation Oncology, Rotterdam, The Netherlands*
[2]*St James's Institute of Oncology- St James's Hospital, Radiation Oncology, Leeds, United Kingdom*

Current plan generation is an iterative trial-and-error procedure in which the planner tries to steer the treatment planning system (TPS) towards an acceptable plan by tweaking of parameters, such as beam angles, goal functions or weights. A plan is generally considered acceptable if it fulfills minimum requirements for tumour and OARs, while significant further improvement of the dose distribution is considered infeasible (within the allotted time). On top of the high workload, the current planning approach leads to suboptimal plan quality: the quality is strongly dependent on the skills and experience of the planner (operator dependence), plan quality is dependent on allotted time, and quality is dependent on subjective preferences and priorities of the planner and the treating physician. Can this variability be reduced? Can treatment planning be standardised? Can we guarantee that each patient will be treated with an individualised, clinically highly favourable (best) treatment plan when generated in an efficient manner? In this presentation, data will be provided demonstrating difficulties that clinicians encounter in evaluating treatment plans. Furthermore, the concept of automated treatment plan generation will be discussed as a procedure that may be used to standardise treatment planning. Examples of the positive impact on plan quality will be presented and consequences for involved personnel and plan quality assurance will be discussed.

SP-0293
Potentials and challenges of automated contouring in treatment planning
S. Pallotta[1]
[1]*University of Florence, Department of Medical Physics, Florence, Italy*

Delineation of targets and normal tissues, typically performed on CT and/or MR images, is still one of the largest sources of variability in radiation therapy treatment plans. In fact, despite well-described guidelines for manual

contouring, substantial intra and inter-observer variations exist. Moreover manual contouring is a time consuming process that, depending on the number and complexity of contours to be delineated, can hinder the implementation of adaptive radiotherapy approach. Current perspectives on contouring procedure suggest that an automated approach could reduce both the contouring time and inter-observer variations. Studies evaluating automated contouring in multiple disease sites have in fact demonstrated the potential to improve efficiency and variability associated with manual segmentation. In practice, automated contour are carried out using atlas-based, model-based or hybrid approaches. In atlas-based segmentation the CT scan of a new patient is segmented using segmented scans of one (single-patient) or more (multi-patient) previously treated patients, called atlases. Methods based on classical deformable models use local image features and automatically adapts the model shape to fit patient's organ. Various implementations of these two principal methods are described in the literature and are available in commercial contouring software. Prior their clinical use automated contouring methods need an accurate validation. This is a challenging task as medical image segmentation lacks a known gold standard in its real world application. Phantoms as well as synthetic images provide an easily identifiable ground truth but are an unrealistic surrogate for patient imaging. Moreover, evaluation methods have also lacked consensus as to comparison metrics. A number of different methods have been utilized for comparing segmentation results. The common metrics used fall into one of two categories: volume based or distance based. Each of the comparison metrics has limitations and thus it is desirable to use multiple metrics where possible. This presentation will discuss the advantage in standardization deriving from the use of automatic contouring and the different approach followed in the implementation and validation of automated segmentation tools in different anatomical districts.

SP-0294

Implementation of new standards in your department: a RTT perspective

A. Baker[1], Y. Tsang[1]
[1]*Mount Vernon Cancer Centre, Deaprtment of Radiotherapy, Middlesex, United Kingdom*

Standardisation of clinical practice is essential for the delivery of safe, accurate radiotherapy treatments. Implementation of new standards can be at both local and national levels and examples of these approaches, from an RTT perspective, will be discussed. New standards should be developed and implemented within a multi-professional team setting. Each profession has a role to play and bring different perspectives to the development and implementation process.

Development of training and competency assessments for the use of new delivery techniques are an essential aspect of implementing any new standards. These assessments can be established locally using national guidelines. For example the UK National Radiotherapy Implementation Group IGRT recommendations1 which was written by a multi-profession team to assist centres in utilising IGRT equipment and details content for IGRT training and competency assessment programmes. This recommendation document has been instrumental in the UK with ensure appropriate utilisation of IGRT for each anatomical site and ensuring quality IGRT is delivered to patients. RTTs are also involved in the preparation of national SABR guidelines, as part of the UK SABR consortium, particularly focusing on the treatment delivery and IGRT sections.

Clinical trials provide a controlled environment where new standards can be developed in a quality assured way. A UK prostate radiotherapy clinical trial utilised both IMRT and IGRT within the context of a study evaluating a number of fractionation schedules. This assisted the centres involved to develop IMRT and IGRT standards within their departments within a quality assured clinical trial. RTTs were able to use IGRT processes clearly defined within the protocol and the support of the QA team for the trial were available for advice and support. This same method is currently being adopted in the UK for a number of adaptive radiotherapy trials and this will assist in establishing new evidence for adaptive radiotherapy and the community will be prepared for routine implementation if the results favour an adaptive approach.

It is important to consider the role of QA together with audit programmes both during the implementation phase and also on a routine basis following the implementation of the new evidence based standards. RTTs are a key component of this process within the multi-professional team.

Conclusion

Utilisation of national recommendations or clinical trial processes ensure that new standards are developed and implemented safely and accurately. There is sometimes a tendency to slowly adopt new technologies and evidenced based practice into routine practice but by having national protocols, quality assurance and multi-centre clinical trials, new standards can be implemented timely, appropriately and safely.

References

1National Radiotherapy Implementation Group Report. Image Guided Radiotherapy. Guidelines for Implementation and use. http://webarchive.nationalarchives.gov.uk/20130513211237/http://ncat.nhs.uk/sites/default/files/work-docs/National%20Radiotherapy%20Implementation%20Group%20Report%20IGRTAugust%202012l.pdf

OC-0295

Improvement of delineation quality of organs at risk in head and neck using the consensus guidelines

R. Steenbakkers[1], C. Brouwer[1], J. Bourhis[2], W. Budach[3], C. Grau[4], V. Grégoire[5], M. Van Herk[6], A. Lee[7], P. Maingon[8], C. Nutting[9], B. O'Sullivan[10], S. Porceddu[11], D. Rosenthal[12], N. Sijtsema[1], J. Langendijk[1]
[1]*University Medical Center Groningen, Radiation Oncology, Groningen, The Netherlands*
[2]*Hospitalier Universitaire Vaudois, Radiation Oncology, Laussane, Switzerland*
[3]*University Hospital Düsseldorf, Radiation Oncology, Düsseldorf, Germany*
[4]*Aarhus University Hospital, Oncology, Aarhus, Denmark*
[5]*Cliniques Universitaires St-Luc, Radiation Oncology, Brussels, Belgium*
[6]*University of Manchester, Centre for Radiotherapy Related Research, Manchester, United Kingdom*
[7]*The University of Hong Kong Shenzhen Hospital, Clinical Oncology, Hong Kong Shenzhen, China*
[8]*Centre Georges-François Leclerc, Radiation Oncology, Dijon, France*
[9]*Royal Marsden Hospital and Institute of Cancer Research, Radiation Oncology, London, United Kingdom*
[10]*Princess Margaret Hospital, Radiation Oncology, Toronto, Canada*
[11]*Princess Alexandra Hospital, Cancer Services, Brisbane, Australia*
[12]*University of Texas M. D. Anderson Cancer Center, Radiation Oncology, Houston TX, USA*

Purpose or Objective: Very recently, the DAHANCA, EORTC, GORTEC, HKNPCSG, NCIC CTG, NCRI, NRG Oncology and TROG consensus guidelines for delineating organs at risk (OARs) in the head and neck region have been published (1). The purpose of this study was to investigate whether these international consensus guidelines improved delineation quality among observers.

Material and Methods: Ten radiation oncologists, considered experts in the field, were asked to delineate 20 different OARs on CT images (2 mm slice thickness) in two delineation sessions. The first session was performed in 2013 without the use of any predefined guidelines. The second session was performed in 2015 just after publication of the consensus guidelines. The observer variation was measured in 3D by measuring the distance between the median delineated OAR and each individual delineated OAR (2). The variation in distance of each OAR was expressed as a standard deviation (SD). Furthermore, to assess the overlap between observers the concordance index (CI) was calculated. The CI has values

ranging from 0 for no overlap to 1 for perfect agreement between all observers (3).

Results: Seven observers delineated most of the contours in the first and second session. Five observers delineated 14 OARs in both delineation sessions. For fair comparison between first and second delineation session, observer variability was only calculated among the five observers who delineated all 14 OARs in both sessions. The average 3D variation in distance for the first and second session was 3.0 mm and 2.1 mm (1 SD), respectively (Table 1).

Table 1. The observer variation for delineation session 1 (without consensus guidelines) and delineation session 2 (with delineation guidelines) expressed in 3-D variation in distance and conformity index for 14 OARs.

OAR	3-D variation (mm) (1 SD)			Conformity index (CI)		
	Without guidelines (Session 1)	With guidelines (Session 2)	Difference	Without guidelines (Session 1)	With guidelines (Session 2)	Difference
Anterior part Eye L	3.5	1.3	2.2	0.06	0.17	0.11
Anterior part Eye R	3.2	1.2	2.0	0.08	0.16	0.08
Posterior part Eye L	2.4	1.4	1.0	0.26	0.52	0.26
Posterior part EyeR	2.5	1.4	1.1	0.26	0.55	0.29
Parotid gland L	2.2	1.4	0.8	0.47	0.57	0.10
Parotid gland R	2.0	1.5	0.5	0.45	0.48	0.03
Submand. gland L	3.5	4.5	-1.0	0.32	0.27	-0.05
Submand. gland R	3.2	3.5	-0.3	0.41	0.36	-0.05
Oral Cavity	5.8	2.1	3.7	0.36	0.67	0.31
Mandible	1.7	1.2	0.5	0.55	0.67	0.12
Pharyngeal constrictor muscles	6.7	4.2	2.5	0.05	0.09	0.04
Thyroid gland	1.6	1.3	0.3	0.58	0.62	0.04
Pituitary	1.9	1.6	0.3	0.17	0.42	0.25
Chiasm	2.1	2.3	-0.2	0.10	0.01	-0.09
Mean	3.0	2.1	1.0	0.29	0.40	0.10

Out of 14 OARs, 11 OARs showed reduced 3D variation (reduction range 0.3-3.7 mm) using the consensus guidelines. The largest reduction of 3.7 mm was seen for the oral cavity, from 5.8 mm to 2.1 mm (Figure 1).

Figure 1. Contours delineated on CT (left) and the 3-D variation (right) of the oral cavity without and with consensus guidelines.

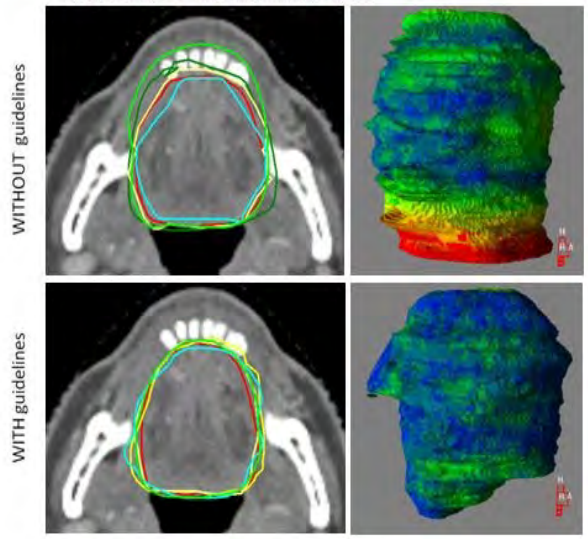

For 3 OARs (i.e. both submandibular glands and the chiasm) the 3D variation was larger using the guidelines (range 0.2-1.0 mm). For the first and second session, the average CI was 0.29 and 0.40, respectively (Table 1). For 11 OARs an improvement of the CI was seen (improvement range 0.03 – 0.31). The largest improvement was again seen for the oral cavity from 0.36 to 0.67. For 3 OARs the CI became worse. For the submandibular glands the differences were however small; 0.05.

Conclusion: The use of the consensus guidelines for head and neck OARs reduced observer variation for most OARs investigated. This stresses the importance to use uniform internationally accepted guidelines in daily clinical practice, to support consistent reporting of dose-volume data and NTCP-models. However, further improvement of delineation quality can be achieved by training and education, and a more consistent use of these guidelines. References: 1. Brouwer et al., Radiother Oncol 2015 aug 13 (ahead of print). 2. Steenbakkers et al., Int J Radiat Oncol Biol Phys. 2006;64:435-48. 3. Hanna GG et al., Clin Oncol. 2010;22:515-525.

Symposium: DNA repair inhibition and radiotherapy: moving towards clinic

SP-0296
Challenges in combining radiation and chemo-radiation with PARP inhibitors

J. Schellens[1]
[1]*Netherlands Cancer Institute Antoni van Leeuwenhoek Hospital, Department of Molecular Pathology, Amsterdam, The Netherlands*

Locally advanced NSCLC is a heterogeneous disease both with regard of the staging and the tumor behavior. In order to improve outcome, combinations of radiation (RT) with cytotoxic drugs to modulate RT-induced cytotoxicity were introduced and are now standard of care. Also in many other malignancies combined modality has shown to improve outcome and has become standard of care. These treatment options are in particular of benefit in patients that can tolerate such treatment regimens. Improvements have been made both in chemotherapy and the radiotherapy. However, co-morbidities and the observed increased normal tissue toxicity limit the use of potent chemoradiotherapy approaches. In order to enhance the therapeutic window, tumor targeted strategies are needed to allow tumor radiosensitization while not affecting normal tissue. This warrants the evaluation of the potential of novel targeted radiosensitizers with tumor targeted properties. The main mechanism by which both radiation and cisplatin kill tumor cells is by an accumulation of un- or misrepaired DNA damage. PARP inhibitors increase radiation and chemotherapy (cisplatin) response in preclinical studies including lung cancer models. PARP inhibitors have been shown to specifically kill homologous recombination deficient tumor cells as single agent. ATM mutations are expected to affect DSB repair and homologous recombination status therefore amplifying damage induced by the combined PARP inhibitor radiation treatment. Thus tumor targeted treatment and radio-chemosensitization in lung cancer could be achieved in the presence of frequently observed ATM gene mutations in lung cancer. Olaparib exhibits low systemic toxicity profiles when given as monotherapy. When combined with cisplatin and RT enhanced toxicity is anticipated, necessitating careful dose- and schedule-finding and development and validation of supporting pharmacodynamic markers. Such approach could also serve as a template for other promising radiosensitizers, for example DNA-PK, ATM and ATR inhibitors of kinases that are key mediators of the so-called DNA damage response (DDR).

SP-0297
Results of phase I trials combining PARP inhibition and radiotherapy in multiple sites

M. Verheij[1], R. De Haan[1], B. Van Triest[1], J. Schellens[2], M. Van den Brekel[3], C. Verhagen[4], C. Vens[4]
[1]*Netherlands Cancer Institute Antoni van Leeuwenhoek Hospital, Radiation Oncology, Amsterdam, The Netherlands*
[2]*Netherlands Cancer Institute Antoni van Leeuwenhoek Hospital, Medical Oncology, Amsterdam, The Netherlands*
[3]*Netherlands Cancer Institute Antoni van Leeuwenhoek Hospital, Head and Neck Surgery, Amsterdam, The Netherlands*
[4]*Netherlands Cancer Institute Antoni van Leeuwenhoek Hospital, Biological Stress Response, Amsterdam, The Netherlands*

Increased understanding of the molecular mechanisms underlying tumour and normal cell radiosensitivity has led to

the identification of a variety of potential targets for rational intervention. These are based on the "hallmarks of cancer", eight biological capabilities acquired during the multistep development of human tumours. Among these, targeting the DNA damage response represents an attractive strategy, especially in tumours that contain mutations in specific components of the DNA repair pathway, such as BRCA1 and BRCA2. In addition to their use as single agents, inhibitors of the DNA damage response, when combined with radiation could increase tumour response while sparing the normal tissue.

Poly(ADP-ribose) polymerase (PARP) inhibitors affect DNA repair and thus are good candidates for combined use with DNA damaging agents. Indeed, PARP inhibitors increase radiation and chemotherapy responses in preclinical studies. As a single agent they have been shown to specifically kill homologous recombination (HR) deficient tumour cells. A large variety of tumour-specific mutations, such as in BRCA or ATM, affect double strand break repair and HR status and therefore amplify the damage induced by the combined PARP inhibitor radiation treatment. We found that the PARP inhibitor olaparib induced radiosensitisation in mouse breast cancer cells and in a panel of human head and neck cancer cell lines at much lower doses than those required for its single agent activity. Importantly, at these low doses olaparib prevented PAR induction by radiation. Also, the extent of radiosensitisation by olaparib depended on the integrity of the HR pathway, as witnessed by the difference in olaparib dose required to induce radiosensitisation in BRCA2-deficient versus BRCA2-complemented cells.

We have designed 3 phase I-II studies evaluating the safety and tolerability of olaparib, in combination with radiotherapy in locally advanced breast cancer, non-small cell lung cancer and head and neck cancer. Dose-escalation according to the TITE-CRM design allows the evaluation of late toxicity and ensures continuous patient accrual. In support of these trials, biomarkers for the radiosensitisation efficacy of PARP inhibitors have been developed and are evaluated. Tumour and normal tissue samples are collected from all patients to measure PARP inhibition and γH2AX foci formation. These measurements will help to guide the dose-escalation strategy used in these trials.

SP-0298

Phase I Results of PARPi (Olaparib) + RT + Cetuximab in LAHNSCC

D. Raben[1], D. Bowles[1], T. Waxweiler[2], S. Karam[2], A. Jimeno[1]
[1]*University of Colorado Health, Medical Oncology, Aurora, USA*
[2]*University of Colorado Health, Radiation Oncology, Aurora, USA*

DNA repair within cancers contributes to radioresistance and is a concept across all histology's. Cancer cells employ rapid and efficient methods for repairing damaged single and double strand DNA breaks from radiation and chemotherapy. Can we take advantage of this survival mechanism? One strategy incorporates the use of poly(ADP-ribose) polymerase (PARP) inhibitors. What do we know about PARP? PARP inhibition sparked interest in oncology based in part on the concept of "synthetic lethality" in which cancer cells with pre-existing deficiencies in homologous-recombination pathways (e.g. BRCA mutations) exhibit highly selective cytotoxicity to single agent PARP inhibitors in contrast to normal cells – a differentiation that radiation oncologists find attractive and might provide an opportunity with radiation based studies for locally advanced cancers. Building upon the synthetic lethality story, PARP inhibitors show promise as radiosensitizers by directly preventing cancer cells from repairing stress induced DNA damage. In the preclinical setting, our data suggested enhanced sensitivity to PARP(I) monotherapy as well as when combined with radiation across a variety of HNSCC lines known to be HPV negative many groups have shown the ability of PARP inhibitors to sensitize a variety of histology's, both p53 wild type and null, to radiation in both in vitro and in vivo settings. The data seems to suggest that the levels of PARP inhibition required to enhance radiation may be significantly lower than when used as a monotherapy. Remarkable activity has been observed in patients with BRCA1/2 mutations using Olaparib (AZD2281), an orally bioavailable PARP inhibitor, recently approved for refractory ovarian cancer with BRCA1/2 mutations. Toxicity with monotherapy has been remarkably low. Is the BRCA mutation story the only predictor of PARP inhibition (I) sensitivity? Perhaps other homologous and non-homologous repair defects may also contribute to PARP(I) sensitivity. Fanconi anemia phenotypes may also relate to sensitivity as well as pathways related to the SMAD family. We assessed the safety, toxicity and early response when combining escalating doses of Olaparib with fixed dose cetuximab and RT in heavy smoker HNSCC patients. We chose this group of patients due to their high local-regional failure rates and hypothesized amplified rates of HR defects that would lend itself to Olaparib sensitivity. We used a TITE-CRM model with a starting Olaparib dose of 50 mg po BID. The TITE-CRM algorithm uses both the length of observation and whether or not a DLT has occurred in each previous patient enrolled on the trial to estimate the probability of a DLT for each dose level, thereby optimizing subsequent dose assignment. We enrolled 13 patients to date. Among these patients, with a median follow-up of ~14 months, two failed distantly and one failed locally. Patients who experienced local/regional failures continued to smoke during treatment. Toxicity was primarily related to grade 3 dermatitis and acneiform rash. Skin toxicities resolved in all patients after treatment concluded; long-term follow up has revealed development of grade 2 fibrosis in the neck areas where dermatitis was most severe in four patients. The optimal timing of PARP inhibitors and radiation remains unknown and with dose enhancement factors seen pre-clinically, might it be possible to investigate radiation de-intensification or perhaps consider novel combinations with checkpoint inhibitors. This discussion will include a review of some of the pertinent pre-clinical studies with radiation, a review of toxicities and cautions as it relates to combinations with radiation and what are the possibilities for future approaches with DNA repair in locally advanced disease.

Symposium: Radiotherapy of prostate cancer: technical challenges

SP-0299

Extreme hypofractionation: indications and results

A. Widmark[1], L. Beckman[1,2], A. Gunnlaugsson[3,4], C. Thellenberg-Karlsson[1], M. Hoyer[5], M. Lagerlund[6], L. Franzen[1], P. Nilsson[3,4]
[1]*Umeå University, Department of Radiation Sciences, Oncology, Umeå, Sweden*
[2]*Sundsvall Hospital, Department of Oncology, Sundsvall, Sweden*
[3]*Skåne University Hospital, Department of Oncology, Lund, Sweden*
[4]*Lund Unversity, Department of Oncology, Lund Sweden*
[5]*Aarhus University Hospital, Department of Oncology, Aarhus, Denmark*
[6]*Kalmar Hospital, Department of Oncology, Kalmar, Sweden*

The α-ß ratio for prostate cancer (PCa) is postulated to be low; < 3 Gy, i.e. even lower than for late normal tissue reactions. Hence hypofractionated radiotherapy (RT) is hypothesized to be advantageous for treatment of localized PCa. Literature data indicating that this is the case for a moderately hypofractionated regimen was first reported from Italy by Arcangeli. This study was however quite small. At ECC 2015 Dearnaley presented the results from the UK three-armed CHHiP-trial comprising 3,200 patients. This three-armed trial showed non-inferiority between the 74 Gy conventional arm (37 fr; 2 Gy/fr) and the 60 Gy moderately hypofractionated arms (20 fr; 3 Gy/fr) while the experimental arm given 57 Gy arm (19 fr; 3Gy/fr.) had lower efficacy. Patients had predominately intermediate risk tumours and most patients received 6 month of neoadjuvant and concomitant castration treatment. Previously published toxicity data from the trial showed similar results for the trial arms. Results from other moderately hypofractionated

schedules have also been reported recently. RTOG 0415 with only low-risk patients, showed that 70 Gy in 28 fr over 5.6 weeks is non-inferior to 73.8 Gy in 41 fr over 8.2 weeks for low risk PCa patients. The Dutch randomised phase III HYPRO trial with 804 evaluable patients with intermediate/high-risk PCa, comparing moderately hypofractionated RT (19 fr; 3.4 Gy/fr.) with conventional RT (39 fr; 2 Gy/fr), showed non-inferiority with comparable toxicity.
Some prospective results of Sterotactic Body RadioTherapy (SBRT) with 5 fractions and 7-8 Gy/fr suggest equal clinical outcome compared to conventional RT and with acceptable toxicity. The Scandinavian multicentre phase III trial "HYPO-RT-PC" was recently closed, with 1200 patients recruited during 2005-2015. All patients had intermediate risk PCa (PSA≤20; one or two of the risk factors; T3, Gleason ≥7, PSA 10-20). No hormones were used. Patients were randomized to either conventionally fractionated RT (39 fr; 2.0 Gy/fr) over 7 weeks, or to a schedule with extreme hypofractionation (7 fr; 6.1 Gy/ fr) in 2.5 weeks (always including two weekends). The two treatment arms are designed to be equieffective for late normal tissue complications assuming α/ß=3 Gy. Primary endpoint will be mature within 2 years, and toxicity data will be reported by late this year.

SP-0300
Focal strategies: ready for prime time?
A.Bossi[1]
[1]*Institut Gustav Roussy, Radiation Oncology, Villejuif, France*

Abstract not received

SP-0301
Brachytherapy as a boost: the way to go?
P. Hoskin[1]
[1]*Mount Vernon Hospital, Northwood Middlesex, United Kingdom*

Brachytherapy has always represented the most focal means on delivering radiationh having the advantages of the inverse square law around the radiation source which ensures delivery of an intense high dose within the implant and a rapid fall dose outside. These characteristics mean that brachytherapy can deliver very high doses to the prostate gland with in the tolerance doses of bladder and rectum and that the characteristics of dose distribution with in the implant mean that the volume receiving 150% and 200% prescribed peripheral dose (the 150 and the 200) are considerably greater than can be achieved with any external beam technique.
Brachytherapy as a boost can be used in two distinct ways. First is as a boost to the whole gland following external beam radiotherapy. There is now grade a level I evidence from randomised controlled trials that both low dose rate and high dose rate brachytherapy achieve effective dose escalation and consequently better biochemical relapse free survival.
There is also increasing interest in the use of brachytherapy to deliver a focal boost to dominant lesions defined on multi-parametric MR scanning and mapping template biopsies. Thus within a whole gland brachytherapy volume sub volumes can be defined within which the dose can be further escalated. Planning studies have confirmed the feasibility of this approach with both low dose rate and high dose rate brachytherapy and the requirements for catheter or seed placement to achieve these endpoints has been described. The clinical application of this approach is still in its infancy although early results confirm its feasibility.
Summary: both low dose rate and high dose rate brachytherapy offer optimal means of focal dose delivery within the prostate gland. The use of this modality for whole gland treatment is now well established sound evidence base. Emerging application sub volume posts to dominant tumour volumes is under investigation.

Debate: This house believes that SBRT should become the standard of care for T1 and small T2 NSCLC tumours

SP-0302
For the motion
K. Franks[1]
[1]*St James Institute of Oncology, Clinical Oncology, Leeds, United Kingdom*

The current standard of care for T1 and small T2 early-stage non-small cell lung cancer (NSCLC) is surgical resection with lobectomy and nodal sampling/resection. There is randomized evidence that wedge resection is an inferior operation to lobectomy [1] but no large series randomized evidence of surgery versus any other curative intervention for early stage lung cancer. In addition, for patients over 71 years there may be no benefit of lobectomy over limited resection[2]. Stereotactic body radiotherapy (SBRT) is not a new treatment and has been used in medically inoperable stage I NSCLC for 20 years[3]. Given the very high rates of local control ~90% at 3-5 years[4], the low rates of acute toxicity and little detriment to quality of life post treatment[5] SBRT is now a standard of care for medically inoperable peripherally located T1 and T2 tumours up to 5cm in diameter. For medically operable patients where the risks of surgery are low, surgery does offer a theoretical advantage over local ablative treatment such as SBRT. Optimum surgery with removal or the tumour and surrounding lobe may remove occult cancer cells outside the treated volume that may not be included in the SBRT treatment volume. In addition, nodal resection may convey an additional survival benefit and for those patients with occult N1/2 disease those patients could further benefit with the addition of adjuvant chemotherapy.
However, the average age at the time of diagnosis of lung cancer is 70, often in patient's with significant medical co-morbidity that precludes lobectomy and reduces the chance of them receiving adjuvant chemotherapy[6]. Surgical mortality at both 30 and 90 days increases with age further reducing the potential benefit from lobectomy and nodal sampling/resection[7]. In addition, with PET/CT staging and minimally invasive techniques (EBUS) for pathologically sampling the mediastinum now routine practice, the chance of missing occult N1/N2 nodal disease is small being <9% in one series[8].
Propensity analysis of patients receiving surgery versus SBRT have been performed on retrospective series with some reports suggesting no difference in survival between the two match groups and others suggesting a benefit with surgery. Randomized controlled trials (RCT) of surgery versus SBRT (STARS/ROSEL) have been attempted but have been closed prematurely due to poor accrual. A recent pooled analysis of the STARS and ROSEL studies showed no significant difference between SBRT and surgery, though a trend for improved survival with SABR but this was based on 58 patients[9].
Given the limited data from STARS/ROSEL and conflicting results from propensity matched analysis there is a need for successful randomized trials of surgery versus SBRT to prove whether SBRT should be the standard of care. Hopefully, the open SABRtooth (UK) and STABLE-MATES (USA) trial combined with other planned trials of SBRT versus surgery will recruit and provide the answer to this key question.

1. Ginsberg, R.J. and L.V. Rubinstein, *Randomized trial of lobectomy versus limited resection for T1 N0 non-small cell lung cancer. Lung Cancer Study Group.* Ann Thorac Surg, 1995. **60**(3): p. 615-22; discussion 622-3.
2. Mery, C.M., et al., *Similar long-term survival of elderly patients with non-small cell lung cancer treated with lobectomy or wedge resection within the surveillance, epidemiology, and end results database.* Chest, 2005. **128**(1): p. 237-45.
3. Blomgren, H., et al., *Stereotactic high dose fraction radiation therapy of extracranial tumors using an accelerator. Clinical experience of the first thirty-one patients.* Acta Oncol, 1995. **34**(6): p. 861-70.
4. Senthi, S., et al., *Patterns of disease recurrence after stereotactic ablative radiotherapy for early stage non-small-cell lung cancer: a retrospective analysis.* Lancet Oncol, 2012. **13**(8): p. 802-9.
5. Lagerwaard, F.J., et al., *Patient-reported quality of life after stereotactic ablative radiotherapy for early-stage lung cancer.* J Thorac Oncol, 2012. **7**(7): p. 1148-54.
6. Ramsden, K., J. Laskin, and C. Ho, *Adjuvant Chemotherapy in Resected Stage II Non-small Cell Lung Cancer: Evaluating the Impact of Dose Intensity and Time to Treatment.* Clin Oncol (R Coll Radiol), 2015. **27**(7): p. 394-400.
7. Powell, H.A., et al., *Early mortality after surgical resection for lung cancer: an analysis of the English National Lung cancer audit.* Thorax, 2013. **68**(9): p. 826-34.
8. Robson, J.M., et al., *Occult nodal disease in patients with non-small-cell lung cancer who are suitable for stereotactic ablative body radiation.* Clin Lung Cancer, 2014. **15**(6): p. 466-9.
9. Chang, J.Y., et al., *Stereotactic ablative radiotherapy versus lobectomy for operable stage I non-small-cell lung cancer: a pooled analysis of two randomised trials.* Lancet Oncol, 2015. **16**(6): p. 630-7.

SP-0303
Against the motion
P. Van Schil[1]
[1]*University Hospital Antwerp, Department of Thoracic and Vascular Surgery, Edegem, Belgium*

For early-stage non-small cell lung cancer (NSCLC) surgical resection remains the treatment of choice providing excellent long-term results (1). Recently, stereotactic body radiotherapy (SBRT) has become an alternative treatment for localized NSCLC (2). SBRT has mainly been applied for functionally in operable patients with severe cardiopulmonary morbidity. Currently, there is an ongoing debate whether SBRT is also a valid oncological treatment for low-risk patients who are operable from a technical and functional perspective. No large randomized studies are available directly comparing SBRT and surgical resection with systematic lymph node dissection. Several trials closed prematurely due to poor accrual.
From a thoracic surgical point of view several concerns emerge when applying SBRT to operable early-stage NSCLC: precise pathology is not obtained in all cases, information on locoregional lymph node involvement is not always available making it difficult to recommend adjuvant chemotherapy in specific cases, and rather troublesome, different criteria are used when comparing results of surgery and SBRT, mainly in relation to local recurrence (3,4). Moreover, thoracic surgeons are more and more dealing with "salvage surgery" after previous radiotherapy when no other therapeutic options are available (5). Technically, these resections may be very challenging due to technical difficulties during dissection of the hilar region not encountered during primary intervention. These procedures should be performed in dedicated thoracic centres with a large experience.
Due to the lack of clear evidence, different opinions are expressed in present-day literature.
In a pooled analysis of two randomised trials comparing SBRT with lobectomy for stage I NSCLC that closed prematurely due to poor accrual, the authors concluded that SBRT can be considered a valid treatment option for operable stage I NSCLC (6). However, because of small patient sample size and short follow-up time, they indicate that further randomized studies should be performed before more definite recommendations can be made (6).
A different conclusion was reached in a recent propensity score analysis matching 41 patients who underwent video-assisted (VATS) lobectomy with 41 patients treated with SBRT for stage I NSCLC (7). Significant differences were found in overall survival, cause-specific survival, recurrence-free survival, local and distant control favouring VATS lobectomy. Conclusion of this study was that VATS lobectomy may offer a significantly better long-term outcome than SBRT in potentially operable patients with biopsy-proven clinical stage I NSCLC.
Another propensity score analysis compared SBRT with sublobar resection for stage I NSCLC in patients at high risk for lobectomy (8). In 53 matched pairs the difference in overall survival was not significant and the cumulative incidence of cause-specific death was comparable between both groups. Conclusion of this study was that SBRT can be an alternative treatment option to sublobar resection for patients with severe comorbidity who cannot tolerate alobectomy due to functional impairment (8).
In June 2015 the "Comité del'Evolution des Pratiques en Oncologie (CEPO) from Québec, Canada published recommendations regarding the use of SBRT (9). For medically operable patients with T1-2N0M0 NSCLC surgery remains the standard treatment due to the lack of high-level evidence and valid comparative data. For medically inoperable patients withT1-2N0M0 NSCLC or medically operable patients who refuse surgery, SBRT should be preferred to external beam radiotherapy. In the latter cases a biological equivalent dose (BED) of at least 100 Gy should be administered. The choice ofusing SBRT should be discussed within a multidisciplinary tumor board. Radiotherapy should not be considered for patients whose life expectancy is very limited because of comorbidities.
In summary, main points are:
· surgical resection remains the treatment of choice for operable early-stage NSCLC
· SBRT may be considered for functionally compromised patients who cannot tolerate lobectomy.
· further high-level evidence is needed which requires close cooperation between radiation oncologists and thoracic surgeons to design comparative trials with clear inclusion criteria and unequivocal definitions of endpoints.

References

1. McCloskey P. Eur J Cancer 2013; 49:1555-64
2. Louie AV. RadiotherOncol 2015; 114:138- 47
3. Van Schil PE. Lancet Oncol 2013;14:e390
4. Van Schil PE. J Thorac Oncol 2013; 8:129-30
5. Van Schil PE. J Thorac Oncol 2010; 5:1881-2
6. Chang JY. Ann Thorac Surg 2015; 99:1122-9
8. MatsuoY. Eur J Cancer 2014; 50:2932-8
9. BoilyG. J Thorac Oncol 2015;10:872-82

Debate: Is brachytherapy the best for partial breast irradiation?

SP-0304
Multicatheter brachytherapy is the best for APBI
V. Strnad[1]
[1]*University Hospital Erlangen, Dept. of Radiation Oncology, Erlangen, Germany*

Accelerated Partial Breast Irradiation (APBI) using multicatheter brachytherapy is an attractive treatment approach not only to shorten the course of radiation therapy from 3-6 weeks to 2-5 days but also to reduce significantly the radiation exposure to the breasts, the skin, the lung and particularly to the heart very effectively.
Over the last 20 years different modalities of APBI have been introduced into clinical practice –multicatheter brachytherapy, single catheter brachytherapy, IORT techniques, different techniques of External Beam Radiation Therapy (EBRT). Unfortunately fact is that the results of APBI trials with IORT using intraoperative electrons or 50 kV photons have been negative. As well Vaidya et al. (TARGIT trial) as Veronesi et al. (ELIOT trial) reported high 5-year recurrence rate after IORT, namely 3.3%-4.4% in IORT groups versus statistically significant lower recurrence rates in control groups 0.4%-1.3%. Possibility of APBI using EBRT is of course very attractive, since this technique is broadly available and easy to perform. Unfortunately, hitherto reported results of phase 3 APBI trials using EBRT are either disappointing (RAPID trial) or with low statistical power (Olivotto et al., Livi et al.). On the contrary, during the last decade number of modern phase 2 and phase 3 APBI trials, using multicatheter interstitial brachytherapy for the delivery of APBI, have demonstrated favorable long-term local control

rates and cosmetic outcomes, comparable to the results of whole breast irradiation (WBI). In the largest phase 3 randomized non-inferiority GEC-ESTRO trial with sufficient statistical power (~1200 pts.), importantly using for APBI solely multicatheter interstitial brachytherapy in 5 days, after median follow-up of 6.6 years the 5-year local recurrence rates were 1.4% in the APBI arm, and 0.9% in the WBI arm (p=0.4), and 5-year disease-free and overall survival were 96-97% in the WBI group versus 97% in the APBI group - all events are without any statistical and clinical significance. The equivalence of local recurrence rates was evident in all age groups, in all histological subgroups and also independent of the type of systemic therapy. Thus it´s the first phase 3 study proving non-inferiority of APBI in comparison to whole breast irradiation for selected early stage breast cancer patients. Undoubted is, that in the light of the landmark UK and Canadian trials comparing 5 versus 3 weeks of WBI the difference in total treatment time between WBI and APBI using multicatheter brachytherapy (4-5 days) has been partially diminished. However the difference between 3 weeks of WBI versus 4-5 days of APBI still remains clinically and socio-economically relevant. Moreover, due to the extreme steep fall-off of dose of Iridum-192, the significant dose reduction of irradiated normal tissues (including the heart and skin) is a unique advantage of interstitial multicatheter brachytherapy, which is hardly ever achievable by other APBI techniques. The remaining, hitherto unreported ongoing APBI trials unfortunately use for APBI only different techniques of EBRT. The results of these trials will therefore particularly contribute to further fine-tuning of selection criteria and to precise requirements for quality assurance of EBRT-based APBI.
In summary: At the present time only the long-term results of APBI using sole multicatheter brachytherapy for appropriate selected patients demonstrate impressive low local recurrence rates – similar as WBI, accompanying with excellent radiation protection of surrounding organs – better as WBI. Consequently "APBI used multicatheter brachytherapy is today a proven and valid alternative treatment option after breast conserving surgery, and can be offered for all low risk breast cancer patients in clinical routine".

SP-0305
IORT is the best for PBI
R. Orecchia[1]
[1]*European Institute of Oncology, Milan, Italy*

Over the past ten years the results of several clinical trials have been published, detailing various approaches of PBI. Among the different techniques used, IORT has increased rapidly in popularity, mainly in Europe, and up to date many thousands of women have been treated in clinical setting. IORT allows to realize a radiation dose to the index quadrant, eliminating the treatment to the tissue remote from the tumour bed, and using only one very high dose (20 Gy or more) in a single session. When single doses above certain thresholds of 10 Gy are given, some additional biological effects on tumor cell killing and from the surrounding microenvironment can be expected. IORT also represents the possibility of overcoming some constraints such as the accessibility to the centres of radiotherapy, the socio-economic impact on the working life and on the personal habits of the patient. Another important advantage is the avoidance of the interactions with the systemic therapy, that may determine delays in the initiation or in the carrying out of the adjuvant treatment. These potential benefits must be balanced with the potential higher risk of recurrence within the untreated gland tissue in the same breast as well as the still unknown long-term results on survival and cosmesis. Two prospective randomized clinical studies establishing the role of IORT in clinical practice have been published up to now. A single-center study, named ELIOT, was performed at the European Institute for Oncology (EIO) in Milan, Italy. Patients with limited size tumor (2.5 cm) and age of 48 years or more were either randomized to a single dose of 21 Gy of IORT with electrons or to standard WBI. The local recurrence rate (LRR) at 5-years was higher in the experimental arm (4.4% versus 0.4%), and just fell within the pre-defined non-inferiority margin of 4.5%. However, in patients with low risk factors like suggested by the ESTRO or ASTRO consensus' criteria, there were not statistically different LLRs in both arms, and also in patients with luminal A molecular subtype the LLR was very low in the IORT arm, about 1%. It was also found that there was no significant difference in the 5-year overall survival rate in two arms, that is, 96.8% in the ELIOT arm and 96.9% in the EBRT arm. For patients with higher risk factors, a new strategy has been now developed, which include a hypofractionated WBI to be given after surgery and ELIOT. The TARGIT-A trial was a multicentric trial. The inclusion criteria were stricter than in the ELIOT trial. It included patients with unifocal small breast cancer with non-lobular histology and tested the concept of risk-adapted single-dose IORT, which was followed by external-beam WBI in patients with additional unfavorable risk factors. The latest published results from the TARGIT-A trial, with a median follow-up of 2 years and 4 months, reported a LRR with IORT of 3.3% and with EBRT of 1.3, meeting the non-inferiority margin of 2.5%, set at the outset. Overall, breast cancer mortality in the IORT arm was 2.6% versus 1.9% in the WBI arm. In addition, non-breast cancer deaths were found to be significantly reduced in the IORT arm: 1.4% versus 3.5%, with p = 0.0086. Toxicity and cosmesis were assessed by different methods in the studies, but in any case a favorable outcome has been shown. The comparison between the current standard or alternative PBI approaches for early stage breast cancer with data coming IORT techniques poses a dilemma as to when preliminary results are sufficiently mature to be allow practitioners and patients to consider a new treatment approach as safe. We know that most data from studies of breast conservation therapy have demonstrated the importance of long-term data (up to 20 years) in determining the ultimate efficacy of a treatment. The level 1 randomized evidence produced by the IORT trials show that this technique is very convenient for the patient, effective and has few side effects, rather than any postoperative treatment or procedures. Patients have every right to be offered an informed choice.

SP-0306
IMRT is the best for PBI
B. Offersen[1]
[1]*Aarhus University Hospital, Dept Oncology, Aarhus C, Denmark*

Several clinically controlled randomized trials on accelerated partial breast irradiation (APBI) are currently being conducted and some of these have now published results. The trials have used different strategies, for example different patient selection criteria, doses and number of fractions, overall treatment time, treated volume and radiation techniques. Many trials have compared the APBI treatment to whole breast irradiation (WBI) 50 Gy/25 fr followed by a boost. External beam APBI is an attractive strategy, because every radiation department will be able to do the dose planning. The demand for technical skills is in principle not higher than for conventional dose planning. Few randomized trials have reported data, but unfortunately the largest one has not been promising.
In the phase III randomized RAPID trial significantly worse cosmetic outcome was reported with median follow up 36 months in 2135 patients randomized 1:1 to APBI based on 3D-CRT with 38.5 Gy/10 fractions, 5 days, versus WBI based on 42.5Gy/16 fr or 50Gy/25 fr +/-boost. Adverse cosmesis was higher in APBI-treated patients compared with WBI patients as assessed by trained nurses (29% vs 17%; p=0.001) and by patients (26% vs 18%; p=0.02). Grade 3 adverse events were seen in 1.4% of APBI patients, and not in WBI patients. With median 5 years follow up data from another phase III trial involving 520 patients randomized to APBI with IMRT using 30 Gy/5 fr versus WBI using 50 Gy/25 fr + boost has been reported by Livi and coworkers. Significantly better results were seen in APBI patients regarding acute (p=0.0001), late (p=0.004) and cosmetic morbidity (p=0.045). Local recurrence was seen in 1.5% of the patients. Thus data from large phase III trials supporting routine use of external beam

APBI at the present time are not available. However, it is to be expected that the UK IMPORT LOW Trial will be able to report data from >2000 patients with median 5 years follow up at the Early Breast Cancer Conference (EBCC) March 2016. In that trial the strategy is based on 40 Gy/15 fr in all 3 arms, where arm 1 is WBI, arm 2 is partial breast irradiation, and arm 3 has a gradual dose using 40 Gy/15 fr to partial volume and 36 Gy/15 fr to residual breast. At EBCC, data on morbidity will also be reported from the DBCG PBI trial, which has included >800 patients and randomized them to APBI versus WBI using 40 Gy/15 fr in both arms. Data from these 2 trials will be presented and discussed at ESTRO 35. If the results from the IMPORT LOW Trial show that PBI using 40 Gy/15 fr is safe, and these data are supported by results from the DBCG PBI trial using the same treatment, then there is support for the statement that *IMRT is the best for PBI*. However, we are also awaiting results from the ongoing NSABP B-39/RTOG 0413 trial, which has accrued >4000 patients, who were randomized to APBI versus WBI. The majority of patients in the APBI arm have been treated with 3D-CRT. Many of the APBI trials were designed and initiated a decade ago, where the local recurrence risk was higher than we see today. Therefore some of these trials are underpowered to support the statement they are investigating. It is to be expected that results from several trials investigating external APBI will be published in the near future, and hopefully results from the trials will be included in meta-analyses to achieve enough statistical power to identify subgroups of patients where APBI is safe and other subgroups where WBI is to be preferred.

SP-0307

Dosimetric pros and cons of available PBI techniques

T. Major[1]
[1]*National Institute of Oncology, Budapest, Hungary*

Partial breast irradiation (PBI) can be performed with various techniques including both **brachytherapy (BT)** and **external beam radiotherapy (EBRT)**. These methods differ from each other regarding technical skill and dosimetric characteristics. Recent developments in imaging, dose calculation algorithms and beam delivery techniques have made all methods clinically feasible, but in most institutions the applied method mostly depends on the physician's preference and the technical availability.

Among all techniques the longest experience exists with **multicatheter interstitial BT** which can provide highly conformal dose distribution, large dose gradient at target edge, but it is quite complex and requires certain manual skilfulness. The possible geometric miss can result in significant under dosage of the target.

Technically, the **intracavitary applicators** are easier to be used and with balloon-type applicators no geometric miss can occur, but proper tissue conformance is not always guaranteed. In dosimetric point of view drawbacks of the Mammosite applicator are the spherical dose distribution, the symmetric margin and the potential high dose to skin, lungs and ribs. In some anatomical situation the balloon can be asymmetric resulting in asymmetric target coverage. The multichannel applicators are more flexible regarding shaping the dose distribution and reducing dose to critical structures without compromising the target volume coverage. With these applicators asymmetric margins can be used to a small degree.

In **intraoperative electronic BT** using spherical applicators the dose distribution is also spherical and a large dose inhomogeneity develops due to the sharp dose fall-off of the low energy X-ray beam. The margin is always symmetric, but the geometric accuracy is always ensured.

At **intraoperative irradiation with electron beams** there is no 3D-defined target volume, modulation possibilities to shape the dose distribution are very limited and conformal radiotherapy cannot be performed.

Linear accelerator based EBRT techniques expose relatively large volumes of non-target breast to high dose mainly due to the extended target volume created from CTV. In three-dimensional conformal radiotherapy (3D-CRT) dose to contralateral breast, lung or heart can be reduced with proper selection of beam orientations. With intensity modulated radiotherapy (IMRT) highly conformal dose distribution can be achieved, but volumes irradiated by low doses can be larger than with 3D-CRT. Regarding the dose to OARs, with multicatheter BT the critical structures can be better spared than with 3D-CRT/IMRT except for the heart whose dose in BT is strongly dependent on the location of the PTV. With image guidance in EBRT the dose to OARs can be significantly reduced. At left sided lesion the dose to heart can be considerably decreased with deep inspiration breath-hold technique.

With special EBRT equipments such as **Cyberknife** or **Tomotherapy** which are equipped with image guidance smaller CTV-PTV margin can applied which reduces the dose to OARs while maintaining proper target coverage. Real-time tracking with Cyberknife can provide better target volume coverage and spare nearby critical organs, but the treatment time is too long.

Proton beam irradiation, due to the more favourable dose characteristics of proton beam, can provide the less dose to organs at risk, but the availability of the technique is sparse.

Symposium: New challenges in modelling dose-volume effects

SP-0308

Evaluating the impact of clinical uncertainties on TCP/NTCP models in brachytherapy

N. Nesvacil[1], K. Tanderup[2], C. Kirisits[1]
[1]*Medical University of Vienna, Department of Radiotherapy-Comprehensive Cancer Center- and CDL for Medical Radiation Research, Vienna, Austria*
[2]*Aarhus University Hospital, Department of Oncology, Aarhus, Denmark*

During the past decade many investigations have been performed to investigate and minimize clinical uncertainties that could lead to significant deviations between the planned and the delivered doses in radiotherapy. Among the sources of uncertainties patient setup plays an important role in EBRT. Analogously, in brachytherapy the geometric uncertainties caused by movement or reconstruction uncertainties of the implant position in relation to the CTV and/or normal tissue can lead to systematic or random variations between prescribed and delivered dose. At the same time interfraction or intrafraction variations of the anatomy, e.g. caused by variations of position, shape and filling status of OARs, during the course of a treatment pose an additional challenge to all types of radiotherapy.

Recent investigations of different types of uncertainties for a variety of treatment sites, including gynaecological, prostate, head and neck, or breast BT, have led to numerous reports on accuracy of image guided brachytherapy. These have triggered the development of the recommendations for reporting uncertainties in terms of their dosimetric impact (GEC-ESTRO / AAPM guidelines, Kirisits et al. 2014, Radiother Oncol 110). Following these guidelines for uncertainty analysis, individual BT workflows can be analysed in order to identify those components of the overall uncertainty budget which will have the largest impact on the total delivered treatment dose. Once identified, strategies for reducing these uncertainties can be taken into consideration, such as repetitive/near treatment imaging, advanced online dose verification tools, etc.

In order to assess the clinical benefit of such uncertainty reduction measures, it is important to understand the interplay between different types of uncertainties and their combined effect on clinical outcome, in terms of TCP and NTCP. In the past, dose-response relationships have been derived from clinical data, which could not take into account the accuracy of the reported dose. For some treatment sites, e.g. for cervical cancer, uncertainty budgets and dose-response relations have been described in the literature in sufficient detail that now allows us to simulate what impact specific clinical uncertainties would have on TCP/NTCP modelling. In addition to that, one can simulate how TCP or

NTCP models would change, if systematic and random dosimetric uncertainties could be reduced.
In this presentation a few such simulation examples will be shown to illustrate the clinical impact of uncertainties for source calibration, applicator reconstruction, interobserver variations and anatomical interfraction variations. Strategies for reducing clinical uncertainties will be discussed.
Finally, we will come one step closer to answering the questions whether reducing our clinical uncertainties is possible and meaningful, and if so, which strategies would have the largest clinical impact. In the future dose prescription may be affected by technological improvements that lead to a reduction of dosimetric uncertainties and a subsequent widening of the therapeutic window. These developments would benefit from a common effort in the BT community to investigate dose-response relationships for various treatment sites, and to simultaneously report uncertainty budgets for the underlying workflows applied for image guided brachytherapy, in our current clinical practice.

SP-0309

Incorporation of imaging-based features into predictive models of toxicity

C. Brink[1,2]
[1]*Odense University Hospital, Laboratory of Radiation Physics, Odense, Denmark*
[2]*University of Southern Denmark, Institute of Clinical Research, Odense C, Denmark*

The probability of local tumor control is limited by the amount of dose deliverable to the tumor, which is limited by the amount of radiation induced toxicity. There is a large, and currently unpredictable, interpatient variation in the amount of observed toxicity. Since the expected patient specific toxicity is not known, the prescribed dose is restricted such that, within the patient population, the number of patients with major or even fatale toxicity is limited. Due to the interpatient variation in toxicity the population based dose limits lead to undertreatment of patients with low normal tissue irradiation sensitivity. This issue could be addressed if, on a patient specific level, it would be possible to classify the patients according to expected toxicity prior to or early during the treatment course – which calls for predictive models of toxicity.
Many clinical factors such as performance status, patient age, and other co-morbidity are associated with observed toxicity, and models based on such factors are today available (e.g. http://www.predictcancer.org/). The models can be a useful tool to optimize the treatment on the population level, but in order to be used on a patient specific level, input of more patient specific information is needed. During planning and delivery of radiotherapy a large number of patient images are acquired. The information content in the images is often reduced to a few figures (e.g. volume of tumor or measurement of patient positioning). The different types of images (CT/SPECT/PET/MR/CBCT) are available for free, and it is tempting to believe that these images could provide more patient specific information, if extracted in a proper way. Also as part of the response evaluation it is likely that imaging could be used to quantify the degree of toxicity. At the end of the day, the overall toxicity level can only be assessed by the patient, who should cope with the toxicity on a daily basis. However, in terms of biological tissue response to the radiation, patient (or oncologist) reported toxicity is likely to underestimate the “true” amount of toxicity since the toxicity effects might be overshadowed by treatment related gains e.g. re-ventilation of obstructed airways due to tumor regression in lung cancer patients, or because the toxicity is assumed to be related to co-morbidity. Disentanglement of such effects is desirable during creation of predictive models of toxicity; which might be feasible by evaluation of follow-up images.
The most used imaging-based feature to predict toxicity is obviously measurement of dose to individual risk organs (e.g. dose to heart or lung). These values are routinely used clinically and typical not regarded as image-based features. More advanced imaging-based features such as homogeneity, texture, or time changes of signals/images has been proposed and showed to be associated with toxicity. It is important to remember that such features, to some extent, might be confounded by more simple factors (e.g. tumor volume or volume of irradiated region). Nevertheless, image based features appears in a number of studies to add independent toxicity information; but it is likely that no single image-based feature (or no single feature at all) will be able to make a perfect patient specific toxicity prediction for the entire population. In many studies the correlation between a specific image-based feature and observed toxicity is relative weak. However, if predictive toxicity models simply are able to identify a subset of patients who are likely to have modest toxicity that would be very beneficial, since this group of patients could then be offered a more aggressive treatment, which hopeful would result in improved local control. Predictive toxicity models should thus not only be evaluated on their overall prediction performance for the entire population, but also on their ability to identify a significant subgroup of patients who are candidates for intensified treatment.
The current lecture will present examples of image-based features and point to their potential clinical impact; but will also focus on the potential use of patient specific toxicity models to select subgroups of patients as described above. Moreover comments on image quality will be made, since high images quality is the foundation for imaged-based features used in predictive models for toxicity.

SP-0310

Growing importance of data-mining methods to select dosimetric/clinical variables in predictive models of toxicity

T. Rancati[1]
[1]*Fondazione IRCCS Istituto Nazionale dei Tumori, Prostate Cancer Program, Milan, Italy*

In the field of toxicity modeling it is common practice to build statistical models starting from analysis of clinical data which are prospectively collected in the frame of observational trials. Modern prospective observational studies devoted to modelling of radioinduced toxicity are often accumulating a large amount of dosimetric and patient-related information, this requires particular attention when normal tissue complication probability modelling is approached. A core issues is related to selection of features, which then influences overfitting, discrimination, personalization and generalizability.
These risks are particularly high in clinical research datasets, which are often characterized by low cardinality - i.e. the number of cases is overall low - and are often strongly imbalanced in the endpoint categories – i.e. the number of positive cases (e.g. toxicity events or loss of disease control) is small, or even very small, with respect to the negative ones. This is obviously positive for patients, it is however a disadvantage for model building.
In this context a possible methods using in-silico experiment approach for toxicity modelling will be discussed together with some applications.
This method aimed at identifying the best predictors of a binary endpoint, with the purpose of detecting the leading robust variables and minimizing the noise due to the particular dataset, thus trying to avoid both under- and over-fitting. It followed, with adjustments, a procedure firstly introduced by El Naqa [IJROBP2006]: the treatment response curve was approximated by the logistic function, while the bootstrap resamplings were performed to explore the recurrence of the selected variables in order to check their stability. A further bootstrap resampling was introduced for the evaluation of the odds ratios of the selected variables.
The in-silico experiment was implemented using the KNIME software (KNIME GmbH, Germany) and consisted in the following processing steps:
1) 1000 bootstrap samplings of the original dataset are created, as suggested by El Naqa [IJROBP2006];
2) backward feature selection based on minimization of residuals is performed on each bootstrap sample;
3) the rate of occurrences and the placement of each variable (selected by the backward feature selection) in the

1000 bootstrapped datasets are used to classify the most robust predictors. A synthetic index, called normalized area, is defined for ranking each predictor: it corresponds to the area under the histogram representing the number of occurrences of each variable (x-axis) at a given importance level in each re-sampled dataset;
4) a basket analysis of the 1000 sets of predictors is used to identify the predictors that appears together with higher probability;
5) the best set of predictors is chosen, with its maximum size determined by the rule of thumb "one tenth of the number of toxicity events";
6) the distribution of odds ratios are determined through 1000 bootstrap re-samplings of the original dataset including the set of predictors selected in the previous step;
7) a logistic model with the best set of predictors and the median odds ratios, calculated from the distributions obtained in the previous step, is defined.
In this approach, logistic regression is enhanced with upstream and downstream data processing to find stable predictors.
The method was tested with satisfactory results on different datasets aimed at modelling radio-induced toxicity after high-dose prostate cancer radiotherapy.

Symposium: Automated treatment plan generation in the clinical routine

SP-0311
Automated treatment plan generation - the Zurich experience

J. Krayenbuehl[1], M. Zamburlini[1], I. Norton[2], S. Graydon[1], G. Studer[1], S. Kloeck[1], M. Guckenberger[1]
[1]*University Hospital Zürich, Department of Radiation Oncology, Zurich, Switzerland*
[2]*Philips, Philips Radiation Oncology Systems, Fitchburg, USA*

Intensity modulated radiotherapy and volumetric modulated radiotherapy (VMAT) involves multiple manual steps, which might influence the plan quality and consistency, for example planning objectives and constraints need to be manually adapted to the patients individual anatomy, tumor location, size and shape [1]. Additional help structures are frequently defined on an individual basis to further optimize the treatment plan, resulting in an iterative process. This manual method of optimization is time consuming and the plan quality is strongly dependent on planner experience. This is especially true for complex cases such as head and neck (HN) carcinoma and stereotactic treatment.
In order to improve the overall plan quality and consistency, and to decrease the time required for planning, automated planning algorithms have been developed [2,3]. In this pilot study, we compared two commercially available automatic planning systems for HN cancer patients. A VMAT model was created with a knowledge based treatment system, Auto-Planning V9.10 (Pinnacle, Philips Radiation Oncology Systems, Fitchburg, WI) [4] and for a model based optimization system, RapidPlan V13.6 (Eclipse, Varian Medical System, Palo Alto, CA) [2]. These two models were used to optimize ten HN plans. Since the aim was to achieve plans of comparable quality to the manually optimized plans in a shorter time, only a single cycle of plan optimization was done for both automated treatment planning systems (TPS). Auto-Planning was additionally used to evaluate the treatment of lung and brain metastases stereotactic treatments.
The results from the planning comparison for HN cancer patients showed a better target coverage with AutoPlanning in comparison to Rapidplan and manually optimized plans ($p < 0.05$). RapidPlan achieved better dose conformity in comparison to AutoPlanning ($p < 0.05$). No significant differences were observed for the OARs, except for the swallowing muscles where RapidPlan and the manually optimized plans were better than AutoPlanning and for the mandibular bones were AutoPlanning performed better than the two other systems. The working time needed to generate clinical accepted plans for both automated TPS was drastically reduced to less than ten minutes.
For the two stereotactic sites evaluated, target coverage and OARs doses differences were not clinically relevant between Auto-Planning and manually optimized plans.
The encouraging results of automatic planning shows that highly consistent treatment plans for complex cases can be achieved with an automated planning process.

SP-0312
Automated treatment plan generation - the Milan experience

A. Fogliata[1]
[1]*Humanitas Research Hospital, Department of Radiation Oncology, Rozzano-Milan, Italy*

A knowledge based planning process, named RapidPlan, has been recently implemented into the Varian Eclipse treatment planning system. The goal of the engine is to generate patient tailored and personalized objectives to input in the optimization process for IMRT or VMAT inverse planning. Data from previously generated high quality plans are used to estimate DVH ranges where the specific DVH of a structure will most likely land according to the prior plans knowledge. Estimate-based optimisation objectives are hence generated. A complete pre-clinical preparation have been established before the clinical implementation of RapidPlan and the configured specific models. The anatomical sites and pathologies chosen for the first models generation in Milan were Head and Neck, and Breast. For the first site the choice was driven by the complexity of the planning phase due to the anatomy and critical structures; the breast was chosen since, beside of its planning complexity, almost one third of our patient population presents breast cancer. For each of the two chosen sites the process of the model generation included different phases. Initially a set of about 100 patients per site, having quite spread anatomical characteristics (as, for example, the breast size) while excluding extreme anatomies, was selected. The selected plans were all clinical plans of high quality, for VMAT (RapidArc) delivery. Those plans were used to train the model for the extraction of the parameters, based on prinicipal component analysis methods and regression models, needed to estimate the DVH for any new patient. The training results were analysed to evaluate possible outliers and their eventual exclusion from the model. Finally the validation process was followed on another group of patients to assess the model reliability and usability. From this last phase improvements in the plan quality when using RapidPlan was assessed. Once the two models were evaluated, a number of head and neck and breast cases were selected for the pre-clinical trial. The planners used to plan without RapidPlan were asked to produce plans using the knowledge based planning models. Two kind of evaluations were felt interesting: on one side the plan quality, for which the same cases were asked to be planned without RapidPlan by the same planner, and on the other side the time required to obtain such plans. The results were very promising, both on the plan quality, and especially on planning time. We are ready to move to the clinical daily use of the automated treatment plan generation.

SP-0313
Fully automated treatment plan generation using Erasmus-iCycle - the Rotterdam experience

M.L.P. Dirkx[1], A.W. Sharfo[1], P.W.J. Voet[2], G. Della Gala[1], L. Rossi[1], D. Fransen[1], J.J. Penninkhof[1], M.S. Hoogeman[1], S.F. Petit[1], A.M. Mendez-Romero[1], J.W. Mens[1], L. Incrocci[1], N. Hoekstra[1], M. Van de Pol[1], S. Aluwini[1], S. Breedveld[1], B.J.M. Heijmen[1]
[1]*Erasmus MC Cancer Institute, Radiation Oncology, Rotterdam, The Netherlands*
[2]*Elekta AB, Physics Research, Uppsala, Sweden*

Aim: Treatment plan generation in radiotherapy is commonly a trial-and-error procedure in which a dosimetrist tries to steer the treatment planning system (TPS) towards an acceptable patient dose distribution. For a single patient, this process may take up to several days of workload. The

quality of the final treatment plan is dependent on the skills and experience of the dosimetrist, and on allotted time. In addition, for the treating physician it is extremely difficult to assess whether the generated plan is indeed optimal considering the unique anatomy of the individual patient. At Erasmus MC, systems for fully automated plan generation have been developed to obtain plans of consistent high quality, with a minimum of workload. This presentation will focus on their clinical implementation and applications.

Materials and methods: An IMRT or VMAT plan is generated fully automatically (i.e., without human interface) by the clinical TPS (Monaco, Elekta AB), based on a ***patient-specific*** template. The patient-specific template is automatically extracted from a plan generated with Erasmus-iCycle, our in-house developed pre-optimizer for lexicographic multi-criterial plan generation (Med Phys. 2012; 39: 951-963). For individual patients of a treatment site (e.g., prostate), automatic plan generation in Erasmus-iCycle is based on a ***fixed*** 'wishlist' with hard constraints and treatment objectives with assigned priorities. The higher the priority of an objective, the higher the chance that the planning aim will be achieved, or even superseded. All plans generated with Erasmus-iCycle are Pareto optimal. In case of IMRT, the system can be used for integrated beam profile optimization and (non-coplanar) beam angle selection. ***Site-specific wishlists*** are a priori generated in an iterative procedure with updates of the wishlist in every iteration step, based on physicians' feedback on the quality of plans generated with the current wishlist version. Also for patients treated at a Cyberknife, either with the variable aperture collimator (Iris) or MLC, the clinical TPS (Multiplan, Accuray Inc.) can be used to automatically generate a deliverable plan, based on a pre-optimization with Erasmus-iCycle.

Results: Currently, automatic treatment planning is clinically used for more than 30% of patients that are treated in our department with curative intent. It is routinely applied for prostate, head and neck, lung and cervical cancer patients treated at a linac. In a prospective clinical study for head and neck cancer patients, treating radiation oncologists selected the Erasmus-iCycle/Monaco plan in 97% of cases rather than the plan generated with Monaco by trial-and-error (IJROBP 2013; 85: 866-72). For a group of 41 lung cancer patients, clinically acceptable VMAT plans could be generated fully automatically in 85% of cases; in all those cases plan quality was superior compared to manually generated Monaco plans, due to a better PTV coverage, dose conformality, and/or sparing of lungs, heart and oesophagus. For plans that were initially not clinically acceptable, it took a dosimetrist little hands-on time (<10 minutes) to modify them to a clinically acceptable plan. In 44 dual-arc VMAT Erasmus-iCycle/Monaco plans for cervical cancer treatment small bowel V45Gy was reduced by on average 20% ($p<0.001$) when compared to the plans that were manually generated by an expert Monaco user, spending 3 hours on average. Differences in bladder, rectal and sigmoid doses were insignificant. For 30 prostate cancer patients, differences between Erasmus-iCycle/Monaco VMAT plans and VMAT plans manually generated by an expert planner with up to 4 hours planning hands-on time, were statistically insignificant (IJROBP 2014; 88(5): 1175-9). Attempts to use acceptable, automatically generated plans as a starting point for manual generation of further improved plans have been unsuccessful. For prostate SBRT, clinically deliverable Cyberknife plans that were automatically generated with Erasmus-iCycle/Multiplan showed a better rectum sparing and a reduced low-medium dose bath compared to automatically generated VMAT plans with the same CTV-PTV margin.

Conclusion: In our department, automatic plan generation based on Erasmus-iCycle is currently widely used, showing a consistent high plan quality and a vast reduction in planning workload. Extension to new target sites (breast, liver, lymphoma, spine, vestibular schwannoma) is being investigated. In addition, the use of automated planning for intensity modulated proton therapy is being explored, making objective plan comparison with other modalities possible.

Symposium: Elderly and radiation therapy

SP-0314

Geriatric assessment is a requirement to effectively provide a quality radiotherapy service to the older person

A. O'Donovan[1], M. Leech[1]
[1]*Trinity Centre for Health Sciences, Discipline of Radiation Therapy, Dublin 8, Ireland Republic of*

Most European countries are currently faced by a major demographic shift that will see increasing numbers of older patients. This represents a corresponding increase in the number of older patients presenting for radiation therapy. It is recognised that this will require "age attuning" of our cancer treatment services to provide a more holistic approach to the care of older patients. Comprehensive Geriatric Assessment (CGA) or Geriatric Assessment (GA) as used in the oncology literature, can identify risk factors for adverse outcomes in older cancer patients. CGA was designed to more accurately detect frailty in older patients, and both the National Comprehensive Cancer Network (NCCN) and International Society of Geriatric Oncology (SIOG) recommend its use in Oncology. CGA includes a compilation of reliable and valid tools to assess geriatric domains such as comorbidity, functional status, physical performance, cognitive status, psychological status, nutritional status, medication review, and social support. The benefits of CGA include greater diagnostic accuracy, reduced hospitalisation and improved survival and quality of life. Benefits for cancer patients include predicting complications of treatment, estimating survival and detection of problems not found using standard oncology performance measures, such as performance status. Cancer treatment is a physiologic stressor, and its impact on older patients is poorly defined in relation to baseline reserve capacity. GA provides a means of quantifying known heterogeneity in older patients, and may identify problems that could potentially be reversed, or better managed, in order to improve outcomes. Despite the evidence demonstrating the benefits of GA in improving the health status of older patients, its adoption in (radiation) oncology has not been widespread. The published literature lacks a standardised approach to GA in Oncology, making interpretation of the current evidence difficult. Exacerbating this issue is the traditional exclusion of older patients from clinical trials. GA has the potential to predict toxicity, survival and quality of life in older patients, and further research is needed to clarify its role. GA is known to be time and resource intensive, and recent studies have sought to develop shorter screening tools specifically for oncology patients, such as the G8. However, none of these approaches have been validated to date, with one obvious drawback being the lack of comparison in the form of a "gold standard" comprehensive approach. One potential solution to resource and time issues is the sharing of responsibility among the multidisciplinary team, with radiation therapists having a valuable role to play as front line staff. Recent focus in policy documents on measures to improve the quality of healthcare for older patients has resulted in a need to adequately prepare qualified health professionals to work together in a more collaborative manner. Many international models of Geriatric Oncology exist, however implementation is institution-specific and must take account of existing resources and infrastructure. In addition, there is currently no formal Geriatric Oncology fellowship scheme in most countries (apart from the US) or education programme in place for oncology professionals on how to best implement geriatric assessment. Many healthcare professionals, do not receive any training in the fundamental principles of geriatric medicine and how they may apply to their profession. The aim of this presentation is to present a critical overview of the current literature on GA in radiation oncology, and previous research by the authors in this field. It will also incorporate aspects of feasibility and requirements for a geriatric oncology service. The latter will include educational aspects and the need for adapted curricula in radiation

oncology to incorporate aspects of aging, optimal treatment and attitudes towards aging.

SP-0315

Treatment choices in the elderly: focus on breast cancer

N. De Glas[1]
[1]*Leiden University Medical Center LUMC, Department of Surgery, Leiden, The Netherlands*

· The evidence for treatment ofolder patients with breast cancer is scarce due to lack of clinical trials andselective inclusion of patients
· Older patients are less willing totrade quality of life for absolute survival gain, but data that can providepatients with information concerning these outcomes are lacking
· The recently performed "FOCUS onChoice" study has shown that older patients choose a mastectomy more frequentlythan younger patients
· Recent trials suggest thatradiotherapy can be omitted in older patients with low-risk tumours
Normal 0 21 false false false FR-BE X-NONE X-NONE

SP-0316

Palliative radiation therapy in geriatric cancer patients

C.Nieder[1]
[1]*Nordlandssykehuset, Department of Oncology and Palliative Medicine, Bodoe, Norway*

Symposium: A Joint session of Young Radiation Oncologists National Societies & YROG

SP-0317

What is the Young ESTRO Committee and what can it do for young radiation oncology professionnals?

J.E. Bibault[1]
[1]*Hôpital Européen Georges Pompidou, Radiation Oncology Department, Paris, France*

The Young Task Force
The first YTF was formed in 2011 at the Anniversary congressbased on the decision of the ESTRO Steering Committee of 16 June 2009. At thebeginning, members of the YTF were appointed by the Board each year. In 2012,at the Agorá meeting, YTF members' term was changed to three years, renewableonce. This meeting allowed for "strategic discussions", bringing young,promising RT scientists / professionals together with the core ESTROleadership. The Agorá meeting provided valuable input for the YTF. Several projectsrealised by the YTF were based on the results of the Agorá meeting.
The first chair of the YTF, Daniel Zips, thought that theaim of the YTF, from the start, was to become a committee and be an integralpart of ESTRO governance contributing to activities and supporting the youngmembers. The Young task force (YTF) is a key structure in securing thelong-term future of ESTRO. The 3rd YTF succeeded in initiating several projects(e.g. revision of YTF structure, involvement in ESTRO committees, improvementof online communication, etc.). To carry on these essential activities, the YTFwas changed to become a full ESTRO Committee in 2015.
Composition of the Young Committee
The Young Committee reflects the diversity andmultidisciplinarity of ESTRO with members from clinical radiation oncology,radiobiology, physics and RTTs. Each member also acts as an observer in one ofthe other standing committee of ESTRO:
• Jean-Emmanuel Bibault (Paris, France): National Societies Committee
• Gerben Borst (Amsterdam, The Netherlands) : Clinical Committee
• Laura Mullaney (Dublin, Ireland): RTT Committee
• Kasper Rouschop (Maastricht, The Netherlands): Radiobiology Committee
• Maximilian Schmid (Vienna, Austria): GEC-ESTRO Brachytherapy Committee
• Mateusz Spalek (Warsaw, Poland): ACROP Committee
• Daniela Thorwarth (Tübingen, Germany): Physics Committee
• Wouter van Elmpt (Maastricht, The Netherlands): Physics Committee
Future vision: carry on the activities initiated by theprevious task Forces and work on new perspectives
Standing committee involvement
Young Committee members' positions as observers allow us torepresent the interests of the young ESTRO members and to evaluate thecontribution and participation of the young members in other standingcommittees' activities.
Young scientist session at ESTRO Forum and Young scientisttrack at numbered ESTRO congresses
The Young Committee is responsible for the organisation,contribution and promotion of the young scientist session / track at all ESTROcongresses. Each year, a young track is held with symposia and teachinglectures aimed at the young radiation oncology professionals, with subjectssuch as "how to build a career", "how to write a good article/abstract". Wealso organize a young reception at the end of the track, which is always a nicemoment to meet other young Europeans and network with each other.
Online services (Facebook, videos, FALCON, DOVE, scientificnetworking)
The 3rd YTF started several projects regarding onlineservices. The main task will be to maintain, promote and communicate theseactivities. The Young Committee will also contribute to ESTRO online serviceslike FALCON, DOVE, etc.
ESTRO Fellow
In regard of the heterogeneous training in the field ofradiation oncology within Europe, the "ESTRO Fellow" was created to achieve ahigh level of education as well as reflect a high dedication towards ESTRO. Ithas become a prestigious mark of distinction.
The next ESTRO fellow exam will take place on April, 29th2016 at ESTRO35 in Turin. The Application deadline is set for March, 29th 2016.
The future
The Young Committee is currently involved in the setup ofthe 3rd Agora Meeting which should take place late 2015 or early 2016. Thismeeting will bring together motivated young ESTRO members to discuss andexchange our vision for our field. A call for applications will be sent in thatperspective.

SP-0318

The Young Radiation Oncology Group of EORTC -ROG

O. Kaidar-Person[1]
[1]*Rambam Health Care Campus- Faculty of Medicine-Technion, Oncology Institute, Haifa, Israel*

The Young Radiation Oncologists Group (YROG) is a working party of the European Organization for Research and Treatment of Cancer (EORTC) -Radiation Oncology Group (ROG). Its members are the "young members" of the ROG.
The YROG was initiated in 2012 with an aim to incorporate radiation oncologists in early phases of their career within the EORTC- ROG activities. This was done to have a new generation of radiation oncologists actively involved in research.
Joining the YROG is an opportunity to present your research and new study proposals and to take part in the discussions held at the different ROG working parties. By being a part of the EORTC-ROG you will learn about designing clinical trials and have a chance to work side by side with world-leaders in oncology.
If you are at the early stages of your career in radiation oncology and are looking for an opportunity to be involved in key research, come to hear about the YROG.

SP-0319

The French Society of Young Radiation Oncologists

T. Leroy[1]
[1]*Centre Oscar Lambret, Lille, France*

Since 2003, the SFjRO (French Society of young Radiation Oncologist) promote radiation oncology teaching in France.

The goals of our society are to promote and ease the teaching of radiation oncology by developing relationships between residents and professors. By creating specific tools, giving access to scientific journals and organizing each year two theoretical courses, the SFjRO aims to give access to a better understanding of current practices in Radiation Oncology. Nowadays our society has more than 200 members. Each year French residents attend one national radiation therapy courses covering each fundamental field of radiation oncology : radioanatomy, radiobiology, radiophysics and brachytherapy and a summer school dedicated to a specific organ. All these courses are available freely on our website which has now a database of more than 300 radiation oncology courses. The SFjRO works with SFRO (French Society of Radiation Oncologists) and organize a young session during the National meeting of Radiation oncology. We also represent resident in front of national organisation such as National cancer Institute (Inca) and National Board of Oncology Teachers (CNEC). Another goal of SFjRO is to promote research among residents and we have published several studies about delineation variability, burnout or mobile technology and social media use by young radiation oncologists. In the future we hope to strengthen our cooperation with European young radiation oncologist societies, and to take part in young sessions such as the YROG sessions.

SP-0320

The Young AIRO (Italian Association of Radiation Oncology) Group

D. Greto[1]

[1]*University of Florence- Azienda Ospedaliera Universitaria Careggi, Sperimental and Clinica Biomedical Sciences, Firenze, Italy*

The Young AIRO group (yAIRO) is a part of the Italian Association of radiation oncology composed by members below 40 years old. The increasing participation of the young member to the AIRO scientific activities resulted in the foundation of the Young group in 2007. The main purpose of the yAIRO was to create a network connections between junior physicians working in different institutions throughout the country, to promote the collaboration with junior groups of other national scientific societies in the field of oncology. Nowadays the Young group has approximately 350 members. Every years there is an annual scientific national event dedicated to young members, a scientific session dedicated to the young members takes place during the AIRO national meeting. One of the main project of the yAIRO is to create collaboration programs with other young specialists involved in the oncology field. In the last years, relationships were created with the young group of the Italian medical oncology association (AIOM), young urologists (SIURO) and young medical radiologists (SIRM). The yAIRO published some collaborative research projects: the INTER-ROMA Project (2011), the BUONGIORNO Project (2013), the PROCAINA part I and II Project (2013), the STYRO Project (2013), the PEDRO project (2015). A project about the history and development of Italian radiation oncology residency programs and one about the pacemaker and implanted cardioverter defibrillator management in radiation therapy are in progress. The fundamental role of young members in the Italian radiation oncology society will induce yAIRO to improve young specialists' participation, involvement and commitment into education, research and clinical care.

SP-0321

The British Institute of Radiology

S. Hafeez[1]

[1]*The Insitute of Cancer Research and The Royal Marsden NHS Foundation Trust, Clinical Oncology, Marsden, United Kingdom*

Abstract not received

Poster Viewing: 7: Physics: Intra-fraction motion management II

PV-0322

Target displacement evaluation for fluoroscopic and four-dimensional cone-beam computed tomography

H. Iramina[1], M. Nakamura[2], Y. Iizuka[2], Y. Matsuo[2], T. Mizowaki[2], M. Hiraoka[2], I. Kanno[1]

[1]*Kyoto University, Nuclear Engineering, Kyoto, Japan*

[2]*Kyoto University, Radiation Oncology and Image-Applied Therapy, Kyoto, Japan*

Purpose or Objective: Four-dimensional cone-beam computed tomography (4D-CBCT) has great capability to provide volumetric and respiratory motion information with one gantry rotation. It is necessary to quantitatively assess, how difference of tumor displacement between actual and 4D-CBCT image exists. In this study, we evaluated the displacement of implanted fiducial markers assumed as tumor on fluoroscopic projection images and reconstructed 4D-CBCT images with different sorting methods.

Material and Methods: We have developed 4D-CBCT utilizing dual source kV X-ray imaging subsystems. Five lung cancer patients with two to four implanted fiducial markers were enrolled in the institutional review board-approved trial. Each patient underwent three consecutive 4D-CBCT imaging. For at least two scans out of three, the imaging parameters were 110 kV, 160 mA and 5 ms, the rotational speed of the gantry was 1.5°/s, rotation time was 70 s, the image acquisition interval was 0.3°, and the rotational angle of 105°. A marker that located the most nearest to the lung tumor was used for surrogate respiratory signal. The marker motion in superior-inferior (SI) direction was used as surrogate respiratory signal for 4D-CBCT image reconstruction. Surrogate respiratory signal were converted eight phase bins with retrospective amplitude- or phase-based sorting. On reconstructed 4D-CBCT images, the marker was contoured on all phases to detect its 3D positions. Meanwhile, the marker positions on two fluoroscopic images obtained simultaneously were converted to 3D position. Evaluation was employed among the displacement on fluoroscopic image (*d*fluoro), that on amplitude-based sorting 4D-CBCT (*d*a-4DCBCT) and that on phase-based sorting 4D-CBCT (*d*p-4DCBCT) in left-right (LR), anterior-posterior (AP), and SI direction. Difference between *d*a-4DCBCT and *d*fluoro (*D*a-f), and difference between *d*p-4DCBCT and *d*fluoro (*D*p-f) were obtained for all patients.

Results: Depending on the sorting methods, the positional difference was up to 2 mm on 4D-CBCT images. Overall mean ± standard deviation of *D*a-f and *D*p-f in LR, AP, and SI direction were -1.5±1.2, -2.9±1.2, -5.1±1.6 mm and -1.4±1.1, -2.3±0.9, -5.2±1.2 mm, respectively (Table 1). 4D-CBCT underestimated displacement of marker by 5 mm on average in SI direction.

Table 1. Means and standard deviations of D_{a-f} and D_{p-f} for LR, AP, and SI direction.

Sorting	Patient	1st			2nd			3rd		
		LR	AP	SI	LR	AP	SI	LR	AP	SI
Amplitude -based	1	-1.0	-3.2	-4.3	-0.5	-5.8	-4.0	-1.5	-3.0	-5.3
	2	-0.2	-3.3	-7.8	-0.7	-1.3	-4.3	-1.3	-2.9	-5.4
	3	-4.2	-1.7	-3.9	N/A	N/A	N/A	-2.8	-2.6	-4.3
	4	-0.4	-1.3	-2.6	N/A	N/A	N/A	-0.9	-2.5	-4.1
	5	-2.0	-2.7	-7.4	N/A	N/A	N/A	-2.9	-3.8	-7.4
	Mean	-1.6	-2.4	-5.2	-0.6	-3.6	-4.1	-1.9	-3.0	-5.3
	SD	1.5	0.8	2.1	0.1	2.3	0.1	0.8	0.5	1.2
Phase -based	1	-1.2	-2.0	-4.3	-0.6	-4.4	-5.4	-0.8	-1.7	-4.8
	2	0.5	-1.8	-5.8	-0.1	-2.0	-5.3	-1.5	-2.0	-5.3
	3	-3.6	-1.3	-4.9	N/A	N/A	N/A	-1.9	-2.1	-4.8
	4	-0.6	-1.6	-3.1	N/A	N/A	N/A	-1.1	-2.6	-4.1
	5	-2.3	-2.8	-6.4	N/A	N/A	N/A	-3.0	-3.8	-8.0
	Mean	-1.5	-1.9	-4.9	-0.4	-3.2	-5.4	-1.7	-2.4	-5.4
	SD	1.4	0.5	1.2	0.2	1.2	0.1	0.8	0.7	1.4

Abbreviations; LR: left-right, AP: anterior-posterior, SI: superior-inferior, SD: standard deviation, N/A: not available
Note: For Patient 3 to 5, 4D-CBCT images at 2nd session was taken for different purpose with different imaging conditions from others.

Conclusion: We performed displacement evaluation of fiducial markers on 4D-CBCT with two sorting methods. Since 4D-CBCT requires convolution of marker motion in eight bins, underestimation of 5 mm on average was observed in SI direction.

PV-0323

Prospective evaluation of markerless tumour tracking using 4D3D registration and dual energy imaging

J. Dhont[1], D. Verellen[1], K. Poels[2], M. Burghelea[1], K. Tournel[1], T. Gevaert[1], B. Engels[1], C. Collen[1], R. Van Den Begin[1], G. Storme[1], M. De Ridder[1]
[1]*Universitair Ziekenhuis Brussel, Radiotherapy, Brussels, Belgium*
[2]*Universitair Ziekenhuis Leuven, Radiotherapy, Leuven, Belgium*

Purpose or Objective: Image registration of Digitally Reconstructed Radiographs (DRRs) and real-time kV images is the only clinically implemented solution to markerless tumor tracking. However, registration still suffers from poor soft tissue visibility, restricting the workflow to only a certain size and density of tumors. The purpose of this study is to evaluate the feasibility of markerless tumor tracking on a clinical system through 4D/3D registration and the use of dual-energy (DE) imaging.

Material and Methods: For 3 patients treated for NSCLC with dynamic tracking on the Vero SBRT system, on average 90 soft-tissue enhanced DE images were created from sequential low- (LE) and high-energy (HE) orthogonal fluoroscopy. All DE images were binned in either inhale, exhale, maximum inhale or maximum exhale, using the amplitude of the synchronous external breathing signal.
For each respective breathing phase, DRR templates were created from the 4D planning CT using the open-source Insight Toolkit (itk).
As such, the localization problem was reduced to 2D/2D registration of 2 orthogonal kV images and 2 DRRs.
Before registration, the currently implanted marker was removed on all images so to not bias the results.
Intensity-based 2D/2D registration was carried out between each DE image and the respective DRR. The same was done with all HE images to evaluate the benefit of using DE imaging..
The implanted marker was recovered and used as a benchmark to quantify the accuracy of the tumor localization. The mean Euclidean distance between the center of the marker in the DE and HE images, and the center of the marker in the matched DRR template was defined as the tracking error (TE).

Results: Table 1 summarizes the localization results for each patient and imaging angle. All TEs remain below 2.5 mm and results between DRR-HE and DRR-DE are similar. However, a significant difference in TE is present for 1 imaging angle. From a qualitative analysis, see Figure 1, it can be observed that for those imaging angles where the tumor is mainly obscured by bony anatomy, tumor localization through intensity based registration is more accurate when dual-energy images are applied.

Figure 1 High-energy (left) and dual-energy (right) images from patient 1. Note that the tumour, indicated by the implanted marker, is obscured by soft tissue only for imager 1 (above), while for imaging angle 2 the tumour is mostly obscured by the ribs.

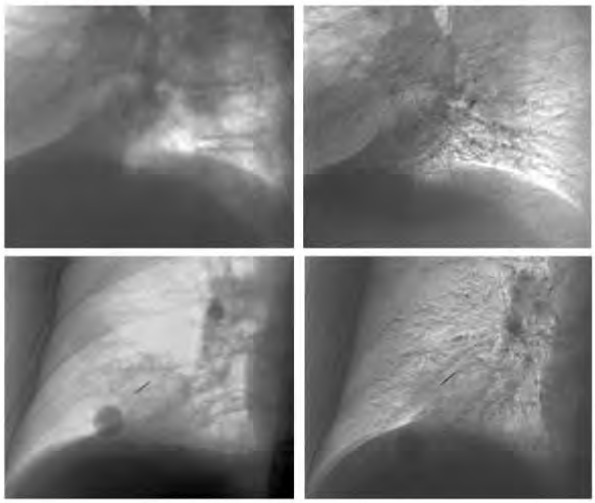

Table 1 Root-mean square (RMS) tracking errors, defined based on the implanted marker distance, from 2D/2D registration between DRR and dual-energy images, and DRR and high-energy images.

	RMS tracking error		
	DRR - DE	DRR - HE	t-test
patient 1 Im. 1 - 10°	1.7 ± 0.8	2.2 ± 0.8	p = 0.08
patient 1 Im. 2 - 100°	1.2 ± 0.6	1.3 ± 0.5	p = 0.83
patient 2 Im. 1 - 70°	1.8 ± 0.7	3.1 ± 1.1	p < 0.01
patient 2 Im. 2 – 340 °	1.4 ± 0.5	1.6 ± 0.8	p = 0.78
patient 3 Im. 1 - 250°	1.3 ± 0.4	1.2 ± 0.4	p = 0.85
patient 3 Im. 2 - 160°	1.3 ± 0.4	2.1 ± 0.5	p = 0.06

Conclusion: The results of this prospective evaluation indicate that for markerless localization of lung tumors through 4D/3D intensity-based registration, using DE images is more accurate than using regular kV images for certain imaging angles. Removing overlying bony anatomy and enhancing tumor visualization prior to registration makes the workflow more robust.

PV-0324

Intra-fraction motion characterisation of head-and-neck tumors using cine-MRI

T. Bruijnen[1], B. Stemkens[1], M.E.P. Philippens[1], L.P.W. Canjels[1], R.H.N. Tijssen[1], T. Schakel[1], C.H.J. Terhaard[1], J.J.W. Lagendijk[1], C.P.J. Raaijmakers[1]
[1]*University Medical Center Utrecht, Radiotherapy, Utrecht, The Netherlands*

Purpose or Objective: Intensity modulated radiotherapy and the recent introduction of the MR-linac emphasize the need for detailed tumor motion characterization for adequate motion management in radiotherapy planning and online MRI-guidance. Hitherto, intra-fraction head-and-neck (H&N) tumor motion has been assessed as the displacement of local

landmarks in cone beam CT or X-ray. The superior soft-tissue contrast of MRI enables characterization of the actual tumor displacement. Here, we investigate the intra-fraction tumor displacement on a sub-second and 10-minute time scale, using cine-MRI.

Material and Methods: Thirteen patients with H&N squamous cell carcinoma underwent pretreatment clinical MR imaging in a radiotherapy immobilization mask. Two 2D sagittal cine-MR scans (balanced steady state free precession; TE/TR = 1.2/2.5 ms; 1.42x1.42mm², slice thickness 10 mm, 500 dynamics), positioned through the tumor were acquired with 8 frames per second and an interval of 10-15 min on a 3.0T MR scanner. Tumor GTVs were delineated by a radiation oncologist.
Image analysis: Tumor motion was estimated by non-rigid image registration over the 1 minute dynamic MRI data using an optical flow algorithm (Fig. 1a). The displacement vectors on the GTV border were combined into a 95th percentile distance (dist95%) for every image. 95% of the range of dist95% over time was used as a measure of tumor displacement. The standard deviation of the GTV border displacement vectors was calculated and averaged over the time series as a measure of tumor deformation. Tumor displacement over 10 minutes was estimated by computing the difference in the average tumor position between the two dynamic series with an equivalent non-rigid registration.

Results: Results of the image registration (Fig. 1c) showed respiratory-induced tumor motion, which was confirmed by a peak at the principle respiratory frequency in a power spectrum analysis. Displacements were relatively small in both directions with a median displacement of 0.60 ± 0.13 mm (range: 0.18–1.44 mm) (AP) and 0.59 ± 0.11 mm (range: 0.32-2.69 mm) (CC) (Fig. 1b), which agreed with visual inspection. For two patients standard deviations within the border pixels were > 0.20 mm, which might imply a deformation of the tumor. The average tumor position differences over 10 minutes were smaller than the tumor displacement in the 1-minute data for both directions, with means of 0.28 mm (range: 0.08-0.99 mm) (AP) and 0.34 mm (range: 0.07-0.99 mm) (CC).

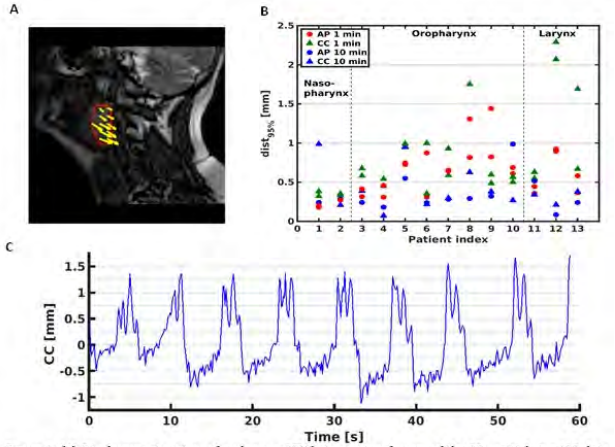

Figure 1. (A) Displacement vectors of a pharynx GTV between two frames of the 2D sagittal cine-MR data. (B) P95 displacement values for the surface pixels of delineated GTVs, red and green markers show the average AP/CC displacement of the tumor during respiration. Blue markers show the difference in average tumor position over 10 minutes. (C) Tumor displacement in CC direction over a single dynamic MRscan.

Conclusion: Tumor displacements on both time scales were relatively small, but varied considerably between patients.

PV-0325
Retrospective self-sorted 4D-MRI for the liver
T. Van de Lindt[1], U. Van der Heide[1], J. Sonke[1]
[1]*Netherlands Cancer Institute Antoni van Leeuwenhoek Hospital, Radiation Oncology, Amsterdam, The Netherlands*

Purpose or Objective: There is an increasing interest in 4D-MRI for MR-guided radiotherapy. 4D-MRI methods are typically based on either an external respiratory surrogate with possible deviations from internal motion or an internal navigator channel which can disturb the image acquisition. Experimental methods, using self-gated strategies based on the center of k-space, lack a quantitative signal and have extensive scan times. To overcome these limitations, a new self-sorted 4D-MRI method was developed for treatment planning and MR-guided radiotherapy of the liver.

Material and Methods: For 3 volunteers, a 2D multi-slice MRI of the upper-abdomen was acquired 30 times (single-shot TSE, slices=25, voxel size=2x2x5mm3, TR=383ms, TE=80ms, dynamics=30) and resulted in a total of 750 axial slices (scan time 4:50min) in an unknown respiratory state. For comparison, a navigator was acquired, outside the FOV, prior to every slice acquisition.
To extract the respiratory signal from the data, first a 3D exhale reference dataset was constructed. As the anatomy predominantly moves in the SI-direction, the average position of every slice is located below the exhale position. Therefore, for each slice, the dynamic with the highest mean correlation with all dynamics of the slice below was selected for the exhale reference set. The exhale data was then interpolated to slices of 1mm. Then all slices of all dynamics were registered to the exhale reference frame in SI-direction, using correlation as an objective function, resulting in a displacement relative to exhale. To obtain a 4D-MRI reconstruction, the resulting respiratory signal was processed to identify inhale positions and sort the data according to phase. This was compared to the navigator signal and associated sorting.

Results: The self-sorting signal (SsS) and the navigator signal (NavS) correlate very well (mean r=0.86). For all volunteers, the SsS and NavS identified the same number of inhale positions with an average mean absolute difference (MD) of 268ms. This is in good agreement with the slice acquisition time. The 10 phase 4D-MRI was on average under-sampled 7% (NavS) and 14% (SsS) and missing slices were linearly interpolated. After reconstruction, the average MD of the LR, SI and AP motion obtained by local rigid registration were 0.3, 0.6 and 0.3mm, respectively. Reconstruction time was ~20s on a 8 Core Intel CPU, 3.4GzH, 16GB RAM PC.

Volunteers		A	B	C
Respiratory signal				
r = corr(NavS,SsS)		0.96	0.74	0.89
Inhale positions				
MD(NavS, SsS)	(ms)	273	284	249
4D reconstruction				
Under-sampling NavS	(%)	2	5	14
Under-sampling SsS	(%)	7	14	15
Motion				
LR: MD(NavS, SsS)	(mm)	0.1	0.3	0.6
SI: MD(NavS, SsS)	(mm)	0.4	0.5	1.0
AP: MD(NavS, SsS)	(mm)	0.2	0.2	0.5

Table1: Comparison between navigator (NavS) and self-sorting signal (SsS) for 3 volunteers

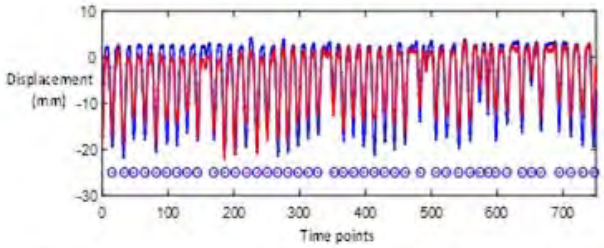

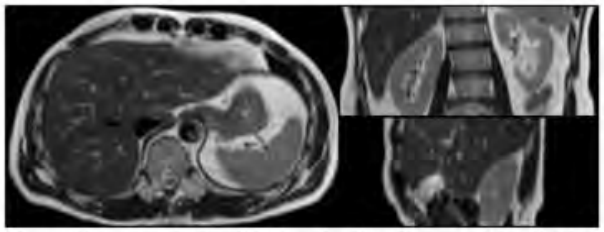

Figure1 (top): Navigator (blue) and self-sorting signal (red). Blue circles at the bottom represent minima derived from the NavS and red dots represent minima derived from SsS.
Figure2 (bottom): Axial, coronal and sagittal slice from reconstructed 4D-MRI. FOV was lowered for minimal interaction with the navigator channel.

Conclusion: A 4D-MRI dataset could be acquired in ~5min and reconstructed by retrospective sorting using a self-sorting signal. The signal correlated very well with an additionally acquired navigator signal. Differences in motion between the reconstructed data using the self-sorting signal and the navigator were minimal. Before clinical implementation, acquisition and reconstruction parameters should be optimized and the method should be verified in more volunteers as well as in patients.

Acknowledgements: This research was partly sponsored by Elekta AB.

PV-0326

Respiratory gating guided by internal electromagnetic motion monitoring during liver SBRT

P. Poulsen[1], E. Worm[2], R. Hansen[2], L. Larsen[3], C. Grau[1], M. Høyer[1]
[1]*Aarhus University Hospital, Department of Oncology, Aarhus, Denmark*
[2]*Aarhus University Hospital, Department of Medical Physics, Aarhus, Denmark*
[3]*Aarhus University Hospital, Department of Radiology, Aarhus, Denmark*

Purpose or Objective: Accurate dose delivery is crucial for stereotactic body radiation therapy (SBRT), but the accuracy is challenged by intrafraction motion, which can be several centimeters for the liver. Respiratory gating can improve the treatment delivery, but may be inaccurate if based on external surrogates. This study reports on the geometric and dosimetric accuracy of our first four liver SBRT patients treated with respiratory gating using internal electromagnetic motion monitoring. We expect to include 10-15 patients in this gating protocol with three new patients being recruited at the time of writing.

Material and Methods: Four patients with liver metastases were treated in three fractions with respiratory gated SBRT guided by the position signal of three implanted electromagnetic transponders (Calypso). The CTV was defined in the end exhale phase of a CT scan and extended by 5 mm (LR/AP) and 7-10 mm (CC) to form the PTV. 7-field conformal or IMRT plans were designed to give a mean CTV dose of 18.75Gy or 20.60Gy per fraction (=100% dose level) and minimum target doses of 95% (CTV) and 67% (PTV). The treatment was delivered in free respiration with beam-on in end-exhale when the centroid of the three transponders deviated less than 3mm (LR/AP) and 4mm (CC) from the planned position. The couch was adjusted remotely if intrafraction baseline drift caused the end exhale position to deviate more than ~2 mm from the gating window center. Log files provided the transponder motion during beam-on in the actual gated treatments and in simulated non-gated treatments with CBCT-guided patient setup. This motion was used to reconstruct the actually delivered CTV dose distribution with gating and the would-be dose distribution without gating. The minimum dose to 95% of the CTV (D95) for each fraction and each course was compared with the planned CTV D95.

Results: Fig. A shows the internal tumor motion at a fraction with large baseline drift of 3mm (LR), 9mm (CC), and 6mm (AP) relative to the pre-treatment CBCT. Fig. B shows the same motion with four drift compensating couch adjustments applied as marked with red lines. The width of the green areas indicates the time of beam delivery. The height indicates the allowed positions for beam-on without (Fig. A) and with (Fig. B) gating. The course mean geometrical error was <1.2mm for all gated treatments, but would have ranged from -2.8mm to 1.2mm (LR), from 0.7mm to 7.1mm (CC), and from -2.6mm to 0.1mm (AP) without gating due to baseline drift. Fig. C shows the CTV D95 reduction relative to the planned D95 versus the 3D mean error for each fraction and course. The mean reduction in D95 for the 12 fractions was 1.1% [range: 0.1-2.1%] with gating and 10.8% [0.9-35%] without gating. The mean duty cycle was 59% [54-70%].

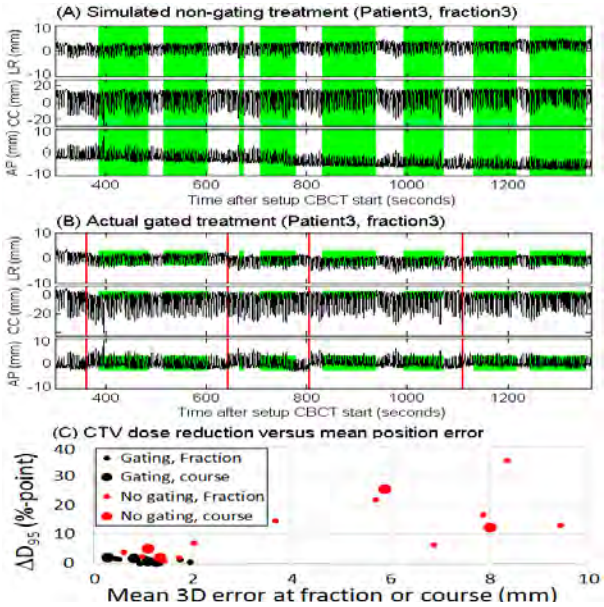

Conclusion: Respiratory gating based on internal electromagnetic monitoring was performed for four liver SBRT patients. The gating added robustness to the dose delivery and ensured a high CTV dose even in the presence of large intrafraction motion.

PV-0327

Patient-specific motion management and adaptive respiratory gating in Pancreatic SBRT

B.L. Jones[1], W. Campbell[1], P. Stumpf[1], A. Amini[1], T. Schefter[1], B. Kavanagh[1], K. Goodman[1], M. Miften[1]
[1]*University of Colorado School of Medicine, Radiation Oncology, Aurora, USA*

Purpose or Objective: Ablative radiotherapy is rapidly emerging as an effective treatment for locally advanced pancreatic adenocarcinoma. However, the pancreas undergoes erratic and unstable respiratory-induced motion, which decreases coverage of the tumor and increases dose to the duodenum. The purpose of this study was to develop and optimize motion management protocols which allow for safe delivery of pancreatic SBRT.

Material and Methods: We analyzed 4DCT and CBCT data from 35 patients who received pancreatic SBRT; the majority were locally advanced tumors receiving 30 Gy in 5 fractions.

In total, the data from 175 treated fractions was analyzed. For each fraction, the daily trajectory of the tumor was reconstructed by calculating a Gaussian probability density function using the location of gold fiducial markers in the CBCT projections. These trajectories represented over 600 samples of the position of the tumor during the course of CBCT acquisition. Using the calculated trajectories, we investigated the dosimetric impact of several respiratory motion management strategies, including gating based on instantaneous kV imaging of implanted fiducial markers.

Results: 4DCT was a poor predictor of pancreatic motion, as the amplitude of daily motion exceeded the predictions of pre-treatment 4DCT by an average of 3.5 mm in the SI direction. In a Fourier-based analysis, these uncertainties were correlated with an increase in low-frequency motion (potentially due to peristalsis of the duodenum). Abdominal compression increased the consistency of motion and reduced the amplitude by 2.7 ± 2.8 mm. On average, respiratory gating decreased the apparent motion even further, with attainable effective motion amplitudes of 2 mm. However, gating based on external surrogates (either phase- or amplitude-based) is greatly hindered in some patients by the inconsistency of pancreatic motion. In these cases, internal gating surrogates are warranted. In a simulated clinical scenario, fiducial-based internal gating using a 2 mm SI window greatly outperformed conventional gating using external surrogates ($p<0.001$), with a mean target D95 of 99±2%, 95% CI 93-100% (conventional gating – D95 97±7%, 95% CI 68-100%). Additionally, we analyzed the dosimetry of motion by convolving the dose distribution with phase-specific motion information. Using these data, we developed a metric that predicts patient-specific consistency, and in a simulated adaptive protocol which adjusted margins based on this metric, there were significant increases in mean target D95 and minimum dose.

Conclusion: Motion management is essential in reducing the size of target volumes and minimizing dose/side effects to the small bowel. Motion uncertainties and patient-specific differences warrant an adaptive approach to respiratory management. Our data shows that using real-time kV imaging of implanted fiducial markers to adapt the gating protocol based on the instantaneous position of the tumor outperforms conventional approaches.

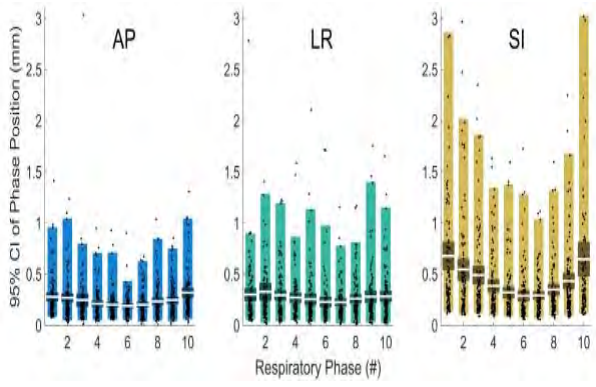

PV-0328

Rectal immobilisation device in stereotactic prostate treatment: intrafraction motion and dosimetry

J. De Leon[1], D. Rivest-Henault[2], S. Keats[1], M. Jameson[1], R. Rai[1], S. Arumugam[1], L. Wilton[3], D. Ngo[1], J. Martin[3], M. Sidhom[1], L. Holloway[1]

[1]*Liverpool Hospital, Liverpool Cancer Therapy Centre, Liverpool, Australia*

[2]*CSIRO Digital Productivity Flagship, The Australian e-Health Research Centre, Herston, Australia*

[3]*Calvary Mater Newcastle, Cancer Therapy Centre, Newcastle, Australia*

Purpose or Objective: PROMETHEUS (UTN: U1111-1167-2997) is a multicentre clinical trial investigating the feasibility of stereotactic radiotherapy (SBRT) as a boost technique for prostate cancer. The objective of this sub-study is to evaluate infraction motion, using cine MRI, and the dosimetric impact when using a rectal immobilisation device (RID).

Material and Methods: The initial 10 patients recruited underwent planning CT and MRI, with and without a RID. Cine MRI images were captured using an interleaved T2 HASTE sequence in sagittal and axial planes with a temporal resolution of 5.4 seconds acquired over 4 minutes, the average time for a single SBRT VMAT fraction. Points of interest (POI) were outlined by a single investigator and a validated tracking algorithm measured displacement of these points over the 4 minutes in the anterior – posterior, superior – inferior and left – right directions (Figure 1).

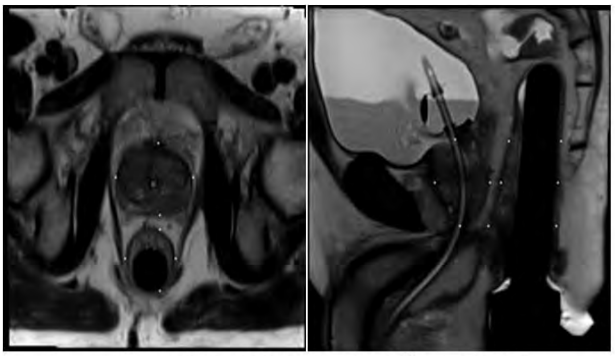

Figure 1: Axial and sagittal MRI slice showing Points of Interest (white dots)

Planning CT and MRI scans were fused and contoured by a single investigator. They were planned using a VMAT technique to 19Gy in 2 fractions by a single investigator. The planning priority set for the non – RID plan was to match the coverage achieved in the RID plan. Dose Volume Histogram results of both plans were analysed.

Results: There was an overall trend for increasing POI displacement in all directions as time progressed when no RID was insitu. POI remained comparatively stable with the RID.
In the sagittal plane, the RID resulted in statistically significant improvement in the range of anterior - posterior displacement over the entire 4 minutes of the inferior anterior and posterior rectal wall (both $p<0.001$), mid anterior and posterior rectal wall (both $p = 0.007$), anterior prostate ($p =0.019$), prostate apex ($p = 0.003$) and prostate base ($p=0.011$).
The RID also resulted in improvement in range of superior - inferior displacement of the inferior posterior rectal wall ($p = 0.002$), mid anterior rectal wall ($p = 0.043$) and posterior rectal wall ($p = 0.023$).
In the axial plane, the RID resulted in statistically significant improvement in the range of anterior - posterior displacement of the anterior rectal wall ($p =0.008$) and posterior prostate ($p=0.011$).
For all these points, the RID approximately halved the range of displacements, with some points moving over 2mm when no RID was insitu.
Dosimetrically, the use of a RID significantly reduced rectal V16 (0.27cc vs 1.71cc; $p < 0.001$), V14 (1.12cc vs 2.32cc; $p =0.02$) and Dmax (15.72Gy vs 18.90Gy; $p < 0.001$), as well as percentage of posterior rectal wall receiving 8.5Gy (7.38% vs 12.20%; $p = 0.003$). There was no statistically significant difference between bladder or urethral Dmax, CTV D98 or conformity index between both plans.

Conclusion: The rectal immobilisation device used in stereotactic prostate radiotherapy leads to reduced intrafraction motion of the prostate and rectum, with increasing improvement with time. It also results in significant improvement in rectal wall dosimetry.

PV-0329

Modulation indexes for predicting interplay effects in lung SABR treatments

J. Puxeu Vaqué[1], V. Hernandez[2], J. Saez[3], P. Saldaña[1], W.H. Nailon[4], A. Sankar[4], M.A. Duch[5]
[1]*Institut Català d'Oncologia, Department of Medical Physics, L'Hospitalet de Llobregat, Spain*
[2]*Hospital Universitari St Joan, Medical Physics Department, Reus, Spain*
[3]*Hospital Clinic de Barcelona, Radiation Oncology Department, Barcelona, Spain*
[4]*Edinburgh Cancer Centre, Department of Oncology Physics, Edinburgh, United Kingdom*
[5]*Universitat Politecnica de Catalunya, Institut de Tecniques Energetiques, Barcelona, Spain*

Purpose or Objective: The purpose of this study was to analyze the modulation indexes proposed in the literature for predicting interplay effects in lung SABR treatments

Material and Methods: 23 SABR plans (4 arcs of 200°-220° for 6MV and 2 arcs for 10 MV FFF) calculated on Eclipse V10.1 (Varian) were analyzed with the Quasar respiratory phantom (Modus Medical Devices) by comparing dose distributions on EBT3 radiochromic film. Static and dynamic irradiation at 0.5 cm amplitude (1 cm peak-to-peak) and 12 breaths per minute (BPM) was used. 18 plans were irradiated in a Silouette LINAC with 6 MV and 5 on a TrueBeam (Varian) LINAC with 6 MV FFF. The acceptance criteria was set to be < 5% of points with γ(3%,3mm)>1 on the comparison between static and dynamic dose distributions. A threshold of 90% was fixed since the aim was to study the influence of the modulation on the ITV. The modulation indexes analyzed were: The Modulation Complexity Score (MCS)-McNiven 2010; the Modulation Index Total (MIt)- Park 2014 which introduces speed and MLC acceleration and finally the Aperture Irregularity (AI) -Du 2014 which analyzes the non-circularity of the MLC apertures. A Matlab (Mathworks) program was developed to calculate them. Finally, the PUMA method, which is based on splitting arcs in the TPS and modeling movements by changing their isocenter positions, was also used. Possible linear correlation between these indexes and radiochromic films was analyzed and a statistical analysis performed.

Results: Modulation indexes are shown in Table 1. A statistical analysis of the goodness of fit was done; which found only significant linear correlation ($p < 0.0001$) between film-PUMA, film-MIt and also between PUMA-MIt A positive plan is considered to be a plan suitable for treatment when evaluating the interplay effect. A value of 0.6 for the MIt index is proposed as the upper limit. This value was selected in order to minimize the number of false negative plans. MIt and PUMA have the same specificity (100%) since both detected all of the failing plans. However, PUMA has a greater sensitivity (95% vs 85%).

Plan	Rad. film (%)	PUMA	MCS	MIt	AI
1	4.3	4.9	0.19	0.83	5.75
2	7.1	9.2	0.20	0.72	5.31
3	3.7	11.7	0.24	0.66	6.68
4	3.6	2.1	0.18	0.70	8.33
5	3.3	1.2	0.24	0.49	4.28
6	8.1	17.8	0.60	1.04	1.69
7	2	0.0	0.45	0.33	1.86
8	2.5	3.2	0.28	0.45	3.49
9	0.2	0.4	0.31	0.54	4.69
10	1.4	0.0	0.41	0.37	3.50
11	0.0	0.0	0.31	0.44	3.08
12	0.0	4.5	0.32	0.44	2.81
13	0.3	0.0	0.42	0.38	2.24
14	3.0	2.0	0.43	0.55	5.11
15	0.2	0.0	0.45	0.38	3.68
16	2.9	0.5	0.34	0.60	3.80
17	2.5	0.5	0.30	0.52	4.21
18	1.6	0.0	0.48	0.37	3.29
19	1.5	0.0	0.43	0.41	2.02
20	15.1	9.0	0.24	0.79	4.31
21	1.7	0.8	0.29	0.48	3.54
22	0.0	0.0	0.41	0.42	2.22
23	3.2	0.0	0.35	0.43	2.76

Table 1. Calculated indexes for the 23 plans.

Conclusion: Most of the modulation indexes proposed in the literature are related to the robustness and modulation of a plan. However, none of them has been conceived to appropriately predict the interplay effect in lung SABR. MIt has been found to be the only published index capable of detecting failing plans. MIt and PUMA have the same specificity since both detected all of the failing plans. However, PUMA has a greater accuracy and sensitivity.

Symposium with Proffered Papers: Uncovering the gap between optimal and actual utilisation of radiotherapy in Europe

SP-0330

Introduction: The HERO data on optimal versus actual utilisation of radiotherapy in Europe

G.Crau[1]
[1]*Aarhus University Hospital, Radiation Oncology, Aarhus C, Denmark*

OC-0331

How many new cancer patients in Europe will require radiotherapy by 2025? An ESTRO-HERO analysis

J.M. Borras[1], Y. Lievens[2], M. Barton[3], J. Corral[4], J. Ferlay[5], F. Bray[5], C. Grau[6]
[1]*Institut Català d'Oncologia, University of Barcelona- IDIBELL, L'Hospitalet de Llobregat, Spain*
[2]*Ghent University Hospital, Radiation Oncology Department, Ghent, Belgium*
[3]*University of South New Wales, CCORE Ingham Institute for Applied Medical Research, Liverpool, Australia*
[4]*Autonomous University of Barcelona, Doctoral Programme in Public Health- Department of Pediatrics- Obstetrics-Gynecology and Preventive Medicine and Public Health, Barcelona, Spain*
[5]*International Agency for Research on Cancer, Section of Cancer Surveillance, Lyon, France*
[6]*Aarhus University Hospital, Department of Oncology, Aarhus, Denmark*

THIS ABSTRACT FORMS PART OF THE MEDIA PROGRAMME AND WILL BE AVAILABLE ON THE DAY OF ITS PRESENTATION TO THE CONFERENCE

OC-0332

Modelled effects of hypofractionation on radiotherapy demand in England

T. Mee[1], N.F. Kirkby[1], K.J. Kirkby[1], R. Jena[2]
[1]*University of Manchester, Institute of Cancer Sciences, Manchester, United Kingdom*
[2]*University of Cambridge, Department of Oncology, Cambridge, United Kingdom*

Purpose or Objective: Current clinical trials and studies are identifying hypofractionation as a viable treatment option when compared with current fractionation regimens. Our work estimates the reduction in the number of fractions prescribed and the potential effect on the overall demand for radiotherapy across the whole of England. With the evidence based estimates of demand for radiotherapy currently outstripping the supply capacity in England, this potential reduction in fraction demand needs to be calculated to assess the potential effects for radiotherapy service and infrastructure planning.

Material and Methods: The Malthus Program, a tool for modelling radiotherapy demand, was used to calculate the potential effect of three hypofractionation studies/trials for the population of England. Well-published and potential clinical indications for hypofractionation have been modelled for prostate cancer, non-small cell lung cancer (NSCLC) and breast cancer. The hypofractionation indications for radiotherapy were mapped into the original Malthus clinical decision trees and simulations completed to study the effects of hypofractionation on demand.

Results: If the CHHiP prostate trial achieves universal uptake throughout England then it has the potential to reduced radiotherapy demand by 3,500 fractions per million population (#pmp). SBRT for medically inoperable (or refusal of surgery) for stage 1 and stage 2 NSCLC has the potential to reduce the demand by a further 700 #pmp. The FAST-Forward trial, using 5# instead of 15# for T1-3 N0-1 M0 breast cancer has the potential to reduce demand by 4,600 #pmp. A potential reduction in modelled demand of 8,800 #pmp arises from these three studies alone. Across the total population of England, this translates to approximately 479,600 fractions per year.

Conclusion: The current clinical indications and trials for hypofractionation have the potential to reduce the evidence-based estimates of demand of radiotherapy sufficiently to be achievable with a modest increase of the current levels of equipment in England. While the presented calculations are for England as a whole, the Malthus program offers the facility to calculate the changes in modelled demand at a regional level within England, enabling a more precise calculation for treatment centres and their local catchment.

SP-0333

Evaluation of radiotherapy utilisation in Belgium: patterns and possible causes of suboptimal use

E. Van Eycken[1], H. De Schutter[1], K. Stellamans[2], M. Rosskamp[1], Y. Lievens[3]
[1]*Belgian Cancer Registry, Brussels, Belgium*
[2]*General Hospital Groeninge, Radiation Oncology, Kortrijk, Belgium*
[3]*Ghent University Hospital, Radiation Oncology, Ghent, Belgium*

Using the evidence-based decision analytic model developed by the Collaboration for Cancer Outcomes, Research and Evaluation (CCORE) (1), the ESTRO-HERO project (2,3) calculated that 53.2% of incident cancer patients in Belgium would require external beam radiotherapy during the course of their disease. In order to find out what is the actual utilization of radiotherapy in Belgium and how it compares with this calculated optimal utilization proportion (OUP), a population consisting of 112,235 patients with a unique invasive cancer diagnosis in the years 2009 and 2010 was evaluated. Tumour categories were defined according to the CCORE methodology. For each cancer, the data set consisted of the incidence date, topography, histology, TNM stage and the treatment recommendations formulated during the multidisciplinary team meetings (MDT), the latter giving an indication on the pattern of radiotherapy prescription in Belgium. Data on reimbursement for external beam radiotherapy, obtained through linkage with the administrative database from the Health Insurance Companies and covering a time period up till 3 years after the year of incidence, provided insight in the actual utilization. Besides overall analyses at the Belgian population level, variability of actual and optimal utilization amongst cancer types was assessed.

For the Belgian cancer population diagnosed in 2009-2010, the actual use of radiotherapy was 35.1%. About 3 in 4 of these patients received radiotherapy within the first 9 months after diagnosis, providing an estimate of those irradiated in the context of the primary treatment strategy. The global result was in line with the percentage of prescribed or recommended radiotherapy series (35.0%) during the MDT.

Radiotherapy uptake varied with primary tumour site. Most of the cancers in Belgium have a lower actual utilization than predicted with the exception of leukaemia, ovarian, thyroid, testicular, colon and liver cancer. Most pronounced differences between optimal and actual utilization were found in less typical radiotherapy indications such as in bladder, brain, lymphoma, myeloma, pancreas and stomach cancer. For more common radiotherapy indications such as breast, head and neck and rectal cancer, the underutilization is about 10-15% while in lung, oesophagus and prostate cancer, the underuse was more pronounced resulting in only about 55-60% of the patients requiring radiotherapy being actually treated.

These data, derived at the unique patient-level, illustrate that even in a country that is well-resourced in terms of radiotherapy staffing and infrastructure, a clear discrepancy can be observed between the optimal and actual radiotherapy delivery. Potential reasons for this may include physician and patient preferences favouring non-radiotherapy regimens in case of competing treatment modalities (e.g. in prostate cancer), deviation from guidelines (e.g. due to comorbidity or low performance status), an overestimation of the real needs by the evidence-based OUP-model and an underestimation of the actual utilisation due to available nomenclature data being limited to 3 years after incidence. These reasons all deserve further evaluation and they must be carefully taken into account when forecasting and planning radiotherapy staffing and infrastructure.

References:

(1) Ingham Institute for Applied Medical Research (IIAMR) – Collaboration for Cancer Outcomes Research and Evaluation (CCORE). Review of optimal radiotherapy utilization rates. CCORE report; 2013. Available from: https://inghaminstitute.org.au/content/ccore (accessed 22/12/2015)

(2) Borras JM, Barton MB, Grau C et al. The impact of cancer incidence and stage on the optimal utilization of radiotherapy: methodology of a population based analysis by the ESTRO-HERO project. Radiother Oncol. 2015 Jul;116(1):45-50. doi: 10.1016/j.radonc.2015.04.021. Epub 2015 May 19.

(3) Borras JM, Lievens Y, Dunscombe P et al. The optimal utilization proportion of external beam radiotherapy in European countries: An ESTRO-HERO analysis. Radiother Oncol. 2015 Jul;116(1):38-44. doi: 10.1016/j.radonc.2015.04.018. Epub 2015 May 14.

SP-0334

Cancer plans in Europe and radiotherapy needs assessment: can we dance a tango?

T. Albreht[1]
[1]*National Institute of Public Health NIJZ, Ljubljana, Slovenia*

European countries have a several decade long history of planning for cancer services and cancer care. The World Health Organization (WHO), whose focus was on middle-income countries, had launched the original initiative. WHO at that time at the beginning of the 1980s also proposed the first comprehensive definition of National Cancer Control Programmes (NCCP): *"A national cancer control programme is a public health programme designed to reduce the number of cancer cases and deaths and improve quality of life of cancer patients, through the systematic and equitable implementation of evidence-based strategies for prevention, early detection, diagnosis, treatment, and palliation, making the best use of available resources."* Cancer control programmes bear different names – cancer plans, cancer control programmes, cancer strategies, etc. They may be national or regional, but in either case they are closely related with the decision-making authorities. They depend on the appropriate allocation of resources and on the legal enactment of regulation of cancer care delivery and all of its services and activities. The rapid growth in cancer incidence coupled with exorbitantly rising costs brought the reflection on the planning of cancer care and its services to the European Union's table. As a result of the conclusions of the Slovenia's Presidency to the Council of the European Union, an initiative called European Partnership for Action Against Cancer (EPAAC) was born and launched by Commissioner Dalli in September 2009. At the same time the European Commission called upon Member States (MS) to develop and adopt national cancer plans (NCPs) or strategies by 2013. In the Joint Action (JA) EPAAC, which acted as the practical implementation of the partnership, the status of the national cancer plan development was revised through a comprehensive survey in all MSs, Norway and Iceland. What should be practical consequences of an NCP? In principle they should be the following: Mapping all the processes belonging to the comprehensive control and management of cancerIdentifying priorities in cancer careDefining clear patient pathways and assuring the necessary resources for themSecuring sufficient financial resources through the implementation of both guidelines and patient pathwaysIntroducing new programmes – therapeutic and screening, treatment approaches and new concepts, such as survivorship.Raising awareness of the different elements in cancer care and management From the point of view of radiotherapy all of the above are relevant and pertinent. The changing epidemiology, treatment patterns and improved survival rates all raise the importance of comprehensive approaches. Radiotherapy has not seen appropriate attention in terms of economic evaluation since a lot of attention lies with the medical, i.e. phamacological treatment. Contrary to the analyses on the innovative therapies and new lines of cancer drugs, radiotherapy does not attract that many health technology assessments. There are at least the following reasons why it should: The greater and rising use of radiotherapy treatments in cancer care.The high cost of initial investment and maintenance – the latter being equally important as the formerThe need for more flexibility in its availability and useThe inherent multi- and interdisciplinarity needed to successfully carry out the radiotherapeutic care For policy makers often the immediate needs and problems are more relevant than rather remote projections. Nevertheless, the need to plan is even more pertinent to the investments needed for radiotherapy than for other types of care. This makes it benefit better from the planning process but also raises the need to better balance the different therapeutic elements in cancer care when adopting and changing guidelines and patient pathways. Consequently, plans may better reflect the future need for investment and for the planning and development of human resources. In that sense and through its dependance on technology, radiotherapy should be even more interested in supporting and contributing to the idea of the national cancer plans. There have been recent challenges for many countries lately. Austerity measures have cut into health care budgets similarly as into other public expenditures. Careful epidemiological analyses that can evaluate the contribution of the different elements of care to patient survival and quality of life are extremely important and may very often offset the costs of complex treatments. Radiotherapy is a vital element of comprehensive cancer care. Given its needs for careful planning, equipment purchases and development of human resources in combination with a rising need for radiotherapy, there is a definite need for clear identification of radiotherapy in national cancer plans. Only through such transparency it is possible to secure all the conditions for further development of cancer radiotherapy.

Debate: Maximising tumour control: crank up the volume or turn off the switches?

SP-0335
For the motion
A Tree[1]
[1]*The Institute of Cancer Research and the Royal Marsden NHS Foundation Trust, Academic Radiotherapy, Sutton, United Kingdom*

SP-0336
Against the motion
J-J Sonke[1]
[1]*Netherlands Cancer Institute, Radiotherapy Department, Amsterdam, The Netherlands*

SP-0337
For the motion rebuttal
B. Wouters[1]
[1]*Ontario Cancer Institute, Princess Margaret Cancer Centre, Toronto, Canada*

SP-0338
Against the motion rebuttal
A. Dekker[1]
[1]*MAASTRO Grow, School for Oncology and Developmental Biology, Maastricht, The Netherlands*

Proffered Papers: Clinical 7: Urology

OC-0339
More acute proctitis symptoms with hypofractionation (3.4 Gy) than 2 Gy fractions
W. Heemsbergen[1], L. Incrocci[2], C. Vens[3], M. Witte[1], S. Aluwini[2], F. Pos[1]
[1]*Netherlands Cancer Institute, Dept of Radiation Oncology, Amsterdam, The Netherlands*
[2]*Erasmus MC Cancer Institute, Dept of Radiation Oncology, Rotterdam, The Netherlands*
[3]*Netherlands Cancer Institute, Division of Biological Stress Response, Amsterdam, The Netherlands*

Purpose or Objective: Several clinical studies investigated hypofractionation schedules with fractions ≥ 3 Gy in prostate cancer. Recovery from rectal radiation damage has been reported to depend on weekly dose rates, implying that acute rectal toxicity is regarded as little fractionation sensitive. A phase 3 randomized trial, with dose delivery of ≈10 Gy/week in both arms, recently reported a significantly higher peak incidence of RTOG grade≥2 gastrointestinal (GI) toxicity in the 3.4 Gy vs the 2 Gy fractions arm. Here, we further analyzed the acute proctitis symptoms of the two schedules with 3.4 Gy or 2Gy fractions delivered with image-guided (IG)-IMRT, and compared it with the incidence of patients receiving 2 Gy fractions delivered with a 3D conformal technique (3DCRT).

Material and Methods: We selected patients treated with IG-IMRT (planning margins 5-8 mm) from a randomized trial for localized prostate cancer, with patients in the Hypofractionation arm (HF, n=303) receiving 3 fractions per week of 3.4 Gy with 48h intervals, during 6.5 weeks. Patients in the standard arm (SF, n=298) received 5 fractions of 2 Gy per week with 24h intervals, for 8 weeks. A third historical group (3DCRT) contained patients from a previous

trial (n=522) treated with 2 Gy/fraction (7-8 weeks), planning margins of 10 mm, and a three-field 3D-conformal technique. Prospectively collected patient-reported symptoms were available for week 4 and week 6. Peak incidences (maximum week 4 & 6) were compared between the groups (chisquare test).

Results: We found a significantly increased risk for acute rectal bleeding in the HF group (15.1% versus 7.6% for SF, **Table 1, Figure 1**), which implies a relative risk of 2.0. Increased risks for HF vs SF ($p<0.05$) were also found for mucus loss, loose stools, and increased stool frequency. **Figure 1** shows the incidences for bleeding and mucus loss (with 1 SE). The increased risks for bleeding in the HF schedule were comparable with the observed risks in the historical 3DCRT cohort. Risks for other toxicities with HF were somewhat lower than for 3DCRT, with no significant differences except for stools≥4 (HF 34.7% vs 3DCRT 42.9%, $p=0.02$). Incidence of diarrhea exceeded that of the 3DCRT schedule, but not significantly ($p=0.1$).

Conclusion: We observed significantly more acute proctitis symptoms in the HF group. These data might point to an underestimated fractionation sensitivity of acute rectal tissue. Our findings suggest that the repair capacity between two fractions was less effective when 3.4 Gy was delivered every other day, compared to daily 2 Gy fractions. The increased damage by hypofractionation is in the same order as the reduction in damage previously achieved with the introduction of IG-IMRT.

Table 1. Acute gastrointestinal symptoms with p for hypo-fractionation (HF, 3.4 Gy) vs standard fractionation (SF, 2 Gy).

GI symptom	Peak incidence W4 - W6 (%)			
	HF N=303	SF N=298	p	3DCRT N=522
Blood loss	15.1	7.6	**0.004**	15.6
Mucus loss	50.8	38.2	**0.002**	57.9
Pain/cramps	46.0	39.4	0.110	51.9
Loose stools	52.5	42.8	**0.025**	56.1
Stools 4+	34.7	25.8	**0.018**	42.9
Incontinence	19.5	14.0	0.100	21.8
Diarrhea	16.5	13.4	0.290	12.6

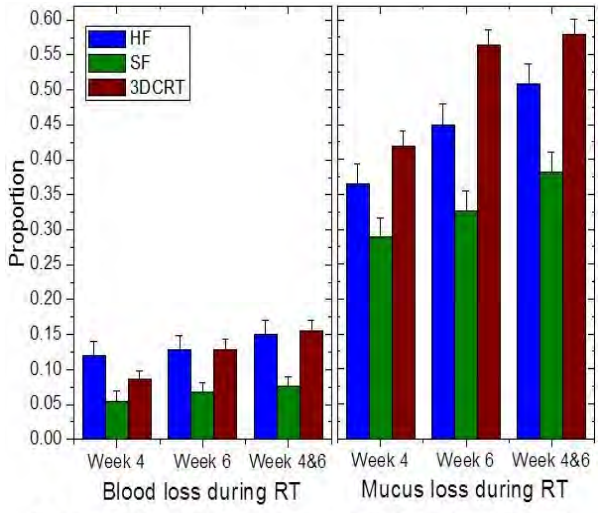

Fig 1. Proportion (1SE) of symptoms with HF (3.4 Gy) and SF (2 Gy) both with IG-IMRT, and a third reference 3DCRT population (2 Gy/fr).

OC-0340

Effect of dose and image guided radiotherapy (IGRT) on erectile potency (EP) in prostate radiotherapy

J. Murray[1], J. Dean[2], H. Mossop[3], E. Hall[3], D. Dearnaley[1], S. Gulliford[2]

[1]*The Institute of Cancer Research and The Royal Marsden NHS Foundation Trust, Radiotherapy and Imaging, London, United Kingdom*

[2]*The Institute of Cancer Research and The Royal Marsden NHS Foundation Trust, Joint Department of Physics, Sutton, United Kingdom*

[3]*The Institute of Cancer Research, Clinical Trials and Statistics Unit, London, United Kingdom*

Purpose or Objective: IGRT enables accurate target volume localisation, potentially permitting reduced treatment margins, which may decrease normal tissue toxicity.
Erectile dysfunction is a common toxicity of prostate RT and the penile bulb (PB) is suggested as a surrogate for undetermined structures critical for erectile function. However, PB dose-volume effects are not well established.
We aim to determine dose-response characteristics of the PB in prostate cancer patients treated using IGRT with standard and reduced margins.

Material and Methods: Men with previously untreated localised prostate cancer were randomised within the multicentre CHHiP (Conventional or Hypofractionated High dose Intensity Modulated Radiotherapy for Prostate Cancer) IGRT sub-study (CRUK/06/16). Men were randomised to receive 2Gy or 3Gy per fraction, delivered either with or without daily online image-guidance, with standard or reduced CTV-PTV margins. Short course hormone therapy (HT) was allowed and details were recorded.
EP was assessed at baseline, pre-RT and at 6 monthly intervals to 2 years, then annually to 5 years post-RT. EP was physician graded as normal erection (G0), decreased (G1), absent (G2) and unknown. Analysis included the subset of men treated with IGRT within the sub-study with an EP assessment at 2 years.
Planning CT scans and reference dose distributions were imported into analysis software (Vodca, MSS GmbH). The PB was retrospectively contoured using established anatomical boundaries (1) and published guidelines (2,3) by one clinician. In-house software was used to convert the hypofractionated plans into equivalent dose in 2Gy per fraction using the Withers formula (α/β = 3Gy). PB dose-volume (DVH) parameters were evaluated against EP at 2 years using atlases of complication incidence (ACI) (Matlab, Mathworks, Natick, MA) for G2 EP. Dose-volume constraints were derived using ROC analysis (Youden index) and assessed against the no information rate.

Results: Between June 2010 and June 2011, 293 men entered the study. Complete dose-EP data sets were available for 129 men treated with IGRT. 14/129 men had G2 EP at baseline and were excluded. At 2 years, 27/52 (52%) men treated with standard margins (IGRTS) and 25/63 (40%) men treated with reduced margins (IGRTR) had G2 EP. HT characteristics between the two groups were similar. The PB volume was 7.1(±2.8)cm^3 in IGRTS group and 6.5(±2.5)cm^3 in IGRTR group. The reduced margins resulted in a reduction in dose to the PB and statistically significant dose-volume constraints for G2 EP were derived for 45, 50, 55, 60 and 65Gy (Table 1). The ACI is presented in Figure 1 and demonstrates a dose-volume response.

		% Penile bulb volume receiving dose										
		20Gy	30Gy	40Gy	45Gy	50Gy	55Gy	60Gy	65Gy	70Gy	Mean dose	Max dose
IGRTS (n=52)	Median	40.8	34.0	24.4	18.0	17.5	10.3	1.6	0	0	20.7Gy	60.0Gy
	IQR	14.9 - 77.5	9.7 - 67.5	0 - 55.8	0 - 49.0	0 - 42.1	0 - 29.7	0 - 26.7	0 - 14.3	0 - 0.03	8.8 - 41.6Gy	37.9 - 69.0Gy
IGRTR (n=63)	Median	15.5	6.0	0	0	0	0	0	0	0	9.1Gy	33.6Gy
	IQR	0 - 39.3	0 - 26.2	0 - 24.0	0 - 12.0	0 - 11.2	0 - 0.1	0	0	0	4.5 - 18.8Gy	16.3 - 55.9Gy
Dose volume constraints					45	28	25	18	9			
AUC (95%CI)					0.61 (0.51 - 0.71)	0.61 (0.51 - 0.71)	0.62 (0.52 - 0.71)	0.59 (0.50 - 0.68)	0.58 (0.50 - 0.66)			
Predictive accuracy (%)					66	67	65	63	63			
p value *					0.009	0.005	0.01	0.04	0.04			

Table 1: Penile bulb dose-volume characteristics in patients treated using IGRT with standard and reduced margins and calculated statistically significant dose-volume constraints with associated parameters

IGRTS: IGRT with standard margins; IGRTR: IGRT with reduced margins; AUC: area under the curve; CI: confidence interval; IQR: interquartile range; *compared to the no information rate

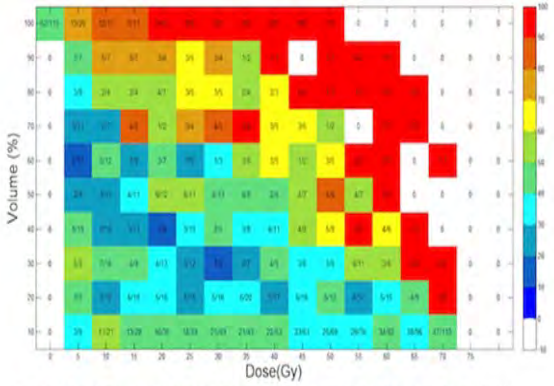

Figure 1: Atlas of complication incidence for grade 2 erectile potency (G2 EP). Each box within the atlas describes dose (EQD2) and percentage volume of penile bulb. The numeric fraction presents the patients whose dose volume histogram (DVH) falls within the box (denominator) and the number of patients whose DVH falls within the range who experienced G2 EP (numerator). The fractional incidence (intervals of 10%) of G2 EP was used to generate a colour for each box (scale: blue (low incidence) to red (high incidence)).

Conclusion: There is evidence to suggest a dose volume effect between the PB and EP. Discriminatory PB dose-volume constraints were found to predict G2 EP. Further analysis is in progress to include patient reported outcomes related to EP.

Ref: (1) Wallner, IJROBP 2002 (2) Perna, Rad Onc 2011 (3) Gay, IJROBP 2012

OC-0341

Anal dose reduction for radiotherapy of prostate cancer does not lead to less rectal incontinence

F. Pos[1], L. Incrocci[2], R. Wortel[2], U. Van der Heide[1], J. Lebesque[1], S. Aluwini[2], M. Witte[1], W. Heemsbergen[1]

[1]*Netherlands Cancer Institute Antoni van Leeuwenhoek Hospital, Department of Radiation Oncology, Amsterdam, The Netherlands*

[2]*Erasmus MC Cancer Institute, Radiation Oncology, Rotterdam, The Netherlands*

Purpose or Objective: Radiation-induced rectal incontinence has a negative impact on Quality of Life in patients irradiated for prostate cancer. Several studies identified dose-effect relationships for the anal canal and lower rectum and hence, dose constraints for treatment planning have been implemented. We studied patient-reported rectal incontinence in a population treated with Image-guided intensity modulated radiotherapy (IG-IMRT) and planned with a dose constraint for the anal canal, and compared it with a reference population treated with 3D-conformal radiotherapy (3D-CRT) with no dose constraint for the anal canal. For that purpose we analyzed data from two large prospective cohorts

Material and Methods: We selected patients treated to 78Gy (39x2Gy) from two trials (CKTO 96-10 and CKTO 2006-08), who completed at least 2 follow-up questionnaires which included questions on pad use and fecal incontinence (IGIMRT group n=242, 3DCRT group n=189). In the IG-IMRT group, mean dose to the anal canal was restricted to 58 Gy per protocol (more strict constraints depended on local planning guidelines). Grade ≥2 (G≥2) incontinence was defined as use of pads for uncontrolled loss of feces or mucus, Grade ≥1 (G≥1) incontinence was defined as any reported fecal incontinence regardless use of pads. Prevalence and cumulative incidences of ≥G2 and G≥1 incontinence were calculated. Cox regression was used to calculate Relative Risks (RR)

Results: Planned mean dose to the anal canal was on average 44.6 Gy (range 17-65) for 3D-CRT and 23.6 Gy (range 3-50) for IG-IMRT (p<0.001). Median follow-up was 60 months. The 5y cumulative incidence of G≥2 incontinence was 15.2% for IG-IMRT vs 14.9% for 3D-CRT (RR=1.02, p=0.9). Prevalence of G≥1 incontinence was ≈ 5% at baseline and in the range of 30% - 40% in the years after treatment, with no significant differences between the groups (Figure 1). Within the 3D-CRT group, previous abdominal surgery was predictive for G≥2 incontinence (RR=2.1, p=0.05), whereas age >70 years at start RT (RR=2.9, p<0.01), diabetes mellitus (RR=2.4, p=0.04), and seminal vesicle dose≥70 Gy vs 0 Gy (RR=9.2, p=0.03) were predictive in the IG-IMRT group. At multivariate analysis, adjusting for the significant baseline factors, RR of mean anal canal dose was 1.00 (p=0.9) for IG-IMRT patients and 1.05 (for each increase of 1 Gy) for 3D-CRT (p=0.04). Acute toxicity G≥2 (mainly proctitis) was predictive (p<0.01) in both groups with a RR of 3.1 (IG-IMRT) and 4.1 (3D-CRT). G≥1 incontinence at any time during follow-up was significantly associated with abdominal surgery in the 3D-CRT group, and with age >70 years, and diabetes mellitus in the IG-IMRT group

Conclusion: IG-IMRT with anal canal dose constraints did not reduce long-term incidence of rectal incontinence in prostate cancer patients, despite significantly reduced dose levels to the anal canal region. Further investigations are needed to understand the mechanisms of radiation damage causing rectal incontinence

OC-0342

Chemoradiotherapy in high-risk prostate cancer (QRT SOGUG trial): Preliminary report

P. Foro Arnalot[1], X. Maldonado[2], M. Bonet[3], J. Jove[4], A. Rovirosa[5], M. Rico[6], A. Bejar[7], G. Sancho[8], M.J. Vega[9], M. Mira[10], M. Martinez[11], M. Algara[12], J. Carles[13]

[1]*Parc de Salut Mar, Radiation Oncology. IMIM Hospital del Mar Medical Research Institute- University Pompeu Fabra, Barcelona, Spain*

[2]*Hospital Universitari Vall d'Hebron, Radiation Oncology, Barcelona, Spain*

[3]*Hospital Universitari Parc Taulí, Radiation Oncology, Sabadell, Spain*

[4]*Hospital Germans Trias i Pujol- Institud Catala d'Oncologia, Radiation Oncology, Badalona, Spain*

[5]*Hospital Clinic Universitari-, Radiation Oncology, Barcelona, Spain*

[6]*Hospital Universitario Virgen de la Victoria, Radiation Oncology, Malaga, Spain*

[7]*Hospital Reina Sofia-, Radiation Oncology, Cordoba, Spain*

[8]*Hospital de la Santa Creu i Sant Pau, Radiation Oncology, Barcelona, Spain*

[9]*Hospital Provincial de Zamora, Radiation Oncology, Zamora, Spain*

[10]*Hospital Universitari Arnau de Vilanova, Radiation Oncology, Lleida, Spain*

[11]*Hospital Universitario Virgen de las Nieves, Radiation Oncology, Granada, Spain*

[12]*Parc de Salut Mar. IMIM Hospital del Mar Medical Research Institute. University Pompeu Fabra, Radiation Oncology, Barcelona, Spain*

[13]*Hospital Universitari Vall d'Hebron, Medical Oncology, Barcelona, Spain*

Purpose or Objective: To assess the toxicity and feasibility of concomitant radiotherapy with low doses of docetaxel plus

standard hormonal treatment in patients with high risk localized prostate cancer.

Material and Methods: Patients were randomly assigned to either arm A (LH-RH analogs every 3 months for 3 years and radiotherapy 74 Gy [2Gy x 37 fractions]) or arm B (LH-RH analogs every 3 months for 3 years, radiotherapy 73.8 Gy [1.8 Gy x 41 fractions] and concurrent weekly docetaxel at 20 mg/m2 for 9 weeks). Chemotherapy was started one week before of radiotherapy. Primary endpoint was PSA relapse according to the Phoenix definition. The planned number of patients was 130 to detect a 15% difference with a power of 80% and an alpha of 0.05 (two-sided).

Results: From 12/2008 to 9/2012, 130 pts were accrued (Arm A: 64, Arm B: 66). Median age was 68 years (61-73). Patients had T3-T4 (82.6%), Gleason Score 8 (76.3%), PSA > 20 ng/mL (26.9%) and pN+ (18.9%). All characteristics were well-balanced between arms. Median dose of radiotherapy was 74 Gy (72–74.8) in arm A, and 73.8 Gy (72-75.6) in arm B. 75.7% of patients received the planned 9 treatments of docetaxel and median number of cycles delivered per patient was 9. After a median follow-up of 29.6 months (9.6-40.2), most common grade 1/2 toxicities (arm A and arm B) were: cystitis (12.5% vs 8.3%), diarrhea (35.9% vs 70%), proctitis (12.5% vs 13.3%), rectal tenesmus (3.1% vs 23.3%), asthenia (23.4% vs 61.6%) and dysuria (28.1% vs 30.0%). Toxicity grade3/4, diarrhea was reported in 8.3% of patients in arm B and 0% in arm A. Grade3/4 lymphopenia occurred less often in arm A than in arm B (3.1% vs 23.3%). %). There was no toxicity-related death.

Conclusion: The QRT SOGUG phase IIb trial shows that standard doses of radiotherapy and concurrent weekly docetaxel can be administered without increasing toxicity profile.

OC-0343

Pattern of intraprostatic recurrence on multiparametric MRI after radiotherapy for prostate cancer

H. Ariyaratne[1], D. Kopcke[2], A. Padhani[2], R. Alonzi[1]
[1]*Mount Vernon Cancer Centre, Clinical Oncology, Northwood, United Kingdom*
[2]*Paul Strickland Scanner Centre, Radiology, Northwood, United Kingdom*

Purpose or Objective: The majority of intraprostatic recurrences after radical prostate radiotherapy occur at the site of initial tumour, in previous reported series. However, there is no published data directly comparing recurrence patterns after different modalities of radiotherapy. The aim of this study was to investigate differences in spatial pattern of intra-prostatic recurrences on multiparametric MRI, after external beam radiotherapy or brachytherapy.

Material and Methods: We identified 382 consecutive patients referred for multiparametric MRI after previous prostate cancer treatment. Patients with post-radiotherapy biochemical recurrence and intraprostatic recurrence on MRI were included in the study. Scans were independently reviewed by two radiologists. The location of recurrence was mapped to prostate sectors based on European consensus guidelines. The chi-square test was used to analyse differences in site of recurrence between modalities of radiotherapy.

Results: 66 patients who had radical radiotherapy between 1997 and 2013 had intraprostatic recurrence on MRI. The D'Amico risk stratification at initial diagnosis was 14% low-risk, 34% intermediate-risk and 52% high-risk. The series consisted of 34 patients after external beam radiotherapy (EBRT), 20 patients after low-dose rate brachytherapy (LDR) and 12 after high-dose rate brachytherapy monotherapy (HDR mono). 68% of the EBRT recurrences had received a dose-fractionation schedule with an EQD2 less than 74 Gy. The mean time between the end of radiotherapy and imaging recurrence was 77 months (95% CI 68 – 85 months) with no significant differences between treatment groups. 80% of patients did not have any associated pelvic bony metastasis or nodal disease. 88% of patients had a contiguous intraprostatic recurrence. The median recurrence size detected on MRI was 2.0 cm (range 0.6 – 4.2 cm). Recurrences after EBRT were more likely to involve multiple sectors of the prostate. 71% of EBRT recurrences involved the apex compared to 30% after LDR and 25% after HDR mono (p = 0.003). In the LDR group, recurrences involved the base of the gland in 60% of cases, compared to 41% after EBRT and 8% after HDR mono (p = 0.016). 21% of patients underwent salvage treatment with cryotherapy, HDR brachytherapy or prostatectomy.

Conclusion: Apical recurrences predominated in patients following EBRT. This highlights the need for MR-fusion during EBRT target definition because the apex is difficult to visualise on CT. Basal recurrences were associated with LDR brachytherapy, which may reflect a tendency of radioactive seed migration away from the base. The use of multiparametric MRI facilitates identification of patients for focal salvage treatment.

OC-0344

Risk of second primary cancers after radiotherapy for prostate cancer

N.S. Hegemann[1], U. Ganswindt[1], J. Engel[2], C. Belka[1]
[1]*Klinikum der Universität München, Department of Radiation Oncology, Munich, Germany*
[2]*Klinikum der Universität München, Munich Cancer Registry of the Munich Tumour Centre- Department of Medical Informatics- Biometry and Epidemiology IBE, Munich, Germany*

Purpose or Objective: The average 5-year survival rate of men diagnosed with prostate cancer (PCa) is 93%. The long life expectancy exposes them to a greater risk of developing second primary cancers. To quantify the risk of radiation induced second primary cancer, we analysed data of PCa patients based on our Cancer Registry.

Material and Methods: We analysed 19.538 patients treated for PCa from 1988 until 2008. They were either treated with surgery (RPE only) or received radiation therapy as primary (RT only) or as postoperative treatment (RT after RPE). Statistical analysis was performed using a stratified Cox proportional hazard model and a chi-square test.

Results: Patients who received RT only were 5 years older (median) than patients who underwent RPE only or RT after RPE. Second primary cancers were observed with 13.1% and 13.6% in the RPE only and in the RT after RPE group and 16.4% in the RT only group (p= 0.0001), respectively. Colon carcinoma was seen in the RPE only and RT only group in roughly 10 percent, whereas in the RT after RPE group in 14.6% (p= 0.2140). Bronchial cancer surpassed 10% in the RT only group (12.5%) vs. 9.7% and 7.8% in the RPE only and the RT after RPE group (p= 0.0552). Bladder cancer was observed with roughly 10% in the RPE only (10.2%) and RT after RPE (10.4%) group versus 15.5% in the RT only group (p= 0.0007). Rectal cancer after treatment of PCa was diagnosed in 5.7%, 7% and 3.1% in the RPE only, RT only and RT after RPE group (p= 0.1037). Within the first 10 – 15 years the cumulative hazard curves for second primary cancers gave no hint to an increased tumor risk due to prior treatment. After 15 years there are hardly any cases left and the occurring events can no longer be reasonably interpreted. Cox proportional hazard ratio revealed that patients with a higher age have a significantly higher risk of developing second primary cancer (Hazard Ratio 1.279 in 60 - <65 year old patients vs. 2.169 in ≥75 year old patients, p <0.0001).

Conclusion: Based on this population with PCa from the PSA era the incidences of second primary cancers did not differ significantly between the three arms apart from bladder and lung cancer that came close to being significantly different. However, these differences cannot reliably be ascribed to radiation, but to other factors such as older age, lifestyle habits like smoking and the well known fact that cancer

survivors generally have an increased risk of new tumor formation.

Proffered Papers: Clinical 8: Adult and paediatric CNS malignancies

OC-0345

Patterns of failure after radiotherapy in pediatric ependymoma: correlation with dose parameters

F. Tensaouti[1], A. Ducassou[2], S. Bolle[3], X. Muracciole[4], B. Coche-dequeant[5], L. Claude[6], S. Supiot[7], C. Alapetite[8], V. Bernier[9], A. Huchet[10], C. Kerr[11], E. Le Prise[12], G. Truc[13], E. Regnier[14], S. Chapet[15], A. Lisbona[7], G. Hangard[2], A. Laprie[2]

[1]*UMR 825 Inserm / Université Toulouse Iii - Paul Sabatier, Research, Toulouse, France*

[2]*Institut Claudius Regaud Toulouse- Iuct Oncopole, Radiotherapy, Toulouse, France*

[3]*Institut Gustave Roussy- Villejuif, Radiotherapy, Paris, France*

[4]*CHU La Timone, Radiotherapy, Marseille, France*

[5]*Centre Oscar Lambret, Radiotherapy, Lille, France*

[6]*Centre Léon Bérard, Radiotherapy, Lyon, France*

[7]*Institut De Cancérologie De L'ouest, Radiotherapy, Nantes, France*

[8]*Institut Curie, Radiotherapy, Paris, France*

[9]*Institut De Cancérologie De Lorraine- Alexis Vautrin, Radiotherapy, Nancy, France*

[10]*CHU Bordeaux, Radiotherapy, Bordeaux, France*

[11]*Institut Du Cancer De Montpellier, Radiotherapy, Montpellier, France*

[12]*Centre Eugène Marquis, Radiotherapy, Rennes, France*

[13]*Centre Georges François Leclerc, Radiotherapy, Dijon, France*

[14]*Institut Jean Godinot, Radiotherapy, Reims, France*

[15]*CHU Tours, Radiotherapy, Tours, France*

Purpose or Objective: The aim of this study was to investigate the patterns of failure after radiotherapy for pediatric intracranial ependymoma and their correlation to dose parameters.

Material and Methods: Between 2000 and 2013, 206 patients with intracranial ependymoma were treated in the 13 french reference pediatric radiotherapy centers . The magnetic resonance imaging obtained at recurrence were registered with the original planning CT for topographic analysis of the patterns failure. Clinical target volume (CTV) and planning target volume (PTV) margins were extracted ; several dosimetric quality indices were derived from Dose Volume Histogram (DVH) to compare relapse with no-relapse patient.

Results: With a median follow-up of 44.81 months (95% CI [36.80; 56.51]), 85 (41.3%) patients presented with recurrence. The topographic analysis of patterns of failure showed 50 (58.8%) patients with local recurrence in the radiation field (LF), 6 (4.1%) in the edge of field (EFG), 6 (7.1%) were loco-regional outside the field (LRF), 8 (9.4%) in spine (SF), 5 supratentorial (SUF) and 10 (11.8%) local and distant (LDF). The median prescription dose was respectively: 55.8 Gy [50.4; 60] in LF, 54 Gy [48.6; 59.4] in EF, 56.7 Gy [50.4; 60] in LRF, 54 Gy [50.4; 59.4] in LDF, 59.4 Gy [48.6-59.4] in SUF and 56.7Gy [54; 60] in SF. The median PTV margins was 0.5 mm [0.3; 1]. The median Coverage index and The Target Coverage index of the PTV were both lower in the relapse group as they were respectively 0.97 and 94.8% in the relapse group compared with 0.98 and 95.99% in the no-relapse group. The median Homogeneity index was 0.097 in the relapse group versus 0.091 in the no-relapse group. The median volume of relapse was 1.29 cc [0.11; 27] in the LF group, with a median dose of 58.81 Gy [50.86; 61.38].

Conclusion: In patients with intracranial ependymoma, local failure in the tumor bed was the major pattern of failure. The preliminary results showed that all dosimetric indices on the PTV were worse in the relapse group. Improving the coverage of target volume may be an effective way to reduce the local failures. Thus a complementary correlation of relapse patterns with dose parameters to PTV and organs at risks and the irradiation techniques is under statistical analysis and final results will be presented at the meeting.

OC-0346

Pediatric diffuse intrinsic pontine glioma re-irradiation: better survival and better time

L. Gandola[1], E. Pecori[1], V. Biassoni[2], B. Diletto[1], E. Schiavello[2], S. Meroni[3], F. Spreafico[2], E. Pignoli[3], M. Massimino[2]

[1]*Fondazione IRCCS Istituto Nazionale dei Tumori, Radiation Oncology- Pediatric Radiotherapy Unit, Milan, Italy*

[2]*Fondazione IRCCS Istituto Nazionale dei Tumori, Pediatric Oncology, Milan, Italy*

[3]*Fondazione IRCCS Istituto Nazionale dei Tumori, Medical Physics, Milan, Italy*

Purpose or Objective: Since 2009 we launched a strategy for children with centrally reviewed MRI diagnosis of diffuse intrinsic pontine glioma (DIPG) implying the intravenous administration of vinorelbine with nimotuzumab –an anti-EGFR monoclonal antibody- weekly, for a total of 12 weeks, during radiotherapy delivery of 54 Gy, 1.8 Gy/fraction daily. After radiotherapy completion, vinorelbine and nimotuzumab were administered any other week until tumor progression or for a total of two years. In the attempt to improve survival and quality of life of our children, a protocol amendment in July 2011 introduced re-irradiation at relapse/progression.

Material and Methods: Local re-irradiation consisted of 19.8 Gy, fractionated over 11 days. A 3DCRT with 5-6 coplanar beams was adopted with a beam geometry possibly not overlapping that of the first line irradiation; the most demanding planning issue of re-irradiation was to meet optic chiasm dose constraints. Three additional children were re-irradiated to distant sites of relapse, spine (2) or ventricular system at doses of 36 Gy or 54 Gy respectively.

Results: Of the 39 patients treated from 8/2009, 28 had local (23) or disseminated (5) progression and 18 were given local (15) or distant (3) relapse re-irradiation at a median of 8 months after first radiotherapy (2.5-19 months). Reasons for not re-irradiating the other 10 children were: progression before July 2011 (4), parents refusal (4), too poor Lansky status (2); median PFS and progression site were not different in the two subgroups. Survival after re-irradiation lasted between two weeks and 14 months, median 6 months, and determined a statistically difference in median OS between the two groups of re-irradiated or not children, being 16 and 12 months, respectively (P=0.004). In 16 radiologically evaluated patients, re-irradiation induced: reduction of tumor volume in 8, stable volume in 3 while 5 had progression; 13 had symptom amelioration and 12 steroid suspension. Volume reductions were obtained in 7/8 children that have shown the same response after first line irradiation while one was obtained after stable disease in first line treatment. No adverse event was reported and all children were re-irradiated as outpatients .

Conclusion: Re-irradiation after relapse/progression represented a significant benefit for both OS and quality of life of children with DIPG with symptom amelioration in 13/18. This option is worth to be offered also in case of disseminated progression.

Partially supported by Associazione Italiana per la Ricerca sul Cancro (AIRC)

OC-0347

Outcome and prognosticators in adult patients with medulloblastoma: a Rare Cancer Network study

B. Atalar[1], M. Ozsahin[2], J. Call[3], A. Napieralska[4], S. Kamer[5], V. Salvador[6], P. Erpolat[7], L. Negretti[2], Y.L. Ramstad[8], C. Onal[9], S. Akyurek[10], G. Ugurluer[1], B. Baumert[11,12], S. Servagi-Vernat[13], R.C. Miller[14], E. Ozyar[1], T. Sio[15]

[11]*Acıbadem University, Department of Radiation Oncology, Istanbul, Turkey*

[2]*Centre Hospitalier Universitaire Vaudois, Department of Radiation Oncology, Lausanne, Switzerland*

[3]Mayo Clinic, Department of Radiation Oncology, Rochester, USA
[4]Maria Skłodowska-Curie Memorial Cancer Center and Institute of Oncology, Department of Radiotherapy, Gliwice, Poland
[5]Ege University, Department of Radiation Oncology, Izmir, Turkey
[6]Catalan Institute of Oncology, Department of Radiation Oncology, Badalona, Spain
[7]Gazi University, Department of Radiation Oncology, Ankara, Turkey
[8]Aarhus University Hospital, Department of Oncology, Aarhus, Denmark
[9]Baskent University, Department of Radiation Oncology, Ankara, Turkey
[10]Ankara University, Department of Radiation Oncology, Ankara, Turkey
[11]Maastricht University (MAASTRO) GROW Research Institute, Department of Radiation Oncology, Maastricht, The Netherlands
[12]MediClin Robert Janker Clinic & Clinical Cooperation Unit Neurooncology, University of Bonn MC, Bonn, Germany
[13]University Hospital of Besancon, Department of Radiation Oncology, Besancon, France
[14]Mayo Clinic, Department of Radiation Oncology, Jacksonville, USA
[15]Mayo Clinic, Department of Radiation Oncology, Phoenix, USA

Purpose or Objective: For the treatment of adult patients newly diagnosed with medulloblastoma, there is no standard to guide multimodality therapy. With a multi-institutional cohort, we investigated and reported the multidisciplinary approach, clinical outcome, and prognostic factors of medulloblastoma in adult patients treated with postoperative radiotherapy (RT).

Material and Methods: Thirteen (13) institutions from the RCN study group among Europe and United States enrolled 206 adult medulloblastoma patients who underwent postoperative RT between 1976 and 2014. All hospitals received their respective Institutional Review Board approval, and extracted data were sent to one investigator (B.A.) for data analyses. Log-rank univariate and Cox-modeled multivariate analyses were performed.

Results: There were 118 men and 88 women, and median age was 29 (range, 16-67). The median follow-up was 31 months. Tumor resection was performed in all patients, and surgery was complete in 140 (68%) of the patients. For those patients with reported residual volume, 83 (66%) achieved <1.5 cm2 after resection. Histological subtype was classic (61%) predominantly. Postoperative RT was given in 202 (98%) patients, and 93% of them received craniospinal irradiation (CSI) to a median dose of 36 Gy, with a median RT boost of 18 Gy to the posterior fossa. Ninety-eight (48%) patients had chemotherapy before, after, or concomitant with RT; the most common chemotherapy regimens were cisplatin and vincristine-based. At 5 and 10 years' marks, the overall survival (OS) rates were 63 and 51%; local control (LC) rates were 60 and 46%; and disease-free survival (DFS) rates were 52 and 38% for all patients, respectively. On univariate analyses, Karnofsky performance status (KPS) ≥ 80%, time between surgery and RT ≤ 47 days), negative CSF, total RT dose ≥ 54 Gy, CSI completion, use of boost field, and chemotherapy were associated with better LC, DFS, and OS. Additionally, complete surgery, <1.5 cm2 residual volume, desmoplastic pathology, and age ≥ 29) were significant favorable prognostic factors for DFS and OS. In multivariate analyses, KPS ≥ 80% (P<0.001) and CSI (P=0.0002) were the remaining significantly favorable prognostic factors for DFS and OS; presence of chemotherapy (P=0.0002) and KPS≥ 80% (p=0.03) correlated with better LC rates.

Conclusion: We retrospectively reported the largest clinical series for the treatment of adult medulloblastoma and elucidated prognostic factors for tumor control and also survival outcomes. For patients with high KPS who also received CSI, their DFS and OS were better. The use of chemotherapy may associate with better local control, possibly due to improved radio-sensitization. This information should serve as the benchmark and provide the basis for future prospective clinical trials in further improving the outcome for this group of adult patients with rare medulloblastoma.

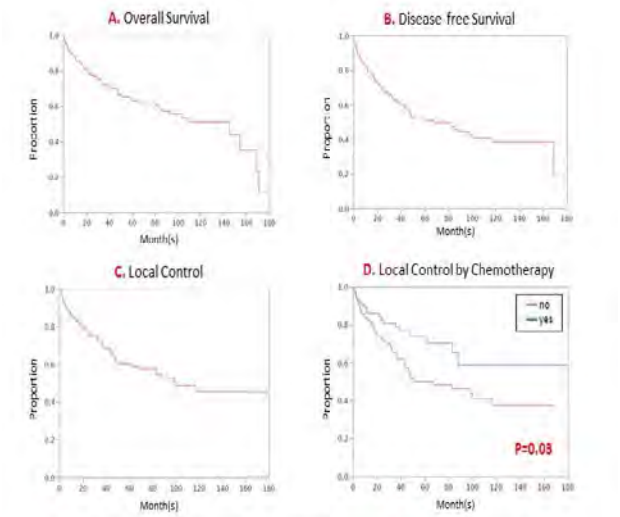

Figure: A. Overall survival of the entire cohort (N=206 patients); B. Disease-free survival, 206 pts; C. Local control rate, also 206 pts; D. Local control as stratified by the use of any adjuvant chemotherapy, P=0.0273, Log-Rank testing

OC-0348

Tumor bed radiosurgery vs. whole brain radiotherapy after surgery of single brain metastasis

L. Kepka[1], D. Tyc-Szczepaniak[2], K. Bujko[2], M. Olszyna-Serementa[2], W. Michalski[3], A. Sprawka[2], B. Trabska-Kluch[4], K. Komosinska[1], E. Wasilewska-Tesluk[1], B. Czeremszynska[1]
[1]Independent Public Health Care Facility of the Ministry of the Interior and Warmian & Mazurian Oncology Centre, Department of Radiotherapy, Olsztyn, Poland
[2]Maria Sklodowska-Curie Memorial Oncology Center and Institute of Oncology, Department of Radiotherapy, Warsaw, Poland
[3]Maria Sklodowska-Curie Memorial Oncology Center and Institute of Oncology, Department of Biostatistics, Warsaw, Poland
[4]Medical University of Lodz, Department of Radiotherapy, Lodz, Poland

Purpose or Objective: A multicenter randomized trial evaluated neurological status (including neurological deaths) and cognitive function of patients with resected single brain metastasis (BM) after stereotactic radiotherapy of the tumor bed (SRT-TB) in comparison with adjuvant whole-brain radiotherapy (WBRT). This study reports a preliminary comparison of pattern of failure and neurological deaths in this trial.

Material and Methods: A planned number of 60 patients was randomly assigned into SRT-TB (30) and WBRT (30) arms. Inclusion criteria were: total or subtotal resection of BM, single BM in the MRI before craniotomy, KPS ≥ 70, life expectancy >6 months. Patients in the SRT-TB arm received linac-radiosurgery of 15 Gy/1 fraction, or 5 x 5Gy if large cavity or proximity of critical structures. WBRT consisted of 30 Gy in 10 fractions. Evaluation at baseline (before RT), eight weeks after RT, and next every three months consisted of EORTC QLQ-C30 - BN-20, MiniMental test, KPS, neurologic status, and MRI of the brain. Neurological death was defined as every death from progression in the brain, toxicity of treatment of BM, and from undetermined cause. Crude rates of neurological deaths and relapses in the brain were compared according to the treatment actually received analysis with chi2 test. Overall survival (OS) and interval free from neurological death (IFFND) rates were compared with log-rank test.

Results: In the SRT-TB arm, six patients were ineligible (new BM detected during RT planning [5], withdrawal of consent [1]), one received WBRT by error, two had rapid extracranial progression (one had no BM treatment, one received WBRT), thus finally 21 (72%) patients received the assigned treatment in this group. In the WBRT arm, 29 (97%) received the assigned treatment. With median follow-up of 12 months (range: 1-36) for 26 living patients, one-year OS rates (intention-to-treat) were 48% (95% CI: 36-60%) and 61% (95% CI: 43-79%) for SRT-TB and WBRT arm, respectively, p=.14. In the intention-to-treat analysis, one-year IFFND rates were 59% (95% CI: 35-84%) and 74% (95% CI: 56-93%) for SRT-TB and WBRT arm, respectively, p=.10. In the treatment actually received analysis, one-year IFFND rates were 62% (95% CI: 37-88%) and 72% (95% CI: 53-90%) for SRT-TB and WBRT arm, respectively, p=.26. There were 9 (41%) and 9 (30%) neurological deaths, in the patients receiving SRT-TB and WBRT, respectively, p= .10.
Ten (45%) of 22 patients treated with SRT-TB had relapse in the brain including 5 (23%) relapses in the tumor bed; 9 (31%) of 30 patients treated with WBRT had relapse in the brain including 7 (24%) relapses in the tumor bed, p=.29.

Conclusion: Our results showed high rate of neurological deaths with omission of WBRT, thus such treatment might not be safe. Planned analysis of the results from our study that will compare neurological and cognitive functions following two treatments will be also helpful in decision making process.

OC-0349

Hippocampal dosimetry predicts the change in neurocognitive functions after whole brain radiotherapy

S.Y. Lin[1], C.C. Yang[2], C.C. Chuang[3], P.C. Pai[1], P.F. Tsai[1], D.L. Tsan[1], C.K. Tseng[1]
[1]Chang Gung Memorial Hospital, Department of Radiation Oncology, Taoyuan, Taiwan
[2]Chang Gung University, Division of Clinical Psychology-Master of Behavioral Sciences- Department of Occupational Therapy, Taoyuan, Taiwan
[3]Chang Gung Memorial Hospital, Department of Neurosurgery, Taoyuan, Taiwan

Purpose or Objective: Whole brain radiotherapy (WBRT) has been the treatment of choice for patients with brain metastases. However, change/decline of neurocognitive functions (NCFs) resulting from impaired hippocampal neurogenesis might occur after WBRT. It is reported that hippocampal sparing would provide the preservation of NCFs. Our study aims to investigate the correlations between hippocampal dosimetry and neurocognitive outcomes in patients receiving hippocampal sparing during WBRT (HS-WBRT).

Material and Methods: Fifty prospectively recruited cancer patients underwent HS-WBRT for therapeutic or prophylactic purposes. Before receiving HS-WBRT, all participants received a battery of baseline neurocognitive assessment, including memory, executive functions and psychomotor speed. The follow-up neurocognitive assessment at 4 months after HS-WBRT was also performed. To deliver HS-WBRT, Volumetric Modulated Arc Therapy (VMAT) with two full arcs and two non-coplanar partial arcs was employed. For each treatment planning, dose volume histograms were generated for left hippocampus, right hippocampus, and the composite hippocampal structure respectively. Biologically equivalent doses in 2-Gy fractions (EQD2) assuming an alpha/beta ratio of 2 Gy were computed. To perform analyses addressing the correlation between hippocampal dosimetry and the change in NCF scores, pre- and post-HS-WBRT neurocognitive assessments were available in 32 patients.

Results: NCF scores were quite stable before and after HS-WBRT regarding hippocampus-dependent memory. For verbal memory, the corresponding EQD2 values of 0%, 10%, 50%, 80% irradiating the composite hippocampal structure with <12.60Gy, <8.81Gy, <7.45Gy and <5.83Gy respectively were significantly associated with neurocognitive preservation indicated by the immediate recall of Word List Test of Wechsler Memory Scale-III. According to logistic regression analyses, it showed that dosimetric parameters specific to left hippocampus exerted an influence on immediate recall of verbal memory (adjusted odds ratio, 4.08; *p*-value, 0.042, predicting patients' neurocognitive decline after HS-WBRT).

Conclusion: Functional preservation by hippocampal sparing during WBRT is indeed achieved in our study. Providing that modern VMAT techniques can reduce the dose irradiating bilateral hippocampi below dosimetric threshold, patients should be recruited in prospective trials of hippocampal sparing during cranial irradiation to accomplish neurocognitive preservation while maintaining intracranial control.

OC-0350

Post-radiation neuronal depletion in hippocampus measured by in-vivo magnetic resonance spectroscopy

P. Pospisil[1], T. Kazda[1], R. Jancalek[2], P. Slampa[1]
[1]Masaryk Memorial Cancer Institute, Radiation Oncology, Brno, Czech Republic
[2]St. Anne's University Hospital Brno, Department of Neurosurgery, Brno, Czech Republic

Purpose or Objective: Ongoing clinical trials are evaluating advantage of hippocampal avoiding whole brain radiotherapy (WBRT), however, further basic research focusing on in-vivo description of radiation injury processes is still needed. Using magnetic resonance spectroscopy (MRS), it is possible to measure specific metabolite concentrations in any region of interest in the brain. N-acetylaspartate (NAA) represents a marker of viable neurons. To describe hypothesized post-WBRT neuronal depletion in hippocampus, we prospectively measured changes in NAA concentrations 4 months after WBRT.

Material and Methods: Patients referred for WBRT with favorable prognosis estimated by graded prognostic assessment and without MRI hippocampal pathology were eligible for study enrollment. Before standard WBRT (two-dimensional planning, 2 laterolateral 6 megavoltage fields, dose 10x3.0 Gy delivered by linear accelerator), hippocampal spectroscopy was performed using GE Medical Systems Discovery MR 750 3T. Region of interest was placed through the whole temporal lobi with the voxel layer position adjusted based on the localization of hippocampi. Specialized software was utilized for measurement of absolute NAA concentration in voxels within right, left and both hippocampi. The controle MRS with the same setup parameters was performed 4 months after the end of course of WBRT. Wilcoxon's signed rank test was employed for calculation of NAA concentration changes.

Results: Thirty-five patients (68% mens, mean age 59.5) were enrolled and underwent baseline MRS while only 18 (51%) of them finished the whole protocol with control measurement (15 died before and 2 refused). The most common primary cancer was lung (44%), kidney (20%) and breast (15%). On average, 9 voxels were analyzed per right and left hippocampus. The mean NAA concentration pre- and post-WBRT was 8.47 [mM] and 7.43 [mM] for the right and 8.80 [mM] and 8.04 [mM] for the left hippocampus, respectively. The statistically significant decrease was observed in the right (-11.4%; 95% confidence interval -6.9 to -15.9; p=0.0003) as well as in the left (-8.5%; 95% confidence interval -2.9 to -14.0; p=0.0034) hippocampus.

Conclusion: Hippocampal MR spectroscopy is feasible and sensitive method for non-invasive measurement of brain radio injury. In our study, we observed correlation between left hippocampal N-acetylaspartate concentration and verbal memory decline with smaller effect of right hippocampus. Robust analysis of pre-irradiation imaging studies may provide valuable predictive biomarkers for decision making for the best radiotherapy approach in the treatment of brain metastases.

Proffered Papers: Brachytherapy 4: Gynae-Breast

OC-0351

MRI-guided brachytherapy in cervical cancer: high doses to small bowel don't predict late morbidity

C. Petit[1], R. Mazeron[1], C. Chargari[1], I. Dumas[1], P. Maroun[1], P. Annede[1], T. Seisen[1], C. Haie Meder[1]
[1]*Gustave Roussy, Radiation Oncology, Villejuif, France*

Purpose or Objective: To establish dose-volume effect correlations for late small bowel toxicities in patients treated for locally advanced cervical cancer with concomitant chemoradiation followed by MRI-guided adaptive brachytherapy.

Material and Methods: In a cohort of patients treated in curative intent and followed prospectively, those who had completed the treatment one year before were retained for this study. The small bowel loops were delineated during the planning process, but no specific dose constraint was applied. The dosimetric data, converted in 2 Gy equivalent (α/ß=3) were confronted to the occurrence of small bowel events: diarrhea, pain, flatulence, bleeding, obstruction, and fistula. Patients were followed every 3 months for the first year then every 6 months, for 3 years, then annually. Late morbidity was defined over the threshold of 90 days from treatment initiation and assessed using the CTC-AE 3.0. Patients who experienced recurrences were censored from the date of their relapse. Dose-effect relationships were assessed using mean dose comparisons (T-pair and Kruskal-Wallis tests), log rank tests on event-free survivals, and probit analyses. The highest graded event, or in cases of similar grade the earliest, was considered for analyses.

Results: One hundred and fifteen patients were eligible. Of them, 94.8% received concomitant chemoradiotherapy; 12.2% extended-field radiotherapy, and 32.2% nodal sequential boost. Their mean age was 47.5 years. The median follow-up was 35.5 months. A total of 522 events was reported. Focusing on the highest grade per patient: 17 had grade 0, 75, grade 1, 20, grade 2 and 3, grade 3. The prevalence of grade 1 events appeared stable during the study period, ranging between 31.2 and 50%. The one of grade 2 events tended to worsen: 2.2% at 6 months, 4.5% at 1 year, 6.9% at 2 years, and 7.0% at 3 years. Incidences of grade 2-4 events were 0.9% at 6 months, 6.6%, 19.0%, and 27.2% at 1, 2, 3 years respectively. The mean D2cm3 and D0.1cm3 were respectively 68.7±13.6 Gy and 85.8±33.1 Gy and did not differ according to grade (p=0.47 and p=0.52). Comparisons of mean D2cm3 and D0.1cm3 according to grade 0-1 versus 2-4 were not significant (68.0±12.4 vs 71.4±17.7 Gy, p=0.38 and 83.7±26.4 vs 94.5±51.9 Gy, p=0.33 respectively). Log rank tests were performed after splitting patients into 4 groups according to D2cm3 levels: > 80 Gy, 70 to 79 Gy, 60 to 70 Gy and < 60 Gy. No difference was observed for grade 1-4 (p=0.52), grade 2-4 (p=0.52) or grade 3-4 (p=0.21). Probit analyses showed no correlation between both dosimetric parameters and the probability of small bowel events grade 1-4, 2-4, or 3-4 (p ranging from 0.19 to 0.48).

Conclusion: No significant dose-volume effect relationships were demonstrated between the D2cm3 and D0.1cm3 and the probability of late small bowel morbidity. These two parameters should not limit the optimization process.

OC-0352

The high doses employed in brachytherapy of cervical cancer counteract hypoxia – a modelling study

E. Lindblom[1], A. Dasu[2], I. Toma-Dasu[3]
[1]*Stockholm University, Medical Radiation Physics, Stockholm, Sweden*
[2]*Linköping University, Department of Radiation Physics and Department of Medical and Health Sciences, Linköping, Sweden*
[3]*Stockholm University and Karolinska Institutet, Medical Radiation Physics, Stockholm, Sweden*

Purpose or Objective: Brachytherapy is a well-established radiotherapy treatment modality that has been employed in treatments of several cancer types for more than a century. One of the most common treatment strategies for cervical cancer today is a combination of external beam radiotherapy, chemotherapy and brachytherapy. Similar to other forms of radiation therapy, pre-treatment imaging of hypoxia is rarely done for cervical cancer. Nevertheless, the clinical outcome is highly positive, despite the fact that hypoxia has been repeatedly confirmed in cervical tumours. It was therefore the purpose of this study to investigate whether the success of brachytherapy in these tumours, seemingly regardless of oxygenation status, could be explained by the characteristics of the brachytherapy dose distributions in comparison to external beam radiotherapy.

Material and Methods: A previously used *in silico* model of tumour oxygenation and radiation response was further developed to simulate the treatment of cervical cancer employing the combination of external beam radiotherapy and intracavitary brachytherapy. Based on the local clinical protocol and using a clinically derived brachytherapy dose distribution and assuming a homogeneous dose delivered by external radiotherapy, survival was assessed on voxel level taking into account the dose-modifying effect of the oxygenation as well as the effects of repair and repopulation of tumour cells during treatment. Two scenarios were considered for brachytherapy: one in which the high dose region was highly conformal to the hypoxic region in the target and one in which they were displaced relative to each other. Overall-response was assessed as Poisson-based tumour control probability (TCP). The interplay between tumour oxygenation and the heterogeneous high-dose distribution was also studied by simulating different spatial and temporal patterns of hypoxia. The results were compared to the case when irradiation was performed only with external beams delivering a homogeneous dose to the target.

Results: Predicted values of *D*50 with respect to the external treatment and assuming reoxygenation were in agreement with the clinically observed high cure rates. Assuming fast reoxygenation, the *D*50 was similar for the different cases of overlap between the brachytherapy dose distribution and the tumour, regardless if the hypoxic fraction was 10% or 25% (Table 1). To achieve 50% control with external RT only, a total dose of more than 70 Gy in 25 fractions would be required for both cases of hypoxic fraction assuming reoxygenation (Figure 1).

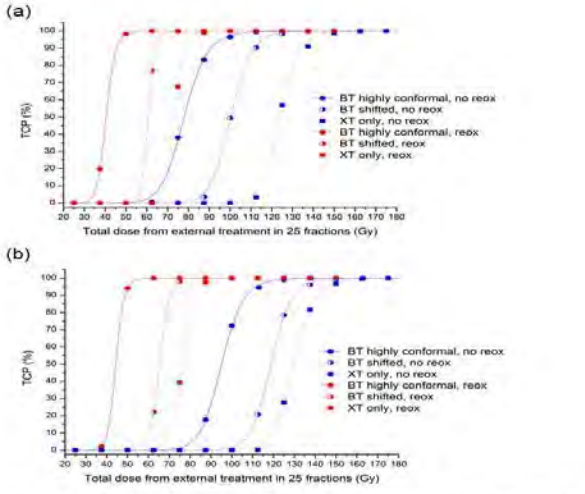

Figure 1. TCP curves for external RT given in 25 fractions for various scenarios for the brachytherapy (BT) dose distribution: highly conformal or shifted relative to the hypoxia area and the corresponding curves for the external RT (XT) only, for a simulated tumour with 10% hypoxia in (a) and 25% hypoxia in (b).

Hypoxic fraction	Oxygenation pattern	D_{50} (Gy)		
		BT highly conformal	BT shifted	XT only
10%	No reoxygenation	77.9	100.3	124.1
	Fast reoxygenation	40.4	60.6	73.4
25%	No reoxygenation	95.1	118.7	129.9
	Fast reoxygenation	44.3	65.4	76.2

Table 1. Values of D_{50} for external RT given in 25 fractions for various scenarios for the brachytherapy (BT) dose distribution: highly conformal or shifted relative to the hypoxia area and the corresponding values for the external RT (XT) only.

Conclusion: Assuming fast reoxygenation, the dependence on the degree and extent of hypoxia has little impact on the outcome and therefore the high doses delivered in brachytherapy could counteract the negative impact of hypoxia.

OC-0353

EBRT and interstitial brachytherapy for recurrent vault carcinomas: Factors influencing the outcomes

R. Engineer[1], S. Chopra[2], U. Mahantshetty[2], A. Maheshwari[1], R. Kerkar[1], R. Phurailatpam[2], J. Swamidas[2], S.K. Shrivastava[2]
[1]*Tata Memorial Centre, Surgical Oncology, Mumbai, India*
[2]*Tata Memorial Centre, Radiation Oncology, Mumbai, India*

Purpose or Objective: Post hysterectomy vaginal vault recurrences have poor outcomes with pelvic control rates ranging from 50-60%. We conducted this prospective study at our centre with an aim to determine the factors influencing the outcomes of these patients treated with external beam radiotherapy (EBRT) and interstitial brachytherapy.

Material and Methods: Ninety patients were accrued between October 2008 and May 2014. All the patients underwent prior hysterectomy and were diagnosed to have recurrent vault cancers with squamous cell carcinomas. Only patients with minimum gap of 6 months between the hysterectomy and recurrence were accrued in the study. All underwent EBRT of 50Gy (2Gy/fraction) to pelvis and simultaneous boost to the pelvic nodes of (10 Gy/5 fraction) if present, using Intensity Modulated Radiotherapy with concurrent chemotherapy of weekly cisplatin (40mg/mt2) followed by HDR Interstitial brachytherapy boost of 20Gy (4Gy/fraction b.i.d).

Results: Eighty (88%) patients were post simple hysterectomy and 20(22%) had Wertheim's hysterectomy, 16 (18%) had pelvic nodes and 46(51%) had parametrial extension upto the pelvic side walls. All the patients completed EBRT and concurrent chemotherapy and 28 (31%) patients had gross residual disease at the time of interstitial brachytherapy. Post brachytherapy 5 patients continued to have persistent disease, 6 had local relapse, 2 had local + distant relapse and 9 patients had only distant relapse. At the median follow up of 42 months for the surviving patients the local control rate was 86% and the 5-year actuarial disease-free survival (DFS) and overall survival (OAS) was 75%, 71%. In univariate analysis OAS was influenced by tumor involving the pelvic side wall (55% vs 84% p=0.004) and large pelvic nodes >1cm (44% VS.73% P=0.01) at presentation and partial vs. complete tumor response to EBRT at the time of brachytherapy (40% vs. 83% p=0.001). On multivariate analysis pelvic nodes at presentation and the tumor response to EBRT were significant factors affecting DFS and OAS. Other factors such as age, disease volume, and vaginal extension did not impact the survivals. Grade III/IV rectal toxicity was seen in 5 (5%) patients, bladder toxicity in 3 (3%) patients, whereas none of the patients developed Grade III small bowel toxicity.

Conclusion: Using EBRT with concurrent chemotherapy and interstitial brachytherapy a majority of the recurrences can be salvaged. An excellent local control and survival is achievable using this technique and 28 (31%) patients had gross residual disease at the time of interstitial brachytherapy.

OC-0354

Artificial neural network for bladder dose interfractional variation prediction in GYN brachytherapy

Z. Siavashpour[1], M.R. Aghamiri[1], R. Jaberi[2], R. Ghaderi[1], C. Kirisits[3]
[1]*Shahid Beheshti University, Medical Radiation Engineering, Tehran, Iran Islamic Republic of*
[2]*Tehran University of Medical Science, Radiotherapy, Tehran, Iran Islamic Republic of*
[3]*Comprehensive Cancer Center- Medical University of Vienna, Radiotherapy and Oncology, Vienna, Austria*

Purpose or Objective: Introducing a fast technique to estimate bladder dose due to interfractional variations.

Material and Methods: 30 cervical cancer patients treated with HDR intracavitary brachytherapy were selected. After applicator insertion all cases pelvic CT scans were performed twice; pre- and post-treatment (15-30 min after dose delivery), with applicator in situ and identical bladder filling protocol. A 3D treatment planning software (TPS) (Flexiplan®, version 2.6, Isodose control, the Netherlands) was used. Applicator (Rotterdam tandem-ovoid) reconstruction and organs contouring were done by the same physicist and physician on both image series. Planning was performed on the pre-treatment CT. Fractional prescription dose was calculated for each patient based on the EQD2 and defined planning aims: 80-90 Gy for D90 of the high-risk clinical target volume and D2cm^3 of bladder, rectum, and sigmoid less than 85, 75, and 75, respectively. DVH parameters (D2cm^3, D0.1cm^3, D10, D30, and D50) were recorded after each planning. 192Ir dwell times were copied manually to the post-treatment CT in the TPS. The recalculations of the DVH parameters showed the interfractional OAR dose variations. Images and structures of each pre- and post-treatment plan were exported in DICOM format to an in-house MATLAB written code. An artificial neural network (ANN) based on the 'back-propagation algorithm' was developed to predict the OARs dose variations. ANN input data was based on the changes of OAR wall distance-to-dwell positions along the applicators, that were extracted from two images series of each case. 25 cases were randomly selected as the training and model validation set (20 cases for training and 5 for validation), and the last 5 one for the resulted ANN model testing. Testing was performed by comparing the interfractional dose variations obtained from TPS calculated DVH and that obtained from ANN-based computing. The performance of the ANN was analyzed by root mean square error (RMSE).

Results: RMSE of the designed ANN was 0.28. RMSE of the testing cases was 0.72. TPS-based interfractional variations for D2cm^3 were -2.9 % ± 18.7 %. As an example of the model performance, relative differences of TPS-calculated and ANN-based interfractional variations for D2cm^3 of the training + validation cases (just the first 25 ones) are presented schematically in the Figure 1. It can be seen that these relative differences are almost less than 3%.

Figure 1: Relative difference of D_{2cm}, interfractional variations of ANN model-based and TPS-based data.

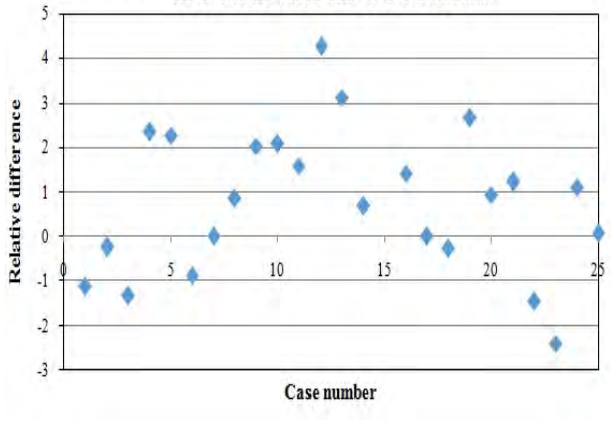

Conclusion: An ANN-based model was introduced which can give a fast prediction of bladder interfractional dose variations during cervical cancer intracavitary brachytherapy independent from TPS based dose calculations. This can serve as a basis for online verification tools in brachytherapy dose delivery.

OC-0355

Long term analysis of electron vs. HDR boost in breast conservation – an Indian experience

S. Saha[1], S. Sarkar[2], A. Mitra[3], A. Ghosh Dastidar[4], S. Chattopadhyay[5], S. Gupta[6]

[1]*Apollo Gleanegles Cancer Hospital, Department of Radiation Oncology, Kolkata, India*

[2]*Calcutta Medical Research Institute, Oncology, Kolkata, India*

[3]*Vivekananda Institute of Medical Science, Paediatrics, Kolkata, India*

[4]*IPGMER, Radiotherapy, Kolkata, India*

[5]*Medical College Hospital, Radiotherapy, Kolkata, India*

[6]*Apollo Gleanegles Cancer Hospital, Department of Surgical Oncology, Kolkata, India*

Purpose or Objective: Last decade has witnessed a revolution in breast conservation (BCS) in India as a consequence of sustained awareness campaigns and detection of early cases. But success of BCS demands not only local control but cosmetic excellence as well. Radiotherapy plays a major role in this treatment and selected high risk cases require boost also . This retrospective analysis aims to explore impact of modality of boost radiotherapy (electron vs. HDR interstitial brachytherapy) on long term cosmesis.

Material and Methods: 194 early breast cancer patients (T1N0, T2N0, T1N1) underwent BCS (Lumpectomy =125, Quadrentectomy = 69) + N3 nodal dissection in our unit between July 2004 and March 2010 after metastatic work up. Clips (4 or 5) were placed in all for subsequent delineation of radiotherapy target. Receptor status (including Her 2 neu) was detected for all. All patients received post BCS adjuvant chemotherapy - FEC for 'low risk' cases and EC X 4 then taxane X 4 for 'intermediate' and 'high risk' cases. Whole breast radiotherapy was given to all (50 Gy/ 25 fractions with CT-based planning). 145/194 patients also received boost - either 15 Gy/ 6 fractions electron or 10 Gy/ single fraction HDR interstitial implant (2 or 3-planes) with individualized CT-based planning and geometrical optimization. DVH was analyzed in each for D90, Coverege index, Dose received by skin, DNR and COIN. Cosmetic outcome was analyzed in each follow up visit using 4-point scale (excellent, good, fair, poor).

Results: Out of evaluable 173/ 194 patients (4 died of metastasis, 17 lost to follow up) with minimum duration of follow up of 36 months, 86 did receive electron boost and 38 received HDR. Local recurrence was in none so far. The PTV differed significantly - median 38 cc with HDR vs. median 90 cc with electron. Cosmetic outcome was significantly different – only 48/86 patients receiving electron boost have 'excellent and good' cosmesis compared to 31/38 receiving HDR brachytherapy (P = 0.008). Grade 1-2 fibrosis was seen in 39/86 (46%) with electron and 6/38 with brachytherapy (P= 0.002). Grade 1-2 telengiectasia was also significantly lower with HDR brachy 3/38 vs 29/86 with electron (P= 0.0019). Arm oedema was negligible in all patients - only 2.8%.

Conclusion: For best cosmetic outcome after BCS, HDR brachytherapy (with CT-based 3D planning) for patients requiring boost radiotherapy appears to be much better option compared to electron unless the tumour is very superficial.

OC-0356

Long terms results of permanent breast seed implants (PBSI) as partial breast irradiation

J.P. Pignol[1], J. Caudrelier[2], C. McCann[3], S. Doggett[4], J. Crook[5]

[1]*Erasmus Medical Center Rotterdam Daniel den Hoed Cancer Center, Radiation Oncology, Rotterdam, The Netherlands*

[2]*The Ottawa Hospital Cancer Centre, Radiation Oncology, Ottawa, Canada*

[3]*Sunnybrook Health Sciences Centre, Radiation Oncology, Toronto, Canada*

[4]*Tustin Radiation Clinic, Radiotherapy, Tustin, USA*

[5]*BCCA Centre for the Southern Interior, Radiation Oncology, Kelowna, Canada*

Purpose or Objective: Since2004 breast cancer patients have been prospectively included in three clinicaltrials using post-operative permanent breast seed implant (PBSI) brachytherapy.We report the long term efficacy results of the technique on patients with lowrisk, small (less than 3 cm) and node negative tumors.

Material and Methods: Thefirst trial was a Phase I/II accruing patient with low risk infiltrating ductalcarcinoma (IDC), the second trial was a Phase II trial DCIS patients, and the thirdtrial was a Multicentre Registry. All patients received PBSI delivering a doseof 90 Gy after CT-simulation and planning. Stranded ^{103}Pd seeds wereimplanted using light sedation, ultra-sound guidance, fiducial needle localization,and using template. Patients werefollow-up annually for 10 years. Overall survival, disease free survival, localrecurrence and ipsilateral recurrence at 5 years were compared to theoreticalones calculated using theIDCTuft University IBTR and DCIS Memorial Sloan Kettering Cancer Center nomograms.

Results: FromApril 2004 to May 2014, a total of 134 patients have been accrued. The median FUof the entire series is 58.6 months [range 1.3 to 121.8 months]. The median ageat surgery was 61.9 years old [41 to 84.5], 91% of patients had an invasivetumor and the remaining were DCIS. All patients were T1-2 N0, grade 1 or 2 butone was found node positive on pathology review. At time of evaluation 119 patientswere without any evidence of disease. The local recurrence free survival at 5years was 98.8% (SD ± 1.20%), which was not statistically significantlydifferent to the theoretical rate of 98.6% for patients receiving whole breastradiotherapy (p=0.23). But this rate was significantly better than the 95.4% theoreticalrisk of local recurrence with surgery alone (RR=0.27, p<0.001), The 5 yearsoverall survival was 97.4% (SD ± 1.91%) and the disease free survival was 96.4%(SD ± 2.07%). In terms of tolerance, 22% of patients had telangiectasia almostexclusively grade I at 2 years. This rate decreases over time to 16% at 8years. Of note 40% of the patients developed a palpable and asymptomaticinduration in the surgical scar.

Conclusion: Long-term results suggest that PBSI is a well-toleratedtreatment, with an efficacy similar to whole breast radiotherapy for wellselected early stage breast patients. This treatment represents a goodtreatment option for patients having difficulties attending prolongedradiotherapy protocols.

Proffered Papers: Physics 8: Dose measurement and dose calculation I

OC-0357

Pilot study of a remote end-to-end dosimetry audit for IMRT and VMAT treatments

P. Wesolowska[1], B. Almady[1], E. Adolfsson[2], A. Carlsson Tedgren[2], D. Georg[3], S. Kry[4], W. Lechner[3], J. Povall[5], M. Tenhunen[6], M. Tomsej[7], J. Izewska[1]

[1]*International Atomic Energy Agency, Section of Dosimetry and Medical Radiation Physics- Division of Human Health-Department of Nuclear Sciences and Applications, Vienna, Austria*

[2]*Linköping University, Department of Radiation Physics and Radiation Physics- Department of Medical and Health Sciences, Linköping, Sweden*

[3]*Medical University of Vienna /AKH Vienna, Division of Medical Radiation Physics- Department of Radiation Oncology, Vienna, Austria*

[4]*IROC Houston QA Center, U.T. M. D. Anderson Cancer Center, Houston, USA*

[5]*St. James's Institute of Oncology- University of Leeds, Radiotherapy Physics Group, Leeds, United Kingdom*

[6]*Helsinki University Central Hospital, Department of Oncology, Helsinki, Finland*

[7]*CHU André Vésale, Radiation Oncology Department, Charleroi, Belgium*

Purpose or Objective: The new methodology for end-to-end remote dosimetric quality audit for IMRT and VMAT treatments for national dosimetry audit networks has been developed within a co-ordinated research project (CRP). The purpose of this audit is to verify the entire radiotherapy chain including imaging, treatment planning and dose delivery for a clinical IMRT treatment executed with either a static or rotating gantry. Overall 16 research groups from 13 countries participate in this CRP. Results of a pilot study involving 6 CRP participants are presented.

Material and Methods: A polystyrene phantom (see Fig. 1) was designed for this exercise with the solid water structures representing PTV and OAR. Each participant received a phantom preloaded with a custom cut EBT3 film and 4 TLDs (2 in PTV and 2 in OAR), extra TLDs for imaging and a set of instructions and datasheets. Participants were asked to scan the phantom, contour the structures, create the treatment plan and irradiate the phantom. The plan was generated as for a patient to deliver 4 Gy to PTV in 2 fractions and limit the dose to OAR to 2.8 Gy (additional target objectives were provided).

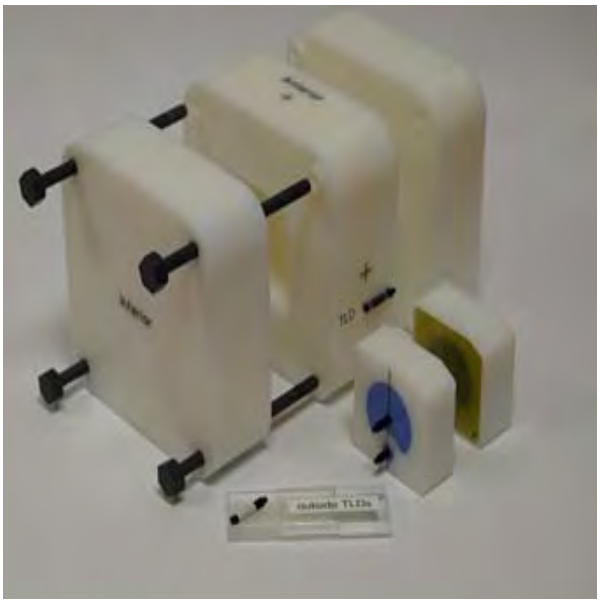

Fig. 1 IMRT phantom with an insert loaded with film and TLDs.

Upon receipt of the irradiated phantom by the CRP organiser, TLDs and film were evaluated. Comparison was performed between the calculated and the film measured dose distributions using a gamma analysis tool (FilmQA ProTM, Ashland). The gamma acceptance criterion of 3%/3 mm over all pixel values exceeding 20% of the maximum dose was adopted. TLD results were presented as ratios of the TLD measured dose and the participant stated dose, D(TLD)/D(stat).

Results: The results were obtained for 6 participants using 6 different accelerator models, 4 MLC models, 3 TPS models and 5 dose calculation algorithms. All participants created treatment plans which fulfilled the dose constraints provided. The results of gamma evaluation were between 93.5% and 100%. TLD results for PTV showed good agreement with the average D(TLD)/D(stat) = 0.995 and 1.2 % standard deviation (SD), whereas for OAR the average D(TLD)/D(stat) was 1.041 and the SD = 4.6%. As OAR was located in a high dose gradient region, even a 1 mm positional shift could cause significant TLD dose difference.

Conclusion: The methodology of this audit, examined through a pilot study, proved to work well. The instructions and datasheets appeared to be clear and straightforward to follow. The results showed good agreement for TLDs in PTV and also between the planned and the film measured dose distributions. However, TLD measurements in the OAR were challenging because of the high dose gradient in this region. The results of the pilot study were used to assess the measurement uncertainties and will help in establishing the acceptance limits for audit results. The study continues with 10 additional research groups involved in the CRP.

OC-0358

Surface doses with FFF VMAT dose delivery for breast cancer

J. Seppala[1], A. Voutilainen[2], J. Heikkilä[1], T. Koivumäki[1], T. Viren[1], M. Vauhkonen[2]

[1]*Kuopio University Hospital, Cancer Center / Radiotherapy dept. 4251, Kuopio, Finland*

[2]*University of Eastern Finland, Faculty of Science and Forestry, Kuopio, Finland*

Purpose or Objective: Flattening filter free (FFF) beams have the potential to speed up breast cancer radiotherapy (RT) treatments and reduce whole body dose of a patient by reducing treatment head leakage. However, the near surface dose data of modulated FFF beams is lacking. In this work the surface doses were studied with various treatment plans for breast cancer RT with both FFF and flattening filter (FF) beams.

Material and Methods: This study was executed with EBT3 films irradiated in a cylindrical phantom (CIRS, ø16cm). The phantom was imaged with CT scanner (slice width 1 mm). PTV and critical organs were contoured to the 3D images (Fig.1). Four clinical treatment plans (photon energy 6 MV, fractional dose 2 Gy) were created for Elekta Infinity accelerator with Agility MLC: 1) tangential open field, 2) tangential IMRT with dynamic MLC (DMLC), 3) tangential VMAT (tVMAT) and 4) continuous VMAT (cVMAT) (Fig.1). Doses were calculated to water with X-ray Voxel Monte Carlo algorithm (XVMC, Monaco v5.00.04, Elekta) with a resolution of 1 mm and STD of 0.5%. Treatment plans were normalized to mean dose of PTV. All irradiations were repeated three times and the calibrated films were scanned in RGB mode. Red channel data was used in analysis with OmniProImRT software (v1.7, IBA, Germany).

Results: Calculated and measured surface dose distributions were compared and are presented for FFF in Fig.1. The overall accuracy of XVMC calculation was good with the largest point dose difference of -11% recorded with FFF DMLC. Line dose analysis was performed in lateral and central parts of the phantom to evaluate surface doses with

respect to beam directions (shown in Fig.1). Compared with measured dose the calculated doses were on average 3% larger at the depths of 0-2 mm (relevant depth for RT induced skin reactions). At 2-5 mm depths the dose deviation was on average 0% (Table 1). Central part surface doses at 0-2 mm were on average 27% higher with open fields than with both VMAT techniques which was also well predicted by the TPS (max error 4%). Within the lateral parts the average surface doses between the techniques deviated less than 8% (range 45% - 48%). An important finding was also that on average the lowest values of surface doses were measured with open fields (lateral parts). No significant differences in surface doses were detected between FFF and FF techniques.

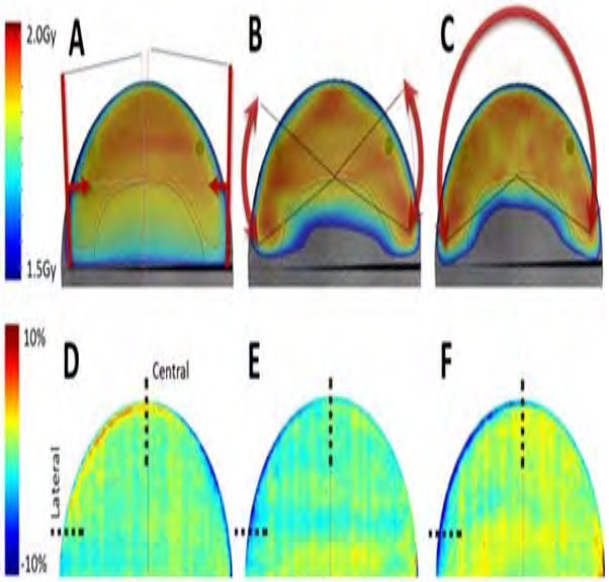

Fig.1: Calculated dose distributions of (A) open field, (B) tVMAT and (C) cVMAT treatment plans with FFF and the corresponding differences against the measured dose distributions (meas-calc) in D, E and F, respectively.

Table 1: Measured and calculated surface doses of FFF and FF (depths of 0-2mm and 2-5mm).

	Open field		DMLC		tVMAT		cVMAT	
FFF	Meas.	Calc.	Meas.	Calc.	Meas.	Calc.	Meas.	Calc.
Lateral 0-2 mm	45 %	50 %	45 %	44 %	46 %	47 %	48 %	52 %
2-5 mm	66 %	73 %	59 %	55 %	62 %	70 %	68 %	76 %
Central 0-2 mm	69 %	66 %	55 %	62 %	55 %	56 %	50 %	52 %
2-5 mm	98 %	94 %	87 %	84 %	89 %	89 %	90 %	84 %
FF	Meas.	Calc.	Meas.	Calc.	Meas.	Calc.	Meas.	Calc.
Lateral 0-2 mm	46 %	50 %	45 %	48 %	44 %	42 %	50 %	48 %
2-5 mm	69 %	66 %	66 %	69 %	63 %	63 %	74 %	75 %
Central 0-2 mm	62 %	71 %	64 %	62 %	62 %	59 %	48 %	49 %
2-5 mm	92 %	88 %	94 %	91 %	96 %	92 %	80 %	82 %

Conclusion: The accuracy of surface dose calculation was acceptable in Monaco TPS. There was no significant difference in surface doses between FFF and FF beams. Based on our results the VMAT techniques produce more homogeneous surface doses when compared to tangential open fields.

OC-0359

Superficial dose verification of four dose calculation algorithms

Y. Cao[1], Z. Yang[1], X. Yang[1], X. Qiu[2]

[1]*Xiangya Hospital Central-South University, Oncology Department, Changsha- Hunan, China*

[2]*University Of South China, School of Nuclear Science and Technolgy, Hengyang-Hunan, China*

Purpose or Objective: The aim of this study is to verify superficial dose calculation accuracy of four commonly used algorithms in commercial available treatment planning systems (TPS) by Monte Carlo (MC) simulation and film measurements.

Material and Methods: EGSnrc (BEAMnrc\DOSXYZnrc) code was performed to simulate the central axis dose distribution of Varian Trilogy accelerator, combined with measurements of superficial dose distribution viaa extrapolation method of multilayer radiochromic films, to verify the dose calculation accuracy of four algorithms of AXB (Acuros XB), AAA (Analytical Anisotropic Algorithm), CCC (Collapsed Cone Convolution) and PBC (Pencil Beam Convolution) in the superficial region which was described in detail by ICRU and ICRP, under the conditions of source to surface distance (SSD) of 100cm, field size (FS) of 10cm×10 cm, solid water size of 30cm×30cm×30cm and the incident angles of 0°, 30° and 60°.

Results: In superficial region, good agreement was achieved between MC simulation and film extrapolation method, with the mean differences respectively less than 1%, 2% and 4% , and the relative skin dose difference were 0.84%, 1.88% and 3.90% for 0°, 30° and 60°; the mean dose errors (0°, 30° and 60°) between four algorithms and MC simulation were AXB (2.41±1.55%, 3.11±2.40%, 1.53±1.05%), CCC (3.09±3.0%, 3.10±3.01%, 3.77±3.59%), AAA (3.16±1.5%, 8.7±2.84%, 18.2±4.1%) and PBC (14.45±4.66%, 10.74±4.54%, 3.34±3.26).

Table 1. Skin dose difference of film measurements and different algorithm calculations (%)

Incident angle	Method				
	Film	AXB	AAA	CCC	PBC
0°	0.84	-0.05	4.07	11.37	22.15
30°	1.88	-0.71	0.15	12.17	20.00
60°	3.94	0.74	-9.51	14.11	11.74

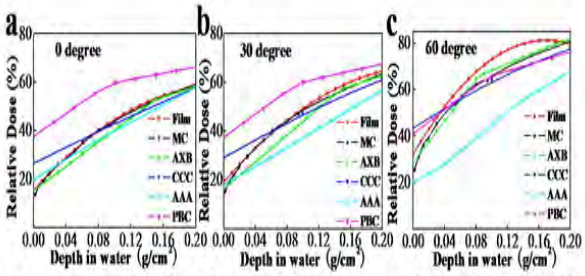

Fig. 1. Superficial dose distributions of film measurements and algorithm calculations with incident angle of 0° (a), 30° (b) and 60° (c) compared with those of MC simulations within the initial 2 mm depth.

Conclusion: Monte Carlo simulation validated the feasibility of the superficial dose measurement via multilayer Gafchromic film detectors. And the rank of superficial dose calculation accuracy of four algorithms was AXB>CCC>AAA>PBC. AAA and PBC algorithms were not applicable for superficial dose calculation.

OC-0360

TomoTherapy tangential breast treatment position uncertainty via exit detector fluence

N. Corradini[1], P. Urso[1], C. Vite[1]

[1]*Clinica Luganese, Radiotherapy Center, Lugano, Switzerland*

Purpose or Objective: To analyze the exit detector fluences from tangential breast treatments in estimation of the breast

position uncertainty of daily IGRT on the TomoTherapy system.

Material and Methods: Twenty patients who received tangential breast radiotherapy on the TomoTherapy system were selected randomly. All patients were aligned daily to the planning-kVCT using MVCT prior to treatment. For each detector measurement, the treatment projection containing the fluence passing through the midpoint of the breast was extracted for analysis in MATLAB. The high fluence gradient indicating the interface between the breast surface and tangential beam flash was easily observed and used for analysis (Fig 1). Each CT detector channel has a nominal width of ~0.76 mm projected at treatment isocenter, therefore absolute position of the projected breast surface was calculated. Separately, a study was performed using the TomoTherapy Cheese phantom simulating breast patient. A radiotherapy plan mimicking that of the breast patients was created. The plan was delivered onto the phantom in the correct treatment position, as well as with known phantom displacements in increments of 1-mm along the x- and z-axes. The analysis described above was subsequently performed on the phantom detector data to correlate the known displacements to those measured from the detector fluence. The correlation fit obtained from the phantom measurements was applied to the patients in estimation of breast surface position.

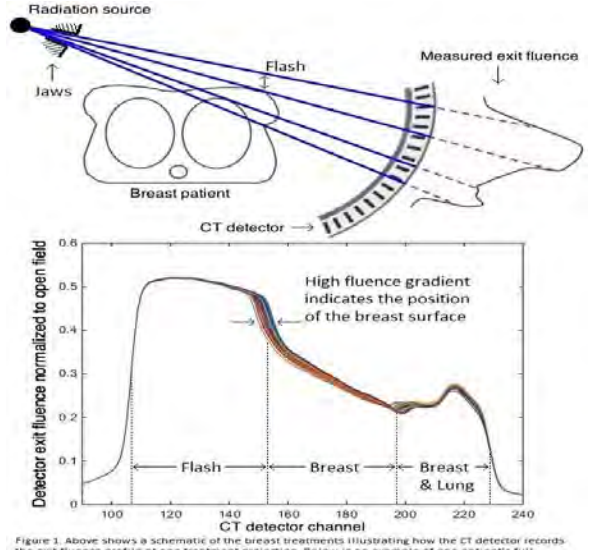

Figure 1. Above shows a schematic of the breast treatments illustrating how the CT detector records the exit fluence profile at one treatment projection. Below is an example of one patient's full dataset, i.e. 25 fluence profiles from one treatment projection, and detailed explanations are added to help interpret the measurement profiles.

Results: The phantom study showed that phantom position was linearly correlated with the exit detector measurements resulting in an r > 0.99. The standard deviation in the measured breast surface position, σ, was 2.28 mm for the 453 analyzed detector fluences (σmin = 1.39 mm, σmax = 4.33 mm). The uncertainty in the detector measurements was estimated to be under one detector channel's width.

Conclusion: The σ results of this study should be an indicator of the overall positioning uncertainty in our IGRT process for these treatments, i.e. kVCT-MVCT image registration, patient movement, and respiratory motion. Even if only one projection of the treatment data was used in the estimation, our results compare very well with similar studies' (von Tienhoven et al (1991), Smith et al (2005), Wang et al (2013)) findings on breast displacement due to respiratory motion. Furthermore, the novelty of this study is its evaluation of the breast position was performed on exit detector fluence of intensity-modulated fields, which we believe to be a first.

OC-0361

Simulation of clinical relevance errors detected by real-time EPID-based patient verification system

T. Fuangrod[1], J. Simpson[2,3], R. Middleton[1], P. Greer[2,3]

[1]*University of Newcastle, School of Electrical Engineering and Computer Science, Newcastle- NSW, Australia*

[2]*Calvary Mater Newcastle, Radiation Oncology, Newcastle-NSW, Australia*

[3]*University of Newcastle, School of Mathematical and Physical Sciences, Newcastle- NSW, Australia*

Purpose or Objective: A a real-time patient treatment verification system using EPID (Watchdog) for clinical implementation was developed as an advanced patient safety tool. However to use Watchdog for treatment intervention we need to understand its response to clinically significant errors. The purpose of this study is to investigate the performance of Watchdog under controlled error conditions.

Material and Methods: The real-time verification system (Watchdog) utilises a comprehensive physics-based model to generate a series of predicted transit cine EPID image as a reference data set, and compares these to measured cine-EPID images acquired during treatment. The agreement between the predicted and measured transit images is quantified using chi-comparison on a cumulative frame basis. To determine the ability of Watchdog to detect clinically significant errors during treatment delivery we used real patient data and simulated dosimetric and patient positional errors. Four study cases were used; dosimetric error in Prostate IMRT, HN patient weight loss, prostate displacement and lung SBRT displacement errors. These errors were introduced by modifying the planning CT scan data and re-calculating the predicted EPID data set. The error embedded predicted EPID data sets were compared to the measured EPID data acquired during patient treatment.

Results: The average % cumulative chi pass-rate across four case studies were 84.0% and 94.5% for 3%, 3mm and 4%, 4mm respectively. In the figures, the cumulative chi pass-rate results based on error simulation are shown. The difference ratio of chi comparison criteria between 3%, 3mm and 4%, 4mm was approximately 13%. As a result, the threshold level should determine based on the criteria and clinical acceptant limit.

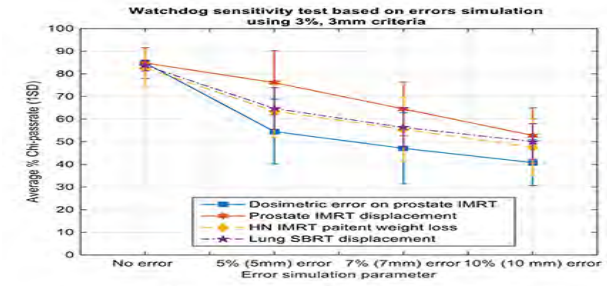

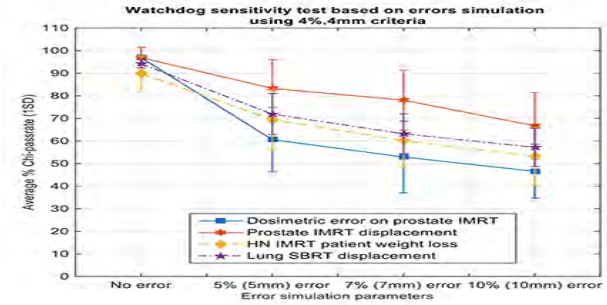

Conclusion: We have evaluated our proposed real-time EPID-based treatment verification system using clinical relevant error simulation in prostate, HN and lung cases. Using either a 3%, 3mm or 4%, 4mm criteria, the real-time EPID-based patient verification system successfully detected simulated errors introduced into patient plan deliveries; including 5% dosimetric errors on prostate IMRT, 5mm prostate IMRT displacement, 5% HN patient weight loss, and 5mm Lung SBRT displacement.

OC-0362

EPID-based in-vivo dosimetry results: a national statistic

A. Piermattei[1], S. Menna[2], F. Greco[2], S. Cilla[3], R. Caivano[4], V. Fusco[4], L. Orlandini[5], G. Benecchi[6], R. Nigro[7], D. Falco[8], A. Fidanzio[1]

[1]*Università Cattolica del Sacro Cuore -Fondazione A. Gemelli, UOC Fisica Sanitaria, Rome, Italy*

[2]*Fondazione A. Gemelli, UOC Fisica Sanitaria, Rome, Italy*

[3]*Fondazione Giovanni Paolo II, UO Fisica Sanitaria, Campobasso, Italy*

[4]*CROB, UOC Radioterapia, Rionero Pz, Italy*

[5]*CFO, U.O. Fisica Medica, Firenze, Italy*

[6]*Azienda Ospedaliero-Universitaria, UOC Fisica Sanitaria, Parma, Italy*

[7]*Ospedale S. Camillo de Lellis, UOC Radioterapia, Rieti, Italy*

[8]*OC S.S. Annunziata, UOC Radioterapia, Chieti, Italy*

Purpose or Objective: The increasing complexity of modern radiation therapy requires major quality control (QC) to ensure safety and reliability of patients' treatments. The large number of QCs requires a considerable amount of work that sometime is responsible of missing controls that may lead to dosimetric errors. In this frame the in vivo dosimetry (IVD) by EPID images has an important role to detect eventual dosimetric discrepancies between planned and delivered doses. The present work reports the results of 7500 IVD tests obtained in the last 2 years in 7 Italian Centers.

Material and Methods: SOFTDISO is an IVD-program distributed by the Best Medical Italy for 3D-CRT ,IMRT and VMAT treatments, and it is based on correlation functions between EPID signals and doses in patient. The software is easy to implement for Varian, Elekta and Siemens linacs, and it is connected with the Record and Verify system of the Center, supplying the results in a few seconds. The method supplies two tests (i) the ratio R=(Diso/Diso,TPS) between the reconstructed and computed isocentre dose, with pass criteria of ±5% and (ii) a 2D γ-analysis between EPID images with the following pass criteria: the percentage of the points Pγ<1 should be higher than 90% for 3DCRT and 95% for IMRT and VMAT; the γ-mean should be less than 0.5 and 0.3 for 3DCRT and IMRT-VMAT respectively.

Results: The percentage of the off-tolerance tests ranged between 10% and 17%, depending on the type of treatment checked. The causes of dosimetric discrepancies, in order of frequency were: setu-up variations, attenuators left in the field, morphological changes, TPS implementation and linac output factor. All the causes of the off-tolerance tests were justified and, once removed, the mean R values of all patients were within 5% and the γ-analysis indexes satisfied the specific pass criteria. The discrepancies due to patient morphological changes triggered new TC or CBCT scans to verify the need of an adaptive plane. Some of these cases have been discussed by radiotherapists and physicists.

Conclusion: The multicenter result proved: (i) the great utility to obtain IVD tests in quasi real time, (ii) the positive role of the physicists during the dose-delivery step, (iii) SOFTDISO allows to understand the causes of dose discrepancies triggering adequate QC, and once the causes of errors were removed all the pass criteria were respected (iv) the role of IVD to intercept patient morphological changes to examine for eventual adaptive radiotherapy strategy.

Proffered Papers: Physics 9: Adaptive RT for inter-fraction motion management

OC-0363

Dose escalation in lung cancer patients, the dosimetric implications of inter-fractional change

L. Hoffmann[1], M. Knap[2], A. Khalil[2], D. Møller[1]

[1]*Aarhus University Hospital, Medical physics, Aarhus, Denmark*

[2]*Aarhus University Hospital, Oncology, Aarhus, Denmark*

Purpose or Objective: To date no satisfactory treatment options exist for locally advanced lung cancer. Based on promising phase II studies, dose escalation gave hope for better local control. However, the phase III RTOG 0617 [1] dose escalation trial showed that treatment related deaths can increase. Strict normal tissue constraints, as well as focus on the actual delivered dose, are essential when aiming for safe dose escalation. For standard doses, adaptive radiotherapy (ART) has mainly been concerned with ensuring target coverage, but with escalated doses anatomical changes during treatment can result in critical over dosage of organs at risk (OARs). Furthermore, it is important to monitor doses to known OARs such as the heart, and other structures as connective tissue and chest wall, where we don't know the risk for high dose RT. The present study investigates the impact of anatomical changes during RT on the escalated dose distribution used in the Danish NARLAL2 dose escalation trial.

Material and Methods: Fifteen patients (pts) with a standard treatment plan and an experimental dose escalation plan were analysed. The standard plan delivered a homogeneous dose of 66 Gy/ 33 fractions (fx) while the experimental plan delivered a heterogeneous escalated dose distribution. The dose escalation was driven by the most FDG-PET active region of the tumour and lymph nodes, with mean doses up to 95 Gy/ 33 fx and 74Gy/ 33 fx, respectively. The dose distribution was limited by constraints to the OARs (Table 1). All pts had a surveillance scan (sCT) at fx 10 and ten pts also at fx 20. The original treatment plans were recalculated on the sCTs to evaluate the impact of inter-fractional changes during the RT course. For most OARs, a maximum dose constraint was set, allowing higher doses for < 1cm3 of the OAR. The number of pts with OARs reaching the maximum dose for the escalation plan, was determined. For some pts, the volume receiving doses above the maximum constraint, increased on the sCT. Volume increments ΔV > 1cm3 were made up.

Organ at risk OAR	Constraint, escalation plan	D > x Gy, pCT #patients	ΔV> 1cm³, sCT #patients
Lung	MLD < 20Gy		
Lung	V_{20Gy} < 35%		
Heart	V_{50Gy} < 20%		
Heart	D_{1cm3} < 74Gy	2	0
Oesophagus	D_{1cm3} < 70Gy	5	1
Trachea	D_{1cm3} < 74Gy	0	0
Bronchi	D_{1cm3} < 74Gy	3	0
Aorta	D_{1cm3} < 74Gy	3	1
Connective tissue	D_{1cm3} < 74Gy	14	7
Chest wall	D_{1cm3} < 74Gy	12	5
Spinal cord	D < 45 Gy	0	0

x=20 Gy for mean lung dose (MLD), 45 Gy for spinal cord, 70 Gy for oesophagus and 74 Gy for all other OARs. Connective tissue: All tissue between the lungs, exclusive the gross tumour volume (GTV) and all OARs delineated.

Results: At least one OAR reached maximum dose constraint on planning CT (pCT) for all pts. Of these, 9 pts showed doses to OARs increasing above maximum dose on sCT, see Table. Heart doses (V50Gy) increased more than 1cm3 (up to 19 cm3) in eight pts and in one pt the oesophagus was over dosed on the sCT. For connective tissue and chest wall, the volume receiving > 74 Gy increased more than 1cm3 on the sCT in 7 and 5 pts, respectively. The anatomical changes leading to higher OAR doses were tumour shrinkage (5 pt), body contour changes (3 pt) and resolving atelectasis (1 pt).The mean dose to the PET-GTVT was 92±3Gy. In six pts, the mean dose decreased more than 1% (up to 10%) on the sCT.

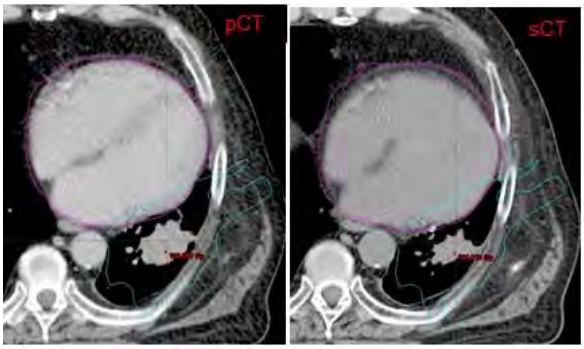

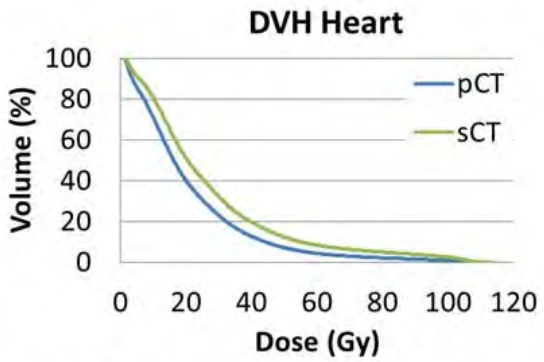

The caudal part of the heart (pink) moves into the high dose region. V_{50Gy} (turquoise) increases from 2.4% to 5.4% and mean heart dose increases from 14Gy to 18 Gy.

Conclusion: Anatomical changes during RT may result in increased doses to OAR. Introduction of dose escalation therefore requires frequent evaluation of treatment plans and ART should be used in order to avoid over dosage of OARs.

[1] Bradley, Lancet 2015

OC-0364

Adaptive radiotherapy for advanced lung cancer ensures target coverage and decreases lung dose

D.S. Moeller[1], M.I. Holt[2], M. Alber[1], M.M. Knap[2], A.A. Khalil[2], L. Hoffmann[1]

[1]*Aarhus University Hospital, Department of Medical Physics, Aarhus C, Denmark*

[2]*Aarhus University Hospital, Department of Oncology, Aarhus C, Denmark*

Purpose or Objective: Effective treatment options are needed for locally advanced lung cancer. Increased treatment precision and decreased treatment volumes are mandatory for more aggressive radiotherapy. Adaptive radiotherapy (ART) was implemented to adjust the treatment plan to positional or volumetric changes of the tumour, and to normal tissue changes like atelectasis. Recently, ART was shown to improve local control without increasing radiation pneumonitis [1]. The present study investigates the dosimetric consequences of ART for 235 patients.

Material and Methods: ART intervention rules were implemented for lung cancer patients treated with definitive chemo-radiotherapy, in concordance with smaller PTV margins and daily online soft-tissue matching. Intervention rules derived from geometrical criteria for normal tissue and tumour changes. Violation of these for three consecutive fractions triggered an evaluation. If the observed change was suspected to lead to an underdosage of tumour/lymph nodes or an overdosage of normal tissue, a CT rescan and a replan were made. The original plan was recalculated on the rescan to evaluate the consequence of replanning for patients receiving a plan adaptation in a cohort of 235 consecutive patients treated with ART. For the first 50 patients, in order to assess the efficacy of the intervention rules, two additional surveillance CT scans were acquired during the RT course and the treatment plans were recalculated on these scans. The change in lung dose due to the implementation of ART was found comparing the treatment plans of the first 50 ART-patients with 50 pre-ART-patients.

Results: Due to ART, the PTV decreased from 569 cm3 to 398 cm3, and consequentially the mean lung dose decreased from 14.1 Gy (SE 0.6) to 12.6 (SE 0.6) Gy. The criterion for the need of adaptation was a decrease in target coverage of CTV>1% or PTV>3%. The cohort of patients with two surveillance scans showed coverage above this in 94% of the cases not replanned. Sixty-one (26%) patients treated with ART had at least one replan. In total 77 adaptations were made. Fifty three adaptations corrected for a decrease in overall target coverage. Figure 1 shows the extent of decrease and designates the reason for replanning. In five patients with several separate targets under dosage of one of the targets were seen. One patient was replanned in order to avoid overdosage of spinal cord. Three patients were replanned due to changes in atelectasis making match evaluation impossible. In 15 patients, target shrinkage or less conformal dose distributions counterbalanced the geometric shifts that triggered adaptation.

Figure 1

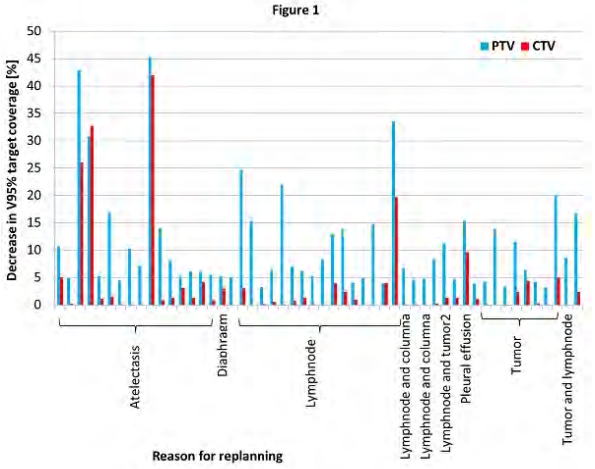

Conclusion: The implementation of soft-tissue match and ART secured high treatment precision and allowed safe margin reduction in terms of persistent target coverage. The reduced margins reduced the mean dose to the lung.

[1] M Tvilum et al. Acta Oncol 2015, Acta Oncol. 2015 Jul 24:1-8.

OC-0365

The need for anatomical landmarks in adaptive rectal cancer boost radiotherapy

J.J.E. Kleijnen[1], B. Van Asselen[1], M. Intven[1], J.J.W. Lagendijk[1], B.W. Raaymakers[1]

[1]*UMC Utrecht, Radiotherapy Department, Utrecht, The Netherlands*

Purpose or Objective: In rectal cancer 15% of the patients show a pathological complete response (pCR) after neo-adjuvant chemo-radiotherapy and these patients show better overall survival. To increase this pCR rate, in several studies a boost dose is given to the tumor. To safely deliver this boost, insight in the tumor position is needed. Currently, online imaging techniques provide no contrast of the tumor. However, since tumors are situated in the rectal wall, which is visible on online imaging like CBCT, the rectal wall position may be used as a surrogate for the tumor position. We therefore investigate the feasibility of tracking a part of the rectal wall close to the initial tumor as a motion surrogate for the tumor, to be used in online adaptive boost radiotherapy in rectal cancer.

Material and Methods: We scanned 16 patients daily on a 1.5T MRI scanner during a one-week short course of radiotherapy (5 times 5Gy). Rectum and tumor were delineated on the T2 weighted scan of each day. All scans were registered on bony anatomy, mimicking daily patient set-up. For both tumor and rectum separately, displacements

from the first day to every other day were determined, by calculating per voxel the shortest distance to each delineation.
To find out how proximate to the tumor we have to define our rectum motion surrogate, we selected that part of the rectum that lies within 1, 3, 5, 7 and 10 mm of the initial tumor (ProximateRectum). For each point on these ProximateRectums, we determined the nearest point of the tumor as corresponding point. Between all the corresponding points of ProximateRectum and tumor, the displacements to every day were correlated to each other. We also determined how much of the variance in tumor motion was explained by each ProximateRectum. These analysis were done for the 1, 3, 5, 7 and 10 mm ProximateRectum separately.

Results: Different motion patterns were found for tumor and ProximateRectums, especially when movement of the tumor is in cranial caudal direction, since no anatomical landmarks are available (see figure 1). We found correlations of ρ = 0.66, 0.64, 0.55, 0.53 and 0.45 (all $\leq$ p 0.001) for ProximateRectum of respectively 1, 3, 5, 7 and 10 mm. This results in only 44%, 40%, 31%, 28% and 20% of the variance of tumor motion being explained by local rectum motion for respectively ProximateRectums of 1, 3, 5, 7 and 10 mm.

Conclusion: Even when the rectal motion surrogate is defined within 1 mm of the tumor, tracking this part of the rectal wall will not result in an accurate tumor positions since only 44% of the variance in tumor motion is explained by tracking the rectal wall. The lack of anatomical landmarks prevents finding the true rectum deformation and thus an accurate tumor position. Especially for motion in cranial-caudal direction, there is poor correlation between tumor and local rectal motion. Therefore, anatomical landmarks are needed for positioning the tumor e.g. direct imaging of the tumor using MRI or indirect imaging of the tumor using implanted markers.

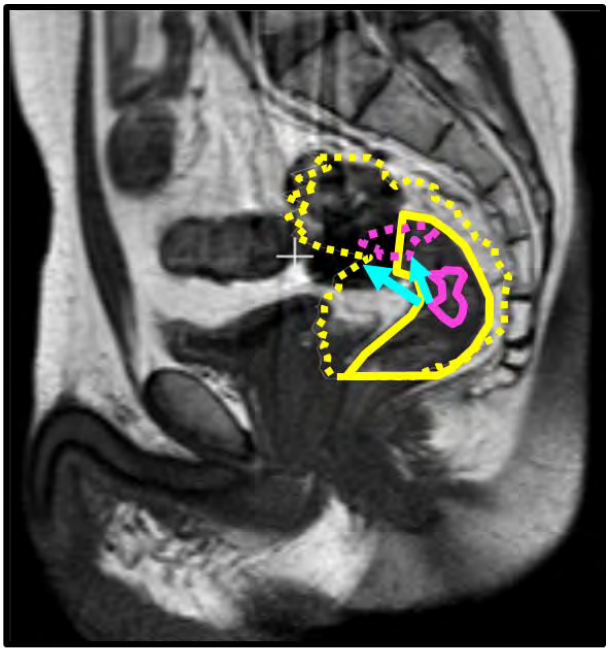

Figure1: Rectum (yellow) and tumor (purple) delineations overlaid on sagittal MRI scan. The dashed delineations are from a different day. Note the difference in motion direction and extent between rectum and tumor (cyan arrows).

OC-0366

Dosimetric benefit of adaptive proton therapy compared to adaptive photon therapy in cervical cancer

A.J.A.J. Van de Schoot[1], P. De Boer[1], K.F. Crama[1], J. Visser[1], L.J.A. Stalpers[1], C.R.N. Rasch[1], A. Bel[1]
[1]Academic Medical Center, Department of Radiotherapy, Amsterdam, The Netherlands

Purpose or Objective: In cervical cancer, adaptive radiation therapy (ART) can be applied to compensate for interfraction target motion. However, organs at risk (OAR) still receive substantial dose when photon-based ART is applied. Adaptive proton therapy (APT) holds the promise to further limit OAR dose while maintaining adequate target coverage. Our aim was to investigate the potential dosimetric advantages of image-guided APT (IGAPT) compared with photon-based image-guided ART (IGART).

Material and Methods: Twelve cervical cancer patients treated with photon therapy were included in this retrospective study. Besides the clinically acquired full bladder planning CT, additional empty bladder planning CT and weekly repeat CTs were acquired for study purposes. Planning CTs were registered based on bony anatomy and multiple interpolated cervix-uterus structures were derived using a point-based non-rigid registration method. For each interpolated structure, a photon (VMAT) and a proton (IMPT) plan was created to build patient-specific plan libraries. All plans were robustly optimized with a prescribed physical CTV dose of 46 Gy-equivalent (GyE) (23 x 2 GyE) for pelvic irradiation or 50.4 GyE (28 x 1.8 GyE) for para-aortic irradiation. For each patient, repeat CTs were registered to the full bladder planning CT based on bony anatomy and IGART and IGAPT treatments were simulated by selecting library plans and recalculating the dose. For each simulated fraction, CTV coverage (V95% > 98%) was assessed and differences in Dmean and D2cc fraction dose and fractionated substitutes of V15Gy, V30Gy and V45Gy parameters (i.e. dose levels divided by the number of fractions) for bladder, bowel and rectum were evaluated and tested for significance (Wilcoxon signed-rank test). Also, fraction dose distributions were accumulated and differences in the overall rectum toxicity related DVH parameter (V30Gy) and normal tissue complication probability (NTCP) for grade 2 acute gastrointestinal toxicity were determined.

Results: In 6 fractions (10.7%), the cervix-uterus structure deviated substantially from the pre-treatment derived structures. Adequate CTV coverage was obtained in 92% (96%) of the remaining fractions for IGAPT (IGART) which resulted in adequate CTV coverage on average per patient. All DVH parameters for bladder, bowel and rectum, except for the fractionated substitute of rectum V45Gy, were improved using IGAPT (Figure). Also, the mean dose to bowel, bladder and rectum was reduced significantly (p<0.01). Compared to IGART, IGAPT indicated a mean reduction of 7% for rectum V30Gy and a mean decrease from 0.33 to 0.18 in bowel NTCP.

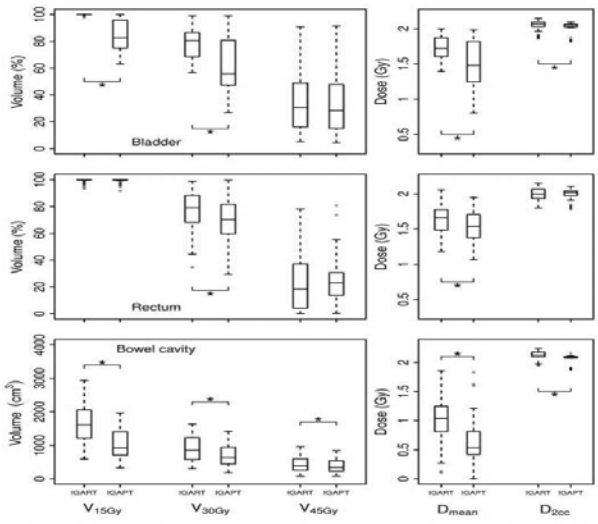

Figure: Boxplots of fraction parameter substitutes over all simulated fractions for bladder (upper), rectum (middle) and bowel cavity (lower). Boxes represent the median value and upper and lower quartiles, whiskers give the lowest and highest data point within 1.5x inter quartile range and the dots show the outliers. Horizontal lines indicate significant differences: * P<0.01.

Conclusion: This study demonstrates the feasibility of IGAPT in cervical cancer using a plan library based adaptive strategy

to compensate for interfraction target motion. Compared to photon-based IGART, IGAPT maintains adequate target coverage while a significant dose reduction in bladder, bowel and rectum can be achieved.

OC-0367

A Neural Network analysis to support Adaptive RT strategies: a multicenter retrospective study

G. Guidi[1,2], N. Maffei[1,2], B. Meduri[3], S. Maggi[4], M. Cardinali[5], V.M. Morabito[4], F. Rosica[6], S. Malara[7], A. Savini[6], G. Orlandi[6], C. D.Ugo[7], F. Bunkheila[8], M. Bono[9], S. Lappi[9], C. Blasi[8], G.M. Mistretta[1], P. Ceroni[1], A. Ciarmatori[1,2], A. Bernabei[1], P. Giacobazzi[3], T. Costi[1]

[1]*Az.Ospedaliero-Universitaria di Modena, Medical Physics, Modena, Italy*
[2]*University of Bologna, Physics and Astronomy, Bologna, Italy*
[3]*Az.Ospedaliero-Universitaria di Modena, Radiation Oncology, Modena, Italy*
[4]*Az.Ospedaliero-Universitaria Ospedale Riuniti, Medical Physics, Ancona, Italy*
[5]*Az.Ospedaliero-Universitaria Ospedale Riuniti, Radiation Oncology, Ancona, Italy*
[6]*AUSL4 Teramo, Medical Physics, Teramo, Italy*
[7]*AUSL4 Teramo, Radiation Oncology, Teramo, Italy*
[8]*Az.Osp.Ospedali Riuniti Marche Nord, Radiation Oncology, Pesaro, Italy*
[9]*Az.Osp.Ospedali Riuniti Marche Nord, Medical Physics, Pesaro, Italy*

Purpose or Objective: The retrospective analysis of anonymous data investigates the benefit of predictive analysis to assess anatomical and dosimetric variations for Adaptive Radiation Therapy (ART) purpose. Within a multicenter research network, clinical outcome were evaluated to determinate eligible patients for re-planning; a time series analysis allows scheduling re-planning during RT. We highlighted advantage and challenges due to the combination of IGRT (MVCT and CBCT), deformable image registration (DIR) and different set-up protocols comparing the multicenter data.

Material and Methods: The retrospective study enrolled 40 head and neck (H&N) anonymous patients from Center-A (MVCT), 20 from Center-B (CBCT), 8 from Center-C (CBCT), 8 from Center-D (CBCT). We have post-processed more than 2100 CT studies obtained by the imaging on board (>200000 slices). We analyzed parotid gland (PG) such as organs most affected by warping during the weeks of therapy. Volume and dose were normalized to the first day of treatment in order to remove bias related to machine/images variability and anatomical dimension. Structures were re-contoured automatically and the doses deformation was performed by RayStation® within an automated ART workflow supported by IronPython® scripting. Using DIR algorithms and GPU fast computing, the daily setup images were analyzed and compared. To support the data-mining; a Neural Network (NN) tool was developed and implemented in MATLAB® to evaluate abnormal clinical cases and re-planning strategies during fractions.

Results: A weekly analysis was carried out to follow and predict variations. After 6 weeks of therapy, PG showed a mean volume decrease of 23.7±8.8%: 25.1±9.2% in Center-A, 23.8±6.6% in Center-B, 21.2±10.3% in Center-C, 24.4±9.8% in Center-D. The NN analysis showed that, during the first 3 weeks, almost the patients' cohort followed a similar trend. Mean PG morphing can be predictable in 86.3% of the center cases: 89.6% A, 92.7% B, 76.0% C, 87.0% D. From the 4th week some challenges appeared. The patients that benefit from a review of the initial plan increased during treatment, highlighting the need of re-planning. Based on PG shrinkage, 53.5% of patients would need a re-planning with an inter-centers variability of 19.7%. An amount of 17.0% of cases is affected by bias due to algorithm and set-up error: 11.5% and 5.5% respectively.

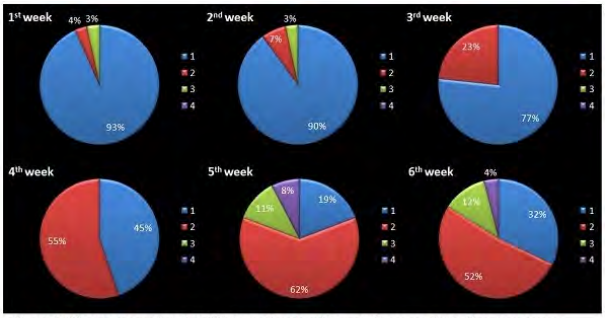

Figure 1: PG outcome predicted by NN during 6 weeks of therapy. Cases are divided into 4 outcomes: 1) patients with normal trend (no re-plan needed); 2) patients with abnormal morpho-dosimetric variations (re-plan suggested); 3) software bias; 4) possible set-up error

Center	Output	Week 1	2	3	4	5	6
A	1 (no re-plan)	92%	92%	85%	41%	19%	21%
	2 (re-plan)	8%	8%	15%	59%	69%	77%
	3 (bias)	0%	0%	0%	0%	8%	2%
	4 (set-up error)	0%	0%	0%	0%	4%	0%
B	1 (no re-plan)	100%	89%	89%	56%	18%	23%
	2 (re-plan)	0%	11%	11%	44%	38%	27%
	3 (bias)	0%	0%	0%	0%	33%	38%
	4 (set-up error)	0%	0%	0%	0%	11%	13%
C	1 (no re-plan)	76%	75%	77%	66%	20%	20%
	2 (re-plan)	10%	10%	23%	34%	72%	77%
	3 (bias)	14%	15%	0%	0%	2%	3%
	4 (set-up error)	0%	0%	0%	0%	6%	0%
D	1 (no re-plan)	100%	100%	61%	52%	29%	66%
	2 (re-plan)	0%	0%	39%	48%	66%	25%
	3 (bias)	0%	0%	0%	0%	0%	4%
	4 (set-up error)	0%	0%	0%	0%	5%	5%

Table 1 Outcome of patients' percentage during 6 weeks of therapy. Data are analyzed by Center (A, B, C, D) and NN output (1, 2, 3, 4)

Conclusion: IGRT and ART techniques ensure a personalization of patients' treatment. A predictive NN tool was implemented and trained in order to detect criticalities in a multi-centric study supporting the feasibility of national data-mining for ART purpose. Based on PG warping and data prediction, a mid-course re-planning could be scheduled in the 4th week to ensure an adequate dose distribution during the treatment course.

OC-0368

Accurate CBCT based dose calculations

R.S. Thing[1,2], U. Bernchou[1,2], O. Hansen[1,3], C. Brink[1,2]

[1]*Institute of Clinical Research, University of Southern Denmark, Odense, Denmark*
[2]*Laboratory of Radiation Physics, Odense University Hospital, Odense, Denmark*
[3]*Department of Oncology, Odense University Hospital, Odense, Denmark*

Purpose or Objective: Cone beam CT (CBCT) based dose calculations are inaccurate due to the image quality of CBCT images acquired for image guided radiation therapy (IGRT). This study demonstrates that a post-processing of the raw projection data can improve the CBCT image quality such that the accuracy of CBCT based dose calculations can be recovered.

Material and Methods: 5 lung cancer patients were selected for analysis, all of whom had a re-simulation CT (rCT) scan performed on the same day as a CBCT scan during their radiotherapy treatment. For each patient, two CBCT reconstructions were computed and used for dose calculation. The first CBCT was a clinical 3D reconstruction of the CBCT images as acquired for IGRT by the Elekta XVI R4.5 system (denoted cCBCT). The second CBCT used the clinical projection images, but was corrected for image lag, detector scatter, body scatter, beam hardening, and truncation artefacts prior to reconstruction using the open-source Reconstruction Toolkit. This second reconstruction is denoted iCBCT.
Although the rCT and CBCT images were acquired on the same day, setup errors and anatomical differences such as

diaphragm and chest wall position were evident when the CBCT images were compared with the rCT. Therefore, deformable image registration was performed with elastix, to eliminate dose differences due to anatomical differences between the scans. Missing anatomy in the CBCT images due to the limited field of view was copied from the rCT image after deformable registration of the CBCT images.
The original treatment plan was recalculated on the rCT, cCBCT, and iCBCT image sets using Pinnacle ver. 9.10. The resulting dose matrices were compared using a 2%/2mm and 1%/1mm gamma analysis with the rCT dose as reference dose. The dose criterion was evaluated as 2% (1%) of the prescribed dose of 66 Gy. A low dose threshold of 10% of the prescription dose was used, and the gamma analysis was only performed in the CBCT volume.
Results: High gamma pass rates were achieved. The cCBCT-based doses resulted in 2%/2mm gamma pass rates between 89.4 and 96.4%, while the iCBCT-based doses resulted in gamma pass rates between 98.4 and 100%. The 1%/1mm gamma analysis yielded pass rates between 77.5 and 80.3% for the cCBCT images, while the iCBCT images provided pass rates between 90.7 and 98.7%. For all patients, the iCBCT images provided superior pass rates compared to the cCBCT images. The table below shows all gamma pass rates for the 5 patients.

γ-criterion	Image	Pt 1	Pt 2	Pt 3	Pt 4	Pt 5
2 %/2 mm	cCBCT	89.4 %	96.4 %	95.8 %	94.7 %	93.1 %
	iCBCT	100 %	98.4 %	99.9 %	100 %	100 %
1 %/1 mm	cCBCT	77.5 %	80.3 %	77.6 %	79.9 %	79.5 %
	iCBCT	98.7 %	90.7 %	98.6 %	98.6 %	95.1 %

Conclusion: CBCT images can recover the image quality necessary for accurate dose calculations through comprehensive artefact corrections. While the iCBCT doses are accurate, further studies are required to determine how this result can be translated into clinical practice where the accurate dose calculation has potentials within adaptive radiotherapy and CBCT-based online planning. The present study is an important step towards the routine use of CBCT images for adaptive radiotherapy.

Proffered Papers: RTT 4: How to increase the knowledge for patients and staff

OC-0369

Video glasses to reduce claustrophobic anxiety in radiotherapy treatment

V. Althof[1], H. Althof[1], E. Dahmen[2], P. Bouma[1]
[1]*Radiotherapiegroep, Deventer, Deventer, The Netherlands*
[2]*Brainspa, Institute for Biofeedback, Zutphen, The Netherlands*

Purpose or Objective: To investigate whether video glasses can reduce the anxiety level in claustrophobic patients in radiotherapeutic treatment. Claustrophobic patients experience a high level of stress and discomfort which can hamper therapeutic procedures and possibly lead to non optimal treatment. The influence of video glasses (Luna5, Cedexis Inc.) on stress level during radiotherapy was measured using the Beck Anxiety Inventory (BAI) and biometrical parameters.

Material and Methods: In radiotherapy, systems may be equipped with a tight bore (CT, Tomotherapy) and the patients are immobilized on the treatment couch. A mild to moderate level of anxiety due to claustrophobia occurs at 10% of the population, a more severe level occurs at 4%. The common method to deal with a claustrophobic patient is to spend time with the patient to simulate treatment or to prescribe a tranquillizer. The idea of the video glasses is to focus patient attention to a movie using images and sounds from nature ('Beter door Beeld' Inc.). Volunteers (n=15) underwent a simulation of a radiotherapy treatment on the Tomotherapy system. Each volunteer filled in the BAI form in advance, which estimates the severity of their anxiety, based on a past individual claustrophobic experience. Severe level of anxiety was present in 11 volunteers, moderate level was found in 4 volunteers. Each volunteer was exposed to 3 runs: one without glasses, one with and the third without to measure a possible effect on habituation. The glasses were placed when the volunteer was on the couch (no immobilization). The volunteer was positioned in the bore of the Tomotherapy system and left alone during 2 minutes. After each run the volunteer filled in the BAI form with reference to the anxiety felt during the last run. Moreover, the volunteer was monitored continuously during each run using the Nexus-10 biofeedback system (MindMedia Inc.) to access the experienced level of anxiety more objectively. Results shown here are based on the detection of the high beta EEG wave.
Results: Reduced level of anxiety (based on the BAI score) was indicated by 13 out of 15 volunteers when using video glasses (see figure 1). This was confirmed by the observed trend in the 'high beta' brain wave amplitude. This brain signal is associated with stress level. The difference in mean amplitude of this wave between the run with and without video glasses is depicted in figure 2.

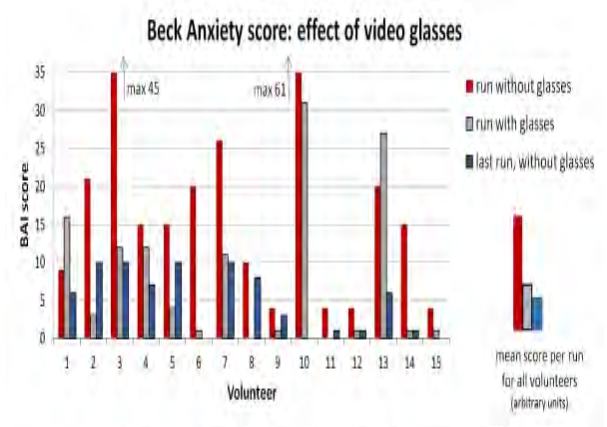

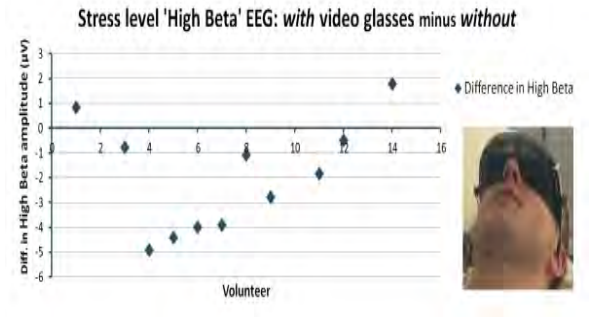

Conclusion: Using video glasses with an especially composed movie using images and sounds from nature during radiotherapy treatment, clearly lowers the level of anxiety of claustrophobic volunteers both subjectively based on the questionnaire as objectively by biometric measurements. Feedback of the volunteers overwhelmingly expressed a preference to undergo treatment with video glasses: "it was much easier to relax, never without glasses!"

OC-0370

The influence of virtual training on pelvic radiotherapy education for the multidisciplinary team

A. Williams[1], U. Shah[1], G. Fury[1], L. Codd[1], M. Brown[1], Y. Tsang[1]
[1]*Mount Vernon Cancer Centre, Radiotherapy, Middlesex, United Kingdom*

Purpose or Objective: Radiotherapy accelerates rapidly and ongoing training is essential to maintain and develop knowledge. A virtual reality environment is one way to provide training.
This study aims to demonstrate how a training package for advanced prostate and cervix radiotherapy can be

implemented effectively in a multi-disciplinary setting using a virtual reality environment.

Material and Methods: The training package consists of a virtual reality training tool (visual demonstration) and workbooks (self filled questions). Each training tutorial is delivered by a senior radiographer and includes identification of pelvic anatomy, review of different radiotherapy treatment planning and delivery techniques (conformal, static field intensity modulated radiotherapy and volumetric modulated radiotherapy), image guided treatment scenarios and radiotherapy related side effects.
The trainees were asked to complete pre and post tutorial questionnaires by grading their knowledge from 1 not confident at all, to 10 being exceptionally confident. These were devised to assess the effectiveness of the training package in terms of the trainees' knowledge and decision-making skills in advanced prostate and cervix radiotherapy. An evaluation of the session was also completed.

Results: The session was presented to 20 attendees comprising of 14 radiographers, 4 physicists and 2 clinical oncologists. In general, all attendees found the session useful and appropriate for their level of experience. All would recommend the training package to their peers.
The results of the pre and post tutorial questionnaires were summarised in table 1 below. Using Wilcoxon signed rank test, significant improvements in scoring were found in all questions ($p<0.05$)

Question	Pre-tutorial score	Post-tutorial score	P value
How confident are you at identifying pelvic anatomy on CT	Median= 7 Range= 3 to 9	Median= 8 Range= 6 to 9	<0.05
How confident are you to decide if a patient is suitable to treat with image matching decision making for prostate and cervix patients using images, DVH and organ at risk tolerance dose information	Median= 6 Range= 1 to 10	Median= 8 Range = 5 to 10	<0.05
Please rate your knowledge of planning for prostate and cervix patients when looking at rapid ARC, IMRT and conventional plans.	Median= 5 Range= 1 to 9	Median= 8 Range= 3 to 9	<0.05

Conclusion: Our analysis of the data suggests the virtual reality teaching tool can enhance learning, influence decision making, improve knowledge and understanding of cervix and prostate radiotherapy for radiographers, physicists and clinicians. To this effect, further training sessions will be held and evaluated with the multidisciplinary team.

OC-0371

Introduction of a consultant radiographer to stereotactic radiotherapy service

Y. Tsang[1], P. Ostler[2], N. Shah[2], J. Kudhail[1], P. Hoskin[2]
[1]*Mount Vernon Cancer Centre, Radiotherapy Department, Northwood Middlesex, United Kingdom*
[2]*Mount Vernon Cancer Centre, Clinical Oncology, Northwood Middlesex, United Kingdom*

Purpose or Objective: The role of a radiotherapy consultant radiographer has been proposed by the government in the United Kingdom with the aim to take advantage of the competencies of radiographers in driving forward the implementation of protocol-based care. With the increasing demand for Stereotactic Radiosurgery and Radiotherapy (SRS/SRT), our institution has appointed a consultant radiographer to lead the service since 2014. This study aims to investigate the impact of a consultant radiographer on the SRS/SRT service.

Material and Methods: A consultant radiographer is defined as someone with the appropriate education and training who is able to provide clinical leadership within a specialism, bringing strategic direction, innovation and influence through practice, research and education to the post. It is acknowledged that the role of a consultant radiographer was introduced to enhance our SRS/SRT service delivery and hence improve patient outcomes by increasing capacity and patient throughput. This helps the service to meet national and cancer targets.
A retrospective review of SRS/SRT patients who were treated in 2013, 2014 and 2015 at our institution was carried out to determine the interval between decision to treat and treatment start dates (INT). Kruskai-Wallis ANOVA was performed to test for any significant difference in INT across the three years.

Results: Between January 2013 and September 2015, 229 patients were included in the study and the descriptive statistics were summarised in the table below.

Year	2013 (Jan - Sept)	2014 (Jan - Sept)	2015 (Jan - Sept)
Number of patients treated	66	74	89
Mean INT (days)	39.4	28.6	22.0
95% Confidence Intervals for Mean INT (days)	32.2-46.7	24.2-32.9	18.9-25.0

A significant difference ($p<0.05$) was found in INT between 2013, 2014 and 2015. The mean INT in 2015 is shortened to nearly half of that in 2013.

Conclusion: This analysis suggests that intervals between decision to treat and treatment start dates of our SRS/SRT patients have been shortened since the consultant radiographer was appointed. The post holder has streamlined the patient pathways that still deliver high quality services but in more resourceful and innovative ways including radiographer led target volume delineations and consent.

OC-0372

Changes in student attitudes following a pre-registration interprofessional learning experience

K. Coleman[1], B. Darlow[2], E. McKinlay[2], P. Gallagher[3], M. Perry[4], L. Beckingsale[5], B. Gray[6], H. Neser[1], S. Donovan[2], J. Stanley[7], S. Pullon[2]
[1]*University of Otago- Wellington, Department of Radiotherapy, Wellington, New Zealand*
[2]*University of Otago- Wellington, Department of Primary Health Care and General Practice, Wellington, New Zealand*
[3]*University of Otago- Wellington, Medical Education Unit, Wellington, New Zealand*
[4]*University of Otago- Wellington, School of Physiotherapy, Wellington, New Zealand*
[5]*University of Otago- Wellington, Department of Human Nutrition, Wellington, New Zealand*
[6]*University of Otago- Wellington, Department of Primary Health Care and General Practice, Wellington, New Zealand*
[7]*University of Otago- Wellington, Biostatistical Group- Dean's Department, Wellington, New Zealand*

Purpose or Objective: Interprofessional Education (IPE) aims to improve collaborative practice by bringing together health professionals from different disciplines who learn about, from and with each other. This study evaluated whether an IPE program changed health professional students' attitudes to interprofessional teams and learning, students' self-reported effectiveness as team members, and students' perceived ability to manage long-term conditions.

Material and Methods: A prospective controlled trial evaluated an eleven-hour IPE program delivered over a four-week period by an interdisciplinary teaching team. The program included an initial three-hour interactive workshop, a home visit in interdisciplinary groups to a person living in the community with long-term conditions, and a peer presentation with facilitated group discussion. Pre-registration students from the disciplines of dietetics (n = 9), medicine (n = 36), physiotherapy (n = 12) and radiation therapy (n = 26) were allocated to either an intervention group (n = 41) who received the IPE program or a control group (n = 42) who continued with their usual discipline

specific curriculum. Attitudes were measured pre- and post-intervention using the Attitudes Toward Health Care Teams Scale (ATHCTS), Readiness for Interprofessional Learning Scale (RIPLS), the Team Skills Scale (TSS), and the Long-Term Condition Management Scale (LTCMS).

Results: Mean post-intervention attitude scale scores adjusted for baseline variation (all on a five-point scale), were significantly higher in the intervention group than the control group for all scales. The mean difference for the ATHCTS was 0.17 (95%CI 0.05 to 0.30; p=0.006), for the RIPLS was 0.30 (0.16 to 0.43; p<0.001), for the TSS was 0.71 (0.49 to 0.92; p<0.001), and for the LTCMS was 0.75 (0.56 to 0.94; p<0.001).

Conclusion: This trial found significant improvement in students' attitudes towards both interprofessional teams and learning as a result of receiving the IPE intervention. It also found significant improvements in intervention group students' self-reported effectiveness as team members and self-perceived confidence, knowledge, and ability to manage long-term conditions. This study indicates that a brief, modular, multifaceted IPE intervention using purpose-developed resources can have immediate positive effects and contribute to the development of health professionals who are ready to collaborate with others to improve patient outcomes.

Darlow, B., Coleman, K., McKinlay, et al. (2015). The positive impact of interprofessional education: a controlled trial to evaluate a programme for health professional students. BMC Medical Education, 15, 98.

OC-0373

IGRTonline: development and evaluation of a free online course on Image Guided Radiation Therapy

I. Mallick[1], R. Achari[1], S. Chatterjee[1], R. Shrimali[1], S. Prasath[1], B. Arun[1], A. Mahata[1]

[1]Tata Medical Center, Department of radiation Oncology, Kolkata, India

Purpose or Objective: Despite the rapid increase in use and availability of highly conformal treatment techniques and image guided treatment delivery, there is a lack of availability of focussed training in Image Guided Radiation Therapy (IGRT) for users in most countries. Online education has the potential to reach a wide audience across geographical regions, and offer flexibility of access. The aim was to develop a free, online, self-paced, interactive course on IGRT catering to the non-expert end-users of IGRT, primarily radiation oncologists and radiation therapists (RTT).

Material and Methods: An online platform for IGRT courses was developed (www.igrtonline.com) on a learning management platform called Moodle. The first course, called 'IGRT: Principles and Practice', was an introductory level online course was developed by radiation oncologists and medical physicists in our center, a tertiary care cancer hospital in India. The teaching material was created in the form of Flash and HTML5 interactive content, compliant with SCORM 1.2 standards. Interactive elements like triggered animation, inline quizzes were used. Nineteen modules were prepared in 3 sections covering the (a) principles of uncertainty, margins and correction protocols, (b) image guidance technology; and (c) clinical application in different anatomical sites. Self-assessment quizzes were prepared for every module with a question bank of > 200 questions, including optional preliminary and final assessment quizzes. Capabilities for downloading course modules to mobile devices was added. At the end of 6 months, course enrolment and participation was audited. A short online feedback survey was conducted.

Results: Course development took 16 months. The course was launched in April 2015. Between 15 April to 10 October 2015, 717 participants (from 44 countries across 5 continents) registered into the learning platform. The 5 most common countries of origin were India 409, USA 75, Brazil 37, UK 19 and Canada 10. The distribution of registrants according to job description consisted of radiation oncologists (49.4%), radiographer/therapists (31.4%) and medical physicists (19.2%). Of the registered students 553 enrolled themselves into the course in question. The number of students who completed > 5 modules was 337 (60.9%). Of the 48 students who completed both the preliminary and final quizzes, the score improved from a mean of 68.25% to 82.75% (p=0.002). A total of 103 responded to the online feedback survey. Results are shown in Table 1.

Table 1. Survey of users of IGRTOnline (total respondents = 103)

	Rad Onc	**RTT**	**Dosimetrist**	**Physicist**	
Job description	53 (51.4%)	15 (14.6%)	3 (2.9%)	32 (31.1%)	
	New	**0-2 years**	**3-5 years**	**> 5 years**	
IGRT Experience	45 (43.7%)	18 (17.5%)	19 (18.4%)	21 (20.4%)	
	Strongly agree	**Agree**	**Neither agree or disagree**	**Disagree**	**Strongly disagree**
Were important topics covered?	53 (51.5%)	48 (46.6%)	2 (1.9%)	0	0
Were you able to understand the content?	62 (60.2%)	41 (39.8%)	0	0	0
Was the course a valuable addition to your knowledge and understanding of IGRT?	64 (62.1%)	39 (37.9%)	0	0	0
	Excellent	**Good**	**Average**	**Poor**	**Very Poor**
Rate Course Design	65 (63.1%)	38 (36.9%)	0	0	0
Rate Overall quality of content	60 (58.3%)	40 (38.8%)	3 (2.9%)	0	0
	Yes	**Maybe**	**No**		
Interested in more online courses on this platform?	102 (99.0%)	1 (1%)	0		

Conclusion: Online education platforms have the capacity to reach a wide audience across geographical boundaries. Quiz results suggest that the online course was successful in improving the student's knowledge and understanding of IGRT. User perception of the course was good and the majority of participants were keen on more online education opportunities.

OC-0374

Use of IV contrast media in pre-treatment radiotherapy planning CT scans: A UK study

K. Williams[1], H. Probst[2]

[1]Clatterbridge Cancer Centre, Radiotherapy, Bebington, United Kingdom

[2]Sheffield Hallam University, Faculty of Health and Wellbeing, Sheffield, United Kingdom

Purpose or Objective: The primary aim analysed adherence to current UK Royal College of Radiologists (RCR) 2004 and 2015 guidelines. The secondary aim identified if current guidelines are adequate for optimum enhancement and image quality or should be redefined to reflect new evidence based practice.

Material and Methods: Questionnaires were sent to 80 UK cancer centres; 34 questions covered a wide range of topics including RCR compliance, contrast timings, cannulation protocols and administration in conjunction with advanced techniques to ensure comprehensive analysis could be performed.

Results: Eighty three percent of centres responded; 22% were excluded from analysis due to incomplete responses or duplication where one questionnaire applied to multiple satellite centres resulting in 52 responses.

Ninety eight percent of centres administer IV contrast to at least one tumour site. However, only 6% of centres administer to all 8 of the RCR 2004 recommended tumour sites (pharynx, neck nodes, lung, oesophagus, stomach, pancreas, cholangiocarcinoma, liver) with 40% of centres administering to 5 sites or less. Sixty two percent of centres routinely administer IV contrast to at least three tumour sites

not supported by RCR 2004; most commonly para-nasal sinus (73%) prostate (62%) and brain (60%).
RCR 2015 compliance was also poor with the most common response to which eGFR formula used was stated as unknown, although 88% of centres do check eGFR for every patient. Fifteen percent of centres did not have an extravasation policy although centres with policies had a wide range of procedures with no standardised requirements.
Only 35% of centres use IV contrast in conjunction with 4DCT, of the centres that don't use IV contrast with 4DCT most patients are dual scanned i.e. IV contrast 3D scan followed by non contrast 4DCT.
Sixty five percent of centres agreed or strongly agreed updated guidelines would be useful.

Conclusion: The results suggest adherence to RCR guidelines is poor. Very little current evidence exists relating to optimal IV contrast protocols both in the UK and internationally. No standardised guidelines exist in relation to 4DCT IV contrast protocols and timings which in some centres is resulting in patients being dual scanned. There are many areas such as flow rates, timings and administration in conjunction with advanced techniques which require further research to enable updated standardised guidelines to be identified. The need for updated guidelines is supported by 65% of respondents of this study.

Poster Viewing: 8: Physics: Inter-fraction motion management II

PV-0375

Comparison of carina- versus bony anatomy-based registration for IGRT in esophageal cancer.

M. Machiels[1], P. Jin[1], C.H.M. Van Gurp[1], J.E. Van Hooft[1], T. Alderliesten[1], M.C.C.M. Hulshof[1]
[1]*Academic Medical Center, Radiation Oncology, Amsterdam, The Netherlands*

Purpose or Objective: In image-guided radiotherapy (IGRT) for esophageal cancer, it is common to use bony anatomy-based registration (BR) for setup verification. A recent study, in which we investigated fiducial marker-based registration relative to BR, indicated marker-based registration to be infeasible due to tissue deformation. In the present study, we investigated the feasibility and geometric accuracy of carina-based registration (CR) for CBCT-guided setup verification in esophageal cancer IGRT.

Material and Methods: Retrospectively, 24 esophageal cancer patients with 65 implanted fiducial markers, visible on planning CTs and follow-up CBCTs, were included in this study. Fiducial markers were considered as standard for tumor position. All available CBCT scans (n=236) were independently rigidly registered to the reference CT with respect to either the bony anatomy or to the carina using XVI software (Elekta Ltd. Crawley) to determine the individual marker displacement relative to the bony anatomy and to the carina, respectively. Automatic registrations were visually checked and manually adjusted when necessary. Subsequently, we assessed and compared per individual marker the mean marker displacement over the treatment course (systematic position error, SE) associated with either BR or CR. Markers were classified into four subgroups based on their locations in the esophagus (proximal, mid-esophagus, distal, cardia) and analysis was similarly as mentioned above performed per subgroup. Comparison between both registration methods was done using a paired Wilcoxon signed-rank test.

Results: The distributions of the absolute mean systematic position error of the individual markers relative to the bony anatomy and the carina are given in Figure 1.A. Overall, a large SE is associated with the use of both bony anatomy and carina, especially in the CC direction. Figure 1.B, illustrates the slightly favorable use of the BR for proximal located markers. Markers located in the mid-esophagus show a smaller SE in CC and AP direction when using the CR, however this difference was not significant. For markers located in the distal esophagus and cardia, the BR is favorable in AP direction ($p<0.001$). Furthermore, the majority of the CRs were more challenging given the low contrast resolution in comparison with the BRs.

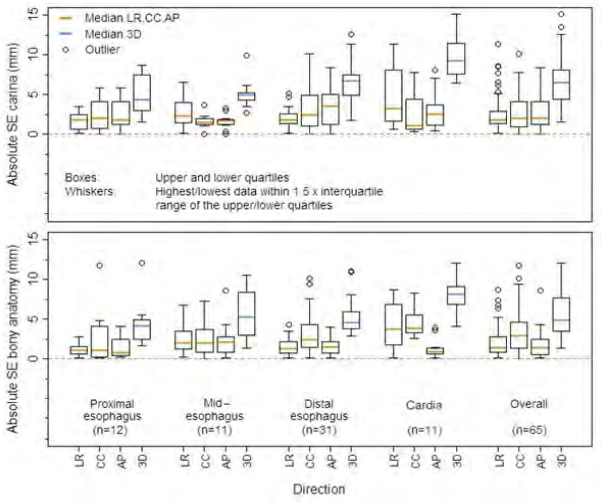

Figure 1.A Distributions of the absolute mean systematic position errors (SE) of the individual markers relative to the carina (upper) and the bony anatomy (lower). The distribution of absolute mean SE is given for each marker subgroup separately as well as for all markers together (Overall). Results are given in the left-right (LR), cranio-caudal (CC), and anterior-posterior (AP) direction as well as in the 3D vector distance (3D).

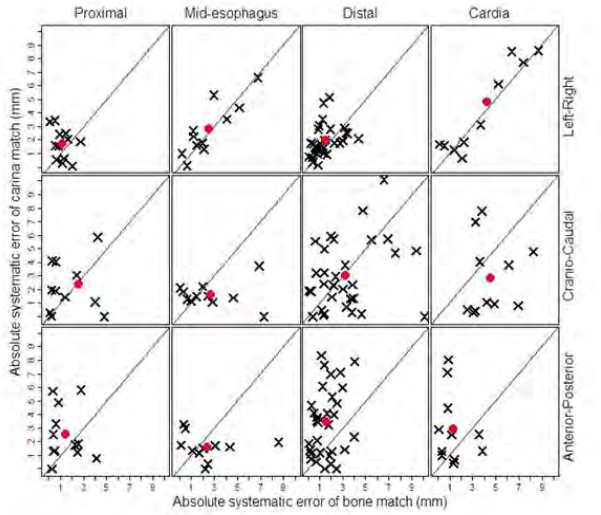

Figure 1.B. Scatterplots of the absolute systematic position errors (SE) of the individual markers relative to the bony anatomy versus the carina. Results are given in 3 directions for all 4 subgroups. Above blue line = preference for bony anatomy-based registration. Underneath blue line = preference for carina-based registration. The red dot indicates the mean absolute systematic error.

Conclusion: The mean marker displacement (SE), residual tumor position error, over the treatment course remains large and is in most directions even slightly larger when using CR compared with BR. Only for tumors located in the mid-esophagus the CR can be slightly favorable. However, esophageal tumors typically extend across regions and the majority of tumors are located distally. Therefore, our data endorse the use of BR over CR for setup verification.

PV-0376

Contrast-enhanced respiration managed cone-beam CT for image-guided intrahepatic radiotherapy

M. Lock[1], N. Jensen[2], R. Kozak[3], J. Chen[4], T. Lee[5], E. Wong[6]
[1]*London Regional Cancer Centre - Victoria Hospital, Department of Radiation Oncology, London- Ontario, Canada*
[2]*Næstved sygehus, Department of Oncology, Næstved, Denmark*
[3]*University of Western Ontario, Medical Imaging, London, Canada*
[4]*University of Western Ontario, Radiation Oncology, London, Canada*

[5]University of Western Ontario, Lawson Imaging, London, Canada
[6]University of Western Ontario, Physics and Astronomy, London, Canada

Purpose or Objective: Contrast enhancement and respiration management are widely used during image acquisition for radiotherapy treatment planning of liver tumors along with respiration management at the treatment unit. However, neither respiration management nor intravenous contrast is commonly used during cone-beam CT (CBCT) image acquisition for alignment prior to radiotherapy. In this study, the authors investigate the potential gains of injecting an iodinated contrast agent in combination with respiration management during CBCT acquisition for liver tumor radiotherapy.

Material and Methods: Five rabbits with implanted liver tumors were subjected to CBCT with and without motion management and contrast injection. The acquired CBCT images were registered to the planning CT to determine alignment accuracy and dosimetric impact. We developed a simulation tool for simulating contrast-enhanced CBCT images from dynamic contrast enhanced CT imaging (DCE-CT) to determine optimal contrast injection protocols. The tool was validated against contrast-enhanced CBCT of the rabbit subjects and was used for five human patients diagnosed with hepatocellular carcinoma.

Results: In the rabbit experiment, when neither motion management nor contrast was used, tumor centroid misalignment between planning image and CBCT was 9.2 mm. This was reduced to 2.8 mm when both techniques were employed. Tumors were not visualized in clinical CBCT images of human subjects. Simulated contrast-enhanced CBCT was found to improve tumor contrast in all subjects. Different patients were found to require different contrast injection protocols to maximize tumor contrast.

Conclusion: Localization of the tumor during treatment is the weak link in IGRT for liver. Respiration managed contrast enhanced CBCT provides a possible solution. Simulation tools for optimal contrast injection, recommended margins for interfraction motion and additional benefits from patient specific tracer kinetics determined from DCE-CT are presented.

PV-0377

Inter-fraction bladder variations in RT of prostate cancer: impact on dose surface maps

A. Botti[1], F. Palorini[2], V. Carillo[2], I. Improta[2], S. Gianolini[3], C. Iotti[4], T. Rancati[5], C. Cozzarini[6], C. Fiorino[2]
[1]Arcispedale S. Maria Nuova, Medical Physics, Reggio Emilia, Italy
[2]San Raffaele Scientific Institute, Medical Physics, Milan, Italy
[3]Medical Software Solutions GmbH, Medical Physics, Hagendorn, Switzerland
[4]Arcispedale S. Maria Nuova, Radiation Ocology Unit, Reggio Emilia, Italy
[5]Istituto Nazionale dei Tumori IRCCS, Prostate Cancer Program, Milan, Italy
[6]San Raffaele Scientific Institute, Radiotherapy, Milan, Italy

Purpose or Objective: Bladder is a hollow and flexible organ exposed to high doses in RT for prostate cancer. Its absorbed dose can be properly described by the dose surface maps (DSM) however, due to its flexible nature, the discrepancy between the planned dose and the dose absorbed during the treatment is a major issue. Present work aims at verifying the robustness of DSMs relative to the daily inter-fraction movement of bladder during RT of prostate cancer.

Material and Methods: 18 patients treated with moderately hypofractionated Tomotherapy were considered (prescription of 70 Gy at 2.5 Gy/fr in 28 fractions and full bladder). All patients underwent daily Image Guided Radiotherapy (through MVCT) with rigid registration on the prostate. After matching, bladder contours were delineated on each MVCT by a single observer and copied on the planning CT: the planned dose distribution was employed to generate DSMs. For each patient, the bladder DSMs from the planned treatment and from each fraction were then computed by unfolding the bladder contours on a 2D plane: they were anteriorly cut at the points intersecting the sagittal plane passing through the center of mass. The DSMs were then laterally normalized and aligned at the bladder base, while cranially they were cut at the minimal extension of the planned DSMs. Discrepancies between planned and treatment DSMs were analyzed through the average map of individual systematic errors, the map of population systematic errors (standard deviation of individual systematic errors) and that of population random errors (average of individual random errors) of dose.

Results: 472 normalized DSM were considered (cranial extension 34 mm): the mean number of available daily MVCTs was 25 (18-28) per patient. The Figure shows the average planned map (panel A), the average map of individual systematic errors (B), the map of population systematic errors (C) and that of population random errors (D). Two main regions can be recognized: 1) the central posterior bladder base (light/dark blue in D) and 2) the region that surrounds it, involving the lateral and the more cranial portion of bladder (orange/red in D). Region 1), which absorbs the highest doses (see A), appears to be the most stable one during the treatment: panel B shows mean values between -1 Gy and 1 Gy in region 1) and around 2-3 Gy in 2). Population systematic (C) and random errors (D) are below 4 and 3 Gy respectively in region 1), while they reach values between 6-11 Gy and 5-7 Gy, respectively, in 2).

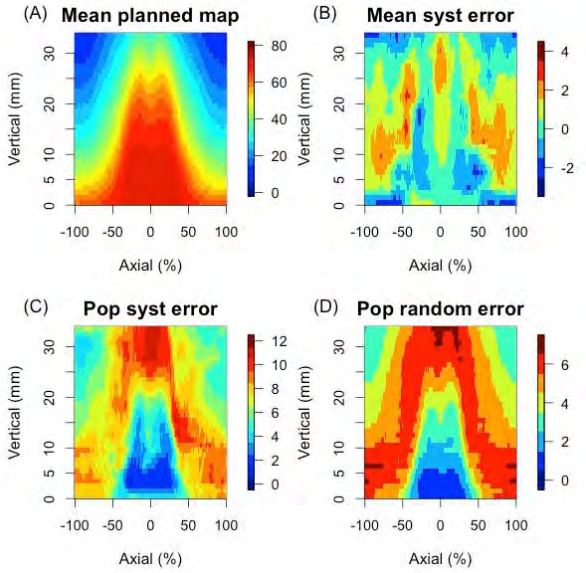

Conclusion: The results show that DSMs are quite stable with respect to changes occurring during daily IGRT for prostate cancer in the high-dose region, in the first 1-2 cm from bladder base. Larger systematic variations occur in the anterior portion and cranially 2.5-3.5cm from the base: these effects may be due to systematic differences in bladder filling and to systematic shits of bladder base between planning and treatment.

PV-0378

CBCT derived CTV-PTV margins for elective pelvic node irradiation of prostate cancer patients

C.A. Lyons[1], R.B. King[1], C.J. Ho[2], J.Y. Sun[2], J.M. O'Sullivan[3], S. Jain[3], A.R. Hounsell[4], C.K. McGarry[4]
[1]Queen's University Belfast, Centre for Cancer Research and Cell Biology, Belfast, United Kingdom
[2]Queen's University Belfast, School of Medicine and Dentistry, Belfast, United Kingdom
[3]Belfast Health and Social Care Trust, Clinical Oncology-Northern Ireland Cancer Centre, Belfast, United Kingdom

[4]Belfast Health and Social Care Trust, Radiotherapy Physics-Northern Ireland Cancer Centre, Belfast, United Kingdom

Purpose or Objective: To derive suitable CTV-PTV margins, using only anatomical information contained within cone beam CT (CBCT) images, for use in prostate external beam radiotherapy (EBRT) with elective pelvic nodal irradiations.

Material and Methods: CBCT images from 20 patients undergoing radical EBRT to the prostate and pelvic nodes were analysed. Each patient had an average of 5 CBCT images (range= 4 – 7) acquired during their treatment. Eclipse (version 13.5) was used to contour the pelvic nodal volumes on the CBCT images and to rigidly register the images to the original planning CT (pCT). Two different image-registration protocols were investigated; a bone match and a soft tissue match to the prostate. All CBCT contours were transferred to a single structure set, accounting for translational shifts in the registration. Boolean logic tools were used to create two composite volumes based on the CBCT contours and the two registration methods.

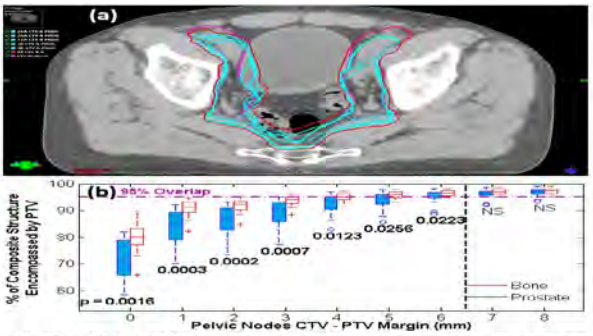

Figure 1 (a) Axial pCT image. Contoured on the image are the pCT nodal CTV volume (purple), 5 CBCT CTV volumes (cyan) and their corresponding composite structure (red). (b) Box-whisker plot of the distribution in % overlap values for each of the CTV-PTV margin sizes for the 20 patients analysed. Annotated on the chart are *p* values from a Mann-Whitney statistical test for each pair of distributions.

Figure1 (a) displays an example axial CT view of CTV contours on the original pCT together with individual prostate-matched CBCT CTVs and their corresponding composite structure. The structures were compared to the original CTV with a uniform margin (0 – 8 mm) applied to generate a PTV. The percentage overlap of the PTV with the composite structures was used to quantify agreement and compare the two registration types. A Mann-Whitney U test was used to evaluate the significance of differences between the distributions of percentage overlap values for the two match options. The margin required to achieve 95% overlap of the grown PTV with each composite volume was interpolated from these results and used to estimate a CTV-PTV margin for each match.

Results: Figure1 (b) displays box-whisker plots for the percentage overlap values from each ofthe CTV-PTV margins for the 20 patients. As expected, a better overlap was generally achieved with a bone match. Results of statistical tests are also included in the plot, where it is observed that the difference between the two distributions is statistically significant ($p < 0.05$) for all margins ≤ 6 mm.
Table 1 summarises results obtained for the sample studied, including an estimate ofthe margins required to achieve 95% overlap with the composite structures for 90% of patients. These margin values were calculated assuming a normal distribution for the frequency of margin size required to achieve 95% overlap.

Table 1. Summary of results obtained for the 20 patients analysed in this study.

		Match Type	
		Bone	Prostate
pCT CTV Volume (cm^3)	Average	370.5	
	Std. Dev.	60.7	
Composite volume / pCT CTV volume	Average	1.19	1.29
	Std. Dev.	0.20	0.24
Margin required to achieve 95% overlap (mm)	Average ($\bar{x}$)	4.00	5.46
	Std. Dev. (σ)	1.48	1.59
Margin required to achieve 95% overlap in 90% of population ($\bar{x}+1.28\sigma$, mm)		5.9	7.5

Conclusion: Using the simple approach outlined, CTV-PTV margins of 6 or 7.5 mm have been calculated for the external beam irradiation of pelvic node volumes when performing online matching to bone or prostate structures respectively. This approach is based purely on anatomical data and does not consider dose coverage or delineation error. The study involved the analysis of an average of 5 CBCT images per patient making the results of particular relevance to SABR fractionation schedules.

PV-0379

4D Cone-Beam CT reconstruction with 60s acquisition and 60s reconstruction

D. Hansen[1], T. Sørensen[2]
[1]Aarhus University Hospital, Oncology, Aarhus, Denmark
[2]Aarhus University, Clinical Medicine, Aarhus, Denmark

Purpose or Objective: Temporally resolved cone-beam CT (CBCT) has many advantages when compared to 3D CBCT for image-guided radiotherapy of lung cancer. E.g. superior set-up accuracy and the possibility to quantify tumour motion.
The 4D CBCT methods currently employed clinically require increased scan times however. In addition, relying on filtered backprojection algorithms for reconstruction, 4D CBCT reconstructions obtain significantly lower quality than 3D CBCT. Several algorithms exist, which improve the image quality of 4D CBCT through iterative image reconstruction, but long reconstruction times have made them unsuitable for setup and online verification purposes.
We present a novel reconstruction algorithm, which allows for iterative 4D CBCT reconstruction in 60s from a 60s acquisition.

Material and Methods: 672 projections were acquired using the onboard imager on a Varian Trilogy linear accelerator using a standard 60s 3D protocol. Initially a standard FDK reconstruction was performed and used as starting point for the iterative algorithm. The respiratory signal was extracted using the RPCA Amsterdam shroud method and the projections respiratory sorted in 10 temporal bins. The 4D CBCT was then reconstructed using prior image constrained compressed sensing (PICCS) based on a novel algorithm combining ordered subsets, Nesterovs method, and the Arrow-Hurwicz algorithm for image denoising.
Reconstruction was performed on a single GPU (Nvidia GTX Titan X). For comparison, we reconstructed the same data using the McKinnon-Bates algorithm (4D filtered backprojection). Both reconstructions with a voxel size of 1x1x3 mm3.

Results: The figure compares a representative axial slice from one temporal phase reconstructed using our fast iterative method and the standard 4D non-iterative method respectively. The standard image is contaminated by significant streaking artefacts and demonstrates poor tumour visibility. The proposed method, on the other hand, does not exhibit streaking and depicts the tumour clearly. The reconstruction time for the iterative method was 63s.

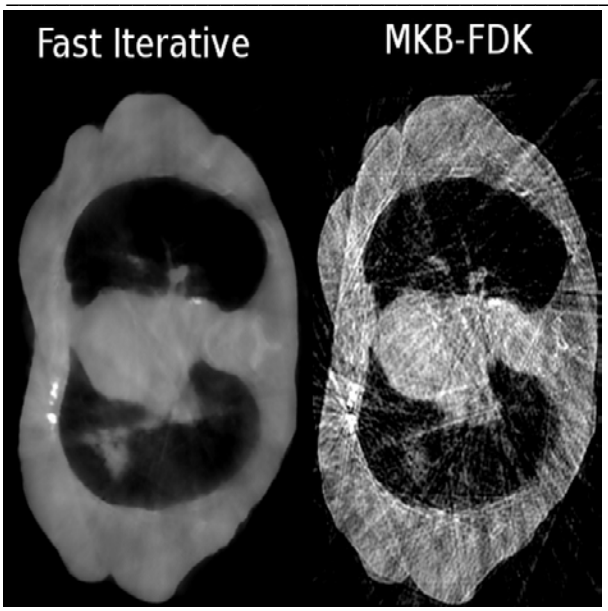

Conclusion: The proposed iterative 4D CBCT reconstruction algorithm is more than an order of magnitude faster than other iterative algorithms described in the literature. It produces sharp, streak free images from standard 60s acquisitions used for 3D CBCT. For purposes such as patient setup and verification of tumour motion, the fast reconstruction algorithm presented enables online usage of 4D CBCT as a part of the clinical treatment routine.

Award Lecture: Academic award: Jack Fowler University of Wisconsin Award

OC-0380

Moving away from binary definition of PTVs: a novel probabilistic approach to PTV definition

H. Tsang[1], C. Kamerling[1], S. Nill[1], U. Oelfke[1]
[1]*Royal Marsden Hospital Trust & Institute of Cancer Research, Physics, London, United Kingdom*

Purpose or Objective: Radiotherapy treatment planning for use with high-energy photon beams currently employs a binary approach when defining the PTV. Current approach using van Herk's 3D margin recipe (VHMR) may require additional modifications if the PTV overlaps with OARs. Our novel approach aims to move away from the binary treatment of PTVs, where each voxel is categorised as either target or non-target, and generate PTVs with voxels that may be considered part PTV and part OAR, providing the optimiser with additional information to more easily tackle conflicting dose constraints. We investigate the impact of this novel approach when applied to prostate radiotherapy treatments, and compare treatment plans generated using our approach and VHMR.

Material and Methods: Following the principles laid out in VHMR, only geometrical uncertainties are considered. We explore the use of 2D margins, motivated by the fact that small displacements in beam direction result in negligible change in dose delivered to the target. Only uncertainties perpendicular to the incident beam direction are considered, and therefore safety margins are generated for each beam direction. The degree of overlap of these beam specific margins is normalised and used to assign a weighting factor defined as the ratio of target-to-OAR content to a specific voxel. The objective function employed in the inverse planning process uses these local weighting factors for voxels of the CTV and OAR, should an overlap occur.
Five prostate radiotherapy plans were generated using IMRT inverse planning. The prostate was given a prescription of 78Gy in 2Gy fractions. Systematic uncertainties of 1.1mm, 1.1mm and 1.5mm in the LR, SI and AP directions, respectively, and 2.2mm, 2.1mm, 3.2mm for the random uncertainties, were used. Plans were generated such that the static dose distribution conforms to requirements outlined in the PACE clinical trial.
A verification tool was used to perform Monte Carlo simulations to model the cumulative dose of the ROI when it is displaced due to the presence of uncertainties; statistics from the tool are used for plan comparison.

Results: We used a population of 50,000 for simulation. We observed a median of 96.7% and 100% of the population CTV receiving D98% > 95% Dpres for our approach and VHMR respectively. Both values are higher than the 90% population requirement as stated in the VHMR derivation, and this is a direct consequence of the imperfect conformality of the dose distribution. When looking at rectal doses, we observed an improvement of 20.2% to 89.2% of the population satisfying D2% < 70Gy using our method; table 1 shows the results of the simulation for the CTV, rectum and bladder for all 5 patients.

Table 1: Results from the Monte Carlo simulation conducted on the ROIs. 50,000 identical ROI samples are modelled in the simulation. Each sample is shifted once following the systematic uncertainty, and from this displacement, shifted again based on the number of fractions to find the cumulative dose the ROI receives in the presence of uncertainties. The table below shows the percentage of the population satisfying a certain DVH requirement.

Patient	CTV $D_{98\%} > 95\%\ D_{pres}$		Rectum $D_{2\%} < 70$ Gy			Bladder $D_{2\%} < 70$ Gy		
	2D	3D	2D	3D	Diff	2D	3D	Diff
1	97.174	99.998	79.782	0.412	79.370	99.196	61.670	37.526
2	94.678	100.000	76.818	1.684	75.134	91.258	20.748	70.510
3	96.432	100.000	82.898	1.286	81.612	100.000	99.986	0.014
4	96.704	100.000	20.196	0.012	20.184	100.000	99.014	0.986
5	98.248	99.996	92.776	3.546	89.230	90.086	41.716	48.370
Median	96.704	100.000	79.782	1.286	79.370	99.196	61.670	37.526
Min	94.678	99.996	20.196	0.012	20.184	90.086	20.748	0.014
Max	98.248	100.000	92.776	3.546	89.230	100.000	99.986	70.510

Conclusion: We observed a significant decrease of high rectal doses delivered whilst maintaining sufficient dose coverage of the CTV, though the amount of sparing depends largely on the patient's anatomy and the objectives chosen for optimisation.

Award Lecture: Company Award Lectures

OC-0381

Perfusion SPECT can quantify radiation-induced changes in the lung after IMRT for NSCLC

K. Farr[1], A. Khalil[1], D. Møller[2], H. Bluhme[3], S. Kramer[3], A. Morsing[3], C. Grau[1]
[1]*Aarhus University Hospital, Department of Oncology, Aarhus C, Denmark*
[2]*Aarhus University Hospital, Department of Medical Physics, Aarhus C, Denmark*
[3]*Aarhus University Hospital, Department of Nuclear Medicine and PET Centre, Aarhus C, Denmark*

Purpose or Objective: This study examines the radiation-induced changes in regional lung perfusion according to the dose level in the lungs in 58 NSCLC patients treated with chemo-radiotherapy (RT). The purpose of the study was to assess dose and time dependence of RT-induced changes in regional lung function measured with single photon emission computed tomography (SPECT) and establish a correlation with the development of radiation pneumonitis (RP).

Material and Methods: NSCLC patients scheduled to receive RT of minimum 60 Gy were included prospectively in the study. Lung perfusion SPECT/CT was performed on a dual-head SPECT/CT camera in the treatment position before and 1, 3, 6 and 12 months after RT. Reconstructed SPECT/CT data were fused with the planning CT using MIM Software. Dose to the whole lung was segmented into regions of 0-5, 5-20, 20-40, 40-60 and >60 Gy. Regional perfusion was calculated from SPECT for each dose bin. Changes (relative to baseline, %) in regional lung perfusion were correlated with regional dose. A total of 58 patients with baseline SPECT were treated with IMRT. Of these 51 had 1 month follow-up (FU) scans, 45 had 3 months scans, 34 had 6 months scans and 23 had 12 months scans. Toxicity was assessed prospectively and graded by CTC-AE version 4 for radiation

pneumonitis. Patients with minimum grade 2 were considered as RP.

Results: Composite perfusion changes were associated with dose. Statistically significant dose-dependent reduction in regional perfusion was observed at 3, 6 and 12 months FU. Comparison of dose-response curves based on their slopes showed a dose-dependent reduction in perfusion at all time intervals (R2=0.8-0.9) except 1 month (R2=0.4). Relative perfusion loss per dose bin was 4% at 1 month, 14% at 3 months, 13% at 6 months and 21% at 12 months FU (Figure 1).

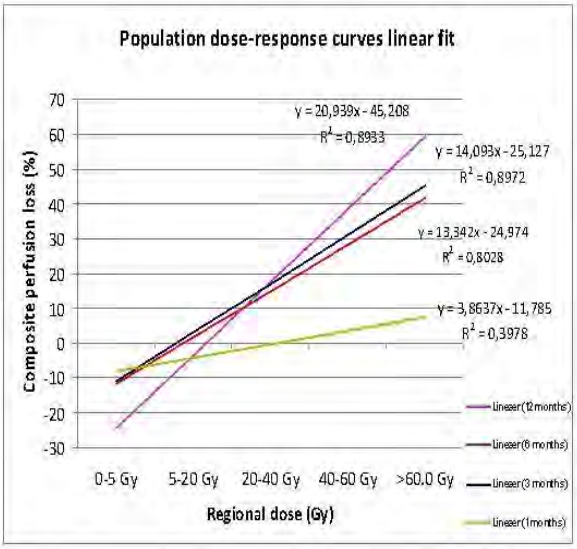

Figure 1. Dose-response curves linear fit for composite perfusion changes 1, 3, 6 and 12 months after radiotherapy

The dose-response relations varied between patients with or without RP. In patients who developed RP, perfusion reduction was larger in 20-40 Gy dose bin at 3 months FU (p=0.04), and in >60 Gy dose bin at 6 months (p=0.03), compared to those without the complication. Low dose regions, on the contrary, revealed larger perfusion increase at 12 months FU in the patients with RP (p=0.002).

Conclusion: Progressive dose dependent perfusion loss was seen on SPECT up to 12 months following IMRT. Patients with radiation pneumonitis demonstrate a larger perfusion loss in the high dose regions, as well as relatively larger perfusion increase in regions receiving low dose, possibly due to function being shunted to these areas.

OC-0382

A novel concept to tumour targeting: inverse dose-painting or targeting the "Low uptake drug volume"

A. Yaromina[1], M. Granzier[1], W. Van Elmpt[1], R. Biemans[1], N. Lieuwes[1], L. Dubois[1], P. Lambin[1]
[1]*MAASTRO clinic, Radiation Oncology, Maastricht, The Netherlands*

Purpose or Objective: There are several potentially radioresistant targets for dose escalation in dose-painting apporoach. Among them tumor hypoxia is a very attractive target. However, 2-3 times higher radiation dose is required to overcome hypoxia-mediated radioresistance in tumors, which is clinically difficult to achieve due to normal tissues constraints. Therefore, we propose a novel treatment approach to combine 1) targeting hypoxic tumor cells with a hypoxia-activated prodrug (HAP) TH302 and 2) at the same time use inverse radiation dose-painting strategy to boost tumor subvolumes with no/low drug uptake. We tested this approach in a rat rhabdomyosarcoma model using 18F-HX4 hypoxia tracer, which is a surrogate of TH302 accumulation in a tumor.

Material and Methods: A clinical PET/CT scanner was used to evaluate 18F-HX4 uptake 3 hrs post injection. Low or high drug uptake volume (LDUV or HDUV) was defined as 40% of the GTV with the highest or the lowest 18F-HX4 uptake, i.e. TH302 accumulation. Within 24 hrs after PET/CT animals (n=9) received either a single dose radiotherapy (RT) uniformly or a dose-painted non-uniform irradiation with 50% higher dose to LDUV or to HDUV. Mean dose in uniform RT was 18.5 Gy similarly to the mean dose in DUV. Mean dose to the GTV in the non-uniform RT scenario was 14.9 Gy. Treatment plans were created using Eclipse treatment planning system. Animals were irradiated on a TrueBeam High Definition 120 Leaf MLC linac. Tumor response was quantified as time required to reach 3-times starting tumor volume (TGTV3).

Results: Non-uniform RT with radiation boost to tumor subvolumes with low TH302 uptake (LDUV) was much more effective than the same dose escalation to subvolumes with high drug uptake (Fig. 1). Noteworthy, dose escalation to LDUV was as effective as uniform RT with 3.6 Gy higher mean dose to GTV.

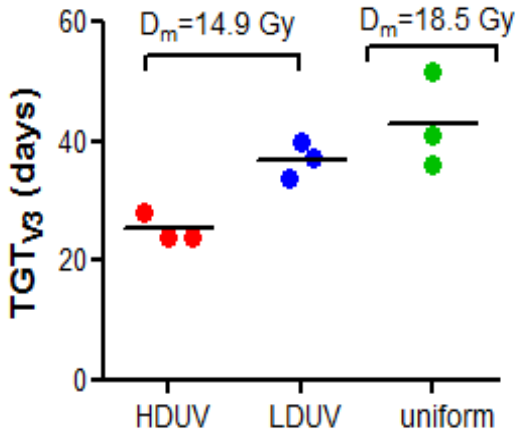

Fig. 1.Time to reach 3-times starting tumor volume (TGTV3) after uniform RT or non-uniform RT with dose escalation to tumor volume with high drug uptake (HDUV) or low drug uptake (LDUV). Mean dose (Dm) to GTV is indicated.

Conclusion: The results of this pilot study support targeted dose escalation in non-hypoxic tumor subvolumes with no/low accumulation of hypoxia-activated prodrugs, which requires further confirmation. This strategy appears to be as effective as a uniform dose escalation of the entire GTV but with greater capacity to spare normal tissues. It is expected that this approach of inverse dose-painting can be combined with other imageable cytotoxic drugs, which warrants further investigations.

Teaching Lecture: How to bring QUANTEC into the 21st century?

SP-0383

How to bring QUANTEC into the 21st century?

C. Fiorino[1]
[1]*San Raffaele Scientific Institute, Medical Physics, Milan, Italy*

The implicit concept behind the title of this lecture concerns the role of “quantitative” data-driven approaches in assessing dose-volume effects in normal tissues in the era of “high-tech” radiotherapy and integration of “omics”. The continuously growing literature regarding dose-volume relationships indirectly reflects the need of improving and refining our knowledge in this field [1]. This seems to be particularly urgent in a number of clinically relevant situations such as, for instance, heart, bowel and bladder. However, the impact of the above mentioned elements (“high-tech & “omics”) on the research issues of this field is increasingly relevant and claims for the development of new research lines and methods that will shortly be overviewed in the lecture.

The occurrence of radiation-induced toxicity is a very complex process that is always modulated by the individual [2]; if two patients receive the "same dose distribution" they will likely have different reactions and possibly one will experience toxicity while the other not. The availability of individual information potentially characterizing the patient response, including the "omics" information, is highly valuable, especially in the "high-tech" era of image-guided/adaptive IMRT in which organs are more efficiently spared: the better sparing reduces the incidence and severity of toxicities and, at the same time, enhances the impact of individual sensitivity factors. This point reinforces the need to create large data bases including individually assessed clinical, biological and genetic information, in addition to the individual dose distribution. As a consequence, the approach of quantitatively modelling dose-volume relationships is increasingly becoming "phenomenological" [3]: robust methods for (dosimetric and non-dosimetric) variable selection able to condense the information in "reliable", friendly to use, predictive models is a major field of research: the adaptation of statistical methods for data-mining and to avoid over-fitting is a pivotal point of the story.

Although the potentials of large data bases and of data sharing platforms on toxicity modelling are clear [4], we should not forget that the creation of large data-bases is not the "aim" but is a (powerful) "tool". The outcome of the process in terms of robustness and reliability of the models will not only depend on the "numbers" (a highly important component) but also (and maybe more importantly) on the "quality" of data. Differently from the "easy" score of the success of a therapy (survival, tumour control), toxicity is a much more complex issue that deserves specific attention and the careful collection of patient-reported and/or physician-reported information, often for years. Well assessed prospective observational studies focused on specific toxicities seem to be the best choice; secondary analyses of high-quality data coming from controlled trials are also very important although they may be limited in some cases by too homogenous protocols restricting the spread of the delivered dose distributions.

At the end of the circle, the external validation of integrated dose-volume models is clearly a crucial component of the next year's research [3]: testing the generalizability of dose-volume models will be a major end-points. In addition, robust results from phenomenological models are expected to feed up mechanistic approaches in a sort of mutual synergy that can further corroborate our knowledge: these two components (mechanistic and phenomenological) will likely cooperate much more in the next future. Relevant developments are expected to impact the quantitative modelling of normal tissue effects also from the side of the dosimetry data. The robust, organ-planning-DVH approach to quantitatively describe the relationship between dose/volume and toxicities should be overcome/refined in many relevant situations by directly looking to the 3D dose distribution, integrating the spatial information lost when using "classical" surrogates like DVH/EUD. Relevant examples are: the direct measurement of dose-map dissimilarities between patients [5], the quantification of local (and organ) effects by imaging biomarkers [6], the interplay between the dose received by different organs, the impact of anatomy changes during therapy and their incorporation into normal tissue predictive models.

Quantitative modelling of normal tissue effects is lively present in current century and seems to have a brilliant future in contributing to rapidly improve the way we treat our patients with the promise to continuously reduce toxicity.

1-Marks LB et al. Int J Radiat Oncol Biol Phy. 2010;76 (Suppl 1):S10-S19.
2-Bentzen SM. Nature Rev Cancer. 2006;6:702-713
3-van der Schaaf A et al. Int J Radiat Oncol Biol Phys 2015;91:468-471
4-Deasy JO et al. Int J Radiat Oncol Biol Phys 2010; 76 (Suppl 1):S151-S154
5-Acosta O et al. Phys Med Biol 2013;58:2581-95
6-Fiorino C et al. Radiother Oncol 2012;104:224-229.

Teaching Lecture: Shared decision making

SP-0384
Shared decision making

D. Tomson[1]
[1]*Institute of Health and Society Newcastle University, Newcastle Upon Tyne, United Kingdom*

Drawing on experience as a practicing GP with a special interest in communication skills and shared decision making, the work of The Health Foundation funded MAGIC (Making Good decisions in Collaboration) programme and most recently on a collaboration with a Danish Oncology Hospital, Dr Dave Tomson will explore recent developments in Shared Decision Making (SDM). Using experience and expertise from the delegates we will

a) check out attitudes and beliefs about the need and rationale for putting SDM centre stage in patient interactions,
b) look at a useful model of SDM both for personal clinical practice and for teaching other clinicians,
c) explore some of the key skills needed and the key challenges in doing better SDM with a particular focus on oncology – the constant changing nature of the evidence base, individualised care in a guideline driven world, dealing with personal bias, unwarranted versus warranted variation in practice, the tyranny of time.
d) share some ideas about possible solutions to these challenges and think about some of the steps needed to both develop personal practice and implement programmes of development within departments and across hospital systems

Teaching Lecture: The study of therapy resistance in genetically engineered mouse models for BRCA1-mutated breast cancer

SP-0385
The study of therapy resistance in genetically engineered mouse models for BRCA1-mutated breast cancer

S. Rottenberg[1], M. Barazas[2], J. Jonkers[2], G. Borst[3]
[1]*University of Bern, Institute of Animal Pathology, Bern, Switzerland*
[2]*The Netherlands Cancer Institute, Molecular Pathology, Amsterdam, The Netherlands*
[3]*The Netherlands Cancer Institute, Division of Radiotherapy, Amsterdam, The Netherlands*

Although various effective anti-cancer treatments have become available over the last decades, therapy resistance remains the major cause of death of cancer patients. Striking examples are patients with tumors that are defective in DNA repair by homologous recombination (HR). Despite initial responses to cancer therapy, resistance of primary or disseminated tumors eventually emerges, which minimizes therapeutic options and greatly reduces survival. The molecular mechanisms underlying this therapy escape are often poorly understood.

A clinically relevant mechanism for the defect in HR is a lack of function of BRCA1. This defect impairs error-free repair of DNA double-strand breaks (DSB) – a feature that can be exploited by the treatment with DSB-inducing agents. Using the *K14cre,Brca1F/F,p53F/F* (KB1P) genetically engineered mouse model for BRCA1-mutated breast cancer, we have shown the success of this strategy. Tumors are highly sensitive to DNA cross-linking agents, or to the inhibition of topoisomerase I/II and poly (ADP-ribose) polymerase (PARP) (reviewed by Rottenberg & Borst, 2012). Despite this sensitivity, tumors are not eradicated and eventually drug-refractory tumors emerge. In several of the resistant tumors we found that the HR defect can be partially rescued by down-regulation or knock-out of additional repair factors, such as 53BP1 (Jaspers *et al.* 2013) or REV7 (Xu *et al.* 2015).

Based on these observations we set out to investigate whether this type of HR restoration can also explain radiotherapy resistance. For this purpose, we treated mice carrying KB1P tumors with high-precision radiotherapy. We

observed that KB1P tumors were initially hypersensitive to fractionated local delivery of radiotherapy, but could not be eradicated: tumors relapsed and eventually acquired stable resistance. To investigate whether HR was restored in the resistant tumors, we studied 53BP1 and RAD51 irradiation-induced foci formation. Surprisingly, while restoration of HR was prominently found in tumors that acquired resistance to PARP or topoisomerase I inhibition, we did not find it in radiotherapy resistant tumors. To investigate this discrepancy more closely, 53BP1 and related repair factors were knocked out in cell lines derived from the KB1P model using the CRISPR/Cas9 technology. Consistent with our *in vivo* data, clonogenic assays showed that the knock-out of 53BP1 conferred strong resistance to PARP1 inhibition. Intriguingly, the lack of 53BP1 sensitized BRCA1-deficient cells to radiotherapy. An *in vitro* competition assay confirmed the selection to maintain a functional 53BP1 allele during radiotherapy treatment. Based on the KB1P model, we therefore hypothesize that resistance mechanisms that frequently occur in response to PARP1 inhibition sensitize cells to radiotherapy. These results, and their significance to human cells, are currently further validated in additional *in vivo* models including patient-derived tumors.

References
- Jaspers *et al.* (2013). Loss of 53BP1 causes PARP inhibitor resistance in Brca1-mutated mouse mammary tumors. 3:68-81.
- Rottenberg & Borst (2012). Drug resistance in the mouse cancer clinic. *Drug Resistance Updates* 15:81-9.
- Xu *et al.* (2015). REV7 counteracts DNA double-strand break resection and affects PARP inhibition. *Nature* 521:541-4.

Teaching Lecture: SBRT/SABR for oligometastatic disease

SP-0386
SBRT/SABR for oligometastatic disease

E. Lartigau[1]
[1]*Centre Oscar Lambret, Lille, France*

Introduction: Stereotactic (ablative) body radiotherapy (SBRT/SABR) has been successfully used in the treatment of metastatic lesions and could be considered as a "curative option" for some oligometastatic patients. Multiple studies have described significant local control in brain, lung and liver metastases of various primary cancers. Results suggest SBRT/SABR could be an effective treatment extending patients' life span.

Study: For example in our retrospective study involved 90 patients, designed to test potential effectiveness of SBRT in the treatment of oligometastases irrespective of primary Between July 2007 and June 2010, 90 patients were treated with robotic SBRT/SABR for hepatic or pulmonary metastatic lesions. A total of 113 liver and 26 lung metastatic lesions in 52 men (58%) and 38 women (42%) were treated. Median follow-up was 17 months. Median age at treatment was 65 years (range, 23-84 years). Primary cancers were 63 GI, three lung, eight breast, four melanoma, three neuro-endocrine tumors, and three sarcomas. Median diameter of the lesions was 28 mm (range, 7-110 mm) for liver and 12.5 mm (range, 5-63.5 mm) for lung. Local control rates at 1 and 2 years were 84.5% and 66.1%, respectively. Two-year overall survival rate was 70% (95% CI: 55-81%). The 1 and 2-year disease-free survival rates were 27% (95% CI: 18-37%) and 10% (95% CI: 4-20%), respectively. Median duration of disease-free survival was 6.7 months (95% CI: 5.1-9.5 months). Observed toxicities included grade 1-3 acute toxicities. One grade 3 and no grade 4 toxicity were reported. High-dose SBRT/SABR for metastatic lesions is both feasible and effective with high local control rates.

Discussion: In the last 4 years, some reports have described the so call abscopal effect described as "*an action at a distance from the irradiated volume but within the same organism.*" Abscopal effect may be more pronounced in response to ablative (> 10 Gy) rather than conventional dosage or fractionation schedules and has been reported mostly in renal cell carcinoma and in melanoma. The effect is attributed to activation of the systemic immune response by increase antigen presentation (neo antigens released after rapid cell necrosis) and enhanced immune response. These concepts may be of clinical value, improving outcomes by inducing systemic abscopal effects and potentially combined SBRT/SABR with immunotherapy or lymphocytes activating agents. Furthermore, these results have raised the question whether classic radiobiological modeling, and the linear-quadratic (LQ) model, are appropriate for large doses per fraction with the possibility of such an additional biological effects resulting from endothelial cell damage, enhanced tumor immunity, or both. These concepts will be discussed at the time of presentation.

Conclusion: SBRT/SABR treatment is well tolerated with low toxicity rates. It could represent an interesting treatment option for oligometastatic patients not amenable to surgery, even when patients had been pre-treated with chemotherapy. The biological models behind the observed clinical efficacy are currently scrutinized. New combined treatment may be driven from such promising results.

Teaching Lecture: Advanced treatment strategies for head and neck cancer

SP-0387
Advanced treatment strategies for head and neck cancer

W. Budach[1]
[1]*University Hospital Düsseldorf Heinrich Heine University Düsseldorf, Düsseldorf, Germany*

Optimal treatment of head and heck squamous cell carcinoma (HNSCC) patients requires well organized interdisciplinary coordination. Standard treatment of locally advanced HNSCC is chemoradiation or surgery followed by chemoradiation. Cisplatin containing chemotherapy remains standard of care in combination with concurrent radiotherapy. Neither neoadjuvant chemotherapy, nor treatments with targeted drugs have changed this standard, although some data suggest that cetuximab can be used as substitute for cisplatin especially in HPV/p16 positive disease. Combinations of cetuximab or other EGFR1 antagonists with chemoradiation did not improve patient's outcome, but added toxicity. Overall, attempts to improve clinical outcome in locally advanced HNSCC with targeted drugs and new cytostatic drugs have not been successful. The situation is different in locoregionally recurrent HNSCC not amenable for local treatment and in metastatic disease. In these patients, the addition of cetuximab to cisplatin and 5FU resulted in a significant survival benefit and consequently is considered as standard of care.

HPV/p16 positive HNSCC represents a distinct entity, which is more sensitive to radiotherapy and cytotoxic drugs. Several strategies testing deescalated treatments are being tested in randomized trials. However, deescalated is not yet recommended outside clinical trials.

Neoadjuvant chemotherapy followed by radiotherapy +/- chemotherapy or cetuximab, and primary chemoradiation have been shown to allow for organ preservation especially in laryngeal cancer in the majority of patients without compromising overall survival. However, adequate selection of patients is critical to obtain organ preservation with good functional outcome.

Recent technological developments in surgery and radiotherapy like transoral robotic surgery and radiotherapy using intensity modulated radiotherapy (IMRT), volumetric modulated arc therapy (VMAT), image guided radiotherapy (IGRT), and stereotactic body radiation therapy (SBRT) have been evaluated in cohort studies and a few randomized trials. These technologies are suitable for decreasing early and late toxicity and improvement of functional outcome, but have not been shown to improve locoregional control, disease free survival, and overall survival.

The available data on the topics addressed above will be shown and discussed.

Teaching Lecture: Dose to water vs. dose to tissue in advanced treatment planning: myths, realities and concerns

SP-0388

Dose to water vs. dose to tissue in advanced treatment planning: myths, realities and concerns

N. Reynaert[1]
[1]*Centre Oscar Lambret, Medical Physics, Lille, France*

Teaching Lecture: Nanodosimetry: from radiation physics to radiation biology

SP-0389

Nanodosimetry: from radiation physics to radiation biology

H. Rabus[1], V. Conte[2]
[1]*Physikalisch-Technische Bundesanstalt PTB, Radiation Effects, Braunschweig, Germany*
[2]*Laboratori Nazionali di Legnaro, Microdocimetry, Legnaro, Italy*

Nanodosimetry is an emerging experimental technique that measures the so-called particle track structure, i.e. the pattern of ionizing radiation interaction with matter on the nanometric scale. In such small dimensions, comparable to the diameter of the DNA double helix, the stochastic nature of ionizing radiation interactions has to be taken into account.

The stochastic quantity of nanodosimetry is the ionization cluster size (ICS), i.e. the number of ionizations produced by a passing particle within a specific nanometric target volume. The frequency distribution of ionization cluster size (ICSD) depends on the size of the target volume and its distance from the primary particle trajectory. The ICSD is a characteristic of the track structure. The statistical moments of the ICSD can be used to establish a new concept of radiation quality that is based on measurable physical quantities of the radiation that are closely related to the biological effects of the radiation.

Three nanodosimeters of different type have been developed for measurement of ICSDs [1-3] in a sensitive volume of a dilute gas which is simulating microscopic targets based on a density scaling principle [4]. They are differing in the operating gas used, the detected particle type (electrons or cations of the target gas) and the size of the equivalent nanometric target in biological matter (a.k.a. site size). Within the European Project BioQuaRT [5, 6] and the adjoint Italian MITRA project [7], the three European nanodosimeters (“StarTrack“, “Ion Counter”, “Jet Counter”) [8-10] have been compared by measuring ion beams with all three nanodosimeters.

Fig. 1 shows a synopsis of particular moments of all measured ICSDs. Each data point represents a measurement of a radiation quality (energy and type of ion) with a particular nanodosimeter simulating a certain nanometric site size. The horizontal axis is the mean ionization cluster size $M_1(Q)$, i.e. the number of ionizations obtained for the combination (indicated by Q) of radiation quality and site size. The vertical axis is the cumulative probability $F_2(Q)$ for obtaining at least two ionizations when measuring this radiation quality with the respective nanodosimeter. These quantities are obtained from the measured frequency $P(\nu|Q)$ of ionization cluster size ν.

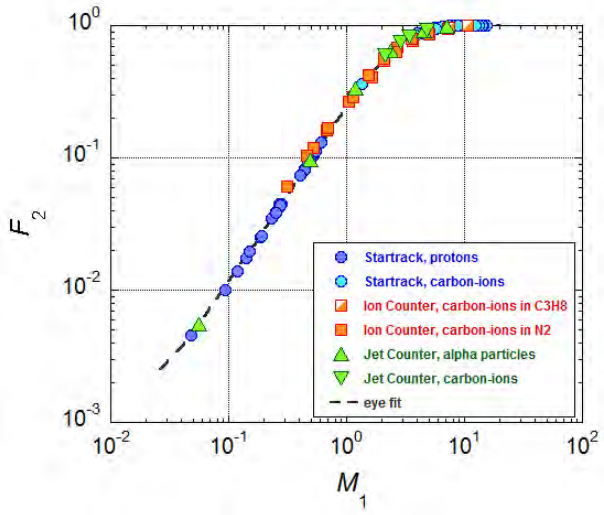

Fig. 1

All data points shown in the Fig. 1 are falling on the same curve indicated by the dashed line. Similar results are also found when cumulative probabilities F_k for a cluster size $\nu \geq k$ are plotted versus M_1. Hence, despite the different operating principles of the nanodosimeters, there seems to be a universal relation between the cumulative probabilities F_k and the mean ionisation cluster size M_1.

The saturation behavior seen in Fig. 1 is found for all cumulative probabilities F_k. Hence, the universal curves have a similarity to the curves expected for the yields of radiobiological endpoints. Fig. 2 illustrates, that this similarity can be exploited to establish a quantitative correlation between nanodosimetric quantities and radiobiological effects.

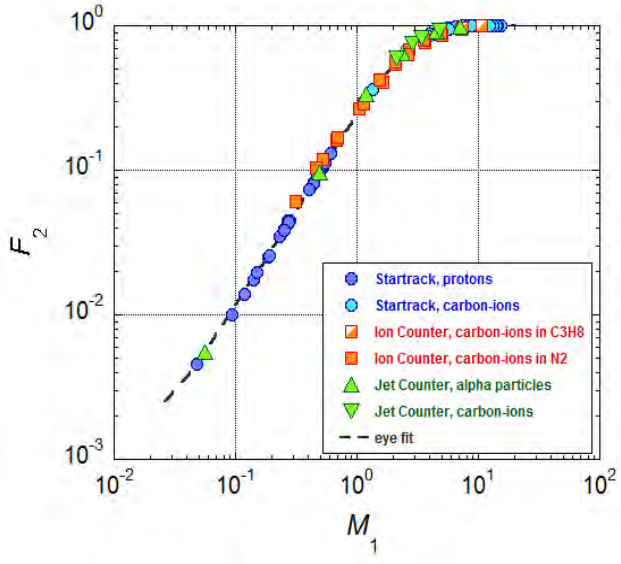

Fig. 2

The colored data points are results from cell experiments using protons (blue) and carbon ions (red). The vertical axis is the cross section for cell inactivation determined from the cell survival curves at 5% survival rate [11, 12]. The horizontal axis is the mean ionization cluster size that was obtained from Monte Carlo simulations. The black data points are mean cluster size and cumulative probability F_2 derived from the simulated ICSDs.

The track structure simulations were carried out for different values of the nanometric site size. The data plotted in Fig. 2 are those for which the nanodosimetric curve indicated by the grey line provides a best fit to the radiobiological data. This best fit is obtained if a site size of 1 nm in liquid water is used, i.e. of about half the diameter of the DNA double helix.

Acknowledgements:

The project BioQuaRT has been funded within the European Metrology Research programme EMRP. The EMRP is jointly funded by the EMRP participating countries within EURAMET and the European Union. The project MITRA has been funded by the Italian Istituto Nazionale di Ficica Nucleare (INFN).
References:
[1] S. Pszona et al., Nucl. Instrum. and Meth. A 447, 601 (2000)
[2] V.Conte et al., New J. Phys. 14, 093010, (2012)
[3] G. Garty et al., Radiat. Prot. Dosim. 99, 325 (2002)
[4] B. Grosswendt, Radiat. Prot. Dosim. 110, 789 (2004)
[5] H Palmans, H Rabus, et al., Br. J. Radiol. 87: 20140392 (2015)
[6] http://www.ptb.de/emrp/bioquart.html
[7] http://www.lnl.infn.it/~microdos/MITRA.html
[8] D. Moro et al., INFN-LNL-Report 239, 178-179 (2013)
[9] G. Hilgers et al., INFN-LNL-Report 240, 129-130 (2014)
[10] G. Hilgers et al., HIL Annual Report 2013, 46-48 (2014)
[11] T. Friedrich et al., Journal of Radiation Research 54, 494-514 (2013)
[12] https://www.gsi.de/bio-pide

Teaching Lecture: Brachytherapy for the pelvic region: status and perspective for the future

SP-0390
Brachytherapy for the pelvic region: status and perspectives for the future - Gynaecology

R. Mazeron[1]
[1]*Institut Gustave Roussy, Villejuif, France*

Brachytherapy in gynaecological cancers, and especially in cervix cancer, has greatly evolved during the last twenty years. For decades, brachytherapy has relied on x-ray orthogonal acquisitions, and prescription has been a matter of systems and schools, making reporting and comparisons difficult. Based on the developments of afterloaders and treatment planning systems, image-guided adaptive brachytherapy has emerged. This high precision technique combines all modern radiation requirements: image guidance, adaptation to tumor response, and short time treatment.
Ten years ago, the GEC-ESTRO, in a will of harmonizing practices, published recommendations in cervical cancers regarding the definition of target-volumes and the reporting. These recommendations were rapidly adopted worldwide. During the last decade, multiple monocentric series, historical cohorts' comparisons, and a prospective multicentric study (STIC trial) demonstrated high local control rates with a limited morbidity in regard to classical data. These data are about to be confirmed by two large studies led by the Gyn GEC-ESTRO: Retro-EMBRACE and EMBRACE, which will establish MRI-guided brachytherapy as a gold standard.
In addition, clear dose-volume effect relationships have been demonstrated between the modern dosimetric parameters and the probability of achieving local control or facing morbidity. The better knowledge of these correlations allowed the launch of EMBRACE II, a prospective study combing the best radiation modalities (EBRT and IGABT), with optimal and ambitious planning aims. In the near future, the large amount of data collected in the EMBRACE study (> 1 500 patients accrued) will allow the development of monograms integrating not only dosimetric parameters, but also criteria on comorbidities, clinical features, and tumor response to external beam radiotherapy. This would be of great help in adapting and personalizing treatment plans.
Longer-term prospects include the development of alternative image modalities for guidance, such as endorectal ultrasound, cheaper and more accessible than MRI, or conversely, a more advanced and sophisticated image modality.
Image-guided brachytherapy is also progressively declined in other gynecologic tumors, such as vagina cancer or non-operable endometrial cancer.

SP-0391
Brachytherapy for the pelvic region: status and perspective for the future - prostate

A. Henry[1]
[1]*St James Institute of Oncology, Radiation Oncology, Leeds, United Kingdom*

Prostate brachytherapy allows radiation dose escalation directly into the gland with minimal dose to adjacent rectum and bladder. Over the last decade improvements in brachytherapy technology have refined dose delivery with the introduction of HDR after loading devices, more sophisticated treatment planning systems and the incorporation of functional imaging into the planning process. This teaching lecture will provide an overview of the techniques, indications, and clinical outcomes for both permanent and High Dose Rate prostate brachytherapy. Recent results from randomised clinical trials will be critiqued and emerging indications including focal and salvage treatments discussed.

Symposium with Proffered Papers: Adaptive radiotherapy for coping with anatomical variations: hope or hype?

SP-0392
Overview of clinical practice of ART for pelvic tumours

S. Thörnqvist[1], L.B. Hysing[1], L. Tuomikoski[2], A. Vestergaard[3], K. Tanderup[3], L.P. Muren[3], B.J.M. Heijmen[4]
[1]*Haukeland University Hospital, Department of Medical Physics, Bergen, Norway*
[2]*Helsinki University Central Hospital, Department of Oncology, Helsiniki, Finland*
[3]*Aarhus University Hospital, Department of Medical Physics, Aarhus, Denmark*
[4]*Erasmus MC Cancer Institute, Department of Radiation Oncology, Rotterdam, The Netherlands*

Introduction: Variation in shape, position and treatment response of both tumour and organs at risk are major challenges for accurate dose delivery in radiotherapy. Adaptive radiotherapy (ART) has been proposed to customise the treatment to these motion/response patterns of the individual patients, but increases workload thus challenge clinical implementation. This presentation presents a review of the clinically implemented ART in addition to *in silico* workflows that have been published on pelvic tumours.

Material and methods: Initial identification of papers was based on searches in PubMed. For each tumour site (prostate, gynaecological [gynae], bladder, ano-rectal), the identified papers were screened independently by two researches for selection of studies describing all processes of an ART workflow: treatment monitoring and evaluation, decision and execution of adaptations. Both brachytherapy (BT) and external beam studies were eligible in the review.

Result: The review consisted of 43 clinical studies and 51 *in silico* studies. For prostate, 1219 patients were treated with offline re-planning workflows, mainly to adapt prostate motion relative to bony anatomy. For gynae 1155 patients were treated with online BT re-planning while 25 ano-rectal cancer patients were treated with offline re-planning, all to account for tumour regression detected by MRI/CT. For bladder and gynae, 161 and 64 patients respectively, were treated with library-based online plan selection to account for target volume and shape variations (Figure). In comparison to non-ART, sparing of rectum (prostate and bladder cancer), bladder (ano-rectal cancer) and bowel cavity (gynae and bladder cancer) was reported with ART.

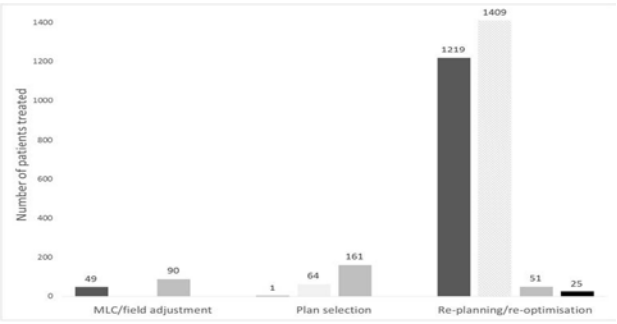

Figure. Number of patient treated with different categories of ART workflows for prostate (dark grey), gynaecological (light grey), bladder (grey) and ano-rectal (black). Patients treated with BT additionally marked with striped pattern.

Conclusion: Implementations of ART were dominated by offline re-planning and online BT re-planning, although recently online plan selection workflows have increased with the availability of cone-beam-CT. Advantageous dosimetric and outcome related patterns using ART was documented by the studies included the review. Despite this, clinical implementations have been scarce, especially regarding prostate and the vast amount of *in silico* studies available. Identified challenges, hindering successful clinical implementations, were re-contouring of target/OARs in addition to patient selection, aiding the focus of the adaptations to the more challenging patients.

SP-0393

The challenges of ART from a physician's perspective

S. Nuyts[1]
[1]*University Hospital Gasthuisberg, Leuven, Belgium*

Currently, with our highly conformal modulated radiotherapy techniques, we are capable of delivering high radiation doses to tumour volumes, whilst minimizing dose to the surrounding structures. However, today's radiotherapy is based on the dogmatic concept of unchanging anatomy of tumors, surrounding normal organs and tissues, where radiotherapy plans solely based on pre-treatment imaging are delivered invariably for several weeks of treatment. Conversely, during a course of curative radiotherapy, tumors and to some extend OARs change. In the field of head and neck cancer, tumor and lymph nodes shrink up to 3% per day, changing size, shape and position. External contour modifications result from loss of weight and muscle mass, altering the geometry of the disease in relation to OARs. This leads to changes in the anatomy of patients, impacting the dose distribution that may differ significantly from what was planned. In this context, considerable efforts have been put on adaptive radiotherapy (ART), i.e. to adapt the treatment delivery on the basis of changes in the tumor and/or normal tissues during the course of radiotherapy. The aim is then to compensate for under-dosage of the target volumes or over-dosage of OARs.
Re-imaging and re-planning evidently result in an extra workload and cost. Therefore, although ART is an appealing concept, it is at present not used on a routine basis for all patients. The optimal implementation strategy regarding selection of patients and timing of imaging/replanning remains to be defined. Several groups are currently investigating these questions, and an overview of the results, from a physician's perspective will be presented.

SP-0394

The practical "costs" of adaptive radiotherapy

C. Rowbottom[1]
[1]*The Clatterbridge Cancer Centre - Wirral NHS Foundation Trust, Medical Physics, Bebington- Wirral, United Kingdom*

Adaptive radiotherapy is an emerging area of radiotherapy. In general there are two categories of adaptive radiotherapy leading to either pro-active or reactive adaptations. As the terms suggest, pro-active adaptation is chosen in advance of the patient commencing treatment, whereas reactive adaptation is unscheduled and arises from an unexpected patient change seen during treatment.
There are 3 distinct categories for which adaptive radiotherapy approaches should be considered. The categories and most appropriate form of adaptation are given in table 1.

Table 1.

Patient Characteristic	Example clinical site	Type of Adaptation	Most likely Adaptive approach	Frequency of adaptation
Daily anatomy change	Bladder	Pro-active adaptation	Based on small number of pre-determined options	Daily
Slowly changing anatomy over treatment course	Head & Neck	Pro-active adaptation	Modified treatment plan based on new patient anatomy information	≤ Weekly
Unexpected anatomy changes	Any	Reactive adaptation	Modified treatment plan based on new patient anatomy information	Unscheduled

Studies of safety in radiotherapy have shown that there is a higher risk of deviation during handoffs between staff groups with tight coupling and when decisions are made under significant time pressure. Deviation rates of <0.5% per fraction have been reported[1-4], leading to deviation rates in the range 1-2% per patient. Adaptive radiotherapy can be seen as increasing the complexity of handoffs and creating more frequent decision making points in the process under time pressure. In this context the introduction of adaptive radiotherapy needs to be made whilst mitigating the risk of significantly increasing deviation rates. .
Justification is required for adaptation from the assessment of risks and benefits from adaptive approaches. As there is currently no clear clinical benefit from adaptive radiotherapy, new risks need to be mitigated to ensure there is an overall patient benefit. Once procedures have been developed for an adaptive approach, changes in personnel, training and workload are likely to be needed to ensure the safe use of adaptive radiotherapy. For example, there are significant training requirements for radiotherapy treatment staff when applying pro-active adaptive radiotherapy techniques where the most appropriate plan must be chosen at each treatment fraction.
Reactive adaptation has organically arisen from the routine use of online image-guidance. For example using cone-beam CT has provided a wealth of information regarding patient anatomy changes during the course of radiotherapy. Inevitably changes in patient anatomy seen during treatment lead to questions regarding the appropriateness of the original treatment plan. It is likely that around 20% of patients receiving radiotherapy will have anatomy changes requiring assessment for appropriateness of their original treatment plan during the course of their treatment. However, modifications to treatments should only be enacted if the patient benefit from the change outweighs the risk of a deviation that could lead to worse patient outcome. Applying this approach is likely to lead to <5% of patients requiring a modification to their treatment. Therefore, at the very least, departments will require efficient processes for the review of treatment plans against changes to patient anatomy.
In conclusion, currently the clinical justification for adaptive radiotherapy approaches is unclear but the adoption rate is likely to continue to rise due to the available technology. In this context there is a requirement to ensure staffing,

training and workload is carefully considered to mitigate risks to patients.
1. Huang G et al. Error in the delivery of radiation therapy: Results of a quality assurance review. Int J Radiat Oncol Biol Phys 2005;61:1590–1595.
2. Kapur A et al. Incident Learning and Failure-Mode-and-Effects-Analysis Guided Safety Initiatives in Radiation Medicine. Front Oncol. 2013 3:305.
3. Kalapurakal JA et al. A comprehensive quality assurance program for personnel and procedures in radiation oncology: value of voluntary error reporting and checklists. Int J Radiat Oncol Biol Phys. 2013 86(2):241-8.
4. Hunt MA et al. The impact of new technologies on radiation oncology events and trends in the past decade: an institutional experience. Int J Radiat Oncol Biol Phys. 2012 84(4):925-31.

OC-0395

Patient selection in head and neck adaptive radiotherapy

C. Brouwer[1], R. Steenbakkers[1], A. Van der Schaaf[1], C. Sopacua[1], L. Van Dijk[1], R. Kierkels[1], H. Bijl[1], J. Burgerhof[1], J. Langendijk[1], N. Sijtsema[1]
[1]*University of Groningen- University Medical Center Groningen, Department of Radiation Oncology, Groningen, The Netherlands*

Purpose or Objective: During the course of head and neck radiotherapy, anatomical changes may lead to underdosage or hotspots in target volumes, and overdosage in organs at risk (OARs). The largest dose differences between planned and actual given OAR dose have been reported for the parotid glands (PGs). Dose increase to the PGs could lead to an increase of radiation induced side effects, justifying adaptive radiotherapy (ART) to reduce the PG dose. Still, ART procedures are labour intensive and only a fraction of patients will benefit. The aim of this study was to develop and validate a method to predict dose deviations from the planned PG mean dose, to select patients for adaptive radiotherapy (ART) up-front.

Material and Methods: Planning and response (6 weeks after RT) CT-scans from 113 head and neck cancer patients (cohort A) were used to estimate deviations between planned and actually given PG mean dose (ΔDmean). Potential pre-treatment selection parameters presented in recent literature were included in the analysis. Uni- and multivariable linear regression analysis for the endpoint PG ΔDmean was performed to select pre-treatment parameters eligible for patient selection. ROC curve analysis was performed to determine cut off values for selecting patients with PG ΔDmean larger than 3 Gy with a sensitivity in the range of 70-100%. The proposed method of patient selection was validated in another patient cohort consisting of 43 head and neck cancer patients who received weekly rescan CTs (cohort B).

Results: In univariable analysis, pre-treatment parameters significantly associated with PG ΔDmean were: BMI, chemotherapy, T-stage, N-stage, volume of the GTV, tumour location, overlap of the PG with the high and low dose PTV, V20, V30, V40 and mean dose of the PG. In multivariable analysis, the initial PG mean dose remained the only significant parameter. ROC results were summarized in Table 1. Selection of patients for dose deviations larger than 3 Gy with a sensitivity of 90% could be obtained by a threshold of the initial PG mean dose of 22.2 Gy (Table 1). This would select 62% of patients for ART in cohort A and 76% in cohort B with a corresponding precision of 29 and 19%, saving 38 and 24% of patients from the labour-intensive ART procedure.

Conclusion: We succeeded to develop a method to select patients for ART up-front by using the initial mean dose to the parotid gland. The labour of ART could be reduced by 24-38% with 87-90% sensitivity, contributing to a more effective allocation of the department resources.

Table 1. Performance of the classification of patients for a parotid gland dose deviation > 3 Gy by using the initial mean dose of the parotid glands (PG D_{mean})

Cut off value PG D_{mean} (Gy)	0	3.6	22.2	24.7	27.0
Cohort A					
Sensitivity (%)	100	100	90	80	70
Specificity (%)	0	33	45	50	60
% selected for ART	100	74	62	56	46
Precision (%)	20	27	29	29	30
Cohort B					
Sensitivity (%)	100	100	87	60	40
Specificity (%)	0	0	19	38	46
% selected for ART	100	100	76	62	51
Precision (%)	18	18	19	17	14

Precision = true positives / (true positives + false positives)

Symposium with Proffered Papers: Time is not on our side: cardiovascular toxicity after radiotherapy

SP-0396

The risk of cardiovascular disease after breast cancer treatment: the clinician's point of view

C. Taylor[1]
[1]*University of Oxford, Clinical Trial Service Unit, Oxford, United Kingdom*

Background: Breast cancer radiotherapy reduces the risk of cancer recurrence and death. However it usually involves some radiation exposure of the heart which may increase the risk of subsequent heart disease. Epidemiological data suggest that the major coronary event rate increases by 7.4% per Gy mean heart dose[1]. Estimates of the absolute risks of radiation-related heart disease are needed to help oncologists plan each individual woman's treatment. The absolute risk for an individual woman depends on her estimated cardiac radiation dose and her background risk of ischaemic heart disease in the absence of radiotherapy. When the risk is known, it can then be compared with the absolute benefit of the radiotherapy.

Methods: Worldwide data on heart doses in breast cancer radiotherapy published during 2003-2013 were collated systematically. Analyses considered the variation in the typical mean heart dose according to various patient and treatment-related factors including laterality, target(s) irradiated and technique[2]. These heart doses were used to predict typical absolute cardiac risks from breast cancer radiotherapy using the dose-response relationship of a 7.4% per Gy increase in the rate of major coronary events.[1] These risks were compared with estimates of the absolute benefits of breast cancer radiotherapy.

Results: In left breast cancer, mean heart dose averaged over 398 regimens in 149 studies from 28 countries was 5.4 Gy (range <0.1-28.6 Gy). In left-sided regimens that did not include the internal mammary chain, the average mean heart dose was 5.6 Gy (range <0.1-23.0) for inverse-planned intensity modulated radiation therapy, 3.4 Gy (range <0.1-12.4) for tangential irradiation, 2.2 Gy (range <0.1-3.8) for brachytherapy and 0.5 Gy (range 0.1-0.8) for proton beam therapy. On average, inclusion of the left IMC doubled the heart dose. In 93 regimens where the left IMC was irradiated, average mean heart dose was around 8 Gy for most photon or electron techniques, and it varied little according to which other targets were irradiated. In right-sided breast cancer, the average mean heart dose was 3.3 Gy based on 45

regimens in 23 studies.[2] Applying these doses to estimated typical absolute cardiac risks[1] showed the absolute risk of a radiation-induced major coronary event for many women today is less than 1%. So for them, the risk of radiotherapy is likely to be much smaller than the benefit. Nevertheless there is considerable variation in predicted absolute cardiac risks, depending on an individual woman's background risk and on her heart radiation dose.

Conclusions: Exposure of the heart from breast cancer radiotherapy has reduced substantially over the past few decades but there is still considerable variation in published heart doses worldwide. In addition, there is variation in the risk of heart disease among patients being considered for radiotherapy. Thus there is likely to be substantial interpatient variability in the cardiac risks of radiotherapy. The population-based dose-response relationship[1] can be used to provide reassurance for many women that their absolute risk of ischaemic heart disease from breast cancer radiotherapy is likely to be small compared with their likely absolute benefit. For other women, for example those with a high predicted heart radiation dose or for those with prior heart disease, the dose-response relationship can be used to identify the minority of women for whom the risk-benefit ratio is less favourable. In these women, consideration may be given to reducing cardiac radiation dose to reduce the radiation-related cardiac risk.

Funding This work was funded by core funding from Cancer Research UK to the CTSU, University of Oxford and the Department of Health, London (project grant RRX 108).
Conflicts of interest None

References

1. Darby SC, Ewertz M, McGale P, et al. Risk of ischemic heart disease in women after radiotherapy for breast cancer. NEJM 2013; 368: 987-998.
2. Taylor CW, Wang Z, Macaulay E, et al. Exposure of the heart in breast cancer radiation therapy: A systematic review of heart doses published during 2003-2013. Int J Radiat Oncol Biol Phys 2015; 93: 845-853.

SP-0397

Predicting cardiac toxicity after breast irradiation: new quantitative data and new challenges

G. Gagliardi[1]
[1]*Karolinska University Hospital, Section of Radiotherapy Physics and Engineering- Dept of Medical Physics, Stockholm, Sweden*

The QUANTEC summary of data on dose-volume-response effect in heart after radiation therapy provided some answers and practical guidelines for the optimization of the dose distribution in breast cancer patients, and left a few problems open. The main dilemma centered on the fact that cardiac serious events are late, requiring long follow-up and rare, requiring large populations. Furthermore, in studies evaluating cardiac toxicities after irradiation the quality of the outcome clinical data was in general different from the quality of the dosimetrical data. Similar considerations still apply to a few studies performed after QUANTEC.
A main step forward is represented by the increased size and design of the studies, e.g. as in the one by Darby *et al* (N Engl J Med 2013) which included about 2.000 women treated in Scandinavia. The paper provided among several results an estimation of the cumulative risk of death from ischemic heart disease for patients treated/not treated with radiation therapy and with different mean heart doses, obtained through reconstruction of the dose planning on a model patient.
Beyond size and type of study population another relevant factor investigated in several analysis is the relationship between fraction size and late cardiac effects. Mahrin (Int J Radiation Oncology Biol. Phys. 2007) performed an analysis on about 3.800 left sided respectively 3700 right sided breast cancer patients treated between 1984 and 2000, compared the different fractionation schedules and concluded that a statistical increase in overall and cardiac-specific mortality could not be found comparing left vs right breast cancer patients. Furthermore the hypofractionated adjuvant RT regimens did not significantly increase the risk of cardiac mortality. The 10 year follow-up of the START - UK Standardization of Breast Cancer Radiotherapy trials of radiotherapy hypofractionation (Haviland JS *et al*, Lancet Oncol 2013) confirmed the 5 years results that "appropriately dosed hypofractionated radiotherapy is safe and effective". A norwegian study with a longer follow-up, but a smaller study population and irradiated in a different way concluded instead than the degree of hypofractionation and parasternal nodes contributed to an increased cardiac mortality in the patient cohort (Tjessem *et al*, Int J Radiation Oncology Biol. Phys 2013).
Another perspective is given by the studies on cardiac dose-volume effects where dose distributions in subregions of the heart are investigated (e.g. Nilsson G *et al*, J Clin Oncol 2012; Johansen S, *Breast cancer: basic and clinical research* 2013). The results from these analyis might be very helpful in the design of treatment protocols.
Finally the technological development has to be taken into account (e.g. gating, DIBH etc), which in some cases might simply by-pass the issue of cardiac irradiation. This approach does not provide answers to the basic question, but provides a convenient solution.

SP-0398

Active surveillance for cardiovascular disease after Hodgkins lymphoma

L. Daniels[1]
[1]*Leiden University Medical Center LUMC, Department of Radiotherapy, Leiden, The Netherlands*

Hodgkin lymphoma is a relatively rare form of cancer, which mainly effects young adolescents and young adults. Over the past decades developments in treatment options for patients with Hodgkin lymphoma have led to improved outcome rates. As a result, there is an increasing number of Hodgkin lymphoma survivors. They are at risk of developing long-term toxicity due to treatment such as secondary malignancies or cardiovascular complications. There is an increased risk of developing valvular heart disease after mediastinal radiotherapy, although risk increases significantly after radiation treatment doses over 30 Gy (1). Recent studies also show a 4-6 fold increased standardized incidence ratio of heart failure and coronary heart disease (CHD), due to anthracycline containing chemotherapy regimens and mediastinal radiotherapy (2). Severe CHD can even be present in the absence of typical symptoms such as chest pain (3). A linear dose-response relationship between mediastinal radiotherapy and CHD has been established with a 2.5-fold increased risk of CHD after receiving a mean heart dose of 20 Gy (4). This implies that even patients treated with current standard radiotherapy doses remain at serious risk of developing radiation induced CHD. At the same time, new strategies for non-invasive screening for CHD have developed, by means of CT coronary angiography, showing encouraging positive and negative predictive values for detecting significant CHD. In this lecture, an overview of recent efforts of screening for coronary artery disease in Hodgkin lymphoma patients is presented, and clinical implications are discussed.
REFERENCES 1. Cutter DJ, Schaapveld M, Darby SC, et al.: Risk of valvular heart disease after treatment for Hodgkin lymphoma. J Natl Cancer Inst 107, 2015 2. van Nimwegen FA, Schaapveld M, Janus CP, et al.: Cardiovascular disease after Hodgkin lymphoma treatment: 40-year disease risk. JAMA Intern Med 175:1007-1017, 2015 3. Daniels LA, Krol AD, de Graaf MA, et al.: Screening for coronary artery disease after mediastinal irradiation in Hodgkin lymphoma survivors: phase II study of indication and acceptancedagger. Ann Oncol 25:1198-1203, 2014 4. van Nimwegen FA, Schaapveld M, Cutter DJ, et al.: Radiation Dose-Response Relationship for Risk of Coronary Heart Disease in Survivors of Hodgkin Lymphoma. J Clin Oncol, 2015

OC-0399

Dose to heart substructures is associated with non-cancer death after SBRT in stage I NSCLC patients

B. Stam[1], H. Peulen[1], M. Guckenberger[2], F. Mantel[3], A. Hope[4], J. Belderbos[1], I. Grills[5], M. Werner-Wasik[6], N. O'Connell[7], J.J. Sonke[1]

[1]*Netherlands Cancer Institute Antoni van Leeuwenhoek Hospital, Department of Radiation Oncology, Amsterdam, The Netherlands*
[2]*University Hospital Zurich, Radiation Oncology, Zurich, Switzerland*
[3]*University Hospital Wuerzburg, Radiation Oncology, Wuerzburg, Germany*
[4]*Princess Margeret Hospital, Radiation Oncology, Toronto, Canada*
[5]*William Beaumont Hospital, Radiation Oncology, Royal Oak, USA*
[6]*Thomas Jefferson University, Radiation Oncology, Philidelphia, USA*
[7]*Elekta AB, National Oncology Data Alliance, Stockholm, Sweden*

OC-0400

Risk estimation of cardiac toxicity following craniospinal irradiation of pediatric patients.

G. Engeseth[1], C. Stokkevåg[2], L. Muren[3]

[1]*Haukeland University Hospital, Department of Medical Physics and Oncology, Bergen, Norway*
[2]*University of Bergen, Department of Physics and Technology, Bergen, Norway*
[3]*Aarhus University Hospital, Department of Medical Physics, Aarhus, Denmark*

Purpose or Objective: Craniospinal irradiation (CSI) plays an important role in the treatment of medulloblastoma and improvement in treatment during the last decades has resulted in good prognosis. CSI is most commonly delivered with photons or a combination of photon/electrons. However, proton therapy is generally indicated as it lowers the dose to normal tissues and potentially reduces the risk of late effect. The aim of this study was therefore to compare the estimated risk of cardiac toxicity following CSI using photons, electrons and protons.

Material and Methods: CSI treatment plans including conformal photons, electrons/photons combined, double scattering protons (DS) and intensity modulated proton therapy (IMPT) were created in the Eclipse treatment planning system [Varian Medical Systems, Palo Alto, CA, USA] for six pediatric patients. The CTV included the brain and the spinal canal, for the protons the CTV was expanded to also include the entire vertebral body to prevent asymmetric growth of the skeleton. During treatment planning a setup uncertainty of 5 mm was taken into account, as well as an uncertainty in the proton range of 3.5 %. The prescribed dose for all techniques was 23.4 Gy(RBE). Dose-risk models derived from two independent pediatric patient cohorts were used to estimate the risk of cardiac toxicity. The excess Relative Risk (ERR – relative to general population) for cardiac mortality was estimated using a linear model [1], while ERR for cardiac failure and disorder were estimated using both a linear and a linear-quadratic [2] (LQ) model. Input parameters were the mean heart dose, and the parameters (with 95 % Confidence Interval (CI)) displayed in Table I. The Relative Risk (RR) was defined as the ratio between ERR for photon /electron, photon/DS and photon/IMPT.

Table I: Dose-response models, parameters and 95 % CI

	Model	Parameter	95 % CI
Mortality	Linear[1]	α: 0.6	0.2; 2.5
Disorder	Linear[2]	α: 0.35	-0.005; 1.2
	LQ	α_1: 0.4	0.002; 1.4
		α_2:-0.00013	-0.01 ;0.1
Failure	Linear[2]	α: 0.09	-0.02; 0.3
	LQ	α_1: 0.19	-0.02; 0.5
		α_2: -0.002	-0.004; 0

Results: Regardless of dose-risk model applied, the conformal photons were ranked with the highest ERR for all cardiac toxicities, whereas IMPT was ranked with the lowest (Figure 1a). For cardiac mortality the ERR for photon was 8.1 (95 % CI: 3.4 to 30.5), while ERR for IMPT were 1.3 (95 % CI: 1.1 to 2.4). For cardiac disorder and cardiac failure the ERR for photon was 5.1 (95 % CI: 0.9 to 15.2) and 2.1 (95 % CI: 0.8 to 4.6), respectively (Linear model). The corresponding results for IMPT were 1.2 (95% CI: 1.0 to 1.7) and 1.1 (95 % CI: 1.0 to 1.2). Similar trends were found using the LQ model. Relative to IMPT, photons lead to a risk of cardiac mortality that was a factor of 6.1 higher (range 5.7 to 7.0), cardiac disorder a factor of 4.3 higher (range 4.1 to 4.9) and cardiac failure a factor of 2.0 higher (range 1.9 to 2.1) (Figure 1b).

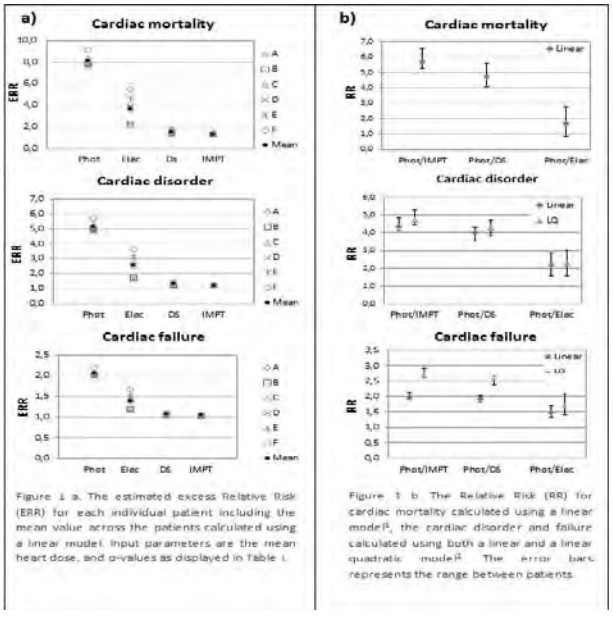

Figure 1 a. The estimated excess Relative Risk (ERR) for each individual patient including the mean value across the patients calculated using a linear model. Input parameters are the mean heart dose, and α-values as displayed in Table I.

Figure 1 b. The Relative Risk (RR) for cardiac mortality calculated using a linear model[1], the cardiac disorder and failure calculated using both a linear and a linear quadratic model[2]. The error bars represents the range between patients.

Conclusion: Across different cardiac morbidity endpoints, and despite different dose-risk models used, the results of our modelling study were consistently in favour of protons.

References:
1. Clin Oncol, 2010: 28 (8): 1308-1315
2. Radiother and Oncol: 2006 (81): 47-56

Symposium: Emerging biomarkers

SP-0401

Circulating tumour cells as biomarkers in lung radiotherapy

K. Haslett[1]
[1]*The University of Manchester, Institute of Population Health, Manchester, United Kingdom*

It has long been hypothesized that the propagation of circulating tumour cells (CTCs) is a pre-requisite for the development of metastases. However, robust technology to reliably isolate CTCs and characterise them at the molecular level has only become available in recent years. Thus repeated blood sampling for CTCs could provide a non-invasive method of serially reassessing tumour status and evolving tumour biology.
Patients with stage I-III NSCLC are at high risk of developing distant metastases after radiotherapy (RT) or chemo-radiotherapy treatment. With the advent of new technologies to enumerate CTCs, the clinical significance of CTCs before, during and after RT has become of great interest. In the current era of targeted therapy and the development of personalised medicine the question still remains as to whether CTCs could be used to identify patients most likely to benefit from radical RT and prevent the delivery of futile cancer treatments and their associated toxicity. Prospective clinical trials have shown the prognostic value of CTC enumeration in patients with non-small cell lung cancer (NSCLC) and small cell lung cancer (SCLC) (1, 2). Although CTCs have been used as a surrogate biomarker in hundreds of clinical trials, as yet none have been incorporated into standard clinical practice. To date there are few published studies evaluating CTC's in patients undergoing radical thoracic RT.
In my talk I will discuss the following:
•novel platforms available for isolation of CTCs
•current data on the evaluation of CTCs as a biomarker in NSCLC and SCLC patients treated with RT
•advantages and limitations of CTCs as a biomarker •future directions and the prospect of using CTCs to stratify patients in clinical trials

References

ADDIN EN.REFLIST 1. Krebs MG, Sloane R, PriestL, Lancashire L, Hou JM, Greystoke A, et al. Evaluation and prognosticsignificance of circulating tumor cells in patients with non-small-cell lungcancer. Journal of clinical oncology : official journal of the American Societyof Clinical Oncology. 2011 Apr 20;29(12):1556-63. PubMed PMID: 21422424.
2. HouJ, Krebs M, Lancashire L, Sloane R, Backen A, Swain R, et al. ClinicalSignificance and Molecular Characteristics of Circulating Tumor Cells andCirculating Tumor Microemboli in Patients With Small-Cell Lung Cancer. Journalof Clinical Oncology. 2012 FEB 10 2012;30(5):525-32. PubMed PMID:WOS:000302622900018. English.

SP-0402

The fall and raise of predictive radiotherapy biomarkers

M. Baumann[1,2,3,4]
[1]*OncoRay – National Center for Radiation Research in Oncology, Faculty of Medicine and University Hospital Carl Gustav Carus- Technische Universität Dresden, Dresden, Germany*
[2]*Helmholtz-Zentrum Dresden - Rossendorf, Institute of Radiooncology, Dresden, Germany*
[3]*German Cancer Consortium DKTK Dresden, and German Cancer Research Center DKFZ, Heidelberg, Germany*
[4]*Department of Radiation Oncology, Institute Faculty of Medicine and University Hospital Carl Gustav Carus-Technische Universität Dresden, Radiooncology, Dresden, Germany*

Radiotherapy is a mainstay of cancer treatment. Due to it high efficacy to inactivate cancer stem cells in the primary tumor and regional metastases as well as its increasing ability to spare normal tissues, it has a proven curative potential in many cancer types. State-of-the-art radiation treatment planning and delivery is fully individualized based on anatomical imaging, precise space-resoluted radiation dose models, tumor control probability- vs. normal tissue complication-models and clinical parameters. These advances in personalized radiation oncology can mainly be attributed to the revolutionary progress in high-precision radiation delivery and planning technology during the past decades and have been rapidly translated into clinical practice. In parallel radiobiological knowledge has significantly improved during the past decades by e.g. unravelling radiobiological mechanisms of radioresistance of tumors and volume-dose relationships for a host of radiation induced effects in normal tissues. This research translated into more efficient radiation schedules on a population base and to NTCP parameters clinically used for treatment planning in individual patients. While several bioassays, including SF2 and plating efficiency determined in human tumor biopsies, provided proof-of-concept of radiobiological mechanisms, these early assays could not be applied to tailor a treatment strategy for an individual patient. Revolutionary advances in biotechnology and tumor biology allow to profile tumors rapidly, thereby providing information on resistance parameters (e.g. hypoxia, stem cell density, radiosensitivity) which can be rationally tested for their prognostic and predictive power for radiotherapy. The same applies for biological imaging which may be of particular relevance for advancing biology-driven individualization of radiation oncology. One uniqueness for the development of personalized radiation oncology is that already a broad biological stratification of patients can substantially enhance individualization as this information adds to the fully anatomically-personalized dose-distributions achieved today. Therefore biomarker driven high precision radiotherapy is in pole position to create a show-case for personalized oncology at large.
This lecture will review preclinical and clinical-translational examples of potential strategies to further personalize radiation oncology by inclusion of biomarkers.

SP-0403

Genomic breast cancer subtype classification for response prediction

N. Somaiah[1]
[1]*The Institute of Cancer Research and The Royal Marsden NHS Foundation Trust, Division of Cancer Biology and Division of Radiotherapy and Imaging, Sutton, United Kingdom*

The advent of genomics has revolutionized our understanding of breast cancer as several biologically and molecularly distinct diseases. New molecular techniques generate data about the intrinsic characteristics of a tumour, thereby providing useful diagnostic, prognostic and predictive information. Commercially available tests have begun to fundamentally change the clinicopathological paradigm of selecting patients for adjuvant systemic therapies in early breast cancer. Several recently published radiosensitivity gene expression signatures aim to predict response to adjuvant radiotherapy. The ultimate aim of biomarker research is to individualise therapies in order to maximise tumour response whilst minimizing overtreatment and toxicities. This talk will review the strengths and limitations of currently available breast cancer-specific molecular tests with a view to response prediction.

SP-0404

Genomic subtypes in prostate cancer and its influence in treatment response

R Bristow[1]
[1]*Princess Margaret Cancer Centre, Radiation Oncology, Toronto, Canada*

Abstract not received

Symposium: SBRT for oligometastatic disease

SP-0405

Combining SBRT and immunotherapy: a promising approach?

F. Herrera[1]
[1]*Centre Hospitalier Universitaire Vaudois, Department of Radiation Oncology, Lausanne Vaud, Switzerland*

Clinical reports of limited and treatable cancer metastases, a disease state that exists in a transitional zone between localized and widespread systemic disease, have been reported and are now termed oligometastasis. SBRT treatment of oligometastases has shown promising local control rates (65-97%), and a good toxicity profile (<5% of serious adverse events) because the delivered doses are ablative and spatially limited. [1, 2] However, most of these patients usually recur at distant sites, outside of the irradiated area, with a median time to progression of 4 to 6 months, indicative of occult metastatic deposits at the time of treatment. Thus, although SBRT is effective in definitively ablating most treated lesions, distant tumors progress highlighting the need for better systemic therapies.[3]

Immunotherapy has emerged as an independent therapeutic modality that can result in objective – even complete – responses and significant amelioration of overall survival in patients with advanced metastatic tumors. There is an emerging opportunity for combining immune therapy together with ablative SBRT for oligometastatic patients, with the final aim of increasing T cell infiltration into the tumor.

***In situ* vaccination during lethal RT of few metastases**

Lethal (high) doses of radiation can induce immunogenic death in cancer cells, i.e. irradiated cancer cells can trigger an antitumor immune response. RT can upregulate the necessary "eat-me" signals that promote the uptake of dying tumor cells by dendritic cells (DCs) and macrophages[4]. However, a systemic immune response against distant lesions (the so-called abscopal effect) is rarely seen. Given the beneficial but limited immune modulatory effects of SBRT, combination of SBRT with simultaneous activation of other immune-pathways could lead to antigen-specific adaptive immunity, a phenomenon called "*in situ* vaccination".[5]An abscopal effect has been observed when RT was combined with immunotherapy and has been proven to be T-cell mediated. [6-8] A recent report of patients with melanoma and renal cell carcinoma treated with SBRT (20 Gy), in combination with IL-2 showed higher than expected abscopal responses.[9] In a phase I trial combination 8 Gy in 2-3 fractions with ipilimumab partial responses were observed in 18% of the patients. When dual checkpoint blockade with both anti-CTLA4 and anti-PD-1 combined with radiation was tested in a B16 melanoma model improved responses and abscopal effects were observed. Even in the presence of dual checkpoint blockade, omission of radiation resulted in high rates of relapse.[10]

The combination of lethal SBRT to few tumor deposits in combination with different immunotherapy strategies triggers antitumor immunity. However, the key question that needs to be answered is which are the best combinatorial strategies, the best timing to combine them and how to increase effective homing of antitumor T cells to the remaining tumor deposits. Modifying the tumor microenvironment in these residual tumors is therefore of major importance to improve therapeutic outcome and finally cure.

References

[1] Rusthoven KE, et al Multi-institutional phase I/II trial of stereotactic body radiation therapy for lung metastases. Journal of clinical oncology : official journal of the American Society of Clinical Oncology 2009, 27:1579-84.
[2] Katz AW, Carey-Sampson M, Muhs AG, Milano MT, Schell MC, Okunieff P: Hypofractionated stereotactic body radiation therapy (SBRT) for limited hepatic metastases. International journal of radiation oncology, biology, physics 2007, 67:793-8.
[3] Tree AC, et al. Stereotactic body radiotherapy for oligometastases. The lancet oncology 2013, 14:e28-37.
[4] Zitvogel L, et al. Immunogenic tumor cell death for optimal anticancer therapy: the calreticulin exposure pathway. Clinical cancer research : an official journal of the American Association for Cancer Research 2010, 16:3100-4.
[5] Formenti SC, Demaria S: Combining radiotherapy and cancer immunotherapy: a paradigm shift. Journal of the National Cancer Institute 2013, 105:256-65.
[6] Golden EB, et al. An abscopal response to radiation and ipilimumab in a patient with metastatic non-small cell lung cancer. Cancer immunology research 2013, 1:365-72.
[7] Postow MA, et al. Immunologic correlates of the abscopal effect in a patient with melanoma. The New England journal of medicine 2012, 366:925-31.
[8] Demaria S, et al. Ionizing radiation inhibition of distant untreated tumors (abscopal effect) is immune mediated. International journal of radiation oncology, biology, physics 2004, 58:862-70.
[9] Seung SK, et al. Phase 1 study of stereotactic body radiotherapy and interleukin-2--tumor and immunological responses. Science translational medicine 2012, 4:137ra74.
[10] Twyman-Saint Victor C, et al. Radiation and dual checkpoint blockade activate non-redundant immune mechanisms in cancer. Nature 2015, 520:373-7.

SP-0406

SBRT for metastatic disease: how far can and should we go?

M. Dahele[1]
[1]*VU University Medical Center, Amsterdam, The Netherlands*

Stereotactic body radiotherapy (SBRT) is attracting substantial interest as a treatment option for selected patients with metastatic disease. It is reasonable to take a step back and take a look at where the field is now and what we can expect from this intervention. This presentation will focus on a number of contemporary clinical issues, including: what can be expected from SBRT at various anatomical sites; definitions of oligo-metastatic disease and their limitations; defining treatment goals in metastatic disease; lessons from published outcome data; a pragmatic approach to decision-making in the clinic; is radiation technology driving the agenda? and; gathering evidence for the future.

SP-0407

Abdominal-pelvic targets

M. Hoyer[1]
[1]*Aarhus University Hospital, Department of Oncology, Aarhus, Denmark*

Patients with oligometastases from colo-rectal carcinoma (CRC) are often considered as candidates for surgical resection, radiofrequency ablation and SBRT and CRC often metastasize to the abdominal organs, especially to the liver. Therefore, abdominal oligo-metastases are often treated with SBRT. A relative large number of publications demonstrate outcome after SBRT for liver metastases that are almost as good as for lung metastases. Local control rates in both lung and liver are most often in the range 70-90% and survival rates are depending on tumor type and the selection of the patients. There are only few publications on SBRT of abdominal, non-liver oligometastases, but the few available publications indicate favourable local control as well for these patients. Most publications on SBRT for abdominal targets report a low risk of morbidity, but there are reports of relatively severe morbidity related to irradiation of the liver and the bowel, most often in terms of severe mucositis or intestinal ulceration. Treatment of abdominal targets is complex due to the multiple organs at risk. Treatment planning is based on a snapshot of the anatomy on a treatment planning CT-scan. 4DCT takes the intrafraction motion motion of the target into account, but we usually do not take the motion of bowel structures into account. CBCT is used to correct for set-up errors of the target, but organs at risk are less often considered. This may lead to unintended high doses to the organs at risk and side effects that were not expected from the treatment planning.

Symposium: Head and neck: state-of-the-art and directions for future research

SP-0408
Molecular targeting with radiotherapy
K. Harrington[1]
[1]*The Institute of Cancer Research and The Royal Marsden NHS Foundation Trust, Radiation Oncology, Sutton, United Kingdom*

Abstract not received

SP-0409
Immunotherapy for HNSCC: an emerging paradigm?
J. Guigay[1]
[1]*Centre Antoine Lacassagne, Nice, France*

Recent progress has been made in oncology with new drug targeting immune system. Ipilimumab which targets CTLA-4 has been the first one approved in melanoma. Another way to block the deleterious cascade of T-lymphocyte inhibition is to block an extracellular target, namely Programmed Death Receptor-1 (PD-1). PD-1 is a cell surface receptor expressed by T cells, B cells, and myeloid cells, and member of the CD28 family involved in T cell regulation. PD-1 pathway is activated by receptor binding to ligands (PD-L1 or PD-L2) and its physiological role is to prevent uncontrolled immune activation during chronic infection or inflammation. In cancer, activation of PD-1 pathway can suppress antitumor immunity. In mouse models, antibodies blocking PD-1/PD-L1 interaction lead to tumor rejection. In clinical trials, targeting PD-1 pathway using human monoclonal antibody such as nivolumab, which blocks binding of PD-1 to PD-L1 and PD-L2, showed promising results in metastatic solid tumors with durability of objective responses, and sustained overall survival (Topalian and al, NEJM 2012). Phase I studies showed a potential better safety profile of anti-PD-1/PD-L1 agents in comparison with ipilimumab. Following, anti-PD-1/PD-L1 drugs have been developed at a phenomenal speed, taking just three years from the first clinical trials to approval. At now, anti-PD-1 nivolumab and pembrolizumab are approved in melanoma and NSLCC... There is a strong rationale for using anti-PD-1/PD-L1 agents in HNSCC. Tumor-infiltrating lymphocytes (TILs) which are required for PD-1 blockade, and PD-L1 expression are present in HPV+ and HPV negative HNSCC. There is a correlation between infiltration by CD8 cells and response to CRT, and between PD-L1 expression and survival. The high number of specific mutations observed in HNSCC could be a mechanism of immunogenicity. Results of phase I studies testing anti-PD-1/PD-L1 agents in HNSCC patients have been recently reported with promising results in terms of efficacy with prolonged responses. During ASCO 2014 meeting, Seiwert et al. presented first results of a phase Ib study of pembrolizumab in recurrent/metastatic (R/M) HNSCC patients. Patients ≥1% with PD-L1 immunohistochemistry expression in tumor cells or stroma were enrolled in the study. The anti-tumor effect was observed both in patients with HPV-positive and HPV-negative tumors. The duration of these responses was impressive, some already lasting over one year (Seiwert TY et al., ASCO 2014, CSS 6011). Updated data on a expanded cohort have been presented at last ASCO 2015 meeting. 132 (81 HPV+) R/M HNSCC patients were treated with prembrolizumab 200 mg Q3W regardless of HPV or PD-L1 status. 78% received at least one line of chemotherapy. Tolerance was good (9.8% of grade 3-5 adverse events). Objective response rate was 25%, stable disease rate was 25% with long-lasting responses (Seiwert TY, et al. J Clin Oncol. 2015;33(suppl): LBA6008). First results of a phase I study evaluating the safety and efficacy of an anti-PD-L1 agent, durvalumab (MEDI4736), have been presented at ESMO 2014 congress (M. Fury M et al., abstr 988PD, ESMO 2014). MEDI4736 is a human IgG1 mAb, engineered to prevent ADCC activity, that blocks PD-L1 binding to PD-1 and CD-80. 50 pts with HNSCC, with median 3 prior treatments received median 3 doses of MEDI4736 10 mg/kg q2w. Treatment-related adverse events were observed in 39% of pts; most frequently nausea (6%), diarrhea, dizziness, and rash (4% each). Dyspnea, syncope, raised GGT and sepsis (each 5%) were the most common grade≥3 AEs. Among 29 evaluable HNSCC pts for efficacy, 4 pts had a partial response. Numerous anti-PD-1/PD-L1 agents are currently tested in HNSCC. First randomized trial with nivolumab vs standard of care in second line after platinum based first line therapy has just closed. Randomized trials testing pembrolizumab and durvalumab in first-line or second-line treatment for R/M HNSCC patients are ongoing. Beside evaluation of efficacy, these studies should help define the best population (HPV status, prior therapies) and more useful biomarkers than threshold of PD-L1 expression, to select patients who can benefit from these new agents. Flare-up reaction with increase of tumor volume and immune-related adverse events may occur: new guidelines are needed to define criteria of response, time to stop treatment and management of toxicities. Some patients may have a fast progression under monotherapy and mechanisms of resistance are unclear. New approaches combining anti-PD-L1/PD-1 agents and other immune-modulators, chemotherapy and radiotherapy are currently explored. Abscopal effect related to anti-PD-L1/PD-1 agents seems promising. For locally advanced HNSCC, trials testing combinations with anti-PD-L1/PD-1 agents in induction regimen and concurrent CRT are ongoing. The story of immunotherapy as a new paradigm in HNSCC is just beginning…

SP-0410
Proton therapy in HNSCC: better than IMRT?
C. Rasch[1]
[1]*Academic Medical Center, Department of Radiation Oncology, Amsterdam, The Netherlands*

Abstract not received

Symposium: SBRT in lung - choices and their impact on related uncertainties

SP-0411
Dosimetric aspects and robustness in treatment plan optimisation of small tumours
A. Ahnesjö[1]
[1]*Uppsala University Hospital Akademiska Sjukhuset, Uppsala, Sweden*

Stereotactic radiation of small brain targets provides high spatial resolution and accuracy for positioning of patient and radiation fields, almost on submillimeter ranges. This is not matched by equally sharp dose gradients, since finite source size, collimator design limitations and transport of electrons in the irradiated tissue all diffuses the dose. Not surprisingly, the dose prescriptions evolving for small brain tumors aimed for a specified dose to the target periphery, accepting whatever resulting dose to the target center. A kind of standard evolved aiming for a ratio of approximately 65% relative dose at the periphery versus the maximum target center dose (or 154% center-to-periphery ratio). This dose heterogeneity was considered favorable, as to more effectively treat presumably hypoxic cells at the tumor center. The stereotactic treatment methodology for brain treatments were in the early 1990s transferred to radiation of liver metastasis. Through use of stereotactic body frame high target positioning reproducibility was achieved, and similar dose prescriptions of heterogeneous dose were applied, with a center-to-periphery dose ratio of approximately 154%. Soon the technique was also applied to peripheral lung tumors.
Following the development of 3D treatment planning systems in the late 1980s, ICRU responded to the need for consistent handling of geometrical uncertainties and launched in 1993 the ICRU 50 report recommending the use of GTV, CTV and PTV to capture the uncertainties. Specifically, the role of PTV was to “ensure that the prescribed dose is actually absorbed in the CTV”. The normal use of the PTV is to plan a

homogenous dose to its interior, through which it is assumed that the CTV gets the same dose as it is located in the PTV. This requires the dose inside the PTV to be both homogeneous and robust with respect to movements involving heterogeneities. The PTV concept was applied also for extracranial stereotactic body treatments, often inheriting a high center-to-periphery prescription. Dose calculations at the time used "class a" algorithms that not account for dose variations due to a varying level of lateral charged particle equilibrium caused by low density regions. Most so called pencil beam algorithms belong to this, class a, category. Accurate dose calculations can now be achieved with "class b" algorithms such as Monte Carlo, Collapsed Cone or Grid based Boltzmann equation solvers. However, for any algorithm that would calculate the dose physically correct, the resulting dose for the PTV is not representative for the CTV when the margin around the latter contains a lower density medium. Hence, the straight forward application of PTV based treated planning together with heterogeneous prescriptions principles (originally inherited from intracranial treatments), has created a confused situation with large uncertainties with respect to the actually delivered doses.

A robust dosimetry can be achieved by realizing that the dose to a CTV surrounded by a low density medium will be independent of movements as long as it is exposed to a uniform fluence. Given that a near homogeneous fluence cover the PTV, dose prescriptions can then be done directly to the CTV based on a dose calculation with a "class b" algorithm (MC, CC or equivalent). As long as the movements of the CTV are kept well inside a PTV with a homogeneous fluence, the dose delivered to the CTV will be much closer to the prescribed dose, thus providing robust dose specification for small tumors. However, tools for optimization of uniform fluence are presently not provided in clinical TPS. Luckily, several workarounds exists that can "cheat" the optimization of homogenous dose to instead yield a effectively homogeneous fluence. From a pure physics point of view, this can be achieved by incapacitating the lateral spread of energy from the rays of the primary beam. In class a algorithms of the pencil beam kind, this can be implemented by changing the pencil beam parameter controlling the lateral spread. In point kernel algorithms such as CC, similar manipulation of kernel data can be done. In essence, in most algorithms fluence is a precursor for dose providing opportunities to access it. Alternatively, the density of the PTV can be set to a high value that shortens the electron transport distance enough to make the dose more fluence like.

In summary, a robust small lung tumor dose can be implemented through a planning process in which the PTV is determined by the common practice addition of a setup margin to a MIP projections ITV, but replacing the common practice dose calculations by a fluence optimization followed by a class b dose calculation with the CC (or similar) algorithm, using absolute dose prescriptions to the CTV rather than the PTV. For a test series of 5 patients this procedure reduced the difference between prescribed and delivered dose to the CTV from 30% to 8% in D98, with a similar reduction for D02.

SP-0412

Does the prescription isodose matter?

M. Guckenberger[1]
[1]*University Hospital Zürich, Department of Radiation Oncology, Zurich, Switzerland*

The current practice of cranial and extra-cranial stereotactic radiotherapy is in many ways influenced by Gamma-Knife Radiosurgery (GN-RS). It has been a key component of GN-RS to treat the target volumes without any safety margins (GTV = PTV) and to use inhomogeneous dose profiles within the target volume. The dose was most frequently prescribed to a low isodose e.g. 50% meaning that substantially higher doses are delivered to the central part of the tumor.

This practice of dose prescription to a low target encompassing isodose line has been adopted in extra-cranial stereotactic radiotherapy (Stereotactic Body Radiotherapy SBRT) despite many differences to GN-RF: (1) safety margins are used in almost all SBRT indications; (2) in lung SBRT, the use of safety margins will result in inclusion of low density lung tissue into the target volume; (3) radiotherapy delivery is today performed using MLC and in many centers intensity-modulated techniques allowing more sophisticated dose shaping; (4) target and organs at risk motion will affect the delivered dose profile as compared the planned dose profile; (5) the composition of the taget volumes in SBRT is very different to GN-RS - Organs-at-risk are not only close by but within the target volume; (6) in the RTOG protocols of SBRT for stage I NSCLC, dose prescription to a wide range of isodose lines is allowed.

Based on these differences between GN-RS and SBRT above, it is obvious that the concept of dose prescription to a fixed isodose line is not sufficient for SBRT practice. The dose profile within the target volume needs to be sufficiently prescribed and reported to achieve better standardization and comparability between institutions, studies and individual patients. Additionally, current SBRT technology allows to adapt the dose profile within the PTV to the patient-specific clinical requirements: homogeneous dose profiles or even cold spots might allow organ at risk sparing; in contrast, an escalation of the dose within the target center might be beneficial for targets without critical normal tissue within the PTV. Recommendations by the ICRU specific for the needs of SBRT are eagerly awaited and future studies will better define how to optimize SBRT dose planning.

SP-0413

To use or not to use the LQ model at "high" radiation doses

W. Dörr[1]
[1]*Medical University of Vienna, Dept. of Radiation Oncology, Vienna, Austria*

In curative SBRT regimen, few large doses per fraction are applied in a highly conformal way. Such protocols, however, usually do not only differ from conventional protocols in the size of the dose per fraction, but also with regard to overall treatment time and total (equieffective) dose. Moreover, large doses per fraction are usually administered to (normal tissue) volumes that are clearly smaller compared to conventional protocols. Hence, all these parameters, i.e. recovery, repopulation, tumour reoxygenation and normal tissue volume effects, need to be included into considerations concerning the biological effect of SBRT protocols – independently for tumor, early and late responding tissues.

The effect of dose per fraction ("recovery") for tumors is – with few exceptions – considered as low, as expressed by a high a/b-value in the linear-quadratic (LQ) model. Recently, a high fractionation effect was shown for prostate and breast tumors, and is also discussed for others. For lung tumours, however, a small capacity for recovery can be assumed. Early responding normal tissues usually display a similarly low fractionation effect, while most late radiation effects have a high sensitivity with regard to changes in dose per fraction. Hence, doses per fraction must be adjusted to the respective tumor type and the expected (late) morbidity pattern in order to achieve the biologically equieffective doses that result in optimum dissociation between treatment efficacy and adverse events.

The linear-quadratic model has been shown to only inadequately describe the effect of large doses per fraction (>6-10 Gy) for cell survival endpoints in vitro (colony forming assay) and in vivo (e.g. intestinal crypt survival assay). Here, the LQ model overestimates the effects of exposure in the high-dose region. It needs to be emphasized, however, that in the vast majority of pre-clinical investigations and analyses of the fractionation effect for morphological and functional endpoints, large doses per fraction and/or single doses were regularly included. In clear contrast to the cell survival based analyses, these studies in general do not show any major difference of the fit of the LQ model for the in- or exclusion of large doses per fraction in the analyses. Moreover, no deviation of the resulting a/b-values from the respective estimates from clinical data was observed. This indicates the applicability of the LQ model also for the calculation of

equieffective doses at high doses per fraction, such as applied in SBRT protocols in the lung. Besides high dose per fraction,
SBRT protocols regularly include a shortening of the overall treatment time (OTT) compared to conventional or moderately hypofractionated protocols. This is associated with less tumour repopulation, which also contributes to the increased tumor effectiveness. With very few fractions in short time intervals, however, tumour reoxygenation may also be less effective, thus at least partly counteracting the benefit of the shorter OTT. It also needs to be noted that SBRT protocols with short OTT are less permissive for regenerative processes in early responding normal tissues. These protocols hence also bear a risk of increased early normal tissue reactions and thus, in certain tissues, of enhanced ("consequential") late effects.
The administration of large doses per fraction and large total doses is mainly facilitated by a strong conformation of the high-dose volume to the target, i. e. a minimization of the normal tissue volumes exposed to these doses, and is associated with very steep dose gradients within the adjacent normal tissues. However, it must be emphasized that in such scenarios, not only the amount of normal tissue effects may be changed, but also their quality, with altered tissue pathophysiology and morbidity endpoints that are usually not observed with conventional or moderately hypofractionated protocols. Prominent examples are the manifestation of atrophic rather than fibrotic processes, or pathologic rib fractures in SBRT of peripheral lung tumors.
In conclusion, administration of large doses per fraction in SBRT may be advantageous for biological reasons. Estimation of biologically equieffective doses may be based on the standard LQ model. However, such treatment strategies not only impact on tissue recovery, but can also affect other radiobiological parameters (radiopathology, repopulation, volume effects) in a complex manner. Therefore, the patients included in such therapeutic protocols need to be monitored carefully not only for treatment outcome, but also for treatment-related morbidity.

Proffered Papers: Physics 10: Functional Imaging I

OC-0414

Assessing 4DCT-ventilation as a functional imaging modality for thoracic radiation therapy

Y. Vinogradskiy[1], L. Schubert[1], T. Waxweiler[1], Q. Diot[1], R. Castillo[2], E. Castillo[3], T. Guerrero[3], C. Rusthoven[1], L.E. Gaspar[1], B. Kavanagh[1], M. Miften[1]
[1]*University of Colorado Denver, Radiation Oncology, Aurora-CO, USA*
[2]*University of Texas Medical Branch, Radiation Oncology, Galveston, USA*
[3]*Beaumont Health System, Radiation Oncology, Royal Oak, USA*

Purpose or Objective: 4DCT-ventilation is an exciting new lung function imaging modality that uses 4DCT data to calculate lung function maps (Fig 1).

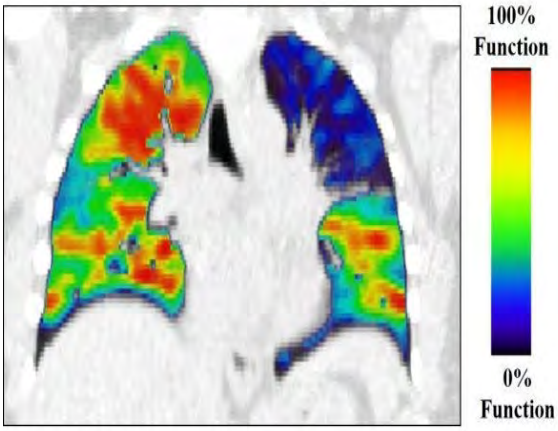

Because 4DCTs are acquired as part of routine clinical care, calculating ventilation from 4DCTs provides clinicians the ability to evaluate spatial lung function without added monetary or dosimetric cost to the patient. Development of clinical trials is underway to use 4DCT-ventilation for thoracic functional avoidance with the idea that preferential radiotherapy (RT) sparing of functional regions may decrease toxicity. Before 4DCT-ventilation is incorporated in a clinical trial; work is needed that assesses the clinical utility of 4DCT-ventilation imaging. The purpose of this study was to evaluate 4DCT-ventilation as a functional imaging tool for RT.

Material and Methods: The study assessed 118 stage III lung cancer patients. 4DCT images, spatial registration and a density-change based model were used to compute a 4DCT-ventilation map for each patient. Full 4DCT-ventilation assessment included: 1) comparison of 4DCT-ventilation against nuclear medicine ventilation (VQ) imaging and pulmonary function tests (PFT) 2) an analysis to determine whether dose to highly ventilated regions of the lung was a better predictor for toxicity than dose alone and 3) an evaluation of the percentage of lung cancer patients with significant ventilation defects. 4DCT-ventilation was compared to VQ imaging and PFTs using radiologist observations, sensitivity and specificity analysis, and correlation coefficients. Bootstrap methods were used to evaluate whether ventilation-based dose-function metrics were a better predictor for grade 3 radiation pneumonitis than dose metrics alone. Radiologists assessed the percentage of patients with significant ventilation defects with the idea that if patients had homogenous ventilation there would be no basis to preferentially spare any regions; conversely functional avoidance can be done for patients with ventilation defects.

Results: Comparing radiologist noted defects between 4DCT-ventilation and VQ imaging, we calculated a sensitivity, specificity, and accuracy of 90%, 64%, and 81% respectively. Correlation coefficients comparing 4DCT-ventilation to PFTs ranged from 0.63-0.72. Bootstrap results suggested an improvement in toxicity prediction using dose-function metrics compared to dose alone (p=0.11). Clinical ventilation defects were noted in 69% of our study cohort.
Conclusion: Our study demonstrates that 4DCT-ventilation provides clinically meaningful lung function information, is a better predictor of toxicity than dose alone, and that a significant portion of patients have substantial ventilation defects. Our work provides the largest and most comprehensive study to fully evaluate 4DCT-ventilation as a thoracic functional imaging tool and presents strong evidence for the incorporation of 4DCT-ventilation into prospective clinical trials.

OC-0415

The effect of breathing motion on CT radiomics feature extraction in oesophageal cancer

R.T.H.M. Larue[1], L. Van De Voorde[1], R.T.H. Leijenaar[1], M. Berbée[1], M.N. Sosef[2], W.J.C. Van Elmpt[1], P. Lambin[1]
[1]*Maastricht University Medical Centre, GROW School for Oncology and Developmental Biology - Department of Radiation Oncology - MAASTRO clinic, Maastricht, The Netherlands*
[2]*Zuyderland Medical Centre, Department of Surgery, Heerlen/Sittard, The Netherlands*

Purpose or Objective: Medical imaging plays a crucial role in response evaluation due to its non-invasive character and wide applicability and availability. Next to the routinely used metrics (e.g. RECIST), extraction of a large number of quantitative radiomics features might unravel more information in these medical images. To quantify the reliability of these features across different phases in the breathing cycle, the stability of 59 radiomics features in respiratory-correlated 4D CT-scans of patients with oesophageal cancer was investigated. Since the tumour does not change during image acquisition, quantitative features derived from it should not change either. Hence, we

hypothesised that 4D-RCCT provides a valuable means to identify the most reliable features.

Material and Methods: Twenty-five oesophageal cancer patients (stage IB-IIIC) who received a 4D-RCCT scan for radiotherapy planning between October 2012 and March 2014 were included in this study. The gross tumour volume (GTV) of the primary tumour was delineated on the 50% exhale (50ex) CT phase using all available diagnostic information. The delineations were copied to the CT images of the other breathing phases: 0in, 25in, 50in, 75in, 100in, 25ex and 75ex. Next 15 first-order statistics and 44 textural radiomics features were calculated for the GTV. For each feature, the pairwise intra-class correlation coefficient (ICC) between all possible phase combinations was calculated. Features with a pairwise ICC-value of at least 0.85 between all phase combinations were considered to have an acceptable stability throughout all phases of the breathing cycle.

Results: Of the 44 textural features, 12 (27%) were not susceptible to breathing motion (ICC>0.85). Also 9 out of the 15 (60%) first-order statistics features turned out to be stable. The statistics-energy and graylevel-nonuniformity (GLN) features, found to be prognostic in both head-and-neck and lung cancer [Aerts et al. Nat. Commun. 5 (2014)], were among the most stable features with minimum ICC-values of 0.98. In general, the highest ICC-values were observed when two adjacent phases (e.g. 50ex-75ex) were compared.

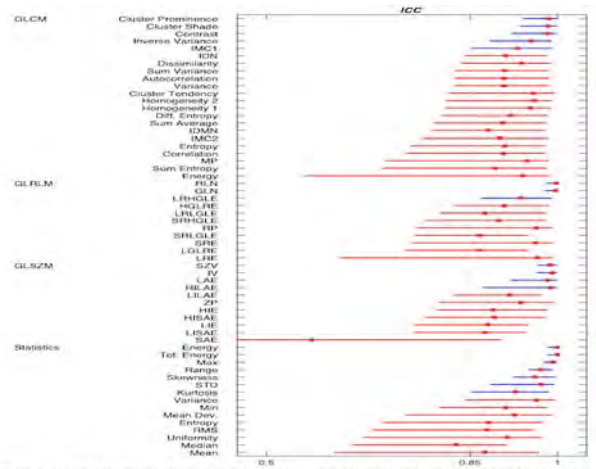

Figure 1. Graphical representations of the pairwise ICCs for all phases of the 4D-RCCT scan. The horizontal lines extend from the minimum to the maximum observed values per feature, and are blue when every ICC > 0.85. The red dots represent the median. Features are, for each feature group, ranked by their minimum ICC-value. Abbreviations for the textural feature groups: gray-level co-occurrence (GLCM), gray-level run-length (GLRLM) and gray-level size-zone (GLSZM).

Conclusion: This study identified nineteen CT radiomics features that were not subject to breathing motion in patients with oesophageal cancer. The remaining features were affected by the differences in breathing phase. This emphasises the importance of tumour-site specific feature selection together with a strict imaging and delineation protocol before using them for further clinical applications.

OC-0416

FDG-PET can objectively quantify esophageal dose-response and toxicity during radiation therapy

J. Niedzielski[1], Z. Liao[2], R. Mohan[1], J. Yang[1], F. Stingo[3], D. Gomez[2], M. Martel[1], T. Briere[1], L. Court[1]

[1]*University of Texas-MD Anderson Cancer Center, Radiation Physics, Houston, USA*

[2]*University of Texas-MD Anderson Cancer Center, Radiation Oncology, Houston, USA*

[3]*University of Texas-MD Anderson Cancer Center, Biostatistics, Houston, USA*

Purpose or Objective: To use FDG-PET uptake during treatment course to objectively quantify esophagitis severity, understand esophageal dose response, and examine the timing of increased PET uptake and esophagitis symptoms for possible early detection of eventual toxicity.

Material and Methods: FDG-PET scans were acquired for 71 NSCLC patients during concurrent chemoradiotherapy, at fraction 23 on average. PET uptake was normalized to the mean SUV of esophageal voxels receiving < 5 Gy, creating normalized PET uptake (nSUV) as a patient specific radiation response. Localized measures of nSUV were correlated to esophagitis grade during PET scan and max treatment grade, scored with CTCAE 4.0, using logistic regression. Performance was measured with AUC from ROC analysis. Voxel esophageal dose response curves of nSUV were created for analysis conducted with DVH metrics. Spearman rank analysis was used to determine the dose correlation to nSUV and toxicity. The timing of nSUV and esophagitis presentation was examined. Preemptive detection of toxicity was studied using asymptomatic patients at time of PET scan, examining these patients esophagitis severity by treatment end, and analyzing any differences in nSUV values or dose response; statistical difference was tested with the Mann Whitney U test.

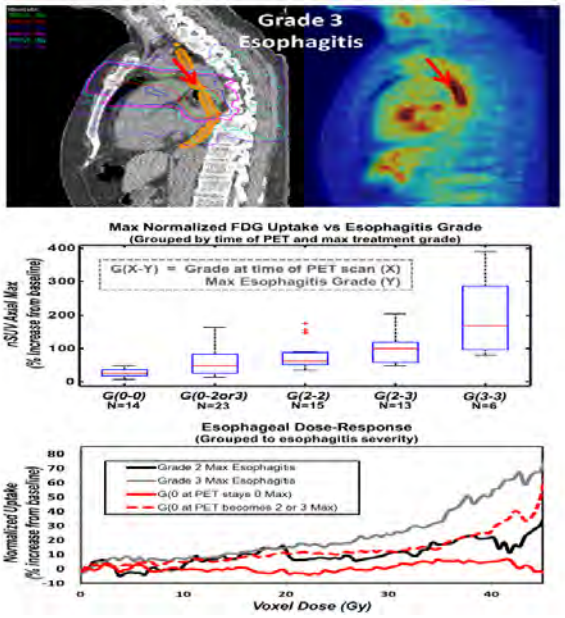

Table 1: Statistical Analysis of nSUV metrics and ≥ grade 2 esophagitis endpoint. Likelihood ratio chi square test was used to calucalte p-values.

Mid-Tx Grade 2			
nSUV Metric	**Pval**	**AUC**	**nSUV 50% NTCP**
NormSUV Mean (%)	2.11E-05	0.84	31.0
nSUV Axial Max 1-Slice (%)	9.78E-05	0.83	150.2
Length ≥ 40% nSUV (mm)	8.16E-05	0.83	28.6
nSUV 90th Percentile (%)	2.42E-05	0.83	89.8
Max Grade 2			
nSUV Metric	**Pval**	**AUC**	**nSUV 50% NTCP**
NormSUV Mean (%)	4.09E-05	0.86	4.9
nSUV Axial Max 1-Slice (%)	1.26E-06	0.90	92.5
Length ≥ 40% nSUV (mm)	6.52E-08	0.91	0.0
nSUV 90th Percentile (%)	1.17E-06	0.91	75.9

Results: Normalized PET uptake was significantly correlated to esophagitis grade both at the time of the PET study and max treatment grade, for both grade 2 and grade 3 endpoints. Increased nSUV occurs before esophagitis presentation. The highest performing nSUV metrics were axial max nSUV, and esophageal length with nSUV 40% increase from baseline, with both $p < 0.001$ and AUC ≥ 0.83 (Table 1). DVH metrics were poorly correlated to nSUV or toxicity and several patients that were grade 0 throughout treatment had DVH values comparable to patients who developed esophagitis, but had low nSUV values. Esophageal dose-response curves grouped according to max esophagitis

grade showed no response in the Grade 0 cohort. Response in grade 2 and grade 3 groups starts at approximately 30-35 Gy and had considerable inter-patient variability. For max esophagitis severity prediction, nSUV metrics and dose-response curves were statistically different between grade 0 patients at time of PET scan that remained grade 0 by treatment completion, and those eventually becoming grade 2, with flat dose-response curve and increasing approximately 2nd order, respectively (Fig. 1c).

Conclusion: Normalized uptake strongly correlates to esophagitis, both at time of FDG-PET scan and by the end of treatment. Normalized uptake gives an objective quantification of esophageal toxicity with geometric information. PET scans acquired early in treatment may predict esophagitis severity.

OC-0417

Functional imaging using dual energy Computed Tomography and its application in radiation oncology

A. Lapointe[1], M.B. Besnier[2], D.B. Blais[1], H.B. Bahig[1], J.G. De Guise[3], J.F.C. Carrier[1], E.F. Filion[1], D.R. Roberge[1], S.B. Bedwani[1]

[1]*Centre Hospitalier de l'Université de Montréal, Radio-oncologie, Montréal, Canada*

[2]*Centre Hospitalier de l'Université de Québec, Radio-oncologie, Québec, Canada*

[3]*Centre de Recherche du Centre Hospitalier de l'Université de Montréal, Laboratoire de Recherche en Imagerie et Orthopédie, Montréal, Canada*

Purpose or Objective: The objective of this project is to evaluate pulmonary and renal relative function by analysing the iodine concentration extracted from a dual energy CT (DECT) scan with injection of a contrast agent. The evaluation of parallel organs' functionality such as kidney and lung is usually derived from DMSA and perfusion scintigraphy. However, such techniques have spatial and temporal resolutions generally inferior to those of a CT scan. Our approach exploits DECT imaging, which allows in a single acquisition to combine the anatomical image to the organ function as determined by its iodine concentration. This functional cartography has a clinical potential to improve the planning of radiotherapy treatments considering new functional constraints.

Material and Methods: Two cohorts of 11 and 8 patients (kidney and lung, respectively) received a scintigraphy and a DECT scan (SOMATOM Definition Flash, Siemens) with intravenous iodine injection. The iodine concentration is evaluated with the principle of the three material decomposition that was implemented in MATLAB (MathWorks). This technique quantifies in each voxel of the DECT scan the proportion of each material defined in a basis specific to a targeted site (kidney and lung for instance). The evaluation of the differential function is also adapted to each type of organ previously segmented by an expert to only consider the presence of iodine relevant to the function. A functional cartography is also generated to segment each organ in regions more or less functional.

Results: The results show that the relative functions obtained by scintigraphy and DECT correlate well with a Pearson of 0.8 for lung. The most functional regions of the lung have an average of 2.68 mg/mL and 0.30 mg/mL for the least functional, whereas for the kidney 8.95 mg/mL and 0.36 mg/mL. In some cases, the absence of iodine in specific locations were easily ascribed to dysfunctional sections of the organ such as cancerous tumors, abnormal pulmonary lobe and kidney cysts. The following figure shows how (left) a mixed image provided by a DECT scan can be converted into (middle) an iodine concentration map and further processed into (right) a map of functional regions.

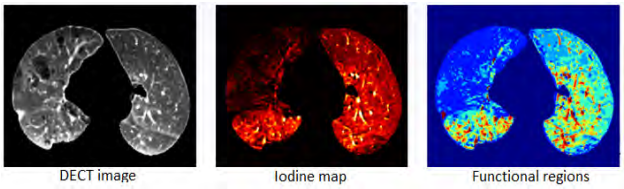

DECT image | Iodine map | Functional regions

Conclusion: The extraction of iodine concentration maps from injected DECT scan was achieved to evaluate the differential function of lungs and kidneys. Therefore, our DECT analysis tool provides functional information in addition to the high resolution DECT images. Further improvement in the analysis tool will include advanced algorithms to perform segmentation and 3D model to address functionality according to specific sections of an organ. Further work will also incorporate the functional information to radiation oncology treatment planning decisions to eventually spare further functional tissue and reduce the toxicity.

OC-0418

Cluster analysis of DCE MRI reveals tumor subregions related to relapse of cervical cancers

T. Torheim[1], A.R. Groendahl[1], E.K.F. Andersen[2], H. Lyng[3], E. Malinen[4], K. Kvaal[1], C.M. Futsaether[1]

[1]*Norwegian University of Life Sciences NMBU, Dept. of Mathematical Sciences and Technology, Ås, Norway*

[2]*Soerlandet Sykehus HF, Dept. of Radiology, Kristiansand, Norway*

[3]*Oslo University Hospital, Dept. of Radiation Biology, Oslo, Norway*

[4]*University of Oslo, Dept. of Physics, Oslo, Norway*

Purpose or Objective: Solid tumors are known to be heterogeneous, often consisting of regions with different treatment response. Early detection of treatment resistant regions can improve patient prognosis, by enabling implementation of adaptive treatment strategies. In this study, K-means clustering was used to group voxels in dynamic contrast enhanced (DCE) MR images of cervical cancer tumors. The aims were to explore the intratumor heterogeneity in the MRI parameters and investigate whether any of the clusters reflected treatment resistant regions.

Material and Methods: Eighty-one patients with locally advanced cervical cancer treated with chemoradiotherapy underwent pre-treatment DCE MRI. The resulting image time series were fitted to two pharmacokinetic models, the Tofts model (*Ktrans* and *ve*) and the Brix model (*ABrix*, *kep* and *kel*). K-means clustering was used to cluster similar voxels based on the pharmacokinetic parameter maps or the relative signal increase (RSI) time series. The association between clusters and treatment outcome (progression-free survival, locoregional control or metastasis-free survival), was evaluated using the volume fraction of each cluster or the spatial distribution of the cluster.

Results: We identified three voxel clusters based on the Tofts parameters, all significantly related treatment outcome. One voxel cluster based on the Brix model was significantly linked to progression-free survival and metastatic relapse. Two RSI based cluster were significantly related to all types of treatment outcome.

Conclusion: Based on either pharmacokinetic parameter maps or relative signal increase time series, we were able to group the voxels into cluster that were associated with treatment outcome. With the exception of one cluster, the spatial distribution rather than the volume fraction of each cluster was significant.

OC-0419

Association between pathology and texture features of multi parametric MRI of the prostate

P. Kuess[1], D. Nilsson[2], P. Andrzejewski[1], J. Knoth[1], P. Georg[3], M. Susani[4], D. Georg[1], T. Nyholm[5]

[1]*Medizinische Universität Wien Medical University of Vienna, Department of Radiation Oncology and Christian Doppler Laboratory for Medical Radiation Research for Radiation Oncology, Vienna, Austria*
[2]*Umea University, Computational Life Science Cluster CliC-Department of Chemistry, Umea, Sweden*
[3]*EBG Med Austron GmbH, Medical Department and Christian Doppler Laboratory for Medical Radiation Research for Radiation Oncology, Wiener Neustadt, Austria*
[4]*Medizinische Universität Wien Medical University of Vienna, Clinical Institute of Pathology, Vienna, Austria*
[5]*Umea University, Department of Radiation Sciences-Radiation Physics, Umea, Sweden*

Purpose or Objective: The aim of this study was to find a correlation between multiparametric (mp) MRI derived quantitative imaging parameters (textual features) and pathological verified tumor occurrence. Textual feature analysis (TFA) as a method for quantifying the spatial distribution of intensities in images has already shown promising results in the field of diagnostic oncology and also as biomarker for treatment response.

Material and Methods: 25 prostate cancer patients which underwent prostatectomy were investigated in this study. Multiparametic MRI were collected prior to the surgical procedure. Along with T2 weighted images, dynamic-contrast-enhanced (DCE-MRI) (KTrans, AUC) and diffusion-weighted MRI (DW-MRI) with its estimated apparent diffusion coefficient (ADC) were recorded. The resected prostate was axial cut in slices of 3-4 mm thickness and the tumor was tagged by a pathologist. On the T2 images delineation of the central gland (CG) and the peripheral zone (PZ) was performed by two physicians. Additional, the prostate was divided into 22 geometrical substructures following the PIRADS classification. Hence, the tagged tumor area on the pathological slices could be assigned to the respective substructure on the MRI where it was scored into distinct levels according to the volume covered by malignant tissue. For each geometrical substructure texture analysis was performed using gray level co-occurrence matrix (GLCM). Additional to the textual parameters also histogram based information (gray value) was investigated. The large amount of information created by the TFA was analyzed with principal component analysis (PCA). For each image modality, the 23 textural parameters were compressed into two principal components, which explained most of the variation found in the data. Prior to analysis, each variable was mean centered and also scaled to unit variance.

Results: The TFA showed a significant difference between substructures in the CG and PZ. A correlation was found between the pathological findings and the texture of the ADC map as shown in fig 1a, where the larger dots represent substructures with confirmed tumor occurrence. For the other investigated modalities the correlation was weaker or absent. Based on the score plot (fig 1a) ROC curves were calculated (fig1b) resulting in an AUC of 0.789 for ADC considering the highest tumor scores only.

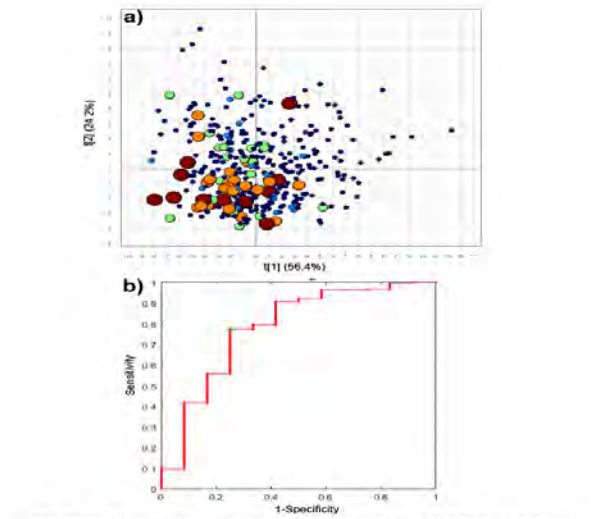

Fig.1 Scatter Plot (a) and resulting receiver operating characteristics curve (b) for textual feature analysis of ADC maps evaluating the PZ of prostate cancer patients. The larger dots in the scatter plot represent geometrical substructures with pathologically confirmed tumor occurrences, where the colors light blue, green, orange and red symbolize the four levels of tumor scores (in increasing order) and blue illustrates structures without tumor. The area under the ROC curve is 0.789.

Conclusion: The current study indicates that ADC mapping is the most promising MRI technique to predict the tumor location in the prostate based on TFA and therefore is absolute prerequisite for dose painting approaches in advanced adaptive radiotherapy (ART).

OC-0420

Radiomics in OPSCC: a novel quantitative imaging biomarker for HPV status?

R.T.H. Leijenaar[1], S. Carvalho[1], F.J.P. Hoebers[1], S.H. Huang[2], B. Chan[2], J.N. Waldron[2], B. O'Sullivan[2], P. Lambin[1]
[1]*Department of Radiation Oncology MAASTRO clinic, GROW - School for Oncology and Developmental Biology- Maastricht University Medical Centre, Maastricht, The Netherlands*
[2]*Department of Radiation Oncology- Princess Margaret Cancer Center, University of Toronto, Toronto, Canada*

Purpose or Objective: Oropharyngeal squamous cell carcinoma (OPSCC) is one of the fastest growing head and neck cancers, for which human papillomavirus (HPV) status has been described as a strongly prognostic factor. Overall, prognosis is favorable for HPV positive (HPV+) patients, which makes this an interesting subgroup for de-escalation protocols. An established, non-invasive, imaging biomarker of HPV status currently does not exist. Radiomics–the high-throughput extraction of large amounts of quantitative features from medical images–has already been shown to be of prognostic value for head and neck cancer. In this study we evaluate the use of a Radiomic approach to distinguish between HPV+ and HPV negative (HPV-) OPSCC patients.

Material and Methods: A total of 542 patients with OPSCC, treated with curative intent between 2005 and 2010 were collected for this study. HPV status was determined by p16 and available for 434 patients. Patients underwent pre-treatment CT imaging and the tumor volume was manually delineated for treatment planning purposes. Images were visually assessed for the presence of CT artifacts (e.g. streak artifacts due to dental fillings) within the GTV, in which case they were excluded from further analysis. In total, 241 Radiomic features were extracted, comprising: a) first-order statistics, b) shape, and c) (multiscale) texture by Laplacian of Gaussian filtering. The Radiomic feature space was first reduced by selecting cluster medoids after hierarchical cluster analysis using correlation (ρ>0.9) as a distance measure. Multivariable logistic regression was performed using least absolute shrinkage and selection operator (LASSO) model selection (100 times 10-fold cross-validated). The area under the receiver operator curve (AUC; 500 times bootstrapped) was used to assess out-of-sample model performance in predicting HPV status.

Results: Out of the patients with known HPV scoring, we identified 211 (49%) patients without visible CT artifacts, of which 134 were HPV positive. The modeling process resulted in an eleven-feature multivariable prediction model. The overall receiver operator curve is shown in Figure 1. The bootstrapped AUC was on average 0.77 (95% CI: 0.73-0.80).

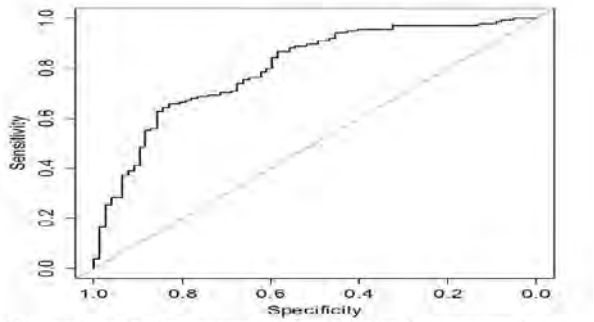

Figure 1: Receiver operator curve for HPV status prediction in OPSCC patients. Bootstrapped (500 times) AUC: 0.77 (95% CI: 0.73-0.80).

Conclusion: Using a Radiomic approach, we were able to distinguish between HPV+ and HPV- OPSCC patients, using standard pre-treatment CT imaging. These results require further validation, but suggest the potential for a novel quantitative Radiomic biomarker of HPV status, facilitating personalized treatment selection.

Symposium: Adaptive treatments in the pelvic region

SP-0421
Brachytherapy pelvic and MRI-Linac combination

C.N. Nomden[1], A.A.C. De Leeuw[1], B.W. Raaymakers[1], J.J.W. Lagendijk[1], I.M. Jürgenliemk-Schulz[1]
[1]*UMC Utrecht, Radiation Oncology, Utrecht, The Netherlands*

MRI guidance for the radiation treatment of patients with cancer in the pelvic region has globally increased during the last two decades. MRI is used for staging, treatment planning, monitoring of treatment response and for disease observation during follow up. Consistent and repetitive use of MRI has provided insight into tumour and surrounding organ anatomy as well as their movements and deformations. In cervical cancer treatment, MRI guidance for brachytherapy treatment planning and dose delivery allowed better tailoring of the dose to the target, with higher tumour doses while sparing the organs at risk (OARs). However, the aimed dose for target and OARs may differ from the actually delivered dose due to movements and deformations of the OARs during HDR or PDR treatments. Several single institution reports describe that dose uncertainties caused by displacement and deformations of OARs are on average small, however individual outliers occur. Especially for the rectum higher delivered doses have been found in individual patients. In case of HDR brachytherapy, re-imaging prior to dose delivery can help to detect unfavourable anatomical changes, allowing for interventions that might help to stabilize dosimetry and prevent morbidity. The availability of MR imaging within the brachytherapy suite is an upcoming innovation that supports these types of adaptive brachytherapy approaches. The aim of the international 'EMBRACE study' (*www.embracestudy.dk)* was to introduce MRI based brachytherapy in a multicentre setting within a prospective observational setting and to correlate DVH parameters with outcome. Preliminary results from EMBRACE, from the retrospective 'Retro-EMBRACE' study (www.retroembrace.com) and from several single institution reports, revealed an increase in local control due to the use of MRI guidance. Brachytherapy treatment allows delivery of sterilizing doses to the primary cervical tumour, however, lymph node disease is getting the dose delivered by external beam radiotherapy treatment (EBRT). The upcoming prospective multicentre 'EMBRACE II study' will focus on advanced Image Guided and Adaptive EBRT (IGART) combined with MRI guided intracavitary/interstitial brachytherapy with the aim to improve loco-regional control and survival, however not at the expense of treatment related morbidity. Besides nodal disease detection, monitoring nodal disease during treatment is stil a remaining challenge. Node positions and volumes can change during the course of treatment asking for EBRT strategies that are able to follow these changes in order to allow tight treatment margins. Unfortunately the visibility of lymph nodes on cone beam CT images is limited and shifted and shrunken lymph nodes can be missed. The superior soft tissue contrast of MRI based position verification as realized in the concept of integrated MRI and linear accelerator (MR-Linac) decreases the uncertainties around nodal disease development during the course of radiotherapy, allows a more precise definition of nowadays accepted elective treatment margins and might allow an additional boost to individual lymph nodes . Currently, an MR-Linac system is built at the radiation oncology department at the UMC Utrecht, bringing the ultimate combination of MRI guided brachytherapy, advanced adapted external beam treatment with concurrent cisplatin based chemotherapy and MR-Linac treatment for nodal disease within reach for the treatment of patients with advanced cervical cancer.

SP-0422
Clinical implementation of ART for cervix

Y. Seppenwoolde[1], M. Buschmann[1], M. Daniel[1], K. Majercakova[1], D. Georg[1]
[1]*Christian Doppler Laboratory for Medical Radiation Research for Radiation Oncology- Medical University Vienna- Austria, Radiation Oncology, Vienna, Austria*

For patients with cervical cancer, despite the improved dose conformity enabled by IMRT and VMAT, sparing of bladder, rectum and small bowel is still challenging because all organs at risk (OAR) in the pelvic area change shape and position on a daily basis due to variations in filling. With the introduction of cone-beam CT scanners it became possible to observe the internal organ variations of patients during each treatment fraction. Theoretically, this enables re-adaptation of plans according to tumour shrinkage and changes in OAR morphology, resulting in reduction of toxicity [1,2] and better target coverage. Full online plan adaptation requires that re-delineation, re-optimizing of dose distributions and repetition of all legally required quality assurance steps should be performed in a few minutes. These workload intensive procedures would require a high degree of automation and workflow-integration that is currently absent in off-the-shelf products.

Nonetheless, by finding a well-balanced compromise between full automation and degree of plan adaptation, it is possible to apply a simplified scheme of adaptation that provides improved treatment. Based on our own experience and that of other research groups [3], patients can be divided into two groups: the first group consists of patients who show uterus motion as a function of bladder filling (called "Movers") and the second group are those patients whose uterus position stays relatively stable, regardless of bladder volume ("Non-Movers"). With a model for the uterus position, a pre-determined set of plans (library) can be constructed for the "Movers" and the most appropriate treatment plan can be selected on a daily basis with the help of CBCT scans, while for the "Non-Movers" a single plan will suffice.

The patient specific relation between bladder filling and the position of the uterus can be assessed by making a set of CT scans with full and empty bladder. A two stage approach, consisting of two treatment plans, one for an empty to half full and one for half full to full bladder, has been shown to give a good level of plan adaptiveness [2], ensuring both a good tumor coverage as sparing of the surrounding healthy tissue.

Commercially available clinical software that is designed for organ contouring and treatment plan optimization does not provide solutions to generate new contours based on a motion model that interpolates between two extreme (filling) positions of an organ. We developed a MATLAB-based tool that allows generating intermediate contours of uterus as well as bladder, according to the available bladder

volumes. Its main purpose was to interpolate linearly between two extreme positions and/or filling states of patient's organ contours. Non-rigid deformation between one organ position and the other was made by matching the outer contour of both structures. To facilitate data handling and DICOM import/export options, the Matlab code was integrated to 3DSlicer/SlicerRT (Freeware for image handling) by using MatlabBridge.
Our first adaptive patient was treated in October 2016 and in this presentation we will discuss our experience we gained since then, the challenges we encountered and the risks that remain with the implemented procedure. Furthermore, dosimetric results of different ART schemes as well as open issues like non-rigid dose addition for evaluation will be discussed.
[1] Bondar L, Hoogeman M, Mens JW, Dhawtal G, De Pree I, Ahmad R, et al. Toward an individualized target motion management for IMRT of cervical cancer based on model-predicted cervix-uterus shape and position. Radiother Oncol 2011;99:240–5.
[2] Heijkoop S, Langerak T, Quint S. Clinical Implementation of an Online Adaptive Plan-of-the-Day Protocol for Nonrigid Motion Management in Locally Advanced Cervical Cancer IMRT. IJORBP 2014;90:673–9.
[3] Ahmad R, Hoogeman MS, Bondar M, Dhawtal V, Quint S, De Pree I, et al. Increasing treatment accuracy for cervical cancer patients using correlations between bladder-filling change and cervix-uterus displacements: Proof of principle. Radiother Oncol 2011;98:340–6.

SP-0423

Implementation of daily plan selection in rectum

R. De Jong[1], L. Lutkenhaus[1], N. Van Wieringen[1], J. Visser[1], J. Wiersma[1], K. Crama[1], D. Geijsen[1], A. Bel[1]
[1]Academic Medical Center, Department of Radiation Oncology, Amsterdam, The Netherlands

The standard of care for non-metastasized locally advanced rectal cancer is chemo-radiotherapy combined with surgery. Sparing the organs at risk (OAR) with the use of state-of-the-art planning techniques like intensity-modulated radiation therapy (IMRT) or volumetric modulated arc therapy (VMAT) is compromised by the large population-based margins that are necessary to compensate for the shape changes of the target volume over the time of treatment. In rectum patients, day-to-day variation in rectum and bladder filling often causes large deformation of the target volume, especially the mesorectal fat (mesorectum), which cannot be corrected for with a table adjustment. Minimizing shape changes with the use of drinking protocols to manage bladder filling or dietary instruction to manage bowel motion have been unsuccessful.
A strategy with multiple plans made prior to treatment tailored to a range of possible shapes can mitigate the variations in target volume, by selecting the best-fitting plan based on daily Cone Beam CT (CBCT) scans. This strategy has been successfully applied in the treatment of bladder and cervical cancer where bladder filling is the predominant factor of shape changes. To create multiple plans a full and empty bladder pretreatment CT scan is acquired from which a patient specific motion model is derived which is used to create intermediate target volume structures.
In rectum cancer, however, shape changes are mostly driven by changes in rectum volume and shape and to a much lesser extent by bladder filling. Because of this creating multiple plans based on varying bladder filling is not useful. Therefor our strategy to create multiple plans for plan selection is to apply different PTV margins to the ventral side of the mesorectum based on a single CT scan. This will also coop with the shape changes that are encountered.
Plan selection based on daily Conebeam CT (CBCT) images require adequate visibility of the regions of interest. In the pelvic region CBCT image quality can be hampered by imaging artefacts caused by moving air or bowel. At the same time identifying the boundaries of a complex target volume such as the target volume for rectum cancer can be challenging. Uniform plan selection is realized by participation in an observer study where all observers perform the selection procedure for a set of patients. Subsequently, the choices are discussed in the group of observers and a set of selection rules is composed. In this lecture we will discuss the plan selection strategy for rectum cancer and its introduction in the clinic.

Poster Viewing : 9: Radiobiology

PV-0424

Cyclin D1 silencing radiosensitises prostate cancer cells by impairing DNA-DSBs repair pathways.

F. Marampon[1], G. Gravina[1], C. Festuccia[1], A. Colapietro[1], E. Di Cesare[1], E. Tombolini[2]
[1]University of L'Aquila, of Biotechnological and Applied Clinical Sciences, L'Aquila, Italy
[2]Policlinico Umberto I "Sapienza" University of Rome, od Radiotherapy, Rome, Italy

Purpose or Objective: Patients with hormone-resistant prostate cancer (PCa) have higher biochemical failure rates after radiation therapy. Cyclin D1 deregulated expression in PCa is associated with a more aggressive disease however its role in radioresistance has not been determined.

Material and Methods: Cyclin D1 levels in the AR-negative, androgen-independent PC3 and AR-positive, androgen-independent 22Rv1 cells were stably inhibited by transfection with Cyclin D1-short hairpin RNA (shRNA). Tumorigenicity and radiosensitivity were investigated using *in vitro* and *in vivo* experiments.

Results: Independently by AR-expression, Cyclin D1 silencing interfered with PCa oncogenic phenotype by inducing growth arrest in the G1 phase of cell cycle and reducing soft agar colony formation, migration, invasion, tumor formation and neo-angiogenesis in xenografted mice. *In vitro* colony formation and *in vivo* tumor growth of the PCa xenografts were significantly inhibited by Cyclin D1 silencing combined with radiotherapy. Cyclin D1 silencing radiosensitizes PCa cells by impairing the NHEJ and HR pathways responsible of the DNA double-strand break repair. Cyclin D1 directly interacts with activated-ATM, -DNA-PKC and RAD51 that are downstream targets of Cyclin D1-mediated PCa cells radioresistance.

Conclusion: Taken together, these observations suggest a Cyclin D1 role in radioresistance mechanism. Cyclin D1 could represents a potential target for radioresistent androgen-sensitive or not prostate cancer cells.

PV-0425

EEF2K promotes progression and radioresistance of esophageal squamous cell carcinoma

H.C. Zhu[1], X. Yang[1], X.L. Ge[1], J.Y. Chen[1], H.M. Song[1], J. Liu[1], Z.L. Pei[1], M.Q. Chen[1], X.C. Sun[1]
[1]The First Affiliated Hospital of Nanjing Medical University, Radiation Oncology, Nanjing, China

Purpose or Objective: We investigated the effects of eukaryotic elongation factor 2 kinase (EEF2K) in esophageal squamous cell carcinoma (ESCC) and its role in radiosensivity.

Material and Methods: We used quantitative real-time polymerase chain reaction and immunohistochemistry analyses to compare expression of EEF2K between paired ESCC samples and nontumor esophageal tissues. Lentivirus was used to overexpress and knockdown of EEF2K gene and stable transmitted cell line of ECA109 and TE13 were made. In vitro cell counting kit 8 and clone formation assay were used to detect cell viability and proliferation. Wound-healing migration assay, transwell invasion assay three-dimensional culture and tube formation assay were used to investigate invasion, metastasis and angiogenesis of ESCC. Radioresponse was primary examined by clone formation assay after exposure of 0, 2, 4, 6, 8 Gy X-ray by a medical accelerator of different stable cell lines. Then apoptosis, cell-cycle arrest, and γ-H2AX expression were examined in 0 Gy and 8 Gy in

the overexpressed and knockdown ESCC cell line by flow cytometer and immunoflourence. Gene-chips and western blot were used to investigate molecular mechanism. In vivo experiments of xenografts were used to confirm the results.

Results: Levels of eEF2K were increased 52.17% of ESCC samples compared with matched nontumor tissues, as well as ESCC cell lines. Increased levels of eEF2K were associated with ESCC survival times of patients ($P<0.05$). eEF2K expression correlated between tumor size and TNM stage in primary ESCC during clinicopathological feature analysis ($P<0.05$). EEF2K promotes ESCC proliferation and tumorgeneity in vitro and in vivo. Improved invasion, metastasis and angiogenesis were also seen in EEF2K overexpressed cells compared with control in TE13 and ECA109 cell lines. An improved radioresponse was detected in eEF2K knockdown cells which could also be induced by NH125, an eEF2K inhibitor. Affymetrix GeneChip were used in EEF2K overexpressed ECA109 and control cells in normal conditions and 8 Gy of irradiation and autophagy pathways were detected by bioinformatic analysis. Improved protein expression of Atg5, mTOR, LC3, and TP53 were confirmed by western blot. In xengraft radiosensivity experiments, an enhancement factor of 1.78 was seen in ECA109 bearing nude mouse by NH125, along with a reduction of tumor doubling time. Immunohistochemistry and immunofluorescence of tumor tissue confirmed the molecular mechanism of autophagy pathway.

Conclusion: EEF2K is overexpressed in ESCC and associated with progression and shorter survival times of patients. Decreased expression of EEF2K correlated with a reduction of malignancy in biological behavior and an improvement of radioresistance in ESCC, which may be mediated by autophagy signaling pathway. Targeting EEF2K may be a potential therapeutic approach of ESCC in the future.

PV-0426

Targeting PI4K for radiosensitisation: a viable model of drug repositioning

I.A. Kim[1], J. Kwon[2], Y. Park[2], D. Kim[3], J. Park[3]
[1]*Seoul National Univ. Bundang Hospital, Radiation Oncology, Seongnam- Gyeonggi-Do, Korea Republic of*
[2]*Seoul National University Graduate School of Medicine, Radiation Oncology, Seoul, Korea Republic of*
[3]*Seoul National Univ. Bundang Hospital, Medical Science Reseach Institute, Seongnam- Gyeonggi-Do, Korea Republic of*

Purpose or Objective: Phosphatidylinositol 4-phosphate (PI4P), upstream regulator of both phospholipase C (PLC)/Protein Kinase C (PKC) and phosphatidylinositol 3-kinase (PI3K) / serine/threonine-protein kinases (Akt) pathways which control the cell motility and proliferation, is produced by phosphatidylinositol 4-kinase (PI4K). Thus, an inhibition of PI4K could inactivate these two PI4P dependent pathways simultaneously. In this study, we tried to identify that which isotype of PI4K may affect a radiosensitivity using RNA interference (RNAi) and also to investigate anti-hepatitis C viral (HCV) agents which are known to inhibit PI4K activity, could be repositioned as a radiosensitizer in human breast cancer, glioblastoma and hepatoma models.

Material and Methods: A panel of human cancer cell lines including U251 malignant glioma cells, BT474 breast cancer cells, and HepG2 hepatocellular carcinoma cells were used. RNAi was used to specific inhibition of each isotype of PI4K and clonogenic assay was performed to assess the radiosensitizing effect of each isotype. To select an anti-HCV agent for pharmacologic inhibition of PI4K, IC50s of nine commercial antiviral agents were determined. Specific inhibitory effect on PI4K isotype was determined by *in vitro* kinase assay. Radiosensitizing effect of the selected anti-HCV agents were tested by clonogenic assay *in vitro* and tumor xenograft model *in vivo*, respectively. Immunoblotting, immunocytochemistry, and invasion/migration assay were performed to identify the mechanism of radiosensitization.

Results: First, we identified that specific inhibition of PI4K IIIα using RNAi increased radiosensitivity in the human cancer cell lines we tested. In contrast, inhibition of other isotypes did not affect a radiosensitivity of these cancer cell lines. Next, *in vitro* kinase assays showed, simeprevir, a selected anti-HCV agent via IC50 assay, inhibited activity of PI4K IIIα in a dose-response manner. Pretreatment of simeprevir induced discernible downregulation of p-PKC and p-Akt and also increased clonogenic survival of U251, BT474, and HepG2 cells *in vitro* and also significantly delayed growth of mouse tumor xenografts *in vivo*. Simeprevir caused prolongation of γH2AX foci after irradiation, decreased invasion / migration and downregulation of PD-L1 expression.

Conclusion: Targeting PI4K IIIα using anti-HCV agent could be a viable drug repositioning approach to enhance the therapeutic efficacy of radiotherapy for breast cancer, glioblastoma and hepatoma. (Work supported by grant #2013R1A1A2074531 from the Ministry of Science, ICT & Future Planning to Kim IA)

PV-0427

Real-time tumour oxygenation changes following a single high dose radiotherapy in mouse lung cancers

C. Song[1], B.J. Hong[2], S. Bok[2], C.J. Lee[2], Y.E. Kim[2], S.R. Jeon[3], H.G. Wu[3], Y.S. Lee[4], G.J. Cheon[4], J.C. Paeng[4], G.O. Ahn[2], H.J. Kim[3]
[1]*Seoul National Univ. Bundang Hospital, Radiation Oncology, Seongnam- Gyeonggi-Do, Korea Republic of*
[2]*Pohang University of Science and Technology, Division of Integrative Biosciences & Biotechnology, Pohang, Korea Republic of*
[3]*Seoul National University College of Medicine, Radiation Oncology, Seoul, Korea Republic of*
[4]*Seoul National University College of Medicine, Nuclear Medicine, Seoul, Korea Republic of*

Purpose or Objective: To investigate serial changes of tumor hypoxia in response to a single high dose irradiation by various clinical and pre-clinical methods in order to propose an optimal fractionation schedule for stereotactic ablative radiotherapy (SABR)

Material and Methods: Syngeneic Lewis lung carcinomas were grown either orthotopically or subcutaneously in C57BL/6 mice and were irradiated with a single dose of 15 Gy to mimic SABR used in the clinic. Serial [18F]-misonidazole (F-MISO) positron emission tomography (PET) imaging, pimonidazole FACS analyses, hypoxia-responsive element (HRE)-driven bioluminescence, and Hoechst 33342 perfusion were performed before irradiation (d-1), at 6 hours (d0), 2 (d2), and 6 days (d6) after irradiation for both subcutaneous and orthotopic lung tumors. For F-MISO, scan was performed 2 hr after the intravenous injection of F-MISO probe and the tumor-to-brain ratio (TBR) was analyzed.

Results: We observed that hypoxic signals were too low to quantitate for orthotopic tumors by F-MISO PET or HRE-driven bioluminescence imaging. In subcutaneous tumors TBR values were 2.87 ± 0.483 at d-1, 1.67 ± 0.116 at d0, 2.92 ± 0.334 at d2, and 2.13 ± 0.385 at d6, indicating that tumor hypoxia was decreased immediately after irradiation and returned to the pretreatment levels at d2, followed by a slight decrease by d6 post-radiation. Pimonidazole analysis also revealed similar patterns. By using Hoechst 33342 vascular perfusion dye and CD31 co-immunostaining, we found that there was a rapid and transient vascular collapse, which may have resulted in poor intratumoral perfusion of F-MISO PET tracer or pimonidazole delivered at d0 leading to decreased hypoxic signals at d0 by PET or pimonidazole analyses.

Figure 1

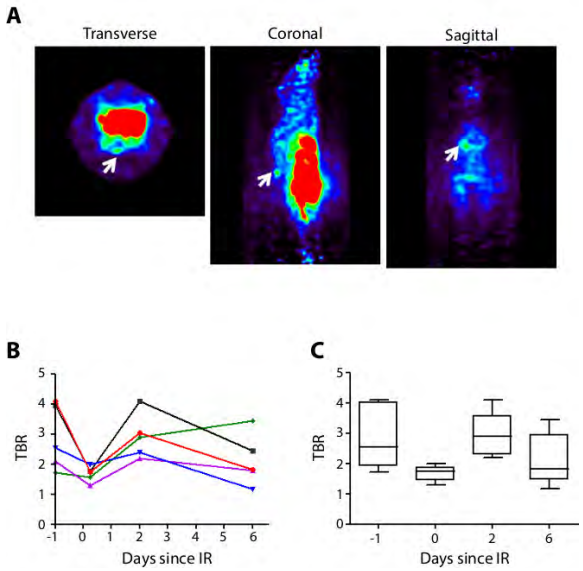

Fig. 1. Temporal changes in tumor hypoxia for subcutaneous tumors by F-MISO PET imaging. (A) Representative PET images demonstrating F-MISO uptake in subcutaneous tumor. Arrows indicate the tumor position. (B) A graph showing TBR values for an individual animal. (C) A graph showing the mean ± s.e.m. of TBR values (n = 5).

Conclusion: We found tumor hypoxia levels to be returned to the pretreatment levels by 2 days after irradiation, hence supporting the current fractionation intervals of SABR being given at least 2 days. Our results also indicate that SABR may produce a rapid but reversible vascular collapse in tumors.

PV-0428

Factor 2.5 radiosensitivity difference determined by ex vivo γH2AX assay in prostate cancer patients

C. De Colle[1,2], A. Menegakis[2,3], A.C. Mueller[2], A. Yaromina[4], J. Hennenlotter[5], A. Stenzl[5], M. Scharpf[6], F. Fend[6], U. Ricardi[1], M. Baumann[7,8,9], D. Zips[2,3]

[1]*Azienda Ospedaliero-Universitaria- Citta' della Salute e della Scienza di Torino- University of Turin, Radiation Oncology, Torino, Italy*

[2]*Medical Faculty and University Hospital- Eberhard Karls University Tübingen, Radiation Oncology, Tuebingen, Germany*

[3]*German Cancer Research Center DKFZ- Heidelberg and German Cancer Consortium DKTK, Partner site Tuebingen, Tuebingen, Germany*

[4]*GROW-School for Oncology and Developmental Biology- Maastricht University Medical Centre, Radiation Oncology Maastro, Maastricht, The Netherlands*

[5]*Medical Faculty and University Hospital- Eberhard Karls University Tübingen, Urology, Tuebingen, Germany*

[6]*Medical Faculty and University Hospital- Eberhard Karls University Tübingen, Pathology, Tuebingen, Germany*

[7]*German Cancer Research Center DKFZ- Heidelberg and German Cancer Consortium DKTK, Partner site Dresden, Dresden, Germany*

[8]*National Center for Radiation Research in Oncology- Faculty of Medicine and University Hospital Carl Gustav Carus- Technische Universität Dresden and Helmholtz-Zentrum Dresden - Rossendorf, OncoRay, Dresden, Germany*

[9]*Faculty of Medicine and University Hospital Carl Gustav Carus- Technische Universität, Radiation Oncology, Dresden, Germany*

Purpose or Objective: In previous study we showed that γH2AX assay in *ex vivo* irradiated tumour samples collected from cancer patients of various types correlates with known differences in radioresponsiveness. In the present study we aimed to apply the assay in a panel of prostate tumour specimens to investigate whether it could allow discrimination of sensitive and resistant tumours of the same type. In addition we aimed to further explore the robustness of the method via investigating the potential impact of the tumour sampling on the reproducibility of the results.

Material and Methods: Tumour biopsies from prostate cancer patients undergone radical prostatectomy were cultivated in media for 24 h before irradiation (IR) with single doses and fixed 24 h post IR. The microenvironmental parameters were determined by addition of BrdU (perfusion) and Pimonidazole (hypoxia) to media prior to IR. Histological sections of previously paraffin-embedded material were stained for γH2AX and the foci were evaluated in viable, well oxygenated tumour areas. To investigate the heterogeneity of radiation response among the different patients, biopsies were irradiated with graded single doses (0, 2, 4, 6, 8 Gy) while to determine the intratumoural sampling variability, biopsies from different tumour locations were irradiated with single dose of 4 Gy.

Results: In all the 15 patients currently analyzed we observed a linear dose-response of residual γH2AX foci. The slope of the dose-response expressed high heterogeneity among the different patients (slope values range: 0.83-2.27). Using the slope of the foci dose-response as a parameter of tumour radiosensitivity we could determine 3 patients subgroups, namely resistant, with slope values lower than the 25th percentile of the slope values distribution (<1.1); moderate, with slope values between the 25 and 75th percentile and sensitive, with slope values above the 75th percentile (>1.8). These results are consistent with previously observed slope values for very sensitive (e.g. seminoma, slope value >2) and resistant (e.g. GBM, slope value ~1) tumour types. ANOVA analysis of the residual foci values post 4 Gy IR evaluated in tumour cells form different parts of the same tumour revealed no significant differences in the foci value distributions.

Conclusion: We herein show for the first time that the γH2AX *ex vivo* assay is clinically feasible and able to detect differences in cellular radiation sensitivity among patients with the same tumour type. Our results suggest that intratumoural heterogeneity (potential source of sampling error) do not significantly affect the results of the assay. Taken together, this assay has a promising potential for individualized radiation oncology and prospective validation in different tumour types in relation to known tumour characteristics and patient's outcome is warranted.

PV-0429

A 3D in vitro cancer model and imaging platform to measure proton radiation-induced cellular damage

T. Long[1], M. Loizidou[1], G. Schettino[2], G. Royle[3], K. Ricketts[1]

[1]*University College London, Division of Surgery and Interventional Science, London, United Kingdom*

[2]*National Physical Laboratory, Radiation Dosimetry Group, London, United Kingdom*

[3]*University College London, Department of Medical Physics and Bioengineering, London, United Kingdom*

Purpose or Objective: The aim of the project is to present an in vitro 3D cellular platform capable of measuring radiation-induced cell damage at the cellular scale, enabling high-resolution image capture of cell response along the proton depth dose.

Material and Methods: A 3D cancer model of dimensions 17 mm x 17 mm x 5 mm (L x W x H) was developed for proton irradiation. The model comprises 1 million uniform distributed HT29 colon cancer cells within a type 1 collagen scaffold. The model was irradiated with 62 MeV proton spread out Bragg peak (SOBP) of 10 mm width. Samples were fixed after irradiation, set within agarose gel, processed via vibratome to 400 nm thickness slices, stained with markers for apoptosis (Caspase-3), DNA double strand breaks (53BP1) and hypoxia (CA9).

Results: Alamar blue assay proves the cell metabolism can maintain 1-5 days depending on seeding density. The cancer cells invade into stroma, form spheroid and show paracrine activity (vascular endothelial growth factor and epidermal growth factor receptor expression) and hypoxia gradients in 3D model. The measurement of DNA double strand breaks is achievable in 2D fluorescent microscopy but less easily resolvable in 3D imaging. The level of cell apoptosis along SOBP can be imaged and correlated to the actual position and dose. Figure below shows 1 million HT29 3D models are irradiated by 5Gy dose and fixed 24 hour after irradiation. The image position located at the proximal edge of the SOBP.

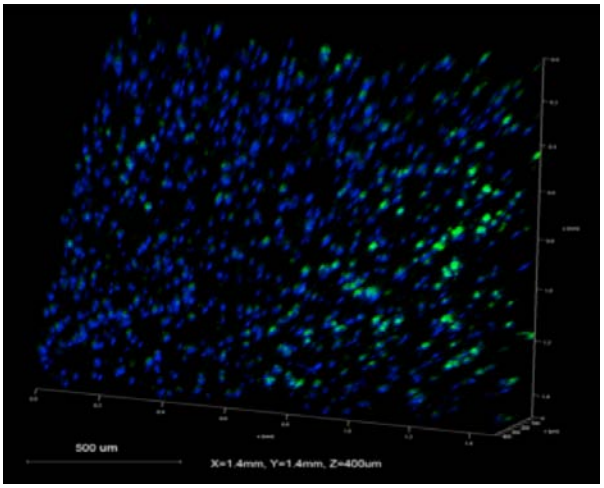

Conclusion: In this novel methodology of sample processing and well-controlled coordination system, correlation between the cell response of the 3D cancer model and proton dose distribution was possible. The fluorescent images show a clear difference in cell apoptosis signal response with depth dose, and in the 3D samples we could image a hypoxia gradient. Further work is underway to model LET within the 3D cancer model to be linked to cell response parameters, and to repeat the experiment under x-ray irradiation.

PV-0430

Late radiation enteropathy: do tissue cytokines play a protective role? A first-in-man study.

M. Reis Ferreira[1], H.J.N. Andreyev[2], K. Mohammed[3], S. Gowan[4], D.P. Dearnaley[1]

[1]*Institute of Cancer Research and Royal Marsden NHS Trust, Academic Radiotherapy, Surrey, United Kingdom*

[2]*Royal Marsden NHS Trust, Gastroenterology, London, United Kingdom*

[3]*Royal Marsden NHS Trust, Statistics and Computing, London, United Kingdom*

[4]*Institute of Cancer Research, Tumour Biology and Metastasis, London, United Kingdom*

Purpose or Objective: Late radiation enteropathy affects 20% of prostate cancer survivors. Inflammatory processes may relate to its occurrence. We aimed to assess differences in the levels of intestinal mucosa cytokines between patients with side-effects after pelvic radiotherapy and healthy controls.

Material and Methods: Patients with GI symptoms developing after prostate radiotherapy and undergoing colonoscopy were recruited for this study. Controls were patients undergoing colonoscopy for polyp surveillance. All participants were free of bowel cancer. Colonoscopy was performed after standard preparation of the bowel with citramag and senna or Kleen prep. Biopsies were obtained for cytokine characterization and pathologic assessment as follows (Fig.1):

- (1) Two endoscopic directed biopsies were taken from an area where mucosal radiation lesion was present; if no mucosal change was obvious, biopsies were taken from the anterior rectal wall.
- (2) A second pair of biopsies was taken from normal looking mucosa as close as possible to the previous sampling site.
- (3) Controls: biopsies were taken from the anterior rectal wall only.

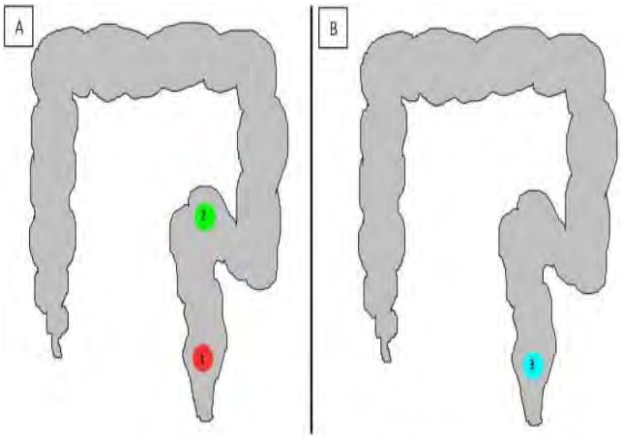

Figure 1: Sampling sites in A – patients with side-effects; B – control patients (1) – Area with enteropathy; (2) – Area without enteropathy; (3) – Controls)

Total sample protein was extracted. Cytokine levels were evaluated using 3 independent panels detecting the presence and concentrations of 30 different cytokines. A histology score for radiation enteropathy (*) was used to characterize the samples. Higher scores reflect worse outcomes.
Significance was studied with the Kruskal-Wallis, Wilcoxon and Student's t-test.

Results: Recruitment ran from April 2014 to January 2015. 9 symptomatic patients, treated with prostate irradiation at least 2 years before and 6 healthy controls were recruited.
Cytokine concentrations were higher in controls and in biopsies taken from normal tissue in the patients. Although patient samples from areas without disease had globally higher cytokine levels when compared to areas with disease, this was not significant. There was a trend to slightly higher histology scores in biopsies from irradiated tissues (table 1).

	Chemokine panel (10 molecules)	Cytokine panel (10 molecules)	Pro-inflammatory panel (10 molecules)	Histology score (*)
Control biopsies (3) *versus* biopsies of area with enteropathy (1)	Concentrations of chemokines higher in controls **p=0.05**	Concentrations of cytokines higher in controls **p=0.001**	Concentrations of pro-inflammatory cytokines higher in controls p=0.14	Score higher in areas with enteropathy p=0.06
Control biopsies (3) *versus* biopsies of area without enteropathy (2)	Concentrations of chemokines higher in controls p=0.16	Concentrations of cytokines higher in controls p=0.06	Concentrations of pro-inflammatory cytokines higher in controls **p=0.01**	Score higher in areas with enteropathy p=0.06
Biopsies of area with enteropathy (1) versus biopsies of area without enteropathy (2)	Concentrations of chemokines higher in area without enteropathy p=0.67	Concentrations of cytokines higher in area without enteropathy p=0.13	Concentrations of pro-inflammatory cytokines higher in area without enteropathy p=0.21	Score higher in areas with enteropathy p=0.6

Table 1: Differences in global cytokine level analysis by panel and histology score.

(*) Reference: Langberg CW, et al. Acta Oncol. 1992;31(7):781-7.

Conclusion: Cytokine levels are decreased in human tissues with late radiation enteropathy. This may reflect a protective function of cytokines, either in the maintenance of the mucosal barrier or in keeping a normal balance of gut microbiota. Pathway analysis and modeling of the inflammatory response will be the object of further analyses.

PV-0431

Changes of the density CD8+ tumour infiltrating lymphocytes after neoadjuvant radiochemotherapy

D. Buka[1], J. Dvorak[2], V. Sitorova[3], I. Richter[4], I. Sirak[1]

[1]*University Hospital Hradec Kralove, Oncology and Radiotherapy Department, Hradec Kralove, Czech Republic*

[2]*Charles University and Thomayer Hospital, Department of Oncology- First Faculty of Medicine, Prague, Czech Republic*

[3]*University Hospital Hradec Kralove, Department of Pathology- Charles University, Hradec Kralove, Czech Republic*
[4]*Regional Hospital Liberec, Department of Oncology, Liberec, Czech Republic*

Purpose or Objective: The aim of this retrospective study is to evaluate the effect of neoadjuvant radiochemotherapy on the density of CD8+ tumor infiltrating lymphocytes (TILs) of rectal adenocarcinoma, by comparison of the density of CD8+ TILs in endoscopical biopsies before and resection specimens after the therapy.

Material and Methods: In total 53 patients with locally advanced rectal cancer were studied retrospectively. Neoadjuvant treatment comprised 50.4 Gy/28 fractions external radiation with continual 5-fluorouracil. Four to six weeks after the radiochemotherapy, surgical resection was performed. Immunohistochemistry was applied to assess CD8+ expression in both the pretreatment biopsies and resected specimens.

Results: During radiochemotherapy 30 patients (57%) had increased the density of CD8+ TILs, in 18 patients (34%) decreased, in 1 patient there was no change, in 4 patients it was not possible to assess the dynamics of the density of CD8+ TILs (in 2 patients due to insufficient amount of tissue for immunohistochemical analysis and in other 2 patients due to pathologic complete response after radiochemotherapy). The median of follow-up was 75 months (6.3 years). In 2 patients resection with microscopic residual tumor (R1) was performed and for 51 patients radical resection with microscopically negative margins (R0) was performed. Downstaging after preoperative radiochemotherapy was observed in 34 patients (64%). Five-year overall survival was 56% (95%CI: 43-70%). The density of CD8+ TILs was not significant in Cox regression analysis (p=0.16) or log-rank test (p=0.16). According to chi-square test (p=0.37) there was no significant impact of the increase of the density of CD8+ TILs after radiochemotherapy on downstaging. The increase of the density of CD8+ TILs after radiochemotherapy was associated with a trend of 2.5 longer overall survival in comparison with patients with the decrease of the density of CD8+ TILs after radiochemotherapy.

Conclusion: In the present study we did not observe any predictive or prognostic significance of the density of CD8+ TILs in endoscopical biopsies before radiochemotherapy, in resection specimens after the radiochemotherapy nor in changes of the density of CD8+ TILs after radiochemotherapy. The limitation of our study is the number of patients (53). It is not excluded that in a larger number of patients predictive or prognostic significance of the density of CD8+ TILs could be detected.

PV-0432

Mechanisms and abscopal effects of combined mRNA-based radioimmunotherapy in a syngenic mouse model.

L. Basler[1], A. Kowalczyk[2], M. Fotin-Mleczek[2], K.J. Kallen[2], D. Zips[1], S.M. Huber[1]
[1]*Universitätsklinikum Tübingen, Department of Radiation Oncology, Tübingen, Germany*
[2]*CureVac AG, CureVac AG, Tübingen, Germany*

Purpose or Objective: Tumor metastasis and tumor immune evasion present major challenges of cancer treatment. Radiotherapy has been demonstrated to overcome the immunosuppressive tumor microenvironment and anecdotal reports suggest that local tumor irradiation alone may also exert systemic or abscopal anti-tumor effects by immune-response stimulation with subsequent control of non-irradiated tumor metastases. This study aimed to assess abscopal effects of radiation alone and in combination with an mRNA-based tumor vaccination in a syngenic mouse model.

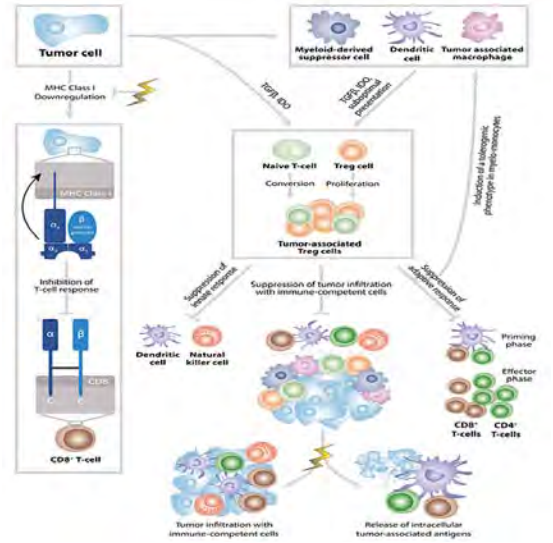

Material and Methods: Syngenic C57BL/6 mice were subcutaneously injected with ovalbumin-expressing murine thymoma cells (E.G7-OVA, 3×105) into the right hind leg of on day -13 and into the left flank on day -9. On days 0, 1 and 2, the primary tumors (right hind leg) were irradiated (IR) with fractions of 2 Gy photons by the use of a linear accelerator. The secondary tumors at the left flank were shielded and received only 1.1 ± 0.3% of the IR dose applied to the primary tumor as confirmed by film dosimetry. Twice per week, tumor length and width were measured by caliper for tumor volume calculation and vaccination groups were intradermally injected with the mRNA-based vaccine RNActive® encoding Ovalbumin beginning day 0. At the end of the experiments, the secondary tumors were analyzed for cytokine abundances by protein microarray.

Results: Primary and secondary tumors of control mice developed with similar growth kinetics. IR and combined radioimmunotherapy significantly delayed tumor growth leading to primary tumor control in 15% and 53% of mice. Importantly, in secondary tumors with starting volumes below 30mm^3 radioimmunotherapy induced a significant growth delay compared to vaccination alone (p=0.002) and control group (p=0.01). IR alone delayed the growth of the secondary, unirradiated tumors in an unsignificant manner. Cytokine microarray analysis of the unirradiated secondary tumors showed significant differences in combined radioimmunotherapy for CCL5/RANTES and CXCL9/MIG expression as compared to the other groups, both suggesting increased T-cell activation. Similar but unsignificant trends could be observed for TNF-α, CCL3, IL-1α, VEGF, M-CSF and other cytokines.

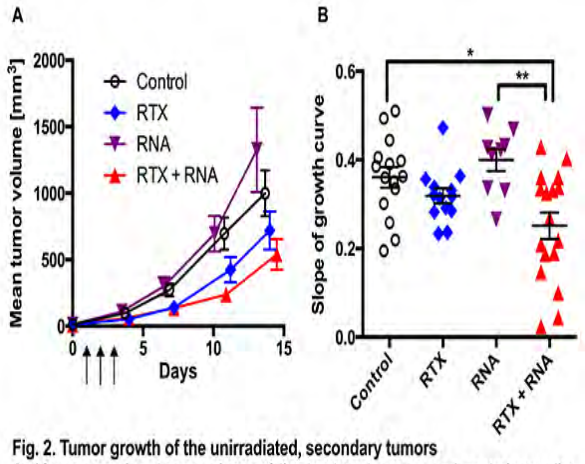

Fig. 2. Tumor growth of the unirradiated, secondary tumors
A. Mean secondary tumor volume of the treatment groups and control over the treatment period of 14 days.
B. Slope of the growth curve of secondary tumors. In secondary tumors with starting volumes below 30mm^3 radioimmunotherapy induced a significant growth delay compared to vaccination alone (p=0.002) and control group (p=0.01).

Conclusion:
Immunotherapy can enhance radiation-induced abscopal effects in small immunogenic tumors. This effect exhibits the potential of a combined radioimmunotherapy for the control of micrometastases. The characterization of the underlying immunological processes has to await further experiments.

Symposium: Modern ART based on functional / biological imaging

SP-0433
Functional imaging for ART; biological bases and potential impact on clinical outcome
B. Hoeben[1]
[1]*Radboud University Medical Center, Radiation Oncology, Nijmegen, The Netherlands*

Developments in high-precision radiotherapy by means of on-board imaging, such as IMRT and stereotactic radiotherapy, have extended the possibilities for dose escalation to tumor localizations, while de-escalating doses to surrounding normal tissues. Advances in imaging technologies allow for better differentiation of tumor extension and target localization. In addition to superior anatomical imaging possibilities, functional and molecular imaging can be utilized to convey information regarding inherent tumor characteristics relevant for prognostication and prediction of therapy response. In many different tumor types, studies have investigated the potential of especially magnetic resonance imaging (MRI) and positron emission tomography (PET) / computed tomography (CT) scan to bring various tumor features to light. Repetitive imaging of malignancies before and during treatment can give rise to response adaptive treatment as has been successfully shown by integrating 18F-Fluorodeoxyglucose (18F-FDG) PET/CT imaging in chemotherapy response evaluation of Hodgkin's Lymphoma, in order to define the eventual radiotherapy target and dose or to avoid radiotherapy altogether. For response evaluation of Hodgkin's Lymphoma on 18F-FDG PET/CT images, application of the internationally accepted Deauville criteria reduce interobserver variability and standardize response criteria.
In many solid tumor types, numerous mostly single-center studies have described a plethora of functional or molecular imaging characteristics for description of tumor features, prognostication and prediction purposes, radiotherapy target delineation or direction of targeted therapy. This illustrates the drive towards personalized medicine in oncology, where individual therapy and therapy adaptation are based on specific patient and tumor characteristics. PET/CT studies concerning prognostic and predictive imaging properties have focused on depiction of tumor characteristics and their changes during therapy; such as metabolism (e.g. 18F-FDG PET), hypoxia (e.g. 18F-fluoromisonidazole PET, 18F-fluoroazomycin arabinosine PET, Blood Oxygen Level-dependent MRI), proliferation (e.g. 18F-fluorothymidine PET), cell membrane synthesis (e.g. 11C-choline PET), tumor cellularity (e.g. Diffusion-weighted MRI) or tumor perfusion (e.g. Dynamic Contrast-enhanced MRI). Clinical and pre-clinical PET/CT studies have illustrated the possibility to quantify presence and abundance of targets for antibody-based therapies, such as radiolabeled cetuximab in the case of the epidermal growth factor receptor. Studies on adaptive radiotherapy based on PET/CT imaging, in e.g. head-and-neck squamous cell carcinoma and non-small cell lung cancer, have mainly focused on definition of radiotherapy-resistant tumor subvolumes relevant for dose-escalation. Longer follow up results of these studies will reveal if these therapy intensifications will lead to better disease outcomes.
What such imaging studies bring forward, is that different imaging modalities with different specific biological markers will define different tumor subvolumes, mostly with different spatial and temporal properties. The challenge is to define the correct individual therapy regulations for the correct tumor within the correct timeframe. Moreover, how can one reliably quantify the imaging signal, delineate radioresistant tumor subvolumes or evaluate therapy response, if most studies use local institutional approaches to manage imaging information for these purposes?
All these issues need to be resolved before widespread implementation into clinical practice can take place. Molecular and functional imaging and its evaluation has to be validated and proven to be useful in multicenter studies. Advanced solutions need to be established to incorporate multiparameter information from e.g. tumor biopsy immunohistochemical analysis and gene-arrays into decision-making processes for specific imaging modalities, individualized treatment and treatment evaluation pathways. The first multicenter studies with these goals in mind are now being established.

SP-0434
Adaptive radiation therapy by the example of head and neck cancer: is there any role for a RTT?
B. Speleers[1], M. Madani[2], M.S. Olteanu[3], I. De Gersem[1], M. Duprez[3], M.S. Vercauteren[3], M.D. Berwouts[3], M. De Neve[3]
[1]*Ghent University, Department of Radiotherapy, Ghent, Belgium*
[2]*University Hospital Zürich, Department of Radiation Oncology, Zürich, Switzerland*
[3]*Ghent University Hospital, Department of Radiotherapy, Ghent, Belgium*

Normal 0 21 MicrosoftInternetExplorer4
Changes in the tumoras well as normal tissues and organs surrounding the tumor during and/or in response to radiation therapy require treatmentadaptation. A need for adaptive radiation therapy (ART) is not obvious for alltumors, but head-and-neck cancer, for which substantial changes in tumor andparotid gland geometry and dosimetry have been shown [1]. Moreover, biologicchanges in the tumor may require treatment adaptationas well [2]. Logistics of ARTis complex and hampered by a lack of personnel and robust technical tools. Theworkflow is usually not well-defined and well-supported by commercial oncologyinformation and treatment planning systems. Nevertheless, an increasing numberof academic centers introduce ART in their practice as has done it inDepartment of Radiotherapy, Ghent University Hospital. In this talk theworkflow of ART for head-and-neck cancer on the example of this particularcenter will be discussed in more detail including the roles of personnel withemphasis on RTTs, their current responsibilities and their possible empowermentin the frame of ART.

References
1. Brouwer CL, Steenbakkers RJ,Langendijk JA, Sijtsema NM. Identifying patients who may benefit from adaptiveradiotherapy: Does the literature on anatomic and dosimetric changes in headand neck organs at risk during

radiotherapy provide information to help?Radiother Oncol 2015; 115: 285-294.
2. GeetsX, Daisne JF, Tomsej M et al. Impact of the type of imaging modality on targetvolumes delineation and dose distribution in pharyngo-laryngeal squamous cellcarcinoma: comparison between pre- and per-treatment studies. Radiother Oncol2006; 78: 291-297.

SP-0435

Dosimetric impact of dose painting and replanning: ARTFORCE project

J.J. Sonke[1]
[1]*Netherlands Cancer Institute, Department of Radiation Oncology, Amsterdam, The Netherlands*

In the ARTForce project, two international clinical trials are conducted. The first trial (NCT01504815) for locally advanced head-and-neck cancer patients is a phase two trial randomizing between standard chemo-radiotherapy, redistributing the dose in the PTV of the primary tumor. Instead of a homogeneous dose of 70Gy in 35 fractions, an inhomogeneous dose is optimized based with a minimum dose of 64 Gy at the edge of the PTV and a maximum dose of 84 Gy around the FDG PET SUVmax location. Additionally, in the experimental arm, the treatment plan is adapted after two weeks to account for anatomical changes. The second phase 2 trial (NCT01024829) for locally advanced lung cancer patients randomizes between dose escalation to the primary tumor >= 72 Gy in 24 fractions and dose escalation to the region of the tumor defined by the 50% of FDG PET SUVmax. Both treatment plans are optimized to have an equal mean lung dose. In this presentation, dosimetric differences between the arms in both trials will be discussed as well as the impact of anatomical changes on the delivered dose and the effectiveness of replanning to mitigate dose discrepancies.

Symposium: Secondary cancer after radiotherapy: from cancer registries to clinical implications

SP-0436

Radiotherapy-related second cancer risks from epidemiological studies, and their application to newer therapies

A. Berrington de González[1]
[1]*Center for Global Health National Cancer Institute, Division of Cancer Epidemiology and Genetics DCEG, Rockville- MD, USA*

Second cancers are an important cause of morbidity and mortality in cancer survivors. One in five cancers diagnosed in the US are now second cancers. The causes of second cancers include lifestyle factors, genetic predisposition and also the treatment for the first cancer, including radiotherapy. In the last decade there have been a large number of new studies that have advanced our understanding of the risk of second cancers after radiotherapy. The most informative studies provide dose-response relationships based on individual dose-reconstruction. These studies suggest that the second cancer risk generally increases linearly with dose, even at organ doses of 60Gy. This is contrary to earlier theories that the dose-response would flatten or even have a down-turn at higher doses because of cell killing. The magnitude of the risk from these fractionated high-dose exposures is, however, 5-10 times lower than the risk from acute exposures of <2Gy among the Japanese atomic bomb survivors. The results from these detailed observational studies provide insights into radiation carcinogenesis from fractionated high-dose exposures, and can be used to develop second solid cancer risk projection models for newer radiotherapy techniques.

SP-0437

Modelling of secondary cancer risks

U. Schneider[1,2]
[1]*Clinic Hirslanden Zürich, Institute of Radiotherapy, Zürich, Switzerland*
[2]*University of Zürich, Institute of Physics- Science Faculty, Zürich, Switzerland*

In developed countries, more than half of all cancer patients receive radiotherapy at some stage in the management of their disease. However, a radiation-induced secondary malignancy can be the price of success if the primary cancer is cured or at least controlled. Therefore, there is increasing concern regarding radiation-related second cancer risks in long-term radiotherapy survivors and a corresponding need to be able to predict cancer risks at high radiation doses. Of particular interest are second cancer risk estimates for new radiation treatment modalities such as intensity modulated radiotherapy, intensity modulated arc-therapy, proton and heavy ion radiotherapy. The long term risks from such modern radiotherapy treatment techniques have not yet been determined and are unlikely to become apparent for many years, due to the long latency time for solid tumor induction. Most information on the dose-response of radiation-induced cancer is derived from data on the A-bomb survivors who were exposed to gamma-rays and neutrons. Since, for radiation protection purposes, the dose span of main interest is between zero and one Gy, the analysis of the A-bomb survivors is usually focused on this range. With increasing cure rates, estimates of cancer risk for doses larger than one Gy are becoming more important for radiotherapy patients. Simple radiation protection models should be used only with extreme care for risk estimates in radiotherapy, since they are developed exclusively for low dose. When applied to scatter radiation, such models can predict only a fraction of observed second malignancies. Better semi-empirical models include the effect of dose fractionation and represent the dose-response relationships more accurately. The involved uncertainties are still huge for most organs and tissues. A major reason for this is that the underlying processes of the induction of carcinoma and sarcoma are not well known. Most uncertainties are related to the time patterns of cancer induction, the population specific dependencies and to the organ specific cancer induction rates. For radiotherapy treatment plan optimization these factors are irrelevant, as a treatment plan comparison is performed for a patient of specific age, sex, *etc*. If a treatment plan is compared relative to another one only the shape of the dose-response curve (the so called risk-equivalent dose) is of importance and errors can be minimized. One of the largest remaining uncertainties is the precision of the dose distribution which is the basic input into all risk-estimate-models. Dose calculation and/or measurement are as precise as approximately 5% in the treated volume of the patient. However, in the periphery dose errors can reach 100% and more. The use of erroneous dose data (see Figure 1) can lead to wrong risk estimates. Therefore a lot of effort is undertaken to produce precise dose computations in the whole patient volume about which is reported. Strategies are discussed how to include relevant dose information into cancer registries.
Figure 1. Two dose comparisons of the same radiation treatment techniques which were used for risk estimates. The resulting risk estimates were highly contradictory.

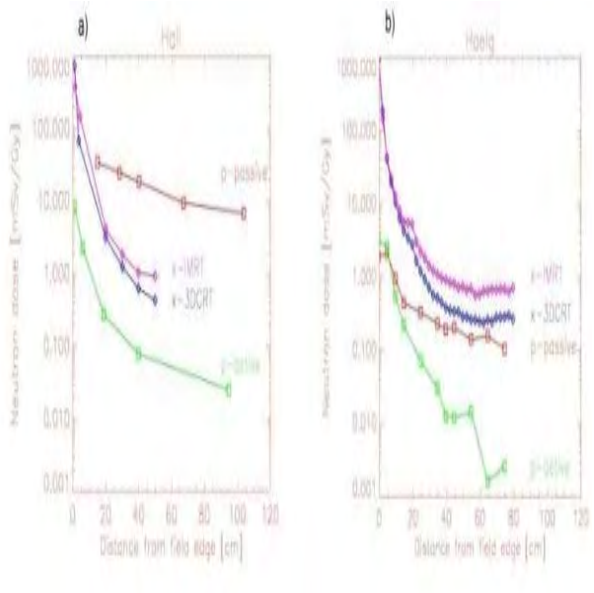

SP-0438

Clinical implications of secondary cancer risks in pediatric and adult patients

D. Hodgson[1]

[1]*Hodgson David, Radiation Oncology, Toronto, Canada*

The association between radiation exposure and cancer risk has been studied for several decades, although in the clinical oncology setting, significant gaps in the understanding and management of radiation therapy (RT) related second cancer risks still exist.

This talk will address the clinical implications of current knowledge relating to treatment- related second cancers, including:

1. Treatment selection: Some clinicians or patients may opt to avoid RT in order to reduce the risk of second cancers. These decisions often reveal important misunderstandings about the impact of age, competing risks of death or other morbidity, and differences between absolute and relative risks. Through a case-based approach, participants will learn to identify scenarios in which over- or under-estimation of second cancer risk may lead to suboptimal treatment choices.

2. Modification of Radiation Treatment: Oncologists are able to deliver dose much more precisely than ever before, but it remains difficult to decide where to deposit excess dose, or if low doses to large volumes are more carcinogenic than high doses to small volumes. The emergence of proton therapy now adds further complexity to these issues. In this session, participants will learn about dose-risk relationships and the clinical implications for radiotherapy planning.

2. Clinical management in follow-up: Survivorship care is of growing clinical concern, and management of second cancer risk is an important feature of this care. Oncologists will be required to have familiarity with guidelines recommending specific screening interventions following RT. Participants will learn about resources and guidelines for management of second cancer risk, and the evidence supporting these guidelines will be reviewed.

Proffered Papers: Radiobiology 4: Molecular biomarkers for patient selection

OC-0439

Localization of p16 expression is an important factor to determine radiotherapy response in HNSCC

R. Dok[1], L. Abbasi Asbagh[2], E. Van Limbergen[3], A. Sablina[2], S. Nuyts[1]

[1]*University Hospital Gasthuisberg, Lab of Experimental Radiotherapy, Leuven, Belgium*

[2]*KU Leuven, Human Genetics, Leuven, Belgium*

[3]*MAASTRO Clinic, Radiation Oncology, Maastricht, The Netherlands*

Purpose or Objective: The influence of HPV positivity on therapy response in head and neck squamous cell cancers (HNSCC) highlights the importance of uniform and robust biomarkers for stratification of HNSCC patients. Our previous report indicates that p16 is not only a surrogate marker for HPV infections but has an active role in modulation of radiotherapy response by impairing DNA damage response and repair, which is a process known to be dominant in the nucleus of the cells. Based on this, we hypothesized that p16 compartmentalization according to nuclear and cytoplasmic expression may have a role in risk stratification.

Material and Methods: p16 expression (immunostaining) and HPV status (GP5+/6+ PCR) was assessed in 241 pretreatment biopsies of oropharyngeal cancer patients treated with chemoradiotherapy. Tumors were classified in nuclear p16 expressing (>10% of tumor cells), cytoplasmic (>10% tumor cells) and p16 negative groups. Statistical analysis was performed to assess the correlation between clinical and tumor characteristics and p16 immunostaining. Influence of p16 localization on radiotherapy response was further assessed by clonogenic and cell survival assays in HPV/p16 negative HNSCC cells transfected with viral construct containing p16-NLS (nuclear localization signal); p16-NES (nuclear exit signal) and p16-WT. The expression and localization of p16 was confirmed by western blotting and immunofluorescence. The response of p16 localization on DNA damage response and homologous recombination repair (HRR) was assessed by gH2AX, RAD51 foci formation and immunoprecipitation.

Results: Nuclear p16 expressing HNSCC showed significant ($p<0.05$) better locoregional control rates (5-year 82%) compared to cytoplasmic p16 positive (5-year 55%) and p16 negative patients (5-year 48%). Only nuclear p16 expression was a significant prognostic factor for locoregional control with a hazard ratio of 0.48 ($p<0.05$; 95% CI: 0.22-1.01). Interestingly, HPV positive patients were significantly enriched in the nuclear p16 expressing group (60%) compared to cytoplasmic p16 expressing group (9%). In concordance with our patient data, cells containing nuclear p16 expression (p16-NLS) showed a higher radiosensitization compared to cells with predominant cytoplasmic p16 expression (p16-NES) or p16 negative cells, indicating a differential role of p16 protein expression depending on its localization. Strikingly, cells expressing nuclear p16 (p16-NLS) -although showing a similar level of gH2AX induction- were characterized with lower number RAD51 foci formation compared to cells expressing cytoplasmic p16 (p16-NES), suggesting an impaired HRR.

Conclusion: Cellular p16 localization is an important factor for stratification of HNSCC patients with nuclear p16 expression showing a superior predictive value for radiotherapy response.

OC-0440

Impact of chemokine receptor CXCR4 and its ligand SDF1 expression on loco-regional control in HNSCC

A. Menegakis[1,2], C. De Colle[1,3], D. Moennich[1,2], F. Fend[4], P.S. Mauz[5], S. Welz[1], I. Tinhofer[6,7], V. Budach[6,7], E. Gkika[8,9], M. Stuschke[8,9], P. Balermpas[10,11], C. Roedel[10,11], M. Avlar[12,13], A.L. Grosu[12,14], A. Abdollahi[15,16,17,18,19], J. Debus[15,17,18,19,20], C. Bayer[21], C. Belka[21,22], S. Pigorsch[21,23], S.E. Combs[21,23], M. Krause[24,25,26], M. Baumann[24,25,26], D. Zips[1,2]

[1]*University Hospital Tübingen Eberhard Karls University Tübingen, Radiation oncology, Tübingen, Germany*

[2]*German Cancer Research Center DKFZ- Heidelberg and German Cancer Consortium DKTK, Partner site Tuebingen, Tuebingen, Germany*

[3]*Azienda Ospedaliero-Universitaria- Citta' della Salute e della Scienza di Torino- University of Turin, Radiation Oncology, Turin, Italy*

[4]*University Hospital Tübingen Eberhard Karls University Tübingen, Pathology, Tübingen, Germany*

[5]University Hospital Tübingen Eberhard Karls University Tübingen, Otorhinolaryngology, Tübingen, Germany
[6]German Cancer Research Center DKFZ- Heidelberg and German Cancer Consortium DKTK, Partner site Berlin, Berlin, Germany
[7]Charité University Hospital- Berlin, Radiooncology and Radiotherapy, Berlin, Germany
[8]German Cancer Research Center DKFZ- Heidelberg and German Cancer Consortium DKTK, Partner site Essen, Essen, Germany
[9]Medical Faculty- University of Duisburg-Essen, Radiotherapy, Essen, Germany
[10]German Cancer Research Center DKFZ- Heidelberg and German Cancer Consortium DKTK, Partner site Frankfurt, Frankfurt, Germany
[11]Goethe-University Frankfurt, Radiotherapy and Oncology, Frankfurt, Germany
[12]German Cancer Research Center DKFZ- Heidelberg and German Cancer Consortium DKTK, Partner site Freiburg, Freiburg, Germany
[13]Clinical Study Section- University of Freiburg, Radiation Oncology, Freiburg, Germany
[14]University of Freiburg, Radiation Oncology, Freiburg, Germany
[15]German Cancer Research Center DKFZ- Heidelberg and German Cancer Consortium DKTK, Partner site Heidelberg, Heidelberg, Germany
[16]University of Heidelberg Medical School and German Cancer Research Center DKFZ, Translational Radiation Oncology, Heidelberg, Germany
[17]University of Heidelberg Medical School and German Cancer Research Center DKFZ, National Center for Tumor Diseases NCT, Heidelberg, Germany
[18]Heidelberg Ion Therapy Center HIT- University of Heidelberg Medical School, Radiation Oncology, Heidelberg, Germany
[19]National Center for Radiation Research in Oncology NCRO- University of Heidelberg Medical School and German Cancer Research Center DKFZ, Heidelberg Institute of Radiation Oncology HIRO, Heidelberg, Germany
[20]University of Heidelberg Medical School and German Cancer Research Center DKFZ, Clinical Cooperation Unit Radiation Oncology, Heidelberg, Germany
[21]German Cancer Research Center DKFZ- Heidelberg and German Cancer Consortium DKTK, Partner site Munich, Munich, Germany
[22]Ludwig-Maximilians-Universität, Radiotherapy and Radiation Oncology, Munich, Germany
[23]TechnischeUniversität München, Radiation Oncology, Munich, Germany
[24]German Cancer Research Center DKFZ- Heidelberg and German Cancer Consortium DKTK, Partner site Dresden, Dresden, Germany
[25]National Center for Radiation Research in Oncology- Faculty of Medicine and University Hospital Carl Gustav Carus- TechnischeUniversität Dresden- Helmholtz-Zentrum Dresden – Rossendorf, OncoRay, Dresden, Germany
[26]Faculty of Medicine and University Hospital Carl Gustav Carus- TechnischeUniversität Dresden, Radiation Oncology, Dresden, Germany

Purpose or Objective: To retrospectively assess the prognostic value of the potential biomarkers, i.e. chemokine receptor CXCR4, its ligand CXCL12 (SDF1), and nuclear EGFR expression in a cohort of 201 patients with locally advanced HNSCC. Patients were treated between 2005 and 2011 in 8 German cancer centers, as part of a multicenter biomarker study of the German Cancer Consortium Radiation Oncology Group (DKTK-ROG). Experimental data and first clinical observations suggest that activation of CXCR4 and SDF1 signaling pathway and nuclear location of EGFR are implicated in tumour cell proliferation, cellular survival, tumour progression, worse overall survival, metastasis and enhanced treatment resistance in different tumour types.

Material and Methods: Patients with locally advanced SCC of the oral cavity, oropharynx and hypopharynx were treated with resection and adjuvant RT and Cisplatin-based CT. Tissue micro-arrays (TMAs) were generated from surgical specimens and evaluated for the expression of the biomarkers by immunofluorescence with a semi-quantative method, based on their cellular location (membranous, intracellular, nuclear), extent of expression on TMA area and staining intensity. The results of the biomarker analysis along with the clinical parameters were then correlated with the clinical outcome.

Results: In univariate analysis, tumours with either SDF1 or CXCR4 intracellular overexpression displayed a significant negative correlation with loco-regional control (LCR) (HR: 2.52, p=0.01 and HR: 1.96, p=0.05 respectively). No correlation was observed for the nuclear expression of EGFR (HR: 0.85, p= 0.67), membranous expression of SDF1 (p=0.73) or CXCR4 (p=0.38). Tumours with intracellular co-expression of both SDF1 and CXCR4 were significantly correlated with poor LRC (HR: 2.72, p=0.01). Previously published data from the same cohort, showed that absence of p16 (negative HPV status) was correlating with poor LRC. Importantly, increased expression of SDF1 or co-expression with CXCR4 could identify a group of patients with significantly worse outcome within the HPV negative group (p=0.01). Multivariate cox regression analysis including HPV status, tumour localisation, tumour volume and the respective biomarkers indicated a significant independent role of SDF1 (HR: 2.20, p=0.04) and co-expression with CXCR4 (HR: 2.19, p=0.05) on LRC.

Conclusion: In summary, pre-treatment overexpression of CXCR4/SDF1 is an independent negative prognostic factor for the outcome of patients with locally advanced HNSCC who receive surgery and standard RT-CT. Further investigation in a cohort of patient receiving primary RT-CT and a prospective validation study is currently ongoing. SDF1/CXCR4 appears to be a promising biomarker for treatment individualization, in particular in HPV negative advanced HNSCC patients and supports strategies using drugable targets against this pathway to enhance efficacy of standard treatment.

OC-0441

Genomic amplification of FancA in HNSCC: mechanisms of radioresistance and clinical relevance

J. Hess[1,2], I. Gimenez Aznar[1], A. Michna[1], D. Klein[3], U. Schötz[4], M. Orth[4], L. Schneider[1,2], H. Braselmann[1], L. Schüttrumpf[4], V. Jendrossek[3], C. Belka[2,4], V. Zangen[1], K. Unger[1,2], H. Zitzelsberger[1,2], K. Lauber[2,4]
[1]Research Unit Radiation Cytogenetics, Helmholtz Zentrum Muenchen - German Research Center for Environmental Health, Neuherberg, Germany
[2]Clinical Cooperation Group 'Personalized Radiotherapy of Head and Neck Cancer', Helmholtz Zentrum Muenchen - German Research Center for Environmental Health, Neuherberg, Germany
[3]Department of Molecular Cell Biology, Institute of Cell Biology Cancer Research- Medical Faculty- University of Duisburg-Essen, Essen, Germany
[4]Molecular Oncology, Department of Radiation Oncology- Ludwig-Maximilians-Universität München, Munich, Germany

Purpose or Objective: Radio(chemo)therapy is a crucial treatment modality for head and neck squamous cell carcinoma (HNSCC). Radiotherapy resistance is a major reason for therapy failure and, therefore, predictive biomarkers for therapy response are urgently needed. DNA gains on chromosome 16q23-24 have been shown to be associated with genomic amplification of the FancA gene and to correlate with reduced progression-free survival of HNSCC patients after radiotherapy. This study aimed to analyze the effects of the potential predictive marker FancA on radiation sensitivity *in vitro*, to characterize the underlying molecular mechanisms, and to evaluate the clinical relevance in HNSCC.

Material and Methods: We generated FancA overexpressing human oral keratinocytes (OKF6/FancA) and analyzed several endpoints upon irradiation. To identify signaling pathways involved in FancA-mediated resistance, global transcriptome analyses were performed after irradiation with 4 Gy or sham-

irradiation followed by pathway enrichment analysis and reconstruction of function interaction networks. The clinical relevance of the cytogenetic marker 16q23-24, the FancA gene and our *in vitro* results was analyzed in data of 113 radiotherapy-treated patients from The Cancer Genome Atlas (TCGA) HNSCC cohort (Nature, 2015).

Results: Overexpression of FancA resulted in enhanced survival after *in vitro* irradiation. Moreover, FancA overexpressing cells demonstrated accelerated DNA damage repair mechanisms paralleled by increased repair fidelity: enhanced p53 and p21 response, accelerated kinetics in the disappearance of γ-H2AX DNA damage repair foci, faster pATM translocation, reduced accumulation of chromosomal translocations, but no increase in FancD2 mono-ubiquitinylation. Global mRNA expression analyses identified interferon signaling as a major candidate pathway, which was affected by FancA overexpression. Functional interaction networks of genes deregulated upon irradiation pointed to pathways exclusively involved in FancA-mediated radioresistance including the *senescence-associated secretory phenotype (SASP)*. Increased levels of basal and irradiation-induced cellular senescence accompanied by enforced SASP formation further support their potential involvement in FancA-mediated radiation resistance. The clinical relevance of our findings was validated in the data of 113 radiotherapy-treated patients of the TCGA HNSCC cohort demonstrating the association of chromosomal gains on 16q24.3 with increased FancA mRNA expression levels and impaired overall survival. Furthermore, the translation of our *in vitro* model derived results into the HNSCC patient specimens revealed similar gene expression changes linked to FancA overexpression.

Conclusion: Our data suggest an important role for FancA in cellular mechanisms of radioresistance in HNSCC.

OC-0442

Does miR-210 predict benefit from hypoxia modification in BCON randomised bladder cancer patients?

C. West[1], J. Irlam-Jones[2], A. Eustance[2], H. Denley[3], P. Hoskin[4], A. Choudhury[5]

[1]*The University of Manchester, Christie Hospital, Manchester, United Kingdom*

[2]*The University of Manchester, Translational Radiobiology Group, Manchester, United Kingdom*

[3]*Central Manchester University Hospitals NHS Foundation Trust, Department of Histopathology, Manchester, United Kingdom*

[4]*Mount Vernon Hospital, Cancer Centre, Northwood, United Kingdom*

[5]*The Christie Hospital NHS Foundation Trust, Department of Clinical Oncology, Manchester, United Kingdom*

Purpose or Objective: The addition of hypoxia modifiers carbogen and nicotinamide (CON) to radiotherapy (RT) improved overall survival in bladder cancer patients enrolled in the BCON phase III clinical trial. We investigated whether the expression of miR-210 in the BCON patient samples reflects hypoxia and predicts benefit from hypoxia-modification.

Material and Methods: The retrospective study involved 183 T1-T4b patients: 86 received RT+CON and 97 received RT alone. Formalin-fixed samples taken prior to radiotherapy were available and RNA extracted. Customised TaqMan plates were used to assess miR-210 expression using quantitative real-time PCR. Patients were classified as low miR-210 (<median expression) or high miR-210 (≥ median). Data on other hypoxia biomarkers were available for comparison.

Results: Patients with high miR-210 had a trend towards improved five-year OS with RT+CON (53.2%) compared with RT alone (37.8%; HR 1.68, 95% CI 0.95-2.95, P=0.08). No benefit was seen with low miR-210 (HR 1.02, 95% CI 0.58-1.79, P=0.97). High expression of miR-210 was also associated with high HIF-1α protein (P=0.0008), CA9 protein (P=0.004), Glut-1 protein (P=0.02), expression of a 26-gene hypoxia signature (P=0.01), tumour necrosis (P=0.04) and concurrent pTis (P=0.03).

Conclusion: High miR-210 expression may reflect tumour hypoxia and should be investigated further as a potential biomarker to identify bladder cancer patients who would benefit from hypoxia-modifying therapies.

OC-0443

Radiotherapy sensitivity in breast cancer is influenced by the DNA cytosine deaminase APOBEC3B

P.N. Span[1], A. Post[1], J.W.M. Martens[2], R.S. Harris[3]

[1]*Radboud University Medical Center, Department of Radiation Oncology, Nijmegen, The Netherlands*

[2]*Erasmus MC Cancer Institute, Department of Medical Oncology and Cancer Genomics Netherlands, Rotterdam, The Netherlands*

[3]*University of Minnesota- Masonic Cancer Center, Department of Biochemistry- Molecular Biology- and Biophysics, Minneapolis, USA*

Purpose or Objective: The DNA cytosine deaminase APOBEC3 proteins catalyze deamination of cytidines in single-stranded DNA, providing innate protection against retroviral replication. Recent studies have implicated APOBEC3B as a major source of mutation in breast cancer, suggesting a role for these enzymes in tumor initiation and/or progression. APOBEC3B expression levels were earlier found to correlate with poor outcomes for patients with estrogen receptor positive breast cancer, especially after Tamoxifen. Given its role in mutagenesis, we set out to assess whether APOBEC3B associates with radiosensitivity in breast cancer.

Material and Methods: MCF7 breast cancer cells were cultured radioresistant by daily 2 Gy treatments or tamoxifen-resistant by continuous culturing in up to 10 uM 4-OH-tamoxifen. The effect of irradiation on expression of APOBECs was assessed by RNAseq and qPCR in radiosensitive and radioresistant MCF7, and by qPCR in radioresistant MDA-MB231 cells. Furthermore, we studied a retrospective cohort of 535 non-systemically treated breast cancer patients. The predictive power of APOBEC3B was assessed in patients that did or did not receive radiotherapy as part of their primary therapy. Next, we suppressed endogenous APOBEC3B in MCF-7L with shRNA, or overexpressed either wt APOBEC3B, or a catalytically dead mutant APOBEC3B.

Results: Radioresistant breast cancer cells had increased baseline APOBEC3B mRNA levels (and not of any of the other APOBEC proteins), and irradiation induced an increase in APOBEC3B expression in both MCF7 and MDA-MB231 cells. In the breast cancer patient cohort we found a strong, statistically significant, independent interaction between APOBEC3B expression and radiotherapy. APOBEC3B predicted a poor prognosis only in those patients that received radiotherapy as part of their primary treatment, also when this analysis was restricted to patients that received a mastectomy (figure). This suggests that APOBEC3B influences radiosensitivity, and does not merely predict efficacy of surgery (as radiotherapy is generally given to lumpectomy patients). The effect of APOBEC3B knockdown and overexpression on radiosensitivity is currently being assessed using colony-forming assays and will be presented.

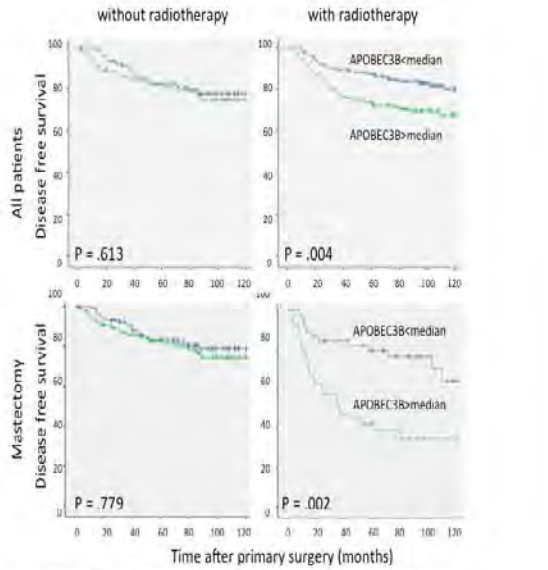

Figure: Kaplan-Meier analyses of non-systemically treated breast cancer patients that did (right panels) or did not (left panels) received radiotherapy as part of their primary treatment. Even in mastectomy patients alone did APOBEC3B predict radiosensitivity.

Conclusion: Our data suggest that the anti-viral APOBEC3B enzyme influences radiosensitivity in breast cancer, and might be a potential target for radiosensitization.

Proffered Papers: Clinical 9: SBRT and oligometastatic disease

OC-0444

Stereotactic body radiotherapy of hepatocellular carcinoma lesions in liver transplant candidates

J. Shiao[1], A. Gutierrez[1], A. Patel[1], A. Harris[1], K. Washburn[2], G. Halff[2], J. Lopera[3], F. Sharkey[4], R. Crownover[1]

[1]*University of Texas Health Science Center San Antonio, Radiation Oncology, San Antonio, USA*

[2]*University of Texas Health Science Center San Antonio, Transplant Surgery, San Antonio, USA*

[3]*University of Texas Health Science Center San Antonio, Radiology, San Antonio, USA*

[4]*University of Texas Health Science Center San Antonio, Pathology, San Antonio, USA*

Purpose or Objective: To determine the radiographic response of Hepatocellular Carcinoma (HCC) lesions treated via stereotactic body radiotherapy (SBRT) in a series of liver transplant candidates and to correlate these findings with pathology after transplant.

Material and Methods: We retrospectively reviewed 17 liver transplant candidates from December 2008 to December 2013 at a single institution with discrete HCC lesions were treated with SBRT for evaluation of local control (LC); other methods of bridging patients to transplant were also available. Peripheral SBRT dose was either 50 Gy in 5 fractions or 45 Gy in 3 fractions with 2 fractions weekly. The records of transplant patients who underwent SBRT for single or multiple hepatomas were reviewed for maximum tumor dimension (MTD) at time of simulation, last imaging before transplant, and gross pathology following transplant. Radiographic LC of the treated lesion was defined as stable or decreasing enhancement on imaging with either triple-phase CT Liver or MRI Liver prior to transplant as demonstrated in Figure 1; this was recorded one month subsequent to treatment and just before the transplant. Pathologic Control (PC) was defined as stable to decreased size in MTD and/or no viable tumor present.

Figure 1. MR Imaging of HCC Lesion prior to (left) and after SBRT (right)

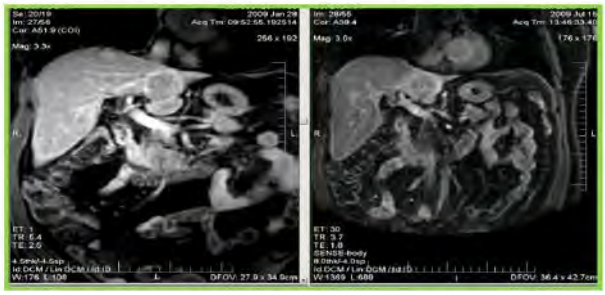

Results: Twelve patients have successfully been transplanted. All patients were male with a median age of 57 years. Of the 12 patients transplanted, there were 17 lesions treated. Median MTD at time of radiation was 3.6 cm (1.1cm - 6.1 cm). Median time to transplant from radiation treatment for 12 patients was 9 months (2mo-18mo). Table 1 summarizes tumor and treatment characteristics. Eight lesions (47%) had no evidence of viable tumor on pathology. Radiographic LC and PC was achieved in all 17 lesions. At a median follow-up of 53 months, disease free and overall survival were 100% with no evidence of disease (NED). Of the remaining 5 candidates, 3 patients awaiting transplant had one lesion, 1 had two lesions, and 1 had three lesions treated via SBRT. No patient experienced significant decrement in liver function nor indication of radiation induced liver disease. One patient experienced Grade 1 abdominal pain and three patients experienced Grade 1 nausea.

Table 1. Tumor and Treatment Characteristics for Patients With HCC Treated With SBRT as a Bridge to Liver Transplantation

Patient	Pre-SBRT Treatment	Tumor Diameter (cm)	Tumor Volume (cm^3)	SBRT Dose (Gy)/ fractions	Time from SBRT to Liver Transplantation (Days)	Explant Pathology/ Tumor Size (cm)/ Tumor volume (cm^3)	Follow-up After SBRT (Months)	Disease Status
1a	None	3.8	n/a	50/5	286	No viable tumor	51	NED
1b	None	4.1	n/a	50/5	286	Residual HCC/ 4.3/ 54.2	51	NED
2	TACE x 1	6.1	11.7	50/5	73	Residual HCC/ 5	45	NED
3a	TACE x 2	4.6	60.9	50/5	541	No viable tumor	15	NED
3b	RFA x 1	1.9	n/a	50/5	541	No viable tumor	15	NED
4a	None	3.5	13.4	50/5	115	Degenerative HCC/ 3.5/21	54	NED
4b	None	2.2	1.9	50/5	115	Residual HCC/ 1.8/ 0.8	54	NED
4c	None	1.1	8.0	50/5	115	Residual HCC/ 1.3/ 2.9	54	NED
5	None	4	46.8	50/5	352	Residual HCC/ 2.2/ 6.7	41	NED
6	None	2.9	7.1	50/5	137	Residual HCC/ 1.8/ 2.8	33	NED
7a	RFA x 2	2.2	4.8	45/3	130	No viable tumor	3	NED
7b	RFA x2	2.4	n/a	45/3	130	No viable tumor	3	NED
8	TACE x 1	2.7	8.0	45/3	374	No viable tumor	17	NED
9	TACE x 1	4.3	43.1	45/3	376	Residual HCC/ 1.5/16.3	41	NED
10	None	4	29.5	50/5	381	Residual HCC/ 3/ 33.6	47	NED
11	TACE x 3 RFA x 1	5.5	2.1	50/5	223	No viable tumor	223	NED
12	TACE x1	5.6	8.4	50/5	321	No viable tumor	15	NED

Conclusion: SBRT for HCC lesions in transplant candidates is an effective means of LC with successful bridging to transplant. Radiologic assessment subsequent to SBRT correlated with pathologic findings after transplant. These promising results suggest a broader role for SBRT in management of limited volume HCC.

OC-0445

Patterns of care and outcome analysis of SBRT for liver metastases - a DEGRO database initiative

N. Andratschke[1], H. Alheid[2], M. Allgäuer[3], G. Becker[4], O. Blanck[5], J. Boda-Hegemann[6], T. Brunner[7], S. Combs[8,9], M. Duma[8], S. Gerum[18], M. Guckenberger[1,10], G. Hildebrandt[11], C. Ostheimer[12], C. Panje[1], A. Papachristofilou[13], C. Petersen[14], T. Schneider[15], R. Semrau[16], S. Wachter[17], D. Habermehl[9]

[1]*University Hospital Zürich, Department of Radiation Oncology, Zurich, Switzerland*

[2]*Strahlentherapie Bautzen, Radiation Oncology, Bautzen, Germany*

[3]*Krankenhaus Barmherzige Brüder, Radiation Oncology, Regensburg, Germany*

[4]*RadioChirurgicum CyberKnife Südwest, Radiation Oncology, Göppingen, Germany*

[5]*Universitätsklinikum Schleswig-Holstein, Radiation Oncology, Kiel/Lübeck, Germany*

[6]*University Hospital Mannheim, Radiation Oncology, Mannheim, Germany*

[7]University Hospital Freiburg, Radiation Oncology, Freiburg, Germany
[8]Klinikum rechts der Isar- Technische Universität München, Radiation Oncology, Munich, Germany
[9]University Hospital Heidelberg, Radiation Oncology, Heidelberg, Germany
[10]University Hospital Würzburg, Radiation Oncology, Würzburg, Germany
[11]University Hospital Rostock, Radiation Oncology, Rostock, Germany
[12]University Hospital Halle, Radiation Oncology, Halle, Germany
[13]University Hospital Basel, Radiation Oncology, Basel, Switzerland
[14]University Medical Center Hamburg-Eppendorf, Radiation Oncology, Hamburg, Germany
[15]Strahlenzentrum Hamburg, Radiation Oncology, Hamburg, Germany
[16]University Hospital of Cologne, Radiation Oncology, Cologne, Germany
[17]Klinikum Passau, Radiation Oncology, Passau, Germany
[18]University of Munich, Radiation Oncology, Munich, Germany

Purpose or Objective: The intent of this pooled analysis as part of the German Society for Radiation Oncology (DEGRO) stereotactic body radiotherapy (SBRT) initiative was to analyse the pattern of care of SBRT for liver metastases in Germany and to derive factors influencing local control and overall survival in a large patient cohort.

Material and Methods: From 17 German and Swiss radiotherapy centers, data on all patients treated for liver metastases with SBRT since its introduction in 1997 was collected and entered into a centralised database as an effort of the SBRT task group of the DEGRO. In addition to patient and tumor characteristics, data on immobilization, image guidance and motion management as well as dose prescription and fractionation was gathered. Besides dose response and survival statistics, time trends of the aforementioned variables were investigated.

Results: In total, 442 patients with 586 liver metastases (median 1 lesion/patient; range 1-4) have been collected from 1997 until 2014. Predominant histologies were colorectal cancer (n=213), lung cancer (n=26) and breast cancer (n=57). All centers employed a SBRT-specific setup (including abdominal compression in 41%). Initially, stereotactic coordinates and CT simulation was used for treatment set-up (55%), but eventually replaced by CBCT guidance (28%) or more recently robotic tracking (17%). High variance in fraction (fx) number (median 1 fx; range 1-13) and dose per fraction (median: 18.5 Gy; range 3-37.5 Gy) was observed, although median BED remained consistently high after an initial learning curve. Median follow-up time was 13 months; median overall survival after SBRT was 24 months. 1 and 2 year local control rate of treated lesions was 77% and 64%; local control increased to 83% and 70%, respectively, if maximum isocenter biological equivalent dose (BED) was greater than 120 Gy EQD2Gy versus below that dose.

Conclusion: After a learning curve with regards to total cumulative doses, consistent biologically effective doses were employed, although with a significant variation in number of fraction, single fraction dose and prescription isodose. A clear dose response was observed with high local control after 1 and 2 years with higher BED. Nevertheless, local control is still inferior compared to lung metastases with a similar distribution of histologies. Therefore, further analysis needs to investigate the influence of image guidance and motion management as well as radiation sensitivity on local tumor control.

OC-0446

Extra-cranial SBRT in patients with oligometastatic disease: a dose-escalation study

F. Deodato[1], G. Macchia[1], S. Cilla[2], M. Nuzzo[1], L. Ronchi[3], A. Ianiro[2], R. Autorino[4], G. Mantini[4], R. Frakulli[3], S. Cammelli[3], G. Compagnone[5], A.L. Angelini[5], G. Frezza[6], L. Caravatta[7], A. Farioli[8], V. Valentini[4], A.G. Morganti[3]
[1]Fondazione di Ricerca e Cura "Giovanni Paolo II"- Catholic University of Sacred Heart, Radiation Oncology Unit, Campobasso, Italy
[2]Fondazione di Ricerca e Cura "Giovanni Paolo II"- Catholic University of Sacred Heart, Medical Physics Unit, Campobasso, Italy
[3]S. Orsola-Malpighi Hospital- University of Bologna, Radiation Oncology Center- Department of Experimental- Diagnostic and Specialty Medicine – DIMES, Bologna, Italy
[4]Policlinico Universitario "A. Gemelli"- Catholic University of Sacred Heart, Radiation Oncology Center, Roma, Italy
[5]S. Orsola-Malpighi Hospital- University of Bologna, Department of Medical Physics, Bologna, Italy
[6]Bellaria Hospital, Radiotherapy Department, Bologna, Italy
[7]P.O. Businco, Radiotherapy Unit- Centro di Radioterapia e Medicina Nucleare, Cagliari, Italy
[8]S. Orsola-Malpighi Hospital- University of Bologna, Department of Medical and Surgical Sciences DIMEC, Bologna, Italy

Purpose or Objective: To define maximum tolerated dose (MTD) of stereotactic treatment (SBRT) performed in different clinical settings.

Material and Methods: This analysis was based on a dose-escalation (Phase I) trial. Patients were enrolled in seven different arms depending on treatment site and previous treatment: 1) intraparenchymal lung tumors; 2) lung tumors near to chest wall or to mediastinum; 3) extra pulmonary tumors; 4) re-irradiation after radiotherapy (< 60 Gy); 5) re-irradiation after radiotherapy (> 60 Gy) or re-irradiation of pelvic and pancreatic tumors; 6) boost after a dose < 50Gy; 7) boost after a dose≥50Gy. SBRT was delivered in 5 fractions. The dose was prescribed at isocenter with a 3D static technique using 4-5 non-coplanar beams or with VMAT technique. PTV was defined as the GTV + 5-15 mm. Considering study arms, the first group of patients received 20 Gy, while other cohorts of patients received doses up to 50 Gy. Grade 3 acute and late toxicities were considered as dose limiting toxicity (DLT). If 2/6 or 4/12 DLT were recorded in one cohort, that dose was considered as MTD.

		1	2	3	4	5	6	7
Level	n° pts	Lung Target	Lung Target with inclusion of mediastinum or chest wall	Extra thoracic target (neck, abdomen, pelvis)	Retreatment: Previous Dose ≤ 60Gy (pancreas and pelvis); Previous Dose>60Gy	Retreatment: Previous Dose≤60Gy	SBRT-boost (Post ERT 45-50 Gy)	SBRT-boost (Post ERT >50Gy)
A	6 §	25 Gy	25 Gy	25 Gy	20 Gy	25 Gy	25 Gy	20 Gy
B	6 §	37.5 Gy	30 Gy	30 Gy	25 Gy	30 Gy	30 Gy	25 Gy
C	6 §	45 Gy	35 Gy	35 Gy	30 Gy*	35 Gy	35 Gy*	30 Gy
D	6 §	50 Gy	40 Gy	40 Gy	35 Gy	40 Gy		
E	6 §		45 Gy	45 Gy	40 Gy	45 Gy		
F	6 §		50 Gy	50 Gy	45 Gy	50 Gy		

On-going dose level is underlined; *: 1 DLT; ERT: external beam radiotherapy

Results: 213 patients were enrolled (M/F: 125/88), median age was 69 years (35-90) and 281 lesions were treated (102 primary tumors or local recurrences, 96 nodal and 83 distant metastases); they were mainly lung cancer (31%), gynaecologic cancer (24%), gastrointestinal neoplasms (22%), urologic tumour (12%), in the following sites: 150 in neck or chest, 70 in abdomen and 61 in pelvis. With a median follow-up of 17 months (3-131) the overall response rate was 82% (Complete Response: 58%; Partial Response: 24%), with only 3% of patients developing disease progression. DLT was recorded only in two patients, both treated with 50 Gy. Two-year and 4-year local control were 71% and 62%, respectively. Two-year and 4-year metastases free survival were 46% and 39%, respectively.

Conclusion: SBRT in five fractions up to a dose of 50 Gy is well tolerated in different clinical settings.

OC-0447

Stereotactic Body Radiotherapy (SBRT) in oligometastatic prostate cancer patients

C.L. Chaw[1], D. Henderson[1], V. Khoo[1], A. Tree[1], R. Eeles[1], N. Van As[1]

[1]*Institute of Cancer Research, Royal Marsden Hospital-Academic Uro-Oncology Department, London, United Kingdom*

Purpose or Objective: Oligometastatic prostate cancer is a state of limited metastatic disease≤(3 sites) that may be amenable to aggressive local therapy to achieve long term survival. The use of SBRT in this clinical setting has been reported to confer local control rate in excess of 90%, and encouraging progression free survival rate with no significant treatment –related toxicities1-4. One of the goals with this approach is to delay initiation of palliative systemic treatment, which can potentially impact negatively on quality of life. This study evaluated the outcomes of SBRT in our cohort.

Material and Methods: Forty five patients diagnosed with oligometastatic prostate cancer (defined as a rising PSA and positive CT/PET choline scan) after definitive local therapy were treated with 1-2 courses of SBRT between July 2011 and July 2015. Over 90% of metastases were situated in lymph nodes or bone. Median dose was 30 Gy in 3 fractions, prescribed to the highest isodose covering the PTV. Retrospective data collection and analysis were performed for these patients. Kaplan-Meier was utilised to estimate progression free survival and overall survival and time to initiation of systemic treatment. Nineteen of the 35 patients with castration sensitive disease were treated with SBRT alone for their oligometastatic disease, 16 patients received SBRT and Androgen Deprivation Therapy (ADT) with median duration of 5 months. 10 patients who were castration resistant at the diagnosis of oligometastases were treated with SBRT with ongoing systemic treatment.

Results: The median follow-up was 29 months (range 6-60 months). Local control rate of lesions following SBRT treatment was 90%, overall progression free survival (PFS) was 38%, overall survival (OS) of 89% at 29 months. A reduction of pre-treatment PSA value of 48% and 75%, respectively was seen in castration sensitive patients who received SBRT alone and SBRT with ADT, and a 25% PSA reduction in castration resistant patients treated with SBRT and ADT. Median time to clinical progression was longer in castration sensitive patients treated with SBRT and ADT compared to SBRT alone (13 months vs 25 months). The median ADT-free survival for castration sensitive patients was 16 months. Median time to initiation of next line therapy in castration resistant patients following SBRT treatment was 6 months. No grade 3 or 4 treatment related toxicities reported.

Conclusion: SBRT can provide a substantial delay to the next initiation of systemic therapy in castration sensitive patients whilst for castration resistant patients, there is a modest prolongation before initiation of subsequent therapy. Phase III data is lacking but will shortly be addressed in the SABR-COMET and CORE trials.

OC-0448

Give me five: extreme hypofractionated IG-IMRT for organ confined prostate cancer

B.A. Jereczek-Fossa[1,2], D. Ciardo[1], S.P. Colangione[3], C. Fodor[1], D. Zerini[1], A. Cecconi[1], A. Surgo[1], M.A. Gerardi[1], M. Muto[1], G. Timon[1], S. Comi[4], F. Pansini[4], A. Bazani[4], D. Maestri[4], M. Garioni[4], V. Scroffi[1], F. Cattani[4], R. Cambria[4], O. De Cobelli[2,5], R. Orecchia[1,2]

[1]*European Institute of Oncology, Department of Radiation Oncology, Milan, Italy*

[2]*University of Milan, Department of Oncology and Hemato-oncology, Milan, Italy*

[3]*European Institute of Oncology, Department of Radiation Oncology affiliation at the time of the study, Milan, Italy*

[4]*European Institute of Oncology, Unit of Medical Physics, Milan, Italy*

[5]*European Institute of Oncology, Department of Urology, Milan, Italy*

Purpose or Objective: Radiobiological findings suggest an improvement in the therapeutic ratio for prostate cancer (PCa) treated with hypofractionation, compared with conventional fractionation. On this basis, in 2012 we activated a prospective study on extreme hypofractionated image-guided intensity modulated radiation therapy (IG-IMRT) in organ-confined PCa. The aim of this study is the assessment of the feasibility of the proposed protocol – Give me five, in terms of acute and late toxicity and biochemical efficacy.

Material and Methods: The study was performed within the Institutional Ethics Committee notification regarding hypofractionated IGRT for PCa. Inclusion criteria were: low to intermediate-risk (according to NCCN risk categories) histologically confirmed PCa; personalized indication for high-risk patients; prostate volume <100cm3; N0 and cM0; age >18 years; specific informed consent. In 10% of patients, multiparametric MRI was used for an improved definition of the patient anatomy, in addition to CT imaging. The nominal prescription dose was 32.5 or 35 Gy scheduled in 5 fractions on alternate days (therefore the name of protocol, "Give me five"), namely 6.5-7 Gy/fraction respectively, corresponding to a normalized total dose delivered at 2-Gy/fraction of 74.3 or 85 Gy, respectively, estimating an α/ß ratio of 1.5 Gy. Dose delivery was performed with VERO®-BrainLab-Mitsubishi or RapidArc®-Varian. No fiducial markers were implanted and set-up verification was performed daily by means of CBCT imaging. Toxicity was evaluated according RTOG/EORTC scales. The study was founded by Associazione Italiana per la Ricerca sul Cancro - AIRC, grant no. 13218.

Results: Between April 2012 and May 2015, 166 patients were eligible. All patients completed the treatment. Median follow-up was 12.5 months (range 6-32.7 months). Fifty-eitght, 83, 24 and 1 patients out of 166 were at low, intermediate, high and unknown risk, respectively. Median age was 74.3 years, median Gleason score was 6. Considering acute toxicity, 89.8%, 7.8%, 2.4% of patients had gastro-intestinal G0, G1, G2 toxicity, respectively; 54.2%, 35.5%, 9.6%, 0.6% of patients had genito-urinary G0, G1, G2, G4 toxicity, respectively. Late toxicity and outcome were assessed in 129 patients (6 months minimum follow-up). Considering late toxicity, 3.1% and 0.8% of patients had gastro-intestinal G1 and G2 toxicity; 12.4%, 6.2% and 0.8% of patients had genito-urinary G1, G2, G3 toxicity, respectively. Clinical and biochemical progression prostate disease was observed in 2/129 of patients; currently, no evidence of prostate disease in 127/129 patients.

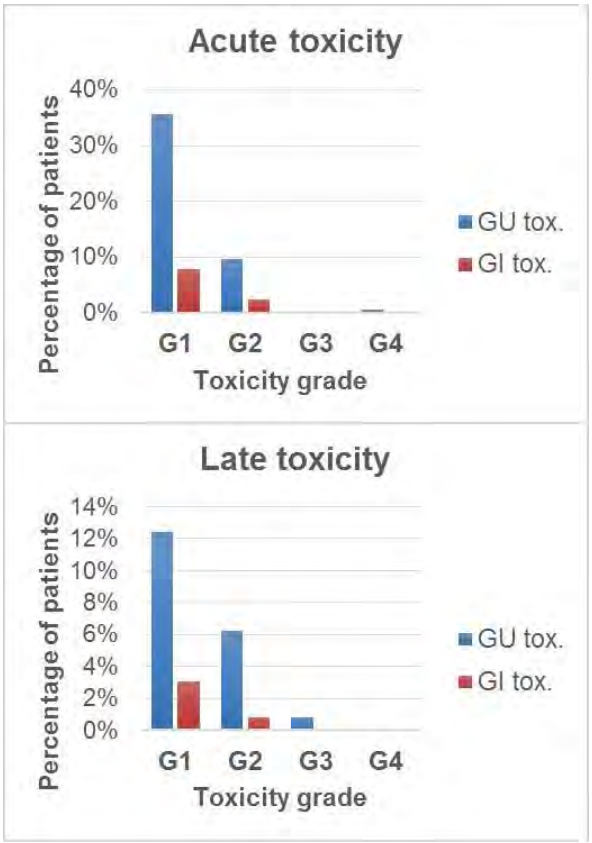

Conclusion: Longer time is needed to corroborate our encouraging early results in terms of toxicity, biochemical control rates, disease-free survival and overall survival. Our report shows that extremely hypofractionated IG-IMRT in localized PCa is feasible, safe and well tolerated with good PSA response and minimal toxicity.

Proffered Papers: Clinical 10: Head and neck

OC-0449

Pattern of failure and disease control in patients treated for glottic cancer in Denmark 1971-2011.

N. Lyhne[1], H. Primdahl[2], C. Kristensen[3], E. Andersen[4], J. Johansen[5], L. Andersen[6], J. Overgaard[1]

[1]*Aarhus University Hospital, Department of Experimental Clinical Oncology, Aarhus C, Denmark*

[2]*Aarhus University Hospital, Department of Oncology, Aarhus C, Denmark*

[3]*Rigshospitalet, Department of Oncology, Copenhagen, Denmark*

[4]*Herlev Hospital, Department of Oncology, Copenhagen, Denmark*

[5]*Odense University Hospital, Department of Oncology, Odense, Denmark*

[6]*Aalborg University Hospital, Department of Oncology, Aalborg, Denmark*

Purpose or Objective: To describe disease control, the pattern of failure, laryngeal preservation, and survival in a large consecutive national cohort of patients with glottic squamous cell carcinomas (scc) treated with primary radiotherapy (RT) and salvage surgery over a period of 41 years.

Material and Methods: Patients diagnosed alive with a scc of the glottic larynx between 1971 and 2011 were included if curative treatment was started. Patients were identified from the DAHANCA database, and crosschecked with the National Cancer Registry. Missing information was obtained from hospitals records and the National Patient Registry.

Results: A total of 5001 patients were identified. 98% of patients had primary RT. The median follow-up was 9.1 years (patients alive) and 5.7 years (patients who died). 10 patients were lost to follow-up. 1511 failures were observed; hereof 93 %, 11 % and 5 % included T- and/or N- and/or M-site, respectively. 5-year incidence of local failure (LF) and loco-regional failure (LRF) was 26 % and 27%, respectively. From the 1970s to the 2000s the 5-year incidence of LF and LRF decreased significantly; 32% vs 19% and 34% vs 21%, respectively. Curative salvage was intended in 1088/1511 patients with failure, hereof 707 achieved ultimate control. In total, 980 patients had a laryngectomy, hereof 11 was primary treatment, 12 were caused by morbidity. The 5-year incidence of laryngectomy was 18%, decreasing from 26 % (1970s) to 10% (2000s). The 5-year incidence of ultimate failure was unchanged over time (range 13-16 %). 5-year estimates of laryngectomy free survival (LFS), Disease free survival(DFS) and Overall survival(OS) was 54%, 63% and 64%, respectively. LFS increased continuously, contrary to DFS and OS, which were stable in the 1970s-1990s but increased in the 2000s. LFS, DFS and OS were significantly higher in the 00s compared to the earlier decades.

Conclusion: As a result of a national strategy with primary RT, a continually improving disease control with concurrent decrease in laryngectomy, was observed in this non-selected national cohort of patients. All survival parameters were significantly better in the 2000s compared to the earlier decades.

Supported by CIRRO and the Danish Cancer Society

OC-0450

Failure pattern and salvage treatment after radical treatment of head and neck cancer

A. Pagh[1], C. Grau[2], J. Overgaard[1]

[1]*Aarhus University Hospital, Department of Experimental Clinical Oncology, Risskov, Denmark*

[2]*Aarhus University Hospital, Department of Oncology, Aarhus, Denmark*

Purpose or Objective: The aim of the study was to test the hypothesis that head and neck cancer (HNC) patients benefits from specialized follow-up (FU), as this strategy ensures timely detection of relapses for successful salvage treatment. This was done by evaluation of the pattern of failure, the temporal distribution of recurrences, and the outcome of salvage treatment in a contemporary cohort of HNC patients

Material and Methods: The study evaluated a population based cohort of 2,062 consecutive patients treated with curative intent from 1 January 2000 to 31 December 2013. The database of DAHANCA contained recordings of recurrent disease in 567 patients with primary tumors of the larynx, pharynx, oral and nasal cavity, para-nasal sinuses and salivary glands. A review of medical records was performed in order to update and supplement the database.

Results: Failures of the 567 patients were T-site failures (65%) followed by N-site (36%) and M-site (22%) failures. The vast majority of the first recurrence occurred within the first years after primary treatment; 62%, 82%, and 91% within the first, second and third year, respectively. Totally, 51% were amenable for salvage treatment, and 44% benefited from salvage in terms of a complete response. Permanent tumor control was observed in 128 patients (23%) after one or two salvage attempts. The highest salvage rate was recorded in patients with primary glottic carcinoma (41%) and the lowest among hypopharyngeal cancers (2%). Asymptomatic recurrence was recorded in 12% of all recurrences and this was found to be a positive prognostic factor for disease-specific survival, as they had significantly better outcome after salvage.

Conclusion: Our data support the usefulness of specialized FU in terms of early detection of recurrent disease. In particular patients with silent recurrences benefitted from early detection, as they had a significantly lower risk ratio of death from primary HNC.

OC-0451

Tumour volume, hypoxia and cancer stem cells as prognosticators for LRC after primary RCT in HNSCC

A. Linge[1,2,3,4], F. Lohaus[1,2,3,4], S. Löck[1,2,3,5], V. Gudziol[6], A. Nowak[7], C. Von Neubeck[1,3], I. Tinhofer[8,9], V. Budach[8,9], A. Sak[10,11], M. Stuschke[10,11], P. Balermpas[12], C. Rödel[12,13], M. Avlar[14,15], A.L. Grosu[14,16], A. Abdollahi[17,18,19,20,21], J. Debus[17,18,19,22,23], C. Belka[24,25], S. Pigorsch[24,26], S.E. Combs[24,26], D. Mönnich[27,28], D. Zips[27,28], G.B. Baretton[1,29,30], F. Buchholz[1,31], M. Baumann[1,2,3,5], M. Krause[1,2,3,5]

[1]*German Cancer Research Center DKFZ, Heidelberg and German Cancer Consortium DKTK partner site Dresden, Dresden, Germany*

[2]*Faculty of Medicine and University Hospital Carl Gustav Carus- Technische Universität Dresden, Department of Radiation Oncology, Dresden, Germany*

[3]*OncoRay – National Center for Radiation Research in Oncology, Faculty of Medicine and University Hospital Carl Gustav Carus- Technische Universität Dresden, Dresden, Germany*

[5]*Helmholtz-Zentrum Dresden – Rossendorf, Institute of Radiooncology, Dresden, Germany*

[6]*Faculty of Medicine and University Hospital Carl Gustav Carus- Technische Universität Dresden, Department of Otorhinolaryngology, Dresden, Germany*

[7]*Faculty of Medicine and University Hospital Carl Gustav Carus- Technische Universität Dresden, Department of Oral and Maxillofacial Surgery, Dresden, Germany*

[8]*German Cancer Research Center DKFZ, Heidelberg and German Cancer Consortium DKTK partner site Berlin, Berlin, Germany*

[9]*Charité University Hospital, Department of Radiooncology and Radiotherapy, Berlin, Germany*

[10]*German Cancer Research Center DKFZ, Heidelberg and German Cancer Consortium DKTK partner site Essen, Essen, Germany*

[11]*Medical Faculty- University of Duisburg-Essen, Department of Radiotherapy, Essen, Germany*

[12]*Goethe-University Frankfurt, Department of Radiotherapy and Oncology, Frankfurt am Main, Germany*

[13]*German Cancer Research Center DKFZ, Heidelberg and German Cancer Consortium DKTK partner site Frankfurt, Frankfurt am Main, Germany*

[14]*German Cancer Research Center DKFZ, Heidelberg and German Cancer Consortium DKTK partner site Freiburg, Freiburg, Germany*

[15]*University of Freiburg, Department of Radiation Oncology- Clinical Study Section, Freiburg, Germany*

[16]*University of Freiburg, Department of Radiation Oncology, Freiburg, Germany*

[17]*German Cancer Research Center DKFZ, Heidelberg and German Cancer Consortium DKTK partner site Heidelberg, Heidelberg, Germany*

[18]*University of Heidelberg Medical School and German Cancer Research Center DKFZ, Heidelberg Institute of Radiation Oncology HIRO- National Center for Radiation Research in Oncology NCRO, Heidelberg, Germany*

[19]*University of Heidelberg Medical School- Heidelberg Ion Therapy Center HIT, Department of Radiation Oncology, Heidelberg, Germany*

[20]*University of Heidelberg Medical School and German Cancer Research Center DKFZ-, National Center for Tumor Diseases NCT, Heidelberg, Germany*

[21]*University of Heidelberg Medical School and German Cancer Research Center DKFZ, Translational Radiation Oncology, Heidelberg, Germany*

[22]*University of Heidelberg Medical School and German Cancer Research Center DKFZ, National Center for Tumor Diseases NCT, Heidelberg, Germany*

[23]*University of Heidelberg Medical School and German Cancer Research Center DKFZ, Clinical Cooperation Unit Radiation Oncology, Heidelberg, Germany*

[24]*German Cancer Research Center DKFZ, Heidelberg and German Cancer Consortium DKTK partner site Munich, München, Germany*

[25]*Ludwig-Maximilians-Universität, Department of Radiotherapy and Radiation Oncology, München, Germany*

[26]*Technische Universität München, Department of Radiation Oncology, München, Germany*

[27]*German Cancer Research Center DKFZ, Heidelberg and German Cancer Consortium DKTK partner site Tübingen, Tübingen, Germany*

[28]*Faculty of Medicine and University Hospital Tübingen- Eberhard Karls Universität Tübingen, Department of Radiation Oncology, Tübingen, Germany*

[29]*University Hospital Carl Gustav Carus- Technische Universität Dresden, Tumour- and Normal Tissue Bank- University Cancer Centre UCC, Dresden, Germany*

[30]*Faculty of Medicine and University Hospital Carl Gustav Carus- Technische Universität Dresden, Institute of Pathology, Dresden, Germany*

[31]*University Hospital Carl Gustav Carus- Technische Universität Dresden, University Cancer Centre UCC- Medical Systems Biology, Dresden, Germany*

Purpose or Objective: To investigate the impact of tumour volume, hypoxia and cancer stem cell (CSC) marker expression on outcome of patients with locally advanced head and neck squamous cell carcinoma (HNSCC) after primary radiochemotherapy.

Material and Methods: In this retrospective multicentre study, 160 patients with squamous cell carcinoma of the oral cavity, oropharynx and hypopharynx were included. All patients received primary cisplatin-based radiochemotherapy (RCT) between 2005 and 2011. Their median follow-up was about 26 months. Primary and nodal gross tumour volume (GTV) segmentations were performed centrally in the computer tomography-based radiation treatment plans. HPV status (p16 overexpression) and CD44 expression were analysed by immunohistochemistry. Gene expression analysis was performed for hypoxia-associated genes and the potential CSC marker SLC3A2. Results of the biomarker analyses, clinical parameters and tumour volume were correlated with the clinical outcome. Primary endpoint was loco-regional control (LRC). Secondary endpoints were distant metastases (DM) and overall survival (OS).

Results: In univariate analysis, tumour volume, HPV status and CSC marker expression were significantly associated with LRC (tumour volume: HR 1.51, p=0.02; HPV: HR 0.30, p=0.02; CD44: HR 2.30, p=0.04; SLC3A2: HR 2.08, p=0.01). Interestingly, hypoxia showed a significant association with LRC in small tumours only (HR 9.26, p=0.04). Multivariate Cox regression analysis including HPV status, tumour localisation, stage, smoking status, tumour volume and hypoxia or the respective CSC marker showed a significant effect of the tumour volume (HR: 1.6-1.8, p<0.01), SLC3A2 (HR 2.03, p=0.02) or CD44 (HR 2.52, p=0.04) on LRC. Tumour hypoxia also reached borderline significance in small tumours (HR 7.86, p=0.06). Interestingly, the tumour volume was an independent variable in all Cox models, a high tumour volume was significantly associated with poor LRC. Tumour volume and CSC marker expression also showed a negative prognostic impact on the secondary endpoints DM and OS.

Conclusion: We have shown that large tumour volume and high CSC marker expression correlate with poor LRC in patients with locally advanced HNSCC who received primary RCT. In small tumours, hypoxia also had a negative impact. After validation of these promising results in the ongoing prospective study of our study group, these biomarkers may help to further stratify patients for individualised treatment escalation or de-escalation strategies.

OC-0452

Prospective randomized adaptive dose-de-escalation in the elective neck: late toxicity and control

J. Schatteman[1], D. Nevens[2], S. Nuyts[2], D. Berwouts[1], W. De Gersem[3], L. Olteanu[3], T. Vercauteren[3], W. De Neve[3], F. Duprez[3]

[1]*Ghent University Hospital, Nuclear Medicine, Ghent, Belgium*

[2]*Leuven University Hospital, Radiotherapy, Leuven, Belgium*

[3]*Ghent University Hospital, Radiotherapy, Ghent, Belgium*

Purpose or Objective: A multicentre prospective randomized phase II trial investigated whether a 3-phase adaptive IMRT-scheme using reduced volumes of elective neck could reduce toxicity without compromising disease control compared to standard non-adaptive IMRT. We report on disease control and toxicity at 6 and 12 months of follow-up.

Material and Methods: All patients were primarily treated with IMRT ± chemotherapy for head and neck squamous cell carcinoma with a 2 Gy-equivalent dose of 40 Gy to the elective neck. The dose to the high-risk volume was not reduced. In the adaptive de-escalation (AD) arm, elective neck volumes were reduced based on a lower theoretical risk of subclinical disease and replanning was done after 2 and 4 weeks. In the control (C) arm, IMRT without adaptations and with standard volumes of elective neck was performed.
All statistics were performed using Fisher's exact test and Kaplan-Meier analysis (SPSS v. 23).

Results: Patiënts, tumor and treatment characteristics can be found in Table 1.
Before 1 year of follow-up, 12 patients deceased due to aspiration (n=1), tumor progression (n=8) or intercurrent disease (n=3).
At 6 months, we observed grade (G)≥2 dysphagia in 3% and 6% (p = 1.0), G≥2 xerostomia in 40% and 34% (p = 0.81) and G≥2 fibrosis in 6% and 6% (p = 1.0) in the AD- and C-arm, respectively. At 12 months, we observed grade G≥2 dysphagia in 17% and 3% (p = 0.09), G≥2 xerostomia in 43% and 28% (p = 0.28) and G≥2 fibrosis in 10% and 9% (p = 1.0) in the AD- and C-arm, respectively.
Local (LC), regional (RC) and distant control (DC) and overall survival (OS) for the whole group are given in Fig. 1. LC, RC, DC and OS were 86%, 84%, 82% and 74% in the AD-arm and 90%, 92%, 86% and 78% in the C-arm, respectively. All p-values were > 0.05. Regional relapse was observed in 8 (AD) and 4 (C) patients: 5/12 were isolated regional relapses (3 in the AD- and 2 in the C-arm) of which 3/5 isolated relapses were seen in the initial GTV of a pathological lymph node, 1/5 in the irradiated elective neck in the C-arm and 1/5 in the AD-arm in a region of the neck that would have been irradiated in the C-arm; salvage neck dissection was successfully performed. Seven regional relapses were combined with local recurrence (n=3) or metastases (n=4).

	AD-arm (n=50)	C-arm (n=50)	p-value
Age (range; in years)	63,0 (38-84)	62,4 (38-83)	
Male/female	39/11	42/8	0.61
Site: - Oropharynx - Hypopharynx - Larynx - Oral cavity	 24 13 10 3	 25 10 14 1	0.56
HPV-status oropharynx - Negative - Positive - Unknown	 5 4 15	 8 5 12	0.76
T-staging - T1 - T2 - T3 - T4a - T4b	 1 16 15 16 2	 3 12 20 12 3	0.55
N-staging - N0 - N1 - N2a - N2b - N2c - N3	 11 2 0 16 19 2	 11 6 1 16 15 1	0.58
Pre-IMRT neck dissection	5	5	1.00
Concomitant systemic therapy - Cisplatin-based - Cetuximab	30 29 1	29 27 2	1.00

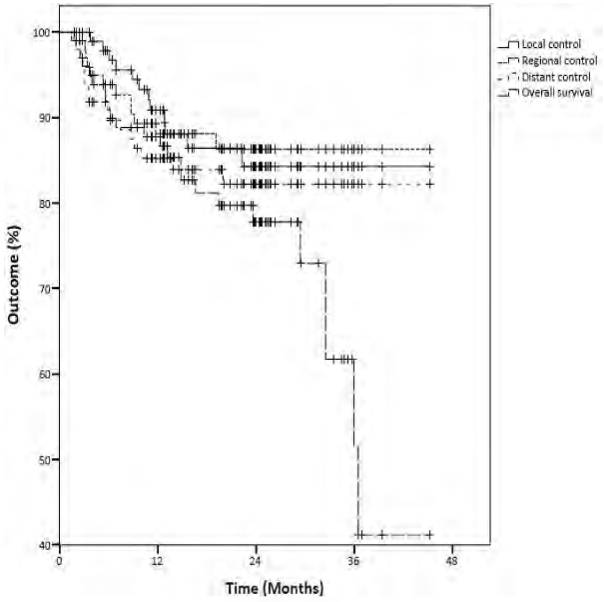

Conclusion: With a minimal follow-up of 1 year, no significant differences in RC, LC or DC or OS were observed between adaptive IMRT with reduced volumes of elective neck versus standard IMRT with non-reduced volumes, although 1 patient had an isolated regional recurrence in the non-treated elective neck. Unfortunately, the volume reduction and adaptive strategy did not result in a better late toxicity profile. We hypothesize that due to the large portion of patients with locoregionally advanced disease the treated neck volumes could not be sufficiently reduced in the whole group to achieve the desired gain in toxicity. Future analysis will now be started to elucidate this problem.

OC-0453

Phase II trial of de-intensified chemoradiotherapy for HPV-associated oropharyngeal cancer

B. Chera[1], R. Amdur[2], J. Tepper[1], B. Qaqish[3], R. Green[1], N. Hayes[4], J. Weiss[4], J. Grilley-Olson[4], A. Zanation[5], T. Hackman[5], W. Funkhouser[6], N. Sheets[7], M. Weissler[5], W. Mendenhall[2]
[1]*University of North Carolina, Radiation Oncology, Chapel Hill- NC, USA*
[2]*University of Florida, Radiation Oncology, Gainesville- FL, USA*
[3]*University of North Carolina, Biostatistics, Chapel Hill, USA*
[4]*University of North Carolina, Medicine- Division of Hematology Oncology, Chapel Hill- NC, USA*
[5]*University of North Carolina, Otolaryngology/Head and Neck Surgery, Chapel Hill- NC, USA*
[6]*University of North Carolina, Pathology, Chapel Hill- NC, USA*
[7]*Rex UNC Healthcare, Radiation Oncology, Raleigh- NC, USA*

Purpose or Objective: We performed a prospective multi-institutional phase II study of a substantial decrease in concurrent chemoradiotherapy (CRT) intensity as primary treatment for favorable risk, HPV-associated oropharyngeal squamous cell carcinoma (OPSCC).

Material and Methods: The major inclusion criteria were: 1) T0-T3, N0-N2c, M0, 2) HPV or p16 positive, and 3) minimal/remote smoking history. Treatment was limited to 60 Gy intensity modulated radiotherapy with concurrent weekly intravenous cisplatinum (30 mg/m2). The primary study endpoint was pathologic complete response rate (pCR) based on required biopsy of the primary site and dissection of pretreatment positive lymph node regions, regardless of radiographic response. Power computations were performed for the null hypothesis that the pCR rate is 87% and N=40, resulting in a type I error of 14.2%. Secondary endpoint measures included physician reported toxicity (CTCAE), patient reported symptoms (PRO-CTCAE), quality of life

(EORTC QLQ-C30 & H&N35), and penetration aspiration scale (PAS) scores for modified barium swallow studies.

Results: The study population is 43 patients. The pCR rate was 86% (37/43). All 6 non-pCR cases were limited to microscopic foci of residual cancer: 1 primary site, 5 nodal. All patients are alive with no evidence of disease (median follow-up 21.3 months, range 4-41 months). Thirty-eight patients had a follow-up of at least one year. The incidence of acute CTCAE Grade 3/4 toxicity and PRO-CTCAE severe/very severe symptoms were: mucositis 34%/45%, pain 5%/48%, nausea 18%/52%, vomiting 5%/34%, dysphagia 39%/55%, and xerostomia 2%/75%. Grade 3/4 hematological toxicities were 11%. Mean pre and 6 month post CRT EORTC QOL scores were: Global 80/71 (lower worse), Pain (mouth, jaw, throat) 19/21 (higher worse), Swallowing 11/16, Coughing 17/26, Dry Mouth 16/68, and Sticky Saliva 6/49. Six months post CRT mean PRO-CTCAE scores for swallowing and dry mouth were mild and moderate, respectively. No patients reported their swallowing or dry mouth symptoms to be severe or very severe. 39% of patients required a feeding tube (none permanent) for a median of 15 weeks (5 - 22 weeks). There were no significant differences in PAS scores for thin, pureed, and solid foods before and after CRT.

Conclusion: Pathological CR rate with decreased intensity of therapy with 60 Gy of IMRT and weekly low-dose cisplatinum is very high in favorable risk OPSCC with evidence of decreased toxicity compared to standard therapies. (ClinicalTrials.gov, NCT01530997)

OC-0454

Clinical outcome in nasopharyngeal carcinoma patients with post-radiation detectable plasma EBV DNA

J.C. Lin[1], W.Y. Wang[2], C.W. Twu[3]
[1]*Taichung Veterans General Hospital, Department of Radiation Oncology, Taichung, Taiwan*
[2]*Hung Kuang University, Department of Nursing, Taichung, Taiwan*
[3]*Taichung Veterans General Hospital, Department of Otorhinolaryngology, Taichung, Taiwan*

Purpose or Objective: To investigate the long-term clinical behavior of nasopharyngeal carcinoma (NPC) patients with persistently detectable plasma EBV (pEBV) DNA after curative radiotherapy (RT) with/without chemotherapy.

Material and Methods: We screened 931 newly diagnosed NPC patients who finished curative RT and found 125 patients (13.4%) with detectable pEBV DNA one week after finishing RT. The clinical characteristics, treatment modality, subsequent failure patterns and survivals were analyzed.

Results: The levels of post-RT pEBV DNA for the studied population were in a very lower copy number (median 21, interquartile range 8-206 copies/mL). After a minimal follow-up of 52 months, the subsequent relapse rate was 64.8% (81/125) with distant failure predominantly and the median time to progression is 20 months for all 125 patients. Thirty-two of 39 (82.1%) patients with post-RT pEBV DNA $\geq$ 100 copies/ml developed tumor relapse later, whereas 57.0% (49/86) patients with post-RT pEBV DNA < 100 copies/ml had tumor relapse (P=0.0065). The 5-year rates of overall survival (OS) were 20.5% and 62.9% for the patients with post-RT viral load $\geq$ and < 100 copies/mL (HR, 0.22; 95% CI, 0.12 to 0.38; P<0.0001). Patients who received adjuvant chemotherapy (AdjCT) with oral tegafur-uracil experienced significant reduction in distant failures (66.2% vs. 31.6%; P=0.0001) but similar locoregional recurrences (P=0.234). The 5-year OS rates were 69.4% for the patients who received AdjCT compared with 33.2% for those of without AdjCT (HR, 0.38; 95% CI, 0.24 to 0.61; P<0.0001).

Conclusion: NPC patients with persistently detectable pEBV DNA after finishing RT have a higher rate of treatment failure. Levels of the post-RT pEBV DNA and administration of AdjCT affect the final outcome. Future trial should consider post-RT pEBV DNA levels as a stratification factor and investigate the role of AdjCT for the target population.

Proffered Papers: Physics 11: Dose measurement and dose calculation II

OC-0455

Development of activity pencil beam algorithm using nuclear reaction for innovative proton therapy

A. Nishio-Miyatake[1], T.N. Teiji Nishio[2]
[1]*Keen Medical Physics Corporation, Medical Physics Research, Yokohama, Japan*
[2]*Hiroshima University, Institute of Biomedical & Health Sciences, Hiroshima, Japan*

Purpose or Objective: Proton therapy is a form of radiotherapy that can be concentrated on a tumor using a scanned or modulated Bragg peak. To use this radiotherapy efficiently in a clinical context, it is necessary to evaluate the clinical proton-irradiated volume accurately. Therefore, a beam ON-LINE PET system (BOLPs) has been developed for activity imaging of various positron emitter nuclei generated from each target nucleus by target nuclear fragment reactions with irradiated proton beam. The purpose of this study is to develop an activity pencil beam (APB) algorithm for a simulation system for proton activated positron-emitting imaging in proton therapy.

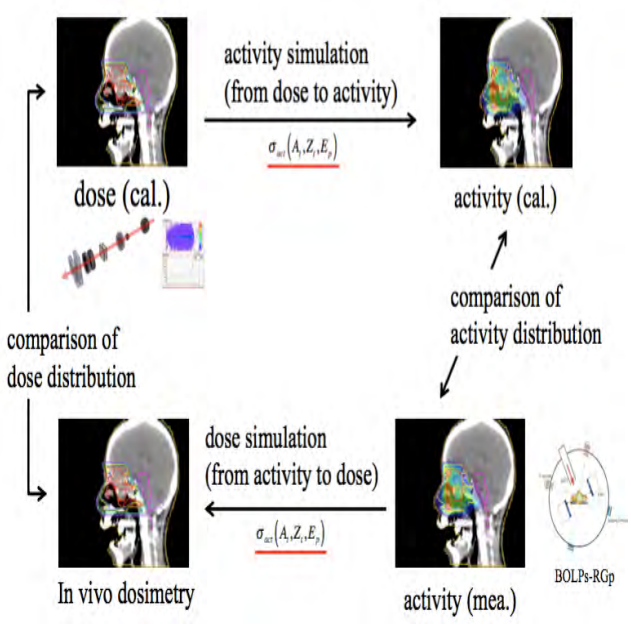

Material and Methods: The APB algorithm was developed as a calculation algorithm of the activity distributions formed by positron emitter nuclei generated from target nuclear fragment reactions. Depth activity data of 12C nuclei, 16O nuclei, and 40Ca nuclei were measured with BOLPs after proton beam irradiation whose energies were 138, 179, and 223 MeV. Measurement time was about 5 h until the measured activity reached the background level.

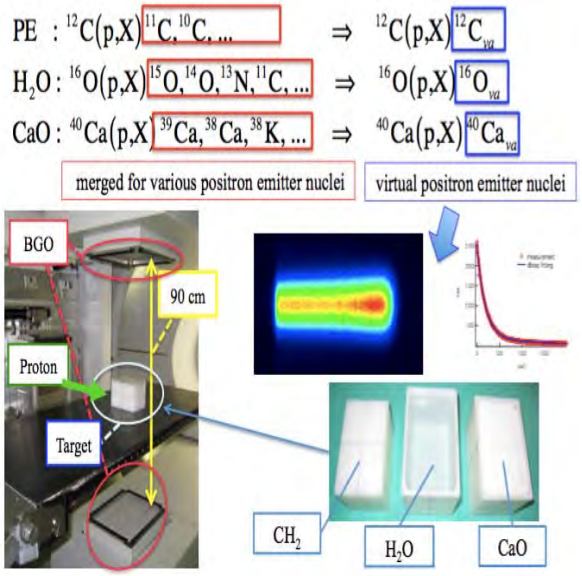

Results: Data of measured depth activity distributions were prepared using the measured depth activity data. Activity pencil beam kernels needed for the APB algorithm were constructed using the data of measured depth activity distributions and calculations in lateral direction. Gaussian form was used for the lateral distribution data to take the effect of multiple Coulomb scattering into consideration.

Conclusion: A method of obtaining the depth activity distributions and the APB algorithm were developed. The simulation system with the APB algorithm can be used in clinical proton therapy.

OC-0456

Translation of a prompt gamma based proton range verification system to first clinical application

C. Richter[1,2,3,4], G. Pausch[1], S. Barczyk[1,2], M. Priegnitz[5], C. Golnik[1], L. Bombelli[6], W. Enghardt[1,2,3,4], F. Fiedler[5], C. Fiorini[7], L. Hotoiu[8], G. Janssens[8], I. Keitz[1], S. Mein[1], I. Perali[7], D. Prieels[8], J. Smeets[8], J. Thiele[2], F. Vander Stappen[8], T. Werner[1], M. Baumann[1,2,3,4]

[1]*OncoRay - National Center for Radiation Research in Oncology, Faculty of Medicine and University Hospital Carl Gustav Carus- Technische Universität Dresden- Helmholtz-Zentrum Dresden-Rossendorf, Dresden, Germany*

[2]*University Hospital Carl Gustav Carus- Technische Universität Dresden, Department of Radiation Oncology, Dresden, Germany*

[3]*Helmholtz-Zentrum Dresden – Rossendorf, Institute of Radiooncology, Dresden, Germany*

[4]*German Cancer Consortium DKTK and German Cancer Research Center DKFZ, Dresden, Germany*

[5]*Helmholtz-Zentrum Dresden – Rossendorf, Institute of Radiation Physics, Dresden, Germany*

[6]*XGLAB S.R.L, Milano, Italy*

[7]*Politecnico di Milano, Dipartimento di Elettronica-Informazione e Bioingegneria, Milano, Italy*

[8]*Ion Beam Applications SA, Louvain-la-Neuve, Belgium*

Purpose or Objective: To improve precision of particle therapy, in vivo range verification is highly desirable. Methods based on prompt gamma rays emitted during treatment seem promising but have not yet been applied clinically. Here we report on the translational implementation as well as the worldwide first clinical application of prompt gamma imaging (PGI) based range verification.

Material and Methods: Focused on the goal of translating a knife-edge shaped slit camera prototype into clinical operation, we first systematically addressed remaining challenges and questions. A robust energy calibration routine and corresponding quality assurance protocols were developed. Furthermore, the positioning accuracy of the system was determined. The slit camera, intentionally developed for pencil beam scanning, was applied for double scattered (DS) proton beams. Systematic phantom experiments with increasing complexity have been performed.

In the next step, the knife-edge shaped slit camera was applied clinically to measure the spatial prompt gamma ray distribution during a proton treatment of a head and neck tumor for seven consecutive fractions. Inter-fractional variations of the prompt gamma profile were evaluated. For three fractions in-room control CTs were acquired and evaluated for dose relevant changes.

Results: In translational phantom experiments it was shown that proton range shifts can be visualized with the camera system for DS proton irradiation, proving its applicability under conditions of increased neutron background. Moreover, prompt gamma profiles for single iso-energy layers were extracted by synchronizing time resolved measurements to the rotation of the range modulator wheel of the DS treatment system. Furthermore, the position precision of the slit camera has been determined to provisionally be 1.1 mm (2σ).

With this preparatory work, the first clinical application of the PGI slit camera was successful. Based on the PGI information, inter-fractional global range variations were in the range of ±2 mm for all evaluated fractions. The results of the iso-energy layer resolved prompt gamma profile analysis were in consistence with the sum profile analysis. Also the control CT based dose reconstruction revealed negligible range variations of about 1.5 mm. No influence of DVH parameters for target volume and organs at risk was found.

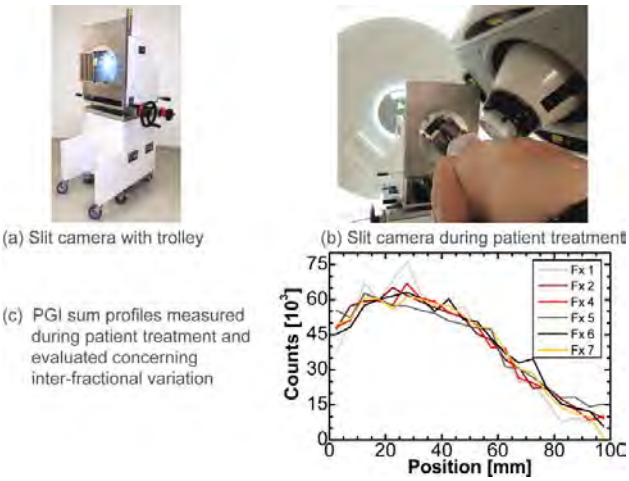

Conclusion: This work demonstrates for the first time that prompt gamma ray based range verification can be applied for clinical treatment of patients. Further plans include the continuation of the clinical study to perform systematic evaluations based on an appropriate patient number. With the translation from basic physics experiments into clinical operation, the authors are confident that a prompt-gamma ray based technology is capable of range verification and can be used in the near future for online quality assurance as well as in midterm for potential margin reduction.

OC-0457

Towards analytic dose calculation for MR guided particle beam therapy

H. Fuchs[1], P. Moser[1], M. Gröschl[2], D. Georg[1]

[1]*Medical University of Vienna, Department of Radiation Oncology & Christian Doppler Laboratory for Medical Radiation Research for Radiation Oncology, Vienna, Austria*

[2]*Vienna University of Technology, Institute of Applied Physics, Vienna, Austria*

Purpose or Objective: The importance of MRI steadily increases in radiation oncology not only as multimodality imaging device but also as an implemented online imaging

technology. Imaging using MRI shows advantages compared to CT or CBCT offering superior soft tissue contrast without additional dose. Also in particle beam therapy integrated MR guided treatment units have great potential. A complete understanding of the particle beam characteristics in the presence of magnetic fields is required. So far, studies in this area are limited.

Material and Methods: Protons (60-250MeV) and carbon ions (120-400MeV/u) in the clinically required energy range impinging on a phantom of 35x35x50cm^3 size were simulated using the MC framework GATE 7. Homogeneous magnetic fields of 0.35T, 1T and 3T perpendicular to the initial beam axis were applied. The beam deflection, shape, and the energy spectrum at the Bragg peak area was analyzed. A numerical algorithm was developed for deflection curve generation solving the relativistic equations of motion taking into account the Lorentz force and particle energy loss. Additionally, dose variations on material boundaries induced by magnetic fields were investigated for 250MeV protons.

Results: Transverse deflections up to 99mm were observed for 250MeV protons at 3T. Deflections for lower field strengths (e.g. future hybrid open-MRI proton delivery systems) yielded 12mm for 0.35T and 34mm for 1T. A change in the dose distribution at the Bragg-peak region was observed for protons. Energy spectrum analysis showed an asymmetric lateral energy distribution. The different particle ranges resulted in a tilted dose distribution, see Fig.1.The numerical algorithm successfully modeled the deflection curve, with a maximum deviation of 1.8% and calculation times of less than 5ms. For a 250MeV proton beam passing in a 3T field through multiple slabs (water-air-water), only a 4% local dose increase at the first boundary was observed in single voxels due to the electron return effect.

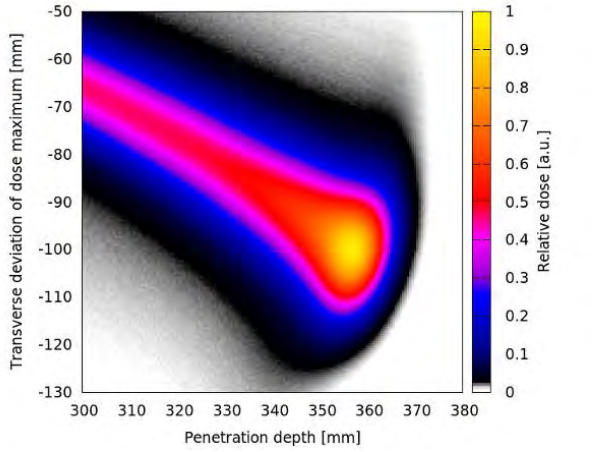

Fig1: Deformed 2D dose distribution at the Bragg peak area for a 250MeV proton beam in a 3T field

Conclusion: Beam deflections in magnetic fields could be described by a numerical algorithm. The observed change in dose distribution in the Bragg-peak region has to be taken into account in future dose calculations. However, local dose changes due to boundary effects seem to be negligible for clinical applications. Current work in progress deals with the inclusion of magnetic field effects in a dose calculation algorithm for particles.

OC-0458

Delivery errors detectability with IQM, a system for real-time monitoring of radiotherapy treatments

L. Marrazzo[1], C. Arilli[1], M. Casati[1], S. Calusi[2], C. Talamonti[1,2], L. Fedeli[2], G. Simontacchi[3], L. Livi[2,3], S. Pallotta[1,2]

[1]*Azienda Ospedaliera Universitaria Careggi, Medical Physics Unit, Firenze, Italy*

[2]*University of Florence, Department of Biomedical-Experimental and Clinical Sciences 'Mario Serio', Florence, Italy*

[3]*Azienda Ospedaliera Universitaria Careggi, Radiation Therapy Unit, Firenze, Italy*

Purpose or Objective: To test the ability of detecting small delivery errors of the Integral Quality Monitoring (IQM) device (iRT Systems GmbH, Koblenz, Germany), a system for online monitoring of Intensity Modulated Radiation Therapy (IMRT) treatments. To evaluate the correlation between the changes in the detector output signal induced by small delivery errors with other metrics, such as the γ passing rate and the DVH variations, which are commonly employed to quantify the deviations between calculated and actually delivered dose distributions.

Material and Methods: IQM consists of a large area ionization chamber, with a gradient in the electrode plate separation, to be mounted on the treatment head, and a calculation algorithm to predict the signal based on the data received from the treatment planning system. The output of the ionization chamber provides a spatially dependent signal for each beam segment. 5 types of errors were induced in clinical IMRT step and shoot plans for head and neck (H&N), prostate and index quadrant planned with Pinnacle (Philips) with an Elekta Precise linac (6 MV), by modifying the number of delivered MUs and by introducing small deviations in leaf positions. The obtained dose distributions, both 'error free' (EF) and 'error induced' (EI) were delivered with the IQM system and the signal variations were recorded. EF and EI dose distributions were also compared in terms of: 1) 3D γ passing rate calculated on the entire dose volume; 2) 2D γ passing rate calculated on planar beam-by-beam dose distributions; 3) DVH metric, by calculating the differences for several significant DVH parameters. The correlation between IQM signal variations and 3D γ, 2D γ and DVH parameters was investigated.

Results: IQM system resulted to be extremely sensitive in detecting small delivery errors. Variations in beam MU down to 1 are detected by the system as well as changes in field size and positions down to 1 mm. In Table 1 the variations in the IQM signal are reported as an example for an H&N plan.

	Variations in IQM counts (%)				
Beam	**1MU/beam**	**2MUs/beam**	**3MUs/beam**	**1mm shift 1 MLC bank**	**1mm shift 2 MLC banks**
1	1,5	2,6	3,4	2,5	4,3
2	1,0	2,1	3,0	3,1	5,8
3	1,0	2,2	3,0	2,5	5,2
4	1,3	2,1	2,8	3,1	5,3
5	1,6	2,1	2,8	3,0	6,0
6	1,4	2,0	3,0	2,6	5,1
7	1,4	2,2	3,5	2,8	5,3
Mean	**1,3**	**2,2**	**3,1**	**2,8**	**5,3**

Table 1. % variations in the IQM signal for each beam of an H&N plan an for the 5 types of induced errors.

In Figure 1 the 2D γ per beam (1%/1mm, th10, local approach) and the PTV D95% and V95% are plotted vs the IQM signal variation for the same H&N example. A good correlation is observed thus suggesting that the IQM signal could be effectively used for quantifying delivery errors.

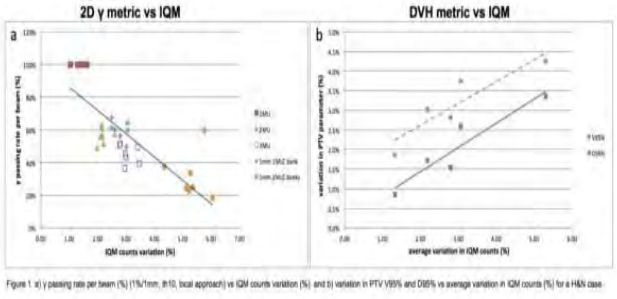

Conclusion: IQM is capable of detecting small delivery errors in MU and leaves position and it shows a sufficient sensitivity for clinical practice. It also exhibits a good correlation with other metrics used to quantify the deviations between calculated and actually delivered dose distributions. Such

correlations are useful in order to identify the alert threshold associated with this kind of monitoring systems.

OC-0459

Small fields output factors and correction factors determination for a linac with circular cones

A. Girardi[1], C. Fiandra[1], E. Gallio[2], F.R. Giglioli[2], R. Ragona[1]
[1]*University of Torino, Department of Oncology- Radiation Oncology Unit, Torino, Italy*
[2]*Azienda Ospedaliero - Universitaria Città della Salute e della Scienza, Medical Physics Unit, Torino, Italy*

Purpose or Objective: The use of small fields is a well-established practice in stereotactic radiosurgery, although it is hard to measure with accuracy the parameters for machine commissioning. This is related to the peculiarities of highly collimated beams, such as high dose gradient, source occlusion and lack of lateral electronic equilibrium, and to the features of the detector, like dimension of the active volume and components with high-Z materials. The first goal of this work was to determine small fields output factors (OF) with several active detectors and one passive detector (Gafchromic EBT3 films) for an Elekta Axesse medical linear accelerator equipped with circular cones. The second one was to determine the correction factors for different active detectors for comparison with passive detector, as suggested in a proposed small field dosimetry formalism. Radiochromic films do not require correction factors and can be then used as reference dosimeter, as demonstrated by Bassinet et al. (C. Bassinet et al., Med. Phys. 2013, 40(7): 071725).

Material and Methods: Small fields beams, ranging from 5 mm to 30 mm in diameter, were defined using circular cones. OF measurements were performed with six active detectors (ionizing microchambers air-filled: Exradin A26, Exradin A16; ionizing microchamber isooctane-filled: PTW microLion; synthetic diamond: PTW microDiamond; plastic scintillator: Exradin W1; diode: Razor IBA) and one passive detector (Gafchromic EBT3 films).

Results: OFs measured with Exradin W1 scintillator were in excellent agreement with EBT3 films (better than 2%) . A significant underestimation between the results obtained by radiochromic films and air-filled microchamber was observed, particularly for the smallest field, up to 12% for Exradin A16. The results obtained with the PTW microLion and the PTW microDiamond indicate instead an opposite behavior: a dose overestimation for the smaller radiation fields, up to 5% and 8% for the 5 mm-diameter field for microLion and microDiamond respectively was noted. The effect decreases with field size. Razor diode was in good accordance with Gafchromic films for very small fields (diameter≤ 10 mm), while a underestimation for larger fields has been observed. The results are shown in the following figures.

Correction factors						
Diameter of circular field (mm)	Exradin A16	Exradin A26	PTW microLion	Exradin W1	PTW microDiamond	IBA Razor
5.0	1.118	1.037	0.951	0.986	0.923	0.961
7.5	1.048	1.029	0.967	0.997	0.944	0.991
10.0	1.036	1.031	0.975	0.996	0.971	1.022
12.5	1.030	1.028	0.985	0.995	0.986	1.036
15.0	1.024	1.027	0.988	0.996	0.993	1.041
20.0	1.021	1.025	0.992	0.998	1.001	1.044
25.0	1.015	1.022	0.991	1.001	1.002	1.040
30.0	1.011	1.018	0.990	1.003	1.001	1.037

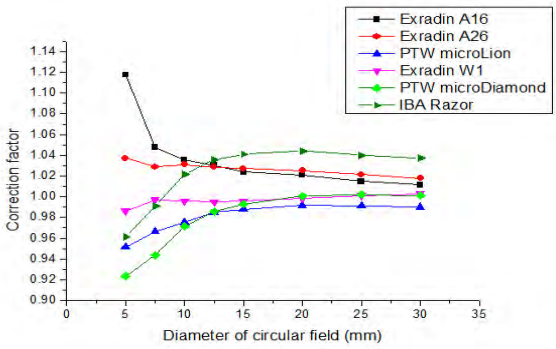

Conclusion: The present study points out that it is crucial to apply the appropriate correction factors in order to provide accurate measurements in small beam geometry. The results show that the Exradin W1 scintillator can be used for small fields dosimetry without correction factors. The correction factors should be employed for the other detectors, in particular for field diameter smaller than 10 mm. The results furthermore demonstrate that effects such as volume averaging, perturbation and differences in material properties of the detectors should be to taken into account in order to avoid large errors in the dose determination process.

OC-0460

Common errors in basic radiation dosimetry and radiotherapy practice

S. Kry[1], L. Dromgoole[1], P. Alvarez[1], J. Leif[1], A. Molineu[1], P. Taylor[1], D. Followill[1]
[1]*UT MD Anderson Cancer Center Radiation Physics, Radiation Physics, Houston- TX, USA*

Purpose or Objective: Dosimetric errors in radiotherapy dose delivery lead to suboptimal treatments and outcomes. Identification and resolution of such dosimetric errors in support of clinical trials is the mission of the Imaging and Radiation Oncology Core office in Houston (IROC Houston). The current study reviews the frequency and severity of dosimetric and programmatic errors identified by on-site audits performed by the IROC Houston QA center.

Material and Methods: IROC Houston on-site audits evaluate absolute beam calibration, relative dosimetry data compared to the treatment planning system calculations, and processes such as machine QA. These evaluations are conducted in a uniform manner. Audits conducted from 2000-present were reviewed, which included on-site evaluations of 1020 accelerators at 409 institutions. Suboptimal conditions that led to IROC Houston recommendations (absolute dose errors >3%, relative dosimetry errors >2%, or sizeable QA deficiencies) were identified, including type of recommendation and magnitude of error when applicable.

Results: A total of 1280 recommendations were made (average 3.1/institution) (Table). The most common recommendation was for inadequate QA procedures per TG-40 and/or TG-142 (82% of institutions) with the most commonly noted deficiency being x-ray and electron off-axis constancy versus gantry angle. Dosimetrically, the most common errors in relative dosimetry were in small-field output factors (59% of institutions), wedge factors (33% of institutions), off-axis factors (21% of institutions), and photon PDD (18% of institutions). Errors in calibration were also problematic: 20% of institutions had an error in electron beam calibration, 8% had an error in photon beam calibration, and 7% had an error in brachytherapy source calibration (Figure). Almost all types of data reviewed included errors up to 7% although 20 institutions had errors in excess of 10%, and 5 had errors in excess of 20%. The frequency of electron calibration errors decreased significantly with time, but all other errors show non-significant trends with time.

Recommendation	# Inst. Receiving rec.	% of Inst receiving rec	# Linacs receiving rec	% of Linacs receiving rec
QA	337	82.4	-	N/A
Small FS dependence	132	59.2	165	50.8
Wedge (FS or depth)	134	32.8	171	16.8
Off-axis factor	87	21.3	109	10.7
Electron calibration	83	20.3	105	10.3
Photon PDD	75	18.3	100	9.8
Update calibration	70	17.1	-	N/A
Electron PDD	47	11.5	57	5.6
Temp/press correction	44	10.8	-	N/A
IGRT coincidence	3	9.4	4	8.0
Beam symmetry	34	8.3	44	4.3

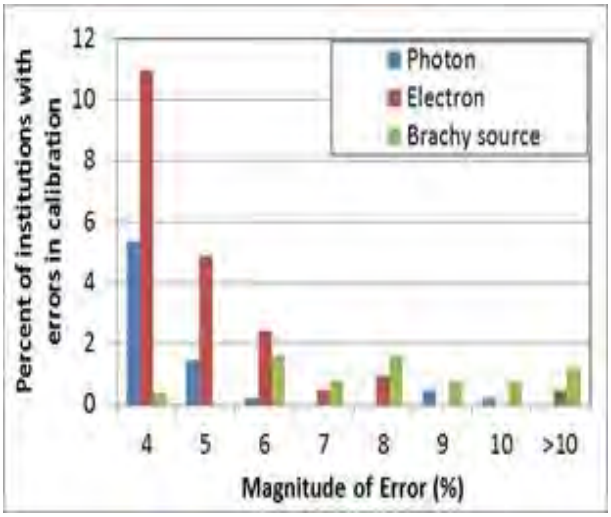

Conclusion: There are many common and often serious errors made during the establishment and maintenance of a radiotherapy program that can be identified through independent peer review. Physicists should be cautious, particularly in areas highlighted herein that show a tendency for errors.

Proffered Papers: Physics 12: Treatment planning: applications I

OC-0461

Does the dosimetric advantage of prone setup persist in small-margin IMRT for gynecological cancer?

S.T. Heijkoop[1], G.H. Westerveld[2], N. Bijker[2], R. Feije[1], A.W. Sharfo[1], N. Van Wieringen[2], J.W.M. Mens[1], B.J.M. Heijmen[1], L.J.A. Stalpers[2], M.S. Hoogeman[1]

[1]*Erasmus MC - Cancer Institute, Radiation Oncology, Rotterdam, The Netherlands*

[2]*Academic Medical Center, Radiation Oncology, Amsterdam, The Netherlands*

Purpose or Objective: In order to reduce dose to the small bowel, some institutions treat patients with gynecological cancer in prone position using a small-bowel displacement device (belly board). This practice is based on dosimetric advantages found in the past for 3DCRT and/or the use of large margins. It is unknown to what extent those advantages are persistent using modern intensity-modulated delivery techniques (e.g. IMRT or VMAT) and adaptive treatment approaches with small CTV-to-PTV margins. The aim of this study is to determine the best patient setup position (prone or supine) in terms of OAR sparing for various CTV-to-PTV margins and modern dose delivery.

Material and Methods: In an IRB approved study, 26 patients with gynecological cancer scheduled for definitive (9) or postoperative (17) radiotherapy were scanned in prone and supine position at the same day. The primary CTV (proximal part of the vagina and intact cervix-uterus or vaginal cuff with paravaginal soft tissue), nodal CTV, bladder, bowel cavity, and rectum were delineated on both scans. Nine PTVs were created, each with a different margin for the primary and nodal CTV (Table 1). Pareto optimal IMRT plans with 20 equi-angular beams to be delivered with dMLC were generated using our in-house system for automated treatment planning. Previously, we demonstrated that 20 beam IMRT is superior to dual arc VMAT. For all primary/nodal margin combinations supine and prone plans were compared considering OAR dose-volume parameters, giving highest priority to bowel cavity. P-values < 0.05 were considered significant. To determine the sensitivity of the dosimetric difference to the needed margin we not only compared supine to prone treatment plans with similar margins, but also compared supine to prone plans for which the supine plans had a smaller margin than for prone. In that way, we assessed the scenario that in prone position a larger margin around the nodal CTV is needed due to increased patient setup variations.

Results: Figure 1 illustrates the comparison between supine and prone position in terms of V45Gy of the bowel cavity for all patients and margins. Prone setup was significantly superior for large margins, but not for the three smallest margin combinations, i.e. 5/5mm, 5/7mm, and 10/5mm (primary/nodal margin around CTV). The rectum Dmean was significantly lower in prone setup: 2.9 Gy ± 0.4 averaged over all margins and patients, while the bladder Dmean was lower in supine setup: 2.5 Gy ± 0.3. The significant advantage for prone setup was not present if prone setup needed a larger margin than supine. In that case the V45Gy of the bowel cavity was on average 27 cc lower in supine setup.

Margin around primary CTV (mm)	Margin around nodal CTV (mm)
5	5
5	7
10	5
10	7
10	10
10	15
20	7
20	10
20	15

Table 1. Nine tested CTV-to-PTV margin combinations

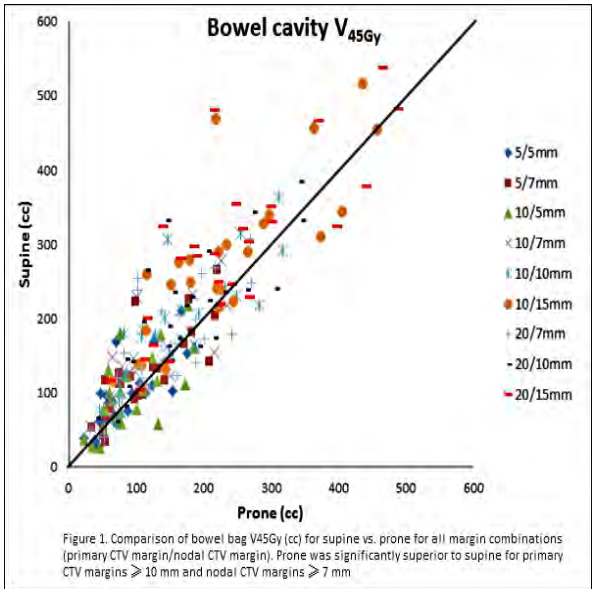

Figure 1. Comparison of bowel bag V45Gy (cc) for supine vs. prone for all margin combinations (primary CTV margin/nodal CTV margin). Prone was significantly superior to supine for primary CTV margins ⩾ 10 mm and nodal CTV margins ⩾ 7 mm

Conclusion: The historically found dosimetric advantages for prone setup will persist if modern dose delivery techniques are used, combined with large margins. However, the advantage is lost for small margins and if prone setup needs a larger margin than supine setup.

OC-0462

Motion induced interplay effects for hypo-fractionated FFF VMAT treatment of liver tumours

A. Edvardsson[1], F. Nordström[2], C. Ceberg[1], S. Ceberg[2]
[1]*Department of Medical Radiation Physics, Lund University, Lund, Sweden*
[2]*Department of Oncology and Radiation Physics, Skåne University Hospital, Lund, Sweden*

Purpose or Objective: The mutual movement of the tumour and treatment delivery during VMAT might cause hotspots and coldspots in the dose distribution, so-called interplay effects. These can be hard to predict and might be of great concern for hypo-fractionated VMAT treatments. The purpose of this study was (1) to develop a method to calculate the absorbed dose to moving tumours for VMAT treatments, (2) verify the proposed method by measurements, and (3) use the proposed method to investigate the dosimetric impact of interplay effects for hypo-fractionated FFF VMAT treatment of moving liver tumours.

Material and Methods: Treatment plans using 6 MV FFF VMAT (1400 MU/min) were created for three liver metastases (TrueBeam and Eclipse, Varian Medical Systems). The prescribed dose was 36 Gy in 3 fractions. The arcs were divided into sub-beams (one for every two control points) using an in-house developed software and the isocenter was shifted for every sub-beam to simulate sinusoidal motion in the superior-inferior direction. The sub-beams were calculated in Eclipse, generating a 4D dose distribution including effects of motion. For each treatment plan, combinations of three different motion amplitudes (5, 15 and 25 mm peak-to-peak) and periods (3, 5 and 7 s) were simulated. To separate the interplay effect from dose blurring, the original 3D dose distribution was convolved with the motion pattern and subtracted from the simulated 4D dose distribution, and the resulting D1%-D99% was calculated for the ITV. To verify the method, simulated treatment plans were delivered in developer mode to the Delta4 phantom positioned on Hexamotion (ScandiDos), which was either static or moving sinusoidally with a peak-to-peak distance of 15 mm and a period time of 5 seconds during irradiation. The measured and simulated dose distributions were compared using gamma analysis (2%/2 mm local dose, cut-off dose 10%) in the Delta4 software. To synchronize the isocenter shifts in the simulations with the motion during the measurements, kV images were acquired asynchronously during beam delivery.

Results: Gamma analysis show good agreement between the simulated 4D dose distribution and the dynamic measurement, comparable to the original 3D dose distribution and the static measurement (table 1). The impact of the interplay effects, expressed as D1%-D99%, varies considerably between targets as well as the combination of tumour amplitude and period time (figure 1), with a maximum difference in D1%-D99% compared to no motion of 2.8 Gy (target 2, 25 mm, 7s).

Table 1 Comparison of static and dynamic measurements with the 4D and original 3D calculated dose distributions, presented as average gamma pass rate [range] for criteria 2%/2mm local dose

	Gamma pass rate (%)
Static measurement vs 3D dose	99.4 [98.7 - 99.7]
Dynamic measurement vs 3D dose	76.5 [66.0 - 83.7]
Dynamic measurement vs 4D dose	99.7 [99.5 - 100.0]

Conclusion: A method to calculate the absorbed dose to moving tumours was developed and verified by measurements. Using this method, it was shown that large interplay effects may occur, with no obvious relation to the motion pattern. Therefore, caution should be taken before using FFF VMAT for moving liver tumours without using motion management techniques.

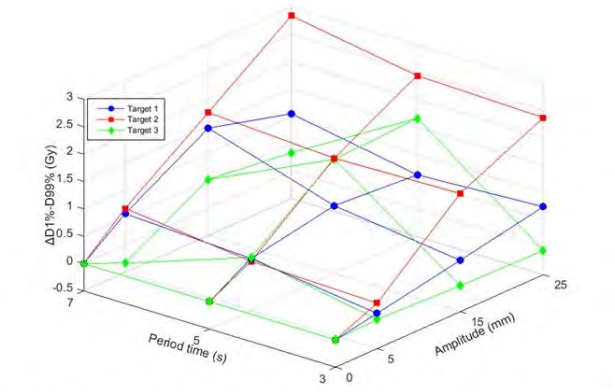

Figure 1 Difference in $D_{1\%}$-$D_{99\%}$ compared to no motion ($\Delta D_{1\%}$-$D_{99\%}$) as a function of tumour amplitude and period time for three targets

OC-0463

Improving treatment plan quality of SBRT lung tumors using a new gradient index

E. Van der Bijl[1], M. Witte[1], C. Van Vliet-Vroegindeweij[1], E. Damen[1]
[1]*Netherlands Cancer Institute Antoni van Leeuwenhoek Hospital, Radiotherapy, Amsterdam, The Netherlands*

Purpose or Objective: In order to assess treatment plan quality a good strategy is to compare plan quality indices for similar patients treated previously. For SBRT treatments the dose gradient is strongly associated with plan quality. Our objective is to introduce and show the merits of a gradient index for (lung) SBRT treatment plans that is, in contrast with existing indices, usable for multiple tumors and is readily interpretable.

Material and Methods: Our gradient index is defined as the relative dose-gradient averaged over the voxels in the first centimeter around the PTV. When a patient has multiple tumors, voxels closer to other tumors are excluded from the average, see inset of Fig. 1. For 100 tumors of lung SBRT patients treated in our clinic we calculated the proposed gradient index as well as other possible quality indices, such as conformity (ratio of volume receiving prescribed dose to volume of PTV) and inhomogeneity (ratio of max and prescribed dose). In addition, we listed geometric parameters such as volume, position in the lung, and distance to various OARs of the GTVs. We establish the mutual correlations of the plan quality indicators and dependencies on geometric factors. To test whether the suggested parameter indeed measures quality we select five low-scoring patients, including a patient with multiple tumors, and try to improve the treatment plans with respect to the suggested gradient index without compromising other constraints.

Results: For peripheral tumors the average relative dose-gradient in the first cm from the edge of the PTV is 5.6 ± 0.6 %/mm, shown in Fig. 1. It is independent of volume, position in the lung and does not correlate with the conformity index, in contrast to other gradient indices. For five low-scoring patients we could improve the dose-gradient on average by 0.5 %/mm without compromising target coverage and conformity. By increasing the gradient in the first centimeter around the PTV the average dose in most OARs was reduced, with an 8% reduction in average dose to the whole patient excluding PTV and an 6% reduction to average dose to healthy lung tissue.

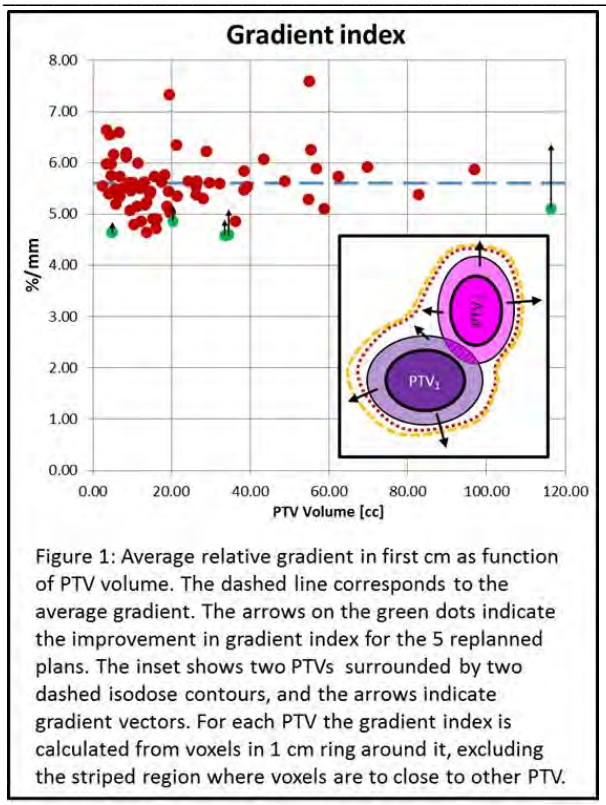

Figure 1: Average relative gradient in first cm as function of PTV volume. The dashed line corresponds to the average gradient. The arrows on the green dots indicate the improvement in gradient index for the 5 replanned plans. The inset shows two PTVs surrounded by two dashed isodose contours, and the arrows indicate gradient vectors. For each PTV the gradient index is calculated from voxels in 1 cm ring around it, excluding the striped region where voxels are to close to other PTV.

Conclusion: We can improve treatment-plan quality for lung SBRT treatments by providing the planner with a quality parameter associated with the dose gradient around the PTV. This index does not depend on GTV volume and position and is suited to compare all patients treated for SBRT without making corrections for size and position of the tumor and is suitable for multiple tumors.

OC-0464

Integration of fMRI and MEG functional maps into a Cyberknife planning system:a feasibility study

E. De Martin[1], D. Duran[2], F. Ghielmetti[1], E. Visani[2], D.R. Sebastiano[2], D. Aquino[3], M. Marchetti[4], D. Cusumano[5], M.G. Bruzzone[3], F. Panzica[2], L. Fariselli[4]

[1]*Foundation Carlo Besta Neurological Institute IRCCS, Health Department, Milan, Italy*

[2]*Foundation Carlo Besta Neurological Institute IRCCS, Neurophysiology, Milan, Italy*

[3]*Foundation Carlo Besta Neurological Institute IRCCS, Neuroradiology, Milan, Italy*

[4]*Foundation Carlo Besta Neurological Institute IRCCS, Neurosurgery- Radiotherapy Unit, Milan, Italy*

[5]*University of Milan, Postgraduate School in Medical Physics, Milan, Italy*

Purpose or Objective: In recent years Magnetoencephalography (MEG) and Functional Magnetic Resonance Imaging (fMRI) have imposed as non-invasive methods providing localization of eloquent brain areas for pre-surgical planning. With the advent of radiosurgery, the impact of these neuroimaging techniques in preventing neurological morbidity is under investigation in the clinical conditions for which radiotherapy is the treatment of choice. This study aimed to develop a method of integrating MEG and fMRI maps into a Cyberknife system to optimize dose planning.

Material and Methods: A patient with a recurrent brain metastasis affecting both the left pre-central and the post-central gyrus underwent functional imaging of the hand motor cortex two weeks prior its scheduled radiosurgery treatment. MEG data were acquired with a 306 sensors whole-head system while the patient performed self-paced motor activation of right hand and index finger. Epochs were extracted in the window ranging from – 3 to +3 seconds with respect to the movement onset and then averaged. Source of the motor-related activity was assessed by means of swLORETA algorithm. A day after MEG acquisition, fMRI was performed using a 3T MR Philips Achieva scanner. Motor activation of right hand and index finger was obtained through a block designed paradigm. Stimulation modality and duration both for MEG and fMRI were chosen to maximize time course signal to noise ratio. Magnetoencephalography and fMRI maps were integrated into a Cyberknife system for treatment planning optimization, considering the boolean sum of activations as organ at risk.

Results: Localization of the hand motor cortex was obtained for both functional investigation methods within close proximity of the lesion.
Integration of the fMRI data into the Cyberknife system was easily achieved through the customary Cyberknife import protocol.
More problematic was the integration of the MEG images, and for the purpose a customized Dicom import software had to be developed.

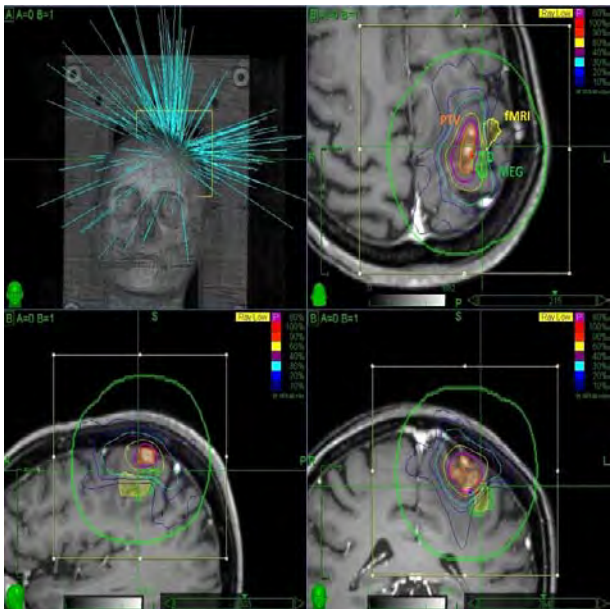

Figure show the results of the MEG and fMRI functional areas implemented into the Cyberknife system: the fMRI area (indicated in yellow) and the MEG area (indicated in green) result partially overlapped.
Only small differences were observed between MEG and fMRI activation areas after image co-registration.
Inclusion of the activation area into the plan optimization process allowed a reduction of 19% of the mean dose to the motor cortex

Conclusion: Nowadays, the availability of advanced neuroimaging techniques is playing a more and more important role in radiosurgical planning strategy. The authors developed an effective method to co-register fMRI and MEG data sets in a Cyberknife treatment planning system.
This additional information can improve dose sparing of eloquent areas, and MEG information in particular might be valuable when BOLD effect is disturbed by pathological vascularization.

OC-0465

Quality of treatment plans in hybrid IMRT and VMAT for prostate radiotherapy

J. Bedford[1], G. Smyth[1], I. Hanson[1], A. Tree[2], D. Dearnaley[2], V. Hansen[1]

[1]*The Institute of Cancer Research and The Royal Marsden NHS Foundation Trust, Joint Department of Physics, Sutton, United Kingdom*

[2]*The Institute of Cancer Research and The Royal Marsden NHS Foundation Trust, Academic Radiotherapy Unit, Sutton, United Kingdom*

Purpose or Objective: The strong directional characteristics of step-and-shoot IMRT beams, and the ability to turn off the beam between segments, may be used to advantage when avoiding critical structures. Consequently, there may be a benefit in delivering selected parts of VMAT plans using IMRT beams. This study investigates such a hybrid approach for the case of prostate radiotherapy.

Material and Methods: Five prostate patients were retrospectively studied. The AutoBeam treatment planning system produced hybrid IMRT / VMAT plans with a prescribed mean dose of 74 Gy in 37 fractions to the smallest of three target volumes, PTV74Gy, PTV71Gy and PTV60Gy. Inverse planning consisted of fluence optimisation using iterative least squares, sequencing, and aperture optimisation. The plans consisted of a single 220º arc with 111 segments arranged in groups of 20°. For each patient, five hybrid IMRT / VMAT plans were constructed, with 0%, 25%, 50%, 75% and 100% of the segment groups sequenced for IMRT, respectively, and the remainder of the segment groups sequenced for VMAT, maintaining the same number of beam segments in all cases. Thus, 0% IMRT corresponded to conventional VMAT and 100% IMRT corresponded to an 11-beam IMRT plan. IMRT groups were selected on the basis of fluence variation in each group, the most complex fluence maps being selected for IMRT delivery at the central gantry angle of the group. Treatment plans were evaluated in terms of PTV dose uniformity (root-mean-square variation) and coverage, critical structure dose, objective value and monitor units. All plans were then delivered as single hybrid beams to a water-equivalent phantom using an Elekta Synergy accelerator with Agility head, and the delivery time recorded. The dose measured using a Farmer ionisation chamber at the centre of the phantom within PTV74Gy was compared with the planned dose. Data were demonstrated by quantile-quantile plots to be normally distributed and compared to the 0% IMRT case using paired Student t-tests.

Results: All plans are clinically acceptable, but increasing the IMRT percentage improves PTV coverage ($p < 0.01$ for 50% or more), reduces the volume of rectum irradiated to 65 Gy ($p < 0.01$) and increases the monitor units ($p < 0.001$) (Table 1). Delivery time also increases substantially, which is clinically relevant due to prostate motion being partly dependent on treatment time. All plans show accurate delivery of dose.

Table 1. Mean ± 1 SD statistics for the hybrid IMRT / VMAT plans

	PERCENTAGE IMRT IN HYBRID PLAN				
	0%	25%	50%	75%	100%
PTV74 uniformity (%)	2.2±0.2	2.1±0.2	1.8±0.2	1.4±0.1	1.3±0.1
PTV71 minimum dose (Gy)	65.2±0.7	65.8±0.4	66.0±0.2	66.1±0.5	66.1±0.5
PTV60 minimum dose (Gy)	56.2±2.2	56.6±2.0	56.7±1.6	56.8±1.4	57.4±1.2
Rectum V30Gy (%)	75.1±10.2	75.7±10.5	77.9±10.0	77.2±9.7	74.9±9.8
Rectum V50Gy (%)	43.7±9.4	42.0±8.0	41.5±8.0	41.1±7.4	40.1±7.4
Rectum V65Gy (%)	18.5±2.8	16.6±2.5	16.2±2.3	16.1±2.4	15.9±2.6
Bladder V50Gy (%)	28.2±11.6	29.2±11.9	30.2±12.8	29.4±12.5	28.8±12.5
Bladder V60Gy (%)	21.6±9.5	21.8±9.4	22.0±9.4	21.7±9.2	21.7±9.2
Femoral joints V50Gy (%)	0.0±0.0	0.1±0.1	0.0±0.0	0.0±0.0	0.0±0.0
Penile bulb mean dose (Gy)	55.2±12.7	56.4±12.7	56.8±13.1	57.0±13.3	57.0±13.4
Objective value	7.6±0.7	7.4±0.6	7.5±0.6	7.4±0.5	7.2±0.5
Total monitor units	345±15	378±14	391±16	404±13	410±12
Delivery time (s)	76±4	201±9	276±16	380±28	439±36
Measured – plan dose (%)	1.6±1.5	1.8±1.7	1.8±1.7	0.9±1.0	0.4±0.7

.

Conclusion: Hybrid IMRT / VMAT can be efficiently planned and delivered as a single beam sequence. Beyond 25% IMRT, the delivery time becomes unacceptably long, outweighing the benefit of the improved plan quality, but 25% IMRT is an attractive compromise. These hybrid plans can be accurately delivered.

OC-0466

Dynamic Wave Arc: initial characterisation, dosimetric benchmark and performance validation

M. Burghelea[1], D. Verellen[1], M. Nakamura[2], K. Poels[3], C. Hung[4], T. Gevaert[1], J. Dhont[1], T. Kishi[2], V. Simon[5], M. Hiraoka[2], M. De Ridder[1]

[1]Universitair Ziekenhuis Brussel, Department for Radiation Oncology, Brussels, Belgium
[2]Kyoto University Graduate School of Medicine, Department of Radiation Oncology and Image-applied Therapy, Kyoto, Japan
[3]University Hospitals Leuven, Department of Radiation Oncology, Leuven, Belgium
[4]Brainlab AG, R&D Radiosurgery, Munich, Germany
[5]Babes Bolyai University, Faculty of Physics, Cluj-Napoca, Romania

Purpose or Objective: Dynamic Wave Arc (DWA) is a clinical approach designed to maximize the versatility of Vero SBRT system by synchronizing the gantry-ring noncoplanar movement with D-MLC optimization. The purpose of this study was to verify the delivery accuracy of DWA approach for SBRT treatments and to evaluate the potential dosimetric benefits.

Material and Methods: A preclinical version of RayStation v4.7 (RaySearch Laboratories, Sweden) was used to create patient specific wave arc trajectories. DWA is an extended form of VMAT with a continuous varying ring position. The main difference in the optimization modules of VMAT and DWA is during the angular spacing, where the DWA algorithm does not consider the gantry spacing, but only the Euclidian norm of the ring and gantry angle that cannot exceed 4°. Thirty-one patients with various anatomical tumor regions were selected from the Vero patient database. It was decided to select some pathologies with a high incidence (prostate and oligometastases) and some more challenging cases from the perspective of organ-at-risk sparing i.e. centrally-located non-small cell lung cancer (NSCLC) tumors and locally-advanced pancreatic cancer (LAPC). DWA was benchmarked against the current clinical approaches and coplanar VMAT to establish the clinical importance of DWA among other treatment approaches. Each plan was evaluated with regards to the target coverage, dose to OAR, MU efficiency and treatment delivery time. The delivery accuracy was evaluated using the Delta4 2D diode array that takes in consideration the multi-dimensionality of DWA.

Results: For prostate and oligometastases, the results showed that all modalities provide comparable plan quality, with no significant difference for PTV coverage or OAR sparing, but with a steeper dose gradient outside the target for DWA. The delivery time per lesion was significant reduced with DWA (Table 1). For centrally-located NSCLC (Figure 1), DWA and VMAT increased target coverage and conformity. The structures that significantly benefited from using DWA were proximal bronchus (Dmax 24.72Gy, 20.57Gy and 22.75Gy) and esophagus (16.6Gy, 12.57Gy and 14.76Gy) for 8-10CRT beams, DWA and VMAT, respectively. The other OARs presented comparable values. In the LAPC cases, DWA achieved similar PTV coverage, along with a significantly improved GTV coverage and improved low dose spillage ($p<0.01$). The delivery time and the number of MU needed to deliver the dose were significantly lower for DWA versus IMRT. The DWA plans presented a good agreement between measured and calculated dose, with an mean γ (3%,3mm) passing rate of 98.17%, 98.72%, 99.2% and 98.1% for the prostate, oligometatstatic cases, centrally-located NSCLC and LAPC, respectively.

Figure 1. Treatment delivery scenarios investigated along with the dose distribution in the axial plane. a) noncoplanar static beams b)DWA treatment using a template-based trajectory c) $_{CDR}$VMAT denotes a coplanar arc solution with MLC filed shape modulation, but constant gantry speed and constant dose rate.

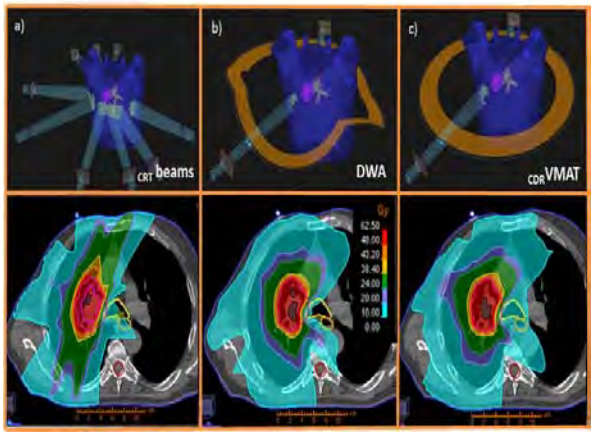

Table 2: Summary of the results of the target volume dose distribution and delivery parameters for all investigated scenarios. The data is presented as average values, standard deviations and p-test value

		CRT/IMRT	DWA	$_{CDR}$VMAT
Prostate n=3	Coverage PTV $D_{95\%}$	0.99 ± 0.01	0.98 ±0.03 (p=0.95)	0.98 ± 0.03 (p=0.90)
	Low dose spillage	3.99 ± 0.21	3.81 ± 0.22 (p=0.66)	4.08 ± 0.58 (p=0.49)
	MU	531 ± 45	495 ± 2.31 (p=0.24)	463 ± 54 (p=0.36)
	Actual time	5.55 ± 0.45	1.69 ± 0.01(p<0.01)	1.23 ±0.11 (p<0.01)
Oligo-metastatic cases n=15	Coverage PTV $D_{95\%}$	0.96 ± 0.1	0.98 ± 0.05 (p=0.27)	0.97 ± 0.07 (p=0.35)
	Low dose spillage	5.98 ± 2.33	4.87 ± 1.23 (p<0.01)	5.03 ± 1.03 (p=0.25)
	MU	975 ± 211	1370 ± 346 (p<0.01)	1320 ± 309 (p=0.29)
	Actual time	5.47 ± 1.04	3.44 ± 0.88 (p<0.01)	3.46 ±0.88 (p=0.94)
Centrally-located NSCLC n=9	Coverage PTV $D_{95\%}$	0.84 ± 0.20	0.91 ± 0.06 (p=0.21)	0.90 ± 0.09 (p=0.26)
	Low dose spillage	5.39 ± 1.24	4.43 ± 1.06 (p<0.01)	4.58 ± 1.02 (p=0.11)
	MU	1885 ± 477	3349± 596 (p<0.01)	3238 ± 809 (p=0.29)
	Actual time	7.08 ± 1.09	8.45 ± 2.32 (p=0.18)	8.59 ± 2.29 (p=0.90)
LAPC n=10	Coverage PTV $D_{95\%}$	0.71 ± 0.23	0.76 ± 0.13 (p=0.59)	0.76 ± 0.15 (p=0.94)
	Coverage GTV $D_{95\%}$	0.81 ± 0.17	0.85 ± 0.15 (p=0.53)	0.86 ± 0.18 (p=0.10)
	Low dose spillage	3.70 ± 0.28	3.25 ± 0.22 (p<0.01)	3.34 ± 0.22 (p=0.90)
	MU	1091 ± 100	644 ± 65 (p<0.01)	704 ± 87 (p=0.10)
	Actual time	6.83 ± 0.41	2.42 ± 0.01 (p<0.01)	2.51 ± 0.28 (p=0.63)

Conclusion: DWA combines direct machine parameter optimization with noncoplanar geometry, allowing additional flexibility in dose delivery, while preserving dosimetrically robust delivery.

Proffered Papers: RTT 5: Optimizing treatment planning and delivery in the pelvic region

OC-0467

Can a VMAT radiotherapy planning solution match brachytherapy in cervical cancers?

E. Buck[1], J. Mcgrane[1], I. Fraser[1], N. Simpson[1]
[1]*Royal Cornwall Hospitals Trust, Medical Physics, Truro, United Kingdom*

Purpose or Objective: Radiotherapy treatment for cervical cancers typically involves external beam irradiation to the whole pelvis followed by an intra-uterine brachytherapy boost to the primary tumour site. The purpose of the current study was 1) to assess dose reduction to OARs using a VMAT treatment technique compared to a conformal four field brick and 2) whether VMAT using sequential or simultaneous integrated boost can provide coverage to the tumour and OARs similar to brachytherapy.

Material and Methods: Ten patients previously treated for cervical cancer were identified (age range 30-78 years). Four plans were retrospectively produced for each patient (3D conformal four field brick, VMAT to the whole pelvis, VMAT boost, SIB) providing a phase one dose of 50.4Gy over 28 fractions. The sequential boost dose varied between patients from 16.5Gy-27.5Gy over 3-5 fractions. An averaged boost dose of 31Gy over 32 fractions, corrected using biological equivalent dose calculations was used for all SIB plans. All data was corrected to EQD2.

Figure1: Typical dose distribution for a VMAT with SIB plan.

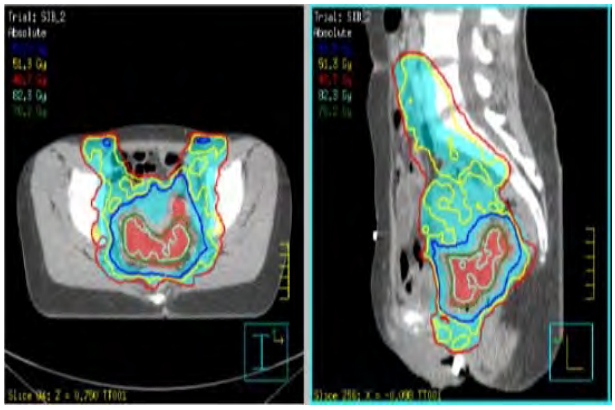

Results: Results demonstrated significantly improved dose homogeneity between the VMAT and four field phase one techniques ($p<0.01$) but failed to find significant dose reductions to the bladder and rectum. Dose to the bowel was reduced at all dose points ($p<0.01$). Comparing the VMAT and brachytherapy boost, significantly increased doses to OARs were identified in the VMAT boost (bladder $p<0.05$; rectum $p<0.01$; bowel $p<0.01$). Dose homogeneity was decreased using an SIB compared to sequential but OAR doses were also decreased ($p<0.05$).

Table 1: Mean and standard deviation of OAR data contained within the SIB and VMAT phase one plus either boost or brachytherapy plan combinations.

		Bladder		Rectum		Bowel	
Plan	Data-Point	Mean/Gy	S.D./Gy	Mean/Gy	S.D./Gy	Mean/Gy	S.D./Gy
VMAT + VMAT boost	D_{2cc}	81.03	10.16	80.14	9.55	84.46	9.11
	D_{50cc}	70.87	11.94	69.92	16.31	74.03	11.42
	D_{Mean}	54.40	17.18	54.79	16.28	59.01	11.48
	D_{100cc}	55.38	9.03	58.25	10.30	54.00	6.96
VMAT + Brachytherapy	D_{2cc}	79.79	7.88	67.03	4.99	70.29	7.07
	D_{50cc}	67.18	5.74	57.45	7.73	62.80	4.05
	D_{Mean}	45.14	18.50	37.30	20.31	55.23	2.57
	D_{100cc}	32.32	21.69	36.09	23.80	51.80	2.47
SIB	D_{2cc}	68.86	9.73	72.34	12.06	69.66	13.24
	D_{50cc}	55.12	9.54	55.96	15.28	57.31	12.94
	D_{Mean}	43.84	8.17	45.82	4.38	49.99	3.11
	D_{100cc}	42.55	6.08	45.17	3.28	48.48	0.89

Conclusion: When treating cervical cancer, VMAT allowed significant improvement in dose homogeneity with overall reductions in doses to OARs. When comparing the feasibility of SIB or sequential EBRT boost instead of brachytherapy the SIB plan produced a better solution with respect to OAR doses. Whilst cervical surface doses with SIB to the high-risk CTV will not match brachytherapy a SIB may offer an alternative option for those patients who refuse/cannot access brachytherapy.

OC-0468

Validation of Mask Based Registration in CBCT pretreatment imaging of locally advanced cervix ca

L. Van den Berghe[1], K. Vandecasteele[1], A.L. Michiels[1], Y. Lievens[1], C. De Wagter[1], E. Bogaert[1]
[1]*University Hospital Ghent, Radiotherapie, Ghent, Belgium*

Purpose or Objective: Online CBCT pre-treatment registration (Elekta, XVI) for locally advanced cervix carcinoma (LACC) is performed by RTT's, using a cubic Clipbox-based Volume of Interest (C-VOI) algorithm. Consecutive manual adaptation in order to fulfill the predefined criteria for LACC-registration, implies large shifts. This is suboptimal regarding setup reproducibility, challenges PTV margins and strongly depends on RTT's experience. The objective is to determine whether the use of a Mask-based VOI (M-VOI) reduces the magnitude of manual shifts and thus is a better starting point.

Material and Methods: Seventeen consecutive image sets (1 representative patient) and 14 sets among them were registered by 2 RTT's and 1 experienced radiotherapist respectively, both using C-VOI and M-VOI methods (identical Gray Value T algorithm). The M-VOI was generated from the primary CTV which includes the uterus and cervix. Within predefined matching criteria, lymph node regions were not taken into account. Four 3D translations were recorded: after C-VOI and M-VOI autoregistration (AR) and after consecutive C-VOI and M-VOI manual registration (MR). Data was analyzed using SPSS software.

Results: M-VOI and C-VOI AR resulted in statistically significant different translations in all 3 directions (paired T-test $p < 0.01$). The manual shifts afterwards cancelled out the significance in all directions (ANOVA, pairwise comparison, Bonferroni corrected $p > 0.05$). All 3 readers converged towards each other. Nevertheless, values of maximal relative shifts between the readers stayed x: 0.47 cm, y: 1.06 cm, z: 1.33 cm and x: 0.76 cm, y: 0.68 cm, z: 1.28 cm after C-VOI and M-VOI MR respectively. Plotting the data stresses the importance of the level of experience in LACC-CBCT registration. Comparison of the vector endpoints of C-VOI and M-VOI MR, shows that the experienced reader is able to move the CBCT towards one and the same endpoint, whereas the less experienced readers produce more fanned out point-by-point clouds and tend to vary around the given solution (which stresses the importance of a good starting point). Analysis of the manual shifts (Δ) reveals a better performance of M-VOI AR, i.e. smaller shifts are applied. This means that criteria for a 'good' match are here inherently taken into account in a better way. Paired T-tests for the shifts either after C-VOI and M-VOI AR for high and low experience levels revealed significances in all groups and directions (see table).

Table: Analysis of manual shifts (Δ) after C-VOI and M-VOI AR for high and low experience levels

	$\lvert\Delta_{\text{after Clipbox}}\rvert$ (cm)		$\lvert\Delta_{\text{after Mask}}\rvert$ (cm)	p
Experienced Reader				
X (left-right)	|0.15|	>	|0.03|	0.043
Y (cranial-caudal)	|-0.39|	>	|0.05|	0.000
Z (ventral-dorsal)	|0.92|	>	|0.15|	0.000
Less Experience Readers				
X (left-right)	|0.06|	>	|-0.03|	0.001
Y (cranial-caudal)	|-0.25|	>	|0.23|	0.000
Z (ventral-dorsal)	|0.94|	>	|0.14|	0.000

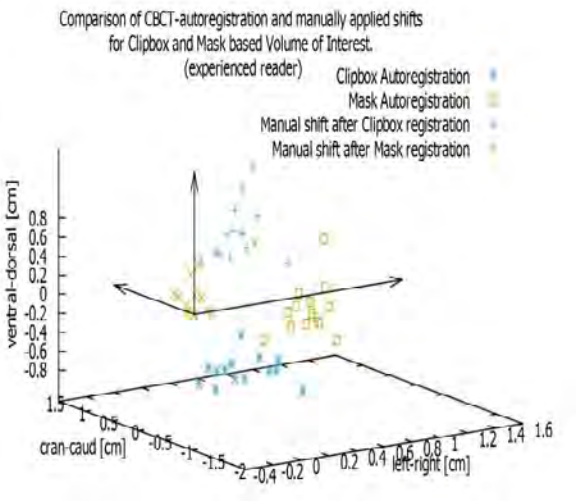

Conclusion: M-VOI AR is a better starting point than C-VOI AR for pre-treatment CBCT registration of the tumor in LACC. In order to minimize the maximal relative shifts, registration experience should be high. To minimize inter- and intrareader variability, manual shifts after AR should be avoided. Therefore Dual Registration (XVI, Elekta ®) combined with a written procedure will be the next step in the study.

OC-0469

Genitalia contouring in anal cancer IMRT; comparisons of volumes with and without a genitalia atlas

C. Brooks[1], V. Hansen[1], D. Tait[2]

[1]*The Institute of Cancer Research and The Royal Marsden NHS Foundation Trust, Joint Department of Physics, Sutton, United Kingdom*

[2]*The Institute of Cancer Research and The Royal Marsden NHS Foundation Trust, Department of Clinical Oncology, Sutton, United Kingdom*

Purpose or Objective: Genitalia as an organ-at-risk in radiotherapy has received little attention in literature. Contours vary widely and IMRT dose constraints in anal cancer (AC) often not met without compromising PTV. Despite IMRT technological advances genitalia toxicity still exists. Study aim: apply a proposed genitalia atlas to a retrospective series of AC patients and quantify the genitalia dosimetric differences between the original genitalia contour as defined by the clinician and the new genitalia contour defined with the aid of the genitalia atlas.

Material and Methods: Sixty AC patients (females *n*=40, males *n*=20) previously treated with IMRT were retrospectively identified. Four sub-groups were defined: female node negative (FNN) (*n*=24), female node positive (FNP) (*n*=16), male node negative (MNN) (*n*=10) and male node positive (MNP) (*n*=10). 'Node negative' and 'node positive' groups are defined as MRI tumour staged with involved nodes. Original genitalia contours for the retrospective treated plan were defined by the clinical oncologist and their interpretation of the departmental protocol. Genitalia were re-contoured following proposed genitalia contouring guidelines. DVH data and genitalia volume of original and new genitalia contours were compared. Statistical significance level of $P < 0.05$* and 0.01** is reported.

Results: Table 1 shows the volume and dosimetric differences between original and new genitalia contours. New contours were significantly larger than original. F genitalia received more radiation than M genitalia. Patients with involved nodal disease received more genitalia irradiation than patients without nodal disease. The majority of genitalia contours failed to meet current genitalia dose constraints hence new achievable dose constraints are recommended (figure 1). Dose constraints are rounded to the

nearest whole number. The median DVH value of new genitalia contours denotes the optimal constraint and the 75th centile denotes the mandatory constraint. Horizontal lines represent current genitalia dose constraints. It can be observed that new recommended dose constraints contrast the current dose constraints highlighting the need for gender and tumour stage specific genitalia dose constraints.

	Genitalia Volume Diffrences: Genitalia Contour (cm^3)		
	Original	New	Difference cm^3/%
All	80.1 (9.6-812.5)	182.2 (55.9-815.5)	102.1 / 127.5**
F	54.4 (9.6-195.4)	123 (55.9-413.6)	68.6 / 126.1**
M	255.8 (153.8-812.6)	391.8 (185.8-815.5)	144 / 56.3**

	Genitalia Dosimetric Differences									
SAMPLE	V20Gy (%)		V30Gy (%)		V40Gy (%)		V50Gy (%)		Mean Dose (Gy)	
	Original	New	Original	New	Original	New	Original	New	Original	New
All	69.6 (1.5-100)	**82.3 (19.7-100)	38.7 (0-100)	**43.7 (5-96.9)	19.4 (0-57.5)	16.8 (0-89.4)	5 (0-74.7)	4.4 (0-26.6)	26.8 (5.1-49.7)	27.7 (14.6-45.5)
FNN	79 (39.3-100)	85.4 (57-100)	32.8 (1.1-100)	38.4 (13.8-91.9	9.9 (0-57.5)	9.3 (1.1-57.8)	0.2 (0-74.7)	2 (0-26.6)	27.4 (19.4-49.7)	28.2 (21.7-41)
FNP	95.4 (21.9-100)	94 (53-98.8)	71.5 (3.6-98.7)	72.2 (17-96.9)	33.1 (0-55)	24.9 (2-89.4)	3.6 (0-22.2)	4 (0-24.5)	36.7 (15.1-46.7)	34 (21.7-45.5)
MNN	32.3 (1.5-57.5)	**47.5 (19.7-64.3)	4.6 (0-19.2)	**15.1 (5-21.8)	0 (0-1.1)	*2.9 (0-10.7)	0 (0-2.7)	*0.8 (0-4.7)	15.7 (5.1-21.7)	*13.5 (15-23.9)
MNP	51.7 (17.1-93)	49.1 (35.2-92.9)	30.8 (2.1-81)	31.8 (13.7-76.1)	10.7 (0-66.5)	13.8 (2.4-60)	0.7 (0-10.8)	1.4 (0.4-11.1)	21.3 (8.3-40.3)	20.7 (14.6-38.6)

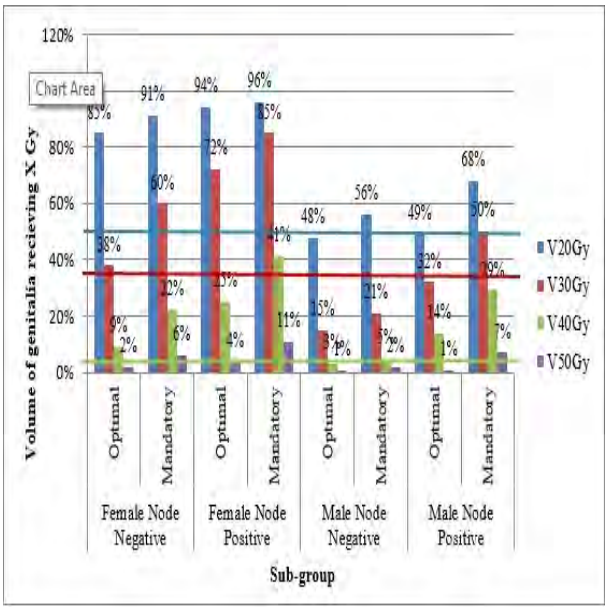

Conclusion: Dosimetric differences exist between genders and between patients with and without involved nodes when defining genitalia contours with aid of an atlas. Current generic set of genitalia dose constraints are inappropriate and gender/tumour stage specific constraints have been recommended.

OC-0470

Library of plans in radiotherapy of rectal cancer: feasible and inter-observer consistent?

S. Van Beek[1], L. Hartgring[1], A. Betgen[1], J. Stam[1], M. Buijs[1], B. Van Triest[1], P. Remeijer[1]

[1]The Netherlands Cancer Institute, Department of Radiation Oncology, Amsterdam, The Netherlands

Purpose or Objective: The clinical target volume (CTV) in rectal cancer is subject to large deformations. These deformations result in large margins when a planning target volume (PTV) is constructed with a population based method. A preferred approach uses a library of plans (LoP) and is expected to result in smaller PTV margins. A LoP requires a selection of the best fitting plan based on a Cone Beam CT (CBCT) scan. This triggers the questions: 'Is the visibility of the target volume sufficient for plan selection? ' and ' Do the plan selection choices of Radiation Therapists (RTT) coincide?' The purpose of this study is to determine feasibility in plan selection for a LoP in radiotherapy of rectal cancer.

Material and Methods: Thirty rectal cancer patients were included in this retrospective study. All patients received a radiation dose of 25 Gy in 5 fractions of 5 Gy, with on-line position verification. Instructions for the patient on the planning-CT were: full bladder and empty rectum The CTV was defined on the planning-CT (pCT) and contained the mesorectum, presacral area, pelvic lymph node areas and gross tumor volume (GTV). From the this single CTV a library of CTVs was constructed with in-house built software using population statistics on daily rectal deformations. The library consisted of five plans: two larger, two smaller and the original plan, see figure. We performed a baseline measurement with 4 observers (all RTTs). The observers separately selected plans on 150 CBCT scans based on a priori set of instructions (Observer study I). The study was followed by multiple consensus meetings with an experienced radiation oncologist to discuss deviating choices and refine the instructions. A golden standard was determined for each scan. After 5 months the observers were asked to reevaluate the same set of scans based on the refined guidelines (Observer study II).

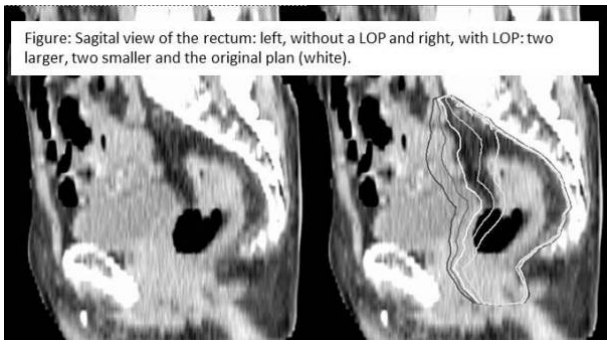
Figure: Sagital view of the rectum: left, without a LOP and right, with LOP: two larger, two smaller and the original plan (white).

Results: Observer study I: The scan quality was determined to be sufficient for plan selection. In 69 % of the cases the observers were in accordance with the gold standard. 29 % of all selections deviated by 1 plan and 2% deviated by 2 plans. The consensus meeting revealed that inconsistency in choices arose from inadequate instructions. For instance, should an air pocket rather far from the GTV also be covered within the CTV? Instructions were clearified, and more specified.Observer study II: In 87% of the cases the observers were in accordance with the gold standard and 13% of all selections deviated by 1 plan.

Conclusion: The observer study showed a good consistency in selecting the plan that would fit best on the anatomy of that day, even given the suboptimal CBCT image quality. Clinically, the occasional selection of a plan that deviates by one from the gold standard is deemed acceptable by the radiation oncologist. Therefore, plan selection based on daily CBCT by RTT for rectum patients is feasible, albeit room for improvement remains.

OC-0471

Influence of rectum volume on fine-tuning of image registration in bladder adaptive radiotherapy

L.S. Sier-Wismeijer[1], L.J. Lutkenhaus[1], K.N. Goudschaal[1], M. Frank[1], M.C.C.M. Hulshof[1], A. Bel[1], N. Van Wieringen[1]

[1]Academic Medical Center, Radiotherapie, Amsterdam, The Netherlands

Purpose or Objective: In our department, bladder cancer patients with solitairy muscle-invasive bladder tumor are standardly treated with adaptive radiotherapy treatment

(ART) to account for daily variations in bladder filling. Prior to each fraction, a conebeam CT (CBCT) is acquired and registered to the planning CT using a Chamfer algorithm (Elekta XVI 4.5). A dedicated RTT chooses the best fitting plan from a library of five plans. When none of the five plans fit the bladder volume, fine-tuning of the bony anatomy registration is performed (tweak), in order to optimize target coverage.
A tweak introduces an inter observer error and is a challenging time consuming part of the online CBCT registration workflow. We hypothesized that the rectum volume had a large influence on fine-tuning. The aim of this study was to investigate whether a significant correlation exists between rectum volume and performed tweak.

Material and Methods: Prior to treatment, the tumor was marked during cystoscopy with lipiodol or hydrogel. Two planning CTs were acquired: full bladder 100%; empty bladder 0%. A structure-based algorithm was used to create five different target volumes: 0%, 33%, 67%, 100%, and 133%, to create five different VMAT plans. The bladder and lymph nodes were treated to 40 Gy, the tumor up to 55 Gy, in 20 fractions using a simultaneously integrated boost. If none of the plans resulted in a good coverage of the bladder volume, the dedicated RTT had three options. The first two options were to instruct the patient to drink more and/or defecate: a 100% bladder filling is preferred. The third option was to perform a tweak.
A tweak should not exceed the PTV margins: 7 mm L-R (X), 8 mm C-C (Y) and A-P (Z) and is restricted by adequate coverage of the high dose area, visible through the lipiodol or hydrogel. This area is considered clinically more important compared to the elective lymph nodes.
189 CBCTs from 10 patients were analyzed. Bladder and rectum volumes from both CT and CBCT were recorded. The differences in rectum volume between CT and each CBCT were calculated, as well as the mean rectum volume (compared to the planning CT) and the vector length of the tweak (see figure 1). The correlation (R^2) between the rectum volume and the tweak vector was calculated.

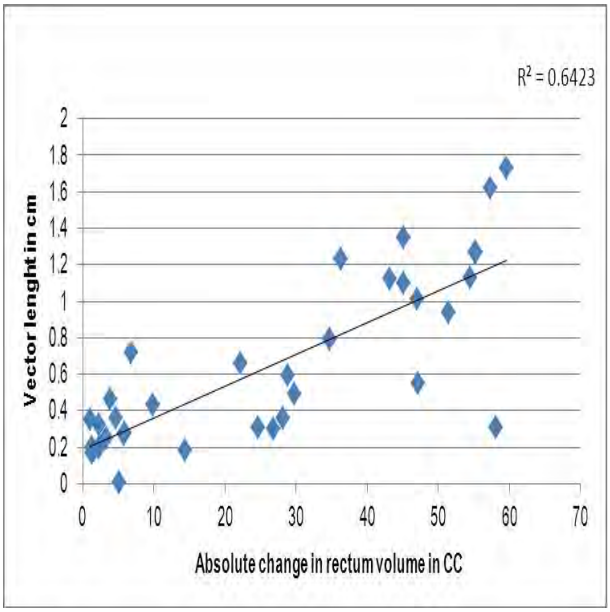

Results: For fractions without a tweak the mean relative rectum volume was 99% compared to 79% for fractions in which a tweak was performed. The number of times each plan was chosen and the times a tweak was performed are shown in Table 1.

VMAT Plan	How many times chosen	Fine tuning performed	R^2
0% (empty bladder)	5	4	0.60
33%	38	14	0.10
67%	89	35	0.64
100% (full bladder)	42	17	0.37
133%	15	3	0.53
Total	189	73	

Conclusion: A significant correlation was found between the vector length of the tweak and rectum volume difference between full bladder CT and CBCT. Also tweaking was necessary less often when the rectum volume remained stable. Further research is necessary to identify a range of rectum volumes that will probably remain stable during the course of treatment.

OC-0472

Patient preference-driven plan optimisation for shared decision making in anal cancer radiotherapy

H.S. Rønde[1], J. Pløen[2], L. Wee[1], A.L. Appelt[2]
[1]*Vejle Hospital, Department of Medical Physics, Vejle, Denmark*
[2]*Vejle Hospital, Department of Oncology, Vejle, Denmark*

Purpose or Objective: The traditional paradigm for inverse planning does not always deliver a Pareto-optimal dose distribution. In addition, trade-offs between different organs at risk are often necessary. In a clinical setting centered on shared decision making (SDM) between patients and their physicians, we suggest that individual preferences could be incorporated into plan selection based on a family of optimal plans. We present interim results from an efficient workflow for plan generation with trade-off selection, based on multi-criteria optimization (MCO).

Material and Methods: In this pilot study, dose plans were retrospectively generated for four representative anal cancer patients. All were treated with intensity-modulated radiotherapy with a standard regimen (60.2 Gy simultaneous-integrated tumor boost with 50.4 Gy to elective nodes, in 28 fractions, *high dose regimen*) and physician-defined organ-sparing priorities. In the first alternative plan generation, we optimized for minimum acceptable target volume coverage and same organ-sparing priorities, but assumed that the patient voluntarily foregoes the last three fractions of the standard regimen (tumor and nodal dose lowered by 6.45 Gy and 5.4 Gy, respectively, *low dose regimen*). Resulting changes in 2-year local tumor control probability were estimated using a model by Muirhead et al (Radiother Oncol 2015;116: 192–196). In the second round of alternative plan generation, we used MCO to search the phase space of optimal plans at the shorter regimen that would maximize sparing of the bowel at the expense of the bladder (*bowel sparing regimen*), and vice versa (*bladder sparing regimen*). In this way, we simulated the maximum span of dose distributions available for individualized patient preferences in regards to toxicity avoidance.

Results: Figure 1 demonstrates dose distributions for a single patient for the high dose, low dose, bowel sparing, and bladder sparing regimen. Dose metrics for bladder and bowel are shown in Table 1. All dose plans had clinically acceptable target coverage, and were deemed satisfactory by a senior oncologist. Considerable reduction of dose to the bowel was possible, not only by reduction in prescription dose (ΔV45Gy=289 ccm) but also further by prioritization of bowel in the plan optimization (ΔV45Gy=308 ccm). This resulted in bladder dose metrics no better than those for the high dose regimen. The reverse was seen for bladder sparing plans.

Overall, the possibility of sparing the bowel at the cost of extra dose to the bladder and vice versa was demonstrated. The estimated change in primary tumor control for high versus low dose regimen was less than 1% for early stage tumors and approximately 5% for late stage tumors.

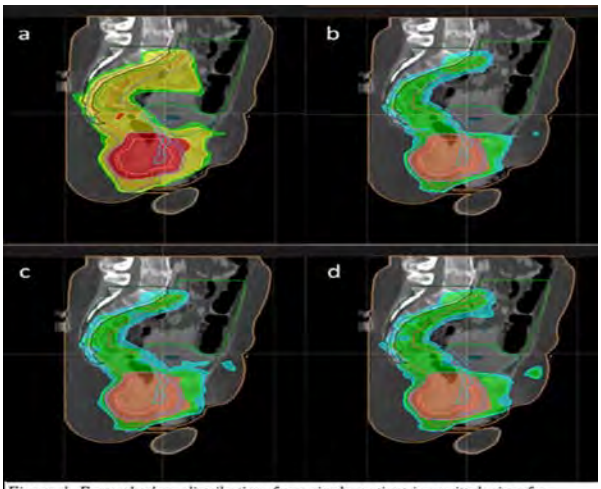

Figure 1. Example dose distribution for a single patient in sagittal view for for the high dose regimen (a), low dose regimen (b), bowel sparing regimen (c), and bladder sparing regimen (d). Dose color wash showing the two dose levels and the 45 Gy bowel dose constraint. Red: 57.19 Gy (95 % of 60.2 Gy). Yellow: 47.50 Gy (95 % of 50.4 Gy). Green: 45 Gy (bowel constraint). Orange: 51.06 Gy (95% of 53.75 Gy). Turquoise 42.75 Gy (95 % of 45 Gy).

	Bladder [%]				Bowel [ccm]			
	Rel. diff [%]		Abs. diff [% points]		Rel. diff [%]		Abs. diff [ccm]	
Plans	V35Gy	V50Gy	V35Gy	V50Gy	V30Gy	V45Gy	V30Gy	V45Gy
High vs. low	0.9	88.0	0.8	9.7	1.9	51.3	30.7	288.6
High vs. low, bladder sparing	27.3	91.3	19.8	10.3	-0.8	35.6	1.8	205.8
High vs. low, bowel sparing	-20.8	83.5	-6.1	8.8	8.0	54.4	86.4	308.1

Table 1. Relative and absolute mean differences for dose to the bladder and bowel for four patients (two men and two women). Dose metrics from the high dose regimen plans are compared to the low dose regimen, bowel sparing regimen and bladder sparing regimen, respectively.

Conclusion: There is room in the optimization space for incorporation of patient outcome and toxicity preferences. This opens for SDM for anal cancer patients. The study is to be expanded, with results for a total of 22 patients to be presented at ESTRO 2016.

Poster Viewing : 10: Physics: Functional Imaging II

PV-0473

Diagnostic and predictive values of quantitative analysis on T2-w and ADC map MRI in prostate cancer

K. Gnep[1], A. Fargeas[2], R.E. Gutiérrez-Carvajal[2], F. Commandeur[2], R. Mathieu[3], J.D. Ospina[2], G. Jimenez[2], T. Rohou[4], O. Acosta[2], R. De Crevoisier[1]
[1]*Centre Eugène Marquis, Radiotherapy, Rennes, France*
[2]*Inserm U1099- University of Rennes 1, LTSI, Rennes, France*
[3]*Centre Hospitalo-Universitaire Pontchaillou, Urology, Rennes, France*
[4]*Centre Eugène Marquis, Radiology, Rennes, France*

Purpose or Objective: To explore the ability of quantitative prostate T2-weighted (T2-w) and apparent diffusion coefficient maps (ADC) MRI using Haralick texture features: i) to differentiate prostate cancer (PC) from healthy tissues; ii) to be correlated with Gleason score; iii) to predict biochemical recurrence after external beam radiotherapy (RT) for prostate cancer.

Material and Methods: Tumor and prostate zones were segmented on co-registered T2-w and ADC on two pre-treatment 3.0T MRI from 83 patients with a median age 67 years (range 50-82 years) and a median pre-treatment PSA of 9.8 ng/ml (range 3.4-48.0 ng/ml). 9 (11%) tumors were localized in the transitional zone (TZ) and 74 (89%) in the peripheral zone (PZ). Tumors were clinically staged as follows: 13% of T1, 46% of T2 and 41% of T3. Gleason scores were as follows: 6 (27%), 7 (51%), 8 (20%) and 9 (2%). They were 2% of low-risk, 33% of intermediate-risk and 65% of high-risk tumors according to D'Amico risk group classification. Almost all patients received standard treatment consisting in IMRT (100%) with IGRT (94%) associated with hormonal therapy in 53% of the patients. After a median follow-up of 47 months (range 19-65 months), 11 patients had biochemical recurrence. A total of 114 grey-leveled features (first order, gradient-based and second order Haralick texture characteristics) and 4 geometrical features (maximal tumor diameter, maximal tumor perimeter, maximal tumor area and tumor volume) were extracted on normalized T2-w and ADC and were analyzed. Statistical analyses were performed using Wilcoxon signed-rank test, Spearman's correlation coefficient, Harrell's C-index, Kaplan-Meier curves and univariate Cox regression analysis.

Results: i) 56 out of 57 T2-w and 46 out of 57 ADC grey-leveled features were significantly different between tumor and prostate tissues in the PZ and 25 out of 57 T2-w and 37 out of 57 ADC features in the TZ ($p<0.05$). ii) 5 T2-w features and 4 ADC features were significantly correlated with Gleason score, all were Haralick texture features. iii) T2-w features that significantly predicted ($p<0.05$) biochemical recurrence were: maximal tumor diameter/perimeter/area/volume, Kirsch gradient operator, normalized mean and standard deviation of signal intensity and 8 Haralick texture features (Difference Variance, Contrast, Inverse Difference Moment, Difference Entropy, Information Measure of Correlation, Sum Average, Sum Variance and Sum of Squares). Only normalized mean value on ADC was significantly predictive of biochemical recurrence.

Conclusion: Quantitative analysis using Haralick texture characteristics on T2-w MRI are good features: i) to differentiate prostate cancer from healthy tissues, ii) for Gleason score assessment and iii) to predict biochemical recurrence after RT. Geometrical characteristics extracted from T2-w are also good predictors of biochemical recurrence after RT.

PV-0474

Comparison of DCE MRI and FMISO-PET kinetic parameters in head and neck cancer patients

U. Simoncic[1,2,3], S. Leibfarth[1], S. Welz[4], N. Schwenzer[5], H. Schmidt[5], D. Zips[4], D. Thorwarth[1]
[1]*University Hospital Tübingen, Section for Biomedical Physics - Department of Radiation Oncology, Tübingen, Germany*
[2]*Jozef Stefan Institute, Medical Physics program, Ljubljana, Slovenia*
[3]*University o Ljubljana, Faculty for Mathematics and Physics, Ljubljana, Slovenia*
[4]*University Hospital Tübingen, Department of Radiation Oncology, Tübingen, Germany*
[5]*University Hospital Tübingen, Department of Diagnostic and Interventional Radiology, Tübingen, Germany*

Purpose or Objective: Tumour hypoxia is associated with poor response to radiotherapy. Comprehensive hypoxia assessment through [18F]-fluoromisonidazole (FMISO) PET imaging requires quantitative techniques, such as dynamic acquisition. However, dynamic FMISO PET protocols might be simplified by using DCE-MRI imaging in addition to static FMISO-PET. The aim of this work was to compare FMISO and DCE-MRI kinetic parameters by means of correlation analysis.

Material and Methods: This study was done on N=6 head and neck cancer patients, who were imaged dynamically with FMISO-PET and DCE-MRI on the same day. Images were registered and analyzed for kinetics on a voxel basis. FMISO-

PET images were analyzed with a two-tissue compartment three-rate constant model with an additional vasculature compartment. Consequently, the model had the following parameters: K1 – FMISO transport rate to the tissue, k2 – FMISO backflow parameter, k3 – rate of FMISO binding in the cells, and Vb – vasculature fraction in the tissue. DCE-MRI images were analyzed with the extended Tofts model with the following parameters: Ktrans – contrast agent transport rate to the tissue, ve – relative volume of the tissue, and vp – vasculature fraction in the tissue. Voxel-wise Pearson correlation coefficients were evaluated on pairs of parametric images for each patient over the tumour volume including lymph nodes and tumour bed, if present. FMISO kinetic parameters were modelled with multivariate linear models of DCE-MRI parameters. The relative likelihood of the models was evaluated using the Akaike information criterion.

Results: Correlations between FMISO and DCE-MRI kinetic parameters, median over all the patients, varied across the parameter pairs from -0.12 to 0.71, with the highest correlation coefficient of 0.71 for Vb-vp pair, while K1-Ktrans correlation was 0.46. Correlations between FMISO and DCE-MRI kinetic parameters varied also across the patients. Among various multivariate models for FMISO parameters, those with more DCE-MRI parameters were more likely. Table 1 shows the correlation matrix for FMISO and DCE-MRI kinetic parameters with the median over all the patients in the lower-left and minimum/maximum in the upper-right triangle.

Table 1: Correlation matrix for FMISO and DCE-MRI kinetic parameters.

		FMISO				Tofts		
		K_1	k_2	k_3	V_b	K^{trans}	v_e	v_p
FMISO	K_1	1	0.80 0.94	-0.39 0.08	-0.08 0.51	0.27 0.59	-0.40 0.33	0.14 0.55
	k_2	0.92	1	-0.35 0.01	0.06 0.58	0.26 0.51	-0.40 0.33	0.29 0.60
	k_3	-0.12	-0.16	1	-0.21 0.24	-0.27 0.35	-0.20 0.06	-0.16 0.22
	V_b	0.18	0.3	0.02	1	-0.31 0.56	-0.41 0.02	-0.17 0.74
Tofts	K^{trans}	0.46	0.39	0.13	0.15	1	-0.06 0.86	0.34 0.87
	v_e	0.09	-0.06	-0.04	-0.12	0.42	1	-0.30 0.76
	v_p	0.42	0.5	0.02	0.71	0.58	0.15	1

Figure 1 shows K1 and Ktrans parametric images for the case with low K1-Ktrans correlation. Additional DCE-MRI kinetic analysis for this case, using the tissue homogeneity model revealed that tumour and tumour bed had different Ktrans because of considerably different permeability surface area product.

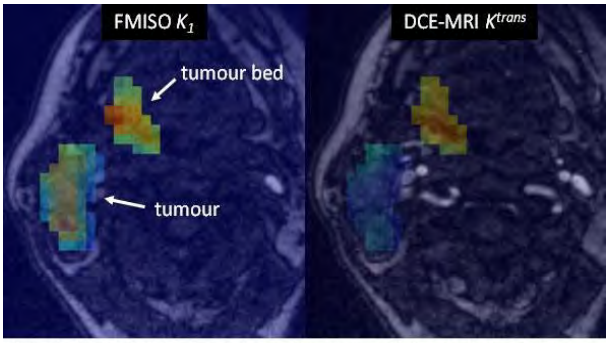

Figure 1: K_1 and K^{trans} parametric images for the case with low K_1-K^{trans} correlation.

Conclusion: Vasculature fractions from DCE-MRI and FMISO-PET are interchangeable up to a scaling factor. Transport rates from DCE-MRI and FMISO-PET can be different; FMISO K1 measures blood flow, whereas the DCE-MRI Ktrans can be notably affected by the blood vessel permeability. Information from any single FMISO kinetic parameter is spread over multiple DCE-MRI parameters.

PV-0475

Probability map prediction of relapse areas in glioblastoma patients using multi-parametric MR

A. Laruelo[1,2], J. Dolz[3,4], S. Ken[1], L. Chaari[2], M. Vermandel[4], L. Massoptier[3], A. Laprie[1,5,6]

[1]*Institut Claudius Regaud, Département de Radiothérapie, Toulouse, France*

[2]*Univ. of Toulouse, IRIT - INP-ENSEEIHT, Toulouse, France*

[3]*AQUILAB Parc Eurasante Lille Metropole, Research, Loos, France*

[4]*Univ. Lille- Inserm- CHU Lille- U1189 - ONCO-THAI, Image Assisted Laser Therapy for Oncology, Lille, France*

[5]*Université Toulouse III Paul Sabatier, Faculté de Médecine, Toulouse, France*

[6]*Institut National de la Santé et de la Recherche Médicale, UMR 825, Toulouse, France*

Purpose or Objective: Despite post-operative radiotherapy (RT) of glioblastoma (GBM), local tumor re-growths occur in irradiated areas and are responsible for poor outcome. Identification of sites with high probability of recurrence is a promising way to define new target volumes for dose escalation in RT treatments. This study aims at assessing the value of multi-parametric magnetic resonance (mp-MR) data acquired before RT treatment in the identification of regions at risk of relapse.

Material and Methods: Ten newly diagnosed GBM patients included in a clinical trial, treated in the reference arm of 60 Gy plus TMZ, underwent magnetic resonance imaging (MRI) and MR spectroscopy (MRSI) before RT treatment and every 2 months until relapse. The site of relapse was considered as the new appearing contrast-enhancing (CE) areas on T1-weighted images after gadolinium injection (T1-Gd). Using a set of mp-MR data acquired before RT treatment as input, a supervised learning system based on support vector machines (SVM) was trained to generate a probability map of CE appearance of GBM. More specifically, T1-Gd and FLAIR image intensities, Choline-over-NAA, Choline-over-Creatine and Lac-over-NAA metabolite ratios, and metabolite heights were used. The resolution of the MRI images was lowered to the one of the MRSI grid by averaging MRI pixel intensities within each MRSI voxel (400 MRSI voxels were considered for each subject). The region of CE was manually contoured on both the pre-RT and post-RT T1-Gd images by experienced medical staff. All voxels that enhanced at the pre-RT exam were excluded from further consideration. The learning system was trained and tested using leave-one-out-cross-validation (LOOCV) with all the patients. A grid-search strategy was employed for parameter optimization.

Results: For comparison purposes, generated probability maps were thresholded with a value of 0.5. Thus, only voxels with values higher than 0.5 on the probability map were considered as relapse. The sensitivity and specificity of the proposed system were 0.80 (±0.19) and 0.87 (±0.09), respectively. For our data, standard Choline-to-NAA index (CNI) achieved a sensitivity of 0.62 (±0.25) and a specificity of 0.63 (±0.13) (an optimal CNI threshold was derived for all the patients). The receiver operating characteristic (ROC) curve also shows that the presented approach outperforms CNI (Fig 1.). In addition, the SVM-based results had lower variation across patients than CNI. An example of a probability map generated by the proposed approach is shown in Fig.2. Relapse areas predicted by the learning scheme are in high accordance with the manually contoured regions.

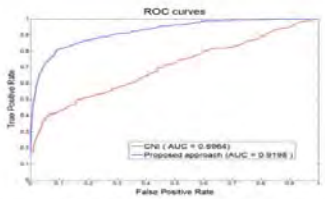

Figure 1 Receiver operating characteristic (ROC) curve for the proposed method (blue) and for the standard CNI approach (red).

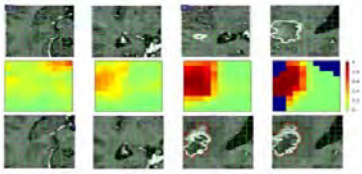

Figure 2 Pre-RT T1-Gd (top), probability maps of GBM relapse generated by the proposed approach (middle) and reference manual contours of the relapse for a given patient (bottom). Each slice represents a slice in the axial view. Dark blue on the probability maps indicate voxels where metabolic information was not available. The areas at risk of relapse predicted by the proposed approach (using MR data acquired before RT) are in clear accordance with the manually contoured relapse regions.

Conclusion: A learning system based on SVM trained with mp-MR data has been presented. Reported results show that this learning scheme can provide a probability map of the area of relapse of GBM in a stable and accurate manner. This study suggests the potential of mp-MR data in addressing specific questions in GBM imaging.

PV-0476

Fractional anisotropy dose-response relationship of the corpus callosum

N. Pettersson[1], H. Bartsch[2], J. Brewer[2], L. Cervino[1], M. Connor[1], A. Dale[2], D. Hagler[2], R. Karunamuni[1], A. Krishnan[2], J. Kuperman[2], C. McDonald[3], N. Farid[2], N. White[2], J. Hattangadi-Gluth[1], V. Moiseenko[1]

[1]*University of California San Diego, Radiation Medicine and Applied Sciences, La Jolla, USA*

[2]*University of California San Diego, Radiology, La Jolla, USA*

[3]*University of California San Diego, Psychiatry, La Jolla, USA*

Purpose or Objective: Diffusion tensor magnetic resonance imaging (DTI) is a non-invasive modality for determination of water diffusion properties. Fractional anisotropy (FA) quantifies the extent of directionality of water diffusion. We investigated absorbed dose as a predictor of FA change in the corpus callosum (CC) following radiation therapy for high-grade glioma.

Material and Methods: Fifteen patients with high-grade glioma underwent DTI scans before, and ten months after radiation therapy to 59.4-60 Gy. Diffusion data were acquired on a 3T MRI scanner. Using an automated white matter fiber tracking technique, 23 fiber tracts were segmented on the baseline and follow-up DTI images. The CT images used for treatment planning and both DTI image sets were aligned using non-linear registration. This way, the baseline FA, the follow-up FA, and the absorbed dose could be determined for each voxel in all 15 patients. For each voxel in the CC, we calculated the FA change as FAfollow-up /FAbaseline and dichotomized the data into a binary outcome variable using 0.5 as cutoff. For all 15 patients, logistic regression was used to determine dose-response curve parameters (D50 and g50) and their confidence intervals (CIs). We used the area under the receiver-operating characteristics curve (AUC) to evaluate the discriminative ability of the voxel dose. Then, we estimated dose-response curve parameters and calculated the AUC for each patient individually.

Results: The median age was 59 (range: 40-85) years. The average CC volume and average CC mean absorbed dose was 62±8 cm3 and 26±14 Gy (1 SD), respectively. Using data from 99 691 voxels, the estimated parameters for the dose-response curve for all patients (upper panel in Figure 1) were D50=88.0±0.1 Gy and γ50=0.80±0.01 (95% CIs). The AUC was 0.71 indicating good discriminative ability. For nine out of 15 patients, the individual AUC was ≥0.60, indicating that higher absorbed dose is associated with higher probability of FA change ≥0.5. Dose -response curves for those patients are shown in the lower panel in Figure 1 and their estimated parameter values in Table 1. Individual D50s varied between 41.3 and 125.9 Gy.

Table 1. Fractional anisotropy and absorbed dose data for the corpus callosum. For patients with an AUC ≥0.6, dose-response curve parameters and their 95% confidence intervals are given.

patient id	# voxels changed ≥0.5	# of voxels	median voxel dose (range) (Gy)	AUC	D_{50} (Gy)	γ_{50}
All 15	**11448**	**99691**	**21.5 (0.5-65.9)**	**0.71**	**88.0±0.1**	**0.80±0.01**
1	*279*	*7037*	*3.0 (0.6-20.1)*	*0.13*		
2	*155*	*6428*	*8.5 (0.7-64.4)*	*0.49*		
3	1159	6417	38.7 (2.5-65.9)	0.69	79.2±0.5	0.80±0.05
4	*777*	*6095*	*21.0 (4.7-64.2)*	*0.57*		
5	533	6605	39.9 (4.1-64.0)	0.68	104.8±0.7	1.06±0.08
6	816	6232	19.6 (1.5-57.9)	0.70	41.3±0.4	1.02±0.05
7	1137	6688	24.7 (1.0-63.6)	0.76	57.9±0.3	0.86±0.04
8	28	6988	6.7 (0.8-36.1)	0.61	125.9±3.7	1.50±0.16
9	377	6982	21.7 (8.0-64.9)	0.72	92.6±0.6	1.12±0.07
10	*113*	*5767*	*9.1 (0.5-44.9)*	*0.56*		
11	749	8149	35.5 (2.0-63.9)	0.77	81.1±0.5	1.26±0.07
12	*1299*	*6501*	*37.8 (5.3-63.1)*	*0.58*		
13	1108	6946	11.2 (1.3-63.0)	0.85	46.0±0.3	0.90±0.04
14	1017	7765	60.9 (7.9-63.1)	0.68	69.1±1.8	3.24±0.42
15	*1900*	*5091*	*25.4 (6.8-42.8)*	*0.59*		

AUC: the area under the receiver-operating characteristics curve; D_{50}: absorbed dose required for 50% probability; γ_{50}: the normalised dose-response gradient.

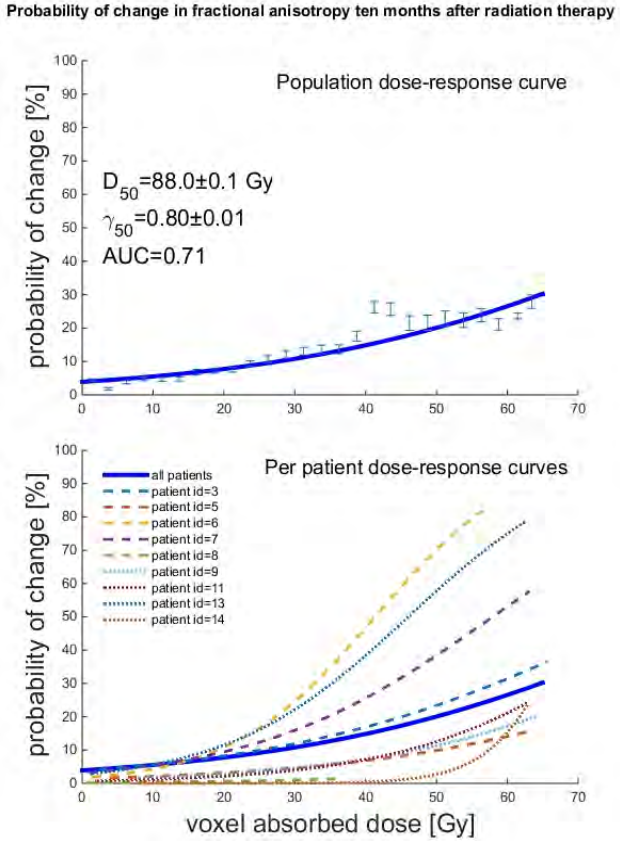

Conclusion: Absorbed dose was a significant predictor of FA change in the CC. This was the case both when all patients were pooled for analysis, and in nine out of 15 patients when analyzed separately. More detailed analyses are needed to better understand the effect radiation has on water diffusion in brain white matter.

PV-0477

Early CT image biomarkers change and xerostomia score are strong predictors for late xerostomia

L.V. Van Dijk[1], C.L. Brouwer[1], R.J. Beukinga[1], A. Van de Schaaf[1], H.P. Van der Laan[1], H.G.M. Burgerhof[2], J.A. Langendijk[1], R.J.H.M. Steenbakkers[1], N.M. Sijtsema[1]

[1]*University of Groningen- University Medical Center Groningen, Radiation oncology, Groningen, The Netherlands*

[2]*University of Groningen- University Medical Center Groningen, Epidemiology, Groningen, The Netherlands*

Purpose or Objective: Radiation induced xerostomia is related to the dose given to the parotid glands (PG).

Nevertheless, substantial unexplained variability remains in the development of late xerostomia. To understand this variation becomes increasingly important with the advent of more conformal radiation techniques. Our hypothesis is that the patient-specific late response to radiotherapy (RT) is associated with changes in CT images and xerostomia scores early after RT.

Material and Methods: Parotid gland (PG) image characteristics were extracted from CTs before (T0) and after RT (6 weeks post RT) of 110 HNC patients. The differences between those two time points resulted in potential Δ CT Image Biomarkers (IBMs). These potential Δ CT IBMs represent geometric (20) and CT intensity (24) changes of the PG. Furthermore, the scored xerostomia of the patients before (XER*baseline*) and 6 weeks post RT (XER*6w_post*), tumour, patient and dose characteristics were included. To identify variables that were associated with the endpoint moderate-to-severe xerostomia 12 months after RT (XER*12m*) whilst reducing multicollinearity, variables were first omitted based on inter-variables correlation. Second, multivariable selection was conducted by bootstrapped forward selection based on log-likelihood performance. The performance of the resulting logistic regression models was evaluated with the area under the ROC-curve (AUC) and Nagelkerke R2 index. All models were internally cross validated.

Results: Multivariable analysis was performed with 23 Δ CT IBMs. The primarily selected IBM was Δ volume (between T0 and 6 weeks post RT) of the PG (figure) ($p<0.001$). Larger volume change was related to a higher chance of XER*12m*. Furthermore, the XER*6w_post* and XER*baseline* were very prognostic. The performance of the multivariable model was high with an AUC of 0.89 and R2 of 0.54 (table). This model showed to be stable when it was internally validated (AUC-cross=0.88, R2-cross=0.53). Moreover, dose parameters did not add to the performance of the model (AUC-cross=0.88, R2-cross=0.52). Δ Volume made dose parameters redundant, suggesting that PG volume changes are related to the patient-specific response to dose.

Table. Model performance measures

	Baseline model	Post RT model	
	PG dose + $XER_{baseline}$	$XER_{w6\ after\ RT}$ + $XER_{baseline}$	$XER_{w6\ after\ RT}$ + $XER_{baseline}$ + Δ volume
2 log-likelihood	111.47	99.55	81.72
Nagelkerke R^2	0.27	0.47	0.54
Discrimination Slope	0.20	0.38	0.45
AUC (95% CI)	**0.76 (0.66-0.85)**	**0.83(0.75-0.91)**	**0.89 (0.82-0.95)**
AUC-cross validation	0.74	0.83	0.88
R^2- cross validation	0.25	0.47	0.53

XER_T: *Patient rated xerostomia at different time points;*
PG dose: *Planned mean dose to contra lateral parotid gland;*
Δ volume: *PG volume change from baseline (T0) to 6 weeks post RT*

Conclusion: Change of PG volume 6 weeks post RT showed to be strongly related to late xerostomia. Moreover, together with xerostomia scores before and 6 weeks after RT, outstanding performance was obtained to predict XER*12m*. We believe that this model can contribute to the understanding of the patient-specific response to RT in developing late xerostomia. Secondly, it can serve as a quantitative measure for late damage to the PG early after treatment. The next step will be to investigate whether Δ PG Volume and xerostomia determined early in treatment can be used to predict late xerostomia, to select patients with a large risk on late xerostomia for proton treatment.

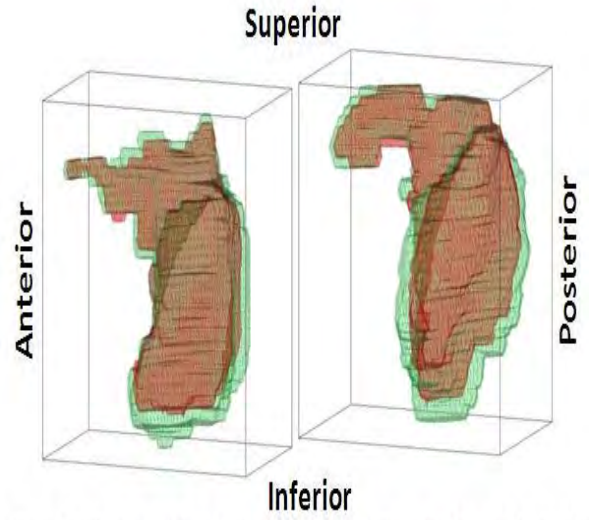

Figure. Examples of PGs with large Δ volume between the start of (green) and 6 weeks after (red) RT

PV-0478

Predicting pulmonary function loss in lung cancer radiotherapy patients using CT ventilation imaging

C. Brink[1,2], J. Kipritidis[3], K.R. Jensen[1], T. Schytte[4], O. Hansen[2,4], U. Bernchou[1,2]
[1]*Odense University Hospital, Laboratory of Radiation Physics, Odense, Denmark*
[2]*University of Southern Denmark, Institute of Clinical Research, Odense, Denmark*
[3]*The University of Sydney, Radiation Physics Laboratory, Sydney, Australia*
[4]*Odense University Hospital, Department of Oncology, Odense, Denmark*

Purpose or Objective: Pulmonary complications remain a major dose limiting factor for lung cancer radiotherapy. Pulmonary function loss is known to correlate with physical lung dose, but better prediction accuracy is desired. This work investigates the potential of 4D CT-based functional imaging to improve the prediction of radiation-induced pulmonary function loss.

Material and Methods: 80 lung cancer patients each received a treatment planning 4D CT scan prior to radiotherapy. To quantify pulmonary functional loss the patients also underwent spirometry measurements of forced expiratory volume (FEV1) and forced vital capacity (FVC) immediately before radiotherapy and at 3, 6, and 9 months follow-up. For each patient, the pre-treatment regional ventilation was evaluated by performing deformable image registration (DIR) between the CT inhale and exhale phase images. The Jacobian determinant (J-1) of the DIR motion field was used as a ventilation surrogate. The functional mean lung dose (fMLD) was then defined as the regional lung dose weighted spatially by the regional ventilation. The physical mean lung dose (MLD) was calculated without ventilation weighting.Logistic regression was used to compare the ability of fMLD and MLD to predict clinical pulmonary function loss, defined as a reduction of the FEV1 and FVC to less than 90% of their initial values at 6-months post treatment. To minimise noise in the spirometry data, the FEV1 and FVC values at 6 months were estimated based on a fit to the available data up to 9 months post-treatment.

Results: Both functional and physical lung dose correlated with the onset of clinical pulmonary function loss. The figure and table show the logistic regression results and model parameters respectively. We observed a 0.7 Gy decrease in the tolerance dose (D50) when using fMLD as opposed to MLD. However, the difference in log-likelihood between the MLD and fMLD based models was not statistically significant different from zero. Thus we did not observe a significant

improvement in the prediction of pulmonary function loss using fMLD as opposed to MLD.

Lung function	Physical dose		Functional Dose	
(95% conf. interval)	D_{50} (Gy)	γ_{50}	D_{50} (Gy)	γ_{50}
FVC	20.5 (17.7-26.6)	1.01 (0.59-1.60)	19.8 (16.5-27.2)	0.83 (0.46-1.32)
FEV1	19.1 (14.5-35.3)	0.55 (0.14-1.06)	17.8 (13.5-30.7)	0.51 (0.18-0.89)

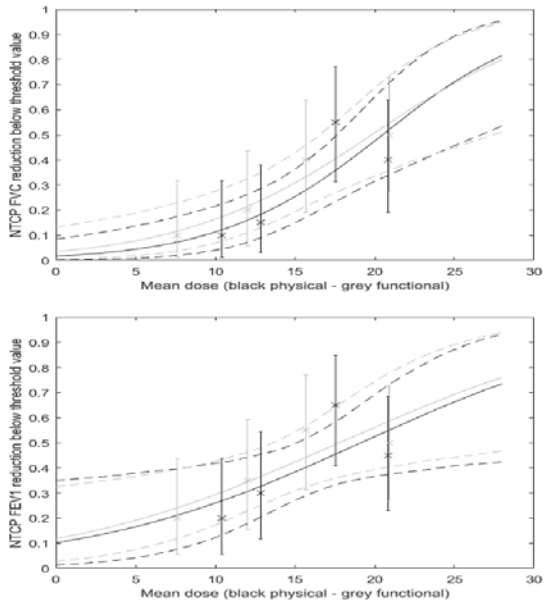

Conclusion: Reduction in lung function, measured by spirometry, can be predicted by functional as well as physical lung dose, but no statistically significant difference in their predictive ability was observed in these patients. The actual biological impact of radiation on normal lung tissue might be underestimated in spirometry data (as well in patient/oncologist reported outcomes) since a significant fraction of the patients actually observe an improved lung function during treatment. This improvement is likely related to re-ventilation of obstructed airways due to tumour regression, which could mask underlying radiation damage. Another possibility is that regional ventilation may vary over a course of treatment. Analysis of 4D cone beam CT scans during treatment, and of post-treatment radiographic changes in follow-up CT scans may help untangle these "competing" effects.

Proffered Papers: Selected randomised trials

OC-0479

Neoadjuvant chemoradiation for fixed cT3 or cT4 rectal cancer: results of a phase III study

K. Bujko[1], L. Wyrwicz[2], A. Rutkowski[3], M. Malinowska[4], L. Pietrzak[1], J. Krynski[3], W. Michalski[5], W. Polkowski[6], R. Stylinski[7], R. Wierzbicki[8], M. Jankiewicz[9], B. Cisel[6], M. Bebenek[10], A. Maciejczyk[11], T. Lesniak[12], J. Zygulska[13], W. Zegarski[14], M. Las[15], L. Kolodziejski[16], A. Radkowski[17], B. Czeremszynska[18], L. Kepka[19], Z. Toczko[20], A. Danek[21], W. Markiewicz[22]

[1]*The Maria Sklodowska-Curie Memorial Cancer Center, Deaptment of Radiotherapy II, Warsaw, Poland*
[2]*M. Sklodowska-Curie Memorial Cancer Centre, Department of Gastroenterological Oncology, Warsaw, Poland*
[3]*The Maria Sklodowska-Curie Memorial Cancer Center, Department of Gastroenterological Oncology, Warsaw, Poland*
[4]*The Maria Sklodowska-Curie Memorial Cancer Center, Deaptment of Pathology, Warsaw, Poland*
[5]*The Maria Sklodowska-Curie Memorial Cancer Center, Bioinformatics and Biostatistics Unit, Warsaw, Poland*
[6]*Medical University, Department of Surgical Oncology, Lublin, Poland*
[7]*Medical University, 1st Department of General Surgery-Transplantology and Nutritional Therapy, Lublin, Poland*
[8]*MSW Hospital, Department of Surgery, Lublin, Poland*
[9]*Medical University and St John's Cancer Centre, Department of Surgical Oncology, Lublin, Poland*
[10]*Silesian Oncological Centre, Department of Surgery, Wroclaw, Poland*
[11]*Silesian Oncological Centre, Departmetn of Radiotherapy, Wroclaw, Poland*
[12]*Bekid Centre of Oncology, Department of Surgery, Bielsko Biala, Poland*
[13]*Beskid Centre of Oncology, Department of Radiotherapy, Bielsko Biala, Poland*
[14]*Oncology Centre, Deapartment of Oncological Surgery, Bydgoszcz, Poland*
[15]*Oncology Centre, Department of Oncological Surgery, Bydgoszcz, Poland*
[16]*Regional Cancer Centre, Department of Surgery, Tarnow, Poland*
[17]*Regional Cancer Centre, Department of Radiotherapy, Tarnow, Poland*
[18]*Warminsko-Mazurskie Centre of Oncology, Department of Medical Oncology, Olsztyn, Poland*
[19]*Warminsko-Mazurskie Centre of Oncology, Department of Radiotherapy, Olsztyn, Poland*
[20]*Regional Hospital, Department of Surgery, Elblag, Poland*
[21]*The Maria Sklodowska-Curie Memorial Cancer Center, Deaptment of Radiotherapy I, Warsaw, Poland*
[22]*Regional Cancer Centre, Department of Surgery, Bialystok, Poland*

Purpose or Objective: The study tested whether preoperative 5x5 Gy and consolidation chemotherapy is more locally efficacious than standard preoperative chemoradiation in "unresectable" rectal cancer.

Material and Methods: Patients with fixed cT3 or cT4 cancer without distant metastases were randomized either to 5x5 Gy and 3 cycles of FOLFOX4 after one week rest (experimental group) or to 50.4 Gy delivered in 28 fractions given simultaneously with two 5-day cycles of 5-Fu 325 mg/m2/day and leucovorin 20 mg/m2/day in bolus during the first and fifth week of irradiation; 5 one-day infusions of oxaliplatin 50 mg/m2 were given once a week at 1, 8, 15, 22, and 29 days of irradiation. 3 cycles of FOLFOX were chosen to keep overall neoadjuvant treatment time similar in the two groups. Postoperative chemotherapy in both groups was optional. For the second study part, because of the new publications, oxaliplatin was delivered to the two groups at the discretion of the participating centre. Both randomized groups underwent surgery about 12 weeks after starting irradiation and about 6-7 weeks after completing neoadjuvant treatment.

Results: 541 patients were randomised and 515 were eligible for analysis; 261 in the experimental group and 254 in the control group of whom pelvic MR at baseline was respectively performed in 66% and 65% of patients. Oxaliplatin was given preoperatively to 70% of patients in the experimental group and to 66% in the control group, p=0.40. The incidence and severity of the neoadjuvant treatment acute toxicity was lower in the experimental group than in the control group, p=0.005; the overall toxicity rate being respectively 75% vs. 83%, grade III-IV 23% vs. 21% and toxic deaths 1% vs. 3%. The postoperative complications rate was 29% of patients in the experimental group and 25% in the control group, p=0.18. R0 resection rates (primary endpoint) and pathological complete response rates were respectively in the experimental group and in the control group 77% vs. 71% (p=0.081) and 16% vs. 12% (p=0.17). Median follow-up was 35 months. At 3 years, rates of overall survival and disease-free survival were respectively in the experimental group and in the control 73% vs. 64.5% p=0.055 and 54% vs. 52%, p=0.69. At 3 years, cumulative incidence of local failure and cumulative incidence of distant metastases were respectively 22% vs. 21%, p=0.82 and 30% vs. 27%, p=0.26. The incidence and

severity of the late complications were not different between the experimental group and the control group, p=0.54; the overall toxicity rate being respectively 20% vs. 21% and for grade III+ complications 9% vs. 6%.

Conclusion: The trial showed no difference in local efficacy between preoperative 5x5 Gy with consolidation chemotherapy and standard preoperative chemoradiation. Lower acute toxicity, lower cost, convenience and a trend towards improved overall survival favour 5x5 Gy with consolidation chemotherapy.

OC-0480

Five-year clinical outcome of the Phase III ACCORD 12 neoadjuvant trial in rectal cancer

J. Doyen[1], S. Gourgou-Bourgade[2], D. Azria[3], I. Martel-Laffray[4], C. Hennequin[5], V. Vendrely[6], G. De Laroche[7], T. Conroy[8], J.P. Gérard[1]

[1]*Centre Antoine Lacassagne, Radiotherapy, Nice, France*
[2]*ICM, Biostatistiques, Montpellier, France*
[3]*ICM, Radiotherapy, Montpellier, France*
[4]*Centre Léon Bérard, Radiotherapy, Lyon, France*
[5]*CHU St Louis AP-HP, Radiotherapy, Paris, France*
[6]*CHU Bordeaux, Radiotherapy, Bordeaux, France*
[7]*ICL, Radiotherapy, St Etienne, France*
[8]*Centre Alexis Vautrin, Oncology, Nancy-Vandoeuvre, France*

Purpose or Objective: The aim of the ACCORD 12 trial was to compare two different regimens of neoadjuvant chemoradiotherapy (nCRT). No significant difference has been found in main end point (pCR rate) . At 3 years there was no significant difference for local control and survival. We report the 5 years outcome.

Material and Methods: Between 11/2005- 07/2008, 598 pts randomized. Inclusion criteria: adenocarcinoma , distal-middle rectum, T3-4, anterior-distal T2 staged using MRI and/or endorectal US. Treatment : CAP 45 : radiotherapy (RT) 45 Gy/25 fr/5 weeks with concurrent capecitabine (800 mg/m2 BID) vs CAPOX 50 : RT 50 Gy/25 fr/5 weeeks with Capecitabine (same) and weekly oxaliplatin (50 mg/m2). A TME surgery was performed after 6 weeks interval. Adjuvant chemotherapy was left to each institution.

Results: Median follow-up time was 60 months with 299 pts in each group. In intent to treat analysis main results are shown in table. In 31 pts T4 confounded the local relapse rate was 11.3%[3.8-31.5].A clinical CR in 24 pts was associated with 81% DFS (p<0.0001) and Sphincter saving or organ preservation in 23. Adjuvant chemotherapy given in 253 pts.

Endpoint	CAP 45 299 pts	CAPOX 50 299 pts	p(log rank)	HR CI 95%
Loc. Rec. 5y	8.8%	7.8%	0.78%	0.92 [0.51-1.66]
Dist. Met. 5y	30%	28%	0.48%	0.89 [0.77-1.15]
DFS 5y	60.4%	64.7%	0.25%	0.86 [0.66-1.11]
Overall Surv. 5y	76.4%	81.9%	0.06%	0.71 [0.50-1.01]
Bowel function (1-7)	5.2	4.9	NS	

Conclusion: At 5 years there was no significant difference for local recurrence, distant metastases, survival and bowel function rates. Both CAP 45 and CAP 50 regimens are feasible and provide acceptable local control rate. More prognostic factors will be available at time of meeting and may generate hypothesis to further improve local control in locally advanced T3 or T4, achieve organ preservation in some T2 or early T3 and reduce toxicity in pts > 75 y old. Gerard Jp et al. J Clin Oncol. 2012 Dec 20;30(36):4558-65

OC-0481

Late toxicity and cosmesis after APBI with brachytherapy vs WBI: 5-year results of a phase III trial

C. Polgár[1], V. Strnad[2], O. Ott[2], G. Hildebrandt[3], D. Kauer-Dorner[4], H. Knauerhase[5], T. Major[1], J. Lyczek[6], J. Guinot[7], J. Dunst[8], C. Gutierrez Miguelez[9], P. Slampa[10], M. Allgäuer[11], K. Lössl[12], B. Polat[13], G. Kovács[14], A. Fischedick[15], T. Wendt[16], M. Hindemith[3], A. Resch[4], P. Niehoff[8], F. Guedea[9], R. Pötter[4], C. Gall[17], W. Uter[17]

[1]*National Institute of Oncology, Center of Radiotherapy, Budapest, Hungary*
[2]*University Hospital Erlangen, Department of Radiation Oncology, Erlangen, Germany*
[3]*University Hospital Leipzig, Department of Radiation Oncology, Leipzig, Germany*
[4]*University Hospital AKH, Department of Radiation Oncology, Wien, Austria*
[5]*University Hospital Rostock, Department of Radiation Oncology, Rostock, Germany*
[6]*Instytut im Marii Skłodowskej- Centrum Onkologii, Brachytherapy Department, Warsaw, Poland*
[7]*Valencian Institute of Oncology, Department of Radiation Oncology, Valencia, Spain*
[8]*University Hospital Kiel, Department of Radiation Oncology, Kiel, Germany*
[9]*Catalan Institute of Oncology, Department of Radiation Oncology, Barcelona, Spain*
[10]*Masaryk Memorial Cancer Institute, Department of Radiation Oncology, Brno, Czech Republic*
[11]*Hospital Barmherzige Brüder Regensburg, Department of Radiation Oncology, Regensburg, Germany*
[12]*University Hospital Bern, Department of Radiation Oncology, Inselspital, Switzerland*
[13]*University Hospital Würzburg, Department of Radiation Oncology, Würzburg, Germany*
[14]*University of Lübeck- UKHS Campus Lübeck, Interdisciplinary Brachytherapy Unit, Lübeck, Germany*
[15]*Clemens Hospital Münster, Department of Radiation Oncology, Münster, Germany*
[16]*University Hospital Jena, Department of Radiation Oncology, Jena, Germany*
[17]*University Erlangen-Nuremberg, Department of Medical Informatics, Erlangen, Germany*

Purpose or Objective: The 5-year local control and survival results of the GEC-ESTRO multicentric accelerated partial breast irradiation (APBI) trial have been reported recently. In this analysis we report the 5-year late toxicity and cosmetic results of patients treated with APBI using interstitial brachytherapy (iBT) compared to those who underwent standard whole breast irradiation (WBI) with a tumour bed boost.

Material and Methods: Between April 2004 and July 2009, 1184 patients aged≥40 years with stage 0, I and IIA breast cancer who underwent breast conserving surgery (BCS) were randomly assigned to receive either 50 Gy WBI with tumour bed boost of 10 Gy or APBI using HDR/PDR iBT. Among these, 5-year follow-up records on late toxicities and cosmetic results were available at 969 patients (82%). Five-year prevalences of toxicities graded by the RTOG/EORTC late radiation morbidity scoring scheme were compared using the Fisher's exact test. The cosmetic results were scored by the patients and treating radiation oncologists using the four-scale (excellent-good-fair-poor) Harvard criteria. The trial is registered with ClinicalTrials.gov, NCT00402519.

Results: There were no grade 4 toxicities. The cumulative incidence of grade (G) 2-3 late skin toxicity at 5 years was 5.7% in the WBI group versus 3.2% in the APBI group (p=0.08), difference: -2.4% (95% CI: -5 – 0.2%). Concerning G2-3 late subcutaneous tissue side effects at 5 years the cumulative risk was 6.3% in the WBI group versus 7.6% in the APBI group (p=0.53), difference: 1.3% (95% CI: -1.9 – 4.5%). The cumulative incidence of severe (G3) fibrosis at 5 years was 0.2% in the WBI group and 0% in the APBI group (p=0.46), difference: -0.2% (95% CI: -0.6 – 0.2%). The cumulative incidence of G2-3 breast pain was low in both arms (3.2%

after WBI; 1.4% after APBI; p=0.04) difference: -2% (95% CI: -3.9 – -0.1%). The rate of excellent/good cosmetic results judged by the patients was 87.2% versus 90.4% (p=0.06) in the WBI and APBI group, and 86.7% versus 88.2% (p=0.07) scored by the physicians.

Conclusion: The 5-year toxicity profile and cosmetic results are similar at patients treated with BCS followed by either APBI using iBT or conventional WBI with tumour bed boost. A non-significant trend towards less late skin side effects and better cosmetic results has been observed in the APBI arm.

Award Lecture: K. Breur Award Lecture

SP-0482
Whither fractionation?

P. Hoskin[1]
[1]*Mount Vernon Hospital, Radiation Oncology, Northwood, United Kingdom*

Traditional delivery of radiotherapy uses daily fractions of 1.8-2Gy building up to a therapeutic dose over 6 to 8 weeks of treatment. This reflects application of the fundamental principles of radiobiology in which repair, repopulation, reoxygenation and redistribution in the cell cycle are considered important in defining the response of tumour and normal tissue. However the relevance of this approach in an era of more precise image guided dose delivery where the exposure of normal tissue is minimised and high individual doses can be delivered must be questioned. There are two scenarios in which single dose radiotherapy has been evaluated and found to be highly effective. The first is in the extensive work which has been undertaken over several decades to establish the role of single dose palliative radiotherapy. The best example of this is in the management of metastatic bone pain where single dose radiotherapy is considered the standard of care but other palliative scenarios in non-small cell lung cancer, oesophageal cancer, rectal, bladder and prostate cancer are also relevant to this approach. The second scenario is that of curative treatment for localised prostate cancer using high dose rate brachytherapy (HDRBT). Dose escalation using HDRBT is well established as an effective therapy in prostate cancer and there is now a substantial database of large published series using HDRBT alone demonstrating high biochemical control rates. It is now feasible to deliver single dose radical radiotherapy using HDR BT with low toxicity and high disease control rates challenging the conventional and modest hypofractionation schedules used with external beam. The relevance of conventional fractionation can now be challenged in the era of modern image guided radiation delivery for both palliative and radical treatment. A sufficiently high dose delivered accurately to the target volume is all that is required.

Joint Symposium: ESTRO-ASTRO: In room adaptive imaging with a focus on MRI

SP-0483
MRI Linac: physics perspective

B. Raaymakers[1], J.J.W. Lagendijk[1]
[1]*UMC Utrecht, Department of Radiation Oncology, Utrecht, The Netherlands*

The MRI linac originates from the desire to bring sight to the radiation oncologist. So to offer truly simultaneous soft-tissue visualization during radiation delivery. In UMC Utrecht, in collaboration with Elekta and Philips, a hybrid 1.5 T MRI radiotherapy system has been developed to facilitate this. Later also other systems emerged; in the Cross Cancer Institute in Edmonton a rotating 0.5 T MRI linac has been developed and the Viewray company has launched a 0.3 T Cobalt 60 system into the clinic. The systems will be briefly presented.

The common ground of the systems is the soft-tissue guidance. As will be shown, MRI offers a wealth of contrasts for anatomical and physiological information but also motion data. Exploiting these data for treatment guidance and treatment adaptation requires a new workflow with more on-line decisions, such as contouring, plan adaptation or full re-planning to initialize the treatment. Moreover, the continuous anatomical imaging during radiation delivery enables new direct anatomical triggers for gating and tracking, but equally important, this imaging can be used for dose reconstruction while accounting for intra-fraction motion. The latter is a valuable input for dose response assessment and can also be used for quality assurance (QA) purposes.

The QA for these systems need to be revisited, not only because of the new on-line plan adaptations but also due to the fact that the dose is delivered in the presence of a (perpendicular or parallel) magnetic field. This will alter the dose distribution which needs to be verified. Also the radiation detectors are potentially affected and their performance need to be validated (and corrected if necessary) for use in the presence of a magnetic field. This implies new machine QA , patient QA and workflow QA procedures.

The promise of hybrid MRI linac technology is to enable real-time plan adaptations in order to maximize the dose to the target while continuously minimizing the dose to the surrounding organs at risk. The efforts to move from pre-treatment planning to once daily (on-line) plan adaptation and ultimately to real-time plan adaptations will be presented.

In conclusion, the technology of hybrid MRI radiotherapy systems is there while the full clinical value needs to be established. This is an exciting new clinical arena and at the same time poses new challenges for on-line and ultimately real-time, adaptive radiotherapy.

SP-0484
First two years clinical experience with low-field MR-IGRT--system practicality and future implications

J.M. Michalski[1], O.L. Green[1], R. Kashani[1], H. Li[1], V. Rodriguez[1], T. Zhao[1], D. Yang[1], J.D. Bradley[1], I. Zoberi[1], M.A. Thomas[1], C. Robinson[1], P. Parikh[1], J. Olsen[1], S. Mutic[1]
[1]*Washington University School of Medicine, Department of Radiation Oncology, Saint Louis- MO, USA*

Purpose: We report on the first two years of clinical operation of the first magnetic-resonance imaging-guided radiation therapy (MR-IGRT) program, experiences with patient treatments, and implications for future developmental and clinical work. We previously reported on initial clinical implementation of this system. = The purpose of this work is to analyze clinical practicality of MR-IGRT and implementation of online adaptive RT.

Methods and Materials: The MR-IGRT system consists of a split 0.35T MR scanner straddling three ^{60}Co heads mounted on a ring gantry, each head equipped with independent doubly-focused multileaf collimators. The MR and RT systems share a common isocenter, enabling simultaneous and continuous MR imaging during RT delivery. The system is also capable of online plan adaptation where patients can be imaged, planned, verified, and treated all in a single treatment session. To assess the clinical practicality of the system, makeup of treated cancer sites, distribution of available treatment techniques, total number of patients, maximum number of patients treated daily, and the utilization of advanced treatment techniques were evaluated. The system was clinically implemented in January of 2014 and data was collected over a 24 month consecutive period. The adaptive feature was clinically implemented in September of 2014.

Results: During the initial 2 years of the operation, more than 20 cancer sites in 263 patients were treated. The maximum number of daily treatments was 18. Top 3 treated cancer sites were breast, lung, and bladder with 22%, 13%, and 9% of the total treatments, respectively. The utilization

of IMRT, SBRT, and 3D treatments was 50%, 28%, and 22%,respectively. More than 150 real time adaptive fractions were delivered to more than 45 patients. We have also demonstrated that the system is capable of determining true delivered doses based on daily MR images.

Conclusions: Based on the first two years of clinical operation, routine MR-IGRT program is practical, with ability of treating a broad spectrum of cancer sites, significant number of patients in a day, and systematic delivery of advanced and adaptive treatments.

SP-0485
MR-linac: Clinical introduction
C. Schultz[1]
[1]*Medical College of Wisconsin, Department of Radiation Oncology, Milwaukee, USA*

The MR-linac combines a 1.5 Tesla MRI and a modern 7MV Linac into a single device that can simultaneously produce diagnostic quality MRI images and deliver highly conformal IMRT based treatments. The introduction of in room MR-linac based imaging allows for superior soft tissue contrast of tumor and surrounding normal tissues. This functionality enables enhanced re-positioning and adaptive radiation therapy to account for inter-treatment positioning errors, organ deformation, organ movement, and tumor response. Additionally, this combined device provides functionality to account for intra-treatment motion and has the potential to acquire multi-parametric functional sequences at the time of treatment.
The addition of the MR-linac to a radiation therapy clinic poses novel challenges related to the the presence of the magnetic field and the configuration of the device. Prevailing regulations concerning room access, shielding, and adjacency to other treatment units and medical equipment must be considered when siting the device. Personnel must possess or acquire the skill sets and competencies to safely operate an MRI and Linac treatment machine. This training should be in place prior to installation of the device. Experience with MRI based simulation and treatment planning is also a prerequisite for MR-linac based treatment delivery. MRI based simulation requires attention to the size and material of patient positioning devices, MRI coil and table top design. Optimal MRI sequences to facilitate region specific tumor and normal tissue delineation that may differ from institutional diagnostic sequences must be developed. Image distortion is routinely managed as part of modern MRI imaging but the use of MRI for simulation and the MR-linac for guidance and treatment requires a QA process that is nuanced to these specific workflows.
It is anticipated that the work flow for the MRI-linac device will be divided into two general scenarios. The first utilizes pre-treatment MRI images for patient repositioning to correct translational and or rotational errors. This is similar to the current cone beam CT image guidance workflow with the addition of superior soft tissue contrast. Additionally, the intra-fraction imaging will provide superior ability to manage tumor motion. The second approach adds plan adaption to the MRI based treatment guidance workflow to account for deformation, volume, and independent motion changes of the targets and organs at risk. The frequency of online or offline adaption will depend on the characteristics of tumor response and anatomical location.
An international research consortium has been formed to allow for an evidence-based introduction of the MR-linac technology and to address how the technology could be used to achieve an optimized radiation treatment approach in terms of tumor control and toxicity. The MR-linac consortium structure is outlined in Figure 1. Nine tumor site groups have been selected to start consortium based clinical studies based on the expected clinical benefit (either increased local control, survival, decreased toxicity or improved quality of life). The first nine consortium-broad tumor sites include: rectum, esophagus, oropharynx, pancreas, prostate, breast, cervix, brain and lung. Each consortium institute coordinates one or more Tumor Site Groups (TSG). To achieve the clinical introduction of the MR-linac in a safe and step wise manner, an adapted version of the IDEAL framework, the R-IDEAL (Radiotherapy, Idea, Development, Exploration, Long-term study) framework, will be used to conduct the proposed prerequisite imaging studies and clinical treatment studies.

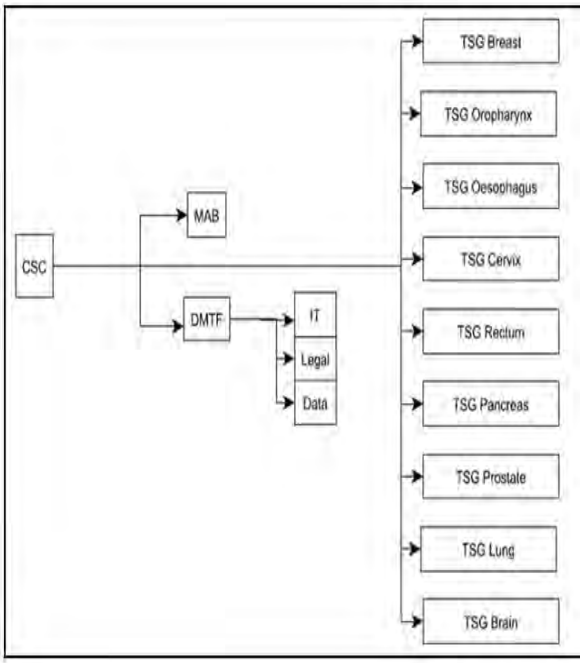

Figure 1. Organizational structure clinical working groups MR-linac Consortium (CSC-clinical steering committee, MAB-methodology advisory board, DMTF-data management task force, TSG-tumor site group)
References: McCulloch P, Altman DG, Campbell WB, et. al. No surgical innovation without evaluation: the IDEAL recommendations. Lancet 2009:374:1105-12

SP-0486
Adaptive planning, dose delivery and verification with MRI based brachytherapy
C. Kirisits[1], R. Pötter[1]
[1]*Medical University of Vienna, Department of Radiotherapy-Comprehensive Cancer Center, Vienna, Austria*

Soon after the introduction of MRI in radiology it became part of treatment planning in radiotherapy and in brachytherapy. Especially in gynecological brachytherapy MRI was used during the process of target definition. But also in other clinical sites MRI before brachytherapy became an essential tool for correct staging, treatment decision making and target volume definition. The important point was the use of MRI with the brachytherapy applicators in-situ. By this process the image series contain both, the delivery device and the anatomy including tumour, target and organs at risk. This enables a real adaptive planning strategy, as the treatment planning is based directly on these image series. Imaging of a fixed geometry of delivery device inside the anatomy is not different to in-room imaging used for external beam with a linac or other device as delivery device outside the patient. The aim of in room imaging is to depict the situation during dose delivery as close as possible. The question is how much change of the target and organs at risk happens between imaging and dose delivery. In external beam this is performed almost simultaneously without essential changes, while in brachytherapy the movement of patients from an imaging room to a treatment room might impose changes. This question was analyzed and debated for years, often using inappropriate methodologies as registration to bony landmarks. Only recently multicenter studies showed that for cervix cancer brachytherapy for example the relation of applicators to target is stable with minor variations. However, more variation may occur for adjacent OARs. Various methods are investigated on how to minimize such uncertainties. One is to perform MRI in-room

imaging comparable to external beam using dedicated set-ups with an afterloader inside the MRI room. On the other side it seems very promising to invest into in-vivo dosimetry methods. Other forms of volumetric imaging in the treatment room may be another alternative. As the MR image series for treatment planning already contains already the delivery device and the anatomy, the situation during dose delivery can be verified with different methods with co-registration and may reach then almost the same accuracy as if performed simultaneously together.
Real in-room US imaging has been performed since long with prostate brachytherapy for direct guidance of needle insertion, target definition and on-line dose planning. Especially HDR techniques applying ultrasound for treatment planning before and during needle insertion, again for verification just before dose delivery, leaving the ultrasound probe in place and finally performing an ultrasound image directly after dose delivery have probably the highest accuracy possible. Combining such methods with MRI may lead to the ultimate accuracy in terms of target definition, OAR localization, treatment planning and dose delivery verification.
Combinations of different imaging techniques with the applicator in place, even generated in different rooms, seem to be the future in brachytherapy. Already by now brachytherapy planning was performed as adaptive procedure, taking into account pre-treatment imaging information and dose optimization based on the situation directly before dose delivery. The adaptive process includes image guided applicator placement. The term "in-room adaptive imaging" in brachytherapy can be extended to an overall definition of a "room" inside the patient visualized via adaptive imaging containing target, OARs and the delivery device in one image.

Symposium: Communication with patients

SP-0487
Patient's Perspective

E. Naessens[1]
[1]*Trinity College Dublin, Dublin, Ireland Republic of*

Good communications are primarily thought to involve skills of articulation. However, this presentations makes the case for listening as the recurrent starting point in patient interactions. Listening is deceptive. Generally viewed as a “soft skill” the challenges of listening are easily overlooked. Engaging requires gaging (active listening, observing, clarifying, and feeding back).
Drawing upon his experience as an oncology patient and his academic background and training in communications and social science, Eddie explains why we are prone to assume we are good listeners despite evidence to the contrary. Demonstrating a number of relevant biases and fallacies, he explains why there is no necessary link between assumption of competence and actual competence. He presents concrete examples from the patient perspective of excellent and poor communications and their positive and negative outcomes. The presentation concludes with an overview of useful ways to reflect upon the issues, improve communications, and enhance overall outcomes.

SP-0488
Healthcare professional's perspective

G. Sancho Pardo[1]
[1]*Hospital de la Santa Creu i Sant Pau, Barcelona, Spain*

Training in communication and interpersonal skills was not considered a relevant part of the training at medical school and during the specialty residency programmes. Medical doctors therefore learned by observation of how their seniors performed. After some time one realizes that effective communication with patients involve both content and style and that being caring, nice and logical is not enough. Based on the available literature, this presentation will look into the factors influencing the patient-healthcare professional communication. I will focus on how healthcare professionals are involved in the process of communication and how they can improve it.
When we are visiting a patient we have to ensure that several aspects are well covered. First we need to identify the patient’s problems and concerns and their impact on their family and daily life. Second, we should give clear information and advice about their disease, their treatment and their prognostic. Giving patients tailored information of what and how you think they want to know might be not enough. In many occasions breaking bad news is unavoidable, and patients may express some strong emotional reactions that you should be able to understand and cope with. One has also to be aware that some patients do not want to know the diagnostic and nothing related to the disease and few patients will move into denial. Third, we should ensure that patients are aware of the situation, that they have not misunderstood the information we have given them and that they trust us. It is of paramount importance to empathise with the patient. Remember that verbal information goes together with visual messages and physical contact. Patient depending factors like race, sex, age, language, culture, socioeconomic status, disability or communication barriers could condition the process of communication. Healthcare professional’s factors such as time, job strain, working conditions, work engagement and personal life may spoil communication with patients.
Doctors have to be aware that patients today have access to information about their disease from their relatives, friends, books, media and the Internet that clearly impacts on the relation with patients and on the communication process. An issue that deserves special attention is the recruitment of patients for clinical trials. Patient recruitment partially depends on a relation of trust with the patient and in the doctor’s ability to communicate the importance of joining a trial. It has been shown that training in communication about trials may influence in the recruitment. However, trial design, especially when one arm offers placebo or less treatment, highly contributes to patients’ decline. It has been suggested that involving patients and patients’ organisations in the design and development of clinical trials could accelerate research and make it more effective.
There is a need for training in communication skills in medical education. Training healthcare professionals how to be more effective in communication with patients will provide a benefit for them as well as for the patients.

SP-0489
RTT/Nurse's perspective: patient is the key element of communication

L. Koevoets[1]
[1]*Dr. Bernard Verbeeten Instituut, Radiotherapy Breda, Tilburg, The Netherlands*

Patient is the key element of communication.
Where do we stand regarding communication with our patients? Our mission statement: we want to give our patients the best possible experience.We really want to connect.
How do we try to achieve this? Personal contact and support as much as possible“Do what you say and say what you do”. Honest and clear information. Information in common words, but also use of visual aids. This is rooted into our Instituut by use of a timeline: who explains what at which particular stage in the treatment and what tools can be used? Example: we inform all our patients in a private briefing before their treatment starts.
The role of the RTT in communication with the patient Explanation of the treatmentConnecting with other disciplines to support the patiëntA person who a patient can approach Provision of personal coaching programme to help patients to quit smoking. We check the satisfaction of our patients on a regular basis.
How do we do that? We try to stay in dialogue with our patients.All staff are trained for giving and receiving feedback.
What do we try to attempt witch our information conversation? The information given before treatment is

aimed at providing patients with more knowledge. Armed with insight, personal behaviour patterns which influence treatment outcomes can be challenged. Our belief is that a well informed patient will be less anxious and insecure. The information that we give is to repress misconception, reduce unrealistic fears and provide predicitive information. The latter is to let the patient know what we do during the ratiation and why, further to inform the patient what side effects the patient can develop after an period of time. We try to support the patient in different areas. We try to meet within the needs in the pyramid of Maslow. It states that a human being among other things is in need of safety and security, need for social contact and is in need of appreciation and recognition. In the conversation we try to acknowledge their fears and and recognize that these may exist and by giving information we try to repress those fears. We try as much as possible to be really in contact with the patient and to connect whith the experiences of the patient. To reassure them and to let them know what we do and why, we try let them feel safer and more certain about the process they will be going through. To give the patient also some sense of control over the radiation we hope to achieve that the patient feels he/she also affects the process and thus have the situation more under control. The information is given with use of an PowerPoint presentation with supports the story the radiation technician is giving. In this presentation he shows pictures that support the story. The radiation technician uses the knowledge that a person remembers 20% of what they read, 35% of what they see and 55% when you combine these two.

SP-0490

Interaction between patients and professionals: a psycho-oncologist's view

E. Van Hoof[1]
[1]*Vrije Universiteit Brussel, Department of Psychology, Brussels, Belgium*

Purpose or Objective: Stress influences our communication: the way how we interpret the world, our communications style we use to interact with our environment and our internal communication. During the presentation, neuropsychological insights into communication will be presented. These insights will be used to introduce some pragmatic intervention to monitor and control communication.

Materials and Methods: a literature review of the impact of stress on our information processing system and hence, our communication and of possible intervention that can positively influence our information processing

Results: Several brain mechanisms can negatively influence our communication. Our knowledge of these mechanisms is key in understanding and identifying possible communication styles. In cancer, we see many patients and their relatives struggling with the information-processing. Coping strategies like avoiding and neglect, for instance, are effective in the short-term but in the long run, flexibility in coping is required to ensure shared decision making in cancer care. Indeed, shared decision making is the priority in cancer care. Caregivers, specialists and the patients collaborate ensure the best possible cancer care. Shared decision making requires an efficient information processing. However, stress has a strong impact on this shared decision making process.
Results from cognitive behavioral interventions and intervention based on positive psychology positively influence information processing and stress-levels. Including these strategies can facilitate emotion regulation and hence, shared decision making in cancer care.

Conclusion: Stress negatively impact our information processing and hence, our communication. On the other hand, communication is the central factor in shared decision making. Caregivers, specialists and patients should always be aware of these possible disruptive factor in order to ensure shared decision making in cancer care.

Symposium: Imaging biology

SP-0491

What do we really see?

D. Zips[1]
[1]*University Hospital Tübingen Eberhard Karls University Tübingen, Tübingen, Germany*

Successful implementation of functional imaging in radiation therapy requires understanding of images. This includes radiobiological interpretation, quantification as well as validation of the prognostic and predicitve value. This talk will reflect on functional imaging and its link to radiobiological mechanisms of radiation response and discuss current knowledge as well as ongoing research in image validation.

SP-0492

Genomics and imaging: a pas-de-deaux in response prediction

H. Lyng[1]
[1]*Oslo University Hospital - Norwegian Radium Hospital, Department of Radiation Biology, Oslo, Norway*

Medical imaging has a fundamental role in radiotherapy planning today, but is almost exclusively used for assessing anatomical features like tumor size, stage and spreading. Introduction of functional imaging provides an opportunity to also consider biological features of disease aggressiveness in the clinical decision making. Recent advances in genomic research have led to promising molecular biomarkers of treatment outcome, but it is not clear how to best translate them into clinical practice and face challenges related to tissue sampling and intratumor heterogeneity. Radiogenomics, which refer to extraction of image features reflecting cancer genomics, allow visualization of molecular biomarkers within the entire tumor and have been proposed as a promising tool for this purpose. Such analyses provide a better understanding of the molecular background of the images and open for the use of imaging in the planning of combination therapies with radiation. In this talk, I will present clinical data on associations between functional MR imaging and biopsy based genomic biomarkers and reflect on the challenge of intratumor heterogeneity for such investigations. I will further discuss the potential of combining functional MR imaging and genomic signatures in the prediction of radiotherapy outcome. Examples will be given from published data and from our ongoing studies on cervical cancer and prostate cancer.

SP-0493 Molecular imaging for radiotherapy optimisation

R. Jeraj[1]
[1]*Jozef Stefan Institute, Ljubljana, Slovenia*

Molecular imaging adds value in each of the steps of the radiotherapy process: (1) Diagnosis and staging, (2) Target definition, and (3) Treatment response assessment. As such, it remains an important tool for optimization of radiation therapy. At the moment there is no general consensus how molecular imaging should be utilized in defining treatment target. A number of automatic and semi-automatic approaches exist, but their use in treatment planning is limited. Dose painting – biologically conformal radiotherapy – is an exciting concept, but still needs further development. Its feasibility has been established in various tumor types, and early efficacy clinical trials are underway. Generally, post-RT molecular imaging, particularly FDG PET/CT has a high negative predictive value (NPV), but rather low/moderate positive predictive value (PPV) for predicting treatment outcome. Early RT molecular imaging response assessment is promising and provides potential for innovative adaptive approaches. High inter- and intra-tumor response heterogeneity remains challenging.

Debate: This house believes that centralised large radiotherapy units will provide the best academia and the best treatment quality

SP-0494
For the motion - SIZE MATTERS
B. Slotman[1]
[1]*VU University Medical Center, Department of Radiation Oncology, Amsterdam, The Netherlands*

The field of radiation oncology has moved away from a generalistic radiotherapy practice to a number of specialized areas where radiation oncologists have broadened their knowledge outside the field of radiation oncology per se to be a better partner in multidisciplinary teams. Most radiation oncologists in the larger centers nowadays have only one or two areas of expertise (commonly around brain, head & neck, breast, lung, upper GI, lower GI, urogenital, gynecology, hematology, palliation, etc.). In these areas, radiation oncologists can be better counterparts for the organ-specialists, which have often left all the non-oncological work in their specialty to other colleagues.
With 2-3 areas of expertise per radiation oncologists and accounting for sufficient back-up, the minimum size of a department treating all categories of patients should be around 8 radiation oncologists. Based on 250 new patients per radiation oncologist and about 500 new patients per linac, the minimum size of a department which covers all areas of expertise should be 4 linacs. This size will also allow physicists and therapists to specialize, although at a size of 6-8 machines, this opportunity may be even better. A minimum size also makes investments of specialized equipped within the department, such as CT, PET-CT or MRI feasible and makes it easier to accommodate machine breakdown or replacement.
The economic lifetime of a linac is generally around 10-12 years. Since the pace of technical innovation is much faster, a department with 4-8 linacs has the opportunity to install the latest technology every 2-3 years. This, in combination with a larger physics group, will allow earlier implementation of new treatments. In Europe, the median size of a radiotherapy department is between 2 and 3 linacs, with on average more than 4 linacs per department in only 6 countries.
Sufficiently sized departments are also better equipped for research and moving the field forward. The multidisciplinary setting and available infrastructure in larger departments will help to work off the beaten track. Studies in various tumor sites have shown that outcome for patients treated in highly accruing (often larger) centers is better.
However, there is probably also a maximum size. For patients, entering a mega-department can be intimidating and beyond a certain size, no further benefits may exist. In addition, geographical circumstances should be taken into consideration. It is well known that easy access to care is related to use of radiotherapy. In more remote areas, satellite centers may be an alternative, especially if infrastructure and staffing can be shared and allow for similar protocols and expertise. Especially where resources are limited, a close collaboration between centers may further improve health care.
A possible disadvantage of subspecialization could be that highly specialized radiation oncologists may lose their overview of the developments in the radiotherapy arena and the transfer of new ideas and solutions from one indication to another may be reduced. For that reason, radiation oncologists working with one leg in the tumor-specific field, should keep their other leg in the radiation oncology field.

SP-0495 Against the motion - against dinosaurs
S. Bodis[1]
[1]*Kantonsspital Aarau, Radiation Oncology, Aarau, Switzerland*

Smart-modular-flexible: The essentials for academic excellence and high quality

NoBodis and nobody can believe that there is a general relationship between physical size and quality neither in biology, politics, industry, administration, culture nor more importantly for this forum, in science. Centralisation on the other hand is often an imposed structural process and has nothing to do with guaranteed high quality performance of high quality research. In organic systems and in most operational business units high quality growth is overwhelmingly present in (early) development i.e. in small structures. Moreover biology (organic) systems have a finite size to protect them from excessive and dysfunctional growth.
Neither data from radiation oncology industry, health care insurance companies, patient advocacy organisations nor from international data banks provide published evidence that large centralised radiation oncology units provide a higher treatment quality compared with small units. Moreover there is no international accepted definition of “small” and “large” RO unit. Large centralised radiation oncology units might produce more academic quantity because it is in their to do list. However academic quality is never a matter of size and/or centralisation. Most breakthrough innovations arise by chance, in small teams of 6-12 researches and fostered by a creative und productive environment (The majority of Nobel prizes laureates are citizens of small countries).
If you have to choose between one monopolistic large radiation oncology department and several smaller units think about similar choices made historically by politics or by evolution. The audience should carefully consider the scientific information provided in this debate not according to the evidence but also by common sense, gut feeling and empathy (e.g. in what type of radiation oncology environment would you like to work and/or be taken care of as a patient: Familial or military?). And by the way Radium, the “potion magique” of radiation oncology, was discovered in a storeroom and introduced into clinics by a handful enthusiastic scientists.
To pave the way for a constructive debate consider this: Based on the existing local health care systems in Europe both types of radiation oncology units (large and small) can co-exist and improve each other by cross-feeding. The IAEA has published recommendations as to how national radiation oncology services should be established, specifically in low- and middle-income countries with little or no RO infrastructure. Their recommendation is to start with small primary centers and step by step establish a network with a few secondary and eventually one tertiary (national reference) RO center(s). Such tailored RO networks allow proper allocation of professional skills and resources to each center including modern communications tools like telemedicine to optimize patient care especially where long distances might prevent patients from reaching the larger center(s).
In a multidisciplinary environment such as a RO clinic, the quality (education, experience, research as commitment for continuous improvement) of the staff will always be more important than quantity.
I would like to acknowledge the following:

Firstname / surname	Institute	City	Country
Staff	Kantonsspital Aarau-Baden	Aarau/Baden	Switzerland
Staff	Swiss Hospital Network Partners		Switzerland
SAKK	National Network Partner	Bern	Switzerland
Swiss Hyperthermia Network	National Network Partner	Aarau	Switzerland
NRG (Interncontinental Group)	International Network Partner	Philadelphia	USA
EORTC	International Network Partner	Brussels	Belgium
Varian Intl.	International Network Partner	Palo Alto/Zug	USA/Switzerland
IAEA	International Network Partner	Vienna	Austria

Joint Symposium: ESTRO-ILROG: Modern radiotherapy in lymphoma

SP-0496

Indications to radiotherapy for lymphoma in 2016: what is standard of care and what remains controversial?

J. Yahalom[1]
[1]*Memorial Sloan Kettering Cancer Center, Radiation Oncology, New York, USA*

The role of radiation therapy (RT) in the management of Hodgkin lymphoma (HL) and various non-Hodgkin lymphomas (NHL) has changed significantly over the last three decades. The indications, the fields and dose recommendations still continue to evolve. Old biases, new outcome data (often conflicting or controversial) as well as availability of tested and untested alternative drugs and a desire to evaluate them in an environment free of other high impact modalities have affected the consideration of radiotherapy in many tried and true indications for RT alone or as a combined-modality. Unfortunately many non-radiation oncologists were trained to believe that RT (even if limited and modernized) is loaded with long-term complications, while more chemotherapy, as an alternative is risk-free. Although radiotherapy remains, as stated by James Armitage, former ASCO president and highly regarded lymphoma leader, “the most effective single agent in the treatment of lymphomas”, the number of patients who are not receiving RT even when most guidelines recommend it has increased over the last two decades. Several 2014-2015 publications documented it in analyzing tens of thousands of patients even in localized stages of common lymphomas. Two themes are repeating in analyses of SEER and the U.S. National Cancer Data Base (NCDB) in early-stage HL (lymphocyte predominant and classical HL), in early-stage follicular lymphomas, in early-stage diffuse large B-cell lymphomas (DLBCL), and primary mediastinal lymphomas: 1. The use of RT is decreasing; 2. Looking at overall survival in multivariate analysis and using propensity scores- Not receiving RT is an independent factor associated with a significantly decreased overall survival. In an era of individualized medicine, one approach or dogmatic concepts without understanding what the other modality may offer your patient does not reflect best care. As radiation oncologists we are often dependent on the “gate keepers” for consulting lymphoma patients and thus our responsibility is to remain up-to-date on the issues relevant to the use of RT, the arguments and the studies for RT exclusion or inclusion, and to inform our colleagues and our patients of what radiation may offer in terms of outcome and avoidance of toxicity. This session will review the controversial issues of the main indications for using RT in lymphoma, mostly in early-stages of HL, DLBCL, and indolent lymphomas. Arguments supporting the role of RT will be highlighted in the talk.

SP-0497

New concepts for lymphoma radiotherapy and the use of advanced technology

L. Specht[1]
[1]*Rigshospitalet- University of Copenhagen, Department of Oncology- Section 3994, Copenhagen, Denmark*

The role of radiotherapy (RT) in the treatment of lymphomas has changed from being the primary treatment. In most situations RT is now part of a combined modality strategy, as consolidary treatment after primary chemotherapy or immunochemotherapy. With modern effective systemic treatments, microscopic disease is efficiently managed, and RT is only needed to treat initial macroscopic disease or residual masses. Moreover, the long-term follow-up of patients treated in the past with extended field RT has demonstrated serious long-term sequelae from the fairly low doses which used to be considered safe. With modern RT for lymphomas only the initially macroscopically involved sites or residual masses are irradiated to the lowest doses necessary for optimal tumour control, and the utmost care is taken to irradiate as little as possible of the surrounding normal tissues, thus minimizing the risk of long term complications.
Modern advanced imaging allows a precise delineation of the involved lymph nodes, and techniques such as image fusion and deformable co-registration allow transfer of target volumes from pre-chemotherapy to post-chemotherapy images for treatment planning. The majority of lymphomas are FDG-avid, and PET/CT-scans for treatment planning are highly recommended. Modern highly conformal planning and treatment techniques, combined in many situations with even lower RT doses, have further reduced the radiation doses to normal tissues. In the past 15 years there has been a veritable paradigm shift in lymphoma RT, from 2-dimensional treatment planning and RT to regions defined by bony landmarks, to 3-dimensional treatment planning and RT to volumes defined by advanced imaging and conforming to the ICRU guidelines, similar to the principles of modern RT of solid tumours. Guidelines for modern radiotherapy of Hodgkin lymphoma, nodal lymphomas, extranodal lymphomas, cutaneous lymphomas, and pediatric lymphomas have been published by the International Lymphoma Radiation Oncology Group (IROG), and they have been implemented by most large centres and cooperative groups worldwide. The new concept of involved site radiation therapy (ISRT) takes into account different scenarios with regard to the quality of pre-chemotherapy imaging, where optimal imaging allowing image fusion allows for RT to the smallest volumes. In other situations somewhat larger margins may be needed to allow for uncertainties in contouring, but the volumes irradiated are still much smaller than in the past.
Estimates of the consequences on long-term toxicity of these modern treatments demonstrate very significant reductions in the risks of second malignancies, cardiovascular disease and other long-term sequelae compared to what has been seen after the extended treatment fields of the past. It is important to realize that these treatments are now obsolete, and that the analyses of long-term sequelae of RT for lymphomas from the era of the extended fields, which have been extensively published, are not directly relevant for patients treated with modern highly conformal RT.
More than 60 different lymphoma diseases have now been defined, and lymphomas may present in all parts of the body, both within and outside of the lymphatic system. Hence, there is great variation in target volumes and critical normal structures from patient to patient. With highly conformal treatments such as intensity modulated radiotherapy (IMRT) or volumetric arc therapy there are many possible variations which may be used in different patients to optimize treatment. An “intelligent” choice of treatment angles for IMRT may allow sparing of particular organs at risk. Treatment of mediastinal or upper abdominal lymphomas in deep inspiration breath hold allows significant sparing of the heart and lungs. Which technique should be used in different patients will depend on the location of the target and considerations of the importance of different toxicities in relation to age, gender, comorbidities, and risk factors for other diseases.

Dose constraints normally used for solid tumour radiotherapy are not optimal for lymphoma RT, as most of the conventional dose constraints for different organs are higher than the RT doses prescribed for lymphomas. Hence, if conventional dose constraints are used uncritically, most plans will be within the limits, even if far from the best plan achievable. Doses to all normal structures should be kept as low as possible. However, combining dose-response data for all relevant normal structures and using mathematical modeling to predict long-term risks of relevant sequelae would allow for a quantitative comparison of different treatment plans in individual patients. Developing a tool for this kind of multispectral plan evaluation would enable further optimization of RT for lymphomas in the future.

SP-0498

Modern imaging and radiotherapy in lymphoma

G. Mikhaeel[1]
[1]*Guy's and St Thomas' Hospital NHS Foundation Trust, Radiation Oncology, London, United Kingdom*

Abstract not received

Joint Symposium: ESTRO-PTCOG: ART in particle therapy

SP-0499

The need for adaptive approaches in proton therapy (compared to photons).

M. Schwarz[1,2]
[1]*Proton therapy centre, Protontherapy, Trento, Italy*
[2]*INFN, TIFPA, Trento, Italy*

The large scale introduction of soft-tissue imaging (e.g. via computed tomography) and the multiyear experience in its use paved the way, at least in radiotherapy with photons, for the development of adaptive treatments, where image datasets acquired during the treatment cycle are used to evaluate and tune the dose distributions actually delivered to the patient.
In proton therapy the presence of range uncertainties, and their effect in terms of dose perturbations, has been tackled so far mostly looking at source of range and dose uncertainties other than anatomy deformation, e.g. range error due to imperfections in the CT scan calibration and setup errors. However, neither improved CT calibration nor the use of sophisticated planning approaches such as robust optimization are coping with dose perturbations due to anatomy changes. As a consequence, proton therapy has for quite some time approached the issue in a defensive way, i.e. focusing on dose indications where anatomy changes are not expected (e.g. the skull) or at least choosing beam directions going through regions of the body where such changes are less likely.
The broadening of the indications considered to be suitable for proton therapy and the increased availability of soft tissue image guidance in proton therapy treatment rooms is slowly allowing for more proactive approaches, where repeat CT scans are actually used to modify the treatment parameters.
Starting from clinical cases, we'll see how adaptive therapy with protons has some peculiarities with respect to adaptive with photons, such as:
- A more prominent impact of anatomy deformation on the dose distribution. The finite range of protons makes the dose distribution sensitive even to anatomy variations that would not be of concern in photons
- Adaptive proton therapy needs to rely on high quality imaging for dose recalculation and optimization. Since CT calibration is an issue even with diagnostic quality CT, any further deterioration of the image quality will in principle impact the accuracy in dose distribution, thus potentially making the treatment adaptation less relevant.
- Given the strict correlation between anatomy and dose distribution, it remains to be seen whether approaches that are successful in photons (e.g. the use of plan libraries) are safe and effective with protons too.

SP-0500

Cone beam CT for adaptive proton therapy

S. Both[1]
[1]*Memorial Sloan-Kettering Cancer Center, Medical Physics Department, New York- NY, USA*

Daily volumetric imaging is essential in adaptive radiation therapy (ART) due to patient related uncertainties which may occur during the course of radiation treatment. The in room Cone-Beam CT (CBCT) imaging has been considered a viable option for photon ART, while CBCT just recently emerged in proton therapy. CBCT deployment in proton therapy has been slow due to technical challenges for design and implementation, lower image quality and more importantly less HU accuracy relative to CT imaging due to scattered x-rays. Therefore, the clinical deployment of CBCT in proton therapy is still in an early phase and currently is limited to treatment setup and detection of potential changes in patient anatomy generated by tissue deformation, weight loss, physiological changes and tumor shrinkage. The HU accuracy of CBCT is more critical in adaptive proton therapy (APT) relative to photon ART, as even small differences in HU could cause significant range and absolute dose errors. As a result, the integrity of the proton dose calculation may be easily compromised. Studies showed that photon dose calculation discrepancy caused by CBCT HU error can be over 10% for raw CBCT image data sets and be within 1% for scatter corrected CBCT. However, no study up to date has demonstrated the feasibility of proton clinical dose calculation or treatment planning on raw CBCT data sets and therefore currently the primary role of CBCT in APT is to trigger the need for CT rescanning for dose adaptation. However, there are two major approaches explored to overcome current CBCT image data sets limitations. The first one employs deformable image registration of the treatment planning CT to the daily verification raw CBCT to generate a CBCT based stopping power distribution. This method has been explored mostly for head and neck dose adaptation. The second one aims to improve the raw CBCT data accuracy via scatter corrections and in its current stage explored the feasibility of raw CBCT based planning on an anthropomorphic phantom. As these methodologies are developing and new ones emerge, CBCT imaging may further evolve and holds the potential to become a viable tool for APT.

SP-0501

Adaptive practice and techniques in proton therapy of the lung

P.C. Park[1], H. Li[1], L. Dong[2], J. Chang[3], X. Zhu[1]
[1]*The University of Texas MD Anderson Cancer Center, Department of Radiation Physics, Houston, USA*
[2]*Scripps Proton Therapy Center, Radiation Oncology, San Diego, USA*
[3]*The University of Texas MD Anderson Cancer Center, Department of Radiation Oncology, Houston, USA*

Adaptive radiation therapy is the practice of modifying initial treatment plan in order to accommodate the changes in a patient's anatomy, organ motion, and biological changes during course of treatment. Within this scope of definition, it can be further classified based on different time scale going from offline (between fractions) to online (prior to a fraction), and to real time (during fraction) modification in beam delivery. The dose distribution of proton is "non-static" relative to the change in patient anatomy because the finite path length of protons is tissue density dependent. Therefore the adaptive radiation therapy is more relevant for proton than photon. For the same reason, for moving target in particular, online or real time adaptation may become more important for proton therapy. During initial treatment planning phase, proton ranges in patient must be determined precisely in order to take the advantage of Bragg peak. Changes in water equivalent thickness along the beam path due to breathing motion must be accounted by robust planning strategies. Any significant changes in proton range from what was calculated should be detected and prompt for an adaptive re-plan. Treatment sites that are likely to change

in anatomy during the course of treatment or during treatment are particularly important. In this regard, lung cancer is one of the most relevant sites to practice adaptive proton therapy. Over 40% of lung tumors move more than 5 mm and 10% moves greater than 10 mm [1] with possibility of changes in breathing pattern during the course of treatment. The change in tumor shape or density and decrease in tumor volume as tumors respond to the radiation also raise another challenge for proton therapy. The protons can travel further without the tumor tissues to stop them in lung. Previous studies found that on average from 0.6 to 2.4% of tumor volume can be reduced per day [2]. Adaptive radiation therapy requires modification in treatment plan through changing contours of targets or organs at risk and beam parameters accordingly and any quality assurance checks that are deemed necessary. Therefore the adaptive radiation therapy requires more resources when compare to the conventional image-guided radiation therapy. In fact, image-guidance can be considered the first step in adaptive practice as it triggers the initial decision to adapt and provide the 3D volumetric images that are necessary for adaptive re-plan. There have been efforts to create techniques and technologies that can facilitate the adaptive planning. In this presentation, we will first discuss the state of art practice of adaptive proton therapy including the experience at our institution. We will review studies assessing the magnitude of intra- and inter-fractional changes and its impact on delivered proton dose distribution with and without adaptive practice. Secondly, we will present the cutting edge ideas and techniques that are developed specifically for adaptive proton lung therapy in the most recent literature.

[1] Liu HH, Balter P, Tutt T, et al. Assessing respiration-induced tumor motion and internal target volume using 4DCT for radiation therapy of lung cancer. Int J Radiat Oncol Biol Phys 2007;68:531-540

[2] Sonke JJ, Belderbos J. Adaptive Radiotherapy for lung cancer. Semin Radiat Oncol 2010 Apr; 20(2):94-106.

SP-0502

In-vivo range estimation and adaptive particle therapy

T. Lomax[1]

[1]*Paul Scherrer Institute PSI, Centre for Proton Therapy, Villingen, Switzerland*

The finite range of protons is a two-edged sword. On one side, it is the *raison d'etre* of proton therapy, on the other, a potential source of uncertainties in-vivo. As such, both in-vivo range estimates and adaptive therapy are being proposed and pursued for mitigating such uncertainties. However, sources of in-vivo range uncertainties are many, ranging from systematic uncertainties in the calibration of CT Hounsfield units to proton stopping power and inaccuracies in dose calculations (for convenience defined here as type I uncertainties) to variations in patient positioning and anatomy changes during the course of treatment (type 2). Whereas, for good quality CT data, type 1 uncertainties can result in range uncertainties of a few percent or millimeters (about 3% or 6mm in the worst case,) type 2 can result in range changes of the order of centimeters. In addition, type 1 uncertainties will, to a good approximation, be similar across all patients of a particular indication and will remain the same throughout the duration of a patient's treatment. Type 2 on the other hand will be patient and (potentially) treatment day dependent. So, what are the roles of in-vivo range measurement and adaptive therapy for dealing with these? It seems to this author that in-vivo range verification perhaps has a role to play in reducing type 1 uncertainties, whereas the best approach to type 2 has to be adaptive therapy. Adaptive therapy (based on regular, if not daily, imaging) must be pro-active (i.e. the treatment should ideally be adapted *before* delivery), whereas in-vivo range verification can only be (at best) reactive (e.g. may be able to provide a reason to interrupt a delivery if an error is detected). As such, the best use of in-vivo range estimation seems to be as part of a population based (commissioning) approach in order to verify that CT calibration and dose calculations are more and more precise, such that type 1 uncertainties resulting from pre-treatment imaging (necessary to mitigate type 2 errors) can then be reduced as much as possible. Such an approach however puts stringent demands on the accuracy and precision of in-vivo range estimates, with in-vivo resolutions in the millimeter range being required in order to significantly improve these uncertainties. Will this ever be achievable?

SP-0503

European strategy

M. Baumann[1,2,3,4]

[1]*OncoRay – National Center for Radiation Research in Oncology, Faculty of Medicine and University Hospital Carl Gustav Carus- Technische Universität Dresden, Dresden, Germany*

[2]*German Cancer Consortium - DKTK Dresden, and German Cancer Research Center - DKFZ, Heidelberg, Germany*

[3]*Helmholtz-Zentrum Dresden - Rossendorf, Institute of Radiooncology, Dresden, Germany*

[4]*Department of Radiation Oncology, Faculty of Medicine and University Hospital Carl Gustav Carus- Technische Universität Dresden, Dresden, Germany*

One of the most exciting areas of basic, translational and clinical research in radiation oncology today is radiotherapy with particles, i.e. with protons or heavier ions. The main advantage of radiotherapy with protons compared to state-of-the-art radiotherapy with photons is a decrease of the volume of normal tissues irradiated to intermediate and low doses, while irradiation of normal tissues to high doses or the conformality of the dose to the tumor are usually similar for protons and photons. Exceptions include situations where critical normal tissues can be excluded by proton therapy from the irradiated volume completely or to a large extent. The most relevant clinical research question is therefore to investigate whether sparing of normal tissue by proton therapy leads to clinical relevant benefits which balance the higher costs of this treatment. After demonstration of relevant sparing of normal tissues, further clinical studies on utilizing dose intensification strategies may become another important research avenue in those tumors where local or locoregional tumor control today are unsatisfactory.

At present only few centers (often with different technologies and patient populations) are active in clinical research using protons, which makes fresh thinking on study design in radiation oncology necessary, as large scale randomized trials will not be feasible in many situations. Model-based approaches are a major component of the trial methodological portfolio, but alternatives (including multicenter stepwise randomized trials, pseudo-randomized trials and prospective matched pair trials) may be superior in different clinical situations. All of these approaches necessitate dedicated clinical research infrastructures and complex high-level network formation to reach the power for meaningful clinical trials. This also plays an important role in terms of radiotherapy stratified by biological parameters, which is anticipated to become a clinical reality in the near future for several tumor entities.

Proton (or other particle) therapy holds particular promise to further advance personalized radiation oncology. However obstacles in trial design, data sampling and integration, or analysis may dilute the effects to such an extent that it may not be possible to demonstrate it according to generally accepted scientific standards. This would be a major hurdle for further implementation and reimbursement of this auspicious technology, and also for sound medical stratification of access of patients in need for this therapy.

The lecture will discuss opportunities and problems of proton therapy in the context of high precision personalized as well as biologically stratified radiation oncology, thereby also touching trial design, technology development and the importance of network formation on a European level.

Symposium: Small animal irradiation

SP-0504

Preclinical radiotherapy technology, dosimetry and treatment planning

K. Butterworth[1], M. Ghita[1], C.K. McGarry[2], S. Jain[3], G.G. Hanna[3], J.M. O'Sullivan[3], A.R. Hounsell[2], K.M. Prise[1]
[1]*Centre for Cancer Research & Cell Biology Queen's Uni, School of Medicine- Dentistry and Biomedical Sciences, Belfast, United Kingdom*
[2]*Northern Ireland Cancer Centre, Radiotherapy Physics, Belfast, United Kingdom*
[3]*Northern Ireland Cancer Centre, Clinical Oncology, Belfast, United Kingdom*

Small animal image guided irradiation platforms are revolutionizing the field of preclinical radiobiology by facilitating the delivery of clinically relevant irradiation protocols under experimental conditions. Our laboratory is developing an in vivo radiobiology research program using the small animal radiotherapy research platform (SARRP, Xstrahl Life Sciences) as a central enabling technology to perform translational studies focussing on biologically optimised radiotherapy, nanoparticle theranostics and novel combination treatments. A major challenge now facing investigators is how to correctly apply the technology to accurately model clinical scenarios in relevant small animal models so that it can be exploited to its full potential in driving translational studies with outcomes likely to impact current standard of care in radiation oncology.
An overview of the current state-of-the-art in preclinical radiotherapy will be presented including recent developments such as integration of bioluminescence imaging, preclinical 4-D CBCT and Monte Carlo based dose calculation methods. Examples of innovative preclinical studies will be highlighted along with experience from our own laboratory from commissioning to experimental design and important considerations for the successful execution of hypothesis-driven investigations using small animal radiotherapy.
Despite certain challenges, small animal radiotherapy has much potential to bridge the translational gap between basic radiobiology and radiotherapy. As the technology develops and investigators gain experience as multidisciplinary scientists, pre-clinical studies that increasingly replicate the clinical scenario will drive new approaches in radiobiology that should ultimately translate to human health gains.

SP-0505

Radiation biology studies with a small animal irradiator: results from the Research Programme at Johns Hopkins University

P. Tran[1]
[1]*Johns Hopkins University The Sidney Kimmel Comprehensive Cancer Center, Department of Radiation Oncology, Baltimore, USA*

Although advances with in-vitro cancer cell culture models have occurred recently, in vivo tumor models are still crucial for the study of novel radiation treatments. This is particularly important for radiation combination approaches that target tumor cell non-autonomous anti-cancer pathways such as the tumor microenvironment or the immune system. In addition, more sophisticated animal studies with radiation are now possible with the advent of technologies that integrate treatment planning, imaging, and radiation delivery capabilities such as with the small-animal radiation platform (SARRP; Fig 1).

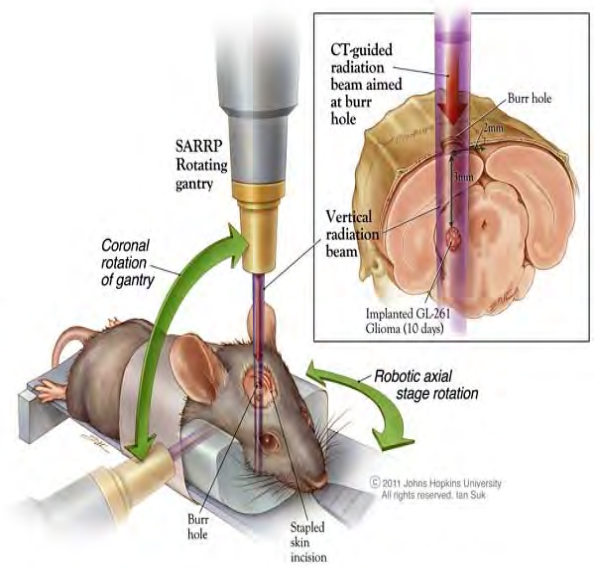

Tumor xenograft models using human-derived tumor models implanted into immune-deficient mice are a mainstay of pre-clinical testing and discovery. Although the majority of in vivo studies involve immunocompromised mice, such as athymic, severe combined immune-deficiency (SCID) or NOD-SCID mice, these models are less ideal with radiation studies because some of these mice have mutations in DNA response and repair pathways. The abnormal DNA repair mechanisms in these mice limit the applicability of results with radiosensitizers given the integral role of DNA damage to the biologic effect of radiation therapy. Furthermore, anti-tumor effects of radiation may be mediated by the immune system. As a result of these limitations, genetically engineered mouse models (GEMMs) are becoming more widely used in preclinical studies with and without radiation. "Co-clinical trials" that use GEMMs that faithfully replicate the mutational events observed in human cancers to conduct preclinical trials that parallel ongoing human phase I/II clinical trials have shown great promise in cancer. This presentation will review published and on-going pre-clinical studies targeting both cancer cell autonomous and cancer cell non-autonomous pathways utilizing the SARRP with both xenograft tumor models and GEMMs at Johns Hopkins.

SP-0506

How do we select meaningful pre-clinical models for studies in radiation biology?

D. De Ruysscher[1]
[1]*MAASTRO clinic, Radiation Oncology, Maastricht, The Netherlands*

Clinical research faces many problems, of which the availability of pre-clinical models that predict the human situation is one of the most important. Pre-clinical tumour models are being used for decades in many cases with the assumption that they are predictive for what will later happen in humans. As such, the use of pre-clinical, mostly mouse, models may limit the exposure of inactive and or toxic treatments in patients. Although there is no doubt that pre-clinical models have been crucial to understand better molecular and other characteristics of carcinogenesis, growth and metastases and were the basis of many currently used cancer therapies, they still have considerable shortcomings. Classical mouse models use tumour cell lines that have been grown in vitro for many years and hence may have altered characteristics compared to *de novo* tumours. These tumour cells are then implanted subcutaneously in mice and tend to grow rapidly and thus do not mimic the much slower doubling times of most human cancers. This faster tumour growth may lead to a higher sensitivity for most chemotherapy drugs and hence erroneous conclusions. Moreover, in some situations, ectopic (out of the normal place) subcutaneously implanted tumours — still a standard methodology — may respond

differently to treatment compared to tumours grown in an orthotopic site, i.e. in their organ or tissue of origin, such as breast cancers in mammary fat pads. The latter may correspond more to the human situation. Moreover, metastases frequently show other responses than primary tumours in patients, and it is only recently that these effects can be mimicked in genetically engineered mouse models. Tumour bearing mice are often treated with drugs at levels, or with pharmacokinetics, that are not relevant to humans. Furthermore, nearly all pre-clinical models have not used tumours that were pre-exposed to another therapy, whereas in many phase I and phase II clinical trials only patients that show tumour progression after one or more systemic treatments are included. With the huge interest in immune therapy, the use of humanised mice has gained even more attention than before. However, these models still face problems with remaining mouse innate immunity and weak human innate and adaptive immunity. Even the best models suffer from the development of wasting disease in highly engrafted humanized mice and poorly developed lymph nodes and germinal centres. It is also unclear if the cell trafficking resembles that of humans.At present, no single mouse models mimics perfectly the human situation. However, models that use injected tumour cells in the organ from which they were derived and which form metastases in organs that are similar to the human situation may be the most appropriate for they bear a micro-environment that resembles that of humans. Spontaneously arising tumours, preferentially in older mice may represent an interesting model for immune therapy.

Symposium: Focus on the pelvic region

SP-0507
Bladder variability for pelvic radiotherapy: its approaches and impact

V. Khoo[1]
[1]*Royal Marsden Hospital Trust & Institute of Cancer Research, Department of Clinical Oncology, London, United Kingdom*

It is clear that the bladder as an organ has marked shape and positional variability due to its function of storing urine before the call of nature. This has obvious repercussions for pelvic radiotherapy depending on the intent of treatment particularly if the bladder itself is the radiotherapeutic target. As an organ-at-risk (OAR) this variability can be important and this can also impact on adjacent organs such as the prostate, rectum and uterus if these latter organs are being treated with radiotherapy. These adjacent pelvic organs can also deform the bladder. In addition the setup position of the patient either supine or prone can also influence on the day-to-day bladder position and shape. Furthermore the kidneys filtered continuously thus there will be steady filling of the bladder with a rate dependant on the hydration status of the patient during radiotherapy delivery. Other factors may also be crucial such as bladder capacity and function as well as disease extent if there is bladder cancer. Therefore the variability of the bladder size and shape is an important consideration for any pelvic radiotherapy. Many investigators have reported on the marked difference in filling of the bladder with variation in bladder size that may range up to 20 mm on different scanning times during a course of fractionated radiotherapy. For primary bladder radiotherapy, identification of the disease extent remains important as both the target and tissue of tolerance is the bladder itself. This can also impact on the manner in which the bladder fills in 3D and be distorted by invasive bladder disease. It can be difficult to maintain daily consistency of the 3D shape and size thus there are several methods developed to deal with this including treatment with either an empty or comfortably full bladder to initiating adaptive planning and image guided delivery methods. Fiducials have been used to better target the main disease for either boosting disease or to incorporate focal therapy strategies. These methods can also permit organ avoidance if the bladder is an OAR and it is critical to minimise dose to it due to poor bladder function and other clinical factors. If the bladder is not the target then it can perform a useful function with intended filling prior to radiotherapy in order to displace other pelvic organs such as the bowel from irradiation such as with treatment of the pelvic nodes. Thus patient and disease related factors will need to be carefully assessed for each case. All these methods including their rationale and effectiveness will be discussed for both situations of the bladder as a target and as an OAR.

SP-0508
An evaluation of GoldAnchor intraprostatic fiducial marker stability during radiotherapy

D. Bodusz[1], L. Miszczyk[1], K. Szczepanik[1], W. Leszczyński[2]
[1]*Maria Sklodowska-Curie Memorial Cancer Center and Institute of Oncology, Radiotherapy Department, Gliwice, Poland*
[2]*Maria Sklodowska-Curie Memorial Cancer Center and Institute of Oncology, Radiotherapy and Brachytherapy Planning Department, Gliwice, Poland*

Background: Implantation of fiducial markers for IGRT (Image Guided Radiation Therapy) of prostate cancer patients increases the treatment accuracy by prostate localization using two orthogonal X-rays images. However the precision of the treatment depends on the stability of the fiducial marker. The aim of this study was to evaluate the migration of fiducial markers during the whole radiotherapy of prostate cancer patients.

Material and methods: An analysis of the intraprostatic fiducials migration during the treatment planning was done on a group of 45 patients on the basis on fusion of kV CBCT (performed during the first week of the treatment) and planning CT. The value of migration during the course of radiotherapy was done on a group of 20 patients treated within IGRT protocol on the basis on the fusion of kV CBCTs, performed weekly. The migration was defined as a shift between central points of markers, measured in three axis.

Results: The average values of the GoldAnchor™ migration during the treatment planning were: 1.1 mm (SD=0.9 mm) in the superior-inferior (SI) direction, 0.5 mm (SD=0.6 mm) in the left-right (LR) direction and 1.1 mm (SD=1.2 mm) in the anterior-posterior (AP) direction. The mean value of the vector of shifts was 1.9 mm (SD=1.3 mm). The average values of the GoldAnchor™ migration during the course of radiotherapy were: 0.1 mm (SD=0.2 mm) in the superior-inferior (SI) direction, 0.1 mm (SD=0.3 mm) in the left-right (LR) direction and 0.2 mm (SD=0.4 mm) in the anterior-posterior (AP) direction. The mean value of the vector of shifts during the treatment was 0.3 mm (SD=0.5 mm).

Conclusions: The analysis of the collected data showed that the marker shifts during the treatment planning seems to have no clinical significance and probably are related to the inaccuracy of the fusion of kV CBCT and planning CT. Position of the marker is stable during the whole course of radiotherapy. Therefore, IGRT based on GoldAnchor™ markers is safe and effective method of prostate cancer patient positioning.

SP-0509
Validation of a prostate cancer decision aid tool for shared decision making

E.J. Bloemen- van Gurp[1], B.G.L. Vanneste[1], A.J. Berlanga[1], D. Rijnkels[1], K. Van de Beek[2], J. Van Roermund[2], P. Lambin[1]
[1]*MAASTRO clinic, Radiation Oncology, Maastricht, The Netherlands*
[2]*MUMC, Urology, Maastricht, The Netherlands*

Purpose: To comply a decision aid tool with the criteria of the International Patient Decision Aid Standards (IPDAS), it is mandatory to follow a systematic and iterative approach to; (a) understand patient's and clinicians decisional needs, (b) create prototypical tools, (c) evaluate these prototypes with patients and clinicians and (d) use these results to improve the tool. We developed and validated a web-based decision

aid (DA) for shared decision making in prostate cancer patients using this approach.

Methods: A prototype of the tool was designed based on the input of an interdisciplinary group. Its clarity and acceptability was tested using a mixed method (interview and technology acceptance questionnaire; 5-Likert scale). The evaluation was performed with physicians (N=19) and patients (N= 16). Professionals from 5 academic and private hospitals (urologists, radiotherapists, specialized nurses and family doctors) gave their perspective about the patients' decisional needs and validated the information about the treatment options, complications and outcomes. The included patients were treated with either external beam radiotherapy, brachytherapy or prostatectomy. Patients who choose not to be treated (active surveillance) were also included. The decisional needs were evaluated during an interview. Afterwards the patients' were guided through the DA and asked to fill in a questionnaire to check the comprehensibility of the tool. A second group of patients (N=8) was included to assess the e-learning effect of the DA and to check if patients were able to use the DA alone (without coaching).

Results: The results were considered to create a new version of the DA. Physicians mentioned the need of information about basic anatomy, contraindications, hospital specific figures, and psychological support. Patients reported that the prototype of the DA provides clear information about the treatment options and their side-effects. Issues about the usability of the DA were reported and enabled us to improve and simplify the DA. The next step is to perform a study to establish the impact of the DA on the decisional conflict and the shared decision making process.

Conclusion: The systematic and iterative approach used to develop and validate the DA, allows to follow a thoroughly development process, and to gain knowledge about decisional needs.

Poster Viewing: 11: Clinical: Breast, head and neck

PV-0510

Evaluation of a breast cancer nomogram to predict local relapse after breast conserving therapy

I. Kindts[1,2], A. Laenen[3], S. Peeters[1,2], H. Janssen[1,2], T. Depuydt[1,2], E. Van Limbergen[1,2], C. Weltens[1,2]

[1]*KU Leuven - University of Leuven, Department of Oncology, B-3000 Leuven, Belgium*

[2]*University Hospitals Leuven, Department of Radiation Oncology, B-3000 Leuven, Belgium*

[3]*KU Leuven - University of Leuven, Leuven Biostatistics and Statistical Bioinformatics Centre L-Biostat, B-3000 Leuven, Belgium*

Purpose or Objective: Van Werkhoven et al. developed a nomogram to predict the 10-years ipsilateral breast relapse (IBR) after breast conserving therapy (BCT) for breast cancer (BC) based on the European Organisation for Research and Treatment of Cancer (EORTC) 'boost no boost'-trial with a concordance probability estimate (CPE) of 0.68 (van Werkhoven E, et al. 2011, Radiother Oncol). The nomogram includes histologic grade, ductal carcinoma in situ (DCIS), tumour diameter, age, tamoxifen, chemotherapy and boost. The aim of this study was to evaluate the performance of that algorithm in an independent cohort.

Material and Methods: We retrospectively identified 1866 BC patients who underwent BCT with radiotherapy from 2000 to 2007.

Two definitions of IBR were considered where simultaneous regional or distant recurrence were either censored (conform EORTC analysis) or included as event.

Patient, tumour and treatment characteristics were evaluated in uni- and multivariable analysis.

Firstly we assessed discrimination, i.e. the extent to which patients predicted to be at higher risk exhibit higher event rates than those deemed at lower risk, by the CPE. The CPE was determined based on a Cox model with time to IBR as outcome and the EORTC nomogram 10-years IBR-free probability as the only covariate. Secondly a calibration plot was drawn, showing the predicted 10-years IBR-free probabilities against observed Kaplan–Meier estimates, to reflect prediction accuracy, i.e. the absence of over- or underestimation.

Results: Median follow-up time was 10.75 years.

Patients were on average older (58 vs 54 years), had a larger average tumour diameter (18 mm vs 15 mm) and were more likely to have received chemotherapy (29.7 % vs 15.7 %), to have a high grade disease (37.0 % vs 23.5 %) and to have a DCIS (69.8 % vs 57.8 %). Twenty-three percent of the patients received tamoxifen in the EORTC group, whereas 81.6 % received hormonal therapy in the validation group. Almost all patients (99.7 %) in the validation group received a boost versus 50.4 % in the EORTC cohort. Noteworthy on the variables not included in the nomogram, patients in the validation cohort had a higher percentage of oestrogen and progesterone receptor positivity (86.4 % vs 71.7 % and 75.9 % vs 64.3 %, respectively) and 10.2 % had HER2 overexpression.

The 10-years IBR-rate was 1.4 %. On multivariable analysis, only the omission of the boost dose was a significant prognosticator of IBR ($p < 0.01$) with a trend for age ($p = 0.06$).

The nomogram demonstrated suboptimal discrimination, with a CPE of 0.54, and suboptimal calibration with an overestimation of the IBR-risk in general (Table 1 – Figure 1).

Table 1: CPE for the two definitions of local relapse.

IBR	Dataset	N cases	N events	CPE * (95 % CI)
First definition	All data	1787	34	0,54 (0,52;0,57)
	Restricted data *	1672	31	0,54 (0,51;0,57)
Second definition	All data	1787	45	0,54 (0,51;0,56)
	Restricted data *	1672	42	0,54 (0,51;0,56)

* Restricted data: excluding values beyond the ranges applied in the EORTC nomogram (age range 27-76 years and tumour size 0-50 mm).

Figure 1: model calibration plot for the two definitions of local relapse.

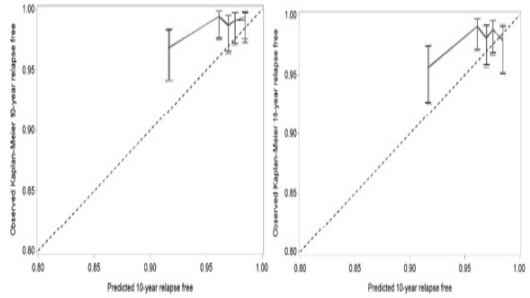

Note: For 5 subgroups of equal size, the model-predicted average relapse-free rate was plotted against the Kaplan-Meier estimated observed rates with 95 % confidence intervals. Black represents 'All data', grey represents 'Restricted data'. The dashed line corresponds to ideal calibration.

Conclusion: The EORTC predictive model for IBR in BC patients lacks accuracy in this more recent study population. Therefore the model should be tested and verified in additional, large patient populations and incorporating molecular subtyping might be needed.

PV-0511

Hypofractionated VMAT for early stage breast cancer: acute toxicity and cosmesis in 840 patients

C. Iftode[1], F. De Rose[1], D. Franceschini[1], A. Fogliata[1], E. Villa[1], A.M. Ascolese[1], P. Navarria[1], G.R. D'Agostino[1], C. Franzese[1], T. Comito[1], A. Tozzi[1], E. Clerici[1], R.L.E. Liardo[1], A. Stravato[1], M. Scorsetti[1]

[1]*Istituto Clinico Humanitas, Radiotherapy and Radiosurgery, Rozzano Milan, Italy*

Purpose or Objective: To evaluate acute toxicity and early clinical outcomes of hypofractionated simultaneous

integrated boost (SIB) approach with Volumetric Modulated Arc Therapy (VMAT) as adjuvant treatment after breast-conserving surgery.

Material and Methods: Patients presenting early-stage breast cancer were enrolled in a phase II trial. Eligibility criteria were as follow: age >18 years, invasive cancer or DCIS, Stage I to II (T <3 cm and ≤N3), breast -conserving surgery, any systemic therapy was allowed in neoadjuvant or adjuvant setting. All patients underwent VMAT-SIB technique to irradiate the whole breast with concomitant boost irradiation of the tumor bed. Doses to whole breast and surgical bed were 40.5 Gy and 48 Gy respectively, delivered in 15 fractions over 3 weeks Acute skin toxicities were recorded according to RTOG scoring criteria, and late skin toxicities according to CTCAE v4.0. Cosmetic outcomes were assessed as excellent/good or fair/poor according to the Harvard scale.

Results: Between August 2010 and January 2015, 840 consecutive patients were treated. Median age was 60 year (range 19-89 years). The median follow up was 16 months (range 6-55). At the end of RT treatment skin toxicity profile was G1 in 49% of the patients, G2 in 13%, and one patients presented G3 toxicity (0.1%). At six months of follow up skin toxicity was G1 in 27% of patients, G2 in 1%, no G3 cases; cosmetic outcome was good/excellent in 94% of patients. At one year skin toxicity was G1 in 13% of patients, 1 patient G2, 1 patient G3; cosmetic outcome was good/excellent in 93% of patients.After an early evaluation of clinical outcomes we have found 12 cases of progression disease, only one patient had an In-Breast-Recurrence.

Conclusion: The 3-week course of postoperative radiation using VMAT with SIB was well tolerated in acute and early late settings. Long-term follow-up data are needed to assess late toxicity and clinical outcomes.

PV-0512

Accelerated partial breast irradiation for Luminal-A breast cancer: analysis from a phase 3 trial

I. Meattini[1], C. Saieva[2], I. Desideri[1], G. Simontacchi[1], L. Marrazzo[3], S. Scoccianti[1], C. De Luca Cardillo[1], V. Scotti[1], P. Bonomo[1], M. Mangoni[1], F. Rossi[4], J. Nori[5], D. Casella[6], M. Bernini[6], L. Sanchez[6], L. Orzalesi[6], S. Pallotta[3], S. Bianchi[7], L. Livi[1]

[1]*Azienda Ospedaliero-Universitaria Careggi, Radiation Oncology Unit- University of Florence, Florence, Italy*

[2]*ISPO Cancer Research and Prevention Institute, Molecular and Nutritional Epidemiology Unit, Florence, Italy*

[3]*Azienda Ospedaliero-Universitaria Careggi, Medical Physics Unit, Florence, Italy*

[4]*S. Maria Annunziata Hospital, Radiation Oncology Unit, Florence, Italy*

[5]*Azienda Ospedaliero-Universitaria Careggi, Senology Radiology Unit, Florence, Italy*

[6]*Azienda Ospedaliero-Universitaria Careggi, Breast Surgery Unit, Florence, Italy*

[7]*Azienda Ospedaliero-Universitaria Careggi, Pathology Unit - University of Florence, Florence, Italy*

Purpose or Objective: Breast cancer (BC) could be classified into four major molecular subtypes: Luminal-A, Luminal-B, triple negative/basal-like, human epidermal growth factor 2 (HER2) enriched. This classification could be based on immunohistochemistry, and may allow the clinicians to optimize treatment management. Luminal-A tumors represent around 40% of BC and are characterized by: estrogen receptor (ER) and/or progesterone receptor (PgR) positive, HER2/neu negative, and low Ki-67 proliferative index. Early luminal-A tumors tend to have an excellent prognosis, with high survival and low recurrence rates. The aim of this analysis was to observe Luminal-A outcome from a phase 3 trial comparing whole-breast irradiation (WBI) to accelerated partial breast irradiation (APBI) using intensity-modulated radiotherapy (IMRT) technique.

Material and Methods: In the whole trial 520 patients were randomized in 1:1 ratio to receive APBI versus WBI after breast conserving surgery for early BC. The primary endpoint was occurrence of ipsilateral breast tumor recurrence (IBTR); the main analysis was by intention-to-treat. This trial was registered with ClinicalTrials.gov, number NCT02104895.

Results: Luminal-A patients represented the 61.5% of the whole series (151 WBI versus 169 APBI). 5-year event rate according to allocated group showed no statistical difference in terms of IBTR (p=0.53). One case (0.9%) versus two cases (1.7%) were observed in the WBI and APBI arms, respectively. Survival events occurrences and IBTR curve are summarized in the Figures.

		WBI (n=151)		APBI (n=169)		
Event	**Total**	**n**	**%**	**n**	**%**	**p-value***
IBTR	3	1	0.9	2	1.7	0.53
Local relapse	1	1	0.9	0	0	0.33
New ipsilateral BC	2	0	0	2	1.7	0.14
Locoregional relapse	4	2	1.7	2	1.7	0.95
Distant metastases	1	1	0.8	0	0	0.33

*p-value from log rank test

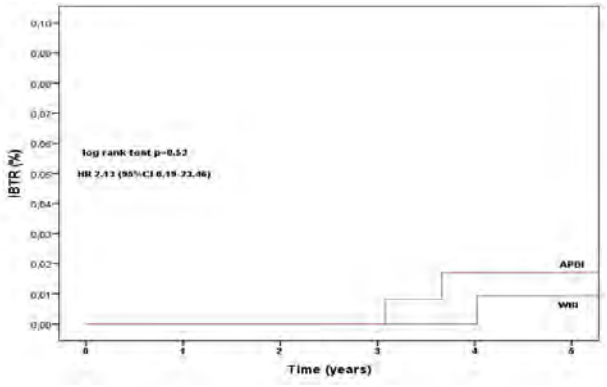

Conclusion: We observed a very low 5-year rate of IBTR for Luminal-A patients treated with APBI. Although these results should be confirmed at a longer follow up time, this approach should be considered for this subset of early BC patients.

PV-0513

The impact of chemotherapy on toxicity in the era of hypofractionated radiotherapy

M.C. De Santis[1], F. Di Salvo[2], F. Bonfantini[3], M. Dispinzieri[1], M. Franceschini[1], F. Soncini[1], E.D. Mantero[1], V. Cosentino[3], D. Postè[3], P. Baili[2], M. Sant[2], E. Pignoli[3], L. Lozza[1]

[1]*Fondazione I.R.C.C.S Istituto Nazionale Tumori di Milano, Radiotherapy and Oncology, Milan, Italy*

[2]*Fondazione I.R.C.C.S Istituto Nazionale Tumori di Milano, Statistical Department, Milan, Italy*

[3]*Fondazione I.R.C.C.S Istituto Nazionale Tumori di Milano, Physical Department, Milan, Italy*

Purpose or Objective: To evaluate toxicity in breast cancer patients treated with anthracycline and taxane based chemotherapy and whole breast hypofractionated radiotherapy, and to identify the risk factors for toxicity.

Material and Methods: From April 2009 to December 2014, 540 patients received radiotherapy after breast conservative surgery (BCS). The dose was 42.4 Gy in 16 daily fractions, 2.65 Gy per fraction. The boost to the tumor bed was administered only in grade 3 patients and in patients with close or positive margins. Acute and late toxicity were prospectively assessed during and after radiotherapy according to RTOG scale. The impact of patients clinical

characteristics and dose inhomogeneities on the occurrence of an higher level of toxicity has been also evaluated by univariate and multivariate analysis.

Results: One hundred and nineteen patients received chemotherapy. Sixty-one patients (11.3%) underwent trastuzumab therapy and four hundred and forty-one (81.6%) hormonotherapy. The mean age was 74 (range 46-91 yrs). Forty seven (8.7%) and two hundred fifty eight (47.5%) patients were affected by diabetes mellitus and hypertension, respectively. G1 and G2/G3 acute skin toxicity were 53.7% and 28.5% in patients received chemotherapy and 63.2% and 18.5% in patients who did not receive it, respectively. No significant difference (p=0.092) was find between the two groups of treatment. The boost administration (p< 0.01), the breast volume (p 0.04), dose inhomogeneities (p<0.01) and boost volume (0.04) were found to be statistically significant as concerns the occurrence of acute skin reaction at the univariate analysis; the boost administration (p< 0.01), and hormonotherapy (p 0.01) at multivariate analysis. Other clinical factors such as diabetes or hypertension were not correlated with the development of acute skin reaction. G1 and G2/G3 late fibrosis were 15.3% and 8.1% in patients received chemotherapy and 12.3% and 3.1% in patients who did not receive it, with a significant difference (p=0.045) between the two groups. Diabetes (p 0.04) and boost administration (p <0.01) were also found to be statistically significant on the occurrence of late fibrosis, but a multivariate analysis adjusted also for clinical tumour characteristics did not show any factors correlated to late fibrosis .

Conclusion: The results of our study, according to the large randomized trials, confirmed that hypofractionated whole breast irradiation is safe, even in patients treated with chemotherapy. Chemotherapy didn't impact on acute toxicity but only on late toxicity; however the percentage of G2-G3 fibrosis is low (8.1 vs 3.1%). Our study confirmed an increase of acute and late toxicity in patients who received additional boost.

PV-0514

Chest wall radiotherapy and complications after flap reconstruction

Y. Rao[1], A. Mull[2], A. Qureshi[2], T. Myckatyn[2], I. Zoberi[1]
[1]*Washington University in St. Louis, Radiation Oncology, Saint Louis, USA*
[2]*Washington University in St. Louis, Plastic Surgery, Saint Louis, USA*

Purpose or Objective: The effect of radiotherapy (RT) on the outcome of autologous reconstruction after mastectomy for breast cancer is unclear. Advances in technique such as the deep inferior epigastric artery perforator (DIEP) flap and IMRT may affect the complication rate. We seek to retrospectively evaluate the outcomes after flap reconstruction at our institution with a focus on radiotherapy variables.

Material and Methods: Patients receiving flap reconstruction after mastectomy at our institution from 2003-2014 were identified in a chart review. Analysis was limited to patients with a coded cancer status and who returned for at least one follow up visit. The outcome variables analyzed were flap loss or any complication (loss, ischemia, hematoma, infection). Descriptive data analyzed included age, tumor stage, flap type, chemotherapy, and radiation. RT specific variables included radiation at an academic medical center vs independent radiotherapy facility, 3D-CRT vs IMRT, and whether radiation was directed to the internal mammary (IM) region. Analyses was on a per-flap basis rather than per patient. Statistics were done in SPSS using logistic regression. Two prognostic models were generated. The first included all patients and analyzed age, stage, flap type, chemotherapy, and radiation therapy. The second model included only those receiving radiation therapy and included significant factors from the first model and the RT variables discussed above.

Results: 291 patients receiving 402 flap procedures met inclusion criteria. Mean age was 47.2 years with median follow up of 339 days. 93 (21.2%) had transverse rectus abdominis (TRAM) flaps, 178 (40.6%) had muscle sparing TRAM flaps, and 121 (27.6%) had DIEP flaps. 128 (29.2%) flaps were done after mastectomy for benign histology; 62 (14.2%) were for DCIS/ LCIS, 69 (15.8%) were for stage I, 88 (20.1%) were for stage II, 52 (11.9%) were for stage III, and 3 (0.7%) were for stage IV disease. 146 (33.3%) received RT and 187 (42.7%) received neoadjuvant chemotherapy. Of those receiving RT, 42 (28.7%) received 3D-CRT, 38 (26.0%) received IMRT, and 66 (44.5%) had unknown RT technique. 28 (6.9%) flaps failed and 64 (15.9%) flaps had a complication. The first model, which included all patients, identified increasing cancer stage (p=0.03) as the most important variable for flap loss with a hazard ratio of 3.4 for DCIS/LCIS, 2.1 for stage I, 7.3 for stage II, and 1.8 for stage III compared to benign pathology. Age was the only variable associated with increased overall complications. In the second model, location of RT, RT technique, and IM directed radiation were not significant predictors of flap loss or complications.

Conclusion: Cancer stage and age are important predictors for flap failure and complications. Use of chest wall radiation therapy was not a significant predictor of flap failure.

PV-0515

GTV delineation of laryngopharyngeal carcinoma on PET is more accurate than on CT and MRI

H. Ligtenberg[1], E.A. Jager[1], J. Caldaz-Magalhaes[1], T. Schakel[1], N. Kasperts[1], F.A. Pameijer[2], N. Kooij[3], L.M. Janssen[4], C.H.J. Terhaard[1], S.M. Willems[3], C.P.J. Raaijmakers[1], M.E.P. Philippens[1]
[1]*UMC Utrecht, Department of Radiotherapy, Utrecht, The Netherlands*
[2]*UMC Utrecht, Department of Radiology, Utrecht, The Netherlands*
[3]*UMC Utrecht, Department of Pathology, Utrecht, The Netherlands*
[4]*UMC Utrecht, Department of Otorhinolaryngology, Utrecht, The Netherlands*

Purpose or Objective: Correct GTV delineation is the basis for accurate radiotherapy treatment. It is important to determine which imaging modality (CT, MRI or FDG-PET) results in most accurate GTV delineation. For clinical assessment, both GTV delineations and target volumes adjusted for delineation inaccuracies were compared with histopathology.

Material and Methods: Twenty-seven patients with a laryngeal or hypopharyngeal tumor (T3/T4) were imaged with CT, MRI and FDG-PET followed by laryngectomy. Imaging was performed in radiotherapy positioning mask. GTV was delineated in consensus by three observers on CT and MRI, while a semi-automatic delineation was performed on FDG-PET using an intensity based threshold method. The true tumor volume was delineated by one pathologist on whole-mount histopathological sections. These slides were digitized and the specimen was reconstructed in 3-dimensions. The tumor contours were non-rigidly transferred to the imaging acquired before tumor resection.
To cover 95% of the outer contour of all tumors, modality dependent target margins were derived and added to the GTV (Fig. 1a). GTVs and target volumes were compared between the modalities.

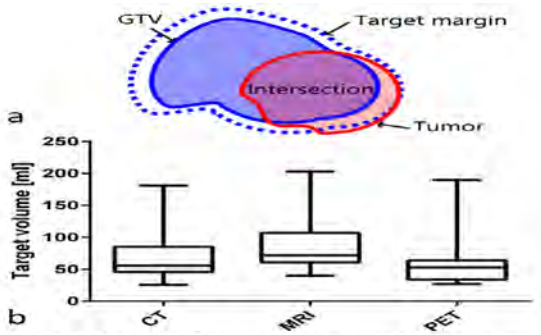

Figure 1: a) A schematic representation of the target margin (blue dotted line) added to the delineated GTV (blue) to cover 95% of the outer surface of the tumor (red). b) Boxplots of target volumes of all patients are shown for the three modalities.

Results: The median tumor volume delineated on pathology was 10.5 ml (range: 3.4 ml – 68.6 ml). Median GTVs delineated on CT, MRI and PET were 17.5 ml, 15.2 ml and 14.8 ml, respectively. None of the GTVs fully covered the pathological tumor volume with a median tumor coverage of 93%, 90% and 87%. In several cases, the position of cartilage invasion was not recognized, which contributed to missing tumor volume.
The modality dependent target margins to cover 95% of the tumor outer contour were 5.6 mm, 8.7 mm and 6.2 mm and resulted in median target volumes of 56 ml, 72 ml and 53 ml for CT, MRI and PET, respectively (Fig. 1b).

Conclusion: In all modalities, delineated GTVs overestimated tumor volume. Nevertheless, some tumor volume was missed in all cases. Automated delineation on PET resulted in the smallest target volume compared to manual delineation on CT and MRI, while covering an equivalent amount of tumor. This study suggests that delineation or segmentation inaccuracies can be corrected using a margin between 5.6 and 8.7 mm.

PV-0516

Guideline development for tumor delineation on MR-images for laryngeal and hypophargeal cancer

E. Jager[1], N. Raaijmakers[1], H. Ligtenberg[1], J. Caldas-Magalhaes[1], T. Schakel[1], F. Pameijer[2], N. Kasperts[1], N. Willems[3], C. Terhaard[1], M. Philippens[1]
[1]UMC Utrecht, Department of Radiation Oncology, Utrecht, The Netherlands
[2]UMC Utrecht, Department of Radiology, Utrecht, The Netherlands
[3]UMC Utrecht, Department of Pathology, Utrecht, The Netherlands

Purpose or Objective: Development of guidelines for the delineation of the gross tumor volume (GTV) on MRI is of utmost importance to benefit from the increased visibility of anatomical details and to achieve a more accurate and precise GTV delineation. In the ideal situation, the GTV corresponds to the histopathologically determined "true tumor volume". In this work we developed and validated guidelines for GTV delineation on MRI by comparison with the tumor outline on histopathology as gold standard.

Material and Methods: Twenty-seven patients with T3 or T4 laryngeal or hypopharyngeal cancer underwent a MRI scan before total laryngectomy. After surgery, whole-mount hematoxylin-eosin stained (H&E) sections were obtained from the surgical specimen. One pathologist delineated all tumor tissue on the H&E sections (tumorH&E). The GTV was delineated on the MR images (T1 w, Gd-T1 w, T2 w) by three independent observers in two sessions. The first session (delineation 1) was performed according to clinical practice. In the second session (delineation 2) the observers used delineation guidelines derived from guidelines for detection of cartilage invasion on MRI: Volumes with increased signal intensity on T2w images and higher signal intensity on Gd-T1w images than that of the tumor bulk were not included in the GTV.
The reconstructed specimen was registered to the MR images in order to compare the GTV to the tumorH&E in 3D. Volumes and overlap parameters were analyzed. Distances between the GTV and the tumorH&E were calculated at locations where the tumorH&E was outside the GTV. Subsequently, a margin that accounted for the underestimation of the tumour was determined. Finally, target volumes were created by applying this margin to the GTV.

Results: The median GTVs of delineation 1 (19.4 cm3) and of delineation 2 (15.8 cm3) were larger than the volume of the tumorH&E (10.5 cm3). However, target margins of 10.2 mm and 8.3 mm were needed for delineation 1 and 2 , respectively, to compensate for the underestimation of the tumor at specific locations. By adding this margin to the GTVs, the target volumes for delineation 1 (median: 117.6 cm3, mean: 125.9 cm3, SD: 53.2 cm3) were significantly larger than those for delineation 2 (median 76.2 cm3, mean 85.7 cm3, SD: 43.3 cm3).

Conclusion: GTV delineation guidelines on MRI decreased the overestimation of the tumour, resulted in a smaller margin around the delineated GTV needed to include all tumor tissue and consequently resulted in smaller target volumes with the same tumor coverage.

PV-0517

Upfront vs. no upfront neck dissection in primary head and neck cancer radio(chemo)therapy

D. Nevens[1], F. Duprez[2], K. Bonte[3], P. Deron[3], W. Huvenne[3], A. Laenen[4], W. De Neve[2], S. Nuyts[1]
[1]KU Leuven-University of Leuven- University Hospitals Leuven, Radiation Oncology Department, Leuven, Belgium
[2]Ghent University Hospital, Radiation Oncology Department, Ghent, Belgium
[3]Ghent University Hospital, Department of Head- Neck & Maxillofacial Surgery, Ghent, Belgium
[4]KU Leuven-University of Leuven, Leuven Biostatistics and Statistical Bioinformatics Centre, Leuven, Belgium

Purpose or Objective: The benefit of upfront neck dissection (ND) in locally advanced head and neck cancer (HNC) treated with primary (chemo-) radiotherapy (CRT) is debated. Therefore, we retrospectively compared outcome and toxicity between patients with and without upfront ND followed by CRT.

Material and Methods: Two-hundred sixty-four consecutive patients with HNC without metastases at diagnosis and with lymph node stage N2-N3 were included in 2 centers. Patients were all treated between January 2002 and December 2012, and received definitive CRT in center 1 and upfront ND followed by CRT in center 2. Clinical data and outcome were assessed retrospectively. Toxicity was scored using the LENT-SOMA scale at 6, 12, 18 and 24 months after the end of treatment.Both patient groups were compared using a Chi-square test for categorical variables or a Mann-Whitney U test for continuous variables. Descriptive statistics on overall survival (OS) is based on Kaplan Meier estimates. For all other time-to-event outcomes, cumulative incidence function (CIF) estimates were calculated. The difference between both groups on the different outcomes was analyzed using multivariable models, including group and prognostic patient- or tumor characteristics on which the 2 groups were different. All tests were two-sided, and a p-value of less than 0.05 was considered statistically significant.

Results: We included 150 patients in the group without ND (center 1) and 114 patients in the group with upfront ND (center 2). The group comparison is given in *Table 1*.

Variable	Statistic	No dissection	Neck dissection	P-value
Sex				
Male	n/N (%)	126/150 (84.00%)	103/114 (90.35%)	0.132
Female	n/N (%)	24/150 (16.00%)	11/114 (9.65%)	
Diagnosis age	N	150	114	0.794
	Mean	58.9	59.0	
	Std	8.78	8.67	
	Median	58.0	58.9	
	IQR	(52.0; 65.0)	(52.4; 65.4)	
	Range	(38.0; 81.0)	(40.1; 86.8)	
T stage				
0	n/N (%)	0/150 (0.00%)	1/114 (0.88%)	0.001
1	n/N (%)	7/150 (4.67%)	12/114 (10.53%)	
2	n/N (%)	36/150 (24.00%)	39/114 (34.21%)	
3	n/N (%)	39/150 (26.00%)	37/114 (32.46%)	
4	n/N (%)	68/150 (45.33%)	25/114 (21.93%)	
N stage				
2A	n/N (%)	8/150 (5.33%)	6/114 (5.26%)	0.182
2B	n/N (%)	63/150 (42.00%)	59/114 (51.75%)	
2C	n/N (%)	73/150 (48.67%)	41/114 (35.96%)	
3	n/N (%)	6/150 (4.00%)	8/114 (7.02%)	
Subsite				
Oral cavitity	n/N (%)	13/150 (8.67%)	6/114 (5.26%)	0.526
Orofarynx	n/N (%)	66/150 (44.00%)	46/114 (40.35%)	
Hypofarynx	n/N (%)	53/150 (35.33%)	49/114 (42.98%)	
Larynx	n/N (%)	18/150 (12.00%)	13/114 (11.40%)	
IMRT				
No	n/N (%)	64/150 (42.67%)	42/114 (36.84%)	0.339
Yes	n/N (%)	86/150 (57.33%)	72/114 (63.16%)	
Overall treatment time radiotherapy	N	150	114	<.001
	Mean	43.4	44.9	
	Std	3.29	2.73	
	Median	43.0	44.0	
	Interquartile range	(41.0; 44.0)	(43.0; 46.0)	
	Range	(37.0; 58.0)	(39.0; 61.0)	
Concomitant treatment				
No	n/N (%)	22/150 (14.67%)	26/114 (22.81%)	0.089
Yes	n/N (%)	128/150 (85.33%)	88/114 (77.19%)	
Type concomitant treatment				
Cisplatinum	n/N (%)	109/128 (85.16%)	83/87 (95.40%)	0.017
Cetuximab	n/N (%)	19/128 (14.84%)	4/87 (4.60%)	
HPV status Oropharynx				
Positive	n/N (%)	13/66 (19.70%)	10/46 (21.74%)	0.752
Negative	n/N (%)	44/66 (66.67%)	31/46 (67.40%)	
Unknown	n/N (%)	9/66 (13.64%)	5/46 (10.87%)	

Table 1. Group comparison on patient/tumor characteristics.

Based on this result, we decided to account for the differences in T stage, overall treatment time and concomitant treatment for the statistical analysis of outcome and toxicity. Mean follow up was 5.68 years in the group without ND and 5.83 years in the group with upfront ND. Local, regional and distant control after 2 years were 91.07% and 85.96% (p = 0.09), 89.22% and 83.27% (p = 0.12) and 76.74% and 75.13% (p 0.92) in the group with and without upfront ND, respectively . We observed worse OS after 2 years in the subgroup with upfront ND (48.01% vs. 70.79%, p = 0.01). The difference in OS can be explained by more secondary primaries in this subgroup with upfront ND and more non-disease related deaths. We did not find a significant difference between both groups regarding edema and atrophy at 6, 12, 18 and 24 months (*Figure 1*). Regarding fibrosis, we found an overall trend towards worse outcome in the ND group at all time-points (p=0.06). A significantly higher proportion of severe fibrosis (grade≥2) was present in the ND group (p=0.01) at all time points (*Figure 1*).

Outcome	OR (95% CI)	P-value
Fibrosis	1.558 (0.982;2.470)	0.0595
Edema	1.251 (0.758;2.063)	0.3810
Atrophy	1.652 (0.644;4.242)	0.2964
Severe fibrosis	2.811 (1.384;5.710)	0.0042

OR: Odds ratio, CI: Confidence interval

OR >(<) 1 means higher (lower) level on scale for Neck dissection group.

Figure 1. The table presents for every toxicity, the effect of group (Neck dissection versus No neck dissection) by means of odds ratios (OR) with 95% confidence intervals at all time-points (6, 12, 18 and 24 months).

Conclusion: Both treatment regimens have a comparable local, regional and distant control. However, fibrosis and more specifically fibrosis grade≥2 is more prominent following upfront ND and CRT when compared to CRT alone.

PV-0518

Phase 1 study of Debio 1143 in combination with Concurrent Chemo-Radiotherapy in LA-SCCHN

Y. Tao[1], C. Le Tourneau[2], H. Bouchaab[3], J. Delord[4], V. Calugaru[2], P. Crampton[5], B. Gavillet[6], E. Rouits[6], C. Zanna[7], C. Schusterbauer[7], E. Deutsch[1], J. Bourhis[8]

[1]*Institute Gustave Roussy, Département de Radiothérapie, Villejuif, France*

[2]*Institute Curie, Department d'Oncologie Médicale, Paris, France*

[3]*Département d'Oncologie UNIL-CHUV, Service de Oncologie Médicale, Lausanne, Switzerland*

[4]*IUTC Oncopole, Oncologie Médicale, Toulose, France*

[5]*Debiopharm International SA, Clinical Research & Development, Lausanne, Switzerland*

[6]*Debiopharm International SA, Translational Medicine, Lausanne, Switzerland*

[7]*Debiopharm International SA, Clinical Research & Development, Lausanne, Switzerland*

[8]*Département d'Oncologie UNIL-CHUV, Service de Radio-oncologie, Lausanne, Switzerland*

Purpose or Objective: Chemo-radiotherapy (CRT) plays a major role in the management of patients with locally advanced squamous cell carcinoma of head and neck (LA-SCCHN). However, loco-regional (LR) failure remains a significant problem due to the resistance to radiotherapy and chemotherapy. Inhibitors of Apoptosis Proteins (IAPs) are expressed in various cancers and are able to block caspase activation and modulate NF-kB signalling pathways. As such, they represent attractive targets to overcome resistance to both chemo- and radio-therapy. Debio 1143 is a potent orally-available IAP antagonist currently in clinical development able to radiosensitize and ameliorate the effects of platinum derivatives in multiple SCCHN models both in vitro and in vivo. A previous phase I study showed Debio 1143 as a single agent was well tolerated up to 400 mg/day q14d21. This Phase I study defined the dose limiting toxicities (DLTs), maximum tolerated dose (MTD), safety, pharmacokinetic (PK) and pharmacodynamic (PD) of Debio 1143 in combination with CRT.

Material and Methods: Treatment-naïve LA-SSCHN (stage III/IV), negative HPV status for oropharynx, were treated with CRT (70 Gy in 7 weeks + cisplatin 100 mg/m2 every 3 weeks) and escalating doses of Debio 1143, administered orally once daily on days 1-14 every 3 weeks for a maximum of 3 cycles. The starting dose of Debio 1143 was 100 mg/day. Doses were escalated using a Bayesian Continuous Reassessment Method (CRM) until MTD, based on dose limiting toxicities (DLTs) observed within the first 9 weeks

from start of study drug administration. Dose escalation decision and recommended dose (RD) were made by an independent safety committee. Blood PK and PD samples were serially drawn along the 3 cycles.

Results: Fourteen patients were included in the study. DLTs per dose level (DL) are shown in the table with 3 patients experiencing more than one DLT. The RD of Debio 1143 to be combined with CRT was 200 mg/day (=MTD). Debio 1143 exposure increased proportionally with dose and did not accumulate over time. Amylase/lipase and ALT/AST increase was associated with higher Debio 1143 exposures. At all dose levels, the PD effect of Debio 1143 was evidenced by the degradation of cIAP1 in PBMCs and a trend in an increase of serum MCP1. 12 patients were evaluable for response by RECIST 10-12 weeks post treatment among which 3 CR, 5 PR and 1 SD.

Debio 1143 DL	DLT evaluable patients N=14	Patients with DLTs N=5	Event (CTCAE)	CTCAE grade	Action	Outcome
100mg	5	1	Amylase increase (Cy1-d3)	3	None	Recovered
			Anemia (Cy3-d8)	4	Drug withdrawn	"
			Esophagitis (Cy3-d14)	4		"
200mg*	6	2	Tubular necrosis (Cy1-d4)	3	Drug withdrawn	Ongoing
			AST/ALT increase (Cy1-d4)	3		Recovered
			Febrile neutropenia (Cy1-d14)	4		"
			Lipase increase (Cy1-d15)	3	None	Recovered
300mg	3	2	ALT increase (Cy3-d22)	3	None	Recovered
			Amylase increase (Cy2-d14)	3	Drug withdrawn**	Recovered
			Lipase increase	4		"

*MTD, established by CRM
** Patient experienced concomitant cerebro-vascular accident G3 (related to cisplatin) and asthenia G3 (related to radiotherapy)

Conclusion: Combination of Debio 1143 with CRT was tolerated, exhibited favourable PK in combination with CRT with significant PD activity. The MTD was found to be 200 mg/day and is now being used in a randomized phase 2 study initiated by GORTEC to evaluate the anti-tumor activity of this combination in LA-SCCHN.

PV-0519

The hypoxic radiosensitizer, nimorazole, in RT of HNSCC: pharmacokinetics, toxicity and compliance

M.A.H. Metwally[1], J. Overgaard[1]
[1]*Aarhus University Hospital, Department of Experimental Clinical Oncology, Aarhus C, Denmark*

Purpose or Objective: Study of pharmacokinetics (PK), toxicity, and compliance with nimorazole (NIM) which is currently investigated for its efficacy in three large randomized clinical trials (NIMRAD, EORTC 1219/DAHANCA 29, and DAHANCA 30)

Material and Methods: The PK of NIM was studied in 63 patients with HNSCC treated in the DAHANCA-5 trial. While the toxicity and compliance were studied in HNSCC patients treated with NIM, in combination with radiotherapy (RT) or chemo-radiotherapy (CRT), in Denmark between 1990 and 2013. Plasma concentration measurements were done using high pressure liquid chromatography following the first day dose; and plasma concentration profiles were subjected to non-compartmental PK analysis using validated PC-based software. The different PK parameters were calculated and correlated with the different patient- and treatment-related variables. Nimorazole was administered as oral tablets in doses of approximately 1.2 g/m² BSA before the first daily radiation treatment. A second dose of 1 g was given before the second RT fraction in the accelerated fractionation regimen (6 fractions/week). The compliance was estimated as the percentage of the initially prescribed dose; and drug-related side effects were reported from the DAHANCA database.

Results: A linear relationship between peak plasma concentration and administered dose was detected. The mean peak concentration was 36.8 ± 1.3 µg/ml, and the time of peak concentration ranged between 30 and 180 min (median 60 min). Plasma elimination occurred with a mean half-life of 3.35 ± 0.09 h. There was a statistically significant correlation between area under the concentration-time curve (mean 191 ± 6 µg·h/ml) and administered dose, especially when expressed as g/m². A statistically significant longer elimination half-life in men relative to women (mean difference 0.40 h; 95% confidence interval 0.77-0.03; P 0.03) was detected. A total of 1049 patients were investigated for toxicity and compliance with NIM. The compliance was fair, with both conventional and accelerated RT as well as CRT schedules, with 58% of patients received the full prescribed total dose. Nausea and vomiting were the major complaints representing 87% of the known side effects that caused dose reduction. All side effects ceased when treatment was interrupted, and neither severe nor long lasting side effects were observed. Female patients, and patients received accelerated CRT were significantly less compliant with NIM, and more likely to have nausea and vomiting; while patients who received less than 1100 mg/m² per day were significantly more compliant, and less likely to have nausea and vomiting.

Conclusion: The current nimorazole administration practice in clinical trials is acceptable, and the compliance to the drug is fair, either with the conventional or accelerated RT as well as CRT, with tolerable acute, but neither persistent nor late, toxicity.

Symposium: Dose painting: those pending issues

SP-0520

The promises of dose painting

W. De Neve[1], L. Veldeman[2], P. Ost[2], F. Duprez[2], K. Vandecasteele[2], K. De Wolf[3], C. Monten[2], D. Berwouts[4], A.M.L. Olteanu[2], T. Vercauteren[2], W. De Gersem[2]
[1]*De Neve Wilfried, Belgium,*
[2]*University Hospital Ghent, Radiation-Oncology, Ghent, Belgium*
[3]*Ghent University, Radiation-Oncology, Ghent, Belgium*
[4]*University Hospital Ghent, Radiology, Ghent, Belgium*

Purpose To demonstrate that dose painting (DP) is a promising tool to decrease overall treatment time (OTT), to reduce toxicity, to improve palliation or enhance tumor control. The present state of DP will be illustrated through 3 types of applications. We will also speculate about the potential of DP to integrate with novel systemic treatment approaches.
Materials and methods
A. Topographical DP (TDP) in breast irradiation. TDP distributes dose as function of the spatial distribution of subclinical cancer deposits nearby the primary tumor in breast cancer. Patients (n=170) were randomized between prone whole breast irradiation (WBI) followed by a boost (WBI-SeqB: OTT=4 weeks) and WBI with simultaneous integrated boost (SIB) using TDP (WBI-TDP-SIB: OTT=3 weeks). Acute moist desquamation rate was the primary endpoint.
B. DP against bone metastasis pain. There is no dose-response relationship above 8 Gy single dose for the control of pain by uncomplicated bone metastases. This observation triggered the hypothesis that cytokine cascades counteracting palliation are activated by radiation and that their activity is function of the irradiated volume. DP was employed to drastically reduce the irradiated volume. Patients (n=45) were randomly assigned (1:1:1) to receive a single fraction of either 8 Gy with conventional radiotherapy (Conv-8Gy) or 8 Gy with DP (dose range 6-10 Gy) (DP-8Gy) or 16 Gy with DP (dose range 14-18 Gy) (DP-16Gy). The trial was designed for selection of the experimental arm worthwhile of continuing in phase III.
C. DP in loco-regionally advanced head&neck cancer. 18F-FDG-PET-guided DP-treated patients enrolled in 3 dose-escalation studies (n = 72) were matched with standard IMRT-treated patients (n=72) irradiated during the same time period. Median dose in the DP-group was 70.2-85.9 Gy/30-32

fractions against 69.1 Gy/32 fractions in the IMRT group. Endpoints were local control, acute and late toxicity.
Results A. Interim analysis (n = 150) showed low rates of moist desquamation, mostly located in the infra-mammary fold (5/75 WBI-SeqB vs 3/75 WBI-TDP-SIB, p =0.5). Trends in favor of WBI-TDP-SIB were observed for breast edema (p=0.08) and pruritus (p = 0.1). B. The volume of normal tissue receiving 4 Gy, 6 Gy and 8 Gy was at least 3, 6 and 13 times smaller in the DP-8Gy arm compared to Conv-8Gy and DP-16Gy (p<0.05). DP-8Gy resulted in a pain response of 80% compared to 53% and 60% for Conv-8Gy and DP-16Gy. Quality of life analysis suggests better outcome for patients treated in the DP-8Gy arm with the scores 'painful characteristic', 'insomnia' and 'appetite loss' reaching significance (p<0.05). C. Local control at 5 y was 83.4% and 75.2% in the DP- and IMRT-treated patients, respectively (p=0.28). Grades of acute dysphagia and mucositis were higher for the DP- than for the IMRT-treated group (p=0.03 and p=0.08, respectively) but differed according to DP-technique and –prescription. Poorly healing mucosal ulcers at the locations of the highest doses were observed in 9 DP- and 3 IMRT-treated patients (p=0.07) and reflect dose-limiting toxicity (DLT). Analysis of all DP-treated patients showed that DP-planning using a linear relation between 18F-FDG voxel-intensity and dose was associated with high risk of DLT if peak-doses were >84 Gy or the volume receiving >80 Gy was >1.75 cc in 30-fraction schedules (OTT = 6 weeks). Discussion and conclusions
The term DP covers a variety of techniques that open a vast spectrum of applications.The use of TDP after breast-conserving surgery allows to integrate boost treatment in WBI without increasing toxicity. In bone metastasis, DP-8Gy was selected as a candidate experimental arm to test the hypothesis of improved palliation by reducing the irradiated volume. A confirmatory phase III trial is underway. In loco-regionally advanced head&neck cancer, DP may open a window for improving local control. However, the safety margin for dose-escalation is narrow. Poorly healing mucosal ulcers at the peak-dose regions are DLT of DP. The dose/volume/DLT relationship casts doubt on the safety of linear 18F-FDG voxel-intensity based DP. A phase III trial using non-linear DP is underway. Tumor heterogeneity – known for decades- supports DP and refutes the use of homogeneous dose distributions. Dose escalation to radioresistant regions in the tumor or decreasing the irradiated volume may be a conceptually naive way to use DP. The insight that ionizing radiation can enhance vascular and immunogenic mechanisms of cell death opens a new field for DP characterized by large fraction doses to small sub-volumes of tumor. In these applications, direct cancer cell kill might be subordinate to other goals of DP including amplifying bystander and abscopal effects or breaking immune tolerance. Combination of DP with immunomodulating drugs or drugs that target vasculature or immune checkpoints are investigated to validate these concepts.

SP-0521
The biological rationale of dose painting: is it realistic?
M. Alber[1]
[1]*Aarhus University Hospital, Department of Clinical Medicine - Department of Oncology, Aarhus, Denmark*

Any additional dose that can be applied without harm will lift tumour control in a patient population. Dose painting (DP) claims to make better use of dose than an indiscriminate or random escalation: by virtue of functional imaging, it should be more effective, more selective and more patient-specific. Still, on a pragmatic level, DP can often be summarized by "we boost because we can". What does it take to go more biological?
Obstacles lie in quantitative functional image acquisition, image interpretation, dose prescription and collection of evidence. Unfortunately, quantitative functional imaging is notoriously capricious. The problems tend to grow the more specific in terms of tumour biology an imaging modality is - which is one of the reasons for the popularity of FDG-PET, being arguably one of the least specific modalities. A specific modality may be more intriguing scientifically, but obviously shows only a narrow aspect of tumour biology, which may create a need for a combination of multiple modalities. Imaging modalities usually operate at length scales far greater than the phenomena to which they are sensitive. This can make the interpretation of images challenging, especially when tracer kinetics need to be considered. Imaging sophistication alone reveals little of the import of some physiological or biological trait for treatment outcome. Only clinical data can fill this gap in biological understanding with some confidence. Further, a single image is just a snapshot of a dynamically evolving tumour, and if taken pre-treatment, says little about the tumour´s response to therapy. Therefore, without any highly suggestive clinical evidence, the prospects for naive (i.e. model-based) DP are bleak.
Accordingly, the majority of DP trials to date are pragmatic in their choice of imaging modality and –protocol, and dose prescription. In addition to being practical, especially in a multi-centric setting, this also ensures that a proof of benefit (of both boosting and imaging) can eventually be made. The essential advantage of "we boost because we can" over sophisticated "dose painting by numbers" is, that it generates the data needed to reach said sophistication.
From this pragmatic standpoint, neither today´s imaging capabilities nor the understanding of their relevance to tumour treatment response are sufficient to speak of an established biological rationale for DP. Some clinical evidence exists in few instances that links certain functional imaging to lack of tumour control or even location of recurrence. Given this, workable DP concepts today are rather shaped by considerations about image sensitivity and specificity and organ mobility, than biology.

SP-0522
Dose prescription and treatment delivery at the voxel scale: a fantasy?
J. Lee[1], D. Di Perri[2], S. Differding[2], X. Geets[2], V. Grégoire[2]
[1]*Université Catholique de Louvain, Box B1-54.07, Brussels, Belgium*
[2]*Universite Catholique de Louvain, Molecular Imaging-Radiotherapy- and Oncology, Brussels, Belgium*

Purpose/Objectives: This work aims at formally identifying the methodological issues that hinder the implementation and adoption of dose painting (DP) in radiotherapy. DP entails the use of functional imaging to set up a non-uniform dose escalation, either with sub-contours or voxel-to-voxel variations. Although theoretically appealing, DP has not succeeded yet in passing from research to clinical use. This work reviews the physical, mathematical, and statistical causes of this delay, in the specific case of DP guided by PET.

Method: The following steps occur in PET-based DP: acquisition of PET images (before and/or during treatment, with one or several tracers), conversion of the uptake(s) into a dose increment, treatment plan optimization, fractionated treatment delivery, accumulation and assessment of the delivered dose, and optional treatment adaptation. Every step or piece of data in this path can be modeled to investigate its shortcomings. All PET tracers are characterized with their specificity and sensitivity as a surrogate of some biological variable of interest in given conditions (e.g., before or during radiotherapy). PET images are described by their resolution and signal-to-noise ratio. Treatment plan quality is assessed by a quality-volume histogram (QVH), namely, a DP-specific dose-volume histogram that considers the ratio planned dose over prescribed dose. Random and systematic patient setup errors are quantified with their respective standard deviation. Non-rigid registration of pre- and per-treatment images is used to approximate the cumulated dose, taking into account patient evolution (tumor regression, possible weight loss).

Results: Our main result is the formal proof that PET-based DP cannot lead to a delivered dose that is strongly correlated with the tracer uptake at the microscopic level. This weak correlation is caused by: i) The limited information conveyed by heterogeneities observed in PET images. Current PET systems have a low resolution and a low signal-to-noise ratio,

which translate into biases and variance in the uptake measurement. Moreover, the tracer has typically a source-to-background ratio that decreases during treatment (e.g. after 3 weeks for FDG). This intrinsically limits the number of interpretable images that can be acquired during treatment. ii) Dose blurring due to treatment fractionation. Daily setup introduces geometrical errors. Random errors blur the planned dose, while systematic ones shift it. A systematic drift can also be caused patient evolution (tumor regression, weight loss), thus making adaptive radiotherapy a desirable prerequisite for DP. All this shows that DP must cope with limited information about the real uptake heterogeneities. If directly converted into a dose prescription, these blurred heterogeneities are likely to be further smoothed or even shifted by random and systematic errors if the delivered dose is considered. While dose blurring is beneficial to uniformity within the targets in usual treatment plans, it is actually detrimental to any form of intended heterogeneity. Dose blurring cannot be compensated for with usual safety margins, since they rely on a model that implicitly assumes dose uniformity and further reinforces it to guarantee coverage. Instead, robust plan optimization must be used, either by modeling the setup errors in the optimizer or by providing a modified prescription, dilated for systematic errors and deconvolved for random errors. It is however noteworthy that ensuring coverage might sound paradoxical in DP: it widens the dose peaks and increases the mean dose, whereas DP precisely aims at a selective and parsimonious escalation.

Conclusions: Advanced treatment techniques such as intensity-modulated radiotherapy make DP technically feasible: a non-uniform dose prescription, with rather sharp gradients, can be accurately delivered at each fraction. Issues are located upstream (poor quality of PET images, which further decreases during treatment) and downstream (dose blurring due to setup errors and patient evolution). These issues lead to delivered doses that are weakly correlated to the underlying microscopic reality. To increase this correlation, an adaptive treatment strategy is a prerequisite to DP. Combined with other confounding factors, this weak correlation also jeopardizes the chances for an evidence-based approach to succeed in differentiating various flavors of DP from each other or from other comparable escalation strategies.

Symposium: ACROP

SP-0523

ACROP: General procedures, SOPs and current status

C. Belka[1]
[1]*Klinik und Poliklinik für Strahlentherapie und Radioonkologie, Radiooncology, Munich, Germany*

Since 2012 the Advisory committee for radiation oncology practice ACROP has taken over the responsibility for the initiation and coordination of ESTRO internal guidelines ae well as multidisciplinary guidelines together with other scientific societies.
During the ESTRO 35 ACROP session C Belka will present the workflow and SOP of ACROP, K Tanderup will give an brief overview of the ongoing and mature guidelines in the areas brachtherapy and physics and Max Niyazi will present the new guideline on Target volume delineation in Glioblastoma.

SP-0524

Clinical guidelines, update and introduction of recent clinical guidelines

M. Niyazi[1]
[1]*Klinik und Poliklinik für Strahlentherapie und Radioonkologie, Department or Radiation Oncology, München, Germany*

The ACROP committee has been established to generate European guidelines on radiotherapeutic topics and therefore, a group of thirteen experts had been selected to draft target delineation guidelines on glioblastoma. This talk will summarize the different steps that were taken to pull together all relevant information and will highlight the most relevant issues having been included within this guideline. In brief, treatment preparation, imaging prerequisites, delineation guidelines and pitfalls, planning objectives and normal tissue constraints will be discussed. The panel members have ensured to update this guidline within a 2 year's time frame and updates will be given as amendments if there are scientific breakthroughs.

SP-0525

Brachytherapy and physics guidelines, update and introduction of recent guidelines

K. Tanderup[1]
[1]*Aarhus University Hospital, Department of Oncology, Aarhus C, Denmark*

GEC ESTRO has a long term tradition for development and publication of guidelines within brachytherapy. These initiatives have grown out of working groups, which have a structure for joint multicenter research and development projects. The working groups have facilitated substantial progress within e.g. imaging, target definition and treatment planning, and this has become the basis of novel guidelines such as the GEC ESTRO recommendations for cervix, prostate, breast, as well as head & neck brachytherapy. The most recent example is the guideline on target definition for accelerated partial breast irradiation (APBI) which was published by the GEC ESTRO breast working group (Strnad et al) in June 2015 in Radiotherapy & Oncology. In parallel, the GEC ESTRO breast working group has been carrying out a randomized study on APBI, and this has further strengthened the impact of the guidelines. The clinical outcome of the study was published in Lancet in October 2015, and this is an excellent example of possible synergy between development of guidelines and related research activities. Other initiatives from GEC ESTRO include the current development of guidelines on bladder brachytherapy (Bradley Pieters), quality assurance of ultrasound in brachytherapy (Frank André-Siebert), as well as an update on head & neck brachytherapy (György Kovács). During the last decade there has been extensive collaboration between ESTRO (in particular the BRAPHYQS working group and AAPM therapy group on joint physics recommendations and guidelines. The underlying idea is that the gathering of experts from different continents improves quality, and that geographically broader views improve the global applicability of guidelines. Examples of recently published joint GEC ESTRO/AAPM guidelines are guidelines for uncertainty analysis (Christian Kirisits), robotic brachytherapy (Tarun Podder), and the report on High Energy Brachytherapy Dosimetry (Jose Perez-Calatayud). Uncertainty analysis is an example of a research field which has been well developed in external beam radiotherapy, but was less developed in brachytherapy for many years – mainly due to the fact that 3D imaging was introduced later in brachytherapy than in external beam radiotherapy. The guidelines for uncertainty analysis (Kirisits) showed therefore big impact on the field, and there is altogether now an increasing attention towards quantification of uncertainties in brachytherapy and considerations about how to improve clinical outcome by decreasing uncertainties. Joint GEC ESTRO/AAPM recommendations currently in progress are: TG - 167 Recommendations by the AAPM and GEC-ESTRO on the use of new or innovative brachytherapy sources, devices, applicators, or applications: Report of Task Group 167 (Ravinder Nath) and Supplement 2 to the 2004 update of the AAPM Task Group No. 43 Report (Mark Rivard). ESTRO physics has published several booklets on QA guidelines. Non-brachytherapy physics guidelines in progress are Quality Management in RT: The use of industry Quality Tools (Crister Ceberg), QA guidelines for CBCT developed together with EFOMP (Alberto Torressin), and also guidelines on Technology for Precision Small Animal Radiotherapy Research (Frank Verhaegen and Dietmar Georg). ESTRO physics committee and AAPM are currently working on a memorandum of understanding (MoU) with the aim of increasing scientific

interactions and strategic relationships between the societies. The MoU will facilitate collaboration across the ocean on e.g. Joint Task Groups, Scientific meetings and Education. The development of reports (e.g. AAPM task group reports, professional guidelines, etc.) should seek collaboration between the two societies where appropriate and feasible. Such collaboration could be achieved by inviting joint membership on appropriate drafting task groups by the initiating society. Both societies have now Standard Operating Procedures (SOP) available for development of guidelines, which gives a good structure for initiating international guidelines and securing high quality reviews - representing both Europe and North America – in upcoming guidelines.

Proffered Papers: Radiobiology 5: Imaging and molecular biomarkers in radiation oncology

OC-0526

Noninvasive imaging of the PD-1/PD-L1 checkpoint in naïve mice and after combined radioimmunotherapy

M. Hettich[1], F. Braun[2], G. Niedermann[1]
[1]*University Clinics Freiburg, Dept. of Radiation Oncology, Freiburg, Germany*
[2]*University Clinics Freiburg, Dept. of Nuclear Medicine, Freiburg, Germany*

Purpose or Objective: There is increasing evidence that antibodies blocking the PD-1 checkpoint (either anti-PD-1 or anti-PD-L1) dramatically increase in-field anti-tumor responses to ionizing radiation and enhance abscopal effects on non-irradiated metastases. Here, we developed PET tracers based on therapeutic surrogate antibodies that enable to non-invasively visualize not only the PD-1 and PD-L1 expression in mice but also the biodistribution of the surrogate checkpoint-blocking antibodies.

Material and Methods: Two novel PET tracers were developed by conjugation of anti-murine PD-1 and PD-L1 surrogate checkpoint-blocking antibodies with the chelator NOTA and labeling with the radioisotope 64Cu. Non-invasive PET imaging was performed on naïve and tumor-bearing mice. Mice bearing s.c. B16 melanomas were treated with hypofractionated radiation therapy (hRT) using two fractions of 12 Gy in combination with CTLA-4 checkpoint blockade several days before PET imaging. PD-1 or PD-L1 knockout mice and PD-L1-deficient B16 cells generated using the CRISPR/Cas technology served as specificity controls.

Results: The newly developed PD-1 and PD-L1 PET tracers allowed the highly specific and high-resolution imaging of PD-1 and PD-L1 expression and of the biodistribution of the two therapeutic antibodies in both naïve and tumor-bearing mice treated with hRT and CTLA-4 checkpoint blockade. Imaging of the respective knockout mice, blocking experiments with an excess amount of unlabeled antibodies, and the analysis of animals bearing both wild-type B16 melanomas and PD-L1-CRISPR knockout melanomas demonstrated the high specificity of the two newly developed PET tracers. The in vivo imaging data were confirmed by ex vivo biodistribution analyses. The targets of the PET tracer antibodies were verified by ex vivo flow cytometric analyses of tumor single-cell suspensions and cell suspensions of secondary lymphoid and other organs. Interestingly, visualization of immune-related adverse events was also possible.

Conclusion: We developed two innovative PET tracers that allow imaging the expression of the receptor/ligand pair of the important PD-1 checkpoint and the biodistribution of surrogate checkpoint-blocking antibodies in fully immunocompetent mice. This technology also enabled whole-body pictures of combination radio/immunotherapies.

OC-0527

Monitoring mitochondrial complex-I using novel PET probe allows early detection of radiosensitivity

C. Murayama[1], A. Kawaguchi[2], A. Kamijo[3], K. Naito[3], M. Kanazawa[4], H. Tsukada[4]
[1]*Tokai University- School of Medicine, Clinical Pharmacology, Isehara, Japan*
[2]*Tokai University School of Medicine, Cell Transplantation and Regenerative Medicine, Isehara, Japan*
[3]*Tokai University, Support Center for Medical Research and Education, Isehara, Japan*
[4]*Hamamatsu Photonics K.K., Central Research Laboratory, Hamamatsu, Japan*

Purpose or Objective: Objectives: Aerobic glycolysis is the main pathway of energy production in tumors (Warburg effect), and ionizing radiation is reported to switch this to mitochondrial oxidative phosphorylation. We developed a novel PET probe,18F-2-tert-butyl-4-chloro-5- {6-[2-(2-fluoro-ethoxy)-ethoxy]-pyridin-3-ylmethoxy}-2H-pyridazin-3-one (18F-BCPP-EF), for imaging mitochondrial complex I (MC-I) activity. In this study, early detection of tumor radiotherapeutic effect was evaluated using 18F-BCPP-EF and compared with 18F-FDG and apoptosis index.

Material and Methods: Methods: Tumor uptake of 18F-BCPP-EF or 18F-FDG was examined in C3H/HeN mice inoculated with murine squamous cell carcinoma SCCVII after a single dose of x-ray irradiation, 0, 6, 15, or 30 Gy. Apoptosis incidence was determined by TUNEL staining in excised tumor tissue.

Results: Results: Tumor growth suppression was dose-dependent; tumor grew 10 fold (0 Gy), 5 fold (6 Gy), 2 fold (15 Gy), and reduced to half in its volume (30 Gy) 14 days after treatment. 18F-BCPP-EF uptake was significantly increased as early as 2 days (15 Gy) or 3 days (30 Gy) after irradiation, at time points when tumor size or apoptosis index showed no difference among radiation doses. In contrast, 18F-FDG uptake was initially increased dose-dependently, remained elevated, and eventually decreased 10 days after 30 Gy when tumor size was already reduced. Apoptosis index was increased after irradiation but failed to correlate with tumor response. The uptakes of 18F-BCPP-EF and 18F-FDG, as well as AI, were plotted against Tvol on day 14 as surrogate of radiotherapeutic effect. Highly significant negative correlations were observed between the uptake of 18F-BCPP-EF and Tvol on day 14, as early as on day 2, and on each day up to day 7, and in all days combined. In contrast, between tumor uptake of 18F-FDG and Tvol on day 14, there was a significant negative correlation on day 2 and positive correlations on day 10 and on day 14, with no correlation in all days combined.

Conclusion: Conclusion: Tumor uptake of 18F-BCPP-EF was increased dose-dependently early after irradiation when 18F-FDG uptake and apoptosis index remained elevated regardless of radiation doses or its efficacy. The results suggest that 18F-BCPP-EF is a promising "positive" MC-I imaging PET probe for early detection of adequacy of tumor radiotherapy.

OC-0528

Modelling tissue radiosensitivity and PET hypoxia image contrast in acute and chronic hypoxia

D.R. Warren[1], M. Partridge[1]
[1]*University of Oxford, CRUK/MRC Oxford Institute for Radiation Oncology, Oxford, United Kingdom*

Purpose or Objective: PET imaging studies with the hypoxia tracer 18F-MISO typically show a heterogeneous distribution within the tumour, and regions of high uptake have been proposed as targets for dose painting. However, there is no widely-accepted method to determine dose prescriptions from hypoxia imaging. Oxygen diffusion distances in tissue (~100 μm) are smaller than the PET resolution (~4 mm) so a range of radiosensitivities may exist within each voxel. Furthermore, the perfused vasculature is not constant over

the course of a fractionated radiotherapy treatment or during a PET study. This work examines how transient perfusion of vessels may influence tissue radiosensitivity (including reoxygenation) and FMISO image contrast, as a guide for dose painting.

Material and Methods: Microscopic oxygen and FMISO distributions are simulated in tissue using bespoke MATLAB software which solves coupled partial differential equations by finite difference methods. Dynamic vasculature is modelled by opening and closing individual vessels at random, with time spent in each state sampled from a normal distribution. Oxygen enhancement ratios are calculated from the resulting PO2 maps. The optimal prescription dose is found by simulating a range of dose levels and determining radiobiological cell kill using the linear-quadratic model with repopulation. A novel approach to modelling reoxygenation is adopted in which a tissue's oxygen consumption in one fraction is reduced by the cell kill in previous fractions.

Results: Predicted FMISO tissue-to-muscle ratios (TMR) are in the range 1.0-2.3, increasing as PO2 decreases to a peak at ~7 mmHg. At very low vascularity, FMISO uptake is limited by perfusion of tracer into the tissue, rather than the oxygen-dependent binding characteristic. No gross differences are observed in TMRs simulated with static or dynamic vascular models. For a representative hypoxic tumour (10 mmHg, intrinsic α=0.3) surviving fractions of 10^-9 are predicted at doses of: 110 Gy (static vasculature, no reoxygenation), 87 Gy (dynamic vasculature changing every fraction) and 71 Gy (reoxygenation by reduced consumption). The effect of vessel dynamics is negligible if significant reoxygenation of chronic hypoxia occurs.

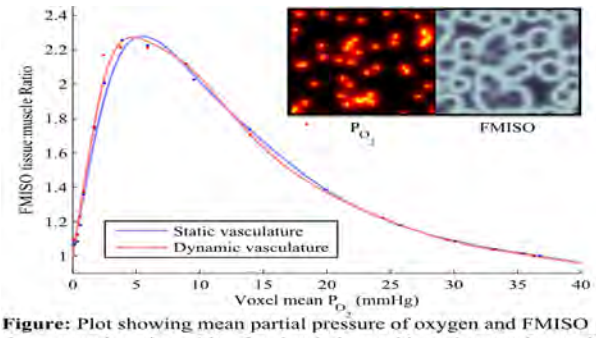

Figure: Plot showing mean partial pressure of oxygen and FMISO tissue:muscle ratio at 4 hrs for simulations with static vascular model and a dynamic model in which vessels randomly open and close. *Inset:* Simulated microscopic distributions of oxygen and FMISO at 4 hours in the same 1 mm^2 of tissue with mean PO_2 = 5 mmHg.

	Static Vessels		Dynamic Vessels		Rexoygenation	
Dose	P_{O_2}	SF	P_{O_2}	SF	P_{O_2}	SF
0 Gy	3.8	1	3.8	1	3.8	1
10 Gy	3.8	2.3×10^{-1}	4.1	2.3×10^{-1}	14.8	2.0×10^{-1}
20 Gy	3.8	6.0×10^{-2}	3.8	5.5×10^{-2}	35.2	2.5×10^{-2}
30 Gy	3.8	1.6×10^{-2}	3.8	1.3×10^{-2}	39.4	2.8×10^{-3}
40 Gy	3.8	1.1×10^{-2}	3.8	8.1×10^{-3}	39.9	8.3×10^{-4}
50 Gy	3.8	8.4×10^{-3}	3.5	5.0×10^{-3}	40.0	2.5×10^{-4}
60 Gy	3.8	6.2×10^{-3}	3.6	3.2×10^{-3}	40.0	7.3×10^{-5}

Table: Simulated surviving fraction (SF) and oxygen partial pressure (PO_2) in mmHg for varying dose delivered in 2 Gy fractions with a static vascular model, a dynamic vascular model and the reduced consumption reoxygenatio model. Parameters: intrinsic radiosensitivity α = 0.3, repopulation kick-off time 21 days and doubling time 5 days.

Conclusion: A model has been demonstrated that predicts realistic FMISO uptake in hypoxic tissue and provides a method for calculating prescription doses with reoxygenation. Individual vessel dynamics do not affect FMISO image contrast at 4 hours, or the prescription dose if global reoxygenation occurs.

OC-0529

A MR-based IGRT platform using the KPC transgenic mouse model of pancreatic cancer

J. Thompson[1], J. Beech[1], D. Allen[1], S. Gilchrist[1], R. Newman[1], P. Kinchesch[1], A. Gomes[1], Z. D'Costa[1], L. Bird[1], K. Vallis[1], R. Boghozian[1], A. Kavanagh[1], O. Sansom[2], I. Tullis[1], R. Muschel[1], M. Hill[1], B. Vojnovic[1], S. Smart[1], E. Fokas[1]

[1]*CRUK/MRC Institute for Radiation Oncology University of Oxford, Department of Oncology, Oxford, United Kingdom*

[2]*Cancer Research UK Beatson Institute- Glasgow, Institute of Cancer Sciences- University of Glasgow, Glasgow, United Kingdom*

Purpose or Objective: With a 5-year survival rate of 5%, pancreatic ductal adenocarcinoma (PDAC) is considered a disease of unmet-need. Preclinical radiobiological research in PDAC has been limited by mouse models that do not recapitulate the human biology and, more importantly, the immense technical challenges in establishing a platform that enables precise irradiation of pancreatic tumours in mice

Material and Methods: Herein we describe the key steps in the development of a state-of-the-art preclinical image-guided radiotherapy (IGRT) platform that enables precise planning and dose delivery in the KRASLSL.G12D/+; p53R172H/+; PdxCretg/+ (KPC), a genetically-engineered mouse model (GEMM) of PDAC. CT (x-ray computerised tomography) does not provide the soft tissue contrast required for accurate and precise RT planning in the mouse. We demonstrate the use of magnetic resonance Imaging (MRI) for RT planning in the mouse abdomen. KPC mice with spontaneous pancreatic tumours were anaesthetised and placed in an MR-CT compatible cradle. A newly-developed respiratory-gated multiple echo contrast scan (8 echoes, TE 6-50 ms) operating at constant TR=3600, was run at 150x150x300 um resolution in a scan time of ca. 9 minutes.

Results: Tumours were undetectable using CT but showed as bright regions on T2-weighted images, as described previously. After registration of the MRI to the CT images RT planning was quite straightforward and beam trajectory and RT dose estimations were performed for a conical arc trajectory. MRI can be used with CT-guided RT system to give soft tissue contrast and enable RT planning. The respiratory gated T2-weighted scans acquired using multiple echoes gave very good contrast, though the scan time was relatively long (ca. 9 minutes). At the expense of SNR this can be reduced to ca. 2 minutes through use of fast spin echo. The different steps will be discussed in detail. Precise beam delivery was confirmed using immunohistochemical staining for γH2AX foci.

Conclusion: Altogether, our IGRT platform represents a novel tool to explore the effects of RT on the biology of PDAC and investigate the mechanisms of treatment resistance. To our best of knowledge, no studies to date have reported such a precise MR-based IGRT platform for preclinical radiobiological research in the KPC model. This platform will enable exploration of the mechanisms of treatment resistance and is expected to provide important radiobiological insight to guide successful future clinical trials that will directly benefit patients with PDAC.

OC-0530

Nanoparticle-enhanced MRI-guided radiation therapy

A. Detappe[1,2], S. Kunjachan[1], O. Tillement[2], R. Berbeco[1]

[1]*Dana Farber Cancer Institute, Radiation Oncology, Boston, USA*

[2]*Institut Lumiere Matiere, Universite Claude Bernard, Lyon, France*

Purpose or Objective: MRI is increasingly used in radiation oncology for target delineation and real-time treatment guidance. The gadolinium-based nanoparticles (GdNP) used in this study are a dual modality probe with MRI contrast and radiosensitization properties. We use a mouse model of pancreatic cancer to demonstrate *in vivo* contrast enhancement, quantification of GdNP concentration, and

significant improvement in survival. By modeling our preclinical study on current clinic workflows, we show clear compatibility with modern patient care, thus heightening the translational significance.

Material and Methods: AGulX (Nano-H, Lyon, France) is a gadolinium-based nanoparticle that has been proposed for an upcoming clinical trial. We performed in vitro cell uptake and radiosensitization studies of a pancreatic cancer cell line in preclinical (220kVp) and clinical (6 MV and 6 MV FFF) beams. MRI was used to monitor tumor uptake and biodistribution. Due to their small size (2-3 nm), the GdNP have good renal clearance and long blood circulation (around 20-30 min in mice).
In vivo radiation therapy studies were performed to characterize the effect of AGulX as a radiosensitizer (n=8/cohort). Histology was performed to measure the increase in damage in the tumor and to evaluate the toxicity in healthy tissues.

Results: The *in vitro* results demonstrate a dose enhancement factor (DEF) of 1.37 ($p<0.005$) when the combination of irradiation and GdNP is used with the 220kV and a DEF of 1.26 for the clinical 6MV FFF. The maximum tumor uptake and tumor/muscle ratio is reached 15 minutes after IV injection. The *in vivo* results demonstrated statistically significant tumor regression ($P<0.001$) and increase in median survival ($p<0.005$) for AGulX combined with radiation vs. radiation alone. There was no observed increase in toxicity in the surrounding healthy organs.

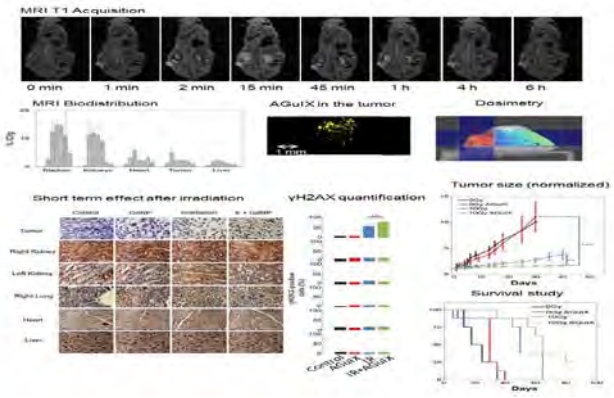

Conclusion: MRI contrast and radiosensitization have been demonstrated in a preclinical pancreatic tumor model. There is a strong translational potential for AGulX with modern and likely future MRI-guided radiation therapy procedures

Proffered Papers: Clinical 11: Health Economics and patient reported outcomes

OC-0531

Time driven activity based costing: a conceptual framework for cost assessment in radiation therapy

N. Defourny[1], P. Dunscombe[2], L. Perrier[3], C. Grau[4], M. Coffey[5], J. Van Loon[6], C. Gasparotto[7], Y. Lievens[8]
[1]*ESTRO A.I.S.B.L., HERO, Brussels, Belgium*
[2]*University of Calgary, Oncology, Calgary, Canada*
[3]*Centre Régional de lutte Contre le Cancer Léon Bérard, Oncology, Lyon, France*
[4]*Aarhus University Hospital, Oncology, Aarhus, Denmark*
[5]*Trinity College Dublin, Oncology, Dublin, Ireland Republic of*
[6]*Maastro Clinic, Oncology, Maastricht, The Netherlands*
[7]*European Society for Radiotherapy and Oncology, HERO, Bruxelles, Belgium*
[8]*Ghent University Hospital, Radiotherapy, Ghent, Belgium*

Purpose or Objective: The value of healthcare can be defined as the additional health outcomes gained for each euro spent. Thus, understanding costs, and their origins, of a medical intervention is key to the estimation of value. Costing studies to date have yielded highly variable results largely due to which and how resources have been analyzed. A rigorous health economics approach requires the cost of the real resources used to be identified (ISPOR, 2007). We report on such an approach to the estimation of the cost of radiation therapy.

Material and Methods: A Time-Driven Activity Based Costing (TDABC) model was created for external photon beam radiotherapy at the national level. The model was developed in an iterative manner by a panel of experts, taking into account current knowledge of resources, products, and clinical processes. The resources were identified through a systematic review of the literature from 1981 to 2015. In TDABC, resource unit costs per minute are defined as the ratio of gross expense to available capacity. The products, defined as courses of treatment for specific tumor indications, were derived from the decision trees developed by the Collaboration for Cancer Outcomes, Research and Evaluation (CCORE). The process map was derived from that developed by the AAPM (2012, Ford).

Results: Resources are organized in 3 categories: personnel, equipment and overhead. Products are grouped per organ site and target volume. For each of these, treatment complexity and diversity are addressed by extending the AAPM process map in three ways:
1. six technique categories, specified as follows: single-field, 2D-RT, 3D-CRT, IMRT, rotational IMRT and stereotactic techniques;
2. eight possible fractionation schedules can be defined;
3. some steps along the patient care pathway are identified separately from the 7 high level steps, see figure.
These, reflecting an additional level of treatment complexity, are optional and hence not necessarily applicable to all treatment courses.
The core input required is the time of personnel's involvement at each process step for every technique and product. This TDABC approach yields two classes of output:
1. costs, at the level of the resources, activities and products, the latter being the sum of the costs of the component process steps; and
2. resource utilization efficiency.

Fig1. HERO Process map

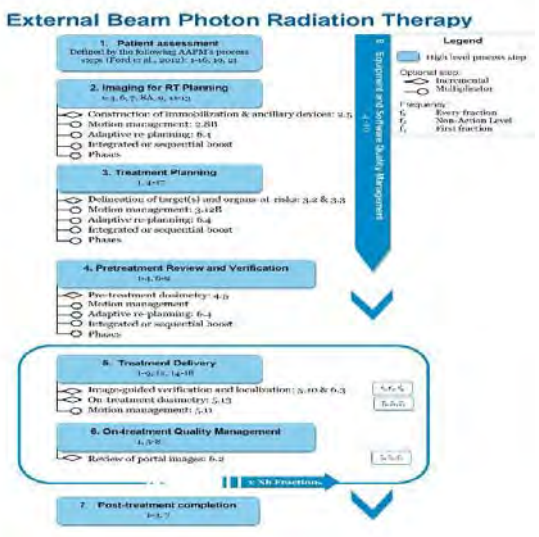

Conclusion: A TDABC model for external photon beam radiotherapy is developed for use at the national level. In the next step, the model is being tested in close collaboration with selected European Radiotherapy Societies, by introducing nation-specific data on the resources consumed, monetary values and resources' time devoted to each step, reflecting complexity. These data generate national cost estimates per course for a range of radiotherapy treatments. The cost estimates and details of the methodology will be presented.

OC-0532

Improved cost-effectiveness of short-course radiotherapy in elderly or frail glioblastoma patients

S. Baker[1], S. Ghosh[2], D. Guedes de Castro[3], L. Kepka[4], N. Kumar[5], V. Sinaika[6], J. Matiello[7], D. Lomidze[8], K. Dyttus-Cebulok[9], E. Rosenblatt[10], E. Fidarova[11], W. Roa[1]

[1]*Cross Cancer Institute and University of Alberta, Radiation Oncology, Edmonton, Canada*
[2]*Cross Cancer Institute and University of Alberta, Medical Oncology, Edmonton, Canada*
[3]*AC Camargo Cancer Center, Radiation Oncology, São Paulo, Brazil*
[4]*Warmia and Mazury Oncology Center, Radiation Oncology, Olsztyn, Poland*
[5]*Postgraduate Institute of Medical Education and Research, Radiotherapy and Oncology, Chandigarh, India*
[6]*N.N. Alexandrov National Cancer Centre of Belarus, Radiotherapy, Minsk, Belarus*
[7]*Irmandade da Santa Casa de Misericórdia de Porto Alegre, Radiotherapy, Porto Alegre, Brazil*
[8]*High Technology Medical Center- University Clinic, Radiation Oncology, Tbilisi, Georgia*
[9]*Maria Sklodowska-Curie Memorial Cancer Centre and Institute of Oncology, Radiation Oncology, Warsaw, Poland*
[10]*International Atomic Energy Agency, Applied Radiation Biology and Radiotherapy Section, Vienna, Austria*
[11]*International Atomic Energy Agency, Radiation Oncology, Vienna, Austria*

Purpose or Objective: Short-course radiotherapy (25 Gy in five fractions) was recently shown in a multi-national randomized phase III clinical trial to be non-inferior to a commonly used regimen (40 Gy in 15 fractions) in elderly and/or frail patients with glioblastoma multiforme, with no difference in overall survival (OS) and progression free survival (PFS). This study compared the cost-effectiveness of the two regimens.

Material and Methods: The direct unit costs of imaging, radiotherapy (RT), and dexamethasone were collected in equitable US dollars (USD) from the five primary contributing countries to the trial, representing 88% of all patients accrued (n = 86) between 2010 and 2013. Effectiveness was measured by the restricted mean overall survival (RMOS) and progression free survival (RMPFS). Irwin's restricted mean method was used to calculate mean survival time in the presence of censoring, and life-years gained and PFS gained. The incremental cost-effectiveness ratio (ICER) was calculated as: Cost per life-year gained = (Difference in direct costs between short-course RT and commonly used RT) ÷ (Difference in life-years gained between short-course RT and commonly used RT). Indirect costs were also estimated for comparison.

Results: There was no OS difference between the two studied populations. The median OSs for the short-course and commonly used RTs were 8.2 (6.1-10.3) and 7.7 (5.5-9.9) months, respectively. Median PFSs were also not different. The differences in the RMOS and the ICER, however, were +0.11 life-years and -USD 3307 per life-year gained, respectively. The differences in the RMPFS and the ICER were +0.02 PFS and -USD 19030, respectively. The negative ICER values indicated improvement in direct cost in addition to life-years gained with the short-course RT. Indirect cost comparison also identified improved survival-to-treatment time ratio and reduced cost for patients and care-givers with short-course RT.

Conclusion: The direct cost account for ICER of -USD 3307 per life-year gained and -USD 19030 per PFS gained indicates that the short-course RT is less costly and more effective compared to the commonly used RT. Indirect cost is also improved with the short-course RT.

OC-0533

TGUGT and G8 tests predicting frailty and radiotherapy compliance and acute toxicity in the elderly

J. Middelburg[1], T. Rozema[2], H. Maas[3], E. Baartman[1], M. Aarts[4], D. Geijsen[5], A. Leest[6], J. Jobsen[7], J. Coebergh[8], H. Struikmans[9]

[1]*Erasmus Medical Center, Radiotherapy, Rotterdam, The Netherlands*
[2]*Institute Verbeeten, Radiotherapy, Tilburg, The Netherlands*
[3]*Tweesteden Hospital, Geriatrics, Tilburg, The Netherlands*
[4]*Netherlands Comprehensive Cancer Organisation IKNL, Netherlands Cancer Registry, Utrecht, The Netherlands*
[5]*Academic Medical Center, Radiotherapy, Amsterdam, The Netherlands*
[6]*University Medical Center Groningen, Radiotherapy, Groningen, The Netherlands*
[7]*Medisch Spectrum Twente, Radiation Oncology, Enschede, The Netherlands*
[8]*Erasmus Medical Center, Public Health, Rotterdam, The Netherlands*
[9]*Medical Center Haaglanden, Radiotherapy Center West, Den Haag, The Netherlands*

Purpose or Objective: On behalf of the LPRO (National organisation for radiotherapy in the elderly):
The incidence of cancer increases with age. Older cancer patients are often underrepresented in clinical trials. Reliable predicting tools for toxicity and compliance of radiotherapy are not yet available. The G8 is a screening tool developed for older cancer patients. The "Timed Get Up and Go Test" (TGUGT) is a validated test for quantifying the degree of mobility. In the current study we aim to quantify to which extend the G8 and the TGUGT are predictive for both radio(chemo)therapy compliance and acute toxicity of curative radiotherapy in elderly cancer patients.

Material and Methods: Patients were recruited in seven Dutch radiotherapy centers: if they were 65 years and older, had newly diagnosed breast/ NSCLC/prostate/head and neck/ rectal and oesophageal cancer, were referred for radio(chemo)therapy with curative intent between April 2015 and the end of October 2015, and had no history of prior radiotherapy. The TGUGT test (normal ≤10 seconds, frail elderly: 11-20 seconds, and needs further evaluation: >20 seconds) and the G8 score (≤14 is indicative of frailty in older cancer patients) were performed before starting the radiotherapy. Compliance with radio- and or radio/chemotherapy and acute toxicity (< 3 months after ending the radiotherapy) were recorded.

Results: A total of 335 patients were included, of which 53% were male. The mean age was 72.8 and 4% were 85 year or older. WHO scores were 0 for 55%, 1 for 36%, 2 for 8%, 3 for 0.3% and unknown in 1%. Patients were motivated to participate, with a mean score of 9.1 and a median of 10, on a ten point scale. Forty-three percent of the patients were considered frail based on the G8 score and 18% based on the TGUGT test. There was an association between the G8 and the TGUGT, with every point increase of the G8 corresponding to walking 0.4 seconds faster. Comorbidity was associated with lower G8 scores, difference 1.3 (95% confidence interval (CI): 08.to 1.8) and slower TGUGT, difference 1.5 (CI: 0.8 to 2.2). Follow-up is still ongoing but will be completed before the end of January 2016. Full results will be presented at the ESTRO 35. Until now (n=57) the compliance is high. All patients completed treatment according to protocol. Acute toxicity is low with 5% grade 3. No grade 4 or 5 toxicity was observed.

Conclusion: We observed an association between the results from G8 and TGUGT. Associations between test results and toxicity and compliance will be presented.

OC-0534

No decline in patient reported outcomes following radiotherapy for breast cancer patients ≥ 60 years

K.R. Charaghvandi[1], D.A. Young-Afat[1], C.H. Van Gils[2], M.L. Gregorowitsch[1], B. Van Asselen[1], M. Van Vulpen[1], H.M. Verkooijen[2], H.J.G.D. Van den Bongard[1]

[1]*University Medical Center Utrecht, Department of Radiation Oncology, Utrecht, The Netherlands*

[2]*University Medical Center Utrecht, Department of Epidemiology, Utrecht, The Netherlands*

Purpose or Objective: The incidence of breast cancer is increasing in women over the age of 60 years. In this group of patients, (age associated) comorbidity is the most important factor influencing survival. The impact of treatment on daily functioning and quality of life may therefore be a more appropriate endpoint for therapy efficacy instead of standard survival outcome. Radiotherapy improves local control in elderly, however its impact on short-term physical and emotional well-being has not been well studied. This study describes patient reported outcomes measures (PROMs) during the first 6 months following radiotherapy in women over the age of 60 years, within a prospective breast cancer cohort. The effect of increasing age on PROMs was evaluated by comparing patients below and at least 70 years of age.

Material and Methods: From October 2013 on, all breast cancer patients referred to the department of Radiation Oncology were invited to enter the UMBRELLA cohort (cohort for multiple breast cancer intervention studies and long-term evaluation). Participants consented to the collection of clinical data and PROMs questionnaires before and at predefined intervals after radiotherapy. For the purpose of this study, changes in quality of life (EORTC QLQ-C30 including fatigue subscale, QLQ-BR23), anxiety and depression (HADS) were evaluated in patients at least 60 years of age, between baseline and 6 months follow-up (FU). Changes in median levels of PROMs between baseline and 6 months follow-up were evaluated with the paired sample t-test. Differences between mean levels of PROMs (continuous scale e.g. 0-100, higher scores indicate better QoL) for the two age groups were evaluated with the independent sample t-test.

Results: Between October 2013 and June 2015, a total of 848 patients were included in the cohort, with 374 patients aged ≥ 60 years. Preliminary analysis was performed in the first 158 patients. At a median FU of 5.5 months after radiotherapy, a decline in mean overall QoL (FU score 75.0, Δ 3.4; p=0.028), improvement of mean anxiety score (FU score 4.6, Δ 0.8; p=0.001) and stable mean fatigue (FU score 74.9, Δ 0.9; p= 0.578) and depression (FU score 3.5, Δ 0.1; p=0.635) scores were observed. No differences between patients 60-69 years and from 70 years of age were observed for overall QoL, anxiety, depression and fatigue scores. Severe anxiety symptoms (HADS anxiety score > 11) were reported in 8.1% and 10% in age groups 60-69 and 70 years or older, respectively.

Conclusion: In the first six months following radiotherapy, no clinically relevant decline in short-term emotional well-being and fatigue have been observed for patients at least 60 years of age. Overall well-being appears to be good in patients below and over the age of 70. Updated and more detailed results (e.g. effect comorbidity and toxicity) with an expected sample size of at least 375 patients will be presented in April 2016.

Patient characteristics	Value in n(%) unless other stated
Median age (range)	
- all patients, n=158	67 (60-85)
- < 70 years, n=102	65 (60-69)
- ≥ 70 years, n=56	73 (70-85)
Median Charlson Comorbidity Index[1] (range)	
- all patients	5 (4-10)
- < 70 years	4 (4-7)
- ≥ 70 years	5 (5-10)
WHO performance status	
- 0	133 (84%)
- 1	23 (15%)
- 2	2 (1%)
Surgery	
- breast conserving	142 (90%)
- mastectomy	16 (10%)
- sentinel lymph node biopsy	140 (89%)
- axillary lymph node dissection	16 (10%)
Disease stage	
- in situ	32 (20%)
- I	86 (54%)
- II	32 (20%)
- III	8 (5%)
Radiotherapy target volumes	
- local: breast or chest wall	129 (82%)
- regional: axillary levels I-II	3 (2%)
- locoregional (axillary levels I-II)	17 (11%)
- locoregional (periclavicular levels / III-IV)	9 (6%)
- median number of fractions (range)	16 (16-23)
- median dose (range)	42.56 (42.56-61.18 Gy)
Systemic treatment	
- neoadjuvant treatment	5 (3%)
- adjuvant chemotherapy[2]	29 (18%)
- adjuvant endocrine therapy[2]	70 (44%)
- adjuvant immunotherapy[2]	2 (1%)
- none	81 (51%)
Acute toxicity[3]	
- at least one grade II episode	36 (23%)
- grade III episode	1 (0.6%)
- > grade III	-
Late toxicity	
- at least one grade II episode	3 (2%)
- > grade II	-

1: age adjusted score 2: overlap in cases with specified treatment 3: toxicity assessed according to Common Terminology Criteria for Adverse Events v4.0, with acute toxicity occurring < 90 days after start radiotherapy and late toxicity ≥ 90 days. Observed toxicities were dermatitis radiation (40%), fatigue (25%), lymphedema of the breast or chest wall (10%), breast pain (8%), pain in extremity (5%), chest wall pain (3%), edema limbs (3%), soft tissue fibrosis (2%), pneumonitis (2%) and esophagitis (2%).

OC-0535

How patient-reported urinary symptoms predict impairment of urinary QoL from RT for prostate cancer

C. Cozzarini[1], F. Badenchini[2], T. Rancati[2], G. Girelli[3], P. Gabriele[4], C. Degli Esposti[5], P. Franco[6], V. Vavassori[7], M. Galeandro[8], C. Bianconi[1], C. Improta[9], F. Palorini[9], R. Valdagni[2], C. Fiorino[10]

[1]*IRCCS San Raffaele Scientific Institute, Radiotherapy, Milano, Italy*

[2]*IRCCS Istituto Nazionale Tumori, Radiotherapy, Milan, Italy*

[3]*Ospedale Civile ASL TO 4, Radiotherapy, Ivrea, Italy*

[4]*Istituto per la Ricerca e la Cura del Cancro- IRCC, Radiotherapy, Candiolo, Italy*

[5]*Ospedale Bellaria, Radiotherapy, Bologna, Italy*

[6]*Azienda U.S.L. Valle d'Aosta, Radiotherapy, Aosta, Italy*

[7]*Cliniche Gavazzeni Humanitas, Radiotherapy, Bergamo, Italy*

[8]*Arcispedale di S.M. Nuova Azienda Ospedaliera, Radiotherapy, Reggio Emilia, Italy*

[9]*IRCCS San Raffaele Scientific Institute, Medical Physics, Milano, Italy*

[10]*IRCCS San Raffaele Scientific Institute, Medical Physiscs, Milano, Italy*

Purpose or Objective: Within a large multi-Institute observational study, patient reported urinary symptoms (PRUS) were available at baseline and at different times intervals after RT: aim of current analysis was to assess the power of the different PRUS in discriminating a severe impairment of urinary QoL.

Material and Methods: Pts treated in 9 Institutes with radical 3DCRT/IMRT for localized prostate cancer with conventional or moderate hypo-fractionation (2.35-2.7 Gy/fr) filled in several questionnaires, including IPSS and ICIQ. Questionnaires are to be filled in at baseline, at RT end, 3 and 6 months after its conclusion, and thereafter every 6 months up to 5 years. Current analysis focused on the IPSS score relative to urinary QoL (item #8, IPSS8) during the first two years after RT, considering a score ≥4 as a severe impairment. At each time interval (i.e.: baseline, RT end, 3, 6, 12, 18, 24 months after RT) the power of the different PRUS, the overall IPSS, single IPSS items (IPSS1 to IPSS7) and ICIQ scores in discriminating patients with ≥4 IPSS8 was assessed by ROC curves: AUCs were calculated for each score at each timing and ROC curves compared to detect significant differences among scores and times.

Results: The available data refer to 499, 449, 412,361, 339, 304, 238 pts at baseline, RT end, 3,6,12,18 and 24 months after RT respectively. Pts with IPSS8≥4 were 50, 126, 25, 24, 23, 28, 21 respectively. The discriminative power of the overall IPSS remained quite constant over time, ranging

between 0.84 and 0.90 without significant differences. Interestingly, the discriminative power of the single IPSS ites was different and dramatically changed over time: only IPSS6 (straining) always showed a poor value at each time (AUC: 0.55-0.65). All the remaining IPSS items showed not significantly (p>0.07) different AUCs at baseline (0.71-0.76), while exhibiting very different patterns after RT. IPSS2 (frequency), IPSS4 (urgency) and IPSS7 (nocturia) showed the highest performances in the acute phase (AUC:0.77-0.87 at RT end and at 3 months). At 24 months, weak stream showed the highest AUC (0.87) while the remaining items ranged between 0.69 and 0.76. Very importantly, the AUC of ICIQ continuously increases from baseline/RT end (AUC=0.62-0.63) up to 24 months (AUC:0.82). In Figure 1a/1b the ROC curves at the different time intervals for overall IPSS and ICIQ are shown; a summary of AUC changes is shown in Figure 1c for all scores at baseline, end RT, 12 and 24 months.

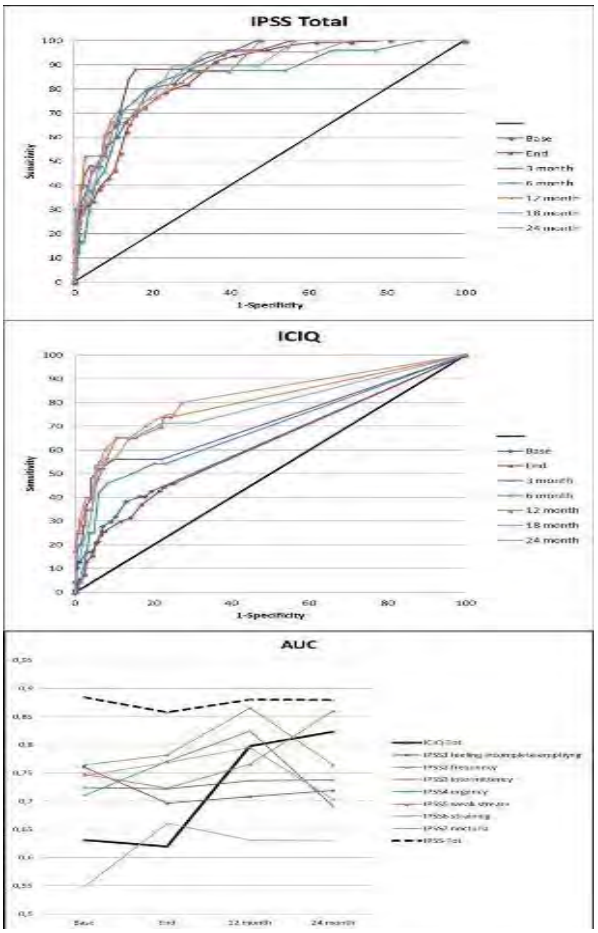

Conclusion: The analysis of a large population of prospectively followed patients with PRUS evaluation showed that the discriminative power of different symptoms in assessing a severely impaired urinary QoL significantly changes over time. As expected, the overall IPSS always captures a very large fraction of these patients, while the predictive value of ICIQ is negligible at baseline and acutely, becoming highly discriminative in the long term.

OC-0536

Course of quality of life after radiotherapy for painful bone metastases

P. Westhoff[1], M. Verdam[2], F. Oort[3], J. Jobsen[4], M. Van Vulpen[5], J.W. Leer[1], C. Marijnen[6], A. De Graeff[7], Y. Van der Linden[6]

[1]*Radboudumc Nijmegen, Radiotherapy, Nijmegen, The Netherlands*

[2]*Academic Medical Center- University of Amsterdam, Medical Psychology, Amsterdam, The Netherlands*

[3]*Academic Medical Center- University of Amsterdam, Research Institute of Child Development and Education-Medical Psychology, Amsterdam, The Netherlands*

[4]*Medical Spectrum Twente, Radiotherapy, Enschede, The Netherlands*

[5]*University Medical Center Utrecht, Radiotherapy, Utrecht, The Netherlands*

[6]*Leiden University Medical Center, Radiotherapy, Leiden, The Netherlands*

[7]*University Medical Center Utrecht, Medical Oncology, Utrecht, The Netherlands*

Purpose or Objective: In patients with painful bone metastases, radiotherapy is an effective treatment. Besides symptom control, quality of life (QoL) is an important endpoint. We focus on the course of QoL after radiotherapy.

Material and Methods: In the Dutch Bone Metastasis Study, 1,157 patients with painful bone metastases were randomized between one fraction of 8 Gray and six fractions of 4 Gray. The study proved equal effectiveness, with a pain response of 74%. Patients filled out weekly questionnaires for 13 weeks and then monthly for two years or until death. Three QoL domain scores (physical, psychosocial and functional) and a visual analogue scoring of general health were studied. Mixed modeling was used to model the course of QoL and to study the influence of several characteristics. An effect size of≥ 0.10/0.20 (binary or continuous variable, respectively) is considered a small effect and therefore clinically relevant.

Results: In general, QoL stabilizes after a month. Psychosocial QoL improves temporarily after treatment. The level of QoL remains stable for a long time, steeply deteriorating at the end of life. For most QoL domains, a high pain score and intake of opioids are associated with worse QoL, with a small effect size (-0.11 to -0.27). A poor performance score is associated with worse functional QoL, with a medium effect size of 0.41.

Figure: The modeled course of QoL after radiotherapy for painful bone metastases, represented in survival groups (patients surviving less than 3, 3-<6, 6-<12, 12-<18 and 18-<24 months after randomization). The x-axis represents the months after treatment, where month 0 is the baseline measurement before treatment and month 1 the first months after treatment. The y-axis reflects the domain score of QoL, where the average is 0, with a standard deviation of 1. The higher the score, the better the QoL.

Table: Influence of baseline and follow-up variables on QoL domains, with effect sizes

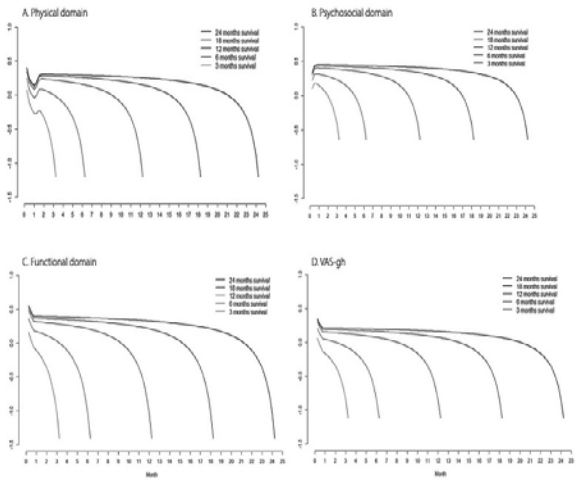

	QoL domains							
	physical		psychosocial		functional		VAS-gh	
variables	effect size	p-value	effect size	p-value	effect size	p-value	effect size	p-value
Baseline:								
age	0.01	0.72	0.03	0.24	**-0.12**	<0.001	0.01	0.65
gender	-0.11	0.26	-0.17	0.11	-0.19	0.02	-0.06	0.45
(reference: male)								
KPS	0.00	0.93	0.06	0.04	**0.41**	<0.001	0.09	<0.001
primary tumor								
(reference: other)								
breast	-0.08	0.43	-0.12	0.28	**-0.27**	0.002	-0.14	0.11
prostate	**-0.20**	0.03	0.18	0.06	**-0.22**	0.003	0.11	0.11
lung	0.06	0.44	-0.04	0.63	-0.10	0.16	0.00	0.95
Follow-up:								
treatment arm	-0.12 - -0.17 *	<0.001	0.06	0.24	0.02	0.57	0.03	0.42
(reference: 1x8Gy)								
pain score	**-0.14**	<0.001	**-0.11**	<0.001	-0.07	<0.001	**-0.24**	<0.001
intake of opioids	**-0.27**	<0.001	-0.05	0.001	**-0.21**	<0.001	**-0.21**	<0.001
(reference: no opioids)								

KPS : Karnofsky performance status, VAS gh: visual analogue scoring of general health

Binary variables (gender, primary tumor, treatment arm and intake of opioids): Effect sizes between -0.19 and 0.19 are considered minor effects and are not clinically relevant. Continuous variables: Effect sizes between -0.09 and 0.09 are considered minor effects and are not clinically relevant. To facilitate interpretation, clinically relevant effects are shown bold.

A positive direction of the effect size means improvement of QoL by increase of the variable / compared to the reference

** The effect size varies each week, ranging from -0.12 (week 4), -0.13 (week 2) to -0.17 (week 3)*

Conclusion: Although radiotherapy for painful bone metastases leads to a meaningful pain response, QoL does not improve after treatment. Initially, it remains stable followed by deterioration towards the end of life.

Proffered Papers: Clinical 12: Rare tumours

OC-0537

p16 and high risk-HPV in node positive cutaneous squamous cell carcinoma of the head and neck

L. McDowell[1], R. Young[2], M. Johnston[1], T. Tan[1], C. Liu[1], M. Bressel[3], V. Estall[1], B. Solomon[4], J. Corry[1]

[1]*Peter MacCallum Cancer Centre, Radiation Oncology Department, East Melbourne, Australia*

[2]*Peter MacCallum Cancer Centre, Research Division, East Melbourne, Australia*

[3]*Peter MacCallum Cancer Centre, Centre for Biostatistics and Clinical Trials, East Melbourne, Australia*

[4]*Peter MacCallum Cancer Centre, Department of Medical Oncology, East Melbourne, Australia*

Purpose or Objective: The incidence of p16-overexpression and the role of human papillomavirus (HPV) in cutaneous head and neck squamous cell carcinoma (cHNSCC) is unclear. In the unknown primary setting, where cHNSCC is a potential putative site, p16 status is being used to guide management despite varying reports of its incidence in non-oropharyngeal sites.

Material and Methods: 143 patients with cHNSCC lymph node metastases involving the parotid gland were evaluated for p16 expression by immunohistochemistry. Detection of 18 high-risk HPV subtypes was performed using HPV RNA in situ hybridization on a subset of 59 patients. Results were correlated with clinicopathological features and outcomes

Results: Median follow up time was 5.3 years. No differences were observed in clinicopathological factors based on p16 status. p16 was positive, intermediate and negative in 45 (31%), 21 (15%) and 77 (54%) of cases, respectively. No high-risk HPV subtypes were identified, irrespective of p16 status. p16 status was not prognostic for overall (HR 1.08 95% CI [0.85 - 1.36], p=0.528), cancer-specific (HR 1.12 95% CI [0.77 - 1.64], p=0.542) or progression-free survival (HR 1.03 95% CI [0.83 - 1.29], p=0.783). Distant metastasis free survival, freedom from locoregional failure and freedom from local failure were also not significantly associated with p16 status.

Conclusion: p16 positivity is common but not prognostic in cHNSCC lymph node metastases. High-risk HPV subtypes are not associated with p16-positivity, and do not appear to play a role in this disease. HPV testing, in addition to p16-status in the unknown primary setting may provide additional information in determining a putative primary site.

OC-0538

Tumor-related leukocytosis associated with poor radiation response and outcome in cervical cancer

Y. Cho[1], K. Kim[1], K. Keum[1], C. Suh[1], G. Kim[1], Y. Kim[1]

[1]*Yonsei Cancer Center, Radiation Oncology, Seoul, Korea Republic of*

Purpose or Objective: To investigate the prognostic significance of tumore-related leukocytosis (TRL) in cervical cancer patients treated with definitive radiotherapy

Material and Methods: Between 1986 and 2012, 2,456 patients with uterine cervical cancer (FIGO stage IA-IB 494, stage IIA-IIB 1530, stage IIIA-IIIB 394 and stage IVA 38) who received definitive radiotherapy (62.6%) or platinum-based chemoradiotherapy (37.4%) consisting of EBRT and ICBT were retrospectively analyzed. TRL was defined as WBC count of ≥9,000/μL on ≥2 occasions at the time of diagnosis and during the course of treatment. The neutrophil/lymphocyte ratio (NLR) was defined as the absolute neutrophil count divided by the absolute lymphocyte count. Locoregional failure free survival (LRFFS) and overall survival (OS) were compared between patients with or without TRL.

Results: Median age of all patients was 55 years (range, 21-87) and the median follow-up time was 65.1 months (range, 0.7-347.8). Among 2,456 patients included in this study, TRL was observed in 398 (16%) at the initial diagnosis. Patients in TRL(+) group were younger in age and had larger tumor, advanced FIGO stage and more common LN metastases (all p < 0.05). TRL (+) group showed relatively lower rate of complete remission (CR) (90% vs. 97%, p = 0.042).The 10-year LRFFS and OS for all patients were 84% and 78%, respectively. Compared to TRL(-) group, LRFFS and OS were significantly lower in TRL(+) group (10-yr LRFFS: 69% vs. 87%, p <0.001; 10-yr OS: 63% vs. 81% p < 0.001). After propensity score matching by age, FIGO stage, tumor size, LN metastasis, histologic subtype and pretreatment hemoglobin (Pre Tx Hb), both groups were well matched. The LR control and OS rate of TRL (+) group was still significantly lower than those of TRL (-) group. In multivariate analysis, advanced FIGO stage, non-SqCCa, larger tumor size and TRL were identified as risk factors for LRFFS and OS (all p < 0.05). In addition, Pre Tx Hb, LN metastasis and high NLR (≥2.5) were also associated with poorer OS (all p < 0.05). Among patients with LRF (n=345), patients with TRL at the time of recurrence accounted for 26% and showed relatively poorer median OS (6 vs. 12 months, p = 0.001).

Conclusion: This study supports the aggressive nature and poor radiation response of cervical cancer with leukocytosis. Given the unfavorable features and higher probability of treatment failure, optimal therapeutic approach and careful monitoring for early detection of recurrence should be considered for these patients.

OC-0539

Stage II testicular seminoma: patterns of care and survival by treatment strategy

S.M. Glaser[1], G.K. Balasubramani[2], S. Beriwal[1]

[1]*University of Pittsburgh Cancer Institute, Radiation Oncology, Pittsburgh- PA, USA*

[2]*University of Pittsburgh School of Public Health, Department of Epidemiology, Pittsburgh- PA, USA*

THIS ABSTRACT FORMS PART OF THE MEDIA PROGRAMME AND WILL BE AVAILABLE ON THE DAY OF ITS PRESENTATION TO THE CONFERENCE

OC-0540

IOERT after gross total resection combined with EBRT in extremity sarcoma: a pooled analysis

F. Roeder[1,2], A. De Paoli[3], I. Alldinger[4], G. Bertola[3], G. Boz[3], J. Garcia-Sabrido[5], M. Uhl[6], A. Alvarez[7], B. Lehner[8], F. Calvo[7], R. Krempien[9]

[1]*German Cancer Research Center DKFZ, Molecular Radiation Oncology, Heidelberg, Germany*
[2]*University Hospital of Munich LMU, Radiation Oncology, Munich, Germany*
[3]*National Cancer Institute, Radiation Oncology, Aviano, Italy*
[4]*University of Heidelberg, Surgery, Heidelberg, Germany*
[5]*University Hospital Gregorio Maranon, Surgery, Madrid, Spain*
[6]*University of Heidelberg, Radiation Oncology, Heidelberg, Germany*
[7]*University Hospital Gregorio Maranon, Radiation Oncology, Madrid, Spain*
[8]*University of Heidelberg, Orthopedics, Heidelberg, Germany*
[9]*Helios Clinic, Radiation Oncology, Berlin, Germany*

Purpose or Objective: In 2009 we reported promising first results of a European pooled analysis which evaluated the use of intraoperative radiation therapy (IORT) in the treatment of soft tissue sarcomas. However, comparison of these results with non-IORT series seemed difficult, mainly because of the inclusion of grossly incomplete resected lesions, patients treated without additional external beam radiation therapy (EBRT) and comparatively short follow-up. Therefore we re-analyzed our data limited to the patients who received IOERT preceeded or followed by EBRT after gross total resection with extended follow-up.

Material and Methods: Three European expert centers participated in the current analysis. Patients with gross incomplete resection, missing documentation of EBRT or primary lesions outside the extremities were excluded, leaving 259 patients for analysis. Median age was 55 years and median tumor size 8 cm. 80% of the patients presented in primary situation with 81% of the tumors located in the lower limb. Stage at presentation was I:9%, II:47%, III:39%, IV:5%. Most patients showed high grade lesions (FNCLCC grade 1:9%, 2:34%, 3:58%, predominantly liposarcoma (31%) and MFH (27%). IOERT was applied to the tumor bed with a median dose of 12 Gy using a median electron energy of 8 MeV. IOERT was preceeded (17%) or followed (83%) by EBRT with a median dose of 45 Gy in all patients. 37% of the patients received additional chemotherapy.

Results: Median follow up was 63 months. Surgery resulted in free margins (R0) in 71% while 29% suffered from microscopic positive margins (R1). We observed 27 local failures, transferring into a 5-year local control rate of 86%. Univariate analysis revealed primary vs recurrent situation and resection margin as significant factors for local control but only resection margin (5-year LC rate 94% vs 70%, HR 3.8) remained significant in multivariate analysis. Distant failure was found in 70 patients, resulting in a 5-year distant control rate of 69%. Factors with significant impact on distant control in univariate analysis were histology, grading, resection margin and stage IV prior/at IOERT, but only grading and stage IV remained significant in multivariate analysis. Actuarial 5-year rates of FFTF and OS were 61% and 78%, respectively. Significant factors for overall survival were only grading and stage IV prior/at IOERT (uni- and multivariate). Secondary amputations were needed in 14 patients (5%) resulting in a final limb-preservation rate of 95%. Good functional outcome was achieved in 81%.

Conclusion: Combination of IOERT and EBRT after limb sparing surgery resulted in encouraging local control and overall survival with excellent rates of preserved limb function in this unfavourable patient group. Our analysis identified resection margin as most important factor for local control while overall survival was mainly influenced by grading and stage IV prior/at IOERT.

OC-0541

Long-term results of the AIEOP MH-89 protocol for pediatric Hodgkin lymphoma

M. Robazza[1], M. Mascarin[1], C. Elia[1], A. Todesco[2], G. Scarzello[3], A. Pession[4], A. Garaventa[5], S. Barra[6], M. Zecca[7], N. Santoro[8], M. Bianchi[9], U. Riccardi[10], F. Locatelli[11], R. De Santis[12], P. Indolfi[13], M. Nardi[14], F. Porta[15], T. Casini[16], C. Consarino[17], S. D'Amico[18], M. Provenzi[19], G.A. Zanazzo[20], P. Farruggia[21], G. Guerrini[22], R. Burnelli[22]

[1]*CRO - Aviano Cancer Center, Pediatric Radiotherapy Unit, Aviano, Italy*
[2]*Azienda Ospedaliera -Universita' di Padova, Clinica di Oncoematologia Pediatrica, Padova, Italy*
[3]*Azienda Ospedaliera -Universita' di Padova, U.O. di Radioterapia, Padova, Italy*
[4]*Clinica Pediatrica-Policlinico Sant'Orsola Malpighi, U.O. di Oncologia ed Ematologia "Lalla Seràgnoli", Bologna, Italy*
[5]*Ospedale Gaslini, U.O. di Ematooncologia Pediatrica, Genova, Italy*
[6]*Istituto Tumori Genova, U.O. di Radioterapia, Genova, Italy*
[7]*Policlinico San Matteo, U.O. di Oncoematologia pediatrica, Pavia, Italy*
[8]*Policlinico di Bari, U.O. di Oncoematologia Pediatrica, Bari, Italy*
[9]*Ospedale Regina Margherita, U.O. di Oncoematologia Pediatrica, Torino, Italy*
[10]*Ospedale le Molinette, U.O. di Radioterapia, Torino, Italy*
[11]*Ospedale Bambin Gesù, U.O. di Ematoncologia Pediatrica, Roma, Italy*
[12]*Casa Sollievo della Sofferenza, U.O. di Oncologia Pediatrica, San Giovanni Rotondo, Italy*
[13]*Università Federico II- policlinico di Napoli, U.O. di Ematooncologia Pediatrica, Napoli, Italy*
[14]*Azienda Ospedaliera - Universita' Pisana Ospedale S. Chiara, U.O. di Oncoematologia Pediatrica, Pisa, Italy*
[15]*Ospedale dei Bambini, U.O. di Oncoematologia Pediatrica, Brescia, Italy*
[16]*Azienda Ospedaliero-Universitaria Meyer, Dipartimento A.I. Oncoematologia SODC Tumori pediatrici e Trapianto di cellule staminali, Firenze, Italy*
[17]*Azienda Ospedaliero Pugliese-Ciaccio, U.O. di Oncologia Pediatrica, Catanzaro, Italy*
[18]*Clinica Pediatrica, U.O. di Oncologia Pediatrica, Catania, Italy*
[19]*Ospedali Riuniti, U.O. di Onco Ematologia Pediatrica, Bergamo, Italy*
[20]*Università degli studi di Trieste Ospedale Infantile Burlo Garofolo, U.O. Emato-Oncologia Pediatrica, Trieste, Italy*
[21]*A.R.N.A.S. Civico di Cristina e Benfratelli, U.O. Oncoematologia Pediatrica, Palermo, Italy*
[22]*Azienda Ospedaliero-Universitaria di Ferrara S.Anna, U.O. di Oncoematologia Pediatrica, Ferrara, Italy*

Purpose or Objective: The AIEOP-MH89 protocol aimed to optimize treatment results in pediatric Hodgkin lymphoma compared to the previous AIEOP-MH83 protocol. Modifications included: involved field instead of extended field radiation therapy (RT) in early-stage patients (pts); anticipated RT for pts with a mass/thorax ratio (M/T)>0.33; enrolment of advanced-stage pts in SIOP HD IV protocol.

Material and Methods: Between 1989-1995, 254 evaluable pts (median age 10 years, range 2-15 years) received the AIEOP-MH89 protocol. The pts were divided into 3 chemotherapeutic groups according to the clinical stage. Group (GR) 1, pts in stages IA and IIA, including those with a mass/thorax ratio (M/T)<0.33, received 3 cycles of adriamycin, bleomycin, vinblastine, and imidazole carboxamide (ABVD). RT was given after completion of chemotherapy. GR 2, pts in stages IEA, IB, IA, IIA with M/T>0.33, IIB, IIEB, IIIA, IIIS, and IIEA, was treated with alternating cycles of nitrogen mustard, vincristine, procarbazine, and prednisone (MOPP)/ABVD. The therapeutic program included 2 cycles of MOPP/ABVD before radiation therapy and 4 cycles MOPP/ABVD after RT. GR 3, pts in advanced stages IIIB, IVA and IVB, was treated according to the SIOP HD IV-87 protocol, with 2 cycles of vincristine, procarbazine, prednisone, adriamycin, (OPPA) and 2 cycles of

cyclophosphamide vincristine, procarbazine, prednisone (COPP) followed by RT. Pts enrolled in GR 1 and 3 were treated with involved field RT. Pts with positive cervical lymph nodes received RT to the neck. In positive axillary lymph nodes, RT included also the sovraclavear region. Pts with mediastinal disease were treated with mediastinum and bilateral supraclavicular fossa RT, whereas pts with involvement of both mediastinum and other supra diaphragmatic lymph nodes stations received the conventional mantle RT. Pts with positive single inguinal lymph node received also comprensive RT to omolateral iliac nodal stations, whereas in case of multiple subdiaphragmatic lymph nodes disease, bilateral iliac nodal stations irradiation was avoided if not directly involved. The radiation doses were established according to response to initial chemotherapy, and were the same in GR 1 and 2: pts in CR and ≥75% PR received 20 Gy, whereas <75% PR received 40 Gy. GR 3 pts with CR or ≥75% PR received 20 Gy, and 36 Gy those with 75% PR.

Results: In table 1 are reported the results in term of Overall Survival (OS) and Event Free Survival (EFS). Long term side effects of treatment were evaluated (median follow-up duration 16 years): 25.6% of the pts developed thyroid complications and 6.6% secondary malignancies.

Table 1: Overall and by Group Risk, Survival (OS) and Event Free Survival (EFS)

time	5 yrs	10 yrs	15 yrs	20 yrs	
OS	97.2%	96.0%	95.5%	94.8%	Risk Group
	99.0%	98.4%	97.9%	97.9%	GR1
	97.2%	96.2%	95.3%	94.5%	GR2
	93.7%	89.2%	89.2%	89.2%	GR3
EFS	89.3%	86.5%	86.5%	86.5%	
	94.9%	92.8%	92.8%	92.8%	GR1
	89.2%	86.8%	86.8%	86.8%	GR2
	75.0%	72.9%	72.9%	72.9%	GR3

Conclusion: The AIEOP-MH89 protocol improves globally OS and EFS. In GR 1 OS and EFS are the same compared to the previous protocol, minimizing radiation exposure. In GR 2 and 3 OS and EFS improved because of therapeutic changes. Analysis of delayed toxicities underlines the importance of long-term monitoring of pts.

OC-0542

Benign tumours among long-term childhood cancer survivors: a DCOG LATER record linkage study

J. Kok[1], J. Teepen[1], H. Van der Pal[2,3], W. Dolsma[3,4], E. Van Dulmen-den Broeder[3,5], M. Van den Heuvel-Eibrink[3,6,7], J. Loonen[3,8], W. Tissing[3,9], D. Bresters[3,10], B. Versluys[3,11], S. Neggers[3,12], M. Van der Heiden-van der Loo[3], F. Van Leeuwen[3,13], H. Caron[3,14], F. Oldenburger[15], G. Janssens[7,16,17], J. Maduro[4], R. Tersteeg[17], C. Van Rij[18], L. Daniels[19], C. Haasbeek[20], The DCOG LATER Study Group[3], A. Gijsbers-Bruggink[21], L. Kremer[1,3], C. Ronckers[1,3]

[1]*Academic Medical Center, Pediatric Oncology, Amsterdam, The Netherlands*
[2]*Academic Medical Center, Medical Oncology, Amsterdam, The Netherlands*
[3]*Stichting KinderOncologie Nederland SKION / Dutch Childhood Oncology Group DCOG, The Hague, The Netherlands*
[4]*University of Groningen/University Medical Center Groningen, Radiation Oncology, Groningen, The Netherlands*
[5]*VU University Medical Center, Pediatric Oncology/Hematology, Amsterdam, The Netherlands*
[6]*Sophia Children's Hospital/Erasmus Medical Center, Pediatric Oncology/Hematology, Rotterdam, The Netherlands*
[7]*Princess Maxima Center for Pediatric Oncology, Utrecht, The Netherlands*
[8]*Radboud University Medical Center, Pediatric Oncology and Hematology, Nijmegen, The Netherlands*
[9]*Beatrix Children's Hospital/University of Groningen/University Medical Center Groningen, Pediatric Oncology/Hematology, Groningen, The Netherlands*
[10]*Willem-Alexander Children's Hospital/Leiden University Medical Center, Pediatric Stem Cell Transplantation, Leiden, The Netherlands*
[11]*Wilhelmina Children's Hospital/University Medical Center Utrecht, Pediatric Oncology and Hematology, Utrecht, The Netherlands*
[12]*Erasmus Medical Center, Internal Medicine, Rotterdam, The Netherlands*
[13]*Netherlands Cancer Institute, Epidemiology, Amsterdam, The Netherlands*
[14]*Academic Medical Center, Peadiatric Oncology, Amsterdam, The Netherlands*
[15]*Academic Medical Center, Radiation Oncology, Amsterdam, The Netherlands*
[16]*Radboud University Medical Center, Radiation Oncology, Nijmegen, The Netherlands*
[17]*University Medical Center Utrecht, Radiation Oncology, Utrecht, The Netherlands*
[18]*Erasmus Medical Center, Radiation Oncology, Rotterdam, The Netherlands*
[19]*Leiden University Medical Center, Radiation Oncology, Leiden, The Netherlands*
[20]*VU University Medical Center, Radiation Oncology, Amsterdam, The Netherlands*
[21]*PALGA Foundation, Houten, The Netherlands*

Purpose or Objective: Childhood cancer survivors (CCS) face high risk for late effects. Aside from malignant neoplasms, it is known that ionizing radiation induces benign tumours of, e.g., the central nervous system and other sites. Record-linkage with pathology report registries provides a unique opportunity to obtain non-selected and uniformly collected benign tumour information. We aim to estimate the incidence of histologically-confirmed solid benign tumours (SBT), to describe clinical characteristics and to quantify the role of radiotherapy (RT).

Material and Methods: The Dutch Childhood Oncology Group – Late effects after childhood cancer (DCOG LATER) is a collaborative effort of all 7 academic paediatric hemato/oncology centres in the Netherlands with clinicians and researchers who focus on optimal patient care and research in CCS. The DCOG LATER cohort includes 6168 five-yr CCS treated between 1963 and 2001 before the age of 18 yrs. The entire DCOG LATER cohort was linked with the nationwide Dutch Pathology Registry (PALGA) to ascertain histologically confirmed SBT (excluding skin) diagnosed between 1990-2014.

Results: We identified 1278 eligible pathology reports in 788 CCS after a median follow up since diagnosis of 22 yrs (max. 52). We excluded reports on SBT diagnosed within 5 yrs after childhood cancer (243 reports); 145 reports without a clear diagnosis in conclusion and 25 reports still to be classified. These preliminary analyses include 865 reports from 578 CCS, of whom 79% had one SBT, and 21% had multiple. Tumour locations included head/neck/CNS (36%), chest (13%), abdomino-pelvic (34%), and extremities (14%). Of 3% location was unclear. Most common SBT types in the head/neck/CNS were meningiomas (44%), often following cranial radiotherapy (RT) (95%); mammary fibroadenomas (49%), 1 in 6 after RT chest; colorectal adenoma (38%), including 1 in 4 after abdominopelvic RT, and female genital tract tumours (leiomyomas and ovarian mucinous cystadenomas) (29%), 1 in 3 after abdominopelvic RT. We will present effects of RT dose, chemotherapy and genetic syndromes.

Conclusion: This preliminary analyses give insight into the amount and types of histologically confirmed SBT in CCS in relation to RT. To our knowledge, this is one of the first comprehensive assessments of subsequent SBT among CCS. In ongoing clinical follow-up studies we aim to gain knowledge about risk factors and clinical characteristics (e.g. meningioma) to help guideline groups decide for or against screening of asymptomatic, high-risk CCS.

Dutch Childhood Oncology Group – Late Effects after Childhood Cancer

Additional members

Aleida Postma[1]
Alida van der Steeg[2,2]
Martha Grootenhuis[3,3]
Hanneke van Santen[4,4]
Andrica de Vries[2,2]
Monique Jaspers[5,5]
Marleen van den Berg[2,7]
Nynke Hollema[1]
Huib Caron[1,8]
Gea Huizinga[2,9]

Patient representative
Jaap den Hartogh[1,10]

Representatives radiation oncology
Berthe Aleman[11]

[1] *Stichting KinderOncologie Nederland (SKION) / Dutch Childhood Oncology Group (DCOG), The Hague, The Netherlands*
[2] *Pediatric Surgical Center of Amsterdam, Emma Children's Hospital AMC and VU University Medical Center, Amsterdam, The Netherlands*
[3] *Dept. of Pediatric Psychology, Emma Children's Hospital/Academic Medical Center, Amsterdam, The Netherlands*
[4] *Dept. of Pediatric Endocrinology, Wilhelmina Children's Hospital/University Medical Center Utrecht, Utrecht, The Netherlands*
[5] *Dept. of Pediatric Oncology/Hematology, Sophia Children's Hospital/Erasmus Medical Center, Rotterdam, The Netherlands*
[6] *Dept. of Medical Informatics, Academic Medical Center, Amsterdam, The Netherlands*
[7] *Dept. of Pediatric Oncology/Hematology, VU University Medical Center, Amsterdam, The Netherlands*
[8] *Dept. of Pediatric Oncology, Emma Children's Hospital/Academic Medical Center, Amsterdam, The Netherlands*
[9] *Dept. of Pediatric Oncology/Hematology, Beatrix Children's Hospital/University of Groningen/University Medical Center Groningen, Groningen, The Netherlands*
[10] *Dutch Childhood Cancer Parent Organisation (VOKK), Nieuwegein, The Netherlands*
[11] *Dept. of Radiation Oncology, Netherlands Cancer Institute, Amsterdam, The Netherlands*

Proffered Papers: Physics 13: New Technology and QA

OC-0543

Technical development and clinical implementation of an MR-guided radiation therapy environment

T. Stanescu[1], S. Breen[1], C. Dickie[2], D. Letourneau[1], D. Jaffray[3]

[1]*Princess Margaret Cancer Centre, Medical Physics, Toronto, Canada*
[2]*Princess Margaret Cancer Centre, Radiation Medicine Program, Toronto, Canada*
[3]*Princess Margaret Cancer Centre, Medical Physcics, Toronto, Canada*

Purpose or Objective: Feasibility study for the clinical implementation of a hybrid radiation therapy system consisting of an MR-on-rails scanner and a linear accelerator.

Material and Methods: A 1.5 T MR-on-rails system (IMRIS, Minnetonka, MN) was configured a) to be used as a standalone MR simulator in a dedicated suite or b) to travel on ceiling-mounted rails to an adjacent linac vault and operate in the vicinity of a 6X FF/FFF TrueBeam therapy system (Varian Medical System, Palo Alto, CA). The in-room MR guidance is intended be used in conjunction with the standard linac's kV imaging for the patient setup verification and treatment delivery. Key aspects of the MR and linac integration were investigated such as: magnetic field coupling of the MR with the linac vault environment, RF noise, RT workflows, safety systems, and QC procedures. Numerical simulations and measurements were performed to establish the magnetic field optimal separation between the MR and linac. A FEM-based simulation space was built and validated to mimic the full-scale MR-linac/couch system; this provided a detailed picture of the magnetic field coupling effects and guided the engineering activities. Field mapping was performed with low/high field Hall probes, and pull forces on couch sub-components were measured via a force gauge for several scenarios. Hysteresis effects on the linac beam performance were quantified by measuring the flatness/symmetry/output vs. gantry angle for short and long-term MR's field exposures. The MR performance was evaluated using procedures available in the service mode of the MR console as well as dedicated methods developed in-house (e.g. B0 mapping). RF noise isolation was achieved by parking the linac behind specially designed RF doors during the MR imaging sessions. An interlocking system was designed and implemented to enforce the safe linac curation (e.g. gantry position, doors statues and table position) prior to MR's travel into the vault.

Results: The MR-linac platform is in the last phase of the assessment. At its pre-defined imaging position in the linac room, the MR was shimmed and configured to work at peak performance. The linac's radiation beam output was also found to be within specifications, being not affected by multiple passive exposures (testing over one year) to the MR's magnetic fringe field. A hybrid MR-kV framework is under development to enable comprehensive RT tools for MR-only RT planning, quantification of organ motion (fast imaging), in-room treatment guidance, and site specific adaptive RT workflows. QC procedures specific to the MR and linac integration were also developed for the mapping and correction of both scanner-related and patient-induced MR image distortions, mutual registration of the MR and linac isocenters, B0 mapping for monitoring the MR performance, 4D MR, and generation of synthetic CT data sets.

Conclusion: Key milestones of the MR and linac integration were achieved, supporting the feasibility of the system for clinical implementation.

OC-0544

Heterogeneous FDG-guided dose escalation of locally advanced NSCLC, the NARLAL2 phase III trial

D.S. Moeller[1], L. Hoffmann[1], C.M. Lutz[1], T.B. Nielsen[2], C. Brink[2], A.L. Appelt[3], M.D. Lund[3], M.S. Nielsen[4], W. Ottosson[5], A.A. Khalil[1], M.M. Knap[1], O. Hansen[2], T. Schytte[2]

[1]*Aarhus University Hospital, Department of Oncology and Medical Physics, Aarhus, Denmark*
[2]*Odense University Hospital, Laboratory of Radiation Physics and Department of Oncology, Odense, Denmark*
[3]*Vejle Hospital, Department of Oncology, Vejle, Denmark*
[4]*Aalborg University Hospital, Department of Oncology, Aalborg, Denmark*
[5]*Herlev Hospital, Radiotherapy Research Unit and Department of Oncology, Herlev, Denmark*

Purpose or Objective: Locally advanced lung cancer lacks effective treatment options and may require aggressive chemo-radiotherapy (RT) with high doses. In the light of the RTOG 0617 trial, multi-centre dose escalation trials should avoid increasing organ at risk (OAR) toxicity and require strict quality assurance (QA). Dose escalation can be performed for sub volumes of the tumour by targeting of the most FDG-PET avid regions, and the planning target volume (PTV) can be reduced by implementing daily soft tissue based image-guidance and adaptive RT. Incorporating these elements, the randomized multi-centre trial NARLAL2 by the Danish Oncologic Lung Cancer Group aims at increasing loco-regional control at 30 months without increasing toxicity.

Material and Methods: In the standard arm, the PTV is treated with a homogenous dose of 66 Gy/33 fractions (fx). In the experimental arm, the dose is escalated heterogeneously to the FDG-PET avid volumes, with mean doses up to 95 Gy/33 fx for the most PET active volumes of the primary tumour, and 74 Gy/33 fx for malignant lymph nodes≥ 4 cm3. The escalation dose is limited in favour of OAR constraints. A standard and an experimental treatment plan are optimized for each patient prior to randomization. Dose to the lung in the experimental plan is kept similar to the lung dose in the standard plan. All enrolment centres were obliged to follow a strict QA program consisting of a treatment planning study, a soft tissue match and adaptive strategy workshop, and QA for PET scanners and FDG-PET volume delineation. In the present study, the dose distributions of the first 20 patients are analysed. The achieved dose escalation is compared to a previously conducted pilot study.

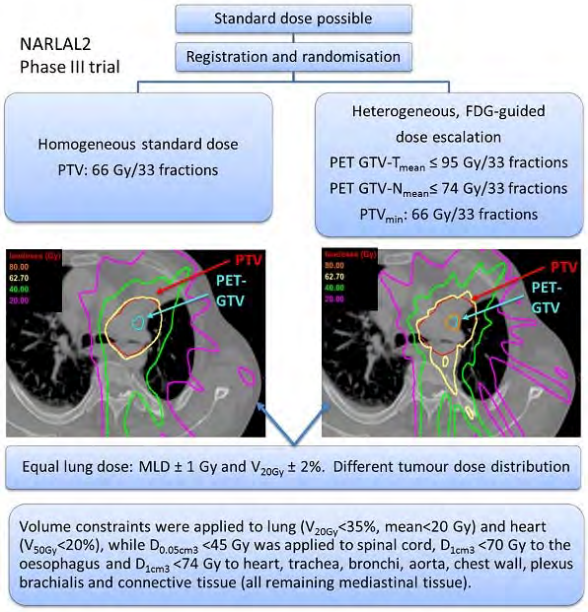

Results: In the pilot study, the dose escalated FDG-PET avid part of tumour (PET GTV-T) and lymph nodes (PET GTV-N) received an average mean dose of 91.9 Gy and 72.1 Gy, respectively. The combined clinical target volume (CTV-total) received an average mean dose of 78.6 Gy. This corresponds to a 16 % estimated increase in loco-regional control at 30 months. For the first 20 patients included, the experimental plan achieved an average mean dose of 92.3 Gy (SD 3.7) to PET GTV-T. A total of 11 large lymph nodes were escalated to an average mean dose of 72.1 Gy (SD 2.7) to PET GTV-N. CTV-total obtained an average mean dose of 75.8 Gy (SD 4.1). Normal tissue doses were similar for the experimental and standard plan (Table 1). The maximum dose for the standard plans was 72.6 Gy (110%). Higher doses were applied for the experimental plans, but only to small volumes respecting the strict normal tissue constraints (see figure).

Table 1: Dose to organs at risk (in absolute dose or percentage) as an average (with standard deviation) for the first 20 patients included.

Organ at risk	Standard (S)	Exp. (E)	E-S
Mean Lung Dose [Gy]	13.7 (3.7)	13.6 (3.8)	-0.1 (0.4)
Lung V$_{20Gy}$ [%]	22.0 (7.2)	21.4 (7.2)	-0.6 (0.6)
Mean Heart Dose [Gy]	8.4 (8.6)	8.2 (8.1)	-0.8 (0.8)
Heart V$_{50Gy}$ [%]	4.2 (3.9)	2.9 (3.9)	-0.6 (1.1)
Oesophagus V$_{35Gy}$ [%]	25.1 (13.7)	24.3 (14.0)	-0.8 (2.0)

Conclusion: A dose escalation trial with strict QA has been set up. Patient enrolment started January 2015. Analysis of the first 20 patients demonstrates that the escalation goals were met for the target and that dose to OARs were similar for the standard and the experimental treatment plans.

OC-0545

Results of a national audit of IMRT and VMAT patient QA

E. Seravalli[1], A.C. Houweling[2], M.P.R. Van Gellekom[3], J. Kaas[4], M. Kuik[5], E.A. Loeff[6], T.A. Raaben[7], J.A. De Pooter[8], J.H.W. De Vries[9], J.B. Van de Kamer[4]

[1]*UMC Utrecht, Department of Radiation Oncology, Utrecht, The Netherlands*
[2]*Academic Medical Center, Department of Radiation Oncology, Amsterdam, The Netherlands*
[3]*Radiotherapiegroep, Department of Medical Physics, Arnhem, The Netherlands*
[4]*The Netherlands Cancer Institute, Department of Radiation Oncology, Amsterdam, The Netherlands*
[5]*Medisch Centrum Alkmaar, Department of Radiotherapy, Alkmaar, The Netherlands*
[6]*Erasmus MC-Cancer Institute, Department of Radiation Oncology, Rotterdam, The Netherlands*
[7]*Medisch Spectrum Twente, Radiotherapy, Enschede, The Netherlands*
[8]*VSL, VSL, Delft, The Netherlands*
[9]*University Medical Centre Utrecht, Department of Radiotherapyy, Utrecht, The Netherlands*

Purpose or Objective: To independently validate patient-specific quality assurance (QA) methods, clinically used in the Netherlands, for IMRT and VMAT plans using the same set of treatment plans for all institutes.

Material and Methods: A set of treatment plans was devised: simple and more complex IMRT/VMAT and a stereotactic VMAT plan, all 6MV for both Varian and Elekta linacs. Ten plans were used for Varian linacs (5 for True Beam and 5 for Clinac) and 9 for Elekta linac(4 for MLCi and 5 for Agility). The plans were imported in the participating institute's treatment planning system for dose computation on the CT scan of the audit phantom (provided by the audit team together with the plans). Additionally, 10x10 cm2 fields were made and computed on both phantoms. Next, the audit team performed measurements using the audit equipment. All 21 Dutch radiotherapy institutes were audited. The measurements were performed using an ionization chamber (PinPoint, PTW), Gafchromic EBT3 film and a 2D ionization chamber array, all in an octagonal phantom (Octavius, PTW). Differences between the measured and computed dose distribution were investigated using a global gamma analysis with a 5%/1mm criterion for the stereotactic VMAT plan and 3%/3mm for the other plans with a 95% pass rate tolerance. Additionally, the participating centres performed QA measurements of the same treatment plans according to their local protocol and equipment.

Results: The average difference between the point measurement, at the centre of the phantom, and the planned dose is below 1% (range: (-4.0 – +2.0)%) independently on the plan type (table 1).

Table 1 Point measurement for all the plans measured with a PinPoint at the centre of the Octavius phantom

	10x10 cm^2 field	Simple IMRT	Simple VMAT	Complex IMRT	Complex VMAT	Stereotactic VMAT
Average ± σ (%)	0.1 ± 1.4	-1.3 ± 1.2	0.1 ± 1.8	-0.9 ± 1.4	-0.9 ± 2.2	-1.2 ± 1.8
Max (%)	0.1	0.4	4.0	1.9	2.7	2.6
Min (%)	-2.2	-3.9	-2.7	-3.3	-3.7	-4.4

As shown in figure 1 the average pass rate obtained from the array measurements is in good agreement (average difference: (0.4 ± 1.0)%) with the average pass rate of the QA measurements provided by the participating institutes performed with their equipment for all the plans except for the simple VMAT plan.

Figure 1 Average pass rate (%) for (3%,3mm) criterion, (5%,1mm) for the stereotactic plan, for measurements obtained with the Octavius phantom and with the participating institute's patient specific QA phantom.

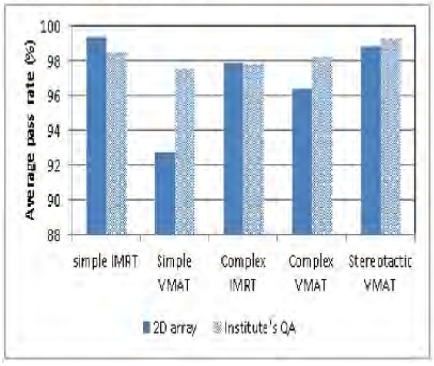

For the latter, the pass rate obtained with the Octavius is influenced by the sensitivity variation of the array as a function of gantry angle. Seven institutes out of 21 had plans that failed the audit gamma analysis pass rate tolerance of

95% while the institute's QA outcome was within tolerance (1 institute two plans, 6 institutes one plan). The film measurement results are still under investigation and therefore not presented in this abstract.

Conclusion: The results demonstrate that such a national QA audit is feasible. The reported in-house QA results were consistent with the audit despite differences in dosimetry equipment and analysis methods. Of the 21 Dutch centres audited, 67% passed the gamma analysis test for all the plans measured with a 2D-array by the audit team showing acceptable implementation of IMRT and VMAT delivery.

OC-0546

The development of proton-beam grid therapy (PBGT)

T. Henry[1], A. Valdman[2], A. Siegbahn[1]
[1]*Stockholm University, Department of Medical Radiation Physics, Stockholm, Sweden*
[2]*Karolinska Institutet, Department of Oncology and Pathology, Stockholm, Sweden*

Purpose or Objective: Radiotherapy with grids has previously been carried out with photon beams. The grid method is used as an attempt to exploit the clinical finding that normal tissue can tolerate higher doses as the irradiated volumes become smaller. In this work we investigated the possibilities to perform proton-beam grid therapy (PBGT) with millimeter-wide proton beams by performing Monte Carlo simulations of dose distributions produced by such grids. We also prepared proton-grid treatment plans with a TPS, using real patient data and beam settings available at modern proton therapy centers.

Material and Methods: Monte Carlo calculations were performed using TOPAS version 1.2.p2 in a 20x20x20 cm3 water tank. The beam grids (each containing 4x4 proton beams arranged in a square matrix) were aimed towards a cubic target at the tank center. A total of 2x2 opposing grid angles were used. The target was cross-fired in an interlaced manner. A beam-size study was carried out to find a suitable elemental beam size regarding beam thinness, peak-to-entrance dose ratio and lateral penumbra along the beam path. Dose distributions inside and outside of the target were calculated for beam center-to-center (c-t-c) separations inside the grids of 6, 8 and 10 mm.
The TPS study was performed with Varian Eclipse. We re-planned two patients (one liver cancer and one rectal cancer patient) already treated in the hospital with photon therapy with the suggested PBGT. The IMPT method was used to prepare these plans. The plan objectives were set to create a homogeneous dose inside the target.

Results: A beam size of 3 mm (FWHM) at the tank surface was found suitable from a dosimetric point of view for the further studies. By interlacing simulated beam grids from several directions, a cubic and nearly homogeneous dose distribution could be achieved in the target (see Figure 1). The c-t-c distance was found to have a significant impact on the valley dose outside of the target and on the homogeneity of the target dose. In the TPS study, a rather uniform dose distribution could be obtained inside of the contoured PTV while preserving the grid pattern of the dose distribution outside of it. The latter finding could be important for tissue repair and recovery.

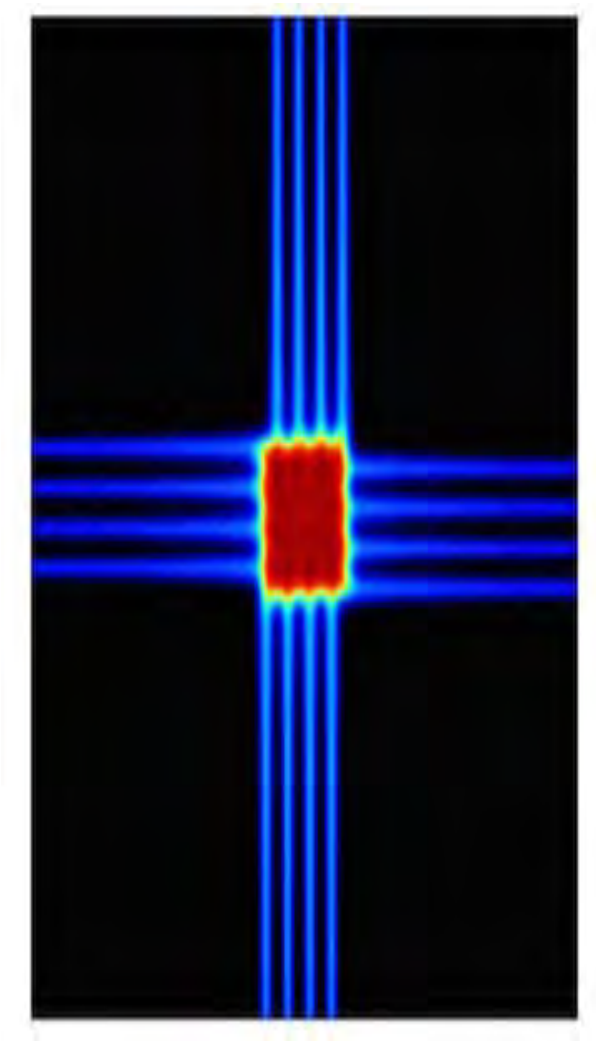

Conclusion: Proton-beam grids with 3 mm beam elements produce dose distributions in water for which the grid pattern is preserved down to large depths. PBGT could be carried out at proton therapy centers, equipped with spot-scanning possibilities, using existing tools. However, smaller beams than those currently available could be advantageous for biological reasons. With PBGT, it is also possible to create a more uniform target dose than what has been possible to produce with photon-beam grids. We anticipate that PBGT could be a useful technique to reduce both short- and long-term side effects after radiotherapy.

OC-0547

Towards Portal Dosimetry for the MR-linac: back-projection algorithm in the presence of MRI scanner

I. Torres Xirau[1], R. Rozendaal[1], I. Olaciregui-Ruiz[1], P. Gonzalez[1], U. Van der Heide[1], J.J. Sonke[1], A. Mans[1]
[1]*Netherlands Cancer Institute Antoni van Leeuwenhoek Hospital, Department of Radiation Oncology, Amsterdam, The Netherlands*

Purpose or Objective: Currently, various MR-guided radiotherapy systems are being developed and clinically implemented. For conventional radiotherapy, Electronic Portal Imaging Devices (EPIDs) are frequently used for in vivo dose verification. The high complexity of online treatment adaptation makes independent dosimetric verification in the Elekta MR-linac combination indispensable. One of the challenges for MR-linac portal dosimetry is the presence of the MRI housing between the patient and the EPID.
The purpose of this study was to adapt our previously developed back-projection algorithm for the presence of the MRI scanner.

Material and Methods: Three steps have been added to our current EPID dosimetry back-projection model to account for the presence of the MRI scanner: i) subtraction of scatter from the MRI to the EPID, ii) correction for the MRI attenuation, iii) compensation for changes in the beam spectrum. The calibration of the algorithm needs a set of commissioning data (from EPID and ionization chamber, both with and without the MRI) to determine the parameters for the back-projection method.
An aluminum block of 12 cm thickness at 15 cm distance from the EPID was used to approximate the effects of the MRI scanner. Measurements were performed using a 6MV photon beam of a conventional SL20i linear accelerator (Elekta AB, Stockholm, Sweden) at 0° gantry.
58 IMRT fields of 11 plans (H&N, lung, prostate and rectum) were delivered to a 20 cm polystyrene slab phantom and portal images were acquired with the aluminum plate in place. For independent comparison with our conventional method the same fields were delivered without the aluminum plate. The EPID images were converted to dose, corrected for the presence of the aluminum plate, back-projected into the phantom and compared to the planned dose distribution using a 2-D gamma evaluation (3%, 3 mm).

Results: The γ_mean averaged over the 58 IMRT fields was 0.39±0.11, the γ_1% was 1.05±0.30 and the %_γ≤1 was 95.7±5.3. The dose difference at the isocenter was -0.7±2.2 cGy. These results are in close agreement with the performance of our algorithm for the conventional linac setup (Table 1).

	γ_{mean}	$\gamma_{1\%}$	$\%\gamma_{\leq 1}$	ΔDose iso (cGy)
Conventional	0.35 ± 0.10	0.94 ± 0.18	98.1 ± 3.8	-1.9 ± 2.3
MR/aluminum	0.39 ± 0.11	1.05 ± 0.30	95.7 ± 5.3	-0.7 ± 2.2

Table 1: γ results (3%,3mm) averaged over the 58 IMRT fields. Our conventional back-projection method was used to back-project portal images acquired without the aluminum plate (top) and our adapted method was used to correct and back-project portal images acquired with the aluminum in place (bottom).

Conclusion: Our EPID dosimetry back projection algorithm was successfully adapted for the presence of an attenuating medium between phantom (or patient) and EPID. Experiments using a 12 cm aluminum plate (approximating the MR-linac geometry) showed excellent agreement between planned and EPID reconstructed dose distributions. This result is an essential step towards an accurate, independent, and potentially fast field-by-field IMRT portal dosimetry based verification tool for the MR-linac.
Part of this research was sponsored by Elekta AB.

OC-0548

Hyperthermia treatment planning in the pelvis using thermophysical fluid modelling of the bladder

G. Schooneveldt[1], H.P. Kok[1], E.D. Geijsen[1], A. Bakker[1], E. Balidemaj[1], J.J.M.C.H. De la Rosette[2], M.C.C.M. Hulshof[1], T.M. De Reijke[2], J. Crezee[1]
[1]Academic Medical Center, Radiotherapy, Amsterdam, The Netherlands
[2]Academic Medical Center, Urology, Amsterdam, The Netherlands

Purpose or Objective: Hyperthermia is a (neo)adjuvant treatment modality that increases the effectiveness of radiotherapy or chemotherapy by heating the tumour area to 41-43 °C. Loco-regional hyperthermia is delivered using phased array systems with individually controlled antennae. Hyperthermia treatment planning is necessary to determine the phase and amplitude settings for the individual antennae that result in the optimal temperature distribution. Current treatment planning systems are accurate for solid tissues but ignore the specific properties of the urinary bladder and its contents, which limits their accuracy in the pelvic region. This may have clinical implications for such treatment sites as the rectum, the cervix uteri, and the bladder itself. The aim of this study is to incorporate a physically correct description of the bladder properties in treatment planning, most notably the presence of convection and the absence of perfusion, and to assess the differences with the conventional model.

Material and Methods: We created a convective thermophysical fluid model based on the Boussinesq approximation to the Navier-Stokes equations; this means we assumed all parameters to be temperature independent except for the mass density in the gravitational term. We implemented this using the (finite element) OpenFOAM toolkit, and coupled it to our (finite difference) in-house developed treatment planning system, based on Pennes' bio-heat equation.
A CT scan was obtained from a bladder cancer patient and an experienced clinician delineated the bladder as part of the standard clinical work-flow. Based on this input, we first performed the treatment planning the conventional way with a muscle-like solid bladder, and calculated the optimal phase and amplitude settings for all four antennae. Next, we redid the temperature calculation with the expanded treatment planning system with a fluid-filled bladder, using the same settings. We subsequently calculated the differences between the two temperature distributions.

Results: The temperature in the bladder with realistic fluid modelling is much higher than without, as the absence of perfusion in the bladder filling leads to a much lower heat removal. The maximum temperature difference was 3.6 °C. Clinically relevant tissue temperature differences of more than 0.5 °C extended to 1.75 cm around the bladder. The temperature distribution according to the convective model and the difference with the solid only model are shown in Figure 1. The difference reflects the homogenizing effect of convection within the bladder and the nett heat transport in the upward direction.

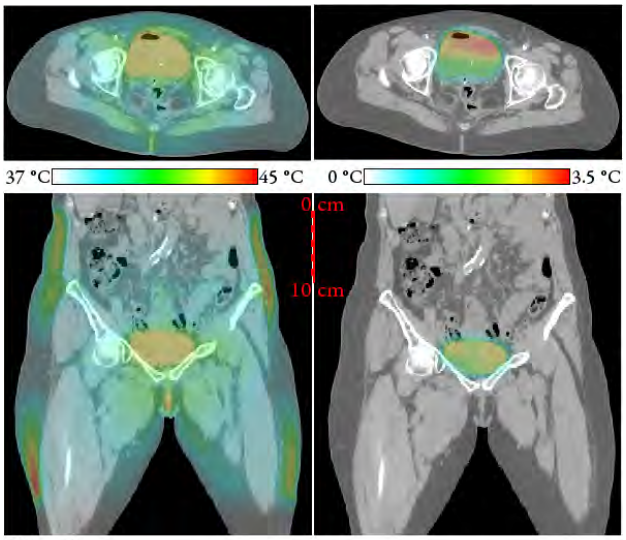

Figure 1.
Left: Temperature distribution at equilibrium according to the expanded treatment planning system with fluid dynamics. Note the homogeneous temperature distribution inside the bladder (top: axial view, bottom: coronal view).
Right: Temperature difference at equilibrium between the expanded treatment planning system with fluid dynamics and the traditional planning system without fluid dynamics. Note that the entire bladder, but especially the top half, is much warmer when fluid dynamics are accounted for. Clinically relevant effects extend to 1.75 cm around the bladder (top: axial view, bottom: coronal view).

Conclusion: The addition of the new convective model to the hyperthermia treatment planning system leads to clinically highly relevant temperature changes. Explicit modelling of fluids is particularly important when the bladder or its direct surroundings are part of the treatment target area.

Proffered Papers: Physics 14: Treatment planning: applications II

OC-0549

The effects of a magnetic field and real-time tumor tracking on lung stereotactic body radiotherapy

M.J. Menten[1], M.F. Fast[1], S. Nill[1], C.P. Kamerling[1], F. McDonald[1], U. Oelfke[1]

[1]*The Institute of Cancer Research and The Royal Marsden NHS Foundation Trust, Joint Department of Physics, London, United Kingdom*

Purpose or Objective: There have been concerns that the quality of highly conformal dose distributions, delivered under active MRI guidance, may be degraded by the influence of the magnetic field on secondary electrons. This planning study quantifies this effect for stereotactic body radiotherapy (SBRT) of lung tumors, conducted either with or without real-time multileaf collimator (MLC) tumor tracking.

Material and Methods: The Elekta Monaco treatment planning software, research version 5.09.07, was used to design treatment plans on the peak-exhale 4DCT phase of nine patients undergoing lung SBRT. The software features a machine model of the Atlantic MR-linac system and allows dose calculation and plan optimization under consideration of a magnetic field.

For each patient, we prepared four different 9-beam step-and-shoot IMRT plans: two for conventional, non-tracked treatment and two for delivery with real-time MLC tumor tracking, each delivered either with or without a 1.5T magnetic field oriented in the superior-inferior patient direction. For the conventional delivery, the internal target volume was defined as the union of the gross tumour volumes (GTV), delineated on each 4DCT phase. For the tracked delivery, the moving target volume was defined as union of all GTVs, each corrected for the center-of-volume shift thus accounting for target deformations. Dose was prescribed according to the RTOG 1021 guideline. Delivery of the respective plans was simulated to all 4DCT phases and the doses were then deformably accumulated onto the peak-exhale phase.

In order to evaluate the effect of the magnetic field and real-time tumor tracking, several dose-volume metrics and the integral deposited energy in the body were compared. Statistical significance of the differences was evaluated using a two-sided paired t-test after verifying normal distribution of them, while correcting for multiple testing for the four primary endpoints.

Results: The table presents the differences in the investigated dose-volume metrics due to either the presence of a magnetic field or real-time MLC tumor tracking. Most prominently, the magnetic field caused an increase in dose to the skin and a decrease of dose to the GTV (see figure). While statistically significant, the magnitude of these differences is small. In all 36 simulated dose deliveries, the dose prescription to the target was fulfilled and there were only minor violations of normal tissue constraints.

Real-time MLC tumor tracking was able to maintain dose coverage of the GTV while reducing the integral deposited energy. This results in a decrease in dose to the skin and normal lung tissue, both with and without a magnetic field.

	Effect of magnetic field during conventional delivery		Effect of magnetic field during MLC tracked delivery		Effect of real-time tumor tracking at 0T		Effect of real-time tumor tracking at 1.5T	
	Difference	p-value	Difference	p-value	Difference	p-value	Difference	p-value
GTV - $D_{99\%}$ [Gy]	−0.83 ± 0.91	0.03	−0.92 ± 0.76	0.0065	−0.04 ± 1.21	0.92	−0.12 ± 0.60	0.53
Skin - $D_{2\%}$ [Gy]	+1.29 ± 0.52	< 0.0001	+1.38 ± 0.55	< 0.0001	−0.45 ± 0.37	0.0064	−0.36 ± 0.47	0.05
Lungs - D_{mean} [Gy]	−0.09 ± 0.17	0.14	−0.15 ± 0.21	0.06	−0.26 ± 0.29	0.03	−0.32 ± 0.28	0.0063
Integral deposited energy [J]	+0.09 ± 1.17	0.84	−0.01 ± 1.72	0.99	−2.30 ± 2.80	0.07	−2.40 ± 2.61	0.05
Great vessels - $D_{2\%}$ [Gy]	+0.75 ± 1.58	0.19	−0.05 ± 1.73	0.91	−0.20 ± 1.02	0.56	−1.00 ± 0.98	0.02
Oesophagus - $D_{2\%}$ [Gy]	−0.58 ± 1.34	0.23	−1.15 ± 2.15	0.15	+0.52 ± 1.27	0.25	−0.06 ± 1.30	0.93
Proximal airways - $D_{2\%}$ [Gy]	−0.06 ± 0.90	0.83	−0.87 ± 1.85	0.20	+0.58 ± 1.09	0.15	−0.23 ± 0.89	0.46
Ribs - $D_{2\%}$ [Gy]	−0.57 ± 0.87	0.06	−0.63 ± 1.39	0.21	−0.71 ± 0.83	0.03	−0.77 ± 1.52	0.17
Skin - D_{mean} [Gy]	+0.10 ± 0.03	< 0.0001	+0.09 ± 0.03	< 0.0001	−0.05 ± 0.04	0.0054	−0.05 ± 0.04	0.007
Spinal cord - $D_{2\%}$ [Gy]	−0.50 ± 1.84	0.44	−0.11 ± 0.33	0.81	−0.50 ± 0.89	0.13	−0.11 ± 0.53	0.53

Changes with standard deviation in the evaluated dose-volume metrics and integral deposited energy due to either the presence of a 1.5 T magnetic field or real-time MLC tumor tracking, averaged over the entire patient cohort. Statistically significant differences are denoted by red font. The changes of the four primary endpoints are shown at the top of this table and were evaluated at a significance level of p = 0.0125. The differences in the dose-volume metrics investigated in an exploratory analysis are presented in the bottom and were evaluated at p = 0.05.

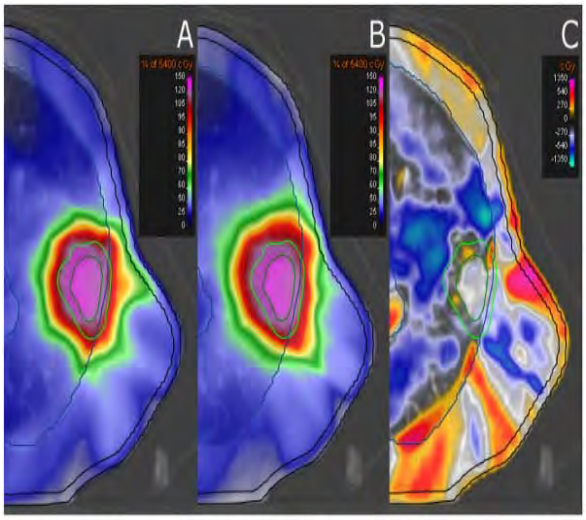

Transversal CT slice of a lung cancer patient. Overlaid are (A) the simulated dose delivered with a 1.5 T magnetic field present, (B) the simulated dose delivered without a magnetic field and (C) the local dose difference. The GTV is contoured in dark green, while the PTV is contoured in light green, the lung in blue and the skin in black.

Conclusion: This study has shown that accounting for the effects of the magnetic field during treatment planning allows for design of clinically acceptable lung SBRT treatments with a MR-linac. Furthermore, it was found that the ability of real-time tumor tracking to decrease dose exposure to healthy tissue was not degraded by a magnetic field.

OC-0550

Investigation of magnetic field effects for the treatment planning of lung cancer

O. Schrenk[1,2], C.K. Spindeldreier[1,2], A. Pfaffenberger[1,2]

[1]*German Cancer Research Center, Medical Physics in Radiation Oncology, Heidelberg, Germany*

[2]*Heidelberg Institute for Radiation Oncology HIRO, National Center for Radiation Research in Oncology, Heidelberg, Germany*

Purpose or Objective: Combining the capabilities of high resolution soft tissue MR imaging and intensity modulated radiation therapy into a hybrid device has the potential to increase the accuracy of radiotherapy. However, it is known that the magnetic field of the MR manipulates the trajectory of the secondary electrons and leads to a deviation of dose especially at the interfaces between high and low density materials. This study aims to introduce a routine for the evaluation of magnetic field effects to dose delivery and plan optimization using Monte Carlo simulations.

Material and Methods: An EGSnrc Monte Carlo environment, based on the egs++ class library, was developed which can be used for the simulation of IMRT treatment plans in the presence of a magnetic field, based on patient CT data. A routine for the processing of treatment planning parameters and Monte Carlo simulation data was implemented into the

in-house open source treatment planning system matRad. In order to basically validate the implementation, dose distributions at 0 T were compared against collapsed cone calculations by the treatment planning system RayStation. The effect of a magnetic field to the dose distribution was investigated for simulations in a porcine lung phantom. Based on Monte Carlo simulations of patient specific beamlets, plan optimization was performed and analyzed.

Results: Comparison showed that the Monte Carlo simulations of IMRT plans at 0 T are in good agreement with RayStation dose calculations. The effect of a 1.5 T lateral magnetic field on the dose distribution showed distinct alteration in tumor dose. Differences appear to be less when an opposing field technique is used. It could further be proven that the routine is capable of performing plan optimization based on Monte Carlo simulated beamlets in the presence of a magnetic field (see figure 1).

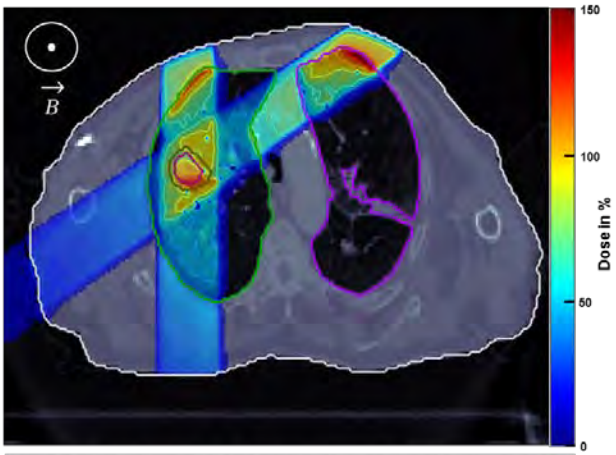

Figure 1: A simplified example of the forward simulation of unmodulated Monte Carlo beamlets in the presence of a lateral 1.5 T magnetic field. Dose hot spots (electron return effect, cf. Raaijkmakers, 2005) are evident at tissue lung interfaces and the tumor boundary.

Conclusion: A routine for dose calculation of IMRT plans with EGSnrc and for plan optimization based on Monte Carlo simulated beamlets using the in-house planning system matRad was developed. This implementation provides the possibility to analyze the effects of a magnetic field during radiotherapy in detail. Additionally it enables the investigation of optimization strategies for an MRI-LINAC system.

Acknowledgments: We thank Dr. Iwan Kawrakow for providing the egs++ magnetic field macro for the EGSnrc code system.

OC-0551

Advantage of IMPT over IMRT in treatment of gynaecological cancer with para-aortic nodal involvement

M. Van de Sande[1], C.L. Creutzberg[1], S. Van de Water[2], A.W. Sharfo[2], M.S. Hoogeman[2]

[1]*Leiden University Medical Center LUMC, Radiation Oncology, Leiden, The Netherlands*

[2]*Erasmus MC Cancer Institute, Radiation Oncology, Rotterdam, The Netherlands*

Purpose or Objective: High costs and limited capacity in proton therapy requires prioritizing according to expected benefit. The aim of this work is to quantify the clinical advantage of robust intensity-modulated proton therapy (IMPT) in terms of sparing of organs at risk (OARs) for three target volumes in treatment of gynaecological cancers compared with state-of-the-art intensity-modulated photon therapy (IMRT), and to evaluate for which target volume the benefit would justify the use of IMPT.

Material and Methods: Three target volumes were included: pelvic region (primary or postoperative treatment; N=10, 6 with boost dose), pelvic and para-aortic region (N=6, all with boost dose), para-aortic region alone (para-aortic recurrence, N=5, all with boost dose). Robust IMPT (minimax method) and 20-beam IMRT plans were generated with an in-house developed system for automated treatment planning. Prescription dose was 48.6 Gy with or without a simultaneous integrated boost to 58.05 Gy. IMPT and IMRT plans were made for wide (15 mm primary CTV/7 mm nodal CTV) and small (5/2 mm) CTV-PTV margins. IMPT plans included range robustness of 3% and setup robustness of 2 mm assuming online setup correction and adaptive radiotherapy. Relevant dose-volume parameters of OARs were used to compare both techniques.

Results: IMPT reduced the dose in all OARs for similar target coverage (>99%). The benefit of IMPT was higher in the lower dose region than in the higher dose region. Figure 1 compares OAR dose-volume parameters per patient. For treatment of the pelvic region, the dose in pelvic bones was on average 27% lower with IMPT; and in femoral heads 5% lower. For treatment of pelvic and para-aortic region, kidney and spinal cord dose was lower for IMPT (left kidney 1.1 Gy vs 7.8 Gy; right kidney 2.4 Gy vs 11.8 Gy; spinal cord 14.5 Gy vs 28.0 Gy). For the para-aortic region alone an important advantage in favour of IMPT was seen (left kidney 4.4 Gy vs 38.6 Gy; right kidney 0.5 Gy vs 5.8 Gy; spinal cord 29.2 Gy vs 39.7 Gy), see Table 1. For all target volumes clinically relevant reductions in V15Gy for the bowelbag were found, reducing V15Gy by 153 cc, 1231 cc, and 523 cc, respectively. Differences in dose to most OARs were similar for wide and small margins, while the advantage of IMPT was more pronounced for rectum, bladder, and sigmoid using small margins.

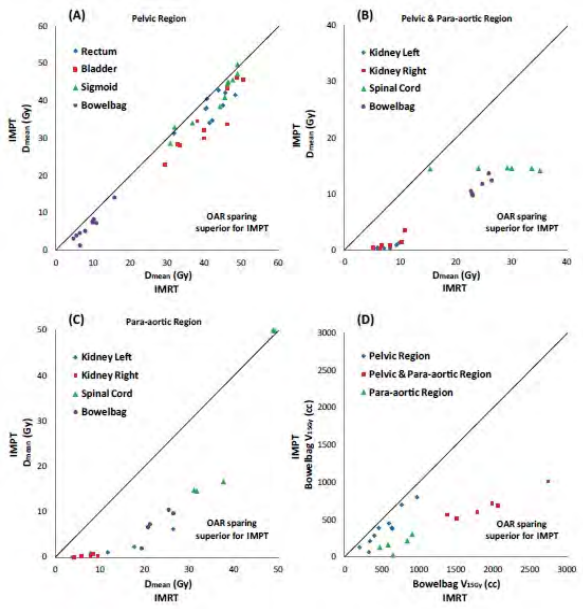

Conclusion: For all gynaecological target volumes, IMPT reduced the dose to all OARs compared with IMRT, mainly in the lower dose region and for both wide and small margins. Considerable reduction of the bowel volume receiving 15 Gy or more was seen. The greatest and clinically relevant advantage of IMPT was found for treatment of macroscopic disease in the para-aortic region, justifying the use of proton therapy for this indication.

OAR	Parameter		Para-aortic region (N=5, including para-aortic boost)* Wide margin IMPT	Wide margin IMRT	Small margin IMPT	Small margin IMRT
Bowelbag	V_{15Gy} (cc)	Mean	172	695	96	583
		Range	[30-308]	[475-913]	[13-165]	[416-818]
		Difference	75%		84%	
	V_{45Gy} (cc)	Mean	48	65	16	31
		Range	[11-96]	[14-127]	[2-35]	[5-62]
		Difference	26%		48%	
Kidney left	V_{15Gy} (%)	Mean	4.4	38.6	1.3	26.4
		Range	[0.0-13.3]	[0.2-85.2]	[0.0-4.9]	[0.2-76.4]
		Difference	89%		95%	
Kidney right	V_{15Gy} (%)	Mean	0.5	5.8	0.0	0.7
		Range	[0.0-1.7]	[0.0-13.3]	[0.0-0.0]	[0.0-1.7]
		Difference	91%		95%	
Spinal cord	D_{max} (Gy)	Mean	29.2	39.7	28.5	36.2
		Range	[14.6-50.0]	[31.1-49.2]	[14.6-49.5]	[23.3-49.0]
		Difference	26%		21%	

OC-0552

Skin-NTCP driven optimization for breast proton treatment plans

L. Cella[1], F. Tommasino[2], V. D'Avino[1], G. Palma[1], F. Pastore[3], M. Conson[3], M. Schwarz[4], R. Liuzzi[1], R. Pacelli[3], M. Durante[2]

[1]*National Research Council CNR, Institute of Biostructure and Bioimaging IBB, Napoli, Italy*

[2]*National Institute for Nuclear Physics INFN, Trento Institute for Fundamental Physics and Applications TIFPA, Trento, Italy*

[3]*Federico II University School of Medicine, Department of Advanced Biomedical Sciences, Napoli, Italy*

[4]*Azienda Provinciale per I Servizi Sanitari APSS, Protontherapy Department, Trento, Italy*

Purpose or Objective: Proton beam therapy represents a promising modality for left breast irradiation due to negligible dose to non-target volume, as heart and lung. However skin toxicity and poor cosmesis inherent to protons physical properties are of major concern. Radiation-induced skin toxicity (RIST) is a side effect impacting on the quality of life in breast cancer patients treated with radiation therapy. Purpose of the present study is twofold: a) to develop a normal tissue complication probability (NTCP) model of severe acute RIST in BC patients treated with conventional three-dimensional conformal radiotherapy (3DCRT) and b) to use the implemented skin NTCP model to guide breast proton therapy plan optimization.

Material and Methods: We evaluated 140 consecutive BC patients undergoing 3DCRT after breast conserving surgery in a prospective study assessing acute RIST. Acute RIST was classified according to the RTOG scoring system. Dose-surface histograms (DSHs) of the body-structure in the breast region were extracted. DSHs of the body were considered as representative of the irradiation in epidermis and dermis layers and extracted by an in-house developed library using the relative complement in the body of its 3D erosion defined by a spherical structuring element of radius r = 3 mm (assumed as mean skin thickness). On such shell, the absolute dose-volume histogram was regularly computed and then divided by r to obtain the DSH. NTCP modeling by Lyman-Kutcher-Burman (LKB) recast for DSHs and using bootstrap resampling techniques was performed. Five randomly selected left BC patients were then replanned using proton pencil beam scanning (PBS). PBS plans were obtained to ensure appropriate target coverage (90% 50 Gy(RBE) prescription dose to the 90% breast) and heart-lung sparing. Different planning objectives for skin were used (Table 1) and two different beam set-ups were tested. The proton plan body DSHs were extracted and the corresponding NTCP values calculated.

Table 1

Planning objectives/ constraints	Plan set up A Single oblique beam	B Single oblique beam	C Tangential beams
CTV	Uniform Dose=50 Gy	Uniform Dose=50 Gy	Uniform Dose=50 Gy
Ipsilateral lung	D_{15}≤20Gy D_{35}≤10Gy D_{40}≤5Gy	D_{15}≤20Gy D_{35}≤10Gy D_{40}≤5Gy	D_{15}≤20Gy D_{35}≤10Gy D_{40}≤5Gy
Contralateral lung	D_{10}≤5Gy	D_{10}≤5Gy	D_{10}≤5Gy
Heart	D_5≤20Gy D_{30}≤10Gy	D_5≤20Gy D_{30}≤10Gy	D_5≤20Gy D_{30}≤10Gy
Skin	Dmax= 50 Gy	Dmax=30 Gy	Dmax=30 Gy
# patient			
1	0.66	0.23	0.19
2	0.62	0.19	0.09
3	0.63	0.20	0.06
4	0.62	0.21	0.03
5	0.65	0.25	0.14
Average skin NTCP ± SD	0.64 ± 0.02	0.24 ± 0.02	0.10 ± 0.06
Average CTV $V_{95\%}$± SD	100.0±0.4%	93±1 %	93±1%
Average CTV D_2± SD	51.0±0.1 Gy	51.5±0.4 Gy	52.0±0.3Gy

Abbreviations: Dx= the minimum dose to x% highest dose volume, Dmax= maximum dose, Vx= volume receiving at least X Gy, NTCP= normal tissue complication probability, CTV= clinical target volume

Results: By the end of 3DCRT, severe (RTOG G3 vs. G0-2) acute RIST was found in 11 out of 140 (8%) patients. Using DSHs for LKB modeling of acute RIST severity (estimated model parameter: TD50=39 ± 4 Gy, m=0.13 ±0.08, n=0.36 ±0.05) a good prediction performance was obtained (Rs= 0.3, AUC= 0.8, p=0.003). When used to guide parameter choice in proton PBS optimization, our NTCP model suggests that the probability of having acute RIST can be on average lowered by a factor 2.7 using a single oblique beam or even by a factor 6 with a tangential-beam set up (Table 1 and Figure 1a) at negligible expense of target coverage (Figure 1b).

Figure 1

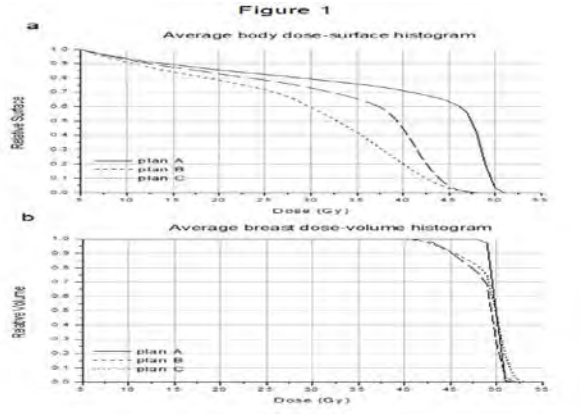

Conclusion: Robust LKB NTCP model with a good prediction performance for acute RIST can be derived using the body DSHs of the irradiated area. The obtained skin NTCP represents a valuable tool for breast proton plan optimization and evaluation in order to reduce the risk of acute skin toxicity.

OC-0553

Relative risks of radiation-induced secondary cancer following particle therapy of prostate cancer

C. Stokkevåg[1], M. Fukahori[2], T. Nomiya[2], N. Matsufuji[2], G. Engeseth[1], L. Hysing[1], K. Ytre-Hauge[3], A. Szostak[3], L. Muren[4]

[1]*Haukeland University Hospital, Department of Oncology and Medical Physics, Bergen, Norway*

[2]*National Institute of Radiological Sciences, Research Center for Charged Particle Therapy, Chiba, Japan*

[3]*University of Bergen, Department of Physics and Technology, Bergen, Norway*

[4]*Aarhus University Hospital- Aarhus, Department of Medical Physics, Aarhus, Denmark*

Purpose or Objective: An elevated risk of secondary cancer (SC) has been observed in prostate cancer patients following radiotherapy (RT). Particle therapy has in general a considerable potential of reducing the irradiated volumes of healthy tissues, which is expected to have a positive effect on radiation-induced cancer. However, the carcinogenic effect of RT in the high dose region is uncertain, and is influenced by fractionation, radio-sensitivity, relative biological effects (RBE) as well as patient-specific patterns in the dose distributions. The aim of this study was therefore to

estimate relative risks (RR) of secondary bladder and rectal cancer using dose distributions from x-ray, proton and carbon(C)-ion therapy as applied in contemporary clinical practice. We also included a model parameter scan to identify the influence of variations in typical values of these parameters.

Material and Methods: Treatment plans for volumetric modulated arc therapy (VMAT, Eclipse), intensity-modulated proton therapy (IMPT; Eclipse) and C-ions (XiO-N) were generated for ten prostate cancer patients. For all three modalities, the primary clinical target volume included the prostate gland and the seminal vesicles, while technique specific boost volumes included the prostate only. Both VMAT and IMPT plans were prescribed to deliver 67.5 Gy(RBE) to the prostate and 60 Gy(RBE) to the seminal vesicles over 25 fractions (assuming fiducial margin based set-up). The C-ion plans comprised 12 fractions with 34.4 Gy(RBE) to the total target volume and 51.6 Gy(RBE) to the boost volume (bony anatomy set-up). Physical dose distributions of the bladder and rectum were used to estimate the RR of radiation-induced cancer (VMAT/IMPT and VMAT/C-ion) using the published malignant induction probability model (J Radiol Prot 2009). The mean RR results presented were calculated by sampling the dose distributions of all ten patients and previously published model input parameters with the listed confidence intervals (CI) (Table I). Subsequently a parameter scan was performed over a wide range of possible RBEs and radio-sensitivity (α and ß) values.

Results: The mean estimated RR (95% CI) of SC for VMAT/C-ion were 1.31 (0.65, 2.18) for the bladder and 0.58 (0.41, 0.80) for the rectum. Corresponding values for VMAT/IMPT were 1.73 (1.07, 2.39) and 1.11 (0.79, 1.45), respectively (Table I). The radio-sensitivity parameter α had the strongest influence on the RR for both the investigated organs; decreasing for increasing values of α (Fig 1). The ß parameter influences the RR significantly only for very low α values (below about 0.2).

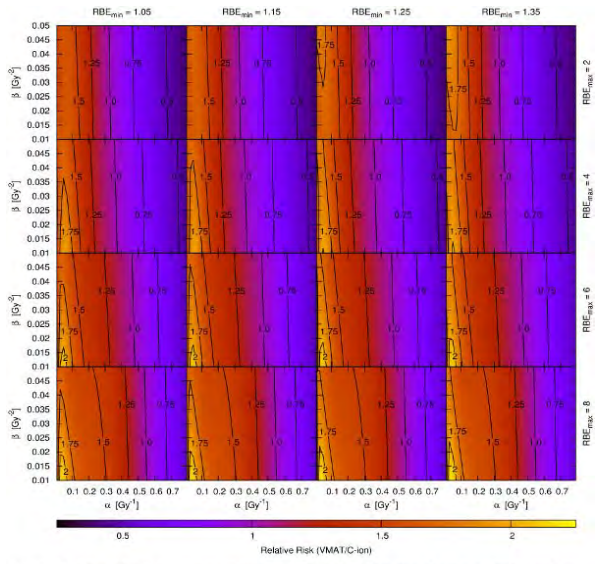

Figure 1. Relative risk (RR) parameter scan for mean bladder dose distribution. RR >1 means higher risk from VMAT compared to C-ions, while RR<1 means higher risk from C-ions compared to VMAT.

Table I. Estimated Relative Risks, model parameters and input distributions

	Bladder	Rectum	CI
RR (VMAT/C-ion)	1.31 (0.65, 2.18)	0.58 (0.41, 0.80)	95%
RR (VMAT/IMPT)	1.73 (1.07, 2.39)	1.11 (0.79, 1.45)	95%
α (Gy^{-1})	0.25 (σ=0.075)	0.25 (σ=0.075)	Gaussian
B (Gy^{-2})	0.033 (σ=0.0055)	0.046 (σ=0.0077)	Gaussian
RBE_{min} (C-ion)	1.25 (1.2, 1.3)	1.25 (1.2, 1.3)	triangle
RBE_{max} (C-ion)	6 (5, 7)	6 (5, 7)	triangle
RBE_{min} (proton)	1.03 (1.01, 1.05)	1.03 (1.01, 1.05)	triangle
RBE_{max} (proton)	1.25 (1.2, 1.3)	1.25 (1.2, 1.3)	triangle

Conclusion: Based on the modest variations in RR across the large spread in parameter values, the treatment modalities are not expected to have very different SC risk profiles with respect to these organs. The α value had the strongest influence on the RR and may change the RR in favour of one technique instead of another (particle vs photons).

OC-0554

Robustness recipe for minimax robust optimisation in IMPT for oropharyngeal cancer patients

S. Van der Voort[1], S. Van de Water[1], Z. Perkó[2], B. Heijmen[1], D. Lathouwers[2], M. Hoogeman[1]

[1]*Erasmus Medical Center Rotterdam, Erasmus MC Cancer Center, Rotterdam, The Netherlands*

[2]*Delft University of Technology, Department of Radiation Science and Technology, Delft, The Netherlands*

Purpose or Objective: Treatment plans for intensity-modulated proton therapy (IMPT) can be robustly optimized by performing 'minimax' worst-case optimization, in which a limited number of error scenarios is included in the optimization. However, it is currently unknown which error scenarios should be included for given population-based distributions of setup errors and range errors. The aim of this study is to derive a 'robustness recipe' describing the setup robustness (SR; in mm) and range robustness (RR; in %) settings (i.e. the absolute error values of the included scenarios) that should be applied in minimax robust IMPT optimization to ensure adequate CTV coverage in oropharyngeal cancer patients, for given Gaussian distributions of systematic and random setup errors and range errors (characterized by standard deviations Σ, σ and ρ, respectively).

Material and Methods: In this study contoured CT scans of 6 unilateral and 6 bilateral oropharyngeal cancer patients were used. Robustness recipes were obtained by: 1) generating treatment plans with varying robustness settings SR and RR, 2) performing comprehensive robustness analyses for these plans using different combinations of systematic and random setup errors and range errors (i.e. different values of Σ, σ and ρ), and 3) determining the maximum errors for which certain SR and RR settings still resulted in adequate CTV coverage. IMPT plans were considered adequately robust if at least 98% CTV coverage (V95%≥ 98%) was achieved in 98% of the simulated fractionated treatments. Robustness analyses were performed using Polynomial Chaos methods, which allow for fast and accurate simulation of the expected dose in fractionated IMPT treatments for given error distributions. Separate recipes were derived for the unilateral and bilateral cases using one patient from each group. The robustness recipes were validated using all 12 patients, in which 2 plans were generated for each patient corresponding to Σ = σ = 1.5 mm and ρ = 0% and 2%.

Results: The robustness recipes are depicted in Figure 1. We found that 1) systematic setup errors require larger SR than random setup errors, 2) bilateral cases are intrinsically more robust than unilateral cases, 3) the required RR only depends on ρ, and 4) the required SR can be fitted by second order polynomials in Σ and σ. The formulas for the robustness

recipes are: SR = $-0.15\Sigma^2 + 0.27\sigma^2 + 1.85\Sigma - 0.06\sigma + 1.22$ and RR = 3% for ρ = 1% and 2% for unilateral cases, and SR = $-0.07\Sigma^2 + 0.19\sigma^2 + 1.34\Sigma - 0.07\sigma + 1.17$ and RR = 3% and 4% for ρ = 1% and 2%, respectively, for bilateral cases. The recipe validation resulted in 22 plans being adequately robust, while for the remaining two plans CTV coverage was adequate in 97.8% and 97.9% of the simulated fractionated treatments.

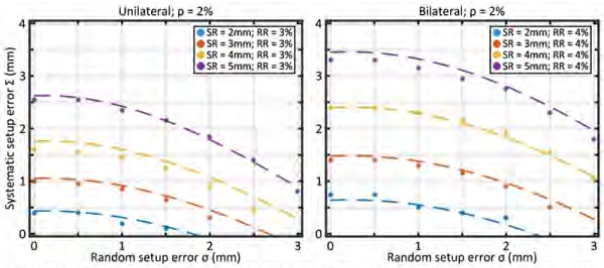

Figure 1. Combinations of systematic (Σ) and random (σ) setup errors that give adequate CTV coverage (V95% ≥ 98%) for 98% of the simulated fractionated treatments for a range error (ρ) of 2% for a unilateral and bilateral patient. In each plot different SR and RR settings are shown. The solid round markers show the obtained data, the dashed lines are a quadratic fit.

Conclusion: Robustness recipes were derived that can be used in minimax robust optimization of IMPT treatment plans to ensure adequate CTV coverage for oropharyngeal cancer patients.

Proffered Papers: RTT 6: Advanced radiation techniques in prostate cancer

OC-0555

Organ at risk dose parameters increased by daily anatomic changes in prostate cancer SBRT

M. Faasse-de Hoog[1], M.S. Hoogeman[1], J.J.M.E. Nuyttens[1], S. Aluwini[1]
[1]*Erasmus MC Cancer Institute, Radiation Oncology, Rotterdam, The Netherlands*

Purpose or Objective: Stereotactic body radiotherapy (SBRT) is increasingly used to treat low and intermediate stage prostate cancer (PC). In our institution, SBRT is delivered in 4-5 fractions of high dose using the CyberKnife system with marker-based tracking. Tracking accurately aligns the treatment beams to the prostate just prior and during the treatment fraction. However, surrounding organs at risks (OARs) may move relative to the prostate, causing the OAR dose to deviate from what was planned. The aim of this work is to quantify the daily dose to OARs in SBRT for PC, and compare it to the planned dose.

Material and Methods: For 9 patients, four to five repeat CT scans were acquired prior to each daily SBRT fraction and were analyzed. The bladder, rectum, anus, and urethra were contoured in the planning and repeat CTs. The urethra was divided in three parts: the cranial and the caudal part of the urethra prostatica (UP) and the membranous urethra (MU, 2 cm caudal to the prostate). The repeat CTs were aligned to the planning CT based on the four implanted markers. Subsequently, the planned dose distribution was projected on the aligned repeat CTs. For each patient, dose-volume parameters of the OARs were recorded, averaged over the 4-5 repeat CTs and compared to planning.

Results: The greatest deviation between the delivered and planned dose was seen for the MU. The planned mean dose of 24.0 Gy was exceeded in the repeat CTs by on average 59±17% (1 SD) and the D5% was increased by 7±3%, from 38.7 to 41.6 Gy (Fig. 1a). For the mean dose of the caudal and cranial UP the deviation from planning was limited: 1±1% and 5±5% respectively. The planned mean and V1cc (dose allowed to 1cc of the organ) rectum dose, 10.9 and 32.8 Gy respectively, was on average 5±5% and 12±11% higher in the repeat CTs (Fig. 1b). The mean dose of the anus increased as well, with 15±24% from 8.7 to 9.8 Gy. The planned V1cc bladder dose (40.2 Gy) was reproducible in the repeat CTs (difference: 1±1%). The planned mean bladder dose (18.4 Gy) was slightly reduced in the repeat CTs (-6±7%).

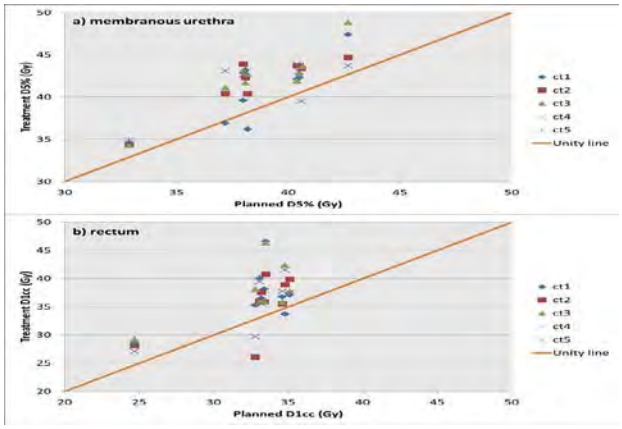

Conclusion: For the membranous urethra, rectum, and anus, the dose in the repeat CTs was higher than was planned. This warrants future research investigating whether increased dose leads to increased incidence of side effects and whether dose increases should be mitigated by treatment adaptations.

OC-0556

Early clinical outcomes of prostate SABR treated with VMAT-FFF

A. Duffton[1], C. Duncanson[1], S. Paterson[1], L. Dallas[1], S. Smith[1], M. McJury[1], C. Lamb[1], N. MacLeod[1], A. Sadozye[1], D. Dodds[1]
[1]*The Beatson West of Scotland Cancer Centre, Radiotherapy, Glasgow, United Kingdom*

Purpose or Objective: Endpoints for this ethically approved clinical study:
- Assess the feasibility of planning SABR for low-intermediate risk prostate cancer using flattening filter free volumetric arc therapy.
- Assess safety of treatment delivery by recording RTOG scoring criteria of acute gastro-intestinal (GI) and genito-urinary (GU) toxicity.

Material and Methods: 25 patients were included, each has 18 week toxicity data.
Inclusion criteria:
Written informed consent, 18 - 80 years, T1-T2 stage, WHO performance status ≤ 2. Initial PSA ≤ 20 ng/ml. Gleason score ≤7 with histologically-proven prostate adenocarcinoma. No pathologic lymph nodes on CT/ MRI scans and no distant metastases. No previous prostate surgery, including transurethral resection of the prostate no TURP in past 6 months. No previous active malignancy within the last 10 years.
A prescription dose of 35Gy in 5 fractions was treated alternate days. This was planned using Rapidarc VMAT planning on Varian Eclipse (V.10), treated using a Varian Truebeam STX.
A clinically acceptable plan was determined by assessing the planned dose to GTV/PTV criteria and achieving dose constraints (table 1).

	Objective	Mean	SD
GTV V95%	>99%	99.8	0.4
PTV V95%	>95%	96.5	1.4
max PTV point dose		108.4	2.3
Rectum V18Gy	<35%	28.0	5.2
Rectum V28Gy	<10%	8.6	2.7
Rectum V32Gy	<5%	4.0	1.7
Rectum V35Gy	<1%	0.0	0.0
Baldder V35Gy	<1%	0.0	0.0
Beam on time (BOT)		120.5	0.2

Table 1. Planning data for first 25 patients

GI, GU and skin toxicity was scored using Radiation therapy oncology group (RTOG) criteria. Baseline data was recorded before treatment commenced (baseline), week 4 and week 18.

Results: Results include first 25 patients.
Age range was 52-78, median 70, initial PSA median 4.3-29.2, median 10.8ng/ml. All patients were successfully planned and treated with VMAT-FFF with plans being deemed clinically acceptable for 100% of patients.
GU and GI toxicity at baseline, week 4 and week 18 is detailed for each grade below, respectively.
GU toxicity:
Grade 0 - 44%, 12%, 48%
Grade 1 - 52%, 56%, 48%
Grade 2 – 4%, 28%, 4%
Grade 3 – 0%, 4%, 0%
For GU toxicity, a statistically significant increase in toxicity was observed from baseline to week 4 (p=<0.01) and a significant reduction from week 4 to week 18 (p=<0.01). No significant difference was observed between baseline and week 18, with toxicity reducing to similar levels as baseline.
GI toxicity (baseline, week 4, week 18):
Grade 0 – 96%, 52%, 72%
Grade 1 – 4%, 40%, 28%
Grade 2 – 0%, 8%, 0%
Grade 3 – 0%,0%, 0%
GI toxicity significantly increased from baseline to week 4 (p=<0.01). From week 4 to week 18, toxicity had reduced (p=<0.05). A significant difference was observed between baseline and week 18 (p=<0.05) with toxicity having reduced, but not having returned to baseline grade.

Conclusion: Highly conformal plans were created for all patients. Toxicity was acceptable throughout, with toxicity at week 18 reducing to that of baseline for GU toxicity, and reducing significantly for GI toxicity. 1 patient experienced grade 3 GU toxicity at week 4, this resolved by week 10. Longer follow-up is required to assess late outcomes.

OC-0557
Feasibility of single fraction HDR brachytherapy in patients with prostate cancer: a planning study
M. Roos[1], C. De Pan[1], I.K.K. Kolkman-Deurloo[1], S. Aluwini[1]
[1]*Erasmus MC Cancer Center, Radiation Oncology, Rotterdam, The Netherlands*

Purpose or Objective: To investigate the feasibility of single fraction High Dose Rate (HDR) brachytherapy (BT) as monotherapy for low risk prostate cancer.

Material and Methods: CT scans of 30 patients were selected from our prostate HDR database. Patients were divided in groups based on prostate volume (< 40cc, 40-70cc and >70cc) and the number of needles used (13-16 and 17-22). The existing needle geometry was used to regenerate new treatment plans for three radiation schemes: 1x19.0Gy, 1x19.5Gy and 1x20Gy. All plans were optimized according to the following objectives:
Prostate V100% ≥ 95% Prostate D90% ≥ 100%
Bladder D1cc < 16.0 Gy Bladder D2cc < 15.5 Gy
Rectum D1cc < 15.5 Gy Rectum D2cc < 14.5 Gy Rectum V100% 0 cc
Urethra D0,1cc < 21.0 Gy Urethra D10% < 20.5 Gy Urethra V120% 0 cc
A total of 90 plans were generated using an inverse planning module. The planning target volume (PTV) was the prostate without margins. The coverage of the prostate was maximized considering the dose constraints for the organs at risk (OAR). The primary end point of this study was the feasibility of above mentioned target coverage and OAR constraints. The secondary end point was to investigate the restricting factors to reach a feasible plan stratified to prostate volume, OAR position and implant geometry.

Results: The average prostate V100% for the 19.0, 19.5 and 20.0Gy schemes was 96.6%, 95.3% and 93.0% respectively with 83%, 57% and 33% of plans meeting this objective. The D90% of the prostate averaged 20.3 Gy , 20.3 Gy and 20.4 Gy respectively. Only 4 plans failed this objective.
The 40-70cc group showed an average prostate V100% of 96.3% an increase of 2.1% and 2.7% compared to the < 40cc and >70cc group respectively.
The number of needles had no influence on prostate coverage and urethra constraints. The rectum and bladder D1cc and D2cc increased for the 17-22 needle group with 5.7%, 8.6% and 3.3%, 5.3% respectively.
The average prostate V100% decreased in patients with a larger distance between the urethra and the posterior border of the prostate.
Prostate V100% increased from 95.7% to 97.5% in patients with a prostate to rectum distance of 2mm or more.

Conclusion: Single fraction HDR brachytherapy as monotherapy in patients with prostate cancer is feasible using our current implant geometry. Considering the OAR constraints, an acceptable D90% was reached in 96% of plans.Prostate volume, implant geometry and OAR proximity have a substantial impact on target coverage.

OC-0558
Automated VMAT planning in prostate cancer patients using a Single Arc SIB Technique
N. Simpson[1], G. Simpson[1], R. Laney[1], A. Thomson[1], D. Wheatley[1], R. Ellis[1], J. Mcgrane[1]
[1]*RCHT, Medical Physics, Truro, United Kingdom*

Purpose or Objective: To evaluate the feasibility of automated single arc treatment planning for prostate cancer patients using a commercially available treatment planning system. We also compared the resultant AutoplanningTM plans with our current institutional inverse planned prostates.

Material and Methods: A technique was created within the AutoplanningTM module of the PinnacleTM treatment planning system using institutional prescription dose/fractionation and OAR constraints to be delivered with a single arc VMAT plan. The Planning Target Volume **PTV1 (74Gy)** encompasses the prostate; **PTV2 (66.6Gy)** encompasses the prostate and the base or full seminal vesicles plus setup margins both delivered simultaneously in 37 fractions. Plans were generated for 10 randomly selected patients with prostate cancer treated at our institution, using the automated treatment technique template. Plan quality was assessed using institutional criteria and ICRU 83 criteria: D98, D2, Conformity Index (CI), Homogeneity Index (HI) and Remaining Volume at Risk (RVR). OAR constraints for rectum D65<30%, Bladder D50<50%, Femoral Heads, D50< 50%. Bowel D50<50cc, D55<14cc and D60< 1cc were assessed. The time for planning was also documented.
The ten AutoplanningTM technique plans were compared with clinical institutional VMAT prostate plans in a blinded study.

Plans were compared by Clinical Oncologists, assessing clinical coverage of the PTVs, OAR sparing and DVH parameters.

Results: Table 1 summarises results of the automated plan generation. The automated technique produced highly conformal plans that met institutional clinical constraints for 7 of 10 plans in a single run. In the 3 cases that failed, overlap of the PTV with rectum or bowel exceeded institutional DVH goals (Fig 1). There were no significant differences between the two planning techniques when comparing CI and HI.

Volume	Dose	Vol (%)	Mean	SD
PTV				
PTV1 (Min)	D63.27	98	99.81	+/-0.395
PTV1 (Max)	D75.48	2	0.13	+/-0.108
PTV2 (Min)	D70.3	98	99.99	+/-0.031
PTV2 (Max)	D70.0	2	0.04	+/-0.005
CI PTV1			1.17	+/-0.06
CI PTV2			1.09	+/-0.02
HI PTV1-2			0.012	+/-0.006
HI PTV2			0.035	+/-0.00
RVR (Mean -Gy)			23.369	+/-4.93
OAR				
Rectum	D65	<30	17.61	+/-3.964
Bladder	D50	<50	17.11	+/-5.748
Femoral Heads	D50	<50	0	+/-0
Bowel	D4.5	<50	18.82	+/-19.44

Table 1 Dosimetric Results for PTV and OAR with Automated Planning Technique

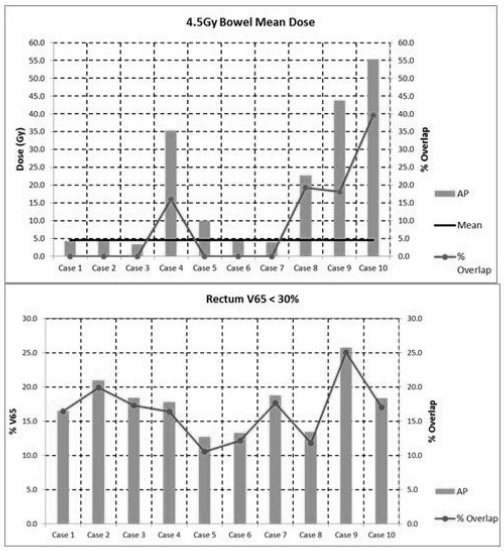

Fig 1. Impact of PTV overlap on Mean OAR doses for automated planning technique.

Conclusion: The automated technique for VMAT planning for prostate cancer is a promising solution which is feasible and may improve efficiency by automating cases that meet institutional dose volume constraints. We will present the results of the blinded plan selection study at the meeting.

OC-0559

The impact of rectal interventions on target motion and rectal variability in prostate radiotherapy

C. Smith[1], B. O'Neill[2], L. O'Sullivan[2], M. Keaveney[2], L. Mullaney[1]

[1]*Discipline of Radiation Therapy- School of Medicine- Trinity Centre Dublin, Radiation Therapy, Dublin, Ireland Republic of*

[2]*St Luke's Radiation Oncology Network- Beaumont Hospital, Radiation Therapy Department, Dublin, Ireland Republic of*

Purpose or Objective: Target position is variable during fractionated prostate radiotherapy, mainly due to rectal changes. Margin reduction is preferable with the advancements of modulated techniques and IGRT. However, geometric uncertainty can persist in the absence of an intervention to minimise rectal motion. The purpose of this study is to retrospectively evaluate the effectiveness of three rectal emptying strategies in maintain rectal stability and reducing target motion during prostate radiotherapy.

Material and Methods: Four cohorts of consented prostate patients (total n=37) underwent different rectal strategies: daily phosphate enema; low-fibre diet and microlax microenema and no intervention (control). Using retrospective CBCT data, (8 CBCTs per patients), inter-fraction PTV motion relative to bony anatomy was measured using automatic bone anatomy registration, followed by an automatic Structure Volume of Interest (SVOI) match. Changes in rectal diameter (RD) at the base, mid and apex of the prostate and rectal volume (RV) were measured using the CBCT data. Frequency of prostate geometric miss was assessed, with a miss defined as any PTV shift in any direction.

Results: PTV displacement was significantly reduced in the anteroposterior (AP) direction in the microlax group (p=0.004), and in the superoinferior (SI) direction in the phosphate enema group (p=0.013) when compared with the control group (Table 1). The frequency of geometric miss was lowest in the microlax group. RD variability at the base of prostate was significantly smaller in the microlax and phosphate enema groups compared to the control group stats, and variation in RV was smallest in the microlax group. PTV motion and rectal variability were largest in the control group.

Table 1: Mean (μ), Systematic (Σ), and Random (δ) PTV displacements (mm) in the anteroposterior (AP), superoinferior (SI) and left-right (LR) directions for each group. Negative values indicate posterior, inferior and left PTV displacements from bony anatomy.

	Daily Phosphate Enema n=9			Microlax Microenema n=8			Low-Fibre Diet n=10			No Intervention (Control) n=10		
	AP	SI	LR	AP	SI	LR	AP	SI	LR	AP	SI	LR
μ (mm)	-1.2*	0.3*	-0.1	-0.7*	-0.6	0.3	-1.1*	-1.3	-0.2	-2.6*	-1.9*	0.3
Σ (mm)	0.8	1.6	0.6	0.6*	0.4*	0.6	1.0	1.1	1.1	1.6*	1.9*	0.7
δ (mm)	1.4	1.0	0.5	0.8*	0.9	0.6	1.5	1.7	0.7	2.0*	1.6	0.9

*Significant difference ($p<0.05$) when compared with the control group statistics.

Conclusion: Microlax microenema is an effective intervention in maintaining rectal stability, and PTV motion during prostate radiotherapy, in patients with large RD (≥4cm) on planning CT.

OC-0560

Plan of the day approach in post prostatectomy radiation therapy

C. Lac[1], A. Sims[1], T. Eade[1,2], A. Kneebone[1,2]

[1]*Central Coast Cancer Centre, Radiation Oncology, Gosford, Australia*

[2]*Northern Sydney Cancer Centre, Radiation Oncology, St Leonards, Australia*

Purpose or Objective: Our primary aim is to investigate the frequency of using smaller margins for post prostatectomy radiotherapy (RT) in conjunction with daily soft tissue image guided radiotherapy (IGRT). Our secondary aim is to assess the feasibility of implementing an adaptive, 'plan of the

day', treatment approach by selecting an appropriate plan on a daily basis which will highly conform to the target and minimise rectal and bladder toxicities.

Material and Methods: Retrospectively identified 19 post prostatectomy patients. Soft tissue matching guidelines were created and split into two categories; patients with or without surgical clips. Soft tissue match was performed on cone-beam CT (CBCT) in offline review program by two radiation therapists and reviewed by two radiation oncologists. The frequency of geographic miss was measured using a planning target volume (PTV) small with a 5 mm clinical target volume (CTV) expansion and PTV large with 10 mm (15 mm anteriorly) CTV expansion. To implement a 'plan of the day' treatment approach, a post prostatectomy soft tissue training module was developed to educate the radiation therapists to perform daily soft tissue alignment. Radiation therapists will then apply an adaptive RT regime that selects from a plan library to account for internal organ inconsistencies of the bladder and rectum.

Results: A total of 135 CBCTs were reviewed on 19 radical post prostatectomy patients including those with lymph node involvement. Retrospective soft tissue match analysis determined that PTV small covered the target for 84% of CBCTs while the PTV large covered the target for 16%. There was no geographic miss outside PTV large in this retrospective analysis. In the matches that resulted in the selection of PTV large, 12% of CBCTs were due to variations in bladder filling and 4% from rectal filling.

Conclusion: PTV small is suitable for use on most CBCTs with PTV large selected for only a small portion of CBCTs. Very small bladders caused a greater amount of bladder and small bowel to fall in the target and increases the chance of side effects but rarely causes a geographic miss. Over filling bladders on CBCTs was undesired as it caused internal pelvic tilt in the superior portion resulting in a selection of the plan with PTV large. A dangerous combination is present if there are inconsistencies to both the bladder and rectum filling causing the CTV prostate bed region to tilt and fall outside of the target. With a high frequency of using PTV small, and a better understanding of the effect of bowel and bladder filling, implementation of 'plan of the day' is feasible. This will result in a highly targeted treatment delivery in conjunction with soft tissue IGRT that will reduce toxicities and increase local control.

Poster Viewing : 12: Physics: Dose measurement and dose calculation III

PV-0561

Validation of an optimised MC dose prediction for low energy X-rays intraoperative radiation therapy

P. Ibáñez[1], M. Vidal[1], P. Guerra[2], J.M. Udías[1]
[1]*Universidad Complutense de Madrid, Física Atómica-Molecular y Nuclear, Madrid, Spain*
[2]*Universidad Politécnica de Madrid, Ingeniería Electrónica, Madrid, Spain*

Purpose or Objective: Low energy X-rays Intra-Operative Radiation Therapy (XIORT) is increasingly used in oncology, predominantly for breast cancer treatments with spherical applicators [1], but also for skin or gastrointestinal cancer [2] with surface and flat applicators. This study aims to validate a fast and precise method [3,4] to calculate Monte Carlo (MC) dose distributions with an optimized phase space file (PSF) obtained from a previously stored database of monochromatic PSF and depth dose curves (DDP) for different INTRABEAM® (Carl Zeiss) applicators. To validate this procedure, we compared dose computed with the PSF with measurements in phantoms designed to prove actual XIORT scenarios.

Material and Methods: PSF were optimized from experimental DDP in water and were employed to calculate dose distributions, first in water, then in validation phantoms such as air gaps or bone inhomogeneities, for all flat, surface and spherical applicators. Measurements with Gafchromic EBT3 films were performed. Irradiated films were scanned with an EPSON Expression 10000XL flatbed scanner (resolution 72 ppi) after a polymerization time of at least 24 h, and the three-channel information corrected for inhomogeneity [5] was used to derive dose. Calibration films were irradiated from 0 Gy to 5 Gy for surface and flat applicators and from 0 Gy to 20 Gy for spherical applicators. Simulations and experimental data were compared in detail.

Results: MC simulations are in good agreement with experimental data, at the 3%-1 mm level (10% dose threshold) for most setups, well within what is needed for XIORT planning. Accuracy of the comparison was mostly limited by the difficulty in assuring geometrical positioning within 1 mm or less of the physical phantoms. An example of dose distribution on a heterogeneous phantom of PMMA and bone for a 3 cm flat applicator is shown in **figure 1**.

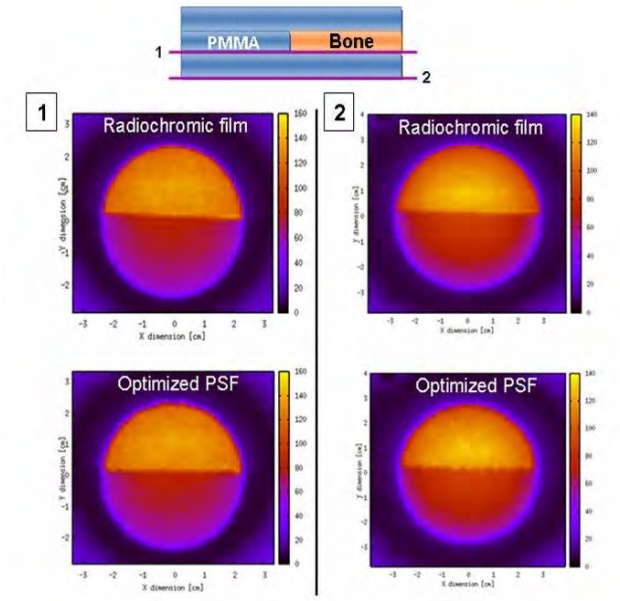

Figure 1. Experimental (top) and simulated (bottom) dose distributions of a PMMA-bone phantom with a 3 cm diameter flat applicator. More than 90% voxels pass the 3%-1mm gamma test.

Conclusion: Preliminary results show that the optimized Monte Carlo dose calculation reproduces dose distributions measured with different applicators, accurately enough for XIORT planning. The method is flexible and fast, and has been incorporated in Radiance® [6], a treatment planning system for intraoperative radiation therapy developed by the GMV company.

[1] Vaidya, J. S. *et al*. 2010. TARGIT-A trial. Lancet, 376, 91-102.
[2] Schneider, F. *et al.* 2014. *J Appl Clin Med Phys,* 15, 4502.
[3] Vidal M. *et al.* 2015. Rad. and Oncol. *115, 277-278.*
[4] Vidal M. *et al.* 2014. Rad. and Oncol. 111, 117-118.
[5] A.Micke *et al*. 2011. Med. Phys.,38(5), 2523-2534.
[6] J.Pascau *et al*. 2012. Int. J. Radiat. Oncol. Biol. Phys. 83(2), 287-295

PV-0562

Hadron-therapy monitoring with in-beam PET: measurements and simulations of the INSIDE PET scanner

F. Pennazio[1], M. Bisogni[2], N. Camarlinghi[2], P. Cerello[1], E. Fiorina[1], M. Morrocchi[2], M. Piliero[2], G. Pirrone[2], R. Wheadon[1]
[1]*Università degli Studi di Torino and INFN, Physics, Torino, Italy*
[2]*Università degli Studi di Pisa and INFN, Physics, Pisa, Italy*

Purpose or Objective: In-beam PET exploits the ß+ activation induced in the patient's body by the hadron-therapy (HT) particle beam to perform treatment monitoring

and dose-delivery accuracy assessment. The INSIDE collaboration is building an in-beam PET and tracker combined device for HT. In this work we focus on the preliminary PET measurements performed at the CNAO (Italian Hadron-therapy National Center) synchrotron facility and on Monte Carlo simulations.

Material and Methods: The PET module block is made of 16x16 Lutetium Fine Silicate scintillator elements 3.2x3.2x20 mm^3 each, coupled one-to-one to a Silicon Photomultiplier matrix, read out by the TOFPET ASIC. The scanner will feature two 10x20 cm2 planar heads, made by 10 modules each, at a distance of 25 cm from the iso-centre. Preliminary tests investigated the performance of one module per head at nominal distance. Monoenergetic proton pencil beams of 68, 72, 84 MeV and 100 MeV were targeted to a PMMA phantom placed inside the FOV of the two detectors. The CNAO synchrotron beam has a periodic structure of 1 s beam delivery (spill) and 4 s interval (inter-spill). Acquisition was performed both in- and inter-spill. A 250 ps coincidence window is applied to find the LORs and reconstruct the image with a MLEM algorithm. Monte Carlo (MC) simulations are used in HT for detector development and treatment planning. In case of 3D online monitoring, they could also be used to compare the acquired image, which is a measurements of the activity, with the expected distribution, and hence to assess the treatment accuracy. Taking into account the detection and digitisation processes, it is also possible to reconstruct the simulated image. MC simulations, performed with FLUKA, were used to assess the expected performance and also compared to the measured activity profiles.

Results: Acquisition has been successfully performed in both inter-spill and in-spill mode. The inter-spill and in-spill Coincidence Time Resolution (CTR) between the two modules, measured without a fine time calibration, is 459 ps and 630 ps σ, respectively. The larger in-spill value is expected and related to background uncorrelated events. The images profile along the beam axis for the 68 and 72 MeV beam energies, which have a range short enough to be stopped by the phantom inside the FOV (5x5x5 cm^3), show the characteristic distal activity fall-off. The expected proton range difference in PMMA for 68 and 72 MeV (3.64 mm) is compatible with the experimental measurement (3.61±0.10 mm), obtained by fitting with sigmoid functions the fall-off of the image profiles (fig. 1). The same behaviour is found in simulated images.

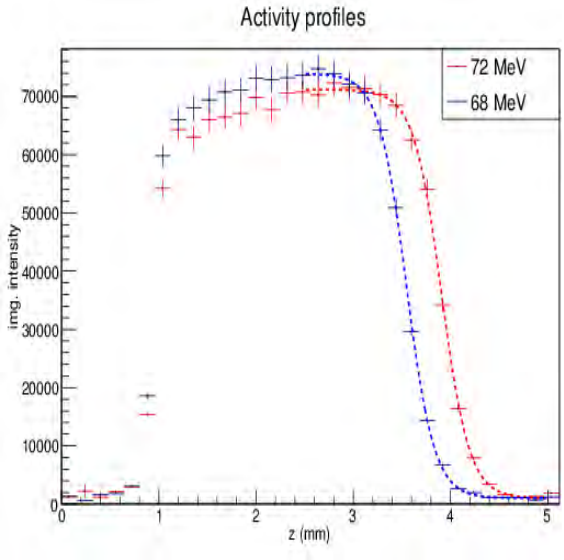

Conclusion: Tests with proton beams and prototype detector modules has confirmed the feasibility of the INSIDE in-beam PET monitoring device. Simulations are in good agreement with data and could be used to calculated the expected activity distribution measured by the PET scanner.

PV-0563

Dosimetric comparisons of 1H, 4He, 12C and 16O ion beams at HIT

T. Tessonnier[1,2], A. Mairani[3,4], S. Brons[4], T. Haberer[4], J. Debus[1,4], K. Parodi[2,4]

[1]*Hospital University of Heidelberg, Department of Radiation Oncology, Heidelberg, Germany*

[2]*Ludwig Maximilians University, Department of Medical Physics, Munich, Germany*

[3]*Centro Nazionale di Adroterapia Oncologica, CNAO, Pavia, Italy*

[4]*Heidelberg Ion Beam Therapy Center, HIT, Heidelberg, Germany*

Purpose or Objective: The interest in particle therapy, with light and heavy ion beams, has grown worldwide, due to their beneficial physical and biological properties. At the Heidelberg Ion beam Therapy Center, four ions are available for irradiation with an active scanning beam delivery system: 1H, 4He, 12C and 16O. While most of the actual studies comparing different characteristics of the ions are based on Monte Carlo or analytical dose calculations, we present here an experimental based comparison for spread-out Bragg peaks (SOBP) and a first clinical-like scenario study, experimentally validated.

Material and Methods: Several SOBP have been planned with 1H, 4He, 12C and 16O ions, at four different clinically relevant positions (5, 8, 15 and 20 cm) and different irradiation volumes (10x10x4 cm^3 / 3x3x2 cm^3). The measurements have been done in a water tank coupled with 24 motor-driven PinPoint ionization chambers. Delivery is applied with an active scanning beam delivery system. Both depth-dose and lateral dose profiles are investigated at different depth for each SOBP. We compare several parameters: the entrance-to-plateau ratio, the lateral penumbra along the depth, the fall-off, and the distal dose due to the fragmentation tail for ions with Z>1. For the clinical case, representing a meningioma treatment, the dose has been biologically optimized for every ion on the target volume. Experimental validations of the calculated physical dose have been made in the same water phantom.

Results: Dosimetrically, the plans doses for the SOBPs and the measured ones are within +/- 5% (figure 1). Measurements show that physically optimized SOBPs present different behavior depending on the ion used, field size and depth. These dosimetric characteristics exhibit several advantages and/or inconvenients depending on the ion used. This may help improving dose distribution during treatment planning. For the clinical-like scenario, the different ions show different characteristics on the dose distributions, impacting either the conformity to the target or the organ at risk sparing. The measurements in the water phantom show agreement within 5% to the physically planned dose.

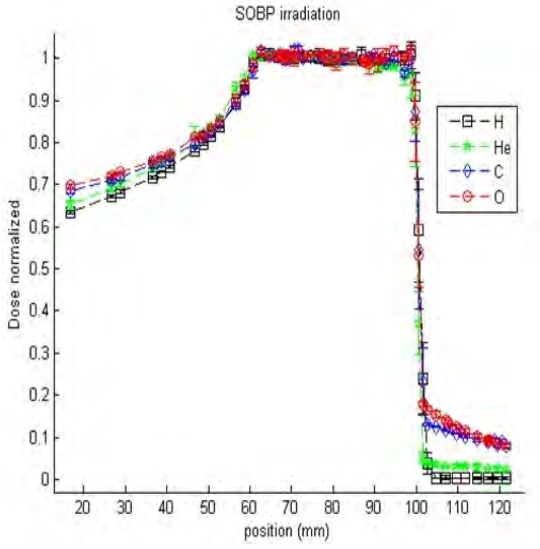

Figure 1: SOBPs measurements for irradiation (at 8cm volume of 10x10x4cm^3) with 1H, 4He, 12C or 16O

Conclusion: Although its therapeutic use had been discontinued after the end of the clinical experience at the Berkeley National Laboratory in 1992, our experimental results indicate 4He as a good candidate for further particle therapy improvements due the favorable physical characteristics, especially due to the smaller lateral scattering than 1H and the very low tail-to-peak ratio compared to 12C or 16O. For the clinical like scenario, 4He present interesting results for organ at risk sparing with a good conformity to the target. But one have to remind that even if the physical dose measured is matching with the planned one, proper validated biological model have to been used for the ions to have a fair comparisons.

PV-0564

Experimental validation of proton stopping power calculations based on dual energy CT imaging

J.K. Van Abbema[1], M.J. Van Goethem[2], J. Mulder[2], A.K. Biegun[1], M.J.W. Greuter[3], A. Van der Schaaf[2], S. Brandenburg[1], E.R. Van der Graaf[1]

[1]University of Groningen- Kernfysisch Versneller Instituut - Center for Advanced Radiation Technology, Medical Physics, Groningen, The Netherlands

[2]University of Groningen- University Medical Center Groningen, Radiation Oncology, Groningen, The Netherlands

[3]University of Groningen- University Medical Center Groningen, Radiology, Groningen, The Netherlands

Purpose or Objective: To improve the accuracy of proton dose calculations using dual energy X-ray computed tomography (DECT) based proton stopping powers.

Material and Methods: The CT densities of 32 different materials (table) have been measured with DECT in a 33 cm diameter Gammex 467 tissue characterization phantom. The phantom has been scanned with a clinical 90 kV / 150 kV (with additional Sn filtration) DE abdomen protocol (CTDIvol = 15.52 mGy) in a dual source CT system (SOMATOM Force). A Qr40 strength 5 ADMIRE kernel with a slice thickness of 1 mm has been used for the reconstruction. Using the method developed by van Abbema et al (Ref), effective atomic number (Z') and electron density ($\rho e'$) images have been derived. A fit from Z' to the logarithm of the mean excitation energy ($\ln(I)$) has been determined based on calculated values for Z' of 80 average tissues described by Woodard and White and measured values for Z' from DECT. Depth dose profiles of 190 MeV protons have been measured using a Markus chamber in a water phantom (figure) with a step size of 0.2 mm in the Bragg peak. The range R80% (distal 80% of the dose) after traversing a material in water has been measured relative to the R80% in water only, for three different depths of the material in water. Geant4 simulations have been performed to obtain depth dose profiles from specified elemental composition and density of the materials. A method has been developed to predict the energy loss in the material from DECT determined values for $\rho e'$ and $\ln(I)$. The derived relative stopping powers (RSPs) for the materials have been compared to RSPs determined from range differences measured in the water phantom.

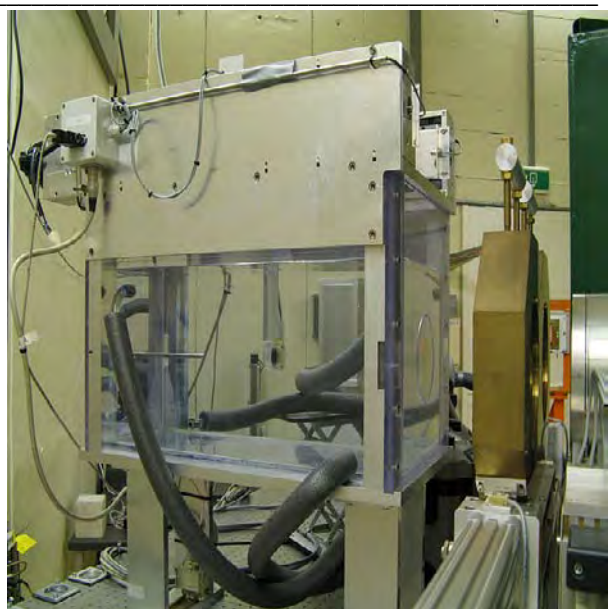

Results: Effective electron densities $\rho e'$ derived from DECT have been determined with accuracy better than -0.9 to 0.7%, except for the inhomogeneous LN-450 material, Teflon and aluminium (table). The fit from Z' to $\ln(I)$ deviates -2.2 to 1.6% from calculated values of the 80 average tissues. For the 32 materials, the fit deviates -2.9 to 2.8% from calculated values (excl. carbon, Teflon, aluminium and Al2O3). Depth dose profiles in water have been measured with a reproducibility of the R80% < 0.1 mm. For 18 analysed materials (151 MeV at sample), RSPs determined from the Geant4 simulations are within 0.2 to 3.5% of the experimental RSPs. The RSPs determined from the Z' and $\rho e'$ derived from DECT are within -0.6 to 4.1% (excl. aluminium) of the experimental RSPs (table).

No.	Material	ρ_e' meas-calc [%]	RSP Sim-Exp [%]	RSP DECT-Exp [%]
1	LN-450 Lung	3.1	0.4	4.0
2	AP6 Adipose	0.5	0.2	1.3
3	BR-12 Breast	0.7	2.7	3.5
4	Solid Water M457	0.1	2.2	2.4
5	LV1 Liver	0.4	2.1	2.7
6	SB3 Cortical Bone	0.6	3.3	4.1
7	n-Pentane	0.1		
8	n-Hexan	-0.5		
9	n-Heptane	-0.2	0.7	-0.6
10	Methanol	-0.4	1.0	0.1
11	Ethanol	0.6	0.5	1.1
12	Propan-1-ol	-0.7	0.8	-0.3
13	Propan-2-ol	0.1	0.9	0.4
14	Oleic acid	0.2	0.9	1.0
15	Ethyl acetoacetate	0.0	0.6	1.9
16	Water	-0.4		
17	Polyethylene glycol 200	-0.6	0.9	0.8
18	Glycerol	-0.9	1.1	1.0
19	Silicon oil Siluron 5000	0.2		
20	Potassium Chloride 4.01%	0.1		
21	Potassium Chloride 7.71%	0.0		
22	Potassium Chloride 11.13%	0.1		
23	Potassium Chloride 20.03%	0.2		
24	Carbon	0.5		
25	UHMWPE	0.6	1.5	1.3
26	Polypropylene	0.0	3.5	2.0
27	Nylon 6.6-101	-0.3		
28	PMMA	-0.2		
29	Polycarbonaat	-0.3		
30	Teflon	-1.4		
31	Aluminium	1.7	2.0	12.0
32	Al_2O_3 99.7%	0.5		

Conclusion: DECT enables accurate $\rho e'$ determination for dose calculations. Combined with a translation of the measured Z' to $\ln(I)$, proton stopping powers can be calculated with high accuracy.

Reference

van Abbema J K, van Goethem M J, Greuter M J W, van der Schaaf A, Brandenburg S and van der Graaf E R 2015 Relative electron density determination using a physics based parameterization of photon interactions in medical DECT *Phys. Med. Biol.* **60**, 3825–46.

PV-0565

Dosimetric response maps of diode and diamond detectors in kilovoltage synchrotron beams

T. Wright[1], D. Butler[1], A. Stevenson[2], J. Livingstone[2], J. Crosbie[3]
[1]*ARPANSA, Radiotherapy Section, Yallambie, Australia*
[2]*Australian Synchrotron, Imaging and Medical Beamline, Clayton, Australia*
[3]*RMIT University, School of Applied Sciences, Melbourne, Australia*

Purpose or Objective: To measure the spatial response of diode and diamond detectors commonly used in radiotherapy to a sub-millimetre beam of kilovoltage synchrotron radiation.

Material and Methods: The spatial dosimetric response of three detectors was measured on the Imaging and Medical Beamline (IMBL) at the Australian Synchrotron. The signals from a PTW 60016 Dosimetry Diode P, PTW 60017 Dosimetry Diode E and the PTW 60019 microDiamond were continuously measured during a series of line scans to create two-dimensional maps of the response of each detector to a sub-millimeter kilovoltage beam. Dosimetric maps were collected for both side-on and end-on orientations. Detectors were also radiographed to help identify internal components.
The radiation beam was a low-divergence, high dose-rate beam of kilovoltage synchrotron x-rays, collimated to 0.1 mm in diameter with a tungsten pinhole. The weighted-average energy was 95 keV. The scanning system and its application to ionisation chambers are described in reference [1].

Results: End-on results show the spatial uniformity of each detector with a resolution of about 0.1 mm. The active volume is clearly seen as a disc in each case. The response is found to vary by 3% across the central 1.5 mm of the two diode detectors. Fig. 1(a) shows an end-on contour map of the electron diode. The central 1.5 mm of the microDiamond contained a sensitive spot where the response was approximately 30% higher than the remaining detector area. Some structure is visible where wires behind the active volume affect the response.
Side-on results show the active volume as a line because the thickness of the active volume (27 microns for the diodes and 1 micron for the diamond) is much less than the scan resolution. Contributions from outside the active area can also be seen. In the photon diode the shield is visible and the active area is recessed from the end surface when compared to the electron diode. The microDiamond response is almost exclusively due to the response in the active detector area. Fig. 1(b) shows a side-on contour map of the electron diode and Fig. 1(c) shows a radiograph of the microDiamond.

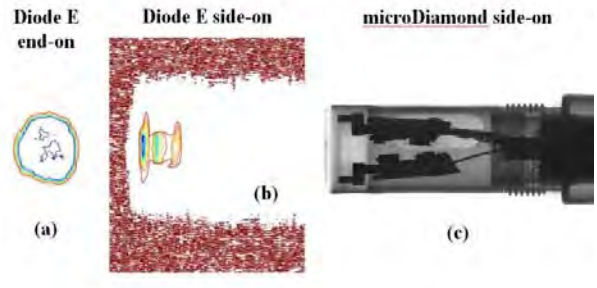

Conclusion: A synchrotron dosimetric scanning technique has been shown to work for common solid state detectors. The technique is able to measure the spatial uniformity and contribution from material around the active region, for kilovoltage beams.

Ref:

[1] DJ Butler et al., "High spatial resolution dosimetric response maps for radiotherapy ionization chambers measured using kilovoltage synchrotron radiation", Phys. Med. Biol. (accepted for publication)

PV-0566

Improving image reconstruction for Compton camera based imaging for proton radiotherapy verification

E. Draeger[1], S. Peterson[2], D. Mackin[3], S. Beddar[3], J. Polf[1]
[1]*University of Maryland Medical Center, Radiation Oncology, Baltimore- MD, USA*
[2]*University of Cape Town, Physics, Cape Town, South Africa*
[3]*University of Texas MD Anderson Cancer Center, Radiation Oncology, Houston- TX, USA*

Purpose or Objective: To improve analysis and reconstruction techniques for data measured with a Compton Camera (CC) imaging system for prompt gamma imaging for proton radiation therapy.

Material and Methods: The CC consists of four detector stages containing CdZnTe (CZT) crystals. Two stages contain crystals with dimensions of 20 mm x 20 mm x 15 mm, while the other two stages have crystals with dimensions of 20 mm x 20 mm x 10 mm. Rather than looking at γ interactions that occur in multiple detector stages, double- or triple-scatter events from γ-rays emitted from a 60Co point source (2 mm full width at half maximum) that occurred in only one detector plane were studied. Using triple-scatter events in a single stage, 2D images of the γ emission were reconstructed. The energy deposited in the first interaction (*Edep1*) as a function of the scatter angle (θ) of the γ was analyzed (see Fig. 1A). Next, the measured triple-scatter data was filtered so that it included only events satisfying the "Compton line" equation,

$$E_{dep1} = E_{\gamma 0}\frac{\alpha(1-\cos\theta)}{1+\alpha(1-\cos\theta)}$$

where α=Eγ0/(me*c^2), *me* is the rest mass of the electron, and *Eγ0* is the initial energy of the γ. Finally, the Compton line filtered triple-scatter data was used to reconstruct 2D images of the γ emission and was compared to the image reconstructed using all triple-scatter events.

Results: There was a dramatic difference in the position reconstruction of the point source, as seen in images reconstructed with all measured triple-scatter interactions in one CC stage (see Fig. 1B) and images reconstructed using only measured triple-scatter interactions in one stage that were within ±10% of the Compton lines (see Fig. 1C). The location of the source in both runs was -40 ± 2 mm along the z-axis. Fig. 1D shows that all measured data gives a reconstructed source position of -21 mm (19 mm from the actual source position), while filtering the data gives a reconstructed position of -41 mm (1 mm from the actual source position and within the uncertainty of the source position). Following tests of the Compton line filtering technique with point sources, initial imaging tests are being completed for measured data of prompt gammas emitted during irradiation of a water phantom with clinical proton therapy beams.

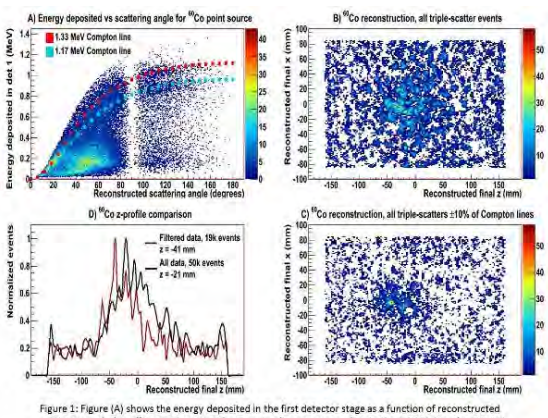

Figure 1: Figure (A) shows the energy deposited in the first detector stage as a function of reconstructed scattering angle for a ^{60}Co point source. The Compton lines corresponding to the 1.17 MeV and 1.33 MeV ^{60}Co γ's are overlaid for reference. Figure (B) and Figure (C) show the reconstructed positions of the ^{60}Co point source for the non-filtered data and filtered data, respectively. Figure (D) shows the z-profiles of the filtered (red) and non-filtered (black) point source reconstructions. The unfiltered reconstruction contained 50,000 events, the filtered reconstruction contained 19,000 events (statistics limited), and the point source was positioned along the z-axis at -40 ± 2 mm.

Conclusion: We have developed a new method of analyzing and filtering data from a Compton camera that can be used to greatly improve the image quality and position reconstruction of prompt gammas. With this new filtering method, the position localization was improved from within 19 mm of the actual source location to within 1 mm of the actual source location for the filtered data.

Teaching Lecture: The new 'Rs' in radiation biology

SP-0567
The new 'R's; in radiation biology

M.C. De Jong[1], M.W.M. Van den Brekel[2], M. Verheij[1]
[1]*Netherlands Cancer Institute Antoni van Leeuwenhoek Hospital, Department of Radiation Oncology and Department of Biological Stress response, Amsterdam, The Netherlands*
[2]*Netherlands Cancer Institute Antoni van Leeuwenhoek Hospital, Department of Head and Neck Oncology and Surgery- The Netherlands Cancer Institute. and Department of maxillofacial surgery- Academic Medical Center-University of Amsterdam., Amsterdam, Th*

Over the last decades the precision of radiotherapy delivery has vastly improved. Using the newest image-guided, intensity-modulated radiotherapy techniques radiation oncologists can be fairly sure that two identical patients with seemingly identical tumors will receive the same radiotherapy dose distribution. In these cases, reasons for radiotherapy failure within the field cannot be found in clinical factors or in the delivery of the radiotherapy, but must be sought in the (heterogeneous) biological makeup of the tumor. Knowledge of an individual tumor's biology could contribute to a better prediction of radiotherapy failure and the design of approaches to radiosensitize resistant tumors.
The classical biological factors influencing radiotherapy response conveniently all start with a ´R´: Reoxygenation, Redistribution, Repair and Repopulation. Intrinsic Radiosensitivity has been added as a fifth factor to describe the difference in radiosensitivity of individual cells. This factor can be broken down into three main mechanisms. Firstly, a difference in radiosensitivity could be explained by a difference in received damage upon irradiation, for example due to different levels of reactive oxygen scavengers. Secondly, a difference in (DNA) repair capability is a well-known cause for variation in intrinsic sensitivity. Thirdly, tumor cells can respond differently to inflicted damage depending on their ability to engage cell cycle or cell death pathways.
In recent years new factors have been added to the list of 'Rs'. The most important new players are cancer stem cells, the tumor microenvironment, the immune response, the cell's energy metabolism, angiogenesis and vasculogenesis. Although new techniques like pre-treatment expression profiling enable us to study different biological processes simultaneously, some major challenges remain in the accurate prediction of radioresponse. The most important relates to (spatial and temporal) tumor heterogeneity: different cells within a tumor could have different properties and all biological factors mentioned (and possible more that are yet to be discovered) could interact with each other, making it difficult to assess the overall effect within a tumor. In addition, little is known about the changes in biological behavior of a tumor during a course of fractionated radiotherapy.
This lecture will address these new R's in radiation biology and their relevance for clinical practice.

Teaching Lecture: Texture analysis of medical images in radiotherapy

SP-0568
Texture analysis of medical images in radiotherapy

E. Scalco[1], G. Rizzo[1]
[1]*Istituto di Bioimmagini e Fisiologia Molecolare, CNR, Segrate Milano, Italy*

The wide availability of tomographic images acquired before, during and after radiation treatment had offered the possibility to improve diagnosis and treatment evaluation in a non-invasive way. Image analysis is widely performed to extract parameters in different contexts, as, for example, for the identification of tumoral tissues with respect to normal tissues, for the correct classification of tumor grade, for the evaluation of treatment efficacy or its side-effects on organs at risks, or for the prediction of radiation-induced toxicities. The classical image analysis methods are based on the evaluation of some geometric features (volume, dimension, short-axis length, …) or the mean gray-level intensity of the organ of interest. Also when functional images are considered (e.g. PET, DWI-MRI, DCE-MRI), the quantitative analysis of functional information is usually carried out in a ROI-based approach, considering only the average value within a region of interest. However, since the spatial organization of a tissue is an important marker both for the identification of abnormal tissues and for the evaluation of radiation-induced variations, it is worth considering the structural patterns of the image, generally lost in a ROI-based approach. For this purpose, texture analysis can be very helpful in extracting features able to characterize the structural information hold in these images. This is true when anatomical images (CT, MRI) are considered, because textural features can directly reflect the structural properties of the region, but also when functional images are analyzed, since the functional behavior of a tissue cannot be properly captured by a simple average value. Texture analysis can be faced in many different ways; the most used in literature are the First-Order statistical method, based on the histogram, the second-order statistical method, based on co-occurrence matrices, the steerable Gabor filter, the fractal-based features, the run length matrices and the Fourier transform. These methods, in general, extract a large number of features, which can be used for classification or prediction models. For this purpose, a selection method able to identify the most significant parameters is required, followed by an automatic classification method (e.g. support vector machine, neural networks, random forests, linear discriminant analysis, Bayesian methods, fuzzy-logic analysis). In this lesson, some of these approaches will be presented, focusing, in particular, on statistical and fractal-based methods and their biological meaning. Moreover, an overview of the different applications of texture analysis in radiotherapic context is presented, considering different image modalities (CT, anatomical MRI, DWI-MRI, DCE-MRI, PET). In fact, many works have applied texture analysis for the characterization of tumoral tissue for an automatic identification of radiation targets and for the discrimination between abnormal/normal tissues. In some cases, it is the power of textural features in capturing information about the spatial organization of the tissue to be fundamental for a correct discrimination between tumoral and normal tissue, rather than the simple mean intensity. Another application of texture analysis was in the evaluation and prediction of radiation-induced effects on tumor and organs at risk. Recently, textural features were also proposed as a modulation index in VMAT.

Teaching Lecture: Biology of high-energy proton and heavy ion particle therapy versus photon therapy: recent developments

SP-0569
Biology of high-energy proton and heavy ion particle therapy versus photon therapy: recent developments

M. Pruschy[1]
[1]*University Hospital Zürich, Department of Radiation Oncology, Zurich, Switzerland*

The rapid introduction of low LET particle therapy worldwide - in particular proton therapy - but also high LET particle therapy contrasts with the scarcity of radiobiologic evidence to support the expansion of new clinical indications. For many years, particle radiobiology research has focused on the determination of generic values for the relative biological effectiveness (RBE) for both proton and heavy ions, to be

applied in the clinics and relevant for both tumor control and radiation effects in the normal tissue. Nevertheless, recent mechanistic-oriented research on the cellular and tissue level reveal differential response patterns on the gene expression, intracellular signaling, tumor and normal tissue level to low and high LET particle therapy and to photon therapy. For example, our own studies at the center for proton therapy at the Paul Scherrer Institute, but also at other proton therapy institutes, reveal a differential requirement of the two major double strand break repair pathways in response to proton- versus photon-irradiation and indicate individual susceptibilities to photon and low LET proton but also high LET particle therapy. This has been demonstrated in accepted models of genetically-defined normal tissue cells and human tumor cells with a defined lack in specific DNA repair capacities. Likewise combined treatment modalities with pharmacologic inhibitors of specific DNA repair machineries sensitize tumor cells for the respective type of ionizing radiation. These results might become relevant for clinical stratification of patients e.g. carrying mutations in specific DNA damage response pathways; ask for the identification of relevant functional biomarkers; and the critical evaluation of generic RBEs to be applied for the different particle-based radiotherapy modalities. Thus, we nowadays realize that the RBE can vary significantly depending on the tissue, cell line or physiological end point investigated and that differential biological processes are induced by photon and particle therapy. Here we will discuss recent radiobiological findings on the subcellular, cellular and tumor microenvironment level in the framework of proton and other particle therapies.

Teaching Lecture: Neuroendocrine tumours – personalised diagnosis and treatment using radiolabelled peptides

SP-0570

Neuroendocrine tumours - personalised diagnosis and treatment using radiolabelled peptides

R.P. Baum[1], J. Strosberg[2], E. Wolin[3], B. Chasen[4], M. Kulke[5], D. Bushnell[6], M. Caplin[7], T. Hobday[8], A. Hendifar[9], K. Oberg[10], M. Lopera Sierra[11], D. Kwekkeboom[12], P. Ruszniewsk[13], E. Krenning[12], E. Mittra[14]

[1]*Zentralklinik Bad Berka, Dept. of Molecular Radiotherapy, Bad Berka, Germany*
[2]*Moffitt Cancer Center, Oncology, Tampa, USA*
[3]*Markey Cancer Center- University of Kentucky-, Carcinoid and neuroendocrine Dept., Lexington, USA*
[4]*University of Texas MD Anderson Cancer Center, Nuclear Medicine, Houston, USA*
[5]*Dana-Farber Cancer Institute, Medical Oncology, Boston, USA*
[6]*University of Iowa-, Nuclear Medicine, Iowa City, USA*
[7]*Royal Free Hospital-, Neuroendocrine tumour NET unit, London, United Kingdom*
[8]*Mayo Clinic College of Medicine, Oncology, Rochester, USA*
[9]*Cedars Sinai Medical Center, Gastrointestinal disease Dept., Los Angeles, USA*
[10]*University Hospital- Uppsala University, Medical Sciences-Endocrin Oncology, Uppsala, Sweden*
[11]*Advanced Accelerator Applications, Nuclear Medicine, New York, USA*
[12]*Erasmus Medical Center, Nuclear Medicine, Rotterdam, The Netherlands*
[13]*Hopital Beaujon, Oncology, Hopital Beaujon- Clichy-France, France*
[14]*University Medical Center, Nuclear Medicine, Stanford, USA*

The strong expression of SSTR2 by neuroendocrine tumors (NETs) enables peptide receptor radionuclide therapy (PRRT), the molecular internal radiation therapy of NETs. In our hospital (certified as ENETS Center of Excellence), a dedicated multidisciplinary team of experienced NET specialists is responsible for the management of NET patients (over 1,200 patient visits per year). Patient selection for PRRT is based on the Bad Berka Score (BBS) which takes into account clinical aspects and molecular features. Frequent therapy cycles (4-6 and up to 10), applying low or intermediate doses of radioactivity are suitable for these relatively slow-growing tumors ("long term low dose, not short term high dose concept"). After each 2 treatment cycles, restaging is performed by morphologic (CT/MRI) and molecular imaging (Ga-68 SSTR PET/CT), blood chemistry and tumor markers. All data are entered in a prospective structured database (over 250 items per patient).

NET Center Bad Berka - Results

Retrospective analysis was performed in 1000 patients (age 4 - 85 years) with metastatic and / or progressive NETs, undergoing 1 - 9 cycles of PRRT at our center using Lu-177 (n=331), Y-90 (n=170) or both (n=499). Median total administered activity was 17.5 GBq. Patients were followed up for up to 132 months after the 1st cycle of PRRT. Well-differentiated NETs (G1-2) accounted for 54 %. Most patients (95.6 %) had undergone at least 1 previous therapy (surgery 86.8 %, medical therapy 55 %, ablative therapy 14.2 % and radiotherapy 3.4 %). The median overall survival (OS) of all patients from the start of PRRT was 52 months (mo). Median OS according to radionuclide used: Y-90 24 mo, Lu-177 55 mo, both (TANDEM or DUO PRRT) 64 mo; according to the grade of tumor: G1 87 mo, G2 55 mo, G3 28 mo, unknown 50 mo; and according to origin of primary tumors: pancreas 45 mo, small intestine 77 mo, unknown primary 55 mo, lung 36 mo. Median progression-free survival (PFS) measured from the last therapy cycle was 22 mo, comparable for pancreatic (23 mo) and small intestinal (25 mo) NETs.The use of a combination of Lu-177 and Y-90 takes this heterogeneity into account. Sequential administration of Y-90 and Lu-177 labeled analogues is useful for the treatment of larger tumors, followed by treatment of smaller metastases, respectively in further treatment cycles.*Conclusions*PRRT lends a significant benefit in progression free survival as well as in overall survival in metastasized and / or progressive G1-2 NETs as compared to other treatment modalities and regardless of previous therapies. Combination of Lu-177 and Y-90 (DUO) based PRRT may be more effective than either radionuclide alone. Up to 10 cycles of PRRT, given over several years were tolerated very well by most patients. Severe renal toxicity can be completely avoided or reduced by nephroprotection applying aminoacids; haematological toxicity is usually mild to moderate (except for MDS which occurs in approx. 3-5% of all patients treated). Quality of life can be significantly improved. PRRT should only be performed at specialized centers as NET patients need highly individualized interdisciplinary treatment and long term care. NETTER-1 is the first Phase III multicentric, randomized, controlled trial evaluating 177Lu-DOTA0-Tyr3-Octreotate (Lutathera®) in patients with inoperable, progressive, somatostatin receptor positive midgut NETs. 230 patients with Grade 1-2 metastatic midgut NETs were randomized to receive Lutathera 7.4 GBq every 8 weeks (x4 administrations) versus Octreotide LAR 60 mg every 4-weeks. The primary endpoint was PFS per RECIST 1.1 criteria, with objective tumor assessment performed by an independent reading center every 12 weeks. Secondary objectives included objective response rate, overall survival, toxicity, and health-related quality of life.Enrolment was completed in February 2015, with a target of 230 patients randomized (1:1) in 35 European and 15 sites in the United States. At the time of statistical analysis, the number of centrally confirmed disease progressions or deaths was 23 in the Lutathera group and 67 in the Octreotide LAR 60 mg group. The median PFS was not reached for Lutathera and was 8.4 months with 60 mg Octreotide LAR [95% CI: 5.8-11.0 months], p<0.0001, with a hazard ratio of 0.21 [95% CI: 0.13-0.34]. Within the current evaluable patient dataset for tumor responses (n=201), the number of CR+PR was 18 (18%) in the Lutathera group and 3 (3.0%) in the Octreotide LAR 60 mg group (p=0.0008). Although the OS data are not mature enough for a definitive analysis, the number of deaths was 13 in the Lutathera group and 22 in the Octreotide LAR 60 mg group (p=0.019 at interim analysis) which suggests an improvement in overall survival.The Phase III NETTER-1 trial provides evidence for a clinically meaningful and statistically significant increase in PFS and ORR, and also suggests a survival benefit in patients with advanced midgut NETs treated with Lutathera.

Teaching Lecture: Radiotherapy for paediatric brain tumours

SP-0571

Radiotherapy for paediatric brain tumours

R.D. Kortmann[1]
[1]*University of Leipzig, Radiation Therapy, Leipzig, Germany*

Introduction

Radiation therapy is an integral component in the management of childhood CNS malignancies. Although high cure rates can be achieved, detrimental long term side effects often hamper the functional outcome.

Technologies

Stereotactic conformal radiation therapy, IMRT, tomotherapy, image-guided radiation therapy and proton therapy are increasingly used to provide an excellent coverage of the target. Multimodality imaging such as MRI, PET and spectroscopy are implemented in treatment planning and permit an exact definition and delineation of the target and organs at risk. Novel fractionation schedules exploit the radiobiological properties of tumour and normal tissue. The selection of treatment modality is based on the tendency of the tumour with respect to local infiltration and leptomeningeal spread. Craniospinal irradiation is the standard of care in medulloblastoma and metastatic germcell tumours. IMRT, tomotherapy and proton therapy provide a high conformality and excellent dose homogeneity throughout the target volume. Especially proton therapy has the ability to decrease the dose exposure to whole body and surrounding normal tissue thereby reducing the risk of acute and late effects. The major developments in radiation therapy of pediatric tumours are aimed to individually tailor radiation therapy to the target especially in irradiation of the tumours site such as ependymoma, low grade glioma. With the increasing complexity of irradiation techniques in the treatment of CNS malignancies formalised systems and comprehensive quality assurance programmes were introduced to provide an optimal and reproducible treatment on a high quality level. To reduce late effects RT parameters can be modified by the investigation of novel radiotherapy dose prescriptions and reducing dose exposure to neighbouring normal tissue with a maximal sparing of normal brain. The introduction of models to predict the impact of radiotherapy dose volume parameters on long-term neuropsychological function will help to further reduce the risk for late effects.

Conclusion

The rapid developments and small patient numbers as well as the lack of appropriate measurement instruments and difficult endpoints like quality of survival preclude the necessity to investigate the role of these new technologies within prospective randomised trials. Paediatric oncologists should therefore not refrain from including new technologies in their prospective trials as part of treatment standards. A detailed assessment of the long-term benefits and side effects is however necessary to define their precise role in the management of childhood CNS malignancies.

Teaching Lecture: Role and validation of deformable image registration in clinical practice

SP-0572

Role and validation of deformable image registration in clinical practice

M. van Herk[1,2]
[1]*University of Manchester, Manchester Academic Health Science Centre, Manchester, United Kingdom*
[2]*The Christie NHS Foundation Trust, Medical Physics, Manchester, United Kingdom*

Image registration is the process of finding the transformation between two image sets. It is used widely in radiotherapy, e.g. for image guidance and target volume delineation. Compared to rigid registration, deformable image registration (DIR) is much more complex as the number of degrees of freedom in a typical DIR system exceeds the ten-thousands versus 6 for rigid registration. To make DIR tractable, registration systems therefore need to make a compromise between image similarity and smoothness of the deformation, attempting to find the ‘smallest’ deformation that still optimizes the image similarity. This compromise is achieved by tuning a large amount of parameters, which is the ‘trick of the trade’. DIR is currently considered the most essential and most complicated component of on- and off-line adaptive radiotherapy and its validation is therefore essential. Validation programmes should look at technical, general, and patient-specific performance. Technical and general QA methods include 4D and anatomically realistic phantoms, natural and implanted fiducials, and manually placed landmarks, potentially using mathematical methods to account for observer variation. Visual verification is an essential patient specific form of QA, but an important caveat of deformable image registration is the inadequacy of visual validation to provide a final verdict on the registration accuracy, as completely different deformable registrations can result in the identical images. This is not a problem for descriptive tasks such as Hounsfield unit correction and autocontouring, where organ boundaries are sought, but is highly detrimental for quantitative tasks such as dose accumulation and treatment adaption around tumour boundaries where anatomical “cell to cell” correspondence is required. Another unsolved issue is that registration performance is poor around sliding tissues and anatomical changes in the patient and specific care should be taken with clinical decisions that depend on dose summation around such regions. I conclude that QA of deformable registration is complex, and that current algorithms lack biological and biomechanical knowledge. I believe that today it is therefore not safe to use them for dose-accumulation and treatment adaptation around shrinking tumours.

Teaching Lecture: VMAT QA: To do and not to do, those are the questions

SP-0573

VMAT QA: To do and not to do, those are the questions

J.B. Van de Kamer[1], F.W. Wittkämper[1]
[1]*Netherlands Cancer Institute Antoni van Leeuwenhoek Hospital, Department of Radiation Oncology, Amsterdam, The Netherlands*

Introduction

With the advent of Volumetric Modulated Arc Therapy (VMAT), Quality Assurance (QA) has evolved to a next step regarding complexity. Different parts of the linear accelerator (linac) move synchronously, resulting in a dose delivery that can be highly modulated in both space and time. In this lecture the practical aspects of QA are discussed, in particular focussed on VMAT.

Machine QA

Prior to implementing VMAT treatments in the clinic, the user should be familiar with the dynamic behaviour of the machine. In particular, features such as the lowest maximum leaf speed and the behaviour of the system under both dose rate changes and accelerations/decelerations of the gantry should be determined. Such machine characteristics need to be incorporated in the treatment planning system (TPS) to avoid devising undeliverable plans. To properly measure the dose delivered by the linac, the used measurement systems need to be dosimetrically accurate and have a high degree of spatial and temporal resolution. Usually different QA devices are needed to achieve this.

Patient-specific QA

Before a treatment plan can be delivered clinically, the medical physics expert (MPE) has to be convinced that the correspondence between calculated and measured dose

delivery is adequate. This can be achieved by performing patient-specific QA, comparing the measured, integral dose with the computed one in a phantom. For this purpose, a high dosimetric accuracy combined with a high spatial resolution is required. Again, different measurement devices are in general needed to meet these demands. The interpretation of the differences between intended an delivered dose distribution, in terms of a gamma analysis, will be discussed. After gaining experience and confidence with a certain class solution for treatment plans, most MPE resort to using only point dose measurements or computer programs for independent validation. When and how to introduce such alternatives will be discussed in the lecture. The value of continuous patient-specific QA will also be addressed.

Conclusion
After the lecture, the participant should have a clear idea what type of detectors should be used for what purpose and how to optimise patient-specific QA in a busy clinical environment.

Teaching Lecture: Optimising workflow in a radiotherapy department - an introduction to lean thinking

SP-0574
Optimising workflow in a radiotherapy department - an introduction to lean thinking

B. Naddy[1]
[1]*Health Service Executive, Clinical Strategy and Programmes, Dublin 2, Ireland Republic of*

Lean Thinking originated from the manufacturing industry in Japan as a method of highly-efficient production. However, Lean Thinking is not confined to manufacturing and as a management strategy focused on improving processes, is applicable to any organisation. It is now well-established in the complex area of healthcare delivery. Lean Thinking has been described as “the dynamic, knowledge driven and customer-focused process through which all people in a defined enterprise work continuously to eliminate waste and to create value” (Rebentisch et al, 2004). For a healthcare organisation, it provides a patient-focused, systematic approach to identifying and eliminating waste (i.e. non-value-added activities) through continuous improvement. The key principle of Lean is distinguishing value-added steps from non-value-added steps, and eliminating waste with the aim that eventually every step will add value to the overall process.
The lean philosophy is not intended to reduce the number of employees working in the hospital. It seeks only to eliminate waste in tasks and processes so that time, materials, resources and procedures can be utilised as efficiently as possible with the aim of dedicating more time and effort to patient care without extra cost to the patient or healthcare organisation.
Using case studies and real-life examples, this talk will introduce the lean concepts, principles and tools that contribute to improving efficiency, quality and patient safety in radiotherapy and healthcare.

Symposium: New concepts of tumour radioresistance

SP-0575
Radiotherapy combined with immunotherapy: present status and future perspectives

P. Lambin[1,2], N. Rekers[1,2], A. Yaromina[1,2], L. Dubois[1,2]
[1]*MAASTRO clinic, Radiation Oncology, Maastricht, The Netherlands*
[2]*Maastricht University Medical Centre, GROW - School for Oncology, Maastricht, The Netherlands*

Radiotherapy is along with surgery and chemotherapy one of the prime treatment modalities in cancer. It is applied in the primary, neoadjuvant as well as the adjuvant setting. Radiation techniques have rapidly evolved during the past decade enabling the delivery of high radiation doses, reducing side-effects in tumour-adjacent normal tissues. While increasing local tumour control, current and future efforts ought to deal with microscopic disease at a distance of the primary tumour, ultimately responsible for disease-progression. This talk will explores the possibility of bimodal treatment combining radiotherapy with immunotherapy. L19 targets the extra domain B (ED-B) of fibronectin, a marker for tumor neoangiogenesis, and can be used as immunocytokine when coupled to IL2. We hypothesize that radiotherapy in combination with L19-IL2 provides an enhanced antitumor effect, which is dependent on ED-B expression.
EXPERIMENTAL DESIGN: Mice were injected with syngeneic C51 colon carcinoma, Lewis lung carcinoma (LLC), or 4T1 mammary carcinoma cells. Tumor growth delay, underlying immunologic parameters, and treatment toxicity were evaluated after single-dose local tumor irradiation and systemic administration of L19-IL2 or equimolar controls.
RESULTS: ED-B expression was high, intermediate, and low for C51, LLC, and 4T1, respectively. The combination therapy showed (i) a long-lasting synergistic effect for the C51 model with 75% of tumors being cured, (ii) an additive effect for the LLC model, and (iii) no effect for the 4T1 model. The combination treatment resulted in a significantly increased cytotoxic (CD8(+)) T-cell population for both C51 and LLC. Depletion of CD8(+) T cells abolished the benefit of the combination therapy.
CONCLUSIONS: These data provide the first evidence for an increased therapeutic potential by combining radiotherapy with L19-IL2 in ED-B-positive tumors. This new opportunity in cancer treatment will be investigated in a phase I clinical study for patients with an oligometastatic solid tumor (NCT02086721). An animation summarizing our results is available at https://www.youtube.com/watch?v=xHbwQuCTkRc .
REFERENCE:. Zegers CM1, Rekers NH2, Quaden DH3, Lieuwes NG2, Yaromina A2, Germeraad WT4, Wieten L5, Biessen EA6, Boon L7, Neri D8, Troost EG2, Dubois LJ2, Lambin P2. Radiotherapy combined with the immunocytokine L19-IL2 provides long-lasting antitumor effects. Clin Cancer Res. 2015 Mar 1;21(5):1151-60.

SP-0576
The contribution of cancer stem cells to tumour radioresistance

A. Chalmers[1]
[1]*Inst. of Cancer Sciences-Univ. Glasgow The Beatson West of Scotland Cancer Center, Department of Clinical Oncology, Glasgow, United Kingdom*

For a number of tumour types there is increasing acceptance that cancer stem cells play an important role in tumour initiation and recurrence after treatment. In line with this model, increasing evidence indicates that cancer stem cells exhibit resistance to conventional cytotoxic agents. In the case of glioblastoma, an incurable primary brain tumour associated with dismal prognosis and devastating effects on quality of life, a series of influential publications have demonstrated that the radiation resistance of glioblastoma stem-like cells (GSC) is associated with constitutive upregulation of the DNA damage response (DDR).
In this presentation I will outline the evidence supporting this model, and present new data that elucidates the relative contributions of DNA repair and cell cycle checkpoints to this phenotype. Subsequently I will investigate the effects of inhibiting various components of the DDR, alone and in combination, and discuss the potential clinical application of a number of promising new small molecule inhibitors.

SP-0577
Novel insights in radioresistance of head and neck cancer

I. Tinhofer-Keilholz[1]
[1]*Charité Campus Virchow Klinikum, Department of Radiooncology and Radiotherapy, Berlin, Germany*

Recent technological advances in DNA sequencing with greater speed and resolution at lower costs has provided new

insights in cancer genetics. The next-generation sequencing (NGS) technology is tremendously facilitating the in-depth genome-wide search for genetic alterations which might significantly contribute to aggressive and/or treatment-resistant phenotypes of cancers, thereby establishing the basis for improvement of cancer treatment. We hypothesized that NGS should also be useful for dissecting the molecular mechanisms of radioresistance in squamous cell carcinoma of the head and neck (HNSCC).
We therefore applied the technology of targeted NGS to clinical samples from two multicenter studies of definitive and adjuvant cisplatin-based chemoradiation of locally advanced HNSCC. We evaluated whether by molecular profiling using targeted NGS it is possible to prospectively discriminate between patients who clearly benefit from chemoradiation and those with poor locoregional control and reduced overall survival after such treatment. Our studies could confirm previous reports of poor efficacy of radiotherapy in HNSCC tumors harboring *TP53* mutations. For the first time, we identified additional mutations in other genes as predictive biomarkers of outcome after chemoradiation.
The talk will summarize the results of NGS studies in HNSCC and other carcinoma models, thereby focusing on studies in which molecular mechanisms involved in radio-/chemoresistance have been addressed. It will present unpublished results from functional studies in preclinical models in which we are evaluating the mode of interaction of distinct genetic variants with radio-/chemoresistance. Concepts of how to integrate the results from NGS into novel personalized treatment strategies for HNSCC will be discussed.

Symposium with Proffered Papers: Towards Personalised Radiation Oncology (PRO)

SP-0578
New technologies for genomic tumour profiling

W. Weichert[1]
[1]*Technical University Munich, Institute of Pathology, Munich, Germany*

Massive parallel sequencing technologies (also: next generation sequencing) have revolutionized our understanding of the genomic and transcriptional makeup of malignomas. Aided by equally impressive developments in sequencing- and chip-based epigenetic tumor profiling and developments in mass spectrometry which allow for a comprehensive proteomic and metabolomic profiling we are now able to draw fairly comprehensive multi –omics landscapes of individual tumors both from tissue but increasingly also from blood or circulating tumor cells. However, many issues remain still challenging when it comes to a translation of these findings into a potential clinical outreach. This includes matters of tumor heterogeneity specifically with respect to tumor evolution in the metastatic setting as well as under therapeutic pressure. Other widely unresolved issues include the usefulness of identified drivers as novel targets for therapy or as predictive biomarkers and strategies to implement broad high throughput genomic testing into individualized patient care. Specifically the latter issue will decide which of these multi-omics technologies will take the step from tools merely for biological research profiling to advanced and modern routine clinical care.

SP-0579
Gene expression profiles in tumours for PRO

J. Alsner[1]
[1]*Aarhus University Hospital, Department of Experimental Clinical Oncology, Aarhus C, Denmark*

Gene expression profiles hold great promises for PRO (Personalized Radiation Oncology), yet very few - if any - are implemented in routine clinical practice and used as predictive biomarkers for treatment decisions in radiation oncology.
Several challenges needs to addressed before a gene expression profile can be approved as a predictive biomarker by regulatory bodies like the European Medicines Agency (EMA) and the US Food and Drug Administration (FDA). In an ongoing trial, EORTC-1219 (ClinicalTrials.gov ID: NCT01880359), a 15-gene hypoxia profile (1,2) is being tested prospectively. One of the primary aims of the study is to provide data for regulatory approval of the gene profile as an accompanying biomarker for the use of the hypoxia modifier Nimorazole.
The development and ongoing validation of this 15-gene profile will be used as a general example of the challenges for implementing gene expression profiles in PRO. Different strategies for identification of relevant gene expression profiles will be discussed together with the challenges of validating the predictive value of a gene expression profile. The requirements for a quick and robust test for the gene expression profile working on simple routine FFPE (formalin-fixed, paraffin-embedded) sections will also be discussed. Finally, some of the regulatory and patent issues related to gene expression profiles will be commented upon.
1. Toustrup et al. Cancer Res. 71(17):5923-31, 2011.
2. Toustrup et al. Radiother Oncol 102(1):122-9, 2012.

SP-0580
GWAS, SNPs and normal tissue toxicity for personalised radiation oncology

C. West[1]
[1]*The University of Manchester, Christie Hospital, Manchester, United Kingdom*

A key challenge in radiotherapy is to maximise radiation doses to cancer while minimising damage to surrounding healthy tissues. As toxicity in a minority of patients limits the doses that can be safely given to the majority, there is interest in developing a test to measure an individual's radiosensitivity before treatment and predict their likelihood of developing toxicity. A biomarker that predicts a cancer patient's risk of toxicity could be used to personalise dose prescriptions or to offer alternative treatments. Many approaches have been studied to measure radiosensitivity. The development of omics technologies underpinned genome wide association studies (GWAS) attempting to identify genetic variants reported as single nucleotide polymorphisms (SNPs). The advantages of the approach include: a genetic test will be easier to implement clinically than a functional assay; a genetic test will not suffer from the poor reproducibility associated with some radiosensitivity testing methods; and SNPs are the most common type of genetic variation and so easiest to identify. Omics technologies offer promise, but to have an impact on radiotherapy practice research must identify biomarkers that replicate across cohorts. Robust replication needs big data, which is only possible with large collaborative efforts. The need for big data was addressed by establishing an international Radiogenomics Consortium. Achievements of the consortium include: pooling cohorts to increase statistical power and identify definitively whether individual SNPs are associated with risk of toxicity; producing guidelines to improve the reporting of radiogenomics studies; identifying approaches for analysing data from heterogeneous cohorts involving different toxicity reporting scales and treatment regimens; and establishing studies collecting standardised data to improve our ability to detect more SNPs. Work over the past three years showed it is possible to pool heterogeneous cohorts and has identified several SNPs associated with risk of toxicity. Large collaborative projects in the cancer pre-disposition field involving analysis of ~100,000 participants shows that sufficient SNPs can be identified to generate a polygenic risk profile for clinical implementation. For example, men in the top 1% of the distribution of a 74-SNP polygenic risk score have a 4.7 fold increased risk of developing prostate cancer. Key challenges for the radiation oncology community are to collect the data in multiple cancers to identify enough SNPs to generate a polygenic risk profile and to increase understanding of the need for endpoint dependent versus independent profiles.

SP-0581

Integrative data analysis for PRO

M.A. Gambacorta[1]
[1]Gambacorta Maria Antonietta, Roma, Italy

Personalized Radiation Oncology (PRO) integrating omics technology is a rapidly developing concept that will have an enormous impact on oncologic treatments and specifically radiation therapy in the near future. Tumor behaviour and outcomes related to oncologic treatments are related to several factors of which connections are nowdays poorly known. Different branches of medicine have developed their own lines of research which are sometimes difficult to be interpreted, difficult to be integrated with classical clinical factors and for these reasons, difficult to be applied in clinical practice. In clinical prediction and decision making process, results provided by omics are rarely used, whereas clinicians usually use clinical and imaging data for understanding tumor behaviour, predicting patients' outcomes and for choosing the the most suitable treatment. The clinical decision is usually based on general guidelines which extrapolate information from randomized clinical trial. Moreover independent factors derived from several RCT are used by the Radiation Oncologist to make his prevision on tumor behaviour and consequently to choose the „right treatment“ for a specific patient. Randomized clinical trials enclose patients with characteristics chosen beforehand and usually omics informations are rarely or never included. This lead to a potential missing of several information that could refine prediction and thus promote personalized treatments and to an erroneous outcomes prediction that can lead to un-appropriate treatment decision for a specific patient. Integrative data analysis has the potential to correlate data of different origins (genetic, radiology, clinic...) with patient’s outcomes and to create a consistent dataset useful to obtain a trustful analysis for the Decision Support System. The DSS can easily be applied in clinical practice helping the Radiation Oncologist to utilize several information that otherwise would be excluded in the process of decision making. The possibility to predict the outcome for a certain patient in combination with a specific treatment with more accuracy, will lead to better identification of risk groups and thus better treatment decisions in individual patients, but it will also stimulate research focused on specific risk groups which try to find new treatment options or other combinations of treatment options for these subgroups. These treatments will be more personalized, which will not only save patients from unnecessary toxicity and inconvenience, but will also facilitate the choice of the most appropriate treatment . The resulting predictive models, based on patient features, enable a more patient specific selection from the treatment options menu and a possibility to share decisions with patients based on an objective evaluation of risks and benefits. Finally, considering the important role that predictive models could play in the clinical practice, clinicians must be aware of the limits of these prediction models. They need to be internally validated taking into account the quality of the collected data. An external validation of models is also essential to support general applicability of the prediction model. Therefore structural collaboration between different groups is crucial to generate enough anonymized large databases from patients included or not in clinical trials.

OC-0582

Gene signatures predict loco-regional control after postoperative radiochemotherapy in HNSCC

S. Schmidt[1,2,3,4], A. Linge[1,2,4,5], F. Lohaus[1,2,5], V. Gudziol[6], A. Nowak[7], I. Tinhofer[8,9], V. Budach[8,9], A. Sak[10,11], M. Stuschke[10,11], P. Balermpas[12], C. Rödel[13,14], M. Avlar[15,16], A.L. Grosu[15,17], A. Abdollahi[18,19,20,21,22], J. Debus[18,20,21,22,23], C. Belka[24,25], S. Pigorsch[24,26], S.E. Combs[24,27], D. Mönnich[28,29], D. Zips[28,29], G.B. Baretton[2,30,31], F. Buchholz[2,32], M. Baumann[1,2,3,5], M. Krause[1,2,3,5], S. Löck[1,2,3,5]
[1]OncoRay – National Center for Radiation Research in Oncology, Faculty of Medicine and University Hospital Carl Gustav Carus- Technische Universität Dresden, Dresden, Germany
[2]German Cancer Research Center DKFZ, Heidelberg and German Cancer Consortium DKTK partner site Dresden, Dresden, Germany
[3]Helmholtz-Zentrum Dresden – Rossendorf, Institute of Radiooncology, Dresden, Germany
[5]Faculty of Medicine and University Hospital Carl Gustav Carus- Technische Universität Dresden, Department of Radiation Oncology, Dresden, Germany
[6]Faculty of Medicine and University Hospital Carl Gustav Carus- Technische Universität Dresden, Department of Otorhinolaryngology, Dresden, Germany
[7]Faculty of Medicine and University Hospital Carl Gustav Carus- Technische Universität Dresden, Department of Oral and Maxillofacial Surgery, Dresden, Germany
[8]German Cancer Research Center DKFZ, Heidelberg and German Cancer Consortium DKTK partner site Berlin, Berlin, Germany
[9]Charité University Hospital, Department of Radiooncology and Radiotherapy, Berlin, Germany
[10]German Cancer Research Center DKFZ, Heidelberg and German Cancer Consortium DKTK partner site Essen, Essen, Germany
[11]Medical Faculty- University of Duisburg-Essen, Department of Radiotherapy, Essen, Germany
[12]Goethe-University Frankfurt, Department of Radiotherapy and Oncology, Frankfurt am Main, Germany
[13]German Cancer Research Center DKFZ, Heidelberg and German Cancer Consortium DKTK partner site Frankfurt, Frankfurt am Main, Germany
[14]Department of Radiotherapy and Oncology, Goethe-University Frankfurt, Frankfurt am Main, Germany
[15]German Cancer Research Center DKFZ, Heidelberg and German Cancer Consortium DKTK partner site Freiburg, Freiburg, Germany
[16]University of Freiburg- Germany, Department of Radiation Oncology- Clinical Study Section, Freiburg, Germany
[17]University of Freiburg, Department of Radiation Oncology, Freiburg, Germany
[18]German Cancer Research Center DKFZ, Heidelberg and German Cancer Consortium DKTK partner site Heidelberg, Heidelberg, Germany
[19]University of Heidelberg Medical School and German Cancer Research Center DKFZ, Translational Radiation Oncology, Heidelberg, Germany
[20]University of Heidelberg Medical School and German Cancer Research Center DKFZ, National Center for Tumor Diseases NCT, Heidelberg, Germany
[21]University of Heidelberg Medical School- Heidelberg Ion Therapy Center HIT, Department of Radiation Oncology, Heidelberg, Germany
[22]University of Heidelberg Medical School and German Cancer Research Center DKFZ, Heidelberg Institute of Radiation Oncology HIRO- National Center for Radiation Research in Oncology NCRO, Heidelberg, Germany
[23]University of Heidelberg Medical School and German Cancer Research Center DKFZ, Clinical Cooperation Unit Radiation Oncology, Heidelberg, Germany
[24]German Cancer Research Center DKFZ, Heidelberg and German Cancer Consortium DKTK partner site Munich, München, Germany
[25]Ludwig-Maximilians-Universität, Department of Radiotherapy and Radiation Oncology, München, Germany
[26]Technische Universität München, Department of Radiation Oncology, München, Germany
[27]Department of Radiation Oncology, Technische Universität München, München, Germany
[28]German Cancer Research Center DKFZ, Heidelberg and German Cancer Consortium DKTK partner site Tübingen, Tübingen, Germany
[29]Faculty of Medicine and University Hospital Tübingen- Eberhard Karls Universität Tübingen, Department of Radiation Oncology, Tübingen, Germany
[30]University Hospital Carl Gustav Carus- Technische Universität Dresden, Tumour- and Normal Tissue Bank-University Cancer Centre UCC, Dresden, Germany
[31]Faculty of Medicine and University Hospital Carl Gustav Carus- Technische Universität Dresden, Institute of Pathology, Dresden, Germany

[32]*University Hospital Carl Gustav Carus- Technische Universität Dresden, University Cancer Centre UCC- Medical Systems Biology, Dresden, Germany*

Purpose or Objective: To determine gene signatures which predict loco-regional control (LRC) and the secondary endpoints overall survival (OS) and freedom of distant metastases (FDM) of locally advanced head and neck squamous cell carcinoma (HNSCC) after postoperative radiochemotherapy.

Material and Methods: A gene expression panel of 216 genes was composed including genes which are involved in proliferation, invasion and metastasis as well as in radio(chemo)resistance associated with tumour hypoxia, cancer stem cell markers, cisplatin-resistance and DNA repair. Gene expression analysis was performed using NanoString technology on a multicentre retrospective patient cohort of 196 patients with HNSCC who received postoperative radiochemotherapy. Gene signatures with a minimal number of contributing genes were extracted, which optimally predict for LRC and the secondary endpoints OS and FDM. For the construction of these minimal signatures, different statistical methods were compared, including Cox regression with forward variable selection, boosting methods and random forests. To assess the performance of the different gene signatures and statistical methods the concordance index (CI) was evaluated using 3-fold internal cross validation.

Results: The resulting gene signatures mostly contained genes related to cellular proliferation, migration, invasion, and tumour hypoxia. For all endpoints and statistical methods a cross-validated CI>0.7 could be obtained, indicating a good performance of the models. Using the linear predictor

$$\Sigma_i \beta_i x_i$$

as a risk variable allowed for splitting the patient cohort into groups of good and bad prognosis. The figure exemplarily shows Kaplan-Meier curves of the total patient cohort split by the median risk variable of the gene signatures determined by Cox regression with forward variable selection for all endpoints. The difference between the survival curves is highly significant (p<0.001).

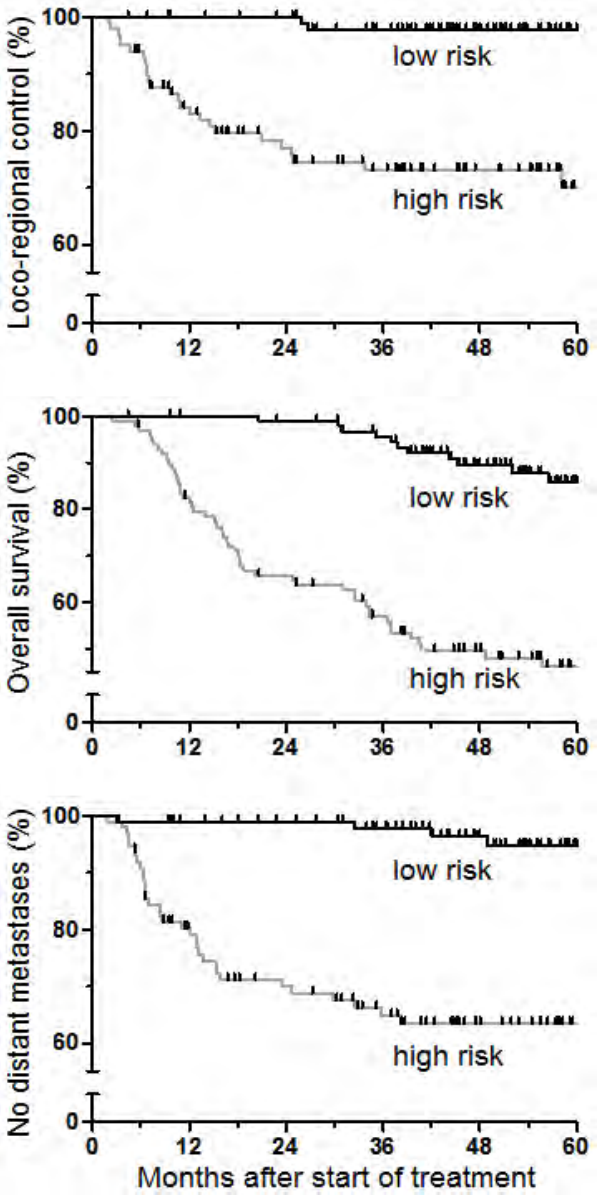

Conclusion: We determined gene signatures for the prediction of LRC, OS and FDM in a cohort of 196 HNSCC patients after postoperative radiochemotherapy. The signatures showed a good prognostic value and were validated by internal cross validation. After validation with an external dataset and in a currently ongoing multicentre prospective trial within the study group, the gene signatures may help to further stratify patients for individualised treatment de-escalation or intensification strategies.

Symposium: The tumour in 3D: the role of tumour microenvironment

SP-0583

Relevance of 3D cultures to address radiation response and novel RT combination strategies

N. Cordes[1]

[1]*OncoRay - Center for Radiation Research in Oncology, Dresden, Germany*

Novel 3D cell culture models enable cell growth in a more physiological environment than conventional 2D cell cultures. Most importantly, cells need to be embedded in a composition of extracellular matrix proteins similarly present in situ to guarantee conservation of the phenotype. As shown by comparative analyses between 2D, 3D and tumor xenografts, various processes such as signal transduction and DNA repair share great similarity in 3D and in-vivo but not 2D.

Based on our long-standing experience, a large variety of endpoints can be determined and many methods can be conducted in 3D matrix-based cell cultures. While this is sometimes not as easy as in 2D and also requires a bit more financial invest, the generated data reflect cell behavior in-vivo and thus have a higher clinically relevance. Further, we are able to address specific tumor features in detail. For example, malignant tumors show great genetic/epigenetic and morphological/cell biological heterogeneity. Here, a prime example is the stiffness of a tumor. Although we know that the stiffness greatly varies in different parts of the tumor, the underlying mechanisms and prosurvival consequences on the genetic/epigenetic and morphological/cell biological level are far from being understood. 3D matrix-based cell cultures models can elegantly support our efforts to gain more knowledge in this field. Another important point is the sparing of animal experiments based on our broad knowledge that human (patho)physiology is significantly different from mice (or other species). Many decades of in-vivo research have demonstrated that only a negligible proportion of therapeutic approaches could be translated from rodents to humans. In conclusion, 3D cell cultures are powerful tools to generate more clinically relevant information. A broader implementation of this methodology is likely to underscore our efforts to better understand tumor and normal cell radiation responses and foster identification of most critical cancer targets.

SP-0584

The potential of normal tissue organoid cultures

R.P. Coppes[1,2]

[1]*University Medical Center Groningen, Department of Cell Biology, Groningen, The Netherlands*

[2]*University Medical Center Groningen, Department of Radiation Oncology, Groningen, The Netherlands*

The response of normal tissues to irradiation is mainly determined by the survival and regenerative potential of the tissue stem cells, and modulated by inflammatory processes, vasculature damage and altered neuronal innervation and fibrosis. Interestingly, transplantation of tissue specific stem cells has been shown to restores tissue homeostasis and prevent late radiation effects. Moreover, the sparing of localized stem cells was predicted to preserve salivary gland function in patients treated for head and neck cancer. Interestingly, mounting evidence indicates that cancer stem cells might contribute to the poor prospects. Recently, we and others have developed methods to culture patient specific organ and tumour stem cell containing organoids (tissue resembling structures). These organoids contain all the tissue/tumor lineages and the tissue/tumor stem cells, as indicated by their secondary organoids self-renewal potential and regeneration/regrowth potential and offer the opportunity to investigate tissue and patient specific assessment of the response of stem cells to (chemo-) radiotherapy. Stem cell survival curves and DNA DSB repair kinetics indicate that the response of organoids to different radiation qualities may differ from tissue to tissue, especially in the low dose regions typically delivered to the normal tissue outside the planning target volume. Therefore, organoids cultures could be used to investigate the mechanism of differences in response of normal and tumour stem cells to irradiation and exploit these for personalized optimisation of (chemo-) radiation treatment and prediction of treatment response.

SP-0585

The impact of a novel 3D cell culture model of glioblastoma on radiation and drug-radiation responses

N. Gomez-Roman[1], A. Chalmers[2]

[1]*Inst. of Cancer Sciences-Univ. Glasgow The Beatson West of Scotland Cancer Cente, Glasgow, United Kingdom*

[2]*Inst. of Cancer Sciences-Univ. Glasgow The Beatson West of Scotland Cancer Cente, Wolfson Wohl Translational Cancer Research Centre, Glasgow, United Kingdom*

Glioblastoma (GBM) is the most common primary brain tumour with dismal prognosis. Tumours exhibit inherent resistance to radiation and chemotherapy which has been attributed to a subpopulation of cancer cells termed 'GBM stem-like cells' (GSC) characterised by multipotentiality and potent tumorigenic capacity. The use of established cancer cell lines in simplified two-dimensional (2D) *in vitro* cultures might explain the observed discrepancy between pre-clinical and clinical responses to cytotoxic treatments. We developed a customised, 3D GSC culture system using a polystyrene scaffold (Alvetex®) that recapitulates key histological features of GBM including high cellularity and sparse extracellular matrix (ECM) and compared it to conventional 2D GSC cultures. 2D and 3D cultures of three different primary GSC lines exhibited similar radiation sensitivities as measured by clonogenic survival. Previous studies have demonstrated radiopotentiating efficacy of the epidermal growth factor receptor (EGFR) inhibitor erlotinib against GBM cell lines in 2D cultures; however it failed in GBM clinical trials. Thus we evaluated the radiation modifying effects of erlotinib on 2D and 3D GSC cultures. Erlotinib enhanced radiosensitivity of 2D GSC cultures but had no effect on radiation responses of 3D GSC or in neurosphere formation assays, where cells grow in 3D conditions devoid of a scaffold or extrinsic ECM. We next examined VEGF inhibition, since anti-VEGF therapy in combination with standard radio-chemotherapy increases progression-free survival of GBM patients. VEGF deprivation was associated with significant radiosensitisation of 3D GSC cultures but had no effect on 2D GSC. Erlotinib treatment of VEGF-deprived 3D cultures increased radiation resistance of 3D cells to the same extent as VEGF addition, indicating epistasis. EGFR has been shown to regulate repair of radiation-induced double-strand breaks by activating the non-homologous end-joining (NHEJ) repair protein DNA-PKcs. A correlation between radiosensitivity, increased gH2AX foci and phospho-DNA-PK nuclear foci after radiation treatment was observed. In contrast, increased numbers of foci of the homologous recombination (HR) repair protein Rad51 were observed in radioresistant populations. Our results show that in the 3D model, VEGF signalling is required for optimal NHEJ activation with fast kinetics. This effect allows access to HR repair proteins at the remaining unrepaired DSBs at later time points, facilitating their repair and conferring radiation protection. Detailed analysis of the signalling pathways involved in the radiation resistance conferred by VEGF and EGFR signalling in the 3D and 2D models respectively demonstrated a radioprotective role of the downstream signaling molecule Akt. Specific inhibition of Akt using the small molecule inhibitor MK-2206 increased radiation sensitivity to the same extent as VEGF deprivation in 3D cells or erlotinib treatment in 2D cells, and no additivity was observed when these agents were combined. Our results for erlotinib treatment and VEGF deprivation in the 3D model recapitulate data from clinical trials, and suggest novel therapeutic targets for GBM. The 3D-specific effects of this panel of molecularly targeted agents strongly support the clinical relevance of this 3D model and its potential value in preclinical studies.

SP-0586

Radiotherapy supports tumour-specific immunity

M. Van den Broek[1]

[1]*University of Zürich, Institute of Experimental Immunology, Zurich, Switzerland*

Tumour-specific immunity occurs in cancer patients but has insufficient potential to control or eliminate the tumour. Strengthening this response through immunotherapy may lead to a durable, systemic response that may also control (development of)metastases.

Radiotherapy - a standard treatment for cancer - acts through induction of DNA damage in cancer cells. Although this treatment was thought to e immuno suppressive for a long time, recent data show that radiotherapy can support tumour-specific immunity. In fact, there is accumulating evidence that immune stimulation is an integral part of this therapy.

Using preclinical cancer models we showed that the efficacy of radiotherapy crucially depends on $CD8^+$ T cells and dendritic cells. Radiotherapy induces activation of tumour-associated dendritic cells and accumulation of $CD8^+$ T cells with protective effect or function within the tumour (1).
These results prompted us to investigate whether similar changes occur in cancer patients and we compared the immune signature in paired biopsies that were obtained from sarcoma patients before and after radiotherapy. Most patients showed a significant upregulation of molecules and cell types associated with protective immunity and a concomitant downregulation of such characteristic for immune regulation/suppression. Importantly, those patients with the strongest changes towards protective immunity survived longer after radiotherapy (2, 3).
Because it is largely unknown how radiotherapy supports tumour-specific immunity, we performed a semi-unbiased transcript analysis to identify pathways that change significantly upon radiotherapy. We found that radiotherapy induces transient and local activation of the classical and alternative pathway of complement in murine and human tumours, which results in local production of the anaphylatoxins C3a and C5a. Complement activation and subsequent production of anaphylatoxins happens downstream of radiotherapy-induced necrosis. The local production of C3a andC5a is crucial to clinical efficacy of radiotherapy and concomitant stimulation of tumour-specific immunity (4).
Radiotherapy influences a plethora of pathways, which we are currently identifying, because we think that selectively promoting or inhibiting particular pathways in the context of radiotherapy may further promote tumour-specific immunity and increase the therapeutic efficacy.Because chronic inflammation is immunosuppressive whereas acute inflation supports immunity, we are comparing chronic radiotherapy (low-dose given in multiple fractions during weeks) with radiotherapy that includes radiation holidays (limited fractions of high-dose given with substantial breaks) with respect to efficacy and immune stimulation.

1. Gupta A, Probst HC,Vuong V, Landshammer A, Muth S, Yagita H, Schwendener R, Behnke S, Pruschy M,Knuth A, van den Broek M. 2012. Radiotherapypromotes tumor-specific effector $CD8^+$ T cells via DC activation.J.Immunol. 189:558-566.
2. Sharma A, Bode B, Wenger RH,Lehmann K, Sartori AA, Moch H,Knuth A, von Boehmer L, van den Broek M. 2011.g-Radiation EnhancesImmunogenicity of Cancer Cells by Increasing the Expression of Cancer-TestisAntigens *in vitro* and *in vivo.* PLoS ONE, e28217.
3. Sharma A, Bode B, StuderG, Moch H,Okoniewski M,Knuth A, von Boehmer L, van den Broek M. 2013.Radiotherapy of human sarcoma promotes an intratumoral immune effector signature. Clin. Cancer Res. 19:4843-4853.
4. Surace L, Lysenko V, Fontana AO, Cecconi V,Janssen H, Bicvic A, Okoniewski M, Pruschy M, Dummer R, Neefjes J, Knuth A,Gupta A, van den Broek M. 2015. Complement is a central mediator of radiotherapy-induced tumor-specific immunity and clinical response. Immunity, 42:767-777.

Symposium: WBRT for brain metastases- the end of an era?

SP-0587
Whole brain radiotherapy for brain metastases - the end of an era?
P. Mulvenna[1]
[1]*Freeman Hospital, Northern Centre for Cancer Care, Newcastle-upon-Tyne, United Kingdom*

Summary: Whole Brain Radiotherapy (WBRT) may be administered with either prophylactic or palliative intent. I will discuss both these approaches and how they fit into our management of metastatic brain disease in the 21st century.

Background: The use of Whole Brain Radiotherapy (WBRT) emerged as standard management for patients with brain metastases during the latter half of the 20th century (1,2,3). This practice is based on reported experience from single institutions.
In the first decade of the 21st century, local control using stereotactic radiotherapy or surgical resection of individual brain metastases has emerged as a clinically beneficial modality for highly selected patients. Whole brain radiotherapy is increasingly seen as a treatment provided in addition to this local control, or is held in reserve for salvage management should new or recurrent brain metastases develop at a later date – without RCT evidence supporting this approach (4,5,6).
The majority of patients with brain metastases, however, are not suitable for stereotactic or surgical approaches and WBRT continues to be seen as the standard of care for this group, particularly if they are perceived to have a durable prognosis (5). Until the MRC QUARTZ trial was undertaken in non-small cell lung cancer (NSCLC) (Mulvenna et al 2016-in press), there were no sufficiently powered randomised controlled trials specifically addressing the utility of WBRT compared to supportive care (7).
Although prophylactic cranial irradiation has enhanced overall survival and reduced incidence of brain metastases for patients with the exquisitely radiosensitive small cell variant of lung cancer, trials addressing this issue in NSCLC and Breast cancer have failed to accrue. This lack of high quality evidence added to the fear of neurocognitive decline remains a potential barrier to applying this technique to other solid tumours with a propensity for metastasising to the brain.

Questions to address:
Can we apply prognostic indices reliably to all solid tumour types?
Do we really know which patients will benefit from WBRT, whether used as a sole palliative modality or as an adjunct to local (stereotactic or surgical) modalities?
If so, how can we best use Image Guided radiotherapy to minimise long term neurocognitive impact?
References:

1. Chao J-H, Phillips R and Nickson JJ.Roentgen Therapy of Cerebral Metastases. Cancer 1954; **7**: 682-689.
2. Order SE, Hellman S, Von Essen CFand Kligerman MM. Improvement in quality of Survival following Whole BrainIrradiation for Brain Metastasis. Radiology 1968; **9**: 149-153.
3. Zimm S, Wampler GL, Stablein D, HazraT, Young HF. Intracerebral metastases in solid-tumor patients: natural historyand results of treatment. *Cancer*1981; **48**(2): 384-94.
4. Khuntia D, Brown P, Li J, Mehta MP.Whole Brain Radiotherapy in the management of Brain Metastasis. J Clin Oncol2006; 24: 1295-1304.
5. Owen S and Souhami L. The Managementof Brain Metastases in Non-Small cell Lung Cancer. Frontiers in Oncology 2014;4: 1-6.
6. Lin X and DeAngelis LM. Treatment ofBrain Metastases. J Clin Oncol 2015; **33**:3475-3484.
7. Tsao MN, Lloyd N, Wong RK, et al.Whole brain radiotherapy for the treatment of newly diagnosed multiple brainmetastases. *Cochrane Database Syst Rev*2012; **4**: CD003869.

SP-0588
Focal radiotherapy for multiple brain metastases
L. Schiappacasse[1]
[1]*Centre Hospitalier Universitaire Vaudois, Department of Radiation Oncology, Lausanne Vaud, Switzerland*

Brain metastases (BM) develop in up to 30% of patients with cancer. There is marked heterogeneity in outcomes for patients with BM, and these outcomes vary not only by diagnosis, but also by diagnosis-specific prognostic factors; we should not treat all patients with brain metastases the same way, treatment should be individualized.
Phase III randomized trials have shown that upfront whole brain radiotherapy (WBRT) may decrease brain recurrence both in terms of better local and improved distant brain tumour control rate, and that neurological death rate may be reduced in patients treated with WBRT + stereotactic

radiosurgery (SRS), but no survival benefit is reached. The EORTC 22952-26001 study (Kocher M et al) shows that adjuvant WBRT fails to improve the duration of functional independence.
The use of SRS in the treatment of multiple BM has increased dramatically during the past decade to avoid the neurocognitive dysfunction induced by WBRT.
One of the biggest (1194 patients) multi-institutional prospective observational studies (JLGK0901, Yamamoto M et al and Watanabe S et al) including patients with multiple BM (even more than 10) have shown that SRS without WBRT in patients with five to ten BM is non-inferior to that in patients with two to four BM in terms of median OS (10,8 months for both groups), 1-year local recurrence (6,5% and 7%), with a very low incidence of side effects (less than 3%). They also concluded that carefully selected patients with 10 or more BM are not unfavourable candidates for SRS alone, having these patients a median survival time and neurological death-free survival times comparables to the group with 9-10 BM; their results suggest also that even among patients 80 years and older, those with modified-RPA Class I+IIa or IIb disease are considered to be favourable candidates for more aggressive treatment of BM.
SRS has been an option for limited (1-3) metastatic brain lesions, and nowadays the updated guidelines (for example, the NCCN panel) have recently added SRS as a primary treatment option for multiple (>3) metastatic lesions.
The exclusive SRS approach for patients with multiple BM is mostly curative for each treated lesion, it can be repeated several times (the limits in terms of median cumulative dose to the normal brain must be explored), and WBRT remains an option as salvage treatment.
Exclusive SRS with frequent magnetic resonance imaging-based follow-ups (every 2-3 months) in order to salvage recurrent BM before symptomatic manifestations, should be routinely offered to selected patients as a treatment option to consider (Lester SC et al). Initial treatment with a combination of SRS and close clinical monitoring should be recommended as the preferred treatment strategy to better preserve learning and memory in good prognosis patients with newly diagnosed BM (Chang EL et al).
The Lausanne University Hospital (CHUV) has created a brain metastases clinic to provide medical and radiation oncology, neurosurgical, and supportive services to this complex patient population. During the first 18 months, 250 cases were discussed, 55% of patients had more than one brain metastases, and focal treatments were proposed in 69% of treated cases (for 50% of them radiosurgery or fractionated stereotactic radiotherapy, FSRT). WBRT was proposed to only 16% of patients (some of them as salvage therapy after sequential treatments with SRS).
Higher BM burden (in terms of size and volume) and higher integral SRS dose to the brain are the main predictive factors for late toxicity after SRS. The cumulative neurocognitive effect of numerous SRS sessions remains unknown. In order to reduce the cumulative median dose to the brain, the SRS technique must be carefully chosen.
At CHUV, we have performed a dosimetric comparison study in cases with multiple brain metastases (up to 10), comparing a radiosurgical planning (same dose and isodose prescription) with Gamma Knife (GK), CyberKnife (CK), VMAT and Helical Tomotherapy (HT). Gradient index was better with GK and CK (3.4 and 4.1, compared to 17.8 and 19), as well as PTV coverage (100% with GK and CK, compared to 97% with VMAT and 90% with HT); brain Dmean was lower with GK (3 Gy) and CK (2.66 Gy), compared to VMAT (6.4 Gy) and HT (6.72 Gy).
SRS alone should be considered a routine treatment option in patients with multiple BM due to favourable neurocognitive outcomes, less risk of late side effects, without adversely affecting the patients performance status.

SP-0589
Role of systemic therapy in the treatment of brain metastases
R. Dziadziuszko[1]
[1]*Medical University of Gdansk, Department of Oncology and Radiotherapy, Gdansk, Poland*

Median survival of patients with brain dissemination in the course of solid tumors typically ranges between 3 and 6 months, depending on several prognostic factors. In order to select patients for most appropriate treatment or best supportive care, several prognostic indices were proposed, of which recursive partitioning analysis (RPA) score and graded prognostic assessment (GPA) are most widely used. In patients with good prognosis and limited number of metastatic lesions, aggressive local treatment, including surgery and radiosurgery is common, with median survival approaching 12 months. Patients in the intermediate group are typically managed with whole brain radiotherapy (WBRT), whereas patients with poor prognosis are typically offered best supportive care. Advances in the systemic therapy of several malignancies have changed this picture, particularly in subsets of patients with driving molecular aberrations, such as *ALK* rearranged non-small cell lung cancer or *BRAF* mutant melanoma. In these patients, long-term responses in the brain and other tumor locations are documented, with series of patients being alive and well for several years after treatment commencement. Penetration of novel targeted agents to CNS becomes its critical feature, as demonstrated by relatively poor intracranial control for ALK inhibitor crizotinib vs. new generation ALK inhibitors such as alectinib. The activity of immunotherapy (anti-CTLA4 and checkpoint inhibitors) in patients with brain metastases is less well documented, but also appears substantial in patients who do not require steroids. Paradoxically, at some point of time, aggressive local treatment strategies and WBRT remain important options in patients with prolonged intracranial control on systemic therapy to improve treatment results even further. The optimal management of these patients remains challenging due to limited evidence-based data and requires multidisciplinary approach.

Symposium: Radiotherapy “autovaccination” with systemic immune modulators for modern immunotherapy

SP-0590
Should the combined treatment be part of our field of knowledge? The "5th R," (immune-mediated) Rejection of Radiobiology
P.C. Lara Jimenez[1]
[1]*Hospital Universitario de Gran Canaria Dr. Negrín, Academic Physics, Las Palmas de Gran Canaria- Ca, Spain*

Radiation therapy is an important part of oncological treatment for advanced and metastatic patients and is widely employed, usually in combination with other treatment modalities. Several strategies have been developed to increase the therapeutic index of radiation therapy, in order to maximize its antitumour activity or radiosensitation and, at the same time, limiting its cytotoxic effects on normal tissues or radioprotection.
Radiation therapy includes new, high precision, low toxicity, treatments as SRS and SBRT. The paradigm of a systemic treatment alone for systemic disease, has been clearly changed over the last decade, as SRS/SBRT achieved unexpectedly (90%) high rates of local control for metastasis and different tumor primary locations. High doses of radiotherapy can now be delivered with high precision and very limited toxicity, therefore increasing the opportunities for treating patients in combination with systemic treatments without compromising tolerance. Such excellent responses do not completely fit the standard radiobiology models, based on well-known classical DNA damage and tumor cell kill, described by the "4 R's" of radiobiology (Reassortment, Reoxygenation, Repair, and Repopulation). Some non-targeted effects seem to be involved and preclinical radiobiological studies have suggested that they may be immune-mediated. Either local bystander or distant abscopal effects could explain part of the unexpected results of radiotherapy. In fact, local radiotherapy appears to be a powerful tool for autovaccinating the patient by modifying the highly immunosuppressive microenvironment of established cancers. These pro-immunogenic effects of ionizing radiation on the tumor microenvironment, include

potentiated innate and adaptive immune responses through release of pro-inflammatory molecules and modifications in MHC and adhesion molecules in cancer cells, stroma and endothelium. Therefore radiation therapy elicits immune responses as part of its role for killing cancer cells.
Unfortunately the abscopal effect is uncommonly observed in clinical practice with radiotherapy alone. Although there is a clear contribution of the immune system to eradication of tumours by novel systemic immunotherapy, only a subset of patients benefit from these therapeutic approaches. The preexisting immune microenvironment seems to be an important predictor of response to such treatments. The increase of productive immune synapses induced by radiation, could be required for the local therapeutic responses to immune agents. In that scenario, changes induced by radiotherapy could modify the immune microenviroment of the tumour, improving response to systemic immune treatments. On the other hand, novel systemic immune treatments could increase the rate of abscopal responses observed after radiotherapy.
Radioimmunotherapy seems to be an excellent approach for cancer. In fact, responses and improved outcomes are continuously reported in highly resistant tumours and could be hypothetized to provide a "broad spectrum" treatment for advanced cancer. In that case, modern systemic immunotherapy could represent the most recent form of radiosensitizing tumour cells and increase the radiation induced abscopal effect.
We could anticipate that in the next few years radiation-driven immunotherapy will be systematically used in combinations with new agents. But, to be responsible of a treatment, we must be aware of the potential acute and late toxicity issues. As for other radiosensitizing treatments, we should also know the best supportive treatment to manage such adverse events. At present anti-CTLA-4 and anti-PD-1/PD-L1 antibodies are becoming increasely used in clinical practice and clinical trials.
Although several reports showed no increase expected toxicity in combination with radiotherapy, these drugs are associated with immune-related adverse events (irAEs). irAEs are believed to arise from general immunologic enhancement and affect the dermatologic, gastrointestinal, hepatic, endocrine, and other organ systems. Temporary immunosuppression with corticosteroids, tumor necrosis factor-alpha antagonists or other agents can be effective treatment.
As oncologists, radioimmunetherapy should be part of our field of knowledge and must be rapidly incorporated to our clinical practice.

SP-0591

Radiotherapy for immunotherapy: optimizing the doses and fractionation

S. Demaria[1]
[1]*Weill Cornell Medicine Medical College, Radiation Oncology and Pathology, New York, USA*

Elimination of virally-infected epithelial cells is mediated by CD8+ T cells and results in life-long protective immunity against reinfection. Similarly, clinical data have shown that CD8+ T cells mediate the rejection of solid tumors and can confer long-term protection from disease recurrence when their activity is unleashed by immune checkpoint inhibitors. Like viral proteins, mutated proteins expressed by an individual tumor are a source of powerful tumor-specific T cell epitopes. However, most of the cancer patients do not develop a sufficient number and repertoire of tumor-reactive T cells and are unresponsive to currently available immunotherapies.
We have pioneered studies to explore the use of local tumor radiotherapy (RT) as a means to release tumor antigens in an immunogenic context. We demonstrated that RT converted an insensitive mouse carcinoma into one responsive to CTLA-4 blockade (Demaria et al., Clin Cancer Res 2005), and have recently shown that this combination is effective in lung cancer patients (NCT02221739), a carcinoma unresponsive to anti-CTLA-4 monotherapy. Unique changes in T cell receptor (TCR) repertoire of intra-tumoral CD8 T cells were observed in the mouse carcinoma after treatment with RT + CTLA-4 blockade. Significant changes in TCR repertoire were also seen in peripheral blood of responding patients, supporting the hypothesis that RT can convert the irradiated tumor into an in situ vaccine.
Immunogenic cell death is induced by radiation in a dose-dependent way, with higher ablative single doses being more effective in vitro (Golden et al., OncoImmunology 2014). However, in vivo the interaction between the dying cancer cells and the pre-existing immune microenvironment determines the ability of RT to prime effective anti-tumor T cell responses. For instance, we have shown that the number of DCs available in the tumor and draining lymph nodes to uptake and present the antigens released by RT is a critical determinant of the magnitude of the immune response elicited (Pilones et al., J Immuntother Cancer 2014). We have recently found that canonical pathways mediating the induction of type I interferon responses in epithelial cells during viral infection are induced by fractionated but not single dose RT. RT-induced cancer cell intrinsic interferon-I production enhanced DCs infiltration and was required for development of tumor-specific T cells capable of rejecting not only the irradiated tumor but also non-irradiated metastases (abscopal effect). This explains, at least in part, the synergy of fractionated RT regimens (8GyX3 or 6GyX5), but not a single ablative RT dose of 20 Gy, with anti-CTLA-4 in achieving abscopal responses against poorly immunogenic carcinomas (Dewan et al., Clin Cancer Res 2009). In addition, we have shown that immunosuppressive mediators such as TGF-beta, which is released in its active form by RT-generated ROS, need to be neutralized to improve DC maturation and activation of T cells capable of rejecting the tumor (Vanpouille-Box et al., Cancer Res 2015).
Overall, optimal RT regimens combined with targeting of dominant immune suppressive pathways enable RT use as a simple, widely available tool for patient and tumor-specific in situ vaccination.
Supported by DOD BC100481P2, NIH R01CA201246, Breast Cancer Research Foundation, and The Chemotherapy Foundation.

SP-0592

Combining immunotherapy and anticancer agents: the right path to achieve cancer cure?

L. Apetoh[1]
[1]*INSERM UMR866, Department of Immunology, Dijon, France*

Recent clinical trials revealed the impressive efficacy of immunological checkpoint blockade in different types of metastatic cancers. Such data underscore that immunotherapy is one of the most promising strategies for cancer treatment. In addition, preclinical studies provide evidence that chemotherapy and radiotherapy have the ability to stimulate the immune system, resulting in anti-tumor immune responses that contribute to clinical efficacy of these agents. These observations raise the hypothesis that the next step for cancer treatment is the combination of cytotoxic agents and immunotherapies. This presentation will discuss the immune-mediated effects of anticancer agents and their clinical relevance, the biological features of immune checkpoint blockers and finally, the rationale for novel therapeutic strategies combining anticancer agents and immune checkpoint blockers.

Joint Symposium: ESTRO-AAPM-EFOMP: Functional / biological imaging and radiotherapy physicists: new requests/challenges and the need for better and more specific training

SP-0593

The role of the medical physicist in integrating quantitative imaging in RT: practical and organisational issues

G.M. Cattaneo[1], V. Bettinardi[2]
[1]*Ospedale San Raffaele IRCCS, Department of Medical Physics, Milan, Italy*
[2]*Ospedale San Raffaele, Nuclear Medicine, Milan, Italy*

The evolution of radiation oncology is based on the increasing integration of imaging data into the design of highly personalized cancer treatments.
Technologically advanced image-guided delivery techniques have made modern radiotherapy treatment extremely flexible in term of optimal sparing of the organs at risk and shaping different prescribed target doses to tumor volumes delineated on the basis of functional imaging information.
In the last 10 years a remarkable development of more sensitive and specific signals (quantitative dynamic contrast-enhanced CT and MRI; diffusion MRI, specific PET tracers, multi-parametric MRI/PET, etc) have contributed to the prescription and design of radiation treatment plan.
The main contribution of new imaging modalities can be summarized:
- Improved delineation of target and normal structures (new hybrid imaging devices offer co-registration of anatomical, functional and molecular information); a further refinement of this approach is the possibility to shape the dose gradually according to the functional parameters (dose painting);
- Adaptation, the radiation technique defined at planning simulation can often require modification not only due to the changes in patient anatomy but because of early variations of certain imaging related parameters surrogates of treatment outcome.
- Predictive biomarkers, the use of more advanced image analysis methods (texture feature parameters) could be a surrogate of important tumor characteristics and have a higher predictive and prognostic power than simpler numeric approaches;
- Radiomics, the extraction of large amount from diagnostic medical images may be used to underlying molecular and genetic characteristics and this genetic profile may change over time because of therapy.
Despite the multiple benefits that the quantitative imaging can offer for radiation therapy improvement, there are a number of technical challenges and organisational issues that need to be solved before its fruitful integration into RT treatment planning process.
The main aspects covered by this lecture will be:
- Standardized procedures for acquisition, reconstruction and elaboration of PET data set;
- Methods for delineation of the PET-related biological target volume (BTV).
- Data acquisition and processing techniques used to manage respiratory motion in PET/CT studies; the use of personalized motion information for target volume definition.
- A procedure to improve target volume definition when using contrast enhanced 4D-CT imaging in pancreatic carcinoma.

SP-0594
Individualised image-guided adaptive therapy in Michigan: lessons learned from clinical trial implementation
J. Balter[1]
[1]*University of Michigan, Ann Arbor, USA*

SP-0595
Training in biological/functional imaging: lacks and opportunities
A. Torresin[1], M. Buchgeister[2]
[1]*Azienda Opsedaliera Ospedale Niguarda Ca'Granda, Department of Medical Physics, Milan, Italy*
[2]*Institution: Beuth University of Applied Sciences Berlin, Department of Mathematics- Physics & Chemistry, Berlin, Germany*

Pubmed references, presentations and posters during a lot of Conferences (ESTRO, EFOMP, ESMRMB, EANM,...) are introducing a lot of biological and functional imaging for radiotherapy applications: MRI, PET, SPECT, functional CT are able to support radiation therapy for target and Organ of Risk definition. Looking at the EUROPEAN GUIDELINES ON MEDICAL PHYSICS EXPERT (RP 174) the competence on biological and functional imaging is not specific item into RT skill and competences. We can find the key activities of MPEs inside the following: Diag.& Therap. NM Internal Dosimetry Measurements(K23: Explain methods for determining patient-specific organ masses including the respective errors and explain the difference between morphological and functional volume of organs), Scientific Problem Solving Service (K36: Explain the physics principles underpinning MR angiography (MRA) and flow, perfusion and diffusion imaging, functional MR imaging (fMRI) and BOLD contrast, MR spectroscopy (MRS), parallel imaging, DCE-MRI) and Clinical Involvement in D&IR (K88: Explain the use of the various modalities for anatomical and functional imaging and K90: Interpret anatomical and functional 2D/3D images from the various modalities and recognize specific anatomical, functional and pathological features). The curricula defines the SKC not specificying how MPE is involved in RT because the functional imaging (in general) and in radiotherapy (in particular), needs a strong interdisciplinary team: MPE expert in radiation oncology and MPE expert in functional imaging should approach the problem together with clinical support. The University and Accreditation training in Europe is not the same and each country differs: in many of them, MPE accreditation in Radiotherapy does not require the accreditation in Diagnostic Imaging. In the next future, requirements of physics application in radiotherapy willneed to include the expertise in diagnostic imaging with particular attention to functional imaging, but the interdisciplinary approach is more effective in the clinical practice. EFOMP and ESTRO working Group is working to define the potential topics for MPE education and training e-learning platform; the knowledge and the expertise in this field will be more and more important.

Symposium: The future of QA lies in automation

SP-0596
The need of automation in QA, state of art and future perspectives
N. Jornet[1]
[1]*Hospital de la Santa Creu i Sant Pau, Medical Physics, Barcelona, Spain*

From the earliest times mankind has struggled to improve his productive means; skills, tools and machines. Aristotle dreamed of the day when “every tool, when summoned, or even of its own accord, could do the work that befits it”. However, we have to wait till 1956 to see the name “automation” appearing in dictionaries. Automation was defined as: “the use of various control systems for operating equipment such as machinery, processes in factories, aircraft and other applications with minimal or reduced human intervention”. In the fifties it was heralded as the threshold to a new utopia, in with robots and “giant brains” would do all work while human drones reclined in a pneumatic bliss. The pessimists pictured automation as an agent of doom leaving mass unemployment and degradation of the human spirit in its wake. Sixty years from those first papers and books in automation we can see that neither the optimistic perspectives nor the most catastrophic views have come true; we still have to wake up to go to work each morning and job have changed but not disappeared. The use of automation in different fields is not homogeneous. For instance, planes, trains and ships are already heavily automated while in our field, radiation oncology and medicine in general, automation has not been fully exploited. Repetitive tasks can be easily automated and this will on one side avoid tedious thinking that must be done without error and on the other side will free time to more creative thinking which will satisfy and give us more joy. Treatment planning, evaluation of treatment planning and QA at treatment unit are areas that are being explored by different research groups. We can automate tasks but automations means much more than this. Automation is a means of analysing, organising and controlling our processes. But how far can we go? Can we design a system able to take complex decisions and not only binary ones such as pass/fail for a quality control test? Yes we can, if we exploit machine learning algorithms. Machine learning will be able to predict the best possible solution for a particular problem and will

form the core of both quality control methods (comparing the predictions with the actual results). One of the side products of automation is standardisation of practice. Let's take treatment planning as an example. Treatment planning is a time consuming task and the resulting plans depend largely on the ability of the planer. Automation in treatment planning has shown to reduce the time needed to achieve plans with less variability and quality. The fact that most vendors offer the possibility of writing scripts to automate checks and to query treatment machine log-files and treatment planning systems data is welcomed and will facilitate the clinical implementation of automation. For management, automation poses the problem of adapting to new concepts and new methods of working and the processes have to be adjusted. Risk analysis has to be re-evaluated and probably different risk mitigation strategies will have to be implemented. For the worker, automation involves changes in the way of working. In particular, clinical medical physicists will have to design performance tests to evaluate these automated systems. To face the challenges that automation brings to our field, medical physics curricula should include IT and also programming. With automation comes a choice between additional leisure and additional products. I would strongly advocate for more time for scientific creative thinking which is needed to contribute to significant advances in medicine and in particular the cure of cancer.

SP-0597

Automated QA for radiotherapy treatment planning

S. Petit[1,2], Y. Wang[1], B. Heijmen[1]
[1]*Erasmus MC Cancer Institute, Department of Radiation Oncology, Rotterdam, The Netherlands*
[2]*Massachusetts General Hospital - Harvard Medical School, Department of Radiation Oncology, Boston MA, USA*

The need of QA for individual treatment plans

The achievable degree of organ sparing with radiation treatment planning is highly dependent on the patient anatomy. Radiation treatment planning with a commercial TPS is an iterative trial and error process. Even for experienced dosimetrists or physicians it is very difficult to judge whether the dose to OARs cannot be lowered further. As a result, the quality of a treatment plan is highly dependent on the available planning time, the experience and talent of the treatment planner and how critically the treatment plan is being reviewed. In a recent study by our group it was shown that after trying to further improve already approved IMRT treatment plans for prostate cancer patients, the rectum dose could be further reduced by on average 6 Gy (range 1-13 Gy), without negative consequences for PTV or other OARs [1]. In conclusion, there is a clear need for treatment planning quality assurance (QA) protocols to guarantee that for each patient the generated plan is indeed optimal for the patient-specific anatomy.

Different strategies for treatment planning QA

In recent years different groups have proposed different strategies for treatment planning QA. The general idea is to predict the lowest achievable dose for OARs and compare the achieved dose of the treatment plan with the predictions. As long as differences between the predictions and the achieved doses to the OARs exceed some predefined action levels, treatment planning should continue, to try to further lower the doses. Most methods rely on a database with plans of prior patients treated for the same tumor site. Because the achievable degree of OAR sparing is highly dependent on patient anatomy only treatment plans of prior patients with anatomies similar as the new patient are selected. Next these prior plans are used to predict achievable DVH metrics for the new patient. The main distinctions between the different methods are (i) the manner in which similarity in anatomy is assessed and (ii) how the dose distributions of the similar prior patients are used to predict DVH parameters for new patients.

Similarity in anatomy can be assessed using distinctive anatomical features. These can vary from very simple such as the percentage overlap of the PTV with an OAR[2]; to an intermediate level of complexity such as the Overlap Volume Histogram that quantifies in 1D the orientation and position of an OAR to the PTV[3]; to more complex such a non-rigid registration based [4]. Also the strategies to predict the dose based on the selected patients vary in complexity: from the lowest achievable dose among all more "difficult" patients [5], to principal component analyses that combine achieved doses of multiple patients and organs to make the predictions [6]. Different models have been successfully applied for prostate, head-and-neck, pancreatic and lung cancer patients [2, 4, 7, 8].

Evaluation of the performance of different treatment planning QA models

An important challenge for the development of treatment planning QA models is that the plans to train and validate the models are often generated with the same trial and error treatment planning process, as where the treatment planning QA models are intended for in the first place. Suboptimal plans used for training and validation could lead to suboptimal models, a bias in the evaluation of the prediction accuracy, suboptimal action levels and difficulties to compare different models that were trained on different patients cohorts. Therefore, recently our group has generated a dataset of 115 Pareto optimal IMRT treatment plans for prostate cancer patients that were planned fully automatically with consistent prioritization between PTV coverage, sparing of organs at risk, and conformality (see abstract Wang, Breedveld, Heijmen, Petit). This dataset has been made publicly available and can be used for objective validation of existing and development of new treatment planning QA models.

Conclusion

There is a need for treatment planning QA models to assess whether a generated treatment plan is indeed optimal for the patient specific anatomy. Different models have been proposed for this purpose that vary in complexity. There are currently some challenges for clinical implementation, but these are likely to be solved in the near future.

References

1. Wang, Y., et al., Radiotherapy and Oncology, 2013. 107(3): p. 352-357.
2. Moore, K.L., et al., International Journal of Radiation Oncology* Biology* Physics, 2011. 81(2): p. 545-551.
3. Kazhdan, M., et al., Med Image Comput Comput Assist Interv, 2009. 12(Pt 2): p. 100-8.
4. Good, D., et al., International Journal of Radiation Oncology* Biology* Physics, 2013. 87(1): p. 176-181.
5. Wu, B., et al., Medical physics, 2009. 36(12): p. 5497-5505.
6. Zhu, X., et al., Medical physics, 2011. 38(2): p. 719-726.
7. Petit, S.F., et al., Radiotherapy and Oncology, 2012. 102(1): p. 38-44.
8. Petit, S.F. and W. van Elmpt, Radiother Oncol, 2015.

SP-0598

Automated QA using log files

V. Hernandez[1], R. Abella[1]
[1]*Hospital Universitari Sant Joan de Reus, Medical Physics, Reus, Spain*

Purpose

The purpose of thispresentation is to show the capabilities of treatment unit log files for QA, aswell as their limitations. To this aim, the implementation of a QA Programbased on Varian dynalogs is presented together with the results obtained. Thepossibility of replacing phantom-based pretreatment QA by log file analysiswill also be discussed during the presentation.

QA Program

The QA Program wasdeveloped with in-house software, in particular with Java (dynalog analysis), MATLAB® (fluence calculation andcomparisons) and MySQL (data storage and reports). Three Varian linacs wereevaluated and >60,000 dynalogs were analyzed, corresponding to both slidingwindow and VMAT techniques.

As part of this QA Program,all IMRT beam deliveries were verified by the following tests:
· Analysis of the RMS (Root Mean Square) values of leaf positionalerrors. RMS values from different deliveries of the same beams were verystable, with differences between different fractions <0.05mm in over 99.9%of the cases. This shows that the MLC positioning is extremely reproducible.
· Analysis of the maximum leaf positioning deviations. Maximumdeviations were typically within 1-1.5mm and depended mainly on the maximumleaf speed.
· Incidence of beam hold-offs and beam interruptions. The meanincidence was 1 hold-off for every 3 dynamic beams deliveries and <1% beamswith interruptions (related to any kind of interlock).
· Comparison of the planned fluence and the actual fluencecomputed from dynalogs. Excellent agreement was obtained, with passingrate>98% for gamma 1%/1mm in practically all cases (>99.9% of the beams).
Limitations and validation of dynalogs
In general, the accuracy oflog files is unclear, especially if they come from non-independent systems.Information in Varian dynalogs comes from the MLC controller, that is, from thesame motor encoders that drive the MLC. For this reason, dynalog files will NOTdetect errors due to MLC calibration parameters (dosimetric leaf gap, offset,skew), motor count losses or backlash. Indeed, Varian dynalogs must becarefully validated by experimentally checking the accuracy of MLC positioning,preferably at different gantry angles and at the end of the treatment day (dueto the cumulative effect of motor count losses since MLC initialization).
Another limitation ofdynalogs is that several aspects of treatment delivery are not recorded in logfiles (beam symmetry, homogeneity, energy…). However, these other aspects arenot specific to IMRT treatments and should be verified as part of the routinestandard QA Program.

Conclusions

Logfile analysis allows exhaustive monitoring of MLC performance and other machineparameters.
Implementing a QA Programbased on dynalogs makes it possible to control data transfer integrity and ALLtreatment deliveries (the entire course of treatment).
Theefficiency of QA can be increased with a fully automated and integrated QAprogram based on log file analysis. Commercial software is available which alsoincorporates independent dose calculations.
Log file analysis providesa useful complement to a general 'conventional' QA program. However, validationof log files against measurements isneeded. In Varian environments, daily experimental verification of theMLC positioning, preferably at different gantry angles and at the end of thetreatment day, is strongly recommended.
Normal 0 21 false false false CA X-NONE X-NONE

SP-0599

Automation in patient specific QA using in vivo portal dosimetry

P. Francois[1]
[1]*Institut Curie, Paris cedex 05, France*

Over the last years, the efficacy of radiation oncology treatmentsimproved dramatically. However, due to the increase in technical complexity anddose escalation, the risk of secondary effects also rises. In vivo dosimetry(IVD) is now widely recommended to avoid major treatment errors and is evenmandatory in several countries.
In this perspective, transit dosimetry using amorphous siliconElectronic Portal Imaging Devices (EPID) appears to be an interesting solutionfor several practical reasons (easy to use, no additional time, no perturbationin the beam, 2D detectors, complex techniques possible, numerical data, etc…). Forall these reasons, daily controls for every patient becomes realistic. However,with constrained resources (staffing, time, etc…), this will become feasible in the clinic by means of automated systems.Medical physics teams will then be able to set and managea permanent survey system:
· To verify the actual radiation dosedelivered to the patient during the procedure
· Detect errors before it is too late
· Anticipate the drifts and be able toassess when deviations are large enough to require adjustments
Such a process will combine "on line" and "off line"procedures (figure 1) giving opportunities to detect and alert for isolatedgross errors, systematic deviations and/or small variations with time. Beyondindividual patients follow up, such databases will bring new perspectives ifproperly designed for automated analysis. Statistical analysis of data per energy,machine, technique, before and after a change in the delivery process (upgrade,new device, etc…) will become possible and help in decision making. Moreover,the frequency and variability in the controlled configurations will go farbeyond any well designed quality control program which could lead to reconsiderour strategies in that domain.

Symposium: Management and optimisation of the daily workflow

SP-0600

Optimising workflow using a workflow management system

A. Vaandering[1], M. Coevoet[1]
[1]*UCL Cliniques Univ. St.Luc, Academic Department of Radiation Oncology, Brussels, Belgium*

It is well known that a concerted effort from an entire radiotherapy (RT) team is needed in order to provide accurate, precise, and effective radiotherapy treatments to patients. And in this process, each member of the RT must perform specific tasks in order to achieve the best possible care for the patient. Throughout the pre-treatment and treatment process, communication and knowledge sharing between the different team members is of paramount importance. Any disruption in the workflow can result in treatment delays and errors and costly repetition of work. In an era where organisations and department are aiming for continuous quality improvement and increased efficiency, optimal workflow management is of uttermost importance.
With the advent of lean management and quality improvement approaches, various types of workflow management softwares are currently being offered or developed in house to improve the radiotherapy departments' workflow. Their overall aim is to facilitate intra and interdisciplinary communication between the RT team members in order to optimise the department's patient flow and safety (1). Nevertheless, to successfully implement these systems, it is important to properly define the department's workflow and processes. These systems also need to be flexible enough to integrate workflow modifications and evolutions resulting from improvement actions or process changes (ie: new treatment modality/new technique/…). Interconnectivity, compatibility with other systems in RT department, user friendliness and ease of access are also features that should characterize these systems.
In the past few years, numerous departments have thus equipped their departments with these workflow management systems. These have proven to be a real asset in the RT departments and their arrival have already ameliorated numerous aspects of patient workflow through standardization of workflow, integration of checklists and forcing functions and task attribution tools. Their use have also allowed for departments to quantitatively monitor their workflow and put into place procedures/modalities that increase the efficiency and safety of their workflow. However, many of the company-based systems are costly and do not allow for the overall visualisation of the status of different patients within the RT workflow at a given time. As a result, certain departments have developed their own workflow management system. One such system is "iTherapy Process" (iTP) which is an internally developed open source software (2). This system provides the user with the quick visualisation of all patients in the pre-treatment and treatment sub processes (Fig. 1).

Fig 1. iTP Process

And in a user friendly environment, allows for the user – RO, MP and/or RTT to quickly visualize the tasks that need to be completed. Through the completion of dedicated and integrated checklists per subprocess, safe and efficient patient workflow is ensured.

Furthermore, ease of access to procedures, staff availabilities and breakdown statistics and information are also valuable tools that can be integrated within workflow management systems.

In conclusion, workflow management systems are fundamental tools for the improvement of quality and safety of patient workflow. These need to be personalized to the department's workflow and user centered. As such, in addition to company developed systems, in house or open source software can provide an ideal solution for radiotherapy department desiring to improve patient workflow in a safe environment.

1. Medina, Angel. In pursuit of Safety: Workflow Management and Error Reporting In Radiation Oncology. [En ligne] 12 06 2012. [Citation : 1 12 2015.] https://www.medicaldosimetry.org/pub/397ad575-2354-d714-51df-7805c51aeab7.

2. Coevoet, Maxime. iTherapy Process - iTP - Checklist workflow manager. [En ligne] 2015. [Citation : 18 12 2015.] https://github.com/mcoevoet/iTP.

SP-0601

Does lean management improve patient safety culture?

P. Simons[1], R. Houben[2], H. Backes[1], P. Reijnders[1], M. Jacobs[1]

[1]*MAASTRO clinic, Department of Radiotherapy and Radiobiology, Maastricht, The Netherlands*

[2]*MAASTRO clinic, Data Centre MAASTRO clinic, Maastricht, The Netherlands*

Introduction: In the field of radiotherapy the importance of a safety culture to maximize safety is no longer questioned. However, how to achieve sustainable culture improvements is less evident. A multifaceted approach is preferrred to improve the safety culture, where multiple safety interventions are combined. Lean management is such an integral approach which aims to improve safety, quality and efficiency. Therefore, lean is expected to improve the safety culture. MAASTRO clinic combined lean intitiatives with structural and cultural elements to promote continuous improvement. They reorganized from managing the different professions to managing multidisciplinary care pathways in January 2011. Executive management discussed the organizations' strategy with all employees to create a shared vision. In 2013, many professionals were engaged in multiple lean projects to improve the entire (flow of the) patient process. The treatment planning system and the accelerators were replaced by new technology from 2011 to 2012. The patient safety culture was measured to evaluate the effects of this multifaceted approach.

Methods: The patient safety culture was evaluated over a three year period using a triangulation of methodologies. The Manchester Patient Safety Framework, implemented as a workshop, was combined with two surveys to evaluate the safety culture /behavior. Incident reports from an incident reporting system (IRS) and interviews with professionals were used to increase understanding of results. The workshops were performed twice. We used the internationallly validated Hospital Survey on Patient Safety Culture (HSOPSC), which measures four overall safety outcomes and ten dimensions of safety climate on a five-point scale, and a new developed factorial survey which measured the intentions for safety behaviour. Surveys were distributed three times in a three year period. In addition, the HSOPSC and the data from the IRS were used to evaluate the sustainability of results in 2015. Averages, chi-square, logistical and multi-level regression were used for analysis.

Results: Although the workshops detected no changes in safety culture between 2011 and 2013, the HSOPSC showed improvements on six out of twelve safety culture dimensions. In 2012, staffing, teamwork across units and handoffs & transitions presented more positive scores than in 2010 (Table 1). Improvements sustained and in 2013 the dimensions feedback & communication about error, experienced management support for safety and the overall perception of patient safety improved. All improvements had sustained until 2015 and teamwork across units improved further. Based on the results from the factorial survey on intentions for safety behavior, the intention to report incidents not reaching patient-level (near misses) decreased from 2010 to 2013 in accordance with the decreasing number of reports in the IRS. However, the intention towards taking action to prevent future incidents (structural improvement), strongly improved in 2013 (B: 1.19 with p: 0.01), especially for the near misses. From 2004 to 2009, the number of reported incidents increased from 510 to 1835 reports on yearly basis (Figure 1). However, the number of reported incidents that reached patient-level (misses) decreased with 27% from 2004 (N=122) to 2009 (N=89). From 2009 the number of reported near misses decreased with 50% from 1746 to 870 in 2013. However, the number of reported misses decreased with about 40% (89 in 2009 to 48 in 2013/ 55 in 2014).The interviewed employees experienced a sustained safety awareness, improved quality of reports and a strong increase in creating structural improvements. Due to improvements in equipment and increased problem solving, the actual number of incidents could have decreased.

Dimensions of HSOPSC	T1 (2010) N=54	T2 (2012) N=53	T3 (2013) N=51	T4 (2015) N=49	p T2–T1	p T3–T2	p T3–T1	p T4–T3
01: Supervisor/manager expectations and actions promoting PS	64	66	74	67	0.379	0.317	**0.050**	0.314
4.1.My supervisor/manager says a good word when he/she sees a job done according to established patient safety procedures.	65	57	71	57	0.250	0.106	0.805	0.148
4.2. My supervisor/manager seriously considers staff suggestions for improving PS	69	77	78	67	0.152	0.780	0.350	0.313
4.3.[R] Whenever pressure builds up, my supervisor/manager wants us to work faster, even if it means taking shortcuts.	63	72	75	71	0.452	0.614	0.322	0.665
4.4.[R] My supervisor/manager overlooks patient safety problems that happen over	59	66	71	74	0.769	0.135	0.071	0.524
02: Organizational learning/ continuous improvement	64	62	70	69	0.687	0.308	0.304	0.796
3.6. We are actively doing things to improve patient safety.	95	85	96	96	0.259	0.133	0.866	0.999
3.9. Mistakes have led to positive changes here.	76	73	84	78	0.296	0.064	0.488	0.449
3.13. After we make changes to improve patient safety, we evaluate their	52	28	29	33	0.434	0.766	0.944	0.429
03: Teamwork within units	70	71	77	82	0.930	0.362	0.304	0.155
3.1.People support one another in this unit.	93	89	92	98	0.427	0.609	0.761	0.362
3.3. When a lot of work needs to be done quickly, we work together as a team to get the work done.	78	70	80	88	0.638	0.181	0.387	0.097
3.4. In this unit, people treat each other with respect.	80	83	90	96	0.367	0.241	0.341	0.455
3.11. When one area in this unit gets really busy, others help out.	32	42	46	47	0.495	0.128	0.348	0.674
04: Communication openness	72	70	78	76	0.724	0.193	0.073	0.778
5.2. Staff will freely speak up if they see something that may negatively affect	94	85	92	94	0.104	0.247	0.639	0.736
5.4. Staff feel free to question the decisions or actions of those with more	50	43	61	57	0.556	0.076	0.062	0.668
5.6.[R] Staff are afraid to ask questions when something does not seem right.	72	83	80	78	0.221	0.586	0.539	0.567
05: Feedback and communication about error	60	62	76	78	0.661	**0.033**	**0.009**	0.714
5.1.We are given feedback about changes put into place based on event	48	47	65	82	0.940	0.067	0.094	0.269
5.3. We are informed about errors that happen in this unit.	65	68	71	71	0.516	0.781	0.747	0.602
5.5. In this unit, we discuss ways to prevent errors from happening again.	67	72	88	82	0.634	0.077	**0.028**	0.463
06: Non-punitive response to error	67	79	78	84	**0.045**	0.978	0.076	0.258
3.8.[R] Staff feel like their mistakes are held against them.	85	91	90	86	0.593	0.858	0.794	0.694
3.12.[R] When an event is reported, it feels like the person is being written up, not	95	85	92	85	0.140	0.512	0.494	0.232
3.16.[R] Staff worry that mistakes they make are kept in their personnel file.	82	69	61	82	0.180	0.559	**0.023**	0.071
07: Staffing	36	44	54	43	0.101	0.12	**<0.001**	0.424
3.2. We have enough staff to handle the workload.	17	45	55	33	**<0.001**	0.323	**<0.001**	0.123
3.5.[R] Staff in this unit work longer hours than is best for patient care.	43	51	55	49	0.082	0.610	0.250	0.833
3.7.[R] We use more agency/temporary staff than is best for patient care.	67	47	63	76	**0.016**	0.122	0.654	0.370
3.14.[R] We work in "crisis mode" trying to do too much, too quickly.	19	32	39	33	0.257	0.644	0.062	0.493
08: Management support for PS	41	42	64	60	0.835	**0.001**	**<0.001**	0.656
8.1.Hospital management provides a work climate that promotes patient safety.	48	51	73	61	0.341	**0.026**	**0.003**	0.334
8.8. The actions of hospital management show that patient safety is a top priority.	40	33	58	54	0.272	**0.032**	**0.049**	0.758
8.9.[R] Hospital management seems interested in patient safety only after an adverse event happens.	33	42	61	67	0.100	0.076	**0.016**	0.213
09: Teamwork across units	34	51	52	73	**<0.001**	0.057	**<0.001**	**0.001**
8.4. There is good cooperation among hospital units that need to work together.	24	47	45	69	**0.043**	0.313	**0.014**	**0.046**
8.10. Hospital units work well together to provide the best care for patients.	43	60	71	82	0.177	**0.045**	**0.001**	0.079
8.2.[R] Hospital units do not coordinate well with each other.	7	15	16	57	**0.032**	0.411	**0.001**	**<0.001**
8.6.[R] It is often unpleasant to work with staff from other hospital units.	61	79	76	86	0.116	0.144	**0.023**	0.239
010: Handoffs and transitions	32	42	50	61	0.051	0.250	**<0.001**	0.142
8.3.[R] Things "fall between the cracks" when transferring patients from one unit to	13	23	31	51	0.050	0.393	**0.001**	0.129
8.5.[R] Important patient care information is often lost during shift changes.	39	53	51	59	0.210	0.826	0.427	0.611
8.7.[R] Problems often occur in the exchange of information across hospital units.	20	32	47	63	**0.002**	0.295	**<0.001**	0.240
8.11.[R] Shift changes are problematic for patients in this hospital.	57	59	69	69	0.389	0.214	0.430	0.868
01: Overall perceptions of PS	57	55	66	64	0.641	**0.033**	**0.018**	0.717
3.15. Patient safety is never sacrified to get more work done.	30	27	34	31	**0.048**	0.646	0.337	0.959
3.18. Our procedures and systems are good at preventing errors from happening.	52	57	68	74	0.399	**0.011**	**0.046**	0.846
3.10.[R] It is just by chance that more serious mistakes don't happen around here.	77	64	78	75	0.313	0.282	0.825	0.933
3.17.[R] We have patient safety problems in this unit.	68	71	82	74	0.953	0.202	0.118	0.131
02: Frequency of reported events	65	55	50	65	**0.048**	0.126	**0.016**	**0.027**
6.1. When a mistake is made, but is caught and corrected before affecting the patient, how often is this reported?	61	42	43	59	0.063	0.244	0.181	0.060
6.2. When a mistake is made, but has no potential to harm the patient, how often is this reported?	52	43	29	45	**0.027**	0.593	**0.036**	0.258
6.3. When a mistake is made that could harm the patient, but does not, how often is this reported?	83	88	77	90	0.773	0.279	0.624	0.203

Positive scores: negative formulations were recoded
p-values ≤ 0.05 are bold

Figure 1. Results from the Incident Reporting System for 2004 until 2014.

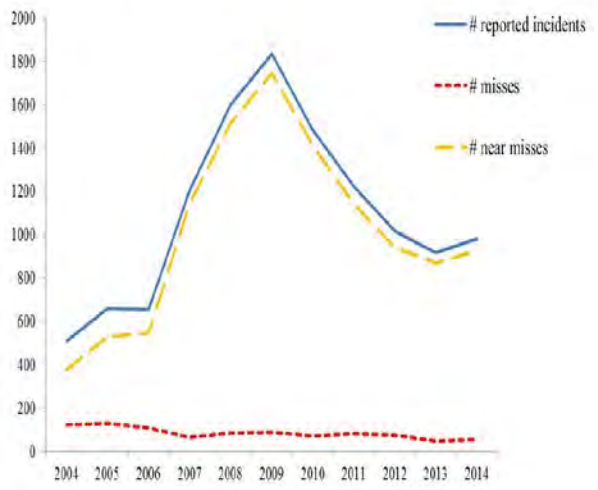

Conclusion: Due to increased problem solving and improvements in equipment, the number of incidents decreased until 2013. Although the intention to report incidents not reaching patient-level decreased, employees experienced sustained safety awareness and an increased intention to structurally improve. The patient safety culture improved in 2013 due to the lean activities combined with an organizational restructure, and actual patient safety outcomes might have improved as well. Results from 2015 proved the sustainability of the realized improvements. We conclude that lean management can help to improve the patient safety culture, but it's success depends greatly on how lean is implemented. In addition to the cultural aspects, structural elements and clinical process improvements should be addressed to create sustainable quality/safety improvements. Measurement of effect is an important foundation for continuous improvement. As patient safety culture is a complex phenomena, quantitative and qualitative measures should be combined to increase understanding in the actual effects. A sufficient level of detail in measures should be reported to not loose the opportunities for improvement.

SP-0602

The impact of demographics trend, cancer incidence and cancer prevalence for planning numbers of treatment units in Austria

A. Osztavics[1], R. Pötter[1]
[1]*Medizinische Universität Wien Medical University of Vienna, Radiotherapy, Vienna, Austria*

Purpose: There are around 38.000 new cancer cases in Austria per year. To generate an optimal patient-centered cancer care are clear formal structures in Austria how to plan the resources in health care. Based on a constitutional law exist a regulation between the national government, the district governments and the social insurances as third party based on which also the resources for radiotherapy are planned. The major method to calculate resources for radiotherapy is to refer treatment units to the population number, which has been formulated according to national guidelines for Austria. This method can also take into account demographics trends. This investigation addresses the additional impact of cancer incidence and prevalence estimates on such calculation models for population based number of treatment units (LIN).

Methods and materials: According to laws and national / regional guidelines (aim: 1 LIN for 100.000-140.000 inhabitants (Austrian Structure plan for Healthcare (ÖSG)) the recommended number of treatments units in radiotherapy were calculated for Austria and the city of Vienna for 2015 (population of 8.6 mill/1.8 mill) and for 2020 and 2030 taking into account expected demographic development. Around 60% of the 38.000 new cancer patient will have a treatment in a radiotherapy department. Based on the figures of the Austrian Cancer registrations the cancer prevalence will increase dramatically in the near future based on the demographic trend, general increased expectation of life in combination with the expectations of higher survival rate of cancer patients. In addition, prognosis for cancer prevalence and cancer incidence were used to calculate the needed number of LIN for the year 2015, 2020 and 2030 for Austria and Vienna.

Results: There is a need for minimum 61 LIN and maximum 86 LIN and present which implies a discrepancy of 18 LIN for the whole country (actual 43 LIN) for 2015. Based on the prognosis for cancer incidence a discrepancy of 14 LIN for Austria (aim 57 LIN) exists for 2015. The cancer prevalence prognosis shows a need for 68 LIN, which is a discrepancy of 25 LIN for the year 2015. For the city of Vienna, the actual situation (12 LIN) seems appropriate, as the discrepancy for 2015 is only 1 LIN. There is one important extra factor for Vienna: about 20% of all treated cancer patient come from Austrian neighbour districts, therefore there is a growing waiting list in Vienna. The entire prognosis until 2030 are general worse, because the results shows 2.01 mill inhabitants and around 8900 new cancer cases gives a need of 16 LIN for Vienna.

Conclusion: There is a minimum discrepancy of 18 LIN for the whole country for 2015. One important factor for precise planning the resources in radiotherapy is the cancer prevalence. Based on the prognosis model with the cancer prevalence is an actual need of 25 LIN for whole Austria and one more in Vienna. To fulfil the constitutional law obligations, the government should immediately start to close the gap of minimum 18 LIN for the whole country. Austria will have in 15 years a shortage of 40 LIN (aim 73 LIN) and this will have a negative impact on waiting time and outcomes of the treatments. Never less in these calculations is not the included the different complexity of treatments in radiotherapy which need different recourses of time, staffing and equipment. A further project should implement these factors to get a much more tailored planning for the formal recommended radiotherapy resources in Austria. .

Symposium: Combining radiotherapy with molecular targeted agents: learning from successes and failures

SP-0603

Interaction of radiotherapy with molecular targeting agents

P. Harari[1]
[1]*University of Wisconsin School of Medicine and Public Health, Madison, USA*

Despite the well established role of radiation in the treatment of solid tumor malignancies, and the rapidly expanding cadre of promising molecular targeting agents in oncology, the systematic investigation of radiation combined with molecular agents remains in an early dawn period. The increased precision of modern day radiation delivery to tumor targets with diminished dose exposure to normal tissues lends itself very favorably to combination with systemic therapies, particularly those tailored to specific molecular tumor targets. The complementary strengths of highly conformal radiation with molecular targeting agents affords a powerful opportunity to advance precision cancer medicine to a new level of impact for the future.
In this presentation, we will review the rationale for combining radiation with molecular targeting agents and consider opportunities for systematic study in both the preclinical and clinical trials setting. Several major clinical trials that examine this combination will be presented and discussed to highlight current findings and future opportunities. Strategies to expand the investigation of radiation/molecular target combination studies will be previewed. In both the curative and palliative oncology setting, it is possible that some of the most compelling

opportunities for improvement in cancer patient outcomes for the future may derive from combinations of radiation with molecular targeting agents.

SP-0604
Challenges combining radiotherapy with immunotherapy
S. Formenti[1]
[1]*Weill Cornell Medical Center of Cornell University, Radiation Oncology, New York- NY, USA*

Both preclinical studies and case reports have described synergistic interactions between local radiation (RT) and different types of cancer immunotherapy, demonstrating the potential for the combination to enhance locoregional efficacy and, by inducing an effective immune response reflect in systemic control. The latter effect, defined as "abscopal" is particularly relevant, since it has re-positioned classical radiotherapy into a treatment modality with systemic effects (1, 2). Our group described a role for RT in enhancing T cell activation and proliferation via antigen cross-presentation in the draining lymph node when combined with a diverse array of immune strategy, including enhancers of the priming phase (Flt-3L, GM-CSF, TLR agonists) or the effector phase (blocking CTLA4, PD-1, or TGF-beta) (3-8). Specifically, when combined with anti-CTLA-4 we demonstrated mechanisms underlying the abscopal effect, including enhanced T cell homing through release of CXCL16 and enhancement of the immunological synapse by release of RAE, the ligand for NKG2D receptor (7,8). We further demonstrated the clonal diversity of T cell immune responses induced by RT alone and RT combined with ipilimumab in patients with metastatic non small cell lung cancer refractory to other treatments, and are currently working at detecting the specific antigens responsible for the immune response to the combination (unpublished data).
However, many challenges remain to best optimize radiation in the context of cancer immunotherapy, both in terms of the choice of dose and fractionation when radiation is combined with immunotherapy as well as how to best block the immunosuppressive effects that accompany the immunogenic properties of radiation.
While we have demonstrated that when combined with anti CTLA-4 radiation best work when hypo-fractionated, it remains unclear whether ablative doses are necessary to sustain this effect (9). Similarly, when radiotherapy is combined with both CTLA-4 and PD- blockade the optimal scheduling remain unknown. Because of the immune-privilege status of established tumors, it is likely for multiple strategies to be necessary to subvert this condition (10). Ideally a rseries of well orchestrated interventions should result in release of neo-antigens, increased permeability of the tumor to enhance access to antigen presenting cells and increased cross presentation (potentially with the addition of TLR agonists). The ensuing effector phase requires the availability of a sufficient number of T lymphocytes, a variable that can be assessed by measuring in the peripheral blood the ratio between neutrophils and lymphocytes (11). Blockade of immune checkpoints is also required to develop and sustain a robust effector response. The concurrent interplay of macrophages is crucial for each of the steps described (12). While preclinical evidence for the therapeutic advantage of reverting macrophage polarization from M2 to M1 is emerging, how to optimally combine radiotherapy remains elusive. Experiments of low dose radiation inducing M1 polarization and recovering response to immune checkpoint blockade are being translated to the clinic (13). Strategies to overcome the immunosuppressive effects of RT have also evolved from preclinical to clinical setting. For instance to overcome RT-induced activation of TGFbeta, the need for additional PD-1 blockade has emerged, and it warrants clinical testing (6). A general barrier to advance the field consists of the complexity of testing multiple immunotherapy agents, often provided by different pharmaceutical companies. While radiation is a standard modality, with well-established, organ-specific acute and longterm toxicities, its use in combination with each immunotherapy agent obeys standard clinical trials safety and feasibility rules, and the pace of clinical testing. To this regard reliable biomarkers of response, ideally to be used as early surrogate endpoints for assessing response are much needed. Our results suggest that as early as at a three weeks interval from RT and ipilimumab, peripheral blood markers predict for development of a clinical objective response to the combination.

1. Demaria, S., B. *et al* (2004) Int. J. Radiat. Oncol. Biol. Phys., 58:862-870.
2. Formenti, S.C & Demaria, S., (2013) 105:256-265.
3. Demaria, S., *et al* (2005). Clin. Cancer Res. 11:728-734.
4. Formenti, S.C. & Demaria, S., (2009) 10(7), 718-726.
5. Dewan, Z., *et al* (2012) Clin Cancer Res, 18(24):6668-6678.
6. Vanpouille-Box C, et al (2015) Cancer Res., 1;75(11):2232-42.
7. Matsumura, S., *et al* (2008) J Immunol, 181(5), 3099-3107.
8. Ruocco, M. G., *et al* (2012), J Clin Invest, 122(10), 3718-3730.
9. Dewan M.Z., *et al* (2009) Clin Cancer Res 15:5379-88.
10. Joyce, J.A, Fearon, D.T. (2015).. Science vol 348, issue 6230, 74-80.
11. Golden E.B., *et al* (2015). Lancet Oncology, 16:795-803.
12. DeNardo DG, *et al* (2009). Cancer Cell 16, 91-102.
13. Klug F, *et al* (2013) Cancer Cell. Nov 11;24 (5):589-602

SP-0605
New strategies to targeting tumour angiogenesis and hypoxia
O.Chinot[1]
[1]*CHU La Timone, Service de Neuro-oncologie, Marseille, France*

Abstract not received

Symposium with Proffered Papers: Radiomics - the future of radiotherapy?

SP-0606
Imaging-genomics: identifying molecular phenotypes by integrating radiomics and genomics data

To be confirmed

SP-0607
PET/CT heterogeneity quantification through texture analysis: potential role for prognostic and predictive models
M. Hatt[1]
[1]*INSERM, LaTIM- UMR 1101, Brest, France*

The use of PET/CT has increased much in the last decade, from a purely diagnostic to a radiotherapy planning and therapy monitoring tool. For these new applications, the quantitative and objective exploitation of PET/CT datasets becomes crucial given the well-established limitations of visual and manual analysis. Within this context, the Radiomics approach which consists in extracting large amount of information from multimodal images relies on a complex pipeline: image pre-processing, tumor segmentation, image analysis for shape and heterogeneity features calculation, and machine learning for robust and reliable features selection, ranking and combination with respect to a clinical endpoint. Although the Radiomics approach has been extensively applied to CT imaging, its use for PET/CT is more recent and less mature. There are however already a large body of published works hinting at the potential value of textural features and other advanced image features extracted from PET/CT in numerous tumour types. However, many methodological issues and limitations specific to PET/CT image properties have been highlighted by recent studies, This presentation aims at presenting both the promises and potential of advanced PET/CT image textural features analysis to build prognostic and predictive models, as well as the numerous pitfalls to avoid in order to further advance research in that promising field.

SP-0608

The potential of radiomics for radiotherapy individualisation

E. Troost[1,2,3,4], K. Pilz[2,4], S. Löck[1,2,3,4], S. Leger[3], C. Richter[1,2,3,4]

[1]*Helmholtz-Zentrum Dresden-Rossendorf, Institute of Radioonkology, Dresden, Germany*

[2]*German Cancer Consortium DKTK, Partner site Dresden, Dresden, Germany*

[3]*Faculty of Medicine and University Hospital Carl Gustav Carus- Technischen Universität Dresden- Helmholtz-Zentrum Dresden-Rossendorf, OncoRay – National Center for Radiation Research in Oncology, Dresden, Germany*

[4]*Faculty of Medicine and University Hospital Carl Gustav Carus- Technischen Universität Dresden, Department of Radiation Oncology, Dresden, Germany*

In the era of tailored medicine, the field of radiation oncology aims at identifying patients likely to benefit from treatment intensification and of those suffering from undesired treatment-related side-effects. In the past, patient selection in oncology was merely based on, e.g., randomisation, immunohistochemical staining of tumour biopsies, on tumour size or stage, or even on preferences. The introduction and increased availability of high-throughput techniques, such as genomics, metabolomics and Next Generation Sequencing, have revolutionised the field.

In radiation oncology, high-quality anatomical and functional imaging is, besides physical examination, the pillar for target-volume delineation, planning and response assessment. Therefore, 'radiomics', referring to the comprehensive quantification of tumour phenotypes through extensive image features analyses, is a logical consequence. Pioneered by the publication of Aerts *et al*. [1], the field is rapidly evolving regarding techniques, tumour sites and imaging modalities assessed.

In this presentation, the status of radiomics for radiotherapy individualisation will be highlighted and possible areas of future research activities outlined.

References: [1] Aerts HJWL, Rios Valezques E, Leijenaar RTH, *et al*. Decoding tumour phenotype by noninvasive imaging using a quantitative radiomics approach. Nature Communications 5, Article number: 4006.

OC-0609

Radiomic CT features for evaluation of EGFR and KRAS mutation status in patients with advanced NSCLC

E.E.C. De Jong[1], W. Van Elmpt[1], L.E.L. Hendriks[2], R.T.H. Leijenaar[1], A.M.C. Dingemans[2], P. Lambin[1]

[1]*Maastricht University Medical Centre, GROW-School for Oncology and Developmental Biology- Department of Radiation Oncology MAASTRO Clinic, Maastricht, The Netherlands*

[2]*Maastricht University Medical Centre, GROW-School for Oncology and Developmental Biology- Department of Pulmonology, Maastricht, The Netherlands*

Purpose or Objective: Molecular profiling is considered standard of care for advanced non-small cell lung cancer (NSCLC) patients. Approximately 25% of adenocarcinoma patients has a *KRAS* mutation; 10-15% has an activating *EGFR* mutation where tyrosine kinase inhibitors (TKI) are approved for first line treatment. *EGFR* and *KRAS* mutations are mutually exclusive. Obtaining enough tissue for molecular analysis may be difficult. Therefore, in this study we investigated whether *EGFR* and *KRAS* mutations can be distinguished from wildtype patients based on features derived from standard CT imaging.

Material and Methods: From a retrospective database of NSCLC patients included between 2004 and 2014, all *EGFR*-mutated (*EGFR*+, only exon 19 deletions or exon 21 L858R) patients, the consecutive *KRAS*-mutated (*KRAS*+) and *EGFR*/*KRAS* wildtype (WT) patients were included. The CT-scan at first diagnosis of NSCLC (i.e. before any treatment) with the primary tumor visible was used for radiomics feature extraction. The primary tumor was delineated using a GrowCut segmentation algorithm (3D Slicer) and manually adapted if needed. 724 CT features were calculated using radiomics software. To test if features were different for *EGFR*+, *KRAS*+ or WT patients one way ANOVA (initially without correction for multiple testing) was performed using a 5% significance level. A pair-wise comparison (t-test) identified significantly different groups.

Results: 51 *EGFR*+, 47 *KRAS*+ and 32 WT patients were included. 41 features were significantly different between *EGFR*+, *KRAS*+ and WT patients. One feature is a first order gray-level statistics feature (7% of feature subgroup total), two are gray-level co-occurrence matrix based (9%), two gray-level size-zone matrix based (18%), one Laplacian-of-Gaussian transform based (0.5%) and 35 are wavelet transform based features (7%). Statistics for the significant features are shown in Table 1. One easy to interpret significantly different feature for *EGFR*+ compared to WT patients was the median Hounsfield Unit (HU). *EGFR*+ patients had a median HU which is on average 54±23 HU higher compared to WT patients, see Figure 1. *KRAS*+ patients did not have a significantly different median HU compared to *EGFR*+ or WT patients.

Table 1: Mean values and standard deviation of *EGFR+*, *KRAS+* and WT patients for the significant simple features.

Feature inside primary tumor	*EGFR+* Mean± std	*KRAS+* Mean ± std	Wild type Mean± std	Different group
GLCM_infoCorr1	-0.12 ± 0.05	-0.15 ± 0.06	-0.15 ± 0.07	*EGFR+* vs. both
GLCM_infoCorr2	0.57 ± 0.13	0.63 ± 0.14	0.66 ± 0.13	*EGFR+* vs. both
GLSZM_lowIntensityEmphasis	3.5 ± 2.10^{-2}	5.0 ± 4.10^{-2}	5.4 ± 6.10^{-2}	*EGFR+* vs. wt
GLSZM_lowIntensitySmallAreaEmp	2.5 ± 2.10^{-2}	3.3 ± 2.10^{-2}	4.1 ± 4.10^{-2}	*EGFR+* vs. wt
LoG_sigma_2_mm_3D_stats_std	65 ± 25	78 ± 34	80 ± 35	*EGFR+* vs. both
Median Hounsfield Unit	31 ± 40 HU	-9 ± 131 HU	-23 ± 124 HU	*EGFR+* vs. wt

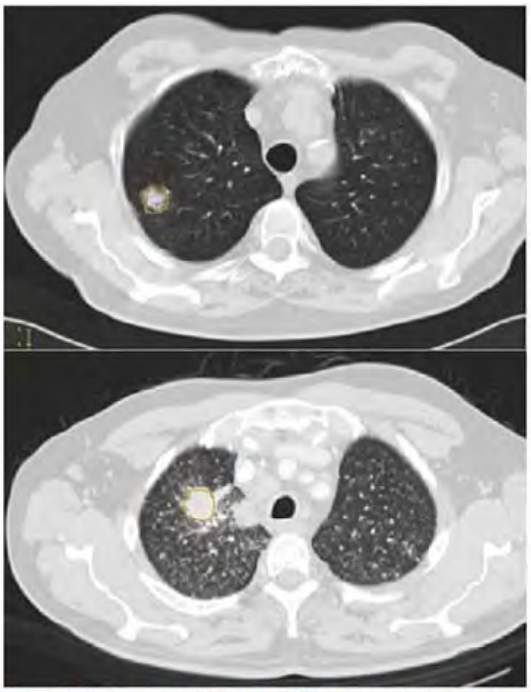

Figure 1: This image shows the difference in intensity between a WT patient (upper, median: -390 HU) and an *EGFR+* patient (lower, median 61 HU).

Conclusion: We showed that there are differences in radiomic CT features between *EGFR*+, *KRAS*+ and WT NSCLC. The next step will be to externally validate (work in progress) a robust radiomic signature, based on standard CT imaging. Also this allows to monitor radiomic signature evolvement under treatment.

Symposium: Radiobiology of proton / carbon / heavy ions

SP-0610

Gene expression alterations to carbon ion and X-irradiation

M. Moreels[1], K. Konings[1], S. Baatout[1]
[1]*SCK-CEN, Radiobiology Unit, Mol, Belgium*

Hadron therapy is an advanced technique in the field of radiotherapy that makes use of charged particles such as protons and carbon ions. The inverted depth-dose profile and the sharp dose fall-off after the Bragg peak offered by charged particle beams allow for a more precise localization of the radiation dosage to the tumor as compared to the conventional used photons. As a consequence, the surrounding healthy tissue receives a much lower dose. Besides this ballistic advantage, the use of high-linear energy transfer (LET) carbon ion beams offers also a biological advantage, i.e. a higher relative biological effectiveness (RBE) as compared to conventional low-LET photon therapy.
Carbon ion radiation is thus more effective in inducing DNA damage, cell cycle arrest and cell death, thereby accounting for highly lethal effects, even in tumors that are resistant to X-ray irradiation.
The response of an irradiated cell depends on the dose, dose-rate, radiation quality, the lapse between the radiation-induced stress and the analysis, and the cell type. In this context, genome-wide studies can contribute in exploring differences in signaling pathways and to unravel 'high-LET-specific' genes. Several studies within SCK•CEN and outside have already compared changes in gene expression induced by different radiation qualities. Overall, the number of differentially expressed genes as well as the magnitude of (dose-dependent) gene expression changes was found to be more pronounced after irradiation with particle beams.
Currently, the Radiobiology Unit of SCK•CEN is deeply investigating the effect of low- and high-LET radiation on the gene expression of different cancer cell lines *in vitro*. Our results clearly demonstrate a dose-dependent downregulation in several genes involved in cell migration and motility after carbon ion irradiation. A higher number of genes as well as more pronounced changes in their expression levels were found after carbon ion irradiation compared to X-rays. Further research are currently investigating whether the observed molecular changes also influence the cellular 'behavior' after irradiation in terms of cell migration and motility after irradiation, since these are prominent characteristics of cancer progression and metastasis.
Assessing both the risks and advantages of high-LET irradiation can contribute to the study of the biological effect on the tumor and will lead to further acceptance and improvement of the clinical outcome of hadron therapy.
Acknowledgements: This work is partly supported by the Federal Public Service in the context of the feasibility study ‘Application of hadrontherapy in Belgium’, which is part of action 30 of the Belgian cancer plan. Carbon ion irradiation experiments (P911-H) were performed at the Grand Accélérateur National d'Ions Lourds (Caen, France).

SP-0611

Normal tissue response in particle therapy

B.S. Sørensen[1]
[1]*Aarhus University Hospital, Exp. Clin. Oncology, Aarhus C, Denmark*

Particle therapy as cancer treatment, with either protons or heavier ions, provide a more favourable dose distribution compared to x-rays. While the physical characteristics of particle radiation have been the aim of intense research, less focus has been on the actual biological responses particle irradiation gives rise to. Protons and high LET radiation have a higher radiobiological effect (RBE), but RBE is a complex quantity, depending on both biological and physical parameters. One of the central questions in particle therapy is whether the tumor and the normal tissue has a differential RBE due to the difference in α/ß ratio. Most of the data to enlighten this is in vitro data, and there is very limited in vivo data available, although this is a more appropriate reflection of the complex biological response.
RBE is often established as measured by cell death, but emerging evidence also demonstrate an altered response in the surviving cells. This is both evident for high LET radiation, but also for proton radiation. This differential biological effect is not only relevant in the tumour, but also in the normal tissue. Current research in particle radiobiology is, in addition to the RBE, focusing on the molecular tissue response, and on the signalling pathways. Gene expression response in a panel of primary human fibroblasts, established from patients with known response to xray radiation in regards to late tissue damage, irradiated in vitro with different radiation qualities, has evaluated the effect of particle irradiation at different positions in the beam. This enlightens the heterogeneity in patient response to proton irradiation, individual biological variations and the differential effect of proton irradiation. This presentation will focus on the available experimental data on normal tissue response after irradiation with protons or heavier ions.
Supported by grants from the Danish Cancer Society

SP-0612

Preclinical studies using protons for high-precision irradiation of small animals

P. Van Luijk[1]
[1]*University Medical Center Groningen, Department Radiation Oncology, Groningen, The Netherlands*

Many technological developments attempt to reduce dose to normal tissues in order to reduce normal tissue damage. However, optimal use of such technologies requires knowledge of mechanisms underlying normal tissue damage. Therefore, normal tissue effects were studied using highly accurate proton irradiation to different regions and volumes in various rat organs.
Rats were irradiated using high-energy protons. Collimator design was based on X-ray imaging (spinal cord), MRI (parotid gland) or CT scans (heart, lung) of age, sex and weight matched rats. This typically resulted in 2-4% uncertainty in irradiated volume of that organ. For partial irradiation of the spinal cord an in-line X-ray imager was used to yield a positioning accuracy of 0.1 mm. Finally, non-uniform irradiations were facilitated by sequential use of different collimators. Hind leg paralysis, breathing frequency chances and salivary flow rate and tissue histo-pathology were used to assess organ response.
Spinal cord: Next to irradiated volume, low doses surrounding small volumes with a high dose effects were found to strongly impact the tolerance dose. In addition, the tolerance dose strongly depended on the shape of the dose distribution, independent of irradiated volume. Taken together this indicates that irradiated volume is not good predictor of toxicity. However, a model including tissue repair originating from non-irradiated tissue over a limited distance could explain the observed effects. Taken together these results suggest that regeneration plays an important role in the response of the spinal cord.
Parotid gland: We demonstrated that the response of the parotid gland critically depends on dose to its stem cells, mainly located in its major ducts. The importance of this anatomical location was confirmed in a retrospective analysis of clinical data. A prospective clinical trial to validate this finding is in progress.
Lung: Volume dependent mechanisms of lung toxicities were observed, where high volumes with low dose limiting early vascular/inflammatory responses inducing pulmonary hypertension and consequential cardiac problems, whereas low volumes displayed high or even no dose limiting late fibrotic response. Moreover, inclusion of the heart in the irradiation field strongly enhanced early lung responses.
In summary, using high-precision proton irradiation of rat organs we elucidated several mechanisms and critical targets for normal tissue damage. In general we found that, rather than dose to the organ, the development of toxicity strongly related to dose to functional sub-structures within the organ or even in other organs. In general, in more parallel organized tissues it seems that a high dose to a small volume

is better that a low dose to a large volume. Maintaining or enhancing the regenerating potential of the normal tissue seems warranted to further optimize radiation therapy.

Symposium: New insights in treating vertebral metastases

SP-0613
Recent progresses in interventional radiology
P. Bize[1]
[1]*Centre Hospitalier Universitaire Vaudois, Department of Diagnostic and Interventional Radiology, Lausanne Vaud, Switzerland*

Treatment of verterbral metastasis can be compex, involving medical treatment, radiotherapy, suregry or newer technique such as thermal ablation and vertebroplasty. The purpose of vertebral metastasis treatment is to rapidly improve the quality of life of the patients and to restore the mechanical properties of the spinal column and to a lesser extend to prevent local tumor growth.
Minimally invasive treatment,such as vertebroplasty, combined or not, with thermal ablation fulfill all these purposes with minimal impact on the patient's quality of life.
Vertebroplasty is efficient in contolling the patient's pain in 89.7% at 1 month and 86.9% at 6 months (ref 1).
Restoration of the mechanical properties of the spinal column is obtaind in 100% of cases after successful vertebroplasty (ref 2)
When combined with thermal ablation (RFA or Cryoablation) the local reccurence rate is very low (ref 3)
While radiation therapy remains the mainstay in the treatment of vertebral metastasis, it does not improve the stability of the vertebral column. A complimentary surgery is often necessary to ensure stability of the treated vertebra.
Minimalliy invasive procedure such as thermal ablation combined with vertebroplasty do offer immediate pain control in addition to local tumor control and restoration of mechanical stability with a minimal impact on the patient's quality of life.

SP-0614
What are the limits of minimally invasive surgery?
F. Zairi[1]
[1]*CHRU Lille Hôpital Salgreno, Department of Neurosurgery, Lille, France*

Abstract not received

SP-0615
How to optimise the potential of SBRT
P. Ost[1]
[1]*University Hospital Ghent, Ghent, Belgium*

Radiotherapy is a well-established treatment for painful vertebral metastases. Multiple prospective studies report pain response rates of 50 to 90%. Based on randomized studies, 8 Gy in a single fraction is the standard of care for painful uncomplicated bone metastases. Despite the lack of a dose response relationship for pain control, there is good rationale for dose escalation with the aim to improve upon existing rates of local tumour control and pain control. Stereotactic body radiotherapy is ideally suited to safely escalate the dose and improve tumour control. In order to optimize the potential of SBRT, adequate patient selection and specific technical considerations should be taken into account.
PATIENT SELECTION
Several considerations should be taken into account before delivering SBRT for vertebral metastases. A first consideration is the life expectancy of the patient, which should be evaluated with validated scoring systems (e.g. NRF score, Recursive partitioning analysis index, PRISM). Patients with a short life expectancy in need for palliative radiotherapy should be managed with short effective radiotherapy courses. In patients with longer life expectancy local control might be an important end point potentially requiring a higher radiotherapy dose. A second consideration is the characteristic of the vertebral metastasis and divides the metastases into uncomplicated or complicated. A systematic review suggested the following working definition for uncomplicated bone metastases: those unassociated with impending or existing pathologic fracture or existing spinal cord compression or cauda equina compression. Although this definition looks straightforward it is still variable to interpretation and might be incomplete. The Spinal Instability Neoplastic Score (SINS) might help us estimate the risk of vertebral fracture limiting SBRT to stable and potentially unstable metastases. Different definitions of spinal cord compression are available with the minimum evidence for cord compression being indentation of the thecal sac at the level of clinical features. Finally, other aspects such as, primary tumour type, other metastases, symptoms, practical considerations, current systemic treatment and previous radiotherapy… should be taken into
TECHNICAL CONSIDERATIONS
For treatment simulation several options are available for patient immobilization. Independent of the system used, the patient must be positioned in a stable position capable for reproducibility of positioning, allowing the patient to feel as comfortable as possible. A typical CT scan length should extend at least 10 cm superior and inferior beyond the treatment field borders (slice thickness of≤2.5 - 3 mm). CT contrast will help visualize the soft tissue and adjacent normal tissues. The International Spine Radiosurgery consortium developed a consensus guideline for target volume definition. MRI images are mandatory for delineation. Axial volumetric T1 and T2 sequences without gadolinium are a standard with ≤3 mm slice thickness. Contouring of normal tissue should be standardized for example: start contouring at 10 cm above the target volume to 10 cm below the target (RTOG 0631). Different fractionation schedules exist with variable total doses. None of the proposed schedules is proven to be superior to another. In case of single fraction, the doses vary between 16 and 24 Gy, with a strong trend for increasing pain relief with higher radiation doses, particularly with doses≥ 16 Gy. In case of fractionated radiotherapy, doses vary between 7-10 Gy for a 3 fraction schedule and between 5-6 Gy for a 5 fraction schedule. Most centers prescribe the dose (Dpr) to a % volume of the PTV. A PTV dose coverage of <80% of the Dpr should be avoided (RTOG 0631). This Dpr. should be prescribed to the isocenter or periphery of target. To minimize the risk for toxicity it is advised to strictly adhere to the published dose-constraints keeping in mind that they are mostly unvalidated. Control and correction of the patient and tumor position should be done with volumetric or stereoscopic X-ray imaging at least before each treatment fraction. Extensive recommendations and guidelines for a stereotactic or high precision QA program, supplementing the QA program for linear accelerators can be found in literature and should be followed (e.g. AAPM TG 101 report).
OUTCOME
The International Bone Metastases Consensus Working Party developed guidelines for the assessment of endpoints of palliative radiotherapy of bone metastases. It is recommended to follow the proposed definitions of pain assessment and pain response. Toxicity should evaluated at follow up visits using standardized criteria such as the National Cancer Institute (NCI) Common Terminology Criteria for Adverse Events (CTCAE) v.4.0.

Symposium: IMRT, the new standard in treatment of gynaecological, lung and breast cancers?

SP-0616
Organ motion: is it an obstacle to the use of IMRT as a standard technique for gynecological cancers?
I. Barillot[1]
[1]*Hôpital Bretonneau, Tours, France*

Intensity-modulated radiotherapy (IMRT) has been introduced in a number of disease in the late nineties for treating complex treatment volumes and avoiding close proximity

organs at risk (OAR) that may be dose limiting. Fifteen years later, in many countries, IMRT is still not considered as a standard technique for treating gynaecological cancers. It is well accepted that, if reducing acute and chronic toxicity are the main endpoints, IMRT may be considered as the ideal technique. By contrast, if disease-related outcomes are considered, there are still insufficient data to recommend IMRT over three-dimensional conformal radiotherapy. Moreover, with the increased accuracy of treatment delivery comes the need for greater accuracy in incorporation of organ motion to prevent geographical misses.

Uterus significantly moves according to the bladder and rectal filling. The majority of motion occurs in the anterior–posterior and superior–inferior directions, with mean interfraction movements of 4–7 mm, but very large displacements up to more than 2 cm may occur with the inherent risk of poor coverage of the posterior part of the cervix or of the uterine fundus. Similarly, during post-operative irradiation, the vaginal CTV changes its position with standard deviation of 2.3 cm into the anterior or posterior direction, 1.8 cm to left or right and 1.5 cm towards the cranial. According to the majority of studies a uniform CTV planning treatment volume margin of 15 mm would fail to encompass the CTV in 5% of fractions in post-op. It rises up to 32%, when the CTV includes the entire uterus. For intact cervical cancer, where gross disease is present, the significant shrinkage in tumour volume of 62% in mean, also contributes to potential unintended doses to normal tissues, but the risk is rather low.

How to deal with motion uncertainties?

It can be helpful to attempt to control rectum and bladder filling, although the compliance with instructions for bladder filling and for rectal emptying does not always result in adequate reproducibility. The construction of an ITV from CT images acquired with empty and full bladder is also another way to account for interfraction motion of the CTV. The implementation of IGRT on a daily basis is essential for judging the effectiveness of the measures previously outlined. However, one must never forget that the cervix or vaginal cuff and surrounding tissues are mobile relative to the bony pelvis, while the pelvic lymph nodes which are also part of the target are relatively fixed. Thus, the shifts to account for motion of the mobile target may move the pelvic lymph nodes out of the PTV. Consequently, care should be taken when shifting to ensure that nodal targets are still within PTV, but keeping CTV to PTV margins to 10-15 mm helps to find a good compromise without jeopardizing the OAR's sparing. The risk of geographical misses does exist, but its level must be appreciated in the light of the dose contribution brought by the additional brachytherapy. Brachytherapy still plays a major role in the treatment of cervix carcinomas. The important dose gradient and the absence of target movements in relation to the inserted radioactive sources allow for dose escalation and 3D image guided adaptative procedure allows for accurate definition of target volumes with definition of dose volume parameters. Consequently a moderate under dosage of a part of CTV during IMRT may be compensated by the high dose delivered by brachytherapy.

The concept of adaptive IMRT seems to be applicable for the management of the complex deformable target motion that occurs during radiation of gynecological cancers. The cervix-uterus shape and position can be predicted by bladder volume, using a patient-specific prediction model derived from pre-treatment variable bladder filling CTscans. Based on that, a strategy called "plan of the day" has been elaborated and is under investigation.

In conclusion, organ motion is not an obstacle to the use of IMRT as standard technique for gynecological cancer, especially when combined with brachytherapy, provided that PTV margins are not reduced and IGRT is adequately used. The participation to prospective studies and/or the registration of patients in database are strongly encouraged.

SP-0617

IMRT for lung cancer: current status and future developments

C. Faivre-Finn[1]

[1]*The Christie NHS Foundation Trust, Institute of Cancer Sciences - Radiation Oncology, Manchester, United Kingdom*

IMRT is a technique that adds fluence modulation to beam shaping, which improves radiotherapy dose conformity around the tumour and spares surrounding normal structures. Treatment with IMRT is becoming more widely available for the treatment of lung cancer, despite the paucity of high level evidence supporting the routine use of this more resource intense and complex technique [Chan. J Thor Oncol 2014]. It allows the treatment of patients with large volume disease, close to critical organs at risk with curative doses.

Very few prospective trials have reported on the use of IMRT. RTOG 0617 was a 2 x 2 factorial design study, in which patients with stage III NSCLC were randomized to receive high dose (74 Gy in 37 fractions) or standard dose (60 Gy in 30 fractions) RT concurrently with weekly paclitaxel/carboplatin with or without cetuximab [Bradley. Lancet Oncol 2015]. The radiotherapy technique (3D conformal RT vs IMRT) was a stratification factor. Disappointingly, there was a significant increase in the risk of death in the high-dose arms (median survival, 19.5 months vs 28.7 months; p=0.0007), and a 37% increase in the risk of local failure in the high-dose arms (hazard ratio, 1.37; p=0.0319). It should be noted that just under half of the patients in this study were treated with IMRT (46.5%). Although patients were stratified by treatment delivery technique and the proportions of patients treated with IMRT were balanced between treatment groups (46.1% in 60 Gy arms and 47.1% in 74 Gy arms), the delivery of 74 Gy was probably challenging, particularly in patients treated without IMRT, given the gross tumour volume (GTV) (mean 124.7 in 60 Gy arms and 128.5 cc in 74 Gy arms).

A subsequent analysis on patient reported outcome demonstrated a significantly worse quality of life on the 74 Gy arms at 3 months after treatment [Mosvas JAMA 1015]. Interestingly, despite minimal differences in clinician-reported side-effects between treatment arms, the decline in quality of life was significantly reduced with the use of IMRT compared to 3DCRT suggesting that the use of improved radiotherapy treatment techniques may be beneficial. Furthermore, baseline QOL was an independent prognostic factor for survival. A further analysis of RTOG0617 compared the outcome of patients treated with 3D-conformal and intensity modulated radiotherapy [Chun. ASTRO 2015]. Survival was the same in both groups in spite of the larger proportion of patients with stage IIIb vs IIIa and larger Planning Target Volume in the IMRT cohort. Moreover the use of IMRT reduced severe pneumonitis, dose delivered to the heart and more patients received chemotherapy in the IMRT cohort.

Population-based studies have not shown any significant difference in overall survival, toxicity or time spent hospitalized following treatment between 3DCRT and IMRT [Harris. Int J Radiat Oncol Biol Phys 2014; Chen. J Thorac Oncol 2014]. The need remains to develop clinical trials that will demonstrate the benefit of IMRT in terms of toxicity, local control, survival or quality of life.

A number of clinical trials are currently recruiting patients. Some are evaluating personalized dose escalation based on dose delivered to organs at risk (NCT01836692, NCT01166204) and others an increase dose to selected parts within the tumour, defined by functional imaging (Dose Painting) (NCT01024829, NCT01507428).

SP-0618

Are there early and late benefits of breast IMRT for improving dose distribution homogeneity?

J.P. Pignol[1]

[1]*Erasmus MC Cancer Institute, Radiation Oncology, Rotterdam, The Netherlands*

In countries with active mammography screening programs, the majority of breast cancers are diagnosed at an early

stage. Those patients are treated with breast conserving surgery followed by adjuvant radiotherapy, which is equivalent to mastectomy in term of survival. The objective of the radio-surgical association is hence primarily cosmetic. Since those patients have excellent outcomes, it is logical to minimise any detrimental effects of the treatment, in term of acute and delayed side effects.
Intensity Modulated Radiation Therapy (IMRT) is a radiation technique where the photon beam intensity is modulated across multiple irradiation fields to achieve a pre-determined goal for the dose distribution, using try and error methods. The goal can be to improve the conformality of the dose distribution or, as it is often the case for the breast, its homogeneity.
There are many cohort studies and randomised clinical trials reporting on the clinical benefit for BIMRT used to improve the dose distribution homogeneity in the breast. A multicentre randomised controlled trial from Canada has demonstrated a large and significant reduction of acute skin toxicity, notably the moist desquamation occurring on the infra-mammary fold. This benefit was not present for large breasted patients. Moist desquamation was significantly associated with a severe pain and a reduction of Health Related Quality of Life (HRQoL). There are several studies reporting significant associations between the occurrence of moist desquamation and delayed side effects like telangiectasia and induration. Several randomised trials have also evaluated the impact of BIMRT on long-term side effect, and two studies from the UK using hypofractionated regimen showed a small but significant improvement of the cosmetic outcome at 5 years. It is important to note that no cosmetic improvement was found at 8 years in the Canadian study using conventional fractionation of 50 Gy in 25 treatments. In the Cambridge and Canadian studies there was no impact of the radiation technique on the long-term HRQoL. In the Canadian study there was a highly significant correlation between the initial pain experience at time of radiotherapy and the occurrence of chronic pain and a reduction in HRQoL at 8 years. Also the occurrence of moist desquamation at the time of radiation treatment was significantly correlated with the occurrence of telangiectasia, fibrosis and a poorer cosmetic outcome on self-evaluation questionnaire. Those studies suggest a complex interplay between the breast volume, the dose-fractionation schedule and the radiation technique. More recently, a study from Ghent demonstrated that for large breasted patients hypofractionated prone BIMRT significantly reduces moist desquamation compared to hypofractionated supine BIMRT.
In summary, there are solid evidences to suggest that BIMRT reduces the occurrence of acute skin toxicity, including moist desquamation and pain. For large breasted women, the use of a prone technique BIMRT appears to significantly reduce moist desquamation. In regards to long-term side effect it seems that BIMRT could improve the cosmetic outcome when using hypofractionation, but its role is less clear when using a standard dose-fractionation regimen. A painful experience of moist desquamation during the initial radiation treatment is significantly associated with chronic pain and poorer HRQoL. Since BIMRT is a technique relatively simple to implement at no cost, outside the USA, it should be used as standard for adjuvant breast radiotherapy.

Symposium with Proffered Papers: Plan of the day (PotD): current status

SP-0619
PotD external beam: overview of current practice

J. Penninkhof[1], S. Heijkoop[1], S. Quint[1], A.P. Kanis[1], A. Akhiat[2], R. Langerak[1], J.W. Mens[1], B.J.M. Heijmen[1], M.S. Hoogeman[1]
[1]*Erasmus MC Cancer Institute, Radiation Oncology, Rotterdam, The Netherlands*
[2]*Elekta AB, Research Physics, Stockholm, Sweden*

Most image guidance strategies today aim at minimizing random and/or systematic geometrical uncertainties by offline or online correction protocols based on either surrogates or the actual tumor position. Corrections are usually limited to translations, and rotational errors, shape change and intra-fractional changes are not corrected for. For targets with a large day-to-day shape variation, or in case of multiple targets with differential motion, generous safety margins have to be used that partly undo the healthy tissue sparing properties of modern radiation techniques such as IMRT and VMAT. Adaptive radiotherapy (ART), e.g. with a Plan-of-the-Day (PotD) strategy has been proposed to overcome this problem. Guidelines for proper selection of patients that need a replanning (e.g. lung, rectum), or implementation of a more labour-intensive PotDworkflow for groups of patients (e.g. cervix, bladder) have been major research topics in recent years.
In this presentation, an overview will be given of current *clinical* implementations of PotD strategies in literature. The library-based PotD procedure as implemented at Erasmus MC for cervical cancer patients will be discussed in more detail. For these patients, a plan library contains 2 or 3 VMAT plans adequate for target shapes and positions corresponding to smaller and larger bladder volumes. Every treatment day, the best fitting plan is selected based on an in-room acquired cone beam CT scan, showing internal anatomy and markers implanted around the primary tumor. The recent PotD implementation in our record & verify system has pathed the way for a more wide-spread application of safe and efficient delivery of library-based PotD strategies, and for more advanced library-based approaches including dynamic plan-library updates.

SP-0620
In-room MR image-guided plan of the day

R. Kashani[1], J. Olsen[1], O. Green[1], P. Parikh[1], C. Robinson[1], J. Michalski[1], S. Mutic[1]
[1]*Washington University School of Medicine, Radiation Oncology, St. Louis, USA*

The clinical implementation of magnetic resonance image-guided radiation therapy (MR-IGRT) has enabled the daily visualization of internal soft-tissue anatomy with the patient in the treatment position. The information provided by the daily MR, which may not be available in some other online imaging modalities such as cone-beam CT, has allowed us to evaluate the impact of geometric variations in the patient on the planned versus delivered dose on a day to day basis. The availability of daily volumetric MR images, in combination with software tools integrated into the MR-IGRT system, and independent quality assurance tools for online patient-specific QA, has allowed for clinical use of online adaptive MR-IGRT since September 2014.
We report on the first year of clinical experience with online treatment adaptation for over 45 patients treated to various sites including abdomen, pelvis, and thorax, having received more than a total of 150 adapted fractions. Here we describe the clinical implementation and workflow for online adaptive MR-IGRT, provide details on decision criteria for daily plan adaptation, and discuss and compare an online plan adaptation approach to a plan library approach where the plan of the day is selected from a group of plans based on previous patient anatomy. We also discuss limitations of current techniques and future improvements.

OC-0621
A population based library of plans for rectal cancer: design and prospects for margin reduction

L. Hartgring[1], J. Nijkamp[1], S. Van Kranen[1], S. Van Beek[1], B. Van Triest[1], P. Remeijer[1]
[1]*Netherlands Cancer Institute Antoni van Leeuwenhoek Hospital, Radiotherapy, Amsterdam, The Netherlands*

Purpose or Objective: The clinical target volume (CTV) in rectal cancer is subject to considerable shape deformations due to rectal and bladder filling changes, which require large planning target volume (PTV) margins when conventional correction strategies based on bony anatomy are used.
To mitigate errors introduced by shape variations, the library of plans (LoP) approach has been successfully applied for cervical and bladder cancer. For those sites, libraries were

created by interpolation of structures of interest defined on CT scans in the full and empty bladder state. However, for rectal patients this approach is not feasible, as a major source of uncertainty is not bladder, but rectal filling.
The purpose of this study was therefore to develop an alternative method for generating structures for a LoP for rectal cancer and to investigate its potential for PTV margin reduction.

Material and Methods: The method proposed is based on 3D population statistics of the shape variation of the rectum CTV, rather than patient specific data derived from several CT scans, allowing the use of only a single planning CT scan for structure generation. The population statistics were derived from shape variation data of thirty three short course radiotherapy (SCRT) patients with daily repeat scans on which the rectum CTV was delineated. Shape variations were defined as standard deviations of (local) perpendicular displacements of the CTV surface, using each patient's planning CT scan as reference.
The LoP CTVs were created by expanding or contracting the planning CTV perpendicular to its surface, proportional to the local statistics of shape variation of the population and a global scaling factor. The scaling factor was tuned such that the largest distance between CTVs was 1 cm. Five CTVs were created; the original CTV, two smaller (max -1, -2 cm) and two larger CTVs (max +1, +2 cm).
To determine the potential of this method, residual errors were calculated by using the most optimal CTV from the library as a reference in computing the shape variation statistics, rather than the original planning CTV. Subsequently, margins were computed for both the conventional and LoP strategy, using a modified version of the van Herk recipe.

Results: An example of the constructed CTV structures is depicted in figure 1a. The original CTV is the middle one; two larger and two smaller CTVs were created using population statistics. Figures 1c and 1d show the required PTV margin for a conventional and a LoP approach, respectively. The difference between the two methods is shown in Figure 1b. The largest reduction was found in the upper anterior part of the CTV: 1.5 cm (≈ 40%).

Conclusion: We have successfully developed a LoP strategy for rectum patients that uses population statistics and scalable expansions, thereby only requiring a single CT scan, as opposed to the current methods for cervix and bladder. Analysis of the residual errors has shown that a potential margin reduction of 40% is possible with this approach.

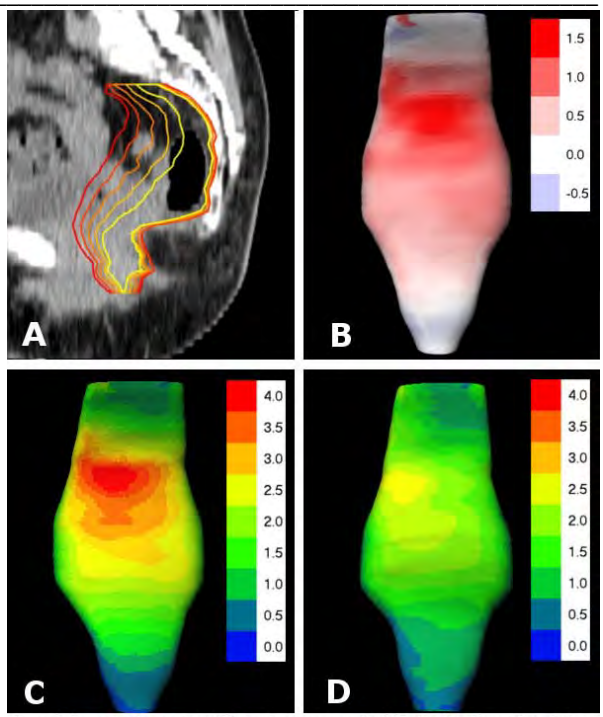

Figure 1. Example of generated LOP structures on a sagittal CT slice (A). Figures B to D depict anterior views of 3D representations of the (average) CTV. Figures C and D present the required margins in the case of bony anatomy based corrections and when using our LoP approach, respectively. Figure B shows the difference between the two methods. All measurements are in cm.

Debate: We don't need better dose calculation, it's doing more bad than good

SP-0622
For the motion
E. Sterpin[1]
[1]*Katholieke Universiteit Leuven, Oncology, Leuven, Belgium*

Advanced dose calculation algorithms have demonstrated excellent performance against measurements for complex treatments and heterogeneous phantoms. Thus, it is natural to consider those as the best candidates for treatment planning. Because the dose calculation is more accurate, so will be the treatment and its outcome improved. This seems intuitively obvious.
However, a broader view on our clinical practice may temper this conclusion. In our clinical practice, we are using dose prescriptions from past experience that was typically based on less accurate dose calculation algorithms. Also, we are using safety margins for geometrical uncertainties that are based on hypothesis that simplify considerably the physics of dose deposition, but yet seem to provide adequate coverage and safety for the majority of the patients.
We will show during this debate that changing the dose calculation algorithm considering our present practice will not necessary have a positive impact for the patients. Therefore, the introduction of such algorithms in clinics should be made cautiously.

SP-0623
Against the motion
T. Knöös[1]
[1]*Lund University Hospital, Malmö, Sweden*

Debate: Are we precisely inaccurate in our adaption?

SP-0624
For the motion
M. Leech[1], M. Kamphuis[2]
[1]*TCD Division of Radiation Therapy, Radiation Therapy, Dublin, Ireland Republic of*

[2]*Academic Medical Centre, Radiotherapy, Amsterdam, The Netherlands*

This debate will critically discuss recent developments in adaptive radiotherapy (ART). Adaptive radiotherapy is being introduced in many departments nowadays and one of the main question is if there is sufficient evidence to safely do so?
In the debate, the inaccuracies of the process will be discussed profoundly. What is the accuracy of the process as a whole? Do delineation errors and dose calculation errors still make ART really worth the effort? Or can these errors safely be corrected for?
Another aspect that will be discussed is risk management. Procedures are often not supported by software released for this purpose. In case of e.g. plan selection, different manual steps are made which are probably prone to human errors. What is the impact of these human errors? On the other hand, do we really have to wait for optimal software to be release and keep patients treated in a sub-optimal manner?
Last but not least is the lack of sufficient knowledge on tumor spread e.g. in the case of gynecological tumors. If we reduce the treatment area, aren't we going to miss our target? Will this in the end increase local relapse rates instead of reducing toxicity? From a different point of view it can be argumented that we will never get knowledge of the exact tumor location if we keep treating patients with a (too) large safety margin.

SP-0625
Against the motion
M. Kamphuis[1]
[1]*Academic Medical Center, Academic Physics, Amsterdam, The Netherlands*

Joint abstract submitted

Debate: Moving away from 2 Gray: are we ready for a paradigm shift?

SP-0626
This house believes that larger fraction sizes will be the standard-of-care for the majority of curative treatments by 2025
J.R. Yarnold[1]
[1]*The Institute of Cancer Research and The Royal Marsden NHS Foundation Trust, Radiotherapy & Imaging Department, Sutton, United Kingdom*

A significant proportion of curative schedules still use fraction sizes ≤2.0 Gy, mostly on a once-daily basis five times per week. These practices are likely to diminish further over the next 10 years, driven independently by advances in biology and physics. Although randomised trials in the 1980s and ‘90s confirmed squamous carcinomas of the head and neck and bronchus to be relatively insensitive to fraction size compared to the dose-limiting late-reacting normal tissues, it is now well established that adenocarcinomas of the breast and prostate share comparable, or perhaps greater, sensitivity to fraction size than the dose-limiting late normal tissues. Hypofractionation is increasingly adopted as a standard of care for women with breast cancer, and practices are changing for men with prostate cancer too, diseases account for 28% and 17%, respectively, of all UK radiotherapy courses. High dose brachytherapy and novel external beam techniques exclude adjacent normal tissues from the high dose zone so effectively that prescribed dose is limited mainly, if not exclusively, by tissues in the paths of entry and exit beams. The impact of stereotactic radiotherapy in common cancers remains to be established, but early results for early stage lung cancer look encouraging, particularly when the benefits of acceleration are factored in. There is therefore ample justification to support a prediction that accelerated hypofractionation will be a standard of care for the majority of curative treatments well before 2025.

SP-0627
Against the motion: This house believes that standard fractionation will remain the standard-of-care for the majority of curative treatments by 2025
J. Overgaard[1]
[1]*Aarhus University Hospital, Radiation Oncology, Aarhus c, Denmark*

Abstract not received

SP-0628
For the motion (rebuttal):It is the *small* fraction sizes that need special pleading, not the large ones.
A. Nahum

Fractionation is a very odd business. The question ought really to be "Why should we deliver curative radiotherapy in a large number of small doses, thereby prolonging the number of treatment days, increasing both patient inconvenience, and overall treatment costs?" Given the significant reduction in doses to non-target tissues achievable by modern conformal external-beam therapy (including intensity modulated photons and spot-scanned protons), and the recent findings for breast tumours, and probably also for prostate, that the α/β for the clonogens is of the same order as that for late normal-tissue complications, there are not many tumour sites where hyperfractionation is justified. In the latter category are only relatively large lung tumours, close to the mediastinum, and those tumours in the head & neck region where 'serial' normal tissues (e.g. spinal cord) are dose-limiting. Otherwise the onus is on the 'hyper-fractionators' to justify, to both administrators and patients, the vast number of daily visits they wish to impose on patients. One can go further - fraction size/number should be tailored to each patient according to the maxim "Deliver the minimum number of fractions compatible with a high rate of local control and a low rate of complications". Software such as 'BioSuite' exists to do exactly this; there are no good excuses for not using it.

SP-0629
Against the motion rebuttal
I.R. Vogelius[1]
[1]*The Finsen centre – Rigshospitalet, Physics, Copenhagen, Denmark*

Abstract not received
I

POSTERS

Poster: Clinical track: Head and neck

PO-0630

Outcomes of induction chemotherapy for head and neck cancer patients

S.Y. Wu[1], L. Kuan-Chou[2], C. Tsung-Ming[3], L. Fei-Peng[3]
[1]*Taipei Medical University Hospital, No.111- Section 3, Taipei, Chinese Taipei*
[2]*Wan Fang Hospital- Taipei Medical University- Taipei-Taiwan, Department of Oral and Maxillofacial Surgery, Taipei, Taiwan*
[3]*Wan Fang Hospital- Taipei Medical University- Taipei-Taiwan, Department of Otorhinolaryngology, Taipei, Taiwan*

Purpose or Objective: To the present, the role of induction chemotherapy has remained a subject of controversy. In this study, we directly compared the survival of patients receiving induction chemotherapy using docetaxel or platinum given before concomitant chemoradiotherapy (CCRT) with upfront chemoradiotherapy alone.

Material and Methods: The National Health Insurance claims database and cancer registry databases from The Collaboration Center of Health Information Application in Taiwan were linked for the analysis. Head and neck cancer patients from January 1, 2002 to December 31, 2011 were included in the study. The follow-up duration was from the index day to December 31, 2013. The inclusion criteria were having a head and neck cancer (identified according to the International Classification of Diseases, Ninth Revision, Clinical Modification [ICD-9-CM] codes 140.0~148.9), being aged > 20 years, being at American Joint Committee on Cancer (AJCC) clinical cancer stage III or IV, and having undergone induction chemotherapy or platinum-based CCRT. Exclusion criteria were having been diagnosed with cancer before the head and neck cancer was confirmed, having distant metastasis, being at AJCC clinical cancer stages I or II, having platinum and docetaxel combined use before radiotherapy (RT), being younger than 20 years, one's gender being unknown, and having docetaxel use during or after RT, induction chemotherapy beyond 8 weeks before RT, only one course of induction chemotherapy before RT, cetuximab use, adjuvant chemotherapy within 90 days after completion of RT, <7000 cGy dose of RT, curative head and neck cancer surgery before RT, nasopharyngeal cancer, carcinoma in situ, a sarcoma, and head and neck cancer recurrence. The total number of enrolled head and neck cancer patients was 30,990 persons.

Results: In total, 10,721 stage III or IV head and neck cancer patients without distant metastasis were included in the study, and the median follow-up duration was 4.18 (interquartile range, 3.25) years. There were 7968 patients in the CCRT group (arm 1); 503 patients in the induction chemotherapy with docetaxel group of arm 2, and 2232 patients in the induction chemotherapy with platinum group of arm 3. We used the CCRT arm as the control arm to investigate the risk of death after induction chemotherapy. After adjusting for age, gender, clinical stage, and comorbidities, the adjusted hazard ratios (HRs) of overall deaths were 1.37 (95% confidence interval [CI], 1.22~1.53) in arm 2 and 1.44 (95% CI, 1.36~1.52) in arm 3. In a disease-specific survival rate analysis, the adjusted HRs of head and neck cancers deaths were 1.29 (95% CI, 1.14~1.46) in arm 2 and 1.47 (95% CI, 1.38~1.56) in arm 3.

Conclusion: Our cohort study showed that induction chemotherapy with docetaxel or platinum did not improve survival and also resulted in more all-causes death and head and neck cancer death risks compared to CCRT.

PO-0631

The prognostication of tumour volume and lower neck lymph nodes in laryngeal cancer treated with IMRT

S.H. Huang[1], J. Su[2], J. Waldron[1], J. Kim[1], A. Bayley[1], S. Bratman[1], J. Cho[1], A. Hope[1], M. Giuliani[1], J. Ringash[1], A. Hansen[3], J. De Almeida[4], L. Tong[1], W. Xu[2], B. O'Sullivan[1]
[1]*Princess Margaret Cancer Centre/University of Toronto, Department of Radiation Oncology, Toronto, Canada*
[2]*Princess Margaret Cancer Centre/University of Toronto, Department of Biostatistics, Toronto, Canada*
[3]*Princess Margaret Cancer Centre/University of Toronto, Division of Medical Oncology, Toronto, Canada*
[4]*Princess Margaret Cancer Centre/University of Toronto, Department of Otolaryngology – Head and Neck Surgery, Toronto, Canada*

Purpose or Objective: Evidence suggests that gross tumor volume (GTV) is a prognostic factor (PF) for laryngeal cancer beyond TNM staging. Lower neck lymph nodes (LWNK-LNs) have been linked to increased risk of distant metastasis (DM) although are generally evident when upper neck disease also exists. We hypothesized that primary GTV (GTV-T) and total lymph node (LN) GTV (GTV-N) may differentially impact overall survival (OS) and DM, and that LWNK-LN may lack independent effect.

Material and Methods: All newly diagnosed laryngeal cancers treated with definitive intensity modulated radiotherapy (IMRT) +/- chemotherapy in 2005-2012 were included. GTV-T and GTV-N were delineated for IMRT treatment (confirmed with staging CT/MRI) and peer-reviewed at quality assurance meetings. Levels IV or Vb LNs were considered LWNK-LNs. GTV-N was the summed LN volume receiving full-prescribed dose (lower doses were occasionally used to spare brachial plexus). OS and distant control (DC) were compared between larger/smaller GTV-T, GTV-N (both dichotomized at median value), and presence/absence of LWNK-LN. Multivariate analysis (MVA) identified PFs for OS and DM.

Results: A total of 635 cases [456 (72%) glottic, 164 (26%) supra- and 15 (2%) sub-glottic cancers] were included. TNM stages were I: 215 (34%), II: 161 (25%), III: 129 (20%), and IV 130 (20%). Gross LNs were present in 131 (21%) patients. LWNK-LNs were present in 55/131 (42%) cases, all of which also had overt LNs in the upper neck (levels 2 +/- 3). Median GTV-T was 4 cc (range: 0.1-234.0) and GTV-N was 8 cc (range: 0.9-178.0). Systemic agents were used in 81 (13%) patients. Larger GTV-T (>=4 cc vs <4 cc) or GTV-N (>8 cc vs <=8 cc), or presence of LWNK-LN had inferior 3-year OS (GTV-T: 65% vs 89%; GTV-N: 37% vs 75%; LWNK-LN: 41% vs 65%, all $p<0.001$) and DC (GTV-T: 87% vs 97%; GTV-N: 71% vs 87%; LWNK-LN: 72% vs 84%, all $p<0.001$). MVA (adjusted for treatment) confirmed that TNM stage was the strongest PF for OS [III/IV vs I/II: HR 2.52 (1.78-3.56), $p<0.001$] and DM [HR 6.24 (2.67-14.57), $p<0.001$]. GTV-T (per 10 cc increment) was also a PF for OS [HR 1.15 (1.07-1.23), $p<0.001$] and DM [HR 1.18 (1.03-1.36), $p=0.015$]. GTV-N was a PF for OS [HR 1.13 (1.07-1.20), $p<0.001$] but not for DM ($p=0.22$). LWNK-LN was not a PF for OS ($p=0.18$) nor for DM ($p=0.67$) although it became significant for OS [HR 1.97 (1.32-2.93), $p<0.001$] when GTV-T and GTV-N were excluded from the MVA model.

Conclusion: The TNM classification remains the strongest PF for OS and DM. GTV-T is also a PF for OS and DM in addition to TNM. GTV-N is a PF for OS but not for DM. Presence of LWNK-LN is always associated with upper neck LN involvement (likely a surrogate for lymph node burden), and seems to lack independent impact on DM and OS if controlling for GTV-T and GTV-N.

PO-0632

A multivariate model predicting grade ≥ 2 neck fibrosis at 6 months after radio(chemo)therapy

D. Nevens[1], A. Laenen[2], F. Duprez[3], J. Daisne[4], W. De Neve[3], S. Nuyts[1]
[1]*KU Leuven-University of Leuven- University Hospitals Leuven, Radiation Oncology Department, Leuven, Belgium*
[2]*KU Leuven-University of Leuven, Leuven Biostatistics and Statistical Bioinformatics Centre, Leuven, Belgium*
[3]*Ghent University Hospital, Radiation Oncology Department, Ghent, Belgium*
[4]*Clinique & Maternité Ste-Elisabeth, Radiation Oncology Department, Namur, Belgium*

Purpose or Objective: Neck fibrosis is an important complication following radio(chemo-)therapy (R(C)T) for head and neck cancer (HNC). The purpose of this study was to find a parameter that could predict late neck fibrosis and to make a multivariate model to predict neck fibrosis grade 2 (fibrosis RTOG2-4) at 6 months following R(C)T for HNC.

Material and Methods: We prospectively included 193 patients in 5 different RT centers for a randomized controlled trial. On this patient-population we tested age, sex, T/N stage, tumor site, concomitant chemotherapy, upfront neck dissection, neo-adjuvant chemotherapy, accelerated RT, smoking (never-former-current), alcohol abuse (never-former-current), the dose prescribed to the elective neck and erythema at the end of treatment for their potential to predict neck fibrosis RTOG2-4 6 months after the end of treatment. Fisher's exact test and Mann-Whitney U test were used for testing the association between fibrosis grade 0-1 versus fibrosis grade 2-4 with categorical or continuous variables, respectively. A stepwise selection procedure was made to determine the best combination of predictor variables for fibrosis RTOG2-4 at 6 months. The area under the ROC curve (AUC) was determined for the selected model. Additionally a bootstrap-corrected AUC value was calculated. This AUC value corrects for over optimism resulting from the fact that model construction and model validation were performed on the same data set. All tests are two-sided; a 5% significance level is considered for all tests.

Results: Upfront neck dissection (p<0.01), erythema at the end of R(C)T ≥ grade 3 (p<0.01), increasing N stage (p<0.01) and cancer of unknown primary (p=0.02) are significantly associated with the incidence of fibrosis RTOG2-4 at 6 months in our patient population in univariate analysis. Upfront neck dissection and erythema grade ≥3 at the end of R(C)T were identified for our model using a stepwise selection procedure. Additionally, increasing N stage was selected as an independent predictor variable (*Table 1*).

Parameter	OR	P-value
Neck dissection vs No neck dissection	159.06 (19.158;1320.7)	<.0001
Acute erythema grade3 vs grade 0-2	129.18 (15.930;1047.6)	<.0001
N-stage (+1 level)	1.446 (1.012;2.068)	0.0430

Table 1: Final model

CI: confidence interval
OR>(<)1 means higher (lower) risk for first category.
OR>(<)1 means higher (lower) risk for higher level.

The AUC for this model containing upfront neck dissection, erythema at the end of treatment and smoking status was 0.92; the bootstrap-corrected AUC was 0.90. The risk for fibrosis RTOG2-4 at 6 months can be calculated using the following formula:

$$\text{risk for fibrosis RTOG2-4 at 6 months} = \frac{e^{\mu}}{1+e^{\mu}}$$

$$\begin{aligned}\mu = \; & -5.3225 + 5.0693\,(\textit{only when upfront neck dissection was performed}) \\ & + 4.8612\,(\textit{when grade} \geq 3 \textit{ erythema is present at the end of treatment}) \\ & + 0.3691\,(\textit{Nstage: N0} = 0; \textit{N1} = 1; \textit{N2a} = 2; \textit{N2b} = 3; \textit{N2c} = 4; \textit{N3} = 5)\end{aligned}$$

Conclusion: A model for the prediction of fibrosis$RTOG_{2-4}$ following R(C)T for head and neck cancer is presented withan AUC of 0.92. Erythema at the end of R(C)T is associated with $RTOG_{2-4}$ fibrosisat 6 months.

PO-0633

Dissection of submandibular glands increases the risk of xerostomia after postoperative radiotherapy

H.P. Van der Laan[1], H.P. Bijl[1], A. Van der Schaaf[1], J.G.M. Vemer-van den Hoek[1], J.A. Langendijk[1], R.J.H.M. Steenbakkers[1]

[1]University Medical Center Groningen, Department of Radiation Oncology, Groningen, The Netherlands

Purpose or Objective: To determine if the remaining submandibular gland volume after surgery is a prognostic factor for late xerostomia after postoperative radiotherapy (PORT) for head and neck cancer (HNC).

Material and Methods: This prospective cohort study consisted of 198 HNC patients who received PORT. The primary endpoint was CTCAE v4.0 grade 2 or higher physician rated xerostomia at 6 months after completing PORT (XERM6). From a set of factors deemed relevant in relation to the endpoint (patient characteristics, treatment details, surgical data, dosimetric data of major and minor salivary glands and oral cavity) a subset of candidate factors was selected, using expert knowledge and model exploration. Manual stepwise logistic regression was performed with the aim to build a strong and valid parsimonious prediction model for XERM6.

Results: XERM6 was observed in 54 patients (27.3%). The number of remaining submandibular glands was 2 (n=42, average remaining volume: 18.7 cm^3); 1 (n=105, average remaining volume: 9.0 cm^3); or 0 (n=51). Patients underwent surgery in the oral region (n=154) or in the hypopharyngeal / laryngeal region (n=44). The multivariable analysis revealed the following independent prognostic factors for the final model: baseline xerostomia≥ grade 1 (OR: 2.978, 95%CI: 1.363-6.504); ipsilateral parotid mean dose (OR: 1.035 per Gy, 95%CI: 1.007-1.065); contralateral parotid mean dose (OR: 1.019 per Gy, 95%CI: 0.984-1.056); and the remaining total submandibular gland volume (OR: 0.908 per cm^3, 95%CI: 0.855-0.964). This model calibrated well with the observed data (Hosmer & Lemeshow test: p = 0.798) and had a good performance (Nagelkerke adjusted R^2: 0.223, and ROC-AUC: 0.758). Effect sizes and performance measures were not significantly different after internal validation using cross-validation.

Conclusion: With a similar dose in the parotid glands, the risk of late xerostomia increased significantly with less remaining submandibular gland volume after surgery. This effect is not accounted for in excisting models for late xerostomia. The proposed model is the first model specifically valuable for predicting late xerostomia in HNC patients receiving PORT.

PO-0634

Body image in irradiated head and neck cancer patients

H. Chiu[1], T.M. Hung[2], J.T.C. Chang[2]

[1]Chang Gung Memorial Hospital, Radiation Oncology, Taoyuan, Taiwan

[2]Chang Gung Memorial Hospital, Radiation Oncology, Taoyuan, Taiwan

Purpose or Objective: To investigate the body image in head and neck cancer patients treated with radiotherapy.

Material and Methods: A cross-sectional survey of 150 patients with head and neck cancer, 60 patients were nasopharyngeal cancer (NPC) treated by definite radiotherapy without surgery, and 90 patients were oral cavity cancer (OCC) treated by radical surgery plus adjuvant radiotherapy. All participants completed a 10-item Body Image Scale (BIS) to assess the body image dissatisfaction. In all patients, the clinical and socio-demographic variables were cancer type, age, gender, partnership, education, and employment. In OCC patients, the socio-demographic variables were the same, and clinical variables were facial skin sacrificed, mouth angle sacrificed, glossectomy, maxillectomy, and mandibulectomy. ANOVA, t-test, and multiple regression were used to evaluate the relationships between these variables and BIS.

Results: In all patients, the cancer type (NPC vs. OCC) was the strongest independent predictor of BIS. The non-surgically treated NPC patients had significantly better body

image outcome than the surgically treated OCC patients. Education was also an independent factor for BIS. In OCC patients, facial skin sacrificed, mouth angle sacrificed, maxillectomy, and mandibulectomy were significantly associated with BIS. Using multivariate analysis, inferior maxillectomy and segmental mandibulectomy were the independent poor prognosticators of body image outcome in OCC patients.

Conclusion: The radical surgery for head and neck cancer patients has a significant impact on body image, especially those with facial bone destruction. These findings could be used to guide psychosocial interventions targeting body image disturbance for patients with head and neck cancer.

PO-0635

Dose to the masseter muscle and risk of trismus after chemoradiation for advanced head & neck cancer

S. Verheijen[1], O. Hamming-Vrieze[1], M. Jonker[1], E. Lamers[1], S.A.C. Kraaijenga[2], L. Van der Molen[2], J.B. Van de Kamer[1], M.W.M. Van den Brekel[2], W.D. Heemsbergen[1]

[1]Netherlands Cancer Institute, Radiation Oncology, Amsterdam, The Netherlands

[2]Netherlands Cancer Institute, Head and Neck Oncology & Surgery, Amsterdam, The Netherlands

Purpose or Objective: Head and neck cancer patients treated with chemoradiation are at risk for developing trismus (reduced mouth opening). Trismus is often a persisting side-effect and difficult to manage. It impairs eating, speech and oral hygiene, affecting quality of life. Although several studies identified the masseter muscle (MM) as one of the main organs at risk, currently this structure is rarely considered during treatment planning. Prospective studies for chemoradiation are lacking. The aim of our study was to quantify the relationship between radiation dose to the MM and development of radiation-induced trismus in an IMRT-VMAT population.

Material and Methods: The 93 patients in this study participated in a prospective preventive exercise program to preserve oral functioning between 2006-2013. All received concomitant high-dose chemotherapy during VMAT- or IMRT-radiotherapy (70 Gy in 35 fractions). Tumor locations were mainly oropharynx (37%) and hypopharynx (33%). Maximum interincisor mouth opening was measured before and approximately 10 weeks after the end of treatment. Bilateral delineations of the MM were available from 2 retrospective studies. Patients were excluded if trismus was present at baseline, or if gross tumor infiltration of the MM was present on CT evaluation. Evaluated outcomes were trismus (mouth opening ≤ 35 mm) and decrease in mouth opening. Logistic regression (using maximum likelihood) was performed.

Results: At the first evaluation, 6-12 weeks post-treatment, fourteen patients had developed radiation-induced trismus (15%). On average, mouth opening decreased with 4.1 mm, or 8.2 % relative to baseline. Mean dose to the ipsilateral MM was a stronger predictor for trismus than mean dose to the contralateral MM, as indicated by the lowest -2 log likelihood (Table 1). Figure 1A shows the correlation between the ipsilateral mean masseter dose and the relative decrease in mouth opening, with trismus cases indicated in red. No trismus cases were observed in 33 patients (35%) with a mean dose to the ipsilateral MM < 20 Gy. The risk of trismus in the other 60 patients (65%) increased with higher mean doses to the ipsilateral MM. Figure 1B shows the fitted NTCP curve as a function of the mean dose, with a TD50 of 55 Gy. The actual incidence (with 1 SE) of trismus cases within 5 dose bins is indicated as well, showing a good correspondence with the NTCP fit with a relatively large uncertainty in the dose area > 50 Gy. Patients with tumors located in the oropharynx were at highest risk.

Conclusion: The risk of trismus can be established with the mean dose to the ipsilateral masseter muscle. The majority of head and neck cancer patients could benefit from dose reduction to the masseter muscles to prevent trismus, especially patients with a mean dose to the ipsilateral masseter > 20 Gy. Further development of a NTCP model could identify dose objectives to guide treatment planning.

Table 1. Results of univariate logistic regression analysis.

Dose parameter	-2 LLH	RR per 10 units	p value
Ipsilateral Masseter			
Volume > 20 Gy (%)	66.5	1.5	0.004
Volume > 40 Gy (%)	69.8	1.4	0.004
Mean dose (Gy)	65.3	2.3	0.001
Contralateral Masseter			
Volume > 20 Gy (%)	66.5	1.4	0.002
Volume > 40 Gy (%)	70.6	1.5	0.007
Mean dose (Gy)	68.2	2.2	0.003

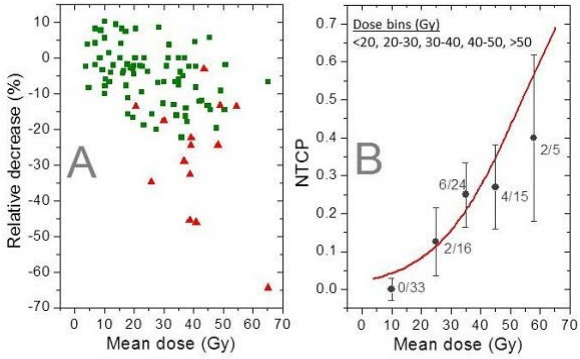

Figure 1. % decrease in mouth opening (A), NTCP for trismus & actual incidence with 1SE (B), both as function of mean dose to the ipsilateral masseter muscle.

PO-0636

Safety profile support efficacy of gingival clonidine tablet to prevent severe oral mucositis in HNC

Y. Tao[1], J. Giralt[2], J.R. Bensadoun[3], R.V. Lalla[4], E.M. Ozsahin[5], G. Pajkos[6], R.D. Kortmann[7], J. Contreras-Martinez[8], P. Céruse[9], X. Zasadny[10], F. Arias de la Vega[11], B. Vasseur[12], L. Houdas[13], M. Henke[14]

[1]Institut Gustave Roussy, Département de Radiotherapie, Villejuif, France

[2]Vall d'Hebron University Hospital, Department of radiotherapy, Barcelona, Spain

[3]Centre de Haute Energie CHE, Department of radiotherapy, Nice, France

[4]University of Connecticut Health Center, Section of Oral Medicine MC1605, Farmington- CT, USA

[5]Centre Hospitalier Universitaire Vaudois, Service de Radio-Oncologie, Lausanne, Switzerland

[6]Bács-Kiskun Megyei Kórház Szegedi Tudományegyetem Általános Orvostudományi Kar Oktató Kórháza Onkoradiológiai Központ-, Radiologia, Kecskemét, Hungary

[7]Universitätsklinikum Leipzig Klinik für Strahlentherapie und Radioonkologie, Radioonkologie, Leipzig, Germany

[8]Hospital Carlos Haya, Radiation Oncology Dept, Malaga, Spain

[9]Groupement Hospitalier Lyon Nord, Service d'ORL et de CCF, Lyon, France

[10]Clinique François Chénieux, Oncology and radiotherapy, Limoges, France

[11]Complejo Hospitalario de Navarra, Radiotherapy, Pamplona, Spain

[12]Onxeo, Clinical Department, Paris, France

[13]Onxeo, Clinical Dept, Paris, France

[14]Universitätsklinikum Freiburg Klinik f. Strahlentherapie, Section Head Clinical Studies, Freiburg-, Germany

Purpose or Objective: Oral mucositis (OM) is the most frequent and severe acute toxicity of chemoradiotherapy (CRT) in head and neck cancer (HNC) patients. In preclinical

studies, topical clonidine shown activity in reducing NF-κB activation and incidence of severe OM (SOM). In a randomized double blind, placebo-controlled study, a novel mucoadhesive buccal tablet (MBT) containing clonidine reduced the incidence of SOM in HNC patients being treated with CRT. We now report overall survival (OS), tolerability and systemic exposure of clonidine of study subjects.

Material and Methods: Clonidine MBT 50µg (n=56), 100µg (n=65) or matching placebo (n=62) were applied to the gum once daily 1-3 days prior to RT and then daily until the end of CRT (1.8-2.2 Gy/d, 5 times/week combined with a platinum based CT). AEs, vital signs and gingival tolerance by Silness-Loe index (global score from 0 to 9) were assessed twice a week; xerostomia and sedation (visual scale from 0 to 10) were evaluated once a week. Blood and saliva samples for clonidine levels were collected Q2 weeks. OS data will be collected until 2 years after last patient last visit. Patients received a median cumulative radiation dose of 66 Gy [min: 4; max: 78]. SOM was reported in 60% [95%CI: 47%; 72%] of placebo patients, 43% [95%CI: 29%; 57%] in clonidine 50µg MBT (p=0.063) and 48 % [95%CI: 35%; 61%] in clonidine 100µg MBT (p=0.169).

Results: All grade AE incidence was 91% in clonidine MBT groups and 98% in placebo group (p<0.10). No difference in heart rate and blood pressure was reported between groups. Reversible hypotension AEs were reported in 7% clonidine MBT 50µg patients, 6% clonidine MBT 100µg and 2% placebo-treated patients (p=ns). Sedation score slightly increased in all groups between week 1 and week 6 (overall from 1.5 ± 2.3 to 3.0 ±2.3) and was similar between groups (p=ns). Xerostomia grade ≥ 2 increased to 41% in clonidine MBT 50µg, 31% in clonidine MBT 100µg and 42% in placebo patients (p=ns). The mean plasma/saliva concentrations of clonidine were 0.087/154.2ng/mL in clonidine MBT 50µg and 0.134/301.1 ng/mL in clonidine MBT 100µg. With a median follow-up of 15 months, the median 1year-OS of 89.3% [95%CI: 73.9; 95.8] placebo and 89.7% [95%CI: 80.4; 94.8] clonidine MBT.

Conclusion: Clonidine MBT daily applied to the gum throughout CRT reduced the incidence of SOM and was well tolerated in HNC patients undergoing postoperative CRT. No significant systemic effects of clonidine were reported in the phase 2 study probably due to its low systemic levels.

PO-0637

RCT pilot study of Therabite vs wooden spatula in amelioration of trismus in H&N cancer patients

R. Lee[1], S.N. Rogers[2], A.L. Caress[3], A. Molassiotis[4], R. Edwards[5], D. Ryder[1], P. Sanghera[6], C. Lunt[1], T. Yeo[5], N. Slevin[7]

[1]*The Christie, Research and Development, Manchester, United Kingdom*

[2]*University Hospital Aintree, Maxillofacial Unit Directorate, Liverpool, United Kingdom*

[3]*University of Manchester, School of Nursing and Midwifery, Manchester, United Kingdom*

[4]*The Hong Kong Polytechnic University, Cancer & Supportive Care, Hong Kong, China*

[5]*Bangor University, The Bangor Health Economics Unit, Bangor, United Kingdom*

[6]*University of Birmingham, Clinical Oncology, Birmingham, United Kingdom*

[7]*The Christie, Clinical Oncology, Manchester, United Kingdom*

Purpose or Objective: Specific objectives of the study were (i) to assess whether prophylactic exercise intervention prevented the worsening of jaw tightening that would be expected following radiotherapy (ii) to assess whether the Therabite® or wooden spatulas intervention improved patients' QOL as measured using validated questionnaires; (iii) to assess issues around power for sample size calculations, compliance and practical aspects of running a full RCT in this group of patients and (iv) whether the intervention reduced the level of post-treatment clinical management/health care utilisation required by mouth cancer patients

Material and Methods: All patients had some sense of subjective jaw tightening prior to study entry. Measurements of jaw opening and QOLs were taken pre and post radiotherapy 3 and 6 months. Patients were instructed to follow the 5-5-30 regimen daily, for 6 months. (5stretches, 5times, 30 second hold).

Results: 37 patients with stage 3/4 oral/oropharyngeal cancers were randomised to receive the therabite device and 34 the wooden spatulas for jaw exercises. The study has shown that mouth openings had increased on average in both groups following the exercise intervention. There was no statistically significant difference between the two interventions. There were problems with compliance. Lessons learnt from the semi structured telephone interviews, (15 patients) which would aid compliance included: (1) Allow patients to have more of a say in the exercise regimen ie reduce to 3 times a day. (2) Allow patients to take a variable break (up to 6 weeks) from the exercises when side effects of radiotherapy are at their worst. Mucositis, soreness and pain in mouth being reported during last few weeks and 4 weeks post radiotherapy. (3) More regular contact with the patients for encouragement and support. The study was designed to give an indication about the benefits of exercises and to inform feasibility to conduct a larger study

Conclusion: Prophylactic exercises during and after radiotherapy treatment can ameliorate trismus for stage 3 and 4 oral/oropharyngeal cancers. Keyword: Trismus, Radiotherapy This abstract presents independent research funded by the National Institute for Health Research (NIHR) under its Research for Patient Benefit (RfPB) Programme (Grant Ref No: PB-PG-0610-22317). The views expressed are those of the author(s) and not necessarily those of the NHS, the NIHR or the Department of Health. Sponsor: The Christie NHS Foundation Trust

PO-0638

Adaptive dose painting by numbers for head and neck cancer: interim analysis of a randomised trial

F. Duprez[1], J. Daisne[2], D. Berwouts[3], W. De Gersem[1], I. Goethals[3], A. Olteanu[1], J. Schatteman[3], T. Vercauteren[1], W. De Neve[1]

[1]*Universitair Ziekenhuis Gent, Radiotherapy, Gent, Belgium*

[2]*Clinique et Maternité Sainte-Elisabeth Namur, Radiotherapy, Namur, Belgium*

[3]*Universitair Ziekenhuis Gent, Nuclear Medicine, Gent, Belgium*

Purpose or Objective: A prospective randomized multi-centre phase II trial comparing standard IMRT (S-IMRT) to 3-phase adaptive dose painting by numbers (DPBN) for head and neck cancer (HNC) is currently recruiting patients. Unlike the fact that the initial dose prescription was derived from a phase I trial, we observed an unacceptable rate of late mucosal ulceration using this dose prescription in the DPBN group. This made us change the dose prescription in two steps. This interim analysis reports on acute and late toxicity and local (LC), regional (RC) and distant control (DC) in almost half of the patients to be included.

Material and Methods: From 2011, Q3 to 2015, Q3 53 patients received primary radio(chemo)therapy for HNC. We report on 45 patients who have ended therapy for 3 months. Patient, tumor and treatment characteristics can be found in Table 1

	3-phase adaptive DPBN (n = 21)	Standard IMRT (n = 24)	*p-value*
Median age (range; in years)	59 (40 – 74)	56 (48 – 68)	
Male / female	19 / 2	19 / 5	0.42
Site: - Oropharynx - Hypopharynx - Larynx	 14 5 2	 13 6 5	0.64
Stage grouping - I - II - III - IVA - IVB	 1 3 3 14 -	 - 2 6 12 4	0.25
T-staging - T1 - T2 - T3 - T4a - T4b	 4 7 5 4 1	 4 11 3 2 4	0.91
N-staging - N0 - N1 - N2a - N2b - N2c	 6 1 1 5 8	 2 7 2 4 9	0.13
Pre-IMRT neck dissection	6	1	0.04
Concomitant cisplatin	13	9	0.14

Fig. 1 demonstrates dose prescription protocols (DPP) of the DPBN- and S-IMRT group

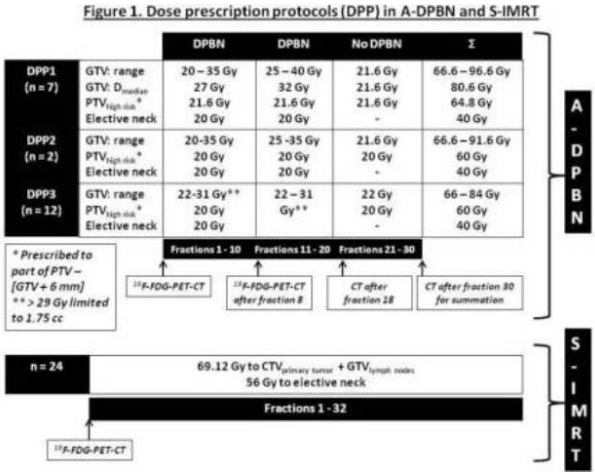

Results: As previously reported (ESTRO 2015) we unexpectedly observed late grade (G)3 and 4 mucosal ulcers in 1/7 and 3/7 DPBN-patients in DPP1, respectively, that healed spontaneously (n = 1), after surgical intervention (n = 2) and is still persisting (n = 1) at 42 months. In order to avoid G4 mucosal late toxicity (LT) the DPBN-DPP has been adapted in 2 steps (Fig. 1): DPP1 used a median dose prescription that can result in increased doses in a GTV with > 50% voxels of low-uptake. This median dose prescription was abandoned in DPP2. In DPP3 the very-high dose region is limited to an absolute volume of 1.75 cc. In DPP2, 1/2 had G3 mucosal LT that healed spontaneously. In DPP3, 2/11 and 1/11 had G3 and G4 mucosal LT, respectively. In S-IMRT, there was no G3-4 mucosal LT (n = 20). Late G3 dysphagia was seen in 2/18 and 3/20 DPBN and S-IMRT patients at month 3, respectively. After 6 months, 6/15 and 2/13 patients had G≥2 dysphagia (p = 0.22) and PEG-tube was needed in 5/15 and 3/13 patients in DPBN and S-IMRT, respectively. G2 xerostomia was present in 6/13 and 7/13 patients in DPBN and S-IMRT, respectively.
Median follow-up is 12 (3-45) months. Nine patients deceased: 5 DPBN-patients (metastases in 3, complications after neck dissection for regional recurrence in 1 and unknown cause in 1) and 4 S-IMRT patients (2 metastases, 1 aspiration pneumonia and 1 cardial event). Local failure was seen in 1/21 (5%) and 4/24 (17%) in DPBN and S-IMRT, respectively. Regional failure was seen in 2/21 (10%) and 2/24 (8%) in DPBN and S-IMRT, respectively. Metastases were seen in 4/21 (19%) and 5/24 (21%) in DPBN and S-IMRT, respectively. At 1 year actuarial LC was 92% and 76% (p = 0.22), RC 86% and 87% (p = 0.9), DC 76% and 86% (p = 0.9) and OS 68% and 90% (p = 0.6) in DPBN and S-IMRT, respectively.

Conclusion: At short term, we did not observe significant differences yet in LC, RC, DC or OS in the first 45 patients. Due to mucosal LT, the DPBN-DPP has been adapted. Since then, G4 mucosal LT was observed in 1/12 patients. Strict follow-up of LT is being performed.

PO-0639

Graves ophthalmopathy: a network meta-analysis of treatments

M.P. Shaikh[1], F. Alite[1], M. Wu[2], J. Welsh[1], B. Emami[1], E. Melian[1], M.M. Harkenrider[1]
[1]*Stritch School of Medicine- Loyola University Chicago, Radiation Oncology, Chicago, USA*
[2]*Loyola University Chicago, Research Methodology, Chicago, USA*

Purpose or Objective: Although several treatments have been evaluated in randomized clinical trials (RCTs) for Graves Ophthalmopathy (GO), many of these treatments have not been directly compared against each other and thus the relative efficacy among them is unclear. We conducted a network meta-analysis (NMA) to compare all regimens simultaneously.

Material and Methods: A systematic review was performed through MEDLINE, Cochrane Central Register of Controlled Trials and meeting abstracts to identify RCTs involving treatments for GO. Treatments included: Radiation 10 Gy in 10 fractions (RT10) or 20 Gy in 10 fraction (RT20), with oral glucocorticoid (RT20POGC), with intravenous glucocorticoid (RT20IVGC), with retrobulbar glucocorticoid injections (RT20RBGC); oral glucocorticoid (POGC); intravenous glucocorticoid (IVGC); surgical decompression (Decomp); somatostatin analogs i.e., Octreotide or Lanreotide (SSanlg); Cyclosporin alone (Cysprn), with oral glucocorticoid (CysprnPOGC); Ciamexone (Ciamex); rituximab (Ritux); peribulbar orbital glucocorticoid injection (BGCI) or no treatment/placebo/sham radiation (NoTx). Success of treatment was determined from overall clinical response, which was provided by most studies. If this was absent, then it was estimated from proportion of patient not needing further treatment, improvement in clinical activity score (CAS), ophthalmopathy index (OI) or proptosis was used in that order. Odds Ratio (OR) was calculated either directly or via standardized mean difference (SMD) in measures. A frequentist NMA was used to compare treatments. Fixed or random effect model was used based on any significant variation among ORs.

Results: 27 studies involving 1216 patients were identified, with 15 distinct treatments including NoTx. Fixed effect model was used, as there was no significant variation among ORs. RT20IVGC was significantly better that BGCI (OR 31.4 [5.1, 195.7]), Ciamex (OR 6.8 [1.4, 33.1]), Cysprn (OR 64.9 [10.6, 398.5]), Decomp (OR 25.8 [1.7, 392.8]), IVGC (OR 4.1 [1.5, 11.6]), NoTx (OR 18.9 [5.69, 62.6]), POGC (OR 11.8 [4.0, 34.6]), RT10 (OR 10.1 [1.9, 52.2]), RT20 (OR 8.4 [2.7, 25.9]), RT20POGC (OR 4.2 [1.3, 12.9]), RT20RBGC (OR 3.5 [1.2, 10.2]) and SSanlg (OR 11.1 [3.0, 40.4]), but did not reach significance compared to CysprnPOGC (OR 3.7 [0.8, 17.8]) or Ritux (OR 5.0 [0.9, 28.9]). IVGC was found to be significantly better than BGCI (OR 7.6), Cysprn (OR 15.7), NoTx (OR 4.6) and POGC (OR 2.9). Also, CysprnPOGC was significantly better than BGCI (OR 8.6), Cysprn (OR 17.7), NoTx (OR 5.1) and POGC (OR 3.2). RT20, RT20POGC and RT20RBGC were all significantly better than Cysprn (ORs 7.7, 15.6 & 18.6 respectively). RT20 and RT20RBGC were better

than NoTx (ORs 2.3 & 5.4 respectively). Also, SSanlg was better than NoTx (OR 1.7).

Conclusion: RT20IVGC is the best treatment followed by IVGC and CysprnPOGC per this NMA. Also, RT20RBGCI and SSanlg were better than NoTx.

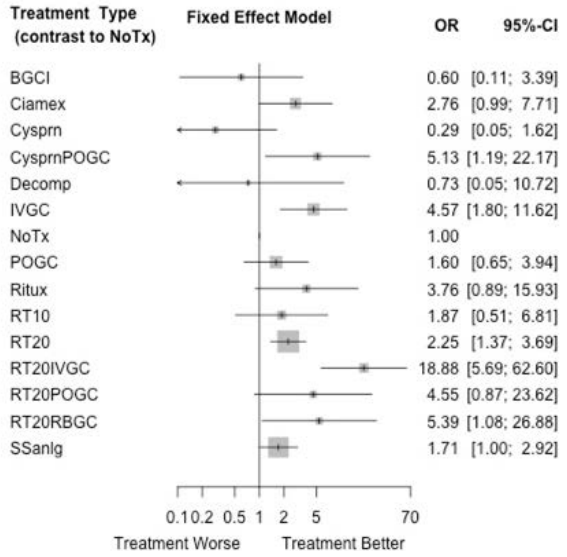

Table: Odds ratios of pair-wise comparisions of treatments for thyroid eye disease synthesized using network meta-analysis

	BGCI	Ciamex	Cysprn	Cysprn POGC	Decomp	IVGC	NoTx	POGC	Ritux	RT10	RT20	RT20 IVGC	RT20 POGC	RT20 RBGC	SSanlg
BGCI	1	0.22	2.06	0.12*	0.82	0.13*	0.6	0.38	0.16	0.32	0.27	0.03*	0.13	0.11*	0.35
Ciamex	4.6	1	9.51*	0.54	3.78	0.6	2.76	1.73	0.73	1.48	1.23	0.15*	0.61	0.51	1.62
Cysprn	0.48	0.11*	1	0.06*	0.4	0.06*	0.29	0.18*	0.08*	0.16	0.13*	0.02*	0.06*	0.05*	0.17
CysprnPOGC	8.55*	1.86	17.66*	1	7.01	1.12	5.13*	3.21*	1.36	2.75	2.28	0.27	1.13	0.95	3.01
Decomp	1.22	0.26	2.52	0.14	1	0.16	0.73	0.46	0.19	0.39	0.33	0.04*	0.16	0.14	0.43
IVGC	7.62*	1.65	15.74*	0.89	6.25	1	4.57*	2.86*	1.21	2.45	2.03	0.24*	1.01	0.85	2.68
NoTx	1.67	0.36	3.44	0.19*	1.37	0.22*	1	0.63	0.27	0.53	0.44*	0.05*	0.22	0.19*	0.59
POGC	2.66	0.58	5.5*	0.31*	2.18	0.35*	1.6	1	0.42	0.86	0.71	0.08*	0.35	0.3	0.94
Ritux	6.27	1.36	12.95*	0.73	5.15	0.82	3.77	2.36	1	2.01	1.67	0.2	0.83	0.7	2.21
RT10	3.11	0.68	6.43	0.36	2.55	0.41	1.87	1.17	0.5	1	0.83	0.1*	0.41	0.35	1.1
RT20	3.75	0.81	7.74*	0.44	3.08	0.49	2.25*	1.41	0.6	1.2	1	0.12*	0.5	0.42	1.32
RT20IVGC	31.46*	6.83*	64.96*	3.68	25.8*	4.13*	18.88*	11.81*	5.01	10.1*	8.39*	1	4.15*	3.5*	11.07*
RT20POGC	7.57	1.64	15.64*	0.89	6.21	0.99	4.55	2.84	1.21	2.43	2.02	0.24*	1	0.84	2.67
RT20RBGC	8.99*	1.95	18.56*	1.05	7.37	1.18	5.39*	3.37	1.43	2.89	2.4	0.29*	1.19	1	3.16
SSanlg	2.84	0.62	5.87	0.33	2.33	0.37	1.71	1.07	0.45	0.91	0.76	0.09*	0.38	0.32	1

* p<0.05

PO-0640

Prognostic factors in definitive salvage RT for recurrent Head and Neck cancer

O. Suzuki[1], R. Oh[2], K. Ogawa[3]

[1]*Osaka University Graduate School of Medicine, Carbon Ion Radiotherapy, Suita, Japan*

[2]*Miyakojima iGRT Clinic, Radiation Oncology, Osaka, Japan*

[3]*Osaka University Graduate School of Medicine, Radiation Oncology, Suita, Japan*

Purpose or Objective: Recurrent head and neck cancer (HNC) after radiotherapy or surgery has many problems about salvage treatment options such as surgery, chemotherapy and radiation therapy. Stereotactic radiotherapy is one of the treatment options for inoperable patients. However, in many cases, salvage radiation (SRT) is considered as a re-irradiation, and the treatment results of salvage radiation with a definitive dose for recurrent HNC are still insufficient. This analysis was done to reveal the treatment results and prognostic factors in SRT for both of locoregional and distant recurrences, with definitive treatment dose.

Material and Methods: One hundred and three patients with 43 local, 23 regional and 36 distant recurrences were treated with stereotactic radiotherapy for definitive treatment purpose. Treatment period was between May 1998 and July 2014. Eighteen to 70 Gy were delivered in 3 to 20 fractions. Treatments were delivered with CyberKnife or Novalis treatment system. There were 59 patients with squamous cell carcinoma, 8 with adenoid cystic carcinoma, 7 with papillary adenocarcinoma and 26 patients with other histlogical type.

Results: Median follow up period of survivors was 17 months (range 0-103), and the median survival time of all patients was 23 months. At 3 years, actuarial overall survival rate (OS) was 37%, 33% and 23%, and median survival time was 30, 26 and 20 months for local, regional and distant recurrence, respectively (p =0.638). OS was significantly better in the patients with oligo-recurrence (p<0.001) or to whom SRT were done for a lesion previously untreated by surgery (p=0.001). Cox regression analysis indicated that factors of oligo-recurrence and histology except for squamous carcinoma had significant influence on OS. The favorable group having both of the two factors (n=23) showed excellent 5 year survival as 73 % compared with 15% of unfavorable group.

Conclusion: This study showed that SRT with definitive dose achieved equivalent survival regardless of recurrent site and revealed two prognostic factors of oligo-recurrence and non-squamous carcinoma in the SRT for recurrent HNC.

Poster: Clinical track: CNS

PO-0641

Radiosurgery for intracranial meningioma. A systematic review and meta-analysis

V. Pinzi[1], E. Biagioli[2], A. Roberto[2], F. Galli[2], F. Chiappa[2], I. Floriani[2], L. Fariselli[1]

[1]*IRCCS Istituto C. Besta, Neurosurgery Radiotherapy Unit, Milan, Italy*

[2]*IRCCS-Istituto di Ricerche Farmacologiche Mario Negri, Laboratory of Clinical Research Department of Oncology, Milan, Italy*

Purpose or Objective: Single session radiosurgery (SRS) and staged radiosurgery (sSRS) have been performed in primary and adjuvant settings for intracranial meningioma. Although, different aspects of SRS and sSRS are still controversial above all regarding timing, prescription doses and fractionation of delivery. So far there are no definitive data about treatment-related symptom control and toxicity and categorization. The aim of this systematic review is to summarize the data on the long-term efficacy and safety of SRS and sSRS for meningioma patients.

Material and Methods: Medline and Embase databases were searched for relevant studies published until April 2015. Experimental and observational studies focused on SRS and sSRS for intracranial WHO grade I and II meningioma were included. Studies enrolling a number of patients inferior to five for each arm (for comparative studies) or overall (for non-comparative studies) were excluded. Studies including patients with malignant meningioma (WHO grade III), radio-induced meningioma or patients who had previously undergone brain radiation therapy were excluded from our review. Studies including both benign and malignant meningiomas were considered eligible, provided that results were reported separately, according to histo-pathological subtype. The primary outcomes were disease control and progression-free-survival. The secondary outcomes were symptom control and radiation-induced toxicity.

Results: Thirty-four studies fulfilled eligibility criteria. Only two studies were about sSRS. The estimate of disease control rate ranged from 87.0% to 100.0% at 5 years and from 67.0% to 100.0% at 10 years. The PFS rate ranged from 78.0% to 98.9% and from 53.1% to 97.2% at 5 and 10 years, respectively. No meta-analysis could be performed.We meta-analyzed symptom control and toxicity data. The overall frequency of symptom control was 92.3% (95% CI:88.4-95.6%), the overall toxicity was 8.1% (95% CI:5.2-11.5%). The overall relative frequency of patients with toxicity of 8.1% (95% CI:

5.2-11.5%), again with high heterogeneity (I2=81.0%) among studies.

Conclusion: All included studies have shown some limitations: most of them were retrospective and all were non-comparative; many of them were carried out in absence of a rigorous methodology and only few reported a measure of variability for the primary endpoint. Despite these limitations, we can conclude that SRS appears safe and effective treatment for intracranial meningioma.

PO-0642

Radiosurgery without whole brain radiotherapy in brain metastases from non-small cell lung cancer

P. Anselmo[1], L. Chirico[1], M. Muti[1], M. Basagni[1], F. Trippa[1], R. Rossi[1], L. Draghini[1], F. Arcidiacono[1], M. Italiani[1], M. Casale[1], S. Fabiani[1], C. Giorgi[2], E. Maranzano[1]

[1]"S. Maria" Hospital- Terni, Radiation Oncology Centre, Oncology Department, Terni, Italy

[2]"S. Maria" Hospital- Terni, Oncology Department, Terni, Italy

Purpose or Objective: patients (pts) with 1-4 brain metastases (BM) from non-small cell lung cancer (NSCLC) submitted to radiosurgery (SRS) alone were retrospectively evaluated.

Material and Methods: 130 pts with 207 BM were identified. Pts were treated with a 5-MV linear accelerator fitted with a commercial dynamic μMLC. Doses were prescribed to isocentre so that at least the 90% isodose line encompassed the target volume. Doses were chosen according to maximum diameter of the tumor as suggested by RTOG Protocol 90-05. Male/female ratio was 90/40, median age was 64 years (range, 31-86). Median KPS was 100% (range, 70-100). 42/130 (32%) pts had extracranial metastases, 83 (64%) pts had a controlled systemic disease, and 47 (36%) progressive disease. Neurologic functional score was generally good (NFS = 0), and only 15 (11.5%) pts had an NFS = 3 or 4. Relapse was defined "in-field" when more than 95% of the recurrence volume was within the original 50% isodose, and "out-field" in the other cases.

Results: In 82 (63%) pts there was only one BM, in remaining 48 (37%) 2-4 BM with a median volume of 0.8cc (range, 0.09-25) Median prescribed dose was 23 Gy (range, 12-25). At a median follow-up of 67 months (range, 24-110), 123 (95%) pts with 197 (95%) BM were evaluable. Local control, evaluated 3 months after SRS, was obtained in 95% of lesions: there were complete remission in 50 (25%), partial remission in 77 (39%), stable disease in 62 (31%), and progression in 13 (5%) BM. During follow up, 63 (51%) pts had no brain progression of disease, 11 (9%) had in-field relapse, 40 (33%) out-field relapse, and 9 (7%) in- and out-field relapse. Of 60 (49%) relapsing pts, 37 (62%) were retreated: 19 with SRS, 15 with whole brain radiotherapy (WBRT), 2 with fractionated stereotactic radiotherapy, and 1 with surgery and WBRT. No SRS-induced late toxicity was registered. At the time of analysis, 119/123 patients (97%) had died, 40 (34%) for brain progression, 72 (60%) for systemic progression and 7 (6%) for non-oncological causes. The median overall survival was 13 months, deaths from brain progression occurred after a median time of 51 months, while from systemic progression after 19 months.

Conclusion: SRS without upfront WBRT is an effective treatment of BM from NSCLC. Since that our results are similar to the best published data on SRS plus WBRT, SRS alone could be considered the treatment of choice in this setting.

PO-0643

Stereotactic hypofractionation in combination with radiosurgery in the treatment of brain metastases

P. Ivanov[1], I. Zubatkina[1], G. Andreev[1]

[1]International Institute of Biological Systems, Radiosurgery, Saint-Petersburg, Russian Federation

Purpose or Objective: To estimate the clinical results of hypofractionated stereotactic radiotherapy (HSR) alone or in combination with stereotactic radiosurgery (SRS) for the treatment of brain metastases using different radiation devices, which provide precise delivery of a high radiation dose to the target.

Material and Methods: Between November 2010 and July 2015, 257 patients with brain metastases were treated by HSR alone or simultaneous application of two stereotactic radiation techniques (SRS plus HSR) at the Radiosurgical Centre of IIBS (Saint Petersburg, Russia). Radiation treatment was performed with Gamma Knife 4C and Perfexion (Elekta AB, Stockholm, Sweden), Cyber Knife (Accuray, Sunnyvale, CA, USA) and linear accelerator TrueBeam STX (Varian Medical Systems, Palo Alto, CA) equipped with the BrainLAB Exac Trac system. The indications for HSR were determined by the presence of large volume lesions or proximity to critical brain structures. Patients with multiple brain metastases were subjected to a combination of HSR and SRS. Radiation schemes were selected depending on the number of metastases, size, location, proximity to critical brain structures, histological type of primary cancer and the patient's general condition. SRS was performed with the marginal dose of 18 – 24 Gy at 40 – 90 % isodose and HSR was performed with the total dose of 24, 27 or 30 Gy in 3 fractions. Following treatment the patients underwent control MRI examination with standard protocols (2 mm T2 and 1 mm T1 with double contrast enhancement) at 8 weeks and then every 3 months. The median follow-up period was 6 months.

Results: The study revealed that the application of hypofractionated stereotactic radiotherapy for the treatment of large volume or critically located brain metastases provides a high level of local control (12-month local control rate was 83 %). Complications in the form of radiation necrosis occured in 15 % of patients at a median of 6 months after treatment. The median overall survival for the entire patient cohort was 9 months. There was no statistically significant difference in the median survival of the patients receiving HSR alone and those receiving HSR plus SRS. The best results were obtained in patients belonging to the first RPA-class who achieved two-year survival in 70 % of the cases. The advantage of combining SRS and HSR is the possibility to deliver high radiation doses to large volume lesions, without exceeding the brain's tolerance. HSR allows one to achieve a rapid shrinkage of large volume tumors, which considerably improves the patient's neurological condition.

Conclusion: High-dose stereotactic radiation is a safe and effective method for controlling brain metastases. A combined application of SRS and HSR is a viable treatment strategy for patients with multiple brain metastases who have at least one large lesion or a lesion located in/near critical brain structures.

PO-0644

Hippocampal sparing brain radiotherapy using VMAT to the primary brain tumour

K.S. Kim[1], C.W. Wee[1], J.Y. Seok[2], J. Hong[2], J.B. Chung[2], K.Y. Eom[2], J.S. Kim[2], I.A. Kim[2]

[1]Seoul National University College of Medicine, Radiation Oncology, Seoul, Korea Republic of

[2]Seoul National University Bundang Hospital, Radiation Oncology, Seongnamsi, Korea Republic of

Purpose or Objective: We hypothesized that hippocampal-sparing radiotherapy using volumetric modulated arc therapy (VMAT) could preserve cognitive function of the patients with primary brain tumor treated with brain radiotherapy.

Material and Methods: We prospectively collected patients who were diagnosed with primary brain tumor and treated with brain radiotherapy from March 2014 to April 2015. Brain radiotherapy was delivered using VMAT planning technique with inclined head position. Optimization criteria for the

hippocampus dose was Dmax less than 17Gy without compromising the coverage of planning target volume (PTV) and other organs at risk were prioritized over hippocampal constraint. The mini-mental state examination (MMSE) and Seoul verbal learning test for total recall, delayed recall and recognition (SVLT-TR, DR, R) were performed at baseline and at 7 and 13 or 16 months after radiotherapy.

Results: A total of 41 patients were accrued. Median age was 48 years (range 26-76) and 51.2 % of the patients were male. Eighteen patients (43.9%) had WHO grade I or II tumor whereas 23 patients (56.1%) had grade III or IV tumor. Median volume of PTV was 192.8 cc (range 33.4-522.6) and median prescribed dose was 60Gy (range 46-66). Concurrent chemotherapy was given to 18 patients (43.9%). Median D100% and Dmax to the contralateral hippocampus were 7.7Gy (range 0.6-24.8) and 16.6 Gy (range 3.56-60.4) respectively. Mean dose to contralateral hippocampus could be spared to less than 21 Gy in 39 patients with median value of 11.6 Gy (range 0.3-37.3) which was lower compared to previous documentation. Median value of maximal dose to lenses and eyeballs were 4.3 Gy (0.4-8.1) and 13.7 Gy (0.5-46.6) respectively. At median follow up of 7.8 months (range 0-14.8), median progression-free survival and overall survival were not reached. Cognitive function tests at 7 months were analyzable in 12 patients. For these patients, MMSE, SVLT-TR, SVLT-DR and SVLT-R at 7 months showed improved results compared to the baseline with 2.0% (95% CI, -0.8% to 4.7%), 11.0% (95% CI, 3.3% to 18.8%), 20.1% (-5.5% to 45.8%) and -0.6% (95% CI, -6.6% to 8.2%) increase respectively. No grade 4 or 5 toxicity was reported.

Conclusion: Hippocampus could be spared effectively in radiotherapy to primary brain tumors using VMAT. Despite limited follow up data, cognitive function tests of the patients showed promising results. Further follow up data would clarify the effect of hippocampal sparing on the cognitive function of the patients treated with radiotherapy for primary brain tumor.

PO-0645

18F-FET PET and MRI for treatment planning in glioblastoma

M. Harat[1], B. Malkowski[2], Z. Okońska[3], R. Makarewicz[4]
[1]*The Franciszek Lukaszczyk Oncology Centre, Radiotherapy, Bydgoszcz, Poland*
[2]*The Franciszek Lukaszczyk Oncology Centre, Nuclear Medicine, Bydgoszcz, Poland*
[3]*The Franciszek Lukaszczyk Oncology Centre, Medical Physics, Bydgoszcz, Poland*
[4]*The Franciszek Lukaszczyk Oncology Centre, Oncology and Brachytherapy, Bydgoszcz, Poland*

Purpose or Objective: To analyze pre-treatment MRI- and 18F-fluoroethylthyrosine-PET- (FET-PET) based target volumes and patterns of failure following radiotherapy (RT) with concurrent temozolomide (TMZ) for primary glioblastoma multiforme (GBM).

Material and Methods: Thirty-four patients with primary GBM were treated using MRI based treatment volumes (GTVrm). Before treatment patients underwent FET PET/CT scans and biological tumor volume (GTVpet) were contoured but not used for target definition. Progression were defined according to RANO criteria. Tumor progression and pre-treatment MRI and PET scans were co-registered to the radiation dose map. Failures were classified based on location of primary GTVs and dose delivered at the site of failure. We investigated volumetric size and uniformity of MRI- vs. FET-PET/CT-derived GTVs and progression patterns assessed by means of FET PET/CT and MRI.

Results: FET-PET based GTVs measured 10 minutes after radionuclide injection (a.r.i.) (median 37.3 cm3) were larger than GTVs measured 60 minutes a.r.i. (median 27,7 cm3). GTVpet were significantly larger than corresponding MRI based GTVs (median 19,3 cm3). The congruence of MRI and FET signals for the identification of glioblastoma GTVs is poor with mean uniformity index of 0.4 (p=0,0). 74% of failures were located inside primary GTVpet. 68% of failures occured within the 95% isodose line, and 9% within 60 Gy isodose.

Conclusion: The size and geometrical location of GTVs differed in a majority of patients. The volume of GTVpet depends on time a.r.i. Tumor progression were mostly inside FET-PET volumes. FET PET better defined failure site then MRI. Finally dose inhomogenity inside GTVpet and GTVrm and favourable tumor control within 60Gy isodose advocates further studies with PET-MR based high-dose radiation therapy of GBM.

PO-0646

Temozolomide during radiotherapy of glioblastoma multiforme: daily administration improves survival

S. Nachbichler[1], G. Schupp[1], H. Ballhausen[1], M. Niyazi[1], C. Belka[1]
[1]*Klinikum der Universität München, Klinik und Poliklinik für Strahlentherapie und Radioonkologie, München, Germany*

Purpose or Objective: Temozolomide (TMZ) based chemoradiotherapy defines the current gold standard for the treatment of newly diagnosed glioblastoma. Data regarding the influence of TMZ dose density during chemoradiotherapy are currently not available. We retrospectively compared outcomes in patients receiving no TMZ, patients receiving TMZ during radiotherapy on radiotherapy days only (5/7) and patients receiving TMZ constantly 7 days a week (7//7).

Material and Methods:
From 2002 to 2012 a total of 432 patients with newly diagnosed glioblastoma received radiotherapy in our department. 118 patients had radiotherapy alone, 210 had chemoradiotherapy with temozolomide (75 mg/m²) daily (7/7 days a week) and 104 chemoradiotherapy with temozolomide only on radiotherapy days (5/7 days a week, Monday till Friday). Radiotherapy was applied in 30 fractions to a total dose of 60 Gy.

Results: Median survival after radiotherapy alone was 9.1 months, compared to 12.6 months with temozolomide 5/7 and to 15.7 months with temozolomide 7/7. The 1 year survival was 33% in the radiotherapy only group, 52% in the 5/7 group and 64% in the 7/7 group. Kaplan Meier analysis showed a significant improvement of temozolomide 7/7 vs. 5/7 (p=0.01 by the log-rank test), while temozolomide 5/7 was still superior to no temozolomide at all (p=0.02).

Conclusion: Our results confirm the findings of the EORTC/NCIC-trial by Stupp et al., establishing the daily temozolomide chemoradiotherapy as standard therapy for glioblastoma. Also a reduced temozolomide scheme can at first prolong the survival of glioblastoma patients, but not as much as the daily application.

PO-0647

Subventricular zones: new key targets for glioblastoma treatment

J. Khalifa[1], F. Tensaouti[2], A. Lusque[3], B. Plas[4], J.A. Lotterie[2], E. Uro-Coste[5], V. Lubrano[4], E. Cohen-Jonathan Moyal[1]
[1]*Institut Universitaire du Cancer de Toulouse - Oncopole, Radiation Oncology, Toulouse Cedex 09, France*
[2]*INSERM, U825, Toulouse, France*
[3]*Institut Universitaire du Cancer de Toulouse - Oncopole, Biostatistics, Toulouse Cedex 09, France*
[4]*CHU Purpan, Neurosurgery, Toulouse, France*
[5]*Institut Universitaire du Cancer de Toulouse - Oncopole, Pathology, Toulouse Cedex 09, France*

Purpose or Objective: We aimed to identify subventricular zone (SVZ)-related prognostic factors of survival and patterns of relapse among patients with glioblastoma.

Material and Methods: Forty-three patients with primary diagnosed glioblastoma treated in our Cancer Center between 2006 and 2010 were identified. All patients received surgical resection, followed by temozolomide-based

chemoradiation (60 Gy, 2 Gy per fraction). Ipsilateral (iSVZ), contralateral (cSVZ), and bilateral (bSVZ) SVZs were retrospectively segmented following two delineation methods: with (TH+) and without (TH-) temporal horns. Dose-volume histograms were retrospectively generated on the original plans. Progression was defined according to the RANO criteria. Multivariate analysis using the Cox proportional hazards model including significant covariates in univariate analysis was assessed to examine the relationship between prognostic factors and time to progression (TTP).

Results: Median age was 59 years (range: 25-85). Median follow-up, OS and TTP were 52.8 months (95% CI 43.4-61.1), 26.2 months (95% CI 20.3-34.2) and 6.4 months (95% CI 4.4-9.3), respectively. On univariate analysis, initial contact to SVZ was a poor prognostic factor for OS (20.5 vs 56.4 months, p = 0.011) and TTP (4.6 vs 12.9 months, p = 0.002). With TH-method, patients receiving mean dose to bSVZ greater than 40 Gy had a significantly improved TTP, as well as patients whose V20 Gy to bSVZ was greater than 84% (17.7 months vs 5.2 months, p = 0.017). On multivariate analysis, initial contact to SVZ and V20 Gy to bSVZ lesser than 84% remained poor prognostic factors for TTP (HR = 3.07, p = 0.012 and HR 2.67, p = 0.047, respectively).

Conclusion: Our results suggest that contact to SVZ, as well as insufficient bSVZ coverage such as a V20 Gy lower than 84%, are independent poor prognostic factors for TTP. Therefore, targeting SVZ is of crucial interest for optimizing glioblastoma treatment.

PO-0648

Pilot study in the assessment of contouring variability in stereotactic radiosurgery

H. Sandstrom[1], C. Chung[2], J. Gårding[3], I. Toma-Dasu[1]
[1]*Stockholm University and Karolinska Institutet, Medical Radiation Physics, Stockholm, Sweden*
[2]*University of Toronto and University Health Network-Princess Margaret Cancer Centre, Department of Radiation Oncology, Toronto, Canada*
[3]*Elekta Instrument AB, Research & Physics- Neuroscience, Stockholm, Sweden*

Purpose or Objective: The accuracy in contouring the target is one of the key factors for the success of stereotactic radiosurgery (SRS). This is particularly important when delivering one large fraction of radiation with small or no margins, since the consequence of not defining the correct clinical target volume can be that intended treatment results are not achieved. Furthermore, accurate contouring of the relevant Organs-at-Risk (OARs) is essential to minimize any normal tissue toxicity. The aim of this study was to analyze and quantify the variability of target and OAR contouring for two lesions in the brain.

Material and Methods: A multicenter analysis of the variability in contouring the target and the OARs for two typical cases of brain disorders, a cavernous sinus meningioma and a vestibular schwannoma was performed. Twelve Gamma Knife centers from around the world have participated in the study by contouring the targets and the OARs. The resulting treatment plans were analyzed with respect to the agreement in target and OARs contouring.
The 50 %-agreement volume, AV50, and the common volume, AV100, together with the encompassing volume, AV100/N, were determined based on a binary analysis method. A novel metric for the variability in delineation defined as the Agreement-Volume-Index was introduced and additionally calculated. The variability of the contoured structures was also analyzed with respect to the position of their centers of mass (COMs).

Results: Substantial disagreement in target delineation was observed with an Agreement-Volume-Index of 0.22 for the meningioma case and 0.50 for the vestibular schwannoma case, respectively. Very high disagreement was also observed for the delineation as OARs of the optic apparatus and cochlea with an Agreement-Volume-Index ranging from 0 to 0.13. The disagreement was observed with respect to the shape, size and position of the contoured volumes. The resulting disagreement in target volumes was highest for the meningioma (range 5.29-7.80 cm3) while a lower disparity was observed for the schwannoma (range 3.56-4.48 cm3). The majority of structures analyzed displayed the highest disagreement of the COM in longitudinal direction. An illustration of the displacement of the COMs together with the common volume and encompassing volume is shown in Figure 1 for the cavernous sinus meningioma case.

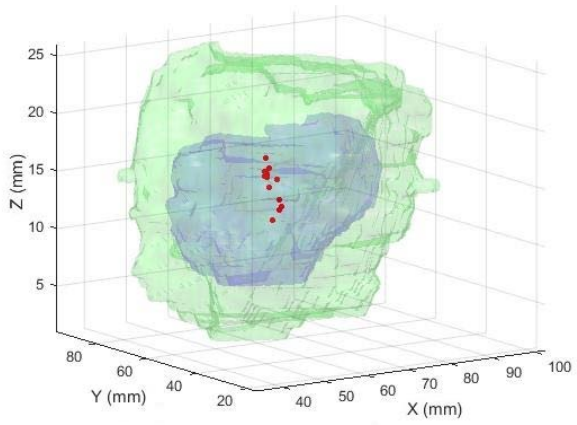

Figure 1. Illustration of the displacement of the COMs (red dots) together with the common volume (blue) and encompassing volume (green) for the cavernous sinus meningioma case.

Conclusion: Differences in target and OARs contouring expressed using different parameters, including a novel metric, emphasize the importance of further investigating and standardizing the contouring in SRS. Therefore, clinically significant differences in target and OARs delineation might lead to the need of better contouring tools, education and standardized protocols in SRS.

PO-0649

Evaluation of distant brain failure among patients undergoing SRS for lung cancer brain metastases

G. Bhattal[1], A. Keller[1], J. Dajac[1], Z. Pavlovic[1], R. Ismail[1], S. Kailas[1], J. Babb[1], T. Buntinx-Krieg[1], T. Do[1], E. Kim[1], A. Sarparast[1], N. Ramakrishna[2]
[1]*University of Central Florida, College of Medicine, Orlando, USA*
[2]*UF Health Cancer Center-Orlando Health, Dept. of Radiation Oncology, Orlando, USA*

Purpose or Objective: The latency, overall extent, and rate, of distant brain failure for non-small cell lung cancer patients undergoing SRS for brain metastases is not well characterized. We evaluated the impact of multiple pre-treatment parameters including age, KPS, extracranial disease status (ECD), initial number of metastases, initial aggregate tumor volume, and histological/molecular subtypes, on distant brain failure. We also evaluated the impact of WBRT performed before, combined with, or after SRS.

Material and Methods: The retrospective study population included 118 NSCLC patients with brain metastases treated with SRS between 11/2008 and 01/2014. The distant brain metastasis-free survival (DBMFS) was defined as latency in months from initial SRS to first subsequent radiographic evidence of new brain metastasis. The extent of overall distant brain failure (ODBF) was defined as the total number of new metastases that developed following initial SRS treatment. The distant brain failure rate (DBFR) was defined as the ODBF/RFI where RFI was defined as the maximum radiographic follow-up interval in months. Kaplan Meir analysis was used to evaluate DBMFS and Log Rank test was used to determine the significance (p-value <0.05 was considered significant). For ODBF and DBFR, Independent

sample t-test and one way ANOVA were used for statistical evaluation.

Results: The median overall DBMFS was 12.9 months. A significant difference in median DBMFS was observed for patients with squamous cell vs. adenocarcinoma primary histology (4.57 months vs. 15.9 months, respectively, p <0.015). The initial number of metastases, total initial metastasis volume, ECD status, KPS scores, EGFR mutation status, or ALK gene rearrangement status, made no significant difference on DBMFS. None of the analyzed parameters displayed significant impact on ODBF. WBRT had no significant effect on DBMFS or ODBF in the study population, but patients with history of WBRT prior to SRS had an increased DBFR (0.396 vs. 0.089) which was borderline significant (p=0.05). There was an insufficient number of patients receiving combined WBRT with SRS to determine an effect on distant brain failure vs. SRS alone.

Conclusion: Characterization of the risk of distant brain failure is important to treatment selection, prognosis and follow-up. Among lung cancer patients with brain metastases treated with SRS, our study found no impact from age, initial number/volume of metastases, EGFR/ALK status, or ECD status, on distant brain failure. However, this study did reveal a significantly shorter latency to appearance (DBMFS) of distant brain metastatic disease for patients with squamous vs. adenocarcinoma histology. The clinical prognostic significance of this histologic subtype-dependent difference on distant brain failure is the subject of further study.

PO-0650

Prognostic value of minimal time to peak in dynamic 18F-FET-PET for high-grade glioma re-irradiation

D.F. Fleischmann[1,3], M. Unterrainer[2], P. Bartenstein[2], C. Belka[1], N.L. Albert[2], M. Niyazi[1]

[1]University Hospital of Munich, Radiation Oncology, Munich, Germany

[2]University Hospital of Munich, Nuclear Medicine, Munich, Germany

[3]German Cancer Consortium (DKTK), German Cancer Research Center (DKFZ), Heidelberg, Germany

Purpose or Objective: Most high-grade gliomas recur after initial multimodal therapy and re-irradiation has been shown to be a valuable re-treatment option in selected patients. We present the prognostic value of dynamic O-(2-18F-fluoroethyl)-l-tyrosine ([18F]-FET) PET for patients treated with re-irradiation ± concomitant bevacizumab. Dynamic [18F]-FET-PET provides useful information to individualize treatment decisions and personalize risk stratification of patients with high-grade glioma recurrence.

Material and Methods: We retrospectively analyzed 72 patients suffering from recurrent high-grade glioma. Static and dynamic [18F]-FET-PET was performed prior to re-irradiation. PET analysis revealed information about the maximal standardized uptake value (SUVmax) of the tumor corrected for the mean background (BG) (SUVmax/BG), the biologic tumor volume (BTV) and the mean tracer uptake within the BTV (SUVmean/BG). Dynamic parameters such as time-activity-curves (TACs) and minimal time-to-peak (TTPmin) were analyzed. Additional analysis was performed for gender, age, KPS, MGMT methylation status, IDH1 mutational status, WHO grading, concomitant bevacizumab therapy and the number of foci. The influence of PET derived and clinical parameters on post-recurrence survival (PRS) was investigated.

Results: TTPmin had a significant impact on PRS both on univariate (p=0.027) and multivariate analysis (p=0.008). Shorter TTPmin was related to shorter PRS after re-irradiation with 6 months for TTPmin <12.5 min, 7 months for TTPmin 12.5 – 25 min and 11 months for TTPmin >25 min (p=0.027). Other factors significantly related to PRS were number of foci (p=0.025), TAC classifications (p=0.019; G1-2 vs G3-5), and gender (p=0.028).

Conclusion: Dynamic [18F]-FET-PET with TTPmin is of high prognostic value for recurrent high-grade glioma and might help to personalize re-irradiation treatment regimens in future either through PET-guided dose escalation or by combination therapy with targeted agents.

PO-0651

Pattern of failure in glioblastoma patients after FET-PET and MRI-guided chemo-radiotherapy

M. Lundemann Jensen[1,2], J. Cardoso Costa[1,3], I. Law[3], A. Muhic[4], S.A. Engelholm[1], P. Munck af Rosenschöld[1,2]

[1]Rigshospitalet, Department of Oncology- Section for Radiotherapy, København Ø, Denmark

[2]University of Copenhagen, Department of Science- Niels Bohr Institute, København Ø, Denmark

[3]Rigshospitalet, Department of Clinical Physiology- Nuclear Medicine and PET, København Ø, Denmark

[4]Rigshospitalet, Department of Oncology, København Ø, Denmark

Purpose or Objective: The aim of this work is to investigate the pattern of failure for patients with glioblastoma, after FET-PET- and MRI-planned volumetric-modulated arc therapy (VMAT) with concomitant and adjuvant temozolomide (TMZ). Our hypothesis; FET-PET volume will better predict the pattern of failure and the inclusion of FET-PET in the radiation therapy target leads to a decrease in marginal failures.

Material and Methods: We analysed the first 66 consecutive patients with histologically confirmed glioblastoma (WHO grade IV), scanned with FET-PET and MRI for post-surgical radiotherapy planning. Residual tumor volume including the resection cavity, denoted GTV(MR), was manually contoured on contrast-enhanced T1-weighted MRI (cT1). Metabolic tumor volume (GTV(PET)) was semi-automatically delineated by including tissue with uptake exceeding 1.6 times the uptake in normal appearing grey matter and subsequently edited to exclude non-tumor tissue. The CTV was created by adding a uniform margin of up to 2 cm to GTV(MR) and if necessary modified to include GTV(PET) and exclude natural boundaries such as the skull. A dose of 60 Gy was prescribed to the PTV (CTV plus 0.2 cm) in 2 Gy fractions, five days a week, using VMAT. TMZ was administered daily with radiotherapy (75 mg/m2) and subsequently in 6 cycles in a 5 days schedule every 28 days (150-200 mg/m2). The recurrence volume (RV) was evaluated radiologically on follow-up cT1 according to the RANO-criteria. Patterns of failure were classified as central, in-field or marginal if >95%, 80-95% or 20-80% of the RV was located within the 95% isodose (D95%). In case of the appearance of any new lesion outside the D95% or if <20% of the RV was within D95%, the failure was defined as distant. The treatment failure overlap (TFO) for three pre-treatment tumor volumes; GTV(MR), GTV(PET) and the union of the two, denoted GTV(MRPET), were calculated as the intersection of each GTV and RV divided by RV. Differences were assessed using Willcoxon signed rank test.

Results: Sixteen patients were excluded due to; no follow-up imaging (n=6), incomplete RT (n=3), whole-brain irradiation (n=1), clinical deterioration but no sign of radiological progression (n=2) and four patients were progression-free at the time of analysis (median follow-up 38.5 months). All patients were FET-positive. The pattern of failure was central, in-field, marginal and distant in 82%, 10%, 2% and 6%, respectively. The TFO were in median 0.73, 0.34 and 0.87 for GTV(MR), GTV(PET) and GTV(MRPET), respectively. All TFO were significantly different (p<0.001).

Conclusion: The inclusion of FET in radiotherapy planning leads to fewer marginal failures compared to previously reported studies. FET-PET alone is not better than MRI to predict the pattern of failure in glioblastoma patients. However, the combination of the two appears better than either of the modalities alone.

PO-0652

SFRT of the resection cavity in patients with one to three brain metastases

A. Bilger[1], H. Lorenz[1], D. Milanovic[1], O. Oehlke[1], A.L. Grosu[1]
[1]*University Medical Center Freiburg, Department of Radiation Oncology, Freiburg, Germany*

Purpose or Objective: In patients undergoing surgical resection of brain metastasis local recurrence is about 60%. Whole brain Radiation Therapy (WBRT) can significantly reduce the risk of local relapse but fails to improve overall survival. The most important side effects of WBRT are neurocognitive deficits, which can reduce quality of life. The goal of this study is to evaluate the role of stereotactic fractionated radiotherapy (SFRT) in patients with one to three brain metastases after surgical resection.

Material and Methods: We performed a retrospective single-institutional study in 60 patients undergoing SFRT of surgical cavity after resection of ≤3 brain metastases (November 2009 - August 2013). The total irradiation dose was 30 Gy (5Gy/d, BED 45 Gy) after complete macroscopical resection and 35 Gy (5Gy/d, BED 52.5 Gy) in patients with macroscopic residual tumour after surgery. Macroscopic residual tumour was defined as contrast enhancement next to the resection cavity on the postoperative T1-MRI. We investigated local control (LC) as a primary endpoint. Intracranial distant intracranial tumour control (DC), overall survival (OS) and side effects were secondary endpoints.

Results: The median follow-up for 52 patients was 8 months (1 to 32 months). 8 patients were lost to follow-up, due to mortality or morbidity. There were 6 (11.5%) local failures and 29 (55.8%) distant failures. Local control was correlated with age (p=0.046). Thirty-seven of 60 (61.7%) patients died during follow-up. Median overall survival was 15 months. Cox regression for survival was significant for KPS score ≤ 70% and size of PTV. No severe side effects were seen. Patients undergoing whole brain radiation therapy (WBRT) as salvage therapy in case of progression had no severe side effects.

Conclusion: SFRT could be an alternative to WBRT after surgical resection of≤3 brain metastasis. We had an encouraging rate of local control. Due to the high rate of distant intracranial failure regular follow-up with MRI is mandatory. No Grade 3, 4 or 5 adverse events were reported in patients undergoing WBRT or additional Stereotactic Radiotherapy as salvage therapy in case of intracranial progression. Prospective studies are warranted.

PO-0653

Surgical interventions after previous SBRT of the spine – increased risk for complications?

J. Roesch[1], J. Cho[2], D.K. Fahim[3], J.C. Flickinger[4], P.C. Gerszten[5], I.S. Grills[3], M.S. Jawad[3], R. Kersh[6], D. Letourneau[7], F. Mantel[8], A. Sahgal[9], J.H. Shin[10], B. Winey[11], M. Guckenberger[1]
[1]*University Hospital Zürich, Department of Radiation Oncology, Zurich, Switzerland*
[2]*Princess Margaret Hospital, Radiation Medicine Programme, Toronto, Canada*
[3]*William Beaumont Hospital, Department of Radiation Oncology, Royal Oak- Michigan, USA*
[4]*University of Pittsburgh Medical Center, Department of Radiation Oncology, Pittsburgh- Pennsylvania, USA*
[5]*University of Pittsburgh Medical Center, Department of Neurological Surgery, Pittsburgh- Pennsylvania, USA*
[6]*Riverside Medical Center, Department of Radiation Oncology, Newport News- Virginia, USA*
[7]*Princess Margaret Hospital, Department of Radiation Oncology, Toronto, Canada*
[8]*University Hospital Würzburg, Department of Radiation Oncology, Würzburg, Germany*
[9]*Sunnybrook Health Sciences Centre, Department of Radiation Oncology, Toronto, Canada*
[10]*Massachusetts General Hospital, Department of Neurosurgery, Boston- Massachusetts, USA*
[11]*Massachusetts General Hospital, Department of Radiation Oncology, Boston- Massachusetts, USA*

Purpose or Objective: Stereotactic body radiotherapy (SBRT) of vertebral metastases has emerged as a promising methodology, offering high rates of symptom relief and local control combined with low risk of toxicity. Nonetheless, local failure or spinal instability may occur, generating the need for subsequent surgery in the irradiated region. This study evaluated whether there is an increased incidence of intra- and post-surgical complications after high-dose radiotherapy.

Material and Methods: Based on a retrospective international database of 704 cases of SBRT for vertebral metastases, 42 patients treated at 7 different institutions were identified who underwent surgery in a previously stereotactic irradiated region. Data regarding surgical characteristics and complications were available for 38 patients.

Results: Twenty women, 13 men, median age 59 years (range 27 to 84 years) underwent SBRT for vertebral metastases followed by surgery. In 18 cases, conventional radiotherapy had been delivered prior to SBRT at a median dose of 30 Gy in median 10 fractions. SBRT was most frequently administered in 1 fraction with a mean prescription dose of 20,9 Gy (mean EQD2/10 = 45,3Gy). The median time until the surgical intervention was performed was 7.5 months after SBRT. The most frequent reason for surgery was progressive pain (n=35) followed by progressive neurological deterioration (N=20) or fracture of the vertebral body (n=16). Therefore, open surgical decompression (n=29) and/or stabilization (n=22) were the most frequently performed surgical procedures. Increased fibrosis complicating the operation was explicitly stated in the surgical report in 5 cases. In 3 patients a durotomy occurred which could be sufficiently sealed during the operation in two cases and required surgical revision in 1 case. Median blood loss was 425 ml, but 5 patients had a blood loss of >1l during the procedure. After the operation, 2 patients suffered from an increased neurological deficit which could be explained by an epidural hematoma in one case. Delayed wound healing was reported in 4 cases. In one patient this lasted for 5 months after surgery until death. One patient died shortly after the surgical procedure due to unknown causes.

Conclusion: In this largest series of surgical interventions following spine SBRT, the overall complication rate was 45%. This appears to be higher when compared to primary surgery without previous SBRT. Therefore, spine surgery after SBRT is technically feasible. However, the decision to perform surgical procedures in these highly complex cases should be made by a multidisciplinary team and their performance in an experienced center may be beneficial.

PO-0654

Hypofractionated StereotaticRS for patients with brain metastases. Outcome evaluation and toxicity

P. Navarria[1], A. Ascolese[1], G. D'agostino[1], E. Villa[1], E. Clerici[1], A. Tozzi[1], C. Iftode[1], F. De Rose[1], L. Liardo[1], T. Comito[1], C. Franzese[1], D. Franceschini[1], F. Pessina[2], M. Riva[2], L. Bello[2], G. Reggiori[1], M. Scorsetti[1]
[1]*Istituto Clinico Humanitas, Radiotherapy and Radiosurgery, Rozzano Milan, Italy*
[2]*Istituto Clinico Humanitas, Neurosurgery, Rozzano Milan, Italy*

Purpose or Objective: Hypofractionated Stereotactic radiosurgery (HSRS) delivered in few fractions, up to 5, has been employed in patients with large brain metastases (BM), alone or after surgical resection on tumor bed, as an alternative to whole brain radiotherapy or to single fraction SRS with the aim to reduce late radiation-induced toxicity while maintaining high local control rate. The aim of this study was to evaluate the outcome and toxicity of patients treated for large brain metastases using HSRS, in terms of local control, incidence of distant brain metastases (DBM) and toxicity

Material and Methods: Between July 20011 and July 2015, 138 patients, 66 men and 72 women, with large brain metastases from different solid tumors have been treated with HSRT, using Volumetric Modulated Arc Therapy Rapid-Arc (VMAT-RA) in flattening filter-free (FFF) beams mode. The total doses prescribed were 30 Gy in 3 fractions or 30 Gy in 5 fractions in relation to the size and site of BM or 30 Gy in 3 fractions on tumor bed in patients underwent surgical resection.

Results: At a median follow-up time of 10.6 months (range 2-53 months) 6 (4%) patients had local relapse at a median time of 8 months (range 2-53 months) and 45 (32%) patients distant brain progression at a median time of 8 months (range 2-26 months). The 1- and 2-year local control rates were 90% and 87% respectively. The 1- and 2-year survival rates were 72% and 42 % respectively. At the last observation time 99 /71.7%) patients were alive and 39 (28.3%) dead. Eighty-five percent of patients succumbed to their extracranial disease and 15% died of progressive intracranial disease. During HSRS no increases of corticosteroid or AED have been needed. No symptomatic radionecrosis was observed. Factors recorded as influencing local failure and worse survival were the presence of metastases at diagnosis, NSCLC histology and impossibility to surgical resection

Conclusion: HSRS is a safe and effective treatment option for patients with large brain metastases. In our series better local control was recorded in case of metachronous BM, breast cancer histology and patients suitable for surgical resection followed by HSRT.

PO-0655

Targeted therapy and stereotactic radiotherapy in brain metastases from renal cell carcinoma

P. Anselmo[1], C. Caserta[2], M. Casale[1], F. Trippa[1], F. Arcidiacono[1], L. Draghini[1], F. Roila[2], E. Maranzano[1]
[1]*Ospedale Santa Maria, Radiotherapy Oncology Centre, Terni, Italy*
[2]*Ospedale Santa Maria, Medical Oncology Centre, Terni, Italy*

Purpose or Objective: To retrospectively evaluate safety and brain control (BC) in patients (pts) with 1-4 brain metastases (BM) from renal cell carcinoma (RCC) submitted to radiosurgery (RS) or fractionated stereotactic radiotherapy (FSRT) with or without target therapies (TTs).

Material and Methods: 46 pts with 74 BM were treated. Male/female ratio was 31/15, median age was 62y (range, 29-76). Median KPS was 100% (range, 50-100), 14 (37%), 27 (59%) and 2 (4%) pts were in RPA class 1, 2 and 3, respectively, and 37 (80%) pts had extracranial metastases. Disease was controlled in 28 (61%) and in progression in 18 (39%) pts. Neurologic functional score was generally good (NFS=0-2) having only 5 (11%) NFS=3. Relapse was defined "in-field" when more than 95% of the recurrence volume was within the original 50% isodose, and "out-field" in the other cases. Median number of irradiated BM per patient was 1 (range, 1-4). 37 (80%) pts with 63 BM (85%) received RS at a median dose of 20Gy (range, 15-25). Remaining 9 (20%) with 11 lesions (15%) were underwent FSRT at a dose of 5x6-7Gy. 21 (46%) pts did not receive TTs, 19 (46%) received concomitant and 6 (8%) post- irradiation TTs (sunitinib, sorafenib, pazopanib, mTOR inibitors, bevacizumab).

Results: At a median follow-up of 19 months (range, 1-51), 41 (89%) pts with 66 (89%) BM were evaluable. Local control was obtained in 96% of BM: there were complete remission in 29 (44%), partial remission in 25 (38%), stable disease in 9 (14%), and progression in 3 (4%) BM. During follow up, 21 (51%) pts had no brain progression, 4 (10%) had in-field relapse, 15 (37%) out-field relapse, and 1 (2%) in- and out-field relapse. Of 20 (49%) relapsing pts, 14 (70%) were retreated with RS, surgery, WBRT and FSRT (8, 3, 2 and 1, respectively). In-field relapse occurred after a median time of 21.5, out-field relapse after a median time of 8 months. At the time of analysis, 39/41 pts (95%) had died, 9 (22%) for brain progression, 30 (73%) for systemic progression. Global median duration of BC was 22 months (range, 3-51) and global median OS from irradiation was 19 months (range, 4-53). No difference in outcome and toxicity was registered comparing pts receiving or not TTs. Deaths due to brain or systemic progression occurred after a median time of 12 and 20 months, respectively.

Conclusion: Effectiveness of RS and FSRT in RCC BM was confirmed. The addition of concomitant TTs, though safety, does not seem to improve outcomes.

PO-0656

Radiosurgery in brain metastases: a mono-institutional experience

E. Pelle[1], E. Trino[1], M. Levis[1], C. Mantovani[1], U. Ricardi[1]
[1]*University of Turin, Radiotherapy, Turin, Italy*

Purpose or Objective: to evaluate the local control and survival in patients with brain metastases treated with stereotactic radiosurgery (SRS) as primary treatment approach and to identify predictors of distant brain failure (DBF)

Material and Methods: from 2010 to 2014 three hundred and eleven brain metastases in 204 consecutive patients were treated with SRS at University of Turin. Patients eligible for SRS had one to five brain lesions, metastases size≤3 cm, Karnofsky performance status≥ 70 and life expectancy ≥ 3 months. A total of 172 patients with 266 brain metastases were analysed. Doses ranged from 18-24 Gy in single fraction related to lesion size. Local control (LC), overall survival (OS) and distant brain failure were estimated using the Kaplan-Meier method. Univariate and multivariate analysis were performed to determine the prognostic factors for treatment outcomes and DBF

Results: the median follow-up was 24.9 months. The 6- and 12- month local control rates were 88.5% and 75.1% respectively. 46 patients recurred locally after SRS on 55 brain metastases, with a median time to local failure of 12.1 months. The median overall survival was 12.8 months, with 6- and 12- months OS rates of 74.5% and 53.8% respectively. On multivariate analysis, no significant prognostic factors were associated with local control and survival outcome, even if RPA class (I versus II) and metastases diameter showed a trend of significance for OS (p=0.11 e p=0.10 respectively). A distant brain failure was observed in 88 patients (43.2%), with a median time to DBF of 5.5 months. 60.8% of these patients maintained an oligometastatic intracranial disease ≤(5 brain lesions), while 39.2% of patients developed multiple brain metastases. Salvage therapy was delivered in 46.5% of DBF patients, consisting of WBRT in 28.4% of cases and SRS on metastases of new onset in 18.1% of patients. However, more than half of patients with DBF (53.5%) did not require any salvage treatment. Prognostic factors significantly associated with prolonged DBF-free survival on multivariate analysis included the number of brain metastases <2 (p=0.000) and breast primary (p=0.026). Tumor size≤ 10 mm, s table extracranial disease and oligometastatic brain failure were significant predictive factors for survival after DBF.

Conclusion: stereotactic radiosurgery is an effective and well-tolerated treatment option in patients with oligometastatic disease. SRS might also represent a valid salvage strategy in patients relapsing in order to delay or completely avoid WBRT.

PO-0657

Does Radiomics have prognostic value in glioblastoma?

I. Compter[1], R.T.H. Leijenaar[1], D.B.P. Eekers[1], J.D. Zindler[1], A. Hoeben[2], B. Küsters[3], J. Beckervordersandforth[3], L. Ackermans[4], O.E.M.G. Schijns[4], M. Anten[5], A.A. Postma[6], P. Lambin[1]
[1]*MAASTRO clinic, Dept. of Radiation Oncology, Maastricht, The Netherlands*
[2]*Maastricht University Medical Centre, Dept. of Medical Oncology, Maastricht, The Netherlands*

[3]*Maastricht University Medical Centre, Dept. of Pathology, Maastricht, The Netherlands*
[4]*Maastricht University Medical Centre, Dept. of Neurosurgery, Maastricht, The Netherlands*
[5]*Maastricht University Medical Centre, Dept. of Neurology, Maastricht, The Netherlands*
[6]*Maastricht University Medical Centre, Dept. of Radiology, Maastricht, The Netherlands*

Purpose or Objective: Radiomics is the high-throughput extraction of large amounts of features from radiographic images and allows to capture intra-tumoral heterogeneity in an non-invasive way. It can therefore have an important role in predicting clinical outcome and has the potential to support personalized medicine for the treatment of different types of cancer. The value of Radiomics has already been shown for head-and-neck- and non-small cell lung cancer. In this study we assess the prognostic value of CT Radiomics in glioblastoma (GBM) patients.

Material and Methods: Clinical data were obtained from 125 patients with a GBM, diagnosed with a biopsy only and treated with radiotherapy +/- TMZ between 2004 and 2015 at our institute. Patients underwent pre-treatment CT imaging and the tumor volume was manually delineated for treatment planning purposes. Pretreatment images from 74 patients were available for analysis. In total, 161 Radiomic features were extracted, comprising: a) first-order statistics, b) shape, and c) (multiscale) texture. Multivariable Cox proportional hazards (Cox PH) regression was performed using least absolute shrinkage and selection operator (LASSO) model selection (100 times 10-fold cross-validated). First, a Cox PH model consisting of only clinical features was fitted. A second model consisted of both clinical and Radiomic features, for which the Radiomic feature space was first reduced by selecting cluster medoids after hierarchical cluster analysis using correlation (ρ>0.9) as a distance measure. Harrell's concordance index (C-index; 500 times bootstrapped) and time dependent AUC curves were used to assess model performance.

Results: At a median follow up of 7.4 months, 8 (11%) of the patients were still alive at time of analysis. Mean age was 64 years (20 – 86). WHO performance status was <2 for 82%. Sixty-six percent of patients was concurrently treated with TMZ. Median overall survival was 6.5 months after treatment. The time-dependent AUC curves for the clinical model (C-index: 0.65) and the model including Radiomics (C-index: 0.71) are shown in Figure 1, Table 1. Incorporation of Radiomic features resulted in an overall higher time-dependent AUC curve and significantly higher C-index.

Table 1: Clinical and combined model for prediction of overall survival in patients with a GBM

Model	Features		C-index
Clinical	Age		0.65
	WHO performance status		
	Radiotherapy dose		
	Temozolomide		
Clinical & Radiomics	Age	GLCM_invDiffmomnor	0.71
	WHO performance status	GLSZM_largeAreaEmphasis	
	Radiotherapy dose	LoG_sigma_1_5_mm_3D_stats_entropyPos	
	Temozolomide	LoG_sigma_1_5_mm_3D_stats_kurtosis	
		LoG_sigma_2_5_mm_3D_stats_mean	
		LoG_sigma_4_5_mm_3D_stats_kurtosis	
		Shape_surface	
		Stats_max	
		Stats_median	
		Stats_skewness	

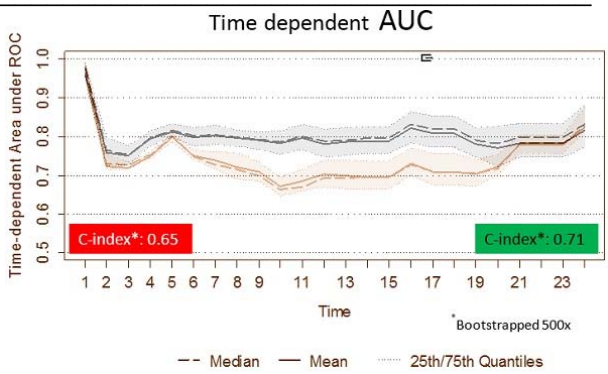

Conclusion: Radiomics has the potential to predict outcome using the pre-treatment CT and possibly identify clinical subgroups which can support personalized treatment for GBM. Additionally the dataset will be expanded to MR imaging, the leading imaging modality in GBM.

PO-0658

Linear accelerator radiosurgery for arteriovenous malformations: a single institution experience

S. Yahya[1], G. Heyes[1], P. Nightingale[2], S. Lamin[2], G. Cruickshank[2], I. Geh[1], D. Spooner[1], P. Sanghera[1]
[1]*Hall-Edwards Radiotherapy Research Group- Queen Elizabeth Hospital, Cancer Center, Birmingham, United Kingdom*
[2]*Queen Elizabeth Hospital, University Hospitals Birmingham, Birmingham, United Kingdom*

Purpose or Objective: Arteriovenous malformations (AVMs) are the leading causing of intra-cerebral haemorrhage. Stereotactic radiosurgery (SRS) is an established treatment for arteriovenous malformations (AVM) and commonly delivered using Gamma Knife. Linear accelerator (LINAC) SRS is often more widely available however there is debate over whether if offer equivalent outcomes. The aim of this project is to evaluate the outcomes using LINAC SRS for AVMs within a large UK neurosciences unit.

Material and Methods: Fifty sequentially treated patients with an AVM were identified from a prospective SRS database at a tertiary university hospital with a neurosciences unit. Planning was performed using BrainLab's BrainScan 5.3.1 treatment planning system, utilising a rigid fixed headframe and radiographic localisation box to determine target co-ordinates. Treatment was performed using multiple co-planar arcs delivered with a Varian600C linear accelerator at 6MV fitted with the BrainLab external stereotactic collimator system (fixed cones 10-35mm diameter). A review of all imaging was undertaken by a neurovascular radiologist to confirm obliteration and post SRS necrosis. A retrospective review of case notes was undertaken to confirm toxicity which was recorded using CTCAE Version 4. All outcomes were correlated prospectively recorded dose metrics.

Results: Forty six patients data analysed with median follow up of 5 years (1-14 years).Median age at first SRS treatment was 37.5 years (15-71 years) with 24 male and 22 female patients. Median lesion volume treated was 1.97cm^3 (mean 2.81cm^3 range 0.11-19.50).The median radiosurgery dose was 19.9Gy (range 13.0 – 28.7). The median normal brain volume V12Gy was 5.86cm3 and the median gradient index was 4.4 (2-9.9). Overall obliteration rate at 3 years was 71.7%. The overall incidence of CTCAE v 4 grade 3 or 4 toxicity was 6.5%. One patient presented with cognitive and mobility decline 3 years after treatment and was diagnosed with hydrocephalus. One patient had recurrent bi-frontal headaches with nausea and vomiting (MRI showed necrosis). One patient had refractory epilepsy (parietal AVM) although no imaging features present to support necrosis.

Conclusion: LINAC based SRS offers similar outcomes in terms of obliteration and toxicity to other platforms. Recent

developments in imaging and technology may further improve the therapeutic index.

PO-0659

Impact of 68Ga-Dotatoc-PET on tumor delineation and outcome in patients with meningioma

H. Fischer[1], K. Kessel[1,2], T. Pyka[3], M. Devečka[1], M. Schwaiger[3], S.E. Combs[1,2]
[1]*Technische Universität München TUM, Department of Radiation Oncology, München, Germany*
[2]*Institute of Innovative Radiotherapy iRT, Helmholtz Zentrum München, München, Germany*
[3]*Technische Universität München TUM, Department of Nuclear Medicine, München, Germany*

Purpose or Objective: Surgery represents the treatment of choice for meningiomas. However, complete resection is often not possible, and recurrence is common. Radiation therapy (RT) can be prescribed as an alternative treatment to surgery for low-grade meningiomas, or in the recurrent/adjuvant setting. Differentiation between normal tissue, i.e. meninges, post-operative changes and residual viable tumor can be difficult using MR and CT imaging alone. We evaluated the impact of 68Ga-Dotatoc-PET imaging on treatment planning including potential benefit in terms of outcome.

Material and Methods: We analyzed 15 patients with WHO I meningiomas of different localizations. All patients were treated with fractionated stereotactic radiotherapy (FSRT) with a total dose of 54 Gy and a single dose of 1.8 Gy. An advanced radiation oncologist delineated gross tumor volume (GTV) independently once based on diagnostic CT and MRI only (GTV_MR/CT), and a second time complemented by data of diagnostic 68Ga-Dotatoc-PET (GTV_PET). For image fusion and target definition BrainLab iPlan RT® software (Munich, Germany) was used. The intersection and union volumes of both GTVs (GTV_inter, GTV_union), were calculated.

Results: In 11 of 15 patients (73%) the additional data gained by 68Ga-Dotatoc-PET led to a lager GTV. In four patients (27%) GTV_PET was smaller than GTV_MR/CT. The mean intersection of both GTVs was 58.6%. Hence, 41.4% of the GTV_PET was contributed only due to information from 68Ga-Dotatoc-PET. About 22.6% of the GTV_MR/CT was not delineated in the GTV_PET volume because no increased tracer enhancement could be detected in these parts. Our first analyses of overall and progression free survival showed no significance in patients with a 68Ga-Dotatoc-PET for tumor delineation during treatment planning.

Conclusion: 68Ga-Dotatoc-PET improves the detection of residual or recurrent tumor cells especially in patients with meningioma of the skull base and the sphenoorbital region. In addition it helps to spare normal tissue in patients with large tissue defects after operation. However, the interobserver variability must be taken into account. The data will now be correlated with OS and further analyzed concerning the standard uptake values (SUV) of the PET-images to assess if a threshold value can be recommended for meningioma detection and delineation.

PO-0660

Evaluation of distant brain failure among patients undergoing SRS for melanoma brain metastases

S. Kailas[1], E. Kim[1], A. Sarparast[1], P. Adedoyin[1], A. Keller[1], G. Bhattal[1], R. Ismail[1], J. Babb[1], T. Buntinx-Krieg[1], J. Dajac[1], T. Do[1], Z. Pavlovic[1], N. Ramakrishna[2]
[1]*University of Central Florida, College of Medicine, Orlando, USA*
[2]*UF Health Cancer Center-Orlando Health, Dept. of Radiation Oncology, Orlando, USA*

Purpose or Objective: The latency, overall extent, and rate, of distant brain failure for patients undergoing SRS for melanoma brain metastases is not well characterized. We evaluated the impact of multiple pre-treatment parameters including age, KPS, gender, extracranial disease status (ECD), initial number of metastases, initial aggregate tumor volume, and B-raf V600E status, on distant brain failure. We also evaluated the impact of WBRT performed before, combined with, or after SRS.

Material and Methods: The retrospective study population included 54 melanoma patients with brain metastases treated with SRS between 11/2008 and 01/2014. The distant brain metastasis-free survival (DBMFS) was defined as latency in months from initial SRS to first subsequent radiographic evidence of new brain metastasis. The extent of overall distant brain failure (ODBF) was defined as the total number of new metastases that developed following initial SRS treatment. The distant brain failure rate (DBFR) was defined as the ODBF/RFI, where RFI was defined as the maximum radiographic follow-up interval in months. Kaplan Meir analysis was used to evaluate DBMFS and Log Rank test was used to determine the significance (p-value <0.05 was considered significant). For ODBF and DBFR, Independent sample t-test and one-way ANOVA were used for statistical evaluation.

Results: The median overall DBMFS was 5.69 months. A significant difference in median DBMFS was observed for patients with KPS<70 vs KPS >70 (2.24 vs. 10.44 months, p <0.022). Females had significantly worse DBMFS than males (5.96 vs. 17.96 months, p<0.009). The initial number of metastases, total initial metastasis volume, ECD status, and B-raf V600E mutation status, were associated with no significant difference in DBMFS. The ODBF was also worse for females than males (P<0.002). The DBFR was worse for females (p<0.049), and those with c-kit mutation (P<0.024). WBRT had no significant effect on DBMFS, ODBF or DBFR in the study population.

Conclusion: Characterization of the risk of distant brain failure is important to treatment selection, prognosis and follow-up. Among patients with melanoma brain metastases treated with SRS, our study found that female gender and a KPS<70 was associated with a significantly decreased latency to distant brain failure. In addition, female gender was associated with greater overall number of distant brain metastases and rate of distant brain failure. Mutations in c-kit but not b-raf were found to be associated with increased distant brain failure. Further study is underway to examine the overall clinical prognostic relevance of these findings.

PO-0661

Gliosarcoma: prognostic and therapeutics factors

J. Castelli[1], L. Feuvret[2], Q. Haoming[3], J. Biau[4], E. Jouglar[5], A. Berger[6], G. Truc[7], F. Llama Guttierrez[8], X. Morandi[9], F. Thillays[5], D. Loussouarn[10], I. Lecouillard[1], G. Crehange[7], D. Antoni[11], E. Vauleon[12], R. De Crevoisier[1], G. Noël[11]
[1]*Centre Eugène Marquis, Radiotherapy, Rennes Cedex, France*
[2]*La Pitié Salpétrière, Radiotherapy, Paris, France*
[3]*University of Rochester Medical Center, Radiation Oncology, Rochester, USA*
[4]*Centre Jean Perrin, Radiotherapy, Clermont Ferrand, France*
[5]*Insitut de Cancérologie de l'Ouest, Radiotherapy, Nantes, France*
[6]*CHU Poitiers, Radiotherapy, Poitiers, France*
[7]*Centre Georges François Leclerc, Radiotherapy, Dijon, France*
[8]*CHU de Rennes, Department of pathology, Rennes, France*
[9]*CHU de Rennes, Department of neurosurgery, Rennes, France*
[10]*CHU de Nantes, Departement of pathology, Nantes, France*
[11]*Centre Paul Strauss, Radiotherapy, Strasbourg, France*
[12]*Centre Eugène Marquis, Oncology, Rennes Cedex, France*

Purpose or Objective: In concern gliosarcoma management, the aims of this multicentre retrospective study were to identify prognostic or therapeutic factors impacting on overall survival.

Material and Methods: The analysis included all the patients treated for gliosarcoma between 1998 and 2014 in seven French academic centres.

Results: Seventy-five patients with a median age of 60 years (range from 23 to 79 years) were treated with a combination of surgery (n=66), radiotherapy (adjuvant for 64 patients and exclusive for 8 patients) and temozolomide based chemotherapy (n=58). Median follow-up was 12 months (range from 2 to 71 months). Two-year overall survival (OS) and disease free survival rates were 12% (95% CI: 4-20%) and 2% (95% IC: 0-6%), respectively. The median OS was 13 months. Treatment at recurrence consisted of chemotherapy (n=38) (bevazicumab for 18 patients, resumed temozolomide for 10 patients), salvage surgery (n=8) and radiochemotherapy (n=1). In univariate analysis, younger age, high total dose of radiotherapy, long time to recurrence and treatment at recurrence increased significantly OS. In multivariate analysis, high total dose of radiotherapy (HR = 0.97, p=0.007) and treatment at recurrence (HR=0.28 p<0.001) were favourable prognostic factor of OS.

Conclusion: High dose of radiotherapy and salvage surgery increase OS of gliosarcoma.

Poster: Clinical track: Haematology

PO-0662

The multi-institutional retrospective study of radiation therapy for NK/T-cell lymphoma in Japan

M. Oguchi[1], Y. Motoko[2], S. Ritsuro[3], S. Keisuke[4], H. Masatoshi[5], E. Yasuo[6], S. Toshinori[7], I. Koichi[8], I. Michiko[9], S. Emiko[10], K. Yasuko[11], H. Arisa[11]

[1]*Cancer Institute Hospital, Radiation Oncology, Tokyo, Japan*
[2]*Mie University Hospital, Hematology, Tsu, Japan*
[3]*Shimane University Hospital, Hematology, Matsue, Japan*
[4]*Juntendo University Hospital, Radiation Oncology, Tokyo, Japan*
[5]*Nara Medical School Hospital, Radiation Oncology, Kashihara, Japan*
[6]*Kobe University Hospital, Radiation Oncology, Kobe, Japan*
[7]*Hyogo Cancer Center, Radiation Oncology, Kobe, Japan*
[8]*Toho University Sakura Hospital, Radiation Oncology, Sakura, Japan*
[9]*Iwata General Hospital, Radiation Oncology, Iwata, Japan*
[10]*Nara Medical School Hospital, Radiation Oncology, Nara, Japan*
[11]*Cancer Institute Hospital JFCR, Radiation Oncology, Tokyo, Japan*

Purpose or Objective: JCOG0211 study demonstrated that the 5-year local control, 5-y OS and 5-y PFS of patients treated with RT-DeVIC were 94, 70 and 63%, respectively. NKEA project (UMIN000015491) conducted a multi-institutional retrospective study to clarify the changing current practice of the treatment for Extranodal natural killer(NK)/T-cell lymphoma nasal type(ENKL) over the first decade of this century in Japan, reviewing detailed information on treatment, clinical features and prognosis of patients with ENKL. The aim of this sub-study is to investigate the relationship between local failure patterns and radiation therapy before and after JCOG0211 study.

Material and Methods: Selection criteria of NKEA survey are newly pathologically diagnosed ENKL, any stage, and any type of treatment and treated from 2000 to 2013. From 32 institutions, more than 384 data of patients with ENKL have been registering in the NKEA project database. Of them, radiation therapy (RT) data, focusing on CTV setting, of 233 patients with localized nasal ENKL were evaluated with the JROSG-lymphoma committee.

Results: The baseline patients characteristics were followings, median age was 58 years old (range 18-88), male dominant (2:1), stage I/II=162/66(2.4:1). The median dose of RT was 50 Gy (range 9-60), delivering median 25 (range 3-33) fractionation over 37 (range 9-106) days. The 3D-CRT (CT based RT planning) was applied in 88% of patients and IMRT in 3%, using shrinking technique; 70%. RT was interrupted with 15% of patients due to hematological and mucosal toxicities. After JCOG0211 study, 49% of RT was designed according to JCOG0211 RT protocol, while 80% or more were not compliant RT protocol before/during JCOG0211. The local control was 74% for all population, 88% of local control rate was observed in patients treated with RT compliant with JCOG0211 RT protocol (extended RT), while 70% in patients not compliant with JCOG RT protocol (small field/limited RT). Based on the results of RT-QA review; we would like proposed the CTV guideline for IMRT/VMAT.

Conclusion: A multi-institutional retrospective survey after prospective clinical trial is important to review how the results of trial influence on the community standard practice of the treatment for rare lymphoma, and observance of radiation therapy guidance. The extended RT had higher local control rate than small limited RT.

PO-0663

Treatment result of primary thyroid lymphoma; a single institute experience

N. Yoshikawa[1], T. Shimbo[1], H. Yoshioka[1], K. Yoshida[1], Y. Uesugi[1], Y. Narumi[1]

[1]*Osaka Medical College, Radiology, Takatsuki, Japan*

Purpose or Objective: Primary thyroid lymphoma (PTL) is a relatively rare entity of extra-nodal lymphoma. There was no randomized clinical trial and the optimal treatment is not established. The purpose of this retrospective study is to verify the effectiveness and safety of our treatment protocol with long term follow-up.

Material and Methods: The stage IE - IIE PTL patients treated with combined treatment including radiotherapy and followed up at least three years were eligible for this retrospective study. We used CHOP or CHOP-like regimens with or without rituximab. Chemotherapy was not administered to the patients who were IEA MALToma treated in or after 2007 or have a contraindication to it. Acute and late toxicities were graded by CTCAE v4.0.

Results: Seventy-two PTL patients were analyzed and median follow-up period was 91 months (37 – 238 m) . The doses of radiotherapy were 36 - 61.2 Gy (median 41.4Gy). Seven-year overall survival and cause specific survival were 98.6 % and 92.2 %, respectively. Recurrences were observed in 7 patients; five of them were retreated (chemotherapy +/- radiotherapy) and four patients achieved complete remission. Three patients died during follow-up; 2 of them due to malignant lymphoma, one due to breast cancer. Grade 3 dermatitis, mucositis and pneumonitis were observed in 11 patients (15.2 %), 4 patients (5.5 %) and 3 patients (4.2 %), respectively. Two patients experienced grade 3 late toxicities (dyspnea and laryngeal edema), but we judged they were less relevant to the treatment. Laryngeal carcinomas which located in field of radiotherapy were appeared in two patients.

Conclusion: Effectiveness and safety of our treatment protocol were excellent. Because PTL patients are expected to have long term survival, we should optimize our treatment strategy to minimize acute and late toxicities and patients' quality of life.

PO-0664

Outcome of radiotherapy for stage I and II follicular lymphoma in patients staged by 18 FDG PET-CT

J.L. Brady[1,2], S.F. Barrington[3], V. Warbey[4], N.G. Mikhaeel[1,2]

[1]*Guy's and St.Thomas' NHS Foundation Trust, Department of Clinical Oncology, London, United Kingdom*
[2]*King's Health Partners, Academic Health Sciences Centre, London, United Kingdom*
[3]*King's College, PET Imaging Centre at St Thomas' Hospital-Division of Imaging Sciences and Biomedical Engineering, London, United Kingdom*

[4]King's College, PET Imaging Centre at St Thomas' Hospital-Division of Imaging Sciences and Biomedical Engineering, London, United Kingdom

Purpose or Objective: The majority of patients with follicular lymphoma (FL) present with advanced disease and are considered incurable. For patients with localised stage I or contiguous stage II, radiotherapy (RT) may be curative, but a significant proportion will relapse, usually at distant sites. Historical series report progression free survival (PFS) rates at 5 & 10 years post RT of 50-60% and 40-50% respectively.
PET-CT using Fluorodeoxyglucose (FDG) is superior to CT for staging of FL, with upstaging reported in 10-60% of patients. PET-CT has recently been recommended as the standard imaging modality for staging of FL.
By measuring outcomes in patients who underwent radical RT for stage I/II FL staged by PET-CT, this study aims to test the hypothesis that more accurate staging improves selection for localised RT and consequent patient outcome.

Material and Methods: A retrospective review was undertaken of all patients who underwent radical RT for stage I and II FL (grade 1, 2, 3a) at our institution from 2006-2014 staged by PET-CT. Patients were newly diagnosed and had not received any prior systemic or radiation therapy. Sex, age, PET-CT stage, LDH level, FLIPI score were recorded and whether a bone marrow trephine (BMT) was performed. RT site and dose were documented. Outcomes included relapse within the radiation field, distant relapse and PFS.

Results: Between July 2006 and November 2014, twenty-seven patients received radical involved field RT for stage I or contiguous stage II FL. 11 were male and 16 female. Median age (range) at RT was 59 years (32-84). 11 patients had grade 1 FL, 5 grade 1-2, 7 grade 2 and 5 grade 3a. 23 of 27 (85.2%) had Ann Arbor stage I disease by PET-CT. 23/27 (85.2%) had a BMT prior to treatment. In 3 cases BMT was not performed and in 1 the sample was inadequate. FLIPI score was 0-1 in all cases. The radiation dose was 24Gy/12# or 30.6Gy/17#, with the majority receiving 30.6Gy (23/27, 85.2%).
With a median follow up of 59.6 months (10.6-104), 23/27 (85.2 %) remain free of relapse either within or outside the radiation field. There have been no in-field recurrences. 4 patients (14.8%) have relapsed at distant nodal sites. The 4 relapses occurred at 3, 3, 9 and 25 months post treatment. 5 year PFS estimate was 84.75% (95% CI 71.01- 98.59) (see figure 1). For patients with stage 1 by PET-CT, 5 year PFS estimate was 90.87% (95% CI 68.2-97.9) and for those with stage 2, 50% (95% CI 6.6-.84.2). All patients were alive at completion of the study.

Figure 1. Progression free survival post radiotherapy

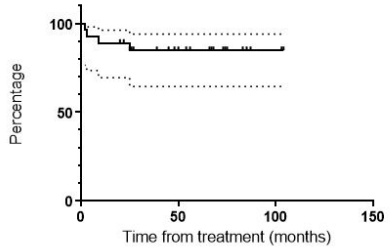

Conclusion: PFS after local RT for stage I/II FL staged by PET-CT appears to be better than for those historically staged by CT. Longer follow up and more patients are needed to confirm our findings, but this study suggests that earlier series from the pre-PET-CT era may have underestimated the efficacy of RT as a curative treatment for truly localised FL.

PO-0665

Compliance with ILROG guidelines in the treatment of extranodal lymphomas; an internal plans review

C. Furlan[1], P. Bulian[2], M. Michieli[2], M. Trovo[1], A. Ermacora[3], M. Spina[4], U. Tirelli[4], F. Franchin[1]

[1]Centro di Riferimento Oncologico, Radiation Oncology, Aviano, Italy
[2]Centro di Riferimento Oncologico, Hematology, Aviano, Italy
[3]Azienda Ospedaliera Santa Maria degli Angeli, Hematology, Pordenone, Italy
[4]Centro di Riferimento Oncologico, Medical Oncology, Aviano, Italy

Purpose or Objective: In 2015 the International Lymphoma Radiation Oncology Group (ILROG) has published guidelines on field and dose for modern radiotherapy in extranodal lymphomas. Involved site radiation therapy (ISRT) is recommended, and for most cases, ISRT results in smaller radiation fields than the involved-field radiation (IFRT) used previously. We analyzed our treatment plans to determine the compliance to ILROG guidelines in extranodal lymphomas.

Material and Methods: This retrospective study is based on the medical records of 62 patients with extranodal lymphoma, who were treated with definitive radiotherapy at our institute between 2011 and 2014. The patients characteristics are shown in Table 1. After evaluating the compliance to ILROG guidelines for each RT plan, Fisher's exact test was performed to determine factors associated with non-standard treatment including tumor site, histology, and radiation technique (IMRT vs. conventional technique). We calculated the progression free survival (PFS) by site and histology, and compared our findings to reference data retrieved from the IELSG trials.

Table 1. Clinical characteristics of patients and treatment modality

Patients	62
Age (range)	65 years (33-86 years)
Sex	
Male	36 (58%)
Female	26 (42%)
Histology	
DLBCL	34 (55%)
T cell anaplastic/large cell	5 (8%)
T cell NK	1 (2%)
MZL	8 (13%)
FL	9 (14%)
Mycosis Fungoides	5 (8%)
Stage	
I-II	47 (76%)
III-IV	15 (24%)
IPI	
0-1	48 (78%)
>1	14 (22%)
Site	
Skin	21 (34%)
Pharynx	7 (11%)
Paranasal Sinuses	3 (5%)
Testis	5 (8%)
Brain	5 (8%)
Bone	4 (6%)
Stomach	4 (6%)
Salivary gland	3 (5%)
Breast	3 (5%)
Orbital	3 (5%)
Soft tissue	3 (5%)
Thyroid	1 (2%)
Comorbidity index (ACE27)	
1	43 (70%)
2-3	19 (30%)
ECOG performance status	
0-1	57 (92%)
2	5 (8%)
Prior chemotherapy	
Yes	34 (56%)
No	28 (44%)
Median radiation dose (range)	30 Gy (24 – 46 Gy)
IMRT	
Yes	19 (30%)
N0	43 (70%)

Results: Forty-four (71%) patients were treated according to ILROG guidelines, and eighteen did not receive a standard teratment, either due to non standard treatment volume (n=13) or due to radiation dose (n=5).The major deviations from ILROG guidelines were observed in patients affected by pharynx lymphoma and orbital lymphoma. All patients with pharynx lymphoma underwent whole-Waldeyer ring RT instead of ISRT, while all patients with orbital lymphoma underwent partial-orbital RT instead of recommended whole-orbital RT. The majority (61%) of patients managed with nonstandard treatment were treated with IMRT technique. PFS by site and histology were similar to those reported in the IELSG trials.

Conclusion: This plans review process resulted in a high compliance to ILROG guidelines (71%). We identified a subset of patients which did not receive a standard treatment, therefore we are revising our treatment policy for pharynx lymphoma and orbital lymphoma.

PO-0666

Comparing the efficacy of low-dose radiotherapy in patients with aggressive and indolent lymphomas

C. Furlan[1], P. Bulian[2], M. Michieli[2], M. Spina[3], A. Ermacora[4], M. Trovo[1], U. Tirelli[3], G. Franchin[1]
[1]*Centro di Riferimento Oncologico, Radiation Oncology, Aviano, Italy*
[2]*Centro di Riferimento Oncologico, Hematology, Aviano, Italy*
[3]*Centro di Riferimento Oncologico, Medical Oncology, Aviano, Italy*
[4]*Azienda Ospedaliera Santa Maria degli Angeli, Hematology, Pordenone, Italy*

Purpose or Objective: Low-dose radiotherapy (LDRT) is a highly effective treatment in indolent non-Hodgkin lymphomas (NHLs). However, a reduced efficacy in aggressive lymphomas has never been demonstrated. We aimed to assess the effect of histologic type on disease response to LDRT.

Material and Methods: Data from a clinical phase-II trial using LDRT for palliation in diffuse large B-cell lymphoma (DLBCL) patients were compared with clinical outcome of patients with follicular lymphoma (FL), marginal zone lymphoma (MZ), and mycosis fungoides (MF) which were treated with LDRT at our Institution in the same period. LDRT consisted of 4 Gy in 2 fractions on symptomatic areas only for both DLBCL and indolent NHLs. Bulky disease was defined as > 5 cm in maximum diameter. Chemoresistance was defined as the failure of chemo to achieve a complete or partial response, or as disease relapse after a complete response. Clinical response was assessed 21 days after LDRT, and was defined as reduction > 50% of maximum diameter of the radiated lesions. Response evaluation was performed with CT-scan or clinical exam for palpable lesion. Toxicity was scored using the CTCAE v3.0.

Results: In all, 35 patients were evaluated. Sixteen were male; histologies were 17 DLBCL, 8 FL, 6 MZ, and 4 MF. Characteristics were generally balanced between the two groups. However, DLBCL patients were more likely to have bulky disease and chemoresistance. Median follow up was 7 months (range, 1 – 49 months). No significative difference was noted concerning overall response rate between DLBCL and indolent NHLs (overall response rate was 70% (12/17) and 83% (15/18) for patients with aggressive and indolent forms, respectively; p = 0.39), but indolent forms were associated with a higher rate of complete response (complete response rate was 61% (11/18) and 35% (6/17) for patients with indolent and aggressive NHL, respectively; p = 0.09). Only 1 case of toxicity was noted (grade 2 nausea). The median duration of response was 7 months (range, 1 – 35 months). Among responders, only 2 patients progressed within the radiated field at the time of last follow-up visit.

Conclusion: Efficacy of LDRT for DLBCL and indolent NHL patients resulted comparable in terms of overall response rate. Complete response rate was higher in the indolent NHL population than in the subset of DLBCL patients included in the phase II trial.

PO-0667

Second malignancies after TBI in AHCT for relapsed follicular lymphoma

S. Tisseverasinghe[1], R. Samant[1], M. Sabloff[2], Y. Xu[3], C. Bredeson[2], L. Huebsch[2], P. Genest[1], P. Cross[1]
[1]*University of Ottawa and The Ottawa Hospital, Radiation Oncology, Ottawa, Canada*
[2]*University of Ottawa and The Ottawa Hospital, Haematology, Ottawa, Canada*
[3]*Ottawa Hospital Research Institute, Epidemiology, Ottawa, Canada*

Purpose or Objective: Follicular lymphoma (FL) is an indolent disease with a progressive relapsing course. Autologous hematopoietic cell transplantation (AHCT) has been proven to be effective in treating recurrences. At The Ottawa Hospital (TOH), AHCT utilizing total body irradiation (TBI) has been used to treat FL patients, who have progressed after at least one course of chemotherapy, for over 20 years. There are concerns in the literature regarding the use of TBI due to the potential for radiation-induced second malignancies. However, we hypothesize that TBI based conditioning regimens should not lead to excessive second cancers. We undertook a review of our large single-institution AHCT experience in order to assess patient outcomes and rates of second malignancy.

Material and Methods: We retrospectively reviewed consecutive patients undergoing AHCT for relapsed FL from July 1991 to February 2013. All patients received treatment at TOH, a regional tertiary center. The most common pre-AHCT conditioning regimen was Etoposide 60 mg/kg / Melphalan 140 mg/m2 / TBI. Patients received TBI on a linear accelerator using high energy photons (10MV or 18MV) and utilizing a translating bed technique. 92% received 5 Gy / 1fraction / 1day, the rest received 12 Gy / 6 fractions / 3 days. Lung attenuators were used for all patients to maintain a homogeneous dose. Patient information was stored in our bone marrow transplant registry database. This includes baseline characteristics, demographics, outcomes, types and dates of second cancers. Descriptive statistics were calculated for all relevant demographic variables. Overall survival of the cohort was estimated using the Kaplan-Meier method. Cumulative incidence of second malignancy was calculated; death was a competing risk.

Results: Overall, we evaluated 174 patients with a median age of 50 years at transplant. There were 106 men and 68 women included, and median follow-up was 6.0 years after AHCT. Overall survival at 1, 5, 10 and 15 years was 93%, 73%, 57% and 47% respectively. The median follow-up among survivors was 8.3 years. Eighteen of 174 patients (10.3 %) developed a second malignancy. Of these, 11 (6.3%) had solid tumors, 2 (1.1%) had AML and 5 (2.9%) developed myelodysplastic syndrome. Median time to second malignancy was 7.2 years, with cumulative incidences of developing second cancer at approximately 4.5% and 8.2% at 5 and 10 years. Solid tumors included breast (2), prostate (3), endometrial (1), skin (4) and lung cancers (1). Furthermore, 82% of patients who developed solid tumors were alive at last follow-up.

Conclusion: Our results with AHCT utilizing TBI in the management of relapsed FL patients have been very good. Indeed, most patients survive more than 10 years after treatment. The risk of second cancers is acceptable and compares favorably with the published literature. Moreover, we suspect screening, particularly for solid tumors post-treatment, may help detect early treatable second malignancies.

PO-0668

Outcome of low and intermediate dose radiotherapy in head and neck MALT lymphoma

F. Rahman[1], J. Brady[1], S. Galli[1], N.G. Mikhaeel[1]
[1]*Guy's and St Thomas' NHS Foundation Trust and King's Health Partners Academic Health Sciences Centre, Department of Clinical Oncology, London, United Kingdom*

Purpose or Objective: Mucosa-associated lymphoid tissue (MALT) lymphoma can present in several sites in the head and neck and is often treated with radiotherapy. MALT lymphoma of the salivary and lacrimal glands is >300 fold more common in patients with Sjogren's syndrome (SS) than in the rest of the population and tends to be a multifocal process. The optimal dose of radiotherapy is not established. The aim of this study is to analyse the outcome of radiotherapy for head and neck MALT lymphoma in patients with and without SS.

Material and Methods: A retrospective review of departmental records identified 26 patients with head & neck MALT lymphoma treated with radiotherapy between 2003-2013. Inclusion criteria were histologically proven MALT lymphoma and complete radiotherapy record. The primary end-points were objective response rate and response

duration. Median age was 61 years (range 30-83). Fourteen patients had confirmed SS. Eighteen patients were female (12 with SS) and 8 were male (2 with SS). Stage of disease includes: stage 1 (17 patients) stage 2 (7), stage 3 (1) and stage 4 (1). Patients with SS were treated with 4Gy and patients without SS were treated with 25.2Gy, unless they had advanced stage. Sites treated include: parotid (13 patients), orbit or conjunctiva (6), thyroid (1), tongue (1), palate (4) & spine (1) Indications for treatment included pain, recurrent inflammation or unsightly mass. 17 patients received 4 Gy in 2 fractions (13 with SS) and 9 patients received 25.2 Gy in 14 fractions (1 with SS).

Results: The objective response rate (ORR= CR + PR, assessed 6 weeks after RT) was 100%. Twenty-two patients (84.6%) remain progression-free at the time of writing with median FU of 89 months (range 22 - 144). Two males (1 with SS) and one female had disease progression in the treated area at 3, 36 and 19 months respectively. All 3 relapses occurred in 4Gy dose group. Two patients were subsequently retreated with further 4Gy/2# and 20Gy/5# and achieved further progression-free survival of 36 and 60 months respectively. One female patient (4Gy/2#) underwent transformation to diffuse large B-cell lymphoma at 36 months. The distribution of relapses is summarised in table 1. Radiotherapy was well tolerated in all patients, with the most common long-term side effect being dry mouth in 3 patients (11.5%), cataract in 1 patient and watery eye in 1 patient. All three patients who reported dry mouth were known to have SS.

Conclusion: Radiotherapy is a very effective treatment for head and neck MALT lymphoma resulting in high response rate, durable local control and minimal toxicity. There were no relapses after 25.2Gy and only few relapses (3/17) after 4Gy, 2 of which had durable remission following re-treatment.

Table 1: distribution of relapses

	SS (no of relapses)	No SS (no of relapses)	Total
4Gy	13 (2)	4 (1, •1)	17
25.2Gy	1	8	9
Total	14	12	26

- transformation to DLBCL

PO-0669

Risk of second malignant neoplasms among long-term survivors of extranodal NK/T-cell lymphoma

B. Chen[1], Y.X. Li[1], W.H. Wang[1], J. Jin[1], S.L. Wang[1], Y.P. Liu[1], Y.W. Song[1], H. Fang[1], H. Ren[1], Q.F. Liu[1], R.Y. Wu[1], Y. Yang[1], X.F. Liu[1], Z.H. Yu[1]

[1]Cancer Hospital- Chinese Academy of Medical Sciences & Peking Union Medical College, Department of Radiation Oncology, Beijing, China

Purpose or Objective: The purpose of this study was to estimate risk and incidence of second malignant neoplasms (SMN) among long-term survivors of early stage extranodal nasal-type natural killer/T-cell lymphoma (NKTCL).

Material and Methods: Between January 1983 and December 2007, 174 patients with stage IE and IIE NKTCL survived 3 or more years after treatment. Of them, 50 patients were treated with radiotherapy alone, 120 patients with combined modality therapy, and 4 patients with chemotherapy alone. The China 2010 population census data and Segi's world population data were used for calculating the age-standardized cancer incidence rates.

Results: Median follow-up time was 8.3 years (range, 3.1 - 35.6 years) for all patients. Nine (5.2%) SMNs were recorded. The median time to SMN was 12.6 years (range, 0.9 - 18.5 years) from diagnosis of NKTCL. Seven patients had solid tumors, and 2 had other type of malignant lymphomas. The cumulative incidence rates at 5-year, 10-year and 15-year were 1.2%, 2.4%, and 13.7% (Figure), respectively. The crude incidence was 531.6/105 person-years, the age-standardized rates by Chinese standard population (ASR China) and by world standard population (ASR world) were 294.5/105 and 243.7/105, and the cumulative incidence rate (0-74 age years old) was 22.4%. All of them were higher than the cancer incidence rates for general population in China in 2010.

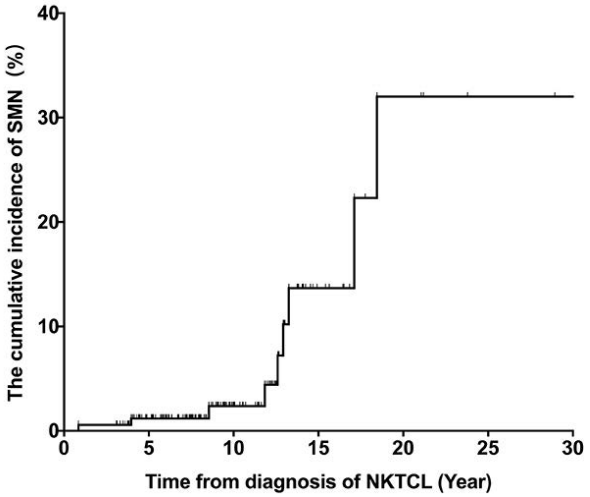

Conclusion: A frequency of SMN in patients with NKTCL is higher than expected in the general population. The patients have more risk for SMN during 10 to 15 years after diagnosis of NKTCL. Patients with long-term survivor are at higher risk of SMN and should be carefully follow-up.

PO-0670

Efficacy of low dose radiotherapy in relapsed or refractory high grade non Hodgkin lymphoma

J.L. Brady[1,2], H. Attallah[3], N.G. Mikhaeel[1,2]

[1]Guy's and St.Thomas' Hospital NHS Foundation Trust, Department of Clinical Oncology, London, United Kingdom

[2]King's Health Partners, Academic Health Sciences Centre, London, United Kingdom

[3]Maadi Military Hospital, Department of Clinical Oncology and Radiotherapy, Cairo, Egypt

Purpose or Objective: Low dose radiotherapy (LDRT) provides effective palliation and local disease control in patients with low grade non Hodgkin lymphoma (LGNHL). Its role in high grade NHL (HGNHL) remains unclear.
The purpose of this study was to evaluate the efficacy of LDRT in relapsed/refractory (RR) HGNHL.

Material and Methods: We performed a retrospective review of all patients undergoing LDRT for RR HGNHL at our institution. LDRT was defined as a total dose of 8Gy or less in 1 or more fractions.
Sex, age, histological type, time from diagnosis to LDRT and number of prior systemic therapies were recorded, along with radiotherapy dose and site treated.
Outcomes included overall response rate (ORR), in field recurrence, time to progression (TTP) and overall survival from completion of RT. Toxicity was also recorded. Analysis was performed by site and by patient as a number of patients had more than 1 site treated at different times.

Results: Between August 2004 and September 2015 15 patients received LDRT for HGNHL. 5 patients had >1 site treated, with LDRT being given to 37 sites in total. Most patients (12/15) had a diagnosis of diffuse large B cell lymphoma, which accounted for 32/37 (86.5%) of all sites. Patient and treatment characteristics are shown in table 1.

Table 1. Patient and treatment characteristics

Patient characteristics	
Total number of patients	15
Total number of sites	37
Sex Male	9
Female	6
Median age at treatment in years (range)	73 (54-88)
Histological subtype	
Diffuse large B cell lymphoma	12 (32 sites)
Mantle cell lymphoma	3 (6 sites)
Median time from diagnosis to LDRT in months (range)	11.8 (0.23-195.1)
Median number of prior systemic therapies (range)	2 (1-7)
Treatment characteristics	
Site treated (n=37)	
Nodal	6
Extra-nodal (parotid, stomach, brain, orbit and oropharynx)	7
Skin	19
Bone	5
Radiotherapy dose/number of fractions	
4Gy/1	1
4Gy/2	15
6Gy/1	1
8Gy/1	2
8Gy/2	16
8Gy/4	2

Overall response rate (ORR) for all sites was 89.2% (33/37 sites). 17 sites (45.9%) achieved a complete response (CR) and 16 sites (43.2%) a partial response. 4 sites (10.8%) did not respond to LDRT. Considering ORR by patient, 11/15 patients (73.3%) had a response to LDRT at all sites, 3/15 (20%) did not respond and 1 patient responded at 2 sites but not the 3rd.
Skin was the most commonly treated site (19/37, 51.4%) and skin sites had the highest ORR at 100%, with 73.7% (14/19) CR. This was statistically significant when compared to all other sites (p=0.046). ORR for nodal sites was 83.3% (5/6) and extra-nodal sites was 85.7% (6/7). Bone sites had the lowest ORR at 60% (3/5 cases) with no CR.
16 sites received a total dose of 4Gy in 1 or 2 fractions. 21 sites received either 6 or 8Gy in total. ORR in both groups was similar (87.5% versus 90.5%, p =1). Toxicity from LDRT was minimal, with no toxicity recorded above grade 2.
Of the 33 initially responding sites there have been 4 infield recurrences (12.1%). Median TTP was 4.8 months (3.1-11.8). 2 sites were retreated with further symptomatic benefit. Median duration of response was 3.6 months (0.5-126.7). 6 sites (2 patients) had responses lasting >30 months. The majority of patients died without documented local recurrence, with median overall survival from LDRT of 2.4 months (0.03-126.7).

Conclusion: LDRT is an effective palliative treatment for patients with RR HGNHL and anticipated short survival, achieving high response rates and excellent local control, with minimal toxicity and inconvenience. A small subgroup of patients with slowly relapsing disease derived durable remissions with LDRT.

PO-0671

Risk of cardiac damage after mediastinal radiotherapy for Hodgkin's disease

M. Buglione[1], F. Trevisan[1], L. Baushi[1], M. Triggiani[2], N. Pasinetti[1], A. Alghisi[1], D. Greco[1], A. Papa[1], L. Spiazzi[3], P. Borghetti[1], S. Nodari[2], S. Magrini[1]
[1]*University and Spedali Civili di Brescia, Radiotherapy Unit, Brescia, Italy*
[2]*University and Spedali Civili di Brescia, Cardiology Unit, Brescia, Italy*
[3]*Spedali Civili di Brescia, Medical Physics, Brescia, Italy*

Purpose or Objective: Hodgkin lymphoma (HL) has become a highly curable lymphoid malignancy. The improved prognosis of HL has been accompanied by increasing incidence of adverse late effects. Mediastinal radiotherapy (RT) and cardiotoxic chemotherapy (CT) with anthracyclines are routinely used to treat HL, but they could be associated with a variety of cardiovascular complications in long-term HL survivors. The aim of this study is to evaluate the late cardiovascular toxicity of a series of 202 patients treated from 1995 to 2012.

Material and Methods: 420 patients (pts) were treated for HL with RT +/- CT at our institution from 1995 to 2012. All the alive patients were contacted and invited to participate to the study. A detailed medical history of the 202 pts who accepted and subscribed informed consent was obtained, collecting events occurred after treatment; they had medical examination, ECG, Echocardiogram TT and blood tests. Treatment features were extracted from medical records. The entire group was divided in two groups: 157 pts received mediastinal RT (cases) and 45 pts did not (controls). The cardiac events were categorized using CTCAE ver. 4.0. A preliminary descriptive statistic using SPSS® software (x2 test) has been performed and here presented. The contouring of the different cardiac structures for dosimetric evaluation is ongoing.

Results: The patients and therapeutic characteristics of the patients are summarized in Table 1. After a median follow-up of 8 years (range 2-20 years) 144 pts (71,3%) manifested cardiac alterations: 1,0% arrhythmia, 2,5% ischemia, 1,5% heart failure and 66,3% valvular fibrosis without statistical differences between cases and controls. Most patients (75,4%) had asymptomatic grade I-II valvular fibrosis; only one had grade III valvular fibrosis. After treatment, with a median follow up time of 11,2 years, (range 4,1-17,8 years), acute myocardial infarction occurred in 5 pts, all in the group of cases.

		CASES	CONTROLS	TOTAL	p value
SEX	M	63 (40,1%)	32 (71,1%)	95 (47%)	<0,001
	F	94 (59,9%)	13 (28,9%)	107 (53%)	
MEDIAN AGE	(range)	35 yy (18-77)			
AGE	<28 y	46 (29,3%)	8 (17,8%)	54 (26,7%)	<0,001
	28-41 y	67 (42,7%)	9 (20,0%)	76 (37,6%)	
	42-64 y	42 (26,8%)	21 (46,7%)	63 (31,2%)	
	>64 Y	2 (1,3%)	7 (15,6%)	8 (4,5%)	
HYPERTENSION	YES	8 (5,1%)	7 (15,6%)	15 (7,4%)	0,018
	NO	149 (94,9%)	38 (84,4%)	187 (92,6%)	
DIABETES	YES	4 (2,5%)	3 (6,7%)	7 (3,5%)	0,183
	NO	153 (97,5%)	42 (93,3%)	195 (96,5%)	
SMOKE	YES	40 (25,5%)	19 (42,2%)	59 (29,2%)	0,029
	NO	117 (74,5%)	26 (57,8%)	143 (70,8%)	
ALCOHOL	YES	42 (26,8%)	24 (53,3%)	66 (32,7%)	0,001
	NO	115 (73,2%)	21 (46,7%)	136 (67,3%)	
FAMILY HISTORY OF CAD	YES	126 (80,3%)	33 (73,3%)	159 (78,7%)	0,317
	NO	31 (19,7%)	12 (26,7%)	43 (21,3%)	
HISTOLOGY	NS	114 (72,6%)	10 (22,2%)	124 (61,4%)	<0,001
	MC	11 (7,0%)	9 (20,0%)	20 (9,9%)	
	NLP	4 (2,5%)	13 (28,9%)	17 (8,4%)	
	LR	1 (0,6%)	3 (6,7%)	4 (2,0%)	
	LD	1 (0,6%)	0 (0,0%)	1 (0,5%)	
	NOS	26 (16,6%)	10 (22,2%)	36 (17,8%)	
STAGE	I-II	119 (75,8%)	35 (77,8%)	154 (76,2%)	0,783
	III-IV	38 (24,2%)	10 (22,2%)	48 (23,8%)	
TREATMENT	RT+CT	149 (94,9%)	33 (73,3%)	182 (90,1%)	0,000
	RT alone	8 (5,1%)	12 (26,7%)	20 (9,9%)	
TREATMENT	RT-CT with anthracyclines	141 (89,8%)	27 (60,0%)	168 (83,2%)	<0,001
	RT-CT no anthracyclines	8 (5,1%)	6 (13,3%)	14 (6,9%)	
	RT alone	8 (5,1%)	12 (26,7%)	20 (9,9%)	
MEDIASTINAL DOSES	0 Gy	0 (0,0%)	45 (100,0%)	45 (100,0%)	<0,001
	< 30 Gy	1 (0,6%)	0 (0,0%)	1 (0,5%)	
	30 Gy	57 (36,3%)	0 (0,0%)	57 (28,2%)	
	>30-36 Gy	44 (28,0%)	0 (0,0%)	44 (21,8%)	
	> 36 Gy	55 (35,0%)	0 (0,0%)	55 (27,2%)	
TOTAL		157 (77,8%)	45 (22,2%)	202 (100%)	

TABLE 1. Legend: NS: nodular sclerosing; MC: mixed-cellularity subtype; NLP: nodular lymphocyte predominant; LR: lymphocyte rich; LD: lymphocyte depleted; NOS: unspecified

Conclusion: The study does not show a direct association between late cardiac toxicity and mediastinal RT. Multi-parametric statistical analysis to evaluate a possible

correlation between the different variables and cardiac damage is ongoing.

Poster: Clinical track: Breast

PO-0672

Ten years experience of breast reconstruction after mastectomy in previously irradiated patients

A. Di Donato[1], E. Ippolito[1], R.M. D'Angelillo[1], A. Sicilia[1], E. Molfese[1], P. Trecca[1], S. Ramella[1], L. Trodella[1], B. Cagli[2], M. Barone[2]
[1]*Campus Bio-Medico University, Radiotherapy, Roma, Italy*
[2]*Campus Bio-Medico University, Plastic and Reconstructive Surgery, Roma, Italy*

Purpose or Objective: To evaluate the rate of complications and the aesthetic outcome in previously irradiated patients who underwent mastectomy and subsequent prosthetic reconstruction in 2 times.

Material and Methods: Eighty-three patients who underwent immediate postmastectomy reconstruction with tissue expander between January of 2003 and June of 2012 at the Campus Bio-Medico University Hospital in Rome were retrospectively divided into two groups: Group A (study group) included 30 patients with previous quadrantectomy and radiotherapy who underwent salvage mastectomy after local recurrence and Group B (control group) included 53 patients submitted to primary radical mastectomy. Patients and disease characteristics were analysed and complications were correlated to treatment group.

Results: The median follow-up time for the whole group was 36 months (range= 12-144 months). Between group A and group B, there were no significant differences in terms of age, body mass index, comorbidities, pathological stage, treatments data (p=NS). In Group A 25/30 patients (83.33%) completed heterologous reconstruction. In 5 patients (16.67%) a conversion to combined or solely autologous reconstruction was needed. In Group B, 52/53 patients (98.11%) completed heterologous reconstruction. In 1 case (1.88%) the expander was removed due to infection and an autologous reconstruction was performed. Revision surgery was needed in 5 patients (9.4%). Autologous salvage reconstruction was more frequent for Group A patients (relative risk 10.4, p=0.02). The overall rate of complications was not different between the two groups (66.6% vs 58.5%; p=0.49) even if major complications (vast necrosis of mastectomy flaps with or without partial implant exposure, with or without implant removal, all III and IV-degree capsular contractures, either requiring or not requiring further surgery) were non significantly higher in the irradiated group (53.3% vs 32.0%; p= 0.07). However, analysing capsular contracture, a significantly higher risk of grade III-IV were recorded in Group A (40% vs 15%; relative risk 3.75, p=0.02). In Group A the median time from RT to reconstruction was 24 months (range= 9-192 months) and the incidence of major complications was not related to time from RT to reconstruction (p=0.313).

Conclusion: Heterologus reconstruction after salvage mastectomy in previously irradiated patients, is still possible with satisfactory results.

PO-0673

Common European mitochondrial haplogroups in the risk of RT-induced breast fibrosis

L. Deantonio[1], S. Terrazzino[2], S. Cargnin[2], L. Donis[1], C. Pisani[1], L. Masini[1], G. Gambaro[1], P. Canonico[2], A. Genazzani[2], M. Krengli[1]
[1]*University Hospital Maggiore della Carità, Radiotherapy, Novara, Italy*
[2]*University of Piemonte Orientale, Department of Pharmaceutical Sciences, Novara, Italy*

Purpose or Objective: Germline polymorphisms in oxidative stress response genes have been postulated to be involved in the development of late normal tissue complications following radiotherapy. Despite the key role of mitochondria in the production of reactive oxygen species, the contribution of mitochondrial DNA variations to clinical radiosensitivity is still largely unknown. In the present study, we evaluated the association between mitochondrial DNA haplogroups and the risk of radiation-induced subcutaneous fibrosis after postoperative radiotherapy in breast cancer patients.

Material and Methods: Subcutaneous fibrosis was scored according to the Late Effects of Normal Tissue-Subjective Objective Management Analytical (LENT-SOMA) scale in 286 Italian breast cancer patients who received radiotherapy after breast conserving surgery. Eight mitochondrial DNA (mtDNA) SNPs that define the nine major haplogroups in the European population were determined by PCR–RFLP analysis on genomic DNA extracted from peripheral blood.

Results: In a Kaplan-Meier analysis evaluated by the log-rank test, carriers of haplogroup H were found at lower risk of grade ³2 subcutaneous fibrosis (P=0.018). In the multivariate Cox regression analysis adjusted for clinical factors (BMI, breast diameter, adjuvant treatment, dose per fraction, radiation type and acute skin toxicity), the haplogroup H emerged as significant protective factor for moderate to severe radiation-induced fibrosis (HR: 0.50, 95% CI 0.27-0.92, P=0.027).

Conclusion: Our results support a protective role of the mitochondrial haplogroup H in the development of radiation-induced fibrosis in breast cancer patients. Further prospective studies with larger sample size and different populations are nevertheless warranted to corroborate the possible influence of mitochondrial haplogroups on late normal tissue radiosensitivity.

PO-0674

Factors influencing patient reported cosmetic outcome: results of the Young Boost Trial

P. Brouwers[1], E. Van Werkhoven[2], J. Van Loon[1], P. Poortmans[3], H. Bartelink[2], L. Boersma[1]
[1]*MAASTRO clinic, Department of Radiation Oncology, Maastricht, The Netherlands*
[2]*The Netherlands Cancer Institute, Department of Radiation Oncology, Amsterdam, The Netherlands*
[3]*Radboud University Medical Center, Department of Radiation Oncology, Nijmegen, The Netherlands*

Purpose or Objective: The Young Boost trial (YBT), a multicenter RCT (NCT00212121), investigates whether a higher boost dose leads to a lower recurrence rate in young patients treated with breast conserving therapy. Cosmetic outcome is the secondary objective. The aim of the current analysis is to investigate the factors influencing the patients' opinion about cosmesis.

Material and Methods: From 2004-2011, 2421 breast cancer patients ≤ 50 yrs were included in The Netherlands, France, and Germany. All patients were treated with lumpectomy, followed by 50 Gy whole breast irradiation. Patients were randomized to receive a standard 16 Gy (n=1211) or a high 26 Gy boost (n=1210) to the tumour bed. Cosmetic outcome data at 4 years of 807 patients were used for the current analysis according to the following two scoring systems:
1. BCCT.core: Digital photographs were analyzed using a software program to extract an overall cosmetic score: excellent, good, fair or poor. This score is based on symmetry, skin color and scar visibility. The 7 features of symmetry in the BCCT.core program are: nipple position (pBRA), level of lower breast contour (pLBC), level of nipple (pUNR), distance from nipple to inframammary fold (pBCE), length of breast contour (pBCD), area of the breast (pBAD) and non-overlapping area between left and right breast (pBOD). 2. Patients' score using a validated patient's questionnaire about the breast appearance, including an overall score: very satisfied, satisfied, not dissatisfied, dissatisfied or very dissatisfied. First, we analyzed the 7 features of BCCT.core in a proportional odds model, to

investigate which parameters were related to the patients' opinion about cosmesis. In addition, we analyzed whether firmness, presence of rib pain or quality of life (QoL) aspects (EORTC QLQ C-30 questionnaire) at 4 years were related to the patients' opinion on cosmetic outcome.

Results: Of the 7 BCCT.core parameters, pBCE and pBCD were significantly related to patients' score at 4 years. Patients with any difference in firmness rated their cosmesis worse than patients without any difference, even when the objective score (i.e. BCCT.core) was similar. This effect was larger by increasing difference. Worse perception of cosmetic outcome was also independently related to lower global QoL, lower emotional functioning and higher scores in the depression scale. The presence of rib pain had no influence.

Conclusion: The patients' opinion on cosmetic outcome was significantly related to objective parameters like distance from nipple to inframammary fold (pBCE) and length of breast contour (pBCD), but also to subjective factors, i.e. severity of firmness, depressive feelings, global QoL and emotional functioning.

PO-0675

Radical radiotherapy in ologometastatic breast cancer patients

M. Trovo[1], C. Furlan[1], M. Berretta[2], L. Militello[2], S. Spazzapan[2], J. Polesel[3], A. Del Conte[4], S. Arcangeli[5], A. Fiorentino[6], G. Franchin[1]
[1]*Centro di Riferimento Oncologico, Radiation Oncology, Aviano, Italy*
[2]*Centro di Riferimento Oncologico, Medical Oncology, Aviano, Italy*
[3]*Centro di Riferimento Oncologico, Epidemiology, Aviano, Italy*
[4]*Pordenone General Hospital, Medical Oncology, Pordenone, Italy*
[5]*San Camillo Hospital, Radiation Oncology, Rome, Italy*
[6]*Sacro Cuore - Negrar, Radiation Oncology, Negrar, Italy*

Purpose or Objective: The primary endpoint of this phase II study was to determine the progression-free survival (PFS) of oligometastatic breast cancer patients treated with radical radiotherapy to all metastatic sites.

Material and Methods: Patients affected by oligometastatic breast cancer were enrolled in this phase II trial. Inclusion criteria were the following: 1) histologically confirmed diagnosis of breast cancer, 2) 5 or fewer metastatic lesions, 3) no brain metastases, 4) primary tumor controlled. Radiotherapeutic treatment was SBRT (30-45 Gy in 3 fractions) or fractionated IMRT (40-60 Gy in 15-25 fractions). Primary endpoint was PFS; secondary endpoints were local-control (LC), overall survival (OS), and toxicity, which was assessed using the CTCAE v4.0 scale.

Results: The analysis was conducted on 37 patients. The median age was 55 years. Twenty-five (68%) had oligometastatic disease at diagnosis, and 12 (32%) had the oligometastatic status induced by systemic treatment. Sixteen (43%) patients had a single metastasis, and 21 (47%) had 2 or more lesions. Thirty-one (84%) patients were treated with SBRT and 6 (16%) with fractionated IMRT. With a median follow-up of 18 months, 1-year and 2-year PFS was 74% and 44%, respectively. No differences was seen in PFS between patients with only 1 metastases vs. those with ≥2 metastases, or between patients treated with SBRT vs. fractionated IMRT. Only two patients experienced local failure. One of these two patients had an isolated local failure for a spinal lesion that was treated with a minimum dose of 17 Gy in 3 fractions (being the spinal cord constraint prior on the PTV coverage). Two-year LC was 96%. Two patients died of disease, and 2-year OS was 96%. The proposed treatment was well tolerated; no Grade≥3 toxicity was documented. Two patients experienced Grade 2 pain, 4 Grade 1 pain, and 2 developed Grade 2 fatigue.

Conclusion: Radical radiotherapy delivered to all the metastatic sites in oligometastatic breast cancer patients led to promising results in terms of local control and progression-free survival. Treatment was well tolerated. The results of this study may motivate for conducting phase III trials.

PO-0676

Impact of IMN irradiation on the right coronary artery and OAR in right-sided post-mastectomy patients

K. Rock[1], A. Barry[1], M. Rahman[1], M. Pintilie[1], C.A. Koch[1]
[1]*Princess Margaret Cancer Centre, Department of Radiation Oncology, Toronto, Canada*

Purpose or Objective: Previous studies have shown an increased risk of ischemic heart disease in breast cancer patients treated with radiotherapy (RT). It has recently been reported that the risk of major coronary events increases per gray of mean radiation dose delivered to the heart for patients undergoing either left- or right-sided breast RT. However, the anatomy of cardiovascular damage related to right-sided breast RT has not been well-described, specifically for radiation dose delivered to the right coronary artery (RCA). This may be of particular relevance for regional nodal irradiation that includes the internal mammary nodes (IMNs). In this prospective planning study, the impact of IMN irradiation on the RCA and organs at risk (OAR) in patients undergoing right-sided post-mastectomy RT (PMRT) was assessed.

Material and Methods: CT simulation scans of 60 right-sided post-mastectomy patients were identified from an institutional database. In 30 cases, the IMNs were contoured from the 1st to 3rd intercostal space with a PTV of 5 mm. The RCA, heart, lungs and contralateral breast were delineated as OARs. A four-field modified wide tangent photon plan was created encompassing the chestwall, IMNs, supraclavicular fossa and axilla. For the remaining 30 patients (control group), a four-field plan that excluded the IMNs was generated. All patients were planned to receive 50 Gy in 25 fractions over 5 weeks. Doses were compared between the two groups utilizing the Mann-Whitney test to determine whether there was a statistically significant difference in dose to OARs between these groups.

Results: In the group with IMN treatment, 95% of prescribed dose to the IMN PTV covered a median volume of 99% (range 90-100). There was a significant increase in dose to the RCA in the IMN treated group compared to the control group. The maximum dose to the RCA (3.33 Gy vs 2.35 Gy, $p<0.0001$) and mean RCA dose (2.41 Gy vs 1.69 Gy, $p<0.0001$) were both increased. Similarly, the mean heart dose (MHD) was increased (1.3 Gy vs 1.09 Gy, $p<0.022$). Inclusion of the IMNs increased lung V20 (18 Gy vs 15 Gy, $p<0.00021$) and mean lung dose (9.1 Gy vs 8.09 Gy, $p<0.00051$). There was a significant increase in the volume of contralateral breast receiving 3 Gy in the group requiring IMN treatment (3.75 Gy vs 0 Gy, $p<0.0001$).

Conclusion: Inclusion of the IMNs in patients undergoing PMRT significantly increases radiation dose to the RCA and MHD. An acceptable dose to the RCA has not been well-established but should be as low as is reasonably achievable. The dose and clinical implications of radiation to the RCA needs further evaluation in prospective studies utilizing techniques to minimize cardiac exposure.

PO-0677

Comparing detailed cardiac structure dose-volume metrics in supine versus prone breast irradiation

C. Luo[1], J. Otton[1,2], V. Batumalai[1,3,4], E.M. Pogson[3,4,5], K. Dundas[3,4,5], L. Holloway[1,3,4,5,6], W. Xuan[4], G.P. Delaney[1,3,4], L. Thomas[1,2], D.H. Tran[2], G. Liney[1,3,4,5], E.S. Koh[1,3,4]
[1]*University of New South Wales, South Western Sydney Clinical School, Sydney, Australia*
[2]*Liverpool Hospital, Department of Cardiology, Sydney, Australia*
[3]*Liverpool Hospital, Cancer Therapy Centre, Sydney, Australia*

[4]*Ingham Institute for Applied Medical Research, Ingham Institute, Sydney, Australia*
[5]*University of Wollongong, Centre for Medical Radiation Physics, Wollongong, Australia*
[6]*University of Sydney, Institute of Medical Physics, Sydney, Australia*

Purpose or Objective: To compare radiation dosimetry of various cardiac structures and other thoracic tissue, such as lung fields and non-treated breast, associated with breast irradiation (left versus right-sided) in supine versus prone treatment positions.

Material and Methods: Twenty-four post-lumpectomy patients (8 left-sided, 16 right-sided) underwent non-contrast 2mm slice thickness radiotherapy (RT) planning CT scans in the supine and prone positions. Optimized tangential breast RT plans were generated. In all cases, prescribed RT dose was 50Gy in 2Gy daily fractions. Twenty specific structures (whole heart, atria and ventricles, major vessels, cardiac valves, epicardial coronary arteries including left anterior descending (LAD), ipsilateral/contralateral lung and non-treated breast) were contoured on each CT dataset based on a published reference atlas. Maximum, minimum, mean doses and volume (cm^3) were compared for all structures in both supine and prone positions. Whole heart V5, V25 and V30 as well as lung V20 were evaluated. The independent two-sample t-test was used to determine the impact of treatment laterality and the paired t-test for the treatment positioning on RT dosimetry respectively, with $p<0.05$ considered significant.

Results: Left compared to right-sided breast irradiation significantly increased maximum ($p<0.001$) and mean ($p<0.001$) whole heart dose, as well as doses to individual cardiac structures, in both prone and supine positions.
Prone versus supine positioning significantly increased maximum whole heart dose 25.8Gy versus 19.2Gy ($p=0.007$) and mean LAD artery 8.4Gy vs. 5.0Gy respectively ($p=0.03$). Whole heart V5 (3.9 vs. 2.5%), V25 (1.4 vs. 0.8%), and V30 (1.1 vs. 0.7%), did not differ significantly between prone and supine positions. Table 1 illustrates comparisons of other individual cardiac structures. As anticipated, maximum dose (48.5 vs. 50.3Gy), mean dose (3.3 vs. 6.5Gy) and V20 (5.3% vs. 11.5%) to the ipsilateral lung ($p<0.001$ for all comparisons) were reduced when patients were treated in the prone versus supine position.

Table 1: Comparison of radiation doses to selected cardiac structures in patients planned for supine (n=24) versus prone (n=24) treatment

	Supine Treatment (n=24)	Prone Treatment (n=24)	*p*-value (* indicates significant values)
Right Ventricle			
Maximum (Gy)	12.5	16.8	0.03*
Minimum (Gy)	0.6	0.6	0.09
Mean (Gy)	1.6	2.5	0.01*
Right Atrium			
Maximum (Gy)	2.9	5.9	0.03*
Minimum (Gy)	0.5	0.6	0.06
Mean (Gy)	1.3	1.6	0.001*
Aortic Valve			
Maximum (Gy)	1.5	1.8	0.001*
Minimum (Gy)	0.7	0.8	0.02*
Mean (Gy)	1.0	1.2	0.006*
Tricuspid Valve			
Maximum (Gy)	2.2	2.3	0.6
Minimum (Gy)	0.9	1.1	0.05
Mean (Gy)	1.4	1.5	0.1
Left Anterior Descending Artery			
Maximum (Gy)	14.2	16.2	0.08
Minimum (Gy)	0.9	0.8	0.43
Mean (Gy)	5.0	8.4	0.03
Left Coronary Artery			
Maximum (Gy)	1.1	1.1	0.9
Minimum (Gy)	0.7	0.7	0.4
Mean (Gy)	0.9	0.8	0.7
Right Coronary Artery			
Maximum (Gy)	2.7	3.2	0.009*
Minimum (Gy)	1.3	1.6	0.001*
Mean (Gy)	2.0	2.4	0.001*

Conclusion: A statistically higher radiation dose was seen to the whole heart and various cardiac structures, including atria, ventricles and LAD artery, for left compared to right-sided breast cancer patients. Furthermore, prone positioning increased maximum whole heart and LAD artery doses, despite its known benefit in reducing dose-volume effects to lung tissue. This is one of few studies to assess differential radiation doses to individual cardiac structures.

Poster: Clinical track: Lung

PO-0678

Do blood-biomarkers enhance clinical models for NSCLC patients treated with radical radiotherapy?

S. Carvalho[1], E.G.C. Troost[2], J. Bons[3], P. Menheere[3], P. Lambin[1], C. Oberije[1]
[1]*GROW – School for Oncology and Developmental Biology- Maastricht University Medical Centre MUMC+, Department of Radiation Oncology - MAASTRO, Maastricht, The Netherlands*
[2]*Institute of Radiooncology, Helmholtz-Zentrum, Dresden-Rossendorf, Germany*
[3]*Maastricht University Medical Centre MUMC+, Laboratory for Immunodiagnostics- Central Diagnostic Laboratory, Maastricht, The Netherlands*

Purpose or Objective: A prognostic model for non-small cell lung cancer (NSCLC) patients with validated clinical variables [gender, World Health Organization performance status, forced expiratory volume in 1 second, number of positive lymph node stations, and total gross tumor volume], and blood-biomarkers related to hypoxia [osteopontin (OPN) and carbonic anhydrase IX (CA-IX)], inflammation [interleukin-6 (IL-6), IL-8, and C-reactive protein (CRP)], and tumor load [carcinoembryonic antigen (CEA), and cytokeratin fragment 21-1 (Cyfra 21-1)] was developed and validated. Finally, the model was extended with alpha-2-macroglobulin (α2M), serum interleukin-2 receptor (sIL2r), toll-like receptor 4 (TLR4), and vascular endothelial growth factor (VEGF).

Material and Methods: The model was developed and validated on respectively 182 and 181 inoperable stage I-IIIB NSCLC patients treated radically with (chemo)radiotherapy. It included the mentioned clinical features, and blood-biomarkers were selected by least absolute shrinkage and selection operator (LASSO). Discrimination was reported by means of internal 10-fold cross-validated (CV) and external concordance index (c-index).

Results: The inclusion of OPN and Cyfra 21-1 (hazard ratios of 3.3 and 1.7) in this clinical model significantly increased the c-index from 0.66 to 0.70 (10-fold CV=0.64 and 0.67; c-index external =0.62 and 0.66). The calibration slope of the prognostic index in the validation cohort was 0.66 ($p<0.01$), therefore requiring re-calibration. Further extension of the model by selecting from the 4 additional blood biomarkers yielded a c-index of 0.67 (10-fold CV = 0.66), TLR4 was left unincluded, and resulted in a better fitting model (likelihood ratio test: p=0.01; Table 1). Hypoxia is known to be present in NSCLC adversely affecting disease progression and response to radiation treatment. Likewise, tumor load is often associated with disease development and prognosis. The value of hypoxia and tumor load associated markers OPN and Cyfra 21-1, was confirmed in this study. Extension of the model included α2M, sIL2r, and VEGF, with higher concentrations of these new markers being associated with a worse prognosis. α2M, a previously identified candidate predictor for radiation pneumonitis was found to be a prognostic factor in NSCLC. IL-2 was already identified as an independent prognostic marker in patients with advanced NSCLC. The correlation of IL-2 with shorter survival was confirmed in these cohorts and may be of relevance for patients receiving IL-2 immunotherapy. Finally, VEGF, the angiogenesis factor found in a variety of solid tumors including NSCLC, was found to be of added value in the extended model.

Table 1 - Multivariable Cox PH regression of the clinical variables and blood-biomarkers fitted on the validation dataset, after a feature selection made by LASSO, by including the offset of the re-calibrated linear predictor and allowing for a selection among the new blood-biomarkers. Performance of the model expressed in terms of internal Harrell's c-index, corrected for optimism by a 10-fold CV (between brackets).

Feature	Hazard Ratio	95% CI HR	p-value	c-index
Calibrated PI	2.4	1.7 – 3.5	<0.01	
α2M	4.6	1.3 – 16	<0.01	0.67
sIL2R	3.1	1.1 – 9.2	<0.01	(0.66)
VEGF	1.4	0.8 – 2.4	0.3	

Conclusion: In conclusion, we improved and validated a clinical model with inclusion of hypoxia and tumor-load related blood-biomarkers. New immunological markers were associated with overall survival. Currently we are aiming to extend these models to include imaging information (Radiomics).

PO-0679

Comparison of toxicity and outcome in stage III NSCLC patients treated with IMRT or VMAT

R. Wijsman[1], F. Dankers[1], E.G.C. Troost[2], A.L. Hoffmann[2], J. Bussink[1]

[1]*Radboud University Medical Center, Radiation Oncology, Nijmegen, The Netherlands*

[2]*Institute of Radiooncology, Helmholtz-Zentrum Dresden Rossendorf, Dresden, Germany*

Purpose or Objective: Intensity-modulated radiation therapy (IMRT) and volumetric-modulated arc therapy (VMAT) are widely used in the treatment of advanced stage non-small cell lung cancer (NSCLC). These techniques deliver conformal dose distributions at the cost of increased target dose heterogeneity (particularly IMRT) and larger volumes of surrounding healthy tissues receiving low doses (particularly VMAT). We evaluated whether these dosimetric differences between IMRT and VMAT are of influence on treatment toxicity and outcome.

Material and Methods: We retrospectively assessed a cohort of 189 consecutive patients with stage III NSCLC having undergone radical (chemo-)radiotherapy using IMRT (until 2011) or VMAT (starting in 2011). Most patients (n=182) received 66 Gy in 33 (once-daily) fractions to the primary tumour and involved hilar/mediastinal lymph nodes based on FDG-PET/CT. Concurrent chemoradiation (CCR; n=122) consisted of 2 courses of etoposide cisplatinum, whereas sequential treatment (n=56) consisted of 3 courses of gemcitabine cisplatinum. Acute and late toxicity were assessed using the RTOG radiation morbidity scoring criteria for esophageal and pulmonary toxicity. Follow-up visits were planned every 3 months (first 2 years), biannually thereafter. Median overall survival (OS) was calculated using Kaplan-Meyer survival analysis. Differences between the groups receiving IMRT and VMAT were statistically tested using the Mann-Whitney-U or Chi-square test, where appropriate.

Results: Gender, age, performance score, clinical (tumour and nodal) stage and radiation dose did not significantly differ between the IMRT (*n*=93) and VMAT (*n*=96) groups. Patients undergoing IMRT, however, received less concurrent chemotherapy compared to patients treated with VMAT (n=51 *vs* *n*=71; *p*= 0.007). Incidences of grade ≥2 and ≥3 acute esophageal toxicity (AET) were significantly lower for IMRT compared to VMAT (28 *vs* 57 patients, *p*<0.001; and 6 *vs* 17 patients, *p*=0.025, respectively). Maximum grade acute and late pulmonary toxicity did not differ between groups (*p*=0.57 and *p*=0.14, respectively). Grade ≥3 late esophageal toxicity was scored in 1 and 3 patients after IMRT and VMAT, respectively. Median follow-up for the patients alive was 32 months (range 2.4-82.1 months). Median OS was 23.9 months (95% CI 19.6-28.1), without a significant difference between the groups (23.9 and 24.9 months for IMRT and VMAT, respectively; *p*=0.70).

Conclusion: Patients treated with VMAT showed significantly higher incidence of Grade ≥2 and ≥3 AET, which may be due to a higher percentage of patients receiving CCR in the VMAT-group. Median OS did not differ between groups. Currently the target volumes and dosimetric data are evaluated for differences between the groups, for we hypothesized that VMAT enables treatment of larger tumour volumes, leading to increased AET.

PO-0680

Predictive models of the extent and CT appearance of radiation induced lung injury for NSCLC

U. Bernchou[1], R. Christiansen[1], J. Asmussen[2], T. Schytte[3], O. Hansen[3], C. Brink[1]

[1]*Odense University Hospital, Laboratory of Radiation Physcis, Odense, Denmark*

[2]*Odense University Hospital, Department of Radiology, Odense, Denmark*

[3]*Odense University Hospital, Department of Oncology, Odense, Denmark*

Purpose or Objective: The purpose of the present study was to investigate the extent and appearance of early radiologic injury in the lung after radiotherapy (RT) for non-small cell lung cancer (NSCLC). Furthermore, the ability of planned mean lung dose to predict the risk of a radiologic response was explored.

Material and Methods: Eligible follow-up computed tomography (CT) scans acquired within 6 months after commencement of radiotherapy were retrospectively evaluated for radiologic injuries in a cohort of 213 NSCLC patients treated to 60 or 66 Gy in 2 Gy fractions at a single institution from 2007 to 2013. Radiologic injuries were divided in two categories based on CT appearance. Category 1 represented ground-glass opacity (GGO) and interstitial changes. Both are characterized by moderately increased densities in the lung parenchyma, but where GGO appears diffuse, amorphous, and with poorly defined vessel structures, interstitial changes are identified by more pronounced vessels and borders. Category 2 indicated patchy or confluent consolidation in the lung. The volume fraction of injured lung corresponding to either category was estimated in each scan. To investigate the relationship between the volume fraction of injured lung and mean lung dose, a logistic regression analysis was performed. Four different cut-points were chosen to define radiologic injury response. These were volume fractions of injured lung larger than 5%, 10%, 15%, or 20%. Both individual and combined categories were investigated.

Results: Radiologic injuries of category 1 and 2 were found in follow-up scans for 81% and 42% of the patients, respectively. The mean volume fraction of injured lung was 6.5% (range 0-95%) and 1.7% (range 0-22%) for category 1 and 2, respectively, and 8.2% (range 0-95%) when the categories were combined. The logistic normal tissue complication probability (NTCP) models are shown in the figure for the combined categories of lung appearance. The risk of radiologic response was found to be significantly associated with mean lung dose. The mean lung dose resulting in 50% risk of radiologic response (D50) increased from 17 to 29 Gy as the cut-point used for dichotomization increased from 5 to 20% of volume fraction of affected lung (see table). A logistic relationship between radiologic response and mean lung dose was also found for the individual categories of lung

appearance (see table). In these cases, increased D50 values were found since the frequency of response was reduced.

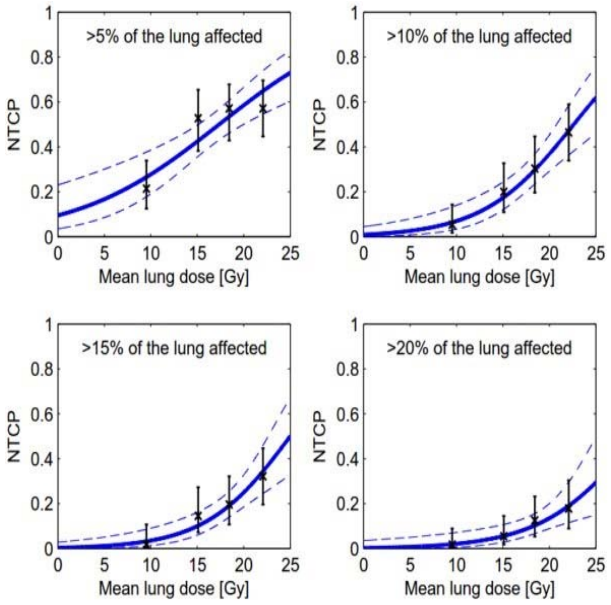

Fraction of lung affected [%]	Category 1 and 2 combined		Category 1		Category 2	
	D_{50} [Gy]	γ_{50}	D_{50} [Gy]	γ_{50}	D_{50} [Gy]	γ_{50}
>5	17 (15-20)	0.6 (0.3-0.8)	21 (15-26)	0.7 (0.4-1.0)	31 (25-59)	1.1 (0.7-1.9)
>10	22 (21-26)	1.2 (0.8-1.7)	24 (21-29)	1.3 (0.9-2.0)	29 (25-49)	2.5 (1.4-8.0)
>15	25 (23-30)	1.4 (1.0-2.0)	28 (23-39)	1.6 (1.1-2.5)	NA	NA
>20	29 (25-42)	1.5 (1.0-2.5)	30 (25-45)	1.7 (1.1-2.9)	NA	NA

γ_{50} is the relative gradient at D_{50}. 95 % confidence intervals are given in the parentheses.

Conclusion: Radiologic injuries were frequently found in follow-up CT scans after RT for NSCLC patients. Logistic relationships between the risk of a radiologic response and increasing mean lung dose were observed both when categorizing the lung injuries in terms of appearance and when combining the categories.

PO-0681

Randomized phase II study of Erlotinib with radiotherapy in irresectable non small cell lung cancer

E. Martinez[1], M. Rico Oses[1], F. Casas[2], N. Viñolas[2], J. Minguez[3], A. Paredes[4], A. Pérez Casas[4], E. Domine[4]
[1]*Complejo Hospitalario de Navarra, Department of Radiation Oncology, Pamplona, Spain*
[2]*Hospital Clinic i Provencial, Radiation Oncology, Barcelona, Spain*
[3]*Hospital Donostia, Radiation Oncology, San Sebastian, Spain*
[4]*Fundación Jiménez Díaz, Radiation Oncology, Madrid, Spain*

Purpose or Objective: Although many studies have confirmed the synergic effects of combining chemotherapy and radiotherapy (RT), clinical data evaluating safety and efficacy of erlotinib in combination with RT in locally advanced non-small-cell lung carcinoma (NSCLC) are limited. This is the first study to determine the feasibility, tolerability, and efficacy of the concurrent addition of erlotinib to the standard conformal thoracic RT in patients with unresectable or locally advanced NSCLC who are not candidates for receiving standard CT by any cause.

Material and Methods: 90 patients (p) with irresectable NSCLC (I-IIIB stage), ECOG < 2 and measurable disease for criteria RECIST were randomized. P assigned to the arm A received RT 3D (66 Gy/33 fractions) and P in the arm B received the same RT with erlotinib 150 mg/d p.o. concurrent up to a maximum of 6 months. The principal aim was the G 3-4 toxicity the secondary aims: OS, PFS, cause-specific survival (CSS), and objective response rate (ORR).

Results: 90 p were included (30 in arm A, 60 in B), 89 were valid for safety analysis and 81 of efficacy. Responses: CR A/B (%): 21,4/ 41,5 (p <0,05). Median of follow-up 17,1 m. OS: 15,3/ 12,9 m (p: NS). CSS: 17,7/ 21,4 m (p: NS). G 3-4 toxicities: A/B (%): pneumonitis: 10,6/3,3; radiodermitis: 3/3,3); esofagitis: 0/0; pulmonary fibrosis: 0/3,3; cardiopathy: 3,4/1,6; rash: 0/13,3; diarrhea: 3,4/6,7; fatigue: 0/8,3. Erlotinib did not increase the toxicity produced by the RT.

Conclusion: The combination of erlotinib with RT produces a scarce clinical benefit in this group of patients, limited to complete responses and longer CSS rate compared with RT alone. Increased toxicity events were associated with combined therapy, mainly cutaneous toxicity. Further studies in molecularly unselected lung cancer patients treated with EGFR TKIs and radiotherapy are not indicated. Use of predictive biomarkers to identify patients most likely to benefit are mandatory

PO-0682

Prognostic factors and patterns of failure after post-op radiotherapy for epithelial thymic tumors

F. Belkhir[1], A. Levy[1], A. Suissa[1], N. Grellier-Adedjouma[1], P. Xu[1], E. Fadel[2], C. Le Péchoux[1]
[1]*Institut Gustave Roussy, Radiation Oncology Department, Villejuif, France*
[2]*Centre Chirurgical Marie-Lannelongue, Surgery, Le Plessis-Robinson, France*

Purpose or Objective: To evaluate the sites of relapse and prognostic factors of outcome in a retrospective series of patients with epithelial thymic tumors (ETT) treated consecutively with surgery and post operative RT.

Material and Methods: Data from 134 ETT patients who were operated according to guidelines in different centres and received RT in Gustave Roussy from 1990 to 2011 was retrospectively analysed. Before 1998, patients had radiotherapy to the thymic region as well as elective nodal radiotherapy (ENRT) to the mediastinum and both supra-clavicular regions. From 1999 on, patients had conformal RT limited to the thymic tumour bed. A 3D-conformal radiotherapy (CRT) with CT-based treatment planning was used from 1995, and Intensity Modulated Radiotherapy has been gradually implemented since 2010

Results: Median follow-up was 8.8 years. Quality of resection was R0 in 75%, R1 in 22%, and R2 in 3% of patients. 16% had neoadjuvant chemotherapy. Classification according to Masaoka-Koga was: stage I/IIA in 17%, IIB in 22%, III in 28%, and IV in 33%. 28 patients (21%) had thymic carcinoma according to WHO classification. The mean (median? delivered dose of RT was 54 Gy (42-66) and 53% patients an ENRT at a dose of 45-50 Gy median dose different between ENI and CRT. Late toxicities were observed in 16% of patients (11 pneumonitis, 9 pericarditis and 6 coronaropathy) but no related toxic-death was reported. Considering patterns of relapse, there were 26 local relapses which could be considered in-field (46% pleura, 27% mediastinum, and 27% to both locations) and 42 regional relapses (88% pleura, 5% mediastinum, and 7% lung) resulting in a locoregional control (LRC) rate of 67%49% at 5/10 years. Distant control rate was 91% at 10 years. ENI (HR: 2.3) and Masaoka-Koga classification > stage IIB (HR: 3.2) were associated with a decreased LRC in the multivariate analysis (MVA). Gender, age, WHO classification, PS, score, R0 status, CRT dose, and boost CRT Were not correlated with LRR in the MVA. The cause specific and overall survivals (OS) at 5 and 10 years were 72% and 63%, respectively (add 5 year results). PS>0 (HR: 2.6), and Masaoka-Koga stage IV (HR: 2.1) correlated with a lower OS in the MVA.

Conclusion: Masaoka-Koga was the main prognostic factor of OS and LRC in this analysis. Indications of RT should be

discussed within a multidisciplinary board. When adjuvant RT is indicated, conformal RT should be used. Patients should be followed up as late recurrences may occur

PO-0683

Multiple training interventions improve PET/CT based target volume delineation in NSCLC RTP

T. Konert[1], W. Vogel[1], M. MacManus[2], S. Everitt[2], D. Thorwarth[3], J. Sonke[4], D. Paez[5], E. Fidarova[5], G. Hanna[6]

[1]*Netherlands Cancer Institute Antoni van Leeuwenhoek Hospital, Nuclear Medicine, Amsterdam, The Netherlands*

[2]*Peter MacCallum Cancer Centre, Radiation Oncology, Melbourne, Australia*

[3]*University Hospital Tübingen, Radiation Oncology, Tübingen, Germany*

[4]*Netherlands Cancer Institute Antoni van Leeuwenhoek Hospital, Radiation Oncology, Amsterdam, The Netherlands*

[5]*International Atomic Energy Agency, Nuclear Sciences and Application, Vienna, Austria*

[6]*Centre for Cancer Research and Cell Biology, Radiation Oncology, Belfast, United Kingdom*

Purpose or Objective: PET/CT based radiotherapy planning (RTP) has been shown to improve the consistency of target volume delineation (TVD) in lung cancer radiotherapy, hopefully leading to improved local control. This study assesses the impact of a standardized delineation protocol and multiple training interventions on PET/CT based TVD in NSCLC.

Material and Methods: Over a one year period, nuclear medicine physicians (NMP) and radiation oncologists (RO) with limited experience in PET/CT based TVD from nine different countries participated in a multicenter study. The first training intervention included a three-day training course, consisting of three contouring assignments which formed the basis of a teaching discussion with the aim of identifying and correcting misinterpretations of practical guidelines, and various lectures on PET/CT based RTP. The second training event contained detailed individual feedback reports about previous performed contouring assignments and a webinar on PET/CT based TVD in NSCLC. Eleven teams consisting of a RO and NMP performed joint gross tumor volume (GTV) delineation of the primary tumor as per a standardized delineation protocol. In-house developed software called Big Brother recorded any user-software interaction, consequently allowing visual inspection of delineation strategies. Six delineation cases were performed before, during and after the training program and were compared with agreed expert contours (GTVexp) to assess delineation performance.

Results: Following the three-day training course overall concordance indices for 3 repetitive cases increased from 0.57±0.11 (SD) to 0.66±0.10. Observer volumes were larger after the training and miss of GTVexp was significantly reduced from 79.01±52.35 cc (SD) to 42.86±38.08 cc. Results are summarized in table 1. After further feedback and the webinar overall concordance indices for another 3 repetitive cases increased from 0.64±0.10 (SD) to 0.80±0.08. A reduction of GTVexp miss from 78.89±44.51 cc (SD) to 30.87±20.26 cc was observed.

Table 1. Comparison of results from contouring the GTV before and after the first training event, and before and after a complete training in the use of a standardized delineation protocol. CI_{expert} = median concordance index between the observers' GTV and expert GTV.

	Expert Volume (cc)	Median Group Volume (cc ± SD)	Miss (cc ± SD)	CI_{expert} (± SD)
Contours before and after the three-day training course				
Before	388.38	282.75 ± 46.28	127.32 ± 42.43	0.67 ± 0.10
After		409.48 ± 115.12	59.94 ± 48.94 (p=0.03)	0.70 ± 0.07 (p=0.34)
Before	50.86	30.58 ± 6.99	20.43 ± 6.09	0.59 ± 0.11
After		51.35 ± 20.94	8.88 ± 9.34 (p=0.03)	0.65 ± 0.10 (p=0.06)
Before	164.46	84.93 ± 11.67	84.26 ± 11.66	0.49 ± 0.07
After		108.49 ±41.23	62.18 ± 23.14 (p=0.05)	0.58 ± 0.12 (p=0.08)
Contours before and after the complete training program				
Before	377.99	280.39 ± 92.41	115.45 ± 52.16	0.68 ± 0.11
After		370.78 ± 37.06	26.73 ± 18.34 (p=0.01)	0.85 ± 0.03 (p=0.01)
Before	254.68	157.99 ± 80.15	103.70 ± 43.86	0.59 ± 0.10
After		220.24 ± 81.53	39.72 ± 25.87 (p=0.04)	0.82 ± 0.10 (p=0. 05)
Before	134.07	83.77 ± 15.95	50.66 ± 10.13	0.61 ± 0.06
After		117.52 ± 30.95	23.32 ± 10.12 (p=0.01)	0.80 ± 0.07 (p=0.01)

Conclusion: Following a training intervention, PET/CT based TVD in NSCLC RTP using a standardized delineation protocol led to significant improvement in delineation performance. A greater improvement in TVD with the use of multiple training events as compared to a single training event was observed.

PO-0684

Does the dose to heart affect survival in NSCLC patient treated with definitive Radiotherapy?

T. Schytte[1], T.B. Nielsen[2], T. Stolberg-Rohr[2], C. Brink[2], O. Hansen[1]

[1]*Odense University Hospital, Department of Oncology, Odense, Denmark*

[2]*Odense University Hospital, Laboratory of Radiation Physics, Odense, Denmark*

Purpose or Objective: High radiotherapy dose to the heart increase the risk of cardiac morbidity and death in early stage breast cancer and lymphoma. Recent reports (1,2) have indicated that an association between overall survival and dose to heart (e.g. V5 for the heart) are observable after radiotherapy of NSCLC patients as well. The objective of this study was to evaluate if overall survival was affected by high V5 to the heart in NSCLC patients treated with definitive radiotherapy (RT).

1) Bradley et al, Lancet Oncology 2015 Feb;16(2):187-99. 2) Belderbos et al, WCLC2015 mini33.03)

Material and Methods: In a single institution, 297 NSCLC patients were treated consecutively with definitive RT from 2001-2007 with at least 60 Gy. Concomitant chemotherapy was not part of the standard treatment initially but became a treatment option later in the study period (weekly docetaxel). RT was delivered as 3D RT without elective nodal irradiation. No constraint on dose to the heart was applied during treatment planning. The heart was delineated retrospectively and heart doses were extracted from the treatment planning system (mean heart dose (MHD) and V5). Patients were stratified in two groups depending on their heart dose being above or below the median value. Survival test was performed using Kaplan Meyer and log-rank test. All patients were followed to death.

Results: Patient and treatment characteristics are summarized in table 1. Median follow-up was 127 months. The overall median survival was 19.1 months with 1, 2 and 5 year survival of 69%, 41%, and 17%, respectively. Median V5 for the heart was 49%. No association between survival and heart dose were observed (p=0.29 see Fig 1). The same was true when including smoking, gender, and concomitant chemotherapy as strata in the analyses. Median MHD was 14 Gy. Survival for patients with MHD ≥14 Gy or <14 Gy was 17% and 21%, respectively (p=0.83).

Table 1		Median	Range	SD
Age (year)		67	34-88	9.29
Heart V_5 (%)		49	0-100	1.83
Mean heart dose (Gy)		14	0.1-47.5	11.4
Follow up (month)		127	81-168	25.7
			N=295	(%)
Gender	Female		118	40
	Male		177	60
Performance status	0-1		239	81
	>1		56	19
Smoking	Yes*		246	83
	No°		49	17
Histology	Sq. cell carcinoma		146	50
	Adeno carcinoma		104	35
	Other		45	15
Dose (Gy)	60		193	65
	66		90	31
	80		12	4
Concomitant chemotherapy			34	12

* Current or ex-smoker within 10 yr. ° Never or ex-smoker at least for 10 yr.

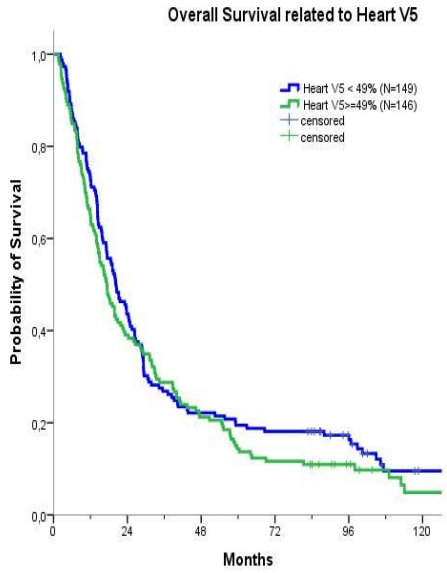

Conclusion: This study did not show that heart V5 or MHD had a negative effect on survival for NSCLC patients treated with definitive radiotherapy. This study differs from recently reports by having a longer follow-up. On the other hand, concomitant chemotherapy was only used in 12% of the patients in this study. The main goal for NSCLC patients is still to achieve better loco-regional control. However, if dose escalation is performed with doses significant above those in the present study, strict dose constraints to the heart might still be advisable based on experience from patients with breast cancer.

PO-0685

Is PET imaging a reliable target for dose painting by numbers in lung cancer?

D. Di Perri[1], J. Lee[1], A. Bol[1], S. Differding[1], G. Janssens[1], D. Labar[1], A. Robert[2], F. Hanin[1], X. Geets[1]

[1]*Université Catholique de Louvain, Institut de Recherche Expérimentale et Clinique IREC - Center of Molecular Imaging Radiotherapy & Oncology MIRO, Brussels, Belgium*

[2]*Université Catholique de Louvain, Institut de Recherche Expérimentale et Clinique IREC - Epidemiology and Biostatistics EPID, Brussels, Belgium*

Purpose or Objective: Since many years, PET has been foreseen as a promising candidate for dose painting. However, the lack of biological specificity of tracers together with the low spatial resolution could call PET into question as a reliable target for voxel-based dose prescription.

To address this issue, we analysed FDG (tumor burden) and FAZA (hypoxia) PET uptake distributions in lung tumours in terms of biological specificity, spatial resolution, and spatiotemporal evolution.

Material and Methods: Twelve patients with locally advanced lung carcinomas treated by concomitant chemo-radiation were prospectively included. These patients underwent 4D PET/CT (FDG and FAZA) with audio coaching at 3 time-points: prior to radiotherapy, and in the second and the third weeks of treatment. All images were reconstructed in their time-weighted mid-position (MidP).

At each time-point, CT-based rigid registration was performed between FDG and FAZA MidP PET/CT while CT-based deformable registration was performed between per- and pre-treatment images.

In order to be compared with native FDG images, simulated PET images (PETsim) were created. To this end, tumours were segmented on FDG images (GTVFDG) using a gradient-based method relying on watershed and clustering. Subsequently, binary images were generated (uniform activity inside and null activity outside GTVFDG) and blurred using a Gaussian kernel of 8-mm FWHM.

PET SUV within the GTV were pairwise compared on a voxel-by-voxel basis using Spearman's correlation (rs) between:

- FDG and FAZA images, to assess their respective specificity
- FDG and PETsim images, to assess to which extent the blurring effect linked to the limited spatial resolution impacts the observed tracer distribution)
- per- and pre-treatment images, to assess the spatiotemporal evolution of the uptake distribution during radiation therapy

Results: At each time point, FDG and FAZA SUVpeak showed high correlation (r = 0.78) (Fig. 1A). FDG and FAZA voxel-by-voxel comparison showed high correlation (rs = 0.75 ± 0.13). This correlation was even higher when the 50% more hypoxic tumours were considered (FAZA SUVpeak = 1.83 ± 0.32 ; rs = 0.80 ± 0.05), compared to the 50% less hypoxic (FAZA SUVpeak = 1.17 ± 0.22 ; rs = 0.69 ± 0.16) (Fig. 1B).

Similarly, high correlation was found between FDG and PETsim images (rs = 0.78 ± 0.14).

Finally, the uptake distribution was spatially stable through imaging sessions for both tracers (FDG: rs = 0.86 ± 0.09; FAZA: rs = 0.82 ± 0.11).

All results were significant (p < 0.01).

Fig 1a. Comparison between FDG and FAZA SUV_{peak}

FDG and FAZA SUV_{peak} showed high correlation (r = 0.78).

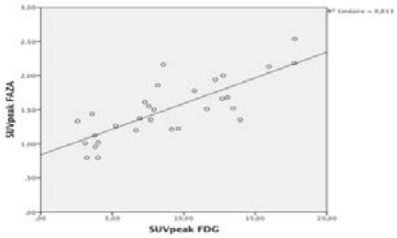

Fig 1b. Voxel-based comparison between FDG and FAZA SUV

FDG and FAZA voxel-by-voxel comparison showed high correlation (r_s = 0.75 ± 0.13). The correlation was higher for the 50% more hypoxic tumors (r_s = 0.80 ± 0.05) than for the 50% less hypoxic (r_s = 0.69 ± 0.16).

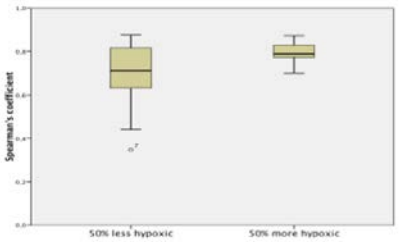

Conclusion: FDG and FAZA PET images share similar uptake patterns, even more for hypoxic tumours. In addition, FDG and FAZA uptake distribution were stable over treatment time. Blurring caused by the limited spatial resolution seems to be the main driver of the observed uptake distributions, as

suggested by the comparison between real and simulated images.
These results question the use of PET imaging as a target for dose painting by numbers in lung cancer.

PO-0686
Locoregional failure in locally advanced non-small cell lung cancer after definitive radiotherapy
E. Jouglar[1], V. Isnardi[2], D. Goulon[3], C. Ségura-Ferlay[4], M. Ayadi[5], C. Dupuy[6], M.A. Mahé[1], L. Claude[7]
[1]*Institut de Cancerologie de L'Ouest Centre René Gauducheau -Site Hospitalier Nor, Radiation Oncology, Saint-Herblain, France*
[2]*Centre Léon Bérard, Nuclear Medicine, Lyon, France*
[3]*Institut de Cancerologie de L'Ouest Centre René Gauducheau -Site Hospitalier Nor, Nuclear Medicine, Saint-Herblain, France*
[4]*Centre Léon Bérard, Biostatistics Unit- DRCI, Lyon, France*
[5]*Centre Léon Bérard, Medical Physics, Lyon, France*
[6]*Institut de Cancerologie de L'Ouest Centre René Gauducheau -Site Hospitalier Nor, Medical Physics, Saint-Herblain, France*
[7]*Centre Léon Bérard, Radiation Oncology, Lyon, France*

Purpose or Objective: To determine the patterns of locoregional failure (LRF) in patients with locally advanced non-small cell lung cancer treated with definitive radiotherapy (RT).

Material and Methods: One hundred and fifty-four patients from the Gating 2006 prospective randomized trial (NCT00349102) were treated with conformal RT with or without respiratory motion management. All patients had a PET-CT with 18FDG in the two months leading up to study inclusion. The recommended protocol prescription was 66 Gy in daily 2-Gy fractions, five days a week. IMRT was not permitted. Patients with a LRF as first event were included. Treatment plannings with simulation CT, pre-treatment 18FDG PET-CT and post-treatment images demonstrating recurrence were registered and analyzed. Measurable LRF was contoured (rGTV) and classified as in-field (if 95% of rGTV volume was within the 95% isodose), marginal (if 20 to 95% of rGTV volume was within the 95% isodose), or out-of-field (if less than 20% of rGTV volume was within the 95% isodose).

Results: Median follow-up was 27.8 months. Forty-eight patients presented LRF. One-year and 2-year locoregional disease-free survival were 77% (95% CI 70-83) and 72% (95% CI 64-79) respectively. Age was the only independent LRF prognostic factor. The median age for patients in LRF was 67 years vs 60 years for the group not in LRF (p=0.009). 79% of the patients with LRF as first event relapsed within the RT field. 32% of patients with LRF had a marginal LRF component. Isolated out-of-field failure occurred in only 3% of all patients. The regions of highest FDG-uptake on pre-treatment PET-CT were located within the recurrence in 91% of patients with in-field LRF.

Conclusion: In-field failure was the most common pattern of failure. Escalated dose RT with high-dose fractions guided by PET parameters warrants further investigation.

PO-0687
Machine learning method for biomarkers identification in lung cancer patients
B.D. Delgado-León[1], J. Moreno[2], J. Cacicedo[3], M. Perez[4], A. Moreno[2], F.J. Núñez[2], L. Delgado[4], S. Pérez[4], J.M. Praena-Fernandez[5], E. Montero[1], J.M. Nieto[1], C. Parra[2], M.J. Ortiz-Gordillo[1], J.L. López-Guerra[1]
[1]*University Hospital Virgen del Rocio, Radiation Oncology, Sevilla, Spain*
[2]*University Hospital Virgen del Rocio, Group of Technological Innovation, Sevilla, Spain*
[3]*Cruces University Hospital, Radiation Oncology, Bilbao, Spain*
[4]*Instituto de Biomedicina de Sevilla, IBIS/HUVR/CSIC/Universidad de Sevilla-, Sevilla, Spain*
[5]*University Hospital Virgen del Rocio, Methodology Unit-Fundación Pública Andaluza para la Gestión de la Investigación en Salud de Sevilla- Sevilla- Spain, Sevilla, Spain*

Purpose or Objective: Treatment of lung cancer (LC) with radiotherapy (RT) is often accompanied by the development of relapse. The significance of biologic markers for predicting recurrence has been increasingly emphasized by recent studies. Highly accurate and reliable machine-learning approaches can drive the success of biomarkers identification in clinical care. We developed a prospective platform to incorporate translational research into the clinical decision making process in LC patients.

Material and Methods: Prospective data from 138 consecutive LC patients with indication of radio(chemo)therapy and diagnosis from January 2013 to August 2014 were available to enable the development of a prediction model. Median age was 62.5 years-old (range, 35-88) and the Karnofsky performance status (KPS) was ≥70 except for 129 cases. The most common histology for non-small cell LC patients (77.5%) was squamous cell carcinoma (52.3%). 73.1 percent of patients had Stage III disease (9 cases were a mediastinum recurrence) and 91 % received platinum-based chemotherapy. Median total dose prescribed was 61.2 Gy. 20 cases also underwent surgery. Data from translational research included genotypes of 4 single nucleotide polymorphisms (SNPs) of the transforming growth factor (TGFB1) gene (rs4803455, rs1800468, rs8179181, and rs8110090) and 3 SNPs of the heat shock protein (HSPB1) gene (rs2868370, rs2868371, and rs7459185).

Results: In univariate analysis, the CA genotype (N=92; 64 relapses [70%]) of TGFB1 rs4803455 was associated with a statistically significantly higher risk of recurrence (OR = 2.09; P = 0.045) compared with the CC genotype (N=46; 24 relapses [52%]). This effect was virtually unchanged after multivariate analysis (OR = 2.31; 95% CI, 1.08– 4.95; P = 0.031). In addition, we performed an ROC curve analysis to determine the strength of the above identified biomarker in predicting relapse. Age was the most important predictor, with an AUC of 0.62. By adding the TGFB1 rs4803455 SNP, the predictive power of the recurrence risk model improved, enhancing the AUC to 0.67 (95% CI, 0.57– 0.76; P = 0.001).

Conclusion: The prediction model for recurrence of patients with LC highlights the importance of combining patient, clinical, treatment, and translational variables. Our results showed that the CA genotype of TGFB1 rs4803455 SNP was associated with a higher risk of relapse in patients with LC treated with radio(chemo)therapy and thus may be used for guiding therapy intensity or as a selection criteria for a clinical trial, which would further the goal of individualized therapy. This tool could be used as a first building block for a decision support system.

PO-0688
Patterns of LR for stage III N2 NSCLC patients after chemotherapy and surgery: implications for PORT
C. Billiet[1], D. De Ruysscher[1], S. Peeters[1], H. Decaluwé[2], J. Vansteenkiste[3], C. Dooms[3], C.M. Deroose[4], M. Hendrikx[5], J. Mebis[6]
[1]*University Hospitals Leuven, Radiation Oncology, Leuven, Belgium*
[2]*University Hospitals Leuven, Thoracic Surgery, Leuven, Belgium*
[3]*University Hospitals Leuven, Respiratory Oncology, Leuven, Belgium*
[4]*University Hospitals Leuven, Imaging and Pathology- Nuclear Medicine, Leuven, Belgium*
[5]*University of Hasselt, Cardiothoracic Surgery, Hasselt, Belgium*
[6]*University of Hasselt, Medical Oncology, Hasselt, Belgium*

Purpose or Objective: To evaluate loco-regional patterns of failure after induction chemotherapy and surgical resection for stage III N2 non-small-cell lung cancer (NSCLC).

Material and Methods: This retrospective study included 151 patients with pathological confirmed diagnosis of stage III-N2 NSCLC from 1998 to 2012, at the University Hospitals Leuven and the Oncologic Center Limburg. All patients were treated with induction chemotherapy and surgical resection. Postoperative radiotherapy (PORT) was only performed in case of incomplete resection (R1/R2) or persistent nodal disease (ypN2). For the non-PORT group, we created a virtual PTV, consisting of the initially involved lymph node stations, N7, the ipsilateral hilum and bronchial stump. All patients were staged with FDG PET-CT and brain imaging. Disease recurrence at the primary affected lobe of the lung, ipsilateral hilum, and/or initially involved mediastinal nodes was considered loco-regional (LR). R2 resections were also seen as LR. Follow-up occurred at 3-month intervals for the first 2 years, every 6 months for the next 3 years, and then annually and included physical examination, blood test and CT scan of thorax and upper abdomen each 6 months.

	2R	2L	3	4R	4L	5,6	7	8,9	10R	10L	Surgical margin	Sites of relapse
PORT group (n = 27)	5	1	2	6	3	5	10	2	13	6	7	N = 60
	19%	4%	7%	22%	11%	19%	37%	7%	48%	22%	26%	
Non-PORT group (n = 32)	9	3	0	19	7	7	20	3	17	7	6	N = 98
	28%	9%	0%	59%	22%	22%	63%	9%	53%	22%	19%	

Results: After a mean follow-up of 46 months, disease recurrence occurred in 96/151 patients. Cumulative LR and distant metastases (DM) were seen in 39% (59/151) and 57% (86/151), respectively. Forty-eight patients (32%) had a LR as first event. PORT was performed in 76 patients. Considering the patients with cumulative LR (n=59), patients who underwent PORT (n=27) had a total of 60 relapse sites (2.2 sites/patient), whereas in the non-PORT group (n=32) a total of 98 sites were documented (3.1 sites/patient)($p<0.05$).
In the PORT-group, the most common site of failure was the hilum, followed by station 7, the bronchial stump, 4R, 2R, 5-6, 4L, 2L, 3 and 8-9. In the non-PORT group, the most common site of failure was station 7, followed by station 4R, the hilum, 2R, 4L, 5-6, the bronchial stump, 8-9 and 2L (table).
In the PORT group, 33% of patients relapsed inside the planning target volume (PTV), 33% had a local relapse both within and outside the PTV. Another 18% of patients had a LR outside the PTV. In the non-PORT group, 66% of patients relapsed inside the virtual PTV, 31% both within and outside the PTV, and only 3% had a LR outside the PTV.

Conclusion: Patients receiving PORT had less sites of LR compared to the non-PORT group. In the non-PORT group, significantly more relapses were seen in nodal station 7, 4R and 4L, which are in the majority of cases irradiated in the PORT group. These data indicate the potential benefit of PORT in stage III N2 NSCLCL treated with induction chemotherapy and surgery.

PO-0689

Outcome predictors for moderate hypofractionated tomotherapy in Malignant Pleural Mesothelioma

A. Fodor[1], S. Broggi[2], I. Dell'Oca[1], M. Picchio[3], C. Fiorino[2], E. Incerti[3], M. Pasetti[1], G. Cattaneo[2], L. Gianolli[3], R. Calandrino[2], N. Di Muzio[1]
[1]*San Raffaele Scientific Institute, Department of Radiotherapy, Milan, Italy*
[2]*San Raffaele Scientific Institute, Medical Physics, Milan, Italy*
[3]*San Raffaele Scientific Institute, Department of Nuclear Medicine, Milan, Italy*

Purpose or Objective: Malignant pleural mesothelioma (MPM) has an aggressive course, high mortality rate and no standard of care. The role of radiotherapy has not been established. In a dose escalation study of moderate hypofractionated tomotherapy(HTT) we obtained statistically significant better local control adding a simultaneous integrated boost (SIB) on FDG-PET positive areas (BTV) (Fodor et al, Strahlenter Onkol 2011). Here we evaluate factors influencing outcome in MPM patients(pts) treated with HTT.

Material and Methods: From May 2006 to April 2014 54 pts with MPM, progressive after previous treatments (surgery + chemotherapy) were treated with salvage HTT. Patient characteristics are presented in the table below. Median survival was 10.2 (1.18-70) months, 4 patients, all treated with SIB, were alive at the last follow up. A univariate analysis was performed to identify which of these factors: BTV boost, volume of BTV, type of surgery, histology, stage, chemotherapy yes/no and volume of PTV influence Overall Survival(OS), Local Relapse(LR) and Distant and Local Relapse(R).

Sex	Men: women = 44:10
Median age	69 years (39-82)
Median follow up	10.2 months (1.18-70)
Histology	Biphasic /sarcomatous: epithelial= 8:46
Location	Right pleura: Left pleura= 29:25
Initial Stage	I:II:III:IV= 10:15:22:7
Induction CT	Yes:no= 48:6
Surgery	Extrapleural pneumonectomy(EPP) vs Pleurectomy (P) vs Biopsy/Talc Pleurodhesis= 2 vs 19 vs 33
Boost on BTV	Yes:No= 40:14
Treated volumes	Median PTV: Median BTV= 3166.7 cc: 196.65 cc

Results: Median survival for initial stage I vs II vs III vs IV was: 10.2: 22.07:9.97:5.72 (p=0.006). Only stage (I-II vs III-IV) was statistically significant in predicting OS: 13.11 vs 8.23 months(mts) (p=0.04) and only surgery yes(EPP/P) vs Biopsy/Talc Pleurodhesis (TP) for LR(p=0.009). SIB on BTV has an impact on survival for stage III-IV (p=0.05), but not for stage I-II (p=0.7). A BTV volume of 353.2 cc was found to be the best cut-off having a statistically significant impact on OS (p= 0.0003). Median OS was 5.84 vs 7.8 vs 11.54 (p=0.04) for pts without SIB vs pts with SIB and BTV volume > cut off vs pts with BTV < cut-off. BTV volume< 353.2 cc significantly influences OS in stage III-IV (p=0.03). In stage III-IV SIB has a role in BTV< 353.2 cc, and pts with higher BTV treated with SIB have similar OS to pts without boost: 11.54 vs 6 vs 4.85 mts (p=0.04). In stages III-IV, type of surgery was significant for OS: EPP vs P vs TP= 1.61: 10.1:8.23 (p=0.001). For pts with TP BTV volume <353.2 cc is a significant predictor of survival (p=0.001) and these pts have a better OS than pts with larger BTV treated with SIB or without SIB: 13.11 vs 7.8 vs 7.74(p=0.04).

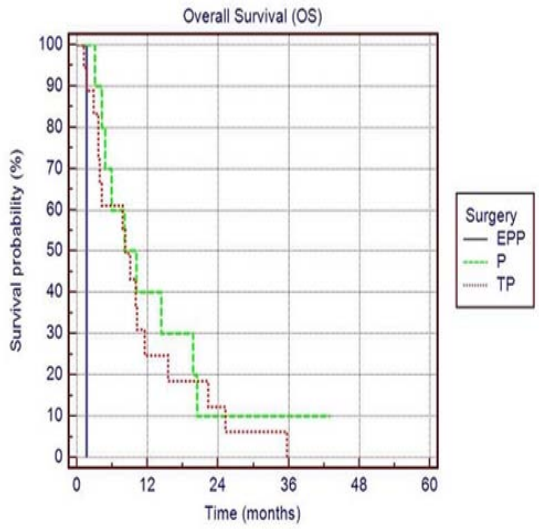

Conclusion: The BTV cut off volume <353.2 cc significantly influences OS in stage III-IV pts , even in those treated with palliative surgery, but irradiated with SIB and can help in patient selection for salvage SIB HTT.

PO-0690

Patient weight loss predicts worse overall survival for stage I lung cancer treated with SABR

G. Cook[1], Y. Xu[2], P. Cross[1], O. Holmes[1], R. Macrae[1], J. Pantarotto[1]

[1]*The Ottawa Hospital Regional Cancer Centre, Radiation Oncology, Ottawa, Canada*

[2]*The Ottawa Hospital Research Institute, Radiation Oncology, Ottawa, Canada*

Purpose or Objective: As per published guidelines, SABR is the recommended curative treatment option for those stage I non-small cell lung cancer patients (NSCLC) who either cannot or will not have surgery. This study investigates whether patient reported weight loss at presentation is a prognostic factor in a retrospective cohort of biopsy-proven stage I NSCLC patients who received SABR at one institution.

Material and Methods: Between January 2009 and December 2013, 314 consecutive patients with histologically proven T1 or T2a N0 NSCLC treated with SABR were entered in a research ethics board approved database. All patients were reviewed for potential surgical resection by a thoracic surgeon and all had FDG-PET/CT staging. Overall survival (OS) by weight loss was evaluated by Kaplan-Meier and log-rank test. Univariate and multivariate of weight loss was performed using a Cox proportional hazard model; adjustment of potential confounders included age, gender, performance status, histology, T-stage, tumor location, SUV max, smoking status and Charlson Comorbidity Index (CCI).. Weight loss was self-reported by patients on a standard intake form prior to oncology consultations under 5%, 5-10% or greater than 10%.

Results: 292 patients (92.9%) in the database had self-reported weight loss. 26 (8.9%) and 27 (9.2%) patients self-reported weight loss of 5-10% or greater than 10%, respectively. Survival differences were significant between weight loss groups especially in those patients with greater than 10% cohort. On univariate analyses, hazard ratio (HR) were 0.86 (95%CI 0.41-1.80) and 2.77 (95%CI 1.61-4.79) for patients with 5-10% and greater than 10% weight loss, respectively. The increased risk of death in patients with greater than 10% weight loss remained significant after adjustment for all confounders HR= 2.52 (95% CI 1.43-4.45). Weight loss overall was a significant risk factor for overall survival (P=0.0059).

Conclusion: Patient reported weight loss is a symptom that predicts shorter survival even in early stage NSCLC treated with SABR.

PO-0691

SABR for central lung tumors: plan quality and long-term clinical outcomes

H. Tekatli[1], S. Senan[1], M. Dahele[1], B.J. Slotman[1], W. Verbakel[1]

[1]*VU University Medical Center, Radiation Oncology, Amsterdam, The Netherlands*

Purpose or Objective: The role of stereotactic ablative radiotherapy (SABR) for central tumors is less well established due to toxicity concerns. Volumetric modulated arc therapy (VMAT) has been used at our center since 2008 to deliver risk-adapted SABR for central tumors. We evaluated plan quality and clinical outcomes for patients with a central tumor.

Material and Methods: We identified 80 consecutive patients with primary NSCLC located within 2 cm from the proximal bronchial tree (PBT) and treated using RapidArc™ between 2008-2013. Patients with prior radiotherapy or lung surgery were excluded. RTOG definitions were used to contour organs at risk (OARs). Compliance to departmental, RTOG 0813 and LungTech criteria was assessed for PTV coverage, high/low dose spillage and doses delivered to OARs. Long-term toxicity results were analysed and overall survival (OS) was compared with 252 peripheral tumors (same exclusion criteria) treated with 3 or 5 fractions during the same period.

Results: PTV V95 was 60Gy in 96% of patients. Median PTV was 66 cm3 (range 9-286). Dmax was ≥60Gy in 40% of patients for PBT, 26.3% for aorta, 55% for heart, and 1.3% for trachea. Esophageal maximum Dmax was 58Gy. Mean total lung V5Gy was 21% and mean total lung V20Gy was 8%. Mean contralateral V5Gy was 6.3%. 54 patients (68%) exceeded RTOG0813 Dmax for organ-at-risk (OAR), with 27 exceeding PBT Dmax. LungTech OARs dose limits were exceeded in 48 patients (60%). 5 of 78 patients (6.4%) with adequate follow-up information had grade 3 toxicity. Grade 4 toxicity was not observed. Treatment-related death was considered possible (n=3) or likely (n=3) in 6 patients (7.5%). With a median follow-up of 47 months, 3-year survival was 53%, compared with 57% for 252 peripheral tumors treated with 3 or 5 fractions SABR in the same period (p=0.369).

Conclusion: Although a substantial proportion of moderately central SABR patients received ≥60Gy to OARs, the 3-year survival was similar to patients with peripheral tumors. OARs tolerance doses continue to be refined and patients should be informed of the potential risks and benefits of central lung SABR. In the meantime, it appears reasonable to limit Dmax in OARs (including inside PTV) and lung doses (e.g. V5), using IMRT/VMAT. It is finally important to note that the outcomes in the present analysis should not be extrapolated to very central tumors, where the toxicity risks may be higher.

PO-0692

A novel endoscopically injected liquid-gel marker for image guided radiotherapy of thoracic tumours

S.R. Mortensen[1], J. Scherman-Rydhög[2], K.R. Larsen[3], P.F. Clementsen[4], G.F. Persson[1], M. Aznar[2], M. Josipovic[2], P.M. Rosenschöld[2], R.I. Jølck[5,6], T.L. Andresen[5], L. Specht[1]

[1]*Copenhagen University Hospital- Rigshospitalet, Dept. of Oncology- Section for Radiotherapy, Copenhagen, Denmark*

[2]*Copenhagen University Hospital- Rigshospitalet/University of Copenhagen, Dept. of Oncology- Section for Radiotherapy/Niels Bohr Institute of physics, Copenhagen, Denmark*

[3]*Bispebjerg Hospital, Dept. of Pulmonary Medicine, Copenhagen, Denmark*

[4]*Gentofte Hospital, Dept of Pulmonary Medicine, Gentofte, Denmark*

[5]*Technical University of Denmark- DTU Nanotech, Dept. of Micro and Nanotechnology- Center for Nanomedicine and Theranostics, Kgs Lyngby, Denmark*

[6]*Nanovi Radiotherapy A/S, Kgs Lyngby, Denmark*

Purpose or Objective: A novel liquid gel fiducial marker (BioXmark®) was developed for use in image guided radiotherapy (IGRT).

The injectable marker is based on three components; sucrose acetate isobutyrate (SAIB), x-SAIB (electron dense SAIB analogue) and ethanol. After injection, the liquid gel matrix rapidly increases viscosity forming a rigid hydrophobic gel.with minimal degradation over months (animal studies).

The marker was developed as an alternative to solid metal fiducial markers, providing a simpler injection procedure and potentially lowering the risk of complications/displacement/marker loss while remaining visible on ultrasound, 2D kV X-ray/CT and MRI images.

In this study, we investigated the safety and feasibility of endoscopic (bronchial) ultrasound (EUS/EBUS) guided injection of the liquid marker into patients with stage III non-small cell lung cancer (NSCLC), and the visibility of the marker throughout the radiotherapy (RT) course.

Material and Methods: Patients with stage III NSCLC referred for concomitant chemo-RT (66 Gy in 33 fractions) were eligible.

Marker injection was done by experienced pulmonologists as an outpatient procedure. Standard EUS and EBUS equipment with a 22G aspiration needle was used for injection.

Marker deposits were injected in the primary tumour (if possible) and affected mediastinal lymph nodes. The

injection was monitored on real-time ultrasound using the probe on the endoscope. Patients were monitored for two hours before discharge.
Daily cone beam CT (CBCT) images and 2D kV fluoroscopy (FS) images at fractions 2, 16 and 30 were acquired for setup and evaluation of marker visibility.
Safety visits were planned twice during the RT course.

Results: 15 patients were included. A total of 35 markers were injected, 1-3 markers per patient, 0.10-0.30 mL per injection.
The marker injections were performed 9-27 days before start of RT
No pneumothorax, haemorrhage or other serious complications to the marker injection were observed during or after the procedure.
29 of 35 placed markers were available for evaluation; 2 markers disappeared and one dispersed into a tumour cavity.
Another three markers were injected in two patients who subsequently did not receive RT; one patient died (not related to the marker) and one patient developed metastatic disease prior to start of RT.
All 29 examined markers remained stable in position relative to original injection site (based on visual assessment) and were visible on planning CT, CBCT and FS images throughout the treatment course (fig.1).
27 of 29 markers were usable for image registration between planning CT and CBCT.
No marker related adverse events were seen during the RT period.

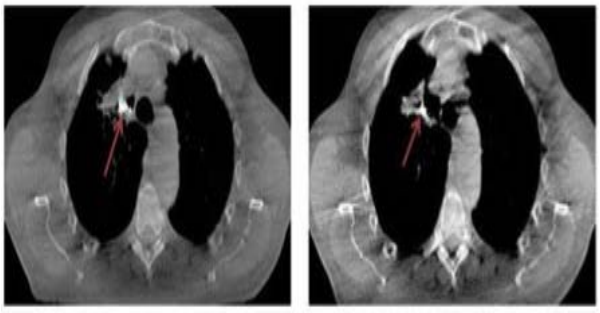

Fig.1 : CBCT images of patient 1 at fraction 2 (left) and fraction 32 (right). Marker indicated by arrow.

Conclusion: The liquid fiducial marker is a safe and clinically useful alternative to solid metal fiducial markers for IGRT of patients with NSCLC and may also be a good alternative for use in IGRT of other solid tumours.

PO-0693

Primary tumor response of locally advanced NSCLC in PET/CTs during radiochemotherapy

T. Schimek-Jasch[1], S. Adebahr[1,2], M. Mix[3], A.L. Grosu[1,2], U. Nestle[1,2]
[1]*University Medical Center Freiburg, Department of Radiation Oncology, Freiburg, Germany*
[2]*German Cancer Consortium DKTK, Partner Site Freiburg, Heidelberg, Germany*
[3]*University Medical Center Freiburg, Department of Nuclear Medicine, Freiburg, Germany*

Purpose or Objective: Standard of care for patients with inoperable, locally advanced non-small-cell lung cancer (NSCLC) consists in combined radiochemotherapy (RCT) with curative intent. Ideally, radiotherapy planning will be performed based on F18-FDG-PET/CT. Additionally, there is great interest in using the biological signal from PET/CT for assessment of treatment response and outcome prediction. Hypothetically, PET/CT may serve as basis for treatment modification such as dose escalation of radiotherapy for poor responders to RCT. The objective of the presented work was the evaluation of the early primary tumor (PT) response during RCT by means of response (R)-PET/CTs during and shortly after radiotherapy and its correlation with survival.

Material and Methods: Between 2011 – 2015, 39 patients with locally advanced NSCLC undergoing conventionally fractionated (2 Gy/day) RCT were prospectively scheduled for three whole-body PET/CT-scans (a radiotherapy planning (RP) PET/CT, a first response PET/CT (1R-PET/CT) 2 weeks after start of RCT and a second response PET/CT (2R-PET/CT) within one week after end of RCT. FDG-uptake of the PT was measured semiquantitatively by means of the maximum standardized uptake value (SUVmax). SUVmax measurements were compared using PERCIST 1.0 criteria*. Here, a response to treatment is defined by a decline of SUVmax of at least 30% (partial metabolic response, PMR). * *Wahl RL, et al.: From RECIST to PERCIST: Evolving Considerations for PET Response Criteria in Solid Tumors, JNM, Vol. 50, No. 5 (Suppl), May 2009*

Results: 39 patients (33% female, 67% male) with a NSCLC (59% SCC, 31% adenocarcinoma and 10% other NSCLC) in UICC-stage IIa (5%), IIIa (51%) und IIIb (44%) received an average total dose of median 68 (58-76) Gy during a median duration of 49 (39-66) irradiation days. Median GTV size was 58 (15-923) ml. SUVmax was median 14 (5.5-28.3) in the RP-PET/CT median 15 (2-37) days before start of irradiation. 33 patients had a 1R-PET/CT median 15 (13-29) days after start of irradiation and at median 22 (16-40) Gy, with a SUVmax of median 10.5 (3.4-23.7)). 36 patients had a 2R-PET/CT median 4.5 (4 days before, 15) days after end of irradiation, with a SUVmax of median 5.45 (1.4-14.3). A PMR was seen in 14/33 (42%) patients in the 1R-PET/CT (PMR1) (compared to the RP-PET/CT), and in 22/30 (73%) patients in the 2R-PET/CT (PMR2) (compared to the 1R-PET/CT). 9/29 (31%) patients reached both a PMR1 and a PMR2 (double PMR), none of these patients experienced a PT-progression during a median follow up of 18 (1.4-53) months after end of irradiation. The 2-year-overall survival rate was 75% as opposed to 54% without a double PMR.

Conclusion: These preliminary data imply that a double PMR measured in response PET/CTs scheduled during and at the end of RCT for NSCLC is associated with a prolonged overall survival rate.

PO-0694

Lung toxicity modelling in thoracic post-operative RT for NSCLC and pleural mesothelioma

A. Botticella[1], G. Defraene[1], C. Billiet[1], C. Draulans[1], K. Nackaerts[2], C. Deroose[3], J. Coolen[4], P. Nafteux[5], S. Peeters[1], D. De Ruysscher[1]
[1]*KU Leuven - University of Leuven- University Hospitals Leuven, Laboratory of Experimental Radiotherapy- Oncology Department, Leuven, Belgium*
[2]*KU Leuven - University of Leuven- University Hospitals Leuven, Respiratory Diseases/Respiratory Oncology Unit, Leuven, Belgium*
[3]*KU Leuven - University of Leuven- University Hospitals Leuven, Department Imaging and Pathology- Nuclear Medicine and Molecular Imaging, Leuven, Belgium*
[4]*KU Leuven - University of Leuven- University Hospitals Leuven, Radiology Department, Leuven, Belgium*
[5]*KU Leuven - University of Leuven- University Hospitals Leuven, Department of Thoracic Surgery, Leuven, Belgium*

Purpose or Objective: Our hypothesis is that NSCLC patients and malignant pleural mesothelioma (MPM) patients treated with thoracic post-operative RT (PORT) are more prone to develop lung toxicity compared to non-surgical NSCLC RT patients. Main objectives are: 1) To quantify the differences in terms of CT lung density changes after PORT for NSCLC and MPM vs. non-surgical RT patients; and 2) To evaluate the correlation between CT lung density changes, dosimetric factors and clinical symptoms (dyspnea).

Material and Methods: Two groups of patients were analyzed: a) SURGICAL GROUP (n=27): stage I-III resectable MPM treated with extrapleural pneumonectomy (EPP) and PORT (n=22) and stage I-III NSCLC treated with pneumonectomy and PORT (n=5); b) NON-SURGICAL GROUP (n=35): stage I-IV NSCLC treated with chemo-radiotherapy.

Patients were treated consecutively in the University Hospitals of Leuven between 2005 and 2014 and their data were retrospectively retrieved. PORT MPM patients were treated with RT doses up to 64 Gy in 2-Gy fractions. PORT NSCLC were treated with RT doses up to 60 Gy in 2-Gy fractions. Non-surgical patients were treated with RT doses up to 66 Gy in 2.75 Gy sequentially with chemotherapy or up to 70 Gy in 2 Gy fractions concurrently with chemotherapy. Dyspnea scores (CTCAE 4.03) before and after RT were retrieved and delta dyspnea was calculated as the difference between the dyspnea after RT (worse at any time point) and before RT. For every patient, 2 CT scans were retrieved: 1) CT0: a free breathing planning CT scan; 2) CT3M: deep inspiration breath-hold diagnostic follow up CT scan 3-6 months after the end of RT. CT0 and CT3M were non-rigidly co-registered in MIM. Differences in Hounsfield Unit (delta HU=HU3M-HU0) were represented as the slope of the dose-dependent delta HU between 0 and 20 Gy (expressed in delta HU/Gy). Primary endpoint was delta dyspnea >= 2. Univariate and multivariate logistic regression analysis were performed in order to identify significant predictors of delta dyspnea >= 2. A p-value of < 0.05 was considered statistically significant.

Results: Delta dyspnea >= 2 was observed in 10/27 patients (37%) in the surgical group and in 7/35 patients (20%) in the non-surgical group (chi-square test 3.38, p=0.06). Mean delta HU/Gy was higher in the surgical group (1.63 vs. 0.67, t-test: p=0.04) (see Figure 1). Outcomes of univariate and multivariate analysis are showed in Table 1. The model with MLD, mean delta HU/Gy and mean heart dose appears to better predict a delta dyspnea >= 2 both in the surgical and non-surgical group (although not significant).

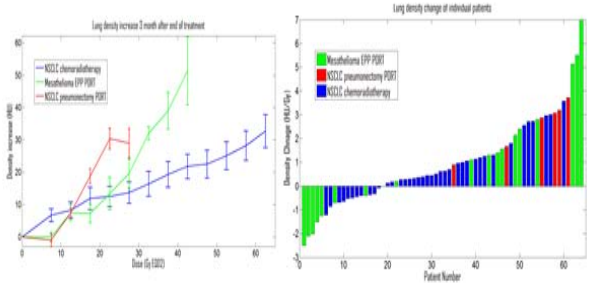

Independent variables	Non-surgical group		Surgical group	
	Logistic regression		Logistic regression	
	C-statistics	P value	C-statistics	P value
Mean delta HU/Gy	0.71	NS	0.62	NS
MLD	0.66	NS	0.55	NS
Mean heart dose	0.64	NS	0.62	NS
MLD - Mean delta HU/Gy	0.73	NS	0.73	NS
MLD - Mean delta HU/Gy – mean heart dose	0.76	0.08	0.75	0.07

Conclusion: Surgical patients after PORT are at higher risk of developing clinically relevant dyspnea (with a delta >= 2) and have a higher increase in lung density (a surrogate of lung damage) compared with non-surgical patients. To strengthen this hypothesis, we will investigate radiation toxicity after more limited surgery (lobectomy) in NSCLC patients. Results will be available by the time of the congress.

PO-0695

Lobectomy vs Stereotactic Ablative Radiotherapy in NSCLC:a multicentric series in four centers

V. Scotti[1], A. Bruni[2], G. Simontacchi[1], I.F. Furfaro[3], M. Loi[1], D. Scartoni[1], A. Gonfiotti[4], D. Viggiano[4], C. De Luca Cardillo[1], B. Agresti[1], L. Poggesi[1], E. Olmetto[1], K. Ferrari[5], M. Perna[1], P. Bastiani[3], L. Paoletti[3], L. Lastrucci[6], P. Pernici[6], G. Carta[1], S. Borghesi[6], S. Bertocci[1], P. Giacobazzi[2], L. Voltolini[4], L. Livi[1]

[1]*Azienda Ospedaliera Universitaria Careggi, Oncology, Firenze, Italy*

[2]*Radiation Oncology, Oncology and Respiratory Disease, Modena, Italy*

[3]*Radiation Oncology, Oncology- Ospedale Santa Maria Annunziata, Florence, Italy*

[4]*Thoracic Surgery, Cardiovascular Department, Florence, Italy*

[5]*II Pneumology, Cardiovascular Department, Florence, Italy*

[6]*Radiation Oncology, Ospedale San Donato, Arezzo, Italy*

Purpose or Objective: Purpose Data from prospective randomized clinical trials are lacking in the comparison between lobectomy (LOB) and stereotactic ablative Radiotherapy (SABR) in operable patients (pts) and on-going trials have troubles in recruiting. In inoperable pts SABR achieves a local control of 64-95% in retrospective and 92-98% in prospective trials particularly when over 100 Gy Biological Equivalent Dose (BED) is delivered.

Material and Methods: From 2010 to 2014, 187 pts with stage I-II NSCLC were treated: 133 were male, 54 female. Mean age was 72 years. Cyto-histological prove of NSCLC was available in 167/187 (89.3%): 111 pts had adenocarcinoma, 51 squamous cell carcinoma and 3 other histologies. 133 pts (71.1%) had stage T1 NSCLC, and 54 (29.9%) stage II NSCLC. Ninety-three (49.8%) pts underwent SABR, while ninety-four (50.2%) were submitted to LOB. Pts who underwent SABR received to 9-20 Gy/die for 3-7 fractions; BED was superior than 100 Gy for all treatments. Response to SABR was evaluated according to RECIST criteria and toxicity according to CTCAE 4.0 scale. To compare LOB vs SABR, we analyzed outcomes in terms of Local Control (LC), Tumor-Specific Survival (TSS), Metastasis Free Survival (MFS) and Overall Survival (OS) using Kaplan-Meier method and log rank tests to evaluate differences in time-to-event outcomes between LOB and SABR.

Results: At a mean follow up of 23 months (range 6-67), LOB showed a better OS (p <0,014) with a 2- and 5-yr OS of 67,6±5,9% and 34.6±15,7% for SABR and 84.1±4.8% and 73.4±6.6% for LOB. SABR achieved the same results in terms of LC with a 2 and a 5 years LC of 92±3.2% and 80.8±7.9% respectively with a p<0,07. Neither significant difference in frequency of distant metastasis nor in TSS was observed between the two treatment groups (respectively p< 0.41 and p<0.50).. In SABR group only 3 G3 lung toxicities were found. No other G3 or G4 acute/late toxicity was found. Toxicity was minor in SABR group (1 fatigue G1,1 dyspnoea G1,1 hemoptysis G1); in surgery group we have recorded 7 atrial fibrillation, 2 bleeding,1 with death, e 6 prolonged air leak.

Conclusion: SABR using high doses (BED>100) shows similar LC than LOB. Very encouraging results in terms of MFS and TSS with very few toxicity and no excess of tumor-related deaths are obtained with SABR compared with LOB. OS is better in LOB group, apparently being strongly influenced by the selection of pts addressed to surgery.

Poster: Clinical track: Upper GI (oesophagus, stomach, pancreas, liver)

PO-0696

Prognostic impact of celiac/supraclavicular node metastasis in locally advanced oesophageal cancer

W.K. Cho[1], D. Oh[1], Y.C. Ahn[1], H. Lee[2], Y.M. Shim[3], J.I. Zo[3], J.M. Sun[4], M.J. Ahn[4], K. Park[4]

[1]*Samsung Medical Center, Radiation Oncology, Seoul, Korea Republic of*

[2]*Kangbuk Samsung Hospital, Radiation Oncology, Seoul, Korea Republic of*

[3]*Samsung Medical Center, Thoracic and Cardiovascular Surgery, Seoul, Korea Republic of*

[4]*Samsung Medical Center, Medicine, Seoul, Korea Republic of*

Purpose or Objective: Most of trials which established the standard treatment of locally advanced oesophageal cancer included M0 stage according to the 6th edition of the AJCC staging system. Now in the 7th edition of AJCC staging system, supraclavicular and celiac lymph node (LN) metastasis are no more classified into M1, but considered same as other regional LNs. We aimed to evaluate the treatment outcomes of NACRT followed by surgery in thoracic

esophageal squamous cell carcinoma (ESCC) patients including this group of tumors that had been excluded in the previous randomized studies.

Material and Methods: A total of 202 patients who were diagnosed with stage II-III thoracic ESCC initiated NACRT between January 2003 and July 2014. Among them, 9 patients refused further treatment during the course of NACRT and finally 200 patients were analyzed. For clinical staging, endoscopic ultrasonography was performed in 116 (58.0%) and FDG PET/CT in all patients. 75 patients (37.5%) had supraclavicular or celiac LN metastasis, which staged as M1a (*N*=54, 27.0%) or M1b (*N*=21, 10.5%) according to the 6th edition of AJCC staging. 168 patients (84.0%) completed both NACRT and surgery, 79 (47.0%) of whom underwent 2 field LN dissection while 89 (53.0%) received 3 field LN dissection. Prognostic factors for survival were assessed using Cox regression.

Results: After the median 17.8 months' follow-up, patients (%) experienced disease progression and (%) died. In all patients, the 2-year locoregional control (LRC), disease free survival (DFS), and overall survival (OS) rates were %, 47.8%, and 67.9%, respectively. Following surgery, the pathologic complete response was achieved in 44 (26.2%) patients. In multivariate analysis, 3 field LN dissection (*p*=0.0439), ypT0 (*p*=0.0380), ypN0 (*p*=0.0024), and negative surgical margin (*p*=0.0037) were favorable prognostic factors for DFS and negative surgical margin (*p*<0.0001) and age < 60 years (*p*=0.0411) were favorable factors for OS. The metastasis to supraclavicular and/or celiac LN was not significant factor for and DFS (*p*=0.5584) and OS (*p*=0.5874).

Conclusion: Celiac and/or supraclavicular LN metastasis did not compromise treatment outcomes significantly following NACRT and surgery in selected patients who tolerates the trimodality treatment.

PO-0697

Neoadjuvant vs. adjuvant treatment of gastroesophageal junction cancer: a retrospective analysis

A. Stessin[1], J. Miccio[2], O. Oladeru[2], S. Ryu[1]
[1]*Stony Brook University Hospital, Department of Radiation Oncology, Stony Brook, USA*
[2]*Stony Brook University Hospital, Stony Brook University School Of Medicine, Stony Brook, USA*

Purpose or Objective: Cancer of the gastroesophageal junction (GEJ) has been rising in incidence in recent years. The role of radiation therapy (RT) in the treatment of GEJ cancer remains unclear, as the largest prospective trials advocating for either adjuvant or neoadjuvant chemoradiotherapy (CRT) combine GEJ cancer with either gastric or esophageal cancer. The aim of the present study is to examine the effect of neoadjuvant versus adjuvant treatment on overall and disease-specific survival for patients with surgically resected cancer of the true GEJ (Siewert type II).

Material and Methods: The Surveillance, Epidemiology, and End Results (SEER) registry database (2001-2011) was queried for cases of surgically resected Siewert type II gastroesophageal junction cancer. The variables obtained for each case include patient demographics (race/ethnicity, sex, age at presentation, year of diagnosis), disease characteristics (histologic grade, surgical stage/extent of disease, nodal status of the disease, presence of distant metastases), and treatment modalities (radiation sequence relative to surgery, type of surgery performed, and type of radiation administered). Patients with metastatic disease, no surgical intervention, and missing data were excluded from the cohort. 1497 patients with resectable GEJ cancer were identified, with 746 receiving adjuvant RT and 751 receiving neoadjuvant RT. Retrospective analysis was performed with the endpoints of overall and disease-specific survival.

Results: Using cox regression and controlling for independent covariates (age, sex, race, stage, grade, histology, and year of diagnosis), we showed that adjuvant RT resulted in significantly lower death risk (hazard ratio [HR], 0.84; 95% confidence interval 0.73-0.97; *p-value*=0.0168) and significantly lower disease-specific death risk (HR, 0.84; 95% confidence interval, 0.72-0.97; *p-value*=0.0211)

Conclusion: This analysis of SEER data showed a survival benefit for the use of adjuvant RT over neoadjuvant RT for the treatment of Siewert type II GEJ cancer. We suggest future prospective studies to compare outcomes of adjuvant versus neoadjuvant treatment for true GEJ cancer.

PO-0698

Integration of radiotherapy to chemotherapy for abdominal lymph node recurrence in gastric cancer

J. Lee[1], S.Y. Rha[2], W.J. Hyung[3], Y.C. Lee[2], J.S. Lim[4], H.S. Kim[2], W.S. Koom[1]
[1]*Yonsei University College of Medicine, Radiation Oncology, Seoul, Korea Republic of*
[2]*Yonsei University College of Medicine, Internal Medicine, Seoul, Korea Republic of*
[3]*Yonsei University College of Medicine, Surgery, Seoul, Korea Republic of*
[4]*Yonsei University College of Medicine, Radiology, Seoul, Korea Republic of*

Purpose or Objective: We hypothesized that selected cases among patients with localized ALN recurrence in gastric cancer (GC) might be salvaged by integration of radiotherapy (RT) in the multimodal treatment.

Material and Methods: We retrospectively identified patients with isolated ALN recurrence from GC between 2005 and 2013. We categorized patients into two groups by treatment approach after diagnosis of ALN recurrence: those who treated with integration of RT to chemotherapy (RCT group) vs. those who received systemic chemotherapy only (CT group).

Results: Of 53 patients with ALN recurrence from GC, 31 patients were classified as RCT group and 22 as CT group. The isolated distant failure (DF; 11/31, 35.5%) was dominant pattern of failure (POF) in the RCT group (median DF-free, 26 months). While local progression (LP) followed by DF (7/22, 31.8%) was dominant POF in the CT group, in which LP (median LP-free, 8 months) occurred earlier than DF (median DF-free, 18 months). RCT group had significantly prolonged median PFS compared with CT group (25 vs. 8 months, p = 0.021). In multivariate analysis, the treatment group was identified as independent prognostic factor related to PFS (p = 0.013). There was a borderline significance in OS between RCT group and CT group (29 vs. 20 months, p = 0.095).

Conclusion: Integration of RT and chemotherapy influenced the pattern of failure, and significantly improved PFS with isolated ALN recurrence in recurrent GC. RT may be considered in the treatment course of isolated ALN recurrence.

PO-0699

Treatment of metachronous esophageal cancer after head and neck cancer

K.H. Fan[1], Y.K. Chao[2], H.M. Wang[3], C.Y. Lin[1], T.C. Chang[1], C.T. Liao[4], C.H. Hsieh[3]
[1]*Chang Gung Memorial Hospital, Radiation Oncology, Taoyuan, Taiwan*
[2]*Chang Gung Memorial Hospital, Thoracic Surgery, Taoyuan, Taiwan*
[3]*Chang Gung Memorial Hospital, Medical Oncology, Taoyuan, Taiwan*
[4]*Chang Gung Memorial Hospital, Otorhinolaryngology- Head and Neck Surgery, Taoyuan, Taiwan*

Purpose or Objective: To review the treatment result of metachronous esophageal cancer (ESC) after head and neck cancer (HNC).

Material and Methods: This study reviewed cancer registry data of our hospital from 2004 to 2012 with following inclusion criteria: ESC were found at least 90 days after HNC in the same patient, and both were diagnosed with pathology of invasive cancer. Patients would be excluded with following criteria: ESC was an extension of HNC or vice versa, and no available information of treatment could be retrieved. Treatment was composed by combinations of radiotherapy, chemotherapy, and surgery depending on disease status and performance status of the patient. The primary end point was overall survival (OS), and the second endpoint was progression-free survival (PFS).

Results: 77 patients were eligible. The median time from HNC to ESC was 32 months (4 – 147 months). Fifty-three patients (60%) were stage III/IV and 15 patients received best supportive care only after diagnosis of ESC. After excluding the BSC group, the 2-year OS were 34.9%. Fifteen patients were alive and one of them still had ESC. Thirty-five, 10, and 2 patients died from ESC, treatment related complications, and other disease, respectively. Univariate analysis revealed that ECOG > 1, tube feeding, anemia, and no esophagectomy correlated with poor OS (p < 0.05). Multivariate analysis showed that lower hemoglobin level, habit of smoking, ECOG score = 2, and no esophagectomy were independent poor prognostic factors (p < 0.05). The 2-year PFS rate for all patients was 30.7%. In the univariate analysis, ECOG > 1, tube feeding, body weight loss > 5%, anemia, no esophagectomy, and ESCstage III/IV were significantly correlated with poor PFS (p < 0.05). In the multivariate analysis, anemia and no esophagectomy were independently correlated with tumor recurrence (p < 0.05). Treatment outcome of patients who received esophagectomy were similar to ESC patients without prior history of HNC. The 2-year OS and PFS were 63.9% and 50.6%, respectively. Both were significantly higher than patients who did not receive esophagectomy (11.8% and 9.9%, p < 0.01).

Conclusion: the treatment result of metachronous ESC after HNC varied with disease and patient status. If esophagectomy was possible, the treatment outcome was not inferior to esophageal cancer without prior head and neck cancer history. But the treatment outcome was poor in patients with unresectable disease or poor performance status. A screening program for metachronous ESC should be considered for high risk patients to detect resectable ESC and improve treatment outcome.

PO-0700

Salvage radiotherapy in the patients with supraclavicular lymph node metastases after esophagectomy

Z.G. Zhou[1], C.J. Zhen[1], P. Zhang[1], X.Y. Qiao[1], J.L. Liang[1], W.W. Bai[1]
[1]*Fourth Hospital of Hebei Medical University, Department of Radiation Oncology, Sijiazhuang- Hebei, China*

Purpose or Objective: Evaluate the salvage radiotherapy outcome in patients with supraclavicular lymph node metastases (SCLN) after esophagectomy.

Material and Methods: A total of 117 patients with esophageal squamous cell carcinoma after initial esophagectomy (R0 resection) were retrospectively analyzed and they were diagnosed supraclavicular lymph node metastases during follow-up time. All patients were divided into salvage radiotherapy group (SR, n=89) and no salvage radiotherapy group (NSR, n=27).

Results: The 1,3,5-year overall survival rates were 81.6%、31.4%、8.6%, respectively. In all patients the 1,3-year survival time after SCLN metastasis (ASMS) rates were 40.2%、14.5%, and the median ASMS time was 10 months. The 1, 3-year ASMS rates were 48.1%、18.9% in SR group and 12.0%、0% in NSR group,respectively (P<0.001). In SR group, the 1, 3-year ASMS rates in the patients with combined radiochemotherapy and single radiotherapy were 62.6%, 33.4% and 41.9%, 16.5% (P<0.001). In the subgroup analysis, in combining visceral metastases group (CVM), the 1,3-year ASMS rates were 35.5% , 0%, and 42.3%, 21.5% in no combining visceral metastases group (NCVM) (P = 0.004). The 3-year ASMS rate with the patients in no combining mediastinal failure group (NCMF) (22.2%) was higher than those in combining mediastinal failure group (CMF) (7.0%) (p=0.041). According to the salvage radiation dose, the 1,3-year ASMS rates were 56.5%, 23.4% in ≥60Gy group and 29.2%, 7.5% in <60Gy group (p<0.001). Multivariate factor analysis revealed that combining visceral metastases, combining mediastinal failure, salvage radiotherapy, salvage radiation dose and salvage treatment model may be considered favourable prognostic factors.

Conclusion: Salvage radiotherapy may improve survival of patients with supraclavicular lymph node metastases after esophagectomy. Combined radiochemotherapy and no combining visceral metastases and a salvage radiation dose ≥60 Gy were associated with a better prognosis for those patients.

PO-0701

Dose-response relationship for locoregional control in esophageal cancer treated with curative CRT

H.J. Kim[1], Y.G. Suh[1], W.S. Koom[1], Y.B. Kim[1], C.G. Lee[1]
[1]*Yonsei University, Radiation Oncology, Seoul, Korea Republic of*

Purpose or Objective: To evaluate the correlation between radiation dose and locoregional control (LRC) for patients with stage II-III esophageal cancer treated with definitive concurrent chemo-radiotherapy (CCRT).

Material and Methods: The medical records of 236 patients with clinical stage II and III esophageal cancer treated with definitive CCRT at the Yonsei Cancer Center between Feb 1994 and May 2013 were retrospectively reviewed. Among these patients, 120 received a radiation dose of < 60 Gy (standard-dose group), while 116 received a radiation dose of ≥ 60 Gy (high-dose group). The median dose of radiation in the standard and high dose groups was 50.4 Gy (range, 45.0-59.4 Gy) and 63 Gy (range, 60.0-66.6 Gy). Concurrent 5-FU/cisplatin (FP) chemotherapy (CHT) was performed in 82.2 % of patients.

Results: The patient characteristics had no differences in age, sex, pathology, grade, tumor length, and clinical stage between the two groups. Patients with high Karnofsky performance status scale and lower thoracic esophageal tumor were included more in standard dose group (p = 0.017 and 0.038). Maintenance CHT was performed more in standard dose group (45% versus 30.2%, p = 0.037) and FP CHT was more frequently used in high dose group (76.7% vs. 87.9%, p = 0.019). The median follow-up time for all patients was 19.2 months (range, 2.2-164.7). Of all patients, 2-yr and 5-yr LRC rate were 60.0% and 48.4%. The median progression-free survival (PFS) and overall survival (OS) were 13.2 months and 26.2 months, respectively. Patients in the high-dose group had a significantly better LRC (2-yr LRC rate, 50.3% vs. 69.1%, p = 0.002), PFS (median, 11.7 vs. 16.7 months, p = 0.029) and OS (median, 22.3 vs. 35.1 months, p = 0.043). The complete clinical response (CR) rate was significantly higher in the high-dose group (44.2% vs. 62.1%, p = 0.007). The treatment-related toxicities did not show a significant difference between the both groups (p = 0.936), although it was difficult to assess due to a retrospective fashion. On multivariate analysis, sex (female), radiation dose ≥(60 Gy) and use of maintenance CHT were independent predictors for improved LRC, and sex (female), clinical stage (stage II vs. III), radiation dose ≥(60 Gy) and use of maintenance CHT were significant predictive factors for OS.

Conclusion: A higher radiation dose of > 60 Gy is associated with increased LRC, PFS and OS for patients with stage II-III esophageal cancer treated with definitive CCRT.

PO-0702

The use of pet texture analysis to predict lymph node metastases in patients with oesophageal cancer

K. Foley[1], B. Berthon[2], C. Marshall[2], E. Spezi[3]
[1]*Cardiff University, Institute of Cancer & Genetics, Cardiff, United Kingdom*
[2]*Cardiff University, Wales Research & Diagnostic PET Imaging Centre, Cardiff, United Kingdom*
[3]*Cardiff University, School of Engineering, Cardiff, United Kingdom*

Purpose or Objective: The prognosis of oesophageal cancer (OC) is poor, with overall 5-year survival approximately 15%. The presence of lymph node metastases (LNMs) is a major prognostic indicator and the ability to identify LNMs is important. Texture analysis of medical images enables additional information to be extracted from routine staging investigations and quantifies intra-tumoural characteristics via non-invasive methods. The aim of the study is to obtain preliminary data investigating the association of texture variables and LNMs.

Material and Methods: A prospectively maintained database including clinical, radiological and pathological details of consecutive OC patients with biopsy proven adenocarcinoma in South East Wales from October 2010 to August 2013 was retrospectively analysed. All patients underwent PET/CT staging. Consecutive patients were grouped into those with and without LNMs on endoscopic ultrasound (EUS), considered the superior staging investigation for loco-regional assessment. Texture analysis of the primary tumour was carried out on the PET images using PET-STAT, software developed and written in the Matlab-based open source software CERR. The tumour was outlined with ATLAAS, a learning algorithm for optimised automatic segmentation developed at Cardiff University. Seventeen variables including SUVmax, metabolic tumour volume (MTV), total lesion glycolysis (TLG) and intensity variability (IV) were calculated. Table 1 details all variables calculated. Patients with primary tumour volume less than 5 ml and distant metastatic disease were excluded. Independent T-tests were used to identify promising texture variables for future study. A p-value <0.05 was considered significant. Primary outcome was LNMs on EUS.

Results: Eighty-one patients underwent staging with PET/CT and EUS [male 67, median age 66 (range 42-82)]. Forty patients were staged as N0 on EUS, with 41 having evidence of regional lymph node metastases. Independent T-tests demonstrated significant differences between patients with and without LNMs for MTV [mean 38.45 v 21.71; t(56.03)=-2.449, p=0.017], TLG [mean 328.72 v 208.66; t(74.721)=-2.023, p=0.047], Coarseness [mean 0.010 v 0.013; t(79)=3.107, p=0.003], Entropy [mean 6.15 v 5.91; t(79)=-2.075, p=0.041] and IV [mean 21.09 v 13.45; t(64.366)=-2.458, p=0.017].

Conclusion: Preliminary results have shown a number of texture variables that have the potential to predict LNMs. On-going work at our institution is investigating the added benefit of texture analysis when developing robust clinical predictive models.

PO-0703

Perioperative chemotherapy versus neoadjuvant chemoradiotherapy for esophageal adenocarcinoma

L. Goense[1], P.C. Van der Sluis[2], P.S.N. Van Rossum[1], S. Van der Horst[2], M. Van Vulpen[1], S. Mook[1], J.P. Ruurda[2], R. Van Hillegersberg[2]
[1]*UMC Utrecht, Radiotherapy, Utrecht, The Netherlands*
[2]*UMC Utrecht, Surgery, Utrecht, The Netherlands*

Purpose or Objective: Perioperative chemotherapy (pCT) and neoadjuvant chemoradiotherapy (nCRT) are well-established therapies to improve survival for resectable non-metastatic esophageal carcinoma. However, the optimal type of treatment for esophageal adenocarcinoma is currently under debate. Until now, limited evidence is available to determine whether pCT or nCRT is most beneficial with regard to toxicity, pathologic outcome and survival. Therefore, the aim of this study was to compare toxicity, pathologic outcome and survival after pCT versus nCRT and surgery in patients with esophageal adenocarcinoma.

Material and Methods: Consecutive patients who underwent pCT or nCRT followed by esophagectomy for cancer between October 2006 and September 2015 in a single institution were analyzed. The pCT regimen consisted of intravenous administration of epirubicin, cisplatin and capecitabin, whereas nCRT consisted of paclitaxel and carboplatin with concurrent radiotherapy. Toxicity of grade 3 or higher was scored according to the National Cancer Institute Common Terminology Criteria for Adverse Events. Data on surgical procedures, complications and follow-up were collected from a prospectively maintained database. Full propensity score-matching was applied to generate matched sets of cases based on pretreatment covariates in order to create comparable groups. Univariable analysis was performed to determine differences between the two groups. Disease-free survival (DFS) and overall survival (OS) were assessed using the Kaplan-Meier method and log-rank test.

Results: A total of 189 eligible patients were identified of whom 19 were discarded after propensity matching; 86 underwent pCT and 84 received nCRT. During preoperative therapy, thromboembolic events occurred more frequently in the pCT group (18% vs. 0%, p<0.001), while leukopenia occurred more frequently in the nCRT group (25 vs. 11%, p=0.013). Complete resection with no tumor within 1 mm of the resection margins (R0) was achieved in 90% of patients in the pCT group, as opposed to 96% in the nCRT group (p=0.103). Pathologic tumor regression was more frequently observed in patients who underwent nCRT compared to pCT (p<0.001). There was no significant difference between the groups with regard to risk of surgical complications, length of hospital stay or in-hospital mortality. Both treatments resulted in comparable 3-year DFS (49% vs. 53% for pCT and nCRT, respectively, log-rank p=0.774) and OS rates (48% vs. 51%, log-rank p=0.842) (Figure 1).

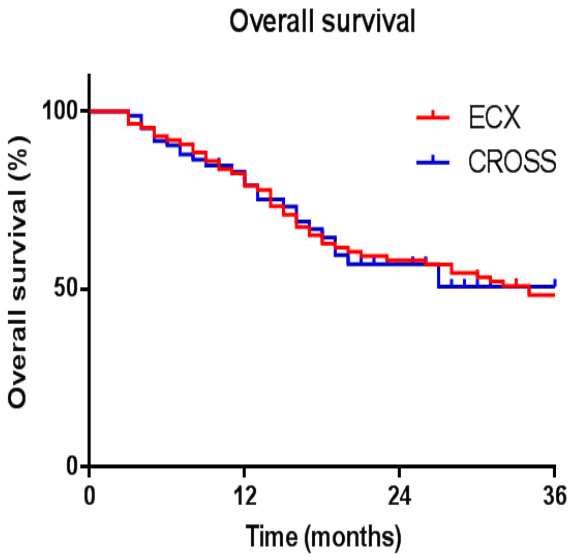

Conclusion: Perioperative chemotherapy (MAGIC) and neoadjuvant chemoradiotherapy (CROSS) were associated with comparable toxicity and postoperative morbidity. Although neoadjuvant chemoradiotherapy was associated with improved tumor regression compared to perioperative chemotherapy, this finding did not translate into improved R0 resection or 3-year survival rates.

PO-0704

Patterns of replase in stage III thoracic esophageal squamous cell carcinoma patients after surgery

Y.X. Wang[1], Q. Yang[1,2], M. He[3], J.F. Yao[3], J. Li[1], S.C. Zhu[1], X.Y. Qiao[1], Z. Qi[3]

[1]*the fourth Hospital of Hebe Medical University, Department of Radiation Oncology, Shijiazhuang, China*
[2]*Handan Central Hospital, Department of Radiation Oncology, Handan, China*
[3]*The fourth Hospital of Hebe Medical University, Department of Thoracic Surgery, Shijiazhuang, China*

Purpose or Objective: To evaluate the patterns of recurrence and its value in target delineation for postoperative radiotherapy(PORT) in patients with stage III thoracic esophageal squmous cell carcinoma(ESCC) after esophagectomy.

Material and Methods: 395 patients with stage III thoracic ESCC treated with radical esophagectomy from Jan, 2008 to Dec, 2011 were enrolled in this study. No patients has accepted preoperative adjuvant therapy. There were 302 males and 93 females; median ages was 60 years old (range 33-83). There were 33 patients located in upper-, 273 in middle- and 89 in low-segment. 375 patents has operated with two-field and 22 with three-field esophagectomy. The median number of dissected lymph nodes were 10 per case (range 1-34). There were 244 with stage IIIA, 106 with IIIB and 45 with IIIC. There were 97 patients received with surgery alone, 212 with postoperative chemotherapy(POCT), 86 with PORT(30 with POCT and PORT). Diagnosis of recurrence was parimarily based on CT images, some of which were biopsy-confirmed. The location and time of tumor recurrences were analyzed.

Results: The overall failure rates was 75.7%(299/395). Locoregional recurrence(LR) was found in 48.4% of patients, distant metastasis(DM) in 16.2%, and LR plus DM in 4.3%; the total rate of LR and DM were 52.7% and 20.5%, respectively. There were 208 patients recurred with LR, 26.9%(56) recurred in supraclavicular/neck(51 in supraclavicular), 69.7% (145) in mediastinum, and 19.7% (41) in upper abdomen (38 in para-aortic lymph node). 92.8% of LR involved locoregional lymph nodes; the rate of anastomotic recurrence was 5.1% (20/395). Further analysis showed that upper-mediastinal recurrence accounted for 88.7% of mediastinal recurrence. The estimated 1-, 3-, and 5-year accumulated LR rates for all patients were 32.2%, 55.1% and 60.1%. Multivariate COX and logistic regression analysis showed that TNM stage and adjuvant therapy were independent factor for LR (p<0.05); PORT could reduce LR, especially in patients with middle-thoracic segment, IIIA and IIIB disease, two-field esophagectomy, less than 6 dissected lymph node or severe adhesion at surgery (p<0.05); but POCT did not decrease LR.

Conclusion: The recurrence rate was very high in stage III thoracic ESCC patients, LR was the main pattern of failure; TNM stage was one of the most important factor for LR. PORT could reduce LR but POCT could not. Upper-mediastinum was the most common site of recurrence, followed by supraclavicular and para-aortic regions; these areas should be consedered the key target of PORT.

PO-0705
Clinical outcomes for inoperable HCC treated with SBRT: results on 71 patients and 102 lesions.
T. Comito[1], C. Franzese[1], E. Clerici[1], F. De Rose[1], A. Tozzi[1], G. D'Agostino[1], P. Navarria[1], C. Iftode[1], E. Villa[1], A.M. Ascolese[1], D. Franceschini[1], R.L.E. Liardo[1], L. Cozzi[1], A. Foglliata[1], A. Stravato[1], F. Zucconi[1], G. Reggiori[1], S. Tomatis[1], M. Scorsetti[1]
[1]*Istituto Clinico Humanitas, Radiotherapy and Radiosurgey, Rozzano Milan, Italy*

Purpose or Objective: Aim of this study is the evaluation of feasibility and efficacy of SBRT in the treatment of unresectable hepatocellular carcinoma (HCC).

Material and Methods: Patients with 1-3 inoperable HCC lesions with diameter ≤6cm were treated by SBRT. Prescription dose was 36-75Gy in 3-6 fractions. SBRT was delivered using the volumetric modulated arc therapy technique with flattening filter free photon beams. The primary end points of this study were in-field local control (LC) and toxicity. Secondary end points were overall survival (OS) and progression free survival (PFS).

Results: From February 2011 and April 2015, 71 patients with 102 HCC lesions were irradiated. All patients had Child-Turcotte-Pugh class A or B disease. Median follow-up was 9 months (range 5-43 months). Actuarial LC at 1 and 2-years was 92% and 81%. An Equivalent Dose >100Gy was a significant prognostic factor for LC in univariate analysis, with a 1-2 years LC rates of 99%-94% for a subgroup of lesions treated with a BED≥100Gy and 58% -29% for lesions treated with a BED <100Gy (p<0.001). Median OS was 25 months. Actuarial OS at 1 and 2 years was 70% and 60%, respectively. Univariate analysis showed that OS is correlated with LC (p<0.02), BED>100 (p<0.05) and Cumulative GTV<5cm (p<0.04). Median PFS was 9 months. Grade≥3 toxicity was observed in 7 patients (18%). No classic RILD was observed.

Conclusion: Our study shows that SBRT is a safe and effective treatment for selected patients with inoperable HCC. Local control rates and toxicity profile were encouraging.

PO-0706
Supraclavicular lymphnode disease is not an independent prognostic factor in esophageal cancer
P. Jeene[1], M.C.C.M. Hulshof[1], E. Versteijne[1], M.I. Van Berge Henegouwen[2], J.J.G.H.M. Bergmann[3], E.D. Geijsen[1], H.W.M. Van Laarhoven[4]
[1]*Academic Medical Center, Academic Radiotherapy, Amsterdam, The Netherlands*
[2]*Academic Medical Center, Academic Upper GI Surgery, Amsterdam, The Netherlands*
[3]*Academic Medical Center, Academic Gastroenterology, Amsterdam, The Netherlands*
[4]*Academic Medical Center, Academic Medical Oncology, Amsterdam, The Netherlands*

Purpose or Objective: In the TNM 7 staging, supraclavicular lymph nodes (SCN) are considered distant metastasis and thus prognostically unfavourable. This is one of the reasons for a generally accepted policy to treat these patients with supraclavicular disease spread and without further distant metastases with definitive chemoradiation (dCRT), irrespective of N stage. However, the worse prognostic value of a supraclavicular disease may be questioned. We analysed the prognostic value of supraclavicular disease in dCRT for esophageal cancer.

Material and Methods: We retrospectively analyzed 207 patients treated between 2003 and 2013 with a standardized protocol of definitive chemoradiation (dCRT) for esophageal cancer to identify the prognostic value of metastasis in the supraclavicular lymphnodes on treatment failure and survival, with special attention to the relation between supraclavicular disease and N stage. All patients were treated with external beam radiotherapy (50.4 Gy in 28 fractions) combined with weekly concurrent paclitaxel 50 mg/m2and carboplatin AUC2.

Results: Median follow up time for patients alive was 43.3 months The median overall survival (OS) for all patients was 17.5 months. OS at 1, 3 and 5 year was 67%, 36.1% and 21.3% respectively. For patients with a metastasis in a supraclavicular lymph node, overall survival was 23.6 months compared to 17.1 months for patients without a metastasis in the SCN (p=0.51). In multivariate analyses , higher cT status, cNstatus and tumor length were found prognostically unfavorable, but a positive supraclavicular lymph node was not of independent prognostic value for survival (p=0.67). The relationship between SCN involvement and N stage was analyzed separately. Median OS for tumors with SCN involvement and N0/1 disease was 49.0 months (15.4-82.6) compared to 17.4 months in patients with N2/3 disease (95%CI 99-24.8 p=0.097). Median diseasefree survival (DFS) for tumors with SCN involvement and N0/1 disease was 51.6 months (95%CI 0-108.5) compared to 8.2 months in the N2/3 group (95%CI 6.2-10.1 p=0.028). No significant difference in

toxicity was seen between patients with SCN involvement and those without,irrespective of the location of the primary tumor.

Conclusion: In esophageal cancer treated with definitive chemoradiation, number of affected lymph nodes is an important prognostic factor, while involvement of a supraclavicular lymph node is not. The supraclavicular lymph node should beconsidered a regional lymph node and treated with curative intend if the total number of involved lymph nodes is limited, irrespective of the site of the primary tumor.

PO-0707

The impact of dose on survival in adjuvant chemoradiation pancreatic cancer

L. De Filippo[1], G.C. Mattiucci[1], A.G. Morganti[2], M. Falconi[3], R.G.P.M. Van STIPHOUT[4], S. Alfieri[5], M. Balducci[1], F.A. Calvo[6], J.M. Herman[7], G. Macchia[8], B.W. Maidment III[9], G. Mantini[1], R.C. Miller[10], W. Regine[11], M. Reni[12], V. Valentini[1]
[1]*Università Cattolica del Sacro Cuore -Policlinico A. Gemelli, Radiotherapy Division, Rome, Italy*
[2]*University of Bologna- S.Orsola-Malpighi Hospital, Department of Experimental- Diagnostic and Specialty Medicine - DIMES Radiation Oncology Unit, Bologna, Italy*
[3]*Università Politecnica delle Marche, Department of Surgery, Ancona, Italy*
[4]*University Medical Centre, Department of Radiation Oncology MAASTRO, Maastricht, The Netherlands*
[5]*Università Cattolica del Sacro Cuore -Policlinico A. Gemelli, Department of Surgery-, Rome, Italy*
[6]*Hospital General Universitario Gregorio Marañón-Complutense University, Department of Oncology, Madrid, Spain*
[7]*Johns Hopkins University School of Medicine, Department of Radiation Oncology and Molecular Radiation Sciences, Baltimore, USA*
[8]*Fondazione di Ricerca e Cura Giovanni Paolo II-Università Cattolica S. Cuore, Department of Radiotherapy, Campobasso, Italy*
[9]*University of Virginia, Department of Radiation Oncology, Charlottesville, USA*
[10]*Mayo Clinic, Department of Radiation Oncology, Rochester, USA*
[11]*University of Maryland Medical Center, Department of Radiation Oncology, Baltimore, USA*
[12]*S. Raffaele Scientific Institute, Department of Oncology, Milan, Italy*

Purpose or Objective: To define the role of radiation dose on overall survival (OS) in pancreatic adenocarcinoma (PAC) patients treated with adjuvant chemoradiotherapy (CRT).

Material and Methods: A total of 518 patients from different centers, completely resected with macroscopically negative margins (R0-1) for PAC (T1-3; N0-1; M0) and treated with adjuvant CRT, were retrospectively reviewed. Patients with metastatic or unresectable disease at surgery, macroscopic residual disease (R2), treated with intraoperative radiotherapy (IORT), dead within 60 days of surgery and without a histological diagnosis of ductal carcinoma were excluded. Only 142 patients received adjuvant chemotherapy.

Results: With 35 months of median follow-up, median OS was 23.0 months after adjuvant CRT with dose ≥ 45 Gy versus 13.0 months with dose < 45 Gy (p < 0.001); 5-year OS was 21.9% versus 3.8%, respectively. Among prognostic factors, higher Ca19-9 levels (>90; p<0.001), higher tumor grade (G3-4, p = 0.017), R1 resection (p = 0.003), higher pT stage (p = 0.002) and positive nodes (p < 0.001) can be identified as negative. Multivariate analysis (HR: 0.52, 0.34-0.77; p = 0.001) proved the positive impact of higher dose.

Conclusion: A significant impact of CRT dose on OS was pointed out by the results of this analysis. The randomized trials on adjuvant CRT in PAC, in which a relatively low-dose of radiation (40 Gy, split course) was used, may have had conflicting results due to this bias.

PO-0708

Advanced age is no contraindication for chemoradiotherapy with curative intent in oesophageal cancer

F. Voncken[1], R. Van der Kaaij[2], K. Sikorska[3], E. Van Werkhoven[3], J. Van Dieren[4], C. Grootscholten[4], P. Snaebjornsson[5], J. Van Sandick[2], B. Aleman[1]
[1]*Netherlands Cancer Institute Antoni van Leeuwenhoek Hospital, Radiation Oncology, Amsterdam, The Netherlands*
[2]*Netherlands Cancer Institute Antoni van Leeuwenhoek Hospital, Surgery, Amsterdam, The Netherlands*
[3]*Netherlands Cancer Institute Antoni van Leeuwenhoek Hospital, Biometrics, Amsterdam, The Netherlands*
[4]*Netherlands Cancer Institute Antoni van Leeuwenhoek Hospital, Gastrointestinal Oncology, Amsterdam, The Netherlands*
[5]*Netherlands Cancer Institute Antoni van Leeuwenhoek Hospital, Pathology, Amsterdam, The Netherlands*

Purpose or Objective: To compare long-term outcomes of chemoradiotherapy between young and elderly (≥70 years) oesophageal cancer patients treated with curative intent.

Material and Methods: Oesophageal cancer patients treated between 1998 and 2013 in our institute with neoadjuvant (nCRT) or definitive (dCRT) chemoradiotherapy were retrospectively analysed. nCRT consisted of 36-50Gy with concurrent 5-fluorouracil/cisplatin or 41.4Gy with concurrent carboplatin/paclitaxel. dCRT consisted of 50Gy with concurrent fluorouracil/cisplatin or 50.4Gy with concurrent carboplatin/paclitaxel. Overall survival (OS), disease-free survival (DFS) and locoregional control (LRC) were compared between older (>70 years) and younger patients (< 70 years). Cox models were used to obtain adjusted hazard ratios (HR) and 95% confidence intervals (CI).

Results: The cohort consisted of 253 patients with a median follow up of 4.3 years. A group of 182 patients (72%) was < 70 years (median age 60). The remaining 71 patients were >70 years (median age 75). The two age groups (younger vs. older) differed significantly regarding smoking (59% vs. 31%; p<0.001), alcohol abuse (64% vs. 46%; p=0.007), Charlson comorbidity index (median 0 vs. 1; p=0.001) and weight loss prior to CRT (median 4 vs. 3 kgs; p=0.038). Most patients had stage IIA-IIIA disease (82%). Distribution of tumour stages was similar in the two age groups (stage IIA: 27% vs. 24%, stage IIB: 4% vs. 4%, stage IIIA: 51% vs. 55%).
Initial treatment was nCRT with the intent to proceed to surgery in 169 patients, whereas 84 patients were planned for dCRT. Although surgery was the intent, 15% of the younger nCRT patients were not operated versus 35% of the older nCRT patients (p=0.01). Reasons to withhold surgery in the younger versus older patients were tumour progression (10% vs. 14%), toxicity (2% vs. 11%) or patient's own choice (3% vs. 11%), p=0.01. At baseline, there was a significant difference in the distribution of the final treatment given (nCRT + surgery, dCRT or nCRT without surgery; p<0.001).
For the entire study population, OS at 3-years was 42%. In the multivariable analysis, no difference was found in OS between the two age groups (old vs. young; HR 0.72, 95% CI 0.49–1.07, p=0.10). In the older age group, DFS (HR 0.66, 95% CI 0.45–0.98, p=0.04) and LRC (HR 0.43, 95% CI 0.23–0.82, p=0.01) were significantly better than in the younger age group.

Conclusion: Elderly oesophageal cancer patients (>70 years) treated with neoadjuvant chemoradiotherapy followed by surgery or definitive chemoradiotherapy had long-term outcomes which did not differ from the outcomes of their younger counterparts. For oesophageal cancer patients, advanced age alone should not be a contraindication for chemoradiotherapy as a part of treatment with curative intent.

PO-0709

Interobserver variation of CT and FDG-PET based GTV for oesophageal cancer: a Dutch nationwide study

M.E. Nowee[1], F.E. Voncken[1], A.N. Kotte[2], L. Goense[3], P.S.N. Van Rossum[3], A.L.H.M.W. Van Lier[2], B.M. Aleman[1], M. Van Vulpen[2], G.J. Meijer[2], I.M. Lips[2]

[1]The Netherlands Cancer Institute, Department of Radiation Oncology, Amsterdam, The Netherlands

[2]University Medical Center Utrecht, Department of Radiation Oncology, Utrecht, The Netherlands

[3]University Medical Center Utrecht, Department of Radiation Oncology and Surgery, Utrecht, The Netherlands

Purpose or Objective: Interobserver variation in target definition is a major contributor to geometric uncertainty in radiotherapy and consistent GTV delineation is crucial in dose escalation studies for oesophageal cancer. The routine use of FDG-PET for target delineation in oesophageal cancer patients treated with chemoradiation is debated in the literature. The aims of this study were to evaluate the interobserver variation of GTV delineation in The Netherlands and the impact of adding FDG-PET to CT images on interobserver variability in patients with oesophageal carcinoma.

Material and Methods: Six cases were included from a prospective database of oesophageal carcinoma patients. All cases underwent a planning FDG-PET/CT scan in treatment position. Twenty upper gastro-intestinal dedicated radiation oncologists from 14 institutes in The Netherlands independently delineated the GTV first on CT, using additional clinical and diagnostic information. Secondly, they adjusted this GTV after CT and FDG-PET images were fused. As general metrics for interobserver variability, volumes and generalized conformity indices were calculated. For visual comparison of interobserver variation observer count maps were generated for each case, i.e. maps of voxels showing the number of enclosing observer delineations. To quantify the interobserver variation at the cranial and caudal border, the distance along the z-axis that contains 5-95% of the observers was used.

Results: Significant differences in delineated GTV volumes were observed in 4 out of 6 cases after addition of FDG-PET to CT (Table 1). In 3 cases there was a significant volume reduction, whereas in one case a significant volume increase was found by PET, caused by unsuspected continuation of the tumour in the stomach. Generalized conformity indices were comparable for CT and FDG-PET/CT (Table 1). Count maps revealed that interobserver variation was mainly located at the cranial and caudal border (Figure 1A). The median observer variation was 26 mm (range 6-36 mm) at the cranial border and 18 mm (range 3-30 mm) at the caudal border (Figure 1B). Even after addition of PET interobserver variation remained more than 20 mm in 4 out of 6 cases (Figure 1B). In 2 cases a reduced interobserver variation was seen with PET/CT at the cranial border and in another 2 cases only at the caudal border. An increased variation was seen with PET/CT compared with CT at the caudal border for the case with the unsuspected FDG uptake in the stomach.

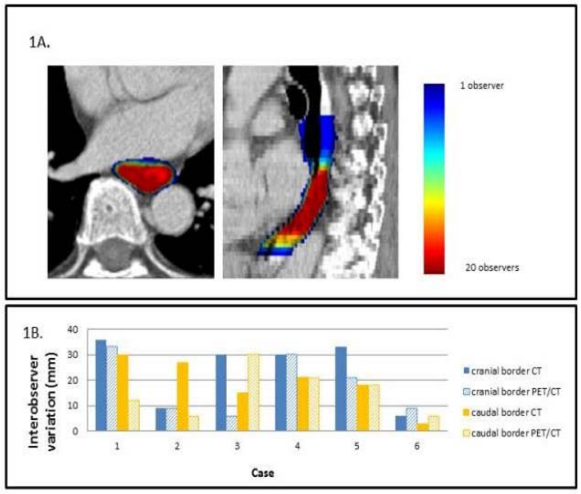

Figure 1A. Observer variation of CT based delineations of 20 observers in case 5, displayed as observer count map overlay on CT. Axial and sagittal view. **1B.** Interobserver variation at the cranial and caudal border of CT based and of FDG-PET/CT based delineations. Interobserver variation was defined as the distance along the z-axis that contains 5-95 % of the observers.

Table 1. Comparison of CT and PET/CT based delineations in 6 oesophageal cancer patients

	Mean volume in cm³ (SD)		CIgen ¹	
Case	CT	PET/CT	CT	PET/CT
1	51.0 (12.3)	53.1 (11.4)	0.67	0.69
2	54.2 (9.4)	49.2 (8.7)*	0.76	0.77
3	65.8 (7.6)	76.7 (12.1)*	0.66	0.69
4	52.0 (13.6)	45.0 (12.7)*	0.62	0.65
5	28.3 (7.5)	26.8 (7.5)	0.58	0.56
6	13.3 (2.3)	12.4 (2.0)*	0.75	0.76

* $p < 0.05$, pairwise t-test

¹ CIgen = generalized conformity index [Kouwenhoven et al. 2009]

Conclusion: This nationwide Dutch contouring study in oesophageal cancer demonstrated that in daily clinical practice considerable GTV delineation variation is present, with variations up to 36 and 30 mm at the cranial and caudal border, respectively. Although FDG-PET significantly impacted the delineated volume in two-thirds of the patients, the addition of PET did not translate into an observer variation below 20 mm in 4 out of 6 cases.

PO-0710

Large interobserver variation of delineated target volumes of pancreatic cancer in the Netherlands

E. Versteijne[1], O. Gurney-Champion[1], A. Van der Horst[1], E. Lens[1], M. Kolff[1], H. Heerkens[2], G. Paardekooper[3], M. Berbee[4], J. Buijsen[5], P. Vande Putte[6], K. Neelis[7], M. Van Herk[8], A. Bel[1], G. Van Tienhoven[1]

[1]Academic Medical Center, Radiation Oncology, Amsterdam, The Netherlands

[2]University Medical Center Utrecht, Radiation Oncology, Utrecht, The Netherlands

[3]Isala Clinics, Radiation Oncology, Zwolle, The Netherlands

[4]Maastro Clincs, Radiation Oncology, Maastricht, The Netherlands

[5]Maastro Clinics, Radiation Oncology, Maastricht, The Netherlands

[6]Catharina Hospital, Radiation Oncology, Eindhoven, The Netherlands

[7]University Medical Center Leiden, Radiation Oncology, Leiden, The Netherlands

[8]University of Manchester, Institute of Cancer Sciences, Manchester, United Kingdom

Purpose or Objective: In pancreatic cancer, the delineation of target volumes on a CT scan can be difficult due to poor contrast between tumour and surrounding tissues. This study quantifies, for pancreatic cancer in the Netherlands, the interobserver variation of delineated gross tumour volume (GTV) and the internal GTV (iGTV: the volume encompassing GTV in all ten phases of the respiratory cycle) on three-dimensional CT (3DCT) and four-dimensional-CT (4DCT), respectively.

Material and Methods: Seven radiation oncologists from six institutions, with an average of 5 irradiated pancreatic patients per year (range: 3–10), delineated pancreatic tumours in four patients with (borderline) resectable pancreatic cancer. First, the GTV was delineated on a contrast-enhanced 3DCT under guidance of an arterial and venous contrast-enhanced diagnostic scan. This contrast-enhanced 3DCT scan was obtained during free breathing, using a GE LightSpeed RT16 scanner. The GTV was expanded with a fixed margin of 5 mm to create the CTV. In the same session, a 4DCT scan, without contrast enhancement, was obtained, during which the respiratory motion of the patient was monitored to reconstruct 10 respiratory phase scans. Second, the iGTV was delineated on the 4DCT, under guidance of the diagnostic CT and expanded with a fixed margin of 5 mm to create an iCTV. Also, a questionnaire concerning experience of the participating radiation oncologists was filled out. We calculated median volumes, encompassing volumes and common volumes of the GTV, iGTV, CTV and iCTV. In addition, the generalized conformity index (CIgen) and overall observer variation were calculated (value of 1 representing full agreement; 0 no agreement). Interobserver variation of 3DCT and 4DCT delineations were analysed and compared.

Results: For all delineated and created volumes, the results of the mean median volumes, encompassing volumes, common volumes and CIgen over all four patients are presented in Table 1. The mean overall standard deviation (SD) (averaged over 4 patients) was 0.54 cm and 0.58 cm on 3DCT and 4DCT, respectively. The CIgen was smaller for 4DCT, indicating larger variations in delineation on 4DCT. Typical differences in delineations between the seven observers are presented in Fig. 1. The radiation oncologists experienced the GTV and iGTV delineations in this study as difficult.

Table 1: The volumes and generalized conformity index CI_{gen} averaged over all 4 patients.

	3DCT GTV	3DCT CTV	4DCT iGTV	4DCT iCTV
Median Volume (cm^3)	20.8	52.2	19.6	48.7
Mean SD (cm)	0.48	0.58	0.42	0.54
Encompassing volume (cm^3)	65.5	129.7	93.9	178.7
Common volume (cm^3)	7.3	22.0	6.1	19.6
CI_{gen}	0.36	0.46	0.27	0.35

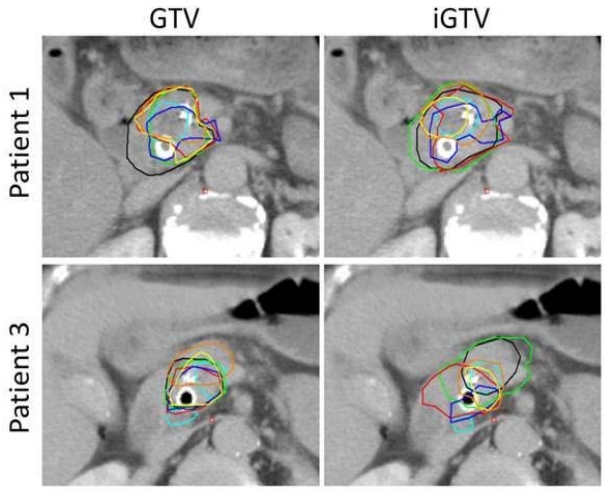

Figure 1: Typical delineations of all seven observers of the GTV and iGTV in two patients projected on the average scan

Conclusion: A considerable interobserver variation in delineation of pancreatic tumours was found, with a mean CIgen of 0.46 for 3DCT (GTV) and 0.35 for 4DCT (iGTV). This indicates a large variation in interpretation of diagnostic CT images and 4DCT images. The limited experience of the observers with delineation as well as the poor contrast between pancreatic cancer and surrounding tissues on CT imaging may have contributed to these results. This should be improved, perhaps by using additional imaging.

PO-0711

Relating CT image heterogeneity to patient outcome in the SCOPE 1 oesophageal cancer trial

R. Carrington[1], E. Spezi[2], S. Gwynne[3], J. Staffurth[4], T. Crosby[5]

[1]*Velindre Cancer Centre, Medical Physics, Cardiff, United Kingdom*

[2]*Cardiff University, School of Engineering, Cardiff, United Kingdom*

[3]*Singleton Hospital, Clinical Oncology, Swansea, United Kingdom*

[4]*Cardiff University, Institute of Cancer and Genetics, Cardiff, United Kingdom*

[5]*Velindre Cancer Centre, Clinical Oncology, Cardiff, United Kingdom*

Purpose or Objective: Heterogeneity is a well recognised feature of malignancy that has been associated with adverse tumour biology (1). There is also initial evidence that it may be a potential prognostic biomarker for oesophageal cancer (2). Using texture analysis, the purpose of this study is to investigate the relationship between CT image heterogeneity and patient outcome in the SCOPE 1 UK wide multi-centre clinical trial on oesophageal cancer.

References

1 Ganeshan B, Miles KA. Quantifying tumour heterogeneity with CT. Cancer Imaging. 2013;13(1):140-9.

2 Yip C, Landau D, Kozarski R, Ganeshan B, Thomas R, Michaelidou A, et al. Primary esophageal cancer: Heterogeneity as potential prognostic biomarker in patients treated with definitive chemotherapy and radiation therapy. Radiology. 2014;270(1):141-8.

Material and Methods: The planning CT images of 215 patients from the SCOPE 1 clinical trial were uploaded to the TexRAD texture analysis software package. The original GTV outlines from the trial were imported on to the relevant DICOM CT images for each patient. Outcome data from the trial (Overall survival (OS) and progression free survival (PFS)) was included for analysis. Texture analysis of the area within

the GTV was undertaken on the images to quantify entropy, uniformity, mean grey-level intensity, kurtosis, standard deviation of histogram and skewness for fine to coarse textures (filters: 0.0-6.0).

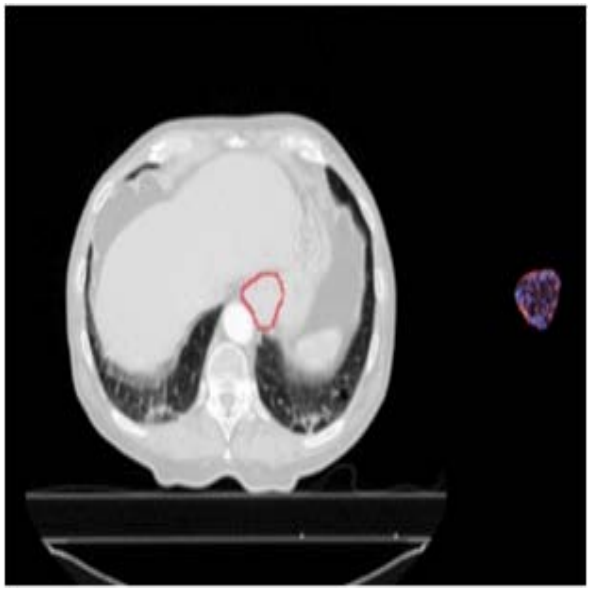

Results: To date, 23 patients from 21 centres entered in the trial have been analysed. Mean Grey Level <399.745, Skewness >2.215, Kurtosis >0.6 were associated with improved PFS (p=0.0227, p=0.0218, p=0.0460 respectively) for medium filter 3.0. For filter 4.0, improved PFS was associated with Mean Grey Level <454.055 (p=0.0227) and Skewness >0.840 (p=0.0371). Mean Grey Levels of <565.535 (p=0.0251) and <542.5(p=0.0251) were associated with improved PFS for filters 5.0 and 6.0 respectively. For OS, mean grey levels of <34.845 (p=0.0182), <399.745 (p=0.0381) and <454.055 (p=0.0381) were associated with improved survival for filters 0.0, 3.0 and 4.0 respectively. An entropy level <5.6 was also found to be significant (p=0.0428) for improved overall survival using filter 2.0.

Conclusion : Normal 0 false false false EN-GB JA X-NONE
We have shown using a 10% sample of the overall database available that CTimage heterogeneity factors are associated with PFS and OS for patients frommultiple centres. Preliminary results therefore suggest that in the future itmay be possible to make clinical treatment decisions based on the CT imageheterogeneity of a tumour volume. This will be confirmed by completing analysison the whole SCOPE 1 database.

PO-0712

Stereotactic body radiotherapy in the treatment of inoperable hepatocellular carcinoma

P. Franco[1], A. Guarneri[1], E. Trino[1], M. Levis[1], F. Giglioli[1], A.R. Filippi[1], R. Ragona[1], U. Ricardi[1]
[1]*Ospedale Molinette University of Turin A.O.U. San Giovanni Battista di Torino, Department of Oncology - Radiation Oncology, Torino, Italy*

Purpose or Objective: To evaluate the feasibility and clinical results of stereotactic body radiation therapy (SBRT) in the treatment of hepatocellular carcinoma (HCC) in patients unsuitable or failing to standard loco-regional therapies.

Material and Methods: Patients with < 3 inoperable HCC lesions with < 6 cm diameter were treated with SBRT. Prescription dose was adapted according to tumor size and global liver function and comprised 48-36 Gy in 3 fractions or 40 Gy in 5 fractions (prescribed on 80 % isodose). Primary endpoint included in-field (LC) local control and toxicity. Secondary endpoints were overall (OS), cancer-specific (CSS) and progression-free survival (PFS).

Results: 82 patients with 120 HCC lesions were treated. Median age was 70 (range 44-90). Most of the patients had Child-Pugh A5-A6 cirrhosis (80.4%), Barcelona Clinic Liver Cancer classification 0-A-B (93%). Median lesion size was 22 mm (range 7-120 mm). Most lesion were in the left lobe (65%). In most patients SBRT was the first local treatment (82%). Up to 7% of patients had portal vein thrombosis. Median observation time was 14 months. Actuarial 1-year LC, PFS, CSS and OS were 76.7% (95%CI:40-92.5%), 13.5% (95%CI:4.9-26-4), 92.1% (95%CI:81.8-96.7%) and 78% (95%CI:66.4-86%), respectively. Up to 18 patients (22%) experienced G3-G4 acute toxicity and 1 case of G5 toxicity was reported. Four cases of classical Radiation-induced liver disease (RILD) were reported, while 21 patients experienced a modification of Child-Pugh classification (25%), mostly of 2-3 points. On multivariate analysis, no factors were predictive for LC while initial Child-Pugh class and > 2 points Child-Pugh classification modification predicted for OS and CSS.

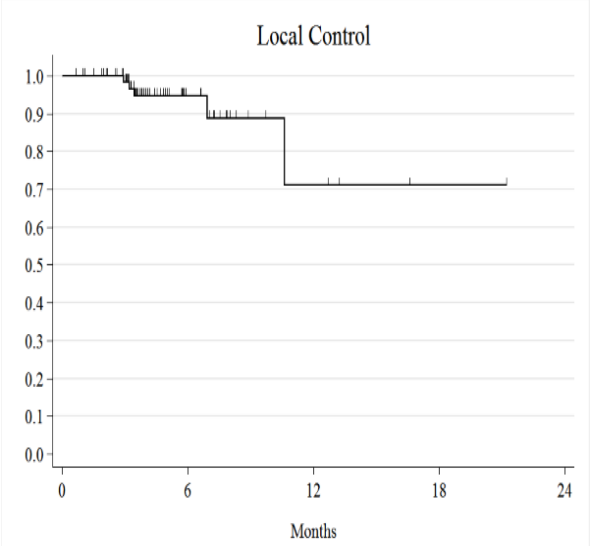

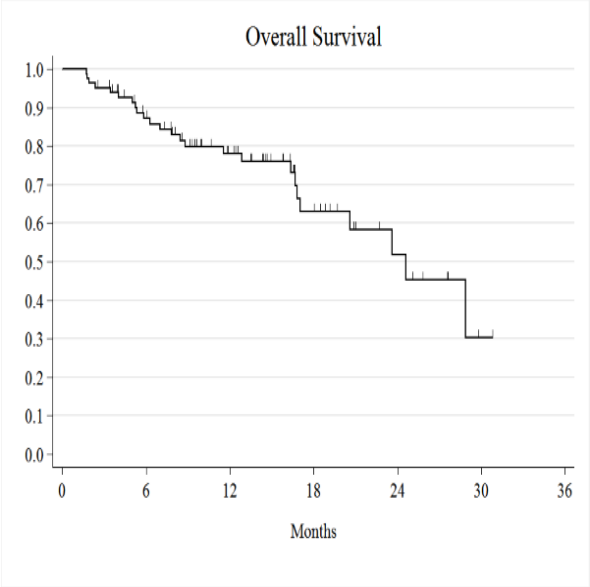

Conclusion: SBRT is a safe and effective treatment option for inoperable HCC, with acceptable LC rate and toxicity profile. Limiting toxic events may have prognostic significance.

PO-0713

Conformity analysis of target-volume definition for margin-directed boost in pancreatic cancer SBRT

D. Holyoake[1], M. Robinson[2], D. Grose[3], D. McIntosh[3], D. Sebag-Montefiore[4], G. Radhakrishna[4], N. Patel[5], S. Mukherjee[2], M. Hawkins[1]

[1]University of Oxford, CRUK/MRC Oxford Institute for Radiation Oncology, Oxford, United Kingdom
[2]Oxford University Hospitals NHS Foundation Trust, Department of Clinical Oncology, Oxford, United Kingdom
[3]The Beatson West of Scotland Cancer Centre, Department of Clinical Oncology, Glasgow, United Kingdom
[4]St James's University Hospital, The St James's Institute of Oncology, Leeds, United Kingdom
[5]Oxford University Hospitals NHS Foundation Trust, Department of Radiology, Oxford, United Kingdom

Purpose or Objective: Margin-directed neoadjuvant pancreatic cancer radiotherapy aims to improve rates of surgical resection with clear margins. The target volume encompasses adjacent/infiltrated vasculature but methods used in its definition have varied and in some cases lacked reproducibility. SPARC (UKCRN ID: 18496) is a CRUK-funded [grant number C43735/A18787] phase 1 study of pre-operative Margin-Intense Stereotactic Radiotherapy for patients with Borderline-Resectable Pancreatic Cancer (BRPC) and incorporates a comprehensive Radiotherapy Quality Assurance protocol to ensure consistency in target definition and radiotherapy delivery.

Material and Methods: On a BRPC test case 'Gold-Standard' structures were defined by two clinical oncologists and one radiologist. A detailed method was specified for derivation of CTV_M, the target structure for the margin-directed boost. GTV_T was contoured to define gross tumour. Conformity analysis metrics were generated to compare structures produced independently by six clinical oncologist investigators with the Gold-Standard.

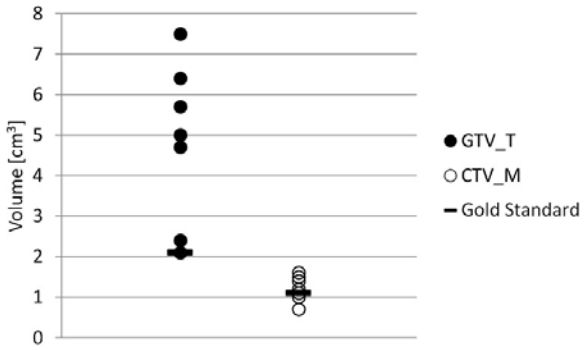

Figure. Absolute volumes of investigator and gold standard structures

Results: Gold-Standard and median investigator volumes for GTV_T were 2.1cc and 5.35cc (IQR 4.1-6.7) respectively, and 1.1cc and 1.3cc (IQR 0.9-1.5) for CTV_M. Median distance between centre of mass of Gold-Standard and investigator volumes was 0.32cm (0.19-0.47cm) for GTV_T and 0.24cm (0.09-0.36cm) for CTV_M. Median DICE conformity coefficients for GTV_T and CTV_M were 0.51 (0.40-0.60) and 0.68 (0.60-0.75), median discordance indices (measurement of over-inclusive contouring) for GTV_T and CTV_M were 0.64 (0.54-0.74) and 0.39 (0.19-0.44).

Conclusion: The investigator CTV_M structures showed less inter-observer variance in volume and less deviation from the Gold-Standard compared with the investigator GTV_T structures. The method of CTV_M definition appears consistently reproducible but accurate delineation of pancreatic malignancies remains difficult and oncologists should have expert radiology support in this task.

PO-0714

Proposal for the delineation of the clinical target volume in biliary tract cancer radiotherapy

J. Socha[1], M. Michalak[2], G. Wołąkiewicz[3], L. Kępka[3]
[1]Regional Oncology Centre Częstochowa, Radiotherapy, Częstochowa, Poland
[2]Independent Public Care Facility of the Ministry of the Interior and Warmian & Mazurian Oncology Center, Diagnostic Imaging, Olsztyn, Poland
[3]Independent Public Care Facility of the Ministry of the Interior and Warmian & Mazurian Oncology Center, Radiotherapy, Olsztyn, Poland

Purpose or Objective: Adjuvant radiotherapy (RT) is frequently used in the treatment of biliary tract cancer (BTC). Accurate target volume delineation is crucial for tumor control and avoiding unnecessary damages. However, there is no consensus on delineation of clinical target volume (CTV) in BTC. The aim of our study is to review the published details of the CTV contouring practice and to propose criteria for the CTV delineation in the adjuvant RT of BTC.

Material and Methods: A comprehensive literature search was performed using the ''PubMed'' and ''Google Scholar'' databases, and articles on BTC radiotherapy that provided descriptions of the CTV contouring were selected. The descriptions were thoroughly reviewed and compared to identify the areas of strong consensus on their inclusion in the CTV among different authors and the areas with more variability that require individual decisions when creating the CTV. Nodal CTV was considered as well as the microscopic tumor spread (MTS) into the liver and along the bile-duct system. Three types of BTC were considered: intrahepatic cholangiocarcinoma (IHC), extrahepatic cholangiocarcinoma (EHC) and gall bladder cancer (GBC). Based on the analyzed data on contouring practice, we proposed a set of guidelines for the CTV delineation.

Results: Out of 52 studies that reported the use of adjuvant RT in BTC, 17 were finally included: one prospective, 13 retrospective and 3 reviews. 1. EHC and GBC (14 relevant studies): the porta hepatic and celiac lymph nodes (LN) were always included into the CTV (100% accordance), the pancreaticoduodenal LN were included in all but one study (93%), whereas for paraaortic LN no agreement exists: four authors (28.5%) mentioned them to be included. Additionally, one author (7%) included the superior mesentery artery nodes for ampullary location. Some data regarding the MTS was reported in three studies: tumor bed was encompassed with 1 cm, 1-1.5 cm and 2-3 cm margin, respectively. One author mentioned 2-4 cm margin to account for MTS along the bile duct. 2. IHC (3 studies): a strong consensus (100% accordance) exists on including the porta hepatic, celiac and pancreaticoduodenal LN into the CTV. Only one author mentioned the para-aortic LNS to be included. Regarding the MTS: two authors used 1 cm margin to cover the tumor bed and resection margin of liver and one author mentioned 2-4 cm margin to account for MTS along the bile duct.

Conclusion:

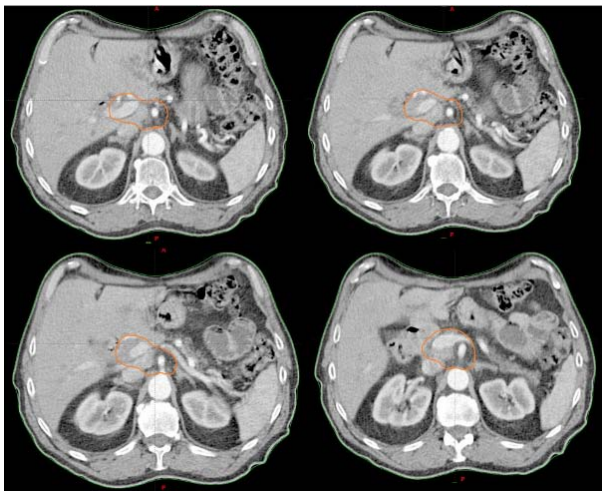

This is the first proposal of the CTV contouring guidelines for adjuvant RT for BTC. We recommend the coverage of porta hepatic, celiac and pancreaticoduodenal LN in all cases of BTC. Para-aortic LN coverage should be considered especially in EHC and GBC, and its use should be individualized. Tumor bed and resection margin of liver should be encompassed

with at least 1cm margin. In view of considerable variability between different authors, there is an obvious need for the international consensus guidelines.

Poster: Clinical track: Lower GI (colon, rectum, anus)

PO-0715

Chemoradiation with concomitant boost in rectal cancer (T4&recurrences): a phase II study

V. Picardi[1], G. Macchia[1], M. Di Bartolomeo[1], M. Giordano[1], M. Nuzzo[1], L. Caravatta[2], M.A. Gambacorta[3], L. Di Lullo[4], A. Guido[5], L. Giaccherini[5], L. Fuccio[6], R. Golfieri[7], D. Cuicchi[6], G. Ugolini[6], S. Cammelli[5], G. Frezza[8], A.G. Morganti[5], V. Valentini[3], F. Deodato[1]

[1]*Fondazione di Ricerca e Cura "Giovanni Paolo II"- Catholic University of Sacred Hea, Radiation Oncology Unit, Campobasso, Italy*

[2]*P.O. Businco, Radiotherapy Unit- Centro di Radioterapia e Medicina Nucleare, Cagliari, Italy*

[3]*Policlinico Universitario "A. Gemelli"- Catholic University of Sacred Heart, Department of Radiotherapy, Roma, Italy*

[4]*"F. Veneziale" Hospital, Oncology Unit, Isernia, Italy*

[5]*S. Orsola-Malpighi Hospital- University of Bologna, Radiation Oncology Center- Department of Experimental- Diagnostic and Specialty Medicine – DIMES, Bologna, Italy*

[6]*S. Orsola-Malpighi Hospital- University of Bologna, Department of Medical and Surgical Sciences - DIMEC, Bologna, Italy*

[7]*S. Orsola-Malpighi Hospital- University of Bologna, Radiology Department, Bologna, Italy*

[8]*Bellaria Hospital, Radiotherapy Department, Bologna, Italy*

Purpose or Objective: Aim of this clinical study was to evaluate resectability and pathological response after preoperative concurrent chemotherapy with 2 different drugs and radiation therapy (RT) intensified with concomitant boost.

Material and Methods: A clinical trial based on two-stage Simon's design was planned. The trial included a first phase with enrolment of 9 patients. If 0/9 patients had complete pathologic response (pCR) the study had to be closed. In case of ≥ 1/9 patients with pCR it was planned to enrol other 8 patients. RT was performed with 3D-conformal technique. The dose to mesorectum and pelvic lymph nodes was 45 Gy (1.8 Gy/fraction). A concomitant boost was delivered to GTV + 2 cm margin with a total dose of 55 Gy (2.2 Gy/fraction). The following concurrent chemotherapy was administered: Raltitrexed (3 mg/m2) and Oxaliplatin (130 mg/m^2) on days 1, 17, 35 of RT. Acute and late toxicities were evaluated according to CTC-AE v.3.0 criteria.

Results: All 9 patients enrolled in the 1st phase underwent radical surgical resection, with 4/9 pCR. Then, 9 additional patients were enrolled for a total of 18 patients (F: 8, M: 10; median age 64.5, range: 45-80; clinical stage: 2 local recurrences, 16 cT4, 6 cN0, 4 cN1, 7 cN2, 1 cN3). Seventeen patients underwent surgical resection (7 anterior resections and 9 abdominal-perineal amputation) while 2 patients did not undergo surgery for early metastatic progression (1) or surgery refusal (1). R0 resection was achieved in all patients who underwent surgery. Overall, 5 patients had pCR and 2 patients showed only microscopic residual disease (pT0-Tmic: 7/17 = 41.2%). Acute grade≥ 3 toxicity was: 1 leucopoenia - neutropenia, 1 liver toxicity, 5 gastro-intestinal toxicities, with an overall incidence of 7/18 patients (38.9%). The actuarial analysis showed the following 2-year results: local control 100%, metastasis-free survival 93.7%, overall survival 92.3%.

Conclusion: The regimen used in this study allowed to achieve complete and near-complete response rate higher than 40%, despite the advanced stage of disease. However, severe acute toxicity was reported in more than 1/3 of patients.

PO-0716

Preoperative chemoradiation with VMAT-SIB in rectal cancer: a phase II study (Grace-Rectum-1)

V. Picardi[1], G. Macchia[1], S. Cilla[2], M. Di Bartolomeo[1], M. Giordano[1], F. Rotondi[3], M.A. Gambacorta[4], F. Deodato[1], L. Ronchi[5], A. Farioli[6], A. Guido[5], G. Siepe[5], G. Compagnone[7], A. Ardizzoni[8], S. Cammelli[5], G. Frezza[9], V. Valentini[4], A.G. Morganti[5]

[1]*Fondazione di Ricerca e Cura "Giovanni Paolo II"- Catholic University of Sacred Heart, Radiation Oncology Unit, Campobasso, Italy*

[2]*Fondazione di Ricerca e Cura "Giovanni Paolo II"- Catholic University of Sacred Heart, Medical Physics Unit, Campobasso, Italy*

[3]*Fondazione di Ricerca e Cura "Giovanni Paolo II"- Catholic University of Sacred Heart, Department of Oncologic Surgery, Campobasso, Italy*

[4]*Policlinico Universitario "A. Gemelli"- Catholic University of Sacred Heart, Department of Radiotherapy, Roma, Italy*

[5]*S. Orsola-Malpighi Hospital- University of Bologna, Radiation Oncology Center- Department of Experimental- Diagnostic and Specialty Medicine – DIMES, Bologna, Italy*

[6]*S. Orsola-Malpighi Hospital- University of Bologna, Department of Medical and Surgical Sciences - DIMEC, Bologna, Italy*

[7]*S. Orsola-Malpighi Hospital- University of Bologna, Department of Medical Physics, Bologna, Italy*

[8]*S. Orsola-Malpighi Hospital- University of Bologna, Department of Medical Oncology, Bologna, Italy*

[9]*Bellaria Hospital, Radiotherapy Department, Bologna, Italy*

Purpose or Objective: Aim of this analysis was to describe the results of a phase II study based on the use of VMAT in preoperative combined treatment of locally advanced rectal cancer.

Material and Methods: A clinical trial based on two-stage Simon's design was planned. The trial includes a 1st phase enrolment of 9 patients. If 0/9 patients had complete pathologic response (pCR) the study had to be closed. In the case of ≥ 1/9 patients with pCR it was scheduled to enrol other 8 patients. Radiation therapy was performed using VMAT-SIB technique. The dose to mesorectum and pelvic lymph nodes was 45 Gy (1.8 Gy/fraction). A concomitant boost was delivered on GTV + 2 cm margin with a total dose of 57.5 Gy (2.3 Gy/fraction). The following concomitant chemotherapy was administered: Capecitabine (825 mg/m^2 twice daily, 5 days/week) and Oxaliplatin (130 mg/m^2 on days 1, 17, 35). Acute and late toxicities were evaluated according to CTC-AE v. 3.0 criteria.

Results: All 9 patients enrolled in the 1st phase underwent radical surgical resection, with 4/9 pCR. Then 9 additional patients were enrolled for a total of 18 patients (F: 7, M: 11; median age 62, range: 39-79); clinical stage: 4 local recurrences, 6 cT4, 5 cT3, 3 cT2, 2 cN0, 7 cN1, 9 cN2). Sixteen patients underwent surgical resection (9 anterior resection, 6 abdominal perineal amputations and 1 trans-anal resection) while 2 patients did not undergo surgery for early metastatic progression (1) or death from acute pulmonary oedema prior to surgery (1). R0 resection was achieved in all patients who underwent surgery. Overall, 4 patients had a pCR and 7 patients only a microscopic residual of disease (pT0-Tmic: 11/18 = 61.1%). Acute grade≥ 3 toxicity was: 1 leukopenia-neutropenia, 1 skin toxicity, 1 genitourinary toxicity and 5 gastrointestinal toxicities, with an overall incidence (considering the patient who died after radio chemotherapy) of 7/18 patients (38.9%). The actuarial analysis reported the following 2-year results: local control 80%, metastasis-free survival 93.7%, overall survival 88.9%.

Conclusion: The regimen used in this study showed excellent results in terms of pathologic responses (pT0-Tmic: 61.1%). However, despite the use of VMAT technique, more than 1/3 of patients had severe acute toxicity.

PO-0717

Serum miR-345-5p predicts pathological response to chemoradiotherapy in local advanced rectal cancer

J. Yu[1], N. Li[1], J. Jin[1]
[1]*Cancer Hospital- CAMS, Radiation Oncology, Beijing, China*

Purpose or Objective: Neoadjuvant chemoradiation(nCRT) has been represented as the standard treatment for locally advanced rectal cancer(LARC). Tumor pathological responses and radiotherapeutic sensitivity alter variously. We aimed to explore the predict value of serum circulating miRNAs, which have already been certificated as potential therapeutic predictors in many cancers for the pathological responses and radiosensitivity after nCRT in LARC patients.

Material and Methods: Six fresh tumor biopsy samples of T3-4/N+ rectal cancer patients were collected before any treatments and these samples were classified as radiation sensitive and resistant groups according to the postoperative pathological analysis assessed by Mandard TRG scale(3 samples of TRG1 vs 3 samples of TRG4). The two groups were strictly matched by clinical features. miRNAs expression profile of the two groups were analyzed by microarray. Predictive value of radiotherapeutic sensitivity of the candidated miRNAs was further validated by 160 serum samples of LARC patients.

Results: 19 miRNAs were identified to have different expression profile between radiation sensitive and resistant groups by microarray analysis (p<0.05). Among these miRNAs, nine miRNAs were down-regulated and ten were up-regulated in radiation sensitive group. miR-345-5p was identified significantly correlated with radiation resistant to nCRT and appeared highly discrepant expression between the two groups (fold change>2). Low expression of miR-345-5p in serum predicted superior pathological responses to radiosensitivity after nCRT (TRG1/2) (AUC=0.69, p<0.001) and favorable LRFS (p=0.02).

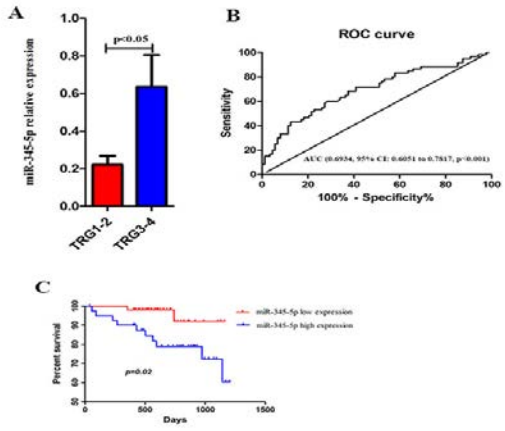

Fig 1. A: Comparison of miR-345-5p expression levels between radiation sensitive and resistant groups Statistical significance was determined by the Mann-Whitney U test; B: Predictive value of pathological responses by miR-345-5p was determined by a ROC curve test; C: Low expression of miR-345-5p was correlated with superior of LRFS.

Conclusion: Serum level of miR-345-5p is associated with favorable pathological responses to neoadjuvant chemoradiotherapy and local-regional control ratio in LARC patients. It presents as a promising biomarker to predict the radiotherapy sensitivity and prognosis.

PO-0718

The significance of postop CEA after preoperative CRT followed by TME in advanced rectal cancer

S. Jeong[1], J.H. Lee[1], S.H. Kim[1], H.M. Cho[2], B.Y. Shim[3], D.Y. Kim[4], T.H. Kim[4], S.Y. Kim[4], J.Y. Baek[4], J.H. Oh[4], T.K. Nam[5], M.S. Yoon[5], J.U. Jeong[5], K. Kim[6], E.K. Chi[6], H.S. Jang[7], J.S. Kim[8], J.H. Kim[9], B.K. Jeong[10]
[1]*St. Vincent Hospital- College of Medicine- The Catholic University of Korea, radiation oncology, Suwon- Kyeonggi-do, Korea Republic of*
[2]*St. Vincent Hospital- College of Medicine- The Catholic University of Korea, surgery, Suwon- Kyeonggi-do, Korea Republic of*
[3]*St. Vincent Hospital- College of Medicine- The Catholic University of Korea, internal medicine, Suwon- Kyeonggi-do, Korea Republic of*
[4]*Research Institute and Hospital- National Cancer Center, Center for Colorectal Cancer, Goyang, Korea Republic of*
[5]*Chonnam National University Hospital, Radiation Oncology, Hwasun, Korea Republic of*
[6]*Seoul National University Hospital- College of Medicine, Radiation Oncology, Seoul, Korea Republic of*
[7]*Seoul St. Mary`s Hospital- College of Medicine- The Catholic University of Korea, Radiation Oncology, Seoul, Korea Republic of*
[8]*Seoul National University Bundang Hospital- College of Medicine, Radiation Oncology, Bundang, Korea Republic of*
[9]*Dongsan Medical Center- Keimyung University School of Medicine, Radiation Oncology, Daegu, Korea Republic of*
[10]*Gyeongsang National University School of Medicine, Radiation Oncology, Jinju, Korea Republic of*

Purpose or Objective: To evaluate the significance of postoperative carcinoembryonic antigen (CEA) level as a predictor for tumor recurrence and as a prognostic factor for survival in locally advanced rectal cancer patients treated with preoperative concurrent chemoradiation followed by curative surgery

Material and Methods: Total 1559 rectal cancer patients staged with cT3-4N0-2M0 received pelvic preoperative chemoradiotherapy (CRT) 50.4 Gy in 28 fractions followed by total mesorectal excision (TME). CEA levels were measured before CRT and after surgery. Clinicopathologic factors which could be associated with tumor recurrence and survival were analyzed.

Results: The cumulative probability of the tumor recurrence showed a steep increase with a cutoff value of 2.5 ng/mL for postoperative CEA, and the gradient decreased as postoperative CEA levels increased above 2.5 ng/mL. After median follow-up time of 46.7 months, patients with postoperative CEA level of > 2.5 ng/mL had significantly lower relapse-free survival (75.6% vs. 65.2%, p<0.001) and overall survival (88.3% vs. 78.1%, p<0.001) at 5 years than patients with CEA level of≤2.5 ng/mL. In the multivariate analysis, postoperative CEA level is the only significant prognostic factors of relapse free survival (HR=1.561 and 95% CI=1.221-1.996, p<0.001) and overall survival (HR=2.073 and 95% CI=1.498-2.869, p<0.001). Increased pre-CRT CEA level is not a significant prognostic factor with consideration of postoperative CEA in multivariate analysis. The postoperative CEA level above 2.5 ng/ml is a significant predictor for distant recurrence (OR=1.689 and 95% CI=1.188-2.402, p=0.004), but not for local recurrence (OR=0.776 and 95% CI=0.389-1.549, p=0.472).

Conclusion: Postoperative CEA level above 2.5 ng/ml is a predictor for tumor recurrence and a negative prognostic factor for survival in rectal cancer patients who received preoperative CRT and curative surgery. Physician can consider intense surveillance after curative resection in these patient.

PO-0719

Target delineation of anal cancer based on MR or PET – an inter-observer, inter-modality study

E. Rusten[1,2], B.L. Rekstad[1], C. Undseth[3], G. Al-Haidari[3], B. Hanekamp[4], E. Hernes[5], T.P. Hellebust[1], E. Malinen[1,2], M. Guren[3]
[1]*Oslo University Hospital, Dept of Medical Physics, Oslo, Norway*
[2]*University of Oslo, Biophysics and medical physics, Oslo, Norway*
[3]*Oslo University Hospital, Dept of Oncology, Oslo, Norway*

[4]Oslo University Hospital, Dept of Radiology, Oslo, Norway
[5]Oslo University Hospital, Dept of Radiology and Nuclear Medicine, Oslo, Norway

Purpose or Objective: Anal cancers are treated by definitive chemoradiotherapy of the primary tumor and pelvic nodes. Although survival is high (5y 75%), locoregional recurrence occurs in 24% of patients. Patients are mostly treated with IMRT and VMAT, and therefore precise dose delivery is important. For target volume delineation typically either PET or MRI is used together with planning CT, but practice varies between institutions. In the current work, we aim to investigate the variability between imaging modalities and oncologists with respect to target volume delineation based on either PET/CT or MRI/CT information.

Material and Methods: Twenty patients with anal cancer referred to chemoradiotherapy were prospectively included. Written informed consent was obtained from all patients and the regional ethics committee approved the study. Prior to therapy, patients underwent a planning CT scan, a PET/CT scan with 18FDG and T2 and diffusion weighted MRI scans at a 3T scanner. At the treatment planning station (Varian Eclipse), all images where co-registered to the planning CT scan. Three oncologists delineated the Gross tumor volume (GTV) independently of each other twice for each patient, once with medical records and images blinded for MRI information, and once blinded for PET information. The CT image information was always available. A randomization scheme of the order of the anonymized patients was used during delineation to minimize intra-observer bias. All volumes were exported from the treatment planning system, analyzed by calculating the DICE coefficients and compared with the Wilcoxon Signed-rank test.

Results: The median volume of the GTV was respectively 27.5 cm3 and 31.0 cm3 for PET and MRI, and there was a high correlation (r=0.94) between the volumes. The DICE coefficient (minimum, median, maximum) was 0.43, 0.81, 0.93 and 0.50, 0.75, 0.89 for PET and MRI. These DICE distributions were significantly different (P=0.03). Half of the patients with low DICE (<0.7) for PET, also gave low DICE for MRI, this indicated difficulties with delineation irrespective of imaging modality. For inter-modality comparison (PET to MRI for same observer), the DICE coefficient was 0.31, 0.75, 0.92, with a significant difference in distribution relative to the inter-observer distribution.

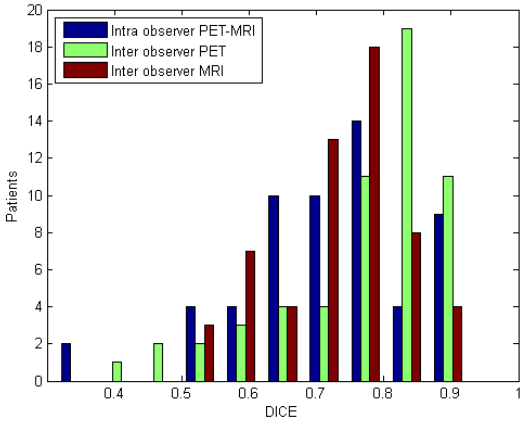

Conclusion: PET and MRI produced similar GTV volumes for radiotherapy planning of anal cancer. However, PET has a significantly lower inter-observer variability in terms of the DICE coefficients. Still, the deviations between PET and MRI were not substantial and may not translate into clinically meaningful differences. This is also supported by the relatively high inter-modality DICE coefficients. Thus, radiotherapy target delineation for anal cancer is performed quite consistently among observers and is not strongly dependent on whether PET or MRI is used.

PO-0720

High tumour glycine concentration – an adverse prognostic factor in locally advanced rectal cancer

K. Redalen[1], B. Sitter[2], T. Bathen[3], K. Grøholt[4], K. Hole[5], S. Dueland[6], K. Flatmark[7], A. Ree[1], T. Seierstad[5]
[1]Akershus University Hospital, Department of Oncology, Lørenskog, Norway
[2]Sør-Trøndelag University College, Department of Health Science, Trondheim, Norway
[3]Norwegian University of Science and Technology, Department of Circulation and Medical Imaging, Trondheim, Norway
[4]Oslo University Hospital, Department of Pathology, Oslo, Norway
[5]Oslo University Hospital, Department of Radiology and Nuclear Medicine, Oslo, Norway
[6]Oslo University Hospital, Department of Oncology, Oslo, Norway
[7]Oslo University Hospital, Department of Gastroenterological Surgery, Oslo, Norway

Purpose or Objective: In locally advanced rectal cancer (LARC), further advances in individualised treatment approaches require identification of robust biomarkers. Although metabolic reprogramming has been regarded essential for cancer cell proliferation, the systematic characterisation of activated metabolic pathways in aggressive cancer is scarce. Hence, by recognising the link between altered tumour metabolism and disease aggressiveness, we aimed to identify associations between pretreatment tumour metabolic profiles and therapeutic outcome in LARC.

Material and Methods: Tumour metabolic profiles were acquired from 54 LARC patients, receiving induction neoadjuvant chemotherapy followed by long-course chemoradiotherapy and surgery, by using high-resolution magic angle spinning magnetic resonance spectroscopy. Metabolite concentrations were correlated to TNM and presence of disseminated tumour cells (DTC) at time of diagnosis, and to ypTN and tumour regression grade (TRG) following the neodjuvant treatment. All patients had either reached 5 years of follow-up or were scored with a progression-free survival (PFS) event at time of analysis. The performance of metabolite concentrations in prediction of PFS was assessed by receiver operating characteristic curves. Univariate Cox regression assessed associations between selected variables and PFS; those being significant were entered into multivariate analysis. Survival differences were assessed by the Kaplan-Meier method.

Results: Pretreatment tumour metabolite concentrations showed no significant associations to TNM, DTC, ypTN or TRG. In univariate regression analysis, high concentrations of glycine, creatine and myo-inositol were significantly associated to poor PFS, with distant metastasis to the lung and/or liver being the main PFS event (87.5% of events). When separating patients above and below the identified cut-off concentrations the respective estimated 5-year PFS were 85% and 50% for glycine, 74% and 29% for creatine and 81% and 50% for myo-inositol. In multivariate analysis, high glycine concentration remained most significantly associated to poor PFS (hazard ratio = 4.4, 95% confidence interval = 1.4–14.3, p = 0.008).

Conclusion: High tumour glycine concentration was identified as adverse prognostic factor for PFS in LARC. In a patient population treated with curative intent but with metastatic disease as main PFS event these results motivate further investigations of glycine as early predictor of metastatic progression and as potential therapeutic target.

PO-0721

Impact of sentinel lymph-node biopsy on staging and treatment in patients with anal cancer

N. Slim[1], C. Gumina[1], P. De Nardi[2], A. Tamburini[2], C. Canevari[3], M. Ronzoni[4], G. Bordogna[4], V. Ricci[1], C. Fiorino[5], R. Rosati[2], N. Di Muzio[1], P. Passoni[1]
[1]*Ospedale San Raffaele IRCCS, Radiation Oncology, Milan, Italy*
[2]*Ospedale San Raffaele IRCCS, Surgery, Milan, Italy*
[3]*Ospedale San Raffaele IRCCS, Nuclear medicine, Milan, Italy*
[4]*Ospedale San Raffaele IRCCS, Medical Oncology, Milan, Italy*
[5]*Ospedale San Raffaele IRCCS, Medical Physics, Milan, Italy*

Purpose or Objective: The prophylactic inguinal lymph-nodes (LNs) radiotherapy (RT) is considered the standard treatment, however it implies more toxicity. Moreover, inguinal recurrence occurs in 0%-12% of T1-T2, and 19%-30% of T3-T4 patients (pts) who did not receive prophylactic inguinal RT. So, 70%-81% of T3-T4 pts are uselessly irradiated, and 0%-12% of T1-T2 pts should be treated. An improvement of staging is mandatory. Aim of this study is to evaluate the role of sentinel lymph-node biopsy (SLNB) in staging and treatment of pts with anal cancer.

Material and Methods: Patients with squamous cell carcinoma of anal canal were staged with physical examination, endoscopy, chest and abdomen CT, pelvic MR, and simulation FDG-PET. Pts without gross inguinal LN metastasis were candidate for the lymphoscintigraphy with 99mTC nanocolloid. The CTV included the GTV (primary tumour and positive LNs), mesorectum, internal and common iliac LNs. As the inguinal RT was considered standard, the radiation oncologists were left free to decide whether irradiate this region independently from the clinical stage and the SLNB histological results. PTV1 and PTV2 corresponded to GTV and CTV, respectively, with a margin of 0.5 cm. Prescribed dose was 50.4Gy in 28 F to the PTV2, and 64.8Gy in 36 F, as sequential boost, to the PTV1. IMRT or Volumetric Modulated Arc Therapy (VMAT) were used. Concomitant chemotherapy consisted of 2 cycles of Mito-C 10 mg/m2, and continuous infusion 5-FU 1000 mg/m2/day for 4 consecutive days.

Results: From 3/2008 to 2/2014, 48 consecutive pts were treated (T1=9, T2=15, T3=16, T4=8). PET was performed in 42 out of the 48 pts, and 27 out of these 42 pts underwent lymphoscintigraphy. Pathologic inguinal uptake was shown in 15/42 (36%) pts. Lymphoscigraphy was performed in 9 out of these 15 pts. Histological examination was performed in 8 pts (SLN not found in 1 pt) and confirmed inguinal metastasis in 3/8 pts (37.5%) but did not confirmed metastasis in 5 pts (62.5%). PET did not show pathologic uptake in 27/42 pts (64%). Lymphoscintigraphy was performed in 18 out of these 27 pts: SLN was not found in 1 pt. Histological examination found metastasis in 2/17 (12%) and confirmed the absence of metastasis in 15 pts (88%). Thirty-one pts received prophylactic or curative RT to the groins, the “Groin group”, and 17 pts did not , the “No groin group”. All the 17 pts of the “No groin group” underwent SLNB procedure: 16 pts had SLNB histologically negative, 1 pt had lymphoscintigraphy negative (SLN not found) and PET negative; two pts with PET positive in right inguinal LN but ipsilateral SLNB negative were not irradiated. No pt in both groups had inguinal relapse or progression. Of note, median follow up duration in the “No groin group” was 41 months (19.2-90.7 months).

Conclusion: SLNB can further improve the PET based staging and select the “true negative” patients for which the inguinal LN irradiation could be avoided.

PO-0722
Stereotactic ablative radiatiotherapy for lung oligometastatic patients with colorectal cancer

L. Agolli[1], V. Maurizio[2], N. Luca[2], D.S. Vitaliana[2], O. Mattia F[2]
[1]*Azienda Ospedaliera Sant' Andrea, Department of Radiation Oncology, Rome, Italy*
[2]*Sant'Andrea Hospital, Radiation Oncology, Rome, Italy*

Purpose or Objective: to evaluate efficacy and tolerability of stereotactic ablative radiotherapy (SABR) in the treatment of patients with colorectal cancer with exclusive oligometastases to the lung.

Material and Methods: we treated 62 lung metastases in 38 patients with oligometastatic colorectal cancer. Inclusion criteria were: primary tumor controlled, ≤ 5 lung metastases, no other active sites of disease at the time of the SABR. Dose prescription was: 23Gy/1 fr per central lesion <30 cc (18 lesions), 30Gy/1fr for peripheral metastases <30 cc (35 lesions), 45Gy/3fr for peripheral lesion >30cc (9 lesions). Twenty patients had 1 metastasis (53%), 14 patients had 2 metastases (37%)and 4 patients tree-to-four metastases (10%). Median BED was 120 Gy. OS, PFS, MFS, local control and toxicity were evaluated.

Results: median follow-up was 24 months (ranged 3-76 mo). Median actuarial survival was 34 months (c.i. 20-47 months). Overall survival (OS) at 1-, 2- and 5-years was 80%, 50.7% and 26.9% respectively. Complete response (CR) was achieved in 22/62 lesions (35.4%). Median disease-free survival (DFS) was 24 months (ranged 13-34 months). DFS at 1-, 2- and 5-years was 79.8% and 40.4% and 22%, respectively. Complete response (CR) was the only prognostic factor significantly correlated with OS, PFS and metastasis-free survival (MFS) (p= 0.001 in each case). Patients with CR had 1-,2- and 5-years OS of 100%, 90.9% and 67.3%, while patients with partial response (PR) and stable disease (SD) had respectively 69.2, 34.6% and 0% and 63.5% at 1 and 2-years and 15.9% at 5-years. Acute G1-2 lung toxicity, according to the CTCAE-V4.0, was 10%, G3 lung toxicity was 1.6%. Late G1-2 toxicity rate was 25%. No late G3 toxicity was found.

Conclusion: SABR has a high rate of local control in the lung metastasis from colorectal cancer and also affect survival. CR statistically correlated with OS, PFS and MFS, even at long-term. There is a need of prospective trials to confirm these data and to identify the right selection criteria and the best timing with systemic therapies.

Poster: Clinical track: Gynaecological (endometrium, cervix, vagina, vulva)

PO-0723
Short time interval between radiation and hyperthermia improves treatment outcome in cervical cancer

C.M. Van Leeuwen[1], A.L. Oei[1], K.W.T.K. Chin[1], L.J.A. Stalpers[1], A. Bel[1], J. Crezee[1], N.A.P. Franken[1], H.P. Kok[1]
[1]*Academic Medical Center, Radiation Oncology, Amsterdam, The Netherlands*

Purpose or Objective: To determine the effect of the time interval between external beam radiotherapy (EBRT) and hyperthermia (HT) treatments on locoregional recurrence and overall survival of patients with cervical cancer.

Material and Methods: This retrospective study included 59 women with locally advanced (stage IB2-IVA) cervical cancer, all treated with radiotherapy and HT. Additional treatment with chemotherapy was reason for exclusion.
Patients received four to five weekly HT treatments concurrent with 23-28 fractions (1.8-2.0 Gy) EBRT and a brachytherapy boost (20-24Gy). On HT treatment days, HT was given after EBRT. The mean time interval between the EBRT and HT treatments that were delivered on the same day was used to characterize the typical time interval for that patient. The median thereof (79.2 minutes) was used to split the cohort in a ‘short’ and ‘long’ time-interval group. Median time intervals were 65.8 minutes (range 33.8-79.2) and 91.7 minutes (range 80.0-125.2) for the short and long time-interval group, respectively.
Locoregional recurrence and overall survival were estimated using Kaplan-Meier analysis, and compared by a log-rank test. To correct for any potential confounding factors, a stepwise Cox regression analysis using backward elimination was used with time-interval group, age, FIGO stage, number of HT treatments, tumour temperature during HT treatment (T90), lymph node status and smoking as covariates.

Results: Locoregional recurrence was significantly lower in the short time-interval group (Fig. 1). Recurrence rate at 2 years was 11% (95%CI 3-36%) in the short time-interval group compared to 49% (95%CI 30-73%) in the long time-interval group. The stepwise Cox regression identified time-interval (a short interval is better), T90 (higher temperatures are beneficial) and age (younger age is unfavourable) as significant prognostic factors, and shows a favourable trend for lower FIGO stage (Table 1).
Overall survival was also significantly better in the short time-interval group (Fig. 1). Overall survival at 2 years was 60% (95%CI 39-75%) in the short group compared to 39% (95%CI 21-56%) in the long time-interval group. The stepwise Cox regression identifies a short time-interval and higher T90 as significant factors for a favourable outcome (Table 1).

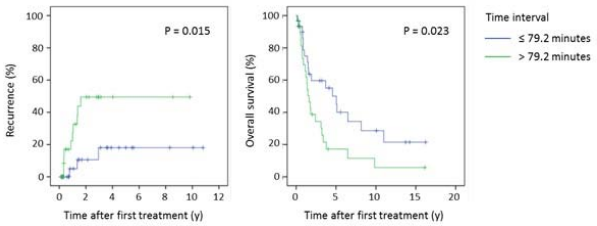

Fig. 1. Kaplan-Meier curves for locoregional recurrence (left) and overall survival (right) after EBRT and HT for advanced cervical cancer, grouped by time-interval between EBRT and HT.

Table 1 Results of the Cox multivariable analysis of locoregional recurrence and survival after radiotherapy and hyperthermia for advanced cervical cancer.

Outcome	Factor	Hazard ratio (95%CI)	P-value
Recurrence	Time-interval	6.7 (1.6-28)	0.008
	T90	0.31 (0.13-0.72)	0.007
	Age	0.93 (0.89-0.97)	0.002
	Stage	4.5 (0.96-21)	0.057
Overall survival	Time-interval	2.2 (1.2-4.2)	0.014
	T90	0.57 (0.38-0.86)	0.008

Conclusion: A short time interval between EBRT and HT results in a significantly lower recurrence and better overall survival for locally advanced cervical cancer patients. Furthermore, a higher tumour temperature during HT is associated with lower locoregional recurrence and better overall survival, stressing the importance of HT quality assurance.

PO-0724

Adjuvant SIB-VMAT in endometrial cancer: a dose escalation study

G. Macchia[1], S. Cilla[2], F. Deodato[1], M. Nuzzo[1], A. Ianiro[2], M. Marucci[1], G. Perrella[1], C. Digesù[1], V. Valentini[3], M. Ferioli[4], F. Bertini[4], A. Galuppi[4], M. Perrone[5], P. De Iaco[5], S. Cammelli[4], G. Frezza[6], A.G. Morganti[4]
[1]*Fondazione di Ricerca e Cura "Giovanni Paolo II"- Catholic University of Sacred Heart, Radiation Oncology Unit, Campobasso, Italy*
[2]*Fondazione di Ricerca e Cura "Giovanni Paolo II"- Catholic University of Sacred Heart, Medical Physic Unit, Campobasso, Italy*
[3]*Policlinico Universitario "A. Gemelli"- Catholic University of Sacred Heart, Department of Radiotherapy, Roma, Italy*
[4]*S. Orsola-Malpighi Hospital- University of Bologna, Radiation Oncology Center- Department of Experimental- Diagnostic and Specialty Medicine – DIMES, Bologna, Italy*
[5]*Sant'Orsola-Malpighi Hospital, Gynecologic Oncology Unit, Bologna, Italy*
[6]*Bellaria Hospital, Radiation Department, Bologna, Italy*

Purpose or Objective: To define the recommended dose in high-intermediate risk endometrial cancer (HIR-EC) patients postoperatively irradiated by simultaneous integrated boost volumetric modulated arc therapy (SIB-VMAT).

Material and Methods: A radiation dose of 45 Gy over 5 weeks, 1.8 Gy/fraction, was delivered to the vagina and the lymphatic drainage (planning target volume, PTV2). Radiation dose was escalated to the upper two thirds of vagina (PTV1) with the SIB-VMAT strategy, after 1 year follow up of the first 15 patients. Two dose levels were planned: Level 1 (PTV2: 45/1.8 Gy; PTV1: 55/2.2 Gy), and Level 2 (PTV2: 45/1.8 Gy; PTV1: 60/2.4 Gy). All treatments were delivered in 25 fractions. Patients were treated according to a Phase I-II dose-escalation study. Toxicity was scored by CTC-AE v. 3.0 scale.

Results: Sixty-six HIR-EC patients were enrolled. The Level 1 group included 38 patients while Level 2 group included 28 patients. Clinico-pathological characteristics of the two groups are reported in Table 1. All patients completed radiation treatment without interruption. No differences were found between the 2 groups in terms of skin, gastrointestinal and genitourinary toxicities.

Table 1: Patients characteristics and toxicity (CTC v 3.0); number in brackets are percentages

		Level 1	Level 2	p
N° Patients (%)		38 (57.5)	28 (42.5)	ns
Age, years (median; range)		64; 45-84	64; 47-82	ns
BMI (average ± DS)		31.5 ± 7.7	29.3 ± 5.1	ns
FIGO Stage				
	IA	6 (15.5)	8 (28.5)	ns
	IB	13 (34.2)	6 (21.5)	
	II	11 (28.7)	6 (21.5)	
	III-IV	8 (21.6)	8 (26.5)	
Grading				
	1	3 (7.9)	2 (7.1)	ns
	2	21 (55.2)	12 (42.8)	
	3	14 (36.9)	14 (50.0)	
Adjuvant CT before RT				
	Yes	15 (39.5)	14 (50.0)	ns
	No	23 (60.5)	14 (50.0)	
Skin Toxicity	Grade			
	0	11 (28.9)	14 (50.0)	ns
	1	21 (55.3)	10 (35.8)	
	2	6 (15.8)	4 (14.2)	
	3	0 (0)	0 (0)	
	4	0 (0)	0 (0)	
Gastro-intestinal toxicity	Grade			
	0	11 (28.9)	3 (10.8)	ns
	1	18 (47.4)	18 (64.2)	
	2	9 (23.7)	6 (21.5)	
	3	0 (0)	1 (3.5)	
	4	0 (0)	0 (0)	
Genito-urinary toxicity	Grade			
	0	14 (36.8)	10 (35.8)	ns
	1	20 (52.6)	8 (28.5)	
	2	4 (10.5)	9 (32.2)	
	3	0 (0)	1 (3.5)	
	4	0 (0)	0 (0)	

BMI= Body Mass Index; CT= chemotherapy; RT: radiotherapy.

With a median follow up of 20 months (range 3-48 months), no dose limiting toxicity was reported, therefore Level 2 was considered as the recommended dose. Three vaginal recurrences were documented at 8, 14 and 19 months after SIB-VMAT in Level 1 group. At two-years local control was 90.4% (Level 1), versus 100% (Level 2), while disease free survival was 85.6% (Level 1) versus 93.3% (Level 2); overall survival was 96.2% (Level 1) versus 100% (Level 2), respectively.

Conclusion: To date, according with this phase I-II study clinical results, SIB-VMAT strategy represents the standard adjuvant treatment in HIR-EC at our Institution. We established the dose of 45Gy/1.8 Gy to pelvic nodes and 60 Gy/2.4 Gy to the upper two thirds of vagina as the recommended doses for further evaluation of SIB- VMAT approaches in this setting.

PO-0725

Pelvic organ motion during radiotherapy for cervical cancer and impact on target coverage

G. Eminowicz[1], J. Motlib[1], S. Khan[1], C. Perna[1], M. McCormack[1]
[1]*University College London Hospital, Radiotherapy Department, London, United Kingdom*

Purpose or Objective: Minimisation of internal organ motion during pelvic radiotherapy (RT) is necessary to ensure accurate reproducible treatment. We analysed bladder and rectal filling during pelvic RT and their impact on CTV coverage.

Material and Methods: Cone beam Computed Tomography scans (CBCTs) taken twice weekly during 3D conformal RT were retrospectively analysed for 10 cervical cancer patients. All patients followed the departmental guidelines; empty bladder then drink 4 cups of water 40 minutes before

scanning/RT; laxatives taken to ensure bowels opening daily, ideally Bristol stool chart type 5. Bladder, rectum and primary CTV were outlined on each CBCT by 2 independent clinicians. Effects of time through RT, chemotherapy administration, and drinking time on bladder and rectal volume were analysed. Volume variation impact on CTV coverage was also investigated using fixed effect logistic regression modelling.

Results: 10 planning scans and 109 CBCTs were reviewed. Bladder volume was 45-578cc during radiotherapy and 73-664cc at planning. Bladder volume increased (approx. 4cc/minute) with waiting time, decreased (average 4cc/day) through RT and was larger (approx. 50cc average) on chemotherapy days. All bladder volumes that deviated >130cc from planning led to CTV being out of PTV. The odds of CTV remaining within PTV reduced by 1.9% for every cc deviation from planning volume, predominantly affecting uterus. Large planning bladder volumes (>300cc) were not reproducible during RT. Rectal anterior-posterior (AP) diameter correlates with rectal volume and displays no pattern through treatment. AP diameter ranged from 2.9-5.3cc at planning and 1.6-8.7cc during RT. The odds of CTV remaining in PTV reduced by 5.8% with every mm deviation from planning rectal AP diameter, predominantly affecting cervix.

Conclusion: Bladder volume changes during RT and with chemotherapy increase the risk of CTV being outside of PTV, especially the uterus. Rectal size changes increase the risk of CTV being outside of PTV, predominantly affecting the cervix. Increasing rectal size correlates with decreasing bladder volume, possibly due to dehydration. We therefore recommend an ideal bladder planning volume of 150-300cc, a shorter waiting time on chemotherapy days and adequate hydration throughout RT. We also recommend regular laxatives to ensure smaller rectal sizes through RT. Even with these recommendations, regular imaging is vital to monitor organ motion when implementing advanced RT techniques for gynaecological cancers.

PO-0726

Stereotactic body radiotherapy for mediastinal and sub-diaphragmatic nodal relapse of ovarian cancer

L. Draghini[1], F. Trippa[1], F. Arcidiacono[1], P. Anselmo[1], M. Casale[1], M. Italiani[1], M. Muti[1], M.L. Basagni[1], L. Chirico[1], R. Rossi[1], E. Maranzano[1]
[1]*Radiation Oncology Centre, Oncology Departement "S.Maria" Hospital Terni, Terni, Italy*

Purpose or Objective: To retrospectively evaluate the effectiveness and toxicity of stereotactic body radiotherapy (SBRT) for localized nodal relapse (NR) of ovarian cancer.

Material and Methods: Between August 2008 and March 2015, eleven patients were treated with SBRT on 16 NR of previous ovarian cancer. All patients at the time of ovarian cancer diagnosis were submitted to surgery and at least 1 line of chemotherapy (range, 1-3). Median age was 64 years (range, 49-74), and primitive histology was siero-papillar and endometrioid carcinoma in 8 (72%) and 3 (28%) patients, respectively. Median interval time between first diagnosis and NR was 83 months (range, 22-148). NR was documented with PET-CT as the only site of disease. Response was evaluated with PERCIST criteria.

Results: Median follow-up was 11 months (range, 2-47), median GTV 5.4 cc (range, 1.8-18.3), median PTV -obtained adding an isotropic margin of 5 mm to the GTV- 16.5 cc (range, 4,2-85.7). There were 11/16 (69%) sub-diaphragmatic, 5/16 (31%) mediastinal NR. Fractionation schemes were: 5 x 8Gy in 10 (62%), 5 x 7Gy in 1 (6%), 5 x 6Gy in 1 (6%) and 5 x 5Gy in 5 (26%) NR. Outcome, evaluated with PET-CT 3 months after SBRT, showed a complete response in all treated NR, with a median duration of response of 17 months (range, 2-47). Six (54%) patients had a subsequent "out-field" progression, 1 nodal and 4 peritoneal progression in sub-diaphragmatic region, 1 nodal progression in mediastinal region. The two cases with nodal progression received another SBRT, while the others chemotherapy. No acute or late toxicity was registered after SBRT. At the time of last follow-up, 9 patients were alive 6 of whom without evidence of disease.

Conclusion: All ovarian cancer patients submitted to SBRT for NR had a durable complete response without toxicity. However, outcome seems less satisfying in patients with sub-diaphragmatic disease because of peritoneal progression in absence of in-field relapse.

PO-0727

Prognostic impact of 18F-FDG PET-CT in patients with locally advanced cervical carcinoma

S. Cima[1], A. Galuppi[2], P. De Iaco[3], M. Perrone[3], S. Fanti[4], G. Compagnone[5], M.C. Valli[1], A. Richetti[1], G. Macchia[6], M. Nuzzo[6], F. Deodato[6], G. Ferrandina[7], F. Bertini[2], A. Farioli[8], S. Cammelli[2], G. Frezza[9], A.G. Morganti[2]
[1]*Oncology Institute of Southern Switzerland, Radiation Oncology Unit, Bellinzona, Switzerland*
[2]*Radiation Oncology Center - S. Orsola-Malpighi Hospital - University of Bologna, Department of Experimental-Diagnostic and Specialty Medicine - DIMES, Bologna, Italy*
[3]*S.Orsola-Malpighi University Hospital, Gynecologic Oncology Unit, Bologna, Italy*
[4]*Nuclear Medicine Unit- S.Orsola-Malpighi Hospital-University of Bologna, Department of Experimental-Diagnostic and Specialty Medicine, Bologna, Italy*
[5]*S.Orsola-Malpighi University Hospital, Department of Medical Physics, Bologna, Italy*
[6]*Fondazione di Ricerca e Cura "Giovanni Paolo II" - Catholic University of Sacred Heart, Radiotherapy Unit, Campobasso, Italy*
[7]*Policlinico Universitario "A. Gemelli"- Catholic University of Sacred Heart, Department of Gynecologic Oncology, Roma, Italy*
[8]*S.Orsola-Malpighi Hospital - University of Bologna, Department of Medical and Surgical Sciences- DIMEC, Bologna, Italy*
[9]*Ospedale Bellaria, Radiotherapy Department, Bologna, Italy*

Purpose or Objective: The primary objective of this study was to evaluate the prognostic value of pretreatment 18-F-FDG PET-CT in patients with locally advanced cervical cancer.

Material and Methods: At pre-treatment staging, 92 patients with histological diagnosis of cervical cancer, underwent 18-F-FDG PET-TC in addition to routine protocol including International Federation of Obstetrics and Gynecology (FIGO) staging and MRI. Patients were treated with concurrent chemoradiation followed by brachytherapy boost.

Results: 18-F-FDG PET-CT identified the presence of para-aortic lymph node metastases in 17 patients (18%). These patients were treated with extended field irradiation (including para-aortic nodes). The results of multivariate analysis showed that 18-F-FDG PET-CT positive para-aortic lymph nodes and advanced FIGO stage were predictive of worse disease-free survival (p=0.01; p=0.001, respectively), and high T SUV max had a negative impact on local control, disease-free survival and overall survival (p=0.02; p=0.01; p=0.01, respectively).
Figure 1. Actuarial local control, Disease free survival and Overall survival for T SUVMAX

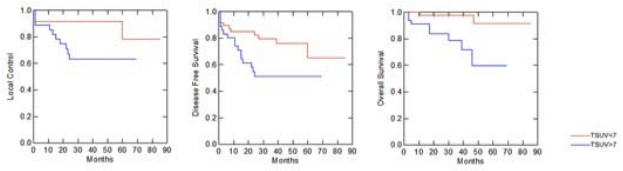

Conclusion: High T SUV (max) showed a strong prognostic impact in these patients. Furthermore, staging 18-F-FDG PET-

CT modified radiotherapy planning in a significant percentage of patients.

PO-0728

Stereotactic Body Radiation Therapy for oligometastatic patients with ovarian cancer

A. Tozzi[1], C.S. Iftote[1], T. Comito[1], C. Franzese[1], F. De Rose[1], E. Villa[1], P. Navarria[1], A.M. Ascolese[1], D. Franceschini[1], R.L.E. Liardo[1], E. Clerici[1], G.R. D'Agostino[1], V. Palumbo[1], M. Scorsetti[1]

[1]Istituto Clinico Humanitas, Radiotherapy and Radiosurgery, Rozzano Milan, Italy

Purpose or Objective: Ovarian cancer is a gynecological malignancy characterized by a dismal outcome for its tendency to metastasize despite aggressive systemic therapies, commonly carboplatin and paclitaxel. Among recurrent ovarian cancer, patients with oligometastatic disease are supposed to have a better prognosis since they could benefit from local approaches besides chemotherapy, considering also the limited alternative regimens of systemic therapy. The aim of our study is to evaluate the role of stereotactic body radiotherapy (SBRT) in terms of LC and toxicity in a setting of patients with oligometastatic recurrent ovarian cancer.

Material and Methods: Between January 2011 and February 2015, 15 patients (20 lesions) with recurrent oligometastatic ovarian carcinoma of any histology underwent SBRT. Toxicity and tumor response was scored using Radiation Therapy Oncology Group/European Organization for Research and Treatment of Cancer Scale. Tumor response was evaluated by CT/ PET, according to Response Evaluation Criteria in Solid Tumors.

Results: Median age at treatment was 60 years and median follow-up was 21 months. The sites of disease were abdomino-pelvic lymphnodes (13 lesions), liver metastasis (4 lesions), lung metastatasis (2 lesions) and para-vaginal mass (1 lesion). The SBRT doses were prescribed based on dimensions of target volumes and organs at risk constraints as follow: for lymphnodal lesions the dose prescription was 36-45 Gy in 6 fractions and only one case treated with 40 Gy in 4 fr; for hepatic lesions 61.89 -75 Gy in 3 fractions, for the pulmonary lesions both cases received 48 Gy in 4 fractions meanwhile in the para vaginal recurrence dose prescription was 36 Gy in 6 fractions. None of the patients had grade 3 /4 acute or late Gu or Gi toxicity. At a median follow-up of 21 months local control was observed in 85%. Complete radiologic response, partial response and progressive disease were observed in 12 (60%), 5 (25%) and respectively 3 cases (15%).

Conclusion: SBRT is a feasible and well tolerated treatment approach in oligo-metastatic ovarian patients, offering a good local control. Certainly, additional patients and longer follow-up are necessary to confirm the impact of local treatment as SBRT in ovarian cancer therapy.

PO-0729

Hematological toxicity of Rth-Chth for cervical cancer: Rth technique and dose given to bone marrow

K. Bialas[1], M. Agnieszka Stefanowicz[1], M. Karolina Osowiecka[1], P. Katarzyna Pawłów – Pyrka[1], P. Lucyna Kępka[1]

[1]SP ZOZ MSW Warmia@Mazury Oncology Centre, Radiation Oncology, Olsztyn, Poland

Purpose or Objective: This is a concern about hematological toxicity (HT) of intensity-modulated radiation therapy (IMRT) technique combined with chemotherapy used in the treatment of gynecological malignancies due to the high volume of low radiotherapy doses given to bone marrow. We aimed to determine if pelvic IMRT increased HT and which dosimetric parameters were predictors of this toxicity.

Material and Methods: Ninety-nine consecutive cervical cancer patients treated with radio-chemotherapy (45-50,4Gy with Cisplatin 40mg/m2/week) between IX2011 and V2015 were included. Fifty patients received three-dimensional conformal radiotherapy (3D-CRT) (4-6 fields) and 49 IMRT with RapidArc. Target volumes were contoured in accordance with RTOG Atlas guidelines. Pelvic bone marrow was defined using a computed tomography density-based autocontouring algorithm. HT was graded by Common Terminology Criteria for Adverse Events, version 4.0 criteria weekly during treatment. The rate of occurrence of grade III-IV HT (overall, anemia, thrombocytopenia, neutropenia, leucopenia) were evaluated in relation with radiotherapy technique, PTV, age, mean dose to bone marrow, volumes of bone marrow receiving 5, 10, 20, 30, and 40 Gy (V5, V10, V20, V30, and V40). The Chi2 test was used to compare HT for each studied parameter dichotomized at the median. Differences between IMRT and 3D-CRT technique were compared with U-Mann-Whitney test.

Results: Patients treated with IMRT had significantly lower V20, V30, V40, mean bone marrow dose, and PTV volume than 3D-CRT patients ($p<.00001$ for each). The both techniques did not differ significantly in age of patients, number of chemotherapy cycles given, V5 and V10. Grade III-IV HT of any kind occurred in 52% of 3D-CRT patients and 30% of IMRT patients, $p=0.03$. Each evaluated threshold of dose given to bone marrow predicted significantly occurrence of HT. Larger PTV was not predictor of higher HT.

Conclusion: Pelvic IMRT decreased HT of radio-chemotherapy for cervical cancer in comparison with 3D-CRT by reduction of volume of doses >20Gy given to bone marrow. Even though a precise dose threshold for bone marrow was not determined, limitation of bone marrow volume defined automatically as bone in patients treated with radio-chemotherapy is warranted.

PO-0730

QOL after postoperative IMRT for cervical cancer: results from matched pair analysis with 3DCRT

S. Chopra[1], S. Mohanty[1], U. Mahantshetty[2], S. Kannan[1], R. Engineer[2], S. Mechanery[1], R. Phurailatpam[1], J. Ghosh[1], S. Gupta[1], S. Shrivastava[2]

[1]Advanced Centre for Treatment- Research and Education in Cancer- Mumbai, Radiation Oncology, Mumbai, India

[2]Tata Memorial Hospital- Tata Memorial Centre, Radiation Oncology, Mumbai, India

Purpose or Objective: Adjuvant intensity modulated radiotherapy (IMRT) for cervical cancer is associated with reduced late gastrointestinal toxicity (GI) however it's impact on quality of life (QOL) is not known. The present matched pair analysis was performed to compare QOL between three-dimensional conformal radiation (3DCRT) and IMRT.

Material and Methods: From Jan,2011- Dec,2013 patients undergoing adjuvant or salvage radiation with 3DCRT or IMRT (with or without concurrent chemotherapy) and vaginal brachytherapy were included. Those who received systemic chemotherapy or extended field radiation were excluded. The study inclusion criteria also necessitated at least 1 year of follow up with QOL assessment at at least 2 time points. At follow up toxicity was documented using CTCAE version 3.0 and QOL was measured with EORTC QLQC-30 and Cx-24 module. The baseline characteristics of two cohorts were compared using chi-square test. Raw scores were converted into final scores using EORTC recommended conversion and linear mixed model was used to evaluate impact of time trends and treatment technique on QOL. A 10-point difference in QOL score and $p\leq0.05$ was considered relevant and statistically significant. All data were analyzed using SPSS, version 20.0 and Graph pad Instat.

Results: A total of 64 patients were eligible. Postoperative IMRT and 3DCRT was used in 40 and 24 patients respectively. The baseline socioeconomic, disease and treatment related characteristics were well balanced in both groups rendering cohorts eligible for a matched pair analysis. At one year there was recovery in most of the QOL domains in both cohorts with objective scores reaching baseline levels. The

recovery in QOL scores over time was deemed statistically significant (p<0.0001). A clinically and statistically significant improvement in physical (78.7 vs. 87.7, p=0.05), emotional (66.5 vs. 78.5, p=0.05) and social functioning (61.5 vs. 82.2) was observed in IMRT cohort. The patients treated with IMRT had fewer patients having symptoms of appetite loss (30.4 vs. 12.1,p=0.01) and diarrhea (24 vs. 9;p=0.04). The use of IMRT was also associated with reduced lymphedema (15.2 vs 3.2; p=0.05). However no difference was observed in sexual and global QOL.

Conclusion: Early results show improved functional scales and reduced symptom scales with use of postoperative IMRT when compared to 3DCRT. Further long term follow up is needed to clearly define the impact of IMRT on patient reported outcomes.

PO-0731

Quality of life of women after endometrial cancer: the role of the vaginal dilator

R. Foerster[1], L. Schnetzke[1], T. Bruckner[2], H. Rief[1], J. Debus[1], K. Lindel[1]
[1]*University Hospital Heidelberg, Department of Radiation Oncology, Heidelberg, Germany*
[2]*University Hospital Heidelberg, Department of Medical Biometry, Heidelberg, Germany*

Purpose or Objective: Pelvic radiotherapy (RT) provides good local control in women with endometrial cancer (EC), but may also cause substantial acute and chronic adverse effects, which in turn may reduce patients' (pts) quality of life (QoL).

Material and Methods: 293 pts who were treated with adjuvant pelvic RT for EC at our department between 2004 and 2012 were asked to fill in questionnaires regarding their QoL (EORTC QLQ-C30, EN24). Median follow-up was 6 years. 112 pts agreed to participate. 42 (38%) used the vaginal dilator (VD; group A) as prescribed, 62 (55%) did not use the VD (group B), 8 (7%) preferred not to answer this question. The values of the function and symptom scales of the pats were statistically analyzed and compared between the two groups as well as compared with reported values of normal populations.

Results: The values of the function and symptom scales are generally lower in our pts compared to an age adapted normal population (NP). Pts reported statistically better values for sexual interest and sexual activity compared to NP (p<.0001), while sexual enjoyment was significantly reduced (p<.0001). Vaginal dryness and pain during intercourse (p<.00001) were the leading complaints. Sexual interest and activity increased with age (p<.0005) in contrast to NP. Pts in group A were younger than in group B (p=.016). Group A reported significantly less pain in the back and pelvis (p=.005) as well as less muscular pain (p=.013). Pts using VD >1 year had better values for sexual interest (p=.0022) and sexual activity (p=.013) compared to 1 year. Pts with vaginal brachytherapy (IVB) only had a better global health status compared to pts with additional external beam RT, while IMRT was better than 3D-conformal RT (p<.0017). Pts with higher acute GI toxicity reported more chronic GI symptoms (p=.002) with diarrhea (p=.009), nausea/vomiting (p=.032) as well as poorer social functioning (p=.036). Pts with higher acute GU toxicity reported more pain during intercourse (p=.044).

Conclusion: Pelvic RT substantially affects QoL even years after treatment. Women participating in our study were more sexually active than the normal population. Therefore sexuality is important for QoL in women after endometrial cancer, even at higher age. The vaginal dilator is capable of improving chronic pelvic pain, sexual interest and sexual activity when used longer than one year. Pts with higher acute toxicities also exhibit more chronic problems. IMRT seems to be beneficial for long-term QoL.

PO-0732

Predictive factors for inter-fraction uterine motion in definitive radiotherapy for cervical cancer

H. Maemoto[1], T.T. Takafumi Toita[1], S.H. Seiji Hashimoto[1], T.A. Takuro Ariga[1], Y.K. Yasumasa Kakinohana[1], J.H. Joichi Heianna[1], S.M. Sadayuki Murayama[1]
[1]*University of Ryukyis, Radiology, Okinawa, Japan*

Purpose or Objective: Uterine motion is a challenging issue in applying intensity-modulated radiotherapy (IMRT) for patients with cervical cancer. In this study we quantified the inter-fraction uterus movement during a course of definitive radiotherapy (RT) to determine the predictive factors affecting uterine motion.

Material and Methods: A total of 343 cone-beam CT (CBCT) scans from 43 patients who underwent definitive RT were analyzed retrospectively. The median age of the patients was 58 years (range, 34-85 years). The FIGO stages were as follows: IB1, 9; IB2, 6; IIA, 1; IIB, 12; IIIB, 10; and IVA, 5. Cervical and corpus movement (mm) were measured for each direction (cranial [C), anterior [A) left [L) and right [R) for the uterine corpus; and A, posterior [P), L, and R for the cervix) by comparing planning CT and CBCT. The mean movement of each patient was analyzed according to the following factors: age; tumor stage; BMI; area of visceral fat in the umbilical plane, as assessed by CT; circumference of abdominal girth; history of abdominal surgery; uterine orientation (anteverted or retroverted); size of the uterus; tumor diameter; and tumor invasion to the corpus.

Results: The mean movement of the corpus was as follows: C, 5.8 mm (range, 0-29.0 mm); A, 5.2 mm (range, 0.3-37.7 mm); L, 2.4 mm (range, 0-10.6 mm); and R, 2.5 mm (range, 0-9.2 mm). The mean movement of the cervix was as follows: A, 3.2 mm (range, 0-11.4 mm); P, 2.4 mm (range, 0-12.5 mm); L, 1.5 mm (range, 0-9.2 mm); and R, 1.6 mm (range, 0-7.3 mm). There was a significant correlation between abdominal girth and anterior movement of the corpus (r=-3.6 and p=0.029). Tumor invasion to the corpus had a negative correlation with posterior movement of the cervix with marginal statistical significance (p=0.05).

Conclusion: The study demonstrated that abdominal girth and tumor invasion to the corpus were predictive factors of uterine motion during definitive RT for patients with cervical cancer.

PO-0733

Treatment response evaluation with ADCmean in cervical cancer patient treated with chemoradiotherapy

C. Onal[1], G. Erbay[2], O.C. Guler[1]
[1]*Baskent Universitesi Tip Fakultesi- Adana Hastanes, Department of Radiation Oncology, Adana, Turkey*
[2]*Baskent University Faculty of Medicine, Deoartment of Radiology, Ankara, Turkey*

Purpose or Objective: The aim of this study is to investigate the ADCmean of the primary tumor to evaluate their correlations with the recurrence and survival rates in patients with primary cervical cancer before and after definitive CRT.

Material and Methods: The data of 44 patients with histologically proven squamous cell carcinoma of cervix was retrospectively evaluated .All patients had multi-parametric pelvic MR imaging (CE-MRI and DW-MRI) and 18F-FDG PET/CT for initial staging prior to treatment and also multi-parametric pelvic MR imaging after treatment at our Institution between February 2009 and May 2014. ADC response was measured by the proportion of ADC changes between pretreatment and posttreatment ADC measured in DW-MRI. The patients were divided into groups based on the pretreatment and posttreatment ADCmean of the primary tumor cutoff values derived from the ROC curves. Disease-

free survival (DFS) and OS rates were calculated using the Kaplan-Meier method. Multivariate analyses were performed using the Cox proportional hazards model.
Results: The median follow-up for all patients and surviving patients was 25 months (range, 3–75 months) and 28 months (range, 15–75 months), respectively. Post-treatment MRI images were taken within a median of 3.2 months (range, 2.8–4.1 months) after the completion of CRT. At post-treatment MRI, 41 patients (93%) exhibited a complete response. The mean pretreatment and posttreatment ADCmean were 0.882±0.096 × 10-3 mm2/sec, 1.159±0.168 × 10-3 mm2/sec, respectively. Median percent ADC change was 33.7% (5.0 – 70.0%). The analyses identified pretreatment ADCmean of the primary tumor cutoff values of 0.878× 10-3 mm2/sec for recurrence (area under the curve [AUC] = 0.818, p<0.001; 95% CI, 0.690–0.946, sensitivity 86.4%, specificity 72.7%), posttreatment ADCmean of the primary tumor cutoff values of 1.132 × 10-3 mm2/sec for recurrence (AUC = 0.810, p<0.001; 95% CI, 0.684–0.936, sensitivity 77.3%, specificity 72.7%), ADC change cutoff values of 32.8% for recurrence (AUC = 0.810, p<0.001; 95% CI, 0.683–0.937, sensitivity 77.3%, specificity 68.2%). In a multivariate analysis, pelvic lymph node metastasis and pretreatment ADCmean were significant prognostic factors for both OS and DFS. Additionally, ADC change between pretreatment and posttreatment DW-MRI was significant factor for OS.

Conclusion: Our findings provide evidence that posttreatment low ADCmean of the primary tumor is a useful clinical prognostic biomarker for recurrence and survival in patients with cervical cancer.

PO-0734
Justgin in the prevention of radio-induced vaginal mucositis
F. Piccolo[1], A. Romano[1], A. Rese[1], E. D'Ippolito[1], F. Pastore[1], P. Romanelli[1], L. Faraci[1], E. Toska[1], V. De Chiara[1], A. Farella[1], R. Solla[1,2], M. Conson[1,2], R. Liuzzi[1,2], L. Cella[1,2], R. Pacelli[1,2]
[1]*Az. Ospedaliera Universitaria Federico II, Dipartimento di Scienze Biomediche Avanzate, Napoli, Italy*
[2]*C.N.R, Istituto di Biostrutture e Bioimmagini, Napoli, Italy*

Purpose or Objective: Radiation therapy on the pelvic region in women may induce disturbing vaginal irritation impacting on patients quality of life. We tested a hyaluronic acid based vaginal washing (Justgin) in the prevention of vaginal mucositis in patients treated with external beam radiation therapy for pelvic neoplasms.

Material and Methods: Fifty eight female patients affected by uterine tumors and undergoing radiation therapy on the pelvic region were considered for the study. Median age was 58. Twenty eight patients were affected by endometrial cancer, while 30 were affected by cervical cancer. Radiation therapy was delivered by 6 MV X ray of a linear accelerator with 4 fields 3D conformal radiation therapy with a dose of 45-50.4 Gy in 25-28 daily 1.8 Gy fractions. Group A (28 patients) used Justgin every other day, and 30 patients (group B) did not use any prophylactic therapy. Patients were visited and interviewed about vaginal discomfort or symptoms every week.

Results: At the end of radiation therapy 13/28 patients of group A and 27/30 of group B, developed vaginal toxicity of any grade (p=0.0005). Overall, however the toxicity was mild or moderate in all patients.

Conclusion: Our study suggests that a vaginal washing with hyaluronic acid (Justgin) can reduce the incidence of the vaginal acute symptoms induced by external beam irradiation in women affected by uterine cancer.

PO-0735
Prognostic value of microRNA-205 in endometrial cancer patients treated with adjuvant radiotherapy.
M. Wilczynski[2], J. Danielska[1], J. Fijuth[3], A. Malinowski[2]
[1]*Medical University of Lodz, Radiotherapy Department, Lódz, Poland*
[2]*Polish Mother's Memorial Hospital Research Institute, Department of Surgical- Endoscopic and Oncologic Gynecology, Lodz, Poland*
[3]*Medical University of Lodz, Radiotherapy Department, Lodz, Poland*

Purpose or Objective: Endometrial cancer (EC) is the leading malignant tumour occurring in the female genital tract. miRNAs are small non-coding RNAs that have a broad impact on cancer progression. The aim of our study was to define tissue miRNA-205 expression levels, which could potentially serve as a prognostic marker in EC. We investigated miRNA-205 profiles in regard to clinicopathological characteristics of patients treated with adjuvant radiotherapy from 2002 until 2014.

Material and Methods: Expression profiling of miRNA-205 was performed in EC tissues from patients who were submitted to adjuvant radiotherapy after hysterectomy, according to the International Federation of Gynecology and Obstetrics (FIGO) guidelines. 90 patients were included in the study. The median follow-up period was 46 months (min.2 months;max.119 months). We analyzed the paraffin-embedded tissue samples and identified the areas of EC. We extracted total RNA from 90 EC samples. The reference group was constituted by 10 paraffin-embedded healthy endometrial tissue samples. Spectrophotometric assessment of the total RNA concentration was performed. cDNA was synthesized from total RNA with high capacity cDNA synthesis kit and miRNA-specific primers (miR-205 and internal control RNU6b). The expression of the miRNA-205 was determined using real-time quantitive PCR. The expression level of miRNA-205 was calculated by $\Delta\Delta$CT values based on the internal control and plotted as relative value (RV).

Results: Our results indicate that the expression of miRNA-205 was significantly higher in EC samples (p=0,000158). The expression of miRNA-205 was differentiated considering different grading levels. The lowest miRNA-205 expression was observed in grade 3 (p=0,02). There was no correlation between FIGO stages of EC and miRNA-205 expression (p=0,23). When we divided patients into two subgroups: advanced EC (III, IV FIGO) and non-advanced EC (I,II FIGO) it turned out that the expression levels of miRNA-205 were significantly lower in the advanced EC patients group (p<0,045). The miRNA-205 expression was lower when there was over 50% invasion of the myometrium (p<0,038). Kaplan-Meier survival curves were generated to examine the relationship between the expression levels of miRNA-205 and patient's survival rate. Its analysis revealed that high levels of miRNA-205 are associated with longer survival (fig.1).

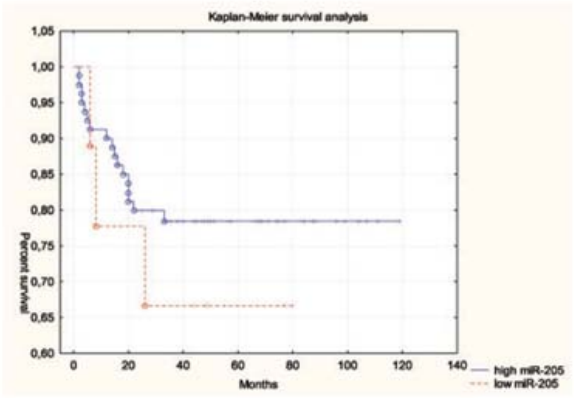

Conclusion: Increased miRNA-205 expression is a positive prognostic factor. Lower levels of miRNA-205 are characteristic of more advanced stages of EC.

Poster: Clinical track: Prostate

PO-0736

Tumour staging using MRI in prostate cancer: improvement of treatment decisions for radiotherapy

F. Couñago[1], E. Del Cerro[1], A.A. Díaz-Gavela[1], F.J. Marcos[1], M. Recio[2], D. Sanz-Rosa[3], I. Thuissard[4], K. Olaciregui[5], J. Castro-Novais[6], J. Carrascoso[2], C. Hayoun[2], R. Murillo[7], J.M. Rodriguez-Luna[8], C. Bueno[8], J. Hornedo[9], R. Perez-Carrion[9], V. Martinez de Vega[2], M. Mateo[10]
[1]*Hospital Quiron, Radiation Oncology, Madrid, Spain*
[2]*Hospital Quiron, Radiology, Madrid, Spain*
[3]*Universidad Europea, Clinical Department- Faculty of Biomedicine, Madrid, Spain*
[4]*Universidad Europea, Department of Research, Madrid, Spain*
[5]*Universidad Europea, School of Medicine, Madrid, Spain*
[6]*Hospital Quiron, Medical Physics, Madrid, Spain*
[7]*Hospital Quiron, Pathology, Madrid, Spain*
[8]*Hospital Quiron, Urology, Madrid, Spain*
[9]*Hospital Quiron, Clinical Oncology, Madrid, Spain*
[10]*Hospital Quiron, Assistant manager, Madrid, Spain*

Purpose or Objective: To assess and validate the incorporation of the multiparametric magnetic resonance imaging (mpMRI) tumor stage (mT-stage) to the conventional clinical tumor stage (cT-stage), in order to guide the radiotherapy (RT) treatment decisions in prostate cancer. In addition, to identify the clinical factors associated to the technique reliability.

Material and Methods: mpMRI was performed in 274 prostate cancer patients in order to refine the treatment decisions according to PSA, Gleason Score (GS) and cT-stage. Comparisons between the cT and mT-stage were performed, as well as the impact on the RT treatment prescription (target volume, doses and hormonal therapy [HT]) independently if it was finally performed. Changes in HT indication for intermediate risk with unfavourable factors were also analyzed. Until 2014, the unfavourable factors according to the initial criteria were a GS of 7 (4+3), or three unfavourable intermediate risk factors (T2b+PSA 10-20 ng/mL + GS 3+4), or T2c by digital rectal exam (DRE)/transrectal ultrasound (TRUS); more recently, unfavourable risk factors have been established according to Memorial Sloan Kettering Cancer Center (MSKCC) criteria: GS 4+3, or at least two intermediate-risk factors, or at least one intermediate-risk factor and a positive prostate biopsies (ppb) percentage greater than 50%. mpMRI validation was performed with pathological staging (n=90 patients finally decided to join surgery). To analyse the relationship between the reliability of mpMRI and the clinical variables, a univariate and multivariate logistic regression analysis was performed.

Results: The mpMRI upstaging range was 86-94% for any PSA value or GS. Following mpMRI, 32.8% of the patients (90/274) were assigned to a different risk group. Compared to cT-stage, mpMRI identified more intermediate-risk (46.4% vs. 59.5%) and high-risk (19.0% vs. 28.8%) prostate cancer patients. This resulted in a higher indication ($p<0.05$) of seminal vesicle irradiation (63.5% vs. 70.1%), inclusion of any extracapsular disease (T3-T4) within the target volume (1.8% vs. 18.2%), higher doses (65.3% vs. 88.3%) and more indication of HT associated to RT (45.6% vs. 62.4%), Table 1. Finally, decisions concerning RT were changed in 43.8% (initial criteria) or 52.5% (MSKCC criteria) of the patients, depending on the criteria applied to indicate HT in intermediate-risk patients. Global reliability of T-staging with DRE/TRUS was 8.8% (8/90), while it was 71.1% (64/90) for mpMRI. cT-stage was associated to a greater occurrence ($p<0.05$) of indication of inadequate RT treatments. mpMRI reliability was independent of PSA or GS or ppb percentage.

Table 1. Impact of mpMRI tumor staging on RT treatment prescription (target volume, doses and hormonal therapy).

Characteristics	DRE/TRUS n (%)	mpMRI n (%)	p value
T1-T2a	239 (87.2)	67 (24.5)	
T2b-T2c	30 (11.0)	157 (57.3)	<0.001
T3-T4	5 (1.8)	50 (18.2)	
Low-Risk (LR)	95 (34.7)	32 (11.7)	
Intermediate-Risk (IR)	127 (46.4)	163 (59.5)	<0.001
High-Risk (HR)	52 (19.0)	79 (28.8)	
Target volume			
VVSS prophylactic	174 (63.5)	192 (70.1)	<0.001
T3a+T3b+T4	5 (1.8)	50 (18.2)	
Doses			
Low	95 (34.7)	32 (11.7)	<0.001
High	179 (65.3)	242 (88.3)	
Hormonal Therapy			
HR and IR (Initial criteria)			
No	182 (66.4)	158 (57.7)	0.035
Yes	92 (33.6)	116 (42.3)	
HR and IR (MSKCC criteria)			
No	149 (54.4)	103 (37.6)	<0.001
Yes	125 (45.6)	171 (62.4)	
Hormonal Therapy in IR patients			
Initial criteria			
No	220 (80.3)	221 (80.7)	0.914
Yes	54 (19.7)	53 (19.3)	
MSKCC criteria			
No	180 (65.7)	144 (52.6)	0.002
Yes	94 (34.3)	130 (47.4)	
Hormonal Therapy in HR patients			
No	222 (81.0)	195 (71.2)	0.007
Yes	52 (19.0)	79 (28.8)	

VVSS seminal vesicles, *DRE/TRUS* digital rectal exam/transrectal ultrasound

Conclusion: mpMRI tumor staging significantly improved the RT treatment decisions in all prostate cancer risk groups. The magnitude of the impact on final RT treatment decisions will depend on the institution's clinical protocol for prostate cancer management.

PO-0737

Predictors of PSA relapse in patients with intermediate risk prostate cancer treated with SBRT

T. Kole[1], S. Guleria[1], H. Koneru[1], O. Obayomi-Davies[1], T. Yung[1], S. Lei[1], B. Collins[1], S. Suy[1], A. Dritschilo[1], S. Collins[1]
[1]*Georgetown University Hospital, Radiation Medicine, Washington, USA*

Purpose or Objective: SBRT has demonstrated favorable outcomes in selected patients with early stage localized prostate cancer. Treatment of patients with intermediate risk disease remains cautionary due to the heterogeneity within this population with respect to risk for occult extraprostatic disease. Here we report an analysis of PSA outcomes following SBRT for intermediate risk prostate cancer and identify disease specific risk factors for biochemical failure.

Material and Methods: Patients treated with SBRT at Georgetown University Hospital for intermediate risk prostate adenocarcinoma, with or without the use of androgen deprivation therapy (ADT), were included in this retrospective analysis. Treatment was delivered using CyberKnife® SBRT with doses of 35 Gy or 36.25 Gy in 5 fractions. PSA failure was defined as a rise > 2 ng/ml above nadir (ASTRO Phoenix definition) and analyzed using the Kaplan Meier method. A Cox proportional hazards model was generated using disease related covariates including T stage, primary gleason pattern, pretreatment PSA, number of positive cores, percent positive cores, maximum single core involvement in order to identify potential predictors of PSA relapse after SBRT. A logrank test was also used to compare patients classified as having favorable vs. unfavorable intermediate risk disease by previously reported criteria of primary gleason pattern 4, 50% cores involved, or ≥2 intermediate risk factors.

Results: Three hund;red and fifty three patients at a median age of 70 years (range, 46 to 90) received SBRT. ADT was initiated prior to SBRT in 16% of patients and the median pre-

treatment PSA was 7.2 ng/ml (range, 0.8 to 19.9). The overall 3-year biochemical relapse free survival (bRFS) was 93.9%. Cox regression identified primary gleason pattern as the only significant predictor of PSA relapse with a HR of 5.84 (1.92 to 17.8, 95% CI) for primary gleason pattern 4 vs. 3. There was no significant difference in bRFS between patients classified as having favorable vs. unfavorable intermediate risk disease, HR 0.39 (0.11 to 1.41, 95% CI). There were no significant benefits observed with respect to ADT in any subgroup.

Conclusion: Early PSA responses after SBRT for intermediate risk prostate adenocarcinoma compare favorably to those reported using other radiation therapy modalities. Primary gleason pattern 4 is predictive of less favorable bRFS, however early rates of PSA control are excellent compared to historical controls. The role of ADT in these patients is still unclear. The current evidence supports SBRT as a standard therapeutic option in intermediate risk disease.

PO-0738

Hydrogel injection prevents long-term rectal toxicity after radiotherapy for prostate cancer

M. Pinkawa[1], V. Schmitt[1], V. Djukic[1], J. Klotz[1], L. König[1], D. Frank[1], B. Krenkel[1], M. Eble[1]
[1]*Uniklinikum RWTH Aachen, Radiation Oncology Department, Aachen, Germany*

Purpose or Objective: The aim of the study was to compare health-related quality of life (QoL) after external beam radiotherapy (RT) for prostate cancer with and without a hydrogel spacer.

Material and Methods: A group of 202 patients with the indication for treatment of the prostate +/- base of seminal vesicles without pelvic lymph nodes was treated in a single institution in the years 2010-2013. Depending on the patient's and responsible radiation oncologist's preference, 108 patients were selected for a hydrogel injection before the beginning of RT. The injection of 10 ml hydrogel was performed under transrectal ultrasound (TRUS) guidance after dissecting the space between prostate and rectum with a saline/lidocaine solution under local anaesthesia. Treatment was performed with a five-field IMRT or VMAT technique with daily ultrasound based image guidance. Only for patients with a spacer the prescription dose was increased from 76Gy to 78Gy, subsequently 80Gy. Patients were surveyed prospectively before RT (time A), at the last day of RT (time B), a median time of two months (time C) and seventeen months after RT (time D) using a validated questionnaire (Expanded Prostate Cancer Index Composite; comprising 50 items concerning urinary, bowel, sexual and hormonal domains). The multi-item scale scores were transformed lineary to a 0-100 scale, with higher scores representing better QoL. Baseline QoL assessment was available from 101 / 66 patients with / without a spacer. Responses to both the baseline and last (time D) questionnaire were available in 94 / 57 cases with / without a spacer.

Results: Apart from higher prescription doses in the spacer group, baseline patient characteristics were well balanced between patients with vs. without a spacer (Table). In particular, baseline QoL was comparable. Acute toxicity (corresponding to QoL changes at times B and C relative to baseline levels) did not differ significantly, with only a tendency for better scores in the spacer group. However, mean bowel bother scores >1 year after RT in comparison to baseline did not change for patients with a spacer (mean change of 0 points) in contrast to patients without a spacer (mean decrease of 7 points). Long-term mean urinary bother scores did not decrease in both groups. At time D, statistically significant differences were found in the function items "bloody stools", "painful bowel movements" and "frequency of bowel movements". Focusing on patients with no problem with bowel symptoms initially, 0% vs. 12% with vs. without a spacer reported a moderate/big problem with bowel symptoms >1 year after RT ($p<0.01$).

		with spacer	without spacer
patient age (years); median (range)		72 (49-82)	73 (53-85)
PTV (cm^3); median (range)		127 (37-335)	123 (36-300)
prescription dose to PTV ≤76Gy / 78Gy / 80Gy; %		64* / 26* / 10*	100* / 0* / 0*
PSA (ng/ml); median (range)		7.6 (2.3-83)	7.3 (1.8-94)
low/intermediate/high risk patients; %		33 / 37 / 30	33 / 42 / 26
urinary bother score; mean	before RT	84	79
	decrease at time B/C/D	18 / 14 / -1	21 / 17 / -2
bowel bother score; mean	before RT	94	93
	decrease at time B/C/D	14 / 3 / 0*	18 / 6 / 7*
sexual bother score; mean	before RT	66	66
	decrease at time B/C/D	6 / 12 / 12	9 / 19 / 17

*p<0.01 (significant differences between groups)
negative decrease corresponds to quality of life improvement

Conclusion: Though acute rectal symptoms are still reported, spacer injection is associated with a significant long-term benefit for patients after prostate cancer RT.

PO-0739

IMRT versus 3D conformal radiotherapy when used in combination with I-125 prostate brachytherapy

A. Yorozu[1], T. Tanaka[1], R. Kota[1], Y. Takagawa[1], Y. Shiraishi[1], K. Toya[1], S. Saito[2]
[1]*Tokyo Medical Centre- NHO, Department of Radiation Oncology, Tokyo, Japan*
[2]*Tokyo Medical Centre- NHO, Department of Urology, Tokyo, Japan*

Purpose or Objective: To compare biochemical outcomes and toxicity of intensity modulated radiotherapy (IMRT) and three-dimensional conformal radiotherapy (3D-CRT) when used in combination with I-125 brachytherapy (BT) for the treatment of unfavorable-risk prostate cancer.

Material and Methods: A retrospective review was performed on 839 patients with localized prostate cancer who received external-beam radiotherapy (EBRT) following BT between 2003 and 2012. Patients were categorized into National Comprehensive Cancer Network risk groups: 616 were unfavorable intermediate-risk (Gleason score 4+3, or Gleason score 3+4 with positive biopsy core rate >1/3), and 223 were high-risk. Treatment begins with BT, followed 6 weeks later by 45 Gy/25 fractions of EBRT. EBRT was delivered via 3D-CRT in 616 men at first and via IMRT technique for 223 men after 2010. The prescription dose for I-125 was 100 Gy, up to 110 Gy after 2009. All patients underwent a CT scan for postplan dosimetry at day 30. The rectal volumes receiving doses higher than 30 Gy, 35 Gy, and 40Gy should be kept under 35%, 25%, and 15%, respectively. Neoadjuvant androgen deprivation therapy was given to 45% of patients. Biochemical failure was defined with the Phoenix criteria, and toxicity was graded according to the National Cancer Institute's Common Terminology Criteria for Adverse Events, prospectively collected. The median (range) follow-up was 7 (2-12) years for the entire cohort; 8.3 years for 3D-CRT, and 4.3 years for IMRT. The biological effective dose (BED) was calculated using an α/β of 2 Gy and the D90 values of the prostate on a day-30 CT scan. Comparisons were made by chi-square test and log-rank test.

Results: The total BED value of the prostate was higher in the IMRT group than in the 3D-CRT group (219 Gy2 vs. 209 Gy2, $p<0.001$). The 5-year actuarial freedom from biochemical failure for the IMRT group vs. the 3D-CRT group were 92.7% vs. 92.6% ($p=0.825$) for all; 95.4% vs. 95.1% for intermediate-risk, and 88.0% vs. 84.8% for high-risk group ($p=0.788$), respectively. Acute gastrointestinal (GI) grade 2+ toxicities occurred in 0.5% of the IMRT group and 2.7% of the 3D-CRT

group (p =0.056), and the 5-year actuarial grade 2+ GI toxicity rate was lower in the IMRT group than in the 3D-CRT group (5.0% vs. 12.1%, p <0.01). A lower incidence of acute genitourinary (GU) grade 2+ toxicities occurred in the IMRT group than in the 3D-CRT group (7.1% vs. 16.4%, p = 0.001). The 5-year actuarial grade 2+ GU toxicity rate for the IMRT vs. the 3D-CRT group was 16.3% vs. 21.7% (p = 0.103), respectively.

Conclusion: IMRT combined with I-125 brachytherapy in prostate cancer patients found a lower incidence of toxicities than 3D-CRT combination, without compromise of biochemical outcomes.

PO-0740

Nodal clearance rate and efficacy of individualised SN-based pelvic IMRT for prostate cancer

A. Müller[1], F. Eckert[1], F. Paulsen[1], D. Zips[1], A. Stenzl[2], D. Schilling[2], M. Alber[3], R. Bares[4], P. Martus[5], D. Weckermann[6], C. Belka[7], U. Ganswindt[8]
[1]*University Hospital Tübingen- Eberhard Karls University, Radiation Oncology, Tübingen, Germany*
[2]*University Hospital Tübingen- Eberhard Karls University, Urology, Tübingen, Germany*
[3]*Aarhus University, Oncology, Aarhus, Denmark*
[4]*University Hospital Tübingen- Eberhard Karls University, Nuclear Medicine and Clinical Molecular Imaging, Tübingen, Germany*
[5]*University Hospital Tübingen- Eberhard Karls University, Institute for Clinical Epidemiology and Applied Biometry, Tübingen, Germany*
[6]*Klinikum Augsburg, Urology, Augsburg, Germany*
[7]*University Hospital Munich- Ludwig-Maximilians-University, Radiation Oncology, Munich, Germany*
[8]*University Hospital Munich- Ludwig-Maximilians-University, Radiation Oncology, Munich, Germany*

Purpose or Objective: Studies on extended or sentinel node (SN) pelvic lymph node dissection (PLND) have shown a higher detection rate compared to standard PLND in high risk prostate cancer (HRPC). In accordance with these findings, we previously demonstrated that ~30% of SNs in HRPC-patients were detected outside of the radiotherapy volume for elective lymph node irradiation. The aim of this study was to assess efficacy of individually SN-guided pelvic intensity modulated radiotherapy (IMRT) by determining nodal clearance rate {(n expected nodal involvement – n observed regional recurrences)/ n expected nodal involvement} in comparison to surgically staged patients.

Material and Methods: Data on 475 HRPC patients were examined. Sixty-one consecutive patients received pelvic SN-based IMRT (5x1.8Gy/week to 50.4Gy (pelvic nodes+individual SN) and an integrated boost with 5x2.0Gy/week to 70.0Gy to prostate + (base of) seminal vesicles) and neo-/adjuvant long-term androgen deprivation therapy; 414 patients after SN-PLND were used to calculate the expected nodal involvement rate for the radiotherapy sample. Biochemical control and overall survival (OS) were estimated for the SN-IMRT patients using the Kaplan-Meier method. The expected frequency of nodal involvement in the radiotherapy group was estimated by imputing frequencies of node-positive patients in the surgical sample to the pattern of Gleason, PSA, and T-category in the radiotherapy sample.

Results: After a median follow-up of 61 months, five year OS after SN-guided IMRT reached 84.4%. Biochemical control according to the Phoenix definition was 73.8%. The nodal clearance rate of SN-IMRT reached 94%. The estimated nodal involvement in the SN-IMRT group was 28.6% (95%-CI:19.3%-37.7%). Retrospective follow-up evaluation is the main limitation.

Conclusion: Radiation treatment of pelvic nodes individualized by inclusion of SN is an effective regional treatment modality in HRPC patients. The pattern of relapse indicates that the SN-based target volume concept correctly covers individual pelvic nodes. Thus, this SN-based approach justifies further evaluation including current dose-escalation strategies to the prostate in a larger prospective series.

PO-0741

Even high-dose radiotherapy requires long-term androgen ablation for high-risk prostate cancer

T.K. Nam[1], D.D. Kwon[2], J.W. Jeong[1], Y.H. Kim[1], M.S. Yoon[1], J.Y. Song[1], S.J. Ahn[1], W.K. Chung[1]
[1]*Chonnam National University Medical School, Radiation Oncology, Gwangju Metropolitan, Korea Republic of*
[2]*Chonnam National University Medical School, Urology, Gwangju Metropolitan, Korea Republic of*

Purpose or Objective: Whether the benefit of androgen ablation therapy (AAT) remains currently unclear in the era of dose escalation and the recent radiation therapy oncology group trials regarding this issue are still under accrual. We tried to evaluate the role of long-term adjuvant AAT for more than 12 months after completion of high-dose intensity modulated radiotherapy (IMRT) for high-risk prostate cancer patients at the single institution retrospectively.

Material and Methods: Between 2005 and 2013, there were 177 high-risk patients treated with radical IMRT. From 2005 to 2009, 25 patients were treated by LINAC-IMRT, and since 2010, remaining 152 patients were treated by helical tomotherapy. High-risk was defined as having one or more among three factors such as pretreatment prostate specific antigen (pPSA) levels > 20 ng/ml, or Gleason score (GS) > 7, or clinical stage ≥ T3a. Ninety-four patients (53.1%) had pPSA levels > 20 ng/ml, and 91 patients (51.4%) had GS > 7. Clinical stage T3 or 4 was diagnosed in 143 patients (80.8%) and 21 (11.9%) had pelvic lymph node metastasis initially. Among all patients, 95.5% received neoadjuvant/concurrent and 91.1% had adjuvant AAT. Median fraction size was 2.2 Gy for prostate plus proximal seminal vesicles with simultaneously integrated boost during whole pelvic irradiation of 1.8 Gy fraction. Most patients (88.1%) received whole pelvic irradiation of a median of 45.0 Gy. Median total nominal dose was 72.6 Gy (66.0 ~ 78.0) which was equivalent to a median of 81.4 Gy α/ß 1.5 (74.2 ~ 86.3) in biologically effective dose of 1.8 Gy fraction. Biochemical failure (BCF) was defined as nadir plus 2 ng/ml.

Results: Follow-up period was ranged from 6 to 117 months (median: 37). Eighteen patients (10.2%) developed BCF and 5-year BCF-free survival rate (BCFFS) was 83.1%. Six out of 18 BCF patients eventually developed clinical failure and 5-year clinical failure-free survival (CFFS) was 93.7%. 5-year cause-specific survival (CSS) and overall survival (OS) was 99.1% and 95.8%, respectively. Several potential prognostic factors were analyzed for each survival endpoints by multivariate analysis. Whether adjuvant AAT or not (p=0.000) and N stage (p=0.016) were significant factors affecting BCFFS but no factors were significant for CFFS, CSS, or OS. Biologically effective dose according to 1.8 Gy ≤80.0 Gy α/ß 1.5 vs. > 80.0 Gyα/ß 1.5) was not a significant factor in all survival endpoints. There was only one patient who suffered urethral stricture of grade 3 late toxicity. No patient suffered grade 3+ in gastrointestinal or grade 4+ in genitourinary late toxicity. s 2 ng/ml.

Conclusion: Based on BCF end point, even high-dose IMRT was an insufficient treatment for high-risk prostate cancer patients if adjuvant AAT was not added. The addition of adjuvant AAT significantly reduced the BCF, although longer follow-up is needed to determine if the combined treatment impacts significantly on other survivals

PO-0742

Image-guided IMRT reduces late toxicity compared to 3D-CRT for prostate cancer

R. Wortel[1], L. Incrocci[1], F. Pos[2], U. Van der Heide[2], J. Lebesque[2], S. Aluwini[1], M. Witte[2], W. Heemsbergen[2]
[1]*Erasmus MC Cancer Institute, Radiation Oncology, Rotterdam, The Netherlands*
[2]*Netherlands Cancer Institute, Radiation Oncology, Amsterdam, The Netherlands*

Purpose or Objective: Image-guided intensity modulated radiotherapy (IG-IMRT) reduces dose to organs at risk (OARs) compared to 3D-conformal radiotherapy (3D-CRT). Currently it is not known to what extent this reduces late toxicity in prostate cancer patients. We previously reported on significant reductions in dose to OARs and acute toxicity. The aim of this study was to assess the therapeutic gain with IG-IMRT in terms of long-term toxicity reductions, and to establish to what extent acute toxicity was associated with late side effects. For that purpose we used prospective data of two randomized trials.

Material and Methods: A total of 242 IG-IMRT patients from a hypofractionation trial (2007-2010) and 189 3D-CRT patients from a dose escalation trial (1997-2003) with ≥2 completed questionnaires were selected. All patients received 78 Gy in 2 Gy fractions. Applied margins were 10 mm for 3D-CRT and 5-8 mm for IG-IMRT, all with 0 mm margin towards the rectum for the 10 Gy boost. The mean dose to the anorectum was 34.4 Gy vs. 47.3 Gy, 23.6 Gy vs. 44.6 Gy for the anal canal and 33.1 Gy vs. 43.2 Gy for the bladder (all significantly reduced with IG-IMRT). Late toxicity was scored using identical questionnaires and case report forms according to RTOG/EORTC scoring criteria. Study endpoints were grade ≥2 (G≥2) gastrointestinal (GI) and genitourinary (GU) toxicity. Cumulative incidences of G≥2 endpoints were calculated. Cox regression was used to determine Relative Risks (RR) for IG-IMRT, adjusted for baseline factors. RRs of acute toxicity as a predictor for late G≥2 endpoints were also calculated.

Results: Median follow-up was 60 months. The five-year (5y) cumulative incidence of late G≥2 GI toxicity was 25.4% for IG-IMRT compared to 36.4% for 3D-CRT (RR=0.62, p=0.009) (Figure 1). This resulted from significantly lower incidences of increased stool frequency ≥6/day (4.3% vs 16.5%, RR=0.24, p<0.001) and non-significant lower incidences of G≥2 (needing medical intervention) rectal bleeding (RR=0.67, p=0.4), rectal pain/cramps (RR=0.59, p=0.13), and proctitis (RR=0.38, p=0.05). G≥2 anal incontinence (with use of pads) was not reduced (RR=1.02, p=0.9). With regard to GU toxicity, a non-significant increase was observed with IG-IMRT with 5y incidences of 46.9% vs. 37.1% for 3D-CRT (RR=1.3, p=0.12). Acute toxicity levels G≥2 (mainly proctitis) were 29% vs. 51% (p<0.01). Acute ≥G2 GI toxicity was predictive for late G≥2 toxicity (RR=2.9 for IG -IMRT, 2.5 for 3D-CRT, both p<0.01), especially for rectal discomfort (RR=7.2, p<0.001) in IG-IMRT, and rectal incontinence (RR≈3.5, p<0.01) in both groups. IG-IMRT patients with acute GU G≥2 complaints had a 1.81 fold (p=0.002) increased risk of late GU G≥2 toxicity, compared to 2.37 (p=0.001) for 3D-CRT.

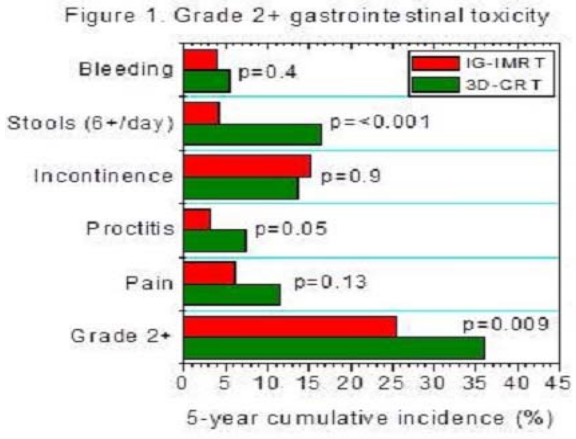

Conclusion: IG-IMRT for prostate cancer was beneficial since it significantly reduced the incidence of long-term GI toxicity, as a result of lower doses to OARs and reduced acute toxicity levels. GU toxicity was not reduced despite significant reductions in bladder dose.

PO-0743

Stereotactic body radiotherapy in recurrent lymph nodes metastases from prostate cancer

F. Trippa[1], E. Maranzano[1], E. Ponti[2], A. Carosi[2], F. Arcidiacono[1], L. Draghini[1], L. Di Murro[2], A. Lancia[2], P. Anselmo[1], R. Santoni[2], G. Ingrosso[2]

[1]Radiation Oncology Centre, Oncology- "S.Maria"- Hospital, Terni, Italy

[2]Radiation Oncology Centre, Diagnostic Imaging- Molecular Imaging- Interventional Radiology and Radiotherapy- Tor vergata- Hospital, Rome, Italy

Purpose or Objective: To assess outcome and toxicity of stereotactic body radiotherapy (SBRT) in prostate cancer patients (pts) with recurrent isolated lymph node metastases (LNM).

Material and Methods: Between September 2008 and December 2014, 40 prostate cancer pts with 47 recurrent isolated LNM, were treated with SBRT. Median age was 74 yrs (range, 58-83), median Gleason score at the primary diagnosis was 7 (range, 5-10). Median and mean time from primary treatment to SBRT were 37.45 and 62.6 m, respectively (range 11.16–216.03). Diagnosis was performed with choline (ch) PET/CT, and the mean and median PSA values before SBRT were 5.6 and 4.2 ng/ml, respectively. Six (15%) pts were treated in different sessions for metachronous metastases, and one (2%) underwent SBRT for two synchronous metastases. 21 (52.5%) pts underwent only SBRT, remaining 19 (47.5%) received also androgen deprivation therapy (ADT). Gross tumor volume (GTV) was delineated using choline uptake and planning target volume (PTV) was defined as the GTV plus a 5-8 mm isotropic margin. Mean and median volume of GTV and PTV were 6.63 cc and 3 cc and 25.03 and 15.03 cc, respectively. In 90% of cases 5 fractions of 6-8 Gy were delivered. Response was assessed with PSA evaluation scheduled every 3 m during the first year and then every 6 m. Pts with a reduction or a stability of PSA level were considered responders. Being evaluation of response with ch-PET-CT not mandatory, it was done in 23 (57.5%) pts.

Results: Mean and median follow-up were 30.18 and 23.8 m, respectively (range 3.73-79.8). Mean time of biochemical progression from the end of SBRT was 15.54 m (range 1.16 - 48.86), and the 2-years biochemical progression free survival (b-PFS) was 44%. We registered a complete concordance between PSA increase and progression of disease shown at ch-PET/CT. Sixteen (40%) of the pts experienced no disease recurrence after SBRT. Of 21 no-ADT pts, 16 (76%) were still free from ADT (mean 26.18 m), whereas remaining 5 (24%) had a mean deferment time of ADT of 13.58 m. At univariate analysis, Gleason score >7 is related with a worse b-PFS (p=0.02). Acute grade 2 diarrhea was registered in 1 (2,5%) case. Grade 3 small bowel late toxicity was observed in only one (2.5%) case 11.76 m after the end of SBRT.

Conclusion: SBRT resulted effective and generally well tolerated by pts. PSA level is a valid tool for response evaluation and ch-PET/CT can be useful for pts with documented biochemical progression.

PO-0744

Effects of IMRT or radical prostatectomy (RP) on serum testosterone in patients with prostate cancer

A. Giraldo Marin[1], X. Maldonado[1], J. Planas[2], M. Hermida[3], M.J. Mañas[1], S. Mico[1], J. Morote[2], J. Giralt[1]

[1]Hospital Universitario Vall d'Hebron, Radiotherapy Department, Barcelona, Spain

[2]Hospital Universitario Vall d'Hebron, Urology Department, Barcelona, Spain

[3]Hospital Universitario Vall d'Hebron, Radiation Physics Department, Barcelona, Spain

Purpose or Objective: Subtle changes in serum testosterone have been noted in prostate cancer patients, without androgen blockade, treated with radiotherapy as well as radical prostatectomy (RP). The significance of these changes

remains unanswered. The aim of the study was to retrospectively review the changes in total testosterone in low risk prostate cancer patients treated with IMRT alone, in comparison with a RP cohort and to assess the correlation between dosimetric parameters for the testes and changes in the level of testosterone.

Material and Methods: From 2009-2012 we studied 115 men in this cross-sectional study. 92 patients underwent RP and 23 patients were treated with IMRT exclusively. The patients were treated with IMRT to the prostate and seminal vesicles for a total dose of 76 Gy (2 Gy/d, 5d/w) with 6 MV photons. We measured serum levels of total testosterone, at baseline and at 3, 12 and 24 months (m) after treatment. We calculated the mean and maximum dose in the testes and the distance between PTV-testes. T –test and Pearson correlation index (PI) were used for statistical purposes.

Results: Patients undergoing RP were younger with IMRT (64.3 vs 72 years, p<0.0001). No differences regarding serum hormonal levels were found at baseline between the two groups. At 3months the testosterone levels were significantly lower in IMRT group (360,3 vs 414,83 ng/dl) in comparison with RP group (p <0,039). At 12 months testosterone levels remained significantly lower (339,89 vs 402,39 ng/dl, p 0,03) in the IMRT group.
In the IMRT group the mean and maximum testes doses (± SD) were 0.472Gy (±0.195) and 0.896 Gy (±0.382) respectively. At 3 months, the mean testosterone reduction was 29.4 ng/dl (± 111.3), without correlation among the mean and maximum dose to the testes (p=0.2). At 12 months, 60% (12/20) of the patients had recovered their basal testosterone levels as well as 61% (11/18) at 24 months. The PI didn´t show any statistical significance related with testosterone kinetics and dosimetric parameters at 12 and 24 months. In the multivariate analyses, we didn´t find any significant relationship regarding: scattered doses in testes; total dose to the prostate; distance between PTV-testes or age, with testosterone recovery.

Conclusion: Despite IMRT for localized prostate cancer leading to low doses to the testes, we observed a decline in total testosterone higher than RP. Nevertheless, it doesn´t seem to correlate with either dosimetric parameters or the scattered dose in testes. More studies are needed to elucidate the role that the prostate may play as an endocrine organ itself.

PO-0745

Significant correlation between prostate volume and obstructive voiding symptom in hypofractionation

S. Pérez Echagüen[1], C.J. Sanz Freire[2], G.A. Ossola Lentati[1]
[1]*Center for Biomedical Research of La Rioja, Radiation Oncology, Logrono, Spain*
[2]*Center for Biomedical Research of La Rioja, Medical Physics, Logrono, Spain*

Purpose or Objective: To investigate the correlation between initial prostate volume and the probability of developing acute Obstructive Voiding Symptoms (OVS) during the course of moderate hypofractionated (HF) prostate RT.

Material and Methods: Data from patients (*n=181*) undergoing IMRT delivered, daily Cone Beam CT guided, HF RT were retrospectively analyzed. Two treatment schedules were considered: HF1 (2.6 Gy/fr, 27 fr; *n=107*) and HF2 (3.15 Gy/fr, 20 fr, 4 days a week; *n=74*). Patients verifying: 1. previous OVS score 3 or greater according the International Prostatic Symptoms Score (IPSS), 2. CTVs encompassing volume outside the prostatic capsule (*i.e.* margin for extracapsular extension or seminal vesicles invasion), 3. presence of central calcification masses or 4. altered RT schedules for reasons other than OVS, were excluded. Measured HF1 and HF2 median prostate volumes as contoured in the simulation CT image were 61.0 cc [18.6, 157.7] and 53.6 cc [18.5, 114.8], respectively. OVS was assessed according the RTOG/CTC v3.0 scale. Development of OVS G2 or greater during treatment was considered as binary end-point. Volume-effect correlation was evaluated by logit analysis, assuming a log-normal distribution.

Results: OVS G2 or greater was found in HF1 (*n=11)* and HF2 (*n=10)* patients. A few patients HF1 (*n=1*) and HF2 (*n=5*) needed urethral catheterization. Some patients (n=12) had their course of treatment modified due to OVS: temporary interruption of treatment (*n=6*), modified fractionation (*n=5*), urinary catheterization at treatment delivery (*n=1*). Logit analysis showed that prostate volume did not correlate with OVS for HF1 patients (*p > 0.05*) but proved to be significantly predictive of OVS for HF2 patients (*p = 0.0002*). For this second arm, normalized gradient of the volume-effect regression curve was found to be γ50=7.8 [3.2-14.7] and ED50% = 95.7 cc [84.7-117.8] (*see Figure*). The Receiver Operating Characteristics analysis (ROC) showed excellent predictive capabilities of the model, with Area Under the Curve AUC=0.94. Based on these findings, a volume cutoff value of 80 cc, corresponding to an acceptable 20% risk of OVS G2 or greater was selected.

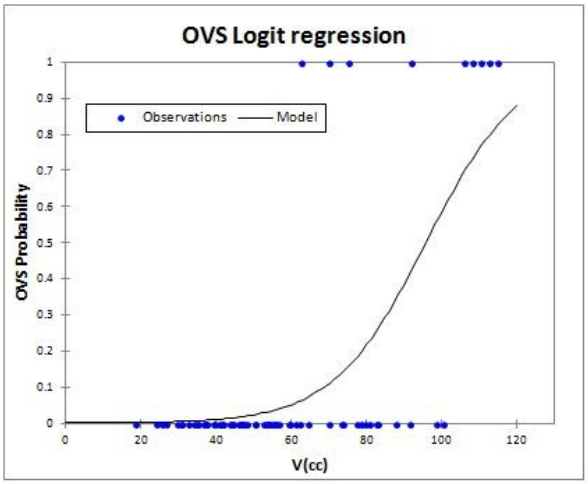

Conclusion: Depending on the HF scheme, patients with larger prostate volume will face an increasing risk of OVS. This may compromise their quality of life and alter the RT treatment schedule. In this work, we successfully correlated OVS to prostate volume. This predictive model can be exploited for decision-making prior to treatment. In our Institution, patients with prostate volume larger than 80 cc will be preferably addressed to the HF1 schedule due to the risk of OVS.

PO-0746

Spanish validation of Charlson Index applied to prostate cancer

F. Casas i Duran[1], F. Ferrer[2], A. Herreros[3], J. Saez[4], C. Camacho[4]
[1]*Hospital Clinic, Radiation Oncology, Barcelona, Spain*
[2]*Hopsital Duran I Reynals, Radiation Oncology, Hopsitalet del Llobregat, Spain*
[3]*Hospital Clinic, Radiation Oncology Physics, Barcelona, Spain*
[4]*Hospital Clinic, Radiation Oncology Physics, Barcelona, Spain*

Purpose or Objective: Comorbidity assessment is essential to triage of care for men with prostate cancer. Specially in these with an expectative of life less of ten years. We made a Spanish validation of comorbid revised Charlson index (RCI) applied to prostate cancer.

Material and Methods: A group of 619 consecutive patients of Prostate Cancer diagnosed between 1994- 2007 were send for clinical assessment at Radiation Oncology Department of Hospital Clinic of Bacelona.
A long the period of follow-up (till November 2014) 69 patients deceased for Prostate Cancer and were excluded in this study in order to determine the risks of mortality associated with comorbidities measured by the RCI.

RCI was classified in three categories 0 to 2 , 3 to 4 and 5 and higher. For this purpose we used Kaplan-Meier method and Cox proportional hazards modeling

Results: Finally 550 patients with prostate cancer were included, with median age of 70 years old (47-85), Mean follow-up time was 136.8 months, between 5,6 and 245,8 months. D'Amico risk classification distribution was for low risk, mediun and high 20.4%, 36,5% and 43,1% respectively. RCI distribution categories was as follows 61,5%, 21,8 and 16,7%. Survival analysis showed significant differences (p<0.001) between RCI groups at 5 and 10 years. Survival probability was 98,2 and 88,5% ; 95% and 79,6% ; and 52,2% and 8,9% was respectively for each RCI category.

Conclusion: RCI allowed for more accurate identification of men at highest risk for other cause mortality.
Our results are in concordance with original RCI .This revised index may be used to aid medical decision making and personalized medecine for men with prostate cancer.

PO-0747

Revisiting guidelines for target definition after prostatectomy when taking MRI study into account

G. Sancho Pardo[1], D. Hernandez[2], D. Gimenez[1], N. Jornet[3], M. Menso[2], E. Umbrarescu[1], F. Benítez[1], G. Gómez de Segura[1], J. Craven-Bartle[1]
[1]*Hospital de la Santa Creu i Sant Pau, Radiation Oncology, Barcelona, Spain*
[2]*Hospital de la Santa Creu i Sant Pau, Radiology, Barcelona, Spain*
[3]*Hospital de la Santa Creu i Sant Pau, Medical Physics, Barcelona, Spain*

Purpose or Objective: The definition of the clinical target volume (CTV) for salvage radiotherapy after prostatectomy is based on clinical and pathologic variables of the tumor and consensus guidelines. Multiparametric-MRI is recommended to evaluate pelvic recurrences after radical prostatectomy when the PSA is low (0.2-2 ng/ml) but the benefit of planning individualised radiation treatment based on the results of MRI is unknown. We analysed whether all suspicious lesions detected with pelvic multiparametric MRI were included in the clinical target volume defined according to four current guidelines and we determined the percentage of missing target if this radiological information was lost.

Material and Methods: We retrospectively reviewed the clinical records and multiparametric MRI studies of 70 patients with PSA recurrence after radical prostatectomy. Salvage radiotherapy of at least the prostate bed was indicated in all cases. On the simulation CT scan of 33 patients who had visible tumor recurrence in the MRI study, we delineated four different CTV according to RTOG, EORTC, PMH and FROGG consensus guidelines for postoperative prostate bed irradiation. We delineated a relapse CTV which included the radiological tumor recurrence plus 5 mm. For the PTV, we added a 5 mm margin. We compared volume size of the CTV and determined the percentage of geographically missed target (relapse PTV not included / relapse PTV).

Results: Multiparametric-MRI was positive in 33/70 patients. Local recurrence occurred in 27 patients, mainly in the perianastomotic area (19). Mutiparametric-MRI detected positive lymph nodes in 7 patients, mostly in the external iliac region. The mean size of the lymph nodes was 10 mm (range 8-16 mm). The mean volumes of the CTV delineated according to the EORTC, RTOG, PMH and FROGG consensus were 81.5, 100.7, 109.3 and 99.7 cc, respectively. In 2 out of 33 cases, the recurrence depicted in the pelvic MRI was not totally enclosed in the CTV, independently of the consensus guidelines used. The missed recurrences were located in the left retrovesical region (patient 1) and at the level of the penile bulb (patient 2) . The volumes of the relapsed PTV were 23.4 and 14.9 cc, respectively. The percentages of relapse PTV out of the PTV created according to each guideline were 41%, 59%, 44 and 44% in patient 1 and 44%, 39%, 39% and 41% in patient 2. In 7 out of 70 patients (10%), lymph node recurrence would have been missed if we had only considered salvage prostate bed irradiation.

Conclusion: Using current guidelines for CTV definition for salvage radiotherapy after prostatectomy, we found that the local recurrences depicted in the pelvic multiparametric MRI were totally covered in most patients. Multiparametric-MRI may help tailor local and lymph node CTV and identify lesions to treat with a higher dose

PO-0748

Escalated-dose IMRT for prostate cancer: long-term toxicity and biochemical outcomes

H. Bettina[1], D. Strauß[1]
[1]*Südharz- Krankenhaus Nordhausen gGmbH- Germany, Department of Radiation Oncology and Radiotherapy, Nordhausen, Germany*

Purpose or Objective: To report the toxicity and preliminary biochemical outcomes with high-dose intensity-modulated radiation therapy (IMRT) to a dose of 82.8Gy in patients prostate cancer.

Material and Methods: Between April 2002 and December 2013, 757 patients with biopsy proven prostate cancer were treated with high-dose IMRT. While 398 patients received a 7 or 8- field -IMRT -sliding window- technique up to a median total dose to the prostate of 77.4 Gy/1.8Gy, 359 patients were treated with a 2 arc-Volumetric Modulated ArcTherapy (VMAT) plans up to a median total dose to the prostate of 82.0Gy/ 1.8Gy. In 264 high-risk prostate cancer patients the pelvic node region was treated to incorporate the nodes at risk. Total doses of 50.4Gy were prescribed to the pelvis. In 29 % of SW patients and 23% of VMAT patients an additional boost of 5 to 16Gy was administered in cases of MRI-staged lymph node metastases. Acute and late toxicities were prospectively scored by the RTOG/ LENT SOMA morbidity grading scales (until 2009) and a modified CTCAEv3.0 score (since 2009), respectively. Biochemical failure was defined according to the Phoenix definition of nadir + 2ng/ml. The median follow- up time was 65 months (range,12-151 months).

Results: The IMRT dose distribution provided excellent PTV coverage and satisfying protection of all the organs at risk, with less than 2% of all patients experiencing grade (G) 3 toxicities, G4 toxicities were not observed at all. In total 40.3 / 11 / 1.1% of patients developed acute G1/ 2/ 3 genitourinary (GU) toxicities. 28%/ 3.1% of patients experienced acute G1/ 2 gastrointestinal (GI) side effects, no patient developed acute > G2 gastrointestinal symptoms. Late GU- and GI toxicity was mild with > 85% of the patients free from any GU/GI toxicity during follow-up and no time trend to increased rates or to higher grade of GU/GI-toxicity. Maximum late GU toxicities were G1/ 2/ 3 for 10/ 2.5/ 1.6% of patients, respectively. Maximum late GI toxicities were G1/2 for 4.9 / 0.4%of patients. The 5-year freedom from biochemical failure (FFBF) was 87.8%for all patients and 95, 79.9 and 83.4% for low-, intermediate-, and high-risk disease.

Conclusion: These data demonstrate that escalated -dose IMRT is a well tolerated technique in prostate cancer patients and the preliminary excellent biochemical control rates are encouraging.

PO-0749

Factors predicting late severe urinary incontinence after postprostatectomy RT: a longitudinal study

B. Noris Chiorda[1], C. Sini[2], C. Fiorino[2], F. Badenchini[3], A. Briganti[4], A. Chiara[1], C.L. Deantoni[1], N. Slim[1], N. Suardi[5], F. Montorsi[4], N. Di Muzio[1], C. Cozzarini[1]
[1]*San Raffaele Scientific Institute, Department of Radiation Oncology, Milan, Italy*
[2]*San Raffaele Scientific Institute, Department of Medical Physics, Milan, Italy*
[3]*Istituto Nazionale Tumori - San Raffaele Scientific Institute, Department of Radiation Oncology, Milan, Italy*

[4]*Vita-Salute San Raffaele University - San Raffaele Scientific Institute, Department of Urology, Milan, Italy*
[5]*San Raffaele Scientific Institute, Department of Urology, Milan, Italy*

Purpose or Objective: The fear of radiotherapy-induced urinary incontinence (URINC) often contraindicates post-prostatectomy RT (POPRT), despite the lack of accurate data about its real incidence and severity. The purpose of this analysis was to analyze clinico-dosimetric factors predicting severe, self-reported URINC 1 and 2 years after POPRT.

Material and Methods: In 2012 a longitudinal, observational study aimed at assessing URINC from POPRT including prophylactic whole-pelvis irradiation (WPRT) was activated at our Institute. For the evaluation of urinary toxicity, 2 validated questionnaires, IPSS and ICIQ-SF, are to be filled-in by pts at baseline, at RT mid-point and end, at 3 and 6 months after RT conclusion, and every 6 months thereafter. This analysis pertains to the first 101 pts correctly filling the questionnaires at baseline and at 12 months (60 also at 2 years). Fifty-four and 47 pts were treated with adjuvant (ADV) and salvage (SALV) intent after a median of 4 and 38 months, respectively, from radical prostatectomy (RP), with either conventional (n=42) or moderately hypofractionated (n=59) regimens, at a median 2-Gy equivalent dose (EQD2) to the prostatic bed of 70 and 74 Gy in ADV and SALV cohort, respectively, and a median EQD2 dose of WPRT of 50 Gy.

Results: The mean baseline ICIQ scores were 7.8 and 4.8 in ADV and SALV cohorts, respectively (p=0.009). The corresponding values at 1 and 2 years were 7.4 vs 7.3 and 8.5 vs 7.9, respectively. Severe URINC (³ 13 points) was recorded in 23% and 19% at 1 year, and in 37% and 21% of pts treated with ADV and SALV intent, respectively (p ≤ 0.20). The 75th quartiles of ICIQ at 12 (ICIQ12) and 24 (ICIQ24) months (12 and 13 points, respectively), were set as end-points for regression logistic analysis. Several clinico-dosimetric factors, including age, diabetes, hypertension, pT and pN stage, # of removed LNs, RT intent, time from RP to RT, fractionation, EQD2, adjuvant androgen deprivation (AAD), IQIQ and IPSS baseline values were analyzed. Variables with a p-value <0.20 at univariable analysis were entered into a backward stepwise multivariable model indicating baseline ICIQ and nocturia (IPSS item #7) and AAD as predictors of ICIQ12 (AUC 94%), while baseline ICIQ and EQD2 predicted ICIQ24 (AUC 89%).

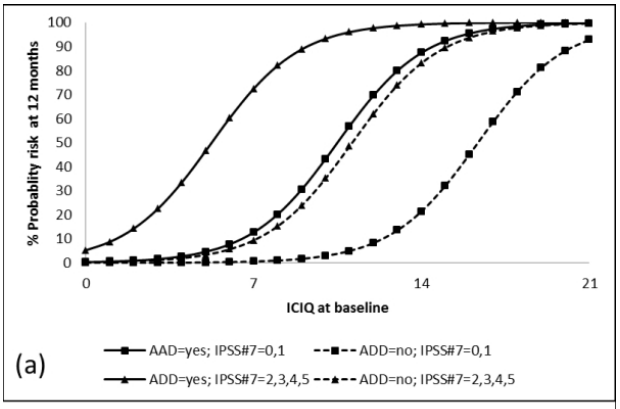

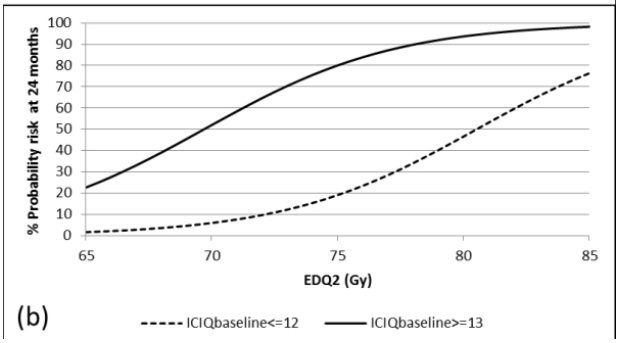

Conclusion: The risk of long-term severe URINC 1 and 2 years after POPRT is strongly modulated by baseline URINC, and by AAD and higher EQD2, respectively (Figure 1).

PO-0750

Conventionally-fractionated VMAT vs. SBRT in prostate cancer:PSA kinetics, toxicity,quality of life

M. Tambas[1], F. Agaoglu[1], A. Iribas[1], M. Guveli[1], Y. Dizdar[1], M. Okutan[2], D. Ozkan[3], N. Tenekeci[3], E. Darendeliler[1]
[1]*Istanbul University Institute of Oncology, Radiation Oncology, Istanbul, Turkey*
[2]*Istanbul University Institute of Oncology, Medical Physics, Istanbul, Turkey*
[3]*Istanbul University Institute of Oncology, Radiology, Istanbul, Turkey*

Purpose or Objective: In the present study, conventionally fractionationed volumetric arc therapy (VMAT) and hypofractionated stereotactic body radiotherapy (SBRT) modalities were aimed to compare in terms of side effects and quality of life (QOL) in patients with localized prostate cancer.

Material and Methods: Patients who admitted to I.U. Institute of Oncology with a diagnosis of localized prostate cancer during the period from March 2010 to December 2013 were included into the study. Patients received radical RT with dose schedules of either 33.5 Gy/5 fr for SBRT or 75.6 Gy/35 fr for VMAT. Acute and late side effects of treatment were evaluated according to CTCAE version 4. IPSS and EORTC QOL-PR25 forms were used to assess QOL at baseline, end of treatment and during follow-up.

Results: Of the 48 patients (28 SBRT, 20 VMAT) who were included into the study, 40 (20 SBRT, 20 VMAT) were evaluated for their QOL status. All demographic and pathological features including median age of the patients, clinical manifestations, and the risk groups were found to be similar between treatment groups. PSA control rates were %100 in both arms during the follow up with a median of 23 months. PSA nadir values were detected to be 0.5 ng/dl in both arms. PSA bounce was observed in 43% and 50% of patients in SBRT and VMAT arms, respectively. The magnitude of PSA bounce value was significantly higher in SBRT arm compared with VMAT (0.8 ng/dl vs. 0.1 ng/dl, p=0.01). PSA decline rate in VMAT arm was found to be significantly higher than in SBRT arm (p = 0.028). Grade 3 rectal toxicity was not observed in any of the treatment arms. Although Grade 3 urinary side effects were not seen in patients treated with VMAT technique, 3 patients (10.7%) in SBRT arm with a history of TURP before RT experienced Grade 3 urinary toxicity. No significant difference was observed between the two arms concerning sexual activity functioning and sexual functioning scores whereas the scores at 10.5 and 13.5 months were found to be significantly decrased compared with baseline in both treatment arms. SBRT and VMAT arms did not differ significantly regarding urinary, incontinence, bowel symptom scores and IPSS obstruction scores. The magnitude of increase in IPSS scores at the end of the treatment compared with baseline were detected to be significantly higher in VMAT arm than SBRT arm (p=0.046). The decrease in hormonal symptom scores at 4.5, 10.5 and 13.5 months compared with baseline was detected to be significantly higher in VMAT arm than SBRT arm (p=0.007, p=0.027, and p=0.021, respectively).

Table 1. Comparison of SBRT and VMAT arms in terms of amount of changes over time relative to baseline EORTC-PR25 functioning (sexual activity and sexual) and symptom (urinary, incontinence aid, bowel and hormonal) scores

	SBRT Mean±SD (Median)	VMAT Mean±SD (Median)	p	SBRT Mean±SD (Median)	VMAT Mean±SD (Median)	p
	Sexual Activity Functioning Scores			**Sexual Functioning Scores**		
RT Completion	-3±29(0)	0,8±39(0)	0,12	0,8±24(0)	0,0±29(0)	0,89
1.5 month	-10±37(0)	-5±41(0)	0,39	-1,7±22(0)	0,8±36(0)	0,56
4.5 month	-8±33(0)	-20±53(0)	0,87	-5,0±29(0)	-15,8±45(-4)	0,54
7.5 month	-13±40(0)	-19±53(0)	0,81	-4,6±29(0)	-16,3±45(-17)	0,40
10.5 month	-29±48(-33)	-28±50(0)	0,63	-20,0±43(-25)	-22,5±47(-17)	0,97
13.5 month	-25±39(-25)	-35±50(-17)	0,61	-19,6±36(-17)	-25,8±44(-21)	0,66
	Urinary Symptoms Scores			**Incontinence Aid Scores**		
RT Completion	-0,2±21(-2)	-3,7±39(0)	0,97	3,3±10(0)	0,0±19(0)	0,67
1.5 month	-0,8±16(0)	-12,7±37(-4)	0,18	3,3±10(0)	-1,7±17(0)	0,32
4.5 month	-6,7±16(-4)	-10,6±34(-6)	0,88	-1,7±8(0)	5,0±27(0)	0,19
7.5 month	-5,6±19(-4)	-10,4±35(-2)	0,81	1,7±17(0)	5,0±27(0)	0,43
10.5 month	-4,6±26(-2)	-6,9±36,7(0)	0,85	5,0±27(0)	5,0±27(0)	1,00
13.5 month	-5,6±27(-4)	-8,3±36,1(0)	0,90	0,0±22(0)	6,7±28(0)	0,26
	Bowel Symptom Scores			**Hormonal Symptom Scores**		
RT Completion	2,9±13(0)	-0,4±19(0)	0,98	3,1±16(6)	-2,8±11(0)	0,08
1.5 month	9,2±22(0)	-2,9±16(0)	0,31	6,1±13(6)	-1,1±15(0)	0,09
4.5 month	0,0±20(0)	-5,8±14(0)	0,42	6,9±17(8)	-5,3±15(0)	*0,007*
7.5 month	-0,4±20(0)	-3,3±20(0)	0,47	6,1±21(8)	-1,9±16(0)	0,10
10.5 month	-2,9±23(0)	-4,2±24(0)	0,76	6,1±21(8)	-5,0±15(-3)	*0,027*
13.5 month	-2,5±24(0)	-10,4±19(0)	0,21	5,6±23(3)	-7,5±14(-6)	*0,021*
	Total IPPS Scores			**IPSS-Obstruction Scores**		
RT Completion	0,1±7(-1)	3,2±6(2,5)	*0,046*	0,3±5(0)	1,2±3(0)	0,30
1.5 month	-1,0±7(-1)	0,3±5(0)	0,63	-0,9±5(-1)	-0,7±3(0)	0,61
4.5 month	-3,8±7(-2)	-2,0±4(-2)	0,50	-2,9±5(-2)	-1,5±3(-1)	0,40
7.5 month	-4,0±7(-2)	-1,4±5(-1)	0,30	-3,0±5(-1)	-1,5±4(-1)	0,46
10.5 month	-2,8±6(-2)	-0,6±8(-2)	0,57	-2,0±4(-1)	-0,9±6(-1)	0,99
13.5 month	-3,1±7(-1)	-2,4±5(-3)	0,92	-2,3±6(-1)	-2,0±3(-2)	0,79

Abbreviations: SBRT=Stereotactic body radiotherapy, VMAT= Volumetric Arc Therapy, SD=Standard deviation, IPSS=International Prostate Symptom Score

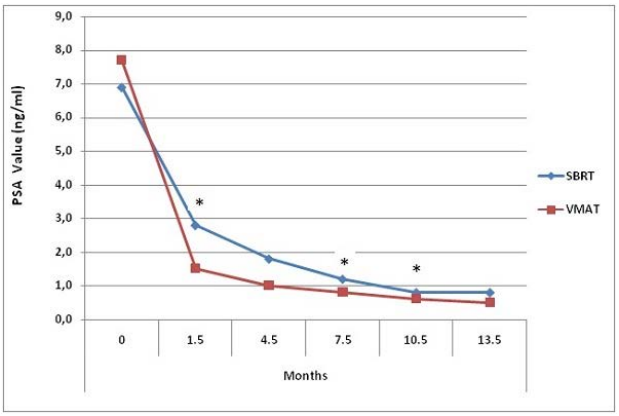

Conclusion: Both SBRT and VMAT treatments were highly successful in terms of PSA control. QOL assessment were found to be mostly similar between treatment modalities. Grade 3 urinary toxicities might be eliminated with careful patient selection for SBRT technique

PO-0751

Predicting recurrence after 3DC Radiotherapy for prostate cancer: proposal for a new classifier

P. Gabriele[1], B. Jereczek-Fossa[2], M. Krengli[3], E. Garibaldi[4], M. Tessa[5], G. Moro[6], G. Girelli[7], C. Bona[8], V. Balcet[9], P. Ferrazza[10], D. Gabriele[11]

[1]Candiolo Cancer Centre FPO-IRCCS, Department of Radiotherapy, Candiolo, Italy
[2]IEO Milan, Radiotherapy, Milan, Italy
[3]Novara H- Univ Avogadro, Radiotherapy, Novara, Italy
[4]Candiolo Cancer Centre FPO-IRCCS, Department of Radiotherapy, Candiolo Turin, Italy
[5]Asti Hospital, Radiotherapy, Asti, Italy
[6]Biella Hospital, Radiotherapy, Biella, Italy
[7]Ivrea Hospital, Radiotherapy, Ivrea, Italy
[8]Verbania Hospital, Radiotherapy, Verbania, Italy
[9]Como Hospital, Radiotherapy, Como, Italy
[10]Pisa Univ Hospital, Radiotherapy, Pisa, Italy
[11]Physiology Turin Univeristy, Neuroscience, Turin, Italy

Purpose or Objective: The aim of this work is to develop an algorithm to predict recurrence in prostate cancer patients treated with radical radiotherapy, getting up to a prognostic power higher than traditional D'Amico risk classification.

Material and Methods: 2493 men belonging to the EUREKA-2 retrospective multi-centric database on prostate cancer and treated with external-beam radiotherapy (3D-CRT and or IMRT) as primary treatment comprised the study population. A Cox regression time to PSA failure analysis was performed in univariate and multivariate settings, evaluating the predictive ability of age, pre-treatment PSA, clinical-radiological staging, Gleason score and percentage of positive cores at biopsy (%PC). The accuracy of this model was checked with bootstrapping statistics. Subgroups for all the variables' combinations were combined to classify patients into five different "Candiolo" risk-classes for biochemical Progression Free Survival (bPFS); thereafter, they were also applied to clinical PFS (cPFS), systemic PFS (sPFS) and Prostate Cancer Specific Survival (PCSS), and compared to D'Amico risk grouping performances.

Results: the Candiolo classifier splits patients in 5 risk-groups with the following 10-years bPFS, cPFS, sPFS and PCSS: for very-low-risk 90%, 94%, 100% and 100%; for low-risk 74%, 88%, 94% and 98%; for intermediate-risk 60%, 82%, 91% and 92%; for high-risk 43%, 55%, 80% and 89% and for very-high-risk 14%, 38%, 56% and 70%. Our classifier outperforms D'Amico risk classes for all the end-points evaluated, with concordance indexes of 71.5%, 75.5%, 80% and 80.5% versus 63%, 65.5%, 69.5% and 69%, respectively.

Conclusion: Our classification tool, combining five clinical and easily available parameters, seems to better stratify patients in predicting prostate cancer recurrence after radiotherapy compared to the traditional D'Amico risk classes. This classifier must be validate by another prostate cancer series.

References: Gabriele D et al: Beyond D'Amico risk classes for predicting recurrence after external beam radiotherapy for prostate cancer: the Candiolo classifier. Radiat Oncol 2015, in press

PO-0752

Outcome of prostate cancer patients treated with 3DCRT: impact of rectal/bladder preparation

A. Maggio[1], E. Garibaldi[2], D. Gabriele[3], S. Bresciani[1], E. Delmastro[2], A. Di Dia[1], A. Miranti[1], M. Poli[1], P. Gabriele[2], M. Stasi[1]

[1]Candiolo Cancer Institute - FPO-IRCCS, Medical Physics, Candiolo, Italy
[2]Candiolo Cancer Institute - FPO-IRCCS, Radiotherapy, Candiolo, Italy
[3]University of Torino, Neuroscience Department- Physiology Unit, Turin, Italy

Purpose or Objective: To test the hypothesis that rectal/bladder preparation is associated with an increase in Cancer Specific Overall Survival (CSOS), in Clinical Disease Free (CDFS) and Biochemical Disease free Survival (BDFS)

Material and Methods: From October 1999 to March 2012, 1080 prostate cancer patients (PCa) were treated with 3DCRT. 761 patients (pts) were treated with empty rectum and comfortable full bladder while for 319 pts no rectal/bladder preparation (NRBP) protocol was adopted. The mean age was 69.2±5.6 years. The mean prescribed dose was 76±2 Gy. The mean followup was 81±39 months. Survival analysis was performed by Kaplan Meier method. Comparison between groups were made with the log-rank test. A Cox proportional hazards model was applied for univariate (UVA) and multivariate analysis (MVA). Hazard Ratio (HR) was used to measure how rapidly an event occurs.

Results: Pts with rectal/bladder preparation (RBP) have significantly lower biochemical and clinical failures rates and lower risk of dying of PCa respect to NRBP pts (log-rank p<0.0001). At 140 months for RBP and NRPB, the CSOS was 95% vs 85%, the CDFS was 81% vs 71%, the BDFS was 64% vs 48 %, respectively. Table 1 shows UVA and MVA results. In MVA, for CSOS the Gleason Score (GS) and RBP predicted for death from PCa, while for CDSF and BDFS the GS, D'Amico Risk Classification, PSA, dose>75 Gy, clinical stage and RBP

predicted for clinical and biochemical failures. MVA indicates that RBP is an independent risk factor for biochemical failure (p=0.003, HR=0.6) while it is the strongest risk factor for clinical failures and PCa deaths (p<0.0001, HR<0.5, regression coefficient b<-0.5). No statistical significant difference in rectal volume between RBP (mean volume 62.4±24.5 cc) and NRPB (mean volume 63.4±27 cc) was observed (chi square p value equal to 0.52)

Cancer Specific Overall Survival	Univariate Analysis			Multivariate Analysis		
	p	b	HR	b	p	HR
% Positive Cores	0.0001	0.020	1.02			
Number of positive Cores	0.0060	0.150	1.16			
Bioptic Gleason Score	<0.0001	0.680	1.98	0.650	<0.0001	1.92
D'Amico Risk Classification	<0.0001	1.020	2.80			
Lymph nodes irradiation	0.0001	1.130	3.10			
Seminal Vesicle irradition	<0.0001	2.180	8.80			
Rectal/Bladder preparation	0.0002	-1.030	0.36	-1.220	<0.0001	0.29
Clinical- radiological Stage	0.0001	0.880	2.42			
Positive lymph node in CT	0.0001	1.300	3.70			
PSA	0.029	0.004	1.00	0.005	0.03	1.01
Biochemical Disease Free Survival	**Univariate Analysis**			**Multivariate Analysis**		
	p	b	HR	b	p	HR
% Positive Cores	<0.0001	0.01	1.01			
Number of positive Cores	<0.0001	-0.09	1.10			
Bioptic Gleason Score	<0.0001	0.32	1.37	0.1	0.027	1.15
D'Amico Risk Classification	<0.0001	0.65	1.92	0.41	<0.0001	1.50
Lymph nodes irradiation	<0.0001	0.81	2.26			
Seminal Vesicle irradition	<0.0001	0.99	2.69			
Rectal/Bladder preparation	<0.0001	-0.65	0.52	-0.60	<0.0001	0.50
Clinical- radiological Stage	<0.0001	0.58	1.79	0.30	0.008	1.34
Positive lymph node in CT	<0.0001	0.81	2.24			
PSA	<0.0001	0.00	1.004	0.002	0.014	1.00
Dose>75 Gy	0.0098	-0.43	0.65	-0.39	0.02	0.67
Clinical Disease Free Survival	**Univariate Analysis**			**Multivariate Analysis**		
	p	b	HR	b	p	HR
% Positive Cores	0.0001	0.01	1.01			
Number of positive Cores	<0.0001	0.14	1.14			
Bioptic Gleason Score	<0.0001	0.45	1.57	0.2400	0.0040	1.27
D'Amico Risk Classification	<0.0001	0.77	2.17	0.550	0.0001	1.73
Lymph nodes irradiation	<0.0001	0.99	2.70			
Seminal Vesicle irradition	<0.0001	1.09	3.00			
Rectal/Bladder preparation	0.0010	-0.52	0.56	-0.4900	0.0030	0.61
Clinical- radiological Stage	0.0002	0.50	1.65			
Positive lymph node in CT	0.0002	0.82	2.28			
PSA	<0.0001	0.00	1.00	0.0034	0.0030	1.00
Age	0.003	-0.04	0.96	-0.041	0.0020	0.96
Dose>75 Gy	0.006	-0.61	0.54	-0.500	0.0200	0.60

Figure 1: Univariate and multivariate Cox regression analysis

Conclusion: We found strong evidence that rectal/bladder preparation significantly decreased (HR<0.6, b<-0.5) the probability of death from PCa, biochemical and clinical failures in patients who were treated with 3DCRT for PCa without daily image-guided prostate localization, presumably because pts with RBP are able to maintain a reproducible empty rectum and comfortable full bladder for all the treatment. These results also emphasize the routinely need of image-guided radiotherapy to improve outcome in prostate cancer patients

PO-0753

Prospective evaluation of urinary function in patients with prostate cancer treated with RT

F. Badenchini[1], C. Cozzarini[2], B. Avuzzi[3], C. Sini[4], A. Fodor[2], T. Rancati[1], R. Valdagni[5], N. Di Muzio[2], C. Fiorino[4]

[1]*Fondazione IRCCS Istituto Nazionale dei Tumori, Prostate Program, Milan, Italy*

[2]*San Raffaele Scientific Institute, Radiation Oncology, Milan, Italy*

[3]*Fondazione IRCCS Istituto Nazionale dei Tumori, Radiation Oncology, Milan, Italy*

[4]*San Raffaele Scientific Institute, Medical Physics, Milan, Italy*

[5]*Fondazione IRCCS Istituto Nazionale dei Tumori, Prostate Program- Radiation Oncology, Milan, Italy*

Purpose or Objective: The aim of the study is to prospectively evaluate urinary symptoms using the International Prostate Symptom Score (IPSS) in patients with localized prostate cancer (CaP) treated with radical (RRT) or postprostatectomy (PRT) radiotherapy delivered with conventional (CONV) or moderately hypofractionated (HYPO) fractionation.

Material and Methods: We considered patients enrolled in the two multicentric prospective observational studies DUE01 (RRT, CONV and HYPO) and IHU WPRT TOX (RRT and PRT, including irradiation of the pelvic lymphnodal area, CONV and HYPO). The IPSS questionnaire, evaluating 7 symptoms (IPSS1-IPSS7) and a quality of life (IPSS8), is filled in before and at the end of RT, then 3 and 6 after treatment end and every 6 months thereafter up to 5 years after the end of treatment. In this preliminary analysis only data relative to first year will be analyzed. Longitudinal trends were assessed by analysis of variance (anova).

Results: The analysis pertains to 146 RRT CONV pts, 104 RRT HYPO pts, 74 PRT CONV pts and 94 PRT HYPO. The median age in the 2 studies was 71 (RRT) and 66 (PRT) years (p = 0.0001). Overall, urinary function was always better in the RRT CONV cohort. Statistically significant differences among the 4 groups have emerged with respect to urinary frequency, urgency, effort, nocturia. When comparing RRT vs PRT, frequency (p = 0.007) and stress (p = 0.01) were significantly more present in PRT, while only a borderline difference in terms of urgency (p = 0.07) was evident. The last item of IPSS shows a significant difference of quality of life between groups, especially at 12 month where RRT cohort, especially CONV, shows a better score than PRT patients. Figure 1 shows the comparison of each group for all IPSS items (incomplete emptyng, urinary frequency, intermittence, urgency, urinary stream, obstruction, nocturia, QoL), evaluating the mean response in the first five time of compilation (Rt start, RT end, 3m, 6m, 12m).

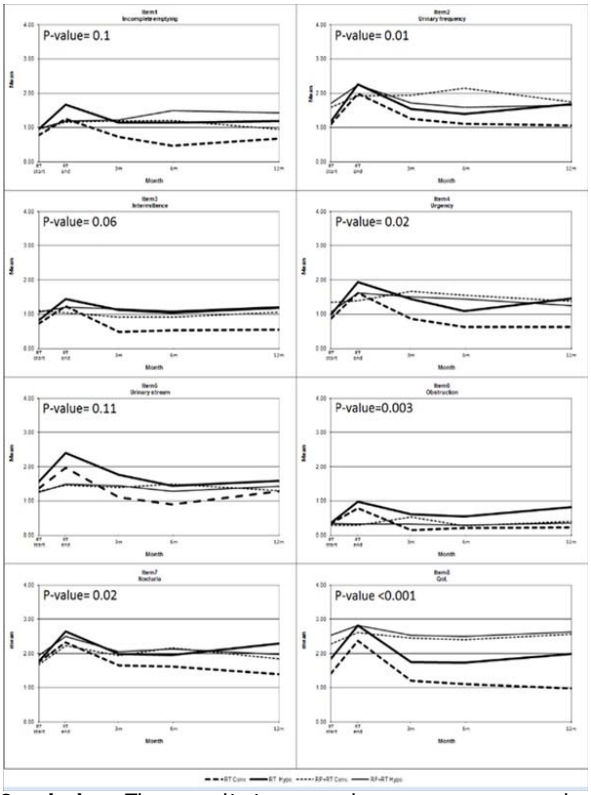

Conclusion: These preliminary results seem to suggest that RRT would result in less deterioration of urinary symptoms over time than PRT, especially RRT with conventional fractionation. Further analyses are ongoing in order to study the effect of baseline urinary situation, age, doses to the bladder and the impact of each urinary symptoms on quality of life.

PO-0754

Whole body Integral dose is associated with radiotherapy related fatigue in prostate cancer

N. Joseph[1], A. McWilliam[1,2], J. Chang-Claude[3], S. Davidson[1,2], K. Johnson[4], T. Rancati[5], C. Talbot[6], A. Webb[6], C. West[2], A. Choudhury[1,2]

[1]*Christie NHS Foundation Trust, Clinical Oncology, Manchester, United Kingdom*

[2]*University of Manchester, Institute of Cancer Sciences, Manchester, United Kingdom*

[3]*German Cancer Research Centre, Cancer Epidemiology, Heidelberg, Germany*

[4]University of Leicester, Clinical Oncology, Leicester, United Kingdom
[5]Fondazione IRCCS Istituto Nazionale dei Tumori Via, Prostate Cancer Program, Milan, Italy
[6]University of Leicester, Medical Genetics, Leicester, United Kingdom

Purpose or Objective: Although intensity modulated radiotherapy (IMRT) permits the delivery of a highly conformal dose to target volumes while sparing dose to identified organs at risk, it results in a higher whole body integral dose due to irradiation of a larger volume of tissue at lower doses. A randomized clinical trial in head and neck cancer comparing IMRT with 3-D conformal radiotherapy, demonstrated higher acute fatigue in the IMRT cohort, raising the possibility of an association with higher integral dose. We hypothesized that a higher integral whole body dose is associated with worsening fatigue and an adverse functional outcome in patients with localized prostate cancer treated with intensity modulated external beam radiotherapy.

Material and Methods: 26 patients with localized adenocarcinoma of prostate treated with intensity modulated external beam radiotherapy were included in this analysis. The integral dose was calculated as the product of mean body dose and body volume and the study cohort was dichotomized using the median integral dose as the cut-off value. The fatigue, physical functioning and role functioning domains of the EORTC QLQ-C30 questionnaire prior to radiotherapy and upon completion of radiotherapy were assessed. The outcome measure was defined as worsening in any of these three domains.

Results: The median integral dose was 119.7 litre-Gy (range 90.5 – 168.1). In the whole population 17/26 (65%) had worsening of fatigue, physical or role functioning. A significantly higher proportion of patients with an integral dose above median had worsening fatigue, physical and role functioning compared with patients with an integral dose below median. (6/13 versus 11/13; z test for proportions p=0.04).

Conclusion: To our knowledge, this is the first study linking acute worsening of fatigue and functional outcome with whole body integral dose. Further validation in a larger cohort and in different tumour sites is necessary and the relationship between integral dose and toxicity merits further investigation.

PO-0755

Intestinal toxicity from WPRT delivered with IMRT is negligible. A multicentric observational trial.

C. Sini[1], E. Garibaldi[2], A. Maggio[3], L. Perna[4], A. Prisco[5], E. Moretti[6], M. Gaetano[7], V. Carillo[8], B. Avuzzi[9], T. Giandini[10], D. Cante[11], E. Petrucci[12], B. Saracino[13], V. Landoni[14], E. Della Bosca[15], P. Salmoiraghi[16], C. Bianconi[17], F. Badenchini[17], C. Fiorino[18], C. Cozzarini[19]
[1]Fondazione Centro San Raffaele, Medical Physics, Milan, Italy
[2]Istituto per Ricovero e Cura a Carattere Scientifico - IRCCS, Radiotherapy, Candiolo, Italy
[3]Istituto per Ricovero e Cura a Carattere Scientifico - IRCCS, Medical Physics, Candiolo, Italy
[4]San Raffaele Scientific Institute, Medical Physics, Milano, Italy
[5]Azienda Ospedaliera Universitaria S.Maria della Misericordia, Radiotherapy, Udine, Italy
[6]Azienda Ospedaliera Universitaria S.Maria della Misericordia, Medical Physics, Udine, Italy
[7]Centro AKTIS Diagnostica e Terapia, Radiotherapy, Napoli, Italy
[8]Centro AKTIS Diagnostica e Terapia, Medical Physics, Napoli, Italy
[9]Istituto Nazionale Tumori, Radiotherapy, Milan, Italy
[10]Istituto Nazionale Tumori, Medical Physics, Milan, Italy
[11]Azienda ASLTO4, Radiotherapy, Ivrea, Italy
[12]Azienda ASL TO4, Medical Physics, Ivrea, Italy
[13]Istituo Nazionale Tumori 'Regina Elena', Radiotherapy, Roma, Italy
[14]Istituto Nazionale Tumori 'Regina Elena', Radiotherapy, Roma, Italy
[15]Cliniche Gavazzeni - Humanitas, Radiotherapy, Bergamo, Italy
[16]Cliniche Gavazzeni Humanitas, Medical Physics, Bergamo, Italy
[17]Fondazione Centro San Raffaele, Radiotherapy, Milano, Italy
[18]San Raffaele Scientific Institute, Medical Physics, Milan, Italy
[19]San Raffaele Scientific Institute, Radiotherapy, Milano, Italy

Purpose or Objective: To prospectively evaluate acute intestinal toxicity (AIT) from RT including whole-pelvis irradiation (WPRT) for prostate cancer by means of a validated questionnaire (IBDQ, Intestinal Bowel Disease Questionnaire), and to investigate the intestinal symptoms that most affect patient quality of life (QoL).

Material and Methods: In 2014 a multicentric, observational trial aimed at assessing IT from RT including WPRT was activated. Prior to study activation, a pilot feasibility study was started in the coordinating Institute. For the study's purpose, the IBDQ is to be filled in by pts at baseline, RT mid-point and end, 3 and 6 months, and thereafter every 6 months up to 5 years. The questionnaire comprises 32 items investigating bowel symptoms (10 items), emotional health (12), systemic symptoms (5) and social function (5). The responses are scored on a seven-point scale in which 7 corresponds to the best function and 1 to the worst. Average per item scores can be calculated for each of the 4 domains. This analysis pertains to the first 144 pts (8 Institutes) with complete data available at baseline, RT mid-point and end. Initially, only pts treated with post-prostatectomy RT with either adjuvant (ADV, n= 71) or salvage (SALV, n=73) intent were enrolled. Pts were treated with static-field IMRT (n=31), Tomotherapy (n=42) and VMAT (n=71), with conventional (1.8-2 Gy/fr, n=78) or moderate hypofractionation (2.15-2.65 Gy/fr, median 2.35, n=66). The median EQD2 dose to the prostatic bed and pelvic lymph-nodal area was 71.2 and 50 Gy, respectively. 58 pts received concomitant androgen deprivation.

Results: Overall, self-perceived intestinal toxicity from WPRT was mild: mean scores for bowel symptoms at baseline, RT mid-point and end were in fact 6.58, 6.09, 5.90 (repeated measures Anova, $p<0.0001$), for emotional health 5.94,5.79,5.69 (0.0003), for social function 6.20, 5.83, 5.65 ($p<0.0001$) and for systemic symptoms 5.95, 5.55, 5.40 ($p<0.0001$), respectively. For the evaluation of acute toxicity, the worst variation (delta) between baseline and RT mid-point or end was considered. With respect to the bowel symptoms, the median score decrease (worsening) was 2 points for only one item (frequent bowel movements), 1 point for loose bowel movements, gas passage, abdominal bloating and urge to defecate, and 0 for abdominal pains and cramps, rectal bleeding, accidental soiling and nausea. Nevertheless, abdominal pain and urge to defecate were the two items with higher predictive power (AUC 72-79% at ROC curve analysis) with respect to a worsening of ≥ 1 point (25th percentile) of either emotional or systemic or social domains, as well as gas passage, urge to defecate and nausea (AUC 72-73%) for emotional.

Conclusion: The self assessed AIT from WPRT delivered by means of modern IMRT technique is negligible. Abdominal pain and urge to defecate are the 2 symptoms mostly correlated with a worsening of patient's QoL.

PO-0756

Choline PET/CT and Stereotactic Body Radiotherapy in oligometastatic prostate cancer patients

F. Pasqualetti[1], M. Panichi[1], A. Sainato[1], F. Matteucci[1], L. Derosa[2], P. Cocuzza[1], G. Coraggio[1], P. Ferrazza[1], S.

Montrone[1], M. Cantarella[1], D. Delishaj[1], A. Cristaudo[1], M. Fabrini[1], C. Greco[3], P. Erba[4]
[1]*Azienda Ospedaliero Universitaria Pisana, Radiotherapy, Pisa, Italy*
[2]*Azienda Ospedaliero Universitaria Pisana, Medical Oncology, Pisa, Italy*
[3]*Champalimaud Centre for the Unknown, Radiotherapy, Lisbon, Portugal*
[4]*University of Pisa, Department of Translational Research and New Technologies in Medicine, Pisa, Italy*

Purpose or Objective: A new entity of patients with recurrent prostate cancer limited to a small number of active metastatic lesions is having growing interest: the oligometastatic patients. Patients with oligometastatic disease could eventually be managed by treating all the active lesions with local therapy, i.e. either surgery or ablative stereotactic body radiotherapy. This study aims to assess the impact of [18F]Choline ([18F]FMCH) PET/CT and the use stereotactic body radiotherapy (SBRT) in patients (pts) with oligometastatic prostate cancer (PCa).

Material and Methods: Twenty-nine pts with oligometastatic PCa ≤3 synchronous active lesions detected with [18F]FMCHPET/CT) were treated with repeated salvage SBRT until disease progression (development of > three active synchronous metastases). Primary endpoint was systemic therapy-free survival measured from the baseline [18F]FMCHPET/CT.

Results: A total of 45 lesions were treated with SBRT. After a median follow-up of 11.5 months (range 3-40 months), 20 pts were still in the study and did not receive any systemic therapy. Nine pts started systemic therapy, and the median time of the primary endpoint was 39.7 months (CI 12.20-62.14 months). No grade 3 or 4 toxicity was recorded.

Conclusion: Repeated salvage [18F]FMCHPET/CT-guided SBRT is well tolerated and could defer the beginning of systemic therapy in selected patients with oligometastatic PCa.

PO-0757
SBRT for prostate cancer using tomotherapy: interim analysis of a prospective trial in 82 patients

V. Macias Hernandez[1], M. Blanco Villar[1], M.J. Fernandez Gomez[2], S. Garcia Repiso[3], P. Soria Carreras[1], A. Nieto Palacios[1], A.I. Rodriguez Gutierrez[1], O. Alonso Rodriguez[1], C. Cigarral Garcia[1], S. Rodriguez Garcia[1], C. Gil Restrepo[4], A. Matias Perez[1], F. Gomez Veiga[5], M. Martin Izquierdo[6], L.A. Perez Romasanta[1]
[1]*Hospital Clínico Universitario de Salamanca, Radiation Oncology, Salamanca, Spain*
[2]*University of Salamanca, Statistics, Salamanca, Spain*
[3]*Hospital Clínico Universitario de Salamanca, Medical Physics, Salamanca, Spain*
[4]*Hospital Provincial de Zamora, Radiation Oncology, Zamora, Spain*
[5]*Hospital Clínico Universitario de Salamanca, Urology, Salamanca, Spain*
[6]*Hospital Clínico Universitario de Salamanca, Radiology, Salamanca, Spain*

Purpose or Objective: 5-fraction SBRT using CyberKnife is a well-established safe alternative treatment for selected low-risk (LR) and intermediate-risk (IR) prostate cancer.
The aim of this study is to determine prospectively the morbidity (CTCAE) and QOL (auto-administered IPSS) of an 8-fraction scheme for high-risk (HR), IR and LR using tomotherapy.

Material and Methods: Exclusion criteria were T3b-4, GS 9-10, PSA ≥50, IPSS ≥20.
Since 2012 eighty-two patients were treated: 41 HR (23/41 with GS≥8 or PSA >20 or T3a, and 18/41 with ≥2 intermediate risk factors), 17 IR (GS 7 or PSA 10-20 or T2b-c), and 24 LR.
57/82 patients received 6-month hormonal therapy (HT).
8 fractions of 5.65 Gy for HR-IR, and 5.48 Gy for LR patients were delivered every other day over about 2.5 weeks. EQD2 is 92.3 Gy (HR, IR) or 87.4 Gy (LR) for prostate cancer (a/b 1.5), and 78.2 or 74.3 Gy for late-responding tissues (a/b 3), respectively.

Results: Median follow-up was 13.7 months (0.3-40.1).
No acute/late grade ≥3 events were observed. Late GU or GI grade 2 toxicities were far bellow 10% (see Table). We observed a slight urinary flare at 18 months.

		During/following SBRT (N=81)	1 month (N=80)	6 months (N=66)	12 months (N=50)	18 months (N=35)	24 months (N=27)
GU toxicity	Grade 1	41 **50.6%**	17 **21.2%**	11 **16.7%**	9 **18%**	3 **8.6%**	2 **7.4%**
	Grade 2	17 **21%**	3 **3.8%**	0 **0%**	0 **0%**	2 **5.7%**	0 **0%**
GI toxicity	Grade 1	26 **32.1%**	8 **10%**	6 **9.1%**	9 **18%**	7 **20%**	1 **3.7%**
	Grade 2	10 **12.4%**	0 **0%**	1 **1.5%**	1 **2%**	1 **2.9%**	2 **7.4%**
GU / GI toxicity	Grade 3+	0 **0%**	0 **0%**	0 **0%**	0 **0%**	0 **0%**	0 **0%**

IPSS scores (Q1-7) and patient satisfaction (Q8) returned to baseline at 6 months (p=0.21), after they significantly worsened at the last fraction (p=0.00), especially the IPSS-obstructive component (see Figure).

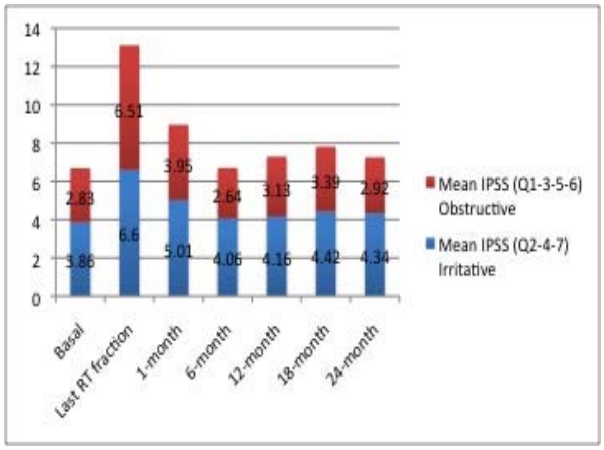

Without HT, PSA nadir has not been reached yet. Mean value at 24 months was 0.66 ng/mL.
With HT, PSA nadir was reached between 1-6 months and then raised up to 0.37 ng/mL average at 18 months (mean testosterone 291 ng/dL), to remain steady afterwards.
No biochemical (nadir+2) /clinical failure was found. One unrelated cancer/treatment death occurred during SBRT.

Conclusion: To our knowledge this is the first communication of SBRT using helical tomotherapy for localized prostate cancer.
The 8-fraction scheme is being well tolerated, with no moderate-severe toxicity, suggesting that this approach is safe.
Longer follow-up is needed to find out whether the delivery of equivalent doses near the plateau of the dose-response curve (>90 Gy) results in better tumour control in this cohort of patients (mostly HR and IR tumours).

PO-0758
Adjuvant or Salvage?10-y results of the AIRO Group on Prostate cancer multicentre prospective trial

F. Maurizi[1], P. Antognoni[1], S. Barra[1], F. Bertoni[1], A. Bonetta[1], G. Bortolus[1], A. Colombo[1], G. Frezza[1], O. Gabriele[1], C. Iotti[1], F. Mattana[1], S. Meregalli[1], G. Moro[1], M. Signor[1], G. Malinverni[1]
[1]*AIRO, AIRO National Working Group on Prostate Radiotherapy, Italy, Italy*

Purpose or Objective: The use of postoperative radiotherapy (RT) in patients (pts) at risk for local recurrence is well established for many tumours. The postoperative subgroup of the AIRO Working Group on Prostate RT carried out a multi-institutional prospective study to evaluate the impact of Adjuvant RT (PORT) and Salvage RT (SART) on biochemical outcomes in prostate cancer pts.

Material and Methods: Between January 2002 and December 2003, data of 440 pts (mean age: 65 years, range 42-81) treated with radical prostatectomy (RP) were collected by 14 Italian RT Departments. Of the 411 pts available for the 10 year analysis (median follow up: 111 months), 284 (69.1%) received PORT (started <6 months after RP) and 127 underwent SART because of increasing PSA level after having been undetectable or persistently elevated PSA (> 6 months after RP). Gleason Score (GS) > 7 and positive surgical margins (SM+) have been shown by 69% pts and 74.5% respectively; 76.5% presented locally advanced disease (pT3-4), 27 (6.7%) positive pelvic nodes; 163 pts (40.2%) revealed seminal vesicles invasion (SVI). All pts received RT to the prostatic fossa (mean dose of 67.8 Gy, range: 60-76). Pelvic RT was delivered to 111 pts (27%). Androgen deprivation (AD) was prescribed to 47,3% pts. Among 127 SART pts, pre-RT PSA level was 1 ng/mL or less in 56 pts (44,1%).

Results: Ten year analysis shows that 259 pts are disease free and 331 are still alive. 10 year (10-y) overall survival and biochemical control (BC) rate are 75.9% and 57.8% respectively. On univariate analysis, PORT versus SART, SVI and GS > 7 significantly influenced 10-y BC rate: 62.7% in PORT group versus 45.6% SART one (p = 0.003), 56.9% in pts with SVI versus 65.6% pts without SVI (p < 0.001), 52.5% if GS > 7 and 69.8% if GS < 7 (p= 0.003). SM+, pathological T and N stages, AD or pelvic RT had no impact on biochemical recurrence rate. SVI and PORT versus SART were variables associated with BC on multivariate analysis. Only pre-RT PSA level significantly influenced disease free survival in SART setting: when the pre-RT PSA was 1 ng/mL or less, 59.8% pts were disease free at 10-y compared with 33.5% of those treated at PSA levels greater than 1 ng/mL (p= 0.017).

Conclusion: Pts in PORT group, pts without SVI and with GS < 7 show better BC rates . Postoperative RT delivered in high risk prostate cancer patients can reduce the impact of other common unfavourable prognostic factors (pT stage, positive surgical margins). Early referral for SART offers better disease control after radical prostatectomy. This prospective multicenter study confirms outcomes of other series.

Poster: Clinical track: Urology-non-prostate

PO-0759

Results of radical radiotherapy with a tumour boost for bladder cancer in patients unfit for surgery

L.J. Lutkenhaus[1], R.M. Van Os[1], A. Bel[1], M.C.C.M. Hulshof[1]
[1]*Academic Medical Center, Radiotherapy, Amsterdam, The Netherlands*

Purpose or Objective: A bladder-preserving strategy, combining transurethral resection of the bladder tumor (TUR-B) with radiochemotherapy, results in a long-term overall survival comparable to cystectomy. However, such a strategy is mostly applied to elderly or unfit patients, but their medical status regularly contraindicates chemotherapy. This leaves the combination of TUR-B and radical radiotherapy as the only treatment option. For this vulnerable patient group, reduction of toxicity is of additional importance, which could be obtained by more conformal treatment plans. It was our aim to retrospectively analyze the treatment outcome and associated toxicity of both conformal and intensity-modulated radiotherapy (IMRT) using a tumor boost, for locally advanced bladder cancer in patients not suitable for cystectomy.

Material and Methods: 119 patients with T1-4 N0-1 M0 bladder cancer were analyzed retrospectively. Median age was 80 years. Patient and treatment characteristics can be found in Table 1. Treatment consisted of either a conformal box technique or IMRT. Patients were treated with 40 Gy in 20 fractions to the elective treatment volumes, and a daily boost of 0.75 Gy to the tumor. This resulted in a tumor boost of either 55 Gy or 60 Gy, the latter in case expected toxicity allowed delivery of two additional 2.5 Gy fractions to the tumor. Cystoscopic placement of fiducial markers aided in tumor delineation. To evaluate response, a cystoscopy was performed two months after treatment and thereafter every six months. To assess toxicity, patients were seen by their oncologist every week during the treatment course, and thereafter with 1-12 month intervals until up to 5 years after treatment. Toxicity was scored according to the CTCAE version 4, with acute toxicity defined as occurring during treatment or within the first three months thereafter. The Kaplan-Meier method was used to estimate survival and locoregional control. Possible predictors for survival were examined in univariate Cox proportional hazard regression analyses. Differences in toxicity between IMRT or conformal radiotherapy were tested using x2 tests.

Table 1: Patient and treatment characteristics

Characteristics	Patients n	(%)
Sex		
Female	28	(24)
Male	91	(76)
Tumor stage		
1	2	(2)
2	37	(31)
3	70	(59)
4	10	(8)
Clinical lymph node involvement		
No	110	(92)
Yes	9	(8)
Tumor size		
2-4 cm	37	(31)
4-6 cm	59	(50)
≥ 6 cm	22	(18)
Unknown	1	(1)
Planned radiotherapy dose		
55 Gy	62	(52)
60 Gy	57	(48)
Elective treatment volume		
Bladder	24	(20)
Bladder and lymph nodes	95	(80)
Boost delivery		
Concomitant	101	(85)
Simultaneously integrated	18	(15)
Radiotherapy technique		
3D-conformal	68	(57)
IMRT	51	(43)

Results: At 3 months, a complete response was seen in 87% of patients. 3-year overall survival was 44%, with a locoregional control rate of 72% at three years (Figure 1). Including pelvic lymph nodes in the elective field increased survival significantly (hazard ratio: 0.58, p = 0.04). Late toxicity was low, with urinary and intestinal toxicity grades ≥ 2 of 14% and 5%, respectively. IMRT reduced late intestinal toxicity grade ≥ 1 from 24% to 7% (p=0.04), as well as acute intestinal toxicity grade ≥ 2 (from 36% to 12%, p = 0.03).

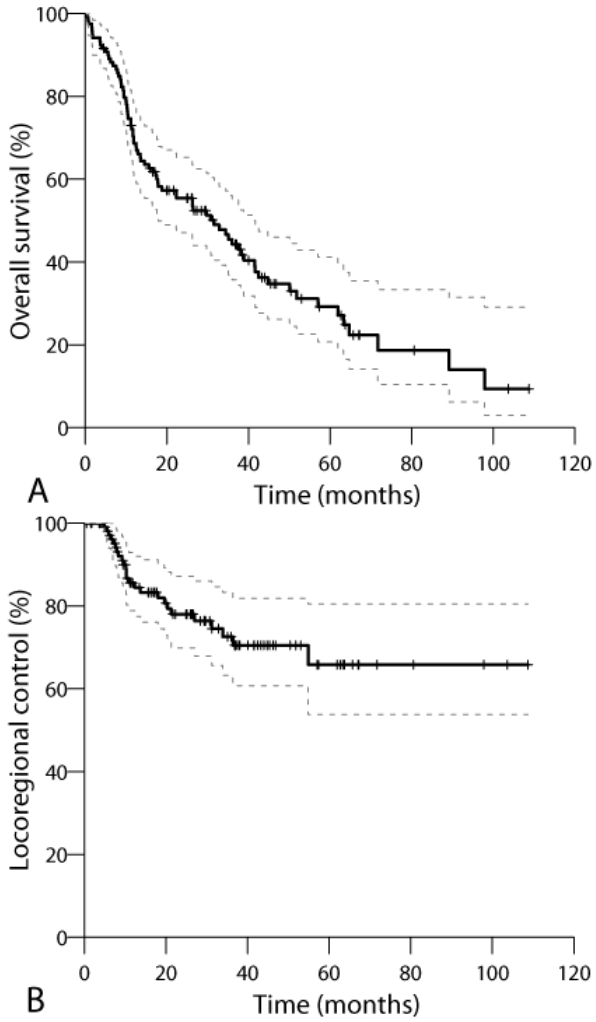

Figure 1: *A*: Overall survival. *B*: Locoregional control. Dashed lines indicate the 95% confidence intervals.

Conclusion: Radical radiotherapy is feasible and effective for elderly or unfit patients. Three-year locoregional control after radical radiotherapy using a boost technique was 72%, with low rates for late urinary and intestinal toxicity. Early and late toxicity rates were reduced by using IMRT.

PO-0760

3D Radiotherapy with concurrent weekly Gemcitabine and Cisplatin for bladder carcinoma

A. Varveris[1], J. Stratakis[2], M. Mazonakis[2], A. Spanakis[1], C. Varveris[1]
[1]*University Hospital of Heraklion, Radiotherapy, Heraklion, Greece*
[2]*University of Crete, Medical Physics, Heraklion, Greece*

Purpose or Objective: We conducted a phase I trial of Gemcitabine (GEM) with concomitant 3D-Conformal Radiotherapy (3D-CRT) and Cisplatin (CDDP) in patients with muscle-invasive bladder cancer who were ineligible for surgery or refused organ loss.

Material and Methods: 28 patients with transitional cell carcinoma, cT2(n=14), cT3(n=8), T4a(n=6), cN0-1, M0, median age 70.5 years were included after maximal transurethral resection. 3D-CRT was administered with a 18MV Linac, 1.8Gy/Fr, 5d/week up to 64.80Gy. The GEM starting dose of 40mg/m2/week was increased by 40mg/m2 increments to 2 levels (80 and 120mg/m2/week) in cohorts of 6 patients. The standard dose of CDDP was 25mg/m2/week given 2 days after GEM infusion. Both drugs were given 30 to 60min before irradiation

Results: All patients were evaluated for toxicity which was evaluated according to the Common Toxicity Criteria and the RTOG/EORTC Score. The DLTs (Dose Limiring Toxicities) were defined as hematologic grade >3 or Non-hematologic grade 3 events, as Abdominal pain/Diarrhea (Proctitis), Dysuria/Urinary frequency (Cystitis), Fatigue/Asthenia, not resolving tro grade 1/2 within 2 days or necessitating the interruption of RT for >1 week, in more than 3 of 6 patients in each cohort. The GEM dose immediately before the level at which the DLT was observed was defined as the Maximum Tolerated Dose (MTD). In 6 patients accrued to GEM dose 40mg/m2/week no grade 3 toxicities were seen. From 6 patients given 80mg/m2/week of GEM, 2 had episodes of grade 3 bladder toxicity, 3 General Weakness and 2 presented with grade 3 hematological sequelae. From 6 patients accrued to GEM dose 120mg/m2/week, 4 had episodes of grade 3 neutropenia and/or thrombocytopenia and 3 showed grade 3 fatigue/malaise. In 4 patients treatment was interrupted for more than 1 week. The 2-year locoregional failure rate was 28% (8/28). 12 of 28 (42%) patients are alive with no evidence of disease progression, 8 patients developed M1 disease and 5 died from this.

Conclusion: GEM given synchronously with 3D-CRT is well tolerated as a bladder preservation schema. The MTD was defined at 80mg/m2/week combined to CDDP and merits evaluation in phase II/III trials.

Poster: Clinical track: Skin cancer / malignant melanoma

PO-0761

Radiation therapy for angiosarcoma of the scalp: total scalp irradiation with X-rays and electrons

M. Hata[1], H. Wada[2], I. Ogino[1], M. Omura[1], I. Koike[1], Y. Tayama[1], K. Odagiri[1], T. Kasuya[1], M. Aihara[2], T. Inoue[1]
[1]*Yokohama City University Graduate School of Medicine, Department of Radiology, Yokohama, Japan*
[2]*Yokohama City University Graduate School of Medicine, Department of Dermatology, Yokohama, Japan*

Purpose or Objective: Wide surgical excision is the standard treatment for angiosarcoma of the scalp, but it is often difficult to completely excise because of the invasive nature and typical multifocal spread of the tumor. Furthermore, many patients are medically inoperable because of old age or coexisting disease. Therefore, we investigated the outcome of radiation therapy with total scalp irradiation for angiosarcoma of the scalp.

Material and Methods: Seventeen patients with angiosarcoma of the scalp underwent radiation therapy with total scalp irradiation with curative intent. Their median age at the time of irradiation was 77 (range, 57–89) years. Four of the 17 patients had tumor invasion into the deep organs, including the skull in three and the temporal muscle in one. Four patients had cervical lymph node metastases, but none had distant metastases. A median initial dose of 50 Gy in 25 fractions was delivered to the entire scalp. Two pairs of lateral X-ray and electron fields were used for total scalp irradiation: 4–6 MV X-rays were delivered through bilaterally opposed ports to the central scalp from the frontal eminence to the suboccipital region, to a depth of 10 mm inside the skull, and 5–9 MeV electrons were delivered through single ports to the bilateral temporal scalp. Subsequently, local radiation boost to the tumor sites achieved a median total dose of 70 Gy in 35 fractions.

Results: All irradiated tumors disappeared or were markedly reduced after radiation therapy; the objective response rate was 100%. However, 14 of the 17 patients developed recurrences during the median follow-up period of 14 months after radiation therapy; seven had recurrences in the scalp, including primary tumor progression in two patients and new disease in five, and 12 patients developed distant metastases. The two patients with primary tumor progression originally had tumor invasion into the skull and temporal muscle, and received a total radiation dose of 70 Gy in 35 fractions. The primary progression-free, scalp relapse-free,

and distant metastasis-free rates were 86%, 67%, and 38% at 1 year and 86%, 38%, and 16% at 3 years, respectively. Thirteen patients died; the cause of death was tumor progression in 10 patients, infectious pneumonia in two, and old age in one. The overall and cause-specific survival rates were both 73% at 1 year and 23% and 44% at 3 years, respectively. The median survival time was 16 months. Although all 17 patients developed grade 1–2 radiation dermatitis, there were no therapy-related toxicities of grade ≥3.

Conclusion: Total scalp irradiation with X-rays and electrons is safe and effective for local tumor control of angiosarcoma of the scalp, but a prophylactic dose of 50 Gy in conventional fractions may be insufficient to eradicate microscopic disease. For gross tumors, a total dose of 70 Gy, and >70 Gy for tumors with deep invasion, is recommended.

PO-0762

Dose-volume predictors of radio-induced effects after SRS for uveal melanoma

C.R. Gigliotti[1], M. Di Nicola[2], L.A. Perna[1], C. Fiorino[1], G. Modorati[2], P. Mortini[3], A. Franzin[3], A. Bolognesi[4], A. Del Vecchio[1], R. Calandrino[1]

[1]*IRCCS San Raffaele Scientific Institute, Medical Physics, Milano, Italy*

[2]*IRCCS San Raffaele Scientific Institute, Ophthalmology, Milano, Italy*

[3]*IRCCS SAN Raffaele Scientific Institute, Neurosurgery, Milano, Italy*

[4]*IRCCS SAN Raffaele Scientific Institute, Radiotherapy, Milano, Italy*

Purpose or Objective: Uveal melanoma (UM) is a life threatening intraocular malignant tumor in adults. Gamma Knife Stereotactic Radiosurgery (GKSRS) is a well assessed strategy for conservative treatment of UM providing satisfactory results in terms of survival, local control and eye preservation. Despite severe side effects following GKSRS have been reported, literature studies designed to investigate dose effect relationship of critical structures are rather poor. The aim of this work is to develop predictive models for radio induced effects in UM patients (pts) treated with GKSRS.

Material and Methods: In our institute 149 pts were treated with exclusive GKSRS for UM between 1994 and 2014. Prospectively collected clinical data are available. For 66/149 pts, 3D dosimetry data of involved critical structures could be recovered: optic nerve (ON), eyeball and posterior part of bulb. For this cohort of pts the median follow up of 2years (6 months-6 years) is available. Cox's analyses were used to identify selected clinical and dosimetric variables as independent risk factor of main side effects: cataract, radiation vasculopathy (RV), radiation papillopathy (RP) and neovascular glaucoma (NVG), visual acuity (VA) reduction > 20% of basal value (VA20%) and complete loss of basal VA (VA100%). ROC curve analysis allowed predicting cut off value of significant variables.

Results: The 2 years incidences from our data were: cataract 39%, RV 10%, RP 12%, NVG 14%, VA20% 59% and VA100% 27%. Age and sex did not result significant. Concerning cataract the volume of whole bulb receiving more than 30Gy (p=0.0004) and tumor thickness (p=0.002) resulted highly predictive; best cut off were respectively 82.2mm3 and 6.6mm. A clear relationship with maximum dose (Dmax) to ON was found for RP (p=0.009 cut off: 14.9Gy) and RV (p=0.0009 cut off: 23.8Gy). For RV, also tumor in the anterior to equator position was predictive (p=0.008). The volume of the posterior bulb receiving more than 20Gy (p=0.0003, cut off: 413.7mm3) and tumor thickness (p=0.0009 cut off: 8.7mm) were predictive for NVG. Multivariate analyses resulted in two variables predictive model both for VA20% (AUC=0.79) and for VA100% (AUC=0.83), including the tumor longest basal diameter and Dmax to the ON. The best cut off values for the tumor longest basal diameter were 11.6mm for VA20% (p=0.02) and 8.98mm for VA100% (p=0.007); the best cut off values for Dmax to the ON were 7.8Gy (p=0.045) for VA20% and 13.2Gy (p=0.002) for VA100%. A summary of the main results are reported in Figure.

	Cataract	*Neo Vascular Glaucoma*	*Radiation Vasculopathy*	*Radiation Papillopathy*	*20% Visual Acuity Reduction* (Model AUC=0.79)	*100% Visual Acuity Reduction* (Model AUC=0.83)
V30 Whole Bulb	p=0.0004 HR=1.007 95%CI: 1.003-1.011 cut-off: 82.2mm³ AUC=0.71					
Dmax Optic Nevre			p=0.0009 HR=1.2 95%CI: 1.07-1.32 cut-off: 23.8Gy AUC=0.86	p=0.009 HR=1.14 95%CI: 1.032-1.258 cut-off: 14.9Gy AUC=0.83	p=0.045 HR=1.04 95%CI: 1.00-1.08 cut-off: 7.8Gy	p=0.002 HR=1.12 95%CI: 1.04-1.21 cut-off: 13.2Gy
V20 Posterior Bulb		p=0.0003 HR=1.12 95%CI: 1.05-1.19 cut-off: 413.7mm³ AUC=0.83				
Position: anterior to equator			p=0.008 HR=0.14 95%CI: 0.04-0.60			
Tumor Longest Basal Diameter					p=0.02 HR=1.15 95%CI: 1.02-1.30 cut-off: 11.6mm	p=0.007 HR=1.36 95%CI: 1.09-1.69 cut-off: 8.98mm
Tumor Thickness	p=0.002 HR=1.35 95%CI: 1.12-1.62 cut-off: 6.6mm AUC=0.64	p=0.0009 HR=2.01 95%CI: 1.33-3.03 cut-off: 8.7mm AUC=0.83				

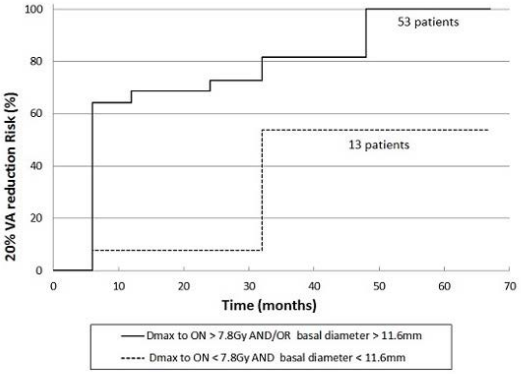

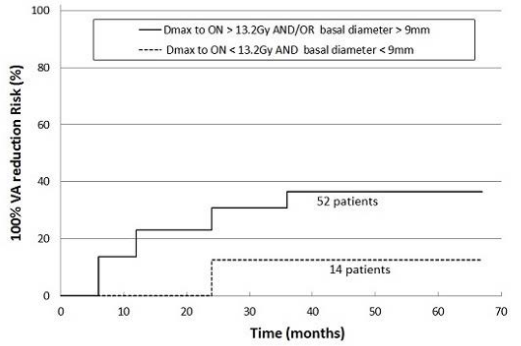

Conclusion: We found clinical and dosimetric variables to clearly predict the risk of the main side effects after GKSRS for UM. These results may provide new dose constraints to critical structures, that once implemented during treatment planning, could reduce radiation toxicities. Further investigation to create bulb dose surface maps highlighting any specific regions more radiosensitive are now under implementation.

PO-0763

Ruthenium-106 brachytherapy for choroidal melanoma: high efficacy with improved visual outcome.

F.P. Peters[1], M. Marinkovic[2], N. Horeweg[1], L. Sommers[1], M. Fiocco[3], J.C. Bleeker[2], M. Ketelaars[1], G.P.M. Luyten[2], C.L. Creutzberg[1]

[1]*Leiden University Medical Center, Department of Radiation Oncology, Leiden, The Netherlands*

[2]*Leiden University Medical Center, Department of Ophtalmology and Melanoma Center, Leiden, The Netherlands*

[3]*Leiden University Medical Center, Department of Biostatistics, Leiden, The Netherlands*

Purpose or Objective: Choroidal melanoma is the most frequent malignant tumour of the eye. Eye-conserving treatment with Ruthenium-106 brachytherapy (RuBT) is a standard treatment for patients with small to intermediate size melanomas. The present study was done to evaluate

efficacy and visual outcomes of a large series of patients with choroidal melanoma (CM) treated with RuBT, and compare the results to those of the preceding protocol in which RuBT was combined with transpupillary thermotherapy (Ru/TTT).

Material and Methods: Outcomes of 449 consecutive CM patients with tumour prominence <8 mm and basal diameter <16 mm treated with RuBT from 2004 to 2011 were analysed. 253 (56.3%) were treated according to the current RuBT protocol (from 2008 onwards) with 130 Gy specified at the tumour apex and minimum and maximum doses to the scleral surface of 300 Gy and 1000 Gy, respectively. 196 (43.6%) were treated using the preceding Ru/TTT protocol with either 400 or 600 Gy to the scleral surface followed by TTT, or 600-800 Gy without TTT for peripheral tumour location. The brachytherapy dose was standardized to a dose rate of 100 Gy per 24 h using a correction factor (2-10% dose correction). Local failure was defined as residual prominence with signs of activity on fluorescence angiography, or regrowth after complete remission.

Results: Median follow-up was 40.1 months; 25.9 months for RuBT and 67.5 months for Ru/TTT; hence 3-year results were analysed. Patients treated with RuBT had smaller and less centrally located tumours and better median visual acuity (VA). VA deteriorated more rapidly in Ru/TTT patients; at 1 year the loss of vision relative to the VA before treatment was -0.1 for RuBT patients vs -0.25 for Ru/TTT, while at 3 years the relative VA decline was similar (-0.30 vs. -0.28). Local failure was detected within 3 years in 4.3% of RuBT patients compared to 11.2% of Ru/TTT patients, for 3-year cumulative incidence rates of 6.4% vs 11.2% (p=0.09). Treatment for local failure consisted of repeated RuBT; TTT; or enucleation. Enucleation was performed in 2.4% of RuBT patients vs. 10.2% of Ru/TTT; of these, 1.6% vs 6.1% were done for recurrence and 0.8 vs 4.1% for complications. Three-year cumulative incidence of distant metastases was 4.8% vs 6.6% for RuBT vs Ru/TTT (p=0.37), and of death 0.5 vs 3.7%. In univariate analyses, most important risk factors for local recurrence and metastases were tumour prominence, tumour diameter and stage, while in multivariate analysis only diameter remained significant for local recurrence. In view of the short follow-up of RuBT, updated results will be presented.

Conclusion: Both protocols for eye-conserving treatment of patients with choroidal melanoma provided excellent rates of local tumour control and eye preservation, with the RuBT protocol confirmed to be best standard of care with 97% eye preservation and significantly longer preservation of visual acuity.

Poster: Clinical track: Sarcoma

PO-0764

Perioperative brachiterapy boost in high grade soft tissue sarcomas

A. Cortesi[1], A. Galuppi[1], E. Shukulli[1], G. Bianchi[2], D.M. Donati[2], S. Cima[3], C. Digesù[4], M. Nuzzo[4], G. Macchia[4], F. Deodato[4], G. Frezza[5], S. Cammelli[1], A.G. Morganti[1]

[1]*Radiation Oncology Center- S.Orsola-Malpighi Hospital-University of Bologna, Department of Experimental-Diagnostic and Specialty Medicine-DIMES, Bologna, Italy*

[2]*Istituto Ortopedico Rizzoli, Muskuloskeletal Oncology Department, Bologna, Italy*

[3]*Oncology Institute of Southern Switzerland, Radiation Oncology Unit, Bellinzona, Switzerland*

[4]*Fondazione di Ricerca e Cura "Giovanni Paolo II"- Catholic University of Sacred Heart, Radiotherapy Unit, Campobasso, Italy*

[5]*Ospedale Bellaria, Radiotherapy Department, Bologna, Italy*

Purpose or Objective: The standard primary treatment for soft tissue sarcoma (STS) is radical surgical resection, preceded or followed by radiotherapy. The purpose of this retrospective study was to assess the efficacy and safety of perioperative brachytherapy (BT) plus postoperative external beam radiation therapy (EBRT) +/- chemotherapy (CT).

Material and Methods: The primary aim of the study was evaluating local control (LC) and overall survival (OS) in a large patients population of treated with combined modality therapy. Secondary objectives were to identify prognostic factors for local recurrence (LR). BT was delivered with Pulsed Dose Rate. Total dose was 20 Gy (0.80 Gy/pulse). EBRT was delivered with 3D-technique by using multiple beams technique. The prescribed dose was 46 Gy (2Gy/fraction). Neoadjuvant and adjuvant chemotherapy was prescribed to patients with potentially chemo-sensitive histological subtypes. Univariate analysis was performed with the log-rank test and multivariate analysis with Cox's proportional hazard model.

Results: From 2000 to 2011, 107 patients (median age 54 years; range 13-85) with high grade primary or recurrent STS were treated with surgery, perioperative BT and adjuvant EBRT +/- CT. Five year LC and OS were 82.2% and 87.8%, respectively. A higher LC was recorded in patients treated for primary tumor, lower limbs, and negative margins STS.

Conclusion: The combination of BT and EBRT was able to achieve high LC and OS rates. A particular risk factor recorded was the disease site. These results warrant further prospective studies to define the role of BT boost in adjuvant therapy of resected STS.

PO-0765

Management of primary cardiac and great vessel sarcomas, The RMH experience 2000-2015.

R. Rieu[1], C. Benson[1], A. Dunlop[1], K. Khabra[1], O. Al-Muderis[1], R. Jones[1], W. Van der Graaf[1], C. Fisher[1], K. Thway[1], C. Messiou[1], I. Judson[1], A. Miah[1], S. Zaidi[1]

[1]*The Royal Marsden, Sarcoma Unit, London, United Kingdom*

Purpose or Objective: Primary cardiac and great vessel sarcomas are a challenging group of cancers with poor prognosis. No consensus management guidelines exist and definitive treatment favours surgery, reserving adjuvant radiotherapy (RT)/chemotherapy (CT) for high-risk patients.

Material and Methods: Retrospective analysis of patients identified from a prospectively collected database Sarcoma Unit, 2000-2014.

Results: 33 patients(19 males) were identified with either primary cardiac(73%) or great vessel sarcomas; median age of 46.9 (range 13-83). Presenting symptoms included dyspnoea(55%), pain(21%), cough/haemoptysis(11%), heart failure(24%), emboli(18%) or pulmonary HTN(12%). Diagnosis was on biopsy(42%) or following resection(58%). Atrial tumours accounted for 58% of cases. Surgery was performed in 66%, with R0(12%),R1(24%) ,R2(24%), or unknown (6%) margins. High grade tumours were seen in 17(52%) cases. Commonest histological subtypes were angiosarcoma (32%), and spindle cell (17%). Localised disease was observed in 18 (55%) cases. Median follow-up was 379 days.
Group A, Radiotherapy: 15 patients received RT (6 males), 10 had operable tumours. 8 patients also received CT. Median time to first treatment was 57.9 days. Patients received 60 Gy/30#(n=4), 59.4 Gy/33#(n=3), 58 Gy/30#(n=1), 50.4 Gy/28#(n=3), 45 Gy/25#(n=1), 35 Gy/15#(n=1), or 20 Gy/5#(n=1). 85% reported toxicity (oesophagitis, cough or fatigue). 8 (53%) patients developed a local recurrence (LR) and 13 patients developed metastatic disease (DM). 2 were long term survivors. Median time to DM for right sided lesions was 116 days, left sided, 1226 days. Overall survival was 2.1 years (R side) and 3.4 years (L side). Median OS was 803 days.
Goup B, Chemotherapy: 13 patients received CT(10 males), 7 had operable tumours. Median time to first treatment was 44 days. Regimens were mainly alkylating/anthracycline/taxane based. 3 patients stopped early (toxicity). 10 patients had LR(77%) and 10 patients developed DM. 2 were long term survivors. Median OS was 296 days.
Group C, Surgery:

5 patients, 1 died 3 days after diagnosis. 4 patients had surgery, 3 developed DM and 1 is a long-term survivor. Median OS was 68 days.

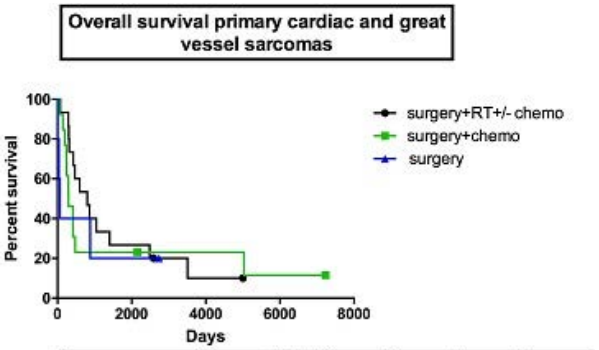

	Surgery+RT+/- Chemo	Surgery+chemo	Surgery
Median survival	803	296	68

Conclusion: These rare sarcomas have variable clinical presentations. Surgery is the central component for successful treatment but complete resection is not always possible. RT may reduce LR (reduced from 77%, group B,to 53%, group A) and chemotherapy is offered if high risk (inoperable, R2 margins, or DM). We still need to define the optimum management.

PO-0766

Is dose de-escalation possible in sarcoma patients treated with extended limb sparing resection?

A. Levy[1], S. Bonvalot[2], P. Terrier[3], A. Le Cesne[4], C. Le Péchoux[5]
[1]*Institut Gustave Roussy, Radiation Oncology department, Villejuif, France*
[2]*Curie, Surgery, Paris, France*
[3]*Gustave Roussy, Pathology, Villejuif, France*
[4]*Gustave Roussy, Medicine, Vilejuif, France*
[5]*Gustave Roussy, radiation Oncology, Villejuif, France*

Purpose or Objective: To evaluate the impact of a dose escalation > 50 Gy in a large series of resected limbs soft tissue sarcomas (STS)

Material and Methods: Data were retrospectively analyzed from 414 consecutive localized limbs STS patients who received irradiation and enlarged surgery at Gustave Roussy from 05/1993 to 05/2012. RT dose level were decided in multidisciplinary staff and depended upon the quality of surgery and margins size.

Results: The median age was 52 years, the median tumor size was 89 mm, most patients had proximal locations (72%), and G-2-3 tumors (79%). Available histologic analyses after surgery retrieved 84% unifocal tumors and free-tumor margins >1 mm in 69% of cases. Radiotherapy (RT) was delivered prior (13%) or after (87%) surgery. Seven patients (2%) had pre- and a postoperative RT boost. Median delivered RT dose was 50 Gy (36-70 Gy), and 40% received >50Gy. At a median follow-up of 5.5 years, the 5-year local relapse rates (LRRs) were 7%, 4%, and 13% in the general population, in patients receiving <50Gy and in those who had >50 Gy ($p<0.001$), respectively. Despite this may due to confounding factors, a dose >50 Gy (HR: 2.6; p=0.04) remained associated with higher LRRs in the multivariate analysis (MVA), as well as histological subtypes (HR: 3.7; p=0.002), and surgical margins<1mm (HR: 3.2; p=0.008). Grade, age, and tumour size were not associated with LRRs in the MVA.

Conclusion: In this retrospective analysis of patients having enlarged and surgery and RT dose escalation did not allow offsetting local relapse in high-risk patients. This should be evaluated in a larger set of patients all having enlarged surgery. A Prospective study allowing dose refinement in this setting is required.

PO-0767

Does fluid collection have an impact on radiotherapy outcomes after excision of soft tissue sarcoma?

N. Choi[1], J.Y. Kim[1], T. Yu[1], H.S. Kim[2], H.J. Kim[1], I.H. Kim[1]
[1]*Seoul National University College of Medicine, Department of Radiation Oncology, Seoul, Korea Republic of*
[2]*Seoul National University College of Medicine, Department of Orthopaedic Surgery, Seoul, Korea Republic of*

Purpose or Objective: Fluid collection of lymph or blood may accumulate at the site of excision after surgery for soft tissue sarcoma, with reported incidence rates from 10-36%. Though small fluid collections have a high probability of being completely covered within the postoperative radiotherapy (PORT) field, large fluid collections may require a more extensive expansion of CTVs. This study is an unprecedented analysis of fluid collection in relation to radiotherapy outcomes after wide excision of soft tissue sarcoma (STS).

Material and Methods: Medical records of 151 patients with STS treated with wide excision followed by adjuvant PORT between 2004 and 2014 were retrospectively reviewed. Only non-recurrent and non-metastatic patients were included. After evaluation of CT and MR images taken at the time of PORT planning, fluid collection was detected in 46 patients (30.5%). Because fluid collection developed more commonly in lower extremity ($p<0.001$) and higher grade tumors (p=0.095), only these patients were included in further analyses (n=76). Fluid collection was present in 35 (46.1%) patients, of which 74.3% and 25.7% had, respectively, either complete or partial coverage in planning target volumes (PTVs) throughout the entire course of PORT.

Results: After a median follow-up of 41 months, patients with and without fluid collection demonstrated local failure rates of 14.3% and 9.8%, and 5-year local control (LC) rates of 83.1% and 86.8%, respectively. The presence of fluid collection had no statistical impact on the clinical outcomes of PORT. Partial coverage of fluid collection showed a low 5-year LC rate of 77.8% compared with 85.5% and 86.8% for patients that had complete PTV coverage or absence of fluid collection, respectively, without statistical significance. Post-PORT complications developed in 5 (6.6%) patients, of which 4 had fluid collection. Wound complication developed in 3 (8.6%) of 35 patients with fluid collection and in 1 (2.4%) of 41 patients without fluid collection.

Conclusion: Fluid collection demonstrated lower LC rates after wide excision and PORT for STS, but with a reasonable wound complication rate of 8.6% when compared with rates of previous studies ranging from 5-17%. Furthermore, partial coverage of fluid collections in PTVs had worse LC rates, thus recommending complete coverage. Future evaluation wth a larger number of cases will be needed for statistical support of our findings.

PO-0768

Evaluation of RT practice for limb soft tissue sarcomas and its impact on prognosis and toxicity

C. Llacer-Moscardo[1], C. Le Pechoux[2], M.P. Sunyach[3], S. Thezenas[4], A. Ducassou[5], M. Delannes[5], G. Noel[6], J. Thariat[7], G. Vogin[8], J. Fourquet[9], F. Vilotte[10], P. Sargos[10], G. Kantor[10], S. Chapet[11], L. Moureau-Zabotto[12]
[1]*ICM - Val d'Aurelle, Radiation Oncology, Montpellier Cedex 5, France*
[2]*Institut Gustave Roussy, Radiation Oncology, Paris, France*
[3]*Centre Léon Bérard, Radiation Oncology, Lyon, France*
[4]*ICM - Val D'Aurelle, Biostatistics, Montpellier, France*
[5]*Institut Universitaire du Cancer, Radiation Oncology, Toulouse, France*
[6]*Paul Strauss, Radiation Oncology, Strasbourg, France*
[7]*Centre Antoine Lacassagne, Radiation Oncology, Nice, France*
[8]*Institut de Cancerologie de Lorraine - Alexis Vautrin, Radiation Oncology, Nancy, France*
[9]*Centre Oscar Lambret, Radiation Oncology, Lille, France*
[10]*Institut Bergonié, Radiation Oncology, Bordeaux, France*
[11]*Hopital Trousseau, Radiation Oncology, Tours, France*

[12]*Institut Paoli-Calmette, Radiation Oncology, Marseille, France*

Purpose or Objective: If radiotherapy (RT) combined with extended resection is part of the standard treatment of high risk extremity soft tissue sarcomas (ESTS), the evidence regarding the optimal target volume of RT ensuring local control (LC) is not very robust. But it is well known that toxicity is directly related to the RT volume and the delivered dose. The development of image-guided radiotherapy and implementation of better target volume conformation could reduce toxicity without compromising outcome. Here we evaluate the definition of RT volume according to clinical, surgical and histological factors.

Material and Methods: Between the 1st January 2008 and the 31th Decembre 2009, 173 patients from eleven centers with ESTS were retrospectively evaluated, all patients having had resection with pre- or post-operative RT. Primary endpoint was to evaluate the target volume and RT dose and their impact on LC and patterns of local relapse (LR). Secondary endpoints were: impact of surgery's quality on LC, patterns of relapse and RT volume. Impact of RT dose on LC and patterns of LR. Impact of histological type on LC and on recurrent pattern. Impact of RT volume on toxicity (CTC V.04).

Results: Median age was 60 years [19-91]. 32% of patients had upper limb and 68% lower limb STS. Median tumor size was 75mm [17-270]. RT was preoperative in 12% and postoperative in 88% of cases. Quality of surgery was R0 in 62%; R0 after second surgery in 11% and R1 in 27% patients. Intraoperative tumor fragmentation rate was 6% in expert centers and 16% in non-expert centers. Most frequent histologic types were liposarcoma (31%) and myxofibrosarcoma (13%). Median dose was 54 Gy [36-70]. Median PTV1 and PTV2 volumes were 864cc [25-5122] and 443cc [20-1613] respectively. LR rate was 11.20% (n=20); 45% within PTV1, 28% in the PTV2, 18% at the edge of the RT volume and 9% outside. 21.4% of patients had a metastatic failure. Regarding toxicity, we observed 19.6% and 15.2% of G1 and G2 fibrosis, 19.6% and 12.5% of G1 and G2 edema, 12.6% and 4.5% G1 and G2 pain, 3.4% and 6.9% of G1 and G2 joint stiffness, 5.2% and 6.9% G1 and G2 neuropathy. Bone fracture occurred in 3.2% of cases. After univariate analysis, intraoperative tumor fragmentation was related to a higher risk of LR (22% vs 8% p=0,004) and distant metastasis (50% vs 17% p= 0,0029). Including scar drainage in the RT field was correlated to a lower LR rate (9% vs 29% p= 0,015). Upper limb location was correlated with higher risk of neuropathy (p=0,049) and lower limb location was correlated with edema (p=0,024). Dose > 60 Gy did not impact on LC but was correlated with pain (p=0,021). No significant correlation with fibrosis could be identified.

Conclusion: As in other studies, the quality of surgery is the most important prognostic factor predicting outcome. Most of LR were within the PTV field translating a correct target volume definition. Toxicity was acceptable. A prospective evaluation is warranted.

Poster: Clinical track: Paediatric tumours

PO-0769

Survival benefit for patients with diffuse intrinsic pontine glioma (DIPG) undergoing re-irradiation

G.O.R.J. Janssens[1], S. Bolle[2], H. Mandeville[3], M. Ramos-Albiac[4], K. Van Beek[5], H. Benghiat[6], B. Hoeben[7], A. Morales la Madrid[8], M. Peters[9], R. Kortmann[10], A.O. Von Bueren[11], D. Van Vuurden[12], C.M. Kramm[13]

[1]*UMC Utrecht, Radiation Oncology, Utrecht, The Netherlands*
[2]*Institut Gustave Roussy, Radiotherapie, Villejuif, France*
[3]*The Royal Marsden NHS Foundation Trust, Clinical Oncology, Sutton- Surrey, United Kingdom*
[4]*Hospital Universitari Vall d'Hebron, Oncologia Radioterapica, Barcelona, Spain*
[5]*UZ Leuven, Radiotherapie-Oncologie, Leuven, Belgium*
[6]*University Hospitals Birmingham NHS Foundation Trust, Oncology, Birmingham, United Kingdom*
[7]*Radboud University Medical Center, Radiation Oncology, NIjmegen, The Netherlands*
[8]*St Joan de Deu, Pediatric Hematology and Oncology, Barcelona, Spain*
[9]*Utrecht Cancer Center, Radiation Oncology, Utrecht, The Netherlands*
[10]*Universitaetsklinikum Leipzig, Klinik und Poliklinik für Strahlentherapie und Radioonkologie, Leipzig, Germany*
[11]*Georg-August-Universität Göttingen, Pediatric Hematology and Oncology, Goettingen, Germany*
[12]*VU Medisch Centrum, Pediatrics, Amsterdam, Germany*
[13]*Georg-August-Universität, Pediatric Hematology and Oncology, Goettingen, Germany*

Purpose or Objective: Radiotherapy remains the cornerstone of treatment for patients with DIPG. Nevertheless, median overall survival of patients initially responding to radiotherapy is poor. The role of chemotherapy as second-line treatment remains elusive. Purpose of this study is to analyze the benefit and toxicity of re-irradiation at the time of disease progression.

Material and Methods: At the time of disease progression 27 children, aged 2 to 16, underwent re-irradiation (10 fractions of 1.8, 2.0 or 3.0 Gy) alone (N=21) or combined with systemic therapy (N=6). At first diagnosis, all patients had symptoms for ≤3 months, ≥2 signs of the neurological triad (cranial nerve deficit, ataxia, long tract signs), characteristic features of DIPG on magnetic resonance imaging or biopsy proven high-grade glioma. An interval of ≥3 months after first-line radiotherapy was required before re-irradiation. A group of 39 patients fulfilling the same diagnostic criteria receiving radiotherapy at primary diagnosis, followed by best supportive care (N=10) or systemic therapy (N=19), were eligible for a matched-cohort analysis.

Results: Median overall survival for patients undergoing re-irradiation was 15.9 months. For a similar median time to first progression (8.1 vs. 7.7 months; *P*=.22), a significant benefit in median overall survival (15.9 [95% CI 13.0-20.0] vs. 10.3 [95% CI 9.4-12.5] months; *P*=<.01) was observed in favor of patients undergoing re-irradiation compared to no re-irradiation. The median overall survival benefit of re-irradiation versus no re-irradiation was most pronounced in patients with a longer interval between end-of-radiotherapy and first progression (3-6 months: 11.1 vs. 8.7; *P*=<.01; 6-12 months: 19.4 vs. 13.8; *P*=.02). On multivariable analysis corrected for age and systemic therapy, re-irradiation remained prognostic for overall survival (HR 0.43 [0.13-81]; *P*=<.01). Clinical improvement after re-irradiation was observed in 15/20 (75%) patients. No grade 4 or 5 acute or late toxicity was diagnosed.

Conclusion: The majority of patients with DIPG, responding to first-line radiotherapy, do benefit of re-irradiation. A prospective data collection, supported by the SIOP-E-HGG/DIPG working group, will start for patients fulfilling the criteria of re-irradiation.

PO-0770

Subsequent colorectal adenomas in childhood cancer survivors: a DCOG LATER record linkage study

J. Teepen[1], J. Kok[1], F. Van Leeuwen[2,3], W. Tissing[3,4], W. Dolsma[3,5], H. Van der Pal[3,6], E. Van Dulmen-den Broeder[3,7], M. Van den Heuvel-Eibrink[8,9], J. Loonen[3,10], D. Bresters[3,11], A. Versluys[3,12], S. Neggers[3,13], A. De Vries[3,8], M. Jaspers[3,14], M. Van den Berg[3,7], H. Caron[1,3], M. Van der Heiden-van der Loo[3], N. Hollema[3], DCOG LATER Study Group[3], F. Oldenburger[15], O. Visser[16], L. Overbeek[17], L. Kremer[1,3], C. Ronckers[1,3]

[1]*Emma Children's Hospital/Academic Medical Center, Pediatric Oncology, Amsterdam, The Netherlands*
[2]*Netherlands Cancer Institute, Epidemiology, Amsterdam, The Netherlands*

[3]Stichting KinderOncologie Nederland SKION / Dutch Childhood Oncology Group DCOG, The Hague, The Netherlands
[4]Beatrix Children's Hospital/University of Groningen/University Medical Center Groningen, Pediatric Oncology/Hematology, Groningen, The Netherlands
[5]University of Groningen/University Medical Center Groningen, Radiation Oncology, Groningen, The Netherlands
[6]Academic Medical Center, Medical Oncology, Amsterdam, The Netherlands
[7]VU University Medical Center, Pediatric Oncology/Hematology, Amsterdam, The Netherlands
[8]Sophia Children's Hospital/Erasmus Medical Center, Pediatric Oncology/Hematology, Rotterdam, The Netherlands
[9]Princess Maxima Center for Pediatric Oncology, Utrecht, The Netherlands
[10]Radboud University Medical Center, Pediatric Oncology and Hematology, Nijmegen, The Netherlands
[11]Willem-Alexander Children's Hospital/Leiden University Medical Center, Pediatric Stem Cell Transplantation, Leiden, The Netherlands
[12]Wilhelmina Children's Hospital/University Medical Center Utrecht, Pediatric Oncology and Hematology, Utrecht, The Netherlands
[13]Erasmus Medical Center, Internal Medicine, Rotterdam, The Netherlands
[14]Academic Medical Center, Medical Informatics, Amsterdam, The Netherlands
[15]Academic Medical Center, Radiation Oncology, Amsterdam, The Netherlands
[16]Netherlands Comprehensive Cancer Organisation, Registration, Utrecht, The Netherlands
[17]PALGA Foundation, Houten, The Netherlands

Purpose or Objective: The risk of colorectal adenomas (CRAs) in childhood cancer survivors (CCS) is unknown. In the general population and in individuals with cancer susceptibility syndromes, CRAs are associated with colorectal carcinoma (CRC) risk and this knowledge is the basis for colorectal cancer screening. To support recommendations for or against CRC screening among asymptomatic CCS, we aim to estimate the risk of histologically confirmed CRAs in a large cohort of 5-year CCS and to quantify the contribution of associated treatment-related factors.

Material and Methods: The Dutch Childhood Oncology Group-Late Effects After Childhood Cancer (DCOG LATER) cohort includes 6,168 five-year CCS treated between 1/1/1963 and 12/31/2001 in one of the seven Dutch pediatric oncology/hematology centers before age 18. Detailed information on prior cancer diagnosis and treatment was collected, including information on radiotherapy (RT) dose, field, and fractionation schedule and chemotherapy (CT) dose per drug. Subsequent CRAs were identified by linkage with the population-based Dutch Pathology Registry (PALGA) for follow-up years 1990-2014, a unique resource for case ascertainment without selection bias from self-reporting. Among patients with CRA we also ascertained the occurrence of CRC based on cancer registry linkage.

Results: At a median follow-up of 23 years (range: 5-52) since childhood cancer diagnosis and a median attained age of 30 years, we identified 60 patients with at least one histologically confirmed CRA, of which 37 had >1 CRA. Most common CRA histology was tubular adenoma, followed by tubulovillous adenoma. Median age at first CRA diagnosis was 39 years and median time from childhood cancer diagnosis to CRA diagnosis was 28 years. Most CRA patients had been treated for leukemia (23.3%) or lymphomas (20.0%). Eight CRA patients also developed a CRC. Preliminary univariate analyses showed an increased risk of CRA associated with abdominal/pelvic RT (odds ratio=2.7; 95% CI: 1.5-4.9).

Conclusion: This study shows a fairly high incidence of histologically confirmed CRAs in a relatively young population. However, these exploratory analyses need further in-depth medical file review to ascertain the potential for surveillance bias. More detailed analyses with multivariable risk models including RT dose and specific CT agents and the role of cancer susceptibility syndromes will be presented during the meeting. Also this study provides the baseline for a longitudinal assessment of CRA and CRC risk, as this population ages.

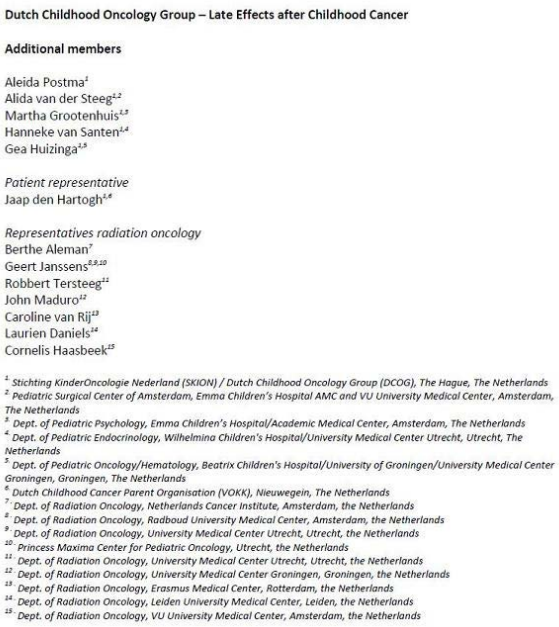

PO-0771

Temporal changes in pediatric radiation oncology: DCOG LATER childhood cancer survivor study

J. Kok[1], W. Dolsma[2,3], E. Van Dulmen-den Broeder[3,4], M. Van den Heuvel-Eibrink[3,5,6], J. Loonen[3,7], W. Tissing[3,8], D. Bresters[3,9], B. Versluys[3,10], H. Van der Pal[3,11], S. Neggers[3,12], N. Hollema[3], M. Van der Heiden-van der Loo[3], F. Van Leeuwen[3,13], F. Oldenburger[14], B. Aleman[15], G. Janssens[6,16,17], J. Maduro[18], R. Tersteeg[17], C. Van Rij[19], L. Daniels[20], C. Haasbeek[21], H. Caron[1,3], The DCOG LATER Study Group[3], L. Kremer[1,3], C. Ronckers[1,3]
[1]Academic Medical Center, Pediatric Oncology, Amsterdam, The Netherlands
[2]University of Groningen/University Medical Center Groningen, Radiation Oncology, Groningen, The Netherlands
[3]Stichting KinderOncologie Nederland SKION / Dutch Childhood Oncology Group DCOG, The Hague, The Netherlands
[4]VU University Medical Center, Pediatric Oncology/Hematology, Amsterdam, The Netherlands
[5]Sophia Children's Hospital/Erasmus Medical Center, Pediatric Oncology/Hematology, Rotterdam, The Netherlands
[6]Princess Maxima Center for Pediatric Oncology, Utrecht, The Netherlands
[7]Radboud University Medical Center, Pediatric Oncology and Hematology, Nijmegen, The Netherlands
[8]Beatrix Children's Hospital/University of Groningen/University Medical Center Groningen, Pediatric Oncology/Hematology, Groningen, The Netherlands
[9]Willem-Alexander Children's Hospital/Leiden University Medical Center, Pediatric Stem Cell Transplantation, Leiden, The Netherlands
[10]Wilhelmina Children's Hospital/University Medical Center Utrecht, Pediatric Oncology and Hematology, Utrecht, The Netherlands
[11]Academic Medical Center, Medical Oncology, Amsterdam, The Netherlands
[12]Erasmus Medical Center, Internal Medicine, Rotterdam, The Netherlands
[13]Netherlands Cancer Institute, Epidemiology, Amsterdam, The Netherlands
[14]Academic Medical Center, Radiation Oncology, Amsterdam, The Netherlands

[15]Netherlands Cancer Institute, Radiation Oncology, Amsterdam, The Netherlands
[16]Radboud University Medical Center, Radiation Oncology, Nijmegen, The Netherlands
[17]University Medical Center Utrecht, Radiation Oncology, Utrecht, The Netherlands
[18]University Medical Center Groningen, Radiation Oncology, Groningen, The Netherlands
[19]Erasmus Medical Center, Radiation Oncology, Rotterdam, The Netherlands
[20]Leiden University Medical Center, Radiation Oncology, Leiden, The Netherlands
[21]VU University Medical Center, Radiation Oncology, Amsterdam, The Netherlands

Purpose or Objective: Pediatric cancer treatment, including radiotherapy (RT) achieves high cure rates, but can cause late health problems. We aim to describe temporal trends of pediatric RT use in the Netherlands based on treatment experience in the DCOG-LATER cohort of five-yr childhood cancer survivors (CCS).

Material and Methods: The Dutch Childhood Oncology Group – Late effects after childhood cancer (DCOG-LATER) is a collaborative effort of all 7 academic paediatric oncology/hematology centres in the Netherlands for optimal patient care and research. The DCOG-LATER cohort includes 6168 five-yr CCS diagnosed 1963-2001 prior to age 18 yrs. Most children were treated according to (inter) national study protocols. Trained data-managers obtained *individual* medical file information on prior cancer diagnosis and treatment including prescribed RT dose, field(s), fractionation schedule, machine and RT technique from data were coded and stored in a web-based database using study coding manuals. Here we summarize trends in RT use by calendar period (1963-1979 vs 1980-2001) and diagnosis group.

Results: In all, 2426 (39%) CCS received external beam RT (EBRT) for a primary tumor or recurrence, most often photons, or, <1989, Cobalt-60. Use of orthovoltage and electrons was limited. Brachytherapy (2%) and radio isotopes (2%) were given, mainly during 1990-2001. RT use decreased substantially for all cancer types; most dramatic changes were seen among CCS of acute lymphoblastic leukemia, Non-Hodgkin lymphoma, neuroblastoma, and nephroblastoma, for whom RT-use declined from 92%, 79%, 59% and 76% (1963-1979), to 15%, 8%, 8%, and 27% (1990-2001), respectively, but also for bone tumors (75%-32%), retinoblastoma (57%-16%), and CNS tumors (82%-47%). Modest declines were seen for CCS of Hodgkin lymphoma (74%-50%), soft tissue sarcomas (57%-36%), and germ-cell tumors (43%-26%). Among 2094 leukemia survivors, 773 had any RT, directed to the cranium (56%), total body (22%), cranio-spinal axis (12%), and testes (4%). Formal trend analyses by childhood cancer type, body compartment, and RT dose will be presented.

Conclusion: The use of RT declined over time for all pediatric cancer types, likely related to improved diagnostic techniques (CT/MRI/pathology) and the introduction of multimodal chemotherapy and enhanced surgical techniques. Temporal changes in treatment exposures document the magnitude of changes, illustrate the heterogeneity of treatment exposures and can be correlated with trends in health outcomes.

Dutch Childhood Oncology Group – Late Effects after Childhood Cancer

Additional members

Aleida Postma[1]
Alida van der Steeg[1,2]
Martha Grootenhuis[1,3]
Hanneke van Santen[3,4]
Andrica de Vries[1,5]
Monique Jaspers[1,6]
Marleen van den Berg[1,7]
Gea Huizinga[1,8]

Patient representative
Jaap den Hartogh[1,9]

Representatives radiation oncology
Irma van Dijk[10]
Peter van der Hulst[11]

[1] Stichting KinderOncologie Nederland (SKION) / Dutch Childhood Oncology Group (DCOG), The Hague, The Netherlands
[2] Pediatric Surgical Center of Amsterdam, Emma Children's Hospital AMC and VU University Medical Center, Amsterdam, The Netherlands
[3] Dept. of Pediatric Psychology, Emma Children's Hospital/Academic Medical Center, Amsterdam, The Netherlands
[4] Dept. of Pediatric Endocrinology, Wilhelmina Children's Hospital/University Medical Center Utrecht, Utrecht, The Netherlands
[5] Dept. of Pediatric Oncology/Hematology, Sophia Children's Hospital/Erasmus Medical Center, Rotterdam, The Netherlands
[6] Dept. of Medical Informatics, Academic Medical Center, Amsterdam, The Netherlands
[7] Dept. of Pediatric Oncology/Hematology, VU University Medical Center, Amsterdam, The Netherlands
[8] Dept. of Pediatric Oncology/Hematology, Beatrix Children's Hospital/University of Groningen/University Medical Center Groningen, Groningen, The Netherlands
[9] Dutch Childhood Cancer Parent Organisation (VOKK), Nieuwegein, The Netherlands
[10] Dept. of Radiation Oncology, Academic Medical Center, Amsterdam, The Netherlands
[11] Dept. of Radiation Oncology, University of Groningen/University Medical Center Groningen, Groningen, The Netherlands

Poster: Clinical track: Palliation

PO-0772

Adequacy of dose volume constraints in stereotactic radiotherapy and radiosurgery of abdominal area

S. Cilla[1], G. Macchia[2], A. Ianiro[1], V. Picardi[2], C. Digesù[2], M. Ferro[2], F. Labropoulos[2], G. Torre[2], M. Nuzzo[2], F. Deodato[2], A. Guido[3], L. Giaccherini[3], L. Manuzzi[3], A. Arcelli[3], D. Balestrini[4], G. Compagnone[5], S. Cammelli[3], M. Campitelli[6], G. Frezza[4], A.G. Morganti[3]
[1]*Fondazione di Ricerca e Cura "Giovanni Paolo II"- Catholic University of Sacred Heart, Medical Physics Unit, Campobasso, Italy*
[2]*Fondazione di Ricerca e Cura "Giovanni Paolo II"- Catholic University of Sacred Heart, Radiation Oncology Unit, Campobasso, Italy*
[3]*S. Orsola-Malpighi Hospital- University of Bologna, Radiation Oncology Center- Department of Experimental- Diagnostic and Specialty Medicine – DIMES, Bologna, Italy*
[4]*Bellaria Hospital, Radiotherapy Department, Bologna, Italy*
[5]*S. Orsola-Malpighi Hospital- University of Bologna, Department of Medical Physics, Bologna, Italy*
[6]*Policlinico Universitario "A. Gemelli"- Catholic University of Sacred Heart, Department of Radiotherapy, Roma, Italy*

Purpose or Objective: To verify the adequacy of dose volume constraints in stereotactic radiotherapy and radiosurgery of abdominal area considering that dose constraints reported in literature are not still validated. This study is based on toxicity recorded in organs at risk (OARs) of patients enrolled in dose-escalation trials and treated in Our Institution.

Material and Methods: Treatment plans of 51 patients (Table 1) who underwent SBRT (30 patients) or SBRS (21 patients) on abdominal neoplasms from March 2007 to May 2014 were retrospectively evaluated. All patients were treated using V-MAT technique. SBRT treatment was delivered in 25-40 Gy in 5 fractions, and 16-30 Gy in single fraction in SBRS treatment. Small intestine and duodenum were the main OARs whose irradiation was virtually limited to 30 Gy in SBRT treatments and 12 Gy in SBRS treatments. Dosimetric data were compared with clinical results in terms of early and late toxicity.

Table 1: Patients' characteristics

		SBRT (N, %)	SBRS (N, %)
N°		30 (59)	21 (41)
M/F		8/22	9/12
Age (range; average)		31-82; 64	39-85; 67
Primary tumor			
	Endometrium	6 (20)	0 (0.0)
	Ovary	5 (16.7)	1 (4.8)
	Cervix	5 (16.7)	1 (4.8)
	Vagina	2 (6.7)	0 (0.0)
	Breast	0 (0.0)	3 (14.3)
	Pancreas	4 (13.3)	1 (4.8)
	Prostate	3 (10)	5 (23.8)
	Colon	3 (10)	3 (14.3)
	Rectum	1 (3.3)	2 (9.5)
	Stomach	1 (3.3)	0 (0.0)
	Other	0 (0.0)	5 (23.8)
Treated lesion			
	Primary tumor	4 (13.5)	3 (14.2)
	Nodal metastases	22 (73)	7 (33.3)
	Distant metastases	4 (13.5)	12 (57.1)

Results: SBRT treatment: maximum small bowel and duodenum dose-volume constraints were exceeded in 5/30 (16.7%) and 2/30 (6.7%), respectively. Dose to OARs was: small bowel: Dmax 31.5-40.5 Gy, V30 0.2-13.4 cc; duodenum: Dmax 35.7-36.6 Gy, V30 2.1-3.7 cc.
SBRS treatment: maximum small bowel and duodenum dose-volume constraints were exceeded in 2/21 patients (9.5%) and 1/21 patient (4.7%), respectively. Dose to OARs was: small bowel: Dmax 15.6-16.3 Gy, V12 1.7-8.5 cc; duodenum Dmax 16.0 Gy, V12 0.1 cc.
With a median follow up of 24 months after SBRT and 18 months after SBRS, no early or late severe toxicity was observed in patients in whom constraints were not respected.

Conclusion: Patients irradiated on small bowel and duodenum did not develop severe toxicity although the administered doses were above constrains proposed in literature. A prolonged follow-up and a larger population are needed to confirm the safety of dose-volume constraints other than those reported in literature about SBRT and SBRS on abdominal area.

PO-0773

Reirradiation by extracranial stereotactic treatment: preliminary results of a dose escalation study

F. Deodato[1], S. Cilla[2], G. Macchia[1], M. Nuzzo[1], C. Annese[1], M. Ferro[1], F. Labropoulos[1], G. Torre[1], V. Picardi[1], A. Ianiro[2], S. Ciabatti[3], G.C. Mattiucci[4], D. Smaniotto[4], S. Luzi[4], G. Siepe[3], E. Shukulli[3], F. Romani[5], L. Caravatta[6], A. Farioli[7], S. Cammelli[3], G. Frezza[8], A.G. Morganti[3]
[1]*Fondazione di Ricerca e Cura "Giovanni Paolo II"- Catholic University of Sacred Heart, Radiation Oncology Unit, Campobasso, Italy*
[2]*Fondazione di Ricerca e Cura "Giovanni Paolo II"- Catholic University of Sacred Heart, Medical Physics Unit, Campobasso, Italy*
[3]*S. Orsola-Malpighi Hospital- University of Bologna, Radiation Oncology Center- Department of Experimental- Diagnostic and Specialty Medicine – DIMES, Bologna, Italy*
[4]*Policlinico Universitario "A. Gemelli"- Catholic University of Sacred Heart, Department of Radiotherapy, Roma, Italy*
[5]*S. Orsola-Malpighi Hospital- University of Bologna, Department of Medical Physics, Bologna, Italy*
[6]*P.O. Businco, Radiotherapy Unit- Centro di Radioterapia e Medicina Nucleare, Cagliari, Italy*
[7]*S. Orsola-Malpighi Hospital- University of Bologna, Department of Medical and Surgical Sciences DIMEC, Bologna, Italy*
[8]*Bellaria Hospital, Radiotherapy Department, Bologna, Italy*

Purpose or Objective: To define the maximum tolerated dose (MTD) of extra-cranial stereotactic treatment (SBRT) in previously irradiated patients.

Material and Methods: In a dose escalation (Phase I) study, previously irradiated patients were enrolled in two different arms depending on treatment site and previous dose: 1) retreatment with previous dose > 60 Gy or retreatment of pancreatic and pelvic tumors, 2) retreatment with previous dose < 60 Gy. SBRT was delivered in 5 fractions with static 3D technique (4 non-coplanar beams) or dynamic arc (VMAT). The dose was prescribed at the isocenter. The Planning Target Volume (PTV) was defined as the GTV + 5-15 mm margin. According to the study arm, the first cohort of 6 patients received a dose of 20 or 25 Gy, and subsequent cohorts of patients received doses up to 40 Gy. The dose limiting toxicity (DLT) was defined as any acute and late toxicity Grade ≥ 3. The MTD was defined a s the dose level with 2/6 or 4/12 DLT.

Results: From September 2004 to December 2014, 51 patients (M/F: 27/24; median age 65, range 44-87), previously irradiated with doses of 30 to 87 Gy (median dose 50 Gy) were enrolled, after 4-228 months from the first treatment (median 11 months). Sixty-six lesions were treated (23 primary lesions or relapses, 43 lymphadenopathies) mainly from gynecological tumors (30%), followed by gastrointestinal tumors (26%) and prostatic tumors (17%). Nineteen of the 66 lesions were in the neck or chest, 22 in the abdomen and 25 in the pelvis. With a median follow-up of 19 months (3-104), an overall response rate of 81% (Complete Response: 55%, Partial Response: 26%), with only 3% of disease progression was recorded. At 40 Gy dose-level, only 1 patient showed DLT (cutaneous fistula in the sacral region). Two-year local control was 75% and 2-year metastasis-free survival was 30%.

Conclusion: SBRT treatment in 5 fractions up to a dose of 40 Gy is well tolerated in previously irradiated patients. This dose escalation protocol is still ongoing (Table 1).

		Retreatment	
Level	n° pts	previous dose ≤ 60 Gy (pancreas e pelvis); previous dose > 60 Gy	previous dose ≤ 60 Gy
1	6 §	20 Gy	25 Gy
2	6 §	25 Gy	30 Gy
3	6 §	30 Gy*	35 Gy
4	6 §	35 Gy	**40 Gy**
5	6 §	40 Gy	45 Gy
6	6 §	**45 Gy**	50 Gy

Current dose level is underlined; *1 DLT

PO-0774

Extra-cranial radiosurgery in oligometastatic disease: a dose escalation study (Destroy-2).

F. Deodato[1], G. Macchia[1], M. Nuzzo[1], C. Annese[1], M. Ferro[1], F. Labropoulos[1], G. Torre[1], V. Picardi[1], S. Mignogna[2], A. Ianiro[3], R. Autorino[4], A. Petrone[4], A. Arcelli[5], I. Mascia[5], E. Farina[5], F. Bertini[5], G. Compagnone[6], S. Pini[6], S. Cammelli[5], G. Frezza[7], V. Valentini[4], A.G. Morganti[5], S. Cilla[3]
[1]*Fondazione di Ricerca e Cura "Giovanni Paolo II"- Catholic University of Sacred Heart, Radiation Oncology Unit, Campobasso, Italy*
[2]*Fondazione di Ricerca e Cura "Giovanni Paolo II"- Catholic University of Sacred Heart, Oncology Unit, Campobasso, Italy*
[3]*Fondazione di Ricerca e Cura "Giovanni Paolo II"- Catholic University of Sacred Heart, Medical Physics Unit, Campobasso, Italy*
[4]*Policlinico Universitario "A. Gemelli"- Catholic University of Sacred Heart, Department of Radiotherapy, Roma, Italy*
[5]*S. Orsola-Malpighi Hospital- University of Bologna, Radiation Oncology Center- Department of Experimental- Diagnostic and Specialty Medicine – DIMES, Bologna, Italy*
[6]*S. Orsola-Malpighi Hospital- University of Bologna, Department of Medical Physics, Bologna, Italy*
[7]*Bellaria Hospital, Radiotherapy Department, Bologna, Italy*

Purpose or Objective: To define the maximum tolerated dose (MTD) of stereotactic extracranial radiosurgery performed in a single session (SBRS) in different clinical settings.

Material and Methods: Based on a Dose Escalation study (Phase I), oligometastatic patients were enrolled in 4 different arms depending on site and treatment purpose: 1) liver metastases, 2) lung metastases, 3) lymph node metastases or liver or lung metastases with a prolonged local control purpose, 4) bone metastases (non-vertebral). Dose was prescribed according to the Rosel protocol (V100 >95%, V90 >99% and Dmax <140% of the prescription) with dynamic

volumetric intensity modulated arc technique (VMAT). The Planning Target Volume (PTV) was defined as the GTV plus a personalized Internal Margin and a 3 mm Set -up Margin. Based on the study arm, the first cohort of 6 patients received a dose of 12-26 Gy, and the subsequent cohorts of patients received doses up to 30 Gy. The dose limiting toxicity (DLT) was defined as any acute and > Grade 3 late toxicity (CTC-AE v. 4.03). In case of 2/6 or 4/12 DLT in the analyzed cohort, this dose was considered as MTD.

Results: From August 2010 to April 2015 92 patients were enrolled (M/F: 50/42; median age: 67 years (40-93); range: 40-93) and 142 lesions were treated (bone: 47, lung: 39, nodes: 33, and liver: 23) mainly from prostatic (28%), gastrointestinal (25%), breast (21%), and gynecological (8%) tumors. With a median follow-up of 11 months (2-58), overall response rate was 70 % (CR: 47%, PR: 23%), with 15% stable disease and only 4% of progressive disease (15 lesions (11%) not evaluable for response at the time of the analysis). No DLT was recorded. Two-year local control at was 77% and 2-year metastases-free survival was 34%. Two-year overall survival was 78%.

Conclusion: SBRS is well tolerated up to a dose of 30 Gy. The dose escalation protocol is ongoing (Table).

Table: Destroy -2: study arms and dose levels

Dose level	Lung	Liver	Bone	Other
1	26 Gy	26 Gy	12 Gy	16 Gy
2	28 Gy	**28 Gy**	14 Gy	18 Gy
3	**30 Gy**	30 Gy	16 Gy	20 Gy
4	32 Gy	32 Gy	18 Gy	22 Gy
5	34 Gy		20 Gy	**24 Gy**
6			22 Gy	
7			**24 Gy**	

The dose level in progress is underlined

PO-0775

Risk stratification of vertebral compression fracture after palliative RT for spinal metastases

T. Yu[1], J.H. Kim[1], K. Kim[1], K. Hak Jae[1], E.K. Chie[1], K.H. Shin[1], H.G. Wu[1], I.H. Kim[1]
[1]*Seoul National University College of Medicine, Radiation Oncology, Seoul, Korea Republic of*

Purpose or Objective: Vertebral compression fracture (VCF) by involvement of metastatic tumor significantly compromises in quality of life of patients. Spinal Instability Neoplastic Score (SINS) is the classification system to predict VCF, but lacks clinical validation. The purpose of this study was to develop a novel simple method predicting the risk of VCF and compare its effectiveness with SINS.

Material and Methods: A total of 225 vertebral segments in 154 patients treated with palliative radiotherapy from Sep 2011 to Aug 2013 were included for analysis. VCF was defined as occurrence or progression of collapse deformity within treated vertebral segments. Each segment was scored by SINS. In addition to 6 SINS components, we also evaluated the impact of paraspinal tumor extension, epidural extension, tumor origin, performance status, and radiotherapy-related factors on VCF risk. Recursive partitioning analyses (RPA) was used to identify optimal classification of risk groups.

Results: The median follow-up was 8.5 months. The 6-month and 12-month VCF-free probability was 83.3% and 77.3%, and median survival was 10 months. Multivariate analysis identified paraspinal tumor extension (P=0.03) and baseline vertebral body collapse (P<0.001) were independent predictors for VCF. All SINS criteria except body collapse were not significant for VCF. The RPA defined 3 risk groups. The lowest risk group (n=96) were vertebrae with less than 50% body involved by tumor and no collapse. The intermediate risk group (n=90) were vertebrae with more than 50% body involved and no collapse, or vertebrae with body collapse and no paraspinal tumor extension. The highest risk group (n=39) were vertebrae with body collapse and paraspinal extension. The 6-month VCF-free probability for each groups were 93.5%, 84.9%, and 53.7%, respectively (P<0.001). According to the SINS classification, the 6-month VCF-free probabilities were 91.9% (stable group, n=78), 81.9% (potentially unstable group, n=122), and 62.8% (unstable group, n=25) (P<0.001).

Conclusion: Not all the components of SINS were significant predictors of VCF. It is feasible to estimate VCF by the simpler RPA stratification.

PO-0776

Radiotherapy for painful bone metastases: clinical predictors of efficacy

N. Bychkova[1], E. Khmelevsky[1], A. Kaprin[1]
[1]*Gertzen Moscow Research Oncological Institute, Radiotherapy Department, Moscow, Russian Federation*

Purpose or Objective: The purpose of this randomized clinical trial was to estimate prognostic factors predicting symptom control after radiotherapy in patients with painful bone metastases.

Material and Methods: 640 cases of symptomatic bone metastases treated with EBRT were analyzed. The primary tumor sites were breast (419), prostate (52), lung (50), renal (37), colon (13), melanoma (8), sarcomas (7) and others including bladder, thyroid, uterus, carcinoid (54). The lesions of spine and pelvis predominated (48% and 30% correspondingly). Pathological fractures in treatment area were observed in 72,3% for spinal metastases and in 22,2% for long bones lesions. The average pain intensity was 2,2 by the four-point verbal scale and proved significantly lower for carcinoid tumors. Treatment schedules included 2, 3 and 4 fractions of 6,5 Gy and standard treatment schedule with 23 fractions of 2 Gy.

Results: The average follow-up period was 70 months. Overall effectiveness of EBRT - 96,1%. Complete response rate (CRR) - 59,1%. The pain relapse rate - 8,7%. CRR for standard treatment schedule was 77,4% and significantly decreased from 64,4% to 47,9% and 43,6% for 4, 3 and 2 fractions of 6,5 Gy correspondingly (p<0,05). There was no correlation between treatment schedules and pain relapse rate. CRR in patients with low initial pain intensity was 87,3%, with moderate pain – 59,8% and intense pain – 42% (p<0,01). CRR for spine and pelvis lesions was 63,4% and 59,3%, for long bones metastases - 48,3% and significantly decreased for sacrum isolated metastases – 27,8% (p<0,01). The frequency of pathological fractures in treatment area detected no correlation with CRR. High radiosensitivity was revealed for bone metastases of carcinoid with CRR 100%, melanoma – 75%, breast cancer – 64%, prostate cancer – 59,6% and sarcomas – 57,1%. Bone metastases of lung, colon, and renal cancer turned to be radioresistance (44%, 30,1% and 27% correspondingly). Analysis of variance (ANOVA) revealed several factors affecting CRR: tumor primary site (p<0,001), total dose (p<0,001), initial pain intensity (p<0,001), localization of metastases in skeleton (p<0,02). In the multifactorial analysis MANOVA tumor primary site and pain intensity before radiotherapy were the only independent prognostic factors of CRR.

Conclusion: Tumor primary site, initial pain intensity, total dose, localization of metastases in skeleton are clinical predictors of radiosensitivity of bone metastases, they significantly affect the CRR.

PO-0777

Evaluation of spinal stability in relation to pain response after radiotherapy for spinal metastases

A.S. Gerlich[1], J.M. Van der Velden[1], A.L. Versteeg[2], H.M. Verkooijen[1], C.G. Fisher[3], F.C. Oner[2], M. Van Vulpen[1], L. Weir[4], J.J. Verlaan[2]

[1]*University Medical Center Utrecht, Radiation Oncology, Utrecht, The Netherlands*

[2]*University Medical Center Utrecht, Orthopedic Surgery, Utrecht, The Netherlands*

[3]*University of British Columbia, Orthopedic Surgery, Vancouver, Canada*

[4]*University of British Columbia, Medicine, Vancouver, Canada*

Purpose or Objective: A substantial number of patients with painful spinal metastases experience no effect of palliative radiotherapy. Besides tumor-induced pain, mechanical spinal instability due to metastatic disease, could be associated with failed pain control following conventional radiotherapy. Early identification of patients who will not benefit from radiotherapy is important, since these patients might benefit more from a surgical approach. This study aims to prospectively investigate the relation between spinal instability, as defined by the Spinal Instability Neoplastic Score (SINS), and the pain response to conventional palliative radiotherapy in patients with symptomatic spinal metastases.

Material and Methods: From two academic centers, data of 155 patients with thoracic, lumbar or lumbosacral metastases was prospectively collected. In all patients, SINS was calculated by a spine surgeon, specialized in spine oncology and blinded for treatment outcome. Images from radiotherapy planning computed tomography (CT) scans were used. The highest SINS was recorded in case more than one lesion was irradiated. Patients who died within four weeks after radiotherapy (n=13, 8%) or had an otherwise unknown pain response (n=18, 12%) were excluded. Pain response, determined using the International Bone Metastases Consensus Working Party, was recorded between 4 to 8 weeks after treatment in 124 patients. Multivariable logistic regression analysis was used to estimate the association between SINS and pain response in patients with spinal metastases.

Results: In total, 81 (65%) patients experienced a pain response. Of the patients who died within four weeks after radiotherapy (n=13), 6 patients had SINS of 7 or higher. Except for Karnofsky performance score, no significant differences in patients and disease characteristics were found between responders and non-responders within the cohort. Median SINS was not significantly different between responding and non-responding patients. In multivariate analysis, SINS was not associated with pain response (adjusted odds-radio 0.94; 95% confidence interval 0.81–1.10; p = 0.449) (Table). SINS improved the prediction of response in addition to other clinical variables only marginally: the area under the receiver operating curve improved from 0.68 (0.60–0.79) to 0.70 (0.60–0.80) (Figure).

Table Association between SINS and response status

SINS	Response (n=81)	No response (n=43)	Odd ratio (95% CI) Unadjusted	p-value	Adjusted[a]	p-value
Continuous SINS[b]			0.91 (0.80–1.04)	0.166	0.94 (0.81–1.10)	0.449
Median (range)	7 (2–15)	8 (2–15)				
Mean ±SD	7.8±2.8	8.6±2.9				
Categorized SINS						
Stable, n (%)	29 (36%)	12 (28%)	1.00		1.00	
Impending unstable, n (%)	46 (57%)	27 (63%)	0.71 (0.31–1.61)	0.405	0.91 (0.37–2.27)	0.841
Unstable, n (%)	6 (9%)	4 (7%)	0.62 (0.15–2.60)	0.514	0.71 (0.15–3.27)	0.708

SINS, spinal instability neoplastic score; CI, confidence interval; SD standard deviation

[a] adjusted for gender, tumor, and performance status

[b] SINS modeled as continuous variable ranging from 0 to 18

Conclusion: In this study no significant relationship between mechanical spinal instability, as reflected by the SINS score, and pain response to conventional radiotherapy could be demonstrated. SINS was developed as a referral tool in patients with spinal metastases, and is not useful as a predictive tool for pain response.

PO-0778

Limited short-term effect of radiotherapy on bone density in metastatic femoral bone

F. Eggermont[1], L.C. Derikx[1], N. Verdonschot[1], G. Hannink[1], R.S.J.P. Kaatee[2], E. Tanck[1], Y.M. Van der Linden[3]

[1]*Radboud University Medical Center- Radboud Institute for Health Sciences, Orthopaedic Research Laboratory, Nijmegen, The Netherlands*

[2]*Radiotherapeutic Institute Friesland, Leeuwarden, The Netherlands*

[3]*Leiden University Medical Center, Department of Radiotherapy, Leiden, The Netherlands*

Purpose or Objective: Bone metastases are frequently treated with radiotherapy (RT) for pain, which also may have a beneficial effect on bone density, and thus bone strength. So far, only one study (*Koswig et al., Strahlenther Onkol, 1999*) compared single fraction (SF) and multiple fraction (MF) RT in terms of remineralization and found a larger response after MF RT. However, they only studied lytic lesions in mostly vertebrae. Although a pathological fracture results in major problems for mobility and self-care, femoral lesions have been studied limitedly for remineralization. Furthermore, little is known about the effect of RT on bone tissue surrounding the lesions. Therefore, the aim of this study was to determine the effect of SF and MF RT on bone density over time in proximal femora and in lytic, blastic and mixed lesions.

Material and Methods: In this prospective cohort study, 42 patients with 47 femora irradiated for 52 metastatic lesions were included from three RT centers in the Netherlands. All patients received SF (1x8Gy) or MF (5 or 6x4Gy) RT, according to Dutch clinical guidelines. Quantitative computed tomography (QCT) scans were obtained before RT and 4 and 10 weeks after RT. MF patients additionally underwent QCT on the final day of RT (after 1 week). Mean bone densities were determined at each time point for each proximal femur and for each lesion (expanded by 6 mm to account for obscure edges). For proper comparison over time, proximal femora and lesions were registered using an automated, objective and accurate registration method. Linear mixed models were used for statistical analysis.

Results: No significant differences in bone density were found between SF and MF RT over all time points (Figure 1A). Blastic, lytic and mixed lesions responded differently to RT over time (Figure 1B). No difference in bone density was found for lytic lesions, whereas bone density in mixed and blastic lesions increased up to 105% (SD 10%) and 121% (SD 17%) after 10 weeks, respectively. Comparably, bone density of the proximal femora with blastic lesions increased to 109% (SD 10%), while proximal femora with lytic and mixed lesions showed no difference in bone density over time.

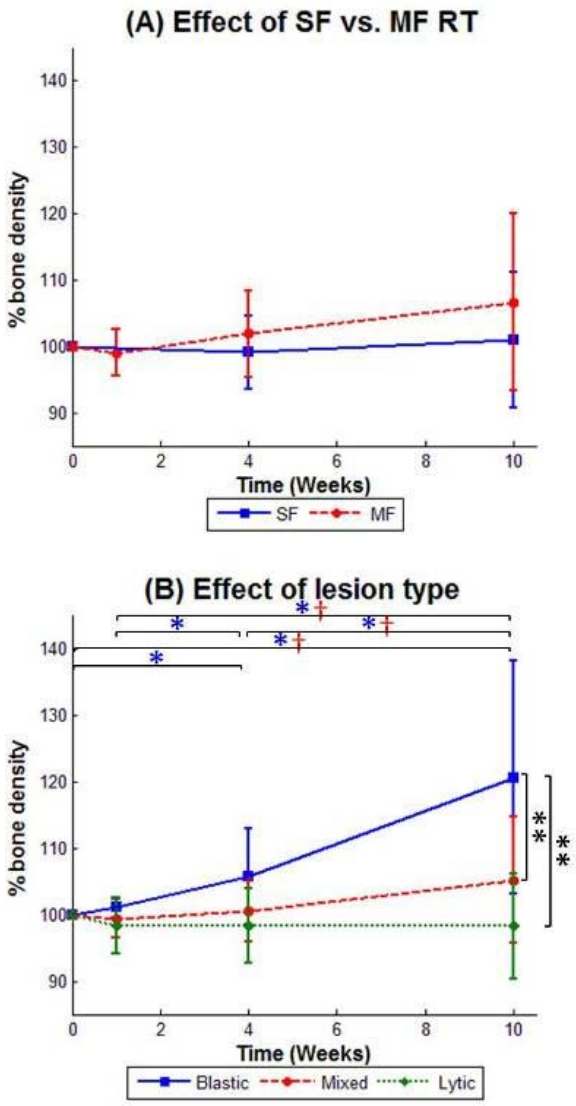

Figure 1: Bone densities (percentage relative to baseline QCT) of the lesions over time, average ± SD; (A) SF vs. MF RT; (B) each lesion type. Symbols indicate significant differences within lesions (*blastic, † mixed), or between lesion types at ten weeks (**).

Conclusion: In general, 10 weeks after RT in patients with femoral metastases a significant increase in bone density was seen in blastic and mixed lesions, but not in lytic lesions. However, the subsequent effect of these changes on femoral bone strength remains unknown. Since higher total doses did not lead to significantly higher bone densities, the clinical relevance of MF over SF for stabilizing femoral bone with metastases can be questioned.

PO-0779

Multicenter study of palliative pelvic radiation for symptomatic primary and recurrent rectal cancer

M. Cameron[1], C. Kersten[1], I. Vistad[2], R. Van Helvoirt[1], K. Weyde[3], C. Undseth[4], I. Mjaaland[5], E. Skovlund[6], S. Fosså[4], M. Guren[4]

[1]*Sørlandet Hospital, Department of Oncology, Kristiansand, Norway*

[2]*Sørlandet Hospital, Department of Obstetrics and Gynecology, Kristiansand, Norway*

[3]*Innlandet Hospital, Department of Oncology, Gjøvik, Norway*

[4]*Oslo University Hospital, Department of Oncology, Oslo, Norway*

[5]*Stavanger University Hospital, Department of Oncology, Stavanger, Norway*

[6]*Norwegian University of Science and Technology, Department of Public Health and General Practice, Trondheim, Norway*

Purpose or Objective: Advanced primary and recurrent rectal cancers (RC) may cause significant pelvic morbidity including pain, dysfunction and hematochezia. Palliative pelvic radiotherapy (PPRT) is often used but symptomatic effects and toxicities are poorly documented and optimal treatment schedules remain undefined. Aims of this prospective multicenter phase-II study were to evaluate changes in symptom severity and explore quality of life (QOL) and toxicity after PPRT of RC using a common palliative radiotherapy regimen.

Material and Methods: Patients with symptomatic pelvic RC (primary or recurrent) prescribed PPRT with 30-39 Gy in 3 Gy fractions were eligible. Treatment volume included primary tumor or recurrence and enlarged pelvic lymph nodes, if indicated. Subjects identified a target symptom (TS) as their principal pelvic complaint requiring palliation. Primary outcome was self-reported TS severity relative to baseline 12 weeks after PPRT. Pelvic symptom burden including toxicity and QOL (EORTC QLQ C30) were assessed before, at the end of, and six and 12 weeks after PPRT.

Results: From Q4/2009-Q3/2015, 51 patients were included at 8/9 Norwegian radiotherapy centers. Thirty-three patients were evaluable 12 weeks after PPRT, and 16 (31%) did not complete the study due to progressive cancer (n=6) and death (n=10). Albumin < 36 g/L (OR=1.31 (95% CI 1.11-1.54)) and age≤ 79 yrs (OR=4.79 (95% CI 0.97 -23.65)) were independent predictors of study drop-out. Median delivered dose was 36 Gy (6–39). Pain (n=24), rectal dysfunction (n=16), and hematochezia (n=9) were the most common TS. 28/33 (85%) evaluable patients reported that their TS had either resolved or improved 12 weeks after PPRT. 4/33 (12%) reported unchanged TS severity, while one patient had worsening TS severity at the 12-week follow-up. Forty-two of the 51 included patients (82%) reported complete resolution or improvement of the TS at at least one of the three follow-up visits. Hematochezia responded most rapidly and consistently with all evaluable patients reporting improvement or resolution. The time course of pain and rectal dysfunction severity was variable. Twelve weeks after PPRT, 10/13 (77%) and 9/10 (90%) of evaluable patients who had identified TS pain and rectal dysfunction, respectively, reported improvement or resolution. Non-target pelvic symptom severity decreased during the study. Median global QOL scores remained stable at follow-up visits. There was no grade 4 toxicity reported. Median survival after PPRT was 9 months (0-51).

Target symptom response and HRQOL compared to baseline

		Proportion of evaluable patients reporting target symptom improved or resolved (95% CI)		
Number of patients with target symptom at Baseline		End of radiotherapy	6 week follow-up	12 week follow-up
Pelvic pain	n=24	14/21 67% (0.46-0.88)	14/18 78% (0.58-0.98)	10/13 77% (0.54-1.0)
Rectal dysfunction#	n=16	4/15 27% (0.04-0.50)	10/12 83% (0.61-1.0)	9/10 90% (0.71-1.0)
Hematochezia	n=9	9/9 100%	9/9 100%	8/8 100%
Other¤	n=2	1/2 50% (0-1.0)	2/2 100%	1/2 50% (0-1.0)
Total	n=51	28/47 60% (0.46-0.74)	35/41 85% (0.74-0.96)	28/33 85% (0.73-0.97)
		Proportion of the evaluable patients (95% CI)		
Global QOL compared to baseline:		End of radiotherapy	6 week follow-up	12 week follow-up
Clinically significant improvement*		17/45 38% (0.24-0.52)	14/35 40% (0.24-0.56)	10/25 40% (0.21-0.59)
Stable**		18/45 40% (0.26-0.54)	10/35 29% (0.14-0.44)	7/25 28% (0.13-0.43)
Clinically significant deterioration***		10/45 22% (0.10-0.24)	11/35 31% (0.16-0.46)	8/25 32% (0.14-0.50)
		HRQOL: Global health status score Median (IQR); p-value^		
	Baseline	End of radiotherapy	6 week follow-up	12 week follow-up
Global QOL score	50 (37.5-67) n=49	60 (50-67) n=45 p=0.146	50 (33-83) n=35 p=0.837	67 (50-83) n=25 p=0.569

CI= confidence interval; HRQOL= health-related quality of life; IQR= interquartile range. # includes rectal obstruction (n=6), diarrhea (n=2), incontinence (n=6), mucous production (n=2); * = Increase ≥ 10 points; ** = Values within 9 points of baseline score; *** = Decrease ≥ 10 points; ¤ = Edema, urinary incontinence; ^ = Score compared to baseline.

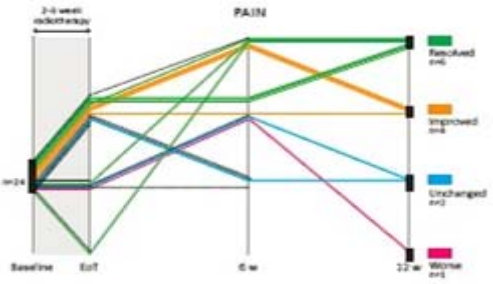

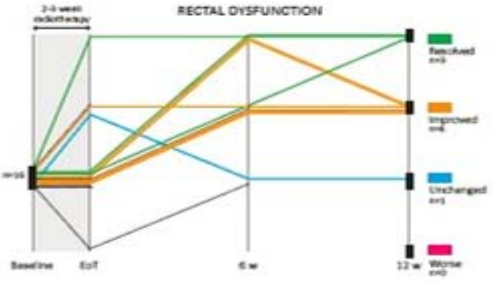

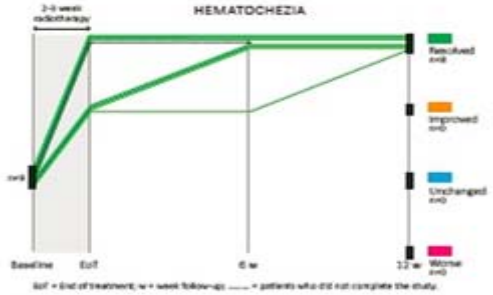

Conclusion: In the majority of patients with symptomatic primary or recurrent RC, PPRT with 30-39 Gy contributes to relief of pain, rectal dysfunction, hematochezia, and other pelvic symptoms, with little toxicity. A large proportion of patients prescribed PPRT of RC have very limited life expectancy and future studies should investigate patient selection and further simplification of PPRT.

Poster: Clinical track: Elderly

PO-0780

An analysis of elderly patients compliance and disease distribution treated with radiation therapy

S.H. Lee[1], L. Seung Heon[1], S. KiHoon[1], C. Young Eun[1], L. Kyu Chan[1], K. Kwang Pil[2]
[1]*GIl Medical Center- Gachon University of Medicine and Science, Department of Radiation Oncology, Inchon, Korea Republic of*
[2]*Gachon University of Medicine and Science, Department of Preventive Medicine, Inchon, Korea Republic of*

Purpose or Objective: In this study, we investigated the disease distribution and analyzed treatment compliance for the elderly patients received radiation therapy (RT).

Material and Methods: Among the patients underwent RT from January 2005 to May 2014 in this hospital, the 670 patients aged over 75 were retrospectively analyzed in this study. We classified the patients for each disease and analyzed the RT compliance for each disease. The RT compliance was determined whether or not the scheduled RT plan was completed. The Chi-squared test and multiple logistic regression analysis were used for the factors (region, economic status, age, gender, disease type, treatment aim, ECOG score) influencing the RT compliance.

Results: The mean age of the patients was 78 years (range; 75~99 years). The disease distribution was as follows; Lung cancer in 127 patients (19.0%), metastasis in 123 patients (18.4%), gastrointestinal (GI) cancer in 116 patients (17.3%), gynecologic cancer in 110 patients(16.4%), head and neck cancer in 53 patients (7.9%), genitourinary cancer in 44 patients (6.6%), breast cancer in 30 patients (4.5%), hematologic cancer in 22 patients (3.3%), skin cancer in 17 patients (2.5%), brain tumor in 9 patients (1.3%), and others in 19 patients (2.8%). The RT compliance in total 670 patients was 82.6% The 116 patients of all patients could not complete their course of scheduled treatment. According to x2 test analysis, the factors found to be related to the RT compliance were; gender(p=0.001), disease type(p=0.014), and patient`s ECOG score(p<0.001). Multiple logistic analysis showed that gender(p=0.016) and patient`s ECOG score(p<0.001) were related to RT compliance.

Conclusion: Based on these preliminary results, more than 80% of elderly patients received RT for lung cancer, metastatic cancer, GI cancer, gynecologic cancer, head and neck cancer, and genitourinary cancer. This study showed that the most significant factor related to RT compliance was the patient's functional status. Further comparative studies with younger patients are also needed.

PO-0781

Hypofractionated or conventional radiotherapy for early glottis cancer. Does age influence?

L. Gutierrez Bayard[1], M. Salas Buzón[1], E. Porras Alonso[2], L. De Ingunza Barón[1], S. Garduño Sánchez[1], I. Villanego Beltrán[1], V. Díaz Díaz[1], E. González Calvo[1], L. Díaz Gómez[1]
[1]*Hospital Universitario Puerta del Mar, Radiation Oncology, Cadiz, Spain*
[2]*Hospital Universitario Puerto Real, Otorrinolaringology, Puerto Real, Spain*

Purpose or Objective: To evaluate the effect of shortening overall treatment time by hypofractionated radiotherapy for cT1-T2N0M0 glottic carcinomas. Results for local control, survival and toxicity were calculated and compared to cT1-

T2N0M0 tumors those received conventionally dose fraction schedule, by age group, less than 65 years old or greater.

Material and Methods: Between 2005 and 2008, 72 patients with cT1N0M0 and 47 with cT2N0M0 glottic cancer were treated with radical conventional radiotherapy (2Gy/fraction, 5 days per week total dose 70Gy and 72 Gy: group 1), 87/119 over 65 years old. Between 2009 and 2013, 34 patients with cT1N0M0 and 31 with cT2N0M0 glottic cancer were treated with radical hypofractionated radiotherapy (2.75Gy/fraction, 5 days per week, total dose 55Gy and 57.75Gy: group 2), 52/65 over 65 years old.Toxicity was evaluated according to RTOG toxicities scale.

Results: The 5-year local control was in group 1 was 86% for T1 and 78% for T2, in group 2 was 90% for T1 and 88% for T2, whereas the 5- year overall survival was in group 1: 72% for T1 and 67.7% for T2 ; in group 2: 73.8% for T1 and 70.7% for T2. The treatment was well tolerated. No significant statistical difference was found between the two groups, or by age group. Only grades 1 and 2 acute skin and dysphonia toxicity with good voice quality were observed and no evidence of severe late toxicity.

Conclusion: Hypofractionated radiotherapy proved beneficial por T1-T2 glottic carcinoma with no increase of toxicity and a good local control, well tolerated in older patients, over 65 years.

PO-0782
Stereotactic body radiation therapy for primary lung cancer in the elderly
L. Larrea[1], E. López[1], P. Antonini[1], V. González[1], M. Baños[1], J. Bea[1]
[1]*Hospital NISA Virgen del Consuelo, Radiation Oncology Department, Valencia, Spain*

Purpose or Objective: To evaluate stereotactic body radiation therapy (SBRT) for primary lung tumors in patients over 75 years old.

Material and Methods: Between 2002 and 2015, 62 elderly patients with 65 lung primary tumors (T1-T2N0M0) were treated using SBRT at our institution. SBRT procedure involved: Slow-scan computed tomography (CT) simulation with immobilization devices, contouring the target volume in 3 sets of CTs, superimposing the volumes in the planning system to represent the internal target volume and dose calculation using heterogeneity correction. Radiation delivery with multiple static planar or non-coplanar beams and arc therapy assured conformal dose distribution and steep fall-off of the radiation. The prescribed dose was 3 fractions of 15 Gy each (90%) over 6 to 10 days or a single 30-Gy fraction (10%). Dosimetric constraints were set for surrounding organs at risk. Repeated cone-beam CT (2 previous and 1 after radiation administration) were used to verify and adjust daily positioning. Toxicity and radiologic response were assessed in follow-up visits, using standardized criteria (RTOG and RECIST) and analyzed retrospectively. Survival rates and toxicities were calculated by the Kaplan-Meier method.

Results: Median patient age was 81 years (75-88). All patients had good performance status at the moment of treatment (ECOG PS 0-1). Because of patient's comorbidities or preferences, none were surgical candidates. The FEV1 was over 30 % of predicted in all cases. 7 % of all patients also received systemic treatment before or after SBRT. 83 % of the patients had 18-FDG PET-CT previous to SBRT. Histology included: epidermoid (48 %), adenocarcinoma (14 %), undifferentiated NSCLC (19 %), microcytic/neuroendocrine (4 %) and PET positive tumors without histology (15%). Mean tumor volume was 28.4 cm3 (1.2-143). Transient grade 1 or 2 acute toxicities (cutaneous erythema, esophagitis or respiratory symptoms) occurred in 18.4% of all cases. No grade > 3 acute or any chronic toxicities were identified. The median follow-up was 24 months (3-65). The overall and cancer-specific survivals were: 80 and 85 % at 1 year and 64 % and 70 % at 2 years. Control in the irradiated volume is 98 %, the only relapse occurring in a patient with neuroendocrine histology.

Conclusion: SBRT is an excellent treatment option for lung tumors in elderly patients in whom other treatment options might be limited. Our encouraging results are in line with those reported in recent literature for younger patients.

Poster: Clinical track: Health services research / health economics

PO-0783
Implementation of a trial outpatient clinic to improve participation and data collection in trials
J. Paulissen[1], C. Offermann[1], R. Houben[1], E. Van Erp[1], M. Brouns[1], H. Backes[1], L. Boersma[1], G. Vreuls[1], R. Lemmen[1], A. Dekker[1], P. Lambin[1], M. Jacobs[1], K. Smits[1]
[1]*MAASTRO clinic, Radiation Oncology MAASTRO Clinic, Maastricht, The Netherlands*

Purpose or Objective: Participation of patients in trials and quality of trial data collection are important factors hampering successful execution of clinical trials. Our aim was to design a system to increase patient participation in clinical radiotherapy trials and to install a process that would lead to a higher quality of data collection during treatment and follow-up.

Material and Methods: In 2013 we implemented a Trial Outpatient Clinic (TOC) for prospective screening of all patients referred to our radiotherapy institute, in order to identify potential trial candidates and to support radiation oncologists during the informed consent procedure and the work-up phase before the patients' treatment within the trial. During treatment and follow-up, dedicated TOC consultations facilitate a rearrangement in trial data collection from radiation oncologists to trial (physician) assistants of the TOC.
Patient inclusion in trials was measured in relation to the total number of radiotherapy treatments in our institute per year from 2005 to 2014. Quality of data collection was subjectively analysed based on completeness of CRF's and consistency of data. In addition, a questionnaire was provided to a random subset of seventeen trial participants to evaluate their satisfaction with the TOC. Interviews with seven radiation oncologists were performed to evaluate their experience with the TOC.

Results: The percentage of trial patients as compared to the total number of treatments declined between 2005 and 2008 from 6.6% to 3.8%. After implementing the TOC, this number increased to 5.3%. In 2014 we observed an increase to 9.3% despite a decline in the number of trials open for inclusion in the last two years. CRF's were found to be more consistent and complete. The participants' questionnaire showed that 82% was very satisfied having one contact person for trial related issues and 71 % thought that the existence of the TOC had added value. Participants did not think it bothersome having additional consultations and experienced an extra benefit by becoming more familiar with TOC personnel. Radiation oncologists were satisfied about the TOC as rearrangement of data recording was beneficial to them and less laborious.

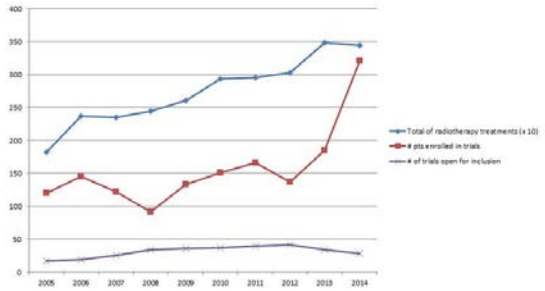

Conclusion: The implementation of our TOC model has led to a higher inclusion in trials, an improved data collection and a higher satisfaction of patients and radiation oncologists involved in clinical trials. The TOC model has led to an optimal infrastructure for well-performed, high-quality clinical trials.

PO-0784

Targeting general practitioners: prospective outcomes of a nationwide GP education programme

L. Morris[1], S. Turner[1], P. Gorayski[2]
[1]*Crown Princess Mary Cancer Centre, Department of Radiation Oncology, Sydney, Australia*
[2]*Radiation Oncology Queensland, Toowoomba, Queensland, Australia*

Purpose or Objective: To report the learning outcomes of a standardised national multicentre education program aimed at improving General Practitioner (GP) knowledge about radiation therapy (RT) and referral pathways to radiation oncologists (RO).

Material and Methods: In 2014, a GP education session was developed through the 'Targeting Cancer: Radiation Oncology' campaign (an initiative of RANZCR, Faculty of Radiation Oncology). The content and structure was developed by a committee of ROs with skills in training and education. The sessions are designed to be held within an RT department and consist of RO-led interactive teaching around two common patient scenarios, followed by a physical tour of the RT department with demonstrations of set up and treatment. Pre- and immediate post-session custom surveys were administered on consented GPs. Four key domains were assessed:
1. Objective and subjective knowledge about RT.
2. Satisfaction regarding referral pathways to ROs.
3. Self-reported referral behaviours.
4. Feedback on quality of the educational session.
A 6 question follow up survey was sent 6-8 months after the session to assess the usefulness of the knowledge gained in the clinical care of cancer patients and ongoing referral behaviours.

Results: 120 GPs attended a total 10 sessions held in RT departments across Australia between October 2014 and 2015. Pre-session, 96% of GPs reported their knowledge of radiation therapy required signficant or some improvement. Post-session, 91% rated their knowledge as "excellent", "above average" or "competent". In concordance with this, the proportion of GPs correctly answering objective knowledge questions rose from 50% to 82%. Over one third of GPs did not know the location of their nearest RT department and 80% wanted improved referral pathways to ROs. Despite this 92% have had patients in their practice who might benefit from palliative RT. However nearly half the GPs indicated they were not comfortable referring directly to a RO. Following the session this rose to 92%. All 120 respondents felt the session improved their understanding of RT and would recommend the session to colleagues. Early data from the 6 month follow up survey shows 100% of GPs felt the knowledge gained at the education session has improved their ability to care for cancer patients and increased their confidence to refer directly to ROs.

Conclusion: A national standardized GP education program can significantly improve GP knowledge of the core RT concepts and likely influence patient referrals for RT.

PO-0785

Improvement strategies and performance enhancement in Healthcare: the reorganisation of Radiotherapy

M. Altini[1], D. Gallegati[2], L. Solinas[2], C. Zani[1], I. Massa[3], A. Romeo[4], V. Turri[1]
[1]*IRCCS - Istituto Scientifico Romagnolo per la Cura e lo Studio dei Tumori, Healthcare Department, Meldola, Italy*
[2]*IRCCS - Istituto Scientifico Romagnolo per la Cura e lo Studio dei Tumori, Planning and Business Management, Meldola, Italy*
[3]*IRCCS - Istituto Scientifico Romagnolo per la Cura e lo Studio dei Tumori, Biostatistic and Clinical Trial Unit, Meldola, Italy*
[4]*IRCCS - Istituto Scientifico Romagnolo per la Cura e lo Studio dei Tumori, Radiotherapy Unit, Meldola, Italy*

Purpose or Objective: Population ageing, changes in epidemiological trends and the development of new treatments are putting strain on National Health Systems, which need to implement performance measurement systems to minimize the impact of expenditure reduction on service quality and to drive value creation for the whole population. We developed a model of healthcare performance evaluation for oncology care whose main focuses are: - specific types of cancers and value for citizens of a catchment area served.
The model synthesizes into a single index the value of a service - outcome and costs for the population – building upon the Italian NHS principles. We applied the model to a Radiotherapy Service before and after IRST IRCCS took over its management in January 2014

Material and Methods: We measured value produced by Radiotherapy Services for the Ravenna district (393,184 inhabitants) before 2013 and after the technological investment in 2014.We considered three performance dimensions:
-clinical outcomes;
-appropriateness;
-accessibility and geographic proximity of services.
An expert panel selected variables, indicators and weights such as waiting times for treatments, % advanced treatment (IMRT, V-MAT), passive migration cases to other areas, average access to treatment. Per-capita cost was computed as direct costs of radiotherapy minus reimbursement for "active" patient migration, plus costs for "passive" patient migration; total costs were divided by age-adjusted population. A composite indicator was computed, whose nominator synthesizes quality indicators and whose denominator accounts for costs. 2013 IRST performance in Forlì-Cesena district was used as benchmark

Results: Value assessed in Ravenna district was lower than that of Forlì-Cesena in 2013 (0.35 and 0.78, respectively), translating into a higher per-capita cost (12 euro vs. 9 euro) and lower service level (4.2 vs. 7.0 quality points). In 2014, performance of Ravenna Radiotherapy Service significantly improved (0.47; +34%): quality points went up from 4.2 to 5.1 as a result of better clinical outcome, improved accessibility and shorter wait times **Fig1**.
Per-capita costs decreased from 12 Euro to 10.8 Euro thanks to a reduction in "passive" patient migration, efficiency gain (fewer radiotherapy sessions for specific regimens) and economies of scale. A return on investment and financial stability were guaranteed by efficiency gain (lower emerging compared to savings from reduced "passive" patient migration) and by increased attractiveness (increased "active" patient migration) **Fig2**.

Fig.1 Populational Performance

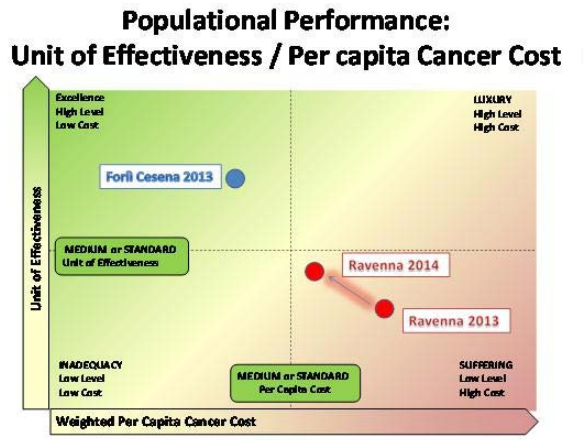

Fig.2 Indicator results

Indicators	2013 Ravenna	2014 Ravenna	2013 Forlì Cesena
Waiting times for treatments (Performance Index to 30 days)	35%	76,9%	31%
% Advanced treatment (V-MAT - IMRT)	23%	48%	53%
Passive migration to other areas	55%	41%	14%
Average access to treatment	19	15	14

Conclusion: Investments in technological upgrades in public services can result in increased efficiency and productivity levels, while improving service quality, decreasing costs and reducing service duplication and overlapping. Our preliminary findings suggest the applicability of our model to the full cancer care pathway

PO-0786

Could a 3-tier teleradiotherapy network provide a cost-effective radiotherapy care in LMICs?

N.R. Datta[1], M. Heuser[1], M. Samiei[2], S. Bodis[1]
[1]*Kantonsspital Aarau, Radio-Onkologie, Aarau, Switzerland*
[2]*International Atomic Energy Agency IAEA, Senior Consultant, Vienna, Austria*

Purpose or Objective: Information and communication technologies (ICTs) have enabled cost-effective eHealth programmes gain wider acceptance in a range of health disciplines. However, this is yet to be evaluated in radiotherapy (RT), especially in low- and middle income countries (LMICs). We explored the use of ICTs to create a 3-tier network of teleradiotherapy centres (RTC), namely - primary (PRTC) with 1 teletherapy (TRT) unit; secondary (SRTC) with 2 TRT units and brachytherapy (BRT); and tertiary RT centre (TRTC) with state-of-the-art RT facilities. The cost-effectiveness of this network was evaluated for 10 adjoining countries in middle and east Africa.

Material and Methods: Seven of the 10 countries (Gabon, Congo Republic, Congo DR, Central African Republic, South Sudan, Rwanda and Burundi) have no RT facilities for their 123.6 million inhabitants. Remaining 3 countries (Uganda, Kenya and Tanzania) have in total 11 TRT and 6 BRT units. Thus, presently, only 2.3% of 262.2 million people have RT access in these 10 countries. Based on the regional population density and location of current centres, 6 PRTCs, 2 upgraded PRTCs (with BRT), 6 SRTCs and upgradation of an existing centre to SRTC are proposed. These could be networked to share the available resources. With DICOM RT compatible data sets, ICTs could facilitate an easy exchange of patient information between centres. Consequently, patients at PRTC with a standalone TRT unit could deliver RT based on treatment plans derived at SRTC. Similarly patients treated at PRTC could receive brachytherapy at SRTC. TRTC could cater to specialized RT techniques not feasible either at PRTC or SRTC. Thus, patients within the 3-tier network would have access to state-of-the-art technology in a shared step-wise manner.

Results: The total cost of the infrastructure, networking, maintenance and incidentals is estimated around US$ 66.25 million. With a total of 32 TRT and 15 BRT units provided in this network, the RT accessibility would enhance from 2.3% to 30.7% (9.2%-76.9%). The mean cost of this investment for the 262.2 million inhabitants would be around US$ 0.69 per inhabitant (US$ 0.12-2.22) while the average cost in terms of individual patients receiving RT is estimated to be US$ 374 (US$ 71.67-508.33). Capacity building could be undertaken through telementoring by linking to regional or international centres of excellence and professional societies through multisectoral collaborative efforts.

Conclusion: The 3 tier-teletherapy network with ICTs could provide cost-effective comprehensive RT care by overcoming the geographical barriers by optimizing resource sharing, pedagogical telementoring and capacity building. This could lead to scalable, equitable, affordable and improved RT access to patients of the region. The approach could be explored for other underserved LMICs and executed with the help of respective national and international stakeholders.

PO-0787

Abstract withdrawn

PO-0788

Predicted patient demand for MRI Linac

B. Sanderson[1], A. McWilliam[2], C. Faivre-Finn[1], A. Choudhury[1], T. Mee[3]
[1]*The Christie NHS Foundation Trust, Department of Clinical Oncology, Manchester, United Kingdom*
[2]*The Christie NHS Foundation Trust, Department of Medical Physics and Engineering, Manchester, United Kingdom*
[3]*University of Manchester, Institute of Cancer Sciences, Manchester, United Kingdom*

Purpose or Objective: MRI offers superior soft tissue delineation compared to CT. When incorporated in to a linear accelerator (MRI Linac), it could improve temporal resolution and dynamic visualisation of the target during treatment allowing for motion compensation and real-time adaptive planning. This study investigated the predicted patient demand for radiotherapy delivered via a MRI Linac for prostate and lung cancer at a large comprehensive cancer centre to ensure that any clinical research will be achievable.

Material and Methods: Local stage data was sourced from hospital databases and the UK NHS CASCADE system. Indications for MRI Linac were obtained by consulting with the specialist clinical leads for prostate and lung cancers. Locally advanced patients where soft tissue definition would be clinically advantageous were identified (T3/4 prostate, stage 2/3 non-small cell lung cancer [NSCLC] including superior sulcus tumours and limited stage small cell lung cancer [SCLC] with good performance status). The Malthus programme was used to estimate the demand for MRI Linac. The Malthus programme is an evidence based, predictive mathematical model, based on regional population and incidence data, mapping around 2,000 clinical decisions relating to radiotherapy for 23 different cancer sites.

Results: The catchment area of the comprehensive cancer centre in the study is approximately 3.2 million people. For prostate, the total projected incidence for 2015 was 1,983 cases, of which 436 high risk patients were predicted to be eligible for MRI Linac. For lung, the total projected incidence for 2015 is 2,634 cases. Of these, a total of 360 patients were identified as suitable for MRI Linac (table 1). Approximately 92 of the NSCLC's were considered superior sulcus tumours.

Table 1. Estimated number of patients eligible for MRI Linac according to stage and type of lung cancer.

Disease & Stage	Estimated number for MRI Linac
NSCLC	
Stage 2	94
Stage 3a	169
Stage 3b	45
SCLC	
Limited	52
Total	360

Conclusion: The potential cohort is estimated at 796 eligible patients for MRI Linac in lung and prostate cancer. In the context of lung and prostate cancer, we estimate during the initial research phase that we will treat around 180 patients per year on one machine. Therefore, the estimated number of eligible patients far exceeds the estimated throughput for a single MRI Linac machine. This has positive implications for its use as a research tool. Even after accounting for patients who will inevitably decline entry to clinical trials, the estimated eligible patient population is such that trials should still have sufficient recruitment; this is especially important for rare indications such as superior sulcus tumours.

PO-0789

Treatment time in breast irradiation: a trade-off between positioning and complexity.

C. Monten[1], L. Veldeman[1], Y. Lievens[1]
[1]*University Hospital Ghent, Radiotherapy, Ghent, Belgium*

Purpose or Objective: In whole breast irradiation (WBI), different approaches are used to spare the organs at risk, including intensity modulation and altered positioning. These may however come at the cost of longer treatment times, which in turn may slow down adoption in daily clinical practice. To document the impact of different approaches, time measurements were performed, following a strict protocol.

Material and Methods: A time-and-motion study was carried out using a 'continuous timing' method (running chronometer with defined intervals), according to the following protocol:
- Positioning time: Patient in bunker - Start Cone Beam CT (CBCT)
- CBCT recording time: Start CBCT - Stop CBCT
- Adaptations: Stop CBCT - Beam on
- Irradiation time: Beam on - Beam off
- Patient recovery time: Beam off - Patient exits bunker

Time measurements were categorized per position, technique and target. Positioning time is reported over all patients, irradiation time per category, in absolute time and, to correct for dose and volume differences, in Irradiation Time per 100MU's (ITcMU). Statistical analysis was performed using parametric testing, i.e. the One Way Anova.

Results: Registration was performed in 86 patients, of which 47 in prone and 39 in supine position. Positioning time was measured in 74 patients, and irradiation time in 86. Results are listed in table 1.

Treatment characteristics (n=86)								
Supine				Prone				
39				47				
Without lymph node irradiation				With Lymph nodes				
65				21				
WBI		SIB		Thoracic Wall		Tumorbed		
36		28		12		10		
IMRT without table rotation		IMRT with table rotation		VMAT		Single-arc VMAT		
52		21		6		7		
Positioning time (per fraction) (n=74)								
Supine (n=28)				Prone (n=42)				Significance (One way Anova)
00:03:52				00:05:03				p=0,01
WBI (n=32)		SIB (n=19)		Thoracic wall (n=9)		Tumorbed (n=10)		
00:04:45		00:04:49		00:03:44		00:04:18		p=0,5
Without Lymph nodes (n=56)				With Lymph nodes (n=14)				
00:04:46				00:03:49				p=0,1
Irradiation time (ITcMU) (n=86)								
Supine (n=37)				Prone (n=45)				p=0,002
00:00:53				00:01:10				
WBI (n=34)		SIB (n=27)		Thoracic wall (n=11)		Tumorbed (n=10)		p=0,1
00:01:06		00:00:54		00:01:02		00:01:11		
IMRT without table rotation (n=48)		IMRT with table rotation (n=21)		VMAT (n=6)		Single-arc VMAT (n=7)		p<0,001
00:01:02		00:01:11		00:01:18		00:00:29		
No LNI (n=37)	LNI (n=11)	No LNI (n=17)	LNI (n=4)	No LNI (n=5)	LNI (n=1)	No LNI (n=3)	LNI (n=4)	
00:00:59	00:01:10	00:01:14	00:00:57	00:01:20	00:01:07	00:00:22	00:00:34	
"WBI only" irradiation time (ITcMU) (n=32)								
Supine (n=5)				Prone (n=27)				p=0,8
00:01:03				00:01:05				
IMRT without table rotation (n=28)		IMRT with table rotation (n=4)		VMAT (n=1)				p=0,08
00:01:04		00:01:21		00:00:40				
"WBI only" irradiation time (per fraction dose 2,67Gy) (n=32)								
Supine (n=5)				Prone (n=27)				p=0,02
00:04:38				00:02:59				
IMRT without table rotation (n=27)		IMRT with table rotation (n=4)		VMAT (n=1)				p=0,08
00:03:07		00:04:34		00:01:30				
"Overall" irradiation time (per treatment) (n=55)								
No LNI						LNI		
Hypofractionation WBI		Hypo-fractionation SIB		Acceleration SIB		Hypofractionation TxW		Acceleration TxW
Supine (n=5)	Prone (n=19)	Prone (n=4)	Supine (n=11)	Prone (n=4)		Supine (n=9)		Supine (n=3)
01:09:39	00:43:35	01:16:56	00:35:37	00:35:46		01:35:16		00:41:55
Acceleration (5 fractions)						Hypofractionation (15 fractions)		
IMRT (n=9)	IMRT with table rotations (n=3)		VMAT (n=1)	Single-arc VMAT (n=3)		IMRT (n=28)	IMRT with table rotations (n=8)	VMAT (n=3)
00:36:50	00:43:20		00:40:40	00:17:10		00:46:46	01:12:45	01:09:45

Abbreviations: WBI = Whole breast irradiation; SIB = Simulatineously integrated boost; IMRT = Intensity modulated radiotherapy; VMAT = Volumetric modulated arc therapy; ITcMU = irradiation time per 100 monitor units.

Positioning time per session was on average 1'11" longer for prone than for supine. This difference is confirmed in "WBI only", simultaneous integrated boost (SIB) and tumor bed irradiation, all three predominantly performed in prone, in contrast to two purely supine positions: thoracic wall and "lymph node included" irradiation.
ITcMU was 17" faster for supine versus prone positioning. Looking into hypofractionated WBI only, no difference was observed in ITcMU, but irradiation time per fraction was 1'40" longer for supine versus prone position. The mean number of gantry positions for prone and supine position was respectively 2 and 5, signifying less complex planning in prone to obtain equivalent dosimetric results.
Single-arc Volumetric Modulated Arc Therapy (VMAT) resulted in less than half of the irradiation time needed compared to IMRT or normal VMAT used for similar target or position.

Conclusion: Prone position comes at the cost of longer positioning time, but reduces irradiation time as a result of less need for complex planning, especially for WBI and sequential boosting. Although fraction time increases when using acceleration, overall irradiation time decreases, which compensates for potentially higher time demands of more complex treatment techniques. Single-arc VMAT reduces longer fraction times. These data will be used for balancing the costs and effects of the different approaches.

Poster: Clinical track: Other

PO-0790

Radiation-induced mesothelioma among solid cancer survivors: an analysis of the seer cohort

A. Farioli[1], L. Ronchi[2], M. Ferioli[2], F. Busi[2], G. Compagnone[3], S. Cammelli[2], M. Ferro[4], F. Labropoulos[4], M. Nuzzo[4], G. Macchia[4], F. Deodato[4], G. Frezza[5], A.G. Morganti[2], F.S. Violante[1]

[1]*Sant'Orsola-Malpighi Hospital- University of Bologna, Department of Medical and Surgical Sciences DIMEC, Bologna, Italy*

[2]*Sant'Orsola-Malpighi Hospital- University of Bologna, Radiation Oncology Center- Department of Experimental-Diagnostic and Specialty Medicine - DIMES, Bologna, Italy*

[3]*Sant'Orsola-Malpighi Hospital- University of Bologna, Department of Medical Physics, Bologna, Italy*

[4]*Fondazione di Ricerca e Cura "Giovanni Paolo II"- Catholic University of Sacred Heart, Radiotherapy Unit, Campobasso, Italy*

[5]*Ospedale Bellaria, Radiotherapy Department, Bologna, Italy*

Purpose or Objective: To investigate the association between external beam radiotherapy (EBRT) and pleural and peritoneal mesothelioma among long-term (>5 years) solid cancer survivors.

Material and Methods: We analysed data from the US Surveillance, Epidemiology, and End Results (SEER) program (1973-2012). We fitted survival models adjusted by age, gender, race, year, surgery, and relative risk of primary mesothelioma in the county of residence (proxy for individual asbestos exposure). We estimated hazard ratios [HR] with reference to non-irradiated patients. We distinguished between scattered and direct irradiation to study the dose-response.

Results: We observed 300 mesotheliomas (264 pleural; 32 peritoneal; 4 others) among 913,873 patients. EBRT increased the risk of mesothelioma (any site; HR 1.36, 95%CI 1.05–1.76). We observed an increased risk of pleural mesothelioma (HR for EBRT 1.35, 95%CI 1.02–1.78), but we did not find signs of a dose-response relationship (HR for scattered irradiation 1.35; HR for direct irradiation 1.36). On the opposite, only direct peritoneal irradiation was associated with peritoneal mesothelioma (HR 2.13, 95%CI 0.96–4.74), particularly for latencies ≥10 years (HR 3.19, 95%CI 1.11–9.18). A competing risks analysis revealed that the clinical impact of radiation-induced mesothelioma was limited by the high frequency of competing events. The cumulative incidence function of mesothelioma after 40 years of observation was very low (non-irradiated patients: 0.00031, irradiated patients: 0.00056).

Conclusion: EBRT is a determinant of mesothelioma. Longer latency periods are associated with higher risks, while the dose-response seems non-linear. The clinical impact of mesothelioma after EBRT for primary solid cancers is very limited.

PO-0791

Motion management and Vero dynamic tracking for SBRT in oligometastatic disease: a prospective trial

R. Van den Begin[1], B. Engels[1], M. Boussaer[1], J. Dhont[1], M. Burghelea[1], C. Collen[1], T. Gevaert[1], D. Verellen[1], G. Storme[1], M. De Ridder[1]

[1]*Universitair Ziekenhuis Brussel, Department of Radiotherapy, Brussels, Belgium*

Purpose or Objective: To evaluate the clinical efficacy and toxicity of stereotactic body radiotherapy (SBRT) with respiratory motion management in patients with oligometastatic cancer.

Material and Methods: Patients with five or less metastases were eligible for this prospective trial. A four-dimensional respiration-correlated CT (4D-CT) was obtained for planning. In metastases with significant motion, a fiducial marker was implanted for dynamic tracking using the gimbaled Vero SBRT system, otherwise an internal target volume (ITV) was defined to encompass the tumor trajectory. ITV-targets were also treated on Vero, unless numbering 4 or more, in which case tomotherapy was used. A dose of 50 Gy in 10 fractions of 5 Gy was prescribed on the 80% isodose line, covering the planning target volume.

Results: We treated 87 metastases in 44 patients, with colorectal cancer as the most common primary origin (65.9%). Metastatic sites were mainly lung (n=62) and liver (n=17). Twenty-seven metastases, of which 12 in lung, 14 in liver and 1 in a kidney, were treated with dynamic tracking, the remaining 60 using the ITV-concept. Three patients (7%) experienced grade ≥3 toxicity, of which one with a liver metastasis invading the major bile ducts with grade 5 cholangitis due to bile duct stenosis. After a median follow-up of 12 months. we report an actuarial one-year local control (LC) of 89% for the whole group (95% CI 77–95%), with corresponding values of 90% and 88% for the metastases irradiated with the ITV-approach and dynamic tracking, respectively. Median progression-free survival reached 6.5 months, one-year overall survival 97%.

Conclusion: This first clinical trial on Vero dynamic tracking shows favorable efficacy. SBRT with respiratory motion management resulted in a high LC and acceptable toxicity profile in oligometastatic cancer patients.

Poster: Physics track: Basic dosimetry and phantom and detector development

PO-0792

Direct dose measurements in contrast enhanced radiotherapy with iodine and gadolinium

A.A. Cherepanov[1], A.A. Lipengolts[2], E.S. Vorobyeva[3], V.A. Klimanov[3], V.N. Kulakov[1], E.Y. Grigorieva[2]

[1]*Burnasyan Federal Medical Biophysical Centre, Department of radiation technologies, Moscow, Russian Federation*

[2]*Russian Cancer Research Center, Institute of Clinical and Experimental Radiology, Moscow, Russian Federation*

[3]*National Research Nuclear University, Department of Experimental and Theoretical Physics, Moscow, Russian Federation*

Purpose or Objective: Contrast enhanced radiotherapy (CERT) has already been shown to be a promising antitumor modality capable to overcome some limitation inherent to conventional beam radiotherapy. Depth dose distribution in CERT is characterized by local dose increase in a volume, which incorporates certain amount of a high atomic number element. Photoabsorption of external X-ray radiation by high atomic number elements (such as iodine, gadolinium, gold etc.) leads to absorbed dose enhancement exactly in the region of the element location. Dose increase is caused by emission of short range secondary radiation such as characteristic X-rays, photoelectrons and Auger electrons. Dose enhancement in CERT for particular high atomic number element is strongly dependent on energy spectrum of external radiation. Calculations of many researchers show that significant part of absorbed dose is caused by Auger-electrons especially in the close vicinity (about 1 um) of emitting atom. Because of their extremely short range in water Auger-electrons are not detectable by most dosimetric tools such as ionizing chambers, radiochromic films etc. However ferrosulfate based dosimeters (Fricke dosimeters) can be used to measure total absorbed dose caused by photoabsorption of external X-ray radiation by high atomic number elements.

Material and Methods: Direct dose enhancement was measured for iodine in the chemical form of iopromide (Ultravist 370, Bayer) and gadolinium in the from of gadolinium sulfate (Sigma-Aldrich). Fricke dosimeter solution was prepared by standard procedure described elsewhere.

Iopromide and gadolinium sulfate solutions were introduced into standard Fricke dosimeter solution for final concentrations of iodine from 2.5 mg I/ml to 50 mg I/ml and gadolinium from 5 mg Gd/ml to 10 mg Gd/ml. Detection of iron (III) ions was performed with spectrophotometer Varian Cary 50. For measurement of iron (III) ions concentration in the presence of iopromide ammonium tiocianate (Panreac) was used as an indicator because optical spectrum of iopromide interfere with optical spectrum of iron (III) ions. Irradiation of Fricke solutions was performed with 110 kVp X-rays through 3.5 mm Al filter at 0.7 Gy/min dose rate.

Results: Dose enhancement in presence of iodine and gadolinium was expressed as dose enhancement factor (DEF), which is the ratio of absorbed dose value in Fricke water solution containing iodine or gadolinium and in pure Fricke water solution. Measured DEF values and corresponded iodine and gadolinium concentrations are presented in Table.

High atomic number element	Concentration, mg/ml	DEF
Gadolinium	5	1.3±0.1
	10	1.5±0.1
Iodine	2.5	1.2±0.1
	5	1.3±0.1
	10	1.7±0.2
	25	3.1±0.3
	50	4.8±0.5

Dose enhancement is proportional to concentration of the element used. DEF value for iodine varies from 1.2±0.1 to 4.8±0.5 for concentration of iodine from 2.5 mg I/ml to 50 mg I/ml respectively.

Conclusion: A new approach for measuring dose enhancement in CERT was proposed. This method can be used as a routing procedure in experimental and clinical practice of CERT dose measurements.

PO-0793

The Advanced Markus ionization chamber is useable for measurements at ultra high dose rates

K. Petersson[1], M. Jaccard[1], T. Buchillier[1], C. Bailat[1], J. Germond[1], M. Vozenin[2], J. Bourhis[2], F. Bochud[1]

[1]*Lausanne University Hospital - CHUV, Institute of Radiation Physics - IRA, Lausanne, Switzerland*

[2]*Lausanne University Hospital - CHUV, Department of Radiation Oncology, Lausanne, Switzerland*

Purpose or Objective: The Advanced Markus ionization chamber from PTW (PTW-Freiburg GmbH, Freiburg, Germany) saturates at high dose rates (Ḋ) and/or at a high dose-per-pulse (DPP). According to PTW, the ion collection efficiency is ≥ 99% at continuous Ḋ < 375 Gy/s and at DPP < 5.56 mGy. At a source-to-surface distance (SSD) of 50 cm, our prototype linac produces a mean Ḋ of ≈ 500 Gy/s, an instantaneous Ḋ of ≈ 2.5 MGy/s, and a DPP of ≈ 5 Gy (far above the chamber datasheet range). In order to use the Advanced Markus chamber for determining the absorbed dose in these intense radiation conditions, we needed to establish a model of its saturation as the Ḋ/DPP increases.

Material and Methods: Two independent methods were used to determine the chamber saturation curve. 1) Measurements in a water phantom at different Ḋ/DPP by varying the SSD and the linac gun grid tension (pulse amplitude). The hypothesis was that if the linac output varies with grid tension in a reproducible way and if the grid tension was varied by the same factor for every SSD then the relative change in chamber response with grid tension should be the same for all SSD if not for the chamber saturation. 2) Simultaneous measurements of chamber and Ḋ/DPP independent radiochromic film (Gafchromic™ EBT3, Ashland Inc., Covington, USA), in a solid water phantom (RW3 slabs, PTW) at various Ḋ/DPP.

Results: The results show how the chamber saturation increases (the ion collection efficiency decreases) as the DPP increases (Figure). These results also show that the chamber saturation is much more dependent on the DPP than the instantaneous Ḋ, as the ion collection efficiency curves for the different pulse widths (= DPP/instantaneous Ḋ) are only slightly separated when plotted against DPP.
A mathematical model of the saturation curves was established by fitting a logistic function (dependent on DPP) to the data points:

$$\frac{1}{k_s} = \frac{1}{\left(1+\left(\frac{0.3}{DPP}\right)^{-2}\right)^{a}} \Leftrightarrow k_s = \left(1+\left(\frac{DPP}{0.3}\right)^{2}\right)^{a}$$

Where ***ks*** is the saturation (ion recombination) correction factor and where ***a*** takes a slightly different value for different instantaneous Ḋ (***a*** = 0.197, 0.192, and 0.184 for pulse widths of 0.5, 1.0, and 1.8 µs, respectively).

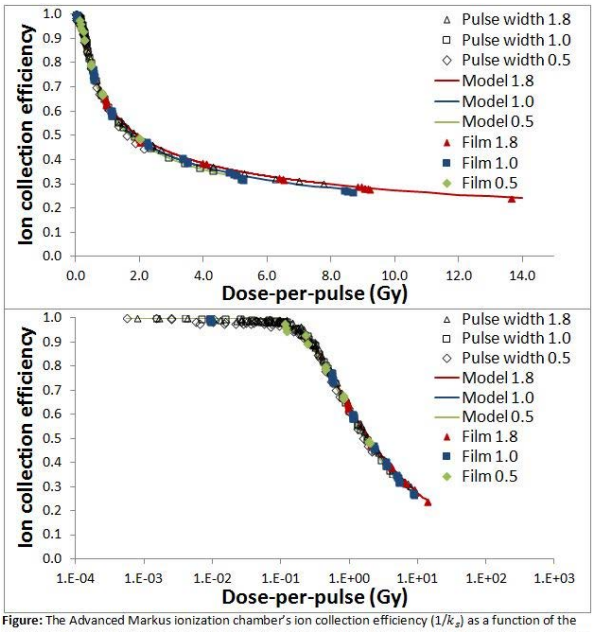

Figure: The Advanced Markus ionization chamber's ion collection efficiency ($1/k_s$) as a function of the dose-per-pulse for the water phantom measurements (unfilled data points), the logistic function model (Eq.1, lines), and for the simultaneous film and chamber measurements (filled data points). Above: a linear dose-per-pulse axis, below: a logarithmic axis. Pulse widths are given in µs.

Results from subsequent dose measurements at various Ḋ/DPP verified that chamber dose values (corrected by the saturation model) were compatible with film and TLD dose values.

Conclusion: We present a saturation model for the Advanced Markus ionization chamber, which was based on dose measurements performed in a water phantom as well as simultaneous film and chamber measurements in a solid water phantom, at various Ḋ/DPP. Chamber dose measurements corrected by the saturation model were compared to independent film and TLD dose measurements. These measurements verified that the Advanced Markus ionization chamber does not completely saturate up to DPP values of 10 Gy and can consequently be used for accurate dose measurements (within 5%) in ultra high Ḋ/DPP irradiation conditions, if the chamber saturation model is applied.

PO-0794

First proton irradiation experiments with a deformable radiochromic 3D dosimeter

E.M. Høye[1], P.S. Skyt[1], P. Balling[2], L.P. Muren[1], J. Swakoń[3], G. Mierzwińska[3], M. Rydygier[3], V. Taasti[1], J.B.B. Petersen[1]

[1]*Aarhus University Hospital, Department of Medical Physics, Aarhus, Denmark*
[2]*Aarhus University, Department of Physics and Astronomy, Aarhus, Denmark*
[3]*Polish Academy of Sciences, Institute of Nuclear Physics, Kraków, Poland*

Purpose or Objective: In proton therapy, anatomical changes may cause considerable deterioration of the delivered dose distributions. Transmission-based treatment verification is generally not possible, making three-dimensional (3D) dosimetry a promising tool for verification of the delivered dose. However, solid state 3D detectors have significant problems related to linear-energy-transfer dependent quenching in particle beams – an under-response of the signal in the Bragg peak. A new deformable, silicone-based, radiochromic 3D dosimeter has recently been developed by our group. The aim of this study was to perform the first proton beam experiments with this detector. Special attention was given to the quenching and dose-rate dependencies in general, relating these effects to the chemical composition of the dosimeter.

Material and Methods: Dosimeters (1 x 1 x 4.5 cm^3) of varying chemical compositions were produced. They contained leuco-malachite green (LMG) dye as the active component, chloroform and silicone elastomer.
Twelve different batches were irradiated with 60 MeV proton beams, using a 40 mm circular collimator, to different doses (0 – 30 Gy). Irradiations were performed with both a low and a high dose rate (0.23 and 0.55 Gy/s). For comparison, depth-dose distributions were measured in water with a Markus-type plane-parallel ionizing chamber. Simultaneously, dosimeters from the same batches were irradiated with 6 MV photon beams in a 10 cm square field on a linear accelerator. All dosimeters were read out before irradiation and four hours after, at a wavelength of 635 nm. The read-out was performed with a home-built 1D-scanner with a depth resolution of 0.2 mm for the proton irradiated dosimeters, while a spectrophotometer was used for the photon read-out. The dose-rate dependency was compared for proton and photon irradiations. The ratio of Bragg-peak to plateau response (at 1 cm) was compared between batches.

Results: The effect of lowering the dose rate was similar for proton and photon beams, although the beam qualities were different. The dose response was higher at a low dose rate, but at increasing dye concentration the effect was reduced. Significant under-response was observed in the Bragg peak. The peak-to-plateau ratio was improved from (2.5 ± 0.1) to (3.0 ± 0.04) by increasing the dye concentration from 0.1 to 0.3 % (w/w). By increasing the curing-agent concentration from 5 to 9 % (w/w), the ratio further improved to (3.7 ± 0.4) and (3.5 ± 0.1) for the same respective dye concentrations.

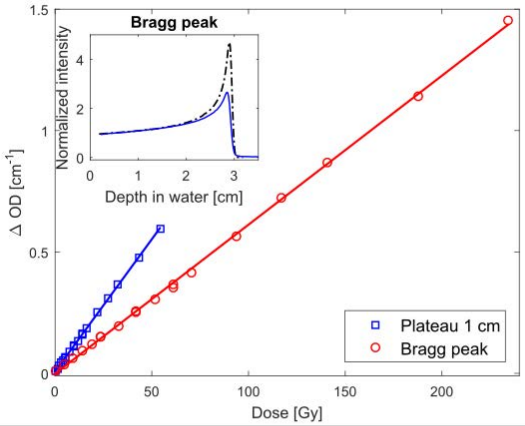

The dose response (change in optical density (Δ OD) vs. dose) for protons has been plotted for the plateau at 1 cm depth (blue squares) and for the Bragg peak (red circles). The lower sensitivity in the Bragg peak is clearly observed. The dose response is linear in both cases; 0.011 cm-1 Gy-1 at the plateau and 0.006 cm-1 Gy-1 at the Bragg peak. The inset shows one example of a measured proton depth–dose profile (blue full line), which has been normalized to the ion chamber measurement (black dashed line) at a depth of 13.1 mm. The example given here is from a batch irradiated with protons at 0.23 Gy/s, where the dosimeters contained 0.23 % (w/w) dye, 1.5 % (w/w) chloroform and 5.0 % (w/w) curing agent.

Conclusion: The 3D radiochromic silicone based dosimeter has for the first time been investigated in proton beams, and it was demonstrated that chemical modifications could influence the dosimeter response.

PO-0795
Dose verification of fast and continuous scanning in proton therapy

G. Klimpki[1], S. Psoroulas[1], M. Eichin[1], C. Bula[1], D.C. Weber[1,2], D. Meer[1], A. Lomax[1]
[1]*Paul Scherrer Institute, Center for Proton Therapy, Villigen PSI, Switzerland*
[2]*University of Zurich, University Hospital, Zurich, Switzerland*

Purpose or Objective: Out of all techniques proposed to mitigate intra-fractional motion in particle therapy, rescanning appears to be the easiest to realize: One simply needs to apply the same field multiple times with proportionally reduced dose to average out interplay patterns (Phillips *et al.* 1992). However, dead times (e.g. energy changes, spot transitions) accumulate which lengthens the overall treatment time. Thus, efficient rescanning – possibly combined with gating and/or breath-hold – requires fast energy changes (~ 100 ms) and fast lateral scanning. The former is already established at Gantry 2 (Safai *et al.* 2012). For the latter, we pursue implementing a faster delivery technique called line scanning, in which we scan the beam continuously along a straight line while quickly modulating the speed and/or current (Schätti *et al.* 2014). In this presentation, we would like to report on the dose verification concept of line scanning.

Material and Methods: With beam current changes in less than 1 ms (Schippers *et al.* 2010) and lateral scanning speeds of up to 2 cm/ms (Pedroni *et al.* 2004), the frequency of speed and current modulation along a line can be exceptionally high. This calls for a verification system that can intervene (almost) in real-time to fulfill current safety standards. Thus, we decided to monitor the beam current and position continuously during the delivery of a single element, since errors in those two parameters directly impair the homogeneity of the delivered dose distribution. In addition to these real-time verification measures, we implemented a final, redundant verification step, in which the overall dose profile of the delivered line is validated.

Results: We investigated time-resolved signals from (a) two planar ionization chambers in the gantry nozzle to monitor the beam current and (b) two Hall probes in the sweeper magnets to verify the lateral beam position. Tolerance bands define acceptable fluctuations of all signals. We

implemented the readout in detector-specific firmware, running at a sampling rate of 100 kHz. This allows us to initiate interlocks in a few ms whenever limits are exceeded. Figure 1 shows the Hall probe signal during the application of a corrupt line. We simulated two position errors of ± 1 mm at iso-center during its application; both clearly visible (peak downwards, peak upwards). In the redundant verification step, we compared the dose profile of each line, measured with a strip chamber in the nozzle, to a forward-calculated expectation.

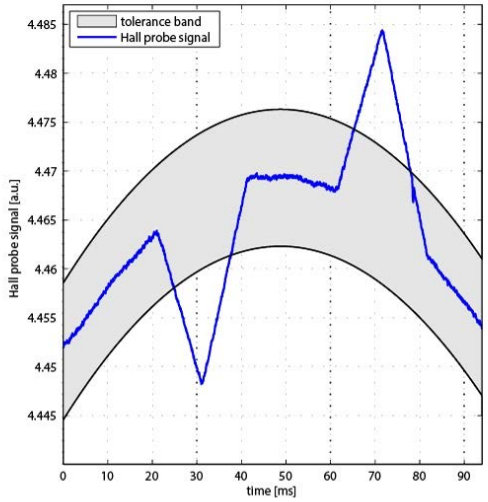

Figure 1: Measured Hall probe signal during the application of a corrupt line. Both delivery errors in position (± 1 mm at iso-center) push the signal outside of the pre-defined tolerance band (here at t_1 = 25 ms and t_2 = 65 ms). Short reaction times in initiating interlocks prevent clinically unacceptable distortions of the delivered dose distribution. The curved signal shape originates from a non-linear correlation between the magnetic field of the sweeper and the actual beam position.

Conclusion: Line scanning is a fast scanning technique; well-suited to rescanning, because it can deliver entire low-dose fields within a few seconds. The combination of real-time verification and dose profile validation ensures safe beam delivery. Interlocks can be initiated quickly during the application of a line if continuously monitored signals exceed pre-defined tolerance limits.

PO-0796

Dose rate dependence of the PTW 60019 microDiamond detector in high dose-per-pulse pulsed beams

J. Pardo-Montero[1], L. Brualla-González[2], F. Gómez[3], M. Pombar[1]

[1]*Clinical Universitary Hospital, Medical Physics, Santiago de Compostela, Spain*

[2]*Hospital General Universitario-ERESA, Medical Physics, Valencia, Spain*

[3]*Universidade de Santiago, Particle Physics, Santiago de Compostela, Spain*

Purpose or Objective: Recombination can affect detectors used for the dosimetry of radiotherapy fields, and should be corrected for. The introduction of FFF accelerators increases the typical dose-per-pulse (DPP) used in radiotherapy, which leads to more important recombination effects.
Diamond detectors provide a good solution for the dosimetry of small fields, due to their low energy dependence and small volume. The group of Università di Roma Tor Vergata has developed a synthetic diamond detector, commercialized by PTW as microDiamond. In this work we present an experimental characterization of the collection efficiency of the this detector, focusing on high-DPP, FFF beams.

Material and Methods: Measurements were performed in a Truebeam linac (Varian) with FF and FFF modalities. The microDiamond chamber was placed in a cubic PMMA phantom at 10 cm depth, the detector axis perpendicular to the beam axis. The source-to-detector distance was varied between 70 cm and 150 cm to change the DPP. The detector was irradiated with different modalities (6MV-FFF, 10MV-FFF, and 10 MV for reference) and monitor unit rates. The detector was pre-irradiated with ~15 Gy, enough to achieve signal stability. Leakage current was measured before and after each irradiation, and was always found to be <0.1 pA. We also performed measurements with a CC13 air ionization chamber (IBA, Belgium) for reference. Collection efficiencies for the microDiamond detector can qualitatively be obtained from ratios of detector readings.

Results: The collection efficiency decreases with DPP, down to 0.978 at 2.2 mGy/pulse. The effect is within 1.1% in the range 0.1-2.2 mGy/pulse, referred to 0.5 mGy/pulse. This dependence is similar to the value reported in the user manual in a narrower dose-per-pulse range (0.05-0.8 mGy).
The collection efficiency versus DPP curve does not show the typical linear dependence observed in the near saturation region for ionization chambers, but an equation based on the Fowler-Attix model provides a good fit. Such different behaviour is not surprising: recombination in diamond detectors is a more complex physical process than it is in ionization chambers, with impurities playing a significant role.
On the other hand, we have found no significant dependence of the collection efficiency on pulse repetition frequency.

Conclusion: The dose rate dependence of the microDiamond is within 1.1% in the range 0.1-2.2 mGy/pulse referred to 0.5 mGy/pulse The dependence, though moderate, can cause some systematic discrepancies when measuring FFF beams with different DPP values and should probably be considered.

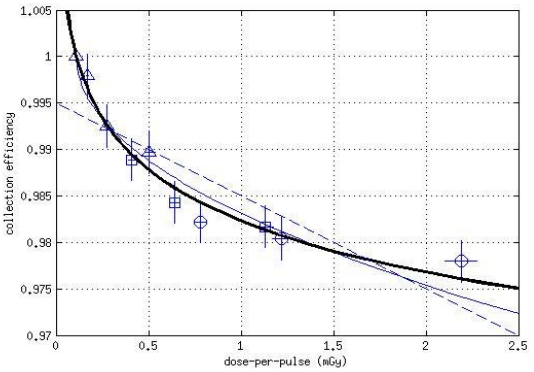

Figure. MicroDiamond collection efficiencies versus DPP: 10 MV (triangles), 6MV-FFF (boxes) and 10MV-FFF beams (circles). Best fits to a linear dependence on the dose-per-pulse (dashed line), an equation with a square root dependence (thin solid line), and the Fowler-Attix expression (thick solid line), are showed.

PO-0797

Advanced Radiation Dosimetry System (ARDOS) - A novel breathing phantom for radiation therapy

N. Kostiukhina[1], A. Sipaj[1], S. Rollet[1], E. Steiner[2,3], P. Kuess[2,3], H. Furtado[3,4], D. Georg[2,3]

[1]*AIT Austrian Institute of Technology GmbH, Health & Environment Department- Biomedical Systems, Vienna, Austria*

[2]*Medical University of Vienna / AKH Vienna, Division Medical Radiation Physics- Department of Radiation Oncology, Vienna, Austria*

[3]*Medical University of Vienna, Christian Doppler Laboratory for Medical Radiation Research for Radiation Oncology, Vienna, Austria*

[4]*Medical University of Vienna, Center for Medical Physics and Biomedical Engineering, Vienna, Austria*

Purpose or Objective: Nowadays an increasing number of techniques that account and compensate for 4D tumor motion are proposed, investigated and implemented into

clinical practice for imaging, treatment planning and dose delivery. Consequently, it is necessary to verify such techniques and/or investigate the related dosimetric improvements under conditions as close as possible to the clinical situation. For this purpose a respiratory motion phantom, i.e. the Advanced Radiation Dosimetry System (ARDOS), was developed and a prototype was realized. This phantom can be used in clinical practice and research to verify dose delivery and image quality of lung cancer patients on a quantitative and reproducible basis.

Material and Methods: The phantom represents an average human torso with a movable tumor insert and comprises a chest wall, ribs, and lungs (Figure 1a). These parts consist of tissue-equivalent materials. Different types of dosimeters can be inserted at the position of the tumor. The phantom's movement is based on an ARDUINO microcontroller and dedicated software allowing to program independent motions: translational motion for all the parts individually, while the tumor additionally can be rotated. Some basic motion types like sinusoidal and quadratic are preprogrammed with the possibility of changing their parameters. Moreover, complex or irregular motions (e.g., patient-specific breathing cycles) can be reproduced.

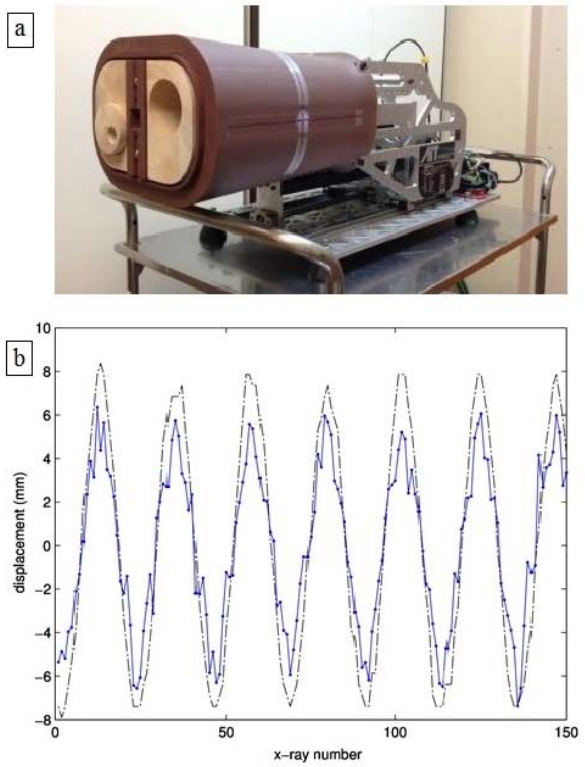

Figure 1: (a) Phantom setup. (b) Tumor motion (blue) tracking in comparison with annotated motion (black) along cranio-caudal direction

Results: To demonstrate the versatility of the phantom first a dosimetric investigation was performed using a clinical stereotactic photon beam treatment plan. The dosimetric study was based on ionization chamber, EBT3 film, and TL dosimetry. The obtained results showed differences (among the dosimeters) in the delivered dose between static and chest-wall-only or ribs-only motion of up to 1.2%. This value increased to 4.3% for tumor-only- and all-of-the-parts motion modes. In the second step real-time 2D/3D image registration software was verified using kV images with the moving tumor, chest wall and ribs in the phantom. Figure 1b shows results obtained from this tumor motion tracking sub-study.

Conclusion: In this pilot study, the anthropomorphic phantom with its specific characteristics (mimicking a tumor, rib cage, and lungs), flexibility, and possibility to offer close-to-real conditions was found to be easily applicable for state-of-the-art research and QA purposes for advanced clinical practice. In the next steps of the project the evaluation of scanned ion beam radiotherapy for a moving target, as well as the development of a 4D QA workflow protocols, and the comparison of measurement data with numerical simulations are envisaged.

PO-0798

Validation of Monte Carlo calculated correction factors for MRI-linac reference dosimetry

D.J. O'Brien[1], D.A. Roberts[2], S. Towe[2], G. Ibbott[1], G.O. Sawakuchi[1]

[1]*The University of Texas MD Anderson Cancer Center, Radiation Physics, Houston, USA*

[2]*Elekta Limited, Linac Platforms, Crawley- West Sussex, United Kingdom*

Purpose or Objective: MRI-guided radiotherapy is an emerging field of considerable interest and has prompted the development of specialized treatment units which integrate MR-imaging systems with radiation sources. Such devices require patients and dosimetry equipment to be immersed in a magnetic (B-)field. Consequently the B-field influences the trajectory of charged particles via the Lorentz force which affects the dose-distribution in water and, critically, the response of the ionization chambers (IC) that are needed for reference dosimetry. To accurately calibrate MRI-RT units it is necessary to correct the chamber readings for these effects. The purpose of this study was to validate Monte Carlo (MC) calculations of IC correction factors against measurements with and without a 1.5 T B-field in an MRI-RT unit.

Material and Methods: Measurements were performed using an Elekta 1.5 T MR-linac located at The University of Texas MD Anderson Cancer Center with and without the B-field. An NE2571 Farmer chamber was placed at isocenter at depths of 10 and 20 cm in a water-equivalent plastic phantom. Three orientations were examined: i) the chamber's long-axis parallel to the B-field; ii) the long-axis rotated 90° clockwise w.r.t. the B-field; and iii) the long-axis rotated 90° anticlockwise w.r.t. the B-field. The long-axis was always perpendicular to the beam. Measured charge readings were corrected for temperature, pressure, polarity and ion recombination using the TG-51 protocol. The ratios of the corrected readings with and without the B-field were compared with those predicted by a Geant4 MC model of the chamber with the energy spectrum from an Elekta MR-linac used as a source.

Results: The measurements indicate that the change in chamber signal due to the B-field ranges from 1.4-2.5% and depends on the chamber orientation which compares to the range of 1.7-3.3% predicted by MC. The ratio of the signal with and without the B-field was within 0.3% of the MC values except for the clockwise perpendicular orientation in which a larger discrepancy of 2.5% was found. However, the two perpendicular orientations differed from each other in both the measured and MC data.

Conclusion: Our MC calculations accurately predict the response of the NE2571 Farmer chamber in the 1.5 T MR-linac beam. Measurements performed in the parallel orientation are the least affected by the B-field and can be accurately corrected. Larger uncertainties exist for perpendicular orientations which are possibly due to uncertainties in the MC chamber geometry.

PO-0799

Beam quality specifiers for an integrated MRI-linac

D.J. O'Brien[1], D.A. Roberts[2], S. Towe[2], G. Ibbott[1], G.O. Sawakuchi[1]

[1]*The University of Texas MD Anderson Cancer Center, Radiation Physics, Houston, USA*

[2]*Elekta Limited, Linac Platforms, Crawley- West Sussex, United Kingdom*

Purpose or Objective: The emergence of MRI-guided radiotherapy has led to the development of new radiotherapy treatment machines with integrated MR-imaging systems. Several designs have emerged such as the 60Co ViewRay system and the different MRI-linac systems developed independently by Utrecht/Elekta, the Cross Cancer Institute in Canada and the Ingham Research Institute in Australia. Magnetic (B-)fields do not alter the photon energy fluence of the beam but they do change the dose distribution in water. Therefore the quantity that is used to specify the beam quality of an MRI-RT device must ideally be insensitive to these changes. The purpose of this study was to investigate the sensitivity of the two most standard beam quality specifiers (%dd(10)x and TPR20,10) to the presence of the B-field.

Material and Methods: Depth dose curves and tissue phantom ratio at depths of 20 and 10 cm (TPR20,10) values with and without a 1.5 T B-field were calculated using the Geant4 Monte Carlo toolkit with the energy spectrum from an Elekta MRI-linac used as a source. For comparison, TPR20,10 values were also measured with a NE2571 Farmer chamber in a water-equivalent plastic phantom on an Elekta MRI-linac with and without the 1.5 T B-field.

Results: The measured and calculated TPR20,10 values agreed within 0.3%. The Lorentz force acts perpendicularly to the direction of motion of the secondary electrons causing them to move in spirals which shortens their range. This reduces the depth of the build-up region and enhances the dose per primary photon at the depth of maximum dose (dmax). On the other hand, the dose at depths where transient charged particle equilibrium (CPE) exist are relatively unaffected by the B-field. Consequently, the photon component of the percentage depth dose at 10 cm depth, %dd(10)x, changes by 2.4% when the B-field is applied because this value is normalized to dmax. However, the calculated and measured values of the TPR20,10 changed by only 0.1% and 0.3% respectively due to the fact that both depths (10 and 20 cm) are in regions of transient CPE.

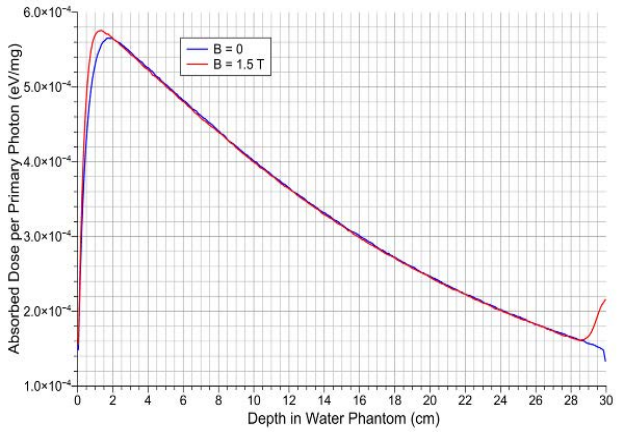

Figure 1: Depth dose curves per primary photon with and without a 1.5 T magnetic field.

	MC PDD Data		$TPR_{20,10}$	
$\lvert\vec{B}\rvert$	$\%dd(10)$	$\%dd(10)_x$	MC	Measured
0	70.4	71.2	0.694	0.695
1.5 T	69.3	69.5	0.695	0.697
% diff	1.6%	2.4%	0.1%	0.3%

Table 1: Measured and calculated TPR20,10 values as well as calculated percentage depth dose data with and without a 1.5 T magnetic field. %dd(10)x is the photon component of the percentage depth dose at 10 cm water depth. %dd(10) contains electron contamination.

Conclusion: The TPR20,10 beam quality specifier is more consistent in the presence of B-fields than the %dd(10)x specifier.

PO-0800

Fricke-type dosimetry for "real-time" 3D dose measurements using MR-guided RT: a feasibility study

H.J. Lee[1], M. Alqathami[1], J. Wang[1], A. Blencowe[2], G. Ibbott[1]
[1]*The University of Texas MD Anderson Cancer Center, Radiation Physics, Houston, USA*
[2]*The University of South Australia, Health Sciences, Adelaide, Australia*

Purpose or Objective: To investigate the feasibility of using 3D Fricke-type gel dosimeters for "real-time" dose observations using the combined 1.5 T MRI – 6 MV linear accelerator system (MRL).

Material and Methods: Fricke-type dosimeters were prepared in 97% w/w Milli-Q water with 3% w/w gelatin (300 Bloom), 1 mM ferrous ion, 0.05 mM xylenol orange, 50 mM sulfuric acid, and 1 mM sodium chloride. The dosimeters were stored at 4 °C prior to irradiation and imaging. For this preliminary study, the dosimeters were irradiated in air, with a part of each dosimeter outside the treatment field to act as a reference. MR imaging was performed with the MRL to observe the change in paramagnetic properties pre and post irradiation using a T1-weighted sequence of TR = 500 ms and TE = 20 ms. MRI during irradiation was done in the MRL using a fast sequence of TR = 5 ms and TE = 1.7 ms.

Results: When exposed to ionizing radiation, ferrous ions are oxidized to ferric ions forming a 1:1 xylenol orange – ferric complex in radiochromic Fricke dosimeters. The corresponding changes in paramagnetic properties can be measured using an MRI. The paramagnetic spin changes, which are dependent on the concentrations of ferrous and ferric ion species, were observable on T1-weighted images due to changes in the spin-lattice relaxation rate (R1 = 1/T1). We observed a mean increase in pixel value of 53% from un-irradiated to irradiated regions of about 20 Gy. The increase in pixel value and corresponding dose was also visible during irradiation using a fast MR sequence with four snapshots included in the figure (in RGB color scale to emphasize the irradiated region). Visibly, the dosimeter underwent a color change from yellow to purple with the formation of the xylenol orange – ferric complex.

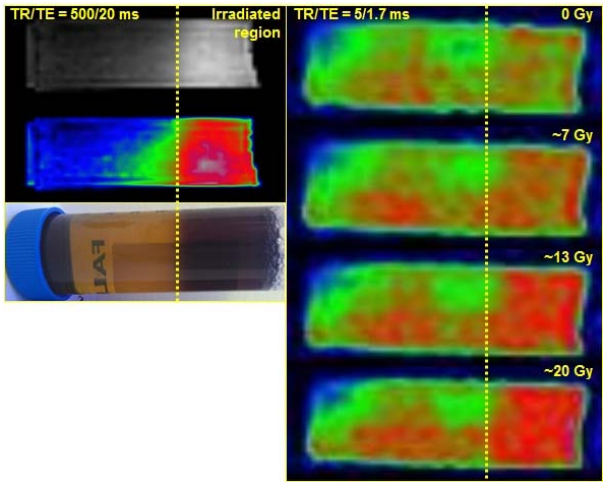

Conclusion: Our Fricke-type dosimeters displayed visible ferric complex formation with xylenol orange after irradiation using the 6 MV linear accelerator component of

the MRL, as well as measurable paramagnetic changes observed using the 1.5 T MRI component of the MRL during and after irradiation. To our knowledge, this is the first time the dose accumulation inside a 3D dosimeter has been visualized in real-time during irradiation using the MRL. The results of this study warrant further investigations into the use of 3D dosimeters for the verification of patient specific radiation therapy treatment plans for the MRL.

PO-0801

Large area 2D polycrystalline CVD diamond dosimeter under intensity modulated beams

C. Talamonti[1,2], A. Baldi[3], M. Scaringella[4], M. Zani[1], D. Pasquini[4], E. Pace[5], L. Livi[1], S. Pallotta[1,2], M. Bruzzi[2,5]
[1]*University of Florence, Dip Scienze Biomediche Sperimantali e Cliniche, Firenze, Italy*
[2]*Istituto Nazionale di Fisica Nucleare, Sezione di Firenze, Firenze, Italy*
[3]*University of Florence, Dip. di Ingegneria Industriale, Firenze, Italy*
[4]*University of Florence, Dip. di Ingegneria dell'Informazione, Firenze, Italy*
[5]*University of Florence, Dip. di Fisica e Astronomia, Firenze, Italy*

Purpose or Objective: In radiotherapy, the development of bidimensional detectors with the suitable dosimetric features for pretreatment quality assurance of the new advanced treatment techniques is of interest. Diamond is a valid candidate as real-time dosimeter since, contrary to silicon, it is an almost tissue equivalent material showing in principle no energy dependence. Furthermore, it is possible to product large-area polycrystalline diamond wafers with suitable electronic properties. In this study we describe the performance of DIAPIX, a large area dosimeter used for pretreatment verification of intensity modulated treatment plans.

Material and Methods: The dosimeter is made of two detector-grade adjacent 2.5x2.5cm2 polycrystalline Chemical Vapour Deposited (pCVD) diamond samples, each equipped with a 12x12 matrix of 144 contacts with a pitch of 2mm, connected to a custom-made electronic read-out system. Tests of the pCVD diamond dosimeter have been performed by means of an Elekta Synergy LINAC, with conventional photon beams, with clinical IMRT fields, from prostate and breast cancer, and with a VMAT lung treatments. The dosimeter was placed at the isocenter and sandwiched inside a phantom of water equivalent material. First set of measurements under a conventional radiotherapy beam aimed to verify the correct behavior of the whole matrix under a flat field and to obtain a flatness correction factor for each pixel were performed. Afterwards dosimetric maps were acquired. Since the area of the prototype under study is smaller respect to a typical IMRT field, the dosimeter was firstly positioned at the isocenter and then shifted in the Latero-Lateral direction. QA plans were computed on the phantom using the Treatment Planning System (TPS) Monaco v3.2., which uses a MonteCarlo algorithm to compute the dose distribution, with a dose grid of 2 mm, and Pinnacle v9.2 which uses a collapsed cone convolution respectively for the VMAT and IMRT plan.

Results: A comparison between the measured maps and the ones predicted by the TPS was performed. As an example, in fig 1 is reported the map collected of lung VMAT plan and the comparison between the measured profiles of some pixels and the ones calculated by Monaco TPS. Dose differences with TPS are in general within 5%, apart in the penumbra region where the dose gradient is high and where the distance-to-agreement is within 3mm.

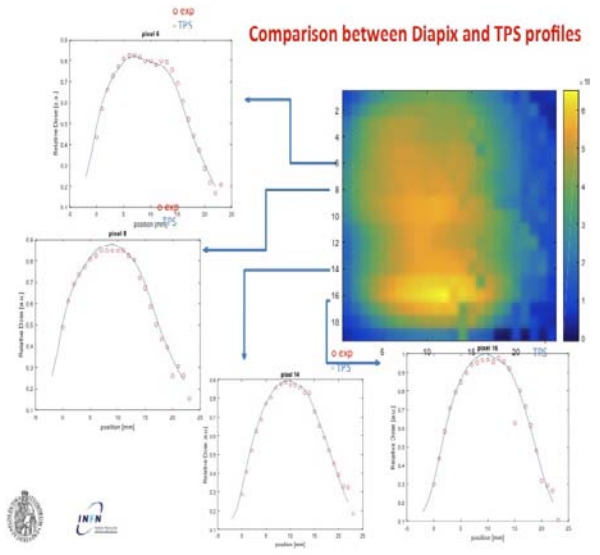

Conclusion: Dose profiles compare favorably with TPS both for IMRT and VMAT. These results demonstrate that the pCVD diamond device is a suitable detector for dosimetric pre-treatment verification analysis in modulated radiation therapy and for conformal beams. This allows for the development of a large area monolithic device with high spatial resolution. In a next future, three samples will be put together in order to realize a matrix with 432 pixels with a total area of 7.5x2.5 cm2.
This work has been supported by the experiments INFN CSN5 DIAPIX and IRPT/MIUR.

Poster: Physics track: Dose measurement and dose calculation

PO-0802

Monte-Carlo based validation of accelerator beam base data measurements

M. Alber[1], M. Söhn[2], M. Sikora[3]
[1]*Aarhus University, Department of Clinical Medicine - Department of Oncology, Aarhus, Denmark*
[2]*University of Munich, Radiation Oncology, Munich, Germany*
[3]*Haukeland University Hospital, Medical Physics, Bergen, Norway*

Purpose or Objective: The quality of beam base data (BBD) is crucial for the accuracy of dose computation, because every measurement error translates into a systematic dose computation error. Despite elaborate guidelines and recommendations, the quality of BBD measurements cannot be verified directly. This constitutes a gap in the clinical QA chain. We present a Monte-Carlo (MC) based method to validate the self-consistency and overall quality of typical BBD measurements.

Material and Methods: BBD are naturally not independent; therefore, self-consistency is a sensitive indicator. Ideally, a full MC simulation, starting with the primary electron beam, would allow benchmarking of individual measurements. This requires that the electron beam properties are known, which can in turn only be determined indirectly from measurements of the photon fields, resulting in a circular problem; not to mention that full linac simulations with a final uncertainty fit for this purpose still require a long time. Thus, we propose: for each accelerator type, a number of electron beam tunes are simulated with BEAMnrc and the phase spaces recorded. The phase spaces are then decomposed into 5 sources and each source is described by a parametric model. The model parameters are naturally highly correlated and yield a unique parameter fingerprint of the beam tune. Given that the photon dose distribution of each source is known, the model parameters of a BBD set can be derived by a fitting process. If a parameter fingerprint of a measurement does not follow

the previously established correlation patterns, the measurement can be considered problematic, and the most probable parameter fingerprint can be determined by mixing the base fingerprints.

Results: Parameter fingerprints for the most frequent energies of Varian and Elekta linacs were generated and used to validate BBD. The method is very sensitive to problems with depth-dose curves (DDC), e.g. incorrect placement of the sensitive volume of the detector, spectral dependencies of the detector for large fields/large depths, partial-volume-, cable- and scatter-effects. Due to the virtually absent scatter in small fields, MC is the ideal method to augment and validate the self-consistency of small field dosimetry. The precision of error detection is in the range of 0.1 mm detector position shifts and 0.3% dose error, for DDC from 5x5 mm² to 400x400 mm². Output factor variations can be detected with a sensitivity of 0.2%, MLC positioning uncertainty with a sensitivity of 0.1 mm. Typical issues with detector types and accelerator models can be identified.

Conclusion: Monte-Carlo derived phase space abstractions can be used to validate the self-consistency and overall quality of base data measurements and thereby fill a gap in the quality assurance chain. Base data can be validated with an accuracy of 0.3%, being one order of magnitude better than potential experimental errors.

PO-0803

Validation of a pre-treatment delivery quality assurance method for the CyberKnife Synchrony System

E. Mastella[1], S. Vigorito[2], E. Rondi[2], G. Piperno[3], A. Ferrari[3], E. Strata[3], D. Rozza[3], B.A. Jereczek-Fossa[3], F. Cattani[2]
[1]*Fondazione CNAO, Medical Physics Unit, Pavia, Italy*
[2]*IEO - European Institute of Oncology, Medical Physics Unit, Milano, Italy*
[3]*IEO - European Institute of Oncology, Department of Radiation Oncology, Milano, Italy*

Purpose or Objective: To evaluate the accuracy of the CyberKnife Synchrony Respiratory Tracking System (RTS) and to validate a method for pre-treatment patient-specific delivery quality assurance (DQA).

Material and Methods: An EasyCube Phantom (Sun Nuclear), consisting of RW3 slabs, was mounted on the ExacTrac (ET) Gating Phantom (Brainlab), which can move along the superior-inferior axis of the patient to simulate a moving target. Eight fiducial markers were implanted in the EasyCube for the treatment set-up and for the tracking. A Gafchromic EBT3 film (Ashland) was positioned between two slabs of the EasyCube, while a PinPoint ionization chamber (PTW) was placed in an appropriate insert. The EBT3 films were calibrated with a 6MV beam (Trilogy, Varian) from 0 to 15 Gy and analysed with the multichannel film dosimetry performed by the FilmQA Pro software (Ashland). Our evaluation was performed in two steps: 1) the films were irradiated with single fields perpendicular to the EasyCube for several collimators (3 fixed collimators: 15, 30, 60mm; 3 IRIS openings: 20, 30 and 40mm) and in different dynamic conditions (e.g. motion amplitude of the ET Phantom from 8 to 28 mm). The delivered and planned dose distributions were compared with the gamma (γ) analysis method. The local γ passing rates (GP) were evaluated using 3 acceptance criteria, varying the local dose difference (LDD), the distance-to-agreement (DTA) and the dose threshold (TH): 3%/3mm TH=10%, 2%/2mm TH=30% and 3%/1mm TH=50%.Dynamic cases were also delivered with purposefully simulated errors (RTS switched off or low coverage of the respiratory correlation model). 2) The DQA plans of 6 clinical patients were delivered in different dynamic conditions, for a total of 19 cases. The measured and planned dose distributions were evaluated with the same γ-index criteria of step 1 and the measured PinPoint doses were compared with the planned mean doses in the sensitive volume of the chamber.

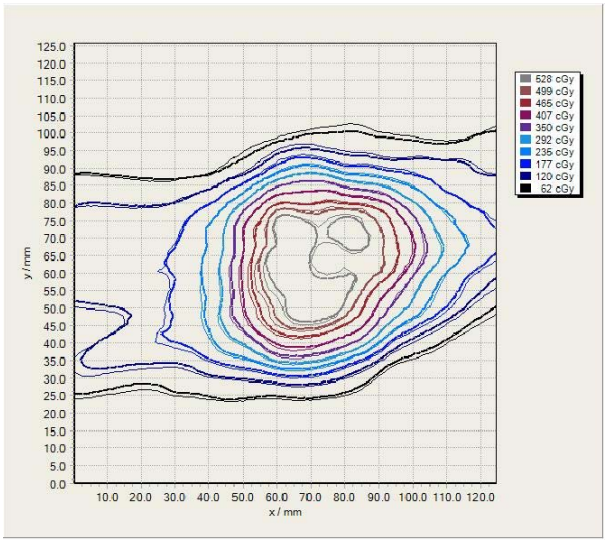

The test was considered passed if the 3 γ analysis criteria yielded a GP>90% or at least 2 criteria yielded a GP>90% and the PinPoint dose difference (ΔD) was <5.0%.

Results: The γ analysis of the collimators showed the need to use more γ-index criteria to detect the simulated errors. Only the stricter DTA criterion drastically failed the test, with GP<70%. All of the DQA plans passed the tests, both in static and dynamic conditions. The mean GP (±σ) were 95.5±5.2% (3%/3mm), 98.6±1.4% (2%/2mm) and 97.8±2.2% (3%/1mm).The mean ΔD was 2.9±1.8%. No significant differences were found between the static and the dynamic cases.

Conclusion: The presented method confirms the ability of the RTS, if used properly, to treat a moving target with great precision. Our pre-treatment patient-specific DQA method was robust, combining PinPoint dose measurements and an evaluation of dose distributions with EBT3 films. However, we found the need of a detailed study of each case, especially when one acceptance criterion does not satisfy the tolerance level.

PO-0804

Clinical applications of a Monte Carlo tool of a proton pencil beam scanning delivery system

F. Fracchiolla[1,2], M. Schwarz[1]
[1]*Azienda Provinciale per i Servizi Sanitari, Protonterapia, Trento, Italy*
[2]*Università di Roma "La Sapienza", Post Graduate School of Medical Physics, Roma, Italy*

Purpose or Objective: Apply a validated Monte Carlo (MC) tool for independent dose calculation in proton PBS to 'patient specific' quality assurance (QA) tasks

Material and Methods: We had developedand validated a MC tool for independent dose calculation[1]. In this work weuse this code for:
- Recalculationof a clinically approved plan from the TPS, to evaluate the quality of our TPSsemi-analytical dose calculation algorithm at the level of the individualpatient
- Recalculationof a treatment session using the Log File coming from the Therapy ControlSystem (TCS), to evaluate differences in 3D dose distribution in patientanatomy taking into account the characteristics of spots (energy, position, MUetc.) as actually delivered by the machine
- Simulationof a 2D patient specific QA (2DQA).

This is aretrospective study on 10 patients done to evaluate the possibility ofsubstituting our actual 2DQA measurement process with a completely automatic andreliable MC based workflow. For each 2DQA TPS and MC dose distributionsrecalculated in water equivalent material, at different depths, were comparedwith measurements performed with an array of 1020 ionization chambers

(IC)detector making use of gamma analysis (3%,3mm): measurement and simulationtimes were compared too.

Results: The table shows a comparison of clinically significant DVH points from TPS dose distribution, MC simulation of the nominal plan and of TCS log file.

ROIs - DVH points	DVH values		
	TPS	MC - Nominal	MC - Log File
PTV - D95	52,63	55,97	52,16
Brainstem - D1	53,37	54,71	53,46
Coclea dx - D1	46,42	46,11	50,67
GTV - D95	53,74	54,88	54,14
GTV - Mean dose	54,46	55,69	55,50
Cerebral Tissue - V33	38,67%	34,82%	35,21%

Table: DVH points comparison between TPS dose distribution, MC recalculated dose from nominal plan and MC dose calculation from TCS log files.

In figure a comparison of TPS and MC planar dose distribution with 2DQA measurements is shown. In our protocol, if the passing rate (PR) is above 95% the field is accepted. If it is between 95 and 90% a justification must be added to the QA report to flag the field as accepted. A passing rate below 90% makes the field unacceptable. In the graph 27 fields belonging to 10 patients are analysed. MC has a PR always greater than 95% for every depth showing a good agreement with measurements. TPS results are always in the "grey" area between 90 and 95%. The execution time of a 2DQA with an array of ICs takes almost 1 hour and half; simulations, that can be performed in parallel, take 11 minutes on average.

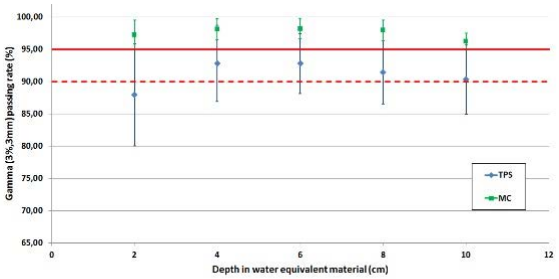

Figure: gamma PR (3%,3mm). Comparison at different depths between TPS (diamonds) and MC (squares) dose distribution with measurements of 27 fields belonging to 10 patients.

Conclusion: We realized a system to verify with an independent calculation algorithm both the nominal plan and the delivered one with the TPS dose distribution. This lets the user to estimate the effects on the dose distribution due to a different algorithm and due to delivery uncertainties of the machine. We proposed a method to drastically reduce 2DQA verification time. Our suggestion is to substitute measurements with simulation that showed a very high accordance in terms of gamma PR (always above 95%); one field per patient may be measured at single depth as an additional safety check.

[1] F Fracchiolla et al,'End to end' validation of a Monte Carlo code for independent dose calculation in a proton pencil beam scanning system Radand Onc, 115, S78-S79, 2015

PO-0805

Proton radiography for the clinical commissioning of the new Gantry2 head support at PSI

L. Placidi[1], S. König[2], R. Van der Meer[2], F. Gagnon-Moisan[2], A.J. Lomax[1], D.C. Weber[3], A. Bolsi[1]

[1]Paul Scherrer Institute PSI- Center for Proton Therapy, Medical physics, Villigen PSI, Switzerland

[2]Paul Scherrer Institute PSI- Center for Proton Therapy, Facility Management, Villigen PSI, Switzerland

[3]Paul Scherrer Institute PSI- Center for Proton Therapy, Radiation oncology, Villigen PSI, Switzerland

Purpose or Objective: The treatment couches for Gantry2 will support new head pieces for head and neck treatments, the BoS HeadframeTM. Thanks to their geometry and composition (a sandwich of thin carbon layers and light foam), they will increase the flexibility of planning, as they should only minimally disturb proton beams passing through it. Therefore there will be no restrictions in the deliverable gantry angles; posterior targets will be treated in supine position, thus increasing patient comfort, safety (especially for children under anesthesia) and the position accuracy (bite block will be used more often). We describe here the measurement of their Water Equivalent Range (WER) and homogeneity.

Material and Methods: Mono-energetic scanned proton layers (12x20cm2) of 129 MeV up to 145 MeV were delivered through the head support, with the proton dose on exit being measured using a scintillating screen/CCD camera device approach. A reference set of measurements were first performed without the head support with 1 MeV discrete energy steps. The measurements were then repeated for three different positions (head, neck and shoulder) of the head support. A second set of measurements were performed with an energy step of 0.2 MeV for energies between 133-139 MeV, to increase the measurement accuracy. For each acquisition, a 2D map of the maximum values among all the layers was generated, from which the WER of the head support in the different positions could be calculated by subtracting the measurements with and without the frame. WER homogeneity was calculated as the standard deviation of sub-regions of the 2D difference maximum value maps. CT images of the head supports were also imported in the TPS and converted to WER (via HU-Relative Proton Stopping Power calibration curve), to estimate if the planned WER corresponded to the measured values (with no need of synthetic CTs).

Results: WER was found to be between 2.4mm and 7.2mm with an accuracy of 1.0mm or 0.5mm, depending on the measurements energy steps (respectively 1.0 MeV and 0.2 MeV) (Fig). In the three different positions, WER in-homogeneity was lower than 1.0mm (respectively 0.36mm, 0.99mm and 0.40mm). The differences of WER between measured and TPS values were also below 0.5 mm (0.2 MeV step) and 1.4 mm (1 MeV step).

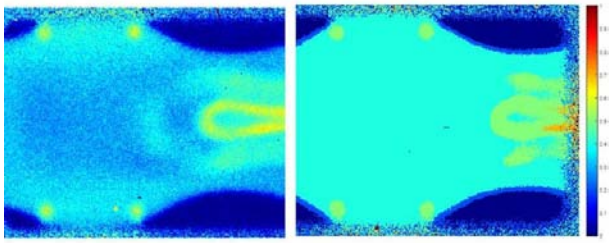

Conclusion: The described method was accurate, fast and reproducible. The results on the thickness and homogeneity of the head frame show that it can be safely and accurately used in clinical operation and the first patients have already been treated.

PO-0806

Optimisation and assessment of the MLC model in the Raystation treatment planning system

A. Savini[1], F. Bartolucci[1], C. Fidanza[1], F. Rosica[1], G. Orlandi[1]

[1]AUSL 4 Teramo, Medical Physics Department, Teramo, Italy

Purpose or Objective: Accurate modeling of the MLC is necessary to achieve a clinically acceptable agreement between dose calculations and measurements in IMRT/VMAT treatment plans. The RayStation TPS uses several parameters to model a MLC but no specific procedure exists on how to perform measurements to optimize them. The aim of this work is to present a fast procedure to optimize the MLC parameters in RayStation v.4.5 and to assess the obtained MLC model.

Material and Methods: A proper set of MLC-collimated fields was designed on a Varian Trilogy linear accelerator equipped with a Millennium 120 MLC. Dose profile scans of those fields

were taken in a motorized water phantom using small detectors (Razor stereotactic diode and PFD, IBA Dosimetry). In addition, MLC transmission was measured using a Farmer ion chamber. MLC model parameters (transmission, offset, leaf tip width, tongue-and-groove) were optimized to maximize the agreement between measurements and calculations. Model assessment was performed using a set of highly intensity-modulated MLC geometrical patterns, designed to enhance tongue-and-groove, transmission and offset/leaf-tip effects. For those fields, planar dosimetry was carried out with GafChromic EBT3 films. Clinical validation was performed evaluating TG-119 cases along with 25 DMLC and 10 VMAT clinical plans. Plan-specific quality assurance was performed with a 2D-array (MatriXX, IBA Dosimetry) and gamma-index metric was used to assess the agreement between planned and measured dose distributions. A 2%/2mm criterion was used with both local (LN) and global (GN) normalization.

Results: Optimized MLC parameters were: transmission 0.018, position-offset 0.04cm, tongue-and-groove 0.05cm, leaf tip width 0.3cm. Average and standard deviation (SD) values of gamma index pass-rates were: for geometrical patterns: 92.8%, SD=5.1%(LN); 95.5%, SD=2.5%(GN). For TG-119 plans: 97.1%, SD=4.4%(LN); 99.7%, SD=0.7%(GN). For DMLC clinical plans: 97.0%, SD=3.7% (LN); 98.8%, SD=2.6%(GN). For VMAT plans 90.1%, SD=4.0% (LN); 96.5%, SD=2.1% (GN). Critical regions dominated by tongue-and-groove and rounded-leaf-tip effect showed a very good agreement between measurements and calculations (see Fig.1).

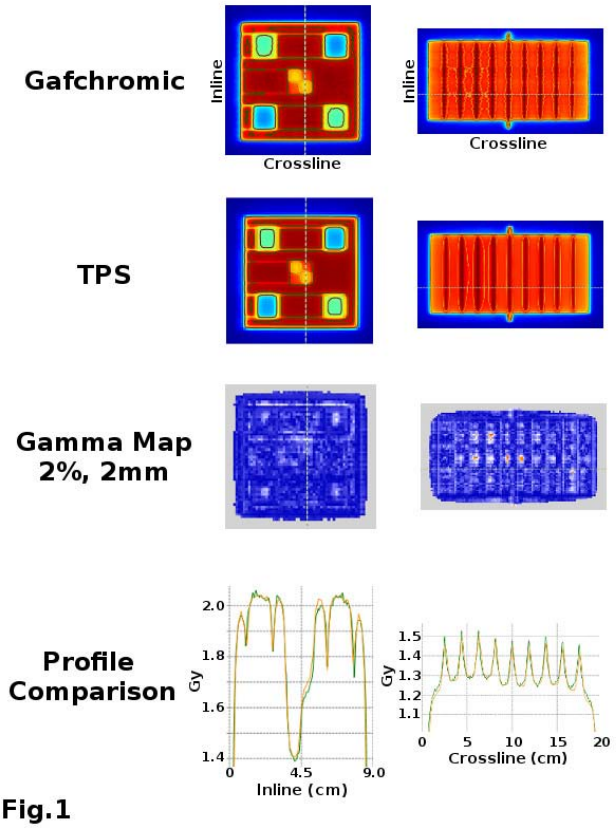

Fig.1

Conclusion: Results demonstrate the followed procedure leads to a proper optimization of the MLC model in RayStation, leading to clinically acceptable gamma index pass-rates. The needed additional measurements can be easily integrated as a subset of the standard measurements required for the commissioning of the RayStation TPS.

PO-0807

3D and 4D dose calculations for tumour-tracking irradiation of lung/liver tumours using gimbaled linac

Y. Iizuka[1], N. Ueki[2], Y. Matsuo[1], Y. Ishihara[1], K. Takayama[3], M. Nakamura[1], T. Mizowaki[1], M. Kokubo[3], M. Hiraoka[1]

[1]Kyoto University, Department of Radiation Oncology and Image-Applied therapy, Kyoto, Japan

[2]Hyogo Prefectural Amagasaki General Medical Center, Department of Radiation Oncology, Amagasaki, Japan

[3]Institute of Biomedical Research and Innovation, Division of Radiation Oncology- Department of Image-based Medicine, Kobe, Japan

Purpose or Objective: To compare dose-volume metrics calculated with the four-dimensional (4D) Monte Carlo (MC) and three-dimensional (3D) dose evaluation systems in dynamic tumor tracking (DTT) irradiation for lung or liver tumors.

Material and Methods: Twenty patients with lung tumors and 15 patients with liver tumors who underwent DTT irradiation using a gimbal-mounted linac were enrolled in this study. During computed tomography (CT) simulation, 4DCT under free breathing and exhale breath-hold CT were performed. Planning target volume (PTV) for DTT was calculated using the gross tumor volume (GTV) delineated on a reference CT scan (exhale phase in the 4DCT or exhale breath-hold CT) by adding asymmetric margins to compensate for possible errors due to the DTT. The 6 to 9 non-coplanar ports of the 6-MV X-ray were set to each PTV. Doses were calculated for the reference CT using a commercially available treatment planning system (TPS). At the same time, 4DMC dose evaluation was performed for 10 respiratory phases of 4DCT using an in-house dose calculation system based on the MC algorithm, considering the gimbal rotation. The doses calculated for 10 phases were accumulated using deformable image registration software for the lung tumor patients, whereas mean values of the dose-volume metrics were evaluated for the liver tumor patients. The difference between the doses calculated with 4DMC (4D doses) and those calculated for the reference CT scan with TPS (3D doses) were investigated for the following dose-volume metrics: the percentage of dose that covers 95% of the GTV (GTV D95), the max dose received by the spinal cord (Cord max), the percentage of lung volume that received more than 20 Gy and 5 Gy irradiation (Lung V20 and Lung V5, respectively) in patients with lung tumors, and the mean dose and percentage of liver volume that received more than 20 Gy irradiation (Liver mean and Liver V20, respectively) in patients with liver tumors.

Results: The mean values of the dose-volume metrics for the 4D doses were as follows: 94.1% (range, 83.8–99.7%) GTV D95, 9.7 Gy (range, 1.8–22.0 Gy) Cord max, 4.9% (range, 1.9–13.7%) Lung V20, 19.2% (range, 7.2–30.7%) Lung V5, 10.0 Gy (range, 5.2–15.2) Liver mean,15.5% (range, 8.2–27.7%) Liver V20 The mean differences in the dose-volume metrics for the 3D and the 4D doses were as follows: 0.5% (range, -7.4–4.8%) GTV D95, 0.1 Gy (range, -2.5–1.8 Gy) Cord max, 0.1% (range, -0.8–1.4%) Lung V20, 0.3% (range, -1.6–2.1%) Lung V5, 0.1 Gy (range, -1.6–1.1 Gy) Liver mean, and -1.0% (range, -1.7–3.1%) Liver V20. There were no statistical significant differences in these dose-volume metrics evaluated by paired t-test.

Conclusion: The 3D doses calculated with TPS for the target tumor and organs at risk were almost equal to those calculated with 4DMC. 3D dose could be used as a substitution for 4DMC calculation. However, the dose to the spinal cord was underestimated by a maximum of 2.5 Gy.

PO-0808

Validation of a clinical peripheral photon dose model: prostate IMRT irradiation of Alderson phantom

B. Sanchez-Nieto[1], L. Irazola[2], M. Romero-Expósito[3], J. Terrón[4], F. Sánchez-Doblado[5]

[1]Pontificia U-dad Catolica de Chile, Insitute of Physics, Santiago, Chile

[2]*Universidad de Sevilla, Departamento de Fisiología Médica y Biofísica- Universidad de Sevilla- Spain, Sevilla, Spain*
[3]*Universitat Autònoma de Barcelona, Departamento de Física, Barcelona, Spain*
[4]*Hospital Universitario Virgen Macarena, Servicio de Radiofísica, Sevilla, Spain*
[5]*Universidad de Sevilla, Departamento de Fisiología Médica y Biofísica, Sevilla, Spain*

Purpose or Objective : Unwanted peripheral doses (PD) from external beam radiotherapy (RT) are associated with increased incidence of second cancers. PD estimations after RT are becoming highly relevant due to the larger cancer incidence as well as survival rates. Additionally, an accurate knowledge of out-of-field doses is of importance when treating children, pregnant patients and those with implantable electronic devices [1]. Our group has developed a novel peripheral photon dose (PPD) model [2] which includes intensity modulated treatments. This model estimates out-of-field doses (i.e., beyond the commercial TPS limits -around 10 cm from the field edge) received by individual patients undergoing any RT isocentric technique.
The aim of this work was the experimental validation of the model in a number of points inside the Alderson Radiation Therapy phantom (ART) irradiated with an IMRT prostate plan. This exercise is part of the process toward the implementation of the model onto a commercial TPS.

Material and Methods: A Siemens Primus linac was used to deliver a 6 MV prostate IMRT treatment (896 MU and 7 incidences, equivalent to 2 fractions of the treatment). TLD-100 pairs of dosimeters were inserted at phantom holders, placed outside the 1% isodose as shown in the coronal plane of the figure. Positions were selected as being representative of cancer-at-risk organs. TLD-100 readings were converted into doses, through a calibration factor which considers the spectral condition outside the field, and then compared to PPD model estimates [2]. Measured leakage outside the field resulted 4 μGy/MU. Peripheral photon equivalent dose (PPED) to organs was also computed using PERIPHOCAL [2] (a MATLAB® GUI piece of software which considers a basic patient model with scaled dimensions from Cristy phantom [3]).

Results: Plot at the figure depicts the estimated and measured photon equivalent doses (mSv) at 11 points for studied case (identified on the coronal plane of the phantom). Uncertainty Range (UR) corresponds to ±2 mSv and the error bars represent the ±6 % global uncertainty estimated for the TLDs in the out-of-field area2.
Figure.

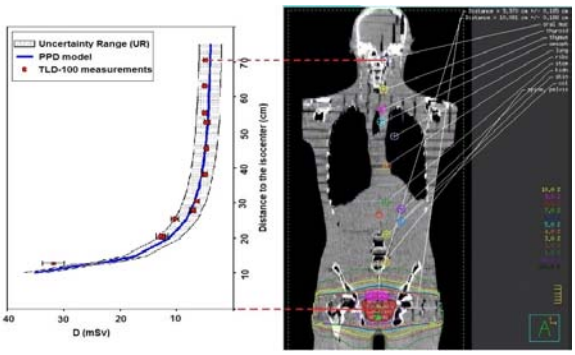

Conclusion: Validation of a PPD calculation model [2] has been carried out in an Alderson phantom for an IMRT prostate treatment using TLD-100 detectors. Very good agreement has been found between the model and the experimental measurements. However, bigger differences have been found between dose to points and PPED to organs, which might suggests that the mathematical phantom and/or the escalation model used for estimating organ location/dimensions are not properly mimicking the anatomy of the Alderson phantom. This issue deserves further investigation before implementing the dose-to-organ model onto a commercial TPS.

Ref.
[1] http://dx.doi.org/10.1118/1.4925789
[2] Analytical model for photon peripheral dose estimation in radiotherapy treatments. Sánchez-Nieto B. et al. Biomed Phys Eng Express 2015: In press
[3] http://crpk.ornl.gov/resources/phantom.html

PO-0809

FFF beams from TrueBeam and Versa HD units: evaluation of the parameters for quality assurance

A. Fogliata[1], J. Fleckenstein[2], F. Schneider[2], M. Pachoud[3], S. Ghandour[3], H. Krauss[4], G. Reggiori[1], A. Stravato[1], F. Lohr[2], M. Scorsetti[1], L. Cozzi[1]
[1]*Humanitas Research Hospital, Radiation Oncology Dept, Rozzano-Milan, Italy*
[2]*University Medical Center Mannheim- University of Heidelberg, Dept. of Radiation Oncology, Mannheim, Germany*
[3]*Hôpital Riviera Chablais, Radiation Oncology Dept, Vevey, Switzerland*
[4]*Kaiser Franz Josef Spital, Radio-Oncology Dept., Vienna, Austria*

Purpose or Objective: Flattening filter free (FFF) beams generated by medical linacs are today clinically used for stereotactical treatments, thanks to their very high dose rate (up to four times the dose rate of the common flattened beams). Such beams differ from the standard flattened beams (FF) in the profile shape, that is strongly peaked on the beam central axis. However, FFF beams are not standard in terms of the parameters describing the field characteristics. Definitions of new parameters as *unflatness* and *slope* for FFF beams have been proposed, based on a renormalization factor for FFF profiles. With those factors the FFF dose fall-off at the field edge is superimposed with the corresponding (in nominal energy) flattened profile commonly normalized to 100% at the beam central axis. The present study aims to provide the renormalization factors for FFF beams of 6 and 10 MV generated by Varian TrueBeam and by Elekta Versa HD linacs. Estimation of the values of the new parameters (unflatness and slope) for the two units are also given.

Material and Methods: Dosimetric data from two Varian TrueBeam and two Elekta Versa HD linacs, all with 6 and 10 MV nominal accelerating potentials, FF and FFF modes have been collected. Renormalization factors were estimated according to Fogliata et al. procedure (Med.Phys. 2012,39) with the third derivative method, and parameters of *RenormFactor=(a+b*FS+c*depth)/(1+d*FS+e*depth)* have been fitted for FFF beams of both units and energies. Unflatness and slope parameters were computed. Dosimetric differences as beam penetration and surface dose were also assessed.

Results: Renormalization factors are summarized in the graphs here presented.

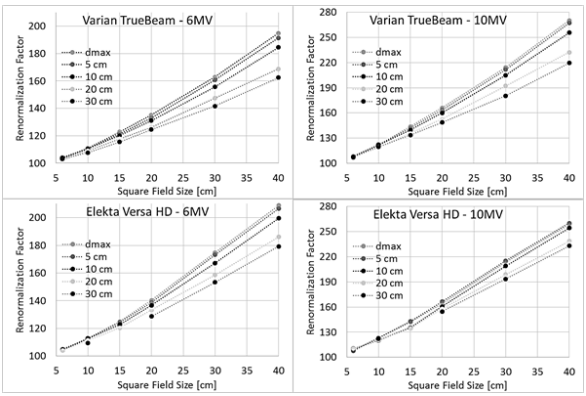

Once the FFF profiles have been renormalized, the unflatness and slope were computed. As an example of unflatness parameter, for a 20x20 cm2 field, it was estimated in the range (from dmax to 30 cm depth) of 1.248-1.317, and 1.304-

1.371 for the 6MV beams, TrueBeam and Versa HD, respectively. The same figure for the 10MV beams were 1.484-1.524, and 1.501-1.543. Concerning beam penetration, TPR20,10 for 6 and 10 flattened and FFF TrueBeam beams were: 0.665, 0.629 (6MV) and 0.738, 0.703 (10MV), while for Versa HD beams are: 0.684, 0.678 (6MV) and 0.734, 0.721 (10MV).

Conclusion: Renormalization factor and unflatness parameters proved to be efficient to describe the FFF beam characteristics. Renormalization factors here presented could be used for all TrueBeam and Versa HD beams, without the need of recalculate them for the site specific conditions.

PO-0810

Implementation of Normalised Dose Difference method for evaluation of VMAT Monte Carlo QA

R.O. Cronholm[1], P. Andersson[2], M. Krantz[2], R. Chakarova[2,3]
[1]*Skåne University Hospital, Radiation Physics, Lund, Sweden*
[2]*SahIgrenska University Hospital, Department of Medical Physics and Biomedical Engineering, Gothenburg, Sweden*
[3]*SahIgrenska Academy at the University of Gothenburg, Department of Radiation Physics, Gothenburg, Sweden*

Purpose or Objective: Monte Carlo calculations are increasingly applied as an independent QA tool for pre-treatment verification of patient plans for complex treatment delivery techniques such as VMAT. The dose obtained is usually imported to the treatment planning system for further analysis. The analysis can encompass visual comparison of dose distributions as well as qualitative and/or quantitative comparison of Dose Volume Histograms for specific structures. More sophisticated quantitative comparison in 3D includes gamma analysis combining dose difference and distance-to-agreement evaluation generating pass/fail maps. The normalized dose difference (NDD) method is considered to be an extension of the gamma-index concept including locally defined, spatially varying normalization factors. The NDD is reported to be insensitive to the dose grid size. Also, it shows which dose distribution has a higher value at the comparison point (has a sign).
The objective of the work is to test the applicability of the NDD method in the Monte Carlo pre-treatment QA procedure, as well as to develop a stand-alone module which will include visual and quantitative analysis.

Material and Methods: Monte Carlo simulations were performed using the EGSnrc/BEAMnrc code system with modifications, capable to compute dose distributions due to a continuously moving gantry, dynamic multileaf collimator and variable dose rate (I.A. Popescu and J. Lobo, Radiother. Onc.2007). A Monte Carlo model of a Varian Clinac iX accelerator was used. Patient treatment plans were generated by Eclipse treatment planning system (Varian Medical Systems, USA) and calculated by the AAA algorithm. NDD formalism has been applied in Matlab (Mathworks®) as described in (Jiang SB, et al. Phys Med Biol 2006).

Results: Dose distributions for patients in different anatomical regions have been obtained; pelvic and head and neck. Example of NDD analysis for a prostate cancer is shown in the figure.

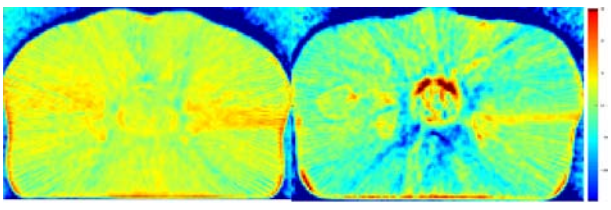

A 3%, 3 mm tolerance criteria is used. The colour scale varies from ±3%, i.e. the region of acceptance. Negative values indicate that the Eclipse dose (AAA) is lower than the Monte Carlo calculated dose. The Monte Carlo simulations include the air surrounding the patient. Therefore the NDD values outside the patient are negative. All the NDD values are within tolerance on the left transversal slice, i.e. there is agreement between Monte Carlo and AAA. On the right transversal slice, the AAA shows higher target dose in small ventral regions and lower dose at some points in the risk organ (rectum). In general the pass-rate observed is > 95%. A slight dominance of the Monte Carlo dose has been observed in the NDD statistics expressed as a shift of the maximum in the NDD distribution.

Conclusion: The NDD method can give important information for pre-treatment verification of VMAT plans, which is complementary to the dose analysis in the treatment planning system.

PO-0811

Patients in vivo skin dosimetry using the Exradin W1 plastic scintillator for proton therapy

F. Alsanea[1], L. Wootton[1], N. Sahoo[1], S. Beddar[1]
[1]*U.T. M.D. Anderson Cancer Center, Radiation Physics, Houston- TX, USA*

Purpose or Objective: To evaluate the usefulness and accuracy of a commercially available plastic scintillator (Exradin W1) for use in *in vivo* proton therapy skin dosimetry.

Material and Methods: Six patients undergoing passive scatter proton therapy for prostate cancer were enrolled in an IRB approved protocol. The Exradin W1 plastic scintillator was used to measure *in vivo* skin dose by attaching the detector to the patient's skin at the central axis of each treatment field (2 laterally opposed treatment fields). Measurements were acquired once per week for the entire treatment course resulting in a total of 93 measurements. The detector was first calibrated on a Cobalt-60 unit, and phantom measurements in the proton beam with the W1 and a calibrated parallel plane ion chamber were used to account for the under-response due to ionization quenching. The average dose difference between the Exradin W1 *in vivo* dose and parallel plane ion chamber in phantom dose over all measurement and per-patient was computed, as well as standard deviations. Furthermore, dose extracted from the treatment planning system was compare to the parallel plane ion chamber. Finally, baseline stability measurements in the cobalt unit were performed weekly for the duration of the study.

Results: The calibrated detector exhibited a 7% under-response for 225 MeV proton beams. The temperature under-response was 4% when used at 37° C (relative to the response at the calibration temperature of 20° C). The detector exhibited a stable response and was within 1% for the duration of the study (144 days). The average dose difference between the Exradin W1 and parallel plane ion chamber over all patient measurements was 0.27 ± 0.67% after applying the temperature and quenching correction factors. The dose difference between the Exradin W1 *in vivo* measurements and parallel plane ion chamber for all six patients treatment fields throughout the study were all within ± 2% with a standard deviation of 0.67% (see figure 1).

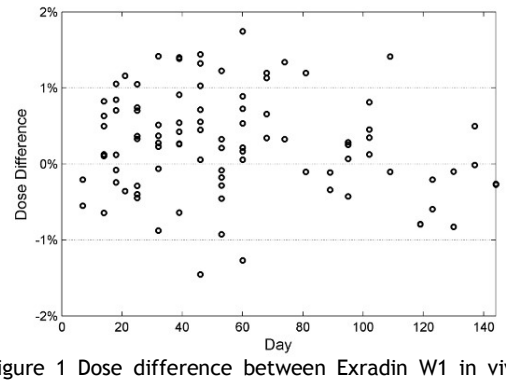

Figure 1 Dose difference between Exradin W1 in vivo dose and parallel plane ion chamber dose for every patient during the study.

Conclusion: The Exradin W1 exhibited a high level of accuracy for *in vivo* skin dosimetry measurements in passively scattered proton beams. The quenching correction and temperature corrections are easy parameters to extract. The detector will be useful as a verification tool for proton therapy patients because plastic scintillators are water equivalent, very small detectors (2mm diameter), accurate, and durable.

PO-0812

Dosimetric accuracy of TPS algorithms for actively scanned proton beams and small target volumes

G. Magro[1], S. Molinelli[2], A. Mairani[2], A. Mirandola[2], D. Panizza[2], S. Russo[2], E. Mastella[2], F. Valvo[3], M. Ciocca[2]
[1]*University of Pavia, Physics Department, Pavia, Italy*
[2]*Fondazione CNAO, Medical Physics Unit, Pavia, Italy*
[3]*Fondazione CNAO, Clinical Directorate, Pavia, Italy*

Purpose or Objective: To evaluate the accuracy of different lateral proton beam spreading models of two commercially available treatment planning systems (TPS) in optimizing proton pencil beam dose distributions for small targets located at increasing depths in water.

Material and Methods: The TPSs analytical algorithms were benchmarked against experimental data and the FLUKA Monte Carlo (MC) code, previously validated for the selected beam-line. We tested the Siemens Syngo and the RaySearch RayStation TPS plan optimization modules for water cubes, by fixing the configurable parameters at clinical standards, with homogeneous target coverage to a 2 Gy (RBE) (Relative Biological Effectiveness) dose prescription as unique goal. An RBE of 1.1 has been used. For shallower targets requiring a range shifter, two different approaches were adopted with Syngo: A) the passive absorber was numerically accounted for its water equivalent thickness only and a single Gaussian approximation was considered for the lateral evolution of the beam; B) the passive absorber was contoured as a body included in the TPS calculation volume, where a double Gaussian modeling for the beam lateral spread is applied. Case B served to directly compare Syngo with the RayStation strategy of accounting the range shifter as a part of patient geometry during pencil beam tracing. Transversal and longitudinal profiles, acquired across target centers, were compared and a γ-analysis was performed within each volume between TPS and MC. Optimized plans were delivered and the dose at each volume center was measured in water with a calibrated PTW Advanced Markus chambers. An EBT3 film was also positioned at the phantom entrance surface for the acquisition of 2D dose maps.

Results: Discrepancies between TPS calculated and MC simulated values were mainly due to the different lateral spread modeling and resulted to be related to the field-to-spot size ratio. Severe limitations were found for Syngo configuration A (clinical scenario), when planning on very small and shallower cubes. The high level of agreement shown between MC and Syngo configuration B and RayStation, regarding these challenging targets, supported the hypothesis that the use of a single Gaussian beam model is one of the main sources of dose deviations for superficial volumes. No major discrepancies were registered in all cases analyzed, either at the volume center or in the penumbra region.

Conclusion: The accuracy of the TPSs was proved to be clinically acceptable in all cases but very small and shallow volumes, when a poor beam lateral spreading model is used (single Gaussian). Satisfactory dose calculation accuracy could be achieved by using either a double Gaussian parameterization or the RayStation version of this algorithm, separately handling the nuclear halo effect, for range shifter modeling in the TPS. In this contest, the use of MC to validate experimental results proved to be a reliable procedure for pre-treatment plan verifications.

PO-0813

Assessing the quality of proton PBS delivery: log file analysis of every treatment at PSI Gantry 2

D. Scandurra[1], F. Albertini[1], R. Van der Meer[1], G. Meier[1], D. Weber[1], A. Bolsi[1], A. Lomax[1]
[1]*Paul Scherrer Institute, Center for Proton Therapy, Villigen PSI, Switzerland*

Purpose or Objective: Pencil beam scanning (PBS) proton therapy requires the delivery of many thousand proton beams, each modulated for position, energy and dose, to provide a highly conformal patient treatment. The quality of the treatment is dependent on the delivery accuracy of each beam and at each fraction. In this work we describe the use of treatment log files, which are a record of the machine parameters for a given field delivery on a given fraction, to investigate the integrity of treatment delivery compared to the nominal planned dose, for all clinical patients treated at Paul Scherrer Institute on Gantry 2.

Material and Methods: The dosimetry-relevant log file parameters are used to reconstruct the 3D dose distribution on the patient anatomy, using a TPS-independent dose calculation system developed at our institute and experimentally validated previously. The analysis was performed for all clinical treatments, both for individual fields and per series, and delivery quality was assessed by comparing the log file dose to the TPS dose, in particular by determining the percentage of voxels within +/- 1% of the nominal dose, as well as gamma index using 1% and 2mm criteria.

Results: The mean +/-1% pass rate on the series-level is 96.4%, though individual fields showed larger variations in pass rate. Furthermore, this work establishes a correlation between the delivery quality of a field and the beam position accuracy. This correlation is evident for all delivered fields regardless of individual patient or plan characteristics. We have also detailed further implementation of log file analysis within our clinical workflow, including the clinical evaluation of patient delivered dose from a problematic fraction delivery, the discovery and diagnosis of systematic issues in treatment planning or delivery workflow, extra TPS quality assurance, and the trending of machine performance following repairs or upgrades.

Conclusion: We have demonstrated the usefulness of treatment log files in PBS proton therapy, particularly in regard to assessing the quality of daily treatment delivery by calculating 3D dose distributions on the patient anatomy and comparing it to the nominal TPS dose. We have presented the results of this analysis for every patient field and series delivered thus far on Gantry 2. Additionally, we have shown that the integrity of treatment delivery is highly correlated with the accuracy of spot position and believe this will be useful for driving machine performance improvements in the PBS field.

PO-0814

Beam quality and perturbation factors of Farmer chambers in magnetic fields

C.K. Spindeldreier[1], O. Schrenk[1], S. Greilich[1], C. Karger[1], A. Pfaffenberger[1]
[1]*German Cancer Research Center, Medical Physics in Radiation Oncology, Heidelberg, Germany*

Purpose or Objective: Hybrid MR-Radiotherapy devices combine radiation treatment and excellent soft tissue contrast imaging, which does not deliver any additional radiation dose to the patient. The permanent magnetic field of the MRI is known to deflect the electrons during irradiation, influencing the dose response of ionization chambers [Meijsing 2009]. This work investigates the effect of the magnetic field on the beam quality and the perturbation factors for six customized Farmer chambers with different sensitive volumes.

Material and Methods: Six ionization chambers, essentially identical in design but varying in radius of the sensitive volume from 0.1 cm to 0.6 cm, were modelled using the C++ class library egspp of the Monte Carlo code EGSnrc [Kawrakow 2009]. In order to calculate the beam quality factors, Monte Carlo simulations were performed placing the chamber models into a water phantom at 10 cm depth using a Siemens PRIMUS phase space [Pena 2007] and at 5 cm water depth using a 60Co-spectrum [Rogers 1987]. The perturbation factors were determined following the process described by [Wulff 2008]. For the calculations, magnetic field strengths from 0.0 T to 3.0 T were used.

Results: The beam quality factors of all chambers differ from the values without magnetic field with a maximum of ±3% depending on the magnetic field strength. The highest influence on the beam quality factor can be found for the replacement and the central electrode perturbation factor. Moreover, these two factors show the highest dependency on the magnetic field strength.

Conclusion: Magnetic field specific perturbation and beam quality factors of six different Farmer chambers were calculated. The results indicate that chambers with a small sensitive volume show less influence of the magnetic field. In order to measure dose with ionization chambers in a magnetic field correctly, beam quality factors have to be determined for every individual chamber and every magnetic field strength.

Acknowledgements: We thank Dr. Iwan Kawrakow (ViewRay) for providing the magnetic field macro for the EGSnrc code system. Detailed information on the geometry of the Farmer chambers given by Dr. Edmund Schüle (PTW) are gratefully acknowledged.

PO-0815

Impact of digitizer response and time averaging de-noising in radiochromic film dosimetry

J.A. Vera Sánchez[1], C. Ruiz Morales[2], A. Gonzalez Lopez[3]
[1]*Hospital Universitari Sant Joan de Reus, fisica medica, Reus, Spain*
[2]*Hospital IMED- Elche, Radioterapia, Elche, Spain*
[3]*Hospital Clínico Universitario Virgen de la Arrixaca, Radioprotección, Murcia, Spain*

Purpose or Objective: To study how noise and digitizer response affect radiochromic film dosimetry. The variations introduced because of these factors in gamma scores is determined.

Material and Methods: Five VMAT treatment plans were analyzed in this work. Two dose planes (coronal and saggital) were verified for every treatment plan, they were irradiated in a MULTICUBE phantom (IBA, dosimetry), measured with the Matrixx chamber array (IBA, Dosimetry) and analyzed with the Omnipro I'm RT (IBA, Dosimetry). Once the plans were accepted for clinical treatment, the analysis of the same dose planes was carried out with radiochromic films and two different algoritms: the multichannel protocol of Mayer et al (MC), that corrects the lateral effect of the digitizer and minimize the amount of noise, and the efficient protocol of Lewis et al (EP), that keeps the corrections included in the multichannel protocol and corrects the digitizer variability with a two point recalibration. Radiochromic film dosimetry is affected by knwon factors as digitizer lateral effect, noise and variability in digitizer response. These factors affect the gamma scores. In particular, when the dose plan obtained from the film is used as the reference distribution in the gamma analysis, the amount of noise and changes in digitizer response may give rise to wrong gamma evaluations. Every film was digitized with three different resolutions (72, 96 and 150 ppp), and twenty digitalizations were obtained for every resolution. For every single digitized image a dose map was obtained with the two mentioned algorithms and, in addition, dose maps from averaged images were analyzed (dose maps 21 to 25) and averaged dose maps were also analyzed (dose maps 26 to 30)

Results: In the figure, results of the passing rate of a prostate VMAT coronal dose plane evaluated with radiochromic film are shown for the 2mm, 2% criteria.

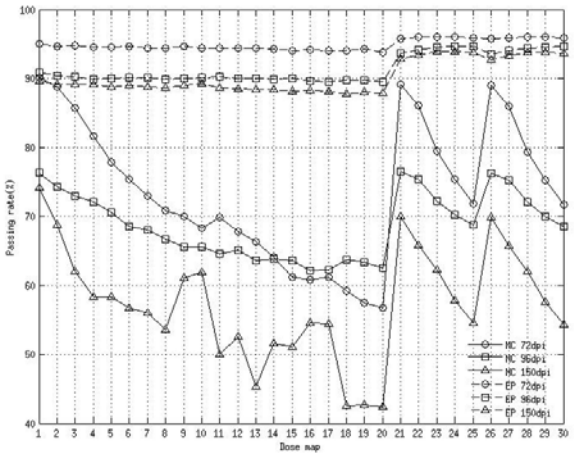

Conclusion: The multichannel protocol is not able to compensate variability in digitizer response, and this is a central issue for radiochromic film dosimetry. The efficient protocol compensates variations of digitizer response, so parameters of the gamma analysis become more stable. The compensation of variability in digitizer response by the efficient protocol may be used for de-noising by time averaging and gamma analysis results may be improved for all resolutions.

PO-0816

Sensitivity and reproducibility of the portal imaging panel for routine FFF QC measurements

A. Willett[1], D. Kelly[1], M. Gilmore[1], C. Rowbottom[1]
[1]*The Clatterbridge Cancer Centre - Wirral NHS Foundation Trust, Physics, Bebington- Wirral, United Kingdom*

Purpose or Objective: The purpose of this work was to see if the EPID is a viable alternative to other QA devices for routine FFF QA measurements.

Material and Methods: Sensitivity measurements were made to assess response to small changes in field size, beam steering, and energy. A series of QA plans were created where field size was varied from baseline values in small increments. Field size: (5-5.5cm, 20-20.5cm) 1mm increments. Beam steering was adjusted by manually altering values in service mode. Beam steering: (Symmetry 0-3%) 1% increments. Symmetry was defined using the maximum variation method (Dx-D-x)max. Energy was varied by placing small quantities of Perspex into the beam path (0-6cm), 2cm blocks. These plans were then measured using the portal imager (aS1200 DMI panel), QA3 (Sun Nuclear), and Starcheck Maxi (PTW). EPID beam data was taken from the Portal Dosimetry module in ARIA and exported into Excel for processing; FFF beam parameters as stated in Fogliata et al [1] were calculated. Starcheck data was also exported to allow for similar analysis. The increment measured by each of the devices was compared to the known increment set by looking at the differences between the baseline (no increment) measurement and the incremented one.
Constancy measurements were then taken on an ad-hoc basis over a period of 5 weeks using all 3 QC devices to measure a MLC defined 20x20cm field and the results were recorded.

Results: Overall the EPID and the Starcheck performed better at detecting changes in field size (Average difference from set offset: EPID = 0.28mm, Starcheck = 0.33mm, QA3 = 0.88mm), with the QA3 performing better when detecting changes in beam symmetry (Average difference from set offset: EPID = 0.10%, Starcheck = 0.20%, QA3 = 0.07%). Energy changes were looked at using the slope parameter (EPID – range 0.295-0.309 %/mm for 0-6cm of Perspex), (Starcheck – range 0.31-0.315 %/mm) or the Energy parameter (QA3 – range 104.7-109.1%).

Daily measurements were examined for consistency and again the EPID and Starcheck performed similarly, with comparable standard deviations, as shown in Table 1.

	Transverse symmetry (%)			Field size X (cm)			Slope (%/mm) / Energy (%)		
Date	EPID	Starcheck	QA3	EPID	Starcheck	QA3	EPID	Starcheck	QA3
15/09/2015	0.5	-	0.04	19.92	-	20.01	0.29	-	107.2
18/09/2015	0.24	-	0.04	19.91	-	20.06	0.29	-	105.9
21/09/2015	0.46	-	0.21	19.91	-	20.01	0.29	-	106.6
23/09/2015	0.36	0.29	0.44	19.91	19.91	20.02	0.29	0.3	106.3
25/09/2015	0.42	0.32	0.33	19.93	19.87	20.05	0.29	0.3	106.6
29/09/2015	0.57	0.33	0.11	19.91	19.94	20.01	0.29	0.3	105.7
08/10/2015	0.42	0.34	0.09	19.91	19.92	20.24	0.29	0.3	104.7
12/10/2015	0.42	0.37	0.09	19.91	19.93	20.24	0.29	0.3	105.4
Std Deviation	0.097	0.029	0.147	0.007	0.027	0.101	0.000	0.000	0.791

Table 1 – Table showing the daily measurements and calculated standard deviations for all three devices taken for Symmetry, Fields size and Energy.

Conclusion: Our results show that for FFF QA measurements such as field size and symmetry, using the EPID is a viable alternative to other QA devices. The EPID performs particularly well on geometric measurements, as it is able to detect small changes in positon (~1mm) with good consistency. This is to be expected due to its high resolution when compared to the other QA devices used (EPID 0.34mm, Starcheck 3mm, QA3 5mm). Therefore the EPID could potentially be used for a wider range of QC measurements with a focus on geometric accuracy, such as MLC positional QA.

References [1] Fogliata, A., Garcia, R., et Al (2012). Definition of parameters for quality assurance of flattening filter free (FFF) photon beams in radiation therapy. *Med. Phys.*, 39(10), p.6455.

PO-0817

Characteristics and performance of the first commercial MLC for a robotic delivery system

P. Prins[1], C. Fürweger[2], H. Coskan[1], J.P.A. Marijnissen[1], B.J.M. Heijmen[1]

[1]Erasmus Medical Center Cancer Institute, Department of Radiation Oncology, Rotterdam, The Netherlands

[2]European Cyberknife Center, Munich, Germany

Purpose or Objective: To assess characteristics and performance of the "InciseTM" MLC (41 leaf pairs, 2.5mm width, FFF linac) mounted on the robotic SRS/SBRT platform "Cyberknife M6TM" in a pre-clinical 5 months test period and to ensure quality of clinical treatments.

Material and Methods: Beam properties were measured with unshielded diodes and EBT3 film. Bayouth tests for leaf / bank position accuracy were performed in standard (A/P) and clinically relevant non-standard positions, before and after exercising the MLC for 10+ minutes. Total system accuracy was assessed in End-to-End tests. Delivered dose was verified with EBT3 film for exemplary and clinical plans. Stability over time was evaluated in Picket-Fence- and adapted Winston-Lutz-tests (AQA) for different collimator angles.

Results: Penumbrae (80-20%, with 100%=2*dose at inflection point; SAD 80cm; 15mm depth) parallel/perpendicular to leaf motion ranged from 2.7/2.2mm for the smallest (0.76x0.75cm2) to 3.7/3.6mm for larger (8.26x8.25cm2) square fields. MLC penumbrae are slightly wider than penumbrae fixed cones (2.1 to 2.8mm for 5 to 60 mm cones). Interleaf leakage was <0.5%. Average leaf position offsets were ≤0.2mm in 14 standard A/P Bayouth tests and≤0.6mm in 8 non-standard direction tests. Pre-test MLC exercise slightly increased jaggedness (range +/-0.3mm vs. +/-0.5mm) and allowed to identify one malfunctioning leaf motor. Total system accuracy with MLC was 0.39+/-0.06mm in 6 End-to-End tests. Delivered dose showed good agreement with calculated dose (typically Gamma(3%,3mm)<1 for >95% of pixels with D > 0.1 Dmax). Picket-Fence and AQA showed no adverse trends (> 1 yr).

Conclusion: The InciseTM MLC for CyberKnife M6TM displays high mechanical stability and accurate dose delivery. The specific CK geometry and performance after exercise demand dedicated QA measures.

PO-0818

Multicentre small field measurements using a new plastic scintillator detector

M. Pasquino[1], S. Russo[2], P. Mancosu[3], E. Villaggi[4], G. Loi[5], R. Miceli[6], G.H. Raza[7], A. Vaiano[8], M.D. Falco[9], E. Moretti[10], F.R. Giglioli[11], R. Nigro[12], C. Talamonti[13], G. Pastore[14], E. Menghi[15], F. Palleri[16], S. Clemente[17], C. Marino[18], G. Borzì[19], V. Ardu[20], S. Linsalata[21], A. Mameli[22], V. D'Alesio[23], F. Vittorini[24], M. Stasi[1]

[1]A. O. Ordine Mauriziano di Torino - Ospedale Mauriziano Umberto I, Medical Physics, Torino, Italy

[2]Azienda Sanitaria di Firenze, Medical Physics, Firenze, Italy

[3]Humanitas, Radiotherapy, Milano, Italy

[4]AUSL Piacenza, Medical Physics, Piacenza, Italy

[5]AOU Maggiore delle Carità, Medical Physics, Novara, Italy

[6]AOU Tor Vergata, Medical Physics, Roma, Italy

[7]Ospedale San Pietro Fatebenefratelli, Medical Physics, Roma, Italy

[8]USL 3, Medical Physics, Pistoia, Italy

[9]Policlinico SS. Annunziata, Radiotherapy, Chieti, Italy

[10]AOU "Santa Maria della Misericordia", Medical Physics, Udine, Italy

[11]AOU Città della Salute e della Scienza, Medical Physics, Torino, Italy

[12]O.G.P. S.Camillo de Lellis, Radiotherapy, Rieti, Italy

[13]AUO Careggi, Medical Physics, Firenze, Italy

[14]Ecomedica, Radiotherapy, Empoli, Italy

[15]I.R.S.T., Medical Physics, Meldola, Italy

[16]AO Parma, Medical Physics, Parma, Italy

[17]IRCCS CROB, Medical Physics, Rionero in Vulture, Italy

[18]Humanitas, Medical Physics, Catania, Italy

[19]Centro REM Radioterapia, Radiotherapy, Catania, Italy

[20]Policlinico San Donato, Radiotherapy, San Donato M.se, Italy

[21]USL Lucca, Medical Physics, Lucca, Italy

[22]Campus Biomedico, Radiotherapy, Roma, Italy

[23]Malzoni Radiosurgery Center, Radiotherapy, Agropoli, Italy

[24]ASL1 Abruzzo, Medical Physics, L'Aquila, Italy

Purpose or Objective: Small field dosimetry standardization is fundamental to ensure that different institutions deliver comparable and consistent radiation doses to their patients. The current study presents a multicenter small field evaluation including: Tissue Phantom Ratio (TPR), dose profiles FWHM and penumbra, and output factors (OF), for the two major linear accelerator manufacturers and different X-ray energies.

Material and Methods: The project enrolled 31 Italian centers, 15 equipped with Elekta Linacs and 16 with Varian Linacs. Each center performed TPR measurement, in-plane and cross-plane dose profile of 0.8x0.8cm2 field and OFs measurements for field sizes ranging from 0.6x0.6 cm2 to 10x10 cm2 defined by both secondary jaws and MLC. Set-up conditions were: 10cm depth in water phantom at SSD 90cm. Measurements were performed using the new Exradin W1 plastic scintillator detector (Standard Imaging). The two canals SuperMAX electrometer (Standard Imaging) to automatically correct for Cherenkov radiation was used. Two identical W1 were used to speed up the data collection.

Results: The analysis included 13 Varian and 13 Elekta centers; 7 centers were excluded due to a condenser problem in an electrometer. As reported in Table 1 for the two most representative linac models, TPR measurements showed standard deviations (SD)=0.6%; penumbra values of dose profiles showed SD=0.5mm, while FWHM measurements showed a greater variability. As illustrated in Figure 1, OF measurements showed standard deviations within 1.5% for field size greater than 2x2 cm2; for field size less than 2x2 cm2 measurements' variability increases with decreasing field size. OF values show no dependence from the effective field size.

Table 1. TPR, FWHM and penumbra values measured with W1 PSD for the two most representative linacs of the multicenter study

Manufacturer	Model	Energy	TPR	FWHM (mm)		Penumbra (mm)	
Varian	Clinac 2100	6	0.670±0.003	8.1±0.4	7.9±0.5	2.3±0.4	2.3±0.2
Elekta	Agility	6	0.688±0.004	9.3±0.4	7.9±0.5	4.2±0.4	2.7±0.2

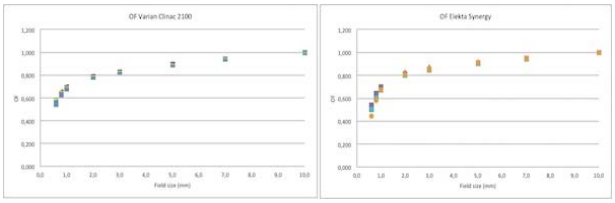

Fig. 1. OF values measured with W1 PSD for the two most representative linacs of the multicenter study

Conclusion: High TPR and penumbra values consistency were obrained over the centers. FWHM and OF showed greater variability, also considering Linac with the same model of the head. Measurements confirm W1 PSD as a good candidate for small field clinical radiation dosimetry in advanced radiation therapy techniques.

PO-0819

Analysis of liquid embolic agents on flattening filter free dose deposition with Monte Carlo method

D. Akcay[1]
[1]*Dokuz Eylul University Medical Faculty, Radiation Oncology, IZMIR, Turkey*

Purpose or Objective: Brain Arteriovenous mal-formation (AVM), in some cases, is treated with Onyx34 liquid embolic system (LES) containing tantalum. Moreover, stereotactic radiosurgery (SRS) may be required when total obliteration is not achieved after embolization. Presence of tantalum in radiation field not only generates artefacts in computed tomography (CT) images but also it could arise dose distribution perturbations. Goal in this study was to analyze the perturbation effect of Onyx34 in flattening filter free (FFF) photon beams using GAMOS Monte Carlo (MC). Artefact cause analysis was also included in the study.

Material and Methods: GAMOS simulations for 6 FFF and 10 FFF photons were done in three different conditions: a) depth dose simulations in a water phantom containing 2x2x2 cm3 Onyx34 (inc. %35wt/vol Ta) medium at 5 cm depth, b) depth dose simulations in the same condition with compact bone instead of Onyx34, c) simulations in homogenous water phantom. Dose and photon flux scorers were used at central beam axis with 5x5x2 mm3 grid sizes. For comparison purposes, photon fluxes were also scored with broad photon beam with single photon energy of 80 keV. All of MC calculations were done with 1.5% and 0.5% statistical noise respectively.

Results: In 80 keV photon simulations, photon flux decreased around 50% at post Onyx34 region relative to homogeneous water simulations. However, for compact bone falloff was around 10% at the same geometry. Also, there was a remarkable flux reduction in pre-Onyx34 region which is not as much as post Onyx34 region. For both 6 and 10 FFF photon beams, around 5% of decrease was seen in photon flux and depth dose after Onyx34 and compact bone inhomogeneties . Pre-Onyx34 region doses were increased by 15% for 6 FFF and 10% for 10 FFF.

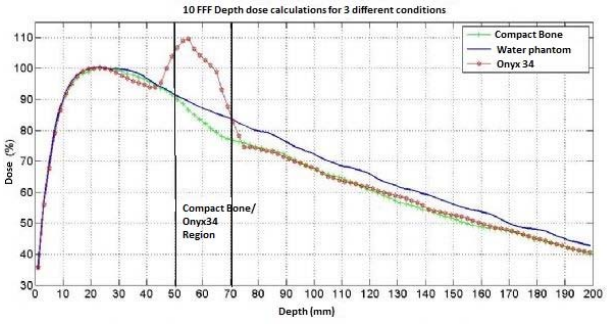

Conclusion: Photon flux calculations for 80 keV beam, showed a considerable photon attenuation and lateral scattering due to presence of Onyx34. As a result, photon starvation causes black-white streak artefacts in CT images. In conclusion, in AVM SRS planning the presence of LES can be taken into account by defining high density artefact region as a compact bone. However in vicinity of critical structures, the possible dose peaks must be considered at pre-Onyx regions which might not be calculated in treatment planning systems.

PO-0820

Volumetric quality assurance of RapidArc plans for multiple intracranial targets using gel dosimetry

N. Khater[1], C. El Khoury[1], M. Sarraf[2], J. Barouky[1], D. Nehme Nasr[1], F. Azoury[1], T. Felefly[1], R. Sayah[1], N. Farah[1], S. Achkar[1], E. Nasr[1]
[1]*Hotel Dieu de France - University of Saint Joseph, Radiation Oncology, Achrafieh, Lebanon*
[2]*Clinatec-Cea-Grenoble, University of Joseph Fourier - University of Saint Joseph, Grenoble, France*

Purpose or Objective: Given the unlimited spatial arrangements of multiple intracranial tumors, an evaluation of a planar sampling for end-to-end test is insufficient as it could provide no information about one or more tumors. Hence, a volumetric approach is needed. Here, we evaluate polymer gel dosimetry for three-dimensional (3D) patient-specific quality assurance (QA) in multiple brain lesions stereotactic radiosurgery (SRS) plans using volumetric modulated arc therapy (VMAT) technique.

Material and Methods: End-to-end test using polymer gel dosimeters was performed for an intracranial SRS case involving two lesions treated with VMAT – single isocenter approach. The following was performed: (1) BANG-3 polymer gel was prepared for two opaque spherical glass phantoms, one for patient plan QA and one for calibration; (2) the patient plan was delivered to the patient phantom and a simple non-modulated plan with predetermined doses was given to the calibration phantom; (3) 1.5T MRI was performed on both phantoms; (4) an in-house program was used to determine the relaxation rate maps (R2) from proton density and T2-weighted images; (5) CT scans were acquired with markers triangulating the isocenter of irradiation setups; (6) CTs were imported into Eclipse treatment planning system for dose computation in corresponding gel phantoms; (7) CTs and MRs were registered in Eclipse and registration transformations used to resample the R2 maps in corresponding CT positions using MATLAB. Then, data analysis was performed using an in-house visual-C++ code which took as input all 3D images, 3D dose, patients' structures exported from Eclipse and performed the following: (8) A calibration was extracted from the calibration gel and used in the patient gel QA; (9) the patients' structures were registered with the patients' gel using CT isocenter marks on the gel phantom and through the isocenter on the patients' plan; and (10) compared measured versus planned 3D isodose, dose volume histogram (DVH) analyses, and multi-slice 2D gamma evaluation.

Results: The measured isodose lines and surfaces were well visualized and qualitatively reproduced the calculated dose distribution (Figure 1). Gamma analysis between the dose matrices were carried out using gamma criteria 3% 3mm and 5% 5mm, % dose difference – distance to agreement combination within the volume enclosed by the 50% and the 80% isodose surface, respectively. Representative transverse slices yielded gamma pass rates of greater than 90%. Measured and planned DVH analyses showed agreement for planning target volume and organs at risk.

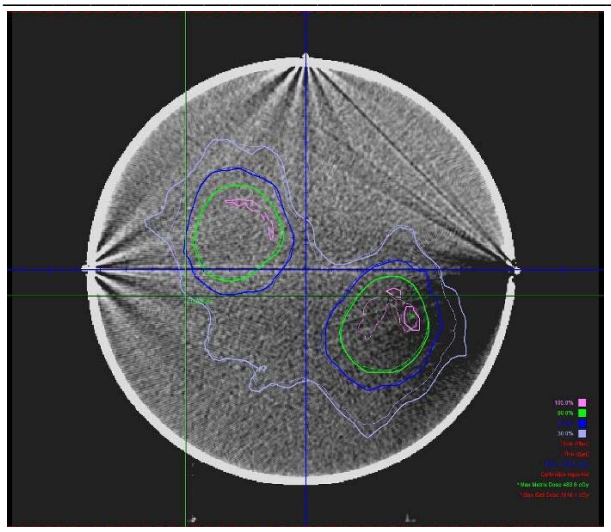

Conclusion: Polymer gel dosimetry shows promise for volumetric patient-specific QA of IMRS dose distributions. It does not present limitations when treatments involve couch rotation and gives a complete 3D assurance. However, it is labor intensive to be applicable in daily clinical practice. Nevertheless, the gel method has an important role during safe implementation of a SRS program.

PO-0821

A comparison between different patient QA devices for IMRT treatments on VERO system

A. Bazani[1], F. Pansini[1], C. Garibaldi[1], S. Comi[1], E. Rondi[1], G. Piperno[2], A. Ferrari[2], B.A. Jereczek-Fossa[2,3], F. Cattani[1]

[1]*European Institute of Oncology, Medical Physics, Milan, Italy*

[2]*European Institute of Oncology, Radiation Oncology, Milan, Italy*

[3]*University of Milan, Radiation Oncology, Milan, Italy*

Purpose or Objective: The purpose of this study was to compare the ability of OCTAVIUS® 4D phantom with 1000 SRS array (PTW) and ArcCHECK® system (SunNuclear) in detecting geometric and dosimetric errors intentionally introduced into the IMRT step-and-shoot treatments delivered with VERO® system (Mitsubishi Heavy Industries and BrainLAB). Moreover, the impact of these errors on the DVH of PTVs and OARs was investigated.

Material and Methods: The treatment plans of 3 clinical cases were considered (prostate, partial breast irradiation PBI and splenic lesion). From each of the original plans, 4 verification plans were created, containing one intentional error per plan: gantry rotation of +3°, ring rotation of +5°, 2% increased number of monitor units and isocenter translation of 3 mm (caudal direction). All the plans were calculated with iPlan 4.5.3 (BrainLAB) with a calculation grid of 2 mm on a mathematical phantom, for OCTAVIUS® 4D system, and on the CT images (plug inserted), for ArcCHECK®. The analysis was executed applying the 3D γ evaluation method (3% local dose-3mm and 2% local dose-2mm, 10% dose threshold), comparing the original calculated distributions with the measured ones (with errors) using the related software (VeriSoft® Patient Plan Verification Software for OCTAVIUS 4D®, coronal projection, and SNC Patient™ Software for ArcCHECK®). The tolerance level considered was 5% for the gamma failure rate (an error was considered detected when the gamma failure rate was higher than 5%). The impact of the errors introduced was evaluated by considering the DVH of PTVs (D98%, D2% and Dmean), rectum (D50% and D5%), ipsilateral lung (D40% and D10%) and spinal cord PRV (Dmax) respectively. The Pearson's correlation coefficient between the variation of the gamma passing rate and the variations of the DVHs points for the PTVs and the OARs considered was also calculated.

Results: The results of the 3D γ evaluation are reported in the figure, both for 3%-3 mm and 2%-2 mm criteria, for the original plans and for the modified ones. Using McNemar's test, the total detection rate detected by ArcCHECK® was higher than that of OCTAVIUS® 4D (p= 0.045), with 3%-3 mm criteria, while it was comparable with 2%-2 mm criteria (p= 0.480).

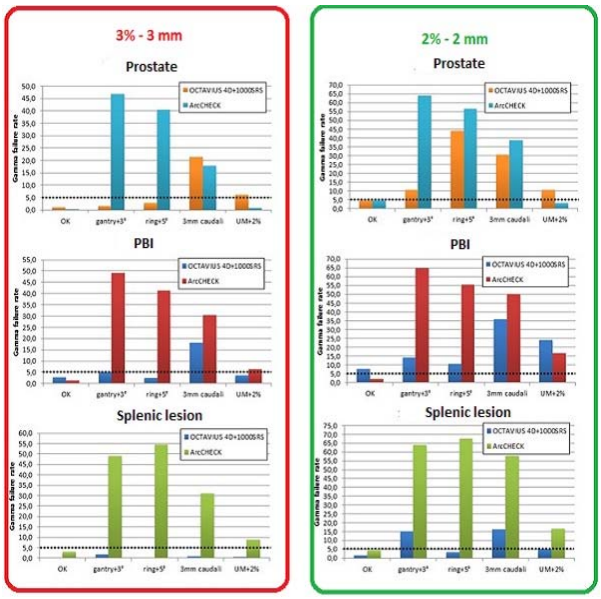

The Pearson's correlation coefficient calculated between the variation of the gamma passing rate and the variations of the constraints for the OARs considered are shown in the table.

OCTAVIUS® 4D + PTW 1000SRS

r					
	PTV			OAR	
Prostate	$D_{98\%}$	$D_{2\%}$	D_{mean}	Rectum $D_{50\%}$	Rectum $D_{5\%}$
3%-3 mm	**0.848**	0.236	0.408	-0.689	**-0.994**
2%-2 mm	0.587	-0.170	0.019	**-0.840**	**-0.936**
PBI	$D_{98\%}$	$D_{2\%}$	D_{mean}	Lung $D_{40\%}$	Lung $D_{10\%}$
3%-3 mm	**0.899**	0.543	0.294	0.226	-0.672
2%-2 mm	0.691	0.057	-0.213	-0.048	-0.472
Spleen	$D_{98\%}$	$D_{2\%}$	D_{mean}	PRV D_{max}	
3%-3 mm	-0.131	0.135	0.248	-0.624	
2%-2 mm	0.249	0.578	0.378	**-0.777**	

ArchCHECK®

r					
	PTV			OAR	
Prostate	$D_{98\%}$	$D_{2\%}$	D_{mean}	Rectum $D_{50\%}$	Rectum $D_{5\%}$
3%-3 mm	0.059	0.651	0.609	**0.900**	0.502
2%-2 mm	0.283	**0.779**	**0.773**	**0.806**	0.294
PBI	$D_{98\%}$	$D_{2\%}$	D_{mean}	Lung $D_{40\%}$	Lung $D_{10\%}$
3%-3 mm	0.092	**0.813**	**0.949**	0.628	-0.332
2%-2 mm	0.238	**0.892**	**0.987**	0.649	-0.427
Spleen	$D_{98\%}$	$D_{2\%}$	D_{mean}	PRV D_{max}	
3%-3 mm	0.576	0.414	**0.874**	0.519	
2%-2 mm	**0.767**	0.687	**0.983**	0.323	

Conclusion: The results showed a different sensitivity to errors for the two systems, in particular in the case of ring and gantry rotations. This variation can be related to the different dose reconstruction methods applied: ArcCHECK® uses both the entry and exit dose, while OCTAVIUS® system the planar dose measured by the inserted detector and the PDD of the beam. Furthermore, no significant correlation was found between the results of the 3D γ analysis and the DVHs variations due to the intentional errors, as shown in literature.

PO-0822

Tumor margin estimation by multiple Bragg peak detection in carbon ion therapy

M.F. Ferraz Dias[1], C.A. Collins Fekete[2], G. Baroni[1], J. Seco[3], M. Riboldi[1]

[1]*Politecnico di Milano University, Dipartimento di Elettronica- Informazione e Bioingegneria - DEIB, Milano, Italy*

[2]*Université Laval, Département de Physique- de Génie Physique et d'Optique et Centre de Recherche sur le Cancer-, Québec, Canada*
[3]*Massachusetts General Hospital MGH, Department of Radiation Oncology, Boston, USA*

Purpose or Objective: Carbon ion therapy is very sensitive to tissue density variations along the beam path. Within the lung region, due to the high-density difference between tumor and lung tissue, these variations are further emphasized, leading to miss the tumor or high-dose deposition in critical structures. Hence, it is crucial to have correct knowledge of tumor margin. If one shoots these structures with a carbon beam with energy high enough to cross the patient and detects their residual range using a range detector, multiple peaks will be present in the acquired signal. This is caused by the fact that carbons from the same beam cross different structures. The purpose of this work is to show that using information from these multiple peaks, it is possible to measure the interface position using just a few irradiation spots, thus minimizing the imaging dose.

Material and Methods: Two approaches are proposed: the single shot approach is a theoretical model, which provides a relationship between the peaks intensity and distance from the interface; such approach only requires one shot around the interface to predict its position. The second approach (inflection point) entails irradiating the interface at two different positions and through an exponential fit compute the exact interface location. Both methods are validated using Monte-Carlo simulations with different interface configurations. A Carbon Digitally Reconstructed Radiography (CDDR) method is implemented in order to assess both methods in two lung tumor cases. Positional shifts to a water density tumor are implemented and the accuracy of the proposed methods is tested.

Results: Results show that both approaches exhibit an error <1mm in determining where the interface is positioned with respect to the beam. The inflection point method showed to be the most reliable, since it allows the determination of the interface when more than two peaks are detected using prior-knowledge information. Both methods offer a low dose approach, which will potentially allow adjustment of the irradiation beam position when a tumor shift occurs.

Conclusion: By measuring the difference between the two generated peaks at an interface, it is possible to determine its exact position with 1mm accuracy. Currently tumor margin positioning/delimitation is being accessed using multiple angle approaches and considering breathing motion effects. Future work will consider applying the same methods to other tumor areas and structures which can be used for patient positioning.

PO-0823

Five-year results of treatment quality assurance using in vivo dosimetry in ocular proton therapy

A. Carnicer Caceres[1], V. Letellier[2], G. Angellier[1], V. Floquet[1], W. Sauerwein[3], J. Thariat[1], J. Hérault[1]
[1]*Centre Antoine Lacassagne, Physics, Nice, France*
[2]*MedAustron, MedAustron, Wiener Neustadt, Austria*
[3]*Universitätsklinikum Essen, Universitätsklinikum Essen, Essen, Germany*

Purpose or Objective: An in-house in vivo dosimetry system based on the measurement of gamma-prompt radiation emission during irradiation was implemented for quality assurance of ocular proton therapy treatments at the Centre Antoine Lacassagne (CAL) in 2011. Based on the last five years results we report the performance and limitations of the system.

Material and Methods: Gamma-prompt radiation is emitted during proton therapy irradiation by collision of protons with beam modifiers all along the optical bench. A correlation was established at CAL between gamma-prompt radiation and the accessories conforming the clinical SOBP (range shifter and modulating wheel), by measuring, for a large set of treatment sessions, the charge cumulated (Q) at a large volume ionization chamber located inside the treatment room at 3 m from the optical bench. A power function was used to fit the dose rate D/MU and Q/D data points, where D is the dose delivered to the patient. The function was introduced to an in-house Visual Basic code to automatically retrieve the differences (d) between calculated and expected D/MU. A tolerance of 5% was established, out-of-tolerance cases requiring systematic SOBP accessories checking. Out-of-tolerance rate was calculated from more than 4000 treatment sessions performed from May 2011 to September 2015. Out-of-tolerance causes were analysed by assessing uncertainties on the ionization chamber measurement acquisition (repeatability test performed in reference treatment conditions (10 s irradiation, 13 Gy and 1.37 cGy/UM)), correlations of d with D, D/MU and Q and the impact of the customized patient accessories located just before the eye (collimators, filters and compensators).

Results: The relative differences were normally distributed and centered on 0.004% with a σ of 3%. 12% of cases were out-of-tolerance, only 2% being larger than 7%. Out-of-tolerance cases were never related to an error on SOBP accessories. More than 60% cases with differences larger than 7% were related to low dose treatments (<7 Gy). Relative differences were not correlated to the use of filters or to the collimator area. Treatments performed with compensator yielded higher differences (doses are below 7 Gy for these treatments). The uncertainty on Q acquisition was estimated to 0.8%. Cumulating Q beyond the treatment time (40 s) increased the relative difference by 2%.

Conclusion: The system is independent of the customized patient accessories located right before the eye. The precision is consistent with in-vivo dosimetry systems and yields results within or very near tolerance limits for most standard treatments performed at CAL (13 Gy). Out-of-tolerance cases could be minimized by limiting the ionization chamber measurement acquisition time. The method perfectly fulfills the goal of SOBP accessories verification, and could be further improved by reviewing the default for low dose treatments.

PO-0824

Treatment couch modeling in Elekta Monaco treatment planning system

C. Huertas[1], C. Ferrer[1], C. Huerga[1], I. Mas[1], A. Serrada[1]
[1]*H.U. La Paz, Radiofísica y Protección Radiológica, Madrid, Spain*

Purpose or Objective: This study describes the modeling of the treatment couch in Elekta Monaco treatment planning system (v. 3.30.01), and the measurements made to validate it for attenuated and skin dose calculation, and 6MV energy beams.

Material and Methods: The iBEAM evo carbon fiber couch has a sandwich design. It consists of a narrow outer layer of electron density ρE=1.7gr/cm3 and a foam core of lower density ρE=0.3gr/cm3.
First modeling was composed of a single contour. CT images were acquired and the couch contoured in each slice. The dimensions were according to vendor specification. The best agreement between experimental and computed dose attenuation was using an effective density of ρE=0.13gr/cm3.However, the comparison failed at the edges of the couch. Therefore, a second contour has been added with the thick of the edges and the density of carbon fiber ρE=1.7gr/cm3. That way, calculations vary slightly with grid size and don't depend on the order of ROIs.
A cylindrical phantom with an ionization chamber CC13 placed in the central insert was used to measure the attenuated dose. The phantom was centered laterally on the couch and the chamber position coincides with linac isocenter. Dose measurements were performed for an open 10x10 field at multiple gantry angles, MΘ, 100 Monitor Units

(MU) were delivered at each angle: The reference dose without couch attenuation is the average dose at 0º,90º and 270º. Gantry angles ranging from 235º to 223º in 1º increments are used to measure the edge attenuated dose. And gantry angles ranging from 220º to 180º in 10º increments to measure the dose attenuation of the central region of the couch.
Skin dose was measured with radiochromic films and FilmQA Pro. Several films were placed between RW3 slabs in different depths.The center of RW3 phantom coincides with linac isocenter.
First,films were located at the surface, 0.5cm and 1.5cm from the surface, and in the center of the RW3 phantom. Then 200MU were delivered with an open 10x10 field and with zero gantry angle. The irradiated films were removed and other films were placed under the phantom, 0.5cm and 1.5cm from the couch and in the center. The opposite beam was delivered, so we measure the effect of the couch to the dose distribution in the buildup region.

Results: Table 1A Comparison results between measured and calculated relative transmitted dose (T%), with and without the couch. Table 1B Evaluation of skin dose increment and comparison results between scanned and calculated increment of skin dose.

TABLE 1A	Monaco						Measurements	
	Without table			With table				
Angle	cGy	T(%)	diff %	cGy	T(%)	diff %	nC	T(%)
0	69	1	0,1	68,1	1,001		2,35	0,999
90	68,7	0,996	-0,4	68,1	1,001	0,2	2,35	0,999
270	69,3	1,004	0,3	67,8	0,997	-0,4	2,35	1,002
235	69	1	4,8	65,7	0,966	1,3	2,24	0,954
234	69	1	5,6	64	0,941	-0,6	2,23	0,947
233	69	1	4,2	65	0,956	-0,4	2,26	0,96
232	69	1	3,1	66,9	0,984	1,4	2,28	0,97
231	69	1	3,1	66,8	0,982	1,3	2,28	0,97
230	69	1	3,5	66,5	0,978	1,3	2,27	0,966
229	69	1	3,5	66,3	0,975	1	2,27	0,966
228	69	1	3,7	66,1	0,972	0,8	2,27	0,965
227	69	1	3,6	65,8	0,968	0,3	2,27	0,965
226	69	1	3,7	65,4	0,962	-0,2	2,27	0,964
225	69	1	3,9	65,2	0,959	-0,4	2,26	0,962
224	69	1	4,1	65,2	0,959	-0,2	2,26	0,961
223	69	1	4,4	65,4	0,962	0,4	2,25	0,958
220	69	1	5,4	65,4	0,962	1,4	2,23	0,948
210	69	1	3,7	65,9	0,969	0,5	2,27	0,964
200	69	1	3,2	66	0,971	0,2	2,28	0,969
190	69	1	2,9	66,1	0,972	0	2,28	0,972
180	69	1	2,9	66,4	0,976	0,4	2,29	0,972
	average difference %		3,3	average difference %		0,4		

TABLE 1B	Monaco		Radiochromics	
AP 10x10 SSD=91cm, 200MU without couch	Dose (cGy)	percentage of Dmax	Dose (cGy)	percentage of Dmax
Over 18cm of RW3 (at the surface)	56,5	**23,7**	49,8	**20,9**
0.5cm from the surface	213	89	205	86
1.5cm from the surface	239	100	238	100
Iso, at 9cm depth	174	73	166	69,8
PA 10x10 SSD=91cm, 200MU with couch	Dose (cGy)	percentage of Dmax	Dose (cGy)	percentage of Dmax
under the phantom, 18cm of RW3	228	**93,8**	221	**92**
0.5cm from the couch	241	99,4	239	99,5
1.5cm from the couch	243	100	240	100
Iso, at 9cm of depth	158	65	163	67,7
Increment of skin dose	3,96		4,4	

Conclusion: The couch model improves the discrepancy between measured and computed attenuated dose. If we take into account the couch in treatment planning calculations, this average difference decreases from 3.3% to 0.4%. The couch increases 4 times the skin dose and the couch model provides an accurate calculated dose in the buildup region.

PO-0825

Characterization of a commercial EPID 3d software for in vivo dosimetry.

M. Esposito[1], P. Bastiani[2], A. Bruschi[1], A. Ghirelli[1], S. Pini[1], G. Zatelli[1], S. Russo[1]
[1]*Azienda Sanitaria Firenze, Fisica Sanitaria, Firenze, Italy*
[2]*Azienda Sanitaria Firenze, Radioterapia, Firenze, Italy*

Purpose or Objective: Dosimetry Check (DC) is a commercial software that allows reconstruction of 3d dose distributions using transit and through-air EPID images. DC is composite of two parts: a deconvolution kernel that converts EPID images to fluence, and a pencil beam algorithm to calculate the dose. It can be used for pre treatment QA verification and for in vivo dosimetry. In this work we evaluated the suitability of DC software for in vivo dosimetry of VMAT treatments.

Material and Methods: DC (v4.10) was used along with Elekta Synergy® Linac (6 and 10 MV beams) equipped with a-Si Electronic Portal Imaging Device (EPID) Iview-GT. Twenty VMAT (5 prostate, 5 whole pelvis, 5 lung, 5 head and neck), elaborated by treatment planning system (TPS) Elekta Monaco® 5.0 were measured. Through-air (EPID T-A) and transit EPID images were used for three dimensional dose maps reconstruction in homogeneous phantoms. Octavius 4D with 729 2D array was used as reference. Gamma analysis at 3% local dose /3mm DTA was performed. Doses from though-air measurements were also reconstructed in the planning CT (T-A in plan TC) and compared with the treatment planning dose maps.Gamma pass rate of DC dose maps were compared with those of 729 in the Octavius 4D.

Results:

Anatomical Site	Energy	Octvavius 4d	EPID T-A	EPID Transit	T-A in plan TC
Prostate1	X10	97.7	92.6	92.5	92.9
Prostate2	X10	95.4	83.3	87.1	81.3
Prostate3	X10	96	91.8	92.5	94.8
Prostate4	X10	96	90.5	89.9	90.2
Prostate5	X10	98.8	94.8	95.4	95.9
Whole Pelvis1	X10	92.5	94.4	95.9	94.5
Whole Pelvis2	X10	88.9	95.2	85.9	93.5
Whole Pelvis3	X10	88.9	91.8	83.6	91.8
Whole Pelvis4	X10	88.1	90.2	84.6	86.3
Whole Pelvis5	X10	89.3	95.5	92.34	95.6
Lung1	X6	97.7	92.0	96.8	89.2
Lung2	X6	98.0	96.8	97.8	85.8
Lung3	X6	96.0	97.5	99.4	79
Lung4	X6	97.2	93.4	98.7	72.8
Lung5	X6	97.0	96.8	97.4	96.3
Head and Nek1	X6	90.3	81.9	72.4	89.7
Head and Nek2	X6	91.2	70.1	73.8	90.6
Head and Nek3	X6	92.9	75.9	73.4	90.7
Head and Nek4	X6	92.5	80.1	83.3	94.5
Head and Nek5	X6	92.6	79.5	86.4	89.8

Table1 Gamma pass rate. EPID T-A are computed in the synthetic Ocatvius 4D phantom,
EPID transit is measured and computed in the homogeneous Octavius II phantom.

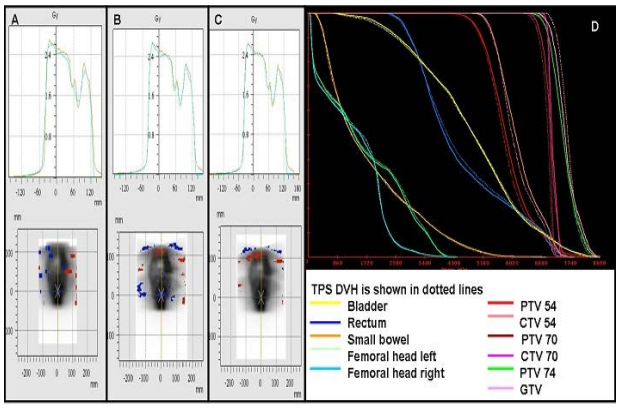

Figure1: Results of a whole pelvis SIB treatment. In the upper part comparison of profiles for Octavius 4D (A), T-A EPID (B) and Transit EPID (C). In yellow the TPS profile. The lower part of the image contains central coronal map of gamma>1 points. In D the comparison of DVH measured by DC in plan CT (solid) versus TPS (dotted lines) is shown.
Gamma pass rates are shown in the table1.The assessment of VMAT plans shows a mean of 93.9% points with gamma<1 for Octavious 4d (3.5% SD), 89.2% and 7.9%SD for EPID T-A, 89% and 8.5% SD for EPID Transit and 89.8% and 6.1%SD for T-A in plan CT. Transit and through-air EPID acquisitions produced similar gamma pass rates.Through-air EPID images computed by DC in the plannning CT showed gamma pass rate in agreement with those of Octavious 4d in the prostate, whole

pelvis and head and neck, in lung instead, gamma pass rates were lower in 4/5 cases.

Conclusion: DC is a suitable tool for VMAT in vivo dosimetry. The pencil beam algorithm can be inaccurate in the presence of low-density inhomogeneities.

PO-0826

Benchmarking computed IDD curves for four proton treatment planning systems against measured data

J. Alshaikhi[1,2], D. D'Souza[2], C.G. Ainsley[3], I. Rosenberg[2], G. Royle[1], R.A. Amos[2]

[1]*University College London, Medical Physics & Biomedical Engineering, London, United Kingdom*

[2]*University College London Hospitals, Radiotherapy Physics, London, United Kingdom*

[3]*University of Pennsylvania, Roberts Proton Therapy Center, Philadelphia, USA*

Purpose or Objective: Accurate beam modelling is an essential function of a treatment planning system (TPS) to ensure that plans can be calculated that are deliverable within clinically acceptable tolerances. The purpose of this work is to evaluate the computed integral depth dose (IDD) curves of four commercially available proton TPSs, benchmarked against measured data. The four TPSs (EclipseTM, XiO®, Pinnacle3, RayStation®) were commissioned using pencil beam scanning data from the University of Pennsylvania (UPenn) facility.

Material and Methods: A water cube phantom (40cm3) was created in each TPS for calculation of IDD curves. Calculation grid size set to 1mm in all TPSs. Individual IDDs for 27 nominal energies, ranging from 100 to 226.7MeV, were calculated by integrating the calculated depth dose distributions. These were all benchmarked against measured data from UPenn, comparing the clinical range at 80% distal dose (D80), Bragg peak width between distal and proximal 80% (D80-P80), range at 0.5% (R0.5), and distal penumbra between D80 and R0.5. Gamma-index analysis with pass criteria of 1mm/1% was also used to compare computed and measured IDDs.

Results: Mean percentage of IDDs with >95% pass rate for 1mm/1% criteria were 96.7% (SD 4.9) for XiO®, 94.1% (SD 8.9) for EclipseTM, 95.4% (SD 8.6) for RayStation®, and 49.2 (SD 26.0) for Pinnacle3. Maximum differences between computed and measured IDD data are shown below. No correlation with nominal energy was observed.

	Maximum differences [mm]			
	Range 80% (D_{80})	Peak width (D_{80}-P_{80})	Distal penumbra (D_{80}-$R_{0.5}$)	Range 0.5% ($R_{0.5}$)
XiO®	0.1	0.1	0.2	0.2
Eclipse™	0.8	0.6	1.1	1.2
RayStation®	0.3	0.4	0.8	0.8
Pinnacle³	0.4	0.6	0.9	1.3

Conclusion: Characteristics of computed IDDs were compared to measured data for four commercially available TPSs. All were within clinically acceptable tolerances, with XiO showing the closest agreement. Differences observed were attributed to TPS specific beam modelling. Further investigation will assess the cumulative impact of these discrepancies on verified clinical treatment plans.

PO-0827

Principal component analysis for deviation detection in 3D in vivo EPID dosimetry

R.A. Rozendaal[1], B. Mijnheer[1], I. Olaciregui-Ruiz[1], P. Gonzalez[1], J.J. Sonke[1], A. Mans[1]

[1]*Netherlands Cancer Institute Antoni van Leeuwenhoek Hospital, Department of Radiotherapy Physics, Amsterdam, The Netherlands*

Purpose or Objective: One of the clinical issues our institute faces regarding in vivo EPID dosimetry is the number of raised alerts. For example, alerts are raised for 49% of the treatments in case of head-and-neck (H&N) VMAT treatments; an alert is raised when dosimetry results are found deviating according to statistics derived from the histogram of 3D γ-analysis results. These alerts are mostly found to be patient-related or attributable to limitations of our back-projection and dose calculation algorithm. After inspection, an intervention is considered for only 0.3% of the treatments. The purpose of this study is to develop a principal component analysis (PCA) based classification method to improve the specificity of our EPID dosimetry system. In particular, in contrast to our current classification method, PCA allows for the spatial distribution of γ-values to be taken into account for deviation detection.

Material and Methods: The input for PCA consisted of 3D γ-distributions (3%/3mm), one per treatment arc per fraction. In total, 2024 3D γ-distributions from 499 H&N VMAT treatment-plans were included. As an initial choice, components describing at least 1% of the variance were selected. The distribution of variances over the components was inspected to validate this choice. Using these components, new 3D γ-distributions were created by projecting each input 3D γ-distribution on only these components and then projecting the result to the original coordinate system of the 3D γ-distributions. If the selected components describe the original γ-distribution well, the new and original γ-distributions will be similar. This similarity was quantified by the root mean square (RMS) d of the difference between the two γ-distributions; a γ-distribution was marked as deviating when d exceeded a threshold. All true positive γ-distributions (n = 2) in the dataset, as identified by experienced medical physicists, were used to determine this threshold for identification of alerts.

Results: The first 16 components were each found to describe at least 1% of the variance; cumulatively, they account for 83% of the variance in the dataset. Figure 1 shows the cumulative variance accounted for as a function of selected components and indicates that the choice for selecting components is reasonable. After finding and applying the appropriate threshold for detecting the identified true positives, a drop in alert rate from 49% to of 11% was observed, corresponding to an increase in specificity from 0.51 to 0.89.

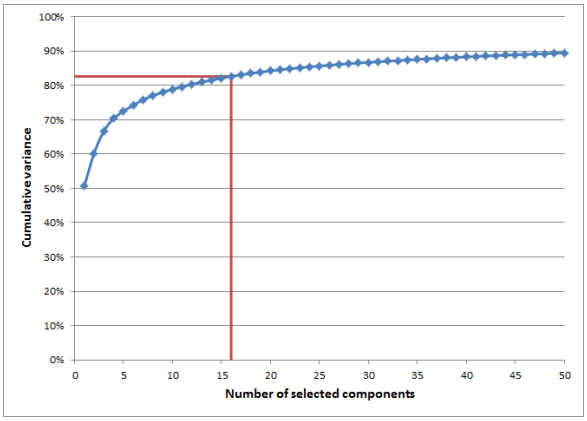

Conclusion: The PCA-based classification method presented in this study enhances the specificity of deviation detection in 3D in vivo EPID dosimetry of H&N VMAT from 0.51 to 0.89, compared to our current clinical γ-histogram based method. Before clinical implemention, a rigorous validation is required.

PO-0828

Dosimetric assessment of a second generation Multi-Leaf Collimator for robotic radiotherapy

P.H. Mackeprang[1], D. Schmidhalter[1], D. Henzen[1], M. Malthaner[1], D.M. Aebersold[1], P. Manser[1], M.K. Fix[1]

[1]*Division of Medical Radiation Physics and Department of Radiation Oncology Inselspital, Bern University Hospital, and University of Bern, Switzerland*

Purpose or Objective: Recently, a second generation Multi-Leaf Collimator (InCise 2™) was released for the CyberKnife® M6™ robotic radiotherapy system. As part of the evaluation and initial characterization, physical, dosimetric and planning parameters were recorded. Further, planning studies on phantoms were performed to compare the InCise 2 to the Iris™ collimator system.

Material and Methods: As part of the InCise 2 validation, leakage, TG-50 picket fence, Bayouth fence and automated quality assurance measurements were performed using radiochromic film. End to end delivery tests were performed for skull-, fiducial-, x-sight spine-, x-sight lung- and synchrony tracking. Ten treatment plans and five QA plans were delivered to phantoms using the InCise 2. Ionization chamber measurements as well as film measurements were compared with dose calculated by the treatment planning system. For dosimetric assessment, treatment plans to water phantoms were generated using the IRIS collimator system and the InCise 2 MLC. On a cylindrical water phantom of a diameter of 20 cm, spherical target volumes of diameters from 5 to 80 mm were drawn. Firstly, the dose optimization algorithm using the MLC was assessed using a simple Optimize Minimum Dose (OMI) objective. Secondly, shell volumes were generated around the target volumes and their coverage was optimized (OCI). 1000 cGy were prescribed to the 80% isodose. Dose distributions, Nakamura's new Conformity Index (nCI) as well as optimization and estimated treatment times were analyzed.

Results: All validation tests were passed within tolerances. Maximum leakage was recorded as 0.44% for all MLC orientations. Mean leaf positioning errors in Bayouth fence tests ranged from -0.043 mm to 0.006 mm, without any individual leaves exceeding the tolerance of ±0.27 mm. All phantom plans were delivered successfully, with recorded dose for QA plans differing 1.94% ±1.03% from calculated dose and gamma analysis (3% / 1mm, 20% dose threshold) showing > 97% agreement. Total end to end tracking errors were below 0.95 mm for all tested tracking methods. Testing the optimization algorithm revealed nCI values for plans optimized based on target volume shells between 1.02 and 1.50 for plans using the InCise 2 and 1.05 and 1.43 for IRIS. MLC optimization times increased as a function of both target size and optimization steps, ranging from 12 s for the 5 mm PTV OMI plan to 7 h for the 80 mm PTV shell based optimization. Estimated treatment times including setup times for the synthetic plans were reduced by a mean of 19.1% when choosing the InCise 2 over the IRIS.

Conclusion: The InCise 2 MLC system passed initial physics evaluation at our site and showed dose distributions comparable to the CyberKnife IRIS collimator system for spherical targets. Estimated MLC treatment times are about 20% lower compared to the IRIS collimator system.

PO-0829

Determining the mechanical properties of a radiochromic deformable silicone-based 3D dosimeter

L.P. Kaplan[1], E.M. Høye[2], P. Balling[1], L.P. Muren[2], J.B.B. Petersen[2], P.R. Poulsen[2], E.S. Yates[2], P.S. Skyt[2]

[1]*Aarhus University, Dept. of Physics and Astronomy, Aarhus C, Denmark*

[2]*Aarhus University/Aarhus University Hospital, Dept. of Oncology, Aarhus C, Denmark*

Purpose or Objective: Recently emerged radiotherapy methods such as intensity-modulated or image-guided radiotherapy are capable of delivering very conformal dose distributions to patients, but their accuracy can be greatly compromised by e.g. the deformation of organs in the patient. The accuracy of deformable registration algorithms developed to correct for this is not well known due to the challenging nature of deformation measurements. A new type of deformable radiochromic 3D dosimeter consisting of a silicone matrix has recently been developed in our group. This dosimeter makes direct dose measurements in deformed geometries possible. The aim of this study was to investigate its mechanical properties in terms of tensile stress and compression.

Material and Methods: The dosimeter contained the SYLGARD® 184 Silicone Elastomer kit (Dow Corning), Leuco-Malachite Green (LMG) dye as the active component and chloroform as solvent and sensitizer. To determine the shape of the dosimeter's stress-strain curve and Young's modulus (Y), tensile stress was imposed on rod shaped samples along their central axis and the resulting strain was observed using a camera. To define Y a linear approximation was made for small strains. This was done at varying times after production, for varying curing agent concentrations and for both irradiated and non-irradiated dosimeters. 10 × 10 cm2 photon fields with beam quality 6 MV were used to deliver a dose of 60 Gy at 600 MU/min. To investigate whether the density of the material is conserved under compression, dosimeters were CT-scanned while placed in a wooden clamp to impose varying degrees of compressive stress. Finally, dosimeters were also partially irradiated while subject to tensile stress to see if the irradiated areas would return to the original geometry once the stress was removed after irradiation.

Results: The measured stress-strain curves did not show hysteresis or plastic deformation, even after multiple deformations. Y was found to be 0.08-0.2 MPa 48 hours after production depending on the amount of curing agent (see figure), and it increased at an exponentially decreasing rate for up to several weeks afterwards due to further hardening. Irradiation prior to imposing tensile stress did not affect the mechanical properties immediately, but it slowed the hardening process in the following days. The volume was found to be conserved during compressive stress of up to 60%. Multiple tests showed that dosimeters irradiated partially under tensile stress returned completely to their original geometries after removing the stress (see table).

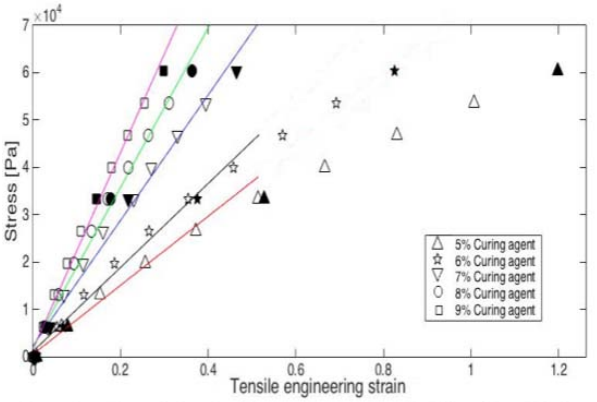

Figure 1: Stress-strain curve for dosimeters with varying curing agent concentrations 48 hours after production. The un-filled markers indicate measurements taken while loading, while the filled markers show measurements taken while unloading. Notice that these coincide well with the un-filled markers, indicating the absence of hysteresis. Linear fits are included for strains smaller than 0.5. Error bars are not included, as they are smaller than the markers.

Tabel 1.1: Dosimeters irradiated under tensile strain. All dosimeters were irradiated with a field 0.5 cm wide.

Original length of irradiated area (no strain)[1](cm)	Length after irradiation(cm)
0.5	0.5
0.44	0.48
0.41	0.41
0.38	0.39
0.34	0.34
0.31	0.32
0.28	0.28
0.25	0.27
0.19	0.21

[1] Due to the setup there was an uncertainty of ≈ ±0.05 cm in determining the original length of the areas to be irradiated.

Conclusion: The dosimeter's deformable properties are not altered significantly by repeated strain or irradiation, its volume is conserved under compression and it displays predictable behavior when being irradiated under strain. These properties makes the dosimeter a very strong candidate for direct dose measurement in deformed geometries.

PO-0830

Correlation of MLC positions detected using log-files with MLC positions detected using the EPID

W. Lechner[1,2], A. Moser[1,2], A. Altendorfer[1,2], D. Georg[1,2]
[1]*Medical University of Vienna, Department of Radiation Oncology, Vienna, Austria*
[2]*Medical University of Vienna, Christian Doppler Laboratory for Medical Radiation Research for Radiation Oncology, Vienna, Austria*

Purpose or Objective: The Purpose of this work was to investigate the long term correlation between leaf positioning errors determined using LINAC log-files with an independent method.

Material and Methods: A picket fence pattern was irradiated on four different LINACs with simultaneous EPID measurement and log-file recording. Measurements were performed on two VersaHD and two Synergy LINACs (Elekta AB, Stockholm, Sweden) over a period of six months on a weekly basis. The picket fence pattern consisted of 5 bands with a width of 2 cm. The positions of bands' centers were -11 cm,-2 cm, 0 cm, 2 cm and 11cm. An in-house developed software was employed to calculate the deviation of the actual leaf positions according to the log-file data from the planned position. The simultaneously acquired EPID images were analyzed using MLCSoft-EPID (PTW, Freiburg, Germany) and provided reference data. The sensitivity of all measurement methods was evaluated by means of implementing leaf errors in the picket fence pattern. The sensitivity of both methods was investigated by artificially introducing leaf positioning errors of 0.5 mm, 1 mm and 2 mm. In order to investigate the correlation between log-file and EPID data, Pearson's correlation coefficient was calculated considering all leafs as unity of each LINAC over the measurement period (henceforth denoted as total correlation coefficient ptot). Additionally, Pearson's correlation coefficient was calculated for each leaf separately (pL). The percentage of the absolute value of pL exceeding 0.6 was reported.

Results: The artificially introduced errors were detected by both measurement systems. The total correlation coefficients for LINAC 1, LINAC 2, LINAC 3 and LINAC 4 were 0.44, 0.06, 0.61 and -0.19, respectively. In contrast to that, only 0%, 2.04%, 6% and 0% of the absolute values of correlation coefficients calculated for each leaf separately exceeded a value of 0.6. These results are summarized in Table 1. In Figure 2 depicts an example of a scatter plot of the data acquired for LINAC 2.

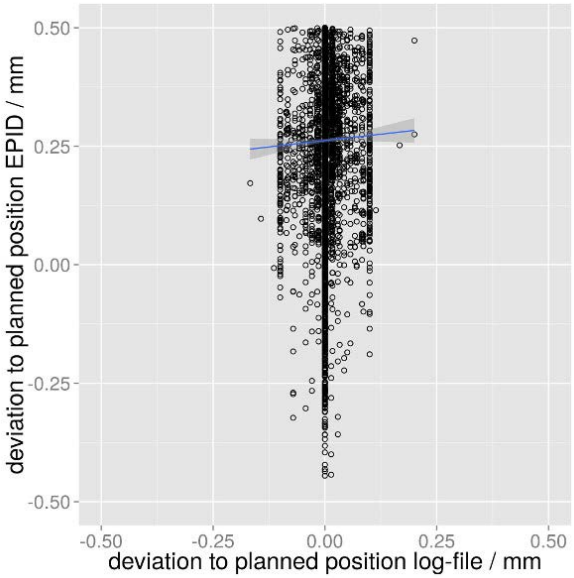

Fig 1: Scatter plot of all simultaneously measured leaf deviations of LINAC 2. The blue line represents a linear fit of the data. The correlation coefficient for this LINAC was 0.06

Table 1:

	LINAC 1 Synergy	LINAC 2 VersaHD	LINAC 3 Synergy	LINAC 4 VersaHD
p_{tot}	0.44	0.06	0.61	-0.19
abs(p_L) > 0.6 (%)	0	2.04	6	0

Conclusion: When investigating the correlation of MLC positioning errors detected with different methods, it is not sufficient to consider correlation coefficients based on sets of leafs, since a bias could be introduced. Such correlations must be investigated for each single leaf separately. This investigation revealed a poor correlation between log-file detected leaf positioning errors with EPID detected leaf positioning errors. However, deviations from planned leaf positions can potentially be detected using log-files, provided that a rigorous MLC quality assurance procedure using an independent system is performed on a regular basis.

PO-0831

Does a single MLC characterization guarantee a high accuracy of RapidArc delivered dose?

A. Scaggion[1], N. Pivato[1], A. Roggio[1], M. Paiusco[1]
[1]*Insituto Oncologico Veneto IOV-IRCCS, Medical Physics, Padova, Italy*

Purpose or Objective: In order to improve the accuracy of RapidArc delivered doses, users of Eclipse TPS commonly are forced to tailor the values of dosimetric leaf gap (DLG) and MLC transmission factor (TF). The aim of this work is to propose a methodology to improve the agreement between planned and delivered dose identifying a suitable group of (DLG,TF) couples.

Material and Methods: The 2D variation of DLG and TF has been measured for a Varian Unique Linac equipped with a Millennium 120 MLC. Using the 2D maps of DLG and TF an optimal couple (DLG,TF) has been computed for 50 treatment plans including H&N, chest and pelvis. A clinical couple (DLG,TF) has been computed as the mean over each optimal couple for the entire group of plans and for subgroups. Pre-treatment QA has been performed using a cylindrical diodes array and analyzed using both gamma index and DVH-oriented metric. QA results of any calculated plan has been correlated with the distance between the clinical couple and the optimal one. Finally a sensitivity analysis has been performed to assess a relation between the results of pre-

treatment QA and the minimum number of clinical couples (DLG,TF) needed to ensure the acceptance of all plans.

Results: The optimal couple of (DLG,TF) was found to vary with MLC motion complexity: as the MLC apertures became smaller and more irregular DLG and TF increase. As a consequence the optimal value of (DLG,TF) vary with district from (2mm,1.7%) for prostate plans to (2.35mm,1.9%) for H&N ones. Despite this rough classification, some differences within the same district can arise when target volumes are significantly different from typical values.Because of this differences the use of a single couple (DLG,TF) can lead to mean dose deviations as large as 5% between planned and delivered dose. In our case three different (DLG,TF) couples were found to be enough to ensure a local gamma (3%,3mm) passing rate larger than 95% for each plan.Once a significant database has been collected the optimal couple (DLG,TF) to be used for a new plan can be a priori decided considering the anatomical district. The choice can be then confirmed after a single optimization process computing the optimal couple for that plan and evaluating the distance from the clinical couple to foresee the expected degree of dosimetric agreement.

Conclusion: Our work shows that a single optimal couple (DLG,TF) can not be found for all possible clinical plans, but three MLC configurations can be enough to ensure the accuracy of delivered dose. A method to identify the group of MLC configurations is proposed together with indications about how to identify the appropriate couple to be used for any plan.

PO-0832

Preliminary scanning water phantom data for beam characterisation of a hybrid MRI-Linac

S. Woodings[1], H. Van Zijp[1], T. Van Soest[1], P. Woodhead[2], M. Duglio[2], N. Marinos[2], S. Pencea[2], D.A. Roberts[2], J. Kok[1], J.W.H. Wolthaus[1], B.W. Raaymakers[1]
[1]*University Medical Center Utrecht, Radiotherapy, Utrecht, The Netherlands*
[2]*Elekta Limited, Linac House, Crawley, United Kingdom*

Purpose or Objective: An Elekta MR-Linac (MRL) prototype has been installed at the author's institute, combining 1.5 T magnetic resonance imaging (Philips) with linear accelerator treatment (Elekta). A novel method for alignment and use of a scanning water phantom has been established. The first data of sufficient precision and quantity to characterize the beam has been acquired in a 1.5 T magnetic field for the purposes of beam modelling and/or beam verification.

Material and Methods: The isocentre is located at 143.5 cm from the linac target and is within an enclosed MRI-like bore which affects the use of a water phantom. A prototype MR-compatible water phantom (PTW) was used to acquire percentage depth doses, inline and crossline scans, relative output factors and collimator scatter factors with a CC04 ion chamber (IBA) and a micro-diamond detector (PTW). An exit PDD showing the electron return effect was also acquired. Position and orientation of the phantom was established using radio-opaque markers and a gantry-mounted electronic portal imaging device.
Linac-specific parameters such as gantry tilt, EPID rotation and isocentre location were independently checked using the water phantom.

Results: The beam energy is consistent with a nominal 7.3 MV photon beam (TPR 0.702), however the depth of maximum dose is 13 mm, closer to the surface than in a standard field due to the 1.5 T magnetic field. Inline profiles are generally consistent with those of a standard flattening-filter-free beam, however the crossline profiles are clearly distinct with an off-axis shift and asymmetric penumbral shoulders and feet due to the Lorentz force of the magnetic field on the secondary electrons. Small field data were acquired taking into account the dose-shift due to the magnetic field. The relative output factors are consistent with those from a standard FFF beam, with no evidence of abnormal variation for small fields.
Final results will be presented.

Conclusion: Practical use of a scanning water tank has been established in an MRL. The data presented here comprises the first substantial collection of MRL data that can be used for beam characterization. The dataset is suitable for calculating relative doses and testing planning system model performance in a 1.5 T magnetic field.

Poster: Physics track: Radiation protection, secondary tumour induction and low dose (incl. imaging)

PO-0833

Measured neutron spectra & dose: craniospinal irradiation on single-room passively scattered proton

R. Howell[1], E.A. Burgett[2], D. Isaccs[2], S.G. Price Hedrick[3], M.P. Reilly[3], L.J. Rankine[3], K.K. Grantham[3], S. Perkins[3], E.E. Klein[3]
[1]*UT MD Anderson Cancer Center Radiation Physics, Radiation Physics, Houston- TX, USA*
[2]*Idaho State University, Nuclear Engineering, Pocatello, USA*
[3]*Washington University, Radiation Oncology, St. Louis, USA*

Purpose or Objective: Secondary neutron dose is of particular concern in proton craniospinal irradiation (CSI) as this treatment is primarily used to treat children and adolescents, who are at significant risk of developing radiation-related late effects. While Monte Carlo techniques have been used to calculate such data for proton CSI, doses that are based on spectra measurements are lacking in the literature. Furthermore, the existing data are only reported for one of the proton beamline manufacturers. Given that doses from externally generated neutrons are highly dependent on the design of the proton therapy machine itself and treatment-specific devices within the beamline, there is a need to report doses for all beamlines used to treat proton CSI. Single-room compact proton systems are particularly noteworthy as many units are currently operational and more are being commissioned and installed. Therefore, the objectives of the present study, for a typical passively scattered proton CSI treatment, were to measure the secondary neutron spectra and calculate dose equivalents for neutrons delivered via a single-room compact system.

Material and Methods: Secondary neutron spectra were measured using extended-range Bonner spheres for three different clinical CSI proton fields, including their respective brass apertures: whole brain, upper spine, and lower spine. For each field, measurements were repeated with an active scintillator and 18 different moderating. Measurements were performed with a water phantom at isocenter and the detector located at 50 cm from the isocenter along the patient plane. For each set of measurements, neutron spectra were determined by mathematical deconvolution of detector count rates. Ambient dose equivalents [H*(10)] were calculated using ICRP-74 conversion coefficients to the fluence spectra.

Results: The measured neutron spectral fluence and H*(10) for each field are shown in Figure 1a and 1b, respectively. The energy distributions for each of the fluence spectra were similar, with a high-energy direct neutron peak, an evaporation peak, a thermal peak, and an intermediate continuum between the evaporation and thermal peaks. Neutrons in the evaporation peak made the largest contribution to the dose equivalent. The, H*(10) in mSv per proton Gy to isocenter were 3.94, 2.79, and 2.71 respectively, for the brain, upper spine, and lower spine fields. Neutron fluence and H*(10) were approximately 1.6 times higher for the brain field than for the spine fields, which is attributed to the greater range and modulation for the brain field than for the spine fields.

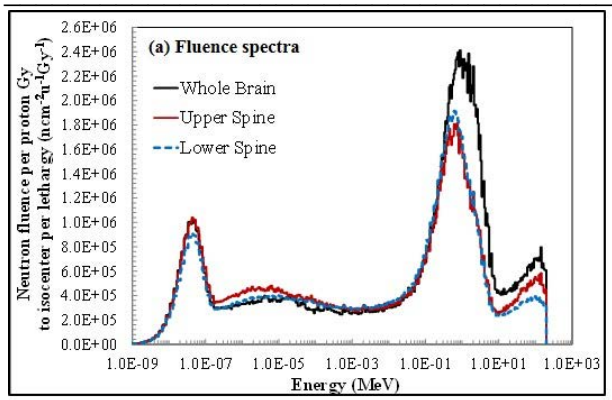

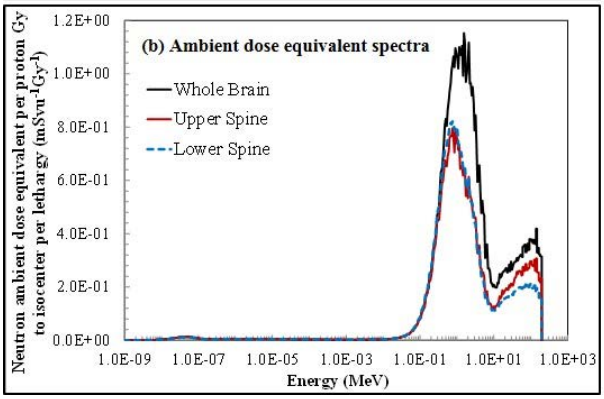

Conclusion: We measured neutron spectra and calculated neutron dose equivalents for a clinical treatment for a single gantry proton system, whose use and planned installations have recently increased. Data reported here are consistent with dose equivalents reported for CSI carried out with other proton therapy beamlines.

PO-0834

Calibrating absolute malignant induction probabilities into life-time attributable risk

A. Madkhali[1,2], C. Timlin[3], M. Partridge[1]
[1]*University of Oxford, CRUK/MRC Oxford Insitute for Radiation Oncology, Oxford, United Kingdom*
[2]*King Saud University, College of Medicine - Department of Medicine, Riyadh, Saudi Arabia*
[3]*University of Oxford, PTCRi, Oxford, United Kingdom*

Purpose or Objective: More than half of cancer patients receive radiotherapy for radical or palliative purposes. Increasing survival rates in cancer patients make it important to study late side-effects, including secondary radiation-induced cancers. Although a number of predictive models exist, the absolute accuracy of these models in the radiotherapy dose range is limited partly due to scarcity of data and partly by extrapolation beyond historical data bounds. The aim of this work is to investigate conversion of malignant induction probabilities, which provide useful relative risk estimates, into absolute life time attributable risk estimates (LAR) and excess absolute risk (EAR) by calibrating and benchmarking our models using published outcome data.

Material and Methods: An in-house modelling tool, which calculates voxelwise risk estimates from patient-specific 3D dose distributions, was modified to generate linear-no-threshold (LNT) model-based risk estimates for the whole body and per organ using organ-equivalent dose. Second cancer risk was calculated for uniform whole-body exposure of 0.1 Gy for comparison with tabulated BIER VII data. Model parameters initially used were taken from existing published reports for the relevant models. The calculated LAR was then compared to the BIER VII results and the linear coefficient, λ, was adjusted to make the model prediction better match the BEIR VII result. A similar calibration of parameters was then performed for the linear quadratic (LQ) and linear model (LIN) malignant induction coefficients. EAR was calculated for a dose range to compare results with published data.

Results: After calibration, calculations of LAR for single uniform exposure of 0.1 Gy produced a value of 837 cases per 100,000 for an exposure at age of 40, in comparison to 824 according to BIER VII report. Averaging over ages at exposure of 20 to 80 produced a value within 5% of the BIER VII report. Calculations of EAR for a dose range relevant to RT of 1-6 Gy using the LIN model were always within the range of uncertainty due to differences in RBE neutron value in the independent published Hodgkin Lymphoma data (Schneider et al, 2008).

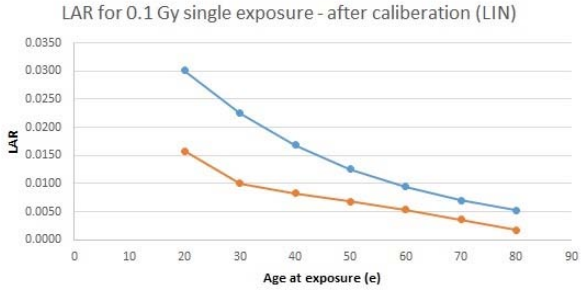

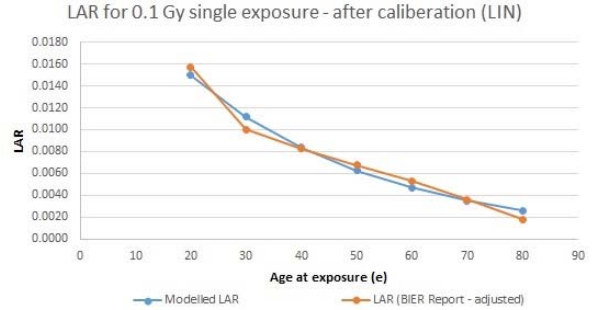

Conclusion: These results show that our models can produce absolute LAR estimates for secondary cancer which are consistent with the values reported in the BEIR VII report for uniform irradiation to 0.1Gy. The comparison of our results of EAR using LIN model to published data showed agreement with independent published data of HL.

PO-0835

A system for measuring and calculating neutron doses in paediatric proton patients

R. Schulte[1], S.D. Clarke[2], E. Pryser[2], B.M. Wieger[2], M. Norsworthy[2], S.A. Pozzi[2], R. Hälg[3], A. Lomax[3], V. Smyth[4], A. Ottolenghi[4]
[1]*Loma Linda University, Division of Radiation Research, Loma Linda, USA*
[2]*University of Michigan, Nuclear Engineering and Radiological Sciences-, Ann Arbor, USA*
[3]*Paul Scherrer Institut, Center for Proton Therapy-, Villigen, Switzerland*
[4]*University of Pavia, Physics, Pavia, Italy*

Purpose or Objective: There is increased use of proton therapy in pediatric cancer patients. In treatment planning, neutrons produced in the treatment delivery system and the patient are usually ignored and not documented. The goal of this ongoing project is to develop and establish a system for measuring and simulating 3D neutron and gamma radiation fields of passively scattered and actively scanned proton beams using representative clinical proton fields impinging on tissue-equivalent phantom materials. Eventually this should lead to a standardized approach for calculating organ neutron doses in paediatric proton patients.

Material and Methods: The neutron dosimetry consists of neutron and gamma fluence measurements with an array of three organic scintillators positioned 70-80 cm lateral to blocks of tissue equivalent materials (soft tissue and compact

bone, CIRS) which are at isocenter and irradiated with therapeutic protons beams. The tissue equivalence of the irradiated materials for neutron doses (per incident proton) and energy spectra has previously been established with Geant4 simulations. Pulse shape discrimination is used to classify each detected pulse as either a neutron or a gamma ray, which allows selective analysis of the neutron and gamma ray spectra. Data are acquired using a digital measurement system based on a CAEN DT5720 waveform digitizer (12 bit, 250 MHz). The response of the scintillators is also simulated using a detection post-processor distributed with a modified version of MCNPX (PoliMi code). To validate the code, the total simulated neutron pulse height distributions scaled to the absolute fluence recorded during the measurements is compared with the measured distributions from the scintillators.

Results: There was good agreement (within 10%) of neutron dose and energy spectra for investigated tissue equivalent materials when compared to ICRP human tissues. So far measurements have been performed at three different proton treatment centers and measurements at two additional centers are planned, thus testing the system on a range of contemporary proton beam accelerators and beam delivery systems. Good agreement was found between the detector responses and Monte Carlo simulations. Using MCPNX, it was shown that the secondary neutron field can be separated into two distinct components; an isotropic, low-energy component and a forward-directed, high-energy component.

Conclusion: The neutron dosimetry system is applicable to any proton facility and will be valuable for prospective data collection of neutron doses and second cancer risk evaluation, thus establishing the dosimetric basis for a prospective clinical data base for paediatric proton patients.

PO-0836

Low dose out-of-field radiation: calculation, measurement and radiobiological impact on cells

M. Kruszyna[1], S. Adamczyk[1], A. Skrobala[2], M. Skorska[1], W. Suchorska[3], K. Zaleska[3], A. Konefal[4], A. Kowalik[1], W. Jackowiak[5], J. Malicki[2]

[1]*Greater Poland Cancer Centre, Medical Physics Department, Poznan, Poland*

[2]*Medical Science University, Electroradiology Department, Poznan, Poland*

[3]*Greater Poland Cancer Centre, Medical Physics Department-Radiobiology Laboratories, Poznan, Poland*

[4]*Silesian University, Department of Nuclear Physics and its Applications- Institute of Physics, Katowice, Poland*

[5]*Greater Poland Cancer Centre, Ist Radiotherapy Department, Poznan, Poland*

Purpose or Objective: The study presented here is three-part work whose primary aims were to determine a) the properties of the scattered radiation responsible for out-of-field doses b) the out-of-field radiation doses at varying distances from the primary beam, and c) the impact of these doses to biological response of in-vitro cells.

Material and Methods: We developed a purpose-designed water phantom to study out-of-field radiation. The phantom consists of seven dual-purpose inserts that can be used to measure doses and to assess radiobiological effects at the same measuring points. The photon (6 MV) energy spectra were calculated at 5 unique positions (at depths of 0.5 1.6, 4, 6, 8, and 10 cm) along the central beam axis (CAX) and at six different off-axis distances. To gain a better understanding of out-of-field doses, we measure the individual contribution of photons and neutrons to the total out-of-field dose for 6 MV and 20MV photons at open beam. Radiation doses were measured at 6 separate points in the phantom with TLD 100, TLD 600, TLD 700, and Gafchromic EBT films. Cells from the human breast cancer line MDA-MB-231 were inserted in a water phantom and irradiated at CAX and off-axis distance, at varying doses (1.5, 2.0, 2.5, 3.0 Gy). Survival fraction, number of DNA double strand-breaks (DNA DSBs), and cleaved PARP levels were determined by clonogenic assay and flow cytometry.

Results: Measured Monte Carlo simulations showed that mean radiation energy levels drop rapidly beyond the edge of the 6 MV photon beam field (Table 1). Simulations showed that the energy level actually increased slightly in some cases as the distance from the field edge increased. At a prescribed dose of 75 Gy to the isocentre, the measured photon dose level in the close-to-field area could reach up to 2.0-2.5Gy for 6MV and 1.5-2.0Gy for 20MV. Although the dose decreased rapidly as the distance from the CAX increased, even distant doses could reach several cGy when photons were used (Fig. 1). The neutron dose for 20 MV photons at a distance of 25 cm from the isocentre was 3.5 mSv/Gy. A slight non-significant decrease of 3-5% in cell SF was observed in cells irradiated outside the primary field.

Table 1. The mean photon energy at depths of 0.5, 1.6, 8 and 10 cm on the central axis (0 cm) and at 10, 15, 20, 25, 30 and 35 cm from the CAX at open (10x10 cm) beam.

	Mean energy [MeV]						
	Distance from beam central axis [cm]						
Depth [cm]	0	10	15	20	25	30	35
0.5	1.514	0.296	0.248	0.295	0.275	0.214	0.279
1.6	1.456	0.319	0.205	0.252	0.221	0.250	0.234
8.0	1.181	0.239	0.241	0.174	0.201	0.204	0.225
10.0	1.178	0.278	0.245	0.186	0.204	0.213	0.247

Figure 1. Dose measurements outside the field of radiation for 20 MV photon energy.

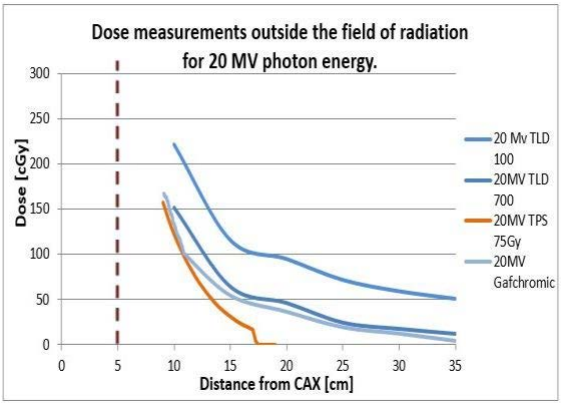

Conclusion: The dose levels measured in this study strongly suggest that out-of-field doses (especially for 20 MV) should be taken in consideration to obtain radiation protection of patients, as these dose levels could increase second cancer risk. Scattered irradiation appears to induce an in vitro biological response on out-of-field cells.

Poster: Physics track: Treatment plan optimisation: algorithms

PO-0837

Automatic treatment planning improves clinical quality of Head and Neck cancer treatments

C.R. Hansen[1], I. Hazell[1], A. Bertelsen[1], R. Zukauskaite[2,3], N. Gyldenkerne[3], J. Johansen[2,3], J.G. Eriksen[2,3], C. Brink[1,3]

[1]*Odense University Hospital, Laboratory of Radiation Physics, Odense, Denmark*

[2]*University of Southern Denmark, Institute of Clinical Research, Odense, Denmark*

[3]*Odense University Hospital, Department of Oncology, Odense, Denmark*

Purpose or Objective: Treatment plans for head and neck (H&N) cancer are highly complex due to multiple dose prescription levels and numerous organs at risk (OAR) close to the target. The plan quality is inter-planner dependent since it is dependent on the skills and experience of the dosimetrist. This study presents a blinded clinical comparison

of automatic (AU) and manual (MA) generated H&N VMAT plans created for clinical use.

Material and Methods: All patients (n=30) referred to curative H&N radiotherapy in August and September 2015 were planned with a MA and AU VMAT plan in Pinnacle version 9.10. Half of the tumours were located in the pharynx (15) and the rest were mixed between larynx (4), oral cavity (3), salivary glands (2), thyroid gland and unknown primary (4). The plans followed national guidelines, and planning techniques were blinded before clinical evaluation of senior oncologists. The MA plans were optimized according to standard clinical practice. The AU plans were created by the Autoplan software available in the Pinnacle planning system. After AU optimisation, slight manual fine-tuning of the plans was performed. To supplement the clinical evaluation the operator time for the dosimetrist was recorded along with DVH parameters and the global detector pass rate (3% and 3mm) of the delivered plans on an ArcCheck phantom. All statistical analyses were performed with a paired Wilcoxon-signed rank test.

Results: In 29/30 plans, the AU plan was chosen for clinical application ($p<0.001$). In terms of DVH parameters similar target coverage was obtained between the two planning methods. As seen in the table, mean OAR doses were significantly reduced in the AU plans for all organs. The mean reduction ranged from 0.5 Gy for the entire patient to 6.5 Gy for the contralateral submandibular gland. Differences in DVH showed significant AU superiority in the dose range 10 Gy to 45 Gy for all organs (Mean DVH example shown in figure). The only manual plan selected for clinical use was a thyroid cancer plan involving level VII lymph nodes and therefore included a large volume of the lung, which had a lower lung dose in the manual plan. The AU plans were more modulated as illustrated by the increase in MUs, which might cause the reduced, but still clinically acceptable, pass rate of 97.7% in ArcCheck measurements. The increased beam-on time of 4 sec is clinically unimportant. Mean operator time spent on MA plans was more than twice that of AU plans. The target homogeneity, conformity and dose fall off were all superior in the AU plans.

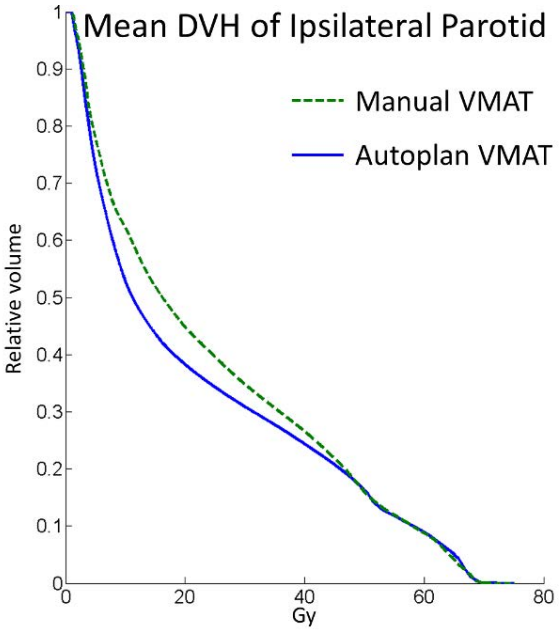

		Autoplan		Manual		
Mean Target dose	Unit	Mean	SD	Mean	SD	P
PTV68	Gy	67.9	0.3	67.6	0.6	0.06
PTV66	Gy	65.9	0.8	65.5	0.8	<0.001
Mean OAR dose						
Spinal cord	Gy	20.2	6.9	22.9	5.8	<0.001
Brainstem	Gy	3.5	4.0	5.1	4.7	<0.001
Oral cavity	Gy	31.6	13.3	34.3	12.8	<0.001
Libs of mouth	Gy	12.3	7.7	15.2	6.8	<0.001
Parotid Ipsi	Gy	23.4	16.4	25.5	15.7	<0.001
Parotid Contra	Gy	18.5	8.1	20.5	8.8	0.004
Submand Ipsi	Gy	53.2	11.4	56.0	7.7	0.014
Submand Contra	Gy	34.0	19.2	40.5	18.9	<0.001
Mandible	Gy	30.2	9.4	32.3	8.9	<0.001
Thyroid	Gy	34.6	13.3	37.1	11.2	<0.001
Larynx	Gy	39.1	9.4	44.8	8.7	<0.001
Body	Gy	9.3	3.0	9.8	2.9	<0.001
Delivery						
MU	MU	435	79	360	56	<0.001
Operator time	Min	64	31	32	26	<0.001
Beam on time	Sec	113.8	22.3	110.1	24.0	0.017
Pass rate (3%,3mm)	%	97.7	1.7	98.4	1.7	0.0011

Conclusion: All AU and MA plans were of acceptable clinical quality, however, AU plans resulted in reduced doses to all OAR and required less operator time in the planning process. AU plans were almost consistently preferred by senior head and neck cancer specialists. The dosimetric superiority of the AU plans was evident.

PO-0838

Impact of dosimetric outliers on the performance of a knowledge-based planning system

A. Delaney[1], J. Tol[1], M. Dahele[1], J. Cuijpers[1], B. Slotman[1], W. Verbakel[1]

[1]*VUMC, Radiotherapy, Amsterdam, The Netherlands*

Purpose or Objective: RapidPlan (Varian Medical Systems) is a knowledge-based planning solution based on a model derived from a library of previous treatment plans. The model utilizes the geometric features and associated dosimetry of these plans to predict a range of achievable dose volume histograms (DVHs) for each organ at risk (OAR) of a new patient. RapidPlan (RP) drives the VMAT or IMRT optimization process by placing a line of optimization objectives along the lower boundary of the DVH prediction range. Planning inconsistencies may lead to sub-optimal plans in the model, which can be identified as dosimetric outliers. Outlier cleaning is advised, however this is time consuming and often subjective. We examined the effect of model cleaning and increasing numbers of dosimetric outliers in a model library, on RP plan quality.

Material and Methods: 70 head and neck cancer treatment plans (planned consistently using the same departmental objective priorities) were used to populate uncleaned ModelUC. Statistical metrics provided by RP were used to identify geometric/dosimetric outliers in ModelUC which were then visually assessed and, if appropriate, removed to create cleaned ModelC. The last 5-40 patients (increments of 5) of ModelC were then re-planned with no attempt to spare the salivary glands, and afterward re-introduced to ModelC, creating Model5-40. All models were used to create plans for a 10 patient evaluation group. Although RP can generate OAR objective priorities, for this study, the same standard priorities were used as for the plans in ModelUC. Plans were compared on the basis of generated prediction ranges, boost/elective target volume homogeneity index (HIB/HIE), mean dose to the oral cavity (OC) and to composite structures comprising the salivary glands (compsal) and swallowing structures (compswal).

Results: On average, outlier cleaning (ModelUC vs ModelC) had minimal impact on HIB/HIE and OAR sparing, although in 1/10 patients, outlier removal resulted in substantial deteriorations to the sparing of two swallowing OAR (>10Gy increase). Adding 5/10 outliers to the model marginally improved average compsal while increasing the number of outliers to 40 led to a 3.9Gy increase in compsal (Table). The increase in OAR dose, even with 40 outlier plans added to the model, was modest compared to the average increase of 14.9Gy in compsal, in the outlier plans themselves. This is due to the placement of optimization objectives along the lower boundary of the DVH prediction range, which progressively widened with the addition of outliers.

Knowledge Based Plan	HI_B(%)	HI_E(%)	Oral Cavity (Gy)	$Comp_{sal}$ (Gy)	$Comp_{swal}$ (Gy)
$Model_{UC}$	9.4 ± 1.5	14.7 ± 1.5	20.5 ± 8.4	21.4 ± 4.7	27.9 ± 6.0
$Model_C$	9.4 ± 1.3	14.3 ± 1.1	20.6 ± 9.0	21.3 ± 4.6	28.3 ± 6.0
$Model_{10}$	9.6 ± 1.6	14.6 ± 1.6	21.1 ± 9.7	20.7 ± 5.0*	27.9 ± 6.0
$Model_{20}$	9.4 ± 1.3	14.6 ± 1.4	20.0 ± 8.5	22.2 ± 5.8	27.6 ± 6.2
$Model_{30}$	8.9 ± 1.3	14.1 ± 1.3	19.6 ± 8.4	23.8 ± 5.8*	27.5 ± 6.0*
$Model_{40}$	9.1 ± 1.2	13.5 ± 1.4*	19.6 ± 8.2	25.2 ± 6.9*	27.4 ± 6.3

Rapidplan results, averaged over the 10 patient evaluation group, using the uncleaned model($Model_{UC}$), cleaned model($Model_C$) and outlier models($Model_{10-40}$). Mean OAR doses are reported.

* Indicates a statistically different ($p \leq 0.05$) value from $Model_C$ plan.

Conclusion: This study reveals that extensive outlier cleaning from this large model comprising 70 consistently made plans had limited impact on the performance of RP. Furthermore, the replacement of >20 plans with those in which the salivary glands were not spared only modestly deteriorated RP performance. In summary, RP demonstrated robustness for moderate proportions of salivary gland dosimetric outliers.

PO-0839

Clinical simulation of nodal boosting in cervix cancer using reduced margin and coverage probability

A. Ramlov[1], M.S. Assenholt[1], M.F. Jensen[1], C. Grønborg[1], R. Nout[2], L. Fokdal[1], M. Alber[1], K. Tanderup[1], J.C. Lindegaard[1]

[1]*Aarhus University Hospital, Department of Oncology, Aarhus C, Denmark*

[2]*Leiden University Medical Center, Department of Radiation Oncology, Leiden, The Netherlands*

Purpose or Objective: We examined the feasibility of reducing PTV margin when using a simultaneous integrated boost (SIB) of pathological lymph nodes in locally advanced cervical cancer. Additionally the clinical performance of a coverage probability (CovP) planning strategy was investigated.

Material and Methods: 25 previously treated patients with regional lymph node metastases were included. All patients were treated with whole pelvic EBRT (45 Gy/25 fx) using IMRT or VMAT. Nodal GTV contouring was based on MRI in supine treatment position. A CTV-N was constructed based on the combined (fused) nodal GTV-N contoured on MRI and PET-CT. Treatment planning was performed in Eclipse with three margin strategies for the SIB: 1) 10 mm GTV-PTV margin (ICRU PTV10mm plan), 2) 5 mm CTV-PTV (ICRU PTV5mm plan) and 3) 5 mm CTV-PTV margin using CovP (CovP plan). Constraints for the ICRU plans (1+2): PTV coverage of 95-107% of prescribed dose. Running a number of CovP plans in the research dose planning software Hyperion developed dose constraints for CovP planning in Eclipse. CovP dose constraints: PTV5mm D98 >90%, CTV D98 > 100% and a soft constraint of CTV D50 > 101.5% of prescribed dose (Figure 1). Dose prescription for SIB was 55 Gy/25 fx in the true pelvis and 57.5 Gy/25 fx above true pelvis. Daily image-guidance with cone beam CT (CBCT) and couch correction based on bony fusion was used systematically. GTV-N was contoured on every second or third CBCT scan and the contour transferred to the planning CT. The accumulated dose for each node was determined in terms of D98 and Dmax. Finally, the volumes of body, bones and bowel receiving >50 Gy (V50) were calculated directly from organs at risk (OAR) contours on the planning CT.

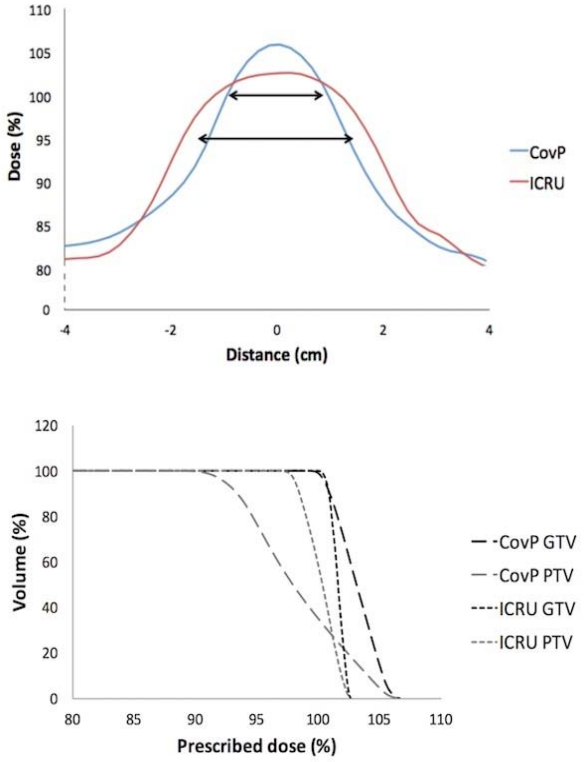

Results: In total 47 lymph nodes were boosted of which 41 (87%) were visible on CBCT. Median number of nodes per patient was 2 (range 1-4). Median GTV D98 and Dmax (%) are listed in Table 1. All nodes treated with ICRU plans had a D98 above 98% and no difference was found between the ICRU plans with regard to target coverage. For CovP the D98 was significantly lower but Dmax significantly higher when compared to the two ICRU plans. Only one node positioned in the true pelvis had a D98 below 95% using CovP. In this patient, bladder filling varied during EBRT, which resulted in large shifts of GTV-N. V50 of body, bones and bowel were significantly lower ($p<0.001$) with the 5mm margin strategy. A further significant reduction was seen with the use of CovP ($p<0.001$).

	ICRU PTV_{10mm}	ICRU PTV_{5mm}	CovP
PTV volume (cm^3)	19.9 (9.2-98.5)	8.4 (2.9-62.7)	-
GTV D98 (%)	100 (98 - 102)	100 (99- 102)	99 (93 - 101)
GTV Dmax (%)	102 (101 - 104)	102 (99 - 103)	104(101 - 107)
Body volume > 50 Gy (cm^3)	75 (32 - 315)	48 (16 - 209)	27 (12 - 122)
Bones volume > 50 Gy (cm^3)	7(0-50)	2 (0-25)	1 (0-8)
Bowel volume > 50 Gy (cm^3)	4 (0-106)	2 (0-68)	1 (0-35)

Conclusion: Pathological nodes are visible on CBCT in the majority of patients with locally advanced cervical cancer. Sequential analysis of CBCT taken during EBRT shows that nodal boosting by use of SIB and CovP is clinically feasible providing an increased central dose in the nodes, full target coverage and a significant reduction in near by OAR volumes treated to high doses. CovP based SIB using the above planning aims are now standard at our institution for nodal boosting and will be implemented in the forthcoming Embrace II study.

PO-0840

Voxel-based ΔTCP distribution:a tool to study the impact of dose distributions in tumour outcome

D. Fabri[1], B. Sánchez-Nieto[1], A. Gago[1], I. Espinoza[1], A. López-Medina[2]

[1]*Pontificia U-dad Catolica de Chile, PHYSICS, Santiago, Chile*
[2]*Galaria-Hospital do Meixoeiro-Complexo Hospitalario Universitario de Vigo, Medical Physics Department and Radiological Protection, Vigo, Spain*

Purpose or Objective: The aim of this study is to create a tool to evaluate the effect of radiosensitivity parameterization and dose distributions on the local Tumour Control Probability (TCP). This tool will be an extension of the ΔTCP method by Sánchez -Nieto and Nahum1 without missing the spatial information associated to the dose volume histograms (DVH)

Material and Methods: In ref [1] it was shown, that the use of a voxel control probability (VCP) distribution is not a correct approach to discretize the effect on TCP of dose inhomogeneity throughout the tumour. Alternatively, the concept of the ΔTCP using the information of the bins of the DVH was proposed and proved to be a better solution.
Based on this concept and due to the advances made on the last 15 years in terms of computational calculation time, access to individual patient information regarding radiosensitivity and 3D dose distribution maps, we propose a ΔTCP voxel-based model.
The first step for generating the mentioned distribution map is to identify, by means of functional images, three regions with different oxygenation status (normoxic, hypoxic and necrotic regions) to which oxygenation histograms [2] are assigned. Secondly, a radiosensitivity value α is initially assigned to the system and modified for every voxel taking into account the oxygen parametrization (α'). Moreover, patient-to-patient variabilities are considered using a σα around the initial value so that the final distribution of effective radiosensitivity values (i.e., including the oxygen status) produce a response curve with a clinically meaningful steepness. Then, VCPs are calculated for the planned dose distribution according to the expression in [1]. A second set of VCPs are calculated for a different reference dose distribution (e.g., a completely homogeneous dose through the tumour or an optimized one after a dose painting approach).
Finally, theΔTCP for every (i,j,k) voxel, representing the impact on the final TCP of that voxel having a tested dose (Dt) instead the reference one (Dr) is computed as:
$\Delta TCP_{ijk}=\Sigma_x TCP(\alpha'x)\,[1-VCP_{ijk}(\alpha'x, Dr)/VCP_{ijk}(\alpha'x, Dt)]$
Where α'x the oxygen-corrected initial α value and TCP(α'x) is calculated as the multiplication of all the VCPs for α'x , for the tested dose distribution.

Results: The tool was tested using a H&N patient from Artfibio project[3]. As a result theΔ TCP distribution shown on the image was obtained. A dose distribution chosen to have a low local control (to highlight the tool functionality) and as reference an homogeneous 2 Gy dose per fraction to the GTV for 32 fractions were used.

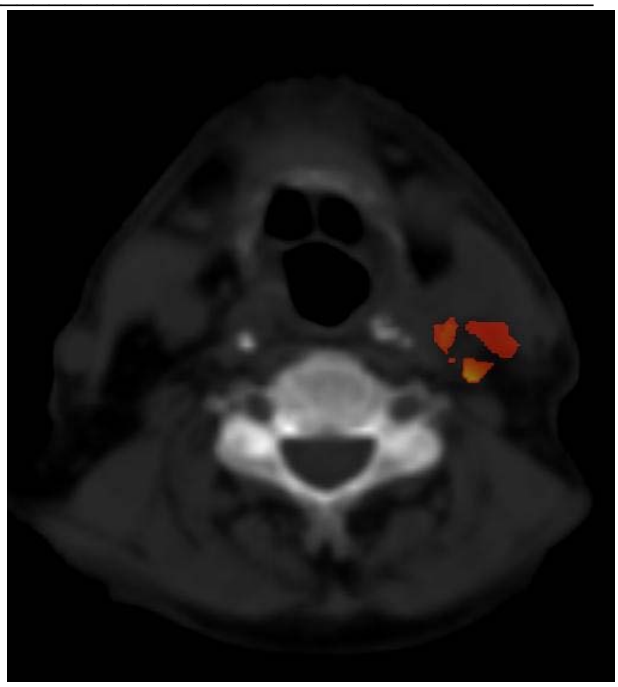

Conclusion: It was shown that this could be a useful tool. As expected due to the small influence of single voxel dose variabilities on the total TCP, it is necessary to think on a future steps using megavoxels define within a certain threshold of oxygen level, dose and any relevant parameter.
References.
1 IJROBP 44(2):369-380,1999
2 Med. Phys. 40, 081703 (2013)
3 Comput Math Methods Med. 2015:103843

PO-0841

Cranial stereotactic trajectory optimization via patient-specific overlap atlas

L. MacDonald[1], J.L. Robar[1,2,3], C. Thomas[1,2,3]

[1]*Dalhousie University, Medical Physics, Halifax, Canada*
[2]*Nova Scotia Cancer Centre, Medical Physics, Halifax- Nova Scotia, Canada*
[3]*Dalhousie University, Radiation Oncology, Halifax, Canada*

Purpose or Objective: This study examines potential dosimetric improvements in cranial stereotactic radiotherapy plan quality by using a geometric optimization approach to reduce dose to organs-at-risk.

Material and Methods: Using previously delivered cranial stereotactic radiotherapy plans treated at the Nova Scotia Cancer Centre (NSCC), we have redesigned the treatment geometry to find an optimal couch rotation position based on a two-step process involving novel algorithms which reduce the presence of dose in surrounding organs at risk of exposure (OARs). Maintaining the gantry start/stop orientation from the conventionally designed treatment, the couch position is optimized based on a cost function analysis of accumulation of overlap score from an equation developed by Yang et al. [2] and refined by MacDonald et al. [1]. The score equations are used to generate 2D patient overlap atlases that are inform trajectory design. The algorithm incorporates factors for depth of both organs at risk (OAR) of exposure and target (PTV) volumes, and radiation dose sensitivities of each OAR. A further step is then implemented to focus on an individual OAR in need of further reduction after initial optimization. This algorithm applies an urgent sparing factor to the specified OAR, whose purpose is to maximize dose gradient between OAR and PTV, while minimally affecting the dose reduction effects to others.

Results: The optimization was conducted recursively on twenty plans for previously treated acoustic neuroma patients. Maximum and mean doses to the OARs were reduced by 37.03% ± 2.48% and 42.25% ± 1.62% respectively

with application of the optimization technique when compared to the clinical treatment plans. Secondary optimization of the brainstem with the urgent sparing factor was able to increase further sparing to the brainstem by up to 9.8%, with a subtle effect on the sparing of the remaining of the structures. In addition, PTV coverage was maintained to the same degree as the delivered treatment.

Conclusion: The geometric optimization method allows enhancement of the existing arc geometries, resulting in significant improvements in OAR sparing, without increase to required treatment planning or delivery time.

Poster: Physics track: Treatment planning: applications

PO-0842

Non-coplanar volumetric-modulated arc therapy for craniopharyngiomas reduces doses to hippocampus

M. Uto[1], T. Mizowaki[1], K. Ogura[1], M. Hiraoka[1]
[1]*Kyoto University Graduate School of Medicine, Radiation Oncology and Image-applied Therapy, Kyoto, Japan*

Purpose or Objective: As patients with craniopharyngiomas make good prognoses and as pediatric patients seem to be more sensitive to radiation than adults, irradiation of normal tissue should be minimized. Recent studies suggest that radiation-induced injuries to the hippocampus play important roles in compromising neurocognitive functioning for patients with brain tumors and it could be important to spare the hippocampus using modern planning methods for patients with craniopharyngiomas. In terms of radiation techniques, 3D conformal external beam radiotherapy delivered using dynamic conformal arc therapy (DCAT) and volumetric-modulated arc therapy (VMAT) are clinically employed to treat for patients with craniopharyngiomas. While the use of non-coplanar beams in VMAT of malignant intracranial tumors has recently been reported, no dosimetric comparison has yet been made between VMAT using non-coplanar arcs (ncVMAT) and VMAT employing only coplanar arcs (coVMAT) among patients with craniopharyngiomas. We performed a planning study comparing dose distributions to the planning target volume (PTV), hippocampus, and other organs at risk (OAR) of DCAT, coVMAT, and ncVMAT.

Material and Methods: DCAT, coVMAT, and ncVMAT plans were created for 10 patients with craniopharyngiomas. The prescription dose was 52.2 Gy in 29 fractions, and 99% of each PTV was covered by 90% of the prescribed dose. The maximum dose was held below 107% of the prescribed dose. CoVMAT and ncVMAT plans were formulated to satisfy the following criteria: the doses to the hippocampus were minimized, and the doses to the OAR were similar to or lower than those of DCAT.

Results: The mean equivalent doses in 2-Gy fractions to 40% of the volumes of the bilateral hippocampus [EQD2(40%hippos)] were 15.4/10.8/6.5 Gy for DCAT/coVMAT/ncVMAT, respectively. The EQD2(40%hippos) for ncVMAT were <7.3 Gy, which is the threshold predicting cognitive impairment, as defined by Gondi et al.. The mean doses to normal brain tissue and the conformity indices were similar for the three plans, and the homogeneity indices were significantly better for coVMAT and ncVMAT compared with DCAT.

Figure.

Coronal plains of dose distributions in a representative case and a comparison of the normalized doses covering 40% of the volume of the bilateral hippocampus using DCAT, coVMAT, and ncVMAT.

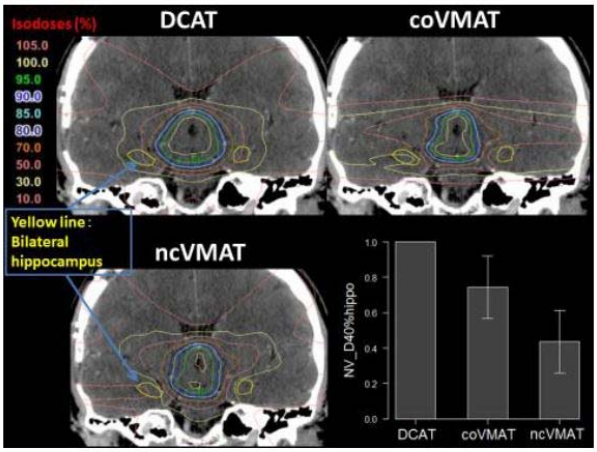

The yellow line shows the contour of the bilateral hippocampus. The normalized value of $D40\%_{hippo}$ indicates that the dose covering 40% of the volume of the bilateral hippocampus was significantly reduced in the following order: ncVMAT, coVMAT, and DCAT (ncVMAT 0.4, coVMAT 0.7, and DCAT 1).

DCAT=dynamic conformal arc therapy, coVMAT=coplanar volumetric-modulated arc therapy, ncVMAT=non-coplanar volumetric-modulated arc therapy, $NV\_D40\%_{hippo}$=normalized value of $D40\%_{hippo}$

Table.

Summary of doses delivered to the bilateral hippocampus and the normal brain and the dose indices, in Gy.

Structure /index	DCAT	coVMAT (Mean±SD)	ncVMAT	P-value (ANOVA)	P-value (DCAT vs. coVMAT)	P-value (DCAT vs. ncVMAT)	P-value (coVMAT vs. ncVMAT)
Bilateral Hippo							
Maximum dose	42.3±9.8	36.2±11.2	30.5±15.0	0.121			
Mean dose	20.7±7.6	15.4±8.1	10.7±8.2	<0.05	0.515	<0.05	0.530
$D40\%_{hippo}$	21.7±8.4	16.2±7.6	10.3±7.9	<0.05	0.406	<0.05	0.326
$EQD_2(40\%_{hippo})$	15.5±7.9	10.8±6.3	6.5±6.0	<0.05	0.41	<0.05	0.51
$NV\_D40\%_{hippo}$	1	0.7±0.2	0.4±0.2	<0.05	<0.05	<0.05	<0.05
Normal brain							
Mean dose	6.8±1.7	6.2±1.5	6.8±1.4	0.563			

If a significant difference was evident when data from the entire cohort were compared via two-way analysis of variance (ANOVA), the Bonferroni post hoc test was performed to compare pairs of modalities.

DCAT=dynamic conformal arc therapy, coVMAT=coplanar volumetric-modulated arc therapy, ncVMAT=non-coplanar volumetric-modulated arc therapy, SD= standard deviation, Hippo=hippocampus.

$D40\%_{hippo}$=dose to 40% of the volume of the bilateral hippocampus.

$EQD_2(40\%_{hippo})$=equivalent dose in 2-Gy fractions (assuming α/β=2) to 40% of volume of the bilateral hippocampus.

$NV\_D40\%_{hippo}$=normalized value of $D40\%_{hippo}$ (the DCAT value was set to unity). The normalized values for coVMAT and ncVMAT were calculated as $D40\%_{hippo}$(coVMAT)/$D40\%_{hippo}$(DCAT) and $D40\%_{hippo}$(ncVMAT)/$D40\%_{hippo}$(DCAT), respectively.

Conclusion: NcVMAT is more appropriate than DCAT and coVMAT for patients with craniopharyngiomas. NcVMAT significantly reduces radiation doses to the bilateral hippocampus (to 50% that of the DCAT) without increasing the doses to normal brain tissue and other OAR.

PO-0843

Dosimetric evaluation of 10 years of treatment planning improvements in head and neck cancer

J. Tol[1], P. Doornaert[1], M. Dahele[1], B. Slotman[1], W. Verbakel[1]
[1]*VU University Medical Center, Radiotherapy, Amsterdam, The Netherlands*

Purpose or Objective: Advances in delivery techniques like intensity modulated radiotherapy (IMRT) and volumetric modulated arc therapy (VMAT) facilitated increased treatment plan complexity, leading to the inclusion of more organs-at-risk (OARs) for sparing. Initial treatment planning

studies typically evaluate whether extra sparing affects boost/elective planning target volume (PTVB/PTVE) dose coverage or homogeneity, sparing of previously included OARs or dose conformity. However, once novel techniques are introduced in routine clinical practice, predicted changes are rarely retrospectively evaluated or confirmed. We therefore analyzed longitudinal changes in plan quality for head and neck cancer (HNC) patients treated at our department from 2005-2015 following the introduction of new technologies and planning techniques.

Material and Methods: 4x30 plans of oropharynx patients were selected from 4 distinct periods (P). P1: 7-field static IMRT plans with parotid gland sparing. P2: Dual arc VMAT plans including submandibular gland sparing. P3: VMAT with swallowing muscle sparing and further attempts to reduce parotid gland / oral cavity doses through manual interactivity during optimization. P4: VMAT with the same OARs as P3, but automatically optimized using in-house developed software. PTVE prescribed doses were 54.25-57.75Gy in P1/P2, and 54.25Gy in P3/P4. 70Gy was prescribed to PTVB for all patients, delivered in 35 fractions as a simultaneous integrated boost. Plans were compared using mean dose to composite salivary glands (Dsal), swallowing muscles (Dswal) and oral cavity (Doc), PTVB/PTVE dose coverage (V95) and homogeneity indices (HI), and V5Gy (volume receiving 5Gy), V30Gy, V50Gy and mean dose to the body contour with PTV subtracted.

Results: The Figure shows mean salivary gland, swallowing muscle and oral cavity DVHs for each period and the Table summarizes the mean dosimetric results. OAR sparing, swallowing muscle sparing in particular (P1=55.0Gy to P4=38.6Gy), gradually improved throughout the periods without compromising PTV dose coverage, homogeneity or conformity indexes. In addition, P3 improved Dsal/Doc over P2 by 6.3/7.5Gy, illustrative of gains facilitated by improved planner experience and planning technique used. Automatically optimized plans (P4) achieved similar OAR sparing, Body-PTV doses and PTV V95/HI values as P3 plans. Although depending on the degree of OAR-PTV overlap, individual OAR sparing could vary between the periods, such differences are inherent to this type of study.

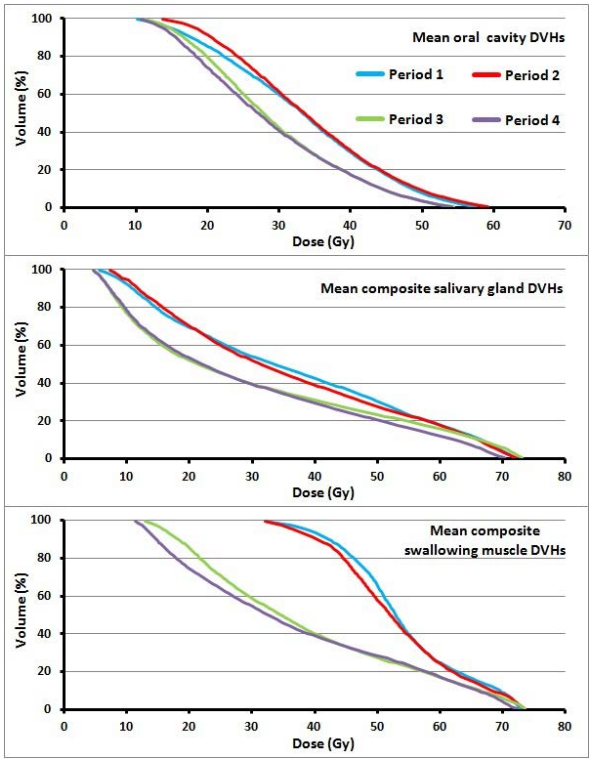

	Period	1 - Parotid gland sparing IMRT	2 - Salivary gland sparing VMAT	3 - Swallowing muscle sparing VMAT	4 - Automatically optimized VMAT
PTVB	V95 (%)	98.1 ± 1.6	98.8 ± 0.9	99.0 ± 0.5 *	98.9 ± 0.2 *
	HI (%)	9.8 ± 1.0	10.0 ± 1.4	10.4 ± 1.1 *	9.7 ± 0.9 #
PTVE	V95 (%)	98.5 ± 1.0	98.2 ± 1.0	97.7 ± 1.2 *	98.2 ± 0.6 #
	HI (%)	13.3 ± 2.1	13.6 ± 2.1	15.8 ± 2.2 * †	13.2 ± 1.4 #
Mean Dose (Gy)	Salivary Glands	41.1 ± 7.1	37.3 ± 7.7	31.0 ± 5.0 * †	31.3 ± 6.4 * †
	Swallowing muscles	55.0 ± 5.7	56.0 ± 8.0	40.8 ± 7.3 *†	38.6 ± 7.9 * †
	Oral cavity	35.3 ± 7.2	36.8 ± 8.2	29.3 ± 7.8 * †	27.5 ± 8.2 * †
Body-PTV	Mean Dose (Gy)	20.5 ± 2.1	20.6 ± 1.9	18.7 ± 1.2 * †	18.9 ± 1.6 * †
	V5Gy (%)	73.8 ± 5.9	79.1 ± 3.1 *	74.5 ± 3.8 †	73.5 ± 4.7 †
	V30Gy (%)	29.7 ± 4.8	29.6 ± 4.9	27.2 ± 2.8 * †	27.2 ± 3.6 * †
	V50Gy (%)	7.4 ± 2.4	7.0 ± 2.4	4.5 ± 0.8 * †	5.3 ± 1.5 * † #

*, †, # : Statiscally significant differences (p<0.05) with respect to period 1, 2 and 3, respectively ANOVA with post-hoc Bonferroni analysis

Conclusion: Successive improvements in radiotherapy technologies and planning techniques substantially improved HNC plan quality. Swallowing muscle sparing did not compromise sparing of other OARs, PTV dose coverage and homogeneity or dose deposition in the remainder of the body. On the contrary, salivary gland doses, HIB/HIE and Body-PTV doses generally decreased in P3/P4 compared to earlier periods.

PO-0844

Dosimetrical advantages of 4D mid-vent: should every LA NSCLC patient be treated this way?

S. Philippi[1], N. Barthelemy[1], M. Devillers[1], P. Nguyen[1], P. Coucke[1], A. Gulyban[1]

[1]C.H.U. - Sart Tilman, Radiotherapy Department, Liège, Belgium

Purpose or Objective: In this study, we aimed to compare the effect of 4D mid-ventilation vs. free breathing 3D CT technique on target volume differences and corresponding dosimetrical changes using intensity modulated radiation therapy (IMRT) for patients with locally advanced non small cell lung cancer (NSCLC). Furthermore, additional investigation was performed to evaluate the possible dosimetrical improvement by using volumetric modulated arctherapy (VMAT) instead of IMRT.

Material and Methods: Twenty-three patients with locally advanced NSCLC were scanned with 4D-CT acquisition for treatment planning purpose. The different breathing phases were analyzed to obtain the tumor motion (direction and amplitude) and to determine which dataset better represents the mid-ventilation phase. Based on the gross tumor volume, two planning target volumes were generated for each patient: One using 15 mm margin in all three directions (PTV-3D) and the other with 12 mm with the margin of 1/4 of the movement (= mid-ventilation approach, PTV-4D). For objective comparison, IMRT plans (3D-IMRT, 4D-IMRT) were made by using Pinnacle v9.0 (Philips, Eindhoven, the Netherlands) with identical optimization parameters. For the 4D mid-vent, additional VMAT plan was generated. All DVH were collected using the VODCA package (Medical Software Solutions, Hagendorn, Switzerland). For the evaluation, the following dosimetric parameters were used: for corresponding PTV coverage using V95%, for lungs-PTV4D (for objective comparison of healthy lung volume) V20Gy and Dmean, for spinal cord Dmax, for oesophagus Dmean, while for heart V35Gy. All 4D plans were verified at the treatment machine following the institutions QA procedure. Differences were tested using the pairwise t-tests with the significance level of $p<0.05$.

Results: Based on the 4D-CT analysis, the average (range) tumor motions were 3.1 (0-11.2) mm for cranio-caudal, 1.7 (0-4.6) mm for antero-posterior and 1.9 (0-4.0) mm for lateral direction. The average PTV volumes were reduced on average with 14% (Table 1).

Mean (SD) cc, % or Gy	3DCT (IMRT)	4DCT (IMRT)	3D vs. 4DCT (IMRT)	4DCT (VMAT)	IMRT vs. VMAT (4DCT)
PTV volume	618 (333)	518 (296)	p<0.01		
PTV V95%	95.2 (3.4)	97.1 (2.7)	p<0.01	97.1 (2.1)	p=0.83
PTV V107%	0.5 (0.5)	0.1 (0.1)	p<0.01	0.2 (0.3)	p=0.06
Lungs-GTV V20Gy	25.6 (5.4)	24.3 (5.5)	p<0.01	22.8 (4.7)	p<0.01
Lungs-PTV4D V20Gy	21.8 (5.3)	20.5 (5.3)	p<0.01		p<0.01
Oesophagus Dmean	21.6 (8.0)	20.9 (8.2)	p=0.02	19.8 (8)	p=0.04
Heart V35Gy	11.8 (10.7)	11.1 (10.2)	p<0.01	8.6 (8.6)	p<0.01

All treatment plans were met the clinically acceptable goals. The 4D-IMRT showed a statistically significant improvement ($p<0.05$) compared to 3D-IMRT in all relevant parameters. The 4D-VMAT plans further reduced all OAR parameters significantly ($p<0.05$), while maintaining identical target coverage. Phantom measurements confirmed that both techniques (IMRT and VMAT) can be safely administered.

Conclusion: By using the 4D-CT acquisition and mid-ventilation target delineation approach, significant PTV volume reduction was obtained. This method is improving PTV coverage and OAR doses using the same technique (IMRT). VMAT technique might further gain additional dosimetric benefits for patients with NSCLC.

PO-0845

Evaluating dosimetric indices in lung SBRT for establishing treatment plan quality guidelines

R. Yaparpalvi[1], M. Garg[1], J. Shen[1], W. Bodner[1], D. Mynamapati[1], H.C. Kuo[1], P.G. Scripes[1], A. Basavatia[1], N. Ohri[1], W.A. Tome[1], S. Kalnicki[1]
[1]*Montefiore Medical Center, Radiation Oncology, Bronx- New York, USA*

Purpose or Objective: We applied a variety of published conventional and stereotactic plan quality dosimetric indices to describe and discern clinically achieved target dose distributions in Lung SBRT.

Material and Methods: Treatment plans of 100 Lung SBRT patients treated were retrospectively reviewed. The targets (n=102) were evenly distributed – right lung (53) and left lung (49). Patients were prescribed to a total dose of 50-60 Gy in 3-5 fractions. Dose optimizations were accomplished with 6 MV using either 2-5 arcs VMAT (90); 8-14 IMRT fields (6) or 10-16 static fields (6). Dose calculations were performed using AAA algorithm with heterogeneity correction. A literature review on dosimetric indices recommended for qualitative analyses of conventional and stereotactic dose distributions in target coverage, homogeneity, conformity and gradient categories was performed. From each patient treatment plan, the necessary parameters for calculating various indices were quantified.

Results: For the study, the mean (±SD) values for indices were: coverage (96.4 (±2.4) %); homogeneity (1.27 (±0.07)); Conformity (1.04 (±0.08)) and Gradient 1.27(±0.30) cm). Geometric conformity (g) strongly correlated with the conformity index (defined by van't Riet /Paddick)($p<0.0001$). All Gradient measures strongly correlated with PTV ($p<0.0001$). Evaluating High Dose Spillage, the average cumulative volume of all tissue outside the PTV receiving a dose of > 105% of prescription dose was 0.94 (± 1.64) %. Considering Low Dose Spillage, the maximum % of prescription dose to any point at 2 cm distance in any direction from PTV was 56.0 (± 11.4) %. The lung volume (total lung volume – GTV) receiving doses of 20 Gy and 5 Gy (V20 and V5) were mean 4.9 % (± 3.1) and 16.9 % (± 9.0). The RTOG lung SBRT protocol advocated conformity guidelines for prescribed dose in all dosimetric evaluation categories were met in ≥94% of cases.

Conclusion: The high-rate of adherence to RTOG protocol dose conformancy guidelines in our study validates that indices derived from our SBRT lung plan dose distributions are a tool for establishing plan metrics in clinical trials, for scoring competing plans and as well as for comparing inter-institutional lung SBRT plan dosimetric data. However, these indices should only be used as an additional tool to grade plan quality once a satisfactory treatment plan has been achieved judged on the basis of clinical expertise, acceptable dose distributions and dose gradients, while respecting critical organ and normal structure doses.

PO-0846

The impact of anatomical changes on the accumulated carbon ion dose in pancreatic cancer patients

A.C. Houweling[1], K. Fukata[2], Y. Kubota[2], H. Shimada[2], C.R.N. Rasch[1], T. Ohno[2], A. Bel[1], A. Van der Horst[1]
[1]*Academic Medical Center, Department of Radiation Oncology, Amsterdam, The Netherlands*
[2]*Gunma University, Gunma University Heavy Ion Medical Center, Maebashi, Japan*

Purpose or Objective: Improvements in overall survival of pancreatic cancer patients after carbon ion radiotherapy have been reported from Japanese clinical trials. Due to the sharp distal dose fall-off, a high dose can be delivered to the tumor, while sparing the nearby healthy organs. However, changes in gastrointestinal gas volumes can greatly influence the carbon ion range.
We evaluated the robustness of carbon ion therapy for pancreatic cancer patients by investigating the impact of interfractional anatomical changes on the accumulated dose when using bony anatomy- and fiducial marker-based position verification.

Material and Methods: Nine pancreatic cancer patients, treated with photon radiotherapy in free breathing, were included in this retrospective planning study. The internal gross tumor volume (iGTV), internal clinical target volume (iCTV), duodenum, stomach, liver, spinal cord and kidneys were delineated on the (average) 4D-CT scan. Intratumoral gold fiducial markers were implanted in all patients to enable position verification using cone beam CT (CBCT).
Treatment plans were created using a 4-beam passive scattering technique. A smearing technique was used to account for patient setup errors; a safety margin of 3 mm was applied to compensate for range uncertainties. Plans were generated to deliver at least 95% of the prescribed dose (36GyE in 12 fractions) to 99% of the iCTV.
To enable dose calculations on the daily CBCTs, the planning CT was deformably registered to each CBCT. The gastrointestinal gas volume visible on each CBCT was copied to the deformed CTs. Next, fraction doses were calculated by aligning the treatment plan according to a bony anatomy- and a fiducial marker-based registration. For both registration methods the resulting fraction doses were rigidly summed to acquire the accumulated dose.
We compared both accumulated doses to the planned dose using dose-volume histograms (DVHs) and calculated DVH parameters for the iGTV and iCTV (Dmean, D2%, D98%) and organs at risk (Dmean, D2cc).

Results: The D98% of the target volumes showed the largest differences (Figure). For the bony anatomy-based registration, D98% reduced significantly from 99.6% ± 0.2% (iGTV; mean ± standard deviation) and 98.6% ± 0.5% (iCTV) as planned to 92.3% ± 3.8% and 81.9% ± 7.7% for the accumulated dose, respectively. For the marker-based registration, this was slightly improved to 95.1% ± 4.0% (iGTV) and 88.6% ± 4.0% (iCTV), which was still significantly different from planned.
For the duodenum, severe deviations were observed in the DVHs between the planned and accumulated dose. Both the direction and magnitude of the deviations differed considerably between patients. The other organs showed minor changes.

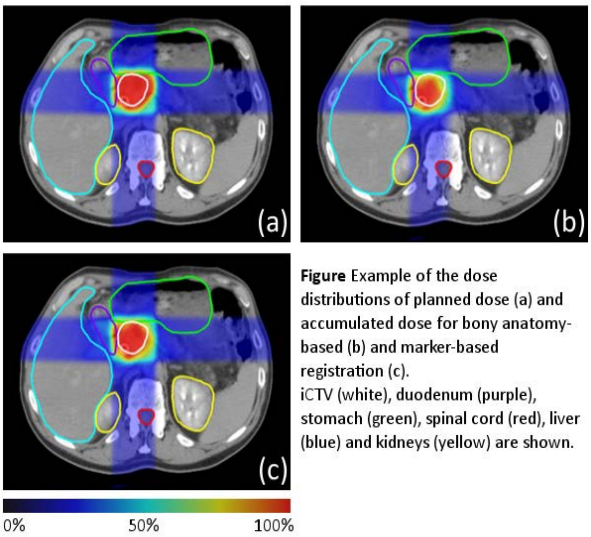

Figure Example of the dose distributions of planned dose (a) and accumulated dose for bony anatomy-based (b) and marker-based registration (c).
iCTV (white), duodenum (purple), stomach (green), spinal cord (red), liver (blue) and kidneys (yellow) are shown.

Conclusion: Severe reductions in target dose coverage were observed as an effect of interfractional anatomical changes. The difference between the position verification methods was a lesser issue compared to the effect of the anatomical changes.

PO-0847

Implementing the new ESTRO guideline for elective breast radiotherapy with the humeral head as PRV

K. Surmann[1], J. Van der Leer[1], T. Branje[1], M. Van der Sangen[1], M. Van Lieshout[1], C.W. Hurkmans[1]
[1]Catharina Hospital, Radiation Oncology, Eindhoven, The Netherlands

Purpose or Objective: The new ESTRO consensus guideline for target delineation for elective breast radiotherapy (Offersen Radiother Oncol. 2015) establish the humeral head and connective tissues 10 mm around it as Planning Risk Volume (PRV). The objective was to implement these guidelines for sparing the humeral head in elective breast radiotherapy with level 1 and 2 (L1/L2) lymph nodes by comparing three different planning techniques.

Material and Methods: Ten patients with left-sided breast cancer were enrolled in a planning study performed in Pinnacle3 v9.8 (Philips). All patients were planned with 16 x 2.66Gy on the breast (PTVp) and the elective L1/L2 lymph nodes (PTVn). We compared three techniques: IMRT with high tangential field (HTF), 6-field IMRT and VMAT. The humeral head PRV (hh+10) was included with an objective of V40Gy < 1cc for all three techniques. Treatment plans were obtained with the inverse planning tool and optimization was achieved by decreasing the dose to the organs at risk (OARs; lungs, heart and right breast) as low as possible while maintaining a PTVp V95% of 97% and PTVn V90% of 95%.
For the high tangential fields, the cranial border of the fields was extended to include PTVn. The leaves of the 5 mm multi leaf collimator were then closed to exclude hh+10 to reduce the dose to the humeral head and the surrounding tissue. This technique is currently used in our clinic. The 6-field IMRT technique consisted of tangential fields and four additional fields (at 330, 20, 80 and 170 degrees) to ensure proper coverage of the cranial part of the breast and the lymph nodes. The cranial border of the tangential fields and caudal border of the four additional fields was set 1cm below the attachment of the clavicle at the sternum. The third technique was a VMAT dualarc from 305 to 180 degrees.

Results: HTF resulted in an average PTVp V95% of 97.2% and an average PTVn V90% of 90.4% (see Table 1). With the additional fields of the 6-field IMRT technique, the coverage of the lymph nodes increased significantly to on average 98.0% ($p = 0.01$) while PTVp did not vary significantly ($p = 0.92$). The doses to the OAR were comparable between the HTF and IMRT technique. The coverage of PTVn increased when using VMAT to an average of 99.5% ($p < 0.01$ compared to HTF and $p = 0.19$ compared to IMRT). The dose to the OAR increased as well. The mean dose to the contralateral breast increased significantly from 0.6Gy with HTF and IMRT to 2.3Gy with VMAT ($p < 0.01$ for both).

Table 1: Dosimetric parameters for the planning target volumes (PTVp and PTVn), planning risk volume (humeral head + 10 mm) and the organs at risk for high tangential fields (HTF), 6-field IMRT and VMAT.
The parameters are given as average (min – max).

	HTF	IMRT	VMAT
PTVp V95% (%)	97.2 (91.8 - 99.5)	97.1 (96.8 - 97.3)	97.0 (96.6 - 97.4)
PTVn V90% (%)	90.4 (73.7 - 98.7)	98.0 (89.5 - 99.9)	99.5 (98.2 - 99.9)
hh+10 V40Gy (cc)	0.45 (0 - 1.02)	0.67 (0 - 1.83)	0.70 (0 - 1.35)
Lungs Dmean (Gy)	4.7 (3.9 - 6.1)	4.8 (3.8 - 5.9)	5.2 (4.2 - 6.8)
Heart Dmean (Gy)	3.3 (1.6 - 6.1)	2.9 (1.6 - 5.7)	3.6 (2.0 - 5.7)
Right breast Dmean (Gy)	0.6 (0.3 - 0.9)	0.6 (0.3 - 0.7)	2.3 (0.6 - 4.2)

Conclusion: The humeral head and surrounding tissues as defined in the new ESTRO guideline can be spared with the 6-field IMRT or VMAT technique. It is not possible through high tangential fields without reducing PTVn coverage.
A 6-field IMRT technique including tangential fields and four additional fields to cover the lymph nodes and the cranial part of the breast leads to adequate coverage of the primary target and the lymph nodes without increasing the dose to the other OARs.

PO-0848

Simultaneous integrated protection (SIP): a new concept for high precision radiation therapy

T. Brunner[1], S. Adebahr[1], E. Gkika[1], A. Zipfel[1], R. Wiehle[1], U. Nestle[1], A. Grosu[1]
[1]Universitätsklinik Freiburg, Department of Radiation Oncology, Freiburg, Germany

Purpose or Objective: Stereotactic radiotherapy near critical serial organs at risk (OAR) requires specific caution to avoid severe toxicity. Current strategies are to (1) to rule out SBRT as a treatment option, (2) to use full dose SBRT and expose patients to higher risks, (3) to homogenously underdose the entire planning target volume (PTV), or (4) to trim PTV margins individually and non-quantifiably. We here describe a novel IMRT prescription method termed simultaneous integrated protection (SIP) for quantifiable and comparable dose prescription to targets very close to dose limiting structures. This work will be focussed on the planning of SBRT.

Material and Methods: For patients with infringement of dose constraints to at least one serial OAR, e.g. central airways, bowel, we defined a planning risk volume (PRV). The intersection volume of the PRV with the total planning target volume (PTV_Σ) was defined as the protection PTV_SIP and the vast non-intersecting majority of PTV_Σ as the dominant PTV (PTV_dom). Radiotherapy treatment planning was performed using IMRT. Dose was prescribed to PTV_dom according to ICRU in 3, 5, 8 or 12 fractions. If in doubt, preference to a higher number of fractions was given as a function of the size of PTV_SIP. D_max was allowed to be up to 130% of the prescribed dose. No specific dose was prescribed to the PTV_SIP but dose was required to stay just within the constraints for the respective OAR. Dose-volume-histogram (DVH) analysis was based on absolute volumes of OARs, not on PRVs.

Results: This method led to a fall off region within PTV_SIP between the PTV_dom and the OAR. We here demonstrate this approach for six patients. Two had lesions in the chest, one in the liver, two in the pancreas and one in the left kidney (Figure 1). Size of the PTVs (PTV_Σ) ranged from 14.5 to 84.9 mL (median 49.2 mL, mean 49.7 mL; Figure 2). Sizes of PTV protection subvolumes (PTV_SIP) ranged from 1.8 - 3.9 mL (median and mean 2.8 mL). Relative PTV_SIP ranged from 2.9% - 13.4% of the size of PTV_Σ (median 7.4%). Noteworthy, the largest ratio, 13.4%, was an absolute volume of 2 mL, only. D_min of the PTV_SIP was significantly lower in patients

1, 2 and 6 due to air within the PTV_SIP volumes compared with the other patients. Safety of the plans was analysed from the absolute volume DVHs (dose to mL). The steepness of dose fall off could be read off by the comparing the doses to the PRVs with those to the OARs. The constraints were respected for the corresponding OARs. All patients had local control at a median follow-up of 9 months and toxicity was low.

Conclusion: SIP-IMRT is shown to result in a median dose of ≥100% to PTV_Σ, to achieve high local control and low toxicity. Longer follow-up is required for verification of these results and a prospective clinical trial is currently testing this new approach in chest and abdomen SBRT.

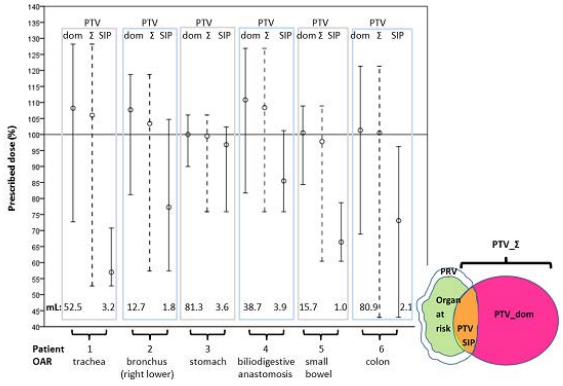

Figure 2
Dose to planning target volumes (PTV) in six patients planned with the SIP concept. For each patient from left to right the non-protection PTV (PTV_dom), total PTV_Σ and protection PTV (PTV_SIP) are shown with minimal, maximal and mean (open circles) relative doses. In plans 1 and 4 maximal doses were asked to be ≤130%. Sizes of PTV_dom and PTV_SIP volumes are shown. Abbreviations: OAR: organ at risk, mL: millilitre, SIP: simultaneous integrated protection.

PO-0849

Heart structures sparing through volumetric modulated arc therapy in mediastinal Hodgkin lymphoma

A.R. Filippi[1], M. Levis[1], A. Girardi[1], C. Fiandra[1], F. Cadoni[1], V. Papurello[1], C. Piva[1], I. Donegani[2], R. Ragona[1], U. Ricardi[1]
[1]*Universita di Torino, Radiation Oncology Department, Torino, Italy*
[2]*Universita di Torino, School of Medicine, Torino, Italy*

Purpose or Objective: Within the frame of further implementing a precise dose delivery in young patients with mediastinal Hodgkin lymphoma, heart sparing appears a crucial endpoint. Recent studies demonstrated a correlation between the occurrence of various late events (e.g. heart failure, myocardial infarction, valve disease) and the dose received by different cardiac substructures, giving insights into a complex mechanism of radiation-induced toxicity. The purpose of this study was to compare the dose received by these substructures either using an optimized multi-arcs volumetric arc therapy (VMAT) or classical 3D-CRT.

Material and Methods: We analyzed the plans of 14 patients (3 males and 11 females) with stage I-IIA mediastinal disease without axillary involvement, treated with involved site radiotherapy; 11 had a bulky presentation at diagnosis. In every patient, a deformable fusion was performed with a dedicated software (Velocity™, Varian) between the planning CT scan and the pre-radiotherapy contrast enhanced CT scan. The following structures were delineated: whole heart; left main, left descending, circumflex and right coronary arteries; aortic, pulmonary, mitral and tricuspid valves; right and left atria; right ventricle, left ventricle and inter-ventricular septum; left ventricular apex, mid cavity, base and lateral wall. Two experienced radiation oncologists contoured target volumes (CTV) and heart structures, after a training session with a cardiologist and a heart radiologist. 3DCRT was planned as AP-PA, while the VMAT approach consisted of multi non-coplanar arcs (the so-called butterfly technique). Mean and max dose received by the single substructures were compared by Student's T test.

Results: Mean and max doses for the different cardiac structures,, according to the technique used, are reported in table 1. Maximum dose resulted similar for almost all the structures except for the whole heart and the right ventricle, where VMAT gave higher doses (probably due to small hotspots in the PTV areas adherent to heart segments, mainly located in the lower anterior mediastinum). Conversely, a lower mean dose was delivered by using VMAT to all structures, reaching a strong significant difference for whole heart (p = 0.025), aortic valve (p<0.0001), mitral valve (p=0.049) and left atrium (p<0.0001). Most significant findings are illustrated in figure 1.

Structure	Dosimetric parameter	VMAT	3D-CRT	p-value
Apex	Maximum Dose (Gy)	3.5	5.0	0.444
	Mean Dose (Gy)	0.9	1.6	0.222
Right Atrium	Maximum Dose (Gy)	25.8	24.8	0.406
	Mean Dose (Gy)	9.4	10.9	0.146
Left Atrium	Maximum Dose (Gy)	25.5	27.3	0.135
	Mean Dose (Gy)	10.2	14.7	< 0.0001
Basal Cavity	Maximum Dose (Gy)	23.6	24.0	0.653
	Mean Dose (Gy)	7.2	8.6	0.358
Circumflex Artery	Maximum Dose (Gy)	20.6	20.4	0.614
	Mean Dose (Gy)	12.1	14.4	0.062
Right Coronary	Maximum Dose (Gy)	23.0	21.8	0.428
	Mean Dose (Gy)	13.1	13.9	0.345
Heart	Maximum Dose (Gy)	30.3	28.7	0.031
	Mean Dose (Gy)	6.1	7.7	0.025
Left Descending	Maximum Dose (Gy)	25.0	25.2	0.181
	Mean Dose (Gy)	14.9	15.4	0.892
Mid Cavity	Maximum Dose (Gy)	9.3	8.5	0.544
	Mean Dose (Gy)	2.2	3.6	0.305
Lateral Wall	Maximum Dose (Gy)	17.2	15.6	0.290
	Mean Dose (Gy)	2.9	4.0	0.374
Interventricular Septum	Maximum Dose (Gy)	24.0	23.1	0.071
	Mean Dose (Gy)	4.1	4.5	0.584
Left Main Trunk	Maximum Dose (Gy)	26.1	25.7	0.947
	Mean Dose (Gy)	20.8	Unassessable	/
Aortic Valve	Maximum Dose (Gy)	24.4	26.8	0.094
	Mean Dose (Gy)	14.8	21.9	0.0001
Mitral Valve	Maximum Dose (Gy)	17.1	14.7	0.678
	Mean Dose (Gy)	7.1	10.0	0.049
Pulmonary Valve	Maximum Dose (Gy)	27.2	26.5	0.174
	Mean Dose (Gy)	23.7	23.1	0.845
Tricuspid Valve	Maximum Dose (Gy)	14.7	15.1	0.824
	Mean Dose (Gy)	8.5	10.8	0.101
Right Ventricle	Maximum Dose (Gy)	27.3	26.0	0.025
	Mean Dose (Gy)	4.8	5.3	0.296
Left Ventricle	Maximum Dose (Gy)	24.0	24.1	0.958
	Mean Dose (Gy)	3.5	4.8	0.238

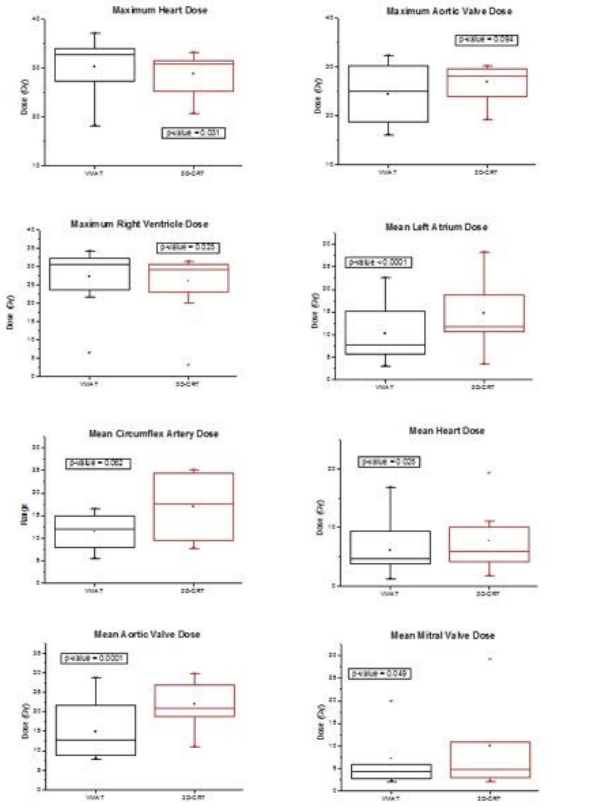

Conclusion: In this preliminary dosimetric comparison, optimized multi arcs VMAT was able to significantly reduce the mean dose to crucial heart substructures such as aortic valve, with a generalized reduction in mean doses received

by other substructures. The potential clinical benefits still need to be demonstrated in expanded cohorts, with prolonged life-long follow-up.

PO-0850

Interplay effect quantification of PBS lung tumour proton therapy with various fractionation schemes

Y. Zhang[1], I. Huth[2], M. Wegner[2], D. Weber[1], A. Lomax[1]
[1]*Paul Scherrer Institut, Center for Proton Therapy, Villigen PSI, Switzerland*
[2]*Varian Medical Systems, Particle Therapy, Troisdorf, Germany*

Purpose or Objective: This study aims to investigate how much fractionation, and the different delivery dynamics of higher dose-per-fraction deliveries, can influence the impact of interplay effects for PBS-based lung tumour treatments.

Material and Methods: For two example lung tumour cases (I and II), three-field 3D plans were calculated on a patient specific range-adapted ITV (rITV) using a spot spacing of 4mm orthogonal to the beam directions. 4D dose calculations were performed, simulating three different fractionation treatments with schemes of (A)2.5Gyx35fx, (B)5Gyx10fx and (C)13.5Gyx3fx, based on machine and delivery parameters of the Varian ProBeam system (lateral scanning speed of 5/20 mm/ms and energy switching time of 700 ms with layer-wise optimized dose rates). 1x- to 10x- layered and volumetric rescanning was simulated to mitigate residual motion effects. The final dose distributions for fractioned treatments were obtained by superposition and normalization of the 4D dose distributions of each field and each fraction with random starting phases sampled from 4DCT (10 different phases with 100 random starts). We used homogeneity index (HI:D5-D95) in the CTV to quantify the resultant 4D dose distributions within the target, while for the normal lung (both lungs minus CTV), V20, mean lung dose (MLD) and D2 were compared.

Results: For single fraction only delivery (shown by error bars with hollow markers in figure a), the normalized HIs are similar for the different fraction doses for both patients, with HI being typically 14/15% higher than the static for case I and II respectively. For the full treatments (solid markers), the normalized HIs of plans under scheme A and B are equal or better than for the static plan, with only ±1.2% variations as a function of starting phase. In addition, whereas for scheme C, HI is 2.5±2.6/4.8±2.3% (Case I/II) higher than the static case, this also reaches comparable homogeneity as the static case once combined with moderate rescanning (<5x). Variability is also reduced to within 1%, independent of the rescanning technique used. Concerning treatment time, for single fractions, nearly no difference can be seen among the different schemes when no rescanning is applied, due to the layer-wise optimized dose rate used by the ProBeam system. For 5x LS or VS, treatment time is increased by 100% and 37% respectively for scheme C in comparison to scheme A, although the absolute treatment time for LS is always less than half that of VS for all schemes. For the whole treatment, more than 75% reduction of time cost can be obtained once fractionation scheme (C) is used.

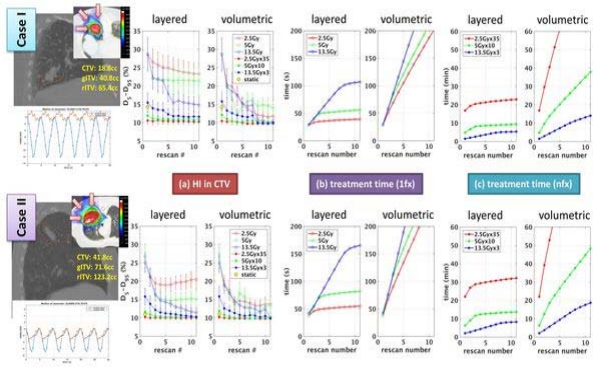

Conclusion: For PBS-based lung tumour proton therapy, fractionation can lead to an improved target homogeneity, and variability as a function of starting phase is only obvious when large fraction doses are used and can be reduced with moderate (<5x) rescanning is applied.

PO-0851

Development of a postoperative image-based treatment planning system for breast IOERT

H.R. Baghani[1], M.E. Akbar[2], S.R. Mahdavi[3], S.M.R. Aghamiri[4], H.R. Mirzaei[2], M. Robatjazi[5], N. Naffisi[2]
[1]*Hakim Sabzevari university, Applied Physics, Sabzevar, Ireland Republic of*
[2]*Shahid Beheshti University of Medical Science, Cancer Research Center, Tehran, Ireland Republic of*
[3]*Iran University of Medical Science, Medical Physics, Tehran, Iran Islamic Republic of*
[4]*Shahid Beheshti University, Radiation Medicine, Tehran, Iran Islamic Republic of*
[5]*Tehran University of Medical Science, Medical Physics, Tehran, Iran Islamic Republic of*

Purpose or Objective: One of the major limitations of IOERT is the lack of a postoperative image based treatment planning, in order to optimize the radiotherapy procedure. The aim of this study is to develop and introduce a postoperative image based treatment planning system for breast cancer IOERT.

Material and Methods; to obtain a postoperative image based treatment planning software, it is necessary to have a postoperative image which includes the anatomical modifications of the tumor bed after the surgery. To this end, a C-arm fluoroscopy system (Zeihm Vision-8000) was employed to obtain a series of 2D images which include the tumor bed together with the IORT applicator and protection disk.In addition to the postoperative images, it is mandatory to have the complete isodose distributions for different combinations of applicator size/energy. To obtain this data, Monte Carlo simulation was employed. The LIAC IORT accelerator was simulated by MCNPX code and then, isodose distributions were extracted using mesh tally inside a water phantom. To develop a graphical treatment planning software, a graphical user interface (GUI) was prepared by an in house program written with MATLAB. At first, the postoperative image is imported to the program. Then, the corresponding isodose distribution file is loaded to the program. Then, the user will specify the applicator edge and program registers the isodose curves to the postoperative image. In order to evaluate the performance accuracy of the implemented postoperative image based treatment plans and delivered dose to the patient, in vivo dosimetry was used. To this end, the delivered dose to the surface of tumor bed was measured by Gafchromic EBT2 film.

Results: The result of intraopertaive imaging and corresponding treatment planning is shown in Fig. 1.

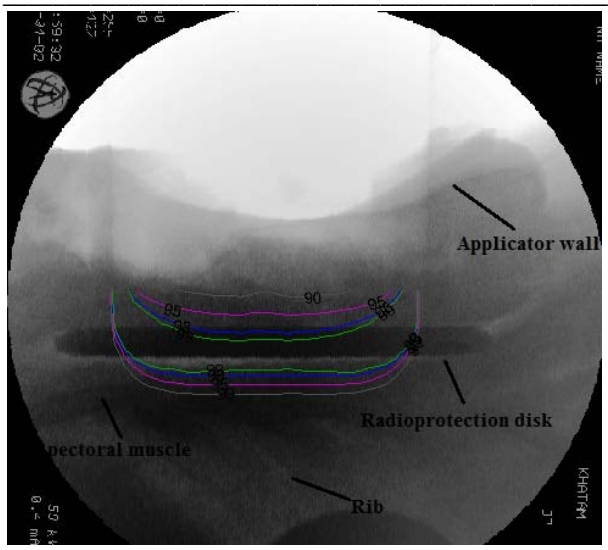

As it can be seen, the developed treatment planning system is able to clearly show the variations of isodose levels at the site of tumor bed. Therefore, treatment team can precisely determine the interested isodose level for the dose prescription.The results of in vivo dosimetry at the surface of tumor bed showed there is no meaningful difference between the measured and expected dose at the surface of tumor bed (P-value=0.92).

Conclusion: The feasibility of intraoperative imaging and development of a postoperative image based treatment planning system during breast cancer IOERT was investigated in this study. The results of in vivo dosimetry confirm the validity of the developed treatment planning system for clinical applications.

PO-0852

The dose in marrow of iliac plates during radiotherapy of cervical and endometrial cancer

A. Jodda[1], T. Piotrowski[2], B. Urbański[3], A. Roszak[3], J. Malicki[2]
[1]*Greater Poland Cancer Centre, Medical Physics, Poznan, Poland*
[2]*Poznan University of Medical Sciences, Electroradiology, Poznan, Poland*
[3]*Greater Poland Cancer Centre, Gynaecological Radiotherapy Ward, Poznan, Poland*

Purpose or Objective: To compare the differences between average doses cumulated in the marrow of iliac plates (PBM), obtained for five different radiotherapy strategies of cervical and endometrial cancer.

Material and Methods: A total of 150 treatment plans were calculated retrospectively for 30 patients with cervical and endometrial cancer.
For each case, 3 different dose delivery techniques were used. It were respectively: (i) 4-field, X15MV, 3DCRT; (ii) 7-field, X6MV, IMRT; and (iii) 2-arc, X6MV, VMAT. Two strategies were used during preparation of the IMRT and VMAT plans. The first take into account (+) PBM during optimization of the dose distribution and the second, do not take it into account (-).
All plans were normalized on the median dose in PTV. The same calculation algorithm (AAA) was used for calculation of the dose for each of plan. The total dose was 50.4 Gy (1.8 Gy in 28 fractions).
Average doses cumulated in PTV, PBM, bladder, rectum, bowels and femoral heads obtained from the evaluated plans were compared. In addition, the doses accumulated in PBM were analyzed in the light of the volume of PTV and/or PBM.
The statistical analysis were performed by Friedman ANOVA with Nemenyi's procedures used as post-hoc tests. In order to find the relationship between doses in PBM and volume of PTV and/or PBM, the Spearman correlation was used. All tests were performed on the significance level equal to 0.05.

Results: Table 1 shows the result of the comparison of the average dose in the light of the generated plans.

Technique	PTV	PBM	Bladder	Rectum	Bowels	FHR	FHL
	Average Dose (Standard Deviation) [Gy]						
3DCRT	50.4 (0.1)	33.3 (1.7)	49.9 (0.4)	47.7 (1.6)	37.6 (2.4)	38.2 (1.2)	38.3 (2.8)
IMRT(-)	50.4 (0.1)	29.9 (1.5)	35.4 (1.7)	36.2 (3.0)	32.6 (1.3)	25.4 (1.3)	27.7 (1.6)
VMAT(-)	50.4 (0.1)	29.4 (2.0)	34.6 (2.4)	35.7 (2.6)	33.2 (1.1)	26.3 (1.8)	28.7 (1.7)
IMRT(+)	50.5 (0.1)	27.7 (1.5)	35.5 (2.9)	36.3 (2.8)	32.6 (1.3)	23.9 (1.4)	24.4 (2.2)
VMAT(+)	50.4 (0.1)	26.4 (1.7)	34.6 (2.8)	35.7 (2.9)	32.9 (1.1)	24.1 (1.2)	25.0 (2.0)
Technique	Similarity/Dissimilarity of the results						
	p = 0.998	p < 0.001	p < 0.001	p < 0.001	p < 0.001	p < 0.007	p < 0.011
3DCRT	A	A	A	A	A	A	A
IMRT(-)	A	B	B	B	B	B	B
VMAT(-)	A	B	B	B	B	B	B
IMRT(+)	A	C	B	B	B	C	C
VMAT(+)	A	C	B	B	B	C	C

PTV - Planning Target Volume; PBM - The bone marrow in the iliac plates; FHR - right femoral head; FHL - left femoral head

The average dose in PTV for evaluated plans was similar. The worst doses in organs at risk were obtained for 3DCRT. Using the PBM during optimization of IMRT and VMAT reduces the average dose in PBM without increasing the doses in bladder, rectum and bowels. Differences between doses in PBM for IMRT and VMAT plans, where PBM was used during optimization, were not statistically significant. The correlation between mean dose in PBM and the volume ratio of PBM and PTV was found for each technique (Figure 1).

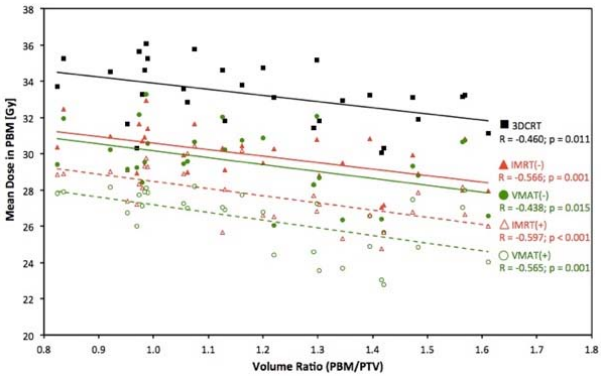

Conclusion: Using the PBM during optimization of the IMRT and VMAT plans effectively reduces the dose in PBM without increasing the dose in bladder, rectum and bowels. The doses, obtained in PBM for IMRT and VMAT are not statistically different. Decreasing the PBM volume in relation to PTV increases the mean dose in PBM.

PO-0853

Impact of CT modality used for treatment planning of lung SBRT

A. Vicedo-Gonzalez[1], T. Garcia-Hernandez[1], L. Brualla-González[1], A. Hernandez-Machancoses[2], D. Granero-Cabañero[1], J. Roselló-Ferrando[1]
[1]*Eresa Valencia, Medical Physics, Valencia, Spain*
[2]*Eresa Valencia, Radiotherapy, Valencia, Spain*

Purpose or Objective: The introduction of lung stereotactic body radiation therapy (SBRT) requires images that allow a more precise delineation of the tumor and its movement. The free breathing CT does not contain information on the variable electron density over time. The objective of this study is to analyze the CT mode that provides the best estimation of the tumor movement and the most appropriate image set for the calculation of the dose distribution image.

Material and Methods: 10 patients were retrospectively investigated. For each patient, a retrospective 4DCT was acquired using a Brilliance 16-slice scanner. From the 4DCT study, 10 respiratory phases, an average CT and a maximum intensity projection (MIP) were reconstructed. The gross tumor volumes (GTV) were delineated in each image set of the 4DCT using a MIM® 6.4 software. Three internal target volumes (ITV) were obtained, one from the union of GTVs delineated in each phase, another from the average CT and the last from the MIP reconstruction. Special care was taken with the window level selection when contouring. The size of the three ITVs was compared. The planning target volume

(PTV) was created adding a margin of 5 mm to the ITV .The dose distribution was optimized on the average CT prescribing a dose of 20 Gy per fraction delivering a total dose of 60 Gy to the PTV. The plans were calculated in a Phillips Pinnacle 9.10 planning system using conformal 3DRT and heterogeneity correction. The parameters obtained in the average CT optimized plan, were copied to the different image sets with identical monitor units to analyze the differences.

Results: The average GTV volume was 1.6 ± 1.1 cc. The ITV size is twice the lesion size in most of the cases except in those with higher breathing amplitude. The ITVs outlined in the average CT were smaller than those outlined in the 4DCT ranging from 0.1 cc, where there hardly was lesion movement, to 0.6 cc. The differences between the volumes were usually found in the cranio-caudal direction due to the higher movement of the lesion in this direction. The ITVs outlined in the MIP CT were equivalent to the 4DCT except in the cases where there was a higher density organ in the vicinity of the tumor. Respect to dose distribution, the dose of the organs at risk shows no significant differences in the different image sets. The V100 of the ITV presents significant variations up to 15% due to the variation in electron densities depending on the CT mode chosen. The V100 of the GTV calculated in each phase is greater than 97%.

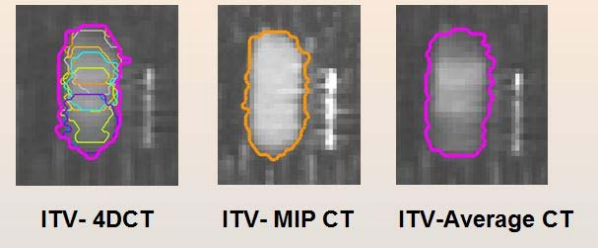

Conclusion: We recommend using the ten phases of the 4DCT study for proper delineation of ITV. If the institution does not have the technology the CT average (low pitch CT) could be used selecting the appropriate window level and increasing margins. There is no significant difference in dose to organs at risk between the images modalities studied. Optimized planning in the average CT provides adequate coverage of GTV at different breathing phases.

PO-0854

Evaluation of a dedicated brain metastases treatment planning optimization for radiosurgery

T. Gevaert[1], F. Steenbeke[1], L. Pellegri[2], B. Engels[1], N. Christian[2], M.T. Hoornaert[2], C. Mitine[2], D. Verellen[1], M. De Ridder[1]

[1]*Universitair Ziekenhuis Brussel, Radiotherapy, Brussels, Belgium*

[2]*Centre Hospitalier Jolimont, Radiotherapy, Jolimont, Belgium*

Purpose or Objective: Stereotactic radiosurgery alone has become a popular treatment option in the management of patients with brain metastases. Multi- or single-isocenter dynamic conformal arcs (DCA) and volumetric modulated arc therapy (VMAT) are two common used delivery techniques. Recently, a dedicated inverse optimized brain metastases treatment planning solution using single isocenter multiple DCA (SIDCA) has been developed, with intend to carefully balance normal tissue protection, target coverage and treatment speed. The purpose of the current study was to investigate the feasibility of this novel software and to benchmark it against well-established multi-isocenter DCA and single isocenter VMAT approaches.

Material and Methods: Ten previously treated patients were selected representing a variable number of lesions (1-8), range of target sizes and shapes most frequently observed in the practice of SRS for brain metastases. The original multi-isocenter DCA (MIDCA) were replanned with both single-isocenter VMAT approach and the novel brain metastases tool (Elements, Brainlab AG, Germany). The treatment dose was 20 Gy at the 80% prescription isodose. For all the plans, the dose to the surrounding healthy brain tissue (brainstem, cochlea, optical nerve, eyes and lens) was optimized to minimize normal tissue complications. The plans were evaluated by calculation of Paddick conformity and gradient index, and the volume receiving 10 and 12 Gy indicating risk of radionecrosis.

Results: All plans were judged clinically acceptable, but differences were observed in the dosimetric parameters. The mean conformity of the automated single-isocenter planning tool (SIDCA) compared similarly to the established MIDCA and VMAT treatment techniques (CISIDCA=0.65 ± 0.08, CIMIDCA=0.66 ±0.07 and CIVMAT=0.67 ±0.16). Comparable mean dose fall off was observed between SIDCA and MIDCA (GISIDCA =3.9 ± 1.4 and GIMIDCA=4.5 ± 1.6). On the other hand, the GI of the VMAT plans (GIVMAT=7.1 ± 3.1) were significantly higher compared to the SIDCA. The V10 and V12 were significantly higher for VMAT plans (V10VMAT=67.9 ±55.9cc, V12VMAT=46.3 ±35.9cc) ($p<0.05$) compared to MIDCA (V10MIDCA=49.0 ±38.1cc, V12MIDCA=35.6 ±26.4cc) and SIDCA (V10=48.5 ± 35.9cc, V12=36.3 ± 27.1cc).

Conclusion: The automated brain metastases treatment planning element, based on an inversely-optimized SIDCA approach, revealed comparable results to the general accepted MIDCA approach. By reducing the time on planning, patient and treatment setup, this software tool improves the planning and delivery efficiency while preserving the plan quality of the MIDCA technique and lowering low dose spread of the VMAT approach, suggesting that this novel software offers the best of both worlds (i.e. efficient single-isocenter DCA delivery).

PO-0855

Flattening Filter Free VMAT for extreme hypofractionation of prostate cancer

M. Ahlström[1], H. Benedek[2], P. Nilsson[2], T. Knöös[2], C. Ceberg[1]

[1]*Lund University, Department of Medical Radiation Physics-Clinical Sciences, Lund, Sweden*

[2]*Skåne University Hospital and Lund University, Department of Oncology and Radiation Physics, Lund, Sweden*

Purpose or Objective: To examine the feasibility of flattening filter free (FFF) volumetric modulated arc therapy (VMAT) for extreme hypofractionation of prostate cancer and investigate the potential decrease in treatment time per fraction while preserving or improving the treatment quality. To investigate the impact of intrafractional prostatic displacement.

Material and Methods: Single arc treatment plans with photon beam qualities 10 MV with flattening filter (FF), 6 MV FFF and 10 MV FFF were created for nine patients treated with conventional fractionation (78 Gy, 2 Gy/fraction) and hypofractionation (42.7 Gy, 6.1 Gy/fraction), respectively. Dose-volume histograms (DVH) for all beam qualities were statistically evaluated using a paired sample Student's t-test. Treatment delivery was evaluated through measurements on a Varian TrueBeam™ using a Delta4 PT system (ScandiDos AB). The beam-on time for each plan was recorded. A motion study, including one FF and one FFF hypofractionated treatment plan, was also performed using the HexaMotion (ScandiDos AB) and with trajectory data from six authentic prostate movement patterns.

Results: All treatment plans were approved by a senior radiation oncologist. Evaluating the DVHs, no significant differences between beam qualities or between fractionation schedules were observed. All objectives were met for all plans. At the treatment delivery all plans passed the gamma criterion 3%, 2 mm with a pass rate of 98.8% or higher. The beam-on time for all conventional treatment plans was 1.0 minute. The mean beam-on time was 2.3 minutes for the hypofractionated 10 MV FF plan, 1.3 minutes for the 6 MV FFF and 1.0 minute for the 10 MV FFF. In the motion study, no or little effect was observed on the pass rate for displacements

≤1mm. The shorter treatment delivery was superior for three patterns, while the longer treatment was preferred in the case of temporal displacement of the prostate.

Conclusion: The treatment time for extreme hypofractionation of prostate cancer is reduced to less than half the time per fraction by combining FFF-technique with VMAT. The treatment plan quality was preserved for the FFF beams. Finally, a shorter beam-on time also seems advantageous for the majority of prostate motion patterns investigated.

PO-0856

Clinical and dosimetric issues of VMAT craniospinal irradiation for paediatric medulloblastoma

S. Meroni[1], T. Giandini[1], B. Diletto[2], E. Pecori[2], C. Chiruzzi[2], V. Biassoni[3], E. Schiavello[3], F. Sreafico[3], M. Massimino[3], E. Pignoli[1], L. Gandola[2]

[1]Fondazione IRCCS Istituto Nazionale dei Tumori, Medical Physics, Milan, Italy

[2]Fondazione IRCCS Istituto Nazionale dei Tumori, Radiation Oncology- Paediatric Radiotherapy Unit, Milan, Italy

[3]Fondazione IRCCS Istituto Nazionale dei Tumori, Paediatric Oncology, Milan, Italy

Purpose or Objective: With increased 5 years survival of children with medulloblastoma, optimization of radiotherapy treatment to avoid iatrogenic sequelae has become a primary issue. Clinical and dosimetric characteristics of VMAT Craniospinal Irradiation (CSI) were studied and compared with the 3DCRT technique in use since 1997 at our institution with excellent clinical results. The impact of a setup error on dose distribution was also studied.

Material and Methods: CT images of 8 pts that received CSI at our institution (23.4 Gy in 13 fractions) were used for the dosimetric study. For each patient, a standard 3DCRT treatment and a VMAT were planned. PTV dosimetric objectives for treatment planning were: D95% >95%, D100% >90%, D5% <107%. The resulting DVHs were analyzed considering: conformity index (CI) and homogeneity index (HI) for PTV, mean dose (Dmean) and D2% for OARs (small bowel, kidneys, heart, liver, stomach, lenses, thyroid, lungs) and V2Gy of non target tissues as an integral dose index. The data were then compared using paired Student's t test. The dependence of dose indexes on patient size was evaluated. A 3 mm longitudinal error in patient setup was simulated for both techniques to evaluate dosimetric impact in the junction region.

Results: Dosimetric objectives were always met. All VMAT treatment plans had better HI and CI independently of patient size. Dmean and D2% of heart and thyroid were significantly lower with VMAT. On average, for heart Dmean was 9.8±3.4 Gy and 6.3±1.0 Gy, and D2% was 20.3±4.1Gy and 10.4±1.7 Gy, for 3DCRT and VMAT respectively, while for thyroid Dmean was 18.2±1.2 Gy and 13.8±1.8 Gy, and D2% was 20.4±1.2 Gy and 17.4±2.0 Gy, for 3DCRT and VMAT respectively. On the contrary, lung dose was higher with VMAT: on average Dmean was 1.8±0.9 Gy for 3DCRT and 3.5±0.8 Gy for VMAT. A 3 mm gap at field junction level resulted in an underdosage of about 20% for VMAT and 50% for 3DCRT, while a 3 mm overlap gave rise to a hotspot on the spine up to 30% for VMAT and 70% for 3DCRT. V2Gy was about 3 times higher for VMAT.

Conclusion: VMAT allowed to achieve a more conformal and homogeneous dose distribution, with greater sparing of most OARs. Considering the risk of iatrogenic cardiopathy, hypothyroidism or secondary tumors to the thyroid, the dose reduction obtained with VMAT was significant. The clinical effect of the increased lung dose is not yet predictable, since absolute dose values were extremely low. VMAT implies a higher MU value for the delivery of the prescribed dose, possibly increasing the risk of secondary tumors. This is an important factor when dealing with pediatric pts. In VMAT, overdosage areas are greatly reduced with respect to 3DCRT, particularly in the junction region. The analysis of simulated gaps and overlaps shows that field junctions are less critical for VMAT, nevertheless junction moving is still mandatory to avoid potentially dangerous hot or cold spots. Partially supported by Associazione Italiana per la Ricerca sul Cancro (AIRC)

PO-0857

GTV-based prescription and Monte Carlo treatment planning in Cyberknife treatments for lung lesions

A. Vai[1,2], P. Bonfanti[1], M. Invernizzi[1], A. Martinotti[1], I. Redaelli[1], F. Ria[1,3], R. Beltramo[1], L.C. Bianchi[1], I. Bossi Zanetti[1], A. Bergantin[1]

[1]Centro Diagnostico Italiano, Cyberknife Department, Milan, Italy

[2]ProgettoDiventerò Grantee, Fondazione Bracco, Milan, Italy

[3P]rogettoDiventerò Alumnus, Fondazione Bracco, Milan, Italy

Purpose or Objective: GTV-based prescription has been proposed as a possible recipe for Monte Carlo treatment planning in Cyberknife SBRT treatments for lung lesions (Lacornerie et al., 2014, [1]). The feasibility of this approach was investigated comparing Ray-Tracing algorithm (Effective Path Length method, EPL) and Monte Carlo (MC) dose calculation.

Material and Methods: A group of 40 consecutive patients from July to October 2015, treated with Cyberknife SBRT using an advanced target tracking system (Lung Optimized Treatment, LOT) was considered. Primary lung cancers and metastatic pulmonary lesions, different tumor size (small: V<14cc, large: V>65cc) and locations (totally air-surrounded, partially air-surrounded), prescription dose and fractionation schemes were included in the group. Treatment plans were optimized using RT algorithm (RT plans), with prescription isodose line of 80% providing 95% PTV coverage (PTV = GTV + 5mm), and re-calculated with MC algorithm (1x1x1 mm3 dose grid, uncertainty=1%), using the same beam angles and monitor units (MCrecalc plans). Dose parameters for RT and MCrecalc plans were evaluated for both GTV, PTV and OARs, in relation to tumor size and position. On a subset of 5 patients, MCrecalc plans were normalized to the isodose line encompassing the 95% of the GTV volume (MCnorm plans) and compared to MC-optimized plans, with dose prescribed to the same isodose line (MCopt plans).

Results: Difference between RT and MCrecalc plans in average percentage volume covered by the prescribed dose for GTV and PTV is 13.5% (RT: 99.6%, MC: 86.1%) and 41.8% (RT: 96.8%, MC: 55.0%) respectively. Dose parameters referred to GTV (Dmean, D50, D98, D2) have a lower variation compared with PTV parameters: excluding D2, D50 shows the lowest variability for the analyzed group. Concerning OARs, difference in V20, V10, V5 for lungs (ipsilateral and contralateral) is 0.6%, 1.4% and 3.4%, respectively.

Table 1

Average difference RT - MC_{recalc}

GTV	$V_{DosePresCovered}$	D_{mean}	D_{50}	D_{98}	D_2
all	13.5%	8.2%	7.9%	13.9%	5.1%
small	15.6%	9.8%	9.3%	17.4%	5.7%
medium	8.6%	5.3%	5.4%	6.9%	4.3%
large	11.8%	4.2%	3.9%	6.6%	2.2%
air-surrounded					
totally	14.2%	3.2%	3.0%	7.5%	0.8%
partially	12.8%	9.6%	9.3%	15.4%	6.5%
PTV	$V_{DosePresCovered}$	D_{mean}	D_{50}	D_{98}	D_2
all	41.8%	12.9%	12.5%	24.6%	5.3%
small	50.8%	16.1%	15.9%	30.3%	6.1%
medium	26.4%	7.2%	6.6%	14.3%	4.2%
large	14.9%	4.0%	3.3%	10.2%	1.7%
air-surrounded					
totally	39.1%	6.6%	6.0%	18.2%	0.9%
partially	41.4%	14.4%	14.0%	26.1%	6.7%
Lungs	V_{20}	V_{10}	V_5		
average	0.6%	1.4%	3.4%		
max	1.5%	7.2%	22.7%		

Average difference RT, MC_{recalc}, MC_{norm}, MC_{opt}

MC_{recalc}-RT		MC_{norm}-RT		MC_{opt}-RT	
D_{50}	D_{mean}	D_{50}	D_{mean}	D_{50}	D_{mean}
-12.8%	-13.7%	0.4%	-0.5%	9.3%	8.3%

MCnorm and MCopt have a value of GTV D50 and Dmean comparable to the RT plan and higher than the MCrecalc plan. At the same time, MCnorm plans could not always be accepted referring to OARs dose constraints respect and target dose conformity (see Fig.1). Results are reported in Table 1.

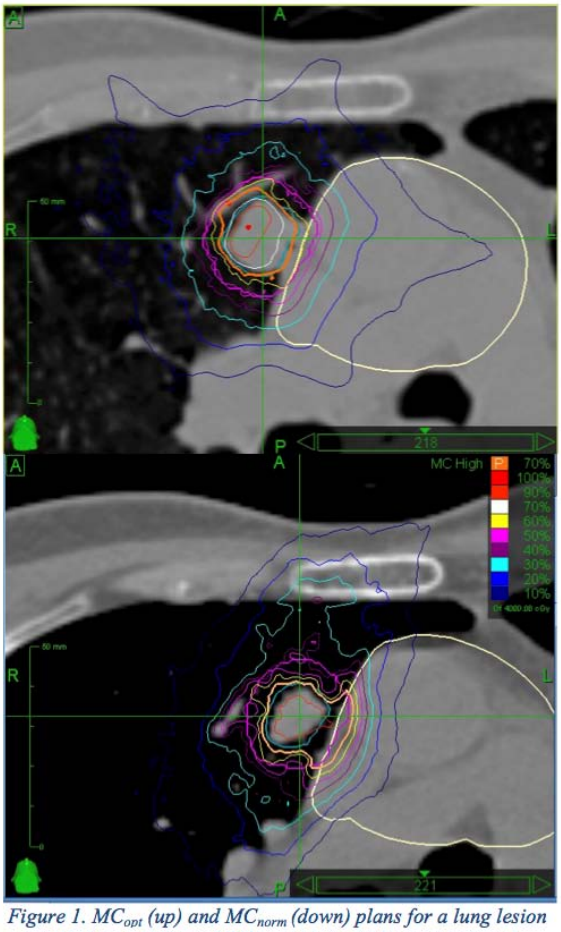

Figure 1. MC_{opt} (up) and MC_{norm} (down) plans for a lung lesion near the heart. GTV and PTV are contoured as a green and purple lines, respectively. Although volume coverage is obtained, dose constraint on the heart (D_{1cc}< 22Gy) is not respected in MC_{norm} plan.

Conclusion: Lower variation of GTV dose parameters compared with PTV, when both RT and MCrecalc treatment plans are evaluated, suggests that GTV should be used for dose normalization and reporting instead of PTV. According to van der Voort van Zyp et al. (2010, [2]), a different prescription dose could be adopted, depending on lesion size and location. Moreover, MCopt plans need to be implemented, adopting a different prescription dose based on GTV D50 and Dmean values [1], as MCnorm plans could not guarantee appropriate target coverage and OARs sparing. Further multivariate analysis is mandatory to determine if there are correlations between the variables (size and location of the lesions, type of tracking adopted) considered for plan comparisons.

PO-0858

Development of dysphagia optimised IMRT for head and neck cancer treatment in the DARS trial

J. Tyler[1], D. Bernstein[1], K. Rooney[2], C. Nutting[3]

[1]*Royal Marsden NHS Foundation Trust, Physics, London, United Kingdom*

[2]*Belfast Health and Social Care Trust, Radiotherapy, Belfast, United Kingdom*

[3]*Royal Marsden NHS Foundation Trust, Radiotherapy, London, United Kingdom*

Purpose or Objective: To develop a dysphagia optimised IMRT (Do-IMRT) technique comparing fixed-field IMRT with VMAT for treatment of head and neck cancer in the DARS clinical trial (CRUK/14/014), which is a phase III randomised multicentre study of Do-IMRT versus standard IMRT (S-IMRT).

Material and Methods: Six oropharynx cases were outlined and planned according to the DARS trial QA guidelines. CTVs were outlined using a volumetric approach with a 10mm GTV-CTV expansion. Pharyngeal constrictor muscles (PCM) were also delineated. The dose levels prescribed were 65 Gy to the primary site and involved nodes and 54 Gy to the elective volume in 30 fractions. Plans were produced according to both arms of the trial using both fixed-field IMRT and VMAT (RapidArc) with an Eclipse treatment planning system (version 11). In the experimental Do-IMRT arm, the aim was to achieve a mean dose of less than 50 Gy to the superior and middle PCMs, excluding the CTV receiving 65 Gy (PlanSMPCM), and less than 20 Gy to the similarly edited inferior PCM (PlanIPCM). These constraints were prioritised over coverage of the PTV receiving 54 Gy (PTV_5400) but not the PTV receiving 65 Gy (PTV_6500). In the S-IMRT arm no attempt was made to reduce PCM doses. Plans were assessed for their clinical acceptability and DVH statistics compared.

Results: Using fixed-field IMRT for Do-IMRT, it was not possible to achieve clinically acceptable plans in terms of both PTV_5400 95% isodose coverage and homogeneity whilst achieving the PCM constraints. However, using VMAT for Do-IMRT a PlanSMPCM mean dose of less than 50 Gy was achieved in all cases, reduced by 8 Gy on average compared to S-IMRT. PlanIPCM mean doses of less than 20 Gy were achieved in the majority of cases, reduced by 30 Gy on average compared to S-IMRT. Do-IMRT plans had decreased but acceptable dose homogeneity and 95% isodose coverage was maintained, only compromising in the region where PCMs and PTV_5400 overlap (as shown in the example in figure 1). Other OAR (spinal cord, brainstem and parotids) doses were increased for Do-IMRT but critical OAR constraints were still achieved in all cases. The results are summarised in table 1.

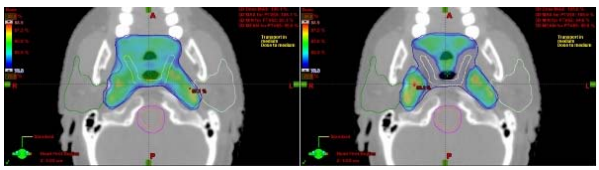

Figure 1: Dose distribution (colour wash displays 95-107% of 54 Gy) of transverse slice showing PTV_5400 (blue) coverage using S-IMRT (left) compared to Do-IMRT (right), where

coverage is compromised in the region of PlanSMPCM (yellow).
Table 1: Comparison of VMAT S-IMRT and Do-IMRT plan dose-volume statistics for PlanPTVs (edited 5mm from body surface and excluding PlanPTV_6500 from PlanPTV_5400), spinal cord, brainstem, contralateral (CL) and ipsilateral (IL) parotids, PlanSMPCM and PlanIPCM.

Dose-volume statistics	Case 1		Case 2		Case 3		Case 4		Case 5		Case 6		Paired t-test
	S-IMRT	Do-IMRT	S-IMRT	Do-IMRT	S-IMRT	Do-IMRT	S-IMRT	Do-IMRT	S-IMRT	Do-IMRT	S-IMRT	Do-IMRT	
PlanPTV_6500 D95 (%)	96.3	95.5	96.2	96.0	97.4	96.4	97.4	96.9	96.7	95.5	96.7	96.3	0.004
PlanPTV_6500 D5 (%)	101.8	102.2	102.4	102.6	101.7	102.0	101.6	102.3	102.0	102.3	101.6	101.9	0.002
PlanPTV_5400 D95 (%)	80.1	74.4	80.0	68.2	80.1	71.2	80.0	66.3	79.9	72.9	79.5	75.8	0.001
SpinalCord max dose (Gy)	44.2	44.5	40.0	42.8	35.2	42.3	37.9	42.6	38.9	38.5	42.5	41.2	0.080
BrainStem max dose (Gy)	45.2	41.2	42.0	42.4	44.1	46.0	38.6	44.1	40.0	39.5	36.4	38.6	0.255
Parotid_CL mean dose (Gy)	23.7	27.3	24.6	26.7	24.2	26.6	25.8	32.0	29.3	29.4	28.3	29.5	0.015
Parotid_IL mean dose (Gy)	24.0	28.3	35.2	36.1	32.1	38.2	37.0	46.0	35.2	29.6	29.6	30.6	0.181
PlanSMPCM mean dose (Gy)	57.9	49.2	56.3	45.6	57.5	48.6	58.3	49.3	56.1	49.6	56.7	50.0	0.000
PlanIPCM mean dose (Gy)	51.6	18.8	50.3	20.0	51.5	19.3	52.6	19.9	45.3	19.9	56.2	29.9	0.000

Conclusion: Do-IMRT can be achieved using VMAT for the DARS trial. Fixed-field IMRT may also be used to reduce constrictor dose, however is unlikely to produce plans acceptable within the DARS trial QA guidelines.

PO-0859

Quantifying and categorizing plan rejections as a part of the clinical process improvement

C. Speirs[1], J. LaBrash[1], S. Mutic[1], Y. Rao[1], S. Rehman[1], M.C. Roach[1], J.M. Michalski[1], S.M. Perkins[1]
[1]Washington University Medical Center, Radiation Oncology, St. Louis, USA

Purpose or Objective: RT plan rejections are defects that cause suboptimal or erroneous treatments if undetected and should be a focus of improvement. Applying the DMAIIC (Define, Measure, Analyze, Improve, Implement, and Control) formalism to clinic workflow provides actionable parameters for feedback and process correction. In our clinic, a web-based treatment planning board shows the real-time workflow and compiles causes of plan rejection, which can be categorized and quantified for subsequent process improvement efforts.

Material and Methods: Data was collected from July 2014-September 2015. 341 (of 673) entries associated with plan rejection were categorized as changes in one of the following: (1) tumor anatomy/patient setup; (2) dose/volume; (3) tumor/OAR constraints; (4) treatment planning modification generated during plan review; and (5) external (patient-, disease-, or hospital/equipment-generated) causes. Each entry was initiated by the physician, physicist, or dosimetrist involved in planning. Analyzed time intervals included the following: (1) dosimetry contours; (2) MD contour approval; (3) dosimetry plan computed; (4) physics plan precheck; (5) MD plan approval; and (6) total time for planning from simulation/planning board entry until MD plan approval (*TMD*). The data was analyzed with Two-way ANOVA, Student T-test, and Pearson correlation.

Results: The mean *TMD* time was 85 hrs (+/- 45). With breakdown by interval, the mean dosimetry contour (16 hrs), MD contour approval (27 hrs), dosimetry planning (12 hrs), physics precheck (4 hrs), and MD approval (11 hrs) times were calculated. The planning modification category was a significant source of variation in planning time ($p<0.0001$). Treatment planning modifications presented the predominant (50%) source of planning delay, followed by constraint (26%), dose/volume (18%), external (4%), and tumor anatomy/patient setup changes (2%). Those with tumor anatomy/patient setup or dose/volume changes resulted in the longest *TMD*, dosimetry contour, dosimetry plan computing, and MD plan approval intervals. 27% of plan modifications were initiated by physicians, 70% by physicists, and 3% by dosimetrists. Entries initiated by physicians on the planning board were associated with shorter *TMD* times than when physicists initiated plan rejection ($p=0.016$).

Conclusion: We report a novel process for quantification of clinical RT plan rejections. In this analysis, tumor anatomy/patient setup or dose/volume changes resulted in the longest treatment *TMD* times. Physician-initiated plan modification entries were associated with shorter *TMD* times, which may denote early, proactive involvement—an optimal approach with complicated or aggressive disease. Though planning delays may depend on department infrastructure and patient population, our method provides a comprehensive census to optimize planning throughput and can be applied as a part of broader process improvement.

PO-0860

Is there a "best technique" available for reducing acute toxicities in craniospinal Irradiation?

M. Devecka[1], M.N. Duma[1,2], S. Kampfer[1,3], C. Hugo[1], K.M. Hofmann[1], B.S. Müller[1,3], C. Heinrich[1], J.J. Wilkens[1,2,3], S.E. Combs[1,2]
[1]Klinikum rechts der Isar- Technische Universität München, Department of Radiation Oncology, Munich, Germany
[2]Institute of Innovative Radiotherapy iRT, Department of Radiation Sciences- Helmholtz Zentrum München, Munich, Germany
[3]Technische Universität München, Physik-Department, Munich, Germany

Purpose or Objective: Craniospinal irradiation is performed rarely in a palliative intention due to concerns of acute toxicities (mostly dysphaghia and bone marrow supression). Therefore the purpose of this study was to evaluate the dosimetric parameters responsible for the acute toxicity in patients with leptomeningeal metastasis of a solid cancer treated with craniospinal irradiation (CSI) by helical tomotherapy (HT), 3D conformal radiotherapy (3D-CRT) and Protons.

Material and Methods: Data of five adult patients previously treated with HT CSI were evaluated. For each patient the initial tomotherapy plan (inHT) was compared to a 3D conformal plan (3D-CRT), a scanning proton beam plan (p-CSI) as well as to a specifically optimized bone marrow (BM) sparing tomotherapy plan (BM-HT). The BM-HT was also optimized to reduce the acute dysphagia. The prescribed dose was 36 Gy. All active bone marrow compartments were delineated separately according to Campbell et al. To analyse the impact of different bone marrow compartments weighted bone marrow exposure (WBME) was used.
WBME Dmean =Σ(proportion (%) of functional bone marrow according to anatomical site x Dmean to anatomical site)
WBME V20=Σ(proportion (%) of functional bone marrow according to anatomical site x V20 to anatomical site)
This calculation was also performed for V30.
Further, the following organ at risks (OARs) were delineated: left and right submandibular glands, the parotid glands, the eyes, the cochlea, the oral cavity, the pharynx, the thyroid gland, the esophagus, the heart, both lungs, both kidneys, the liver, the bowel, and the pancreas. For all of these structures the Dmean in all four treatment plans were analyzed.
Descriptive statistics were used to analyze the results.

Results: p-CSI results in the best sparing of the organs at risk (OARs) including the active bone marrow compartments. BM-HT achieved better results as inHT and 3D-CRT regarding bone marrow sparing (see Figure 1.). Dose to the crucial OARs responsible for dysphagia was also reduced with BM-HT. The trade off for this was an slightly increased lung and kidney dose.

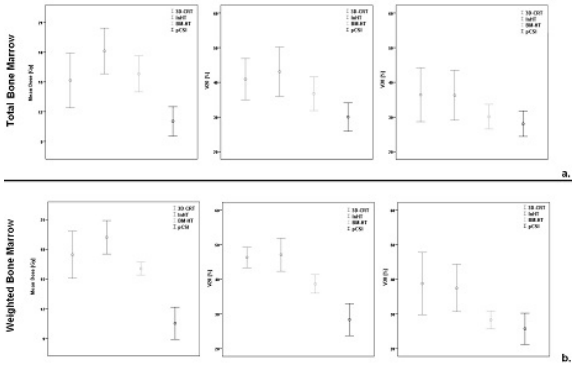

Figure 1. Total bone marrow and weighted bone marrow dosimetry (presented are averages and 95% confidence intervals).

Conclusion: With the use of the novel techniques such as p-CSI and BM-HT quality of life impairing acute side effects such as cytopenias and dysphagia can be reduced. We propose WBME to better assess the impact on active bone marrow.

PO-0861

Whole lung irradiation using VMAT – dosimetric and NTCP benefits vs. second cancer risks

P. Clarke[1], S. Padmanaban[1], M. Partridge[2], T. Foord[3], D. Cutter[3]

[1]*Oxford Cancer Center, Radiotherapy Physics, Oxford, United Kingdom*

[2]*CRUK/MRC Oxford Institute for Radiation Oncology, Gray Laboratories- University of Oxford, Oxford, United Kingdom*

[3]*Oxford Cancer Center, Clinical Oncology, Oxford, United Kingdom*

Purpose or Objective: Whole lung irradiation (WLI) of 12 to 18 Gy is used as treatment for lung metastases in patients with Ewing sarcoma and Wilms tumour. This results in irradiation of normal tissues including heart and breast. Conventionally this treatment has been delivered with standard AP-PA fields. To minimise cardiac radiation dose and reduce the risk of subsequent late complications, we validated the use of VMAT to deliver WLI without increasing the predicted risks of secondary breast cancers compared to AP-PA fields.

Material and Methods: Five female patient datasets (ages ranging from 3 to 18 years) were used for this retrospective study. The planning target volume (PTV) included total lung volume with a 1 cm margin (and adjacent vertebrae for three patients). Organs at risks included were heart, breast bud/tissue, liver and thyroid. 6 MV AP-PA (with segments) and RapidArc (2 or 3 full arcs) plans were created using the Eclipse treatment planning system (Version 11). Plans were calculated using the anisotropic analytical algorithm (AAA). The prescribed dose was either 15 Gy in 10 fractions or 18 Gy in 12 fractions based on the patient's age. PTV D2%, D98% and D50% and mean and maximum doses for heart and breast were obtained. The absolute excess risk (AER) of cardiac mortality at 15 years post treatment was calculated for each plan based on an age-at-exposure adjusted relative risk per Gy obtained from published data (1,2,3,4) combined with contemporary UK population-based absolute risks. The risk of breast cancer induction was calculated using the model proposed by Schneider et al. (2011) (5).

Results: The VMAT plans resulted in a similar minimum PTV coverage when compared to the AP-PA plans whilst reducing the PTV D2% by an average of 6.1% (4.1 – 9.1). The use of VMAT reduced the heart and breast mean dose by an average of 19.1% (11.7 – 30.5) and 16.2% (-2.2 – 30.4) respectively when compared to the AP-PA plans. The difference in AER of cardiac mortality at 15 years was lower for the VMAT plans by an average of 0.48% (0.11 – 0.98). The average excess absolute risk (EAR) for breast cancer induction across all plans decreased by 2.9% (-0.8 – 6.8) when compared to the conformal plans (assuming α/β = 3 Gy, α = 0.067 Gy-1, R = 0.62, μ = 4.8/10000PY/Gy).

Table: Calculated mean dose, AER and EAR per patient.

			Heart			
			Mean Dose [Gy]		AER [%]	
Patient	Age	Dose [Gy]	AP-PA	VMAT	AP-PA	VMAT
1	17	18	18.6	12.9	3.19	2.21
2	18	18	18.5	13.7	3.29	2.43
3	13	15	15.5	13.1	2.07	1.75
4	3	15	15.4	13.6	0.98	0.87
5	3	15	15.4	13.6	0.98	0.87

			Breast			
			Mean Dose [Gy]		EAR [#/10k/yr]	
Patient	Age	Dose [Gy]	AP-PA	VMAT	AP-PA	VMAT
1	17	18	18.2	14.2	26.5	24.7
2	18	18	13.5	10.4	22.0	22.1
3	13	15	12.5	8.7	21.8	20.4
4	3	15	14.3	13.1	24.9	24.2
5	3	15	13.6	13.9	24.6	24.7

References

1. Tukenova, M., et al., 2010. *J Clin Oncol*, 28:1308-1315.
2. Aleman, B. M., et al., 2003. *J Clin Oncol*, 21:3431-9.
3. Darby, S.C. and Taylor, C. American Society of Clinical Oncology Annual Meeting. Chicago, 2007.
4. Hancock, S.L., Tucker, M.A., Hoppe, R. T., 1993. *JAMA*, 270:1949-55.
5. Schneider, U., et al.2011. *Radiation Oncol*, 6:67.

Conclusion: VMAT achieved highly conformal plans and reduced cardiac late normal tissue complication probability whilst also reducing (or achieving similar) predicted risk of second cancer induction in breast tissue.

PO-0862

Comparison of Monte-Carlo computed 50 kV X-rays radiation therapy and EBRT for rectal cancer.

M. Vidal[1], M. Gautier[1], O. Croce[2], J.P. Gerard[1], K. Benezery[1]

[1]*Centre Antoine Lacassagne, Radiotherapy, Nice, France*

[2]*Institute for Research on Cancer and Aging of Nice IRCAN, INSERM U1081 - CNRS UMR 7284 - UNS, Nice, France*

Purpose or Objective: Traditionally, patients with rectal cancer (T2 anterior low rectum, T3-T4 N0-N+) are treated with preoperative radiotherapy or chemoradiation (CAP 50 regimen). 3D Conformal Radiation Therapy is conventionally delivered: 44 Gy more 6 Gy as a sequential boost to the high risk target volume (total dose 50 Gy). Another strategy would be to use the Contact Therapy technique [1] using 50 kV X-rays (CXRT) to deliver higher dose (30 Gy) to the high risk target volume in addition to 44 Gy. The present study first describes CXRT dose computation with Monte-Carlo simulations and then compares the resulting dose (EBRT+CXRT) with the conventional treatment (EBRT only).

Material and Methods: The CXRT machine Papillon 50™ installed in Centre Antoine Lacassagne (Nice, France) delivers a 50 kV X-ray beam with a dose rate close to 15 Gy/min, allowing treatment delivery more comfortable for the patients [2]. The system is currently used for treating skin and rectal cancers. The detailed geometry of the Papillon 50™ machine [3] was fully generated in Monte-Carlo code PenEasy based on PENELOPE [4] and the resulting simulations were validated against measurements in water (depth dose curves and transverse dose profiles) for all applicators used for rectum cancer. For 10 patients with T2-T3 nodes smaller than 3 cm, dose distributions were calculated to irradiate the high risk target volume. For each patient, 30 Gy CXRT dose was computed with Monte-Carlo simulation in 3DCT patient data acquired in a position close to the rectal cancer CXRT position (genupectoral position). 6 Gy EBRT treatment was computed with the commercial TPS Isogray (Dosisoft) in the 3DCT scan acquired in supine position. Both dose distributions were compared in terms of dosimetric indices computed for target volumes (conformity and homogeneity indices) and dose to organs at risk.

Results: Monte-Carlo penEasy simulations are in good agreement with the Papillon50TM measurements in water for

all rectum applicators. Simulations in patients 3DCT scan allowed us to evaluate CXRT dose to organs at risk and to the target volume. The comparison of dosimetric indices of EBRT and CXRT treatment delivery for the high risk target volume showed that the CXRT technique delivers higher dose to the target volume for the same dose, or even less for some cases, to the organs at risk.

Conclusion: Monte-Carlo simulations are useful to compute accurate dose distributions in 3DCT patient data for the CXRT treatment delivery. Moreover, this comparative study between the EBRT and CXRT techniques confirms the role of CXRT in curative treatment with organ preservation for early rectal cancers.

Bibliography:
[1] Gérard JP, et al. Int J Radiat Oncol Biol Phys. 2008 Nov 1;72(3):665-70.
[2] Gérard JP, *et al*. Expert Rev Med Devices. 2011 Jul;8(4):483-92.
[3] Croce O, *et al.* Rad Phys and Chem, 2012;81(6):609-617.
[4] Sempau J, *et al.* Med Phys. 2011 Nov;38(11):5887-95.

PO-0863

Localizing the benefit of a hydrogel rectum spacer for prostate IMRT within the ano-rectal wall

B.G.L. Vanneste[1], F. Buettner[2], M. Pinkawa[3], P. Lambin[1], A.L. Hoffmann[4]
[1]*MAASTRO clinic, Radiation Oncology, Maastricht, The Netherlands*
[2]*European Bioinformatics Institute, European Molecular Biology Laboratory, Hinxton- Cambridge, United Kingdom*
[3]*Radiation Oncology, RWTH Aachen University, Aachen, Germany*
[4]*University Hospital Carl Gustav Carus at the Technische Universität Dresden, Radiotherapy, Dresden, Germany*

Purpose or Objective: In previous studies the dosimetric impact of an implanted rectum spacer (IRS) in prostate cancer patients undergoing intensity-modulated radiation therapy (IMRT) has been assessed by dose-volume histograms (DVHs) and dose-surface histograms (DSHs) obtained from 3D dose distributions of the ano-rectal wall (ARW). Unfortunately, spatial information is lost when analyzing DVHs or DSHs. This hampers to study the correlation between the shape and location of the ARW dose distribution and clinical outcome. Dose-surface maps (DSMs) have been suggested as a valuable tool for taking the spatial-dosimetric information into account.The purpose of this study is to assess spatio-dosimetric differences in DSMs obtained from planned ARW dose distributions in patients receiving IMRT with and without IRS (IMRT+IRS; IMRT-IRS, respectively).

Material and Methods: In 26 patients with localized prostate cancer a hydrogel rectum spacer (SpaceOAR®, Augmenix) was injected under transrectal ultrasound guidance in Denonvilliers' space between the prostate and the rectal wall. Per patient, two IMRT treatment plans (78 Gy in 39 fractions) were designed, based on CT scans acquired before and after hydrogel injection. DSMs of the ARW were generated from the planned 3D dose distributions by virtual unfolding the rectum contour as described in Buettner et al. (Fig. 1a-b).

Figure 1a
Rectal wall DSM (in Gy) without IRS (left) and with IRS (right). Vertical axis corresponds to superior-inferior direction. Horizontal axis represents circumferential direction: P, posterior; L, left; A, anterior; R, right.

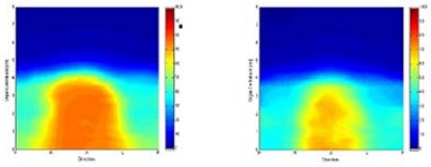

Figure 1b
Anal wall DSM (in Gy) without IRS (left) and with IRS (right).

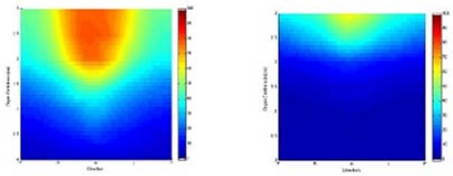

Various shape-based dose measures were extracted from the DSMs. First, dose clusters were generated by thresholding the DSMs at 38 dose levels ranging from 5-79 Gy. Then, for each dose level an ellipse was fitted to the largest dose cluster. Lateral (posterior-anterior-posterior) and longitudinal (superior-inferior) extents were quantified by projecting the major and minor axes of this ellipse to the main axes of the DSMs. The non-circularity of the dose clusters was described by the eccentricity of the ellipse. The contiguity of the ARW dose distribution was assessed by the contiguous-DSH (cDSH), reflecting the single largest contiguous ARW area fraction as function of the dose threshold at the given level. Statistical differences were assessed with a one-sided paired Wilcoxon signed rank test.

Results: Lateral extent, longitudinal extent as well as cDSH were significantly lower in IMRT+IRS than for IMRT-IRS at high-dose levels. Largest significant differences were observed for cDSH at dose levels >50Gy, followed by lateral extent at doses >57Gy, and longitudinal extent. For these three features, no significant differences were observed for low to medium dose levels. For eccentricity no significant differences were found, independent of the dose level.

Conclusion: Significant spatio-dosimetric differences in ARW DSMs exist between prostate cancer patients undergoing IMRT with and without IRS. The IRS particularly reduces the lateral and longitudinal extent of high-dose areas (>50 Gy) in anterior and superior-inferior directions.

PO-0864

A planning study investigating different planning techniques for SBRT of NSCLC.

C. Moustakis[1], I. Ernst[1], F. Ebrahimi Tazeh Mahalleh[1], U. Haverkamp[1], H.T. Eich[1], M. Guckenberger[2]
[1]*University Muenster, Radiation Oncology, Münster, Germany*
[2]*University Zurich, Radiation Oncology, Zürich, Switzerland*

Purpose or Objective: SBRT is a novel treatment procedure, which is used for the particular localization of the tumor to deliver targeted high doses with greatly precise fields. Different irradiation techniques provide a wide spectrum of therapy options. The aim of this work was to evaluate the clinical benefits and potential dosimetric of different planning methods against each other for the treatment of NSCLC.

Material and Methods: In this study, three diagnosed patients with NSCLC metastasis, were chosen. One had a peripheral metastasis in the left lung , the other had a metastasis in the right lung, and the last one had a central metastasis located near to vertebral body. The delineated structures (PTV and OARs) on CT were shared among 22 clinics with the request to generate an irradiation plan with their own internal criteria. Three fractions of 15 Gy were prescribed to the PTV-enclosing 65%. All together it was

assembled 78 treatment plans, that they were generated, 36 IMAT, 18 3DCRT, 3 IMRT, 9 helical irradiation and 12 robotic radiosurgery. All gathered data were finally imported into one treatment planning system for evaluating different planning strategies.

Results: In all plans, the dosimetric coverage of the target volume and the dose to OARs were within clinical limits. The coverage of the PTV were disclosed: CICRU =1.0(0.9-1.1); CI65 =0.7(0.4-1.0); HI=0.3(-0.3-0.5); Dmin/Dmax=0.6(0.5-0.7); D2%,=64.6(47.5-71.3)Gy; D98%=47.2(39.5-68.6)Gy; Dmiddle=57.8(47.3-65.8)Gy.
In the 3DCRT Plans, the mean dose in the PTV was on average, 3 Gy higher than dynamic techniques; MU and irradiation time were by the factor of 2-3 higher in the dynamic techniques. Dose to the OARs for the 1st and 2nd patient is as bellows: Dmedi, ipsilat. lung = 4.9 (3.2-8.8)Gy; Dmax, esophagus =7.7(0.4-16.1)Gy. V35Gy, rips =10(0.6-43.7). For the 3rd one: Dmedi., ipsilat. lung = 8.3(6.8-10)Gy; Dmedi.,contralat. lung = 2.3(1.4-4.7)Gy Dmax, esophagus=20.7(11.3-27.7)Gy.
Picture shows the Dmax for the spinal cord.

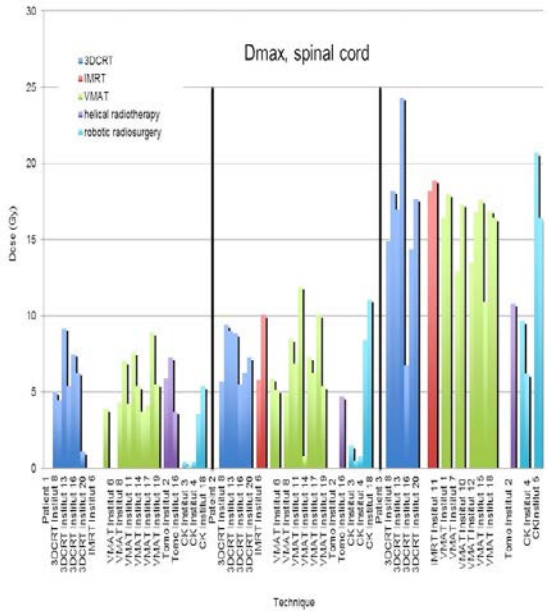

Conclusion: All irradiation techniques were applicable for clinical use, the resulting dose distribution were quite similar. By comparison, the statistically significant differences between the users were greater than the differences between the techniques. This demonstrate that strict constrains and works like the DEGRO reference paper (Guckenberger et al) are necessary to homogenize the SBRT planning at a national level.
This study reports the results of the irradiation planning for the treatment of NSCLC with SBRT depends largely on the user.

PO-0865
Developing sciatic nerve-sparing stereotactic radiotherapy for re-irradiating the pelvic sidewall
M. Llewelyn[1], E. Wells[2], A. Taylor[1]
[1]*Royal Marsden NHS Foundation Trust, Department of Gynaecology, London, United Kingdom*
[2]*Royal Marsden NHS Foundation Trust, Department of Radiotherapy, London, United Kingdom*

Purpose or Objective: Management of pelvic sidewall recurrence in gynaecological cancers is a challenging clinical scenario. Sciatic nerve involvement may exclude surgery and cause intractable symptoms that are difficult to palliate. In the context of re-irradiation, high doses of radiation without consideration of the sciatic nerve can cause irreversible nerve damage, yet this has not traditionally been included as an OAR.
The aims of this study were to develop dose target constraints for re-irradiation of the sciatic nerve, and to assess the impact of nerve-sparing optimisation on target volume coverage and OAR sparing with stereotactic radiotherapy techniques.

Material and Methods: Cumulative dose constraints for re-irradiation were derived assuming prior pelvic radiotherapy of 50Gy (EQD2) and allowing nerve recovery values of 50% and 100%. Treatment plans were produced for 10 patients with recurrent gynaecological cancer delivering 30 Gy in 5 fractions. Two normalisation methods were assessed: ICRU 83 type normalisation and prescription (ICRU); and stereotactic radiosurgery convention of prescribing to the isodose covering 95% PTV allowing maximum doses of ~125% (SRS). For each method, plans were optimised with and without sciatic nerve sparing targets. Sciatic nerve roots were contoured from sacral foramina until the nerve exits the pelvis. Nerve sparing plans were optimised to minimize dose to nerve PRV while maintaining PTV coverage. Doses to GTV, PTV, OAR and sciatic nerve were compared.

Results: All 40 plans met the PTV targets with >95% PTV coverage by the specified isodose. The sciatic nerve was involved in 3 patients, close proximity (<5 mm) in 4 patients and more than 5 mm distant from PTV in 3 patients. The dose targets were Dmax 32 Gy when there was nerve involvement and 21.9 Gy when the nerve was distant from tumour. For all patients, the sciatic nerve dose was reduced with each technique: median Dmax with ICRU from 28.8 Gy to 22.3 GY and with SRS from 28.7 Gy to 19.9 Gy. For patients with overt nerve involvement, median Dmax was reduced from 34.9 Gy to 32.1 Gy with SRS. Nerve sparing was achieved without significantly decreasing GTV mean doses or increasing bowel doses.

Conclusion: The sciatic nerve should be an OAR for re-irradiation of sidewall recurrence. Optimisation using a sciatic nerve PRV can significantly reduce dose to nerve by up 40% (EQD2-2) while having minimal effect on GTV coverage or bowel doses. Feasible dose targets depend on proximity of nerve to GTV and clinical scenario.

PO-0866
Evaluation of three planning RT techniques for boost phase in pediatric medulloblastomas
A.R. Figueira[1], A.R. Lago[1], A. Monteiro[1], D. Monteiro[2], D. Inácio[1], L. Osório[1], M.J. Fontes[1], P. Varzim[1], G. Pinto[1]
[1]*Hospital de São João, Radiotherapy, Porto, Portugal*
[2]*University of Lleida, Medicine, Lleida, Spain*

Purpose or Objective: Over the last half century we have seen remarkable improvements in the survival of pediatric cancer patients. Therefore, the impact of cancer and its treatment must be assessed. Furthermore, the radiotherapy technique must be well selected in order to minimize the secondary effects. Since hearing loss is a common late effect of radiotherapy, the purpose of this study was to compare three different treatment techniques and to evaluate the dose to the cochleas and supretentorial brain, in children treated with radiotherapy for medulloblastoma.

Material and Methods: A total of 121 children were treated in our department with radiotherapy for CNS tumors, between January 2000 and December 2014. Those who were diagnosed with medulloblastoma were included. A total of 29 children fulfilled these criteria. The adopted treatment plan consisted of a first phase with three-dimensional conformal radiotherapy (3D-CRT) to the craniospinal region (prescribed doses from 23.4 to 36.0 Gy) followed with a boost to the PTV (posterior fossa/tumor bed) with prescribed doses of 18.0 or 31.6 Gy depending on the clinical risk-group, high or standard risk respectively . For each child, three different treatment plans were prepared for the boost phase: one with conventional 2 parallel opposed fields (CRT), one more complex with 3D conformal radiotherapy (3D-CRT) and

another with IMRT. The original plans delivered to the patients were not considered in this study because treatment techniques have been changing since 2000 and were not uniform within the selected group. All plans assured PTV coverage according to ICRU 83 criteria. Cochleas and supratentorial brain mean doses, as organs , were analyzed using QUANTEC values and compared for each plan.

Results: Among 29 children, 22 were males. The median age at diagnosis was 8.66 years. At the beginning of treatment, their age range from 3.26 to 15.47 years old. The average mean dosesto the OAR analyzed are presented in Table 1.
Table 1: Average Mean Doses to OARs

Mean Dose (Gy)	High Risk			Standard Risk		
	CRT	3D-CRT	IMRT	CRT	3D-CRT	IMRT
Right Cochlea	17,6	11,0	10,0	29,3	18,0	16,4
Left Cochlea	17,4	11,0	9,0	29,0	19,0	15,0
Supratentorial Brain	6,0	4,5	4,9	10,0	7,5	8,2

Conclusion: The plans for the CRT technique, with 2 parallel opposed fields, produced worst results for both OARs. The IMRT technique was slightly superior to the 3D-CRT in terms of mean dose of cochleas but conducted, in average, to higher dose values to the supratentorial brain. Based on these results we decided to adopt the 3D-CRT technique for the boost phase in high-risk group and IMRT for the standard-risk group, considering the higher potencial impact in the cochleas mean doses in this risk-group.

PO-0867

Treatment planning study for spatially fractionated mini-beam radiotherapy

A. Alexander[1], C. Crewson[1], W. Davis[2], M. Mayer[3], G. Cranmer-Sargison[1], V. Kundapur[4]
[1]*Saskatchewan Cancer Agency - Saskatoon Cancer Centre, Medical Physics, Saskatoon, Canada*
[2]*University of Saskatchewan, Physics and Engineering Physics, Saskatoon, Canada*
[3]*University of Saskatchewan, Small Animal Clinical Sciences, Saskatoon, Canada*
[4]*Saskatchewan Cancer Agency - Saskatoon Cancer Centre, Radiation Oncology, Saskatoon, Canada*

Purpose or Objective: This work is to present the treatment planning workflow and delivery technique for the first application of linac based spatially fractionated mini-beam radiotherapy within a clinical trial of canine brain tumor treatments. The motivation for this investigation originates from work performed using synchrotron generated micro-beams (MRT) which have shown promising results in preserving brain architecture while killing tumor cells. Spatial fractionation of radiation using arrays of parallel micro-planar beams is a developing technique with many unknowns and limitations. To further research this technique and to potentially enable MRT for human treatments, a mini-beam collimator has been designed for use with a linac and a Monte Carlo (MC) beam model has been commissioned for clinical treatment planning.

Material and Methods: Patient population was selected from client-owned canines with spontaneously occurring brain tumors. Patients were placed under general anesthesia and positioned prone within stereotactic immobilization equipment during imaging and treatment delivery. CT and MRI images were used for contouring. The planning technique utilized an arrangements of static mini-beams. Beam angles were chosen such that the treatment depth was within 20% for each beam to minimize beam broadening with depth and blurring of the peak and valley doses. Beam apertures were defined with the MLC leaves set 3 mm back from the PTV. The mini-beam collimated dose distributions were calculated to a statistical uncertainty of ±1.0 % within a voxel size of 0.5 mm. Beam weighting was equalized and the plan normalized such that the prescription dose was delivered to an ICRU dose reference point within the PTV. Deliver quality assurance (DQA) was performed by measuring the absolute dose from each beam using an ion chamber within a solid water phantom.

Results: Contouring and beam arrangement, which included MLC placement, was performed within the clinical treatment planning system (TPS). The DICOM plan was then exported to the MC treatment planning system for mini-beam dose calculation. The distribution was reviewed and DVHs assessed for normal tissue tolerances. The final step was to transcribe the calculated MUs back to the original TPS. Planning turnaround time was 2 days. The MC calculations were initiated overnight at the end of day 1. Day 2 was spent reviewing the plan, generating the DQA plan, and finalizing the treatment parameters into the record-and-verify system (RVS). DQA output measurements of the treatment fields agreed with the calculated dose to within 1.5%. An image of the patient dose distribution and setup is shown in figure 1.

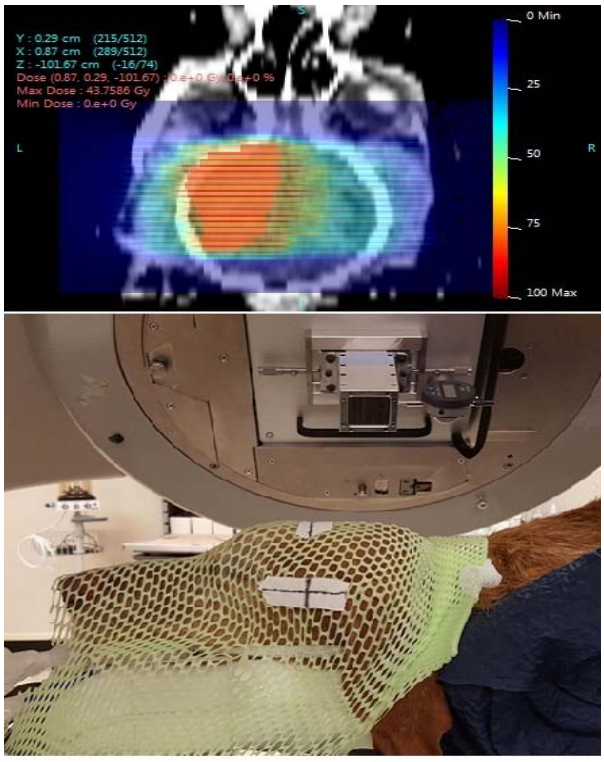

Figure 1: Colorwash display of mini-beam dose distribution (top), photo of patient setup with mini-beam collimator (bottom)

Conclusion: A workflow for mini-beam treatments that includes the planning technique, MC dose calculation method, DQA process, and data integration into a RVS has been established. This clinical dataset represents the first treatment planning study of linac based mini-beam patients.

PO-0868

A method to define isodose-based structures in Dose Painting treatment of GBM in Tomotherapy.

M. Orlandi[1], A. Botti[1], E. Cagni[1], L. Orsingher[1], R. Sghedoni[1], P. Ciammella[2], C. Iotti[2], M. Iori[1]
[1]*Arcispedale S. Maria Nuova, Fisica Medica, Reggio Emilia, Italy*
[2]*Arcispedale S. Maria Nuova, Radioterapia, Reggio Emilia, Italy*

Purpose or Objective: The aim of this study is to investigates different strategies in choosing, in a mathematical way, the structure set that best fit a Dose Painting (DP) distribution, based on ADC maps, to be submitted to the optimization process within the TomoTherapy TPS.

Material and Methods: Hypofractionated Stereotactic Radiation Therapy plans in 5 fractions of intracranial GBM for six patients were retrospectively realized.

A non-uniform Dose Painting By Numbers Dose Distribution (DPBN) was obtained from an ADC map of each patient registered with the planning CT scan. The pixels values within the CTV of the registered ADC maps were converted to dose values through the function of Eq. 1, where Dmin = 25 Gy, Dmax = 50 Gy, Imin = 500 mm2/s e Imax = 1500 mm2/s.
According to Deveau et al., (Acta Oncol. 2010) 9 isodose levels of the DPBN should be converted into structures in order to restrict the number of planning structures in the TPS optimization step. Four different methods to select the isodose levels were implemented.
IsoDose Method (IDM). The dose interval prescription is divided in 9 equal sub-intervals (Fig. 1.a). In this way the sub-intervals are dependent on the dose prescription interval only.
IsoVol Method (IVD). The volume of the CTV structure is divided in 9 equal subvolumes (Fig. 1.b). The absolute DVH of the DPBN of the CTV allows to associate to each volume value (cm^3) a dose value. These are used as the isolevels to be converted in structures.
IsoVD Method (IVDM). An arbitrary function, indicated as ΔDV, was defined in Eq. 2 where Dmin and Dmax are the minimum and maximum prescribed dose, Vmax is the total volume of the CTV, Di and Vi are the dose and the volume at the point i in the DVH line. Dividing the ΔDV(Di) function in 9 equi-spaced interval, as in Fig. 1.c, the corresponding dose values, from which derive the sub-structure for the optimization, were found.
minQF Method (mQM). Starting from a structure set of 9 isolevels obtained from DPBN, it is possible to calculate a Dose Painting By Contours Dose Distribution (DPBC), assigning to each voxel pertaining to the isolevels *k* a uniform dose of value *Dk*. This method imposes that the Quality Factor (QF), in Eq. 3-4 (Vanderstraeten et al., Phys. Med. Biol. 2006), between the DPBN and the DPBC be as close as possible to zero, using a genetic minimization algorithm (Matlab).
In order to estimate which method returns the DPBC more consistent with the DPBN, the QF and the QVH were computed for each method.

$$D(I) = \begin{cases} D_{max} & I < I_{min} \\ D_{min} + \frac{I - I_{min}}{I_{max} - I_{min}} \cdot (D_{max} - D_{min}) & I_{min} < I < I_{max} \\ D_{min} & I > I_{max} \end{cases} \quad \text{Eq. 1}$$

$$\Delta DV(D_i, V_i) = (D_i - D_{min}) \cdot (V_{max} - V_i) \quad \text{Eq. 2}$$

$$D_i \in [D_{min}, D_{max}]$$

$$V_i \in [0, V_{max}]$$

$$QF = \frac{1}{n} \Sigma_i |Q_i - 1| \quad \text{Eq. 3}$$

$$Q_i = \frac{DPBC_i}{DPBN_i} \quad \text{Eq. 4}$$

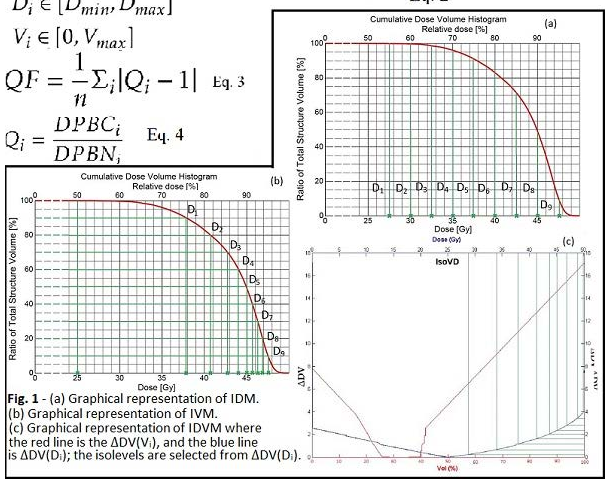

Fig. 1 - (a) Graphical representation of IDM. (b) Graphical representation of IVM. (c) Graphical representation of IDVM where the red line is the ΔDV(Vi), and the blue line is ΔDV(Di); the isolevels are selected from ΔDV(Di).

Results
Comparing the four methods, the results in Table 1 show that the mQM provides QF values closest to zero for six patients and that only in one patient the IVD is better than the mQM only of about 1 %. Also QVHs show lines more about to 1 for the mQM.

Method		Pz1	Pz2	Pz3	Pz4	Pz5	Pz6
IsoDose	(IDM)	0.0236	0.0309	0.0150	0.0362	0.0328	0.0181
IsoVol	(IVM)	0.0230	0.0330	0.0144	0.0432	0.0322	0.0209
IsoVxD	(IVDM)	0.0279	0.0398	0.0238	0.0509	0.0410	0.0259
minQF	(mQM)	0.0226	0.0283	0.0145	0.0310	0.0317	0.0161

Table 1

Conclusion: A robust and mathematical method in order to select the structure set that better fit a Dose Painting distribution was found in the mQM method. This method could be employed regardless the way used to obtained the Dose Painting distribution.

PO-0869
Comparing Varian EDGE and Gamma Knife for brain metastases radiosurgery. Preliminary results
S. Tomatis[1], P. Navarria[2], D. Franceschini[2], L. Cozzi[2], P. Mancosu[1], F. Lobefalo[1], G. Reggiori[1], A.M. Ascolese[2], A. Stravato[1], F. Zucconi[1], G. Maggi[2], M. Scorsetti[2]
[1]*Istituto Clinico Humanitas, Medical Physics Service of Radiotherapy- Radiotherapy and Radiosurgery Department, Rozzano Milan, Italy*
[2]*Istituto Clinico Humanitas, Radiotherapy and Radiosurgery Department, Rozzano Milan, Italy*

Purpose or Objective: Brain metastases occur in 20-40 % of patients affected by primary solid tumors. Radiosurgery (SRS) was demonstrated to be safe and efficient for the brain metastases control. SRS can be delivered with dedicated equipment, like GammaKnife, or with conventional LINAC. Few comparative studies have been conducted. In our institution we designed a phase III randomized trial to evaluate cerebral side effects following SRS delivered by Gamma Knife Perfexion and Linac EDGE

Material and Methods: Patients with 1 to 4 brain metastases, from any primary except for small cell lung cancer (SCLC) or Lymphoproliferative disease, suitable for SRS were randomized to receive the treatment with GammaKnife or Linac. Primary end point was the symptomatic radionecrosis incidence; brain LC, DFS and OS were secondary end points. Planning parameters, including target coverage for accepted surface dose levels, paddick conformity index (PCI), gradient index (GI), homogeneity index (HI), maximum and minimum dose to the target were determined. Beam on time (BOT) was also recorded

Results: Until now, 26 patients with 39 metastases (range 1-3) were enrolled in this phase III trial (12 GK, 14 Linac-EDGE). Median prescribed dose was 24 GY (range 21-24 Gy). Most common primary cancers were breast and melanoma. At the time of analysis 3 patients died. Follow up evaluation was available in 12 cases. No local progression was observed, 4 patients had a further intracranial progression. Until now, no radionecrosis was recorded. PCI was better for linac-based plans (0.93 vs 0.82), in contrast, a better GI for gamma knife was observed (2.5 vs 3.5). Due to the specific characteristics of the two delivery systems, HI was lower for linac (0.14 vs 0.80). BOT was lower for linacs (within 2 min for each target vs 35 min). In our center, linac based immobilization was made by an open mask setup (qfix); CBCT-based IGRT was applied; patients were monitored by optical surface monitoring system (OSMS) during the delivery. Gamma knife immobilization was performed by the traditional stereotactic head frame by Elekta. For this reason, no specific online imaging or tracking device was required

Conclusion: These are very preliminary results of a randomized phase III trial recently started in our institution. No significant clinical data can be provided yet, because of the short follow up time and the small number of enrolled patients. On the dosimetry side, the two systems have different characteristics and markedly different ways to prescribe dose. For linacs, a better dose distribution was obtained on the target rather than for normal tissues, even though no specific side effects were reported. In addition,

data suggested a better comfort for the patient for linac-based therapy, due to the shorter treatment time and the non-invasive immobilization system. Dosimetric data for the patients treated according to this protocol suggest a substantial balance between Gamma Knife and Linac EDGE treatments

Poster: Physics track: (Radio)biological modelling

PO-0870

Fitting data of relapse-free survival after post-prostatectomy RT with a comprehensive TCP model

C. Fiorino[1], S. Broggi[1], N. Fossati[2], C. Cozzarini[3], G. Goldner[4], T. Wiegel[5], W. Hinkelbein[6], J.R. Karnes[7], S.A. Boorjian[7], K. Haustermans[8], S. Joniau[9], S. Shariat[10], F. Montorsi[11], H. Van Poppel[9], N.G. Di Muzio[3], R. Calandrino[1], A. Briganti[2]

[1]*San Raffaele Scientific Institute, Medical Physics, Milano, Italy*

[2]*San Raffaele Scientific Institute, Division of Oncology/Unit of Urology, Milano, Italy*

[3]*San Raffaele Scientific Institute, Radiotherapy, Milano, Italy*

[4]*Medizinische Universitat Wien, Klinik fur Radioonkolgie, Wien, Austria*

[5]*University Hospital Ulm, Department of Radiation Oncology, Ulm, Germany*

[6]*Charitè Universitats Medizin- Campus Benjamin Franklin, Department of Radiation Oncology, Berlin, Germany*

[7]*Mayo Clinic Rochester, Department of Urology, Rochester, USA*

[8]*University Hospital Leuven, Department of Radiotherapy, Leuven, Belgium*

[9]*University Hospital Leuven, Department of Urology, Leuven, Belgium*

[10]*Medical University of Vienna- Vienna General Hospital, Department of Urology, Wien, Austria*

[11]*San Raffaele Scientific Institute, Department of Oncology/Unit of Urology, Milano, Italy*

Purpose or Objective: By pooling data of five large prospective studies/Institutional series, a large data base of pT2-pT3, pN0 patients treated either in the adjuvant or in the salvage setting with conventionally fractionated (1.8-2.0 Gy/fr) 3DCRT post-prostatectomy radiotherapy (RT) was available. The aim of the study was to fit individual data of biochemical-recurrence-free survival (bRFS) with a comprehensive Poisson-based TCP model.

Material and Methods: Considering pre-RT PSA as a surrogate of the number of clonogens, 5-year bRFS was expressed as a function of the dose depending on radiosensitivity (α_eff), number of clonogens for pre-RT PSA=1ng/mL (C) and the fraction of patients that relapses due to clonogens outside the treated volume, assumed to linearly depend on pre-RT PSA (K=1-BxPSA), according to:

bRFS = (1-B x PSA) x [1 - exp (-α_eff D)]^CxPSA.

In addition, the impact of Gleason score (GS) was included by performing separate fits for different sub-groups, depending on GS (<7,=7,>7). In total, complete data regarding bRFS, dose, pre-RT PSA (between 0.01 and 2.0 ng/ml) and GS of 894 hormono-naive patients treated with adjuvant (n=331) or salvage (n=563) intent with a minimum follow-up of 3 years were available. Patients with GS<7, =7 and >7 were 392, 383, and 119 respectively. Best-fit procedures were performed with the sequential quadratic programming, using the sum of the squared residuals error as loss function (SPSS v.17, SPSS Inc., Chicago, IL). The 95% CI of the parameter's best-fit values were calculated by bootstrap. The performance of the resulting model was assessed by calibration plot.

Results: The median follow-up was 72 months; median pre-RT PSA and dose were 0.25 ng/mL (inter-quartile range: 0.1-0.5) and 66.6Gy (range:59.4-77.4Gy) respectively. The fit converged in all situations: depending on GS, best-fit values were in the range 0.20-0.22 Gy-1 and 10^6 for α_eff and C respectively; the maximum obtainable bRFS was reduced by 1.7, 4.9 and 5.6% for each 0.1ng/ml PSA increment for GS<7, =7 and >7 respectively. The calibration plot showed an excellent agreement between predicted and expected values (R2=0.96) and the AUC was 0.69 (95% CI: 0.66-0.73). The bRFS curves as estimated by the model vs prescribed dose for different pre-RT PSA (between 0.1 and 1.0 ng/ml) and for the three GS groups are plotted in the figure.

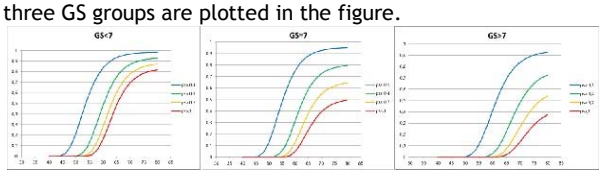

Conclusion: Long-term bRFS data of a large multi-centric data base of post-prostatectomy patients could be fitted by a radiobiologically consistent TCP model, showing a dose-effect critically depending on pre-RT PSA and GS. The model suggests that most relapses occur in patients with clonogens outside the treated volume, indirectly supporting lymph-nodal irradiation and/or systemic therapy for specific risk groups, depending on pre-RT PSA and GS. Early RT is preferred over delayed RT as the detrimental effect due to a PSA increase can never be compensated by increasing the dose, more dramatically evident for patients with GS ≥7.

PO-0871

Radiation-induced lung damage: beyond dose-volume histogram analysis

S. Monti[1], G. Palma[2], V. D'Avino[2], M. Conson[3], R. Liuzzi[2], M.C. Pressello[4], V. Donato[5], J.O. Deasy[6], R. Pacelli[3], L. Cella[2]

[1]*IRCCS SDN, Naples, Italy*

[2]*National Research Council, Institute of Biostructure and Bioimaging, Naples, Italy*

[3]*Federico II University School of Medicine, Department of Advanced Biomedical Sciences, Naples, Italy*

[4]*S. Camillo-Forlanini Hospital, Department of Health Physics, Rome, Italy*

[5]*S. Camillo-Forlanini Hospital, Department of Radiation Oncology, Rome, Italy*

[6]*Memorial Sloan Kettering Cancer Center, Department of Medical Physics, New York, USA*

Purpose or Objective: Traditional normal tissue complication probability (NTCP) models rely on dose-volume histogram (DVH) analysis, which disregards any spatial dose distribution information and possible inhomogeneity in regional organ radio-sensitivity. We propose a voxel-based (VB) approach to correlate local lung dose and radiation-induced lung damage (RILD).

Material and Methods: An inter-institutional database of 115 Hodgkin lymphoma survivors treated with sequential chemo-radiotherapy (with 18 RILD cases after treatment) were included in the study. Sixteen patients were excluded due to an inadequate CT coverage of the lungs.

Each patient dataset was first normalized to a common template. Pre-registration steps were based on a binary mask extrapolated from the organ at risk segmentations of the treatment plan. For each patient, the mask, computed as the union and dilation (spherical structuring element of radius 30 mm) of heart and lung structures, was used to crop the field-of-view, allowing a coarse alignment of the structures of interest. CT images were masked accordingly in order to hide some anatomical inter-individual differences, and allowed the registration algorithm to work more efficiently on tissue contrast inside the chest. The median lung-volume patient was chosen as reference image in the non-rigid registration and a log-diffeomorphic approach [1] was used. The obtained deformation fields were then used to map the dose of each patient to the common coordinate system of the reference patient.

A voxel-wise two-sample t-test was then performed on the normalized dose maps and statistically significance of the differences between groups was displayed as p-value map.

Results: The robustness of co-registration process was assessed both by visual inspection (Fig. 1a-b) and by Dice scores for the lungs (Fig. 1c). On the whole population, the median Dice value was 0.94 (range: [0.87; 0.95]). As shown in

Fig. 1d-f, a significantly ($p < 0.01$) higher dose was delivered to RILD patients nearby the basal portion of the right lung and the submantellar region of the left lung. The average dose delivered to this volume (9.4% of the lungs) was of 5.3 Gy in RILD patients and 2.6 Gy in non-RILD patients.

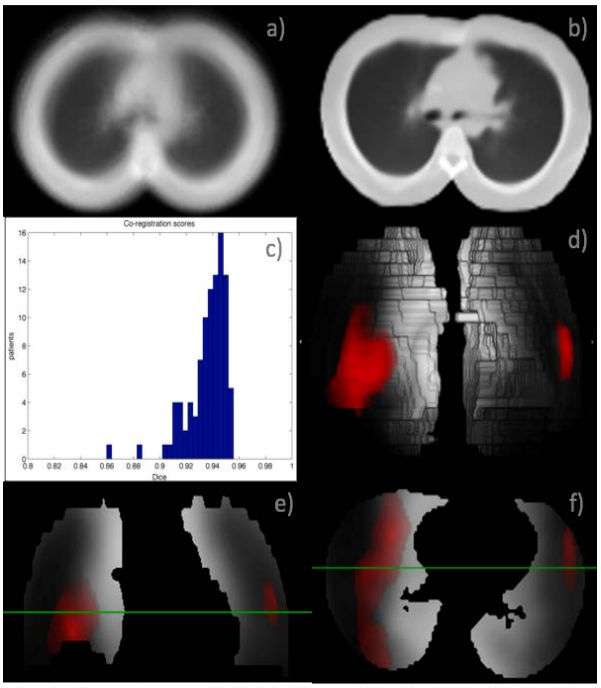

Figure 1. a) Average of the pre-registration CTs. b) Average of the post-registration CTs. c) Lung Dice scores distribution. d) 3D anteroposterior volume rendering of the mean RILD patients' dose (gray scale) with in red the *p*-value map (masked for $p < 0.01$). e) Coronal view of the mean RILD patients' dose (gray scale) with in red the *p*-value map (masked for $p < 0.01$). f) Axial view of the mean RILD patients' dose (gray scale) with in red the *p*-value map (masked for $p < 0.01$).

Conclusion: By a VB approach we were able to highlight local dose-RILD relationship in the lungs. Interestingly, a significantly different dose was delivered in the low-dose (~ 5 Gy) parenchymal regions, in agreement with previous DVH analyses showing that the volume exceeding 5 Gy is consistently more predictive than other dosimetric variables.
In order to obtain more powerful insights on local lung radiosensitivity, this preliminary results should be enriched by applying the VB approach to larger databases evaluating RILF in heterogeneously treated lungs.

[1] Vercauteren T, Pennec X, Perchant A, Ayache N. Symmetric log-domain Diffeomorphic registration: A demons-based approach. In lecture notes in computer science: Vol 5241. MICCAI 2008

PO-0872

The variability of the RBE in proton therapy: can we base it on empirical clinical data?

A. Lühr[1,2,3], C. Von Neubeck[1,2,3], M. Baumann[1,2,3,4,5], M. Krause[1,2,3,4,5]

[1]*German Cancer Consortium DKTK, Partner Site Dresden, Dresden, Germany*
[2]*OncoRay - National Center for Radiation Research in Oncology, Faculty of Medicine and University Hospital Carl Gustav Carus- Technische Universität Dresen- Helmholtz-Zentrum Dresden-Rossendorf, Dresden, Germany*
[3]*German Cancer Research Center DKFZ, Heidelberg, Germany*
[4]*University Hospital Carl Gustav Carus- Technische Universität Dresden, Department of Radiation Oncology, Dresden, Germany*
[5]*Helmholtz-Zentrum Dresden - Rossendorf, Institute of Radiooncology, Dresden, Germany*

Purpose or Objective: Particle therapy has the potential to improve radiotherapy due to the increase in dose conformity and RBE. The RBE depends on multiple factors including cell type, dose, particle type and energy. Accordingly, a variable RBE is clinically applied for carbon ion therapy, in contrast to a prescribed constant RBE = 1.1 in proton therapy jeopardizing part of its accuracy. Therefore, it is the aim to enhance proton therapy by translating a more realistic RBE description into the clinic directly based on clinical (and preclinical) experience gained with photons and heavier ions such as helium and carbon ions.

Material and Methods: The RBE is considered to depend on a) the dose response of the biological endpoint and b) the heterogeneity of the dose distribution on the cellular level (similar to the local effect model). The heterogeneity is determined by the clinically accessible (prescribed) dose D and the beam quality $Q = Z^2/E$ (varying within the patient), where Z and E are the ion charge and kinetic energy, respectively. We propose an approach to obtain proton RBE by interpolating between the biological effectiveness of a homogeneous dose distribution for photons and an increasingly heterogeneous distribution for heavier and slower ions. Based on the linear-quadratic (LQ) model and the dose heterogeneity an analytical description of the radiobiological effect was derived. It suggests a linear increase of the LQ parameter for particle irradiation αP with beam quality Q. *In vitro* RBE data from the literature for different ion types, cell lines, and within clinically relevant LET ranges (below the RBE maximum) were analyzed.

Results: The considered RBE data seem to depend directly on beam quality Q (Figure 1a). In contrast, particle type together with LET appear as a surrogate for beam quality Q (Figure 1b). In accordance with the derived description, the LQ parameter αP increases linearly with Q (Figure 1c) and the RBE (Figure 1d) as well as αP could be approximated for all considered ions and cell lines with a simple formula depending on Q, D, and the photon LQ parameters αX and βX. The deviations between prediction and experiment are mostly within 10 - 20% and therefore on the order of uncertainties often associated with RBE experiments. The variation of βP with Q was much weaker and less conclusive.

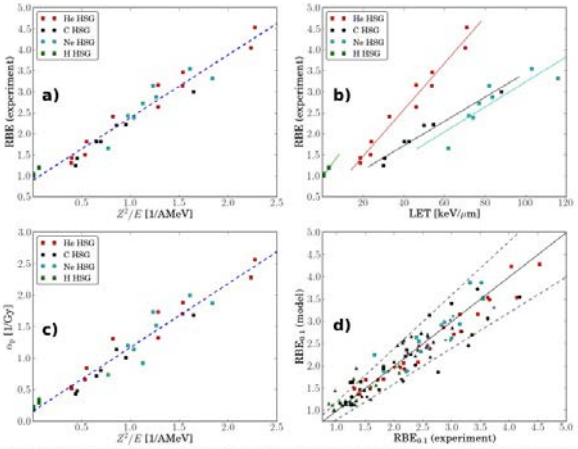

Figure 1: Biological effectiveness for different beam qualities, beam energies, and ion types: green, proton; red, helium; black, carbon; cyan, neon. The same in vitro RBE data for human salivary gland tumor (HSG) cells as a function of a) beam quality $Q = Z^2/E$ and b) LET. c) Linear LQ parameter as function of Q for HSG cells. d) Modeled compared to measured RBE values for about 125 different combinations of cells, ion types and energies. The dashed lines visualize a 20% spread around the solid identity line. All lines are just to guide the eye.

Conclusion: As long as cells "experience" a comparable microscopic dose distribution they cannot distinguish between different ion beams confirming that RBE variability also exists in proton therapy. More realistic RBE values for proton therapy may be directly obtained from available empirical RBE data for heavier ions considering the same beam quality Q and endpoint or, alternatively, by interpolating between empirical data from photon irradiation and heavier ions. Experimental preclinical (and clinical) data should be gathered in order to validate the proposed strategy to enhance proton therapy.

PO-0873

Modelling severe late rectal bleeding in a large pooled population of prostate cancer patients

A. Cicchetti[1], T. Rancati[1], M. Ebert[2], C. Fiorino[3], A. Kennedy[2], D.J. Joseph[2], J.W. Denham[4], V. Vavassori[5], G. Fellin[6], R. Valdagni[1]

[1]*Fondazione IRCCS Istituto Nazionale dei Tumori, Prostate program, Milan, Italy*
[2]*Sir Charles Gairdner Hospital, Radiation oncology, Perth, Australia*
[3]*San Raffaele Scientific Institute, Medical Physics, Milan, Italy*
[4]*University of Newcastle, School of Medicine and Public Health, New South Wales, Australia*
[5]*Cliniche Humanitas-Gavazzeni, Radiotherapy, Bergamo, Italy*
[6]*Ospedale Santa Chiara, Radiotherapy, Trento, Italy*

Purpose or Objective: To develop a model for grade 3 (G3) late rectal bleeding (LRB) after radical radiotherapy (RT) for prostate cancer, in a pooled population from two large prospective trials.

Material and Methods: The trials included patients (pts) treated with a conventional fractionated 3DCRT at 66-80Gy. Planning data were available for all pts. G3 LRB was prospectively scored using the LENT/SOMA questionnaire, with a minimum follow-up of 36 months. Rectal dose-volume histograms were reduced to an Equivalent Uniform Dose (EUD) distribution calculated with volume-effect parameter, n, derived by 3 studies: n=0.018 (Defraene IJROBP2011), n=0.05 (Rancati RO2011) and n=0.06 (Rancati RO2004). EUD was inserted into a multivariable logistic (MVL) regression together with clinical and treatment features. Irradiation of seminal vesicles (SV), irradiation of pelvic nodes, hormonal therapy, hypertension, previous abdominal surgery (SURG), use of anticoagulants, diabetes, cardiovascular diseases and presence of acute toxicity were considered as potential dose-modifying factors. Goodness of fit was evaluated with Hosmer Lemeshow test (HL), calibration through fitting slope, while the AUC was used for the discrimination power.

Results: A total of 1337 pts were available: 708 from first trial and 669 from the second one. G3 LRB was scored in 95 pts (7.1%): 62 and 33 in the first and second trial, respectively. EUD calculated with the volume parameter n=0.06 was the best dosimetric predictor for G3 LRB. A 4-variable MVL model was fitted including EUD (OR=1.07 p=0.02), SV (OR=4.75 p=0.01), SURG (OR=2.30 p=0.02) and cardiovascular disease (OR=1.42 p=0.18). This model had an AUC=0.63, a calibration slope=0.99 (R^2=0.89) and a p for HL=0.43.
Figure 1 shows dose response relationship (model vs observed toxicity rates) as a function of SV irradiation, cardiovascular disease and abdominal surgery.
Inclusion of acute toxicity (OR=2.34 p<0.001) slightly improved AUC (0.65), confirming a possible role of consequential injury.

Variables	Coefficient	Standard Error	P>|z|	Odds Ratio
Cardiovascular disease	0.35	0.26	0.18	1.42
Previous abdominal surgery	0.83	0.36	0.02	2.3
Irradiation of seminal vesicles	1.55	0.6	0.01	4.7
EUD with n=0.06	0.07	0.028	0.02	1.07

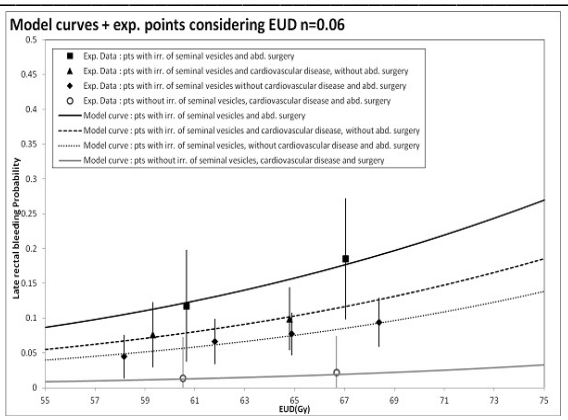

Conclusion: EUD with n=0.06 was predictive of G3 LRB in this pooled population, confirming the importance of sparing the rectum from high doses. Irradiation of seminal vesicles together with the presence of cardiovascular disease and previous abdominal surgery were relevant dose-modifying factors highly impacting the incidence of G3 LRB.

PO-0874

Dose prescription in carbon ion radiotherapy: how to compare different RBE-weighted dose systems.

S. Molinelli[1], G. Magro[2], A. Mairani[1], A. Mirandola[1], N. Matsufuji[3], N. Kanematsu[3], A. Hasegawa[3], S. Yamada[3], T. Kamada[3], H. Tsujii[3], F. Valvo[1], M. Ciocca[1], P. Fossati[4], R. Orecchia[5]

[1]*Fondazione CNAO, Medical Physics, Pavia, Italy*
[2]*Università degli studi di Pavia, Fisica, Pavia, Italy*
[3]*National Institute of Radiological Science, Research Center for Charged Particle Radiotherapy, Chiba, Japan*
[4]*Fondazione CNAO, Radiotherapy, Pavia, Italy*
[5]*Istituto Europeo di Oncologia, Radiotherapy, Milan, Italy*

Purpose or Objective: In carbon ion radiotherapy (CIRT), mainly two calculation models are adopted to define relative biological effectiveness (RBE)-weighted doses (D*RBE*): the Japanese Kanai model and the Local Effect Model (LEM). Taken the Japanese longest-term clinical data as a reference, the use of a different RBE model, with no correction for the Gy (RBE) scale, leads to deviations in target absorbed dose (D*abs*) with a potentially significant impact on tumor control probability. In this study we validate a conversion method linking the two D*RBE* systems, confirming D*RBE* prescription dose values adopted in our LEM-based protocols.

Material and Methods: The NIRS beamline was simulated with a Monte Carlo (MC) code, according to design information about elements position, size and composition. Validation went through comparison between simulated and measured pristine and Spread Out Bragg Peaks, ridge filter based, in water. CT scan, structure set, plan and dose files of 10 treatment fields delivered at NIRS were exported in DICOM format, for prostate (3.6 Gy (RBE) per 16 fractions), Head & Neck (4 Gy (RBE) per 16 fractions) and pancreas (4.6 Gy (RBE) per 12 fractions) patients. Patient specific passive system geometries (range shifter, MLC, compensator, collimator) were implemented, for each field, to simulate delivered Dabs distributions. The MC code was then interfaced with LEM to calculate D*RBE* resulting from the application of a different RBE model to NIRS physical dose. MC and TPS calculated D*abs* and D*RBE* were compared in terms of dose profiles and target median dose. Patient CT and structure sets were also imported in a LEM-based commercial TPS where plans were optimized prescribing the non-converted and converted D*RBE* values, respectively.

Results: The agreement between MC and measured depth dose profiles in water demonstrated beamline model accuracy. Patient dose distributions were correctly reproduced by MC in the target region, with an overall target median dose difference < 2%. MC median D*RBE* resulted 16% higher than NIRS reference, for the lower prostate dose level,

10% for head and neck and 4.5% for pancreas, in agreement with respective LEM-based prescription doses, adopted in our protocols. Deviations are expected to be close to zero around a prescription D*RBE* = 5 Gy (RBE). Target under-dosage was shown in LEM-based optimized plans, when uncorrected D*RBE* were prescribed.

Conclusion: The delivery of a voxel by voxel iso-effective plan, if different RBE models are employed, is not feasible; it is however possible to minimize differences in dose deposited in the target. Dose prescription is a clinical task which ultimately depends only on the radiation oncologist clinical decision; in this study we made an attempt to avoid systematic errors which could potentially compromise tumor control. Initial clinical data on local control of adenoid cystic carcinoma treated in our facility confirms the validity of this approach.

PO-0875

Multivariable models for urinary symptoms at 6-24 months after radical RT of prostate cancer

F. Palorini[1], T. Rancati[2], A. Cicchetti[2], I. Improta[1], C. Cozzarini[3], V. Casanova Borca[4], C. Degli Esposti[5], P. Franco[6], E. Garibaldi[7], G. Girelli[8], A. Maggio[9], R. Micera[10], M. Palombarini[11], A. Pierelli[12], E. Pignoli[13], N. Simoni[10], V. Vavassori[14], S. Villa[15], R. Valdagni[16], C. Fiorino[1]

[1]*San Raffaele Scientific Institute, Medical Physics, Milan, Italy*

[2]*Istituto Nazionale dei Tumori IRCCS, Prostate Cancer Program, Milan, Italy*

[3]*San Raffaele Scientific Institute, Radiotherapy, Milan, Italy*

[4]*Ospedale ASL9, Medical Physics, Ivrea, Italy*

[5]*Ospedale Bellaria, Radiotherapy, Bologna, Italy*

[6]*Ospedale Regionale U. Parini - AUSL, Radiotherapy, Aosta, Italy*

[7]*Istituto Candiolo - Fondazione del Piemonte per l'Oncologia IRCCS, Radiotherapy, Candiolo, Italy*

[8]*Ospedale ASL9, Radiotherapy, Ivrea, Italy*

[9]*Istituto Candiolo - Fondazione del Piemonte per l'Oncologia IRCCS, Medical Physics, Candiolo, Italy*

[10]*Arcispedale S. M. Nuova - IRCCS, Radiotherapy, Reggio Emilia, Italy*

[11]*Ospedale Bellaria, Medical Physics, Bologna, Italy*

[12]*Cliniche Gavazzeni - Humanitas, Medical Physics, Bergamo, Italy*

[13]*Istituto Nazionale dei Tumori IRCCS, Medical Physics, Milan, Italy*

[14]*Cliniche Gavazzeni - Humanitas, Radiotherapy, Bergamo, Italy*

[15]*Istituto Nazionale dei Tumori IRCCS, Radiation Oncology 1, Milan, Italy*

[16]*Istituto Nazionale dei Tumori IRCCS, Prostate Cancer Program and Radiation Oncology 1, Milan, Italy*

Purpose or Objective: To assess clinical and dose factors affecting the incidence of urinary symptoms between 6 and 24 months after therapy completion in patients treated with radical RT for prostate cancer.

Material and Methods: This study examined the dataset of a prospective study with patients treated with conventional (74-80 Gy at 1.8-2 Gy/fr) or moderately hypofractionated RT (65-75.2 Gy at 2.2-2.7 Gy/fr) in 5 fractions per week. Clinical factors were collected for each patient: comorbidities, drugs, hormone therapies, previous surgeries, smoking, alcohol, age, and body mass index. Bladder DVHs were corrected with alfa/beta=3Gy. Urinary symptoms were evaluated through the IPSS (International Prostate Symptom Score) and ICIQ (International Consultation on Incontinence Modular Questionnaire short form) questionnaires filled in by the patients at start/end of RT and every 6 months until 5 years of follow up. We considered the sum of the 7 IPSS questions and the sum of questions 3-4 of ICIQ for the two endpoints: 1) IPSS≥15 and 2) ICIQ34>=4 at least once between 6 and 24 months after RT. The best predictors to be included in the logistic regression model were identified through backward feature selections on 1000 bootstrap resamplings (the reported NArea identifies the weighted occurrences of the variables at the leading positions); then multivariate regressions on 1000 bootstrap resamplings were employed to compute the odds ratio distributions of the selected variables.

Results: 539 patients were enrolled: dose parameters and toxicity data at baseline and between 6-24 months were available for 195 (IPSS) and 197 (ICIQ) patients. 158/195 (81%) and 150/158 (95%) patients did not show toxicity at baseline (IPSS<=12 and ICIQ3=0, respectively). At 6-24 months, the incidence of IPSS>=15 was 42/158 (27%) and of ICIQ34>=4 was 34/150 (23%). A 6-variable model (AUC=0.86) was considered for IPSS: basal IPSS (NArea=0.72, OR=1.51) and the change of IPSS at RT end (deltaIPSS) (NArea=0.74, OR=1.16) were the leading risk factors. V62Gy was also a risk factor (NArea=0.36, OR=1.04), while the analogues and antiandrogens in hormone therapies were found protective (NArea=0.34, OR=0.38) and risk parameters (NArea=0.29, OR=2.57), respectively. For ICIQ, a backward feature selection was employed: antiaggregants (OR=2.16, p=0.11), antiandrogens (OR=2.03, p=0.08) and age (OR=1.09, p=0.04) were found as risk factors, whereas none dose parameter was found correlated with toxicity.

	Coefficient	Median OR (5°perc - 95°perc)	Narea
IPSS>=15 (basal IPSS<=12)			
AUC 0.86 (0.79 - 0.93)			
Delta IPSS	0,15	1,16 (1,09-1,25)	**0,74**
Basal IPSS	0,41	1,51 (1,32 - 1,8)	**0,72**
Lymph node irradiation	1,15	3,17 (1,38 - 6,9)	**0,58**
Volume receiving 62 Gy (%)	0,04	1,04 (1,01 - 1,07)	**0,36**
Hormone therapy with analogues	-0,97	0,38 (0,14 - 0,8)	**0,34**
Hormone therapy with antiandrogens	0,94	2,57 (1,23 - 6,02)	**0,29**
constant	-6,05		

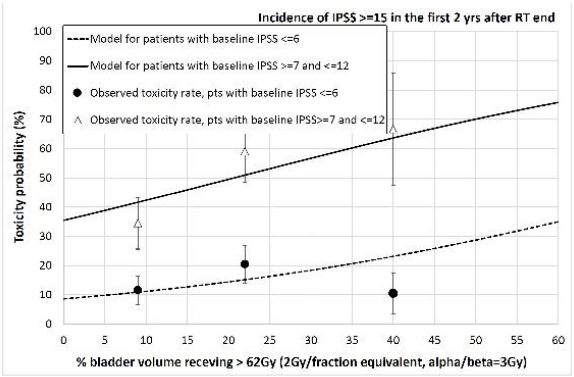

Conclusion: The analysis shows an important correlation of urinary toxicities at 6-24 months with the patient urinary condition at baseline and, also, with the acute worsening of symptoms. Interestingly, hormone therapies with analogues (protective) and antiandrogens (risk) showed an opposite behaviour for late toxicities. The absence of correlation of incontinence with dose might be due to the very low number of severe toxicities registered.

PO-0876

Voxel-by-voxel NTCP model for lung density changes after IMRT

M. Avanzo[1], S. Barbiero[1], M. Trovo[2], J. Stancanello[3], C. Furlan[2], C. Cappelletto[1], E. Capra[1]

[1]*Centro di Riferimento Oncologico, Medical Physics Unit, Aviano, Italy*

[2]*Centro di Riferimento Oncologico, Radiation Oncology Department, Aviano, Italy*

[3]*General Electric, MRI Applications and Workflow, Buc, France*

Purpose or Objective: Differential diagnosis between benign changes on follow-up CT from progression or recurrence is a difficult task in highly conformal RT because areas of dense consolidation usually develop around the treated tumor. The

prediction of radiation-induced changes in lung density on follow-up CT can be of help with differential diagnosis. The goal of this work was to develop a Normal Tissue Complication Probability (NTCP) model for voxel by voxel prediction of changes in lung density on CT scans of patients treated with IMRT.

Material and Methods: 20 patients were treated with fractionated IMRT (60 Gy/25 fractions) or SBRT with Helical Tomotherapy (40-52 Gy in 5-10 fractions) for lung tumors.Follow-up CT scans were acquired at 6 months after the end of RT and were registered with pre-treatment scans using rigid (6 degrees of freedom) followed by a b-spline (> 27 degrees of freedom) deformable registration performed using the 3D Slicer freeware software suite. Registration accuracy was assessed by comparing the calculated displacement at bifurcation points with the displacement measured on unregistered images. Registration was repeated when the difference was more than 1 cm. Voxels Hounsfield units were converted into relative electron density (RED) using in-phantom measured CT-RED curves. The change in RED between the two images was calculated for each voxel within the healthy lung tissue, defined as combined lungs after subtraction of PTV, among all the patients. Voxels RED changes versus absolute dose were fitted among all patients using a function similar to Lyman NTCP model. Model parameters were *D0.5*, the dose giving 0.5 increase in relative electron density and *m*, the slope of the dose-response curve. No correction was used for fractionation of the treatments. Predictive power of model was assessed by a test of correlation of measured and predicted RED changes.

Results: The dose giving an increase of 0.5 RED estimated from fitting of lung density changes was *D0.5* = 99.5 Gy (95%CI = 84.0-114.9 Gy). Slope of dose response, *m*, was 0.338 (95%CI = 0.296-0.380). The correlation test shows that predicted and measured RED changes were statistically strongly correlated ($p<0.001$).

Conclusion: The model describes well the change in RED in follow-up CT scans of IMRT patients and can be used to generate maps of predicted RED to be visualized on follow-up CT scans, as a support for differential diagnosis between benign changes from progression or recurrence.

PO-0877

Baseline CT image and isodose shape features improve prognostic models for dyspnea after RT in NSCLC

G. Defraene[1], W. Van Elmpt[2], D. De Ruysscher[3]
[1]*KU Leuven - University of Leuven, Experimental Radiation Oncology, Leuven, Belgium*
[2]*Maastricht University Medical Centre, Department of Radiation Oncology Maastro-Clinic, Maastricht, The Netherlands*
[3]*University Hospitals Leuven, Department of Radiation Oncology, Leuven, Belgium*

Purpose or Objective: Lung toxicity prediction models currently rely on dosimetric factors as mean lung dose (MLD) or V20 (volume of lung receiving more than 20 Gy), and clinical factors (e.g. age, smoking history). With a consistently reported area under the curve (AUC) around 0.6 these models are limited in discriminating between low- and high-risk patients before treatment. The present study aims at designing a better prognostic model by broadening the search for prognostic factors using a radiomics approach both on the imaging and dosimetric level. For this, CT image features of lung tissue and isodose shape measures were explored to predict the endpoint of dyspnea.

Material and Methods: 80 stage I-IV non-small cell lung cancer patients were included. Prescription dose was 66Gy, in fractions of 2.75 Gy sequentially or 2 Gy concurrent with chemotherapy. Maximal increase in CTCAE 4.0 dyspnea score in the first 6 months after the end of radiotherapy was retrospectively recorded with respect to baseline status.
30 lung image features were extracted from the baseline free-breathing planning CT: 10 intensity-based features (derived from the histogram of intensities), and the mean value and standard deviation of 10 texture features (from the co-occurrence matrix, neighbourhood gray tone difference matrix (NGTDM) and neighbouring gray level dependence matrix (NGLDM) categories). All features were calculated within each of the isodose volumes V5, V20 and V40 of the lung excluding the GTV structure. Additionally 15 shape and location features of these isodose volumes were collected: volume, bounding box dimensions, centroid coordinates and compactness. Other features included age, smoking status, chemotherapy regimen, treatment modulation, heart Dmax and Dmean.
All combinations of the 5 most significant features resulting from a univariate logistic regression analysis were tested in multivariate setting (likelihood ratio test between nested models).

Results: Dyspnea increase grade >= 2 was present in 13.8% of patients. For an increase of at least 1 grade, this was 38.8%.
In univariate modeling, several image and isodose shape features performed significantly better than MLD for both endpoints (Table 1). The resulting classifier for dyspnea increase grade >= 1 was based on the texture feature 'small number emphasis' and the V40 isodose antero-posterior dimension (AUC=0.71). The dyspnea increase grade >= 2 classifier was based on mean heart dose and antero-posterior dimension of the V20 isodose (AUC=0.71).

Feature	AUC
Dyspnea increase grade ≥1	
Texture small number emphasis (NGLDM): mean in V_{20}*	0.66
Texture small number emphasis (NGLDM): SD in V_{20}	0.66
Texture Deviation: mean in V_{20}	0.63
Shape: V_{40} bounding box relative antero-posterior dimension*	0.62
Intensity histogram in V_{20}: 75th quantile	0.60
Mean Lung Dose	*0.51*
Dyspnea increase grade ≥2	
Texture Strength (NGTDM): mean in V_{40}	0.70
Texture Coarseness (NGTDM): mean in V_{20}	0.69
Texture Complexity (NGTDM): mean in V_{20}	0.67
Mean heart dose*	0.66
Shape: V_{20} bounding box absolute antero-posterior dimension*	0.65
Mean Lung Dose	*0.57*

*selected as covariate in the best multivariate model

Table 1 Area under the curve (AUC) of univariate logistic regression models for the 5 most prognostic features. A mean lung dose-based model performance is given as reference.

Conclusion: A radiomics analysis with image and isodose features yielded promising prognostic models for dyspnea compared to the classical MLD-based model. Validation on a recently available large multicentric database will be performed by the time of the congress, which will allow the selection of the most robust model.
This project has received funding from the European Union's Seventh Framework Programme under grant agreement no 601826 (REQUITE).

Poster: Physics track: Intra-fraction motion management

PO-0878

The effect of rectal retractor on intra-fraction motion of prostate

A. Vanhanen[1,2], M. Kapanen[1,2]
[1]*Tampere University Hospital, Department of Oncology, Tampere, Finland*
[2]*Medical Imaging Center and Hospital Pharmacy, Medical Physics, Tampere, Finland*

Purpose or Objective: Intra-fraction motion of the prostate is a known phenomenon that degrades the delivered dose to

the target. Rectal retractor (RF) which main purpose is to separate the rectum from the prostate in order to decrease the rectal dose is commonly suggested to fixate the prostate [1]. In the current study the effect of RF on intra-fraction motion of the prostate was investigated using real-time electromagnetic tracking system.

Material and Methods: A total of 22 conventionally fractionated (39 x 2 Gy) or moderately hypofractionated (20 x 3 Gy) prostate cancer patients were investigated. RF (RectafixTM, Scanflex Medical AB, Sweden) was used in 15/39 and 10/20 first fractions to study its effect on prostate motion. In the RF method the rectum-prostate separation is achieved by rectal rod that is inserted into the rectum and manually pushed posteriorly. Intra-fraction motion of the prostate was recorded with electromagnetic tracking system RayPilot (Micropos Medical AB, Sweden). The system consists of a transmitter implanted into the prostate and a receiver plate positioned on the treatment couch. The system provides transmitter 3D position in real-time. Intra-fractional prostate motion of a total of 260 RF fractions and 351 non-RF fractions were tracked and analyzed. Absolute prostate displacement after image guidance was calculated in all directions. Unidirectional and 3D motion distributions within 10 min treatment time were evaluated by the means of percentage time at displacement≥ 1, 2, 3, 4, 5 and 6 mm. Motion patterns between the RF and non-RF fractions were compared individually and over the whole patient population.

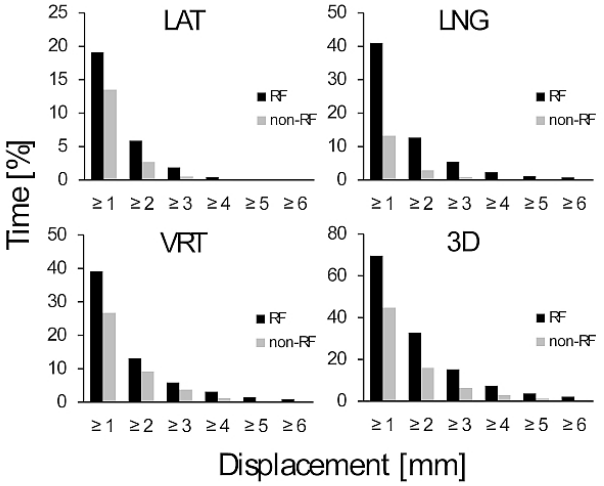

Figure 1. Average percentage time of lat, lng, vrt and 3D prostate displacements

Results: The average percentage time was larger in RF data compared to non-RF data in every direction (fig 1). The greatest increase in motion was seen in superior, inferior and posterior directions (table 1). Differences between the datasets in these directions, as well as 3D motion, were statistically significant ($p < 0.03$). Individually, the 3D motion of the prostate was significantly larger ($p < 0.05$) with RF than without it for 13 patients. For two patients significant ($p \leq 0.04$) stabilizing effect with the RF was observed.

Table 1. Average percentage time of unidirectional and 3D prostate displacements ≥ 1, 2, 3, 4, 5 and 6 mm

		≥1	≥2	≥3	≥4	≥5	≥6
3D	RF	69,6	32,8	15,3	7,5	3,8	2,2
	non-RF	44,8	16,0	6,4	2,9	1,4	0,5
Left	RF	9,4	3,5	1,6	0,4	0,0	0,0
	non-RF	7,5	1,8	0,5	0,2	0,0	0,0
Right	RF	9,7	2,4	0,3	0,1	0,0	0,0
	non-RF	6,0	0,9	0,1	0,0	0,0	0,0
Superior	RF	6,0	2,4	1,1	0,3	0,1	0,0
	non-RF	3,8	1,5	0,6	0,1	0,0	0,0
Inferior	RF	35,0	10,3	4,4	2,0	1,0	0,8
	non-RF	9,4	1,4	0,3	0,0	0,0	0,0
Anterior	RF	8,6	4,1	2,1	0,9	0,2	0,1
	non-RF	9,3	3,6	1,5	0,8	0,4	0,2
Posterior	RF	30,5	9,1	3,8	2,3	1,3	0,9
	non-RF	17,5	5,6	2,2	0,4	0,1	0,0

Conclusion: The use of RF increased the intra-fraction motion of the prostate on average and for most of the patients. The reason for larger motion could be increased muscular tension due to uncomfortableness of the RF and the anatomical changes that the retraction creates at the prostate-rectum surface. Our results indicate that the use of RF requires larger treatment margins or application of real-time tracking and dose gating. As the RF increases the prostate motion its use is questionable and should be evaluated against desired rectum dose sparing.

References:

[1] Nicolae A. et al. Radiat Oncol (2015) 10:122

PO-0879

Real-time prostate tracking in prostate cancer radiotherapy using autoscan transperineal ultrasound

X. Qi[1], X.S. Gao[1], H. Yu[1], S.B. Qin[1], H.Z. Li[1]
[1]*Peking University First Hospital, Radiation Oncology, Beijing, China*

Purpose or Objective: More recently, noninvasive 4D transperineal ultrasound (4D-TPUS) has been introduced in tracking interfraction, as well as intrafraction prostate motion in radiotherapy. Compared to other tracking method, the ultrasound has its own advantage in precise identification of soft tissue without invasive procedure or extra radiation dose. Several studies have reported the tracking data that confirming its accuracy in monitoring prostate motion and 4D-TPUS is nowadays gradually accepted as a monitoring option in prostate cancer radiotherapy. However, rare experience of this new technology with Asia populations has been reported. In this study, we report our clinical experience and tracking data using 4D-TPUS to monitor both inter- and intra-fraction prostate motion.

Material and Methods: Fifteen prostate cancer patients were enrolled in a prospective study and treated to a total dose of 76Gy in 38 fractions using IMRT. For each patient, before treatment delivery, prostates were localized using US and CBCT respectively to determine setup offsets relative to the patient skin tattoos. In the treatment protocol, adjustment of couch was guided by CBCT images. During the treatment, real-time ultrasound images were acquired and data was collected for direct monitoring of 3D motion of the prostate.

Results: A total of 221 fractions were evaluated. The means (μ) and standard deviations (SD) of inter-fraction prostate motion, as evaluated using CBCT and US, averaged from all patients and fractions, were [μ US = (4.62, 4.75, 4.37) mm, SD US = (4.21, 5.17, 5.52) mm], and [μ CBCT = (2.49, 2.26, 3.27) mm, SD CBCT = (2.15, 1.83, 2.89) mm] in the left-right, superior-inferior and anterior-posterior directions, respectively. The median (5% to 95% percentile) of 221 intra-fraction prostate motions in the L−/R+, S+/I− and A+/P− were

0.1 mm (-1.13 to 1.64 mm), -0.1 mm (-1.89 to 1.90 mm), and -0.3mm (-2.88 to 1.25 mm). There were 70/221 (32%) fractions with deviation exceeded 2 mm in any direction, with an average duration of 26% of treatment time. While, there were 19/221 (8.6%) fractions with deviation exceeded 3 mm in any direction with an average duration of 6.3% of treatment time.

Conclusion: 4D-TPUS provides an accurate and noninvasive method for real-time tracking of prostate in radiation treatment. We reported the first tracking data from Asia populations. These data can help to understand the intrafraction motion of the prostate, and may allow a reduction of treatment margin.

PO-0880

Clinical implementation of 5DCT workflow

D. Low[1], D. Thomas[1], T. Dou[1], P. Lee[1], J. Lewis[1], D. O'Connell[1]
[1]*UCLA Medical Center, Department of Medical Physics, Los Angeles, USA*

Purpose or Objective: To implement a quantitative clinical breathing motion characterization technique that employs a 5D motion model.

Material and Methods: We have employed a research breathing motion model and CT acquisition technique into clinical service, supporting lung cancer radiation therapy. The workflow employs 25 fast helical CT scans that are acquired using low mA, fast rotation (0.28s) and a pitch of 1.2 to scan the lungs in approximately 1 s, acquired alternately head to foot and foot to head. A breathing surrogate device, consisting of a hollow sealed bellows-shaped tube, is stretched around the abdomen. The air pressure in the tube is measured using a pressure transducer and the transducer voltage is used as the surrogate. Each slice is assigned a breathing phase according to the breathing surrogate measured at the point in time the scan was acquired. The breathing amplitude and the breathing rate define the breathing phase, allowing the model to explicitly manage breathing amplitude variations as well as breathing hysteresis. The scans are deformably registered to the first scan, arbitrarily assigned as the reference scan. The deformation vectors along with the breathing phases are coupled with a breathing motion model that linearly relates breathing motion to the amplitude and rate of breathing. The 25 scans are averaged at the reference phase geometry to reduce image noise, and the averaged scan deformed to user-defined breathing phases. For the first clinical implementation, we provide 8 static images at breathing phases corresponding to equally spaced breathing amplitude percentiles from the 5th percentile to the 95th percentile and back in equally spaced steps. The model is used to reconstruct the original 25 scans and compare the reconstructed to original scans using deformable image registration, providing a measure of model error. The clinician is provided not only the phase images for planning but estimates of the motion model error presented as colormaps of the model discrepancy.

Results: The protocol provides artifact-free images for contouring and previous research studies have shown that the overall accuracy of the proposed workflow is approximately 2 mm, with severely irregularly breathing patients having only slightly reduced accuracy. The protocol allows the clinician, for the first time, to access quantitatively validated breathing gated CT scans that are related to the overall breathing pattern statistics and that come with accuracy estimates.

Conclusion: While the clinical 5D protocol increases the quantitation available to clinicians, it is only the first step in the next generation of breathing motion modeling and breathing motion mitigation strategies made possible by the quantitative nature of the protocol. Further automation will enable the clinic to greatly increase the efficiency and efficacy of selecting and evaluating competing motion mitigation strategies.

PO-0881

Patient selection for DIBH technique for left sided breast cancers: Impact of chest wall shape

S. Chilukuri[1], D. Adulkar[1], S. Subramaniam[1], N. Mohammed[1], A. Gandhi[1], M. Kathirvel[1], T. Swamy[1], K. Kiran Kumar[1], N. Yadala[1]
[1]*Yashoda Cancer Institute, Department of Radiation Oncology, Hyderabad, India*

Purpose or Objective: Deep inspiratory breath hold (DIBH) technique delivers less dose to heart and left lung during radiotherapy for left sided breast cancers. But the benefit is not uniform in all patients. We analyzed the impact of shape of the chest wall (CW) in predicting benefit with DIBH technique.

Material and Methods: All patients of left sided breast cancer undergoing radiotherapy at our centre in the last one year were analyzed. All the patients underwent 2 sets of planning scans-one in DIBH phase and the other in free breathing (FB) phase. DIBH patients were monitored in prospective mode with the help of Varian real time position management system system. For patients who underwent mastectomy, the shape of the CW was assessed on visual inspection and confirmed on the FB planning CT (pCT). For patients with intact breast, the CW excluding the breast was contoured on the FB pCT to evaluate the shape. CW angle (CWA)-angle measured at mid chest level and is made by the tangent to the most curved portion of chest wall with any line parallel to the couch was computed.

Results: 36 patients were found to have curved CW and 17 (32%) were found to have flat CW. All the 17 patients with flat CW had CWA<30 and all with curved CW had CWA>30. In patients with curved CW mean left lung V20 (V20), mean heart dose (MHD) and mean left anterior descending artery (LAD) dose were significantly less with DIBH technique compared to FB plans, (12% vs. 19%, p=0.001, 1.2Gy vs. 5.5Gy, p<0.000, 16.6Gy vs. 29.1Gy, p<0.000 respectively). In patients with flat CW, there was no benefit seen with DIBH scans compared to FB scans with respect to V20, MHD and mean LAD {21% vs. 22.3% (p=0.78), 5.9Gy vs. 6.5Gy (p=0.19) and 29.1Gy vs. 28.9Gy (p=0.9)} respectively. In patients with curved CW, the NTCP for cardiac mortality was less compared to FB plans (0.25% vs. 4.5%, p<0.001) which was not the case in flat CW patients (4.2%, p=0.86)

Conclusion: Patients with curved CW had a significant benefit with DIBH technique compared to flat CW. CW shape, which is easy to determine, is an effective tool to identify patients suitable for DIBH technique. For patients with flat CW other techniques should be explored to address cardiac doses.

PO-0882

Abdominal organ motion during breath-hold measured in volunteers on MRI: inhale and exhale compared

E. Lens[1], O.J. Gurney-Champion[1,2], A. Van der Horst[1], D.R. Tekelenburg[1], Z. Van Kesteren[1], M.J. Parkes[3], G. Van Tienhoven[1], A.J. Nederveen[2], A. Bel[1]
[1]*AMC Amsterdam, Radiation Oncology, Amsterdam, The Netherlands*
[2]*AMC Amsterdam, Radiology, Amsterdam, The Netherlands*
[3]*University of Birmingham, School of Sport- Exercise & Rehabilitation Sciences, Birmingham, United Kingdom*

Purpose or Objective: Breath-hold (BH) techniques, used to eliminate respiratory-induced tumor motion, are in radiotherapy often implemented without clear feedback and characterization of the residual geometric uncertainties. We measured the motion of the pancreatic head and of the diaphragm during four different 1-minute BHs (2 inhale and 2 exhale) in healthy volunteers using MRI. The aim was to investigate which BH type produced the most stable anatomy

and to establish whether the diaphragm could be used as a surrogate for pancreatic motion.

Material and Methods: We studied 12 healthy volunteers (4 males), with a mean age of 33 y, mean height of 172 cm, mean weight of 63 kg and a mean vital capacity of 3.2 L. Each attempted to perform three 1-minute BHs in end-inhale (completely inflated lungs), deep-inhale (lung volume of ~70%), deep-exhale (lung volume of ~30%) and end-exhale (completely deflated lungs). During BH, we used a 3T MRI to dynamically (1.7 Hz) acquire a thick (8 mm) high resolution (0.9×0.9 mm2) 2D coronal slice including both the pancreatic head and the diaphragm.
For each BH, the motion (i.e. displacement in all successive images relative to the first image) of the pancreatic head and of the diaphragm in the inferior-superior (IS) direction was determined using a 2D image correlation algorithm. The Wilcoxon signed-rank test was used to test the differences in maximum displacement during BH between the different BH types. To investigate the correlation between the intra-BH motion of the pancreas and of the diaphragm, we determined the Pearson correlation coefficient (r). As the achieved BH duration varied, only the data acquired during the first 30 seconds of each BH were included in our analysis.

Results: We observed substantial motion in the IS direction in the form of drifts of the pancreatic head and of the diaphragm during all BH types (Figure and Table). We observed significantly larger maximum displacements for the pancreatic head during deep-inhale compared with deep-exhale (P=0.012) and end-exhale (P=0.045). For the diaphragm, we observed a significant difference in maximum displacement between each of the inhale BHs compared with each of the exhale BHs (P≤0.019), the mean displacement was always larger during the inhale BHs than during the exhale BHs.
A strong correlation (r≥0.8) between the motion of the pancreas and of the diaphragm was observed in only 60 out of the 141 analyzed BHs and a moderate correlation (0.6≤r <0.8) in 34 BHs. Both strong and moderate correlations were found most often for the deep-inhale BHs (Table).

Conclusion: We observed substantial intra-BH motion in IS of the pancreatic head and of the diaphragm. Exhale BH seems more stable and might therefore be preferred for radiotherapy. The diaphragm is not a suitable surrogate for pancreatic motion during BH, especially when the observed motion is small. The intra-BH displacements could have a high clinical impact if not taken into account during radiotherapy under BH conditions.

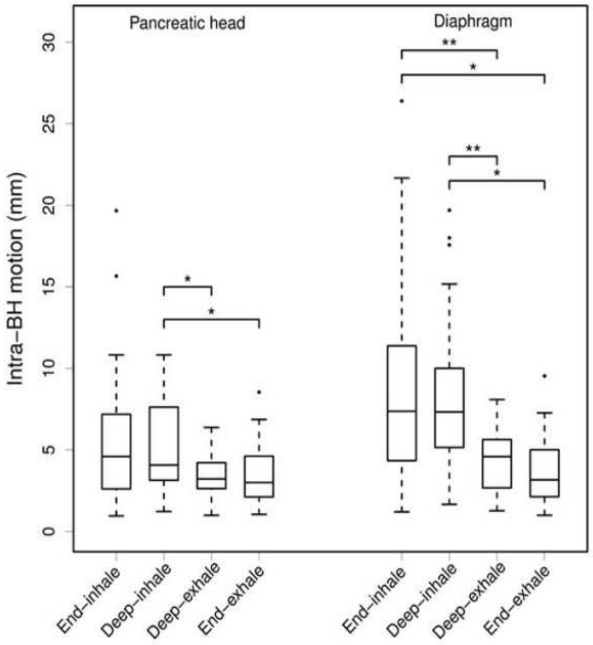

Figure: Boxplots of the intra-breath-hold (intra-BH) motion magnitudes of pancreatic head and diaphragm in the IS direction for the different breath-holds. Significance: * P<0.05 and ** P<0.01. The boxes indicate the median value and upper and lower quartiles, whiskers give the lowest and highest data point within 1.5× inter quartile range and the dots show the outliers.

Table: Intra-breath-hold motion in the IS direction during 4 different breath-holds in 12 volunteers.

	End-inhale	Deep-inhale	Deep-exhale	End-exhale
Pancreatic head motion				
Mean (mm)	5.5	5.1	3.4	3.4
Range (mm)	1.0–19.7	1.2–10.8	1.0–6.4	1.1–8.5
Standard deviation (mm)	3.4	2.5	1.0	1.4
Diaphragm motion				
Mean (mm)	8.7	8.2	4.4	3.6
Range (mm)	1.2–26.4	1.7–19.7	1.3–8.1	1.0–9.5
Standard deviation (mm)	4.8	4.6	1.5	1.8
# r ≥0.8 / # breath-holds[†]	19/36	23/36	3/36	15/33
# 0.6≤ r <0.8 / # breath-holds[‡]	26/36	31/36	12/36	25/33
Mean breath-hold duration (s)	60	59	59	51

[†]Number of times a strong (r ≥0.8) correlation between pancreatic and diaphragm motion was observed out of the total number of analyzed breath-holds.
[‡]Number of times a moderate (0.6≤ r <0.8) correlation between pancreatic and diaphragm motion was observed out of the total number of analyzed breath-holds.

PO-0883

Quantification of Duodenum motion: analysis from respiratory phase guided radiotherapy planning scan

T. Basu[1], T. Kataria[1], D. Gupta[1], S.S. Bisht[1], A. Abhishek[1], S. Goyal[1], S. Krishnan[2], K. KP[1], K. Narang[1], S. Sambasivam[1], S. Banerjee[1]
[1]*Medanta The Medicity, Radiation Oncology, Gurgaon, India*
[2]*Medanta The Medicity, Radiology, Gurgaon, India*

Purpose or Objective: In the era of stereotactic body radiotherapy (SBRT) radiation induced changes in duodenum (D) is an important concern. The tortuous and curvy anatomy often indistinguishable from adjoining organs led to the publication of RTOG upper abdominal normal structure contouring guidelines. The current study assesses the impact of respiration (expiration, inspiration and free breathing) on D and its parts with quantification of planning organ at risk (PRV) volume from respiratory phase guided radiotherapy planning CT scans (RPRTP).

Material and Methods: Ten cases of liver tumors (eight: primary hepatocellular, two: liver metastasis) were selected for RPRTP. After breath hold training in end expiration (E) and end inspiration (I),1mm slice thickness RPRTP along with free breathing (FB) contrast scans were obtained. Three image sets per patient were imported in contouring workstation (Focal Sim) with E as primary. D as a whole structure was contoured by single radiation oncologist in E, I and FB phases of respiration. Following the RTOG and our D

contouring guidelines the first (D1), second (D2), third and fourth (D3) parts were contoured separately in E, I and FB phases creating twelve image sets per patient. Motion variation for each structure was calculated by the difference in all three (XYZ) co-ordinates. Mean variations in position of D, D1, D2 and D3 with respect to E, I and FB phases were noted. The difference between E/I, E/FB and I/FB for D, D1, D2 and D3 were analyzed. Final data had 36 sets of values for mean and standard deviation per patient.

Results: Mean variations (cm) of D motion between E and I in XYZ co-ordinates were: 0.38(±0.53), 0.61(± 0.56), 0.53(± 0.72); between E and FB: 0.47(± 0.53), 0.49 (± 0.52), 0.49(± 0.74); between I and FB 0.35(± 0.49), 0.62(± 0.39), 0.61(± 0.81). The next step was the motion calculation for different parts of D in XYZ co-ordinates. For D1: between E and I 0.31(± 0.25), 0.65(± 0.71), 0.44(± 0.38), between E and FB: 0.31(± 0.17), 1.0(± 1.35), 0.66(± 0.84); between I and FB 0.22(± 0.15), 1.05(± 1.39), 0.66(± 0.88). For D2: between E and I; 1.18(± 1.26), 2.4(± 2.65), 0.55(± 0.76); between E and FB 1.01(± 1.07), 2.28(± 2.29), 0.45(± 0.6), between I and FB: 0.29(±0.22), 0.46(± 0.44), 0.18(± 0.16). Similarly for D3 between E and I; 0.77 (± 1.01), 1.5(± 2.13), 0.52(±0.65), between E and FB: 0.48(± 0.41), 1.48(±2.76), 0.2(± 0.16) and between I and FB: 0.9(± 1.11), 2.4(±2.99), 0.62(± 0.83).

Conclusion: D moves maximally in cranio-caudal (CC) direction and minimally in lateral direction in different phases of respiration. Relatively fixed D1 moves maximally in anterio-posterior (AP) direction (range: 0.1-2.3 cm), while mobile parts D2 and D3 in CC directions (range: 0.5-4 cm) between E and I. Keeping in mind the precision of SBRT, a PRV for duodenum 3mm radial and 5 mm CC with respiratory phase guidance will cover the range of motion. Differential margin for D1-D3 with validated delineation guideline should be evaluated in a larger cohort.

PO-0884

Respiratory motion models from Cone-Beam CT for lung tumour tracking

A. Fassi[1], E. Tagliabue[1], M. Tirindelli[1], D. Sarrut[2], M. Riboldi[1], G. Baroni[1]

[1]*Politecnico di Milano, Dipartimento di Elettronica Informazione e Bioingegneria, Milano, Italy*

[2]*Centre Léon Bérard, Department of Radiotherapy - CREATIS, Lyon, France*

Purpose or Objective: To develop and evaluate a patient-specific respiratory motion model obtained from time-resolved Cone-Beam CT (CBCT) and driven by a surrogate breathing signal. The motion model is proposed for the real-time tracking of lung tumors, accounting for interfraction motion variations.

Material and Methods: The motion-compensated CBCT reconstruction algorithm [1] was used to derive a time-resolved CBCT scan sorted into ten breathing phases. Tumor position was identified on each CBCT phase volume by non-rigidly propagating the GTV contours defined on the planning CT scan. GTV coordinates associated to each CBCT volume were linearly interpolated to obtain the patient-specific motion model, describing the 3D tumor position over the mean respiratory cycle of the CBCT scan. The phase parameter given as input to the respiratory model was estimated from diaphragm motion computed from CBCT projections. The proposed motion model was tested on a clinical database of six lung cancer patients, including two CBCT scans acquired per patient before and after setup correction. The first CBCT scan was used to build the motion model, which was tested on the second scan after correcting model coordinates for the applied setup shifts. Tumor positions estimated in 3D with the motion model were projected at the corresponding angle and compared to the real target position identified on CBCT projections by using a semi-automatic contrast-enhanced algorithm [2].

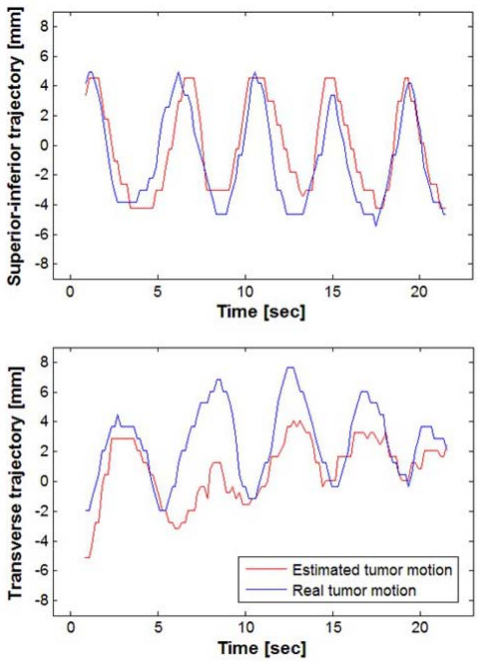

Figure 1. Comparison between real and estimated tumor trajectories obtained for patient P4. Only CBCT projections in which lung tumor was detectable are represented in the Figure.

Table 1. Absolute tracking errors between tumor trajectories estimated from CBCT motion model and real tumor motion identified on CBCT projections along the superior-inferior and transverse directions. Results are expressed as median value [25th - 75th percentiles].

Patient	Superior-inferior tracking error (mm)	Transverse tracking error (mm)
P1	1.0 [0.4 - 1.8]	1.2 [0.8 - 2.8]
P2	1.2 [0.4 - 2.0]	2.4 [1.2 - 3.6]
P3	1.2 [0.4 - 2.0]	2.8 [1.2 - 4.0]
P4	1.2 [0.8 - 2.0]	2.0 [0.8 - 4.0]
P5	2.0 [1.2 - 2.8]	2.4 [1.2 - 3.6]
P6	2.0 [0.8 - 2.8]	1.6 [0.8 - 2.4]

Results: Twenty-five seconds of CBCT scan, corresponding to about 135 CBCT projections, were analyzed on average for each patient. Figure 1 depicts exemplifying results of tumor trajectories along the vertical image direction, which corresponds to the projection of the superior-inferior tumor motion, and along the horizontal image direction, which represents the combination of antero-posterior and medio-lateral tumor motion. A significance correlation (p-value < 0.05) was found between real and estimated tumor trajectories, with Spearman correlation coefficients of 0.71 and 0.68 on average for superior-inferior and transverse directions, respectively. As reported in Table 1, the median value of absolute tracking errors did not exceed 2.0 mm for the single direction of tumor motion.

Conclusion: A novel approach for intrafraction tracking of lung tumors was investigated, exploiting a patient-specific respiratory motion model derived from time-resolved CBCT images. Compared to CT-based motion models, the proposed method does not need to compensate for interfraction motion variations that can occur between planning and treatment phases. An external breathing surrogate obtained from non-invasive optical surface imaging is envisaged to be used to drive the motion model during treatment.

[1] Rit S *et al*, Med Phys 2009;36:2283-96.

[2] Fassi A *et al*, Radiother Oncol 2011;99:S217.

PO-0885

Brain motion induced artefacts in microbeam radiation therapy: a Monte Carlo study

M. Donzelli[1], E. Braeuer-Krisch[1], U. Oelfke[2]
[1]*European Synchrotron Radiation Facility, Biomedical Beamline ID17, Grenoble, France*
[2]*The Institute of Cancer Research and The Royal Marsden NHS Foundation Trust, Joint Department of Physics, London, United Kingdom*

Purpose or Objective: Microbeam Radiation Therapy (MRT) is a relatively new approach in radiation oncology exploiting the dose-volume effect by using orthovoltage X-rays on a microscopic scale [1]. Arrays of plane parallel beams of typically 50 µm width with spacings of a few hundred µm show extraordinary normal tissue sparing, while still being capable to ablate tumours in preclinical research [2].
Organ motion has not been an issue in MRT, as long as preclinical research was carried out in small samples, such as cell cultures and rodents. The possible future treatment of human brain tumours using microbeam radiation however may be affected by cardio-synchronous tissue pulsation. This pulsation, with amplitudes in the order of 100 µm [3], induces translational movements of the brain tissue causing a blurring of the planned plane-parallel dose pattern of microbeams in case of extended exposure times.

Material and Methods: A Monte Carlo study to quantify these effects was performed using the Geant4 toolkit. Dose was scored in a homogeneous cubic water phantom of 15 cm size on a grid with 5 µm resolution perpendicular to the beam. The sensitive volume was chosen to have an extension of 1 mm along the beam direction in 20 mm depth from the surface, which corresponds to the reference dosimetry conditions in MRT. The relative statistical uncertainty of the dose (1 standard deviation) per voxel was between 1% and 1.5% in the peak region and between 6% and 9% in the dose valley, depending on the evaluated beam configuration and could be further reduced by appropriate binning of the raw data.

Results: Monte Carlo calculations for different geometrical microbeam configurations and employed dose rates revealed significant changes of the planned dose patterns when compared to the static case. The chosen quality indicators of our study like peak dose, peak-to-valley dose ratio (PVDR), microbeam width, spacing, and penumbra were observed to be highly degraded, e.g. the PVDR being reduced by up to 35%.

Conclusion: We have demonstrated that the effect of even small organ motions occurring at heart rate frequencies in the brain can only be tolerated at high dose rates of approx. 10 Gy/s. For example, a dose rate of 12.3 kGy/s can be given as a threshold value if one wants to apply a high peak entrance dose of 300 Gy in 3 mm depth for 50 µm wide microbeams and a primary beam size of 500 µm perpendicular to the scan direction. For lower dose rates the observed deterioration of the microbeam dose patterns is likely to destroy the intended dose sparing effect for healthy tissues.
For interlaced microbeam geometries an appropriate gating technique could be applied in the future based on the phase of the cardiac cycle.

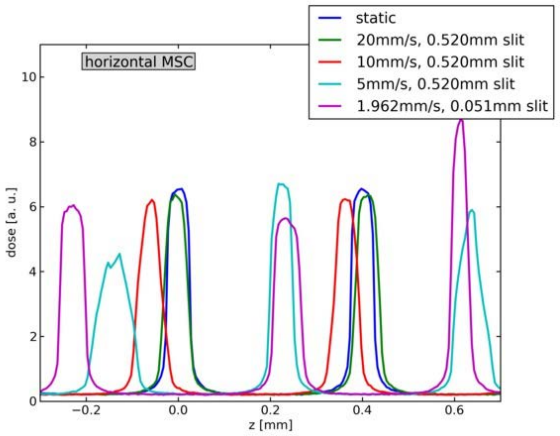

[1] Bräuer-Krisch et al. Mutation Research 704 (2010) 160-166
[2] Laissue et al. International Journal of Cancer 78 (1998) 654-660
[3] Soellinger et al. Magnetic Resonance in Medicine 61 (2009) 153-162

PO-0886

Does lung capacity influence the geometrical reproducibility in DIBH radiotherapy of NSCLC patients?

P. Sibolt[1,2], W. Ottosson[2], C.F. Behrens[2], D. Sjöström[2]
[1]*Technical University of Denmark, Radiation Physics- Center for Nuclear Technologies, Roskilde, Denmark*
[2]*Herlev Hospital, Radiotherapy Research Unit- Department of Oncology, Herlev, Denmark*

Purpose or Objective: Deep-inspiration breath-hold (DIBH) mitigates the breathing motion, and thereby reduces the treated volume. This yields less dose to adjacent organs-at-risk, and enables dose escalated radiotherapy of locally advanced non-small cell lung cancer (NSCLC) patients. However, DIBH can potentially introduce an extra uncertainty as reproducibility of DIBH can be affected by e.g. arching or unwanted motion during inspiration. This study was designed to investigate the feasibility and geometrical reproducibility of the anatomy, when utilizing DIBH in radiotherapy of locally advanced NSCLC patients.

Material and Methods: Seventeen NSCLC patients scheduled for curative radiotherapy were enrolled. One 4DCT in free-breathing (FB) and one 3DCT in DIBH, both with intravenous contrast, were acquired prior to (pre), in the middle of (mid), and after (post) the course of treatment. Furthermore, cone-beam CTs (CBCTs) both in FB and DIBH were acquired weekly throughout the course of treatment. A marker-based optical breathing signal (RPM, Varian Medical Systems, CA, USA) was utilized both for phase sorting into 10 phases during 4DCT and for visual guidance in DIBH 3DCT/CBCT. Changes in relative lung volumes (DIBH over FB) and in gross tumor volumes (GTVs) over the course of treatment were analyzed. Furthermore, the feasibility of DIBH for locally advanced NSCLC patients was analyzed based on the average breath-hold times and average number of breath-holds required to complete a CBCT acquisition.

Results: Compared to FB, the total lung volume increased in DIBH by, on average, a factor of 1.84, 1.81 and 1.86 for the pre, mid and post treatment scans, respectively. A correlation between relative total lung volume (DIBH/FB) and mean amplitude during DIBH CT was observed (Figure 1). No statistically significant changes in lung volume during the courses of treatment were discovered. In the middle of the treatment course the GTV had decreased with 34 % and 26 %, while at the end of treatment the decrease from the original GTV was 42 % and 43 % for DIBH and FB, respectively. On average 2.1 breath-holds, with an average breath-hold time of 43 seconds, were required for a patient to complete a DIBH CBCT acquisition. However, among the patients this varied between 1 to 11 breath-holds with breath-hold times ranging from 4 to 74 seconds. For each patient, no statistically significant changes in breath-hold times or

number of breath-holds required were observed during the courses of treatment.

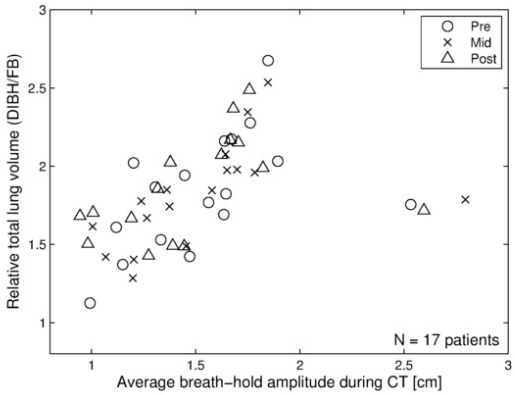

Figure 1. Relative total lung volume (DIBH/FB) as a function of average breath−hold amplitude during CT; pre (circles), mid (crosses) and post (triangles) course of treatment.

Conclusion: Breath-hold capabilities are highly individual and generally not observed to be changing during the course of treatment. The ratio between DIBH and FB total lung volume was observed to be stable during the course of treatment, while systematic decreases in GTV were observed both in DIBH and FB. DIBH radiotherapy of locally advanced NSCLC patients is considered to be feasible with geometrical reproducibility.

PO-0887

Latency characterisation of gated radiotherapy treatment beams using a PIN Diode circuit

M. Lempart[1], M. Kügele[1,2], F. Nordström[1], L. Ambolt[1], B. Blad[1]
[1]*Skåne University Hospital, Department of Oncology and Radiation Physics, Lund, Sweden*
[2]*Lund University, Department of Medical Radiation Physics, Lund, Sweden*

Purpose or Objective: The aim of radiotherapy is accurate delivery of dose to target volumes within a patient, while minimizing dose to the surrounding healthy tissue. Respiratory motion is still a significant problem in many radiotherapy treatments. Recent developments in the treatment of breast cancer have focused on "gating" the delivery of the treatment beams. With this technique, the effect of patient motion during treatment is reduced and the separation between the target volume and organs at risk (OAR) increased. Rapidly switching the treatment beam on or off, depending on the patient breathing cycle is the basic principle of gating. It is therefore important that the characteristics of gated treatments such as latency are known.

Material and Methods: For this study, an in-house built electrical PIN diode circuit was designed to function as a tool for quality assurance (QA). Beam latency timing properties were measured on a TrueBeam™ (Varian, Palo Alto) linear accelerator and its internal gating system. Pulses of radiation, triggered within a predefined gating window, were measured with the PIN diode and the results compared to measurements of current through the linac target. A phantom consisting of the electrical circuit coupled to a moving stage was used to simulate a binary pattern to produce fast beam triggering. Processing of the beam pulses and calculation of the latency timings was performed by an Atmega328P microcontroller (MCU). All measurements were performed with photon energies 6MV and 10MV and a dose rate of 600MU/min (equivalent to a reference dose in water of 6 Gy/min). For every measurement, a total of 50 data points were collected and the results compared by calculating the arithmetic mean value and the standard deviation.

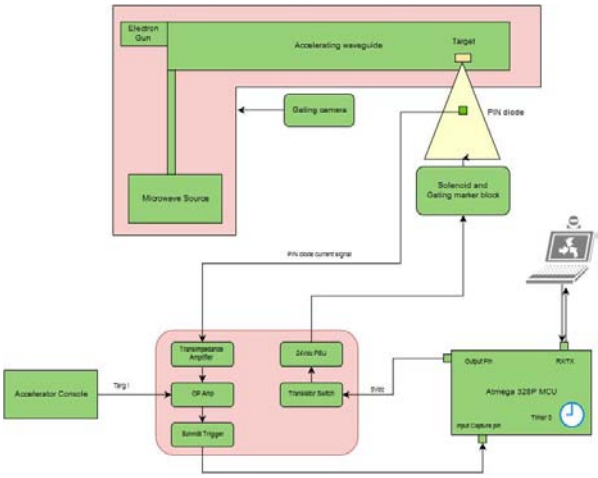

Results: The results of the beam latency measurements are shown in the table below.

	Beam on latency (ms)		Beam off latency (ms)	
Energy	***Target I***	***PIN diode***	***Target I***	***PIN diode***
6 MV	2.13 ±1.15	2.11 ±1.05	57.33 ±10.01	57.69 ±9.59
10 MV	2.15 ±1.06	2.12 ±1.09	56.01 ±10.10	57.73 ±10.06

Conclusion: Measuring beam gating latencies of a linear accelerator via beam pulse analyses with the help of a PIN diode and the in-house built electrical circuit is a useful method in good agreement with measurements from the accelerator target current signal. The PIN diode circuit provided a good response when using different beam energies and can be a useful tool to perform QA on different types of linear accelerators and gating systems. This could potentially lead to improvements in the gated radiotherapy treatments.

PO-0888

The influence of breathing motion on the precision of delivered dose to breast cancer patients

S. Agergaard[1], A. Bertelsen[1], E.L. Lorenzen[1,2], K.L. Gottlieb[1], C. Brink[1,2]
[1]*Odense University Hospital, Laboratory of Radiation Physics, Odense, Denmark*
[2]*University of Southern Denmark, Institute of Clinical Research, Odense, Denmark*

Purpose or Objective: Respiration motion during radiotherapy of breast cancer patients will perturb the delivered dose. The accuracy of the delivered dose can be measured by *in vivo* EPID dosimetry. The respiration motion can be reduced by use of the Active Breathing Coordinator (ABC) produced by Elekta. This study investigates whether a difference in EPID measured acceptance pass rate is associated to the use of ABC and whether the residual breathing variation while using the ABC system is associated to the measured pass rate.

Material and Methods: 15 ABC and 10 non-ABC breast cancer patients were monitored by EPID dosimetry for up to five fractions during the treatment. In total 185 and 82 tangential fields were available for analysis for ABC and non-ABC groups, respectively. The *in vivo* EPID dosimetry system (Wendling et al. Med Phys 2006) back projects the dose to a plane parallel to the EPID panel that includes the prescription point. The dose is compared to the planned distribution using a gamma analysis (3%, 3mm) and defines the pass rate as the fraction of gamma values less than one. Since pass rates are not normally distributed comparison between the ABC and non-ABC group was performed by a Mann-Whitney U test. The ABC system measured the amount of actual inhaled air at each treatment session and during the treatment planning CT. At breath-holds during treatment, deviation in inhaled air

(Vol_dif = Vol_treatment – Vol_CT) could potentially influence the pass rate negatively. Association between Vol_dif and gamma pass rates was analysed by linear regression between the gamma pass rates and Vol_dif squared. In order to adjust at least partially for the residual setup uncertainty, the regression was performed including the fraction number as predictor variable since fields within a fraction are assumed to have the same setup uncertainty.

Results: Difference between pass rates for the ABC and non-ABC group was highly statistically significant ($p<0.001$), with median pass rates of 84.7% and 76.1%, respectively (see figure). However, within the ABC group no significant association was observed between pass rates and deviation of inhaled air relative to the reference from the planning CT. EPID images were used to evaluate patient positioning prior to treatment and only accepted if deviations were less than 5 mm. Thus, it seems likely that the residual positioning uncertainty is the dominant uncertainty relative to the uncertainty in breath-hold volume when using ABC.

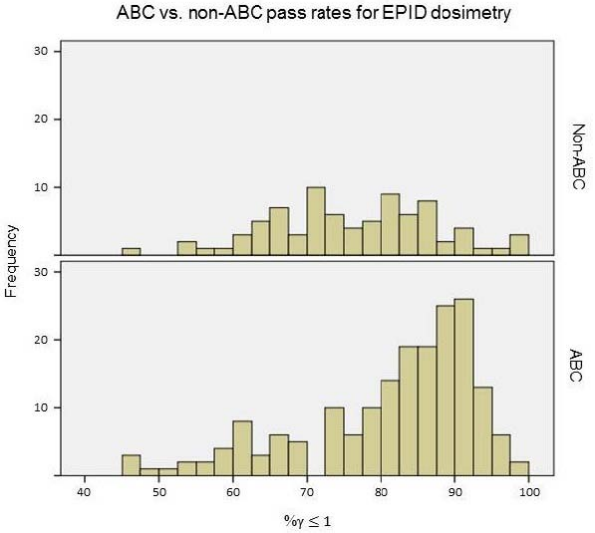

Conclusion: Breast cancer patients treated with the use of ABC showed an improved EPID dosimetry pass rate, reflecting an improved accuracy of dose delivery. However, a potential patient selection bias exists since no randomization between groups was performed. No significant association was observed between Vol_dif and pass rate within the ABC group. The ABC system therefore performs as intended and errors in breath-hold volumes are not of concern given the residual setup uncertainties.

PO-0889

Intra-fraction re-setup with Triggered Imaging allows for margin reduction in prostate treatments

L. Van der Weide[1], M.A. Admiraal[1], T.S. Rosario[1]
[1]*VU University Medical Center, Department of Radiotherapy, Amsterdam, The Netherlands*

Purpose or Objective: Intra-fraction motion of the prostate during irradiation requires large PTV margins. The recently released imaging application Triggered Imaging (TI, Varian Medical Systems, Palo Alto CA) allows to generate 2D kV images at predefined intervals during irradiation. The application can automatically detect implanted fiducial markers and initiate beam interrupt. Our previous work shows that re-setup was justified for almost half of the beam interrupts based on a 6mm tolerance. This study describes how applying TI and re-setup in the clinical workflow resulted in the reduction of the PTV margin.

Material and Methods: A total of 96 prostate cancer patients with implanted gold seeds were treated on the Truebeam with two RapidArc beams (Software version 2.0, Varian Medical Systems, Palo Alto, CA). For patient setup, the gold seeds are lined up using two orthogonal 2D kV images. After the setup procedure, TI is applied during both beams at an interval of 3 seconds, resulting in 41 images per fraction.In the plannings CT, the center of gravity of each seed is defined as a Marker. During treatment, each seed is automatically detected on each acquired Triggered Image and its center of gravity is marked with a cross. A circular overlay centered at the Marker position is projected on each Triggered Image. The radius of this circle indicates the maximum allowed seed deviation and is referred to as the TI limit. A color coding is used to indicate whether the seed is in or outside the TI limit (Fig 1).If one or more gold seeds exceed the limit for more than 6 seconds the beam is manually paused, while TI continues at the same gantry angle. If the deviation persists for another 6 seconds, the beam is interrupted and re-setup is performed using two orthogonal 2D kV images.For a first group of patients (n=27) TI was used, with the TI limit set to 6mm which corresponds to the PTV margin. For a second group of patients (n=32) the TI limit is set to 5mm, with an unchanged PTV margin of 6mm. For a third group (n=37) the PTV margin was reduced to 5mm, along with a TI limit of 5mm.

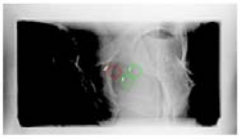

Figure 1. In this figure the auto-detection shows three coloured circles. Green indicates the gold seed is projected within the TI limit, red indicates the gold seed is outside the TI limit.

Results: For the total of 1434 fractions, 134 fractions showed excessive intra-fraction motion of one or more gold seeds leading to 173 beam interruptions and re-setups. Translations applied in re-setup were on average: 3mm, 3mm and 1mm in ventrodorsal, longitudinal and lateral directions, respectively. Overall, the average shift magnitude was 5mm (SD: 2.2mm) with a maximum of 13mm. Shift magnitudes exceeding the PTV margin were considered justified. Table 1 shows that a TI limit that equals the PTV margin leads to about 45% of justified interruptions.

Group (PTV margin/TI limit), n=96	Fractions	Interruptions	Average Shift magnitude (max)	Justified interruptions
Group 1 (6mm/6mm), n=27	305	4.3%	5 (10) mm	46.2%
Group 2 (6mm/5mm), n=32	615	14.0%	5 (12) mm	27.5%
Group 3 (5mm/5mm), n=37	514	14.4%	5 (13) mm	42.5%
Total	1434			

Table 1: Overview of the interrupts and shifts resulting from intra-fraction monitoring with TI.

Conclusion: Triggered Imaging in combination with auto-detection provides a powerful tool to monitor tumor motion during treatment for patients with implanted fiducial markers. We have developed a strategy for intra-fraction re-setup allowing for PTV margin reduction with limited increase in workload.

PO-0890

Homogeneous versus inhomogeneous dose prescription in liver SBRT: effect on delivered CTV-dose

A.T. Hansen[1], P.R. Poulsen[1], E.S. Worm[1], M. Hoyer[1]
[1]*Region Midtjylland, Medicinsk Fysik, Aarhus N, Denmark*

Purpose or Objective: In SBRT it is typical to prescribe a lower dose to an isodose-line encompassing the PTV rim rather than prescribing a uniform PTV dose. This strategy may allow for a higher central tumor dose than achievable by conventional homogenous dose prescription while maintaining an acceptable risk of normal tissue toxicity. However, the tumor dose may deteriorate because of intra-fraction motion. The aim of this study was to determine an optimal dose prescription strategy when explicitly considering the effects of intra-treatment motion in liver SBRT.

Material and Methods: Six patients received liver SBRT in 3 fractions. The PTV was generated from the CTV by adding margins of 5mm (LR,AP) and 10mm (CC). The 3-D motion of an implanted gold marker was monitored throughout each fraction by fluoroscopic kV and MV imaging. Later, five VMAT treatment plans with different PTV dose coverage were

produced for each patient. All plans had a mean CTV dose of 18.75 Gy per fraction (=100% dose) and 95% minimum CTV dose coverage. The PTV was covered by 50%, 67%_S, 67% (our standard), 80%, and 95% of the prescribed dose, respectively. The 67%_S plan was an alternative to the standard 67% plan made with maximum conformity, i.e. as steep as possible dose gradient from 95% to 67% outside the CTV. The 50%, 67%_S, 80%, and 95% plans were renormalized to be isotoxic with the standard 67% plan, i.e. to give the same risk of radiation induced liver disease (RILD) according to the NTCP-model of Dawson *et al*. (Acta Oncol., 2006). For each patient and plan, the dosimetric effects of the observed intrafraction motion were investigated by calculating the delivered dose by an in-house developed method for motion-including dose reconstruction.

Results: The figure shows the CTV mean dose and D99 for each plan type and each patient as planned (start of each arrow) and as delivered with the known tumor motion (end of each arrow). The mean values over all patients are presented in Table 1. The planned CTV dose decreased markedly from 63.3Gy to 47.0Gy (average mean dose) and from 60.5Gy to 44.9Gy (average D99) as the prescription level to the PTV rim was increased from 50% to 95%. Although intrafraction motion reduced this CTV dose difference the CTV dose of plans with high PTV prescription levels remained inferior to isotoxic plans with low PTV prescription levels even when motion was included in the dose calculations, see Table 1. The absolute dose delivered to the liver was almost unaffected by intrafraction motion as seen in Table 1.

Figure 1

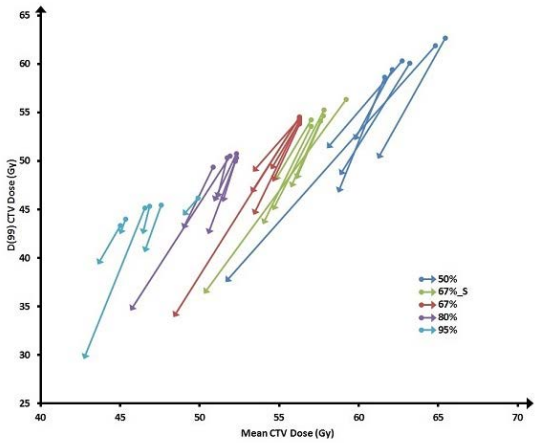

Mean dose (horizontal axis) and D99 (vertical axis) for CTV for each plan type for each patient as planned (start of each arrow) and as delivered with the known tumor motion (end of each arrow). Each color represent a plan type.

Conclusion: The dose level at the PTV rim has a large effect on the risk of RILD. Using a low dose at the PTV rim, where the probability of CTV presence during treatment was low, allowed for higher CTV dose for iso-toxic conditions in 50% and 67%_S plans. Although these plans were less robust to intra-fraction motion, their CTV dose remained superior to the 80% and 95% plans when motion effects were included.

Table 1

PTV prescription dose	Planned mean CTV dose (Gy)	Delivered mean CTV dose (Gy)	Planned mean CTV D_{99} dose (Gy)	Delivered mean CTV D_{99} dose (Gy)	Planned mean liver dose (Gy)	Delivered mean liver dose (Gy)
50%	63.3	58.0	60.5	47.8	10.91	10.53
67%_S	57.7	54.2	54.7	44.7	11.03	10.80
67%	56.3	52.9	54.3	45.5	10.97	10.66
80%	52.0	49.7	50.2	43.0	11.05	10.72
95%	47.0	45.5	44.9	39.8	11.13	10.93

PO-0891

Clinical implementation and experience with real-time anatomy tracking and gating during MR-IGRT

O. Green[1], L. Rankine[2], L. Santanam[1], R. Kashani[1], C. Robinson[1], P. Parikh[1], J. Bradley[1], J. Olsen[1], S. Mutic[1]

[1]*Washington University School of Medicine, Radiation Oncology, St. Louis, USA*

[2]*University of North Carolina, Radiation Oncology, Chapel Hill, USA*

Purpose or Objective: To describe the commissioning process and initial experience using real-anatomy, real-time tracking and gating with MRI-guided radiation therapy.

Material and Methods: An MR-IGRT system was commissioned to enable real-time anatomy tracking and gating. The imaging rate is 4 frames per second; the radiation shuts off when the anatomy of interest is automatically detected outside a pre-defined treatment region. The specific commissioning tests were driven by the goal of compensating for the inherent system latency such that there would not be an increase in treatment margins (i.e., GTV to PTV expansion). Dosimetric and geometric accuracy was evaluated by using both a commercial and an in-house motion phantoms with film and ionization chamber dosimetry. Clinical procedures were developed to maintain the established accuracy during actual patient treatments.

Results: Since initial clinical implementation, 51 patients have been treated using the gating and tracking capability of the MR-IGRT system (out of a total of 193). Based on system characteristics established during commissioning tests, the standard-of-care GTV to PTV expansion was maintained (e.g., 5 mm for abdominal tumors). Dosimetric accuracy was established via ionization chamber measurements that showed a 1.28%±1.7% average difference when comparing gated (with motion) vs. non-gated (without motion) delivery for typical IMRT and open field plans. Spatial accuracy was established via film dosimetric measurements and spatial integrity measurements to be on the order of 2 mm. This level of accuracy is maintained during patient delivery by using the following procedure: setting up to an exhale breath-hold position and using a gating boundary around the region of interest that's 2 mm less than the PTV of interest (e.g., 3 mm expansion of the GTV if a 5-mm expansion to PTV). Depending on the location of the tumor (or other anatomy of interest), duty cycles so far have ranged from about 50% (especially for tumors close to diaphragm) to about 80% (for pancreatic lesions and other abdominal sites excluding liver). Examples are shown in figure below.

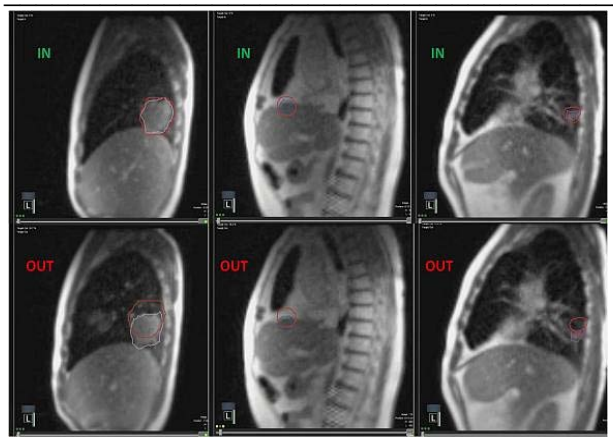

Conclusion: We have clinically demonstrated the practicality of real-time, real-anatomy tracking and have shown that clinical parameters can be selected which allow efficient treatment delivery. This work will be used as a foundation for evaluating options for treatment volume reduction.

PO-0892

Assessment of respiratory and cardiac motion to supplement MRI based tracking of hilar lymph nodes

L.P.W. Canjels[1], M.E.P. Philippens[1], T. Bruijnen[1], B. Stemkens[1], D.C.P. Cobben[1], S. Sharouni[1], J.J.W. Lagendijk[1], A.L.H.M.W. Van Lier[1], R.H.N. Tijssen[1]

[1]UMC Utrecht, Department of Radiation Oncology, Utrecht, The Netherlands

Purpose or Objective: In current radiotherapy for hilar or mediastinal lymph node metastases large treatment margins are used. Online MRI guidance will offer direct visualization of the lymph nodes, allowing highly conformal treatments using gating or tracking techniques. However, both respiratory and cardiac induced motion are expected to cause significant displacements. In this study we have assessed the relative contributions of the heart and respiration to the motion of hilar lymph nodes in order to find the optimal motion compensation strategy on the MR-Linac.

Material and Methods: Five healthy subjects were imaged during free-breathing using cine-MRI on a 1.5T MRI scanner. Sagittal and coronal scans, positioned through the center of the hilar lymph nodes, were acquired interleaved using a balanced Steady-State Free-Precession (bSSFP) sequence, providing T2/T1 contrast; Tacq = 1:08 min, TE/TR = 1.92/0.96 ms, 1.38 x 1.38 mm2, 7 mm slices, at a rate of 4 frames/sec. The motion in the region of the hilar lymph nodes was estimated using an optical flow algorithm [1]. As the cardiac induced motion manifests as a modulation of the respiratory motion waveform, power spectra were calculated to assess the relative contribution of each source of motion. The respiratory-to-cardiac power ratios were determined from the power spectrum by dividing the respiratory peak by the cardiac peak.

Results: Typical results of optical flow analysis on sagittal and coronal slices in Figs. 1A-B. Cardiac motion is shown to have significant contributions in left-right (LR) and anterior-posterior (AP) directions as shown by the power spectra (Fig. 1C). The mean lymph node displacements and respiratory-to-cardiac power ratios are listed in Table 1. The mean displacement was largest in CC direction. The respiratory-to-cardiac power ratio was largest in CC direction, while in LR direction the lowest values are observed. This implies that cardiac induced motion contributes most in LR direction, whereas respiratory induced motion dominates most in CC direction.

Conclusion: These preliminary results in five volunteers showed that cardiac motion has a significant contribution on the motion of hilar structures. This indicates that the cardiac component cannot be ignored when implementing motion compensation strategies. Soon, this study will start with the inclusion of lung cancer patients with lymph nodes metastases. The power spectra will be used to separate the cardiac from the respiratory signal to determine the exact cardiac induced displacement.

Tabel 1: Motion characteristics

	Craniocaudal direction		Left-Right direction		Anterior-posterior direction	
	Mean lymph node displacement (mm)*	respiratory-to-cardiac power ratio**	Mean lymph node displacement (mm)*	respiratory-to-cardiac power ratio**	Mean lymph node displacement (mm)*	respiratory-to-cardiac power ratio**
Subject 1	3.2	32	2.1	1.1	2.4	9.2
Subject 2	5.9	4.1	1.0	1.5	1.8	3.0
Subject 3	4.8	7.9	1.5	1.2	1.3	2.3
Subject 4	8.2	50	1.8	3.4	3.3	5.5
Subject 5	3.9	21	1.6	1.2	0.9	4.4
Average	5.2	23	1.6	1.8	1.9	4.4

* The mean lymph node displacement was calculated using a 95% confidence interval to exclude outliers
** The respiratory-to-cardiac power ratios were determined from the power spectrum by dividing the respiratory peak by the cardiac peak.

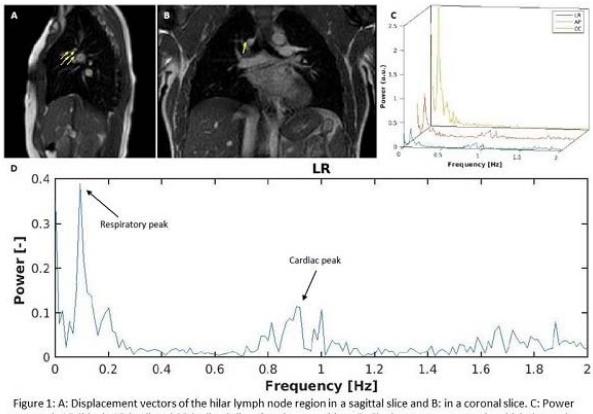

Figure 1: A: Displacement vectors of the hilar lymph node region in a sagittal slice and B: in a coronal slice. C: Power spectra in LR (blue), AP (red) and CC (yellow) directions in one subject. D: Single power spectrum in which the peaks used for the peak-to-peak ratio are indicated.

PO-0893

Direct comparison of electromagnetic guided couch and MLC tracking on a TrueBeam accelerator

R. Hansen[1], T. Ravkilde[1], E.S. Worm[1], J. Toftegaard[2], C. Grau[2], K. Macek[3], P.R. Poulsen[2]

[1]Aarhus University Hospital, Department of Medical Physics, Aarhus C, Denmark

[2]Aarhus University Hospital, Department of Oncology, Aarhus C, Denmark

[3]Varian Medical Systems, Imaging Laboratory, Baden, Switzerland

Purpose or Objective: Couch and MLC tracking are promising methods for real-time motion compensation for moving targets during radiation therapy. Couch and MLC tracking experiments have mainly been performed by different research groups, and no direct comparison of couch and MLC tracking of VMAT plans has been published. Varian TrueBeam 2.0 includes a prototype tracking system with selectable couch or MLC compensation. This study provides a direct comparison of the two tracking types with an otherwise identical setup.

Material and Methods: Several experiments were performed to characterize the geometric and dosimetric performance of electromagnetic guided couch and MLC tracking on a TrueBeam linear accelerator. The tracking system latency was determined without motion prediction as the time lag between sinusoidal target motion and the compensating motion of the couch or MLC as recorded by continuous MV portal imaging. The geometric and dosimetric tracking accuracy was measured in tracking experiments with motion phantoms that reproduced four prostate and four lung tumor trajectories. A Kalman filter was used for prediction in these experiments. The geometric tracking error in beam's eye view was determined as the distance between an embedded gold marker embedded and the circular MLC aperture in continuous MV images. The dosimetric tracking error was quantified as the Delta4-measured 2%/2mm gamma failure rate of a low and a high modulation VMAT plan delivered with the eight motion trajectories and using the static dose distribution as reference.

Results: The mean MLC tracking latency was consistently around 146ms while the couch tracking latency increased from 187ms to 246ms with decreasing sinusoidal period length due to limitations in the couch acceleration. The mean root-mean-square geometric error was 1.26mm (couch tracking) and 0.67mm (MLC tracking) parallel to the MLC leaves and 0.84mm (couch) and 1.74mm (MLC) perpendicular to the leaves. The motion-induced mean gamma failure rate was in mean 30.4% (no tracking), 0.1% (couch tracking), and 8.1% (MLC tracking) for prostate motion and 41.2% (no tracking), 2.9% (couch), and 2.4% (MLC) for lung tumor motion. The dose errors with tracking were largest for high modulation VMAT (see figure). The errors were mainly caused by fast lung tumor motion for couch tracking and by inadequate leaf fitting to prostate motion perpendicular to the MLC leaves for MLC tracking.

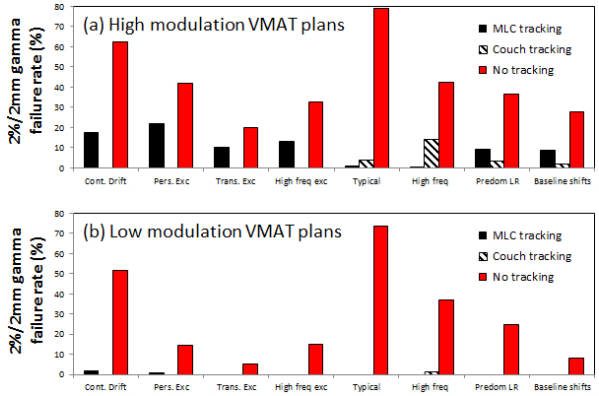

Conclusion: Both MLC and couch tracking markedly improved the geometric and dosimetric treatment accuracy. However, the two tracking types have different strengths and weaknesses. While couch tracking can correct perfectly for slowly moving targets such as prostate, MLC tracking has limitations when adapting to motion perpendicular to the MLC leaves. Advantages of MLC tracking include faster dynamics with better adaptation to fast moving targets, the avoidance of moving the patient, and the potential to track target rotations and deformations.

Poster: Physics track: Inter-fraction motion management (excl. adaptive radiotherapy)

PO-0894

Evaluation of daily setup errors in VMAT for craniospinal irradiation of paediatric patients

C. Constantinescu[1], Y. Bahadur[2], R. Al-Wassia[2], M. Hussain[1], V. Josephjohn[2]

[1]*King Faisal Specialist Hospital, Bio-Medical Physics, Jeddah, Saudi Arabia*

[2]*King Abdulaziz University Hospital, Radiology, Jeddah, Saudi Arabia*

Purpose or Objective: To retrospectively evaluate setup errors in craniospinal irradiation (CSI) with volumetric-modulated-arc-therapy (VMAT) for paediatric patients using daily cone-beam-computed-tomography (CBCT), and assess adequate planning-target-volume (PTV) margins.

Material and Methods: Ten paediatric patients with median age 10 years (range 3-14 years) undergoing CSI by VMAT were included in this study. All patients were immobilized by five-point thermoplastic mask with shoulder fixation and Vac-Lock cushions and treated in supine position, using 6 MV photons and 2 longitudinally aligned isocenters. Radiation beams were covering the brain and upper spine, and the lower spine respectively. The dose distribution at their virtual junction was optimized by inverse planning. Three patients (age ≤ 6 years) received general anesthesia and 1 patient was sedated during positioning and treatment procedures. Daily kV CBCTs were acquired before treatment for both the upper and lower segments of craniospinal axis. CBCT scans were registered to the planning CT using bony anatomy and setup shifts were determined. Inter-fraction shifts were retrospectively evaluated as systematic (Σ) and random (σ) errors in the antero-posterior (AP), lateral (LR), cranio-caudal (CC) and directions. PTV margins were calculated for a minimum CTV dose of 95% for 90% of patients. Setup errors of upper and lower craniospinal axis were compared by a 2-tailed t-test and a p value <0.5 was considered significant.

Results: A total of 376 CBCT image registrations were assessed.

Table 1. Summary of setup errors for upper and lower segments of craniospinal axis for all patients.

	Upper segment			Lower segment		
	AP	LR	CC	AP	LR	CC
M (mm)	0.2	-0.2	0.8	1.4	-0.7	0.1
Min (mm)	-5.	-9.	-5.	-10.	-14.	-6.
Max (mm)	11.	8.	15.	10.	8.	9.
Σ (mm)	0.9	0.6	1.	1.6	2.8	0.8
σ (mm)	2.1	4.5	4.9	4.1	5.2	4.3
Margin (mm)	3.7	4.7	5.9	6.9	10.6	5.1

The largest setup error occurred in the CC and LR direction, for the upper and lower segment of craniospinal axis, respectively. Statistical significant difference was found between upper and lower segment of craniospinal axis in CC (p=0.032) and LR (p=0.009) directions, due to different immobilization devices.

Fig. 1. Distribution of setup errors in all directions, for upper and lower segment of craniospinal axis.

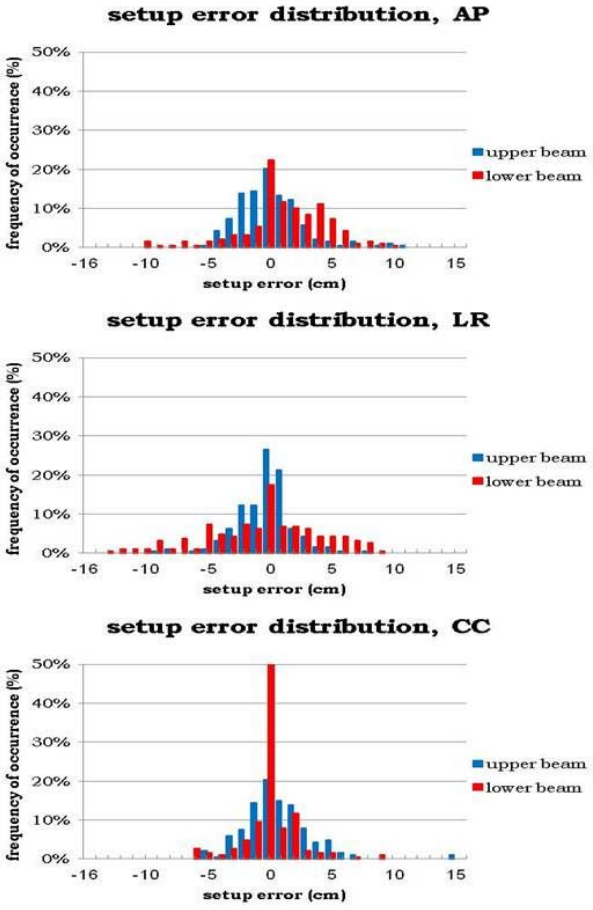

Conclusion: For paediatric patients undergoing CSI by VMAT, the main setup variation occurs in the CC and LR direction, for the upper and lower segment of craniospinal axis, respectively. Despite of specific immobilization methods, large PTV margins are required to reduce the setup

uncertainty. Our data recommend daily kV CBCT imaging and setup corrections for this group of patients.

PO-0895

Intraprostatic calcifications as IGRT fiducial markers: analysis of 646 CBCT images in 35 patients

P. Antognoni[1], D.P. Doino[1], L. Pozzi[2], S. Gottardo[1], P. Stucchi[2], C. Bianchi[2], M. Monciardini[2], L. Cerizza[1], M. Molteni[1], R. Novario[2]
[1]*Ospedale di Circolo Fondazione Macchi, Department of Radiotherapy, Varese, Italy*
[2]*Ospedale di Circolo Fondazione Macchi, Department of Medical Physics, Varese, Italy*

Purpose or Objective: To review CBCT images of 35 pts receiving radical irradiation for localized prostate cancer, according to an IGRT protocol based on the use of intraprostatic calcifications as natural fiducial markers for the evaluation of inter-fraction organ motion.

Material and Methods: Between 2013 and 2014, 646 KVCBCT images of 35 pts radically irradiated with moderately hyopofractionated VMAT (2.5 Gy/fract.- 70 Gy in 28 fract.) for localized prostate cancer were acquired according to an IGRT protocol aimed at evaluating the role of intraprostatic calcifications as natural fiducial markers. All the evaluated pts presented at least 3 calcifications of >2 mm located inside or at the borders of the CTV and contoured on high resolution CT-simulation scans and on each CBCT (mean: 18 CBCT/patient). In order to assess the internal stability of the calcifications the distances between them were measured for each patient on both CT-simulation scans and each CBCT, then mean ± SD of differences between distances was calculated. Distances between calcifications and the center of mass of CTV were also calculated in 21 patients by drawing CTV on 360 CBCT images, contoured by a same physician. The center of CTV mass spatial coordinates (X, Y, Z) was determined for each CTV and finally the distances between the center of the CTV and the center of each calcification were measured. Stability of calcifications in respect of CTV was assessed by calculating mean values ± SD of measured distances.

Results: The mean value of differences in distances between calcifications was -0.04 mm ± 1.54 SD, with 95% of values contained inside 3 mm (μ ± 2SD). The mean value of differences in distances between calcifications and center of mass of CTV (Fig. 1) was -0.03 mm ± 1.55 SD, with 95% of values contained inside 3 mm (μ ± 2SD).

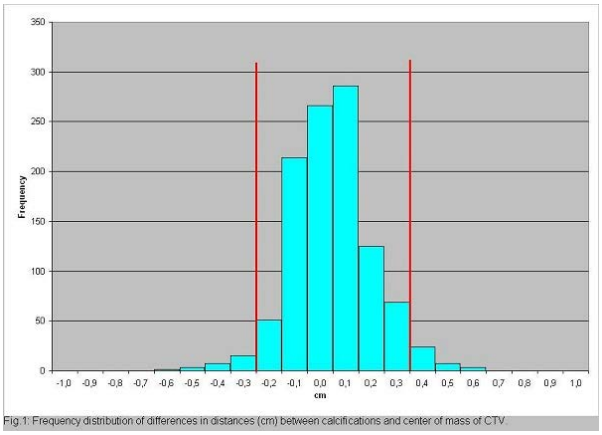

Fig.1: Frequency distribution of differences in distances (cm) between calcifications and center of mass of CTV.

Conclusion: Our results derived from the analysis of a large data set of CBCT images confirm that intraprostatic calcifications, when >2 mm and present at least Nr.=3, properly selected and contoured, can be used as very reliable natural fiducials, with potential reduction of iatrogenic risks and costs associated with the implantation of fiducial markers for prostate cancer IGRT.

PO-0896

The effect of bladder volume on bowel dose in the treatment of anal cancer using IMRT

K. McDonald[1], L. Wells[1], H. Phillips[1], C. McLean[1], L. Carruthers[1], W. Nailon[1]
[1]*Edinburgh Cancer Centre, Radiotherapy Physics, Edinburgh, United Kingdom*

Purpose or Objective: Bony anatomy is used to match anal cancer patients treated using volumetric modulated arc therapy (VMAT). Only extreme volume changes due to bladder, rectum or bowel filling are currently highlighted to the responsible clinician. This study aims to determine the impact that changes in bladder volume has on the dose to the small bowel over the course of the treatment by comparing the dose to volumes outlined on cone-beam CT (CBCT) to the initial planned dose statistics. A more representative value of accrued dose to the small bowel over the course of treatment can also be gained.

Material and Methods: Ten patients who were treated with VMAT for anal cancer were selected for this study. Weekly cone beam CT images were acquired to monitor extreme changes in bladder and rectum filling. Patients were asked at both planning CT and treatment to have a comfortably full bladder. The bladder and small bowel (contained within the scan) were outlined on three CBCTs by one clinician; week one, mid treatment and final week. The bladder volumes were compared over the course of the treatment and the maximum small bowel dose, amount of small bowel receiving 30Gy (V30Gy) and 40Gy (V40Gy) were recorded.

Results: The results in Table 1 show the variation in bladder volume. The V40Gy bowel volume was plotted against the difference between the bladder volume at CBCT and the initial planning scan with the intercept for the linear trends set to the planning CT volume for each patient (see Fig. 1). A similar trend was found for the V30Gy measurement. There was less impact on maximum dose to small bowel with changing bladder size.

Table 1 - *Bladder Volumes*

Patient	1	2	3	4	5	6	7	8	9	10
Planning CT bladder volumes [Range from CBCTs] (cm3)	579 [426-618]	196 [75-628]	278 [146-225]	140 [57-248]	157 [31-70]	170 [80-232]	182 [146-215]	247 [65-227]	239 [79-154]	161 [81-191]

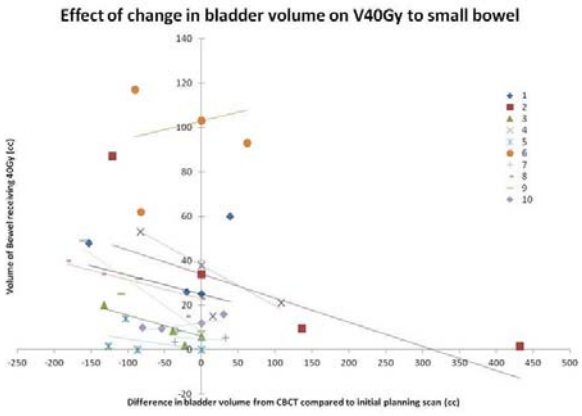

Conclusion: In eight cases a smaller bladder at CBCT resulted in a greater volume of small bowel receiving clinically relevant doses compared to the initial planning CT. There were two patients where the trend indicated that a larger bladder increased small bowel dose. Limitations of this study

include poor visibility of the small bowel on the CBCTs, smaller field of view meaning less volume and variation between initial planning clinician and clinician outlining CBCTs. CBCT is now widely used for adaptive planning techniques and in this case has provided evidence for implementing a stricter bladder filling protocol to improve the accuracy of bowel dose statistics at planning.

PO-0897

Comparison of hippocampus sparing extent according to the tilt of a patient head during WBRT

S. Moon[1], M. Yoon[1], M. Chung[2], W. Chung[2], D. Kim[2]
[1]*Korea University, Department of Bio-convergence Engineering, Seoul, Korea Republic of*
[2]*Kyung Hee University Hospital at Gangdong, Department of Radiation Oncology, Seoul, Korea Republic of*

Purpose or Objective: We report the results of our investigation into whole brain radiotherapy using linear accelerator-based intensity-modulated radiation therapy and volumetric-modulated arc therapy in cancer patients with a high risk of metastasis to the brain. Concretely, we assessed the absorbed dose and the rate of adverse effects for several organs at risk according to the tilt of a patient's head.

Material and Methods: From data regarding patients who had previously received WBRT, we arbitrarily selected five cases where measurements were made with the patients' heads tilted forward and five cases without such tilt. We set the entire brain as the planning target volume, and the hippocampi, the lenses, the eyes, and the cochleae as the main OAR, and formulated new plans for IMRT (coplanar, non-coplanar) and VMAT (coplanar, non-coplanar). Using the dose-volume histogram obtained from the treatment plans, we calculated and compared the effective uniform dose and normal tissue complication probability of the OAR. In order to compare the extent of hippocampal sparing, we also analyzed the mean and the maximum doses.

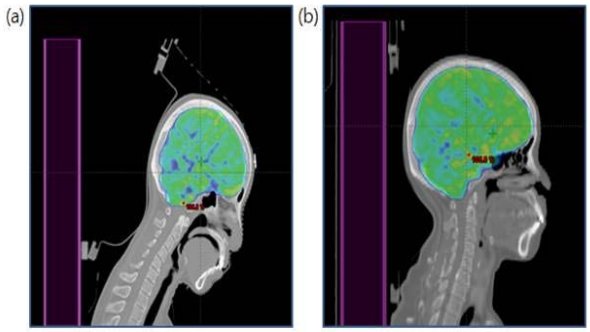

Results: When a patient received coplanar IMRT with the head tilted forward, the EUD and NTCP values for the hippocampus decreased by 13% and 81%, and the mean dose and maximum dose decreased by 8% and 7%, respectively. When the patient received non-coplanar treatment, the hippocampal EUD and NTCP values decreased by 2% and 15%, and the mean dose and maximum dose decreased by 2% and 4%, respectively. For coplanar VMAT treatment, the EUD values decreased by 20%, the NTCP values decreased by 92%, and the mean dose and the maximum dose decreased by 10% and 13%, respectively. For non-coplanar treatment as well, the EUD values decreased by 14%, the NTCP values decreased by 81%, and the mean dose and the maximum dose decreased by 14% and 10%.

			CVI	CI	HI
IMRT	Coplanar	Tilt	0.98 ± 0.01	0.91 ± 0.02	0.09 ± 0.02
		Non-tilt	0.99 ± 0.00	0.90 ± 0.02	0.07 ± 0.01
	Noncoplanar	Tilt	0.99 ± 0.01	0.91 ± 0.01	0.08 ± 0.02
		Non-tilt	0.99 ± 0.01	0.90 ± 0.02	0.07 ± 0.01
VMAT	Coplanar	Tilt	0.98 ± 0.01	0.90 ± 0.01	0.09 ± 0.01
		Non-tilt	0.98 ± 0.01	0.90 ± 0.02	0.09 ± 0.02
	Noncoplanar	Tilt	0.98±0.01	0.90±0.01	0.10±0.01
		Non-tilt	0.98 ± 0.01	0.90 ± 0.01	0.10 ± 0.01

Conclusion: If the patient tilted the head forward when receiving the Linac-based treatment, for the same treatment effect in the PTV, we confirmed that a lower dose entered the OAR, such as the hippocampus, eye, lens, and cochlea. Also, the damage to the hippocampus was expected to be the least when receiving coplanar VMAT with the head tilted forward, and we showed that damage to OAR, including the hippocampus, was the least overall when the head was tilted forward. Accordingly, if patients tilt their heads forward when undergoing Linac-based WBRT, we anticipate that a smaller dose would be transmitted to the OAR, resulting in better quality of life following treatment.

PO-0898

Inter-fraction position of the tongue in postoperative radiotherapy of tongue cancer

E. Dale[1], C. Salamonsen[1], K. Angelvik[2], S. Gjølme[2], B. Bø[2]
[1]*Oslo University Hospital - Radium, Department of Oncology, Oslo, Norway*
[2]*Oslo and Akershus University College of Applied Sciences, Department of Life Sciences and Health, Oslo, Norway*

Purpose or Objective: Postoperative radiotherapy (PORT) of tongue cancer is associated with side-effects such as acute mucositis. Our department previously used intraoral stents to depress the tongue to minimize the dose to the palate. However, the stents were not always very well tolerated and there were also reproducibility issues. Therefore, the intraoral stents were omitted. In order to still ensure target coverage, we have included the air gap (if present) above the tongue in the target volume (CTV tongue including the surgical bed) on the planning CT. We wanted to investigate whether the air gap is a systematic phenomenon over all treatment fractions, so that the size of the CTV could be reduced avoiding irradiating the palate.

Material and Methods: We have so far included 10 patients with T1-T2 N0 M0 squamous cell carcinoma of the tongue referred to PORT. Nine patients were treated with 50 Gy in 2 Gy fractions, and one patients with 60 Gy in 2 Gy fractions with concurrent chemotherapy (cisplatinum) because of positive surgical margins. All patients underwent daily kV cone-beam CT (CBCT). From each CBCT we obtained three distance measures from the sagittal images: The caudo-cranial air gap from the cranial border of the tongue to the palate on the 1) lateral left, 2) midline and 3) lateral right side.

Results: Two of 10 patients had air gaps between the tongue and palate systematically present over the treatment period (Figure, mean air gaps 6 mm and 8 mm) indicating that a caudo-cranial reduction of the CTV for these individuals could be safe. However, for the remaining 8 patients the tongue was mostly located cranially towards the palate. It was not possible to identify a relationship between the size of the air gap and clinical parameters such as resected volume, tumor size, infiltration depth, patient age or gender.

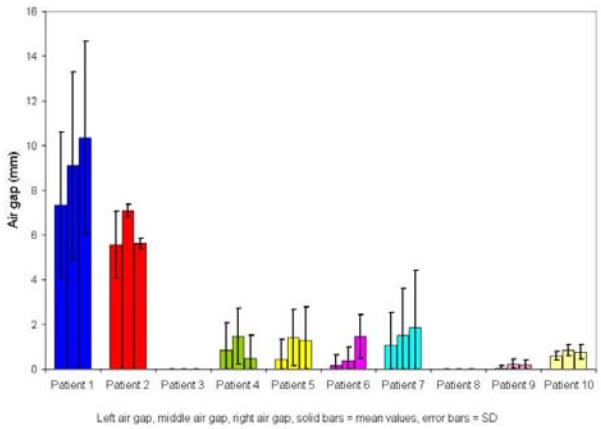

Conclusion: PORT for tongue cancer without intraoral stent is best planned with the target volume extending towards the palate to allow for inter-fractional movement of the tongue.

PO-0899

Robustness of fractionated photon RT for pancreatic cancer: Dosimetric effects of anatomical changes

A. Van der Horst[1], A.C. Houweling[1], J. Visser[1], G. Van Tienhoven[1], A. Bel[1]
[1]*Academic Medical Center, Radiation Oncology, Amsterdam, The Netherlands*

Purpose or Objective: Anatomical changes taking place over the course of radiation therapy (RT) result in a difference between planned and delivered dose. For pancreatic cancer, we investigated the robustness of clinical treatment plans by quantifying the dosimetric effects of changes in gas volumes, body contour and interfractional target displacement. In addition, we compared the dosimetric effect of anatomical changes between use of bony anatomy and use of intratumoral fiducial markers for patient positioning.

Material and Methods: Nine pancreatic cancer patients were included who had intratumoral markers for daily cone-beam CT (CBCT)-based position verification. The clinical plans (10 MV; 1 arc VMAT; internal CTV (iCTV) to PTV margin = 10 mm) were used for dose calculation. To enable fraction dose calculations on CBCT, the planning CT was deformably registered to each CBCT (13–15 CBCTs per patient); air volumes visible on the CBCT were copied to the deformed CT.
Calculations were done for marker-based registration (as clinically used) and for bony anatomy-based registration. For both methods, doses were rigidly summed to yield the accumulated doses on the planning CT. For each patient, all DVHs were normalized to yield for the planned dose to the PTV: V98% = 95% (100% = 36 Gy).
To evaluate target coverage, we defined an iCTV+5mm volume, i.e. the iCTV expanded with a 5 mm margin to account for remaining uncertainties including delineation. We analysed D98%, Dmean and D2% for iCTV+5mm and iCTV and examined DVH differences for duodenum and stomach, the organs at risk closest to the iCTV.

Results: For the iCTV+5mm, D98% changed from mean 96.3% (range 95.5–97.8%) for the planned dose to 96.7% (96.4–97.0%) for marker-based accumulated dose (Table 1).

Table 1. Target dose for the 9 patients.

		Planned		Marker-based		Bony anatomy-based	
		mean	(range) [%]	mean	(range) [%]	mean	(range) [%]
iCTV+5mm	$D_{98\%}$	96.3	(95.5–97.8)	96.7	(96.4–97.0)	95.3	(**85.8**–97.9)*
	D_{mean}	98.7	(97.8–101.1)	99.0	(98.2–100.0)	98.8	(96.7–100.1)
	$D_{2\%}$	100.9	(99.2–104.5)	101.2	(99.7–103.3)	100.6	(98.8–102.4)
iCTV	$D_{98\%}$	96.3	(95.5–98.0)	96.7	(96.4–97.1)	97.1	(**93.6**–98.6)*
	D_{mean}	98.6	(97.8–101.1)	99.0	(98.1–100.0)	99.0	(97.6–100.2)
	$D_{2\%}$	100.7	(99.1–104.5)	101.0	(99.7–103.2)	100.5	(98.8–102.2)

* Doses <95% in **bold**.

For each patient, the DVH of the PTV of the planned dose distribution was normalized to $\mathbf{D_{98\%} = 95\%}$; all other DVHs of planned and accumulated doses were scaled accordingly. For the group, this yielded a PTV $D_{2\%}$ of mean 100.8% (range 99.3–104.3%).

These relatively small differences indicate a limited dosimetric effect from changes in gas and body contour, even though the amount of gas visible on CBCT showed large variations (avg. 166 ml, SD 145 ml).
In contrast, D98% decreased to 95.3% (85.8–97.9%) for bony anatomy registration, due to systematic errors inherently associated with bony-anatomy patient positioning. Changes for stomach and duodenum depended strongly on the direction of these errors, with large increases in D2% for some (error in direction of organ) and large decreases for others. Differences were largest for the stomach (e.g. D2% from 72.7% (planned) to 82.4% (bony anatomy-based accumulated)). For marker-based positioning, the dosimetric effects for stomach and duodenum were limited (<0.5 Gy in 8 out of 9 patients).

Conclusion: Photon irradiation of pancreatic tumours is robust to variations in body contour and gastrointestinal gas, with dose coverage only mildly affected by these anatomical changes. However, when using bony anatomy for patient positioning, dose coverage declines due to interfractional tumour position variations. Therefore, the use of fiducial marker-based daily position verification is essential in RT for pancreatic cancer.

PO-0900

Dosimetric analysis of organ deformation during prostate IMAT with cone beam CT imaging

D. Foley[1], B. McClean[2], P. McBride[2]
[1]*UCD, School of Physics, Dublin, Ireland Republic of*
[2]*St. Luke's Radiation Oncology Network, Physics, Dublin, Ireland Republic of*

Purpose or Objective: Patients undergoing prostate intensity modulated arc therapy (IMAT) were retrospectively investigated using the CBCT images acquired for setup purposes to determine the volumetric variability of the target and organs at risk and the dosimetric implications of these changes.

Material and Methods: IMAT plans from 11 patients were designed to deliver 74 Gy in 37 fractions to the target. The CTV consisted of the prostate and seminal vesicles, while the PTV was the CTV plus a margin of 10 mm in all directions except posteriorly, where a 5 mm margin was used. For between 9 and 14 of the 37 fractions, the patients were scanned using an on-board CBCT imager to verify the setup. These images were retrospectively registered to the planning CT using an in-house registration algorithm to determine the transformations between the images. The calculated transformation vector field was used to deform the planning CT so that the plan could be recalculated with the original MU on this new adapted CT. This allowed the determination of the dosimetric impact of the change in anatomical information from the time of acquisition of the planning CT to immediately prior to a given treatment fraction. The imaged fractions were treated as though they were representative of the entire treatment and were weighted equally for dose accumulation purposes.

Results: Over the course of the patients' treatments, the changes in CTV volume compared to the plan were from a decrease of 25% up to a maximum increase of 6%. Their bladder volumes ranged from -10% to 10% of their respective volumes on the planning CT. The rectal volume decreased for all patients, with 5% less than the planning volume the smallest reduction and 34% being the largest volume shrinkage.
The dosimetric impact of these anatomical changes varied for each structure. The minimum dose received by the CTV varied by less than 1% for all patients, with full coverage of the CTV achieved in all fractions.
The mean dose delivered to the bladder averaged over each patients treatment resulted in variation of between -4% and 17% of their respective planned mean doses. This did not result in a break of the dose-volume constraints (DVCs) for the bladder at any fraction, for any patient.
The rectum received a higher mean dose than the planned value for all patients. This ranged from an increase of 7% up to 38%. It was found that the rectum frequently broke multiple DVCs, resulting in the rectum being overdosed in 79% of the fractions examined.

Conclusion: Analysis of the anatomical condition of the patient on the day of treatment can give an indication of how suitable the original plan for their treatment is. For these patients, although the variability in the anatomy did not

result in any significant under-dosing of the target, the observed differences showed that the rectum broke our institutional DVCs during treatment. This is important data required to evaluate the robustness of institutional procedures for the planning and delivery of patients' treatments.

PO-0901

Investigation of a fast CBCT protocol for supine accelerated whole breast Irradiation

E. Bogaert[1], C. Monten[1], C. De Wagter[1], W. De Neve[1]
[1]*Ghent University Hospital, Radiotherapy, Ghent, Belgium*

Purpose or Objective: Acceleration in breast cancer treatment might become the new standard. As fraction dose rises, the importance of correct positioning increases. CBCT is time consuming and uses (low dose) radiation. Increasing interval between positioning and actual treatment reduces precision. We therefore investigated a CBCT technique with lower dose and faster acquisition.

Material and Methods: Both standard and fast pre-treatment CBCT imaging (STAND and FAST) were performed on XVI Elekta ® in a 5-fractions supine and whole breast irradiation scheme (5 x 5.7 Gy). The main difference between protocols was gantry speed (Table 1). Central dose was measured with PTW equipment in a CTDI32 phantom. High resolution (HR) and contrast were measured on a Catphan Phantom. Breast contour appearance was assessed on a polystyrene breast phantom. Fifteen clinical CBCT-images for three patients to which FAST or STAND was randomly assigned, were blindly scored by a skilled oncologist. A three-level answer had to be formulated regarding visibility of 1) *all* clips, 2) e*ntire* breast contour, 3) lung/thorax wall edge and 4) excision cavity. Answers were decoded: 0: *Not at all*; 1: *Yes, but only with guidance of reference CT*; 2; *Yes clearly, without reference CT*.

Results: FAST operated at only 53% and 61 % of dose and time of STAND. A low HR (3 lp/mm) was the same for FAST and STAND. Contrast was assessed for STAND through visibility of the largest (15mm) 1% contrast nodule. For FAST, no nodules could be distinguished. There was excess-tissue on cranial and caudal CBCT breast phantom slices, but to the same extent in STAND and FAST. In mid position, breast edge was sharp and coincided with reference CT.
The Patient study reflected a difference in the overall low soft tissue contrast for the two protocols. The excision cavity was never scored 2, more 1 for STAND and more 0 for FAST and was less visible with higher breast density (patient 3). Breast contours showed step-wise artifacts near inframammary and axillary folds for both protocols. Lung/thorax wall edges were scored 2 and 1 but the dependency was larger for patient anatomy than for scan protocol. All clips were visible: the rather poor HR is however sufficient. Streak artifacts due to beam hardening and undersampling were apparent in both protocols (Figure 1).
Even though the noisy and artifact-rich appearance of the images, effect on clinical decision making for registration is minimal. The stepwise artifacts appear very localized and are easily corrected for in the observer's mind. Additional information by outer breast contour and lung-thoracic wall edge compensates for this. Distinction between real artifacts and excision cavity can be done by comparison with reference CT. Clips are always visible and of special importance in high density and/or voluminous breasts.

Figure 1: a) STAND CBCT image with step-wise artifacts (arrow 1); b-c) STAND mid and caudal breast phantom image sets (green-purple representation), tissue excess (arrow 2); d) STAND CBCT image with streak artifacts (arrow 3) and clip (arrow 4); e-f) FAST CBCT and reference CT image of the same patient with boost CTV volume (red) where visibility of excision cavity was scored 1.

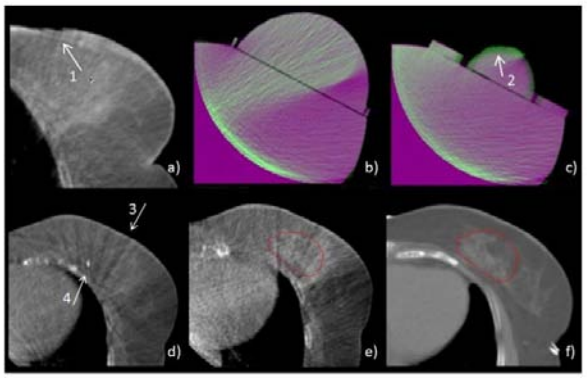

Table 1: Standard and fast pre-treatment CBCT imaging protocols

	STAND		FAST	
	left	right	left	right
*Protocol parameters**				
Acquisition angle [degrees]	205	200	205	200
gantry speed [degrees/min]	180	180	360	360
N° of frames	376	367	188	183
Dose and Time measurements				
Dose Length Product£ [mGy.cm]	30.7	35.1	16.1	19.0
CBCT-acquisition time [s]	79	76	49	45

* *all: 120kV; mA/frame=20; ms/frame=32; 5.5 frames/s*
£ *Dose Length Product: dose measured over 10 cm long pencil chamber @ central hole of CTDI32 phantom*

Conclusion: FAST allows the oncologist to register breast CBCT. However, with high density or voluminous breasts, clips are recommended with the use of FAST.

PO-0902

Improving frameless intracranial stereotactic setup with 6DOF couch using two pre-treatment CBCTs

I. Gagne[1], A. Mestrovic[1], S. Zavgorodni[1]
[1]*BC Cancer Agency - Vancouver Island Cancer Centre, Medical Physics, Victoria, Canada*

Purpose or Objective: The primary goal of this study was to evaluate the residual inter-fraction positioning errors of our intra-cranial frameless stereotactic treatment following a six-degree of freedom (6DOF) correction based on automatic bone anatomy matching. A secondary goal was to evaluate the intra-fraction motion.

Material and Methods: Since the implementation of the stereotactic program at our centre, 13 patients were treated with frameless intra-cranial fractionated radiotherapy on a Varian TrueBeam STx linear accelerator. All patients had a planning CT scan with an immobilization system that comprised of a CIVCO head cup, customizable pillow and thermoplastic shell. To guide setup, nose to forehead pitch was calculated using CT information and reproduced at treatment using a digital level. Roll was measured as the difference in height at the level of the anterior ear notch and reproduced at treatment using the in-room lasers. Two pre-treatment CBCTs were acquired; the first to correct using 6DOF bone anatomy matching the initial inter-fraction positioning error and the second to assess the residual inter-fraction error post 6DOF correction. Since our initial experience with the first 3 patients, revealed residual inter-fraction setup errors greater than 1mm, the residual inter-fraction setup error post 6DOF correction was measured and corrected prior each treatment for all remaining 10 patients. Due to the technical limitations of Varian's 6DOF couch (i.e. maximum 3 degrees pitch and roll), the correction of the residual inter-fraction error was carried out using 4DOF automatic bony anatomy matching (i.e. excluding pitch and roll due to 3degree limitation). A post-treatment CBCT was acquired to determine the intra-fraction motion using 6DOF bone anatomy matching.

Results: Datasets from 10 patients were obtained for a total of 705 CBCT scans – the first 3 patients were excluded from the study due to changes in methodology partly through treatment. The mean 3D vector of residual setup error post first correction (6DOF) was 0.7 ± 0.4 mm (mean ± SD) and the maximum 3D vector was 2.2mm. The mean 3D vector of residual setup error post second correction (4DOF) was 0.2 ± 0.1mm and the maximum 3D vector was 0.8mm. The mean 3D vector of intra-fraction motion was 0.4 ± 0.2mm and the maximum 3D vector was 1.3mm.

Conclusion: Incorporating a second correction pre-treatment significantly reduced the residual inter-fraction setup error from 0.7 ± 0.4 mm to 0.2 ± 0.1mm. The intra-fraction motion for this cohort of patients was twice as large as the residual inter-fraction setup error. Efforts are currently underway to reduce this intra-fraction motion by focusing on improvements to the immobilization system.

PO-0903

IGRT for a highly conformal VMAT-technique for simultaneous treatment of the breast and lymph nodes

B. Houben-Haring[1], M. Admiraal[1]
[1]*VU University Medical Center, Department of Radiotherapy, Amsterdam, The Netherlands*

Purpose or Objective: Recently we introduced an improved hybrid treatment planning technique for breast with simultaneous irradiation of axillary and supraclavicular lymph nodes (level I-IV). This technique combines tangential open fields with VMAT (RapidArc®, Varian Medical Systems) and results in a highly conformal coverage of the lymph node region, with a steep dose fall-off towards esophagus and thyroid. The purpose of this study is to evaluate the validity of this conformal planning technique, with the required setup and image guidance.

Material and Methods: Ten patients were included, of which 8 were treated in Free Breathing and 2 were treated in Deep Inspiration Breathhold. Fractionation was 16 x 267 cGy for both elective breast and lymph node regions. PTV-margin of level I-IV lymph nodes is 5 mm to the medial direction and 8mm for all other directions (image 1). Daily online setup was performed on bony anatomy with 2 orthogonal kV-images and subsequent verified with medio-lateral MV field imaging. At the level of the PTVnodes setup deviation up to 3mm was allowed in lateral direction, in all other directions and for the humeral head 5mm was allowed. At the first 3 fractions and weekly a CBCT was acquired for verification of the PTV-coverage of the lymph nodes. All CBCT's were used offline for analysis of the reproducibility of level I-II nodes, level III-IV nodes, humeral head and bony anatomy. All 160 fractions were used for evaluation of the efficiency of the setup and imaging procedure.

Image 1: 95% dosewash: $CTV_{nodes\ level\ I-IV}$ (green) $PTV_{nodes\ level\ I-IV}$ (thick red) and PTV_{total} (thin red)

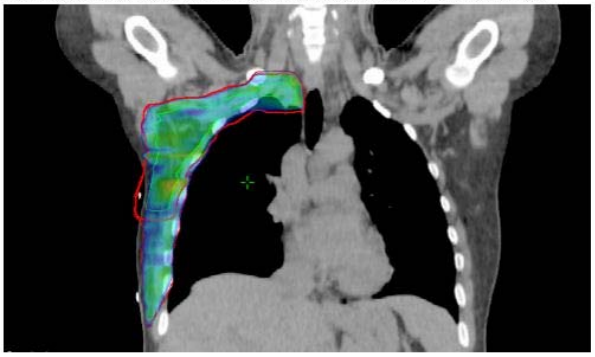

Results: A t-test showed a significant relation between the position of the humeral head and all the nodes in cranio-caudal direction (p=<0.001) and for level III-IV also in lateral direction (p=0.01). Repositioning was required in 31 fractions (19%). This was reduced to 19 fractions (12%) by excluding 1 patient with positioning problems. Based on the CBCT's, we found that only in 2% of all cases, an off-set of the humeral head less than 8mm lead to a deviation of the nodal PTV of more than 5mm. Analysis of the CBCT's also showed that the remaining average setup error for level I-II nodes and level III-IV nodes was less than 2mm in all directions with SD of max 1.6mm in AP direction (Table 1).

Table 1: Residual setup error of the lymph nodes and humeral head after bony anatomy match on 2 orthogonal kV-images

	Level I-II lymph nodes				Level III-IV lymph nodes				Humeral head			
	vrt(mm)	lng(mm)	lat(mm)	Rot(dgr)	vrt(mm)	lng(mm)	lat(mm)	Rot(dgr)	vrt(mm)	lng(mm)	lat(mm)	Rot(dgr)
MEAN	0,19	0,14	0,14	0,8	0,17	0,15	0,13	0,6	0,31	0,23	0,22	1,8
SD	0,16	0,13	0,09	0,6	0,15	0,15	0,09	0,5	0,32	0,15	0,19	1,9
MIN	0,02	0,00	0,01	0,1	0,01	0,00	0,01	0,0	0,31	0,23	0,22	1,8
MAX	1,26	0,90	0,52	3,8	0,82	0,74	0,38	2,3	1,77	0,66	0,88	8,3

Conclusion: The positioning of the lymph nodes level I-IV can be well addressed by the position of the surrounding bony anatomy and the humeral head. For the adequate treatment of both the lymph node regions and the breast, two orthogonal kV-images and MV field imaging are sufficient.

PO-0904

Bladder changes assessment using daily cone-beam computed tomography

O. Casares-Magaz[1], V. Moiseenko[2], A. Hopper[2], N. Pettersson[2], M. Thor[3], L. Cerviño[2], R. Knopp[2], M. Cornell[2], J.O. Deasy[3], L.P. Muren[1], J. Einck[2]
[1]*Aarhus University Hospital, Department of Medical Physics, Aarhus, Denmark*
[2]*University of California San Diego, Department of Radiation Medicine and Applied Sciences, San Diego, USA*
[3]*Memorial Sloan Kettering Cancer Center, Department of Medical Physics, New York, USA*

Purpose or Objective: Late genitourinary (GU) and gastrointestinal (GI) toxicities are the main dose limiting factors prostate radiotherapy plans. However, no predictive models, and consequently, no consensus guidelines have been reported for GU toxicity. One possible explanation is that the plan dose-volume histogram (DVH) is not representative of the accumulated bladder dose throughout the treatment given variability in bladder filling status, motion and set-up uncertainties. Modern image guidance techniques, in particular the use of cone beam computed tomography (CBCT), facilitates reconstruction of the accumulated dose. The aim of the study was to compare planned with accumulated dose and volume data for the bladder with the latter assessed from daily CBCT imaging and deformable image registration (DIR).

Material and Methods: Eight subjects presenting with RTOG GU Grade 2+toxicity were selected from a cohort of 287 patients treated for prostate cancer in 2006-2013. Prescribed dose was 81Gy in 45 fractions. The 8 subjects were each matched to 3 patients without GU toxicity by the following criteria: pretreatment GU symptoms (IPSS score), age ± 5y, risk group (low, intermediate, high), whole pelvis vs. prostate, and use of neoadjuvant ADT. Treatment required adherence to a full bladder and empty rectum protocol. Daily CBCT was used for patient realignment and to assess bladder and rectal filling status. Dose from planning CT was rigidly registered to CBCT using recorded daily shifts followed by bladder contour propagation from plan CT to the first day CBCT and then to the remaining CBCTs using an intensity-based deformable image registration (DIR) algorithm. Bladder contours were corrected manually and the accumulated D10 and D20 (defined as the highest dose received by a volume up to 10 and 20 cm3 of the bladder, respectively) were compared to corresponding values from the planned DVH. All registrations and DVHs computations were done using MIM Maestro 6.4.4 (Mim Software Inc. Cleveland, OH, US).

Results: In the analyzed patients, the bladder volumes in the daily CBCTs were found to vary between 62% and 256% of that from the planning CT, with a mean difference in volume ranging from 63% to 20%. Differences in the compared DVH were also observed where D10 was ±2.7%, and D20 ±11.2% of the corresponding planned metrics.

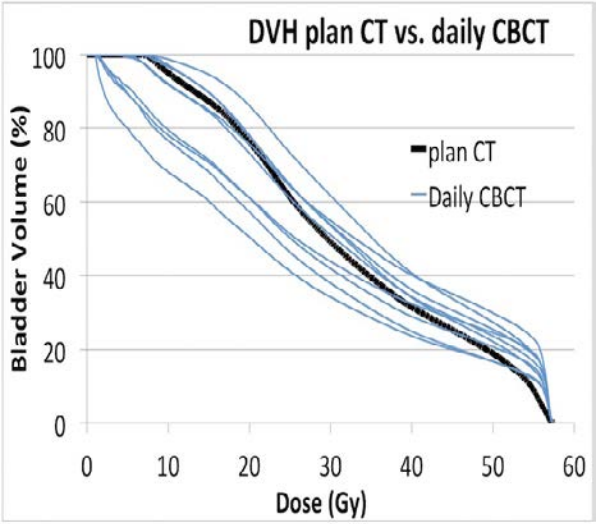

Figure 1. Bladder DVH's for the plan CT and for the daily CBCTs throughout the treatment course, and obtained after the image registration and contour correction.

Conclusion: We found considerable variation in bladder dose and volumes throughout the treatment course. Inclusion of inter-fractional bladder deformations should, therefore, likely be considered in future dose-response modeling of GU toxicity.

Poster: Physics track: Adaptive radiotherapy for inter-fraction motion management

PO-0905

Preparation for the first in man on the MR-Linac: virtual couch shift and on line plan adaptation

I.H. Kiekebosch[1], E.N. De Groot[1], C.N. Nomden[1], G.H. Bol[1], B. Van Asselen[1], G.G. Sikkes[1], L.T.C. Meijers[1], A.N.T.J. Kotte[1], B.W. Raaymakers[1]

[1]University Medical Center Utrecht, Radiation Oncology, Utrecht, The Netherlands

Purpose or Objective: The MR-Linac (MRL) combines a linear accelerator and a 1.5T MRI scanner, which provides the possibility for on line adaptation on the current anatomy. In the current workflow, compensation for discrepancies between pre-treatment and daily treatment geometry is performed using couch translations. On the MRL it is not possible to shift the couch in left-right and anterior-posterior direction. Instead a Virtual Couch Shift (VCS) is applied: the pre-treatment dose distribution is shifted to cover the target volume by moving the MLC aperture. After VCS, it is also possible to perform Segment Weight Optimization (SWO) and Segment Shape Optimization (SSO). The first in man on the MRL will be a patient with vertebral metastases. The purpose of this study was to assess the accuracy and usability of VCS and possibly subsequent optimization for palliative treatment of patients with vertebral metastases.

Material and Methods: Three patients with repeated CT scans of the thoracic spine were included. A CTV of one thoracic vertebra was delineated, a PTV was created with an isotropic margin of 5 mm around the CTV. A clinical reference plan with a prescription dose of 800cGy (single fraction) was created in a research version of Monaco (Elekta)(figure 1). The second CT scan was used to mimic daily imaging at the MRL. The second CT was shifted in left-right and superior-inferior direction from -5 to 5 cm and in the anterior-posterior direction from -1 to 1 cm. VCS plans were created for each shift resulting in 60 plans. These were further optimised by SWO (60 plans) and by both, SWO and SSO (60 plans).
To determine the accuracy of all 180 plans, the dose distributions and DVH's were evaluated and compared with the reference plan. Plans were acceptable if V107<2cm^3, the V99 decreased less than 2%, the V95 decreased less than 1% and the Dmean differed maximal 1% from the reference plan. Also time was evaluated to determine the usability in an online situation at the MRL.

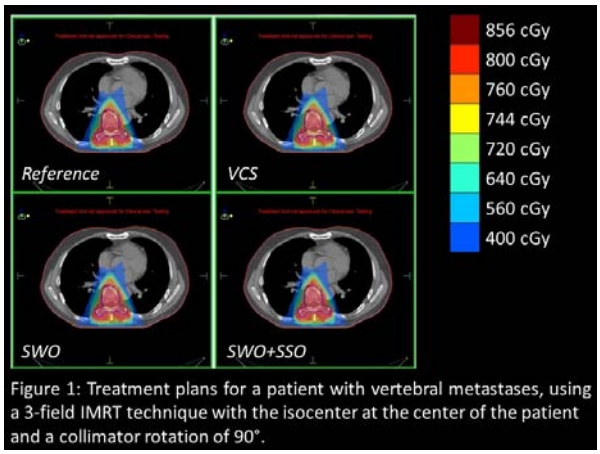

Figure 1: Treatment plans for a patient with vertebral metastases, using a 3-field IMRT technique with the isocenter at the center of the patient and a collimator rotation of 90°.

Results: In total, 52% of the VCS plans were acceptable. Left-right shifts resulted mainly in an unacceptable V107. Superior-inferior shifts resulted mainly in lower coverage. With SWO, 63% of the plans were accepted, the unaccepted plans had a V107>2cm^3. With SWO+SSO, 98% of the plans were accepted. The last 2% failed due to minimal hotspots in the PTV. The average calculation time to create a reference plan was 205 sec. The mean calculation time of a VCS plan, SWO plan and SWO+SSO plan was 125 sec, 9 sec and 507 sec, respectively.

Conclusion: VCS seems to work well for half of the cases, further optimization results in acceptable plans. The time to create VCS plans and SWO plans is compatible with an online setting. SWO+SSO results in stable plans. However, this takes long time in comparison with creating a new plan. To determine for what extent of shifts, acceptable plans can be created, more plans will be made. Then a trade of can be made when to create a VCS/SWO(+SSO) plan or start a new plan.

PO-0906

NTCP differences between planned and delivered dose in treatment for head and neck cancer

J. Heukelom[1], C. Fuller[2], M. Kantor[2], K. Kauweloa[2], C. Rasch[3], J.J. Sonke[1]

[1]The Netherlands Cancer Institute, Department of Radiation Oncology, Amsterdam, The Netherlands
[2]MD Anderson Cancer Center, Radiation Oncology, Houston, USA
[3]Academic Medical Center, Department of Radiation Oncology, Amsterdam, The Netherlands

Purpose or Objective: During the 7 weeks of radiation therapy, the anatomy of head and neck cancer patients changes, resulting in a difference between planned and delivered dose. Currently, the allocation of adaptive radiotherapy (ART) is often based on visual inspection on repeated imaging or dosimetric criteria and thus only implicitly on changes in treatment outcome. Normal Tissue Complication Probability (NTCP) is a metric that translates the treatment dose distribution to treatment outcome. The goal of this study was to assess the impact of anatomical changes over the course of radiation therapy and the consequential difference in NTCP.

Material and Methods: For 36 squamous cell head and neck cancer patients treated in a single tertiary cancer center, daily in room CT scans were made in treatment position using CT on rails. In post-treatment analysis, the original beam set up was used to calculate dose of the day. Additionally, the daily CT was deformably registered to the planning CT (pCT). These daily doses were propagated to the pCT and

accumulated to estimate the delivered dose after which the dose-volume histograms were calculated on the pCT using the original contours. Treatment plan adaptations applied in clinical practice were ignored in this analysis, assuming that ART does not affect anatomic changes. NTCP calculations were done based on the LKB model for both planned and delivered dose, using input parameters based on work by Burman et al. and Emami et al. (1,2) OAR were contoured if deemed at risk and subsequently peer-reviewed by a team of experienced head and neck radiation oncologists. The overall NTCP per patient was calculated by multiplication of the chance of no toxicity i.e.

$$1 - \prod_{n=1}^{N} (1 - NTCP_n)$$

,for both the planned and delivered dose.

Results: On average, 6 OAR per patient were contoured. In 8 patients (22%), the difference in overall NTCP between planned and delivered dose was >3%. In half of them, NTCP of delivered dose was lower than planned. The largest difference in overall NTCP was 14% (Figure 1). The patients with the largest differences in overall NTCP could not be identified based on largest absolute dose differences for the OAR. Of the 8 patients that received ART clinically, 3 had an overall NTCP difference >3%.

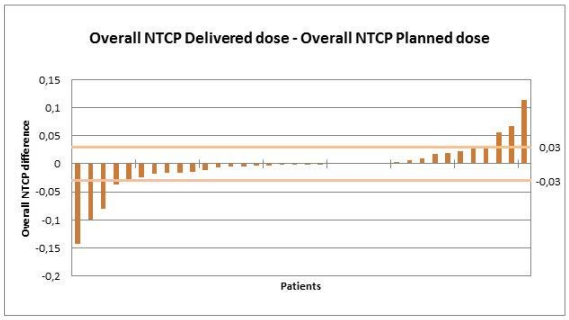

Figure 1. Difference in overall NTCP between delivered and planned dose. A value > 0 means delivered dose NTCP was higher than planned dose NTCP.

Conclusion: Differences >3% in overall NTCP between planned and delivered dose occur in about 1/4th of the head and neck cancer patients. Both increases and decreases in NTCP were observed, stressing the need for ART to either reduce NTCP or allow dose escalation. Expert opinion does not identify the same patients for ART as NTCP calculations do. A model to select patients for ART, however, should not only be based on changes in NTCP but should also include possible changes in TCP. Thus, further research is warranted to timely identify patients in which these differences occur, and on how to optimize the allocation of ART.

1 C Burman et al, *IJROBP*, 1991
2 B Emami et al, *IJROBP*, 1991

PO-0907

Effect of weight loss in head and neck patients in the presence of a magnetic field

A. McWilliam[1,2], M. Culley[2], M. Van Herk[1]
[1]*Institute of Cancer Sciences, University of Manchester, Manchester, United Kingdom*
[2]*The Christie NHS Foundation Trust, Christie Medical Physics and Engineering, Manchester, United Kingdom*

Purpose or Objective: Head and neck patients experience weight loss in a predictable pattern during treatment. CTV volumes typically reduce in volume by a third, as do the parotid glands. Adaptive methods for these patients focus on an offline protocol where the patient is rescanned and planned at two-to-three weeks through treatment, resulting in significant reduction in parotid doses. The MR linac (Elekta, AB, Stockholm, Sweden) will provide excellent soft tissue contrast which may be desirable for this group of patients, e.g., for tumour response monitoring. The presence of the magnetic field results in the Lorentz force causing electrons exiting the patient to spiral and be incident on the exit surface. This may potentially result in an increased dose to superficial tissues, i.e. the parotid glands. This effect can be controlled in plan optimisation. It is unknown, however, whether the presence of the magnetic field makes it necessary to adapt the plan at an earlier stage or more frequently during treatment. It is therefore the purpose of this paper to evaluate the effect of the magnetic field on need for adaptive radiotherapy in the head and neck.

Material and Methods: Five patients were selected from the clinical archive that had shown significant weight loss during treatment and required a repeat CT. Both the initial planning CT and the repeat CT were fully contoured including spinal cord, brainstem, left and right parotids. An initial plan was created for the planning CT using Monaco, Elekta AB Stockholm, Sweden, which met the departmental constraints for OAR dose. This plan was optimised with the B field set to 1.5T and then re-calculated at 0T, allowing the segmentation to remain constant. Plans were calculated with a 1% statistical uncertainty with the GPUMCD algorithm. The plans were transferred onto the re-scan CT and re-calculated. The magnitude of the change in dose to the OARs due to weight loss was compared between the 0T and 1.5T plans.

Results: Table one shows the results of the analysis for the five initial patients investigated. Spinal cord, brainstem and parotid glands are included in the table. Entries in red show that the magnitude of change in the OAR dose is greater, resulting in a larger dose to that OAR compared to the complementary plan. The spinal cord and brainstem do not show a trend, with the 0T and 1.5T plans showing increase dose in an equal number of plans. However, for the parotid glands the magnitude of the change in dose is greater with the 1.5T field present with the majority of plans showing an increase.

		Pt1		Pt2		Pt3		Pt4		Pt5	
		0T	1.5T	0T	1.5T	0T	1.5T	0T	1.5T	0T	1.5T
BS PRV	Max	-113	33	340	66	47	250	-494	-616	1126	1557
	Dose to 1cc	-233	-23	524	244	241	295	-663	-806	1039	1355
SC PRV	Max	33	140	1105	814	103	204	2084	1882	92	-374
	Dose to 1cc	-97	72	1060	742	174	141	1766	1409	-77	-498
LT PAROTID	Mean	85	309	143	301	462	564	-437	-644	-160	-184
RT PAROTID	Mean	-	-	-636	-431	67	133	2143	2255	-73	49

Table1. Increase in cGy for each OAR when the plan optimised for the original planning scan is delivered onto the scan displaying weight loss, entries in red show that the magnitude of change to dose is greater than the complementary plan.

Conclusion: The results from these patients indicate that weight loss in head and neck patients results in a greater increase in dose to the parotid glands when treated in a magnetic field. Adaptive protocols for these patients therefore require more frequent adaption than the current mid-treatment approach.

PO-0908

Inter-fraction OAR dose variation in pancreatic SBRT using contrast-enhanced in-room diagnostic CT

C. Papalazarou[1], M.S. Hoogeman[1], V. Gupta[1], B.J.M. Heijmen[1], J.J.M.E. Nuyttens[1]
[1]*Erasmus Medical Center Rotterdam Daniel den Hoed Cancer Center, Radiotherapy, Rotterdam, The Netherlands*

Purpose or Objective: In SBRT for Locally Advanced Pancreatic Carcinoma (LAPC), the nearby organs of the GI tract are dose limiting. Given the daily positional variation of those OARs, the planning approach is conservative, often leading to concessions in the PTV coverage. The purpose of this study is to evaluate the daily variation in abdominal organ dose.

Material and Methods: For this study, 5 patients were treated for LAPC with SBRT on a Cyberknife to a prescribed dose of 40 Gy in 5 fractions. During treatment, respiratory tracking was applied using implanted fiducials for real-time alignment of the treatment beams to the target. Planning constraints for the OARs included a maximum of 5 cc to

receive a dose above 35 Gy for the stomach, bowel and duodenum, and 15 Gy for the kidneys. For each patient, CT scans with intravenous contrast were obtained prior to the first three fractions using a sliding-gantry in-room CT. Directly after imaging, the patient was automatically transported by the robotic manipulator of the treatment couch to the treatment location in no more than 45 seconds. Each of the daily CTs was matched to the planning CT using automatic deformable image registration that allowed the fast (<1 min) adaptation of OAR contours to match daily anatomy. The OAR contours were manually adjusted by a radiation oncologist. To evaluate the dose to the OARs, each daily CT was matched to the planning CT using a combination of spine and fiducial matching, as performed at treatment. The same transformation was applied to the planned dose distribution, and the dose was evaluated on the new OAR contours.

Results: For the stomach, duodenum and small bowel, we evaluated the maximum dose, as well as the volume exceeding 35 Gy. The Dmax is shown in Figure 1. In all 15 (3x5) imaged fractions, the Dmax to at least one of these OARs was higher than the planned Dmax. The volume above 35 Gy was between 0 and 0.3 cc at planning, and increased or remained constant during treatment. For two patients, a clinically significant increase was observed, i.e. to 4.7 cc for bowel and 4.4 cc for duodenum, respectively. However, the clinical constraint of 5 cc was not violated. Dose to the kidneys remained well within constraints. The PTV volume receiving 95% of prescribed dose was ≥99% for 3 of the 5 patients. For two patients with high OAR dose at planning (Pt3 & Pt4), the planned coverage was 83% and 66%, resp, demonstrating the current limitations imposed by OAR constraints.

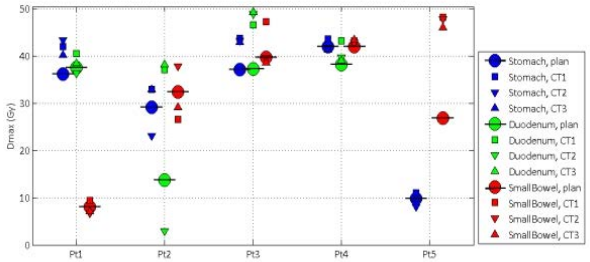

Figure 1 - Dmax for stomach, duodenum, and small bowel for the 5 patients. Note that for patient 5, duodenum is absent due to surgical resection.

Conclusion: In this study, we have employed in-room CT, combined with fast deformable image registration, to evaluate OAR dose constraints on a daily basis. We have observed clinically significant differences in the maximum dose to critical OARs, due to anatomical variations. This observation, even in this small patient group, demonstrates the need for further research on developing adaptive strategies to improve CTV coverage while keeping OAR dose within the clinical constraints.

PO-0909

Merging proton radiographies with treatment planning CT for adaptive radiation therapy

C. Gianoli[1], G. Dedes[2], S. Meyer[2], L. Magallanes[2], G. Landry[2], R. Nijhuis[3], U. Ganswindt[3], C. Thieke[3], C. Belka[3], K. Parodi[2]
[1]*Ludwig Maximilian University of Munich, Department of Experimental Physics - Medical Physics- Department of Radiation Oncology, Garching bei Munchen, Germany*
[2]*Ludwig Maximilian University of Munich, Department of Experimental Physics - Medical Physics, Garching bei Munchen, Germany*
[3]*Ludwig Maximilian University of Munich, Department of Radiation Oncology, Munich, Germany*

Purpose or Objective: Ion CT imaging (iCT), as obtained from tomographic reconstruction of ion radiographies, can be considered an emerging modality for adaptive radiation therapy (ART) in ion beam therapy due to accurate characterization of the in-room/in-beam anatomy in terms of tissue ion stopping power. The purpose of this work is to investigate ART feasibility, by limiting the number of low-dose scanned beam proton radiographies obtained in the treatment room, for different detection configurations of list mode and integration mode, in combination with high resolution anatomical information from the initial treatment planning X-ray CT.

Material and Methods: Proton radiographies obtained from Monte Carlo simulations (MCRs) are calculated based on patient CT images. For each pencil beam, 100 primary protons are delivered and the energy at the detector plane is converted to Water Equivalent Thickness (WET) relying on the *Bethe-Bloch* formula. List mode is reproduced by tracking each proton according to the Maximum Likelihood Path (MLP) and assigning each WET value along the estimated trajectory, while in integration mode only the most probable WET value of the raster point is assigned to a straight trajectory. To simulate inter-fractional anatomical changes, the patient CT, which is assumed to represent the in-room/in-beam scenario, is warped according to three-dimensional (3D) rigid and/or Gaussian deformation fields in head-neck and thoracic-abdominal sites, thus leading to a modified CT (mCT), which provides a theoretical representation of the treatment planning CT. Digitally Reconstructed Radiographs of mCT (mDRRs) are generated and two-dimensional (2D) deformable and/or rigid image registration is applied between corresponding mDRR and MCR in projection domain. By means of dedicated tomographic reconstruction algorithms, which rely on estimating the deformation in projection domain, high resolution anatomical information from mDRR is merged with accurate tissue stopping power from MCR, thus leading to combined iCT-CT. In this study, the DRRs of CT are used as the gold standard for 2D geometrical quantification. The methodological framework is reported in Fig. 1.

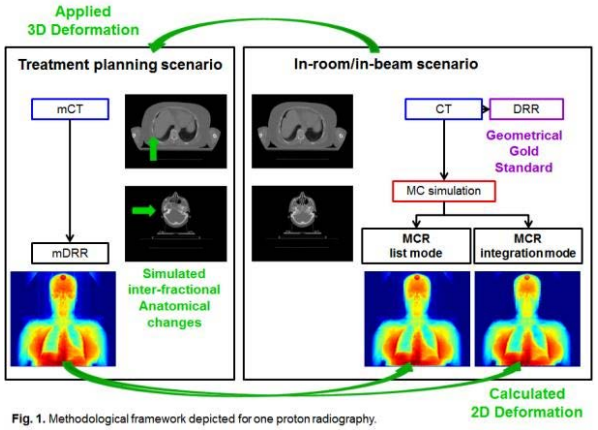

Fig. 1. Methodological framework depicted for one proton radiography.

Results: Performance for list mode was slightly better than integration mode but for both configurations difference were always <35 Hounsfield Unit (HU), translating into maximum 8% error in Relative Stopping Power (RSP), according to the approximate HU-RSP calibration curve. The comparison between list mode and integration mode as a function of different number of primaries will be presented, considering different inter-fractional anatomical changes. Quantification in image domain of combined iCT-CT will be performed as a function of different numbers of radiographies.

Conclusion: Both configurations enable accurate image registration for ART purpose. Conclusions about achievable dose reduction for acceptable quality of iCT-CT will be drawn.

Acknowledgements BMBF (01IB13001, SPARTA); DFG (MAP); DFG (contract no.VO 1823/2-1)

PO-0910

Potential increase in dose delivered on a fraction by fraction basis by adapting to daily OAR DVCs

D. Foley[1], B. McClean[2], P. McBride[2]
[1]*UCD, School of Physics, Dublin, Ireland Republic of*

[2]St. Luke's Radiation Oncology Network, Physics, Dublin, Ireland Republic of

Purpose or Objective: The feasibility of a technique using analysis of on-board CBCT images to adapt the dose to the target on a fraction by fraction basis was investigated. The new approach involves using the dose volume constraints (DVCs) as the objective to be met at each fraction. The dose to be delivered could be adapted such that dose to the target is maximised each day without any organ at risk (OAR) DVCs being broken.

Material and Methods: An in-house registration algorithm based on phase correlation was used to register CBCT images to the planning CT to determine the transformations and deformations in the patients' anatomy. This allowed the original plan to be recalculated on the registered CT image that provided the position of the target and organs at risk (OARs) for that fraction. With this new dose distribution, the DVHs and dose volume constraints (DVCs) values were determined for each fraction and accumulated by tracking throughout the treatment.
To determine how the dose could be changed, the DVCs were used as limits such that the dose that could be delivered would result in the tightest constraint being just met. Therefore, the dose was increased until that point or, if a DVC was already broken for a given fraction, the dose could be reduced by the minimum amount required to ensure that the DVC was within tolerance.
11 patients who underwent prostate treatment were retrospectively investigated for this feasibility study. IMAT plans consisting of 2 arcs were designed to deliver 74 Gy in 37 fractions of 2 Gy each to the target. The patients were imaged prior to treatment with an on board CBCT imager for between 9 and 14 fractions (121 in total). The relevant DVCs can be found in Table 1.

OAR	Bladder	Rectum
$V_{50\ Gy}$	-	60 %
$V_{60\ Gy}$	-	50 %
$V_{65\ Gy}$	50 %	30 %
$V_{70\ Gy}$	35 %	20 %
$V_{75\ Gy}$	25 %	15 %
$V_{80\ Gy}$	15 %	-

Results: Three of the patients investigated could have received higher doses during their treatment without breaking their OAR DVCs. In the remaining 8 patients, for only 3 fractions (out of 88) could an increase in dose been given while staying below the DVC limits.
The largest individual increase possible for all the imaged fractions was of 0.560 Gy. If all changes were made, the accumulated increase in dose possible for the three patients were 3.98 Gy, 6.89 Gy, and 7.70 Gy, weighting all fractions equally and assuming the imaged fractions were representative of the patients' entire treatment.

Conclusion: Analysis of the anatomical condition of the patient on the day of treatment can give an indication of how suitable the original plan for their treatment is. Adapting the dose to be delivered to the patient on a fraction by fraction basis has the potential to allow for significant dose escalation while staying within institutional DVCs. This could be particularly useful in the hypofractionation of treatments. Although it is unlikely that in the clinic the dose level would be reduced below 2 Gy per fraction, it was also included in the calculations here to see how it could theoretically impact the treatment.

PO-0911

Optimal adaptive radiotherapy strategy in head and neck to spare the parotid glands

J. Castelli[1,2,3], P. Zhang[2,3,4,5], A. Simon[2,3,4], B. Rigaud[2,3], J.D. Ospina Arango[2,3], M. Nassef[2,3], C. Lafond[1,2,3], O. Henry[1], P. Haigron[2,3], B. Li[6,7], H. Shu[4,7], R. De crevoisier[1,2,3]
[1]Centre Eugène Marquis, Radiotherapy, Rennes CEDEX, France
[2]Université de Rennes 1, LTSI, Rennes, France
[3]INSERM, U1099, Rennes, France
[4]INSERM, Centre de Recherche en Information médicale sino-français, Rennes, France
[5]North University of China, National Key Laboratory for Electronic Measurement Technology, Taiyuan, China
[6]Shandong Cancer Hospital, Department of Radiation Oncology, Jinan, China
[7]Southeast University, Laboratory of Image Science and Technology, Nanjing, China

Purpose or Objective: In the context of head and neck cancer (HNC) adaptive radiation therapy (ART), this study aimed to quantify the dosimetric benefit of various replanning frequencies and timings with regard to sparing the parotid glands (PG).

Material and Methods: Fifteen locally-advanced HNC patients had one planning then six weekly computed tomography (CT) scans during the seven weeks of IMRT. Weekly doses were recalculated without replanning or with replanning to spare the PGs as at the planning. A total of 63 ART scenarios were simulated by considering all the combinations of numbers and timings of replanning. The cumulated doses corresponding to "standard" IMRT (no replanning) and ART scenarios were estimated using deformable image registration. Finally, these doses were compared to each other and the planned dose by using a Wilcoxon Signed-Rank-Test.

Results: The median PG overdose using "standard" IMRT, compared to the planned dose, was 1.24 Gy, with a maximum of 9.45 Gy.
The table represents the best scenario for each number of replannings, the corresponding mean (min – max) cumulated dose, the difference between the planned and the cumulated delivered dose. Each ART scenario is better than the planned or delivered dose ($p < 0.05$).

Number of replanning	Best week(s) for replanning	Cumulated dose (Gy) Mean (Min-max)	P value
0	NC	32.00 (8.83 – 57.63)	NC
1	w_1	29.39 (6.14 – 50.58)	$p < 0.05$
2	w_1, w_2	28.59 (4.93 – 50.58)	$p < 0.05$
3	w_1, w_2, w_5	27.73 (4.57 – 50.58)	$p < 0.05$
4	w_1, w_2, w_5, w_6	27.34 (4.57 – 50.58)	$p < 0.05$
5	w_1, w_2, w_4, w_5, w_6	27.11 (4.50 – 50.58)	$p < 0.05$
6	w_1, w_2, w_3, w_4, w_5, w_6	27.06 (4.48 – 50.58)	$p < 0.05$

Table : Best scenario by number of replannings. The mean PG planning dose was 30.94 Gy (9.26 – 54.64)

Comparing with the standard IMRT scenario, the most effective ART scenario was the one with six replannings, leading to a decrease of 4.94 Gy (12.22Gy max.)
86 % of this benefit was obtained with 3 replannings only (at week 1-2-5).
If only one replanning should be applied, it should be done at the first week.

Conclusion: Each supplementary replanning leads to a decrease of the mean PG dose.
Early replanning proved the most beneficial for sparing the PG. Considering the maximum benefit obtained with six replannings, almost 90% of this benefit was obtained with only three replannings (Weeks 1-2-5), thus representing an attractive combination for ART in locally-advanced HNC.

Poster: Physics track: CT Imaging for treatment preparation

PO-0912

MRI-only based RT: adopting HU conversion technique for pseudo-CT construction in various body parts

J. Korhonen[1], L. Koivula[1], T. Seppälä[1], M. Kapanen[1], M. Tenhunen[1]
[1]*Helsinki University Central Hospital, HUCH Cancer Center, Helsinki, Finland*

Purpose or Objective: MRI is increasingly applied for radiotherapy target delineation. Recent studies have demonstrated a possibility to omit CT imaging from the radiotherapy treatment planning workflow by developing methods enabling the entire process by relying on MRI only. The HU conversion technique has been shown to construct heterogeneous CT-representative (pseudo-CT) images for prostate cancer patients by transforming the intensity values of an in-phase MR image into HUs with separate conversion models for soft and bony tissues. The technique has been implemented into a routine MRI-only based radiotherapy treatment planning workflow in our clinic. This study aims to investigate whether the pseudo-CT construction technique could be adopted for different patient groups, also in different body sites in addition to the male pelvis.

Material and Methods: The examinations were conducted by investigating the correspondence between the MR image intensity values and CT image HUs for different tissues. The data were applied to develop HU conversion models to transform the MR image intensities into appropriate HUs. In the absence of air cavities, the method was applied as a dual model HU conversion technique with separate conversion models within and outside of a bone segment obtained by atlas and threshold -based segmentation methods. An additional air segment was constructed in the presence of air cavities. An ultra-short echo-time sequence was applied to recognize boundaries between air and bone cortex with an intensity threshold. The constructed HU conversion models were employed with a medical image processing software, and applied for head (10 patients), pelvis (10), abdomen (2), and limbs (2). The obtained pseudo-CT images were tested by comparisons against standard CT images. The tests included evaluation of HU uncertainty and photon dose calculation accuracy.

Results: The HU conversion technique enabled construction of heterogeneous pseudo-CT images for various body sites. The duration of MR image intensity value transformation into HUs was roughly 30 seconds for each image series. Figure 1 shows examples of the resulted pseudo-CT images with the original MR images. Table 1 presents the local HU differences between those in pseudo-CT images and those in standard CT images. The target volume mean dose differences between those in pseudo-CT images and those in standard CT images were within 1% in all cases.

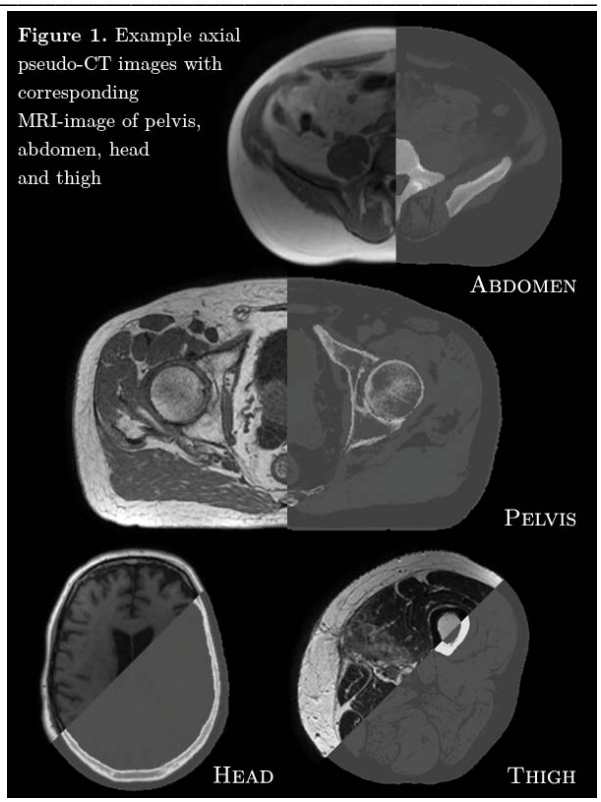

Figure 1. Example axial pseudo-CT images with corresponding MRI-image of pelvis, abdomen, head and thigh

Table 1. Local HU differences between those in pseudo-CT images and those in standard CT images as mean±SD

Site	Bony tissues	Soft tissues
Pelvis	-10±139	-1±13
Abdomen	-173±195	-2±35
Limbs	-3±37	-4±16
Head	31±109	6±20

Conclusion: The HU conversion technique can be adopted for various body sites to enable construction of heterogeneous pseudo-CT images for MRI-only based radiotherapy treatment planning. The conversion models should be adjusted for each site separately to improve pseudo-CT image quality; e.g. for abdomen. Further examinations are ongoing.

PO-0913

Clinically applicable T2-weighted 4D Magnetic Resonance Imaging with good abdominal contrast

D. Tekelenburg[1], O. Gurney-Champion[1], E. Lens[1], A. Van der Horst[1], A. Nederveen[2], A.K. Biegun[3], A. Bel[1], Z. Van Kesteren[1]
[1]*Academic Medical Center, Department of Radiation Oncology, Amsterdam, The Netherlands*
[2]*Academic Medical Center, Department of Radiology, Amsterdam, The Netherlands*
[3]*University of Groningen, KVI-Center for Advanced Radiation Technology, Groningen, The Netherlands*

Purpose or Objective: The main drawback of CT is poor soft tissue contrast. This research aims to develop an accurate respiratory-correlated four-dimensional MRI (4D MRI) method analogous to 4D CT with a clinically relevant acquisition time and superior contrast for abdominal structures.

Material and Methods: We developed a 4D MRI method by alternating a fast (0.6 seconds per 2D slice) T2-weighted turbo spin echo image acquisition (resolution: 1.3 x 1.6 mm^2; 5 mm thickness) with a 1D navigator acquisition. The navigator obtained the diaphragm position prior to each slice acquisition. The total acquisition was done continuously during free breathing for 6 minutes, covering multiple respiratory cycles and yielding 60 image frames per slice over a volume of 11 slices.

After acquisition, each image was coupled to a navigator signal and assigned to a respiratory bin with either phase or amplitude binning. A complete 4D MRI consisted of 110 assigned image states (10 bins, 11 slices).
For phase binning, bins are determined by dividing each end-exhale peak to peak position into evenly distributed bins. For amplitude binning, bins were determined according to the navigator based breathing amplitude range. The range was defined per volunteer and divided into bins. The minima and maxima were the mean values of end-inhale and end-exhale amplitudes, respectively.
The two strategies were used to reconstruct 4D MRI images for 5 volunteers (4 female, mean age 30 years) obtained on a 3T scanner. The position and superior–inferior (SI) motion of the diaphragm were quantified by registering the diaphragm to the begin-inhale image of a series (bin 1). Sorting images into respiratory bins often resulted in multiple images assigned to the same state. From this set, the image with the median diaphragm position was selected for 4D MRI reconstruction. Sometimes, when no images could be assigned to a state, an incomplete 4D MRI resulted.
The 4DMRIs were evaluated on data completeness (filled states of 4D MRI data set) and intra-bin variation of diaphragm position (mean standard deviation (SD) and maximum SD). The variation was calculated over all bins from 3 central slices covering the largest diaphragm motion.

Results: 4D MRI data sets were acquired using a T2-weighted sequence, facilitating abdominal tissue contrast. Figure 1 shows for one volunteer the SI position of the diaphragm for all bins for one central slice, the selected median showing a representation of the respiratory motion. Table 1 summarizes mean and maximum SD of the intra-bin variation as well as data completeness. Phase binning resulted in a more complete (6.9%) dataset, whereas amplitude binning had lower variation (difference of 1.6 (3.5) mm for mean (max) SD).

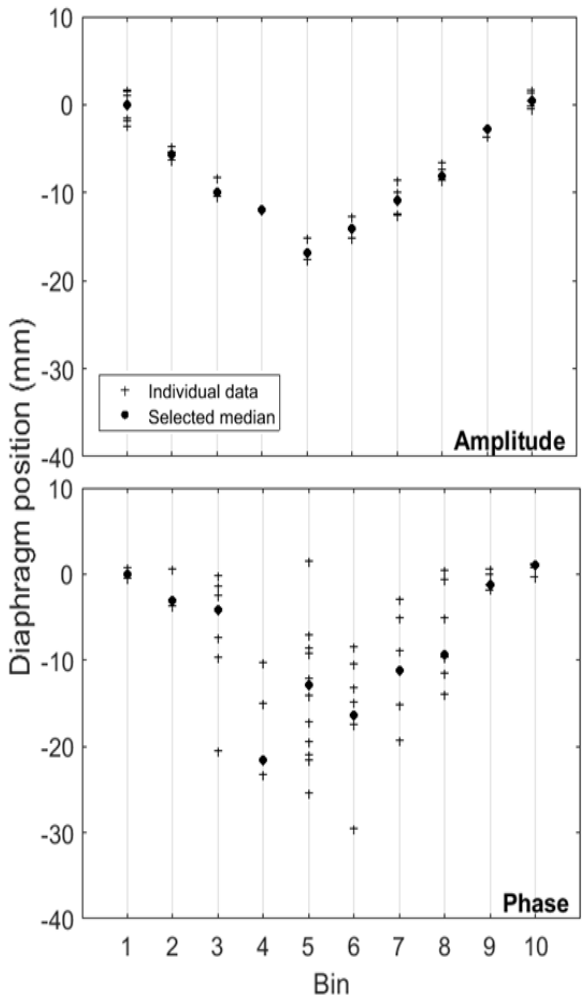

Figure 1: The intra bin variation and inter bin diaphragm (SI) motion is shown for amplitude and phase binning for a representative slice (volunteer 3). Bin 1, 6 and 10 represent data from begin-inhale, begin-exhale and end-exhale respectively.

Table 1: Data completeness (D.C.) and intra bin variation for all volunteers. Mean SD and maximum (Max) SD were calculated over all bins for 3 central slices.

Volunteer	Amplitude Binning			Phase Binning		
	DC (%)	Mean SD (mm)	Max SD (mm)	DC (%)	Mean SD (mm)	Max SD (mm)
1	96.4	0.6	1.6	100	0.9	2.1
2	90.9	0.9	1.9	100	4.6	13.7
3	90.9	0.4	5.0	100	1.3	2.2
4	90.0	0.8	1.7	98.2	2.0	5.0
5	95.5	0.8	1.3	100	2.5	6.2
Mean	92.7	0.7	2.3	99.6	2.3	5.8

Conclusion: We demonstrated the feasibility of 4D MRI as an alternative for 4D CT by creating fast T2-weighted 4D volumetric images. The more accurate amplitude binning can lead to 4D MRI that can be implemented in the clinical workflow.

PO-0914
Adjustment of CT calibration in presence of titanium implants by pencil beam proton radiography
R. Righetto[1], A. Meijers[2], F. Vander Stappen[2], P. Farace[1]
[1]*Centro di Protonterapia, Proton therapy, Trento, Italy*

[2]*Ion Beam Applications IBA, IBA, Louvain-la-Neuve, Belgium*

Purpose or Objective: To implement an adjustment method for conversion of CT numbers to stopping power ratio (SPR) for proton therapy planning in presence of titanium implants, using pencil beam proton radiography (PR) that is acquired by utilizing a multilayer ionization chamber (MLIC).

Material and Methods: A head phantom containing a titanium implant in the cervical region was used. Lateral PR was obtained by delivering spots uniformly positioned at 5.0mm distance in a square of 11x11 spots and collecting the exit dose by MLIC. Spot by spot, the integral depth dose (IDD) measured by MLIC was compared with the reference IDD in air (i.e. without the phantom in the beam path) to assess the corresponding water equivalent thickness (WETMLIC). CT scan of the head phantom was acquired, based on which SPR map was determined (through mass density), to compute the corresponding WET along the beam path (WETCT), assuming a Gaussian spot with uniform size of about 3 mm along the path. CT numbers to mass density conversion was conventionally obtained by scanning a number of tissue equivalent materials (TEM) of known properties. To this multiline curve, an additional extrapolated point and one titanium point were added. Mass density to SPR conversion was performed by published relationships (Fippel and Soukup, Med Phys 2004;31:2263-73) tuned on human tissue properties. Since the titanium caused CT image to be saturated, an artificial mass density was initially assigned to the maximum value supported by the CT scanner, so that the corresponding SPR is equal to the SPR of titanium. The mass density of this point in the calibration curve was varied and the corresponding WETCT computed. The optimal calibration was selected by comparing the corresponding WETCT with the measured WETMLIC.

Results: The values of the initial and the optimal calibrations are reported in Table. The corresponding differential WET maps (WETMLIC-WETCT) are shown in figure. By the initial calibration (fig.B) the WET of the implant was overestimated. The WET error was around 6-8 mm in the thicker portion of the implant along the lateral direction. On the contrary, the optimized CT calibration showed small difference on the differential WET map (fig.C). In fig.A a maximum intensity projection of the CT scan was computed to show the box were the PR was acquired.

CT numbers to mass density calibration curves

	CT numbers (HU)	Mass density (g/cc)	
air	-1024	0.001	
Lung (inhale)	-823	0.20	
Lung (exhale)	-497	0.50	
Adipose	-76	0.96	
Breast	-24	0.99	
Muscle	48	1.06	
Liver	56	1.07	
Trabecular bone	212	1.16	
Dense bone	919	1.53	
Extrapolated	1817	2.00	
Titanium	3071	4.10*	2.70**

* initial value; **optimized value

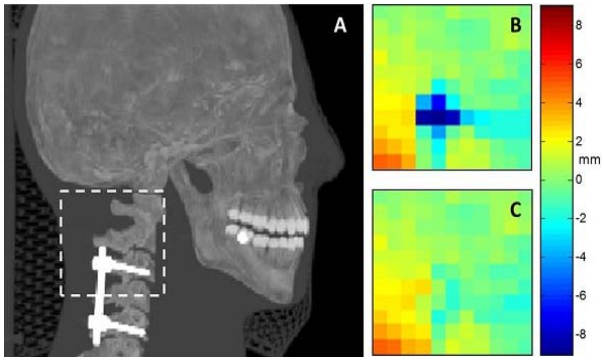

Conclusion: It has been previously reported that the size of the titanium implants can be overestimated on CT scans (Huang et al, Phys Med Biol 2015;60:1047). This can produce range overshooting in phantoms (Farace et al, Phys Med Biol 2015;60:N357-67). In patients, it can cause considerable errors when the proton beam crosses through the implants before stopping close to an organ at risk. With the described method, the potential errors were compensated by an optimized calibration so that a more accurate range can be computed in treatment planning.

PO-0915

Evaluation of a metal artifact reduction algorithm for radiotherapy CT scans

L. Rechner[1], D. Kovacs[1], A. Bangsgaard[1], A. Berthelsen[1], M. Aznar[1]

[1]*Rigshospitalet, Department of Oncology, Copenhagen, Denmark*

Purpose or Objective: The purpose of this study was to investigate the appropriateness of a new commercial iterative metal artifact reduction reconstruction (MAR) algorithm (iMAR, Siemens Healthcare) for use in radiotherapy (RT) CT scans in our clinic.

Material and Methods: A combination of phantom and patient scans were used for analysis. Phantom scans were performed with and without metal and MAR reconstruction. Phantoms used included an electron density phantom and home-made phantoms with removable metal and low contrast objects. The HU values and geometric accuracy of low contrast objects were evaluated. The artifact index (AI) was calculated as the ratio of artifact pixels to total pixels, where artifact pixels were defined as greater than noise after subtracting a no artifact scan from an artifact scan. Differences in dose calculation were also determined in one phantom scan (hip) and for 10 patient scans with metal implants (2 bilateral hips, 1 unilateral hip, 2 shoulder, 1 dental, 4 spine).

Results: HU values were found to be improved with MAR relative to no MAR, and the accuracy of low contrast object next to the metal implant that was previously obscured by artifact was within 1 mm with MAR. In a phantom scan with a hip prosthesis, the use of MAR reduced the AI from 0.62 to 0.35 and the median error of artifact pixels from 155 to 41 HU. The difference in dose between calculation on the MAR phantom scan and the scan with no metal was 0.3%. For the patient scans, the mean difference in dose calculated on the MAR scan and the original scan with HU override of artifacts was 0.06% (range -0.47 to 0.92%) (figure 1). However, when the MAR algorithm was incorrectly applied (e.g. “dental” MAR setting applied to a spine implant) it was observed that new artifacts can be introduced, including new streaking or loss of image contrast near metal. These induced artifacts could potentially cause inaccuracies in the dose calculation or contouring.

Conclusion: The MAR algorithm tested was found to be suitable for use in RT CT scans and has been implemented in our clinic. It increases our confidence in contouring near metal artifacts and reduces the time required during contouring for manual correction of HU values. However, due

to the possibility of induced artifacts or loss of information that we observed, a visual comparison of each MAR scan with the original scan is performed, and the HU values in the artifact-reduced area are spot checked for reasonability relative to known tissue HU values. Future studies will investigate the impact of this type of MAR on contouring variability and accuracy.

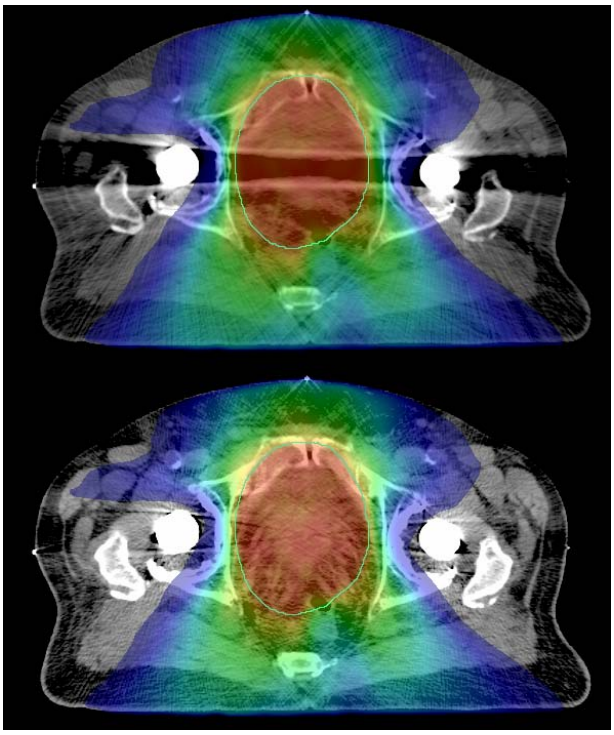

Figure 1: Example of a plan for a patient with bladder cancer and double hip prostheses without (top) and with (bottom) MAR, where the PTV identical in both images (colorwash 15-68 Gy). In the top image, the dose was calculated after manual override of artifact to 0 HU. The mean dose to the PTV was 63.8 Gy and 64.0 Gy, respectively.

PO-0916

MR-based treatment planning for intracranial glioma patients

M.A. Palacios[1], M. Bennis[1]
[1]*VU University Medical Center, Radiation Oncology Department, Amsterdam, The Netherlands*

Purpose or Objective: To assess the dosimetric accuracy of CT-substitute attenuation correction (AC) maps generated from existent clinical MR data for radiation treatment planning in glioma patients.

Material and Methods: CT substitute AC maps were obtained with Statistical Parametric Software (SPM) software applied on 3D T1-weighted Inversion Recovery scans (IT 650 ms; TR/TE 4.6/2.0 ms). Three probability maps (PM) were obtained: air, tissue and bone. To derive corresponding AC maps, air-PM was multiplied by -1000, tissue-PM by 30 and bone-PM by 1000 and 300 when the probability for bone tissue was >0.8 and <0.8, respectively. A composite AC map (MR-based CT) was obtained by summing up all the PM multiplied by the aforementioned values. Difference in bone between clinical CT and MR-based CT was quantified with the Dice Similarity Coefficient (DSC).
MR-based CT were read into Eclipse Treatment Planning System (Varian Medical Systems, Palo Alto CA) and clinical Volumetric Modulated Arc Therapy (VMAT) plans were recalculated with a 0.1 cm dose calculation grid size for 10 patients. All plans were calculated with Accuros XB dose calculation algorithm for a prescription dose of 60 Gy and consisted of two arcs with a different collimator angle to minimize tongue and groove effect.
Differences between both plans were assessed according to the D2%, D98%, Dmean and γ-index (3%/3mm) for the relevant structures: CTV, PTV, brainstem and optical system.

Results: MR-based CTs were generated for 10 patients using SPM software and current clinical MR examinations without the need of adding extra sequences to the clinical protocol. Bone segmentation exhibited an average DSC of 0.81±0.07 (SD) between clinical CT and MR-based CT segmentation, detecting SPM software less bone than in the clinical CT. Recalculated VMAT plans on the MR-based CTs exhibited a very good agreement with the clinical plans. Average Dmean, D2% and D98% for CTV and PTV differed less than 0.5%. Difference in D2% for brainstem and optical system between the clinical plans and recalculated plans using an MR-based CT were 0.4% and 1.1%, respectively. All metrics were found not significantly different ($p>0.05$) from the clinically approved plans.
3D-dose distributions for the CTV and PTV in MR-based plans resulted in γ-passing rates higher than 0.99±0.01 for both structures. Average γ-value for CTV and PTV was 0.16±0.08 and 0.23±0.16, respectively.

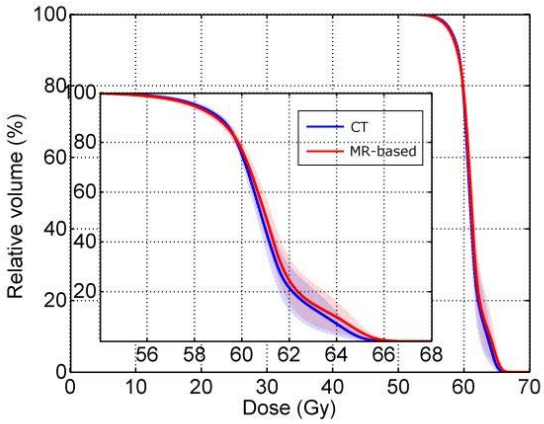

Average DVH of PTV for CT (blue) and MR-based (red) planning for 10 glioma patients. Shaded blue and red areas highlight standard deviations in the DVHs for CT and MR-based plans, respectively.

Conclusion: MR-based CTs were generated using SPM software on 3D MR T1-weighted Inversion Recovery scans with more than 80% agreement for bone segmentation. MR-based VMAT plans exhibited a very good agreement with the clinical plans based on a standard CT as measured by the D2%, D98%, Dmean and γ-index metrics for all relevant structures.
It is feasible a clinical workflow for radiation treatment planning purposes for glioma patients based only on MR without the need of CT or adding additional MR sequences to the clinical protocol for bone segmentation.

PO-0917

The impact of irregular respiratory patterns on tumour volumes in 4DCT

E. Huizing[1], E.B. Van Dieren[2], R. Bruggink[1], D. Woutersen[2], C.H. Slump[3]
[1]*University of Twente, Biomedical Enginering and Technical Medical MIRA, Enschede, The Netherlands*
[2]*Medisch Spectrum Twente, Radiotherapy, Enschede, The Netherlands*
[3]*University of Twente, Robotics and Mechatronics, Enschede, The Netherlands*

Purpose or Objective: Current clinical practise in radiotherapy CT scanning of lung tumours takes into account movement due to breathing. However, the accuracy of used scan protocols is usually validated for phantoms with fairly regular movements, and the effects of breathing irregularity are unclear. Aim of this study is to establish the impact of clinically occurring irregularities on delineated treatment volumes determined using 4DCT images.

Material and Methods: Respiratory patterns, as recorded during CT scanning, were (anonymously) obtained for 50 lung

ca. patients treated in our institution. First, pattern statistics were compared to population data in literature to establish validity of the data used for testing. Second, patterns representing highest irregularity were selected: variance in amplitude (1), periodicity (2), and a pattern with a baseline drift (3). A periodical computer generated sinusoid (4) was used for comparison.
Patterns were fed into a QUASAR™ Respiratory Motion Phantom (Modus Medical), with "lung tumour insert" (cork/polystyrene). Each pattern was scanned 5 times using a 16 slice lightspeed RT series scanner (General Electric). "Lung tumour" contours were extracted using auto segmentation of average (AVE) and MIP CT data. Contour volumes were compared using Dice coefficients (DC) and to expected volumes.

Results: The average breathing amplitude in our patient population was 8.70± 3.0 mm. The average period was 3.99 ± 1.0 seconds per breath. Both compared well with literature values.
Based on repeat CT data, DC was ≥ 0.90 for group (1) and (3) and (4). However, DC for group 2 ('irregular periodicity), was only 0.83, which is significantly lower (p=0.002). Computed volumes were nearer to expected volumes using AVE CT, but using AVE CT always leads to underestimation. Volumes computed in MIP CT reconstructions cover the expected volumes better, but there is a chance of overestimation of up to 20% in volume.

Conclusion: Even though 4D CT scanning has been around quite some time, this is one of the first studies to address the effects of clinically found breathing irregularities. The selected test data seem to be adequate for lung ca. patients, and selected types of irregularities are commonly seen by therapists operating CT scanner and linac.
The study indicates that irregular respiratory patterns introduce the element of "chance" in the position and size of delineated tumour volumes, depending on amount and type of irregularity. Therefore, it is recommended to always take into account effect of breathing pattern irregularity in scanning and treatment planning for lung tumours.
Since 4D imaging typically consists of scanning while tracking a marker position, the recommendation probably holds for every CT scanner used in radiotherapy, and possibly also for PET and MRI scanners.

PO-0918

Validation of freeware-based mid-ventilation CT calculation for upper abdominal cancer patients

S. Vieira[1], J. Stroom[1], K. Anderle[2], B. Salas[1], N. Pimentel[1], C. Greco[1]
[1]*Fundação Champalimaud, Radiotherapy, Lisboa, Portugal*
[2]*GSI Helmholtz, Center for Heavy Ion Research, Darmstadt, Germany*

Purpose or Objective: Most institutes use the ITV approach to account for breathing motion into treatment planning, generally yielding too large treatment volumes. Recent publications showed that use of a mid-ventilation CT (midV-CT, representing the mean breathing phase) and treating remaining breathing motions as a random error, led to high tumor control and overall survival for hypo-fractionated treatments. However, the midV-CT is not available commercially yet. In this work we perform a marker-based validation of our open-source software to generate a midV-CT for upper abdomen cancer patients.

Material and Methods: Planning data from 12 upper abdominal cancer patients (8 liver- and 4 pancreatic patients) were used for this study. These patients were treated with the ITV approach using hypo-fractionated schemes (ranging from 5x7.5 Gy to 1x24 Gy). Each patient had a gold marker implanted close to the CTV center of mass (COM). 4DCT data consisted of 10 amplitude-based breathing phases (CT BrillianceTM, Phillips). In our planning system (EclipseTM,Varian), the position of the marker was measured by hand for each breathing phase and patient. In the open-source medical imaging 3DSlicer, B-spline deformable registration was used to register the plan CT and the different phases of the 4DCT. The resulting transformation matrices were then used by our 3DSlicer modules to automatically generate the midV-CT and the COM motions of any planning volume or marker. Subsequently, the marker position in the midV-CT was compared to the average marker position in Eclipse. Furthermore, the Eclipse marker motion curves and amplitudes were compared with the marker and CTV motions from 3DSlicer. Additionally, treatments plans were generated for one patient using the midV-CT and compared with our ITV-based clinical plan.

Results: The mean CTV volume was 24.7±22.0 cc (1SD) and the mean marker to CTV COM distance was 12.7±6.2mm (1SD). The midV CTs are generated by 3DSlicer within 30 minutes using a PC. Motion validation results are shown in Table 1. Differences in the mean COM of the marker in Eclipse and in midV-CT are within 1 mm, indicating an accurate midV-CT generation by our software. Average amplitude differences are within 1 mm but Eclipse motions tend to be slightly larger, possibly due to the uncertainty of manually finding the marker in the 4D phases. Correspondingly, RMS differences between motion curves of Eclipse and 3DSlicer were therefore 0.2-0.6 mm, whereas the RMS differences between marker and CTV motion in 3DSlicer only 0.1-0.2 mm (Fig 1a). The latter suggests that well-placed markers can estimate CTV motions. Fig 1b shows differences in dose volume histograms between the ITV and the midV-CT approach.

	LR(mm)		AP(mm)		IS(mm)	
	mean	SD	mean	SD	mean	SD
Δmarker(midV - Eclipse)	-0.1	0.4	-0.2	0.6	-0.4	0.9
AMPLITUDES						
Marker Eclipse (ME)	1.4	1.1	2.4	1.1	5.6	2.8
Marker Slicer (MS)	1.2	0.9	1.9	1.1	5.2	2.7
CTV Slicer (CS	1.2	1.1	1.8	1.0	5.0	2.7
Δ(ME - MS)	0.2	1.0	0.5	0.8	0.4	1.4
Δ(ME-CS)	0.2	1.3	0.6	0.7	0.6	1.3
MOTION CURVES RMSE						
Δ(ME - MS)	0.4	0.3	0.4	0.2	0.6	0.4
Δ(ME-CS)	0.4	0.2	0.4	0.2	0.6	0.3
Δ(MS-CS)	0.1	0.1	0.1	0.1	0.2	0.2

Tablel. Mean and variation of breathing motion data of all patients for the marker and CTV position as measured in 3DSlicer (MS and CS, respectively), compared to marker motions as measured in Eclipse (ME).

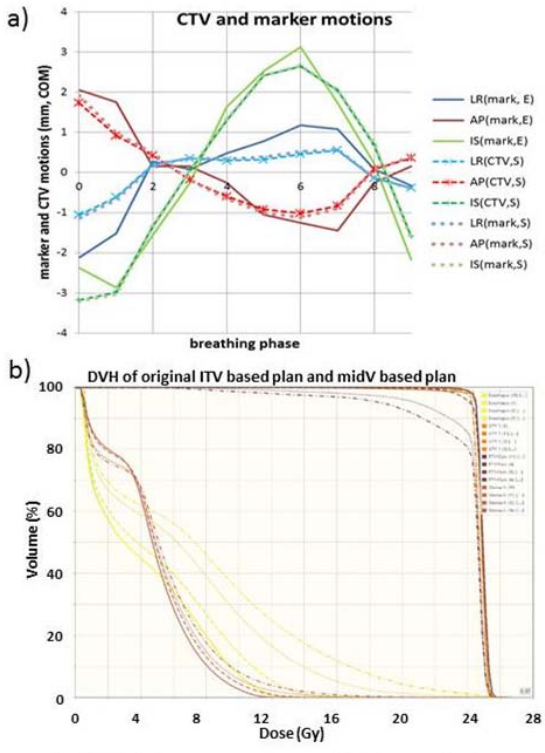

Figure 1. (a) Breathing motion curves of marker and CTV for Eclipse (E) and 3DSlicer (S) for patient 6. (b) Dose volume histograms using midV CT and the ITV-based irradiated plans for patient 1. Although asymmetric ITV margins can compensate for a planning CT in an extreme phase, OARs might truly get a different dose than expected based on the planning DVHs (esophagus). The solid line refers to the irradiated plan with clinical contours; the dashed line to the calculated midV CT plan using clinical contours; the dotted line to the irradiated plan with midV CT contours; and the dashed dotted line to the midV CT-based plan with midV CT contours.

Conclusion: Accurate midV-CT can be generated using freeware. This opens the prospect for its use in our clinical practice, allowing treatments in the upper abdomen with more adequate CTV-to-PTV margins. For lung cancer patients the approach should work even better due to the higher contrast images.

Poster: Physics track: (Quantitative) functional and biological imaging

PO-0919

Optimal respiratory gated FDG-PET for characterizing intra-tumour heterogeneity in lung cancer

J. Bussink[1], W. Grootjans[2], F. Tixier[3], C. Van der Vos[2], D. Vriens[4], C. Cheze Le Rest[5], W. Oyen[2], L.F. De Geus-Oei[4], D. Visvikis[6], E. Visser[2]
[1]*Radboud University Medical Center, Radiation Oncology, Nijmegen, The Netherlands*
[2]*Radboud University Medical Center, Department of Radiology and Nuclear Medicine, Nijmegen, The Netherlands*
[3]*University Hospital Poitiers-, Department of Nuclear Medicine-, Poitiers, France*
[4]*Leiden University Medical Center, Department of Radiology and Nuclear Medicine, Leiden, The Netherlands*
[5]*University Hospital Poitiers-, Department of Nuclear Medicine, Poitiers, France*
[6]*University of Brest, INSERM- UMR1101- LaTIM, Brest, France*

Purpose or Objective: Radiotracer uptake patterns in FDG-PET through computation of textural features vcan be used to improve characterization of lung cancer lesions for disease prognostication and response monitoring and tumor delineation purposes. Respiratory motion artefacts cause lesion blurring resulting in loss of intra-tumour heterogeneity. We have investigated the effect of respiratory gating on the recovery of intra-tumour heterogeneity.

Material and Methods: FDG-PET/CT imaging was performed in 70 lung cancer patients. Amplitude-based optimal respiratory gating (ORG) was performed on bed positions covering the thorax. The duty cycle (percentage of the total PET data) used for image reconstruction of ORG images was 35%. Non-gated images were reconstructed using 126 seconds of PET data, yielding similar noise characteristics as ORG. Lesion segmentation was performed using the fuzzy locally adaptive Bayesian (FLAB) algorithm. Four heterogeneity parameters (entropy, dissimilarity, zone percentage (ZP), and high energy emphasis (HIE)), which have previously shown to be robust and associated with survival in lung cancer, were calculated in non-gated and ORG images.

Results: Respiratory gating did not result in statistically significant differences in the heterogeneity parameters. Sub-group analysis revealed a significant effect of ORG on the heterogeneity parameters of lesions in the lower lobes. The mean increase for entropy, dissimilarity, ZP and HIE, considering lesions in the lower lobes was 1.3±1.5% (p=0.02), 11.6±11.8% (p=0.006) 2.3±2.2% (p=0.002), and 16.8%±17.2% (p=0.006) respectively. For the centrally located lesions, the mean increase for entropy, dissimilarity, ZP and HIE was 0.58±3.7% (p=0.6), 5.0±19.0% (p=0.4) 0.59±4.0% (p=0.9), and 4.4±27.8% (p=0.4), respectively. Lesions in the upper lobes showed a mean increase of -0.35±1.8 (p=0.3), -1.0±7.7% (p=0.3), -0.4±2.7% (p=0.5), -1.7±13.2% (p=0.4), for entropy dissimilarity, ZP and HIE, respectively. There was no significant correlation between lesion volume and the change in parameters between non-gated and ORG images.

Conclusion: Results from this study indicate that ORG significantly impacts characterisation of intra-tumour heterogeneity, particularly for lesions in the lower lung lobes. This suggests that adequate management of respiratory motion artefacts is important for improving characterisation of intra-tumour heterogeneity in PET.

PO-0920

Early prediction of individual response in neo-adjuvant adaptive Radiochemotherapy for rectal cancer

R. Raso[1], P. Passoni[2], A. Palmisano[3], C. Fiorino[1], G.M. Cattaneo[1], F. De Cobelli[3], A. Esposito[3], P. Mangili[1], N. Slim[2], N.G. Di Muzio[2], R. Calandrino[1]
[1]*San Raffaele Scientific Institute, Medical Physics, Milano, Italy*
[2]*San Raffaele Scientific Institute, Radiotherapy, Milano, Italy*
[3]*San Raffaele Scientific Institute, Radiology, Milano, Italy*

Purpose or Objective: Developing a radiobiologically consistent model predicting individual outcome for rectal cancer patients (RCPs) treated with an adaptive boost approach during neo-adjuvant radiochemotherapy (RCH).

Material and Methods: Forty-two RCPs were treated within a prospective observational study. CH consisted of oxaliplatin (on days: -14, 0, 14) and 5-fluorouracil (from day -14 to end) being day 0 the start of RT. All patients were treated with Helical Tomotherapy (18x2.3Gy) with an adaptive concomitant boost technique delivering 3Gy/fr on the residual gross tumor volume (GTV) in the last 6 fractions (fr), based on MRI imaging taken at fr 9. GTVs were contoured by a single radiologist on axial T2 MRI images acquired for initial planning (V_PRE), at fr 9 for the adaptive planning (V_MID) and before surgery, after a median time of 8.9 weeks after the end of RCH (V_POST). Based on a Poisson-like tumor regression model and neglecting repopulation and inter-patient variability of the removal kinetics of killed cells, the parameter (1-ΔV(D))^V_PRE was taken as a surrogate of tumor control probability (TCP), where ΔV(D)=V_MID/V_PRE or V_POST/V_PRE, considering D at fr 9 (TCP_MID) or at the end of RCH (TCP_POST). The discriminative power of TCP_MID/POST in predicting the pathological complete remission (pCR, n=14) was assessed by the AUC of the corresponding ROC curves. Then, two-variables logistic (LOG) models including V_PRE and ΔV(D) as covariates were also considered and the ROC curves of the four models (TCP_MID,TCP_POST,LOG_MID, LOG_POST) were compared. In addition, an estimate of the residual cells at surgery (V_S) was robustly taken as the product of the pathologically assessed fraction of viable cells and V_POST. Spearman correlation rank test was used to evaluate the correlation between the models and V_S.

Results: All models showed a high discriminative power in predicting pCR (p-value<0.0001). AUCs for TCP_ MID was 0.87 (specificity: 71.4%, sensitivity: 96.4%, best cut-off: 5.85), higher than TCP_POST (0.82), although the difference did not reach significance (p=0.18). TCP_MID/TCP_POST were also highly correlated with V_S (R=0.77 and 0.74,p<0.0001). Similar performances were found for LOG_MID/LOG_POST with AUC=0.90/0.87 and R=0.79/0.77. No significant differences were found when comparing TCP models against the corresponding LOG models.

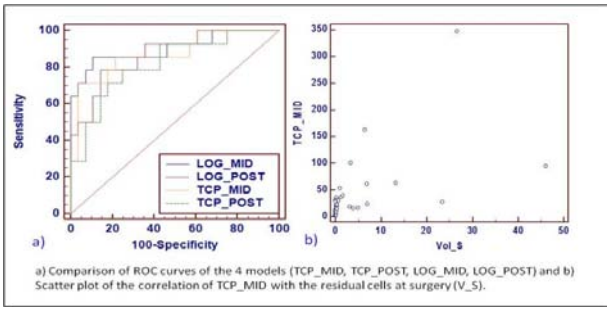

a) Comparison of ROC curves of the 4 models (TCP_MID, TCP_POST, LOG_MID, LOG_POST) and b) Scatter plot of the correlation of TCP_MID with the residual cells at surgery (V_S).

Conclusion: A radiobiologically consistent model including early regression (TCP_MID) measured on T2-MRI images well predicts pCR and is strongly correlated with the estimated residual cells number after adaptive RCH; similar performances were obtained with a logistic model including V_PRE and V_MID/V_PRE. The corresponding models using V_POST showed a slightly, statistically not significant, worse

discriminative power. The results showed that MRI volumes measured before and during RCH have a great potential to better individualize adaptive RCH.

PO-0921

Free-breathing dynamic contrast enhanced MRI of lung cancer

S. Kumar[1,2,3], G. Liney[1,2,3,4], R. Rai[3], D. Moses[5,6], C. Choong[7], L. Holloway[1,2,3,4,8], S. Vinod[1,3]

[1]*The University of New South Wales, South Western Clinical School, Sydney, Australia*

[2]*Ingham Institute of Applied Medical Research, Medical Physcis, Sydney, Australia*

[3]*Liverpool and Macarthur Cancer Therapy Centre, Radiation Oncology, Sydney, Australia*

[4]*University of Wollongong, Centre for Medical Radiation Physics, Wollongong, Australia*

[5]*Prince of Wales Hospital, Department of Medical Imaging, Sydney, Australia*

[6]*The University of New South Wales, School of Computer Science and Engineering, Sydney, Australia*

[7]*Liverpool and Macarthur Cancer Therapy Centre, Radiation Oncology, Liverpool, Australia*

[8]*University of Sydney, Institute of Medical Physics, Sydney, Australia*

Purpose or Objective: Dynamic contrast enhanced (DCE) MRI is becoming an increasingly important tool for assessing tumour response in Radiotherapy (RT). Important characteristics are spatial and temporal resolution and in lung this is further complicated by the effects of respiratory motion. A common approach is to acquire fast gradient-echo imaging utilising k-space sharing to provide optimum temporal resolution and to collect data during short 'windows' of breath-holds over the time course. However patient compliance during breath hold manoeuvres can lead to tumour displacement and introduce error in analysis. Radial acquisitions can alleviate motion by oversampling the centre of k-space albeit with reduced temporal resolution. The purpose of this study was to evaluate whether such a 'stack-of-stars' acquisition can be used with high enough resolution for the DCE sequence to provide a complete free breathing RT planning protocol in lung patients.

Material and Methods: Institutional review board approval was obtained. Two patients receiving lung radiotherapy underwent DCE-MRI on our dedicated wide bore 3 Tesla system (Skyra, Siemens) using an 18 channel flexible coil and 32 channel table coil. Patients were positioned as per treatment setup with their hands above their head. Two DCE protocols were examined; a fast gradient-echo sequence employing k-space sharing (TWIST) acquired as 5 breath-hold periods of 20s each with a spatial and temporal resolution of 1.5 mm/3 s; and a completely free breathing scan performed using a radial acquisition (StarVIBE) with a resolution of 1.8 mm and 14 s. The acquisition time was approximately 6 minutes for both sequences. In both cases a rapid pre-contrast measurement of T1 was acquired using the same sequence and two flip angles. Analysis included calculation of T1 map and a two-compartment model fit to the data (Tissue4D, Siemens) to provide pixel-by-pixel maps of the perfusion rate constant.

Results: Figure 1 shows images and analysis taken from both sequences. Viewing DCE data in a cine loop revealed large movement between frames for TWIST compared to StarVIBE. A comparison of signal-time plots shows a typical result where failure to maintain and reproduce breath hold has produce large variation and discontinuities in the dataset. As a result the goodness-of-fit (chi2) was better for StarVIBE (0.05) than the corresponding value using TWIST (0.16). Although temporal resolution is much poorer with the StarVIBE sequence, it was sufficient to sample the early upslope phase of the contrast agent. General image quality was assessed with radial and motion artefacts scored as being negligible.

Figure1

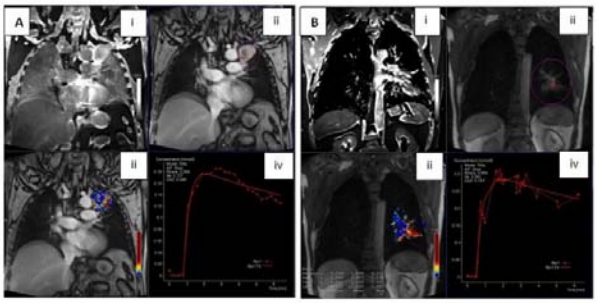

(A) StarVIBE, (B) TWIST (i)T1 map; (ii), DCE image; (iii), Ktrans; (iv), Time-enhancement curve

Conclusion: These initial results show that use of a radial k-space trajectory as a method of motion compensation provides a DCE scan of sufficient image quality and temporal resolution which can be used as part of a complete free breathing lung protocol.

PO-0922

Are planning CT radiomics and cone-beam CT radiomics interchangeable?

J.E. Van Timmeren[1], R.T.H. Leijenaar[1], W. Van Elmpt[1], P. Lambin[1]

[1]*Maastricht University Medical Centre, GROW-School for Oncology and Developmental Biology - Department of Radiation Oncology - MAASTRO clinic, Maastricht, The Netherlands*

Purpose or Objective: Radiomic image features derived from conventional treatment planning CT images have already been shown to have prognostic information. For cone-beam CT (CBCT) imaging during radiotherapy this has not yet been described. Due to the fact that a CBCT image is acquired prior to each fraction it has the potential to monitor response to treatment. The goal of this study was to investigate the stability and the correlation between radiomic features derived from planning CT vs. CBCT and between CBCTs of different fractions.

Material and Methods: A total of 27 stage II-III NSCLC patients who received radiation therapy were included in this study. For each patient a treatment planning CT scan was acquired and CBCT scans were obtained prior to each fraction. The planning CT (CT1), the CBCT of the first (CBCT-FX1) and second fraction (CBCT-FX2) were used in this study. CBCT images were registered to CT1 using automatic rigid registration prior to feature extraction. In total, 149 radiomic image features were extracted of different feature groups: I) tumor intensity, II) texture, III) Laplacian of Gaussian. The third group consists of filtered first order features and the group was subdivided into 10 groups, according to different LoG filter standard deviations ranging from 0.5 mm to 5 mm with a 0.5 mm interval. Since a rigid registration was used, features related to shape and volume were not analyzed. The correlation between features derived from (1) CT1 and CBCT-FX1 and (2) CBCT-FX1 and CBCT-FX2 were analyzed. Correlations were calculated using an intraclass correlation coefficient ICC(2,1). An ICC-value above 0.9 was considered a good agreement.

Results: For 26% of the 149 analyzed radiomics features, the ICC-value was higher than 0.9 for CT1 compared to CBCT-FX1 (Figure). The ICC-value was above 0.9 for 81% of the features when comparing CBCT-FX1 to CBCT-FX2. Specifically for the feature group 'texture', one of the 44 features had an agreement between CT1 and CBCT-FX1 that was higher than 0.9, but 35 out of 44 did show agreement for CBCT-FX1 vs. CBCT-FX2. For 'tumor intensity', 2 out of 15 features showed a large correlation between CT1 and CBCT-FX1 higher than 0.9, whereas 10 out of 15 features showed agreement higher than 0.9 between CBCT-FX1 and CBCT-FX2 (ICC>0.8 for all). All features with ICC above 0.9 for CT1 vs. CBCT-FX1 also showed high correlation between CBCT-FX1 and CBCT-FX2.

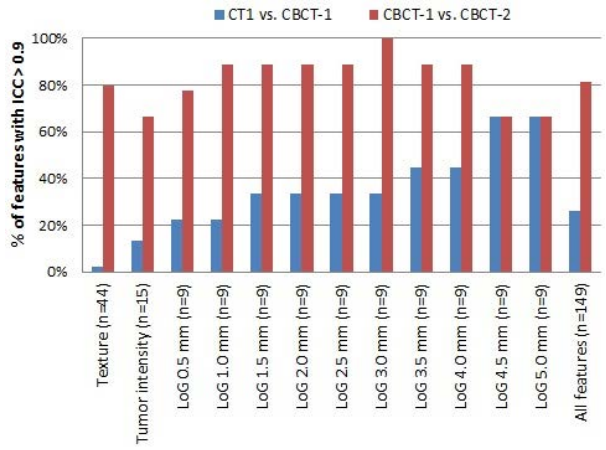

Figure: Percentage of features with ICC>0.9 for CT1 vs. CBCT-1 and CBCT-1 vs. CBCT-2, displayed for each feature group.

Conclusion: For 26% of the radiomics features there is good agreement between CT1 and CBCT. 81% of the image features show high correlation between CBCT-FX1 and CBCT-FX2 where no large differences are expected. In the future, radiomic features derived from CBCT images will be investigated to monitor changes of CBCT features over the course of treatment. One has to be careful with mixing radiomic features derived on planning CT and CBCT scans.

PO-0923

Comparing FMISO and FDG positive tumour sub-volumes for PET-based dose escalation in SCCHN

D. Mönnich[1], S. Leibfarth[1], S. Welz[2], C. Pfannenberg[3], D. Zips[2], D. Thorwarth[1]

[1]*Section for Biomedical Physics - Department of Radiation Oncology, University Hospital Tübingen, Tübingen, Germany*

[2]*Department of Radiation Oncology, University Hospital Tübingen, Tübingen, Germany*

[3]*Department of Diagnostic and Interventional Radiology, University Hospital Tübingen, Tübingen, Germany*

Purpose or Objective: Tumour sub-volumes for dose escalation can be defined using different PET tracers. This study compares hypoxic volumes defined by FMISO PET and metabolically active volumes defined by FDG PET for patients with advanced squamous cell carcinomas of the head and neck (SCCHN).

Material and Methods: Imaging data of 14 patients was used, which were included in a phase II FMISO dose escalation study. Pre-therapy FMISO PET/CT images were acquired four hours post tracer injection. FDG PET/CT imaging was performed according to the institutional diagnostic protocol. The planning CT and the GTV of the primary tumour were available. Datasets were deformably co-registered using the CT images. Metabolically active sub-volumes were segmented in FDG PET images based on a source-to-background method with an adaptive threshold. Hypoxic sub-volumes were defined using a tumour-to-muscle threshold of 1.4. Expanding the volumes by an isotropic margin of five millimeters resulted in PTV-prim and potential dose escalation volumes PTV-FMISO and PTV-FDG. We analyzed the overlap between PTV-FMISO and PTV-FDG.

Results: Mean dose escalation volumes were 19.7 cm^3 (0.0-57.3 cm^3) for PTV-FMISO and 39.3 cm^3 (17.5-91.9 cm^3) for PTV-FDG. On average PTV-FDG covered 73.5% of PTV-FMISO (4.9-100.0%). Only for two out of fourteen patients (14%) PTV-FMISO was completely covered by PTV-FDG. Vice versa 36.3% of PTV-FDG overlapped with PTV-FMISO (0.0-97.4%). PTV-prim from treatment planning was 111.1 cm^3 (57.1-201.2 cm^3). Detailed results of the overlap analysis for all patients are given in Table 1.

Patient	Volumes			Overlap PTV_{FDG} and PTV_{FMISO}		
n=14	PTV_{prim} / cm^3	PTV_{FDG} / cm^3	PTV_{FMISO} / cm^3	cm^3	% of PTV_{FDG}	% of PTV_{FMISO}
006	65.8	35.6	10.3	9.5	26.8	92.7
007	118.7	42.4	27.1	7.6	17.8	28.0
008	81.6	43.6	54.0	39.4	90.4	73.0
009	142.8	47.6	0.0	0.0	0.0	
010	106.6	34.5	12.1	9.0	26.0	74.0
011	57.3	36.5	0.0	0.0	0.0	
013	74.9	26.6	22.5	21.4	80.3	95.0
014	69.2	21.2	5.9	5.9	27.8	100.0
015	196.3	91.9	33.5	25.5	27.8	76.2
016	201.2	17.9	16.0	0.8	4.4	4.9
017	166.4	43.4	4.8	4.8	11.0	100.0
018	57.1	17.5	13.8	11.4	65.0	82.5
019	117.0	39.1	57.3	38.0	97.4	66.4
020	100.4	51.7	19.3	17.2	33.2	89.0
Mean	111.1	39.3	19.7	13.6	36.3	73.5
Min	57.1	17.5	0.0	0.0	0.0	4.9
Max	201.2	91.9	57.3	39.4	97.4	100.0

Conclusion: PTV-FDG typically covers PTV-FMISO only partially and is on average two times larger. Therefore, a dose escalation in the metabolically active sub-volume partially misses the hypoxic sub-volume. The large volume difference suggests that a substantially higher dose escalation is feasible in PTV-FMISO than in PTV-FDG. Clinical trials are required to compare the efficacy of both methods.

PO-0924

Histogram analysis of ADCs from DWMRI predicts tumour response and survival for rectal cancer

K. Bakke[1], T. Seierstad[2], K.H. Hole[2], S. Dueland[3], K. Flatmark[4], A. Hansen Ree[1], K. Røe Redalen[1]

[1]*Akershus University Hospital, Department of Oncology, Lørenskog, Norway*

[2]*Oslo University Hospital, Department of Radiology and Nuclear Medicine, Oslo, Norway*

[3]*Oslo University Hospital, Department of Oncology, Oslo, Norway*

[4]*Oslo University Hospital, Department of Gastroenterological Surgery, Oslo, Norway*

Purpose or Objective: Patients with locally advanced rectal cancer (LARC) are commonly treated with neoadjuvant chemoradiotherapy (CRT) followed by radical surgery. However, tumor responses vary considerably and about one third of the patients experience poor disease outcome due to metastatic progression. We aimed to investigate if apparent diffusion coefficients (ADCs) quantified from diffusion-weighted MRI (DWMRI) predicted histologic tumor response to the neoadjuvant treatment and long-term survival. Recognizing the tumor heterogeneity we specifically aimed to explore if histogram analysis of tumor ADC may reveal more useful information than the commonly used mean ADC measure.

Material and Methods: Data from 23 prospectively enrolled patients receiving induction neoadjuvant chemotherapy (NACT) followed by CRT and radical surgery was analyzed. DWMRI was acquired at baseline and after NACT. Tumor volumes contoured in T2-weighted MR images were transferred to tumor ADC maps calculated with b-values 300 and 900 s/mm2, before ADCs were extracted from all tumor voxels and presented as histograms. The predictive information contained in the histograms was evaluated using receiver operating characteristic (ROC) curve analysis of each percentile from 1-100. Study endpoints were histologic tumor regression grade (TRG) and 5-year progression-free survival (PFS).

Results: Using the change in tumor ADC from baseline to NACT completion, we identified a histogram area below median (20th–40th percentiles) to be associated with both TRG and PFS. By using the 20th percentile, an increase in

ADC predicted poor histologic tumor response (TRG3–5 versus TRG1–2) with 91% sensitivity and 83% specificity (area under curve (AUC)=0.89, 95% confidence interval (CI)=0.74–1.0, p=0.001). Using the 30th percentile, an increase in ADC predicted poor PFS with 89% sensitivity and 71% specificity (AUC=0.75, 95% CI=0.54–0.95, p=0.051). Univariate regression analysis also revealed that the ADC increase was significantly associated to poor PFS (hazard ratio=9.7, 95% CI=1.21-78.30, p=0.033).

Conclusion: By ADC histogram analysis of DWMRI acquired during NACT of LARC we identified low histogram percentiles as predictive of histologic tumor response in particular, but also long-term survival. The results require validation in larger, independent cohorts, but are promising for identification of patients that may benefit from individualized treatment approaches for improved disease outcome.

PO-0925

Simulation of FMISO diffusion-retention in a three-dimensional tumor model

L.J. Wack[1], A. Menegakis[2], R. Winter[1], S. Böke[2], D. Mönnich[1], D. Zips[2], D. Thorwarth[1]

[1]*University Hospital Tübingen, Department of Radiation Oncology- Section for Biomedical Physics, Tübingen, Germany*

[2]*University Hospital Tübingen, Department of Radiation Oncology, Tübingen, Germany*

Purpose or Objective: Tumor hypoxia is prognostic for poor outcome after radiotherapy (RT). A method for non-invasive assessment of hypoxia is PET using hypoxia radiotracers such as FMISO. The goal of this study was to develop and evaluate a tool to simulate 3D oxygen distribution and the resulting FMISO accumulation on realistic vessel architectures, which can be compared to measured PET activities in small animal experiments.

Material and Methods: Two FaDu tumors (human HNSCC) were grown on the right hind leg of nude mice. Imaging was performed after a growth phase of about 5 weeks. FMISO was injected into the tail vein of the anesthetized mice with an activity of ~12MBq for dynamic PET/MRI. ROIs inside the left ventricle and in the tumor were chosen to determine blood and tumor time activity curves (TACs). After image acquisition tumors were excised, snap frozen and cut into consecutive sections (20µm). Sections were stained with immunoflourescence-labeled antibodies for endothelial marker CD31 and scanned with a Zeiss Axioplan 2 fluorescence microscope. Obtained immunofluorescence images were rigidly registered, manually adjusted and thresholded to create a binary 3D vessel map. These maps were used to simulate 3D oxygen distributions based on a Michaelis-Menten relation. Using the oxygen distribution and the dynamic activity in the left ventricle as input, FMISO retention was simulated on the same vessel maps. A tumor ROI was selected and its average activity at different time points post-injection (p.i.) compared against the measured activity in the same region on the PET scan (tumor TAC). To compare 3D and 2D simulations, the simulation were repeated in 2D on the individual sections, and 2D-based oxygen histograms and TACs were determined.

Results: O2 histograms showed a large difference between 2D and 3D simulations, with much lower values for 2D simulations than for 3D (5.94 mmHg vs 26.57 mmHg). Mean values were closer together (8.9 mmHg vs 13.2 mmHg). This is due to the large amount of anoxic voxels (pO2 < 1 mmHg) in the 2D simulation, which made up 17.5% of all simulated voxels in 2d, but less than 1% in the 3D simulations (see Table 1). Visually, the 3D simulations result in a TAC with a similar overall shape compared to the TAC measured with small animal PET, but with a 20.7% overestimation of activity. However, the 2D simulations severely overestimated the total activity by 99.2% (2D) when compared against measured activity in the tumor after 90min as determined by PET.

	2D simulation	3D simulation	Small animal PET image
Tumor 1			
Median oxygen content (mmHg)	2.11	26.03	n.a.
Mean oxygen content (mmHg)	12.28	15.65	n.a.
Anoxic fraction (<1mmHg)	14.1%	0.0%	n.a.
FMISO activity at 90 min p.i. (kBq/ml)	535.2	460.2	425.3
Tumor 2			
Median oxygen content (mmHg)	9.78	27.79	n.a.
Mean oxygen content (mmHg)	14.14	26.57	n.a.
Anoxic fraction (<1mmHg)	20.9%	1.0%	n.a.
FMISO activity at 90min p.i. (kBq/ml)	1339.0	653.7	491.2

Conclusion: 3D simulations based on real 3D vessel architecture is feasible. Our FMISO simulations showed large discrepancies between 2D and 3D simulation approaches, with the 3D values being closer to the PET measurements. Verification of 3D tracer accumulation patterns in additional tumors against pimonidazole stainings is still necessary to validate and calibrate the method, with PET scans in the same test subject to confirm observed activity.

PO-0926

Voxel-based PSMA-PET/histopathology analysis in patients with primary prostate cancer

C. Zamboglou[1], F. Schiller[2], T. Fechter[1], V. Drendel[3], C.A. Jilg[4], P.T. Meyer[2], M. Mix[2], A.L. Grosu[1]

[1]*Universitätsklinik Freiburg, Klinik für Strahlenheilkunde, Freiburg, Germany*

[2]*Universitätsklinik Freiburg, Klinik für Nuklearmedizin, Freiburg, Germany*

[3]*Universitätsklinik Freiburg, Institut für Pathologie, Freiburg, Germany*

[4]*Universitätsklinik Freiburg, Klinik für Urologie, Freiburg, Germany*

Purpose or Objective: Tumorcontrol of primary prostate cancer (PC) is dose dependent. Dominant index lesions (DIL) within the prostatic gland are responsible for local and distant failure. Radionuclide-labelled inhibitors of prostate-specific membrane antigen (PSMA-PET) showed promising preclinical and clinical results in detection of primary prostate cancer. We correlated PET/histopathology using a new coregistration approach, which allows pixel-wise evaluation of the tracers performance in prostatic tissue. Aim of this work is to evaluate the diagnostic accuracy of 68Ga-PSMA-PET/CT and to determine potential SUV-thresholds enabling a focal dose escalation on DIL delineated by PET.

Material and Methods: 10 patients with primary PC and 68Ga-PSMA-PET/CT were enrolled. After prostatectomy, thorough histopathological preparation and anatomical-based coregistration between in-vivo and ex-vivo material was performed. Simulated PET-images were generated out of blurred 3D histopathological tumor distribution (histoPET). The coregistration was further optimized by matching histoPET information with the in-vivo PET signal. The tracer performance was evaluated by coefficient of determination (R^2) between histoPET/PSMA-PET patterns and SUV-values within different tissue types.

Results: 1 patient was excluded due to imprecise pathological preparation. Mean R^2 value was 60 % (± SD 15.2, range: 42.5-81.6). SUVmax of PSMA-PET was located in non resolution adapated / resolution adapted PC-tissue in 80%/90% of patients. Mean SUVmean in non resolution adapted PC and non-PC tissue was 6.1 (range: 2 – 21) and 2.7 (range: 1.3 – 8.2), respectively. The ratio between SUVmean in PC / non-PC was 2.2 (SD ± 0.6).

Conclusion: Using a sophisticated approach for PET/histopathology coregistration PSMA-PET/CT yielded high R^2-values which can be translated in excellent overlap with PCa. Furthermore, we were able to provide SUV-guidance values for PSMA-PET/CT which opens the opportunity for SUV-based GTV-delineation techniques using PSMA-PET as a base for focal dose escalation on DIL.

PO-0927

Bone texture analysis as predictive of bone radiation damage in patients undergoing pelvic RT.

V. Nardone[1], M. Biondi[2], P. Tini[1], L. Sebaste[1], E. Vanzi[2], G. Battaglia[1], P. Pastina[1], L.N. Mazzoni[2], F. Banci Buonamici[2], L. Pirtoli[1]
[1]*Azienda Ospedaliera Universitaria Senese, U.O.C. Radioterapia, Siena, Italy*
[2]*Azienda Ospedaliera Universitaria Senese, U.O.C. Fisica Sanitaria, Siena, Italy*

Purpose or Objective: To assess the potential role for a CT-based, bone texture analysis as a predictive factor of bone radiation damage in patients undergoing radiotherapy (RT) for pelvic malignancies.

Material and Methods: We performed a retrospective analysis of suitable patients treated with RT for pelvic malignancies from January 2010 to December 2014. The DICOM CT data acquired for RT planning were collected, and used for a homemade ImageJ macro analysis. Two region of interest (ROI) were selected: the L5 vertebral body and the femoral heads. Typical texture analysis (TA) parameters were retrospectively evaluated: mean (M), standard deviation (SD), skewness (SK), kurtisis (K), entropy (E) and uniformity (U). The patients who developed bone RT-related damages (i.e.: pelvic bone stress fracture, radiation osteitis, insufficiency fractures) during the follow-up constitute the study patients (SP) group. The TA data were collected for a comparative analysis also in a control group of patients (CP: 2:1 ratio, with respect to SP) not developing bone damages. The CPs were matched taking into account: age, sex, type of tumor, intent of postoperative treatment, comparable doses to the considered organs-at-risk. As for the statistical comparisons, we performed a univariate analysis (Pearson correlation) and a multivariate analysis (logistic regression) using the SPSS software 17.0.

Results: Twenty-four SPs and 48 CPs are the subject of this report. Out of SPs, postoperative RT was delivered for cancer: of the digestive tract (anal or rectal) in thirteen patients (54%); of the female reproductive organs (endometrial or cervical) in 9 (37%); and of the excretory apparatus (prostate or bladder) in 3 patients (9%). In the comparison between SP and CP groups, the univariate analysis showed a significant correlation of the ROI parameters of L5: SD (p: 0,012); K (p<0,001), E (p: 0.001); U (p: 0,008), and of the femoral head: M (p<0,001); SD (p<0,001), with the development of bone damage. The logistic regression highlighted a significant correlation with the ROI parameters of L5: E (p:0.004); U (p:0,014), and femoral head M (p:0,022); and -SD (p:0,042), with an Overall Model Nagelkerke R Square of 0,590.

Conclusion: These results (with the limit of a small series) and those reported in previous related studies deserve some interest, since the knowledge of predictive factors of bone radiation damage might help in patients' selection for pelvic RT, and in identifying suitable dose constraints for the bony pelvis in RT planning for patients at risk.

PO-0928

Impact of fuzzy-thresholding of 18F-FDG PET images for cervical cancer recurrence prediction

G. Roman Jimenez[1], A. Devillers[2], J. Leseur[2], J.D. Ospina[3], H. Der Sarkissian[4], O. Acosta[1], R. De Crevoisier[2]
[1]*Laboratoire Traitement du Signal et de l'Image - INSERM U642, Université de Rennes 1, Rennes, France*
[2]*Centre Eugène marquis, Department of Radiotherapy, Rennes, France*
[3]*Escuela de Estadìstica, Universidad Nacional de Colombia, Medellìn, Colombia*
[4]*Keosys medical imaging, Department of medical imaging, Saint-Herblain, France*

Purpose or Objective: In case of cervix cancer irradiation, parameters extracted from initial 18F-FDG-PET images can be used to predict recurrence. FDG PET parameters are classically computed among voxels binary selected in the segmentation step. We proposed the use of fuzzy-threshold, providing tumor membership probability map, and present a generalization of the computation of FDG PET parameters by weighting each PET voxel by its tumor membership probability. The goal of the study was to evaluate the relevance of fuzzy-threshold based weighted parameters in prediction of tumor recurrence, in comparison with a "standard" fixed or hard threshold based parameters.

Material and Methods: This study included 53 patients treated for locally advanced cervical cancer by external beam radiation therapy with concurrent chemotherapy, followed by brachytherapy and ± surgery. All patient underwent 18F-FDG PET/CT exam before the treatment. Different tumor membership probability maps were extracted from 18F-FDG PET images using fuzzy-thresholding defined by a threshold Th and a level of fuzziness ΔTh (both expressed in % of the maximum uptake value) using a Zadeh's standard function. Fuzzy-thresholding were tested with Th=41%, 50% and 70% and ΔTh from 0% to 40% (ΔTh=0% corresponding to hard-thresholding). Using the fuzzy-thresholding, we computed weighted analogs of four standard 18F-FDG PET parameters; the maximum uptake averaged by its 26 neighbors (SUVpeak), the average SUV inside the tumor region (SUVmean), the metabolic tumor volume (MTV) and the total lesion glycolysis (TLG). The recurrence was defined based on clinical examination, MRI and PET imaging. Median follow-up was 49 months [range: 7-83]. A total of 16 patients developed disease recurrence. The predictive capability of the PET parameters to predict 3 year overall recurrence were evaluated using the area under the receiver operating characteristic curve (AUC) and the p-value of the logistic regression model.

Results: The figure shows the predictive values (AUC and p values) of the weighted parameters depending on the threshold Th and the fuzzy-level Δth used. SUVpeak and SUVmean were not predictive for any of the segmentations tested. TLG and MTV extracted through hard-thresholding (ΔTh=0%) were highly predictive with Th=41% (AUC=0.74, p=0.012) and Th=50% (AUC=0.77, p=0.006) but not with Th=70%. Weighted parameters were discriminative (p<0.05) at Th=41% with Δth = [0% - 22%], at Th=50% with Δth = [0% - 32%] and at Th=70% with Δth = [0% - 32%] indicating a lower sensitivity to the choice of threshold.

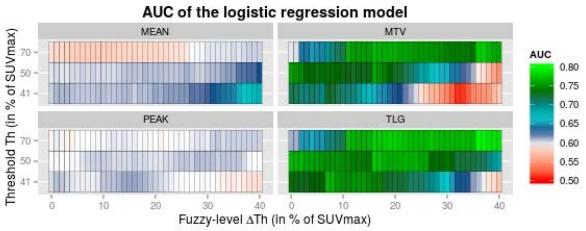

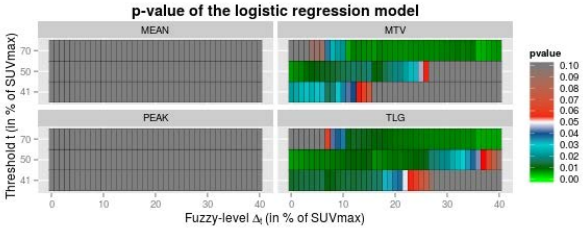

Conclusion: PET weighted parameters including voxels tumor membership probability can be used to predict tumor

recurrence in cervical cancer. Weighted PET parameters were less sensitive to the choice of threshold than standard parameters computed through hard-thresholding, all tested threshold TLG and MTV parameters becoming statistically predictive.

PO-0929

Dual Energy CT imaging of tumour vasculature in NSCLC: an intra-patient comparison with DCE-CT

A.J.G. Even[1], M. Das[2], B. Reymen[1], P. Lambin[1], W. Van Elmpt[1]
[1]*Maastricht University Medical Centre, GROW - School for Oncology and Developmental Biology - Department of Radiation Oncology - MAASTRO clinic, Maastricht, The Netherlands*
[2]*Maastricht University Medical Centre, Department of Radiology, Maastricht, The Netherlands*

Purpose or Objective: Quantification of vasculature is frequently performed by dynamic contrast enhanced CT (DCE-CT) or MRI imaging. However, there are some limitations to this technique: DCE-CT requires a detailed kinetic fitting procedure, a prolonged acquisition time with increased dose to the patient, has a limited FOV and is not easy to implement in clinical routine. Dual Energy CT is an evolving field in CT image analysis that allows quantification of contrast material uptake using a single acquisition, making it easily implementable in a clinical workflow. Therefore we investigated the correlation between the DCE-CT derived vasculature parameters, blood flow and blood volume, with iodine related attenuation measured on a Dual Energy CT acquisition for non-small cell lung cancer patients.

Material and Methods: The same imaging protocol was followed for 13 patients on a Dual Energy CT scanner (Siemens Definition Flash). The protocol consisted of a Dual Energy CT scan (either 80/140kVp or 100/140kVp; 70 ml of iodine 300 mg/ml) of the entire thorax and a DCE-CT acquisition (65 ml of iodine 300 mg/ml; 33 frames @ 1.5sec for a total of 50 sec) in a 13 cm FOV centred around the primary tumour. Kinetic analysis was performed using commercial software (Siemens VPCT body) allowing the assessment of blood flow (unit: ml/100ml/min) and blood volume (unit: ml/100ml) in every voxel. Dual Energy CT images were analysed using in-house developed software for iodine contrast quantification. Iodine related attenuation was calculated by subtracting the Hounsfield units of the CT scan acquired at high energy from the scan acquired at low energy. A comparison was performed on 1) the entire tumour and 2) on a sub-volume level, defined by the upper 50% of the volume-of-interest. Correlation on tumour level was assessed by the Pearson correlation coefficient; overlap of sub-volumes with a DICE coefficient.

Results: There was a significant positive correlation between average contrast enhancement on Dual Energy CT and blood flow ($r=0.615$, $p=0.025$) and blood volume (average $r=0.742$, $p=0.004$) on a patient (i.e. tumour) level. Furthermore, the volumes defined by the highest 50% contrast enhanced uptake and 50% elevated perfusion coincided well (see Figure), with DICE scores of 0.72±0.10 (range 0.58-0.87) and 0.71±0.13 (range 0.50-0.91), for the blood flow and volume, respectively.

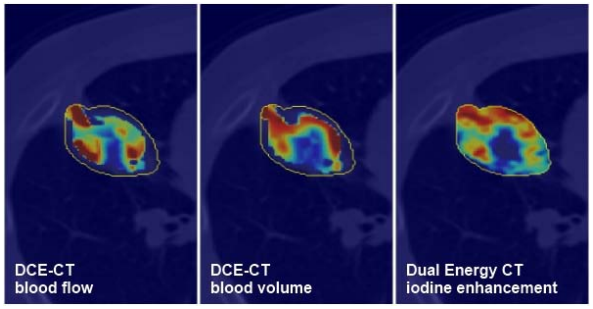

Figure: Example of a patient showing a heterogeneous vasculature; the DICE coefficients for this patient, between the Dual Energy CT iodine enhancement and DCE-CT blood flow and blood volume, were respectively 0.87 and 0.91.

Conclusion: We observed high agreement between Dual Energy CT derived iodine enhancement and DCE-CT derived kinetic parameters, both on a tumour and sub-volume level. This may allow wider implementation of vasculature imaging of tumours using the simplified Dual Energy CT acquisition protocol.

PO-0930

PET based response assessment of lung toxicity - assessment of two approaches for dose response

A. Abravan[1], I. Skjei Knudtsen[1], H. Eide[2], A. Helland[2], P. Van Luijk[3], E. Malinen[1]
[1]*University of Oslo, Department of Physics, Oslo, Norway*
[2]*Oslo University Hospital, Department of Oncology, Oslo, Norway*
[3]*University Medical Center Groningen- University of Groningen, Department of Radiation Oncology, Groningen, The Netherlands*

Purpose or Objective: Patients with lung cancer given external radiotherapy are at risk of radiation induced lung toxicity (RILT). In many studies, mean density changes from CT (in Hounsfield units) have been used as a surrogate for radiation-induced alterations in the lung. However, a combination of mean density changes from CT scans with corresponding standard deviations has been shown to be a more sensitive method. In the current work, we explore whether such a combined approach is feasible for 18F-FDG PET data as well.

Material and Methods: 13 patients with advanced non-small cell lung cancer, participating in a phase II trial on combined radiation and erlotinib therapy, were included. The patients were examined by 18F-FDG-PET/CT at three sessions; prior to, one week into, and six weeks after fractionated radiotherapy (3 Gy × 10). For each patient, lung was delineated in the planning CT images. The RT dose matrix was co-registered with the PET image series. For each PET image series, mean (μ) and standard deviation (σ) map were calculated based on cubes in the lung (3×3×3 voxels) and were further used to quantify local structure (S). The spread in μ and σ was characterized by a local covariance ellipse (in pre-therapy PET series) in a sub-volume of 3×3×3 cubes. The distance of individual cube values to the origin of the ellipse is then calculated using Mahalanobis distance method to form S maps. ΔS and $\Delta\mu$ maps are derived by subtracting pre-therapy maps from maps of mid- and post-therapy. A detection threshold was calculated based on three patients with two sets of pre-therapy PET scans who were not included in the study.

Results: The structure difference maps (ΔS) identified new areas of interest in the lungs of individual patients compared to the mean difference maps ($\Delta\mu$) (Figure 1 A). On a population level, both ΔS and Δm were significantly different ($P<0.05$) from the respective threshold level, irrespective of dose (Figure 1 B). The inter-patient relative variation in ΔS and $\Delta\mu$ were 57% and 88%, respectively, indicating that the ΔS approach yielded less heterogeneous results. 18F-FDG dose response was analyzed up to total dose of 15 Gy by first order linear regression. The relative slopes of the regression lines were 0.036, 0.018, 0.052, and 0.061 for $\Delta\mu$ (mid-pre), ΔS (mid-pre), $\Delta\mu$(mid-pre), and ΔS (post-pre), respectively. A significant dose response was only seen for the ΔS taken between post and pre-therapy PET.

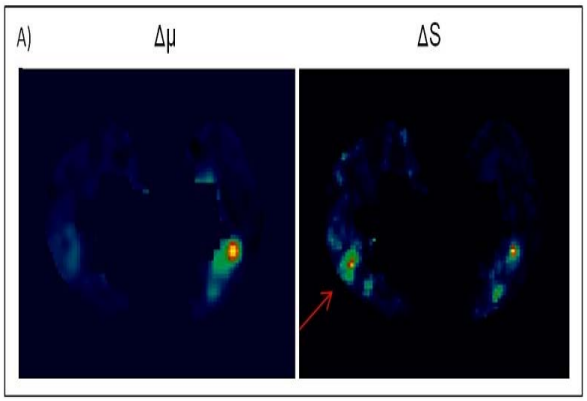

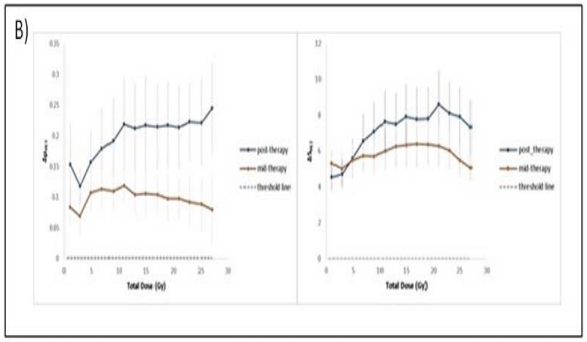

Conclusion: The new method based on local structures in 18F-FDG PET images was a feasible approach. This method is more sensitive in terms of providing a clearer 18FDG uptake dose response six weeks after initiation of treatment compared to standard image subtraction, and may be valuable in future studies addressing RILT.

PO-0931

Onset and recovery of neuronal injury following proton radiotherapy

C.L. Teng[1], M. Mix[1], B.K.K. Kevin[1], C. Ainsley[1], W. Sumei[2], K. Manoj[2], H. Poptani[2], R. Wolf[2], L. Sloan[1], T. Brown[1], N. Thorne[1], S. Avery[1], Z. Tochner[1], C. Hill-Keyser[1], S. Mohan[2], T. Solberg[1], C. Armstrong[3], M. Alonson-Basanta[1]

[1]*University of Pennsylvania, Radiation Oncology, Philadelphia, USA*

[2]*University of Pennsylvania, Radiology, Philadelphia, USA*

[3]*The Children's Hospital of Philadelphia, Neuron-Oncology, Philadelphia, USA*

Purpose or Objective: To quantify the time course and the extent of radiation-induced neuronal changes following skull base (cohort I) or brain (cohort II) proton radiation therapy (PRT).

Material and Methods: We analyzed 4 cohort I and 4 cohort II patients, who completed 2 year follow-up magnetic resonance imaging (MRI) and neurocognitive (NC) study. Apparent diffusion coefficient (ADC) and fractional anisotropy (FA) from diffusion tensor imaging were used to evaluate neuronal and white matter injury at 1.5, 6, 12 and 24 m following PRT. All MR images for each patient were co-registered to the planning CT using rigid image registration, enabling patient-specific contours (ROIs) to be transferred. Each ROI thus encoded time-dependent MR parameters. The biologically effective doses to GTV ranged from 52 to 70 Gy. Dose-related neuronal changes were compared between the two cohorts as well as within each patient. Cohort I typically received a left-right symmetric PRT with higher dose to the temporal lobes and brainstem, and cohort II a unilateral PRT with a significant higher dose to only hemisphere. ROIs were hippocampus, cerebellum, corpus callosum, temporal lobes, GTV, brainstem and the whole brain. NC testing used 8 memory indices that are radiation-sensitive and insensitive, based on prior series of studies: visual or verbal, semantic or perceptual memory (encoding, retrieval, and reaction time to recognize).

Results: ADC is an inverse measure of cellular density. After PRT, average ADC first increased and then decreased; the peaks of the average ADC were detected at 1.5 m and 12 m after PRT for cohort I and II patients. Further, variations in the ADCs were correlated with the mean doses. This dose dependence had different temporal course between the two cohorts. For cohort I, the dose relationship disappeared 12 m after RT. For cohort II, the dose relationship was the strongest at 12 m after RT. ΔADC/ADC (%/Gy) = [0.16, 0.15, 0, -0.06] and [0.16, 0.19, 0.37 0.09] at 1.5, 6, 12 and 24 m after PRT for cohort I and I.FA is a measure of neural connectivity in the brain. On average, no consistent changes in FA were observed for ROIs receiving a mean dose < 40 Gy. In ROIs that received > 40 Gy mean dose, FA decreased consistently. The largest reduction of FA was observed at 1.5 m following PRT. <ΔFA/FA>(%) = [-7.5, -5.3, 2.9, -1.4] at 1.5, 6, 12 and 24 m after PRT for both cohorts. Among NC tests, only changes in verbal and visual semantic retrieval were significant. Decline occurred 1.5 m after PRT (visual semantic reaction time: $p<0.005$; verbal semantic retrieval: $p<000$). Recovery occurred 6 m after PRT, and reached baseline at 24 m.

Conclusion: ADC and FA are sensitive measures to quantify radiation-induced neuronal injury following PRT. Both ADC and FA showed changes at 1.5 m and a recovery similar to the time course of changes in NC functions.

Poster: Physics track: Images and analyses

PO-0932

Preliminary clinical study to evaluate an interactive system to segment OARs in thoracic oncology

J. Dolz[1,2], H.A. Kirisli[1], T. Fechter[3], S. Karnitzki[3], U. Nestle[3], M. Vermandel[2], L. Massoptier[1]

[1]*AQUILAB Parc Eurasante Lille Metropole, Research, Loos, France*

[2]*Univ. Lille, Inserm- CHU Lille- U1189 - ONCO-THAI - Image Assisted Laser Therapy for Oncology, Lille, France*

[3]*University Medical Center of Freigburg, Department of Radiation Oncology, Freigburg, Germany*

Purpose or Objective: Radiotherapy aims at delivering the highest possible dose to the tumor while minimizing the irradiation of surrounding healthy tissue, and especially to the organs at risk (OARs). Therefore, accurate delineation of OARs is required for radiation treatment planning (RTP). In thoracic oncology, delineation of some OARs remains manual, making the task time consuming and prone to inter observer variability. Various (semi-) automatic approaches have been proposed to segment OARs on CT but the task still remains challenging. Here, a system to interactively segment OARs in thoracic oncology on CT images is presented and its clinical acceptability evaluated.

Material and Methods: The proposed framework has been implemented using MITK platform. User interaction lies in the easy definition of few manual seeds for the OARs and background using a 'paintbrush' tool, which can be interactively added in any view (axial, sagittal or coronal), and is subsequently propagated within the whole volume. Once the user is content with the seeds placement, the system automatically performs the segmentation. If the outcome is not satisfying, the user can modify the seeds, which involves adding and/or removing existing seeds, and perform again the automatic segmentation. Number of tries has been limited to five in the current study. If after the five modifications the segmentation result is not sufficient to be usable in the RTP, the user shall reject it; otherwise, he shall accept it. A hybrid approach combining watershed transformation and graph cuts is used for the segmentation task.

Results: The system was evaluated on multivendor CT datasets of 10 patients presenting from early stage to locally advanced NSCLC or pulmonary metastases. OARs taken into consideration in this study were: heart, lungs, oesophagus, proximal bronchus tree, spinal canal and trachea. Interactive contours were generated by a physician using the proposed system. Delineation of the OARs obtained with the presented system was approved to be usable for RTP in more than 90% of the cases, excluding the oesophagus, which segmentation was never approved (Fig 1). On the accepted reported cases, more than 90% of the interactive contours reached a Dice Similarity Coefficient higher than 0.7 with respect to manual segmentations (Fig 2). Therefore, our interactive delineation approach allows users to generate contours of sufficient quality to be used in RTP up to three times faster than manually.

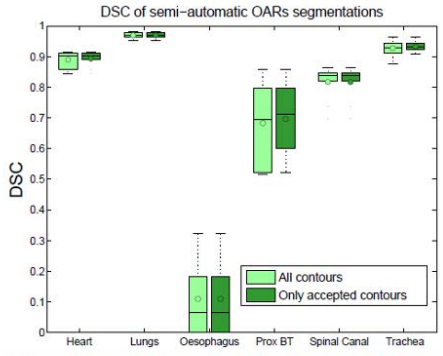

Figure. 1. Dice Similarity Coefficients (DSC) of semi-automatic OARs segmentation.

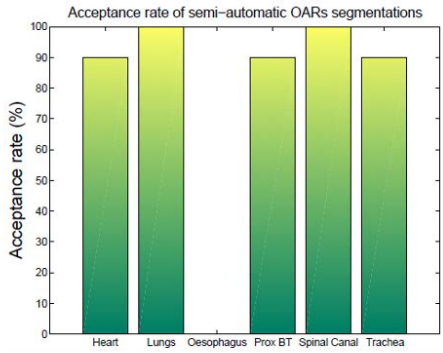

Figure. 2. Acceptance rate for the semi-automatic segmentations

Conclusion: An interactive, accurate and easy-to-use computer-assisted system for OARs segmentation in thoracic oncology was presented and clinically evaluated. The introduction of the proposed approach in clinical routine might offer a valuable new option to radiation therapists (RTTs) in performing OARs delineation task. Consequently, further experiments will be carried out on larger databases and with the participation of additional RTTs to investigate its potential use in daily clinical practice.

PO-0933

Towards standardisation of PET auto-segmentation with the ATLAAS machine learning algorithm

B. Berthon[1], C. Marshall[2], E. Spezi[3]

[1]*Cardiff University, Wales Research and Diagnostic PET Imaging Centre, Cardiff, United Kingdom*

[2]*Cardiff University, Wales Research & Diagnostic PET Imaging Centre, Cardiff, United Kingdom*

[3]*Cardiff University, School of Engineering, Cardiff, United Kingdom*

Purpose or Objective: Positron Emission Tomography (PET)-based -auto-segmentation (PET-AS) methods have been recommended for accurate and reproducible delineation of tumours. However, there is currently no consensus on the best method to use, as different methods have shown better accuracy for different tumour types. This work aims to evaluate the accuracy of a single segmentation model trained for optimal segmentation on a variety of different tumour corresponding to different anatomical sites.

Material and Methods: ATLAAS, an Automatic decision-Tree based Learning Algorithm for Advanced Segmentation was developed and validated in previous work. ATLAAS (patent pending PCT/GB2015/052981) is a predictive segmentation model, trained with machine learning to automatically select and apply the best PET-AS method, according to the tumour characteristics. The ATLAAS model was trained on 500 simulated PET images with known true contour. The PET-AS used in the model included adaptive iterative thresholding, region growing, watershed-based segmentation, deformable contours, and clustering with K-means, fuzzy C-means and Gaussian Mixture Models, applied to the detection of 2 to 8 clusters. In this work, ATLAAS was applied to the segmentation of PET images containing synthetic tumours generated using the fast PETSTEP simulator. The data included 5 Head and Neck (H&N), 5 lung, 5 abdominal and 5 brain tumours. The contours obtained with ATLAAS were compared to the true tumour outline using the Dice Similarity Coefficient (DSC). DSC results for ATLAAS were compared with results obtained for thresholding at 42% (RT42) and 50% (RT50) of the maximum intensity.

Results: ATLAAS contours were closer to the true contour for all cases. The DSCs obtained with ATLAAS were 5.3% to 123% higher across cases than DSCs obtained for RT50 and 4.1% to 74% higher than for RT42. The largest differences between ATLAAS and relative thresholding were obtained for lung images, the smallest differences for H&N and Brain tumours. The minimum conformity of ATLAAS contours on the whole dataset was 0.81 DSC compared to 0.38 and 0.47 for RT50 and RT42 respectively.

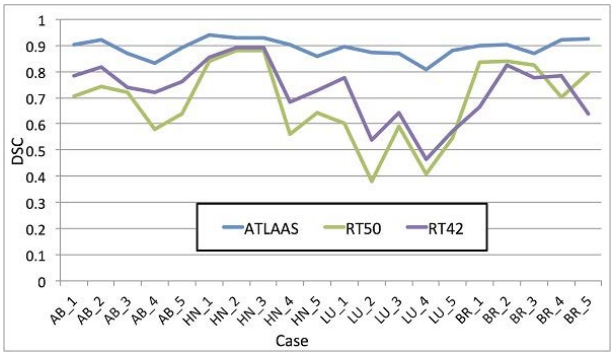

Conclusion: Our results show that ATLAAS is capable of providing highly accurate segmentation for different tumour sites, largely outperforming single-value thresholding methods. The ATLAAS machine learning algorithm represents a standardized approach to PET auto-segmentation. The robustness and adaptability of ATLAAS makes it a very promising tool for PET segmentation in radiotherapy treatment planning.

PO-0934

Cardio-respiratory motion compensation for 5D thoracic CBCT in IGRT

S. Sauppe[1], A. Hahn[1], M. Brehm[2], P. Paysan[2], D. Seghers[2], M. Kachelrieß[1]

[1]*German Cancer Research Center, Medical Physics in Radiology, Heidelberg, Germany*

[2]*Varian Medical Systems, Imaging Laboratory, Baden-Dättwil, Switzerland*

Purpose or Objective: Accurate information about patient motion is essential for precise radiation therapy, in particular for thoracic and abdominal cases. Patient motion assessment based on daily on-board CBCT images immediately before treatment potentially allows accounting for organ motion during the treatment. Especially for patients with tumors close to organs at risk, the organ positions need to be precisely known as a function of time. In case of the heart 5D

CBCT images are required. Since simple double gating yields severe sparseness artifacts we propose a 5D motion compensation (MoCo) algorithm dedicated to cardio-respiratory CBCT in IGRT.

Material and Methods: Clinical patient data acquired with the TrueBeam™ CBCT system (Varian Medical Systems, Palo Alto, CA) have been used for our study. For the intrinsic respiratory and cardiac motion signal detection, about hundred overlapping regions of interests are automatically evaluated in projection space, thus yielding a robust approach independent on the anatomy shown in the projection images. In addition to respiratory gating (4D CBCT) cardiac gating is applied to obtain initial volumes. We compensate respiratory and cardiac motion in a two-step procedure. First, respiratory motion is estimated and compensated using respiratory phase binning only. Then, cardiac motion estimation is performed using respiratory-compensated images with cardiac gating. The motion estimation algorithm is based on a deformable intensity-based 3D-3D image registration method. Combining the obtained motion vector fields for respiratory and cardiac motion allows us to compensate motion for any arbitrary respiratory and cardiac target phases.

Results: Either 5D double-gated or respiratory-compensated plus cardiac-gated images both contain strong streak artifacts and high noise levels. Our 5D MoCo algorithm is able to significantly improve the image quality while maintaining the same high temporal resolution for respiratory and cardiac motion as achieved with simple double gating. Because all sparse projection streak artifacts are removed, small structures can be delineated even in areas where motion is high. The noise level of patient data is the same as that of 3D CBCT due to making use of 100 % of the projection data for each reconstructed frame.

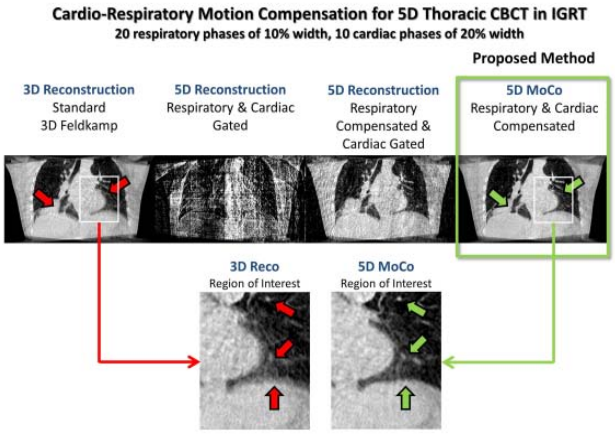

Conclusion: This work presents a reconstruction method for true 5D imaging in IGRT. Our patient data demonstrate that good image quality is achievable at identical x-ray dose levels and at acquisition times as for today's 3D CBCT. Treatments of regions close to the heart should be able to benefit from our approach.

PO-0935

Correcting diffusion weighted MR images for signal pile-up and distortions near gas pockets

L.D. Van Buuren[1], D. Polders[1], M. Milder[1], F.J. Pos[1], S.W. Heijmink[1], B. Van Triest[1], U.A. Van der Heide[1]
[1]*The Netherlands Cancer Institute, Department of Radiation Oncology, Amsterdam, The Netherlands*

Purpose or Objective: Diffusion weighted (DW) MRI is used in RT to improve tumor delineation and monitor treatment response. To minimize scan time, echo-planar imaging (EPI) is employed, but variations in the magnetic field (B0) distort EPI images due to a low pixel bandwidth in the phase-encoding (PE) direction. Geometric distortions can be corrected using a measured B0 map or by combining EPI images obtained with opposite gradients (ref. 1). However, near gas pockets B0 varies strongly. Here signal pile-up can occur, when signals from distinct, possibly non-neighboring, voxel locations are reconstructed into the same voxel. Our objective is to fully correct DW-EPI images using a combination of the above methods.

Material and Methods: On a 3T MRI (Philips Achieva), we acquired EPI images with opposite PE gradients and a dual gradient echo sequence to map B0. Both EPI images are corrected for geometric distortions by the standard correction method using the B0 map. For the new correction method, the B0 map also identifies voxels containing signal pile-up. The distortion-corrected images are averaged into a single image rejecting voxels with signal pile-up. These voxels contain data from only one EPI image. We demonstrated the correction method in a water phantom including an air cavity. The PE gradients had band widths ranging from 6 to 17 Hz/mm, comparable to clinical protocols. The corrected image was compared to raw EPI images and images corrected with the standard method. In a region-of-interest containing only pure water and signal pile-up, improvement was quantified as signal homogeneity using the coefficient of variation (CoV defined as standard deviation divided by signal mean). We applied the same method in two patients (prostate and rectal cancer), who underwent an MRI exam before radiotherapy and compared the raw images with the results of the standard correction and our full correction.

Results: With the standard correction method, distortions and intensity variations were removed in the EPI phantom images, but signal pile-up and signal loss were still visible. These were strongly reduced in our method, which was confirmed by the change in CoV in regions with signal pile-up. Here, the coefficient was 0.34 and 0.35 for the raw EPI image and B0 corrected image, respectively, and decreased to 0.12 after applying the proposed correction. Patient data are shown in the figure below. Here, rectal gas was present causing distortions and clear signal pile-up in the EPI images. After applying the correction, the signal pile-up was removed resulting in improved images.

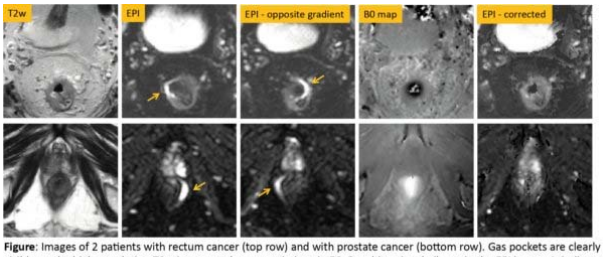

Figure: Images of 2 patients with rectum cancer (top row) and with prostate cancer (bottom row). Gas pockets are clearly visible on the high-resolution T2w images and cause variations in B0. Resulting signal pile-up in the EPI images is indicated by arrows. The black regions on the corrected EPI images result from an amplitude threshold on the B0 signal to mask out regions where B0 is unknown.

Conclusion: Our method has shown improvements in correcting EPI images, both in phantom and clinical data. It does not only correct for geometric distortions, but also for possible signal pile-up near gas pockets. Corrected DW-EPI images can improve tumor delineation and response monitoring near these regions.

Ref 1: Jezzard, P., NeuroImage 62 (2012), 648–651

PO-0936

Evolved Grow-cut: A PET based segmentation algorithm for heterogeneous tumors

H.M.T. Thevarthundiyil[1], D. Devakumar[2], Danie Kingslin Heck[2], Sasidharan Balu Krishna[3], I. Rabi Raja Singh[3], Regi Oommen[2], E. James Jebaseelan Samuel[1]
[1]*VIT University, Photonics Nuclear and Medical Physics Division School of Advanced Sciences, Vellore, India*
[2]*Christian Medical College, Department of Nuclear Medicine, Vellore, India*

[3]Christian Medical College, Department of Radiation Oncology, Vellore, India

Purpose or Objective: The purpose of the study was to evaluate the consistency, accuracy and timesaving of a grow-cut segmentation algorithm for heterogeneous tumor volumes.

Material and Methods: We present a new PET segmentation method, which is developed as a combination algorithm of Otsu and the Grow-cut segmentation algorithms and henceforth referred to as Otsu_GC. An initial contour of the tumor was defined using Otsu algorithm, which sets the threshold to minimize the intra-class variance of the tumor and its background. A concentric 3D shell was defined around the initial tumor contour at a distance of twice the slice thickness and extends up to four times the slice thickness. The space between the initial tumor contour and the inner edge of the shell ensured that the background voxels did not include the spill over voxels. The segmentation then employs the Grow-cut algorithm with the initial tumor contour and the 3D shell as the foreground and background seed respectively. The images underwent preprocessing, which included resampling to thinner slices with smaller in-plane voxel sizes that equal the CT slices. Edge preservation and contrast enhancement was achieved by convolution of high boost filter kernel in spatial domain and denoising with Gaussian blur (σ = 1pixel) filter. The implementation of preprocessing was in MATLAB and the segmentation was with SlicerRT and Grow-cut modules from 3D Slicer. The algorithm was tested on 11 heterogeneous NSCLC tumors (coefficient of variance: mean 0.35 ± 0.04) from 9 retrospective patient data. The manual contour of the PET uptake by the treating clinician was used as the ground truth for validation using Dice Similarity coefficient (DSC) and absolute volume difference as the evaluation metrics. The true contours were also compared to adaptive threshold (T*adaptive*) and 40% SUVmax threshold (T*40*) based isocontours. The PET(*Otsu-GC)* contours were also provided as the initial contour that was edited for final gross tumor volume (GTV) definition, which included composite information from CT and PET. The time taken for manual GTV contouring versus the time to edit the PET(*Otsu-GC)* contours was assessed as a measure of efficiency in this approach.

Results: Otsu_GC segmentation produced consistent contours, which were comparable to those delineated by the clinician (DSC: mean+ Std: 0.82 ± 0.062); while T*adaptive* performed reasonably well (0.80 ± 0.137) and T*40* fared poorly (0.61 ± 0.197). Compared with manual volumes Otsu-_GC volumes showed an overall overestimation (mean+ Std: 2.05 ± 4.51 cc); volumes with T*adaptive* had slight underestimation (-1.17 ± 7.33 cc) and large underestimated volumes were seen with T*40* (mean -14.49 ± 13.42 cc). The mean time of 5.72 minutes for manual GTV definition was reduced to 2.8 minutes (35%) with Otsu_GC.

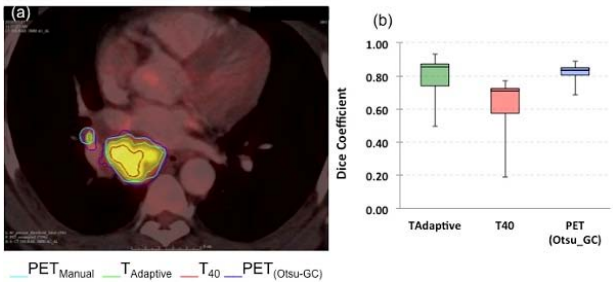

Conclusion: The proposed cellular automata based algorithm show promising results, robust enough to handle complex shaped tumor volumes with inhomogeneous tracer uptake.

PO-0937

Sound speed reconstruction in full wave ultrasound computer tomography for breast cancer detection

M. Perez-Liva[1], J.L. Herraiz[1], E. Miller[2], B.T. Cox[3], B.E. Treeby[3], J.M. Udías[1]

[1]Universidad Complutense de Madrid, Física Atómica-Molecular y Nuclear, Madrid, Spain
[2]Tufts University, Electrical & Computer Engineering, Medford- MA, USA
[3]University College London, Medical Physics and Biomedical Engineering, London, United Kingdom

Purpose or Objective: Ultrasound computer tomography (USCT) is an emerging medical imaging modality in which the acoustical properties of the tissues in the body are studied. Among these properties, the speed of sound has a close correlation with the tissue density [1], providing similar structural information to X-ray mammograms. Therefore, the sound speed maps could be employed to detect breast tumors, avoiding the use of compression and radiation. The potential of these systems as a main diagnostic tool is currently limited by the large computational cost required for image reconstruction, especially when full-wave inversion (FWI), the method that provides the best image quality, is employed [2]. In this work, we present a code based in FWI to reconstruct sound speed maps for USCT.

Material and Methods: The implemented code is based on the Adjoint Method [3] which allows finding the expression of the functional gradient of the global error norm between experimental and simulated data (Eq 1):

$$\nabla_F \varepsilon(r) = \frac{1}{{c_o}^2} \int_0^T \frac{\partial p(r,t)}{\partial t} \frac{\partial p^*(r,t)}{\partial t} dt \qquad (1)$$

$$n(r) = n^j(r) - \alpha_j \nabla_F \varepsilon^j(r) \qquad (2)$$

Here p and p* are the direct and adjoint pressure fields respectively. The functional gradient of the error is used to update the speed of sound distribution Eq 2.
The code was implemented in c++ and a CUDA version of the software k-wave [4] was employed to perform the forward and backward wave propagation. Noisy simulated data were employed to test the algorithm (Fig 1D). A reconstruction with bent-rays was used as initial guess. The simulated setup was a circular ring of detectors of 256 point elements with a field of view of 128 mm and 500 kHz of central frequency. A 2-dimensional numerical phantom representing a coronal slice of breast with 4 different tissues (fat, fibroglandular tissue, benign and malignant tumors) was studied.

Results: The reconstruction took around 9 minutes using 2 iterations with 15 subsets in an Intel Xeon 16-CPU @2.4GHz with Nvidia GEForce GTX 660. We obtained adequate recovery of the shape and values of the several structures included in the phantom and very good quality parameters in general.

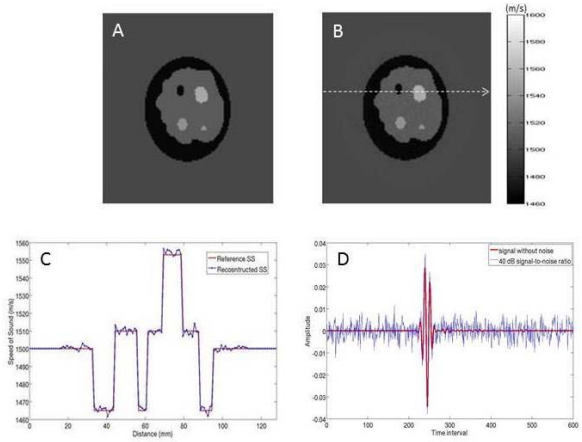

Fig. 1 A) Actual numerical breast phantom. B) Reconstructed image C) Profiles comparison D) Example of noisy reference signal.

Conclusion: A full wave code was implemented in time domain for USCT. The obtained images employed simulated data and present adequate quality parameters. The calculation time was around 9 minutes which is very fast for this modality. These results are encouraging and we are currently working on the reconstruction of real data and other acoustical properties to validate and improve the applicability of the code.

PO-0938

Estimation of system-related geometric distortion in 7T MRI using a 3D anthropomorphic head phantom

J. Peerlings[1]

[1]*Maastricht Radiation Oncology MAASTRO GROW - School for Oncology and Developme, Radiation Oncology, Maastricht, The Netherlands*

Purpose or Objective: Morphological 7 Tesla (7T) MRI is a high-resolution imaging modality offering excellent soft-tissue contrast and promising visualization of micro-vascularization. It shows potential value to be used for improved target volume definition in radiation therapy planning of glioblastoma (GBM) over 1.5T and 3T MRI. However, system- and object-related geometric distortion (GD) of 7T MRI could compromise the spatial accuracy required for high-precision image-guided radiotherapy (IGRT) of GBM. Hence, quantitative evaluation of GD for 7T MRI is mandatory before integration into IGRT. A phantom study was performed to measure system-related GD in clinically relevant 7T MR pulse sequences.

Material and Methods: To assess the GD, a new anthropomorphic head-phantom (CIRS Model 603A) with a rigid 3D grid (3mm rods, spaced 15mm apart) was used. Images were acquired with a Siemens Magnetom 7T whole-body scanner in combination with a Nova Medical 32-channel head coil. Scan protocols with clinically relevant T2-GRE and MP2RAGE pulse sequences were used with and without automatic GD correction. For both sequences, 436 points of interests (POIs) were defined by manual reconstruction of the 3D grid points in the respective images. A global and a local measure of GD were estimated: MADglobal is the mean absolute difference (MAD) between the measured and the true Euclidian distances of all unique combinations of POIs, whereas MADlocal is the MAD between the measured and the true Euclidian distances of all POIs relative to the magnetic field isocenter.

Results: MADglobal and MADlocal ranges from 0.88–1.72 mm and from 0.28–1.76 mm in uncorrected GRE images, respectively. For uncorrected MP2RAGE images, MADglobal and MADlocal ranges from 0.83–1.62 mm and from 0.26–2.04 mm, respectively. Overall GD (MADglobal) is present in both uncorrected images and is shown to be sequence-independent. Larger values for MADlocal are observed with increasing distance from the magnetic field isocenter, with a maximum of 2.04 mm in uncorrected MP2RAGE near the edges of the phantom (Figure 1). At equal distance from the isocenter, GD was found to be anisotropic with the principal component in the superior-inferior direction (MADlocal = 1.38 mm in uncorrected MP2RAGE). In corrected images, MADglobal is respectively lower in both sequences as B0 inhomogeneity was corrected for. MADlocal for GRE and MP2RAGE ranges from 0.22–1.01 mm and 0.21–0.97 mm, respectively. This means that most GD could be reduced within clinically acceptable limits (≤1mm) by the automatic GD correction method.

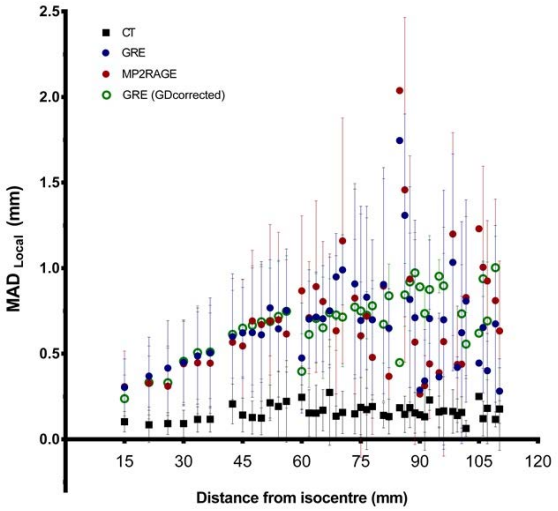

Conclusion: With 7T MRI, the system-related geometrical uncertainty of GD-corrected GRE and MP2RAGE pulse sequences is less than 1 mm and may thus render integration of 7T MRI for IGRT of GBM feasible. The next step will be to quantify and correct object-related GD for clinical implementation.

Poster: Physics track: Implementation of new technology, techniques, clinical protocols or trials (including QA & audit)

PO-0939

The dosimetric consequences of delineation variation for cervical external beam radiotherapy

G. Eminowicz[1], V. Rompokos[1], C. Stacey[1], M. McCormack[1]

[1]*University College London Hospital, Radiotherapy Department, London, United Kingdom*

Purpose or Objective: Target volume delineation variation is of emerging importance with more advanced conformal radiotherapy delivery such as Intensity Modulated Radiotherapy (IMRT). We investigate delineation variation and consequent dosimetric variation for external beam cervical radiotherapy.

Material and Methods: Two INTERLACE trial test cases were outlined by 21 different UK centres. A gold standard clinical target volume (GSCTV) was created by consensus agreement and validated using the STAPLE algorithm. Volume, Jaccard conformity index (JCI) and anatomical areas included (compared with protocol recommendations) were analysed for each centre's CTVs. Individual RapidArc plans were created for each centre's planning target volumes (PTVs). For each centre a gold standard PTV (GSPTV) was created by applying the margins used by that centre to the GSCTV. Comparisons were made with GSPTV dose volume histograms (DVH) parameters including D98%, D95%, D2% (dose delivered to 98%, 95% and 2% volume) and V95% (percentage volume receiving 95% dose). A qualitative review was also performed.

Results: Combined primary and nodal CTV volume varied by up to 1.99 fold. JCI ranged from 0.51 to 0.81 overall. No CTVs demonstrated poor concordance (JCI<0.5). 13% and 32% achieved good concordance (JCI≥0.7). The largest variation in anatomical areas included within CTV was seen in obturator, pudendal and pre-sacral nodal regions. Up to 4cm variation was seen in the superior slice delineated (aortic bifurcation) and up to 3.5cm variation in inferior slice (mid-vagina). Acceptable coverage was achieved for all centres' PTVs but no plans achieved acceptable GSPTV coverage. GSPTV V95%>95% prescribed dose was not achieved for all plans. GSPTV V95%>90% prescribed dose was not achieved in 67% of plans and V95%>80% was not achieved in 9% of plans. GSPTV V95% is on average 10-15% lower than planned and D95% is 10

to 20% lower than planned. Most common anatomical areas not receiving 95% dose were vagina, obturator and external iliac nodes for both cases and superior nodal aspect for case 1. The DVH below shows the gold standard PTV coverage for each centre's RapidArc plan.

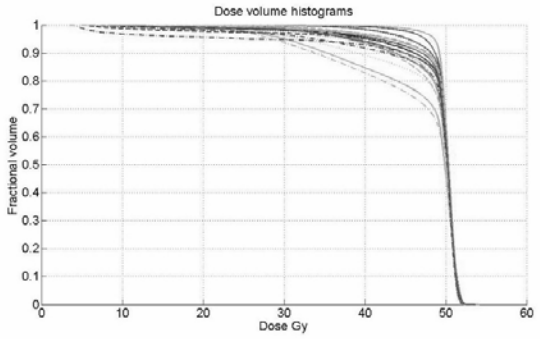

Conclusion: This quality assurance exercise demonstrates that, using IMRT, CTV delineation variation leads to potentially clinically important PTV dosimetric variations. Therefore, as IMRT use increases, the importance of accurate target volume delineation also increases.

PO-0940

The problems found within the on-site dosimetry audits of radiotherapy centres in the Czech Republic

I. Koniarova[1], I. Horakova[1], V. Dufek[1]
[1]*National Radiation Protection Institute, Department of Radiotherapy and X-ray Laboratory, Praha, Czech Republic*

Purpose or Objective: The aim of the study is to report the most important problems found within the on-site dosimetry audits of radiotherapy centres. On-site audits of therapeutic units are performed by our institute after commissioning and acceptance test for each external radiotherapy and brachytherapy unit in the Czech Republic since 1997. They are performed with the same dosimetry equipment by the same persons to reduce the uncertainty in the results. The system of on-site audits includes the basic audit aimed at the verification of selected mechanical and dosimetric parameters, advanced audit to verify selected functions of TPS, and end-to-end audit to check the whole radiotherapy chain from planning to delivery. When high deviation is found (not only exceeding tolerance level), the auditors always try to find the reason, rectify the problem on-site, or give appropriate recommendations to the particular centre. The results of the audits are reported to the national regulatory body.

Material and Methods: The results from on-site basic, advanced, and end-to-end audits have been reviewed and analysed. Statistical process control (SPC) has been performed where appropriate.

Results: We report important errors that might lead to the radiological accident if not revealed by the on-site audit. In early years, the main typical errors were caused by incorrect input data in the TPS after the acceptance test. Of the main importance were: incorrect determination of dose rate for 60Co unit; incorrect output factors or wedge factors; using ionisation data instead of dose data measured with ion chamber for electron beams; incorrect SSD for measurement; incorrect detector; not taking into account couch attenuation etc. These types of errors are not so frequent but still observable nowadays, regardless the high quantity of published recommendations and literature on that topic. Currently, with new algorithms implemented in the TPS, various errors were found due to the lack of training, in particular for Monte Carlo (MC) algorithms. The TPSs were not commissioned i.e. with MC input data used in clinical practice but with data calculated for highest accuracy to comply with the measurements. End-to-end audit enabled to reveal insufficient patient QA, inaccuracy in TPS calculations for non-reference material, incorrect CT numbers to RED calibration curves, not following the ICRU and other international reports.

Conclusion: All the examples can serve as a learning system. In early years, the main cause of errors was a lack of time for measurements evaluation and verification. More recently, the other cause of the errors is a lack of time to get familiar with new equipment, especially with the software (TPS). In all cases, the errors were found at centres with a lack of clinical medical physicists with sufficient continual professional development.This work was supported by the project No. TB04SUJB001.

PO-0941

3D printed bolus for chestwall radiation therapy

J. Robar[1], J. Allan[2], R.L. Macdonald[3], R. Rutledge[1], T. Joseph[4], J. Clancey[2], K. Moran[4]
[1]*Dalhousie University, Radiation Oncology, Halifax, Canada*
[2]*Nova Scotia Health Authority, Medical Physics, Halifax, Canada*
[3]*Dalhousie University, Physics and Atmospheric Science, Halifax, Canada*
[4]*Nova Scotia Health Authority, Radiation Therapy, Halifax, Canada*

Purpose or Objective: 3D printing technology introduces the potential for improved accuracy of bolus in conforming to patients and may provide efficiency gains through automation of production based on planning CT data. The objectives of this study are i) to compare build-up depth dose characteristics of solid and flexible 3D printed bolus material to both Solid Water and standard sheet bolus material, ii) to assess the fit of 3D printed bolus to chestwall anatomy based on CT imaging compared to sheet bolus, and iii) to examine dosimetric accuracy of the treatment plan compared to OSLD measurements with 3D printed bolus.

Material and Methods: Depth dose measurements were performed with a Markus parallel plate chamber for polylactic acid (PLA) and flexible (Ninjaflex) 3D printing materials, and results were compared to both standard sheet bolus (Superflab) and Solid Water. For three chestwall patients, ballistics gel molds of the chestwall were fabricated to produce spatially realistic phantoms with plasticity similar to that of tissue. 5 mm thick, 3D printed chestwall boluses were fabricated for these phantoms based on CT data. CT imaging was then used to assess conformity to the surface and presence of air cavities. Optically Stimulated Luminescent Dosimetry (OSLD) was used to measure dose under both 3D printed and sheet bolus at nine locations on the chestwall surface for typical field-in-field treatment deliveries.

Results: In the build-up region, PLA and Ninjaflex bolus material exhibit similar depth dose characteristics. Both types of 3D bolus yield a greater dose compared to Solid Water, however differences remain below 5%. CT imaging of gel phantoms show an improved fitting of 3D printed bolus, with air cavities below the bolus reduced by 9% to 321% compared to standard sheet bolus. Treatment planning studies show better uniformity of skin dose for 3D printed bolus compared to sheet bolus, with the former giving a standard deviation of 1.8% compared to 4.2%. On average, the agreement of OSLD-measured to planned dose was similar between sheet bolus and 3D printed bolus, however standard sheet bolus shows greater variability in the measured-to-planned dose ratio (15% range for sheet bolus compared to 6% for 3D printed bolus).

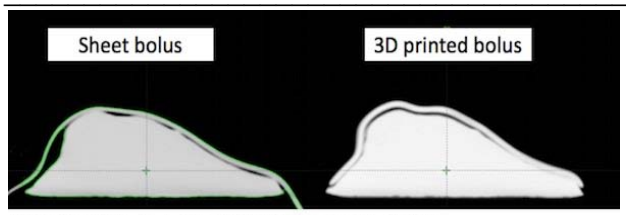

3D bolus reduced total air gap volume by 9% to 321% compared to conventional sheet bolus.

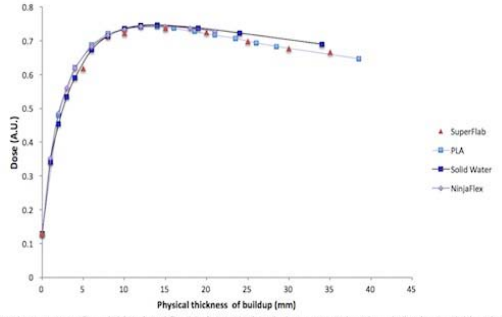

Depth dose characteristics for solid (PLA) and flexible (NinjaFlex) 3D bolus compared to sheet bolus (SuperFlab) and Solid Water.

Conclusion: Rigid (PLA) and flexible (Ninjaflex) bolus materials provide build-up characteristics within 5% of Solid Water. When incorporated into treatment planning calculations, planned dose for 3D bolus agrees with OSLD measured dose to within 2% on average, and 3D printed bolus gives lower variability in the agreement of the delivered to planned dose. In summary, 3D printed chestwall bolus may be produced in an automated fashion and gives improved consistency of delivered dose accuracy compared to standard sheet bolus.

PO-0942

VMAT planning and treatment preparation process adapted for failure mode and effect analysis

N. Khater[1], F. Azoury[1], D. Nehme Nasr[1], N. Farah[1], T. Felefly[1], J. Barouky[1], C. El Khoury[1], R. Sayah[1], E. Nasr[1]
[1]Hotel Dieu de France Hospital - Saint Joseph University, Radiation Oncology, Beirut, Lebanon

Purpose or Objective: Mitigating risks in radiotherapy is paramount for patient safety. A volumetric modulated arc therapy (VMAT) adapted to failure mode and effect analysis (FMEA) and implemented through workflow-integrated checklists is presented. This work is in line with efforts done by organizations to integrate a culture of patient safety into radiotherapy processes.

Material and Methods: VMAT is currently being offered to our patients using RapidArc®, Eclipse® 11, Aria-11®, and TrueBeamTM; all by Varian Medical Systems (Palo Alto, CA). All systems went clinical in February 2013. Three months into the VMAT program, we realized our operation may be optimized by using the new Workflow feature introduced in Aria® version 11. Consequently, a workgroup consisting of 2 physicists, 3 radiation oncologists, one radiation therapist and one IT was created to identify modes-of-failure in our VMAT planning and preparation process; and to implement a workflow that mitigates their risks. A process-centered risk analysis for VMAT employing FMEA was performed. Risk priority numbers (RPN) for occurrence, severity and detection, were assigned for identified modes of failure based on a simplified model of the AAPM TG100 scoring. FMEA for one task in our VMAT process (Figure 1) is presented as example in Table1. Mitigation actions were implemented into Aria-11® Workflow via integrated checklists where e-signatures are enforced. Risk mitigation strategies employing redundancy, implementation of related policies-and-procedures, documentation, and peer-review were hardwired into the VMAT process.

Results: A VMAT workflow (Figure 1) was designed and included 114 potential-modes-of-failure distributed into 4 groups: (1) 59 modes recurring redundantly, (2) 3 decision-type modes forcing re-planning, (3) 33 recurring modes aimed for enhancing communication, and (4)19 modes occurring only once; some with residual RPN's necessitating implementation of policies-and-procedures. In the 18 months period leading up to this study, more than 600 VMAT planning and preparation processes were delivered conforming to the workflow in Figure 1. No aberrations in treatments occurred. Shortcomings in e-chart preparations were virtually eliminated.

Conclusion: An adaptation of the VMAT planning and preparation process to FMEA using the Aria-11® workflow was presented. Risk analysis was performed, and risk mitigation was achieved through hardwiring appropriate checklists into the VMAT planning tasks. The adaptation to FMEA resulted in marked improvements in patient safety, process control and process documentation. The presented workflow adaptation to FMEA could serve as a reference or model for clinics offering VMAT.

RapidArc Planning Workflow adapted to FMEA

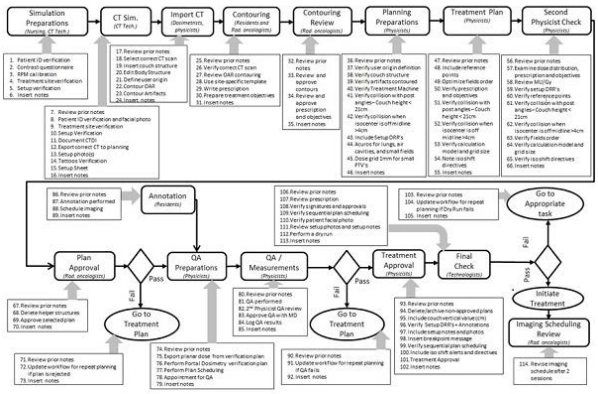

TABLE 1: FMEA for the "Planning Preparations" task is shown with associated checklist-items as mitigating actions. The owners usually of this task are physicists and dosimetrists.

Potential Failure Mode (checklist-item)	Potential Effect of Failure	Pre-mitigation Severity RPN	Potential Cause of Failure	Pre-mitigation Occurrence RPN	Existing detection Mode before risk mitigation actions	Pre-mitigation Detectability	RPN	Action(s) Taken Or Risk Mitigation Control(s)	Post-mitigation Severity RPN	Post-mitigation Occurrence	Post-mitigation Detectability RPN	Residual RPN
36. Review prior notes	Could be serious in case an important note or directive is overlooked.	7	Operator error	4	none	7	196	* Checklist-item in Planning Preparations task	7	1	1	7
37. Verify User Origin definition	Serious. Could cause an offset in treatment isocenter.	7	Operator error	4	CT import Checklist: Define User Origin	1	28	* Checklist-item to verify User Origin on simulation tattoo (redundancy)	7	1	1	7
38. Verify couch structure	Wastes planning time to correct.	4	Operator error	4	CT import Checklist: Insert couch struct.	1	16	* Checklist-item to Insert Couch Structure depending on technique (redundancy)	4	1	1	4
39. Verify artifacts contoured	Inaccurate distribution at and near artifacts.	2	Operator error	4	none	9	72	* Checklist-item to define artifacts	2	1	1	2
40. Verify machine	Wastes planning time and beam scheduling inconveniences to patients.	1	Operator error	2	May be detected in later tasks or at first session	2	4	* Beam energies are matched * Include machine in prescription * Include checklist-item to verify machine	1	1	1	1
41. Check for potential collision with posterior angles – Couch height <21cm	Ranges from serious as in patient injury to waste of time for re-planning.	9	Operator error	4	Could go undetected till later tasks which would waste time.	7	252	* Checklist-item to verify potential collision with posterior angles. Couch height should be less than 21cm * Dry-run check in the later Verify Check tasks reduced the residual RPN to 7	9	2	2	36
42. Check for potential collision when isocenter is off midline >4cm	Ranges from serious as in patient injury to waste of time for re-planning.	9	Operator error	4	Could go undetected till later tasks which would waste time.	7	252	* Checklist-item to verify potential collision when isocenter is off midline by greater than 4cm * Dry-run check in the later Final Check task reduced the residual RPN to 7	9	2	2	36
43. Include setup fields and DRR's	Wastes planning time to correct.	2	Operator error	4	Will be detected at a later stage in the process	2	16	* Checklist-item to include setup fields and DRR's right after isocenter placement and potential collision check.	2	1	1	2
44. Select Acuros for lung and air cavity sites and in small volumes e.g. SRS	Slight distortion in dose representation.	4	Operator error	4	none	9	144	* Select Acuros for calculation model	4	1	1	4
45. Reduce dose grid to 1mm for small PTV's	Slight distortion in dose representation.	2	Operator error	4	none	10	80	* Checklist-item to set dose grid to 1mm for small PTV's	2	1	1	2
46. Insert notes relevant for later tasks and users	Information about the task remains undocumented and non-disseminated.	4	Operator error	4	none	10	160	* Include checklist-item for workflow notes documenting directives	4	1	1	4

PO-0943

Dutch national head and neck plan comparison significantly improved treatment planning quality

W. Verbakel[1], C. Raaijmakers[2], L. Bos[3], M. Essers[4], C. Terhaard[2], J. Kaanders[5], P. Doornaert[1]
[1]VU University Medical Center, Radiation Oncology Department, Amsterdam, The Netherlands
[2]University Medical Center Utrecht, Radiation Oncology, Utrecht, The Netherlands
[3]Medical Center Alkmaar, Radiation Oncology, Alkmaar, The Netherlands
[4]Bernard Verbeeten Instituut, Radiation Oncology, Tilburg, The Netherlands
[5]Radboud University Medical Center, Radiation Oncology, Nijmegen, The Netherlands

Purpose or Objective: The National Platform RT Head and Neck Cancer (HNC, Landelijk Platform Radiotherapie Hoofdhals Tumoren, LPRHHT) is a working party of the Dutch Society of Radiation Oncology, and is engaged in regulating and improving RT for HNC. One of the objectives of the LPRHHT is to evaluate the variation in treatment plan (TP) objectives and possibly improve treatment planning by increased organ at risk (OAR) sparing and reduction of variation between institutes.

Material and Methods: A survey was conducted in all 14 Dutch RT centers treating HNC to identify how a typical TP for oropharynx cancer was generated and judged in terms of PTV coverage, dosimetry requirements and OAR sparing. To this purpose, a CT-scan of an oropharynx cancer patient with delineation of PTVs and OARs was sent to each department. Planning aims were low mean doses of individual salivary glands, swallowing structures and oral cavity, with PTVboost/elective coverage V95%>98%. Prescription dose was 70Gy/35 fractions for the boost, 54.25Gy for PTVelective, using a simultaneously integrated boost. Results were presented anonymously, and the 4 centers with lowest OAR doses were asked to share planning tips and tricks with other centers. Centers were asked to undertake a second attempt to lower the OAR dose, using the suggestions of the other centers. In a third step, after evaluating the results, all centers were asked to plan a new case, using their improved planning protocol.

Results: Five different intensity modulated planning systems/techniques were used. Table 1 shows planning aims and averaged plan results. The initial variation in OAR dose was high, with a mean dose range of 20-46 Gy for combined swallowing structures and 18-49 Gy for the submandibular gland. Using the suggestions of best performing departments significantly improved the overall plan quality and reduced the variation in the 2nd phase without loss of PTV coverage. E.g. the submandibular gland mean dose±SD reduced from 35.4±9.3 to 28.0±7.6 Gy. The SD is a measure of variation between institutes. Average combined salivary/swallowing mean doses (±SD) decreased from 30.3±5 / 36.6±8Gy to 26.0±3.3 / 29.0±6.3Gy. The more consistent OAR sparing was confirmed by the reduced variations in the plan comparison for the new patient in the 3rd step.

Table. Planning aims and results averaged for the 14 centers plus variation for step 1 and step 2. Since step 3 involved planning of a different patient, only the variation (SD) is shown here.

	Aim	Step 1, mean ± SD	Step 2, mean ± SD	Step 3, SD
Contralateral parotid	Mean dose ↓	21.8 ± 4.3 Gy	18.5 ± 2.5 Gy	3.1 Gy
Combined salivary glands	Mean dose ↓	30.3 ± 5.0 Gy	26.0 ± 3.3 Gy	2.4 Gy
Combined swallowing muscles	Mean dose ↓	36.6 ± 8.0 Gy	29.0 ± 6.3 Gy	5.0 Gy
PTVboost V95%	V95% > 98%	99.0 ± 0.7 %	98.8 ± 0.6 %	0.5%
PTVboost V107%	V107% < 5%	0.6 ± 1.4 %	0.7 ± 1.4 %	0.6%
PTVelective V95%	V95% > 98%	97.2 ± 2.5 %	97.3 ± 1.8 %	0.9%

Conclusion: Despite many years experience with IMRT for HNC in all centers, treatment plans from all 14 Dutch RT centers showed great variation using the same set of contours. The centers with the highest original OAR doses benefited from the plan evaluation, and the tips and tricks from the best performing centers, resulting in significantly lower OAR dose in subsequent optimizations. Such exercise, initiated by a national radiation oncology working party, can significantly improve plan quality and reduce variation between institutes.

PO-0944

Stability in leaf position of 3 generations of optical digitally controlled Multi Leaf Collimators

A. Bertelsen[1], C.R. Hansen[1], N.K. Olsen[1], C. Brink[1,2]

[1]*Odense University Hospital, Laboratory of Radiation Physics, Odense, Denmark*

[2]*University of Southern Denmark, Institute of Clinical Research, Odense, Denmark*

Purpose or Objective: To investigate random and systematic uncertainties of MLC-leaf positions for three generations of Elekta MLCs to determine whether highly accurate and precise calibration is possible.

Material and Methods: MLCs of six Elekta accelerators were evaluated; two MLCi, two MLCi2 and two Agility. Details of the heads can be found elsewhere [e.g. Bedford et al J.A.C.M.P, v14, 2013, pp172]. The precision and accuracy over time of the MLC leaf positions were evaluated using the Electronic Portal Imaging Device, measuring a series of rectangular field with MLC positions moving in steps of 40 mm from -120 mm to 80 mm. Analysis of the images were performed by in-house developed software using steepest gradient analysis and compensating for head rotation inaccuracies.

Random uncertainties were assessed by repeating the above described procedure sequentially five times for each MLC. The random variation was measured as standard deviation of each leaf within a given leaf position, creating a distribution of variances for each MLC. Aggregated random variations for each MLC were calculated as the Root Mean Square of all the individual standard deviations.

Systematic uncertainties or time dependent drift was measured by calculating the average position of the five repeated scans. This average was then subtracted from the similar value measured previously, at the last calibration of the MLC, creating a distribution of drifts between the two time points. The aggregated drift was calculated as the standard deviation of the drift distribution.

Statistical differences of the distributions and differences in median were tested by Kruskal-Wallis tests and differences in the width were assessed by Levenes test.

Results: For all generations of MLC both random and systematic errors are found less than 0.15 mm which is small compared to the EPID pixel size of 0.25 mm and the smallest possible MLC-leaf adjustment of the control systems of 1/12mm (Table and figure).

The systematic difference was measured over a time period shown in the table in which no calibrations was performed on the MLC. Both random and systematic errors are statistically significant improved for each generation of MLC ($p<0.001$).

For the latest generation, the Agility, the development has resulted in a random error of 0.03 mm. The systematic error for Agility was found to be 0.07 mm when evaluated more than 79 days after calibration.

All measurements are made relative to radiation iso-centre, thus the group median drift (table and figure) is a combination of stability of MLC and radiation iso-centre. The small values in group median reflect high stability of both radiation iso-centre as well as MLC.

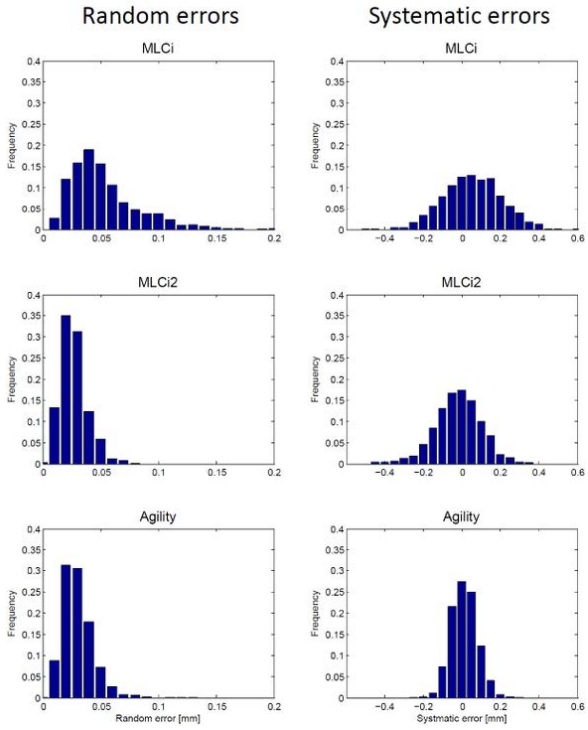

Tabel	MLCi	MLCi2	Agility
Daily variation			
Random error [mm]	0.06	0.03	0.03
Long Term Error			
Group Median [mm]	0.06	-0.02	0.01
Systematic error [mm]	0.15	0.12	0.07
Minimum days since calibration	88	30	79

Conclusion: All three generations of MLC are found to be highly stable with a significant improvement in stability for each generation. Thus, it is possible to make a highly accurate and precise calibration of the Elekta MLCs if an adequate calibration procedure is available.

PO-0945

Modeling and simulation of simultaneous using of two superficial hyperthermia antennas

A. Di Dia[1], S. Depalma[2], S. Bresciani[1], A. Maggio[1], A. Miranti[1], M. Poli[1], P. Gabriele[3], E. Garibaldi[3], M. Stasi[1]
[1]*istituto di Candiolo- IRCCS, Medical Physics, Candiolo, Italy*
[2]*Politecnico di Torino, Dipartimento di Elettronica e telecomunicazioni, torino, Italy*
[3]*istituto di Candiolo- IRCCS, Radiotherapy Department, Candiolo, Italy*

Purpose or Objective: Hyperthermia is a powerful radiosensitizer for treatment of superficial tumors. The purpose of this study is the 3D-modeling and simulation of the simultaneous using of two antennas of our equipment. In particular, geometric and functional characterization of the antennas as a function of various tissues characteristics (skin, fat and muscle) were investigated.

Material and Methods: The hyperthermia device is equipped with double arms, operating at a radiofrequency of 434 MHz, with a water automatic superficial cooling device. For temperature measures, it is equipped with an integrated Multichannel thermometer. The antennas are designed to cover areas from 7.2 × 19.7 cm2 up to 20.7 × 28.7 cm2. The applicators geometry have been reproduced in the CAD environment with a professional software based on the FDTD processing methods. In order to identify the distribution of specific absorption power rate in different types of tissues, several simulations have been performed, varying the relative thicknesses of a model consisting of skin, fat and muscle. Working incident power has been set equal to 100 watt. Waterbolus temperature is assumed to be equal to 38 °C

Results: The numerical model of the applicator has been coupled to various models of tissue, the incident maximum power of 100W for 60 minutes, with a thickness of waterbolus equal to 10 mm. In particular, as the fat thickness is gradually increased, muscle layer temperatures decrease of about 0.04 °C per mm of fat layer. Setting the skin thickness, as the fat thickness increases, the maximum temperature and the penetration depth reached in the muscle decrease; increasing skin thickness, if the fat thickness increases, consequently the maximum temperatures reached in the muscle and the depth of penetration decrease. In particular, increasing the fat thickness, temperatures in the underlying muscles were gradually reduced (approximately 0.2 °C for 5 mm fat raise). In the underlying muscle layer, maps were more homogeneous, with an approximately uniform power intensity decrease on the section plane. By varying waterbolus thickness, from 10 to 20 mm, the adaptation of the applicator coupled to tissue model undergoes small changes of the reflected power and, at the operating frequency, the model with thickness 17.5 mm showed to have the best reflection coefficient (-31.35 dB). The simultaneous use of the two antennas showed that only the 10% isoSAR are overlapping, and it demonstrates that it is possible to use both antennas in safety without possibility of hot spots in the tissue, varying also the thickness of the bolus.

Conclusion: The numerical simulation allows to know in detail the temperature distribution to different levels of depth, in particular it demonstrate that it is possible the simultaneous using of two antennas to treat more lesion in the same hyperthermia treatment session without hot spot in the tissue.

PO-0946

A new liquid fiducial marker formulation for image-guided pencil beam scanning proton radiotherapy

J. Scherman Rydhög[1], R. Perrin[2], R. Irming Jølck[3], T. Lomax[2], F. Gagnon-Moisan[2], K. Richter Larsen[4], S. Riisgaard Mortensen[1], G. Fredberg Persson[1], D. Weber[2], T. Andresen[3], P. Munck af Rosenschöld[1]
[1]*Rigshospitalet, Oncology, Copenhagen, Denmark*
[2]*Paul Scherrer Institut, Center for Proton Therapy, Villigen, Switzerland*
[3]*DTU Nanotech, Dept of Micro and Nanotechnology, Copenhagen, Denmark*
[4]*Rigshospitalet, Department of Pulmonary Medicine, Copenhagen, Denmark*

Purpose or Objective: The purpose of this work was to test the dosimetric impact of using a novel liquid fiducial marker (BioXmark®) in a proton spot scanned system.

Material and Methods: In order to test the clinical applicability of the new fiducial marker for proton therapy we measured the relative proton stopping power (RSP) of the liquid fiducial marker. Second, we measured the dose perturbation of a clinical pencil beam scanning proton beam of the liquid fiducial marker and three other commercially available solid markers for comparison by introducing them in a gelatin phantom. Dose perturbation was measured for several proton energies between 90 and 101 MeV at several distances after the markers in order to evaluate potential dose perturbation directly behind the markers, in the Bragg peak and after the Bragg Peak. Finally, we created proton therapy plans on five patients with locally advanced lung cancer and with the liquid fiducial marker implanted. Each treatment plans had 3-4 intensity modulated proton (IMPT) beams. We examined the markers impact on the dose distribution caused by the fiducial markers. This was done by first calculating the dose with no marker correction, secondly by matching the RSP of the fiducial marker with the experimental results, and subsequently with the RSP matching soft tissue and comparing changes in the dose distributions.

Results: The RSP of the liquid fiducial marker was determined to be 1.164 and 1.174 experimentally and theoretically, respectively. The dose perturbation of the liquid fiducial marker showed no effect directly after the marker itself and only had an effect on the proton range (Figure 1). By introducing the fiducial markers, we estimated a median range deviation of 1.2 (range: 0.7-1.9 mm) of the proton beam as compared to soft tissue. On the clinical lung cancer IMPT plans with the correct RSP manually introduced, the spinal cord max dose, lung V20, PTV V95, CTV V95 and GTV V95 were all modified by less than 1% by introducing the markers.

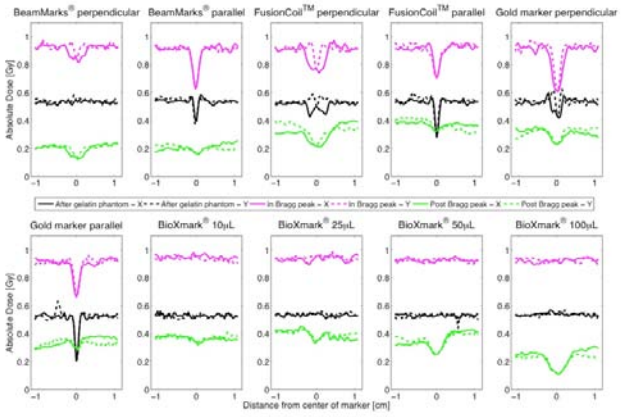

Conclusion: The experimentally determined RSP of the liquid fiducial marker was in good agreement (within 1%) of the theoretical calculation. The investigated liquid fiducial marker introduced smaller dose perturbation than the solid fiducial markers. The liquid fiducial marker shows promise for use in image-guided proton therapy of locally advanced lung cancer, as the risk of altering the clinical dose distribution is minimal.

PO-0947

VMAT-based grid for spatially fractionated radiation therapy

S. Gholami[1], M. Severgnini[2], H.A. Nedaie[3], F. Longo[4], A. S.Meigooni[5]

[1]*Tehran University of Medical Sciences, Department of Medical Physics and Biomedical Engineering, Tehran, Iran Islamic Republic of*

[2]*A.O.U. Ospedali Riuniti, Department of Medical Physics, Trieste, Italy*

[3]*Tehran University of Medical Sciences, Radiation Oncology Department- Cancer institute, Tehran, Iran Islamic Republic of*

[4]*University of Trieste and INFN Trieste, Department of Physics, Trieste, Italy*

[5]*Comprehensive Cancer Centers of Nevada, Las Vegas-Nevada, USA*

Purpose or Objective: The purpose of this study is to investigate about feasibility of using volumetric modulated arc therapy (VMAT) technique to provide a Grid dose distribution with the therapeutic ratio (TR) advantage similar to the block-based Grid.

Material and Methods: A series of cylinders with hole diameters of 1.3 cm and 1 cm height was created in a phantom as the boost volume within a larger volume target. The Monaco® 5 treatment planning system was used to plan the phantom. Four arcs, with collimator angles at 00 and 180 0 were used. The cost functions were defined to deliver 17 Gy dose to the boost volume and 6 Gy dose to the target volume. A dose profile from treatment plan was utilized to calculate TR for the VMAT-based Grid. In addition, for an available Grid block in our department the TR value was calculated from dose profile using EBT Gafchromic film. The Hug-Kellerer (H-K) radiobiological model (Equation 1) which is more appropriate at doses higher than 12 Gy was used to calculate survival fraction of cell lines under a single hole of the both Grids. The values of α/β ratios for tumor cells and normal cells were considered to be 10 Gy and 2.5 Gy, respectively.

Equation 1:

$$\begin{cases} SF = \sum V_i \, e^{(-k_1 D_i + k_2 (1 - \exp(-k_3 D_i)))} \\ \alpha = k_1 - k_2 . k_3 \qquad \beta = k_2 . k_3^2 . (\ln(2) - 1/2) / (\ln(2))^2 \end{cases}$$

Where the *Vi* represents the relative cell numbers receiving the same dose ranging from *Di* and *Di+1*. The therapeutic advantage of the Grid irradiation was considered in terms of the normal tissue cell survival ratio (Grid/open field ratio) for the same tumor cell survival. The therapeutic ratio (TR) was calculated for both VMAT-based and block-based Grids.

Results: Figure 1 shows a 2D dose distribution of VMAT-based and block-based Grids at the center of the phantom. The VMAT plan generated a highly spatially modulated dose distribution in the volumes. D95% and D50% for the cylinders and the target in Gy were 16.5, 17 and 6, 10 respectively. The valley to peak ratio of the VMAT-based and block-based Grid was 19% and 22% respectively. The Therapeutic ratio for VMAT-based and block-based Grid was obtained 1.25 and 1.38 respectively.

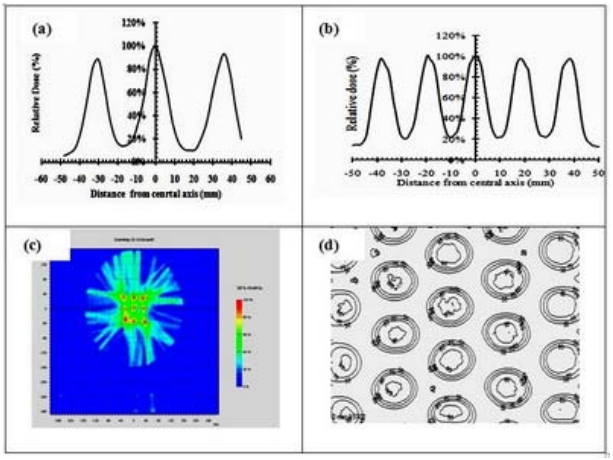

Figure 1-The beam profile for (a) the VMAT-based Grid and (b) the block-based Grid. Dose distributions of (c) VMAT-based Grid from treatment plan and (d) block-based Grid from EBT Gafchromic film.

Conclusion: The therapeutic ratio value obtained for VMAT-based Grid demonstrated the feasibility of volume arc therapy to deliver spatially fractionated radiation therapy technique which can help the treatment time with the additional potential advantage of reducing dose to the normal tissues.

PO-0948

A comprehensive evaluation of intracranial SRS treatment accuracy

T.A. Van de Water[1], P. Remeijer[1], F. Wittkämper[1], C. Schneider[1], M. Frantzen-Steneker[1], E. Damen[1], C. Panneman[1], J. Geuze[1], J. Kaas[1], R. Van Schie[1], A.M. Van Mourik[1]

[1]*The Netherlands Cancer Institute, Department of Radiation Oncology, Amsterdam, The Netherlands*

Purpose or Objective: This study provides a comprehensive overview of our geometric accuracy of frameless, linac-based intracranial SRS treatments. It is currently used to evaluate and further improve SRS treatment accuracy at our institute. Moreover, for other institutes, the overview may be used as reference material to supplement the more coarsely defined tolerance limits available in guidelines. To our knowledge, this is the first study that presents an overview of MRI/CT-to-RT treatment accuracies in such detail, combining regular QA data with clinical data, for a specific treatment.

Material and Methods: Our intracranial SRS treatments are based on a non-coplanar dual arc VMAT technique (table 0° and ±90°), in combination with an extensive online IGRT protocol with table correction verification and a post treatment CBCT. We systematically evaluated precision of the main elements of this SRS chain. We gathered patient set up data and image registration data, evaluated the imaging, treatment planning and QA protocols that were used, measured small fields (≤3 cm²) and compared this data with the TPS beam fit, and analysed QA data of the last couple of

years, including EPID-based Winston Lutz tests, table rotation inaccuracy measurements, leaf and jaw position accuracies and kV-MV isocenter measurements.

Results: Table 1 summarizes the precision of the separate elements in our intracranial SRS treatment chain. The largest inaccuracies of about a mm are found for imaging, delineation and treatment planning. Image registration, machine QA and patient setup show high sub mm accuracy. Resulting accuracies are in compliance with the SRS tolerances as mentioned in international and national guidelines (AAPM TG 142, NCS 22 and 24). The TPS dose grid will be adjusted to 2 mm (recommendation by AAPM TG 101). Furthermore, setup and image registration data are in good agreement with literature [1]. In addition to the upper tolerance limits from guidelines, this table provides detailed reference material regarding realistic machine and treatment accuracies for frameless, linac-based intracranial SRS.

	Accuracy [mm]						Type			Effect		Data based on	
	LR	CC	AP	SD_{LR}	SD_{CC}	SD_{AP}	estimated	tolerance	measured	shift	blur	# patients	# systems
Imaging													
CT voxel size	0.65	1.00	0.65						x				
CBCT voxel size	1.00	1.00	1.00						x				
MR													
voxel size	0.23	0.90	0.23						x				
gradient distortion	≤1	≤1	≤1				x			x			
Water/Fat-shift	≤1	≤1	≤1						x	x			
Image registration													
CBCT-CT translation error	0.02	0.02	-0.03	0.14	0.14	0.15			x	x		50	
MR-CT translation error	0.02	0.02	-0.03	0.14	0.14	0.15	x			x		50	
Delineation													
inter observer variability GTV	1	1	1				x			x			
Treatment planning													
Dose grid resolution	3.0	3.0	3.0						x		x		
Beamfit accuracy small fields [%/mm]	1/1	1/1	1/1						x		x		1
QA machine													
MLC position													
typical value Agility					0.12				x		x		3
typical value MLCi2					0.16				x		x		6
Leave bank/jaw positions													
centering (walkout)					0.4				x		x		9
Cross-hair centering (walkout)		≤0.25						x			x		
Mechanic-isoc – gantry 0° vs 180°		0.9-1.2							x		x		9
MV-isoc – 6MV FF R95%		0.86			0.2				x		x		9
XVI – typical KV/MV-isoc		0.2			0.3				x	x			5
Table													
rotation inaccuracy		0.5			0.2				x	x			6
residual translation error	0.3	0.5	0.5				x			x			
Setup													
Residual error				0.4	0.5	0.5			x	x		42	
Intrafraction motion				0.4	0.4	0.3			x	x		42	
Clinically applied margin GTV-PTV	2.0	2.0	2.0										

Table 1. Precision of the separate elements in our intracranial SRS chain. 'Effect' specifies whether the inaccuracy results in a *shift* or *blur* of the delivered dose distribution. It is important to note that the summed value of these separate inaccuracies does not correctly represent the total uncertainty in treatment delivery, but will give an overestimation (as values are correlated or maximum values and in the total treatment chain errors can compensate one another).

Conclusion: This method to comprehensively map and evaluate SRS treatment accuracy has allowed us to identify the most relevant sources of treatment delivery uncertainties and indicate items that require further investigation. Currently, relevant treatment uncertainties are further investigated and an end-to-end test is developed to further define and improve our accuracy. This approach can be extended to other stereotactic sites and techniques as well as to other institutes. We believe that comparing this kind of comprehensive data over institutes will also help to improve evaluation of treatment outcome as the actually delivered dose highly depends on the treatment accuracy.

[1] Seravalli E. et al., Radiotherapy and Oncology, 2015, Vol.116(1); pp. 131-8.

PO-0949

Automated approval of a pre trial benchmark RTTQA case. The ARISTOTLE experience.

L.N. Sweeney[1], E. Spezi[2], N. Cole[1], D. Sebag-Montifiore[3], R.A. Adams[1]

[1]*Velindre Cancer Centre, Clinical Oncology, Cardiff, United Kingdom*

[2]*Velindre Cancer Centre, Medical Physics, Cardiff, United Kingdom*

[3]*St James Institute of Oncology, Clinical Oncology, Leeds, United Kingdom*

Purpose or Objective: To demonstrate the feasibility of using a statistical algorithm, MDC-OVER-UNDER, as an automated assessment tool of a test case for radiotherapy outlining. If feasible, this efficient technique could be used to screen submissions for significant errors in outlining a radiotherapy quality assurance (RTTQA) pre-trial test case.

Material and Methods: UK centres submitted a neoadjuvant radiotherapy rectal cancer test case, prior to recruitment to the phase III ARISTOTLE trial. CERR (a computational environment for radiotherapy research) software platform was used for assessment. Previous pilot work using conformity indices to evaluate target volume delineation (TVD) in this trial had limitations. An MDC value of +/- 0.2mm from a single line reference volume calculated from ROC curve analysis, gave high sensitivity and specificity for slices which were over/under outlined. We were unable to satisfactorily validate this system owing to areas of "accepted" discrepancy from the reference standard (RS). In this work, a RS (non-margin generated) CTV with a minimum and maximum extent was created by two clinicians involved in the RTTQA process (fig 1). This was based on previous single line RS and iterative review of submissions from several centres. MDC-OVER-UNDER on a slice by slice basis, was applied to the individual institution submitted CTV. *For any slice of the volume to pass the automated assessment, both following criteria had to be met.* NB. An outline difference of 0.1mm is visually perfect.

1) For CTV MAX extent: MDC Over (mm) - 0.1mm = ≤ 0mm 2) For CTV MIN extent: MDC Under (mm) + 0.1mm = ≥0mm.

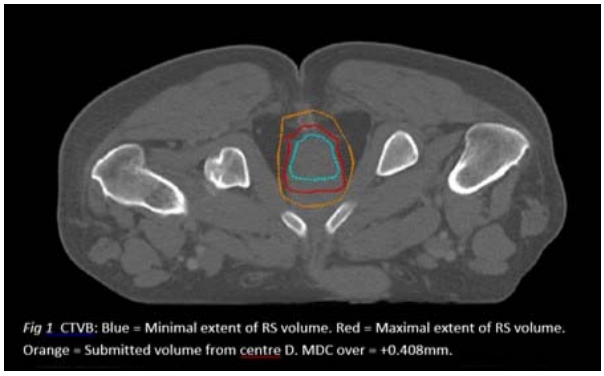

Fig 1 CTVB: Blue = Minimal extent of RS volume. Red = Maximal extent of RS volume. Orange = Submitted volume from centre D. MDC over = +0.408mm.

Results: We analysed 16 submissions from 10 centres. Data was saved in CERR format with uniform naming convention. The RS CTV ranged from maximum extent slices 30-53 (24 slices); minimum extent slices 31-52 (22 slices). Assessment of a submission was complete within seconds. The algorithm identified and quantified deviation for every outlined slice as expected. There was a quantifiable improvement in TV delineation in 75% of centres who had more than one submission, post feedback. Extra/missing slices were always associated with an MDC value greater then +/- 0.5mm respectively. Superior and inferior portions of the volume showed most discordance as reflected in the MDC values, with a tendency to over outline superiorly. Data was simply presented in Excel (see table) for review by centre and reviewer, highlighting and quantifying slices for revision.

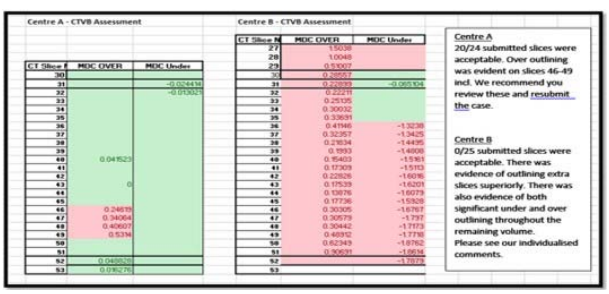

Conclusion: The MDC-OVER-UNDER analysis as an assessment tool, has the potential to reduce labour, reduce inter/intra observer variability and provide rapid quantified feedback. Consistently failing volumes would trigger protocol review in the first instance. Wider application in an RTTQA or educational setting requires a consensus min/max extent volume for several operator defined volumes by the TMG from the outset, supported by the STAPLE algorithm.
(Excluding spaces <2500 characters on word.)

PO-0950

QA and dummy-run results of the TRENDY randomized trial on SBRT vs. chemoembolization for HCC

S.J.M. Habraken[1], B.J.M. Heijmen[1], J. Buijsen[2], W.F.A.R. Verbakel[3], C.J.A. Haasbeek[3], M.C. Ollers[2], G.H. Westerveld[4], N. Van Wieringen[4], O. Reerink[5], E. Seravalli[5], P.M. Braam[6], M. Wendling[6], T. Lacornerie[7], X. Mirabel[7], R. Weytjens[8], L. Depuydt[8], S. Lang[9], O. Riesterer[9], K. Haustermans[10], T. Depuydt[10], A. Méndez Romero[1]

[1]*Erasmus MC - Cancer Institute, Radiotherapy - Physics and Instrumentation, Rotterdam, The Netherlands*
[2]*MAASTRO Clinic, Department of Radiation Oncology, Maastricht, The Netherlands*
[3]*VU University Medical Center, Radiation Oncology, Amsterdam, The Netherlands*
[4]*Academic Medical Center, Radiotherapy, Amsterdam, The Netherlands*
[5]*University Medical Center Utrecht, Department of Radiotherapy, Utrecht, The Netherlands*
[6]*Radboud University Medical Center, Radiation Oncology, Nijmegen, The Netherlands*
[7]*Oscar Lambret Comprehensive Cancer Center, Academic Radiation Therapy Department, Lille, France*
[8]*GZA Sint-Augustinus, Radiotherapy, Wilrijk, Belgium*
[9]*University Hospital Zürich, Department of Radiation Oncology, Zürich, Switzerland*
[10]*University Hospital Gasthuisberg, Radiation Oncology, Leuven, Belgium*

Purpose or Objective: The TRENDY trial is an international multi-center phase II study in which patients with hepatocellular carcinoma (HCC) are randomized between transarterial chemoembolization in the standard arm and stereotactic body radiation therapy (SBRT) in the experimental arm. SBRT is delivered in six fractions with a total target dose of 48-54 Gy. Since the treatment is technologically challenging, an extensive quality assurance (QA) program has been established. The main goal is to ensure high quality treatments in order to achieve an optimal clinical outcome.

Material and Methods: QA guidelines and recommendations are outlined in a separate QA protocol, which also defines minor and major protocol deviations. Treatment is not allowed with a major deviation. If possible minor deviations must be avoided. Centers can only start entering patients with a successfully completed external dosimetry audit. Prior to patient inclusion, a QA questionnaire should be filled out with regards to imaging modalities, treatment planning, patient setup, margins, breathing-motion management and treatment delivery. Besides that, centers are requested to complete a dummy run, including contouring and treatment planning. Contours are evaluated by comparison with golden contours, based on consensus within an expert panel. Treatment plans are evaluated using the constraints and objectives outlined in the treatment protocol, including an NTCP for the healthy liver. During patient accrual, the QA protocol accommodates prospective feedback for the first patients from each center.

Results: Ten participating institutes completed and submitted the dummy-run. All contours were considered acceptable, although variation in both liver and GTV contours was substantial as shown in the figure below. Both individual feedback and general recommendations regarding delineations have been provided. The results of the treatment planning round are summarized in the table below. Two centers (III and VII) did not meet the NTCP constraint initially and re-planned the dummy-run patient after feedback had been provided. Dose homogeneity and conformity vary substantially, with some institutes aiming at a high target dose allowing for large dose gradients in the GTV-PTV margin, and others optimizing for a smoother, more homogeneous, dose distribution.

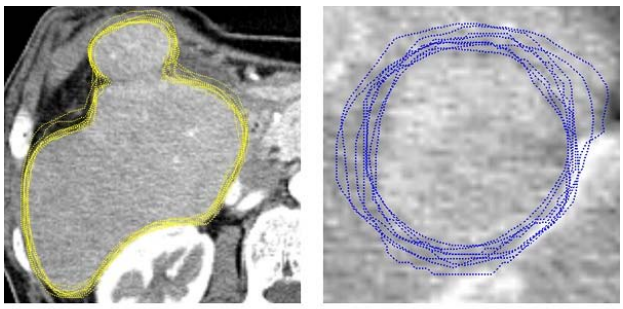

Item	Protocol	I	II	III	III*	IV	V	VI	VII	VII*	VIII	IX	X
D_{mean} CTV [Gy]	≥60	71.2	65.7	67.5	70.1	70.5	65.2	69.4	72.0	68.9	70.3	71.0	70.3
D_{mean} PTV [Gy]	≤72	71.1	65.7	67.5	70.6	70.5	65.2	69.3	72.0	68.9	70.4	70.9	70.3
PTV > 48 Gy [%]	>95	100	100	100	100	100	100	100	100	99.3	100	99.7	100
D_{mean} Liver – GTV [Gy]	≤ 22	15.9	15.7	16.9	14.9	15.9	15.4	17.1	18.4	14.2	17.1	14.7	17.2
Liver-GTV<23.4 Gy [cc]	>800	942	943	914	965	982	954	924	875	947	924	974	920
Liver-GTV NTCP [%]	≤5	2.5	3.2	7.0	0.8	2.1	1.2	3.9	22.7	0.2	4.4	0.5	4.5
D_{max} Stom/Bow [Gy]	<39	18.3	18.0	22.9	14.7	20.8	17.0	19.5	19.5	14.7	19.1	16.7	19.2
V_{3000} Stom+Bow [cc]	<5	0	0	0	0	0	0	0	0	0	0	0	0
D_{max} Esophagus [Gy]	≤36	1.9	2.2	1.3	1.7	1.8	2.0	3.9	5.5	4.1	3.9	1.6	3.9
D_{max} Spinal Cord [Gy]	<24	6.9	8.9	14.7	12.2	5.6	7.2	8.8	6.2	5.7	8.8	7.7	8.8
$D_{2/3}$ right Kidney [Gy]	$D_{2/3}$<19.2	2.9	3.4	3.8	1.0	3.8	3.0	3.0	1.4	3.8	2.0	0.7	3.0
$D_{2/3}$ left Kidney [Gy]	$D_{2/3}$<19.2	0.9	2.7	0.5	2.7	5.4	0.7	2.0	3.2	1.1	3.7	2.8	2.0
Avoidable hotspots	none	none	none	none	none	none	none	none	none	none	none	none	none

Above: Axial slices with liver (left) and GTV (right) contours of the participating institutes. Below: Protocol requirements and planning dummy-run results. Roman numbers (I, II, …) refer to the institutes and replannings are indicated with an asterisk (*).

Conclusion: As part of the TRENDY randomized trial, an extensive QA program has been implemented including a dummy run. Individual feedback and general recommendations have been provided to the participating centers, and will continue to be provided while patients are included.

PO-0951

Radiation beam alignment and baseline dosimetry measurements for the Australian MRI-linac program

J. Begg[1,2], L.C. Holloway[2,3], G. Liney[2], B. Dong[2], S. Alnaghy[4], T. Causer[4], T. AlHarthi[5], A. George[1], G. Goozee[1], P. Vial[1], S. Arumugam[1], L. Glaubes[6], B. Whelan[7], B. Oborn[8], P. Metcalfe[4], D. Thwaites[9], P. Keall[2,7]

[1]*Liverpool hospital, Liverpool and Macarthur Cancer Therapy Centres, Sydney, Australia*
[2]*Ingham Institute, Medical Physics, Sydney, Australia*
[3]*Sydney South West Area Health Service, Liverpool and Macarthur Cancer Therapy Centres, Sidney, Australia*
[4]*University of Wollongong, Centre for Medical Radiation Physics, Wollongong, Australia*
[5]*Unviersity of Sydney, Institute of Medical Physics, Sydney, Australia*
[6]*University Hospitals Bristol NHS Foundation, Medical Physics, Bristol, United Kingdom*
[7]*University of Sydney, Radiation Physics Laboratory- School of Medicine, Sydney, Australia*
[8]*Illawarra Cancer Care Centre, Medical Physics, Wollongong, Australia*
[9]*University of Sydney, Institute of Medical Physics, Sydney, Australia*

Purpose or Objective: To develop and assess methodologies necessary for baseline alignment and dosimetry measurements for a fixed horizontal radiation beam as may occur in heavy ion and proton facilities and is the case for the Australian MRI-linac program (AMP)

Material and Methods: The AMP utilises a fixed horizontal beam which is parallel to the magnetic field. To maximise flexibility the entire linac system (a linatron and independent millennium MLC system, Varian Inc) can be moved on a rail

system towards or away from the isocentre position, which is defined by the isocentre of the MRI scanner. The rail system enables the linatron to be placed at 8 different positions from the linatron ranging from a SSD of 190-336cm. To verify alignment of the radiation beam for the different linac rail positions, radiation profiles were acquired in air at different distances from the target. From the profiles the central axis position (CAX) was used to establish the alignment of the radiation beam. To verify MLC alignment to the CAX without the ability to rotate the collimator, a series of half blocked fields were used, with abutting fields and picket fence tests used to verify positional accuracy. Standard scanning water tank systems can not be used within the MRI scanner due to both ferromagnetic components and lack of physical space. To enable a comparison of baseline data once the magnet is installed, water dosimetry measurements were compared with measurements within an adjustable solid water phantom.

Results: CAX measurements were successfully used to establish the alignment of the radiation beam for different linac positions. The reproducibility of the central position of the radiation beam was within 2 mm for all positions and the radiation beam alignment for all positions was within 0.5 degrees, demonstrating that the radiation beam was horizontal and not misaligned within that plane. MLC alignment was within 0.5mm of the CAX beam position at a source to surface distance (SSD) of 100cm and within 6.5mm at a SSD of 277cm. The solid water phantom set-up achieved comparable dosimetry with the water tank set-up, enabling future measurements to be undertaken safely within the confines of the MRI scanner.

Conclusion: We have developed a generalised methodology appropriate for the commissioning a fixed radiation therapy beam line. We have taken baseline (no magnetic field) alignment and dosimetry measurements for the AMP beamline, demonstrating that the rail system and MLC alignment are within tolerance. We have also demonstrated the equivalency of a solid water approach with a conventional water tank enabling future dosimetry measurements within the MRI scanner.

Poster: Physics track: Professional and educational issues

PO-0952

Blended teaching reduces interobserver contouring variability: first results of the FALCON project

B. De Bari[1], C. Salembier[2], M. Palmu[3], S. Rivera[4], J. Eriksen[5], S. Kaylor[6], A. Boyler[6], C. Verfaillie[3], V. Valentini[7]
[1]*Centre Hospitalier Universitaire Vaudois, Department of Radiation Oncology, Lausanne Vaud, Switzerland*
[2]*Europe Hospitals, Department of Radiation Oncology, Brussels, Belgium*
[3]*European SocieTy for Radiation and Oncology, ESTRO, Brussels, Belgium*
[4]*Institut Gustave Roussy, Department of Radiation Oncology, Paris, France*
[5]*Odense University hospital, Department of Oncology, Odense, Denmark*
[6]*RadOnc, eLearning Center- Inc., Fremont- CA, USA*
[7]*Catholic University, Department of Radiation Oncology, Rome, Italy*

Purpose or Objective: Interobserver contouring variability is one of the most important sources of uncertainty in radiotherapy. Blended learning techniques are formal educational programs in which students learn, at least in part, through delivery of content and instruction via digital and online media with some element of student control over time, place, path, or pace. In 2009, ESTRO launched the FALCON (Fellowship in Anatomic deLineation and CONtouring) project. This web-based project aims at the improvement of the skills and homogeneity in contouring among professionals and/or trainees in the field of radiation oncology by organizing live and online contouring workshops. This study reports the first results of interactive teaching during live workshops.

Material and Methods: We analyzed the contours of 66 participants to 2 live FALCON workshops and covering 2 clinical situations: the contouring of prostate cancer (35 participants) and the contouring of some Organs At Risks (OARs - brachial plexus, esophagus, trachea and proximal bronchial tree, 31 participants). In all the analysed workshops, delineations were done before and after interactive teaching. Variability of clinical target volumes (CTVs) contoured by participants and the impact of teaching courses was evaluated using the DICE indexes. Moreover, for the prostate case, 3 sub-regions were retrospectively identified and analyzed separately : the prostate base (upper 5 slices, total length: 1 cm), the mid-prostate (following 15 consecutive slices) and the prostate apex (five lower slices, total length: 1 cm).

Results: Table 1 summarizes data of the 2 workshops. Mean CTV DICE indices for the workshops ranged overall from 15% to 84.1% before the teaching lecture, and from 23.4% to 86.1% after teaching, but with large interobserver variations. Usually, a significant improvement in delineation was observed on DICE indices among participants compared to experts' delineations after the teaching lecture (two-tailed t-test P value ranging between 0.04 and <0.001). An improvement was also noted at a more qualitative analysis, with the contours being much more homogeneous amongst participants after teaching.

STRUCTURE	AVERAGE PRE-TEACHING DICE (%)	AVERAGE POST-TEACHING DICE (%)	AVERAGE DIFFERENCE (%)	P-VALUE
WHOLE PROSTATE	84.1	86.1	+2	<0.0001
PROSTATE BASE	57.3	68.9	+11.6	<0.0001
MID-PROSTATE	88.3	89.3	+1%	0.01
PROSTATE APEX	48.5	50.3	+1.8	0.35
TRACHEA AND PROXIMAL BRONCHIAL TREE	73.3	76.4	+2.1	0.33
OESOPHAGUS	65.1	77.1	+12	0.1
BRACHIAL PLEXUS	15	23.4	+8.4	0.03

Conclusion: Evaluation of the immediate impact of teaching contouring is feasible and FALCON teaching methods reduce interobserver variability in CTV delineation at workshops. ESTRO is strongly committed in the further development of the current and of the future live and online FALCON workshops. The long-term impact of the FALCON workshops will be further evaluated in the context of well designed ad hoc research projects.

Poster: Brachytherapy track: Breast

PO-0953

Intraoperative multicatheter implant for APBI or boost in conservative surgery of breast cancer

M. Cambeiro[1], F. Regueira[2], N. Rodriguez-Spiteri[2], B. Olartecoechea[3], J. Idoate[4], L. Pina[5], R. Martinez-Monge[1]
[1]*Clinica Universitaria de Navarra, Radiation Oncology, Pamplona, Spain*
[2]*Clinica Universitaria de Navarra, General Surgery, Pamplona, Spain*
[3]*Clinica Universitaria de Navarra, Ginecology, Pamplona, Spain*

[4]Clinica Universitaria de Navarra, Pathologist, Pamplona, Spain
[5]Clinica Universitaria de Navarra, Radiologist, Pamplona, Spain

Purpose or Objective: To assess the safety, feasibility and efficacy of free-hand intra-operative multi-catheter breast implant and peri-operative high-dose rate brachytherapy (FHIOMBI-PHDRBT program) in early breast cancer treated by breast conservative surgery (BCS).

Material and Methods: Patients with early breast cancer who were candidates for BCS and potential accelerated partial breast irradiation (APBI) were prospectively enrolled for the FHIOMBI-PHDRBT program. Patients suitable for APBI received PHDRBT (3.4 Gy BID for 10 in five days). Patients not suitable for APBI received PHDRBT as anticipatory boost (3.4 Gy BID for 4 in two days) followed by whole breast irradiation (WBI).

Results: From November 2008 to January 2015, a total of 119 patients were treated and 122 FHIOMBI procedures were performed. Median duration of FHIOMBI was 25 minutes. A median of 8 catheters (range 4-14) were employed. No intraoperative complications were observed. Severe early postoperative complications (bleeding) were documented in 2 patients (1.6%), wound healing complications in 3 (2.4%), and infection (mastitis or abscess) in 2 (1.6%). Late mammogram follow-up revealed oil cysts in 56% of patients but symptomatic fat necrosis in only 2 patients (1.6%). PHDRBT was delivered as APBI in 88 patients (74%) and as a boost in 31 (26%). The median CTV-T was 40.8 cc (range 12.3-160.5), median D90 of 3.32 Gy (range 3.11-3.85), median DHI 0.72 (range 0.48-0.82) median D10 in high-risk skin zone 1.94 Gy (range 0.92-3.37). With a median follow-up of 35 months (range 5.9-80.9) in the whole group and 37.7 months (range 7.6-80.9) in APBI patients, no local, elsewhere or regional failures were observed, only one distant failure in PHDRBT boost was documented. Cosmetic outcomes were evaluated in APBI patients as excellent (42.0%), very good (46.0%), fair (10.0%) or poor (2.0%).

Conclusion: The FHIOMBI-PHDRBT program does not add complications to conservative surgery, it adapts to breast size and location of the tumor, fulfilling at the same time prescription requirements and constraints. It allows an exquisite selection of APBI patients and offers excellent results in disease control and cosmetics. It also offers logistic advantages as it dramatically shortens the time of local treatment and avoids further invasive procedures.

PO-0954

Early results of a multi-center trial of IORT using electronic brachytherapy for breast cancer

P. Costa[1], A.M.N. Syed[2], H. Chang[3], B. Schwartzberg[4], A. Bremner[5], S. Boylan[6], C. Lopez-Penalver[7], C. Vito[8], M. Davis[9], W. Dooley[10], A.B. Chakravarthy[11], C. Coomer[12], G. Proulx[13], S. Golder[14], O. Ivanov[15], K. Fernandex[16], M. Farha[17], V. Gonzalez[18], A. Bhatnagar[19], G. Neuner[20], K. Kopkash[21], S. Rahman[22], C. Corn[23]
[1]Instituto CUF, Radiation Oncology, Porto, Portugal
[2]Long Beach Memorial Medical Center, Todd Cancer Institute, Long Beach, USA
[3]UCLA, Revlon Breast Center, Los Angeles, USA
[4]Rose Medical Center, Sarah Cancer Research Institute, Denver, USA
[5]Breastlink, Surgical Oncology, Murietta, USA
[6]Sentara Northern Virginia, Radiation Oncology, Woodbridge, USA
[7]Doctors Hospital, Oncology, Miami, USA
[8]City Of Hope National Medical Center, Surgical Oncology, Duarte, USA
[9]Swedish Medical Center, Radiation Oncology, Englewood, USA
[10]Oklahoma University, Surgery, Oklahoma City, USA
[11]Vanderbilt University, Radiation Oncology, Nashville, USA
[12]Staten Island University Hospital, Comprehensive Breast Center, Staten Island, USA
[13]Exeter Hospital, Radiation Oncology, Exeter, USA
[14]Parkridge Medical Center, Shannon Cannon Cancer Center, Chattanooga, USA
[15]Florida, Department of Surgery, Orlando, USA
[16]MedStar Health, Breast Center, Baltimore, USA
[17]MedStar Health, Breast Center, Baltimore MD, USA
[18]University of Arizona, Radiation Oncology, Tucson, USA
[19]Cancer Treatment Services, Radiation Oncology, Casa Grande, USA
[20]Greater Baltimore Medical Center, Radiation Oncology, Baltimore, USA
[21]Rush University, Surgery, Chicago, USA
[22]Diablo Valley Oncology Hematology Medical Group, Radiation Oncology, Pleasant Hill, USA
[23]Phoenix Baptist Hospital, Department of Surgery, Phoenix, USA

Purpose or Objective: To describe early observations of a multi-center study utilizing a single fraction of intra-operative radiation therapy (IORT) using the Xoft® Axxent® Electronic Brachytherapy System® (eBx®) immediately following surgical resection of early stage breast cancer.

Material and Methods: 727 subjects have been treated at 25 hospitals. Upon meeting entry criteria, patients underwent partial mastectomy. While in the operating room a balloon applicator was placed in the lumpectomy cavity and inflated with saline (30–75 cc). The skin was closed over the balloon, a balloon surface-to-skin distance of >1.0 cm was confirmed, and a single fraction of IORT was delivered to the lumpectomy cavity. The prescribed dose was 20 Gy at the balloon applicator surface; the mean treatment time was 10.3 minutes. After treatment, the balloon was deflated and removed, and skin sutured.

Results: 726 subjects received the prescribed dose of 20 Gy; one received 21 Gy. 56 are removed from the primary analysis post-IORT due to subsequent whole breast irradiation (N=37), positive lymph nodes (N=7), positive surgical margins (N=4), re-excision (N=4), inadequate skin bridge (N=2), inadequate balloon conformance (N=1), and other (N=4). These subjects will be followed for the duration of the study. An additional 60 subjects have withdrawn, leaving 667 active subjects. The mean patient age is 65 years (44-88). 148 subjects (20%) had ductal carcinoma in situ, 550 (75%) had invasive ductal carcinoma, 28 (5%) were unknown. DCIS nuclear grade was high (N=55), intermediate (N=64) and low (N=27); 2 were unknown. Invasive cancer was Grade 1-2 in 465/550 cases. 93% (N=676) had T1 lesions, 7% (N=51) had T2 lesions. Mean tumor size is 10.53 mm ± 8.3 mm. Mean follow-up is 336 days (4-1096). Only 125/926 (13.5%) of the reported adverse events were Grade 2 or higher. The most frequent AEs are seroma (15.4%), breast pain (14.1%), erythema (10.7%), and induration (8.5%). Cosmesis was excellent-to-good in over half (65%) of the cases. There have been six (6) deaths (aortic aneurysm; heart attack; pneumonia; liver cancer; 2 unknown causes) and only one (1) recurrence reported to-date.

Conclusion: IORT using the Xoft System as part of the conservative treatment of breast cancer is safe, with low morbidity. Early results from this multi-center trial demonstrate this short, convenient course of radiation therapy for select patients with early stage breast cancer has excellent-to-good cosmetic results and a low rate of low-grade adverse events.

PO-0955

PBI with interstitial HDR brachytherapy: acute and late toxicities & cosmetic results.

V. Cerboneschi[1], M. Mignogna[2], S. Linsalata[3], M. Mignogna[1]
[1]Ospedale San Luca, Radioterapia, Lucca, Italy
[2]Student Of Medicine, University, Pisa, Italy
[3]Ospedale San Luca, Fisica Sanitaria, Lucca, Italy

Purpose or Objective: Purpose: The study we report is for early stage breast cancer and is a multicentre clinical investigation of PBI achieved by interstitial HDR brachytherapy with intraoperative placement of catheters.

The aim of this study is to evaluate feasibility, acute and late toxicities and cosmetic results with a long follow-up.

Material and Methods: Methods and materials: From January 2005 to December 2013 a total of 445 patients were enrolled in the study, implanted during surgery and treated using a microSelectron-HDR brachytherapy Unit. The median age of the patients was 65 years (range 48-88 years). All those enrolled had an infiltrating ductal carcinoma in the absence of an extensive intraductal component and with clear surgical margins. Sentinel node biopsy was positive in 19,9% of patients and the 76,7% of patients have had estrogen therapy, 15,9% have had adjuvant chemotherapy. In the 95.75 of patient the histology was ductal infiltranting carcinoma, in the 51% of cases the stage was T1b, in the 35% was T1c. Adjuvant chemotherapy was given to 15,9% of patients and hormone therapy to 76,7% of patients. The reference dose is taken as 85% of the mean basal dose. A reference dose of 35 Gy (3.5 Gy in two fractions per day) was delivered to 17% and a dose of 32 Gy (4 Gy in two fractions per day) to 83%. The average time of overall treatment was five days (76,8% in 4-5 days and 23,2% in 6-7 day); the difference is due to festivity and hospital provenience. Catheters were implanted (average of 14) guided by templates in most cases with distance between holes of 16 mm, in a double or triple-plane arrangement in 99% of patients. The mean volume surrounded by the prescription-isodose was 69,2 cc (range 13-129 cc). The treatment plans were evaluated in terms of skin dose, natural dose-histogram, quality (mean 2,15 - range 1-3.04) and uniformity (mean 2.53 and range 1-3.54) index.

Results: Results: The average overall treatment time is five/six days starting from implant commencement. The incidence of acute and late toxicities are given in Table I. Cosmetic results were excellent/good in 81% of patients. In a follow-up of 96 months we observed a local control of 7,7% and in 1,5% metastatic disease.
Table II. Acute and late toxicities.

toxicity	*acute*	*late*
Erythema, grade III	4,1	
Dehiscence	4,4	
Reversible oedema	4,1	
Infection	2,7	
Sieroma	3,4	
Fever	3,1	
Highly pigmented skin		8,4
Telangiectasia		5,6
Moderate fibrosis		8
Medium fibrosis		2
Scarring Keloids		0,4
Fat necrosis		1,7

Conclusion: Conclusions: The initial data demonstrates that an interstitial perioperative brachytherapy implant is a feasible method of treatment with good tolerance and good cosmetic results.

Poster: Brachytherapy track: Gynaecology

PO-0956
Audit of 100 consecutive cervical cancer patients treated with HDR CT guided brachytherapy

M. Zahra[1], L. White[1], L. Bleakley[1], W. Keough[2]
[1]*Western General Hospital- Edinburgh Cancer Centre, Clinical Oncology, Edinburgh, United Kingdom*
[2]*Western General Hospital- Edinburgh Cancer Centre, Medical physics, Edinburgh, United Kingdom*

Purpose or Objective: To assess the outcome of patients treated with CT guided HDR brachytherapy for cervical cancer

Material and Methods: The records for 100 consecutive patients treated in our centre were reviewed. All patients prior to treatment had a biopsy for diagnosis, and a staging pelvic MRI and whole body PET scan. Treatment comprised of EBRT to a dose of 45Gy in 25 fractions given to the pelvis ± para-aortics with concurrent cisplatin chemotherapy. The brachytherapy was delivered in 3 fractions using a ring and tandem applicator with CT planning of each individual fraction and using information from a pre-implant planning MRI. The aim is to achieve HRCTV d90 of >80Gy whilst staying within the published parameters for the OARs. The outcomes in terms of survival and pattern of relapse were recorded and correlated with the HRCTV d90 and volume, and the dose to the OARs. The unpaired t-test and pearson correlation coefficient were used with 2-tailed significance testing level of 0.05.

Results: The median follow up was 32 months with a median age at time of treatment of 44 years (21 – 85 years). Most patients were diagnosed with squamous cell carcinoma (77) or adenocarcinoma (17), 3 patients had an adenosquamous carcinoma and there were 4 cases with unusual histological findings of small cell, serous papillary (2) or neuroendocrine carcinomas. At the time of follow up 78 patients are alive, 21 died from disease and 1 died from unrelated causes. The median time to relapse was 8 months (range 1-23 months). There were 2 cases of isolated pelvic central recurrences, 11 cases of pelvic and distant metastases and 8 cases with only distant disease. The median d90 was 83.9Gy and the mean HRCTV volume was 32.3cm3 (range 9.0 – 83.9cm3). There was a statistically significant difference in d90 between patients with relapse v.s. no relapse ($t= 2.49$, $p=0.019$) and there was a strong negative correlation between the HRCTV volume and the d90 ($r= -0.48$, $p<0.0001$). The median doses to the OARs: rectum 60.3Gy (46.8 – 74.1Gy), sigmoid 66.9Gy (46 – 76.5Gy), small bowel 59.1Gy (43.7 – 75Gy) and bladder 75Gy (51.4 – 93.9Gy). There were 3 cases with grade 3-4 toxicity that could be related to the brachytherapy: 1 vesico-vaginal fistula, 1 recto-vaginal fistula, and 1 post treatment hydronephrosis.

Conclusion: CT guided cervical brachytherapy allows the delivery of adequate radiation doses to the HRCTV as shown by our acceptable local control and toxicity rates. The pattern of distant disease in the majority of relapses indicates that despite optimal staging investigations and adequate radiation doses to the HRCTV, distant undetected microscopic disease will still determine the outcome in a proportion of cases.

PO-0957
Focal boost to GTV in interstitial and intracavitary cervical brachytherapy - a feasibility study

N. Groom[1], N. Thiruthaneeswaran[2], G. Lowe[1], P. Hoskin[2]
[1]*Mount Vernon Hospital, Radiotherapy Physics, Northwood Middlesex, United Kingdom*
[2]*Mount Vernon Hospital, Cancer Centre, Northwood Middlesex, United Kingdom*

Purpose or Objective: Image guided plan optimisation with MRI and CT for interstitial and intracavitary brachytherapy is an established technique in treating cervical cancer. The purpose of this current study is to assess the feasibility of boosting the dose to GTV(BT) to 140% of the HRCTV prescription dose, while keeping critical structure dose volume histograms within tolerance.

Material and Methods: 14 MRI/CT guided treatment plans were analysed in this study. Patients were treated using either Vienna-style ring applicator or Fletcher-style applicator, with or without interstitial catheters. The median age of the patients was 51.5 years (range 25-80.2 years). One patient had FIGO Stage IB cancer, 10 had stage IIB cancer and 3 had stage IIIB cancer. All received IMRT external beam

radiotherapy (50.2Gy/27#, 50Gy/25# or 45Gy/25#) followed by brachytherapy (26Gy/4# or 28Gy/4# to HRCTV). In the current study the original treatment plans were re-optimised, using Brachyvision Version 11. The aim was to escalate the GTV(BT) dose to 140% of the original HRCTV prescription dose (8.4Gy and 9.8Gy/# respectively), keeping the HRCTV coverage and organ at risk DVH values within the tolerance which had been accepted for the original clinical plans. GTV (BT) and HRCTV were drawn according to GEC-ESTRO recommendations. The relationship between the volumes can be defined by the following equation. HRCTV2 = HRCTV1 – GTV(BT) The quality of the re-optimised plans was quantified by using dose volume histogram parameters.

Results: Table 1 shows a comparison of the original and the re-optimised plan parameters.In 10 out of the 14 cases (71.4%) more than 90% of the GTV(BT) was covered by the 140% isodose after re-optimisation.The HRCTV1 V100% was reduced for the re-optimised plans by an average of 2.95% (range 0.7-6.01%).Average coverage of HRCTV2 with the prescription isodose was 94.5% for the 6Gy plans, and 81.7% for the 7Gy plans.In 12 out of the 14 cases (85.7%) the treatment time was reduced with the boost plan.

6Gy/#	Original clinical plan				Re-optimised plan			
Patient number	HDRHR-CTV V100% of vol	HDR Bladder D2cc (Gy)	HDR Rectum D2cc (Gy)	HDR Sigmoid D2cc (Gy)	HDRHR-CTV V100% of vol	HDR Bladder D2cc (Gy)	HDR Rectum D2cc (Gy)	HDR Sigmoid D2cc (Gy)
1	97.7	5.3	3.9	4.0	95.1	5.5	3.8	3.9
2	90.8	7.5	3.1	3.7	86.8	7.6	3.2	3.9
3	99.3	5.0	2.8	2.3	93.3	4.3	1.8	2.0
4	97.3	5.3	1.5	3.8	95.2	5.4	1.6	3.7
5	99.0	5.1	2.2	4.1	98.5	4.9	2.2	4.0
6	99.7	3.9	3.1	4.1	97.7	3.1	1.9	3.7
7	97.9	4.8	2.1	4.1	97.2	4.2	2.6	4.1

Patient number	Number of needles inserted into GTV(BT)	IU inserted into GTV(BT)	$V_{100\%\ CTV2}$ (%)	$V\ 8.4_{Gy\ CTV2}$ (%)	GTV(BT) V8.4Gy (%)
1	4	0	94.8	48.60	98.8
2	1	0	88.0	65.60	89.6
3	0	1	92.4	65.70	97.8
4	3	0	93.4	61.80	92.8
5	Needles in close proximity to GTV(BT)	1	98.5	79.80	99.1
6	3	1	98.0	81.10	81.4
7	1	1	96.3	58.00	93.3

7Gy/#	Original clinical plan				Re-optimised plan			
Patient number	HDRHR-CTV V100% of vol	HDR Bladder D2cc (Gy)	HDR Rectum D2cc (Gy)	HDR Sigmoid D2cc (Gy)	HDRHR-CTV V100% of vol	HDR Bladder D2cc (Gy)	HDR Rectum D2cc (Gy)	HDR Sigmoid D2cc (Gy)
8	36.1	4.3	1.5	3.5	36.1	4.3	1.5	3.5
9	76.6	5.0	2.5	3.5	95.6	5.1	2.9	4.5
10	90.8	5.7	1.5	2.2	85.1	5.9	0.9	2.4
11	99.3	4.9	4.2	4.8	97.3	4.9	3.3	4.8
12	96.3	5.5	1.9	4.7	95.1	5.4	1.7	4.6
13	99.6	5.5	3.3	2.9	91.1	5.5	2.0	2.2
14	89.0	6.6	4.6	1.6	88.8	6.4	4.4	1.6

Patient number	Number of needles inserte into GTV(BT)	I inserte into GTV(BT)	V $7_{Gy\ CTV2}$ (cc)	V $9.8_{Gy\ CTV}$ (cc)	GTV(BT) V9.8Gy (%)
8	0	1	27.0	16.8	42.9
9	0	1	94.3	62.1	97.7
10	0	0	84.6	66.0	66.1
11	0	0	94.9	56.4	92.6
12	0	1	94.8	72.6	100
13	0	1	89.3	64.9	100
14	Needles in close proximity to GTV(BT)	1	87.0	42.7	95.5

Table 1: Reporting parameters for the standard and re-optimised GTV (BT) boost plan

Conclusion: It is possible to boost the prescription dose to the GTV(BT) to 140% for treatment plans with interstitial catheters and IU within the GTV(BT) volume. Plans without both interstitial catheters and IU in the GTV(BT) are most likely to be suboptimal. This planning study demonstrates that dose escalation to the GTV(BT) is feasible if clinically indicated, and further work into clinical application and outcome should be considered.

PO-0958

Locally advanced cervical cancer treated with IGABT: impact of the D90 HR-CTV on patterns of relapse

C. Chargari[1], R. Mazeron[1], P. Maroun[1], I. Dumas[1], F. Martinetti[1], A. Tafo-Guemnie[1], E. Deutsch[2], P. Morice[3], C. Haie-Meder[1]
[1]*Institut Gustave Roussy, brachytherapy, Villejuif, France*
[2]*Institut Gustave Roussy, Radiotherapy, Villejuif, France*
[3]*Institut Gustave Roussy, Surgical Oncology, Villejuif, France*

Purpose or Objective: Locally advanced cervical cancer patients with a bulky high-risk clinical target volume (HR-CTV) get the largest benefit of dose escalation in terms of local control. But the expected survival benefit could be lessened by a higher metastatic risk. We examined the patterns of relapse according to the HR-CTV and to the ability to reach the target dose.

Material and Methods: Pts treated with chemoradiation between 04/2007 and 02/2012 were included if they had a disease limited to the pelvis after an exhaustive primary staging (PET/CT plus primary laparoscopic para-aortic lymphadenectomy) and if they had received concurrent chemotherapy. Pts received pelvic irradiation (45 Gy) then a PDR brachytherapy boost +/- a pelvic sequential boost for PET positive pelvic lymph nodes. First sites of relapse were examined.

Results: 109 pts were included, with median follow-up of 39 months. Median D90 HR-CTV was 73.5 Gy in case of HR-CTV ≥ 30 cm3 (n = 28) *versus* 86.4 Gy in case of HR-CTV < 30 cm3 (p < 0.001). Pts with a not-bulky HR-CTV (< 30 cm3) experienced local failure in 5/81 (6.2%), *versus* in 6/28 (21.4 %) in case of bulky HR-CTV (p =0.03), but the HR-CTV volume did not correlate with the risk of local failures as only events. Pts with a bulky HR-CTV volume had a higher risk of distant failures: 10/28 (35.8 %) *versus* 7/81 (8.6 %) in case of not-bulky HR-CTV (p = 0.002). Local failures were seen in 3/47 (6.4 %) for pts with a D90 HR-CTV ≥ 85 Gy and in 8/62 (12.9 %) for pts with a D90 HR-CTV < 85 Gy, respectively (p=0.055). Distant failures were seen in 1/47 (2.1 %) and in 16/62 (25.8 %), respectively (p<0.001). This higher frequency of distant events in pts with a D90 HR-CTV < 85 Gy remained significant after exclusion of local failures: 0/44 (0 %) *versus* 11/54 (20.4 %), respectively (p < 0.001).

Conclusion: The inability to reach the target dose seems correlated with a higher propensity to metastases. Strategies integrating the metastatic risk are mandatory for maximizing the benefit of dose escalation.

PO-0959

Dosimetric outcome and perioperative toxicity using Utrecht applicator in cervical brachytherapy

F.J. Celada Alvarez[1], J. Burgos[2], S. Roldán[2], R. Chicas[2], D. Farga[2], M. Pérez[2], I. Paredero[3], J. Pérez-Calatayud[4], A. Tormo[2]
[1]*Universidad de Valencia, Programa de Doctorado de Medicina, Valencia, Spain*
[2]*Hospital Universitari i Politecnic La Fe, Oncología Radioterápica, Valencia, Spain*
[3]*Hospital Doctor Peset, Oncología Médica, Valencia, Spain*
[4]*Hospital Universitari i Politecnic La Fe, Radiofísica, Valencia, Spain*

Purpose or Objective: GEC-ESTRO recommendations for IGRT in brachytherapy, the incorporation of MRI in the planning and new MRI-compatible applicators have improved our treatments. But, in big tumours, intrauterine applicators don´t seem enough in order to reach a good coverage. Interstitial CT-MRI Utrecht (Elekta®) applicator with plastic needles lets improve HR-CTV and IR-CTV coverage sparing organs at risk. However, a further complication using interstitial applicators may be gynaecological bleeding during the withdrawal of the applicator.
The purpose of this study is to review perioperative toxicity and dosimetry in patients with cervix tumours using interstitial CT-MRI Utrecht applicator.

Material and Methods: Retrospective review of the records of 122 cervical cancer patients treated in our institution from

February´10 to September´15. To be included in the study, the treatment had to fulfill the criteria: (1) include a previous treatment of at least 45Gy of EBRT to the pelvis concomitant with cisplatin; (2) the BT boost consisted in insertion of interstitial Utrecht applicator under spinal anesthesia and individualized MRI planning. Each treatment was composed of 2 applications (7 days apart), with 2 separated fractions (in 24 hours) of nominal 7 Gy (the aim is to obtain the HR-CTV and IR-CTV D90 higher than 85 and 65 Gy EQD2 respectively keeping the OAR doses as low as possible with limits of D2cc of rectum and sigmoid lower than 70 Gy EQD2 and 85 Gy EQD2 in case of bladder). Applicator withdrawal was performed at the surgical theatre. Toxicity score (gynaecological bleeding) were defined by CTCAE v4.0.

Results: 110/122 (90.16%) patients were IIB stage or bigger, and in 68% of patients 6 needles were inserted in both applications. Median tumour volume at diagnoses was 39.8 cc (8.79-205) and median HR-CTV volume at first application was 18.01 cc (7.36-116.59). The final median biologically equivalent doses (EQD2) were D90 HR-CTV = 89.75 Gy10 (78.50-94.00) and D90 IR-CTV = 67.90 Gy10 (58.60-77.40).
For the first application, needles were used in all patients, and 4 (3.2%) patients required vaginal tamponade and/or stitch (Grade 2 CTCAE v4.0), and 2 (1.6%) patients required transfusion and/ or endoscopic intervention (Grade 3 CTCAE v4.0).
For the second application, needles were used in 114 patients, and 5 (4.3%) patients required vaginal tamponade and/or stitch (Grade 2 CTCAE v4.0) without bigger toxicities.

Conclusion: Our results suggest that interstitial IGBT as recommended by the GEC-ESTRO, is a safe option without life-threatening consequences due to bleeding, and dosimetric results compare favorably with the traditional technique.

PO-0960

Making MR-guided cervix cancer brachytherapy efficient: Are plan adaptation & daily planning needed?

J. Skliarenko[1], M. Carlone[2], K. Han[1], A. Beiki-Ardakani[2], J. Borg[2], J. Croke[1], R. Ujaimi[1], W. Levin[1], A. Rink[2], J. Xie[1], A. Fyles[1], M. Milosevic[1]
[1]*Princess Margaret Cancer Centre, Radiation Oncology, Toronto, Canada*
[2]*Princess Margaret Cancer Centre, Radiation Physics, Toronto, Canada*

Purpose or Objective: MR-guided brachytherapy (MRgBT) improves local control and survival in patients with cervical cancer. It is expected that MRgBT will be standard of care within 5 years. MRgBT is more demanding of resources and optimized processes will be of great importance in assuring its widespread availability. Our aim was to determine the value of imaging and adaptive replanning prior to each MRgBT fraction compared to a less resource intensive approach tailored to specific technique considerations.

Material and Methods: A total of 20 patients with cervical cancer who received external beam radiotherapy (EBRT: 45-50.4 Gy in 1.8-2 Gy fractions) and high dose rate MRgBT (28 Gy in 4 fractions using 2 insertions) were included in this study. A tandem/ring applicator (TR) was used in 9 patients, and a TR with interstitial needles in 4 patients for all 4 fractions. In 3 of these 4 patients, further plan adaptation with increase in number of needles was performed for fractions 3 and 4. In the remaining 7 patients, a TR alone was used for fractions 1 and 2 and a TR plus needles for fractions 3 and 4 to improve target coverage or OAR sparing. All patients underwent MR imaging, contouring and planning prior to each fraction. To simulate a more efficient approach with only one plan per insertion, optimized fraction 1 plan was applied to fraction 2 anatomy, and optimized fraction 3 plan was applied to the fraction 4 anatomy. To assess value of plan adaptation, projected total dose from first insertion was compared to the final total dose following plan adaptation.

Results: There was no systematic change in the high-risk clinical target volume (HRCTV) across fractions (mean range 41-44 cm3). Mean cumulative HRCTVD90 with daily plan optimization was 92 Gy10, and the mean rectal, sigmoid and bladder D2cc doses were 67, 65 and 83 Gy3 respectively. There were no clinically significant changes in the mean HRCTV or OAR D2cc doses with only two plans prior to fractions 1 and 3. The GEC-ESTRO HRCTV target dose >85 Gy10 was achieved in 16/20 patients with either daily plan optimization or planning only twice. All GEC-ESTRO OAR target doses (rectum <75 Gy3, sigmoid <75 Gy3, bladder <90 Gy3) were achieved in 14/20 patients with optimized daily replanning, and this was maintained when only two plans were used. Plan adaptation with addition of interstitial needles for second insertion resulted in improved HRCTVD90 dosimetry in 6/10 cases and in improved OAR dosimetry in 4/10 cases.

Conclusion: MRgBT can potentially improve outcomes of cervical cancer patients but is more resource intensive. This study suggests that improvements in efficiency can be achieved through process analysis and optimization. While adaptive MR-based replanning is fundamental to achieving the benefits of MRgBT, replanning at strategic intervals may be as effective as daily replanning with considerable savings in resources.

PO-0961

Retrospective dosimetric comparison of TG43 and a commercially MBDCA for gynecological brachytherapy

S. Pinto[1], A. Pereira[1], T. Viterbo[1]
[1]*Instituto Português de Oncologia do Porto Dr. Francisco Gentil Porto, Medical Physics, Porto, Portugal*

Purpose or Objective: To compare dosimetric plans using a commercially model based dose calculation algorithm (MBDCA) following TG186 recommendations, and the conventional TG43 method in an 192Ir high dose rate (HDR) gynaecological brachytherapy (BT) procedures using two types of cylindrical applicators.

Material and Methods: We analyzed the data of six patients with cervical carcinoma, receiving a 192Ir HDR brachytherapy treatment. The dose was delivered with a micro-Selectron afterloader. A treatment plan was performed using both the TG43 and TG186 dose calculation methods of the Oncentra Brachy v4.5 treatment planning system (TPS). Two cylindrical applicators, of 30 mm and 35 mm diameter were used: the Vaginal Applicator Set and the Shielded Cylindrical Applicator Set, by Nucletron. The treatment dose is prescribed at 0.5 cm distance from the cylinder wall (prescription point), with a treated extension of 3 cm. Analysis included dose volume histograms (DVH) for bladder and rectum and prescription point, according to American Brachytherapy Society (ABS) consensus guidelines (2012). The TG186 results were obtained using the standard accuracy level option of model-based algorithm (Oncentra Brachy-Advanced Collapsed cone Engine (ACE), Elekta), resulting in calculation times on the order of 40 s.

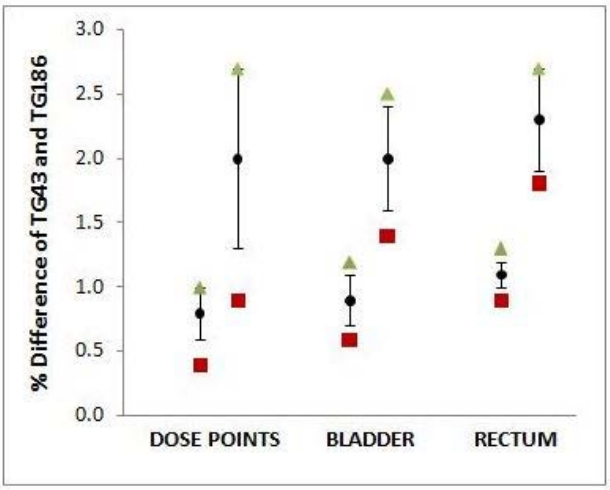

Figure 1 - Mean (point), maximum (triangle) and minimum (square) value and standard deviation (line) of the difference between TG43 and TG186 results, for the dose points, bladder and rectum.

Results: In all cases, the obtained dose following the TG186 method was lower than that obtained with the TG43 recommendations. Moreover, differences were found between the two described applicators (that had never been noticed with the TG43). The prescribed dose and the dose to 2cc of the bladder and rectum varied as follows (figure 1): between 0.4% and 2.7% for the prescribed dose, between 0.6% and 2.5% for the bladder and between 0.9% and 2.7% for the rectum.

Conclusion: Differences were found between the dosimetry plans obtained with the TG43 and our model based dose calculation algorithm following TG186 recommendations. A deeper knowledge of this new algorithm and its applications in a more accurate dose calculation will be the future of this work.

PO-0962

Adjuvant brachytherapy as a part of a multimodal treatment for high-grade uterine sarcoma

P. Annède[1], P. Maroun[1], C. Petit[1], R. Mazeron[1], I. Dumas[1], C. Genestie[2], P. Pautier[3], C. Chargari[1], C. Haie-Meder[1]
[1]*Gustave Roussy, Radiation Oncology, Villejuif, France*
[2]*Gustave Roussy, Pathology, Villejuif, France*
[3]*Gustave Roussy, Gynecology, Villejuif, France*

Purpose or Objective: To assess the loco-regional efficacy and toxicity of a multimodal strategy including brachytherapy (BT) as part of the adjuvant treatment of localized high-grade uterine sarcoma.

Material and Methods: A single center retrospective analysis of patients (pts) treated from 1985 to 2015 was conducted. 104 pts with high-grade uterine sarcoma were identified. 80 pts had leiomyosarcomas, 17 undifferentiated sarcomas, 3 rhabdomyosarcomas and 1 high grade adenosarcoma. 10 pts had a microscopic (n = 8) or macroscopic (n = 2) positive surgical margins.

Results: The median follow-up time was 5.4 years. 57 pts underwent perioperative chemotherapy. 102 pts underwent postoperative external beam radiation therapy (EBRT) followed by a BT boost, and 2 pts received BT without EBRT. The median pelvic EBRT dose was 45 Gy (range 25-50.4). 69 pts were treated with HDR BT (median dose = 10Gy), 33 with LDR (median dose = 15Gy), and 2 with PDR without EBRT (median dose = 60Gy). The 5-year local-regional failure-free survival and overall survival rates were 93% (CI 95% = 87-99%), and 73%(CI 95% = 0.63-0.84%) respectively. Only 5 vaginal recurrences were identified. 2 pts presented grade 3 late toxicity, all other side effects were grade 2 or less.

Conclusion: Adjuvant BT included in a multimodal treatment was associated with a high loco-regional control rate and acceptable acute and late toxicity in patient with localized high-grade uterine sarcoma.

PO-0963

Effectiveness of week 5 MRI virtual preplanning for Image-Guided Brachytherapy for cervical cancers

A. Chang[1], F. Cheung[2], T. Wong[2], E. Wong[3], F. Cho[3], C. Yip[1], I. Soong[1], A. Law[1], M. Lee[2], R. Yeung[1]
[1]*Pamela Youde Nethersole Eastern Hospital, Clinical Oncology, Hong Kong, Hong Kong SAR China*
[2]*Pamela Youde Nethersole Eastern Hospital, Medical Physics, Hong Kong, Hong Kong SAR China*
[3]*Pamela Youde Nethersole Eastern Hospital, Radiology, Hong Kong, Hong Kong SAR China*

Purpose or Objective: This study aims to demonstrate effective and non-invasive virtual pre-planning using week 5 MRI without the need of applicator in-situ for image-guided cervix brachytherapy.

Material and Methods: 15 patients with stage IB2-IVA cervical cancers were treated at our institution in January to October 2015 using chemoradiation and brachytherapy. All patients received whole pelvic radiotherapy 45Gy in 25 fractions over 5 weeks, with concurrent weekly cisplatin 40mg/m^2 for up to 6 cycles, followed by additional parametrial boosting 10-16G in 5-8 fractions over 1-2 weeks. HDR brachytherapy using Ir-192 was performed in all patients at week 6 and 7, using Vienna schedule[3] of 2 weekly insertions with 2 consecutive fractions per week, and first insertion was approximately 4-7 days after completion of whole pelvic radiotherapy. Treatment aim was 7Gy to HRCTV D90 each for 4 fractions. Week 5 MRI was performed in all patients, and $HRCTV_{wk5}$ was contoured. Virtual preplanning was done with proposed applicators according to pre-brachytherapy clinical assessment of dedicated oncologist. An estimated D90 for HRCTV ($D90_{wk5}$) was then compared with the actual D90 HRCTV at week 6 and week 7. Maximum diameter for HRCTV at week 6 were measured, and plans with suboptimal coverage after brachytherapy was regarded as having cumulative D90 HRCTV </= 83.9Gy.

Results: All 15 patients completed chemoradiation with schedule indicated. The choice of applicators was dependent on geometry of tumor (tandem and ovoids or ring or cylinder). Five patients were noted to have suboptimal tumor coverage, with cumulative D90 HRCTV dose ranging from 40.7 to 70.7 Gy. The corresponding maximum diameter of week 6 HRCTV was found to have significant correlation with cumulative HRCTV D90, and a cut-off value of tumor diameter 4.63cm could predict cumulative dose of 83.9 Gy. Based on the initial results, 2.5cm tumor radius from midline was decided to be the cut-off for using interstitial needles to improve dosimetry. With the implementation of interstital needles in September 2015, one patient received needle insertion based on virtual preplanning with estimated needle position and depth of insertion from week 5 MRI. Estimated HRCTV $D90_{wk5}$ tumor radius from midline was 3.6cm. Improvement of HRCTV $D90_{wk5}$ from 4.9Gy and 8.33 Gy was noted before and after virtual needle insertion. The subsequent week 6 and 7 brachytherapy using the preplanning information showed excellent correlation in terms of HRCTV D90 dosimetry, with cumulative $HRCTV_{actual}$ 89.2Gy (dose per fraction was 7.8, 7.5, 8.6 and 8.6Gy respectively).

Conclusion: This study demonstrates the effectiveness of a non-invasive method using week 5 MRI for virtual pre-planning, with accurate estimation of HRCTV, that can guide needle insertion diligently. Tumor radius of 2.5cm was proven to be a good reference to select patients for interstitial needle insertion.

Poster: Brachytherapy track: Head and neck

PO-0964

High-dose-rate interstitial brachytherapy as monotherapy for locally limited mobile tongue cancer

K. Yoshida[1], H. Yamazaki[2], T. Takenaka[3], T. Kotsuma[4], K. Masui[2], H. Akiyama[5], Y. Uesugi[1], T. Shimbo[1], N. Yoshikawa[1], H. Yoshioka[1], E. Tanaka[4], Y. Narumi[1]
[1]*Osaka Medical College, Radiology, Takatsuki, Japan*
[2]*Kyoto Prefectural University of Medicine, Radiology, Kyoto, Japan*
[3]*National Hospital Organization Himeji Medical Center, Radiology, Himeji, Japan*
[4]*National Hospital Organization Osaka National Hospital, Radiation Oncology, Osaka, Japan*
[5]*Osaka Dental University, Oral radiology, Osaka, Japan*

Purpose or Objective: In order to evaluate the usefulness of high-dose-rate interstitial brachytherapy (HDR-ISBT) as monotherapy for locally limited mobile tongue cancer, we analyzed our clinical experience.

Material and Methods: We investigated 29 locally limited mobile tongue cancer treated by HDR-ISBT as monotherapy at National Hospital Organization Osaka National Hospital between February 2001 and August 2012. The median age of the patients was 60 years (range: 34–84 years). All patients had histologically confirmed squamous cell carcinoma. According to the UICC classification of 2007, 3 T1, 18 T2 and 8 T3 were classified, respectively. The median tumor thickness of the patients was 10 mm (range: 2–45 mm). Ten (34%) medically poor risk patients (more than 80 years of age or severe intercurrent disease) were included. One patient had previous irradiation history. All but one patients received 54 Gy in 9 fractions. The other patient reduced his treatment doses (48 Gy in 8 fractions) because of previous irradiation history. We used three-dimensional planning for later 7 patients and delivered the prescribed doses to CTV (clinical target volume). Gross tumor volume (GTV) was defined with metal markers positions, applicator positions, intraoral ultrasonography and CT image. The GTV was equal to the CTV.

Results: The median follow-up time was 47 months (range; 10-171 months). The median V100(CTV) were 100%prescribed dose (range; 99.6-100%) for 7 evaluable patients. The 4-year local control rates were 100%, 73% and 88% for T1, T2 and T3. The 4-year overall survival rates were 67%, 66% and 31% for T1, T2 and T3. The 4-year local control rates were 88%, 83% and 60% for tumor thickness of <10 mm (12 patients), 10-19 mm (12 patients) and ≥20 mm (5 patients). The 4-year overall survival rates were 63%, 67% and 40% for tumor thickness of <10 mm, 10-19 mm and ≥20 mm. Four (14%) patients showed moderate to severe radiation ulcer.

Conclusion: Our treatment result of HDR-ISBT as monotherapy showed good local control result although there were many medically poor risk patients. Overall survival rate was worse for patients who had T3 tumor or tumor thickness of ≥20 mm.

PO-0965

125I seeds implantation under ultrasound guidance for local recurrent tumor of head and neck

P. Jiang[1], J. Wang[1], W. Ran[2], Y. Jiang[1], S. Tian[1], H. Sun[1]
[1]*Peking University Third Hospital, Radiation Oncology Department, Beijing, China*
[2]*Peking University Third Hospital, Ultrasound Department, Beijing, China*

Purpose or Objective: To evaluate the efficacy and safety of interstitial permanent low dose rate 125I seeds implantation under ultrasound guidance for local recurrent tumor of head and neck.

Material and Methods: A total of 70 patients (median age, 60years; range, 4–94 years) with malignant mass in head and neck were retrospectivel -y studyed (from Jan. 2004 to Oct. 2014). 6 were lost to follow-up, and 64 met the inclusion criteria. 81 lesions in head and neck implanted 125I seeds were evaluated. And 54 of 81 lesions were diagnosed cervical lymph node recurrence and another 27 lesions were local recurrence of primary or residual after first management. All the patient underwent 125I seed implantation guided by ultrasonography (Color Doppler Ultrasound with high frequency probe and guiding stabilization devices, Alokaα-10, Figure 1) with adequate local anesthesia. Postoperative dosimetry was routinely performed by TPS (3D treatment planning system; Beijing Fei Tian Industries, Inc.) for all patients. The actuarial D90 of the implanted 125 I seeds ranged from 100Gy to 160Gy (median:130Gy). The activity of 125 I seeds ranged from 0.3mCi to 0.8mCi (median: 0.69mCi). The total number of seeds implanted ranged from 3 to 89 (median: 20). The follow-up period ranged from1 to103.5 months (median: 14months).The survival and local control probabilities were calculated by the Kaplan-Meier method (SPSS 16.0).

Results: Among all the 81 lesions, totally response rate was 80.2% , 22 lesions had complete remission CR (27%) and 43 had partial remission PR (53%) . The 1- ,3-and 5-year tumor control rates were all 75.2% , 73% and 69.1%respectively. The results of cervical lymph node recurrence shows better than the recurrence or residue of primary head and neck neoplasm, with the local control of 5 year was 72.7% and 39.9% respectively. As of the date of follow-up, 22 of 64 patients still alive , The 1- and 3-,5-year overall survival rates were 57.4% , 31%, 26.6% respectively, with a median survival of 20 months. Grade 4 side effects of skin ulceration was seen in 2 patient; grade 1 or 2 skin reactions were seen in 11 patients (17%) who had received external beam radiation therapy before. Other severe complications were not seen.

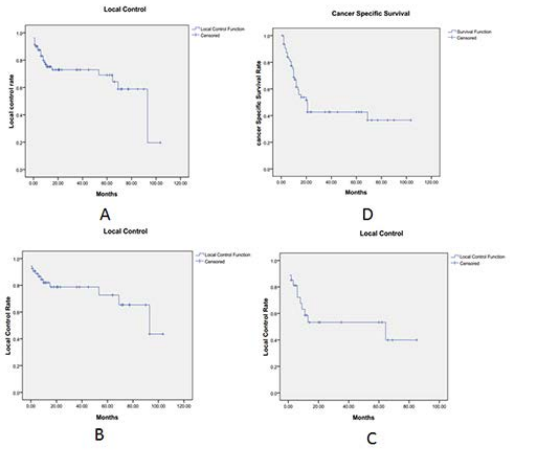

(A) Local control curve of 81 lesions, (B)) Local control curve of 54 cervical lymph node recurrences, (C) Local control curve of 27 recurrence or residue of primary, (D) Cancer specific survival curve of 64 patients

Conclusion: Interstitial permanent implantation of 125 I seeds under ultrasound guidance is feasible, efficacious and safe for refractory head and neck metastasis or recurrence.

Poster: Brachytherapy track: Physics

PO-0966

Dose planning of intraluminal brachytherapy for esophageal cancer using MR imaging

R. Reci[1], D. Förnvik[1], L. Lundgren[1]
[1]*Skåne University Hospital, Radiation Physics, Lund, Sweden*

Purpose or Objective: A new methodology using magnetic resonance (MR) imaging for brachytherapy dose planning of esophageal cancer has been developed. The main objective

have been to determine an MR sequence capable of visualising the tumour and finding a suitable esophageal applicator that can be visualised on the MR images.

Material and Methods: A total of six patients were included in this study. Each patient was scanned with one of two T2-weighted sequences, inversion recovery fast spin echo (IR FSE) or fast recovery fast spin echo (FRFSE). To reduce the motion artefacts in the images, the scanning was only triggered when the diaphragm was at the end-exhale position. The imaging was performed on a 3.0 T MR (GE Healthcare). Dose planning on the obtained MR images was performed using two different methods 1) dose was prescribed at 10 mm from the applicator's centre, which is the method currently used at Skåne University Hospital for treatment based on 2D images 2) dose planning was performed by manual optimisation, i.e. the dwell times were manually adjusted until adequate tumour coverage was reached. To our knowledge, an MR-safe esophageal applicator could not be found at the time of this study. Instead a modified duodenal tube was used. Different contrast agents were studied with the purpose to render the tube's visibility on the MR images.

Results: The esophageal tumour was successfully visualised and delineated on T2-weighted images with the FRFSE sequences, whereas the tumour in the MR images from the IR FSE sequences was difficult to visualise due to poor image quality. Furthermore, improved dose coverage to the tumour was observed when the dose planning was manually optimised to the tumour volume, where V100% to the tumour was increased from 70% to 95% and D90% was increased by 34%. Moreover, the esophageal applicator (duodenal tube) was filled with a saline solution, which was successfully visualised on the MR images.

Conclusion: Brachytherapy dose planning for esophageal cancer with MR imaging enhances tumour visibility and the ability to optimise the dose to the tumour volume and organs at risk.

PO-0967

Current practice in quality assurance of the Papillon50 contact X-ray brachytherapy system in the UK

L. Humbert-Vidan[1], T. Sander[2], C. Clark[3,4]
[1]*Guy's & St Thomas' NHS Foundation Trust, Radiotherapy Physics, London, United Kingdom*
[2]*National Physical Laboratory, Radiotherapy Physics, Teddington, United Kingdom*
[3]*National Physical Laboratory, Radiotherapy Physics, Teddington, United Kingdom*
[4]*Royal Surrey County Hospital, Radiotherapy Physics, Guildford, United Kingdom*

Purpose or Objective; Papillon50 contact brachytherapy has been used for early rectal cancer treatment in the UK since 1993. Currently there are four centres treating and a few more are in the process of implementation. The National Institute for Health and Care Excellence has issued guidance on safety and efficacy from a clinical perspective. However, there is currently no guidance on quality assurance (QA) testing. This review assessed any significant differences in machine QA practice between the current UK Papillon50 users. This is the first step towards standardising QA tests, tolerances and procedures in order to ensure that the accuracy of this technique is maintained at a high level across the UK.

Material and Methods: Each centre provided in-depth information regarding their QA programme. Details on machine-specific design characteristics were also taken into account. An inter-departmental comparison was made with regards to the QA tests performed, the frequency of each test, the accepted accuracy of the results with respect to the set baselines, the setup for each test and the equipment used.

Results: Significant differences were seen between centres in the QA tests in terms of types of test, frequency and acceptable accuracy. A tolerance variation of 10% versus 2% in the beam quality check and a difference of 2 mm versus 0.5 mm in the radiation field size check were observed. The manufacturer provides a calibration jig with which all four centres carry out radiation output measurements. However, each centre uses its own HVL jig design. There are significant design differences between these jigs with respect to the source-to-detector distance (SDD), the narrow beam geometry achieved and the backscatter conditions. All centres use the 1996 IPEMB CoP for the determination of absorbed dose for x-rays below 300 kV generating potential and its Addendum (2005) as a reference for the determination of the radiation output. However, the reference conditions stated in the CoP were generally not met due to the inherent design of the calibration jig used.

Conclusion: Significant differences exist between centres in the level of accuracy and extent of the QA programme. The very-low energy and short SDD in the Papillon50 system result in a very rapid dose fall-off. Differences in the design of the HVL jig may play an important role in the definition of the beam quality in such conditions. An extension of the CoP Addendum may be needed to include the achievable Papillon50 measurement conditions. This review highlights the need to carry out an independent audit in order to assess whether the inter-departmental variations observed could result in differences in the treatment received by patients.

PO-0968

Development of a fluorescent screen based QA system for dose verification of afterloading HDR unit

T.L. Chiu[1], B. Yang[1], H. Geng[1], W.W. Lam[1], C.W. Kong[1], K.Y. Cheung[1], S.K. Yu[1]
[1]*Hong Kong Sanatorium & Hospital, Medical Physics & Research Department, Happy Valley, Hong Kong SAR China*

Purpose or Objective: To develop and assess the feasibility of an in-house developed fluorescent screen based system on dose distribution verification of HDR brachytherapy treatment delivery.

Material and Methods: The QA system consisted of a solid water block with various thicknesses on top of a fluorescent screen (Kodak, Lanex regular screen) and a PMMA block below the screen. The fluorescent signal light was reflected by a mirror below the transparent PMMA to a CCD camera. The whole system was contained in a light tight box. Dose linearity was examined in a previous experiment. In measurement, an Ir-192 source was loaded to an applicator positioned on top of the solid water block. Single source dose distribution without entrance dose effect was first acquired to help obtain a universal light deconvolution kernel. It will then be used in subsequent image processing. Two source dwell positions were placed in each measurement with equal weighting. Source intervals were 5 mm and 10 mm. Four different measurement distances were selected, ranging from 5 mm to 30 mm away from the applicator. Various dwell times ranging from 0.8s to 8s were assigned at different depth to produce the optimal light output. Captured images were then processed by applying a median-filter and the deconvolution kernel to remove radiation induced noise and deconvolute the acquired image, respectively. After the image processing, images were normalized and a region of interest (ROI) (16 cm^2) was selected. Gamma index comparisons were performed between acquired dose distributions and the respective depth calculated by TPS (Elekta, Oncentra). Two profiles which cross the central line of the source dwell positions were obtained.

Results: The system can obtain a dose distribution with resolution 0.257 mm per pixel. Gamma index comparisons, (3% dose difference/1 mm DTA) were performed on all 8 conditions. Results were tabulated in Table 1.

Measurement distances (Dwell time for 5 mm interval, Dwell time for 10 mm interval)	5 mm source interval	10 mm source interval
5 mm(0.8s, 1s)	96.20%	97.40%
10 mm(2s, 2s)	100.00%	98.60%
20 mm(4s, 4s)	99.90%	99.80%
30 mm(8s, 8s)	99.50%	99.00%

Table 1 Gamma index passing rate for various distances away from the applicator.

All gamma indexes have passing rate above 95%. At measurement distances 10 mm to 30 mm, areas which failed to meet the gamma index criteria were, mostly, on the peripheral of the ROI. Gamma index near the source dwell position is well below 1. At measurement distance 5 mm away from source, the discrepancy between measurement and TPS calculation is the most severe. Both cases have points fail to meet the gamma criteria on the entrance path of the source. In particular, for 10 mm source separation, while assigning equal weighting for both dwell positions, measured data has two uneven signal peaks, as shown in Fig. 1 (d)-(f).

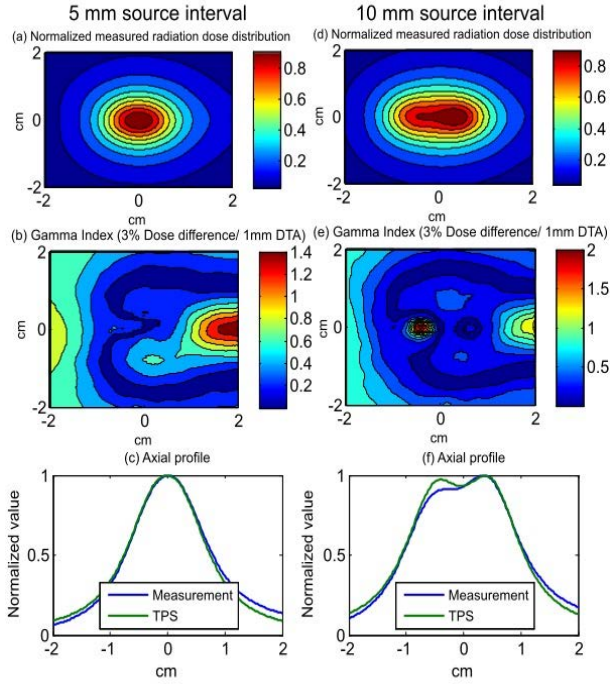

Figure 1 Measurement at 5 mm distance.

Conclusion: The system measured dose distributions agreed closely with TPS calculations, gamma index (3% dose difference/1 mm DTA) passing rates are all above 95% despite a high dose gradient near the source. Hence, this system can serve as a dose verification tool in afterloading brachytherapy. Besides, transit dose is detectable by this system but insignificant in a brachytherapy treatment.

PO-0969

Development of dose measurements close to brachytherapy sources in the German standard DIN 6803

F. Hensley[1], N. Chofor[2], A. Schönfeld[2], D. Harder[3]

[1]*previously University Hospital Heidelberg, Department of Radiation Oncology, Dossenheim, Germany*

[2]*Medical Campus of the Carl-von-Ossietzky University of Oldenburg, Clinic of Radiotherapy and Radiation Oncology – University Clinic of Medical Radiation Physics- Pius-Hospital, Oldenburg, Germany*

[3]*Georg-August University Goettingen, Prof. em.- Medical Physics and Biophysics, Göttingen, Germany*

Purpose or Objective: Due to the steep dose gradients close to a radiation source and the properties of the changing photon spectra, dose measurements in Brachytherapy usually have large uncertainties and are therefore scarcely performed in clinical routine. On the other hand, recommendations for experimental measurements are traditionally part of dosimetry protocols which in Germany are formulated in DIN standards. Within the revision of the outdated DIN standard for clinical brachytherapy dosimetry a working group (DIN 6803-3) was charged to formulate recommendations for brachytherapy dosimetry incorporating recent developments in brachytherapy in the description of radiation fields as well as new detectors and phantom materials. The Goal is to prepare methods and instruments e.g. to verify the emerging new dose calculation algorithms, for clinical dose verification and for in-vivo dosimetry.

Material and Methods: After an analysis of the distance dependent spectral changes of the radiation field surrounding a brachytherapy source, the energy dependent response of a number of typical brachytherapy detectors was examined with Monte Carlo simulations. A dosimetric formalism was developed which allows the correction of the energy dependence as a function of the source distance for a Co-60 calibrated detector. A number of phantom materials were examined with Monte Carlo calculations for their specific influence on the brachytherapy photon spectrum and on their water equivalence.

Results: A simple description of the energy dependence of a detector in the vicinity of a brachytherapy source was found by defining an energy correction factor kQ for brachytherapy in the same manner as in existing dosimetry protocols. The factor can be calculated as a polynomial of the distance from the source. Volume averaging and radiation field distortion by the detector are incorporated into kQ. Materials for solid phantoms were identified which allow precise positioning of a detector close to a source together with small correctable deviations from absorbed dose to water. Recommendations for the selection of detectors and phantom materials are being developed for different measurements in brachytherapy.

Conclusion: The introduction of an energy correction factor kQ for brachytherapy sources may allow more systematic and comparable dose measurements. In principle, the corrections can be verified or even determined by measurement in a water phantom and comparison with dose distributions calculated using the TG43 dosimetry formalism.

PO-0970

On the water equivalence of thirteen commercially available phantom materials in 192Ir brachytherapy

A. Schoenfeld[1], D. Harder[2], B. Poppe[1], N. Chofor[1]

[1]*Carl von Ossietzky Universität Oldenburg, Medizinische Strahlenphysik, Oldenburg, Germany*

[2]*Georg-August University Goettingen, Medical Physics and Biophysics, Goettingen, Germany*

Purpose or Objective: Thirteen commercially available phantom materials have been tested by Monte Carlo simulations of a typical 192Ir therapy source with regard to their suitability as water substitutes in high energy brachytherapy.

Material and Methods: The radial dose-to-water profiles in differently sized cylindrical water substitute phantoms surrounding a centric and coaxially arranged Varian GammaMed afterloading 192Ir brachytherapy source were compared to the corresponding dose-to-water profiles in equally sized water phantoms in order to evaluate the water equivalence of each phantom material within the clinically relevant source center distances up to 10 cm in the transversal plane. Monte Carlo simulations were performed in EGSnrc. The studied phantom materials are RW1, RW3 (both PTW, Germany), Plastic Water (as of 1995), Original Plastic Water (as of 2015), Plastic Water DT, Plastic Water LR (all CIRS, USA), Solid Water, HE Solid Water (both Gammex, USA), Virtual Water (Med-Cal, USA), Blue Water (Standard Imaging, USA), polyethylene, polystyrene and PMMA.
Phantom sizes were varied between diameters and heights of 10 cm and 60 cm to study the effect on the dose contribution by scattered photons. The radial variations of the total

spectral photon fluence and of the fluence contributions by scattered and primary photons were evaluated. The effects of phantom material composition, especially of the organic polymer density and of the amount of inorganic additives, were also studied in terms of the resulting linear attenuation coefficient μ.

Results: Significant differences were seen in the degree of water equivalence between the phantom materials covered by this study. While RW1, RW3, Solid Water, HE Solid Water, Virtual Water, Plastic Water DT and Plastic Water LR phantoms show dose deviations of less than 1.4% in all phantom sizes, Original Plastic Water (2015), Plastic Water (1995), Blue Water, polyethylene and polystyrene produce deviations up to 8.1 %. The role of PMMA is unique, showing deviations up to 4.3 % in phantoms with radii below 10 cm, but below 1 % in larger phantoms. Scattered photons with energies reaching down into the 25 keV region dominate the photon fluence at source distances exceeding 3.5 cm. The degree of water equivalence of a phantom material is correlated with the equivalence of its linear attenuation coefficient μ with that of water over a large energy range.

Conclusion: The key feature of a suitable water substitute material is the agreement of its linear attenuation coefficient μ with that of water over a large range of photon energies. This precondition provides water equivalence with regard to the attenuation of the primary photons, the release of low-energy photons by Compton scattering and their attenuation by a combination of the photoelectric and Compton effects. The instrument to achieve this goal is a balanced content of inorganic additives in a plastic phantom material.

PO-0971

Production of Gd-153 as a source isotope for use in rotating shield high dose rate brachytherapy

G. Famulari[1], A. Armstrong[2], T. Urlich[3], S. Enger[1]
[1]*McGill University, Medical Physics Unit, Montreal, Canada*
[2]*McMaster University, McMaster Nuclear Reactor, Hamilton, Canada*
[3]*McMaster University, Medical Physics & Applied Radiation Sciences, Hamilton, Canada*

Purpose or Objective: Brachytherapy (BT) can be administrated by low (E < 50 keV), intermediate (50 keV < E < 200 keV) or high (E > 200 keV) energy sources. For the lower energy sources, the photoelectric effect dominates the energy deposition and the dose distribution decreases rapidly as the inverse of the distance from the source. For the intermediate and high energy sources, Compton scattering is the dominant photon interaction. The attenuation in tissue is compensated by the photon scatter build-up of the dose. Radiation sources used in high dose rate (HDR) BT have conventionally provided near-isotropic or radially symmetric dose distributions, delivering very high doses to tumours but often with poor tumour dose conformity due to the asymmetric shape of the tumours. Rotating shield brachytherapy (RSBT), is a HDR BT technique delivered through shielded, rotating catheters, providing unprecedented control over radiation dose distributions. However, its application in clinical practice has been limited due to lack of an appropriate radiation source. In this work, gadolinium-153 (153Gd) was produced as source isotope for use in RSBT.

Material and Methods: A sample of isotopically enriched 152Gd with precisely known mass was irradiated in the reactor core at McMaster Nuclear Reactor (MNR) site. The radioactive 153Gd formed was counted on a high purity germanium detector to determine the effective neutron capture cross-section of 152Gd. A sample of natural gadolinium oxide powder was heated at 1000 °C in a muffle furnace to make it more compact. Radioactive gadolinium with known activity was loaded on a series of solid substrates and the remaining activity in the substrate was measured to determine the loading capacity for each sorbent. The maximum specific activity of 153Gd produced from enriched 152Gd at MNR was predicted by modelling studies. Finally, a prototype of the 153Gd source was encapsulated in a titanium casing.

Results: The effective thermal neutron capture cross-section was determined to be 500 b. The maximum density of gadolinium oxide after heating was 2.2 g/cm3, significantly lower than the literature value of 7.4 g/cm3, which refers to the metal oxide state. Dowex 50x6 resin was found to have the greatest loading capacity for gadolinium at 219.6 mg/g sorbent. 153Gd could be produced with a maximum achievable specific activity of 150 Ci/g of 152Gd at MNR after 3 months of continuous irradiation. 153Gd emits 40-100 keV photons with a dose distribution similar to that of iridium-192 (192Ir) due to its intermediate energy, but with much lower shielding requirements (TVL of 3.7 mm in platinum).

Conclusion: We have developed a means of immobilizing and encapsulating a 153Gd source for potential use in brachytherapy. A 153Gd BT source can be used in combination with a shielding system to deliver RSBT.

PO-0972

Clinical application and validation of a collapsed cone based algorithm for brachytherapy

A. Guemnie Tafo[1,2], I. Dumas[1], S. Koren[3], C. Tata-Zafiarifety[1], C. Petit[1], C. Haie-Meder[1], C. Chargari[1], R. Mazeron[1], F. Monnot[1], D. Lefkopoulos[1]
[1]*Gustave Roussy, Radiotherapy, Villejuif, France*
[2]*INSERM, U1030, Villejuif, France*
[3]*Rabin Medical Center, Radiation Oncology, Petach Tikva, Israel*

Purpose or Objective: In this study we evaluated the Advance Collapsed cone Engine (ACE) algorithm for clinical application to Brachytherapy. To this purpose, we followed 3 main objectives: 1) commission the ACE algorithm, 2) Validate this algorithm as compared to measurement and Monte Carlo simulation and 3) quantify the dosimetric differences observed as compared to TG43 for 3 common clinical indications.

Material and Methods: We followed the AAPM TG186 guidelines for MBDCA commissioning. This task group recommends to commission the dose calculation algorithm by 1) performing calculation in simple geometry 2) verifying dose calculation with hand calculation 3) comparing dose calculation results in complex geometries with a MC based algorithm. We developped a dedicated 6 source positions phantom allowing homogeneous dose distribution at the point of measurement in order to perform dose calculation and measurements in air and liquid water with or without heterogeneities introduced (Air, PMMA, Lead, Cortical Bone). Based on this phantom, we performed measurement using 3 different detectors, a A1SL detector, a Farmer chamber and TLD measurements. Measurements have been compared to dose calculated using ACE, TG43 and validated MC (MCNPX and Fluka). Finally ACE algorithm has been used on 19 Gynecologic, 11 Lips and 21 Penis patients where clinical common indicators (V250%, V100%, D2cc, V100%CTV ...) have been compared to TG43 and MC calculated dose distribution.

Results: Simple geometries with a uniform phantom have shown agreement within 0.3% between ACE and TG43 for both point and line sources. Using dedicated phantom, TG43 vs ACE in air and in water measurements with lead heterogeneity showed up to 95% difference and 86% respectively. ACE vs measurements showed an agreement within 3% in air and 0.3% in liquid water using several heterogeneity media (Table1).

	D_{TLD} (Gy)	Dm (Gy)	D_{TG43} (Gy)	D_{TG186} (Gy)	D_{TG186}/Dm	D_{TG186}/D_{TLD}	D_{TLD}/Dm
Without Heterogeneities	1,024	1,018	1,000	1,018	0,02%	0,61%	0,63%
PMMA	0,999	0,996	1,000	0,998	0,25%	0,06%	0,31%
Air	1,123	1,155	1,000	1,152	-0,29%	-2,52%	-2,80%
Lead	0,291	0,298	1,000	0,231	-22,40%	25,87%	-2,33%

Comparison between dose calculation with TG43 and TG186 and dose measurement with Ionisation chamber and TLD using Equal ESTRO phantom setup

For clinical cases, few differences have been observed between ACE and TG 43 in Gynecologic cases (up to 2.75% differences on the CTV and up to 1%,2% and 6% for D2cc of sigmoid, rectum and bladder respectively. For Penis cases large differences in glans volume covered by the 200% isodose up to 70% have been observed, and up to 10% for the 100% isodose volume in lips cases.

Conclusion: We have demonstrated that the use of an advance algorithm for Brachytherapy dose calculation is clinically and physically feasible. It shows good agreements with measured data. The use of such algorithms opens questions regarding the prescription and tolerances allowed in clinical use.

PO-0973

A novel approach to locating source dwell positions in HDR brachytherapy gynaecological applicators

R. Franich[1], M. Hanlon[1], R.L. Smith[1,2], C. Demsey[3], J.L. Millar[1,2]

[1]*RMIT University, School of Applied Science, Melbourne, Australia*

[2]*The Alfred Hospital, Alfred Health Radiation Oncology, Melbourne, Australia*

[3]*Calvary Mater Newcastle Hospital, Department of Radiation Oncology, Newcastle, Australia*

Purpose or Objective: Accurately locating the source dwell positions within HDR brachytherapy applicators is essential to ensure accurate reconstruction of the radioactive source path within the applicator for commissioning. Traditional approaches using radiochromic film are inefficient and limited to one or few dwell positions per film. The aim of this study was to develop a filmless procedure using a flat panel detector (FPD) source tracking system to accurately determine every dwell position and to correlate these with radio-opaque markers.

Material and Methods: The method was applied to two gynaecological HDR treatment applicators, incorporating interuterine tube/ovoids and an interuterine tube/ring combination. The disassembled applicators were fixed to the FPD. Auto-radiographs were captured by the FPD while the HDR source was dwelled at each available position. The location of the source was determined from these images. Using an external x-ray source, a radiograph was also captured, acquiring a combined exposure image. A subtraction method was then used to visualise the physical source in the applicator channel. Radiographs were also acquired with radio-opaque markers installed. Results of this new method were compared to traditional radiochromic film methods for distal dwell positions to compare commissioning approaches.

Results: The double-exposure image subtraction technique provided a method for visualising the active source and accurately determining its true location for all available dwell positions in each applicator channel (see Figure 1). Furthermore, determining the source dwell positions from the radiograph alone agreed with this projection-subtraction technique to < 1.0 mm for 34 out of the 35 available dwells of the ring channel (as an example). One position differed by 1.4 mm having been influenced by a high contrast feature in the radiograph. Distance to coincidence between the actual source positions and three positions identified by radio-opaque markers in the ring (dwells 1, 16, and 30) were measured and shown to differ by 0.7 mm, 1.0 mm and 0.7 mm respectively.

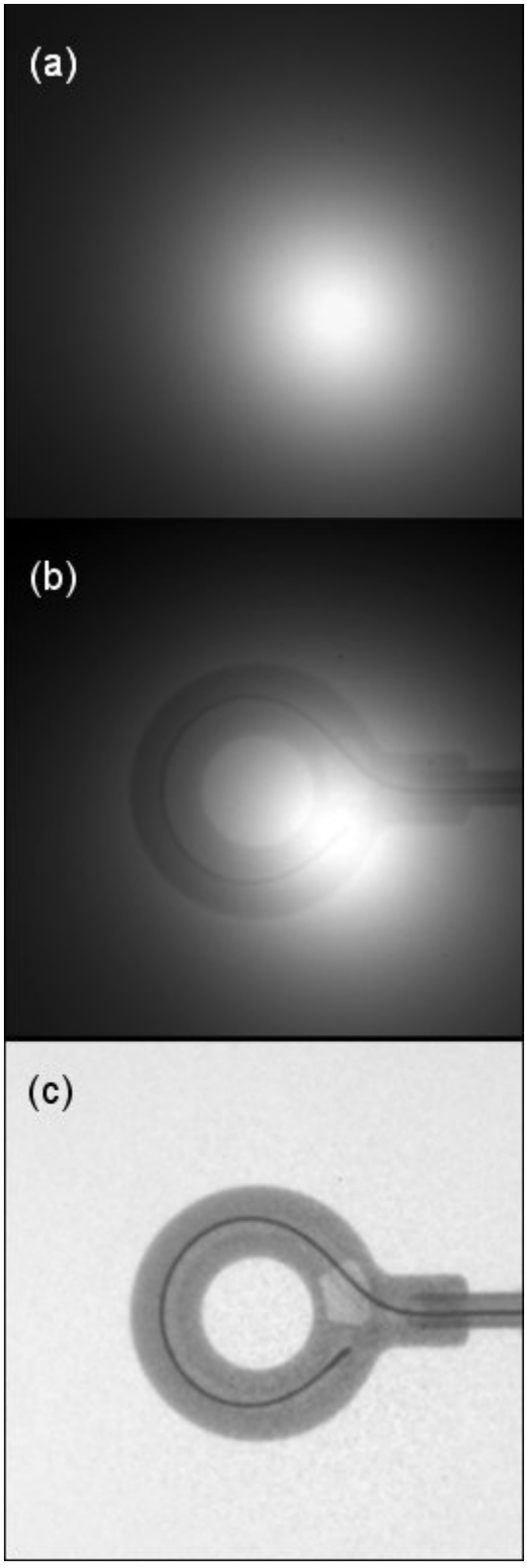

Figure 1: (a) Autoradiograph (source radiation) captured by the FPD. (b) Simultaneous external x-ray exposure and source

autoradiograph. (c) The subtracted image clearly showing the physical position of the source in the applicator and path of the drive cable through the applicator lumen.

Conclusion: We have demonstrated a filmless approach to determining actual source positions corresponding to each dwell position in each channel of two gynaecological HDR brachytherapy applicators. Accuracy is generally sub-millimetre and can also be used to quantify the accuracy of using marker-wire defined positions for reconstructing applicators in planning. The flat panel detector method is efficient and provides additional information not possible with radiochromic film.

Poster: Brachytherapy track: Prostate

PO-0974

Urethral and bladder dose of total and focal salvage brachytherapy: toxicity and dose constraints

M. Peters[1], J.R.N. Van der Voort van Zyp[1], C.J. Hoekstra[2], H. Westendorp[2], S. Van de Pol[2], M.A. Moerland[1], M. Maenhout[1], R. Kattevilder[2], M. Van Vulpen[1]
[1]*UMC Utrecht, Radiation Oncology Department, Utrecht, The Netherlands*
[2]*Radiotherapiegroep, Radiation Oncology Department, Deventer, The Netherlands*

Purpose or Objective: Salvage Iodine-125 brachytherapy (I-125-BT) constitutes a curative treatment approach for patients with organ-confined recurrent prostate cancer after primary radiotherapy. Currently, focal salvage (FS) instead of whole-gland or total salvage (TS) is being investigated, to reduce severe toxicity associated with cumulative radiation dose. Differences in urethral and bladder dosimetry and constraints to reduce late (>90 days) genitourinary (GU) toxicity are presented here.

Material and Methods: Dosimetry on intraoperative ultrasound (US) of 20 FS and 28 TS patients was compared. The prostate, bladder, urethra (figure 1) and bulbomembranous (BM) urethra were delineated. Toxicity was assessed using the CTCAE version 4.0. Dose constraints to reduce toxicity in TS patients were evaluated with receiver operating characteristic (ROC) analysis.

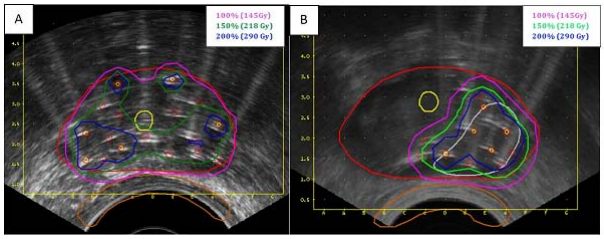

Figure. 1. Urethral (= yellow) D10 difference for TS (A) compared FS (B). The urethral D10 in A was 270 Gy versus 100 Gy in B.

Results: FS I-125 BT significantly reduces bladder and urethral dose compared to TS. Grade 3 GU toxicity occurred once in the FS group. For TS patients late severe≥grade 3) GU toxicity was frequent (38% in the total 61 patients and 56% in the 27 analyzed patients). TS patients with ≥grade 3 GU toxicity showed higher bladder D2cc than TS patients without toxicity (median 43 Gy) (p = 0.02). The urethral V100 was significantly higher in TS patients with several toxicity profiles:≥grade 3 urethral strictures,≥grade 2 urinary retention and multiple ≥grade 2 GU toxicity events. Dose to the BM urethra did not show a relation with stricture formation. ROC-analysis indicated a bladder D2cc <70 Gy to prevent ≥grade 3 GU toxicity (AUC 0.76, 95%CI: 0.56–0.96, p = 0.02). A urethral V100 <0.40 cc (AUC from 0.73–0.91, p = 0.003–0.05) could prevent other late GU toxicity.

Conclusion: FS I-125 BT reduces urethral and bladder dose significantly compared to TS. With TS, there is an increased risk of cumulative dose and severe GU toxicity. Based on these findings, bladder D2cc should be below 70 Gy and urethral V100 below 0.40 cc.

PO-0975

External beam radiotherapy with HDR brachytherapy boost in prostate cancer: 5- and 8-year results

R. Soumarova[1,2,3], T. Blažek[1], L. Homola[1]
[1]*Hospital Nový Jičín a.s., Department of radiation and clinical oncology, Nový Jičín, Czech Republic*
[2]*Agel Research and Educational Institute- o.p.s. – Nový Jičín Branch- Nový Jičín Hospital a.s., Oncology Department, Nový Jičín, Czech Republic*
[3]*Medical Faculty- Ostrava University, Department of Internal Medicine, Ostrava, Czech Republic*

Purpose or Objective: To report 5 and 8-year clinical outcomes, early and late complications in 226 patients with prostate cancer treated with high-dose-rate brachytherapy (HDR-BT) in combination with external-beam radiotherapy (EBRT).

Material and Methods: Between 2004 and 2010, 226 patients underwent HDR-BT in combination with EBRT as a treatment for their low, intermediate or high risk prostate cancer. The HDR-BT procedure was performed using ultrasound-based transperineal implantation. The total HDR-BT dose was 16 - 18Gy in 2. The EBRT technique used by treatment was 3D-CRT (70.3%) or IGRT/IMRT (29.7%) with daily correction of set up errors. Total dose of EBRT for low risk patients was 45Gy in 25 fractions of 1.8Gy within 5 weeks. For intermediate and high-risk patients the dose was 50.4Gy in 28 of 1.8Gy within 5 weeks. Patients were stratified by risk factors in to risk groups – 67 (29.5%) low, 87 (38.5%) intermediate and 72 (32.0%) high risk patients. Neoadjuvant hormonal therapy was applied in patient of intermediate or high risk of recurrence. High risk patients recieved adjuvant hormonal therapy.

Results: 5-year results after a mean follow-up of 70 months of the 226 patients the freedom from biochemical failure was 92.5%. 17 patients (7.5%) showed prostate specific antigen progression according to the Phoenix definition. In 9 patients clinical progression (bone or lymph node metastases) was documented. 8-year results after a mean follow up of 96 months of the 130 patients the freedom from biochemical failure was 82%. 23 patients (18.0%) showed prostate specific antigen progression. In 11 patients clinical progression was documented. Cancer specific survival during 5-year and 8-year follow up was 99.1% and 96.8% respectively. Toxicity was scored using the EORTC/RTOG score system. During follow up we haven´t observed any consequential toxicity or relationship between acute and late toxicity respectively. Higher incidence of GU and GIT toxicity was observed in patients treated by 3D-CRT technique. Acute and late gastrointestinal toxicity (GIT) was very low. Toxicity grade 2 was observed in 1.3% No grade 3 or 4 GIT toxicity was observed. Acute GU toxicity in most cases was grade 1 (40.2%) or grade 2 (10.6%). Late GU toxicity was also in most cases grade 1 (32.7%) or grade 2 (10.1%). Grade 3 toxicity was observed only in 2.2%. Grade 4 toxicity didn´t occurred. We have detected a trend that higher grade late GU toxicity was observed after longer period of treatment than lower grade. Mean time of occurrence for grade 3 and 2 was 64 and 23 months respectively, compared to mean time 12 months for grade 1.

Conclusion: Combination of external beam radiotherapy with high-dose-rate interstitial brachytherapy boost is safety and effective option in treatment localized prostate cancer. Our results show a low incidence of acute and late complications with favorable oncologic outcome after 5 and 8 year follow up.

PO-0976

HDR prostate brachytherapy: 3-D planned simultaneous integrated boost to the peripheral zone

R. Hepp[1], L. Herberholz[1], A. Petry[2], T. Eggert[3], L. Piotrowski[2], C. Morgenstern[1], G. Schabl[1], R. Galalae[1]
[1]*Evangelische Kliniken Gelsenkirchen, Klinik für Radioonkologie und Strahlentherapie, Gelsenkirchen, Germany*
[2]*Gemeinschaftspraxis Urologie Gelsenkirchen, Urologie, Gelsenkirchen, Germany*
[3]*Urologische Praxis, Urologie, Haltern am See, Germany*

Purpose or Objective: Radiotherapy (RT) is one of the most important curative options for treating localized prostate cancer (PC). At low α/β ratio of prostate tumors, HDR-brachytherapy (HDR-BT) represents a way to perform an absolute and radiobiologic dose escalation. When using 3-D real-time planning systems it is possible to optimize treatment plans generating dose distributions with an integrated boost (SIB) to peripheral zone (PZ) without substantially increasing the dose to the organs at risk (OAR), especially the urethra.
Aim: to analyze the dosimetric parameters (DP) and the acute toxicity of 30 consecutive patients (pts) treated with HDR-BT and a SIB to the PZ.

Material and Methods: From January 2014 to September 2015, 20 pts with intermediate/high risk PC were treated with combined external beam RT (EBRT 50 Gy/25 f) and HDR-BT (2 x 9 Gy in the 2nd and 4th week of the EBRT). In the same period, 10 pts with low risk PC were treated with HDR-BT monotherapy (3 x11.5 Gy, every 2nd week). In all implants a SIB of 20% (EBRT+HDR-BT) or 15% (HDR-BT monotherapy) to the PZ was planned. Equivalent dose at 2 Gy / fraction (EQD2), using α/β of 1.5 for target volumes and 3 for OAR, were calculated.

Results: Median age was 68 years (range 56-76). DP are presented in table 1. In 33/40 implants in pts with EBRT+HDR-BT dose-escalation to the PZ was reached (range 6 -44% of the prescribed dose). The median V100 for the prostate was 94.5% (CI ±1.6%). in 26/30 of the implants in pts with HDR-BT monotherapy the intended dose-escalation was reached (range 6 – 40% of the prescribed dose). The median V100 for the prostate was 92.8% (CI ±2.2%). No grade ≥3 toxicity was observed. Grade 2 toxicity was 13% and resolved within 1 month in 90% of the pts.

Table 1. Dose distribution parameters

Dose distribution parameters	Median	95 CI (±)
D90 Prostata (Gy)	9,8	0,2
D90 Boost (Gy)	12,0	0,3
Boost Factor (%)	123,9	3,6
D2cc Rectum (Gy)	6,6	0,4
D2cc Bladder (Gy)	5,4	0,4
D0.1cc Urethra (Gy)	11,5	0,4
EQD2 Prostata (Gy α/β 1.5)	112,1	2,1
EQD2 Boost (Gy α/β 1.5)	141,2	3,6
EQD2 Rectum 2 cc (Gy α/β 3)	75,1	2,1
EQD2 Bladder 2 cc (Gy α/β 3)	67,6	2,4
EQD2 Urethra 0.1 cc (Gy α/β 3)	117,2	3,1

Combined EBRT + HDR-BT (n: 20 pts, 40 implants)

Dose distribution parameters	Median	95 CI (±)
D90 Prostata (Gy)	11,8	0,4
D90 Boost (Gy)	14,0	0,3
Boost Factor (%)	119,1	3,6
D2cc Rectum (Gy)	7,6	0,6
D2cc Bladder (Gy)	6,5	0,6
D0.1cc Urethra (Gy)	14,9	0,4
EQD2 Prostata (Gy α/β 1.5)	135,6	6,4
EQD2 Boost (Gy α/β 1.5)	185,4	6,2
EQD2 Rectum 2 cc (Gy α/β 3)	51,3	4,9
EQD2 Bladder 2 cc (Gy α/β 3)	39,4	5,0
EQD2 Urethra 0.1 cc (Gy α/β 3)	154,9	6,0

HDR-BT monotherapy (n: 10 pts, 30 implants)

Conclusion: HDR-BT with SIB to the PZ is feasible in both combined and monotherapy settings. Acute toxicity was mild. Local control and late toxicity profile should be investigated prospectively.

PO-0977

Ten year patient reported Quality of Life following I-125 prostate brachytherapy monotherapy

A. Henry[1], B. Sethugavalar[1], T. Witteveen[1], B. Al-Qaisieh[1], P. Bownes[1], J. Smith[1], B. Carey[1], K. Franks[1], D. Mitchell[1], D. Bottomley[1]
[1]*St James Institute of Oncology, Clinical Oncology, Leeds, United Kingdom*

Purpose or Objective: This prospective longitudinal study quantifies patient reported Quality of Life (QoL) pre-treatment and up to ten years following permanent I-125 prostate brachytherapy delivered as monotherapy in a single institution

Material and Methods: 120 patients were asked to complete the Expanded Prostate Cancer Index Composite (EPIC) questionnaire, a comprehensive validated QoL tool designed to evaluate patient function and bother after prostate cancer treatment. Men completed the EPIC questionnaire before brachytherapy and at 8 time points after treatment (6 weeks; 6,10 and 18 months; 2,3,5, and 10 years). At each time point clinically relevant small, moderate and severe declines in QoL were defined as 0.2-0.5 times SD, 0.5-0.8 times SD and > 0.8 times SD of baseline function for each of urinary, bowel and sexual domains respectively.

Results: Response rates in the first two years were >90% but thereafter dropped to 75% at 5 years and 48% at 10 years. 50 patients (41.6%) responded at all stages. Maximal deterioration in mean urinary and sexual summary scores was noted 6 weeks after implant with severe urinary symptoms and moderate bowel/sexual symptoms at that point. At 6 months urinary and bowel QoL had improved to mild impairment which then fully resolved by 10 months. Sexual QoL remained mildly impaired throughout the 10 years. At 10 years new mild impairment of urinary and bowel QoL was also found.

Conclusion: Clinically mild changes in urinary, bowel and sexual QoL are found 10 years after I-125 monotherapy. The impairment in sexual function persists from treatment but urinary and bowel symptoms are new at 10 years and may be either a late effect of brachytherapy or due to increasing age.

PO-0978

Image-guided impact on the brachytherapy prostate treatment quality.

V. Cerboneschi[1], V. Ravaglia[2], M. Paoluzzi[3], M. Mignogna[4], M. Mignogna[1]
[1]*Ospedale San Luca, Radioterapia, Lucca, Italy*
[2]*Ospedale San Luca, Fisica Sanitaria, Lucca, Italy*
[3]*Ospedale San Luca, Urologia, Lucca, Italy*
[4]*Student, University, Pisa, Italy*

Purpose or Objective: Purpose: to evaluate the impact of the "image-guided" technology evolution on the implant quality in the interstitial brachytherapy with 125I seeds in the treatment of the prostate cancer.

Material and Methods: Methods and materials: from April 2004 until May 2014 we treated 306 patients with prostate cancer with permanent brachytherapy implants of radioactive 125I seeds with a prescription dose of 145 Gy. The technology is changed during the years and we identify 4 groups relative to each different image-guided method. Group 1: 107 implants from April 2004 until January 2007 using ultrasound guide in the transverse plane, fluoroscopic check and planning with 3D Prowess TPS; Group 2: 76 patients until October 2008 with Variseed 8.0 TPS and ultrasound both for transverse and longitudinal guide; Group 3: 43 patients until February 2010 with a "real-time" ultrasound guide both for transverse and longitudinal guide; Group 4: 80 patients with a new delivery system to assembly seed trains (Quicklink, BARD). For each group we calculate the mean D90 in the "postplanning" (evaluated on CT images after 60 days) and the difference between planning and postplanning in terms of D90 and V100 (dose fall-off). In the last group we evaluate also the difference, in terms of D90, V100 and maximum urethra dose between the theoretical planning and the effective implant, evaluated in the operating room on the ultrasound images at the end of the surgery.

Results: Results: in the 4 groups the results in terms of D90 are respectively 123±32Gy, 146±28Gy, 153±23Gy, 166±17Gy, as shown in Figure 1. The dose fall-off in terms of D90 is respectively 58Gy, 43Gy, 37Gy, 21Gy (as shown in Figure 2) and in terms of V100 17%, 10%, 8%, 4%. In the last group the mean theoretical D90 and V100 are 187Gy and 99%, against a real implant evaluation of 186Gy and 99%and the maximum urethra dose is 210Gy in the planning and 219Gy at the end of the implant. In the 30% of the patients of the "real-time" group we changed the number of seeds or needles composition during the implant, to reach the desired constraints and PTV coverage.

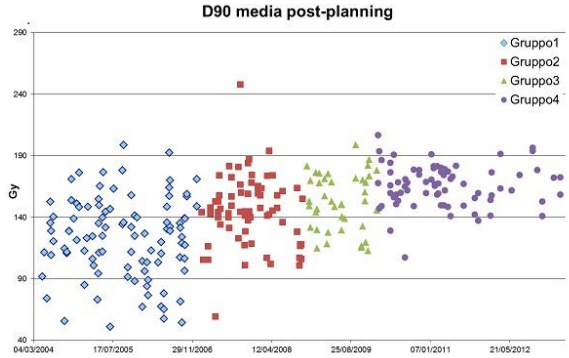

Conclusion: Conclusion: our work shows the impact of the "image-guided" technology evolution on the dose fall-off both in terms of D90 and V100. Moreover, we show how the "real-time" method allows to change the "theoretical" plan during the implant, to reach the recommended constraints and PTV coverage [1].

PO-0979

LTB control and toxicity for Favorable and Intmed Risk pts using real time IO-PSI prostate BT alone

A. Raben[1], A. Sarkar[1], A. Hanlon[2], H.C. Chen[1], F. Mourtada[1], A. Glick[3], M. Lobis[3], S. Terranova[3], T. Desperito[3], D. Cozzolino[3]

[1]*Helen F. Graham Cancer Center, Radiation Oncology, Newark- DE, USA*

[2]*University of Pennsylvania, Department of Nursing, Philadelphia, USA*

[3]*Brandywine Urology Consultants, Urology, Newark, USA*

Purpose or Objective: We initially reported biochemical control rate of 97% at 4 years of followup (Brachytherapy, 2009), which highlighted our methodology of limiting needle trauma, relying on Intra-operative, Real-Time computer assisted IO (Inverse Optimization) to reduce the number of sources and total activity without compromising dosimetric quality. This update was performed to confirm our earlier favorable BFFS outcomes.

Material and Methods: Between 2001 and 2013, 491 patients underwent real-time IO-PSI. Only patients with a minimum of 2 years of follow-up treated without supplemental IMRT were the subject of this analysis (N=315). Our dose objectives and constraints for real-time IO-PSI have previously been published and remain unchanged. The main dose objective intra-operatively was to achieve a V100 > 95% (Volume receiving > 95% of the prescribed dose). Patients were implanted with either ^{125}I (PD=145 Gy) or ^{103}Pd (PD =120 Gy). Toxicity was prospectively scored using the Radiation Oncology Group Toxicity scale and the International Prostate Symptom Score questionnaire. Biochemical control was determined using the nadir+2 ng/ml definition.

Results: The mean and median followup was 58 and 54 months respectively (range: 24-110 months). The NCCN risk classification for FR and IR patients were used. ^{125}I sources were used for 93% of the implants, and ^{103}Pd for 7%. 89% of patients presented with FR disease while 10% presented with IR, and in 2 cases HR. (1%). The median number of sources and total activity implanted were 65 and 999MBq, respectively. The median prostate volume implanted was 36 cc. The median V100 was 95%. Absolute BNED was 97%. The 10 year actuarial probability of biochemical control rate for all patients was 95%, with no difference observed between FR or IR patients (97% and 95% respectively) Late Gu and GI Grade 2 and higher toxicity was very low. With a minimum follow-up for 2 years, the late Grade 2 and Grade 3 GU toxicity was 19% and 1% respectively. The late Grade 2 and 3 rectal bleeding rate was 1% and 0% respectively, with no Grade 4 toxicity observed.

Conclusion: With extended follow-up of 10 years, real-time IO-PSI demonstrated excellent biochemical control rates with low incidence of toxicity confirming the validity of our original hypothesis and methodology of Inverse planning in real time for PSI, and comparing favorably to other alternatives at lower cost in the USA.

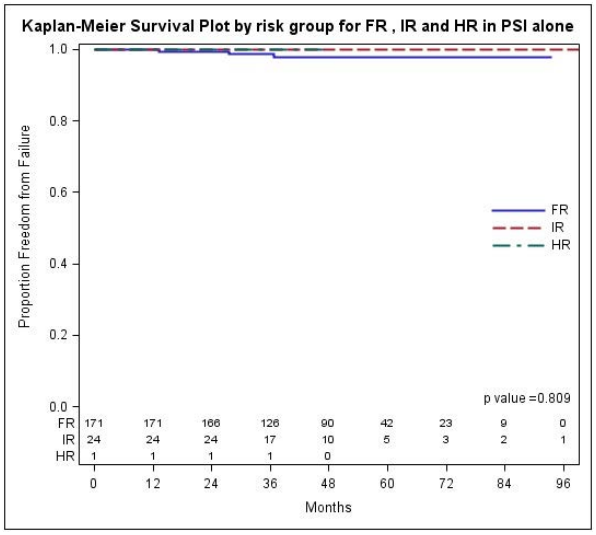

Poster: Radiobiology track: Molecular targeted agents and radiotherapy

PO-0980

Inhibition of STAT3 enhances the radiosensitising effect of Temozolomide in Glioblastoma model

I.A. Kim[1], T. Han[2], B. Cho[3], E. Choi[3], S. Song[2], S. Paek[4]

[1]*Seoul National Univ. Bundang Hospital, Radiation Oncology, Seongnam- Gyeonggi-Do, Korea Republic of*

[2]*Seoul National University, Graduate School of Medicine, Seoul, Korea Republic of*

[3]*Seoul National Univ. Bundang Hospital, Medical Science Research Institute, Seongnam- Gyeonggi-Do, Korea Republic of*

[4]*Seoul National University Hospital, Neurosurgery, Seoul, Korea Republic of*

Purpose or Objective: Despite aggressive treatment with radiation therapy plus temozolomide (TMZ), the prognosis for glioblastoma remains poor. We investigated the potential of targeting signal transducer and activator of transcription-3 (STAT3) to improve the therapeutic outcome of glioblastoma.

Material and Methods: We evaluated the preclinical potential of a STAT3 inhibitor, Cpd188 combined with temozolomide and radiation in vitro assays using two established glioblastoma cell lines (U251, U87) and two patients-derived glioblastoma cell lines (GBL12, GBL28) and in vivo studies using nude mice bearing intracranial U251 xenografts.

Results: Cpd188 potentiated the radiosensitizing effect of TMZ in U251 cell which has high levels of p-STAT3 expression. Increased radiosensitizing effects of TMZ were associated with impaired DNA damage repair, apoptosis and the reversion of epithelial-mesenchymal transition (EMT). Cpd188 delayed in vivo tumor growth both alone and in combination

with radiation and TMZ. We also confirmed the radiosensitizing effect of Cpd188 of GBL28 cell which was originated from a patient with high level of STAT3 expression and unmethylated MGMT.

Conclusion: Targeting STAT3 using Cpd188 could be a viable therapeutic approach to improve the outcome of current standard therapy for glioblastoma patients having high p-STAT3 expression regardless of MGMT methylation status.
Work supported by the grant (#2013R1A1A2074531) from the Ministry of Science, ICT & Future Planning to In Ah Kim.

PO-0981

Activation of immune cells and enhanced efficacy of radiotherapy by anti-TIP1 antibodies in cancer

D. Hallahan[1], V. Kapoor[2], D. Thotala[2], H. Yan[2]
[1]*Washington University School of Medicine, Radiation Oncology, St. Louis, USA*
[2]*Washington University, Radiation Oncology, St. Louis, USA*

Purpose or Objective: Purpose: Stress responses in cancer cells are exaggerated over that of normal tissues include signal transduction pathways such as GRP78, PKC, PLC, Rho and others. Many of these regulators of cell viability translocate of the cell membrane during the stress response. Mechanisms of protein transport include motor and scaffold proteins such as Tax Interacting protein-1 (TIP-1), which translocates to the surface of the cell membrane of cancer cells following exposure to ionizing radiation. TIP1 is a scaffold protein that moves proteins to and from the cell membrane. It is over expressed in poor prognosis cancers.

Material and Methods: Methods: We studied radiation induction of TIP1 by western immunoblot and flow cytometry. We used siRNA to knock down TIP1 in human GBM and NSCLC cell lines. We utilized Anti-TIP1 antibodies administered IV to mouse models of human cancer xenografts. We measured tumor growth delay. To assess the ability of mouse NK cells to target and kill anti-TIP1 antibody-opsonized lung cancers, we cultured H460, or LLC cells in 96-well plates at 37oC. After 40 hr., cells were irradiated with 3 Gy (or shield) to induce TIP1 expression. Cells were continued in culture for 4 hr. 10 ug/ml 2C6F3, NMIgG, or media were added and incubated for an additional 2 hr. Murine NK cells were added and Incubated for 16 hr. Cytotoxicity was then determined by cancer cells cytolysis. anti-TIP1 antibodies (Ab) that bind to the PDZ domain of this protein were administered IV to mice bearing irradiated human cancers.

Results: Results: Membrane protein western blots showed a significant increase in the expression of TIP-1 protein at 4 and 24 hrs following irradiation with 3 Gy as compared to 0 Gy untreated control tumors. Significant levels of the TIP-1 membrane protein were also present in the irradiated tumors, but not in untreated controls, as demonstrated by immunohistochemistry. Near-infrared imaging studies showed significant targeting and binding of anti-TIP-1 Ab to irradiated tumors compared to untreated tumors and IgG controls at 72 hrs. Knockdown of TIP1 and blocking Abs that bind to the PDZ domain of TIP1 enhance cytotoxicity in cancer but not normal tissues. Anti-PDZ-domain Abs significantly enhanced cytotoxicity in D54, H1299, H460 and A549 human cancer cells. We studied the mechanisms by which the Abs enhance cytotoxity and improve tumor control. Abs activate caspases 2, 3/7 in irradiated cancers. Moreover, Anti-TIP1 antibodies bound to the surface of cancer cells activated immune effector cells. In mouse models of human cancers, Anti- TIP1 Abs enhanced tumor growth delay after radiotherapy when administered IV to mouse models of human cancer.

Conclusion: Conclusion: Anti- TIP1 antibodies activate immune effector cells and enhance the efficacy of radiotherapy specifically in cancer without enhancing the response in normal tissues. TIP1 is a molecular target for the development of novel radiation sensitizing agents.

PO-0982

Therapeutic potential of the YB-1/Notch-3 interaction in prostate cancer

N. McDermott[1], A. Meunier[1], C. Haynes[2], A. Flores[2], A. O'Callaghan[1], L. Marignol[1]
[1]*Division of Radiation Therapy- School of Medicine, Radiation Therapy, Dublin, Ireland Republic of*
[2]*Mount Sinai School of Medicine, International Health, New York, USA*

Purpose or Objective: YB-1, a protein increasingly associated with tumour progression and treatment resistance in prostate cancer, is the only known ligand of the Notch-3 receptor. The Notch pathway is an evolutionarily conserved signaling system whose inhibition is under scrutiny as a novel therapeutic approach. We have previously identified elevated Notch-3 mRNA expression in high grade prostate cancer. This study investigated the anti-tumour properties of the YB-1 inhibitor Fisetin, a dietary flavonoid, in an isogenic model of radioresistant prostate cancer cells *in vitro*.

Material and Methods: An isogenic model of radioresistance was generated in 22Rv1 prostate cancer cells through exposure to 30 x 2-Gy dose fractions. YB-1 and Notch-3 expression were determined by western blotting in parent, aged-matched and radioresistant cells following irradiation (5Gy) and/or 60uM Fisetin treatment (24hrs). Patterns of expression were related to modification in cell cycle distribution through analysis of PI staining by flow cytometry and clonogenic survival. The anti-tumour effects of fisetin were compared to those of two notch inhibitors DAPT and Batimastat.

Results: Following a cumulative total dose of 60Gy, the resulting subline RR22Rv1 was associated with a significant increase in clonogenic survival (1.3 fold increase in survival after 2Gy and 2.2 fold increase after 10Gy) when compared to both parent 22Rv1 and aged-matched controls. YB-1 was detected in the cytoplasm of all three lines. Expression levels were elevated following irradiation (4Gy) in RR22Rv1. Radiation (5Gy) inhibited activation and nuclear translocation of Notch-3. Fisetin treatment led to a loss of Notch-3 cytoplasmic expression in RR22Rv1 cells. DAPT and Batimastat did not affect clonogenic survival of 22RV1 and RR22Rv1 cells. Fisetin induced G2 cell cycle arrest and significantly reduced clonogenic survival in untreated and 5-Gy irradiated parent and RR22Rv1 cells.

Conclusion: This study identifies potential role of the YB-1-Notch-3 interaction in the radioresistance of prostate cancer cells, and highlights fisetin as a novel therapeutic agent for the management of prostate cancer.

PO-0983

Nanoparticle mediated tumor vascular disruption: A novel strategy in radiation therapy

S. Kunjachan[1], A. Detappe[2], R. Kumar[3], S. Sridhar[3], G.M. Makrigiorgos[2], R. Berbeco[2]
[1]*Harvard Medical School- Brigham and Women's Hospital-Dana-Farber Cancer Institute, Department of Radiation Oncology- BWH/DFCI/HMS, Boston, USA*
[2]*Harvard Medical School- Brigham and Women's Hospital-Dana-Farber Cancer Institute, Radiation Oncology-BWH/DFCI/HMS, Boston, USA*
[3]*Nanomedicine Science and Technology Center- Northeastern University, Department of Physics, Boston, USA*

Purpose or Objective: More than 50% all cancer patients receive radiation therapy. Despite recent innovations, clinical delivery of curative radiation doses is strictly restricted by the proximal healthy tissues. Chemical/ biological agents to augment the radiosensitization of cancer cells are limited by severe off-target toxicity concerns. We propose a dual-targeting strategy using tumor vascular-targeted gold nanoparticles (which amplify radiosensitization) combined with the conformal image-guided radiation therapy to induce tumor vascular disruption. This is a unique concept with a clear translational path.

Material and Methods: Chemically synthesized, RGD-/PEG-functionalized gold nanoparticles (RGD:AuNP; ≈2 -3 nm) were characterized using STEM, TEM, and LIBS imaging. Following clonogenic assay, radiation damage was induced in Panc1 xenografts with 10 Gy and 220 kVp (Xtrahl, Inc). γ-H2AX, 3D-(confocal) vessel imaging and IHC were performed.

Results: Tumor vessel-targeted gold nanoparticles were subjected to conformal image-guided irradiation in Panc-1 tumor xenograft to induce tumor vascular disruption. By specifically targeting the early angiogenic tumor endothelium, RGD:AuNP circumvent the dense stromal diffusion pathways that often limits the penetration and permeation of anti-cancer drugs/ nanoparticles to the cancer cells - a limitation of current radiosensitization approaches. *In vitro* testing in HUVEC displayed ≥3 -fold difference (***P<0.0001) in radiation damage in the +RGD:AuNP/+IR compared to the controls. More to it, the sub-millimeter accuracy of image-guided radiation therapy facilitated improved therapeutic efficacy (95%-100% tumor dose distribution) and less off-target toxicities. Quantification of the DNA-strand breaks (by γH2AX) showed ≈3 -fold increase (P<0.001) in the radiation specific DNA damage in the 'nanoparticle-radiation' cohort (+RGD:AuNP/+IR: 57%) compared to the 'radiation' group (−RGD:AuNP/+IR:19%) and almost ≈10 -fold difference (P<0.001) compared to (+RGD:AuNP/−IR: 6% and −RGD:AuNP/−IR: 6%).

Conclusion: This dual-targeting strategy holds great translational potential in radiation oncology. The resulting vascular disruption substantially improved the therapeutic outcome and subsidized the radiation/ nanoparticle toxicity, extending its utility to intransigent/ non-resectable tumors that barely respond to standard therapies. This abstract presents the first in-depth experimental investigation of tumor vascular disruption with nanoparticles, a novel strategy in radiation therapy.

PO-0984

Combined inhibition of Chk1 and Wee1 kinases for cancer treatment

S. Hauge[1], G. Hasvold[1], M. Joel[1], C. Naucke[1], G.E. Rødland[1], R.G. Syljuåsen[1]
[1]*DNR - Norwegian Radium Hospital, Department of Radiation Biology, Oslo, Norway*

Purpose or Objective: Inhibition of checkpoint kinases Wee1 or Chk1 causes G2-checkpoint abrogation and mitotic catastrophe, particularly in p53 defective tumors. Based on this, Wee1 and Chk1 inhibitors are currently in clinical trials, combined with radiation or chemo-therapy. However, our previous work has shown that inhibition of Wee1 or Chk1 also causes DNA breakage in S-phase, largely due to high Cyclin-Dependent-Kinase (CDK)-activity followed by unscheduled replication initiation. Furthermore, recent work by others has shown synergistic anti-cancer effects after combined Wee1 and Chk1 inhibition. The aim of this study was to investigate whether S-phase DNA damage may contribute to the synergistic effects after combined Chk1/Wee1 inhibition.

Material and Methods: Osteosarcoma U2OS and lung cancer A549, H460 and H1975 cells were exposed to the Wee1 inhibitor MK1775 and/or the Chk1 inhibitors AZD7762, LY2606368, MK8776 and UCN01. The DNA damage marker gH2AX was analyzed in S-phase cells by flow cytometry. DNA damage signaling and inhibitory phosphorylation of CDK1 and CDK2 were examined by immunoblotting, and cell survival by clonogenic survival assays. CDK activity was measured in S-phase cells by a novel flow cytometry barcoding method. In this method, CDK-dependent phosphorylations (antibodies to phospho-BRCA2 S3291, phospho-bMyb T487 and phospho-Mpm2) versus DNA content (Hoechst staining) were examined in individual cells. Barcoding with Pacific Blue was included to reduce sample-to-sample variations. Loading of the replication initiation factor CDC45 was measured by a similar flow cytometry method and by immunoblotting after removal of unbound proteins by extraction with salt and detergent.

Results: We observed a strong synergy in induction of S-phase damage after combined Wee1 and Chk1 inhibition. Also, clonogenic survival was strongly decreased after the combined treatment. Surprisingly, this synergy could not be explained by increased CDK-activity, as S-phase CDK-activity did not correlate with induction of DNA damage after Wee1 and Chk1 inhibition. Wee1 inhibition caused a bigger increase in CDK-activity than Chk1 inhibition. However, Chk1 inhibition caused more S-phase damage and loading of the replication factor CDC45. The combination of Wee1 and Chk1 inhibitors further increased the CDC45 loading, and the extent of CDC45 loading correlated with DNA damage induction.

Conclusion: We have shown for the first time that combined Wee1 and Chk1 inhibition causes synergistic S-phase DNA damage, due to distinct effects of Wee1 and Chk1 kinases in regulation of CDK activity and CDC45 loading, respectively. This synergy can explain the synergistic anti-cancer effects obtained by simultaneous Chk1/Wee1 inhibition. We propose that combined Chk1/Wee1 inhibition may be useful together with radiation therapy to eliminate radioresistant S-phase cells.

PO-0985

Anti-GRP 78 antibodies bind specifically to cancers enhance efficacy of radiotherapy in cancer

D. Dadey[1], V. Kapoor[1], D. Thotala[1], D. Hallahan[1]
[1]*Washington University, Radiation Oncology, St. Louis, USA*

Purpose or Objective: Purpose: Glioblastoma demonstrates progression of disease within the high dose region of radiotherapy, in nearly all cases. The physiologic response within glioblastoma to radiation is in part dependent upon a pro-survival signaling. GRP78 was first described to regulate cellular stresses, including hypoglycemia, hypoxia and the ER stress response. GRP78 is an important regulator of cell stress, and binds to several pro-survival proteins. Antagonists to GRP78 include Kringle-5 and PAR4 which induce apoptosis in tumor vasculature endothelium and cancer cells. The molecular events that result from the ER stress response can enhance cell viability. GRP78 is overexpressed in poor prognosis cancers and is a molecular therapeutic target in poorly differentiated cancers.

Material and Methods: Methods: We studied radiation induction of GRP78 by western immunoblot and flow cytometry. We used siRNA to knock down GRP78 in human GBM and NSCLC cell lines. In order to study the potential relationship between radiation dose and induction of ATF6 activity, we treated D54 cells with 3 Gy and 6 Gy and analyzed GRP78 protein expression 48h after irradiation. We utilized Anti-GRP78 antibodies administered IV to mouse models of human cancer xenografts. We measured tumor growth delay using subcutaneous implants of human cancer xenografts.

Results: Results: We found that radiation induces the expression of GRP78 in glioblastoma. Antibodies to GRP78 enhanced radiation-induced cytotoxicity in glioblastoma but not normal cells. We found that radiation induced GRP78 expression is regulated through the ER stress response, and that ATF6 is responsible for the transcriptional induction of GRP78. Knockdown of ATF6 abrogates GRP78 induction and enhanced cytotoxicity from radiation. Moreover interruption of GRP78 signaling enhances therapeutic effects of radiation. GRP78 antibodies enhanced cytotoxicity from radiation in human glioblastoma and NSCLC cell lines. We found that the levels of GRP78 protein were elevated at the 48 and 72h time points. Knockdown of ATF6 was sufficient to abrogate GRP78 induction. We observed dose dependent increases in GRP78 levels, which were reproducible when the experiment was repeated with LN827 cells. Similar changes were observed in GRP78 mRNA levels 48h after IR, where a 75% and 100% increase was observed in D54. Anti-GRP-78 antibodies bind specifically to irradiated cancers enhanced the efficacy of

radiotherapy in human cancer models in vitro and in mouse xenografts.

Conclusion: Conclusion: GRP78 is a molecular target for the development of novel radiation sensitizing agents. Anti-GRP78 antibodies enhance the efficacy of radiotherapy when administered IV to mouse models of human cancer.

Poster: Radiobiology track: Tumour biology and microenvironment

PO-0986
MiR-143 inhibits tumour progression by targeting STAT3 in esophageal squamous cell carcinoma

B. Li[1], S.C.H.&I. Jia liu[1], S.C.H.&I. Yu Mao[1]
[1]*Shandong Cancer Hospital and Institute, Departments of Radiation Oncology Chest Section- Shandong Cancer Hospital and Institute, Jinan, China*

Purpose or Objective: The objective of this study was to investigate the biological role of miR-143 in esophageal squamous cell carcinoma (ESCC) progression and its underlying mechanism.

Material and Methods: Surgical tumor tissue samples were obtained from 40 patients. MiR-143 and STAT3 protein expression levels in these clinical samples and three ESCC cell lines were determined by quantitative RT-PCR and western blot. The relationship between expression level of miR-143 and clinical parameters were explored by one-way ANOVA. The specific targeting site of miR-143 in the 3'-UTR of STAT3 was identified using dual-luciferase reporter assays. Then, the effects of ectopic miR-143 or STAT3 expression on proliferation, cell cycle distribution, migration and invasion were determined in colony-forming assay, flow cytometry and transwell assay. The effect of miR-432 on tumor progression in vivo was determineded by performing tumor formation assay in nude mice. The role miR-143 in regulating cell cycle signaling, epithelial-mesenchymal transition and MMP up-regulation through repressing STAT3 was explored by analyzing the expression level of the downstream proteins.

Results: MiR-143 expression was downregulated in 90% of the ESCC clinical samples and its expression level was associated with the lymph node metastasis(LNM), invasion and TNM stage in ESCC patients. Functional experiments showed that ectopic expression of miR-143 could inhibit tumor cell proliferation, migration and invasion by supressing STAT3 in vitro. Animal experiments showed that the size of subcutaneous tumors derived from miR-143 overexpressing cells were significantly smaller than that of empty vector expressing cells. Further studies verified that miR-143 might regulate cell cycle, EMT and MMP up-regulation by targeting STAT3 and hence, lead to the suppresion of ESCC cell proliferation, migration and invasion.

Conclusion: Our study showed that miR-143 could act as a tumor suppressor through the inhibition of proliferation, migration and invasion by directly targeting STAT3 and subsequently mediates the downstream proteins. Thus, miR-143 has significant value in clinical and may serve as a prognostic marker and therapeutic target in the future.

PO-0987
MiR-432 inhibits tumor progression by targeting IGSF3 in esophageal squamous cell carcinoma

J. Liu[1], Y. Mao[1], B. Li[1]
[1]*Shandong Cancer Hospital and Institute, Department of Radiation Oncology- Shandong Cancer Hospital and Institute, Jinan, China*

Purpose or Objective: The objective of this study was to investigate the biological role of miR-432 in esophageal squamous cell carcinoma (ESCC) progression and its underlying mechanism.

Material and Methods: Surgical tumor specimens and adjacent tissue samples were obtained from 40 patients. Pearson correlation coefficients and linear regression model were used to explore the bivariate correlations between miR-432 and IGSF3 expression levels and one-way ANOVA were used to estimate the relationship between expression level of miR-432 and clinical parameters. Then the effects of ectopic miR-432 or IGSF3 expression on proliferation and apoptosis were determined using miR-432 over-expression or knockdown cells in colony-forming assay and flow cytometry, and the effects on cell migration and invasion were determined using a transwell assay. On the other hand, bioinformatic analysis were performed to assess the relationship between IGSF3 and miR-432, and this relationship was identified using a dual-luciferase reporter assay. Finally, the biological consequences of miR-432-mediated suppression of IGSF3 expression in ESCC cell lines were also determined by performing colony-forming assay, flow cytometry and trasnswell assay.

Results: MiR-432 expression was downregulated in 93% (37/40) of the ESCC clinical samples and its expression level was associated with LNM and TNM stage in ESCC patients. Functional experiments showed that over-expression of miR-432 induced an inhibition of cell proliferation, promotion of apoptosis and suppression of cell migraion and invasion in vitro by targeting IGSF3.

Conclusion: In conclusion, our results established a functional link between miR-432 and IGSF3 expression in esophageal cancer, demonstrating that IGSF3 was directly repressed by miR-432, which subsequently effects the tumor biological process. Collectively, this finding not only helped us understand the molecular mechanism of esophageal carcinogenesis, but also gave us a strong rationale to further investigate miR-432 as a potential biomarker and therapeutic target for esophageal cancer.

PO-0988
Combined treatment strategies for microtubule interfering agent-resistant tumors

A. Broggini-Tenzer[1], A. Sharma[1], S. Bender[1], K. Nytko-Karouzakis[1], M. Pruschy[1]
[1]*University Hospital Zürich, Department of Radiation Oncology, Zurich, Switzerland*

Purpose or Objective: Tumor cells are the major targets for classic anticancer treatment modalities. At the same time other cell types within the tumor microenvironment are also targeted and co-determine the treatment response. Resistances to specific treatment modalities are therefore not only linked to the mutated genetic background of the tumor cells but also to the interaction of tumor cells with the tumor microenvironment. Thus targeting of important elements of the microenvironment is a promising strategy to overcome treatment resistances in solid tumors. Here we mechanistically investigate in different clinically relevant microtubule-stabilizing agent (MSA)-refractory tumor models the potency of combined treatment modalities of MSAs, inhibitors of angiogenesis and ionizing radiation to overcome MSA-resistance.

Material and Methods: Rationally designed single and combined treatment regimens of ionizing radiation, microtubule stabilizing (taxane, epothilone) and de-stabilizing agents and anti-angiogenics compounds were investigated in genetically defined MSA-sensitive and MSA-resistant lung and colon adenocarcinoma cell lines in vitro and in the corresponding tumor xenografts in vivo.

Results: While MSAs potently inhibited A549wt and endothelial cell proliferation, no anti-proliferative effect was observed in the corresponding mutated MSA-resistant tumor cells. Importantly, MSAs did not block anymore pro-survival auto- and paracrine signaling from resistant tumor cells by downregulation of HIF1-alpha transcriptional activity and subsequent secretions of HIF-1alpha-mediated growth factors and cytokines like VEGF. Thereby continuous pro-survival

signaling from these resistant tumor cells resulted in an additional level of treatment resistance towards the combined treatment modality of MSAs and ionizing radiation in vivo. However, combined treatment of MSAs with clinically relevant mTOR-signaling- or VEGF-antagonists strongly re-sensitized MSA-resistant tumors (lung and colon carcinoma models) to the corresponding MSA. Interestingly, a novel clinically relevant microtubule-destabilizing agent, which is still active in MSA-resistant tumors, successfully overcame MSA-resistance in the lung and colon carcinoma models, downregulated the HIF1-alpha related aggressive tumor phenotype and strongly sensitized for ionizing radiation (bolus and metronomic scheduling).

Conclusion: These data demonstrate that the interaction between the tumor cell compartment and the tumor microenvironment strongly determines the tumor response to the combined treatment modality of ionizing radiation and microtubule interfering agents. A combined treatment modality of microtubule interfering agents with antiangiogenic agents is potent to overcome tumor cell-linked MSA-resistance and should be considered as clinical strategy for MSA-refractory tumor entities alone and in combination with radiotherapy.

PO-0989

Hypoxic and perfusion effects of Trastuzumab in a HER2+ oesophageal adenocarcinoma xenograft model

C. Yip[1,2], A. Weeks[1], G. Cook[1], D. Landau[1], V. Goh[1]
[1]*King's College London, Department of Cancer Imaging-Division of Imaging Sciences & Biomedical Engineering, London, United Kingdom*
[2]*National Cancer Centre Singapore, Department of Radiation Oncology, Singapore, Singapore*

Purpose or Objective: We aimed to evaluate the pathological hypoxic and perfusion effects of Trastuzumab (**T**) and/or Cisplatin (**C**) in HER2+ oesophageal adenocarcinoma xenograft (OE19) which may potentially direct future clinical adjunctive therapy.

Material and Methods: SCID mice (n=17) bearing subcutaneous OE19 tumours were treated with either (i) Cisplatin 4mg/kg once a week, (ii) Trastuzumab 20mg/kg twice a week or (iii) Cisplatin and Trastuzumab for 2 weeks. Intraperitoneal Pimonidazole (**Pm**), an exogenous hypoxic marker, and intravenous Hoechst 33342 (**Ho**), a perfusion marker, were injected 2 hours and 1 minute prior to tumour excision, respectively. Tumours were immediately snap-frozen and 10µm frozen sections were obtained for immunofluorescence study. Following fixation, non-specific binding was blocked using 10% normal goat serum. The sections were then incubated overnight at 4°C with primary Pimonidazole FITC labelled mouse monoclonal antibody at 1:25 concentration. Propidium iodide (**PI**) was used as a counterstain to highlight morphology. Tumour sections were scanned using different filters for Pm (green), Ho (blue) and PI (red) on a fluorescence microscope at x100 magnification (**Figure 1**).

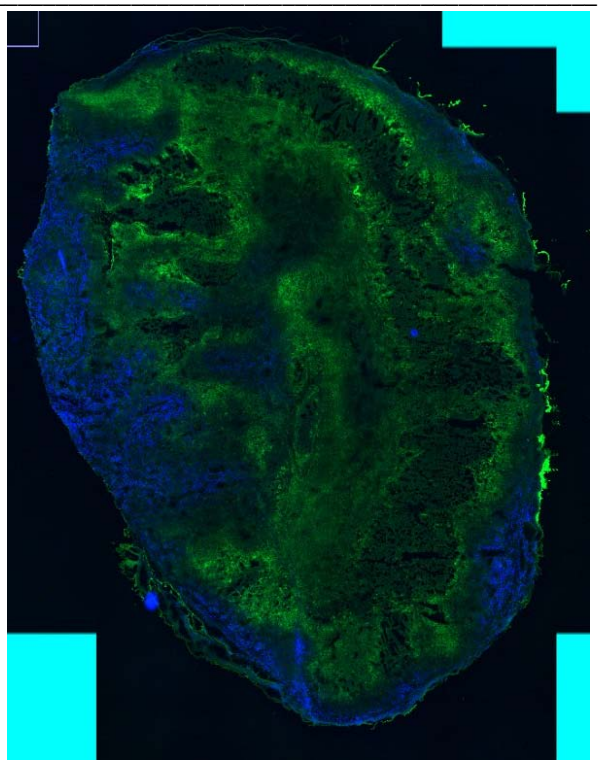

Image analysis was performed using the ImageJ software. Percentage areas stained with Pm (hypoxic fraction/**HF**) and Ho (perfusion fraction/**PF**) were derived and mean (%) ± SD are presented. Difference in the HF and PF between Trastuzumab (**T**) and non-Trastuzumab (**NT**) treated animals were analysed.

Results: Overall, tumour periphery was better perfused in most tumours but there was no consistent hypoxic intratumoral spatial localisation. There was an inverse spatial relationship between Pm and Ho fluorescence in 10/17 tumours, colocalisation in 3/17 and no relationship found in 4 tumours. Trastuzumab-treated tumours (HF 38%±17) were less hypoxic compared to the NT group (HF 50%±13) and these tumours were also better perfused (PF: T 46%±25, NT 39%±16). Cisplatin-treated tumours had the highest HF (50%±13) and lowest PF (39%±16) compared to Trastuzumab (HF 34%±13, PF 48%±26) and combination therapy (HF 41%±21, PF 45%±27).

Conclusion: Trastuzumab appeared to exert the predominant proangiogenic effect with improved perfusion and reduced intratumoral hypoxia, although these effects were diminished with combination therapy. These data suggest that the addition of hypoxia-modifying agents might be tested as an adjunctive therapy, particularly in those not eligible or fit for Trastuzumab therapy.

Poster: Radiobiology track: Normal tissue effects: pathogenesis and treatment

PO-0990

Impact of Ramipril on rat spinal cord after high- and low-LET irradiation

M. Saager[1], E.W. Hahn[2], P. Peschke[3], S. Brons[4], P.E. Huber[3], J. Debus[5], C.P. Karger[1]
[1]*DKFZ, Medical Physics in Radiation Oncology, Heidelberg, Germany*
[2]*The University of Texas- Southwestern Medical Center, Department of Radiology, Dallas- Texas, USA*
[3]*DKFZ, Clinical Cooperation Unit Molecular Radiooncology, Heidelberg, Germany*
[4]*Heidelberg Ion Beam Therapy Center, HIT, Heidelberg, Germany*
[5]*Heidelberg University Hospital, Department of Clinical Radiology, Heidelberg, Germany*

Purpose or Objective: In radiotherapy of head and neck cancer the central nervous system is the dose limiting factor. Late side effects may occur which severely impair the patient's quality of life. Thus, to improve the therapeutic ratio, radioprotective drugs receive increasing interest. In the optimal case, they could protect the normal central nervous system without influencing the tumor response to irradiation. A lot of studies using various approaches with e.g. melatonin, pentoxifylline, growth factors, Amifostine or Angiotensin converting enzymes inhibitors (ACEi) were performed focusing on mitigation or, ideally, on protection from late side effect in central nervous system (brain, optic nerve or spinal cord).

Material and Methods: Within our study the impact of ACEi Ramipril on prevention from the late side effect radiation-induced myelopathy (forelimb paresis grade II) was tested. The cervical spinal cord of female Sprague Dawley rats was irradiated with either 6 MeV photons or carbon ions (12C-ion) (a linear energy transfer (LET) of 45 keV/µm and a 6 cm spread-out Bragg Peak was used). Immediately after irradiation (RT) Ramipril (2 mg/kg/day) was given via the drinking water for 300 days. A total of four groups were used: (1) photon RT + Ramipril (n = 24), (2) photon RT only (n = 20), (3) 12C-ion RT + Ramipril (n = 20) and (4) 12C-ion RT only (n = 20). For each group a complete dose-response curve after single dose irradiation was established and TD50-values (dose at 50% complication probability) were determined for the development of paresis grade II within 300 days.

Results: Preliminary analysis of the data shows no marked shift of the TD50-values related to administration of Ramipril after 12C-ion or photon RT, however, a prolongation of latency time for both irradiation modalities was found. At a dose level of 21 Gy the minimum latency time after 12C-ion RT was 160 d compared to 191 d after 12C-ion RT + Ramipril administration. Whereas, at a dose level of 26 Gy the minimum latency time after photon RT was 191 d compared to 225 d after photon RT + Ramipril administration. Overall the latency time after 12C-ion RT was shorter compared to photon RT.

Conclusion: Ramipril administration after 12C-ion or photon RT exhibits a prolongated latency time. However, to find an ideal radiomitigator further examinations of the underlying pathological mechanisms leading to radiation-induced myelopathy are necessary. Additionally, since it is unclear how Ramipril interfers the pathological mechanism(s) of radiation-induced damage, it is important to understand the underlying mechanism. Thereby it would be possible to compensate potential weak points in inhibition by combination with other compounds.

PO-0991

p53 and in vitro radiation response of fibroblasts from RT-sensitive and -resistant patients

C. Herskind[1], O. Nuta[2], N. Somaiah[3], S. Boyle[3], M.L.K. Chua[4], L. Gothard[3], K. Rothkamm[5], J. Yarnold[3]

[1]*Universitaetsmedizin Mannheim- Medical Faculty Mannheim-Heidelberg University, Department of Radiation Oncology, Mannheim, Germany*

[2]*Public Health England, Centre for Radiation- Chemical and Environmental Hazards, Chilton, United Kingdom*

[3]*Institute of Cancer Research, Division of Radiotherapy and Imaging, Sutton, United Kingdom*

[4]*National Cancer Centre- Duke-NUS Graduate Medical School, Division of Radiation Oncology, Singapore, Singapore*

[5]*Department of Radiotherapy and Radiation Oncology, University Medical Center Hamburg-Eppendorf, Hamburg, Germany*

Purpose or Objective: To test the association between the molecular and functional radiation response of fibroblasts *in vitro* and breast cancer patients' risk of late reaction after radiotherapy.

Material and Methods: Fibroblast cultures were established by outgrowth from biopsies taken with informed consent from selected breast cancer patients with minimal (RT-resistant, n=15) or marked breast changes (RT-sensitive, n=19) after breast conserving therapy. The clinical risk of RT- sensitive patients was further ranked according to severity relative to external risk factors. Early-passage cultures were irradiated *in vitro* with 4Gy or sham irradiated. Molecular markers p53, p21/CDKN1A, p16/CDKN2A, α-sma, and Ki-67, were detected by immunofluorescence microscopy at 2h, 2 and 6 days after irradiation (IR). Plating efficiency (PE) and surviving fraction after 4 Gy (SF4) were determined by the colony formation assay. Non-parametric analysis of differences between fibroblasts from RT-sensitive and RT-resistant patients was performed with the Wilcoxon/Mann-Whitney test, and correlations using the Spearman's ρ rank correlation test.

Results: The basal level of p53 without irradiation was significantly higher in fibroblast cultures from RT-sensitive relative to RT-resistant patients (P=0.02). p53 was upregulated 2h - 2 days after IR in all cells but decayed more slowly on day 6 in fibroblasts from RT-sensitive patients. Further, explorative analysis showed strong early upregulation of p53 2h after irradiation in fibroblasts from high-risk patients (P=0.002). RT sensitivity showed no significant correlation with p21/CDKN1A, p16/CDKN2A, a-sma, and Ki-67, or functional endpoints, PE and SF4. However, proliferation activity (Ki-67 index) appeared to have a confounding influence on the effect of p53. Thus risk was correlated with basal levels of p53 (P<0.001) in unirradiated cultures with lower Ki-67 whereas it correlated with early upregulation at 2h (P<0.001) in cultures with higher Ki-67. Furthermore, correlations of p21/CDKN1A with p53 or p16/CDKN2A were markedly different in fibroblasts from RT sensitive and RT-resistant patients.

Conclusion: In this cohort, patient selection was performed to enhance the contrast between RT-resistant and RT-sensitive patients, including rare patients with severe late reaction. p53 levels in fibroblast cultures *in vitro* were significantly correlated with the risk of developing late breast changes after radiotherapy, and high-risk patients' fibroblasts showed strong early upregulation of p53 after irradiation which depended on the proliferation index. We suggest that a relation between p53 and the risk of late reaction exists in a subgroup of RT-sensitive patients, possibly via enhanced genetic instability and partial dysregulation of the DNA damage response.

PO-0992

The role of HIF-1 in the neo-vascularization of the rectal mucosa after radiation therapy.

L. Eusebi[1], I. Kurelac[2], A. Guido[3], A. Farioli[1], L. Giaccherini[3], L. Frazzoni[1], G. Gasparre[2], F. Bazzoli[1], A. Morganti[3], L. Fuccio[4]

[1]*S.Orsola-Malpighi Hospital- University of Bologna, Department of Medical and Surgical Sciences, Bologna, Italy*

[2]*S.Orsola-Malpighi Hospital- University of Bologna, Medical Genetics Unit, Bologna, Italy*

[3]*S.Orsola-Malpighi Hospital- University of Bologna, Division of Radiation Oncology, Bologna, Italy*

[4]*S.Orsola-Malpighi Hospital- University of Bologna, Department of Medical and Surgical Sciences, Bologna, Italy*

Purpose or Objective: Rectal bleeding after radiation therapy (RT) for prostate cancer has been observed in up to 40% of patients and it is mainly due to multiple rectal angiectasias developed after RT. Soon after the beginning of RT, there is an acute mucosal reaction that can evolve into a more severe condition with prominent vascular involvement, evidence of vasculitis, arteriolar thrombosis and subsequent ischemia and angiogenesis. Recently, attention to the role of hypoxia has contributed to the understanding of radiation-induced late normal tissue response. Under hypoxic conditions, the diverse hypoxia-driven genes (e.g., VEGF) are regulated by a transcriptional factor, hypoxia-inducible factor-1 (HIF-1). *In vivo* and *in vitro* studies have shown that the HIF-1 expression increased soon after irradiation, reaching the highest level after 30 days and preceding the expression of VEGF.

Aim of this prospective study is to evaluate the expression of HIF-1 after RT and correlate it with the development of rectal mucosal angiectasias and bleeding.

Material and Methods: Patients with histological proof of prostate cancer without distant metastases, undergoing a standard course of external beam radiation therapy (3D-RT), were considered eligible. Each patient underwent a rectosigmoidoscopy with bioptic sampling prior to and one month and one year after RT. The development of rectal mucosal angiectasias was graded according to the Vienna Rectoscopy Score (VRS). HIF-1 was evaluated by immunohistochemistry and western blot analysis; the mean number of blood vessels per field was also assessed. Radiation-induced side effects (e.g. rectal bleeding) were recorded during follow-up visits.

Results: Thirty-one patients were enrolled (median age 72 years, IQR 67-75). After the end of a median follow-up of 19.8 months (IQR 18.4-20.9), 10 patients (32.3%) developed rectal bleeding needing intervention. All these patients presented a grade II or III VRS (p=0.03). The difference in the mean number of blood vessels between bleeders and not bleeders was not significantly different (p=0.47). The expression of HIF1 in bleeding patients was down regulated in 2 cases, unchanged in 3 and up regulated in 4 cases (p>0.99); in one case it was not feasible to determine the expression. There was no correlation between the expression of HIF1 and the VRS.

Conclusion: The expression of HIF1 does not correlate with the development of rectal mucosal angiectasias and bleeding in patients irradiated for prostate cancer.

Poster: Radiobiology track: Biomarkers and biological imaging

PO-0993

Genetic profiles of glioblastoma in proximity to the subventricular zone receiving chemoradiation

S. Adeberg[1], C. Koelsche[2], D. Kehle[1], S.B. Harrabi[1], A. Unterberg[3], A. Von Deimling[2], J. Debus[1], S. Rieken[1]
[1]*University Hospital Heidelberg, Department of Radiation Oncology- Im Neuenheimer Feld 400, Heidelberg, Germany*
[2]*University Hospital Heidelberg, Department of Neuropathology- Im Neuenheimer Feld 224, Heidelberg, Germany*
[3]*University Hospital Heidelberg, Department of Neurosurgery- Im Neuenheimer Feld 400, Heidelberg, Germany*

Purpose or Objective: Subventricular zone-infiltrating (SVZ-infiltrating) glioblastomas (GBMs) with subependymal spreads along ventricle walls are associated with decreased patient survival. The heterogeneity in patient survival and recurrence patterns of GBM with SVZ infiltration might be related to neuronal therapy resistant stem cells, located in the SVZ. It has not been systematically investigated if specific molecular genetic patterns of SVZ-infiltrating GBMs exist, and therefore are responsible for the unfavorable course after chemoradiation.

Material and Methods: The current study assessed the molecularbiologic profile of 55 primary GBM cases that underwent chemoradiation. GBMs with SVZ infiltration and subependymal tumor spread (n = 24; 43.6 %) and peripherally located GBMs (n = 31; 56.4 %) were included. Genome methylation patterns were determined and copy number profiling was performed using an Illumina Infinium HumanMethylation450K (450K) Array, and the prognostic influence on progression and survival was evaluated.

Results: The majority of patients showed the characteristics of a "classic" GBM subtype, independent of the tumor localization in regard of the SVZ, demonstrating a chromosome 7 gain and chromosome 10 loss, as well as deletion of Cyclin-Dependent Kinase Inhibitor 2A (CDKN2A) and amplification of Epidermal Growth Factor Receptor (EGFR). Second, RTK I subtype, showing Platelet-Derived Growth Factor Receptor Alpha (PDGFRA) amplifications, could be detected equally in both groups. However, SVZ-infiltrating GBMs with subependymal spreading showed a decreased overall survival (OS) compared to their peripheral counterparts.

Figure: Genome wide copy number profiling of a classic primary gliolblastoma with chromosome 7 gain and chromosome 10 loss

Conclusion: Genome methylation patterns were distributed independently of tumor localization in regard of the SVZ, suggesting that the biological entities in both GBM groups are identical. However, survival rates of GBMs with proximity to the SVZ were inferior and therefore the central localization seems to be responsible for the poor clinical courses.

PO-0994

Assessment of [11C]-metformin PET for identification of patients suitable for metformin treatment

A. Iversen[1], M. Vendelbo[2], L. Gormsen[2], N. Jessen[3], M. Horsman[1], M. Busk[1]
[1]*Aarhus University Hospital, Department of Experimental Clinical Oncology, Aarhus C, Denmark*
[2]*Aarhus University Hospital, PET Centre, Aarhus C, Denmark*
[3]*Aarhus University Hospital, The Department of Molecular Medicine, Aarhus C, Denmark*

Purpose or Objective: Evidence to support a role for the antidiabetic drug metformin in the prevention and treatment of cancer has emerged over the last decade. In particular, recent studies demonstrate that metformin enhances tumor response to radiation in experimental models. Metformin may therefore be of utility for nondiabetic cancer patients treated with radiation therapy. Despite being in clinical use for almost 60 years, the underlying mechanisms for metformins action remain elusive. We have therefore applied a novel PET-tracer, [11C]-metformin, to determine the uptake mechanism and elimination of the drug *in vitro* and in *vivo*.

Material and Methods: To verify transporter-mediated uptake of metformin in tumor cells, a selection of cell lines were incubated with [11C]-metformin in the absence or presence of blocking unlabelled metformin. Two tumor models A549 (lung) and SiHa (cervix) was chosen for *in vivo* experiments. Mice bearing subcutaneous tumors in the lower back were administered ~10 MBq [11C]-metformin and dynamically PET scanned for 90 minutes. As a "proof of principle" experiments using PET/CT with [11C]-metformin organ specific uptake of [11C]-metformin was determined in healthy humans. Dynamic whole-body PET was performed on four healthy volunteers (2 male). Two minutes before scan start, a bolus injection of ~200 MBq [11C]-metformin was injected and five consecutive whole-body scans with increasing frame durations were obtained: 1, 1.5, 2, 2.5 and 3 minutes per bed position. Time intervals for the PET scans were 2-8, 9-18, 19-32, 33-48 and 49-67 minutes (see figure 1). Source organs for the dosimetry calculations were the liver, kidneys, salivary glands and the bladder.
Results: *In vitro* metformin uptake varied widely but a high and inhibitable uptake was observed in A549 and SiHa cells.

Imaging with [11C]-metformin in tumor bearing mice showed a large uptake in the kidneys and excretion through the bladder, as expected for metformin. An uptake of [11C]-metformin was seen in both A549 (lung) and SiHa (cervix) tumors and autoradiography supported this finding. Biodistribution of metformin in humans is shown in figure 1 with visible uptake in liver, kidney and the salivary glands, but no detectable uptake in brain, muscle or adipose tissue.

Conclusion: It is possible to visualize distribution of [11C]-metformin *in vivo*. In xenograft models uptake in tumor was seen. It will be of great interest to investigate whether it is possible to visualize an uptake in human tumors, which will be done in a planned study in prostate cancer patients.

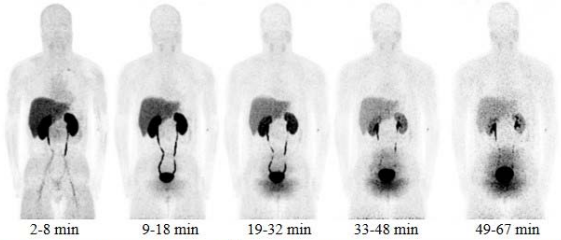

Figure 1: Tissue distribution of [^{11}C]-metformin. Healthy subjects given 200 MBq [^{11}C]-metformin i.v. Time denotes min after injection.

Poster: Radiobiology track: Cellular radiation response

PO-0995

Osteopontin expression in glioblastoma – a promoter of the cancer stem cell-like phenotype?

S. Rogers[1], R. Grobholz[2], J. Berberat[3], A.R. Fathi[4], S. Bodis[1]
[1]*Kantonsspital Aarau, Radiation Oncology, Aarau, Switzerland*
[2]*Kantonsspital Aarau, Pathology, Aarau, Switzerland*
[3]*Kantonsspital Aarau, Neuroimaging, Aarau, Switzerland*
[4]*Kantonsspital Aarau, Neurosurgery, Aarau, Switzerland*

Purpose or Objective: A high level of circulating osteopontin (OPN) at the end of radiotherapy (RT) is an adverse prognostic factor in patients with glioblastoma (GBM) and other tumours including rectum cancer. Recent mechanistic studies demonstrated HIF2α-mediated OPN/CD44 promotion of the glioma stem cell-like phenotype in a mouse model. Using unique paired tumour samples from patients with GBM, we investigated changes in levels of OPN protein expression following RT and compared these with rectum cancers from patients irradiated with the same pre-operative fractionation.

Material and Methods: 3 patients with histologically confirmed GBM received pre-operative RT in an ethics-approved Phase I trial. 2.5 Gy b.d. was delivered using IMRT over 5 days. Maximal safe tumour resection was performed at 3, 5 and 10 days post RT in patients 1, 2 and 3 respectively. Immunohistochemistry was performed on the paired diagnostic biopsy and irradiated resection specimen using validated antibodies (rabbit polyclonal antibody to OPN: clone PA1-38332, Thermo Fisher Scientific) and an automated immunostainer. The staining was scored by a board-certified pathologist.

Results: Levels of OPN in GBM tumour cells were high at baseline as compared with rectum adenocarcinoma. There was marked increase in OPN expression in response to RT in all three GBM tumours (Fig 1). Expression of Glut-1, a marker of intrinsic hypoxia and a target of HIF-2α, was not induced. Ki67 levels were reduced although levels of cyclin D1 expression were unchanged. A dynamic contrast-enhanced (DCE) MRI performed on the last day of RT did not detect any change in tumour perfusion in any of the GBMs. Resection specimens from 3 rectum cancer patients irradiated preoperatively with the same schedule showed very low level induction of OPN.

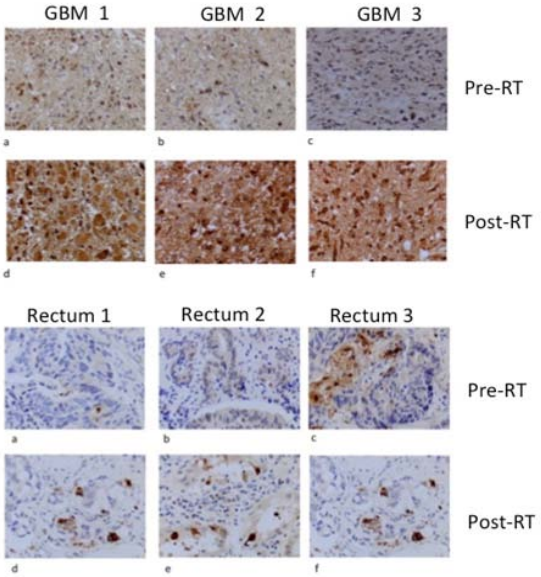

Conclusion: RT increased the levels of OPN expression in GBM tumour cells. This may be a direct effect or related to RT-induced changes in the hypoxic tumour microenvironment that were not detectable on a DCE-MRI or by Glut-1 expression. Although RT significantly increases overall survival compared with surgery alone, particularly when combined with temozolomide, it may promote the cancer stem cell-like phenotype of residual GBM cells. Enhanced OPN/CD44 signalling in the perivascular niche is associated with resistance to therapy and blockade of this signalling pathway may prove of clinical benefit. The relative lack of induction of OPN expression in rectum cancer may explain the success of short course pre-operative RT in this tumour type.

PO-0996

Distinct radiation responses after mtDNA depletion are potentially related to oxidative stress

M.W. Van Gisbergen[1], A.M. Voets[2], R. Biemans[1], G.R.M.M. Haenen[3], M.J. Drittij-Reijnders[3], R.F. Hoffmann[4], I.H. Heijink[4], H.J.M. Smeets[2], K.M.A. Rouschop[1], L. Dubois[1], P. Lambin[1]
[1]*Maastricht University, Radiation Oncology, Maastricht, The Netherlands*
[2]*Maastricht University, Genetics and Cell Biology, Maastricht, The Netherlands*
[3]*Maastricht University, Toxicology, Maastricht, The Netherlands*
[4]*University of Groningen, Pathology and Medical Biology, Groningen, The Netherlands*

Purpose or Objective: In process like reactive oxygen production and apoptosis mitochondria play an important role and both processes play also a significant role in radiotherapy (RT) response. Repair of RT induced damage is dependent on mitochondrial energy supply suggesting a role for mitochondrial DNA (mtDNA) in RT. mtDNA variations, such as mutations or depletion, might therefore influence RT response, as for example found in cisplatin-treated patients. Therefore carefully elucidating the effect of these processes in radiation response might be important. Hence, we hypothesize that reduced mitochondrial function enhances the radiation response as a consequence of reduced ATP production and increased cellular ROS exposure (Fig.1).

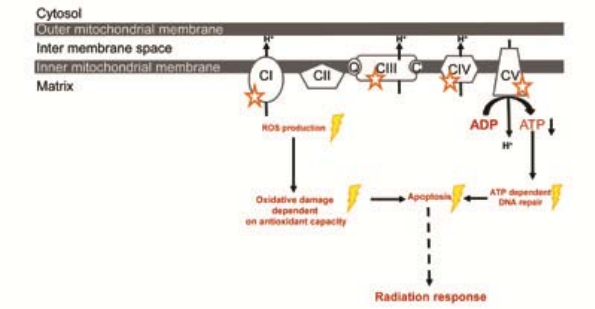

Fig 1. We hypothesize that reduced mitochondrial function caused by mtDNA variations, such as mtDNA depletion, enhances the radiation response as a consequence of reduced ATP production and increased cellular ROS exposure. Oxidative phosphorylation complexes that are encoded by the mtDNA are indicated by the orange stars. Through disruption of these complexes and thereby interfering with free radical and ATP production, radiation responses could potentially be altered. Lightning signs indicate processes that are also involved in radiotherapy.

Material and Methods: Three cell lines were depleted from their mtDNA by ethidium bromide. BEAS-2B immortalized bronchial epithelial, A549 lung adenocarcinoma and 143B osteosarcoma cell lines and their mtDNA depleted counterparts (ρ0) were metabolically characterized using the XF96 Seahorse. Changes in radiosensitivity were assessed by clonogenic survival (0, 2, 4, 6 and 8Gy). ROS production (by dihydrorhodamine FACS analysis), ATP (Cell-TiterGlo Luminescent cell viability test) and glutathione levels (in cell lysate) as well as γH2AX immunostainings were assessed 24 hours post irradiation.

Results: mtDNA depletion resulted in a significant ($p<0.05$) decreased proliferation (64 ± 7%) for all cell lines. Compared to their respective controls, increased clonogenic survival was observed for the BEAS-2B ρ0 cells ($p=0.004$) after irradiation, while both tumor ρ0 lines were more radiation sensitive ($p=0.013$), mainly at higher irradiation doses. ROS formation at baseline (0Gy) was similar ($p=0.878$) for BEAS-2B parental and ρ0, while reduced for A549 and 143B ρ0 ($p=0.021$) cells, compared to their parental counterparts. 24 hours after irradiation ROS levels were significantly ($p<0.05$) increased for all parental cell lines, while levels for the ρ0 cells remained equal. Glutathione levels were lower for the A549 and 143B ρ0 cell lines compared to the parental lines under any experimental condition but no changes were found for the BEAS-2B cells. In agreement, increased residual DNA damage was observed upon mtDNA depletion for A549 and 143B cells. Depletion of mtDNA reduced cellular ATP levels only for the BEAS-2B cell line ($p=0.046$), but not for the A549 and 143B cell lines in high glucose culture medium.

Conclusion: The observed differences in dependence on mitochondrial function for radioresponsiveness appear to be associated with the balance in ROS levels and the antioxidant status of the cells. Currently, the levels of MnSOD and GPX1 and the effect of ROS scavenging on radiotherapy response are investigated in our lab.

PO-0997

Interferon response genes in breast cancer resistance to endocrine treatment and radiotherapy

A.E.M. Post[1,2], A.P. Nagelkerke[1,2], J.W.M. Martens[3], J. Bussink[1], C.G.J. Sweep[2], P.N. Span[1]

[1]Radboud University Medical Center, Radiation Oncology, Nijmegen, The Netherlands

[2]Radboud University Medical Center, Laboratory Medicine, Nijmegen, The Netherlands

[3]Erasmus MC Cancer Institute, Medical Oncology and Cancer Genomics Netherlands, Rotterdam, The Netherlands

Purpose or Objective: We have previously shown that lysosome-associated membrane protein-3 (LAMP3), a protein involved in the unfolded protein response pathway, is involved in resistance to both endocrine (tamoxifen) treatment and radiotherapy in breast cancer patients. We have created subclones of the MCF7 breast cancer cell line that are resistant to either treatment. In these subclones, we investigated common mechanisms between tamoxifen- and radioresistance, and the possible role of LAMP3 therein.

Material and Methods: The estrogen receptor positive breast cancer cell line MCF7 was grown to tamoxifen resistance (MCF7TAM) by culturing with gradually increasing concentrations of 4-OH-tamoxifen up to 10 μM. Additionally, MCF7 cells were exposed to multiple fractions of 2 or 4 Gy irradiation, adding up to a total dose of at least 50 Gy (MCF7RT). Changes in expression profiles in MCF7TAM and MCF7RT cells compared to parental MCF7 cells were investigated by RNA sequencing. Pathway analysis software was used to find pathways involved in tamoxifen- and radioresistance. QPCR was used to confirm the RNA sequencing data, and to investigate the changes in genes of interest after tamoxifen treatment and irradiation.The role of LAMP3 in these treatment resistance pathways is being elucidated by performing LAMP3 gene silencing by siRNA and CRISPR-Cas mediated gene knockout.

Results: The MCF7TAM cells were completely resistant to treatment with 10 μM 4-OH-tamoxifen. Remarkably, these cells had also become resistant to irradiation, with a surviving fraction at 4 Gy (SF4) of 19.7%, compared to 8.3% for the parental MCF7 cells. MCF7RT cells were less sensitive to irradiation with a SF4 of 9.6% compared to 3.9% for the parental cells. RNA sequencing of MCF7TAM and MCF7RT cells revealed an increase of genes involved in the antiviral response, including classic interferon response genes such as IFI6 (shown in figure, left), IFI27, STAT1, OAS1 and DDX60. These genes were increased in parental cells following 4 Gy irradiation (figure, right) or tamoxifen treatment as well.

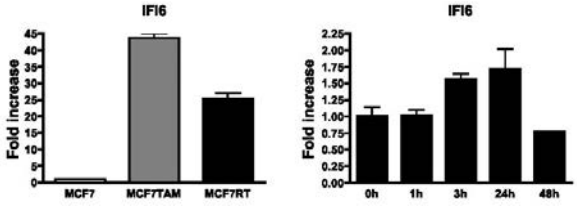

Conclusion: MCF7 cells resistant to tamoxifen treatment are also less sensitive to irradiation,suggesting a common mechanism in the resistance to these diverse types of treatment. Using an unbiased approach, we here show that interferon response genes are increased in both MCF7TAM and MCF7RT cells. Interestingly, others have shown LAMP3 to be a regulator for this pathway. We are currently investigating the role of LAMP3 in our treatment resistant breast cancer clones.

PO-0998

The Robo1-receptor is involved in the migration of irradiated glioblastoma cells

H. Bühler[1], P. Nguemgo-Kouam[1], A. Kochanneck[1], H. Hermani[1], K. Fakhrian[1], I.A. Adamietz[1]

[1]Marienhospital Herne- Ruhr-Univers., Klinik für Strahlentherapie und Radio-Onkologie, Herne 1, Germany

Purpose or Objective: The brain tumor glioblastoma multiforme (GBM) is highly malignant with a very short OS due to rapid recurrences adjacent to the primary tumor. Even radio-chemotherapy extends the survival only for a few months. In this project we tested whether or not the Slit2/Robo1 axon guidance system might be involved in the migration of metastatic GBM cells and whether irradiation with photons might modify this putative effect.

Material and Methods: The experiments were performed with 2 human GBM cell lines (U87 and U373) and in parallel after irradiation with 0.5, 2, or 8 Gy photons. The motility/migration of the cells was analyzed by time-laps videography. Travelling cells were tracked and the parameters accumulated distance and Euclidean distance were determined. The expression of Slit2, Robo1, and FAK (focal adhesion kinase) was tested by Western blot and qRT-PCR. In addition, the cells were transfected either with a Robo1 expression-vector or with a siRNA construct and analyzed similarly.

Results: Irradiation with low doses enhanced the motility of the cells. Slit2 as well as Robo1 was extremely low expressed in the cell line with higher motility (U87). Irradiation reduced the expression even more. On the other hand, a stable overexpression of Robo1 decreased significantly the migration of the cells and suppressed the increase in motility observed after irradiation. In contrast, the siRNA mediated knockdown of Robo1 increased the migratory potential of the cells. The analysis of FAK, a key player in cellular migration, revealed a decreased expression in Robo1-overexpressing cells.

Conclusion: Our data indicate a role for Robo1 in the migration of malignant GBM cells. The expression of Robo1 reduced the migration of these cells and was also able to impede the increase in motility observed after irradiation with photons.

Poster: Radiobiology track: Radiobiology of protons and heavy ions

PO-0999

Reduced side effects by proton minibeam radiotherapy in a mouse ear model

T.E. Schmid[1,2], S. Girst[3], C. Greubel[3], J. Reindl[3], C. Siebenwirth[2,3], K. Ilicic[2], D.W.M. Walsh[2,3], G. Dollinger[3], J. Wilkens[2], G. Multhoff[2], S.E. Combs[1,2]
[1]*Helmholtz Zentrum München, Institute of Innovative Radiotherapy iRT, Neuherberg, Germany*
[2]*Klinikum Rechts der Isar- Technische Universitaet Muenchen, Radiooncology, Muenchen, Germany*
[3]*Universität der Bundeswehr, Institut für Angewandte Physik und Messtechnik, Neubiberg, Germany*

Purpose or Objective: Proton minibeam radiotherapy aims to minimize normal tissue damage in the entrance channel while keeping tumor control through a homogeneous tumor dose due to channel widening with increasing track length. Side effects of proton minibeam irradiation were examined in an in-vivo mouse model to account for immune system, vasculature and higher complexity. Here, we report on our comparative study of minibeam and broad beam irradiation in the ear of Balb/c mice, to prove this hypothesis of reduced adverse effects in normal tissue.

Material and Methods: At the ion microprobe SNAKE, 20 MeV protons were administered to the right ear of 2-3 months old, female Balb/c mice, using an average dose of 60 Gy in a field of 7.2 x 7.2 mm2 in the central part of the ear, in two irradiation modes, homogeneous and minibeams. The 4 x 4 minibeams of 180 x 180 µm2 size were set in a distance of 1.8 mm, resulting in a dose of 6000 Gy in the channels, but with negligible dose in between. Inflammatory response, i.e. ear swelling and skin reactions were monitored for 90 days following irradiation, as well as genetic damage and release of inflammatory proteins.

Results: No ear swelling or other skin reaction was detected after the minibeam irradiations, while significant ear swelling (up to 4-fold), erythema and desquamation (crust formation) developed in homogeneously irradiated ears 3-4 weeks after irradiation. Loss of hair follicles was only detected in the homogeneously irradiated fields after 4-5 weeks.

Conclusion: Our results prove that proton minibeam radiotherapy leads to reduced side effects compared to conventional broad beam irradiation and could become an option in clinical proton and/or heavy ion therapy.
Supported by the DFG Cluster of Excellence: Munich-Centre for Advanced Photonics.

PO-1000

Effect of X-rays and carbon ions on cell survival and expression of Hh pathway genes in cancer cells

K. Konings[1], M. Moreels[1], A. Suetens[1], A. Gonnissen[2], S. Isebaert[2], K. Haustermans[2], S. Baatout[1]
[1]*SCK-CEN, Radiobiology, Mol, Belgium*
[2]*KU Leuven, Laboratory of Experimental Radiotherapy, Leuven, Belgium*

Purpose or Objective: Metastasis is an important cause of mortality in cancer patients and evidence shows that irradiation could actually increase the formation of metastasizing cells. An important pathway implicated in the process of metastasis is the Hedgehog (Hh) signaling pathway. Recent studies demonstrated that activation of this pathway can lead to radioresistance. So far, the impact of high-LET radiation on the Hh pathway is still unknown. In the present study the impact of different radiation qualities (e.g. X-rays and carbon ions) on Hh gene expression was investigated in prostate cancer cells (PC3) and medulloblastoma cells (DAOY).

Material and Methods: *In vitro* models used for prostate cancer and medulloblastoma were PC3 and DAOY, respectively. Colony survival assays were performed to analyze the effect of radiation on cell survival. The impact of radiation on the expression of the different Hh signaling pathway components (SHH, PTCH, SMO, GLI1, GLI2, GLI3 and SUFU) was investigated by means of RT-qPCR. Experiments with X-rays were performed at SCK•CEN (Mol, Belgium) whereas carbon ion irradiation (LET = 33.7 KeV/µm) experiments were performed at the Grand Accélérateur National d'Ions Lourds (GANIL) (Caen, France).

Results: Colony survival assays showed that DAOY cells were more radioresistant than PC3 cells (respectively D10=5.3 Gy and D10=4.2 Gy). Evaluation of the Hh signaling pathway showed that basal gene expression is present in both PC3 and DAOY, although very low. However, basal gene expression of the Hh components differed between both cell lines. Moreover, the more radioresistant cell line DAOY had higher expression levels of Gli1 compared to the PC3 cells. Preliminary RT-qPCR results show that different radiation qualities induce different changes in the expression of the Hh signaling components.

Conclusion: In conclusion, radiation exposure can induce changes in the Hh pathway. Future experiments will address whether modulation of the Hh pathway also affects the radio-responsiveness of cancer cells.

Poster: RTT track: Strategies for treatment planning

PO-1001

Dosimetric impact of flattening filter and flattening filter-free beams on IMRT planning of NSCLC

S.W.Y. Lee[1], K.M.K. Or[2], Y.P.J. Kwong[3], Y.H.S. Choy[4], C.Y.K. Kwong[5], H.K. Keung[6], V.W.C. Wu[1]
[1]*The Hong Kong Polytechnic University, Health Technology and Informatics, Kowloon, Hong Kong SAR China*
[2]*Queen Elizabeth Hospital, Clinical Oncology, Kowloon, Hong Kong SAR China*
[3]*Queen Mary Hospital, Clinical Oncology, Hong Kong, Hong Kong SAR China*
[4]*Princess Margaret Hospital, Clinical Oncology, Hong Kong, Hong Kong SAR China*
[5]*Prince of Wales Hospital, Clinical Oncology, Hong Kong, Hong Kong SAR China*
[6]*Pamela Youde Nethersole Eastern Hospital, Clinical Oncology, Hong Kong, Hong Kong SAR China*

Purpose or Objective: This retrospective study aimed to compare and determine the potential dosimetric benefits of intensity-modulated radiotherapy (IMRT) treatment plans with (FF) and without flattening filter (FFF) as well as to explore the dosimetric differences in 6MV FFF and 10MV FFF plans for non-small-cell lung carcinoma (NSCLC).

Material and Methods: Ten cases of CT data were selected from NSCLC patients. 4 sets of 5-field-IMRT plans were computed with FFF beams (X6FFF, X10FFF) and flattened beams (X6FF, X10FF) with the prescription of total 60Gy in 30 fractions. Planning constraints were based on the Radiation

Therapy Oncology Group (RTOG) protocol 1306. Determination of isocentre, beam arrangement and dose constraints were kept constant in each case. All plans were computed using Varian Eclipse version 11.0 treatment planning system. The plans were then evaluated based on the target coverage, homogeneity, conformity, number of monitor units (MU) to be delivered and dose-volume constraints for various organs at risk (OARs).

Results: All plans exhibited comparable PTV homogeneity (HI ≤ 7.5) and conformity (CI > 96%) with a steep dose fall-off outside the PTVs but at the expense of increased MUs by 39.4% (p=0.007) and 44.7% (p=0.005) for FFF beams at 6 MV and 10 MV respectively. FFF beams offered better dose sparing of OARs than flattened beams. Spinal cord+5mm and volume of 'whole lung (WL) – Gross tumour volume (GTV)' (WL-GTV) that received 20Gy (V20) were reduced by 2% (p=0.017) and 2.8% (p=0.016) respectively in X10FFF plans when compared with X10FF plans. There was also a 16.4 % dose reduction to brachial plexus in X10FFF plans than X6FFF plans.

Conclusion: The application of FFF IMRT for NSCLC yielded quantitatively comparable dosimetric distribution with better sparing of the OARs including 'spinal cord+5mm', V20 of 'WL-GTV' and brachial plexus than using FF beams.

PO-1002

A comparison of outcomes using VMAT and 3DCRT in treatment of esophageal cancer

E. Jimenez-Jimenez[1], J. Font[2], P. Mateos[2], F. Romero[2], J. Pardo[1], N. Aymar[3], I. Ortiz[3], M. Vidal[3], S. Sabater[4]

[1]*Hospital Universitari Son Espases, Radiation Oncology Department. Research Group IDISPA, Palma de Mallorca, Spain*

[2]*Hospital Universitari Son Espases, Medical Physics Department, Palma de Mallorca, Spain*

[3]*Hospital Universitari Son Espases, Radiation Oncology Department, Palma de Mallorca, Spain*

[4]*Complejo Hospitalario Universitario de Albacete, Radiation Oncology Department, Albacete, Spain*

Purpose or Objective: There are few studies comparing 3-dimensional conformal radiation therapy (3DCRT) and volumetric modulated arc therapy (VMAT) in treatment of esophageal cancer. These studies often compare 3DCRT unsophisticated, with few treatment beams, which is not common in clinical practice.
Our aim was to compare a modern 3DCRT plan with VMAT using dose volume histograms (DVH) and evaluate the dosimetric profile.

Material and Methods: We evaluate 7 patients with esophageal cancer (4 medium, 2 distal and 1 upper neoplasms). All were contoured using PET-CT and treated with radio-chemotherapy. Target volumes for primary lesions (50-50,4 Gy) and electively treated regions (45 Gy) were contoured.
Every patient had 2 dose-plans, one with 3DCRT (8-10 beams) and other with VMAT (2 arcs) techniques. For each technique, we evaluate the coverage target, homogeneity index of PTV (HI), conformity index (CI), monitor units and DVH metrics of lungs, heart and spinal cord.

Results: VMAT plans reduced total lung volume treated above 20 Gy (V20) and mean lung dose (MLD), but volume treated above 5 Gy (V5) were higher than 3DCRT. VMAT improved total heart volume treated above 20 Gy and 40 Gy (V20, V40) and maximum dose to cord.
Monitor units (MU) were higher with the 3DCRT. HI and CI are better with VMAT technique. Coverage target was very high with both schemes. Statistically meaningful differences were observed (Table 1).

Conclusion: Our results suggest that VMAT for radical treatment of esophageal cancer is useful for decreasing dose in organs at risk. It can play a more important role in some locations, such as cervical cancer. Nevertheless, VMAT increases low-doses in lung and this may contribute increase pulmonary complications.
A complex multibeam technique -3DCRT preserves constraint of organs at risk with high conformity and homogeneity of the target.

		3DCRT	VMAT	p-value
Target	Coverage (%)	98,1 ± 1,4	95,4 ± 1,1	< 0,05
	HI	0,083 ± 0,016	0,047 ± 0,006	< 0,05
	CI	1,62 ± 0,15	1,00 ± 0,03	< 0,05
Lung	V5 (%)	80,5 ± 11,0	83,9 ± 12,0	< 0,05
	V20 (%)	24,5 ± 4,9	14,5 ± 10,0	< 0,05
	MLD (Gy)	15,03 ± 2,13	12,78 ± 2,72	< 0,05
Heart	V20 (%)	48,8 ± 23,2	28,2 ± 22,6	< 0,05
	V40 (%)	16,4 ± 15,8	3,7 ± 4,1	< 0,05
Spinal cord	Maximum dose (Gy)	40,2 ± 3,7	33,0 ± 4,1	< 0,05
	1 cm^3 dose (Gy)	36,3 ± 4,6	30,1 ± 3,6	< 0,05
Monitor units		588 ± 98	558 ± 127	0,499

PO-1003

Does level of DIBH amplitude correlate to reduction in cardiac dose in left breast cancer patients?

D. Ledsom[1], A. Reilly[2], H. Probst[3]

[1]*Clatterbridge Cancer Centre, Radiotherapy, Bebington, United Kingdom*

[2]*Clatterbridge Cancer Centre, Physics, Bebington, United Kingdom*

[3]*Sheffield Hallam University, Faculty of Health and Wellbeing, Sheffield, United Kingdom*

Purpose or Objective: The aim was to investigate whether the amplitude level achieved during DIBH impacted on the mean cardiac dose and V30 reduction in 30 women treated for a left sided breast cancer during radiotherapy.

Material and Methods: Patients were dual scanned in free breathing and DIBH. Varian Real-time Position Management (RPM) was used to record and monitor breathing. Plans were virtually simulated with field borders following IMPORT high guidelines. Pinnacle treatment planning software was used for dosimetric calculation; all plans conformed to ICRU 62. Spearman's Rank correlation and statistical analysis was performed using SPSS v22. All patient data was annonymised. To improve reliability and assess validity of the researcher, 10 of the 30 patients were chosen at random, re-outlined and re-planned to confirm consistency and intra-rater reliability. The heart was also re-contoured for one patient 5 times to calculate the error in heart contouring.

Results: All patients achieved decreased cardiac V30 and mean cardiac dose reduction using DIBH technique. Moderate positive correlation between DIBH amplitude and cardiac V30 reduction was statistically significant (p=0.007, R=0.48). Ratio increase from free breathing to DIBH and cardiac V30 reduction was also positively correlated and statistically significant (p=0.04, R=0.38). Twenty seven percent of patients achieved full cardiac V30 reduction and 73% of patients achieved over 90% reduction. Ratio of amplitude increase from free breathing to DIBH ranged from 4-27 times with ratios of at least 15 times free breathing all achieving 100% cardiac V30 reduction. However 100% cardiac V30 reduction was observed with amplitude of ratio increase as low as 6.25 times free breathing.
Positive correlation between DIBH amplitude and mean cardiac dose reduction was statistically significant (p=0.003, R=0.523). Seventy seven percent of patients achieved over 50% mean cardiac dose reduction with DIBH amplitudes of 1.04-5.46cm. Correlation of ratio of amplitude increase from free breathing to DIBH and mean cardiac dose reduction was not statistically significant (p=0.316, R=0.189).

Conclusion: A 100% reduction in cardiac V30 can be achieved with a DIBH amplitude increase 15 times free breathing, yet full reduction can also be achieved at much lower levels (6.25 times free breathing in the current study) suggesting patients unable to achieve a large amplitude increase may

still be able to achieve 100% reduction. DIBH amplitudes of 1-5cm reduce cardiac mean dose by at least 50%.

PO-1004

Optimising breast dosimetry: improving homogeneity through the application of angled IMRT fields

M. Squires[1], S. Cheers[1]
[1]*Radiation Oncology Centres, Gosford, Gosford, Australia*

Purpose or Objective: Studies have demonstrated significant side effects associated with dose inhomogeneity and low dose integral splay. Several techniques seek to maximise dose uniformity whilst minimising regions of low dose. The angled segment technique offers two additional options, each allowing for control over homogeneity (HI) and low dose conformity (CI).

Material and Methods: Tangent fields of twenty previously optimised plans were copied. Two re-optimisation methods were applied. Firstly, a single medially angled off inversely planned (I-IMRT) beam was appended to the existing beamset. The plans were further optimised and normalised (PTV V47.5 = 99.00%). Secondly, an additional acutely laterally angled off I-IMRT beam was added, reoptimised, and normalised.

Results: The addition of the single I-IMRT beam resulted in a statistically similar average absolute maximum dose (Dmax 54.55Gy vs. 54.71Gy, p=0.33) but a markedly reduced V107% (14.71cc vs. 23.17cc, p<0.01). Low dose (V1) integral splay was maintained (6410.04cc vs. 6402.45cc, p=0.44), but was reduced marginally contralaterally (V1 splay over midline 6.60cm vs. 6.80cm, p=0.04). Dose to the ipsilateral lung was slightly reduced (5.23Gy vs. 5.33Gy, p=0.04). The additional duel angled off I-IMRT fields reduced the average maximum dose (Dmax 53.79Gy vs. 54.71Gy, p=0.03) and the V107% size substantially (1.90cc vs. 23.17cc, p<0.01). Homogeneity was improved (HI= 0.11 vs. 0.13, p=0.03), whilst the ipsilateral mean lung dose was unaffected (5.33Gy vs. 5.33Gy, p=0.48). The volume of the low dose (V1) integral splay increased by an average of 1.5% (6501.14cc vs. 6402.45cc, p=0.04), and appeared further contralaterally (8.40cm vs. 6.80cm over midline, p=0.02).

Conclusion: The application of additional acutely angled fields provides scope to reduce regions of high dose and improve breast homogeneity while controlling integral dose splay.

PO-1005

Dosimetric effect of US versus CT delineation on postplanning I-125 treatment

J. Van der Klein[1], M. Mast[1], P. Koper[1], P. Rietveld[1], J. Van Wingerden[1], H. De Jager[1]
[1]*Haaglanden Medical Centre Location Westeinde Hospi, Radiotherapy Centre West, Den Haag, The Netherlands*

Purpose or Objective: Since 2000 we have been treating low- and intermediate-risk prostate cancer patients with permanent Iodine-125 implants. After 6 weeks postimplant dosimetry (PID) was performed using the Pro-Qura technique (Allen et al, 2008). In a previously performed study in our institute (cohort of 394 patients), we found that the dosimetric quantifier V100 was not correlated with biochemical relapse. Therefore, we examined the PID method to obtain more detailed information on the quality of the PID parameters. From the literature it appeared that in PID many uncertainties affect the quantifiers: delineation, source identification and imaging modalities (De Brabandere et al, 2012). In 2014 we started working with an automated seed reconstruction system (Elekta) to eliminate uncertainties in source identification. However, the other uncertainties still remained. Furthermore, the craniocaudally length of the Ultrasound (US) prostate contour was distally more extended compared to the contour on the postplan CT-scan. This could be explained by the deformation of prostate by the US probe. The main purpose of this study was to determine the differences in PID based on US- or CT-contours.

Material and Methods: For 71 patients in supine position an axial CT-scan (1 mm slice thickness) was made of the prostate. One radiation therapist (RTT) performed the PID using the US prostate contour fused with the postplan CT-scan. The apex area was defined as the volume derived from a quarter of the base-apex distance. We analyzed the V100 of the apex area and selected the patients with a coverage of less than 67%. Thereafter, we randomly selected 2 groups of patients: Group A: 5 patients with an optimal postplan implantation in the apex area conform Pro-Qura.Group B: 5 patients with an inferior implantation result in the apex area, a coverage of less than 67%. For each patient, one radiation oncologist delineated the prostate on the CT-scan, trying to ignore the seeds. With that new delineated prostate the RTT performed a PID and these CT-based results were compared to the original results. To see the difference in length of the prostate on both modalities, we defined the last slice of the visible apex on both US and CT.

Results: Between the US- and CT-scan volume an absolute difference was found of 12% (SD 2%). In both groups we found, in four out of five patients, that the apex on CT was positioned less caudally compared to the US-scan, figure. This was 4 and 10mm for group A and B respectively.

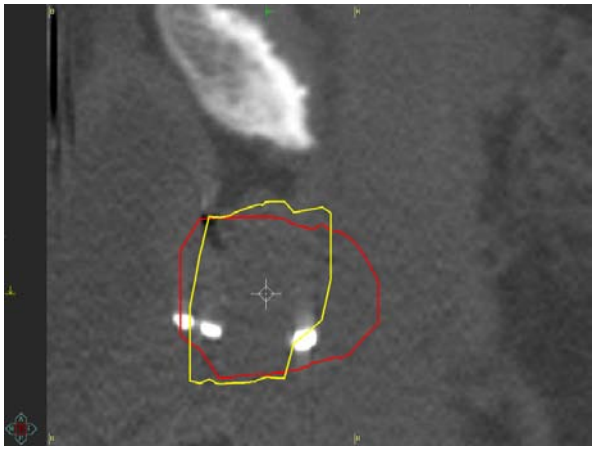

Figure: Delineated prostate volumes. Red: US; Yellow: CT.
For all patients, we found in both groups a significantly higher V100 using the prostate contours of the CT-scan.

Conclusion: The volume of the prostate depends on the image modality. Consequently, the PID results differ as a function of image modality. This needs to be studied in a larger cohort of patients and could help to define on which modality the delineation and the PID needs to be performed.

PO-1006

A breath-hold friendly, hybrid 3DCRT/IMRT technique for locoregional breast irradiation

K. Hunnego[1], D. Martens[1], D. Steeneveld[1], A. Dijkhuizen[1], L. McDermott[1], F. Gescher[1], G. Speijer[1]
[1]*HagaZiekenhuis, Radiotherapy, The Hague, The Netherlands*

Purpose or Objective: IMRT optimises not only the planned dose, but also the clinical preparation and treatment delivery. Until recently, our hospital used a standard 3DCRT for the breast, thoracic wall and lymph nodes ranging from level I to IV, including the parasternum. This usually leads to inconsistent OAR sparing, PTV coverage and conformity, abutting region from multiple fields and long treatment times due to many, high-MU fields. The objective of this study was to develop a hybrid 3DCRT-IMRT technique for locoregional breast irradiationl, which is also “breath-hold friendly” i.e. fewer MUs and fields. This technique should optimise planning and treatment times, maintain or reduce dose to OAR, improve PTV homogeneity, avoid the use of wedges and minimise the number of abutting beams.

Material and Methods: 25 Patients were included, with regional nodes level I-IV. Twelve were left-sided with breath-hold treatments. All were planned with both original 3DCRT and a new hybrid 3DCRT-IMRT techniques. Delineations were made according to ESTRO guidelines. Comparison was based on DVH parameters for OARs, namely lung, heart, oesophagus, contra-breast (eg V20, Dmean) and the PTV (V95%, D2%, D98%, conformity). Analysis was performed using SPSS. Further analysis focussed on the efficacy for breath-hold treatments and efficiency in planning and delivery.

Results: The hybrid plan required extra structures to help avoid hotspots, which is especially important for heart-sparing breath-hold treatments. In general, hybrid plans were superior to 3DCRT plans. An exception was the slightly higher, but acceptable, average dose to selected OAR. Resulting clinical recommendations are as follows: for level I/II, where the delineation of lymph nodes in the cranial direction are limited to lateral side, an optimal plan may be created from 2-3 3DCRT open fields and 2-4 IMRT fields. For level I-IV (also with parasternal lymph node involvement), plan as for level I/II above, with an abutment involving no more than 2 fields. Previously 3DCRT treatments required 10-12 fields, hybrid plans require at most 7 fields (each 3 segments) and only half of the MUs.

Conclusion: Hybrid 3DCRT-IMRT plans are a major improvement on the current 3DCRT technique, with fewer hotspots and more control over the dose to OARs and the target. Planning objectives were achieved, with fewer fields, MUs and field abutments, without the need for wedges. In addition, the treatment length has been reduced, making this hybrid technique more suitable for breath-hold delivery.

PO-1007

Optimizing the overlap sector for patients undergoing cranio-spinal irradiation by VMAT

M. Willemsen - Bosman[1], G.O.R. Janssens[1], E. Seravalli[1]
[1]*UMC Utrecht, Radiation Oncology Department, Utrecht, The Netherlands*

Purpose or Objective: Volumetric modulated arc therapy (VMAT) techniques for cranio-spinal irradiation (CSI) allows radiation delivery without any field junction. Junctions are replaced by sectors in which arcs of two consecutive isocenters overlap. The dose contribution from each arc in this sector is automatically accounted for by the treatment plan optimization process. Inaccurate patient positioning during treatment in this area of overlap between arcs belonging to different isocenters, causes regions of over- or underdosages.
The purpose of this analysis is to find an optimal length of overlap between the overlapping arcs,to minimize the dose deviations that can be attributed to patient setup inaccuracies.

Material and Methods: Five (n = 5) patients undergoing CSI were planned using the Monaco 5.1 (Elekta Ltd,Crawly, UK) treatment planning system. Each plan consisted of 2 isocenters, with an overlap sector at the mid-cervical level. For the head a full clockwise-counterclockwise (cw-ccw) arc was used, while for the spine two cw-ccw partial arcs (180-260 ° and 100-181 °).
In order to assess the optimal overlap length, plans were generated for overlap sectors of 4, 6, 8 and 10 cm. Afterwards, plans were recalculated without re-optimization for a superior isocenter shift of +0.5 cm in cranio-caudal direction and a -0.5 cm in the left-right direction ,mimicking a potential patient setup error. Dose distributions of the generated plans with isocenter shift were compared to the original plans based on V90%, V95% ,V110% of the Planning Target Volume (PTV) and Conformity Index (CI).

Results: The introduction of a shift in the superior isocenter causes a 3% decrease in the V90% of PTV independently of the overlap length (Table1).

Table 1

Average (n=5) relative differences (Δ) of V90%, V95%, V110% and CI of the PTV between the shifted isocenter and the original plans.

Overlap length (cm)	ΔV90 (%)	ΔV95 (%)	ΔV110 (%)	ΔCI (%)
4	-3	-11	-50	-31
6	-3	-10	+39	-25
8	-3	-10	+58	-31
10	-3	-14	+373	-39

A decrease in PTV coverage (V95%) is also observed and the effect is larger for the 10 cm overlap length. The volume receiving ≥110% of the prescribed dose increases when the length of the overlap becomes larger than 4 cm. The relative difference of the CI between the shifted and original plan is the smallest for the 6 cm overlap length. The smallest relative dosimetric deviations from the original non shifted plan are obtained for 6 cm overlap length.

Conclusion: To reduce the impact of setup errors during CSI by VMAT, the optimal length of the overlap sector using the Monaco 5.1 treatment planning system, should be around 6 cm.

PO-1008

In silico implementation of MRI-60Co RT. A dosimetrical comparison in cervical cancer (SIMBAD-02)

N. Dinapoli[1], L. Boldrini[1], E. Placidi[2], L. Azario[2], G.C. Mattiucci[1], D. Piccari[1], S. Teodoli[2], M.A. Gambacorta[1], S. Chiesa[1], A. Piermattei[2], V. Valentini[1]
[1]*Università Cattolica del Sacro Cuore -Policlinico A. Gemelli, Radiation Oncology, Rome, Italy*
[2]*Università Cattolica del Sacro Cuore -Policlinico A. Gemelli, Medical Physics, Rome, Italy*

Purpose or Objective: The ViewRay MRI-60Co hybrid system (MRIdian) allows MRI based targeting, structure autosegmentation and direct planning for numerous anatomical districts. Our department is implementing this technology and, up to date, we are testing QA planning procedures compared to our clinical standards in order to define which districts could take advantage from the use of the MRI-60Co technology. Aim of this investigation was to assess the impact of the implementation of the ViewRay magnetic resonance imaging (MRI)-guided 60Co radiation therapy system through an in silico planning analysis for cervical cancer treatments.

Material and Methods: Patients affected by cervical cancer (cT3; cN0, cN+) were manually segmented on Eclipse TPS v11. RapidArc (6-15 MV arcs) and 5 beams (6-15 MV) sliding window IMRT treatment plans were calculated according to our usual QA protocols by skilled planners. The PTV1 (CTV1+7/10 mm margin) was represented by the tumor, the PTV2 (CTV2+7 mm margin) by drainage pelvic nodes. The OaRs considered for this analysis were the body, the bowel bag and the bladder. The total prescribed dose for PTV2 was 39.6/1.8 Gy and 50.6/2.3 Gy for PTV1 through simultaneous integrated boost. The PTV V95 and OaRs QUANTEC dose constraints on the DVHs and Wu's homogeneity indexes (HI) were then analyzed to ensure the dosimetrical reliability of the plans. The structure sets were then uploaded on the MRIdian workstation and a 60Co plan was calculated by beginner planners after a specific training session. The DHVs and HI were then compared to the RapidArc and IMRT gold standard in order to evaluate MRIdian's performances.

Results: We calculated ten sets of three plans (MRI-60Co, RapidArc and 5 beams static IMRT) for ten consecutive patients. The MRI-60Co system showed a better HI when compared to the other techniques for PTV1, while this advantage could not be appreciated for PTV2, even if a better PTV2 V100 (39.6 Gy) was observed. Comparable mean doses for the bladder were registered, while a higher bowel V45 was observed (even if still in the constraints limits). Low dose body V5 was higher for the MRI-60Co system. The results are summarized in table 1.

Mean	MRIdian	RapidArc	IMRT
V95 PTV1 [%]	98.9	95.7	96.0
V105 PTV1 [%]	0.1	0.0	0.1
V95 PTV2 [%]	98.4	98.0	95.4
V100 PTV2 [%]	70.4	52.2	56.1
V105 PTV2 [%]	21.6	10.3	8.8
V5 Body [cc]	14615	12883	12617
V20 Body [cc]	7003	5004	6086
V45 Bowel Bag [cc]	9.5	6.3	6.9
Mean Dose Bladder [Gy]	37.2	36.2	37.0
Homogeneity Index PTV1	1.5	1.9	2.1
Homogeneity Index PTV2	7.8	5.5	6.0

Standard Deviation	MRIdian	RapidArc	IMRT
V95 PTV1 [%]	0.4	1.8	1.3
V105 PTV1 [%]	0.1	0.1	0.3
V95 PTV2 [%]	0.5	1.1	2.0
V100 PTV2 [%]	1.5	11.4	8.4
V105 PTV2 [%]	3.5	6.5	3.6
V5 Body [cc]	3837	3537	3598
V20 Body [cc]	1857	1620	1235
V45 Bowel Bag [cc]	18.1	13.1	14.1
Mean Dose Bladder [Gy]	3.7	1.9	2.5
Homogeneity Index PTV1	0.2	0.7	0.6
Homogeneity Index PTV2	0.4	1.4	1.0

Conclusion: We registered an higher PTV dose coverage between MRIdian's and the RapidArc and IMRT plans for cervical cancer, with a HI advantage for the PTV1. Differences were described for OaRs, especially for low dose areas (V5 Body). The MRIdian's planning platform showed to be user friendly and allowed to reach dosimetrical goals comparable to RapidArc and IMRT gold standards. The evaluation of a possible reduction in PTV margins and a proper target coverage by MRI based gating will be analyzed when the system will become operative.

PO-1009

VMAT planning approach to avoid superficial underdosage for accelerated partial breast irradiation

F. Zucconi[1], P. Mancosu[1], G. Reggiori[1], F. Lobefalo[1], A. Stravato[1], A. Gaudino[1], V. Palumbo[1], L. Paganini[1], F. De Rose[2], S. Tomatis[1], M. Scorsetti[2]

[1]*Humanitas Clinical and Research Center- Rozzano- Milan-Italy, Medical Physics Unit of radiation therapy, Rozzano, Italy*

[2]*Humanitas Clinical and Research Center- Rozzano- Milan-Italy, Departement of Radiotherapy and Radiosurgery, Rozzano, Italy*

Purpose or Objective: Accelerated Partial Breast Irradiation (APBI) is a RT approach that treats only the lumpectomy bed plus a margin, rather than the whole breast. The dose fluence outside the breast contour to account for breathing and residual motions can be manually increased with RapidArc/VMAT. At this aim, a 10 mm virtual expansion of the breast with soft-tissue equivalent HU is usually applied to the CT series (CT_E) and the optimization is performed on the APBI target expanded along the anterior/lateral directions. However, the dose recalculated on the original CT series (CT_O) could underdose the superficial target volume. In this study, a simple technical strategy to increase the target superficial dose is presented.

Material and Methods: Ten patients treated by APBI were randomly selected from the internal database (41 patients since 06/14). PTV_O was defined on CT_O as the tumor bed + 1-2cm, cropping it of 5 mm to the body. Dose prescription was 30 Gy in 5 fractions. Plans were normalized to PTV_O mean dose. PTV_E was defined on CT_E, expanding PTV_O of 10 mm in anterior/lateral directions. PTV_E was subdivided in three parts: PTV_EI (PTV_E cropped of 7 mm from the CT_O body - internal), PTV_ES (PTV_E cropped 5-7 mm - superficial), PTV_EE (PTV_E minus PTV_EI and PTV_ES - external). Two plans were optimized on the CT_E: (i) prescribing the same dose to the three PTVs, (ii) PTV_EI = 30 Gy, PTV_ES = 32 Gy, PTV_EE = 33 Gy. Final dose calculations for the two optimizations were performed on the CT_O. Plan objectives were: D98% (dose received by 98% of the target volume) > 95% and D2% < 107% for PTV, minimizing the homogeneity index (HI=D2%-D98%); V15Gy (volume of the organ receiving 15Gy) < 50% for breast minus PTV; V10Gy < 20% for ipsilateral lung; V5Gy < 10% for controlateral lung; V3-5Gy < 10% for heart, Dmax < 1-2 Gy for controlateral breast. Plans were compared in terms of dosimetric plan objectives findings.

Results: Figure 1 shows the different dose distribution for the two optimizations on the CT_O and CT_E. Opposite dose distributions outputs were obtained on the two CT series. On the CT_E, D98%, D2%, and HI were favorable to the (i) (respectively, 94.9% vs 94.5%, 103.7% vs 105.9%, 8.8% vs 11.5%). On the CT_O, D98%, D2%, and HI were favorable to the (ii) (respectively, 92.3% vs 94.2%, 104.3% vs 104.2%, 12.1% vs 10.1%). In particular, the superficial volume (i.e. PTV_ES) was the region of highest underdosage (D98%= 85.4 ± 3.3% for the first approach). Regarding the OAR, minimal changes were found between the two approaches.

Conclusion: A virtual overdosage on the superficial part of the APBI target is required to account for involuntary motions. A simple procedure was showed to fully cover the target.

Poster: RTT track: Head and neck reduction of margins and side effect

PO-1010

Partial delegation in 2-D match set-up evaluation for H&N IGRT treatment: preliminary results

A.R. Alitto[1], A. Pesce[1], S. Menna[1], M. Massaccesi[1], S. Manfrida[1], A. Pacchiarotti[1], A. Castelluccia[1], F. Miccichè[1], N. Dinapoli[1], G.C. Mattiucci[1], R. Autorino[1], F. Catucci[1], L. Azario[1], S. Luzi[1], V. Valentini[1], M. Balducci[1]

[1]*Università Cattolica S Cuore, Radiation Oncology Department- Gemelli-ART, Rome, Italy*

Purpose or Objective: Aim of this study was to determine the magnitude of discrepancies between radiation oncologists and radiation therapists to define a partial delegation of verification when 2-D orthogonal Kilovoltage (Kv) images are evaluated for daily set-up verification in head and neck cancer patients.

Material and Methods: Daily on-line kV-images of patients with head and neck cancer were evaluated for set-up verification both on-line by one of 7 radiation therapists (RTT) with adequate training, and off-line by a radiation oncologist (RO). All patients were treated by volumetric-modulated arc therapy (VMAT), by a LINAC 6 MV photon beam equipped with Millenium 120 MLC and on-board imaging system (VARIAN Medical System). Manual bone anatomy matching was used to determine translational displacements in all three axes (x, y, z) and discrepancies between RTT and RO were calculated. The concordance of decisions between RTT and RO were calculated, in particular for differences inferior, equal and superior to 3 mm. Results are presented as mean values, population systematic (Σ) and random (σ) errors. ANOVA test was used to test differences between groups. SPSS software was used for the statistical analysis.

Results: In this analysis 33 consecutive patients treated from March to September 2015 were included. Nine hundred ten (910) kV images were obtained and 2730 measures were made by the RO and RTT. A total agreement between RO and RTT was observed in 12.2% of cases. An inter-observer discrepancy of ±3mm or less and ±4 mm or less on at least one direction was recorded respectively in 98.4% and 99.3%

kV images. Mean displacements on all the three axes were about 1mm and 79% of differences in craniocaudal direction, 82% in lateral direction and 81% in ventrodorsal direction were between -1mm and 1mm. ANOVA test shows significant differences between the mean displacements of the samples ($p < 0.05$). In AP, CC and ML directions, systematic discrepancies were 0.33, 0.32, and 0.42 mm and random discrepancies were 1.25, 1.42, 1.21 mm, respectively. Mean radial discrepancy was 1.78 mm (range 1.11-2.88 mm). By van Herk's formula CTV-PTV margins needed to account for such inter-observer variability were 1.70, 1.80 and 1.90 mm in AP, CC and ML directions, respectively.

Conclusion: The study showed a small inter-observer variability between the RO and RTT's observations after an adequate training, which allows a partial delegation of daily kV control, if the displacements were not superior to PTV margins.

Poster: RTT track: Elderly and radiation therapy

PO-1011

Radiotherapy of brain metastases. Relationship with patients age an Karnofsky Index

J.L. Monroy Anton[1], J. Albestain Maria[2], M. Cuenca Torres[3], M. Lopez Muñoz[4], M. Soler Tortosa[4]
[1]*Hospital Universitario De La Ribera, Radiation Oncology, Madrid, Spain*
[2]*Universidad Catolica De Valencia, School Of Nursing, Alzira, Spain*
[3]*Hospital Universitario De La Ribera, Research Department, Alzira, Spain*
[4]*Hospital Universitario De La Ribera, Radiation Oncology, Alzira, Spain*

Purpose or Objective: Brain metastases are common secondary lesions in several types of neoplasms. Survival is poor, so the treatment with external radiotherapy has as main goal to improve the quality of life of patients by decreasing the possible symptoms that may have.
Our objective is to analyze age and general condition of the patients and their possible influence on the response to treatment with radiation therapy in terms of survival.

Material and Methods: We evaluated 84 patients with brain metastases treated with external radiotherapy .
Karnofsky Performance Status (KPS), was the tool to evaluate functional status the first day of treatment. We divided the population in two KPS groups: <70 vs ≥ 70
We also distinguish two age groups: <70 years vs 70 years (elderly population)

Results: Global mean survival: 5,2 months; median: 3 m
Survival <6months: 27patients (32,1%)
6-12 m: 11pts (13%)
>12 m: 9pts (10,7%)
Karnofsky Performance Status(KPS):
<70: 28 patients (33,3%) mean survival: 5,4 m; median: 3 m
<6m: 23 (82,1%)
6-12m: 4 (14,3%)
>12m: 1 (3,5%)
≥ 70: 56 pts (66,6%); mean survival: 5,4m; median: 3 m
<6m: 34 (60,7%)
6-12m: 14 (25%)
>12m: 8 (14,3%)
Age:
<70years: 58 patients (69%) mean survival: 5,1 m; median: 3 m
<6m: 41 (70,7%)
6-12m: 10 (17,2%)
>12m: 7 (12%)
≥ 70y: 26 (31%) mean survival: 5,3m; median: 3 m
<6m: 16 (61,5%)
6-12m: 8 (30,7%)
>12m: 2 (7,7%)

Conclusion: There are no significant differences in survival (months) depending on the age or the KPS in the analyzed population.
Survival in patients with KPS <70 is poor and less than six months in most cases. Most patients under 70 years have a survival <6mSurvival >12m is higher in KPS ≥70.
Survival in elderly patients (> 70years) is also less than six months. 6-12 months survival is higher in the elderly patients compared to the younger group, although survival >12m is slightly higher in the group of younger patients (<70y)
With these results we can consider applying hypofractionated treatment schemes (developed in few sessions) in the group of patients with KPS <70 or age ≥70 years, where poor survival is expected.

Poster: RTT track: Adaptive treatments in the pelvic region

PO-1012

Can we adequately irradiate bladder cancer without daily on line adaptive treatment?

J. Noordermeer[1], M. Mast[1], J. Egmond van[1], P. Koper[1], E. Kouwenhoven[1], H. Jager de[1]
[1]*MCH Westeinde, RCWEST, Den Haag, The Netherlands*

Purpose or Objective: Standard pattern of care for muscle-invasive T2-T3 bladder cancer is surgery. However, some patients are not eligible for surgery because of age, co-morbidity or non-resectability of the tumour. These patients are treated with radiation therapy. In the literature a large internal motion of the bladder has been reported. Therefore a portion of the Clinical Target Volume (CTV) can be missed during daily treatments. Our current treatment margins have been adjusted according to the findings of these studies. Reduction of margins is important for sparing the bowel. In the present study we investigated the influence of the bladder size and shape as well as the location of tumour itself on the margins.

Material and Methods: From 2013 to 2015, ten patients with solitary bladder cancer were treated. In five patients the tumour was marked circumferentially around the tumour bed using intravesical lipiodol injection. In the other five patients the tumour was not visible anymore after resection of the tumour and no lipiodol was used. As part of our routine treatment protocol, patients were instructed to have a full bladder during simulation and irradiation. They received instructions to void one hour prior to CT simulation or treatment and drink 250 cm3 of liquid. We acquired ConeBeam CT (CBCT) scans daily in the first week of the treatment and thereafter weekly. The bladder and lipiodol volumes were delineated on the CBCT. A bouding box and the centre of mass (COM) was calculated for the bladder and the tumour volumes on both the reference CT and all CBCT's for further analysis. Finally, a comparison of margins was carried out.

Results: In ten patients 93 CBCT-scans were analysed. Despite the full bladder protocol individual deviations were found in the bladder volume, mean volume 203 (SD 93ml), figure. Of the six anatomical directions the movement in the cranial and anterior direction were the largest and appeared to correlate with the volume of the bladder.

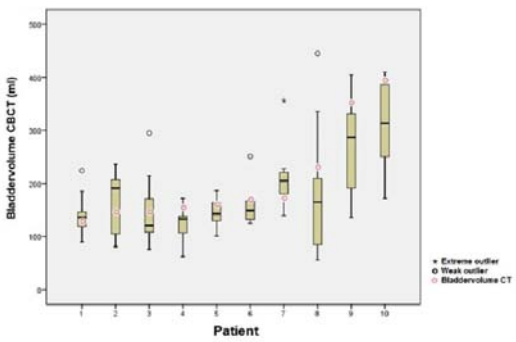

Figure: Boxplot of the bladder volumes for each patient
In the five lipiodol patients we found that the COM of the lipiodol depended on the bladder volume and the location of the lipiodol in the bladder. Based on this correlation we developed a model to predict the position of the lipiodol using the bladder volume. We calculated a margin based on the actual position of the lipiodol, and subsequently we calculated a margin based on the difference between the actual and the predicted position, Table.

	COM lipiodol					
	Actual position			Predicted position		
	LR	AP	CC	LR	AP	CC
	X	Y	Z	X	Y	Z
mean of means	-1.2	5.0	1.2	-0.2	0.1	0.0
stdev mean	3.1	5.2	6.0	0.5	0.5	0.2
mean stdev	2.2	5.2	5.6	2.8	4.2	4.6
Margin	9.2	16.6	18.9	3.2	4.1	3.7

Conclusion: As confirmed in the literature the full bladder protocol does not result in a stable bladder filling, and the displacement in cranial-anterior direction was the largest. Taking the predicted location of the tumour volume into account in preparing the treatment plans of the day, a considerable reduction in margin is achieved. Therefore, we need daily on-line adaptive treatment to adequately treat the bladder.

PO-1013

Adaptive radiotherapy in prostate cancer patients: concepts for Individualized Radiotherapy (iRT)

F. Fuchs[1], G. Habl[1], M. Devečka[1], S. Höfel[1], S. Kampfer[1], S. Combs[1,2], K. Kessel[1,2]
[1]*Technische Universität München TUM, Department of Radiation Oncology, München, Germany*
[2]*Institute of Innovative Radiotherapy iRT, Helmholtz Zentrum München, München, Germany*

Purpose or Objective: To evaluate interfraction volume changes and dose variations of organs at risk (OAR) and to develop individualized radiotherapy (iRT) concepts with movement compensation. This work analyzes the potential benefit of adaptive planning in patients with prostate carcinoma.

Material and Methods: We analyzed 16 patients with prostate cancer treated with helical IMRT and daily image guidance. Eight patients received radiation after prostatectomy with a total dose of 68 Gy in 34 fractions (group A), and eight a definitive irradiation with a total dose of 76.5 Gy in 34 fractions (group B). OAR rectum and bladder were delineated on daily Megavoltage (MV)CTs With the Planned Adaptive software by Tomotherapy® (Accuray Inc., Sunnyvale, CA) we performed dose recalculations on the single fractions CTs and compared the summation dose with the original planned dose. Dose variations were analyzed by means of Dmedian, Dmean, Dmax, Dmin, V30, V40, V60, V70, V75, as well as the OAR volume.

Results: Our evaluation is still ongoing. During treatment, rectum volume ranged from 62-223% (A: 62-157%, B: 63-223%) of its initial volume; bladder from 22-375% (A: 30-311%, B: 22-375%). The mean of the Dmean in the rectum was 30.7 Gy and 37.2 Gy in group A and B, respectively; and for the bladder 26.4 Gy and 40.8 Gy. The dose statistics for the rectum was as follows: V30 22.2-90.2%, V40 14.2-80.5%, V60 0.1-46.9%, only for group A: V70 1.0-22.3% and V75 0-7.2%. The statistics for the bladder are: V30 15.6-100.0%, V40 10.9-100.0%, V60 3.8-89.8%, only for group A: V70 1.6-28.0%, V75 0.5-19.4%.

Conclusion: For patients with prostate cancer, relevant variations in volume of OAR, such as rectum and bladder, can be observed. Hence, corresponding dose variations occur. Adaptive replanning approaches have the potential to reduce the dose to OAR. However, which concept, e.g. “plan of the day” or fast online recalculation, will be the suitable solution for routine patient treatment needs to be assessed in further evaluations.

PO-1014

Long time follow-up experience after IMRT for anal cancer: clinical outcomes and late toxicities

M. De Meric de Bellefon[1], P. Fenoglietto[1], D. Azria[1], C. Llacer-Moscardo[1], O. Riou[1], N. Pirault[1], E. Combettes[1], N. Aillères[1], F. Castan[1], C. Lemanski[1]
[1]*Centre Val d'Aurelle - Paul Lamarque, Hérault, Montpellier, France*

Purpose or Objective: To assess outcomes of patients with anal canal cancer treated with Intensity-Modulated Radiation Therapy (IMRT) after a long time follow-up.

Material and Methods: From July 2007 to September 2015, 233 patients were treated by IMRT for anal squamous cell carcinoma. In 2009, Volumetric Modulated Arc Therapy RapidArc (VMAT RA) rapidly became our usual way of radiation for this cancer. Radiotherapy consisted in delivering 45 Gy in 1.8 Gy daily-fractions, 5 days a week, to the primary tumor and the risk area including pelvic and inguinal nodes (PTV1). A second plan of 14.4-20 Gy was administered to the primary tumor (PTV2) in 1.8-2 Gy daily-fractions, also 5 days a week (Image 1), or by pulsed-dose rate interstitial brachytherapy for some T1 and T2. PTV1 and PTV2 were treated continuously without gap and without Simultaneously Integrated Boost (SIB). Concurrent chemotherapy based on 5FU-mitomycin (MMC) or cisplatin was added for locally advanced tumors. Toxicities were evaluated according to the Common Toxicity Criteria for Adverse Events 4.0 scale. The survival estimates and their associated CI95% were calculated using the Kaplan-Meier method. We present here the first 166 patients’ outcomes.

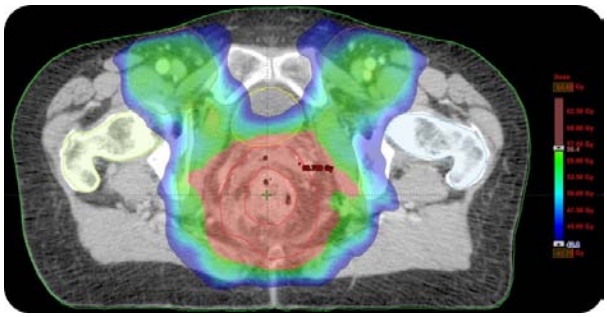

Results: Median follow-up was 46,7 months CI95% [41,2-51,6]. 124 women (75%) and 42 men (25%) were analysed. Median age was 61 years (range, 36-92). Tumors were classified as stages I, II, III and IV in 13%, 25%, 57% and 4% of the cohort, respectively. 13 patients were immunocompromised, 10 of those were HIV-positive (6%). Radiochemotherapy (RCT) or radiotherapy alone (RT) was delivered in 132 (80%) and 34 (20%) patients, respectively: 104 (79%) MMC, 25 (19%) cisplatin and 3 (2%) other regimens. 21 patients (13%) had the PTV2 treated by brachytherapy. 162 patients (97,6%) were complete responders. 36 patients (21.7%) had a relapse : 20 local (56%) among which were 3 synchronous metastatic failures, 4 locoregional (11%) and 12 metastatic without any local failure (33%). 33 patients (20%) had a colostomy following radiotherapy : 17 (46%) for local relapse, 12 (32%) for radiation toxicity, 3 (8%) for an uncomplete response, 1 (2,7%) for tumor complications during RCT. Concerning late toxicities: no grade 4 was observed; grade 3 were diarrhea (1 patient), proctitis (11), vaginal stricture (5), hematuria (1), fecal incontinence (4), chronic radiodermatitis (2 patients); 28 cases of grade 2 occurred among those clinical categories. About the hematologic late toxicity, there wasn’t any significative difference between the blood count prior to treatment and the recent one (p=0.23). The 3-year overall survival rate was 85.5% CI95% [78.7-90.3], cancer-specific survival 89,0% CI95% [82,5-93,1], disease-free survival 74.6% CI95% [67-80.8],

relapse-free survival 79.6 % CI95% [72.1-85.2] and colostomy-free survival 81.2% CI95% [74.0-86.6].

Conclusion: IMRT is emerging as a standard therapy for anal cancer. A dosimetric analysis will be done to complete this study.

Poster: RTT track: Other topics for RTTs

PO-1015

Virtual training in patient information sessions prior to external beam radiotherapy

A. Stewart-Lord[1], M. Brown[2]
[1]*London South Bank University, School of Health and Social Care, London, United Kingdom*
[2]*Barking- Havering & Redbridge University Hospitals NHS Trust, Cancer & Clinical Support Division, London, United Kingdom*

Purpose or Objective: The aim of the study was to explore the prostate patients' perceptions of Virtual Environment for Radiotherapy Training (VERT) as an information giving resource prior to radiotherapy delivery.
The objectives were:
• To determine the level of knowledge of those patients who attended (VERT) for a pre-treatment talk
• To explore patients perceptions who utilised (VERT) as an information giving resource prior to radiotherapy treatment
• To identify the benefits and limitations of using VERT as pre-treatment information giving resource

Material and Methods: A survey design was utilised to address the aims and objective of the study. The study was conducted over 2 phases: Phase 1 - participants were invited to attend a (VERT)patient information session four weeks prior to their planning CT scan. Phase 2 – patients were asked to complete a questionnaire two weeks after start of radiotherapy treatment. The questionnaire was designed to collect data on the prostate cancer patient's knowledge attitudes and beliefs regarding pre-treatment information provided prior to their radiotherapy treatment. A total population sample was used for this study. All patients being referred for radical radiotherapy to the prostate were invited to participate, over a five month data collection period (March – August 2015). A total of n=40 patients were included in the sample

Results: Statistical package SPSS (Version 21) was used for data analysis. Descriptive statistics and frequency tables were the first steps in the data analysis. Thereafter, Chi-squared tests were used to analyse the data further. Open ended questions were analysed thematically.
Results are currently being analysed however preliminary results are very positive, a summary of the preliminary results are outlined below (the final presentation will include frequency tables):
•Most patients found the (VERT) session to be very helpful
•Most patients stated that the session helped them to understand the importance of following bowel and bladder instructions prior to treatment and enhanced their knowledge about radiotherapy side effects
•The sessions were highly recommended for other patients and future recommendations included family members and carers to be included.
•Most patients were comfortable being part of a group during the presentation.
•Patients believed the sessions reduced their anxiety and stress about their upcoming treatment.

Conclusion: Patient perceptions on the use of (VERT) as information giving tool prior to radiotherapy treatment were very positive. The sessions enable patients to understand the potential impact of treatment volumes if the internal organ shape and location differed from that originally planned, enabling them to comply with radiotherapy treatment instructions.

PO-1016

Radiotherapy students' perceptions of skills training simulation using a bariatric suit

R.N.M. Khine[1], D. Flinton[1], P. Cherry[1], R. Thorne[1]
[1]*City University London, Radiography, London, United Kingdom*

Purpose or Objective:
Aim: The question posed is *"Can simulation training improve/enhance student knowledge and skills in dealing with bariatric patients?"*
Context: Accurate patient positioning, immobilisation and the delivery of precisely targeted radiation treatment are key stages in the radiotherapy process and bariatric patients present a unique challenge in achieving these stages. Radiotherapy for obese patients is a major challenge, both for the patient and the radiographer. There are practical limitations of radiation therapy equipment such as treatment couch weight limits and computed tomography (CT) scan aperture limits. Daily setup potentially is difficult. In addition, it also impacts on the safe manual handling on both staff and this group of patients.

Material and Methods: As part of their professional practice clinical skills sessions, the Year one undergraduate radiotherapy students (n=32) took part in a simulation session involving a bariatric suit. During each session, the radiotherapy lecturer wore the bariatric suit whilst the students working in pairs were required to position the lecturer (acting as the patient) on the couch.
After each simulation session, students were asked to complete a 10 point Likert scale questionnaire which permitted them to rate their experience of using the bariatric suit. A response rate of 100% was achieved.
They were asked to consider the following 3 areas:
•Whether it aided their learning in positioning patients'
•Whether it increased their awareness to deal with different patient groups
•Whether it increased their knowledge on the importance of accuracy and precision
In addition, they were asked to write a short reflection to identify what they learnt from the session.

Results: Students gave favourable feedback in all 3 areas investigated with a mean score above 4.5 (range -5 to +5)
The written reflective feedback supported the above quantitative scores by acknowledging the benefits of simulated training

Conclusion: The feedback from the students suggests that simulation training using a bariatric suit has had a positive impact on their learning. In addition, the sessions have assisted them in appreciating aspects as such as accuracy, precision, communication and manual handling issues. Most significantly students have acknowledged that the sessions have prepared them for their clinical placements.

PO-1017

Survey of image-guided radiation therapy use in Australia

V. Batumalai[1,2], L. Holloway[1,2,3,4], S. Kumar[1,2], K. Dundas[1], M. Jameson[1,4], S. Vinod[1,2], G. Delaney[1,2]
[1]*Liverpool Cancer Therapy & Ingham Institute, Radiation Oncology, NSW, Australia*
[2]*South Western Clinical School, University of New South Wales, NSW, Australia*
[3]*Institute of Medical Physics, University of Sydney, NSW, Australia*
[4]*Centre for Medical Radiation Physics, University of Wollongong, NSW, Australia*

Purpose or Objective: Image-guided radiation therapy (IGRT) utilises various imaging modalities for target and organs at risk delineation, tumour localisation, and patient setup. Although there is considerable development in IGRT technologies in Australia, little is known about their current clinical applications. The aim of this survey was to evaluate imaging technologies currently in use for planning and delivery of radiotherapy (RT) in Australia.

Material and Methods: An online survey was developed and sent to all 73 RT departments in Australia in August 2015. The survey inquired about imaging practices during both planning and treatment delivery processes. Respondents were asked about the types of IGRT technologies used, reasons for implementation, current utilisation rates, and future plans for IGRT use in their department.

Results: Responses were received from all states and territories, with a response rate of 71%. All respondents had access to CT simulators and regularly used image registration to fuse or co-register the following scans to the RT planning CT to aid tumour delineation; diagnostic CT (50%), diagnostic MRI (95%), planning MRI (34%), planning PET (26%) and diagnostic PET (97%). All respondents used some type of IGRT for in-room setup/tumour localization. The percentage of respondents using ultrasound, MV planar, kV planar, kV CBCT, and MVCT (Tomotherapy) were 9%, 77%, 89%, 97%, 6%, respectively. For other modalities, the percentage of respondents using spirometer, infrared, optical, and radio-frequency systems were 17%, 31%, 9% and 6%, respectively. Figure 1 displays the cumulative adoption of each IGRT modality based on reported years of adoption. Most centres used a combination of modalities for each tumour site depending on the treatment technique used. Table 1 shows rationale for in-room IGRT implementation. The main reasons or contributing factors for under-utilisation of in-room IGRT use were; lack of equipment capability (53%), insufficient funding (38%), concerns about imaging dose (34%), physicist availability for commissioning (28%), radiation oncologists availability to assess images (28%), and radiation technologists availability for image assessment (25%). The number of departments planning to increase use of IGRT for target delineation and in-room set-up/tumour localisation was 46% and 55%, respectively. No current users planned to decrease or cease use of IGRT.

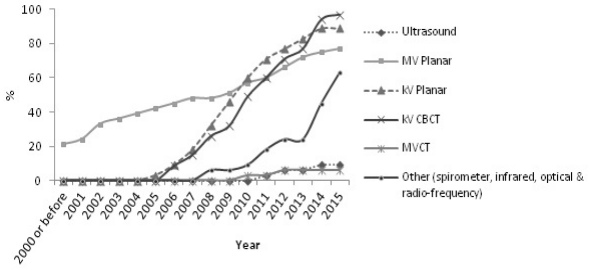

Reasons for implementation	Percentage of respondents
Use of highly conformal techniques	100
Workflow enhancement	77
Use of hypofractionated regimen	57
To minimize normal tissue toxicities	89
To decrease CTV to PTV margin	63
Use of adaptive radiotherapy	54
Clinical trial requirement	43

Conclusion: This survey provides an insight into the IGRT technologies currently in use in Australia. IGRT is widely used among radiotherapy centres in Australia for both planning and treatment delivery. To our knowledge, this is the first study to assess the overall use of IGRT in Australia.

PO-1018

Increase efficiency and quality? Yes please! Use project management, participation and ownership

P.E. Tødenes[1]
[1]*Ålesund Hospital, Academic Physics, Ålesund, Norway*

Purpose or Objective; In Norway about 30,000 Norwegians get cancer each year. Approximately 230,000 Norwegians are living with cancer. The numbers are increasing rapidly. With population growth, longer life expectancy and elderly wave, Norway will have a need to streamline their health care.

Material and Methods: In Norway it has been common that each treatment attendance is set to 15 minutes (one PVE - Patient Visits Equivalent) by default. Normal opening hours are from 08:00 a.m. to 3:30 p.m. In other words 30 PVE per machine per day. Norway has strong union movement and strong culture of cooperation and involvement of employee representatives and employees. From management theories we know that change processes are easier to achieve if the changes are requested by the employees, owned by the employees and that employee representatives are included in the process. Radiation therapists and physicists are concerned with quality. Streamlining should not come at the expense of quality. One must therefore find efficiency measures that both improve quality while offering a more efficient operation.In autumn 2014 began management of the department to look at measures to increase quality and improve operational efficiency. One had thought of several possible ways; extended opening hours, logistics efficiency, LEAN processes, dressing stalls, automatic gantry and field execution, change PVE. We organized the work as a project where we included employee representatives and employees. The group consisted of a total of 4 people. They got a project that consisted of; background, mandate, goals, objectives, organization and budget. Important keywords were; Quality, time and cost. The order was that the group would come with concrete suggestions to increase the quality and efficiency. It was pointed out that efficiency should not compromise on quality. The order was both open and linked to direct questions.The group leaves after a few months forward its proposals. The proposals were discussed in a meeting between management and the group. The group then got feedback on what they could work on and discard. A new meeting was scheduled and we together agreeing on measures. The measures were then presented for all workers at the department. The project was then closed down and implements regular operation.

Results: We increased opening hours by 30 minutes without changing working hours or labor costs. Standard PVE was changed from 15 minutes to 10 minutes. One will thus be able to increase patient meetings with around 60% per treatment machines without increasing staffing levels of radiation therapists and physicists. The increase will be gradual and in close dialogue with employee representatives and employees.

Conclusion: Project management is a good work method to introduce changes. All employees now have ownership of the changes that the department must gradually take over the coming years.

PO-1019

Reflective practice: What is its impact on therapy radiographers practice?

J. Rodgers[1]
[1]*Rodgers John, Academic Physics, Manchester, United Kingdom*

Purpose or Objective: Reflective practice is a well-established aspect of professional development within radiotherapy. It is believed to improve patient care by assisting in workplace learning and providing more competent radiotherapy practice. The aim of the study was to investigate how therapy radiographers perceive how engaging in reflective practice impacts upon their work practice

Material and Methods: A closed question format Likert questionnaire formulated to investigate therapy radiographer's opinions on how reflection impacts on their work practice was distributed to therapy radiographers in The Christie NHS Foundation Trust radiotherapy department and its satellites. Focus groups were employed to investigate

questionnaire findings, in order to provide a deeper understanding of the processes involved and allow a separate methodology to either reinforce or reject findings.

Results: Questionnaire response rate was 78%. 81.8% of radiographers who participated agreed that reflection is an essential part of their professional learning.
Of the radiographers who responded 96% said they could recall engaging in informal reflection. Fewer could recall recently practicing formal reflection. When asked if they feel their work practice improved after reflecting informally 89.5% of radiographers agreed. Compared to informal reflection, less agreed that engaging in formal structured reflection had improved their work practice (76.4%).
Focus group data results suggest that radiographers believe informal reflection is an essential element of their professional learning, and that it has a direct beneficial impact on their patient care. There is a lack of consensus on the practice of formal reflection, with many radiographers citing barriers such as lack of time, training and evidence to support its use.

Conclusion: This study has found that therapy radiographers within the Christie NHS Trust believe engaging in reflective practice directly benefits their professional work and, by inference, improves patient care. Informal refection is considered more effective and easier to employ. It should therefore be acknowledged by educators and professional bodies as the dominant reflective process.
To encourage the adoption of formal reflective practice, researchers and theorists should work on unifying the paradigm around a more simplistic, focused approach. Further research investigating the impact of an appropriate reflective model within the radiotherapy clinical setting using a robust qualitative study design is recommended.

PO-1020

Occurrence of visual phosphenes during radiation therapy of the head

A. Timmers[1], W.J.M. De Kruijf[1], T. Rozema[1]
[1]*Institute Verbeeten, Klinische Fysica & Instrumentatie, Tilburg, The Netherlands*

Purpose or Objective: We investigated the occurence of visual phosphenes during the irradiation of the head. Visual phosphenes may occur because of direct stimulation of the retina by ionising radiation or by the Cerenkov irradiation that is generated in the eyeball. These are 2 different physical processes with their own characteristic visual sensation for the patient. We hypothesise that the direct stimulation of the retina is perceived as flashes of light, whereas the Cerenkov effect is perceived as a coloured light source. These are also the 2 main visual phosphenes that patients report. The first objective of the research is to establish what percentage of patients perceives light flashes or coloured light. The second objective is to determine, if it is perceived, what percentage of treatment fractions the patient perceives light flashes or coloured light. The third objective is to determine whether there is a relation between the perception of light flashes and the dose to the retina, or whether such a relation exists between the perception of coloured light and the dose to the eyeball.

Material and Methods: The inclusion criteria for the study were: treatment on the head, treatment plan with at least 3 fractions, and an informed consent. The patient was asked to complete a survey after each treatment fraction. We specifically ask for the occurrence of flashes of light and/or the occurrence of coloured light. Moreover, we ask for a description of the perception. We distinguish between 6 MV (59 patients) or 10 MV (15 patients) treatment plans. The dose relation has been investigated for a subgroup of 17 patients.

Results: 1) Approximately 60% of the patients with 6 MV plans and about 70% of the patients with 10 MV plans observe light flashes or coloured light at least once during their treatment. Often both light flashes and coloured light are observed at the same fraction. However, it also occurs that only light flashes are observed or only coloured light is observed. 2) If light flashes or coloured light are perceived this occurs in approximately 70% of all treatment fractions for 6 MV beams, approximately 80% of treatment fractions for light flashes in 10 MV beams and approximately 90% of treatment fractions for coloured light in 10 MV beams. 3) The subgroup is too small to establish a dose relationship. However, below an average dose of 25 cGy on both retinas and both eyeballs almost no phosphenes are observed. For plans with an average dose of more than 150 cGy in one retina and more than 100 cGy in one eyeball, the patients in our subgroup perceive both phenomena at every fraction.

Conclusion: We have characterized the occurrence of visual phosphenes in our clinic. A relatively large number of patients perceives these phenomena. A dose relationship cannot be established but seems to exist.

PO-1021

Implementation and clinical use of a digital log regarding the Traffic Light Protocol in daily IGRT

R. Verhage[1], S. Van Beek[1], A. Smit[1], M. Broekhof[1], P. Remeijer[1]
[1]*The Netherlands Cancer Institute, Department of Radiation Oncology, Amsterdam, The Netherlands*

Purpose or Objective: With the introduction of a decision protocol for anatomical changes as observed on ConebeamCT (CBCT) images (traffic light protocol (TLP)), data such as, for example, actions in response to certain anatomical changes have been recorded in the open text area of the patient's electronic treatment chart on a daily basis. Recording the data in this way is manageable for keeping track of changes during a treatment, but this method cannot easily be used for retrospective analysis for e.g. research purposes. Therefore, we have introduced a dedicated digital TLP log within the patient's dossier, that enabled a clear and structured overview of the information gathered from the CBCT scans. In a retrospective study, the efficacy of this log was evaluated.

Material and Methods: The TLP digital log was implemented and accommodated in the Mosaiq Oncology Information Management System. The log contains a separate format for each of the major target areas on which the TLP is used and does not contain any free text entry fields. For every CBCT acquisition a log entry is created. Within the log the user can register the relevant anatomical changes seen on the CBCT, by using drop down lists with fixed entries (e.g. bladder filling or tumour regression and the action taken (see figure). The actions are categorised by colour: Green (no action), Yellow (notification of the Medical Docter (MD) optional), Orange (action needed by the MD before next fraction) and Red (immediate action needed from the MD). During the period of data gathering the digital TLP was made available for five target areas: Breast, Sarcoma, Lung, Gynaecology and Urology. The digital log was retrospectively evaluated on 120 patients (40 for urology, 20 for all other target areas) with a CBCT imaging protocol treated from January 2013 to December 2013. The use of the digital log in clinical practice was evaluated using a questionnaire filled in by the RTTs. During the data gathering, a total of 1806 CBCT scans were reviewed and registered in the digital log. All of these scans were assessed with the TLP to determine the course of action. In this period, all action codes were registered and recorded.

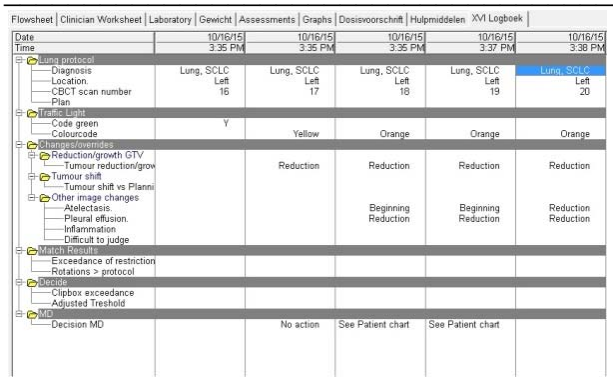

Results: Using the digital log, the data concerning the TLP can be stored in a structured way, rather than in open text parts of a patient's dossier. The action codes regarding the anatomical changes that are present in the log showed a clear overview of possible variations during treatment. The RTTs scored an average of 7.8/10 in the questionnaire on the digital log overview. In succession, this overview showed a clear course of action regarding these anatomical changes using the TLP.

Conclusion: The implementation and use of a digital log improves the overview of the anatomical changes observed on CBCT during radiotherapy. Moreover, the data gathered within the log can retrospectively be used for clinical or research questions regarding clinical IGRT decisions for a specific target area.

PO-1022

Robotic radiosurgery for vestibular schwannomas - the early tumor response and treatment tolerance

I. Wzietek[1], A. Namysl-Kaletka[1], A. Napieralska[1], D. Gabrys[1], S. Blamek[1]

[1]*Maria Sklodowska-Curie Memorial Cancer Center and Institute of Oncology III Dept, Radiotherapy Department, Gliwice, Poland*

Purpose or Objective: Vestibular schwannomas (acoustic neuromas) are common benign tumors that arise from the Schwann cells of the vestibular nerve. Management options include observation with neuroradiological follow-up, microsurgical resection or stereotactic radiotherapy (SRS). The aim of the study was to evaluate tumor size and treatment tolerance of patients treated with CyberKnife (CK) radiosurgery for vestibular schwannoma (VS).

Material and Methods: Between 2011 and 2014, 96 patients with 100 vestibular schwannomas were treated with SRS using CK. The vestibular schwannomas of 5 patients were associated with type II neurofibromatosis. Twenty patients were operated on before radiosurgery. All patients had more than one year follow-up. The median age at the time of treatment was 59 (range 21-88 years). Median tumor diameter was 18 mm (range 3-48 mm) and the median prescribed dose was 16 Gy (12-21 Gy). In 29 patients, single dose of 12-18 Gy was delivered, in 31 total dose of 12-16 Gy was delivered with two fractions and the remaining 40 patients were treated with 15-21 Gy delivered in 3 fractions baseline. Hearing was classified according to the Gardner Robertson grading scale (48% of patients had serviceable hearing).

Results: At 12 month after SRS we observed that :15% of tumors slightly expanded, in 8% patients slight expansion of tumor followed by regression, 11% of tumors increased in size, but then remained stable, 58% were stable in size and 8% responded to therapy. Overall, tumor swelling was, thus, observed in 34% of patients. At first year no patient required neurosurgical intervention due to tumor progression or brainstem compression symptoms. 77% patients had stable level of hearing after SRS, 9% declared improvement and 14% worsening of hearing. The rate of complications was very low, with most consisting of a transient worsening of preexisting symptoms. At the last assessment, full facial and trigeminal nerve function was preserved in 95% and 98% of patients, respectively; the only facial deficit (House-Brackmann grade III) occurred in patient who received a single dose of 18 Gy in one fraction early in our experience, the remaining were mild, grade II dysfunctions. None of the patients treated with doses lower than 13 Gy experienced facial or trigeminal neuropathy.

Conclusion: Cyber Knife radiosurgery is a safe and effective treatment for VS characterized by high probability of retaining functional hearing and facial and trigeminal nerve function preservation. In about one third of patients a tumor swelling after treatment is observed but reliable tumor control and persistence of neural dysfunctions assessment requires longer follow-up.

Poster: RTT track: Position verification

PO-1023

Quality assurance for IMRiS phase II study of IMRT in sarcomas: a survey of limb immobilisation

R. Simões[1], E. Miles[1], F. Le Grange[2], R. Bhat[3], B. Seddon[2]

[1]*Mount Vernon Hospital, RTTQA group- Radiotherapy Physics, London, United Kingdom*

[2]*University College of London Hospital, Sarcoma Unit, London, United Kingdom*

[3]*Cancer Research UK, UCL Cancer Trials Centre, London, United Kingdom*

Purpose or Objective: Soft tissue sarcomas are rare malignancies, commonly arising in limbs, with an annual incidence of 3,298 cases in the UK in 2010. Their rarity leads to a lack of published data and experience in limb immobilisation for radiotherapy planning. The IMRiS trial is a phase II study of intensity modulated radiotherapy (IMRT) in primary bone and soft tissue sarcoma, due to open in late 2015. As part of a pre-trial quality assurance (PT QA) programme, we report on the current UK practice of limb soft tissue sarcoma (LSTS) immobilization and the significance for multi-centre trial recruitment.

Material and Methods: A facility questionnaire (FQ) was circulated to 29 IMRiS centres to investigate variation in immobilisation devices (ID), planning techniques, and imaging protocols. A workshop was held to address limb sarcoma immobilisation and patient set up. Robustness of patient setup at each centre was evaluated based on setup audits, frequency of imaging and the number of patients (pts) treated per centre per annum.

Results: 27 questionnaires were returned. Less than 1/3 of the responders routinely treat their pts with IMRT (8/27). The remaining 2/3 have little or no experience with IMRT for LSTS. Vacuum bags are currently the most popular ID (9/27), followed by thermoplastic shells (7/27), limb boards (5/27), other devices (3/27) of which 2 used in-house developed and customisable devices, and 1 used common positioning pads. 2 centres combined the use of vacuum bag and shell. 9 centres had audited their setup. However, only 4 had calculated their setup margins on the basis of systematic and random error. The majority of centres follow the recommendations to perform imaging on days 1 to 5 and then weekly. 6 centres perform daily imaging (all 6 treat LSTS with IMRT). Of 6 centres with a high level of setup robustness, 3 are IMRT centres. On average centres treat 24 pts annually (range 3-53). Currently over half the centres treat less than the calculated average number of pts.

Conclusion: The results from the FQ and workshop demonstrate variations in treatment modality, ID and imaging frequency across the UK. 70% of IMRiS participating centres will be implementing or further developing IMRT in order to treat LSTS in the study. This will require a change in treatment modality (from 3DCRT to IMRT) in 9 centres. Comprehensive PT QA is required to ensure quality in a trial to be run at centres with such different levels of experience.

Robustness of patient setup is important to decrease variability arising from different ID. The PT QA program will encourage centres to assess robustness of setup through audit and calculation of centre specific margins. The majority of centres will need to review treatment verification as daily imaging is mandated for the trial. We anticipate that centres with less robust setup systems may need more support to safely implement IMRiS, and in response to this a discussion group will be created to allow centres to share their experience.

PO-1024

Residual interfraction error after orthogonal kV in stereotactic RT. Analyses from 139 CBCT scans

S. Manfrida[1], A. Castelluccia[1], M. Massaccesi[1], V. Frascino[1], M. Ferro[1], C. La Faenza[1], A. Petrone[1], N. Dinapoli[1], C. Mazzarella[1], M. Vernaleone[1], G. Macchia[2], G.C. Mattiucci[1], L. Azario[1], S. Luzi[1], V. Valentini[1], M. Balducci[1]

[1]Gemelli-ART- Università Cattolica S.Cuore, Radiation Oncology Department, Rome, Italy

[2]Fondazione di Ricerca e Cura " Giovanni Paolo II"- Università Cattolica S.Cuore, Radiation Oncology Unit, Campobasso, Italy

Purpose or Objective: To quantify residual interfraction error after two-dimensional (2D) orthogonal kV set-up correction using cone-beam CT (CBCT) and 6DOF robotic couch for target localization in patients undergoing stereotactic radiotherapy.

Material and Methods: After clinical setup using in-room lasers and skin/cradle marks placed at simulation, patients were imaged and repositioned according to orthogonal kV registration of bony landmarks to digitally reconstructed radiographs from the planning CT. A subsequent CBCT was matched to the planning CT using also soft tissue information and the resultant residual error was measured and corrected before treatment. Absolute averages, statistical means, standard deviations, and root mean square (RMS) values of observed error were calculated.

Results: From June 2014 to October 2015 a total of 45 patients with intracranial (15 pts), intrathoracic (19 pts) and abdominal (11 pts) lesions received 139 fractions of SBRT. 2D kV images revealed a vector mean setup deviations of 0,9 mm (RMS). Table 1 shows residual translational shifts observed with CBCT. Means of pitch, roll and yaw errors were 0,18° , 0,27° and 0,05°, respectively. Pitch, roll, and yaw errors were lower than 1° in 92%, 88% and 82% of images, respectively. According to tumor site, residual setup deviations seemed to be higher for abdominal lesions (RMS 1,4 mm) compared with intrathoracic (RMS 1,1 mm) and intracranial lesions (RMS 1,0 mm).

		AP (mm)	SI(mm)	ML(mm)
Overall	Mean	-0,8	-4,0	-0,9
	Mean M	3,3	3,1	3,4
	SD	5,1	5,1	5,0
	RMS	1,3		
Intracranial lesions	Mean	-0,7	-0,1	-0,7
	Mean M	1,1	1,6	1,7
	SD	5,3	5,1	4,9
	RMS	1,0		
Intrathoracic lesions	Mean	-0,8	-0.2	-0,7
	Mean M	5,0	4.2	3,6
	SD	5,2	5.0	4,9
	RMS	1,1		
Abdominal lesions	Mean	-0,8	-0,3	-1,2
	Mean M	3,8	3,2	4,8
	SD	5,1	5,1	4,9
	RMS	1,4		

Tab. 1: Residual translational shifts detected by CBCT after repositioning according to kV registration.
Abbreviation: AP= anterior-posterior, SI= superior-inferior, ML= medial lateral, Mean M= mean value in magnitude, SD= standard deviation, RMS= root mean square .

Conclusion: These data confirm the importance of CBCT to reduce interfraction errors, expecially when high dose per fraction is delivered. Residual interfraction shifts for intracranial lesions is lower than for other tumor sites, probably as consequence of poor relevance of organ motion in this site.

PO-1025

Reproducibility of prone immobilization in breast treatment – a retrospective study

N. Rodrigues[1], A. Francisco[1], S. Vieira[1], J. Stroom[1], M. Coelho[2], D. Ribeiro[1], C. Greco[1]

[1]Fundação Champalimaud, Radiotherapy, Lisboa, Portugal

[2]Mercurius Health, Radiotherapy, Lisboa, Portugal

Purpose or Objective: Many studies have been conducted regarding the dosimetric advantages of prone positioning systems for breast radiotherapy treatments, especially for pendulous breasts. However, there is a shortage of publications considering the reproducibility of such systems. This study performs a retrospective patient set-up analysis of a prone positioning system. An estimation of the required safety margin was also calculated in an attempt to predict if patients undergoing breast irradiation in prone position could be safely treated without an online correction protocol.

Material and Methods: A group of 21 patients with localized breast cancer were treated in prone position (New Horizon™ Prone Breastboard, CIVCO Medical Solutions) with a fractionation scheme of 3.2 Gy x 15 to the boost and simultaneously 2.7 Gy x 15 to the whole breast. An online correction protocol based on CBCT imaging was applied and the initial set-up deviations (i.e. the first registration data for each fraction) were used in this study. The overall mean population error (μ) for each translational direction was calculated, as well as the population systematic (Σ) and random (σ) components. These outcomes were subsequently compared to the results derived from an equally numbered group of patients treated in supine position (C-QUAL™ Breastboard, CIVCO Medical Solutions) with the same fractionation scheme.

In both treatment positioning systems CBCT matching criteria was prioritized according to: 1 - Breast contour; 2 - Boost position; 3 - Chest wall.

The mean number of repositioning for each population was also considered.
Geometrical margins were calculated according to the following margin recipe:

$$M_{Geo}=2.1\sum+0.8\sigma$$

Results: Results regarding the evaluated overall mean population error (μ), population systematic (Σ) and random (σ) components and estimated safety margin (Mgeo), for both immobilization techniques, are displayed in Table 1.
A 5 mm safety margin is used in our institute and an online protocol is followed. However if an off-line protocol would be applied (50% reduction of systematic errors) the resulting Mgeo, for the prone positioning, would be of 7,6 mm (SI), 8,2 mm (ML) and 5,6 mm (AP) and the applied margin would be insufficient.
Regarding workload, patients in prone position are, on average, repositioned 4 times during the 15 fractions against 1 repositioning for patients in supine position, which we consider to be acceptable when considering the dosimetric gains for PTV coverage and OAR.

	μ (mm)			Σ (mm)			σ (mm)			M_{Geo} (mm)		
	SI	ML	AP	SI	ML	AP	SI	ML	AP	SI	ML	AP
Prone	1,2	-1,3	-1,1	4	4,8	2,4	4,2	3,9	3,8	10,4	12,2	9,1
Supine	-0,3	-1,5	1,7	2,6	1,9	2,3	2,5	1,9	2,7	8,7	6	7,1

Table 1 - Results for the overall mean population error, systematic and random components and estimated safety margins.

Conclusion: Comparing with supine, prone positioning is more unstable and suffers from larger set-up errors, due to both systematic and random components. Additionally, without an online imaging protocol it requires larger safety margins. However, given the dosimetric advantages of prone immobilization, we conclude that this type of positioning can be safely used as long as an adequate margin is applied and especially if an online imaging protocol is followed.

PO-1026

Setup accuracy of DIBH for breast treatment with a simultaneous integrated boost.

B. Kraan[1], M. Admiraal[1]
[1]*VU medical Center, Radiotherapy, Amsterdam, The Netherlands*

Purpose or Objective: This study aimed to quantify the setup accuracy of voluntary Deep Inspiration Breath Hold irradiation of the left breast with a simultaneously integrated boost (SIB). We investigated the additional effort required to achieve the same accuracy as in non-breath hold SIB treatment.

Material and Methods: Thirty patients with breast cancer were selected for retrospective setup analysis, 15 patients were treated in free breathing (FB), and 15 patients were treated with Deep Inspiration Breath Hold (DIBH).
Patients in the breath hold group were trained to perform a voluntary DIBH in advance of CT scanning. Breathing motion was monitored using the Real-time Position Management System (RPM, Varian Medical Systems, Palo Alto CA). An in-house developed visual feedback system was available to display the live RPM signal to the patient, both at CT and at the linac. All patients were treated in 21 fractions, each delivering a dose of 200cGy to the whole breast and a 267cGy boost to the tumor bed. Plan setup was similar for all patients, with two tangential open fields and 4 additional IMRT fields to minimize inhomogeneity and to boost the tumor bed.
Setup at the linac was based on two 2D-kV images (Varian Medical Systems, Palo Alto CA), either in free breathing (FB group) or in breath hold (DIBH group). All images were matched such, that the surgical clips deviated no more than 5mm in all directions, and the ventral bony anatomy was within 8mm. If these two limits could not be achieved in one match, re-positioning was performed.
We analyzed residual setup error in bony anatomy and clips separately, by re-matching the images twice: focusing either only on the bony anatomy, or only on the clips. We also scored the time between the first setup image and the first treatment field (setup-time).

Results: Deviation of the bony anatomy and clips with respect to the online match were small, and not different between the FB group and the DIBH group (table1).

	ventro-dorsal (cm)	cranial-caudal (cm)	lateral (cm)
FB_{bone}	0.3	0.3	0.2
$DIBH_{bone}$	0.3	0.2	0.2
Fb_{clips}	0.1	0.1	0.1
$DIBH_{clips}$	0.1	0.1	0.1

***Table 1**: average offset with respect to the online match for bone match (top rows) and clip match (bottom rows) for FB group and DIBH group .*

The average setup-time was 6 and 8 minutes for the FB group and DIBH group respectively, with re-setup in 8 out of 135 fractions (6%) for the FB group, and 7 out of 55 fractions (13%) for the DIBH group.

Conclusion: In treatment of left sided breast patients with a simultaneous integrated boost the same setup accuracy can be reached in DIBH as in treatment in FB. To reach this accuracy, the DIBH group needs re-positioning more often than the FB group. Consequently, the online setup in DIBH will require additional time.

E-POSTERS

Electronic Poster: Clinical track: Head and neck

EP-1027

Re treatment in previously irradiated neck. The different problems of relapsed and second cancers

C. Krzisch[1], E. Ecker[1], S. Gabriel[1], A.R. Henry[1], A. Coutte[1]
[1]*CHU Amiens - Hôpital Sud, Radiation Oncology, Salouel, France*

Purpose or Objective: Owing to legitimate fears concerning potentially devastating complications, the treatment of head and neck cancer in previously irradiated patient has been based on surgery for the best cases and chemotherapy for the inoperable ones. We review our series of 84 routinely re-(chemot)irradiated patients since 2000.

Material and Methods: Patients : 84 consecutive patients, mean age 60.47, previously treated by radio(chemo)therapy with a median delay between the the two irradiations of 36.3 months have been treated. 54 patients with relapses and 30 patients presenting second cancers . The mean follow-up is 66.45 months.
Methods : 42 patients were operated upon, (chemo)radiotherapy being used postoperatively for poor prognostic factors. 42 inoperable patients have been treated exclusively by radiochemotherapy. Before 2007, patients were treated by 2D techniques then by IMRT. 44 received concomitant platinum-based chemotherapy, 23 cetuximab and 17 radiotherapy alone.

Results: Results : median overall survival for the entire population is 19.61 months. Specific survival 23 months.Death causes : 40 the cancer itself, 9 patients complications et 11 other causes. Prognostic factors : age, sexe, performance status, Charlson score, location, type of resurgence (local, nodal or both), surgery, chemotherapy antecedents, type of concomitant treatment during the reirradiation, previous disabilities (tracheostomy, nasogastric tube) have been investigated. Only the type of resurgence is discriminant with a median survival time of 16.49 months for patients treated for a relapse and 32 months for those treated for a second cancer (Logrank p=0.00464). Complications : 9 deceased : 1 carotid blowout (with evolutive tumor), 3 late pneumoniae (patient NED), 3 tumoral hemorrhages (evolutive tumors) and 2 unknown complications. Late sequellae: 10 radionecrosis (7 osteoradionecrosis), 7 persistant dysphagia, 8 long term fistulas.

Conclusion: Conclusion :The survival in our series restricted to the second cancers is similar to that obtained in not previously irradiated patients and confirm some data of the literature. Thereby it is our belief that, if the acceptance of this strategy of treatment may merit further clinical trials for the relapsing tumor (however the results compare favorably with palliative chemotherapy), it becomes unethical not to give this chance for the second cancers in spite of the risk of severe complication.

EP-1028

The role of adjuvant external beam radiation therapy for advanced papillary thyroid cancer

C.Y. Kim[1], N.K. Lee[1], K.Y. Jung[2], S.K. Baek[2]
[1]*Korea University Anam Hospital, Radiation Oncology, Seoul, Korea Republic of*
[2]*Korea University Anam Hospital, Otolaryngology–Head and Neck Surgery, Seoul, Korea Republic of*

Purpose or Objective: the purpose of this study was to investigate the prognostic implication of adjuvant external beam radiation therapy on the locoregional control in patients with either locally advanced thyroid papillary carcinoma or cervical lymph node involvement.

Material and Methods: retrospective analysis was performed on 165 patients with locally advanced thyroid papillary carcinoma (T4) or cervical lymph node involvement (N1b), who were treated between 2002 and 2011. Of these, 32 patients were treated with total thyroidectomy followed by adjuvant external beam radiation therapy and radioactive iodine treatment, and 133 patients were treated with total thyroidectomy followed by radioactive iodine treatment.

Results: The median follow-up time was 223 months (range, 93 to 421 months). The 10-year disease-free survival and locoregional relapse-free survival rates were significantly better than unirradiated controls. 10-year disease-free survival rates for patients in the radiation therapy and no radiation therapy groups were 84.3% and 56.7%, respectively (p = 0.049). 10-year locoregional relapse-free survival rates for patients in the radiation therapy and no radiation therapy groups were 83.9% and 60.8%, respectively (p = 0.037). The overall survival rate and distant relapse-free survival rate were not different between the two groups. Multivariate analysis showed that adjuvant radiation therapy was an independent prognostic factor for locoregional relapse-free survival (p = 0.044).

Conclusion: adjuvant external beam radiation therapy should be considered in patients with either pT4 disease or cervical lymph node involvement.

EP-1029

20 v. 25-35 fractions in Oropharyngeal Carcinoma chemoIMRT: Could fraction number be de-escalated?

B. Cheng[1], H. Benghiat[2], J. Glaholm[2], H. Mehanna[1], P. Sanghera[1], A. Hartley[1]
[1]*InHANSE, Radiotherapy Quality Assurance, Birmingham, United Kingdom*
[2]*Hall-Edwards Radiotherapy Research Group, Queen Elizabeth Hospital, Birmingham, United Kingdom*

Purpose or Objective: Highly conformal dose distributions produced by rotational IMRT reliably delivered with daily IGRT raise the possibility that radical chemoIMRT for oropharyngeal carcinoma could be delivered in fewer fractions (#) for certain subgroups. The purpose of this study was to compare two cohorts of patients with oropharyngeal carcinoma treated within a single centre: the first treated with a 20# (4 weeks(wk)) schedule, the second with 25-35# (5-7wk) schedules.

Material and Methods: Patients undergoing radical chemoIMRT between June 2009 and May 2012 were treated with 55Gy/20# over 25 days to PTV1 with synchronous carboplatin or cetuximab (20# cohort). Similar patients were treated between June 2012 and April 2014 with one of three schedules 64Gy/25# over 32 days, 65Gy/30# over 39 days or 70Gy/35# over 46 days to PTV 1 with synchronous cisplatin or cetuximab (25-35# cohort). The local control (LC) and overall survival (OS) of these two cohorts were compared using the log-rank test.

Results: The minimum time elapsed from treatment in all patients was 18 months. There were 86 patients in the 20# cohort: median age 58 years; p16+ 60 (70%); T4 28 (33%); N2C/N3 16 (19%). There were 77 patients in the 25-35# cohort: median age 59 years; p16+ 54 (70%); T4 24 (32%); N2C/N3 16 (22%). The 18 month local control in the two cohorts respectively was 86% v. 88% (p=0.69). The 18 month overall survival was 85% v. 89% (p=0.41). If the two cohorts were restricted to those patients who were p 16+ve, T1-3, no neo-adjuvant chemotherapy and platinum agent used synchronously the corresponding figures (n= 26 for 20# cohort v. n=38 for 25-35# cohort) for local control were 92% v. 95% (p=0.34) and for overall survival 96% v 100% (p=0.22).

Conclusion: Although further follow up and late toxicity data is required, the similarity in results seen between the two cohorts in this study warrant the testing of the 20# schedule with synchronous cisplatin in a randomised setting in good prognosis oropharyngeal patients. This similarity in the endpoints studied is evidence against synchronous chemotherapy acting to reduce accelerated repopulation

during chemoradiation and further models to account for the effect of synchronous chemotherapy should be investigated.

EP-1030

Sentinel lymph node biopsy in clinically N0 laryngeal cancer: validation and application

V. Rudzianskas[1], E. Korobeinikova[1], E. Padervinskis[2], M. Kaseta[2], S. Vaitkus[2], N. Jurkiene[3]
[1]*Kaunas Medical University Hospital, Oncology and Hematology, Kaunas, Lithuania*
[2]*Kaunas Medical University Hospital, Department of Otorhinolaryngology, Kaunas, Lithuania*
[3]*Kaunas Medical University Hospital, Department of Radiology, Kaunas, Lithuania*

Purpose or Objective: Cervical lymph node dissection for laryngeal cancer patients without clinical and radiologic evidence of regional metastasis (N0) is controversial. Aim of our study was to validate sentinel lymph node biopsy (SLNB) procedure and evaluate its applicability in early T1-2 N0 laryngeal SCC.

Material and Methods: A prospective study conducted at the Lithuanian University of Health Sciences Hospital, with the permission of institutional review board. Inclusion period 2010 – 2013y. Patients with histologically confirmed laryngeal SCC T1-2, N0 were involved. Two phase design: validation phase - SLNB and selective neck dissection (SND) were performed simultaneously; application phase - SND was performed according to SLNB outcome. The end points for SLNB validation phase: sensitivity, specificity, negative-predictive value (NPV). Patients from both phases were followed-up after treatment and compared for recurrence-free survival (RFS). Sentinel lymph nodes (SLN) were located by 99mTc lymphoscintigraphy and gamma probe. Pathological evaluation included hematoxylin and eosin staining and immunohistochemistry. Statistical analysis was performed by using SPSS® v20.0, Clinical Calculator 1, ©Richard Lowry 2001-2015.The Pearson X2 was used for categorical data. Significant p-value <0.05. RFS was investigated performing a log-rank test.

Results: Clinicopathological features presented in table 1. In SLNB validation period we involved 16 pts. The mean number of SLNs per patient was 2.3. Four patients had positive SLN, no false positive results found. 12 pts had negative SLN, one of them had positive SND histological findings. The prevalence of positive lymph nodes was 0.31 (95% CI 0.12-0.58), overall sensitivity was 0.8 (95% CI 0.29-0.98), specificity was 1 (95% CI 0.67-1). NPV of SLNB equal to 0.91 (95% CI 0.59-0.99). During whole study period 46 pts were involved. The median of SLN removed per patient was 2.2. The total neck control rate was 87% and did not differ between validation and application groups (p=0.4). In a mean follow up period of 24 months, mean RFS time for validation group was 42 months (95%CI 37.36-48.28) *vs* 40 months in application group (95%CI 32.02-48.13), with no significant difference (p=0.43).

Conclusion: More comprehensive study with a larger group of patients and longer follow-up is needed in order to confirm SLNB applicability, however preliminary data revealed SLNB as sensitive and specific with no negative influence on recurrence-free survival.

EP-1031

Does oral mucosa OAR dose predict duration of G3 mucositis following IMRT for oropharynx cancer?

S. Yahya[1], H. Benghiat[1], P. Nightingale[1], M. Tiffany[1], P. Sanghera[2], A. Hartley[2]
[1]*Hall-Edwards Radiotherapy Research Group, Queen Elizabeth Hospital, Birmingham, United Kingdom*
[2]*InHANSE, University of Birmingham, Birmingham, United Kingdom*

Purpose or Objective: Various methods have been described to delineate the oral mucosa organ at risk (OAR). Due to uncertainty in the literature, the purpose of this study was to examine whether dose delivered to two versions of this OAR correlated to the duration of acute grade 3 mucositis in patients with oropharyngeal carcinoma treated with intensity modulated radiotherapy (IMRT).

Material and Methods: 66 patients previously treated with IMRT (55GY in 20 fractions over 25 days to the high dose volume; 46 in 20 fractions to areas at risk of harbouring microscopic disease) and synchronous carboplatin or cetuximab were included in this study. The duration of CTCAE version (v) 3 grade 3 mucositis (G3M) and the duration of strong opiate use (a surrogate for CTCAE v4 G3M) had been prospectively recorded at the time of treatment. Standard and modified oral mucosa OARs were contoured and the following dose parameters derived: mean dose, V55, V50, V45, V40 and V30.
Spearman's correlation was used to investigate for a relationship between the duration of v3 G3M or strong opiate use and these dose parameters for each OAR and 6 additional patient factors: pre-radiotherapy haemoglobin, weight, age, smoking status, use of neo-adjuvant chemotherapy and synchronous chemotherapy (carboplatin v. cetuximab).

Results: No statistically significant correlation of v3 G3M or duration of strong opiate use was noted with the tested parameters with the exception of a trend towards significance with pre-treatment weight (p=0.053). Duration of opiate use was found be to be approximately proportional to pre-treatment weight.

Conclusion: This study failed to show a relationship between dose to the standard or modified oral mucosa OAR and the duration of CTCAE v3 G3M or duration of opiate use in patients undergoing IMRT for oropharyngeal cancer. Further work is required to test these models with particle therapy where lower dose distributions to oral mucosa may be achievable. The utility of CTCAE v4 G3M as an endpoint if confirmed in larger studies to be related to pre-treatment weight is questioned by this study.

EP-1032

Unilateral neck radiotherapy in HPV-related tonsillar carcinomas

K. Thippu Jayaprakash[1], K. Geropantas[1], K. Sisson[2], T. Roques[1]
[1]*Norfolk and Norwich University Hospitals Foundation Trust, Department of Oncology, Norwich, United Kingdom*
[2]*Norfolk and Norwich University Hospitals Foundation Trust, Department of Pathology, Norwich, United Kingdom*

Purpose or Objective: Unilateral neck radiotherapy is considered a standard treatment for well-lateralized squamous cell carcinomas of the tonsil related to a HPV infection. Well-lateralized tumours are defined as T0-T2 N0-N2b M0 and not invading the base of tongue nor extending more than 1 cm into the soft palate. We performed a retrospective review aiming to assess the risk of a contralateral neck recurrence in this group of patients with a particular focus on those diagnosed with N2b disease.

Material and Methods: Fifty patients with T0-T3 N0-2b M0 disease (only two had T3 tumours) were treated with unilateral 3DCRT between February 2004 and July 2011. All 50 patients had p16-positive tumours. They all received chemotherapy (concomitant, induction or both) apart from two. Twenty-six patients presented with N2b disease. Median follow-up was 54 months.

Results: Four patients relapsed in the contralateral neck with no evidence of local or ipsilateral regional failure; one with recurrent contralateral retropharyngeal nodes and the rest with contralateral level II-IV nodes. Median time to a contralateral recurrence was 32 months (range, 22-47 months). All 4 patients initially presented with T1 N2b M0 disease. Upon recurrence, 2 of these patients were treated with a salvage neck dissection followed by chemoradiation and 2 with re-irradiation. Both re-irradiation patients developed a further recurrence and one of them died of his

disease. Using the Kaplan-Meier method, the estimated 5-year contralateral recurrence-free survival (CRFS) was 90.7% for the total population and 81.3% for the N2b subgroup (*p=0.038*). There was no statistical difference in overall survival (OS) between the N0-2a and N2b subgroups (91.5% *vs* 86.9%, *p=0.654*).

Conclusion: In view of the high risk of a contralateral neck recurrence, bilateral neck radiotherapy should be considered for well-lateralized, T0-T2, HPV-related squamous cell carcinomas of the tonsil presenting with N2b disease.

EP-1033

Pattern of radiation induced thyroid changes in NPC patients in first 3 years post-chemoradiotherapy

W.C.V. Wu[1], Z. Lin[2]
[1]*Hong Kong Polytechnic University, HTI, Kowloon- Hong Kong-SAR, China*
[2]*Shantou University Medical College, Cancer Hospital, Shantou, China*

Purpose or Objective: Thyroid gland is often irradiated in radiotherapy (RT) of nasopharyngeal cancer (NPC) patients leading to radiation induced thyroid disorder. This study aimed to evaluate the pattern of thyroid gland changes in the first 3 years after the completion of chemoradiotherapy.

Material and Methods: Adult NPC patients treated by concurrent chemo-RT (Cisplatin and 5 Fluorouracil) between 2007 and 2011 were recruited. A 7-beam intensity modulated radiotherapy (IMRT) plan was delivered using 6 MV photons. 70 and 66 Gy were prescribed to the PTVs of the nasopharynx and neck lymphatics respectively. Mean thyroid dose was obtained from dose volume histogram using the treatment planning system. Before RT, apart from planning CT, baseline thyroid hormone levels of each patient, comprising free T3 (fT3), free T4 (fT4) and TSH were established by extracting 6 ml of blood. Repeated measurements of the fT3, fT4, TSH and CT were taken at 3, 6, 12, 18, 24, 30 and 36 months after completion of RT. Readings of the 3 hormone levels and thyroid volume obtained from CT at each time interval were recorded. Trend lines of each parameter were plotted. The incidence of hypothyroidism was recorded based on the hormonal findings. The association between the mean thyroid dose and hypothyroidism was evaluated.

Results: 21 patients (M = 13, F = 8) completed the 3-year follow up. The mean thyroid dose ranged from 18.3-61.5 Gy (average 42.8±9.6 Gy). The average volume of the thyroid gland decreased from 17.6 cm3 at pre-RT to 12.3 cm3 at 18 months and remained stable afterward. The average level of fT4 decreased rapidly in the first 6 months, then slowed down and remained stable after 24 months (Fig 1). The average TSH level showed a significant rise between 6 to 18 months and became steady afterward. The level of fT3 remained constant throughout the study period. The incidence of hypothyroidism increased from 7.8% at 3 months to 34.4% at 18 months and remained relatively steady thereafter. Significant association was found between mean thyroid dose and incidence of hypothyroidism.

Conclusion: Our study demonstrated that 18-24 months after chemoradiotherapy was a critical time interval where 1) shrinkage of thyroid gland was stabilized; 2) decrease of fT4 and increase of TSH levels became steady; 3) incidence of hypothyroidism started to rise. All the parameters reached a relatively steady state after 36 months. Applying dose constraints to the thyroid gland in RT treatment planning was recommended to reduce the risk of hypothyroidism.

EP-1034

Cachexia induces head and neck changes in locally advanced oropharyngeal carcinoma

R. Mazzola[1], F. Ricchetti[1], A. Fiorentino[1], S. Fersino[1], N. Giaj Levra[1], G. Sicignano[1], R. Ruggieri[1], F. Alongi[1]
[1]*Ospedale Sacro Cuore Don Calabria, Radiation Oncology, Negrar - Verona, Italy*

Purpose or Objective: Cancer cachexia is a paraneoplastic syndrome characterized by weight loss (WL) and sarcopenia. Aim of the study was to assess the impact of cachexia on head and neck changes during definitive cisplatin- image-guided volumetric modulated arc radiation therapy (VMAT) in a series of locally advanced oropharyngeal cancer.

Material and Methods: Volume variations of sternocleidomastoid muscle (SCM) were considered as surrogate of muscle changes related to sarcopenia. For the purpose of the study , two head and neck diameters, encompassing the cranial limits of II and III neck nodal levels (here defined as "head-diameter" and "neck-diameter", respectively), were measured. All parameters analyzed were defined retrospectively by means of on-board cone beam computed tomography (kV-CBCT) images at 1th , 8th, 15th, 22th radiotherapy fraction (fx) and at the end of treatment. Cachexia was defined as WL > 5% during treatment. Statistical analysis was conducted correlating the parameters changes with three WL ranges: < 5%, 5-9% and > 10%.

Results: 30 patients, underwent to definitive cisplatin-VMAT, were retrospectively evaluated . A total of 150 contoured SCMs and 300 diameters were collected. Median WL of patients during treatment was 6.5% (range, 0-16%). The most significant SCM shrinkage was recorded at 15th fx (mean reduction of 1.6 cc), in correlation with WL 5-9% and WL > 10% (p 0.001). For "head-diameter" the peak reduction was recorded at the 15th fx (mean reduction of 8 mm), statistically correlated to WL > 10% (p 0.001). The peak reduction of "neck-diameter" was registered at the 22th fx (mean value of 6 mm). "Neck-diameter" gradually reduced until the end of treatment for WL > 5%.

Conclusion: The head and neck volume changes here analyzed showed to be potentially related to cancer cachexia. Present data could provide relevant adaptive radiation therapy implications for further investigations.

EP-1035

Predictors of mucositis in volumetric modulated radiotherapy for oropharyngeal-oral cavity cancer

F. Ricchetti[1], R. Mazzola[1], S. Fersino[1], A. Fiorentino[1], N. Giaj Levra[1], S. Naccarato[1], R. Ruggieri[1], F. Alongi[1]
[1]*Ospedale Sacro Cuore Don Calabria, Radiation Oncology, Negrar - Verona, Italy*

Purpose or Objective: to assess predictors of mucositis in oropharyngeal and oral cavity cancer after definitive or adjuvant volumetric modulated arc radiotherapy (VMAT) +/- chemotherapy.

Material and Methods: For the purpose of this retrospective analysis, inclusion criteria were: age ≥ 18 years, histologically proven carcinoma of the oropharynx and oral cavity, no dysphagia at baseline, radical and adjuvant treatment with VMAT (RapidArc®, Varian Medical System, Palo Alto, CA, USA). Fifty patients were evaluated. Statistical Analysis was performed for the following parameters as potential predictors of mucositis ≥ G2: total oral mucosa (OM) and OM minus target high-low radiation dose regions (PTVs), mean dose (Dmean) and maximum dose (Dmax), chemotherapy, weight loss, dysphagia.

Results: mucositis ≥ G2 was related to total OM Dmean ≥ 50 Gy (p .02, CI 95%: 0.1-1.3) and Dmax ≥ 65Gy (p .04, CI 95%: 0.1-1.3). At logistic regression, for Dmean ≥ 50 Gy and Dmax ≥ 65 Gy, the risk of mucositis ≥ G2 increased around 4 times (p .04). Considering OM minus target PTVs, the following volumetric constraints were related to mucositis ≥ G2: V45Gy > 40 % (p .04, CI 95%: 0.9-2.3), V50Gy > 30 % (p .009, CI 95%: 0.6-1.4), V55 Gy > 20 % (p.003, CI 95%: 0.5-1.2). At logistic regression, for OM minus target PTVs V45 > 40, V50 > 30 and V55 > 20 the risk of mucositis≥ G2 increased around 5 times (p .05). A ratio between total OM and OM minus target PTVs > 2.5 is related to G3 mucositis (p .03, CI 95%: 0.8-1.8).

Conclusion: new parameters were found as predictors of moderate-severe mucositis.

EP-1036

Glottic carcinoma stage T1 radiotherapy

G.J. Dickie[1], J. Askew[2], L. Tripcony[1], T. Ha[1]
[1]*Royal Brisbane and Women's Hospital - Cancer Care Centre, Department of Radiation Oncology, Brisbane, Australia*
[2]*Royal Brisbane and Women's Hospital, ENT, Brisbane, Australia*

Purpose or Objective: Retrospective review of results of radiotherapy for stage T1 glottic carcinoma.

Material and Methods: A retrospective review was done of all patients with squamous cell carcinoma of the glottis stage T1 treated with radiotherapy between 1960 and 2012 inclusive. There were 995 patients identified. All patients were treated with wedged lateral or angled anterior oblique technique. The main site of relapse was local and hence the main end point for anaysis was local control at 5 years. Survival curves were calculated using Kaplan Meier method and log rank test used to comparer differences.

Results: Overall the 5 year freedom from relapse was 88%. The only factor which influenced outcome was time period of radiotherapy with those between 1960 and 1980 had a 84% relapse free rate, significantly worse than the latter time period. Other factors examined included sex, age, substage T1a and T1b, grade, radiation dose, radiation field size and duration of radiation, and none of those factors had a significant effect on outcome. There were 121 relapses, most in the primary alone and most within the first two years.

Conclusion: The overall 5 year freedom from relapse was 88%.

EP-1037

Dysphagia and irradiation of constrictor pharyngeal muscles: a clinical-dosimetric correlation

F. Deodato[1], S. Cilla[2], F. Grifa[1], G. Macchia[1], G. Sallustio[3], M. Nuzzo[1], M. Ferro[1], F. Labropoulos[1], S. Mignogna[4], B. Corvari[5], F. Marazzi[5], A. Veraldi[6], M. Pieri[6], S. Ciabatti[6], U. Caliceti[7], S. Cammelli[6], G. Frezza[8], V. Valentini[5], A.G. Morganti[6]
[1]*Fondazione di Ricerca e Cura "Giovanni Paolo II"- Catholic University of Sacred Heart, Radiation Oncology Unit, Campobasso, Italy*
[2]*Fondazione di Ricerca e Cura "Giovanni Paolo II"- Catholic University of Sacred Heart, Medical Physics Unit, Campobasso, Italy*
[3]*Fondazione di Ricerca e Cura "Giovanni Paolo II"- Catholic University of Sacred Heart, Radiology Unit, Campobasso, Italy*
[4]*Fondazione di Ricerca e Cura "Giovanni Paolo II"- Catholic University of Sacred Heart, Oncology Unit, Campobasso, Italy*
[5]*Policlinico Universitario "A. Gemelli"- Catholic University of Sacred Heart, Department of Radiotherapy, Roma, Italy*
[6]*S. Orsola-Malpighi Hospital- University of Bologna, Radiation Oncology Center- Department of Experimental- Diagnostic and Specialty Medicine – DIMES, Bologna, Italy*
[7]*S. Orsola-Malpighi Hospital- University of Bologna, Unit of Otolaryngology- Department of Specialist Surgery and Anesthesiology, Bologna, Italy*
[8]*Bellaria Hospital, Radiotherapy Department, Bologna, Italy*

Purpose or Objective: To correlate clinical late dysphagia with the dose received by the constrictor pharyngeal muscles in patients receiving induction chemotherapy (ICT) and radiochemotherapy (RT-CT) with SIB-VMAT technique.

Material and Methods: Between July 2010 and January 2015, 51 patients with locally advanced head and neck cancer underwent ICT and subsequent RT-CT with concurrent weekly Cisplatin. The superior, middle, and inferior (S, M, and I) pharyngeal constrictors muscles (CM) were delineated and the correlation between dosimetric parameters and late pharyngeal toxicity was analyzed.

Results: 51 patients [M/F: 41/10, median age 56, range 30-77, stage III: 10 (20%), stage IV: 41 (80 %)] were included in this analysis. The tumor site was: oropharynx in 21 (40%) patients, epipharynx in 10 (20%), oral cavity in 9 (18%), larynx in 5 (10%), and hypopharynx in 6 (12%). ICT in the majority of cases (74%), was based on Cisplatin - 5 -Fluorouracil, with the addition of Docetaxel in 26% of cases. The dose delivered to the primary tumor was 67.5 Gy (in 8 patients, 16 %) and 70.5 Gy (in 43 patients, 84 %); 60 Gy and 55.5 Gy were delivered on high and low risk lymph node levels, in 30 fractions with SIB-VMAT (2 arcs) technique, respectively. With a median follow-up of 11 months (range 3-44), late G1 dysphagia was recorded in 6 patients (12%) and late G2 dysphagia was observed in 2 patients (4%) (CTC-AE v. 4.3). Other late toxicities are reported in the Table 1. G3-4 toxicities were not recorded. In DVH analysis, the median dose received by CM was 66.2 Gy (S: 67.4 Gy, M and I: 67.2 Gy), with V50 being 96.9 % (S: 97.4%, M: 98.3%, and I: 95.9 %), and V60 being 82.4% (S: 86.8%, M: 90.1 %, and I: 73.8%). The median dose received by the larynx was 63.5 Gy (V50: 94.1 %, and V60: 66.2 %). No statistically significant difference between the group of patients with and without late dysphagia was observed.

Table 1: Late toxicity (CTC - AE v. 4.3)

	G0	G1	G2	G3	G4
Hyperpigmentation (%)	0 (0)	9 (18)	1 (2)	0 (0)	0 (0)
Xerostomia (%)	0 (0)	16 (31)	5 (10)	0 (0)	0 (0)
Subcutaneous fibrosis (%)	0 (0)	8 (16)	1 (2)	0 (0)	0 (0)

Conclusion: No statistically significant correlation between dose delivered to the constrictors muscles and late dysphagia was observed in this patients cohort. This result may depend on tolerability of the treatment and then by the small number of recorded adverse events.

EP-1038

IMRT/VMAT-SIB technique chemoradiation in locally advanced head and neck cancer: toxicity results

F. Deodato[1], S. Cilla[2], G. Macchia[1], F. Grifa[1], G. Torre[1], M. Nuzzo[1], G.C. Mattiucci[3], G. Sallustio[4], L. Di Lullo[5], F. Micciché[3], L. Tagliaferri[3], F. Monari[6], M. Ntreta[6], C. Parmeggiani[7], A. Cortesi[6], A. Farioli[8], S. Cammelli[6], G. Frezza[9], V. Valentini[3], A.G. Morganti[6]
[1]*Fondazione di Ricerca e Cura "Giovanni Paolo II"- Catholic University of Sacred Heart, Radiation Oncology Unit, Campobasso, Italy*
[2]*Fondazione di Ricerca e Cura "Giovanni Paolo II"- Catholic University of Sacred Heart, Medical Physics Unit, Campobasso, Italy*
[3]*Policlinico Universitario "A. Gemelli"- Catholic University of Sacred Heart, Department of Radiotherapy, Roma, Italy*
[4]*Fondazione di Ricerca e Cura "Giovanni Paolo II"- Catholic University of Sacred Heart, Radiology Unit, Campobasso, Italy*
[5]*"F. Veneziale" Hospital, Medical Oncology Unit, Isernia, Italy*
[6]*S. Orsola-Malpighi Hospital- University of Bologna, Radiation Oncology Center- Department of Experimental- Diagnostic and Specialty Medicine – DIMES, Bologna, Italy*
[7]*S. Orsola-Malpighi Hospital- University of Bologna, Department of Medical Physics, Bologna, Italy*
[8]*S. Orsola-Malpighi Hospital- University of Bologna, Department of Medical and Surgical Sciences DIMEC, Bologna, Italy*
[9]*Bellaria Hospital, Radiotherapy Department, Bologna, Italy*

Purpose or Objective: To evaluate the toxicity of intensity modulated radio-chemotherapy with simultaneous integrated boost technique (SIB) after induction chemotherapy in patients with locally advanced head and neck (H&N) cancer.

Material and Methods: The IRMA studies are described in the table. Patients with stage III-IV H&N cancer, without progressive disease after induction chemotherapy (IC), underwent radio-chemotherapy with weekly Cisplatin 30

mg/m2 (IRMA 1, 2, 3, 5) or Cetuximab 400 mg/m2 (IRMA 4). A dose of 67.5 Gy in 30 fractions (IRMA 1, 2, and 4) or 70.5 Gy in 30 fractions (IRMA 3, 4, and 5) was delivered to primary tumor and involved nodes, 60 Gy were delivered to high risk and 55.5 Gy to low risk lymph node areas. Static (IMRT) or volumetric (VMAT) intensity modulated technique with simultaneous integrated boost was used.

Results: 107 patients (median age 56 years, range 30-78, UICC stage III: n = 18, IV: n = 89) were included in this analysis. IC was performed with Cisplatin + 5-Fluorouracil in 65 (61%) patients and with Docetaxel + Cisplatin + 5-Fluorouracil in 42 (39%) cases. Concomitant Cisplatin and Cetuximab were administered in 84% and in 16% of patients, respectively. 51% (n = 55) of cases were irradiated with step & shoot IMRT-SIB technique (7 beams), while 49% (n = 52) of patients were irradiated with VMAT-SIB (two arcs) technique. During radio-chemotherapy, 23 (21%) patients developed mucositis, 12 (11%) G3 dysphagia and 10 (9.3%) G3 hematological toxicity. Even 1 (0.9%) G4 leukopenia and 3 (2.8%) G5 (2 neutropenia and one fatal myocardial infarction) adverse events were observed. The overall response rate after radio-chemotherapy was 82.2%. Two-year local control and survival were 64.2% and 64.6% (IRMA 1), respectively, 57.8% and 56.2% (IRMA 2), 66.4% and 75.5% (IRMA 3), 70.1% and 66.7% (IRMA 4), and 76.5% and 82.4% (IRMA 5), respectively.

Table IRMA and studies related toxicity

IRMA* 1	IRMA* 2	IRMA* 3	IRMA* 4	IRMA* 5
3 CF → C+IMRT/VMAT (67,5-60-55,5 Gy/30 fx)	3 DCF → C+IMRT/VMAT (67,5-60-55,5 Gy/30 fx)	3 DCF → C+IMRT/VMAT (70,5-60-55,5 Gy/30 fx)	3 CF → Cetuximab+IMRT/VMAT (67,5/70,5 -60-55,5 Gy/30 fx)	3 CF → C+IMRT/VMAT (70,5-60-55,5 Gy/30 fx)
n° pts = 28	n° pts = 16	n° pts = 26	n° pts = 17	n° pts = 20
Mucositis: G3: 29% G4: 0% Disfagia: G3: 11% G4: 0% Haematological toxicity G3: 25% G4: 0% G5: 3% Myocardial infarction G5: 3%	Mucositis: G3: 19% G4: 0% Disfagia: G3: 12% G4: 0% Haematological toxicity G3: 37% G4: 12% G5: 0%	Mucositis: G3: 15% G4: 0% Disfagia: G3: 7% G4: 0% Haematological toxicity G3: 4% G4: 0% G5: 4%	Mucositis: G3: 29% G4: 0% Disfagia: G3: 18% G4: 0% Haematological toxicity G3: 6% G4: 6% G5: 0%	Mucositis: G3: 15% G4. 0% Disfagia: G3: 10% G4: 0% Haematological toxicity G3: 5% G4: 0 G5: 0%)
OR**: 86%	OR: 75%	OR: 92%	OR: 65%	OR: 85%
2-year LC***: 64.2% 2-year OS****:64.6%	2-year LC: 57.8% 2-year OS: 56.2%	2-year LC: 66.4% 2-year OS: 75.5%	2-year LC: 70.1% 2-year OS: 66.7%	2-year LC: 76.5% 2-year OS: 82.4%%

* IRMA : Intensified Radiotherapy by multimodality Association in H&N cancer
CF: Cisplatin + 5Fluoruracile ; C: Cisplatin (30 mg / m2) ; DCF: Docetaxel + Cisplatin + 5Fluoruracile; Cetuximab (400 mg / m2): ** OR: Overall response; ***LC: Local control; ****OS : Overall survival.

Conclusion: In our experience moderately hypofractionated and accelerated radio-chemotherapy after induction chemotherapy was feasible. Intensive patient monitoring and supportive strategies during chemoradiation are necessary to manage of side effects.

EP-1039

H&N IMRT: correlation of dysphagia/xerostomia to dose/volume parameters of involved OARs

L. Deantonio[1], M. Paolini[1], L. Masini[1], F. Pia[2], M. Brambilla[3], M. Krengli[1]
[1]*University Hospital Maggiore della Carità, Radiotherapy, Novara, Italy*
[2]*University Hospital Maggiore della Carità, Otolaringology, Novara, Italy*
[3]*University Hospital Maggiore della Carità, Medical Physics, Novara, Italy*

Purpose or Objective: To analyse the frequency and severity of dysphagia and xerostomia in patients affected by nasopharyngeal and oropharyngeal cancers treated by intensity-modulated radiotherapy (IMRT) and the correlation with volumetric variations and dosimetric data of pharyngeal constrictor muscles and parotid glands.

Material and Methods: Fifty patients, who underwent adaptive IMRT for nasopharyngeal and oropharyngeal cancers, were included in the present study. Eighty-four percent of patients (42/50) received concurrent radio-chemotherapy and 92% (44/50) were in locally advanced stage. Dose-volume parameters related to constrictor muscles (superior constrictor muscle, SCM; middle constrictor muscle, MCM; inferior constrictor muscle, ICM and whole pharyngeal constrictor muscle, CM), and parotid glands were analyzed using dose-volume histograms (DVHs). All patients underwent replanning CT scan after 5 weeks of radiation therapy and the target and OARs were re-contoured on fusion images after co-registration. The volumetric variations of pharyngeal constrictor muscles and parotid glands were measured. Volumetric variations and dose-volume parameters were associated to acute and late dysphagia and xerostomia according to RTOG score, quality of life questionnaires (PSS-H&N e QLQ-H&N35), and oesophageal transit .

Results: Volumetric variations and dose-volume parameters of pharyngeal constrictor muscles and parotid glands are reported in Table 1. Adaptive IMRT achieved a good sparing of parotid glands (mean dose 24.9 Gy) and constrictor muscles (mean dose 51.2 Gy). Acute dysphagia, was scored as grade 0-1 in 18/50 patients (36%) and as grade 2-3 in 32/50 (64%). Acute xerostomia, was scored as grade 0-1 in 21/50 patients (42%) and as grade 2-3 in 29/50 (58%). Volumetric variations and dose-volume parameters of the constrictor muscles and parotid glands did not correlate with acute toxicity ($p>0.05$). At 2 years median follow-up (range 6-67 months), late dysphagia was scored as grade 0-1 in 40/50 of patients (80%) and as grade 2-3 in 10/50 (20%). Late xerostomia was scored as grade 0-1 in 42/50 of patients (84%) and as grade 2-3 in 8/50 (16%). The analysis of the correlation of volumetric variations and dose-volume parameters with clinical data (RTOG score for late toxicity, quality of life questionnaires and oesophageal transit) is ongoing.

OAR	Median Volume (cc)	Replanning median Volume (cc)	Δ volume (%)	Median maximum dose (Gy)	Median mean dose (Gy)
SCM	6.9	8.5	+20	71.9	62.7
MCM	2.1	2.6	+17	65.2	51.5
ICM	3.1	3.7	+11	60.1	42.9
CM	12.0	14.7	+17	71.9	51.2
Right parotid gland	25.0	17.8	-24		24.9
Left parotid gland	22.6	16.2	-32		24.9

Conclusion: During radiotherapy, pharyngeal constrictor muscles and salivary glands underwent volumetric variations. Volumetric variations and dosimetric findings did not correlate with acute toxicity, probably because of the complexity and multifactorial pathogenesis of acute dysphagia and xerostomia. The ongoing analysis on the correlation of late toxicity data with volumetric variations and dose-volume parameters may help in the optimization of IMRT treatment planning.

EP-1040

Development of a CT-based prognostic model for regional control in head and neck cancer after RT

D. Nevens[1], O. Vantomme[1], A. Laenen[2], R. Hermans[3], S. Nuyts[1]
[1]*KU Leuven-University of Leuven- University Hospitals Leuven, Radiation Oncology Department, Leuven, Belgium*
[2]*KU Leuven-University of Leuven, Leuven Biostatistics and Statistical Bioinformatics Centre, Leuven, Belgium*
[3]*KU Leuven-University of Leuven- University Hospitals Leuven, Radiology Department, Leuven, Belgium*

Purpose or Objective: At our center, the need for neck dissection (ND) after radiotherapy (RT) is determined based on the nodal response on the post-RT Computed Tomography (CT) study 4 months after the end of treatment. We want to report the outcome of this approach and investigate whether characteristics on pre- and post- RT CT studies can predict the necessity of post-RT ND.

Material and Methods: Between 2002 and 2012, 183 consecutive patients with lymph node-positive head and neck cancer (HNC) were treated with RT or concurrent chemoradiotherapy (CRT) without planned ND. CT studies pre- and post-treatment were reviewed for lymph node size and presence of necrosis, extracapsular spread and calcifications. At patient level, data were correlated with 3 year regional control (RC), metastasis free survival (MFS), disease free survival (DFS) and overall survival (OS). At nodal level, data were correlated with relapse of the individual lymph nodes (LNR). A stepwise selection procedure was followed to construct a multivariable prediction model for regional relapse (RR) within 3 years. The area under the ROC curve (AUC) was determined for the selected model. Additionally a bootstrap-corrected AUC value was calculated. This AUC value corrects for overoptimism resulting from the fact that model construction and model validation were performed on the same data set.

Results: The median follow-up was 60 months. 3-year outcome rates were as follows: LC of 84%, RC of 80%, MFS of 74%, DFS of 61%, OS of 63%. Pre-treatment nodal size at patient- and nodal level and presence of necrosis at patient level were associated with a poorer outcome. This was also the case for post-treatment lymph node size and presence of necrosis and extracapsular spread (Table 1). Based on our results we developed a multivariate model for RR prediction. After performing a stepwise selection procedure pre-RT T stage (p=0.02), post-RT necrosis (p=0.03) and post-RT largest nodal diameter (p=0.01) were included in the model. The AUC of this model was 0.78 (95% CI 0.63;0.84); the bootstrap-corrected AUC was 0.74 (95% CI 0.67; 0.89). The risk for RR within 3 years can be calculated using the following formula:

$$RR\,(\%) = \frac{e^{\mu}}{1 + e^{\mu}}$$

$$\mu = 0.085 * largest\ axial\ diameter\ (mm) + 0.6749 * (T\ stage) - 4.8482 + (only\ when\ necrosis)\ 1.1384$$

Table 1: Predictive value of post-treatment CT characteristics for outcome

CT characteristic	Outcome	OR/HR (95% CI)	p-value
∑ nodal volume			
	RR	OR 1.262 (1.072;1.486)	0.0051
	MFS	nonlinear trend	
	DFS	HR 1.051 (1.028;1.074)	<0.0001
	OS	HR 1.056 (1.035;1.078)	<0.0001
∑ nodal volume 2cm³ vs 1cm³	MFS	HR 1.152 (1.054;1.259)	0.0018
Largest diameter			
	RR	OR 1.108 (1.047;1.172)	0,0004
	MFS	HR 1.043 (1.014;1.072)	0.0036
	DFS	HR 1.059 (1.035;1.083)	<0.0001
	OS	nonlinear trend	<0.0001
Largest diameter > 31.8 mm	OS	HR 5.764 (2.851;11.651)	<0.0001
Necrosis			
	RR	OR 5.960 (2.410;14.738)	0.0001
	MFS	HR 2.203 (1.186;4.092)	0.0124
	DFS	HR 2.668 (1.671;4.262)	<0.0001
	OS	HR 2.406 (1.529;3.785)	0.0001
Calcifications			
	RR	OR 0.643 (0.167;2.483)	0.5189
	MFS	HR 0.950 (0.373;2.421)	0.9143
	DFS	HR 0.843 (0.404;1.759)	0.6494
	OS	HR 0.863 (0.430;1.729)	0.6772
ECS			
	RR	OR 3.451 (1.056;11.283)	0.0404
	MFS	HR 2.482 (1.144;5.385)	0.0214
	DFS	HR 2.343 (1.275;4.303)	0.0061
	OS	HR 1.800 (0.971;3.337)	0.0620

Abbreviations: CT = computed tomography; OR = odds ratio; HR = hazard ratio; CI = confidence interval; ∑ = sum; RR = regional recurrence; MFS = metastasis-free survival; DFS = disease-free survival; OS = overall survival; ECS = extracapsular spread.

Conclusion: Characteristics on the post-RT CT study can predict the likelihood of residual lymph node disease and outcome. Characteristics on the pre-therapy CT study seem less useful for this purpose. A CT-based multivariate prognostic model based on our findings was developed which can aid in predicting RR.

EP-1041

Evaluation of dysphagia in head and neck cancer patients undergoing Intensity Modulated Radiotherapy

I. Bashir[1], K. Bansal[1], K. Chufal[1]
[1]*Batra Hospital and Medical Research Centre, Radiation Oncology, New Delhi, India*

Purpose or Objective: With the success of Intensity Modulated Radiotherapy (IMRT) techniques in reducing the severity of xerostomia in head and neck cancer (HNC) patients, efforts should be made to improve swallowing dysfunction, which is potentially even more discomforting and incapacitating side effect and adversely affects the quality of life. This is a clinical dosimetric study to investigate the correlation between radiation doses delivered to organs at risk for radiation induced swallowing dysfunction (SWOARs) and severity of dysphagia following concurrent chemoradiotherapy to HNC patients and evaluate various factors which assume importance in determining the risk of dysphagia/aspiration.

Material and Methods: 60 Head and Neck cancer patients (Oropharynx 28, Hypopharynx 12 and Larynx 20) were enrolled between May 2013 and June 2014 for this prospective longitudinal study after prior approval from the hospital ethics and review committee. Patients were treated with curative intent by radiotherapy using IMRT and concurrent chemotherapy using cisplatin (40 mg/m2) on weekly basis. Delineation of SWOARs was done using RTOG guidelines and following structures were contoured: superior, middle and inferior pharyngeal constrictor, cricopharyngeal muscle, esophageal inlet muscle, cervical esophagus, base of tongue, supraglottic and glottic larynx. Dysphagia endpoints included both patient-reported (EORTC Head and Neck Quality of Life instrument and MD Anderson Dysphagia Inventory) and observer-rated scores (Common Terminology Criteria for Adverse Events- CTCAE v4.0 and RTOG/EORTC Late Radiation Morbidity Scoring). Patients were assessed weekly during radiation and at 1 month and 3 months after completion of treatment. Correlation between dysphagia and radiation doses to SWOARs was assessed.

Results: With an increase in the mean dose to the SWOARs, the grades of dysphagia also increased. After 3 months of completion of treatment, 27% patients had persistent dysphagia of grade 3 or grade 4. Significant correlation was observed between patient reported dysphagia scores and the mean doses to the superior and middle pharyngeal constrictor as well as glottic and supraglottic larynx ($p<0.05$). Observer rated dysphagia scores correlated significantly with mean superior pharyngeal constrictor dose and not with dose to other SWOARs. Two patients of carcinoma hypopharynx developed stricture which correlated significantly with dose to esophageal inlet muscle.

Conclusion: Radiotherapy plans sparing SWOARs should be generated and implemented to prevent the problem of dysphagia. The structures whose damage may cause dysphagia and aspiration are the pharyngeal constrictors and the glottic and supraglottic larynx. Further studies are required to evaluate dose constraints to these SWOARs to reduce the incidence of radiation induced dysphagia and thus further improve the quality of life in HNC patients.

EP-1042

Risk-factors in pT1-2N0M0 squamous cancers of the oral cavity and the role of adjuvant radiotherapy

I. Mallick[1], S. Bhaumik[1], K. Sarkar[1], P. Arun[2], K. Manikantan[2], P. Roy[3], I. Arun[3], D. Dabkara[4], S. Chatterjee[1]
[1]*Tata Medical Center, Department of Radiation Oncology, Kolkata, India*
[2]*Tata Medical Center, Department of Head and Neck Surgery, Kolkata, India*
[3]*Tata Medical Center, Department of Pathology, Kolkata, India*

[4]*Tata Medical Center, Department of Medical Oncology, Kolkata, India*

Purpose or Objective: Prognostic factors in early stage resected oral squamous cell cancers (OSCC) are not well understood. The aim of this audit was to identify factors influencing recurrence in pT1-2N0M0 patients with a view to determine the role and indications for adjuvant radiotherapy (adjRT).

Material and Methods: Between Aug 2011 to May 2014, 120 patients were determined to have pT-2N0M0 disease following histopathological examination after primary surgery for oral cancer. Primary sites included oral tongue (66, 55%), buccal mucosa (31, 26%), gingiva (10, 8%), retromolar trigone (9, 7%) and lip (4, 3%). AdjRT was advised to 46 (38%) patients on an individual basis in a multidisciplinary meeting, determined by the presence of one or a combination of known risk factors. Patients with close or positive margins always received chemoradiation. AdjRT was delivered with 3D conformal or intensity modulated techniques to a dose of 60Gy/30Fr/6weeks to the tumor bed and 54-60Gy/30Fr/6weeks to the resected but uninvolved nodal levels. Disease –related outcomes were calculated, and pathological prognostic factors were assessed using univariate and multivariate analyses. The impact of adjRT in reducing disease recurrence was assessed.

Results: The median age was 55 (25-82) years. The median tumor size was 2.2 cm. The median depth of infiltration was 6mm. The incidence of known pathological prognostic factors is listed in Table 1. The median follow up was 23 months (2-44 months). A total of 13 patients had recurrence (local 8; nodal 4, distant 3, including overlapping failures). All locoregional failures were within the RT volumes. The 2yr and 3 year disease-free-survival (DFS) was 89% and 82% respectively. On univariate analysis pT2 tumors, lymphovascular invasion (LVI), perineural invasion (PNI) and depth of invasion >=5mm were statistically significant prognosticators for DFS (Table 1). Primaries of the oral tongue showed a trend towards shorter DFS. None of these factors were independently prognostic on multivariate analysis. A scoring system using the number of risk-factors was created. Patients were grouped as Low risk (0-1 factor); Intermediate risk (2-3 factors) and High-risk (4-7 factors). There was significant difference in DFS of patients in different risk groups (Fig 1). RT was considered unnecessary in Low risk patients (none of 39 received RT, 3 yr DFS 97.1%). In High risk patients, prognosis was poor despite RT (22/25 received RT, 3 yr DFS 68.5%). In the Intermediate risk group, 24/54 patients received RT, but this made no difference to the risk of disease recurrence (2 local failures each in RT vs. no RT cohorts, 3 yr DFS 85.1% vs 72.1%, p=0.75).

Table 1. Incidence and impact of risk factors on disease-free-survival (by univariate analysis)

Factor	n (%)	3 yr DFS	p
Tongue Primary (vs. Others)	66 (55%)	76.0% (vs. 91.7%)	0.1
pT2 (vs. pT1)	67 (56.3%)	72.5% (vs. 95.6%)	0.039
Lymphovascular invasion (vs. absent)	10 (8.3%)	58.3% (vs. 83.6%)	0.024
Perineural invasion (vs. absent)	38 (31.7%)	75.0% (vs. 85.6%)	0.013
Depth of invasion ≥ 5mm (vs. < 5mm)	72 (61%)	73.8% (vs. 97.5%)	0.017
Poorly differentiated cancer (vs. moderately or well-differentiated)	10 (8.3%)	88.9% (vs. 81.2%)	0.956
Close or positive margins (vs. clear margins)	7 (5.8%)	83.3% (vs. 80.9%)	0.854

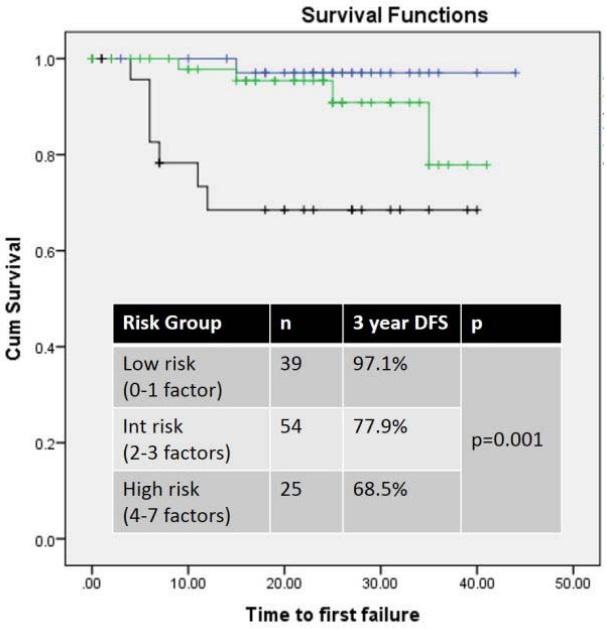

Conclusion: Several pathological risk factors alone and in combination impact disease related outcomes even in pT1-2N0 OSCC. Standard AdjRT did not have a clear effect on reducing recurrence in our cohort in patients with up to 3 risk factors.

EP-1043

Clinical and volumetric prognostic factors in external beam radiotherapy for head and neck cancer

K. Takeda[1], H. Matsushita[2], T. Ogawa[3], S. Dobashi[1], Y. Ishizawa[1], K. Chida[1], N. Kadoya[2], K. Ito[2], M. Chiba[2], M. Kubozono[2], R. Umezawa[2], Y. Shirata[2], Y. Ishikawa[2], T. Yamamoto[2], M. Kozumi[2], T. Tanabe[2], N. Takahashi[2], Y. Katagiri[2], S. Tazaka[2], K. Takeda[2], K. Sato[1], Y. Katori[3], K. Jingu[2]

[1]*Tohoku University School of Medicine, Health Sciences-Course of Radiological Technology, Sendai, Japan*

[2]*Tohoku University School of Medicine, Department of Radiation Oncology, Sendai, Japan*

[3]*Tohoku University School of Medicine, Department of Otorhinolaryngology-Head and Neck Surgery, Sendai, Japan*

Purpose or Objective: To investigate clinical and volumetric prognostic factors in head and neck cancer (HNC) patients (pts) treated with curative external beam radiation therapy (EBRT).

Material and Methods: Sixty-four oropharyngeal squamous cell carcinoma (OSCC) pts and 79 hypopharyngeal squamous cell carcinoma (HSCC) pts treated with curative EBRT were enrolled in this retrospective analysis. No pt had previously undergone surgery for HNC. The median total EBRT dose was 70 Gy (range, 60–72 Gy). For planning EBRT, computed tomography (CT) images were acquired prior to EBRT initiation and at 3–5 weeks after the initiation of EBRT for replanning in each pt. We assessed the gross tumor volume (GTV) reduction rate (GTVRR) on the basis of the results from the initial and replanning CT images. Initial cervical body volume (CBV) was measured from the initial CT images. For induction chemotherapy (IC), seven pts received docetaxel (DOC), cisplatin (CDDP), and 5-fluorouracil (5-FU) (TPF regimen). One course of CDDP plus 5-FU and two courses of TPF regimen were delivered to one pt. In total, 125 pts (87.4%) received concurrent chemotherapy (CC) using the following regimen: TPF in 55 (38.5%) pts; another CDDP-based regimen in 43 (30.1%) pts; another DOC-based regimen in 22 (15.4%) pts; cetuximab in 3 (2.0%) pts; nedaplatin and 5-FU in 1 (0.7%) pt; and S-1 (tegafur, gimeracil, and oteracil) in 1 (0.7%) pt. The disease stage was I in 5 (3.5%) pts, II in 20 (14%) pts, III in 24 (16.8%) pts, and IV in 93 (65%) pts.

Progression-free survival (PFS) and overall survival (OS) were estimated by the Kaplan–Meier method. Cox regression was performed to explore parameters in association with PFS and OS. The potential variables that were examined included age; gender; primary site; UICC stages; serum albumin, C-reactive protein (CRP), albumin–globulin ratio, body weight (BW) and body mass index prior to treatment; initial CBV and GTV; GTVRR during EBRT; IC; and CC.

Results: The median follow-up period was 23 months (range, 2–95 months). The 2-year PFS and OS rates were 51.3% [95% confidence interval (CI), 40.2–55.7] and 71.0% (95% CI, 58.4–72.6), respectively. PFS was associated with age [hazard ratio (HR): 1.029 (95% CI, 1.001–1.058), p = 0.04]; stage IV disease [HR: 3.755 (95% CI, 1.810–7.788), p < 0.001]; pretreatment CRP [HR: 1.077 (95% CI, 1.008–1.152) p = 0.029]; initial GTV [HR: 1.004 (95% CI, 1.000–1.007), p = 0.026]; and GTVRR during EBRT [HR: 0.99 (95% CI, 0.982–0.998), p = 0.016]. OS was related to stage IV disease [HR: 3.669 (95% CI, 1.667–8.071), p = 0.001]; GTVRR during EBRT [HR: 0.986 (95% CI, 0.975–0.997), p = 0.012]; and pretreatment BW [HR: 0.927 (95% CI, 0.892–0.963), p < 0.001].

Conclusion: This study suggested the prognostic value of clinical and volumetric status. Clinical stage, age, pretreatment CRP and BW, initial GTV, and shrinkage of GTV during treatment appear to be critical in the HNC treatment strategy.

EP-1044

Relations between cancer-related communication and dyadic adjustment in head and neck cancer patient

Y.P. Chen[1], B.S. Huang[1], J.T.C. Chang[1]
[1]*Chang-Gung Memorial Hospital, Radiation Onclogy, Taoyuan City, Taiwan*

Purpose or Objective: Head and neck cancer patients suffered from swallowing and speaking difficulties, neck pain and stiffness, and cosmetic disfigurement, resulting in interpersonal relationship troubles and social and emotional adaptation issues. Discussing cancer and the quality of communication when facing stress would affect partner's adaptation to cancer and quality of relationship. This study investigated the (Cancer-related) communication pattern, effect of disease characteristics in head and neck cancer. We used dyadic analysis to investigate the impact and process of communication pattern on quality of relationship.

Material and Methods: This study is cross-sectional design, and subject were the male patients who completion of cancer treatment more than 3 months and their partners with head and neck cancer, included 131 patient-partner dyads. Each participant completed the basic information questionnaire, Communication Pattern Questionnaire, Dyadic and Adjustment Scale.

Results: By treatment, there are no difference on cancer-related communication pattern for both patient and partner. Both patient and partner, their perception of mutual constructive communication was associated with more quality of relationship, Demand-withdraw communication and mutual avoidancewas associated with less quality of relationship. Using the Actor-Partner interdependence model (APIM), result reveled that although each person's cancer-related communication pattern is the strongest predictor of their own quality of relationship, partner's perception of communication pattern also play significant role on patient's quality of relationship. According to APIM, only the partner perceived communication pattern could be accounted for by their influence on quality of relationship.

Conclusion: We found that cancer-related communication and interaction of relationship among couples play an important role in the head and neck adjustment process. Thus, except the medical care, clinicians concern with interaction between patient and partner can be enhance their psychological adjustment and illness, particularly the partner's perception of communication pattern, which may improve the quality of relationship and life adaptation of both couples when they are dealing with head and neck cancer.

EP-1045

Phase I study for evaluation of the safety of high-dose hypofractionated RT in early glottic cancer

T. Yu[1], H.G. Wu[1], K. Jin Ho[1], K. Taek-Gyun[2]
[1]*Seoul National University College of Medicine, Radiation Oncology, Seoul, Korea Republic of*
[2]*Seoul National University College of Medicine, Otorhiolaryngology, Seoul, Korea Republic of*

Purpose or Objective: Reducing overall treatment time has advantages for patient convenience, but also for local control as shown by former studies. Critical organs in the neck causes concern in relation to long-term morbidity and quality of life, but with recent advances with high-precision image-guided and intensity-modulated radiotherapy (IMRT) techniques, avoidance of the organs at risk has become possible. The purpose of this study is to develop an image-guided high-dose hypofractionated vocal cord irradiation technique to treat patients with early stage glottic cancer.

Material and Methods: Eligible patients with early stage glottic cancer provided with informed consent will receive hypofrationated radiotherapy to the larynx with a simultaneous boost to the gross tumor. The fraction size will be stepwise increased from 3.5Gy (total dose 59.4Gy) to 9Gy (total dose 45Gy). To proceed to the next dose level, at least 7 patients should be confirmed that they have no toxicity more than grade 2 after 3 month post-RT. The organs at risk include the larynx, contralateral vocal cord, arytenoids, carotid arteries, inferior pharyngeal constrictor muscle, and spinal cord.

Results: Four patients were enrolled to receive 59.4Gy with 3.5Gy per fraction until July 2015. None of the patients developed toxicity more than grade 2 after 1 month post-RT. The mean equivalent dose in 2Gy fractions (EQD2) to contralateral arytenoid, thyroid gland, inferior pharyngeal constrictor muscle, and larynx were in average 69.5Gy, 12.3Gy, 50.8Gy, and 66.5Gy, respectively. No portion of the carotid arteries were irradiated more than 50 Gy (EQD2) in the IMRT plan. After 3 months of follow-up, all 4 patients demonstrated no more than grade 3 toxicities. Also, all patients showed complete remission by laryngoscopy.

Conclusion: The high-dose hypofractionated IMRT technique provided good sparing of critical structures and resulted in no severe toxicity after a short term follow up. We will continuously perform this phase I clinical trial to stepwise increase the fraction size up to 9Gy.

EP-1046

High dose-low energy intraoperative radiotherapy in the treatment of malignant H&N tumors

B. Emami[1], R. Borrowdale[2], M. Choi[1], E. Thorpe[2], A. Sethi[1], B. Chinsky[1], W. Small[1]
[1]*Loyola University Medical Center, Radiation Oncology, Maywood, USA*
[2]*Loyola University Medical Center, Otolaryngology, Maywood, USA*

Purpose or Objective:

Objective: The aim of this study was to investigate the feasibility of high dose-low energy intraoperative radiation (IORT) therapy using INTRABEAM© (Carl Zeiss Surgical, Oberkochen, Germany) in the treatment of malignant Head & Neck tumors.

Methods and Materials: Between March 2014 and July 2015, 12 patients with head and neck cancers (seven with primary malignant parotid tumors and five patients with previously treated recurrent head and neck cancer) received intraoperative radiation therapy after surgical resection at Loyola University Medical Center (Maywood, IL). The median dose prescription was 6Gy (range, 5-14Gy) prescribed to 5mm

depth in a single fraction delivered with cylindrical shaped flat applicators attached to a 50kV x-ray energy source (INTRABEAM). The flat applicator (sizes 3-6cm) was placed at the high-risk area within the surgical cavity, which was delineated by the surgeon as the area with high likelihood for close or positive margins. The average IORT delivery time was 20 minutes. The single IORT fraction was the sole treatment for all patients with recurrent, previously treated patients and in one patient with parotid tumors, while the remaining six patients with parotid malignancies received additional external beam radiotherapy(EBRT) (median dose 50Gy) four weeks after surgery. Decision for EBRT were based on review of final pathology.

Results: All patients underwent successful completion of intraoperative radiotherapy. With follow up time of 5 to 18 months, there have been no acute side effects or complications related to IORT. All patients with parotid tumors are currently NED; in patients with recurrent tumors, 1 of 5 has re-recurred.

Conclusion: IORT with low kv x-rays appears to be an excellent choice for selected patients with H&N cancers, both primary(parotid) and recurrent disease.
We are now in the process of initiating a prospective trial evaluating the use of IORT as part of primary management of parotid tumors at our institution.
Detailed results will be presented.

Corresponding author:
Emami, M.D, FACR, FASTRO Professor
Dept. of Radiation Oncology
Loyola University

EP-1047

Volume, FDG-PET and ADC responses could predict a similar prognostic benefit as HPV status

Z. Gouw[1], M. La Fontaine[1], O. Hamming-Vrieze[1], A. Al-Mamgani[1], P. Van Houdt[1], J.J. Sonke[1]
[1]Netherlands Cancer Institute Antoni van Leeuwenhoek Hospital, Department of Radiation Oncology, Amsterdam, The Netherlands

Purpose or Objective: Patients treated with concurrent chemoradiation (CCRT) for head and neck cancer (HNC) with HPV(+) associated tumours have a significantly better prognosis compared to those with HPV(-) tumours. Similarly, better prognosis was associated with changes during-treatment consisting of either a reduction in tumour volume, or FDG-PET SUV, or an increase in ADC. This study investigated a possible association between these imaging biomarkers and HPV status. Our hypothesis was that HPV(+) tumours show a stronger ADC increase and a larger volume and SUV decrease.

Material and Methods: 13 Patients with HNC stadium III-IVA underwent CCRT (11 oropharynx, 1 hypopharynx and 1 oral cavity). HPV status was assessed using P16 staining. Patients received FDG-PET and MRI imaging before the start of the treatment and at the end of the second week. The region of interest consisted of the GTV and was delineated by dedicated radiation-oncologists. The volume and the median SUV and ADC were measured pretreatment and during treatment. Relative responses were calculated by subtracting the pretreatment from the during treatment value, which was then normalized to the pretreatment value. A new variable (pooled response) was computed consisting of the average of the relative SUV and volume decrease and ADC increase. A one tailed independent samples t-test compared the average responses between the HPV(+) and HPV(-) tumours. Voxel-based Pearson correlation coefficients between baseline and response maps were calculated for ADC and FDG-PET. A Fisher's z-transformation was used to compare the correlation coefficients between HPV(+) and HPV(-) tumours.

Results: 7 out of 13 tumours were HPV(+) and 6 HPV(-). Comparing HPV(+) to HPV(-), GTV volume decreased 42% vs 28% (p=0.080), SUV decreased with 32% vs 5% for (p=0.074) and ADC increased 24% vs 7% (p=0.058) (figure 1). The total response was significantly higher for HPV(+) tumours (33% vs 13%, p=0.012). Correlation coefficients between baseline and response maps did not differ significantly for HPV(+) and HPV(-) tumours (PET: z= 1.05 vs 1.08 p=0.85, ADC: z=0.47 vs 0.51, p=0.78).

Conclusion: Volume, ADC and FDG-PET individually showed a trend towards a higher response in the HPV(+) tumours at the end of the second week CCRT. The total response was significantly higher for HPV(+) tumours, demonstrating a significant association between HPV-status and imaging biomarkers. The similar correlation coefficients of the response maps indicate the spatial distribution does not depend on HPV status. This study emphasises the importance of reporting HPV status in imaging response biomarker studies for HNC patients. A validation of the prognostic value of imaging response biomarkers within HPV(+) and (-) cohorts is warranted.

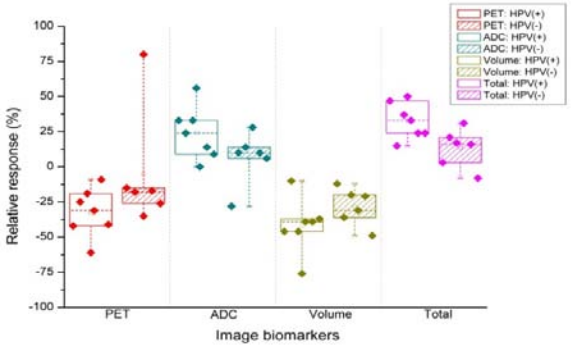

Figure 1: Box plots of relative responses at the end of the second week CCRT. Individual patients are represented as data points. Negative values represent a decrease, positive an increase.

EP-1048

Phase I trial of a novel metalloporphyrin radiosensitiser (MTL005) in head and neck cancer

S. Schipani[1], B. Foran[2], T. Guerrero Urbano[3], H. Jürgens[4], C. Beattie[5], J. Caldwell[5]
[1]Institute of Cancer Sciences University of Glasgow, Radiation Oncology, Glasgow, United Kingdom
[2]Clinical Trials Centre, Academic Unit of Clinical Oncology Western Park Hospital, Sheffield, United Kingdom
[3]Guy's and St Thomas' Hospitals, Radiation Oncology, London, United Kingdom
[4]Tartu University Hospital, Radiation Oncology, Tartu, Estonia
[5]MorEx Development Partners LLP, MorEx, London, United Kingdom

Purpose or Objective: MTL005 is a novel metalloporphyrin that demonstrated efficacy as a radiosensitizer in oxic and hypoxic pre-clinical models, increasing tumour doubling times by 50-90% depending on radiation dose. MTL005 achieved higher concentrations in tumour tissue compared with normal tissues (6:1 ratio), and these higher levels were retained for up to 62 days post administration. We developed a first-in-human phase I, open label, dose escalation, multicenter clinical trial to evaluate the safety and tolerability of single dose MTL005 in combination with radiotherapy (Part 1) and cisplatin chemo-radiotherapy (Part 2) in patients with locally advanced head & neck cancer treated with palliative and curative intent respectively. The results of Part 1 of the study are reported.

Material and Methods: In Part 1 of the study MTL005 was administered 1 week prior to palliative radiotherapy as i.v. injection in 38-76 minutes. Two dose levels were explored (2 and 4 mg/kg). Patients were immobilised in a thermoplastic mask and a contrast enhanced CT scan was used to define the PTV and the organs at risk. Radiotherapy was delivered with IMRT with a total dose of 50Gy to the PTV in 25 consecutive

fractions for 5 days a week. Toxicity was recorded using the CTCAE v4.0 to define a Dose Limiting Toxicity (DLT) and a Maximum Tolerated Dose (MTD) of MTL005.

Results: A total of 8 patients, 7 males (88%) and 1 female (12%), were enrolled, 4 in each of the 2 dose level cohorts. Six patients, all male with median age of 65 (54-77), were dosed with MTL005 successfully, 3 in each cohort. Dosing failures were due to an unexpected severe pain reaction (1 patient) and a technical problem with the infusion line (1 patient). In the 6 evaluable patients the following adverse events were recorded. Grade ≤2 oral mucositis and dysphagia were recorded in 3 (50%) and 4 (67%) patients respectively. Grade 1 pain in site of MTL005 injection was assessed in 1 (17%) patient. Grade ≤2 other toxicities (anaemia, dysgeusia) occurred in 3 (50%) patients. Grade 3 (dyspnoea, pneumonitis, oral haemorrhage, back pain, hyperuricemia) and Grade 4 toxicity (sepsis) were recorded in 4 (67%) and 1 (17%) cases respectively requiring hospitalisation and being considered as Serious Adverse Events (SAE). None of the SAE was assessed as directly related to MTL005 so DLT/MTD was not defined.

Conclusion: We completed Part 1 of the study and MTL005 DLT/MTD was not defined. Part 2 has been commenced with a MTL005 starting dose of 4mg/kg and is currently ongoing.

EP-1049

Prognostic role of 18F-FDG PET/CT in head and neck cancers treated with radical radio-chemotherapy

I. Sandler[1], P. Castellucci[1], S. Fanti[1], U. Caliceti[2], R. Frakulli[3], A. Milani[3], S. Cammelli[3], F. Deodato[4], M. Nuzzo[4], G. Macchia[4], G. Frezza[5], A.G. Morganti[3]

[1]Nuclear Medicine Unit- S.Orsola-Malpighi Hospital-University of Bologna, Department of Experimental-Diagnostic and Specialty Medicine-DIMES, Bologna, Italy

[2]Unit of Otolaryngology- S.Orsola-Malpighi University Hospital, Department of Specialist Surgery and Anesthesiology, Bologna, Italy

[3]Radiation Oncology Center- S.Orsola-Malpighi Hospital-University of Bologna, Department of Experimental-Diagnostic and Specialty Medicine-DIMES, Bologna, Italy

[4]Fondazione di Ricerca e Cura "Giovanni Paolo II"- Catholic University of Sacred Heart, Radiotherapy Unit, Campobasso, Italy

[5]Ospedale Bellaria, Radiotherapy Department, Bologna, Italy

Purpose or Objective: To assess the prognostic role of 18F - FDG PET/CT based response evaluation after primary concomitant radio-chemotherapy (RCT) for loco regionally advanced Head and Neck squamous cell carcinoma (HNSCC).

Material and Methods: 150 patients were included in this retrospective study. Mean age was 59 years (107 males and 43 females). The sites of HNSCC were oropharynx (53%), nasopharynx (14%), oral cavity (10%), hypopharynx (7%), larynx (7%), salivary glands (5%) and paranasal sinuses (4%). All patients underwent 18F-FDG PET/CT between 2006 and 2013 to assess treatment response; 62% of patients also had a pre-therapy 18F -FDG PET/CT scan. 18F -FDG PET/CT was performed from 6 to 36 weeks (median 21 weeks) after the end of RCT. Patients were divided in three groups: 18F -FDG PET/CT performed from 6 to 14 weeks after the end of RCT (group I: 30 patients), from 15 to 23 weeks (group II: 89 patients) and from 24 to 36 weeks (group III: 31 patients). 18F -FDG PET/CT scans were performed according to standard procedure, then they were visually analysed by 2 expert physicians and categorized as negative ("score 1"), doubt negative ("score 2"), doubt positive ("score 3") and positive ("score 4"). Patients were followed-up, based on clinic and radiological and/or histological findings. Median follow up was 38 months (range, 12-60 months). At the end of the follow-up 18F-FDG PET/CT were classified as true positive (TP), true negative (TN), false positive (FP) and false negative (FN).

Results: Group I showed "score 1" in 14 patients, "score 4" in 11 patients and therefore 18F-FDG PET/CT sensitivity was 69%, specificity 83%, VPP 82%, VPN 72%, and accuracy 0.76. This group showed 5 doubt scans (16%) as "score 2" that were find out to be 2 negatives and 3 positives. No "score 3" was observed in this group. Group II showed "score 1" in 55 patients, "score 4" in 27 patients and therefore 18F-FDG PET/CT sensitivity was 87%, specificity 98%, VPP 96%, VPN 93%, and accuracy 0.94. This group showed 7 (8%) doubt scans: 3 scans (3.5%) as "score 2" that in follow-up were 1 negative and 2 positives and 4 scans (4.5%) as "score 3" that were found out to be 2 negatives and 2 positives. Group III showed "score 1" in 24 patients and "score 4" in 6 patients and therefore 18F-FDG PET/CT sensitivity was 86%, specificity 100%, VPP 100%, VPN 96%, and accuracy 0.97. This group showed only 1 doubt scan (3%) as "score 2" that was find out to be negative.

Conclusion: According to our data, PET/CT with 18F-FDG showed an excellent prognostic value of treatment response to primary concomitant RCT if performed at least 14 weeks after the end of RCT. We also observed that the numbers of "doubt scans" significantly decrease 14 weeks after the end of RCT.

EP-1050

Volume definition in radiotherapy planning for thyroid cancer: a retrospective observational study

E. Farina[1], S. Cammelli[1], A. Arcelli[1], G. Zanirato[1], R. Frakulli[1], L. Tagliaferri[2], A.G. Morganti[1], S. Fanti[3], F. Monari[1]

[1]Radiation Oncology Center- Sant'Orsola-Malpighi Hospital-University of Bologna, Department of Experimental-Diagnostic and Specialty Medicine- DIMES, Bologna, Italy

[2]Policlinico Universitario "A. Gemelli"- Università Cattolica del Sacro Cuore, Department of Radiotherapy, Roma, Italy

[3]Nuclear Medicine Unit- Sant'Orsola-Malpighi Hospital-University of Bologna, Department of Experimental-Diagnostic and Specialty Medicine- DIMES, Bologna, Italy

Purpose or Objective: The role of post-operative external beam radiotherapy (EBRT) in differentiated thyroid carcinomas is still discussed considering the low clinical aggressiveness and the possibility to perform a radioiodine ablation (RAI). However, there are dedifferentiated tumors that, over time, lose their capacity to capture Iodine. The aim of this study is to evaluate the utility of 18F-FDG PET/CT in volumes defining and the clinical response rate after EBRT in these patients.

Material and Methods: Patients with locally recurrent thyroid cancer, treated with radical EBRT from October 2011 to March 2015 after total thyroidectomy and RAI, were included in the study. When EBRT was planned, thyroglobulin (HTG) was detectable and there was negative post-RAI whole body scintigraphy (WBS) and no surgical indications. All patients underwent a pre-treatment 18F-FDG PET/CT that resulted positive: 3 in loggia, 3 in loggia and lymph nodes, 9 in lymph nodes, 1 in lymph nodes and in lung. EBRT was delivered with IMRT-SIB technique: a dose of 66 Gy (2.2 Gy/fr) to increased FDG-uptake areas, 60 Gy (2 Gy/fr) to ipsilateral lymph nodes and 54 Gy (1.8 Gy/fr) to contralateral ones, in 30 fractions, 1 fr/die. A revaluation 18F-FDG PET/CT and HTG dosage during the follow-up (range: 5-43 months) was performed. Acute and late toxicity were assessed with CTCAE v. 4.03 and EORTC-RTOG scales respectively, the metabolic, clinical and instrumental response with PERCIST and RECIST criteria. Local control (LC) and overall survival (OS) were analysed with Kaplan-Meier method.

Results: Sixteen patients were treated and analyzed consecutively [M / F: 8/8; median age: 71 years; range: 36-81; histology: 15 papillary carcinomas and 1 follicular carcinoma; UICC stage: III-IV]. Post-EBRT 18F-FDG PET/CT showed CR in 7 (43.8%), PR in 5 (31.2%), SD in 4 (25.0%) patients and unknown lung metastases in 2 patients (12.5%). HTG decreased in agreement with PET/CT results. 4 patients (25.0%) had G3 skin acute toxicity and no one showed G4 late toxicity. LC and OS rates were 100% at last follow-up (median F-UP: 12.3 months).

Conclusion: 18F-FDG PET/CT is useful to target volumes delineation for radiotherapy planning, allowing a clear definition of GTV, not detected with 131I WBS. Disease response and local control justify future prospective studies.

EP-1051

Long-term quality of life and second tumours in T1N0 glottic cancer treated with radical radiotherapy

R. Benlloch Rodríguez[1], J. Romero Fernandez[1], D. Rincón Cruz[1], G. Martín Hernández[2], J.R. García-Berrocal[3], B. Vaquero Barrón[1], I. Zapata Paz[1], O. Alvarez montero[3], S. Gonzalo Ruiz[1], A. De la Torre Tomas[1]

[1]*Hospital Universitario Puerta de Hierro, Radiation Oncology, Madrid, Spain*

[2]*Complejo Asistencial de Ávila, Radiation Oncology, Ávila, Spain*

[3]*Hospital Universitario Puerta de Hierro, Otolaringology, Madrid, Spain*

Purpose or Objective: To evaluate long-term results, prognostic factors, quality of life (QoL) and voice and thyroid toxicity and risk of second tumors in T1N0M0 glottic carcinoma.

Material and Methods: A total of 100 patients with stage T1N0M0 histologically proven squamous cell glottic carcinoma treated between 2000 and 2012 were retrospectively analyzed. Mean age: 62.14 years; 90 males, 10 female; stage: T1a:80, T1b:20. Treatment: radical external radiotherapy with a mean dose of 70 Gy (2Gy/fraction). Statistical analysis: Kaplan-Meier method and Chi-square test. In 35 patients, we prospectively evaluated the Voice Handicap Index (VHI 30) and the QoL with (EORTC)–QLQ C30 questionnaire and organ-specific EORTC-Head & Neck-35 module. In the functional and QoL scales of the QLQ C30 questionnaire a higher score represent better functioning and quality of life, whereas in symptoms scales of both questionnaires a high score implies a higher level of symptoms. The last two questions in QLQ C30 represents a QoL scale ranging from 1 ("very poor") to 7 ("excellent"). Blood determination of TSH, T4, T3 levels was performed in 19 patients. Second primary tumors were defined as those originated outside the head and neck area.

Results: Median follow-up: 91.5 months. Five-and 10-year actuarial OS and disease free survival were 83% and 70%, and 70% and 57% respectively. Five- and 10-year actuarial LC and metastasis free survival were 84% and 77%, and 97% and 94% respectively. Eighteen patients had recurrent disease. Mean time to local recurrence was 80 months. Sex, stage, grade and Overall Treatment Time were not statistically significant prognostic factors. Mean score (MS) for the VHI30 was 19.16, which is considered as a minimal amount of voice handicap. Patients reported excellent QoL in the C30 questionnaire which showed functional scores above 93 and symptoms scores below 14. The global health status and QoL scale were 5.93 and 6, respectively, which should be considered as "good" or "very good". In the H&N 35 questionnaire the worse scores were dry mouth and thick saliva (MS 30.6 for both). Most patients have no problems in open mouth, swallowing, speaking and social contact (MS of 0, 6.9, 18.6 and 16.6, respectively). There were no patients with clinical or subclinical hypothyroidism. Mean TSH, T3, and T4 were 2.32, 3.16 and 1.31, respectively. Mean TSH was not statistically different from normal values (P: 0.34) Eighteen patients (18%) had second tumors: 11 lungs, 2 prostates, 5 others. Ten years probability of second lung cancer was 28%.

Conclusion: In our series radical radiotherapy for T1 glottic cancer was well tolerated and achieved excellent tumor control comparable to surgery. In our opinion radical radiotherapy should be the standard treatment of these patients given the excellent results in QoL and voice preservation. The high probability of second lung cancer could justify performing thoracic CT scan during follow-up.

EP-1052

Treatment outcome of induction bio-chemotherapy followed by IMRT in advanced NPC patients

P.J. Lin[1], W.Y. Wang[2], Y.C. Liu[3], J.C. Lin[3]

[1]*Tung's Taichung MetroHarbor Hospital, Department of Radiation Oncology, Taichung, Taiwan*

[2]*Hung Kuang University, Department of Nursing, Taichung, Taiwan*

[3]*Taichung Veterans General Hospital, Department of Radiation Oncology, Taichung, Taiwan*

Purpose or Objective: We investigated the treatment outcome of induction bio-chemotherapy followed by IMRT for advanced nasopharyngeal carcinoma (NPC) and the prognostic impact of plasma EBV DNA viral load.

Material and Methods: Forty-two NPC patients with previously untreated, stage III/IV received induction chemotherapy of weekly P-FL (cisplatin 60 mg/m2 d1, [5-fluorouracil 2500 mg/m2 + leucovorin 250 mg/m2] d8) ± docetaxel 50 mg/m2 or gemcitabine 1000 mg/m2 d15, for 10-12 weeks and concurrent Cetuximab 400 mg/m2 day 1, then weekly 250 mg/m2. Conventional (70 Gy/35fr) or hyperfractionated (76.4 Gy/64fr for T4 tumor) RT were delivered by IMRT technique. Plasma EBV DNA levels were measured before, during and after treatment regularly.

Results: Baseline characteristics are median age=44; male/female=28/14; performance status ECOG 0/1=13/12; stage III/IV=22/20, and pathological type (WHO) IIa/IIb=20/22. Each patient received a mean of 11 weekly cetuximab. During induction bio-chemotherapy period, cetuximb-associated toxicity included 100% skin rashes (grade 50% III/IV), 64.3% (27/42) dry skin, 52.4% (22/42) paronychia, and 28.6% (12/42) hypomagnesia. Grade III/IV conventional toxicities were rare (11.9% leucopenia, 9.5% anemia, 2.4% thrombocytopenia, and 2.4% mucositis). Response after induction bio-chemotherapy revealed 50% CR and 50% PR. After a median follow-up of 24 months, there were 1 local, 1 regional, and 5 distant failures. The 3-year local failure-free, neck failure-free, distant metastasis failure-free (DMFS), progression-free survival (PFS), and overall survivals (OS) were 96.6%, 96.0%, 87.4%, 79.9%, and 92.1% respectively. Patients with high pretreatment plasma EBV DNA predict significantly lower PFS and DMFS (P=0.0108 and P=0.004) but not OS (P=0.6291). Patients with detectable plasma EBV DNA after bio-chemotherapy had a significantly lower OS, PFS, and DMFS (P=0.0294, P=0.0078, and P=0.0082). Patients with persistently detectable plasma EBV DNA one week after IMRT predict a significantly lower PFS (P=0.0258).

Conclusion: Induction Bio-chemotherapy followed by IMRT is a highly effective protocol with very low toxicity in advanced NPC. Plasma EBV DNA monitoring are the most important prognostic factors in outcome prediction.

EP-1053

Toxicity and clinical outcome for patients treated for advanced head and neck cancer with VMAT-SIB

E. Villa[1], C. Franzese[1], A. Fogliata[1], D. Franceschini[1], G.R. D'Agostino[1], E. Clerici[1], P. Navarria[1], T. Comito[1], F. De Rose[1], C. Iftode[1], A.M. Ascolese[1], A. Tozzi[1], R.L.E. Liardo[1], P. Mancosu[1], M. Scorsetti[1]

[1]*Istituto Clinico Humanitas, Radiotherapy and Radiosurgery, Rozzano Milan, Italy*

Purpose or Objective: The choice of fractionation scheme in radiotherapy of head and neck cancer (HNC) is still debated. In fact it is well known that a shorter overall treatment time and a dose escalation, may improve loco-regional control of disease by reducing cell repopulation. Nevertheless, shortening overall treatment time can result in worse acute toxicity.Volumetric modulated arc therapy (VMAT) with Simultaneous Integrated Boost (SIB), allowing hypofractionation with a better sparing of the organs at risk, has showed promising results in terms of outcome and pattern of toxicity.In this study we retrospectively analyzed a series of patients with stage III-IV HNC treated with VMAT-SIB

radiotherapy, with the aim to verify possible correlations between the planned dose distributions to the main dose limiting structures and the observed levels of toxicity like mucositis, xerostomia and dysphagia.

Material and Methods: Data of hystologically confirmed advanced HNC patients, in stage III and IV (AJCC), were reviewed in a retrospective dosimetric and clinical evaluation. Patients were treated with VMAT (RapidArc) and SIB in 33 fractions for a total dose of 69.96 Gy to the tumor and positive-nodes, and 54.45Gy to the elective volume, respectively. Toxicity was graded according to CTCAE3.0 Correlation was explored between OAR dose parameters and related acute and late toxicities.

Results: From December 2008 to August 2014, 102 patients were treated. Acute mucosal and swallowing toxicities higher than grade 3 were reported in only 11% and 6% of patients, respectively; late morbidities (G1-G2) were present in only 3% of cases. No G3 Toxicity was reported. A statistically significant correlation was found between the dosimetric parameters of oral cavity V30Gy, V40Gy, and V70Gy, and mucosal toxicity (p = 0.01, 0.03, and 0.05, respectively). Concerning salivary glands, late toxicity profile was worse compared to acute side effects, with 19% of persisting late grade equal or higher than 2. Regarding the constrictors and the swallowing toxicity, most of the dosimetric parameters of the inferior constrictor muscle (mean dose, D1/2V, D1/3V, D2/3V) were significant at the univariate analysis, while no correlations were found for middle and superior constrictors. With a median follow-up of 19 months (range 1-61 months), Overall Survival (OS) at 3 and 5 years was 83%±4% and 73%±10%. Mean OS was 51±3 months. Disease Free Survival (DFS) at 3 and 5 years was 71%±7%, and 34%±16%. Mean DFS was 43±3 months.

Conclusion: Volumetric modulated arc therapy (VMAT) with Simultaneous Integrated Boost (SIB), that allow a shorter overall treatment time, a dose escalation, associated with a better sparing of OARs, showed a good toxicity profile. From our analysis toxicity to dose-limiting structures was significantly correlated to the dosimetric parameters explored.

EP-1054

Temporal patterns of patient-reported trismus and associated mouth-opening distances in RT of HNC

M. Thor[1], C.E. Olsson[2], J.H. Oh[3], J. Hedström[4], N. Pauli[4], J.O. Deasy[3], C. Finizia[4]

[1]*Memorial Sloan Kettering Cancer Centre, Department of Medical Physics, NYC, USA*

[2]*Institute of Clinical Sciences- the Sahlgrenska Academy at the University of Gothenburg, Department of Radiation Physics, Gothenburg, Sweden*

[3]*Memorial Sloan Kettering Cancer Center, Department of Medical Physics, NYC, USA*

[4]*Institute of Clinical Sciences- Sahlgrenska Academy at the University of Gothenburg, Department of Otorhinolaryngology- Head and Neck Surgery, Gothenburg, Sweden*

Purpose or Objective: To investigate the association between temporally robust domains of patient-reported trismus symptoms with mouth-opening ability as assessed by maximal interincisal opening distance (MIO) in head and neck cancer (HNC) patients treated with radiotherapy (RT).

Material and Methods: The study included 196 patients previously treated with primary state-of-the-art RT for HNC in 2007-2012. A five answering-category-based (no/mild/moderate/severe/very severe symptom) patient-reported trismus questionnaire (Gothenburg Trismus Questionnaire, GTQ) was completed pre-RT, and at 3, 6, and 12 months post-RT. This study focuses on the 14/21 potentially RT-induced physical trismus symptoms from GTQ. At each follow-up, symptom domains were generated by means of factor analysis and these symptoms were correlated with MIO (categorized into five intervals (mm): 1: >50; 2: >40-≤50; 3: >35-≤40; 4: >25-≤35; 5: ≤25) for each follow-up using Pearson's correlation coefficient (Pr).

Results: The three symptom domains *Jaw aches/pains*, *Jaw-related problems*, and *Eating limitations* were identified at each follow-up, and included one, two and three temporally robust symptoms, respectively. Correlations between MIO and these symptoms were weak to modest (Pr= 0.22-0.58; *Table*) with the overall stronger correlations for 'Opening mouth difficulty' and 'Current mouth-opening ability' in the *Jaw-related problems* domain at 6 and at 12 months post-RT (Pr=0.49-0.58; *Figure*).

Table. Symptom domains with symptom importance and prevalence for a moderate+ symptom severity, as well as correlations (Pr) with MIO.

Baseline N=196				3m post-RT N=189				6m post-RT N=158				12m post-RT N=153			
Symptom	Symptom importance	Prevalence (%)	Pr	Symptom	Symptom importance	Prevalence (%)	Pr	Symptom	Symptom importance	Prevalence (%)	Pr	Symptom	Symptom importance	Prevalence (%)	Pr
Jaw aches/pain															
Jaw aches/pain*	1	11	0.34	Jaw aches/pain*	1	30	0.37	Jaw aches/pain*	1	25	0.32	Jaw aches/pain*	1	26	0.42
Jaw muscle pain/soarness	2	8	0.43					Jaw muscle pain/soarness	2	25	0.34	Jaw muscle pain/soarness	4	23	0.36
Jaw fatigue/stiffness	3	12	0.44					Jaw fatigue/stiffness	4	15	0.45	Jaw fatigue/stiffness	3	32	0.47
				Pain moving jaw	2	34	0.35	Pain moving jaw	3	27	0.48	Pain moving jaw	2	24	0.27
				Noises from jaw	2	15	0.27					Noises from jaw	5	14	0.25
								Clenching teeth habit	5	22	0.32			
								Pressing tongue habit	6	19	0.36			
Jaw-related problems															
Current mouth-opening ability*	1	11	0.49	Current mouth-opening ability*	3	44	0.49	Current mouth-opening ability*	2	35	0.49	Current mouth-opening ability*	1	30	0.52
Opening mouth difficulty*	2	18	0.47	Opening mouth difficulty*	2	45	0.37	Opening mouth difficulty*	1	49	0.55	Opening mouth difficulty*	2	40	0.58
				Jawring difficulty	1	34	0.31								
				Jaw muscle pain/soarness	4	31	0.27								
Eating limitations															
Problems eating soft food*	1	7	0.21	Problems eating soft food*	1	32	0.23	Problems eating soft food*	3	25	0.35	Problems eating soft food*	1	20	0.25
Problems eating solid food*	2	13	0.37	Problems eating solid food*	2	58	0.22	Problems eating solid food*	1	50	0.37	Problems eating solid food*	2	41	0.30
Problems getting food in mouth*	3	13	0.40	Problems getting food in mouth*	4	41	0.32	Problems getting food in mouth*	2	39	0.41	Problems getting food in mouth*	3	31	0.39
Problems biting off	4	8	0.27	Problems biting off	3	32	0.23					Problems biting off	4	25	0.32

*Temporally stable symptom, i.e. present in a symptom domain at each follow-up

Note: Prob.30, and Pr=0.36-0.67 regarded as a weak, and modest correlation, respectively

Figure. The prevalence of the *Jaw-related symptom* 'Opening mouth difficulty' at 6m post-RT, and the distribution of MIOs.

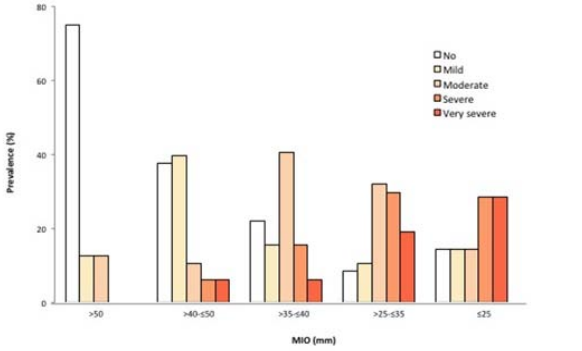

Conclusion: Mouth-opening distances can be explained in terms of associated patient-reported symptom severities on jaw-related problems. Translating the patient's experience into objective measurements and vice versa widens possibilities to monitor and possibly prevent progression of trismus symptoms after RT.

EP-1055

Determination of EGFR in lesions of the oral cavity and evaluating the role of Gefitinib

V. Umesh[1]

[1]*All India Instutute Of Medical Sciences-New Delhi, Radiation oncology, New Delhi, India*

Purpose or Objective: Determination of expression of EGFR in premalignant and malignant lesions of the oral cavity and evaluating the role of Gefitinib in the same

Material and Methods: 130 Patients with premalignant and malignant lesions of oral cavity from JK cancer institute, Kanpur were selected. EGFR status evaluation was done in all the patients. Premalignant lesions over expressing EGFR were observed for transformation into malignant lesions and were given Tab Gefitinib 250 mg OD daily. Malignant lesions with over expression of EGFR were randomly divided into 2 groups first group consisted of patients who were given CCRT(cisplatin). The other group had the same regimen but with the addition of Tab Gefitinib 250 mg daily

Results: Out of 130 patients registered 53 were premalignant out of which EGFR(+) positive in 73%(39) patients. EGFR(++)over expression were in 8%(4)patients, EGFR negative in 18%(10) patients. 77 were malignant lesions EGFR positive in 89%(51) patients. EGFR(+)in 38%(27) of patients, EGFR(++)in 40%(28) patients ,EGFR(+++) were expressed by 11%(11) patients. EGFR negative in 11%(11 patients)

Total of 40 Malignant Lesions were Randomized into the two arms 19patients(total 22) in CCRT+ gefitinib arm have shown complete response in comparison to 11patients(total 18) in CCRT arm

Conclusion: EGFR status evaluation in premalignant can be used as a screening tool for detection of transformation into malignant lesions. We can prevent this transformation by EGFR inhibitors. In malignant lesions it can be really important for the role of EGFR inhibitors .Eg Gefitinib has shown good results when combined with the conventional CCRT.

EP-1056

Treatment delays are associated with disease upstaging in oropharyngeal squamous cell carcinoma

S. Baker[1], R. Banerjee[2], B. Debenham[1]
[1]*Cross Cancer Institute, Radiation Oncology, Edmonton, Canada*
[2]*Tom Baker Cancer Centre, Radiation Oncology, Calgary, Canada*

Purpose or Objective: Increasingly limited health care resources coupled with a rising incidence of oropharyngeal squamous cell carcinoma (OPSCC) is resulting in longer wait times for definitive treatment. Our objectives were to determine the impact of treatment delays on disease upstaging and outcomes in OPSCC.

Material and Methods: Demographic features, number of days from diagnosis until surgery, and clinical and pathological staging information were determined for 139 patients diagnosed with OPSCC between January 2006 and November 2011. Patients were stratified on the basis of whether or not their disease was upstaged between clinical and pathological T, N or M stage. Statistics were performed using MedCalc Statistical Software.

Results: A total of 62 (45%) of patients were upstaged. Upstaged patients had a longer median time to surgery compared to non-upstaged patients (81 vs 68 days, p=0.017) and 21% (n=13) were upstaged to T ≥ T3 or N ≥ N1. There was a trend to higher incidence of margin positivity in upstaged patients (19%, n=12) compared to non-upstaged patients (9%, n=7) (p=0.141). Groups did not differ in the rate of nodal extracapsular extension (50% and 41%, p=0.363). Median overall survival (OS) for upstaged patients was 5.82 years and was not reached for non-upstaged patients. There was a trend to lower OS in upstaged patients (p=0.0746).

Conclusion: Longer duration between diagnosis and surgery is associated with significant pathological upstaging. Allocating resources to reduce treatment delays may result in overall health care savings due to a reduced rate of requirement for adjuvant treatment, reduced patient morbidity, and improvement in disease outcomes.

EP-1057

Impact assessment of Sankol drug on the excretion of radioiodine-131 from patients DTC

S. Saadatmand[1]
[1]*Radiotherapy Sadra Center Qom, Department of Medical Physics and Engineering Isfahan University of Medical Sciences and Healthcare Isfahan- Iran, qom, Iran Islamic Republic of*

Purpose or Objective: The aim of this study was to investigate the impact assessment of Sankol drug on the excretion of 131I from patients with differentiated thyroid cancer (DTC).

Material and Methods: Fifty-four patients with DTC who had normal renal function in two groups of control and intervention were included in this study. The herbal diuretic was given orally to the intervention group from 3 hours after the 131I administration, and then every 8 hours for 24 hours. The control patients received placebo with the same timing. The radioactivity of the urine samples from each maturation was measured and expressed as the percentage of the administered dose. Exposure from patients were measured after the drug administration and then at the time of 3, 9, 15, 21 and 24 hours after the patient isolation.

Results: The obtained mean percentage of activity excreted during 24 hours after intake of radioactive iodine in the urine in the intervention and control group were 68.85±4.3, 59.11±5.3 with p<0.001 respectively. The obtained percentage of residual activity in the body after 24 hours was 25.17±4.6, 19.56±3.6 with p < 0.001, respectively. Radiation dose rate at 300cm after 24 hours for the intervention and control group were 9.52±3.4 µSV/h, 11.92 ± 6.0µSV/h with p > 0.05, respectively.

Conclusion: : Our results demonstrated that Sankol given as an adjuvant medication in the patients with DTC was caused a significant increase in urinary excretion of radioiodine and shorten the hospital stay.

EP-1058

Organ preservation in locally advanced larynx and hypopharynx cancer: non surgical strategy

P. Cucarella Beltran[1], M.A. De la Rúa Calderon[1], J.R. Alonso Pantiga[1]
[1]*Hospital Universitario Central de Asturias, Radiation Oncology, Oviedo, Spain*

Purpose or Objective: To present protocol larynx preservation results in patients treated for carcinoma of the larynx or hypopharynx in stage III and IV.

Material and Methods: Data from a serie of 50 patients treated under the guidance of larynx preservation protocol implemented at our institution in 2007 were analyzed. Treatment protocol is divided into two phases. Patients meeting the inclusion criteria receive CDDP and 5FU cycle. At 3 weeks CT evaluation is performed. If the answer is > 50% are included in the arm radiochemotherapy : CDDP every 3 weeks and RT 70Gy 2 Gy per session 5 days a week. Those who do not respond or <50% are scheduled to total laryngectomy + neck dissection. If indicated received postoperative RT. The cases analyzed belong the period 2007-2012 (minimum three years follow-up). All patients were considered evaluable.

Results: The serie includes 50 patients with a median age of 56 years. 42 men and 8 women with tumors in the larynx (28) and hypopharynx (22); 27 stage III and 23 stage IV. 22 not reached a sufficient response (<50%) and yes they got 27; in one case we missed the information. Laryngectomy was performed in 19 patients out of 22 unanswered (3 refused). Among the 27 respondents, received RT / CT, 6 LT for recurrences were performed. Larynx preservation was achieved in 50% of patients. The survival of the entire group was 51% at 5 years and 62.6% cause-specific survival. The specific survival at 5 years with RT / CT was 60% compared to 65% of total laryngectomy gupo (p = 0.568).

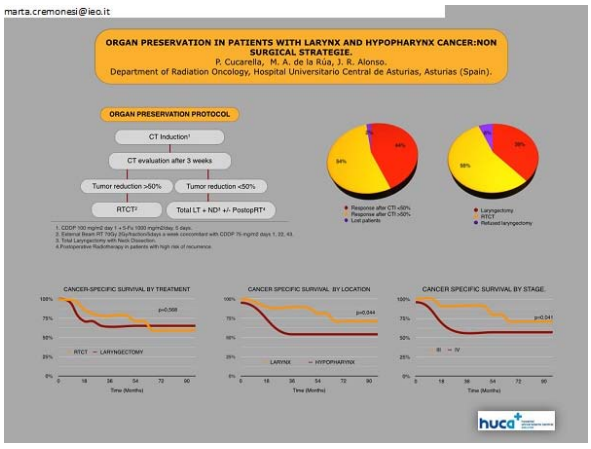

Conclusion: The larynx preservation protocol achieves the same survival rates that total laryngectomy, contributing 50% of preservation of organ function. It is necessary more cases for a final evaluation.

EP-1059

Structured assessment of radiation-induced fibrosis following treatment for head and neck cancer

G. Adigbli[1]
[1]*University College London, Surgery and Interventional Science, London, United Kingdom*

Purpose or Objective: To robustly assess features of radiotherapy-induced fibrosis in patients within the reconstructive/plastic surgery clinic and establish a baseline for comparison against following treatment.

Material and Methods: Patients awaiting fat-graft treatment for radiotherapy-induced fibrosis were assessed with regard to their symptomatology using a quality of life questionnaire. They also underwent clinical examination for functional impairment secondary to the fibrotic process and assessment of the microcirculation and mechanical properties by speckle contrast blood flow assessment and themographic imaging, durometry and skin cutometry respectively. The results were compared against age-matched healthy controls.

Results: Health-related quality of life in these patients was impaired, with 36% of patients overall rating their quality as "fair" or "very poor". On clinical assessment, movement of the neck was impaired with approximately 50% reduction in flexion and rotation movements. 100% of patients had sensory impairment in the fibrotic region. Microcirculatory changes were seen with increased flux (mean = 411.47 vs. 348.83 contralaterally) and temperature (mean difference of 1.3°C vs. control) in the regions of fibrotic change compared with the contralateral side and with controls respectively. Significant differences in hardness of skin and subcutaneous tissues of the neck were seen between treated and untreated areas and between patients and controls (51.5 vs. 16.8 durometer units). Significant increases in the firmness and fatiguability of the skin were seen on cutometry and non-significant decreases in elasticity.

Conclusion: Our methods provide us with important baseline information about how affected our patients are by radiotherapy-induced fibrosis. This baseline can be compared post-operatively to quantify benefits afforded by fat-graft treatment and guide future research into the underlying mechanisms.

EP-1060

Can reduced CTV margin for IMRT in Head and Neck cancers improve therapeutic outcomes?

T.P. Chitradurga Abdul Razack[1], U.K. Annasagara Srinivasa[1], V. Chandraraj[2], A. Shenoy[3], L. Jacob[4], N. Ramar[5], P. Anchineyan[6], L. Vishwanath[1], N. Thimmiah[1], S. Palled[1], S. Patil[7], C.N. Patil[8]
[1]*Kidwai Memorial Institute Of Oncology, Radiation Oncology, Bangalore, India*
[2]*Kidwai Memorial Institute Of Oncology, Radiation Physics, Bangalore, India*
[3]*Kidwai Memorial Institute Of Oncology, Head And Neck Oncology, Bangalore, India*
[4]*Kidwai Memorial Institute Of Oncology, Medical Oncology, Bangalore, India*
[5]*Apollo Cancer Institute, Radiation Physics, Bangalore, India*
[6]*Health Care Global, Radiation Physics, Bangalore, India*
[7]*Health Care Global, Medical Oncology, Bangalore, India*
[8]*Apollo Cancer Institute, Medical Oncology, Bangalore, India*

Purpose or Objective: To assess efficacy & toxicity of reduced CTV margins in the IMRT of head and neck cancers

Material and Methods: Between 2010 and 2015, 83 consecutive patients with locally advanced Head & Neck squamous cell cancers, treated with a radical intent with chemoradiation by IMRT, with reduced CTV margins were analysed for local control, toxicity, compliance & survival. Nodal delineation was as per DAHANCA guidelines.Toxicity was assessed by CTCAE version 4.0

Results: Median age of the cohort was 58 years (32-76) with 65 males & 18 female patients. Hypopharyngeal cancers were 47% followed by oropharyngeal (27%) and laryngeal (26%) cancers. TNM stage grouping in the cohort was IVA in 72% followed by IVB & III. CECT based delineation of the involved primary and nodal volumes were expanded uniformly by 5 mm to create the high risk CTV and this expanded by 5 mm to create the PTV1. Similarly the involved nodal level was considered as intermediate risk (PTV2) and remaining nodal levels as low risk (PTV3). Inverse planning was performed using Varian Eclipse planning system with dose constraints to OAR's as per guidelines. SIB-IMRT was delivered to a dose 70, 63 and 56Gy in 35 fractions to high, intermediate and low risk volumes respectively. Median overall treatment time was 49(40-70) days. 24% of the patients received 6 fractions per week. Weekly Cisplatin (40mg/sqm) was given concurrently with IMRT except in 10 patients receiving Carboplatin (2AUC), 90% received a minimum of 4 cycles. Grade 3 mucositis was seen in 40%, grade 3 dysphagia in 6%, radiation dermatitis was predominantly grade 2, Xerostomia was predominantly grade 1 in 93%, 10% required placement of nasogastric tube and treatment interruption. Myelosuppression of grade 3 was seen towards completion of treatment in 24% of the cohort, predominantly in total leukocyte count. A complete response of 90% and 86% was seen in primary and nodal disease at the end of the treatment and eventually in 100% and 94% in first three months. 3 patients needed neck dissection and showed residual disease. At a median follow up of 2 years, 62 patients are controlled with an overall survival of 74.7%. Deaths are due to distant metastasis in 4% and 8% due to other medical causes.

Conclusion: Reduction of CTV margin to 5 mm seems to be appropriate, with good loco-regional control, reduced overall treatment time, better compliance, reduced toxicity & superior outcomes. This study forms basis for a prospective controlled randomised study to generate further evidence.

EP-1061

Progressive resistive exercise training for shoulder function: a randomised controlled trial

V. Murthy[1], M. Chatterjee[2], S. Kannan[3], T. Gupta[1], A. Budrukkar[1], S. Ghosh Laskar[1], J. Agarwal[1]
[1]*Advanced Centre for Treatment- Research and Education in Cancer- Mumbai, Radiation Oncology, Mumbai, India*
[2]*Advanced Centre for Treatment- Research and Education in Cancer- Mumbai, Physiotherapy, Mumbai, India*
[3]*Advanced Centre for Treatment- Research and Education in Cancer- Mumbai, Biostatistics, Mumbai, India*

Purpose or Objective: Significant shoulder dysfunction persists in a majority of the oral cancer patients after surgery even on performing active exercises. Progressive Resistive Exercise Training (PRET) involves gradual and incremental increase in resistance for improved muscular rehabilitation. This randomized controlled trial was done to compare active shoulder exercise and PRET with active exercises for shoulder dysfunction in patients undergoing Radiation Therapy (RT).

Material and Methods: Ninety four eligible patients with shoulder abduction Active Range of Motion (AROM) ≥90° were randomized to either active shoulder exercises only (n=47) or PRET plus active shoulder exercises (n=47). Resistance was gradually progressed over 6 weeks according to the capacity of patients in PRET arm. AROM was measured at week 0, 2, 4, 6 and 6 months. Shoulder Pain and Disability Index (SPADI) was also measured in both arms at the base line and after completion of the intervention at the end of 6th week.

Results: Results: Improvement in shoulder abduction AROM was significantly greater in the PRET Arm (mean = 73.3° ± 14.3° at baseline to 132.5° ± 28.5° at 6 weeks) than in standard arm (mean = 74.8° ± 12.5° at baseline to 97.1° ±

22.4° at 6weeks, p<0.001). The SPADI pain and disability score also indicated significant improvement in PRET arm at 6 weeks when compared to standard arm (p < 0.05)

Conclusion: Early institution of PRET program provides maximal benefit to the post surgical oral cancer patients undergoing RT than active exercises only and should be considered the standard of care.

EP-1062

Primary (chemo)radiation therapy in organ-sparing treatment of tongue squamous cell carcinoma

A. Gevorkov[1], A. Boyko[1]
[1]*Moscow Research Gerzen Oncology Institut, Radiation Oncology, Moscow, Russian Federation*

Purpose or Objective: To evaluate the efficacy of primary (chemo)radiation therapy in a organ-sparing combined or radical nonsurgical treatment modality for tongue squamous cell carcinoma.

Material and Methods: From January 2003 to January 2015 166 consecutive patients with histologically proven the base (49 pts, 30%) and the mobile part of the tongue (MOT) cancer (117 pts, 70%) received radiotherapy +/- chemotherapy (concomitant) to the dose of 50Gy in the preoperative mode treatment and to 70Gy as radical irradiation. Most of them suffered from III (39%) and IV (35%) staged tumors, with the invasive nature of growth at 88 % and regional metastases in 70%. Patients with base of tongue (BOT) cancer had locally advanced process more often (92% vs 66%), especially stage IV (69% vs 20%). Nonresectable process was diagnosed in 38% patients with BOT cancer and in 23% cases of MOT cancer primary tumor. We also assessed tumors for potential biologic predictors of treatment effectiveness (p53, COX-2 , VEGF, Ki67, E-cadherin , p21 , Bcl- 2 and others). Radiomodification with 5FU/cisplatin or cisplatin/cetuximab was performed in 133 (80%) cases. All patients started with photon external beam radiation to the dose of 50Gy with subsequent decision of necessity of surgery by applying our prognostic model (combined clinical and biological predictive model with multivariate analysis, p<0,05). Nonsurgical treatment was performed in 56 (34%) cases. Patients with BOT primary tumor underwent conservative therapy more often (62% vs 22%). Combined treatment with surgery was performed to 110 (66%) patients, with the preservation of the organ in 76 (69%) cases. Organ-sparing surgery was possible in 89 (76%) cases of MOT cancer and only in 16 (33%) cases of BOT cancer.

Results: After irradiation we observed complete response in 21% cases of BOT cancer and 7% of MOT cancer, partial response in 79% and 82% respectively. Stabilization and progression was diagnosed in 8% and 3% of cases MOT cancer. Complete morphological response in surgically removed tissues was obtained in 48% of BOT cancers and 22% of MOT cancers. 5-year general and disease-free survival were 70% and 58% respectively and there was not reliable difference between localizations. Surgical treatment for local relapse were performed 30 of 62 (48%) patients.

Conclusion: In our single experience primary (chemo)radiation therapy has been shown to be feasible and resulted in high probability of organ-sparing treatment with reliable locoregional control, survival and better quality of life.

EP-1063

Patient reported voice outcomes after laser surgery or radiotherapy for T1 laryngeal cancer

R. Simcock[1], D. Walker[2], A. Addison[2], M. Harries[2]
[1]*Brighton and Sussex University Hospitals NHS Trust, Sussex Cancer Centre, Brighton, United Kingdom*
[2]*Brighton and Sussex University Hospitals NHS Trust, Otolaryngology, Brighton, United Kingdom*

Purpose or Objective: Disease free survival and overall survival figures for early laryngeal cancer (T1) are excellent regardless of treatment modality used; either laser surgery or external beam radiotherapy. Randomised controlled trials of laser versus radiotherapy have failed to recruit. In comparing treatment modalities we must therefore look for other comparators including cost efficacy and patient reported outcomes (PROMS) . Voice outcomes are an important PROM in larynx cancer treatment.

Material and Methods: A retrospective review of all patients treated at a regional Head and Neck centre over a 7 year period with T1a and T1b laryngeal cancers and subsequently followed up in the voice clinic. Patients were routinely asked to complete the Voice Handicap Index 10 (VHI-10) as part of standard care. The VHI-10 is an abbreviated version of the VHI which gives a subjective score of the degree of handicap experienced by the patient due to voice quality (Rosen 2004). The abbreviated score is validated and consistent. High scores indicate greater disability due to voice effects. VHI-10 scores and data on disease status were collected. Patients were treated with either Type 1,2 or 3 carbon dioxide laser cordotomy (as per ELS classification) by a single surgeon or external beam radiotherapy to 55Gy in 20 fractions in 26 days with 6MV photons to a CT planned volume to the larynx only (no elective nodal irradiation)(PTV = CTV+5mm). Patients treated with radiotherapy usually had contraindications to laser surgery (tumour position or access).

Results: 44 patients were identified with follow-up VHI data, 30 of these had been treated with laser surgery (28 with T1a) and 14 with radiotherapy (8 with T1a). Mean follow up was 3.01 years (0.5-5 years). Recurrence occurred in two patients after laser. One patient underwent further laser excision and the other received radiotherapy. There was 100% disease specific survival. The results were analysed by a General Linear Regression model with multiple imputations to address response gaps, using an SBS analysis tool. Both groups showed a statistically significant increase in mean VHI-10 scores over time and from pre-treatment baselines. VHI scores were higher for the radiotherapy treated cohort in the first year of follow up. Return to a VHI score of less than 10 was 6-9 months for laser and 9-12 months for radiotherapy.
Graph shows average VHI score from pre-treatment up to 62 months post treatment.

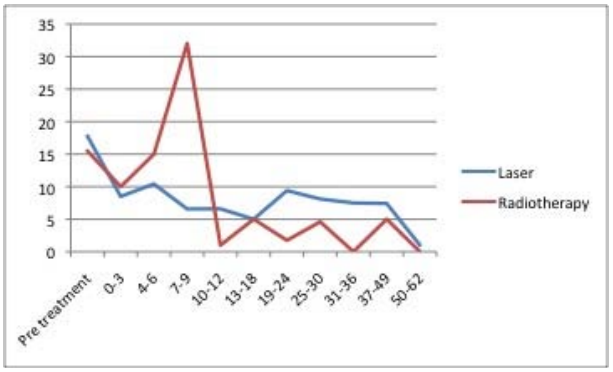

Conclusion: PROMs are an appropriate way to compare treatment modalities with similar disease outcomes. The VHI-10 is an appropriate PROM for patients treated for laryngeal cancer. In an unselected retrospective population subjective voice outcomes are no worse with laser than with radiotherapy and therefore laser may be a preferred option due to lower cost and greater convenience.

EP-1064

Reirradiation results in head and neck tumours

L. Gutierrez Bayard[1], M. Salas Buzón[1], L. De Ingunza Barón[1], S. Garduño Sánchez[1], E. González Calvo[1], I. Villanego Beltrán[1], V. Díaz Díaz[1], L. Díaz Gómez[1]
[1]*Hospital Universitario Puerta del Mar, Radiation Oncology, Cadiz, Spain*

Purpose or Objective: The treatment of choice for recurrences or second tumors of head and neck area, in areas

previously irradiated surgery is not always feasible. The poor results obtained exclusive chemotherapy.We have the objective to study treatment outcome in these tumors recurrent head and neck, previously irradiated.

Material and Methods: We evaluated 57 patients with recurrent disease, between 2005 to 2014.27 larynx, 6 nasopharynx,12 oropharynx, 6 hypopharynx and 6 oral cavity. The initial dose received between 50 and 70 Gy, 25/57 received radical radiotherapy,17 /57 radical chemoradiation; other adjuvant radiotherapy, of which 8 / 57 was combined with chemotherapy. In 24 / 57 nodal recurrence (N1-N2), local 18/57 (T2-T4),6/57 local+nodal recurrence, 9/57 seconds tumor,. Reirradiation with external 3D conforma/IMRTl techniques/ and dose between 50 Gy and 70 Gy. Time between initial treatment and relapse: 11 to 72 months.

Results: 39/57 cases were complete response, 8 / 57 partial response, 7/57 stabilization, 3/57 progresion. Late toxicity: xerostomia (G: 2 26/57, G: 3 4/57), moderate fibrosis (6 /57, one case trismus), 2 osteoradionecrosis fistula required surgical treatment. Local control: 80%, median survival one year and 50% 2 years free of disease, two died of distant metastasis greater than 35 months after second treatment.

Conclusion: This type of treatment, once considered contraindicated, after analyzing various authors, the potential has not seen a high incidence of severe damage expected in healthy tissues. Aggressive treatment of this disease recurring, allowing long survival, even in extensive disease is superior to best supportive care.

EP-1065

Post-treatment FDG-PET CT in detecting residual disease in head & neck squamous cell carcinoma

J. Price[1], A. Pascoe[1], C. Weston[1], S. Kathirgamakarthigeyan[1], M. Griffin[1], R. Ganatra[2], J. Christian[1]
[1]*Nottingham City Hospital, Department of Oncology, Nottingham, United Kingdom*
[2]*Queens Medical Centre, Department of Radiology and Nuclear Medicine, Nottingham, United Kingdom*

Purpose or Objective: Head and neck squamous cell carcinoma (HNSCC) is the 6th most common cancer worldwide, and both the disease and its treatment are associated with high morbidity. FDG-PET CT imaging can be performed approximately 12 weeks following IMRT to exclude persistent disease at the primary tumour site and/or local neck nodes. This report considers how post-treatment PET CT scans may be utilised to inform the follow up of patients treated for HNSCC.

Material and Methods: A retrospective review of HNSCC patients treated with IMRT with radical intent between December 2010 and February 2013 and who underwent a post-treatment PET CT scan. Overall, relapse-free and loco-regional relapse-free survival calculated from date of biopsy to date of death, relapse or last follow up. PET CT reports were noted and categorised as follows:
'Low-risk' - normal scan
'Intermediate-risk' – showing post-treatment change or inflammation
'High-risk' – in keeping with or highly suspicious of residual disease

Results: 100 patients were identified. Median follow up was 2.8 years (range 58 days to 3.9 years). On review of PET CT reports, 47 patients were categorised as low-risk, 27 as intermediate-risk and 26 as high-risk. 13 of the 26 high-risk patients underwent a subsequent biopsy, with residual disease in 3. 6 of the 27 intermediate-risk patients underwent biopsy, with residual disease in 1.
3-year overall survival was 93.3% (95% C.I. 80.7 to 97.8%) for the low-risk group, 79.3% (95% C.I. 56.7 to 91.0%) for the intermediate-risk group and 38.8% (95% C.I. 18.3 to 58.9%) for the high-risk group [p <0.0001].
3-year relapse-free survival was 78.5% (95% C.I. 60.1 to 89.1%) for the low-risk group, 74.0% (95% C.I. 50.1 to 87.7%) for the intermediate-risk group and 33.9% (95% C.I. 15.3 to 53.6%) for the high-risk group [p <0.0001].
3-year loco-regional relapse-free survival was 91.4% (95% C.I. 78.6 to 96.7%) for the low-risk group, 81.6% (95% C.I. 56.5 to 93.0%) for the intermediate-risk group and 71.5% (95% C.I. 49.1 to 85.3%) for the high-risk group [p = 0.0310, figure]

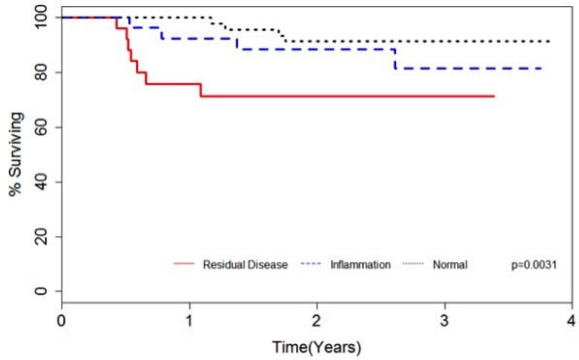

Conclusion: This report confirms the value of the 12-week post-treatment PET CT scan in identifying the risk of loco-regional relapse and death following IMRT treatment for HNSCC. This information could be used to identify patients in a good prognostic group who may benefit from entering follow-up protocols aimed at addressing psychosocial and survivorship issues, with high-risk patients undergoing more intensive follow-up aimed at detecting relapse of disease.

EP-1066

Low FDG-PET detection rate of the primary tumor for patients with cervical lymph node metastases

E. Dale[1], J.M. Moan[1], T.V. Bogsrud[2]
[1]*Oslo University Hospital Radium, Avdeling for Kreftbehandling - Radiumhospitalet, Oslo, Norway*
[2]*Oslo University Hospital Radium, Department of Nuclear Medicine, Oslo, Norway*

Purpose or Objective: FDG-PET is perceived as a valuable diagnostic tool for patients with cancer of unknown primary (CUP). In the literature, detection rates are approximately 30% for pooled patient populations. Patients with isolated neck lymph nodes of squamous cell carcinoma, are usually examined by an ENT specialist with panendoscopy, sampling blind biopsies, CT or MRI of the neck, sometimes ultrasound of the neck and a chest CT. After these examinations have been performed without finding the primary cancer, FDG-PET detection rates are reported to be approximately 25%. For our head and neck cancer patient population with CUP intended for definitive radiochemotherapy, we hypothesize that the previously reported FDG-PET detection rates are too high.

Material and Methods: In our hospital during 2007-2013, 361 head and neck cancer patients had an FDG-PET-CT examination in fixation mask as part of the radiotherapy treatment planning. In this group, 31 patients had cervical lymph node metastases of squamous cell carcinoma of unknown origin.

Results: Two (cancer of the vallecula and esophagus) of these 31 patients had their primary cancer detected by FDG-PET-CT giving a detection rate of 6.5% (95% C.I.: 2%, 21%).

Conclusion: The FDG-PET detection rate of the primary cancer for patients with cervical lymph node metastases of squamous cell carcinoma, who have been through the standard diagnostic work-up, is lower than previously reported. FDG-PET may be less useful for this purpose than what has been anticipated.

EP-1067

Assessing the outcome in 3D and IMRT head and neck (H&N) cancer patients: are we doing well?

I. Prieto[1], J. Luna[1], J. Olivera[1], J. Vara[1], A. Perez[1]
[1]*Fundación Jimenez Díaz, Radiation Oncology, Madrid, Spain*

Purpose or Objective: IMRT is the standard of care in the treatment of H&N carcinoma based on level 1 evidence. However, today there is a greater chance of missing the tumor due to uncertainties in target volume definition by the clinician that is demanded by the highly conformal planning process involved with IMRT. The aim of this work is to compare the outcome in 3D and IMRT treatments in our first two years using IMRT.

Material and Methods: From January 2011 to December 2014, 152 head and neck cancer patients were treated with adjuvant or radical radiotherapy at the Fundacion Jimenez Diaz Radiation Oncology Department. Patients received standard treatments with surgery and chemotherapy following international guidelines. Most of them were locally advanced cancer patients with extensive fields of treatment and high doses of radiotherapy. We have analyzed retrospectively the outcome of these patients regarding local/regional control. Data from technique of treatment employed (3D/IMRT), failure location (infield/outfield) and time to failure (persistence/early recurrence or before 6 months/late recurrence or after 6 months) were collected and compared with spss tools. Employed technique depended on the year and the availability. Our department started IMRT techniques in March 2013.

Results: In this group of 152 patients, 30 (19%) recurrences were found: 21 (20%) in the group treated with 3D techniques (101 patients) and 9 (17%) in the group treated with IMRT (51 patients). 21 recurrences were in field, 2 of them in the elective nodal radiation field. Seven (23%) of the recurrences infield were included the IMRT group, and 21 (66%) in the 3D group. Tumor persistence was identified in 6 (20%) patients treated with 3D and 4 (13%) with IMRT. Recurrences outfield were similar in both techniques, lightly higher in the IMRT group (28% vs 33%). However, this data has no relevance keeping in mind he number of patients in each group. In the 3D group there were found 6 patients with early recurrence (before 6 months) and no patients in the IMRT group.

Conclusion: In this group, recurrences were mostly infield, regardless of the employed technique. These data confirm conclusions previously published in large series with 3D radiotherapy. The IMRT group showed lower treatment failures and no early recurrences. However, it is needed to go on checking the IMRT implementation in the departments: to review possible uncertainties in target volume, to define the target with the best image techniques and to assess retrospectively the outcome.

EP-1068

Impact of pretreatment primary tumor volume on survival of patient with T4a larynx cancer

A. Mohamed[1], J. Shiao[1], J. Messer[1], W. Morrison[1], M. Zafereo[1], A. Hessel[1], S. Lai[1], M. Kies[1], R. Ferrarotto[1], A. Garden[1], R. Weber[1], D. Rosenthal[1], C.D. Fuller[1]
[1]*MD Anderson Cancer Center, Radiation Oncology, Houston, USA*

Purpose or Objective: To determine the impact of CT-determined pretreatment primary tumor volume on the overall survival (OS) in T4a laryngeal squamous cell carcinoma (LSCC) patients.

Material and Methods: We retrospectively reviewed patients with proved diagnosis of T4a (AJCC 7th) LSCC from 1983 to 2011 at MD Anderson Cancer Center under an approved IRB protocol. Primary tumors were manually contoured on pretreatment diagnostic CT scans for all patients with available scans then total tumor volumes were recorded. Cox regression multivariate analysis was done to investigate the impact of the following variables (age, sex, ethnicity, LSCC subsite of origin, performance status, nodal stage, surgical treatment, radiation use and dose, chemotherapy use, and tumor volume) on OS. Recursive partitioning analysis (RPA) was used to determine cut point of tumor volume associated with OS then Kaplan-Meier curves were plotted for groups above and below the RPA-derided cut point and log-rank tests was used to compare OS in both groups.

Results: A total of 124 patients were included. Median follow-up was 68 months, and median age at the time of diagnosis was 58 years. Table 1 summarizes patients, disease, and treatment characteristics.

Table 1 – Patients, Disease, and Treatment Characteristics

Sex [n(%)]	
Male	101 (83)
Female	23 (17)
Ethnicity [n(%)]	
African American	26 (21)
White	75 (60)
Hispanic	21 (17)
Other	2 (2)
Disease Site [n(%)]	
Glottic	30 (24)
Subglottic	3 (2)
Transglottic	26 (21)
Supraglottic	65 (53)
Nodal Staging [n(%)]	
N0	41 (33)
N1	5 (4)
N2A	2 (2)
N2B	26 (21)
N2C	27 (22)
N3	2 (2)
Smoking History [n(%)]	
Yes	120 (97)
No	4 (3)
Treatment Method [n(%)]	
Total Laryngectomy followed by Post-Operative Radiotherapy (TL-PORT)	41 (33)
Larynx Preservation (LP) with Radiotherapy (RT)	83 (67)
Radiotherapy Dose	60 (40-72)
Fractionation	30 (12-42)
Chemotherapy Use	
No chemotherapy	56 (45)
Concurrent	46 (37)
Induction	5 (4)
Induction and chemoradiotherapy	17 (13)

A total of 83 patients (67%) received total laryngectomy followed by postoperative radiotherapy (TL-PORT), and 41 patients (33%) received larynx preservation (LP) with radiotherapy (RT). The distribution of sex was 101 males (81%) and 23 females (19%). On multivariate analysis, the only independent predictor of OS was tumor volume (HR 2.6; 95% CI 1.5-4.5, p=0.0006). RPA derived the cutpoint at 21cc. Patients with tumors ≥ 21cc had significantly worse 5-year OS compared to <21cc (44% vs. 64%, p=0.003) as in Figure 1.

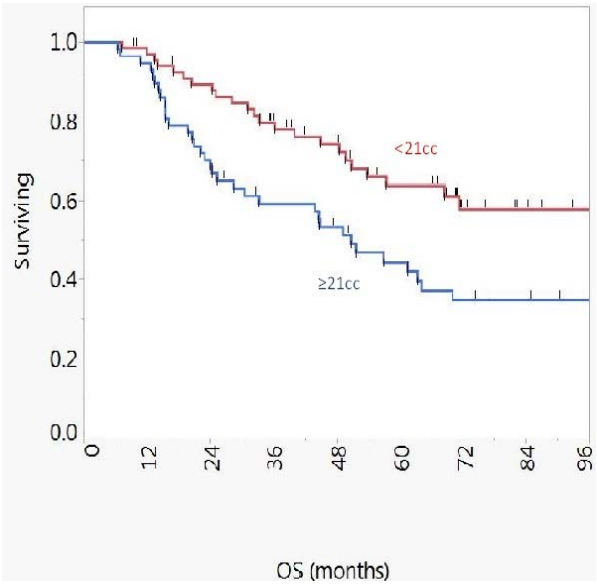

Conclusion: Our results suggest that pretreatment primary tumor volume was the only independent predictor of OS in T4a LSCC patients. We recommend the routine measurement

of primary tumor volume for its prognostic impact and for treatment stratification in future clinical trials.

EP-1069

Nasopharyngeal carcinoma screening by plasma EBV DNA and serum antibodies in an outpatient clinic

C.W. Twu[1], J. Jin-Ching Lin[1], W. Wen-Yi Wang[2]
[1]*Taichung Veterans General Hospital, Otolaryngology-Head and Neck Surgery, Taichung, Taiwan*
[2]*Hung Kuang University, Department of Nursing, Taichung, Taiwan*

Purpose or Objective: To investigate the role of plasma EBV (pEBV) DNA and serum antibodies tests in nasopharyngeal carcinoma (NPC) screening.

Material and Methods: From Feb. 2008 to Nov. 2009, a total of 467 subjects coming to an otorhinolaryngology outpatient clinic were enrolled in a prospective screening study. Paired serum and plasma samples were collected and subjected to an immunofluorescence assay for IgA antibodies against the viral capsid antigen (VCA) and early antigen (EA) and a real-time quantitative polymerase chain reaction assay for pEBV DNA measurement. Nasopharyngoscopy was done for subjects with risk factors associated with NPC or abnormal reports of blood tests. Biopsy was performed for suspected lesions to confirm the diagnosis.

Results: We divided the studied population into three subgroups- group A (n=139, symptoms/signs mimicking NPC, presence of family history of NPC, or abnormal antibody tests at other hospital), group B (n=191, symptoms/signs not related to NPC), and group C (n=137, healthy volunteers). After a minimal follow-up of five years, 9 of 467 screened subjects were proven to have NPC. All NPC patients were found in the group A. The sensitivity, specificity, positive predictive value, and negative predictive value for the pEBV DNA test were 100%, 99.8%, 90.0%, and 100%. The sensitivity, specificity, positive predictive value, and negative predictive value for the VCA-IgA test were 77.8%, 88.9%, 12.1%, and 99.5%. The corresponding numbers for the EA-IgA test were 33.3%, 97.6%, 21.4%, and 98.7%.

Conclusion: The pEBV DNA test is a useful screening tool in the detection of NPC. Both VCA-IgA and EA-IgA antibody tests have a low sensitivity and positive predictive value in clinical practice.

EP-1070

Prognostic role of FDG-PET performed before or during radiotherapy in head and neck cancer

M. Min[1], P. Lin[2], M. Lee[1], I. Ho Shon[2], M. Lin[2], D. Forstner[1], M.T. Tieu[3], A. Chicco[2], V. Bray[4], A. Fowler[1]
[1]*Liverpool Hospital, Radiation Oncology, Liverpool, Australia*
[2]*Liverpool Hospital, Nuclear Medicine, Liverpool, Australia*
[3]*Calvary Mater Newcastle, Radiation Oncology, Newcastle, Australia*
[4]*Liverpool, Medical Oncology, Liverpool, Australia*

Purpose or Objective: The aim of this study is to evaluate the prognostic value of metabolic parameters derived from 18F-FDG PET-CT performed before definitive radiation therapy (RT) (prePET) in patients with mucosal-primary head and neck squamous-cell-carcinoma (MPHNSCC) and to assess the additive prognostic values of 18F-FDG PET-CT performed during RT (iPET).

Material and Methods: One hundred consecutive patients who had radical RT for MPHNSCC and underwent staging prePET and iPET performed during the third week of treatment, were retrospectively analysed. The maximum-standardised-uptake-value (SUVmax), metabolic-tumour-volume (MTV) and total-lesional-glycolysis (TLG) of primary tumour were analysed for both prePET and iPET, and results were correlated with oncological outcomes including loco-regional-recurrence-free-survival (LRFS), disease-free-survival (DFS), metastatic-failure-free survival (MFFS) and overall-survival (OS), using Kaplan-Meier analysis. Optimal-cutoffs (OC) were derived from Receiver-Operating-Characteristic curves for the best combined sensitivity and specificity.

Results: Median age was 61 years (range 39-81), median follow-up of 20 months (range 4-70, mean 27), and AJCC 7th Edition clinical stage II, III and IV were 8, 24 and 68 patients respectively. All patients in this study received definitive RT using IMRT or TomoTherapy®: 15 patients were treated with RT only; 68 patients with chemoradiotherapy; 17 patients with RT and concurrent Cetuximab; and 17 patients received induction chemotherapy. Addition of iPET significantly improves the prognostic values of all three metabolic parameters. Metabolic values below cutoffs in both prePET and iPET (comPET) were found to be associated with significant improvements in DFS ($p<0.01$), LRFS ($p<0.05$) and OS ($p<0.05$). In addition, patients with SUVmax above the OC in comPET were associated with worse MFFS ($p = 0.011$) and confirmed on both univariate ($p=0.019$) and multivariate analyses ($p=0.04$).

Conclusion: The predictive value of FDG-PET is significantly improved by addition of iPET. ComPET is found to be predictive of oncological outcomes including MFFS and can potentially be used in future adaptive local and systemic therapy trials.

EP-1071

Maintenance metronomic chemotherapy for recurrent/metastatic nasopharyngeal carcinoma

C. Wu[1], W.Y. Wang[2], C.W. Twu[3], P.J. Lin[4], Y.C. Liu[5], J.C. Lin[5]
[1]*Changhua Show-Chwan Memorial Hospital, Department of Radiation Oncology, Changhua, Taiwan*
[2]*Hung Kuang University, Department of Nursing, Taichung, Taiwan*
[3]*Taichung Veterans General Hospital, Departments of Otorhinolaryngology, Taichung, Taiwan*
[4]*Tungs' Taichung MetroHarbor Hospital, Department of Radiation Oncology, Taichung, Taiwan*
[5]*Taichung Veterans General Hospital, Department of Radiation Oncology, Taichung, Taiwan*

Purpose or Objective: The prognosis of recurrent/metastatic nasopharyngeal carcinoma (r/m NPC) after curative radiotherapy is very poor. We aim to investigate the survival impact and toxicity of maintenance metronomic chemotherapy in patients with r/m NPC.

Material and Methods: Patients with r/m NPC were first salvaged by iv cisplatin-based or gemcitabine-based chemotherapy. Local therapy (either radiotherapy or surgery) was administered for suitable patients and feasible disease (local tumor or oligometastasis) as a local consolidation boost therapy. We started to give maintenance chemotherapy with oral tegafur-uracil (two capsules per day) with/without oral cyclophosphamide 50 mg per day for at least 12 months or until disease progression/intolerable toxicity/patient's refusal in our hospital since 2005. A total of 89 patients were collected. We analyzed the treatment outcome between patients with (n=45) and without (n=44) maintenance chemotherapy.

Results: Baseline patient characteristics at diagnosis of recurrence/metastasis (age, sex, pathological type, performance status, disease extent) and response to antecedent iv salvage chemotherapy were comparable in both arms. The median overall survival for patients with and without maintenance chemotherapy were 26 and 11 months, respectively ($P<0.01$). We observed 5 and 1 patients with biopsy-proven distant metastasis surviving more than 5 years and no evidence of disease in patients with and without maintenance chemotherapy. The toxicities during maintenance oral chemotherapy period were usually mild and no occurrence of grade 3/4 non-hematolocal toxicity.

Conclusion: Maintenance metronomic chemotherapy strategy significantly improves overall survival and has low toxicity in patients with r/m NPC after iv salvage chemotherapy.

EP-1072

Early stage hypopharyngeal cancer: treatment outcome and treatment strategy

N. Kim[1], K.H. Kim[1], J. Lee[1], C.G. Lee[1], K.C. Keum[1]
[1]*Yonsei University, Radiation Oncology, SEOUL, Korea Republic of*

Purpose or Objective: Hypopharyngeal squamous cell carcinoma (HPSCC) is rarely diagnosed in early stage due to the nonspecific nature of early symptoms. Since its rarity, few reports regarding the treatment outcome are available and the most optimal treatment for early stage HPSCC has not yet been clarified. We assessed patterns of failure and factors that influence failures.

Material and Methods: total of 36 patients with pathologically confirmed stage I (n = 10) and II (n = 26) treated between January 1992 and March 2014 were retrospectively reviewed. Ten patients (28%) received definitive RT delivered with a median fraction dose 2.1 Gy(range, 1.8–2.3 Gy) to median total dose 69.1 Gy (range, 60.8–70.2 Gy) (R group). Nineteen patients (53%) underwent surgery only (S group). Seven patients (19%) treated with surgery followed by postoperative RT with a median fraction dose of 1.8 Gy (range 1.8–2.3 Gy) to median total dose was 63.0 Gy (range, 54.0–66.6 Gy) (PORT group). Twenty-six patients received surgery included mass excision/partial pharyngectomy (n = 20), total laryngectomy with partial pharyngectomy (n = 4), and total pharyngolaryngectomy (n = 2). Additionally, 4 of S group had no elective neck node dissection, seven patients had ipsilateral and eight patients had bilateral dissection. All of 10 patients in the R group and in the PORT group received elective bilateral neck irradiation.

Results: At a median follow-up of 48 months, the 5-year locoregional control rate (LRC) was 65%. Of the 36 patients, 5 patients had local failure (LF), one had regional failure (RF), three had combined locoregional failure (LRF) and two had distant failure. No differences were observed in the 5-year LRC among three groups (R, S, and PORT = 67%, 52%, and 100%;, *P* = 0.17). In the RT group, 3 patients experienced LF without RF. In the S group, 7 patients experienced LRF; 2 LF, 1 RF, and 3 combined LRF. There was no LRF in the PORT group though resection margin status of patients in the PORT group were more risky than in the S group (Close/Positive margin 85% vs. 32%; *P* = 0.03) Patients with pyriform sinus apex extension showed a trend toward lower LRC (38% vs. 76%; *P* = 0.09). Patients with bilaterally treated neck (Treated neck group) showed lower trend of RF rate (4% vs. 27%; *P*= 0.08). Of the 10 patients who experienced LRF, 9 patients were successfully salvaged and 5-yr LRC after salvage treatment was 80%. Although late events of gastrostomy or tracheostomy were observed in 8 patients; 2 patients in the untreated or ipsilaterally treated neck group, 6 patients in the treated neck group (18% vs. 24%; *P* = 0.70)

Conclusion: Multimodal approach achieved favorable locoregional disease control despite of the risk factor. There is no difference in LRC between R group and S group. Prophylactic treatment of lymph nodes in the neck improves regional control in selected early HPSCC. Future research in the significance of tumor extension and elective neck treatment will be necessary to define the optimal treatment.

EP-1073

The usefulness of 18F-FDG PET and PET-based considerations in locally advanced nasopharyngeal cancer

H.I. Yoon[1], K.H. Kim[1], J. Lee[1], Y.H. Roh[2], M. Yun[3], B.C. Cho[4], C.G. Lee[1], K.C. Keum[1]
[1]*Yonsei Cancer Center- Yonsei University, Department of Radiation Oncology, Seoul, Korea Republic of*
[2]*Yonsei University College of Medicine, Biostatistics Collaboration Unit, Seoul, Korea Republic of*
[3]*Yonsei University College of Medicine, Department of Nuclear Medicine, Seoul, Korea Republic of*
[4]*Yonsei University College of Medicine, Department of Internal Medicine, Seoul, Korea Republic of*

Purpose or Objective: We investigated 18F-fluorodeoxyglucose positron emission tomography (PET)-derived parameters as prognostic indices for disease progression and survival in locally advanced nasopharyngeal carcinoma (NPC) and the effect of high-dose radiotherapy for a subpopulation with PET-based poor prognoses.

Material and Methods: Ninety-seven stage III and IVa-b NPC patients who underwent definitive treatment and PET were reviewed. For each primary, nodal and whole tumor, maximum standardized uptake value, metabolic tumor volume, and total lesion glycolysis (TLG) were evaluated. The primary endpoint was progression-free survival (PFS). PFS was calculated from the treatment start date to the date of disease progression, relapse, death from any cause, or last contact. Overall actuarial survival (OS) was calculated from the treatment start date to the date of death or the last follow-up. PFS and OS were calculated using the Kaplan-Meier method. The Contal and O'Quigley method was performed to determine the cut-off value for the most useful PET parameter from the C-index and iAUC to allow for dichotomization in an objective manner.

Results: The median follow-up duration among surviving patients was 47 months (range, 8–127). Based on the C-index (0.666) and iAUC (0.669), the whole tumor TLG was the most useful predictor for progression-free survival (PFS); the whole tumor TLG cut-off value showing the best predictive performance was 322.7. The low-whole tumor TLG group showed significantly higher 5-year PFS (77.0% vs. 43.0%, P < 0.001), overall survival (OS) (85.7% vs. 54.0%, P = 0.003), loco-regional failure free survival (77.0% vs. 49.1%, P = 0.001) and distant-failure free survival (81.6% vs. 60.3%, P = 0.012) rates than the high-whole tumor TLG group. The whole tumor TLG was one of the significant prognostic factors for PFS (HR, 0.29; 95% CI, 0.13–0.64; P = 0.002) and OS (HR, 0.29; 95% CI, 0.11–0.79; P = 0.02) in multivariate analysis. Patients with low-whole tumor TLG showed higher 5-year PFS in the subgroup for only patients receiving intensity-modulated radiotherapy (77.4% vs. 53.0%, P = 0.01). In the subgroup of patients with high-whole tumor TLG, patients receiving an EQD2 ≥70 Gy showed significantly greater complete remission (71.4% vs. 33.3%, P = 0.03) and higher 5-year OS rates (74.7% vs. 19.6%, P = 0.02).

Conclusion: Our findings demonstrated that the whole tumor TLG could be an independent prognostic factor and high-dose radiotherapy could improve outcomes for NPC showing high whole tumor TLG.

EP-1074

Circulating cell free DNA: dynamics in patients with head and neck cancer during radiochemotherapy

K. Zwirner[1], F. Hilke[2], C. Schroeder[2], O. Rieß[2], D. Zips[1], S. Welz[1]
[1]*Department of Radiation Oncology, Medical Faculty and University Hospital- Eberhard Karls University Tübingen, Tübingen, Germany*
[2]*Institute of Medical Genetics and Applied Genomics, Medical Faculty and University Hospital- Eberhard Karls University Tübingen, Tübingen, Germany*

Purpose or Objective: The analysis of circulating cell free DNA (cfDNA) in plasma samples of cancer patients ('liquid biopsy') is an upcoming option in detecting cancer characteristics, dynamics, prognosis and recurrence. Combining quantitative analysis, genetic information and clinical data appears as a promising tool in personalised medicine.

Material and Methods: In a prospective pilot study a total of 9 patients with head and neck cancer (median age 64.7 years) receiving primary radiochemotherapy were analysed regarding cfDNA dynamics and genetic alterations. Blood samples were taken prior to therapy, during therapy (week 1,4,6) and 6 weeks after end of treatment.

Results: Sequencing results of the tumours in the first three analysed patients showed somatic alterations of the cell cycle (*TP53, CDKN2B*), PI3K; AKT; RAS signaling cascades (*ERBB3, HRAS, VHL, MTOR*), chromatin regulation (*TET2, ARID1A, KMT2A, EZH2, MEN1*), Notch signaling (*FBXW7, NOTCH1*) and DNA damage response (*BRCA1/2, MLH1*). The amount of cfDNA varied among patients and during treatment. Quantitatively, in 5 patients the amount of cfDNA increased during therapy (after week 1). In 4 patients no initial relevant change could be seen (stable after week 1). Currently patients are in follow up for evaluation of clinical outcome.

Conclusion: Our initial results suggest that monitoring cfDNA identifies different patient subsets. As a proof of concept, detection of cfDNA is feasible and a potentially promising tool to identify tumour specific 'finger prints'. Perspectively we hope to use cfDNA as a liquid biopsy and biomarker to identify individual tumour signatures to personalise treatments, detect mutations for targeted therapies and to monitor treatment response.

EP-1075

Squamous cell carcinoma of maxillary sinus : 25-years experience in a single institution

S.H. Jeon[1], H.G. Wu[1], J.H. Kim[1], C.I. Park[1]
[1]*Seoul National University Hospital, Radiation Oncology, Seoul, Korea Republic of*

Purpose or Objective: To evaluate the clinical outomes to find optimal treatment and analyze prognostic factors for squamous cell carcinoma of maxillary sinus.

Material and Methods: Between January 1990 and December 2014, 97 patients with histoligcally proven squamous cell carcinoma of maxillary sinus without distant metastasis, treated with either radical surgery and adjuvant radiotherapy(Op+RT) or radical radiotherapy(RT). Median age at diangnosis was 61. There was no stage I patient and only 5 patients were stage II, all treated with Op+RT. Among twenty-three patients with stage III disease, fifteen patients were treated with Op+RT and eight patients were treated with RT. For stage IVA cancer, thirty-three patients received Op+RT, and twenty-eight patients were treated with RT. All eight patients with stage IVB cancer were treated with RT. Neoadjuvant chemotherapy and concurrent chemotherapy were used in fourty-five and nineteen patients, respectively.

Results: Median follow-up period after diagnosis was 30 months for all patients. For stage III cancer, Op+RT showed better outcomes than RT (5-year OS : 63.8% vs. 29.2%, p=0.12; 5-year PFS : 43.2% vs. 18.8%, p=0.16), although not statistically significant. For stage IVA cancer, however, two treatment options showed comparable results (5-year OS : 52.6% vs. 51.3%, p=0.80; 5-year PFS : 37.6% vs. 28.6%, p=0.53). Local failure was the most common pattern of failure, found in fourty-two of ninty-seven patients (43.3%). Proportion of regional failures in initially node-positive patients was 21.4% (three out of fourteen). For initially node-negative cancer, regional failure was not observed in fifteen patients who received either neck dissection or neck irradiation, but in 14.7% (ten out of sixty-eight) who did not received neck treatment. In multivariate analysis, age younger than 60, positive resection margin and masticator space invasion were bad prognostic factors in Op+RT group. Masticator space invasion and subcutaneous tissue of cheek invasion were bad prognostic factors in RT group.

Conclusion: In squamous cell carcinoma of maxillary sinus, radical surgery followed by adjuvant radiotherapy should be recommended for stage III disease. For stage IVA, however, radical radiotherapy can be a good alternative option to surgery. Prophylactic neck treatment for initially node negative patients can prevent regional recurrence, with absolute risk reduction of about 15%. Masticator space invasion was found to be a bad prognostic factor for both treatment arms.

EP-1076

Phase II study of prophylactic radiotherapy in cN0 HNSCC patients based on sentinel node(s) SPECT/CT

E. Longton[1], G. Lawson[2], B. Bihin[3], S. Deheneffe[1], I. Mathieu[4], J. Installé[4], T. Vander Borght[5], M. Laloux[6], J.F. Daisne[1]
[1]*Clinique et Maternité Sainte-Elisabeth, Radiation Oncology, Namur, Belgium*
[2]*CHU Dinant-Godinne, Head and Neck Surgery, Yvoir, Belgium*
[3]*Namur Research Institute for Life Sciences Narilis, Unit of Biostatistics, Namur, Belgium*
[4]*Clinique et Maternité Sainte-Elisabeth, Nuclear Medicine, Namur, Belgium*
[5]*CHU Dinant-Godinne, Nuclear Medicine, Yvoir, Belgium*
[6]*Clinique et Maternité Sainte-Elisabeth, Head and Neck Surgery, Namur, Belgium*

Purpose or Objective: Due to a risk of 18 to 45% of occult nodal metastases in cN0 HNSCC patients, prophylactic neck irradiation is often mandatory. Anyway, it leads to a large irradiation of normal tissues because bilateral drainage is the rule in only 30 to 50 % of individuals. Moreover, 15 to 30 % of the tumors drain in unpredicted nodal basins (risk of geographical miss). SPECT/CT lymphoscintigraphy of sentinel lymph nodes (SLN) could help individualizing prophylactic irradiation levels in cN0 patients and, hence, reduce irradiated volume and improve quality of life (QoL). This ongoing prospective phase II study investigates its oncological safety.

Material and Methods: Twenty-six patients with newly diagnosed cN0 SCC of the oral cavity, oropharynx, larynx or hypopharynx were included. All patients were imaged with SPECT/CT after 99mTc nanocolloid injection around the tumor. The neck levels containing up to four hottest SLN were identified and selected for prophylactic irradiation (CTVn-LS) by volumetric modulated arc therapy. A comparative virtual planning was performed with volumes selected according to international guidelines (CTVn-IG). QoL was assessed using EORTC C30 and HN25 scales.

Results: Migration was observed in all of the 26 patients (one with gamma probe only) with an average of 2.8 sentinel nodes detected per patient. CTVn-LS was totally encompassed by CTVn-IG in all patients but two with an unpredicted drainage in homolateral retropharyngeal levels. More than half of the patients has only a unilateral drainage. CTVn-LS and related PTV were systematically smaller than IG ones, by a factor of two on average. This led to significant dose decrease in identified OAR as well as remaining volume at risk. With a median follow-up of 24 months, no regional relapse was observed while 3 patients had a local one (11%). Crude overall survival rate is 89%. QoL preliminary data will be presented.

Conclusion: SPECT/CT lymphoscintigraphy of SLN allows individualizing prophylactic node CTV in cN0 HNSCC patients eligible for definitive radiotherapy. Both CTV and PTV are significantly reduced, which results in a significant dose decrease in OAR. At a median follow-up of 24 months, no regional relapse was observed but further follow-up and recruitment are necessary to ensure the oncological safety. QoL data are being analyzed.

EP-1077

Could site, age and stage be clinical factors for development of adaptive RT in head-neck cancer?

L. Lastrucci[1], S. Bertocci[1], S. Nanni[1], V. Bini[2], S. Borghesi[1], A. Rampini[1], G. Buonfrate[1], R. De Majo[1], P. Pernici[1], P. Gennari[1], C. Ceccarelli[1]
[1]*San Donato Hospital Radiotherapy Unit, Oncology Department, Arezzo, Italy*
[2]*University of Perugia, Department of Medicine Section of Internal Medicine Endocrine & Metabolic Sciences, Perugia, Italy*

Purpose or Objective: The aim of this study is to identify prognostic factors of treatment related toxicity after

concomitant radiochemotherapy in patients affected by head and neck cancer.

Material and Methods: 226 patients, 38 female and 188 male, with head and neck cancer, treated with chemoradiotherapy from 1995 to 2014 at our department, were retrospectively reviewed. 59,7% of patients were younger than 60 years. The anatomical sites of cancer were: 36 nasopharynx, 63 oropharynx, 34 oral cavity, 51 larynx, 26 hypopharynx, 16 others sites. 64 patients underwent to post-operative treatment and 162 to radical treatment. They were treated with 2D-3DCRT (80%) or IMRT technique (20%). The mean dose administered was 68 Gy (range 60-74). The schedule of chemotherapy most used included cisplatin and 5-FU. Acute and late toxicity are assessed according to CTCAE v.4.0 scale. Age, gender, tumor/nodal stage, primary site, tumor grading, RT technique and dose were assessed as potential prognostic factors influencing treatment toxicity.

Results: Acute dysphagia and mucositis G2-3 were observed in 82,7% and 84,9% respectively of patients and were related with young age (p=0,03 and p=0,02), pharynx site (p=0,004 and p<0,003) and advanced stage (p=0,02 and p=0,009). Acute xerostomia G2-3 (15%) was associated with oropharyngeal and oral cavity sites (p=0,03) and RT technique (p=0,004). Late xerostomia G2-3 (25,2%) was related with oropharyngeal site (p=0,04) and late fibrosis (14,1%) with nodal stage (p=0,005). Acute and late hearing loss (4,8%) was observed more frequently in nasopharyngeal cancer (p=0,03 and p=0,001 respectively). 3,5% of patients had acute neurotoxicity and 4,8% late neurotoxicity; this adverse effect was associated with nasopharyngeal site (p=0,03 and p=0,03 respectively).

		Gender	Age	Pharynx site	Stage	Nodal stage	Grading	Dose	RT technique
dysphagia	acute	p=0,6	p=0,03	p=0,004	p=0,02	p=0,9	p=0,6	p=0,1	p=0,9
	late	p=0,1	p=0,8	p=0,3	p=0,9	p=0,9	p=0,4	p=0,1	p=0,6
mucositis	acute	p=0,6	p=0,02	p<0,003	p=0,009	p=0,2	p=0,1	p=0,1	p=0,9
xerostomia	acute	p=0,6	p=0,9	p=0,03	p=0,08	p=0,04	p=0,08	p=0,7	p=0,004
	late	p=0,1	p=0,2	p=0,04	p=0,9	p=0,6	p=0,7	p=0,6	p=0,5
neurotoxicity	acute	p=0,8	p=0,8	p=0,03	p=0,4	p=0,09	p=0,7	p=0,4	p=0,7
	late	p=0,7	p=1	p=0,03	p=0,7	p=0,5	p=0,01	p=0,1	p=0,8
hearing loss	acute	p=1	p=0,5	p=0,03	p=0,7	p=0,5	p=0,6	p=0,8	p=0,5
	late	p=1	p=0,2	p=0,001	p=0,1	p=0,5	p=0,6	p=0,5	p=0,8
fibrosis	late	p=0,9	p=0,8	p=0,6	p=0,3	p=0,005	p=0,2	p=0,6	p=0,2

Conclusion: Clinical and technical data may be predictive of severe toxicity. Younger patients with pharynx cancer are more susceptible to dysphagia, mucositis and xerostomia. In this subset of patients it's critical evaluate strategies of adaptive radiotherapy with the aim to decrease the toxicity.

EP-1078

Nasopharyngeal Carcinoma: prognostic factors analysis in patients treated with IMRT and chemotherapy

N.A. Iacovelli[1], A. Cavallo[2], E. De Ponti[3], P. Bossi[4], S. Alfieri[4], G. Rossi[1], S. Naimo[1], C. Bergamini[4], S. Tana[1], L. Licitra[4], E. Pignoli[2], C. Fallai[1], E. Orlandi[1]

[1]Fondazione IRCCS Istituto Nazionale dei Tumori, Radiotherapy 2, Milan, Italy

[2]Fondazione IRCCS Istituto Nazionale dei Tumori, Medical Physics Unit, Milan, Italy

[3]AO San Gerardo, Medical Physics Unit, Monza, Italy

[4]Fondazione IRCCS Istituto Nazionale dei Tumori, Head And Neck Medical Oncology Unit, Milan, Italy

Purpose or Objective: To analyze clinical outcome and prognostic factors in a consecutive series of 160 non-metastatic nasopharyngeal carcinoma (NPC) patients (pts) treated curatively with intensity modulated radiotherapy (RT) techniques (IMRT, Intensity Modulated Radiation Therapy or VMAT, Volumetric Modulated Arc Therapy) and chemotherapy (CT).

Material and Methods: Pts were treated between October 2004 and April 2014 at our institution. Median age at diagnosis was 49 years (range 18-92). According to WHO, 144 patients (90%) were suffering from undifferentiated NPC, 5 patients (3.1%), 3 patients (1.9%) and 8 patients (5%) were respectively affected by squamous cell carcinoma G1, G2 or G3. One pt was in stage I (0.6%), 31 pts (19.4%) were in stage II, 47 pts (29.4%) in stage III, 31 pts (19.4%) in stage IVA and 50 pts (31.2%) in stage IVB. Seven pts (4.4%) received RT alone: 1 pt in stage I and 6 pts in stage II. Of the remaining 153 pts (95.6%) (25 pts with stage II and 128 pts with stage III and IV) 34 patients (21.2%) received CT concomitant to RT and 119 patients (74.4%) were treated with induction CT followed by RT-CT. IMRT was given with standard fractionation at a total dose of 70 Gy. In 134 patients (83.75%) circulating plasma EBV-DNA has been measured before treatment using quantitative PCR. A dedicated software (VODCA, www.vodca.ch) was used to collect and analyze dosimetric parameters in 137 pts.

Results: With a median follow up of 55.7 months (range 3.8 - 118.7) actuarial rates at 2 and 5 years were respectively: overall survival (OS) 92.36% and 82.81%, disease-free survival (DFS) 83.1% and 77.2%, local control (LC) 92.17% and 90.43%, locoregional control (LRC) 94.78% and 93.04% and distant control (DC) 89.57% and 86.96%. At univariate analysis N stage (N0+N1+N2+N3a vs N3b) was found to be a prognostic factor for DM (p = 0.029). At multivariate analysis conducted on the following parameters: T stage, N stage, stage, RT technique , V95%, Dmean and D99% (relative to High Risk PTV), the stage of T (T1+T2+T3 vs T4) was found to be a prognostic factor for LRC (p = 0.035). Both at univariate and multivariate analysis the stage of T was found to be a prognostic factor for LC (p = 0.004 and .011 respectively) and N stage (N0+N1+N2 vs N3) for DM and RC. Pts with a V95% > 90% had better LC (p=0.004) and DFS (p=0.047). Pts with a Dmean > 69 Gy had better LC (p=0.029). Pts with a D99% > 64 Gy had better LC (p=0.008) and OS (p=0.004). The threshold value of 45 cc of GTV T (Gross Tumor Volume of the primary tumor) was prognostic for LC (p = 0.0095). The threshold value of 1500 copies of EBV-DNA was prognostic for DC (p = 0.048).

Conclusion: The intensified treatment of CT-IMRT / VMAT achieves excellent clinical outcomes. Besides traditional prognostic factors, we demonstrated the prognostic value of dosimetric parameters. Finally, for the first time in a non-endemic area threshold values of GTV T and EBV-DNA prognostic for LC and DC respectively have been confirmed.

EP-1079

Clinical outcomes in locally advanced oropharyngeal cancer 18FDG PET-guided dose escalation IMRT-SIB

A. Chiara[1], C. Fiorino[2], M. Picchio[3], A. Fodor[1], S. Broggi[2], M. Pasetti[1], E. Incerti[3], P. Mapelli[3], F. Zerbetto[1], C. De Antoni[1], M. Azizi[1], R. Calandrino[2], I. Dell'Oca[1], N. Di Muzio[1]

[1]IRCCS San Raffaele Scientific Institute, Radiotherapy, Milano, Italy

[2]IRCCS San Raffaele Scientific Institute, Medical Physics, Milano, Italy

[3]IRCCS San Raffaele Scientific Institute, Nuclear Medicine, Milano, Italy

Purpose or Objective: Technological advances have enabled clinicians to explore dose escalation strategies in various tumor sites. Intermediate and high risk oropharyngeal cancers have unsatisfactory 3 year outcomes. The simultaneous integrated boost (SIB) technique with dose per fraction slightly higher than 2Gy offers the advantages of shortening the treatment time and increasing the biologically equivalent dose to the tumor. This retrospective study is aimed to evaluate the clinical outcome of radiation dose escalation to 18FDG PET/CT positive tumor and nodal sub volumes using the Simultaneous Integrated Boost (SIB) IMRT technique by means of Helical Tomotherapy (HT) in locally advanced Oropharyngeal cancer patients (pts).

Material and Methods: 37 pts, median age 59 years (range: 41-81), treated between 2005 and 2014, were evaluated. Reported stage were III-IVAB (4 and 33 respectively). HT was delivered with the SIB technique at different dose levels: 69Gy (2.3 Gy/day) to the PET-positive volume (GTV-PET), 66

Gy (2.2 Gy/day) to the clinical target volume for tumor and metastatic nodal station, 54 Gy (1.8 Gy/day) to the clinical negative neck region concomitantly in 30 fractions. Concurrent chemotherapy was given to 32 pts (cisplatin 75-100 mg/m²/21 days for 25 pts, cisplatin 30-40 mg/m²/week for 5 pts and Cetuximab for 2). Possible correlation between Overall Cancer specific (OS) and GTV-PET Volumes (GTV-T+N, GTV-T, GTV-N) was also considered.

Results: The median follow-up was 39.2 months (range: 3-125); 27%, 62% and 11% pts has respectively never smoked, a smoking history of more than 10 packs/year and not assessed. 36 pts completed the treatment as scheduled. Temporary treatment interruption due to acute toxicity, mainly mucosae, was observed in 5 patients. No grade 4 acute mucosae and skin toxicity was reported. Seventeen pts (46%) experienced grade 3 toxicity, mostly dermatitis and mucositis. Late grade 3 and 2 xerostomia was seen respectively in 3% and 32% pts. No grade 4 late toxicity was observed. The 3-year OS, Local disease-free Tumor (LTC), Local disease-free Nodal (LNC) and distant metastasis-free (DMFS) survivals were 87%, 83%, 89% and 92% respectively. Multivariate Cox regression analyses revealed that GTV-T+N and GTV-T are predictors for OS with a best-cut-off value equal to 30.9 cc (p=0.005) and 22.4 cc (p=0.038).

Conclusion: The slightly accelerated dose escalation in oropharyngeal cancers to 18FDG-PET positive tumour sub-volumes is likely to be safe even with concurrent chemotherapy. Very interesting 3-year OS and loco-regional disease control rate are obtained. The results of the present study suggest that GTV-PET has a predictive value for the SIB-HT outcome. These findings may constitute the basis for more personalized treatments.

EP-1080

Definitive or adjuvant IMRT for locally advanced sinonasal tumors: outcome and prognostic factors

E. Orlandi[1], A. Cavallo[2], E. De Ponti[3], N.A. Iacovelli[1], P. Bossi[4], P. Nicolai[5], P. Castelnuovo[6], M. Guzzo[7], G. Calareso[8], S. Naimo[1], C. Bergamini[4], L. Locati[4], L. Licitra[4], E. Pignoli[2], C. Fallai[1]

[1]*Fondazione Irccs Istituto Nazionale Dei Tumori, Radiotherapy 2, Milan, Italy*
[2]*Fondazione Irccs Istituto Nazionale Dei Tumori, Medical Physics Unit, Milan, Italy*
[3]*AO San Gerardo, Medical Physics Unit, Monza, Italy*
[4]*Fondazione Irccs Istituto Nazionale Dei Tumori, Head And Neck Medical Oncology Unit, Milan, Italy*
[5]*AO Spedali Civili, Otorhinolaryngology, Brescia, Italy*
[6]*Ospedale Di Circolo E Fondazione Macchi, Otorhinolaryngology, Varese, Italy*
[7]*Fondazione Irccs Istituto Nazionale Dei Tumori, Otorhinolaryngology Unit, Milan, Italy*
[8]*Fondazione Irccs Istituto Nazionale Dei Tumori, Radiology Department, Milan, Italy*

Purpose or Objective: There are limited and heterogeneous data on prognostic factors of locally advanced epithelial non glandular sinonasal cancer (ESNC) treated with multimodal treatment strategy. Prognosis of ESNC remains poor, with an overall 5-year survival rate of 30–50%. We analyzed a retrospective series of consecutive patients (pts) treated with IMRT at our institution, with a specific focus on the prognostic implications of clinical and treatment-related factors.

Material and Methods: Since 2007, 49 pts with ESNC staged III and IVA-IVB were treated at our Institution. Histology was squamous cell carcinoma (SCC) in 22 pts (44.9%), undifferentiated carcinoma (SNUC) in 20 pts (40.8%) and neuroendocrine carcinoma (SNEC) in 7 pts (14.3%). Prevalent primary site was ethmoid sinus (24 pts, 49%). Thirteen pts (26.5%) had N stage≥2b and 12 (24.5%) had positive retropharyngeal nodes (RPNs). Orbital apex invasion (OAI), nasopharyngeal involvement, gross nerves involvement (GNI) and positive surgical margins (R1) were found in 24 (49%), 12 (24.5%), 10 (20.4%) and 5 (10.2%) pts respectively. Thirty (61.2%) and 19 (38.8%) pts received definitive and postoperative IMRT, respectively. Thirtyfive pts (71.5%) received induction chemotherapy before surgery or RT and/or concomitant CHT. Thirtyeight pts (77.5%) received concomitant CHT. IMRT was given with standard fractionation at a total dose of 65-72 Gy in definitive cases and 54-66 Gy in adjuvant cases, according to histological findings. Gross tumor volume (GTV) was defined in all radical pts, and dose-volume histograms to all targets were analyzed in all pts.

Results: Median follow up was 22.4 months (range 6-85). Three-year overall survival (OS), disease free survival (DFS) and locoregional control (LRC) were respectively 66.5%, 55.4% and 66.3% for the entire cohort. OS and DFS were statistically better in pts with SCC or SNUC compared to pts with SNEC, in pts with ethmoid primary compared to other sites, in pts with N0 compared to pts with N stage ≥ 2b, in pts with RPNs compared to pts without RPNs (see Fig. 1), in pts with OAI compared to pts without OAI and in pts with GNI compared to pts without GNI. LRC was better even though statistically not different in pts without R1 compared to pts with R1. A multivariate analysis showed that ethmoid as primary origin site was a positive independent prognostic factor on OS, whereas RPNs positivity and OAI were negative independent prognostic factors for OS. For pts receiving definitive IMRT, pts with GTV <79.7cc had better OS, DFS and LRC compared to pts ≥79.7 cc, even if the difference was not statistically significant. Dosimetric factors were not found to have any prognostic role.

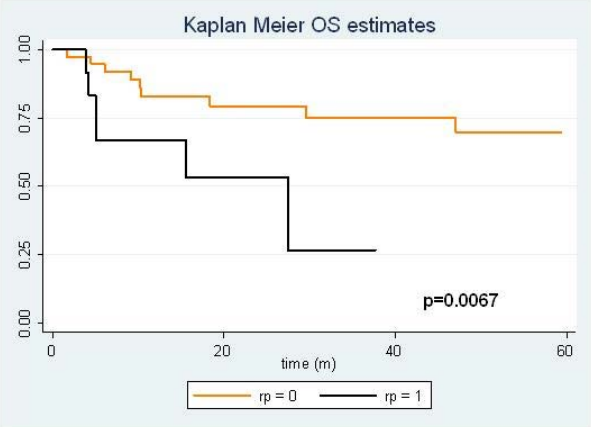

Conclusion: In a monoinstitutional series of locally advanced ESNC we obtained a 66.5% 3-yr OS and a 55.4% 3-yr DFS. We were able to identify RPNs involvement, ethmoid primary site and OAI as independent prognostic factors.

EP-1081

Advanced head and neck ca - chemoradiotherapy with conventional fraction and accelerated fraction

H.A. Gaffor[1], F. Ruzina[1], C.H. Sridhar[2]

[1]*Father Muller Medical College, Radiation Oncology, Mangalore, India*
[2]*Father Muller Medical College, Radiation Physics, Mangalore, India*

Purpose or Objective: To compare early tumor response and compliance of locally advanced head and neck cancer patients receiving concurrent chemo-radiation, weekly Cisplatin with conventional fractionation versus weekly Cisplatin with accelerated fractionation and to assess toxicity profile

Material and Methods: Patients with histologically confirmed primary head and neck squamous cell carcinoma, stage III and IV (Oral cavity, oropharynx, hypopharynx and larynx) attending the department of Radiotherapy, Father Muller Medical College Hospital, Mangalore Between November 2013 to April 2015.
Total of 64 patients were recruited and randomized into conventional and accelerated arm each having 32 patients.

Both the arms received concurrent chemo-radiation. Chemotherapy with inj Cisplatin 35 mg/m² weekly IV infusion was given as a radiosensitizer before Radiotherapy for 6 cycles and external beam radiotherapy 69.99-70Gy in 33-35 fractions 2 - 2.121Gy/fraction using Linear accelerator of 6MV photons by Conventional arm received standard regimen 5 fractions/week with overall treatment time of 6 weeks and Accelerated arm received 6fractions/week with overall treatment time of 7weeks.
Patients were evaluated in both the arms for early tumor response and acute Toxicities

Results: The mean age of patients were 53.44 years,76.60%were male and 23.4% were female .
Concurrent chemoradiation using accelerated fractionation showed higher percentage of complete response rate , in stage III-100%, IVA-88.50%and IVB- 50%,were as in conventional fractionation it was in stage III-87.50% and IVA-80.00%.
According to site complete response rate in oral cavity 87.50%and 50.00% , oropharynx 92.90% and 72.70% in accelerated fractionation and conventional fractionations respectively.
Total number of cycles of chemotherapy received were same in both the arms. There was significant weight loss during treatment in accelerated fractionation compared to conventional fractionation arm.

Conclusion: In our study, Locally advanced head and neck cancers showed better early tumor response with acceptable acute toxicities when treated with concurrent chemoradiation using accelerated fractrationation compared to conventional fraction and the quality of life was not stastically different in both the arms.

EP-1082

Interim 18F-FDG-PET/CT during chemoradiotherapy for early outcome prediction of head and neck cancer

C. Garibaldi[1], S. Ronchi[2], M. Cremonesi[1], M. Ferrari[3], L. Gilardi[4], L. Travaini[4], D. Ciardo[2], F. Botta[3], G. Baroni[5], C. Grana[4], B.A. Jereczek-Fossa[6], R. Orecchia[7]
[1]*European Institute of Oncology, Radiation Research, Milan, Italy*
[2]*European Institute of Oncology, Radiation Oncology, Milan, Italy*
[3]*European Institute of Oncology, Medical Physics, Milan, Italy*
[4]*European Institute of Oncology, Nuclear Medicine, Milan, Italy*
[5]*Politecnico di Milano, Elettronica Informazione e Bioingegneria DEIB, Milano, Italy*
[6]*European Institute of Oncology- University of Milano, Radiation Research- Department of Health Sciences, Milan, Italy*
[7]*European Institute of Oncology- University of Milano, Radiation Oncology- Department of Health Sciences, Milan, Italy*

Purpose or Objective: It is established that in the management of locally advanced head and neck cancer (HNC) patients, 18F-FDG-PET/CT (FDG) plays a significant role in the pre-treatment setting to predict outcome and prognosis and at the end of the chemo-radiotherapy (CRT) to assess the tumor response. This systematic review aims to evaluate the use of FDG acquired during CRT, ad interim FDG (FDGint), with the aim to identify tumor responsiveness in an early stage of the treatment in order to allow modification of the treatment plan and/or to setup alternative therapeutic strategies to enhance the therapeutic ratio.

Material and Methods: Data search was performed in PubMed for full original papers published from 2005 up to August 2015, written in English and based on the use of 3D hybrid PET/CT only, with eight different combination of keywords. The literature search brought 568 articles. Twenty-one original papers fulfilled the inclusion criteria: 8 studies investigated the predictive role of FDGint assessing correlations between metabolic variations and clinical outcomes, 7 studies draw conclusions about a potential role of response assessment during RT for treatment adaptation without reporting any correlation with the clinical data, and 6 studies were focused on the use of FDGint for biology-guided adaptive RT.

Results: The results of the analysis considering only the papers focusing on the predictive role of FDGint are reported in the table. All patients underwent at least a FDG at baseline, and one at a dose in the range of 10-20 Gy (early PETint), or in the range of 40-50 Gy (late PETint). Most of the studies reported a qualitative or semi-quantitative method of delineation of the FDG uptake, using a threshold value of the SUVmax, usually 40% or 50%. All the studies have in common the SUVmax and its variation as the main parameters considered for FDG evaluation, although the largest and first study evaluating all metabolic parameters of FDGint, found that tumor lesion glycolysis was a better and statistically more significant predictor of outcome than SUVmax. Two papers comparing FDGint with FLTint revealed that reduced FLT SUV preceded reduced FDG uptake, suggesting that FLTint is expected to assess the therapeutic response much earlier than FDGint.

Table. Statistics of cohort characteristic

	Value
N° of papers included	15
N° of patients	431
N° of patients/study (median, range)	29 (8 - 72)
Chemotherapy	Different schedules and pharmaceuticals
Radiotherapy	3D-CRT or IMRT
Total dose (range)	T = 60-78 Gy
	N^+= 60-66 Gy
	N^- = 50-56 Gy
Studies with *early* FDG_{int}	4
Dose at which *early* FDG_{int} is acquired (median, range)	20 (10-35)
Studies with *late* FDG_{int}	5
Dose at which *late* FDG_{int} is acquired (median, range)	49 (40-66)
Studies with both *early* and *late* FDG_{int}	6
Studies PRO prognostic value of FDG_{int}	4/8
Studies CONTRA prognostic value of FDG_{int}	2/8
Studies comparing FDG_{int} with FLT_{int}	2/8

Conclusion: Most of the works confirmed the value of FDGint in predicting the response to CRT, while few highlighted the poor prognostic value of FDGint compared to FDG acquired 2-3 months after the end of CRT which revealed a strong correlation with local and regional control and with survival. Although the best timing to assess tumor response during RT remains a matter of debate, the two week time point seems most favorable, also because there is still sufficient opportunity for adaptation of the treatment strategy. Such contradictory findings deserve to be further analyzed and confirmed in a more numerous and homogeneous series according to the tumor site and radio-chemotherapy schedules.

EP-1083

Usefulness of PET/CT in definition of treatment volumes of head and neck tumors

L.P. Luigi Perrone[1], A.D. Anna Destito[1], R.M. Rosa Molè[1], E.M. Elvira Mazzei[1], M.S. Mariaquila Santoro[1], M.A.M. Maria Angela Molinaro[1], D.P. Domenicantonio Pingitore[1], C.B. Cataldo Bianco[2]

[1]*Hospital Pugliese-Ciaccio, Department of Hemato-Oncology-Operative Unity of Radiotherapy and Radiobiology, 88100 Catanzaro, Italy*
[2]*University of "Magna Graecia", Department of Clinical and Sperimental Medicine, 88100 Catanzaro, Italy*

Purpose or Objective: The radiation therapy of head and neck tumors is burdened by high toxicity to organs at risk (OARs) with consequent administered dose limitations to the target and compromised clinical outcome. We investigated the contribution of functional/biological imaging obtained by Positron Emission Tomography (PET/CT) in Gross Tumor Volume (GTV) and Clinical Target Volume (CTV) definition of primary tumor and regional lymph nodes in head and neck cancer, for a more accurate target delimitation resulting in lower toxicity to OARs.

Material and Methods: From March 2103 to June 2014 we examined 51 patients with head and neck cancer and defined clinical volumes with the aid of only morphological CT images and with the aid of diagnostic PET/CT images. Then we evaluated, through tests of statistical significance, the overlap of GTV and CTV obtained with each of the two methods respectively. Moreover usefulness of PET/CT in preventing geographic errors for a more accurate target definition, resulting in peritumoral tissues preservation and less toxicity to the OARs, was evaluated as well. The influence of two different imaging techniques in TNM staging, which is important for treatment planning, was investigated.

Results: In 33 of 51 patients the TNM staging obtained by PET/CT was similar to that performed by CT images, but in 39% of the cases the primary tumor GTV defined by PET/CT was significantly smaller and restricted compared to that defined by CT only ($p < 0.016$). Due to the better GTV definition in terms of size and location, the OARs are potentially better preserved. In 12 patients the more accurate definition of tumor margins made possible by PET/CT produced a different T than that obtained with CT evaluation only; in 6 patients PET/CT identified metastases to regional lymph nodes not assessed with CT images only. It was not observed significant variation of the nodal volumes.

Conclusion: The use of PET/CT imaging allows the realization of more precise target volume and better defined clinical volumes, with a possible better preservation of the OARs and lower toxicity. Functional imaging PET/CT helps the radiation oncologist not only in the process of treatment planning, but has the advantage of identify treatable disease not highlighted on morphological CT images. It is therefore recommended to use a PET/CT scan in the radiotherapy planning process in order to achieve a more appropriate treatment planning in head and neck tumors.

EP-1084

Elderly patients concomitant radiotherapy + cetuximab in locally advanced head and neck cancer

A.T. Falk[1], C. Hébert[2], M. Paquet[3], A. Tran[4], F. Peyrade[2], E. Saada[2], J. Reure[2], O. Dassonville[5], G. Poissonnet[5], A. Bozec[5], J. Thariat[1], A. Leysalle[1], M.E. Chand[1], K. Benezery[1]
[1]*Centre Antoine Lacassagne, Radiation Therapy, Nice, France*
[2]*Centre Antoine Lacassagne, Medical Oncology, Nice, France*
[3]*Centre Antoine Lacassagne, Nuclear Medicine, Nice, France*
[4]*Hôpitaux Pédiatriques de Nice CHU Lenval, Medical, Nice, France*
[5]*Institut universitaire de la face et du cou, Service de cancérologie ORL, Nice, France*

Purpose or Objective: Concomitant radiotherapy + cetuximab association has shown superiority to exclusive radiotherapy for locally advanced head and neck cancers (LAHNC). Data on this association are scarce for the elderly despite its rising incidence. Initial clinical trials that led to its approval have not included patients>70 years. The objective of this study was to assess efficacy and toxicity of concomitant radiotherapy and cetuximab for patients aged>70 years with LAHNC

Material and Methods: A retrospective monocentric data collection was performed in the Antoine Lacassagne center, France. Inclusion criterias were: age>70 years at time of diagnosis, histologically proven LAHNC, treated with radiotherapy combined with cetuximab. Non-inclusion criterias were: previous radiotherapy and metastases at time of diagnosis

Results: Thirty-five patients were included between 2008 and 2012. Median follow up was 22 months. Median age was 74 years (70-86). Median performance status was 1(0-2). Female/male sex ratio was 0.34. Tumor sites were: Oropharynx(57.1%), larynx(20%), hypopharynx(14.3%), oral cavity(2.9%), rhinopharynx(2.9%), lymph node with unknown primary(2.9%). Using TNM classification, tumors were: T1(5.9%), T2(35.3%), T3(35.3%), T4(22.9%), N0(28.6%), N1(8.6%), N2(48.6%), N3(14.3%). Median radiotherapy dose was 70 Gy(60-70). 40% of patients were treated with intensity-modulated radiotherapy, the rest were treated with conventional 3D radiotherapy. 94.3% of patients paused radiotherapy due to toxicity. 29% had a cetuximab dose-reduction and 1 patient had a definitive interruption. Median survivals were respectively: 49 months for overall survival(Standard-Error (SE)=8) and 32 months for relapse free survival(SE=10). Two-year local-regional relapse and metastatic relapse free survivals were respectively 59%(SE=10) and 74%(SE=10). Median body mass index (BMI) was 24.6(17.3–38) before treatment and 23, 24 after treatment(16.3–34.7). Median weight variation was 4 kilograms(-16 to +6). Ninety-four percent of patients had nutritional support: 37.8% had oral nutritional supplements only, 56.8% had enteral nutrition and 2.7% parenteral nutrition. Skin reaction and mucositis were the major toxicities recorded. Toxicities details are reported in table 1

Type	Total incidence (%)	G1 (%)	G2 (%)	G3 (%)	G4 (%)
Skin toxicities	80	8.6	8.6	62.9	0
Mucositis	74.3	5.7	37.1	31.4	0
Xerostomia	20	0	2.9	17.1	0
Dysgeusia	11.4	0	5.7	5.7	0
Anorexia	8.6	0	0	8.6	0
Constipation	8.6	2.9	5.7	0	0
Esophagitis	8.6	2.9	2.9	2.9	0
Pain	5.7	5.7	0	0	0
Dysphagia	5.7	0	0	5.7	0
Nausea	2.9	2.9	0	0	0

Table 1

Conclusion: Concomitant radiotherapy and cetuximab seems to be an effective therapy in the elderly population with encouraging results similar to the literature concerning its efficacy and toxicity. This treatment should be considered for patients > 70 years.

EP-1085

EGFR expression in head and neck cancer : does it have a role as prognostic factor in radiotherapy?

D. Alterio[1], A. Ferrari[2], F. Maffini[3], G. Marvaso[2], L. Santoro[4], C. Fodor[2], M. Cossu Rocca[5], M. Ansarin[6], S. Dicuonzo[2], M. Muto[2], D. Zerini[2], S. Chiocca[7], R. Orecchia[1,8], B. Jereczek-Fossa[1,8]
[1]*European Institute of Oncology, Radiation Oncology, Milano, Italy*
[2]*European Institute of Oncology, Radiation Oncology, Milan, Italy*
[3]*European Institute of Oncology, Pathology, Milan, Italy*
[4]*European Institute of Oncology, Epidemiology and Biostatistics, Milan, Italy*
[5]*Europian Institute of Oncology, Medical Oncology, Milan, Italy*
[6]*European Institute of Oncology, Head and Neck Surgery, Milan, Italy*
[7]*European Institute of Oncology at the IFOM-IEO, Experimental Oncology, Milan, Italy*
[8]*University of Milan, Health Sciences, Milan, Italy*

Purpose or Objective: In an era of personalized treatment there is a great interest in identifying factors which might help to predict patient response to RT. EGFR role in this

setting remains still controversial, despite the large consensus as a promising candidate to become a biomarker that could further improve application and efficacy of radiation therapy (RT) in head and neck squamous cell carcinoma (HNSCC). Moreover, most of the studies refer to series of patients who underwent RT alone or in combination with Cetuximab. We performed a retrospective analysis on the prognostic value of EGFR expression in HNSCC treated with surgery and postoperative RT.

Material and Methods: We analyzed 69 patients with an histological diagnosis of HNSCC who underwent adjuvant RT after surgery in our Institute from 1997 to 2003. A 3D conformal RT was delivered with a 6MV accelerator using a conventional fractionation (median 60 Gy, range 34.2-70 Gy) Median follow-up was 3.73 years (range 0.17-12.25 ys). None of these patients were treated with postoperative concomitant chemotherapy. Tumor samples used for the determination of EGFR were obtained from surgical specimens. Membrane features (intensity, extension, distribution) and percentage of EGFR expression were evaluated and a statistical analysis (univariate) was conducted to correlate these parameters with Overall Survival (OS) and Disease Free survival (DFS).

Results: EGFR was overexpressed in 45,5% of our patients (median value used as threshold). No significant correlation (p value= 0.90) has been found between patients with an overexpression of EGFR and OS or DFS. Among patients with laryngeal carcinoma, those with overexpressed EGFR have showed a lower OS (not statistically significant) and DFS (p=0.05). Considering separately the membrane features, the intensity of the EGFR staining has been found statistically correlated with both OS (p= 0.03) and DSF (p=0.001). Moreover, a stratification of patients was performed combining extension and intensity of EGFR immunolabelling in tumour cell membranes, and their distribution following a three-point score: patients with 3+ score (intense and complete labelling and patchy distribution) presented the lowest OS and DFS and the difference was highly significant for both OS and DFS (p= < 0.0001). The same result was observed in the subgroup of patients with a diagnosis of larynx carcinoma.

Conclusion: Based on our results it is still reasonable that the analysis of EGFR expression, especially referring to membrane features, might be a prognostic value for OS and DFS in locally advanced HNSCC treated with adjuvant RT. A clinical validation in prospective trials of the suggested three-point score system could be useful to select patients with worse prognosis that might benefit from more aggressive treatments.

EP-1086

Finding the right threshold for determining hypoxic subvolumes in F-MISO-PET/CTs for HNSCC

H. Kerti[1], L. Majerus[1], A. Bunea[1], N. Wiedenmann[1], M. Mix[2], C. Stoykow[2], P.T. Meyer[2], A.L. Grosu[1]
[1]*University Hospital Freiburg, Department of Radiation Oncology, Freiburg, Germany*
[2]*University Hospital Freiburg, Department of Nuclear Medicine, Freiburg, Germany*

Purpose or Objective: Tumor hypoxia is a common feature of locally advanced head and neck cancer (HNSCC) that is associated with higher malignancy and increased radioresistance. Tumor-to-blood ratios≥1.2 are generally thought to indicate hypoxia. Nevertheless, previous studies use various thresholds to define tumor hypoxia. The following analysis tries to elucidate which threshold may be the most appropriate to determine hypoxic volume in respect to treatment success.

Material and Methods: A prospective study was performed to determine changes in tumor hypoxia during primary chemoradiation (pRCTx) of HNSCC at our institution. Tumor hypoxia was non-invasively assessed by [18F]-Fluoro-Misonidazole (F-MISO) PET/CT 2.5 h p.i. at baseline (week 0) and in week 2 and 5 of treatment, respectively. Hypoxic volumes (HV) were generated using thresholding at different levels of 1.2, 1.3, 1.4, 1.5 multiplied with the background-uptake, which was defined as SUVmean within the ipsilateral trapezium muscle, as advised by a nuclear-medicine specialist. Δ-values of decrease of HV (ΔHV) during treatment were obtained in weeks 0, 2 and 5 and correlated with local failure. As four patients showed local failure (LF), two groups of four patients each were made: four showing LF, four patients showing complete remission (CR). Before t-test analysis normal sample distribution was confirmes with Shapiro–Wilk test. Significance-level was defined as $p<0.005$.

Results: We analysed 4 patients without local failure in comparison to 4 patients with LF to show differences **Δ**f -values in weeks 0 to 2, 2 to 5 and 0 to 5 of the HV. All patients primarily treated for HNSCC with dRCTx were included. Each patient received a total dose of 70Gy in 35 fractions. Concomitant cisplatin chemotherapy was administered in weeks 1, 4 and 7. The mean follow-up time was 16.9 months (range: 10-22 months). Mean time to LF was 9.5 months (range: 6-15 months). For patients in CR allΔ -HV (mean) show proportional decrease in weeks 0 to 5. This is true for every threshold factor from 1.2 to 1.5. In those patients showing LF,Δ -HV (mean) demonstrates not only a decrease in HV but also some increase at each of the time increments. There is a general decrease (p=0.0073) between week 0 and 5, while between week 0 and 2 and 2 and 5, a rise inΔ -HV(mean) can be shown (p=0.2339, p=0.0649, respectively).

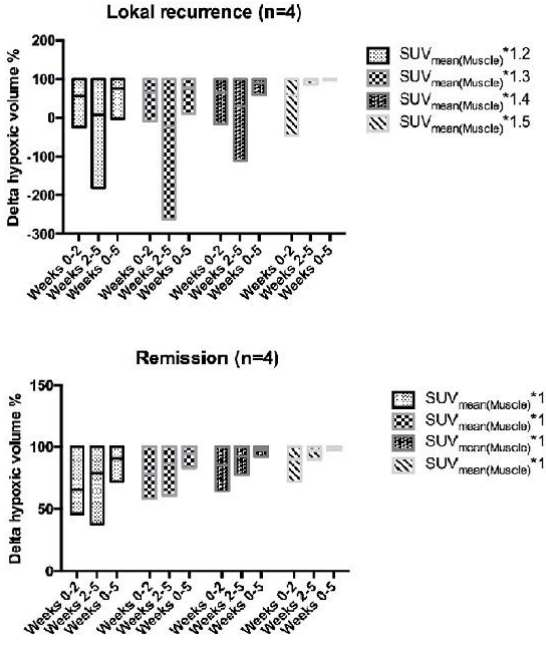

Conclusion: A decrease inΔ -HV (mean) was shown at any time point, for any factor the tumor-to-background-ratio was multiplied with, in patients with CR. In patients with LF, the hypoxic volume showed inconsistence over time, at least at one time of measurement there was an increase in hypoxic volume. The choice of the threshold for determination of hypoxic volume in FMISO-PET/CT remains a crucial question that could not be answered at this point. To elucidate this larger patient numbers are needed.

EP-1087

Screening for symptoms in HNC: Italian translation and validation of a patient-reported outcome

M. Maddalo[1], M. Buglione[1], L. Costa[1], N. Pasinetti[1], S. Tonoli[1], M. Urpis[1], L. Pegurri[1], S. Ciccarelli[1], F. Foscarini[1], F. Frassine[1], D. Tomasini[1], S.M. Magrini[1]
[1]*University and Spedali Civili- Brescia - Italy, Radiation Oncology, Brescia, Italy*

Purpose or Objective: The aim of this prospective observational study was to: (1) linguistically validate the Italian translation of the Vanderbilt Head and Neck Symptom Survey (VHNSS), a patient-reported outcome measure to screen for symptoms in the head and neck cancer (HNC) patients (pts) population; (2) perform a pilot test on the translated survey (VHNSS-IT) to assess the feasibility and utility, both for clinicians (cls) and for pts, of its administration in clinic as a symptoms' screening procedure.

Material and Methods: A multi-step linguistic process was conducted to generate and validate the VHNSS-IT: a forward translation, a backward translation and a patient testing (n = 35). For the pilot test 6 cls and 38 pts were recruited. Each pts completed the survey before the scheduled visit with the cls. Time to completion (TC), caregiver help (CH) and VHNSS-IT scores distribution reflecting symptom's intensity (SI) were recorded. The visit of the first three pts of each cls was performed per standard of care and the cls had to review the VHNSS-IT after the visit; time of revision (TR), perception regarding the acceptability of time burden, ease of use, and identification of potential problems that were previously unrecognized were reported. For the last three pts, cls were allowed to review the questionnaire during the visit, reporting the global perceived utility (GU).

Results: Two intermediate Italian versions were created during the process: the first Italian version derived from a reconciliation of three forward translations and the second Italian version derived from changes in the first version after the backward translation step. During the patient testing step only 2 pts reported problems with items comprehension and the rate of comprehension problems per single item was lower than expected: 2,9% in 16 items and 5,7% in 1 item. Pts could give suggestion in order to make items clearer and easier to understand: 43% of pts proposed a revision of the survey and most of these suggestions were retained. For the pilot test median TR was 2'15'. Time burden was perceived to be acceptable for all cls; they all also found the questionnaire easy to use. The rate of GU was 100%. Reviewing the survey, 4 of 6 cls identified symptoms unaddressed during the visit (swallowing problems, xerostomia, mucus, pain, speech and hearing problems). 30% of pts requested CH: these pts were significantly older (p < 0.001). Median TC was 6'57''. TC was related to age (p = 0.02), educational level (p = 0.023) and employment status (p = 0.004). Time after the start of the radiotherapy course (< 6 months vs > 6 months) and surgery (yes versus no) were considered as variables that could possibly influence average SI scores per subscale. Figure 1 shows relevant findings.

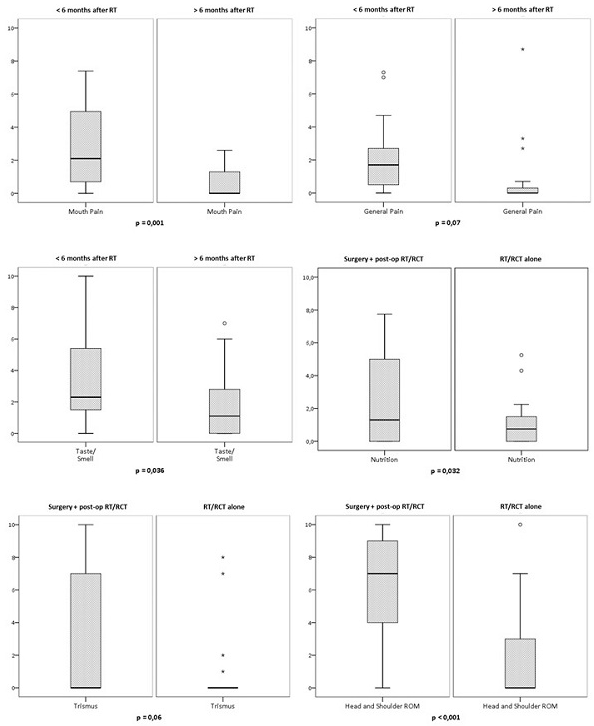

Conclusion: The VHNSS-IT represents a suitable instrument to screen for symptoms in Italian HNC pts treated with surgery and radio-chemotherapy and it can help cls to identify symptoms that require referral, education or intervention.

EP-1088

Is time from symptom to treatment a prognostic factor in stage III-IV head and neck cancer patients?

C. Furlan[1], J. Polesel[2], C. Gobitti[1], E. Minatel[1], E. Vaccher[3], L. Barzan[4], G. Grando[5], G. Franchin[1]

[1]*Centro di Riferimento Oncologico, Radiation Oncology, Aviano, Italy*

[2]*Centro di Riferimento Oncologico, Epidemiology and Biostatistics, Aviano, Italy*

[3]*Centro di Riferimento Oncologico, Medical Oncology, Aviano, Italy*

[4]*Centro di Riferimento Oncologico, Oncologic Surgery, Aviano, Italy*

[5]*Azienda Ospedaliera Santa Maria degli Angeli, Otorhinolaryngology, Pordenone, Italy*

Purpose or Objective: The impact of time from symptoms to treatment on survival of head and neck squamous cell carcinoma (HNSCC) patients has been investigated with conflicting results. This might be explained by the heterogeneity of studies with respect to stage and treatment modality. To reduce bias, this study focused on patients diagnosed with stage III-IV HNSCC managed with definitive chemo-radiotherapy to assess the effect of total interval and treatment delay on survival.

Material and Methods: Asingle-centre retrospective cohort analysis on 185 patients with stage III-IVHNSCC of oropharynx (n = 124), larynx (n = 36), and hypopharynx (n = 25)managed with definitive chemo-radiotherapy between 2008-2014 was performed. Patientscharacteristics included sex, age, smoke, Adult Comorbidity Evaluation (ACE-27),stage, tumor site, and HPV status (table 1). Treatment modalities includedconcomitant chemoradiation (CCRT, n = 33) for stage III patients, and inductionchemotherapy followed by radiotherapy (IC-CRT, n = 152) for stage IV patients.Total interval (time from first symptoms to the start of treatment) andtreatment interval (interval between the date of the pathology report and thestart of treatment) were defined in accord with the Aarhus StatementGuidelines. We chose

median total interval and median treatment interval as cutoff points to divide patients. Univariable and multivariable Cox proportional hazard model was used to evaluate overallsurvival (OS).

Table 1. Patients characteristics and treatment modalities

Patient parameter		
Sex		
Female	37 (20%)	
Male	148 (80%)	
Age		
= 65 y	134 (73%)	
> 65 y	51 (27%)	
ACE-27 comorbidity grade		
0-1	133 (72%)	
2-3	52 (28%)	
Tobacco		
Yes	143 (77%)	
No	42 (23%)	
T stage		
T1-2	62 (34%)	
T3-4	123 (66%)	
N stage		
N0-1	56 (30%)	
N2-3	129 (70%)	
TNM stage		
III	48 (26%)	
IV	137 (74%)	
HPV status		
Positive	39 (21%)	1
Negative	41 (22%)	
Unknown	105 (57%)	
Treatment parameter		
PET for staging		
Yes	100 (54%)	
No	85 (46%)	
IMRT		
Yes	210 (79%)	
No	55 (21%)	

Results: At a median follow up of 37 months, the 3-year OS for the entire cohort was 63%. Median total interval and treatment interval were of 98 days and 29 days, respectively. Patients with longer total interval were more likely to be patients with a low comorbidity grade (ACE-27 grade 0-1). On multivariable analysis a longer total interval was associated with a reduced risk of dying (hazard ratio 0.37, 95% CI 0.13 – 1,01; p = 0.05). No association of longer treatment interval with OS was noted on univariable and multivariable analysis. Longer treatment interval resulted associated with the use of PET for staging (p = 0.13), and with the use of CCRT for treatment (p = 0.05). In the subgroup analysis by treatment modality, no difference in OS according to treatment interval was noted.

Conclusion: In HNSCC patients with stage III-IV at diagnosis, a reduction of total interval and of treatment delay does not ameliorate survival. Development of fast track referral strategies should be aimed at increasing the ratio of stage I-II patients.

EP-1089

Accelerated hypofractionated IMRT-IGRT and concurrent chemotherapy in oropharyngeal cancer

B. Meduri[1], E. D'Angelo[1], P. Barbieri[1], L. Rubino[1], A. Ghidini[1], F. Bertolini[1], R. Depenni[1], P. Giacobazzi[1], F. Bertoni[1]
[1]*University Hospital of Modena, Radiation Oncology, Modena, Italy*

Purpose or Objective: In head and neck cancer absolute improvements in locoregional control rate and overall survival rate are achieved when radiotherapy is accelerated. Concurrent chemotherapy also have been used to improve outcomes at the cost of increased toxicity. The use of IMRT for head and neck cancer has been associated with reduced acute toxicity. Clinical experience with accelerated IMRT-SIB with concurrent chemotherapy for advanced oropharyngeal squamous cell carcinoma (LAOC), however, is limited. Objective of our study is to evaluate efficacy and toxicity of an accelerated hypofractionated SIB-IMRT with Tomotherapy and concurrent chemotherapy in LAOC.

Material and Methods: Between July 2009 and February 2014, 59 consecutive patients with LAOC received accelerated hypofractionated radiotherapy with tomotherapy and concurrent chemotherapy. The disease was stage III in 8% and stage IVa in 92% of patients. Prescribed doses to primary tumor and involved nodes was 66 Gy at 2,2 Gy/fraction, high risk and low risk nodes received simultaneously 60 Gy and 54 Gy at 2,0 Gy and 1,8 Gy/fraction, over 6 weeks. Acute toxicity was scored according to RTOG and late toxicity according to CTCAE-4 criteria. The disease free survival (DFS), local disease free survival (local-DFS), metastasis free survival (MFS) and overall survival were calculated using the Kaplan-Meier method.

Results: With median follow-up of 38 months (range 14-70) the estimated 3-years local-DFS rate, MFS, DFS and OS were 88%±0.04SE, 91%±0.04SE, 82%±0.05SE, and 83%±0.04SE, respectively. The complete response rate was 88%. All the patients completed the radiotherapy; the median treatment duration was 43 days, six patients have temporarily discontinued treatment (median: 5 days) because of toxicity. No grade 4 acute toxicitiy was observed, maximal acute toxicities were G3: mucosa 31%, skin 15%, dysphagia 24%, leukopenia 5%. Maximal late toxicities were: xerostomia G2 36%, mucosa G2 23%, skin G2 12%, laryngeal G2 17%, dysphagia G2 14%, osteoradionecrosis 3%, trismus 9%.

Conclusion: This analysis shows that a moderatly accelerated hypofractionated IMRT-SIB in tomotherapy and concurrent chemotherapy achieved high tumor local control and acceptable toxicity compared with previous chemoradiotherapy treatment with standard fractionation. Based on these results we elaborate a randomized clinical trial with a more hypofractionated regimen in order to obtain a better local control without increasing toxicity.

EP-1090

Overall treatment time is not a prognostic factor in chemoradiation for nasopharyngeal carcinoma.

E. Netto[1], M. Ferreira[2], I. Sargento[2], J. Cabeçadas[3], A. Mota[4], F. Pires[4], T. Alexandre[2], P. Montalvão[2], M. Magalhães[4], M. Roldão[4]
[1]*Nova Medical School, Medicine - Radiation Oncology, Lisboa, Portugal*
[2]*Instituto Português de Oncologia de Lisboa Francisco Gentil-EPE, Medical Oncology, Lisboa, Portugal*
[3]*Instituto Português de Oncologia de Lisboa Francisco Gentil-EPE, Pathology, Lisboa, Portugal*
[4]*Instituto Português de Oncologia de Lisboa Francisco Gentil-EPE, Radiation Oncology, Lisboa, Portugal*

Purpose or Objective: Overall treatment time (OTT) is an important factor in head and neck radiotherapy of squamous-cell carcinoma, the authors investigate its role in a nasopharyngeal carcinoma (NPC) population.

Material and Methods: We reviewed 109 patients charts with NPC. Pathological, clinical and dosimetric data were retrieved. All patients received concomitant chemo-radiation (CCRT) with IMRT-SIB with 69.96Gy to GTVs, 59.4 and 54Gy to CTVs in 33 fractions (RTOG0615). Cisplatin-based chemotherapy (CT) was prescribed as per Intergoup 0099. OTT was recorded from the first day of radiation through the last day of CCRT regardless adjuvant CT. Per protocol treatment was defined as OTT < 7 weeks. Any interruption was recorded as well its length and cause. Kaplan-Meier curves were created by SPSS (IBM Statistics), log-rank test was applied to detect differences and Cox regression model was adjusted to compare variables.

Results: From 109 patients, median age was 53; 74% male; 71% were WHO grade III; 43% T1; 14% T2; 18% T3, 25% T4; 17% N0; 17% N1; 39% N2; 27% N3. With a median follow up of 22 months, 2-year local control was 95,9%, freedom from metastases was 88% and overall survival was 79,8%. 9

patients were excluded because didn't receive CT (T1N0). From the remaining 100, 95 received concomitant plus adjuvant CT and 5 concurrent CT. We found a median OTT of 49 days (range: 11-83 days). 39 patients completed CCRT in more than 7 weeks (50-83 days) from which 31 (79%) in 8 weeks and the remaining 8 (21%) in more than 8 weeks. Interruption causes were by medical indication in 6 (15%), and non-clinical reasons in 33 (85% - patient no show, machine breakdown, and mis-coordination between departments). Compensations were performed at the discretion of the treating physician in the 8 patients with OTT longer than 8 weeks. No difference in local control (LC, p= 0.766), overall survival (OS, p=0.855) or metastases free survival (p= 0.131). Cox regression confirmed age, N stage, local control and distant metastases status as prognostic factors however no impact was found for OTT (p = 0.890 for < 7 weeks; p = 0.959 for < 8 weeks; and p = 0.960 for > 8 weeks).

Cox Regression – Overall Treatment Time vs. Survival
Variables in the Equation

	B	SE	Wald	df	Sig.	Exp(B)
Age	,079	,024	10,454	1	,001	1,082
NStage			10,159	3	,017	
NStage(1)	-2,102	1,004	4,387	1	,036	,122
NStage(2)	-1,661	,742	5,007	1	,025	,190
NStage(3)	-1,851	,722	6,571	1	,010	,157
LCSTATUS	-2,219	,998	4,943	1	,026	,109
MetsStatus	-1,670	,653	6,543	1	,011	,188
OTTime (<7 weeks)			,232	2	,890	
OTTime (7-8 weeks)	8,344	161,761	,003	1	,959	4206,337
OTTime (>8 weeks)	8,055	161,762	,002	1	,960	3149,082

Conclusion: In our study, we found no differences in LC and OS regardless OTT. These data must be interpreted with caution due to the high number of patients receiving CT that may compensate the unplanned interruptions in such a sensitive entity. Further studies with longer follow up are necessary to recommend or not withholding compensations in this setting.

EP-1091

Stratifying patients of head and neck cancer into risk groups for local control: predictive models

B. Dua[1], K. Chufal[2], G. Jadhav[1], A. Thakwani[2], A. Bhatnagar[2]
[1]*Apollo Hospital, Radiotherapy, Delhi, India*
[2]*Batra Hospital, Radiotherapy, Delhi, India*

Purpose or Objective: There have been numerous studies that have shown the importance of tumor volume as an independent prognostic factor over and above the T stage in head and neck cancer. However, data from the Indian subcontinent is sparse, even more so in patients treated by IMRT. This merits further study owing to possible differences in the biology of Indian head and neck cancer compared to its western counterpart. Ours was a prospective study that attempted to elucidate the role of tumor volume as a prognostic factor in locally advanced oropharyngeal and hypopharyngeal cancer.

Material and Methods: We enrolled 87 patients of Stage III-IV squamous cell cancer of the hypopharynx(30), and oropharynx(57), who subsequently received definitive concurrent chemo radiation with IG-IMRT. The tumor volume was the gross tumor volume (TV) delineated on the planning CT scan and was calculated by the volume algorithm in the treatment planning system. The impact of TV on Locoregional relapse free survival (LRFS), Response to chemo radiation (RR), overall survival (OS),local control(LC) and regional control was assessed over a follow up of 2 years. The Shapiro wilk test was done for assessing normality. Survival analysis was by kaplan meir method with log rank testing for assessing significance between groups Univariate analysis was done by mann-whitney/chi square/fisher's exact test , multiariate analysis was done by logistic regression forward stepwise method and a model to predict LC was generated .An ROC curve analysis was done for estimation of cut offs.

Results: The 2 year OS, LRFS, RR, LC& RC were 64%, 56%, 65%,63% and 83% respectively .The T stage distribution was T2, T3&T4 (5/41/41).The TV was not normally distributed and the mean TV was 48 cc (5-167cc) with mean TV in T3 /T4 patients of 39.9/60.9 cc. The mean TV in locally controlled patients was 35.4cc vs 70.8cc in uncontrolled patients .While the TV was a significant prognostic predictor for the OS , LRFS ,RR, and LC on univariate analysis , on the multivariate analysis only the TV predicted for LC. ROC curve analysis found cut off of 38 cc with 2 year LC of 84 % / 40% for TV<38cc / >38cc respectively with log rank p=0.001 with AUC of 0.759(0.653-0.865) and sensitivity/specificity of 82%/64%. ROC curve analysis of our oropharyngeal subgroup revealed similar results with a cut off of 38cc with AUC of 0.770 (0.644-0.896) and sensitivity / specificity of 80%/66%.with 2 year LC of 79%/30% for TV<38cc / >38cc (p=0.001). The likelihood of local failure increased by 3 % for 1cc increase in TV for the entire cohort & 3% for our oropharyngeal subgroup.

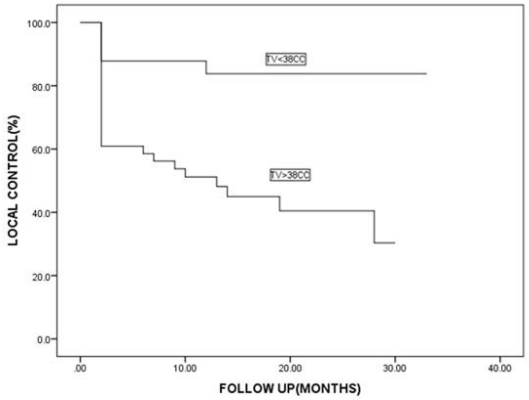

Figure: Kaplan Meir curve for patients with TV < 38 cc and >38cc

MULTIVARIATE LOGISTIC REGRESSION MODEL FOR LC

ODDS OF LOCAL FAILURE (P): LOG (P) =2.036 + 0.030 X TV (ALL PATIENTS)

ODDS OF LOCAL FAILURE (P): LOG (P) =1.857 + 0.032 X TV (OROPHARYNX PATIENTS)

Conclusion: TV is an independent prognostic factor in patients with head and neck cancer in predicting local control. Implications for existing management paradigms include, stratification according to TV in future randomized trials, consideration of altered fractionation and/or dose escalation to the primary disease for patients with TV>38cc.

EP-1092

Intensive radiotherapy in locally advanced head and neck squamous cell cancer- is it worth the pain?

A. Pascoe[1], C. Weston[2], J. Christian[1], M. Griffin[1], J. Price[3]
[1]*Nottingham University Hospitals NHS Trust, Department of Oncology, Nottingham, United Kingdom*
[2]*University of Nottingham, School of Medicine, Nottingham, United Kingdom*
[3]*Derby Teaching Hospitals NHS Foundation Trust, Department of Oncology, Derby, United Kingdom*

Purpose or Objective: With increasing evidence for combined modality treatment in locally advanced squamous cell cancer of the head and neck (HNSCC), there remains debate about the best treatment approach for patients with T4 disease. Local control in HNSCC is extremely important due to the morbidity and mortality associated with local recurrence. However treatment itself can be associated with significant morbidity. The purpose of this review is to determine both overall survival (OS) and local control rates for patients with T4 tumours treated with Intensity Modulated Radiotherapy (IMRT) with or without prior surgery.

Material and Methods: Retrospective review of all patients with T4 HNSCC treated with IMRT at our centre, between December 2010 and February 2013. Overall, relapse free and local relapse-free survival were calculated from date of biopsy to date of death, relapse or last follow up.

Results: Of the 69 patients with T4 tumours, 73.9% were male and median age was 69 (41-84). 50.7% were oropharyngeal tumours and 73.9% were node positive. Primary resection was performed in 18 patients. Eighteen patients underwent radiotherapy alone and 51 received concurrent chemotherapy (45 cisplatin, 6 cetuximab). Median follow up was 3.0 years (range = 3 months to 3.9 years). 28 patients died; 22 related to HNSCC, 6 from other causes. Overall survival at 3 years was 58.0% (95% CI: 44.6 to 69.1). 28 patients (40.6%), relapsed with median time to relapse of 8 months. 20 patients (29.0%) relapsed locoregionally and 11 patients (15.9%) developed distant metastatic disease. For 8 patients, distant metastases were the only site of relapse. Surgical salvage was performed in 6 patients with locoregional relapse only, 2 of whom have since died from causes related to HNSCC. Relapse free survival at 3 years was 54.0% (95% CI: 40.5 to 65.8) and loco-regional relapse free survival at 3 years was 65.5% (95% CI: 51.2 to 76.5). Nineteen patients (27.5%) had residual disease on PET scan 12 weeks post treatment. These patients were at greater risk of relapse and death with 3 year overall survival of 37.0% (95% CI 15.4 to 59.0) and 3 year relapse free survival of 40.5% compared to 3 year overall survival of 85.7% (53.9 to 96.2) and 3 year relapse free survival of 79.0% (47.9 to 92.7) in patients with normal PET scans.

Conclusion: There is a significant risk of relapse and death in T4 HNSCC tumours, particularly in those with residual disease following radiotherapy. However, IMRT, either alone or in combination with chemotherapy or surgery, achieved 3 year locoregional control of 65.5% (95% CI 51.2%-76.5%). This is a meaningful local control rate for locally advanced disease in which local relapse confers significant morbidity.

EP-1093

Impact of comorbidity, polypharmacy and HPV status in elderly patient with oropharyngeal cancer

F. Caparrotti[1], S. Huang[1], J. Ringash[1], Y. Song[2], A. Bayley[1], S. Bratman[1], J. Cho[1], M. Giuliani[1], A. Hope[1], J. Kim[1], J. Waldron[1], A. Hansen[3], D. Goldstein[4], B. Perez-Ordonez[5], I. Weinreb[5], L. Tong[1], W. Xu[2], B. O'Sullivan[1]
[1]*Princess Margaret Cancer Centre/University of Toronto, Radiation Oncology, Toronto, Canada*
[2]*Princess Margaret Cancer Centre/University of Toronto, Biostatistics, Toronto, Canada*
[3]*Princess Margaret Cancer Centre/University of Toronto, Medical Oncology, Toronto, Canada*
[4]*Princess Margaret Cancer Centre/University of Toronto, Otolaryngology - Head and Neck Surgery, Toronto, Canada*
[5]*Princess Margaret Cancer Centre/University of Toronto, Pathology, Toronto, Canada*

Purpose or Objective: To investigate the role of HPV status, comorbidity and polypharmacy on outcomes of elderly patient with oropharyngeal carcinoma (OPC).

Material and Methods: We retrospectively reviewed a prospectively compiled cohort of elderly patients (>70 years) with newly diagnosed OPC treated with curative radiotherapy (RT)+/- systemic therapy in 2000-2013. Tumor HPV status was assessed by p16 staining. Comorbidities were quantified by Charlson Comorbidity Index (CCI). The Comorbidity-Polypharmacy Score (CPS), a validated predictor of outcome for older trauma patients, was used to take into account the number of medications as a surrogate of the severity of comorbidities. Overall survival (OS), and relapse-free survival (RFS) were calculated and compared between HPV-positive [HPV(+)] and HPV-negative [HPV(-)] cohort. Two multivariate analysis (MVA) models [one included CCI (MVA-CCI), one included CPS (MVA-CPS)] were used to confirm the prognostic value of HPV, CCI or CPS, pack-year (PY) smoking, ECOG performance status (PS), and age for OS adjusted for disease extent (T, N).

Results: Tumor HPV status was ascertained in 229 of 287 (80%) patients revealing 115 HPV(+) and 114 HPV(-). Median age was 74.8 years (range 70-93). Systemic agents were given in 48 (21%) patients [chemo 17; EGFR inhibitor 31). RT incompletion [5 (4%) vs 8 (7%), p=0.41) and unplanned RT break rates [22 (19%) vs 28 (25%), p=0.34] were similar between HPV(+) vs HPV(-) cohorts. No significant difference in distribution of CCI (p=0.30) or CPS score (p=0.22) between HPV(+) vs HPV(-) cases. CCI and CPS have a moderate correlation (Kappa: 0.51). Median follow-up was 4.6 years. HPV(+) patients had better 5-year OS (59% vs 32%, p<0.001) and RFS (75% vs 54%, p<0.001) compared to HPV(-). MVA adjusted for T and N-category confirmed HPV(+) status was the strongest prognostic factor (PF) for OS [MVA-CCI: HR 0.52 (95% CI 0.34-0.79), p=0.002; MVA-CPS: HR 0.56 (0.36-0.85), p=0.007]. CPS was also a PF for OS [HR 1.05 (1.00-1.11), p=0.044]. CCI was not significant (p=0.17). ECOG PS was also a PF [MVA-CCI: HR 2.31; MVA-CPS: HR 2.32, both p<0.001]. Smoking (>20 PY) was prognostic in MVA-CCI (HR 1.62, p=0.035) and marginally prognostic in MVA-CPS (HR 1.56, p=0.056). Age was not significant in MVA-CCI (p=0.16) or MVA-CPS (p=0.65) models.

Conclusion: In elderly patients with OPC, HPV status is a strong PF for OS. Neither chronologic age nor CCI is prognostic. Higher CPS is correlated with poorer OS, which implies that inclusion of polypharmacy in addition to comorbidity might be a better reflection of competing mortality risk in this population, and attention to competing mortality causes may influence outcome for this complex patient group. Further validation of prognostication of CPS in elderly OPC population is warranted.

EP-1094

Total tumour volume predicts response in head and neck cancer: regression tree analysis and models

B. Dua[1], K. Chufal[2], G. Jadhav[1], A. Thakwani[2], A. Bhatnagar[2]
[1]*Apollo Hospital, Radiotherapy, Delhi, India*
[2]*Batra Hospital, Radiotherapy, Delhi, India*

Purpose or Objective: While the total tumor volume(TTV) has been extensively analyzed in literature as a prognostic factor in head and neck cancer, there exist no studies to date that have analysed the impact of TTV on response to chemo radiation(CCRT), particularly from the Indian subcontinent and in patients treated with IMRT. We did a prospective study that attempted to elucidate the role of total tumor volume as a prognostic factor in locally advanced oropharyngeal and hypopharyngeal cancer.

Material and Methods: We enrolled 87 patients of Stage III-IV cancer of the oropharynx(57),and hypopharynx(30) , who received definitive CCRT with IMRT. The TTV was the sum of the gross tumour volume and the nodal volume delineated on the planning CT scan. The impact of TTV on Locoregional relapse free survival (LRFS), response to chemoradiation (RR) and overall survival (OS) was assessed over a follow up of 2 years. Survival analysis was by kaplan meir method with log rank testing for assessing significance between groups Univariate analysis was by mann-whitney/chi square test ,multivariate analysis was by logistic regression forward stepwise method and a model to predict response was generated .ROC curve analysis was done for calculating cut offs. A classification tree for Response was generated using CART analysis (CHAID method).

Results: The 2 year OS, LRFS, and RR were 64%, 56% & 65%. The T stage distribution was T2(5) , T3(42) ,T4(42) & N stage was N0 (11),N1(28),N2A(10),N2B (17),N2C(17) & N3(4).The mean TTV was 67.4 cc (8-191)cc. The mean TTV in Responders/ non responders was 51.9 cc / 95.5cc.On multivariate analysis, the TTV was a significant prognostic factor for RR & LRFS but not for OS. ROC curve analysis found cut off of 48 cc for RR with AUC of 0.778(0.672-0.884) ans sensitivity/specificity of 87% /60%.The RR for the <48cc and

>48cc group was 90% vs 46% (chi square p =.001). ROC curve analysis of our oropharyngeal subgroup revealed similar results with a cut off of 48cc with AUC of 0.802 (0.677-0.927) and sensitivity / specificity of 86%/70%.The RR for the <48cc and >48cc group was 88% vs 40% (chi square p =.001). The likelihood of not responding increased by 1.8%% for 1cc increase in TTV for the entire cohort and by 2.4% for our oropharyngeal subgroup.

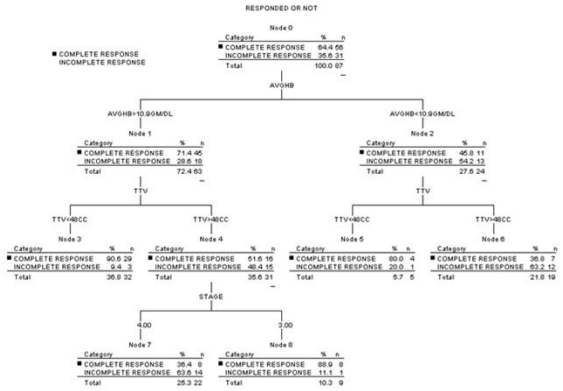

Figure .Classification tree for response according to prognostic factors.
AVGHB = average hemoglobin during treatment; TTV= total tumor volume

MULTIVARIATE LOGISTIC REGRESSION MODEL FOR RESPONSE

ODDS OF NON RESPONDING (P):LOG(P) = 4.075 + 0.018 X TTV – 0.478 X AVGHB – 1.375(IF STAGE 3)

Conclusion: Our study shows that the TTV is a significant and independent prognostic factor in patients with locally advanced head and neck cancer in terms of predicting local control. Implications for existing management paradigms include, stratification according to TTV in future randomized trials and consideration of altered fractionation and/or dose escalation to the primary disease for patients with TTV>48cc.

EP-1095

Prognostic role of FDG PET-CT performed before and during radiotherapy for nasopharyngeal cancer

P. Lin[1], M. Min[2], M. Lee[2], L. Holloway[3], D. Forstner[2], V. Bray[2], A. Fowler[2]
[1]*Liverpool Hospital, Nuclear Medicine and PET, Liverpool, Australia*
[2]*Liverpool Hospital, Cancer Therapy Centre, Liverpool, Australia*
[3]*Liverpool Hospital, Ingham Institute of Applied Medical Research, Liverpool, Australia*

Purpose or Objective: To evaluate the prognostic value of 18F-FDG PET-CT performed prior to (prePET) and during the third week (iPET) of radiation therapy (RT) in patients with newly diagnosed nasopharyngeal carcinoma (NPC).

Material and Methods: Thirty patients with newly diagnosed NPC treated with radical RT and Cisplatin-based chemotherapy underwent prePET and iPET. The median follow up was 26 months (range 8-66.9). AJCC staging included 12 patients in stage II, 8 in stage III and 10 in stage IV. The maximum standardised-uptake-value (SUVmax), metabolic-tumour-volume (MTV) and total-lesional-glycolysis (TLG) of primary tumour (PT), the index-node (IN) (defined as lymph node with highest TLG), total lymph nodes (TN) and combined primary tumour and nodal (PTN), and their % reductions in iPET were analysed, and results were correlated with 2-year loco-recurrence-free-survival (LRFS), regional-failure-free-survival (RFFS), distant-metastatic-failure-free-survival (DMFFS), disease-free-survival (DFS), and overall-survival (OS), using Kaplan-Meier (KM) analysis. Optimal-cutoffs (OC) were derived from Receiver-Operating-Characteristic curves for the best combined sensitivity and specificity.

Results: For LRFS, the only statistically significant predictor was reduction in primary tumour MTV by >50% in iPET (95.2% vs 75.0%, p=0.024). For other treatment outcomes, only nodal or combined PTN predicted treatment outcomes. The IN SUVmax (pre-PET OC=10.45g/mL and iPET OC=8.15g/mL) and TLG (pre-PET OC=90g and iPET OC=33.4g) provide the overall best predictor of outcome, with significant associations with RFFS (iPET only), DMFFS (prePET), DFS (prePET and iPET) and OS (prePET): For RFFS, iPET IN SUVmax and TLG were best predictors: the 2-year KM survivals were 100% vs. 50%, p<0.001 and 100% vs. 44%, p=0.032 respectively. For DMFFS, prePET IN SUVmax and TLG were best predictors: 100% vs. 51.9%, p=0.004 and 100% vs. 47.6%, p=0.002. For DFS, prePET IN TLG and iPET IN SUVmax were best predictors: 87.5% vs. 33%, p=0.045 and 78.7% vs. 20%, p=0.01. For OS, prePET IN TLG and iPET IN TLG were best predictors: 100% vs 72.7%, p=0.048 and 91.7% vs 68.6%, p=0.05. The IN metabolic parameters demonstrated stronger correlation with outcome than PT or PTN, and equivalent correlation to the TN except IN was better in predicting OS.

Conclusion: The metabolic parameters of prePET and iPET can provide complementary prognostic biomarkers of patient outcomes, These parameters may have a role in adaptive therapy for NPC, and identifying the best treatment strategy for precision individualised chemo-radiotherapy combinations. We have demonstrated IN to be a useful novel imaging biomarker for predicting all treatment outcomes, and offers additional potential advantage of ease of generation and reproducibility compared to TN or PTN.

EP-1096

Prognostic value of pretreatment FDG-PET features in laryngeal cancer patients treated with RT

R. Kabarriti[1], P.N. Brodin[1], A. Ginsburg Berkowitz[1], A. Ingber[1], N. Ohri[1], K.P. McGovern[1], C. Modi[1], T.J. Ow[2], A. Tassler[2], S. Packer[3], B.A. Schiff[2], R.V. Smith[2], M. Haigentz[3], C. Guha[1], S. Kalnicki[1], W.A. Tomé[1], M.K. Garg[1]
[1]*Montefiore Medical Center- Albert Einstein College, Radiation Oncology, New York, USA*
[2]*Montefiore Medical Center- Albert Einstein College, Otolaryngology- Head & Neck Surgery, New York, USA*
[3]*Montefiore Medical Center- Albert Einstein College, Medical Oncology, New York, USA*

Purpose or Objective: Statistical image features from computed tomography (CT) and positron emission tomography (PET) scans are being investigated for the potential prognostic value in predicting outcome for various clinical indications. Here, we analyze primary tumor image features from pretreatment FDG-PET and the relation to clinical outcomes in patients treated with definitive radiation therapy (RT) for laryngeal cancer.

Material and Methods: We identified 83 consecutive patients with laryngeal squamous cell carcinoma treated with definitive RT with available pretreatment PET/CT scans at our institution. Clinical variables related to disease and patient characteristics, treatment information, and clinical outcomes data were collected for each patient. Pretreatment PET/CT scans were used for image feature analysis of the primary tumor volume for each patient. Multiple statistical image features were computed, along with several measures related to the standardized uptake value (SUV). Redundant image features were excluded based on a strong correlation with parameters commonly reported as important such as metabolic tumor volume (MTV) and maximum SUV value (SUVmax). A LASSO procedure was applied to select appropriate variables to include in Cox proportional hazard models for local control (LC) progression-free survival (PFS) and overall survival (OS). The concordance index or "C-index" was computed to evaluate the discriminative ability of each model, both on the training data set (apparent C-index) and using bootstrap cross-validation (bCV). Correction for

multiple testing in statistical analysis was done using the Benjamini-Hochberg method.

Results: With a median follow up of 34 months, the 3-year LC, PFS and OS (with 95% confidence intervals) were 64% (53% - 75%), 51% (39% - 62%) and 77% (67% - 87%), respectively. No image features were significantly correlated with LC or PFS and adding image features to the clinical variables did not improve the performance of the Cox model in the bCV setting, as seen in Table 1 where the C-index is highlighted in bold if adding image features improved performance.

Patient #	Minimum distance (Cord to Thecal sac) [mm]	% of Cord closer than 1mm from Thecal sac [%]	Potential max point dose to Cord (SBRT) [Gy]	Potential max point dose to Cord (EQD2) [$Gy_{3/2}$]	Estimated potential myelopathy risk [%]
1	1.71	0.0	18.2	36.6	4.6
2	0.02	13.3	21.9	50.7	10.0
3	2.07	0.0	17.4	33.8	4.1
4	1.01	0.4	19.7	42.1	6.0
5	0.64	5.5	20.5	45.3	7.2
6	1.65	0.0	18.3	37.0	4.7
7	0.92	1.9	19.9	42.9	6.2
8	0.49	4.2	20.8	46.5	7.7
9	0.96	0.6	19.8	42.6	6.2
10	0.59	3.8	20.6	45.7	7.3
11	0.60	5.3	20.6	45.6	7.3
12	1.53	0.0	18.5	37.9	4.9
13	0.02	16.0	21.9	50.8	10.0
14	0.67	5.6	20.4	45.0	7.1
15	0.02	8.7	21.9	50.7	10.0

MTV was the image feature most closely related to OS and for OS the addition of image features did improve the predictive performance of the Cox model. Figure 1 shows the effect of dividing the patient population based on the statistically most important variables, where it is clear that Karnofsky performance score and MTV affect the OS.

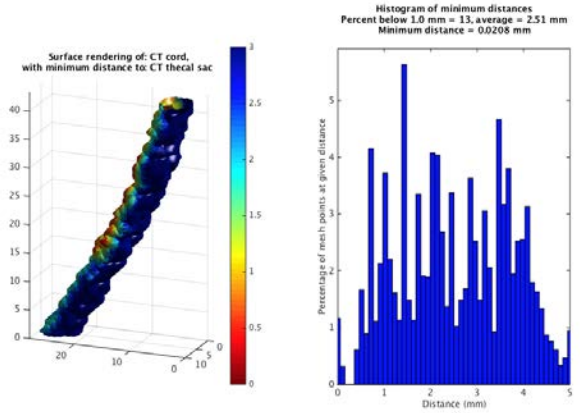

Conclusion

Adding image features to complement clinical parameters was seen to improve the prognostic value for OS. Although no significant image features were found related to LC and PFS, we found that a smaller MTV was predictive of improved OS.

EP-1097

Comparison of outcomes and toxicities between IMRT and SIB-IMRT in cancers of hypopharynx

M.S. Raghunathan[1], R. Subramaniam[1], A. Vaz[1], N. Senthil Kumar[1]

[1]*Kovai Medical Center And Hospitals, Department Of Radiation Oncology, Coimbatore, India*

Purpose or Objective: Among cancers of head and neck, hypopharyngeal cancers tend to have an aggressive clinical course. Chemoradiation has become the standard of care for patients who are candidates for an organ preservation strategy. IMRT planning has incorporated a simultaneous integrated boost (SIB-IMRT) in order to efficiently develop comprehensive radiation therapy plans and also potentially lessen treatment time and toxicity. Outcomes and toxicites of patients with hypopharyngeal cancers treated in a single institute with standard IMRT and SIB-IMRT schedules were analyzed retrospectively.

Material and Methods: A total of 86 patients with hypopharyngeal squamous cell carcinomas were treated between September 2010 and December 2014. Among 44 patients who were treated using SIB-IMRT, 8 received neoadjuvant chemotherapy (NACT) and 42 received concurrent chemotherapy. Among 42 patients who were treated using IMRT with conventional fractionation (IMRT),16 received NACT and 40 received concurrent chemotherapy. The dose for SIB-IMRT group was 65 Gy in 30 fractions to gross and high risk disease and 54 Gy in 30 fractions to low-risk nodes. The dose in IMRT group was 66-70 Gy to gross disease, 60 Gy to high risk nodes and 50 Gy to low risk nodes in 1.8-2 Gy per fraction.

Results: At a median follow-up of 16.5 months (6-56 months) the median OS of entire cohort was 38.9 months. The mean OS was 37.5 months and 38.3 months (p=0.91) for SIB-IMRT and IMRT respectively. The mean treatment duration for SIB-IMRT and IMRT groups was 42 days (range: 38-51 days) and 48.4 days (range: 45-73 days) respectively. 98 % in SIB-IMRT and 93 % patients in IMRT group completed the intended treatment. Complete response was noted in 89 % and 93 % in SIB-IMRT and IMRT groups respectively. The estimated 1 year, 2 year LR control and 2-year DFS were 81%, 66.6%, 67.4% in SIB-IMRT and 84%, 74%, 62% (p<0.81) in IMRT groups respectively.Grade 3 mucositis occurred in 10 (23%) and 12 (28%), grade 3 dermatitis in 9 (20.5%) and 12 (28%) of SIB-IMRT and IMRT patients respectively. Grade 2 xerostomia occurred in 11 patients (27%) and 15 patients (34%) in IMRT and SIB-IMRT groups. Grade 3 soft-tissue fibrosis and esophageal stricture rates were 2 (4.7 %) and 5 (11.4%) in SIB-IMRT and IMRT groups.

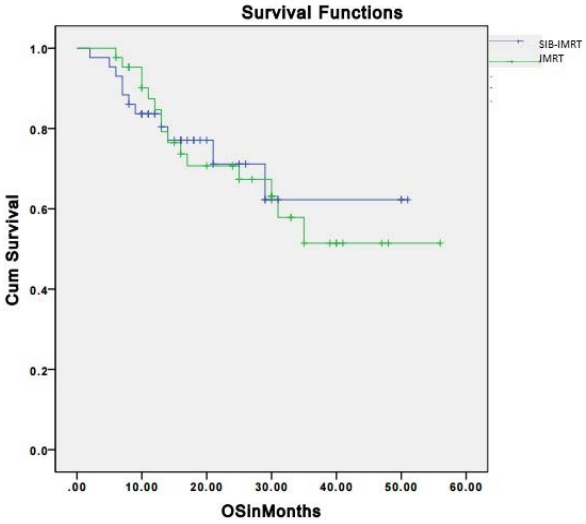

Conclusion: Clinical outcomes, acute and late toxicities of chemo-radiation with SIB-IMRT were comparable with IMRT. Overall treatment duration was reduced and more patients completed intended treatment in SIB-IMRT group with relatively lesser acute toxicities.

EP-1098

Radiation induced brachial plexopathy in head and neck carcinoma (acute and chronic)

S. Yahya[1], M. Hickman[1], A. Hartley[1], P. Sanghera[1]

[1]*Hall-Edwards Radiotherapy Research Group- Queen Elizabeth Hospital, Cancer Center, Birmingham, United Kingdom*

Purpose or Objective: Radiation Therapy Oncology Group (RTOG) guidelines recommend brachial plexus dose constraints ranging from 60-66Gy in 2Gy per fraction (BED = 120-132Gy2). However there remains limited data on brachial plexus (BR.P) toxicity and furthermore the dose limits are

often below those required to control gross disease. This study was done to explore the incidence of brachial plexus injury following radical (chemo) radiotherapy in the IMRT era.

Material and Methods: Patients with head and neck cancer that had completed IMRT to unilateral or bilateral neck with a minimum of 2 years of follow up were identified from a prospective database. All patients underwent clinical review as per local protocol which was commonly 6 weekly. The brachial plexus was contoured based on RTOG Atlas. Maximum dose (Dmax) to brachial plexus was recorded from DVH. All doses were converted to BED using an α/ß ratio of 2. A review of electronic records was performed to determine brachial plexus toxicity using CTCAE v 3.0.

Results: Seventy five patients met the inclusion criteria. Ten patients were excluded due to insufficient dose metric data. Of sixty five patients analysed, 37 patients were treated for oropharyngeal, 2 for nasopharyngeal, 6 for Hypopharyngeal, 9 for Larynx, 8 for oral cavity cancers and 3 for unknown primary site. Forty five patients had concurrent chemotherapy (31 cisplatin, 8 carboplatin and 6 cetuximab). Brachial plexus dosimetry is given in table 1. Maximum point BED to brachial plexus reached 149.5Gy2 (41.3-149.5). There were no reported symptoms of brachial plexopathy during this period.

Dose and Fractionation	Dmax Left BR P (*BED)	Dmax Right BR P (*BED)
55 Gy in 20# (n=11/65)	57.5 (*140Gy2) (*63- 130.2)	59.8(*149Gy2) (*41.3-132.1)
64Gy in 25# (n=3//65)	62.4 (*140 Gy2) (*107.6-149.5)	58.4(*127Gy2) (*103.6-121.9)
67.2 Gy in 28# (n=1/65)	62.6 (*132Gy2)	61.1 (*128Gy2)
60 Gy in 30# (n=20/65)	58.5 (*115Gy2) (*43.6 – 133.8)	60.3(*121Gy2) (*56.5- 136)
65Gy in 30# (n=30/65)	59.3 (*118Gy2) (*86.9 – 141.1)	60.0 (*120Gy2) (*129.7- 144.1)

Table 1: Showing the dose and number of fractions delivered and Dmax to brachial plexus

Conclusion: It is often necessary to accept higher than conventional maximum point doses to the brachial plexus to ensure adequate PTV coverage for head and neck cancers. Although longer term follow-up is required ideally with nerve conduction studies, such an approach of exceeding conventional limits appears to be acceptable. Further data will be presented for patients exceeding conventional constraints.

EP-1099

Re-irradiation for head and neck tumors: efficacy versus late toxicity in 137 patients

W. Bots[1], S. Van den Bosch[1], L.C. Verhoef[1], E.M. Zwijnenburg[1], T. Dijkema[1], G. Van den Broek[1], W. Weijs[1], G.O. Janssens[2], J.H.A.M. Kaanders[1]

[1]Radboud university medical center, Department of Radiation Oncology, Nijmegen, The Netherlands

[2]UMC Utrecht, Department of Radiation Oncology, Utrecht, The Netherlands

Purpose or Objective: To present long-term results on disease control and late toxicity in both primary and post-operative re-irradiation in the head and neck region.

Material and Methods: Retrospective single center analysis of 137 patients re-irradiated between 1986 and 2013 for a recurrent or second primary malignancy. Inclusion criteria were a prescribed dose of at least 45 Gy in first treatment and re-treatment and histological proof of disease. Exclusion criteria were age under 18 years, the presence of metastatic disease and the use of brachytherapy. Endpoints were locoregional control (LRC), disease-free survival (DFS), event-free survival (EFS), overall survival (OS) and grade 3 late complications according to EORTC/RTOG criteria. EFS includes both disease recurrence and late treatment complication as an event.

As 3D-dose distribution data was not available for all patients, a descriptive approach was used to determine the highest cumulative dose in radiation overlap and organs at risk (spinal cord, larynx, mandible and optical nerve).

Results: Patient and tumor characteristics are presented in table 1.

Table 1

Patient characteristics (n=137)		%
Age (range)	65 (31-87)	
Median follow-up in months (range)	16 (2-128)	
Median time between radiation treatments (years)	1.8	
Median re-irradiation dose in Gy (range)	60 (45-70)	
Median cumulative dose in Gy (range)	126 (70-138)	
Concurrent chemotherapy at re-irradiation	7	5.1%
IMRT use at re-irradiation	60	44%
Tumor characteristics		
Tumor location		
Larynx	73	53%
Oral cavity	19	14%
Oropharynx	17	12%
Other	28	21%
Histology		
Squamous cell	118	86%
Other	19	14%
T-stage		
0	1	1%
1	33	24%
2	60	44%
3	23	17%
4	20	15%
N-stage		
N0	88	64%
N+	49	36%

The median re-irradiation and cumulative radiation dose were 60 Gy (range 45-70) and 126 Gy (range 68-138) respectively. Two- and five-year LRC were 52% and 40%, two- and five-year DFS were 38% and 28% respectively (figure 1). There were 17 observations of serious late toxicity in 11 patients (actuarial 26% at 5 years): chondronecrosis (n=1), osteoradionecrosis (n=8), soft tissue necrosis (n=3), arterial blowout (n=3), and stricture/fistula (n=2). Three cases of treatment-related death were reported. Multivariate analysis revealed IMRT as re-irradiation technique to be protective of late complications (HR, 0.10; 95% CI, 0.01-0.96). The five-year actuarial EFS was 18%.

Figure 1

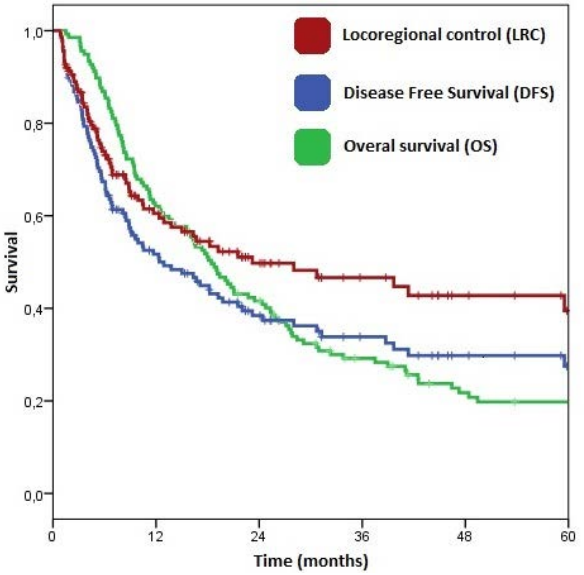

One-hundred-and-seven patients (78%) were re-irradiated post-operatively and had a better LRC in comparison to re-irradiation alone (actuarial 5-yr 46% *vs* 16%, p<0.05). Of patients re-irradiated alone without surgery, patients re-irradiated for a second primary tumor had significant better LRC-rates in comparison with patients re-irradiated for

recurring tumors (actuarial 5-yr 44% *vs* 0% p<0.05). Four cases of mandibular osteoradionecrosis were seen (cumulative dose range 106-128 Gy). Fifty-three patients received a cumulative dose of 100 Gy or higher. The actuarial 5-year mandibular necrosis rate in this group was 26%.

Conclusion: Re-irradiation in the head and neck region for a recurrent or second primary malignancy is associated with LRC-rates of 40%. Results in patients re-irradiated post-operatively are more favorable. Approximately one in six patients survived at 5 years without a recurrence or a serious late toxicity. The most important limitation for re-irradiation is late toxicity, which can be limited with current IMRT techniques.

EP-1100

External validation of a mixture NTCP model of radiation-induced hypothyroidism (HT)

M.F. Roenjom[1], C. Brink[2], S. Bentzen[3], L. Hegedüs[4], J. Overgaard[5], J. Petersen[6], H. Primdahl[7], J. Johansen[1]

[1]*Odense University Hospital, Department of Oncology, Odense, Denmark*

[2]*Odense University Hospital, Laboratory of Radiation Physics, Odense, Denmark*

[3]*Division of Biostatistics and Bioinformatics- University of Maryland Greenebaum Cancer Center and, Department of Epidemiology and Public Health- University of Maryland School of Medicine, Baltimore, USA*

[4]*Odense University Hospital, Department of Endocrinology and Metabolism, Odense, Denmark*

[5]*Aarhus University Hospital, Department of Experimental Clinical Oncology, Aarhus, Denmark*

[6]*Aarhus University Hospital, Department of Medical Physics, Aarhus, Denmark*

[7]*Aarhus University Hospital, Department of Oncology, Aarhus, Denmark*

Purpose or Objective: We have previously developed a mixture NTCP model for radiation-induced HT in a cohort of patients with head and neck cancer treated at the Department of Oncology, Odense University Hospital (OUH), Denmark. The model was validated in an independent cohort of patients treated at the Department of Oncology, Aarhus University Hospital (AUH). One plasma TSH assessment after RT was used in the external validation cohort and the latency time function of the model could therefore not be validated. The aim of this study was to validate the latency function by including repeated thyrotropin (TSH) measurements and a longer follow-up in the validation cohort.

Material and Methods: Initially, 198 patients were included in the validation cohort. From July 2012- October 2014 further TSH measurements were collected in 171/198 patients, increasing the median follow-up from 22 to 38 months after RT. The endpoint, HT, was defined as TSH>4.0 mU/l. Data were analyzed using a mixture model taking both thyroid volume (Vthyroid) and dose (Dmean) into account. From the repeated blood samples, latency was estimated and both the latency time function and NTCP models in AUH were compared to OUH. Validation was performed using a calibration plot of binned groups of patients showing the clinically observed outcome in the validation cohort compared with the predicted outcome from the original NTCP model.

Results: With the additional follow-up, 40 patients (20%) developed HT (19 after one TSH assessment). Dmean and Vthyroid were still significant risk factors for HT, OR=1.11 (1.06-1.19) and OR=0.85 (0.74-0.93), respectively. The cumulative events showed that 94% (59-100%) of the events would develop within the first five years after RT in the validation cohort, in line with the original cohort's 97% (85-100%). Mean thyroid volumes were 17.4 (OUH) and 17.3 (AUH) cm3, and tolerance estimates around this level showed TD25 =38 Gy and 34 Gy, respectively, at 15 cm3 and 48 Gy and 42Gy, respectively, at 20 cm3. The calibration plot (Fig. 1) showed good agreement between the observed incidences of HT in the validation group versus the expected probability of HT from the original model. Thus, the NTCP model has external validity in the cohort with multiple blood tests.

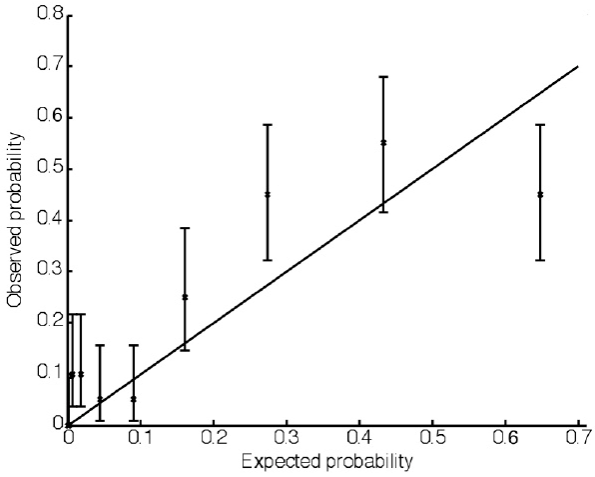

Conclusion: Increasing thyroid dose and a decreasing thyroid volume were confirmed as significant risk factors for radiation-induced HT, which likely develops within the first five years after RT. The calibration plot shows that the original NTCP model has external validity, supporting that risk estimates from the NTCP model may be used to support clinical treatment planning decisions relating to development of hypothyroidism after RT to the neck area.

EP-1101

Knowledge of HNC risk factors and symptoms – a survey among 1903 young Polish respondents

E. Sierko[1], A. Krentowska[1], A. Skoneczny[1], A. Strzałka[2], W. Pietruszewska[3], M.Z. Wojtukiewicz[4], E. Sierko[4]

[1]*Medical University of Bialystok, Students' Scientific Association in the Department of Oncology, Bialystok, Poland*

[2]*Medical University of Lodz, Student's Scientific Association in the Department of Otolaryngology and Laryngological Oncology, Lodz, Poland*

[3]*Medical University of Lodz, Department of Otolaryngology and Laryngological Oncology, Lodz, Poland*

[4]*Medical University of Bialystok, Department of Oncology, Bialystok, Poland*

Purpose or Objective: Head and neck cancer (HNC) is the sixth most common type of cancer in Europe. Its early symptoms are usually non-specific and easy to miss, which in many patients lead to late presentation and diagnosis. Main risk factors of HNC include alcohol consumption and smoking. Both of them are usually present in young people, thus health education in this group is of great importance. The aim of the study was to assess the level of HNC awareness among young population in Poland.

Material and Methods: An anonymous online survey about HNC was conducted among 1903 people in the age of 18-35 years, mainly students of high schools and universities. The closed-ended questions concerned HNC risk factors, symptoms and prognosis. Participation in the study was voluntary.

Results: 85% of respondents had heard about HNC. The main source of information was the Internet (57%). Seventy-eight percent of participants associated smoking with HNC development, but alcohol consumption was mentioned by less than a half, and human papillomavirus (HPV) infection by approximately ⅓ of them. The main risk factors mentioned by students of non-medical schools included smoking (66%), stress (33%), and excessive sunbathing (32%). One fourth of the respondents (38% when excluding medical students) were unaware of any HNC early symptoms. The symptoms mentioned most often included chronic hoarseness (55%), lump in the neck (52%), and chronic sore throat (51%). Over ¾ of medical students and half of other respondents were aware that early diagnosis is associated with a great chance

of cure. In contrast to that, if they noticed the symptoms in themselves, as much as 5% of medical students and 9% of students of other schools would seek medical advice only when they made everyday functioning impossible.

Conclusion: The level of HNC cancer knowledge among young population is alarmingly low. A large number of students of non-medical schools and universities are unaware of its risk factors and early symptoms. This group would benefit from increasing the number of educational campaigns, which would lead to earlier presentation, diagnosis and treatment of HNC.

EP-1102

Parotid toxicity in head and neck cancer patients treated with IMRT

G. Mantello[1], G. Capezzali[1], F. Cucciarelli[1], L. Vicenzi[1], M. Giacometti[2], M. Valenti[2], S. Maggi[2], M. Cardinali[1]
[1]*Azienda Ospedaliero Universitaria Ospedali Riuniti, Radiotherapy Department, Ancona, Italy*
[2]*Azienda Ospedaliero Universitaria Ospedali Riuniti, Physics Department, Ancona, Italy*

Purpose or Objective: The aim of this study was to evaluate the parotid glands toxicity and its relationship with the dose in a cohort of head and neck cancer patients treated with IMRT.

Material and Methods: 78 patients out of 110 treated in our department between January 2011 and October 2015 were included in the analysis. Criteria to select patients were: at least 6 months follow up, the omo-lateral parotid (OP) close to the high (HR) and / or intermediate (IR) risk CTV. Characteristics of the studied patients population are shown in Table1.The GTV, whenever present, CTV HR (regions at high risk of microscopic disease), CTV IR (regions at intermediate risk) and CTV LR (regions at low risk) were contoured on each slice. The targets were expanded 3 mm to obtain the PTVs. The prescribed dose was 66-70 Gy (2 – 2.13 Gy /fr) to PTV HR, 59.4 – 66 Gy (1.8 – 2 Gy/fr) to PTV IR; 56.1Gy (1.7 Gy/fr) to PTV LR. IMRT with Simultaneous Integrated Boost (SIB) technique was used (41patients were treated with Tomotherapy and 36 with VARIAN 21EX). The OP and the CP were contoured; PTV SV1 OP and SV2 CP were defined as overlapping volumes of PTVs and glands. Priority was given to PTV when OP was partially included. The dose limit (Dmean) was <= 25 Gy to the whole contralateral gland (if not close to GTV N) and < 24 Gy to the volume of CP not included in the PTV (external CP). Salivary gland toxicity was assessed weekly, during RT, and at 3,6,9,12,18,24 months after RT and was graduated using the RTOG toxicity scale.

Age (y), mean (range) 62 (39–82)		
Gender	Female	15 (19.2%)
	Male	63 (79.8%)
Tumor site	Nasopharynx	8 (10.2%)
	Oral cavity	26 (33.3%)
	Oropharynx	28 (36.0%)
	Larynx	16 (20.5%)
Adjuvant Chemotherapy	Yes	6 (7.7%)
	No	72 (92.3%)
Concurrent Chemotherapy	Yes	37 (47.4%)
	No	41 (52.6%)
PreRadiotherapy surgery	Yes	50 (64.1%)
	No	28 (35.9%)
Stage (TNM staging system)	I–II	20 (25.6%)
	III–IV	58 (74.4%)

Table 1. Patient and tumor characteristics (n = 78). Values are number (percentage)

Results: The dose delivered to the PTVs was 67.9 Gy (range 66-70) 2.02 Gy/fr (1.9 -2.2) to PTV HR, 62.3 Gy (range 58-66) 1.86 Gy/fr (1.7-2) to PTV IR, 55.9 Gy (range 51-60) 1.68 Gy/fr (1.65-2) to PTV LR. The mean dose was 41.56 Gy (range 17.8 - 66.8) to OP and 24.9 Gy (range 4.7-39.7) to CP; the external CP received 21.7 Gy mean dose. 36 (46.1%) patients experienced mouth dryness, thickened saliva and altered taste (31 G1 and 5 G2) during RT. At a median follow up of 24 months (range 6-56.2) 19 cases with xerostomia were recorded, 15 (19%) G1 and 4 (5,1%) G2. No G3 was observed. The symptom was recorded on an average of 8 months (range 6-15) after RT. Only 13/36 patients with acute salivary problems experienced late xerostomia.

Conclusion: In our experience 25 Gy mean dose to the whole contra-lateral parotid, with <24 Gy mean dose to the external CP, even with sacrifice of the OP, allowed our patients to maintain an adequate salivation. 24% of cases experienced G1 and G2 xerostomia. No G3 toxicity was observed.

EP-1103

Review of thyroid ablation rates with RAI based on I131 uptake in differentiated thyroid carcinoma

M. Keys[1], C. Faul[1], O. Boychek[1]
[1]*St. Lukes Radiation Oncology Network, Radiation Oncology, Dublin 6, Ireland Republic of*

Purpose or Objective: Recent studies show that low activity (1.1GBq) of RAI is as effective as high activity (3.7GBq) in treating those with low-intermediate-risk differentiated thyroid cancer (DTC). The purpose of our study was to retrospectively review post-operative I131 uptake and ablation rates in those with DTC.

Material and Methods: Data was obtained from St. Luke's Radiation Oncology Network (SLRON) patient registry. Selection criteria included histologically proven DTC; post-thyroidectomy; pre and post RAI ablation scan and RAI ablation in SLRON. There were 68 cases of DTC treated with RAI identified between 2005-2007 that were suitable for analysis and met criteria and follow up of ≥5 years

Results: Of the cases analysed 73% were female and 27% male with a mean age of 44 years. The predominant histological subtype was papillary (73%), followed by follicular (22%). Most had early stage disease; Stage I (65%), Stage II (22%), Stage III (13%), 39 cases were pN0 and 29 had pN1 disease. Regarding surgery performed 39 patients had a complete excision CE, 22 had residual disease and there was no information for 7 cases. Thirty seven (37) cases had microscopically positive margins, 26 were negative and it was unknown in 5. Pre RAI ablation, Post op. RAI (I131) uptake in these patients was an average of 3.6 % in pN1 disease and 5.1% in those with pN0 disease. The max uptake was 28%. The extent of the surgery tended to influence the trend of uptake. There was a trend to a higher mean uptake in those who didn't have a CE with an uptake of 0.1-17%, and mean of 6.3%. Patients that had a CE had an uptake of 0-28%, and mean of 3.9%. In the SLRON there was no standard protocol for RAI dosage at the time the patients were treated The mean and range of doses of RAI administered was looked at based on pre-ablation uptake scans. Group 1 had a pre-ablation uptake of <4% and group 2 >4%. For group 1 the mean dose was 3.9GBq with a range 2.2-7.4GBq, and group 2 had a mean of 3.7GBq with a range of 2.8-7.4GBq. Post-ablative RAI131 scans showed an average of 0.07% uptake with the majority of patients (33) having <0.1% uptake. At the time of analysis 23 patients remained disease free, 10 had metastases (M1) and 2 had died from metastatic disease.

Conclusion: In those that received RAI ablation, high ablation rates ≥90% were shown despite variability in post -op. I131 uptake and dose of RAI administered. There didn't appear to be an association between those with recurrent or metastatic disease and their pre-ablation uptake rates, it was more associated with original stage.

EP-1104

Role of perfusion CT in evaluation of tumour response after radiochemotherapy in H&N cancer

P. Ferrazza[1], P. Cocuzza[1], F. Pancrazi[2], D. Delishaj[1], L. Fatigante[1], A. Cristaudo[1], L. Faggioni[2], F. Orlandi[1], F. Matteucci[1], S. Ursino[1]
[1]*Azienda Ospedaliero Universitaria Pisana, Department of Radiation Oncology, Pisa, Italy*
[2]*Azienda Ospedaliero Universitaria Pisana, Department of Diagnostic and Interventional Radiology, Pisa, Italy*

Purpose or Objective: The aim of this prospective study is the comparison of perfusion parameters changes (ΔCTPp) before and after radio-chemotherapy (RCT) and their correlation with maximum standard uptake values variations (ΔSUV max) among patients (pts) with head and neck tumor (HNT), in order to evaluate the prognostic value of perfusion CT parameters (CTPp) in predicting response to RCT.

Material and Methods: We enrolled pts with intermediate and advanced stage of HNT (stage III-IV), candidated to RCT with curative intent. All pts underwent to a pretreatment diagnostic and staging workup including perfusion CT (CTP) and FDG-PET/CT total body. Pts also perform a CTP 3 weeks after the end of RCT (CTP3w) and both CTP and PET/CT 3 months after the end of RCT (CTP3m and PET/CT repectively). We analised variations of following CTPp: Blood Flow (BF), Blood Volume (BV), Mean Transit Time (MTT) and Permeability-surface product (PS). All RCT treatments were performed using intensity modulated radiotherapy technique with simultaneous integrated boost. Prescribed doses were 66 Gy at 2.2 Gy per fraction to high risk volume PTV and 60-54 Gy at 2.0- 1.8 Gy per fraction respectively to intermediate (optional) and low risk PTVs, delivered in 30 daily fractions. Concurrent weekly Cisplatin 40 mg/ m2 or Cisplatin 100 mg/m2 day 1, 22 an 43 was offered to all pts.

Results: From July 2012 to July 2015 25 pts affected by stage III/IV HNT candidate to RCT were enrolled in our study. FDG-PET/CT 3 months after the end of RCT showed a complete metabolic response in 16 pts (64%), a partial metabolic response in 7 pts (28%), a stable metabolic disease in 1 pts and progression metabolic disease in 1 pts (according PERCIS criteria). A significant reduction of all CTPp was observed from baseline CTP to CTP3w, except for MTT that did not show a significant variation (p=0,722). The analysis of differences between baseline CTP and CTP3m showed a significant reduction of all CTPp (p<0,001), including MTT (p=0,001). PET/CT response resulted statistically correlated to reduction of all CTPp both at 3 weeks and at 3 months after the end of RCT, except for MTT (p=0,998 and 0,692). At the multivariate analysis the PS was the only parameter that maintain a statistical significance at CTP3m (p=0,037) with a significant trend also at CTP3w(p=0,099).

Conclusion: The induced damage on the intratumor microvascularization and low resistance flow of neoplastic vessels, explain the decrease of BV and BF whereas the reduction of neoangiogenesis phenomenon could explain the observed decrease of PS.Despite poor sample size, our preliminary results seem to be promising for a potential role of CTP to predict tumor response. PS seems the most valuable to predict the FDG-PET/CT tumor response. Due to the small sample size and short follow up, our results need to be confirmed in other series. Both funcional and morphological datas of the CTP can be usefull in order to reduce as much as possible the rate of false positive.

EP-1105

Impact of waiting time for treatment initation on glotic T1N0M0 cancer radiotherapy results

A. Mucha-Małecka[1], K. Urbanek[1], A. Chrostowska[1], J. Jakubowicz[2], P. Hebzda[1], K. Małecki[3]
[1]*Centre of Oncology - Institute MSC Kraków, Head and Neck Cancer, Krakow, Poland*
[2]*Centre of Oncology - Institute MSC Kraków, Clinic of Oncology, Krakow, Poland*
[3]*University Children's Hospital of Cracow, Radiotherapy of Children and Adults, Krakow, Poland*

Purpose or Objective: The goal of this study is was to evaluate the results of treatment of T1N0M0 glottic cancer with irradiation, with emphasis on the influence of time from diagnosis to the beginning of radiation therapy.

Material and Methods: We performed the retrospective analysis of the group of 539 patients with T1N0M0 glottic cancer, treated with radiation therapy in one institute between 1977 and 2004. In 481 cases (89%) the tumor was limited to single vocal cord and in the remaining 58 involved both of them. Anterior commisure involvement was observed in 173 (32%) of the patients. According to the radiotherapy technique and fractionation scheldule, we have divided patients into three separate groups: I - two oblique fields, TD 60 Gy/24 - 277 patients (51%); II - two opposite fields, TD 60 Gy/30 - 160 (31%); III - one lateral photon-electron beam, TD 60 Gy/30 - 102 (19%). The average time from laryngeal biopsy to the beginning of radiotherapy was 56 days (range: 3 -145 days).

Results: The 5-year OS and 10-year OS were 84% and 69%, 5- and 10-year DFS were 90% and 88%, and the 5- and 10-year LC rates were 89% and 87%, respectively. One- dimensional analysis revealed following prognostic factors for LC and DFS: tobbaco smoking, radiotherapy technique, and the anterior commisure involvement. The 5- and 10-year LC rates in the group of patients smoking less than 20 cigarettes a day were 90% and 87%, compared to 76% and 70%, respectively, in the group smoking more than 20 cigarettes a day (p=0,01). Considering the RT technique, the lowest 5- and 10-year LC rates were observed in the group treated with opposite beams (80% and 78%, respectively), and the highest when the oblique fields were used - 91% and 88%, respectively (p=0,002). The tumor involvement of the anterior commisure decreased 5-year LC by 15% (92 to 77%), and 10- year LC rate by 19% (89 to 70%, respectively, p=0,000). The waiting time for the beginning of RT longer than 30 days from the biopsy was statistically significant poor prognostic factor for DFS and LC. 5- and 10- year LC rates in the group of patients who started RT during the period of 30 days from the biopsy were 92% and 90%, respectively, and in the group which started treatment after that time, these LC rates were 84% and 82%, respectively (p=0,01).

Conclusion: Radiation therapy is efficient method of treatment the T1N0M0 glottic cancer. Prolonged time of waiting for the beginning of RT decreases the LC and DFS rates

EP-1106

A prospective novative docetaxel-based neoadjuvant chemotherapy for advanced head and neck cancer

Y. Ting Shih[3], Y.C. Liu[1], M.D. Po-Ju Lin[2], M.D.-P.D. Jin-Ching Lin[1]
[1]*Taichung Veterans General Hospital, RadioOncology Department, Taichung, Taiwan*
[2]*Tung's Taichung MetroHarbor Hospital, Radiation Oncology Department, Taichung, Taiwan*
[3]*St. Martin De Porres Hospital, Radiation Oncology Department, Chiayi, Taiwan*

Purpose or Objective: To evaluate the overall response rate and access the toxicity for patients with locally advanced squamous cell carcinoma of head and neck (HNSCC) receiving a novative docetaxel-based outpatient neoadjuvant chemotherapy regimen.

Material and Methods: The inclusion criteria for this prospective study are (1)Age≧20 years old (2) Histologically proven squamous cell carcinoma of the oral cavity, oropharynx, hypopharynx, or larynx (3)Stage III or stage IVA or IVB without distant metastasis, (4) No prior chemotherapy given for HNSCC (5) Physician's intention to treat with docetaxel- baed induction therapy (6) Patients' informed consent will be obtained. Tumor response for induction chemotherapy will be evaluated in patient with measurable disease according to institutional guidance. The induction chemotherapy regimen is a novative outpatient regimen. This regimen consists of cisplatin 60mg/m2 on day 1, docetaxel 50 mg/m2 on day 8, 5-Fu 2500 mg/m2 and leucovorin 250 mg/m2 on day 15, and methotrexate 30 mg/m2 and epirubicin 30 mg/m2 on day 21, cycles will be repeated for a total 3 to 4 cycles followed by surgery or radiotherapy. Responses rate will be reported using *Response Evaluation Criteria In Solid Tumors* (RECIST) criteria in patients with at least one measurable lesion. Toxicity will be recoreded using the NCI-CTC v.4.03.

Results: From September 2011 to December 2013, 80 patients were enrolled and two patients withdrew consent, finally 78 patients included for analysis. There were 73 male and 5 female. There were 96.2% of them had 0-1 WHO ECOG. For the primary site, 23(29.5%) patients were oral cavity, 26 (33.3%) patients were oropharynx, 24(30.8%) patients were hypopharynx, and 5 (6.4%) patients were larynx. Treatment compliance was well. There were 92.3% patients completed planned schedule. After the induction chemotherapy, the overall response rate were 92.3%, which included 37.2% complete response and 55.1% partial response, respectively. Only 2(2.6%) patients had stable disease and 1(1.3%) patient had progression disease. The response rate of oral cavity, oropharynx, hypopharynx, and larynx were 82.6%, 92.3%, 100%, 100%, respectively. There were 47.4% grade 3 or 4 neutropenia and 20.5% grade 3 anemia. Only 6 severe adverse event were report, including 4 febrile neutropenia with sepsis, one osteomyelitis, and one massive bleeding.

Conclusion: This outpatient docetaxel-based neoadjuvant chemotherapy regimen is a effective regimen in locally advanced squamous cell carcinoma of head and neck.

EP-1107

Impact of waiting time for treatment initation on glotic T1N0M0 squamous cell carcinoma RT results

A. Mucha-Malecka[1], K. Urbanek[1], A. Chrostowska[1], K. Malecki[2], P. Hebzda[1], J. Jakubowicz[1]
[1]*Center of Oncology, Head and Neck Department, Kraków, Poland*
[2]*University Children's Hospital of Krakow, Department of Radiotherapy of Children and Adults, Krakow, Poland*

Purpose or Objective: The goal of this study is was to evaluate the results of treatment of T1N0M0 glottic cancer with irradiation, with emphasis on the influence of time from diagnosis to the beginning of radiation therapy.

Material and Methods: We performed the retrospective analysis of the group of 539 patients with T1N0M0 glottic cancer, treated with radiation therapy in the Center of Oncology in Cracow between years 1977 and 2004. In 481 cases (89%) the tumor was limited to single vocal cord and in the remaining 58 involved both of them. Anterior commisure involvement was observed in 173 (32%) of the patients. According to the radiotherapy technique and fractionation scheldule, we have divided patients into three separate groups: I - two oblique fields, TD 60 Gy/24 - 277 patients (51%); II - two opposite fields, TD 60 Gy/30 - 160 (31%); III - one lateral photon-electron beam, TD 60 Gy/30 - 102 (19%). The average time from laryngeal biopsy to the beginning of radiotherapy was 56 days (range: 3 -145 days). The overall survival (OS) and disease- free survival (DFS) were calculated using the Kaplan - Meier method. Log - rank test was used to calculate differences between each groups, and the independent prognostic factors were selected by the Cox multiparameter analysis.

Results: The 5-year OS and 10-year OS were 84% and 69%, 5- and 10-year DFS were 90% and 88%, and the 5- and 10-year LC rates were 89% and 87%, respectively. One- dimensional analysis revealed following prognostic factors for LC and DFS: tobbaco smoking, radiotherapy technique, and the anterior commisure involvement. The 5- and 10-year LC rates in the group of patients smoking less than 20 cigarettes a day were 90% and 87%, compared to 76% and 70%, respectively, in the group smoking more than 20 cigarettes a day (p=0,01). Considering the RT technique, the lowest 5- and 10-year LC rates were observed in the group treated with opposite beams (80% and 78%, respectively), and the highest when the oblique fields were used - 91% and 88%, respectively (p=0,002). The tumor involvement of the anterior commisure decreased 5-year LC by 15% (92 to 77%), and 10- year LC rate by 19% (89 to 70%, respectively, p=0,000). The waiting time for the beginning of RT longer than 30 days from the biopsy was statistically significant poor prognostic factor for DFS and LC. 5- and 10- year LC rates in the group of patients who started RT during the period of 30 days from the biopsy were 92% and 90%, respectively, and in the group which started treatment after that time, these LC rates were 84% and 82%, respectively (p=0,01). Tumor interior commisure involvement was proven to be an independent prognostic factor affecting DFS and LC.

Conclusion:

1. Radiation therapy is efficient method of treatment the T1N0M0 glottic cancer
2. Prolonged time of waiting for the beginning of RT decreases the LC and DFS rates
3. The tumor involvement of anterior laryngeal commisure proved to be an independent adverse prognostic factor for LC and DFS

EP-1108

Chemoimmunotherapy with hyperfractionated radiotherapy in head and neck carcinoma.

R. Carmona Vigo[1], J.M. Blanco[1], M. Lloret[1], R. Cabrera[1], P.C. Lara[1]
[1]*Hospital Dr. Negrín, Radiation Oncology, Las Palmas de Gran Canaria, Spain*

Purpose or Objective: The aim of the present study is to analyze clinical outcomes and toxicity in patients with locoregionally advanced head and neck carcinoma treated with concurrent hyperfractionated radiotherapy with Cetuximab and Carboplatin.

Material and Methods: Forty-one patients (8 cases ST.III and 33 cases ST.IV) were prospectively included in this study from September 2009 to November 2014. Radiotherapy consisted in hyperfractionated radiotherapy: 1.15-1.20 Gy/fraction, BID, 5 days/week during 7 weeks. The average dose administered was 80.2 Gy (79.2-80.5). Carboplatin was administered 5 mg/m2 before each fraction of radiotherapy. Cetuximab was administered 400 mg/m2 one week before hyperfractionated radiotherapy and then 250 mg/m2 weekly while radiotherapy. Seven patients were not evaluable for response (in 3 patients, Capecitabine was added to the treatment; in 1 patient nodal metastases came from a papillary thyroid carcinoma; 3 patients were not evaluable for response because 2 patients died within 30 days after treatment and 1 patient has not enough follow-up to be evaluated for response).

Results: All but 2 of the 34 evaluable patients showed objective response (19 complete responses). The local relapse-free survival, cause specific survival, and overall survival was 58.7%, 57%, 49% at 5 years, respectively. Severe (GradeII/III) acneiform rash resulted predictive of Clinical Response (p=0,005), Local relapse (p=0,008), distant metastases (p=0,012) and tumour related dead free survival (p<0,0001). Severe (Grade III) acute cutaneous and mucosal toxicity was present in almost 60% of the cases.

Conclusion: This protocol induces a high rate of clinical responses and excellent survival figures in patients developing an strong immune response after combined radio-chemoimmunotherapy.

EP-1109

Role of adjuvant EBRT for papillary thyroid carcinoma invading the trachea: a single-instn study

Y.S. Kim[1], J.H. Choi[2], K.S. Kim[2], G.C. Lim[3], J.H. Kim[3], H.S. Song[4], S.A. Lee[5], G. Koh[5], C.L. Hyun[6], G.E. Kim[1]
[1]*Jeju National University Hospital, Department of Radiation Oncology, Jeju, Korea Republic of*
[2]*Jeju National University Hospital, Department of Surgery, Jeju, Korea Republic of*
[3]*Jeju National University Hospital, Department of Otorhinolaryngology, Jeju, Korea Republic of*
[4]*Jeju National University Hospital, Department of Nuclear Medicine and Molecular Imaging, Jeju, Korea Republic of*
[5]*Jeju National University Hospital, Department of Internal Medicine, Jeju, Korea Republic of*

[6]*Jeju National University Hospital, Department of Pathology, Jeju, Korea Republic of*

Purpose or Objective: The current standard of care for newly diagnosed papillary thyroid carcinoma invading the trachea is surgical resection followed by radioactive iodine therapy (RAI) and thyroid stimulating hormone suppression. However, the local recurrence rate is high. Several studies reported adjuvant external beam radiotherapy (EBRT) reduced the local recurrence. The benefit of adjuvant EBRT remains controversial. We evaluated the effect of adjuvant EBRT on local control in a single institution database.

Material and Methods: Between May 2003 and October 2013, 36 patients with locally advanced papillary thyroid carcinoma invading the trachea (pathologic stage T4) were treated with surgical resection. After surgery, 16 patients received adjuvant EBRT using intensity modulated radiation therapy followed by RAI, and 20 patients were treated with RAI alone. The age range was 36-87 years (median 64 years). EBRT doses ranged from 30-66 Gy (median 60 Gy). There was no statistically significant difference in terms of clinical characteristics between the EBRT and no EBRT groups.

Results: Median follow up was 26.6 months (range, 16.5-40.1) in EBRT group, and 43.9 months (range, 13.9-117.6) in no EBRT group. There was no local or distant failure in EBRT group during the follow up. There were five local failures and one distant failure in no EBRT group. The two-year & five-year local failure free survival rates were 95.0% and 49.8% in no EBRT group. There were acute grade 2 esophagitis (n=1) and grade 2 skin reaction (n=3). There were no grade 2 late complications in EBRT group.

Conclusion: Adjuvant EBRT was found to be an effective treatment for local control in papillary thyroid carcinoma invading the trachea with tolerable complications, in a study at a single institution. Longer follow up will be required to demonstrate outcomes for tumor control and complications

EP-1110

Combination of RT and cetuximab for aggressive, high-risk CSCC of h&n: a propensity score analysis

A. Raben[1], J.D. Palmer[2], J. Strasser[1], A. Hanlon[3], M. Dzeda[1], N. Hockstein[4], C.J. Schneider[5]

[1]*Helen F. Graham Cancer Center, Radiation Oncology, Newark- DE, USA*

[2]*Sidney Kimmel Medical College at Thomas Jefferson University, Radiation Oncology, Philidelphia, USA*

[3]*University of Pennsylvania, Department of Nursing, Philadelphia, USA*

[4]*Helen F. Graham Cancer Center, Medical Oncology, Newark-DE, USA*

[5]*Helen F. Graham Cancer Center, Surgery, Newark- DE, USA*

Purpose or Objective: Locally advanced, high-risk cutaneous squamous cell carcinoma (CSCC) of the head and neck are typically aggressive and treated with combined modality therapy. These patients tend to be older, frail with multiple comorbidities which makes chemotherapy difficult to tolerate. Cetuximab is a monoclonal antibody against the EGFR receptor and has demonstrated activity in CSCC. We investigate the safety and efficacy of combined therapy in advanced, high risk CSCC with the addition of cetuximab.

Material and Methods: Patients were identified with locally advanced CSCC with high risk or very high risk features who were treated with cetuximab and radiotherapy between 2006 and 2013. A matched cohort over the same time period was identified who were treated with radiation. Propensity score analysis was performed with weighted factors including: Charlson Comorbidity Index score (age-adjusted), age. KPS, primary location, T and N stage, recurrent status, margin status, LVSI, PNI and grade. Overall survival, progression free survival and freedom from local or distant recurrence were evaluated with the Kaplan-Meier method for both the un-adjusted and propensity score adjusted groups. Multivariate analysis was performed using cox proportional hazard models.

Results: 29 patients were in the cetuximab and 39 in the control group. Median follow-up for alive patients was 30 months. Patients in the cetuximab group were more likely to have advanced N stage, positive margins and recurrent disease. After propensity score matching the groups were well balanced. OS was not statistically significant between the two groups but depicted in Table 1 below there were approximately 20% more long term survivors in the cetuximab group after matching. Local control was 76% and 79% in the cetuximab and control groups, respectively. The rate of distant metastases was lower in the cetuximab group 6.8% versus 10%. The incidence of grade 2-3 toxicity was 41% in the cetuximab group. There was one grade 3 cetuximab acneiform rash, one grade 4 dysphagia and no grade 5 toxicity.

Table 1 Overall Survival Probabilities by year in both unadjusted and Propensity Score Adjusted Cohorts

Years:		1	2	3	4	5
Unadjusted	Cetuximab	96%	74%	74%	74%	74%
	No Cetuximab	93%	85%	75%	69%	69%
Propensity Score Adjusted	Cetuximab	98%	80%	80%	80%	80%
	No Cetuximab	81%	73%	66%	61%	61%

Conclusion: Although limited by small numbers, we found that there were more long-term survivors and less distant metastasis in the cetuximab group. This is the largest report of CSCC patients treated with cetuximab. In the absence of prospective data, we believe this data reveals that the addition of cetuximab is well tolerated and reveals signs of efficacy in this typically poor performing group of patients and should be pursued in clinical trials.

Electronic Poster: Clinical track: CNS

EP-1111

A cut point for Ki-67 proliferation that predicts for poorer survival in high-grade glioma

E. Wong[1], P. Sundaresan[2], W. Varikatt[3], V. Gebski[2], N. Nahar[2], T. Ng[3], J. Jayamohan[2]

[1]*The University of Sydney, Sydney Medical School, Sydney, Australia*

[2]*Crown Princess Mary Cancer Center- Westmead, Radiation Oncology, Sydney- NSW, Australia*

[3]*Westmead Hospital, Department of Tissue Pathology & Diagnostic Oncology, Sydney, Australia*

Purpose or Objective: Ki-67 index is used to assess cell proliferation during histopathological assessment of various tumours including high grade gliomas (HGG): Anaplastic astrocytoma, Anaplastic Oligodendroglioma and Glioblastoma Multiforme (GBM). We aimed to determine if there is a correlation between percentage staining of Ki-67 and overall survival in patients with HGG and determine a cut-point for percentage staining of Ki-67 that predicts for poorer survival.

Material and Methods: Records of adult patients diagnosed with HGG on histopathological specimens examined at the Institute of Clinical Pathology and Medical Research at Westmead Hospital, NSW, between 1st of January 2002 and 30th of July 2012 were identified. The specimens of these patients were examined for quantification of Ki-67 staining by two independent pathologists. Patient, disease, treatment and survival data were collected from hospital and cancer care service records. Descriptive statistical analyses were performed on the patient, disease and treatment data. Survival curves were constructed using Kaplan Meir methods. Using the minimum p value approach we obtained a cut-point for Ki-67 percentage staining that predicts for poorer survival.

Results: Of the eligible 78 patients (median age = 57, range 18 - 87) 46 (59 %) were males and 32 (41%) were females. 59 (76%) patients were of ECOG performance status 0 -1. Seven patients had anaplastic astrocytoma or anaplastic

oligodendroglioma and the rest had GBM. There was a clear inverse correlation between Ki-67 percentage staining and overall survival. In patients with Ki-67 ≤ 30% (n=18), 5 year survival was approximately 50% compared to those with Ki-67 >30% (n=60) with survival of 10% (logrank P-value 0.02, HR 0.39, 95% CI 0.17 – 0.88).

Conclusion: There appears to be a correlation between percentage staining of Ki-67 and overall survival in patients with HGG. Percentage staining of Ki-67 > 30% appears to predict for poorer survival in HGG.

EP-1112

Optic toxicity in radiation treatment of meningioma: a retrospective study in 213 patients

M. Farzin[1], M. Molls[1], S. Kampfer[1], S. Astner[1], R. Schneider[2], K. Roth[1], M. Dobrei[3], S. Combs[1], C. Straube[1]
[1]*Klinikum rechts der Isar- TU München, Radiation- Oncology, München, Germany*
[2]*Paul Scherrer Institute, proton therapy, zurich, Switzerland*
[3]*Kliniken Kreis Mühldorf am Inn, Innere Abteilung, Mühldorf, Germany*

Purpose or Objective: Background and purpose:In this retrospective evaluation, we correlated radiation dose parameters with occurrence of optical radiation-induced toxicities.

Material and Methods: Patients and methods:213 meningiomapatientsreceived radiation between 2000 and 2013. Radiation dose and clinical datawere extracted from planning systems and patients' files. The range of follow-up period was 2-159 months (median:75 months).

Results: Results:Median age of patients was 60 years (range: 23-86). There were163 female and 50 male patients. In 140 cases, at least one of the neuro-optic structures (optic nerves and chiasm) was inside the irradiatedtarget volumes. We found 15 dry eye (7%) and 24 cataract (11.2%) cases. Median dose to affected lachrymal glands was 1.47Gy and median dose to affected lenses was1.05Gy. Age and blood cholesterol level in patients with cataract were significantly higher. Patients with dry eye were significantly older. Only 2 patients with visual problems attributable to radiation treatment (RION) were seen. They did not have any risk factors. Maximum and median delivered doses to neuro-optic structures were not higher than 57.30Gy and 54.60Gy respectively.

Conclusion: Conclusion:Low percentages of cases with radiation induced high grade optic toxicities show that modern treatment techniques and doses are safe. In very few patients with optic side effects, doses to organs at risk were higher than the defined constraint doses. This observation leads to the problem of additional risk factors coming into play. The role of risk factors and safety of higher radiation doses in high grade meningiomas should be investigated in more comprehensive studies.

EP-1113

Light seeing in radiotherapy of patients with brain tumours and head and neck malignancies

M. Farzin[1], M. Molls[1], S. Astner[1], S. Reitz[1], K. Kreiser[2], S. Kampfer[1]
[1]*Klinikum rechts der Isar- TU München, Radiation- Oncology, München, Germany*
[2]*Klinikum rechts der Isar- TU München, Department of Neuroradiology, München, Germany*

Purpose or Objective: Evaluating the radiation doses delivered to different parts of the visual pathway for better understanding of light vision in radiotherapy patients.

Material and Methods: 20 patients with brain tumors and head and neck malignancies who received radiotherapy and experienced any kind of light or color vision during radiation treatment. All the components of visual pathway including lenses, eyeballs, retinas, optic nerves, chiasm, optic tracts, optic radiations and visual occipital cortexes were contoured.

Results: 11 patients were male (55%) and 9 were female (45%). Age median was 56 years. The range of dose/fraction and total prescribed dose were 1.8-3 Gy and 36-70.4 Gy respectively. Twelve patients reported white, 11, blue, 2, yellow and 2, gray color visions. Seven patients experienced more than one color, while 2 patients did not attribute any special color to their light seeing experiences. Four patients had a kind of smell experience and 1 patient had a taste experience.

Conclusion: Cherenkov radiation in eye ballsmay be the origin of light seeing experiences in patients receiving radiation treatment for head and neck malignancies, since treatmentsareperformed with ionizing radiations with energycapable to produce this effect. Also this effectmay be due to phosphenes produced by radiation treatment in different parts of the visual pathway (from retina to visual cortex). In order to investigate the mechanism of this phenomenon in patients and to define a radiation dose threshold – if the origin of this phenomenon is phosphenes produced in visual pathway – larger studies are needed.

EP-1114

Clinical outcomes in modern management of infratentorial ependymoma

R. Allison[1], D. Remonde[2], S. Salenius[3], A. Hnatov[1], C. Ballenger[1], C. Mantz[4], E. Fernandez[4], D. Dosoretz[4], S. Finkelstein[5]
[1]*21st Century Oncology, Radiation Oncology, Greenville, USA*
[2]*East Carolina University, The Brody School of Medicine, Greenville, USA*
[3]*21st Century Oncology, Research, Fort Myers, USA*
[4]*21st Century Oncology, Radiation Oncology, Fort Myers, USA*
[5]*21st Century Oncology, Radiation Oncology, Scottsdale, USA*

Purpose or Objective: Ependymomas are central nervous system (CNS) tumors that due to their rare prevalence have considerable controversy regarding their prognostic factors and clinical management. As such, many of the reported series involve accumulation of patient data that spans many decades, making current management decisions difficult. In this study, we report the outcomes and possible prognostic factors of patients with histologically confirmed infratentorial ependymomas treated in the modern era.

Material and Methods: A retrospective chart review of our patient registry was conducted to identify 15 patients diagnosed with infratentorial ependymoma between 2007—2013. Mean age at diagnosis was 29 years (range 1.0—79.0 years). There were 8 males and 7 females, with headache being the most common presenting symptom among the entire cohort. Eleven were newly diagnosed with ependymoma and the remaining 4 were recurrent patients who had failed primary therapy. Of the newly diagnosed patients, all received surgery and post-operative radiation therapy (RT) with a mean dose of 54.3 Gy (range 45.0—59.4 Gy). Two also received chemotherapy. Patients in the recurrent group experienced only local recurrences after initial treatment and underwent salvage RT with a mean dose of 45.6 Gy (range 15.0—59.4 Gy).

Results: With a mean follow-up time of 15 months (range 1.4—61.7 months) for the cohort, a significant difference in overall survival (OS) was found between primary and recurrent patients (p=0.0082). Overall, 9 patients (60%) had no acute complications with the remainder Grade I or II following initial treatment. All were free of late complications throughout follow-up. Moreover, there were no statistically significant differences in OS or local control when tumor size or RT dose were analyzed.

Conclusion: Our findings indicate that recurrence is a prognostic factor for decreased OS in patients with infratentorial ependymomas. Involved field radiation therapy following surgical resection of these tumors offers high local

control rates and may ultimately improve OS. The combination of surgery followed by RT appears to be the current standard of care.

EP-1115

Stereotactic radiosurgery for brain metastases: neuropathological report of three autopsy cases

M. Sakuramachi[1], H. Igaki[2], A. Nomoto[1], N. Sekiya[1], W. Takahashi[1], K. Ookuma[1], M. Ikemura[3], H. Yamashita[1], K. Nakagawa[1]
[1]*Tokyo University, Radiology, Tokyo, Japan*
[2]*National Cancer Center, Radiation Oncology, Tokyo, Japan*
[3]*Tokyo University, Pathology, Tokyo, Japan*

Purpose or Objective: To elucidate the radiobiological effects of stereotactic radiosurgery (SRS) on brain metastases using autopsy cases.

Material and Methods: From 1995 to 2013, 9 brain specimens from 3 patients were available. They underwent autopsy after SRS in our hospital. These specimens were all brain metastases. The timing of autopsy was from 7 days to 20 months (median 10 months) after SRS. The 9 tumors received a margin dose of 16–20 Gy (median 20 Gy) at the 40–75% isodose line (median 40%), with a maximal dose of 16–50 Gy (median 45 Gy). Histopathological investigations were performed. The specimens were fixed in 20% neutral buffered formaldehyde and embedded in paraffin. Hematoxylin-eosin, Azan-Mallory, and Bodian stains were used. Immunohistochemical reactions included glial fibrillary acidic protein, alpha-smooth muscle actin, CD34, and CD68 antigens. Ki67 and p53 reactions were also used.

Results: The first case was a 59-year-old man diagnosed with 2 brain metastases from renal cell carcinoma. Both lesions were irradiated with SRS. He received SRS 4 times after the first SRS. At 1 week after the last SRS, he died from carcinomatous lymphangiosis. The second case was a 63-year-old man diagnosed with 2 brain metastases from lung cancer. Both lesions were irradiated with SRS plus whole brain radiotherapy (WBRT). Seven months later, he died from carcinomatous peritonitis. The third case was a 35-year-old woman diagnosed with 2 brain metastases from breast cancer. Both lesions were irradiated with WBRT plus SRS. When one of the lesions enlarged 1 year later, repeated SRS was performed. At 7 months after reirradiation, she died from carcinomatous lymphangiosis. In the first case, necrosis and viable tumor cells were observed mainly in the center of the lesion at 1 week after SRS, while apoptosis and fibrosis were observed in a small part of the lesion. Glial cells and neutrophilic leukocytes had accumulated around the lesion. In the lesions at 2 months after SRS, tumor cells and fibrosis were not observed; only macrophages and glial cells were observed in the SRS irradiated field. In the second case, fibrosis was observed at the periphery of the center necrotic region at 7 months after SRS. In the third case, almost all parts of the lesions were replaced with fibrosis at 19 months after SRS, while small foci of viable tumor cells, a large number of glial cells, and macrophages were observed around the fibrotic area.

Conclusion: In the tumors, apoptosis was only observed at 1 week after SRS. The time of fibrosis initiation varied in each case. Around the tumors, neutrophilic leukocytes and glial cells accumulated within 1 week after SRS. Macrophages accumulated at least 2 months after SRS. Stromal changes remained for a considerable period of time. It was remarkable that fibrosis occurred very soon after SRS, and other observations were generally compatible with previous reports.

EP-1116

Staged radiosurgery for petroclival meningiomas: preliminary results

V. Pinzi[1], M. Marchetti[1], I. Milanesi[1], E. De Martin[2], L. Fariselli[1]
[1]*IRCCS Istituto C. Besta, Neurosurgery Radiotherapy Unit, Milan, Italy*
[2]*IRCCS Istituto C. Besta, Health Department-, Milan, Italy*

Purpose or Objective: The goal of surgical treatment of meningiomas is the total resection of the tumour. The complete removal of petroclival meningiomas can be difficult because of their proximity to cranial nerves. Stereotactic radiosurgery (SRS) is a well established treatment for many patients with intracranial meningiomas, either in the exclusive or adjuvant setting. However, SRS of large meningiomas might be associated with significant morbidity. Under these circumstances s-SRS has the potential to deliver sharply focused high doses per fraction without increasing the risk of toxicity.The aim of this study is to prospectively evaluate the feasibility of s-SRS for petroclival meningiomas, including large volume lesions.

Material and Methods: Between September 2011 and October 2013 at our Institute, s-SRS using the CyberKnife was prospectively performed on 30 patients (24 women and 6 men, men, mean age 57 years) with petroclival meningiomas. Patients with atypical or malignant meningiomas and those who had received prior radiotherapy were excluded. The average tumor volume was 11,86 cm3 (range 2,2–126,3 cm3); the average tumor prescription dose was 24,4 Gy, the number of fraction was 4 or 5.

Results: After a median follow-up of 30 months (range 13-36 months) the overall tumour control rate was 100% (25 patients with stable disease, 3 patients with partial response and 2 patients with complete response). Tumor control rates at 2 and 3 years was 100%. Among 28 patients who were symptomatic before staged radiosurgery, neurological follow-up showed an improvement in 43%, stable clinical course in 43% and a persistent deterioration of clinical symptoms in 14% of the patients. A transient neurological deterioration was observed in 11% of patients within the first year after treatment.

Conclusion: Our findings show that s-SRS using the CyberKnife is a safe and effective option in the treatment of large-volume petroclival meningiomas. A good tumour control and a low morbidity rate was achieved in our series, either as a primary or adjuvant approach. Long-term follow-up is warranted to confirm these results.

EP-1117

Frameless radiosurgery for acoustic schwannoma: a five-year experience

S. Payano Hernandez[1], O. Hernando Requejo[1], M. Lopez Gonzalez[1], E. Sanchez Saugar[1], M. Garcia-Aranda Pez[1], J. Valero Albarrán[1], A. Montero Luis[1], R. Ciervide Jurio[1], A. Rodriguez[1], R. Alonso[1], X. Chen[1], C. Rubio Rodriguez[1], R. Guimaraes Domingos da Silva[1]
[1]*Hospital Universitario Madrid Sanchinarro - Grupo Hospital de Madrid, Oncologia Radioterápica, Madrid, Spain*

Purpose or Objective: Frameless radiosurgery (SRS) plays an important role in the management of acoustic neuromas. This retrospective study aims to evaluate tumor control using this technique.

Material and Methods: Thirty four patients with unilateral acoustic neuromas (vestibular schwannomas) who underwent linear accelerator-based frameless SRS at low dose (12 Gy) to the tumor from July 2008 to February 2015 were evaluated. Twenty-one patients were male and 13 patients were female. The median age was 62 years (range 23-84) with a median follow-up period of 12.4 months (range 1-60). Treatment volume was 0.1 to 3.8 cm3 (median 0.93 cm3).

Results: Preliminary results from follow-up magnetic resonance imaging (MRI) showed: the tumor of 15 patients decreased in diameter, no changes was found in 14 and the tumor increased slightly in only one patient. All patients are alive, except for 1p who died from intercurrent disease 2 years after radiosurgery. Among 23p with acufeno, full improvement was demonstrated in four. There were no reported complications related to treatment.

Conclusion: We experienced excellent short term local control and low incidence of complication for acoustic schwannomas undergoing frameless SRS treatment. Our data compare favorably with the literature. Additional follow-up will be necessary to evaluate long term results of treatment.

EP-1118

Impact of susceptibility-weighted imaging MRI on radiosurgery for melanoma and RCC brain metastases

A. Klimov[1,2], S. Rogers[2], L. Boxheimer[3], S. Bodis[2]
[1]*Saint Petersburg State University, Faculty of Surgery, Saint Petersburg, Russian Federation*
[2]*Canton Hospital Aarau, Institute of Radiation Oncology, Aarau, Switzerland*
[3]*Canton Hospital Aarau, Department of Neuro-radiology, Aarau, Switzerland*

Purpose or Objective: A patient with malignant melanoma and 4 visible lesions on a gadolinium (Gd)-enhanced T1 MRI scan of the brain was reported at the tumor board as having at least 7 probable metastases on the basis of the matching susceptibility-weighted imaging (SWI). SWI detects cerebral microbleeds and may therefore be more sensitive than Gd-T1 MRI in the detection of small haemorrhagic metastases and prediction of future sites of intra-cranial relapse. Our aim was to explore the potential usefulness of SWI in 1) the selection for radiosurgery and 2) the follow-up of patients with brain metastases from malignant melanoma and renal cell carcinoma (RCC).

Material and Methods: At the time of referral for radiosurgery, a 3-D Gd-T1 MRI was evaluated at the neuro-oncology multidisciplinary tumor board to determine the number of brain metastases. We retrospectively analysed the synchronous SWI sequence to explore any difference in the number of detectable lesions and hence putative metastases. Subsequent enhanced T1-weighted MRIs were evaluated for new metastases at the site of SWI abnormalities.

Results: T1 MRI scans detected 16 metastases in a sample of 11 patients with melanoma and RCC who were treated with primary or postoperative linear accelerator-based radiosurgery in our center. 25 regions of signal change were detectable on the matching SWI sequences. The scans were reviewed by a board-certified neuro-radiologist who confirmed that the 9 additional SWI lesions were non-metatastic. To date, none of the additional lesions have developed into enhancing brain metastases. Indeed, additional SWI changes on postoperative imaging resolved completely on subsequent imaging. Thus the 16 SWI changes with metastatic features correlated perfectly with the 16 metastases on Gd-T1 MRI. (Figure 1)

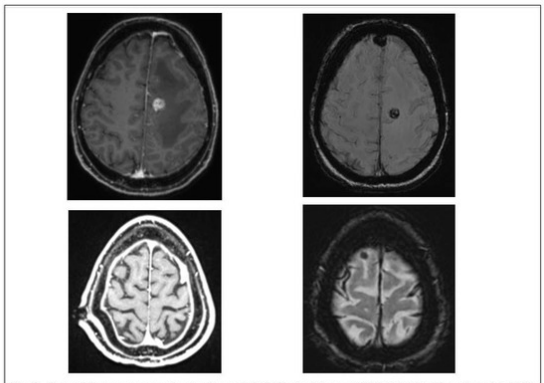

Fig 1. Top: Melanoma metastasis on T1 MRI (left) and SWI (right). The frontal SWI change is falcine calcification. Bottom: The SWI signal change (right) has no T1 correlate (left) and represents postoperative blood.

Conclusion: SWI sensitively detects blood products in primary and secondary brain tumours, but also in veins, vascular malformations and postop-operative bleeding and calcification. An expert neuro-radiology opinion in the context of the tumour board is essential for the accurate interpretation of SWI to avoid "overdiagnosis" of metastases, particularly in the post-operative setting. Occasionally however, additional lesions that are highly suspicious for metastases may be detected on SWI. The sensitivity and specificity of SWI for metastases should be determined in a larger cohort as it may assist patient selection for radiosurgery in borderline cases.

EP-1119

Treatment of Subependymal giant cell astrocytoma (SEGA): Is there a place for radiotherapy?

R. Atef Kamel[1]
[1]*Universitair Ziekenhuis Brussel, Department Radiotherapy, Brussels, Belgium*

Purpose or Objective: SEGA is a WHO grade I glioma that is almost exclusively seen in young patients with tuberous sclerosis complex (TSC). Despite the benign histology, SEGA can be severely symptomatic as it typically arises intraventricularly and can cause obstructive hydrocephalus. The current standard treatment of SEGA includes surgical resection and chemotherapy, the m-TOR inhibitor everolimus. Based on expert opinion, there is an international consensus that radiotherapy should not be used in the treatment of SEGA.
Here, we present a case of a patient with TSC, with inoperable bilateral ventricular SEGA. Years long before the availability of everolimus or its approval for treating SEGA, we treated this patient exclusively with radiotherapy.

Material and Methods: With stereotactic fractionated radiotherapy, a dose of 60 Gy in 30 fractions of 2 Gy, was delivered on the GTV. The patient was afterwards followed up with MR imaging. We did volumetric assessment of tumour size on each follow up MRI and tracked the changes in tumour size after radiotherapy.
We performed an extensive literature study to verify the sources of the consensus against radiotherapy in treatment of SEGA.

Results: The patient tolerated the treatment very well. No acute or chronic side effects were seen. A follow up over a period of 8 years, using MR imaging, showed about 70% decrease in tumour volume.
We found that the advice against radiotherapy appears to be based on very little, if any, evidence.

Conclusion: Radiotherapy can be a potential useful tool in the treatment of SEGA. The slow but progressive response of SEGA to radiotherapy resembles what is seen in other benign brain tumors e.g. meningioma. Radiotherapy has been discarded prematurely as a therapeutic option for SEGA and could be very well used to consolidate effect of everolimus. Prospective registration of patients and treatment outcome is needed to enhance knowledge.

EP-1120

Experience with robotic SBRT in treatment of intraspinal tumours

R. Garcia[1], A. Velazquez-Pacheco[1], I. Marrone[1], I. Santa-Olalla[1]
[1]*Instituto Madrileno de Oncologia, Centro de Radioterapia y Radiocirugía Robotizada Cyberknife, Madrid, Spain*

Purpose or Objective: The role of radiotherapy in the treatment of intraspinal tumors constitutes a paradigm, justified by tolerance of spinal cord. Advances in SBRT (Stereotactic Body Radiation Therapy) as robotic and image-guided treatments have revolutionized in this group. The aim of this study is to analyze our preliminary experience treating intraspinal tumors using robotic SBRT.

Material and Methods: Clinical and dosimetric data on 19 patients between 2011 and 2015 were reviewed, patients with lesions in spinal canal including intramedullary and intradural extramedullary were selected solely. All patients were treated with robotic SBRT image-guided in real time (Cyberknife).

Results: A total of 26 lesions were included in the analysis. Median follow-up was 14 months (3-41 months). Thirteen were metastatic lesions with histology as breast cancer, medulloblastoma, adenoid cystic among others. Response rates were: 31% complete response and partial response / stable at 69%. 13 benign lesions highlighting arteriovenous malformations, neurofibroma and melanocytoma. Response rates for this group: complete response in 8%, partial response / stable at 92%. During the follow-up time only 5 patients had relapsed 100% to distance. Median overall average dose was 21 Gy (14-35 Gy), the median was three fractions (1-5 Fractions), median prescription isodose was 83% (77-88%) with an average coverage of 97.27% (93.13-100%). There were no data as myelopathy Grade II associated to treatment in the whole cohort, the most common symptom after treatment was fatigue.

Conclusion: The treatment of intraspinal tumors with image-guided robotic SBRT, has proven to be a feasible,safe and effective option for treatment, where treatment options are scarce. In our experience, the data are encouraging and comparable with those reported by other authors.

EP-1121

Treatment outcome of adult brain stem Glioma: a single institution experience

S. Chaudry[1], A. Rashid[1], S. Butt[1], A. Rashid[1], S. Hameed[1], A. Jamshed[1]

[1]*Shaukat Khanum Memorial Cancer Hospital, Radiation Oncology, Lahore, Pakistan*

Purpose or Objective: Adult brain stem gliomas are rare accounting for 1-2% of adult gliomas. They are heterogeneous with varying clinical and radiological presentation. Prognosis remains poor because of limited surgical options and radiotherapy still remains the main treatment option. We report our clinical experience of treating brain stem glioma.

Material and Methods: A Retrospective review was made to analyze the clinical presentation, diagnosis, treatment outcome and survival in adult brain stem glioma patients treated at Shaukat Khanum Memorial Cancer Hospital Lahore. Between July 2007 and August 2014.

Results: 46 patients were identified from Hospital record system. Diagnosis was mostly based on radiological findings with MRI brain and biopsy was done only in 11 patients. 98% of the patients were treated with radiotherapy as a first line treatment on presentation and 1 patient was kept under close surveillance which was treated on progression. Median radiotherapy dose used ranged between (20-60Gy) with a median dose of 51Gy. Age of the patients ranged from 18 to 72 years (median 33 years) with a Male to female ratio of 3:1.Median follow up duration was 9 months (range 1-72). Radiological response was seen in 65% (13% partial & 52% stable) of the patients. The median overall survival (OS) for entire cohort was 10 months. One and two year OS rates were 46% and 25% respectively. Radiological Low grade Glioma showed a median survival of 11.5 months and was found to be 9.5 months for High grade Glioma. (p=0.864). ECOG Performance status 0,1,2 and 3 showed median survival of 13.6, 11.5, 6 and 3 months respectively (p=.02)

Conclusion: Survival still remains dismal despite high radiotherapy dose. The role of cytogenetics and chemotherapy should be explored to improve outcome.

EP-1122

Efficacy and safety of stereotactic reirradiation for recurrent brain metastases.

F. Meniai-Merzouki[1], S. Maillard[1], B. Coche-Dequéant[1], T. Boulanger[2], E. Tresch[3], F. Crop[4], T. Lacornerie[4], E.F. Lartigau[1]

[1]*Centre Oscar Lambret, Radiation oncology, Lille, France*

[2]*Centre Oscar Lambret, Medical Imaging Department, Lille, France*

[3]*Centre Oscar Lambret, Methodology and Statistics Department, Lille, France*

[4]*Centre Oscar Lambret, Medical physicist, Lille, France*

Purpose or Objective:

Background: Brain metastases (BM) are the most common CNS malignancies. They represent an important cause of morbidity and mortality in cancer patients. In the literature, few studies have evaluated the efficacy of stereotactic reirradiation (SRT) for recurrent brain metastases as a salvage treatment option after a prior radiotherapy.

Objectives: This study reports the clinical outcome and tolerance of repeat irradiation with CyberKnife robotic stereotactic delivery in patients with recurrent brain metastases and a history of prior cerebral radiotherapy. Overall survival (OS), intracranial progression-free survival (PFS), local control (LC) and prognostic factors associated with overall survival (OS) were evaluated.

Material and Methods: Patients treated from April 2010 to January 2015 for recurrent brain metastases were retrospectively included. Univariate and multivariable analyses included age, performance status, recursive partitioning analysis (RPA), extratracranial disease control, and time from initial RT to SRT. The prior radiotherapy was WBRT for 27 patients (dose from 30 Gy to 45 Gy) , radiosurgery with Gamma knife for 8 patient (dose from 18 Gy to 25 Gy) and hypo fractionated stereotactic radiotherapy in 2 patients. The tumor size ranged from 1to 4 cm (median 2 cm).

Results: In total, 37 Patients with 53 recurrent brain metastases and a median age of 58 years (Range 33-82 years) were included. The median number of metastases per patient was 2 (range 1-4), treated with a median dose of 21 Gy (range 10-36) per treatment, with a median of 3 fractions (range 1-9) per patient. The median follow-up was 10,1 months (range 1-19 months). The OS rate from the SRT was 57,2%(IC 95%: 34.6-74.6). Two (5%) of 12 deaths were from neurologic causes. The median PFS was 5.8 months (IC 95%: 3.6-9.3). On multivariate analysis, controlled extracranial disease is correlated with better overall survival 31% (IC 95%: 15-50; p= 0,005). Adverse radiation events developed was acceptable.

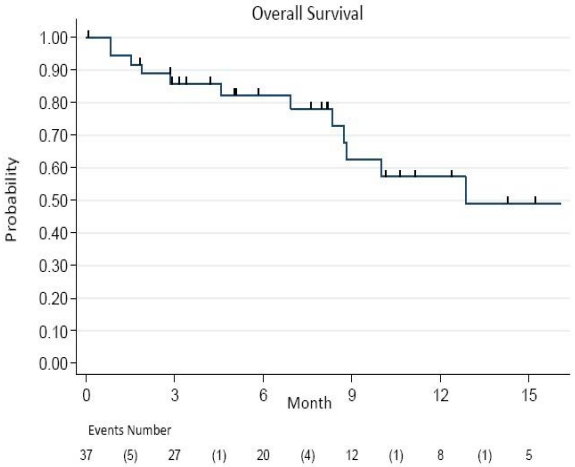

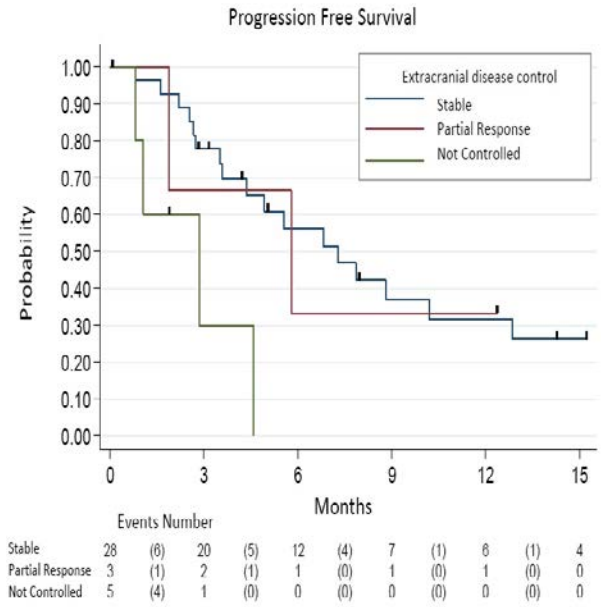

Conclusion: Stereotactic reirradiation with CyberKnife for recurrent brain metastases, seems to be a safe and effective approach in selected patients. However, in the absence of prospective trials, no recommendation can be strongly established.

EP-1123

New aspects regarding the radiation of thalamic gliomas

E. Boelke[1], W. Budach[1], C. Matuschek[1], A. Hayman[2]
[1]*University Hospital Düsseldorf Heinrich Heine University Düsseldorf, Radiation Oncology, Düsseldorf, Germany*
[2]*University of Texas- MD Anderson Cancer Center, Radiology, Houston, USA*

Purpose or Objective: Thalamic tumours represent 5.2% of all intracranial tumours and are typically diagnosed in the paediatric population. These tumors arise from glial cells with an aggressive behavior and a high grade histology. They have a poor prognosis. The aim of this study was to find new approaches for defining the clinical target volume for these tumors.

Material and Methods: Clinical data were collected form archived files of 30 patients diagnosed with thalamic gliomas based on pathologic and radiologic criteria.

Results: Three patterns of tumor spread were found. The first pattern followed the thalamic tributaries of the posterior part of the internal cerebral veins. These were the anterior and superior thalamic veins. For the second pattern the close proximity of the internal cerebral vein branches of the superior thalamic veins was a potential route of spread between the medial surfaces of the thalami. In addition to spread across the midline tumours could also spread along the adjacent tectal, pineal and/or vermian veins. The third pattern of thalamic tumor spread was found in gliomas which use the anterior tributaries of the internal cerebral venous architecture of the posterior and inferior branches from the basal vein of Rosenthal.

Conclusion: Thalamic gliomas spread upon the peritumoral architecture of the perivenous/subglial Scherer structures and this knowledge should be used for redefining the clinical target volume for radiation therapy in thalamic gliomas

EP-1124

Outcomes of patients with 4 or more cerebral metastases treated with stereotactic radiosurgery

H. Benghiat[1], A. Hartley[1], A. Kapadia[1], G. Heyes[1], P. Sanghera[1]
[1]*Queen Elizabeth Hospital, Hall-Edwards Radiotherapy Research Group- The Cancer Centre, Birmingham, United Kingdom*

Purpose or Objective; Evidence for the use of stereotactic radiosurgery (SRS) to 1-3 brain metastases (BM) can be derived from historic prospective trials. With improvements in the ability to control systemic disease, better access to SRS and concerns with WBRT associated neurocognitive toxicity many institutions now offer SRS to patients with greater than 3 metastases. The purpose of this study was to review local control and survival outcomes of patients with 4 or more BM treated with SRS.

Material and Methods: Patients with BM treated with SRS for 4 or more lesions between June 2011 and April 2015 were identified from a prospective database. Patients were deemed suitable for SRS if they had preserved Karnofsky performance status (> 70), controllable systemic disease and an estimated prognosis of > 6 months with a total intracranial metastatic volume of < 20 cm3. Local control and overall survival rates were estimated using Kaplan Meier curves.

Results: A total of 16 patients (median age 54 years) with 85 lesions were treated with primary pathology as follows: breast 3 (18.6%); lung 5 (31.3%); melanoma 6 (31.3%) and others 2 (12.5%). Median number of lesions treated was 5, with median total volume of BM per patient of 1.63cm3. Minimum follow up post SRS in all patients was 6 months. Six (37.5%) patients had received previous WBRT. Eight patients (50%) experienced distant intracranial relapse, 6 (75%) of whom had not received prior WBRT. Of these 6 patients; 3 (50%) received salvage WBRT, 2 (33.3%) were suitable for further SRS and 1 (16.7%) refused further intervention. Of the 10 patients who had not received WBRT prior to SRS, 6 had confirmed distant relapse. The median whole brain radiotherapy free survival (i.e. time from initial SRS to either salvage WBRT or death) was 6.1 months. Eleven lesions (12.9%) recurred locally after a median of 226 days (range 85 – 235) post SRS. Median overall survival was 8.3 months (range 21 – 548).

Conclusion: The median survival in this series suggests there may be a group of patients with greater than 3 metastases that could benefit from SRS. Although patient numbers are small, this data may suggest that durable whole brain free survival (an important quality of life outcome) may be achievable in patients initially treated with SRS only.

EP-1125

Survival, clinical response and prognostic factors in the reirradiation of recurrent brain tumors

M.S. Mariaquila Santoro[1], M.A.M. Maria Angela Molinaro[1], A.P. Armando Pingitore[1], L.R.F. Lucia Rachele Fabiano[1], A.C. Angelo Chirillo[1], A.S. Angela Saccomanno[1], L.P. Luigi Perrone[1], M.L. Marianna Lacaria[1], E.M. Elvira Mazzei[1], R.M. Rosa Molè[1], A.D. Anna Destito[1], D.P. Domenicantonio Pingitore[1]
[1]*Hospital Pugliese-Ciaccio- Via Pio X- 88100 Catanzaro, Department of Hemato-Oncology- Operative Unity of Radiotherapy and Radiobiology-, Catanzaro, Italy*

Purpose or Objective: The primary objective of the study is to assess the survival and quality of life after re-irradiation of relapsing malignant brain tumors. The second objective was to evaluate the influence of some prognostic factors on survival.

Material and Methods: Fifteen patients received radiation re-treatment for relapse in primary brain tumor between October 2011 and May 2015. The interval between two consecutive treatments was at least 1 year. Treatment was carried out with Conformal Radiotherapy (3D-CRT). The total dose radiation of the first treatment was 60 Gy, while the second treatment was 40-50 Gy. During follow-up, patients were evaluated at regular intervals both in taking drugs and corticosteroids for the performance status. Radiological response was evaluated by examining all available imaging

modalities, namely CT and MRI. Potential prognostic factors in survival were evaluated in the univariate analysis that multivariate analysis.

Results: An objective clinical response (ie clinical improvement) was observed in 24% of patients. Of the evaluable patients, almost one third showed a complete radiological response (8%) or partial (22%). The median overall survival (OS) and progression-free survival (PFS) after retreatment were 10.9 and 8.6 months, respectively. By multivariate analysis, we have identified four independent prognostic factors for survival: (1), the first perfomance status of reprocessing (P = 0.002), (2), the duration of the interval between treatments (P 0.008) (three), histology of the tumor and (4), the response to initial treatment (P values, 0.04). The median survival for patients with perfomance status = 0-1 and <2 was of 14.0 and 7.4 months, respectively. Patients with oligodendrogliomas showed a median OS of 27.5 months while patients with astrocytoma had a median OS of 6.9 months after retreatment. There were no long-term complications of reprocessing. Quality of life after reprocessing and to clinical progression, however, was good: all patients remained able to ambulate independently and were able to take care of itself.

Conclusion: Re-irradiation in selected patients with relapsed brain tumors seems feasible option.

EP-1126

Postoperative hypofractionated stereotactic radiotherapy to the resection cavity in brain metastases

M. Lopez Gonzalez[1], X. Chen[1], O. Hernando-Requejo[1], A. Muniz[2], S. Paredes[3], R. Ciervide Jurio[1], A. Montero Luis[1], E. Sanchez Saugar[1], M. García-Aranda[1], A. Ortiz de Mendevil[4], J. Valero[1], C. Rubio Rodriguez[1]

[1]Hospital Universitario Madrid Sanchinarro - Grupo Hospital de Madrid, Radiation Oncology, Madrid, Spain

[2]Hospital Universitario Marques de Valdecilla, Radiation Oncology, Santander, Spain

[3]Hospital Clinico Universitario Lozano Blesa, Radiation Oncology, Zaragoza, Spain

[4]Hospital Universitario Madrid Sanchinarro - Grupo Hospital de Madrid, Radiology, Madrid, Spain

Purpose or Objective: Whole brain radiotherapy is the standard treatment after resection of brain metastases however due to its neurotoxicity some other treatments such as stereotactic radiotherapy are under investigation. Our purpose is to evaluate the acute toxicity and efficacy of postoperative hypofractionated stereotactic radiotherapy to the resection cavity in brain metastasis.

Material and Methods: From october 2011 to september 2015, we treated and analyzed 20 patients diagnosed with intracranial metastasis who were treated by resection followed by postoperative hypofractonated stereotactic radiotherapy. All treatment decisions were based on a multidisciplinary approach, all patients signed consent form before treatment. In all cases countouring was based on MRI and CT fused images, and three different fractionation schemes were used : 7 x5 Gy (n=10), 5x6Gy(n=7) and 10x4Gy (n=3). Treatment has been performed using the Novalis ExacTrac image guided system which consists of a non invasive frame-based mask system that allows us to perform stereotactic treatments. Treatment plan was performed on Iplan-net (v. 4.1) with either multiple non coplanar conformal beams or dynamic conformal arcs, using 3Dconformal radiation therapy or IMRT if it was needed. On treatment room the Novalis IGRT is based on two X-ray orthogonal images that fuse bone structures with DRR reconstructed from CT simulation scan. A Robotic 6D coach corrects with submillimeter accuracy translational both and rotational errors before treatment.

Results: The median age was 57 years. Seven patients were male and 13 female. The most frecuent primary tumor was lung in 65%, followed by breast in 25%, and ovary and hepatocarcinoma in 5%. All the patients received treatment with desxametasone during the treatment and maintained it for at least two weeks after the treatment completion. 85% of patients remained asymptomatic during treatment. 15% had grade I toxicity. Local control was achieved in 85% of patients with a median follow up of 13 months. Intracranial median free survival was 11,9 months. Median survival time was 12 months (range 1- 34months). 30% had new brain metastases who were treated with whole-brain radiation therapy or radiosurgery.

Conclusion: Stereotactic hypofractionated radiotherapy after resection brain metastasis seems feasible and well tolerated. No significant toxicity was observed. Whole brain radiotherapy can be reserved in cases of progression.

EP-1127

Combined chemotherapy and craniospinal irradiation of adults medulloblastoma and PNET tumors.

E. Nowicka[1], W. Bal[1], M. Jarząb[1], M. Gawkowska-Suwińska[1], H. Grzbiela[1], B. Bobek-Billewicz[2], R. Tarnawski[1]

[1]Center of Oncology MSC Memorial Institute, 3rd Radiotherapy and Chemotherapy Department, Gliwice, Poland

[2]Center of Oncology MSC Memorial Institute, Department of Radiology, Gliwice, Poland

Purpose or Objective: Medulloblastoma and central nervous system PNET are rare primary brain tumors in adults. The role of chemotherapy as a part of standard treatment in adult patients is not defined. We aimed to evaluate the toxicity and early results of combined treatment: surgery, multiagent chemotherapy followed by craniospinal irradiation in adult patient.

Material and Methods: From January 2011 to December 2014, 13 adult patients:6 women and 7 men, with medulloblastoma or PNET were treated. Median age was 30,4 years (20,8-46,7). All patients underwent surgery. There were five PNET and eight medulloblastomas, including desmoplastic variant in 2 pts, anaplastic in 1 pt, nodularis in 2 pts and the no specific type in remaining. Neuraxis MRI performed after surgery showed active tumor and spinal metastases in three pts, tumor in operated site in 5 and no signs of disease in 5 pts. There were 6 standard and 7 high risk patients. All patients were treated with multiagent chemotherapy including cisplatin, cyclophosphamide, etoposide and vincristine and received G-CSF as a primary prevention of febrile neutropenia. After chemotherapy the craniospinal irradiation was performed using conformal radiotherapy (8 pts) or tomotherapy (5 pts) with the mean dose 32,7 Gy (14,4-36 Gy) to the craniospinal axis and mean boost dose of 18,8Gy (18-23,4 Gy) to the primary tumor location. MRIs were performed after treatment to monitor response. All patients completed the whole protocol.

Results: Ten patients received 2 courses, 2 patients 3 courses and one patient received only one course of chemotherapy. Chemotherapy was given on time. The hematological toxicity of chemotherapy was: neutropenia WHO IV in 2 and WHO III in 4 pts after the first course and WHO IV in 4 and WHO III in 3 pts after the second course of chemotherapy. There was no febrile neutropenia. Radiological complete and partial response were recorded in 2 and 4 pts respectively in those with previous active disease. Two patients progressed while waiting for radiotherapy. Mean time of radiotherapy was 1,6 mo. During radiotherapy hematological toxicity was observed: leucopenia – WHO II in 5 pts that started in second week of irradiation and WHO III in 2 pts in the third and forth week, thrombocytopenia - WHO I in 5 pts, WHO II in 3 pts and WHO III in one. Five patients required treatment interruptions with median duration of 12 days. Median overall treatment time was 6,4 mo. Median follow up was 17,9 mo. Six patients relapsed after median time of 13,1 mo, four of them locally and two disseminated via cerebral fluid. Five patients died in spite of salvage treatment. Median time of DFS and OS were 13,3 mo and 17,9 mo respectively. One and 2 year OS and DFS are 92% and 45% and 68% and 42% respectively.

Conclusion: Sequential chemotherapy and radiotherapy in adult medulloblastoma/PNET tumors is feasible with acceptable toxicity. High relapse rate in our patients indicate the need of treatment intensification with better coordination of combined therapy.

EP-1128

Outcome of high grade glioma patients: To prioritise dose to primary tumour or organs at risk?

F.C.J. YIM[1], L. Howell[2], S.Y.Y. Pan[3], V.S. Kumar[3], S.R. Kennedy[3]

[1]*University of Manchester, School of Medicine, Manchester, United Kingdom*

[2]*University of Central Lancashire, School of Health, Preston, United Kingdom*

[3]*Lancashire Teaching Hospitals NHS Trust, Rosemere Cancer Centre, Preston, United Kingdom*

Purpose or Objective: Glioma is a primary brain tumour arising from the glial cells. High grade glioma, defined as grade III and IV, have poor survival rates. Glioblastoma multiforme is the commonest, but is also, the most aggressive type of glioma and is associated with a poor prognosis. Median survival of patients after treatment with debulking surgery followed by concurrent chemoradiotherapy and adjuvant chemotherapy is 14.6 months. Currently, post-operative fractionated radiotherapy is prescribed to a range of 54 to 60 Gy in fractions of 2 Gy.
Organs at risk (OARs) including optic chiasm, optic nerves and the brain stem, may lie within, or in close proximity to the PTV. Neuropathy and/or necrosis has been shown to occur when the maximum dose exceeds 55Gy in the optic chiasm and 54Gy to the whole brainstem. The standard practice at Rosemere Cancer Centre is to prioritise the OARs at the expense of the total dose, therefore prescribing to a dose of 54Gy whenever the OARs is included in the PTV, which may have repercussions on tumour control and ultimately, overall survival.
This retrospective analysis aims to compare patient outcomes between the 54Gy/57Gy and 59.4Gy/60Gy regimes, to determine if compromising the dose to spare OARs is detrimental to tumour control and survival.

Material and Methods: The data of all glioma patients treated with radiotherapy between December 2012 and December 2014 at Rosemere Cancer Centre, were collected from our electronic databases. A total of 167 patients were identified. Patients with low grade glioma and those treated with a palliative intent were excluded. Fifty eight patients were included in the analysis.

Results: Twenty one patients were on a lower dose radiotherapy regime of 54Gy or 57Gy. The remaining 37 were on a higher dose regime of 59.4Gy or 60Gy. There was a statistically significant difference (p=0.05) in patients treated with the higher dose regime comparatively, of an additional 7.2 months median overall survival (mOS) benefit. The mortality hazard for the higher dose regime is 37% lower than the lower dose regime.

Conclusion: The outcome of patients treated with the 59.4/60Gy dose regime has shown to be statistically significant with a mOS benefit and lower mortality hazard. It is therefore clear that maintenance of the higher dose (59.4/60Gy) should be a priority, either at the expense of the OARs or to as much of the tumour volume as possible, whilst still observing the OARs constraints.

EP-1129

Pre and post-irradiation hypothalamic-pituitary axis dysfunction in adults treated for brain tumours

N. Taku[1], A. Powlson[2], M. Romanchikova[3], A. Hoole[3], A. Bates[1], J. Hale[2], R. Jena[1], M. Gurnell[2], N. Burnet[1]

[1]*Addenbrooke's Hospital - University of Cambridge, Department of Oncology, Cambridge, United Kingdom*

[2]*Addenbrooke's Hospital - University of Cambridge, Institute of Metabolic Science, Cambridge, United Kingdom*

[3]*Addenbrooke's Hospital - University of Cambridge, Department of Medical Physics, Cambridge, United Kingdom*

Purpose or Objective: Collateral irradiation of normal structures during whole brain radiotherapy increases the risk of secondary toxicities, including dysfunction of the hypothalamic-pituitary axis (HPA). In studies of children treated for intracranial neoplasms, Merchant et al. showed that upwards of 66% of patients had pre-irradiation endocrinopathies and that HPA dosimetry data can be used to predict the dose-volume effects of radiation on growth hormone (GH) secretion. However, no comparable endocrine studies have been performed in adult populations. Evidence exists to suggest that hypopituitarism is an independent risk factor for mortality in adults treated with whole brain radiotherapy. Increased collaboration between radiation oncologists and endocrinologists is needed to amalgamate dosimetry data with the results of endocrine testing and better characterize HPA dysfunction. The purpose of this study is to determine the presence of baseline HPA dysfunction as well as the time to onset and dose-dependence of post-irradiation HPA dysfunction in adults treated for non-pituitary brain tumours.

Material and Methods: Twelve patients, 3 males and 9 females, have been enrolled in our prospective clinical study that will continue to recruit until 2017. Primary diagnoses included meningioma (7), pineal tumor (3), and glioma (2). Median patient age is 52 (range 23-71). Enrolled patients have undergone comprehensive baseline endocrine testing of the thyroid, gonadotropins, cortisol, prolactin, and GH prior to initiation of radiotherapy. Patients have received daily image guidance imaging with positional correction and 50-60 Gy of radiation to the tumour bed. Parametisation of available dosimetry data was performed to determine the maximum, minimum, and mean radiation doses. Endocrine testing is being repeated at 6 month intervals following radiotherapy. Patient reported outcome measures are also collected during follow-up encounters. Reviewing endocrinologists have been blinded to dosimetry data.

Results: Three patients (25%) demonstrated pre-irradiation endocrinopathies, including 2 cases of primary hypothyroidism and 1 case of primary hypogonadism. Furthermore, one patient exhibited temporary HPA suppression secondary to exogenous steroid use. Median length to endocrinology follow-up is still short at only 3 months (range 0-18). We present analyzed dose data for 10 of the 12 patients. Mean radiation doses to the hypothalamus and pituitary were 35 Gy (range 20-55) and 31 Gy (range 13-50), respectively. No cases of new, radiation-related HPA dysfunction have been identified to date.

Conclusion: The incidence of pre-irradiation HPA dysfunction underlines the need for baseline endocrinology studies. The range of radiation doses to the HPA should allow for identification of dose-volume responses.

EP-1130

Hair-sparing whole brain radiotherapy with simultaneous integrated boost using high density bolus

S. Velázquez Miranda[1], E. Montero-Perea[2], R. Dorado-Dorado[1], M. Rubio[2]

[1]*Hospital Universitario Virgen Rocío, Radiofisica, Sevilla, Spain*

[2]*Hospital Universitario Virgen Rocío, Radioterapia, Sevilla, Spain*

Purpose or Objective: Present and retrospectively evaluate our protocol of WBRT + SIB regarding radiation-induced alopecia

Material and Methods: We use masks type 35764 / 2MA / M Orfit a subnet mask with eXaskin and compatible base resonance (eXaFrame). A similar number of slices is used in the images of CT and MRI, both acquisitions with identical position and immobilization and slice thickness of 1 mm. This is possible thanks to eXaFrame, resulting in excellent quality

fusion. The treatment was designed with SmartArc with multiple arches made with Synergy. The dosage regimen used is Lagerwaard one: [RCT (20 Gy) + SIBmts (40 Gy)] / 5 frac. Positioning of the patient was checked daily with conebeam. Before starting the optimization we must be contoured 3mm ring around the calote we call follicles, and a contraction of the outer contour of 12mm we call volume CPE. We define two arcs (VMAT CCW 178 ° -60 ° and 300 ° -182 °), with the following objectives: follicles (DSEmax = 16 Gy, weight = 20; DSEmax = 5 Gy, weight = 1), brain-CPE (Dmax = 21Gy, weight = 100 and Dmin = 20 Gy, weight = 50), eyes (Dmax = 10 Gy, weight = 1). Later, we focus on separate metastases: optimization blocked prophylaxis (Optimization Type None) and create three structures: VI1 = PTV (MTS1) 5 mm VI2 = PTV (m2) 5 mm Epx = brain-VI1-VI2 . The objectives were PTVI (Dmax = 44Gy, despite Dmin = 100 and = 40 Gy weight = 50), Epx (Dmax = 30 Gy) and brainstem (Dmax = 23Gy), follicles (DSEmax = 16 Gy, weight = 20 ; DSEmax = 5 Gy, weight = 1)
Verifying treatment was performed with the Compass software, and the Matrixx detector with gamma (4%, 1 mm) conditioning.

Results: So far we have treated 15 patients, the differences in the images of fusion of less than 1 mm and the average correction IGRT of 1.24mm. No acute toxicity. Nor alopecia, or temporary removal,

Conclusion: If we consider our VMAT optimization alopecia in WBRT + SIB with eXaFrame and eXaSkin, produce optimal aesthetic results.

EP-1131

Hypofractionated Radiotherapy with temozolomide in poor prognosis glioma: a retrospective study

E. Pelle[1], E. Trino[1], M. Levis[1], M. Magistrello[2], C. Mantovani[1], U. Ricardi[1]
[1]*University Of Turin, Radiotherapy, Turin, Italy*
[2]*University Of Turin, Neuro-Oncology, Turin, Italy*

Purpose or Objective: To describe clinical outcomes of hypofractionated radiotherapy, either in combination or not with temozolomide (TMZ) in poor performance status glioblastoma (GBM) patients

Material and Methods: We retrieved the charts of 96 patients treated with hypofractionated radiotherapy plus/minus TMZ for GBM at our Institution

Results: Patients characteristics were summarized in Table 1.

Variables	N (%)
Total	96
Gender	
Female	41 (42,7%)
Male	55 (57,3%)
Age at diagnosis (years)	
Median	66
Range	25-81
≥ 65	53 (55.2%)
KPS at presentation	
< 70	26 (27.1%)
≥ 70	70 (72.9%)
Extent of surgical resection	
Gross total resection	4 (4.2%)
Partial resection	66 (68.8%)
Biopsy	26 (27.1%)
Type of adjuvant treatment	
Short-course radiotherapy alone	57 (59.4%)
Short-course RT plus concomitant TMZ	7 (7.3%)
Short-course RT plus concurrent and adjuvant TMZ	12 (12.5%)
Short-course RT followed by adjuvant TMZ	20 (20.8%)
Patients on corticosteroids	
Yes	16 (16.7%)
No	80 (83.3%)

Among elderly patients, 38 (71.6%) were treated with RT alone, 9 patients (16.9%) with adjuvant TMZ, while 6 patients (11.3%) with a KPS ≥70 received hypoRT plus concurrent TMZ, followed by adjuvant chemotherapy in 3 (5.6%) of these cases. The median follow up time of the entire cohort was 13.6 months (range 1-47 months). A significant improvement in KPS from baseline to the end of radiation therapy was observed in 73 patients (76%). The median overall survival time was 6.7 months, reducing to only 2.5 months and 4 months respectively in elderly and younger patients with low performance status (KPS<70). The 6 months and 1 year survival rates were respectively 56.4% and 29.1%. In multivariate analysis, concomitant Temozolomide (HR:0.38, 95% CI 0.16-0.85,*p=.020*) and adjuvant TMZ (HR:0.28,95% CI 0.14-0.56,*p=.000*) emerged as significant indices of longer OS rates, while weaning from steroids (*p=.18*), extent of surgical resection (*p=.17*) and tumor site (*p=.10*) were not significant predictors of overall survival but showed a positive trend. Patients who received concomitant TMZ had a median survival time of 12.5 months compared with 6.3 months for those treated with RT alone (*p=.017*). Also the use of adjuvant chemotherapy resulted in improved survival compared to no sequential Temozolomide (10.8 *vs* 5.2 months, *p=.001*). In the elderly cohort, patients treated with adjuvant TMZ had median OS of 8.15 months as opposed to 6.4 months of those not receiving adjuvant chemotherapy (*p=.001*). A stronger impact of adjuvant TMZ has been reported in younger patients, with a median OS of 13.5 months in adjuvant TMZ group compared to 3.7 months (*p=.001*) in the other group. Moreover, younger patients receiving concurrent Temozolomide showed a significantly longer OS of 20 months compared to 5.1 months in patients not having TMZ (*p=.006*). Acute tolerance to radiotherapy was generally good. No grade 3-4 acute toxicity was observed.

Conclusion: Our findings seem to suggest that frail elderly patients with KPS at baseline < 70 do not benefit of an active treatment and could be carefully offered best supportive care. In the presence of a good functional status and a wide surgical resection, patients older than 65 years may take advantage of hypo-fractionated radiotherapy, followed by adjuvant TMZ. In younger patients with poor performance status, the significant survival gains obtained with combined modality treatment suggest that a maximum resection followed by combined radiation and chemotherapy should be recommended.

EP-1132

Application of IMRT technique in treatment of malignant gliomas: assessment of treatment tolerance

K. Urbanek[1], A. Mucha-Małecka[1], P. Hebzda[1], K. Kisielewicz[2], K. Małecki[3], E. Góra[2], J. Jakubowicz[4]
[1]*Centre of Oncology - Institute MSC Kraków, Head and Neck Cancer, Krakow, Poland*
[2]*Centre of Oncology - Institute MSC Kraków, Medical Physics, Krakow, Poland*
[3]*University Children's Hospital of Cracow, Radiotherapy of Children and Adults, Krakow, Poland*
[4]*Centre of Oncology - Institute MSC Kraków, Clinic of Oncology, Krakow, Poland*

Purpose or Objective: Assessment of tolerance of combined modality therapy of patients with malignant gliomas irradiated using IMRT technique. We compared dose distribution in IMRT and conformal 3D treatment plans.

Material and Methods: Between 2009 and 2013 in the Oncology Center in Krakow 60 patients with malignant gliomas received combined modality treatment. Mean age was 53 years (range 24–72 years). All patients were in good performance status (WHO 0–1). There were 48 patients with glioblastoma multiforme and 12 with anaplastic astrycytoma. 48 patients underwent complete resection and 12 partial resection. Patient were irradiated using IMRT technique with a total dose of 60Gy in 30 fractions. All patients concurrently received temozolamide in the dose of 75mg/m2. In all patients we performed additional plans using 3D conformal

radiotherapy (3D-CRT) techniques and compared with IMRT plans. The 3D-CRT plans were prepared using 3–4 fields and IMRT plans consisted of 7–8 fields. The primary objective was to treat the planning target volume and to minimize the dose to organs at risk (OAR). Volumetric analysis, target coverage and conformity of prescribed doses were used in plan comparison.

Results: Treatment tolerance was very good in all patients. Only 12 patients needed steroids during treatment. Adjustment of the dose distribution to the target volume was improved and the critical structures were better spared in the IMRT plans than in 3D-CRT plans. For all patients the mean dose and the maximum dose to OAR were significantly reduced in IMRT plans. With respect to target volume, IMRT technique reduced the maximum dose while increasing the minimum dose, resulting in improved conformity. In same patients with tumors located very close to OAR it was impossible to give 60Gy for target volume with 3D-CRT technique because of not acceptable doses in OAR.

Conclusion: The IMRT technique combined with concurrent temozolamide is well tolerated and offers significant advantages comparing to 3D-CRT. Application of IMRT allows dose reduction at OAR without compromising target coverage.

EP-1133

Long-term follow-up and prognostic factors in low-grade glioma (WHO II) postoperatively irradiated.

K. Urbanek[1], A. Mucha-Małecka[1], K. Małecki[2], A. Chrostowska[1], J. Jakubowicz[3]
[1]*Centre of Oncology - Institute MSC Kraków, Head and Neck Cancer, Krakow, Poland*
[2]*University Children's Hospital of Cracow, Radiotherapy of Children and Adults, Krakow, Poland*
[3]*Centre of Oncology - Institute MSC Kraków, Clinic of Oncology, Krakow, Poland*

Purpose or Objective: There is little consensus about the optimal treatment for low-grade glioma (LGG), and the clinical management of LGG is one of the most controversial areas in neurooncology. Radiation therapy is one option for treatment of patients with LGG whereas other options include postoperative observation. The aim of the study is to report the long-term follow-up of a cohort of adult patients with LGG post-operatively irradiated in one institution, and to identify prognostic factors for progression free survival.

Material and Methods: Between 1975 and 2005, 180 patients with LGG (WHO II) received postoperative irradiation after non radical (subtotal or partial) excision. Patients had to be 18 years of age or older, and have histologic proof of supratentorial fibrillary (FA), protoplasmic (PA) or gemistocytic astrocytoma (GA). Radiotherapy was given within 3 to 10 weeks after surgery. The treatment fields were localized and included the preoperative tumor volume, with a 1-2 cm margin, treated to a total dose of 50 to 60 Gy in 25 to 30 fractions over 5 to 6 weeks.

Results: Actuarial ten- year progression free survival (APFS) in the whole group was 19% . The worse prognosis was reserved for patients with GA. Ten-year APFS rates for GA, PA and FA were 10%, 18% and 22% respectively.

Conclusion: The findings from our long-term cohort of 180 patients with LGG confirmed by uni- and multivariate analysis demonstrated that only astrocytoma histology significantly determined the prognosis. The best survival is reserved for patients with the fibrillary variant, and the worst for the gemistocytic one.

EP-1134

Proton therapy re-irradiation for large-volume recurrent high-grade gliomas

D. Amelio[1], L. Widesott[1], F. Maines[2], F. Fellin[1], R. Righetto[1], S. Vennarini[1], B. Rombi[1], M. Cianchetti[1], F. Dionisi[1], D. Donner[3], U. Rozzanigo[4], M. Schwarz[1], F. Chierichetti[3], E. Galligioni[2], M. Amichetti[1]
[1]*Centro di Protonterapia, U.O. Protonterapia- Azienda Provinciale per i Servizi Sanitari - Trento, Trento, Italy*
[2]*Ospedale S. Chiara, U.O. Oncologia Medica- Azienda Provinciale per i Servizi Sanitari - Trento, Trento, Italy*
[3]*Ospedale S. Chiara, U.O. Medicina Nucleare - Azienda Provinciale per i Servizi Sanitari - Trento, Trento, Italy*
[4]*Ospedale S. Chiara, U.O. Radiologia - Azienda Provinciale per i Servizi Sanitari - Trento, Trento, Italy*

Purpose or Objective: To report preliminary results of re-irradiation with proton therapy (PT) for large-volume recurrent high-grade gliomas (rHGG).

Material and Methods: Between January and September 2015 eight patients (pts) with rHGG (7 glioblastoma - GBM, 1 anaplastic oligodendroglioma - AOD) were re-irradiated with PT. Age at re-irradiation was between 40 and 64 years while Karnofsky performance status was 60-100%. Minimum time between prior radiotherapy and PT was 8 months. Target definition was based on CT, MR, and 18F-DOPA PET imaging. GTV included any area of contrast enhancement at MR imaging after contrast medium administration plus any uptake regions at PET imaging. CTV was generated by adding to GTV a 3-mm uniform margin manually corrected in proximity of anatomical barriers. CTV was expanded by 4 mm to create PTV. PTV volume varied between 55 and 260 cc. The patient with AOD received 50.4 GyRBE in 28 fractions (fx) while GBM pts 36 GyRBE in 18 fx. Four GBM pts also received concomitant temozolomide (75 mg/m2/day, 7 days/week). All pts were treated with active beam scanning PT using 2-3 fields with single field optimization technique.

Results: All pts completed the treatment without breaks. Registered acute side effects (according to Common Terminology Criteria for Adverse Events versione 4.0) include skin erythema with pruritus, alopecia, fatigue, conjunctivitis, and headache. All the side effects were grade 1 or 2. There were no grade 3 or higher toxicities. One patient developed grade 1 neutropenia. Three pts started PT under steroids (2-8 mg/day); two of them reduced the dose during PT, one kept the same steroids dose. None of remaining pts needed steroids therapy. During follow-up two pts developed radionecrosis (diagnosed at imaging) with mild symptoms controlled with steroids. All pts are alive. Four pts have stable disease one months after PT, three pts have stable disease three months after PT, and one pts progressed five months after PT.

Conclusion: PT re-irradiation of large volume rHGG is feasible and safe even with concomitant chemotherapy administration. Longer follow-up is necessary to assess definitive efficacy.

EP-1135

Hypofractioned Stereotactic Radiation Therapy for cavernous sinus meningiomas

F. Meniai-Merzouki[1], B. Coche-Dequèant[1], T. Boulanger[2], F. Crop[3], T. Lacornerie[3], E. F.Lartigau[1]
[1]*Centre Oscar Lambret, Radiation Oncology, Lille, France*
[2]*Centre Oscar Lambret, Radiology Imaging Department, Lille, France*
[3]*Centre Oscar Lambret, Medical Physicis, Lille, France*

Purpose or Objective: We evaluate the tolerance and efficiency of robotic hypo fractionated stereotactic radiotherapy (hSRT) for patients with Cavernous sinus meningiomas in our Institution.

Material and Methods: We retrospectively reviewed patients who were treated with robotic hSRT for Cavernous sinus meningioma. Multidisciplinary staff approved treatment. A dose of 36 Gy was prescribed in 9 fractions. Treatment was delivered every other day.

Results: Between 2010 and 2013, 18 evaluable patients with a total 18 lesions were treated in our institution with hSRT

with median follow up of 18 months (6-40 months). Six patients had prior surgical resection of tumor, 12 received treatment as first line. The majority (60 %) of lesions were close to the optic pathway with median values for GTV volume was 9,4 cm3 (0,38-55,66 cm3). The control rates at tow years were favorable with stable disease in 100 % patients, vision was preserved and improved symptoms in 65% patients. We observed no grade 3 or 4 toxicity. The most frequent being grade 1 retro-orbital pain (20%). No late toxicity was reported and no death during the follow – up period.

Conclusion: Robotic Hypo-fractionated stereotactic radiotherapy for Cavernous sinus meningioma is feasible and provides a satisfactory local control with acceptable tolerance, either as a first line treatment or as adjuvant to incomplete surgery or relapse. Although this type of tumor has a slow evolution, extended follow-up is mandatory.

EP-1136

Treatment with radiosurgery (stereotactic radiotherapy) in single session in brain metastases

P. Vargas Arrabal[1], J. Expósito[1], I. Tovar[1], M. Zurita[1], R. Del Moral[1], R. Guerrero[1], I. Linares[1], C. Prieto[1], S. Rodríguez[1], A. Ruiz[1]
[1]*Hospital Universitario Virgen de las Nieves, Radiation Oncology, Granada, Spain*

Purpose or Objective: Until the advent of stereotactic radiotherapy, the main treatment option consisted of cranial radiation for palliation. With a more radical intent, and only in selected patients, surgical resection and adjuvant radiotherapy was indicated later. The purpose of this study is to evaluate the results obtained after treatment with single-session radiosurgery.

Material and Methods: Between 2002 and 2014, has collected a representative sample of 592 patients with histological diagnosis of brain metastases, of which 340 were men and 252 women. The average age in this group was 55.67 years (14-82 years) and with a KPS of 90 in 58.3% of patients. The most common location of these was lung 51%, followed by 17.1% mom. The most frequent pathological study adenocarcinoma was 23.5%, followed by squamous 10.6%. In most 63.2% no surgery was performed. The most common site was the frontal 24.4%. All patients were treated with radiosurgery (stereotactic radiotherapy) single session with a median dose of treatment of 18 Gy.

Results: With a median follow-up of 7 months, median survival was 14.23 months in a range of 0-117 months. In terms of toxicity, only 3.5% of the presented radiation necrosis (21 patients), while the cerebral edema was reported in 10.8% (64 patients).

Conclusion: The single session radiosurgery is a conservative but with a radical purpose, offering technical and few side effects is very convenient for the patient.

EP-1137

Volumetric Modulated Arc Therapy (VMAT) and simultaneus boost for brain metastases patients

A. Papaleo[1], D. Russo[1], E. Donno[1], E. Cavalera[1], F.P. Ricci[1], G. Di Paola[1], M. Santantonio[1]
[1]*Vito Fazzi Hospital ASL LE, Radiation Oncology, Lecce, Italy*

Purpose or Objective: To access treatment toxity and patients' survival after Volumetric Modulated Arc Therapy, a novel rotational Intensity Modulated RadioTherapy (IMRT) technique, with Simultaneus in-field Boost (SIB) for patients with brain metastases.

Material and Methods: Between November 2010 and March 2015, 26 patients with 1-3 brain metastases were treated with SIB-IMRT in the Department of Radiation Oncology at V. Fazzi Hospital (maximum diameter of largest metastasis≤ 3 cm, KPS≥ 70, RPA < III). Mean age was 61 ± 7.5 years. Patients were neurologically stable. Extracranial disease well-controlled (6-month estimated median life expectancy). Patients will undergo contrast-enhanced TC scan of the brain for radiotherapy planning purposes. The macroscopic (gross) tumor volume (GTV) was drawn on the MRI images. The prescription isodose line was generally 3 mm larger than the GTV. Patients will be treated with WBRT/SIB using VMAT, delivering a total of 30 Gy in 10 fractions to the whole brain and SIB doses to brain metastases were 40 Gy to lesions >or= 2.0 cm and 50 Gy to lesions <2.0 cm in diameter, delivered once daily on working days. Following therapy completion, patients will be seen every 3 months for the 1st year, then every 6 months thereafter. Patients will have MRI brain at 3 months and 1 year, and every 6 months after the first year. Any toxicity was recorded according to the RTOG.

Results: The median follow-up interval was 9 months (range, 2 months- 16 months). The median overall survival time was 11 months, and 3 of patients died of disease progression. The 6-month overall survival was 91%. After SIB-IMRT treatment of 42 brain lesions, 35 lesions demonstrated complete responses, 5 lesions demonstrated partial responses, 2 lesion demonstrated stable disease. Actuarial local tumor control rates at 6 months, 1 year and 2 years were 93.9, 82% and 54%, respectively. Thirty-eight patients did not have any adverse events >grade1. The majority of common adverse events were grade 2 headaches (4 patients), grade 2 motor neuropathy (2 patients), and grade 2 lethargy (2 patient). One patient developed a grade 3 headache 5 months after receiving SIB-IMRT.

Conclusion: The delivery of 40/50 Gy in 10 fractions to 1 - 3 BM using VMAT provides a high level of tumor control with minimal toxicity. Therefore, we believe there is a need for a larger prospective study to establish dosing guidelines for SIB-IMRT and to pave the way for a randomized trial to compare SRS/STS plus WBRT with this approach.

Electronic Poster: Clinical track: Haematology

EP-1138

Evolution of radiation techniques in the treatment of mediastinal lymphomas: single center experience

N. Besson[1], S. Zefkili[1], V. Pernin[1], S. Horn[1], D. Peurien[1], N. Fournier Bidoz[1], Y. Kirova[1]
[1]*Institut Curie, Radiothérapie, Paris, France*

Purpose or Objective: To evaluate radiation techniques in the treatment of Hodgkin's Lymphoma (HL) and Non-Hodgkin's Lymphoma (NHL) with mediastinal disease over 10-year period, and the toxicity.

Material and Methods: Between 2003-2015, 173 patients (pts) with stage I-III nodal lymphoma were treated in our institution: some of these patients were irradiated for HL or NHL with mediastinal disease. Some of the patients were treated by 3DCRT, others by IMRT

Results: We studied 26 men and 43 women with a median age of 26 years. The median follow-up was 43 months. Forty nine pts were treated by 3DCRT and 20 pts-by IMRT. The median dose received by patients treated for NHL was 40 Gy (range: 36-44 Gy) and the median dose received by pts with HL was 30 Gy (range: 30-36 Gy). Between 2003-2006, 16 pts were treated by 3DCRT vs. 0 by IMRT. Between 2007-2009, 16 pts received 3DCRT and 1-IMRT. Between 2010-2015, 19 pts received IMRT, and no patients 3DCRT. Eleven of the 20 patients (55%) treated by IMRT and 35/49 pts (71.4%) treated by 3DCRT experienced acute toxicity. Among the patients treated by 3DCRT, 1 patient experienced grade 1 radiation pneumonitis and 2 patients experienced grade 1 acute mucositis. No late toxicity was observed in the patients treated by IMRT.

Conclusion: Improvement of radiation techniques for HL and NHL appears to have improved acute and late clinical safety. Longer follow-up is necessary to evaluate very late toxicity.

EP-1139

Clinical results of radiation therapy for localised gastric lymphoma

H. Ihara[1], K. Katsui[1], K. Hisazumi[1], N. Katayama[1], M. Takemoto[2], M. Iwamuro[3], Y. Kawahara[3], H. Okada[3], S. Kanazawa[1]

[1]*Okayama University Hospital, Radiology, Okayama, Japan*
[2]*Japanese Red Cross Society Himeji Hospital, Radiology, Okayama, Japan*
[3]*Okayama University Graduate School of Medicine- Dentistry- and Pharmaceutical Sciences, Gastroenterology and Hepatology, Okayama, Japan*

Purpose or Objective: To report the outcome of localized gastric lymphoma treated with radiation therapy.

Material and Methods: This study included 27 patients (14 men, 13 women; median age 67 years, range 37 – 83 years) with localized gastric lymphoma and who received radiation therapy between January 2005 and December 2014 at our institution. Patients with a follow-up period < 6 months were excluded. Twenty-three patients were mucosa-associated lymphoid tissue (MALT) lymphoma, and 4 patients were diffuse large B-cell lymphoma (DLBCL). The stage was classified by Lugano international conference classification. All patients with MALT lymphoma were Stage Ⅰ. In DLBCL, 2 patients were Stage Ⅰ, and 2 patients were Stage Ⅱ1. The median radiation dose in MALT lymphoma was 30Gy (range, 7.5–30), and in DLBCL was 40.5Gy (range, 30–40.5). All MALT lymphoma patients with Helicobacter pylori-positive were received eradication therapy before radiation therapy. All patients with DLBCL were treated with chemotherapy followed by radiation therapy. Acute and late adverse events were evaluated in accordance with Common terminology criteria for adverse events, version 4.0. The local recurrence rate was calculated using Kaplan-Meier analysis.

Results: The median follow-up period was 58 months (range, 6.0–120.0). Local recurrence occurred in only 2 patients with MALT lymphoma. No distant recurrence was observed. Local recurrence rate in MALT lymphoma was 91% at 1 year, 91% at 3 years. In acute adverse events, 5 patients had grade 3 white blood cell decreased, 1 patient had grade 4 white blood cell decreased and platelet count decreased, and 1 patient had grade 3 anorexia. One patient with MALT lymphoma could not achieve the planned radiation therapy because of grade 4 white blood cell decreased and platelet count decreased. There was no grade 3 or greater late adverse events. One patient with MALT lymphoma suffered from gastric cancer, and underwent endoscopic excision. No patients died of gastric lymphoma. One patient died of lung cancer.

Conclusion: Radiation therapy for localized gastric lymphoma was safe and effective. Our result was similar to previous reports.

EP-1140

Role of radiotherapy in treatment of Hodgkin and non Hodgkin lymphomas - our experience

D. Scepanovic[1], A. Masarykova[1], M. Pobijakova[1], M. Fekete[1], A. Hanicova[1], M. Masar[1], Z. Dolinska[1]

[1]*National Cancer Institute, Radiation Oncology, Bratislava, Slovakia*

Purpose or Objective: Radiation therapy (RT) is an important component of therapy for patients with Hodgkin (HL) and non Hodgkin lymphomas (NHL).
In our retrospective analyze we showed the role of radiotherapy in treatment of lymphomas and its influence on disease free (DFS) and overall survival (OS) of patients.

Material and Methods: From 2000 to 2010, we treated 347 patients (pts) with lymphomas (Hodgkin - 286 and non Hodgkin - 61). There were 24 pts with stage I, 186 with stage II, 40 with stage III and 36 pts with stage IV of Hodgkin lymphoma. Among group of pts with non Hodgkin lymphoma there were 20 pts with stage I, 17 with stage II, 7 with stage III and 17 pts with stage IV. Sixty-nine percent of pts had favorable HL and 81% of pts nodular sclerosis as histological type. Sixty-four percent of pts with NHL had aggressive disease. Three dimensional conformal radiotherapy has been planned by computed tomography (CT) alone or by 18-FDG positron emission tomography/CT (18-FDG PET/CT). Mostly, patients received chemotherapy (95%) before RT. However, 67% of pts with NHL did not receive rituximab.Whole group of our pts have been irradiated by involved field radiotherapy (IFRT). Most of patients received 36Gy (1.8-2Gy daily) (71%) and 29% more than 36Gy, in both groups.

Results: Median follow-up time was 8 years. Among patients with HL, 33 pts (12%) had relapse and 11 pts (18%) with NHL. Relapses occur most often outside of irradiated volume in both groups of pts. Twenty five percent with HL patients had toxicity, most commonly pulmonary and 7% pts with NHL. During the median time of 13.5 years the incidence of a secondary malignancies (SM) was 3% in pts with HL and 2% with NHL. In group who had HL 91% of these pts lived and 74% in group with NHL. Ten-years DFS was 89% (HL) and 74% (NHL) and 10-years OS was 91% (HL) and 82% (NHL).

Conclusion: Radiotherapy had an important place in the treatment of our patients with HL, as well as in a group of NHL with acceptable toxicity and incidence of secondary malignancies.

EP-1141

Second cancer in Primary Mediastinal Lymphoma treated with MACOP-B ± R and mediastinal radiotherapy

V. De Sanctis[1], M. Alfò[2], A. Di Rocco[3], A. Ansuinelli[3], E. Russo[3], M. Osti[1], M. Valeriani[1], G. Minniti[1], L. Grapulin[4], D. Musio[4], S. Bracci[1], A. Spagnoli[1], M. Moleti[3], V. Tombolini[4], M. Martelli[3]

[1]*Sapienza Università di Roma, Department of Medicine and Surgery and Translational Medicine, Rome, Italy*
[2]*Sapienza Università di Roma, Department of Statistical Sciences, Rome, Italy*
[3]*Sapienza Università di Roma, Department of Cellular Biotechnologies and Hematology, Rome, Italy*
[4]*Sapienza Università di Roma, Department of Radiological-Oncological and Anatomo-pathological Sciences, Rome, Italy*

Purpose or Objective: To assess the incidence of second cancer in a mono-institutional cohort of long-time surviving Primary Mediastinal B Cell Lymphoma (PMBCL) patients treated with combined radio-chemo-immunotherapy.

Material and Methods: Between 1991 and December 2006, 107 consecutive untreated patients (pts) with PMBCL were treated at our Departments. Ninety-two/107 pts were evaluable for the second cancer incidence. All patients were treated with standard Methotrexate, Adriamycin, Cyclophosphamide, Vincristine, Prednisone and Bleomycin (MACOP-B) ± Rituximab; all patients underwent mediastinal radiation therapy (RT) at a dose of 30-36 Gy.

Results: At the end of combined treatment, the overall response rate (ORR) including CR+Cru/PR was 91.3% while 7 (7.6 %) patients showed progressive disease. Nine/84 (9.7%) patients relapsed within 10 months (range 3-10 months) from the end of therapy. After a median follow-up of 142 months (1-212 months), the actuarial 15-year OS and PFS were 87% and 84%, respectively. We recorded secondary malignancies in 3/80 long-surviving patients (3.75%) with cumulative incidence of thyroid and A acute myeloid leukemia of 3.47 at 15 years and with a 20-year second cancer-free survival of 82%. We observed 2 papillary thyroid cancers with a Standardized Incidence Ratio of 7.97 and with an Absolute Excess Risk of 17. 84. Moreover, we observed 1 Acute Myeloid Leukemia (AML) versus 0.015 expected cases with a SIR of 66.53 and with an AER of 10.05. No breast cancer occurred

Conclusion: Combined modality treatment of chemotherapy± with/without Rituximab and mediastinal RT was related to a

statistically significant SIR and AER for thyroid cancer and acute myeloid leukemia.

EP-1142

Role of radiotherapy(RT) in patients undergoing haemopoetic stem cell transplant(HSCT) for lymphoma

M. Singhera[1], M. Kazmi[2], N. Mikhaeel[1]
[1]*Guy's and St Thomas' NHS Foundation Trust and King's Heath Partner's Academic Heath Sciences Centre, Radiotherapy, London, United Kingdom*
[2]*Guy's and St Thomas' NHS Foundation Trust and King's Heath Partner's Academic Heath Sciences Centre, Haematology, London, United Kingdom*

Purpose or Objective: Despite the use of RT before or after salvage haemopoeitic stem cell transplant for relapsed and refractory lymphoma, the indications, timing and benefit of radiotherapy are not well established and it is unlikely that these questions will be tested in a randomised study. We present the outcomes of a retrospective analysis of the benefit of radiotherapy given before or after HSCT for lymphoma.

Material and Methods: We reviewed our transplant and radiotherapy databases to identify patients. Inclusion criteria were patients who underwent HSCT from 2004-2010 for refractory or relapsed lymphoma. Primary end point was progression-free survival (PFS) and secondary end point was overall survival (OS). Risk of relapse and death was compared for those who received radiotherapy and those who did not using Cox' proportional hazards ratio using age at diagnosis as an independent predictor. Rates of death were analysed using Fisher's exact test.

Results: We identified 330 patients who underwent HSCT from 2004-2010 for relapsed lymphoma.72 patients had Hodgkins's and 258 patients had non-Hodgkin's lymphoma. The median age at diagnosis was 46.5 years (14.6-72 years). The median age at transplant was 50.6 years (17.4-73.2 years). 121 patients (36%) underwent an allogeneic and 209 patients (64%) underwent an autologous transplant. Median follow-up was 1.8 years (0.0-10.0 years).
94 patients (28%) underwent radical RT before or after transplant (excluding TBI). 58 patients underwent radiotherapy before HSCT and 36 subsequent to HSCT. Of those who underwent RT before HSCT 64% were in remission going to HSCT compared with 75% of those who received RT after HSCT. There was a trend towards a shorter PFS for those who did not receive RT (HR1.72, 95% CI 0.96-3.67). There was no difference in mortality at 3 years between the two groups (p=0.78). There was no difference in OS between the two groups (HR=0.98, 95% 0.67-1.56). We are currently analysing the pattern of relapse and the impact of different variables on relapse and overall survival.

Conclusion: Peri-transplant RT seems to offer a progression free survival benefit in patients with relapsed/refractory lymphoma undergoing HSCT although confirmation is required.

EP-1143

Splenic irradiation as treatment modality in neoplastic hematological disorders

L. Díaz Gómez[1], A. Seguro Fernandez[2], J. Jaen Olasolo[1], I. Villanego Beltran[1], V. Diaz Diaz[1], E. Gonzalez Calvo[1], L. Ingunza Baron[1], L. Gutierrez Bayard[1], M.C. Salas Buzon[1], S. Garduño[1]
[1]*Hospital Universitario Puerta del Mar, Department of Radiation Oncology, Cadiz, Spain*
[2]*H.U. Rey Juan Carlos, Medical Physics, Mostoles Madrid, Spain*

Purpose or Objective: Splenic irradiation has been used as first treatment for several hematological neoplasm, including chronic leukemia or myeloid malignancies, but with the availability of new drugs its application was restricted. In selected cases, not only with palliative intentions, irradiation can be useful treatment modality

Material and Methods: Our study included 11 patients: 5 with chronic lymphocytic leukemia, 5 with high-grade B-cell lymphoma and 1 with diagnose of polycythaemia Vera. In 5 patients the treatment was with radical intention (all of them with high grade lymphoma) and the rest were palliatives as treatment of pain or normalization of red blood cell that allows more time between transfusions. The doses were generally low with range between 5 and 10 Gy in 0.5Gy daily fractions because doses higher than 10Gy did not provide benefits according to literature.

Results: We got 5 complete responses confirmed by PET but after 2 years 2 of them relapsed and were treated with radiotherapy again with the same scheme and obtain the same response to the present day. In terms of palliative intention, splenic irradiation provided a relief of pail from 6 to 12 months, and in 4 patients the disease progressed without new splenic symptoms. One patient received 3 courses of radiotherapy for painful splenomegaly with a gap of 12, 9 and 6 months without acute toxicity and died due to non-splenic leukemia progression.

Conclusion: In selected patients who are not responsive, not suitable for systemic treatment or palliatives, splenic irradiation can be an efficient therapy with little toxicity and sustained response over time. f of pail from 6 to 12 months, and in 4 patients the disease progressed without new splenic symptoms. One patient received 3 courses of radiotherapy for painful splenomegaly with a gap of 12, 9 and 6 months without acute toxicity and died due to non-splenic leukemia progression.

Electronic Poster: Clinical track: Breast

EP-1144

Clinical outcomes according to molecular subtypes in locally advanced breast cancer patients

H. Kim[1], W. Park[1], S.J. Huh[1], D.H. Choi[1], J.M. Noh[1]
[1]*Samsung Medical Center, Radiation Oncology, Seoul, Korea Republic of*

Purpose or Objective: We evaluated the tumor response and clinical outcomes according to molecular subtypes in locally advanced breast cancer patient who received neo-adjuvant chemotherapy (NAC) followed by surgery and radiotherapy.

Material and Methods: We retrospectively reviewed 400 patients with clinical stage II-III breast cancer who received NAC followed by surgery and radiotherapy in Samsung Medical Center, between 2007 and 2011. Among these, 329 patients who completed recommended therapy were analyzed on clinical outcomes and prognostic factors, with focusing on the molecular subtypes. Luminal A and B, HER2-enriched, and triple-negative subgroups were identified according to the hormone receptor (ER and PR), HER2, and Ki-67 receptor status.

Results: Overall pathologic complete response (pCR) rate after NAC were 20.1% and HER2- enriched subgroup was associated with the highest rates of pCR (43.6%), whereas luminal A showed the lowest rates of pCR (4.6%). A significant correlation was found between pathologic response (pCR vs. non-pCR) and molecular subtypes (*p* value <0.001). The median follow-up duration was 55 months (range, 5 to 98 months). The 5-year overall survival (OS) and disease-free survival (DFS) rates were 88.9% and 72.9%, respectively. In subgroup analysis, according to the pathologic response (pCR vs. non-pCR), triple-negative subtype proved significant difference in 5-year OS rate (100.0% vs. 71.6%, *p* value =0.005) and 5-year DFS rate (93.1% vs. 55.1%, *p* value <0.001). HER2-enriched subtype also showed significant difference in 5-year OS rate (100.0% vs. 79.1%, *p* value =0.05). A distinct survival difference according to molecular subtypes was found especially in non-pCR group (5-year OS and DFS, *p* value <0.001, respectively), in contrast, pCR group did not show a statistical difference of survival according to molecular subtypes. When compared

with luminal A, only triple-negative breast cancer was significantly related with decreased 5-year OS and DFS rate (p value <0.001, respectively).

Conclusion: Non-pCR group showed significantly decreased 5-year OS and DFS rates than pCR group, especially in triple negative and HER2-enriched breast cancer patients. In the case of pCR, there was no difference in survival rates regardless of molecular subtypes. While a significant difference between survival rates and molecular subtypes was found in the patients who failed to attain pCR. Compared to luminal A, only triple-negative subtype was associated with distinctly decreased 5-year OS and DFS rates.

EP-1145

EBRT vs IORT for breast conserving therapy A large mature single institution matched-pair evaluation

V. Vanoni[1], S. Bou Selman[1], S. Mussari[1], L. Menegotti[2], A. Ferro[3], A. Caldara[3], M. Nagliati[1], G. Berlanda[4], C. Prezzi[4], L. Tomio[1]

[1]Ospedale Santa Chiara di Trento, Radiation Oncology, Trento, Italy

[2]Ospedale Santa Chiara di Trento, Medical Physics, Trento, Italy

[3]Ospedale Santa Chiara di Trento, Oncology, Trento, Italy

[4]Ospedale Santa Chiara di Trento, Surgery, Trento, Italy

Purpose or Objective: Comparative outcome data after intraoperative radiotherapy (IORT) and external beam radiotherapy (EBRT) for breast cancer at >5ys median follow-up are rare. We present a large, mature single-institution matched-pair-comparison reporting survival and relapse-rates in patients treated with either modality.

Material and Methods: Complete datasets for 258 IORT-pts treated between 2000 and 2010 were matched with 258pts postoperatively treated with EBRT by age/histology/tumor size, grading/lymph-node-status/hormone-receptors/type of adjuvant therapy/surgical margins/treatment-date. EBRT was performed with 2 tangential fields to whole breast (50Gy/25fractions) and with 9-12MeV direct-electron-field-boosts to tumor bed (10-16Gy/5-8 fractions). A non-dedicated Linac (green-line-setup) with direct 8-12MeV electron fields (21Gy prescribed to 90%-isodose) delivered IORT. Relapse at surgical intervention site was classified as true local recurrence(LR). All recurrences in the treated breast (any quadrant) were classified as Ipsilateral Recurrence(IR).

Results: Median follow-up was 79 months (12-156) for both groups. IR were 11 after IORT and 6 after EBRT. LR for IORT and EBRT groups were 8 and 3, respectively. Cumulative incidence of IR at 5ys were 2.3%(IORT) and 1.4%(EBRT), (p=n.s., HR 1.8 CI 95% 0.69-5). Cumulative incidence of LR at 5ys was 1.5%(IORT) and 0.8%(EBRT), (p=n.s., HR 3.1 CI 95% 0.8-11.3) Overall survival(OS) at 3/5ys was 98.8%/96.1%(IORT) and 98.8%/95.3%(EBRT), (n.s.). Disease-free survival(DFS) at 3/5 ys was 97.2%/93.2%(IORT) and 98%/93.5%(EBRT) (n.s). Between IORT and EBRT, no differences in non-breast-cancer-related-deaths or second-cancer-incidence were recorded. When analyzed according to ASTRO-criteria for accelerated-partial-breast-irradiation(APBI), outcome was better in the APBI-suitable group than in the entire cohort and the APBI-unsuitable group. The IR at 5ys for APBI-suitable/cautionary/unsuitable were 0%/2,7%/8% respectively

Conclusion: In line with published randomized-trial-data, IR-rate was higher after IORT than after EBRT if no stringent patient selection was performed. Non-breast-cancer-mortality and second-cancer-incidence did not differ between IORT and EBRT. In patients suitable for APBI according to ASTRO-criteria, similar IR-, LR- and OS-data indicate that IORT is a viable alternative to EBRT.

EP-1146

Non-surgical therapy of early breast cancer with novel enzyme-targeting radiosensitisation

K. Kobayashi[1], A. Nishioka[2], Y. Ogawa[3], T. Yamagami[1]

[1]Kochi Medical School, Department of Radiology, Nankoku, Japan

[2]Kochi Health Sciences center, Radiation Oncology, Kochi-city, Japan

[3]Hyogo Prefectural Kakogawa Medical center, Radiology, Kakogawa-city, Japan

Purpose or Objective: The current standard treatment for early breast cancer is a combination of conserving surgery and endocrine therapy or that of endocrine therapy and chemotherapy or chemotherapy alone. Even after remarkable technical advances in breast cancer surgery, physical and mental invasion for patients after surgery is a problem to be solved. Also patients of dying from breast cancer for surgery denial exist. In this study, we evaluated the usefulness and safety of novel non-operative enzyme-targeting radiosensitization: Kochi Oxydol-Radiation Therapy for Unresectable Carcinoma, type II (KORTUC II) with endocrine therapy for stage I and II breast cancer.

Material and Methods: From October 2006 to September 2013, radiation therapy was performed for 44 women (median age 63years ranging from 37 to 88 years) of breast cancer (Stage 0; n=2, Stage I; n=19, and stage II; n=23). All patients refused both surgery and systemic chemotherapy. Radiation therapy performed was 44Gy/ 16fr/ 3.5W for total breast with field-in-field technique, then electron beam boost 9Gy / 3fr / 3days was added to the tumor bed. We injected the sensitizer (0.5% hydrogen peroxide solution + 0.83% sodium hyaluronate) under ultrasound guidance, before radiation therapy twice a week. Median follow-up period was 51 months (21-104 months). After the treatment, both PET-CT and breast MR were performed every year.

Results: About adverse event no skin symptoms more than grade3 was observed Beauty effect was excellent or good in all cases. Local recurrence was seen in only 2 case (4.5%). Distant metastasis was not observed. Only one patient died from other disease.

Conclusion: From the results of this study it was suggested that KORTUC II followed by endocine therapy is effective and safe as the therapy for stage I and II breast cancer.

EP-1147

Hypofractionated vs conventional radiotherapy: is there a difference in local recurrence?

R. Yadav[1], P. Lal[1], S. Agrawal[1], M. Verma[1], S. Misra[1], K. Maria[1], S. Senthil Kumar[1], S. Kumar[1]

[1]Sanjay Gandhi Post Graduate Institue Of Medical Sciences, Radiotherapy, Lucknow, India

Purpose or Objective: Randomized trials have established the role of hypofractionated radiation therapy (HFRT) in early breast cancer. HFRT allows for less costly and more accessible treatment. However, there is paucity of data for HFRT in locally advanced breast cancer (LABC). We report the impact of HFRT in unselected breast cancer patients (all stages except metastatic, both BCS /MRM) and compared with CFRT for any differences in outcomes.

Material and Methods: 463 patients of BCS/MRM treated between Jan'08 and July'13 with CFRT (50Gy/ 25fr) or HFRT(42.4Gy/16 fr or 40Gy/15) to the breast/chest wall (CW) ± SCF ± Ax, treated in 2 time periods were retrospectively reviewed. RT was given by direct electron field/ bitangential photons to the CW and by latter to the breast. SCF ± Ax RT was given by enface photons (when indicated). All patients of BCS received a tumor bed boost. Statistical analysis to compare the 2 groups for survival outcomes, was done in Sept'15. The primary endpoint was to compare the differences in loco regional recurrences (LRR) between the 2 groups.

Results: Of the 463 patients, 209 received CFRT and 254 received HFRT. Median age was 48yrs (IQR:40-56),premenopausal(CFRT:23%vs HFRT 39%,p=0.005), and LABC presentation(CFRT36% vs HFRT 52%, p=0.01) was seen in higher proportion of patients receiving HFRT. The commonest pathology was IDC (81%) with grade III tumors (45%),ER (+) was seen in 44%,TNBC in 34% and Her2Neu (3+) were seen in 27%. 254 patients(54.5%)had undergone BCS and 209 patients (45%) MRM. 54% had left sided cancer and neoadjuvant chemotherapy(NACT) was given in 38%.The grade, HR status, laterality, NACT administration, BCS/MRM were similar in the 2 arms. For MRM patients, enface electrons were used in 88% patients treated with CFRT and 76% patients with HFRT. LN RT was delivered in 76% vs 64% in patients receiving CFRT vs HFRT respectively (p=0.005). With a median follow-up of 40mo in CFRT (IQR:14-55) and 29 mo in HFRT (IQR 17-38), 9/209 (4.3%) patients in CFRT and 7/254 (2.7%) in HFRT had LR .On univariate analyses, the 2yr actuarial LRFS in CFRT vs HFRT was 95% vs 97% (p=0.37). The 2yr OS in CFRT vs HFRT was 81% vs 85%(p=0.035) and 2year DDFS was 80% vs 83 % (p=0.15)respectively.

Conclusion: The risk of local recurrence among patients of breast cancer treated with HFRT after BCS or MRM was not worse when compared to conventional radiation therapy despite a younger population with locally advanced clinical presentation in HFRT.

EP-1148

A comparison study of whole breast irradiation of hypo- and conventional fractionation

K.H. Shin[1], S.W. Lee[1], Y.J. Kim[2], K. Kim[1], E.K. Chie[1], H.G. Wu[1], S.W. Park[3], H.J. Yoo[4]

[1]Seoul National University Hospital, Radiation Oncology, Seoul, Korea Republic of

[2]National Cancer Center, Center for breast cancer, Goyang, Korea Republic of

[3]Chung-Ang University Hosptial, Radiation Oncology, Seoul, Korea Republic of

[4]Korea Institute of Radiological and Medical Sciences, Radiation Oncology, Seoul, Korea Republic of

Purpose or Objective: This investigation retrospectively compared early-stage breast cancer patients treated with accelerated hypofractionation (AHF) to the age- and stage-matched patients treated with conventional fractionation (CF).

Material and Methods: Three hundred seventy-nine early-stage (pT1-2 and pN0-1a) breast cancer patients who received radiation therapy (RT) with AHF after breast-conserving surgery (BCS) were included. These patients were matched by the years in which BCS was performed, age (±3 years), and stage to the 379 corresponding patients in a different center, who received BCS and RT with CF. The AFH regimen was delivered as 39Gy in 13 fractions to the whole breast and consecutive 9-12Gy in 3-4 fractions to the tumor bed. The CF was composed of whole breast irradiation up to 50.4Gy in 28 fractions and then boost to the lumpectomy cavity with 9-14Gy in 5-7 fractions.

Results: The median follow-up time was 75 months (range: 3.8-110.8 months). There was no statistically significant difference in the age, T and N stage, resection margin, and histologic grade. There were five ipsilateral breast tumor relapse (IBTR) in the AHF group compared with seven in the CF group. Seven and eight loco-regional relapse (LRR) was observed in the AHF and the CF group, respectively. The 7-year rates of IBTR-free survival (IBTRFS), LRR-free survival (LRRFS), and disease-free survival (DFS) were 98.9%, 98.4%, and 97.1% in the AHF arm and 98.1%, 97.9% and 96.0% in the CF arm, respectively ($p > 0.05$). Among AHF patients, no risk factors including histologic grade or molecular subtype were associated with IBTR. The incidences of mild, grade 1 edema, hyperpigmentation, and wet desquamation at the end of RT were observed higher in the CF group.

Conclusion: While reducing fraction number, AHF radiotherapy of 39Gy whole breast plus 9Gy boost in 16 fractions is comparable to CF radiotherapy with excellent tumor control and tolerable skin toxicity in patients with early-stage breast cancer.

EP-1149

Changing practice patterns for breast cancer radiotherapy: hypofractionation in KFSYSCC at Taiwan

Y.C. Tsai[1], J.J. Jian[1], S.H.C. Cheng[1], B.L. Yu[2], C.M. Chen[2], C.F. Horng[3]

[1]Koo Foundation Sun Yat-Sen Cancer Center, Radiation Oncology, Taipei, Taiwan

[2]Koo Foundation Sun Yat-Sen Cancer Center, Surgery, Taipei, Taiwan

[3]Koo Foundation Sun Yat-Sen Cancer Center, Clinical Research Office, Taipei, Taiwan

Purpose or Objective: Hypofractionated whole breast irradiation (HF-WBI) following breast conserving surgery has produced excellent outcomes, but utilization remains limited. We evaluated the impact of the landmark study (START) in the adoption of HF-WBI in Sun Yat-Sen Cancer Center (KFSYSCC) at Taiwan.

Material and Methods: Information was obtained from the institutional breast cancer data base with stage I to III breast cancer receiving adjuvant whole-breast radiotherapy between 2012 and Aug 2015. Patients treated with palliative intent, accelerated partial breast radiation were excluded. HF-WBI was defined as ≤21 fractions with a dose/fraction ≥2.5 Gy.

Table 1 Baseline characteristics of patients treated in the study

		HF-WBI	CF-WBI	Total patients	HF-WBI/CF-WBI (%)
Year	2012	6	180	186	3.2
	2013 Jan-June	7	145	152	4.6
	2013 July-Dec	46	94	140	32.8
	2014	208	147	355	58.6
	2015 Jan-Aug	144	65	209	68.9
Age	< 40 y/o	48	80	128	37.5
	40-49 y/o	120	181	301	39.9
	50-59 y/0	140	196	336	41.7
	>60 y/o	103	174	277	37.2
T stage	Tis	100	108	208	48.1
	T1	204	255	459	44.4
	T2	67	74	141	47.5
	T3	40	194	234	17.1

CF-WBI: Conventional whole breast irradiation

Results: We identified 1042 patients meeting inclusion criteria. HF-WBI utilization increased significantly from 4% before July 2013 to 57% afterwards. The adoption of HF-WBI reach 77% since July 2015. The reimbursement structure here is based on “course” rather than “number” of treatment, the increased adoption of HF-WBI saved an estimated $700,000 annually in our Cancer Center.

Fig1: The rate of breast hypofractionation utilization is graphed over time between 2012 and Aug 2015. A substantial increase in adoption of hypofractionated whole breast irradiation (HF-WBI) in July 2013

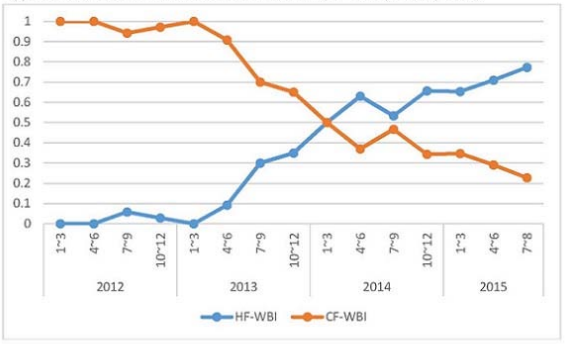

CF-WBI: Conventional whole breast irradiation

Conclusion: We found that the publication of START A and B trials in 2013 substantially increased adoption of HF-WBI for breast cancer at KFSYSCC , which increased the use of HF-WBI by 19-fold. The reimbursement structure allow us to quick adopt state of art and standard care for early stage breast cancer.

EP-1150

Patient quality of life treated with IORT during BCS followed by whole breast radiotherapy (WBI)

B. Urbanski[1], A. Roszak[1], K. Bratos[1], P. Milecki[2], A. Karczewska-Dzionk[2], M. Litoborski[3], S. Adamczyk[4]

[1]Greater Poland Cancer Centre, Radiotherapy and Gynecological Oncology, Poznan, Poland

[2]Greater Poland Cancer Centre, Radiotherapy Ward I, Poznan, Poland

[3]Candela, Candela, Warsaw, Poland

[4]Intra Op, Intra Op, Sunnyvale, USA

Purpose or Objective: The aim of the study was to report quality of life and others aspects based on EORTC questionnaire intraoperative radiotherapy (IORT) given as a boost during breast conserving surgery (BCS) followed by adjuvant whole breast radiotherapy (WBRT).

Material and Methods: Between 2008 and 2011 in 150 breast cancers patients treated in Greater Poland Cancer Centre. Intraoperative radiotherapy as a tumor bed boost was applied using mobile electron accelerator Mobetron 1000 (IntraOp Medical, Inc.). IORT boost (10 Gy) was followed by 50 Gy whole-breast external beam radiotherapy (EBRT). Chemotherapy, if indicated, was given before EBRT. The observation period was 1,5-5,5 years. The data was assessed by EORTC questionnaires (QLQ-C30 and QLQ-BR23) 1 month after RT, 6 months, 1 year, 2 years, 3 years and 4 years.

Results :

Tab 1. QLQ-C30 questionnaire data

SCALE	1 month	6 months	1 year	2 years	3 years	4 years	Reference EORT score	P value
Global health status	64,2	66	62	57,5	66,2	69	61,8	0,2143
Physical functioning	77	78,6	71	78,3	75,6	81	78,4	0,0242
Role functioning	81,3	85	85,3	89,6	84,3	90,2	70,9	0,0195
Emotional functioning	63,8	66	59,6	65,3	52	62	68,6	0,3969
Cognitive functioning	77,6	78	72,6	77	61,3 61,3	79 79	81,5	0,0195
Social functioning	79,6	84,3	85,3	78,6	81,3	86,2	77,0	0,0312
Fatigue	37	36	39,6	36	39,6	40,2	33,3	0,7320
Nausea and vomiting	5	2,3 2,3	8,66	7,7	12,6 12,6	9,2	7,7	0,0002
Pain	20,7	19,7	23,7	22,7	23	20,8	28,7	0,8887
Dyspnoea	21,3	19,7	25,3	26	29,3	27,2	18,1	07499
Insomnia	43	45	39,3	48,3	62,7	54,8	29,8	0,0063
Appetite loss	20,3	17	18,7	11	18,7	16,2	18,5	01591
Constipation	26,3	24,7	30	30	37,7	32,6	17,4	0,3677
Diarrhoea	5,3	8,7	8,7	5	10,3	9,2	5,9	0,3370
Financial difficulties	27	22,3	29,3	20	37,7	39,2	18,3	01880

There was no statistical significance change in quality of life in any follow-up period based on Friedman test analysis (p=0,2143).

Tab 2. QLQ-BR23 questionnaire data

SCALE	1 month	6 months	1 year	2 years	3 years	4 years	Reference EORT score	P value
Body image	70,2 70,2	81 81	79,3	77	74,3	79,2	82,7	0,008
Sexual functioning	10,3 10,3	18,3	18	23,6	26,3 26,3	29,2 29,2	19,5	0,000
Sexual enjoyment	8 8	22,3 22,3	16,3 16,3	22,6	31 31	37 37	53,1	0,000
Future perspective	34,2	39,8 39,8	37,5 37,5	45,3	46,2	49,1 49,1	47,3	0,000
Systemic therapy side effects	32,3	25	31,3	30,8	33,6	29,8	15,5	0,256
Breast symptoms	33,3 33,3	19 19	23,6 23,6	19,3	22,6	17,2	16,2	0,000
Arm symptoms	27,6	20,6	22,6	24,3	24,6	21,3	18,7	0,944
Upset by hair loss	21,6	13,1	17,6	20,3	26,3	22,1	5,0	0,854

There was statistical significance change in body image between 1 and 6 months after radiation therapy (p=0,008), but it was lower than EORTC reference score. Sexual enjoyment was lower than EORTC reference score in any follow up period time. Systemic therapy side effects was higher than EORTC control group in any follow up period time.

Conclusion: Intraoperative radiotherapy is proved to be tolerable and perspective treatment procedure with no statistical significance influence on quality of life.

EP-1151

Lymph flow guided irradiation of internal mammary lymph nodes

S. Novikov[1], S.V. Kanaev[1]
[1]*Prof. N.N. Petrov Research Institute of Oncology, Radiotherapy and Nuclear Medicine, St. Petersburg, Russian Federation*

Purpose or Objective: to analyze possible clinical value of lymph flow visualization as the guide for irradiation of IMLN.

Material and Methods: On the first stage of the study we combined data of 8 published studies that analyzed lymph flow from primary BC (4541 patients) after intra- peritumoral injection of nanosized 99mTc-colloids. Using this data we determined probability of lymph flow from BC of internal/central or lateral localization to IMLN. In 7 studies (4359 women) axillary staging was accompanied by biopsy of sentinel lymph nodes localized in internal mammary region. This data made it possible to estimate probability of IMLN metastatic invasion in relation with the status of axillary LN. At the final stage of the study we calculated probability of IMLN invasion by BC in 4 randomized and 2 observation studies that analyzed effect of IMLN irradiation on overall survival. Additionally, we tried to calculated possible additional gain in survival if patients from this 6 (4+2) trials would be treated according to lymph flow guided irradiation of IMLN.

Results: According to results of 8 published studies lymph-flow from lateral BC to IMLN was detected in 16% (727/4541), from internal/central lesions – in 35% (1589/4541).Evaluation of 7 studies (4359 women) showed that in patients with noninvolved axillary LN metastases in IMLN were revealed in 7.8%, in patients with positive axillary nodes - in 38.1% cases. In all 6 studies that evaluated clinical value of IMLN irradiation, calculated probabilities of IMLN metastatic invasion in "high risk patients" didn't exceed 10%. If IMLN irradiation would be performed only in patients with lymph flow to IMLN about 72.1%-76.8% of "high risk patients" would escape RT to IM region. In remained 23.2%-28.9% patients with visualized internal mammary sentinel lymph nodes their irradiation would improve overall survival from 1.6%-3.3% to 6.9%-14.2%.

Conclusion: visualization of lymph flow from breast cancer after intratumoral injection of 99mTc-nanocolloids make decision about irradiation of IMLN more precise and efficient. Irradiation of visualized IMLN can significantly (6.9%-14.2%) improved overall survival in this group of patients with BC.

EP-1152

Impact on late toxicity of IMRT with concomitant boost after breast conserving surgery

C. Digesù[1], M. Pieri[2], G. Macchia[1], M. Nuzzo[1], F. Deodato[1], S. Cilla[3], A. Ianiro[3], G. Tolento[2], F. Bertini[2], I. Ammendolia[2], M. Taffurelli[4], C. Zamagni[5], G. Compagnone[6], D. Balestrini[7], S. Cammelli[2], G. Frezza[7], V. Valentini[8], A.G. Morganti[2]
[1]*Fondazione di Ricerca e Cura "Giovanni Paolo II"- Catholic University of Sacred Heart, Radiation Oncology Unit, Campobasso, Italy*
[2]*S. Orsola-Malpighi Hospital- University of Bologna, Radiation Oncology Center- Department of Experimental- Diagnostic and Specialty Medicine - DIMES, Bologna, Italy*
[3]*Fondazione di Ricerca e Cura "Giovanni Paolo II"- Catholic University of Sacred Heart, Medical Physics Unit, Campobasso, Italy*
[4]*University of Bologna, Department of Medical and Surgical Science, Bologna, Italy*
[5]*S. Orsola-Malpighi Hospital- University of Bologna, SSD Medical Oncology, Bologna, Italy*
[6]*S. Orsola-Malpighi Hospital- University of Bologna, Department of Medical Physics, Bologna, Italy*
[7]*Bellaria Hospital, Radiotherapy Department, Bologna, Italy*
[8]*Policlinico Universitario "A. Gemelli"- Catholic University of Sacred Heart, Department of Radiotherapy, Roma, Italy*

Purpose or Objective: To assess the feasibility of Simultaneous Integrated Boost in Intensity Modulated Radiotherapy (SIB-IMRT) for breast cancer (BC) in the attempt to reduce the radiation treatment time. Results in terms of late toxicity and local control were compared with a control group (CG) of patients treated with 3-dimensional (3-D) conformal radiotherapy plus sequential boost.

Material and Methods: MARA-2 was conceived as a single arm phase I-II trial. Patients with moderate-high risk BC were enrolled and treated with forward-planned IMRT technique. Whole breast and tumor bed received a total dose of 50 Gy and 60 Gy (10 Gy concomitant boost) in 25 daily fractions, respectively. In CG group, prescribed dose to the breast was 50.4 Gy in 28 fractions with a sequential 10 Gy boost to the tumor bed in 4 fractions. Late skin and subcutaneous toxicity were evaluated using EORTC/RTOG scoring scale.

Results: Four hundred and fifty one patients were included in our study (MARA-2: 321; CG: 130). Median follow up was 52 months (range: 3-115). G1 and G2 late skin toxicities were acceptable without significant differences between the two groups. No G≥3 late skin toxicity was observed in MARA-2. At univariate analysis, late G1 and G2 subcutaneous toxicities were significantly higher in MARA-2 ($p<0.001$). 5-year G1 subcutaneous late toxicity free-survival (LTFS) were 73.4% and 38.5% in CG and MARA-2, respectively; moreover, 5-year G2 subcutaneous LTFS were 96.5% and 80.0% in CG and MARA-2, respectively. 5-year G3 subcutaneous LTFS was 0.9% in MARA-2 and 0% in CG, respectively. No differences were found in term of loco-regional control (LC) with a 5-LC of 96.7% and 97.6% in CG and MARA-2, respectively ($p=0.676$).

Conclusion: The use of SIB-IMRT technique in postoperative radiotherapy of BC allowed to reduce overall treatment time without significantly increasing the incidence of G>2 late effects.

EP-1153

Hypofractionated radiotherapy and simultaneous boost in breast cancer: preliminary result in elderly

N. Giaj-Levra[1], A. Fiorentino[1], R. Mazzola[1], S. Fersino[1], F. Ricchetti[1], G. Sicignano[1], S. Naccarato[1], R. Ruggieri[1], F. Alongi[1]
[1]*Ospedale Sacro Cuore - Don Calabria, Radiation Oncology, Negrar - Verona, Italy*

Purpose or Objective: To evaluate the feasibility and toxicity profile in elderly women, with a diagnosis of early stage breast cancer, underwent to adjuvant hypofractionated Volumetric Modulated Arc Therapy (VMAT) and simultaneous integrated boost (SIB) after conserving surgery (CS).

Material and Methods: Between September 2013 to March 2015, 50 consecutive women with a diagnosis of early stage of breast cancer were treated with SIB-VMAT after CS in our Institution. Inclusion criteria were: age ≥ 65 years, pT1 -2 disease, pN 0-1, no neoadjuvant chemotherapy, no-metastatic disease. A dose prescription of 40.5 Gy in 15 fractions was prescribed to the whole breast (PTVbreast) and an additional radiation dose of 48.5 Gy in 15 fractions to the tumour bed was prescribed (PTVboost). Hypofractionated treatment was purposed in patients with negative margins after surgery (> 1 mm). All patients were followed with periodic clinical evaluation. Acute toxicity were scored using EORTC/RTOG radiation morbidity score system. Both patient and physician recorded cosmetic outcome evaluation with a subjective judgment scale at the time of scheduled follow-up.

Results: Median follow-up was 20 months. At the time of the analysis, overall survival and local control rates were 100%. All patients completed the SIB-VMAT without interruptions. Acute skin toxicity was recorded as follow: grade 0 in 22 patients (44%), grade 1 in 24 cases (48%), grade 2 in 4 patients (8%). Regarding late adverse events, skin toxicity was registered as follow: grade 0 in 40 patients (80%), grade 1 in 10 cases (20%). No toxicity≥ grade 2 was registered. In

terms of cosmetic results, 99% and 1% of patients considered the result as good/excellent and as fair after RT, respectively. No patients had a poor cosmetic outcome.

Conclusion: These results support the feasibility and good tolerability of SIB-VMAT in elderly patients with a diagnosis of breast cancer following CS with acceptable acute and late treatment-related toxicity. These preliminary results justified continuing the clinical study with the goal to establish the impact of hypofractionated SIB-VMAT in elderly patients with diagnosis of early stage breast cancer.

EP-1154

Post mastectomy radiotherapy and periprosthesic capsule contraction: a clinico-pathological analysis

C. Digesù[1], G. Macchia[1], M. Nuzzo[1], F. Deodato[1], M. De Ninno[2], C. Lagreca[3], M.G. Fiorino[3], A. Ianiro[4], G. Tolento[5], I. Ammendolia[5], A. Arcelli[5], L. Ronchi[5], A.L. Angelini[6], S. Ciabatti[5], S. Cammelli[5], C. Zamagni[7], G. Frezza[8], M. Taffurelli[9], S. Manfrida[10], A.G. Morganti[5]

[1]Fondazione di Ricerca e Cura "Giovanni Paolo II"- Catholic University of Sacred Heart, Radiation Oncology Unit, Campobasso, Italy

[2]Fondazione di Ricerca e Cura "Giovanni Paolo II"- Catholic University of Sacred Heart, Pathology Unit, Campobasso, Italy

[3]Fondazione di Ricerca e Cura "Giovanni Paolo II"- Catholic University of Sacred Heart, Surgical Oncology Unit, Campobasso, Italy

[4]Fondazione di Ricerca e Cura "Giovanni Paolo II"- Catholic University of Sacred Heart, Medical Physics Unit, Campobasso, Italy

[5]S. Orsola-Malpighi Hospital- University of Bologna, Radiation Oncology Center- Department of Experimental- Diagnostic and Specialty Medicine – DIMES, Bologna, Italy

[6]S. Orsola-Malpighi Hospital- University of Bologna, Department of Medical Physics, Bologna, Italy

[7]S. Orsola-Malpighi Hospital, SSD Medical Oncology, Bologna, Italy

[8]Bellaria Hospital, Radiotherapy Department, Bologna, Italy

[9]University of Bologna, Department of Medical and Surgical Science, Bologna, Italy

[10]Policlinico Universitario "A. Gemelli"- Catholic University of Sacred Heart, Department of Radiotherapy, Rome, Italy

Purpose or Objective: To investigate the pathogenesis of peri-prosthesic capsule contraction (CCPP) related to post mastectomy radiotherapy in breast cancer patients undergoing breast reconstruction with heterologous material.

Material and Methods: Patients developing (early or late) CCPP after breast reconstruction were enrolled in this study. CCPP was clinically evaluated by Baker score in order to define pain, rigidity, firmness and dislocation of implant. CCPP was analysed considering pathological aspect after sub-total capsulectomy with anterior removal of peri-prosthesic capsule. Patients were split into two groups according to radiotherapy administration. Group 1 accounted for irradiated patients (50 Gy, 2 Gy per fraction on chest wall, using tangential field-in-field technique). Group 2 included not irradiated patients. Baker Score and microscopic observation (simil-synovial reaction, hyalinosis, vascular reaction, giant cells) of the two groups were compared by univariate and multivariate analysis.

Results: Analysis was performed on 26 patients who developed CCPP (29 capsulectomy, because 3 bilateral) in the period between April 2012 and February 2015 (34 months). All patients developed CCPP within 1 year from first reconstructive surgery. Characteristics of both groups are reported in Table 1.

	GROUP 1	GROUP 2
N° (%)	12	14
Median age (range)	47.5 (37-63)	48 (40-60)
Median BMI (range)	22.7 (16.5-33.6)	26.3 (22.10-46.5)
Histology		
Ductal Infiltrating Carcinoma (G1, G2, G3)	5	6
Lobular Infiltrating Carcinoma (G1, G2, G3.)	4	5
Invasive Mix Carcinoma	3	3
Reconstructive procedure		
Immediate monolateral	1	3
Immediate bilateral	0	2
In two operating sessions Monolateral	11	8
In two operating sessions Bilateral	0	1
Adjuvant treatment		
Chemotherapy	3	3
Hormone therapy	0	6
Chemotherapy + Hormone therapy	8	1
No adjuvant therapy	1	4

Univariate analysis showed a positive association between Baker Score and radiotherapy (OR: 1.65), and hyalinosis and radiotherapy (OR: 1.2). Multivariate analysis confirmed association between CCPP and radiotherapy (OR: 17.9); chemotherapy (OR: 4.3) and hormone therapy (OR: 48.44) in terms of contraction grade and simil-synovial reactions respectively.

Conclusion: Radiotherapy after breast reconstruction significantly influenced onset and severity of CCPP, although other variables contributed to CCPP multifactorial aetiology. In particular, hormone therapy and chemotherapy played a role in modifying capsular architecture.

EP-1155

Radiation-induced morbidity evaluated by high-frequency ultrasound: a pilot study

L.M. Schack[1], J. Overgaard[1], B.V. Offersen[2], J. Alsner[1]

[1]Aarhus University Hospital, Experimental Clinical Oncology, Aarhus C, Denmark

[2]Aarhus University Hospital, Department of Oncology, Aarhus C, Denmark

Purpose or Objective: Evaluation of radiation- induced morbidity is routinely done as an integrated part of treatment response follow-up, and can be scored according to clinical assessment tools such as the CTCAE or LENT-SOMA. Objective measures in this evaluation would be valuable given their quantitative nature, facilitating comparison across cohorts and treatment institutions. High-frequency ultrasound (US) is a high-precision, objective tool to measure dermis thickness of the skin. We aimed to analyze dermis thickness in a cohort of women following radiotherapy (RT) for breast cancer with various grades of induration and edema.

Material and Methods: The cohort was recruited from the DBCG HYPO/PBI RT protocols and comprised 15 women treated for early breast cancer during 2009–2013 with lumpectomy and RT 50 or 40 Gy +/- systemic therapy. Clinical morbidity follow-up of induration and edema was done at baseline and annually according to the LENT-SOMA scale. Dermis thickness was measured in mm using high-frequency US. Points of measurement were 3 cm from the areola in four quadrants in both irradiated and contralateral non-irradiated breasts. Differences in mean dermis thicknesses were tested by two-tailed paired t-test. The US scanner utilized was a high-resolution 20 MHz DermaScan® C from Cortex Technology ApS. This device is optimized for recognizing structures at 60 µm, corresponding to tissue microstructures sized like collagenous fibres.

Results: Median follow-up time was 3.0 years (range 1.0 – 4.6). Overall, mean dermis thicknesses were 2.22 mm (1.78 - 2.66) in the irradiated (I) breast and 1.26 mm (95% CI: 1.08 - 1.44) in the contralateral (C) breast. Mean difference between breasts was 0.96 mm (0.49 - 1.43, $p<0.001$). Dermis thickness was distributed in quadrants as follows: Lower lateral I: 2.62 (1.92 – 3.31) C: 1.11 (0.96 - 1.26), lower medial I: 2.64 (2.06 – 3.21) C: 1.45 (1.18 - 1.72), upper lateral I: 1.55 (1.33 – 1.78) C: 1.17 (1.01 – 1.34), upper medial I: 2.08 (1.49 – 2.67) C: 1.31 (1.09 – 1.53). In patients without clinical edema, the mean difference in dermis thickness for grade 1 induration was 0.35 mm (-0.46 - 1.16, $p=0.21$) and for grade 2 induration 0.71 mm (-0.01 - 1.43, $p>0.05$). In patients with clinical edema, only one patient had grade 1 induration (dermis thickness difference 1.34 mm). In

patients with clinical edema and grade 2 induration, mean difference in dermis thickness was 1.61 mm (0.27 - 2.95, p=0.03). Edema was associated with a more diffuse signal and an indistinct demarcation against the subcutaneous tissue. This was more pronounced in the lower quadrants (Figure).

Conclusion: High-frequency US has potential to measure increased dermis thickness associated with radiation-induced induration in breast cancer patients. Edema may increase dermis thickness and lead to a more diffuse US signal.

High-resolution ultrasound images of two patients without- and with edema. Both have grade 2 fibrosis.

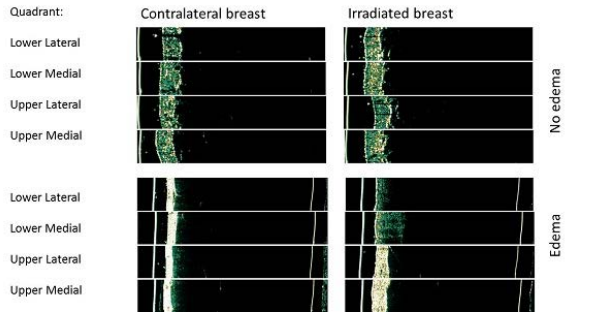

EP-1156

Radiotherapy for ductal carcinoma in situ: patterns of recurrence and risk factors stratification

I. Meattini[1], L. Livi[1], P. Bastiani[2], V. Scotti[1], L. Paoletti[2], C. De Luca Cardillo[1], R. Barca[2], D. Greto[1], F. Martella[3], G. Simontacchi[1], G. Tinacci[3], J. Nori[4], H. Smith[3], L. Sanchez[5], L. Galli[3], L. Orzalesi[5], S. Fondelli[2], S. Bianchi[6], F. Rossi[2]

[1]Azienda Ospedaliero-Universitaria Careggi, Radiation Oncology Unit- University of Florence, Florence, Italy
[2]S. Maria Annunziata Hospital, Radiation Oncology Unit, Florence, Italy
[3]S. Maria Annunziata Hospital, Breast Unit, Florence, Italy
[4]Azienda Ospedaliero-Universitaria Careggi, Radiology Senology Unit, Florence, Italy
[5]Azienda Ospedaliero-Universitaria Careggi, Breast Surgery Unit, Florence, Italy
[6]Azienda Ospedaliero-Universitaria Careggi, Pathology Unit - University of Florence, Florence, Italy

Purpose or Objective: Ductal carcinoma in situ (DCIS) represents around 20% of breast cancers (BC). Standard treatment after breast conserving surgery is still adjuvant radiotherapy (RT). Several randomized trials and meta-analysis showed a 50% risk reduction in LR after adjuvant RT. The aim of our analysis was to evaluate the LR rate and possibly to identify a risk groups stratification for DCIS treatment optimization.

Material and Methods: We analyzed 457 patients that underwent BCS and adjuvant RT between 1990 and 2012. Median dose to the whole breast was 50 Gy in 25 fractions; patients with positive/close final surgical margins received a tumor bed boost. We stratified patients in low risk group using well known risk factor for LR (n=203; age ≥50 years, surgical margins ≥10 mm, nuclear grade 1 -2, pT≤25 mm), and intermediate-high risk group (n=254; age <50 years, surgical margins <10 mm, nuclear grade 3 or pT >25 mm). We performed also a patient startification according to Van Nuys Prognostic Index. Estrogen and progesterone receptors status, nuclear grade, and Ki-67 proliferative index were available for most patients.

Results: The mean age was 57 years (range 33-80). Hormonal status was positive in 92% of patients, 83 cases (18.2%) received adjuvant endocrine therapy. All patients received postoperative RT, 198 cases (43%) received also a RT boost on tumor bed.
At a median follow up time of 12 years (range 3-23), we observed 26 LR (5.6%). Following risk groups stratification, we observed seven LR (3.4%) in low risk group and nineteen LR (7.4%) in intermediate-high risk group (p<0.001).

Conclusion: Our experience evidenced a significant difference in LR incidence after adjuvant RT based on our risk factors stratification.
This confirms the wide heterogeneity of DCIS. Identification of clear subgroups of patients following risk factors is still lacking. Waiting for results from ongoing clinical phase 3 trials and genomic studies, postoperative RT still remains a mainstay in adjuvant treatment for DCIS.

EP-1157

Abstract withdrawn

EP-1158

Should breathing adapted radiation therapy also be applied for right-sided breast irradiation?

M. Essers[1], P.M. Poortmans[2], K. Verschueren[3], S. Hol[3], D.C. Cobben[3]

[1]Dr. Bernard Verbeeten Instituut, Department of Medical Physics, Tilburg, The Netherlands
[2]Radboud University Medical Centre, Radiation Oncology, Nijmegen, The Netherlands
[3]Dr. Bernard Verbeeten Instituut, Radiation Oncology, Tilburg, The Netherlands

Purpose or Objective: Voluntary moderate deep inspiration breath-hold (vmDIBH) is widely used for patients with left sided breast cancer. The purpose of this study was to investigate the utility of vmDIBH in local and locoregional radiation therapy (RT) for patients with right-sided breast cancer.

Material and Methods: For fourteen patients with right-sided breast cancer, forward IMRT plans were calculated on free-breathing (FB) and vmDIBH CT-scans, for local- as well as locoregional breast treatment, with and without internal mammary lymph nodes (IMN). We compared dose volume parameters to estimate the reduction in the risk of radiation pneumonitis, the influence on pulmonary lung function tests and the risk of secondary lung cancer with the use of vmDIBH.

Results: For local breast treatment, no relevant reduction in mean lung dose (MLD) was found. For locoregional breast treatment without IMN, the average MLD reduced from 6.5 to 5.4 Gy (p<0.005) for the total lung and from 11.2 to 9.7 Gy (p<0.005) for the ipsilateral lung. For locoregional breast treatment with IMN, the average MLD reduced from 10.8 to 9.1 Gy (p<0.005) for the total lung and from 18.7 to 16.2 Gy (p<0.005) for the ipsilateral lung. We also found a reduction in mean heart dose between 0.6 and 2.6 Gy in four patients; with a mean of 0.4 Gy for all 14 patients together (p=0.07). We estimate that 1 out of 100 patients will not develop radiation pneumonitis when breath-hold is applied during locoregional right-sided breast cancer treatment. For ever-smoking women, the risk of secondary lung cancer might also be reduced by vmDIBH.

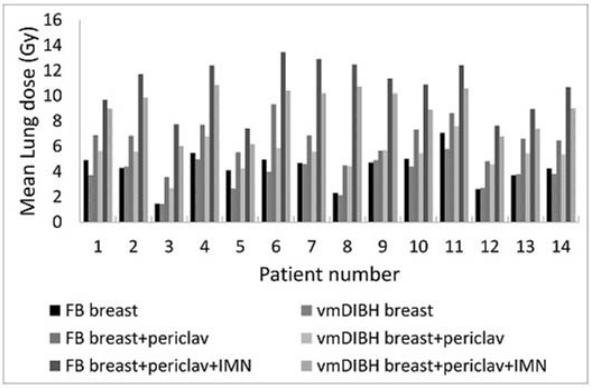

Conclusion: Breathing adapted radiation therapy in patients with left-sided breast cancer is becoming widely introduced. As a result of the slight reduction in lung dose found for

locoregional right-sided breast cancer treatment in this study, a slightly lower risk of pneumonitis and secondary lung cancer (in ever-smoking patients) can be expected. In addition, we estimate that for 10-25% of the patients the heart dose will also be reduced. We therefore suggest to also apply breath-hold for locoregional irradiation (with and without IMN) of patients with right-sided breast cancer.

EP-1159

Does a SPECT-CT improve the delineation of internal mammary nodes for breast cancer patients?

M. Essers[1], K. Van der Klugt[2], R.H. Tijssen[3], R. Pijpers[4], B. Oei[2], P.M. Poortmans[5]
[1]*Institute Verbeeten, Department of Medical Physics, Tilburg, The Netherlands*
[2]*Institute Verbeeten, Radiation Oncology, Tilburg, The Netherlands*
[3]*University Medical Centre Utrecht, Medical Physics, Utrecht, The Netherlands*
[4]*Institute Verbeeten, Nuclear Medicine, Tilburg, The Netherlands*
[5]*Radboud University Medical Centre, Radiation Oncology, Nijmegen, The Netherlands*

Purpose or Objective: A large recent study(1) has shown that in patients with early-stage breast cancer, irradiation of the regional (internal mammary and medial supraclavicular) nodes improves disease-free and distant disease-free survival, while breast-cancer mortality is reduced. However, internal mammary nodes (IMN) are usually delineated using anatomical landmarks, e.g. using the ESTRO delineation atlas (2), since the nodes are not visible on CT. We studied the impact of SPECT-CT lymphoscintigraphy on the localisation of IMN and on the subsequent treatment planning and dose distribution.

Material and Methods: For 10 breast cancer patients (5 right, 5 left), SPECT-CT lymphoscintigraphy of the IMN was performed. Using the Eclipse TPS (Varian), the SPECT-CT and planning CT images were co-registered. The 70% of the maximum uptake value was used to contour the IMN on SPECT-CT images. Using the ESTRO atlas, the IMN were also contoured on the planning CT images. The localisation of IMN based on the SPECT-CT images and based on the ESTRO atlas were compared, as well as treatment plans based on the two contouring methods.

Results: For 2 patients, no drainage to the IMN was visible. For 6 out of the remaining 8 patients, the caudal border of the IMN based on SPECT-CT was situated at the second intercostal (IC) space, whereas the ESTRO atlas prescribes to include the third or fourth IC space depending of the position of the tumour in the breast. In the lateral direction, the lymph nodes mostly follow the veins, but for one patient, the position on SPECT-CT was more medial (and missed by the ESTRO atlas) and for one more lateral. On treatment planning, for one patient only 50% of the IMN seen on SPECT-CT would have been covered following contouring using the ESTRO atlas. The mean heart dose (MHD) increased by 0.8 Gy for one patient and decreased by 1.0 Gy for one patient and the mean lung dose (MLD) decreased by 2 Gy for one of the patients following SPECT-CT based delineation. For the other patients, the differences in MHD and MLD were less than 0.5 Gy.

Conclusion: Delineation of the IMN using SPECT-CT lymphoscintigraphy is easier and less user dependent than using the delineation atlas. In general, the agreement between atlas and SPECT-CT based delineation is good. However, the caudal border of the IMN was overestimated in 6 out of 8 patients. Differences in the medial border were also observed, resulting in underdosage of the IMN in 1 and overdose to lung and heart in 1 other patient. SPECT-CT lymphoscintigraphy might be applied for patients with a high heart dose, to investigate whether the caudal and medial border of the IMN may be reduced.

(1) Poortmans PM, et al. Internal Mammary and Medial Supraclavicular Irradiation in Breast Cancer. N Engl J Med 2015; 373:317-327.
(2) Offersen BV, et al. ESTRO consensus guideline on target volume delineation for elective radiation therapy of early stage breast cancer. Radiother Oncol 2015 Jan;114(1):3-10.

EP-1160

What drives post-mastectomy radiation therapy receipt in T2N0 patients?

C. Fisher[1], R. Rabinovitch[1], J. Jagar[1], A. Amini[1], P. Kabos[1]
[1]*University of Colorado Denver, Radiation Oncology, Aurora-CO, USA*

Purpose or Objective: Increased biological information on individual tumors can be obtained with 21-gene recurrence score (RS) testing, which has revolutionized receipt of chemotherapy. Similar biological drivers of outcomes may be useful in determining who might benefit from post-mastectomy radiation, as is being investigated in the SUPREMO and other trials. This study aimed to determine who was getting post-mastectomy radiation in a T2N0 cohort, as well as whether the recurrence test score affected radiation radiation therapy receipt.

Material and Methods: The National Cancer Data Base captures about 75% of all US cancer patients and was queried for breast cancer patients from 2004-2012. 5302 T2N0 post-mastectomy patients were identified. Multivariate logistic regression analysis was used to estimate the covariates associated with test utilization and impact on radiation therapy decisions (see table). Z-test was used to measure the difference between radiation receipt for those who had the test and those who did not.

Results: Post-mastectomy radiation was delivered for 431 patients (8.1%) of the 5302 included patients. Multivariate statistics were used to investigate potential radiation drivers including age, race, insurance status, grade, recurrence score, and presence of cells in the nodes on immunohistochemical staining (N0i+ versus N0i-). The strongest association with receipt of radiation therapy was N0i+ status ($p<.002$) versus N0. Age, race, insurance status, grade, and actual recurrence score did not predict for receipt of post-mastectomy radiation therapy.

Conclusion: As expected, radiation was used in a minority of this cohort. Presence of cells in a lymph node was the largest driver, even though the disease burden in the nodes was very low to be T2N0i+. In patients where the recurrence score was ordered, it also predicted for non-receipt of radiation therapy as a rationale de-escalation of care. The biggest driver of radiation was Noi+ status, where at least a small number of cells reached the lymph nodes and radiation might be expected to have an impact. Interestingly, increasing recurrence score reflecting aggressive biology and poorer outcomes did not drive PMRT receipt in this population. In the future, use of the recurrence score may help select patients in whom personalized use of local therapy is possible.

EP-1161

Does sentinel-node biopsy affect the use of supine MRI for regional breast radiotherapy?

T. Van Heijst[1], D. Eschbach-Zandbergen[1], B. Van Asselen[1], J.J.W. Lagendijk[1], M. Van Vulpen[1], H.M. Verkooijen[2], R.M. Pijnappel[3], A.J. Witkamp[4], T. Van Dalen[5], H.J.G.D. Van den Bongard[1], M.E.P. Philippens[1]
[1]*UMC Utrecht, Radiotherapy, Utrecht, The Netherlands*
[2]*UMC Utrecht, Epidemiology, Utrecht, The Netherlands*
[3]*UMC Utrecht, Radiology, Utrecht, The Netherlands*
[4]*UMC Utrecht, Surgery, Utrecht, The Netherlands*
[5]*Diakonessenhuis, Surgery, Utrecht, The Netherlands*

Purpose or Objective: Regional radiotherapy (RT) is replacing axillary lymph node (LN) dissection in breast-cancer patients with tumor-positive sentinel node(s) (SNs). In regional RT, only part of the LNs can be visualized using

computed tomography (CT); consequently, LN levels are delineated according to vessels and muscular boundaries. Magnetic resonance imaging (MRI) allows high resolution and high contrast images for explicit LN visualization in supine RT position. The purpose of the study was to assess effects of sentinel-node-biopsy (SNB) on MRI detection rate and on patient endurance, and relate MRI detection rate to CT.

Material and Methods: Currently, 8 of in total 25 female early-stage breast-cancer patients (cT1-3, N0) have been enrolled, scheduled for SNB and breast-conserving surgery (BCS). Additional to standard postoperative CT for RT planning, all patients were scanned on 1.5 T MRI, before and after BCS. CT and MRI were performed in supine RT position, with both arms abducted and supported. MRI comprised two T1-weighted (T1w) spoiled gradient echo techniques, two T2w fast spin echo methods, and diffusion-weighted MRI, all covering the axillary and periclavicular areas using posterior and anterior 16-array coils. MRI acquisition was limited to 20 minutes per session. Patient endurance to undergo MRI was monitored qualitatively. A radiation oncologist delineated LN levels on both MRI and CT (levels I-IV, interpectoral) according to ESTRO contouring guidelines. By inspection of all MRI scans acquired in one session, individual LNs were delineated. The detection rate, i.e. number of LNs identified, was determined for CT and for each MRI session. The pre- and postoperative MRI detection rates were compared to assess influence of SNB, and also compared to CT. For each LN, the corresponding LN level was denoted.

Results: The number of LNs on postoperative MRI exactly matched the preoperative number for all 8 patients (range: 19 – 42), when adding the excised SNs. All SNs were retrospectively identified in level I on preoperative MRI. In 7 out of 8 patients, spatial correspondence of all other LNs between MRI sessions was established. In one patient, a post-SNB seroma was visible, but detection number was unaffected. The majority of LNs were located in the LN levels, while up to 7 were found outside (up to 6 mm). LN detection on CT (7 – 21 LNs) was much lower than MRI. Endurance was excellent and unaffected by BCS/SNB.

	Numbers of LNs					*Location of LNs*					
Patient number	Preop MRI	Postop MRI	Postop CT	Pre- vs. postop MRI	SNs excised	Level I (SNs)	Level II	Level III	Level IV	Level IP	Ext.
1	28	27	21	1	1	15 (1)	7	1	2	0	3
2	42	40	21	2	2	28 (2)	6	3	3	0	2
3	35	33	16	2	2	22 (2)	3	1	2	2	5
4	26	25	10	1	1	13 (1)	4	3	0	2	4
5	34	33	7	1	1	18 (1)	8	1	0	0	7
6	30	29	8	1	1	20 (1)	2	2	0	3	3
7	19	18	7	1	1	13 (1)	2	0	1	3	1
8	23	22	10	1	1	10 (1)	2	2	0	3	6

Table 1: Numbers of LNs found in each patient, on pre- and postoperative MRI, and postoperative CT. The difference between MRI sessions is denoted, as well as the number of SNs excised during SNB. Numbers of LNs per axillary contour, or outside, are listed. IP = inter-pectoral. Ext. = exterior LNs, i.e. those located outside of the standard levels.

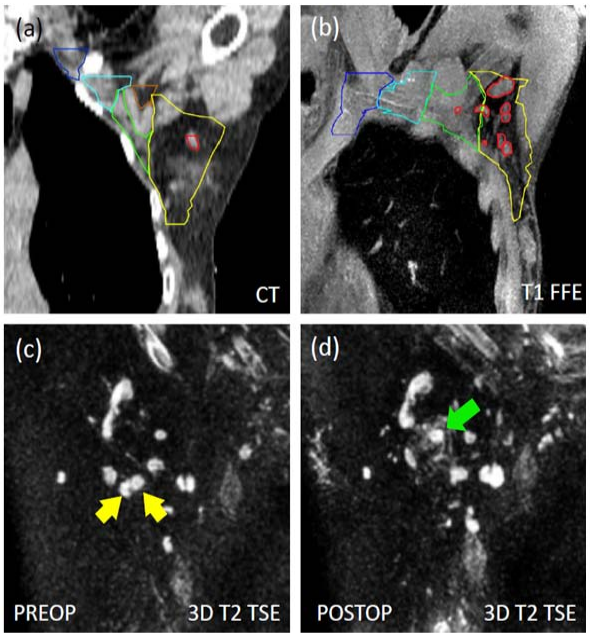

Figure 1: (a) Coronal CT scan with axillary levels contoured (axillary levels I-IV are yellow, green, sky blue, dark blue; inter-pectoral level is brown), according to ESTRO delineation guidelines. (b) Coronal T1-FFE MRI scan with in red individually delineated axillary LNs. (c) Preoperative coronal 3D T2 TSE scan where individual LNs are clearly visible (showing hyper-intense signal). The yellow arrows point to the two SNs which are excised during SNB. (d) The corresponding postoperative 3D T2 TSE; the SNs are now absent, while seroma due to the SNB is visible, as indicated by the green arrow.

Conclusion: MRI after SNB is able to identify the exact numbers of LNs as found on pre-SNB MRI. CT detection rate is much lower than MRI. SNB does not affect patient endurance. All excised SNs were identified on preoperative MRI. Some LNs were located just outside the LN levels. MRI in RT planning may lead to better target definition compared to CT. In future studies, we will study personalized RT using MRI guidance, possibly leading to reduced target volume. Based on current patient inclusion rate, updated results on all 25 patients are expected soon.

EP-1162

Cyberknife stereotactic partial breast irradiation for early stage breast cancer

O. Obayomi-Davies[1], S. Rudra[1], L. Campbell[1], S.P. Collins[1], B.T. Collins[1]

[1]*Georgetown University Hospital, Radiation Oncology, Washington DC, USA*

Purpose or Objective:

Background: Partial breast irradiation (PBI) is an attractive treatment option for well selected women undergoing breast conserving therapy for early stage breast cancer. In properly selected women, outcomes following PBI are comparable to conventional whole breast radiation. The CyberKnife linear accelerator may offer meaningful technical improvements to existing PBI techniques. We report our experience with CyberKnife stereotactic accelerated partial breast irradiation (CK-SAPBI).

Material and Methods: Between 11/2008 and 09/2015, CK-SAPBI was attempted on 21 patients with early stage breast cancer. Four to six gold fiducials were implanted around the lumpectomy cavity prior to treatment. Fiducials were tracked in real-time using the CK Synchrony tracking system. Prior to 2014, the clinical target volume (CTV) was defined on contrast enhanced CT scans using surgical clips and the obvious post-operative cavity. A 5 mm uniform expansion was added to generate the planning treatment volume (PTV). Starting in 2014, the CTV was defined on contrast enhanced CT scans as the lumpectomy cavity plus a 10 mm uniform expansion confined to the breast tissue. A 3-5 mm uniform expansion was added to generate the PTV. All patients received 30 Gy in five fractions delivered to the PTV. Dosimetry was assessed per institutional protocol, the National Surgical Adjuvant Breast and Bowel Project B-39

guidelines, and TG-101. Cosmesis was assessed using the Harvard Breast Cosmesis Scale.

Results: Twenty patients were treated successfully. At a median follow-up of 18 months (1-78), all patients remain locally controlled (100%) and no significant adverse events have occurred. All patients continue to experience good-excellent cosmetic outcomes. At least 3 fiducials were tracked in 85% of cases. Fiducial tracking was not successful in one patient. The mean number of beams delivered was 145 (77-196). The mean treated PTV30Gy was 74 cm3 (15-142 cm3) with a mean prescription isodose line of 82% (75-86%). 99% of the PTV30Gy received the prescription dose (95-100%) with a mean maximum dose of 36 Gy (34.5-40Gy). The mean ipsilateral breast V30Gy and V15Gy were 12% (3-26%) and 30% respectively (8-58%) sparing significant amounts of normal breast tissue. Patient tolerance was excellent and acute toxicity was rarely observed. 2 patients experienced grade 1 localized dermatitis at the initial 4 week follow-up visit.

Conclusions: CyberKnife stereotactic accelerated partial breast irradiation is a suitable radiotherapy technique for the delivery of partial breast irradiation. The CK platform produces highly conformal treatments with excellent normal tissue sparing and offers improvements over existing PBI techniques. Our experience indicates that CK-SAPBI delivered in five fractions is well tolerated with excellent short term local control and breast cosmesis. Longer follow-up is needed for assessment of late toxicity and oncologic outcomes.

EP-1163

Selection of patients with left breast cancer for Deep-Inspiration Breath-Hold Radiotherapy Technique

B. Czeremszynska[1], S. Drozda[2], M. Górzyński[1], L. Kępka[1]
[1]*Independent Public Health Care Facility of the Ministry of the Interior, Radiotherapy Department, Olsztyn, Poland*
[2]*University of Warmia and Mazury, Faculty of Mathematics and Computer Science, Olsztyn, Poland*

Purpose or Objective: The voluntary deep-inspiration breath-hold radiotherapy technique (DIBHRT) in the treatment of left breast cancer has the ability to reduce doses to heart left anterior descending coronary artery (LAD) and lung. Before introduction of DIBHRT into routine clinical practice, we conducted a prospective study to assess the extent of dosimetric benefit of this technique in order to select a group of patients for whom this technique should be routinely applied

Material and Methods: Thirty one consecutive patients qualified for whole breast irradiation (WBI) with tangential fields following breast conserving surgery for left-sided early breast cancer were included. All patients underwent breath-hold training, free-breathing (FB) and DIBH planning-CT. Separate radiotherapy treatment plans for WBI in total dose of 39.9Gy in 15 fraction were prepared based on both planning-CT. Doses like mean heart, heart V20Gy, maximum LAD, left lung V20Gy were calculated for each plan and the difference of respective values (delta) for FB and DIBH were calculated. If relative improvement of at least 20%for any evaluated dosimetric parameter were found for DIBH plan without significant worsening of other measures, this plan was selected for treatment. Daily tree-dimensional surface imaging (VisionRT) and weekly electronic portal imaging were performed. The data distribution were assessed using chi^2 test, correlations were analyzed using the Pearson test. Furthermore, receiver operating characteristic (ROC) analysis was performed.

Results: In 30 of 31 patents a reduction at least 20% in one or more evaluated parameters (i.e.mean heart, heart V20Gy, maximum LAD and left lung V20Gy in 29, 29, 26, and 7 patents respectively)was achieved. The relative worsening of left lung V20Gy was found for in 10 and cases and of maximum LAD in 2 cases. Eventually 25 patients were qualified to DIBHRT. Mean delta(Gy) were:mean heart 1.51 (range:0.06-6.45),heart V20Gy:3.0 (range:0.0-6.59),maximum LAD:18.5(range:-3.29-36.68), left lung V20Gy:1.7(range:-2.71-8.7). Correlations between delta values of mean heart, maximum LAD, heart V20Gy with length of cardiac contact distance (CCD) ($p< 0.05$, AUC>0,6) and maximum LAD, heart V20Gy with Body Mass Index (BMI)($p<0.05$;AUC>0.6) were found. ROC analysis showed that a 2.5 cm of CCD is a threshold for reduction at least 20% in one or more parameters. For BMI no specific threshold for predefined improvement of any dosimetric parameter was identified, which means that despite correlation of dosimetric cardiac benefit with higher BMI, some patients with low BMI may also have cardiac doses reduced with DIBHRT.

Conclusion: In our center we have prospectively confirmed an ability of DIBHRT for heart and LAD but not for lung-sparing. We are going to use this technique routinely for left-sided breast cancer patients with CCD above 2.5 cm

EP-1164

Outcomes of postmastectomy radiotherapy in patients with 1 to 3 positive nodes in single institute

Y. Kumai[1], M. Oguchi[1], Y. Miyagi[2], Y. Ito[2], T. Iwase[2], F. Akiyama[3], K. Yoshida[4], A. Harada[1], H. Okubo[1], T. Asari[1], K. Murofushi[1], T. Toshiyasu[1], T. Kozuka[1], M. Sumi[1]
[1]*Cancer Institute Hospital, Radiation Oncology, Tokyo, Japan*
[2]*Cancer Institute Hospital, Breast Oncology Center, Tokyo, Japan*
[3]*Cancer Institute Hospital, Division of Pathology, Tokyo, Japan*
[4]*Showa General Hospital, Radiology, Tokyo, Japan*

Purpose or Objective: Post-mastectomy radiation therapy (PMRT) is standard care for breast cancer patients with high risk for locoregional recurrence after mastectomy. The indication for PMRT in patients with 1 to 3 positive nodes has been in discussion. We reported that patients concomitantly with 1 to 3 positive nodes and extensive lymphatic invasion, who had not been treated with PMRT from 1990 to 2000, had 13.1% (12/92) of locoregional recurrence rate. Since then we have performed PMRT for patients with 1 to 3 positive nodes and extensive lymphatic invasion.
To investigate the effectiveness of PMRT for patients with 1 to 3 positive nodes and extensive lymphatic invasion.

Material and Methods: Between 2005 and 2013, 639 patients were treated with PMRT and 277 patients of those have not been without neoadjuvant chemotherapy until the lymph node dissection. Among these patients, 81 were diagnosed with 1 to 3 positive nodes pathologically, 65 were with 1 to 3 positive nodes and extensive lymphatic invasion. The 3-D conformal RT, using the partial wide tangent technique to the chest wall, internal mammary lymph nodes and supra-clavicular nodes, was applied for all patients, delivering 50 Gy in 25 fractionation over 5 weeks. In the patients with positive surgical margin, 10 Gy of electron boost to the tumor bed was added. We retrospectively reviewed and compared locoregional recurrence rates of 65 patients with 1 to 3 positive nodes and extensive lymphatic invasion treated with PMRT and that of 92 patients without PMRT.

Results: Baseline patient characteristics; the median age of these patients was 47 years old (range; 34-76). Survivals; the median duration of overall survival was 114 months (30 to 121 months), the five-year survival rate is 97%, and the median progression-free survival time after PMRT was 93 months (7.0 to 110 months). Of the 65 patients in the current analysis, 58 patients (89%) were alive and free of cancer. Initial failure patterns; the locoregional recurrence was observed in 3 patients (4.6%), classifying into 1 chest wall, 1 regional lymph node, and 1 both. All patients with locoregional recurrence were developed the distant metastases then after. As toxicity; radiation induced pneumonitis graded 1 was observed in 9 patients, nor been graded 2 or more observed. Acute radiation induced dermatitis was observed almost all patients at least grade 1, grade3 was observed in 9 patients. One patient denied continuing PMRT at dose of 46Gy, 7 months later her chest wall recurrence was observed.

Conclusion: The 4.6% of local recurrence rate of PMRT cohort registered from 2005 to 2013 was lower than 13.1% (12/92) of non-PMRT cohort registered from 1990 to 2000.

EP-1165

Impact of nodal status on clinical outcome of breast cancer patients: a monoinstitutional experience

C. Cefalogli[1], M. Trignani[1], L.A. Ursini[1], A. D'Aviero[1], M. Di Tommaso[1], S. Di Santo[1], A. Pamio[2], M. Di Nicola[2], D. Genovesi[1]
[1]*Ospedale Clinicizzato S.S. Annunziata, Radiotherapy, Chieti, Italy*
[2]*Laboratory of Biostatistics, Biomedical Science, Chieti, Italy*

Purpose or Objective: The aim of our study was to determine the impact of nodal status and other prognostic factors on clinical outcome of patients with breast cancer treated with surgery and adjuvant radiotherapy.

Material and Methods: A total of 774 breast cancer patients treated between 2001 and 2013 were retrospectively analyzed. Qualitative and quantitative characteristics were summarized as frequencies and percentages, average and standard deviations. The rates of Overall Survival (OS), disease free survival (DFS), and loco-regional recurrence (LR) were calculated at 36 and 60 months with the Kaplan-Meier method. Multivariate analysis was also performed and a p value of 0.05 was considered statistically significant.

Results: We identified 774 patients treated with adjuvant RT of which 595 patients (75.4%) without nodal involvement (pN0), 118 (14.9%) pN1-3 and 61 (7.75%) with more than 3 positive lymph nodes (pN>3). In our sample, supra-clavicular region was irradiated in 62 patients (13 pN>3, 17 pN1-3, 32 pN0). Median follow-up was 36 months (range 1-144 months). There were 14 cases of LR, of which 13 in pN0 and 1 in pN1-3 patients. A total of 31 patients developed distant metastases (48.4% in pN0, 19.4% in pN1-3, 32.2% in pN>3 group). The mortality rate was of 2.8% (68.1% pN0, 18.2% pN1-3 and 13.6% pN>3). There were no statistically significant differences in terms of OS, DFS and MFS among the three treatment groups. Multivariate analysis showed that clinical outcomes were significantly correlated with margin status (p-value: 0.00), T-stage (p-value: 0.053), Her2-neu gene amplification (p-value: 0.00), Ki-67 (p-value: 0.00) and SCRT (p-value:0.00). Variables such as age, surgery, ER and PgR expression and grading, were not significant.

Conclusion: In our study we observed higher rates of events in pN0 and pN1-3 patients, but none statistically significance was demonstrated between pN0, pN1-3 and pN>3 in terms of OS, DFS and MFS. Furthermore pN0 was in this experience the bigger group and this certainly influenced statistical analysis. In breast cancer, nodal status plays a key role both in the prognostic evaluation and in the therapeutic choice, and the clinical outcome of patients pN1-3 is comparable to pN>3 patients; so in this group (pN1-3) it is also necessary the evaluation of other prognostic factors such as receptor status, Ki 67 and surgical margins. Nodal status alone seems incapable to really guide treatment choice, with particular regard to the SCRT appropriateness.

EP-1166

Management of chest wall irradiation in patients with breast reconstruction

S. Falivene[1], F.M. Giugliano[1], R. Di Franco[1], A. Argenone[1], D. Borrelli[2], V. Borzillo[1], E. Esposito[3], M. D'Aiuto[3], P. Muto[1]
[1]*Istituto Nazionale Tumori Fondazione Pascale, Radioterapia, Napoli, Italy*
[2]*Emicenter, Radiotherapy, Napoli, Italy*
[3]*Istituto Nazionale Tumori Fondazione Pascale, Chirurgia Senologica, Napoli, Italy*

Purpose or Objective: The aim of this study was to evaluate treatment related complications and patient satisfaction in women with locally advanced breast cancer who received post-mastectomy radiation therapy after breast reconstruction.

Material and Methods: Between 2009 and 2014, 65 patients, median age 48 years, with locally advanced breast cancer who underwent mastectomy with breast reconstruction in the same time, received post-mastectomy radiation therapy. Two patients received excision of local recurrence, 46 patients nipple sparing mastectomy, 10 skin sparing mastectomy and 7 modified radical mastectomy. Post-mastectomy radiation therapy was delivered to the chest wall with a dose of 50 Gy in 25 fractions over 5 weeks (57 with 3Dconformal RT and 8 with tomotherapy).

Results: A patient interrupted radiation therapy to 20 Gy for severe acute toxicity with rejection of implants (delayed removal of the prosthesis). Acute dermal toxicity G2 for erythema, telangiectasia (1 patient) and edema was relieved in 26 patients, G1 toxicity in 36 patients, G0 in 2 patients and G3 in 1 patient. Two patients in systemic progression were not considered for local evaluation. At median follow-up of 35 months: 43 patients presented late toxicity G1 due to hyperpigmentation, edema, periprothetic fibrosis. 7 patients referred sense of tension or pain and not satisfaction about the final aesthetic result. Two patients presented arm lymphedema. Two patients received replacing of the implants after 36 months due to contraction, encapsulation, dislocation, swelling.

Conclusion: Radiotherapy can be safely delivered after breast reconstruction, with a low complication rate and good patient satisfaction. Further randomized studies are needed to better define the optimal management of breast reconstruction and post-mastectomy radiation therapy.

EP-1167

Radiation therapy and breast reconstruction: outcomes and complications in our experience

M. Gatti[1], G. Belli[1], A. Salatino[1], A. Maggio[2], G. Cattari[1], S. Squintu[1], A. Rivolin[3], R. Ponzone[4], P. Gabriele[1]
[1]*FPO-IRCCS Candiolo, Radiotherapy, Candiolo, Italy*
[2]*FPO-IRCCS Candiolo, Medical Physics, Candiolo Italy*
[3]*FPO-IRCCS Candiolo, Plastic Surgery, Candiolo, Italy*
[4]*FPO-IRCCS Candiolo, Oncological Gynecology, Candiolo, Italy*

Purpose or Objective: The impact of adjuvant therapy on the surgical outcomes following breast reconstruction is poorly understood. The purpose of this work is to evaluate surgical outcomes following autologous and prosthetic reconstruction in the setting of post-mastectomy radiation therapy (PMRT) and adjuvant chemotherapy. We assessed the outcome and complications of irradiated patients in our department.

Material and Methods: From May 2015 to July 2015 we analyzed acute, late toxicity and cosmetic results of 76 patients with a median age of 50 ± 10 years undergoing mastectomy with immediate recostruction with prosthesis (79.7%), autologous technique (7.2%) or expander-implant (13%) following adjuvant radiotherapy. 24 patients underwent to Nac- Sparing Mastectomy, 10 of witch with periareolar pexy. 31 patients underwent to Skin reducing Mastectomy and 5 patients to Skin Sparing Mastectomy. The radiotherapy dose was 50 Gy to chest wall and supraclavicular limphnodes when indicated with 6 MV X-ray delivered with Linac (60pt), or with tomotherapy (16pt).

Results: With a median follow-up of 25±24 months utilizing RTOG toxicity scale we observed a grade I acute toxicity in 74.6% of patients, grade II in 6% of patients while in 19.4% of patients was not observed any sign of toxicity. Late toxicity was not observed in 68.7% of patients while in 28.4% of patients a grade I late toxicity was noted. No post-operative complications was observed in 62.3% of patients while in 15.9% a capsular contracture was responsible in 20.3% of patients of explantation of prosthesis. None of patients developed post-operative skin ulcers. Cosmetic results was analyzed with Harvard Scale and was excellent in 4.5% of patients, good in 32.8%, fair in 16.4% and poor in 46.3%. The chi-test showed no correlation between early or late toxicity or cosmetics results with type of surgery (p>0.1). Univariate

analysis showed no relationship between cosmetic result and age (p>0.13).

Conclusion: Our experiences is limited to a low number of cases but confirm that adjuvant radiotherapy is not controindicated when reconstructive surgery is expected. The patient must be informed about the possible radiation sequelae.

EP-1168

Phase II trial of hypofractionated VMAT treatment for early stage breast cancer: 2-years outcomes

F. De Rose[1], D. Franceschini[1], A. Fogliata[1], C.S. Iftode[1], E. Villa[1], A.M. Ascolese[1], P. Navarria[1], C. Franzese[1], T. Comito[1], A. Tozzi[1], E. Clerici[1], R.L.E. Liardo[1], F. Lobefalo[1], G.R. D'Agostino[1], M. Scorsetti[1]

[1]*Istituto Clinico Humanitas, Radiotherapy and Radiosurgery, Rozzano Milan, Italy*

Purpose or Objective: To report 2-years toxicity and clinical results of hypofractionated simultaneous integrated boost (SIB) tecnique with Volumetric Modulated Arc Therapy (VMAT) as adjuvant treatment after breast-conserving surgery.

Material and Methods: Patients presenting early-stage breast cancer were enrolled in a phase II trial. Eligibility criteria: age>18 years, invasive cancer or DCIS, Stage I-II (T<3 cm and N≤3), breast-conserving surgery without oncoplastic reconstruction, any systemic therapy was allowed in neoadjuvant or adjuvant setting. All patients underwent VMAT-SIB technique to irradiate the whole breast and the tumor bed. Doses to whole breast and surgical bed were 40.5Gy and 48Gy, respectively, delivered in 15 fractions over 3 weeks. Acute and late skin toxicities were recorded based on RTOG scoring criteria and CTCAE v. 4.0, respectively. Cosmetic outcome was assessed as excellent/good or fair/poor, according to the Harvard scale.

Results: The present study focused on long-term results of a cohort of 144 patients with a minimum follow-up of 24 months (median 37, range 24-55 months). Median age was 62 y.o. (range 30-88). At one year, the highest reported skin toxicity was G1, in 14% of the patients; this data dropped to 4% at the last follow-up, after more than 2 years. Breast pain was recorded in 21.6% of the patients 6 months after treatment, while it was present in 3.5% of the patients at the last follow-up, showing a significant improvement with time. No correlation with liponecrosis as recorded from ultrasound exam, nor with dosimetric data. Skin toxicity was correlated with breast volume. No pulmonary or cardiological toxicities were recorded. After an early evaluation of clinical outcomes, only one case presented disease relapse, as liver metastases.

Conclusion: The hypofractionated VMAT-SIB course as adjuvant treatment after breast-conserving surgery showed to be safe and effective with optimal local control. This approach requires validation with long-term follow-up data.

EP-1169

The effect of escalating boost dose in breast cancer patients with involved resection margin

S. Park[1], S.D. Ahn[1]

[1]*Asan Medical Center, Radiation oncology, Seoul, Korea*

Purpose or Objective: To investigate the impact of the boost dose escalation on ipsilateral breast tumor recurrence (IBTR), for breast cancer patients with involved surgical margins after breast conserving surgery.

Material and Methods: Between January 1998 and December 2010 at Asan Medical center, among 4275 breast cancer patients who were treated with breast conserving therapy (BCT), a total 192 patients were treated with boost dose over 10 Gy for involved resection margin. We retrospectively analyzed the outcomes in 192 patients who had whole breast irradiation of 50.4 Gy followed by median boost dose 15.0 Gy (range, 12 - 16 Gy) for breast cancer with involved resection margin. Surgery preceded referral for radiotherapy with a 1-2 mm margin of macroscopically normal tissue. The resection margins were evaluated by pathologist for the presence of invasive carcinoma or ductal carcinoma in situ at the inked margin. Neoadjuvant chemotherapy was done in 3 patients (1.6 %). Adjuvant chemotherapy was given in 93 patients (48.4%). 157 patients (81.8%) received systemic hormone therapy. The median age was 46 years (range, 25-73 years). 182 patients (94.8%) were stage 0 to II and 10 patients (5.2%) with stage III breast cancer were also included. The boost dose delivered with electrons or tangential fields given in daily fractions of 1.5 to 2.5 Gy. The boost volume was described as the site of the primary tumor with a margin of 1.5 cm to the field borders after breast conserving surgery.

Results: The median follow-up duration for all patients was 6.7 years. IBTR were considered as any local failures on ipsilateral breast regardless of the location. The 5-year cumulative risk of ipsilateral breast tumor recurrence as a first event was 5.4%. The 5-year local relapse free survival (LRFS) was 94.4%. IBTR occurred as a first failure in 13 of 192 patients. In boost field recurrences were found in 11 patients (85%). 5 patients (39 %) were out-of boost field failures and 3 of them were both failures. On univariate analysis, age, cell type, pT stage, pN stage, extensive intraductal component (EIC), multiplicity and location of resection margin were prognostic factor for IBTR (p <0.05). In multivariate analysis only young age (<40 years old) and positive radial resection margin were unfavorable prognostic factor for LRFS (p =0.037, p=0.021 respectively). pT stage was marginally significant prognostic factor for IBTR. (p=0.088)

Conclusion: Median boost dose of 15 Gy is comparable to historical boost research results for local control in breast cancer patients with involved resection margin after BCT. Young age (<40 years old) and positive radial resection margin rather than superficial or deep margin were important risk factors for ipsilateral breast tumor recurrence. More than 80% of local recurrences were in boost field, more boost dose escalation needs to be considered.

EP-1170

Onset of fatigue during and after radiotherapy in breast cancer patient

M.S. Mariaquila Santoro[1], M.A.M. Maria Angela Molinaro[1], A.P. Armando Pingitore[1], R.M. Rosa. Molè[1], A.C. Angelo Chirillo[1], M.L. Marianna Lacaria[1], L.R.F. Lucia Rachele Fabiano[1], V.M. Vita Margheriti[1], D.P. Domenicantonio Pingitore[1]

[1]*Hospital Pugliese-Ciaccio- Catanzaro Via Pio X- 88100 Catanzaro, Department of Hemato-Oncology- Operative Unity of Radiotherapy and Radiobiology, Catanzaro, Italy*

Purpose or Objective: Cancer-related fatigue is one of most prevalent symptom among women submitted to radiotherapy (RT) for breast cancer (BC). Despite its prevalence the mechanism of onset is unknown still: one possible mechanism is activation of the immune system, through the mediation by proinflammatory cytokines interleukin (IL), IL1-b,, IL-6, and tumor necrosis factor-*a* (TNF-*a)* as host response to tissue damage determined by the radiant treatment. To purpose of this study was to determine the level of fatigue in a group of BC patients its relation to anxiety, depression, serum cytokines, cortisol and blood count levels

Material and Methods: Between October 2013 and May 2015 twenty-eight patients who received adjuvant RT after breast conserving surgery were studied. The patients' subjective feeling of fatigue intensity was measured according to with two standardized self-assessment instruments the Fatigue Assessment Questionnaire (FAQ) and a visual analog scale (VAS) on fatigue intensity before the start and weekly during RT, as well as 14 days and 3-6 and 12 months after RT. In addition, a differential blood cell count and the serum levels of the cytokines- IL1-b,, IL-6, and TNF-*a,* were determined in parallel to the fatigue assessments.

Results: 60% of patients reported non presence of fatigue before the start of RT Fatigue intensity as assessed with the VAS increased gradually during radiotherapy, 14 days after the end of radiotherapy, the fatigue intensity was still higher than before treatment, but 3 months later, fatigue was lower than at the pre-treatment level. Fatigue measured with the FAQ did not increase significantly during treatment, but the subscores on physical and cognitive fatigue were elevated during treatment weeks 4 and 5. IL-1b, IL-6, and TNF-*a,* and hemoglobin levels did not change during therapy. Peripheral blood cell levels declined significantly during therapy and were still low 3 months after treatment. Until treatment week 5, lymphocytes were reduced to almost 50% of their initial values. Patients that introduce fatigue had significantly lower serum levels of cortisol than the nonfatigued patients as well as differences in two lymphocyte populations, at 3-6 and 12 months after the end of radiotherapy

Conclusion: This study has shown that significant fatigue is common in patients receiving breast irradiation and is precipitated during radiotherapy in some patients but not other. In the patients that show an increase of the fatigue during adjuvant RT, fatigue returned to pre-treatment levels 3 months after treatment. In our study, no evidence was found that anxiety, depression, serum levels of IL1-b, IL6, TNF-*a* and hemoglobin levels were correlate with treatment induced fatigue. The results of our observation suggest the existence of a mechanism among activation of the immune system and alteration in cortisol and lymphocyte subsets.

EP-1171

The impact of body mass index on organs at risk in breast axillary nodal radiotherapy

L. Pettit[1], A. Welsh[1], C. Puzey-Kibble[1], M. Williams[1], J. Santos[1], G. Wardle[1], S. Khanduri[1]

[1]*Shrewsbury and Telford Hospital NHS Trust, Lingen Davies Cancer Center- Royal Shrewsbury Hospital, Shrewsbury, United Kingdom*

Purpose or Objective: There has been recent move within the U.K. to contour the nodal CTV for patients receiving adjuvant radiotherapy for breast cancer. Axillary radiotherapy (ART) following a positive sentinel lymph node biopsy is becoming more common for certain groups of patients. Organs at risk (OAR) should be delineated and considered during the planning process. Body mass index (BMI) has been shown to impact upon spinal cord and brachial plexus doses in irradiation of the supraclavicular fossa. The impact upon the OAR in the axilla has not yet been well documented.

Material and Methods: Patients undergoing ART between 01/04/15–01/10/15 were identified. Non - contrast radiotherapy planning CT scans were taken. External beam radiotherapy was planned with extended tangents using a field in field approach with an additional low weighted anterior oblique field if deemed appropriate for adequate dose coverage. Dose delivered was 40.05 Gy in 15 fractions.BMI was calculated by: weight(kg)/height (m)2. CTV's were contoured in accordance with the RTOG contouring atlas.OAR including ipsilateral lung, humeral head and brachial plexus were delineated.

Results: Fifteen patients were identified. Six patients had a BMI between 20–25, 3 between 25–30, 5 between 30–40 and 1 BMI>40. Mean ipsilateral lung V12 was 10.44% (range 2.3%–14.33%). Mean V12 did not vary with BMI (BMI 20–25;mean V12=9.33%, BMI 25–30; mean V12=8.52%, BMI 30–40;mean V12=9.51%, BMI>40 mean V12=6.38%, p=0.55 Chi-Squared). The mean humeral head maximum dose was 35.2 Gy (range 1.2–41.5 Gy). Mean humeral head maximum dose did not vary with BMI (BMI 20–25; mean=34.2Gy, BMI 25–30;mean=27.8Gy, BMI 30–40; mean=40.3Gy, BMI>40; mean=38.2Gy,p=0.49 t-test). The ipsilateral brachial plexus D2 mean was15.6Gy (range 1.2–37.4 Gy). Mean ipsilateral brachial plexus D2 dose did not vary with BMI(p=0.21 t-test).

Conclusion: BMI did not significantly impact upon OAR dosage although this series is limited by a small sample size. Ipsilateral lung and brachial plexus were comfortably within departmental tolerance. A planning risk volume of 10 mm around the humeral head has now been adopted within the department. It is recognised that intravenous contrast provides better quality images for delineating OAR in particular for the brachial plexus. However, this impacts upon resources in terms of radiographer scanning time. Adequate time needs to be allocated in consultant and physics teams job plans to enable high quality delineation and subsequent radiotherapy plans to be produced.

EP-1172

Thyroid tolerance in adjuvant supraclavicular fossa nodal radiotherapy in breast cancer

L. Pettit[1], A. Welsh[1], S. Khanduri[1]

[1]*Shrewsbury and Telford Hospital NHS Trust, Lingen Davies Cancer Center- Royal Shrewsbury Hospital, Shrewsbury, United Kingdom*

Purpose or Objective: Hypothyroidism is the most commonly reported long-term toxicity following radiotherapy to structures near to the thyroid gland. Emami suggested the thyroid gland tolerance as 45Gy (TD 5/5) although a much wider range of 10–80 Gy has been reported in the literature. When irradiating the supraclavicular fossa (SCF) in adjuvant radiotherapy for breast cancer, it is inevitable that the thyroid gland will receive a high dose of radiation due to its proximity to the target volume. Recently there has been a move to CT based delineation of the CTV and organs at risk (OAR) in patients requiring nodal radiotherapy for breast cancer compared with the previous bony land mark/field based techniques. Dose received by the thyroid gland and subsequent late toxicity has not yet been well studied in breast cancer.

Material and Methods: Patients undergoing external beam radiotherapy to the breast or chest wall plus SCF between 01/04/15–01/10/15 were identified. Radiotherapy planning contrast enhanced CT scans were taken. External beam radiotherapy was planned with tangents using a field in field approach with a matched direct anterior field. A low weighted posterior field was added if deemed appropriate for adequate dose coverage. Angle corrections were used as appropriate. A dose of 40.05 Gy in 15 fractions prescribed at depth was employed. CTV's were contoured in accordance with the RTOG contouring atlas.The thyroid gland was prospectively delineated and D5% was recorded.

Results: Seventeen patients undergoing adjuvant SCF radiotherapy were identified. T stage was as follows: T1:2 patients,T2:9 patients,T3:4 patients, T4a:1 patient,T4d:1 patient. N stage; N1:1 patient, N2:14 patients, N3:2 patients. Fourteen were hormone receptor positive, 3 hormone negative. Twelve were HER2 negative, 5 HER2 positive. Mean D5% thyroid was 37.9Gy (range 7–42.7 Gy). Excluding one patient with a previous hemi-thyroidectomy, the mean D5% thyroid was 39.8 Gy (range 16–42.7 Gy). An abnormality requiring referral to a surgeon for was discovered in one patient.

Conclusion: Our departmental tolerance for the thyroid gland was set as 40Gy (for 2.67Gy per fraction). It is hard to achieve this without compromise of the CTV. The effect modern chemotherapy/targeted agents may have on this prior to receiving radiotherapy is inknown. Baseline TSH recording is desirable. Long-term follow up to detect clinical or biochemical thyroid dysfunction is needed to inform practice but would present challenges with capacity in busy oncology departments.

EP-1173

10-years results of accelerated hypofractionated RT for breast cancer

I. Gladilina[1], O. Kozlov[1], L. Klepper[2], M. Chernykh[1], E. Makarov[1], A. Petrovskiy[1], M. Nechushkin[1]

[1]NN Blokhin Cancer Research Center, RadioSurgery Brachytherapy, Moscow, Russian Federation
[2]Central Economic Mathematical Institute Russian Academy of Sciences, Computer Engineering, Moscow, Russian Federation

Purpose or Objective: The aim of the survey – to compare the results of different regimen of whole-breast irradiation (accelerated hypofractionated and standard radiation treatment) following breast-conserving surgery for breast cancer I-IIA stages.

Material and Methods: From 2000 till 2005 203 patients aged R54 years received whole-breast irradiation following breast-conserving surgery (lumpectomy + axillary and internal lymphatic dissection). The most commonly seen invasive ductal carcinoma (55%), the rare - invasive lobular carcinoma (27%), invasive ductal cancer with extensive in situ component (3%) and special forms (15%). Metastasis in ipsilateral axillary lymph nodes fixed in 17,4% cases. All patients received whole-breast irradiation over a five-day period with different regimens RT: first group - accelerated hypofractionated (AHRT: 3 Gy per fraction over 2,5 weeks, total dose of 39 Gy, N=112) and second group - standard radiotherapy (SRT: 2Gy per fraction over 5 weeks, total dose of 50 Gy, N=91). We used three dimensional CT-based treatment planning, two traditional tangential fields 6-18 MV, changing the gantry angle, collimator angle, blocks to result in coverage of the breast while excluding the heart from the treatment fields and minimized dose to the lung. A LQM to predict rate of tumor control, late normal tissue effects and cosmetic outcome was used in our research. For tumor control the value α/ß was 4 Gy, acute toxicity – 10 Gy, side effects - 3,1 Gy, cosmetic outcome - 3,6 Gy (for AHRT EQD2 53,0/44,4/46.7/46,0). We calculate (LQM) following formula for AHRT:

$$BED = (1+ d/\alpha/\beta) - k(T-T_k)$$

Tumor: k=0,7, Tk=21.

Results: Local recurrence at 5y/10y: 1/3 (1 group) vs 0/1 (2 group) (p>0.05). Overall survival 5y/10y: 99,1%/95,0% (1 group) vs. 97,8%/85,0% (2 group), (p<0.05).. Only 8% of the patients of the 1 group developed grade 2 erythema and 14,3% of the patients of the 2 group (p<0,048). No complications at heart, complications at the lungs (only 1 degree) 5y/10y: 7(7,7%)/7(7,7%) vs. 6 (5,4%)/6(5,4). The other results are presented in Table 1.
Table 1 (5 and 10 year outcome).

Regimen RT	SRT 5 years	SRT 10 years	AHRT 5 years	AHRT 10 years
tumor control	1 (1,1 %)	3 (3,3 %)	0 (0 %)	1 (0,9 %)
side effects (skin)	6 (6,6 %)	8 (8,8 %)	5 (5,5 %)	8 (7,1 %)
side effects (fibrosis)	11 (12%)	16 (17,6 %)	12 (10,7 %)	15 (13,4 %)
cosmetic outcome (good or excellent)	74,6 %	74,6 %	79,5 %	79,5 %

Conclusion: AHRT decrease adverse effects, increase five and ten-year event free survival and cosmetic results vs. SRT. We had confirmed our calculations with clinical results. AHRT had been proved to be a successful parameters combination of a dose for fraction, durations of an irradiation and the common dose. Prominent feature of this regimen is increase of the tumor control in comparison with SRT, thus early and late reactions are essentially decreased

EP-1174

Interobserver variation in CT vs. MRI based delineation of the lumpectomy cavity

N. Al-Hammadi[1], S. Divakar[1], M. Riyas[1], P. Caparrotti[1], S. Chandramouli[1], M. McGarry[1], S. Sheim[1], R. Hammoud[1], P. Petric[1]
[1]National Center for Cancer Care & Research A member of Hamad Medical Corporation, Radiation Oncology, Doha, Qatar

Purpose or Objective: To assess the magnitude of inter-observer contouring uncertainties on CT- and MRI-based boost volume contouring in breast cancer patients without clips in lumpectomy cavity.

Material and Methods: CT and MRI data-sets of 12 consecutive patients, treated with surgery (no clips in lumpectomy cavity) and postoperative irradiation were included. Five experienced radiation oncologists independently contoured the boost clinical target volume (CTVb) on CT. Three weeks later contouring was repeated on MRI. Finally, expert consensus (EC) contours were created on both modalities by combining the opinions of all 5 experts. Contour Analysis software Tool 1 (CAT 1) was used for global volumetric computations and assessment of local contouring variation for each case and contouring approach. Inter-observer volumetric conformity index (VCI) was calculated for all pairs of observer's delineations and the EC contour. In topographic analysis, absolute inter-delineation distances (IDDs) between observers' and EC delineations were measured in contouring plane (Figure). Paired sample t-test was used to for statistical analysis of differences between contouring approaches.

Results: None of the observed differences in results were statistically significant (p>0.05). Mean CTVb size was 154 +/- 26 cm3, and 152 +/- 16 cm3, for CT and MRI, respectively. Mean relative standard deviation (rSD) revealed higher spread of volumes for CT (18 %) when compared with MRI (11 %). Mean ratio between the smallest and largest volume was comparable (CT: 0.7 +/- 0.1; MRI: 0.8 +/- 0.1). Mean VCI was non-significantly higher for MRI (0.81 +/- 0.04) than CT (0.76 +/- 0.07). MRI-based mean VCI was superior to CT-based approach in 10 (83 %) cases. In one case, mean VCI was identical (0.88 +/- 0.1), and in one case CT-based VCI (0.81 +/- 0.04) was slightly superior to MRI (0.8 +/- 0.05). Analysis of mean IDD values revealed non-significantly superior results for MRI when compared to CT (3 +/- 0.5 mm vs. 4 +/- 1.5 mm) (Figure). Mean rSD for IDDs was lower on MRI than CT contouring (49 % vs. 61 %). In contouring plane, predilection regions of variation were in the direction of breast parenchyma, while agreement was highest at the breast-chest wall and breast-air interface (Figure).

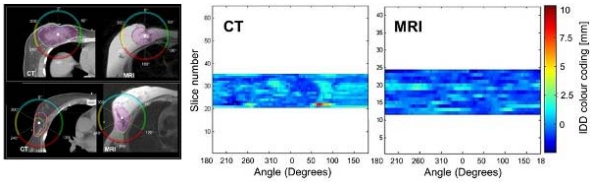

Figure. Example of coordinate system (left) and distance maps (right) or topographic assessment of variation.

Conclusion: Although statistically insignificant, superiority of MRI over CT for accurate boost delineation in patients without clips in lumpectomy cavity may be clinically important. We recommend using information from both modalities, pre-treatment imaging and clinical information to arrive at best results.

EP-1175

Accelerated Partial Breast Irradiation using Carbon-iron Radiotherapy for stage I breast cancer

K. Karasawa[1], T. Omastu[2], M. Wakatsuki[2], S. Shiba[2], S. Fukuda[2], T. Kamada[2], N. Yamamoto[3], T. Ishikawa[4], M. Saito[5]
[1]Tokyo Women's Medical University, Radiation Oncology, Tokyo, Japan
[2]National Institute of Radiological Sciences, Research Center Hospital for Charged Particle Therapy, Chiba, Japan
[3]Chiba Cancer Center, Breast Surgery, Chiba, Japan
[4]Tokyo Medical University, Breast Surgery, Tokyo, Japan
[5]Juntendo University, Breast Surgery, Tokyo, Japan

Purpose or Objective: Our institute started a clinical study on radical C-ion RT for patients with low risk T1N0M0 invasive

ductal carcinoma in 2013. The idea is to develop a short course C-ion RT to be finished in one week, which, we believe, could replace surgery and more than 5 weeks of radiotherapy. The purpose of this report is to evaluate preliminary treatment results.

Material and Methods: There are 2 treatment studies. One is phase I/II clinical trial and the other is "general treatment protocol" (GP). In clinical trial, candidates are patients with low-risk stage I breast cancer who are suitable for APBI in ASTRO consensus statement. A dose escalation study was designed as a phase I clinical trial. Total dose is 48.0 GyE, 52.8 GyE and 60.0 GyE in 4 fractions within 1 week. In phase I, patients planned to undergo surgery for pathological evaluation 90 days after C-ion RT and then received endocrine therapy. In phase II, patients had C-ion RT at recommended dose and then received endocrine therapy. Three-field C-ion beams with 290 MeV/n energy are used by means of passive broad beam methods using individual collimators and a compensation bolus absorber. Irradiation is performed using respiratory gating. The other study, GP is for the patients desiring to receive C-ion RT but ineligible to enroll in the clinical trial due to minor variance or refusal to enroll in the clinical trial. The first 2 patients of this GP were treated by 52.8 GyE and the others by 60 GyE. All patients were suitable for endocrine therapy after RT.

Results: From April 2013 to October 2015, 18 patients were treated. There were 3 cases of 48 GyE and 52.8 GyE and 1 case of 60 GyE of phase I, and 2 cases of 52.8 GyE and 9 cases of 60 GyE of GP. Median age was 66 (44 ~ 81). Median tumor size was 12 mm (4 ~ 20 mm). Median f/u period was 12 mos. No normal tissue adverse events were observed except for grade 1 skin reaction of CTC-AE v4 in 9 cases. At the time of analysis, 7 patients underwent surgery and 2 of them reached pCR. Of the GP patients, 6 reached CR, 4 reached PR and 1 developed PD on MRI. It took 3 months to 2 years with a median of 6 months to reach CR on MRI. So the pathological evaluation in phase I trial after 3 months must be too early for evaluation. The PD patient with basal subtype tumor was successfully salvaged by mastectomy.

Conclusion: C-ion RT for primary tumor of breast needed long time to reach CR on MRI. Low grade stage I breast cancer has a potential to cure by accelerated partial breast irradiation with C-ion RT.

EP-1176

Abstract withdrawn

EP-1177

Hypofractionated radiotherapy with concomitant boost for breast cancer: a dose escalation study

C. Rinaldi[1], E. Ippolito[1], M. Fiore[1], P. Matteucci[1], A. Di Donato[1], P. Trecca[1], S. Ramella[1], R. D'Angelillo[1], L. Trodella[1]
[1]*Campus Biomedico University, Radiotherapy, Roma, Italy*

Purpose or Objective: to test the maximum tolerated dose (MTD) of a concomitant boost to the tumor bed for patients at high risk of recurrence treated with whole breast radiotherapy (RT). The secondary endpoints are to evaluate the acute and late toxicity and the cosmetic result recorded by appropriate scales.

Material and Methods: between June and August 2014 we selected 9 patients with histologically proven breast cancer with pathological stage pT1-2 and at least one of the following risk factors for local recurrence: N1 disease, lymphovascular invasion, extensive intraductal component, close margins, non hormone sensitive disease, grading G3. All patients were treated with hypofractionated RT to whole breast to a dose of 40.05 Gy in 15 fractions. The dose escalation to the tumor bed was delivered through a daily concomitant boost technique at 3 levels of dose: 48 Gy (3.2 Gy/die), 50.25 Gy(3.35 Gy/die) and 52.5 Gy (3.5 Gy/die) for the first, second and third level, respectively. We included 3 patients for each step (3 additional patients if a dose limiting toxicity (DLT) Grade≥ 2 occurred); dose escalation to a higher step was allowed if all patients of the lower one had completed the treatment without DLT. MTD was defined as the dose level below the dose induced DLT in at least 3 patients treated at a given dose level. A clinical evaluation of the patients was carried out before treatment, 2 times a week during RT, at the end of the same, at 3, 6 and 12 months after the end of RT. In addition to skin toxicity a cosmetic evaluation was performed by radiation oncologist, an in-training physician and by the patient herself. The latter also filled the EORTC QLQ - C30 / BR23 on quality of life at each evaluation.

Results: we enrolled a total of 9 patients (3 for each dose level) with a median age of 62 years (range 44-83). Patients' characteristics are reported in Table 1. No dose limiting toxicity Grade ≥ 2 occurred. The maximum toxicity collected during RT was G2 skin toxicity in 7 (77%) patients (2 patients with brisk erythema and 5 with moist desquamation). This toxicity resolved at the first follow up. At a median follow up of 11 months we recorded G2 induration/fibrosis in 3 (33,3%) patients, one for each level of dose. There was a worsening in the self perception of cosmetic outcome at the end of treatment in 6 cases (66%) even if with no statistical significance. Moreover, patients at the end of treatment, reported a worse (not statistically significant) cosmetic outcome compared to that expressed by the in-training physician and the radiation oncologist. The evaluation of QoL found an improvement of the score at the end of treatment compared to initial in 7 of 9 patients (77%), above all in elderly patients (≥ 62 years).

CHARACTERISTICS	NUMBER OF PTS	PERCENTAGE
Adjuvant chemotherapy	4	44%
ER +	9	100%
PgR+	8	88%
HER2 +	2	22%
Ki 67 >20%	4	44%
lymphovascular invasion	1	11%
N1	5	55%
G1	1	11%
G2	4	44%
G3	4	44%
extensive intraductal component	3	33%
Lobular Carcinoma	1	11%
Ductal carcinoma	8	88%

Conclusion

The 3-week course of postoperative RT with dose escalation to the tumor bed to 52,5 Gy has been achieved without dose limiting toxicities. Long-term follow-up data are needed to assess late toxicity and clinical outcomes.

EP-1178

Predictive factors of patient compliance for breath-holding during radiotherapy for breast cancer

R. Walshaw[1], C. Robinson[1], S. Yousif[1], E. Young[1], M. Hogg[1], S. Susnerwala[1], A. Hindley[1], C. Lim[1], F. Danwata[1], D. Williamson[1]
[1]*Royal Preston Hospital, Rosemere Cancer Centre, Preston, United Kingdom*

Purpose or Objective: Radiation to the heart during radiotherapy (RT) for breast cancer may lead to increased risk of ischaemic heart disease years afterwards. A proposed method of reducing cardiac dose is with breath-holding techniques. Patients undergoing adjuvant breast RT form a heterogenous group in terms of demographics and co-morbidities. We aimed to determine what proportion of patients from an unselected group eligible for adjuvant RT would be able to comply with a simple breath-holding technique pre-treatment, and whether any individual characteristics may help predict success or failure.

Material and Methods: We prospectively identified all patients due to receive adjuvant RT to left breast after surgery for early breast cancer, and offered participation. After RT planning scan patients were kept in treatment position and asked to hold their breath for 20 seconds twice, with one minute between attempts. Demographics and patient factors were recorded. Treatment was subsequently delivered as normal with no breath-holding used.

Results: Fifty-eight patients were included, median age 60.0 years (range 35.1-85.2), median body mass index 26.8 (18.1-39.3). WHO Performance status was 0-1 in 56, and 2 in 2 patients; 3 patients had mobility issues, 2 were unable to climb on the scanner couch unaided. Seven patients had a diagnosis of chronic respiratory disease, 7 using inhalers regularly. Twenty patients were ex-smokers, 7 current smokers, 31 never smoked. At diagnosis, 6 patients (10%) had ductal carcinoma in-situ, 36 (62%) T1, 15 (26%) T2, and 1 (2%) T3 disease; 9 (16%) had nodal disease; 7 (12%) had full axillary node clearance and 16 (28%) had chemotherapy prior to RT. Fifty three (91%) were successful in breath-holding for both 20 second periods, 2 (3%) were unsuccessful on both attempts. Two (3%) were unsuccessful first, but successful a minute later; 1 (2%) was successful for the first period but not the second.

Conclusion: The vast majority of patients from an unselected cohort of patients due to undergo adjuvant RT to the breast or chest wall were able to maintain breath-hold successfully for two 20-second periods one minute apart in a simulated treatment position. No consistent patient factors were identified that would reliably predict success or failure to breath-hold. We anticipate most patients will tolerate breath-holding techniques during breast RT should they be employed more in the future. In the era of stereotactic ablative RT, breath-holding may also become important in other patient cohorts.

EP-1179

Preoperative parallel PET/MR predicts the disease free survival in patients with breast cancer

I. LIM[1], J. Park[1], W.C. Noh[2], H.A. Kim[2], K.W. Park[3], H. Seol[4], J.K. Myung[4], I.O. Ko[1], K.M. Kim[1], B.H. Byun[1], B.I. Kim[1], C.W. Choi[1], S.M. Lim[1]

[1]Korea Institute of Radiological And Medical Sciences, Nuclear Medicine, Seoul, Korea Republic of

[2]Korea Institute of Radiological And Medical Sciences, Surgery, Seoul, Korea Republic of

[3]Korea Institute of Radiological And Medical Sciences, Radiology, Seoul, Korea Republic of

[4]Korea Institute of Radiological And Medical Sciences, Pathology, Seoul, Korea Republic of

Purpose or Objective: The aim of this study was to determine whether PET/MR could predict disease-free survival (DFS) in patients with operable breast cancer.

Material and Methods: Seventy-eight patients with breast cancer were enrolled. All patients underwent preoperative parallel PET/MR: whole body PET/CT at 1 h after 18F-FDG injection, breast dynamic contrast enhanced MR, and breast PET/CT at 2h after 18F-FDG injection sequentially in prone position. All patients were analyzed by diverse parameters (maximum SUV at 1 h [SUV1], maximum SUV at 2 h [SUV2], retention index of SUVmax [RI], metabolic tumor volume [MTV], total lesion glycolysis [TLG], initial slope of the enhancement curve [IS], transfer constant [Ktrans], reflux constant [Kep], extravascular extracellular space volume fraction [Ve], and initial area under the curve [iAUC]) . A relationship between covariates and DFS after operation was analyzed using Kaplan-Meier method and multivariate Cox proportional-hazard regression method.

Results: The median follow-up of 78 patients was 55 months (31-67 months), and 9 (11.5 %) patients developed recurrence or metastasis. Among parameters, higher RI (p = 0.0010), lower Ktrans (p = 0.0046), and lower Ve (p = 0.0035) were significantly associated with poorer DFS. In contrast, SUV1, SUV2, MTV, TLG, IS, Kep, and iAUC were not. On multivariate analysis, RI (p = 0.016; HR = 5.20; CI 1.4-19.7), and Ktrans (p = 0.035; HR = 0.22; CI 0.054-0.89) were found as independent predictors of DFS. Patients with higher RI and lower Ktrans revealed a significantly higher recurrence rate (66.7 %) than the rest of patients (6.9 %, P<0.0001).

Conclusion: RI and Ktrans measured by preoperative parallel PET/MR can predict DFS in patients with operable breast cancer. The combination of these parameters could make improvement of patients care because tailored surveillance would be applied for high risk group.

EP-1180

Postoperative IMRT with helical tomotherapy for breast cancer: outcome and toxicity analysis

J. Fourquet[1], F. Crop[1], T. Lacornerie[1], E. Tresch[2], F. Le Tinier[1], S. Horn[1], F. Vasseur[1], E. Lartigau[3], D. Pasquier[3]

[1]Centre Oscar Lambret, Academic department of Radiation Oncology, Lille, France

[2]Centre Oscar Lambret, Unité de Méthodologie et de Biostatistique, Lille, France

[3]Centre Oscar Lambret, Academic department of Radiation Oncology- Université de Lille- CRISTAL UMR CNRS 9189, Lille, France

Purpose or Objective: Radiation therapy (RT) plays a key role in the management of breast cancer. Intensity-modulated radiotherapy (IMRT) has been shown to provide a more homogeneous dose distribution and to decrease skin toxicity. It covers a wide spectrum of techniques, ranging from static IMRT to helical tomotherapy (HT). HT could be relevant for complex volumes and/or difficult anatomies, but it needs to be evaluated since clinical data are still limited. The objective of this retrospective study is to investigate the short-term outcome and toxicity in a series of patients treated with adjuvant breast HT.

Material and Methods: Patients with an indicated breast adjuvant radiotherapy using an IMRT technique were included after a staff discussion. The treatment was performed with HT with concomitant boost if needed: 50 Gy (2 Gy/fraction) over the breast or the chest wall and lymph nodes, 60 Gy (2.4 Gy/fraction) on the tumor bed, 58 Gy (2.33 Gy/fraction) on the mastectomy scar if indicated. Toxicities were evaluated according to the NCI-CTCAE v4.0. A search for factors related to toxicity was conducted using univariate and multivariate analysis.

Results: 98 patients were treated between January 2013 and September 2014. The following target volumes were irradiated: breast (53.4%) or chest wall (46.6%), locoregional lymph nodes i.e. internal mammary chain, infra and supraclavicular levels (79.6%). 54.4% of them were treated for left side breast cancer. The acute toxicities were mainly skin toxicity (grade (gr) 1: 63.1%; gr 2: 28.2%; gr 3: 3.9%) and esophagitis (gr 1: 42.9%; gr 2: 15.3%). Other acute toxicities were gr 1 laryngitis (2.0%); gr 2 pneumonitis (1.0%); gr 1 (3.1%) and gr 2 (1.0%) cough. With a median follow-up of 8.4 months (1.1-20.7), there were skin toxicity (gr 1: 41.2%, gr 2: 2.1%) and dysphagia (gr 1: 1.0%). No local recurrence occurred, two metastatic relapse occurred and one patient died (death related to cancer). Factors significantly (p<0.05) correlated with toxicity in multivariate analysis were: breast size and average skin dose for acute skin toxicity; chemotherapy, esophageal D2%, average esophageal dose, esophageal V30Gy and V45Gy for esophagitis. For the short-term skin toxicity, PTV volume, PTV D2% and average PTV dose were associated with toxicity.

Conclusion: In this retrospective study with a short follow-up, postoperative breast HT is a well-tolerated treatment for patients in need of a complex irradiation. Several clinical and dosimetrical parameters related to toxicity have been identified.

EP-1181

Prostheses irradiation in breast cancer: clinical and aesthetic outcomes in retrospective series

D. Smaniotto[1], V. Masiello[1], F. Beghella Bartoli[1], L. Boldrini[1], G. Mattiucci[1], F. Marazzi[1], S. Manfrida[1], A. Di Leone[2], G. Franceschini[2], R. Masetti[2], V. Valentini[1]

[1]*Policlinico Universitario Agostino Gemelli- Catholic University, Radiation Oncology Department - Gemelli ART, Roma, Italy*

[2]*Policlinico Universitario Agostino Gemelli- Catholic University, UOC Breast Surgery, Roma, Italy*

Purpose or Objective: Post-mastectomy radiation therapy (RT) is a prophylactic adjuvant treatment for high risk patients with breast cancer. Mammary prostheses or expanders often do not tolerate RT causing a reduction of aesthetic profile and, even more, an exposure to clinical risks or new surgery. In this retrospective study clinical and aesthetic results were quantified in patients who did or did not undergo adjuvant RT after reconstruction for breast cancer

Material and Methods: Patients who underwent mastectomy with immediate mammary reconstruction for breast cancer and who had a follow-up (FUP) period of at least six months were selected for this retrospective study. Two subgroups were defined between irradiated or not patients. All the patients were submitted to the scheduled surgical and oncoplastic FUP and the irradiated ones underwent also a RT FUP program. For both groups local infection rate (IR), lipofilling rate (LR), reconstruction with DIEP flap rate (DIEPR), local control (LC) and distant failure rate (DFR) were analyzed. All chi square tests were performed on MedCalc. For the irradiated patients acute and late toxicities were also registered according to CTCAE v4.0 scale

Results: From January 2012 to April 2015, 152 patients underwent mastectomy with prostheses or expanders. Out of them, 76 pts were candidates to standard adjuvant RT for high risk factors, according to NCCN guidelines. Mean age was 48 years (range 32-74). Median FUP was 28 months (range 6-44). IR, LR, DIEPR are reported in Table 1. 21% of not irradiated pts underwent second surgery to replace the expander with the prostheses. LC was equal in both group. High risk pts had higher DFR than low-medium risk ones (5.26% vs 0 with $p<0.05$). Regarding irradiated patients acute skin toxicities G0, G1, G2 and G3 were 38%, 40%, 12% and 9.8% respectively. We reported late skin toxicities rates of: G0 20%, G1 28%, G2 42% and G3 10% (Figure 1).

	Adjuvant RT	No adjuvant RT	Chi square test
Lipofilling rate	10 (13,1%)	16 (21%)	1.2 (p<0,01)
DIEP flap rate	15 (19,7%)	7 (9,2%)	2.5 (p<0,01)
Infection rate	1 (1.3%)	1 (1.3%)	0

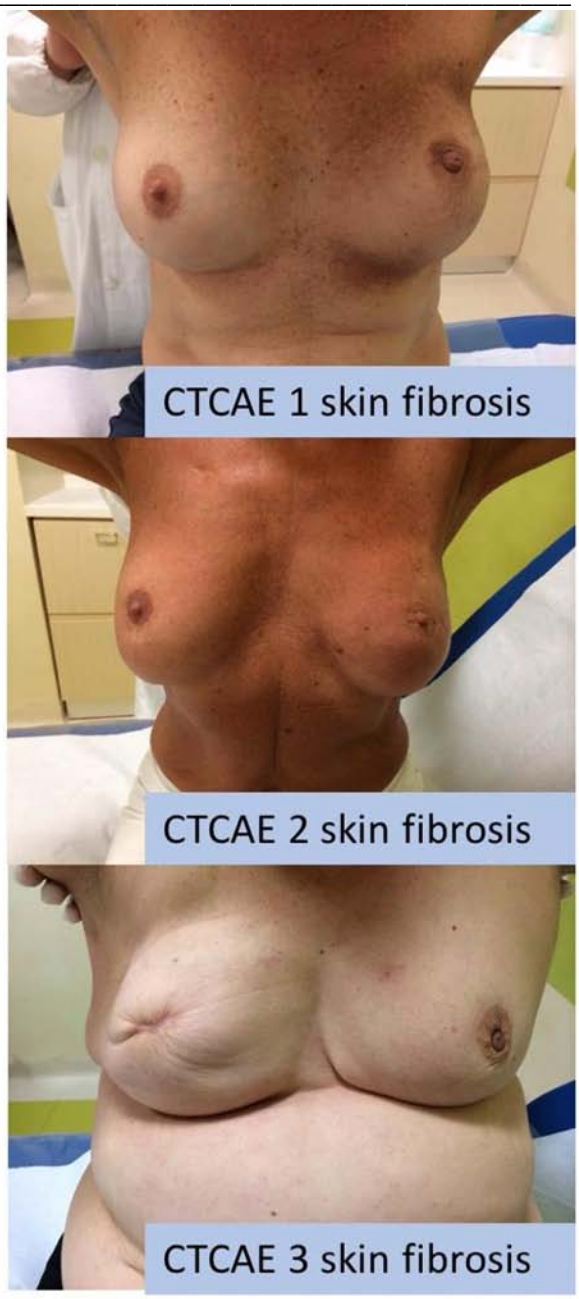

Conclusion: In this preliminary analysis RT after mastectomy with breast reconstruction resulted well tolerated and can ensure to high risk patients local control rates comparable to low-medium risk patients in the early FUP. A longer period of observation and specific Quality of Life questionnaires are needed to better describe the results

EP-1182

Prone whole breast irradiation: multimodal imaging for target delineation

A. Huscher[1], M. Centurioni[1], L. Donadoni[1], D. Santus[2], A. Soregaroli[2], C. Bassetti[3], A. Zaniboni[4], M. Bignardi[1]

[1]*Poliambulanza Foundation, Radiation Oncology Unit, Brescia, Italy*

[2]*Poliambulanza Foundation, Radiology Department, Brescia, Italy*

[3]*Poliambulanza Foundation, Medical Physics, Brescia, Italy*

[4]*Poliambulanza Foundation, Oncology Department, Brescia, Italy*

Purpose or Objective: Whole breast clinical target volume (CTV) contouring rules have been defined for supine set-up. The same indications do not seem to fit properly for prone set-up and no clear definition could be found nowadays in

literature. This study was planned first to evaluate definition of prone CTV (pCTV) based on breast glandular tissue (BGT) distribution on diagnostic MRI, and then to analyse MRI/CT image fusion for treatment planning.

Material and Methods: We first analyzed BGT distribution in 30 diagnostic MRI in respect to the following structures: major and minor pectoralis muscles, caudal edge of clavicular head, sternum, skin, medial and lateral thoracic arteries and infra-mammary fold. Reference structures were derived from the latest ESTRO contouring guidelines for supine irradiation.The anatomical region including BGT in all cases was defined as pCTV. After that MRI and CT were acquired for treatment planning in 10 patients, planned for prone irradiation. Eight channel contrast-enhanced MRI was acquired. Axial T2 IDEAL sequences were used for pCTV definition. CT for treatment plan was acquired with 3 mm thickness and step, with dedicated prone breast board (New Horizon Breastboard - CIVCO Medical Solutions). pCTV was defined on MRI according to the above described references and transferred to CT with a dedicated deformable fusion workflow (MIM 6.4.9 - MIM Software Inc.).

Results: Mean age of patients was 46 year. The well-known distinction in BGT distribution pattern (intermingled and centralized) was confirmed. pCTV could be defined superiorly by the caudal edge of clavicular head, inferiorly 3 mm above infra-mammary fold, medially by the medial thoracic artery (or if not visible 3 mm laterally to the sternal margin) laterally by a plane passing through the lateral surface of the pectoralis muscles and perpendicular to the skin, posteriorly by the anterior surface of pectoralis muscles and anteriorly 3 mm from skin. Image fusion performed easily and transferred pCTV was consistent with anatomy on CT slices. Visualization of BGT on MRI images allowed more precise definition of volumes and the limits chosen for pCTV definition on MRI fit adequately on CT.

Conclusion: Although derived from a small sample, the above reported contouring suggestions could be of aid in defining pCTV; we confirm the superiority for BGT visualization on MRI, The good consistency between MRI and CT anatomy seems to suggest that MRI criteria could be transferred on CT in everyday workflow for pCTV definition

EP-1183

Investigation on the absorbed dose to organs at risks using an IOERT planning software

H. Ozcan[1,2], M. Ghorbanpour Besheli[1,2], C. Matuschek[1], S. Mohrmann[3], C. Illana[4], R. Rodriguez[4], E. Boelke[1], W. Budach[1], I. Simiantonakis[1,2]

[1]University Hospital, Department of Radiotherapy and Radiation Oncology, Duesseldorf, Germany

[2]Heinrich-Heine University, Faculty of Physics/Medical Physics, Duesseldorf, Germany

[3]Medical Faculty- University Hospital, Department of Gynecology, Duesseldorf, Germany

[4]GMV, R&D, Madrid, Spain

Purpose or Objective: In the intraoperative electron radiotherapy (IOERT), as a part of breast-conserving therapy, a single high dose is applied on the tumor bed in order to eradicate the residual tumor cells. Currently, dose profiles obtained by radiochromic films are used to estimate the applied energy. The energy is selected by measuring the distance to the rib as dose limiting organ at risk by intraoperative ultrasound. This method is fast and practical for clinical applications but it is not possible to estimate the absorbed dose on critical organs like heart and lung. Therefore, an IOERT planning system was tested in order to evaluate the adsorbed dosage for organs at risk.

Material and Methods: The dedicated mobile IOERT accelerator, NOVAC7 (SIT, Vicenza/Italy) was used for electron beam generation. The dose calculation was performed in Radiance (GMV, Madrid/ Spain) IOERT treatment planning software. Before dose calculation, the Radiance system was configured based on the measured data obtained from the electron beams. Dose calculation was performed based on the CT images registered a few days after IOERT irradiation (post-operative CT image). The absorbed dose in lung, heart and ribs were shown by DVHs and documented quantitatively. From a database of irradiated 53 patients n=6 patients were selected who developed fibrosis grade 2, edema grade 2, pneumonitis and suspicious heart effect (not confirmed).All of the patients received whole breast irradiation with 50,4 Gy/1,8 Gy SD. Dose constrains of the dose plans showed no exceeding the threshold doses.

Results: Calculated dose resulted for ribs, heart and lung are presented in table 1. As it is shown, the absorbed dose at the ribs varied from 3.8 Gy to 9.2 Gy. This is partially higher than our tolerance dose of 7 Gy. The calculated dose values of different organs depend on the applied energy, the location of the tumor bed, the number of ribs located in the treatment field and the distance of the organ from the tumor bed. The overdoses resulted for ribs imply that the evaluation method of absorbed dose to rib in clinical practice should be optimized. On the other hand, these overdoses could be due to the uncertainty arising from the planning procedure. Because in this investigation a so-called off-line planning through a post-operative image was performed. This makes the actual applicator position and tumor bed localization in relation to the patient's anatomy during the planning procedure difficult.

Table 1: Investigated patients and calculated doses on ribs, lung and heart

Patient	Side effect	Energy [MeV]	Applicator	Estimated dose on ribs [Gy]	Dose on ribs [Gy]	Dose on lung [Gy]	Dose on heart [Gy]
1	fibrosis grade 2	7	40mm, 0°	4,4	5,9	4,3 (right)	0
2	fibrosis grade 2	7	40mm, 0°	5	6,4	5,8 (right)	0
3	fibrosis grade 2	5	40mm, 22.5°	5,5	8,3	6,6 (left)	0
4	edema grade 2	5	40mm, 0°	5,5	8,2	3,0 (left)	0
5	heart effect	7	40mm, 22.5°	5	5,2	6,1 (left)	1,1
6	lung effect	7	50mm, 22.5°	6 – 7	9,7	7,2 (right)	0

Conclusion: No direct relation was observed between the side effects and the absorbed dose on heart and lung. Intraoperative imaging is highly recommended in order to increase the accuracy of the planning procedure and consequently the estimation of the calculated absorbed dose in patient.

EP-1184

Radiotherapy on nodal areas after breast conserving surgery according to histopathological features

G. Lazzari[1], G. Silvano[1], G. Della Vittoria Scarpati[1], R. Marchese[1], M. Soloperto[1], A. Nikolaou[1], A. Terlizzi[2], F. Perri[3]

[1]Azienda Ospedaliera SS. Annunziata Presidio Osped, Radiology, Taranto, Italy

[2]Azienda Ospedaliera SS. Annunziata Presidio Osped, Physician Department, Taranto, Italy

[3]Azienda Ospedaliera SS. Annunziata Presidio Osped, Oncology, Taranto, Italy

Purpose or Objective: To examine locoregional and distant recurrence rate (LLR and DR) in breast cancer patients treated with breast conserving surgery and adjuvant radiotherapy on whole breast and nodal areas according to histological subtype and prognostic characteristics.

Material and Methods: Between 2004 and 2013, 500 breast cancer patients *(*pts*)* were reviewed for this analysis. All pts received breast conserving surgery and adjuvant radiotherapy extended to nodal area because of pN+: 210 pts with pT1-2

pN1 stage, 190 pts with pT1-2 N2 while 100 pts with pT1/2 pN3 stage. Hystological subtype was luminal A (lA=Er+/ Pr+ , Her neg G1-G2) in 164 pts; luminal B (lB= Er+/Pr+, Her2 neg G3) in 170 pts; triple negative (TN= Er- Pr- Her2 neg) in 166 pts. Mean age was 65 yrs (range: 40-72 yrs). Patients were treated with chemotherapy according to prognostic features. All patients received whole breast radiotherapy witha a totale dose of 50 Gy + 10 Gy boost and 48-50 Gy on supraclavicular fossa. In case of medial tumors, the internal mammary chain was included. Kaplan-Meyer and paired t-test were used for statistical analysis.

Results: The 5-year LRR and DR were obtained with a median of 6.3 years. The 5-year LRR was 1.9% in lA, 2.8 % in l B , 2.1% in TN (*p*= .72). The 5-year DR was in lA 2%, lB 4.5%, 8 % in TN (*p*<.001) According to nodal status LRR was 1.7% in N1, 2.3% in N2 and 3.8% in N3 status (*p*= .005). The 5-year DR in N1 lA was 2.4 %, for lB was 3%, for TN was 3.5% (*p*= .82) while in N2 lA it was 3 %,for lB was 5% and for TN it was 7.3% (*p*= .06); for N3 lA was 3.5%, for lB was 4.8%, for TN was 8.5%; overall DR of pN1 versus pN2/N3 was statistically significant (*p*= .02). On multivariate analyses high risk of LRR was related to T size (T>2 cm), presence of lymphovascular invasion, lobular hystology; high risk of DR was observed for N> 4 nodes, presence of ECE, Ki 67> 30% and age <50 years.

Conclusion: *:* In this analysis triple negative breast cancer patients with pN1 seem to benefit by nodal radiation, but further studies are necessary

EP-1185

Male breast cancer - outcome with adjuvant treatment

B. Yadav[1], S. Sharma[1], R. Singh[1], S. Ghoshal[1]
[1]*PGIMER, Radiation Oncology, Chandigarh, India*

Purpose or Objective: To analyze outcome with adjuvant treatment in male breast cancer (MBC) patients.

Material and Methods: From 1991 to 2013, 68 men with breast cancer were retrospectively analyzed for demographic, clinico-pathological and treatment outcomes. Disease-free survival (DFS) was defined as time duration from diagnosis to first recurrence. Overall survival (OS) was defined as time duration from pathologic diagnosis to death or last follow-up with any death defined as an event. DFS and OS were estimated using Kaplan-Meier method and compared between patients receiving and not receiving adjuvant treatment using log-rank test.

Results: Mean age was 55 years (range 30-76). Right, left and bilateral BC was seen in 37(54%), 30(44%) and 1(1%) men respectively. Mean duration of symptoms was 25 months (range 1-240). Comorbidity was present in 22(36%) patients. Family history was present in 3(4%) patients. Mean tumor size was 5x5cm (range 1x1-10x10cm). Nipple was involved in 24(35%) men. Early, locally advanced and metastatic disease was seen in 27(39%), 29(43%) and 13(19%) patients respectively. Majority 51(84%) had IDC histology. In radically treated 56 men, NACT with FAC regimen was given to 10(18%) patients; with CR in 4(40%) and PR in 6(60%) patients. Mastectomy was done in 48(86%) and WLE in 8(14%) men. Margins and nodes were positive in 13(23%) and 30(54%) men respectively. ER, PR and Her2neu positive were 22(39%), 12(22%) and 2(3.5%) patients respectively. Adjuvant radiotherapy, chemotherapy and tamoxifen was received by 45(80%), 25(45%) and 37(66%) men respectively. Median follow up was 52 months (range 1-278). Local recurrence occurred in 8(14.5%) and distant metastasis in 18(33%) men respectively. DFS and OS at 10 year was 41% and 49% respectively. DFS and OS was significantly better in men with adjuvant radiation (53% vs 12%, p=0.002 and 57% vs 22%, p=0.005 respectively) and hormonal therapy (58% vs 14%, p=0.004 and 58% vs 39%, p=0.036). Chemotherapy had no impact on DFS and OS.

Conclusion: Adjuvant radiotherapy and hormonal therapy significantly improve DFS and OS in male patients with breast cancer. Chemotherapy had no impact on DFS and OS.

EP-1186

Late side effects and cosmetic outcome after intraoperative electron radiotherapy in breast cancer

C. Matuschek[1], E. Boelke[1], K. Halfmann[1], M. Ghorbanpour[1], J. Hoffmann[2], T. Fehm[2], W. Budach[1], S. Mohrmann[2]
[1]*University Hospital Düsseldorf Heinrich Heine University Düsseldorf, Radiotherapy and Radiooncology, Düsseldorf, Germany*
[2]*University Hospital Düsseldorf Heinrich Heine University Düsseldorf, Gynecology, Düsseldorf, Germany*

Purpose or Objective: The intraoperative boost radiotherapy is a validated method to irradiate the tumor bed immediately after surgery with an effective dose. The most homogeneously dose can be achieved with electrons (intraoperative radiotherapy with electrons = IOERT). Because of the high individual dose are chronic side effects of particular interest. Therefore we investigated the late side effects with a median of 31 months (5-54 months).

Material and Methods: From 10/2010 until 12/2013 n=138 patients received IOERT (NOVAC 7, New Radiant Technology, Aprilia, Italy) with 1x10 Gy covering the 90% isodose followed by whole-breast radiotherapy with 50.4 Gy/1.8 Gy SD. 58 patients were re-evaluated regarding late side effects and cosmetic outcome until 10/2015. The energy was determined by measuring the distance from the surface tot he rib by intraoperative ultrasound. We investigated the radiogenic side effects according to the LENT-SOMA criteria. Furthermore, we evaluated the cosmetic results (subjective / objective).

Results: Pain in the irradiated breast was denied by 81% of all patients. Pain grade 1 was reported by 15.5% and grade 2 by 3.4% of the patients. There was no breast edema detectable in 91.4%. We found an edema grade 1 in 5.2% and grade 2 in 3.4% oft he patients. There was no significant correlation between edema and pain (p = 0.326). A lymph edema grade 1 in the arm occurred in 5.2%. A retraction of the scar was not recorded for 91.4%, a retraction grade1 in 6.9% and a retraction grade 2 in 1.7%. None of the patients developed a radiogenic ulcer. Fibrosis was not recorded in 75.9%, a fibrosis grade 1 in 20.7%, a fibrosis grade 2 in 3.4% .Telangiectasia's have not occurred in 96.6%. No visible hyperpigmentation was found for 70.7%, and 29.3% had a grade 1 hyperpigmentation 1. One patient showed inhomogenities in the heart MRT, which was performed to rule out heart disease. One patient developed pneumonitis. The cosmetic results (patient's view) was very good in 41.4%, good in 41.4%, moderate in 10.3% and bad in 3.4%. The assessment of the physician (physician`S view) was in 48.3% very good, good in 34.5%, moderate 6.9% and bad in 1.7%. Moderate or bad results mostly occured in patients with small breasts and large tumor size.

Conclusion: IOERT followed by whole-breast radiotherapy by 50.4Gy/1.8 Gy SD is associated with a low incidence of late side effects. The cosmetic outcome is after objective and subjective assessment in the majority (82.8%) of patients very good or good.

EP-1187

T-lysyal based cream (Repalysyal) in the prevention of acute skin toxicity in breast cancer patients

A. Rese[1], E. D'Ippolito[1], F. Piccolo[1], P. Romanelli[1], A. Romano[1], L. Faraci[1], E. Toska[1], F. Pastore[1], V. De Chiara[1], L. Coppa[1], G. Salzano[1], A. Farella[1], R. Solla[1], M. Conson[1], L. Cella[2], R. Pacelli[1]
[1]*University of Naples "Federico II", Advanced Biomedical Sciences, Naples, Italy*
[2]*National Research Center, Institute of Biostructures and Bioimaging, Naples, Italy*

Purpose or Objective: Acute skin toxicity is a frequent side effect of breast irradiation affecting quality of life of breast cancer patients. Ameliorating these unwished events may have a positive impact on the therapeutic course of the patients. In this study we tested a thymine-lysine-hyaluronic

acid based cream in the prevention of radiation induced skin toxicity (RIST).

Material and Methods: Patients undergoing breast irradiation after conservative surgery for breast cancer were considered for the study. The patients were randomly assigned to use T-lysyal (repalysyal, a thymine-lysine-hyaluronic acid based cream) vs. patients using a moisturizing cream. The patients were stratified for age, breast size, and phototype. Radiation therapy was delivered with 3D conformal radiation therapy, with 20 fraction of 2.25 Gy (concomitant boost dose 2.5 Gy) on the residual breast for a total dose of 45 Gy in 4 weeks (50 Gy boost dose to the tumoral bed). The appearance of any grade of skin toxicity was the endpoint of our study. RIST was assessed weekly from the beginning of treatment and graded according to the RTOG acute skin toxicity scale.

Results: Fifty two consecutive patients undergoing radiation therapy after breast conserving surgery for breast cancer were randomized to have the skin treated with 2 daily application of Repalysyal or a simple moisturizing cream. Median age of the patients was 54. At the end of treatment (4 weeks) 15/26 patients in the Repalysyal group vs. 26/26 patients in the control group had any grade of skin toxicity (p=0.0001). Moreover, among patients that developed skin toxicity, 3/15 vs. 18/26 developed G2 toxicity in Repalysial and control group, respectively (0.0036).

Conclusion: Repalysyal ameliorates the acute skin toxicity profile of patients undergoing radiation therapy after conservative surgery for breast cancer.

EP-1188

The protective role of lipofilling in women subjected to radiotherapy.

N. Costantino[1], V.M. Margheriti[1], M. Santoro[2], E. Mazzei[2], M.A. Molinaro[2], R. Mole'[2], A. Destito[2], D. Pingitore[2], C. Bianco[1]

[1]*University Of Catanzaro "Magna Graecia", Oncology Radiotherapy, Catanzaro, Italy*

[2]*Hospital Of Catanzaro "Pugliese-Ciaccio", Oncology Radiotherapy, Catanzaro, Italy*

Purpose or Objective: Many authors suggest, when the patients is suitable, the complete reconstruction of the breast which has undergone radiation by autologous tissue, discouraging prosthetic placing because of the high level of post-radiotherapic complications observed. The aim of this study is the assessment of radiation-induced outcomes in women with breast cancer who have been subjected to radiotherapy after reconstruction.

Material and Methods: Between January 2011 and March 2013 we chose 17 patients, median age of 45 years; 15 of these had undergone a radical mastectomy and 2 a quadrantectomy. During the mastectomy 7 patients were given an immediate prothesis, 9 underwent reconstruction by lipofilling by way of classical breast expander and following prothesis , 1 quadrantectomy and breast remodelling by lipofilling. All the patients received adjuvant chemiotherapy and/or hormonotherapy, conformational radiotherapy on the thoracic wall or residue breast(total dose of 50 Gy) and local prophilactic therapy so as to minimize the radiation-induced adverse effects. All patients have gone thruogh a clinical-instrumental follow-up over an median time of 12 months and an assessment of cutaneous toxicity according to the SOMA-LENT scale.

Results: It was observed in 2 of the cases capsular contracture of the prothesis of high grade which needed further replacing and apperance of cutaneous ulcers (grade 2) in 1 patient ;in the remaining cases of prosthetic reconstruction erythema and edema were found (grade2). A tolerable erythema was observed in the patients with expander and simultaneous lipofilling without late fibrosis. No complications were found in the patients with rimodelling by lipofilling post quadrantectomy, with conservation of the shape and simmetry of the breast.

Conclusion: The grafting of the autologous fat, high in stamina cells, represents an alternative technique in breast reconstruction with complete functional recovery of the tissue , so improving the the surrounding tissue and therefore the capacity to heal in the irradiated tissues. The use of lipofilling is becoming an ever increasing importance as a coadjuvant in the breast reconstruction and avoids radiotherapy-induced complications. This gives notable psychophysical benefits and improves the quality of life in the patients.

EP-1189

Hypofractionated RT with or without boost in breast cancer: an institutional analysis of toxicity

C. Mariucci[1], A.M. Podlesko[1], E. Perrucci[1], L. Falcinelli[1], V. Bini[2], M. Di Benedetto[1], E. Arena[1], S. Nucciarelli[1], V. Lancellotta[1], I. Palumbo[1], C. Aristei[1]

[1]*Ospedale Santa Maria della Misericordia, Radiotherapy, Perugia, Italy*

[2]*Ospedale Santa Maria della Misericordia, Internal Medicine Endocrin and Metabolic Sciences, Perugia, Italy*

Purpose or Objective: Whole breast irradiation (WBI) is the gold standard after breast conserving surgery (BCS), followed by an additional boost when negative prognostic factors are present. WBI can be administered with hypofractionated schedules, on the basis of the relatively low α/ß ratio for breast cancer (BC). The aim of our study was to investigate the effects of an additional hypofractionated boost (HB) in terms of acute and short-term late skin and subcutaneous tissue toxicity.

Material and Methods: Between March 2014 and April 2015 156 women, median age 62 years (range 34-88) with early BC (pT1-pT2, N0-N1) underwent hypofractionated RT (single dose of 2.65 Gy to 42.4 Gy in 16 fractions over 3 weeks) ± HB (single dose 2.65 Gy to 10.6 Gy in 4 fractions). The study enrolled 71 patients (pts) without HB (45.5%) and 85 with HB (54.5%). The additional HB was delivered if risk factors such as young age, positive nodes, negative hormonal receptors, high Ki67 or HER2/neu overexpression were present. According to the risk of relapse chemotherapy (CT) and/or Hormonal Therapy (HT) and/or Trastuzumab were administered. For the analysis of the acute and late toxicity CTCAE 4.03 scale was used. Pts had physical examination at 5th, 10th, 16th and 20th day of RT and then 1 and 6 months after the end of treatment. Statistical analysis was carried out by the Chi-square test and the Mann–Whitney's U-test was used to compare continuous variables.

Results: HB group characteristics were: younger age (median 56 *vs* 67), longer time gap between surgery and RT (median time 20 weeks *vs* 16), more advance stage (43.6 % stage II *vs* 14.1%), CT (37 pts *vs* 2), HT (71 pts *vs* 48). Hypofractionated RT was well tolerated with or without HB and no G3 overall toxicity was documented. HB did not contribute to major skin toxicity; at the end of the treatment only 14 cases had G2 dermatitis *vs* 5 which did not receive HB (p = 0.073).One month after RT HB and CT significantly impacted upon edema occurrence: 15.5% HB group *vs* 1.5% no HB (p = 0.008) and 18.4 % CT group *vs* 6.2% no CT (p = 0.016). Furthermore, CT emerged as a risk factor for hyperpigmentation 6 months after RT: 37.0% *vs* 10.4% (p = 0.003). Attached Table summarizes the toxicity time-related events.

TOXICITY EVENTS

		WITHOUT BOOST (71 pts)					WITH BOOST (85 pts)					
		5 days	10 days	16 days	1 month	6 months	5 days	10 days	16 days	20 days	1 month	6 months
G1	Dry Skyn	0	0	0	3	0	0	1	0	1	2	1
	Hyperpigmentation	0	0	1	39	8	0	3	5	5	47	12
	Induration/fibrosis	0	0	1	3	6	0	0	0	0	3	14
	Pruritus/itching	0	0	3	2	0	1	2	3	3	2	0
	Desquamation	0	1	6	5	0	0	0	3	10	4	0
	Rash: dermatitis	6	21	42	13	0	8	30	49	51	11	3
	Teleangiectasia	0	0	0	0	0	0	0	0	0	0	0
	Skin ulceration	0	0	0	0	0	0	0	0	1	0	0
	Burn	0	0	0	0	0	0	0	0	0	0	0
	Edema	3	1	3	1	6	11	15	12	12	13	8
G2	Dry Skyn	0	0	0	0	0	0	0	0	0	0	0
	Hyperpigmentation	0	0	0	1	0	0	0	0	1	2	0
	Induration/fibrosis	0	0	0	0	0	0	0	0	0	0	0
	Pruritus/itching	0	0	0	0	0	0	0	0	0	0	0
	Desquamation	0	0	0	0	0	0	0	0	1	0	0
	Rash: dermatitis	0	1	5	0	0	0	0	5	14	0	0
	Teleangiectasia	0	0	0	0	0	0	0	0	0	0	0
	Skin ulceration	0	0	0	0	0	0	0	0	0	0	0
	Burn	0	0	0	0	0	0	0	0	0	0	0
	Edema	0	0	0	0	2	0	0	0	0	1	0

Conclusion: Administration of an additional HB is feasible, safe and well tolerated in terms of acute and short-term late skin and subcutaneous toxicity even though it seems to have a role in the edema occurrence. Although G2 dermatitis occurred in 16.47% of pts receiving HB vs 7.04% not receiving it, the difference was not significant, probably due to few observed events. Long term follow up data and a larger sample size are needed to confirm these data, assess late toxicity and clinical outcomes.

EP-1190

Boost volume assessment in breast cancer: preop tumor volume vs clips used in oncoplastic surgery

A. Altinok[1], M. Doyuran[1], M. Caglar[1], D. Canoglu, (1), E. Kucukmorkoc[1], H. Acar[1], N. Kucuk, (1), H. Caglar[1]
[1]*Medipol University, Radiation Oncology, Istanbul, Turkey*

Purpose or Objective: The aim of this study was to compare the volumes obtained with surgical clips during breast conserving surgery of breast cancer patients with volume determined using FDG positive tumor volumes outlined in pre-operative PET-CT imaging and find out the deviations that arise.

Material and Methods: For initial diagnostic PET-CT requested by the surgeon, the patients were positioned on the breast board with the arm on the ipsilateral side up. Those without metastatic tumors and applicable for breast conserving surgery went under operation in compliance with oncoplastic surgery principles. 4 clips were placed at the tumor lodge. For 15 of the patients, before continuing with further therapy, the tumor volume outlined with the surgical clips and that contoured using the area with FDG affinity viewed on the PET-CT were determined. Results were statistically analyzed with SPSS software.

Results: This study determined that methods used in oncoplastic surgery (such as flap shifting) resulted in displacements of the tumors from their original locations. For statistics we apply paired t test to the results that we have from these different techniques and found the values respectively for x,y,z as 0.929, 0.119, 0.991. Even the p value that we found is higher than 0.05 and not seems to be significant when we evaluate the center of mass deviation that we measure with these two techniques makes us to have an impact in overall results.

Conclusion: Determination of boost volume using pre-op tumor volume is not trustable in cases where tumor volume is not marked using clips during oncoplastic surgery of breast cancer and may result in geographical misses.

EP-1191

Pattern of metastasis in different molecular sub-types of locally advanced carcinoma breast

A.D. Sharma[1], J. Poddar[1], S. Patel Shah[1], U. Suryanarayan[1], M. Mehta[1], P. Nandwani Patel[1], J.P. Neema[1], A. Parikh[1], R.K. Vyas[1]
[1]*GCRI, Radiation Oncology, Ahmedabad, India*

Purpose or Objective: To investigate the association between the molecular sub-types and the pattern of distant metastasis in carcinoma breast.

Material and Methods: 400 patients of locally advanced breast carcinoma, without any distant metastasis, both clinically or by imaging were studied retrospectively.(Jan 2010- Dec 2011) The ER/ PR and HER-2neu status of the patients was noted and the patients were classified into luminal A/B, Triple negative, Her2/neu enriched and Luminal/Her.
All patients had received the treatment for carcinoma breast as per the standard protocols i.e. Cuarative treatment with surgery, Chemotherapy, and radiotherapy followed by hormonal therapy as per the indications.
All the patients were followed up for local as well as distant failure and pattern of failure was co-related with the molecular subtypes.
The major sites of distant metastasis were lungs, liver, bones and brain.

molecular subtypes	bone	Liver	Lungs	brain	local recurrence
Luminal A/B	16/30	10/30	2/30	6/30	4/30
Her 2 Neu enriched	28/66	30/66	20/66	20/56	18/56
Luminal Her	16/28	11/28	2/28	8/28	6/28
Triple Negative	7/19	6/19	7/19	4/19	0/19

Results: Brain was the most common site of metastasis in Her 2 /neu enriched subtype.
Bone is the most common site of metastasis in all subtypes

Conclusion: A strong association of different metastatic sites with the molecular status suggests vigilance about the symptoms (metastatic) beforehand. Organ specific metastasis may depend on the molecular subtype of the cancer. High rate of bone metastasis might be due to the role of bone marrow as a homing organ for the cancer cells. Early treatment of Her-2/ neu patients withTrastuzumab might reduce the rate of metastasis. Tailored strategies against distant metastasis concerning the molecular subtypes in breast cancer may be considered.

EP-1192

Management of the axilla after neoadjuvant systemic therapy in breast cancer: A systematic revision

A. Manterola[1], G. Asín[1], F. Arias[1], M. Errasti[1], M. Barrado[1], M. Campo[1], I. Visus[1], M. Domínguez[1]
[1]*Complejo Hospitalario de Navarra, Oncol Radioterápica, Pamplona, Spain*

Purpose or Objective: Worldwide, breast cancer is the most common invasive cancer in women. The management of breast cancer depends on multiple factors. The purpose of this work is review the currently management of the axilla after neoadjuvant systemic therapy in breast cancer especially from the point of view of an oncology radiotherapist

Material and Methods: In May 2015, we searched clinical trial registers, the Cochrane Central Register of Controlled Trials, Web of Science, EMBASE and MEDLINE and reviewed reference lists. Further hand searches were conducted of relevant journal proceedings. At the end, we principally reviewed both meta-analyses regarding the results of the SNB following NAC in patients with a diagnosis of clinically negative axillae, the results of NSABPB-18 and NSABP B-27

Trials, The ASCO recommendations about SNB, The Canadian SN FNAC and German SENTINA, The MD Anderson trials, and the ACOSOG Z 1071 and AO11202 ALLIANCE (NCTO 1901094)

Results: For patients treated with NAC, patients with advanced stages (T3-4 /N2-3) should receive RT after independent NAC response. In early stages, it would be reasonable to receive treatment if there were residual disease; if doubts exist in cases of pRC, such cases should be assessed individually. It seems clear that patients with clinical regional involvement who present affectations of the lymph nodes following NAC will benefit from locoregional RT, but it is less clear in those who are pN0 following the NAC, as their risk of LRR is low.

Conclusion: The benefit of locoregional RT is not clear in patients with pN0 following the NAC The ongoing NSABPB-51 /RTOG1304 (NRG 9353) study has been designed to answer this question. We must wait for the results of this important trial. Until these results, we must follow the recommendations previously prescribed.

EP-1193

ABPI with 3D-CRT, and image-guided IMRT, after BCS – 4 year results of a phase II trial

N. Mészáros[1], G. Stelczer[1], T. Major[1], Z. Zaka[1], C. Polgár[1]
[1]*National Institute of Oncology, Radiotherapy, Budapest, Hungary*

Purpose or Objective: To present the clinical results of ABPI using 3D-CRT and IG-IMRT following breast-conserving surgery (BCS) for early-stage breast cancer.

Material and Methods: Between 2006 and 2014, 104 low risk breast cancer patients were treated with postoperative APBI given by means of 3D-CRT (n=44) using 3-5 non-coplanar, izocentric wedged fields, or IG-IMRT (n=60) technique using KVCBCT guidance for each fractions. The total dose of APBI was 36.9 Gy (9 x 4.1 Gy) using twice-a-day fractionation for 5 consecutive days. Survival results, side effects, and cosmetic results were assessed.

Results: At a median follow-up of 48 months (range: 25-112) one (0.9%) local recurrence was observed. Two patients (1.9%) died of internal disease. One (0.9%) contralateral recurrence and three (2.8%) secondary tumours were observed. Neither regional nor distant failure was detected. Acute side effects included grade 1 (G1) and G2 erythema in 54 (51.9%) and 2 (1.9%), G1 parenchymal induration in 43 (41.3%), G1 and G2 pain in 26 (25%) and 2 (1.9%) patients. No ≥G3 or higher acute side effect occurred. Late side effects included G1 telangiectasia in 10 (9.6%) G1, G2, and G3 fibrosis in 26 (25%), 3 (2.8%) and 1 (0.9%) patients respectively. Asymptomatic (G1) fat necrosis occurred in 8 (7.7%) patients. The rate of excellent/good and fair/poor cosmetic results was 96 (92.3%), 8 (7.7%) respectively.

Conclusion: Both 3D-CRT and IG-IMRT for delivery the ABPI is feasible and the 4 years clinical results and toxicity profile is comparable to other results using multicatheter APBI brachytherapy.

EP-1194

Cardiac toxicity after breast cancer patients treatment

D. Gabrys[1], A. Piela[2], A. Walaszczyk[3], R. Kulik[4], A. Namysł-Kaletka[1], I. Wziętek[1], K. Trela-Janus[1], S. Blamek[1]
[1]*Maria Sklodowska-Curie Memorial Cancer Center and Institute of Oncology, Radiotherapy Department, Gliwice, Poland*
[2]*Maria Sklodowska-Curie Memorial Cancer Center and Institute of Oncology, Oncological and Reconstructive Surgery Department, Gliwice, Poland*
[3]*Maria Sklodowska-Curie Memorial Cancer Center and Institute of Oncology, Center for Translational Research and Molecular Biology, Gliwice, Poland*
[4]*Maria Sklodowska-Curie Memorial Cancer Center and Institute of Oncology, Radiotherapy and Brachytherapy Department, Gliwice, Poland*

Purpose or Objective: Radiation and anthracyclines are known to induce cardiac damage. Despite the use of 3D planning the heart is still irradiated with non-negligible doses, therefore this problem needs further investigation. We perform an analysis of cardiac function in the left sided breast cancer survivors. Patients were treated with surgery alone (S), additional radiation (RT), additional anthracycline based chemotherapy (A) or both (RA).

Material and Methods: A total of 140 patients were subjected to cardiological evaluation more than 8 years after primary treatment. We performed ECG and ECHO (in a part of patients we also had an ECG and ECHO performed before surgery), blood tests, chest X-ray. We also collected additional relevant information on patients (history, comorbidities, current treatment, etc.). Distribution of patients was as follows 50% RA arm, 18% S, 8% RT, 24% A. The mean time from the beginning of the treatment to examination was 12.2 years (8-15.9) in S, 11.7 (8-16.9) in A, 10.7 (8-15.3) in RT, 10.1 (8.1-14.5) in RA. The majority of patients were treated with amputation (74%), the remaining with BCT. In chemotherapy arms 47% were treated with FAC, 31% with CAF, 19% with AC, and 3% with TE. Hormonal treatment was given to 64% of patients, in the majority of them it was Tamoxifen-based. Radiotherapy dose varied between 50 and 70 Gy.

Results: There was no significant difference in ejection fraction (EF) between the groups: median 56 (47-65) in S, 50 (25-65) in A, 55 (47-62) in RT and 54 (35-67) in RA. Other evaluated parameters like size of the right and left ventricle, left atrium, thickness of septum and posterior wall also did not differ between groups. In the whole group in 21% of patients we observed chronic cardiac insufficiency. In 58% of patients there were other cardiovascular disorders as hypertension, hypercholesterolemia, atherosclerosis, arrhythmias, and valvular disorders. Only in one patient treated with radiation and chemotherapy we found impaired heart function without other additional causes.

Conclusion: In the current series no unequivocal association between treatment regimen and long-term cardiac dysfunction could be found. Further studies in a well-balanced patient population are needed to elucidate the impact of contemporary anthracycline-based systemic treatment and modern irradiation techniques on cardiac outcome.
The research received funding from National Science Center Poland under grant no. N N 402 685640

EP-1195

Active breathing coordinator in left-sided breast cancer radiotherapy: dosimetric comparison study

N. Pasinetti[1], L. Pegurri[1], R. Cavagnini[1], L. Costa[1], P. Vitali[1], L. Bardoscia[1], B. Bonetti[1], L. Spiazzi[2], B. Ghedi[2], S.M. Magrini[1]
[1]*University and Spedali Civili Brescia, Radiation Oncology, Brescia, Italy*
[2]*Medical Physics Spedali Civili Brescia, Radiation Oncology, Brescia, Italy*

Purpose or Objective: Incidental radiation dose to the heart and lung during left breast radiation therapy (RT) has been associated with an increased risk of cardiopulmonary morbidity especially in patients treated with antracyclin as neoadjuvant/adjuvant chemotherapy schedules after surgery. We conducted two different dosimetric analyses (by NTCP and Bio-DVH) to determine if left breast RT with the Active Breathing Coordinator (ABC) can reduce heart/left anterior descending artery (LAD) and lung dose without target coverage impairment.

Material and Methods: Patients with stages 0-III left breast cancer (LBC) were enrolled and underwent simulation with both free breathing (FB) and ABC for comparison of dosimetry. ABC was used during the patient's RT course if the heart exposition was V(30)≥ 12%. The prescription dose was 50 Gy plus a boost in 88% and 2,75 Gy up to 44 Gy plus a boost in 22%. The primary endpoint was the magnitude of

heart reduction dose when comparing ABC to FB. Analysis was performed with BIOPLAN (BiOlogical evaluation of PLANs) PC based user-friendly software (evaluation of Dmax, Dmin, Dmean) and home-made Planning Reporting Orienteering (PRO)-DVH software. PRODVH produced Bio-DVH (Equivalent Dose Volume histograms for 25 fractions) that allowed the comparison regardless of the treatment schedule and that were used to calculate the average DVH for each set up. Secondary endpoints included dose reduction to the lung and procedural success rate.

Results: Between May 2012 to February 2015, 50 patients with LBC are selected for receiving RT using ABC after both FB and ABC simulation. Procedural success was good, all patients have sufficient compliance and are been selected for this procedure. The primary endpoint was achieved: use of ABC reduced LAD/heart exposition ($p < 0.01$ T-student test). There was no significant difference between the free-breathing and moderate deep inspiration breath-holding in the target volume coverage. The volume of the ipsilateral lung in the free-breathing technique was smaller than the moderate deep inspiration breath-holding techniques. All these data were confirmed with both software.

Conclusion: ABC was well tolerated and significantly reduced heart/LAD dose without impairment in target volume coverage. No difference was find in lung dose reduction. Use of the ABC device during RT should be considered to reduce the risk of ischemic heart disease in populations at risk.

EP-1196

Atlas-based segmentation for delineating the locoregional node levels during breast radiotherapy

C. Pirson[1], P.V. Nguyen[1], M. Baiwir[1], P.A. Coucke[1], F. Lakosi[1], A. Gulyban[1]
[1]*C.H.U. - Sart Tilman, Radiotherapy Department, Liège, Belgium*

Purpose or Objective: Proper multi-atlas automated delineation can streamline clinical routine only when the proposed volume determination reasonably approximates the manual delineation. In this investigation we aimed to evaluate the automatic atlas-based segmentation of supraclavicular and level 3 lymph nodes for loco-regional irradiation of breast cancer. Further analysis were performed on the final plan's dose coverage to the automated clinical target volume.

Material and Methods: Between June and September 2015 five consecutive breast cancer patients with clinical indication for loco-regional irradiation were selected. Pre-defined breast delineation atlas of Mirada RTx (version 1.6.2, Mirada Medical, Oxford, United Kingdom) software were used to generate automated clinical target volumes (CTVauto) including the supraclavicular and the axillary level 3 lymph nodes. Responsible radiation oncologist delineated the reference CTV (CTVref) for each individual patients as well. Comparison metrics of Dice similarity (DI) and commonly contoured volume (CCV) were used. Furthermore the CTVauto was expanded with 1,2,3,4 and 5 mm uniform margin consecutively followed by an evaluation of the volumetric coverage of CTVref. Finally clinical plans were created expanding CTVref with 5 mm uniform margin using either direct antero-posterior beam or multi-beam IMRT. Dose coverage of the 95% of prescribed dose (V95) were compared for both CTVs.

Results: The average CTVref was 35.1 cc (Standard deviation = 10.2), while for the CTVauto 42.1 cc (SD = 12.1). Mean DI and CCV were 0.73 (SD: 0.26) and 0.72 (SD: 0.28) respectively. Expanding the CTVauto up to 5 mm in 1 mm increments covered the CTVref with 53.9%, 77.9%, 88.1%, 90.9% , 92.7% and 95.7% respectively. (Figure 1). For two patients single direct ante-posterior (AP) beam were used for the loco-regional treatment, while for the other three cases 6 beam IMRT were used. Average V95% dose coverage of CTVref was 98.5% (SD: 3.0) which lowered to 92.0% (SD: 9.1%) for CTVauto. For the two patient with single AP field the CTVref were 93.0% and 99.5%, which dropped to 79.8% and 99.4% for CTVauto. The multi-beam IMRT cases showed 100%, 99.9% and 99.8% CTVref_V95 and 100%, 88.5% and 94.0% CTVauto_V95.

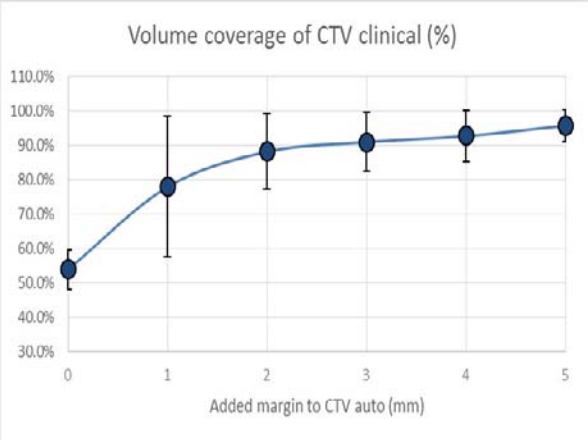

Conclusion: CTV delineation using an atlas-based auto-segmentation shows promising results even in a small complicated volume delineation such as the loco-regional lymph nodes of breast. Further improvement of the delineation accuracy is expected by adding more cases to the initial multi-atlas (with 3 provided cases).

EP-1197

Hypofractionated radiotherapy in locally advanced breast cancer

A.C. Carvalho[1], P. Fernandes[1], J. Casalta-Lopes[1], A. Cleto[1], M. Borrego[1]
[1]*Hospitais da Universidade de Coimbra, Radiation Oncology, Coimbra, Portugal*

Purpose or Objective: Locally advanced breast cancer (LABC), clinically classified as cT4, is mostly identified in elderly patients, typically featuring unfavorable prognosis. It is usually associated with ulceration, bleeding and local pain, with prolonged course. Radiation therapy (RT) shows an important role in local control and symptomatic control. Hypofractionation radiotherapy scheme, with a dose of 13 Gy in two fractions with an interval of 48 hours (also known as RT-FLASH), allows acceptable results. With this study we aim to evaluate the response of the patients treated with RT-FLASH.

Material and Methods: LABC patients treated from 2001 to 2015 with RT-FLASH were retrospectively included. Local response was clinically assessed. Kaplan-Meier method was used for locoregional progression-free survival (LPFS) and overall survival (OS) analysis. Type I error of 0.05.

Results: 63 patients were included, with a median age of 78 years (39-92 years), 61.9% with Karnofsky≤80% and median progression time of 13.5 months (2-180 months). Carcinoma not otherwise specified (NOS) was the most common histological type (84.1%), with estrogen receptor-positive in 71.4%. Most of the tumors were cT4b (50.8%) and cT4c (36.5%) with cN+ in 60.3% and cM1 in 44.4%. At the initial evaluation 46.0% had bleeding injuries. Two RT-FLASH were performed in 65.1% of the patients. During treatment there was no record of toxicity. There was reduction of bleeding (81.5%), size (69.8%) and ulceration (39.6%). Surgical conditions were acquired in 23.8% of the patients. Patients cM1 received chemotherapy more often than cM0 (57.7% vs. 17.6%; p=0.001). Of the 63.9% patients that received hormone therapy (HT), 77.5% had 2 RT-FLASH (p=0.002 vs. non-HT), with a greater dimensional reduction in patients undergoing HT (81.1% vs 43, 8%, p = 0.010). LPFS at 2 and 5 years was 76.6% and 66.1%, respectively. The 2-year OS was 39.7% and 5-year OS was 19.5%, higher in cM0 patients (p<0.001), patients subjected to 2 RT- FLASH (p=0.003), or under HT (p=0.001). Multivariate analysis showed significant

impact of HT and cM1 (p=0.018 with HR =0.593 and p=0.006 with HR=2.574, respectively). In the multivariate analysis of LPFS, HT and 2 RT-FLASH had prognostic impact (p=0.039 with HR=0.297 and p=0.036 with HR=0.257, respectively).

Conclusion: In the context of LABC, with poor prognosis, RT-FLASH improves the quality of life, without registration of acute toxicity, and with reasonable OS. HT and the absence of metastasis at diagnosis had a positive impact on prognosis, significantly. LPFS was significantly higher in patients who underwent two RT-FLASH or HT.

EP-1198

Evaluation of pulmonary acute/ subacute toxicity after different techniques of breast radiotherapy

B. Serarslan[1], Y. Sanlı[2], M. Fayda[1], C. Türkmen[1], M. Erelel[3], N. Dönmez Kesen[4], N.S. Küçücük[1]
[1]*Istanbul University- Faculty of Medicine, Department of Radiation Oncology, Istanbul, Turkey*
[2]*Istanbul University- Faculty of Medicine, Department of Nuclear Medicine, Istanbul, Turkey*
[3]*Istanbul University- Faculty of Medicine, Department of Pulmonary Medicine, Istanbul, Turkey*
[4]*Istanbul University, Department of Medical Physics, Istanbul, Turkey*

Purpose or Objective: The increase in the local control and survival of breast cancer patients with postoperative radiotherapy(RT) has been demonstrated by many of randomized trials and metaanalysis. Because of this longer life expectancy; quality of life and minimizing of treatment toxicity have gained importance. More homogenous dose distribution in the treatment field and reduction of side effects is possible with new RT techniques. The aims of our study are to evaluate acute/subacute pulmonary effects and their differences with different RT modalities of postoperative breast RT via pulmonary function tests (PFT) and single photon emission computer tomography (SPECT) based lung perfusion scintigraphy (SLPS), and to exhibit optimum lung dose constraints data for breast cancer RT. Additionally this study enables to detect early pulmonary toxicity in the asymptomatic period and to treat it, if necessary.

Material and Methods: In our study, voluntary breast cancer patients eligible for postoperative RT, who completed adjuvant systemic chemotherapy were separated equally into two groups of different RT techniques [3D conformal RT (3D-CRT) and intensity-modulated radiotherapy (IMRT)]. To assess the acute/subacute pulmonary toxicity, we performed PFT and SLPS just before RT (baseline) and after 3 months of RT (control). After 1 month of RT patients were rechecked with only PFT. We assessed the relation between dosimetric data and the study changes (Figure1).

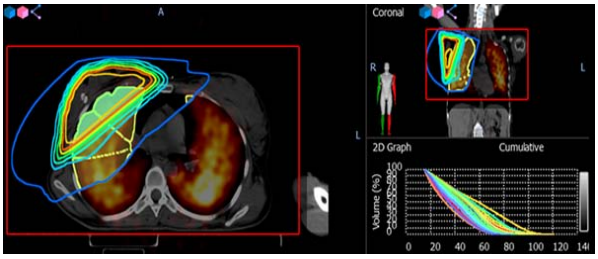

Figure 1: Fusion of single photon emission computer tomography (SPECT) based lung perfusion scintigraphy (SLPS) images and radiotherapy plans via VelocityAI® programme

Results: Mean lung doses and lung volumes receiving ≥20Gy (V1, V5, V10, V20) were significantly higher in IMRT group ($p<0.001$) (Figure 2). There was no significant difference in PFT changes after RT between the two RT techniques ($p>0.05$). Higher lung doses ($p<0.001$) and more significant mean reduction of scintigraphic uptake were observed in low dose volumes with IMRT ($p<0.05$). In 3D-CRT group, the mean reduction of scintigraphic uptake was higher in the lobe, that receives the highest mean dose (ipsilateral lobe) ($p<0.05$). Furthermore, even though right supraclavicular area, which effects the upper lung zone was irradiated, frequently the right middle lobe received more radiation, not right upper lobe. Eventually, none of the patients had grade ≥2 LENT - SOMA lung toxicity. We didn't find any relationship between patient characteristics (smoking history, age, chemotherapy type, surgery type, tumor location, RT field and technique) and radiation induced pulmonary toxicity.

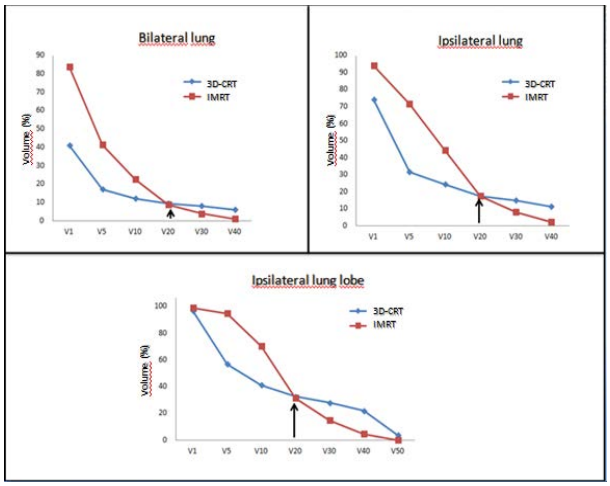

Figure 2: Bilateral lung, ipsilateral lung ve ipsilateral lung lobe mean V1, V5, V10, V20, V30, V40, V50 values

Conclusion: We found that V20 volume of lung is a similar parameter for evaluation of different breast RT techniques and evaluation of low and high dose volumes can be more feasible. Larger group of patients and longer follow-up can lead to more significant results.

EP-1199

Cardiac dose delivered by left sided tumour bed electron boost; a potential source of toxicity

V. Gajapathy[1], L. Hill[1], S. Cleator[1]
[1]*Charing Cross Hospital, Radiotherapy, London, United Kingdom*

Purpose or Objective: Cardiac dose delivered during tangential radiotherapy is increasingly scrutinized, but the cardiac dose delivered during electron boost is not routinely calculated. We retrospectively reviewed cases in which an electron boost was employed to deliver a phase 2 to a tumour bed (TB) overlying the heart to establish the proportion of cases and type of cases in which this treatment delivered a significant cardiac dose.

Material and Methods: A cohort of left sided breast cancer cases receiving radiotherapy in a single treatment centre over a 4 month period were reviewed. Those patients receiving a phase 2 electron boost to a TB in the mid/ lower part of the left breast were identified. For those in which an electron beam was incident on the heart, fully commissioned Monte Carlo dose calculation was used to derive the dose delivered to whole heart and left anterior descending artery assuming a boost dose of 16Gy in 8 fractions to the 100%.

Results: A total of 24 patients received a boost to a TB in the mid/ lower part of the left breast. Of these, 15 were treated with an electron beam incident on the heart. In 6/15 (40%) the mean heart dose delivered by the boost component was 0.5Gy. The maximum mean heart dose was 1.02Gy. In all 6 cases, the energy employed was >9MeV.

Conclusion: The heart dose delivered by an electron boost with beam incident on the heart can be significant, especially if an energy >9MeV is employed. In such cases, mini-tangential treatment in deep inspiratory breath hold is recommended.

Electronic Poster: Clinical track: Lung

EP-1200

Evaluation of response to stereotactic body radiation therapy for non-small cell lung cancer

K. Jingbo[1], D. Rui[1], F. HengHu[1], Z. Xinhong[1], W. JuYi[1], L. YingKui[1]

[1]*Department of Radiation Oncology and Integrative Oncology- Navy General Hospital, Department of Radiation Oncology and Integrative Oncology- Navy General Hospital, Beijing, China*

Purpose or Objective

Recommendations for surveillance after stereotactic body radiation therapy (SBRT) for early stage non-small cell lung cancer (NSCLC) are not well defined. Recently, PET response criteria in solid tumors (PERCIST) have been proposed as a new standardized method to assess radiotherapeutic response metabolically and quantitatively. The aim of this study was to evaluate therapeutic response to Stereotactic Body Radiotherapy for Early Stage Non-small Cell Lung Cancer, comparing PERCIST with the currently widely used response evaluation criteria in solid tumors (RECIST).

Material and Methods

Forty-nine patients with locally early Stage Non-small Cell Lung Cancer who received Stereotactic Body Radiotherapy were studied. Radiotherapeutic lesion responses were evaluated using CT and 18F-FDG PET according to the RECIST and PERCIST methods. The PET/CT scans were obtained before SBRT and about 3 to 6 month after SBRT. Associations were statistically analyzed between overall survival and clinicopathologic results (histology, tumor location, tumor size, lymphatic invasion, clinical stage, radiotherapeutic responses in RECIST and PERCIST).

Results

Median follow-up was 30 months. Thirteen patients had stage IA, 9 stage IB, 10 stage IIA, and 17 stage IIB biopsy-proven NSCLC. Three-year overall survival was 79.6%. CT scans indicated 3 regional recurrences. PET/d-chest indicated 3 regional recurrences and distant metastasis. There was a significant difference in response classification between RECIST and PERCIST (Wilcoxon signed-rank test, P=0.0041). Univariate analysis showed that clinical stage, RECIST and PERCIST were significant factors associated with overall survival in this study, while by multivariate analysis PERCIST was the only predictor of overall survival in early NSCLC patients. In fact, SMD, PMD/PMR, CMR in PERCIST criteria was indicative of a 9.900-fold increase in the risk of overall survival in early NSCLC patients [RR 9.900 (95% CI 1.040, 21.591), P=0.001].

Conclusion

RECIST based on the anatomic size reduction rate did not demonstrate the correlation between therapeutic responses and prognosis in patients with Early Stage NSCLC receiving SBRT. However, PERCIST was found to be the strongest independent predictor of outcomes. PERCIST might be considered more suitable for evaluation of radiotherapeutic response to NSCLC than RECIST.

EP-1201

Impact of low skeletal muscle mass on survival after SBRT for non-small cell lung cancer

Y. Matsuo[1], T. Mitsuyoshi[1], A. Nakamura[1], Y. Iizuka[1], T. Kishi[1], W. Mampuya[1], H. Hanazawa[1], M. Hiraoka[1]

[1]*Kyoto University, Department of Radiation Oncology and Image-applied Therapy, Kyoto, Japan*

Purpose or Objective: Sarcopenia is a syndrome characterized by low muscle mass and low muscle function. Several authors reported that low skeletal muscle mass (SMM) was associated with decreased survival in cancer patients. The purpose of the present study was to retrospectively evaluate impact of SMM on survival and cause of death after stereotactic body radiotherapy (SBRT) for primary non-small cell lung cancer (NSCLC).

Material and Methods: Of consecutive 253 patients who received SBRT for primary NSCLC between 2004 and 2013, 186 patients whose abdominal CT before the treatment was available were enrolled into this study. SMM was evaluated through total psoas area (TPA) at a level of the third lumbar vertebra according to a method proposed by Jones *et al.* (*Colorectal Dis* 2015;17:O20). TPA was estimated by multiplying the greatest anterior/posterior and transverse muscle diameters and then normalizing for patient height. The patients were divided into two groups of SMM according to gender-specific thresholds for TPA. Regression analysis was done for the cumulative incidence function for competing risks of death from lung cancer and from other causes. Evaluated variates were SMM, age, gender, performance status, body mass index (BMI), Charlson comorbidity index (CCI), operability, modified Glasgow prognostic score (mGPS), recursive partitioning analysis (RPA) class, and histology. In multivariate analysis, step-wise selection was applied to identify potential factors.

Results: edian TPAs were 293 and 240 mm^2/m^2 in male and female, respectively, and these values were used as the gender-specific thresholds. Patients with lower SMM tended to be elderly and lean in BMI compared with the higher SMM. A potential median follow-up period was 55.6 months. Overall survival at 5 years was 41.1% and 55.9% in the lower and higher SMM groups, respectively (P = 0.115). Cumulative incidence of non-lung cancer death was significantly worse in the lower SMM (31.3% at 5 years compared with 9.7% in the higher SMM, P = 0.006). Multivariate regression analysis identified SMM and operability as significant factors for non-lung cancer death (**Table**). Impact of SMM on lung cancer death was not significant with cumulative incidence of 27.6% and 34.4% at 5 years in the lower and higher SMM groups, respectively (P = 0.332).

		Univariate		Multivariate	
		HR	P-value	HR	P-value
SMM	Lower vs higher	2.60	0.006*	2.66	0.004*
Age	>75y vs ≤75y	2.01	0.078	1.96	0.094
Gender	Male vs female	1.88	0.140		
PS	1 vs 0	0.78	0.042*		
	2–3 vs 0	2.68			
BMI	Lean vs normal	2.43	0.046*		
	Obese vs normal	1.09			
CCI	1–2 vs 0	5.75	0.059	3.71	0.096
	≥3 vs 0	9.10		6.24	
Operability	inop vs operable	2.60	0.015*	2.22	0.040*
mGPS	1–2 vs 0	1.45	0.260		
T-stage	1b vs 1a	1.00	0.702		
	2a vs 1a	0.72			
RPA class	II vs I	1.27	0.460		
Histology	Sq vs Ad	1.13	0.987		
	Others vs Ad	1.03			
	Unproven vs Ad	1.14			

Table. Univariate and multivariate regression analysis for non-lung-cancer death

Abbreviations: SMM = skeletal muscle mass, PS = performance status, BMI = body mass index, CCI = Charlson comorbidity index, mGPS = modified Glasgow prognostic score, RPA = recursive partitioning analysis

BMI was classified into lean (<18.5), normal and obese (≥25.0). RPA class I is female or patients with T1a. mGPS of 0 was defined as CRP<0.3 mg/dL and albumin>3.5g/dL.

Conclusion: Low SMM is a significant risk factor for non-lung cancer death after SBRT for NSCLC.

EP-1202

CBCT in Lung FFF-SABR: predictive parameters of early response

F. Alongi[1], R. Mazzola[1], F. Ricchetti[1], N. Giaj Levra[1], S. Fersino[1], G. Sicignano[1], A. Fiorentino[1], R. Ruggieri[1]
[1]*Ospedale Sacro Cuore Don Calabria, Radiation Oncology, Negrar - Verona, Italy*

Purpose or Objective: aim of the study was to analyze tumor volume variations, by contouring on cone-beam computed tomography (CBCT) images, to evaluate early predictive parameters of Flattening Filter Free Stereotactic Ablative Radiation Therapy (SABR) treatment response.

Material and Methods: the prescribed dose of SABR varied according to the tumor site (central or peripheral) and maximum diameter of the lesions using a strategy of risk-adapted dose prescription with a range of dose between 48 and 70 Gy (3-10 consecutive fractions). For the purpose of the analysis, gross tumor volume (GTV) was re-contoured for each patient at first and last CBCT using two lung levels/window: 1) -600/1000 Hounsfield Units (HU) and 2) -1000/250 HU. Statistical analysis was performed to evaluate correlations between target variations on CBCT, using the two window-levels, and treatment response three months after the end of SABR. The analysis was conducted considering the following variables: number of fractions≥ 5, BED 95-110, BED > 110 and GTV volume pre-SABR > 6 cc.

Results: 41 lung lesions were evaluated. The median follow-up was 14 months (range, 5 - 43 months). For both the CBCT level/windows, GTV shrinkage of at least 20% was associated to the probability of achieving a disease complete response (CR) at 3 months. The probability of CR ranged between 6 and 8 times higher, in respect to the CBCT lung level adopted, comparing to patients without a GTV decrease of 20%. This cut-off value was confirmed for all the variables analyzed.

Conclusion: according to current findings, a tumor shrinkage cut-off of at least 20% at last session of SABR is predictable for CR

EP-1203

Stereotactic raditherapy for oligometastases or oligorecurrence within a mediastinal lymph node

H.H. Wang[1], M.B. Meng[1], X.L. Zeng[1], F.T. Li[1], L.J. Zhao[1], Z.Y. Yuan[1], P. Wang[1], Y.C. Song[1]
[1]*Tianjin Cancer Hospital, Department of Radiation Oncology, Tianjin, China*

Purpose or Objective: This study *was t*o evaluate the safety and efficacy of stereotactic radiation therapy (SRT) in the treatment of patients with oligometastases or oligorecurrence within a mediastinal lymph node (MLN).

Material and Methods: Between October 2006 and May 2015, patients with oligometastases or oligorecurrence within MLNs originating from different primary tumor were enrolled and treated with SRT at our hospital. The primary end-point was MLN local control (LC). Secondary end-points were: time to symptom alleviation; overall survival after SRT (OS); and toxicity using the Common Terminology Criteria for Adverse Events (CTCAE v4.0).

Results: Eighty-five patients with 98 MLN oligometastases or oligorecurrence were treated with SRT. For the entire cohort, the 1-year and 5-year actuarial LC rates were 97.3% and 77.2%, respectively. Symptom alleviation was observed in 28 patients (28/32, 87.5%), with symptomatic lesions after a median of 5 days (range, 3-30 days). The median OS were 27.17 months for all patients and 32.20 months for those with NSCLC. Univariate and multivariate analyses revealed that an interval between diagnosis of primary tumors and SRT and MLN PTV volume were independent prognostic factors for OS in patients with NSCLC. CTCAE v4.0Grade 3 toxicities occurred in six patients (7.06%), with Grade 5 in three patients (all with radiotherapy history to MLN station 7).

Conclusion: SRT is a safe and efficacious treatment modality for patients with oligometastases or oligorecurrence to MLN, except for patients who received radiotherapy history to MLN station 7. Further investigation is warranted to identify the patients who benefit most from this treatment modality.

EP-1204

Predicting toxicity after lung stereotactic radiation therapy

J.E. Bibault[1], X. Mirabel[1], T. Lacornerie[1], E. Tresch[2], E. Lartigau[1]
[1]*Oscar Lambret Cancer Center, Academic Radiation Therapy Department, Lille, France*
[2]*Oscar Lambret Cancer Center, Biostatistics Department, Lille, France*

Purpose or Objective: Lung SBRT has shown excellent local control rates for inoperable patients with early-stage lung cancer without lymph node involvement. The reported toxicity is low, but factors associated with toxicity such as pneumonitis or lung fibrosis have not been well documented.

Material and Methods: All inoperable patients treated in our institution between August 2007 and April 2013 with SBRT for peripheral early-stage lung cancer were included. Endpoints of the study were rib fracture, acute pneumonitis, lung fibrosis, hemoptysis. Univariate binary logistic regressions were used to look for statistical associations between binary (eg, gender), ordinal (eg, age, dose per fraction, total dose, number of treatment session, V20, mean lung dose, volumes) or nominal (eg tracking method, previous treatment) variables and the study endpoints. Multivariate logistic regression was to be performed if more than 1 factor was associated with 1 of the outcomes of interest with a P value of less than .2. Treatment fractionation regimens were adapted according to tumor localization.

Results: 205 patients with 214 lesions were included in the study (67 central and 147 peripheral). 73 patients (36%) had toxicities: 14 patients (6.8%) had acute pneumonitis and 56 lung fibrosis (27.3%) without clinical effects. Two patients had a rib fracture (1%) and 1 patient had rib cage pains. No other toxicities were observed. In univariate analysis, a lower number of treatment sessions (p=0.018) and higher dose per fraction (p=0.011) were associated with more toxicity. Longer treatment sessions were associated with more acute pneumonitis (p=0.001). Lung fibrosis was associated with a higher dose per fraction (p=0.027). Tracking was also associated with a higher rate of lung fibrosis, but patients treated with tracking had bigger tumors (mean diameter : 21.9 mm vs 28 mm). Tumor localization (central vs peripheral) was not a predictive factor of toxicity.

Conclusion: A higher dose per fraction and fewer treatment sessions were associated with more toxicity. Tumor localization was not associated with toxicity, suggesting that treatment regimens adapted for central tumors are efficient in minimizing toxicity.

EP-1205

Resected pN1 non-small cell lung cancer: recurrence patterns and nodal risk factors

P. Borghetti[1], F. Barbera[1], M. Bonù[2], P. Vitali[1], F. Trevisan[2], S. Ciccarelli[2], M. Maddalo[2], L. Triggiani[2], N. Pasinetti[2], S. Pedretti[1], B. Bonetti[1], G. Pariscenti[3], A. Tironi[4], A. Caprioli[5], M. Buglione[2], S. Magrini[2]
[1]*Spedali Civili di Brescia, Radiation Oncology, Brescia, Italy*
[2]*Brescia University, Radiation Oncology, Brescia, Italy*
[3]*Spedali Civili di Brescia, Thoracic Surgery, Brescia, Italy*
[4]*Spedali Civili di Brescia, Pathology, Brescia, Italy*
[5]*Spedali Civili di Brescia, Pneumology, Brescia, Italy*

Purpose or Objective: To describe the pattern of recurrence in resected pN1 non-small cell lung cancer (NSCLC), aiming to identify clinical, pathological, treatment and nodal factors predicting an increased risk of locoregional recurrence (LR) or distant metastasis (DM), in order to define a selected population who may benefit of postoperative radiotherapy (PORT).

Material and Methods: All patients who underwent surgery for NSCLC with pathologically confirmed N1 disease at the Spedali Civili Hospital of Brescia between 2001-2011 were identified. Patients with positive surgical margins, undergoing neoadjuvant treatment or PORT were excluded. LR was defined as first event of recurrence at the surgical bed, ipsilateral hilum or mediastinum, other sites were considered as DM. Kaplan-Meier actuarial estimates of overall survival (OS), progression free survival (PFS), freedom-from LR (FFLR) and freedom-from DM (FFDM) in different subgroups were compared with the log-rank test. The Cox proportional hazard regression model was used for multivariate analysis.

Results: Among 285 patients who underwent surgery during the interval, 202 met the inclusion criteria. Clinical pathological, treatment and nodal factors are reported in table 1. Twenty four percent received adjuvant chemotherapy. The median follow-up was 39 months. The total number of recurrences was 118 (64.4%): 44 (24%) and 74 (40.4%) for LR and DM, respectively. 5-year OS and PFS rates were 39,2% and 33,3%, respectively. Patients with recurrences experienced a statistically worse OS than patients without recurrences (p<0.001) and patients with DM had in turn OS rates significantly worse than those with LR (Figure 1). At multivariate analysis, extra capsular extension (ECE) (RR 2.10 p 0.01) and lymph nodal ratio (LNR)> 0:15 (RR 1.68, p = 0.015) were associated with a worse PFS. ECE and LNR> 0,15 were significantly related to a worst FFLR (RR 3.04 and 4.42, respectively), adenocarcinoma to an unfavorable FFDM (RR 1.97, p = 0.013).

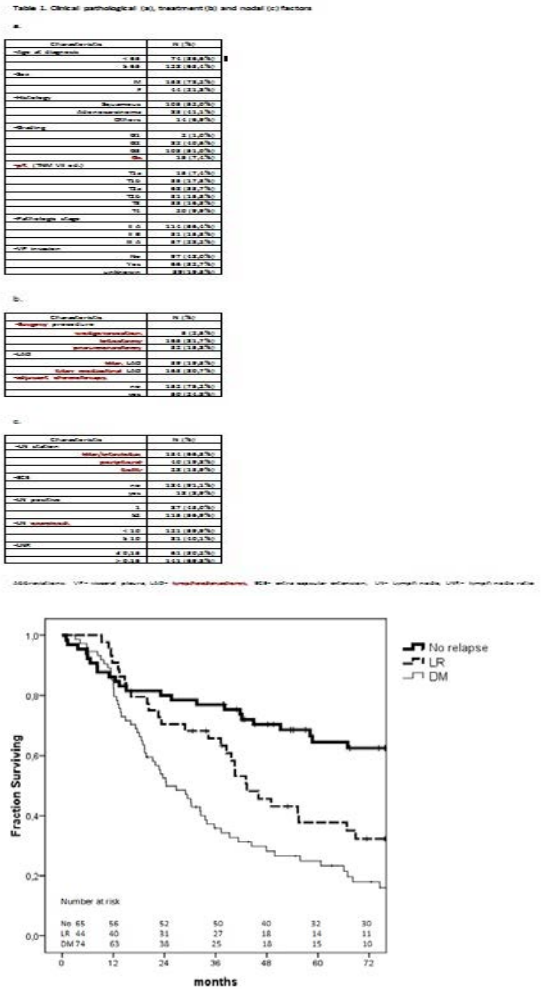

Conclusion: LR are common in pN1 NSCLC patients. Nodal factors as high LNR and ECE can predict an increased risk of worse FFLR and PFS. Prospective data on selected patients, treated with modern radiotherapy techniques, need to be collected to re-evaluate the role of radiotherapy.

EP-1206

Adequacy of dose/volume constraints in stereotactic radiotherapy and radiosurgery of thoracic area

F. Deodato[1], S. Cilla[2], A.G. Morganti[3], C. Annese[1], G. Macchia[1], A. Ianiro[2], V. Picardi[1], C. Digesù[1], M. Ferro[1], F. Labropoulos[1], G. Torre[1], M. Nuzzo[1], N. Dinapoli[4], V. Valentini[4], A. Veraldi[3], A.G.M. Zanirato[3], F. Romani[5], M. Zompatori[6], S. Cammelli[3], A. Ardizzoni[7], G. Frezza[8]

[1]*Fondazione di Ricerca e Cura "Giovanni Paolo II"- Catholic University of Sacred Heart, Radiation Oncology Unit, Campobasso, Italy*

[2]*Fondazione di Ricerca e Cura "Giovanni Paolo II"- Catholic University of Sacred Heart, Medical Physics Unit, Campobasso, Italy*

[3]*S. Orsola-Malpighi Hospital- University of Bologna, Radiation Oncology Center- Department of Experimental- Diagnostic and Specialty Medicine – DIMES, Bologna, Italy*

[4]*Policlinico Universitario "A. Gemelli"- Catholic University of Sacred Heart, Department of Radiotherapy, Roma, Italy*

[5]*S. Orsola-Malpighi Hospital- University of Bologna, Department of Medical Physics, Bologna, Italy*

[6]*S. Orsola-Malpighi Hospital- University of Bologna, Radiology Department, Bologna, Italy*

[7]*S. Orsola-Malpighi Hospital, Department of Medical Oncology, Bologna, Italy*

[8]*Bellaria Hospital, Radiotherapy Department, Bologna, Italy*

Purpose or Objective: To verify adequacy of dose volume constraints reported in literature about stereotactic radiotherapy (SBRT) and radiosurgery of thoracic area. This study is based on the toxicity recorded in organs at risk (OARs) of patients enrolled in dose-escalation trials.

Material and Methods: This is a retrospective study evaluating treatment plans of neoplasms in thoracic area. All 55 patients were treated between November 2009 and December 2013 using SBRT (37 pt) or SBRS (18 pt). Prescribed doses were 30-35 Gy in 5 fractions in SBRS treatments and 16-28 Gy in single fraction in SBRS treatments. All patients underwent radiotherapy with V-MAT technique. Main OARs were heart, oesophagus, and ribs with suggested Dmax of 35 Gy, 32.5 Gy and 32.5 Gy in SBRT treatment, respectively, and 22 Gy, 15 Gy and 30 Gy in SBRS treatment, respectively. Plans were evaluated by DVH analysis. Dosimetric data were compared with clinical data on early and late toxicity.

Table 1: Patients' characteristics

		SBRT (N, %)	SBRS (N, %)
N°		37 (67.3)	18 (32.7)
M/F		28/9	6/12
Age (range; media)		45-86; 65	37-75; 56
Primary tumor			
	Lung	19 (51.4)	3 (16.7)
	Rectum	4 (10.8)	0 (0)
	Colon	3 (8.1)	2 (11.1)
	Breast	2 (5.4)	8 (44.4)
	Endometrial	1 (2.7)	2 (11.1)
	Prostate	1 (2.7)	2 (11.1)
	Other	6 (16.2)	2 (11.1)
Treated lesion			
	Primary tumor	12 (32.4)	0 (0)
	Nodal metastases	9 (24.3)	6 (33.3)
	Distant metastases	16 (43.3)	12 (66.7)

Results: SBRT treatment: considering heart, oesophagus and ribs, Dmax constraints were exceeded in 7/37 patients (18.9%), 4/37 (10.8%) and 16/37 (43.2%) respectively. In these patients results about OARs were as follow: heart Dmax 36.6-50 Gy, V35 0.5-4.7 cc; oesophagus Dmax 35.7-41.3 Gy, V32.5 0.1-0.9cc; ribs Dmax 35.7-52.5 Gy, V32.5 0.1-7.9cc. SBRS treatment: dose on heart and ribs exceeded Dmax constraints in 1/18 patients (5.6%) with a Dmax of 23.3Gy (V22=0.6cc) and 33.6Gy (V30=0.3cc) respectively. With a median follow up of 18 months considering SBRT treatment and 16 months considering SBRT, no Grade >2 (CTCAE 4.3), early or late toxicity of heart or ribs was reported. In SBRT group, 1 grade 2-oesophagus toxicity in a patient exceeding DMax constraint was registered.

Conclusion: Patients irradiated did not develop severe toxicity on heart, oesophagus, and ribs although the administered doses were above constrains proposed in literature. A prolonged follow up and a larger population are needed to confirm the safety of dose-volume constraints

other than those reported in literature about SBRT and SBRS on abdominal area.

EP-1207

Can DIBH technique be used for SABR of large and mobile tumors of lung and liver? A clinical study

C. Srinivas[1], S. Subramaniam[1], N. Mohammed[1], A. Gandhi[1], M. Kathirvel[1], T. Swamy[1], K. Kiran Kumar[1], A. Jotwani[1], N. Yadala[1]

[1]Yashoda Cancer Institute, Department of Radiation Oncology, Hyderabad, India

Purpose or Objective: To assess clinical feasibility, local control and toxicity of deep inspiratory breath hold (DIBH) technique for delivery of SABR for large and mobile tumors of lung and liver.

Material and Methods: All patients suitable to undergo SABR, underwent respiratory training consisting of DIBH on demand for 15-25 seconds at a time. Patients underwent 2 sets of immobilization and imaging, one in DIBH phase and other in free breathing (FB) phase. Respiratory monitoring was performed using Varian RPM system and a 4mm gating threshold window was allowed. Set-up verification was performed using KV imaging and gated cone beam CT both taken in DIBH. All patients were planned with 2-4 arc VMAT using 6MV flattening filter free (FFF) photon beams to a dose of 60Gy in 5 fractions.

Results: 12 patients of lung tumors and 9 patients of liver tumors were treated with DIBH based SABR. In patients with lung tumors, DIBH resulted in 1.53 times higher mean lung volumes (3937 cc vs. 2576 cc, p=0.003). Compared to ITV based contours, PTV volumes were 1.48 times smaller for lung and 1.38 times smaller for liver tumors in DIBH CT compared to FB CT (36.15 cc vs. 53.83 cc, p=0.002, 57.76cc vs. 79.78, p=0.03). All the plans accepted for delivery met the standard criteria (ROSEL for lung and RTOG 1112 for liver) for both target and OAR constraints. On an average, V20 was reduced by 30%(18-38) in DIBH plans compared to FB plans. Time taken to deliver each session in DIBH phase with FFF beams was longer by an average of 2 minutes due to interruptions (maximum 4 interruptions/arc each lasting <10 seconds). Mean setup errors in cm quantified on CBCT were 0.1, 0.2 and 0.1 in vertical, longitudinal and lateral dimensions respectively and a uniform margin (based on Van Herk's formula) of 4mm appears to be safe. Except for 1 patient with symptomatic grade 2 pneumonitis and 1 patient with grade 2 chest wall pain, none had any major toxicities. With a median follow-up of 16 months, 18 month local control was 95%.

Conclusion: DIBH based SABR is clinically feasible and effective and should be considered standard for treating mobile and especially large tumors of lung and liver provided patient is suitable for treatment with DIBH technique. DIBH-CBCT based verification appears to be reproducible and effective to reduce setup errors. A margin of 4 mm appears to be safe in DIBH setting with 4 mm gating threshold window. Despite minimal increase in treatment time, DIBH is an effective way to deliver high throughput high quality SABR.

EP-1208

Radiation-induced pulmonary function change after postoperative radiotherapy in NSCLC

H. Kim[1], N. O Kyu[1], O. Young-Taek[1], C. Mison[1], K. Sang-Won[1], C. Oyeon[1], H. Jaesung[1], K. Mi-Hwa[1], P. Hae-Jin[1]

[1]Ajou University Hospital, Radiation Oncologist, Suwon City, Korea

Purpose or Objective: We aimed to establish the model predicting radiation-induced pulmonary function change after postoperative radiotherapy (PORT) in non-small cell lung cancer (NSCLC).

Material and Methods: From March 2003 to December 2011, 37 patients with NSCLC who underwent PORT were analyzed. All patients took the forced expiratory volume in 1 second (FEV1) at the beginning of PORT and follow-up FEV1 within 6-36 months after the completion of PORT. We calculated mean lung dose (MLD) as a dosimetric parameter of the lung. Simple linear correlation and regression model were implemented to establish the prediction model between MLD and radiation-induced pulmonary function change.

Results: The median absolute value of FEV1 at the beginning of PORT, and follow-up FEV1 were 1.76 L (range, 0.90-3.05),and 1.66 L (range, 0.93-3.08), respectively. Radiation-induced pulmonary function change (follow-up FEV1 minus FEV1 at beginning of PORT) ranged from -0.71 to 0.40 L (median, 0.06). The median MLD of PORT was 12.3 Gy (range, 0.5-20.4). Radiation-induced FEV1 change and MLD showed statistically significant correlation (correlation coefficient = -0.357, p = 0.030). PORT-induced FEV1 change could be predicted by simple linear regression model [FEV1 change (L) = 0.295 – 0.026 MLD (Gy)].

Conclusion: Radiation-induced FEV1 change was significantly correlated with MLD in patients with NSCLC who underwent surgery followed by PORT. Follow-up FEV1 after the completion of PORT can be predicted by simple linear regression model using this correlation.

EP-1209

WBRT plus SRT versus WBRT alone or SRT alone for brain metastases from non-small cell lung cancer

R. Suwinski[1], B. Jochymek[2]

[1]Maria Sklodowska-Curie Memorial Cancer Center and Institute of Oncology- Gliwice Branch, Radiotherapy and Chemotherapy Clinic and Teaching Hospital, Gliwice, Poland

[2]Maria Sklodowska-Curie Memorial Cancer Center and Institute of Oncology- Gliwice Branch, Radiation Oncology, Gliwice, Poland

Purpose or Objective: The benefits of addition of whole brain radiotherapy (WBRT) to stereotactic radiotherapy (SRT) with respect to overall survival of patients with brain metastases from non-small cell lung cancer (NSCLC) are unclear. Most of the published studies addressing this issue recruited the patients with diverse histology and primary sites, with only few focusing on NSCLC. We addressed this issue by evaluating institutional experience in efficacy of SRT plus WBRT vs. SRT alone or WBRT alone in patients with NSCLC.

Material and Methods: The analysis encompassed 143 patients with brain metastases from NSCLC, including 65 with squamous-cell cancer (45.5%), 53 adenocarcinoma (37.1%), 25 NOS (17.4%). SRT alone was used in 52 patients (36.4%), WBRT alone in 33 patients (23.1%) and WBRT plus SRT in 58 patients (40.5%). Two chief subgroups were considered: those with 1-3 brain metastases (121 patients, 84.6%) and those with >3 metastases (22 patients, 15.4%). WBRT doses ranged from 20-30 Gy in 3.0-4.0 Gy per fraction, SBRT was given in 1-6 fractions (median 1 fraction) of 6-22 Gy (median 15 Gy).

Results: 1-year actuarial overall survival was 8%, 6% and 27% for SRT, WBRT and SRT+WBRT respectively. The difference in overall survival among 143 patients treated with SRS+WBRT vs. SRS or WBRT was highly significant (p<0.0001). The difference in overall survival between SRS+WBRT vs. SRS or WBRT was also apparent in a subgroup of patients with 1-3 metastases (1-year OS of 9%, 0% and 26%, respectively). By contrast, the differences in OS according to treatment were not significant among the patients with >3 metastases. A multivariate analysis showed that out of several variables considered only WBRT alone or SRT alone (HR=1.85, p=0.001) and age over 70 years (HR=2.08, p=0.005) were associated with unfavorable survival.

Conclusion: Although conclusions from this study are limited by nonrandomized selection of the treatment schedule and some heterogeneity in prescription practice the data presented suggest that combination of WBRT and SRT vs. WBRT alone or SRT alone result in considerably improved

survival among the patients with 1-3 brain metastases from non-small cell lung cancer.

EP-1210

Definitive Radiotherapy with or without chemotherapy for T4N0-1 Non-small Cell Lung Cancer

Y.J. Kim[1], S.Y. Song[1], S.Y. Jeong[2], S.W. Kim[3], J.S. Lee[3], S.S. Kim[1], W. Choi[4], E.K. Choi[1]

[1]*Asan Medical Center- Univ of Ulsan, Radiation Oncology, Seoul, Korea*

[2]*Asan Medical Center- Univ of Ulsan, Institute of Innovative Science, Seoul, Korea*

[3]*Asan Medical Center- Univ of Ulsan, Medical Oncology, Seoul, Korea*

[4]*Gangneung Asan Hospital, Radiation Oncology, Gangneung, Korea*

Purpose or Objective: To know the failure patterns and survival of T4N0-1 non-small cell lung cancer (NSCLC) treated with definitive radiotherapy.

Material and Methods: Ninety five patients with T4N0-1 NSCLC who received definitive radiotherapy with or without chemotherapy from May 2003 to Oct 2014 were retrospectively reviewed. Standard radiotherapy scheme was 66 Gy in 30 fractions. Main concurrent chemotherapy regimen was weekly Paclitaxel 50 mg/m2 combined with Cisplatin 20 mg/m2 or Carboplatin AUC 2. Primary outcome was overall survival (OS). Secondary outcomes were failure patterns and toxicities.

Results: The median age was 64 (range, 34-90). Eighty eight percent (n=84) of patients had ECOG performance status 0-1 and 42% (n=40) experienced pretreatment weight loss. Sixty percent (n=57) of patients had no metastatic regional lymph nodes. The median radiation dose was EQD2 67.1 Gy (range, 56.9-83.3). Seventy one patients (75%) were treated with concurrent chemotherapy. Among them, 13 patients were also administered neoadjuvant chemotherapy. At the median follow-up of 21 months (range, 1-102), 3-year OS was 44%. Three-year cumulative incidence of local recurrence and distant recurrence were 48.8% and 36.3%. Pretreatment weight loss and combination of chemotherapy were significant factors in OS. Acute esophagitis over grade 3 was occurred in 3 patients and only one grade 3 chronic esophagitis was reported. There was no grade 3-4 radiation pneumonitis.

Conclusion: Definitive radiotherapy for T4N0-1 NSCLC resulted in favorable survival with acceptable toxicity rates and local recurrence was a major pattern of recurrence. For improving local tumor control, the application of intensity modulated radiotherapy and radio-sensitizing agents would be needed.

EP-1211

Prognostic factors in patients with Stage I NSCLC treated with 3-D noncoplanar conformal RT

K. Karasawa[1], K. Ito[1], Y. Shibata[1], S. Hayakawa[1], H. Tanaka[1], T. Shimizuguchi[1], Y. Machitori[1], M. Fujii[1], K. Nihei[1], K. Fuse[1], T. Kawamoto[1], H. Kuramoto[1]

[1]*Tokyo Metropolitan Komagome Hosp., Department of Radiology, Tokyo, Japan*

Purpose or Objective: Stereotactic Body Radiation Therapy has become one of the standard treatments in Stage I NSCLC. However, there exists the problem of reoxygenation for large tumors and BED for serial organs locating near the central lung. Therefore, we have been treating especially these cases by decreasing the fraction dose while increasing overall treatment time and total dose (so-called hypofractionated 3-dimensional noncoplanar conformal radiation therapy). To clarify the prognostic factors of this treatment method, we carried out this investigation.

Material and Methods: Eligibility criteria were as follows: maximum tumor diameter not greater than 5cm, PS between 0 and 2, and no limitation regarding age and pulmonary function. Radiotherapy was given with 6MV photon beam by fixed 10 non-coplanar conformal beams to a total dose of 75Gy in 25 fractions in 5 weeks. Irradiation was aiming at the ITV with proper margins. No ENI was given. Between Jan. 2002 and Jan. 2011, 109 eligible cases were treated. Age ranged from 53 to 93 (median 78). The male/female ratio was 79/30. There were 100 PS 1 and 9 PS 2 cases. There were 22 low risk operable cases, 31 high risk operable cases (surgeons recommended RT), and 56 inoperable cases. There were 63 T1 tumors and 46 T2. Forty-six cases were central tumors and the other 63 were peripheral tumors. Seventy tumors were adenocarcinoma, 23 tumors were squamous cell carcinoma, and 16 others. Regarding tumor markers, pretreatment CEA was elevated (>5ng/ml) in 36 cases. Using these 8 parameters, multivariate analysis (MVA) for overall survival (OS) and local control (LC) was performed by Cox's Proportional Hazard Model. Median follow-up period was 67 months.

Results: Five-year LC and OS rates were 84% and 50%, respectively. As for LC, MVA revealed that histology (p=0.0279) was prognostic and PS (p=0.0541) and pretreatment CEA (p=0.0560) had a tendency. As for OS, MVA revealed that gender (p=0.0081) and pretreatment CEA (p=0.0189) were prognostic and operability (p=0.0520) and histology (p=0.0913) had a tendency. On the other hand, age, T-stage or tumor location was not prognostic regarding neither LC nor OS.

Conclusion: Our overall results of this method were promising considering the status of the patients. Regarding LC, adenocarcinomas were better controlled compared with other histologies, and patients with good PS and tumors with normal pretreatment CEA tended to be better controlled. Regarding OS, female patients, patients with normal pretreatment CEA survived better than their counterpart, and operable cases and adenocarcinoma cases tended to survive better than their counterpart, respectively. Unlike other reported series, T2 stage and central tumors did not carry worse prognoses with this treatment method.

EP-1212

Are the encouraging SABR results for NSCLC reproducible outside of pioneering academic institutions?

C. Peedell[1], E. Aynsley[1], D. Shakespeare[1], J. Green[1], P. Summers[1], J. Reynolds[1], K. Burke[1], H. Bayles[1], C. Huntley[1], N. Richmond[1]

[1]*The James Cook University Hospital, Radiotherapy and Oncology, Middlesbrough, United Kingdom*

Purpose or Objective: Stereotactic ablative radiotherapy (SABR) is an internationally accepted standard of care in the management of early stage medically inoperable NSCLC [1]. However, the issue of whether the excellent results of SABR for lung cancer can also be achieved when patients are treated outside pioneering academic institutions remains a pertinent one [2]

South Tees NHS Trust is a large general hospital with a non-academic cancer centre, serving a population of 1.1 million in the North-East of England. In 2009, we became the first non-academic cancer centre in the UK to establish a SABR programme. To date, over 200 patients have been treated with SABR.

We present outcome data of 167 patients with Stage IA-IIB lung cancer, all of whom have at least 6 months of follow up and CT assessment of response.

Material and Methods: Data was collected prospectively between Sept 2009 – Sept 2015. Only patients with stage IA-IIB histologically proven NSCLC or PET +ve growing lesions, and at least 6 months of follow up, were included in the analysis. All patients were treated according to local protocols based on the national guidelines of the UK SABR Consortium.The following risk adapted treatment schedules were used depending on size and location of the tumour: 54Gy in 3 fractions (40patients), 55Gy in 5 fractions (105pts), 60Gy in 8 fractions (15pts), or 50Gy in 10 fractions (7pts)

Follow up was with CXR at 6months followed by CT at 6 months and clinical follow up, 3 monthly.

Results: 167 patients with stage IA-IIB disease treated. 55% histologically proven.There were 4 (2.4%) radiologically confirmed local recurrences giving a local control rate of 97.6%. Median survival was 43.2months. 3 year Overall Survival was 56.4% (see Fig 1). Treatment was well tolerated with minimal G3 toxicity (5 patients).

Conclusion: Our results suggest that SABR for medically inoperable NSCLC can be safely and effectively implemented in a non-academic institution with appropriate equipment and training.Clinical outcomes are comparable with internationally published series [3}, with encouraging 3yr OS rate of 56%. Toxicity is minimal. Longer term follow-up is required to confirm findings and provide data regarding long-term toxicity.

References:

[1] NCCN Clinical practice guidelines in oncology. NSCLC. 2012. http://www.tri-kobe.org/nccn/guideline/lung/english/non_small.pdf
[2] Senan S,Palma D A,Lagerwaard F J. Stereotactic ablative radiotherapy for stage I NSCLC: Recent advances and controversies. *J Thorac Dis.* 2011 September; 3(3): 189–196.
[3] Timmerman R et al. Stereotactic Body Radiation Therapy for Inoperable Early Stage Lung Cancer *JAMA.* 2010;303(11):1070-1076

EP-1213

Changes in pulmonary function after single-fraction carbon-ion radiotherapy for stage I NSCLC

W. Takahashi[1], N. Yamamoto[2], M. Nakajima[2], M. Karube[1], H. Yamashita[1], K. Nakagawa[1], H. Tsuji[2], T. Kamada[2]
[1]*University of Tokyo, Department of Radiology, Tokyo, Japan*
[2]*National Institute of Radiological Sciences, Research Center Hospital for Charged Particle Therapy, Chiba, Japan*

Purpose or Objective: In patients with inoperable stage I non-small cell lung cancer (NSCLC) or for those refusing surgery, stereotactic body radiotherapy and particle radiotherapy have become therapeutic options. We conducted a Phase I/II study on single-fraction carbon ion radiotherapy (SF-CIRT) for stage I NSCLC that yielded a 3-year survival rate of 75.5% for 218 patients. Until now, the effect of hypofractionated CIRT on pulmonary function (PF) has not been well documented. The purpose of this study was to assess the long-term impact of SF-CIRT on PF in stage I NSCLC patients.

Material and Methods: A review of prospectively collected data from SF-CIRT-treated patients was performed. Patients underwent PF tests (PFT) (or: underwent a PF test) immediately before, and at 6, 12, and 24 months after irradiation. Patients who relapsed or needed adjuvant treatment were excluded as these events might affect PF.

Results:

Patient characteristics (n = 40)

Median age		75 (51-89)
Male/Female		26 / 14
Stage	T1 (IA)/T2 (IB)	25 / 15
Histology	Adeno./Squamous/NSCLC	30 / 9 / 1
Location	Left upper/Lower	12 / 11
	Right upper/Middle/Lower	9 / 2 / 6
Medical inoperability		19 (47.5%)
COPD*		13 (32.5%)
Dose prescription	44/46/48/50 GyE in single fraction	13 / 12 / 6 / 9

* FEV1/FVC ratio <70%

Forty patients treated between 2007 and 2012 fulfilled the inclusion criteria. According to the dose escalation study protocol, a median prescribed single-fraction dose of 46 GyE (range, 44-50 GyE) was delivered. All treatment-related complications were self-limited, without any grade 3-5 toxicities. Two years post-CIRT, the mean values of forced expiratory volume in 1 sec (FEV1) [-8.4% ± 11.9% ($p < 0.001$)] and the FEV1 per unit of forced vital capacity (FEV1/FVC) [-8.9% ± 11.7% ($p < 0.001$)] were less than the pre-CIRT values. There were no significant overall changes in total lung capacity, vital capacity, FVC, and residual volume before SF-CIRT and 2 years after SF-CIRT. At 6 months post-treatment, the diffusion capacity of the lung for carbon monoxide (DLCO) was significantly less than the pretreatment value (86.7 ± 32.7% vs. 78.1 ± 31.1%; $p = 0.002$); however, at 24 months post-treatment, the mean DLCO recovered to pretreatment levels (86.9 ± 30.5%). This might have been due to recovery from non-symptomatic radiation pneumonitis and/or smoking cessation.

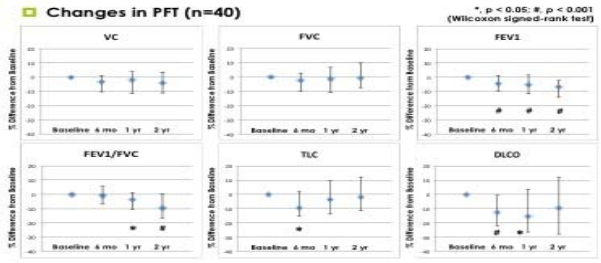

Conclusion: We found stage I NSCLC patients had good long-term preservation of PF after SF-CIRT. Follow-up PFT revealed the following: Declines in FEV1 and FEV1/FVC were statistically significant but clinically trivial, DLCO decreased temporary, thereafter it tended to recover to pretreatment levels within 2 years.

EP-1214

Radiotherapy as adjuvant or definitive treatment method in thymic tumours

A. Napieralska[1], L. Miszczyk[1]
[1]*Maria Sklodowska-Curie Memorial Cancer Center and Institute of Oncology, Radiotherapy Department, Gliwice, Poland*

Purpose or Objective: An evaluation of thymic tumors patient radiotherapy results.

Material and Methods: 93 patients (54F [58%], 39M [42%]) aged from 3 (6 children) to 77 (median 48) treated for thymic tumors since 1981. 84 patients (90%) were diagnosed with thymoma, 9 (10%) with thymic carcinoma. Masaoka stage was assessed in 93% (56% stage II, 31%-III, 6%- IV). All patients were irradiated. In 76 cases radiotherapy (RT) followed surgery – in 41 patients after radical and in 35 after incomplete resection. In 17 cases RT was definitive treatment, combined in 14 patients with chemotherapy. Patients were irradiated with fraction dose of 1.1-4.0Gy (median 2.0) to the total dose of 20-68Gy (median 49.5). Patient- and treatment-related factors potentially affecting survival and local control (LC) were evaluated with log-rank test. Survival analysis was performed with Kaplan-Meier method.

Results: Tumors relapsed in 17 patients. Metastases occurred after 6-129months (median 10.1) in 12 patients (in 8 in lungs). During the follow-up 17 patients died due to progression(13) or recurrence(4) of the disease. Median overall survival (OS) in the whole group (since diagnosis) was 140.2months. OS was significantly longer in patients with WHO B1 type(p=0.02), in good performance status (PS)(p=0.0005), without radiation-induced pulmonary fibrosis(p=0.02) or second cancer(p=0.03). Difference in OS between patients treated with radical surgery+RT, non-radical surgery+RT and definitive RT was of borderline significance(p=0.065). Factors significantly decreasing LC were: male sex(p=0.04), WHO B2 type(p=0.01), bad PS(p=0.0007), presence of metastases(p=0.003) and second cancer(p=0.03).

Conclusion: Obtained results do not permit to form robust conclusion concerning role of RT in the management of thymic tumors patient. Besides clear, unquestionable bad prognostic factors as bad PS, low differentiation, presence of local relapse, lung fibrosis, second malignancy or distant metastases, we found only one more - male sex, decreasing LC.

EP-1215

Do higher doses of palliative radiotherapy still prolong survival in stage III/IV NSCLC?

A. Price[1], K. MacLennan[1], S. Campbell[1], S. Erridge[1], F. Little[1], T. Evans[1]
[1]*Western General Hospital- Edinburgh Cancer Centre, Edinburgh Cancer Centre, Edinburgh, United Kingdom*

Purpose or Objective: In a UK Medical Research Council trial carried out before the widespread use of chemotherapy or CT-PET, palliative thoracic radiotherapy delivering 39 Gy in 13 daily fractions conferred an overall survival (OS) benefit when compared to 17 Gy in 2 weekly fractions in good performance status patients with radically treatable NSCLC. To determine whether this benefit persisted with contemporary standards of staging and systemic therapy, we studied the outcomes of patients with locally advanced/metastatic NSCLC receiving palliative radiotherapy in our centre over a 2 year period.

Material and Methods: The case records of 176 patients who received palliative thoracic radiotherapy in 2011 or 2012 were reviewed retrospectively. Data collected included age, stage, performance status, dose/fractionation, additional treatments and survival.

Results: 36 patients received high dose thoracic radiotherapy (HDTRT, 36-40 Gy in 12-15 fractions) and 140 received a lower dose (LDTRT), 20 Gy in 5 fractions. Median OS in the HDTRT group was 8.5 months and 5.5 months in the LDTRT group (hazard ratio 0.6, p <0.01). 12 patients received chemotherapy and HDTRT with median OS 12m *vs* 7m in the 25 patients receiving chemotherapy and LDTRT. In those who received HDTRT alone, median OS was 6.5m *vs* 4m for LDTRT alone. In patients with stage II-III disease median OS was 9.6m *vs* 6m for LDTRT. In those with stage IV disease, median OS was 8m for HDTRT *vs* 5m for LDTRT. In patients with performance status 0-2 median OS was 9m for HDTRT *vs* 6m for LDTRT, while in the two patients with performance status 3 who were irradiated it was 1m with HDTRT *vs* 3m with LDTRT.

Conclusion: This audit of contemporary practice suggests that the survival benefit of high dose palliative radiotherapy reported by Macbeth (Clin Oncol (R Coll Radiol). 1996;8:167-75) persists with modern staging and systemic therapy practices, and may also extend to patients with small volume stage IV disease excluded from that trial, but not those with poor performance status.

EP-1216

Differential diagnosis between toxicity and recurrence after SBRT in early stage inoperable NSCLC

R. Frakulli[1], F. Salvi[2], D. Balestrini[2], M. Palombarini[3], S. Cammelli[1], G. Macchia[4], M. Zompatori[5], A.G. Morganti[1], G. Frezza[2]
[1]*Radiation Oncology Center- Sant'Orsola-Malpighi Hospital-University of Bologna, Department of Experimental-Diagnostic and Specialty Medicine - DIMES, Bologna, Italy*
[2]*Ospedale Bellaria, Radiotherapy Department, Bologna, Italy*
[3]*Ospedale Bellaria, Medical Physics Unit, Bologna, Italy*
[4]*Fondazione di Ricerca e Cura "Giovanni Paolo II"- Catholic University of Sacred Heart, Radiotherapy Unit, Campobasso, Italy*
[5]*Sant'Orsola-Malpighi Hospital- University of Bologna, Radiology Department, Bologna, Italy*

Purpose or Objective: SBRT is the standard treatment of early stage inoperable NSCLC. Parenchymal changes (PC) after SBRT make it difficult the differential diagnosis between treatment effects and disease recurrence. The purpose of our study was to identify the radiographic features (High Risk Features: HRFS) with high specificity (SP) and sensitivity (SE) for early detection of recurrence.

Material and Methods: We retrospectively evaluated patients treated with SBRT for inoperable early stage NSCLC. Median dose was 50 Gy in 5 fractions (range, 45-60 Gy /3-12 fractions) prescribed to 80% isodose. All patients underwent chest computed tomography (CT) before SBRT and after 3, 6, 12 months (thereafter annually). Using a chest CT scan radiological aspects according to Huang et al. classification (Huang et al., Radiother Oncol 2013;109:51-57) were evaluated. 18F FDG-PET was used in case of suspected tumor recurrence.

Results: Forty-five patients were included, 34 males and 11 females; mean age was 75.7 years (range, 60-86 years); 77.8% of patients had stage IA disease and 22.2% stage IB with a mean follow-up of 21 months, local control was 69%. Benign acute CT changes (up to 6 months after SBRT) were observed in 34 patients (patchy consolidation was the most frequent) and late changes (after 6 months) in 44 patients (mass-like fibrosis was the most frequent). HRFs were identified in 20 patients, enlarging opacity at primary site in 9 patients, enlargement after 12 months in 20 patients, bulging margin in 7 patients, disappearance of linear margin in 2 patients, loss of air bronchogram in 18 patients and cranial-caudal growth in 15 patients. These HRFs were individually significantly associated with local recurrence of the disease. The better predictor of relapse was enlargement opacity at 12 months (p <0.001) with SE: 84.6% and SP: 71.8%. The presence of > 1 HRFS demonstrated a higher SE (93.3%) (p <0.02) with SP: 59.4%.

Conclusion: Detection of HRFS is predictive of relapse with a SE increasing with the number of observed HRFs. This observation allows to better define the diagnostic algorithm in follow-up, suggesting to perform further exams only in patients with > 1 HRFS.

EP-1217

Effect of overall treatment time in dose escalatation for radiotherapy of NSCLC. BED-time analysis

J. Cabrera[1], A. Torres[1], A. Ruiz[1], A. Corbacho[1], M.A. Gonzalez[1], J. Quiros[1], F. Ropero[1], J. Muñoz[1]
[1]*Hospital Infanta Cristina, Radiation Oncology, Badajoz, Spain*

Purpose or Objective: Because there is a positive correlation between radiation dose and local control (LC) in non-small cell lung cancer (NSCLC) although with no impact on overall survival (OS) our institutional protocol allowed moderate radiotherapy dose escalation up to 70 - 74 Gy (BED: 84 - 88.8 Gy) on the standard 60-66 Gy (BED: 72 - 79.2 Gy) providing that organs-at-risk are keep in tolerance. This retrospective study aims to assess the impact of dose escalation in clinical outcome when the duration of radiotherapy is taken in to account through the use of BED model corrected by time (tBED)

Material and Methods: 78 consecutively patients with unresectable NSCLC were retrospectively analyzed. All were PET-CT staged and were treated with platinum-based chemotherapy (either concomitant or sequential) and 3DCRT. Two groups were compared according to prescribed dose level: Standard Dose Group (SD) n = 38 those receiving nominal prescribed BED ≤ 79.2 Gy and Escalated Dose Group (ED) n = 40 those receiving > nominal prescribed BED >79.2 Gy. For both groups actual administered dose corrected for the duration of treatment (tBED) was calculated using the formula *[tBED (Gy) = n d (1+d/ α/β) – KT] (Sinclair, IJROBP 1999. 44:381)* Multivariate Cox regression analysis was performed to identify significant predictors of OS, Disease Free Survival (DFS) and Thoracic Progression Free Survival (TPFS). For purposes of comparison a nominal prescribed dose of 60 Gy @2Gy in 39 days have a tBED = 44, 7 Gy.

Results: For the entire group median follow-up and overall survival (OS) were: 17.7 months (mo) (IQR: 10.3-27.9) and 19.1 mo (95% CI 13.9-24.3). Median tBED for entire group was 45.8 Gy (IQR 40.5-49) tBED in SD and ED group were 42.2 (IQR 37.4-45.2) and 48.9 Gy (IQR 45.7-49.7) Univariate analysis by groups: Actuarial median OS: SD vs. ED was: 17 mo (95% CI 13.6-20.3) vs. 22.3 mo (95% CI 9.6-35) p = 0.18. Actuarial median DFS SD vs. ED was: 8.3 (95% IC 7.2 – 9.3) vs. 12.8 mo (95% IC 3 – 22.7) p = 0.009. Actuarial median TPFS (mo) SD vs. ED was: 8.4 (95% CI 7.2-9.5) vs. 21.8 (95% CI 13.2-30.5) p = 0.003.
On multivariate analysis significant predictors for OS, DFS and TPFS are depicted on table: radiotherapy dose was found not to be a significant factor.

Variable	OS. HR (95% CI)	DFS. HR (95% CI)	TPFS. HR (95% CI)
PS [0-1 vs. 2]	19,03 (2,48 – 145,6)	17,13 (2,9 – 98,66)	2,49 (1,31 – 4,75)
Mediastinoscopy [-/+]	0,64 (0,005 – 0,93)	0,12 (0,25 – 0,66)	
Weight loss (no /yes)		3,85 (1,73 – 8,6)	

Conclusion: On univariate analysis, but not on multivariate, ED associated statistically significant better DFS and TPFS and non-statistically significant better OS, even when adjusted to overall treatment time. Due to treatment time delays SD group received a suboptimal dose of radiotherapy and ED group received a tBED which virtually match nominal 60 Gy. Our data in agreement with those resulting from randomized trials strongly support that 60 Gy @2 Gy with stringent control of time delays is the gold standard in the radiotherapy for NSCLC.

EP-1218

Salvage radiotherapy for locoregionally recurrent non-small cell lung cancer after resection

E. Kim[1], J.S. Kim[1]
[1]*Seoul National University Bundang Hospital, Radiation Oncology, Seongnam, Korea Republic of*

Purpose or Objective: Radiotherapy with or without chemotherapy is commonly used for isolated loco-regional recurrence of non-small cell lung cancer (NSCLC) after initial surgery. This study was undertaken to evaluate the outcomes and complications of curative radiotherapy for locoregionally recurrent NSCLC.

Material and Methods: Medical records of 57 patients who received curative radiotherapy for locoregionally recurrent NSCLC without distant metastasis after surgery from 2004 to 2014 were retrospectively reviewed. At the time of recurrence, the median age was 67 years (range 34-81 years), and most patients (84.2%) have good ECOG performance status. All patients initially received a curative intent operation, and the median disease-free interval was 14 months. For locoregionally recurrent lung cancer, forty-two patients were treated with concurrent chemoradiotherapy (CCRT), and 15 patients with radiotherapy alone. Radiation dose ranged from 45 Gy to 70 Gy (median 66 Gy) by a three-dimensional conformal technique. Lung function change after radiotherapy was evaluated by comparing pulmonary function tests before and after radiotherapy.

Results: Median follow-up after recurrence was 20 months. Six patients showed a complete response, and 39 patients showed a partial response. The median survival was 30 months. Two-year locoregional recurrence-free survival (LRFS), distant metastasis-free survival (DMFS), disease-free survival (DFS) and overall survival (OS) rate were 46.1%, 37.2%, 31.9%, and 65.1%, respectively. Eleven patients showed disease progression within the radiation field after radiotherapy. Pulmonary function decreased meaningfully after radiotherapy, and radiation pneumonitis of any grade was seen in 19 patients. In the multivariate analysis, age under 70 years was associated with good OS (p=0.047); concurrent chemoradiotherapy with good OS (p=0.014), and DFS (p=0.003); and single-station recurrence with good OS (p=0.01), DFS (p=0.022), and LRFS (p=0.01).

Conclusion: Patients who have locoregionally recurrent NSCLC showed favorable survival outcomes with salvage radiotherapy. However, lung function should be carefully evaluated before and after radiotherapy. Young age, single site recurrence, and the use of CCRT were good prognostic factors of overall survival. In patients with good prognostic factors and suitable for curative radiotherapy, CCRT could be considered to improve treatment outcomes.

EP-1219

Utilisation of new functional imaging in NSCLC radiotherapy: Can we use DW-MRI?

M. Al Daly[1], R. Hani[1], M. Fayec[2], S. Talima[1], H. Khafagy[1], M. Kmal[3], M. Hassan[1]
[1]*Cairo University- Fac. of Medicine, Clinical Oncology, Cairo, Egypt*
[2]*Cairo University- Fac. of Medicine, Radiodiagnosis, Cairo, Egypt*
[3]*Cairo University- Fac. of Medicine, Medical physics, Cairo, Egypt*

Purpose or Objective: Precise delineation of primary lung cancer mass and involved mediastinal LN is very important requirement in order to improve radiotherapy outcome and minimize treatment toxicity. Diffusion weighted MRI (DW-MRI) is a recently introduced functional imaging modality, having higher sensitivity and specificity than CT to differentiate lung cancer from post-obstructive lobar collapse . And also able to pinpoint lymph nodes with and without metastasis. The apparent diffusion coefficient (ADC) is the quantitative parameter of DW-MRI with cut off value 1.4 x 103 mm2/s which can be used as a good tool to contour Target volumes in lung cancer.
the aim is to study the feasibility of using the images of DW-MRI and data of ADC map for radiotherapy contouring purposes

Material and Methods: Twenty cases of newly diagnosed lung cancer patients underwent CT chest with contrast and respiratory gatted DW-MRI with b value of 0, 500, 1000s/mms . Both studies were obtained in the same position, respiratory phase and slice thickness (5mm) in order to allow proper image fusion. For each patient, we've delineated GTV for primary lung mass and GTV- LN for involved mediastinal LN on both CT scan (guided by size) and DW-MRI (guided by T2W and the ADC map) together with delineation of the nearby risk structures. Auto margins were taken for the CTV and the PTV. The impact of using MRI on stage and different treated volumes was assessed and compared.

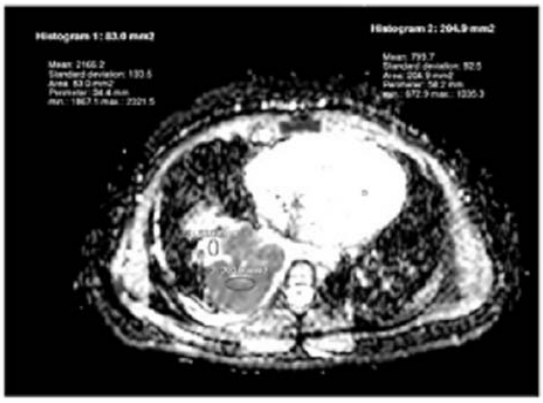

the ADC values in differentiating the lung lesion and the nearby consolidation/collapse.

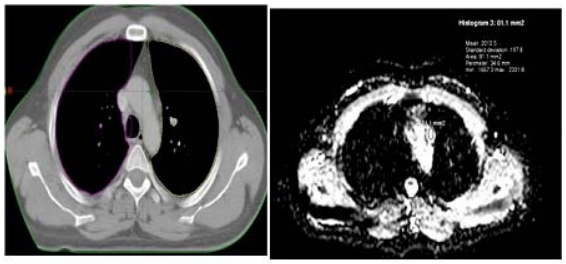

Case #4: shows level 6 LN station positive in both the CT scan but on the ADC image, the mean value 2.01 indicating non malignant involvement (?? Inflammatory)

Results: The main result was the reduction in primary and nodal volumes due to better definition of lung mass and nearby lung Collapse , the latter could be easily defined in 14 cases on the DW-MRI vs. 7 cases only by CT scans (P=0.016). Median GTV total (sum of 1ry and nodal GTV), on MRI Diffusion compared to that on the CT scan was 354 and 386 cm3 respectively (P= 0.009). In 15 cases, a mean decrease in the GTV total of 34% ±56% (median, 9%; range, 0.2- 32.5%) by using DW-MRI. only in three other cases a mean increase in the GTV total of 12.7% ±14.9% (median, 9.7%; range, 0.4-221%). was found. The median PTVs on the CT scans vs. the MRI Diffusion were 1623 (range, 493–2965 cm3) & 1419 (range, 542–3158 cm3) respectively which was statistically non significant (P= 0.391).

Conclusion: This pilot prospective study concluded that DW-MRI as a functional image can aid in proper definition and delineation of the target volumes after fusion of DWI and the CT images . GTV Total decreased in most cases due to exclusion of collapse, consolidation, reactionary and inflammatory LN, however GTV total was increased in 3/20 patients due to better nodal detection and better visualization of borders adjacent to the mediastinum and chest wall. DW MRI could be a future good tool for proper staging and guidance of radiotherapy in NSCLC cases indicated for chemo/radiation.

EP-1220

Postoperative hypofractionated radiotherapy of non-small cell lung cancer: pattern of the relapses

V.M. Sotnikov[1], V.A. Solodkiy[1], V.M. Kcharchenko[1], G.A. Panshin[1], V.D. Chhikvadze[2], S.D. Trocenko[1], A.A. Morgunov[3]
[1]*Russian Scientific Center of Roentgenoradiology, Radiation Therapy, Moscow, Russian Federation*
[2]*Russian Scientific Center of Roentgenoradiology, Surgery, Moscow, Russian Federation*
[3]*Russian Scientific Center of Roentgenoradiology, Scientific, Moscow, Russian Federation*

Purpose or Objective: Purpose: The aim of this work was to compare the patterns of NSCLC relapses after combined modality therapy with postoperative hypofractionated and conventionally fractionated radiotherapy and after sugery

Material and Methods: Material/methods. We treated 528 patients between January 1990 and January 2014 (men – 445, women – 83) aged 27-78 years (median age 59) with morphologically proven NSCLC (adenocarcinoma - 161, squamous cell cancer– 289, other types – 70 patients); stage I-126, stage II - 117, III - 111. All patients were operated: pnevmonectomy -180, lobe/belobectomy – 304, segmentectomy – 30, wedge resection -11. 227 patients received neoadjuvant or adjuvant platinum-based chemotherapy. Three groups were retrospectively analyzed: group I - 174 patients without postoperative radiotherapy (PORT), group II - 180 patients with postoperative hypofractionated radiotherapy with daily dose 3Gy up to the total dose 36Gy-39Gy (EQD2=43-47Gy, α/β=3) and group III - 174 patients with postoperative radiotherapy with daily dose 2Gy up to the total dose 44Gy. Bronchial stump, involved regional lymphatic nodes and uninvolved groups (2R, 2L, 3a, 3p, 4R, 4L, 5, 6, 7 according to IASLC classification) were included in the CTV. The groups were comparable in the following parameters: age, ECOG status, stage, T- and N - classification and the proportion of the patients treated with chemotherapy. The duration of the follow-up was 0,33-16,0 years, median - 2,25 years. The relapses were classified as local (in bronchial stump), regional, or distant. In the cases of mixt relapses (local ± regional ±distant) they were included in each category.

Results: Results. 263(49,8%) patients relapsed: 231 (43,8%) had distant metastases, local relapse – 51 (9,7%), regional relapse – 54 (10,2%). The pattern of the relapses in each group is presented in the table.

Category of the relapse	Group I	Group II	Group III	P (two-sided test)
Local	33 (19,0%)*	10 (5,6%)*	8 (4,6%)	*0,0001
Regional	38 (21,8%)*	8 (4,4%)*	8 (4,6%)	*0,0000
All locoregional	55 (31,6%)*	13 (7,6%)*	12 (6,9%)	*0,0000
Distant only	49 (28,2%)*	66(36,7%)*	68(39,0%)	*0,0924
All distant	81 (46,6%)*	74 (41,1%)*	76 (43,7%)	*0,2978
Relapsed patients	104(59,8%)*	79(43,9%)*	80(46,0%)	*0,0042

Conclusion: Conclusion. Hypofractionated postoperative radiotherapy (daily dose 3Gy, total dose 36-39Gy) significantly decrease the probability of local and regional relapse in NSCLC patients as well as the total number of the relapses without any effect with regard to distant metastases. Hypofractionated PORT is equally effective as conventional PORT (daily dose 2Gy, total dose 44Gy) with regard to locoregional control but has the clear logistical advantage.

EP-1221

Accelerated hypofractionated three-dimensional conformal radiation therapy (AHRT) for NSCLC

N. Rodriguez de Dios[1,2,3], X. Sanz[1,2,3], P. Foro[1,2,3], A. Reig[1,2], I. Membrive[1,2], A. Ortiz[1], J. Quera[1,2,3], E. Fernández-Velilla[1,2], O. Pera[1,2], M. Algara[1,2,3]
[1]*Hospital de la Esperança, Department of Radiation Oncology, Barcelona, Spain*
[2]*Hospital del Mar Medical Research Institute IMIM, Oncology, Barcelona, Spain*
[3]*Pompeu Fabra University UPF, Department of Experimental and Health Sciences, Barcelona, Spain*

Purpose or Objective: Increasing the radiotherapy dose can result in improved local control for non-small-cell lung cancer (NSCLC) and can thereby improve survival. This can be compromised by accelerated repopulation of tumour cells during radiotherapy. Accelerated hypofractionated radiotherapy (AHRT) can expose tumors to a high dose of radiation in a short period of time. We have employed this approach in two groups of NSCLC: 1) early stage NSCLC patients who cannot tolerate the SABR treatment process (for example, extended periods in the treatment position) or who cannot travel to a centre with SABR; and 2) stage III NSCLC unfit for concurrent chemotheraphy.
This study was performed to evaluate the feasibility of utilizing AHRT for these patients.

Material and Methods: 76 patients (46 stage I-II and 30 local advanced NSCLC) were included. All patients had FDG-PET scan. Only the primary tumour and the positive mediastinal areas on the pre-treatmement FDG-PET scan were irradiated. Mean age was 77.9 ± 7.9 years. The performance status (PS) was > 2 in 50% of cases. The radiotherapy was delivered in 2.75 Gy fractions, once daily to a total dose of 66 Gy (BED10: 84 Gy). Sequential chemotheraphy (mainly platinum and vinorelbine) was administered in 95% of stage III patients. Acute/late toxicity was evaluated using the RTOG criteria.

Results: After a mean follow-up of 2 years, the median overall survival (OS) and cause specific survival (CSS) were 23 and 54 months, respectively. On multivariate Cox regression analysis, PS >2 was an independent risk factor for OS ($p<0.0001$) and CSS ($p<0.0001$). The major acute adverse reactions were grade 2 dermitis (18%), grade 2 esophagitis (10%) and grade 1 pneumonitis (26%). There were 34 patients with grade 1 late pneumonitis.

Conclusion: AHRT is a reasonable alternative to conventional fractionated radiotherapy in stage I-II NSCLC without access to SABR and in stage III patients unfit for concurrent chemotheraphy. In both groups, treatment was well tolerated without grade 3 or higher treatment-related toxicity. PS >2 was an independent risk factor for OS and CSS.

EP-1222

Lung SBRT with Dynamic Tracking (DT) on the VERO (Brainlab-Mitsubishi) system

G. Jimenez[1], O. Gallocher[1], C. Chevelle[1], P. Dudouet[1], D. Franck[1], I. Latorzeff[1], M. Ducassou[1], D. Marre[1], N. Mathy[1], J. Mazurier[1], P. Navarro[1], D. Zarate[1]
[1]*Clinique Pasteur Bât. Atrium, Department of Radiotherapy, Toulouse Cedex 3, France*

Purpose or Objective: Since 2014, the VERO system equipped with dynamic tracking DT has been used in our center for lung SBRT.The purpose of this work is to compare 2 compensation techniques for lung SBRT, DT and a method based on the definition of an ITV, in terms of PTV volume reduction and treatment time.

Material and Methods: The VERO is an O ring system equipped with a gimbaled linac allowing pan and tilt rotations and with a stereoscopic dual-source kV X-ray imaging allowing the guidance of the tracking. A 4DCT is done to measure the range of the target movements with the breath: if the amplitude is < 7mm, an ITV is determined on the MIP images and if it is > 7mm, the DT method is preferred. A gold marker (Visicoil, IBA) is then implanted in the lesion and a new 4DCT is realized 1 week later. The GTVDT is drawn on the exhale phase and the PTVDT is defined with a 5mm margin. The dose is prescribed on the isodose covering 95 % of the PTV (Monte Carlo): the peripheral tumors receive 3x17 Gy, near the thoracic wall 4x12 Gy and near the mediastin 8x7,5 Gy. The metastatic diseases received 5x10 Gy. For DT, treatments are delivered with 6-8 no coplanar beams.

Results: 77 patients were treated with lung SBRT, including 22 patients treated with DT. Among these 22 patients, the PTVITV was however estimated: the average size of the PTVDT was 28.8cc(6.5 - 14.3 cc) and that of the PTVITV was 46.4cc(10.4 in 139 cc), so a 40 % reduction of the PTV volume. The average session length in DT was 35 min, the same as with the ITV method. The breathing rate of the patients was often irregular during the session and especially compared with the reference 4DCT. It did not affect the treatment delivery neither the guidance of the tracking. The clinical tolerance during and after the SBRT with tracking was excellent: 1 patient that was already treated for interstitial pulmonary fibrosis developed symptomatic radiation pneumonitis (RP). 5 other patients had radiological RP on the CT done during their first 6 months follow up period ; all of them received corticosteroid therapy and did not show any symptoms. There was no chest wall toxicity. Over a 16 months follow-up,1 patient did not benefit from treatment with DT SBRT and had a progressive disease.

Conclusion: With a 40% reduction of the PTV, this DT technique makes it easy to monitor all the patients breathing motion, including very irregular rates, in a treatment time equivalent to more classical techniques based on the ITV.

EP-1223

Local failure after radical radiotherapy of NSCLC in relation to the pre-therapeutic PET/CT

M. Kandi[1], L. Hoffmann[2], J. Fledelius[3], K.P. Farr[1], D.S. Moeller[2], M.M. Knap[1], A.A. Khalil[1]
[1]*Aarhus University Hospital, Oncology, Aarhus C, Denmark*
[2]*Aarhus University Hospital, Department of Medical Physics, Aarhus C, Denmark*
[3]*Herning Central Hospital, Department of Nuclear Medicine, Herning, Denmark*

Purpose or Objective: Local failure in lung cancer is associated with extremely poor survival. This study tested whether the pattern of failure is associated with the most PET avid volume in the pre-therapeutic PET/CT scan.

Material and Methods: Patients with inoperable NSCLC treated in our department between 2008 and 2010 were reviewed. Forty patients, who received radiotherapy (RT) for NSCLC and had an accessible pre-therapeutic FDG PET/CT scanning, were included. Fifteen of the patients developed local failure as the first event. Patient and tumour characteristics for patients with recurrences are presented in Table 1. The peak SUV area in the pre-therapeutic PET/CT scan in both tumor and lymph nodes were identified by an experienced nuclear physician who delineated the volume encompassing 50% of the maximum SUV (SUVmax50) in all fifteen patients. All patients were followed by CT scans every third month. The CT scans which showed recurrences (rCT) were imported to the Eclipse treatment planning system (Varian MS) and the recurrence gross tumor volume(s) (rGTV) was delineated. A rigid registration between pre-therapeutic PET/CT and treatment planning CT (pCT) was performed using a soft tissue match on the tumor or the lymph nodes in SmartAdapt (Varian MS). The SUVmax50 volumes were copied to pCT using the rigid registration. The rCT with the defined rGTV were also fused with the pCT using a rigid registration based on normal tissue nearby the rGTV but excluding the rGTV. The vertebral column or the aortic arch was found to be preferable. Two radiation oncologists assessed the rigid registration between pCT and rCT.

Results: The patients received conventionally fractionated RT with a total dose of 60-66 Gy. Planning target volumes (PTV) ranged from 169 cm3 to 1065 cm3 (mean = 678 cm3). Median time to local progression was seven months (95% CI 5-9 months). In twelve patients, the recurrences of the primary tumor appeared inside the PTV. In three cases, the recurrences were both inside and outside the PTV. These three recurrences outside the PTV appeared in mediastinal lymph node region. The rGTV overlapped with the pre-therapeutic PET sub-volumes in twelve patients (Figure 1). In one case, rGTV was near the PET sub-volume area without overlapping. In one patient, part of the target was missed because an atelectasis obscured the PET/CT signal and made the delineation of GTV less optimal.

Table 1
Patient and Tumour characteristics

Characteristic	Number of patients N=15
Median age year (range)	65 (59-77)
Gender	
Male	12
Female	3
WHO performance status	
0	8
1	7
Tumour Location	
Central	7
Peripheral	8
Histology	
Adenocarcinoma	4
Squamous cell carcinoma	8
Other NSCLC	3
T classification	
T1	1
T2	6
T3	4
T4	4
N classification	
N0	2
N1	2
N2	10
N3	1
Stage (UICC 7th edition)	
IIIA	11
IIIB	4
Concurrent chemotherapy	5
Sequential chemotherapy	9
No chemotherapy	1

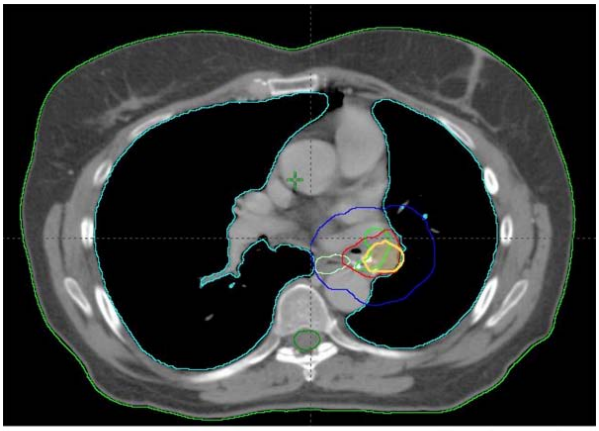

Figure 1: Rigid registration between pre-therapeutic PET/CT, pCT and rCT. Mediastinal window shows overlapping between SUVmax50 (Yellow line), recurrence (Green line). GTV and PTV are red and Blue.

Conclusion: This retrospective study shows that the SUVmax50 pre-therapeutic signal correlates with the post-therapeutic recurrences in the majority of patients. Pre-therapeutic PET/CT or planning PET/CT is a useful tool to guide the future dose escalation studies.

EP-1224

An Australian radiotherapy decision support system with contextual justification

M. Barakat[1], M. Field[1], D. Stirling[2], L. Holloway[3], A. Ghose[4], M. Bailey[5], M. Carolan[5], A. Dekker[6], G. Delaney[3], G. Goozee[3], J. Lehmann[1], T. Lustberg[6], J. Van Soest[6], J. Sykes[7], S. Walsh[6], S. Vinod[3], D. Thwaites[1]

[1]*University of Sydney, Medical Physics, Sydney- NSW, Australia*

[2]*University Of Wollongong, SECTE, Wollongong, Australia*

[3]*Liverpool Hospital, Cancer Therapy Centre, Liverpool, Australia*

[4]*University Of Wollongong, SCSSE, Wollongong, Australia*

[5]*Illawarra Cancer Care Centre, Wollongong Hospital, Wollongong, Australia*

[6]*MAASTRO Clinic, Knowledge Engineering, Maastricht, The Netherlands*

[7]*Westmead Hospital, Westmead Cancer Therapy Centre, Sydney, Australia*

Purpose or Objective:

Background: There is great potential to utilise a large range of retrospective clinical data as an evidence base in decision support systems (DSS) for cancer prognosis and subsequent personalised treatment decisions. Recently, there were several DSSs built for this purpose using machine learning tools, mainly regression models, Bayesian Networks (BN) and Support Vector Machines (SVM). These machine learning tools provide only a prediction of a class (decision), based on input attributes that were used to build the model, without providing additional information to clinicians about how and why this prediction was made.

Objective: To investigate the performance of an alternative machine learning tool in building a lung cancer radiotherapy DSS that provides clinicians with an estimated prediction together with the influencing attributes and their values (evidence) in supporting the decision reached. This will provide contextual justification to clinicians regarding the decisions, which will further help them in deciding whether to adopt the machine prediction or not.

Material and Methods: A Non-Small Cell Lung Cancer 2 year survival prediction model was built, using data at Liverpool Cancer Therapy Centre in NSW, Australia. The attributes used to predict the survival were age, gender, ECOG, GTV and FEV1. The machine learning tool used is a Decision Tree which automatically extracts rules from the training data and formulates these as if-then-else patterns. A report of the used rules during the prediction process indicates the effective attributes used to reach the decision. SVM, Regression models and BN were built and tested using the same data set; however, BN possess less, and SVM/Regression models possess none, of this reporting capability as they are learned by analysing probabilities and numerical distances among data points associated with prediction class.

Results: The DSS was learnt within the Liverpool Clinic with an unfiltered cohort of 4650 4686 patients. After filtering out patient records with missing values for the used attributes the cohort was reduced to 97 patients treated radically. The area under curve of the Decision Tree, SVM, Regression Model and BN when tested using a rigorous 10 fold cross-validation method respectively was 0.62, 0.62, 0.63 and 0.6. There is no significant difference in the performance between the four tools examined, however, the decision tree also generates an understandable context with every prediction made as a list of supporting attributes like the example in Figure 1.

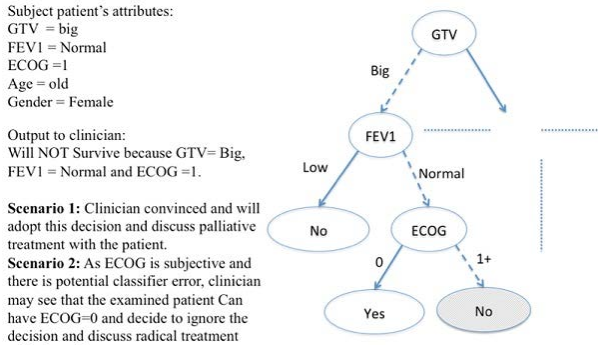

Figure1: Part from the decision tree and the trace of example input patient and expected scenarios

Conclusion: It is possible to build a DSS for NSCLC data that provides a prediction with additional information justifying the decision with similar performance as the commonly utilised SVM, BN and regression tools. To improve the performance and avoid over fitting, more diverse and complete training data is needed by incorporating data from other centres to the learning process using distributed learning.

EP-1225

MRI-defined GTV change during SBRT for unresectable or oligometastatic disease of the central thorax

L. Henke[1], D. Przybysz[1], R. Kashani[1], O. Green[1], C. Robinson[1], J. Bradley[1]

[1]*Washington University School of Medicine, Radiation Oncology, Saint Louis, USA*

Purpose or Objective: Stereotactic body radiotherapy (SBRT) is an attractive modality for the definitive treatment of oligometastatic or unresectable primary lung malignancies. Proximity of the tumor to adjacent organs-at-risk (OAR) may limit delivery of a sufficiently ablative dose. The ability to adapt to tumor response during treatment may improve OAR sparing and/or allow dose escalation. This study aimed to evaluate the degree of daily interfractional variation in gross tumor volume (GTV) during SBRT for patients with oligometastatic or unresectable primary malignancy of the central thorax using a magnetic resonance image guided radiotherapy (MR-IGRT) treatment system.

Material and Methods: Eleven patients with unresectable primary or oligometastatic malignancy of the central thorax were treated at our institution with extended fractionation SBRT on a clinical MR-IGRT system. Treatment regimens consisted of 60 Gy in 12 fractions (n=8) or 62.5 Gy in 10 fractions (n=3). For each treatment fraction, low-field (0.35 Tesla) MR setup imaging was acquired as part of routine clinical practice. Daily GTV was retrospectively defined on MR image sets for all patients at each of 10 or 12 fractions, using initial GTVs from CT simulation as a template. Daily tumor volumes were then recorded and compared for each patient to evaluate for interfractional change in tumor volume.

Results: All patients demonstrated on-treatment reduction in MRI-defined GTV (Figure 1). Average reduction in tumor size from treatment initiation to completion of therapy was 51.0% (median 52.1%) and ranged from 30.5-70.8%. At a time point of fraction six, average reduction in GTV size was 38.2% (median 34.8%). Linear correlation across median values at each time point suggested a consistent decline over time of approximately 4% per day, with the most pronounced changes occurring between the 5th and 6th fractions.

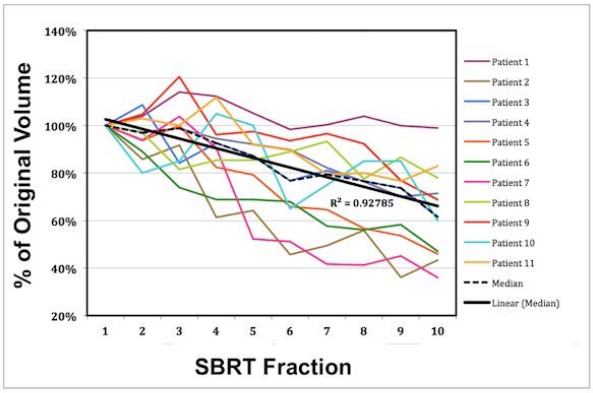

Figure 1. On-treatment change in gross tumor volume (GTV) as defined on daily magnetic resonance (MR) set up imaging at each of 10 fractions for patients treated with SBRT to the central thorax.

Conclusion: Tumor volume decreased considerably during treatment for most patients undergoing lung SBRT. The dosimetric impact of this degree of MRI-defined tumor volume change during the course of therapy has yet to be assessed. However, adaptive planning during the course of SBRT may be dosimetrically advantageous for sparing of surrounding critical structures, particularly for disease involving the central thorax.

EP-1226

Quality of life in locally-advanced non-small cell lung cancer patients: a systematic review

L. Van der Weijst[1,2], W. Schrauwen[3], V. Surmont[4,5], Y. Lievens[1,2]

[1]*Ghent University Hospital, Radiation Oncology, Ghent, Belgium*
[2]*Ghent University, Radiation Oncology, Ghent, Belgium*
[3]*Ghent University Hospital, Medical Oncology, Ghent, Belgium*
[4]*Ghent University Hospital, Respiratory Medicine, Ghent, Belgium*
[5]*Ghent university, Respiratory Medicine, Ghent, Belgium*

Purpose or Objective: Non-small cell lung cancer has a substantial impact on health-related quality of life (HRQoL) of affected patients. Measuring HRQoL in lung cancer patients is an important approach to forecast and assess the relative risks and benefits of a treatment as experienced by patients. A systematic literature review was performed to provide an overview of prospective studies measuring HRQoL in patients with locally-advanced non-small lung cancer (LA-NSCLC) receiving treatment with curative intent, published over the last 10 years.

Material and Methods: The literature search was performed in four electronic databases: PubMed, ScienceDirect, MEDLINE and Embase. The inclusion criteria for the studies were: English language, clinical trial, study population with LA-NSCLC, treatment with curative intent, HRQoL assessment, full text availability and published over the last 10 years.

Results: Only 5 studies out of the 225 potentially eligible studies matched our inclusion criteria. Four of these were randomized controlled trials; one was a prospective cohort study. All studies included radiotherapy at least in one of the evaluated treatment arms. Details of the studies and the analyzed parameters are shown in the table. HRQoL was a secondary endpoint in four studies and a co-primary endpoint in one. No significant treatment-related improvement or deterioration in HRQoL has been reported in the included studies. Variability has been observed in terms of use of HRQoL instruments and statistical analysis.

Conclusion: Evaluation of HRQoL in patients with LA-NSCLC receiving curative intent treatment remains scarce. Reporting and statistical analysis of HRQoL data lacks standardization. More research is needed to address these issues in both clinical trials and daily care of patients receiving radiotherapy as part of their primary treatment for LA-NSCLC. Based on these considerations, a prospective cohort study has been launched in our institute, which aims to evaluate HRQoL, treatment-induced toxicity and neurocognitive functioning in patients with unresectable LA-NSCLC receiving radiotherapy, all or not in combination with concurrent or sequential chemotherapy.

EP-1227

Salvage radiotherapy for regional lymph node recurrence after surgery of non-small cell lung cancer

K.H. Seol[1], J.E. Lee[1], M.K. Kang[2], J.C. Kim[1], I.K. Park[2]

[1]*Kyungpook National University Hospital, Radiation Oncology, Daegu, Korea Republic of*
[2]*Kyungpook National University Medical Center, Radiation Oncology, Daegu, Korea Republic of*

Purpose or Objective: To evaluate clinical outcomes of salvage radiotherapy for regional lymph node (LN) recurrence developing after radical surgery of non-small cell lung cancer (NSCLC).

Material and Methods: Between 2008 and 2013, out of patients with NSCLC who achieved complete response (CR) after definitive treatment (surgery with or without chemotherapy), 31 patients developed regional LN (mediastinum, hilum, and supraclavicular area) recurrence (median age, 66 years; stage Ⅰ, n = 17; stage Ⅱ, n = 7; stage ⅢA, n = 7). The median time from definitive surgery to recurrence was 12 months (range, 3-80). Fifteen patients (48.4%) had single LN recurrence and others had multiple LN recurrence. All patients were irradiated to the recurred LN area with daily fractions of 2.0 Gy (n = 27), 2.5 Gy (n = 2), or 3.0 Gy (n = 2) by 3D-conformal radiotherapy. The median total dose for recurred LN was 66 Gy (BED 79.2 Gy10; range, 65.1-79.2 Gy10). Sixteen patients received chemotherapy either.

Results: The median follow-up was 14 months (range, 3-76). After salvage radiotherapy, 16 patients (51.6%) achieved CR, 9 patients (29.0%) partial response, and 6 patients (19.4%) stable disease. After salvage radiotherapy, one- and two-year in-field local control rate was 88.4% and 75.8%, respectively. Only two patients experienced an out-of-field mediastinal recurrence. One- and two-year progression-free survival rate from initial salvage radiotherapy was 73.1% and 50.9%, respectively. Progression site was predominantly distant. Overall, ten of 31 patients (32.3%) were successfully salvaged as CR state. Recurred LN size (<3 vs. ≥3 cm) was a significant prognostic factor for progression-free survival (p = 0.03). Pneumonitis requiring conservative treatment (grade 2 or more) occurred in 5 patients (16.1%). There was no radiation-related mortality.

Conclusion: Salvage radiotherapy for regional LN recurrence after radical surgery was suggested to be an effective treatment option with an acceptable level of toxicity. The recurred node size (3 cm cutoff value) was a strong predictor of progression-free survival. Aggressive salvage radiotherapy should be considered as a front-line treatment in regional LN recurrence of NSCLC.

EP-1228

Pulmonary toxicity after 3D-CRT or VMAT-based stereotactic radiotherapy for early stage lung cancer

A.R. Filippi[1], S. Badellino[1], R. Ragona[1], C. De Colle[1], A. Guarneri[1], U. Ricardi[1]

[1]*Universita di Torino, Radiation Oncology Department, Torino, Italy*

Purpose or Objective: To compare patterns of acute and late clinical/radiological lung toxicity following either 3D or image-guided VMAT stereotactic radiotherapy for stage I non-small cell lung cancer (NSCLC).

Material and Methods: In this observational study, we included 148 patients from a prospective mono-institutional SBRT series (time interval 2004-2014). All subjects had peripheral tumors and a prescription BED10Gy (at 80%) in the range 100-120 Gy. The first 95 patients (2004-2010) were planned with 3D-CRT, using multiple non-coplanar fields; a stereotactic body frame was used with CTV-PTV margins of 5 mm (antero-posterior and latero-lateral) and 10 mm (cranio-caudal). The second cohort (2010-2014) included 53 patients, planned with volumetric IMRT, using a single/multi arcs VMAT technique, on a PTV generated with 3 mm margins from a patient's specific ITV (obtained from 4D-CT), with a frameless approach through cone-beam CT guidance. Clinical acute and late toxicities were scored according to RTOG scales; radiological acute (<6 months from SBRT) and late (>6 months post SBRT) toxicity on the basis of modified Kimura and Koenig's classifications, respectively. Student's T test was used to compare clinical characteristics, and Pearson's chi square test to compare the incidence of any grade lung toxicity.

Results: Patients and tumors' characteristics were similar and well matched between the groups. PTV volumes were also comparable (35.1 cc for 3D-CRT vs. 40.3 cc for VMAT,, p=0.16). Moreover, no significant difference was detected in Mean Lung Dose, converted in 2 Gy equivalent (11.7 vs. 10.4 Gy for 3D-CRT and VMAT, respectively, p=0.13). Frequencies of acute and late clinical toxicity (all grades) were superimposable between 3D-CRT and VMAT (acute: 10.5% vs. 22.6%, p=0.28; late: 4.2% vs. 13%, p=0.09, respectively). The crude rate of RTOG acute grade 3 radiation pneumon itis was 2.1% after 3D-CRT and 3.8% after VMAT. Acute and late radiological toxicity patterns were also similar between the two cohorts. Figures 1 and 2 depict the incidence and grade of both, according to different treatments. As expected, late radiological toxicity occurred in approximately 60% of patients, with modified conventional (25% after 3D-CRT vs. 32.6% after VMAT) and mass-like (19.6% after 3D-CRT vs. 17.4% after VMAT) patterns as the most commonly observed findings.

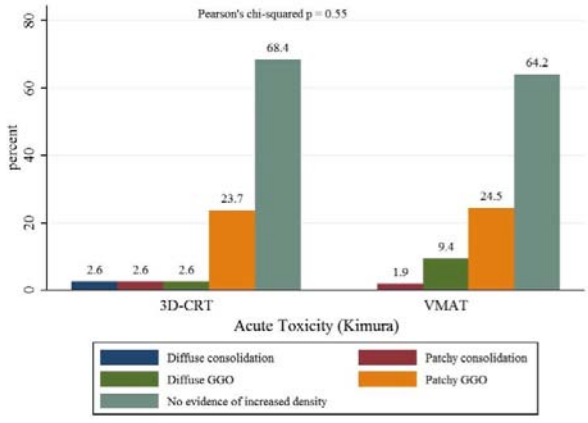

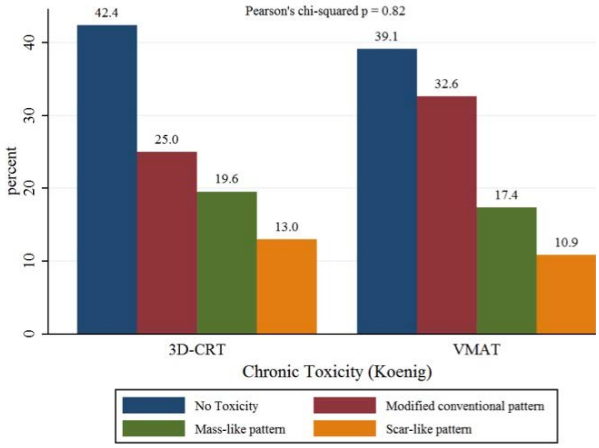

Conclusion: Results of the present study indicate that the pattern of clinical and radiological toxicities following SBRT in peripheral early stage NSCLC treated with comparable BED10Gy is not influenced by the different techniques used for planning and delivery.

EP-1229

Non-small cell lung cancer: marked difference in first failure site depending on histology

L. Nygaard[1], I. Vogelius[1], K. Håkansson[1], S. Langer[2], G. Persson[2], S. Bentzen[3]

[1]*The Finsen Center - Rigshospitalet, Department of Oncology- Section of Radiotherapy, Copenhagen, Denmark*

[2]*The Finsen Center - Rigshospitalet, Department of Oncology, Copenhagen, Denmark*

[3]*University of Maryland Greenebaum Cancer Center, Division of Biostatistics and Bioinformatics, Baltimore, USA*

Purpose or Objective: Inoperable non-small cell lung cancer (NSCLC) comprises several histological subtypes, with squamous cell carcinoma (SCC) and adenocarcinoma (AC) being most frequent. The prognosis is poor with current chemo-radiation strategies and treatment intensification is limited by patient tolerance. It is therefore relevant to target experimental therapeutic approaches to a patient's risk of local versus distant failure. The purpose of the current study was to compare the pattern of first relapse after chemo-radiation for locally advanced pulmonary SCC and AC.

Material and Methods: We retrospectively included 193 patients with locally advanced NSCLC treated with chemo-radiotherapy from 2009 to 2012. Patients with initial stage IV (n=17) disease and/or patients with histology other than AC or SCC (n=22) were excluded leaving 155 patient for the analysis. Patients were identified and grouped according to first event as either: loco-regional (LR) failure; intra-cranial distant metastases (ICDM), extra-cranial distant metastases (ECDM); dead without evidence of disease (Dead, NED), with the remaining patients being Alive, NED at latest follow-up in August 2015. The cumulative incidence of events was compared across the histology subtypes, using the competing risk method of Fine and Gray.

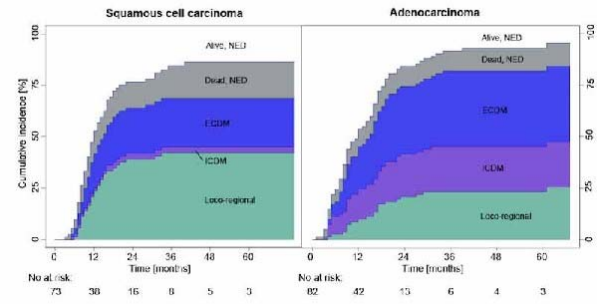

Table 1 Pattern of distant failure in AC and SCC

	ICDM	ECDM	Total
AC	18 (37.5%)	30 (62.5%)	48
SCC	2 (10.5%)	17 (89.5%)	19
Total of DM	20	47	67

Results: Patients received sequential (n=49, 32%) or concomitant (n=93, 60%) chemo-radiotherapy. Eleven patients received radiotherapy alone.. Competing risks analysis found a significantly higher rate of ICDM in the AC group compared to SCC (p= 0.0004) but no significant difference in incidence of ECDM (p=0.08). LR failure was higher in SCC than in AC (p=0.01). There was no significant difference between the two histology groups in the proportion dying without evidence of disease (p=0.3), see Figure. Restricting the analysis to patients with distant metastases as first site of failure, there was a significantly higher rate of cerebral metastases in AC than in SCC (p= 0.04), cf. Table 1.

Conclusion: The pattern of first failure in inoperable NSCLC differs among patients with AC and SCC with intra-cranial distant metastases being more common in AC than in SCC and LR relapse being much more frequent in SCC than in AC. Experimental treatment strategies should be targeting different relapse patters in various histological subtypes. Intensification of local therapy for example may yield a worse risk/benefit ratio in AC compared to SCC.

EP-1230

Clinical outcomes of stereotactic ablative radiotherapy in pulmonary oligometastases

B.S. Jang[1], H.J. Kim[1], B.H. Kim[1], D.W. Kim[2], Y.T. Kim[3], Y.W. Kim[4], H.G. Wu[1]

[1]*Seoul National University Hospital, Department of Radiation Oncology, Seoul, Korea Republic of*

[2]*Seoul National University Hospital, Department of Internal Medicine, Seoul, Korea Republic of*

[3]*Seoul National University Hospital, Department of Thoracic and Cardiovascular Surgery, Seoul, Korea Republic of*

[4]*Seoul National University Hospital, Department of Internal Medicine and Lung Institute of Medical Research Center, Seoul, Korea Republic of*

Purpose or Objective: In addition to its curative use in early stage lung cancer, stereotactic ablative radiotherapy (SABR) can also potentially be indicated for pulmonary oligometastatic disease. This study aims to retrospectively analyze treatment outcomes and develop nomograms to predict survival.

Material and Methods: From September 2012 to April 2015, treatment outcomes and toxicities for 85 cases of SABR in 72 patients retrospectively reviewed. Prognostic factors were analyzed via multivariate analyses using Cox proportional hazards regression. Using factors that demonstrated to be significant in the Cox regression model, nomograms were constructed and validated internally.

Results: After a median follow-up of 15 months, only 1 patient showed local failure within the radiation field. The local failure-free survival (LFFS) rate at 2 years was 98%. The 1-year and 2-year progression-free survival (PFS) and overall survival (OS) rates were 62% and 48%, and 90% and 72%, respectively. Multivariate analyses demonstrated that controlled primary cancer (p = 0.01), absence of extrapulmonary metastatic disease (p = 0.03), and disease-free interval (DFI) longer than 1 year (p < 0.01) favorably affects PFS. Furthermore, the absence of extrapulmonary metastatic disease (p < 0.01) and lower performance status (p = 0.03) increased OS as well. In terms of internal validation, nomograms for PFS and OS revealed C-index of 0.75 and 0.81, and showed a well-fitted calibration curves, respectively. Grade 1 or 2 radiation pneumonitis was found in 37 cases, and grade 1 chest wall pain was found in 1 case. Any grade 3 or higher toxicities were not identified.

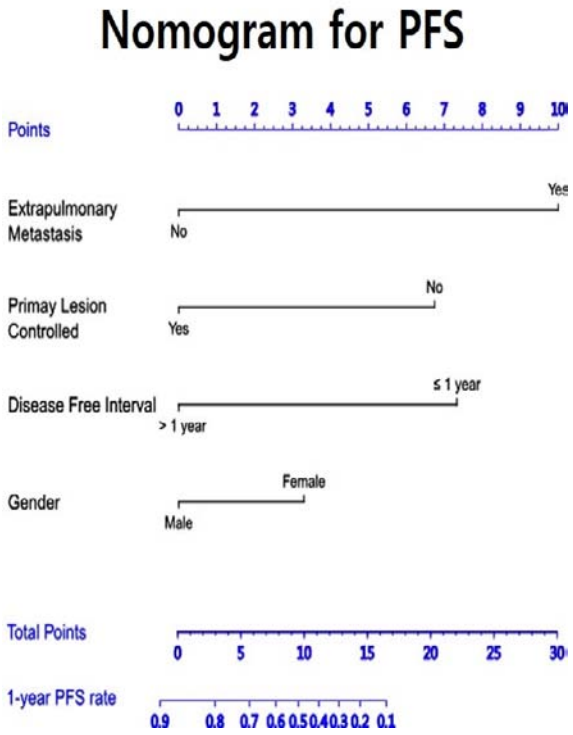

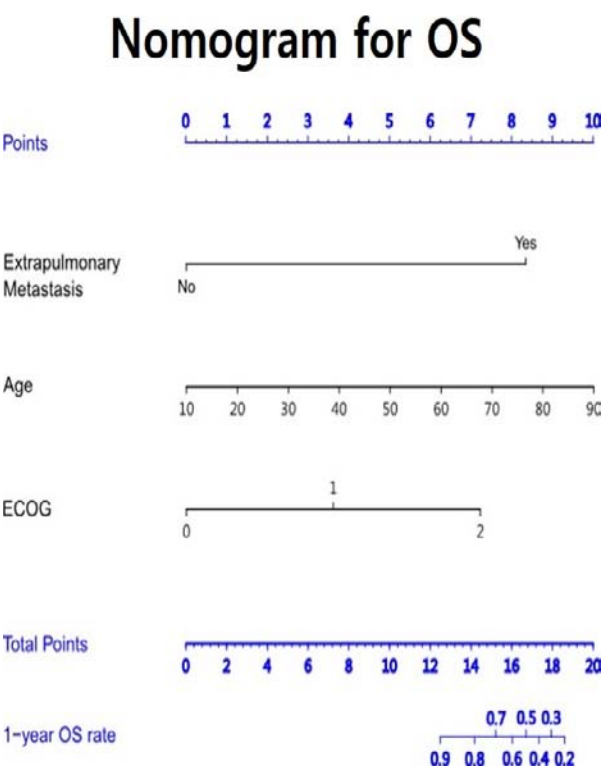

Conclusion: SABR demonstrated good local control with tolerable adverse effects for pulmonary oligometastases. Several factors were predictive for survival. Based on these factors, nomograms presented in this study can potentially be a useful tool for the prediction of progression-free and overall survival rates.

EP-1231

Proton and Carbon ion for stage I non-small cell lung cancer: a meta analysis

J. Tian[1], Q. Zhang[1], X. Wang[1]

[1]*Gansu Cancer Hospital, Department of Radiotherapy, Lanzhou, China*

Purpose or Objective: To synthesize and compare available evidence to compare the Long-Term clinical outcomes of proton therapy (PT) with those of carbon ion therapy (CIT) for stage I non-small cell lung cancer (NSCLC).

Material and Methods: Clinical trials were searched for in Cochrane Library, PubMed, EMBASE,Web of Science and Chinese Biomedical Literature Database through Dec 2014. Additional articles were identified from searching bibliographies of retrieved articles. Two reviewers independently selected studies and extract data. Outcomes were analyzed by random-effects model meta-analysis and reported as odds ratio (OR) with 95% confidence intervals (CI). The meta-analysis was conducted with STATA 12.0 software.

Results: Three retrospective studies were included, the meta analysis showed that there were no difference between proton therapy and carbon ion radiotherapy for stage I non-small cell lung cancer in the one year progression-free survival(PFS) was OR=1.13(95%CI:0.71,1.79), two years PFS was OR=1.25(95%CI:076,2.06),three years PFS was OR=1.02(95%CI:0.58,1.79),four years PFS was OR=0.73(95%CI:0.36,1.46),five years PFS was OR=0.50(95%CI:0.19,1.30), the one year overall survival(OS) was OR=1.01(95%CI:0.65,1.55),two years OS was OR=0.93(95%CI:0.59,1.46),three years OS was OR=0.94(95%CI:0.62,1.41) and four years OS was OR=0.65(95%CI:0.36,1.19),but there was difference in five years OS was OR=0.37(95%CI:0.16,0.90).

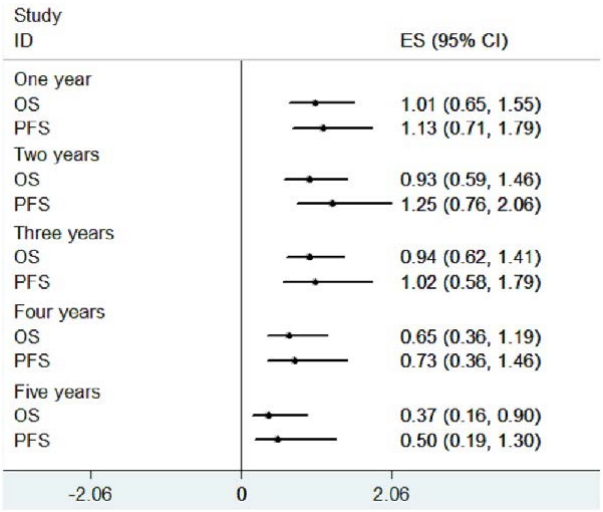

Conclusion: Our data suggest that the clinical outcomes of stage I NSCLC patients treated with PT and CIT may be similar. PT may improve 5-year OS compared with CIT. However, no firm conclusion concerning the difference in clinical outcomes between these two partical therapies can be made because of the limitations of retrospective studies; more homogeneous prospective data, large multicentric and randomized trials are needed to compare the efficacy of PT with CIT for stage I NSCLC.

EP-1232

Interim 18F-FDG-PET/CT for early outcome prediction during chemoradiotherapy of thorax malignancies

M. Cremonesi[1], L. Gilardi[2], C. Garibaldi[1], L. Travaini[2], M. Ferrari[3], S. Ronchi[4], D. Ciardo[4], F. Botta[3], G. Baroni[5], C. Grana[2], B.A. Jereczek-Fossa[4], R. Orecchia[6]

[1]*European Institute of Oncology, Radiation Research, Milano, Italy*

[2]*European Institute of Oncology, Nuclear Medicine, Milano, Italy*

[3]*European Institute of Oncology, Medical Physics, Milano, Italy*

[4]*European Institute of Oncology, Radiation Oncology, Milano, Italy*

[5]*Politecnico di Milano, Elettronica- Informazione e Bioingegneria DEIB, Milano, Italy*

[6]*European Institute of Oncology- University of Milan and Centro Nazionale di Adroterapia Oncologica CNAO, Radiation Oncology- Department of Health Sciences, Milano, Italy*

Purpose or Objective: Lung and esophageal cancer are characterized by aggressiveness and comprehend the majority of thorax malignancies. In both pathologies, the possibility to stratify patients (pts), early during radiotherapy (RT) or chemoradiotherapy (CRT) with interim 18F-FDG-PET/CT (FDGint) is extremely appealing to optimize treatments. CRT-responding pts could benefit from further preoperative treatment, while non responding pts should discontinue CRT, to avoid toxicity, and not to delay surgery. Although controversial findings have been reported on the early value of FDGint in thorax cancer, some notable results support therapeutic decision based on its analysis. Reviews specifically addressing FDGint in thorax cancer are lacking. The purpose of this study is to evaluate where and whether FDGint may offer predictive and prognostic potentials.

Material and Methods: A comprehensive review of the last decade literature was made, assembling studies on FDGint in pts affected by lung or esophageal malignances. Six different searches were completed on PubMed using keywords combined by Boolean operators (and, or). Studies inherent to FDGint for adaptive RT (aRT) were also included. Restrictions were: papers in English; 3D hybrid PET/CT studies; original papers only. Cross-references of the studies selected were also manually checked to complete the literature pursuit.

Results: 1121 items in lung cancer and 193 in esophageal cancer were found. After the steps of process selection, 17 studies were extracted for lung cancer (5 related to change of FDG uptake, 9 correlation with response and prognosis, 3 aRT) reporting on 488 pts, and 8 studies for esophageal cancer (7 correlation with response and prognosis, 1 aRT) reporting on 318 pts. The main metabolic parameters correlated with outcomes, progression free survival, locoregional control, overall survival were the standardized uptake value, metabolic tumor volume, total lesion glycolysis and their variations. Lung studies did not give special emphasis to statistical analysis, while 6/8 esophageal studies reported the results of statistical ROC analysis (Figure). Among the 17 lung studies, 14 advocated the predictivity of FDGint, 3 showed the improvements by aRT. Among the 8 esophageal studies, 4 sustained predictivity, 3 did not find any correlation, 1 showed the feasibility of aRT.

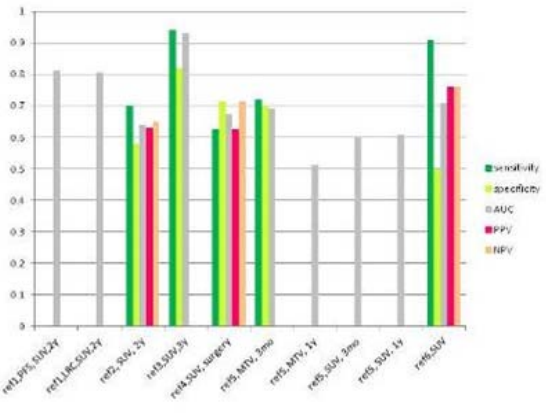

Figure: Sensitivity (dark green), specificity (light green), AUC (area under the curve, gray), PPV (positive predicted value, red), and NPV (negative predicted value, pink) as percent for the various studies related to the predictivity of FDG_{int} in esophageal cancer. SUV = maximum standardized uptake value from FDG_{int}. References 1, 2, and 3 sustained correlation; References 4, 5, and 6 concluded a lack of correlation.

Conclusion: Despite heterogeneity, the studies comprised in this review denoted FDGint as promising and challenging tracer for early assessment of outcomes during CRT. In lung cancer papers, all the authors sustain the predictivity of response and prognosis of FDGint. In esophageal cancer instead, its predictive and prognostic value cannot be

definitively established due to some controversial findings, the possible reasons of which demand further research with prospective and uniform protocols and analysis, great number of pts and adequate follow-up period.

EP-1233

Carbon ion radiotherapy for stage I non-small cell lung cancer: A Meta-analysis of 369 patients

Q. Zhang[1], J. Tian[1], X. Wang[1]
[1]*Gansu Cancer Hospital, Department of Radiotherapy, Lanzhou, China*

Purpose or Objective: To synthesize and compare available evidence considering the effectiveness of carbon-ion radiotherapy for stage I non-small cell lung cancer.

Material and Methods: To synthesize and compare available evidence considering the effectiveness of carbon-ion radiotherapy for stage I non-small cell lung cancer. Methods: A comprehensive search was conducted in the Cochrane Library, PubMed, EMBASE,Web of Science and Chinese Biomedical Literature Database (from inception to Feb 2015). Selection of studies, and extracting data were performed by two reviewers independently. Outcomes were analyzed by random-effects model meta-analysis and reported as odds ratio (OR) with 95% confidence intervals (CI). The meta-analysis was conducted with STATA 12.0 software.

Results: Eight trials(369 patients) were included, the meta analysis showed that the one year local control rate(LCR) was OR=0.89(95%CI:0.81,0.90),two years LCR was OR=0.81(95%CI:0.72,0.89),three years LCR was OR=0.64(95%CI:0.55,0.73),four years LCR was OR=0.23(95%CI:0.13,0.33) and five years LCR was OR=0.70(95%CI:0.67,0.73).the one year overall survival(OS) was OR=0.94(95%CI:0.88,0.99),two years OS was OR=0.85(95%CI:0.70,1.00),three years OS was OR=0.64(95%CI:0.50,0.78), four years OS was OR=0.29(95%CI:0.18,0.40) and five years OS was OR=0.34(95%CI:0.19,0.49).the one year progression-free survival(PFS) was OR=0.79(95%CI:0.69,0.89), two years PFS was OR=0.63(95%CI:0.52,0.75),three years PFS was OR=0.39(95%CI:0.28,0.51),four years PFS was OR=0.20(95%CI:0.10,0.29) and five years PFS was OR=0.08(95%CI:0.02,0.15).the recurrence was OR=0.46(95%CI:0.39,0.53) and distant metastasis was OR=0.20(95%CI:0.14,0.26).

Conclusion: Carbon beam radiotherapy, which is an excellent new modality in terms of a high local control and survival, may be a valid alternative to surgery for Stage I cancer, especially for elderly and inoperable patients.

EP-1234

VMAT based lung ablative radiotherapy: primary lesions and metastases

D. Farga[1], J.A. Burgos[1], F.J. Celada[1], F.J. Martínez[1], M.D. Badal[1], J. Bonaque[2], J. Gimeno[2], R. Chicas[1], M.J. Pérez[1], E. Cuervo[1], J. Pérez[2], A. Tormo[1]
[1]*Hospital La Fe, Radiotherapy Oncology, Valencia, Spain*
[2]*Hospital La Fe, Radiophysics, Valencia, Spain*

Purpose or Objective: Stereotactic ablative radiotherapy is an emerging non-invasive technique for the treatment of lung lesions. Both primary lesions and metastases may benefit from this approach, even in patients with low respiratory reserve. This work describes and evaluates institutional experience of SABR in lung location.

Material and Methods: From May´12 to November´14, 82 lesions in 67 patients were irradiated. 57 lesion were primary lung tumors and 25 metastases. Immobilization systems used in each patient was abdominal compressor and vacuum cushion o head-and-shoulders mask. An ITV was defined using three CT scans in three different phases of the respiratory cycle or with 4D RPM-Varian® system. The PTV was obtained by uniformly 5 mm ITV expanding. BED prescription was always over 100 Gy10 in 3-8 fractions following a risk-adapted protocol. 8 patient treatments were performed on a Clinac iXTM and 74 treatments on a TruebeamTM with high definition MLC. Volumetric modulated arc therapy (RapidArcTM) was mostly used, and image-guided RT was performed with cone-beam CT (CBCT). Intra-fraction movement was controlled by post-treatment CBCT and infra-red ExacTrac.

Results: Median age was 75y.o.(44-89). The median GTV/PTV size was 3.2/27.15cm3 (0.2-129.9/5.90-263.90). Intra-fraction movement in all cases was less than 5mm according to post-treatment CBCT. At a median follow-up of 7(1-30) months, overall l local control was 92.7%, 89.5% for primary lesions and 100% for metastases. Mean overall survival was 18 months for primary lesion (14.7-21.33 [95%]). No toxicities over G3 have been collected.

Conclusion: VMAT based ablative radiotherapy achieves excellent control rates in both primary lesions and metastases. Overall survival also depends on specific characteristics of the patient.

EP-1235

Necrosis / Fistulae occurring in temporal association with chest irradiation

S. Adebahr[1,2], S. Braasch[1], T. Schimek-Jasch[1], A.L. Grosu[1], U. Nestle[1,2]
[1]*University Medical Center Freiburg, Radiation Oncology, Freiburg, Germany*
[2]*German Cancer Consortium DKTK, Partner Site Freiburg, Freiburg, Germany*

Purpose or Objective: Receiving Radio(chemo)therapy [R(C)T] for pulmonary tumors some patients have or develop necrosis or fistulae (N/F) within the area of the treated tumor. Partially such N/F result in fatal complications like mediastinitis or pneumonia whereas other affected patients achieve good local control rates with long term survival after R(C)T. By retrospectively analyzing such cases we are aiming at identifying factors that might have an impact on the course of disease and should pre-therapeutically be considered in future.

Material and Methods: Retrospective analysis of patients coming up with N/F in temporal association with chest RT applied at the University Medical Center Freiburg from 2006 to 2013. Clinical and radiation parameters have been evaluated, acute and late toxicity, complications, clinical and imaging follow up have been assessed and will be analyzed with respect to local control and overall survival.

Results: We identified 40 patients irradiated for pulmonary malignancies (mainly centrally located NSCLC, UICC IIIB/IV; 16 female, 24 male; median age 64 years; 15 squamous cell-, 15 adenocarcinoma, 10 other) who developed N/F in temporal association with chest RT. Intention of treatment was curative in 31 and palliative in 9 patients. 25 patients received R(C)T, 15 received RT alone with a median total dose of 54 Gy (14-72Gy). 26 patients revealed a necrotic primary tumor, 6 additionally necrotic lymph node metastases (LNM), 8 necrotic LNM, exclusively. In 34 lesions necrosis was found previous to RT, in 3 cases it occurred during, in 3 cases after RT.14 patients showed fistulae, all fistulae with esophageal or mediastinal involvement emerged after RT. For 16 patients G3, for 6 G4 toxicities have been reported, one patient died in consequence of an esophago-tracheal fistula. All patients with N/F-connection to the esophagus revealed toxicities≥G3, whereas some patients with centrally necrotic tumor and fistula without esophageal involvement revealed excellent long term follow ups. Median survival was 12,6 months (median FU 6,9 months). All patients with esophago-tracheal fistula died before reaching the median. Histology and location of the necrotic lesions didn't show any significant impact on survival.

Conclusion: R(C)T of pulmonary malignancies for patients with N/ F can be associated with high toxicity. One essential factor with impact on the clinical course seems to be the

involvement of the esophagus. Without, courses with low complications and good local control are possible.

EP-1236

Does a localized NSCLC treated with SBRT affect the survival in COPD patients?

S. Jeppesen[1,2], N.C.G. Hansen[3], T. Schytte[1], M. Nielsen[4], O. Hansen[1,2]

[1]*Odense University Hospital, Department of Oncology, Odense, Denmark*

[2]*University of Southern Denmark, Institute of Clinical Research, Odense, Denmark*

[3]*Odense University Hospital, Department of Respiratory Medicine, Odense, Denmark*

[4]*Odense University Hospital, Laboratory of Radiation Physics, Odense, Denmark*

Purpose or Objective: The most common reason for patients (pts) with localized NSCLC to be deemed medical inoperable is Chronic Obstructive Pulmonary Disease (COPD). COPD is associated with severe morbidity and mortality. It is not known if the prognosis of COPD pts is so poor that diagnosed localized lung cancer may only have little impact on survival. The aim of this study was to compare survival in SBRT treated COPD pts unfit for surgery and COPD pts without a malignant diagnosis.

Material and Methods: Data for the group of SBRT treated NSCLC pts from our institution were prospectively recorded from 2007 until 2013. The non-malignant control group was retrospectively selected among pts referred to the Department of Respiratory Medicine from 2005 until 2011 due to suspected lung cancer, which was subsequently ruled out. From both groups pts were selected for the present analysis if spirometry fulfilled the criteria for COPD defined as the ratio between forced expiratory volume in 1 second (FEV1) and forced vital capacity (FVC) less than 70%. The COPD was classified according to international GOLD criteria as mild, moderate, severe, or very severe based on FEV1 in percent of predicted (FEV1%pred). Propensity score matching (PSM) was performed to reduce confounding between the two groups based on age, gender, and FEV1%pred. The treatment survival outcome variable was calculated using the Kaplan-Meier method. Log rank test was used for testing differences in survival rates.

Results: 102 SBRT treated pts (NSCLC group) and 573 pts without malignant disease (non-malignant group) were enrolled after a spirometry revealed COPD. No SBRT-related deaths were observed. Pts in the NSCLC group were older ($p<0.05$) and had worse FEV1%pred ($p<0.05$). PSM identified 102 pts from each group with similar characteristics: mean age of 72.7 years, FEV1%pred of 52, and 54 women. In the matched comparison a significant difference in the median overall survival was observed, 57 months vs. 87 months in the NSCLC and non-malignant groups, respectively $p<0.05$ (figure 1). Subgroup analyses of pts with mild/moderate COPD and pts with severe/very severe COPD showed that the difference in mOS in the unmatched and matched comparison was more pronounced in pts with mild/moderate COPD.

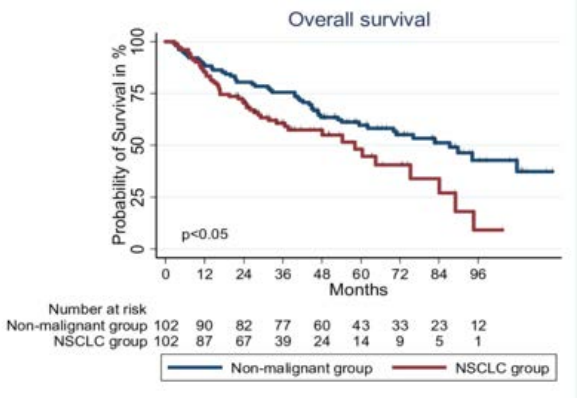

Conclusion: In a matched comparison, SBRT treated COPD pts with localized NSCLC had worse survival compared with COPD pts without a malignant diagnosis. Despite the serious prognosis of COPD, a diagnosis of localized NSCLC affected the survival in COPD pts.

EP-1237

Cyberknife Radiosurgery for spinal metastasis from lung cancer

I. Jung[1], S.Y. Song[1], S.D. Ahn[1], J.H. Kim[1], S.W. Lee[1], S.M. Yoon[1], Y.S. Kim[1], J.H. Park[1], S.S. Kim[1], E.K. Choi[1]

[1]*Asan Medical Center- Univ of Ulsan, Radiation Oncology, Seoul, Korea Republic of*

Purpose or Objective: To evaluate efficacy and safety of Cyberknife radiosurgery (CKRS) in patients with spinal metastasis from lung cancer.

Material and Methods: From July 2011 to October 2014, 64 patients received CKRS for spinal metastasis from pathologically confirmed lung cancer. Medical record of 75 lesions in 64 patients retrospectively reviewed. Pain control, radiological tumor control, especially epidural mass, and treatment related complications such as vertebral compression fracture and pain flare were assessed. Radiologic response was assessed following RECIST criteria. Pain response was defined according to International Bone Metastases Consensus Working Party palliative RT endpoints.

Results: Median age of patients with bone metastasis was 61 years (36-81 years). 42 patients (63.6%) had bone metastasis at initial diagnosis. Mean tumor diameter was 2.59 cm (1.2 cm-8.3cm), and 16 patients had epidural extension. was found in 16 patients (21.3%). Radiation dose were 14 – 32 Gy per 1-4 fx (BED(α/β=10): 28.8-57.6 Gy, median 41.6 Gy). Radiologic evaluation with CT or MR after CKRS was done at 54 lesions (72.0%). Pain response was assessed in 59 lesions (78.7%). With median follow-up of 10.5 months (1 – 40 months), local tumor progression was found in 9 lesions (12.0%), and median time to progression was 10.1 months. 1 year and 2 year local progression free survival rate was 84.6% and 79.7%. Among 16 lesions with epidural extension, 11 lesions had evaluated by CT or MR, and the tumor regression achieved in 8 lesions (72.7%). Pain response rate after CKRS was 83.1% (CR : 28.6% , PR : 71.4% , SD : 20.4%). All patients tolerated the CKRS course well. Compression fracture was found in 31 lesions (41.3%) but only 13 lesions(17.3%) collapsed among 54 lesions(72.0%) with osteolysis.

Conclusion: Cyberknife radiosurgery is an effective for local control and safe treatment modality to osteolytic spinal metastasis from lung cancer.

EP-1238

Thoracic re-irradiation following curative intent radiotherapy for non-small cell lung cancer

S. Scobie[1], G.G. Hanna[2], K. Franks[3], J. McAleese[4], S. Harrow[5]

[1]*Edinburgh Cancer Centre, Clinical Oncology, Edinburgh, United Kingdom*

[2]*Centre for Cancer Research and Cell Biology + Northern Ireland Cancer Centre, Queen's University of Belfast + Belfast City Hospital, Belfast, United Kingdom*

[3]*St James's Institute of Oncology, Leeds Cancer Centre, Leeds, United Kingdom*

[4]*Northern Ireland Cancer Centre, Belfast City Hospital, Belfast, United Kingdom*

[5]*Beatson West of Scotland Cancer Centre, Beatson West of Scotland Cancer Centre, Glasgow, United Kingdom*

Purpose or Objective: Following curative intent radiotherapy, up to 50% of patients with non-small cell lung cancer (NSCLC) experience local recurrence. This may be associated with significant symptomatology such as airways obstruction, haemoptysis and pain. Re-irradiation may be useful to palliate symptoms and to attempt cure, but little is known about effectiveness, usage rates, techniques used and clinical outcome. We report the incidence of thoracic re-irradiation following curative intent thoracic radiotherapy.

Material and Methods: Using the institutional databases of 3 large UK Cancer Centres (Belfast, Glasgow and Leeds), patients who had curative intent thoracic radiation for NSCLC during 2010 were identified. Baseline demographics were collated, along with details of initial irradiation, relapse and subsequent management. Summary statistics were generated detailing the incidence of re-irradiation, treatment intent of re-irradiation and dose fractionation used.

Results: In total, 351 patients were identified who had curative intent radiation. Of these, 188 (54%) relapsed, 60 with local relapse only. Eleven patients (18% of those with local relapse) received palliative re-irradiation to thorax for specific symptoms, with fractionation schemes including 8Gy/1 fraction, 16Gy/2 fractions, 20Gy/5 fractions and 30Gy/10 fractions. Four patients (6%) received radical re-irradiation with curative intent using 55Gy/20 fractions (3 patients) or 55Gy/5 fractions (1 patient). Thirty-five patients (58%) had no treatment at relapse and most were categorised unfit. Four patients had salvage radical surgery. The remainder had systemic therapy or palliative supportive care. Median time between initial radiotherapy and local relapse was 13.5 months (3-49 months). Median time from initial radiation and re-irradiation was 24 months (6-41 months). No excessive radiation related toxicity was reported.

Conclusion: In this selected cohort, re-irradiation is used routinely for patients with NSCLC, both with palliative and curative intent for local failure following radical thoracic radiotherapy. Further investigation of re-irradiation is warranted to assess toxicity, optimise techniques used and improve patient accessibility.

EP-1239

Clinical outcome of SBRT of central, apical or paracostal tumors in the lung, a retrospective study

C. Kristiansen[1], S.S. Jeppesen[1,2], M. Nielsen[3], T.B. Nielsen[3], T. Schytte[1], O. Hansen[1,2]

[1]Department of Clinical Oncology, Odense University Hospital, Odense, Denmark

[2]Instiute of Clinical Research, University of Southern Denmark, Odense, Denmark

[3]Laboratory of Clinical Research, Odense University Hosptial, Odense, Denmark

Purpose or Objective: Stereotactic body radiotherapy (SBRT) of lung tumors gives excellent local control but with higher rates of toxicity for organs at risk located close to the tumor. Treating centrally located tumors with SBRT with 3 fractions increases the risk of severe side effects especially when located near the proximal bronchial tree (PBT) known from earlier studies. We aimed to evaluate our current practice using 56 Gy in 8 fractions for tumors located centrally in the lung or close to other organs at risk (OAR) located more peripherally in the lung.

Material and Methods: Medically inoperable patients treated with 56 Gy in 8 fractions from the 1th of June 2012 until the 1th of September 2014 were reviewed and analyzed. The patients were deemed unfit for SBRT in 3 fractions or normally fractionated radiotherapy. For three patients this treatment was part of the Nordic Hilus Study

Results: Fifty patients were treated with a median follow up of 23.7 months (12.5-38.4). For baseline characteristics, see table 1. Not all tumors were centrally located; some tumors were close to columna, the apex of the lung or invaded the thoracic wall. Six patients had a locally recurrence (12%) and 15 distant recurrence (30%). Twenty-seven patients had died by the end of data analysis. Thirteen patients died of recurrent lung cancer. One patient died of another cancer. Two patients died suddenly without obvious cause. Eight patients died of other reasons, primary due to infections and/or known heart disease. Three patients died of hemoptysis probably due to bleeding from the main bronchus. Only one of these patients had an autopsy. This patient was re-irradiated with 30 Gy in 10 fractions because of recurrence overlapping the initial site. The 1 year survival was 76%, 2 year survival 41% and the 3 year survival was 38%. The median overall survival was 21.1 months (3.1 – 37.0).

Table 1: Patients characteristics

	Patients
Women	21 (42%)
Men	29 (58%)
Age, median (range) in months	74.0 (50.0 – 90.5)
Location[a]	
Centrally < 2 cm of the PBT	22 (44%)
Heart/pericardium	14 (28%)
Aorta or great vessels	34 (68%)
Vertebral body	13 (26%)
Apex of the lung	5 (10%)
Costae	19 (38%))
Histology	
Adenocarcinoma	21 (42%)
Squamous cell carcinoma	19 (38%)
Other	7 (14%)
Not known	3 (6%)
Performance status	
0	6 (12%)
1	24 (48%)
2	18 (36%)
3	2 (4%)
Median GTV (cm^3)	12.1 (0.9 – 145.3)
Toxicity any	
Pulmonary	
Dyspnea	3 (6%)
Atelectasis in minor degree	4 (8%)
Fatal hemoptysis	3 (6%)
Pains	5 (10%)
Fracture	1 (2%)
Plexus palsy	1 (2%)

a: tumors can be located close to more than one site

Conclusion: SBRT with 56 Gy in 8 fractions for lung cancer in relation to OAR are tolerable with an acceptable local recurrence of 12%. The three patients who died of hemoptysis had their tumor located close to the main bronchus. Treatment of SBRT close to the PBT is known to cause damage to the bronchus. Due to the retrospective format of the trial some side-effects may be underreported. It is challenging to treat tumors close to organs at risk and in particularly the bronchial three with a dose to achieve local control and without harming the PBT or close to OAR.

EP-1240

Normal tissue exposure in SBRT: Retrospective QA on a prospective cohort - what have we learned?

S. Adebahr[1,2], J. Hinck[1], R. Wiehle[1], T. Schimek-Jasch[1], E. Gkika[1], A.L. Grosu[1], U. Nestle[1,2]

[1]University Medical Center Freiburg, Department of Radiation Oncology, Freiburg, Germany

[2]German Cancer Consortium DKTK, Partner Site Freiburg, Freiburg, Germany

Purpose or Objective: Technique and indication of stereotactic fractionated radiotherapy (SBRT) has emerged rapidly during the last decade. Delineation, dose specification and constraints have been adjusted to updated evidence. Retrospective Quality Assurance (QA) of available prospective data was performed in order to reconsider recommendations and might reveal important insights for future treatment strategies.

Material and Methods: Within a prospective monocenter phase II study (STIPRE) 100 patients, elderly or unfit for surgery, have been treated with SBRT for 120 pulmonary lesions ≤5cm between 02/2011 and 12/2014. Applied doses were 3X12.5 Gy (85 lesions), 5X7Gy (30),7X5Gy (1) 4X6.5 Gy (1), 5X6.5 Gy (1), 8X7.5 Gy (1), 12X4.5 Gy (1), prescribed to 60% isodose in all but 2 patients. Delineation of organs at risk (OARs) was requested, however not specified in a detailed way in the trial protocol. Applying a moderate dose no constraints were provided in the protocol but derived from the evidence available at that time. SBRT plans had been evaluated by at least two experienced radiation oncologists before treatment. Within the retrospective QA process of the trial we now evaluated the maximal dose applied to OARs and analyzed those data with respect to the dose constraints of the recently launched EORTC 22113-08113 Lungtech trial. If

constraints were violated we re-checked correspondence of the structures to the delineation standards of the Lungtech protocol. Association of violations and the prospectively recorded toxicity was evaluated.

Results: According to DVHs 111 SBRT plans did not violate any of the dose constraints requested in the Lungtech trial. For 7/100 patients SBRT plans exceeded the Lungtech dose constraint for the proximal bronchial tree of EqD2=74.8Gy to > 0.5cc, one of them additionally for the esophagus of EqD2=64 Gy. 6/7 patients showed an increase in dyspnea, 2 of them died 3 and 9 months after SBRT, one after hemoptysis and subsequent pneumonia, the other after being hospitalized for unclear progressive dyspnea; in both cases association of G5 toxicity to SBRT cannot be excluded.

Conclusion: Despite the lack of detailed specific constraints within the STRIPE trial OAR exposure did not largely differ from current practice in modern SBRT. However, these preliminary results underline the importance of the dose constraints for the main airways within the Lungtech trial and the necessity to continuously review and adjust treatment procedures to upcoming evidence, especially when employing new techniques.

EP-1241

Relationship of dosimetric findings and toxicity following SABR for lung cancer

K. Johnson[1], A. Morenc[2], T. Sridhar[2], L. Aznar-Garcia[2]
[1]*University Of Leicester, Cancer Studies, Leicester, United Kingdom*
[2]*University Hospitals Leicester, Oncology, Leicester, United Kingdom*

Purpose or Objective: SABR for primary NSCLC is becoming increasingly popular as evidence is mounting for its equivalent long-term clinical outcomes and good overall tolerability. We review our toxicity against dosimetry and achievement of dose constraints (SABR UK Consortium). We suggest that dosimetric constraints alone cannot be used to prevent SABR related side effects.

Material and Methods: Patients with stage I NSCLC treated with SABR between January 2014 and August 2015 were included in this single centre cohort study. They were planned using relaxed breathing 4D CT then treated using VMAT. Baseline and dosimetric data was retrospectively collected by a clinical oncologist or physicist from the radiotherapy records. Patients were followed up at 4 weeks then at 3 monthly intervals until 1 year. CT scans were performed 3 and 12 months post radiotherapy. Prospective data collection was performed at follow up visits for clinical outcomes and acute and late normal tissue toxicity (scored using CTCAE v 3.0).

Results: 28 patients were included in the study with a median follow up of 10.4 months. 19 patients have attended for post radiotherapy CT scans with 84.2% showing radiological response as per RECIST. All patients were assessed for acute toxicity data, 3.5% (1/28) noted grade 2 reaction. Data on late toxicity was available for 19 patients: 26.3% (5/19) experienced grade 2-3, no grade 4 or 5 reactions were recorded. When adjusted for baseline function (late toxicity score minus baseline score) this fell to 15% (3/19). Other than chest wall (CW) tolerances all dosimetry criteria were met. 10.7% of plans exceeded tolerance to 30cc CW (>30/32) with no recorded episodes of grade 2 CW pain in these patients. 71.4% of plans exceeded dose constraint to 0.01cc CW (>37/39) only 5% (1/20) complained of CW pain. Dosimetric analysis for this patient revealed dose to 30cc of CW was 25.8 Gy (<32), dose to 0.01 cc of CW was 59.1 Gy (<39), volume of PTV and CW overlapping was 0.03 cc and % of PTV-CW overlapping was 0.21%.

Conclusion: We are achieving low rates of moderate or severe toxicity. Despite achieving dose constraints, a small cohort of patients developed toxicity grade 2-3. We hypothesize that these patients could develop radiotherapy toxicity due to other idiosyncratic factors (genetic polymorphisms, microenvironment). Further studies are currently running to investigate other causative factors.

EP-1242

Stereotactic body radiation therapy for early stage NSCLC: clinical outcomes

A. Iurato[1], A. Carnevale[1], E. Ippolito[1], M. Fiore[1], C. Greco[1], L.E. Trodella[1], A. Di Donato[1], S. Ramella[1], R.M. D'Angelillo[1], L. Trodella[1]
[1]*Policlinico Universitario Campus Biomedico, Radioterapia Oncologica, Roma, Italy*

Purpose or Objective: The aim of this study is to evaluate efficacy and toxicity of stereotactic body radiation therapy in early stage medically inoperable non-small lung cancer.

Material and Methods: Data from patients affected by medically inoperable stage I NSCLC treated with stereotactic body radiation therapy (SBRT) were prospectively recorded. Treatments were planned employing 4D-CT . The prescribed dose was modulated according to location of the lesion and tolerance of the surrounding organs at risk: 54 Gy in 3 fractions for peripheral lesions, 60 Gy in 4 fractions for lesions adjacent to the chest wall, 60 Gy in 8 fractions for central lesions. The primary endpoints were local control and toxicity, secondary endpoint was survival. The follow-up examinations were performed with CT and/or PET-CT at 1, 3, 6, 9 and 12 months after treatment and every 6 months subsequentely. Acute and late side effects were recorded according to RTOG morbidity Scoring Scale.

Results: From 2009 to 2014, 65 patients were treated. Mean patients' age was 74 years (range 62-86). The lesions had a mean maximum diameter of 20 mm (range 10-36). All but seven patients were staged by PET-CT. 83% of cases lung cancer was histologically proven: 34 cases were adenocarcinoma, 15 squamous cell carcinomas, 5 undifferentiated carcinomas. In the last 11 patients biopsy was not performed because of high risk features for complications and/or patient's refusal. In this last group 81% had a positive PET-CT and lesion growth documented at subsequent CT and just two patients had only lesion growth. Lesion's location were as follow: RUL 25/65 (38%), RML 2/65 (3%), RIL 7/65 (11%), LUL 22/65 (34%) and LIL 9/65 (14%). Median follow-up in 61 evaluable patients was 40 months. Five local failure (8%) were recorded at a mean of 11,5 months from the end of treatment (range 5.3-22). PET-CT SUV was the only parameter predictive for local failure, with a mean value of 14,2 in the recurrence group versus 6,1 in the recurrence-free group, respectively; p=0.03. Local control at 1 and 2 years were 89.6% and 86%. Median DFS was 22.2 months and 1y-, 2y- and 3y- DFS were 66%, 47% and 40%, respectively. Lesions' location according to treatment group was related to distant progression, which was significantly higher in peripheral location (p=0.004). Overall survival at 1y-, 2y- and 3y were 97%, 77% and 66%, respectively. Treatment was well tolerated. G1 asymptomatic pulmonary toxicity was observed in 18% of cases (11/61), G2 pulmonary toxicity was recorded in 3% of patients. There were no pulmonary toxicity grade 3-4. No other toxicities were reported.

Conclusion: SBRT is an effective and safe treatment for patients with medically inoperable stage I NSCLC. Local recurrence predictive value of PET-CT SUV could be investigated in bigger series.

EP-1243

A multicentre clinical trial using 3DCRT to reduce toxicity of palliative radiation for lung cancer

R. McDermott[1]
[1]*St Luke's Radiation Oncology Center, Radiation oncology, Dublin, Ireland Republic of*

Purpose or Objective: Radiation therapy in the palliation of intra-thoracic symptoms from locally advanced non-small cell lung cancer (NSCLC) is a significant component of workload in most radiotherapy departments. While most trials have

concentrated on optimizing dose schedules, we proposed a study demonstrating that using more technically advanced techniques would result in equivalent symptomatic relief and reduce symptomatic oesophagitis.

Material and Methods: Thirty-five patients with symptomatic locally advanced or metastatic NSCLC were treated using a three-dimensional conformal technique and standardized dose regimens of 39Gy in 13 fractions, 20Gy in 5 fractions or 17Gy in 2 fractions. Treatment plans sought to minimize oesophageal dose and oesophagitis was recorded during and at one month and three months following radiation therapy where applicable. Mean dose to the irradiated oesophagus was calculated for all treatment plans.

Results: At follow-up of one month after therapy for all patients accrued, there were no grade three or higher oesophageal symptoms of oesophagitis or dysphagia reported. Four patients (11.4%) had experienced grade 2 toxicity. All patients in the study derived clinical benefit from the radiation therapy course.

Conclusion: Use of three-dimensional conformal radiation techniques is widely practiced for treating intra-thoracic symptoms in the setting of NSCLC, however no direct study exists proving its superiority in reducing toxicity. This trial is the first of its kind showing that such techniques do provide patients with lower rates of oesophageal toxicity whilst yielding acceptable rates of symptom control. (Sponsored by the All-Ireland Cooperative Oncology Research Group (ICORG). Trial registration number 06-34)

EP-1244

Radiotherapy for loco-regional recurrence of non-small-cell lung cancer after complete resection

K. Terashima[1], M. Inamori[2], A. Matsunobu[3], H. Hirata[1], K. Sakamoato[1], K. Okabayashi[4], A. Furuya[2], M. Hirakawa[1]
[1]*Kyushu University Beppu Hospital, Department of radiology, Beppu, Japan*
[2]*Fukuoka Higashi Medical Center, Department of radiology, Fukuoka, Japan*
[3]*SAGA-HIMAT Foundation, Ion Beam Therapy Center, Tosu, Japan*
[4]*Fukuoka Higashi Medical Center, Department of Thoracic Surgery, Fukuoka, Japan*

Purpose or Objective: Although there is no standard treatment for postoperative recurrence of non-small-cell lung cancer (NSCLC), radiotherapy is occasionally used in the treatment of loco-regional recurrences. The objective of this study is to analyze clinical results of curative intent radiotherapy for loco-regional recurrence of NSCLC after complete surgical resection.

Material and Methods: A total of 38 patients, who had developed loco-regional recurrence after complete resection and received curative intent radiotherapy between 1999 and 2014, were retrospectively analyzed. There were 29 male patients and 9 female patients. The age range was 47-89 years (median 70 years). 25 patients had adenocarcinoma, thirteen patients squamous cell carcinoma. There were 29 patients with regional lymph nodes recurrence, and 10 patients with local recurrence at primary or anastomotic sites with or without lymph nodes recurrence. No patient had distant metastasis at presentation. The clinical endpoints included overall survival, progression-free survival, loco-regional recurrence within the irradiated field, and any other recurrence. The overall survival and local control rate were calculated from the day of radiotherapy completion and estimated by Kaplan-Meier method.

Results: The median total dose of radiotherapy was 60 Gy (range, 50–70 Gy). Thirteen of the 38 patients were treated with concurrent chemotherapy. The median follow-up time after radiotherapy was 30.4 (2.9–151) months. 1-5-year survival rates were 81.2, 69.6, 55.7, 48.5 and 39.6%, respectively. The 5-year progression-free survival, and local control rate were 32.6%, and 67.6%, respectively. Eight patients have survived more than 5 years. There was no significant difference between patients with lymph nodes recurrence and those with local recurrence in overall survival.

Conclusion: Radiation therapy for loco-regional recurrence after complete resection provides acceptable disease control. Curative intent radiation therapy can be the treatment of choice if no evidence of metastasis is observed.

EP-1245

BED <100Gy and ITV≥20cc predict local relapse after stereotactic radiation therapy for lung cancer

A. Suissa[1], A. Levy[1], F. Belkhir[1], N. Grellier-Adedjouma[1], P. Xu[1], F. Martinetti[1], C. Le Péchoux[1]
[1]*Gustave Roussy, Radiation Oncology, Villejuif, France*

Purpose or Objective: To determine predictive factors of local recurrence (LR) after Stereotactic Body Radiotherapy (SBRT).

Material and Methods: Data were retrospectively analyzed from 136 consecutive patients and 156 lung tumors treated with curative intent SBRT between April 2012 and December 2014 at our institution. Most patients had early lung cancer (76%). SBRT was also included in the treatment strategy for locally advanced (3%) or oligometastatic (21%) patients with an intent to complete response.

Results: The median follow-up was 21.8 months (2.4-70.8 months). The median age at diagnosis was 66,5 years (33-89 years) and median performance status was 0,5 (range 1-3). 54% patients had a smoking history with a median VEMS of 62,2%. Histological confirmation was obtained in 67%: 35% adenocarcinoma, 21% squamous cell carcinoma, 5% undifferenciated NSCLC and 5% other. Molecular markers were known in 27 tumors (17%): negative markers in 10%, KRAS mutation in 6%, other in 2%. Tumor location was central in 28%, peripheral in 48%, and intermediate in 24%. Median SUVmax at diagnosis was 7,1. Median ITV was 31,7 cc (0,56-104,8 cc) and median Biological effective dose (BED) was 123,8 Gy (72-151,2 Gy, α/β=10). 11 LR occurred resulting in a 2 year LR rate of 8% [CI 95%: 3-14%]; median: not reached; mean time to LR: 38.4 month [CI 95%: 36-39.6]. BED ≤100Gy (HR=5 [CI 95%: 1.1-22]; p=0.03), and Internal Target Volume (ITV) ≥20cc (HR=4.9 [CI 95%: 1.3 -18.5); p=0.02) were associated with a decreased LR in the multivariate analysis (MVA). Histology (squamous cell carcinoma), central location, and SUVmax of the treated lesion > 8 were not associated with local control in the MVA. Delay from diagnosis to SABR and molecular markers were not correlated with LR results in the univariate analysis. Two years overall survival and progression free survival rates were respectively 74% (IC 95%: 65-83%) and 62% (IC 95%: 52-72%).

Conclusion: BED should carefully be taken into account, particularly in case of tumors that exceed 20 cc

EP-1246

Is there a different dose-effect relation between the tumour and involved lymph nodes in NSCLC?

L. Van den Bosch[1], G. Defraene[2], S. Peeters[1], C. Dooms[3], W. De Wever[4], C. Deroose[5], D. De Ruysscher[1]
[1]*University Hospitals Leuven, Radiation Oncology, Leuven, Belgium*
[2]*University Hospitals Leuven, Experimental Radiation Oncology, Leuven, Belgium*
[3]*University Hospitals Leuven, Respiratory Oncology, Leuven, Belgium*
[4]*University Hospitals Leuven, Radiology, Leuven, Belgium*
[5]*University Hospitals Leuven, Nuclear Medicine, Leuven, Belgium*

Purpose or Objective: It is unknown whether dose-response for the primary tumor is different from that of the involved lymph nodes (LN). As the recurrence rate is much lower in LN, we hypothesized that involved LN need a lower radiation dose than the primary tumor.

Material and Methods: A retrospective analysis of prospective data was performed on patients with locally advanced NSCLC treated with radiotherapy. Three dose groups were defined based on EQD2,T (A: < 50 Gy, B: 50-55 Gy, C: > 55 Gy). The primary endpoint was involved nodal relapse (INR). An actuarial Kaplan-Meier analysis was performed to evaluate the cumulative proportion of INR and primary tumor progression per dose group.

Results: From 2006 to 2010, 75 consecutive patients were included in this study. Groups A, B and C consisted of 22, 24 and 29 patients respectively. Median follow-up was 7 months. All patient characteristics were well balanced between the 3 dose groups. A total of 142 lymph nodes were included in the analysis (A: 49; B: 36; C: 57). Any relapse (locoregional/distant) occurred in 58 patients (77%). INR was observed in 18% in group A, 8% in group B and 14% in group C. No dose-response relationship was observed in the involved LN (p=0.35). Primary tumor progression was seen in 55%, 42% and 28% in group A, B and C respectively. A significant dose-response relationship was observed in the primary tumor (p=0.02). Baseline nodal diameter was not associated with INR (HR 1; p=0.82).

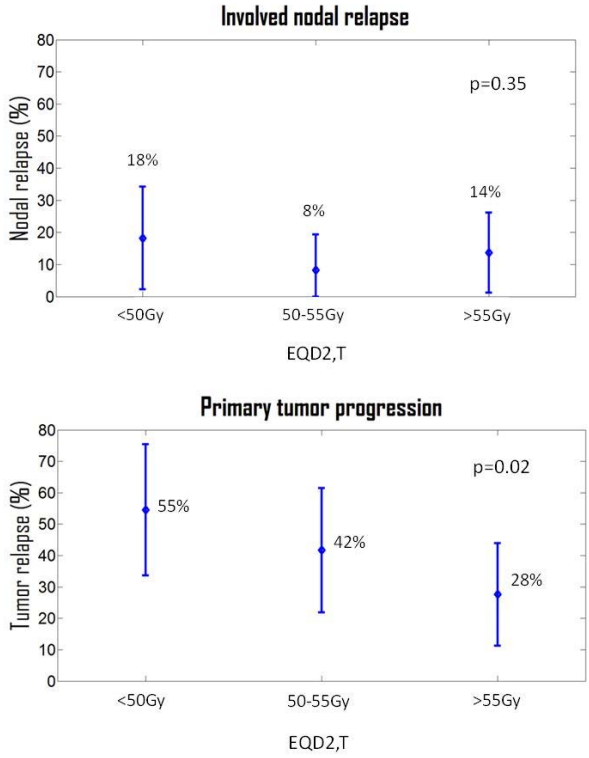

Conclusion:
The results of this study suggest that LN control can be achieved at lower radiation dose than needed for the primary tumor. Prospective dose de-escalation studies on LN are needed to decrease incidence of severe oesophagitis without compromising local control.

EP-1247

Is CC Chemokine Ligand 18 a biomarker for the prediction of radiation induced lung disease?

E. Gkika[1], S. Adebahr[1], T. Schimek-Jasch[1], A. Brenner[1], T. Brunner[1], A. Prasse[2], G. Ziessel[3], A.L. Grosu[1], U. Nestle[1]
[1]*Uniklinik Freiburg, Radiation Oncology, Freiburg, Germany*
[2]*Uniklinik Hannover, Pulmonology department, Hannover, Germany*
[3]*Uniklinik Freiburg, Pulmonology department, Freiburg, Germany*

Purpose or Objective: The CC Chemokine Ligand 18 (CCL18) is produced by alveolar macrophages in patients with fibrosing lung disease and its concentration is increased in various inflammatory and fibrotic lung diseases. In this study we aimed to analyze the role of CCL18 as a potential prognostic biomarker for the development of radiation induced lung disease (RILD) after thoracic irradiation.

Material and Methods: Between August 2011 and February 2012, 60 patients were enrolled prospectively in the study. Forty-six patients were treated for lung cancer; thirteen had an esophageal cancer and one a thymoma. Patients were treated either with conventionally fractionated (n=47) or hypo-fractionated (n=13) radiotherapy, 9 patients were treated adjuvant, 3 neoadjuvant, 4 with palliative intent and 44 with a definitive radiochemotherapy. The CCL18 levels in serum were quantified with ELISA (enzyme-linked immunosorbent assay) at predefined time points; before treatment, after 30 Gy, after 60 Gy (for conventional fractionation), at 6 weeks after completion of treatment and 3 months after therapy. These results were then correlated with clinical signs of RILD routinely performed computed tomographies (CTs) at 6 weeks and 3 months after the last treatment.

Results: Twenty three patients developed radiologic signs of RILD but only three of them developed symptoms. The mean CCL18 levels, for the whole group of patients, were before treatment 110 ng/ml (standard deviation, + 53) and at the end of treatment 85 ng/ml (+ 73). During the first (6 weeks after treatment) and second follow-up (3 months after treatment) the mean CCL18 levels were 93 ng/ml (+ 57) and 104 ng/ml (+ 49), respectively. The CCL18 concentrations in serum were not significantly elevated in the group of patients who developed a RILD. The mean CCL18 levels at six weeks and three months after treatment were in the RILD-group 94 ng/ml (+ 62) and 104 ng/ml (+ 61) and in the non-RILD-group 93 ng/ml (+ 54) and 103 ng/ml (+ 39). Patients with elevated CCL18 over the mean had a slightly worse local control (p=0,047) and a slightly worse overall survival which didn't reach statistical significance.

Conclusion: These findings do not suggest that the chemokine CCL18 is involved in the development of RILD in patients undergoing radiotherapy for chest tumors.

EP-1248

Lung re-irradiation with stereotactic body radiation therapy (SBRT)

P. Bonome[1], C. Scaringi[1], M. Valeriani[1], V. De Sanctis[1], G. Minniti[1], M.F. Osti[1]
[1]*Azienda Ospedaliera Sant' Andrea, Institute of Radiation Oncology, Rome, Italy*

Purpose or Objective: In the present study we have evaluated local control, overall survival (OS) and toxicity of re-irradiation with stereotactic body radiation therapy (SBRT) in patients with recurrent/progressive primary or secondary lung tumors after previous radical radiation therapy or SBRT.

Material and Methods: Between August 2011 and December 2014, 9 patients (6 men and 3 women) received a second course of SBRT in single (23 Gy or 30 Gy) or multiple fractions (15 Gy x 3). The median volume was 19.8 cc (range 3,7 - 46,8 cc). The median interval from previous irradiation was 18 months (range 12 - 47 months). Previous treatment included radical radiation therapy (60 Gy) in 33% of lesions and single-fraction SBRT (23 Gy or 30 Gy) in 67% of lesions.

Results: The median follow-up was 11 months (range 2 – 38 months). The median OS after the second course of SBRT was 12 months (range 3 – 39 months). The 6- and 12-months survival rates were 100% and 88%, respectively. No patient developed grade≥ 2 t oxicity. Complete response was observed in 2 patients (22%) and stable disease in 6 patients (66%). One patient died for progressive systemic disease.

Conclusion: Re-irradiation with SBRT for recurrent/progressive primary or secondary lung tumors is a feasible treatment associated with good local control and acceptable toxicity

EP-1249

Neoadjuvant chemoradiation in locally advanced NSCLC: impact of histology and drugs on results.

B. Floreno[1], R.M. D'Angelillo[1], M. Fiore[1], C. Greco[1], E. Molfese[1], C.G. Rinaldi[1], L.E. Trodella[1], A. Iurato[1], L. Trodella[1], S. Ramella[1]

[1]*Policlinico Universitario Campus Biomedico, Radiotherapy, Roma, Italy*

Purpose or Objective: Locally Advanced Non-Small Cell Lung Cancer (LA-NSCLC) or stage (St) III disease accounts for about 30% of patients with NSCLCs. Treatment strategies include definitive chemoradiation or induction treatment (IT) followed by radical surgery. The main end-points of inductive treatment are resection rate with pneumonectomy rate, and pathological downstaging.

Material and Methods: Pooled data from four consecutive trials published on patients receiving radiochemotherapy from 1992-2007 have been analyzed. The study group comprised 199 patients (87% males, 63±9 mean age, 48% squamous cell carcinoma (SCC), 65% cStIIIA). Patients have been treated with involved field radiotherapy and concurrent carboplatin or cisplatin + 5-FU (old drugs), weekly Gemcitabine only at 300mg/m2(GEM) and Cisplatin at systemic dose plus weekly Gemcitabine at 300mg/m2 (P-GEM).

Results: Present series confirms the impact on survival endpoints (OS, DFS, DSS) of surgical resection, pathological downstaging and tumor response. The indication for resection (HR = 2.7 [95%CI: 1.9; 3.7]; p<0.0001), together with response to radiochemotherapy (HR = 2.3 [95%CI: 1.6; 3.3]; p<0.0001) were the strongest predictors of OS. The most significant predictors of DSS were surgery (No resection vs Resection - HR: 2.0 [95%CI:1.3; 2.9], p<0.001), and the presence of response to induction radiochemotherapy (No response vs Partial Response - HR: 2.0 [95%CI:1.2; 3.1], p<0.004).Concurrent compounds influenced pathological downstaging (4% pStage 0 with old drugs vs. 23% with GEM vs. 36% with P-GEM; p=0.01), response rate (79% and 80% of partial response with GEM and P-GEM vs. 68% with old drugs; p= 0.002) and pneumonectomy rate (33% of patients treated with old drugs, 29% of those treated with GEM, and 19% of those treated with P-GEM). Squamous histology influenced response rate (80% vs. 69%; p=0.009) and disease specific survival (median DSS time was 30 months vs. 20 months).

Conclusion: The roles of major survival predictors (particularly, surgery, pathological downstaging) are discussed. The availability of reliable surrogate end-points (e.g.: pathological downstaging) may drive clinical strategy in the short time combining concurrent compounds and tumor histology.

EP-1250

Outcome after stereotactic radiotherapy for brain metastasis of lung cancer: a retrospective study

N. Grellier Adedjouma[1], A. Levy[1], A. Suissa[1], F. Belkhir[1], P. Xu[1], F. Martinetti[1], D. Planchard[2], B. Besse[2], C. Le Péchoux[1]

[1]*Institut Gustave Roussy, Radiation Oncology, Villejuif, France*

[2]*Institut Gustave Roussy, Medical Oncology, Villejuif, France*

Purpose or Objective: The aim of our study was to evaluate the efficacy and safety of brain stereotactic radiotherapy (BSRT), and potential interactions with mutational status/systemic therapies of patients treated in our Institute.

Material and Methods: We conducted a retrospective study of 85 patients (150 lesions) receiving SRT for brain metastases (mets) of lung cancer between 01/2012 and 03/2015.

Results: 90% patients were smokers and the most frequent histology was adenocarcinoma (ADK: 74%). In 99 patients with mutational analysis: 35%, 8%, and 56% had EGFR/ALK, others (KRAS/PI3K), or no mutations, respectively. The median GPA-DS score was 2.5 (0.5-3.5). The median estimated biologic equivalent dose (BED) was 57.6 Gy (16,7-57,6). 35 patients (41%) had a whole brain radiation therapy (WBRT) prior or after SABR. The median follow-up from SRT was 1.6 years. The 2-year local control (LC) was 54% (95IC: 40-68%). Histology (non-ADK: HR=7.2) and others mutations (KRAS/PI3K: HR=5.8) were associated with lower LC in the multivariate analysis (MVA). The type of systemic treatment, or its delay before BSRT, as well as other variables (history of WBRT, GPA, number of brain mets) did not correlate with LC in the MVA.

Conclusion: In our study, K-Ras mutational status seemed to be associated with poorer local control. The impact of mutational status should be evaluated in a larger set of patients.

EP-1251

Stereotactic Body Radiation Therapy (SBRT) for recurrent lung cancer following prior radiation

J. Wurzer[1], M. Mackowsky[2]

[1]*Atlanticare Cancer Institute, Radiation Oncology, Linwood, USA*

[2]*New Jersey Health Network, Raidation Oncology, Linwood, USA*

Purpose or Objective: Patients with recurrent lung cancer following prior thoracic radiation therapy have limited therapeutic options. This study analyzes the efficacy and morbidity associated with fractionated stereotactic body radiation therapy (SBRT) in the treatment of locally recurrent lung cancer following prior radiation therapy with or without concurrent chemotherapy or prior surgery.

Material and Methods: 37 patients diagnosed with recurrent local lung cancer recurrence following prior thoracic radiation therapy were treated with stereotactic body radiation therapy between June 2009 and December of 2013 at AtlantiCare Cancer Institute. Patients were treated with either robotic-assisted linear accelerator based stereotactic body radiation therapy with 4-D CT simulation and image guidance with cone beam CT or CyberKnife robotic radiosurgery utilizing Synchrony respiratory tracking. SBRT doses included 5400 cGy in 3 fractions and 5000 cGy in 5 fractions depending on normal tissue dose constraints. Patients underwent routine imaging with PET/CT and CT for surveillance.

Results: With a median follow-up of 3 years, the in-field local control was 92%. The actuarial overall survival was 46% with a progression free survival of 27%. Worsened dyspnea was noted in 13% of patients, 5% experienced esophagitis, 5% noted chest wall pain, and 8% experienced clinical pneumonitis. There was no grade 4 or 5 toxicity.

Conclusion: For patients experiencing local recurrence following prior thoracic radiation, robotic SBRT offers both excellent local control and limited toxicity. Despite these favorable results, progressive failure outside of the local therapy field and competing co-morbidities continue to pose a significant challenge.

EP-1252

Oligometastatic NSCLC: long-term results show efficiency of radical approaches in selected patients

A. Bunea[1], D. Schiebahn[1], D. Schanne[1], T. Schimek-Jasch[1], E. Gkika[1], S. Wiesemann[2], J. Rawluk[3], C. Waller[3], A.L. Grosu[1], U. Nestle[1]

[1]*Universitätsklinik Freiburg, Klinik für Strahlenheilkunde, Freiburg, Germany*

[2]*Universitätsklinik Freiburg, Chirurgische Klinik-Thoraxchirurgie, Freiburg, Germany*

[3]*Universitätsklinik Freiburg, Medizinische Klinik, Freiburg, Germany*

Purpose or Objective: Basing on the concept of oligometastases, i.e. less than 5 distant metastases, it was previously described that local, radical treatment of the

primary and/or its metastases in patients with non-small-cellular-lung-cancer (NSCLC) can lead to a favourable progression-free- (PFS) and overall-survival- rates (OS). An analysis made for patients treated between 2008 and 2012 at our institution already showed encouraging results. We extended this group of patients to those treated till 2015.

Material and Methods: Between 2008 and 2015 a total of 58 patients at our centre with an initial stage IV NSCLC with a maximum of 4 metastases at time of diagnosis received local radical treatment to all tumor sites. Method of treatment was indicated by the centre's interdisciplinary tumor board review. This retrospective analysis acquired data using our comprehensive cancer centre's patient-databases, that collected the patients' data and by contacting the patients' GP or their oncologists outside our institution.

Results: Between 2012 and 2015 a total of 58 patients (43 men (74%) and 15 women (26%)) where diagnosed with stage IV NSCLC, having less than 5 distant metastases. The median age at the time of diagnosis was 59 (range 48-86 years). The Karnofsky Performance Score (KPS) at a median of 90% (70-100%). The staging was completed by, MRI, CT and/or PET/CT (47 cases; 81%) as well as by histopathological examination. A biopsy was available in all patients. 43 (74%) had an adenocarcinoma, while 15 patients (26%) had a squamous cell carcinoma. Mutation analyses of epidermal growth factor receptor (EGFR) was determined in 26 patients, of which 4 (15%) showed a mutation. The patients underwent either surgery (74%) or radiotherapy (100%) of the primary or its metastases or a combination of both. Main target volumes were the primary, the mediastinum, brain metastases or bone metastases. Total cumulative doses at the site of the primary had a median of 60 Gy (30-68Gy). 45 patients (78%) were systemically treated. Out of these, 16 patients (28%) received a combined radio-chemotherapy with cisplatin, whereas 29 individuals obtained chemotherapy alone (50%) at some point in their history. Radiotherapy was generally well tolerated. One patient had grade three pneumonitis, requiring hospitalisation. Grade one toxicity occurred in four cases. During cytotoxic treatment one patient suffered grade three nausea. Mild to moderate cytopenia occurred in four patients. Median follow-up-time (FU) was 12.3 months, median PFS 6 months (95%, CI: 3.378-6.622%), while mean OS was 20 months, median OS was 15 months (95%, CI: 7.068-16.932%).

Conclusion: In line with literature, our analysis showed that radical treatment of patients with oligometastatic NSCLC may lead to an improvement of PFS and of the OS. Appropriate groups of patients with high KPS might benefit the most. Treatment modalities are generally well tolerated.

EP-1253

Local control and toxicity for centrally located NSCLC: SABR in no fly zone

C. Menichelli[1], G. Pastore[2], A. Fanelli[1], S. Grespi[1], P. Ferrazza[1], A. Chella[3], I. Petrini[4], F. Casamassima[1]
[1]*Research Institute "Ecomedica", Department of Radiation Oncology, Empoli, Italy*
[2]*Research Institute "Ecomedica", Department of Radiation Physics, Empoli, Italy*
[3]*AOU Pisana, Cardiothoracic Department, Pisa, Italy*
[4]*AOU Pisana, Department of Medical Oncology, Pisa, Italy*

Purpose or Objective: Only few experiences had investigated the use of SABR for locally advanced NSCL centrally located. The RTOG 0236 Trial warns about the risks of SBRT in NSCLS located within 2 cm of the bronchial tree, the edophagus, heart and pericardium. The aim of this study is to evaluate the use of hypofracionated ablative radiotherapy in this setting of disease in terms of local control, toxicities and overall survival (OS).

Material and Methods: Between Jun 2011 and March 2015 36 patients (pts) were treated with Hypofrationated Image guided-Volumetric Modulated Arc Therapy (IGRT-VMAT) for centrally located NSCLC stage III-IV or centrally recurrent NSCLC biopsy-proven. Target was contoured using volumetric mdc enhanced CT and PET/CT scan and OAR according RTOG 0236 Trial criteria. Dose Constraints used were: Single lung V10<20%, Dmax bronchus 38 Gy, Dmax esophagus 35 Gy, Spinal Cord 22.5 Gy, Heart and pericardium 38 Gy. The dose was prescribed to 80% isodose. The VMAT treatment was delivered by 6MV beam modulator Linac with 4 mm MLC and in breath hold using ABC device. Patient set-up and isocenter position was controlled before each fraction by CBCT. Target volume ranged from 21 to 150 cm3 (median 49.5). Median delivered dose was 40 Gy/5fx (median BED 10 of 100 Gy). Toxicities were assessed by CTCAE 4.0 criteria and the response was evaluated 2 months after the end of SBRT and every 4 month successively by CT and PET/CT.

Results: Median follow-up was 18 months (range 3 – 45). 25 pts are still alive (69.5%) and 8 of them have NED. 19/36 (52.8%) of treated lesions show complete respons and 10 (27.7%) partial response. Local control was 89% at 12 months and 67% at 18 months. OS was 84% and 73% at 12 and 18 months respectively. Acute toxicity worse than G2 was observed only in 1 pt. Late toxicity G3 was observed in 3 pts (esophageal stenosis in 1 case and bronco-esophageal fistula in 2 pts). Both fistulas occour in the same site of local recurrence

Conclusion: In our experience hypofractionated treatment with ablative dose for NSCLC locate in "no fly zone" is safe if dose constraints for OAR are respected. The two major late toxicities observed occurred in the same site of local recurrence. The treatments with BED 10 values of 100 Gy or more are effective leading to LC rate of 89% and 67% at 12 and 18 month respectlively. Although OS is not the primary endpoint of this study, beacuse include also metastatic and recurrent disease, nevertheless shows interesting values (84% at 12 months and 73% at 18 months)

EP-1254

Updated outcomes for patients treated with SABR for lung cancer at the Leeds Cancer Centre

P. Murray[1], K. Spencer[1], P. Dickinson[1], M. Snee[1], P. Jain[1], K. Clarke[1], K. Franks[1]
[1]*St James' Institute of Oncology, Clinical Oncology, Leeds, United Kingdom*

Purpose or Objective: To report ongoing longer-term outcomes of a large cohort of patients undergoing SABR for primary stage I lung cancer at the Leeds Cancer Centre.

Material and Methods: Patients were prospectively selected and received SABR for medically inoperable peripheral early stage lung cancer between May 2009 and January 2014. Electronic records were reviewed for baseline characteristics, treatment details and recorded toxicity and outcomes.

Results: 572 patients underwent SABR treatment, with 43 of these patients receiving 2 or more treatments, either concurrently or sequentially. Median follow-up 24 months (IQR 14-35 months, range 0-76 months). Kaplan-Meier (KM) estimated Median Overall Survival (OS) was 33 Months (S.E. 2.43 Months), and estimated 5-year OS 29.5% (S.E. 6%). 128 patients had clinical and radiologically reported recurrence. 26 patients (4.5%) developed local recurrence, 25 (4.3%) developed nodal recurrence, with 77 patients developing distant disease (13.5%). One, two and three-year K-M local control rates were 98.7% (S.E. 0.5%), 95.8% (S.E. 1.0%), and 92.3% (S.E. 1.6%) respectively. 94(21.2%) patients had a radiological report of pneumonitis (G1), 31(6.6%) patients had a clinical diagnosis of pneumonitis recorded (G2) and 2 (0.4%) patients had an episode of Grade 3 pneumonitis. 37 patients had a radiologically reported rib fracture, 14 symptomatic (2.9%) and 23 (4.8%) were asymptomatic (G1-2). There was no other reported ≥3 toxicity. Cox regression analysis showed that factors significantly associated with survival were poorer performance status (P=0.002) and increasing tumour size (p=0.008). Other factors such as histology, treatment related fibrosis, tumour lobar location,

clinical or radiological pneumonitis did not reach statistical significance (P<0.05).

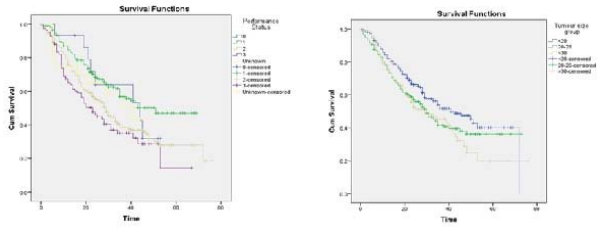

Conclusion: SABR for primary lung cancer performed at the Leeds Cancer Centre continues to show excellent local control rates, with low toxicity and has comparable overall 5-year survival rates to other published series. Poorer performance status and larger tumour size were associated with a negative effect on overall survival.

EP-1255

SABR and FDG-PET in lung cancer: a SUV cut-off value before treatment to predict local control.

S. Vagge[1], M. Marcenaro[2], G. Timon[2], G. Siffredi[2], R. Corvò[2]
[1]*IRCCS San Martino IST, Radiation Oncology, Genova, Italy*
[2]*IRCCS San Martino IST, Radiation Oncology, Genoa, Italy*

Purpose or Objective: To investigate the prognostic value of [(18)F] fluorodeoxyglucose positron emission tomography (FDG-PET) uptake before stereotactic ablative radiotherapy (SABR) for stage I non-small-cell lung cancer (NSCLC).

Material and Methods: From August 2009 to December 2014, 80 medically inoperable patients with proven Stage I NSCLC or FDG-PET-positive primary lung tumors were analyzed retrospectively. SABR consisted of 48-50 Gy delivered in 4 to 5 fractions, respectively by two or one fraction per week. Maximum standardized uptake value (SUV (max)) of the treated lesion was assessed before SABR. Patients were subsequently followed at regular intervals using computed tomography (CT) and FDG-PET scans. Association between post-SABR SUV (max, at minimum of 12 weeks after treatment) and local control (LC), overall survival (OS) was examined.

Results: Median follow-up time was 20 months (range, 9-55 months). Median lesion size was 20 mm (range, 8-50 mm). Due to statistical evaluations around the median range of SUV (max), a pre SABR SUV (max) 5.0 was selected as a cut-off to analyze LC and OS. The 2-year LC was 61.2% versus 78.7% for higher or equal than 5.0 versus lower than 5.0 SUV (max), yielding an adjusted sub-hazard ratio (SHR) for high pre SABR SUV (max) of 5.3 (95% confidence interval [CI], 1.3-25.5; p = 0.057). Two-year OS was 80.6% versus 76.6% respectively (hazard ratio [HR], 1.4; 95%; p = 0.46). No differences were observed between fractionation schedules or different tumor volumes.

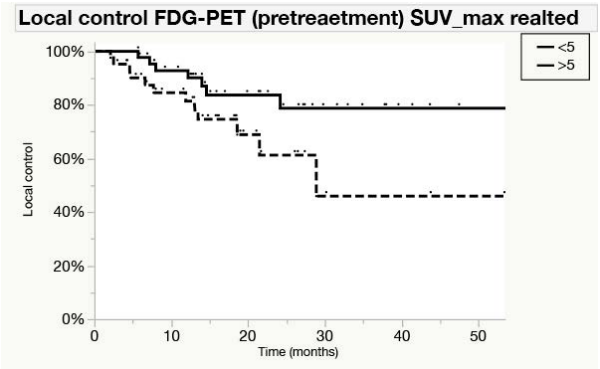

Conclusion: FDG uptake (SUV (max) ≥5.0) before SABR signifies reduces risk of local failure. These results from single institution might stimulate a large accrual from multicenter prospective analysis, due to controversial results already published.

Electronic Poster: Clinical track: Upper GI (oesophagus, stomach, pancreas, liver)

EP-1256

Stereotactic body radiation therapy for liver metastases using RapidArc technique

E. Del Cerro[1], A.A. Diaz Gavela[1], F. Couñago Lorenzo[1], F. Marcos Jimenez[1], E. Pardo Perez[2], Y. Molina Lopez[2]
[1]*Hospital Quiron Madrid, Radiation Oncology, Pozuelo de Alarcon- Madrid, Spain*
[2]*Hospital Quiron Madrid, Radiophysics, Pozuelo de Alarcon-Madrid, Spain*

Purpose or Objective: To report our initial experience in stereotactic body radiation therapy (SBRT) delivered using RapidArc (RA) technique with or without flattening filter beam in terms of toxicity and clinical outcomes.

Material and Methods: From September 2013 to September 2015, 16 consecutive patients with 27 metastatic hepatic lesions were treated with SBRT in a TrueBeam unit using RA technique. 6 lesions received a Volumetric Modulated Arc Therapy (VMAT) treatment using 6Mv RA with flattening filter and 21 were treated without flattening filter (flattening filter free beam- FFF) with an energy of 10Mv. GTV was defined using multi-phase CT scans, PET/CT and/or MRI. The lesions were marked with a radiopaque coil to localize them in the verification CBCT (ConeBeamCT) that was performed daily. ITV (internal target volume) was calculated in gated modality with internal coil tracking by 2D imaging. Prescribed doses ranged from 30-60Gy in 3-5 fractions to ITV. The dose was downscaled in cases of not full achievement of dose constraints. 99.5% of the target volume was covered by 100% of the prescription dose. Initially, we followed the constraints proposed by Timmerman: Three fractions constraints for organs at risk were: 700cc of liver free from the 17.1Gy isodose, Dmax< 24Gy for stomach and duodenum, D5cc< 15Gy for duodenum, Dmax< 30Gy for heart, D1.2cc< 11Gy and D0.25Gy< 18Gy for spinal cord. Five fractions constraints for organs at risk were: 700cc of liver free from the 21Gy isodose, Dmax< 32Gy for stomach and duodenum, D5cc< 18Gy for duodenum, Dmax< 38Gy for heart, D1.2cc< 13.5Gy and D0.25Gy< 22.5Gy for spinal cord. Nowadays we are following the constraints proposed by the Spanish Society of Radiation Oncology: Liver: 700cc of liver free from the 15Gy isodose, V21<30%, V15<20Gy, Mean dose: <15Gy for three fractions and <20Gy for five fractions; D5cc<15Gy for duodenum; V30<1cc and V21<5cc for heart; Dmax<18Gy for spinal cord.

Results: Mean age of the patients was 59 years and the mean following time since the end of SBRT was 9.14 months. ITV mean volume was 41.78cc. The most frequent side effect was acute asthenia and we identified two cases of asymptomatic increase in liver enzymes. No patient experienced acute toxicity greater than Grade 2. In relation to the local response, we used RECIST and/or PERCIST criteria to reevaluate the lesions. We found 15 complete and 1 partial responses, 1 progression, 5 stable lesions and 2 pseudo progressions. 2 patients (4 lesions) were lost in the long-term clinical follow up. No differences between both treatment modalities (with or without FF) were found in terms of local control or side effects (either acute or chronic).

Conclusion: SBRT for liver targets delivered by means of RapidArc resulted to be a feasible technique, with few side effects and good rates of local response in metastatic liver targets.

EP-1257

Stereotactic radiotherapy for recurrent pancreatic adnocarcinoma at stump or abdominal lymph nodes

H.H. Wang[1], H.H. Wang[1], M.B. Meng[1], Z.Q. Wu[1], Y.C. Song[1], H.Q. Zhuang[1], D. Qian[1], L.J. Zhao[1], Z.Y. Yuan[1]

[1]*Tianjin Cancer Hospital, Department of Radiation Oncology, Tianjin, China*

Purpose or Objective: To evaluate the efficacy and safety of stereotactic radiation therapy (SRT) in the treatment of patients with recurrent pancreatic adnocarcinoma at the stump or abdominal lymph node after surgery.

Material and Methods: Between October 1 2011 and May1 2015, patients with recurrent pancreatic adnocarcinoma at the stump or abdominal lymph nodes after surgery were enrolled and treated with SRT at our hospital. The primary end-point was overall survival after SRT (OS). Secondary end-points were: local control rates (LC), time to symptom alleviation, and toxicity using the Common Terminology Criteria for Adverse Events (CTCAE v4.0).

Results: Twenty-four patients with 24 lesions (17 abdominal lymph nodes and 7 stumps) were treated with SRT. Among these patients, five patients were presented with abdominal lymph node and synchronous metastases in liver and lung. For the entire cohort, the median OS from diagnosis and SRT were 28.93 months and 12.20 months, respectively. The 6-month, 12-month, and 24-month actuarial LC rates were 95.2 %, 83.8% and 62.1% respectively. Symptom alleviation was observed in 11 of 14 patients reported symptoms (78.6%) with a median of 8 days (range, 1-14 days) after SRT. Nine patients (37.5%) experienced CTCAE v4.0 Grade 1 to 2 acute toxicities; one patient experienced grade 3 acute toxicity due to thrombocytopenia.

Conclusion: SRT is a safe and efficacious treatment modality for patients with recurrent pancreatic adnocarcinoma at the stump or abdominal lymph nodes after surgery. Further studies are needed before SRT can be recommended routinely.

EP-1258

Concurrent high-dose (60-70 Gy) radiation and chemotherapy for esophageal cancer: long-term results

T. Kondo[1], Y. Shibamoto[1], A. Hayashi[1], A. Miyakawa[1], T. Murai[1], T. Yanagi[1], C. Sugie[1], Y. Ogawa[1]
[1]*Nagoya City University Graduate School of Medical Sciences, Department of Radiology, Nagoya, Japan*

Purpose or Objective: Based on the results of the intergroup-0123/RTOG 94-05 trial that demonstrated no benefit of dose escalation over 50.4 Gy in definitive chemoradiotherapy (CRT) for esophageal carcinoma, 50.4 Gy appears to be accepted as a standard dose. Radiobiologically, however, higher radiation doses, if safely delivered, could lead to better local control. We have used combination of standard FP (5-fluorouracil [5-FU] and cisplatin) chemotherapy and radiation with dose ≥60 Gy in the treatment of non-metastatic esophageal cancer. We report clinical outcome of the treatment protocol.

Material and Methods: Between 2002 and 2014, 86 patients with stage I-III or IV (M1 LYM) esophageal cancer were treated with CRT. Median age of the patients was 68 years (range: 46 to 84); 76 were men and 10 were women. Histology was squamous cell carcinoma in 98%. Patients were divided into 4 groups according to the stage and operability; Group 1: stage I patients (n = 10); Group 2: stage II-III operable patients (n = 20); Group 3: stage II-III (non-T4) inoperable patients (n = 21); and Group 4: stage III-IV (T4/M1 LYM) patients (n = 35). Chemotherapy protocols were either cisplatin (70 mg/m2) plus 5-FU (700 mg/m2 x 4 days) administered every 4 weeks or low-dose daily cisplatin (4 mg/m2) and 5-FU (200 mg/m2). Radiation was given by 10-MV X rays with a daily fraction of 1.8-2 Gy. Treatment volume included primary tumor plus regional lymph nodes. A total dose between 60 and 70 Gy was chosen depending on the treatment volume. Median radiation dose was 64 Gy (range: 50-70 Gy; 5 patients could not complete planned treatment). Failure was confirmed by pathology or findings of progressive disease on serial endoscopy and/or imaging studies. Overall survival (OS) and locoregional control (LC) rates were calculated by the Kaplan-Meier method. Toxicities were evaluated by the Common Terminology Criteria for Adverse Events version 4.0.

Results: For all 86 patients, the 3-year LC and OS rates were 65% and 29%, respectively; they were 100% and 100%, respectively, in Group 1, and 72% and 42%, respectively, in Group 2. The 2-year LC and OS were 53% and 14%, respectively, in Group 3, and 69% and 25%, respectively, in Group 4. Overall response rate was 78% (complete response in 31 and partial response in 36). Grade 3 or higher acute toxicities, mainly hematological, were observed in 37% of the patients and 10% experienced grade 3 or higher late toxicities.

Conclusion: CRT with FP and 60-70 Gy of radiation appears to be tolerable for patients with esophageal cancer. Although outcome of this treatment in inoperable patients is not satisfactory, the 3-year LC of 100% for stage I patients and 76% for stage II-III operable patients appear promising. Further investigation is warranted to clarify the optimal radiation dose in CRT for esophageal cancer.

EP-1259

Clinical significance of lymphocyte count before chemoradiotherapy in resected pancreatic cancer

J. Heo[1], O.K. Noh[1], H.W. Lee[2], M. Chun[1], Y.T. Oh[1], J. Kim[3]
[1]*Ajou University School of Medicine, Radiation Oncology, Suwon, Korea Republic of*
[2]*Ajou University School of Medicine, Hemato-oncology, Suwon, Korea Republic of*
[3]*Dankook University College of Medicine, Radiation Oncology, Cheonan, Korea Republic of*

Purpose or Objective: The objective of this study was to investigate the prognostic value of circulating lymphocyte level at the beginning of postoperative chemoradiotherapy (CRT) in pancreatic adenocarcinoma.

Material and Methods: From 2007 to 2014, 41 patients treated with postoperative CRT were analyzed. The median dose of radiotherapy was 50.4 Gy (range, 45 – 59.4) and chemotherapy was administered after surgery. Absolute lymphocyte counts (ALC) was obtained from complete blood count tests performed prior to CRT. We analyzed blood lymphocyte count as well as clinical parameters to identify prognostic factor

Results: With a median follow-up of 16.9 months, 32 patients had cancer recurrence and 28 died from the disease. The median overall survival (OS) and disease free survival (DFS) were 19.7 months and 9.8 months. The median OS of high postoperative ALC (>2.074 $\times 10^3$/ μL) group was significantly longer than that of the lower ALC group (32.0 months versus 17.0 months, p = 0.007). In multivariate analysis, high postoperative ALC was a good prognostic factor for OS. (Hazard Ratio = 0.341, CI, 0.149 – 0.778, p = 0.011). High ALC at the beginning of postoperative CRT was also a prognostic factor for DFS in multivariate analysis (Hazard Ratio = 0.452, CI, 0.215 – 0.946, p = 0.035).

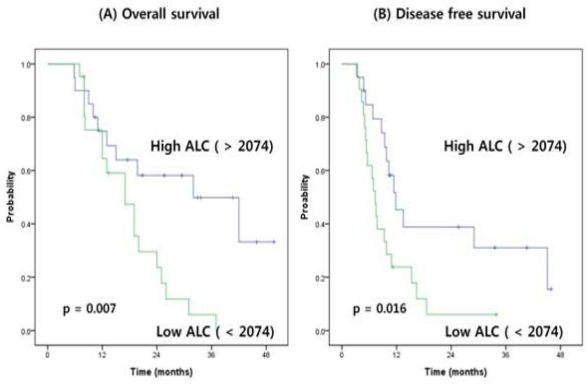

Conclusion: Postoperative ALC is a significant prognostic factor for resected pancreatic cancer patients. Postoperative immune status might help to predict survival outcome and to stratify group that is effective in CRT for resected pancreatic cancer.

EP-1260

Prognostic factors in hepatoma patients treated with radiotherapy for lymph node metastasis

C.W. Wee[1], K. Kim[1], E.K. Chie[1], S.J. Yu[2], Y.J. Kim[2], J.H. Yoon[2]
[1]*Seoul National University College of Medicine, Department of Radiation Oncology, Seoul, Korea Republic of*
[2]*Seoul National University College of Medicine, Department of Internal Medicine, Seoul, Korea Republic of*

Purpose or Objective: To investigate prognostic factors for overall survival (OS) in hepatocellular carcinoma (HCC) patients treated with external beam radiotherapy (RT) for lymph node (LN) metastasis.

Material and Methods: Between 2004 and 2015, 105 HCC patients underwent palliative RT for LN metastasis. The median age was 60 years (range, 30–82). Biologically effective radiation doses of 39–75 Gy10 (median, 59.0 Gy10) were delivered. The median follow-up period was 5.7 months.

Results: The median OS was 5.8 months. On univariate analysis, young age, symptoms related to LN metastasis, poor performance status, Child-Pugh class B–C, uncontrolled intrahepatic disease, non-nodal distant metastasis (DM), multi-station LN metastasis, biologically effective dose <60 Gy10, lack of local response to RT, and stable or increased post-RT alpha-fetoprotein levels compared to pre-RT levels were significant prognostic factors predicting poor OS (all $p<0.05$). On multivariate analysis among pre-RT factors, symptoms related to metastatic LNs (HR, 2.93), Child-Pugh class B–C (HR, 2.77), uncontrolled intrahepatic disease (HR, 2.74), and non-nodal DM (HR, 1.62) were significant prognostic factors for poor OS (all $p<0.05$). Risk stratification in 4 groups by the number of risk factors had a significant predictive value for OS, with patients having 0, 1, 2, and 3–4 risk factors demonstrating median OS intervals of 18.0, 11.7, 5.7, and 3.0 months, respectively ($p<0.001$).

Conclusion: Our risk stratification model can be used effectively in assessing the life expectancy of the HCC patient before initiating palliative RT for LN metastasis. Moreover, the presence of symptoms related to LN metastasis was shown to be the most powerful indicator of poor OS.

EP-1261

Impact of sarcopenia on adverse effects in trimodality therapy for esophageal carcinoma

C. Panje[1], L. Höng[2], G. Henke[2], T. Ruhstaller[3], M. Guckenberger[1], V. Baracos[4], L. Plasswilm[2]
[1]*University Hospital Zürich, Radiation Oncology, Zurich, Switzerland*
[2]*Kantonsspital St. Gallen, Radiation Oncology, St. Gallen, Switzerland*
[3]*Kantonsspital St. Gallen, Medical Oncology, St. Gallen, Switzerland*
[4]*University of Alberta, Oncology, Edmonton, Canada*

Purpose or Objective: Sarcopenia is a major hallmark of cancer cachexia and associated with increased treatment toxicity and worse overall survival in cancer patients. The aim of the study is to investigate the incidence and course of sarcopenia in patients undergoing curative trimodality therapy for locally advanced esophageal cancer and to correlate skeletal muscle mass with treatment complications during neoadjuvant treatment and surgery.

Material and Methods: A subset of 31 patients treated in a prospective trial for locally advanced esophageal cancer with induction chemotherapy, neoadjuvant chemoradiation and surgical resection were identified at two institutions and clinical data was analyzed for treatment-related adverse events and consequent additional hospitalizations. Skeletal muscle mass was obtained by a second analysis of staging CTs before, during and after curative trimodality therapy and analyzed based on previously established threshold values for sarcopenia.

Results: Fourteen patients (45%) were characterized as sarcopenic at the initial staging. Unplanned hospitalizations occurred significantly more frequently in sarcopenic patients (71% vs. 29%, $p = 0.03$) with a significantly longer total duration of hospital stay including postoperative stay (median 33.5 vs. 21.3 days, $p < 0.05$). During neoadjuvant therapy with a median duration of 3.5 months, patients showed a statistically significant reduction of of skeletal muscle mass of 10.1% ($p < 0.01$) resulting in an increase in the prevalence of sarcopenia from 45% to 74%.

Conclusion: CT-based assessment of sarcopenia demonstrates a significant decline of muscle mass during curative trimodality therapy for locally advanced esophageal cancer and can predict toxicity-related unplanned hospitalization. Based on these findings, CT-based measurement of muscle mass may serve as objective parameter to identify frail patients in need of intensified supportive therapy.

EP-1262

Survival and symptom relief after salvage radio(chemo)therapy for recurrent esophageal cancer

P.G. Kup[1], A. Gitt[1], H. Bühler[1], I.A. Adamietz[1], K. Fakhrian[2]
[1]*Marien Hospital Herne- Ruhr-University Bochum, Radiation Oncology, Herne, Germany*
[2]*Marienhospital Herne- Ruhr-University Bochum, Radiation Oncology, Herne, Germany*

Purpose or Objective: Loco-regional recurrence of esophageal cancer (REC) after initial treatment remains a dominant cause of death. Treatment options for REC are limited. This study was realized to assess the survival and symptom relief after salvage radio(chemo)therapy for recurrent esophageal cancer.

Material and Methods: Data from 259 patients from 3 centers were retrospectively reviewed to screen for eligible patients. 194 patients were excluded because of following criteria: 1) no pathologically confirmed squamous cell carcinoma or adenocarcinoma; 2) distant metastasis; 3) no dose-volume histogram (DVH) data available; 4) salvage resection after REC; 5) Brachytherapy in the initial or current treatment. Between January 1998 to December 2014 sixty-five patients with REC after curative intended treatment (primary RCT or surgical resection with or without neoadjuvant radiochemotherapy) met our inclusion criteria retrospectively. The recurrence was diagnosed by computed tomography (CT) and/or upper gastrointestinal endoscopy. The initial treatment was as follows: surgical resection in 47 patients (72%), neoadjuvant RCT (median 50,4Gy, range 45-50,4Gy) plus surgery in 12 (19%) patients or definitive RCT (median 60Gy, range 50,4-64 Gy) in 6 patients (9%). The median time to recurrence from initial treatment was 16 months (range 3-101 months).

Results: Median follow-up time for surviving patients was 27 months (5-150 months). The 1-year and 2-year survival rates were 58 ± 6% and 27 ± 6%, respectively. Subjective symptom relief was achieved in 25 of 34 symptomatic patients (74%). The most common toxicities were leukopenia, nausea, vomiting and gastritis. RT Doses ^{3} 50Gy and ECOG-PS (1-2 vs. 3) associated with better median survival time (MST) and prognosis, respectively ($p=0.003$;$p=0.001$).

Conclusion: Salvage radio(chemo)therapy for recurrent esophageal cancer is a reliable option in patients suffering from REC. In particular therapy of symptoms caused by the tumor can be managed by salvage-RCT. The toxicity is in an acceptable range. Long-term survival is possible in some patients.

EP-1263

Survival and symptom relief after palliative radiotherapy for esophageal cancer

P.G. Kup[1], J. Welsch[1], H. Bühler[1], H. Hermani[1], I.A. Adamietz[1], K. Fakhrian[1]
[1]*Marien Hospital Herne- Ruhr-University Bochum, Radiation Oncology, Herne, Germany*

Purpose or Objective: The aim of this study was to assess the 6-months dysphagia-free survival, improvement in swallowing function, complication rate, and overall survival in patients with incurable esophageal cancer treated with palliative radiotherapy.

Material and Methods: We retrospectively reviewed data from 139 patients (median age 72 years) with advanced/recurrent incurable esophageal cancer, who were referred to 3 German radiation oncology centers for palliative radiotherapy between 1994 and 2014. Radiotherapy consisted of external beam radiotherapy (EBRT) with 30 - 40.5 Gy/2.5 - 3 Gy per fraction, brachytherapy alone (BT) with 15 - 25 Gy/5 - 7Gy per fraction/weekly and EBRT + BT (30 - 40.5 Gy plus 10 - 14 Gy with BT) in 65, 46, and 28 patients, respectively. Dysphagia-free survival (Dy-PFS) was defined as the time to worsening of dysphagia for at least one point, a new loco-regional failure or death of any cause.

Results: Median follow-up time was 6 months (range 0.57-6.0 months). Subjective symptom relief was achieved in 72 % of patients with median response duration of 5 months. The 1-year survival rate was 30%. The 6-months Dy-PFS time for the whole group was 73 ± 4%. The 6-months Dy-PFS was 90 ± 4% after EBRT, 92 ± 5% after EBRT + BT and 37 ± 7% after BT, respectively ($p<0.001$). Five patients lived for more than 2 years, all of them were treated with EBRT ± BT. Ulceration, fistula and stricture developed in 3, 6 and 7 patients, respectively.

Conclusion: Radiotherapy leads to symptom improvement in the majority of patients with advanced incurable esophageal cancer. The present results favor EBRT ± BT over BT alone. Due to the retrospective nature of this study, imbalances in baseline characteristics might have contributed to this finding, and further trials appear necessary.

EP-1264

Patterns of recurrence in stage pT3N0M0 thoracic ESCC patients after two-field esophagectomy

Y.X. Wang[1], L.L. Wang[1,2], Z.S. Li[1], M. He[3], Q. Yang[1,4], J. Li[1], Z. Qi[3], S.C. Zhu[1], X.Y. Qiao[1]
[1]*The Fourth Hospital of Hebei Medical University, Department of Radiation Oncology, Shijiazhuang, China*
[2]*the People Hospital of Pizhou, Department of Radiation Oncology, Pizhou-Jiangsu Province, China*
[3]*The Fourth Hospital of Hebei Medical University, Department of Thoracic Surgery, Shijiazhuang, China*
[4]*Handan Central Hospital, Department of Radiation Oncology, Handan- Hebei Provincre, China*

Purpose or Objective: To evaluate patterns of recurrence and identifyits related factors among patients with Stage pT3N0M0 thoracic esophageal squmous cell carcinoma (ESCC) after two-field esophagectomy.

Material and Methods: 249 patients with Stage pT3N0M0 thoracic ESCC after radical esophagectomy administered in 2008 and 2009 were identified and enrolled into this study. There were 171 men and 78 women; median age was 60 years-old(33 – 78). The distributions of tumor sites were 39 in upper-, 166 in middle- and 44 in lower-thoracic segment. The median lesion length was 5 cm with a range of 2 to 12 cm. Among them, there were 98 patients received with surgery alone, 20 with radiotherapy (RT), 110 with chemotherapy alone (CT), and 21 with radiotherapy and chemotherapy (CRT). Their locoregional recurrence (LR) of tumor and distant metastasis (DM) as the endpoints were analyzed.

Results: The overall recurrence rates was 43.4% (108), LR occurred in 23.7%, DM in 10.4%, and combined recurrence in 9.2%, respectively. For 82 patients with LR, there were 15.9%(13/82) recurred in supraclavicular, 87.8% (72/82) in mediastinum, 9.8% (8/82) in upper abdomen. The rate of LR in upper-mediastinal and supraclavicular was 80%(66/82). The rate of LR were 53.8% in upper-, 33.1% in middle- and 13.6% in low-thoracic ESCC, respectively. Multivariate analysis indicate, site of lesion was the independent factors for total recurrence and LR.

Conclusion: The recurrence rate was very high in pT3N0M0 thoracic ESCC patients, LR was the mainly cause and most of it was occurred in supraclavicular and upper-mediastinum. Site of lesion was the mainly factor effected on LR. PORT should be strongly suggest in upper- and recommend in middle-, but not in low-thoracic ESCC.

EP-1265

Salvage chemoradiation for locoregional recurrences of esophageal cancer after curative treatment

P.M. Jeene[1], E. Versteijne[1], E.D. Geijsen[1], M.I. Van Berge Henegouwen[2], J.J.G.H.M. Bergmann[3], K. Muller[4], H.W.M. Van Laarhoven[5], M.C.C.M. Hulshof[1]
[1]*Academic Medical Center, Academic Radiotherapy, Amsterdam, The Netherlands*
[2]*Academic Medical Center, Academic Surgery, Amsterdam, The Netherlands*
[3]*Academic Medical Center, Academic Gastroenterology, Amsterdam, The Netherlands*
[4]*Radiotherapiegroep Deventer, radiation oncology, Deventer, The Netherlands*
[5]*Academic Medical Center, Academic Medical Oncology, Amsterdam, The Netherlands*

Purpose or Objective: Locoregional recurrence pattern after curative treatment for patients with esophageal cancer has changed since the introduction of preoperative chemoradiation as standard part of curative treatment. The aim of this study was to determine the outcome of salvage definitive chemoradiation (dCRT) for a locoregional recurrence outside previously irradiated areas.

Material and Methods: We retrospectively reviewed 41 patients treated between January 2005 and December 2014 for locoregional recurrent esophageal cancer outside previously irradiated areas. All patients were treated with external beam radiotherapy (50.4 Gy in 28 fractions) combined with weekly concurrent paclitaxel and carboplatin.

Results: The median follow up period was 30 months (range 1.7-120 months). dCRT was completed according to protocol in 90%. The 1-, 3- and 5-year overall survival rate after treatment for recurrence was 74%, 35% and 30% respectively . The median local recurrence free survival (LRFS) and overall survival (OS) time was 27 and 22 months respectively. Median OS was 14.4 months for squamous cell carcinoma (SCC) and 22.0 months for adenocarcinoma (AC) ($p=0.81$). Median survival after salvage dCRT for a lymph node recurrence was 48 months versus 14 months for a recurrence at the anastomosis ($p= 0.009$). Sixteen patients (39%) developed a locoregional recurrence after salvage dCRT, 8 out of 20 SCC and 8 out of 21 AC patients. Only 2 LR after salvage dCRT were solely outfield. In 8 of the 16 LR patients there were synchronous distant metastasis (43%).

Conclusion: Definitive chemoradiation is an effective treatment for recurrent esophageal cancer outside a previously irradiated area, and should be given with a curative intent. This holds true for recurrences of both squamous cell carcinoma and adenocarcinoma. Lymph node recurrences have a markedly better prognosis than recurrences at the anastomotic site. Locoregional failures after salvage treatment occur almost solely infield, at the site of the first recurrence.

EP-1266

Acute health-related quality of life changes after liver stereotactic ablative radiotherapy

H. Chung[1], J. Helou[1], I. Thibault[1], W. Chu[1], D. Erler[1], K. Chan[1], E. Chow[1], R. Korol[1], M. Davidson[1], L. Zhang[1]
[1]*Odette Cancer Centre - Sunnybrook Health Science, Radiation Oncology, Toronto, Canada*

Purpose or Objective: Stereotactic ablative radiotherapy (SABR) for liver metastases is currently accepted as a standard treatment option for patients with liver metastases. Multiple studies have demonstrated high rates of local control and low risk of serious toxicities. However, there is limited prospective patient-reported health-related quality of life data (HRQoL). Herein, we report the acute HRQoL changes in patients treated with SABR for liver metastases.

Material and Methods: A prospective study was performed to measure HRQoL changes in patients treated with SABR to 1-3 hepatic metastases. Doses of 30- 60 Gy in 3-5 fractions were delivered as per institutional policy depending on tumor location, histology and size. Changes in patients' self-reported HRQoL were measured using the European Organisation for Research and Treatment of Cancer (EORTC) Quality of Life Questionnaire–Core 15 Palliative (C15) at baseline (T0) and first follow-up (T1: 6 - 8 weeks post-SABR). The C15 consists of 15 questions; 2 multi-item symptom scales along with 5 single item symptom scales and a final overall QoL question. A significant change in HRQoL was defined as [T0 score-T1 score] > 0.5SD, where SD was the standard deviation of baseline values for each scale. For the overall QoL question, a significant change was defined by a 10-point or greater change from baseline.

Results: Fifty patients were included. Median age at treatment was 65 (40-88) years. Median BED10 was 98 Gy. The 4 most common primary sites of cancer were: gastro-intestinal (29), breast (9), renal cell (4) and lung (4). All patients were Child-Pugh score A. Nine patients had previous hepatectomies for liver metastases. Thirty-one patients had oligometastatic disease≤5(metastases) and 19 had oligoprogression ⩽5 metastases progressing). Forty -seven patients filled the C15 at T1 (94%). The majority of patients did not report a significant change in any of the C15 scales (table 1). For the overall QoL, 64% of the patients reported no significant change at T1, 24% had deterioration and 13% had an improvement.

	Significant Change from Baseline		
C15 Scales	No Significant Change	Improved	Worsen
Physical Functioning	32 (68.09%)	7 (14.89%)	8 (17.02%)
Emotional Functioning	31 (65.96%)	8 (17.02%)	8 (17.02%)
Overall QOL	16 (34.04%)	6 (12.77%)	25 (53.19%)
Pain	18 (38.30%)	16 (34.04%)	13 (27.66%)
Fatigue	26 (55.32%)	7 (14.89%)	14 (29.79%)
Nausea / Vomiting	38 (80.85%)	3 (6.38%)	6 (12.77%)
Appetite loss	34 (72.34%)	6 (12.77%)	7 (14.89%)
Dyspnoea	33 (70.21%)	8 (17.02%)	6 (12.77%)
Insomnia	22 (46.81%)	18 (38.30%)	7 (14.89%)
Constipation	33 (70.21%)	6 (12.77%)	8 (17.02%)
Specific Q7 Scale	30 (63.83%)	6 (12.77%)	11 (23.40%)

Conclusion: SABR offers a non-invasive option for liver metastases ablation. Acute patient-reported outcomes, as measured by C-15, for patients with liver metastases treated with SABR seem favourable. Longer follow-up is needed.

EP-1267

Induction chemotherapy followed by chemoradiotherapy in locally advanced pancreatic adenocarcinoma

J. Reure[1], J. Doyen[1], A. Falk[1], D. Lam Cham Kee[1], L. Evesque[1], P. Follana[1], E. François[1], K. Benezery[1]
[1]*Centre Antoine Lacassagne, Radiotherapy, Nice, France*

Purpose or Objective: Treating locally advanced pancreatic cancer (LAPC) remains a challenging issue. Chemotherapy or chemoradiotherapy alone have not demonstrated their efficacy. A strategy combining chemotherapy and chemoradiotherapy seems promising. Our retrospective analysis aims to evaluate effectiveness and tolerability of induction chemotherapy with Folfirinox followed by chemoradiotherapy in patients with LAPC.

Material and Methods: Nineteen patients treated for LAPC between Mars 2010 and February 2015 were retrospectively identified. These patients with unresectable disease, were initially treated with Folfirinox and then received a chemoradiotherapy with capecitabine or gemcitabine in case of stable disease. Survival was estimated with Kaplan Meier method.

Results: Median number of cycles achieved for Folfirinox was 5. Following chemotherapy, all patients had stable disease and received chemoradiotherapy with capecitabine (53%) or gemcitabine (47%). Majority of patients (63%) received radiotherapy at a dose of 50.4 Gray in 28 fractions. Toxicities are acceptable: three cases of grade 3 nausea / vomiting, three cases of grade 3 asthenia and three cases of grade 3 diarrhea were described during chemotherapy. No grade 3 toxicity was identified during chemoradiotherapy. The median follow-up time was 9 months (1-43 months). Survival rates were 93.8% at six months, 52.7% at 1 year and 21.1% at 2 years. Disease free survival rates were 35.3% at six months, 7.8% at 1 year and 0% at 2 years. Local recurrence free survival rates were 75.3% at six months, 47.3% at 1 year and 31.6 at 2 years. Distant recurrence free survival rates were 34.3% at six months, 18.3% at 1 year and 9.2% at 2 years. At the end of the therapeutic procedure, one patient received surgical resection.

Conclusion: Induction chemotherapy with Folfirinox followed by chemoradiotherapy in locally advanced pancreatic adenocarcinoma seems effective and allows very promising overall and progression free survival rates. Larger studies would be needed to conclusively confirm these observations.

EP-1268

Dosimetric parameters predict toxicity in chemoradiotherapy with nelfinavir for pancreatic cancer

D. Holyoake[1], J. Wilson[1], M. Partridge[2], T. Brunner[3], S. Mukherjee[4], M. Hawkins[1]
[1]*CRUK/MRC Oxford Institute for Radiation Oncology, Advanced Radiation Oncology Group, Oxford, United Kingdom*
[2]*CRUK/MRC Oxford Institute for Radiation Oncology, Radiotherapy Physics Research Group, Oxford, United Kingdom*
[3]*University of Freiburg, Department of Radiation Oncology, Freiburg, Germany*
[4]*Oxford University Hospitals NHS Foundation Trust, Department of Clinical Oncology, Oxford, United Kingdom*

Purpose or Objective: Gastrointestinal (GI) toxicity impedes dose escalation in radiotherapy for pancreatic cancer and limits local tumour control. Clinical data on tolerance doses for the organs of the proximal digestive system remain sparse. We analysed patterns of toxicity in patients treated with concomitant chemoradiotherapy (gemcitabine and cisplatin) with nelfinavir (hypoxia modifier) to identify associated dosimetric factors and establish predictive cut-off values to inform radiotherapy planning.

Material and Methods: Dose-volumes and acute toxicity data were analysed for 21 patients treated for locally-advanced pancreatic cancer in a prospective phase II clinical trial (ARCII, EudraCT 2008-006302-42). Radiotherapy comprised 50.4Gy in 28 daily fractions to the tumour and elective lymph nodes followed by a sequential boost to the primary tumour of 9Gy in 5#. Univariate analysis was performed to investigate association of the dose-volume received by stomach and duodenum with RTOG upper GI toxicity symptoms, and of small-bowel with diarrhoea. Receiver Operating Characteristic analysis was used to identify

strongest predictive factors and to derive optimum cut-off values for predicting likelihood of toxicity incidence.

Results: Grade ≥2 acute RTOG upper GI toxicity attributed to treatment was seen in 11 patients (52%), grade ≥3 in 3 (14%); grade ≥2 diarrhoea was recorded in 3 patients (14%), grade ≥3 in 2 (10%). In patients who experienced grade ≥2 toxicity, stomach V15-55 Gy (absolute volume of stomach receiving 15-55 Gy, in cm3) were significantly larger when compared to those without ($p<0.05$, Mann-Whitney). Differences in V35 Gy and V40 Gy remained significant after Bonferroni correction ($p<0.004$) and ROC analysis was performed to identify the most predictive cut-off values: V35 Gy 55.7cm3 and V40 Gy 43.6 cm3 (both sensitivity 0.82, specificity 0.80, Youden index = 0.62). Significant associations were not seen between duodenal dose-volume and acute toxicity, nor between small-bowel dose-volume and incidence of treatment-related diarrhoea.

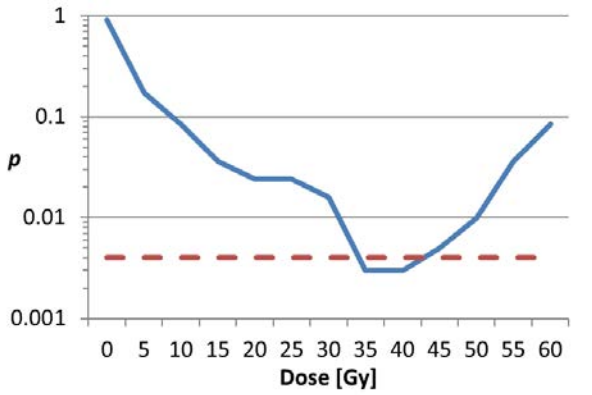

Figure. Results of Mann-Whitney comparison of stomach dose-volume according to grade ≥2 toxicity, showing that $V_{35\,Gy}$ & $V_{40\,Gy}$ are statistically significant predictors

Conclusion: In concomitant chemoradiotherapy with nelfinavir for pancreatic cancer, stomach dosimetric parameters were associated with clinically important acute radiotherapy toxicity and thresholds were derived for predicting toxicity risk. Stomach V35 Gy and V40 Gy were most strongly predictive of acute grade ≥2 side effects.

EP-1269

Dose tolerance of small bowel in patients treated with radiochemotherapy for pancreatic cancer

L. De Filippo[1], G.C. Mattiucci[1], N. Dinapoli[1], M. Boccardi[2], V. Pollutri[1], M. Bianchi[1], R. Canna[1], S. Chiesa[1], G. Macchia[2], A. Morganti[3], V. Valentini[1]

[1]*Università Cattolica del Sacro Cuore -Policlinico A. Gemelli, Radiotherapy Division, Rome, Italy*

[2]*Fondazione di Ricerca e Cura Giovanni Paolo II-Università Cattolica S. Cuore, Department of Radiotherapy, Campobasso, Italy*

[3]*Department of Experimental- Diagnostic and Specialty Medicine - DIMES - University of Bologna- S.Orsola-Malpighi Hospital, Radiation Oncology Unit, Bologna, Italy*

Purpose or Objective: Tolerance of small bowel is the dose limiting factor in radiation therapy for abdominal neoplasms. Bowel constraints for treatment planning in abdominal radiotherapy derive from scientific publications of pelvic tumors. This study has the aim to evaluate dose tolerance of small bowel detecting acute toxicities in patients with pancreatic cancer treated with radiochemotherapy.

Material and Methods: Patients with pancreatic cancer were treated between 2009 and 2014 with 3D-conformal radiotherapy with a total dose of 5040 cGy and conventional fractionation. Chemotherapy with gemcitabine or fluoropyrimidine was simultaneously administered. Nausea, vomit and loss of weight, as acute upper gastrointestinal (GI) toxicities, were scheduled using RTOG scale. In all patients small bowel loops and bowel sac were contoured using QUANTEC guidelines and DVHs were analyzed for this structures using R statistical software (http://www.R-project.org).

Results: Forty-three patients with a median age of 66 years (range 42-79), 14 resected and 29 unresected, were analyzed. Fourteen (32%) patients reported no upper GI toxicity; on 8 (19%), 12 (28%) and 9 (21%) patients were observed respectively grade 1, 2 and 3 toxicity. No grade 4 toxicity was recorded. Nineteen patients discontinued radiotherapy but all of them completed the treatment. Analyzing V Dose on DVHs by logistic regression, small bowel loops V36 Gy resulted as the parameter which most influenced upper GI G1 or higher Toxicity ($p<0.05$). Multivariate analysis showed no impact of surgery on upper GI toxicity.

Conclusion: Our preliminary analysis suggests that new constraints for radiochemotherapy in upper GI cancer could be upgraded. Our study has to be confirmed on a larger sample.

EP-1270

SBRT for liver metastases from low grade neuroendocrine tumors

M. Bignardi[1], A. Huscher[1], M. Centurioni[1], M.M. Colangione[1], D. Barbieri[1], M. Galelli[2], A. Zaniboni[3]

[1]*Fondazione Poliambulanza, Radiation Oncology Unit, Brescia, Italy*

[2]*Fondazione Poliambulanza, Medical Physics, Brescia, Italy*

[3]*Fondazione Poliambulanza, Oncology Department, Brescia, Italy*

Purpose or Objective: Specific results of SBRT for liver metastases from rare tumors have been reported scarcely. This applies also to metastases from low grade neuroendocrine tumors (NET), either derived from gastrointestinal organs or from an unknown primary site. Here we report two cases of multiple liver metastases from low grade NET repeatedly treated by means of SBRT, achieving the outcome of long-term local control.

Material and Methods: From March 2011 to September 2015 49 SBRT courses were delivered to 39 patients for liver metastases from different primaries. All courses were given by VMAT with 6 MV photons, image guided by CBCT in every fraction. Since 2013, deep inspiration breath hold was adopted in order to control organ motion. Two patient had metastases from well differentiated neuroendocrine tumors, one from an unknown primary (patient A), the other from a pancreatic primary (patient B). Patient A underwent two SBRT courses, both in 2011, the first one on segment 6 (CTV volume 25 ml, CTV dose 75 Gy, PTV 50 Gy, in 3 fractions), the second one on two adjacent metastases, respectively in segment 7 and 8 (total CTV volume 54 ml, CTV dose 60 Gy, PTV 50 Gy, in 3 fractions).Patient B received three courses, respectively in 2013, 2014 and 2015. The first SBRT was delivered on segment 6 (CTV volume 38 ml, CTV dose 50 Gy, PTvV45 Gy, in 5 fractions), the second on segment 8 (CTV volume 30 ml, CTV dose 50 Gy, PTV 45 Gy, in 5 fractions), the last on segment 4 (CTV volume 44 ml, CTV dose 50 Gy, PTV 45 Gy, in 5 fractions). Patient A was found to be somatostatine receptor-negative, thus he was followed up mainly by serial CT scans; also, his disease status matched well to trends of two biomarkers (chromogranin A and gastrin). Patient B was followed up by alternating CT scans and PET/CT-68Ga-DOTATOC.

Results: At last follow up patient A achieved long-term local control in S6 metastasis (45 months) as well as in S7-8 (42 months), while showing disease progression at a new liver site at 45 months after first SBRT. At last follow up patient B achieved local control in all sites (S6: 30 months; S8: 13 months; S4: 6 months) with a durable partial PET response in S8 and S4 and a complete PET response in S6. Disease progression took place in two bone sites at 30 months after first SBRT, without any concomitant liver progression.

Conclusion: these favorable results in large volume liver metastases from low grade NET, although derived from only two anedoctal cases, give support to the concept that the outcome of SBRT is relatively independent from tumor type, being mainly mediated by an ablative effect. Also they represent a typical example showing how repeat liver SBRT may lead to a a significant delay in disease progression although without achieving a definitive cure.

EP-1271

Stereotactic body radiation therapy for malignant tumours of the pancreas

X. Chen[1], E. Sanchez[1], A. Montero[1], O. Hernando[2], M. Lopez[1], J. Garcia[3], J.M. Perez[4], R. Ciervide[1], J. Valero[1], M. Garcia-Aranda[1], R. Alonso[2], D. Zucca[3], M.A. De la Casa[3], B. Alvarez[1], S. Payano[1], J. Marti[3], L. Alonso[4], P. Fernandez-Leton[3], C. Rubio[1]

[1]Hospital Universitario HM Sanchinarro, Radiation Oncology Department, Madrid, Spain
[2]Hospital Universitario HM Puerta del Sur, Radiation Oncology Department, Madrid, Spain
[3]Hospital Universitario HM Sanchinarro, Medical Physics Department, Madrid, Spain
[4]Hospital Universitario HM Puerta del Sur, Medical Physics Department, Madrid, Spain

Purpose or Objective: To review stereotactic body radiation therapy (SBRT) safety and local control utility in malignant tumor of the pancreas based in a single center experience since February 2014.

Material and Methods: A systematic review was done. Thirteen patients were treated with SBRT. Eleven patients had a primary pancreatic tumor and two patients had metastatic affectation of the pancreas. In those patients with primary pancreatic cancer, four patients were treated with a radical intent, five as a part of a neoadjuvant treatment and four patients with a palliative intent. All of the treated tumors had a diameter bigger than 2 cm. At least 2 fiducials were located into the tumor, guided by endoscopic ultrasound. All the treatments included CT or PET-CT for GTV delineation, intensity-modulated radiation therapy (IMRT) and image-guided radiation therapy (IGRT) with intrafraction control of tumor motion with a Novalis Exactrac Adaptive Gating System. 50 Gy in 10 fractions were prescribed in eleven patient, one patient was treated with 35Gy in 5 fractions and one patient was treated with 40Gy in 10 fraction.

Results: Pancreatic SBRT was very well tolerated in our cohort of patients. No grade 3 or higher toxicity was observed. Only 3 patients developed grade 2 epigastric pain and/or grade 2 nausea/vomiting. The median patient age was 62 years old (range 36 – 86 years) and the median follow-up was 14 months (range 2 – 18 months). Five patients under went surgery after SBRT. The median overall survival was 14.5 months (range 2.4 – 18.2 months), with 65.3% survival at one year. Median survival time is 15 month (range 12 – 17 months). Median time to local progression has not been reached.

Conclusion: In our experience, gating SBRT for pancreatic tumor is a well-tolerated feasible treatment. Most patients are free from local progression, but overall survival remains poor. Prospective studies are needed to define the role of SBRT for pancreatic tumors.

EP-1272

Stereotactic radiotherapy in pancreatic cancer. Review of two different treatment approaches

E. Gkika[1], S. Kirste[1], S. Adebahr[1], T. Schimek-Jasch[1], R. Wiehle[1], K. Zirlik[2], U. Wittel[3], U. Nestle[1], A.L. Grosu[1], T. Brunner[1]

[1]Uniklinik Freiburg, Radiation Oncology, Freiburg, Germany
[2]Uniklinik Freiburg, Medical Oncology, Freiburg, Germany
[3]Uniklinik Freiburg, Departmet of Surgery, Freiburg, Germany

Purpose or Objective: Stereotactic body radiotherapy (SBRT) in pancreatic cancer can be limited by its proximity to critical organs at risk (OAR) of the upper abdomen. In this study we evaluate the toxicity and efficacy of two different treatment approaches.

Material and Methods: Patients with recurrent or oligometastatic pancreas cancer were treated with SBRT. The planning target volume (PTV) was created through a 4 mm expansion of the internal target volume (ITV) based on a four dimensional CT (4D-CT). All patients were treated with intensity modulated radiation therapy (IMRT). In some cases we created a sub-volume, in order to reduce the risk of toxicity in critical adjacent OARs without compensating the whole PTV. This sub-volume was defined as a simultaneous integrated protection (SIP) PTV. The SIP consisted of the interface of the PTV with the planning risk volume (PRV) of a specific vulnerable structure at which we prescribed a pre-defined reduced dose.

Results: Between 2009 and 2014, 18 patients with 23 lesions were treated in our institution. Seven patients were treated for a local recurrence, nine were treated for oligometastases (liver, lymph nodes) and two patients were treated for both. Of these lesions 11 were treated with SIP and 12 were treated without SIP. The median follow up was 10.8 months (range 1.2-40.3 months). The freedom from local progression (FFLP) at 6 and 12 months was 90% and 84% respectively. The overall survival (OS) rates at 6 months and 12 months after SBRT were 77% and 54%, respectively. Two patients (11%) experienced grade >3 acute toxicity (mechanical ileus, gastrointestinal bleeding) and 2 patients (11%) experienced a grade > 3 late toxicity (cholangitis, bleeding).

Conclusion: Local control and overall survival after SBRT in this high risk group of patients with pancreatic cancer were excellent despite of dose sacrifice in half of the patients when OARs were close to the PTV, with overall favourable toxicity.

EP-1273

Clinical results of stereotactic ablative radiotherapy in the treatment of liver metastases

M. Fiore[1], P. Trecca[1], L. Trodella[1], C. Rinaldi[1], P. Matteucci[1], S. Silipigni[1], A. Iurato[1], S. Ramella[1], R. D'Angelillo[1], L. Trodella[1]

[1]Università Campus Biomedico, Department of Radiation Oncology, Roma, Italy

Purpose or Objective: To evaluate the efficacy and feasibility of stereotactic ablative radiotherapy (SABR) in the treatment of liver metastases.

Material and Methods: We retrospectively analyzed patients with 1-2 secondary liver lesions treated with SABR. The total dose prescriptions were 30 Gy, 37.5 Gy and 45 Gy on three consecutive days in 42.8%, 22.8% and 34.4% of patients respectively. The dose was prescribed to the 80% isodose line covering the PTV. The primary endpoints were in field local control and toxicity; the secondary endpoint was survival rates.

Results: Between March 2007 and May 2015, 30 patients (17 males, 13 females) with 36 liver metastases were treated. The mean age was 66 years (range, 40-90 years). Twenty-five patients (83.3%) had a single hepatic lesion and the remaining 5 patients (16.7%) two hepatic lesions. Twenty patients (64.5%) had extrahepatic stable disease. The most frequent sites of primary tumor were colorectal (58%) and breast (20%). The majority of the lesions treated (75.6%) had a diameter of less than 3 cm. With a median follow-up of 21 months (range 2.3-69.8 months) for all patients, "in field" local response rate was 90%. No patient developed a toxicity greater than grade 2 according to CTC scale v4.02 and no radio-induced liver disease (RILD) was recorded. One-year LC and two-year LC were 62% and 39% respectively. One-year and two-year PFS were 46% and 25% (median, 11 months). One-year, two-year and three-year OS were 89%, 69 and 42%

respectively, with a median survival time, calculated from the date of metastasis and last follow-up or death, of 29.8 months.

Conclusion: These data suggest that stereotactic ablative radiotherapy (SABR) is a safe, non-invasive and effective option in the treatment of liver metastases.

EP-1274

Prognostic factors of gastric cancer treated with adjuvant radiochemotherapy

M. Martin Sanchez[1], M.A. Perez Escutia[2], M.C. Peña Sanchez[2], D. Lora Pablos[3], S. Guardado Gonzalez[2], S. Pedraza Fernandez[2], T.C. Chavez Jimenez[2], A. Moreno Hurtado[4], M. Casado Jimenez[5], J.P. Perez-Regadera Gomez[2]
[1]*Hospital Ramón Y Cajal, Radiation Oncology, Madrid, Spain*
[2]*Hospital 12 De Octubre, Radiation Oncology, Madrid, Spain*
[3]*Hospital 12 De Octubre, Investigation, Madrid, Spain*
[4]*Grupo Imo, Radiation Oncology, Madrid, Spain*
[5]*Hospital De La Princesa, Radiation Oncology, Madrid, Spain*

Purpose or Objective: The aim of this study was to investigate the outcome and prognostic factors for patients with locally advanced gastric cancer (LAGC) treated with adyuvant radiochemotherapy, according Macdonald scheme.

Material and Methods: Between May 2004 and October 2014, a total of 106 patients, 70 men and 36 women, with locally advanced gastric cancer were treated in the University Hospital 12 de Octubre, Spain. The mean age was 57 years .The mean follow-up was 96.48 months. The most common tumor location was antrum (29.25%). The majority of tumors were T3 (52.83%) or T4 (22.64 %) and 86.79 % had nodal metastases, with an average of 8.24 nodes involved. Predominant histological subtype was diffuse (43.4%) and poorly differentiated (grade 3, 50%). Complete resection (R0) was achieved 84.91%, whereas microscopic residual disease (R1) was found in 13.21%. Survival was calculated by Kaplan-Meier and method and differences were assessed by the Log-rank test. Multivariate analysis was used Cox proportional hazards regression model.

Results: A total of 50 (47.16 %) patients relapsed; 16 (15.09%) locoregional, 13 (12.26%) peritoneal, 18 (16.98%) distant metastases and 3 (2.83%) unknown. The overall survival (OS), disease-free survival (DFS), locoregional failure-free survival (LFS) rates to three years were 48.75%, 46.27% and 76.72% and to five years were 32.11%, 38.78%, 69.67% respectively. In univariate analysis, T stage (T1-T2), N negative stage and R0 resection were associated with better survival ($p<0.05$) for OS and only N negative stage for DFS and LFS. In the multivariate analysis indentified only R0 resection as an independent predictor of better survival ($p<0.05$) for OS and DFS.

Conclusion: In this study, the prognostic factors associated with better survival in patients with LAGC treated with adyuvant radiochemotherapy were: T stage (T1-T2), N negative stage and R0 resection ($p< 0.05$). Complete R0 resection also can be considered as independent prognostic factor of better survival ($p<0.05$)

EP-1275

Influence of pretreatment blood parameters on the outcome of gastric cancer patients.

A. Namysl-Kaletka[1], J. Wydmanski[1], A. Tukiendorf[2], E. Wolny-Rokicka[3], I. Wzietek[1], D. Gabrys[1]
[1]*Maria Skłodowska-Curie Memorial Cancer Center and Institute of Oncology- Gliwice Branch- Poland., Radiotherapy Department, Gliwice, Poland*
[2]*Maria Skłodowska-Curie Memorial Cancer Center and Institute of Oncology- Gliwice Branch- Poland., Department of Epidemiology and Silesia Cancer Registry, Gliwice, Poland*
[3]*Karol Marcinkowski Regional Hospital, Department of Radiotherapy, Zielona Góra, Poland*

Purpose or Objective: Activation of coagulation and fibrinolysis are found among gastric cancer patients. The ones with non-metastatic gastric cancer are at risk for thrombotic events due to the combined increase in fibrinogen plasma levels and thrombin formation. It could be associated with a higher risk of local invasion and might be important poor predictive and prognostic factor. In our study, we sought the associations between blood parameters and outcome

Material and Methods: The study examined eighty-nine patients with biopsy-proven, operable gastric adenocarcinoma, with no evidence of distant metastases. Pre-operative fibrinogen, PT, APTT and INR levels were measured before surgery . Complete blood count were also collected before initiation of therapy . All patients underwent surgery as a primary treatment. The survival function was computed using Kaplan-Meier method. The overall survival (OS), Diseases- free survival (DFS), time to distant metastases (DM) and locoregional control (LRC) were calculated from the date of surgery. Multivariate analyses and characteristic (ROC) have been done.

Results: In Multivariate Cox analysis higher level of WBC was associated with worse local control ($p=0,0024$), and shorter overall survival ($p=0,0035$). Shorter Prothrombin Time was correlated with better overall survival ($p=0,0280$). Higher Fibrinogen level has caused better local control ($p=0,0280$). No other correlation between DFS, LRC, DM and OS and other blood parameters were observed in multivariate analyses.

Conclusion: The level of White Blood Cells, Fibrinogen and Prothrombin Time were found to be useful prognostic factor which influenced overall survival and local control. However, further prospective investigations are necessary to assess the predictive value of those factors.

EP-1276

Stereotactic robotic body radiotherapy for patients with unresectable hepatic oligometastases.

P. Berkovic[1], P. Viet Nguyen[1], A. Gulyban[1], D. Dechambre[1], P. Martinive[1], N. Jansen[1], P.A. Coucke[1]
[1]*C.H.U. - Sart Tilman, Radiotherapy Department, Liège, Belgium*

Purpose or Objective: To evaluate the feasibility, efficacy and toxicity of robotic SBRT for the treatment of unresectable hepatic oligometastases.

Material and Methods: Between 09/2010 and 01/2013, 15 consecutive patients (12 female, 3 male, median age at treatment: 70.5, range: 57-85 years) with up to 3 synchronous or metachronous hepatic oligometastases were referred for Cyberknife treatment (Accuray Incorporated, Sunnyvale, CA) at our center. In order to enable tumor tracking, gold fiducial markers were inserted around the lesion 2 weeks prior to each treatment. The treatment was delivered using the Synchrony Respiratory Tracking System to continuously track fiducial position and adjust for respiratory motion during treatment. Treatment planning was performed using the Multiplan TPS (v4.6, Accuray) with Raytracing algorithm, and was retrospectively recalculated using a Monte Carlo dose calculation algorithm (v5.1). The primary endpoint of this study was local control (LC), assessed with either contrast enhanced spiral CT or MRI. Secondary endpoints were liver and distant progression free-survival (liverPFS and DFS), overall survival (OS) and treatment toxicity, evaluated using the Common Terminology Criteria for Adverse Events v4.0. (Institute NC, NIH publication 2009). Statistical analysis was performed using R software (3.1.1, R Development Core Team 2010).

Results: A total of 20 metastatic lesions were treated from primary colorectal (7), breast (7), unknown primary (3), melanoma (2) and stomach (1) cancer. The mean GTV and PTV volumes were 23.8cc (Standard deviation (SD):23) and 74.5cc (SD:45.3) respectively. All treatments were delivered 3x/week in a median three fractions (range: 3-6) to a median dose of 45 Gy (range: 30-45), prescribed to the 80% isodose line. This corresponds to an equivalent 2-Gy dose of 93.75Gy,

when considering a α/ß ratio of 10. The mean GTV and PTV D98% and D50% were 41.6Gy (SD:7.7) and 46.5Gy (SD:6.8) ,39.3Gy (SD:7) and 46.1Gy (SD:6.6) respectively. Each treatment was delivered by an average of 158 beams. All dose constraint parameters proposed by Timmerman were respected (Semin.Radiat.Oncol.2008). Furthermore, the average difference between the Raytracing and the Monte Carlo algorithm was 0.43% on these values. At a median follow up of 30.9 months (range: 5.7-50.3), the 1 and 2-year LC rates remained stable at 83.5%.The 1 and 2-year liver PFS and the DFS rates were 57.1%, 46.1% and 75.5%, 64.4% respectively. The 2 year OS was 60.6% (Figure 1). No acute grade 2 toxicities were observed. Three patients reported late grade 2 gastro-intestinal toxicities. No late grade 3 nor 4 toxicities were reported.

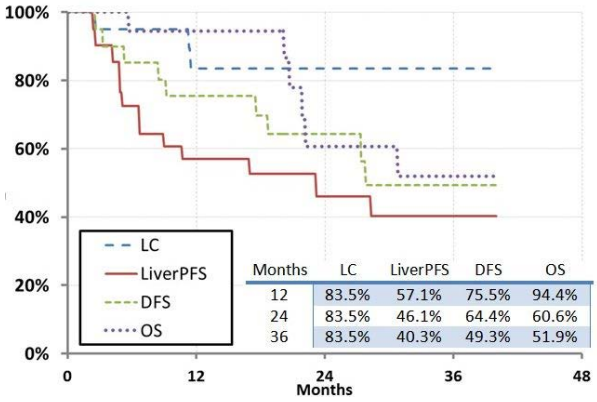

Months	LC	LiverPFS	DFS	OS
12	83.5%	57.1%	75.5%	94.4%
24	83.5%	46.1%	64.4%	60.6%
36	83.5%	40.3%	49.3%	51.9%

Conclusion: Robotic SBRT is feasible, safe and very well tolerated for the treatment of hepatic oligometastases. Our outcome results compare favorably from previous published studies of SBRT. It could represent a valid treatment option in the multimodality treatment of unresectable hepatic oligometastases.

EP-1277

Adyuvant chemoradiation for resected gallbladder cancer: single center 25-year experience

C. Solé[1], V. Solé[2]
[1]*Instituto de Radiaciones Médicas, Radiotherapy, Santiago, Chile*
[2]*Universidad San Sebastian, Medicine School, Santiago, Chile*

Purpose or Objective: Patients with locally advanced gallbladder cancer (LAGC) have a dismal prognosis. We investigated outcomes and risk factors for overall survival (OS) in patients treated with radical surgery and adyuvant chemoradiotherapy (CRT).

Material and Methods: A total of 212 patients with LAGC [⩾cT3 59% and/or cN+ 52%) were studied. For survival outcomes potential associations were assessed in univariate and multivariate analyses using the Cox proportional hazards model. We constructed a risk scoring system in which points were assigned to each risk factor by dividing each ß coefficient in the final model by the lowest ß coefficient and rounding to the nearest integer.

Results: Median follow-up was 46.2 months (2-235). Five-year OS for the entire cohort was 50.2%. In multivariate analysis higher pT stage [HR 1.73, p = 0.01], R1 resection [HR 5.06, p < 0.01], and number of surgical procedures [HR 1.41, p = 0.05] were associated with an increased risk of death. A risk model was generated to determine a prognostic index for individual patients with LAGC.

Conclusion: Overall results after multimodality treatment of LAGC are promising. Classification of risk factors for death has contributed to propose a prognostic index that could allow us to guide risk-adapted tailored treatment

EP-1278

CCRT with or without surgery using Helical Tomotherapy or IMRT for esophageal cancer patients

P.Y. Hou[1], W. Le-Jung[1], H. Chen-Hsi[1], S. Pei-Wei[1]
[1]*Far Eastern Memorial Hospital, Radiation Oncology, New Taipei City, Taiwan*

Purpose or Objective: To retrospectively review the treatment outcome of esophageal cancer in our hospital, and compare the radiotherapy efficacy and toxicity of helical tomotherapy with step-and-shoot Intensity Modulation Radiation Therapy (IMRT).

Material and Methods: Between 2007 and 2012, 108 consecutive patients with locally advanced esophageal cancer, cT2-4N0-3M0-1, received neoadjuvant concurrent chemoradiotherapy (CCRT) followed by esophagectomy or definitive CCRT treatment course respectively. The radiotherapy was delivered with helical tomotherapy in 56 patients, and with conventional IMRT in other 52 patients. We had evaluated outcomes with radiation dose, overall survival rate (OS), disease-free survival rate (DFS), and toxicity of radiation pneumonitis.

Results: The median follow-up duration was 16 months. The median time of overall survival among all patients was 15 months. The treatment modality with neoadjuvant CCRT followed by esophagectomy had favorable OS (47.6% : 10.4%, p = 0.014), DFS (42.9% : 23.9%, p = 0.013), and local recurrence (33.3% : 50.7%, p = 0.574) comparing with definitive CCRT. No significant difference outcome of OS was found between tomotherapy and conventional IMRT. The patients using tomotherapy had less incidence and severity of radiation pneumonitis (only one patient with less than grade 3 radiation pneumonitis in tomotherapy group; 5 patients < grade 3 and 2 patients > grade 3 radiation pneumonitis in conventional IMRT group).

Conclusion: In our study, the treatment outcomes of neoadjuvant CCRT followed by esophagectomy for esophageal cancer are better in OS, DFS, and local control than definitive CCRT. Tomotherapy may reduce lung dose, and probably reduce incidence and severity of radiation pneumonitis when compared with conventional IMRT.

EP-1279

SABR in inoperable liver oligometastatic patients and radioresistant primary tumors.

E. Clerici[1], T. Comito[1], L. Cozzi[1], A. Fogliata[1], A. Tozzi[1], C. Iftode[1], C. Franzese[1], P. Navarria[1], G.R. D'Agostino[1], P. Mancosu[1], F. Lobefalo[1], S. Tomatis[1], M. Scorsetti[1]
[1]*Istituto Clinico Humanitas, Radiotherapy and Radiosurgery, Rozzano Milan, Italy*

Purpose or Objective: To evaluate the feasibility and efficacy of Stereotactic Ablative Body Radiotherapy (SABR) in the treatment of liver metastases from radioresistant primary tumors.

Material and Methods: Patients with inoperable liver metastases from renal cancers, melanoma and sarcomas, not amenable to other locoregional therapies, treated with SABR were included in this retrospective study. Inclusion criteria were: Karnofsky Performance Status of 70; no evidence of progressive or untreated gross disease outside the liver; maximum tumor diameter less than 6 cm; no more than 3 liver lesions; normal liver volume greater than 1000 cm3; adequate liver function. Dose prescription ranged from 75 to 50.26Gy in 3 consecutive fractions, delivered with RapidArc VMAT, with 10MV FFF photons. Local control was defined according to RECIST criteria.Toxicity was classified according to the Common Toxicity Criteria (CTC) version 3.0.

Results: From April 2010 to October 2015, 20 patients were treated with SABR for a total number of 24 lesions. Median follow-up was 21 (range 6–58) months. In field progression was observed in 1 patient for a total of 2 lesions. One and 2

years actuarial local control (LC) rates were 100% and 88%, respectively. Median overall survival (OS) was 24 months. Actuarial OS rates at 1 and 2 years were 83% and 38%, respectively. Median progression-free survival (PFS) was 7 months. No patients experienced radiation-induced liver disease (RILD) or grade >3 toxicity.

Conclusion: SABR is an effective, safe and non-invasive alternative for the treatment of inoperable liver metastases from radioresistant tumor.

Electronic Poster: Clinical track: Lower GI (colon, rectum, anus)

EP-1280

Preoperative short vs. long course chemoradiation with delayed surgery for rectal cancer patients

M.J. Chung[1], W.K. Chung[1], D.W. Kim[1], S.H. Lee[2], S.K. Jeong[3], J.K. Hwang[4], C.S. Jeong[5]

[1]*Kyung Hee University Hospital at Gangdong, Department of Radiation Oncology, Gangdong-Gu- Seoul, Korea Republic of*

[2]*Kyung Hee University Hospital at Gangdong, Department of Surgery, Gangdong-Gu- Seoul, Korea Republic of*

[3]*Yang Hospital-Seoul, Department of Surgery, Seoul, Korea Republic of*

[4]*Yang Hospital- Namyangju, Department of Surgery, Seoul, Korea Republic of*

[5]*Hansol Hospital, Department of Surgery, Seoul, Korea Republic of*

Purpose or Objective: To compare the clinical outcomes between short course chemoradiotherapy (SCRT) and long course chemoradiotherapy (LCRT) with delayed surgery for locally advanced rectal cancer patients retrospectively.

Material and Methods: Seventy two patients, staged cT3-4N0-2M0, had participated in a multicenter study. With regard to the SCRT arm, a total dose of 25 Gy of radiotherapy was delivered in 5 fractions and chemotherapy was given on days 1-3 and delivered 5-Fluouracil and Leucovorin 400mg/m²by bolus injection on day 1 and 5-Fluouracil 1200mg/m²by continuous infusion on day 2 and 3. And additional two cycles of chemotherapy was administered before the surgery. With regard to the LCRT arm, a total dose of 50.4Gy of radiotherapy was delivered in 28 fractions. Chemotherapy was a bolus injection of 5-Fluouracil and leucovorin for the first and last week of radiotherapy. Surgery was performed during 6 - 8 weeks after completion of the radiotherapy in the both group.

Results: From 2010 to 2015, 19 patients were treated using the SCRT and 53 patients were treated using the LCRT. Median Follow-up was 25.0 months (range, 3.0-58.0 months). The patient characteristics of the both arms were not significantly different. The sphincter saving rate (89.5 %, 94.3%), complete remission (21.1%, 13.2%), downstaging (47.4%, 26.4%), treatment complications including wound dehiscence, bowel adhesion, hematologic toxicities of the SCRT were not inferior results to those of the LCRT. Locoregional recurrence was seen in 1 (5.3%) patients in the SCRT, 1 (1.9%) in the LCRT (p=0.442). Distant metastasis was ween in 1 (5.3%) patients in the SCRT, 12 (22.6%) patients in the LCRT (p=0.162). The 2-year disease free survival, overall survival in the SCRT and LCRT arms were 93.8% and 74.0% (P =0.338), 90.0% and 91.2% (P =0.448), respectively.

Conclusion: The preopeative SCRT was a effective and safe modality. We got a comparable clinical outcomes to the LCRT for locally advanced rectal cancer. We get a further study for randomized clinical study to compare between SCRT and LCRT.

EP-1281

DVH relationships in rectal cancer: effects of contouring methods and patient positioning

N. Bennion[1], Y. Lei[1], V. Verma[1], A. Bhirud[1], G. Blessie[1], C. Lin[1]

[1]*UNMC, Radiation Oncology, Omaha, USA*

Purpose or Objective: Preoperative chemoradiation for rectal cancer may cause acute bowel toxicity. Efforts to reduce such side effects include tracking bowel DVH relationships and proper patient positioning to minimize the risks. Our aim is to quantify volume and DVH relationship differences between prone and supine positioning as well as compare different contouring methods to account for such changes.

Material and Methods: Nineteen patients undergoing preoperative chemoradiation for rectal cancer were simulated supine and prone for plan comparison. Thirty-eight plans were compared, 19 prone, and 19 supine. Correlating prone and supine plans were constructed with similar target volumes, beam energies and arrangements. A single physician contoured the bowel bag (BB) and individual bowel loops (BL) with the superior border 1 cm above the PTV per RTOG guidelines. If the RTOG recommended boundaries fell short of the 5 Gy isodose line, additional CT slices were contoured on BB and BL structures to the 5 Gy isodose line and labeled as extended contours. Tabular dose-volume histograms were utilized to assess the volume of bowel receiving 5-50 Gy in 5 Gy intervals. Wilcoxon signed rank test as well as Spearman's correlation tested all variables.

Results: The target volumes showed no statistical differences between supine and prone positioning (p = 0.7344, 0.8203, 0.3594). The median reduction in volumes from supine to prone contours for the extended contour BB, extended contour BL, RTOG BB, and RTOG BL was 316 cc, 156 cc, 324 cc, and 115 cc respectively. Wilcoxon signed rank sum test showed significantly reduced volumes at each dose level (5-45 Gy at 5 Gy intervals) in the prone group compared to supine (range p = 0.0039- 0.0391). All combinations of contours (RTOG and extended contours of BB and BL) showed similar statistically significant reductions in volumes receiving each dose (except 50 Gy) in the prone position. All RTOG defined BB and BL volumes required additional contours to account for the entire volume receiving 5 Gy. RTOG contours required a median of 359 cc to the BB (range 209-1375 cc) and 113 cc to BL (range 37-271 cc).

Conclusion: Volume of bowel was less for nearly all dose levels (5 – 45 Gy) if the patient was positioned prone. Bowel loop contours correlated with bowel bag contours; suggesting they can be used interchangeably. BB and BL contoured volumes, by the RTOG definition, consistently fell short of the 5 Gy isodose line where the "extended contours" were a more complete DVH representation.

EP-1282

Does blood glucose level normalisation improve PET-based response prediction in rectal cancer?

I. Joye[1], A. Debucquoy[2], A. Wolthuis[3], A. D'Hoore[3], E. Van Cutsem[4], V. Vandecaveye[5], X. Sagaert[6], C. Deroose[7], K. Haustermans[1]

[1]*KU Leuven/University Hospitals Leuven, Department of Radiation Oncology, Leuven, Belgium*

[2]*KU Leuven, Department of Oncology, Leuven, Belgium*

[3]*University Hospitals Leuven, Department of Abdominal Surgery, Leuven, Belgium*

[4]*University Hospitals Leuven, Department of Digestive Oncology, Leuven, Belgium*

[5]*University Hospitals Leuven, Department of Radiology, Leuven, Belgium*

[6]*University Hospitals Leuven, Department of Pathology, Leuven, Belgium*

[7]*University Hospitals Leuven, Department of Nuclear Medicine, Leuven, Belgium*

Purpose or Objective: The standard treatment for locally advanced rectal cancer (LARC) is preoperative chemoradiotherapy (CRT) followed by total mesorectal excision (TME). The tumoral response to CRT is highly heterogeneous and about 15-30% of the patients achieve a pathological complete response (pCR). 18F-FDG PET/CT is

promising in response prediction and a reduction in maximal standardized uptake value (SUVmax) has been correlated with therapy response. In a prospective study, we investigated whether PET-based response prediction improves with blood glucose level (BGL) normalization.

Material and Methods: Eighty-five patients with LARC were treated with CRT (45 Gy in 1.8 Gy fractions, 5-FU (225mg/m²)) followed by TME after 6-8 weeks. Patients underwent 18F-FDG PET/CT scans at three time points: prior to CRT, after 10-12 fractions and prior to surgery. PET data were normalized to the BGL measured before FDG injection. Three normalization methods were compared: linear correction according to Janssen et al (SUVnormalized= SUVmax*(glycemia/100)), and two corrections suggested by Keramida et al (SUVnormalized = (SUVmax*glycemia)/SUVmeanliver and SUVnormalized = SUVmax*e(0.099*glycemia)). Treatment response was classified as pCR, ypT0-1 and ypT0-2. PET parameters were compared with pathological response using Mann-Whitney U tests. ROC analysis was employed to investigate the performance of the glycemia corrected and uncorrected PET parameters. A p-value ≤0.05 was considered statistically significant.

Results: Thirteen patients achieved pCR while ypT0-1 and ypT0-2 response was observed in 23 and 50 patients respectively. While the value of PET obtained prior to (SUVmaxpre) and during (SUVmaxduring, RI SUVmaxduring) CRT was limited, presurgical scans (SUVmaxpost, RI SUVmaxpost) appeared useful for response prediction (see Table and Figure). The performance of PET-based response assessment increased with a less stringent definition of tumor response. There were no major differences in the predictive performance of PET-based response parameters before and after BGL normalization and between different normalization methods.

Table: Correlation of PET-based parameters with treatment response.

	pCR	ypT0-1	ypT0-2
	p-value	p-value	p-value
$SUVmax_{pre}$			
Uncorrected	0.5798	0.0971	**0.0207**
Linear correction	0.7554	0.3045	0.1407
Correction to $SUVmean_{liver}$	0.7217	0.5616	0.1541
Exponential correction	0.8637	0.2491	0.0714
$SUVmax_{during}$			
Uncorrected	0.1861	**0.0171**	**0.0219**
Linear correction	0.4282	**0.0309**	0.1517
Correction to $SUVmean_{liver}$	0.2213	**0.0126**	0.0800
Exponential correction	0.2808	**0.0183**	0.0767
$SUVmax_{post}$			
Uncorrected	**0.0406**	**0.0003**	**0.0003**
Linear correction	0.0512	**0.0005**	**0.0015**
Correction to $SUVmean_{liver}$	0.0600	**0.0014**	**0.0013**
Exponential correction	**0.0434**	**0.0003**	**0.0008**
RI $SUVmax_{during}$			
Uncorrected	0.5506	0.3507	0.7351
Linear correction	0.4282	0.3394	0.7968
Correction to $SUVmean_{liver}$	0.3784	0.2988	0.7769
Exponential correction	0.7445	0.4847	0.9141
RI $SUVmax_{post}$			
Uncorrected	**0.0158**	**0.0004**	**0.0004**
Linear correction	**0.0134**	**0.0002**	**0.0006**
Correction to $SUVmean_{liver}$	**0.0097**	**0.0004**	**0.0018**
Exponential correction	**0.0119**	**0.0002**	**0.0006**

Figure: Area under the curve (AUC) of response prediction

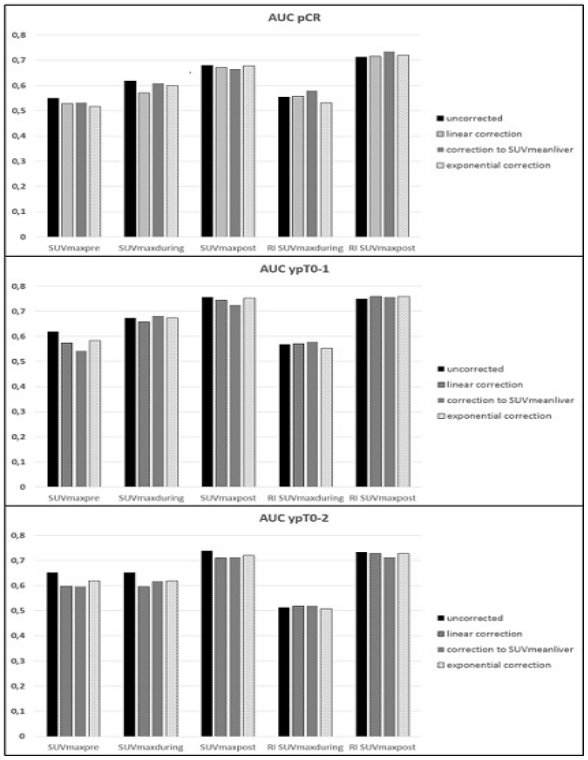

Conclusion: Especially presurgical 18F-FDG PET/CT is useful for the prediction of the tumoral response to CRT in rectal cancer. Blood glucose level normalization has little effect on the performance of PET-based response prediction and there is no large difference in performance between normalization approaches.

1 Janssen et al, Radiother Oncol 2010; 95(2):203-8.
2 Keramida et al, Eur Radiol 2015; 25(9):2701-8.

EP-1283

Outcomes and toxicities in advanced anal cancer treated with radical VMAT chemoradiotherapy

E. Jiad[1], D. Woolf[1], N. Pasha[1], S. Ball[1], S. Raouf[1]
[1]*Queen's Hospital, Oncology, London, United Kingdom*

Purpose or Objective: To investigate the outcomes of advanced anal carcinoma treated with radical Volumetric Modulated Arc Therapy (VMAT) chemoradiotherapy.

Material and Methods: From January 2013 – March 2015, twenty patients (median age 64; Range 46-83; M:F 4:16) with advanced anal carcinoma (T3-T4 or N1-N3) were treated with radical VMAT chemoradiotherapy at our hospital.
The clinical target volume (CTV) included the anal canal, primary tumour, mesorectum, presacral nodes, interior iliac nodes and inguinal nodes. All Patients were prescribed Mitomycin C (12mg/m2 D1; capped at 20mg) and capecitabine (600mg/m2 BD D1-14 and D22-35) chemotherapy concurrently with radiotherapy.

Results: All patients had histologically confirmed squamous cell carcinoma. Treatment was completed in all patients. The standard dose prescription was 50.4Gy in 28 fractions for T3 tumours (8 patients). T4 or node positive cancers received either a simultaneous integrated boost of 2.8Gy to a total dose of 53.2 Gy in 28 fractions (9 patients) or up to a further 3 fractions to a maximum total dose of 56Gy (3pts).
At time of analysis (Median follow up 22.3 months) one patient (5%) had a local recurrence and two patients (10%) had developed metastatic disease, all of which are currently being managed with palliative intent.
The only significant toxicities recorded were local skin erythema and desquamation. Additionally one patient (5%) developed secondary myelodysplastic syndrome which was

presumed to be related to his chemotherapy; and died of neutropaenic sepsis.

Conclusion: Our study shows VMAT chemoradiotherapy delivers excellent local control in the treatment of advanced anal cancers. Treatment was well tolerated and all patients completed the prescribed course of radiotherapy. More data is needed and longer term follow-up to confirm clinical outcomes.

EP-1284

Predictive factors of tumour response after neoadjuvant chemoradiation for rectal cancer

F. Lopez Campos[1], A. Hervas[1], C. De la Pinta[1], J.A. Dominguez[1], E. Fernández[1], M. Martin[1]
[1]*Hospital Ramon y Cajal, Clinical Oncology, Madrid, Spain*

Purpose or Objective: Neoadjuvant chemoradiation followed by surgery is the standard of care for locally advanced rectal cancer (LARC).
The aim of this study was to identify predictive factors of tumor responsiveness.

Material and Methods: A retrospective study was carried out on a series of 243 patients with histologically proven LARC treated between 2000 and 2014 by preoperative chemoradiation before total mesorectal excision. The radiation dose was 45-50.4Gy with fluoropyrimidine-based chemotherapy regimens. The influence of tumor characteristics and treatment regimen in tumor downstaging and regression grade (TRG) was tested using Mandard scoring system on surgical specimens.

Results: Median age (range 33-85) was 67 years. The predominat cancer stages were stage II (38%) and stage IIIB (56%). Tumor downstaging occurred in 167 patients (69%), including 48 (19.8%) with ypT0 (documented T0 at surgery) and 166 (68.3%) with a satisfactory tumor regression grade, defined as TRG1-3. Identified predictive factors for pathologic complete response (pCR) included a planning target volume receiving 50.4Gy (PTV 50.4) and tumor location: PTV 50.4≤600cc (p=0.049) and upper rectal tumor location (p=0.004) were associated with higher pCR by univariate analysis. Multivariate analysis revealed a positive association of the TRG1-3 rate with longer intervals from chemoradiation to surgery (p=0.008): 5.4% at ≤5 weeks, 43.4% at 6-8 weeks and 51.2% at≥9 weeks. Actuarial 3 and 5 years survivals were 95% and 90% for the group as a whole. Among ypT0 cases, the overall survival and relapse-free survival were 97% and 94%, respectively with a median follow-up of 49.4 months, significantly different compared with the remaining group 89% and 74% respectively. There were no treatment-associated fatalities. Thirty-two of the 243 patients (13%) experienced Grade III or IV toxicities (proctitis (8.6%), epithelitis (3.7%) and neutropenia (0.8%) during preoperative treatment.

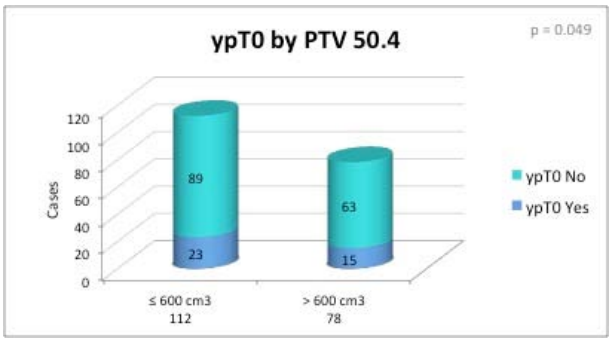

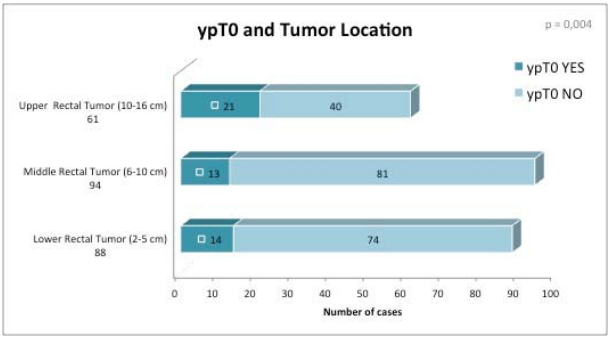

Conclusion: PTV50.4Gy and tumor location were identified as predictive factors of pCR for LARC treated with preoperative chemoradiation. PTV50.4 ≤600cc and upper rectal tumors are more likely to develop complete responses.
Delay in surgery was identified as a favourable predictive factor for TRG1-3, Innovative strategies incorporating further time extension of the surgical interval can be safely explored.

EP-1285

Is watch and wait policy after chemoradiotherapy for rectal cancer detrimental to outcome?

N. Pasha[1], D. Woolf[1], E. Jiad[1], S. Ball[1], S. Raouf[1]
[1]*Queen's Hospital, Clinical Oncology, Romford, United Kingdom*

Purpose or Objective: Neo-adjuvant chemoradiotherapy (CRT) is considered a standard approach for locally advanced rectal cancer. In this study we assessed the outcomes of patients who declined surgery following standard CRT in comparison to those who received surgery.

Material and Methods: We evaluated all patients who received CRT for rectal cancer between February 2012 and December 2014 at our centre. All patients received 50.4Gy in 1.8Gy fractions with concurrent capecitabine chemotherapy (825mg/m2 BD) daily throughout treatment. 61 patients received surgery (total mesorectal excision), performed 8-12 weeks after completion of CRT (Group A). 12 patients received CRT alone and declined definitive surgery (Group B). These patients were monitored on a watch and wait approach. The primary end point of this study was disease free survival (DFS), with local recurrence being a secondary end point.

Results: Group A comprised of 19/61 (31%) females and 42/61 (69%) male, median age of this group was 66 years. 59/61 (96.7%) patients showed an imaging response (defined as any improvement in disease) following CRT. Group B comprised of 6/12 (50%) male and female, median age of this group was 75 years. 9/12 (75%) patients showed an imaging response following CRT. Group A showed a local recurrence rate of 5/61 (8%) and a distant recurrance rate of 9/61 (15%) . Group B showed a recurrence rate of 4/12 (33%), all of which were local recurrences. There was no significant difference in overall recurrance rates between the two groups (t =0.90; p = 0.37). The disease free survival, using the Kaplin-Meier methodology, for Group A was 88% at one year and 80% at two years. For Group B it was 91% at one year and 66% at two years; the difference between the two groups being non-significant (log rank chi-square 1.35; p=0.245)

Conclusion: This study suggests that a watch and wait approach after CRT is associated with increased risk of local relapse and a shorter disease free survival interval. The difference was not significant which might be due to small numbers in the watch and wait group. We continue to advocate surgery as the standard approach post CRT and await the results of prospective studies evaluating a watch and wait approach, as well as the use of imaging biomarkers to enable better prediction of outcome.

EP-1286

Does dose-escalated neo-adjuvant radiotherapy improve pathological response in rectal cancers?

N. Pasha[1], D. Woolf[1], M. Martinou[1], K. Williams[1], S. Ball[1], S. Raouf[1]

[1]*Queen's Hospital, Clinical Oncology, Romford, United Kingdom*

Purpose or Objective: Neoadjuvant chemoradiotherapy (CRT) is considered a standard approach for locally invasive rectal cancer. Several phase 3 studies have shown an improvement in local control with combined radiotherapy and capecitabine / 5-fluorouracil. There is good evidence that increased dose of radiotherapy is associated with both better pathological response and survival in many malignancies, although the data in rectal cancer is less convincing. In this study we assessed the impact of dose-escalated radiotherapy on pathological outcome.

Material and Methods: We evaluated all patients who received chemo-radiotherapy for rectal cancer and subsequently had an anterior resection/ abdominoperineal resection with a total mesorectal excision (TME) between February 2012 and December 2014. Patients received 50.4Gy 1.8Gy fractions, and more recently those who have T3/4 disease with a threatened circumferential margin had a simultaneous integrated boost of the primary tumour to a total dose of 53.2Gy, with concurrent capecitabine chemotherapy (825mg/m2 BD) daily throughout treatment. Treatment was initially using 3-D conformal radiotherapy but more recently has been using a VMAT technique with cone beam CT used during treatment. Surgery was performed 8-12 weeks after completion of CRT.The primary end point was pathological response (Dworak score 0-4) of the operative specimen. Scores of 0-2 were considered to be non-pathological responders and scores of 3-4 were considered to be pathological responders.

Results: A total of 73 patients received neoadjuvant chemoradiotherapy. 61 patients weretreated with a standard radiotherapy fractionation of 50.4Gy in 28 fractions (Group A) and 12 patients were treated with a dose escalated fractionation to the primary tumour of 53.2Gy in 28 fractions (Group B). The rate of pathological response was 39.3% in Group A and 86.7% with Group B (t=3.55, p<0.001).

Conclusion: This study demonstrates the beneficial effects of dose-escalated radiotherapy and wetherefore recommend this regime be considered for inclusion in future phase 2 studies.

EP-1287

Radiation-induced rectal toxicity in prostate cancer: a proctoscopy evaluation

E. Ippolito[1], M. Nuzzo[2], G. Macchia[2], F. Deodato[2], S. Cilla[3], M. Ingrosso[4], L. Fuccio[5], A. Farioli[5], G. Mantini[6], V. Valentini[6], G.C. Mattiucci[6], G. Siepe[7], M. Ntreta[7], S. Cammelli[7], A. Guido[7], M. Pieri[7], A. Arcelli[7], F. Bertini[7], L. Ronchi[7], A.G. Morganti[7]

[1]*Campus Biomedico University, Radiotherapy Unit, Roma, Italy*

[2]*Fondazione di Ricerca e Cura "Giovanni Paolo II"- Catholic University of Sacred Heart, Radiotherapy Unit, Campobasso, Italy*

[3]*Fondazione di Ricerca e Cura "Giovanni Paolo II"- Catholic University of Sacred Heart, Medical Physics Unit, Campobasso, Italy*

[4]*Fondazione di Ricerca e Cura "Giovanni Paolo II"- Catholic University of Sacred Heart, Endoscopy Unit, Campobasso, Italy*

[5]*Sant'Orsola-Malpighi Hospital- University of Bologna, Department of Medical and Surgical Sciences - DIMEC, Bologna, Italy*

[6]*Policlinico Universitario "A. Gemelli"- Università Cattolica del Sacro Cuore, Department of Radiotherapy, Roma, Italy*

[7]*Radiation Oncology Center- Sant'Orsola-Malpighi Hospital-University of Bologna, Department of Experimental-Diagnostic and Specialty Medicine - DIMES, Bologna, Italy*

Purpose or Objective: Early proctoscopy (1 year) can predict late rectal mucosa changes and therefore can be used as surrogate end-point for late rectal toxicity. The aim of this study was to retrospectively analyze data of patients treated at a single institution, consecutively enrolled in different prospective clinical trials, trying to determine a correlation between treatment parameters and VRS (Vienna Rectoscopy Score) recorded at 1-year proctoscopy.

Material and Methods: Patients with prostate adenocarcinoma treated with curative or adjuvant RT underwent endoscopy one year after RT; 195 patients were included in this analysis. Correlations between VRS > 2 and several treatment parameters were investigated by univariate and multivariate logistic analysis.

Results: Patients treated with an EQD2 dose > 75 Gy, with hypofractionatied schedule and radiosurgery boost had a higher incidence of VRS > 2 (p= < 0.001). On the contrary, previous surgery and 3D-conformal radiotherapy (vs IMRT) were associated with a lower incidence of rectal mucosal changes (p=< 0.001; p= 0.003, respectively). At multivariate analysis radiosurgery boost was associated with the highest odd ratios for the risk of developing a VRS > 2 (OR: 4.143; CI: 1.24-13.81; p=0.001). Even surgery showed a significant correlation with VRS > 2 (OR: 0.39; CI: 0.17-9.94; p=0.037, Table 1).

Table 1. Univariate and multivariate logistic regression for VRS score =2.

	Univariate			Multivariate		
Variable	OR	CI95%	P	OR	CI95%	p
Surgery	0.265	0.130-0.539	**<0.001**	0.397	0.167-0.944	**0.037**
IMRT/VMAT	2.588	1.356-4.942	**0.004**	2.097	0.960-4.581	0.063
EQD2 dose > 75 Gy	3.833	1.742- 8.437	**0.001**	-	-	-
Seminal vesicles irradiation	3.801	1.254- 11.528	**0.018**	2.075	0.577-7.463	0.264
Radiosurgery boost	8.250	2.822- 24.117	**<0.001**	4.143	1.243-13812	**0.021**

Conclusion: Prolonged patients follow-up is needed to "clinically" confirm the increased rectal toxicity produced by radiosurgery boost.

EP-1288

Sphincter function and dose of radiation in rectal cancer. A Single-Institutional study

F. Arias[1], C. Eito[1], G. Asín[1], I. Mora[1], K. Cambra[2], F. Mañeru[3], B. Ibáñez[2], L. Arbea[4], M. Errasti[1], M. Barrado[1], M. Campo[1], I. Visus[1], J. García-Escobedo[1], C. Torres[1], M. Ciga[5]

[1]*Complejo Hospitalario de Navarra, Department of Radiotherapy-Oncology, Pamplona, Spain*

[2]*Complejo Hospitalario de Navarra, Statistics Department, Pamplona, Spain*

[3]*Complejo Hospitalario de Navarra, Department of Physics, Pamplona, Spain*

[4]*Clínica Universidad de Navarra, Department of Radiotherapy-Oncology, Pamplona, Spain*

[5]*Complejo Hospitalario de Navarra, Department of Surgery, Pamplona, Spain*

Purpose or Objective: The objective of the study is to determine the correlations among the variables of dose and the sphincter function (SF) in patients with locally advanced rectal cancer treated with preoperative capecitabine/radiotherapy followed by Local Anterior Resection(LAR) +TME.

Material and Methods: We have retrospectively reviewed 92 consecutive patients with LARC treated at our center with LAR from 2006 and more than 1 year free from disease. We re-contoured the anal sphincters (AS) of patients with the help of the radiologist. SF was assessed with the Wexner scale (0-20 points, being punctuation inversely proportional to SF). All questionnaires were filled out between January 2010 and December 2012. Dosimetric parameters that have been studied include: V20 V30, V40, V50, mean dose (Dmean), mínimum dose (Dmin), D90 (dose received by 90% of the sphincter) and D98 Statistical analysis: the correlations

among the variables of dose and SF were studied by the Spearman correlation coefficient. Differences in SF related to maximum doses to the sphincter were assesed by the Mann-Whitney test.

Results: Wexner scaleMean Wexner score was 5.5 points higher in those patients with V20>0 compared to those for which V20=0 (p=0.008). In a multivariate regression model, results suggest that the effect of V20 on poor anal sphincter control is independent of the effect of distance, with an adjusted OR of 3.42 (1.09, 10.72).

Conclusion: In order to improve the SF, the maximum dose of radiation to the AS should be limited, when possible, to < 20 Gy

EP-1289

Anal squamous cell carcinoma; a retrospective case series

O. Houlihan[1], S. O'Sullivan[2], M. Dunne[2], O. Salib[2], C. Gillham[2], G. McVey[2], C. Faul[2], M. Cunningham[2], J. Armstrong[2], D. McNamara[3], B. O'Neill[2]
[1]*Beaumont Hospital, Medicine, Dublin, Ireland Republic of*
[2]*St Luke's Radiation Oncology Network, Radiation Oncology, Dublin, Ireland Republic of*
[3]*Beaumont Hospital, Surgery, Dublin, Ireland Republic of*

Purpose or Objective: Anal cancer is a relatively rare cancer, making up approximately 0.4% of all new diagnoses of cancer. In 2011, there were 1,175 new cases of anal cancer diagnosed in the UK. The current standard treatment is radical chemoradiotherapy. We conducted a retrospective case series of anal squamous cell carcinoma treated in the regional radiation oncology network between 2008 and 2014 inclusive to examine recent management practice and outcome of anal squamous cell carcinoma.

Material and Methods: Patients were identified from the regional radiation oncology cancer database. Data was collected retrospectively from ARIA® oncology information system and patient charts. Information was collected in relation to demographic details, radiotherapy dose and regimen, chemotherapy regimen, persistence and recurrence of disease, salvage surgery rates, and survival analysis. Statistical analyses were carried out using IBM® SPSS® statistical software version 21.0.

Results: 79 cases of anal squamous cell carcinoma were identified. Mean age at commencement of radiotherapy was 60.2 years (+/-13.2 years). 29 patients were male (36.7%) and 50 (63.3%) were female. 8 (10.1%) patients had documented HIV infection. 74 (93.7%) patients were treated with radical chemoradiotherapy. The most common total radiotherapy dose delivered was 50.4 Gy in 28 fractions (N=58; 73.4%) (see table 1). The majority of patients (N=67; 84.8%) received combination chemotherapy with mitomycin C and 5-FU. 2 (2.5%) patients who received radical treatment had persistent disease following radiotherapy. 5 (6.3%) patients had loco-regional recurrence and 3 (3.8%) patients developed solid organ metastases following complete treatment response at the primary. 4 patients had salvage surgery. Survival was measured from the initiation of radiotherapy treatment using the Kaplan-Meier method. Overall survival was 98%, 90%, 83% and 83% at 1, 2, 3 and 4 years respectively. Disease free survival was 91%, 77%, 74% and 74% at 1, 2, 3 and 4 years respectively (see fig. 1).

Table 1 Total delivered radiotherapy dose and fraction

Radiotherapy Dose (Gy)/Fraction	Number of Patients (%)
50.4/28	58 (73.4)
54/30	11 (13.9)
59.4/33	5 (6.3)
57.6/32	2 (2.5)
60/30	1 (1.3)
54.8/31	1 (1.3)
50/25	1 (1.3)

Censored	Observed	Total	Number at risk			
			12 months	24 months	36 months	48 months
65	14	79	52	31	21	12

Fig. 1 Disease free survival shown on Kaplan-Meier curve

Conclusion: Our study found that the majority of patients in our radiation oncology network were treated with chemoradiotherapy in line with international guidelines. In our study, chemoradiotherapy in the treatment of anal squamous cell carcinoma was associated with a high complete response rate and a low treatment failure rate. Treatment and outcomes in our study are consistent with international trial data.

EP-1290

A review of grade 3 bowel toxicity in patients treated with chemoradiotherapy for rectal cancer

J.A. King[1], L. Davidson[1], N. Alam[1], C. Arthur[1], C. McBain[1], A. Mirza[1], M. Saunders[1], V. Misra[1]
[1]*The Christie NHS Foundation Trust, Clinical Oncology, Manchester, United Kingdom*

Purpose or Objective: Concurrent chemoradiotherapy (CRT) is the standard treatment for locally advanced rectal cancer to downstage disease prior to definitive surgery. Previous studies report≥ grade 3 (G3) bowel toxicity of 3 -4%; QUANTEC recommend small bowel V45 <195 cm3 to reduce G3 toxicity. We noted an increase in G3 bowel toxicity in the period Sept – Dec 2014 in our institution and aimed to determine the cause.

Material and Methods: We retrospectively identified patients who received pre-operative long-course CRT for rectal cancer between Sept – Dec 2014 and Jan - April 2014 (control), and reviewed case notes and radiotherapy (XRT) plans. Small bowel V45 was calculated for each patient. G3 toxicity was defined as per the CTCAE grading system for diarrhoea, abdominal pain and vomiting.

Results: Fifty patients were identified: Jan – April cohort (n=28) was compared to Sept – Dec cohort (n=22). Both groups were similar for patient demographics, CRT treatment volumes and doses, patient positioning and XRT delivery technique. Two of 28 patients (9%) in Jan – April cohort had G3 bowel toxicity; both were admitted for symptom control. Six of 22 patients (27%) in Sept – Dec cohort developed G3 bowel toxicity; 5 (23%) required admission.
G3 toxicity occurred after a minimum of 16 fractions (range 16-21). All patients had normal bowel function prior to

treatment; 1 had an ileostomy. Two patients (25%) required prolonged admission, 1 was admitted to critical care with neutropenic colitis. Capecitabine was discontinued in 6/8 (75%); 5 (63%) required a break in XRT. Two patients (25%) discontinued XRT altogether. Mean small bowel V45 for patients who did and did not develop G3 toxicity was 38.6 cm3 (range 0 – 178.8) and 113.0 cm3 (38.4 – 222.4) respectively. Two patients had a small bowel V45 >195 cm3, both developed G3 bowel toxicity.

Conclusion: In this series, incidence of G3 bowel toxicity in patients receiving chemoradiotherapy for rectal cancer was not influenced by gender, age, pre-treatment bowel habit or body habitus. PTV size, patient positioning and radiotherapy delivery technique did not alter the risk. Patients who developed G3 toxicity had a larger volume of small bowel receiving ≥45 Gy. Based on this, we now routinely calculate dose to small bowel, thus identifying patients who are at higher risk of developing G3 toxicity and review or change the treatment plan, including chemotherapy dose, to mitigate this risk.

EP-1291

Can mucosal criteria estimate response in rectal cancer treated with neoadjuvant chemoradiotherapy?

A. Garant[1], T. Niazi[1], A. Gologan[1], A. Spatz[1], J. Faria[1], N. Morin[1], C. Vasilevsky[1], M. Boutros[1], T. Vuong[1]
[1]*Jewish General Hospital, Radiation Oncology, Montreal, Canada*

Purpose or Objective: The past decade in rectal cancer research has raised questions about complete pathological response (pCR) after neoadjuvant therapy. In this context, there has been much hype to identify patients with clinical complete response (cCR) who could eventually be candidates for nonoperative cancer care. So far, experts have published stringent criteria to define cCR, which remain to be validated with surveillance strategies. The purpose of our study is to review pathological mucosal changes after neoadjuvant combined chemoradiation therapy (CRT) for rectal cancer.

Material and Methods: This retrospective review was conducted in a tertiary referral center. Histopathology reports were retrieved for rectal cancer patients treated with neoadjuvant CRT. Exclusion criteria included recurrent rectal cancer, stage IV disease, rectal cancer in the context of IBD or FAP, patient enrollment under clinical trials with chemotherapy or other treatment schemes, and patients who were not operated. The macroscopic mucosal appearance of the specimen was compared with the final pathological staging.

Results: Eighty-eight patients met our inclusion criteria and had complete staging and pathological data with gross mucosal descriptions. These included 59 male and 29 female patients with a median age of 63 years (range 29-83). The staging proportions were: 3.4% stage cI, 15.9% stage cII, and 80.7% stage cIII; 93.2% of patients were cT3/cT4 and 75% were cN+. Clinical CRM was involved in 30 patients. All patients were treated with neoadjuvant CRT consisting of 45 Gy in 25 fractions to the pelvis with a tumour bed boost of 5.4 Gy in 3 fractions using 3D conformal radiotherapy; chemotherapy was 5-FU based. Total mesorectal excision (TME) was performed in all patients. The median time between the last day of radiotherapy and surgery was 58 days (range 32-308). As a result, 15 patients (17.0%) were staged as ypT0N0 (pCR); 12 patients (13.6%) remained CRM+ on surgical pathology evaluation. Eighty-seven patients (98.9%) had residual mucosal abnormalities incompatible with cCR: most changes seen were ulceration and, less often, stenosis. Of the 70 patients with microscopic residual tumor, 7 patients had no macroscopic tumor visualized but an ulcer in its place. There was no statistically significant association between time from CRT to surgery and pCR.

Conclusion: Most patients undergoing neoadjuvant CRT have residual mucosal abnormalities two months after CRT. There are needs to define criteria for clinical endoscopic evaluation to define cCR.

EP-1292

Association between obesity and local control of rectal cancer after surgery and radiotherapy

Y.S. Choi[1]
[1]*Busan Paik hospital, Radiation Oncology, Busan, Korea Republic of*

Purpose or Objective: The association between metabolism and cancer has been recently emphasized. This study aimed to find the prognostic significance of obesity in advanced stage rectal cancer patients treated with surgery and radiotherapy (RT).

Material and Methods: We retrospectively reviewed the medical records of 111 patients who were treated with combined surgery and RT for clinical stage II-III (T3 or N+) rectal cancer between 2008 and 2014. The prognostic significance of obesity (body mass index ≥25 kg/m2, according to Asian classification) in local control was evaluated.

Results: The median follow-up was 27.3 months (range, 3.3-82.1 months). Twenty-five patients (22.5%) were classified as obese. Treatment failure occurred in 33 patients (29.7%), including local failures in 13 patients (11.7%), regional lymph node failures in 5, and distant metastases in 24. The 3-year local control, recurrence-free survival, and overall survival rates were 88.6%, 72.6%, and 87.3%, respectively. Obesity (n=25) significantly reduced the local control rate (p=0.049, 3-year local control 75.8%), especially in women (n=37, p=0.026). Segregation of local control was best achieved by body mass index of 25.6 as a cutoff value.

Conclusion: Obese rectal cancer patients showed poor local control after combined surgery and RT. More effective local treatment strategies for obese patients are warranted.

EP-1293

Intensified neo-adjuvant chemoradiotherapy in locally advanced rectal cancer: long-term follow-up

F. De Felice[1], D. Musio[1], A.L. Magnante[1], N. Bulzonetti[1], I. Benevento[1], R. Caiazzo[1], V. Tombolini[1]
[1]*Policlinico Umberto I- "Sapienza" Università di Roma, Radioterapia, Roma, Italy*

Purpose or Objective: To report long-term follow-up data and determine the toxicity rate in patients with locally advanced rectal cancer (LARC) treated with intensified neo-adjuvant regimen.

Material and Methods: Patients with histologically proven adenocarcinoma of the rectum, stage III-IV, were included and treated with a tri-modality approach. Baseline patient characteristics are shown in Table 1.
Intensified neo-adjuvant treatment (CRT) consisted of RT total dose of 50.4/54 Gy and concomitant OXP (50 mg/m2/ week) and 5-FU (200 mg/m2/ five daily continuous infusion). Surgery was planned 7-9 weeks after the end of CRT. Adjuvant chemotherapy was recommended in those patients with lymph-node metastasis at diagnosis.

Results: One hundred patients (median age 64 years) were eligible, between January 2007 and December 2014. Overall, the 5-years OS and DFS were 76.4% and 74.5%, respectively. Local recurrence was recorded in 9 patients (9%) and 23 patients (23%) presented distant metastasis. CRT was well tolerated, with only 17% grade 3/4 acute toxicity. Twenty-four patients (24%) had a pathologic complete response (pCR) and only 1 patient peri-operative metastasis. The 5-year OS rate was 95.7% for patients with pCR and 70.4% without pCR (p = 0.0489). The 5-year DFS were 95.7% and 66.7% for pCR and no-pCR tumor histology, respectively (p=0.0275) (Figure1).

Conclusion: Distant metastasis remains the major issue in the management of LARC. This study demonstrated improvement in pCR, as well as the potential to achieve higher survival rates, including DFS. Waiting for randomized phase III trials long-term follow-up data, OXP should be considered as feasible and valid neo-adjuvant treatment option. The low rate of severe toxicity and the effective benefit on pCR and peri-operative metastasis support this concomitant CHT schedule for LARC.

EP-1294

Total mesorectal excision vs. local excision following preoperative RT for "early" cT3 rectal cancer

Y. Shin[1], J.H. Park[1], J.C. Kim[2], C.S. Yu[2], T.W. Kim[3], J.H. Kim[1]
[1]*University Of Ulsan College Of Medicine, Radiation Oncology, Seoul, Korea Republic Of*
[2]*University Of Ulsan College Of Medicine, Surgery, Seoul, Korea Republic Of*
[3]*University Of Ulsan College Of Medicine, Oncology, Seoul, Korea Republic Of*

Purpose or Objective: To compare the oncologic outcome of total mesorectal excision (TME) to local excision (LE) in "early" clinical T3 rectal cancer patients who received preoperative radiation therapy.

Material and Methods: "Early" clinical T3 patients, who underwent preoperative radiation therapy followed by TME or LE at Asan Medical Center between January 2007 and December 2013 were retrospectively analyzed. "Early" clinical T3 was defined as extramural extension 5mm, circumferential resection margin negative and lateral lymph node negative in pretreatment magnetic resonance imaging. A one-to-one propensity case-matched analysis was used with covariates of baseline characteristics. Local recurrence free survival (LRFS), disease free survival (DFS), overall survival (OS) were compared between the matched two groups.

Results: A total of 425 patients were identified; 366 underwent TME and 59 underwent LE. The median follow-up period was 47 months. After propensity score-matching, we obtained 55 matched pairs. There were no significant differences in 3-year LRFS (95.8% vs 94.2%, p=0.927), DFS (85.7% vs 90.8%, p=0.473), OS (96.2% vs 100%, p=0.987) between TME and LE groups.

Conclusion: In "early" clinical T3 rectal cancer, local excision could be a feasible alternative to mesorectal excision after preoperative chemoradiation.

EP-1295

Anal cancer as a second human Papillomavirus-related presentation after cervical dysplasia/neoplasia

A. Yates[1], S. Pendlebury[2], E. Segelov[3]
[1]*Yates Angela, St Vincent's Hospital- Darlinghurst NSW 2010 Australia, Annandale NSW, Australia*
[2]*St Vincent's Hospital, Radiation Oncology, Darlinghurst, Australia*
[3]*St Vincent's Hospital, Medical Oncology, Darlinghurst, Australia*

Purpose or Objective: Cervical intraepithelial neoplasia (CIN) and anal squamous cell carcinoma (SCC) are both causally associated with human papilloma virus infection (HPV). Women who have an HPV infection of the cervix are at a higher risk of HPV infection of the anal canal with the same HPV subtype(1). The incidence of HPV infection and related cancers is increasing in developed nations(2). Until the impact of widespread HPV vaccination is manifest, presentation with multiple HPV related malignancies will become a more common clinical scenario. Our objective was to identify the proportion of women with anal cancer who had a history of CIN or invasive cervical cancer (ICC) and discuss the implications for future practice.

Material and Methods: The medical records and histopathology of all consecutive women treated definitively for anal cancer at our centre between January 2004 and July 2015 were reviewed. A case was defined as a woman reporting a history of CIN or ICC treated with either a cone biopsy or hysterectomy. We extracted treatment details of both the anal cancer and CIN or ICC, demographic and outcome data. Women with a previous abnormal pap smear or low grade cervical dysplasia were not included as a case.

Results: Eight cases (25%) were identified; Stage III (63%), I, II, IV (each 12.5%). The women were HIV negative, aged 36-62 years and diagnosed with HPV positive anal SCC 10-40 years after their initial diagnosis. Of the remaining 24 women, Nine had no prior history, Four had a previous abnormal pap smear, one a partial hysterectomy for unknown reason, two a hysterectomy for benign uterine disease and eight no recorded gynaecological history. Seven women had definitive chemoradiotherapy and one had sequential chemotherapy and radiotherapy (Stage IV). All were alive and disease free at follow up.

Conclusion: One quarter of women with anal SCC had a previous history of CIN or ICC. This may be an underestimate as a gynaecological history was missing in 25% of patients. There are several implications for practice: the importance of specifically elucidating a history of HPV-related disease such as warts, CIN or ICC on history; secondly, to have a high index of suspicion when these women present with bowel symptoms; third, that this represents a high risk group of women who may benefit from participation in anal pap screening programs similar to that being investigated in high risk men.

EP-1296

A correlation between PTV dosimetric criteria and pathological responsein rectal cancer patients

A. Franzetti Pellanda[1], P. Urso[1], S. Gianolini[2], B. De Bari[3], G. Ballerini[1], L. Negretti[1], C. Vite[1], N. Corradini[1]
[1]*Clinica Luganese, Department of Radiation Oncology, Lugano, Switzerland*
[2]*Medical Software Solutions GmbH, Medical Software Solutions GmbH, Hagendorm, Switzerland*
[3]*CHUV, Radiotherapy department, Lausanne, Switzerland*

Purpose or Objective: To test the relationship between dosimetric data and pathological response in a series of 52 patients treated with combined pre-operative chemoradiation (CRT) for local advanced rectal cancer..

Material and Methods: We studied 52 consecutive patients treated with pre-operative CRT for locally advanced rectal cancer (T3-4N0M0 or any TN+M0, G1-3). Total dose prescribed was 44 Gy (2 Gy/fx) (Group 1, n = 10) or 45 Gy (1.8 Gy/fx) (Group 2, n = 42), delivered using helical Tomotherapy (HT). A concomitant Capecitabine-based chemotherapy was also delivered. All patients underwent surgery 6 to 8 weeks after the end of CRT. Surgery consisted of low anterior resection (LAR) or abdominoperineal excision (APR), depending on the tumor distance from anal margin. For all patients, we calculated pathological response through difference between TNM clinical staging and TNM pathological staging such as by pathological Dworak tumor regression score (TRG). We tested the relationship between pathological response and planning target volume (PTV) dosimetric criteria in agreement with ICRU 83 and internal guidelines. Selected parameters were: Dmax, Dmin, Dmean,D98,D95, D2, V95,V100 ,V107, V110 and target volume (cc). Non-parametric statistical analysis (Wilcoxon, U-Mann-Whitney, Kruskal-Wallis tests) was performed using SPSS.21 software (significant level $p < 0.05$). Planning dosimetric data were extracted from patient archives using VODCA 5.4.0.

Results: Results: A significant reduction in TNM staging was observed post-treatment ($p < 0.001$ and $p < 0.010$ for T & N, respectively). Furthermore, 3 patients presented a total remission (5.8%) and 30 remained stable (57.7%). For Group 1, average values and standard deviation of Dmean, Dmin and Dmax (Gy) were 44.5 ± 0.4, 30.4 ± 3.6, and 47.2 ± 0.3, while for Group 2 were 45.1 ± 0.3, 33.1 ± 3.5, and 48.1 ± 0.6. Dose

fractionation was not significant for both TNM and TRG ($p > 0.100$). Among dosimetric parameters, Dmin resulted statistically different depending on the patient T staging variation ($p < 0.005$). Specifically, focusing on the 21 patients with favourable pathological response, significant correlation was found with the T index variation (ρSpearman = -0.667, $p = 0.001$), with higher Dmin related to patients undergoing total remission. No other dosimetric parameters resulted associated with clinical tumor regression outcomes.

Conclusion: In this series we found a statistically significant correlation between T staging regression and the Dmin to the PTV. Patients with partial or complete pathological response showed a higher Dmin when compared to patients with no change in TNM staging. Further studies are needed to understand if there is any relation between the site of underdosages and the tumor site.

EP-1297

Impact of 18F-FDG-PET/CT in evaluating the response to neadjuvant chemoradiotherapy in rectal cancer

S. Pedraza Fernández[1], M. Pérez-Escutia[1], D. Sánchez-Fuentes[2], P. Nenclares[1], S. Ruiz-Solís[2], M. Peña[1], D. Lora[3], J. Pérez-Regadera[1]

[1]*Hospital 12 Octubre, Radiation Oncology, Madrid, Spain*
[2]*Hospital 12 Octubre, Nuclear Medicine, Madrid, Spain*
[3]*Hospital 12 Octubre, Investigation and Statistics, Madrid, Spain*

Purpose or Objective: The standard treatment for locally advanced rectal cancer (LARC) is neoadjuvant chemo-radiation (CRT) followed by mesorectal excision. However, surgical specimen histopathology demonstrates a complete pathological response (pCR) in almost 30% of cases. In consequence, these patients (pts) may benefit from conservative management.
The aim of this study is to evaluate the role of 18F-FDG-PET/CT in pts with LARC in the prediction of pCR after treatment with CRT.

Material and Methods: From September 2009 to May 2014, 39 pts (mean age: 62 years, range 40-83) with LARC underwent 18F-FDG-PET/CT for staging and radiotherapy (RT) treatment planning. Tumour location within rectum: superior: 17 (43.85%); middle: 14 (35.89%); inferior: 8 (20.51%). Histology: adenocarcinoma: 37 (94.87%); mucinous adenocarcinoma: 2 (5.13%). Tumour staging: II: 7 (17.95%); III: 31 (79.48%); IV (resected liver metastases disease): 1 (2.56%).
All pts received conformal RT (Nodal PTV: 4500 cGy, Tumor PTV: 5040 cGy) with concurrent Capecitabine, before undergoing either low anterior resection (32pts-82.05%) or abdomino-perineal resection (7pts-17.95%).
The tumour regression grade (TRG) according to Mandard´s criteria was assessed by the pathologist. Pts were classified into two groups: responders (TRG 1 and 2) and non-responders (TRG 3 to 5). The TRG was correlated with 18F-FDG-PET/CT parameters (tumour volume, tumour SUVmax and nodal SUVmax).

Results: Following CRT, 7/39 pts (17.94%) showed no evidence of residual tumour in the surgical specimen (pCR). By TRG status, 14 pts (35.9%) were classified as responders and 25 (64.10%) as non-responders. When analyzing 18F-FDG-PET/CT parameters, no significant difference was found between responders and non-responders for: tumour volume *(*mean: 5.84cm3 vs 6.24 cm3, *p=0.35);* tumour SUVmax (21.95 vs 20.73, *p=0.61);* nodal SUVmax *(4.73 vs 7.56, p=0.12)* or staging *(6.71 vs 7.56, p=0.23).* Histopathological responders had better overall survival compared to non-responders, however this was not statistically significant (617 vs 269 days, *p=0.37*).

Conclusion: In our cohort, 18F-FDG-PET/CT parameters cannot predict the tumour response to CRT. Nevertheless, higher levels of SUVmax and bigger tumour volumes are found in the non-responders group and also worst overall survival. Stronger conclusions should be established in this matter in order to select patients for an organ-preservation safely.

EP-1298

Stereotactic radiotherapy in oligometastatic patients with lung metastasis from colon-rectal cancer

S. Montrone[1], C. Vivaldi[2], G. Coraggio[1], M. Cantarella[1], B. Manfredi[1], C. Laliscia[1], G. Masi[2], F. Loupakis[2], A. Falcone[2], M.G. Fabrini[1], A. Sainato[1], F. Pasqualetti[1]

[1]*Azienda Ospedaliero Universitaria Pisana, Radiotherapy, Pisa, Italy*
[2]*Azienda Ospedaliero Universitaria Pisana, Medical Oncology, Pisa, Italy*

Purpose or Objective: The approach to patients with lung metastasis from primary colon-rectal cancer is based on systemic therapy and the role of stereotactic body radiotherapy (SBRT) is still to be investigated. The present work aims to study the impact of SBRT in oligometastatic patients with lung metastasis from colon-rectal cancer.

Material and Methods: From May 2010 to March 2015, 33 consecutive patients (median age 66 years, range 31-88) with lung metastasis from colon-rectal cancer were treated with SBRT. All patients were treated using Image Guided Radiotherapy (IGRT) and stratified according to K-RAS and B-RAF genotype. The systemic progression free survival and local control were the primary and secondary endpoint evaluated respectively.

Results: A total of 56 active lesions were treated. After a median follow-up of 12.6 months, median OS was 10.5 months. The radiotherapy dose delivered and the schedule adopted were 24-27 Gy as a single fraction and 27-42 Gy/3 fractions. Nineteen out of 33 patients were affected by rectal cancer while 14 patients by colon cancer. Median Planning Target Volume value was 21.45 cc (range 6-156). Mean local relapse was recorded in 23 lesions (41.1%) at a median interval of 19.3 months (range 5-37). By the way, 23 out 33 patients (69.7%) experienced systemic progression after a mean time of 12.6 months (1-24) from SBRT. No differences of local or systemic control were observed considering K-RAS and B-RAS genotype. Severe toxicity were not recorded.

Conclusion: The results of this study suggest that SBRT could represent a safe and valid approach to oligometastatic patients with lung metastasis from colon-rectal cancer. However, further studies are needed in order to better characterize patients potentially suitable for SBRT.

EP-1299

Tomotherapy for anal cancer: analysis of toxicity and response in a dual institution experience

P. Bonomo[1], B. Meduri[2], E. D'Angelo[2], A. Galardi[1], C. Delli Paoli[1], C. Tata[2], G. De Marco[2], I. Desideri[1], F. Bertoni[2], L. Livi[1]

[1]*University of Florence, Radiation Oncology, Firenze, Italy*
[2]*University Hospital of Modena, Radiation Oncology, Modena, Italy*

Purpose or Objective: The purpose of our study is to report on the acute toxicity and response to treatment in patients affected by squamous cell anal carcinoma (SCAC) that underwent tomotherapy (TO) at 2 institutions.

Material and Methods: A cohort of 39 patients affected by SCAC and treated with TO between December 2009 and July 2015 was retrospectively analyzed. Concurrent chemotherapy (CT) was always administered except in patients unfit for intensive therapy due to comorbidity and/or with early stage disease (T1-T2N0). The choice of CT regimen was left to the discretion of the treating institution, as well as the IMRT schedule adopted. The dose/fractionation prescribed to PTV1 (high-risk volume), PTV2 (intermediate-risk volume) and PTV3 (low-risk volume) ranged between 66– 50 Gy, 50.4 – 45 Gy and 46.2 – 36 Gy, respectively, at a corresponding dose per fraction range of 2.2 – 1.8 Gy for PTV1, 2 – 1.67 Gy for PTV2, and 1.65 – 1.5 Gy for PTV3, delivered in a range of 25-33 daily fractions. Acute toxicity was scored according to NCI – CTCAE v.4. Response was assessed at 12 weeks after the end of treatment via digital rectal exam and anoscope.

Morphologic and/or metabolic imaging re-assessment was performed between 12 and 26 weeks after treatment. Disease-free survival (DFS) was calculated from the end of treatment to the date of first event of disease recurrence. Overall survival (OS) was calculated from the end of treatment to the date of death from any cause or of last follow-up.

Results: All patients are evaluable for acute toxicity assessment while clinical outcome has been analyzed in 29/37 (79,4%) patients, with a median follow-up of 8 months (range 3-69). Baseline clinical features of the whole cohort are summarized in table 1. Concurrent CT was given in 30 patients (81.1%) and in 23 of them (76.6%) the preferred regimen consisted of 5 – fluoruracil – mitomycin C combination. A sequential IMRT schedule was delivered in 9 patients (24.3%) while 28 (75.7%) underwent IMRT-SIB. In 22 patients (60%) treatment was completed without any interruptions while the median duration of treatment breaks was 7 days (range 1-16) in the remaining group. In terms of acute toxicity, the rate of G3+ diarrhea and dermatitis was 8.1% and 13.5%, respectively. No G3+ GU and hematological toxicities were reported. Complete response was achieved in 21/29 patients (72.4%), partial response/stable disease in 7 (24.1%) and local disease progression in 1 (3%). All patients were alive at last follow-up. The 1-year OS, DFS, and colostomy-free survival were 100%, 85%and 96%, respectively.

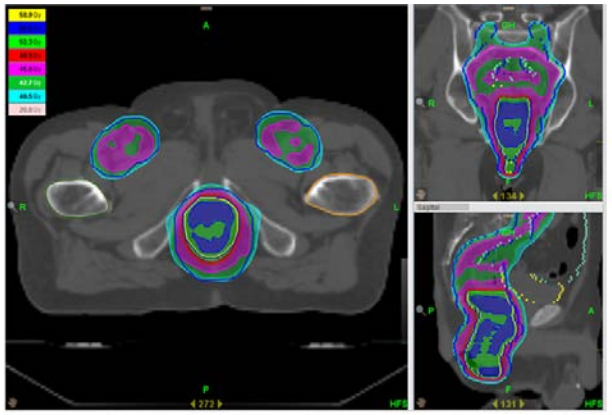

Typical dose distribution in a cT2cN0 patient treated with 55/45 Gy SIB schedule. Yellow and blue lines represent PTV 55 and PTV 45 respectively.

Patient and tumor characteristics

Characteristic	No. of patients (%)
Institution	
A	18 (49)
B	19 (51)
Gender	
Male	10 (27)
Female	27 (73)
ECOG Performance Status	
0	21 (57)
1	14 (38)
2	2 (5)
Charlson Comorbidity Index	
2-3	11 (30)
4-5	20 (54)
6-8	6 (16)
Smoke	
≤ 10 pack/years	29 (78)
11-20 pack/years	3 (8)
> 20 pack/years	5 (14)
HIV status	
Positive	2 (5)
Negative	35 (95)
Tumor category	
T1	6 (16)
T2	16 (43)
T3	9 (25)
T4	6 (16)
Nodal stage	
N0	17 (46)
N1	9 (24)
N2	8 (22)
N3	3 (8)
Stage	
I	3 (8)
II	14 (38)
IIIA	5 (13)
IIIB	15 (41)

Conclusion: In our dual institution experience, concurrent chemo-radiation with TO for SCAC was associated with a favorable acute toxicity profile, in line with published experiences. Considering the prevalence of very advanced loco-regional disease in our cohort, early response assessment is noteworthy, although a longer follow-up is needed to confirm the long-term benefit and to evaluate the incidence of late toxicity.

EP-1300

Preoperative, Adaptive Radiotherapy with Tomotherapy concomitant with chemotherapy in rectal cancer

P. Passoni[1], N. Slim[1], C. Fiorino[2], C. Gumina[1], M. Ronzoni[3], F. De Cobelli[4], A. Palmisano[4], V. Ricci[3], A. Fasolo[3], A. Tamburini[5], P. De Nardi[5], S. Di Palo[5], C. Staudacher[5], R. Rosati[5], R. Calandrino[2], N. Di Muzio[1]

[1]*Ospedale San Raffaele IRCCS, Radiation Oncology, Milan, Italy*
[2]*Ospedale San Raffaele IRCCS, Medical Physics, Milan, Italy*
[3]*Ospedale San Raffaele IRCCS, Medical Oncology, Milan, Italy*
[4]*Ospedale San Raffaele IRCCS, Radiology, Milan, Italy*
[5]*Ospedale San Raffaele IRCCS, Surgery, Milan, Italy*

Purpose or Objective: To report the clinical results of six years experience with Adaptive Radiotherapy concomitant with chemotherapy in the preoperative treatment of rectal cancer.

Material and Methods: Patients (pts) with T3/T4N0 or any TN+ rectal adenocarcinoma were enrolled in an observational trial. Chemotherapy consisted of Oxaliplatin 100mg/m2 on the days -14, 0, +14, and continuous infusion 5-FU 200mg/m2/day from day -14 to the end of radiotherapy. Concomitant Radiotherapy (RT) started on the day 0, was delivered with Tomotherapy, and consisted of 41.4 Gy in 18 fractions (frs) (2.3 Gy/fr) to the PTV defined as CTV, the tumor and regional lymph-nodes contoured on the initial simulation CT and MRI, with a margin of 0.5 cm. Simulation CT and MRI were repeated after two cycles of chemotherapy and 9 frs of RT for the planning of the adaptive RT phase:

PTVadapt was generated by adding a margin of 5 mm to the residual tumour visible on the intermediate MRI images (GTVadapt). A simultaneous integrated boost of 3.0 Gy/fr was delivered to PTVadapt on the last 6 frs of RT until a total dose of 45.6 Gy in 18 frs.

Results: From September 2009 to September 2015, 56 pts completed the preoperative treatment. Toxicity. No G4 toxicity occurred. G3 toxicity was only gastrointestinal: diarrhoea in 9/56 pts (16%), and proctitis in 3/56 (5%). Diarrhoea started before the adaptive RT phase in all the cases. Treatment feasibility. Two pts interrupted radiotherapy after 7 and 13 fractions, respectively, the remaining pts (54/56=96%) completed the treatment; the median duration of RT was 25 days (22-36 days). 47/56 pts (84%) and 45/56 pts (80%) received the full dose of oxaliplatin and 5-FU, respectively: 18% of pts received moderately reduced doses (60%-90%), and only two pts (2%) received less than 60% of the planned dose. Responses. Two pts achieved clinical complete response (cCR) and refused surgery, 1 pt was lost, 1 pt had early distant progression. Fifty-two pts underwent surgery (49 R0, 3 R1). Fifteen pts (29%) had pathological complete response (pCR); 24/52 (46%) had Tumor Regression Grade 3 response: 14/52 (27%) and 6/52 (12%) had <5%, and 6 -10% residual viable cells, respectively. Regarding the two patients with cCR who refused surgery, 1 pt is still in cCR after 69 months, 1 pt had local relapse and underwent transanal resection 1 year after the preoperative treatment.

Conclusion: This study confirms that adaptive Radiotherapy with Tomotherapy concomitant with oxaliplatin based chemotherapy in the preoperative treatment of rectal cancer is feasible, has an acceptable G3 toxicity rate and a very encouraging tumour response rate. A further dose escalation to the PTVadapt could be feasible and could increase the pCR and/or cCR rates.

EP-1301

Neoadjuvant treatment intensification in cT4NXM0 rectal cancer: long-term outcome analysis.

F. Calvo[1], E. Sagarra[2], J. Garcia-Sabrido[2], E. Del Valle[2], M. Rodriguez[2], E. Alvarado Vasquez[3], C. Sole[1], M. Gomez-Espi[3], M. Lozano[3], R. Obregon[2]
[1]*Hospital General Universitario Gregorio Maranon, Oncology, Madrid, Spain*
[2]*Hospital General Universitario Gregorio Maranon, Surgery, Madrid, Spain*
[3]*Hospital General Universitario Gregorio Maranon, Radiation Oncology, Madrid, Spain*

Purpose or Objective: To evaluate the contribution of components for intense multimodal local treatment to the most adverse loco-regional staging scenario of M0 rectal cancer.

Material and Methods: From 1/00 to 12/13, 95 cT4NXM0 patients were treated with radical intent. 54 completed preoperative intensified chemo-radiation (all had post-resection intraoperative electron pelvic boost, IOERT). Adjuvant systemic chemotherapy was recommended considering individualized risk features. Incomplete and complete pre and intra-operative treatment cohorts were comparable in characteristics: male (44/55%); age >70 (44/33%); PS 0 (46/62%); inferior segment (42/41%); grade 2 (67/62%); cN+ (75/83%).

Results: With a median follow-up time of 62 months overall, disease-free (DFS) and loco-regional relapse-free survival were superior in the cohort of complete intensification (75% vs 51%, p=0.009; 67% vs 54%, p=0.03; 77% vs 71%, p=0.01), respectively. IOERT significantly improved presacral control rates. Multivariate analysis indicated that uninvolved surgical margin and intense tumour regression grade assessed response, were protective for DFS.

Conclusion: Multimodal preoperative approach contributed to remarkable cancer-control outcomes and survival in cT4M0 rectal patients, if components of therapy are feasible to be maximized (including free surgical margins) and an intense pathological disease response is described.

EP-1302

The utility of Squamous Cell Carcinoma SCCAg as a marker for treatment response or relapse

L. Pietrzak[1], K. Bujko[1]
[1]*The Maria Sklodowska-Curie Memorial Cancer Center, Radiotherapy, Warsaw, Poland*

Purpose or Objective: The utility of SCCAg as a marker for treatment response or relapse is unknown in anal cancer.

Material and Methods: This is a retrospective analysis of 28 patients in whom SCCAg serum level was increased prior to treatment (mean 6,4 ng/ml, range 1,6-19,6 ng/ml). In all patients, measurement of SCCAg was performed at baseline, after completion of chemoradiation and at each visit during follow-up (median 35 months, range 7-81). All patients were treated radically.

Results: In 27 (96%) patients SCCAg level decreased to normal level after treatment. One remaining patient had persistent unreseceble tumor confirmed by pathology and persistent high SCCAg level. Only one of 27 patients with normalization of SCCAg after chemoradiation had persistent ulceration in the anal canal and persistent enlarger inguinal lymph node. This patient underwent abdominoperineal resection with inguinal lymphadenectomy. On pathological examination only a few cancer cells were found in the inguinal nodes and the primary tumour site was free of cancer.. In six patients, increase of SCCAg was observed during follow-up. In one of these 6 patients, locoregional recurrence was also detected clinically at the same time. In 4 patients, the diagnostic examinations performed because of elevated SCCAg reveled locoregional recurrence (n=2) or distant metastases (n=2). In one remaining patient the diagnostic examinations were negative; distant metastases were detected 5 months thereafter. The remaining 20 patients had both: sustained clinical complete regression and normal SCCAg level.

Conclusion: This study suggests utility of SCCAg in the monitoring of response to chemoradiation and in the detection of recurrence

EP-1303

Radiotherapy dose-escalation in rectal cancer: preliminary results of a pooled analysis.

M. Lupattelli[1], V. Picardi[2], F. Navarria[3], M.A. Gambacorta[4], M. Osti[5], G. Macchia[2], E. Palazzari[6], A.M. Podlesko[6], A. Re[4], L. Nicosia[5], A. De Paoli[3]
[1]*Santa Maria della Misericordia Hospital, Radiotherapy, Perugia, Italy*
[2]*UCSC Campobasso, Radiotherapy, Campobasso, Italy*
[3]*CRO Aviano, Radiotherapy, Aviano, Italy*
[4]*UCSC Rome, Radiotherapy, Rome, Italy*
[5]*S. Andrea Hospital, Radiotherapy, Rome, Italy*
[6]*Perugia University Santa Maria della Misericordia Hospital, Radiotherapy, Perugia, Italy*

Purpose or Objective: Preoperative radiotherapy (RT), alone or in combination with chemotherapy (CT) is the standard of care in patients (pts) with locally advanced rectal cancer (LARC). Nevertheless in those tumors in which the down-sizing and down-staging are necessary, (cT3 MRF - / + N0 of lower rectum or cT3-4 MRF + / N0-2) preoperative chemo-radiotherapy (CT-RT) is recommended. There is a correlation between RT dose and response and the tumor regression grade (TRG) represents an independent prognostic factor. The aim of the study is to analyze the role of RT dose intensification in the preoperative treatment of LARC in terms of feasibility, toxicity and pathological response grade.

Material and Methods: We have retrospectively analyzed 69 pts with histological diagnosis of LARC (stage II-III) treated in five Italian Radiotherapy centres. The treatment programme included: intensity-modulated radiotherapy (IMRT) delivered

to total mesorectum and pelvic lymphatic drainage with simultaneous integrated boost (SIB) to the tumor bed and adjacent mesorectum. Fluoropirimidine-based CT was administered. The acute toxicity was evaluated according to CTCAE 4.0 scale.

Results: Pts characteristics: median age 63.5yy (range 29-84), median tumor distance-IAS 50 mm (range 0-100), median tumor size 50 mm (range 25-120), MRF involvement 24 pts, Stage IIA 7 pts – III 62 pts. All of the pts completed the RT; 45 Gy were delivered to total mesorectum and lymphatic drainage with median SIB dose of 55 Gy (range 52.5-57.5). Forty-nine (71%) pts received concomitant CT with capecitabine alone and 17 (25%) capecitabine plus oxaliplatin. Globally, 16/69 (23%) pts did not complete CT for haematological (5) or, gastrointestinal toxicities (5) and other causes (6). Fourteen (20%), 33 (48%) and 23 (33%) pts experienced grade 1-2 haematological, gastrointestinal and genitourinary toxicity, respectively. Two out of 69 (3%) pts developed grade 3 haematological toxicity and 9/69 (13%) grade 3 gastrointestinal toxicity. Forty-three pts underwent surgery (LAR 28, APR 10, local excision 5 pts) but definitive histology is not yet available in 7 pts. Twenty-six pts are waiting for surgery. The tumor downstaging was documented in 29/36 (80.5%) pts. Forty-four rate (16/36) of surgical cases achieved pathologic complete response.

Conclusion: Despite the limitations related to the heterogeneity of the treatment delivery (SIB dose and concomitant CT), the RT dose-escalation in the preoperative treatment of LARC seems feasible, well tolerated and effective in terms of tumor downstaging and pathological complete response. Nevertheless, this results need to be confirmed on a larger cohort.

EP-1304

Image guided intensity modulated radiotherapy for anal cancer: a multi institutional study

B. De Bari[1], L. Lestrade[2], A. Franzetti Pellanda[3], R. Jumeau[1], M. Kountouri[1], O. Matzinger[4], N. Corradini[5], M. Biggiogero[3], G. Ballerini[3], J. Bourhis[1], R. Miralbell[2], M. Ozsahin[1], T. Zilli[2]
[1]*Centre Hospitalier Universitaire Vaudois, Department of Radiation Oncology, Lausanne Vaud, Switzerland*
[2]*Hopitaux Universitaires de Genève, Department of Radiation Oncology, Genève, Switzerland*
[3]*Clinica luganese, Department of Radiation Oncology, Lugano, Switzerland*
[4]*Riviera-Chablais Hospital, Department of Radiation Oncology, Vevey, Switzerland*
[5]*Clinica luganese, Medical Phisics, Lugano, Switzerland*

Purpose or Objective: To report the results of a retrospective pooled analysis of anal carcinoma (AC) patients treated with IMRT, VMAT, helical tomotherapy (HT) and daily image-guided RT (IGRT) in 3 Swiss radiotherapy centers.

Material and Methods: Local control (LC) and grade 3 or more toxicity rate (CTCAE v.4.0) were the primary endpoints. Overall (OS), disease-free (DFS), distant metastasis-free (DMFS) and colostomy-free survival (CFS) were also studied. Volumes were defined as follows: CTV1 : Anal canal, mesorectal, pelvic, and inguinal nodes. CTV2 : anal tumor and clinically positive nodes. Planning target volumes were obtained by adding 5-mm margin to the CTV (PTV1 and PTV2, respectively). PTV1 received 36 Gy (1.8 Gy/fraction) delivered with IMRT (n = 44), VMAT (n = 16) or HT (n = 100), while PTV2 received a sequential boost up to a total dose of 59.4-60 Gy (1.8-2 Gy/fr), delivered with IMRT (n = 16), VMAT (n = 18) , HT (n = 59) or 3D-conformal RT (CRT, n = 67).

Results: From 03.2006 to 04.2015, 160 patients were treated; 30, 68, 60 and 2 patients presented stage I, II, III, and IV, respectively. Median age was 62 years (range: 35-89). A planned gap was used in 130 patients. Median gap duration was 10 days (range, 5-24). Concomitant chemotherapy (CTX) was delivered in 149 patients, mainly using mitomycine C combined with fluoropyrimidines (i.v. or oral, n = 139). Median follow-up was 45 months (range: 3-97). Four-year LC, OS, DFS, DMFS and CFS rates were 83.6%, 82.3%, 82.7%, 93.4% and 88%, respectively. Time to progression for relapsing patients was 29 months (range: 1-78). A total of 24 patients presented a recurrence (local only in 14, locoregional in 1, locoregional and distant in 1, local and distant in 3, regional only in 2, and distant only in 3 patients). Fourteen patients underwent a colostomy because of local recurrence (n = 12) or pretreatment anal sphincter dysfunction (n = 2). Grade 3 acute toxicity was observed in 30 patients (18.4%), usually as erythema (23/30) or diarrhoea (10/30). No late G3 cutaneous toxicity was recorded. At the time of analysis, 150 patients presented more than 6 months of follow-up and were considered evaluable for late toxicity. Data about late toxicity were not available for 6 patients, followed in other Institutions. Looking at the final 144 patients, 3 of them patients presented a late G3 gastrointestinal toxicity (anal incontinence). No G4 acute or late toxicity was recorded. No significant differences were observed in terms of local control or acute G3 toxicity between IMRT and 3D-CRT boost techniques.

Conclusion: A total dose of 59.4/60 Gy to the anal tumor and involved nodes, including 36 Gy to the elective nodal regions , is effective and safe when delivered using modern IMRT techniques and daily IGRT. Thus, VMAT or HT and concurrent CTX are the standard of care in our institutions.

EP-1305

Impact of time from neoadjuvant treatment and surgery in rectal cancer: a monoinstitutional report

L. Belgioia[1], A. Bacigalupo[1], I. Chiola[1], G. Blandino[1], G. Lamanna[1], S. Vagge[1], S. Scabini[2], E. Romairone[2], R. Murialdo[3], A. Ballestrero[3], R. Corvò[1]
[1]*IRCCS AOU San Martino-IST, Radiation Oncology, Genoa, Italy*
[2]*IRCCS AOU San Martino-IST, Surgery Department, Genoa, Italy*
[3]*IRCCS AOU San Martino-IST, Medical Oncology, Genoa, Italy*

Purpose or Objective: The aim of the study was to analyze if time from neo-adjuvant chemoradiotherapy (CTRT) to radical surgery influences oncologic outcomes in locally advanced rectal cancer.

Material and Methods: We performed a retrospective analysis of 132 consecutive patients with rectal cancer treated at our Institute from March 2006 to March 2013 who underwent to neoadjuvant therapy followed by radical resection. Of these, 12 patients were excluded as lost at follow up, 3 patients for peritoneal carcinosis detection at surgery time and 3 patients refused surgery after neoadjuvant treatment. The remaining patients were analyzed and divided into two groups according to time to surgery (group A≤ 8 weeks and group B > 8 weeks) after completion of CTR

Results: A total of 114 patients underwent total mesorectal excision (TME) after neoadjuvant treatment for stage II and III rectal cancer between 0 and 15 cm from anal verge. There were 51 (45%) patients in group A (interval ≤ 8 weeks) and 63 (55%) in group B (interval > 8 weeks). Median time from chemo-radiotherapy and surgery was 7 weeks (range 1-8) and 12 weeks (range 9-17), respectively, in group A and B. In group B there was a major number of patients with no involvement of circumferential resection margin (CRM), 60 vs 48, and a higher number of major pathologic responce (pT0 – pT1), 19 vs 9. Disease free survival (DFS) at 5 years was 85.7% vs 75.9% and overall survival (OS) at 5 years was 83.7% vs 92% in group A vs group B.

Conclusion: In our analysis we did not reach statistical significance difference as regards DFS and OS in the two groups of patients; however we observed a favorable trend in the group of patients that underwent to surgery after 8 weeks from neoadjuvant treatment in terms of pathological responce and free radial margin.

EP-1306

Helical Tomotherapy with daily image guided radiotherapy for neoadjuvant treatment of rectal cancer

B. De Bari[1], A. Franzetti Pellanda[2], A. Saidi[1], G. Ballerini[2], M. Biggiogero[2], L. Negretti[2], A. Durham[1], J. Bourhis[1], M. Ozsahin[1]
[1]*Centre Hospitalier Universitaire Vaudois, Department of Radiation Oncology, Lausanne Vaud, Switzerland*
[2]*Clinica Iuganese, Department of Radiation Oncology, Lugano, Switzerland*

Purpose or Objective: Intensity modulated radiotherapy (IMRT), including helical Tomotherapy (HT), has been only recently introduced in the treatment of locally advanced rectal cancer (LARC) patients. We retrospectively assessed acute toxicity and efficacy of concomitant chemo-radiotherapy (CRT) delivered with HT and daily image-guided RT (IGRT) for non metastatic LARC patients in 2 Swiss institutions.

Material and Methods: We analyzed acute grade 3+ toxicity (CTC-AE v.4.0) and local control (LC) rates. Late toxicity 3+, Overall (OS), disease-free (DFS), and colostomy-free survival (CFS) were also studied and reported. Tumor Regression Rate (TRG) after CRT was scored using the Mandard score. Volumes were defined as follows: CTV1: rectum + mesorectum + internal iliac nodes + presacral nodes + obturatory nodes. In one of the 2 institutition, a CTV2 was also defined: rectal GTV + corresponding mesorectum (with a 2-cm margin in the cranio-caudal direction) + nodal GTV (if N+ patients). Planning target volumes were obtained by adding 5-mm margin to the CTV (PTV1 and PTV2, respectively). PTV1 received 44-45 Gy (1.8-2 Gy/fraction), while PTV2 received a simultaneous integrated boost up to a total dose of 50 Gy (2 Gy/fr).

Results: From 01.2010 to 01.2015, 118 patients were treated; 35, 9, 61, 12 and 1 patients presented a stage II, IIIA, IIIB, IIIC and IVa, respectively. Median age was 65 years (range, 32-85). All patients received concomitant CTX with fluoropyrimidine (i.v. or oral). After a median time of 53 days (range, 1-142), all patients received a radical surgery. Mean follow-up was 21 months (range: 1-62). No Grade 3 acute toxicity was observed. Acute grade 1-2 toxicity was observed in 22% of patients. Three-years LC, OS, DFS, and CFS rates were 95,2%, 82.4%, 83% and 69%, respectively. Median time to any progression for relapsing patients was 23 months (range: 5-66). At the time of analysis, 108 patients presented more than 4 months of followup and were considered evaluable for late toxicity. Data about late toxicity were not available for 48 patients, followed in other Institutions after RT-CT. Looking at the final 60 patients, only 2 of them patients presented a late G3 gastrointestinal toxicity (anal incontinence). Looking at 3-year LC, at univariate analysis, patients operated in the 66 days after the end of the treatment (98.8% vs 83.6%, Log-rank test: p = 0.022) and those without endovascular invasion at final pathology (98.6% vs 83.3%, p = 0.022) presented better LC rates. Concomitant boost did not improve 3-year LC, but increased the rate of TRG1 and TRG1-2 patients (Pearson's chi-squared test : p = 0.002 and p = 0.04, repsectively).

Conclusion: CRT delivered using HT and daily IGRT is safe and effective in the treatment of LARC patients. Longer followup time and prospective series are needed to confirm our results. Concomitant boost increase the rate of complete or nearly complete pathological response. The impact of TRG on the LC could probably assessed on after a longer followup time.

EP-1307

Chemoradiation in anal cancer with using VMAT: toxicity and early outcome.

D. Russo[1], E. Donno[1], A. Papaleo[1], E. Cavalera[1], C. Capomolla[2], D. De Luca[2], G. Di Paola[1], F.P. Ricci[1], M. Santantonio[1]
[1]*Vito Fazzi Hospital ASL LE, Radioterapia, Lecce, Italy*
[2]*Vito Fazzi Hospital ASL LE, Fisica Sanitaria, Lecce, Italy*

Purpose or Objective: To evaluate safety and feasibility of SIB-IMRT with VMAT combined with chemotherapy as exclusive treatment in patients with anal cancer. Early response is a secondary endpoint.

Material and Methods: From November 2010 to June 2015, 16 consecutive patients with histological diagnosis of anal squamous cells carcinoma underwent to chemoradiation in our center. Patients' characteristics are described in Table 1. Radiation schedule consisted of 52-58 Gy in 2-Gy daily fractions to High Risk Volume (HR), 49.95-54 Gy to Intermediate Risk Volume (IR) and 45-48 Gy to Low Risk Volume. Daily dose fraction was around 1.65 and 1.75 for LR and IR respectively. One patient received a radiation boost up to 66 Gy after 60 days from the end of chemoradiation due to a poor objective response. HR, IR and LR delineation was performed according to AIRO guidelines published in 2012 and reviewed in 2014. Organs at Risk (OAR) were: bladder, bilateral femoral heads and small bowel. All treatment plans were obtained with VMAT technique. SIB was calculate by Oncentra Inverse Planning System. In the first 3 patients was performed a split course radiation schedule to reduce toxicity risk. Target objectives were minimum coverage by 95% isodose and maximum dose of 107% within the volume. OARs' constraints were those suggested by AIRO guidelines (femoral heads: V52<10%; small bowel V45< 195cc; bladder: V60<50%). Median follow-up was 13 months (3-55). Concomitant chemotherapy is described in table 1.

Patient characteristics	
Age	Range 45-83
Sex	F: 12 M: 4
Stage (TNM)	I: 1 II: 5 IIIA: 4 IIIB:6
Concomitant Chemotherapy Schedule	Mytomicin/5 FU: 4 Mytomicin/Xeloda: 6 CDDP/ 5 FU: 2 5FU: 2 Xeloda: 2

Table 1: Description of patients'characteristics and concomitant chemotherapy schedules.

Acute Toxicity, according to RTOG criteria, was weekly recorded during radiotherapy course and monthly in the first three months of follow-up.

Results: Target coverage and organ at risk sparing were optimal in all plans (fig1).

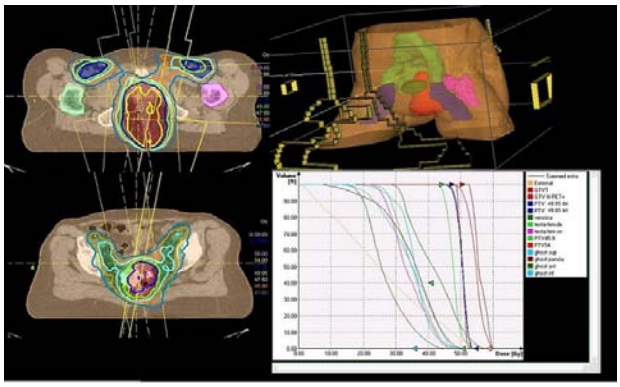

Fig 1: Example of treatment plan. Prescriptio doses werw 54 Gy to HR, 49.95 Gy to IR and 45.9 Gy to LR. Treatment was delivered in 27 fractions.

During chemioradiation none of patients developed G3 Gastroenteric toxicity (6 G1; 7 G2) and Genitourinary side effects were extremely rare (1 G1; 1 G2). Skin toxicity was the most important adverse event registered (8 G2; 4 G3). All chemotherapy schedule were well tolerated such the

incidence of hematologic toxicity was low (1 G1; 1G2). Early response evaluated by instrumental re-staging after 3 months from the end of treatment was encouraging, since 8 patients achieved complete response and 8 a partial response. Among the 6 patients with at least 2 years of follow up, 3 patient developed a progression disease (1 local relapse an 2 distant metastasis) and 1 patient died of disease after 3 years from treatment. The patient who underwent to radiation boost after chemoradiation developed anal stenosis which required a permanent colostomy.

Conclusion: SIB with VMAT combined with chemotherapy is quite feasible in anal cancer treatment. It easily allows different dose delivering to target at different risk of disease involvement. Split course schedule has not be more used because of acceptable acute toxicity profile, which was confirmed in conventional fractionation. A larger patient number and a longer follow-up are required to confirm our data.

EP-1308

Effect of prone and supine positions on setup and organ-at-risk sparing using VMAT for rectal cancer

A. Kim[1], A. Karotki[1], J. Foster[2], K. Yip[2], J. Presutti[2], S. Wong[3], W. Chu[3]
[1]*Sunnybrook Health Sciences Centre University of Toronto, Medical Physics, Toronto, Canada*
[2]*Sunnybrook Health Sciences Centre University of Toronto, Radiation Therapy, Toronto, Canada*
[3]*Sunnybrook Health Sciences Centre University of Toronto, Radiation Oncology, Toronto, Canada*

Purpose or Objective: Radiation treatment for rectal cancer is usually given in the prone position on a belly board with the aim to move the small bowel away from the treatment volume. In practice, this position is sometimes difficult to set up reproducibly and is poorly tolerated for some patients. With the increasing conformality and accuracy of using VMAT and cone beam CT (CBCT), we asked if there was any dosimetric advantage of treating rectal patients prone—it may be that patients can be better treated in the supine orientation. The two aims of this study are 1) to investigate setup reproducibility of rectal cancer patients treated in the prone and supine positions, and 2) to compare dose-volume histogram (DVH) metrics for the bladder and small bowel for both treatment positions.

Material and Methods: Eighteen consecutive patients with rectal cancer who received neoadjuvant chemoradiation were selected for this study. 9 were treated supine and 9 in the prone position. Patients were prescribed a total dose of 50.4 Gy in 1.8 Gy daily fractions according to institutional protocol and were planned with a VMAT posterior half arc. To determine setup reproducibility, weekly CBCTs were acquired and matched to bone. The CBCT-determined translational and rotational shifts were recorded. Clinically relevant dose-volume histogram values were generated for the small bowel and bladder.

Results: The CBCT-determined rotational setup error ranges for the prone position in pitch, roll, and yaw were [-3.6° 4.7°], [-4.2° 3.2°], and [-1.4° 1.1°] respectively. For the supine position the corresponding ranges were [-4.8° 2.0°], [-2.4° 1.3°], and [-1.0° 3.2°]. 7 patients exhibited >±3° rotational errors in the prone versus only 2 in the supine position, indicating better setup reproducibility in the supine position. Translational errors were generally <±1 cm in all directions for both positions. The small bowel V45 and mean dose for prone was 7.3±9.9% and 16.9±6.8 Gy (± values represent standard deviations) respectively; for supine the values were 6.8±7.6% and 19.6±6.4 Gy. The bladder V30 and mean dose for prone were 64.4±14.3% and 36.8±4.1 Gy respectively; for supine, these values were 68.7±18.5% and 37.3±4.1Gy.

Conclusion: There may be increased rotational instability in the prone position, but no apparent dosimetric advantage for small bowel sparing was observed. Rectal cancer patients who undergo neoadjuvant radiation using VMAT and CBCT may not need to be treated prone on a belly board.

EP-1309

Predictive value of FDG-PET in rectal cancer: correlation with tumour characteristics and response.

L. Turri[1], F. Apicella[1], A. Caroli[1], R. Grasso[1], S. Torrente[1], E. Puta[2], D. Ferrante[3], G.M. Sacchetti[2], M. Brambilla[4], M. Krengli[1]
[1]*University Hospital Maggiore della Carità, S.C. Radioterapia, Novara, Italy*
[2]*University Hospital Maggiore della Carità, S.C. Medicina Nucleare, Novara, Italy*
[3]*University Hospital Maggiore della Carità, Biostatistica ed Epidemiologia Clinica, Novara, Italy*
[4]*Università del "Piemonte Orientale", Dipartimento di Medicina Traslazionale, Novara, Italy*

Purpose or Objective: The present study analyses the correlation of pre-treatment (18)F-fluorodeoxyglucose Positron Emission Tomography/Computed Tomography (FDG-PET/CT) standardized uptake value (SUV) and total lesion glycolysis (TLG) with tumour characteristics and clinical response in a series of rectal cancer patients treated with neoadjuvant chemo-radiotherapy.

Material and Methods: Fifty-six patients were included in the present analysis. Pre-treatment PET maximum SUV (SUVmax), mean SUV and TLG of primary tumour were calculated for each patient. The total dose of pelvic radiotherapy was 45-50.4 Gy, 1.8 Gy/fraction. Chemotherapy was delivered with capecitabina or 5-fluorouracil. Six to eight weeks after RT-CT, 44 patients (78.6%) had anterior rectal resection and 12 patients (21.4%) had abdominal pelvic resection (Miles).
Tumor Regression Grade (TRG) (Mandard, 1994) was defined on surgical specimen. Complete regression (TRG1) was observed in 10/56 (17.9 %).The correlation between PET/CT results and histopathological data and tumour response was analyzed.

Results: At the level of the primary tumour, SUVmax ranged from 4.17 and 54.06 (mean 22.46, median 18.96), SUV mean ranged from 6.22 and 32.64 (mean 13.42, median 11.09) and TLG ranged from 7.96 and 3158.23 (mean 350.21, median 183.55).
SUVmax (p=0.05) and TLG (p=0.002) significantly correlated with T-stage. Median SUVmax was significantly higher (p = 0.05) for lesions with partial response (PR, 46/56, 82.1%) than for lesions with complete response (CR, 34/54, 17.9%). Median TLG was significantly higher (p=0.034) for lesions with partial response (PR, 45/54, 83.3%) than for lesions with complete response (CR, 9/54, 16.7%).
SUVmean was not significantly correlated with T-stage (p=0.074). Median SUVmean was higher for lesions with partial response (PR, 45/54, 83.3%) than for lesions with complete response (CR, 9/54, 16.7%) but without statistical significance (p =0.18).

Conclusion: Our data suggest that pre-treatment FDG-PET/CT SUVmax and TLG are strongly associated with tumour primary tumour stage. Furthermore they correlate with prediction of tumour response after neoadjuvant treatment.

EP-1310

PV of FDG-PET SUV in rectal cancer pts: correlation with tumor characteristics/response to neoadj RT

L. Turri[1], F. Apicella[1], A. Caroli[1], R. Grasso[1], S. Torrente[1], E. Puta[2], D. Ferrante[3,4], G. Sacchetti[i2], M. Brambilla[5], M. Krengli[1]
[1]*AOU Maggiore della Carità, Radiotherapy, Novara, Italy*
[2]*AOU Maggiore della Carità, Nuclear Medicine, Novara, Italy*
[3]*AOU Maggiore della Carità, Biostatistica ed Epidemiologia Clinica, Novara, Italy*
[4]*Università del "Piemonte Orientale"-, Dipartimento di Medicina Traslazionale, Novara, Italy*
[5]*AOU Maggiore della Carità, Fisica Medica, Novara, Italy*

Purpose or Objective : The present study analyses the correlation of pre-treatment (18)F-fluorodeoxyglucose

Positron Emission Tomography/Computed Tomography (FDG-PET/CT) standardized uptake value (SUV) and total lesion glycolysis (TLG) with tumour characteristics and clinical response in a series of rectal cancer patients treated with neoadjuvant chemo-radiotherapy

Material and Methods: Fifty-six patients were included in the present analysis. Pre-treatment PET maximum SUV (SUVmax), mean SUV and TLG of primary tumour were calculated for each patient. The total dose of pelvic radiotherapy was 45-50.4 Gy, 1.8 Gy/fraction. Chemotherapy was delivered with capecitabina or 5-fluorouracil. Six to eight weeks after RT-CT, 44 patients (78.6%) had anterior rectal resection and 12 patients (21.4%) had abdominal pelvic resection (Miles).
Tumor Regression Grade (TRG) (Mandard, 1994) was defined on surgical specimen. Complete regression (TRG1) was observed in 10/56 (17.9 %).The correlation between PET/CT results and histopathological data and tumour response was analyzed.

Results: At the level of the primary tumour, SUVmax ranged from 4.17 to 54.06 (mean 22.46, median 18.89), SUV mean ranged from 6.22 to 32.64 (mean 13.42, median 11.09) and TLG ranged from 7.96 to3158.23 (mean 350.21, median 183.55).SUVmax (p=0.05) and TLG (p=0.002) significantly correlated with T-stage. Median SUVmax was significantly higher (p = 0.05) for lesions with partial response (PR, 46/56, 82.1%) than for lesions with complete response (CR, 34/54, 17.9%). Median TLG was significantly higher (p=0.034) for lesions with partial response (PR, 45/54, 83.3%) than for lesions with complete response (CR, 9/54, 16.7%).
SUVmean was not significantly correlated with T-stage (p=0.074). Median SUVmean was higher for lesions with partial response (PR, 45/54, 83.3%) than for lesions with complete response (CR, 9/54, 16.7%) but without statistical significance (p =0.18).

Conclusion: Our data suggest that pre-treatment FDG-PET/CT SUVmax and TLG are strongly associated with tumour primary tumour stage. Furthermore they correlate with prediction of tumour response after neoadjuvant treatment

Electronic Poster: Clinical track: Gynaecological (endometrium, cervix, vagina, vulva)

EP-1311
Chemoradiotherapy followed by surgery in patients with locally advanced cervical carcinoma

J. Anchuelo Latorre[1], A. Kannemann[1], A.S. Garcia Blanco[1], M. Ferri Molina[1], P. Galdos Barroso[1], A. Muniz Garcia[1], J.C. Menendez Garcia[1], J. Cardenal Carro[1], R. Fabregat Borras[2], H. Vidal Trueba[3], R. Jimeno Mate[4], S. Hermana Ramirez[5], J. Estevez Tesouro[6], P. Prada Gomez[1]
[1]*Hospital Universitario Marques De Valdecilla, Radiation Oncology, Santander, Spain*
[2]*Hospital Universitario Marques De Valdecilla, Physics, Santander, Spain*
[3]*Hospital Universitario Marques De Valdecilla, Radiology, Santander, Spain*
[4]*Hospital Universitario Marques De Valdecilla, Medical Oncology, Santander, Spain*
[5]*Hospital Universitario Marques De Valdecilla, Patology, Santander, Spain*
[6]*Hospital Universitario Marques De Valdecilla, Gynecology, Santander, Spain*

Purpose or Objective: To evaluate pathological response and clinical outcomes in women with locally advanced cervical cancer treated with radiochemotherapy and surgery in a tertiary hospital.

Material and Methods: In this retrospective analysis we have included 59 patients with cervical cancer (FIGO stages IB2-IVA) who were treated between December 2004 and July 2015 with concurrent chemoradiation therapy (CCRT) followed by surgery. The patients were treated with pelvic external beam radiotherapy at 46-50,4 Gy, 1,8-2 Gy/day. Based on CT or PET CT if aortic nodes were demonstrated, extended external beam radiotherapy was performed. We boosted nodes or parametria if they were affected (60-68 Gy, 2 Gy/day). After four weeks of treatment, patients received brachytherapy from 15 to 26 Gy in 3-6 fractions with 2D planification or 3D planification (n=28), with a total tumour dose between 85 and 90 Gy. Concurrent chemotherapy with weekly platin and in some cases oral fluoropirimidine was administrated. Overall treatment time did not exceed 8 weeks. All patients completed surgery between 4-15 weeks after CCRT.

Results: The median age was 52 years (range 30 and 77). Squamous cell carinoma was the most common subtype (81%). All patients received hysterectomy. 7 patients (12%) underwent lymphadenectomy. In global, 32 patients (54%) had a complete response, 20 (34%) a partial response and 7 (12 %) patients had residual microscopic disease in the pathologic analysis. With a median follow up of 53 months (range from 2 to 128 months) overall survival was 85% and disease free survival 81%

Conclusion: Our results show that CCRT followed by surgery gets excellents outcomes with acceptable toxicity and may reduce local recurrences. Besides it enables assessment of the pathological response.

EP-1312
Measurement of GTV delineation uncertainty for centrally recurrent gynaecological cancers

D. Bernstein[1], M. Llewelyn[1], A. Taylor[1], S. Nill[1], U. Oelfke[1]
[1]*Royal Marsden Hospital Trust & Institute of Cancer Research, Department of Medical Physics, London, United Kingdom*

Purpose or Objective: To quantify the magnitude of clinician uncertainty in GTV delineation for patients with recurrent gynaecological cancers.

Material and Methods: GTV delineation uncertainty was retrospectively investigated in patients previously treated in our institution for centrally recurrent gynaecological cancer. In order to record clinician delineation uncertainty, clinicians were asked to draw 3 outlines per GTV; an inner GTV (GTV_I) corresponding to the innermost boundary the GTV is likely to have, an outer GTV (GTV_O)corresponding to the outmost boundary the GTV is likely to have and a clinical GTV (GTV_C) outlined in accordance with local treatment protocols. For GTV_C, each observer submitted a confidence score from 1 to 5, with 1 being no confidence in drawn and 5 complete confidence. For each patient, the 3 GTV's were delineated on a co-registered CT-MR, using a local rigid soft tissue registration, as well as on MR images only in order to identify how the co-registered CT information affects the decision process. Paired T Tests (p) were used to test for significance and Pearson correlation coefficient (r) for correlations.

Results: To date, 18 recurrences from 17 patients were investigated by a single observer. For all 17 MR only contours and for 15 out of the 17 CT-MR contours, the GTV_O and GTV_C were identical. GTV_C ranged from 6.3 to 192.9cm3 for CT-MR contours and from 5.5 to 180.1cm3 for the MR only contours, with a mean ± standard deviation of 53.3±44.7cm3 and 39.3±40.4cm3 respectively. The reduction in GTV_I relative to GTV_C was 19.6±12.4cm3 ($p<0.01$) for CT-MR contours and 13.3±9.8cm3 ($p<0.01$) for MR only contours. For GTV_C, MR only contours were consistently smaller than CT-MR contours by 14.0±11.4cm3 ($p<0.01$). For GTV_I, MR only contours were smaller for 13 out of the 17 cases, with differences of 7.9±7.7cm3 ($p<0.01$). The 3D difference in the centre of mass (COM) between GTV_O and GTV_C was 2±2mm for the CT-MR contours and 2±1mm for the MR only contours. Scoring of GTV_C was significantly lower ($p<0.01$) for CT-MR contours relative to MR only contours, with scores of 2.8±0.6 and 3.6±0.7 respectively.

Conclusion: Uncertainty exists in defining the boundary of the GTV for this patient cohort resulting in uncertainty in

both the volume and centre of the GTV. The process of using co-registering MR-CT images increases the uncertainty and leads to larger volumes when compared to GTV delineation using MR only. Data from additional observers will help quantify the magnitude of GTV delineation uncertainties. The limitation of having outlines from a single non-expert observer will be addressed in the final publication.

EP-1313

Short course post operative IMRT on vaginal vault of endometrial tumor at low-risk of recurrence

G. Macchia[1], S. Cilla[2], F. Deodato[1], M. Nuzzo[1], A. Ianiro[2], D. Catani[1], V. Valentini[3], G. Ferrandina[4], A. Galuppi[5], M. Ferioli[5], S. Cammelli[5], L. Ronchi[5], S. Cima[5], M. Perrone[6], P. De Iaco[6], F. Romani[7], G. Frezza[8], A.G. Morganti[5]

[1]*Fondazione di Ricerca e Cura "Giovanni Paolo II"- Catholic University of Sacred Heart, Radiation Oncology Unit, Campobasso, Italy*

[2]*Fondazione di Ricerca e Cura "Giovanni Paolo II"- Catholic University of Sacred Heart, Medical Physic Unit, Campobasso, Italy*

[3]*Policlinico Universitario "A. Gemelli"- Catholic University of Sacred Heart, Department of Radiotherapy, Roma, Italy*

[4]*Policlinico Universitario "A. Gemelli"- Catholic University of Sacred Heart, Department of Gynecologic Oncology, Roma, Italy*

[5]*S. Orsola-Malpighi Hospital- University of Bologna, Radiation Oncology Center- Department of Experimental- Diagnostic and Specialty Medicine – DIMES, Bologna, Italy*

[6]*S. Orsola-Malpighi Hospital, Gynecologic Oncology Unit, Bologna, Italy*

[7]*S. Orsola-Malpighi Hospital- University of Bologna, Department of Medical Physics, Bologna, Italy*

[8]*Bellaria Hospital, Radiotherapy Department, Bologna, Italy*

Purpose or Objective: To evaluate long-term clinical results after intensity modulated radiotherapy technique (IMRT) on vaginal vault in post-operative low-risk endometrial cancer patients.

Material and Methods: Patients enrolled in two sequential trials (June 2006-October 2014) were analysed. A radiopaque methacrylate vaginal applicator was placed in the vagina. Patients were planned in supine position and immobilized using a vacuum cushion. Each patient was instructed to follow a protocol of controlled bladder filling and rectal emptying. Three radiopaque markers (1 mm diameter) fixed on the applicator allowed to improve visualization on portals imaging. Radiotherapy was delivered on the upper two thirds of the residual vagina (CTV), daily identified by the radiopaque markers. A 5 mm isotropic margin was added to the CTV in order to define the planning target volume (PTV). A 7 beams step and shoot IMRT technique was used by means of Plato Sunrise and Ergo++ treatment planning systems. 25Gy/5Gy *per* fraction in the first trial and 30Gy/6Gy in the second one were the doses delivered to PTV. Toxicity was scored by the CTC-AE v.3.0 scale.

Results: 23 patients (median age 63 years, range 49-88; stage IA: 69.6%, IB: 21.7%, II: 8.7%; grading G1: 3; G2: 17; G3: 3) were included in this analysis. Seven patients received 25Gy/5Gy and 16 received 30 Gy/6Gy *per* fraction. Proctitis and dysuria were the most common toxicities. Twelve patients (52.2%) developed late mild toxicity (G2: 1 rectal bleeding and 1 atrophic skin with plaque lesions). The most common late toxicity was G1 vulvar telangiectasia (26%), while 3 patients developed G1 vaginal stenosis (Table 1).

Table 1: Toxicity (CTC-AE Scale v.3.0)

Acute Toxicity				
Type	N° pt (%) Grade 1	N°pt (%) Grade 2	N° pt (%) Grade 3	N° pt (%) Grade 4
Skin reaction	5(21.7)	2 (8.6)	0 (0)	0 (0)
Proctitis	11(47.8)	3 (13.0)	0 (0)	0 (0)
Dysuria	8(34.7)	4 (17.3)	0 (0)	0 (0)
Mucosal inflammation	2 (8.6)	2 (8.6)	0 (0)	0 (0)
Late Toxicity				
Type	N° pt (%) Grade 1	N°pt (%) Grade 2	N° pt (%) Grade 3	N° pt (%) Grade 4
Skin reaction	1(4.3)	1(4.3)	0 (0)	0 (0)
Proctitis/Rectal bleeding	2 (8.6)	1(4.3)	0 (0)	0 (0)
Dysuria	3 (13.0)	0(0)	0 (0)	0 (0)
Atrophic mucosae	1 (4.3)	0(0)	0 (0)	0 (0)
Vulvar telangiectasia	6 (26.0)	0(0)	0 (0)	0 (0)
Vaginal Stenosis	3(13.0)	0(0)	0 (0)	0 (0)

With a median follow-up of 52 months (range 4-103) no vaginal recurrence was observed (5-year local control: 100%), while 4 patients developed pelvic or distance relapse (5-year disease-free survival: 86.4%). Five-year overall survival was 100%.

Conclusion: Endovaginal brachytherapy studies reported 0-5.2% late severe toxicity. Most toxicities were vaginal and urethral stenosis or rectal vaginal fistula, not observed in our study. In conclusion postoperative IMRT on vaginal vault showed promising clinical long-term results.

EP-1314

External beam boost for cancer of the cervix in patients unable to receive brachytherapy

H. Kim[1], Y.S. Kim[2], K.Y. Eom[3], W. Park[4], J.H. Kim[5], J.H. Lee[6], Y.S. Kim[7], S.H. Lee[8], K. Ahn[9], Y.B. Kim[10], M.Y. Lee[11], S.K. Chang[12]

[1]*Hallym University Dongtan Sacred Heart Hospital, Department of radiation oncology, Hwaseong, Korea Republic of*

[2]*Asan Medical Center- University of Ulsan College of Medicine, Department of Radiation Oncology, Seoul, Korea Republic of*

[3]*Seoul National University Bundang Hospital, Department of Radiation Oncology, Seoungnam, Korea Republic of*

[4]*Samsung Medical Center- Sungkyunkwan University School of Medicine, Department of Radiation Oncology, Seoul, Korea Republic of*

[5]*Dongsan Medical Center- Keimyung University School of Medicine, Department of Radiation Oncology, Daegu, Korea Republic of*

[6]*St. Vincent's Hospital- The Catholic University of Korea College of Medicine, Department of Radiation Oncology, Suwon, Korea Republic of*

[7]*The Catholic University of Korea, Department of Radiation Oncology, Seoul, Korea Republic of*

[8]*Gacheon University Gil Hospital, Department of Radiation Oncology, Incheon, Korea Republic of*

[9]*Inje University College of Medicine, Department of Radiation Oncology, Busan, Korea Republic of*

[10]*Yonsei Cancer Center- Yonsei University College of Medicine, Department of Radiation Oncology, Seoul, Korea Republic of*

[11]*Hallym University Sacred Heart Hospital, Department of Radiation Oncology, Anyang, Korea Republic of*

[12]*CHA Bundang Medical Center- CHA University, Department of Radiation Oncology, Seongnam, Korea Republic of*

Purpose or Objective: The current study aims to evaluate the outcomes in patients treated with radical radiotherapy for cervical cancer who received external beam radiotherapy (EBRT) boost in place of intracavitary brachytherapy (ICBT).

Material and Methods: We performed a multicenter retrospective study on the patients with cervical cancer treated with external beam boost as a substitution of ICBT during the period of January 2005 through October 2012 in 11 participating radiation oncology centers in Korea. Treatment outcome, prognostic factor, and toxicity were evaluated.

Results: Seventy-five patients were identified. The median age of the patients was 58 years (range, 33-92 years). The clinical stages were I in 6, II in 34, III in 18, and IVA in 17 patients. Concurrent chemotherapy was performed to 64 patients (85.3%). Radiation doses were median 46 Gy (range, 40-54 Gy) for whole pelvis and 24 Gy (range, 9-35 Gy) for tumor boost. Three-dimensional radiotherapy (in 24 patients) or intensity-modulated radiotherapy (in 51 patients) was used for tumor boost. On images taken 3-6 months after radiotherapy, 46 patients showed complete response (CR), 24 had partial response, and 2 were found to have progressive disease. The median follow-up time was 33 months. Disease progression was found in 30 patients (40.0%). Among these patients, 21 (28.0%) showed local progression with a median time to progression of 29 months (range, 3-101 months). The 5-year local progression-free survival (LPFS) rate was 70.0%. On uni- and multivariate analyses, treatment response at 3-6

months after radiotherapy was a significant factor for LPFS. Patients with CR had higher LPFS rate than the patients without CR (88.6% vs. 30.8%, at 5-year, p<0.01). Grade 3 toxicity was found in 8 patients (5 hematologic, 2 urinary, and 1 skeletal) and grade 5 bowel toxicity was found in 1 patient.

Conclusion: In radical radiotherapy for cervical cancer, EBRT can be an option for tumor boost in cases where ICBT cannot be performed. Tumor response at 3-6 months after radiotherapy was a significant prognostic factor for local control.

EP-1315

Abdominopelvic Radiotherapy for advanced endometrial cancer after surgery and chemotherapy: results

V. Rodriguez Gonzalez[1], J. Perez-Regadera[2], D. Lora[3], A. Campos[2], C. Chavez[2], B. Gil[2], R. Prados[2], M. Colmenero[2]
[1]*Rodriguez Gonzalez Virginia, Radiation Oncology, Madrid, Spain*
[2]*Hospital Doce de Octubre, Radiation Oncology, Madrid, Spain*
[3]*Hospital Doce de Octubre, Epidemiology, Madrid, Spain*

Purpose or Objective: Patients with advanced endometrial cancer are a very heterogeneousgroup of patients in which theprognosis is influenced by thenumber of extrauterine locations,abdominal and nodal spread, typeof surgery, tumor residue and histology.

Material and Methods: We studied 47 patients treated with SQTWAPI. The FIGOstaging was IIIAin 6 patients, IIIC in 22 and IVB in 16. The meanfollow-up for disease-freesurvival (DFS) was 32 months.In 26 patients werefound ≤3 extrauterine locations (≤3LE) and in 21 >3LE. Abdominal spread was presentin 26 and was not in 21, negative lymph nodespread in 11 (G-), positivein 33 (G +) andunknown in 3 (G?). Combination of abdominal dissemination and lymph node spread (AG) was observed in19 patients, only abdominalin 7 (SA), single nodal in 17 (SG) and noabdominal or nodal in 4 (NAG). In 23 ovarian surgery was performed and in 24 it was suboptimal.In 8 patients remained tumor residue and 39 did not remain. 19 patients hadendometrioid histology and 28 had a different one. Histological grade 1-2 in 11 and G3 in 36.

Results: The 5-year DFS was respectively ≤3LE patients was69% vs 30%in> 3LE (p= 0.0445). Withabdominal spread 73%vs 35% without(p = 0.05).Group (G-) 90%,group (G+) 47% andGroup (G?) 0%, (p = 0.0062).No residue 54%vs 34% (p = 0.11). Group (AG) 22%, group(SG) 65%, group(SA) 85%,Group (NAG) 100% (p = 0.0185). With ovarian protocolsugery 42% and without it 62% (p = 0.23).

Conclusion: The number of extrauterine locations, lymph node spread, abdominal dissemination and the combination of both influenced the SLE.

EP-1316

Value of imaging modalities in predicting pelvic lymph node metastases for uterine cervical cancer

W.K. Jung[1], K.J. Lee[1], J.H. Lee[1], Y.J. Kim[1], J.Y. Kim[1], H.J. Yoon[2], B.C. Kang[3], S.C. Kim[4], H.S. Moon[4], W. Ju[4], Y.H. Kim[4], K.R. Park[1]
[1]*Ewha Womans University, Radiation Oncology, Seoul, Korea Republic of*
[2]*Ewha Womans University, Nuclear Medicine, Seoul, Korea Republic of*
[3]*Ewha Womans University, Radiology, Seoul, Korea Republic of*
[4]*Ewha Womans University, Obstetrics and Gynecology, Seoul, Korea Republic of*

Purpose or Objective: The only imaging modalities without pathological confirmation are used to assess lymph node (LN) metastases and to perform radiation therapy (RT) planning for patients with uterine cervical cancer treated with concomitant chemoradiotherapy (CCRT) or RT alone. The aim of this study was to evaluate the accuracy of computed tomography (CT), magnetic resonance imaging (MRI) and positron emission tomography-computed tomography (PET/CT) in predicting pelvic LN metastases.

Material and Methods: From January 2009 to March 2015, one hundred fifty six patients with International Federation of Obstetrics and Gynecology (FIGO) Stage IA1-IIB uterine cervical cancer who underwent radical hysterectomy and pelvic lymphadenectomy, and CT, MRI and PET/CT before surgery were included in this study. The Criteria for LN metastases were a LN diameter of 1cm or more at CT and MRI and a focally increased FDG uptake greater than SUVmax 3.0 at PET/CT. The sensitivity, specificity, positive predictive value (PPV), negative predictive value (NPV) and accuracy for pelvic LN metastases were estimated on the basis of imaging and postsurgical pathological findings. Chi square test and McNemar's test was used to compare the sensitivity and specificity of imaging modalities for the detection of metastatic pelvic LN. A P ≤0.05 value was considered statistically significant.

Results: Among 156 patients, 35 (22%) had pelvic LN metastasis on postsurgical pathological findings. There was no pelvic LN metastasis for stage IA. The rates of pelvic LN metastasis on pathological findings for stage IB, IIA and IIB were 19%, 45%, 67%, respectively. The sensitivity, specificity, PPV, NPV and accuracy for detection of pelvic LN metastases were 48%, 87%, 39%, 91% and 81% for CT; 28%, 97%, 59%, 89% and 87% for MRI; and 43%, 90%, 43%, 90% and 83% for PET/CT, respectively. The sensitivity was highest for PET/CT, the specificity, highest for MRI and the accuracy, highest for MRI. The difference between single and multiple metastases on image studies to predict LN metastasis was not statistically significant (P=0.271).

Conclusion: CT, MRI and PET/CT showed low sensitivity and high specificity. The accuracies (greater than 80%) of the three imaging modalities were acceptable for RT planning for patients treated with CCRT or RT alone. More efforts are necessary to improve sensitivity in predicting pelvic LN metastases.

EP-1317

Prognostic and predictive factors in endometrial cancer

K. Boudaoud[1], S. Taleb[2], A. Brihmat[3], L. Beddar[4], H. Boudaoud[5], R. Aissani[2], S. Boussouf[2], A. Boukaaba[2], T. Filali[6], A. Djemaa[2]
[1]*Scientific research laboratory of molecular biology and genetics- Faculty of Medicine- University Constantine 3., Radiation oncology-, Constantine, Algeria*
[2]*Faculty of Medicine- University Constantine 3., Radiation oncology-, Constantine, Algeria*
[3]*CAC Batna Hospital, Radiation oncology-, Batna, Algeria*
[4]*Scientific research laboratory of molecular biology and genetics- Faculty of Medicine- University Constantine 3., Laboratory of pathological anatomy and cytology, Constantine, Algeria*
[5]*Ain Touta Hospital, Surgery, Batna, Algeria*
[6]*Scientific research laboratory of molecular biology and genetics- Faculty of Medicine- University Constantine 3., Medical oncology-, Constantine, Algeria*

Purpose or Objective: The outcomes among patients with endometrial cancer (EC) are generally favorable. However, certain risk factors, such as age, comorbidities, FIGO stage, histology type, myometrial infiltration and histology grade, may influence survival and prognosis. The aim of this study was to analyze the impact of prognostic factors on disease-free survival (DFS) and overall survival (OS) in patients treated with adjuvant radiotherapy.

Material and Methods: We reviewed the records of patients diagnosed with EC and received adjuvant radiation therapy. The period of recruitment was from January 2001 to December 2014. This included epidemiological, clinical and treatment characteristics. Statistical analyses, survival curves were generated using the Kaplan-Meier technique, and differences were tested with the log-rank test. Multivariate

analysis of prognostic factors was performed using the Cox proportional hazards model and logistic regression analysis.

Results: 155 eligible patients had their data analyzed for this work. The median age was 58.7 years (range 31-86). 55 patients suffered from coexisting comorbidities. All patients underwent surgery; a total abdominal hysterectomy plus bilateral salpingo-oopherectomy in 92.2%. Lymphadenectomy was realized in only 23 patients.They were classified according to FIGO stage on (91 I, 24 II, 29 III, 10 IVA). Myometrial invasion was > 50 % in 80%. Type1 endometrial carcinoma represents the most common type (134 patients). Histologic low-grade (G1–2) was found in 77.4%. 154 patients received radiotherapy; in 79 cases external beam Radiation therapy (EBRT) was associated with vaginal brachytherapy (VB). After median follow up of 72 months (2 -144 months) loco-regional recurrence occurred in 10 patients (5.1%) and metastasis in12 patients (7.7%), the 5-year overall survival (OS) and the Disease Free Survival (DFS) was 88,4%, and 76,1% respectively. DFS was highly significant for: histologic type 1*vs* 2 (p=0.005), histology grade 1-2 *vs* 3 (p= 0.03) and stage I-II *vs* III-IV (p= 0.04), The addition of VB to EBRT revealed statistically significant effect on DFS (p= 0.02).

Conclusion: In our study, tumor's histology type, grad, and FIGO stage are the important prognostic factors and should be considered when making treatment decisions. Delivery of adjuvant EBRT+VB seems to be a significant independent predictor for improved survival and pelvic control. Further studies on larger cohorts are necessary for the validation of those results.

EP-1318

Presence of lymph nodes and survival in cancer cervix: audit from tertiary care hospital in India

S. Singh[1], J. Lamin[1], D. Kapoor[2], A. Rani[2], N. Rastogi[1], S. Kumar[1]

[1]*Sanjay Gandhi Postgraduate Institute of Medical Sciences, Dept of Radiotherapy A-Block- SGPGIMS, Lucknow UP, India*

[2]*Sanjay Gandhi Postgraduate Institute of Medical Sciences, Dept of Gynecology- General Hospital- SGPGIMS, Lucknow UP, India*

Purpose or Objective: The present study was done to evaluate the impact of lymph node on survival outcome of cancer cervix treated by chemo-radiotherapy in a tertiary care hospital in a northern part of India

Material and Methods: Between Jan 2008- Dec 2011, 300 cervical cancer patients were registered. Medical records were retrieved and documented for various host and treatment related parameters and outcomes. Local disease free survival (LDFS) and overall survival (OS) was calculated from time of registration and computed by Kaplan–Meier method. Death due to any cause or loss to follow-up was considered as an event for survival analysis i.e. assuming the worst case scenario.

Results: Of 300 patients, 72 (24%) did not report after first consultation while 64 (21%) were referred for brachytherapy from outside medical facilities. For present analysis, 164 (55%) patients who received treatment with either radical or palliative intent in our department were studied. Of 164 cases, 76%, 15% and 9% presented as de novo cervical cancer, post-operative and stump carcinoma respectively. The median age (range) at presentation was 52years (26–90), 75% were postmenopausal. MRI was preferred pre staging imaging modality in half followed by ultrasound .FIGO stage I–IV was 17%, 37%, 30% and 16% respectively with more than half having bulky disease and a third presenting with regional lymph nodes and 10% had para-aortic lymph nodes seen on imaging at presentation. 93% patients were treated with radical while 7% with palliative intent. Two thirds received concurrent platin based chemoradiotherapy. Brachytherapy was taken by 80% cases. Patients were kept on clinical follow up and imaging was done as and when required.
At the time of analysis 38% are disease free and alive, 21 % dead while 40 % were lost to follow-up with or without disease. At median follow up of 24 months (0-90), LDFS for stage I, II, III and IV was NR (not reached), NR, 17 and 0 months, p=0.000 while median OS was NR, NR, 17 and 8, p=0.000 respectively. The median OS stage-wise with or without lymph node presence was - Stage I 27m vs. NR; Stage II 46m vs.NR; Stage III 14m vs. 17m and Stage IV 9m vs 2m; p=0.000 respectively. Those receiving chemotherapy in presence of lymph nodes had a better survival outcome median 21m vs 5m p=0.001.

Conclusion: Cervical cancer presented in bulky advanced stages with regional and metastatic spread at time of presentation. The presence of lymph node decreased survival in all stages. The addition of chemotherapy improved survival outcome.

EP-1319

Clinicopathological characteristics of patients with synchronous ovarian and endometrial cancers

S. Chaudry[1], T. Sadaf[1], S. Butt[1], A.A. Syed[2], N. Siddique[3], A. Jamshed[1], A. Kazmi[3]

[1]*Shaukat khanum Memorial Cancer Hospital, Radiation Oncology, Lahore, Pakistan*

[2]*Shaukat khanum Memorial Cancer Hospital, Surgical Oncology, Lahore, Pakistan*

[3]*Shaukat khanum Memorial Cancer Hospital, Medical Oncology, Lahore, Pakistan*

Purpose or Objective: Synchronous primary endometrial and ovarian cancers are infrequent. The objective of this study is to evaluate clinicopathological characteristics and treatment outcomes of synchronous endometrial and ovarian cancer treated in our institution.

Material and Methods: The clinicopathological characteristics of 12 patients with synchronous ovarian and endometrial cancer treated at SKMCH from July 2005 to July 2015 were reviewed retrospectively. Their medical records and pathology reports were reviewed in depth from hospital database. The histologic determination was followed by the World Health Organization Committee classification, and cancer stage was based on FIGO.

Results: The median age at the time of diagnosis was 50 years (Range23-66).The incidence of synchronous primary endometrial and ovarian cancers was 2.01 % in patients with endometrial cancer. A total of 7 patients were menopausal (58%), 8 patients were nulliparous (66%) the median BMI was 29 kg/m2 (range, 20–38). The most common presenting symptom was abnormal uterine bleeding. According to FIGO stage 10 cases of endometrial were I /II (88%) and 2 cases were stage III (16%). Of the ovarian cancers, 9 cases were stage I/II 83.3% and 2 cases were stage III (16.7%). Endometroid cancer was the main pathological type in uterine carcinoma (86%) followed by serous carcinoma (14%) and similarly for ovarian cancer endometroid was the most common pathology 67 % followed by serous/clear cell 16% and mucinous 16.7%. Most endometrial and ovarian primaries in our series were grade I and II tumors, 83% and 66% respectively.
8 patients (66%) had similar histology in both primaries while 4 patients (44%) had different histology. All patients underwent surgical intervention. Only one patient did not receive any postoperative adjuvant therapy. 10 patients received platinum-based adjuvant chemotherapy and six patients received adjuvant radiotherapy

Conclusion: Synchronous primary endometrial and ovarian cancers are infrequent and distinct set of patients. Abnormal PV bleed was the most common symptom which helped in early detection. Majority of the patients belong to concordant endometroid histology, low grade, had younger age and High BMI. Treatment should be tailored to the stage, histology, and grade of the individual tumors.

EP-1320

Postoperative radiotherapy results of serous endometrial carcinoma: 34 cases during 2003-2014

K. Holub[1], A. Rovirosa[2], G. Oses[1], L. Castilla[1], J. Mansilla[3], R. Llorente[1], K. Cortes[1], J. Garcia[1], S. Garrido[1], A. Huguet[1], C. Castro[1], J. Sola[1], J. Ordi[4], J. Pahisa[5], A. Biete[1]
[1]*Hospital Clínic i Universitari, Radiation Oncology Dpt, Barcelona, Spain*
[2]*Hospital Clinic i Provincial, Radiation Oncology Dpt, Barcelona, Spain*
[3]*Hospital Rebagliati, Radiation Oncology Dpt, Lima, Peru*
[4]*Hospital Clínic i Universitari, Pathology Dpt, Barcelona, Spain*
[5]*Hospital Clínic i Universitari, Ginecological cancer Unit, Barcelona, Spain*

Purpose or Objective: To evaluate post-operative treatment results of serous endometrial carcinoma (SEC) comparing two histological subtypes (with and without an endometrioid component) and its impact on overall survival (OS), local control, distant relapses in patients treated from 2003-2014.

Material and Methods: Thirty-four patients (p) with SEC were treated with post-operative radiotherapy at our centre. All the patients were divided into two groups according to the histological subtype: 21p with pure SEC in Group 1, 13p with mixed SEC with endometrioid cells in Group 2. All patients were staged using 2009-FIGO classification. Group 1: 10-IA, 5-IB, 1-IIIA, 4-IIIC1, 1-IIIC2. Group 2: 2-IA, 7-IB, 2-IIIA, 1-IIIB, 1-IIIC1. Pathology. Group 1: Grade (G): G2- in 5p, G-3 in 16p. Group 2: Grade: G1 in 1p, G2- in 3p, G-3 in 9 p. Myometrial invasion was presented in 10p in Group 1 and 3p in Group 2. Median tumour size was 3.6cm in Group 1 and 3.9cm in Group 2. Vascular and lymphatic space invasion was presented in 5p (23.8%) in Group 1 and in 6p (46.2%) in Group 2. Radiotherapy: all p received high-dose-rate brachytherapy (1-3 fractions of 4-7 Gy), and 17/21p in Group 1 and 12/13p in Group 2 received external beam irradiation (mean dose of 45.2Gy in Group 1 and 44.6 Gy in Group 2, after 3D planning and 4-field technique tailored to surgical results). Chemotherapy: 4-6 cycles of carboplatin + paclitaxel in 8/21 pts in Group 1 and 6/13 pts in Group 2.

Results: Mean age: 68.7 years (57-81) in Group 1, 70.3 years (63-83) in Group 2. Mean follow-up (months): in Group 1: 57 (7.8-153), in Group 2: 63 (12-117.8). Relapses: No vaginal relapses were developed; only 3/34p (8.8%) presented loco-regional relapse (2p in Group 1 and 1p in Group 2); 8/34 p (23.5%) had distant metastasis (3/21 in Group 1 and 5/13 in Group 2) and 13/34p (38.2%) had died at the time of the last control. The mean OS (months) was 58.9 (range 22.9-138.8) in Group 1 and 37.1 (range 12-84.8) in Group 2. The mean survival time to metastasis (months) was 38.4 (range 8.2-70.7) in Group 1 and 19.6 (range 9.5-53) in Group 2. The mean survival time to loco-regional relapse (months) was 27.5 (10.9-16.6) in Group 1 (2p) and 13 in Group 2 (only 1p).

Conclusion: At the time of the last control 61.8%p were alive. The main cause of relapse was distant metastases followed by loco-regional relapse with no patient showing vaginal relapse. The mean OS was substantially longer in patients with the pure SEC subtype (58.9 vs. 37.1 months) as was the mean survival time to metastasis (38.4 vs. 19.6 months) possibly due to the higher number of IA stage patients. Comparisons of two histological subgroups are scarce in the literature.

EP-1321

Postoperative treatment results of clear-cell endometrial carcinoma: 20 cases from 2005 to 2014

G. Oses[1], K. Holub[1], A. Rovirosa[2], L. Castilla[1], J. Mansilla[3], R. Llorente[1], K. Cortes[1], J. Ordi[4], J. Pahisa[5], M. Arenas[6], S. Sabater[7], A. Biete[1]
[1]*Hospital Clínic i Universitari, Radiation Oncology Dpt, Barcelona, Spain*
[2]*Hospital Clinic i Universitari, Radiation Oncology Dpt, Barcelona, Spain*
[3]*Hospital Rebagliati, Radiation Oncology Dpt, Lima, Peru*
[4]*Hospital Clínic i Universitari, Pathology Dpt, Barcelona, Spain*
[5]*Hospital Clínic i Universitari, Gynecological Cancer Unit, Barcelona, Spain*
[6]*Hospital sant Joan de Reus- Tarragona, Radiation Oncology Dpt., Reus, Spain*
[7]*Hospital General de Albacete, Radiation Oncology Dpt., Albacete, Spain*

Purpose or Objective: To evaluate treatment results in the post-operative treatment of Clear-cell endometrial carcinoma (CCEC) related to overall survival (OS), local control and distant relapses from 2005 to 2014

Material and Methods: Twenty patients (pts) with CCEC were treated at our centre with post-operative radiotherapy. All patients were staged after surgery using the 2009-FIGO classification: 6-IA, 4-IB, 2-II, 1-IIIA, 4-IIIC1, 2-IIIC2, 1-IVA. Pathology. Grade (G): G-I in 2pts, G2- in 5pts, G-3 in 13pts. Myometrial invasion was observed in 40% of pts. Median tumour size was 3.6cm (range 1.2-6.5cm). Vascular and lymphatic space invasion was presented in 25% of pts. Histological subtypes: clear cell in 11 pts (55%), clear cell mixed with endometrioid in 9 pts (45%). Radiotherapy: all pts received high-dose-rate brachytherapy (1-3 fractions of 7-4 Gy) and 18/20 pts received external beam irradiation (mean dose of 45 Gy (44-46Gy) after 3D planning and 4-field technique tailored to surgical results). Chemotherapy: 4-6 cycles of carboplatin + paclitaxel in 8 pts (40%).

Results: The mean age: 67 years (51-79). Mean follow-up: 4.34 years (range 0.96-9.75 years). Relapses: No pts developed vaginal relapse; 6/20 pts (33%) presented loco-regional relapse, 4/20 (20%) pts had distant metastasis (two with pelvic relapse 2/20 (10%); all 6 pts with relapse died (33%). The mean OS of 33.6 months (range 16.3-74.4 months). The mean survival to metastasis was 38.4 months (range 8.2-70.7 months) and 20.64 months (8.2-32months) to loco-regional relapse. No patient was lost to follow-up.

Conclusion: At the time of the last control 70% of patients (14/20) were alive and without relapse. The main cause of relapse was loco-regional followed by distant metastases, with no patients showing vaginal relapse. The results of this study seem to be similar to those reported in the literature.

EP-1322

Effects of upfront radiotherapy on isolated para-aortic lymph node metastasis in cervical cancer

J.H. Kim[1], K.Y. Eom[2], I.A. Kim[2], H.G. Wu[1], H.J. Kim[1]
[1]*Seoul National University Hospital, Department of Radiation Oncology, Seoul, Korea Republic of*
[2]*Seoul National University Bundang Hospital, Department of Radiation Oncology, Bundang, Korea Republic of*

Purpose or Objective: To evaluate the clinical features and treatment outcomes of isolated para-aortic lymph node (PALN) recurrence in cervical cancer patients, and analyze prognostic factors for overall survival

Material and Methods: Between 1992 and 2014, 1302 cervical cancer patients received radiotherapy at two institutions, Seoul National University Hospital and Seoul National University Bundang Hospital. Of these, 29 had isolated PALN recurrence. The median age at recurrence was 62 years (range, 34-81 years). Twenty-seven of 29 patients received salvage treatment: 16 received sequential or concurrent chemoradiotherapy, 6 radiotherapy to the para-aortic region, 4 chemotherapy alone, and 1 chemotherapy followed by salvage operation.

Results: The median follow-up duration after salvage treatment was 17.4 months (range, 1.1-139.2 months). Treatment failure after salvage treatment occurred in 10 of 27 patients. The 5-year progression-free and overall survival rates of all patients were 25.1% and 30.5%, respectively. Disease-free interval >=24 months and upfront radiotherapy (or chemoradiotherapy) were good prognostic factors for

overall survival in multivariate analysis. As to progression-free survival, disease-free interval, PALN size, and upfront radiotherapy (or chemoradiotherapy) were significant prognostic factors in multivariate analysis. Acute grade 3 gastrointestinal and hematologic toxicities developed in 3 patients.

Conclusion: For isolated PALN recurrence of cervical cancer, upfront radiotherapy (or chemoradiotherapy) should be considered as a salvage treatment, especially in patients with long disease-free interval.

EP-1323

Clinical audit of cervical cancer records from Kidwai Memorial Institute of Oncology, South India

S. Palled[1], U.K. Annasagara Srivinasa[2], N. Thimmiah[2], V. Raghu[3], T. Chitradurga Abdul Razack[2], N. Srinath[2], V. Chandraraj[2], S. Goyal[2], L. Vishwanath[2], G. Hosahalli Boriah[2], S. Poojr[2], G. G Venkata[2], J. Kunigal Puttaswamy[2]
[1]*Kidwai Memorial Institute Of Oncology, Radiation Oncology, Bangalore- Karnataka, India*
[2]*Kidwai Memorial Institute Of Oncology, Radiation Oncology, Bangalore, India*
[3]*Kidwai Memorial Institute Of Oncology, Medical Biostatistics, Bangalore, India*

Purpose or Objective: To present the long term outcomes and results of the clinical audit of cervical cancer cases treated at our cancer centre in the year 2010.

Material and Methods: A clinical audit of case records of cervical cancer treated at our centre in the year 2010 was analysed. Out of the 306 patients evaluated for Cervical Cancer, case records for demographics, treatment methodology, long term toxicity and survival data was analysed using the SPSS. The variables were compared using the Chi-square test, the survival by Log-Rank test.

Results: Out of a total of 306 patients with a median age group of 50 years (range-30-80) evaluated for various symptoms pertaining to cervical cancer, 204 underwent concurrent chemoradiation and 102 patients received only radiation alone. In the total cohort, FIGO stage grouping was stage II in 36% (n=111), stage III in 56% (n=172) and stage IVA in the remaining. Radiation was delivered to a dose of 75Gy to point A, external beam radiotherapy (dose of 45-50Gy) being delivered predominantly on the Telecobalt and followed with low dose rate brachytherapy. Cisplatin based concurrent chemotherapy was delivered as weekly at a dose of 40 mg/sqm in 76% of the patients, while in the rest it was delivered as three-weekly regimen. In the weekly chemotherapy arm, 70% of them received atleast 4 cycles. Median overall treatment time (OTT) was 8.4 weeks (40-95 days). At a median follow up of 36 months, 5 year overall survival in the entire cohort was 30%. The OS in the concurrent chemo radiation arm was better (34% Vs. 29%, p=0.036). The OS in the two chemotherapy arms did not show a difference (log rank, p=0.46). The survival difference between the two stage groups demonstrated a superior outcome in patients with stage II (40% vs 32%, p=<0.05). Multivariate analysis showed stage, type of chemotherapy and overall treatment (OTT) time were significant for OS. Acute hematologic, GI, GU and skin toxicity was higher in chemoradiation arm. Difference in long term toxicity between the two treatment arms was not statistically significant.

Conclusion: Our clinical audit of cervical cancer cases treated at our cancer centre, although demonstrates slight inferior survival outcome compared to available literature, might be accounted for the lower Point A dose, longer overall treatment time, and suboptimal chemotherapy dose. These factors have been taken care in our current clinical practice.

EP-1324

High risk early stage endometrial cancer: lymphadenectomy with brachytherapy as alternative to EBRT

R.L. Fabiano[1], M. Molinaro[2], M. Santoro[2], E. Mazzei[2], R. Molè[2], A. Destito[2], D. Pingitore[2], C. Bianco[3]
[1]*Magna Graecia University, Radiotherapy, marina di strongoli, Italy*
[2]*Ciaccio Hospital, Radiotherapy, Catanzaro, Italy*
[3]*Magna Graecia University, Radiotherapy, Catanzaro, Italy*

Purpose or Objective: Endometrial cancer (EC) is the most common gynecologic malignancy in developed countries, affecting 40,000 women/year. Recent studies have shown the therapeutic benefit of pelvic lymphnode dissection in order to determine the extent of desease and establish adiuvant therapies. Several trials have also shown that adiuvant radiotherapy(RT) in early stage EC reduces the risk of local recurrence without improving overall survival (OS). However the role of both lymphnode dissection and adiuvant RT in high risk early stage EC is not clearly defined. The aim of our retrospective study is to evaluate the validity of linfadenectomy with intravaginal brachiterapy (IVRT) as therapeutic option in high risk early stage EC, compare it with adjuvant external beam radiotherapy (EBRT) and determine which one determine the best results in terms of Reccurrence Free Survival (RFS) and OS.

Material and Methods: Were evalueted 85 patients with EC treated between January 2007 and January 2012 with 36 months of follow-up. Of these, 47 had low risk early stage (G1 with myometrial infiltration less than 50% or G2 with myometrial infiltration less than one third) treated with bilateral histerosalpingovariectomy without any adjuvant therapy; 38 were patients with high risk early stage (G1 with more than 50% of myometrial invasion, G2 with more than one third of myometrial infltration and G3) treated with bilateral hysterosalpingo-oophorectomy and then submitted to pelvic lymphadenectomy (n. 22 pts) plus IVRT or EBRT (n. 16 pts) based on age, comorbidities, tumor grade, histotype, tumor size, presence of lymphovascular invasion space, depth or myometrial infiltration.

Results: The recurrence rate was respectively of 4% (n.2 pts) among the low risk patients with a RFS of 96% and of 19% (n.11 pts) among the high risk patients with a RFS of 81%. Considering the high risk group, the 45% of recurrence (n.5pts) occurred among patients treated with EBRT and the 55%(n.6pts) among those who received lymphadenectomy with IVRT. The mortality rate was respectively 0% (n.0 pts) among patients treated with EBRT and 0% (n.0 pts) among those who received lymphadenectomy with IVRT.

Conclusion: Our study shows that in high risk early stage EC there is no significant difference in terms of RFS among patients who received pelvic lymphadenectomy with IVRT and those which had been treated with EBRT. There was also no statistically significant difference for OS between the two groups.

EP-1325

Phase I/II study of weekly cisplatin plus paclitaxel and radiotherapy for primary cervical cancer

L. Zhu[1], W. Jiang[1], S. Tian[1], A. Qu[1], H. Wang[1], X. Li[1], A. Liao[1], Y. Jiang[1], J. Wang[1]
[1]*Peking University Third Hosiptal, Radiation Oncology, Beijing, China*

Purpose or Objective: To determine the maximum tolerated dose (MTD) and effectiveness of weekly PTX plus DDP concurrent with whole pelvic irradiation in Chinese women with locally advanced cervical cancer.

Material and Methods: Between November 2008 and March 2015, a total of 36 patients with primarycervical cancer cervical cancer, FIGO stage IB1 to IIIB, confirmed by histology, negative para-aortic lymph nodes were enrolled into this phase I / II trial. Chemotherapy agents were

administered in escalating doses to cohorts of three patients at each dose level. Phase II was then assessed at the selected maximum tolerated dose (MTD). The patients were monitored for acute toxicity using the Common Toxicity Criteria, version 3.0 and late toxicity using the RTOG/EORTC.tween November 2008 and March 2015, a total of 36 patients with primary carcinoma of the cervix, FIGO stage IB1 to IIIB, confirmed by histology, negative para-aortic lymph nodes were enrolled into this phase I / II trial. Chemotherapy agents were administered in escalating doses to cohorts of three patients at each dose level. Phase II was then assessed at the selected maximum tolerated dose (MTD). The patients were monitored for acute toxicity using the Common Toxicity Criteria, version 3.0 and late toxicity using the RTOG/EORTC.

Results: Of the 36 patients, 18 enrolled on phase I study. The MTD was confirmed to be paclitaxel 40mg/m2 and cisplatin 40mg/m2 administered weekly for six cycles with 3D conformal external beam radiotherapy. There were additional 18 evaluable patients for the phase II analysis, yielding a total of 21 patients at the MTD. 3° (9/21) hematologic, principally neutropenia, occurs late cycles. All patients finished 5-6 cycles chemotherapy and radiotherapy in 7 weeks. The median follow-up was 24 months (5-58). At 4 months, 18 CR (1 pCR), 3 PR. At 24 months local control rate was 90.4％（19/21）. 18/21 patients (85.7%) are still survive (1 was loss of follow-up). 2 of 2 recurrent or metastasis patients have died. Late toxicities did not appear during follow-up.

Conclusion: Combination PTX and DDP administered concurrently with pelvic EBRT can be safely administered at the MTD of DDP 40 mg/m2 and PTX 40 mg/m2 weekly for six cycles in Chinese women. Primary result showed a good clinical outcome. We need continue follow-up. Further development to determine if the combination will help yield a survival benefit.

EP-1326

The role of PET CT in the IMRT of cervical cancer: the experience of the Institute of Candiolo

G. Cattari[1], S. Squintu[1], E. Delmastro[1], E. Garibaldi[1], S. Bresciani[2], P. Scapoli[3], S. Cauda[3], C. Bracco[2], T. Varetto[3], P. Gabriele[1]
[1]FPO-IRCCS CANDIOLO, Radiotherapy, Torino, Italy
[2]FPO-IRCCS CANDIOLO, Medical Physics, Torino, Italy
[3]FPO-IRCCS CANDIOLO, Nuclear Medicine, Torino, Italy

Purpose or Objective: This paper evaluates the impact of of FDG CT-PET in the treatment of cervical cancer by volumetric radiation and chemotherapy.

Material and Methods: From June 2010 to October 2015, 38 patients (pts) with cervical cancer were treated by radiotherapy, 21 with curatively (4 recurrences) and 17 with postoperatively (5 with positive margins). The mean age was 58 years (range 32-88). The histology was: squamous cell carcinoma (26 pts), adenocarcinoma (9 pts), adenosquamous carcinoma (3 pts). The grading was: G3 in 14 pts, G2 in 23 pts, G1 in 1 pt. The FIGO stage was: IB1 in 7 pts, IB2 in 3 pts, IIA1 in 5 pts, IIA2 in 2 pts, IIB in 13 pts, IIIA in 2 pts, IIIB in 2 pts, IIIB2 in 1 pt, IIIC2 in 1 pt and IVA in 2 pts. 24 pts received concurrent chemotherapy (CHT), 3 neoadjuvant CHT and 1 neoadjuvant and concomitant CHT. 3 pts were treated with IMRT by LINAC, 34 pts with image-guided IMRT-SB-IGRT using Helical Tomotherapy; 1 patient received exclusive High Dose Rate (HDR) brachytherapy. Tumor doses were ranged from 54 to 70.4 Gy in 30-32 fractions (fr); dose to the pelvis were from 50.4 to 54 Gy / 25-30 fr. In 5 pts was treated lumbar-aortic chain (51 Gy/30 fr); 14 pts received a boost on PET positive lymph nodes with dose range from 54 to 66 Gy/30 fr). 24 pts were treated with HDR boost with dose/fraction of 6-15 Gy in 1-3 frs.

Results: 37 pts received a PET-CT to staging and planning (Philips GEMINI TF), 33 of these had a PET-CT evaluation post RT. PET –CT changed the previous stage of disease in 6/37 cases (16%). 33 pts received also Magnetic Resonance (MRI) to staging, of these 10 showed positive lymph-nodes, conversely PET CT showed positive nodes in 20 pts (20%). 26 pts underwent a PET CT after RT: 18 pts showed a complete response (CR), 7 a partial response (PR), 1 pt a local persistence of lesion and a distance progression disease (PD). The time from end of treatment to PET evaluation was variable from 1 to 15 months (mean 4.3 months). About 6 pts with PR, 3 showed CR at the following PET-CT (8,12 and 14 months), 1 local stable disease (SD) and distance metastases and 2 showed local and distance PD.

Conclusion: FDG-PET changed tumor stage in 6/37 cases (16%) allowing a dose escalation on lymph-nodes detected and finally showed to be a sensitive and reliable method in the evaluation of radio-chemotherapy treatment response. The optimal timing of execution remains to be defined by further studies.

Acknowledgment: Research was supported by 5 x Mille 2008 Ministero della Salute - FPRC onlus and - 5 x Mille 2009 Ministero della Salute - FPRC Onlus

EP-1327

Clinical outcomes of dose escalation using simultaneous integrated boost in cervical cancer

R. Verges Capdevila[1], A. Varo[2], M. Mañas[1], A. Giraldo[1], J. Giralt[3]
[1]Hospital Universitario Vall d'Hebron, Radiation Oncology, Barcelona, Spain
[2]Hospital Universitari Vall d'Hebron, Medical Physics, Barcelona, Spain
[3]Hospital Universitari Vall d'Hebron, Radiation Oncology, Barcelona, Spain

Purpose or Objective: To evaluate the toxicity and outcome of dose escalated radiotherapy using a simultaneous integrated boost (SIB) technique in patients with locally advanced cervical cancer at primary diagnosis or at nodal recurrence.

Material and Methods: Sixteen patients with FIGO Stage IB2-IIIB N1 were treated with intensity modulated radiation therapy utilizing a SIB technique for gross disease in the para-aortic and/or pelvic nodal regions (8/16) or for microscopic disease after laparoscopic pelvic and para-aortic lymphadenectomy (8/16). Women were treated to 50.4 Gy in 1.8 Gy fractions to the tumor region and the pelvic and / or para-aortic lymph node areas, and a simultaneous boost with 59.36 Gy in 2.12 Gy fractions to the boost region. The boost volum was defined as 18FDG-PET/CT positive lymph nodes. Pulse-dose-rate brachytherapy was performed in eleven of sixteen and concurrent chemotherapy consisted of weekly cisplatin 40 mg/m2 in twelve patients. Acute and late toxicity, local control in the treated volumes, distant metastases and disease-free survival were assessed.

Results: With a median follow-up of 22 months (range 3 -40), rates of acute > grade 2 gastro-intestinal (GI), genitourinary (GU), and hematologic toxicities were 19%, 0%, and 30%, respectively.There were no grade 4 acute toxicities. One patient developed a small bowel obstruction requiring surgical intervention at 16 months. The 2-year actuarial rate of grade ≥3 GI toxicity was 6%. There were no grade 3 or 4 late GU or hematologic toxicities. All patients achieved complete remission in areas treated with high doses with SIB. Two patients presented a local recurrence at 6 and 30 months of follow-up. Three cases of sixteen (19%) relapsed in this area when you analyzed with 18FDG-PET/CT, that resulted positive, but not present disease in the pathologic anatomy of the salvage lymphadenectomy in two of them. On the other hand, two of sixteen patients (12.5%) presented systemic disease (lung metastases) at 27 and 35 months of follow-up, for each patient respectively. And one patient presented a second neoplasm in urinary tract ten months after the initial treatment of the cervix neoplasm. The 2-year actuarial disease-free survival was 62.5% but noting that only one patient presented recurrence in the area of the SIB (6.25%).

Conclusion: Dose escalated radiotherapy for node positive locally advanced cervical cancer at primary diagnosis or at nodal recurrence using a SIB results in acceptable rates of acute and late toxicity. And although our small size population, the present results contribute that the SIB technique is a good treatment for the patients with nodal regional disease.

EP-1328

Phase I study of weekly PTX/DDP, and postoperative radiotherapy for early cervical cancer in Chinese

L. Zhu[1], W. Jiang[1], S. Tian[1], A. Qu[1], H. Wang[1], X. Li[1], J. Wang[1]
[1]*Peking University Third Hosiptal, Radiation Oncology, Beijing, China*

Purpose or Objective: To determine the maximum tolerated dose (MTD) and dose-limiting toxicity (DLT) of weekly PTX and DDP concurrent postoperative radiotherapy in Chinese women with high- and intermediate-risk early cervical cancer.

Material and Methods: Women with high risks postoperative cervical carcinoma, negative para-aortic nodes, KPS≥60 were eligible. Pelvis RT (6/10MV-X, 3D-CRT, DT40Gy/20f, para-metrial boost 10~20Gy/5~10f) was followed by 2~4f brachytherapy applications (192Ir, 5Gy/f). Concurrent weekly chemotherapy was started at DDP 20mg/m2/W and PTX 10mg/m2/W, and escalated in three-patient cohorts according to 3+3 methods. Serious Adverse Event (SAE) was defined as grade 4 hematologic toxicity (excluding anemia) within 30 days of treatment, or grade 3/4 non-hematologic toxicity (excluding alopecia, nausea/anorexia, vomiting).
Table 1.Chemotherapy Dose Level Schema

DDP mg/m2/W	PTX mg/m2/W			
	10	20	30	40
20	DL1	DL2		
25		DL3	DL4	
30			DL5	
35			DL6	
40				DL7

Results: 25 patients were enrolled and treated over seven doses levels until dose-limiting toxicity (DLT) was reached. Median age was 48 years (range, 34-66). All of patients finished RT in 6 weeks. Grade 3/4 non-hematologic toxicities were diarrhea and observed in two patients (4 cycles, DLT) at level VII. 3/4° hematologic, principally neutropenia, and occurs late cycles. One grade IV WBC and NEUT was observed at dose level VI but not seen in three additional patients. No one was delayed treatment time by concurrent chemotherapy. The 1st patient finished 3 cycles due to 2° diarrhea at level I; 1 patient for 5 cycles at level III; 4 patients finished 6 cycles at level VII. Median follow-up is 56 months. 2 recurrent or metastasis patients have died. 1 patient has died of acute pneumonia (30.5 months). Late toxicities did not appear during follow-up.

Conclusion: Combination PTX and DDP administered concurrently with pelvic EBRT can be safely administered at the MTD of DDP 35 mg/m2 and PTX 30 mg/m2 weekly for six cycles in Chinese women with postoperative cervical cancer.

EP-1329

Vaginal and pelvic recurrences of endometrial carcinoma with BT HDR alone or in combination with EBRT

S. Gribaudo[1], U. Monetti[1], A. Mussano[1], S. La Sala[1], E. Madon[2], V. Richetto[2], A. Sardo[2], A. Rossi[3], M. Tessa[4], F. Moretto[4], A. Ruggieri[4], E. Delmastro[5], G. Cattari[5], - Katsaros[6], P. Gabriele[5], A. Urgesi[1]
[1]*A.O.U. "Città della Salute e della Scienza di Torino" P.O. Sant Anna, Radiotherapy, Torino, Italy*
[2]*A.O.U. "Città della Salute e della Scienza di Torino" P.O. Sant Anna, Physics, Torino, Italy*
[3]*A. O. "Ordine Mauriziano di Torino" P.O. Umberto I, Radiotherapy, Torino, Italy*
[4]*A.S.L. AT P.O. Cardinal Massaia, Radiotherapy, Asti, Italy*
[5]*Candiolo Cancer Center IRCCS-FPO, Radiotherapy, Torino, Italy*
[6]*A.O.U. "Città della Salute e della Scienza di Torino", Surgical Sciences- Gynecologic Oncology, Torino, Italy*

Purpose or Objective: In order to verify the results in a population of patients (pts) staged with CT and MR and treated with HDR BT and modern EBRT techniques, we review our experience in the treatment of vaginal or pelvic recurrences of endometrial adenocarcinoma.

Material and Methods: April 1997-October 2012 181 pts. 161 (89%) endometrioid, 12 adenosquamous and 8 clear cell. 30% G1, 42% G2, 25% G3, 10% G unknown. Median age 70 years (range 41-83). First line treatment: surgery alone 134 pts, surgery plus EBRT 27 pts, surgery plus CTH 18 pts and EBRT alone 2 pts. TAH&BSO 145 (80%) pts (36 with pelvic lymph-node sampling), Piver II and pelvic lymphadenectomy 36 pts. Median time to relapse 27 months (range 3-221). 126 pts had vaginal recurrences (66 limited to the dome and 60 with extension to the mid and/or lower third). 45 had a pelvic mass (31 centropelvic, 14 lateral wall); 10 pts had a vaginal recurrence with synchronous extra pelvic disease (6 lung mts and 4 LA nodes). 27 pts had prior adjuvant EBRT after surgery: dose range 32.4-57 Gy; no pts had received VBT. VBT: we use vaginal, shielded cylinders, Miami applicator and vaginal ovoid; interstitial BT in addition to VBT in 11 patients with sub urethral infiltration. HDR BT alone in 68 pts and in combination with EBRT in 113 pts. EBRT doses: range 30.6-50.4 Gy. VBT HDR doses: range 15-25 Gy when used in combination with EBRT and 30-44 Gy when used alone; fraction size: range 4-6 Gy. Interstitial BT: 2-2.5 Gy fr, 2 frs/day, total dose 20-25 Gy. Prescriptions for VBT were at depths ranging between 5 and 10 mm, according with the lesion size.

Results: Clinical CR 170 pts (94%). Median f-up 102 months (range 32-168). 38 pts DOD (14 lung mts, 8 with peritoneal mts without local failure and 16 with local failure, peritoneal and/or lung mts); 18 AWD and 125 (69%) NED. 27 local recurrences: median time to relapse 20 months (range 5-36); we retread, 12 of these, with further VBT HDR and five achieved a new CR. Late complication: 98 pts (54%) G0, 45 pts vaginal stenosis and/or severe mucosal dystrophy, 18 mild proctitis (G1), 5 severe proctitis (G2), 2 (G3) small bowel fistula that required surgery; 12 urine incontinence. Two developed a severe necrosis of the mucosa of the inferior third of the vagina that resolved after medical therapy.

Conclusion: Treatment of local recurrences of endometrial adenocarcinoma in a population of pts staged with CT and MR and treated with HDR BT and modern EBRT is effective and safe; severe complications are rare even in pre-irradiated pts.

EP-1330

Single center experience with definitive radiotherapy for vaginal cancer

H. Westerveld[1], J.J. Den Haan[1], E.C.M. Rodenburg[1], J. Wiersma[1], G.G. Kenter[2], B.R. Pieters[1], L.J.A. Stalpers[1]
[1]*Academic Medical Center, Radiation Oncology, Amsterdam, The Netherlands*
[2]*Academic Medical Center, Obstetrics and Gynaecology, Amsterdam, The Netherlands*

Purpose or Objective: Vaginal cancer is the most rare gynecological malignancy. Consequently, few dose effect data are available. The main objective of our retrospective study was to analyze the outcome of all patients treated at our department with definitive (chemo-)radiotherapy for primary vaginal cancer, with a focus on local failure.

Material and Methods: Thirty-four patients were included in a period from 1994 until 2013. Patients' charts were reviewed to obtain patients', treatment and tumor characteristics. DVH parameters were analyzed after reconstruction of the original brachytherapy plan plus delineation of intermediate risk CTV (CTVIR) and organs at risk. The target volume at time of BT was the GTVres and was defined by the treating doctor based on clinical examination and CT scan. The CTVIR was defined by the tumor extension at time of diagnosis. Survival rates were calculated using the Kaplan-Meier method. Morbidity was scored by CTCAE v3.0.

Results: Nine (26%) patients had FIGO stages I; 13 (38%) II; 5 (15%) III and 7 (21%) IVA. Median age at diagnosis was 68 years (33-91). Median follow-up was 37 months (3-224). Thirty-two patients received whole pelvic external beam radiotherapy (EBRT) to a median dose of 46 Gy (45-50.4 Gy), followed by BT in 31 patients; two patients received BT alone. The median D90 and D98 of the GTVres were 68 Gy and 67 Gy respectively, with a median V100 of 88%. The median D90 and D98 of the CTVIR were 65 Gy and 61 Gy respectively, with a median V100 of 62%. Complete remission at 3 months was achieved in all but one patient. Overall survival (OS) rates at 2- and 5-years were respectively 76% and 41%. Eight (24%) patients had any grade ≥3 toxicity. Local recurrences were seen in seven (21%) patients of whom three had an isolated local recurrence. Patients' and treatment characteristics of this group are shown in Table 1. Although the coverage of the GTVres seemed adequate, in retrospect it was often disputable if the tumor at BT was fully covered due to poor visibility of the tumor on CT scan.

Figure 1

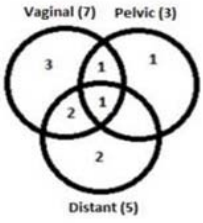

Table 1

Table 1. Patient tumour and treatment characteristics of 7 patients with local recurrence.
LN: lymph node, LF= Local failure, SCC: squamous cell carcinoma, AC= adenocarcinoma, CT= chemotherapy

	Year of diagnose	Age	Histology	FIGO stage	LN	Location	Treatment	Applicator
Local failure #1	2005	56	SCC	IVa	yes	entire length of the vagina, bladder invasion	EBRT+BT+chemo	interstitial needles
Local failure #2	2004	73	SCC	IVa	yes	entire length of the vagina	EBRT+EBRT boost+chemo	No BT
Local failure #3	2005	82	SCC	II	no	entire length of the vagina	EBRT+BT	intra-uterine tandem + interstitial needles mould
Local failure #4	2008	59	SCC	II	no	upper and middle third of the vagina	EBRT+BT+chemo	
Local failure #5	2009	34	AC	I	no	lower third of the vagina	Surgery+BT	Interstitial needles
Local failure #6	2009	61	SCC	I	no	lower third of the vagina	EBRT+BT	Multichannel-cylinder
Local failure #7	2011	63	SCC	III	yes	lower and middle third of the vagina	Excision LN, EBRT+EBRT boost+BT+chemo	Multichannel-cylinder

Conclusion: The combination of EBRT and BT with or without concomitant chemotherapy provides reasonable outcomes in terms of tumor control and toxicity. However, there is still room for improvement. This study was too small to illustrate clear dose-effect relationships. In general, the prescribed dose on target at time of BT (GTVres) seemed low. In addition, coverage of the CTVIR was poor, which can however be explained by the fact that until recently our target at BT was exclusively based on GTVres. Finally, the use of MRI at time of BT seems necessary to better define the target.

EP-1331

Cancer of uterine cervix: PET-CT, IMRT and HDR.

M. Garcia-Aranda[1], X. CHEN[1], A. Montero[1], J. Valero[1], R. Alonso[2], D. Zucca[3], R. Ciervide[1], M. Lopez[1], B. Alvarez[1], S. Payano[1], E. Sanchez[1], O. Hernando[2], C. Rubio[1]
[1]*Hospital universitario HM Sanchinarro, Radiation Oncology Department, Madrid, Spain*
[2]*Hospital universitario HM Puerta del Sur, Radiation Oncology Department, Madrid, Spain*
[3]*Hospital universitario HM Sanchinarro, Medical Physics Department, Madrid, Spain*

Purpose or Objective: To evaluate the treatment results, and complication rates in patients with locally advanced cervical cancer after external beam radiotherapy (EBRT) and high-dose rate (HDR) brachytherapy with dose escalation.

Material and Methods: All patients with locally advanced cervical cancer (FIGO: IB 7 patients, II 10 patients, III 7 patients, IV 4 patients) treated with radical radiotherapy in our center from 2007 to October 2015 were reviewed. Twenty eight patients were treated with EBRT using intensity-modulated radiation therapy (IMRT) technique following by HDR brachytherapy +/- chemotherapy. Planification included CT (50%) or PET-CT (50%) for GTV delineation. The most common prescription was 50.4 Gy (1.8Gy per fraction) for pelvic lymph nodes +/- paraaortic lymph node with concomitant boost up to 60, 48 Gy (2,16Gy per fraction) for macroscopic nodal disease and parametrium affectation. HDR brachytherapy was applied using tandem (25 Gy in 5 fractions) in most patients. Toxicity was assessed according to RTOG-EORTC criteria. All statistical analysis was performed using SPSS vs 22.0.

Results: There was no grade 3 acute toxicity associated with EBRT. Only one case of grade 4 acute toxicity was observed after HDR gynecological brachytherapy. The median age was 51 years (range 39 – 81). The median of follow up was 30 months (range 4 – 85). The actuarial progression-free survival was 77% at 36 months. Median time to local progression has not been reached. The median overall survival was 30 (range 4-85) month.

Conclusion: Radical radiotherapy +/- chemotherapy is still a standard treatment in locally advanced uterine cervical cancer with good local control and global survival. Dose escalation is possible using PET-CT and IMRT which allow *better conformation and better tolerance.*

EP-1332

Clinical results of Nimotuzumab Plus DDP and concurrent radiotherapy for primary cervix cancer

L. Zhu[1], S. Tian[1], A. Qu[1], H. Wang[1], X. Li[1], Y. Jiang[1], H. Sun[1], L. Lin[1], J. Wang[1]
[1]*Peking University Third Hosiptal, Radiation Oncology, Beijing, China*

Purpose or Objective: To determine clinical efficacy and toxicity of weekly nimotuzumab plus cisplatin concurrent with intensity-modulated radiotherapy in Chinese women with locally advanced cervical cancer.

Material and Methods: Between December 2013 and July 2015, a total of 27 patients with primary carcinoma of the cervix, FIGO stage IB1 to IVa, squamous cell carcinomas confirmed by histology were enrolled into this study. 26 patients received intensity modulated radiotherapy and 5 ~ 6 fractions HDR brachytherapy, 1 patient received intensity modulated radiotherapy followed by surgery because she had rectum carcinoma at the same time. Chemotherapy scheme was 200 mg nimotuzumab and 40 mg/m2 cisplatin weekly for six cycles. 2 patients (ages: 78 ~ 79) received only 200 mg nimotuzumab weekly for six cycles. The patients were

monitored for acute toxicity using the Common Toxicity Criteria, version 3.0 and late toxicity using the RTOG/EORTC.

Results: 3° (9/27) hematologic toxicity, principally neutropenia (9/27) and thrombocytopenia (2/27), occurs late cycles. No grade 4 toxicity occurred. 2 patients (ages: 78–79) finished 200 mg nimotuzumab weekly for six cycles with 1° hematologic. Others finished 5 ~ 6 cycles chemotherapy. All of patients finished radiotherapy in 7 ~8 weeks. The median follow-up was 9.5 months (3 ~ 22). At 4 months, 24 patients had attained complete response (23 CR, 1 pCR), 3 patients had achieved partial response (PR). 2 of 3 patients who had PR appeared local recurrent at 8 months and 9 months respectively. Local control rates were 92.6 %（25/27）. All of patients are still survive. 1 patient had haemorrhagic radiation proctitis at 7 months.

Conclusion: Combination nimotuzumab 200 mg and DDP 40 mg/m2 weekly for six cycles concurrently with intensity-modulated radiotherapy can be safely administered in Chinese women. Primary result showed a good clinical outcome. We need continue follow-up. Further development to determine if the combination will help yield a survival benefit.

Electronic Poster: Clinical track: Prostate

EP-1333

PSA kinetics after hypofractionated stereotactic body radiotherapy for localised prostate cancer

H. Kim[1], J.H. Phark[1], W.C. Kim[1]
[1]*Inha University Hospital, Radiation Oncology, Inchon, Korea Republic of*

Purpose or Objective: stereotactic body radiotherapy (SBRT) has emerged as an effective treatment for localized prostate cancer. However, prostate-specific antigen (PSA) kinetics after SBRT has not been well characterized. The objective of the current study is to analyze the rate of PSA decline and PSA nadir following hypofractonated SBRT in low- and intermediate-risk prostate cancer.

Material and Methods: From 2008 to 2014, thirty-six patients newly diagnosed, low- and intermediate-risk (NCCN definition) prostate cancer were treated with SBRT using Cyberknife. Total dose of 36.25 Gy in 5 fractions of 7.25 Gy were administered. No one received androgen deprivation therapy (ADT). PSA nadir and rate of change in PSA (slope) were calculated and compared.

Results: With a median follow-up of 52 months (range, 13-71), the median rates of decline of PSA were -0.359, -0.199 and -0.127 ng/mL/month, respectively, for durations of 1, 2 and 3 years after radiotherapy, respectively. The decline of PSA was maximal in the first year and continuously decreased for durations of 2 and 3 year. The median PSA nadir was 0.27 ng/mL after a median 33 months. 5-year biochemical failure (BCF)-free survival was 100% for low- and intermediate-risk patients.

Conclusion: In this report of low- and intermediate-risk prostate cancer, continuous decrease of PSA level for duration 1, 2 and 3 year following SBRT using Cyberknife resulted in lower PSA nadir. Also, SBRT leaded to long-term favorable BCF-free survival in low- and intermediate-risk prostate cancer.

EP-1334

PSA kinetics following SBRT versus conventionally fractionated EBRT for localised prostate cancer

H. Kim[1], J.H. Phark[1], W.C. Kim[1]
[1]*Inha University Hospital, Radiation Oncology, Inchon, Korea Republic of*

Purpose or Objective: Hypofractionated stereotactic body radiotherapy (SBRT) has emerged as an effective treatment for localized prostate cancer. However, prostate specific antigen (PSA) kinetics after SBRT has not been well characterized. The purpose of this study was to compare the PSA kinetics between SBRT using Cyberknife and conventionally fractionated external beam radiotherapy (CF-EBRT) in low- and intermediate-risk prostate cancer.

Material and Methods: A total of sixty-nine patients with low-and intermediate-risk prostate cancer were enrolled. 34 patients were treated with SBRT (36.25Gy in 5 fractions) using Cyberknife and 35 patients treated with CF-EBRT (45 Gy whole pelvis EBRT and boost of 25.2-30.6 Gy in 1.8 Gy fractions). PSA nadir and rate of PSA decline in PSA (slope) were calculated and compared.

Results: With a median follow-up of 53.6 months (range, 14-74), the median PSA nadir and median slope for SBRT were 0.23 ng/mL and -0.430, -0.199, -0.127 and -0.094 ng/mL/month, respectively, for durations of 1, 2, 3 and 4 years following radiotherapy. Similarly, for CF-EBRT, the median PSA nadir and median slopes were 0.37 ng/mL and -0.529, -0.138, -0.109 and -0.056 ng/mL/month, respectively. The slope of CF-EBRT was significantly different with a greater median rate of change for 1 year post radiotherapy than that of SBRT (p=0.018). Contrastively, the slopes of SBRT for duration for 2, 3 and 4 year tended to be continuously greater than that of CF-EBRT (p=0.028, p=0.058 and p=0.128, respectively). The significantly lower PSA nadir was observed in SBRT (median nadir 0.23 ng/mL) compared with CF-EBRT (median nadir 0.37ng/mL) (p=0.011). 5-year biochemical failure (BCF) free survival were 100% for SBRT and 80.8% for CF-EBRT (p=0.031).

Conclusion: Patients treated with SBRT using Cyberknife experienced a lower PSA nadir and tended to be continuously greater rate of decline of PSA for duration 2, 3 and 4 years than CF-EBRT. The improved PSA kinetics of SBRT over CF-EBRT leaded to favorable BCF-free survival. Further studies with more patients and longer follow-up duration are required.

EP-1335

Prostate cancer hypofractionation: impact of prostate gland dimension in genitourinary toxicity

S. Fersino[1], N. Giaj Levra[1], R. Mazzola[1], A. Fiorentino[1], F. Ricchetti[1], R. Ruggieri[1], F. Alongi[1]
[1]*Ospedale Sacro Cuore Don Calabria, Radiation Oncology, Negrar - Verona, Italy*

Purpose or Objective: to analyze predictors of genitourinary (GU) toxicity in a cohort of prostate cancer (PC) patients treated with moderate hypofractionation and simultaneous integrated boost (SIB) using volumetric modulated arc therapy (VMAT) technique.

Material and Methods: Clinical and dosimetric data were prospectively collected and retrospectively analyzed. Patients were stratified into low (43%), intermediate (30%) and high-risk (27%) groups. Target volumes (expanded to define the planning volumes (PTV)) were clinical target volume (CTV) 1: prostate; CTV2: CTV1 + seminal vesicles; CTV3: CTV2 + pelvic nodes. Low-risk patients received 73.5 Gy to PTV1; intermediate-risk 73.5 Gy to PTV1 and 60 Gy to PTV2; high-risk 73.5 Gy to PTV1, 60 Gy to PTV2, and 54 Gy to PTV3. All treatments were in 30 fractions. Androgen deprivation therapy (ADT) was prescribed upfront in intermediate and high risk patients. Rectal and GU toxicities were scored according to Common Terminology Criteria for Adverse Events v4.0 scoring system.

Results: From January 2012, 60 patients with localized PC were recruited in an internal protocol of moderate hypofractionation SIB schedule using VMAT technique with definitive intent. The median follow-up was 24 months (range 10 - 36 months). GU acute toxicity was recorded as follow: G0 = 16/60 (27%), G1 = 18/60 (30%); G2= 26/60 (43%); no case of toxicity≥ G3 was registered. GU late toxicity was recorded as follow: G0 = 20/60 (34%); G1 = 29/60 (48%); G2 = 11/56 (19%); no case of toxicity ≥ G3 was registered. The risk

of acute G2 GU toxicity was about 3 times if the prostate volume is ≥ 80 cc (p-value 0.004; 95% CI: 1.05 - 9.5). In the adjusted prediction model using the logistic regression, the probability of acute G2 GU toxicity was about 60% with the same prostate volume cut-off (p-value 0.001; 95% CI: 0.13 - 0.46), with an attitude to develop a moderate toxicity in the first 3 weeks from the beginning of treatment. In the late setting, a trend to significance (p=0.076) to develop an acute GU toxicity ≥ G1 was found for bladder V60 Gy ≥ 15%.

Conclusion: In moderate hypofractionation in 30 fractions for prostate cancer, a prostate gland volume greater than 80 cc resulted as predictor of moderate acute GU toxicity.

EP-1336

Hypofractionated salvage radiotherapy after radical prostatectomy

P. Bulychkin[1], S. Tkachev[1], A. Mikhailova[2]
[1]*Federal State Budgetary Institution "N. N. Blokhin Russian Cancer Research Center" the Ministry of Health of the Russian Federation, radiation oncology, Moscow, Russian Federation*
[2]*Federal State Budgetary Institution "N. N. Blokhin Russian Cancer Research Center" the Ministry of Health of the Russian Federation, medical physics, Moscow, Russian Federation*

Purpose or Objective: We have created and implemented in our department a new scheme of hypofractionated salvage volume modulated arc therapy with simultaneous integrated boost for patients with recurrence of prostate cancer (PCa) after radical prostatectomy (RP). The aims of our research are to evaluate toxicities and biochemical response rate.

Material and Methods: Patients with recurrence of PCa after RP have been treated by hypofractionated (HF) salvage radiotherapy (SRT). Characteristics of HF radiotherapy were as follows: the prescribed dose to the regional lymphatic nodes was 46.8 Gy of 1.8 Gy per fraction, to the prostate bed - 61.1 Gy of 2.35 Gy per fraction in case of biochemical recurrence (BR) and if region of clinical recurrence (CR) was identified - 65 Gy of 2.5 Gy each, in 26 fractions with pretreatment imaging; VMAT (two arcs: CW (185°-175°), CCW (175°-185°) technology with SIB was used. Toxicities were scored using RTOG/EORTC Radiation Toxicity Grading.

Results: 41 patients were treated by the HF SRT. Median follow-up was 22 months (10 - 30). Biochemical control rate – 37 (90.2%) patients, locoregional control rate – 41 (100 %) patients. No grade 3 or greater acute toxicities were observed.

Conclusion: We would like to suggest a new scheme of HF SRT with SIB in 26 fractions for patients with recurrence of PCa after RP. The toxicities and early biochemical response rates were comparable with conventional fractionation SRT.

EP-1337

PSA Kinetics: HDR prostate brachytherapy boost in combination with external beam radiotherapy

S. Rodda[1], F. Sun[1], A. Henry[1], K. Franks[1], D. Bottomley[1]
[1]*St.James Oncology Institute, Clinical Oncology, Leeds, United Kingdom*

Purpose or Objective: The Aim of this study is to evaluate PSA kinetics in men with intermediate and high risk prostate cancer treated with HDR brachytherapy boost in combination with external beam radiotherapy (EBRT) and short term androgen deprivation therapy (ADT).

Material and Methods: Data from 134 consecutive patients treated with HDR brachytherapy boost in combination with external beam radiotherapy was extracted from a prospectively maintained database. All the patients had a minimum follow up of 4 years. Patients who were on androgen deprivation therapy for over 12 months were excluded from the analysis. After exclusion we had 95 evaluable patients. All patients received either 17 Gy in 2 fractions or 15 Gy in single fraction of HDR brachytherapy boost followed by external beam radiotherapy 37.5 Gy in 15 fractions. 70% of patients received Androgen deprivation therapy (ADT) for less than or equal to 6 months, 15% received for 6- 12 months, and 15% received no hormones. 3-6 months of ADT was given neoadjuvantly. Date of HDR boost was considered as time=0. Benign PSA bounce was defined as PSA rise of >0.2ng/ml followed by subsequent decline to pre bounce level.

Results: Median follow-up was 4.3 years. At the time of median follow up the median PSA was 0.19. PSA bounce was seen in 32.6% (n=31). Magnitude of PSA bounce was <1ng/ml in 55% (n=17), 1-2ng/ml in 13% (n=4), >2ng/ml in 32% (N=10). In 16 out of 17 patients with a PSA bounce of <1ng/ml was due to a benign bounce. 50% of patients with a PSA bounce between 1-2ng/ml had a benign bounce and the remaining 50% developed biochemical failure. In 9 out of 10 patients who had a PSA bounce of >2ng/ml subsequently developed a biochemical failure . Most common
time for benign PSA bounce was between 6 and 18 months.

Change in PSA over time

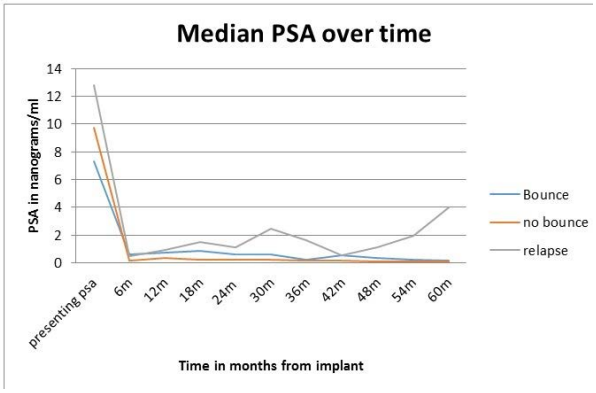

Conclusion: PSA bounce is a common phenomenon which occurs in about a third of men who were treated with short term ADT in combination with HDR boost and EBRT. Benign PSA bounce tends to have a smaller magnitude of rise in PSA <1ng/ml. However patients who developed biochemical failure had PSA bounce of larger magnitude >2ng/ml. Investigators at the time of submission of the abstract are examining variables which predict PSA bounce.

EP-1338

Delay Haematuria after prostatic radiotherapy: do it mean always radiation cystitis?

S. Rodríguez Villalba[1], M. Santos Ortega[1], M. Depiaggio[1], A. Fuster[2], P. Torrus[2], J. Martinez[2], J. Canovas[2], L. De la Torre[2], J. Moreno[2], J. Richart[1], A. Otal[1], J. Perez Calatayud[1]
[1]*Clinica Benidorm, Radiotherapy Department, Benidorm, Spain*
[2]*Hospital Marina Baixa, Urology Department, Villajoyosa-Alicante, Spain*

Purpose or Objective: A retrospective analysis in 368 consecutives organ confined prostate cancer (PC) patients has been made for evaluating the rates of haematuria, etiology and onset time. All these patients have been treated from September 2001 to December 2013 with different multimodality radical radiotherapy approaches: Intensity Guided Modulated radiotherapy (IGRT), Low dose rate brachytherapy (LDR BT) exclusively, LDR BT plus External radiotherapy (EBRT) or High dose rate Brachytherapy (HDR-BT) plus EBRT.

Material and Methods: Median age of the whole group was 70,5 years (range 60-81y). Median PSA at diagnostic of the prostate cancer was 9.3 ng/ml (range 4,67-95 ng/ml). Median Gleason 6 (range 2-10). 20 patients (41,47%) had received IGRT radiotherapy treatment, 4 patients (8%) LDR BT, 10 patients (21%) LDR plus EBRT and 14 patients (30%) HDR-BT plus EBRT. In 17 patients (35,4%) the complete pelvis (L5-S1)

was irradiated receiving 50,4 Gy. The comorbidities associated were: 21% diabetes, 62,5% High blood pressure, 40% cardiac pathology and 33 % were with anticoagulant treatment. All our haematuria patients have been handled following the next algorithm: Blood Test (Including platelets and liver parameters) and Urine Culture. If both are negative: Ultrasound (Kydney, urether and bladder). If haematuria goes on: Cystoscopy.

Results: With a median follow-up of 52.5 months (range 5-122 m), 48 patients (13%) have had haematuria. As etiological factors we have been found: Urine Infection 12 p (25%. Time 32 months (12-70 m), Bladder cáncer 10 p (21%. Four of them a recurrence of a previous treated bladder tumour. Time: 32 months (3-120 m), RADIATION CYSTITIS 10 p (21%. Time: 13 months (6 – 38 m), Lithiasis 4 p (8%. Time: 25.5 months (26-30 m), Local progression of Prostate cancer 1 p (2%). Time: 72 months), Autolimited haematuria (Culture and image studies negatives. It does not repeat.): 9 p (19%. Time: 58 months (25-80 m) and Fatal haematuria (Exitus. Not known etiology): 2 p (4%. Time: 78 and 84 months).

Conclusion: In our experience, haematuria is a frecuent pathology in patients treated with radiotherapy of prostate cancer. The etiology of it spreading in similar proportions, across the different causes founded. The time of it presentation is important for the diagnostic. In the mind of the specialist must be different causes of it, NOT ONLY radiotherapy Cystitis taking in account that if it is due to radiotherapy it appears mainly, in the first two years after radiotherapy treatment.

EP-1339

Influence of leaf thickness on prostate VMAT about dosimeto-volumetoric and delivering parameters

H. Nagano[1], H. Yokoyama[1], H. Hashimoto[1], M. Watanabe[1], M. Nakanishi[1], Y. Kishida[1], T. Ogawa[1], T. Kawasaki[1], M. Katou[2], T. Shimo[2], K. Ishizuka[1]

[1]*Shonan Fujisawa Tokushukai Hospital, Radiation Oncology Department, Fujisawa, Japan*

[2]*Tokyo West Tokushukai Hospital, Radiation Oncology Department, Tokyo, Japan*

Purpose or Objective: Volumetric modulated arc therapy (VMAT), a complex treatment strategy for intensity-modulated radiation therapy, has been established clinically. While 5 mm thick MLC (**L50**) is a usual for VMAT, we have been using 2.5 mm thick MLC (**L25**) from 2012 to treat the prostate cancer. So we compared dosimetric, volumetric and dose delivering parameters between **L25** and **L50**.

Material and Methods: Twenty four cases were selected from our database. Those patients were treated for the prostate carcinoma in the feet-first prone position. Gantry angle range was 182 deg. to 178 deg. and collimation angle was set 0 deg. SmartArc system of Pinnacle3 was used with 6MVX physical data of Novalis Tx (**L25**) and 6MVX Siemens® ARTISTE physical data loaded on Varian Clinac-21 Ex (the base machine of Novalis) virtually (**L50**). The same consolidations for optimization were used. For example, Min Dose, D95 and Max Dose of PTV were 76 Gy, 80 Gy and 84 Gy, respectively. Rectal V40 was set to 20%. Wilcoxon rank sum test was applied to D98, D95, D50 and D02 of PTV, rectal V40, irradiation time and MU. To analyze relationships between these values and ROV grouped by **L25** or **L50**, linear regression model was employed with analysis of covariance for the regression coefficients.

Results: Mean values of D98, D95, D50 and D02, V40, Time and MU were 75.8 Gy, 77.5 Gy, 81.2 Gy, 84.2 Gy, 20.3%, 82.7 sec and 646.6 for **L25**, and were 75.6 Gy, 77.3 Gy, 81.0 Gy, 83.8 Gy, 19.6 %, 149.9 sec and 741.6 for **L50**, respectively. Only those mean values of D02, V40 and Time were significantly different between **L25** and **L50** by Wilcoxon test (Table).

Table p values of statistical analyses

Variables	Wilcoxon rank sum test (L25/L50)	Analysis of covariance for the regression coefficients		
		ROV	L25/L50	ROV*L25/L50
D98	NC	<0.001	NC	NC
D95	NC	<0.01	NC	NC
D50	NC	NC	NC	NC
D02	<0.01	NC	<0.01	NC
V40	<0.05	<0.05	<0.05	NC
Time	<0.001	<0.01	<0.001	<0.05
MU	NC	<0.001	<0.05	NC

D98, D95, V40, Time and MU depended on ROV significantly. Slopes of valuables grouped by **L25** and **L50** were very similar in the all except Time and MU (Table and Figure).

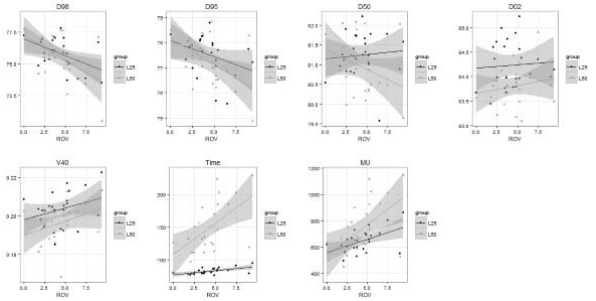

Conclusion: L25 and **L50** plans were very similar from the dosimetric point of view (difference of D02 was significant but very small in value; 0.4Gy, **L25**>**L50**). From the volumetric (V40) point of view, difference was small (0.7%, **L25**>**L50**) but significant. In terms of dose delivery (Time), differences were remarkable and largely depend on the ROV especially in the cases of **L50**. We may use **L50** with the expense of treatment time compared to **L25**.

EP-1340

Nomograms predicting the probabilities of having indications for adjuvant prostatic radiotherapy

M. Ma[1], X. Gao[1], Z. Zhou[2], B. Zhao[1]

[1]*Peking University First Hospital, Radiation Oncology, Beijing, China*

[2]*Hebei Cancer Hospital, Radiation Oncology, Shijiazhuang, China*

Purpose or Objective: For patients with clinically localized prostate cancer with high probabilities to undergo adjuvant radiotherapy after radical prostatectomy(RP), radical radiotherapy may be a proper treatment option for saving time and medical costs. Our purpose is to develop nomograms combining PSA level, clinical T stage, and biopsy Gleason Score to predict probabilities of having indications for adjuvant radiotherapy including extraprostatic extension, positive margin, Gleason Score 8-10 and to provide data for individualizing initial treatment options.

Material and Methods: We analyzed 214 men treated with RP between August 2013 and August 2015 at our hospital. Average age was 66 years. Men who enrolled in this study had a preoperative PSA level assessed before or at least 4 weeks after prostate biopsy, biopsy Gleason Score, pelvic MRI and clinical T stage (TNM 2009 classification). Men were excluded for preoperative treatment with neoadjuvant hormonal therapy, or transurethral resection of the prostate because of potential influence on pathologic stage or PSA level. Preoperative predictors included PSA level, clinical T stage (T2a/b, T2c, T3a, T3b), and biopsy Gleason score (5-6, 3+4=7, 4+3=7, 8-10). These predictors were used in multivariable logistic regression analysis based nomograms to estimate the probabilities of extraprostatic extension, positive margin, Gleason Score 8-10 after RP, respectively. The predictive accuracy and discriminative ability of the

nomogram were determined by concordance index(C-index) and calibration curve.

Results: 47% of the patients had extraprostatic extension, 36% had positive margin, and 20% had Gleason Score 8-10. Nomograms were developed for the predicted probabilities of having the indications of adjuvant radiation therapy(Fig1ABC). The calibration curve for probabilities showed good agreement between prediction by nomogram and actual observation (Fig 1DEF). The C-index of the nomograms for predicting extraprostatic extension disease, positive margin, and Gleason Score 8-10 were 0.799, 0.746, 0.879, respectively. The risk of having one of the indications of adjuvant radiation therapy increased with increases in predictors except for T stage for predicting Gleason Score 8-10(p=0.25).

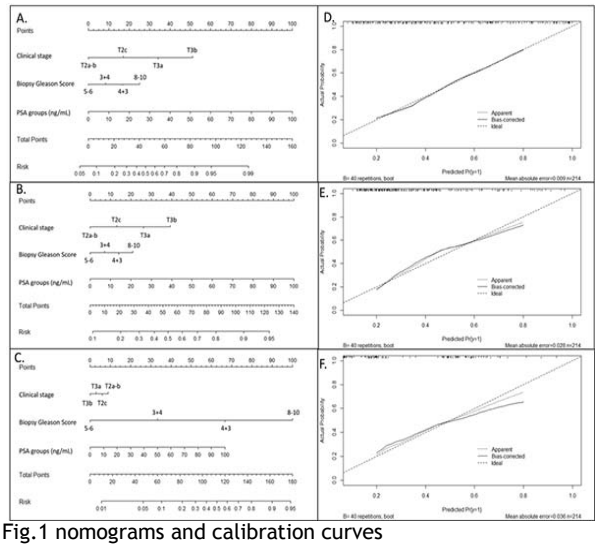

Fig.1 nomograms and calibration curves

Conclusion: We produced nomograms that may accurately predict the probabilities of having indications for adjuvant radiation therapy after RP in men with localized prostate cancer, which may contributes to properly selecting initial treatment option.

EP-1341

Single-nucleotide polymorphisms associated with toxicity to radiotherapy in prostate cancer patients

G. Spagnoletti[1], P. Frisani[1], M. Natalicchio[2], M. Enfasi[1], G. Cocco[1], G. Nardella[1], G. Plotino[1], G. Bove[1]

[1]Az. Osp.-universitaria Ospedali Riuniti, Struttura Complessa di Radioterapia, Foggia, Italy

[2]Az. Osp.-universitaria Ospedali Riuniti, II Laboratorio Analisi, Foggia, Italy

Purpose or Objective: Together with surgery, radiotherapy (RT) is a cornerstone in the treatment of prostate cancer. Despite similar prognostic factors, a wide inter-patient variability was observed in tumour response and side effects. Many studies have been made to understand molecular behaviour of tumours exposed to ionizing radiation. It has been hypothesized that single-nucleotide polymorphisms (SNPs) impact response and adverse reactions for patients (pts) receiving RT. We focused on the analysis of some candidate SNPs in pts treated with RT for prostate cancer.

Material and Methods: Between January and September 2014, 66 pts with prostate cancer underwent RT with radical or adjuvant intent. RT was delivered using 4-6 coplanar 10-18 MV beams at a dose of 70-80 Gy (2.5-2 Gy/fraction). At baseline and weekly during treatment, acute gastrointestinal (GI) and genitourinary (GU) toxicities were scored by a fixed questionnaire. The RTOG toxicity scale served as a basis, but additional symptoms were evaluated as well. Genotyping was performed from whole blood samples at the beginning of RT. DNA was purified with the QIAamp DNA Mini Kit. Assays of samples were performed using the "Radiotherapy response" kit (Diatech Pharmacogenetics, Italy). Pyrosequencing analysis was carried on the PyroMark Q96 ID (Biotage, Sweden). Status of candidate SNPs (GSTP1 A313G, RAD51 G135C, XRCC1 G28152A, XRCC3 A4541G and XRCC3 C18067T) was unknown to interviewers and participants.

Results: Treatments were delivered successfully without any interruption. Grade 1, Grade 2 and Grade 3 GI toxicities were observed in 33%, 12% and 3% of the pts, respectively, during the whole period. Grade 1, Grade 2 and Grade 3 GU toxicities were seen in 50%, 32% and 15% of the pts. Eight items of GI toxicity and six items of GU toxicity were used to calculate, for each patient, his own toxicity score. Time of onset of side effects was taken into account too. Using R statistical program, no significant relation was found between total toxicity or precocity of side effects and the mutational status of our 5 candidate loci, except for GSTP1 and toxicity. Kruskal-Wallis test demonstrated that GSTP1 status (wild-type, heterozygous and mutant) is a strong predictor of GI effects, especially diarrhea (p=0.01), frequency of stools (p=0.01), incontinence (p=0.01) and rectal blood loss (p=0.02).

Conclusion: Overall, RT is a well tolerated therapy for prostate cancer. Five SNPs were analyzed in four genes of relevance for RT. GSTP1 showed to be the most important SNP regarding GI toxicity to RT in pts treated for prostate cancer. Other examined SNPs did not prove to play a significant role in this particular subset of pts. Our findings require validation in larger replication studies and open to future clinical trials. One of the next steps will be evaluate if GSPT1 is associated with response to RT too. This would permit personalization and optimization of RT for each prostate cancer patient.

EP-1342

F-18Fluorcholine-PET/CT guide salvage therapy in biochemical failure of prostate cancer

M. Barrado[1], A. Sola[1], P. Navarrete[1], E. Villafranca[1], M. Rico[1], M. Errasti[1], M. Campo[1], I. Visus[1], S. Flamarique[1], M. Rodríguez[2], E. Martínez[1]

[1]Complejo Hospitalario de Navarra, Oncología Radioterápica, Pamplona, Spain

[2]Clínica Universitaria de Navarra, Medicina Nuclear, Pamplona, Spain

Purpose or Objective: To describe the F-18Fluorocholine PET/CT (cPET/TC) activity after biochemical failure in localized prostate cancer. To analyze the response to cPET/TC-guided salvage therapy.

Material and Methods: N: 80 patients(p) with cPET/TC between 2006-2012, 64p at time of biochemical failure.
At diagnosis 15p T1 (18.5%), 37p T2 (46.4%), 23p T3 (28.8%) and 5p T4 (6.3%). N0 (87.5%). Gleason score: 6: 30p (37.6%), 7: 27p (33.8%),≥ 8: 20p (25.1%), missing: 3p (3.8%). Baseline median PSA 9.0 ng/ml. [0.9-114.5]
Initial treatment: 45p (56.4%) prostatectomy, 13p (16.3%) radiotherapy and hormones 2.5 years, 11p (13.8%) radiotherapy and hormones 6 months, 7p (8.8%) radiotherapy alone and 4p (5%) had hormones alone.
cPET/TC -guided salvage treatments were: 23 radiotherapy (36%), 2 brachytherapy (3.1%), 8 radiotherapy and hormones (12.5%), 29 hormones (45.3%), 1 chemotherapy (1.6%) and 1 radical protatectomy (1.6%).

Results: Median time from diagnosis to cPET/TC failure: 44.03 months [2.37-126.83]. Median PSA values were 1.69 ng/ml [0.1-70.6].
cPET/TC local failure(LF) occurred in 39p (60.9%), nodal failure(NF) in 15p (23.4%) and metastasic failure(MF) in 10p (15.6%).
With a median follow up of 55 m after rescue treatment, 15p (23.4%) had biochemical failure again. At 5 years biochemical relapse free survival (BRFS) was 65%. Overall survival 5y: 91% (median: 119 months).
BRFS was 59% without LF vs 83% with LF (p 0.26)
BRFS was 75% without NF vs 30% with NF (p 0.065)

BRFS was 77% without MF vs 17% with MF (p 0.001)
BRFS was: PSA 0.2-1: 83%; 1.1-2: 66%; 2.1-10: 39%; >10.1: 37%. p: 0.02

Conclusion: cPET/TAC detect initial local and regional relapses that can be treated with local radiotherapy with or without hormonal therapy with good results.

EP-1343
PET-CT-related treatment changes in high risk and recurrent prostate cancer
A. Müller[1], D. Zips[1], D. Wegener[1], G. Reischl[2], K. Nikolaou[3], C. La Fougère[4], C. Pfannenberg[3]
[1]*University Hospital Tübingen- Eberhard Karls University, Radiation Oncology, Tübingen, Germany*
[2]*University Hospital Tübingen- Eberhard Karls University, Department of Radiology- Preclinical Imaging and Radiopharmacy, Tübingen, Germany*
[3]*University Hospital Tübingen- Eberhard Karls University, Department of Radiology- Diagnostic and Interventional Radiology, Tübingen, Germany*
[4]*University Hospital Tübingen- Eberhard Karls University, Department of Radiology- Nuclear Medicine, Tübingen, Germany*

Purpose or Objective: To prospectively evaluate the impact of Choline/ PSMA PET-CT imaging on management of patients with prostate cancer (PC).

Material and Methods: Fifty patients with high risk or recurrent PC received a 11Choline and/or a 68Ga-PSMA-PET-CT before radiation treatment planning within a prospective register study. Main subgroups were identified and only patients with a conventional staging before PET-CT were evaluated to compare treatment management decisions before and after PET-CT with regard to treatment intent, target volume (TV) definition, radiation dose and duration of androgen deprivation therapy (ADT).

Results: The three main subgroups fulfilling the mentioned conditions above were high risk (HR, n=17), recurrence after prostatectomy (R, n=12) and R plus salvage radiotherapy (RSR, n=7). In HRPC, TNM-changes (n=12/17) led to treatment changes (n=14) including TV-changes (n=12). In R, TNM-changes (n=8/12) resulted in treatment changes (n=8) including TV-changes (n=7). In the group after RSR, TNM-changes (n=6/7) resulted in treatment changes (n=6).
Management was changed in 82% (HRPC), 66%(R) and 85%(RSR). Of these groups (n=36) only two patients were initially stratified as M1. PET-CT led to downstaging (M0) or diagnosed only oligometastatic disease enabling curative treatment in both patients. However, in 12 patients initially planned for curative treatment detection of N1-disease (n=3/9) or newly diagnosed M1-disease (n=9/11) shifted treatment allocation to palliative therapy.
Taken together, curative treatment could be offered to initially diagnosed M1-patients (n=2). Since patients with RSR were usually in the palliative situation, PET-CT enabled in further 28% (2/7) of patients disease localization and curative treatment. However, of initially curatively planned patients (27/29) with R or HRPC, PET-CT facilitated to avoid overtreatment in ~30% (8/27) of patients due to early visualization of incurable disease. Main limitation is the absence of histological verification.

Conclusion: PET-CT had a pronounced impact on decision making and management in this group of patients with high-risk or recurrent prostate cancer. Therefore we suggest that PET-CT should be considered in the work-up in specific clinical situations.

EP-1344
Influence of surgical margins on the biochemical and radiological characteristics of the recurrence
L.G. Sapienza[1,2], J.D. Panichella[1], R.C. Camargo[1], A. Ernani[1], J.P. Dos Reis Junior[1], G.A. Pavan[1], H.A. Salmon[1]
[1]*Clínicas Oncológicas Integradas COI-RJ, Radiation Oncology, Rio de Janeiro, Brazil*
[2]*A. C. Camargo Cancer Center, Radiation Oncology, São Paulo, Brazil*

Purpose or Objective: To evaluate the possible impact of positive margins (PM) after surgery for prostate cancer on: I) biochemical parameters of recurrence (immediate failure rate and the time to development of biochemical recurrence) and II) the incidence of macroscopic disease at magnetic resonance image (MRI) realized before salvage radiation therapy (SRT).

Material and Methods: Data from 101 prostate cancer patients treated between 2012-13 was analyzed. Fifty (49.5 %) had MRI before SRT. PSA failure was defined has a value greater than 0.2 ng/ml after 6 weeks after prostatectomy. Cases with PSA >0.2 at the first measure 6 weeks after the surgery were categorized (no vs yes) and considered separately for the analysis of immediate failure. Categorical analysis were done using chi-square test. The time to the development of biochemical recurrence was presented in Kaplan Meier and log-Rank test was used to compare PM vs negative margins (MN) group. Mann-Whitney-Wilcoxon test was used to compare the PSA means between groups (PM vs NM / macroscopic recurrence present vs absent). The statistical analysis was done using SPSS V.20.

Results: The basic characteristics of this population were: age 66.8 years (median), initial PSA 8.0 ng/ml (median), 52.6% pT2 and 34.7% pT3. The proportions of each pathological risk group were 7%, 42% and 51% (low-risk, intermediate risk, high-risk) and 43,6% had PM (n=44). Those with PM had an increased chance of immediate PSA failure (p=0.004) and an earlier development of biochemical recurrence (23.4 months vs 49 months, p = 0.001). The mean PSA of the recurrence was 1.4 (+/- 1.7) ng/ml vs 2.6 ng/ml (+/- 6.1) (p = 0.839), for NM and PM respectively. Patients with macroscopic recurrence had a greater pre-SRT PSA: 3.5 (+/- 1.7) vs 0.8 (+/- 0.7) ng/ml. The incidence of biochemical recurrence with prostatic nodule in the MRI was not influenced by margin status (p=0.108) and marginally not influenced by pathological status (low or intermediate risk vs high risk) (p=0.062).

Conclusion: PM patients have had an earlier development of biochemical recurrence but our series did not find a significant impact of margin status on the incidence of nodule on prostatic bed. A possible delay in the detection of the recurrence in margin negative patients should be evaluated in next studies.

EP-1345
SBRT in low- and intermediate-risk prostate cancer: results of a phase II study
G. D'Agostino[1], E. Villa[1], C. Franzese[1], R. Liardo[1], G. Reggiori[1], P. Navarria[1], C. Iftode[1], F. De Rose[1], D. Franceschini[1], A. Tozzi[1], T. Comito[1], A. Ascolese[1], S. Tomatis[1], M. Scorsetti[1]
[1]*Istituto Clinico Humanitas, Radiotherapy and Radiosurgery, Rozzano Milan, Italy*

Purpose or Objective: Recent evidences has fostered the emergence of Stereotactic Body Radiation Therapy (SBRT) as a promising treatment modality for the management of localized prostate cancer. In fact, given the low alpha/beta ratio of prostate cancer, the delivery of very high radiation doses in few fractions, may even improve the therapeutic ratio in the treatment of this disease. This phase II study was aimed to evaluate the efficacy and toxicity of SBRT in a series of patients with low or intermediate risk prostate cancer.

Material and Methods: Biopsy confirmed prostate cancer patients were enrolled in this phase II trial, provided that they had the following characteristics: iPSA < 20 ng/ml, Gleason Score < 7, IPSS < 7. The treatment schedule was 35 Gy in 5 fractions, delivered every other day with VMAT technology in FFF modality. Toxicity was recorded according

to CT-CAE criteria v3.0. Biochemical failure was calculated according to the Phoenix definition.

Results: Between December 2011 and March 2015, 90 patients were enrolled (53 low risk, 37 intermediate risk). The median age was 71 years (range 48 – 82 y). The median Gleason Score was 6 (range 6-7) and the median initial PSA was 6.9 ng/ml (range 2.7 – 17.0). Acute toxicity was mild, with 32.2 patients presenting a G1 urinary toxicity and 31.1% of patients presenting a G2 urinary toxicity, mainly represented by urgency, dysuria and stranguria. A rectal G1 toxicity was found in a 15.5% of patients, while a rectal G2-toxicity was recorded in 6.6% of patients. Regarding late toxicity, a G1 proctitis was recorded in 11.1% of patients and a G1 urinary (urgency, cystitis) in 38.8%; only 2 events of G2 urinary toxicity were observed (transient urethral stenosis, resolved by a 24-hour catheterization). At a median follow up of 27 months (range 6 - 62 months) only two intermediate risk patients experienced a biochemical failure (22 and 24 months after radiotherapy, respectively). PET Choline revealed a nodal recurrence in one patient who underwent a further stereotactic radiotherapy and is now free of disease. In the other patient a local recurrence was diagnosed, associated to bone progression (rib), therefore the patient started ADT. Compliance to treatment was good, as reported by the EPIC questionnaires, which revealed a slight worsening in the urinary domains during treatment, with a return to baseline three months after treatment.

Conclusion: Stereotactic Body Radiotherapy seems to be a valid therapeutic option in low and intermediate risk prostate cancer patients, warranting an adequate control of disease, with mild toxicity profiles and good patient-reported quality of life perception.

EP-1346

Intraoperative radioterapy (IORT) in the multimodality treatment of locally advanced prostate cancer

M. Krengli[1], D. Beldì[1], G. Apicella[1], G. Marchioro[2], C. Pisani[1], E. Ferrara[1], C. Perotti[1], G. Loi[3], A. Volpe[2], C. Terrone[2]
[1]*University of Piemonte Orientale, Radiotherapy, Novara, Italy*
[2]*University of Piemonte Orientale, Urology, Novara, Italy*
[3]*University of Piemonte Orientale, Medical Physics, Novara, Italy*

Purpose or Objective: The treatment for locally advanced prostate cancer is still a controversial issue and multimodality treatment can lead to treatment optimization. The aim of this study is to describe technical and clinical aspects of intra-operative radiotherapy (IORT) in patients with locally advanced prostate cancer.

Material and Methods: Between September 2005 and September 2015, a total of 110 patients were enrolled. The statistical analysis was performed in 95 patients with follow up > 12 months. Inclusion criteria were: patients age < 76 years, KPS > 90, initial PSA (iPSA) > 10 ng/ml, clinical staging > cT2c according with TNM, probability of organ-confined disease < 25% according to MSKCC nomogram. Median age was 66.9 years (range 51-83), median iPSA was 14.6 ng/ml (range 2.0-80) and median Gleason Score (GS) was 8 (range 4-10). After surgical exposure of the prostate, IORT was delivered by a dedicated linear accelerator (Mobetron, Intraop, Sunnyvale, CA) with 30° beveled collimator, using an electron beam of 9 or 12 MeV to a total dose of 12 Gy. IORT was followed by radical prostatectomy and regional lymph node dissection. Rectal dose was measured "in vivo" by radio-chromic films placed on a rectal probe. All cases with pathological staging pT3a, positive margins (R1) or metastatic lymph nodes (N1) received postoperative external beam radiotherapy (EBRT), delivered to surgical bed with 3D conformal technique or intensity modulated radiation therapy to a total dose of 46-50 Gy (2Gy/fraction). Patients with pT3 or pT4 disease and/or N1 received adjuvant hormonal therapy.

Results: IORT procedure lasted in average 30 minutes (range 15-50). No major intra- or post-operative complication occurred. Median dose to the anterior rectal wall was 4.32 Gy (range 0.06-11.3). Pathological stage was: 30 pT2, 60 pT3, 5 pT4. 55/95 (57.9%) patients were R1 and 27/95 (28.4%) patients were N1. Median post operative PSA was 0.06 ng/ml (range 0-4). Post-operative radiotherapy was delivered to 73/95 patients (76.8%) with pathological staging pT3a or R1. Hormone therapy was prescribed to 61/95 patients (64.2%). Acute toxicity was: 16 G2 (9 GU; 7 GI), 2 G3 (1 GU; 1 GI). Late toxicity was: 11 G2 (5 GU, 6 GI), 4 G3 (2 GU; 2 GI). No G4 acute or late toxicity was observed. Four patients died of prostate cancer. With a median follow-up of 61.5 months (range 12-108), 26/95 patients experienced biochemical failure. Overall biochemical free survival (BFS) was 50% at 5 years. 5 years BFS was 78% and 42 % in high and very high risk classes according to NCCN classification. No evidence of failure in the prostate surgical bed was observed.

Conclusion: IORT during radical prostatectomy is a feasible procedure and allows to deliver safely post-operative EBRT to surgical bed without a significant increase of toxicity. With a median follow-up of 61.5 months, biochemical control seems to be optimal in particular for high risk patients.

EP-1347

Could "radical" RT be a reasonable choice in bone oligometastatic prostate cancer patients?

C.L. Deantoni[1], C. Cozzarini[1], A. Fodor[1], B. Noris Chiorda[1], P. Mangili[2], M. Picchio[3], E. Incerti[3], I. Dell'Oca[1], P. Passoni[1], C. Fiorino[2], R. Calandrino[2], N. Di Muzio[1]
[1]*IRCCS San Raffaele Scientific Institute, Radiotherapy, Milano, Italy*
[2]*IRCCS San Raffaele Scientific Institute, Medical Physics, Milano, Italy*
[3]*IRCCS San Raffaele Scientific Institute, Nuclear Medicine, Milano, Italy*

Purpose or Objective: To evaluate toxicity, clinical outcome and predictive response factors in patients with prostate cancer (PCa) oligometastatic (<2 lesions) to the bone at diagnosis, simultaneously treated with curative radiotherapy (RT) to primary tumor/prostatic bed (PB) and bone metastases.

Material and Methods: From February 2009, 33 patients with oligometastatic PCa (OPC), 18 of whom previously treated with radical prostatectomy and pelvic lymphadenectomy, underwent RT at "radical" dose to bone metastases (median 2-Gy equivalent dose, EQD2, >40 Gy, for α/ß=2,2), to the pelvic ± lomboaortic nodes (51,8 Gy for α/ß=1,5), and to the PB (median EQD2 72,4 Gy) or the prostate (median EQD2 88 Gy) within the same RT course in association with androgen deprivation therapy (ADT). To evaluate the possible role of adding a local treatment (radical dose RT to all sites of disease) to ADT, the biochemical relapse-free survival (bRFS), clinical failure-free survival (CFFS) and freedom from distant progression (FFDP, when the disease occurred in a different site from that treated) were considered, starting from the first day of RT.

Results: After a median follow-up of 20.2 months, 3 patients died, 1 were lost to follow-up, 2 showed in-field and 7 out-of-field progression, 3 have ended ADT and are still free from any progression. Acute toxicity was very mild with no Grade >2 events, and only 2 serious late events, 1 G3 and 1 G4 late urinary toxicity, only in the hypofractionated postoperative cohort. With respect to bone irradiation, no Grade toxicity were reported. Median bRFS, CFFS and FFDP were 15,8 months, 16,9 months and 17,2 months, respectively. When considering FFDP, the most significant clinical end-point to evaluate the role of RT in this subset of patients, the most predictive factors were: PSA at diagnosis (iPSA>24,2 ng/ml, most-informative cut-off, AUC 77%, p=0,008) (HR=4.2, p=0,05), 2 vs 1 metastasis (HR=2.87, p=0,1), and no previous prostatectomy (HR=3,19, p=0,08), while no role emerged for the site of metastases (pelvic or not). When stratifying

patients by the presence of 0-1 or 2-3 risk factor, the 2-year actuarial FFDP was 100% and 49% respectively (p=0,01, Fig 1).

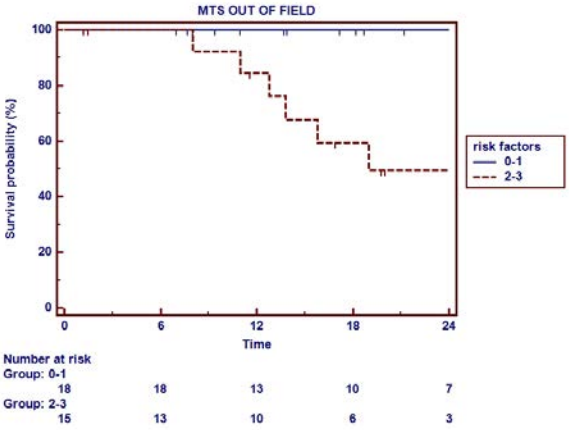

Conclusion: Although with a small cohort and a limited follow-up, these results seem to suggest that radical dose RT to all localization of disease is a valid approach in osseous OPC patients in association with ADT, also considering the low toxicity profile. Our predictive model aiming at identifying which patients may benefit of this kind of treatment seems to show that the ideal candidate could be a previously operated patient, with a iPSA≤24,2 ng/ml and with only one bone metastasis.

EP-1348

Endoscopic evaluation of late rectal toxicity after radiotherapy in 597 prostate cancer patients

M. Nuzzo[1], G. Macchia[1], S. Cilla[2], M. Ingrosso[3], C. Digesù[1], L. Di Lullo[4], E. Ippolito[5], F. Deodato[1], G. Siepe[6], M. Ntreta[6], M. Pieri[6], S. Cammelli[6], R. Schiavina[7], G. Martorana[7], A. Di Lallo[8], A.L. Angelini[9], G. Frezza[10], V. Valentini[11], A.G. Morganti[6]

[1]*Fondazione di Ricerca e Cura "Giovanni Paolo II"- Catholic University of Sacred Heart, Radiation Oncology Unit, Campobasso, Italy*

[2]*Fondazione di Ricerca e Cura "Giovanni Paolo II"- Catholic University of Sacred Heart, Medical Physic Unit, Campobasso, Italy*

[3]*Fondazione di Ricerca e Cura "Giovanni Paolo II"- Catholic University of Sacred Heart, Endoscopy Unit, Campobasso, Italy*

[4]*"F. Veneziale" Hospital, Medical Oncology Unit, Isernia, Italy*

[5]*Campus Biomedico University, Radiotherapy Unit, Roma, Italy*

[6]*S. Orsola-Malpighi Hospital- University of Bologna, Radiation Oncology Center- Department of Experimental- Diagnostic and Specialty Medicine – DIMES, Bologna, Italy*

[7]*S. Orsola-Malpighi Hospital- University of Bologna, Department of Medical Physics, Bologna, Italy*

[8]*"A. Cardarelli" Hospital, Oncological Urology Unit, Campobasso, Italy*

[9]*S. Orsola-Malpighi Hospital- University of Bologna, Department of Urology, Bologna, Italy*

[10]*Bellaria Hospital, Radiotherapy Department, Bologna, Italy*

[11]*Policlinico Universitario "A. Gemelli"- Catholic University of Sacred Heart, Department of Radiotherapy, Roma, Italy*

Purpose or Objective: Late rectal toxicity (LRT) is one of the main limitations of external radiotherapy (RT) for prostate cancer (PC). Purpose of this study was to evaluate the impact of various parameters on LRT, in a large cohort of patients undergoing radical or adjuvant RT in a series of clinical trials.

Material and Methods: 597 patients were selected (median age: 70 years; range: 43-88; NCCN risk class: 59 low, 199 intermediate, 339 high). Impact on grade ≥2 (RTOG) LRT of a series of parameters was analysed: previous radical prostatectomy, RT technique, type and duration of any adjuvant hormone therapy, RT dose and fractionation, acute rectal toxicity. LRT free survival curves were estimated according to the Kaplan Meier method. Univariate analysis was performed using log-rank test. Multivariate analysis was performed using "Cox's proportional hazard models".

Results: Table 1 shows the results of the analysis. Overall, grade > 2 LRT free survivals was respectively 89.5% and 84.9% at 2 and 5 years. At univariate analysis only acute rectal toxicity was significantly related to LRT (p <0.001) while there was a negative trend in patients receiving adjuvant hormone therapy, especially with LH-RH analogues. Multivariate analysis confirmed only the correlation between acute rectal toxicity and LRT (p: 0.006).

Table 1: Grade ≥ 2 late rectal toxicity free survival (%)

		Patients	2-year	5-year	Univariate analysis (log-rank), p:	Multivariate analysis (Cox), p:
Previous R.P.	no	403	88.6	81.1	0.175	
	yes	194	91.6	91.6		
Technique	3D	155	91.1	87.3		
	IMRT	418	88.4	80.1	0.878	
	VMAT	23	95.0	n.v.		
A.O.T. type	no	49	100.0	87.5		
	LH-RH analogue	287	86.8	83.7	0.065	0.991
	Bicalutamide	239	90.8	86.5		
A.O.T. duration	no	49	100.0	87.5		
	6 months	250	86.6	85.3	0.539	
	24 months	298	90.5	85.5		
Dose	≤ 70 Gy	378	90.0	90.0	0.303	
	> 70 Gy	219	88.7	83.1		
ENI	no	75	85.7	70.6	0.268	
	yes	522	90.5	89.9		
Fractionation	≤ 2 Gy/fr.	227	89.0	83.6	0.413	
	> 2 Gy/fr.	370	89.7	89.7		
Acute toxicity	G 0-2	571	90.3	85.6	<0.001	0.006
	G > 2	10	50.6	50.6		

R.P: radical prostatectomy; A.O.T.: adjuvant hormone therapy; ENI: elective nodal irradiation.

Conclusion: The results of this analysis showed no correlation between treatment parameters and LRT. This unexpected result is likely to be related to the use of modulated RT techniques in the majority of patients and to the distribution of the analysed parameters. For example, patients who have previously undergone radical prostatectomy, or treated with a hypofractionated regimen, generally received a lower total dose. The close correlation between acute and late toxicity seems to confirm the existence of a "consequential late toxicity" in radiation-induced damage to the rectum. This seems to suggest the utility of close endoscopic monitoring in the follow-up of patients with severe acute rectal toxicity.

EP-1349

Long term results of a phase I-II study of moderate hypofractionated IGRT in prostate cancer

N. Di Muzio[1], A. Fodor[1], B. Noris Chiorda[1], S. Broggi[2], P. Mangili[2], R. Valdagni[3], I. Dell'Oca[1], M. Pasetti[1], C. Deantoni[1], A. Chiara[1], G. Berardi[1], A. Briganti[4], R. Calandrino[2], C. Cozzarini[1], C. Fiorino[2]

[1]*San Raffaele Scientific Institute, Department of Radiotherapy, Milan, Italy*

[2]*San Raffaele Scientific Institute, Medical Physics, Milan, Italy*

[3]*Fondazione IRCCS Istituto Nazionale dei Tumori, Radiotherapy, Milan, Italy*

[4]*San Raffaele Scientific Institute, Department of Urology, Milan, Italy*

Purpose or Objective: To report long term clinical outcomes in prostate cancer patients (pts) treated with IGRT Moderate Hypofractionated Simultaneous integrated boost (SIB) by Tomotherapy in a phase I-II study.

Material and Methods: Between 2005 and 2011, 211pts were treated with IGRT Moderate Hypofractionated SIB in a phase I-II study . A subgroup of 128 pts (55 low- risk[LR], 33 intermediate- risk [IR] and 40high-risk[HR]) with 5 years minimum follow up were considered for this analysis. IR and HR pts received 51,8 Gy on pelvic lymph-nodes (LN) and concomitant SIB to prostate up to 74,2Gy in 28 fr; LR pts were treated to the prostate to 71,4Gy in 28fr. Androgen deprivation (AD) was delivered to 27% LR/57% IR/87% HR pts for a median time of 12.5, 13.7 and 15,5 months (m) respectively. Biochemical relapse free (bRFS) survival (Phoenix definition), cancer-specific (CCS) and overall survival (OS) actuarial curves were assessed. Selected clinical/dosimetry variables were tested as potential predictors of GI /GU toxicity and of BCR/CCS/OS (Cox test) .

Results: Median follow and median age were 75 m (range: 60-99) and 74 y (57-84) respectively, while median Gleason score(GS) was 6 (3-10):GS<7: 75; GS=7: 39; GS>7: 13 ; missing:2. 73 pts were staged as T1, 46 as T2: 6 as T3; and for 3 pts the stage was unclear (Tx). The median initial Psa (iPsa) was 7.8 (1.2-826). The 75-m bRFS was 92.5% (LR: 94.2%; IR: 96.9%; HR: 84.5%); OS was 94.6% (LR:95.9%; IR: 95.8%; HR: 91.1%) and CSS was 97.4% (LR: 100%;IR:94.5%;HR: 97.1%). AD and class risk were not correlated with bRFS/OS/CSS. The incidence of G3 toxicity was around 6% with drastically reduction of the prevalence at the last follow-up for both ≥G2 and ≥G3 toxicities indicating that symptoms were recovered in most patients.

Conclusion: The combination of pelvic LN irradiation and high dose to the prostate, (EQD2=88Gy) delivered with daily image-guided, intensity-modulated, moderate hypofractionation resulted in an excellent 75-m outcome, even in IR/HR patients. This encouraging result seems to be without correlation with AD considering the long time elapsed between the end of the AD and the last follow up of pts. The toxicity profile was acceptable

EP-1350

Postoperative radiation therapy following radical prostatectomy

J.A. Dominguez Rullan[1], A. Hervás[1], T. Muñoz[1], F. López[1], C. Vallejo[1], D. Candini[1], C. De la Pinta[1], D. Ordoñez[1], M. Martín[1], S. Sancho[1]
[1]*Hospital Ramón y Cajal, Radiation Oncology, Madrid, Spain*

Purpose or Objective: To compare clinical results of adjuvant and salvage radiotherapy after radical prostatectomy for prostate cancer and to determinate prognostic factors of biochemical relapse free survival (BRFS).

Material and Methods: 302 patients were treated at our institution over a 12-year period. Overall survival and biochemical-relapse free survival were analized using Kaplan-Meier and multivariate Cox regression analysis was used to assess differences between groups.

Results: Mean age at diagnosis was 65 years (42-80). All patients underwent radical prostatectomy combined with pelvic lymphadenectomy in 47.1% of cases. Neoadjuvant androgen deprivation before surgery was given to 36.5% . Mean pre-RT PSA of 0.46ng/ml (0-12.8 ng/ml). Adjuvant RT (ART) was performed in 113 patients and salvage RT (SRT) in 183 (9 for local recurrence) and mean dosis to surgical bed was 70 Gy (60-76 Gy). The distribution of patients by pT stage was pT2a/b (30.3%), pT2c (35%), pT3 (29%) and pT4 (2.3%). Upgrade in Gleason Score between transrectal biopsy and prostatectomy was experienced by 46.7% of patients. Positive surgical margins were reported in 56.5% of cases. Mean follow-up was 58.85 months (1-153 months). Overall survival at 5 and 10 years was 98.1% and 94.3%, respectively and BRFS at 5 and 10 years was 76.5% vs. 61.8%, respectively. The timing of RT (ART vs. SRT) and pre-RT PSA <0.5 ng/ml were significant predictors of longer BRFS.

GLEASON SCORE		PROSTATECTOMY					
		5	6	7	8	9	10
BIOPSY	5	1	1	0	0	0	0
	6	0	37	61	3	0	0
	7	1	5	57	16	13	1
	8	0	1	4	5	5	0
	9	0	0	0	0	2	0

Conclusion: Postoperative radiation therapy provides excellent long-term overall survival results with an aceptable BRFS with pre-RT PSA <0.5 ng/ml and adjuvant radiotherapy as predictors of better outcomes.

EP-1351

Developing a prostate decision aid tool considering patients and clinicians decisional needs

A.J. Berlanga[1], B.G.L. Vanneste[1], E. Bloemen[1], D. Rijnkels[1], P. Lambin[1]
[1]*MAASTRO Clinic, GROW School for Oncology and Developmental Biology- Maastricht University Medical Centre, Maastricht, The Netherlands*

Purpose or Objective: To facilitate shared decision making, we aim to develop a decision aid tool that helps prostate cancer patients to understand the benefits and side-effects of the treatments offered by their clinicians.
The tool should follow the International Patient Decision Aid Standard, and therefore patient's and doctor's views on decisional needs must be considered. The tool should have a new slant on existing tools: it should personalize the information, guide patients to identify their preferences, and help doctors to understand patients' preferences.

Material and Methods: Patients and clinicians were interviewed to assess their decisional needs. A prototypical tool was developed. Its clarity and acceptability was evaluated by the technology acceptance questionnaire (5-Likert scale).

Results: Prostate cancer patients already treated (N=16) mentioned the need of visual and free of medical jargon information about prostate cancer, treatments, side-effects, and treatment experience. Medical specialists (N=8; radiation oncologists, urologists, nurses) mentioned the need of information about basic anatomy, contraindications, hospital specific figures, and psychological support. Results about comprehensibility of the prototypical tool showed that most the patients fully agree (69%) or agree (31%) that the prototypical tool provides clear information about treatments, their side-effects, the differences between treatments, and eases comparison. Likewise, most of the patients fully agree (69%) or agree (31%) on using the tool if it would became available, and will recommend it to others (67% fully agree; 33% agree).
After considering the views of patients and medical specialists, the result is an alpha version of a web-decision aid tool for prostate cancer patients (http://www.treatmentchoice.info). The tool personalizes information for each patient. It assists patients to decide what their preferences regarding quality of life and treatment experience are, and to think how important are the side-effects for them. It provides a printed report of patients' preferences to be using during consultation. Fig below gives an impression.

Conclusion: The alpha version of the tool is a first step towards its implementation in the clinical practice. The tool will be tested further by patients, to investigate whether it (a) influences the quality of the decision; (b) can be used without support. The tool is available in Dutch, English and Italian. Future efforts include the development of decision tools for other primary tumors.

EP-1352

Early clinical experience from MRI-only based radiotherapy of localised prostate cancer

M. Tenhunen[1], J. Korhonen[1], M. Kapanen[2], T. Seppälä[1], J. Collan[1], K. Saarilahti[1], H. Visapää[1]
[1]*Helsinki University Central Hospital, Cancer Centre, Helsinki, Finland*
[2]*Tampere University Central Hospital, Department of Oncology, Tampere, Finland*

Purpose or Objective: The increased use of magnetic resonance imaging (MRI) for radiotherapy (RT) target delineation has encouraged method development to enable the entire RT treatment planning workflow based on MRI only. Earlier we have presented a procedure for MRI only based treatment planning replacing planning CT in all phases of RT including simulation, target volume definition, dose calculation based on a pseudo-CT image set generated from MRI, and image guidance where comparison between MR or pseudo-CT reference set and MV/kV planar images or cone-beam CT is performed. The method has been applied clinically for RT planning of localized prostate cancer since November, 2012. Here we present our early clinical experience.

Material and Methods: We have followed n = 125 patients treated with MRI only procedure with serum prostate-specific antigen (PSA) at the beginning (baseline) and end of the RT course. As a reference, similar group of patients has been chosen where RT were planned with similar irradiation technique, margins, dosage (prostate 76 Gy in 2 Gy fractions, seminal vesicles 66 Gy in 2 Gy fractions) and image guidance method (gold seeds + daily kV/MV imaging), but where CT planning image set has been used as a primary data set in treatment planning and IGRT, and MRI images were registered to CT for target delineation. For the reference group, equal number of patients with additional antiandrogen therapy (n = 100) or RT only (n = 25) were chosen.

Results: Mean PSA values for all the patient subgroups are presented in Table 1. The two methods show equal early response in PSA. No difference in early toxicity was noticed between the MRI only and CT+MRI groups.

Patient group	PSA baseline (ng/ml)	PSA at the end of RT (ng/ml)
MRI based planning, monotherapy 76 Gy, n = 25	8.1	5.1
CT based planning, monotherapy 76 Gy , n = 25	8.5	5.9
MRI based planning, hormone + RT 76 Gy, n = 100	1.2	0.2
CT based planning, hormone + RT 76 Gy, n = 100	1.3	0.3

Conclusion: MRI only based RT treatment planning gave expected and equivalent results after RT compared with CT (MRI registered) based treatment planning procedure. Longer follow-up is needed to confirm the clinical equivalence related both to tumour response and normal tissue toxicity.

EP-1353

Phase I/II study of hypofractionated Tomotherapy with CT-MRI planning for prostate cancer

A. Spera[1], M. Mannino[2], G. Mortellaro[1], V. Figlia[3], G. Caminiti[1], G. Iacoviello[4], N. Luca[3], F. Cuccia[3], R. Mazzola[3], G. Ferrera[1]
[1]*Ospedale A.R.N.A.S-Civico, U.O. Radioterapia Oncologica, Palermo, Italy*
[2]*University of Sussex, Genome Damage and Stability Centre, Brighton, United Kingdom*
[3]*Università degli Studi di Palermo, Scuola di Specializzazione Radioterapia, Palermo, Italy*
[4]*Ospedale A.R.N.A.S-Civico, U.O. Fisica Sanitaria, Palermo, Italy*

Purpose or Objective: On the basis of radiobiological studies suggesting a low α/β ratio for prostate adenocarcinoma, hypofractionation has been proposed to improve outcome in localized prostate cancer. STIP trial is a single center prospective phase I/II trial, with the aim of investigating feasibility and safety of moderate hypofractionation in low and intermediate risk (LR and IR) prostate cancer with Helical Tomotherapy (HT). We report early results in the first twelve recruited patients.

Material and Methods: Inclusion criteria are: histologically confirmed adenocarcinoma, age ≥ 18 and ≤ 85 years, LR and IR according to NCCN, performance status (Karnofsky) ≥ 60, no clinical or radiological sign of metastasis, International Prostate Symptom Score (IPSS) ≤ 19, no previous cancer history.The addition of short-term Androgen Deprivation Therapy to radiation is prescribed for IR patients and performed for 6 months. CT/MR simulation and all treatment sessions were performed with empty rectum and comfortably full bladder. Clinical target volume (CTV) 1 comprised the prostate gland in 11 LR patients, CTV2 also included the seminal vesicles in one IR patient. Planning target volumes (PTV) 1 and 2 were defined, respectively, as CTV1 and 2 plus a 0.5 cm margin. Total doses of 60 Gy and 54 Gy were delivered, in 20 fractions, to PTV1 and 2, respectively. To compare CTVs and PTVs obtained with CT and MRI, these volumes were contoured on CT scans and then on the merged image sets. Before each fraction, daily megavoltage tomography (MCVT) was performed to reduce interfraction uncertainties.

Results: Median follow-up was 12 months (range 3-20 months). Mean dose to PTV1 was 60.15 Gy (range 59.98-60.27), mean dose to PTV2 was 54.65 Gy. According to CTCAE 3.0 scale, acute G1 and G2 gastrointestinal toxicity occurred in 3 (25%) and 1 (8%) patients, respectively; no patients experienced G3 toxicity. G1 genitourinary toxicity occurred in 6 (50%) patients and no G2 or higher grade side effects were observed. According to the Expanded Prostate Cancer Index Composite (EPIC) questionnaire, urinary function declined 3 months post-treatment but it was similar to baseline at 12 months; bowel related quality of life remained stable during follow-up. IPSS remained similar to baseline for all patients. The contoured volume analysis showed that CTV and PTV based on MRI were always lower than CT based volumes (mean 38.07-87.10 vs 50.84-106). No patients experienced biochemical failure during follow-up.

Conclusion: Our preliminary data support the safety of a 20-fraction hypofractionated schedule delivered with HT in patients with localized prostate cancer.

EP-1354

Meta analysis of carbon ion therapy prostatic cancer

Q. Zhang[1], J. Tian[1], X. Wang[1]
[1]*Gansu Cancer Hospital, Department of Radiotherapy, Lanzhou, China*

Purpose or Objective: Carbon ion is characterized by unique physical and biological properties which is expected to be suitable to treat localized prostate cancer. In order to assess validate the feasibility and efficacy of carbon-ion radiotherapy for prostatic cancer, we synthesize and

compare available evidence of carbon ion therapy prostatic cancer by meta analysis.

Material and Methods: PubMed,Embase,The Cochrane Library,Web of Science,the Chinese Biomedical Literature Database were systemically searched from 1980 to May 2015 by heavy ion,carbon ion,carbon and 12C6+,to collect clinical study of carbon-ion radiotherapy for prostatic cancer.Two reviews independently screened citation extracted basic information of local control rate,overall survival rate and phase of clinical study,the related data were analyzed by Stata 12.0.

Results: Three phase II clinical trials,four phase I/II clinical trials and one retrospective study were included,which included 1307 patients.the meta analysis showed 3-,4-,5-,and 8-year overall survival rates were 0.934(95%CI:0.901,0.968),0.909(95%CI:0.866,0.951),0.872(95%CI:0.844,0.899) and 0.839(95%CI:0.793,0.884) and the 4-, 5-year local control rate were 0.989(95%CI:0.973,1.004) and 0.99(95%CI:0.969,1.01), respectively(Figure 1).

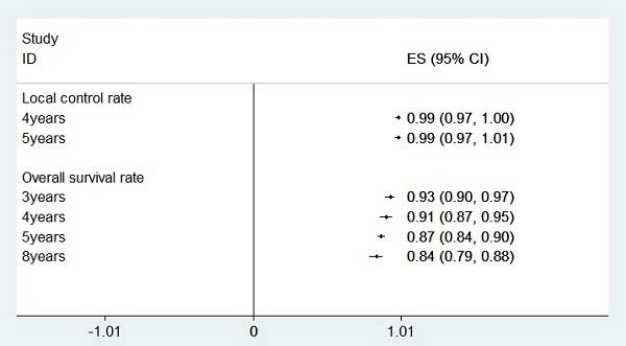

Conclusion: Carbon ion therapy is suitable and tolerable for the treatment of prostate cancer, in the future,more evidence is required before carbon ion therapy can become internationally the standard treatment for prostate cancer patients.

EP-1355

Combined and modulated adjuvant therapy in prostate carcinoma: a phase I-II trial

M. Nuzzo[1], V. Frascino[2], A.R. Alitto[2], G. Mattiucci[2], B. Fionda[2], M. Vernaleone[2], F. Catucci[2], P. Bassi[3], G. Macchia[1], F. Deodato[1], G. Siepe[4], M. Ntreta[4], A.G. Morganti[4], S. Cammelli[4], A. Arcelli[4], F. Bertini[4], E. Ippolito[5], G. Frezza[6], G. Mantini[2], V. Valentini[2]

[1]*Fondazione di Ricerca e Cura "Giovanni Paolo II"- Catholic University of Sacred Heart, Radiotherapy Unit, Campobasso, Italy*

[2]*Policlinico Universitario "A. Gemelli"- Università Cattolica del Sacro Cuore, Department of Radiotherapy, Roma, Italy*

[3]*Policlinico Universitario "A. Gemelli"- Università Cattolica del Sacro Cuore, Department of Urology, Roma, Italy*

[4]*Radiation Oncology Center- S.Orsola-Malpighi Hospital-University of Bologna, Department of Experimental-Diagnostic and Specialty Medicine - DIMES, Bologna, Italy*

[5]*Campus Biomedico University, Radiotherapy Unit, Roma, Italy*

[6]*Bellaria Hospital, Radiotherapy Department, Bologna, Italy*

Purpose or Objective: EORTC trial 22911 showed 75% 5-year biochemical disease-free survival (BDFS) in patients with prostate carcinoma (PCa) treated with radical prostatectomy (RP) followed by postoperative radiotherapy (RT). Aim of this study was to improve this outcomes by using a combined-intensified-modulated-adjuvant (CIMA) treatment, based on RT and adjuvant hormone therapy (AHT).

Material and Methods: The study hypothesis was that CIMA treatment may improve 5-year BDFS from 75% to 90%. The study was planned based on Simon's phase II design. We needed to study 100 experimental subjects to be able to reject the null hypothesis that the success rates for standard and experimental treatments are equal with probability (power) 0.8. The Type I error probability associated with this test of this null hypothesis is 0.05. We used an uncorrected chi-squared statistic to evaluate this null hypothesis. Some over-recruitment was planned to allow for a continuous drop-out process of up to 20% during the follow-up period. Enrolled patients were < 80 years old, with histological diagnosis of PCa, without known metastases, stage pT2-4 N0-1, not previously treated and with ECOG performance status of 0-2. All patients had at least one of these pathologic features: capsular perforation, positive surgical margins, seminal vesicle invasion. Standard dose to the tumor bed was 64.8 Gy. According to the pathological stage patients received a higher dose (70.2 Gy; 85.4%) and/or prophylactic irradiation of pelvic lymph nodes (57.7%) and/or adjuvant hormonal therapy (69.1%).

Results: One-hundred-twenty-three patients were enrolled in the study and completed the planned CIMA treatment. Median preoperative and postoperative PSA were 8.8 and 0.06 ng/dL, respectively. Proportion of patients with pathologically involved nodes and positive resection margin was 14.6 % and 58.5%, respectively. Median follow-up was 67 months (interquartile range: 48.0-98.0 months). Actuarial 5-year BDSF was 92.9%. Actuarial 5-year local control and metastasis-free survival were 99% and 96%, respectively. Actuarial 5-year overall survival was 95%.

Conclusion: CIMA therapy, compared to studies based on standard adjuvant radiotherapy, resulted in an improved 5-year BDFS, although patients with nodal metastatic disease and detectable postoperative PSA were enrolled in the study. A prolonged follow-up will be needed to confirm this improvement even in terms of disease-free survival and overall survival.

EP-1356

Postoperative radiotherapy in pT3a R1-resected prostate cancer patients

N.S. Hegemann[1], S. Morcinek[1], C. Belka[1], U. Ganswindt[1]

[1]*Klinikum der Universität München, Department of Radiation Oncology, München, Germany*

Purpose or Objective: Despite 3 large randomized studies on adjuvant radiotherapy (RT) proving a significantly improved biochemical recurrence free survival in patients (pts) with advanced prostate cancer (PCA), there is still an dispute regarding the need for adjuvant RT in those pts. The risk of recurrence in these advanced stages may reach 30% to 60%. Nevertheless many of those pts are not referred to adjuvant RT. We therefore performed a retrospective analysis of 94 pts with pT3a pN0/cN0 R1-resected PCA in order to investigate the natural history of the disease and the benefit of adjuvant or salvage RT.

Material and Methods: We included 94 pts with pT3a pN0/cN0 R1-resected PCA that had undergone prostatectomy no later than 2009. In 91 pts lymphadenectomy was performed with an average of 10 removed lymph nodes. Gleason-Score was mainly 7a in 33, 7b in 24 and 8 in 19 pts. Statistical analysis was performed using a Cox proportional hazard model and Kaplan Meier survival analysis. Median follow up was 80 months.

Results: 71 pts had a PSA <0.07ng/ml after surgery. 35 of them experienced a biochemical relapse (Group 1). In 30 pts this occurred within the first 80 months. 28 of the pts with biochemical relapse received early salvage RT. PSA before salvage RT was in median 0.24ng/ml and after RT in 23 pts <0.07ng/ml. 36 pts were PSA negative after surgery and did not have any PSA relapse (Group 2). Nevertheless 14 of these pts received an additive RT treatment within the first 15 months after surgery. At the last date of contact all 36 pts were still PSA negative. 23 pts were PSA positive after surgery (Group 3). 18 pts received an early salvage RT with a PSA in median of 0.4ng/ml (0.12-4.58). After RT PSA was 0.28ng/ml (0.0-4.58). 5 pts in Group 1, 1 patient in Group 2 and 9 pts in Group 3 received androgen deprivation therapy (ADT) after radiotherapy until the last date of contact.

Conclusion: In total 60 of 94 pts (63.8%) with homogenously pT3a pN0/cN0 R1 resected PCA received radiotherapy highlighting the need of adjuvant/salvage treatment in those pts. The efficacy of radiotherapy is documented by the fact that the median PSA of all irradiated pts at 80 months of follow up was 0.01ng/ml (0.0 – 204.9). This may be blurred by the influence of ADT (15 pts). However, even our small retrospective cohort demonstrates a biochemical recurrence rate of originally postoperatively PSA negative pts of 49.2%. Furthermore, 65.7% of these pts could be rendered at least temporarily PSA-free by postoperative radiation.

EP-1357

Moderately hypofractionated IGRT / IMRT-SIB in prostate carcinoma: toxicity and QoL in 300 patients

M. Ntreta[1], G. Siepe[1], A. Galuppi[1], S. Cammelli[1], M. Nuzzo[2], G. Macchia[2], F. Deodato[2], S. Cilla[3], G. Mantini[4], A. Farioli[5], A. Arcelli[1], F. Bertini[1], M. Pieri[1], L. Ronchi[1], G. Martorana[6], A.G. Morganti[1], G. Frezza[7]

[1]Radiation Oncology Center- S.Orsola- Malpighi Hospital-University of Bologna, Department of Experimental-Diagnostic and Specialty Medecine-DIMES, Bologna, Italy
[2]Fondazione di Ricerca e Cura " Giovanni Paolo II"-Catholic University of Sacred Heart, Radiotherapy Unit, Campobasso, Italy
[3]Fondazione di Ricerca e Cura " Giovanni Paolo II"-Catholic University of Sacred Heart, Medical Physics Unit, Campobasso, Italy
[4]Policlinico Universitario "A. Gemelli"-Catholic Univerity of Sacred Heart, Department of Radiotherapy, Roma, Italy
[5]S.Orsola- Malpighi Hospital- University of Bologna, Department of Medical and Surgical Sciences-DIMEC, Bologna, Italy
[6]S.Orsola- Malpighi Hospital- University of Bologna, Department of Urology - Department of Medical and Surgical Sciences-DIMEC, Bologna, Italy
[7]Ospedale Bellaria, Radiotherapy Department, Bologna, Italy

Purpose or Objective: Aim of this study was to evaluate the safety, in terms of acute and late toxicity and QoL in patients (pts) with prostate carcinoma (PCa) treated with moderately hypofractionated IGRT/IMRT-SIB using fiducial markers.

Material and Methods: Three-hundred consecutive PCa pts were treated with daily on-line IGRT based on 2D (6MV) orthogonal images. Low risk pts received 62.1 Gy in 23 fractions to PTV1 (prostate). Intermediate risk pts with probability < 15% of lymph nodes involvement (Roach's equation) received 67.5 Gy and 56.25 Gy in 25 fractions to PTV1 and PTV2 (seminal vesicles). In high risk patients with probability > 15% of lymph nodes involvement, pelvic lymph nodes (PTV3) received 50 Gy. Acute and late toxicities were prospectively recorded using RTOG-EORTC scale and AUA score. Survival curves were calculated using the Kaplan-Meier method. Androgen suppressive therapy was prescribed based on risk categories.

Results: GI and GU G ≥ 3 acute toxicity were 0.7 % and 2.0 %, respectively. With a median follow-up of 30 months (range: 12-72), late GI ad GU toxicity were recorded in 4 and 18 pts, respectively. Based on IPSS score, no pts reported severe urinary symptoms, and 7.7% of pts reported moderate symptoms only. In terms of QoL, 91.3% declared to be "pleased", 5.7% "mostly satisfied" and 1.3% "mixed" (1.7% not evaluable).

Conclusion: Our experience confirms the safety of moderate hypofractionation delivered with IGRT/IMRT-SIB and a moderate impact on QoL in pts with PCa. Prolonged follow-up is needed to evaluate the results in terms of patients outcome.

EP-1358

Prospective evaluation of PSA kinetics during salvage radiotherapy as a predictor for outcome

A. Gunnlaugsson[1], E. Kjellen[1], R. Blom[1], O. Bratt[2], G. Ahlgren[3], P. Nilsson[1]

[1]Skåne University Hospital and Lund University, Department of Oncology and Radiation Physics, Lund, Sweden
[2]Cambridge University Hospitals NHS Foundation Trust, Department of Urology, Cambridge, United Kingdom
[3]Skåne University Hospital and Lund University, Department of Urology, Lund, Sweden

Purpose or Objective: The aims of this prospective observational trial was to study early PSA kinetics by weekly PSA measurements during salvage radiotherapy (RT) for patients with recurrent prostate cancer in order to develop a predictive model for treatment outcome.

Material and Methods: This prospective study included patients with a biochemical recurrence after prostatectomy referred for curative salvage RT. No previous or present anti-hormonal treatment was allowed. All patients were prescribed 70 Gy in 35 fractions to the prostate bed. PSA was measured at baseline and then weekly during RT. A PSA follow-up was scheduled at 3, 6, 12, 18 and 24 months after RT and yearly thereafter. Treatment response was defined as PSA <0.1 ng/ml at these time points (PSA_RESP_3/6/12/18/24). Bivariate analyses of the association between response and clinical factors as well as PSA during RT were performed. Here we report the results for end-point PSA_RESP_6.

Results: Since Sept 2012, 151 patients have reached six months follow-up after RT. PSA_RESP_6 was achieved in 89 (59%) of the cases. Significant predictive clinical factors were proportion of positive biopsies, Gleason score, lymph node extirpation and surgical borders. However PSA during therapy was the single strongest predictive factor for PSA_RESP_6 with a ROC AUC up to 0.92 (95% CI 0.86 – 0.95).

Conclusion: We propose that PSA monitored during salvage RT can be used as a predictive factor for treatment outcome and subsequently for personalized patient management.

EP-1359

A randomized trial comparing bladder volume consistency during EBRT in postoperative prostate cancer

K. Braide[1], J. Kindblom[1], U. Lindencrona[2]

[1]Göteborg University Sahlgrenska University Hospital, Department of Oncology, Göteborg, Sweden
[2]Göteborg University Sahlgrenska University Hospital, Department of Physics and Biomedical Engineering, Göteborg, Sweden

Purpose or Objective: There are different guide lines about delineating the post-operative prostatic fossa before EBRT. They all recommend that the patients should have a half full or comfortably filled bladder at the planning CT and at each fraction in order to ensure a consistent bladder volume throughout the whole treatment course. The aim of this study was to compare bladder volume variations between 1) a specific bladder filling protocol and 2) a simple instruction to the patients to keep a comfortably filled bladder before each treatment fraction.

Material and Methods: Twenty-nine patients (median 65 y) with PSA-relapse planned for salvage radiation therapy were randomised in two groups, with different preparation instructions:
1. Drinking 300 ml and empting the bladder one hour before planning CT and treatment fractions. (13 patients)
2. A comfortably filled bladder before planning CT and treatment fractions. A pre-treatment drinking volume according to patient's preference. (16 patients)
Treatment was prescribed to 70 Gy/35/2. As a complement to positioning to bony anatomy a CBCT was performed once a week to calculate the bladder volumes.

Results:

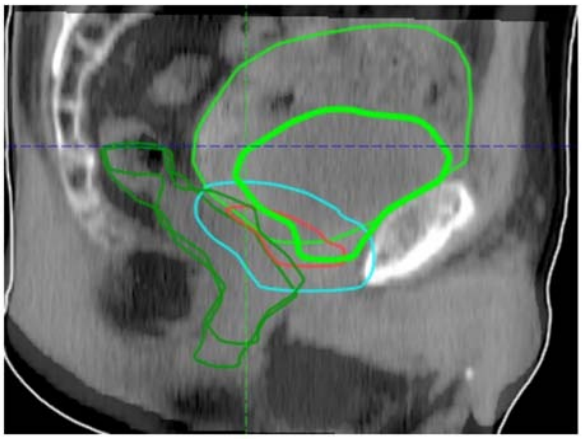

Figure 1. An example of a patient with large variation in bladder filling between planning CT (thin light green) and CBCT before a treatment fraction (thick light green). The planning-CT and CBCT are matched to bony anatomy. (Red =CTV, blue=PTV, dark green= rectum)

The bladder volumes varied widely both within each patient (see example in Fig. 1), between patients in the same group and between the groups.

The individual patient mean bladder volume varied from 79±23 to 269±90 ml in group 1 and between 64±19 to 309±110 ml in group 2.

Furthermore, there was no difference in the group mean bladder volume between the groups, 138±82 ml in group 1 and 150±92 ml in group 2 (p-value 0,59).

Conclusion: The findings indicate that the use of a strict bladder protocol is not superior to a comfortably filled bladder-regime to ensure a consistent bladder volume throughout the whole treatment course. The conclusion would be to let the patient prepare according to his own preference with a comfortably filled bladder. This could result in an easier patient setup due to a more relaxed patient. The impact of the wide variations in bladder volume on toxicity and dose distribution is further to be determined.

EP-1360

Comparing patient and physician-reported GI effects in locally advanced prostate cancer radiotherapy

M. Thor[1], C.E. Olsson[2], S. Hansen[3], P.M. Petersen[4], H. Lindberg[5], M.M. Kempel[6], L. Dysager[3], M. Høyer[7], J.O. Deasy[1], L. Bentzen[7]

[1]*Memorial Sloan Kettering Cancer Center, Department of Medical Physics, NYC, USA*

[2]*Institute of Clinical Sciences- the Sahlgrenska Academy at the University of Gothenburg, Department of Radiation Physics, Gothenburg, Sweden*

[3]*Odense University Hospital, Department of Oncology, Odense, Denmark*

[4]*Copenhagen University Hospital, Department of Oncology, Copenhagen, Denmark*

[5]*Herlev Hospital, Department of Oncology, Copenhagen, Denmark*

[6]*Aalborg University Hospital, Department of Oncology, Aalborg, Denmark*

[7]*Aarhus University Hospital, Department of Oncology, Aarhus, Denmark*

Purpose or Objective: To compare patient-reported outcomes (PROs) with physician-assessed outcomes (PAOs) on gastrointestinal (GI) dysfunction pre- and post-radiotherapy (RT) for locally advanced prostate cancer.

Material and Methods: Adverse GI effects were assessed in 80 subjects treated with intensity-modulated RT for locally advanced prostate cancer (78 Gy/56 Gy in 39 fractions to the prostate/pelvic lymph nodes) in 2011-2012. A study-specific PRO and CTCAE.v.3-based PAOs were completed pre- and post-RT (end, 3, 6, 12, and 24 m). This study focuses on the 18 (PROs) and 8 (PAOs) potentially RT-induced GI symptoms. Symptomatic subjects were considered as having PRO>Grade 1 and PAO>Grade 0 symptom severity. Relative risk ratios (RR) with related 95% confidence intervals (95%CI), and p-values (two-sided 5% significance level) were calculated for each symptom and follow-up time post-RT, with pre-RT symptom severity as the reference.

Results: Across all follow-up times, significant RRs were observed for in total 4/18 (RR: 2-25; p<0.001-0.02) PROs and 1/8 (RR: 2; p=0.0001-0.02) PAO (Table). Defecation urgency and Obstruction yielded the tightest 95%CI among the PROs, and Flatulence among the PAOs. The RR indicated that the PROs acknowledged both acute (12 symptoms) and late (3m: 5; 6m: 4; 12m: 7; 24m: 9 symptoms) RT-induced effects, and that the PAOs typically focused on acute rather than late effects (7 vs. 1-3 symptoms).

Table. Prevalence (%), relative risk ratio (RR), and 95% CI (ps0.05) at each follow-up time for each PRO (upper) and PAO (lower) symptom.

		End of RT N=79			3m post-RT N=79			6m post-RT N=80			12m post-RT N=77			24m post-RT N=74		
GI domain	**PRO**	**%**	**RR**	**95%CI**	**%**	**RR**	**95%CI**	**%**	**RR**	**95%CI**	**%**	**RR**	**95%CI**	**%**	**RR**	**95%CI**
Defecation urgency	Time to defer defecation	54	7	3-15	33	4	2-9	28	3	2-8	36	5	2-10	31	4	2-9
	Re-defecate<1h after last defecation	53	4	2-7	32	**2**	1-4									
	Forcing toilet visit	58	5	3-9	42	3	2-7	35	**3**	2-6	44	4	2-7	39	**3**	2-6
Fecal leakage	Liquid stools	25	3	1-8							25	3	1-7	20	3	1-6
	Solid stools															
	Protective pads use	15	24	2-400							12	19	1-310	12	19	1-320
	Nocturnal bowel movements	24	9	2-38												
	Soiling underwear										47	2	1-6	51	**2**	1-3
Obstruction	Incomplete evacuation	44	4	2-9	30	**3**	1-6	21	**2**	1-5	29	**3**	1-6	34	3	2-7
	Difficulty passing stools	13	20	1-340												
	Strain@defecation	27	**2**	1-5										27	**2**	1-5
Pain	@Defecation	22	6	2-18												
	Anal/rectal	25	3	1-6												
Stool content	Mucous	33	25	4-180	15	11	2-85	21	16	2-120	16	12	2-88	16	12	2-91
	Blood													11	8	1-63
	PAO	**%**	**RR**	**95%CI**	**%**	**RR**	**95%CI**	**%**	**RR**	**95%CI**	**%**	**RR**	**95%CI**	**%**	**RR**	**95%CI**
Fecal leakage	Diarrhea	49	6	3-14	22	3	1-7									
	Incontinence	14	11	1-81	11	9	1-66				12	9	1-68			
Flatulence	Flatuelence	59	**2**	2-4	48	**2**	1-3	51	**2**	1-3	49	**2**	1-3	45	**2**	1-3
Pain	Abdominal	14	4	1-12												
	Bloating	18	5	1-15												
	Rectal	19	7	2-31												
Proctitis	Proctitis	13	5	1-22				13	5	1-21						

Conclusion: This study indicates that the number of symptoms and temporal patterns of RT-induced GI dysfunction in locally advanced prostate cancer depend on the applied assessment method. Physician-assessed outcomes according to CTCAE.v.3 captured acute effects, and in particular flatulence, whilst patient-reported outcomes captured both acute and late effects mainly related to defecation urgency and obstruction.

EP-1361

Prognostic factors in 1080 prostate cancer treated with radical external beam radiotherapy

E. Garibaldi[1], D. Gabriele[2], A. Maggio[3], M. Garibaldi[2], E. Delmastro[4], S. Bresciani[5], A. Sottile[6], M. Stasi[7], P. Gabriele[5]

[1]*Candiolo Cancer Centre FPO-IRCCS, Radiotherapy Department, Candiolo, Italy*

[2]*Physiology Unit, Neuroscience Department, Turin, Italy*

[3]*Candiolo Cancer Center FPO-IRCCS, Medical Physic Units, Candiolo Turin, Italy*

[4]*Candiolo Cancer Centre FPO-IRCCS, Radiotherapy Deaprtment, Candiolo Turin, Italy*

[5]*Candiolo Cancer Centre FPO-IRCCS, Radiotherapy Department, Candiolo Turin, Italy*

[6]*Candiolo Cancer Centre FPO-IRCCS, Laboratory Analysis, Candiolo Turin, Italy*

[7]*Candiolo Cancer Centre FPO-IRCCS, Medical Physic Units, Candiolo Turin, Italy*

Purpose or Objective: The aim of this paper is to analyze, in prostate cancer patients treated with external beam radiotherapy (EBRT), the prognostic factors and their impact on the outcome in terms of Cancer Specific Overall Survival (CSOS), Biochemical Disease Free Survival (BDFS) and Clinical Disease Free Survival (CDFS).

Material and Methods: From October 1999 and March 2012 we treated by EBRT, 1080 prostate cancer patients. The mean age was 69.2 years. Pretreatment staging examinations were: digital rectal examination (DRE), pretreatment PSA (iPSA), abdominal ultrasound, abdominal CT scan and bone scan. The 87% of patients were classified as < cT2, 87% had a

Gleason Score (GS) < 7; the mean of iPSA was 18 ng/mL; the rate of clinical positive nodes was 1%. The ADT was prescribed to 69% of patients in neoadjuvant setting, 65% in concomitant setting and 34% in adjuvant setting. The mean follow-up was 81 months.

Results: The prognostic factors resulted statistically significant for all groups of patients at both, univariate and multivariate analysis, were the GS and the iPSA. In intermediate and high/very-high risk patients at multivariate analysis the prognostic factors for CSOS were: GS (p=0.001), positive lymph nodes on CT scan (p=0.05) and rectal preparation during the treatment (p=0.005); for the BDFS were: GS (p=0.008), patient risk classification (p=0.037), positive lymph nodes on CT scan (p=0.004), iPSA (p=0.001) and rectal/bladder preparation during the radiation treatment (p=0.001); for the CDFS were: number of positive core on biopsy (p=0.003), GS (p=0.0003), positive lymph nodes on CT scan (p=0.015), iPSA (p=0.0056) and RT dose (p=0.001). In high/very-high risk patient group at multivariate analysis the prognostic factors for CSOS were: biopsic Gleason Score, clinical/radiological stage, RT dose; for BDFS were: biopsic Gleason Score, adjuvant ADT, clinical/radiological stage, iPSA and RT dose>77.7 Gy; for CDFS were: biopsic Gleason Score, clinical/radiological stage, iPSA and RT dose>77.7 Gy.

Conclusion: Our results confirm several prognostic factors already described by literature, adding a new prognostic factor represented by the rectal/bladder preparation, generally known for its effect on toxicity but not yet on outcome. We believe that in the future a new nomogram should include also some therapeutic variables (as RT dose, RT technique and ADT), to help clinicians in decision-making.

EP-1362

Hypofractionated Simultaneous Integrated Boost IMRT in high risk prostate cancer – A novel approach

S. Sashidharan[1], K. Beena[1], P. Chelakkot G[1], R. Madhavan[1], D. Menon[1], D. Makuny[1]
[1]*Amrita Institute Of Medical Sciences, Radiation Oncology, Kerala, India*

Purpose or Objective: We aim to evaluate the biochemical failure free survival (BFFS) and morbidity in high risk prostate cancer patients treated with long term androgen deprivation therapy (ADT) and hypofractionated Simultaneous Integrated Boost (SIB) IMRT. Recent advances in techniques enable us to deliver a higher dose of radiation to the prostate with limited dose to the adjacent rectum and bladder. Earlier studies have estimated prostate cancer to have low α/β of 1.5. Thus hypofractionated schedules in theory should confer better local control and cancer specific survival (CSS). Due to the long natural history of prostate cancer it becomes imperative to reduce rectal and bladder morbidity. Also BFFS has shown to be a predictor of CSS. Most of the studies with whole pelvic RT and long term ADT have used conventional fractionation schedules. Data on the benefit of hypofractionated SIB IMRT with long term ADT is limited.

Material and Methods: Retrospective analysis of 100 high risk prostate cancer patients treated between 2010-2012. All patients received SIB IMRT with 70Gy in 28 fractions to the prostate and seminal vesicles (if involved) and 50.4 Gy in 28 fractions to the pelvic nodal stations with neoadjuvant hormonal therapy for a duration of 3-6 months prior to radiation and adjuvant hormonal therapy for a duration of 24-36 months. They were followed up with serial PSA values and clinical examination. Biochemical failure was defined as serum PSA >nadir + 2 (ASTRO Phoenix definition). Acute rectal and bladder toxicity was scored with the RTOG toxicity criteria. Chronic rectal toxicity (proctitis) and chronic bladder toxicity (cystitis) were assessed using the CTCAE 4.0. Patients without biochemical failure were censored at last follow-up/last PSA check or death. BFFS was calculated by the Kaplan-Meier method.

Results: At a median follow up of 45 months (20-87 months), there were 13 cases of biochemical failure (13 %) . 5 year BFFS was 78.6% .There was no Grade 3 or 4 acute rectal or bladder toxicity . Chronic toxicity has been listed in the table below. Urethral stricture developed in 7 patients, of whom 6 had prior TURP showing significant correlation (6/15,p<0.001).

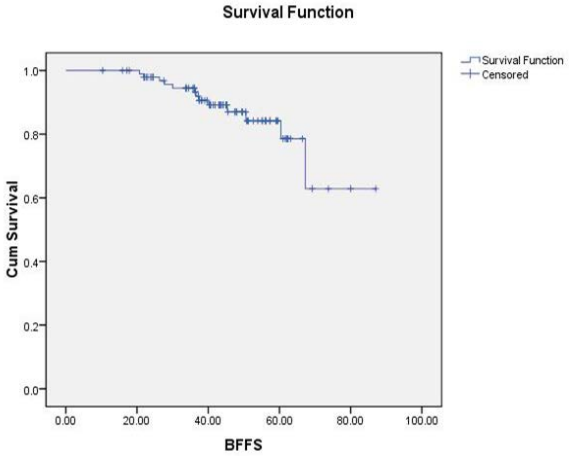

	Grade 2	Grade 3	Grade 4
Proctitis	12	2	0
Cystitis	7	0	0

Conclusion: This study therefore concludes that long term ADT and SIB IMRT provides a feasible alternative to conventional radiation therapy with good biochemical control and acceptable toxicity. Longer follow up of these patients would provide data on cancer specific survival and late morbidity.

EP-1363

Salvage SBRT in isolated nodal oligo recurrence from prostate cancer: UPMC San Pietro FBF experience

M.C. Barba[1], F. Aquilanti[1], F. Bianciardi[2], B. Nardiello[1], G. Raza[2], R. El Gawhary[2], A. Rinaldi[1], C. D'Ambrosio[2], P. Gentile[2]
[1]*UPMC S. Pietro Fatebenefratelli, Radiotherapy, Roma, Italy*
[2]*Ospedale S. Pietro Fatebenefratelli, Radiotherapy, Roma, Italy*

Purpose or Objective: A status of disease with a limited number of distant lesions and a controlled primitive tumor is recently defined as oligo-recurrence: this group of patients is more favorable than the other with a high number of metastases and, in prostate cancer, often is represented by a single node.The objective of this retrospective study was to evaluate the acute and late toxicity rates, in salvage stereotactic body radiation therapy (SBRT) as a treatment modality in nodes oligo-recurrence, from prostate cancer.

Material and Methods: Between February 2013 and March 2015, 21 patients, for a total of 29 isolated lymph nodes from prostate cancer, were treated with SBRT, delivered with Truebeam Stx (Varian®), at UPMC San Pietro FBF radiotherapy center of Rome.The median age at primitive diagnoses was 65 (range 50-74) years. For the primary treatment, radical prostatectomy and postoperative irradiation, exclusive radiotherapy or prostatectomy was performed in 12 (57%) patients, 7 patients (33%) and 2 patients (10%), respectively. Median previous RT dose was 72 Gy/35 fractions.Median PSA at the time of recurrence was 2.04ng/ml.All patients with arising PSA underwent a [11C] choline-positron emission tomography before SBRT, in order to exclude other sites of disease. The SBRT dose varied from 27 to 30 Gy, in 1-5 daily fractions, according to the previous RT treatment for the primitive lesion or a close organ at risk. A daily cone-beam CT and X-ray (BRAINLAB ExacTrac®) scans were acquired before each treatment session, for every

patient. Acute and late toxicity were analyzed, according to CTCAE toxicity scale (v. 4.0).

Results: The median follow-up was 14.5 months. Most of patients received 30 Gy, in 3 fractions, on alternative days: all the patients completed the prescribed SBRT treatment.Fifteen patients (71%) received androgen deprivation therapy concomitant to SBRT.SBRT was well tolerated: only 1 patient experienced G2 acute rectal toxicity but we didn't observe any severe acute or late toxicity (≥G3). Despite the short follow up, local control was 100%, distant control was 79% (6/21).All these recurrences were nodal and all out of SBRT field: in 2 of these 6 patients a new SBRT course was delivered (30 Gy in 3 fractions) while in the other hormonal therapy was proposed. At the moment of analysis, all patients were alive.

Conclusion: Our experience shows that SBRT for isolated nodal relapse from prostate cancer is a safe treatment, offering a low toxicity profile and an excellent tumor local control. More data and a longer follow up are needed.

EP-1364

Role of choline PET/CT in Cyberknife treatment planning for recurrent prostate cancer following EBRT

I. Bossi Zanetti[1], A. Bergantin[1], A.S. Martinotti[1], I. Redaelli[1], P. Bonfanti[1], M. Invernizzi[1], A. Vai[1], L.C. Bianchi[1], G. Beltramo[1]
[1]*Centro Diagnostico Italiano, Cyberknife, Milano, Italy*

Purpose or Objective: Most studies demonstrate that local salvage therapy after EBRT may provide long-term local control in appropriately selected pts, although toxicity is often significant.In these pts, PET/CT with [11C]choline may accurately detect the presence of recurrence.We investigated the role of [11C]choline PET/CT for target volume selection and delineation in pts with recurrent prostate cancer following EBRT for a salvage tailored Cyberknife Stereotactic Hypofractionated Radiotherapy(SBRT) treatment.

Material and Methods: From December 2012 to April 2015,22 pts with initial disease category defined as low(2),intermediate(6) high (14),in accordance with NCCN 2008 guidelines,median age of 74 years(range 62-89) and an history of locally-recurrent prostate cancer following EBRT were referred to our Department for salvage Cyberknife SBRT. The diagnosis of a clinically evident recurrence of prostate cancer was based on biochemical progression and imaging studies. Median iPSA was 22,7 ng.ml(4,9-88 ng.ml),EBRT doses ranged from 74 to 79.2 Gy(median 76Gy) and the median interval time between relapse diagnosis and salvage Cyberknife treatment was 60 months(range 19-139).The median pre-reirradiation PSA was 4,64 ng/ml (range 2,23-13,04 ng/ml). CT scan and MRI with T1-T2 sequences were performed and [11C]choline PET/CT images were fused for prostate target volume delineation.5 pts received 3 fractions of 10 Gy (total dose 30 Gy), 17 pts received 3 fractions of 12 Gy (total dose 36 Gy) delivered to the PET positive prostate node (median volume of 14,3 cc-range 5,75-65,04) in the respect of organ at risk constrains.

Results: The treatment was well tolerated with no RTOG grade 3 acute or late toxicity. With a median follow up of 17 months (range 6-35) we observed the following results: no in field recurrence, with a local control of 100%. In 4 pts, respectively at 11, 14, 16 and 22 months after treatment (median time 15 Months), a [11C]choline PET/CT detect a local recurrence with the evidence of a new positive prostate node outside the irradiated field requiring a second Cyberknife salvage treatment.

Conclusion: Advances in modern imaging show promises in the management of prostate cancer at the different stage (diagnosis, treatment planning and follow up). According to available literature [11C]choline PET/CT is not clinically recommendable to plan target volume, nevertheless ,our promising data suggest a potential role of [11C]choline PET/CT as an image guide tool for the focal irradiation of prostate cancer relapse.

EP-1365

Dosimetric predictors for rectal toxicity with two hypofractionated schedules for prostate cancer

T. Zilli[1], M. Kountouri[1], M. Rouzaud[1], A. Dubouloz[1], D. Linero[2], S. Jorcano[2], L. Escudé[2], R. Miralbell[3]
[1]*Hôpital Cantonal Univ. Genève, Radiation Oncology, Geneva, Switzerland*
[2]*Teknon Oncologic Institute, Radiation Oncology, Barcelona, Spain*
[3]*Hôpital Cantonal Univ. Genève and Teknon Oncologic Institute, Radiation Oncology, Geneva and Barcelona, Switzerland*

Purpose or Objective: To analyze the dosimetric impact on long term gastro-intestinal (GI) toxicity of two sequential dose escalation regimens of twice weekly 4 Gy/fractions hypofractionated intensity-modulated radiotherapy (IMRT) delivered within a protracted overall treatment time of 6.5 and 7 weeks, respectively.

Material and Methods: Clinical and dosimetric data on 96 prostate cancer patients with cT1c-T3a disease and nodal involvement risk ≤20% (Roach index) treated twice-weekly to the prostate +/- seminal vesicles with two sequential dose-escalated IMRT schedules of 56 Gy (14 x 4 Gy, n=28) from 2003 to 2007 and 60 Gy (15 x 4 Gy, n=68) from 2006 to 2010 were analyzed. The corresponding NTD2Gy for an α/ß ratio of 1.5 and 3 Gy were 88 and 78 Gy for the 56 Gy group, and 94 and 84 Gy for the 60 Gy group, respectively. The planning target volume (PTV) consisted of an anisotropic expansion of 10 mm around the prostate, except 6-mm posteriorly. Patient repositioning was made with bone-matching on portal images or body markers registration. GI toxicities were scored using the CTCAE v3.0 grading scale.

Results: Among the 96 analyzed patients, the 5-year grade ≥2 late GI toxicity-free survival was similar in patients treated with 56 Gy compared to those treated with 60 Gy (92.6±5.1% vs. 85.0±5.1%, p=0.533). Mean volumes of rectum receiving more than 50 Gy (V50Gy, equivalent to V70Gy NTD2Gy, α/ß=3 Gy) and 54 Gy (V54Gy, equivalent to V75Gy NTD2Gy) were 15.8% vs. 20.9% (p=0.001) and 4.2% vs. 13.8% (p=0.0001) for the 56 and 60 Gy groups, respectively. A V50Gy19% (median 19.2%, range 4.4%-37.8%) was achieved in 67.9% and 38.2% of the patients treated with 56 and 60 Gy, respectively. A V50Gy >19% correlated with a 5-year grade ≥2 late-GI toxicity-free survival of 80.8±6.3%, significantly worse than patients with a V50Gy ≤ 19Gy (95.3±3.2%, p=0.031).

Conclusion: Independently from the dose prescription, a V50Gy ≤ 19% may result in a better long term rectal toxicity profile in patients treated with a hypofractionated IMRT schedule of 56 or 60 Gy in 4 Gy fractions. As for normofractionated schedules the QUANTEC dose constraint V70Gy<20% for the rectum seems to be a strong predictive factor of late GI toxicity for hypofractionated regimens as well.

EP-1366

Hypofractionated prostate EBRT with simultaneously integrated boost: mono-institutional report

J. Hermesse[1], X. Werenne[1], J. Vanderick[1], F. Lakosi[1], A. Gulyban[1], P. Coucke[1]
[1]*C.H.U. - Sart Tilman, Radiation therapy, Liège, Belgium*

Purpose or Objective: To report early outcome of hypofractionated radiotherapy for prostate cancer patients using a simultaneous integrated boost strategy (SIB) focusing on acute genitourinary (GU) and acute and late gastrointestinal toxicity (GI).

Material and Methods: Between 01/2012 and 06/2014 ninety-seven low (n=13) -, intermediate (n=22) - and high-risk (n=45)- prostate cancer patients were treated with hypofractionated radiotherapy using VMAT/IMRT and SIB. It

consisted of 65.75 Gy to the prostate gland+seminal vesicles (2.63 Gy/fx) and 45 Gy to the pelvic nodes (1.8 Gy daily) when needed, delivered in 25 fractions. All patients underwent daily image guidance with cone-beam computed tomography. Sixty-six percent of the patients received implanted gold markers (64/97). Acute and late gastrointestinal- and genitourinary toxicity was recorded according to the Common Terminology Criteria for Adverse Events 4.0. Chi-square test and univariate regression analysis were used to determine correlation of categorical and continuous data at the p<0.05 significance level.

Results: During a median follow-up of 23 (range: 4-44) months, 7/97 biochemical failures (7%) were observed. The frequency of ≥Gr. 2 acute gastrointestinal (GI) and genitourinary (GU) toxicities were 8% (8/97) and 45% (44/97) including 6% Gr. 3 bladder urgency and nycturia (6/97). Late ≥Gr. 2 GI toxicities of 14 % (13/97) were mainly rectal bleeding and chronic proctitits. Correlation was found between lymph node irradiation (p=0.008) and late rectal toxicities, while for other patient characteristics including the presence of gold markers (p=0.097) or smoking (p=0.99) did not appear to affect such adverse event. d univariate regression analysis were used to determine correlation of categorical and continuous data at the p<0.05 significance level.

Conclusion: Our experiences suggest that moderate hypofractionation with SIB technique is safe with moderate acute side effects. Longer follow-up and higher number of patients is warranted to confirm these results in long term. 8) and late rectal toxicities, while for other patient characteristics including the presence of gold markers (p=0.097) or smoking (p=0.99) did not appear to affect such adverse event. d univariate regression analysis were used to determine correlation of categorical and continuous data at the p<0.05 significance level.

EP-1367

IMRT from 70 Gy to 80 Gy in prostate cancer: clinical and dosimetric predictors of late toxicity

M. Jolnerosvki[1], J. Salleron[2], V. Beckendorf[1], D. Peiffert[1], A.S. Baumann[1], V. Bernier-Chastagner[1], V. Marchesi[3], S. Huger[3], G. Vogin[1], C. Chira[1]
[1]*Institut de Cancérologie de Lorraine, Radiation Oncology, Vandoeuvre les Nancy, France*
[2]*Institut de Cancérologie de Lorraine, Biostatistics, Vandoeuvre les Nancy, France*
[3]*Institut de Cancérologie de Lorraine, Physics, Vandoeuvre les Nancy, France*

Purpose or Objective: Evaluate grade ≥ 2 overall late rectal and bladder toxicity in patients (pts) with localized prostate cancer (CaP) treated by IMRT. Identify predictors of radiation-induced toxicity and analyze biochemical progression free survival (bPFS).

Material and Methods: A total of 276 pts were treated between 2000 and 2010 with 70Gy (10.8%), 74 Gy (63.9%) and 80 Gy (25.3%), using static 5-field IMRT without pelvic irradiation. Short or longue-course deprivation (ADT) was prescribed in 25.4 % and 20.7%, respectively. The toxicity was described using the Common Terminology Criteria for Adverse Events (CTCAE) v4.0 scale. Cox regression models addressed tumor (T stage, Gleason score, PSA) and patient characteristics (age, diabetes, previous abdominal or pelvic surgery, transurethral prostate resection, anticoagulation treatment, hypertension, coronary insufficiency and International Prostate Symptom Score-IPSS) as well as dosimetric predictors of late grade ≥ 2 overall toxicity.
An analysis of dosimetry data was only performed in the 74-Gy arm. Our institutional HDV constraints for rectal wall (maximal dose ≤74 Gy, V68Gy <25%, V45Gy <45%) and bladder wall (maximal dose ≤74 Gy; V50Gy <40%, V65Gy <25%) were tested as potential predictors for late toxicity.
Biochemical progression free survival was analyzed only in pts without ADT.

Results: The median follow-up was 53.1 months (range, 6-150). There was no grade≥ 4 toxicity. The use of ADT was not found to be predictive. The 5-year rectal and bladder toxicity-free survival was 93.8 % (95% CI, 89.8%-96.2%) and 75.2 % (95% CI, 68.7%-80.5%) respectively.
In multivariate analysis (MvA) only the dose (80Gy vs 74 Gy and 70Gy) increased the risk of overall rectal toxicity (hazard ratio [HR]=2.96; 1.07- 8.20). The non-compliance to our constraints on rectal wall was not a significant predictor of rectal toxicity.
IPSS at baseline ≥ 8 (hazard ratio [HR]=2.60;1.47 -4.62), delivered maximum dose (Dmax) ≥ 74Gy (HR=2.09;1.04 -4.17) and dose delivered ≥in 2% of bladder (D2%) ≥ 73Gy (HR=3.33;1.37-8.07) were found to be predictors of bladder toxicity.
The 5-year bPFS was 81.0% (74.5%; 86.0%). D'Amico low (HR=0.09; 0.01- 0.69]) and intermediate risk group (HR=0.49; 0.28-0.88) as well as PSA nadir≥ 0.2 ng/ml (HR =1.79; 1.01 - 3.21) were predictive of biochemical relapse.

Conclusion: The rate of late rectal toxicity increased with higher doses, while Dmax≥ 74Gy, D2% ≥ 73Gy and baseline IPSS ≥ 8 increased bladder toxicity.

EP-1368

A novel decision support method to estimate the value of a rectum spacer: 'Virtual Rectum Spacer'

S. Van der Meer[1], B.G.L. Vanneste[1], W. Van Elmpt[1], C. Schubert[2], M. Pinkawa[2], P. Lambin[1]
[1]*MAASTRO clinic, Department of Radiation Oncology- GROW - School for Oncology and Developmental Biology- Maastricht University Medical Center, Maastricht, The Netherlands*
[2]*University Hospital RWTH Aachen, Department of Radiation Oncology, Aachen, Germany*

Purpose or Objective: A relative new method to decrease the risk of rectal complications during prostate radiotherapy treatments consists of the implantation of a device, an absorbable hydrogel or saline filled balloon, between the prostate and the anterior rectum wall: so called rectum spacers (RS). Nevertheless the implantation of a RS is relatively expensive and invasive. Therefore a decision support system to identify beforehand whether a specific patient will benefit from a RS and whether it will be cost efficient would be very beneficial. We have developed a novel method to predict the CT images with a 'virtual' RS through non-rigid deformations based on a CT scan without RS to be integrated into a decision support system.

Material and Methods: A patient dataset consisting of 16 prostate cancer patients with CT imaging prior and 3-5 days after a gel RS implantation (SpaceOAR™ System, Augmenix Inc.) was used. The median inserted gel volume was 10.5 cc. Gel contours of the first 8 patients were used as a training set to derive the spatial deformation model of the RS. The contours of the RS were registered rigidly according to their centre and an average deformation map was created. The overlapping volumes of RS of different patients having a probability of >3 contour corresponded with a volume of 10 cc, and was used to derive the deformation model of the RS. From this model, a deformation field was calculated that mimics the expansion of the RS between the prostate and the rectum. The CT images of the remaining 8 patients were used to validate the virtual RS model, for this the distance between the rectum and the prostate was compared for the virtual RS and the actual RS .

Results: An example of the virtual RS is shown in the figure where the contours of the real RS and virtual RS show a good overlap (DICE = 0.63). The average minimum distances between the prostate and rectum of all 8 patients in the validation set increased with 3.7±2.4 (1SD) mm when the virtual RS was applied. For the real RS the average increase in minimum distance was 5.4±2.7 mm. The mean distances between the prostate and rectum without RS was 15.8±3.2 mm, with the virtual RS this was 19.5±3.3 mm comparable to the real RS 22.0±4.3 mm.

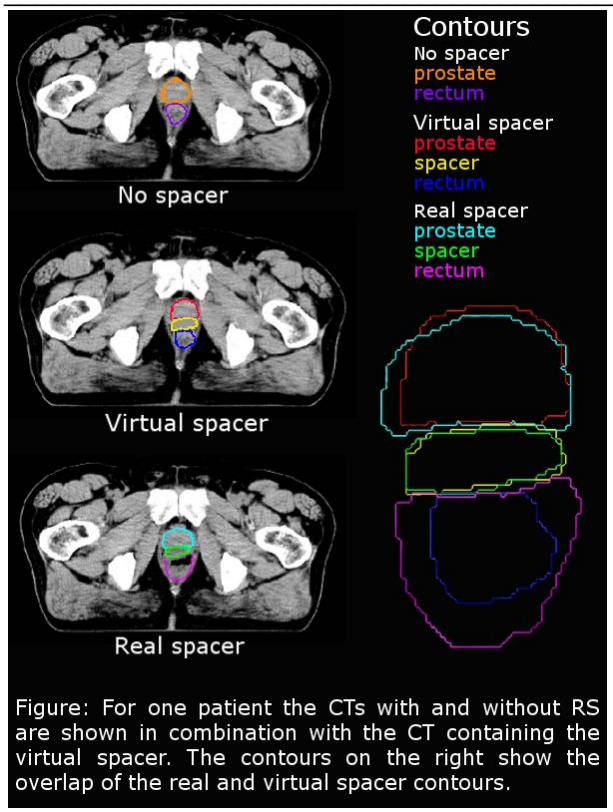

Figure: For one patient the CTs with and without RS are shown in combination with the CT containing the virtual spacer. The contours on the right show the overlap of the real and virtual spacer contours.

Conclusion: We have developed a novel method to simulate a model based virtual RS that is a useful tool to identify patients with a potentially high benefit of a RS implantation. The volume of the virtual RS can be estimated through the use of different deformation fields. In future, a dose comparison study is necessary to extend into a full decision support system using the virtual RS approach.

EP-1369

Toxicity profile with hypofractionated RT for localized prostate cancer: compared 3D-CRT vs VMAT

A. Magli[1], C. Fontanella[2], F. Tonetto[3], M. Crespi[4], T. Ceschia[1], M.R. Malisan[4], G. Chiaulon[1], G. Parisi[1], M. Polsinelli[1], A. Prisco[1], M.A. Signor[1], M. Guernieri[4], E. Moretti[4], C. Foti[4], C.T. Sacco[2], G. De Giorgi[5], V. Ficarra[5]

[1]*University Hospital Udine, Radiation Oncology, Udine, Italy*
[2]*University Hospital Udine, Medical Oncology, Udine, Italy*
[3]*University HospitalPadova, Radiation Oncology, Padova, Italy*
[4]*University Hospital Udine, Medical Physics, Udine, Italy*
[5]*University Hospital Udine, Urology, Udine, Italy*

Purpose or Objective: The escalation dose in the treatment of prostate cancer with external beam radiation therapy has proved the winning way in the biochemical control of the tumor. But the dose escalation to the whole prostate gland, which is considered as clinical target volume in external beam radiotherapy, is limited by the tolerance of the surrounding tissue. We have compared the toxicity profiles between patients treated with moderate hypofractionated 3-dimensional conformal radiotherapy (3D-CRT) collated with volumetric-modulated arc therapy (VMAT), both with image-guided radiotherapy (IGRT) by implanted fiducial markers in prostate gland (FMs) .

Material and Methods: Between 2009 and 2011, 41 patients with prostate cancer were treated with 3DCRT-IG to a dose of 70 Gy 2.5 Gy/fr with daily online correction of the target position based on MV/MV. This group of patients was compared with a similar cohort of 39 patients who were treated between 2012 and 2014 with VMAT-IG to the same prescription dose with daily online correction of the target position based on MV/KV imaging. The clinical characteristics of these two patient populations are shown in Table 1. Radiation Therapy Oncology Group/European Organization for Research and Treatment of Cancer late morbidity RTOG/EORTC scores were used for acute and late effects. The median follow-up time was 3 years (range, 1-6 years). The rectal and bladder dose parameters were also included in the statistical analysis.

Table. 1 Patient characteristics

	3DCRT-IG (n = 41)		IMRT-IG (n = 39)	
Patient demographics	n	%	n	%
Pretreatment PSA (ng/mL)				
< 10	30	73	32	82
10-20	11	24	4	10
>10	0		3	8
Total Gleason Score				
<7	13	31	11	28
7	28	69	21	54
>7	0		7	18
T stage				
T1c-T2a	28	68	25	64
T2b	7	17	10	26
>T2b	6	15	4	10
Age				
< 70	15	37	11	28
>70	26	62	28	72
NCCN risk				
Low	0		8	21
Intermediate	41	100	22	56
High	0		9	23
Neoadjuvant ADT				
Yes	37	90	32	82
No	4	10	7	18

ADT = androgen deprivation therapy; NCCN = National Comprehensive Cancer Network; PSA = prostate-specific antigen.

Results: The rectal acute and late toxicity was low for both treatment groups and no significant reduction was observed for VMAT-IG patients compared with the 3DCRT-IG patients (P = 0.33). The likelihood acute genitourinary toxicity for the VMAT-IG and 3DCRT-IG cohorts were 14.5% and 18.0%, respectively (p = 0.61). Only for ≥ grade 2 acute genitourinary toxicity, the analyses showed a trend better but non significative result on behalf of VMAT-IG (P=0,09). Finally, no significant correlation was observed between the dose parameters and genito-urinary and rectal late toxicity The PSA relapse-free survival in according to Phoenix criteria (nadir plus 2 ng/ml) for 3D-CRT and VMAT were similar (98% vs. 96%; p = 0.34).

Conclusion: Moderate hypofractionated IGRT is associated with a lower rate of genito-urinary and rectal toxicity for both treatment 3D-CRT and VMAT. These data suggest that, the placement of fiducial markers and daily online correction of target positioning may represent the preferred mode of external-beam radiotherapy delivery for the patients treated by definitive radiotherapy.

EP-1370

Stereotactic body radiotherapy in 117 oligometastatic lymph node recurrent prostate cancer patients

G. Fanetti[1,2], B.A. Jereczek-Fossa[1,2], C. Fodor[1], C.M. Francia[1,2], D. Zerini[1], A. Surgo[1,2], M. Muto[1,2], M.A. Gerardi[1,2], S. Dicuonzo[1,2], R. Cambria[3], C. Garibaldi[3], F. Pansini[3], A. Bazani[3], O. De Cobelli[2,4], R. Orecchia[2,5]

[1]*European Institute of Oncology, Advanced Radiotherapy Center, Milano, Italy*
[2]*University of Milan, University of Milan, Milano, Italy*
[3]*European Institute of Oncology, Medical Physics, Milano, Italy*
[4]*European Institute of Oncology, Urology, Milano, Italy*

[5]European Institute of Oncology, Medical Imaging and Radiation Sciences, Milano, Italy

Purpose or Objective: To evaluate the outcome of stereotactic body Vero® linac- or Cyberknife®-based radiotherapy (SBRT) for oligometastatic lymph node recurrent prostate cancer.

Material and Methods: Between 05/2012 and 09/2015 117 patients were treated (180 lymph nodes). Median age, initial PSA (iPSA), pre-SRT PSA and Gleason score (GS) were 70.3 years, 10.3 ng/mL, 4.4 ng/mL and 7, respectively. Any previous treatment was allowed. In all but 4 patients, [11C]choline-positron emission tomography/computer tomography was performed. SBRT consisted in re-irradiation and first radiotherapy for 29 (16%) and 151 (84%) lesions, respectively. Median dose was 24 Gy/3 fractions. Cyberknife-SBRT or Vero linac-SBRT was applied in 20 (11%) and 160 (89%) lymph nodes, respectively. In 56 (48%) patients androgen deprivation was added to SBRT (median duration 13.9 months), some patients were heavily pre-treated and castration-resistant. Biochemical failure was defined as post-SBRT PSA increase over pre-SBRT value. Toxicity was evaluated using Radiation Therapy Oncology Group/European Organization for Research and Treatment of Cancer (RTOG/EORTC) criteria.

Results: All patients completed planned SBRT. The median follow-up was 19.7 months. Acute toxicity included urinary (7 G1 events) and rectal complications (2 G1 events). Late toxicity included only urinary complications (2, 2, and 2 G1, G2, and G4 events, respectively). Both G4 events were temporary and were observed in pts receiving re-RT, with no dose to bladder from SBRT. Complete or partial biochemical response was observed in 68(68%) out of 100 evaluable patients. PSA stabilization was seen for 7(7%) patients and in 24(24%) cases PSA progression was reported. Clinical progression during follow up was observed in 65(65%) patients after a median time of 9 months (range: 1 – 33.1 months) from SBRT. In-field progression was observed in 13(13%) cases. 31(31%) patients had distant metastases and 34(34%) showed regional lymph node progression. All events of clinical failure were preceded by biochemical progression. At the time of the analysis (October 2015), 17(14.5%) patients are alive with no evidence of disease, 79(67.5%) are alive with clinically evident disease, 4(3.5%) died of disease and 17(14.5%) are not evaluable (due to short follow-up).

Conclusion: Our series including 117 unselected pts showed that Vero Linac- or Cyberknife-based SBRT is feasible for oligometastatic lymph node recurrent prostate cancer offering excellent in-field tumor control and low toxicity profile. Further investigation is warranted in order to identify the patients that benefit most from this treatment modality. The optimal combination with androgen deprivation or other systemic treatments should also be defined.

EP-1371

Role of 11C choline PET/CT in the management of prostate cancer patients with biochemical relapse

R. Frakulli[1], G. Siepe[1], M. Ntreta[1], S. Cammelli[1], G. Tolento[1], G. Macchia[2], F. Deodato[2], A. Arcelli[1], F. Bertini[1], L. Ronchi[1], G. Di Gioia[1], V. Dionisi[1], M. Pieri[1], G. Martorana[3], S. Fanti[4], D. Balestrini[5], C. Degli Esposti[5], A. Galuppi[1], A.G. Morganti[1], G. Frezza[5]

[1]Radiation Oncology Center - S.Orsola-Malpighi Hospital - University of Bologna, Department of Experimental-Diagnostic and Specialty Medicine - DIMES, Bologna, Italy

[2]Fondazione di Ricerca e Cura "Giovanni Paolo II" - Catholic University of Sacred Heart, Radiotherapy Unit, Campobasso, Italy

[3]S.Orsola-Malpighi Hospital - University of Bologna, Department of Urology, Bologna, Italy

[4]Nuclear Medicine Unit - S.Orsola-Malpighi Hospital - University of Bologna, Department of Experimental-Diagnostic and Specialty Medicine - DIMES, Bologna, Italy

[5]Ospedale Bellaria, Radiotherapy Department, Bologna, Italy

Purpose or Objective: The aim of our retrospective study was to analyze the role of [(11)C]choline-Positron Emission Tomography/Computed Tomography (cho-PET/CT) in the management of patients (pts) with biochemical failure after curative surgery in patients with prostate cancer.

Material and Methods: We reviewed all patients referred to our department with biochemical failure and without evidence of recurrence on standard imaging (pelvic MRI + total body CT-scan) after curative surgery for prostate cancer. All patients underwent cho-PET/CT scans between 2010 and 2014.

Results: Thirty-four patients fulfilled the inclusion criteria and were included in this study. Previous surgical procedure was: radical prostatectomy (19 pts), radical prostatectomy with pelvic lymph node dissection (8 pts) and radical prostatectomy with lymph node sampling (9 pts). Thirty-six scan cho-PET/CT studies were performed on 34 patients. Median PSA level before cho-PET/CT was 1.7 ng/mL (range 0.2 to 7.6). Cho-PET/CT showed 21 uptakes in prostate bed, 4 in prostate bed and pelvic lymph nodes, 1 in prostate bed and paraaortic lymph nodes, 5 in pelvic lymph nodes, 1 in retroperitoneal lymph nodes (4 exams were negative). Eleven pts underwent salvage radiotherapy, 21 pts salvage radiotherapy and androgen deprivation therapy and 1 patient androgen deprivation therapy only. With a median follow-up of 15 months, 27 showed complete biochemical response to salvage therapy (PSA <0.04 ng\ml), and are still free from biochemical recurrence. Two pts showed biochemical failure, 3 developed lymph node recurrence and 2 patients developed bone metastases.

Conclusion: Cho-PET/CT was able to detect macroscopic disease in prostate cancer pts with biochemical failure after surgery allowing individualized salvage treatment.

EP-1372

Salvage image-guided stereotactic re-irradiation of local recurrence in prostate cancer

G. Timon[1], D. Zerini[1], C. Fodor[1], F. Bazzani[1], A. Maucieri[2], S. Ronchi[2], D.P. Rojas[2], S. Volpe[2], A. Vavassori[1], F. Cattani[3], C. Garibaldi[3], S. Comi[3], R. Cambria[3], O. De Cobelli[4], R. Orecchia[2], B.A. Jereczek-Fossa[1]

[1]IEO - European Institute of Oncology, Radiotherapy division, Milano, Italy

[2]University of Milan, Health Science department, Milano, Italy

[3]IEO - European Institute of Oncology, Medical Physics division, Milano, Italy

[4]IEO - European Institute of Oncology, Urology division, Milano, Italy

Purpose or Objective: To retrospectively evaluate external beam re-irradiation (re-EBRT) delivered to either the prostate or prostatic bed for local recurrence after radical or adjuvant/salvage radiotherapy.

Material and Methods: Between February 2008 and March 2015, 59 patients received re-EBRT. Median age was 63.8 years (range 47.1-81.7) and median PSA at the time of relapse was 20.2 ng/ml (range 4.4-110). All patients had clinical and/or radiological local relapse in the prostate or prostatic bed and no distant metastasis at the time of re-EBRT. A concomitant hormonal treatment was administered to 18 patients. Re-EBRT was delivered with image-guided stereotactic technology including Rapid Arc®, VERO® and Cyberknife® to a total dose of 15-32 Gy in 3-6 fractions. Toxicity was evaluated using RTOG/EORTC Criteria. Biochemical control was assessed according to Phoenix definition.

Results: Only one patient experienced an acute GI event >G3, while two patients had late ≥G3 urinary toxicity.
At a mean and median follow-up of 24.1 and 19.8 months respectively (range 2-65.5), 27 patients (45%) show no evidence of disease, 26 (44%) are alive with biochemical or clinical disease and 2 have been lost at clinical follow-up. 4

patients (7%) died: 2 of disease progression and 2 of other causes. Mean and median time-to-progression are 12.1 and 9.8 months respectively (range 2-53).

Conclusion: Re-EBRT using stereotactic approach is a feasible option for local prostate cancer recurrence, achieving tumour control in 45% of the patients and an acceptable progression-free interval. Toxicity of re-EBRT appeared to be very low. Future studies are needed to identify those patients who would benefit the most from this treatment.

EP-1373

Hypofractionated radiotherapy and androgen deprivation in intermediate risk prostate cancer

S. Bracci[1], M.F. Osti[1], L. Agolli[1], L. Bertaccini[1], V. De Sanctis[1], M. Valeriani[1]
[1]*Azienda Ospedaliera Sant' Andrea, Department of Radiation Oncology, Rome, Italy*

Purpose or Objective: to evaluate the outcomes in intermediate risk prostate cancer treated with hypofractionated radiotherapy (HyRT)

Material and Methods: Between March 2007 and March 2015, 145 patients affected by intermediate risk (T2b–T2c prostate cancer or Gleason Score equal to 7 or pre-treatment PSA value ranging from 10 to 20 ng/mL) prostate cancer were treated with HyRT. The median age at diagnosis was 74 years (range 53-88). A pre-treatment CT scan with 2.5 mm slices was obtained. MRI was used to better delineate the Clinical Target Volume (CTV) when available. The CTV1 included the prostate plus seminal vesicles (SSVV) and the CTV2 the prostate alone. Planning Target Volumes (PTV1 and PTV2, respectively) were generated with 8 mm margin in all directions except posteriorly where a 6 mm expansion was adopted in the first 36 patients. A 5 mm expansion in all direction was used in the other patients as daily kv Cone Beam CT was used to verify the patient position because of an implementation of the linear accelerator. A 3D-CRT and a 15 MV photons linear accelerator was used to deliver the treatment. The PTV1 received 43.8 Gy in 12 fractions and the PTV2 received 54.75 Gy in 15 fractions, three times a week in order to avoid an excess of acute toxicity. Neoadjuvant, concomitant and adjuvant ADT was administered for a total of 9 months and was started 3 months before RT.

Results: After a median follow-up of 52.4 months (range 7 to 95 months), 11 patients (7.6%) died, of whom 9 for intercurrent disease and 2 (1.3%) for PCa. The 5-year OS was 90.1% (95%CI 84.2-97.6%) and the 5-year CSS was 98.6% (95%CI 95.4-100%). Fourteen patients (9.7%) developed biochemical recurrence after a median follow up of 30.5 months (95% CI 28.5 to 32.5 months). Of these patients, thirteen (9.0%) had also a clinical detectable disease while the remaining patient presented only biochemical recurrence. The 5y-bRFS was 88.8% (95%CI 82.8-95.4%). Among the 13 patients with clinical recurrence, 7 (53.8%) had local recurrence, 2 (15.4%) developed distant metastases, and 4 (30.8%) had both local recurrence and distant metastases. Acute genito-urinary (GU) toxicity of grade 1 occurred in 74 patients (51.0%), grade 2 in 15 patients (10.3%) and grade 3 in 2 patients (1.3%). Acute gastro-intestinal (GI) toxicity of grade 1 were observed in 27 patients (18.6%), grade 2 in 12 patients (8.2%). None developed acute GI toxicity of grade 3 or 4. Late GU toxicity occurred as follows: grade 1 in 51 patients (35.2%), grade 2 in 12 patients (8.2%), grade 3 in 2 patients (1.3%). Late GI toxicity of grade 1 was observed in 18 patients (12.4%), grade 2 in 6 patients (4.1%) and grade 3 in 1 patient (0.7%).

Conclusion: The hypofractionated schedule used is well tolerated with a low rate of acute and late ≥grade 2 gastrointestinal and genitourinary toxicities. Hypofractionation is useful to obtain high rate of tumor control but a longer follow-up is needed for definitive conclusion.

EP-1374

Contouring guideline optimisation for prostate pts undergoing carbon ions/photons combined treatment

T. Giandini[1], M. Carrara[2], E. Pignoli[2], N. Bedini[3], S. Morlino[3], D. Bosetti[3], B. Avuzzi[3], S. Villa[3], A. Hasegawa[1], S. Russo[4], B. Vischioni[5], M. Ciocca[4], F. Valvo[5], B. Jereczek-Fossa[1], D. Ciardo[1], D. Zerini[1], S. Colangione[1], C. Fodor[1], F. Cattani[1], R. Valdagni[3], R. Orecchia[1]
[1]*European Institute of Oncology, Radiotherapy Division, Milan, Italy*
[2]*Fondazione IRCCS Istituto Nazionale dei Tumori, Medical Physics, Milan, Italy*
[3]*Fondazione IRCCS Istituto Nazionale dei Tumori, Radiation Oncology 1, Milan, Italy*
[4]*Fondazione CNAO, Medical Physics Unit, Pavia, Italy*
[5]*Fondazione CNAO, Clinical Radiotherapy Unit, Pavia, Italy*

Purpose or Objective: In the context of the multi-institutional research project "Carbon ions boost followed by pelvic photon intensity modulated radiotherapy for high risk prostate cancer", Contouring Guidelines (CG) for target volumes and Organs At Risk (OARs) were commonly defined based on National/International standards and local experiences. Intra- and inter-institutional variability was evaluated within a contouring dummy-run and a graphical tool was developed to assist the Radiation Oncologists (ROs) in the standardization of the contouring.

Material and Methods: CT and MR images of 5 prostate patients were randomly chosen. Seven ROs belonging to the three Institutes involved in the project were assigned to independently contour targets (prostate (GTV-P), seminal vesicles (CTV-VS) and pelvic lymph nodes (CTV-N) and OARs (rectum (R), bladder (B), femoral heads (FH), small bowel (SB) , penile bulb (PB) and anal canal (AC). The registration between CT and MR images was only used to contour GTV-P and PB. The contours were compared by means of the DICE Index (defined as $2*(A \cap B)/(A+B)$, where A e B are the volumes in comparison), as provided by the commercial software VODCA (MSS, v.5.4.0). For each structure, the Global DICE Index (GDI) was calculated as the average value for all the ROs and the patients and then compared with the DICE Index of the individual ROs: an individual DICE Index lower than the corresponding GDI (or lower than a threshold value of 0.9 for GDI > 0.9) was recorded as "disagreement" and reported in a graphical tool (Figure 1) that qualitatively shows intra- and inter-institutional variability.

Results: The resulting GDI are reported in Table 1. A visual analysis of the contours on the CT images showed that the poor quality GDI for CTV-VS and AC were due both to a not strict application of the CG by the ROs of the different Institutes and to the small volume of those structures. The other results were instead attributable to random variation in the contouring. The graphical tool clearly showed that inter-institutional variability was predominant compared to intra-institutional variability both for targets and OARs. Nevertheless, some disagreement was found even between ROs of the same Institute.

Table 1 – *Mean values and standard deviations of the Global DICE Index for the contoured structures*

Structures	Global DICE Index
Prostate	$0,87 \pm 0,02$
Seminal Vesicles	$0,49 \pm 0.06$
Pelvic Lymph Nodes	$0,75 \pm 0.01$
Rectum	$0,80 \pm 0.02$
Bladder	$0,959 \pm 0.003$
Femoral Heads	$0,936 \pm 0.005$
Small Bowel	$0,78 \pm 0.10$
Penil Bulb	$0,71 \pm 0.02$
Anal Canal	$0,52 \pm 0.06$

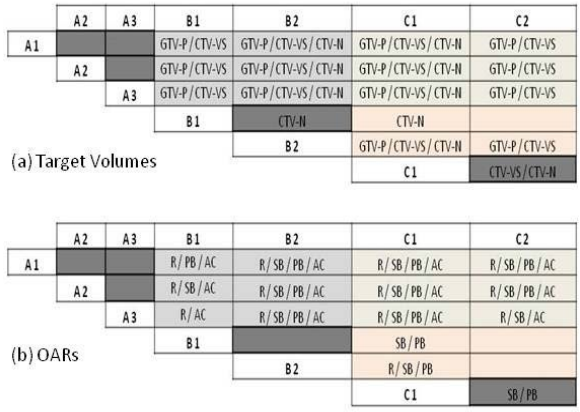

FIGURE 1 – Graphical tool showing the disagreements between ROs belonging to Institute A (A1,A2,A3), B (B1,B2) and C (C1,C2), for target volumes (a) and OARs (b).
Dark grey cells show intra-Institutional variability, whereas the other cells show inter-Institutional variability

Conclusion: The dummy-run showed that the most significant deviations were obtained when ROs did not precisely apply the CG. Such systematic deviations in the contouring could have a dosimetric impact both for target coverage and OAR sparing, especially for particle therapy. The ROs were provided with the developed graphical tool in order to easily identify their deviations and take corrective actions. The graphical tool could also be useful for the optimization of the contouring strategies within individual Institutes.
This work was partially funded by Associazione Italiana per la Ricerca sul Cancro AIRC (grant N-14300)

EP-1375

Adjuvant androgen deprivation therapy and postoperative radiotherapy in prostate cancer: our data

G. Lazzari[1], A. Terlizzi[2], G. Della Vittoria Scarpati[1], R. Marchese[1], M. Soloperto[1], A. Nikolaou[1], G. Silvano[1]
[1]*Azienda Ospedaliera SS. Annunziata Presidio Osped, Radiology, Taranto, Italy*
[2]*Azienda Ospedaliera SS. Annunziata Presidio Osped, Physic Department, Taranto, Italy*

Purpose or Objective: To evaluate the role of adjuvant androgen deprivation therapy (ADT) in combination with postoperative radiotherapy (PORT) on biochemical-relapse-free-survival (b-NED) and metastatic-progression-free-survival (mts-NED) in high risk prostate cancer patients (pts).

Material and Methods: Between 2004 and 2012 370 high risk prostate cancer pts received PORT : 120 pts had stage pT3a pN0, 150 pts pT3b pN0 , 100 pts pT2c/pT3 R1 and post surgical PSA > 0.2 ng/ml detected in 50 pts. Mean age was 72 years (55-78 yrs). PORT on pelvis and surgical bed was delivered in 150 pts while 220 pts were treated on surgical bed . Dose to pelvis was 45-50 Gy, while dose on surgical bed was 66- 72 Gy. *ADT was administerd in 250* pts and consisted of LH-RH analog in monotherapy (70 pts), BAT (60 pts) and bicalutamide 150 mg (120 pts). Timing of ADT ranged six months to 3 years. ADT was administered during and after PORT with a median of 35 months. Kaplan-Mayer b-Ned and mts-Ned survivals , X-square ($p< 0.05$) and paired t-test for univariate and multivariate analyses ($p< 0.001$) were calculated.

Results: Three – hundred were evaluable at 64 months with a median of 5 years. Two groups were identified: ADT (210 pts) and no ADT (90 pts). One-hundred and twenty pts (120) relapsed: 40 pts in the no ADT group (5 with a biochemical relapse and 35 pts with a metastatic relapse) and 70 pts in the ADT group (20 pts with a biochemical relapse and 50 pts with a metastatic). The 5- year biochemical relapse free survival was 80% for ADT group and 78% for no ADT group ($p = 0.34$); the 5-year metastatatic progression free survival for ADT group was 82 % vs 65% ($p< 0.05$)for no ADT group. In the ADT group, radiotherapy dose <70 Gy and PSA >0.2 ng/ml were indipendent factors related to high risk of biochemical-relapse while metastatic-relapse-free-survival was influenced by primary component 5 of the Gleason Score (GS) , no use of LH-RH analog and time of ADT<2aa . In the no ADT group, PSA > 0.2 ng/ml, radiotherapy dose <70 Gy and R1 disease, were factors influencing the biochemical relapse, while metastastic relapse was influenced by a value of 5 in the Gleason Score.

Conclusion: The role of ADT in adjuvant setting prostate cancer is still unclear; our results suggest a benefit of ADT in metastatic-progression-free-survival, especially in case of primary component 5 in the GS , post-operative PSA >0, BAT<2 years.

EP-1376

Long term patient reported urinary function following external beam radiotherapy for prostate cancer

S. Chin[1], A. Hayden[1], V. Gebski[1], S. Cross[1], S. Turner[1]
[1]*Westmead Hospital, Crown Princess Mary Cancer Centre Westmead, Westmead, Australia*

Purpose or Objective: This study reports long-term patient reported urinary function, toxicity and related quality of life (QoL) after external beam radiotherapy for localized prostate cancer.

Material and Methods: 574 men underwent definitive 3D conformal radiotherapy to 74Gy ± androgen deprivation therapy between 2000 and 2009 with a median follow-up of 42 months. Patients were evaluated at baseline and post treatment using the International Prostate Symptom Score (IPSS) and RTOG CTC.

Results: For patients with mild (48%), moderate (40%) and severe (12%) baseline total IPSS, median IPSS at baseline was 3,12, and 24. Median IPSS was 4, 9, and 12 at 6 months and 3, 9 and 14 at 48 months respectively. Late grade 2 genitourinary toxicity incidence was 7%, 20% and 33% and late grade 3 genitourinary toxicity was 1%, 2% and 1% respectively. At 48 months, 80%, 49% and 16% of patient with baseline mild, moderate and severe IPSS respectively demonstrated stable IPSS, 5%, 39% and 72% reported improving IPSS ≥5, and 14%, 12% and 6% had a worsening IPSS ≥5. 82% of patients with mild baseline IPSS had mild IPSS scores. 95% of patients with moderate baseline IPSS had mild or moderate IPSS scores, with 43% improving to mild IPSS scores. 75% of patients with severe baseline IPSS scores had improved to mild (28%) or moderate (47%) IPSS scores. 68% of the cohort reported good baseline urinary QoL (score 0-2), with 89% of these patients maintaining good urinary QoL at 48 months. 71% of patients with poor baseline urinary QoL (score 3-6) had improved to good urinary QoL.

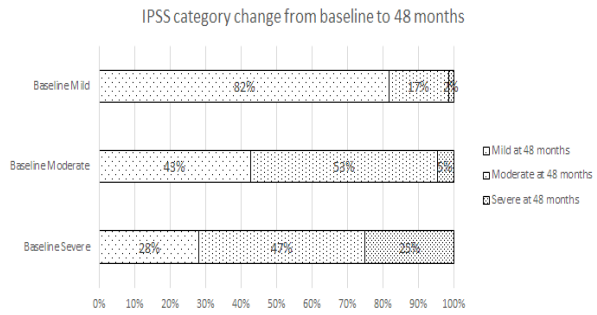

Conclusion: The majority of men undergoing definitive radiotherapy for prostate cancer report stable or improving late urinary symptom burden and urinary quality of life, even with severe urinary symptoms or poor urinary quality of life at baseline.

EP-1377

Consistency of cone beam CT-derived bladder volume and inflow during localized prostate cancer IMRT

C.J. HO[1], C.K. McGarry[2], J.Y. Sun[3], C.A. Lyons[4], R.B. King[4], S. Jain[5], A.R. Hounsell[4], J.M. O'Sullivan[5]

[1]*Queen's University Belfast, School of Medicine- Dentisty and Biomedical Sciences, Belfast, United Kingdom*

[2]*Belfast City Hospital, Medical Physics, Belfast, United Kingdom*

[3]*Norwich university hospital, Radiology, Norfolk, United Kingdom*

[4]*Centre for Cancer Research and Cell Biology, Advanced Radiotherapy, Belfast, United Kingdom*

[5]*The Northern Ireland Cancer Centre Belfast City Hospital, Radiotherapy, Belfast, United Kingdom*

Purpose or Objective: Consistency of bladder volume (BV) during radiotherapy (RT) planning and treatment is important in maintaining the position of the prostate and the surrounding organs at risk, thus minimising RT-related tissue toxicity. This retrospective study evaluated the effectiveness of bladder-filling instructions in achieving a consistent and reproducible bladder volume at the time of planning CT and during the course of radical RT for prostate cancer. This study also assessed the rate of bladder filling (inflow) during the course of RT.

Material and Methods: 28 men with localized prostate cancer were instructed to void their bladder and then drink 500 ml of water before proceeding to RT planning scan 45 minutes later. This bladder filling process was repeated daily before each RT session. BV was assessed during planning CT and at four chronological phases of RT (fractions 1-9, 10-19, 20-29 and 30-37) via cone beam CT (CBCT). Each patient had between four to ten CBCTs taken during his RT sessions and the average BV at each phase was calculated. Inflow was assessed using delineated BV post-treatment in 20 patients. Inflow was calculated by taking the difference in BV between pre-RT CBCT and post-RT CBCT and dividing by the time between the scans. All patients were treated with 74 Gy in 37 fractions via intensity modulated radiotherapy (IMRT).

Results: The mean BV for all treatments (mean= 223.62 ml, range= 57.18– 871.85 ml, SD= 138.08 ml) was significantly lower (p=0.007) than the mean BV at the time of planning (mean= 318.88ml, range= 93.96 – 821.37 ml, SD= 165.10 ml). During RT, 68%, 50% and 38% of pre-treatment BV had >50ml, >100ml and >150 ml difference respectively when compared with their volume at the time of planning. When assessing the BV at different treatment time points, the mean BV for RT fractions 1-9 (239.31ml) was 25% lower than the mean planning volume (p= 0.025). The mean BV for RT sessions 30-37 (203.65 ml) was 36% lower than the mean planning volume (p<0.001).

Inflow over 128 fractions was significantly correlated (r=0.558, p<0.0001) with pre-RT BV. The mean inflow did not differ significantly over the course of RT. The mean inflow of RT sessions 1-9 (3.86 ml/min, SD= 2.50 ml/min) was not significantly higher (p=0.24) than that of RT sessions 30-37 (3.29 ml/min, SD=2.46 ml/min).

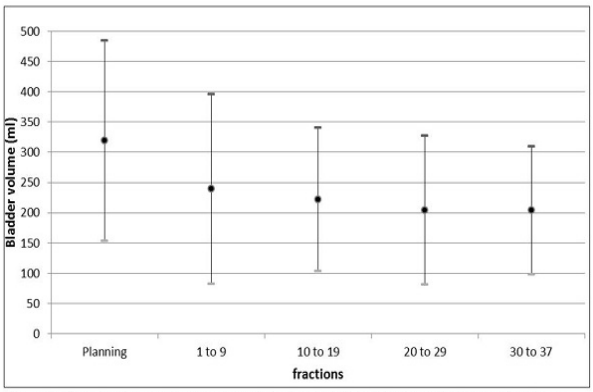

Figure 1: Mean bladder volume measured at planning CT and during radiotherapy fractions, with error bars indicating one standard deviation (SD).

	Planning	1 to 9	10 to 19	20 to 29	30 to 37
Mean bladder volume (ml)	318.88	239.31	222.31	203.93	203.65
SD (ml)	165.10	156.87	118.35	122.78	105.51
% volume difference to planning bladder volumes	0	-24.95	-30.28	-36.05	-36.14
Mean Inflow (ml/min)	-	3.86	4.00	4.02	3.29
SD (ml/min)	-	2.50	2.54	2.95	2.46

Table 1: Table summarizing the bladder volume (mean, SD and % volume differences to planning) and inflow (mean and SD) at planning and during radiotherapy.

Conclusion: A difference in BV was found between planning and during the course of radiotherapy. The mean BV decreased most during the first two weeks of radiotherapy. The large decrease in BV at the early phase of RT suggests a systematic difference in bladder filling at the time of planning compared with treatment. This process has been reviewed and a further analysis will be performed. Inflow from pre- and post-CBCT scans was found to be correlated with pre-RT BV. Inflow information may help to reduce bladder filling variations during treatment.

EP-1378

Should pelvic radiotherapy be tailored to early patient-reported gastrointestinal toxicity?

M. Reis Ferreira[1], S. Gulliford[2], K. Thomas[3], L. Truelove[4], H. McNair[5], D.P. Dearnaley[1]

[1]*Institute of Cancer Research and Royal Marsden NHS Trust, Academic Radiotherapy, Surrey, United Kingdom*

[2]*Institute of Cancer Research, Radiotherapy Physics Modelling, London, United Kingdom*

[3]*Royal Marsden NHS Trust, Statistics and Computing, London, United Kingdom*

[4]*Institute of Cancer Research, Bob Champion Unit, London, United Kingdom*

[5]*Royal Marsden NHS Trust, Radiotherapy, London, United Kingdom*

Purpose or Objective: Whole-pelvic radiotherapy (WPRT) is a cornerstone of the treatment of high-risk prostate cancer. However, late gastrointestinal (GI) toxicity is the major dose-limiting factor in this treatment. There are concerns that dose escalation and aggressive treatment regimens may result in increased acute toxicity, which may modulate long-term side-effects of radiotherapy, a phenomenon known as consequential late effects. The purpose of this work was to evaluate if late GI side-effects are related to acute toxicity using long-term patient-reported outcomes (PRO) of a previously unreported large, prospective phase I/II trial of IMRT for whole-pelvic treatment of prostate cancer.

Material and Methods: 496 patients were recruited between August 2001 and September 2013. Treatment consisted of

WPRT with intensity modulation techniques and long-term androgen-deprivation therapy. Strict radiotherapy dose-volume constraints were used for treatment planning to minimize the risk of serious toxicity.
PRO data (UCLA-Prostate Cancer Index scale) was available for 450 patients. Patients with less than 2 year follow-up data and any patients without acute (10 week after RT initiation) data were excluded, giving 251 patients for analysis. Median follow-up was 5 years. Only bowel habit outcomes were included for this analysis (questions 17 to 21). Data from patients with positive toxicity scores at baseline was excluded on an endpoint-by-endpoint basis.
We separated patients according to acute toxicity into two groups using question-specific toxicity grade cut-offs which differed between each PRO question. We then assessed if the group with acute toxicity had more toxicity in the late setting by calculating the odds-ratios (OR); we also computed p-values using Fisher's exact test. seline was excluded on an endpoint-by-endpoint basis.

Results: We found that patients with positive self-reported acute GI toxicity at 10 weeks have an increased risk of developing serious late GI problems, while patients without toxicity are more likely to be free of chronic toxicity (table 1). as excluded on an endpoint-by-endpoint basis.

UCLA-PCI bowel habit item *Grade cut-off*	OR	95% CI	p-value
Rectal urgency *More than once a week or higher*	2.0	1.1 - 3.6	0.0163
Loose stools *Half the time or higher*	4.6	2.7 - 8.1	<0.0001
Bowel distress *Moderate/Severe*	3.8	2.1 - 7.1	<0.0001
Crampy abdominal pain *Several times a week or higher*	6.9	3.5 - 14.1	<0.0001
Bowel problem *Moderate/Severe*	6.0	3.2- 12.1	<0.0001

Table 1: Odds ratios for late patient-reported gastrointestinal toxicity according to early toxicity.
Equal cut-off points were used for early and late outcomes.

Conclusion: Patients with moderate to severe acute bowel toxicity are at increased risk of serious late GI problems which impact quality of life, potentially reflecting a consequential late effect. Tailoring treatment with the modification of treatment planning according to early clinical outcomes may prove to be necessary to tackle this problem.

EP-1379

SBRT in the treatment of bone metastases in hormone refractary prostate cancer

S. Grespi[1], C. Menichelli[1], A. Fanelli[1], P. Ferrazza[1], G. Pastore[1], F. Casamassima[1]
[1]*Ecomedica, Radiotherapy, Firenze, Italy*

Purpose or Objective: Evaluate the utility of SBRT in terms of local control (LC), global survival (OS), compliance to the treatment and toxicity in patient with oligometastatic and hormone refractary prostate cancer, limited to the skeletal structures.

Material and Methods: 46 patients with bone metastases from prostate cancer, were treated with SBRT between January 2009 and August 2015. At diagnosis 15/46 patients presented bone metastases. Bone lesions irradiate were 131 (range 1-4). Median age was 68 years (range 54-85). Median PSA pre-treatment was 168,1 ng/ml (range 0,23 -1.470). Patients received a median dose of 30 Gy (range 8-40 Giy) in 3 fractions (range 1 -5). The treatment was delivery by LINAC 6 MeV (Elekta Synergy-S) using technical IGRT-VMAT. All patients received some form of androgen-deprivation therapy (ADT) after completing SBRT. 18/46 patients was submitted systemic chemotherapy treatment.

Results: Median follow-up was 22 months (range 1-78). LC was 100% and OS 50,2% at 5 years. 22/46 patients were died for progression disease, 24/46 patient were still alive, of these 14 were disease free and 10 were in progressione disease. The first post-SBRT PSA was lower than pre-treatment levels in 30 patients (65,2%) and continued to decline or remain undetectable in 23 patients (50%) at follow-up of 6 months. Median PSA post-treatment was 32,4 (range 0,29-196). No severe acute or late toxicity of grade >2 was observed.

Conclusion: SBRT is a safe and effective treatment for prostate cancer metastases, presenting excellent LC and an acceptable toxicity profile in selected patient with hormone refractary disease. More importantly, half the patient achieving reductions in serum PSA values.

EP-1380

Primary focal prostate radiotherapy: do all patients really need whole-prostate irradiation?

B.A. Jereczek-Fossa[1,2], D. Ciardo[1], G. Petralia[3], M. Bellomi[2,3], O. De Cobelli[2,4], R. Orecchia[1,2]
[1]*European Institute of Oncology, Department of Radiation Oncology, Milan, Italy*
[2]*University of Milan, Department of Oncology and Hemato-oncology, Milan, Italy*
[3]*European Institute of Oncology, Department of Radiology, Milan, Italy*
[4]*European Institute of Oncology, Department of Urology, Milan, Italy*

Purpose or Objective: Primary focal therapy has been explored for 20 years now, and more than 2000 patients have been treated so far with several techniques but only limited data have been published on the primary focal radiotherapy (FRT). From the technical point of view, primary FRT can be performed through either focal brachytherapy or external beam radiotherapy. The majority of series include both low-dose-rate (LDR) and high-dose-rate (HDR) brachytherapy, and only recently the feasibility of primary FRT by external beam irradiation has been reported. The current review aims to assess the available evidence for primary FRT performed either by the means of brachytherapy or external beam radiotherapy.

Material and Methods: Inclusion criteria were: Medline search for full paper in English language on primary FRT for early prostate cancer including review articles, planning studies or patient series (clinical outcome available) published before May 31, 2015.

Results: Twenty-two papers have been found: 11 review articles, 4 planning studies and 7 patient series. Eleven review articles were dedicated to all types of focal therapy including FRT and 2 to FRT only. All planning studies were performed on cohort of 5-10 patients and included brachytherapy both HDR (24 patients overall), and LDR (9 patients). All studies underline the significant organs-at-risk dose reduction as well as the higher sensitivity to systematic set-up error as target volume decreases from whole-gland to hemi-gland and to ultra-focal target. Patient series included together 715 patients (range 8-318, 99% treated with brachytherapy). Median follow-up period was 33.6 months (range 2-61 months). Promising tumour control was highlighted in low-risk cancer. In intermediate-risk tumours, FRT might be suboptimal (see Table 1). Moreover, some reports on consensus criteria are already available in literature.

First author, Journal (year)	Population (risk factor)	Technique	N. Pts	Dose prescription	Median follow-up	Toxicity & Outcome
D'Amico, IJROBP (1998)	- T1cNxM0; - PSA < 10 ng/mL; - Biopsy Gleason score ≤ 3+4; - MRI stage T2 disease	MR-guided ^{125}I implant	9	Min. dose to peripheral zone = 160 Gy.	2 months	Minimal acute morbidity.
Albert, Cancer (2003)	MRI-guided BRT: - T1c; - PSA < 10 ng/mL; - Biopsy Gleason score ≤ 3+4; - MRI T2 disease; MRI-guided BRT + EBRT: either PSA > 10–13 or ≥ 50% positive biopsies or MRI evidence of extracapsularity.	MRI-guided BRT or MRI-guided BRT + EBRT	201	MRI-guided BRT: min. dose to peripheral zone = 160 Gy. MRI-guided BRT + EBRT: min. dose to peripheral zone = 77 Gy; 45 Gy with 3D-CRT	2.8 years	Mono-therapy vs. combined modality therapy: Rectal bleeding: G1 80% vs. 85% (Pvalue ns), G2 18% vs. 22% (Pvalue ns), G3 8% vs. 30% (Pvalue = 0.0001). Erectile dysfunction: 82–93%. Bladder/urethral dysfunction: no late events after monoth. Cystitis in 2 patients after combined-modality therapy.
D'Amico, Urology (2003)	- T1c; - PSA < 10 ng/mL; - Biopsy Gleason score ≤ 3+4; - No perineural invasion on biopsy.	Prostatectomy vs. MR-guided BRT	322 vs. 196	< 100% of the PD to anterior base and zone anterior to urethra; > 100% of the PD to peripheral zone	4.2 years vs. 3.95 years	5-year estimate of PSA control: 93% vs. 95% (ns) after RP or brachytherapy, respectively.
Vainshtein, Radiation Oncology (2012)	- Gleason score ≤ 6; - PSA ≤ 10; - T1c-T2a; - Excluded if on androgen deprivation therapy	Standard EBRT (S-IMRT) vs. urethral sparing IMRT (US-IMRT)	16	75.85 Gy in 41 fractions	56 months	No differences in EPIC urinary domain HRQOL summary or subset scores. No differences in the bowel, sexual, hormonal, or satisfaction domain scores. Mean PSA nadir 1.5 vs. 0.78 ng/ml (p=0.05) in US-IMRT vs. S-IMRT. 2-year PSA failure rate: 25% in US-IMRT, 0% in S-IMRT.
Barret, European Urology (2013)	- T2a or less - PSA < 10 ng/ml; - Gleason sum ≤ 6; - Unilateral disease; - Fewer than 3 positive biopsies.	^{125}I-BRT (12 pts), HIFU (21 pts), VTP (23 pts), cryotherapy (50 pts)	106	145 Gy	9 months	13% treatment-related complications: 2 G3b. Median IIEF-5 = 14, median IPSS = 6.
Cosset, Brachytherapy (2013)	- life expectancy superior to 10 years - T1c or T2a - PSA < 10 ng/mL - Gleason score ≤ 7 (3+4) - Unilateral disease - No individual biopsy core with more than 50% involvement. Total of prostate volume < 60 cc - IPSS ≥15	^{125}I-BRT	21	145 Gy	28 months	Mean IPSS: 5.4, 11.8, 6.6, 6.1 @ baseline, 2-6-12 mo. No rectal toxicity at 6 and 12 mo. Mean IIEF: 20.1, 18.6, 19.1, 19.8 @ baseline, 2-6-12 mo. Mean PSA: 6.9, 5.5, 3.2, 2.6 ng/mL @ baseline, 2-6-12 mo. Negative biopsies in 5 pts, a Gleason 6 (3+3) lesion <1mm in one patient contra-laterally.
Nguyen, The Journal of Urology (2015)	- T1c - PSA < 15 ng/ml - Biopsy Gleason score ≤ 3 + 4	Monotherapy with MRI-guided ^{125}I-BRT or MRI-guided ^{125}I-BRT + EBRT (61 pts)	318	Monotherapy: prescribed dose = 137 Gy. MRI-guided ^{125}I-BRT + EBRT: 45 Gy in 1.8 Gy/fr to prostate and seminal vesicles, followed by a BRT boost to 90 Gy.	61 months	Using nadir +2 with PSA >0.75ng/ml per year, PSA failure-free survival 91.9% at 5 years and 86.2% at 8 years. For intermediate risk cases: failure-free survival 73.0% at 5 years and 66.4% at 8 years. Distant metastases developed in 1 patient.

Conclusion: Despite the numerous publications on focal therapy in prostate cancer, primary FRT is largely unexplored. Radiotherapy appears to be particularly suitable as a focal approach, since it has an established biological basis, known tumoricidal activity, possibility of dose differentiation, large availability of high-precision dose delivery techniques, limited or no invasiveness and familiarity to radiation oncologists and urologists. However, when applied as primary FRT, its use remains investigational since numerous questions remain unmet: consensus on the initial diagnostic tools, the optimization of technical parameters for therapy delivery, follow-up exams and scheduling, tumour control and toxicity profile, response evaluation and failure definition, salvage therapy and cost-benefit.

EP-1381

ADC of prostate tumour and normal tissue during radiotherapy after neoadjuvant hormone therapy

L. Kershaw[1], A. McPartlin[2], A. Choudhury[2], M. Van Herk[3]
[1]*The Christie NHS Foundation Trust, CMPE, Manchester, United Kingdom*
[2]*The Christie NHS Foundation Trust, Oncology, Manchester, United Kingdom*
[3]*University of Manchester, Institute of Cancer Sciences, Manchester, United Kingdom*

Purpose or Objective: Changes in prostate and tumour ADC values during radiotherapy (RT) may aid prediction of response to treatment. Intermediate and high risk patients are likely to receive neoadjuvant hormone therapy (NA-HT) prior to RT, causing reduction in prostate and tumour volume and changes in ADC values. It is unclear how this affects further ADC changes during subsequent treatment. We assessed ADC values in prostate tumour and normal tissue during RT after NA-HT.

Material and Methods: Fifteen patients with≥T2b disease who were due to receive RT (60 Gy in 20 fractions) were recruited after 3 months of NA-HT. Patients underwent three 1.5 T MRI examinations: post NA-HT (one week prior to RT), at the end of the third week of treatment, and eight weeks after RT completion. The imaging protocol included T2 weighted and diffusion weighted imaging, acquired using the cardiac coil (EPI with TR/TE 8000/70 ms, b = 100, 400, 800 s/mm²). ADC maps were processed offline (ADCmap for Osirix). Normal central gland (CG), peripheral zone (PZ) and tumour were outlined on T2w images by a radiologist expert in prostate MRI, with pre-NA-HT imaging (T2w and DWI) available in 12 patients to aid identification. If disease was not clearly visible, clinical findings and biopsy results were used to aid delineation. CG, PZ and tumour regions were transferred to the ADC maps and median values extracted along with interquartile ranges. A Mann-Whitney U test was used to analyse differences between tumour and normal tissue regions at the three time points.

Results: 13 patients completed all scans, 2 patients missed 1 and 2 scans respectively. After NA-HT, there was a significant difference between median tumour and PZ (p=0.009) and tumour and CG (p=0.002) (median values plotted in figure 1). At the other time points, there was no difference between tumour and normal tissue ADCs.

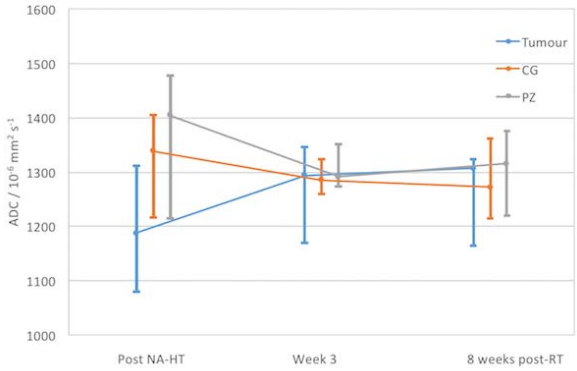

Conclusion: The ADC values display a similar pattern to that seen in previous studies for patients receiving RT alone. The difference between tumour and normal tissue was smaller at baseline than has been seen in other work without NA-HT. This may be due to a reduction in normal tissue ADC during induction therapy, whilst tumour ADC values could have increased due to tumour shrinkage. Variation in imaging protocol for ADC measurement compared to previous studies may also play a role. The reduced magnitude of changes in tumour ADC seen during RT after NA-HT may make its use as a predictive tool for treatment response more challenging in this group of patients.

EP-1382

PET/CT and MRI guided salvage radiotherapy after prostatectomy for prostate cancer

S. Kirste[1], J. Bons[1], N. Volegova-Neher[1], C. Zamboglou[1], K. Henne[1], W. Schultze-Seemann[2], H.C. Rischke[3], A.L. Grosu[1]
[1]*Universitätsklinik Freiburg, Radiooncology, Freiburg, Germany*
[2]*Universitätsklinik Freiburg, Urology, Freiburg, Germany*
[3]*Universitätsklinik Freiburg, Nuclear Medicine, Freiburg, Germany*

Purpose or Objective: At the time of a biochemical recurrence after prostatectomy it is important to distinguish patients who have a local recurrence from patients with distant metastasis. PET/CT and MRI are important imaging modalities that can be used in this scenario. The purpose of this study was to investigate the outcomes and toxicities of patients in a large single-institution cohort treated with salvage radiotherapy (sRT) and dose escalation up to 72 Gy. Boost planning was based on MRI or PET/CT.

Material and Methods: From 2008 to 2012 290 patients who received sRT were included into the analysis. Patients with a PSA > 1 ng/ml or a PSA doubling time > 3 months received a Choline PET/CT before the start of radiotherapy. Additionally, in most patients MRI of the pelvis was conducted. If there was a macroscopic tumor recurrence, defined as local recurrence in the prostate bed in MRI or PET tracer uptake, radiation therapy to the prostatic bed was

complemented by a boost to local recurrence to a total dose of 72 Gy. In case of no macroscopic tumor recurrence the total dose was 66.6 Gy.

Results: MRI was performed in 233 patients and PET/CT was performed in 169 patients. A local recurrence in the prostate bed could be detected in 123 patients with a median volume of 0.5 ml (range, 0.03 – 125.00 ml). The median follow-up time after RT was 49.4 months (range, 7.3 – 86.1 months). A total of 85 patients experienced a biochemical failure with a median time of 19.8 months (range, 1.9 – 76.1 months) after sRT. Median PSA level at the time of recurrence was 0.91 ng/ml (range, 0.01 – 2224.00 ng/ml). The median BRFS after radiation therapy was 73 months. The estimated 3- and 5-year bRFS was 72% and 55%, respectively. On multivariate analysis, Gleason Score (hazard ratio, 6.946; p = 0.006) and pre-RT PSA level (hazard ratio, 2.265; p = 0.022) were statistically significant predictors for bRFS. bRFS was similar in patients with a macroscopic recurrence in either MRI or PET/CT compared to patients without a macroscopic recurrence. 5-year overall survival was 91% and 5-year cancer-specific survival was 96%. Grade 3 gastrointestinal toxicity was observed in 4 patients and 3 patients showed grade 3 genitourinary toxicities. No grade 4 gastrointestinal or genitourinary side effects were reported.

Conclusion: Gleason score and pre-RT PSA were important predictors for bRFS. The dose in salvage radiotherapy should be increased to 72 Gy to prevent an early recurrence after sRT in patients with a macroscopic recurrence. A higher total dose of up to 72 Gy was well tolerated in this cohort of patients.

EP-1383

PSA kinetics in prostate cancer patients after SBRT radiotherapy using CyberKnife.

M. Konkol[1], A. Galuba[1], P. Milecki[1], A. Skrobala[2], A. Jodda[2], M. Adamczyk[2], J. Litoborska[2]
[1]*Greater Poland Cancer Centre, Oddzial Radioterapii I I Radiotherapy Dept., Poznan, Poland*
[2]*Greater Poland Cancer Centre, Department of Medical Physics, Poznan, Poland*

Purpose or Objective: The aim of the study was to assess the kinetics of the Prostate-Specific Antigen (PSA) in prostate cancer patients after stereotactic body radiotherapy using CyberKnife System.

Material and Methods: 44 localized prostate adenocarcinoma patients (33 low and 11 intermediate risk) without hormonal therapy, were irradiated using the CyberKnife Radiosurgical System. The prescription dose was 36,25 Gy in five fractions. During the 1-year follow-up all the patients had at least six PSA measurements – before the treatment (1-2 months before RT), during RT (after the 4th fraction) and 1, 3, 6, 12 months after RT.

Results: The mean initial PSA value among the patients was 6,25 ng/ml (range from 3,02 to 17,46 ng/ml). During the treatment we observe the PSA increase – the mean value was 11,89 ng/ml (4,13-30,68ng/ml, 155% of the initial PSA in average). In every case we noticed the PSA nadir 12 months after the treatment with a mean value of 1,50 ng/ml (0,10-4,56 ng/ml). The mean slope of the PSA was 0,56 ng/ml/month (median 0,46 ng/ml/month). No biochemical failure was observed.

Conclusion: The PSA kinetics after treatment can reflect the biological effect of radiation on prostate cancer and potentially correlate with a clinical outcome. Especially the lower value of PSA nadir (<0,5 ng/ml) is considered to associate with an increased freedom from biochemical failure. The interpretation of PSA slope is more controversial however some studies indicates a correlation with clinical outcome. Our results are similar to other SBRT studies and significantly better than in conventionally-fractionated technics. The rapid decline in PSA is particularly worth to be underlined. The further follow-up will probably confirm the expected good clinical outcome.

EP-1384

Acute toxicity hypofractionated-IMRT vs standard radiotherapy in prostate cáncer: comparative study

J. Valero Albarran[1], R. Guimaraes Domingos da Silva[2], S. Payano[1], A. Montero[1], E. Sánchez[1], X. Chen[1], O. Hernando[1], M. García Aranda[1], R. Ciervide[1], M. Lopez[1], M. Rubio[1]
[1]*Hospital University HM Sanchinarro, Radiation Oncology, Madrid, Spain*
[2]*Institute National of Cancer, Oncology Radiation, Rio of Janeiro, Brazil*

Purpose or Objective: To describe and compare acute toxicity rate in three different radiotherapy (RT) protocols for prostate cancer (PC): hypofractionated radiotherapy intensity modulated and image-guided radiation therapy (Hypo-IMRT-IGRT) group A: 21 fractions/3Gy and group B: 28 fractions/2.5Gy) and three-dimensional conformal radiotherapy standard fractionation (3DCRT) group C: 39 fractions/2Gy.

Material and Methods: Patients with the diagnosis of PC treated with RT between January 1st 2011 to June 30th 2015 were included. Hypo-IMRT-IGRT were performed using internal marker and ExacTrac-X-Ray-system. In 3DCRT group not employed internal marker. Acute genitourinary (AGUT) and acute gastrointestinal toxicity (AGIT) were assessed according to RTOG-EORTC criteria. A p value<0.05 was considered significant. Results were expressed as median (IQR). Categorical and continuous variables were compared with X2 and kruskal-Wallis ran sum test respectively. All statistical analysis was performed using R package. The institutional review board approved this study.

Results: 242 consecutive patients were retrospectively analyzed (group A: 39, group B: 128 and group C: 74). No baseline characteristic differences were found (age, PSA, TNM, PTV total, bladder and rectal volume). Maximal bladder doses and V60 rectal were different within the three groups (p=<0.01). AGUT (n): in group A was grade 0: 18; grade 1: 9, grade 2: 12; group B grade 0: 35; grade 1: 86; grade 2: 7; and group C grade 0: 23; grade 1: 38; grade 2: 13 (p=<0.01). AGIT was in group A grade 0: 38; grade 1: 1; grade 2: 0; group B grade 0: 121; grade 1: 7; grade 2: 0; and group C grade 0: 65; grade 1: 6; grade 2: 3 (p=0.07) Table 1. Comparative AGUT between A+B vs. C did not differ. AGIT in A+B group was less frequent than C group (p=0.017). AGUT from group A was different from group B (p=<0.01). AGIT from A group was not different from B group (p=0.75).There were no events > grade 3 reported in any group.

GRADE n(%)	0	1	2	p
AGUT				<0.01
Group A	18(46)	9(23)	12(31)	
Group B	35(27)	86(67)	7(5)	
Group C	23(31)	38(51)	38(51)	
AGIT				0.07
Group A	38(97)	1(3)	0(0)	
Group B	121(95)	7(5)	0(0)	
Group C	65(88)	6(8)	3(4)	

Conclusion: Hypo-IMRT-IGRT was associated to lower AGIT rate than 3DCRT. Hypo-IMRT-IGRT 21 fractions/3Gy was inferior to Hypo-IMRT-IGRT 28 fractions in terms of AGUT.

EP-1385

A comparative study between radical RT and radical prostatectomy in locally advanced prostate cancer

P. Gupta[1], N. Rastogi[1], K. Sharmad[2], K. Das[1], R. Kapoor[2], A. Mandhani[2], S. Kumar[1]
[1]*Sanjay Gandhi Postgraduate Institute of Medical Sciences, Department of Radiation Oncology, Lucknow UP, India*

[2]*Sanjay Gandhi Postgraduate Institute of Medical Sciences, Department of Urology, Lucknow UP, India*

Purpose or Objective: For the locally advanced prostate cancers (LAPC) dose escalated external beam Radiotherapy (dEBRT) with androgen deprivation therapy (ADT) for 2-3 years is the current standard of care. The role of radical prostatectomy (RP) for high-risk prostate cancer is still debated. Better outcomes with RP as compared to dEBRT especially <69 years of age has been reported. However there is no data available from India to compare dEBRT and RP. We did a retrospective study to compare dEBRT or RP in patients with LAPC.

Material and Methods: Medical records of 77 high risk LAPC treated between 2008-2013 were analysed. All biopsy proven adenocarcinoma of prostate with high risk category (PSA>20ng/ml or Gleason score (GS) >7 or T2c-T4) were included. Patients either underwent dEBRT with image guided RT (IGRT) (group 1) or RP (group 2) along with ADT for 2-3 years. Group 1 and 2 had 37 and 40 patients respectively. The primary end points of the study were biochemical relapse free survival (bRFS), bladder and rectal toxicity, urinary incontinence (UI) and secondary end point was cancer specific survival (CSS).

Results: Median age and median pre-treatment PSA in 2 groups were comparable (66 and 65years) and (22 and 23 ng/ml) respectively. Radiologically T3/T4 lesions were present in 65% and 68% and nodal metastasis was seen in 22% and 30% respectively. Median GS was 8 and 7. Positive surgical margins was seen in 70% in group 2. dEBRT dose was 76Gy with conventional fractionation using IGRT using fiducial marker matching . With a median follow up of 3 years, 5-year bRFS was 78% and 72%. (p=0.12) .Median bRFS was not reached in group 1 and in group 2, it was 79 months. Post treatment UI was seen in 0 and 6(15%)(p=0.03). Radiation Therapy Oncology Group (RTOG) grade III-IV bladder toxicity (hematuria and bladder neck contracture requiring incision) was seen in 2(6%) and 7(18%) respectively and rectal toxicity in 2(6%) and peroperative rectal injury occurred in 2(5%) in group 2. Five year CSS was 65% and 87% respectively (p=0.086). Median CSS was not reached in any group. Six (16%) and 7(18%) patients were lost to follow up. Distant metastasis was seen in 8(22%) and 1(3%) (p=0.14).

Conclusion: UI is the complication associated with RP. Dose escalated IGRT for LAPC is no different from RP in terms of bRFS however there was a trend towards better CSS and distant DFS. Further long term follow up is needed to assess the effect on distant disease free survival and CSS.

Electronic Poster: Clinical track: Urology-non-prostate

EP-1386

Adjuvant pelvic radiotherapy for pathological high-risk muscle-invasive bladder cancer

P. Sargos[1], I. Latorzeff[2], A. Fléchon[3], G. Roubaud[4], V. Brouste[5], R. Gaston[6], T. Piéchaud[6], M. Orré[1]
[1]*Institut Bergonié, Radiotherapy, Bordeaux, France*
[2]*Clinique Pasteur, Radiotherapy, Toulouse, France*
[3]*Centre Léon Bérard, Radiotherapy, Lyon, France*
[4]*Institut Bergonié, Medical Oncology, Bordeaux, France*
[5]*Institut Bergonié, Epidemiology and Clinical Research Unit, Bordeaux, France*
[6]*Clinique Saint Augustin, Surgery, Bordeaux, France*

Purpose or Objective: Radical cystectomy (RC) and pelvic lymph-node dissection (PLND) are standard procedures in the management of non-metastatic muscle invasive bladder cancer (MIBC). Loco-regional recurrence (LRR) is a common early event associated with a poor prognosis. The aim of this study is to evaluate adjuvant radiotherapy (RT) for pathological high-risk MIBC.

Material and Methods: We retrospectively reviewed data from patients treated by RC from 3 institutions. Inclusion criteria were MIBC, histologically proven urothelial carcinoma treated by RC and adjuvant RT. Patients with conservative surgery were excluded. LRR free-survival, overall survival (OS) and metastasis-free survival (MFS) were evaluated. Acute toxicities were recorded according to CTCAE V4.0 scale.

Results: Between January 2000 and December 2013, 57 patients with a median age of 66 years (45-84) were included. Post-operative pathological staging was pT2, pT3 and pT4 in 16%, 44%, and 39%, respectively. PLND revealed 28% of pN0, 26% of pN1 and 42% of pN2. For 2 patients, no PLND was performed. Median number of lymph-nodes retrieved was 10 (2-33). Forty-eight patients (84%) received platin-based chemotherapy, 7 in neo-adjuvant and 41 in adjuvant setting. For RT, clinical target volume 1 (CTV 1) encompasses pelvic lymph nodes for all patients. CTV 1 also included cystectomy bed for 37 patients (65%). Median dose for CTV 1 was 45 Gy (4-50). Dose complement of 16 Gy (5-22) corresponding to CTV 2 was achieved in 53 of cases, depending on pathological features. Intensity Modulated RT was performed in one third of patients. With a median follow-up of 40.4 months, LRR occurred in 8 patients (14%) that appeared concomitantly with metastasis in two-third of cases. Three-year loco-regional free survival, MFS and OS were 45% (IC 95% 0.30-0.60), 39% (IC 95%, 0.25-0.52) and 49% (IC 95%, 0.33-0.63), respectively. Acute grade≥3 toxicities were observed in 5 patients (9%). One patient died with intestinal fistula in septic context. No survival or toxicity predictive factor was identified.

Conclusion: Adjuvant radiotherapy for pathological high-risk MIBC is safe and may have oncological benefits. Thus, new prospective trials evaluating this approach with modern RT techniques should be undertaken.

EP-1387

Outcomes after recurrent bladder cancer and (chemo)radiotherapy post TUR-B vs cystectomy

S. Knippen[1], C. Kelling[1], M. Henke[1], A. Grosu[1], T. Brunner[1]
[1]*Universitätsklinik Freiburg, Department of Radiation Oncology, Freiburg, Germany*

Purpose or Objective: To analyze patients treated for recurrent urothelial cancer with radiation therapy with or without concomitant chemotherapy after surgical intervention that was treated from 2000 to 2012 at our centre.

Material and Methods: Our inclusion strategy was to first identify patients treated for the relevant ICD-10 codes. A number of 270 patients matched the ICD-10 criteria (see CONSORT diagram). In a second step, patients that were treated at other sites than the pelvis, treated for distant metastasis, patients suffering from renal cell cancer and cancer of the renal pelvis were excluded. In a third step patients treated with radiation doses that are typical for palliation (<45Gy) were excluded from the analysis. After this, a number of 57 patients remained at the database for further analyses. All patients were treated for recurrent urothelial cancer of the bladder, of the ureter or of the urethra. All patients were treated using 3D conformal radiation therapy. Mean prescribed dose was 54.22Gy (range 45-72Gy). Mean time from first diagnosis to radio(chemo)therapy was 22.9 months (range one week to 276 months). In 24 cases (42.1 %) a concomitant chemoradiotherapy was applied.

Results: Mean survival from the beginning of radiation treatment was 39.2 months (CI 95 % 24.7 – 53.69 months; median survival 14 months CI 95% 6.8 -21.1). Tumor stage at the time of surgical intervention did not show an impact on overall survival (p=0.96). Patients were divided into three subgroups, depending on the surgical intervention prior to radiation therapy: most patients were treated by TUR(n=38) before the indication to radiation therapy was made, 13 patients had a TUR followed by cystectomy in their further history and in 6 patients early cystectomy was the first type

of treatment. Patients treated with TUR-B followed by radiotherapy were significantly older compared to patients with cystectomy before radiotherapy and were less likely to receive chemotherapy. There was no significant difference for the length of the interval between first treatment and radiotherapy for the three groups. Despite of this, type of surgical procedure before radiotherapy did not show an impact on overall survival (p = 0.86).

Conclusion: In our study we found equal survival of patients treated with (chemo)radiotherapy after TUR-B only compared to patients with cystectomy prior to radiotherapy. Younger age and more concomitant chemotherapy of the latter group was not able to prolong survival.

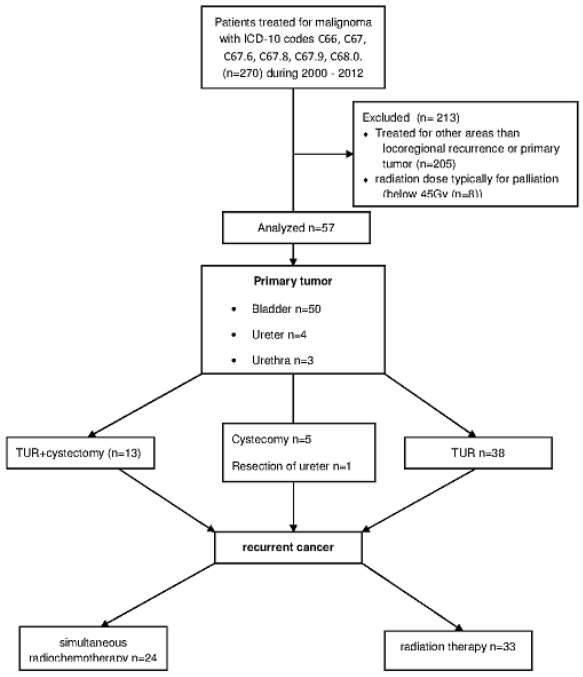

EP-1388

Primary penile cancer: role of adjuvant RT for extracapsular extension in lymph nodes

P. Johnstone[1], G. Diorio[2], R. Djajadiningrat[3], M. Catanzaro[4], D. Ye[5], Y. Zhu[5], N. Nicola[4], S. Horenblas[3], P. Spiess[2]

[1]*Moffitt Cancer Center, Radiation Oncology, Tampa, USA*
[2]*Moffitt Cancer Center, Urology, Tampa, USA*
[3]*Netherlands Cancer Institute-Antoni van Leeuwenhoek Hospital, Urology, Amsterdam, The Netherlands*
[4]*Fondazione IRCCS Istituto Nazionale Tumori, Urology, Milano, Italy*
[5]*Fudan University Shanghai Cancer Center, Urology, Shanghai, China*

Purpose or Objective: In cancers of the head and neck (HNCa), lymph node (LN) status is a critical prognostic factor. Further, the presence of extracapsular extension (ECE) has been shown prospectively to be a criterion for the addition of chemotherapy to postoperative radiation therapy. Limited data exist regarding ECE in inguinal or pelvic LNs from primary penile cancer (PeCa).

Material and Methods: We retrospectively analyzed outcomes of patients with PeCa and pathologically confirmed LN across four international tertiary referral centers. Clinical and demographic characteristics were compared of outcomes (local control and overall survival) by ECE status and between those who had received adjuvant RT or not.

Results: Records of 93 patients were available. Median age at time of LND was 65.3 years (range 35.9–90.2 years). Median follow up was 9.4 months (IQR: 5.3-19.4). The median number of involved ILNs was 4 (range 1-12), and median PLNs positive was 2 (range 1-21). 72% of patients had ECE in the inguinal area and 49% had ECE in the pelvis. Infield failure occurred in 26/87 sites with ECE and 8/64 sites without ECE (p = 0.015). In the presence of ECE, patients receiving RT experienced infield failure in 17/50 cases and in 10/38 patients not receiving RT (P=NS). Absent ECE, patients failed infield in 5/40 cases after RT and 3/24 cases without RT (p=NS). RT was not associated with improved OS (p=0.073) or recurrence (p=0.492) on multivariate analysis. Chemotherapy was significant on multivariate analysis for recurrence (p = 0.009) but not survival (p=0.334).

Conclusion: ECE is associated with increased likelihood of local recurrence in PeCa patients. Contrary to the experience in HNCa, adjuvant RT has no impact on local control. Prospective studies are needed to validate this unusual finding and further develop the timing and roles of RT and chemotherapy for PeCa patients with advanced disease.

EP-1389

Stereotactic radiotherapy for oligometastatic patients with renal cell carcinoma

A. Cecconi[1,2], G. Piperno[3], A. Ferrari[3], E. Rondi[4], S. Vigorito[4], D. Zerini[3], F. Cattani[4], F. Nolè[5], O. De Cobelli[2,6], B.A. Jereczek-Fossa[2,3], R. Orecchia[1,2]

[1]*European Institute of Oncology, Scientific Direction, Milan, Italy*
[2]*University of Milan, University of Milan, Milan, Italy*
[3]*European Institute of Oncology, Radiotherapy, Milan, Italy*
[4]*European Institute of Oncology, Medical Physics, Milan, Italy*
[5]*European Institute of Oncology, Division of urogenital tumours medical treatment, Milan, Italy*
[6]*European Institute of Oncology, Division of urologic surgery, Milan, Italy*

Purpose or Objective: the aim of this study was the evaluation of local control (LC) and toxicity in oligometastatic patients with renal cell carcinoma (RCC) who had undergone stereotactic radiotherapy (SRT) with CyberKnife (Accuray, Sunnyvale, CA) or Vero™ (BrainLab) for cranial and extracranial metastases.

Material and Methods: between January 2012 and September 2015, 23 patients (30 lesions) with metastases of RCC were treated with SRT alone to the new site of disease (if limited disease) or to residual disease during the maximal response in systemic therapy. Disease control was evaluated with serial imaging. Toxicity was recorder according to the Common Toxicity Criteria version 4.0.

Results: after a median follow-up of 10 months (range 0 - 36 months) 20 patients were alive. Ten patients received SRT alone and 13 patients received that during the maximal response of systemic therapy. The median equivalent of the dose (EQD2) was 50.6 Gy delivered with a median of 2.7 fractions (range 1-5) and the median biological equivalent dose (BED) was 51 Gy assuming α/ß =10 for tumour. Six patients are lost in follow-up. Clinical and radiological response was thus evaluated in 17 patients and the their LC was 100% (57.1% of patients received SRT alone and the others patients are still undergoing systemic treatment. 27.7% of patients had more than 12 months follow-up and the LC was again 100%.). Progression of disease in the other sites was observed in all cases. No toxicity was observed.

Conclusion: SRT is a feasible approach that offer an excellent LC with low toxicity profile in the treatment management of oligometastatic patients with RCC with or without the association of systemic therapy. Further investigation is warranted to identify the patients who would probably benefit from this approach.

EP-1390

Cystoman in the prevention of acute radio-induced urinary toxicity in irradiated pelvic region

E. D'Ippolito[1], A. Rese[1], F. Piccolo[1], A. Romano[1], L. Faraci[1], P. Romanelli[1], F. Pastore[1], E. Toska[1], V. De Chiara[1], L. Ghidelli[1], R. Telesco[1], R. Solla[1,2], A. Farella[1], M. Conson[1,2], R. Liuzzi[1,2], R. Pacelli[1,2]

[1]University of Naples "Federico II", Department of Biomedical Sciences Advanced, Naples, Italy
[2]C.N.R., Institute of Biostructures and Bioimaging, Naples, Italy

Purpose or Objective: Acute urinary unwished effects of pelvic irradiation may impact on quality of life of patients undergoing radiation therapy on the pelvis. Neoplasms such endometrial, cervical, rectal, and anal cancer requires irradiation of relevant pelvic volumes. In this study we tested Cystoman, a dietary integrator of D-mannosium, cranberry and vitamin C, as prophylactic therapy for the development of acute urinary side effects.

Material and Methods: Fifty five patients undergoing pelvic irradiation were randomly assigned to take 2 tablets/day of Cystomann or not from the beginning of radiation therapy. Radiation therapy consisted of 45 - 50.4 Gy on the pelvis given by 1.8 Gy daily fractions with 3D conformal radiation therapy. The patients were weekly checked for urinary symptoms. Urine colture was performed before and after the treatment.

Results: Between November 2014 and September 2015, 55 consecutive patients were enrolled in the study. Median age was 65 year, 11 were affected by cervical cancer, 9 endometrial, 31 rectal, and 4 anal cancer. Twenty two patients were treated preoperatively and 33 postoperatively. Urinary toxicity appeared at the second week in 3/28 patients in Cystoman group and 11/27 in the control group (p=0,02). However by the end of the treatment 8/28 and 13/27 patients had urinary toxicity in the Cystoman and control group, respectively (p=0.1).

Conclusion: Our study suggests that Cystomann delays the radio-induced acute urinary toxicity presentation and could ameliorate the toxicity profile of the pelvic irradiation.

Electronic Poster: Clinical track: Skin cancer / malignant melanoma

EP-1391

Total skin irradiation using helical tomotherapy: a novel experience and report of three cases

K. Okuma[1], A. Haga[1], T. Imae[1], R. Takenaka[1], M. Sugaya[2], K. Nakagawa[1]
[1]University of Tokyo Hospital, Radiology, Tokyo, Japan
[2]University of Tokyo Hospital, Dermatology, Tokyo, Japan

Purpose or Objective: Description of three cases of total skin irradiation for cutaneous T-cell lymphoma using helical TomoTherapy (Accuray, Sunnyvale, CA).

Material and Methods: In 2015, three patients with refractory T-cell lymphoma underwent total skin irradiation using invers-planned helical tomotherapy. The first case was a 25-year-old man diagnosed as mycosis fungoides with multiple tumors occurring on the extremities, face, and trunk. The second case was a 73-year-old woman diagnosed as primary cutaneous gamma delta T-cell lymphoma. She had received 24 Gy of irradiation in 12 fractions with total skin electron beam irradiation technique 10 years ago, and some parts of her skin were irradiated with 24 Gy in 12 fractions with local electron beam irradiation within 3 years. The third case was a 52-year-old man diagnosed as mycosis fungoides. No bolus was added around the body. Because of the long length of treatment of the body in TomoTherapy, treatments were delivered to three parts of the body (trunk, head and neck, and legs). Irradiation was not performed in two or three parts on the same day. Each plan was generated with a prescription dose of 10 Gy in 10 fractions. The planning target volume (PTV) was the body surface with 5mm margins of internal and external lesions of the skin. The third patient had several swelling lymph nodes, so the PTV was the body surface and swelled lymph nodes with their margins.

Results: TomoTherapy technique was created that enabled delivery of the prescription dose to PTV with a relatively sharp drop-off of dose at depth. The calculated mean doses for the organs at risk were 1.96, 2.08, 2.12, 2.19, and 2.27 Gy for the lung, heart, liver, kidneys, and bones, respectively. Using the couch-indexed Vac-Lok cushion and head mask, inter- and intra-fractional patients motions were minimized. All three patients experienced edemas of fingers and toes, and lost much of their hair. Myelosuppression occurred in two of the three patients. Because of grade 4 myelosuppression, the second patient who was treated total skin electron beam irradiation 10 years ago, was treated with blood transfusion during the treatment. All tumors were reduced during and after the treatment.

Conclusion: Using the TomoTherapy technique in total skin irradiation, we were able to achieve good coverage of the PTV and good sparing of organs at risk, including the bones. This treatment method, including the prescription dose and treatment duration, will be needed further research.

EP-1392

The abscopal effect:efficacy of radiotherapy in patients on progression after ipilimumab 3 mg/kg

A.M. Grimaldi[1], P.A. Ascierto[1], E. Simeone[1], D. Giannarelli[2], S. Falivene[3], V. Borzillo[3], F. Giugliano[3], F. Sandomenico[4], A. Petrillo[4], M. Curvietto[1], A. Esposito[1], M. Paone[1], M. Palla[1], G. Palmieri[5], C. Caraco[1], G. Ciliberto[6], N. Mozzillo[1], P. Muto[3]
[1]Istituto Nazionale Tumori Fondazione Pascale, Melanoma-Cancer Immunotherapy and Innovative Therapy Unit, Naples, Italy
[2]Regina Elena National Cancer Institute, Statistical Unit, Rome, Italy
[3]Istituto Nazionale Tumori Fondazione Pascale, Radiotherapy, Naples, Italy
[4]Istituto Nazionale Tumori Fondazione Pascale, Radiology, Naples, Italy
[5]National Research Council, research, Sassari, Italy
[6]Istituto Nazionale Tumori Fondazione Pascale, Scientific Direction, Naples, Italy

Purpose or Objective: After more than 30 years, Ipilimumab was the first agent which showed a survival benefit for the treatment of metastatic melanoma. However, only about the 20% of patients have a long-term survival benefit. The combination of ipilimumab with other therapies might improve its efficacy. Abscopal effect refers to a regression of metastatic lesions distant from the primary site of radiotherapy (RT). This systemic response is observed in patients who received ipilimumab. Here we reported the outcomes from patients treated in the ipilimumab Italian expanded access program (EAP) who received RT after ipilimumab progression.

Material and Methods: Patients with advanced melanoma who had received RT after ipilimumab progression were eligible for analysis. Radiotherapy was available upon physician request for patients who failed ipilimumab therapy and for whom no other therapeutic options were available.

Results: 21 out of 95 patients treated with ipilimumab in the Italian EAP were eligible for the analysis. The median age was of 58 years (range 21-77); the progression free survival (PFS) from ipilimumab treatment was 4 months (range 3-6), while the time from the end of treatment with ipilimumab and RT was of 5 months (range 4-8). RT was performed on brain in 13 patients: 8 were treated with whole-brain RT and 5 patients with stereotactic RT. Other RT treatment included bone, metastatic distant lymph nodes, sub-cutaneous metastasis, spinal cord metastatis. The median doses was 30 Gy (range 30-50). A local response to RT was detected in 13 patients while 8 patients did not show any local regression. The abscopal response has been detected in 11/21 patients: in details, we observed 9 abscopal partial response , 2 abscopal stable disease , and 10 progression . The median of occurrence of the abscopal response was of 1 month (range 1-4). The median overall survival (OS) for all the 21 patients was of 13 months (range 6-26). The median OS for patients

with and without abscopal responses was respectively of 22.4 months (range 2,5-50,3) and 8,3 months (range 7,6-9.0). 11 out of 13 patients with local response showed an abscopal effect.

Conclusion: The RT after ipilimumab treatment may be an option for further potentiate its effect. Local response to RT might be predictive for the abscopal response and outcome. Further studies are warranted in this field to better understand and define the role of RT in combination or sequencing with ipilimumab treatment.

EP-1393

Radiological responses of melanoma brain metastases to radiosurgery and patient prognosis

I. Zubatkina[1], P. Ivanov[1], D. Tumarova[1], G. Andreev[1]
[1]*International Institute of Biological Systems, Radiosurgery, Saint-Petersburg, Russian Federation*

Purpose or Objective: The aim of this study was to analyze differences in radiological responses of melanoma brain metastases after Gamma Knife radiosurgery and their correlation with patient survival.

Material and Methods: We retrospectively analyzed 78 patients treated with Gamma Knife radiosurgery for melanoma brain metastases between 2009 and 2015 in the Radiosurgical centre (Saint-Petersburg, Russia) and subjected to follow-up MRI examinations. Patients receiving BRAF inhibitor therapy or ipilimumab were not included in the study. The study group consisted of 39 men and 39 women with a mean age of 52 years. The median KPS was 80 %. According to RPA, 14 patients were in Class I, 61 patients in Class II, and 3 patients in Class III. Most of the patients presented with multiple brain metastases (87 %). Radiosurgery was performed with Gamma Knife 4C and Perfection units; the mean dose delivered to the tumor margin was 20 Gy at 50 % isodose. After treatment, the patients underwent control MRI examination with standard protocols (2 mm T2 and 1 mm T1 with double contrast enhancement) at 8 weeks and at regular 3-month intervals thereafter. MR images were analyzed with Gamma Plan software. Volumetric measurements of metastases on pre- and post-treatment images were performed in order to determine different types of radiological response. We divided the patients into groups according to the type of radiological response and compared Kaplan-Meier survival curves in these groups with the long-rank test.

Results: We found that patients with melanoma brain metastases had different radiological reactions to Gamma Knife radiosurgery. We distinguished several types of radiation response: sustained decrease in tumor volume, prolonged stabilization of tumor volume, transient increase in tumor volume due to intratumoral bleeding with subsequent decrease in tumor size, transient increase in tumor volume due to radiation-induced necrosis followed by tumor shrinkage. Statistical analysis revealed that a rapid decrease in tumor volume was associated with poor prognosis. Median overall survival of this group of patients was about two times less compared with patients whose radiation response developed slowly after the first 2 months of radiosurgery ($p < 0.0001$). Stratification to RPA classes revealed that patients with a rapid response have poorer survival prognosis than those with a slow response in the corresponding RPA classes.

Conclusion: Melanoma brain metastases showed different radiological responses to radiosurgery. Rapid shrinkage of brain metastases is associated with poor survival, which may indicate more aggressive biological behavior of this tumor subtype. Different radiation sensitivity of melanoma brain metastases to Gamma Knife radiosurgery may be associated with molecular characteristics of cell subpopulations, which determine biological tumor behavior and affect patient prognosis.

EP-1394

Radiotherapy for adult T-cell leukemia-lymphoma: a single institutional experience

K. Tomura[1], T. Ohguri[1], M. Sakagami[1], K. Yahara[1], H. Imada[2], Y. Korogi[1]
[1]*University of Occupational and Environmental Healt, Radiology, Kitakyusyu, Japan*
[2]*Tobata Kyoritsu Hospital, Cancer Therapy Center, Kitakyushu, Japan*

Purpose or Objective: Adult T-cell leukemia–lymphoma (ATLL) is a rare disease and a peripheral T-cell malignancy associated with human T-cell lymphotropic virus type I (HTLV-1) infection. ATLL treatment is based on subclassification, and intensive multidrug chemotherapy regimens are often used for aggressive subtypes. However, disease progression occurs in most of patients. There are only a few reports for the radiotherapy in patients with ATLL. Therefore, the role of radiotherapy for ATLL is not well investigated even for the palliation. The purpose of this study was to evaluate the efficacy and toxicity for the radiotherapy in patients with ATLL.

Material and Methods: Between April 1983 to October 2013, 44 patients with 205 ATLL tumor lesions were treated with radiotherapy at our institution. Sites of tumor lesions were as follows; 184 lesions were in the skin, 13 lesions in the lymph nodes, 6 lesions in the central nerves system, and 2 lesions in the bone. Acute type on ATLL subtypes was seen in 8 patients, chronic type in 7 patients, lymphoma type in 10 patients, smoldering type in 15 patients and others in 4 patients. Median total dose of radiotherapy was 29Gy (range, 2-60Gy), and the median fractionated dose was 3Gy (range, 1-7Gy). For the skin tumor lesions, 45Gy in 15 fractions was selected in 33 lesions, 30Gy in10 fractions in 38 lesions, 28Gy in 4 fractions in 21 lesions and 20Gy in 5 fractions in 19 lesions and others in 73 lesions. Only 4 of 44 patients were treated with total skin irradiation, and the remaining 40 patients received conventional radiotherapy for local tumor. Efficacy and toxicity of the radiotherapy for ATLL were retrospectively evaluated, and the predictors of a long-term survival were analyzed.

Results: The median follow-up period was 206 days. Objective tumor response rates were 98%. Four of 6 tumor lesions with stable disease or progressive disease on objective tumor response were associated with aggressive subtypes or tumor sites of the central nerves system. In-field recurrence after radiotherapy was recognized in 3 (2%) lesions. Two-year and 5-year overall survival rates were 76% and 44%, respectively. Median overall survival time in patients with indolent subtypes (chronic or smoldering type) of ATLL was 23 months, while that in patients with aggressive subtypes (acute or lymphoma type) was 6 months, and the difference was significant. Acute toxicities of Grade 2 dermatitis were seen in 3 patients. Acute toxicity of Grades 3–5 was not observed. Late toxicity of≥Grade 2 was also not recognized.

Conclusion: Radiotherapy for ATLL was mainly used for the skin lesion and well tolerated, and could achieve excellent local tumor control without inducing severe toxicity. Radiotherapy should be selected to improve the quality of life, and be incorporated into combined modality therapy for ATLL.

EP-1395

Choroidal melanoma: is radiosurgery more efficient?

L. Larrea[1], E. Lopez[1], P. Antonini[1], V. Gonzalez[1], M. Baños[2], J. Bea[2], M. Garcia[2], T. Sanchez-Minguet[3], J. Tomas[3]
[1]*Hospital NISA Virgen del Consuelo, Radiation Oncology Department, Valencia, Spain*
[2]*Hospital NISA Virgen del Consuelo, Physics Department, Valencia, Spain*
[3]*Hospital NISA Virgen del Consuelo, Ophtalmology Department, Valencia, Spain*

Purpose or Objective: To evaluate local control, enucleation-free survival, toxicity and cost-effectiveness in patients with choroidal melanoma treated with linac-based stereotactic radiosurgery (SRS). GammaKnife® radiosurgery has report very good results for this melanoma treatment.

Material and Methods: Between 2003-2014, 6 patients with choroidal melanoma were treated at NISA Virgen del Consuelo Hospital in Valencia, Spain. Mean age was 59 years (range 43-79). Three were men and three women. Metastatic disease was ruled out in all cases. Two patients had small tumors, two medium sized lesions and two had large lesions according to Collaborative Ocular Melanoma Study Classification. Mean tumor volume was 0,49 cm3 (range 0,17-0,93). Three tumors were localized in the right eye. Visual field previous to treatment was normal in 5 cases and one patient presented complete hemianopsia of the affected eye. Central vision was preserved in all cases. The procedure was made under sedation and retrobulbar blockage, the eye muscles were fixed to Leksell G-Frame with silk sutures. Magnetic resonance (MRI) and computed tomography (CT) were used to contour lesion. CTV minimal marginal dose is 30 Gy, encompassed the 80 % isodose line in 4 patients and the 60% and 55% isodose lines in the other cases. All were treated with 6 MV linac, one isocenter and cone-colimation. Global cost of this method is around 8.000 € (range 7.000-12.000). It is an ambulatory procedure with a total duration of 3 hours or less.

Results: Median follow-up is 19 months (range 1-69). Follow up includes MRI and ophthalmoscopy every 6 months. Complete response in one patient, maximal partial response (≥ 50%) in three patients, partial response (≤ 50%) in other patient and it's too early for response evaluation (less than 6 weeks) in the last one. For lens and optic nerve, the dose constraints were 4 and 18 Gy, respectively. Up to date, no patient has local or distance progression. Enucleation has not been necessary in any patients. Five years after treatment one patient presented retinal scarring in irradiated area. Glaucoma start 9 month after SRS in one patient with previous cataract surgery. No other toxicities were observed.

Conclusion: In our experience, linac SRS is effective eye and vision-sparing method to treat patients with a minimally invasive, safe and cost-efficient alternative to brachytherapy and enucleation in choroidal melanoma with high local control rates and low incidence of toxicities.

EP-1396

Radiosurgery/Stereotacticradiotherapy with Cyberknife and immunotherapy in melanoma brain metastases

V. Borzillo[1], R. Di Franco[1], S. Falivene[1], G. Totaro[1], V. Ravo[1], P.A. Ascierto[2], A.M. Grimaldi[2], F. Cammarota[1], P. Muto[1]
[1]*Istituto Nazionale Tumori Fondazione Pascale, U.O.C Radioterapia, Napoli, Italy*
[2]*Istituto Nazionale Tumori Fondazione Pascale, Struttura Complessa Oncologia Medica Melanoma Immunoterapia Oncologica e Terapie Innovative, Napoli, Italy*

Purpose or Objective: The immunotherapy improves survival in patients (pts) with metastatic melanoma, but there is insufficient data on the efficacy in pts with brain metastases. SRS and SRT allow greater local control in pts with melanoma brain metastases, with not significant impact on prognosis. Our analysis evaluated survival and local control in pts treated with SRT/SRS with Cyberknife® system and Immunotherapy.

Material and Methods: From November 2012 to September 2015 we treated 47 pts (26 M and 21 F) with melanoma brain metastases. The median age was 59 years (28-81y). 28 pts received immunotherapy pre (pre-RT), concomitant and post radiation treatment (post-RT). 26 pts received Ipilimumab: 14 pts pre-RT, 5 pts concomitant-RT, 7 pts post-RT; 2 pts received Nivolumab: 1 pt pre-RT and 1 pt concomitant-RT; 11 pts received Pembrolizumab: 3 pts pre-RT, 4 pts concomitant RT, 4 pts post-RT. we treated 91 lesions of average size 13.5 mm (2-36). Based on the number of lesions, size and location, 69 lesions were treated with SRS (10-24Gy), 22 with SRT (18-24Gy/2-3-5 fractions). We evaluated the local response according to RECIST criteria (complete response CR: disappearance of the lesion; partial response PR: at least a 30% decrease in the diameter of lesion; progression disease PD: increase in the diameter of the lesion > 20%; stable disease SD: everyone else). We assessed overall survival, local control (LC) as the sum of CR, PR and SD, and the impact on LC of the association Radiotherapy (RT) and immunotherapy.

Results: 41 pts were evaluable for follow-up (FU). The 6-month survival was 58%. 11 patients died and 11 pts received Whole Brain RT for progression disease. At two months FU, of the 39 pts evaluable (24 treated with RT and immunotherapy), 85% had LC; at four months FU, of 29 pts evaluable (20 treated with RT and immunotherapy), 81% had LC; at six months FU, the 24 pts evaluable (15 treated with RT and Immunotherapy) 100% had LC.

Conclusion: Our analysis seems to confirm the literature data in terms of overall survival. The results showed a good disease local control in pts treated with SRT/SRS and immunotherapy, demonstrating a potential role of immunotherapy in the treatment of melanoma brain metastases. the recruitment of a greater number of pts, a longer follow-up and new prospective studies of combination RT and immunotherapy are needed to demonstrate the immunotherapy role in the treatment of melanoma brain metastases.

EP-1397

Patterns of failure in patients treated with adjuvant radiotherapy post lymphadenectomy for melanoma

L. Keenan[1,2], S. O'Sullivan[1], A. Glynn[1], M. Higgins[3], S. Brennan[1,2]
[1]*St Luke's Hospital, Radiation Oncology, Dublin, Ireland Republic of*
[2]*St James's Hospital, Radiation Oncology, Dublin, Ireland Republic of*
[3]*Cork University Hospital, Radiation Oncology, Cork, Ireland Republic of*

Purpose or Objective: Adjuvant radiotherapy is proven to prevent lymph-node field relapse after therapeutic lymphadenectomy for melanoma, but does not improve overall survival. Risk factors for lymph-node field recurrence include presence of extracapsular extension, number and size of lymph nodes at dissection. This study reports patterns of failure in patients treated with adjuvant radiotherapy post lymphadenectomy for melanoma.

Material and Methods: This retrospective study included all patients in three institutions treated with adjuvant radiotherapy post lymphadenectomy for melanoma between June 2012 and March 2015.
Patients who received radiotherapy were those with high risk of lymph node field recurrence, as per the findings of Burmeister et al in 2012. Patients received radiotherapy to the head & neck (55%), groin (30%) and axilla (15%). All were staged with PET or CT. Both IMRT (50%) and 3D conformal (50%) techniques were used.

Results: 20 patients were treated during this period (see table). Median follow up was 16 months (range 6.7 - 32 months).
There were no lymph node field recurrences.
Local recurrence rate was 10%.
Distant recurrence rate was 35%, all occurring within 4 months from completion of radiotherapy.
Distant recurrence rate was 53.8% in patients with extracapsular extension.
All patients with local or distant relapse had extracapsular extension.
71% of patients with distant recurrence had PET staging.
8% of patients experienced grade 3 radiotherapy toxicity.

Age	Primary	Adjuvant RT region	No of positive nodes	ECE	Site of recurrence	Time to recurrence post RT	Mortality post recurrence
64	Neck	Neck	6/61	No	-	-	-
57	Unknown	Neck	1/29	Yes	-	-	-
81	Cheek	Neck	2/31	Yes	Distant	4 months	RIP at 4 months
43	Leg	Groin	9/25	No	-	-	-
41	Back	Axilla	3/16	No	-	-	-
19	Neck	Neck	1/35	Yes	Distant	1 month	Alive at 25months
79	Eyelid	Neck	1/58	Yes	Local + Distant	3.5 months	Alive at 22months
69	Auricular	Neck	4/50	Yes	-	-	-
68	Unknown	Neck	1/64	Yes	-	-	-
65	Cheek	Neck	1/24	No	-	-	-
75	Unknown	Neck	4/45	Yes	Distant	4 months	RIP at 1 month
73	Neck	Neck	0	No	-	-	-
62	Leg	Groin	5/10	No	-	-	-
70	Leg	Groin	13/33	No	-	-	-
57	Foot	Groin	3/8	Yes	Local + Distant	0 months + 2.8 months	RIP at 10months
80	Cheek	Neck	38/42	Yes	Distant	1 month	RIP at 7months
48	Unknown	Axilla	13/33	Yes	-	-	-
57	Hand	Axilla	13/33	Yes	Distant	2 months	Alive at 8months
63	Leg	Groin	2/25	Yes	-	-	-
37	Leg	Groin	1/9	Yes	-	-	-

Conclusion: Radiotherapy was well tolerated and effective as no patient developed lymph node field relapse. However patients are at risk of early local and distant relapse, especially those with extranodal extension. Consideration should be given to the use of routine PET CT for high risk patients.

Electronic Poster: Clinical track: Sarcoma

EP-1398

Acute gastro-intestinal toxicities after pre-operative tomotherapy for retroperitoneal liposarcoma

P. Sargos[1], B. Henriques de Figueiredo[1], C. Kintzinger[1], E. Stoeckle[2], M. Delannes[3], G. Ferron[3], A. Giraud[4], C. Dupouy[4], M.A. Mahé[5], A. Mervoyer[5], M. Antoine[6], B.N. Bui[7], C. Bellera[4], G. Kantor[1]

[1]*Institut Bergonié, Radiotherapy, Bordeaux, France*
[2]*Institut Bergonié, Surgery, Bordeaux, France*
[3]*Institut Universitaire du Cancer Toulouse Oncopole, Radiotherapy, Toulouse, France*
[4]*Institut Bergonié, Clinical and Epidemiology Research Unit, Bordeaux, France*
[5]*Institut de Cancérologie de l'Ouest, Radiotherapy, Nantes, France*
[6]*Institut Bergonié, Physics Unit, Bordeaux, France*
[7]*Institut Bergonié, Medical Oncology, Bordeaux, France*

Purpose or Objective: Surgery is the cornerstone in the management of sarcomas. The aim of this study was to evaluate intensity-modulated radiotherapy (RT) with tomotherapy followed by surgery in terms of acute gastro-intestinal (GI) toxicities, especially regarding the high-level of prescribed dose (54 Gy/30 fractions/6weeks).

Material and Methods: From April 2009 to September 2013, 48 patients were included in a prospective multicenter study. Feasibility of tomotherapy, acute toxicities and local control at 3 years were the principal and secondary objectives. Inclusion criteria were operable, biopsy-proven, retroperitoneal liposarcoma. Patients with non-operable tumors validated after multi-disciplinary team evaluation, other histology or metastatic disease were excluded.Clinical Target Volume (CTV) and mains organs at risk (contralateral kidney, duodenum, bowel bag) were systematically delineated with the surgeon. Dose constraints to the bowel bag were defined as V45 Gy<33% and V30 Gy<50%. Surgery was planned 4 to 8 weeks after RT. Clinical visits were performed weekly during RT, before surgery, and 2 and 6 months after surgery. Toxicity was recorded according to CTCAE V4.0 scale.

Results: For acute GI toxicity, 46/48 patients were evaluable. All patients completed the radio surgical schedule without dose reduction. Mean age was 62 years (36-82). All patients were OMS≤2 except one (OMS=3). Mean CTV was 2954 cc (920-4989. Mean small bowel and duodenal volumes were 2725 (1355-4090) and 73 cc (33-113), respectively. Monobloc exerese was systematically achieved and all patients underwent homolateral nephrectomy. Twenty-nine patients underwent bowel resection, including large bowel (28/29), small bowel(4/29) and duodenum (1/29). Mean weight loss during RT was 5,4 kg (about 8% of mean body weight) and 8,9 kg at the first visit after surgery. At 2 months, grade 3 toxicities included duodenal stenosis (1/46), intestinal fistula (1/46) and enterocolitis (1/46) and grade 4 toxicity included GI fistula (1/46). At 6 months, no GI toxicities were observed. Three patients died within 6 months after surgery, 2 of which were related to treatment: one respiratory disorder 6 days after surgery and 1 duodenal perforation with necrosis and infection 4 months after surgery.

Conclusion: For patients with retroperitoneal liposarcoma, preoperative 54 Gy RT appears feasible. Due to the low rate of severe complications, no statistic correlations with dose in digestive structure were performed.

EP-1399

Safety of concurrent adjuvant radiotherapy and chemotherapy for locally advanced soft tissue sarcoma

D. Greto[1], I. Giacomelli[1], M. Loi[1], C. Muntoni[1], R. Grassi[1], A. Mancuso[1], C. Ciabatti[1], R. Capanna[2], D. Campanacci[2], G. Beltrami[2], G. Scoccianti[2], A. Franchi[3], L. Livi[1]

[1]*Azienda Ospedaliero Universitaria Careggi, Radiotherapy, Firenze, Italy*
[2]*Azienda Ospedaliero Universitaria Careggi, Orthopaedic Oncology, Firenze, Italy*
[3]*Azienda Ospedaliero Universitaria Careggi, Surgery and Translational Medicine, Firenze, Italy*

Purpose or Objective: The standard treatment of high grade soft tissue sarcoma (STS) is surgery followed by adjuvant radiotherapy (RT); chemotherapy (CT) can be an option in selected patients due to reported benefit in terms of disease free survival. The association of RT with CT might increase tissue reactions with the consequent risk of unplanned treatment interruptions resulting in an increased risk of treatment failure. This retrospective study analyze the safety and feasibility, respectively in terms of additional toxicity and compliance, of concurrent chemoradiotherapy (CTRT) in adjuvant treatment of STS.

Material and Methods: Data of 84 STS patients treated with surgery and adjuvant RT from June 1994 to November 2014 at the University of Florence, were retrospectively collected. Anthracycline-based CT was performed in high risk patients. Acute and late local toxicity of RT treatment were assessed respectively by Common Terminology Criteria for Adverse Events (CTCAE) 4.0 and RTOG/EORTC criteria for the Late Radiation Toxicity. CT-related hematological Toxicity was assessed by CTCAE 4.0.

Results: Twenty-four (28.6%) patients received CTRT. Mean follow-up was 5.6 years (range 0.4-18.8). At the time of our analysis 8 (9,5%) patients had a local relapse, 17 (19.8%) developed distant metastases, and 14 (16.7%) died of metastatic disease. Local Recurrence Free Survival (LRFS), Distant Relapse Free Survival (DRFS) and Overall Survival (OS) were respectively 83.4%, 70% and 69.5%. Grade ≥3 leucopenia occurred in 6 CTRT patients, resulting in early interruption of the CT treatment in 3 cases. Skin acute toxicity was developed in 59 (70,2%) of patients ; G3 skin toxicity occurred in 19 (22.6%) cases and determined treatment interruption in 15 (17.9%) patients with a mean treatment

delay of 10 days (range 4-20 days). No wounds complication occurred. Grade 1-2 fibrosis, joint stiffness and limb edema occurred in respectively 27 (32.1%), 9 (10.7%) and 18 (21.4%) patients. Age > 60 years was the only predictor of LR at multivariate analysis (HR: 5.26; 95% CI: 1.11-25.05; p=0.037) and correlated with impaired DRFS (86.1% vs 39.9%; p=0.006). No statistical significant parameters influencing OS. No correlation was found between CTRT and acute local toxicity (p= 0.75), and in any case the association determined a definitive interruption of the treatment. There was no difference in acute (p=0.25) and late toxicity (p=0.78) incidence in the IMRT and 3DCRT group.

Conclusion: Concurrent CTRT is a well tolerated treatment option with no additional toxicity compared to exclusive RT or sequential CTRT, resulting in adequate compliance to treatment. Combined postoperative CTRT could reduce the gap between surgery and RT in high risk patients eligible for CT. Further studies are needed to assess the optimal timing and sequence of adjuvant therapies.

EP-1400

Combined modality management of myxofibrosarcomas: a single-institution experience

D. Greto[1], M. Loi[1], C. Ciabatti[1], A. Mancuso[1], C. Muntoni[1], R. Grassi[1], I. Giacomelli[1], R. Capanna[2], D. Campanacci[2], G. Beltrami[2], G. Scoccianti[2], A. Franchi[3], L. Livi[1]

[1]*Azienda Ospedaliero Universitaria Careggi, Radiotherapy, Firenze, Italy*

[2]*Azienda Ospedaliero Universitaria Careggi, Orthopaedic Oncology, Firenze, Italy*

[3]*Azienda Ospedaliero Universitaria Careggi, Surgery and Translational Medicine, Firenze, Italy*

Purpose or Objective: Myxofibrosarcomas are a historically heterogeneous group of tumors that exhibit a propensity for local recurrence. The objectives of this study were to analyze the prognostic factors and outcomes of patients with MFS treated.

Material and Methods: We retrospectively reviewed the records of 41 patients with pathologically confirmed MFS, who underwent surgery and radiotherapy from November 1995 to June 2014. Clinicopathologic features, treatments, and patient outcomes were reviewed.

Results: Fourty one patients were identified, of whom 19 were men (46 %) and 22 were female (54%). The median age was 66 years (35-89). Mean follow-up was 3.9 years (0.3-13.9). Stage I and II disease was present respectively in 21 (51.2%) and 20 (48.8%) patients. Most patients (73%) had a high histological grade disease. Primary tumor was located at the extremities in 36 cases (88%) and at the trunk in 5 (12%); 21/41 (51%) were superficial lesions. Surgery was performed in our center on 33 (80%) patients while 8 (20%) patients underwent reoperation after prior surgery in an non-referring center; 31 (75%) had a radical surgery while 10 (25%) had a marginal resection. Four patients received Anthracycline-based adjuvant chemotherapy.
Radiotherapy was delivered to all 41 patients, as pre-operative treatment in 3 cases (7%, median dose: 50Gy) and as adjuvant treatment in 38 patients (93%, median dose 60Gy). Twenty-two patients underwent radiotherapy within 90 days since surgery. At a median follow-up of 3.9 years, there were 8 (20%) local recurrence (LR), 11 (27%) distant metastatic (DM) relapse and 10 (25%) deaths. A significant difference on Local recurrence - Free survival (DFS-LR) emerged in favour of post-operative radiotherapy compared to neoadjuvant radiotherapy (0% vs 72.8%, p=0.0001). Multivariate analysis confirmed pre-operative radiotherapy as a major predictor of LR (HR=18.6; 95% CI 3.7-93.7; p=0.0001). Tumor site was correlated with distant metastasis free-survival (DFS-DM), showing higher incidence of metastatic recurrence for deep lesion compared to superficial lesion (72.1% vs 32.4 % p=0.034), as confirmed by Cox univariate analysis (HR 3.8; 95% IC 1.01-14.36; p=0.049). LR occurrence was the only predictor of impaired overall survival, as confirmed by Cox regression univariate analysis (HR 4.44; 95% CI 1.28-15.45; p=0.019).

Conclusion: In our series adjuvant radiotherapy yielded superior local control compared to neoadjuvant irradiation. Deep localization was correlated with an increased risk to develop distant metastasis; local recurrence was a major predictor of OS. Improvement in local treatment is required to increase local control of disease in order to prevent both recurrence and metastatic dissemination.

EP-1401

Surgery, IOERT and EBRT in recurrent extremity sarcomas: long term results

L. Saleh-Ebrahimi[1,2], F. Roeder[2,3], B. Lehner[4], I. Alldinger[5], G. Egerer[6], P. Huber[7,8], G. Mechtersheimer[9], J. Debus[1,8], M. Uhl[8]

[1]*German Cancer Research Center DKFZ, Radiation Oncology, Heidelberg, Germany*

[2]*University Hospital of Munich LMU, Radiation Oncology, Munich, Germany*

[3]*German Cancer Research Center DKFZ, Molecular Radiation Oncology, Heidelberg, Germany*

[4]*University of Heidelberg, Orthopedics, Heidelberg, Germany*

[5]*University of Heidelberg, Surgery, Heidelberg, Germany*

[6]*University of Heidelberg, Hematology- Oncology and Rheumatology, Heidelberg, Germany*

[7]*German Cancer Research Center, Molecular Radiation Oncology, Heidelberg, Germany*

[8]*University of Heidelberg, Radiation Oncology, Heidelberg, Germany*

[9]*University of Heidelberg, Pathology, Heidelberg, Germany*

Purpose or Objective: To report our long-term results with surgery, IOERT and EBRT in recurrent soft-tissue sarcomas of the extremities.

Material and Methods: We performed a retrospective analysis of 41 patients suffering from recurrent soft-tissue sarcoma of the extremities, who received IOERT, surgery and EBRT at our institution after prior resection without additional radiation. 11 patients (27%) had more than one prior resection. Median age was 60 years (28-89) and 49% were male. Median tumor size at recurrence was 5 cm and 69% of the tumors were located in the lower limb. Stage in recurrent situation (UICC 7th) was as follows: Ia:2%, Ib:7%, IIa:39%, IIb:10%, III:32%, IV:10%. The majority of patients showed high grade lesions (FNCLCC G1:10%, G2:20%, G3:71%), predominantly liposarcomas (32%) and MFH (29%). Gross total resection was achieved in all patients with free margins in 51% and microscopically positive margins in 49%. IOERT was applied to the tumor bed with a median dose of 15 Gy, using electron energies of 6-8 MeV and a median cone size of 8 cm. IOERT was preceeded (10%) or followed (90%) by EBRT with a median dose of 45 Gy. 20% of the patients also received pre- and/or postoperative chemotherapy.

Results: The median follow up was 73 months (9-231) for the entire cohort and 93 months (16-231) in survivors. 9 patients (22%) showed local failures, resulting in estimated 5-year and 10-year local control rates of were 74% and 68%, respectively. 15 patients (37%) showed distant failures, transferring into estimated 5-year and 10-year distant control rates of 62% and 55%, respectively. Overall treatment failure was observed in 23 patients (56%), of whom 7 failed locally only, 15 distant only and 1 combined, resulting in 5- and 10-year estimated FFTF rates of 44% and 32%, respectively.15 patients have deceased, transferring into estimated 5-and 10-year overall survival rates of 74% and 60%, respectively. Severe postoperative complications were observed in 14% of the patients, mainly as wound complications. Severe late toxicity was found in 19% of the patients. Preserved limb function without impairment in activities of daily living was achieved in 81% of the patients.

Conclusion: Combination of surgery, IOERT and EBRT resulted in good local control and overall survival in recurrent soft tissue sarcomas of the extremities, although the results are worse than reported for primary situation. Given the high

rate of failures, evaluation of treatment intensification by systemic components maybe warranted in patients with recurrent soft-tissue sarcomas.

EP-1402

Surgery, IOERT and EBRT in upper extremity sarcomas: long term results

F. Roeder[1,2], B. Lehner[3], I. Alldinger[4], L. Saleh-Ebrahimi[2,5], G. Egerer[6], P. Huber[1,7], G. Mechtersheimer[8], J. Debus[5,7], M. Uhl[7]
[1]*German Cancer Research Center DKFZ, Molecular Radiation Oncology, Heidelberg, Germany*
[2]*University Hospital of Munich LMU, Radiation Oncology, Munich, Germany*
[3]*University of Heidelberg, Orthopedics, Heidelberg, Germany*
[4]*University of Heidelberg, Surgery, Heidelberg, Germany*
[5]*German Cancer Research Center DKFZ, Radiation Oncology, Heidelberg, Germany*
[6]*University of Heidelberg, Hematology- Oncology and Rheumatology, Heidelberg, Germany*
[7]*University of Heidelberg, Radiation Oncology, Heidelberg, Germany*
[8]*University of Heidelberg, Pathology, Heidelberg, Germany*

Purpose or Objective: To report our long-term results with surgery, IOERT and postoperative EBRT in patients with soft-tissue sarcomas of the upper extremity.

Material and Methods: We performed a retrospective analysis of 37 patients suffering from soft-tissue sarcomas of the upper extremity, who received surgery, IOERT and postoperative EBRT at our institution. Median age was 61 years (28-83) and median tumor size was 6 cm (1-15). 26 patients (70%) presented in primary situation. Stage at presentation (UICC 7th) was as follows: IIa:43%, IIb:8%, III:43%, IV:5%. All patients suffered from high grade lesions (FNCLCC G2: 27%, G3:73%), predominantly MFH (51%). Gross total excision was achieved in all patients with free margins in 51% and microscopically positive margins in 49%. IOERT was applied to the tumor bed with a median dose of 15 Gy, using electron energies of 6-8 MeV and a median cone size of 8 cm. All patients received postoperative EBRT with a median dose of 45 Gy. 30% of the patients also received pre- and/or postoperative chemotherapy.

Results: The median follow up was 78 months (6-231) for the entire cohort and 94 months (6-231) in survivors. Local failures were observed in 6 patients (16%), resulting in estimated 5-year and 10-year local control rates of 80%. 9 patients (24%) showed distant failures, transferring into estimated 5-year and 10-year distant control rates of 71%. Overall treatment failure was observed in 14 patients (38%), of whom 5 failed locally only, 8 distant only and 1 combined, resulting in 5- and 10-year estimated FFTF rates of 55%.11 patients have deceased, transferring into estimated 5-and 10-year overall survival rates of 82% and 70%, respectively. Severe postoperative complications were rare (3%). Severe late toxicity was found in 11% of the patients. Preserved limb function without impairment in activities of daily living was achieved in 79% of the patients.

Conclusion: Combination of surgery, IOERT and postoperative EBRT resulted in good local control and overall survival given the high rate of microscopically positive resections in this unfavourable patient cohort. Severe postoperative complications were rare compared to other sites.

EP-1403

Radiation of cardiac and large vessel sarcoma

M. Wygoda[1], L. Appelbaum[2], O. Shapira[3], A. Meirovitz[4], A. Wygoda[4]
[1]*Hadassah - Hebrew University Medical Center, Oncology - Radiotherapy Unit, Ein-Kerem Jerusalem, Israel*
[2]*Hadassah - Hebrew University Medical Center, Oncology-Radiotherapy Unit, Ein Kerem- Jerusalem, Israel*
[3]*Hadassah - Hebrew University Medical Center, Cardiothoracic Surgery, Ein-Kerem Jerusalen, Israel*
[4]*Hadassah - Hebrew University Medical Center, Oncology Radiotherapy Unit, Ein-Kerem Jerusalem, Israel*

Purpose or Objective: Cardiac and large vessel sarcomas are extremely rare neoplasms exhibiting aggressive behavior. Surgery is the most widely accepted treatment modality, but local recurrence and metastatic spread are common.The role of radiation ("definitive" or adjuvant) and chemotherapy is poorly-defined. In particular sparse data exists on the benefit of radiotherapy, and on the dose and technique required to achieve maximal benefit, with minimal toxicity.

Material and Methods: Five patients with primary cardiac and great vessel sarcomas, diagnosed between 2010and 2013, were identified in our radiation oncology department database.
We present here their clinical characteristics,dosimetric data, and outcomes.

Results: All Patients analyzed had high grade sarcoma with various histologic subtypes and without metastatic spread.Sites of origin were left atrium (2), SVC, pulmonary artery and descending thoracic aorta.Four patients had positive margins after curative-intent surgery, while one was considered inoperable. Surgery included reconstruction with a graft in three cases (PTFE / Gore-Tex) and heartautotransplantation technique in one.One patient received neoadjuvant and adjuvant chemotherapy.All patients received fractionated radiotherapy utilizing IMRT with Simultaneous Integrated Boost (SIB) to a maximal dose of 60-65Gy, except for one who received 54 Gy utilizing a3D technique. Mean PTV was 419.23 (range: 163.99cm3-631.95cm3).All patients completed the full course of treatment. Acute toxicity consisted mainly of fatigue and mild dysphagia, while long termevents were significant for NSTEMI in one patient (with local recurrence), and mild-moderate pleural and pericardial effusions in another patient. With a median follow-up of 25 months (range:24-31), 4/5 pts remain loco-regionally controlled (including the patient treated with definitive radiotherapy) and one had local recurrence (the patient who received 54Gy).One patient remains NED, three others developed metastatic disease, and one died of his local recurrent disease.

Conclusion: Based on our experience, radiotherapy to a dose of 60-65Gy using IMRT/SIB can achieve very good local control in the adjuvant and possibly definitive setting in cardiac and large vessels HG sarcomas. This schedule is feasible and generally well tolerated.

EP-1404

Early results of proton beam therapy in sarcomas at the West German Proton Therapy Center Essen

S. Frisch[1], M. Christiaens[2], F. Guntrum[2] S. Bauer[3], C. Blase[4], G. Fleischhack[5], C. Bäumer[1], D. Geismar[2], B. Timmermann[2]
[1]*West German Proton Therapy Center Essen, University Hospital Essen, Essen, Germany*
[2]*West German Proton Therapy Center Essen, Clinic for Particle Therapy / University Hospital Essen, Essen, Germany*
[3]*Sarcoma Center / West German Cancer Center, University Hospital Essen, Essen, Germany*
[4]*AnästhesieNetz Rhein-Ruhr ARR, West German Proton Therapy Center Essen, Bochum, Germany*
[5]*Paediatrics III, University Hospital Essen, Essen, Germany*

Purpose or Objective: Proton beam therapy (PT) is an attractive tool in multimodality cancer care and of increasing interest especially for tumors in close proximity to critical structures or in particular sensitive tissues. First clinical results of patients with sarcomatous tumors treated at the West German Proton Therapy Center Essen (WPE) with regard to early toxicity are presented.

Material and Methods: Between May 2013 and Oct 2015, 101 patients (aged 0.9-84.6 y (median 13.8 y); 56% male) with sarcomas were prospectively enrolled in the registry studies “KiProReg” and “ProReg” at WPE. Histologies were rhabdomyosarcoma (n=38), chordoma/chondrosarcoma (n=28), EWING sarcoma (n=10), synovial sarcoma (n=4), osteosarcoma (n=3), malignant rhabdoid tumors (n=3), and miscellaneous (n=15). In 79% of the cohort, residual disease

was still present when starting PT after incomplete resection or biopsy only. Treatment sites were head and neck/base of skull (n=59), pelvis (n=19), spinal/paraspinal area (n=23). The median PT dose administered was 55.8 Gy (45.0 - 74.0 Gy) with a median number of 31 fractions (range 25-41). Mixed beam technique was delivered in 2 patients only. In 53.5% of the patients (48 children, 6 adults) concomitant chemotherapy was applied. Treatment related side-effects were classified according to CTCAE V4.0 grading system and were assessed weekly during PT and in all follow-up visits.

Results: Median follow-up after first diagnosis was 10.6 months (range 3.3 months to 10.5 years). During PT no or only mild to moderate (grade 1 to 2) additional acute side-effects were documented in the majority of patients (n=79); predominantly erythema, alopecia, mucositis, fatigue, pain, and hematotoxicities when compared to baseline. In 28 children, additional grade 3 side-effects occurred during PT; aplasia (n=10; all receiving concomitant chemotherapy), mucositis (n=7; all receiving concomitant chemotherapy), general disorder (n=5), nausea, skin ulceration, headache, diplopia, anorexia, and arthralgia (each n=1). Additional grade 4 side-effects during PT were only seen in one patient for blood/bone marrow (n=1) while receiving concomitant chemotherapy. So far, nine patients failed due to systemic (n=6) or local (n=3) recurrence or progression. Five of these patients died due to disease.
In 73 patients, information on early-late effects after at least 3 months is available. In this group one new grade 3 side effect (fatigue) revealed and one new hematotoxicity was documented while receiving concomitant chemotherapy. No grade 4 or 5 toxicity was observed.

Conclusion: Current prospective and standardized data in sarcomatous tumor patients from WPE registry suggest good feasibility of the treatment even when high doses are administered at critical sites and sensitive tissues. However, longer FU is needed to understand the clinical benefit both in terms of late side effects and local control.

EP-1405

Chemoradiation with pegulated Liposomal Doxorubicin and Cisplatin for patients with Uterine Sarcomas

C. Varveris[1], A. Varveris[1], A. Spanakis[1], J. Stratakis[2], M. Mazonakis[2]
[1]*University Hospital of Heraklion, Radiotherapy, Heraklion, Greece*
[2]*University of Crete, Medical Physics, Heraklion, Greece*

Purpose or Objective: Uterine Sarcomas represent 3-7% of Uterine Carcinomas. Stage, Grade, Histology and Lymph Nodes are important prognostic factors. Non metastatic patients had reduced local-regional failure (LRF) with radiotherapy. We evaluated 23 patients treated with 3D-Conformal Irradiation (3D-CRT), Brachytherapy (BT), and Chemotherapy.

Material and Methods: 23 PATIENTS WITH Stage I – III (FIGO 2009) were analysed after TAH/BSO and peritoneal washings sampling. 15 patients with Malignant Mullerian Tumors (MMT), 2 Leiomyosarcomas (LMS), 1 grade 3 Stromal Sarcoma received adjuvant concurrent chemoradiation (CCRT). 5 patients (3 MMT and 2 LMS) were treated for local relapse (Pelvic and/or Nodal involvement). 3D-CRT was given with a 18MV Linac (59.40Gy in 1.8Gy/Fr, 5d/w). All patients received 1 MDR intracavitary insertion with 15Gy at the surface of the applicator. Concomitant Caelyx (12mg/m2) and CDDP (25mg/m2) were given the 1st and 4th day of each week respectively for a total of 6.6 weeks. In addition, Caelyx (20mg total) or CDDP (50mg total) were given simultaneously with MDR Brachytherapy depending on the hematologic toxicity of each patient.The above drugs were used as adjuvant treatment in every case for 4-6 Cycles after CCRT completion.

Results: patients were deemed eligible for the study. The median age was 66 years. For the adjuvant treatment, 13(72%) and 5(27%) patients were Stage I and II respectively. There have been 3/18(17%) locoregional relapses combined with lung metastases in 2 of them (LMS patients who died at 24 and 26 months). Of the 5 patients with documented LRFs 2 patients died at 24 and 31 months with disease progression. Overall 16/18(88%) with stage I/II and 3/5(60%) wth stage III are alive and disease free at a median follow up of 3 years (range 2-8 years). Leucopenia and CCRT enteritis/colitis were the most commonly reported toxicities.

Conclusion: CCRT given for Uterine Sarcoma patients as adjuvant treatment or at LRF is a tolerable and effective treatment which needs verification in large phase II/III trials.

EP-1406

Cardiac sarcomas: update of an evolving multidisciplinary approach with focus on radiation therapy

A. De Paoli[1], C. Lestuzzi[2], F. Santini[3], G. Boz[1], R. Innocente[1], F. Navarria[1], G. Miolo[4], S. Scalone[4], V. Canzonieri[5], A. Buonadonna[4]
[1]*Centro di Riferimento Oncologico, Radiation Oncology, Aviano, Italy*
[2]*Centro di Riferimento Oncologico, Cardiology, Aviano, Italy*
[3]*University, Cardiosurgery, Genova, Italy*
[4]*Centro di Riferimento Oncologico, Medical Oncology, Aviano, Italy*
[5]*Centro di Riferimento Oncologico, Pathology, Aviano, Italy*

Purpose or Objective: Primary cardiac sarcomas are extremely rare and unfavourable malignancies. Surgery, although technically challenging, remains the mainstay of treatment. Only few data are available on the use of chemotherapy (CT) and radiotherapy (RT) for advanced disease. Basing on experiences with combined surgery, RT and CT in extremities sarcomas, we explored the feasibility of this multimodality approach in cardiac sarcomas. An update on tolerance and safety of treatment with focus on RT program is reported.

Material and Methods: A retrospective analysis of a consecutive series of patients (pts) with unresectable disease referred to our Institute is reported. After oncologic-cardiologic evaluation, anthracyclin-based CT was considered, followed by RT. IMRT-IGRT (Helical Tomotherapy) was used for more accurate tumor-conformal treatment while sparing the no-tumor-bearing surrounding heart tissue and to reduce the risk of radiation-induced heart disease (RIHD). Echocardiography was used in the treatment planning for organ motion and target-volume margin definition. Full-dose RT with 45 Gy/25 frs with SIB up to 54 Gy was planned. Individualised dose constraints to left and right ventricles were included.

Results: Between June 1998 and March 2013, 17 consecutive pts (M/F: 11/6, median age: 53yrs (25-72) with M0 cardiac sarcoma were referred to our Institute. Tumor location was right atrium in 8 pts, left atrium in 6, left ventricle in 2, pulmonary artery in 1pt; most common histologic type was angiosarcoma (62%). 8 pts had unresectable disease and 9 had complete resection. 12 pts received 4 cycles of full-dose epirubicin 120mg/m2 and Ifosfamide 9g/m2 and G-CSF; 2 pts 3 cycles of weekly Taxol 80 mg/m2. All pts underwent RT, median dose 54Gy (45-59.4Gy). Only 1 pt had moderate acute pericarditis and 2 had late toxicity (mild ejection fraction reduction). 3 pts with major response to CT-RT underwent successful complete surgical resection. At a median follow-up of 40 months (12-137), 9pts are alive and 6 are disease-free.

Conclusion: In our experience, RT for cardiac sarcomas appeared to be feasible, also when combined with CT and surgery. Technological advances in RT planning and delivery and further insight into RT cardiac tolerance are crucial in minimizing the risk of RIHD. Further experience is needed to confirm these encouraging results.

EP-1407

Surgical spacer for sacral chordoma carbon ion treatment at CNAO

B. Vischioni[1], M. Fiore[1], P. Fossati[1], V. Vitolo[1], A. Iannalfi[1], E. Ciurlia[1], M. Bonora[1], D. Panizza[2], M. Ciocca[2], L. Cobianchi[3], A. Peloso[3], T. Dominioni[3], D. Bugada[3], P. Dionigi[3], F. Valvo[1], R. Orecchia[1]

[1]*Fondazione CNAO, Radiation Oncology, Pavia, Italy*
[2]*Fondazione CNAO, Medical Physics Unit, Pavia, Italy*
[3]*IRCCS Policlinico san Matteo, Surgery 1, Pavia, Italy*

Purpose or Objective: Since the beginning of clinical activity in 2011, approximately 600 patients has been treated with hadrons in CNAO (National Center for Oncological Hadrontherapy), among which 42 were sacral chordoma undergoing carbon ion radiotherapy (CIRT) with a radical intent. The aim of the current study is to analyze the feasibility of the insertion of a newly customized spacer prior CIRT in sacral chordoma patients, in terms of procedure validation and patient tolerance, in selected cases where the sacral chordoma is contiguous to the rectum or the bowel loops in order to safely escalate the dose to the tumor target.

Material and Methods: Since 2014 , 6 consecutive sacral chordoma patients (3 males and 3 females) eligible for active scanning beam delivery CIRT at CNAO (prescribed dose 70.4 GyE in 16 fractions), were enrolled for spacer placement at IRCCS Policlinico San Matteo – Dept. of General Surgery. For each patient silicone spacer was shaped according to intraoperative findings from a 10x10 cm silicone sheet with a width of 1 mm (Distrex, Padua, Italy). Prior to the surgery and clinical use, a variety of measurements was performed to evaluate the physical stability of the spacer during and after irradiation, as well as its main properties when exposed to carbon ion beams. During CIRT, at the end and each 3 months afterwards, patients were followed up for acute and late CIRT toxicity with clinical visit and high field magnetic resonance (MRI).

Results: Three patients underwent laparotomic and 3-laparoscopic spacer placement. A representative CIRT plan recalculation performed on one of the enrolled patient CT performed before spacer insertion showed that during CIRT the presence of the spacer keeps digestive tract far away from the irradiated area, thus the radiation field is unaffected by rectum filling or intestine movement. Patient enrolled in the study did not show any gastrointestinal toxicity during CIRT or at follow up. Patient imaging during follow up did not show anatomic variations.

Conclusion: Silicone spacer placement is a valuable tool for safe dose escalation in sacral chordoma patients undergoing CIRT.

EP-1408

Adjuvant concurrent chemoradiotherapy in soft tissue sarcomas of the limbs: an effective strategy.

A. Ducassou[1], T. Valentin[2], T. Filleron[3], M. Delannes[1], G. Ferron[4], S. Le Guellec[5], P. Rochaix[5], B. Boulet[6], C. Chevreau[2]

[1]*Institut Claudius Regaud - IUCT-Oncopôle, Radiotherapy, Toulouse, France*
[2]*Institut Claudius Regaud - IUCT-Oncopôle, Oncology, Toulouse, France*
[3]*Institut Claudius Regaud - IUCT-Oncopôle, Biostatistics, Toulouse, France*
[4]*Institut Claudius Regaud - IUCT-Oncopôle, Surgery, Toulouse, France*
[5]*Institut Claudius Regaud - IUCT-Oncopôle, Pathology, Toulouse, France*
[6]*Institut Claudius Regaud - IUCT-Oncopôle, Radiology, Toulouse, France*

Purpose or Objective: To determine the efficacy and the morbidity of the post-operative concurrent chemoradiotherapy in patients with advanced localized soft tissue sarcomas (STS) of the limbs : results of a retrospective analysis.

Material and Methods: From 1991 to 2012, 68 patients with primary high grade STS of the limb were treated in our institution with an adjuvant concurrent chemoradiotherapy, following limb sparing surgery The median age was 47.5 years (range, 19 to 74). The most common location was the thigh (56%). The resection was complete (R0) and marginal (R1) in 46 (68%), and 22 (32%), respectively. The median tumor size was 6 cm (range, 8 to 20cm), deep in 83% of cases, and grade was 2 (FNCLCC) in 28 patients (42%) and 3 in 38 (58%), 2 missing. Adjuvant radiotherapy was delivered by brachytherapy (BRT) plus external radiotherapy (EBRT) in 26 patients (38%) and by EBRT alone in 42 (62%). The median dose of BRT and EBRT were respectively 20Gy (range 12 to 30Gy) and 60Gy (range, 45 to 70). The median time between surgery and EBRT was 48 days (range, 20 to 140). Concurrent chemotherapy (CT) was a combination of doxorubicin (60 mg/m2 total dose (TD) and ifosfamide (7,5 g/m2 TD), with a median number of 4 cycles (range, 1-4).

Results: With a median follow-up of 105 months (CI95% 89-125), the 5-year disease-free survival and overall survival rates were 67%(CI95 53.9-77) and 81%(CI95 68-89); 25 relapses were observed (6 local, 18 distant, and 1 local and distant). A severe (grade 3-4) hematologic toxicity was observed in 32% of cases, mainly leucopenia; 13 patients (20%) experienced a dose reduction of CT. Severe non hematologic complications occurred in 15 patients (22%), mainly acute cutaneous toxicity (14 patients, 21%). Six patients (10%) experienced an EBRT interruption. Severe wound complications were very rare (2 absesses), without secondary operation for wound care. In univariate analysis, median EBRT dose was a prognostic factor for hematologic severe complications, the median dose being 64Gy in patients with grade 3-4 toxicities vs 56Gy in patients with grade 1-2 toxicities;p=0.01. Tumor location was a prognostic factor for grade 3-4 wound complications and acute dermatitis. Indeed, 50% of complications were grade 3-4 (5/10) when tumor was located in upper limb, vs 17% in inferior limb (10/58); (p=0.035). No correlation between age, sexe, tumor size, and toxicity was found.

Conclusion: Adjuvant concurrent chemoradiotherapy is efficient, feasible and well-tolerated in soft tissue sarcomas of the limbs.

EP-1409

Neuropathic pain a secondary-effect in Classic Kaposi Sarcoma patients treated witth radiotherapy

I. Nieto[1], A. Gonzalez[1], V. Ochagavia[1]

[1]*MEDTEC, Department of Radiation Oncology- OncoRay ? Centre for Radiation Research in Oncology, Vigo Pontevedra, Spain*

Purpose or Objective: Kaposi sarcoma (KS) is a vascular tumor that can affect the skin and the mucosa of the digestive, respiratory and urinary tracts, as well as the lynphatic system. It is associated to human herpes virus 8 (HHV-8). There are three principal variants: Classic KS which affects older people (mediterranean and jewish askenazi); Endemic KS which mainly affectss african children, is a fulminant lymphadenopathic desease, and HIV- associated KS which affects homosexual men. Patients with Classic KS have skin macules on the legs that enlarge and coalesce into plaques and nodules. Radiotherapy is an effective treatment for localized lesions.

Material and Methods: We retrospectively analized patients with classic KS treated in our department between 2004 and 2014. Until 2012, all our patients were treated with a 3 Gy per fraction, 30 Gy total dose treatment schedule. After this date most of our patientes were treated with a 2 Gy per fraction, 40 Gy total dose treatment schedule. All patients were treated with the same technique: two paralel-opposed 6 Mv photom fields on both legs submerged into water, in order to homogenize the dose on the entire surface, and as a bolus effect. We observed that some patients treated with 3 Gy per fraction schedule, had neuropathic pain in both legs,

after the end of the radiation treatment, which required the use of high dose-opioid and gabaergic pain relievers, chronically. In fact, this was the main factor to consider in our study. Local control was analized too.

Results: Eight patients were treated with 3 Gy /fraction, four of them suffered neuropathic pain in radiation field that required chronic drug treatment. (RR 50%). None of the five patients treated with the 2 Gy per fraction technique had neuropathic pain in legs.

Conclusion: Our preliminary results indicate that the 2 Gy per fraction treatment avoids the onset of neuropathic pain after the radiation treatment. Althoug the patient recruitment was low, we can afirm that both radiation techniques were very useful in the classic KS local control. The 2 Gy per fraction treatment was not associated to neuropathic pain, compared with the hypofractioned radiation treatment.

EP-1410

BBRT in the treatment of metastases from soft tissue sarcoma (STS): Single-institution Experience

C.H. Canova[1], A. Levy[1], F. Martinetti[1], F.G. Riet[1], C. Le Pechoux[1]
[1]*Institut Gustave Roussy, Department of Radiation Oncology, Villejuif, France*

Purpose or Objective: To evaluate the results of stereotactic ablative radiotherapy (SABR) in selected metastatic sarcomas patients

Material and Methods: Outcomes of 21 consecutive metastatic STS patients (32 consecutive lesions) receiving SABR between 2012 and 2015 at our center were retrospectively analyzed.

Results: Most patients (85%) had a performance status of 0-1 and the median age at treatment was 62.4 years. Metastases treated were localized in lung (37,5%), brain (37,5%), liver (9,5%), soft-tissue (12,5%) and pancreas (3%). The median size of the treated lesion was 2.1 cm. The median biologic equivalent dose delivered was 120 Gy (range, 52.7-213.8 Gy) delivered in a median number of 5 fractions (range, 1-13). The majority of patients received systemic agents prior SABR (16/21). With a median follow-up of 18 months, the 2 years local control rate was 86% (CI 95%: 51-100%; median: not reached), with four progressives lesions. Only one patient experienced a grade 3 toxicity consisting of an ear bleeding. Two years overall survival and progression free survival rates were respectively 72% (CI 95%: 47-96%) and 39% (CI 95%: 15-63%).

Conclusion: SABR in metastatic sarcoma seems to be an effective tool in local control that might be used as an alternative to other local treatments in highly selected patients.

Electronic Poster: Clinical track: Paediatric tumours

EP-1411

Evaluating the utility of 18F-DOPA-PET imaging for neurosurgical planning of pediatric gliomas

A. Arnett[1], Y. Zhang[1], M. Seaberg[1], D. Pafundi[1], D. Brinkmann[1], C. Giannini[2], N. Wetjen[3], D. Daniels[3], A. NageswaraRao[4], N. Laack[1]
[1]*Mayo Clinic, Radiation Oncology, Rochester, USA*
[2]*Mayo Clinic, Pathology, Rochester, USA*
[3]*Mayo Clinic, Neurosurgery, Rochester, USA*
[4]*Mayo Clinic, Pediatric Oncology, Rochester, USA*

Purpose or Objective: MRI characteristics and extent of disease in glioma is important for surgical planning. However, MRI may not adequately guide biopsy location in non-enhancing tumors. Furthermore, post-radiation changes are difficult to differentiate from progressive tumor. We previously demonstrated the PET tracer 3,4-dihydroxy-6-[18F]fluoro-l-phenylalanine(FDOPA) has a sensitivity for gliomas and may improve neurosurgical planning in adults. This study evaluates the utility of FDOPA-PET/CT imaging in biopsy and resection planning in pediatric patients.

Material and Methods: MR/CT and FDOPA-PET/CT images were obtained in 5 patients with primary or recurrent malignant gliomas. Regions of interest were defined based on areas of MRI contrast enhancement (CE) and FDOPA uptake to include both concordant (MRI-CE and high-FDOPA) and disconcordant (MRI-non-CE and high-FDOPA, MRI-CE and low FDOPA) regions. Ratios of maximum tumor SUV (SUVmax) normalized to mean SUV (SUVmean) of normal brain tissue (T/N) were determined using the SUVmax from each biopsy coordinate and the SUVmean from contralateral normal brain tissue.

Results: The FDOPA-PET images guided biopsy site selection in four patients. One patient with contrast enhancement in an eloquent location near a region of prior radiotherapy did not undergo biopsy after FDOPA-PET failed to show increased uptake. Average tumor SUVmax was 2.135 (range 2.92-1.27), and the T/N average T/N ratio was 1.6 (range 1.92-1.18). Biopsies within the region of highest uptake were performed in 3 patients and were consistent with Grade III or Grade IV, despite lack of contrast enhancement 1 patient. In one patient, SUVmax was in an eloquent region of thalamus and was deemed an unsafe location for biopsy. Biopsy from an adjacent region revealed infiltrating glioma, non-diagnostic for grade. Regions of increased FDOPA uptake extended beyond those identified with MRI in two patients.

Conclusion: FDOPA-PET imaging appears to have utility in guiding biopsy region selection and may assist with identifying regions of higher-grade disease in pediatric patients with astrocytomas.

EP-1412

Respiration-induced organ motion in children during image-guided radiation therapy

S. Huijskens[1], I.W.E.M. Van Dijk[1], M.A.J. De Jong[1], J. Visser[1], R. Dávila Fajardo[1], C.R.N. Rasch[1], T. Alderliesten[1], A. Bel[1]
[1]*Academic Medical Center, Radiation Oncology, Amsterdam, The Netherlands*

Purpose or Objective: Respiration-induced organ motion is one of the main contributors to intrafractional motion, limiting the maximum achievable accuracy in radiation therapy (RT). Knowledge on respiration-induced organ motion in children during RT is extremely scarce and urgently needed for better definitions of abdominal and thoracic safety margins. It also allows to assess whether developments and introduction of child-friendly breathing exercises and/or coaching during the treatment course could have an added value to control and minimize respiration-induced organ motion. Therefore, the aim of this study is to investigate how respiration influences the diaphragmatic motion, as indicative of organ motion in the abdomen and thorax, during image guided RT (IGRT) in children and to find possible relationships with age and height. In addition, we investigated trends in the respiration-induced diaphragmatic motion during the treatment course.

Material and Methods: This retrospective study consisted of 15 patients with a mean age of 10.6 years (range 2.2-16.9 years) and a mean height of 140 cm (range 90–167 cm), treated at our institute between 2006 and 2015, for whom for setup correction routinely acquired evaluable images of the thorax were available. This amounted to a total of 15 reference CT (refCT) scans and 86 Cone Beam CT (CBCT) scans. CBCTs were reconstructed for the inhale and exhale respiratory phases and registered to the refCT using Elekta XVI software. First, the vertebrae were aligned. Subsequently, the diaphragm was manually aligned in cranio-caudal (CC) direction only. The result yields the mean peak-to-peak (PP) motion (i.e., magnitude of motion) of the diaphragm in the CC direction, derived from registration outcomes of the inhale and exhale CBCTs to the refCT.

Possible time trends were investigated by analyzing the derived PP motion from daily CBCTs as a function of treatment day. The reproducibility of the PP motion was measured as the standard deviation (SD) over the mean PP motion per patient. We used a linear regression model to analyse the relationship between these outcomes and age and height.

Results: Over all patients, PP motion was on average 8.6 mm (range 4-15 mm) and varied largely within and between patients. Time trends differed between patients. PP motion correlated with age and height (*p<0.05*). PP motion increased by 0.42 mm for every yearly increase in patients' age and for every 1 cm increase in height the PP motion increased 0.07 mm (Figure 1). The SD ranged from 1-3.7 mm and correlated with age and height (*p<0.05*) (Figure 1).

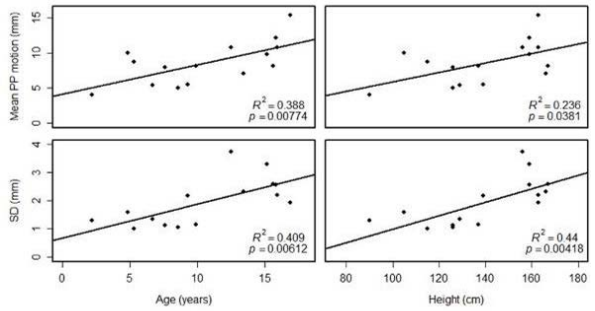

Figure 1. Scatterplots with regression lines describing relationships between mean PP motion and reproducibility of the PP motion (SD) with age (left column) and height (right column) (*p<0.05* was considered as statistically significant).

Conclusion: Respiration-induced diaphragmatic motion in children during IGRT is correlated with age and height, however irregular breathing patterns were found. PP motion was variable throughout the treatment. Therefore, introducing child-friendly breathing exercises and/or coaching techniques may be beneficial to minimize PP motion and to enhance its reproducibility.

EP-1413

Second neoplasms in survivors of childhood acute lymphoblastic leukemia treated with radiotherapy

W.S. Looi[1], J.W.J.C. Koh[2], F.K.C. Chin[1], Y.H.J. Teh[1], A.M. Tan[3]

[1]National Cancer Centre Singapore, Radiation Oncology, Singapore, Singapore

[2]National University of Singapore, Yong Loo Lin School of Medicine, Singapore, Singapore

[3]KK Women's and Children's Hospital, Haematology/Oncology Service, Singapore, Singapore

Purpose or Objective: Second malignant neoplasms (SMNs) are a concern in survivors of childhood cancer. Chemotherapy forms the mainstay of treatment for acute lymphoblastic leukaemia (ALL), but radiotherapy has a role in certain situations. As both chemotherapy and radiotherapy can be carcinogenic, patients treated with both modalities may be at a higher risk of SMNs. This study aims to investigate the incidence of SMNs in patients treated with both chemotherapy and radiotherapy at KK Women's and Children's Hospital, Singapore.

Material and Methods: We performed a retrospective review of ALL patients treated in the largest maternal and children's hospital in Singapore. Children aged 16 years and below diagnosed with ALL from 1993 to 2014 were identified in the Childhood Cancer Registry. Manual and electronic medical records were reviewed for information on demographics, management and SMNs.

Results: A total of 64 patients treated with both chemotherapy and radiotherapy were identified. Seventeen (26.6%) were female and 47 (73.4%) were male. The median follow-up was 9.2 years (range, 1.1-22.0 years). The median age at diagnosis was 5.3 years (range, 0.3-14.6 years). The median age at which radiotherapy was given was 6.6 years (range, 2.9-15.4 years).

SMNs were noted in 3 of 64 (4.7%) patients. Two of 3 patients had a SMN within the radiation field (both cranial). The histological diagnoses were basal cell carcinoma and cerebral PNET. The remaining patient had an ovarian immature teratoma outside the radiation field. The median latency period was 9.4 years (range, 8.3-13.3 years) from date of diagnosis to development of SMN. The estimated 10-year cumulative incidence was 4.3%, 95% CI [0.01, 0.13] using a competing risks analysis.

Radiotherapy data was available in 63 patients. Fifty-one of 63 (81.0%) received cranial irradiation, of which 3 (5.9%) also received spinal irradiation. Total body irradiation was performed in 20 of 63 (31.7%), and testicular irradiation in 17 of 63 (27.0%) patients. The orbit was targeted in 3 of 63 (4.8%) patients.

Conclusion: Long term survivors of ALL treated with both chemotherapy and radiotherapy may have a significant risk of second malignant neoplasms, which may occur years after the initial diagnosis.

EP-1414

Using a DVH registry standardizes IMRT-CSI planning and reduces V20 in non-target tissues

M. Létourneau[1], J. Kildea[2], W. Parker[2], A. Joseph[2], C. Freeman[3]

[1]CHU de Québec, Department of Radiation Oncology, quebec, Canada

[2]McGill University Health Centre, Department of Medical Physics, Montréal, Canada

[3]McGill University Health Centre, Department of Radiation Oncology, Montreal, Canada

Purpose or Objective: An intensity-modulated radiation therapy technique for craniospinal irradiation (IMRT-CSI) delivered on the Tomotherapy unit has been used at our centre since 2008. Defining and prioritizing dose constraints to target and organs at risk (OAR) are time-consuming. To facilitate and standardize the planning process, we developed a dose-volume histogram (DVH) registry and tested its usefulness with two cohorts of patients treated to different doses of CSI.

Material and Methods: The registry consists of a back-end MySQL database and front-end webpages that are served via a web-server internal to the clinic. Approved plans are added to the DVH registry via a filter that standardizes the names of the OARs. Dose constraints for planning are established based on previous aggregate data and planners graphically compare DVH data for a new treatment plan with existing aggregate data without submitting the new data to the registry. We evaluated two cohorts of IMRT-CSI patients: (1) CSI dose 36 Gy in 20 fractions and (2) CSI dose 23.4 Gy in 13 fractions and compared the findings with an earlier cohort of patients that were planned before we started using the registry.

Results: Eighteen patients, age 3 to 17 years, were included in the registry. Eleven were treated to a dose of 36 Gy in 20 fractions and seven to a dose of 23.4 Gy in 13 fractions. Most (56%) had medulloblastoma. Significantly smaller variations were achieved for OAR for patients treated at 36 Gy using the DVH registry compared with patients in the earlier cohort, making the registry a very useful tool for the treating team. V20 were lower for all OARs except the trachea.

Conclusion: The results confirm that the DVH registry standardizes the planning process of IMRT-CSI patients. We will use constraints obtained from the 7 patients treated at 23.4 Gy to start planning new cases and evaluate the benefit of our DVH registry for this regimen.

EP-1415

Cranial irradiation and sleep disorders in children with brain tumour: a case-control study

C. Pilotto[1], E. Coassin[2], E. Passone[1], M. Robazza[1], S. Birri[3], E. Bidoli[3], A. Nocerino[1], M. Mascarin[2]
[1]*AOUD Santa Maria della Misericordia, Clinica Pediatrica, Udine, Italy*
[2]*Centro di Riferimento Oncologico, SOS di Radioterapia Pediatrica, Aviano, Italy*
[3]*Centro di Riferimento Oncologico, SOS Epidemiologia e biostatistica, Aviano, Italy*

Purpose or Objective: Brain tumours as many other neurological diseases may cause sleep problems interfering with the delicate mechanisms of sleep regulation. The presence of a disturbed sleep may have material daily performance effects. In growing subjects this aspect may determine emotional and behavioral problems. The prevalence of sleep disorders (SD) in children with brain tumours is unknown. The main aim of this study is to compare the prevalence of SD in children affected by brain tumours and treated with radiotherapy to the prevalence of SD in children treated only surgically.

Material and Methods: A retrospective case-control study was performed from October 2014 to April 2015 in a Pediatric Department and in a Pediatric Radiotherapy Centre. "Cases" included patients 2 to16 years old with a diagnosis of CNS tumour at least 3 months after treatment conclusion (surgery and radiotherapy and/or chemotherapy). "Controls" were children 2 to 16 years old with CNS tumours treated only surgically. Children's sleep quality was assessed with a questionnaire administered to parents (Child's Sleep Habits Questionnaire, CSHQ). The sleep was considered disturbed if at least one of the following events was present: sleep delay, sleep duration, sleep-related anxiety, night waking, parasomnias and respiratory disorders. The risk of SD was estimated by the Odds Ratio (OR) and their 95% confidence intervals (95% CI) through logistic regression models.

Results: We enrolled 14 cases and 14 controls, for a total of 28 subjects. 9 out of 14 children in "case" group were treated with surgery, radiotherapy and chemotherapy. Our results highlighted a prevalence of SD of 57.4% among cases and 42.9% in controls. A statistically significant difference between the two groups (OR= 1.78 CI: 0.40-7.94) was not reached.

Conclusion: Cranial irradiation is required to treat many brain tumours in children. Some studies involving only children with midline tumours show that high-dose cranial irradiation in midline site in childhood is associated to objective and subjective changes in the sleep-wake rhythm in adulthood. Our study failed to show a statistically significant difference in SD between the two groups, but there is evidence of a greater prevalence among children treated with radiotherapy. Limitations of the study include the small number of patients involved and the lack of irradiation details, as dose and site. We expect that a relationship between cranial irradiation and SD will be statistically confirmed increasing the number of involved patients. We hope to better define the relationship with irradiation dose and site, as brain tumour position and consequent irradiation may have a role on SD development.

EP-1416

Analysis of childhood brain tumours treated with radiosurgery/stereotactic fractionated radiotherapy

J. Paiva[1], T. Santana[1], V. Zaccariotti[1], J. Arruda[1], L. Oliveira[1], V. Araújo[1], L. Goulart[1]
[1]*Hospital Araújo Jorge, Radiation Therapy, Goiânia, Brazil*

Purpose or Objective: The aim of the study is to evaluated data from radiosurgery (RS) and fractionated stereotactic radiotherapy (FSRT) performed in patients from 0 to 14 years of age in Hospital Araújo Jorge, Goiânia, Goiás, Brazil, treated between 2000 to 2013.

Material and Methods: The authors retrospectively assessed medical reports of 65 patients from 0 to 14 years of age with diagnosis of brain tumors and who underwent RS/FSRT from 2000 to 2013. The analysis concerns age at diagnosis, primary location of the tumor, size of the tumor, risk assessment, and employment of either RS or FSRT.

Results: From the 65 records, 42 were included in the analysis for having all the information desired. Of those patients, 46.3% were male and 69.0% were diagnosed with malignant tumors. 29.3% of the patients were between 0 to 6 years, 31.7% between 7 to 10 years, and 39.0% between 11 to 14 years of age. The most frequent histophatological diagnoses were medulloblastoma (19.0%), arteriovenous malformation (14.3%), and glioma (11.9%). As for the treatment, 78.5% underwent to FSRT and 21.5% underwent to RS. The median total radiation dose prescribed dose was 54Gy for the FSRT and 18Gy for the RS. The most frequent prescription dose curves were 90% and 95%, respectively, whilst the conformity index for the RS varied from 1.23 to 2.04. It resulted in 42.9% of the patients having partial response to the performed treatment and 78.6% not having distant disease progression. The overall survival was 58.1 months for patients from 0 to 6 years, 69.3 months for those from 7 to 10 years, and 90.2 months for those in the 11 to 15 years range (p=.0037).

Conclusion: The results show a 13 years experience on treating pediatric tumors with RS/FSRT of that single institution. High precision conformal stereotactic techniques with RS/FSRT employing conservative margins than conventional radiotherapy in childhood tumors appears to be safe based on our experience. Long term prospective trials are required to test their real potential in sustaining local control and minimising treatment related acute and late morbidity.

EP-1417

ANDANTE: second cancers from neutrons following proton therapy: preliminary epidemiological results

K. Perstorfer[1], L. Walsh[1]
[1]*Bundesamt für Strahlenschutz Federal Office for Radiation Protection, AG-SG 1.3, Neuherberg, Germany*

Purpose or Objective: Survivors of childhood cancer generally have an increased risk of developing secondary cancers associated with the treatment for the first primary cancer. Proton therapy represents a highly effective treatment technique for some types of childhood cancers but scattered radiation from secondary neutrons is an unwanted by-product.

Material and Methods: The ANDANTE project investigates the relative risk of neutrons compared to photons for tumorigenesis, as a function of dose and energy. The approach is multidisciplinary, including physical measurements and modeling, molecular biology, radiobiology and epidemiology. Based on stem cells irradiated in vitro with either photons or neutrons, a corresponding predicted model of the relative risk of cancer induction from photons or neutrons following pediatric radiotherapy is developed and tested on clinical data, leading to a proposal for a prospective epidemiological study to validate the relative risk of neutrons on the tumorigenesis in humans. The progress on the epidemiological aspects of this current work is reported here.

Results: In order to validate the dose-risk model developed earlier in the project, a feasibility study with clinical data from the Loma Linda University Medical Centre (LLUMC) was performed. A cohort of 242 patients was constituted in August 2013. Those patients were treated between 1991 and 2013, diagnosed with arteriovenous malformation (AVM) (n=108) or low grade astrocytoma (n=134) before the ages of 30 years, and were followed up later. All variables for statistical analyses are available but data extraction has not been finished yet. Results of this feasibility study will provide a basis for the development of the prospective

epidemiological study, and will be used to test the validity of a predictive risk model based on values of neutron RBE which will be derived from the physics task in the ANDANTE project. Based on the experience from the feasibility study at LLUMC, a proposal for a prospective epidemiological study using pediatric proton therapy data collected from multiple proton centers world-wide is prepared. For this purpose, published results of epidemiological studies on second malignant neoplasms (SMN) after radiotherapy in childhood are reviewed. Up to now, 57 papers were identified from 2001 until present with the objective to estimate the magnitude of the effect of radiation exposure on the occurrence of SMN. Furthermore, European proton therapy centers were contacted in order to assess the feasibility of creating a prospective database on pediatric patients. Five out of thirteen proton therapy centers already replied, showing great interest in preliminary participation in discussion on forming a future prospective study.

Conclusion: This will be essential for investigating the far reaching goal to enhance our understanding of the link between radiation exposure to proton therapy and the risk of SMNs.

EP-1418

Proton therapy in paediatric oncology – An Irish perspective

K. Lee[1,2], C. O'Sullivan[1,2], M. Capra[2]
[1]*St Luke's Radiation Oncology Network, Radiation Oncology, Dublin, Ireland Republic of*
[2]*Our Lady's Children's Hospital Crumlin, Paediatic Oncology, Dublin, Ireland Republic of*

Purpose or Objective: To: (1) produce a descriptive study of Irish children referred abroad for proton therapy (PT), and (2) to discuss the case for PT in general.

Material and Methods: A retrospective review of all children referred for PT before October 2015 was performed. Information was gathered regarding general demographics, diagnosis, tumour grade, other treatments, the PT referral timeline, relapse where relevant, side effects attributable to PT, current status and cost of treatment to the Irish state. Additionally, a review of the relevant literature was performed.

Results: Sixteen children treated in Ireland have been referred abroad for PT to date, with numbers increasing yearly. The largest number referred was in the 0-4 year old group. At initial diagnosis the median age was 5.0 years. Four patients were referred for treatment of rhabdomyosarcoma, 3 for craniopharyngioma, 6 for intracranial ependymoma and 1 each for treatment of meningioma, germinoma and ATRT. The average cost per child has been approximately €52,000. Two patients suffered relapse of their disease - 1 has proven fatal and the other is alive with disease. Four patients have encountered PT-related adverse effects. The time from referral to treatment has improved from 11 to 6 weeks approx.

Conclusion: Despite the fact that >100,000 patients worldwide have been treated with PT, the current level of published evidence to support superiority over conventional treatment remains low. Planning studies have clearly demonstrated superior conformality and reduced risk to normal tissues. It is debated that randomised control trials in this area would be inconsistent with the principle of *clinical equipoise*. In contrast, there is a call for level 1 evidence to justify such drastic changes in patient care, particularly in the light of recent reports of unexpected toxicities.If PT were more widely available, the question remains in which clinical situations would it be likely to show substantial clinical and cost benefit? As no firm conclusions can be derived from the literature, the answer is somewhat speculative. In time, careful evaluation, follow-up and clinical trials will likely support the argument for the preferential use of proton therapy in children. Our challenge remains: how best to use it in the meantime?

EP-1419

Proton irradiation in childhood and adolescence at RINECKER Proton Therapy Center (RPTC)

R. Richter[1], M. Herbst[1], A. Haidenberger[2], M. Walser[1], I. Teichert- von Lüttichau[3], A. Wawer[3], K. Beutel[3], S. Burdach[3], B. Bachtiary[1]
[1]*Rinecker Proton Therapy Center, Radiation Oncology, Munich, Germany*
[2]*Hospital Agatharied, Radiation Oncology, Hausham, Germany*
[3]*Children´s Hospital of Munich Schwabing/ Technical University of Munich, Paediatric Haematology and Oncology, Munich, Germany*

Purpose or Objective: In the multimodal treatment concept for pediatric tumors the implementation of radiotherapy with protons gains more and more importance due to their outstanding radiobiological, physical and technical characteristics. In particular the fact, that about 60% of the irradiated volume of conventional radiotherapy are not burdened by proton therapy, results in a considerable reduced incidence of side effects with lowering the negative impact on growth and development and a lower rate of secondary malignancies. The German Society for Radiation Oncology (DEGRO) clearly recommends preferably proton therapy in the treatment of pediatric patients.

Material and Methods: Analysis of children and adolescents undergoing proton radiation therapy since start of the RPTC 2009 (time period from Jun 2009 to Sep 2015). A highly complex three-dimensional electromagnetic proton beam control system (spot scanning) can applies the tumor dose only to the planned target volume and spares surrounding healthy tissue without significant neutron exposure to the whole body. There is a wide range of free variety of dose intensity to each spot.

Results: From 06/2009 to 07/2015 a total of 82 patients were previously treated at the RPTC in 88 cases. The mean age at start of irradiation was arithmetically 7.9 years (min. 11mo.; max. 17y. 7mo.). These were mostly rhabdomyosarcomas (RMS; n = 26 [29.5%]), of which 10 were alveolar and 16 were embryonal RMS. In the field of central nervous system, 14 patients with low grade gliomas [16%], 11 high grade gliomas [12.5%], 10 ependymomas [11%] and 2 medulloblastomas were treated. From 12 cases with rare tumor types, 8 were also localized in the CNS. 6 patients had chordoma and chondrosarcoma, 5 Ewing tumors and 2 rare types of soft tissue sarcomas.

Conclusion: At the field of pediatric oncology radiotherapy with protons using spot scanning technology is certainly feasible and a highly effective treatment method with significantly lower toxicity of normal tissue. There is a close cooperation with the Children's Hospital of the Municipal Hospital Munich/ Hospital of Munich Technical University for the integration of multimodal therapy studies or to treat in analogy with rule-based case discussions in interdisciplinary tumor conferences.

EP-1420

Cyberknife® radiotherapy for recurrent or oligometastatic tumours in children and adolescents

S. Gaito[1], F. Saran[1], H. Taylor[1], E. Wells[1], S. Mowat[1], H. Burland[1], C. Jones[1], L. Welsh[1], H. Mandeville[1]
[1]*The Royal Marsden Hospital, Department of Radiotherapy, London, United Kingdom*

Purpose or Objective: Despite the increasing availability of stereotactic ablative body radiotherapy (SABR) and stereotactic radiosurgery (SRS) there remains a lack of evidence regarding their indications and role in the treatment of recurrent & oligo-metastatic tumours in children, teenagers & young adults (TYA).

Material and Methods: A retrospective review of paediatric and TYA patients (age ≤24 years) treated with SRS or SABR at The Royal Marsden Hospital from 2010 to 2015 was

performed. Data collected included: tumour type, technique, dose, number of fractions, prescription isodose, acute and late toxicity (CTCAE v4.0), local control (LC) and progression free survival (PFS).

Results: 12 patients were identified: 8 males and 4 females; median age 14.5 years [5-20 years]. Cranial SRS was delivered to 9 sites in 7 patients, and extracranial SABR was delivered to 8 sites in 5 patients. All patients had a Lansky/ Karnofsky score ≥70. All SABR and SRS treatments were performed using the Cyberknife® platform; 8 treatments prescribed as a single fraction (median dose 19 [18-24] Gy), 4 treatments were given in 3 fractions (median dose 28.5 [27-42]Gy) and 5 treatments in 5 fractions (median dose 30 [30-35]Gy). The median prescribing isodose was 79% [70-81%]. For 5 patients SRS was delivered post surgical resection with no macroscopical residual disease at the time of treatment. The treatment for 9 (75%) patients was to previously irradiated sites. After a median follow up of 14.5 [0.9-36.2] months 9 pts (75%) were alive, 2 died from disease progression and 1 died from unclear cause. MRI response assessment was performed at a mean time of 6 [3-17] weeks; 1 patient had a complete response, 10 had stable disease (83 %); 1 was not assessed due to a rapid clinical deterioration. LC was 100 % and 85.7% at 1 and 2 years respectively. PFS was 82.5% at 1 year and 61.9 % at 2 years. 3 reirradiated patients reported symptomatic grade 3 radionecrosis, requiring medical therapy.

Conclusion: In this cohort, SABR and SRS with Cyberknife® have proven feasible in the subset of paediatric & TYA patients with recurrent or oligo-metastatic tumours. It achieved good local control even in pre-irradiated patients. However optimal patient selection for such a treatment approach remains as yet to be determined via an international consensus.

EP-1421

Radiotherapy for pediatric patients from 2006 to 2015 in a large health care region

E. Waldeland[1], T. Hellebust[2], H. Magelssen[3], P. Brandal[3]
[1]*Oslo University Hospital, Academic Physics, Oslo, Norway*
[2]*Oslo University Hospital, Dep. of Medical Physics, Oslo, Norway*
[3]*Oslo University Hospital, Dep. of Oncology, Oslo, Norway*

Purpose or Objective: Particle therapy is not available in our country yet, however, quite a few patients are sent abroad for such therapy. In the largest health trust, covering a population of 2.9 million, 25-40 pediatric patients (< 18 years) are treated with radiotherapy (RT) yearly. We wanted to analyze this group of patient with respect to RT technique and diagnosis.

Material and Methods: All pediatric patients treated between January 2006 and June 2015 were identified and included. The treatment techniques were categorized as follows: total body irradiation (TBI), whole CNS RT, IMRT/VMAT, stereotactic RT (SRT), 3D conformal RT (CRT), kV RT and extracorporal irradiation (ExCRT). Additionally, the pediatric patients referred for proton RT abroad were registered.

Results: 302 pediatric patients were treated with RT in the period. The mean age at treatment were 11.3 ± 4.6 years. 69 patients (25%) had brain tumors, whereas 50 (18%) and 43 (16%) patients were diagnosed with lymphoma and leukemia, respectively.
The figure gives the distribution of the treatment techniques trough the whole period (upper panel), showing that more than 50 % of the patients have been treated with CRT. The lower panel in the figure shows the distribution in 2006 (left) and 2014 (right), indicating that the proportion of patients receiving CRT has decreased from 50 to 38 %. However, the number of patients only reduced from 18 in 2006 to 15 in 2014. The number of patients treated with advanced techniques (IMRT/VMAT, SRT) did not change significantly. On the other hand, 20 % of the patients were referred for proton RT abroad in 2014, while no one received such treatment in 2006. The number of patients where the whole CNS were treated reduced from 8 (25%) in 2006 to 3 (8%) in 2014.
In the whole period 31 patients (10%) were treated with TBI and the number of patients per year did not changed significantly from 2006 to 2014.

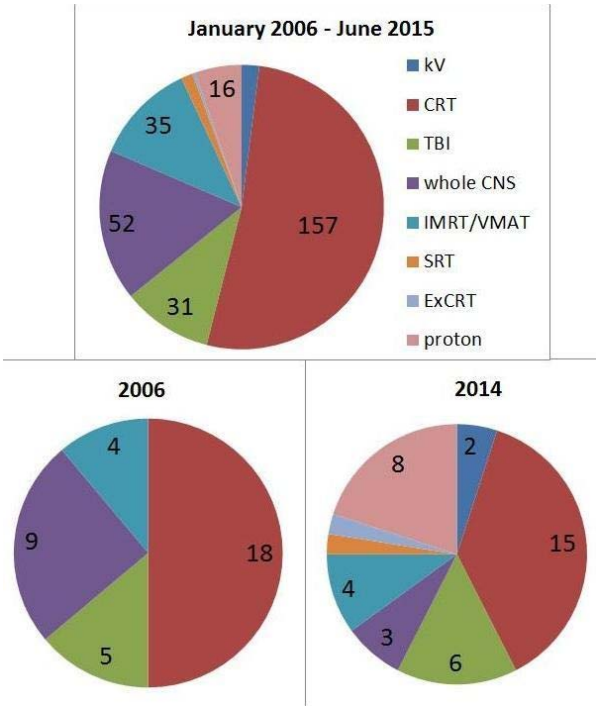

Conclusion: An official agreement was established with proton centers abroad in 2013. The reduction in whole CNS treatment throughout the period is due to this agreement. Except TBI, kV RT and ExCRT, all the other techniques should be replaced with proton RT when such treatment becomes available.

Electronic Poster: Clinical track: Palliation

EP-1422

Contemporary management of bone metastases from breast cancer: Who is getting long course RT?

C. Nieder[1], B. Mannsåker[1], A. Pawinski[1], E. Haukland[1]
[1]*Nordlandssykehuset HF, Dept. of Oncology and Palliative Medicine, Bodoe, Norway*

Purpose or Objective: The Norwegian Breast Cancer Group provides national guidelines regarding systemic therapy for metastatic breast cancer. While our center adheres to these recommendations, use of palliative radiotherapy (PRT) for bone metastases is less standardized. Despite general recommendations for short course PRT for uncomplicated metastases, many physicians prefer ≥10 fractions (long course, LC). Our aim was to analyze factors associated with prescription of ≥10 fractions.

Material and Methods: This retrospective study included 118 female patients (all received systemic therapy including bone-targeting agents in accordance with national guidelines).

Results: Median age was 61 years, and median survival 13 months. Long-course PRT was prescribed in 60% of patients, while 21% had PRT with 8 Gy single fraction to at least one target. Reirradiation rate was numerically higher after 8 Gy (9%, compared to 5% after LC PRT and 6% after 4 Gy x5, not significant). Patients with favorable baseline characteristics were significantly more likely to receive LC PRT. These characteristics included absence of lung metastases and/or

pleural metastases/effusion, normal serum hemoglobin, CRP, LDH and albumin (surrogate markers of disease extent), early PRT within 6 months from diagnosis of metastases, age <65 years, and good performance status (ECOG PS). Biological subtype (Her2 and hormone receptors), comorbidity and reirradiation to a previously treated volume did not correlate with fractionation. Rate of LC PRT remained unchanged over time. In line with imbalances in prognostic factors, survival was significantly longer after LC PRT in univariate analysis. However, after correcting imbalances in multivariate analysis no survival difference was found. Prognosis was influenced by biological subtype (worse for triple negative status), extraskeletal disease extent, presence of anemia and abnormal CRP. Even patients with PS3 had median survival of 3 months, which indicates that they life long enough to experience clinical benefit after PRT.

Conclusion: The likelihood of receiving LC PRT was significantly higher in younger patients, those with good PS, limited disease extent, and shorter time interval after diagnosis of metastatic disease. Educating physicians about these factors might contribute to optimal resource utilization. The limited need for reirradiation after single fraction PRT might encourage physicians to prescribe this convenient regimen, which is also suitable for PS3 patients.

EP-1423

Hypofractionated radiotherapy for complicated bone metastases in patients with poor performance

M. Silva[1], G. Marta[2,3], F. Lisboa[4], G. Watte[5], F. Trippa[6], E. Maranzano[6], N. Motta[4], E. Chow[7]

[1]*Hospital Universitário de Santa Maria, Radiation Oncology, Santa Maria, Brazil*

[2]*Instituto do Câncer do Estado de São Paulo, Radiation Oncology, São Paulo, Brazil*

[3]*Hospital Sírio Libanês, Radiation Oncology, São Paulo, Brazil*

[4]*Universidade Federal de Ciências da Saúde de Porto Alegre, Radiation Oncology, Porto Alegre, Brazil*

[5]*Liverpool Heart and Chest Hospital NHS Foundation Trust, Department of Radiology, Liverpool, United Kingdom*

[6]*"S. Maria" Hospital, Department of Radiation Oncology, Terni, Italy*

[7]*Sunnybrook Odette Cancer Centre, Radiation Oncology, Toronto, Canada*

Purpose or Objective: To evaluate the efficacy of hypofractionated radiotherapy (16 Gy in 2 fractions one week apart) in pain relief in patients with complicated bone metastases and poor performance status.

Material and Methods: This was a phase 2 multicenter study of patients with complicated bone metastases and Karnofsky performance status from 30 to 60 who underwent 2 fractions of radiotherapy with 8 Gy each one week apart. Pain response and quality of life (QOL) were measured using the International Consensus on Palliative Radiotherapy Endpoints and EORTC QOL Pal 15 and BM 22 questionnaires. Complete response was defined as a pain score of 0 at treated site with no concomitant increase in daily oral morphine equivalent (OMED). Partial response was defined as pain reduction of 2 or more on a scale of 0 to 10 scales without analgesic increase, or analgesic reduction of 25% or more from baseline without an increase in pain. Pain progression as an increase in pain score of 2 or more above baseline with stable OMED, or an increase of 25% or more in OMED compared with baseline with the pain score stable or 1 point above baseline, and others were indeterminate. The study was registered on clinicaltrial.gov (NCT02376322)

Results: Thirty patients were enrolled from 4 centres in Brazil, Italy and Canada during July 2014 to September 2015. There were 14 male and 16 female patients. The median age was 58 years old (range 26 - 79). Twenty-two (73%) had extraosseous soft tissue component, 4 neuropathic pain, 2 post-surgical intervention, and 2 impending fracture in weight bearing bone. The most common primary cancer sites were breast (n = 7) and lung/prostate (n = 4 each). The most commonly irradiated areas were lumbosacral spine (n = 10), pelvis/hips (n = 8), thoracic spine (n = 7), cervical spine (n = 3), and superficial bones (n = 2). The median pre-treatment worst pain score was 8 (range 1 to 10) and the median daily OMED was 40 mg (range 0 to 360). The median follow up was 3.7 months (range 0.3 to 9.6). At 2 months, 20 patients were alive (66%). Eleven (55%) had complete or partial response, 4 (20%) progressive disease and 5 (25%) indeterminate response. A statistically significant improvement ($p < 0.0001$) was seen in the painful sites and physical functioning for the BM22 while the other items in BM 22 and C15-PAL remained stable. No patient suffered from spinal cord compression or pathologic fracture, and re-irradiation was not required.

Conclusion: The 2 fractions of radiotherapy with 8 Gy each one week apart appears to be well tolerated without serious side effects in patients with complicated bone metastases and poor performance status. QOL remained stable. The efficacy was similar in patients with uncomplicated bone metastases treated with hypofractionated radiotherapy.

EP-1424

Palliative short-course radiotherapy in rectal cancer: a phase II study.

V. Picardi[1], F. Deodato[1], G. Macchia[1], A. Guido[2], L. Giaccherini[2], M. Nuzzo[1], L. Fuccio[3], D. Cuicchi[3], G. Ugolini[3], A. Farioli[3], S. Cilla[4], F. Cellini[5], S. Cammelli[2], A.F.M.K. Uddin[6], M.A. Gambacorta[5], M. Buwenge[2], T. Salah[7], G. Poggioli[3], V. Valentini[5], A.G. Morganti[2]

[1]*Fondazione di Ricerca e Cura "Giovanni Paolo II"- Catholic University of Sacred Heart, Radiotherapy Unit, Campobasso, Italy*

[2]*S. Orsola-Malpighi Hospital- University of Bologna, Radiation Oncology Center- Department of Experimental- Diagnostic and Specialty Medicine - DIMES, Bologna, Italy*

[3]*S. Orsola-Malpighi Hospital- University of Bologna, Department of Medical and Surgical Sciences - DIMEC, Bologna, Italy*

[4]*Fondazione di Ricerca e Cura "Giovanni Paolo II"- Catholic University of Sacred Heart, Medical Physics Unit, Campobasso, Italy*

[5]*Policlinico Universitario "A. Gemelli"- Catholic University of Sacred Heart, Department of Radiotherapy, Roma, Italy*

[6]*United Hospital Limited, Department of Radiation Oncology, Gulshan- Dhaka, Bangladesh*

[7]*Assiut University, Faculty of Medicine, Assiut, Egypt*

Purpose or Objective: The aim of this phase II study was to evaluate the symptomatic response rate of short course radiation therapy (SCRT) in patients with advanced rectal cancer not amenable for curative treatment and with obstructive symptoms.

Material and Methods: Patients unfit for surgical resection due to synchronous metastases, age and/or comorbidities, were eligible. The sample size was calculated based on the two-stage design by Simon. SCRT was delivered with an isocentric four-field box technique (total dose: 25 Gy; 5 Gy per fraction in 5 days). No chemotherapy was allowed during SCRT. Clinical outcome measures were symptomatic response rate, toxicity, colostomy-free survival and overall survival.

Results: From October 2003 to November 2012, 18 patients (4 females and 14 males; mean age 77.5 years) were enrolled. The median follow up was 57 months (range: 23-132 months). Symptomatic response was: 5.5% no change, 66.7 % partial response, 27.8% complete response. No patients stopped treatment for gastrointestinal or genitourinary toxicities: 27.8% patients had grade 1-2 toxicity and 16.7% had grade 3 toxicity; only 1 patient had haematological grade 2 toxicity. One and 2-year colostomy-free survival were 100% and 71.4% (median: 30 months), respectively. Reduction/resolution of pain and bleeding was 87.5 % and 100 %, respectively. One and 2-year actuarial overall survival were 66.3% and 53% (median: 25 months), respectively.

Conclusion: In this phase II study based on SCRT in patients with symptomatic rectal cancer not eligible for curative treatment an improvement of initial symptoms with

acceptable incidence of side effects was recorded. Furthermore, it was possible to avoid colostomy in a significant proportion of patients.

EP-1425

Phase I study on hypofractionated accelerated radiotherapy for bone metastases from prostate cancer

G. Torre[1], G. Macchia[1], M. Nuzzo[1], F. Deodato[1], F. Labropoulos[1], V. Picardi[1], S. Cammelli[2], J. Cappuccini[2], A. Guido[2], M. Ntreta[2], G. Siepe[2], A. Arcelli[2], G. Compagnone[3], R. Schiavina[4], G. Martorana[4], A.G. Morganti[2]

[1]*Fondazione di Ricerca e Cura "Giovanni Paolo II"- Catholic University of Sacred Heart, Radiation Oncology Unit, Campobasso, Italy*

[2]*S. Orsola-Malpighi Hospital- University of Bologna, Radiation Oncology Center- Department of Experimental- Diagnostic and Specialty Medicine – DIMES, Bologna, Italy*

[3]*S. Orsola-Malpighi Hospital- University of Bologna, Medical Physic Unit, Bologna, Italy*

[4]*S. Orsola-Malpighi Hospital- University of Bologna, Department of Urology, Bologna, Italy*

Purpose or Objective: To define the Maximum Tolerated Dose (MTD) of Middle Half Body (MHB) Radiotherapy (RT) delivered with a conformal 3D technique and twice daily fractionation in prostate cancer (PC) multiple bone metastases.

Material and Methods: A phase I trial was designed with two level of dose: 13 Gy (3.25Gy *per* fraction) and 15 Gy (3.75 Gy *per* fraction). Eligibility criteria were: histological confirmed PC, symptomatic and or impending for fracture multiple bone metastases, ECOG performance status 0-4, expected survival >3 months, and adequate bone marrow function. Radiotherapy was delivered using a 3D conformal technique twice daily in 2 sequential days, with at least 8 hours interval between fractions. Cohort of 6-12 patients were recruited in order to define the MTD (any acute toxicity > grade 3 of RTOG scale). Pain and quality of life were recorded using analogue-visual scales (VAS and CLAS). Clinical target volume was defined as pelvic bones, involved femurs + lumbar spine. Planning target volume was defined as the CTV + 1 cm.

Results: From June 2010 to November 2014, 22 patients (median age 73 years; range 58-86) were enrolled. In Figure 1 treatment volumes are described.

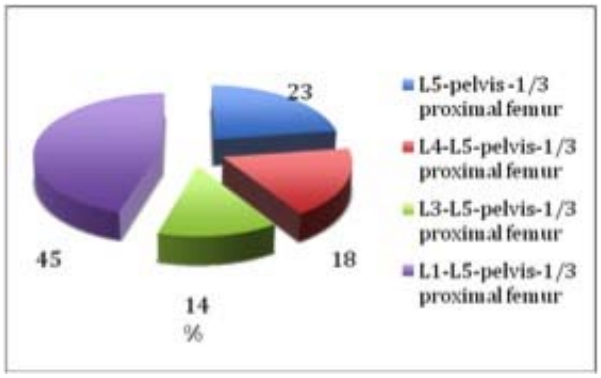

At diagnosis, all patients (100%) reported pain. Clinical pain remission (complete or partial) was observed in 95% of patients. Six patients (27.3%) had a complete symptoms resolution and 15 (68.2%) had a partial symptom control. Pain worsening after radiation treatment was recorded only in 1 patient. On the basis of analogue-visual scales a significant decrease of pain was recorded (mean VAS pre RT *versus* post RT: 4.6 *versus* 3,0; p=0.034; mean pain score pre RT *versus* post RT: 3.1 *versus* 1,9; p=0.069; mean drug score pre RT *versus* post RT: 3.9 *versus* 2,5; p=0.088). Skin and gastrointestinal acute toxicities were only grade 1-2. With a median follow up of 6 months (range 1-26) no late toxicity was recorded.

Conclusion: An accelerated MHB RT treatment with twice daily fraction on bone metastases from PC was well tolerated up to 15 Gy. A phase II study is ongoing to confirm efficacy on pain control and quality of life.

EP-1426

Analysis of treatment response and survival of patients with superior vena cava syndrome (SVCS)

L.G. Sapienza[1,2], A. Aiza[1], B.B. Da Silva[1], R. Fogaroli[1], D.G. Castro[1], M.J.L. Gomes[3], A.C. Pellizzon[1]

[1]*A. C. Camargo Cancer Center, Radiation Oncology, São Paulo, Brazil*

[2]*Clínicas Oncológicas Integradas COI-RJ, Radiation Oncology, Rio de Janeiro, Brazil*

[3]*Hospital Federal dos Servidores do Estado do Rio de Janeiro HFSE-RJ, Radiation Oncology, Rio de Janeiro, Brazil*

Purpose or Objective: To evaluate the factors associated with treatment response (relieve of SVCS) and overall survival.

Material and Methods: Thirty one patients with SVCS between 2012-2015 were analyzed. The end points were: overall survival and SVCS resolution. SVCS resolution was determined as the absence of symptoms related to the compression of superior vena cava. The variables tested were: sex (male vs female), age (<50 years vs > 50 years), primary site (lung vs others), KPS (<70 vs >/= 70), previous palliative RT (no vs yes), BED Gy10 dose (<25 vs > 25), more than 1 year of the initial diagnosis (no vs yes), tumor size (<10 cm vs >/= 10 cm), and number of previous chemotherapy (CT) lines (0 or 1 vs 2 or more), presence of: bone mets (no vs yes), central nervous system (SNC) mets (no vs yes), lung mets (no vs yes), liver mets (no vs yes), lymph node mets (no vs yes) and SVCS resolution (no vs yes).

Results: The mean follow-up time of the patients alive was 376 days (median 241 days). The 6-months and 1-year OS survival were 31.5 % and 18 %, respectively. Factors influencing positively the survival in univariate analysis were: KPS >/= 70 (p=0.001), 0 or 1 previous CT lines (p=0.012), diagnosis <1y (p=0.007), no bone mets (p=0.010), no lung mets (p=0.011), no liver mets (p=0.031) and SVCS resolution (p<0.001). In multivariate analysis only SVCS resolution (p=0.005) remained significant and no lung metastasis was marginally related (p=0.060). The overall SVCS resolution rate was 84% (12/25 cases). Nineteen patient were treated with radiotherapy (RT), four patient with chemotherapy and 2 patients with RT + CT. Six cases receive no treatment (3 because of extremely low KPS and 3 because of the risks of re-irradiation) and were excluded from the efficacy and multifactorial analysis. None of the variables tested influenced the treatment response rate.

Conclusion: Treatment response rate was more than 80 % and it was the strongest factor associated with overall survival. This fact encourages the indication of treatment even in patients with low performance status or previous cervico-thoracic radiotherapy, after a risk-benefit analysis.

EP-1427

Vertebral compression fracture of spinal metastasis from colorectal cancer after radiotherapy

J. Lee[1], W.J. Rhee[1], K.C. Keum[1], W.S. Koom[1]

[1]*Yonsei University College of Medicine, Radiation Oncology, Seoul, Korea Republic of*

Purpose or Objective: The aim of this analysis was to determine the risk of vertebral compression fracture (VCF) following spine radiotherapy (RT) specific to colorectal cancer (CRC) spinal metastases, and to determine clinical predictors

Material and Methods: We retrospectively reviewed 267 spinal segments (176 metastatic and 91 non-metastatic vertebras) in 66 patients, which were irradiated for pain palliation between 2007 and 2014. The primary endpoint was development of a VCF following RT, either a de novo VCF or

progression of a baseline VCF. Each metastatic spinal segment was also evaluated according to the six Spinal Instability Neoplastic Score (SINS) criteria (location, pain, bone lesion type, spinal alignment, posterolateral element involvement, bone lesion type, presence of a baseline fracture) to evaluate the predictive significance.

Results: The median spine RT total dose, dose per fraction, and number of fractions was 30 Gy (range, 8-60 Gy), 3 Gy (range, 1.2-18 Gy), and 10 fraction (range, 1-25), respectively. The median follow-up for the entire cohort was 10 months. Nine percent (23/267) had been previously irradiated, 8% (20/267) had a baseline VCF, and 47% (83/176) were lytic tumor. In all spinal segments, 33 VCF (33/267, 12%) were observed following RT, including 21 de novo fractures and 11 progressive fractures, and the median time to VCF was 4 months. The 1-year fracture free probability (FFP) was 85%. Multivariate analysis identified sex (p = 0.005), metastatic involvement (p = 0.012), prior RT (p = 0.006), and baseline VCF (p < 0.001) as predictors of VCF. Among 176 metastatic spinal segments, we observed 32 fractures (32/176, 18%) with 1-year FFP of 78.1%. Multivariate analysis showed that the risk of VCF in metastatic spine segments was statistically significant in patients with SINS class II/III with or without pre-existing baseline VCF (p < 0.001) and prior RT(p < 0.001).

Conclusion: The risk of VCF is higher in women patients with a baseline VCF and prior RT. Additionally, in metastatic spine segments, the risk of VCF is significant in patients with SINS class II/III with or without pre-existing baseline VCF and prior RT. SINS criteria can be used as an option for predicting VCF risk before performing RT specific to spinal metastases from CRC.

EP-1428

Routine Whole Body MRI of bone metastases may reduce the incidence of spinal cord compression

I. Bhattacharya[1], D.K. Woolf[1], A. Makepeace[1], M. Kosmin[1], A. Makris[1], P. Hoskin[1], A. Padhani[1]
[1]*Mount Vernon Cancer Centre, Clinical Oncology, Northwood, United Kingdom*

Purpose or Objective: Metastatic spinal cord compression (MSCC) is a common oncological emergency resulting in significant morbidity and detrimental functional outcome. Population studies suggest an incidence of 3-7% in men with metastatic castrate resistant prostate cancer. In our centre, therapy monitoring of established bone disease in breast and prostate cancer is undertaken with whole body MRI scanning (WB-MRI). WB-MRI includes a dedicated spinal examination and diffusion weighted sequences that can aid in earlier detection of disease progression or response to treatment. The aim of this cross-sectional hypothesis generating study was to identify if routine WB-MRI reduces the rates of symptomatic MSCC in metastatic breast and prostate cancer patients.

Material and Methods: Patients with metastatic breast and prostate cancer who underwent≥2 WB -MRI scans between 2010-2014 were identified and cross-referenced with patients receiving emergency radiotherapy for symptomatic MSCC. The number of breast & prostate cancer patients, who had ≥2 WB-MRI scans and received emergency radiotherapy for MSCC were recorded.

Results: 63 patients with breast cancer and 89 patients with prostate cancer received emergency radiotherapy for MSCC between 2010-2014. Of the 365 patients with breast cancer who had ≥2 WB -MRI scans, only 1 (0.3%) patient underwent emergency radiotherapy for MSCC. 102 patients with metastatic prostate cancer had≥2 WB -MRI scans of which 2 (2.0%) had emergency radiotherapy for MSCC.

Conclusion: Rates of symptomatic MSCC in this series of patients undergoing regular WB-MRI scans for therapy monitoring of bone disease are low. Routine WB-MRI may aid in the early detection of disease progression in the bones, allowing earlier change in systemic therapy or the use of prophylactic radiotherapy particularly for incipient cord compression. This data generates the hypothesis that WB-MRI may prevent progression of bone disease and development of symptomatic MSCC. This has the caveats that the population studied was selected and in particular had relatively stable disease that permitted the routine use of WB-MRI. It is possible that the morphological spinal MRI examination component, rather than the diffusion weighted sequences, may provide much of the utility of the WB-MRI examination. Further prospective studies are required to confirm our findings.

EP-1429

Phase II study of short-course accelerated palliative radiation therapy for advanced H&N tumours

L. Caravatta[1], F. Deodato[2], J. Capuccini[3], G. Torre[2], A. Farioli[4], M. Buwenge[3], G. Macchia[2], S. Manfrida[5], S. Cilla[6], S. Mignogna[7], W. Tigneh[8], A.F.M.K. Uddin[9], T. Salah[10], D. Dawotola[11], A. Woldemariam[8], P.A. Banu[12], M. Moroni[13], A. Veraldi[3], A. Arcelli[3], F. Bertini[3], S. Cammelli[3], V. Valentini[5], A.G. Morganti[3]
[1]*Centro di Radioterapia e Medicina Nucleare- P.O. Businco, Radiotherapy Unit, Cagliari, Italy*
[2]*Fondazione di Ricerca e Cura "Giovanni Paolo II"- Catholic University of Sacred Heart, Radiotherapy Unit, Campobasso, Italy*
[3]*Radiation Oncology Center - S.Orsola-Malpighi Hospital-University of Bologna, Department of Experimental - Diagnostic and Specialty Medicine - DIMES, Bologna, Italy*
[4]*S.Orsola-Malpighi Hospital- University of Bologna, Department of Medical and Surgical Sciences-DIMEC, Bologna, Italy*
[5]*Policlinico Universitario "A.Gemelli"-Catholic University of Sacred Heart, Department of Radiotherapy, Rome, Italy*
[6]*Fondazione di Ricerca e Cura "Giovanni Paolo II"- Catholic University of Sacred Heart, Medical Physics Unit, Campobasso, Italy*
[7]*Fondazione di Ricerca e Cura "Giovanni Paolo II", General Oncology Unit, Campobasso, Italy*
[8]*Black Lion Hospital, Department of Radiotherapy, Addis Ababa, Ethiopia*
[9]*United Hospital Limited, Radiation Oncology Department, Gulshan- Dhaka, Bangladesh*
[10]*Assiut University, Faculty of Medicine, Assiut, Egypt*
[11]*Radiotherapy and Oncology Center, Department of Radiotherapy, Abuth- Zaria, Nigeria*
[12]*Delta Medical Center, Radiation Oncology Department, Dhaka, Bangladesh*
[13]*Fondazione Seragnoli, Hospice Bentivoglio, Bentivoglio, Italy*

Purpose or Objective: To assess the effectiveness of a SHort-course Accelerated RadiatiON therapy (SHARON) in the palliative treatment of patients with advanced primary or metastatic H&N tumors.

Material and Methods: A phase II clinical trial was planned based on optimal two-stage Simon's design. Eligibility criteria included patients with an Eastern Cooperative Oncology Group performance status of ≤3. Twenty-three patients were treated with H&N radiotherapy at 20 Gy (5 Gy per fraction) in 2 days with a twice daily fractionation. The primary endpoint was the assessment of efficacy in terms of symptoms relief.

Results: Characteristics of the enrolled patients were: male/female: 9/14; median age: 83 years (range: 40-98). Eastern Cooperative Oncology Group performance status was <3 in 11 patients (47.8%). Grade 1-2 acute skin (60.9%) and mucositis (39.1%) toxicities were recorded. Only one patient (4.3%) experienced grade 3 acute mucositis. With a median follow-up time of 4 months (range, 1-32 months) 3 skin grade 1 and 2 skin grade 2 late toxicities have been observed. Of the 23 symptomatic patients, 21 showed an improvement or resolution of baseline symptoms (overall palliative response rate: 91.3%). Three-month overall survival was 89.7% (median survival time: N.R.). Median survival without symptoms

progression was 5.0 months (95%CI: 1.8-8.1). In 22 patients with pain, a significant reduction of this symptom was recorded in terms of VAS (mean baseline VAS vs mean VAS at follow-up: 4.6 versus 3.1, p<0.001).

Conclusion: Short-course accelerated H&N radiotherapy (20 Gy in twice daily fractions for 2 consecutive days) is tolerated and effective in terms of symptom relief. A phase III comparison against a standard palliative regimen (30 Gy in 10 fractions) has been planned in this patient population.

EP-1430

Phase II study of short-course accelerated palliative radiation therapy for advanced thoracic tumors

J. Capuccini[1], L. Caravatta[2], F. Deodato[3], G. Torre[3], A. Farioli[4], M. Buwenge[1], G. Macchia[3], S. Manfrida[5], S. Cilla[6], S. Mignogna[7], W. Tigneh[8], A.F.M.K. Uddin[9], T. Salah[10], D. Dawotola[11], A.A. Woldemariam[8], P.A. Banu[12], M. Moroni[13], A. Veraldi[1], A. Arcelli[1], F. Bertini[1], S. Cammelli[1], V. Valentini[5], A.G. Morganti[1]

[1]*Department of Experimental- Diagnostic and Specialty Medicine - DIMES- University of Bologna, Radiation Oncology Center, Bologna, Italy*

[2]*Centro di Radioterapia e Medicina Nucleare- P.O. Businco, Cagliari, Italy*

[3]*Fondazione di Ricerca e Cura "Giovanni Paolo II"- Università Cattolica del Sacro Cuore, Radiotherapy Unit, Campobasso, Italy*

[4]*S. Orsola-Malpighi Hospital- University of Bologna-, Department of Medical and Surgical Sciences - DIMEC, Bologna, Italy*

[5]*Policlinico Universitario "A. Gemelli"- Università Cattolica del Sacro Cuore, Department of Radiotherapy, Roma, Italy*

[6]*Fondazione di Ricerca e Cura "Giovanni Paolo II"- Università Cattolica del Sacro Cuore, Medical Physics Unit, Campobasso, Italy*

[7]*Fondazione di Ricerca e Cura "Giovanni Paolo II"- Università Cattolica del Sacro Cuore, General Oncology Unit, Campobasso, Italy*

[8]*Black Lion Hospital, Department of Radiotherapy, Addis Ababa, Ethiopia*

[9]*United Hospital Limited, Radiation Oncology Department, Dhaka, Bangladesh*

[10]*Assiut University, Faculty of Medicine, Assiut, Egypt*

[11]*Radiotherapy and Oncology Centre- Abuth- Zaria, Department of Radiotherapy, Abuth- Zaria, Nigeria*

[12]*Delta Medical Center, Radiation Oncology Department, Dhaka, Bangladesh*

[13]*Fondazione Seragnoli, Hospice Bentivoglio, Bologna, Italy*

Purpose or Objective: To assess the effectiveness of a SHort-course Accelerated RadiatiON therapy (SHARON) in the palliative treatment of patients with primary or secondary thoracic neoplasms, symptomatic, and not susceptible of surgery or radical radiotherapy.

Material and Methods: A phase II clinical trial was planned based on optimal two-stage Simon's design. Eligibility criteria included patients with an Eastern Cooperative Oncology Group (ECOG) performance status of 3 and an expected survival > 3 months. Twenty-five patients were treated with radiotherapy (total dose: 20 Gy, 5 Gy per fraction) in 2 days with twice daily fractionation. The primary endpoint was to evaluate symptoms response rate.

Results: Characteristics of the 25 enrolled patients were: male/female: 18/7; median age: 73 years (range: 46-93). ECOG performance status was <3 in 24 patients (96%). Two G1 skin (8%), 7 G1 haematological (28%) and 4 G1 pulmonary (16%) toxicities were recorded. No patient experienced ≥2 acute toxicities. With a median follow-up time of 6 months (range, 1 to 16 months), of the 25 symptomatic patients, 24 showed an improvement or resolution of baseline symptoms (overall palliative response rate: 96%). Three months overall survival was 87.5% (median survival time: 6 months; 95% CI 5.3-6.6 mo). Median survival without symptoms progression was 3 months (95% CI:2.2-3.7mo). In 24 patients with pain, a significant reduction of this symptom was recorded in terms of VAS (5.0 vs 2.9, p=0.02).

Conclusion: Short-course accelerated thorax radiotherapy (20 Gy in twice daily fractions, 2 consecutive days) is tolerated and effective in terms of symptom relief. A phase III comparison against a standard palliative regimen (30 Gy in 10 fractions) has been planned in this patient population.

EP-1431

SBRT for patients with spine metastases using LINAC

Y. Mironova[1], D. Bentsion[1], S. Bayankin[1]

[1]*Regional Oncology Clinic, Radiotherapy, Ekaterinburg, Russian Federation*

Purpose or Objective: Modern technologies of radiotherapy (SBRT,SABR) are utilized to treat patients with solitary spine metastases. Clinical studies have shown the efficacy of image-guided SBRT for pain control, local tumor control, as well as improvement of the life`s quality for these patients. In our clinic we have been using this method since 2013 for primary and re-irradiation treatment.

Material and Methods: We have treated 32 pts (20 primary, 12 reirradiation), 44 lesions. Eligible criteria were ECOG 1-2, spine metastases confirmed by MRI, the number of lesions were less than 3, adequate control of the primary tumor. Mean age 55.8 y.o. (47-72); gender distribution: 12 men and 20 women. Option of the radiation dose and limit critical organs were installed according to the recommendations Elekta Spine Radiosurgery Research Consortium (ESRRC) and RTOG 0631. The prescribed dose was 12-24 Gy in 1-3 fr. For re-irradiation we have used the recommendations of Nieder et al.(2006): BED of each course - 98Gy, total BED -135.5Gy, the interval between two treatments was more than 6 months. In these cases the prescribed dose was 20Gy in 5 fr. The procedure was performed by VMAT on a linear accelerator Elekta Synergy S, equipped with a 4-mm MLC, image-guided system (Elekta XVI), 6D robotic positioning system table (HexaPod). Overall duration of procedures was 20-45 min. The follow-up was every 3 months from treatment time. It was assessed the pain intensity on a 10-point VAS, analgesics, performed MRI control.

Results: Toxicity of SBRT was assessed by using CTC AE (v.4.0). Nausea gr.1 was observed in 3 (9.4%) pts, vomiting gr.1 - 1 (3.1%) pt. Toxicity gr.3-4 has not been observed. There were no cases of therapy interruption due to poor tolerability. Hematological toxicity during follow-up period was not revealed. In average of the period of 3 weeks all patients showed relief of pain syndrome with moderate (4-6 points) to the minimum (1-3 points). The overall response to treatment (decrease of pain syndrome, local tumor control by MRI) was 90.6%, including a complete pain relief - 8 (25%) pts, stabilization - 21 (65.6%), lack of response to the treatment- 3 (9,4%). One patient had a pathological compression fracture of the vertebra at 4 months after irradiation, which required surgical intervention (installation of the fixing system). According to one patient`s MRI after 3 month of treatment, we have revealed soft tissue component of tumor (MRI).

Conclusion: SBRT was well tolerated. We did not observe any clinically significant toxicity. Reduction of the overall treatment time was comfortable for patients and increase capacity of LINAC. Further research is necessary to evaluate the efficacy and toxicity of the treatment and the development of criteria for the selection of patients.

EP-1432

Predicting pain response after conventional radiotherapy in 1018 patients with bone metastases

J.M. Van der Velden[1], H.M. Verkooijen[1], A.L. Versteeg[2], A.S. Gerlich[3], J.J. Verlaan[2], L. Zhang[3], M. Tsao[3], C. Danjoux[3], E. Barnes[3], M. Van Vulpen[1], E. Chow[3]

[1]*University Medical Center Utrecht, Radiation Oncology, Utrecht, The Netherlands*

[2]University Medical Center Utrecht, Orthopedic Surgery, Utrecht, The Netherlands
[3]Sunnybrook Odette Cancer Centre, Radiation Oncology, Toronto, Canada

Purpose or Objective: Many patients with advanced cancer develop bone metastases, with pain as a common, devastating consequence. Adequate treatment is important to maintain quality of life. Radiotherapy is the standard treatment for patients with painful bone metastases. Meta-analyses of radiotherapy trials have consistently shown a pain response rate of approximately 60% implying that many patients are treated insufficiently. It would be worthwhile to identify patients who will not respond to radiotherapy as these patients might be candidates for other treatments. Furthermore, better understanding and identification of the patients who do not respond to radiation, might help in the development of innovative treatments as alternative or addition to standard (radiation) treatment options. We studied the relationship between patient and treatment characteristics and pain response in patients with metastatic bone disease, with the aim to construct a prediction model to guide individualized treatment decision-making.

Material and Methods: We analyzed all prospectively collected data on pain response from a palliative radiotherapy clinic in an academic hospital. Patients were considered responders if they reported a decrease in pain score of at least 2 points with stable analgesic use within 3 months after treatment. A multivariable logistic regression model was developed with age, gender, primary tumor, Karnofsky performance status (KPS), painful localization, presence of visceral metastases, previous systemic treatment, analgesic use at baseline, and baseline pain score. For variable selection, we started with the full model and applied backward stepwise selection with a selection criterion of $p < 0.20$. Performance of the model was quantified using the c-statistic and corrected for optimism. A worst case scenario (assuming no response in patients who were lost to follow up) was added as sensitivity analysis.

Results: A total of 1018 patients treated between January 1999 and November 2007 were included. Outcome was recorded in 588 (58%) patients, of which 394 (67%) reported a response. Primary tumor, KPS, baseline pain score, and analgesic use were predictive for response with a corrected c-statistic of 0.59 (Table). Assuming non-response in the 430 patients without follow up (worst case scenario), there was still an association between response and primary tumor, KPS, and baseline pain score.

Conclusion: Primary tumor, performance status, baseline pain score, and analgesic use are associated with pain response in patients with bone metastases. However, combining these factors in a prediction model showed poor discrimination limiting its use in clinical practice. Response rates after radiotherapy are moderate, and its prediction is difficult, which shows the need for development of innovative treatments for patients with bone metastases.

EP-1433

Comparison of single fraction versus long course RT treating bone metastasis with cobalt machines

O. Spahiu[1], G. Bardhi[1], E. Kozma[1], E. Hafizi[1], E. Karaulli[1], F. Pupuleku Kraja[1], A. Sallaku[1]
[1]"Mother Theresa" University Hospital Center, Department of Radiotherapy- Oncology Service, Tirana, Albania

Purpose or Objective: To present the observed comparative advantages of the single fraction versus long course radiation therapy in the palliative treatment of bone metastasis, in the conditions of technological resources limited to one national center equipped with only cobalt machines.Purpose: To present the observed comparative advantages of the single fraction versus long course radiation therapy in the palliative treatment of bone metastasis, in the conditions of technological resources limited to one national center equipped with only cobalt machines.

Material and Methods: The Radiation Therapy of Mother Theresa University Hospital Center, the unique public center providing RT in the country, performed a study comparing single dose of 8 Gy/1fr. versus 20 Gy/5fr. and 30gy/10fr. enrolling 110 patients during a time period of five years (2007 – 2012). Factors for the treatment choice between available options were age, pain level, effect of narcotics and need for assistance as well as time and cost effectiveness. Pain relief was assessed based on the patient perception expressed during the follow up visits, 2 weeks, 4 weeks and 12 weeks after the treatment and subsequently every 12 weeks for a period of 48 weeks. Qualitative data from the follow up visits were classified in a scale of 10 points.

Results: The complete pain relief was attained for 90 patients or 81.8% out of 110 patients, subject to this study. From this number, 33 patients were treated with single shot, 31 with 20 Gy/5 fraction and 46 with 30Gy/10fr. The percentage of patients benefiting partial pain relief varied from 17.4 to 19.5 which indicate also similar results from the available treatment regimes. Therefore, it wasn't evidenced significant difference between the treatment options as regard to the patients achieving complete or partial pain relief. Further, the toxicity level scored 2-3 grade for all the treatment regimes used. In addition, the patients demonstrated similar median survival from 8 to 10 months for the three options.

Conclusion: The findings of the study indicate that single fraction 800cGy/1fr is a treatment option with similar effects with the multiple fractions 20Gy/5fr and 30Gy/10fr. It can be used as more time and cost effective standard treatment especially for patients presenting higher level of pain and more in need for assistance including elder and those more distant from the treatment centers.

EP-1434

Phase II study of short-course accelerated palliative radiotherapy for complicated bone metastases

G. Torre[1], L. Caravatta[2], F. Deodato[1], J. Capuccini[3], A. Farioli[4], M. Buwenge[3], G. Macchia[1], S. Manfrida[5], S. Cilla[6], S. Mignogna[7], W. Tigneh[8], A.F.M.K. Uddin[9], T. Salah[10], D. Dawotola[11], A.A. Woldemariam[8], P.A. Banu[12], M. Moroni[13], M. Giordano[1], A. Arcelli[3], F. Bertini[3], S. Cammelli[3], V. Valentini[5], A.G. Morganti[3]
[1]Fondazione di Ricerca e Cura "Giovanni Paolo II"- Catholic University of Sacred Heart, Radiotherapy Unit, Campobasso, Italy
[2]Centro di Radioterapia e Medicina Nucleare- P.O. Businco, Radiotherapy Unit, Cagliari, Italy
[3]Policlinico Universitario S. Orsola Malpighi- University of Bologna, Department of Experimental- Diagnostic and Specialty Medicine - DIMES, Bologna, Italy
[4]Policlinico Universitario S. Orsola Malpighi- University of Bologna, Department of Medical and Surgical Sciences - DIMEC, Bologna, Italy
[5]Policlinico Universitario "A. Gemelli"- Catholic Univesity of Sacred Heart, Department of Radiotherapy, Roma, Italy
[6]Fondazione di Ricerca e Cura "Giovanni Paolo II"- Catholic University of Sacred Heart, Medical Physics Unit, Campobasso, Italy
[7]Fondazione di Ricerca e Cura "Giovanni Paolo II"- Catholic University of Sacred Heart, General Oncology Unit, Campobasso, Italy
[8]Black Lion Hospital, Department of Radiotherapy, Addis Ababa, Ethiopia
[9]United Hospital Limited, Radiation Oncology Department, Gulshan- Dhaka, Bangladesh
[10]Assiut University, Faculty of Medicine, Assiut, Egypt
[11]Radiotherapy and Oncology Centre, Department of Radiotherapy, Abuth- Zaria, Nigeria
[12]Delta Medical Center, Radiation Oncology Department, Dhaka, Bangladesh
[13]Fondazione Seragnoli, Hospice Bentivoglio, Bologna, Italy

Purpose or Objective: To assess the efficacy of a SHort-course Accelerated RadiatiON therapy (SHARON) regimen in the palliative treatment of complicated bone metastases.

Material and Methods: A phase II clinical trial was planned based on optimal two-stage Simon's design. Eligibility criteria included patients with an Eastern Cooperative Oncology Group (ECOG) performance status ≤3. The primary endpoint was to evaluate the symptoms response rate produced by a radiotherapy regimen based on the delivery of 4 radiotherapy fractions (5 Gy per fraction) with a twice daily fractionation in two consecutive days.

Results: Twenty-nine patients were enrolled in this trial. Characteristics of the patients were: male/female: 16/13; median age: 66 years (range: 46-87). ECOG performance status was <3 in 25 patients (86.2%). With a median follow-up time of 5.0 months (range, 1 to 36 months), 9 G1-2 gastro-intestinal (31%), 2 G1 haematological (6.8%) and 6 G1 skin (20.7%) toxicities were recorded. Only 1 patient (3.4%) experienced G3 acute gastro-intestinal toxicity. Of 29 symptomatic patients, 27 showed an improvement or resolution of baseline symptoms (overall palliative response rate: 92.6%). Three-month overall survival was 92.2% (median survival time: not reached). In 25 patients with pain, a significant reduction of this symptom was recorded in terms of Drug Score (mean baseline Drug Score vs mean Drug Score at follow-up: 5.3 vs 4.0; p=0.04).

Conclusion: Short-course accelerated radiotherapy on complicated bone metastases (20 Gy in twice daily fractions for 2 consecutive days) is tolerated and effective in terms of symptom relief. A phase III comparison against a standard palliative regimen (30 Gy in 10 fractions) has been planned in this patient population.

EP-1435

Radium223 in castration resistant prostate cancer with bone metastases: preliminary clinical results

G. Zanirato Rambaldi[1], M. Ferioli[1], G.C. Montini[2], P.G. Di Tullio[3], C. Pettinato[4], M. Di Bartolomeo[1], V. Panni[1], A. Ardizzoni[3], M. Marengo[4], S. Fanti[2], G. Frezza[5], A.G. Morganti[1], F. Monari[1]

[1]Radiation Oncology Center- S.Orsola -Malpighi Hospital-University of Bologna, Department of Experimental-Diagnostic and Specialty Medicine-DIMES, Bologna, Italy

[2]Nuclear Medicine Unit - S.Orsola -Malpighi Hospital-University of Bologna, Department of Experimental-Diagnostic and Specialty Medicine-DIMES, Bologna, Italy

[3]S.Orsola -Malpighi Hospital- University of Bologna, Oncology Unit, Bologna, Italy

[4]S.Orsola -Malpighi Hospital- University of Bologna, Department of Medical Physics, Bologna, Italy

[5]Ospedale Bellaria, Radiotherapy Department, Bologna, Italy

Purpose or Objective: More than 90% of patients with metastatic castration resistant prostate cancer (CRPC) have radiologic evidence of bone metastases. Radium-223 dichloride therapy showed improved overall survival, quality of life and symptom control in patients with symptomatic bone metastases. Aim of the present study is to evaluate clinical course of patients treated in our centre including biochemical and imaging response.

Material and Methods: Since November 2014 we started the treatment of symptomatic bone metastatic CRPC patients with Radium-223 dichloride (50kBq/kg, every 4 weeks). Before and after every administration the following parameter were recorded: PSA and alkaline phosphatase (ALP) values, pain numerical rating scale (NRS), performance status (ECOG scale), analgesic therapy and side effects (graded according to the CTCAE v. 4 classification). A whole body scintigraphy was performed before and one month after the treatment.

Results: Twenty patients (total: 70 administrations) were treated. All patients showed increased PSA value and reduced ALP values. Performance status, evaluated with ECOG scale, was improved in all patients. Pain control was excellent, with reduction of NRS and analgesic therapies in all patients. Most patients showed only G1 toxicity: anaemia (15 pts), fatigue (3 pts), diarrhea (1 pt), nausea (1 pt), and pain flare-up (6 pts). Eight patients completed the 6 planned cycles of therapy. Six patients discontinued treatment due to adverse events: anaemia (2 pts), pathological fracture of the femur (1 pt), severe bleeding (2 pts) and complications in uncontrolled diabetes (1 pt). The other patients are still under treatment. Whole body scintigraphy performed one month after the end of the treatment demonstrated in all patients a reduced intensity and number of uptake areas without correlation with PSA values.

Conclusion: Treatment with Radium 223 in patients with CRPC and symptomatic bone metastases was tolerated in the majority of patients. High response rates in terms of symptom control and QoL improvement were recorded.

EP-1436

The superior vena cava syndrome (SVCS): role of the radiotherapy

M.S. Mariaquila Santoro[1], M.L. Marianna Lacaria[1], M.A.M. Maria Angela Molinaro[1], L.R.F. Lucia Rachele Fabiano[1], A.D. Anna Destito[1], N.C. Natascia Costantino[1], V.M. Vita Margheriti[1], D.P. Domenicantonio Pingitore[1]

[1]Hospita Pugliese-Ciaccio, Department of Hemato-Oncology-Operative Unity of Radiotherapy and Radiobiology, 88100 Catanzaro, Italy

Purpose or Objective: To determine the results of 55 patients with Superior Vena Cava Syndrome (SVCS) treated with radiotherapy.

Material and Methods: Between September 2009 and September 2014, 55 patients with SVCS were treated at Operative Unity of Radiotherapy and Radiobiology, "Hospital Pugliese-Ciaccio", Catanzaro. Of these 21 were women and 34 men, with a median age at diagnosis of 61 years (range 33-77 years).The most predominant symptoms were face or neck swelling (85%), upper swelling extremity *(73%), dyspnea (70%), cough (62%), neck and vein distension (45%).* Radiotherapy (RT) has been the only treatment in 6 of 11 patients in which the rapidly progressive symptoms has not allowed to submit to a histologic diagnosis. For the patients which the histo-pathological diagnosis was known and for those in which to effect it, the treatment has included both the chemotherapy and the radiotherapy. The fractionation schedule usually has included initial fractions of 300-400 cGy (2-4 fractions) followed by conventional fractionation of 180-200 cGy. The RT total dose delivered is varied by 2000 cGy to 5000 cGy

Results: With regard radiotherapy delivered, in 5 (9%) of the 55 patient essays we have observed a complete regression of the SVCS, while in 27 (49%) the response has been partial, stability of illness has been underlined in 15 (27%) patients and disease progression in 8 (15%) patients.

Conclusion: In summary, in the SVCS the clinical symptoms often requires an urgent intervention. Survival depend on the status of patient's disease and on the histologic type of the tumor. Radiotherapy is effective in the treatment of the initial SVCS and in the patients that relapsed or with recurrent illness. The radiotherapy produces a good control of the symptoms. There is no necessity of ample fractions in the initial treatment. In the reirradiation, the radiotherapy on mediastinum is one of the most greater components of the palliation. Moreover, in presence laryngeal stridor the radiotherapy can be administered before the histological diagnosis is available.

EP-1437

Radiofrequency, Cementoplasty and Radiotherapy: combined strategy in patients with bone metastases

A. Daidone[1], F. Verderame[2], A. Toscano[3], C. Rinaldi[4], S. Montalbano[5], T. Angileri[2]

[1]U.O Radioterapia Oncologica Villa Santa Teresa, Radioterapia Oncologica, Bagheria, Italy

[2]U.O. Diagnostica per Immagini Villa Santa Teresa, Diagnostica Per immagini, Bagheria, Italy

[3]Istituto Ortopedico Rizzoli, Ortopedia, Bagheria, Italy

[4]U.O. Fisica Medica Villa Santa Teresa, Radioterapia Oncologica, Bagheria, Italy
[5]Servizio di Anestesia, Diagnostica per immagini e Radioterapia, Bagheria, Italy

Purpose or Objective: To evaluate the feasibility and effectiveness of combining radiofrequency (RF), cementoplasty (CP) and Radiotherapy (RT) for pain treatment of bone metastasis (mts) in oligo-metastatic patients (pts).

Material and Methods: From April 2015 to September 2015 twelve pts. (9 men, 3 women; median age 64 years) with 12 injuries to bones (vertebral column n = 9; femur, n = 1; sacrum, n = 2) were treated. Diagnosis of bone mts and then its treatment should be based on the combination of different elements: clinical evaluation, CT, MRI and nuclear medicine patterns. The mini-invasive treatment of oligo-metastatic pts aims pain relief that improving the quality of life; treat biomechanical stability of the spine; and an antineoplastic effect - cytoreductive. RF ablation was performed with the pts under sedation a CT - guidance, and was followed by cement injection. Pain relief was valuated with visual analogue scale (VAS) score. After 10 days on average, the patient was subjected to Stereotactic-RT or Volumetric Modulated Arc Therapy (VMAT) technique and a total dose of 20-30 Gy.

Results: Technical success and pain relief was archived in all pts. Pain rating with the VAS decrease from a mean of 9 to a mean of 4, and after 3 month was detected a mayor decrease (2,5). We recorded an overall improvement in the quality of life measured with a suitable test There was no particular toxicity. At present no patient died for progression of disease.The evolution of the disease will be evaluated with the use of MRI.

Conclusion: Our data showing the importance of a multi-disciplinary approach oligo-metastatic patients. RF with CP and RT carried out by experts is effective for pain relief and functional recovery in patients with painful bone metastases and can significantly improve quality of life.

EP-1438

Radiosurgery to the resection cavity of brain metastasis: Long term efficacity

A. Leysalle[1], J. Doyen[1], K. Benezery[1], F. Almairac[2], D. Fontaine[2], V. Bourg[3], J. Darcourt[4], P.Y. Bondiau[1]
[1]Antoine Lacassagne Center, Radiotherapy, Nice, France
[2]CHU Pasteur, Neuro Surgery, Nice, France
[3]CHU Pasteur, Neurology, Nice, France
[4]Antoine Lacassagne Center, Nuclear Medecine, Nice, France

Purpose or Objective: Few phase II trials have been performed to analyse the efficacy of post-operative stereotactic ablative radiotherapy (SABR) for brain metastases. The aim of the present study was to analyse outcome of this strategy in another cohort.

Material and Methods: Between September 2011 and February 2015 a total of 49 patients (49 lesions) were treated and available for analysis. Eligibility criteria included histologically confirmed malignancy with 1 intra parenchymal brain metastase, age≥18 years, Karnofsky performance status (KPS) ≥70 and controlled extracranial disease. Fourty-two patients have been treated with a single fraction of 18 Gy, and 7 patients with 5 fractions of 5-7 Gy (median dose of 31 Gy) if tumor size was more than 3 cm. SABR treatment was prescribed to the 80% isodose. Survival was evaluated with the Kaplan Meier method.

Results: The median follow-up was 14 months (range, 2-45). SABR to the surgical bed was performed 41 days (13-105) after surgery. Overall, there were 8 local failures (LF) resulting in a 6 months, 1- and 2-year local control rates of 97.9%, 86%, and 74.9%, respectively. The 1- and 2-year overall survival rates were 62.6% and 39%. The 6 months, 1- and 2-year encephalic control rates were 72.9%, 56.7%, and 34.6%, respectively. The Biological Effective Dose, histology, and time interval between surgery and SABR did not correlate with LF in univariate analysis (p> 0.05, Log-Rank).Tumor maximal diameter >3 cm was associated with an increased rate of LF in comparison with smaller tumors (one-year rate LF of 30% vs 7.1%, p=0.02, Log-Rank). Seventy percent of patients died because of extra cranial disease progression while 30 % of patient because of intracranial disease progression. For 14patients with multiple recurrent brain metastases, the whole brain radiotherapy was performed 294 days (126-812) after SABR.

Conclusion: In this cohort postoperative SABR was associated with high rates of local control and encephalic tumor control, especially for brain metastases <3 cm.

EP-1439

Percutaneous pedicle screw fixation for the treatment of unstable spinal metastases

J.J. Verlaan[1], A.L. Versteeg[1], P. De Baat[2], T. Jiya[3], C.H. Diekerhof[4], G. Van Solinge[5], F.C. Oner[1]
[1]University Medical Center Utrecht, Orthopedics, Utrecht, The Netherlands
[2]Catharina Hospital, Orthopedics, Eindhoven, The Netherlands
[3]VU University Medical Center, Orthopedics, Amsterdam, The Netherlands
[4]St. Elisabeth Hospital, Orthopedics, Tilburg, The Netherlands
[5]Isala Clinics, Orthopedics, Zwolle, The Netherlands

Purpose or Objective: Unstable spinal metastases require surgical stabilization often followed by radiotherapy for local tumor control. However, surgical stabilization and radiotherapy are not very compatible treatment modalities. A frequent complication of surgical stabilization after irradiation is disturbed wound healing which can have a devastating impact on quality of life. Advancements in surgical techniques has led to the development of less invasive surgical (LIS) procedures. LIS procedures aim to achieve similar clinical outcomes, as compared with open procedures, but with less approach related morbidity. Additionally, improved wound healing after LIS procedures may allow earlier administration of adjuvant treatments. However, little is known concerning the complications after LIS procedures for the treatment of spinal metastases. Therefore the aim of this study was to determine the incidence and characteristics of complications after percutaneous pedicle screw fixation (PPSF) for the treatment of unstable spinal metastases.

Material and Methods: An ambispective multicentre cohort study of patients who underwent PPSF between 2009 and 2014 for the treatment of unstable spinal metastases was performed. Data regarding demographics, tumor histology, surgical treatment, neurological status, complications and survival were systematically collected.

Results: A total of 101 patients were identified, 45 males and 56 females with a mean age of 60.3 years (± 11.2). The most common primary tumors (in hierarchical order) were breast cancer (25%), multiple myeloma (25%), lung cancer (13%) and renal cell carcinoma (10%). Ninety-three per cent of the patients were neurologically intact at the time of surgery. The median operating time was 122 minutes (range 55 – 325) with a median blood loss of 100 ml (N=41). The overall median survival was 11.0 months (range 0-70 months) with 79 (78%) patients being alive three months postoperative. Eighty-seven per cent of the patients was ambulatory within three days postoperative. A total of 30 complications occurred in 18 patients. Non-surgical adverse events (9%) were most commonly encountered. Wound complications occurred in 4 patients, including 2 deep wound infections with one requiring surgical debridement. Prolonged operating was associated with increased risk of post-operative complications (P=0.041). No relation between the administration of pre- or postoperative radiotherapy and the occurrence of complications could be determined.

Conclusion: A complication rate of 18% was found after less invasive surgery for the treatment of spinal metastases. Promising clinical outcomes were demonstrated in terms of minimal blood loss, high rates of early post-operative ambulation and few wound complications, which may allow earlier administration of adjuvant oncological treatments.

EP-1440

Tokuhashi Scoring and Karnofsky Scale: correlated with prognosis in spinal cord compression?

D. Esteban[1], J.P. Marin[1], I. Prieto[1], A. Idoate[1], W. Vasquez[1], A.M. Pérez Casas[1]
[1]*Hospital Universitario Fundación Jiménez Díaz, Oncologia Radioterápica, Madrid, Spain*

Purpose or Objective: Functional evaluation is crucial in the approach of patients, and the most commonly used functional evaluation tool in cancer patients has been the Karnofsky Scale (KS). A KPS of less than 50% suggests a high mortality risk within 6 months. The Tokuhashi scoring system (TS) is a survival prediction in patients with spinal metastasis. For patients with total TS of 8 or less points, TS predicts a survival of 6 months or less. This study aims to compare KPS and TS for life expectancy in palliative patients with spinal cord compression.

Material and Methods: A sample of 79 patients with cord compression diagnosed from 2007 to 2014 was obtained by consecutive sampling, and KPS and TS were calculated for each patient. The analysis was performed retrospectively, with survival data registered until October 2014. Percentage of patients with KPS≤ 50% and TS ≤ 8 are shown and compared with the survival percentage.

Results: With an average follow up of 4 months (range 0-45), 52.5% of the sample showed KPS ≤ 50% and 80.8% TS ≤ 8. At dead line, 10.3 % continued walking, 2.6 % needed wheelchair, 48.7 % died and 38.5 % were lost in follow up. For patients with follow up, 90% with TS≤ 8 livedless than 6 months and 90% of patients with KPS≤ 50% lived less than 6 months.

Conclusion: Both prognostic scoring systems show similar survival rates in groups KPS≤50% and TS≤ 8%, adding evidence to the Tokuhashi scale as a predictor of survival.

Electronic Poster: Clinical track: Elderly

EP-1441

IMRT in elderly woman with breast cancer: are comorbidities related to toxicity?

A. Fiorentino[1], R. Mazzola[1], N. Giaj Levra[1], S. Fersino[1], R. Francesco[1], R. Ruggieri[1], S. Naccarato[1], F. Alongi[1]
[1]*Sacro Cuore Don Calabria Hospital, Radiation Oncology Department, Negrar, Italy*

Purpose or Objective: To investigate the feasibility, the tolerability and the impact of comorbidity assessment on the compliance of adjuvant Intensity Modulated Radiation Therapy (IMRT) and simultaneous integrated boost (SIB) in elderly patients with a diagnosis of breast cancer after breast-conserving surgery (BCS).

Material and Methods: Between 09/2011 to 02/2014, 40 consecutive women with a diagnosis of early stage breast cancer were treated with SIB-IMRT after BCS in our Institution. Inclusion criteria were: age≥ 70 years, pT1 -2 disease, pN0-1, no neoadjuvant chemotherapy, non-metastatic disease. A dose prescription of 50 Gy in 25 fractions was prescribed to the whole breast (PTVbreast) and an additional dose of radiation on the tumour bed was prescribed (PTVboost). A dose prescription of 60 Gy in 25 fractions to PTVboost was used in patients with negative margins after surgery, whereas if the margins were close (< 1 mm) or positive (without a new surgical resection) a dose of 64 Gy was prescribed. Charlson Comorbidity Index (CCI) was used for comorbidity scoring. All patients were followed with periodic clinical evaluation. Acute and late toxicity were scored using the EORTC/RTOG radiation morbidity score system. Both patient and physician recorded cosmetic outcome evaluation with a subjective judgment scale at the time of scheduled follow-up.

Results: Median follow-up was 36 months. At the time of the analysis, OS and LC rates were 100%. All patients completed the SIB-IMRT without interruptions. Acute skin toxicity was recorded as follow: grade 0 in 5 patients (12.5%), grade 1 in 25 cases (62.5%), grade 2 in 10 patients (25%). Regarding late adverse events, skin toxicity was registered as follow: grade 0 in 27 patients (67.5%), grade 1 in 13 cases (32.5%). No toxicity ≥ grade 2 was registered. At statistical analysis, the presence of comorbidities and the breast volume > 700cc were related to skin grade 2 acute toxicity (p=0.01, p=0.04). In terms of cosmetic results, 98% and 2%of patients considered the result as good /excellent and as fair after RT, respectively. No patients had a poor cosmetic outcome.

Conclusion: These data support the feasibility and safety of SIB-IMRT in elderly patients with a diagnosis of breast cancer following BCS with acceptable acute and late treatment-related toxicity. Moreover, the absence of comorbidity reduced the risk of acute radiation side effects.

EP-1442

Oligometastatic colorectal cancer in elderly patients: role of stereotactic body radiation therapy

D. Franceschini[1], E. Clerici[1], L. Cozzi[1], A. Tozzi[1], C. Iftode[1], C. Franzese[1], T. Comito[1], F. De Rose[1], P. Navarria[1], G.R. D'Agostino[1], E. Villa[1], L. Rocco Luca[1], A.M. Ascolese[1], F. Zucconi[1], M. Scorsetti[1]
[1]*Humanitas, Radiotherapy And Radiosurgery, Rozzano, Italy*

Purpose or Objective: To report about clinical outcome of stereotactic body radiation therapy (SBRT) in the treatment of oligometastatic disease in elderly patients affected by colorectal cancer.

Material and Methods: Patients with 1–4 inoperable metastases were treated with SBRT. Dose prescription ranged from 40 to 75Gy in 3–8 fractions. SBRT was delivered using the volumetric modulated arc therapy technique with flattening filter-free photon beams. The primary end points were in-field local control (LC) and toxicity. Secondary end points was overall survival (OS).

Results: 52 patients with 57 total metastases were treated. Mean age was 79.85 years (range 73.57-88.56). 47 patients (90.4%) had a single lesion; the remaining had 2 lesions. 34 lesions (59.6%) were located in the liver, 18 (31.6%) in the lungs and the remaining 5 (8.8%) were nodal or adrenal metastases. Local response was observed for 35 lesions (61.4%), with 19 complete responses and 16 partial responses, while local progression in 18 lesions (31.6%); stable disease was recorded in 4 cases (7%). Actuarial 1, 2 and 3 year LC was 92%, 78 % and 71%. At time of analysis, with a mean follow up of 2.2 years (range 0.2-4.9), 38 patients (73,1%) were still alive, while 14 (26.9%) died (11 patients died for disease progression). Actuarial 1, 2 and 3 year OS were 98%, 89% and 61,1% respectively. Treatment-related Grade 2 toxicity was observed in two patients (3.8%); Grade 1 toxicity in five patients (9.6%) and no toxicity was observed in 86.6% of the cases. No G3-4 toxicity was recorded.

Conclusion: SBRT is a safe and effective therapeutic option for the treatment of oligometastatic disease in the elderly affected by colorectal cancer with acceptable rates of LC and low treatment related toxicity. The use of SBRT for oligometastatic disease in the elderly can be considered as a valuable approach, particularly for patients with fragile status or refusing other approaches.

EP-1443

Radical hypofractionated VMAT-RA for stage III NSCLC in the elderly: feasibility and toxicity.

A.M. Ascolese[1], D. Franceschini[1], F. De rose[1], L. Cozzi[1], P. Navarria[1], A. Tozzi[1], C. Iftode[1], E. Villa[1], C. Franzese[1], T. Comito[1], G. D'agostino[1], S. Tomatis[1], L. Liardo[1], M. Scorsetti[1]
[1]*Istituto Clinico Humanitas, Radiotherapy and Radiosurgery, Rozzano Milan, Italy*

Purpose or Objective: Purpose: To analyze feasibility and toxicity of radical hypofractionated RT schedules in elderly patients with NSCLC

Material and Methods: Material and methods: Elderly patients (≥70 years old) affected by stage III inoperable NSCLC were treated in our institution with radical IMRT (VMAT RA) according to moderately hypofractionated schedules: 56 Gy/20 fractions or 55 Gy/22 fractions or 50 Gy/20 fractions depending on dose constraints of adjacent organs at risk. Patients underwent simulation CT in supine position, immobilized with a thermoplastic mask. PET CT was performed for simulation and coregistered with CT. Primary end point of this analysis were acute and late toxixcities, secondary end points were local control and overall survival.

Results: Results: 41 patients, treated between January 2013 and April 2015, were included in this analysis. Mean age was 78.59 years (range 70-86). 22 patients were staged IIIA, 19 patients IIIB. All but one patients had pathological nodal involvement (N1:5, N2: 24, N3: 11). Most of patients were unsuitable for chemotherapy for comorbidities and poor general conditions. 15 patients received chemotherapy before RT, concomitant RT-CHT was not allowed. Acute G1-2 toxicity was recorded in 25 patients(61), mostly esophagitis, dyspnea and dry cough. Late toxicity was recorded in 13 patients, the most reported side effects were pneumonitis and dyspnea. No G3 or G4 acute or late toxicity were recorded. A complete response was obtained in two patients, 26 showed a partial response, while progressive disease was recorded in 2 cases. At time of analysis, with a mean follow up of 9.89 months (range 1.08-25.43), 17 patients died for disease progression, one patient died for other causes, 8 patients were alive with distant metastases and 15 were alive without distant progression. Actuarial OS at 1 and 2 years were 51.3% and 35.1% respectively. Mean estimated OS was 15.12 months (range 12.02-18.22). Actuarial local control at 1 and 2 years were 72%. 10 patients experienced local progression. Mean estimated LC was 12.4 months (range 9.6-15.1).

Conclusion: Conclusion: Radical hypofractionated IMRT (VMAT RA) is a valid treatment for locally advanced inoperable NSCLC in elderly frail patients . Our study shows that this approach is safe and feasible also in a fragile elder population. Survival data are satisfactory.

EP-1444

Short-course accelerated palliative radiation therapy for advanced solid cancers in elderly patients

L. Caravatta[1], G. Torre[2], F. Deodato[2], J. Capuccini[3], A. Farioli[4], M. Buwenge[3], G. Macchia[2], S. Manfrida[5], S. Cilla[6], S. Mignogna[7], W. Tigneh[8], A.F.M.K. Uddin[9], T. Salah[10], D. Dawotola[11], P.A. Banu[12], M. Moroni[13], M. Pieri[3], A. Arcelli[3], F. Bertini[3], S. Cammelli[3], V. Valentini[5], A.G. Morganti[3]
[1]*Centro di Radioterapia e Medicina Nucleare- P.O. Businco, Radiotherapy Unit, Cagliari, Italy*
[2]*Fondazione di Ricerca e Cura "Giovanni Paolo II"-Catholic University of Sacred Heart, Radiotherapy Unit, Campobasso, Italy*
[3]*Radiation Oncology Center- S. Orsola-Malpighi Hospital-University Of Bologna, Department of Experimental-Diagnostic and Specialty Medicine-DIMES, Bologna, Italy*
[4]*S. Orsola-Malpighi Hospital- University Of Bologna, Department of Medical and Surgical Sciences-DIMEC, Bologna, Italy*
[5]*Policlinico Universitario "A. Gemelli" - Catholic University of Sacred Heart, Department of Radiotherapy, Roma, Italy*
[6]*Fondazione di Ricerca e Cura "Giovanni Paolo II"-Catholic University of Sacred Heart, Medical Physics Unit, Campobasso, Italy*
[7]*Fondazione di Ricerca e Cura "Giovanni Paolo II"-Catholic University of Sacred Heart, General Oncology Unit, Campobasso, Italy*
[8]*Black Lion Hospital, Department of Radiotherapy, Addis Ababa, Ethiopia*
[9]*United Hospital Limited, Radiation Oncology Department, Gulsha- Dhaka, Bangladesh*
[10]*Assiut University, Faculty of Medecine, Assiut, Egypt*
[11]*Radiotherapy and Oncology Center, Department of Radiotherapy, Abuth- Zaria, Nigeria*
[12]*Delta Medical Center, Radiation Oncology Department, Dhaka, Bangladesh*
[13]*Fondazione Seragnoli, Hospice Bentivoglio, Bologna, Italy*

Purpose or Objective: To assess the efficacy and safety of a SHort-course Accelerated RadiatiON therapy (SHARON) regimen in the palliative treatment of locally advanced or metastatic cancers in elderly patients.

Material and Methods: Eligibility criteria of this analysis (pooled analysis of 3 phase II studies) were: patients with histologically confirmed solid cancers, age ≥ 80 years, patients with an expected survival > 3 months and Eastern Cooperative Oncology Group (ECOG) performance status of ≤ 3. The primary endpoint was to evaluate the symptoms response rate produced by a radiotherapy regimen based on the delivery of 4 radiotherapy fractions (5 Gy per fraction) with a twice daily fractionation in two consecutive days

Results: Twenty-four patients were included in this analysis. Characteristics of the patients were: male/female: 17/7; median age: 87.0 years (range: 80-98). ECOG performance status was < 3 in 16 patients (66.7%). Six patients (25.0%) had locally advanced thoracic cancers, 13 patients (54.2%) had advanced primary or metastatic H&N tumors and 5 patients (20.8%) had complicated bone metastases. With a median follow-up time of 5.0 months (range, 1 to 8 months), eleven G1-G2 acute skin (45.9%) and G1-2 mucositis (12.5%) toxicities were recorded. One patient (4.2%) experienced G1 acute gastro-intestinal toxicity and only 1 patient (4.2%) experienced G3 acute mucositis. Of 24 symptomatic patients, 19 showed an improvement or resolution of baseline symptoms (overall palliative response rate: 79.2%). Three-months overall survival was 89.7% (median survival time: 7.0 months; 95%CI 5.4-8.6 mo). Median survival without symptoms progression was 5.0 months (95%CI: 2.5-7.5 mo). In 23 patients with pain, a significant reduction of this symptom was recorded in terms of VAS (mean baseline VAS vs mean VAS after treatment: 3.9 versus 1.7, p=0.001).

Conclusion: Short-course accelerated radiotherapy in locally advanced or metastatic cancers is effective in terms of symptom relief and well tolerated even in older patients.

EP-1445

The role of radiotherapy in the conservative treatment in bladder cancer elderly patients

M.S. Mariaquila Santoro[1], M.A.M. Maria Angela Molinaro[2], A.P. Armando Pingitore[2], L.R.F. Lucia Rachele Fabiano[2], A.C. Angelo Chirillo[2], L.P. Luigi Perrone[2], E.M. Elvira Mazzei[2], A.S. Angela Saccomanno[2], R.M. Rosa Molè[2], A.D. Anna Destito[2], M.L. Marianna Lacaria[1], D.P. Domenicantonio Pingitore[1]
[1]*Hospital Pugliese-Ciaccio- Via Pio X, Department of Hemato-Oncology- - Operative Unity of Radiotherapy and Radiobiology-, 88100 Catanzaro, Italy*
[2]*Hospital Pugliese-Ciaccio- Via Pio X- 88100 Catanzaro, Department of Hemato-Oncology- - Operative Unity of Radiotherapy and Radiobiology-, Catanzaro, Italy*

Purpose or Objective: The optimal treatment of bladder cancer has been a subject of continuous controversy. In North America, as well as in Europe, the radical cistectomy as the standard option for invasive bladder cancer. In the western countries the elderly ones constitute the part of the population in more rapid growth and, insofar, the group to

taller risk to develop a cancer. The elderly patients, because of the presence of concomitant pathologies, they set to the clinician particular problems and limitations in the therapeutic planning. Several groups have reported the value of combination of conservative surgery and radiochemotherapy or radical radiotherapy alone in patients affected by bladder cancer. In this study we have retrospectively analyzed the prognostic factors influencing survival and relapse free-survival after radiotherapy following transurethral resection (TURB) for bladder cancer.

Material and Methods: Between May 2013 and December 2014, 33 patients with bladder cancer have been treated at the Operative Unity of Radiotherapy and Radiobiology, Hospital of Catanzaro. Of these, 19 patients were treated with radiotherapy alone (RT) and nine with platin based radio-chemotherapy (RCT) after TURB. Overall survival (OS) and Relapse-Free Survival (RFS) were analyzed with the Kaplan and Meyer methods. Comparisons were made using the log-rank test. In the analysis, we proposed the following prognostic factors as affecting the development of relapse after initial treatment: Univariate analysis was performed for age, grade, R-status after initial TURB, T-category relevant to the endpoints initial response, survival and bladder preservation.

Results: Median age was 78 years (range 66-90 years), while the median follow-up is 15 months (range 5-42 months). All patients were treated with three-dimensional conformal therapy (3D-CRT). The total dose of radiotherapy ranged 5040 cGy to 6000 cGy. Complete remissions were achieved at 57% after RT and TURB. Toxicity was acceptable. Further significant prognostic factors were pT-category and R-status. For all patients survival was 31% after 2 years and 25% at 4 years, while the relapse-free survival rates were 19% and 15% at 2 and 4 years, respectively. In the univariate analysis the only significant factor for survival and relapse-free survival and bladder preservation was the R-status after initial TURB

Conclusion: In conclusion, treatment of bladder cancer by TURB and RT alone is an alternative to primary cystectomy, for the elderly patients. Initial TURB is recommended to be as radical as possible.

EP-1446

Multifraction radiotherapy for painful bone metastases in elderly patients: 20 Gy versus 8 Gy

F.M. Giugliano[1], L. Iadanza[2], R. Di Franco[3], D. Borrelli[1], A. Pepe[4], F. Francomacaro[1], P. Muto[3]
[1]*Emicenter, Radioterapia, Casavatore NA, Italy*
[2]*INT "Fondazione G.Pascale", Fisica Medica, Napoli, Italy*
[3]*INT "Fondazione G. Pascale", Radioterapia, Napoli, Italy*
[4]*Studio di Radiologia Prof V. Muto, Radioterapia, Napoli, Italy*

Purpose or Objective: to compare 2 multifraction radiotherapy (RT)schedules in the palliation of painful bone metastases in elderly patients, assessed at baseline with the Cumulative Illness Rating Scale for Geriatrics (CIRS-G).

Material and Methods: 132 elderly patients were analyzed. Seventy-seven patients received a single 8Gy in single fraction and 55 received 20 Gy in 5 fractions. The choice of the treatment schedule was related to comorbidity, disability, target size and compliance. Pain intensity was measured with Numeral Rating Scale (NRS: 0 = no pain; 10 = high pain). Complete response was defined a pain reduction > 3 of three points, partial response as a pain reduction ≥2 (2 ≤ pain reduction ≤ 3), no response was defined by pain score < 2. Pain evaluation was recorded at baseline and at 1-4-8 weeks after completing RT.

Results: overall response: 90.3% in 8 Gy arm (49.8% complete and 40.5% partial), 94.6% in 20 Gy arm (44.6% complete and 50%partial). No high grade toxicity were reported. The relief of pain was attained faster with single fraction (p-value ~ 0.2). We observed maximum response of pain control after 8 weeks and no significant differences were noted between two groups. The re-treatment rate was 17.6% vs 11.1% respectively.

Conclusion: no significant differences between the two arms in terms of pain response, pain control and toxicity. Our experience showed that not influenced by age, but in the elderly, life expectancy, comorbidities evaluated with the CIRS-G, and compliance, are crucial in selecting of shorter treatment.

EP-1447

Lung stereotactic body radiation for oligometastasis treatment in the elderly

L. Larrea[1], E. López[1], P. Antonini[1], V. González[1], M. Baños[1], J. Bea[1]
[1]*Hospital NISA Virgen del Consuelo, Radiation Oncology Department, Valencia, Spain*

Purpose or Objective: To evaluate stereotactic body radiation therapy (SBRT) for oligometastatic lung tumors in patients 75 years old or older.

Material and Methods: Between 2002 and 2015, 24 elderly patients with 34 lung metastases were treated using SBRT at our institution. SBRT procedure involved: Slow-scan computed tomography (CT) simulation with immobilization devices, contouring the target volume in 3 sets of CTs, superimposing the volumes in the planning system to represent the internal target volume and dose calculation using heterogeneity correction. Radiation delivery with multiple static planar or non-coplanar beams and arc therapy assured conformal dose distribution and steep fall-off of the radiation. The prescribed dose was 3 fractions of 15 Gy each (90%) given in 6-10 days or a single 30-Gy fraction (10%), with at least 95 % of the ITV covered by the 95% isodose line. Dosimetric constraints were set for surrounding organs at risk. Repeated cone-beam CT were used to verify daily positioning. Toxicity and radiologic response were assessed in follow-up, using standardized criteria (RTOG and RECIST) and analyzed retrospectively. Survival rates and toxicities were calculated by the Kaplan-Meier method.

Results: Median patient age was 79 years (75-85). The origin of the metastases was: non-small cell lung cancer (53 %), colorectal adenocarcinoma (24 %), urotelial tumors (8.5 %), thyroid carcinoma (8.5 %), endometrial adenocarcinoma (3%) and parotid tumor (3%). All patients had good performance status at the moment of treatment (ECOG PS 0-1). Fifty-six percent of all patients also received systemic treatment before or after SBRT. Mean tumor volume was 10.7 cm3 (0.5-106). The only acute toxicity reported was rib pain, grade 2, in 1 patient. No grade > 3 acute or any chronic toxicities were identified. The median follow-up was 11 months (1-60). The 6, 12 and 18 month overall survivals were 97, 88 and 85 %. Local control in the irradiated volume is 97 %, the only failure occurring in a patient who also had distal progression from colon adenocarcinoma.

Conclusion: SBRT is an excellent treatment option for lung oligometastasis in elderly patients. Our encouraging results are in line with those reported in recent literature for younger patients.

EP-1448

Outcomes and tolerance of larynx preservation treatment in the older population

M. Keys[1], S. Brennan[1], O. McArdle[1], I. Fraser[1], N. El Beltagi[1]
[1]*St. Lukes Radiation Oncology Network, Radiation Oncology, Dublin 6, Ireland Republic of*

Purpose or Objective: Some recent data has questioned the impact of larynx preservation strategy on overall survival. The median age of patients in most major larynx preservation trials was 55-60 years with little representation of the older age group. The aim of this study is to review the tolerance and outcomes of larynx preservation treatment in the older population (≥ 65).

Material and Methods: Data was obtained from the St. Luke's Radiation Oncology Network patient registry. Patients with stage III & IV non-metastatic laryngeal cancer who were fit for radical intervention and offered larynx preservation treatment were identified between 2008-2014. Those who were aged ≥ 65 years at the time of treatment were included in this study.

Results: A total of 68 patients were identified who met the selection criteria. The majority of patients were male (88%) and between 65-74 years, with a median age of 70. Of the patients identified 6% of patients were changed from radical to palliative intent and received a radiation dose of ≤40Gy. Currently, 45% of patients are still alive with 10% having required salvage surgery in the form of total laryngectomy post treatment for local recurrence. Of those studied, 60% of patients received radiotherapy only and 40% received combined chemoradiation. Patients who had combined modality treatment had significant toxicity from chemotherapy related to myelosuppression and febrile neutropaenia. Among those who received chemotherapy 51% did not complete the prescribed chemotherapy course secondary to toxicity. There were 17 patients (25%) who required enteral feeding via a gastrostomy tube and 2 requiring NG feeding during their treatment course.

Conclusion: Patients who are 65 years or greater seem to tolerate combined chemoradiation poorly. The appropriate selection of patients suitable for larynx preservation treatment in this age group is vital in achieving comparable survival and outcomes to the published major trials.

EP-1449

Personalizing cancer care in elder early-breast-cancer patients after conservative surgery

M.D. De las Peñas-Cabrera[1], P.M. Samper Ots[1], E. Amaya Escobar[1], M. Hernández Miguel[1], A. Seguro Fernández[2], R. García Marcos[2], G. Ruíz Galán[2], A.B. Cuesta Cuesta[3], M. De Matías Martínez[3], S. Hoyos Simón[4], M.R. Noguero Meseguer[3]
[1]*Hospital Rey Juan Carlos, Radiation Oncology, Mostoles - Madrid, Spain*
[2]*Hospital Rey Juan Carlos, Radiophysicist, Mostoles - Madrid, Spain*
[3]*Hospital Rey Juan Carlos, Oncology Gynecology, Mostoles - Madrid, Spain*
[4]*Hospital Rey Juan Carlos, Oncology, Mostoles - Madrid, Spain*

Purpose or Objective: To evaluate the use of a new algorithm for making decisions in elderly early breast cancer patients after tumorectomy plus hormone therapy.

Material and Methods: This is a prospective preliminary study stating in June 2014. According to the recommendation of the "Innovation and Best Practices" of the "IDC-Salud health group", a new algorithm to manage elderly (> 70 years) patients with early breast cancer after conservative surgery was designed. This procedure considered the results of the CALGB 9343 randomized trial for counseling patients about the convenience or not to use radiotherapy. Inclusion criteria included patients older than 70 years, early breast cancer (T≤ 2cm, clinical N0), treated by tumorectomy. In order to decide whether or not to indicate external radiotherapy, the new algorithm took into account the following parameter: life expectation estimated by a specialist in Geriatric Oncology using primarily patients' age and the Charlson Comorbidity Index Score. Decision was against to indicate radiotherapy in women fulfilling the following conditions: life expectation ≤ 5 years. Those patients were managed according to both the Canadian nomogram (www.tuftsmedicalcenter.org/ibtr/) which calculates the 10-years local recurrence risk; and the MD Anderson nomogram (www3.mdanderson.org/app/medcalc/bc_nomogram5/index.cfm?pagename=opcs), which calculates the risk of mastectomy at both 5 and 10 years in elderly patients. The criteria to decide whether or not indicate radiation therapy in these patients was based on the calculated reduction in the rate of either local recurrence or mastectomy as follows: ≤ 5% radiotherapy was not indicated; reduction between 5-10% individualize case, reduction≥ 10% radiotherapy should be always indicated. All patients signed a consent form to participate in the study and to assume the risks of local recurrence and/or further mastectomy.

Results: Since June 2014,191 women with breast cancer were attended. 14 for them, (7.3%) were older than 70 years. From them seven fulfill the inclusion criteria (3.6%) and were eligible for the study. They all accepted to be included in the study. Data related to decision making are shown in Table 1 and 2.
After a detailed discussion explaining in depth that the benefits of the treatment was below +/- 5% and the potential risks and side effects, 37.5% (3/7) declined to be treated being surprisingly those who potentially could be more benefited from this therapy as they were at higher risk of recurrence.

Conclusion: Patients fulfilling the criteria represent a low proportion of breast cancer patients. This preliminary study suggests that cultural and psychological aspects should be taken into account when counseling elderly patients with breast cancer in early stages.

Electronic Poster: Clinical track: Health services research / health economics

EP-1450

Incremental radiotherapy treatment complexity: the effect on daily patient treatment times

A. Munshi[1], T. Ganesh[1], B. Mohanti[1]
[1]*Fortis Memorial Research institute, Radiation Oncology, Haryana, India*

Purpose or Objective: Modern day radiation oncologists have multiple options of treatment techniques including 3 D conformal radiotherapy (3 D CRT), Intensity modulated radiotherapy (IMRT) (Step shoot and dynamic) and volumetric modulated arc therapy (VMAT). This study assessed the effect of incremental treatment complexity on patient treatment times and the treatment times for first day and subsequent day treatments.

Material and Methods: From Nov 2014 to Feb 2015, data of all the patients treated in our department with all techniques (3D CRT, IMRT, and VMAT) was analyzed using the Mosaiq system. Treatment time as computed by Mosaiq is the difference between the time at which the patient record is opened in Mosaiq Sequencer for treatment and the time at which the activity is captured after all treatment fields are completed. Treatment time on the first day and subsequent days for each technique was separately analyzed. Data was analyzed using SPSS software.

Results: All timings were recorded in minutes. *First day treatment sessions:* For 18 first day sessions of 3 D CRT, the average treatment time was 30.37 (SD ±11.57). For 81 first day VMAT treatments the average time was 29.49 (SD ± 35.27) while the corresponding time for 5 dynamic and step/shoot IMRT sessions was 13.81 (SD ±7.72). *Subsequent daily treatments:* For 240 sessions of daily treatments of 3D CRT, the average treatment time was 15.53(SD ±12.31). For 2412 daily treatment VMAT sessions, the average treatment time was 15.82 (SD ±15.37). For combined dynamic (117 sessions) and step/shoot IMRT (33 sessions), the average treatment time was 19.62 (SD ± 5.77). Overall daily treatment times were similar for VMAT as compared to 3 DCRT ($p > 0.05$). The difference in treatment times for first day treatment versus subsequent first day treatment were statistically significant for 3D CRT as well as VMAT.($p<0.05$)

Conclusion: More complex radiotherapy techniques like VMAT require nearly same treatment times compared to 3 D conformal techniques on a daily basis. However, first day treatment times for all treatment techniques are significantly

more than their corresponding subsequent daily treatment times. Radiation oncologists need to be cognizant of these issues in everyday management of their patients.

EP-1451

Workflow Management: Impact on the ergonomics of a Radiotherapy department in a developing country

R. Miriyala[1], P. Thakur[1], A.O. Singh[1], A. Gupta[1], B.S. Yadav[1], N. Kumar[1], R. Rattan[1], S. Ghoshal[1]
[1]*Post Graduate Institute of Medical Education and Research, Radiotherapy, Chandigarh, India*

Purpose or Objective: Integration of multiple technical aspects like treatment prescription, planning, delivery and quality assurance is paramount for smooth and efficient functioning of any radiotherapy department. In the developing world, bearing 60% of global cancer burden, efficient management of available resources assumes even greater importance. Workflow management software is a tool available for effective resource management in radiotherapy. The purpose of this audit is to evaluate the impact of implementation of workflow management on the organisational ergonomics of our department.

Material and Methods: Workflow management software (Aria v 11.0™) has been in use in our department since October 2014. Prior to that, on-paper documentation was the predominant mode of communication between physicians and physicists for all forms of conformal treatment planning. Case records of patients who were treated with conformal radiation in the two month period prior to and after the implementation of workflow management were retrospectively evaluated. Proportion of cases for which treatment was started on the day of appointment was taken as a surrogate for work efficiency, which was the primary end point in this study. Other variables, like time available for target delineation (Td), treatment planning (Tp) and plan evaluation (Te) were analysed for different conformal techniques as secondary end points.

Results: Of the 343 cases analysed, 190 were treated before implementation of workflow management (group 1), while 153 were treated after that (group 2). The mean gap between planning CT scans and date of treatment (overall planning time, To = Td + Tp + Te) was 5.25 days for group 1 and 6.53 days for group 2 (p=0.104).
Among 3D-CRT plans, 29% were not started on the day of appointment in group 1, while 20% were not started on time in group 2 (p= 0.13). However, mean time available for planning and evaluation (Tp + Te) increased from 1.3 days in group 1 to 2.8 days in group 2 (p<0.01), without significant increase in overall planning time (To).
In group 1, 71% of IMRT plans were not started on time, while only 27.2% were not started on time in group 2 (p<0.0001). Overall planning time (To) for IMRT decreased from a mean of 9.4 days to 5.9 days, after workflow management (p=0.013), without significant compromise in the time available for planning and evaluation (Tp + Te).
On multivariate analysis, workflow management was an independent factor determining work efficiency (p=0.04) irrespective of the diagnosis, physician or physicist.

Conclusion: Implementation of workflow management resulted in significant improvement in work efficiency, as evidenced by an increase in proportion of cases started on time; this improvement was more substantial for IMRT planning. Time available for planning and evaluation also significantly increased with workflow management. Such improvements in work efficiency are essential for resource management in developing countries.

EP-1452

The impact of individual surgeons on the likelihood of mastectomy in breast cancer

I. Boero[1], A. Paravati[1], R. Matsuno[1], E. Gillespie[1], J. Einck[1], L. Mell[1], J. Murphy[1]
[1]*University of California San Diego, Radiation Medicine and Applied Sciences, San Diego, USA*

Purpose or Objective: Substantial variations exist in the use of mastectomy and breast-conserving surgery (BCS or lumpectomy) to treat invasive cancer. No recent analysis has queried the broader role of individual surgeons play in the decision making process for BCS or mastectomy. The goal of this study was to evaluate the impact of individual surgeons on surgical procedures for definitive treatment of breast cancer in a large cohort of Medicare beneficiaries.

Material and Methods: 36,068 women with non-metastatic breast cancer undergoing primary surgery (either BCS or mastectomy) were identified from Surveillance, Epidemiology, and End Results-Medicare linked database from 2000 to 2009. Medicare claims were used to determine surgery type and provider. Health service area stratified, multi-level, multivariable logistic models clustered by surgeon were used to determine the impact of surgeons on the likelihood of mastectomy while controlling for a patient's clinical and demographic covariates.

Results: 8,327 women were treated with mastectomy. 20.9% of the variation in the likelihood of mastectomy was due to the individual surgeon; 18.8% of this variation in surgery was due to a patient's clinical and demographic status. The median odds ratio, which allows for a direct comparison between the effect of the cluster variable (surgeon) and the odds ratio (OR) of fixed covariates, was 2.43. The only variables with a greater impact than surgeon were regional lymph node surgery (OR 3.0, 95% confidence interval [CI]: 2.79, 3.23) and primary tumor size 2-5 centimeters (OR 2.79, 95% CI: 2.62, 2.97).

Conclusion: Surgeons have a substantial impact on a woman's likelihood of mastectomy for the treatment of invasive breast cancer. Further research should clarify the role of the patient in the decision making process.

EP-1453

Analysis on research and cooperation status of heavy ion

J. Tian[1], Q. Zhang[1], X. Wang[1], H. Zhang[2]
[1]*Gansu Cancer Hospital, Department of Radiotherapy, Lanzhou, China*
[2]*Chinese Academy of Science, Institute of Modern Physics, Lanzhou, China*

Purpose or Objective: To analyze the status of research on heavy ion using the social network analysis methods and analytical methods bibliometric methods.

Material and Methods: We searched PubMed database by ("heavy ion radiotherapies"[Title/Abstract] OR "heavy ion radiotherapy"[Title/Abstract] OR "heavy ion therapy"[Title/Abstract] OR "heavy ion therapies"[Title/Abstract] OR "heavy ion radiation therapies"[Title/Abstract] OR "heavy ion radiation therapy"[Title/Abstract] OR "carbon ion radiotherapies"[Title/Abstract] OR "carbon ion radiotherapy"[Title/Abstract] OR "carbon ion therapy"[Title/Abstract] OR "carbon ion therapies"[Title/Abstract] OR "carbon ion radiation therapies"[Title/Abstract] OR "carbon ion radiation therapy"[Title/Abstract] OR "Heavy Ion Radiotherapy"[Mesh]) OR (("hellion ion"[Title/Abstract] OR "hellium ion"[Title/Abstract] OR neno[Title/Abstract] OR "carbon ion"[Title/Abstract] OR "carbon ions"[Title/Abstract]) AND (Radiotherapy[Title/Abstract] OR radiotherapies[Title/Abstract] OR "radiation therapy" [Title/Abstract] OR "radiation therapies" [Title/Abstract] OR ("radiotherapy" [Subheading] OR "Radiotherapy"[Mesh])),to collect all relevant research on heavy ion. The related software was used to extract the information of author, country, year of publication, publication year,MeSH terms and journal name. SPSS17.0 was used to analyze the frequency and percentage. NetDraw software was used to draw the social network plot.

Results: 907 studies were retrieved, The number of studies on heavy ion were increased from 1975 to 2014, the author

mainly came from Japan, Germany and China,the number of research on carbon ions were more than the number of research on neon ion and helium ion(Figure1); the published paper focused on the clinical research on the effectiveness of heavy ion for cancer,at the same time, heavy ions of animal,tumor cells and equipment design were also concered,30 kinds of tumor were researched.Cooperation degree of different researchers is not enough(Figure1).

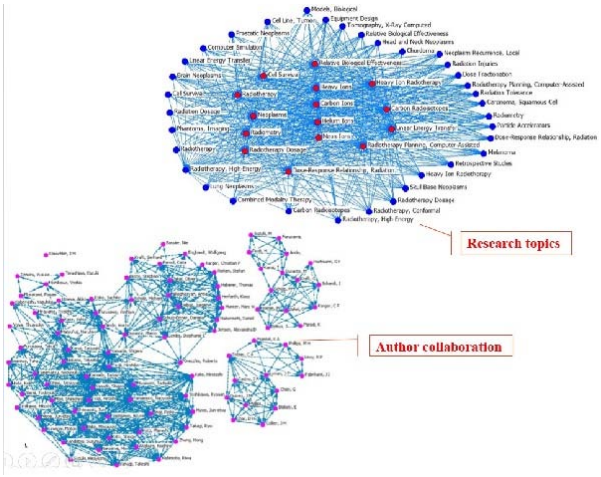

Conclusion: The number of research on heavy ion are increased, but there is an imbalance in regional development,the research topic focused on the clinical research and basic research topics,at the same time, the equipment and design of heavy ion are concered.

EP-1454

Analysis on research status of proton

X. Wang[1], J. Tian[1], Q. Zhang[1]
[1]*Gansu Cancer Hospital, Department of Radiotherapy, Lanzhou, China*

Purpose or Objective: To analyze the status of research on proton using the social network analysis methods and analytical methods bibliometric methods.

Material and Methods: We searched PubMed and EMBASE database by "proton OR proton radiation OR proton beam therapy OR proton beam radiotherapy OR proton irradiation",to collect all relevant research on proton. The related software was used to extract the information of author, country, year of publication, publication year,MeSH terms and journal name. SPSS17.0 was used to analyze the frequency and percentage. NetDraw software was used to draw the social network plot.

Results: 2637 studies were retrieved, The number of studies on proton from one study in 1975 to 556 studies in 2014.Figure shoewd the research in the global distribution.As for different parts of the tumor, mainly for urinary reproductive system tumor (n=349), soft tissue tumor (n=37), skin tumor (n=100), the reticular endothelial cell tumor (n=85), respiratory system tumor(n=232), pelvic tumors (n=10), nervous system tumors (n=531), thoracic and the chest tumor (n=15), the lymphatic system (n=85), the motor system tumor (n=150), the hematopoietic system tumor(n=14), head and neck cancer (n=269), digestive system tumors (n=318), cardiovascular system tumor (n=18), breast tumor (n=211), and abdominal tumor (n=12).As for benign tumors, mainly for epidermoid tumor, epidermoid cyst, ventricle meningioma, cystadenoma, dyeing neoplasia, choroid plexus papilloma, chondroma, cartilage tumor, cavernous hemangioma, inverted papilloma of the mammary gland, mammary gland fibroma and breast fibroadenoma, adenoma and acoustic neuroma.As for type of study, conference abstract (48.24%), conference paper (1.93%) ,study (38.36%), review (7.61%), letter (1.22%) and comments (1.22%), editor's note (0.59%), short-term observation (1%), and conference review(1%).

Conclusion: the number of studies on proton are increased,but the research in the global distribution is imbalance,many studies focuse on the nervous system tumor, urogenital system tumor and digestive system tumor.about 50% published papers were conference abstract/paper.

EP-1455

Impact of the implementation of the radiotherapy workflow optimization software RT-Flow

F. Crop[1], J. Alquier[2], T. Lacornerie[1], Y. Grondin[2], X. Mirabel[3], S. Besson[2], E. Lartigau[3]
[1]*Centre Oscar Lambret, Physics Department, Lille, France*
[2]*Surgiqual Institute, Clinical Applications, Grenoble, France*
[3]*Centre Oscar Lambret, Radiotherapy, Lille, France*

Purpose or Objective: Workflow in radiotherapy involves a lot of different actors and different steps. Subsequently, the management of agendas, schedules and prioritization becomes difficult in a busy department. This results in delays and (first) sessions being delayed or cancelled without being able to be replaced. RT-Flow is a workflow optimization and visualization application (web based), supporting different workflows and clinical prioritization schemes. Our department works with both conventional retro scheduling and industry-based ConWip (management of a Constant Work-In-Progress rather than agendas) workflow [1].

Material and Methods: RT-Flow was implemented in 2014 (3 tomo's, 2 clinacs and 1 cyberknife). All evaluations were performed by year-to-year comparison: between 01/08 of 2013, 2014 and 2015 (+-2500 patients/year). All numbers have been normalized to worked days, excluding breakdowns, holidays and maintenances for fair comparison. Productivity gain was evaluated for the following parameters: machine occupancy and number of first treatment sessions being delayed. Time between CT and prescription finalization has been evaluated before and after implementation of RT-Flow.

Results: Total machine utilization (fractions per worked day, excluding maintenances and failures) rose with >2% in saturated machine conditions. The number of delayed first sessions (all 6 machines combined, all reasons confounded) was halved from 23.6/month to 12.2/month. This was an indirect gain of productivity, as the time slot was most of the time not recovered from late delays. For the specific ConWIP organized Cyberknife, machine utilization raised with 6% (on top of the earlier 30% increase due to the ConWIP organization [1]). This increase was due to the better specific workflow and occupation management by RT-Flow, but also due to a slight change in case mix (3% less liver treatments for example). Mean time between CT and prescription

finalization was reduced by respectively 0.7 and 0.9 days for the conventional and ConWIP (no patient appointment) workflows. The implementation of RT-Flow reduced greatly the delays of MDs generally having prior long delays.

Conclusion: Implementation of the workflow optimization software RT-Flow has reduced the delays and improved productivity, whilst giving users better control over work and better prioritization for patients. Both conventional workflow and ConWip workflows but also personnel stress levels have proven to be improved. Future work will focus on population TCP optimization and booking curves.

[1] Crop, F., Lacornerie, T., Mirabel, X. & Lartigau, E. Workflow optimization for robotic stereotactic radiotherapy treatments: Application of Constant Work In Progress workflow. Oper. Res. Heal. Care 6, 18–22 (2015).

EP-1456

What is the cost of reducing cardiac morbidities when treating breast cancers with radiotherapy?

M. Arunsingh[1], A. Mahato[1], A. Sadhukan[1], R. Achari[1], I. Mallick[1], R.K. Shrimali[1], S. Chatterjee[1]
[1]*Tata Medical Centre, Department of Radiation Oncology, Kolkata, India*

Purpose or Objective: There is no threshold limit for radiation induced cardiac toxicity, making it especially relevant for cardiac sparing radiation delivery in adjuvant breast radiotherapy. Deep inspiratory breath hold (DIBH) technique is one method for reducing the heart dose, however, it is resource intensive. This study analyses the cost of cardiac sparing using DIBH and its associated benefits.

Material and Methods: DIBH technique using Varian RPM, was used to deliver radiotherapy for 50 consecutive patients of left sided breast cancer. The time required in minutes and the number of personnel involved during each step of the planning and the treatment (40Gy in 15 fractions) were recorded. Weighted person hours (WPH) for each step were calculated and all the steps were summed up to arrive at the WPH for each patient. Radiographers, medical physicists and radiation oncologists were given a weightage of 1, 2 and 3 respectively for calculating the WPH. The data was analysed to see if experience reduces the time required. We also calculated the average WPH required for reducing the heart dose by 1 Gy.

Results: The mean age was 51 years. 14 patients were known hypertensive on medications while none of them were known ischemic heart disease patients. Three were suffering from COPD. Twenty nine patients had breast conservation surgery while the remaining 21 patients underwent mastectomy. The mean WPH was 21.49 for the entire cohort. The average mean heart dose (MHD) in the free breathing (FB) technique was 380.96cGy and 160.61cGy in the DIBH technique (p =0.002). Average WPH required for the DIBH planning process was 13.09 and 8.39 for delivery. Patients were divided into 2 cohorts, of 20 and 30 respectively, to assess if practice allowed reduction in DIBH WPH and this showed a decreasing trend of the WPH in the second cohort (22.2 vs 21.0, p=0.36). The average WPH required to reduce the MHD by 2.2 Gy was 22.54 WPH. The average person hours of the oncologist required to reduce the MHD by 2.2 Gy was 0.39 hours, while that of medical physicists and radiographers were 2.89 and 15.9 hours respectively.

	Radiographer	Medical Physicist	Radiation Oncologist
Average Person Hours required for a patient treated by DIBH technique	15.9 person hours	2.89 person hours	0.39 person hours
Formulas Weighted Person Hours = (Weightage x Person involved x Time in Minutes)/60 Person Hours = (Person involved x Time in Minutes)/60			

Conclusion: Although a resource intensive procedure, with practice the time required reduces with experience. On an average 10.25 WPH is required to reduce the MHD by 1 Gy, with 0.18 person hours of the oncologist versus 1.31 person hours of physicist and 7.23 person hours of radiographers time.

EP-1457

Delineation of radiation treatment volumes: a regional network based on the software Radiotherap-e

P. Franco[1], F. Arcadipane[1], J. Di Muzio[1], U. Ricardi[1]
[1]*Ospedale Molinette University of Turin A.O.U. San Giovanni Battista di Torino, Department of Oncology - Radiation Oncology, Torino, Italy*

Purpose or Objective: Modern radiotherapy is able to provide highly precise and focused dose delivery with simultaneous target volume coverage and normal tissue avoidance. Proper selection and accurate definition of treatment volumes is of paramount importance. Anatom-e (Anatom-e Informations System Ltd, Houston, Tx) is a new platform able to drive, simplify, accelerate and standardize the contouring process in different oncological scenarios. Radiotherap-e is an online upgraded version providing the possibility to create an online network to share, discuss, control and optimize clinical cases, radiological images, radiotherapy contours and treatment approaches. We worked on the implementation of the aforementioned software in the Oncological Regional Network of Piedmont, Italy.

Material and Methods: Four pilot centers within the Oncological Regional Network of Piedmont, Italy were connected with the online Radiotherap-e platform. Challenging clinical cases (head and neck, lung, esophageal and rectal cancers) were exchanged within the system (Figure 1). Treatment choices and volume delineation strategies were analyzed and compared before and after the use of the software.

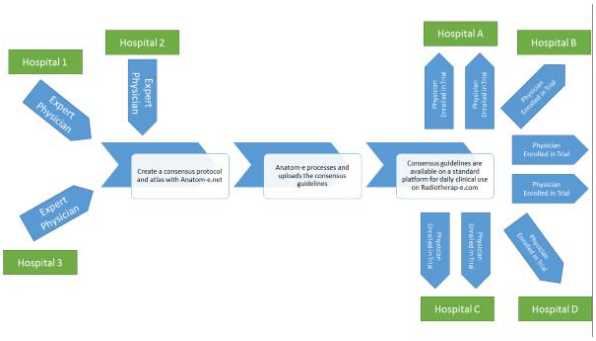

Results: The use of a unified distribution platform was able to eliminate compatibility issues based on different equipment or different treatment planning systems from site to site. Creation of consensus guidelines and common approaches took about 4 hours. Variation of treatment policies and contouring approaches due to platform use is under evaluation.

Conclusion: The online software Radiotherap-e provided a common platform to share clinical, radiological and radiotherapic informations and allowed standardization and optimization of contouring strategies within a regional oncological network.

EP-1458

CBCT-Based On-site Simulation, Planning, and Delivery (OSPD) for whole brain radiotherapy

A. Pompos[1], A. Le[1], R. Timmerman[1], S. Jiang[1], H. Choy[1]
[1]*University of Texas Southwestern Medical Center, Radiation Oncology, Dallas, USA*

Purpose or Objective: To demonstrate the feasibility of a CBCT-based on-site simulation, planning, and delivery (OSPD) for whole brain radiotherapy, in which all steps from imaging, planning to treatment delivery are performed at the treatment unit in one appointment time slot. This work serves as the proof of concept for future OSPD single fraction radiation therapy.

Material and Methods: An integrated on-site imaging, planning and delivery workflow was developed and tested for whole brain radiotherapy. An automated two-opposed-oblique-beam plan is created by utilizing the treatment planning system scripting and simple field-in-field IMRT. The IMRT plan is designed with maximum 8 control points to cover the target volume consisting of the brain to C1/C2 of the spinal cord, with dose homogeneity criteria from -5% to +7% of the prescription dose. Due to inaccuracy of reconstructed Hounsfield unit numbers in CBCT images, the dose distribution is calculated with non-heterogeneity correction introducing only clinically insignificant dose discrepancy. A coherent and synchronized workflow was designed for a team of attending physician, physicist, therapists, and dosimetrist to work closely with the ability to quickly modify, approve, and implement the treatment.

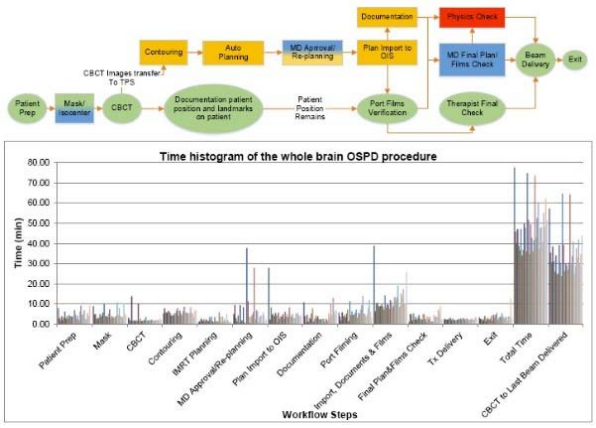

Results: Thirty-one patients have been treated with this OSPD treatment, without compromising the plan quality compared to our regular clinically used parallel apposed 2D plans. The average time for these procedures are 48.02 ±11.55 minutes from the time patient entered the treatment room until s/he exited, and 35.09 ±10.35 minutes from starting CBCT until last beam delivered. This time duration is comparable to the net time when individual tasks are summed up during our regular CT-based whole brain planning and delivery.

Workflow Steps	Time (min) $\bar{x} \pm \sigma$
Preparation/Setup	4.25 ± 2.29
Mask	5.11 ± 2.28
CBCT	2.76 ± 2.59
Contouring	5.89 ± 1.24
IMRT planning	2.28 ± 1.23
MD approval (include re-planning)	5.90 ± 7.86
Plan import, documents & films	12.18 ± 6.34
Plan Import to OIS	5.25 ± 4.49
Documentation	4.27 ± 2.95
Port filming	5.89 ± 2.79
Final plan& films checks	3.56 ± 1.80
Beam Delivery	2.54 ± 0.36
Exiting	3.56 ± 1.98
Total (patient enters and exits)	**48.02 ± 11.55**
Total (CBCT to last beam delivered)	**35.09 ± 10.53**

Conclusion: The OSPD whole brain treatment has been tested to be clinically feasible. The next step is to further improve the efficiency and to streamline the workflow. Other disease sites will be also tested with this new technology.

EP-1459

Testing the self-sufficiency of the Radiotherapy Department of Ospedali Riuniti Marche Nord

F. Maurizi[1], C. Blasi[1], G. Moroni[1], M. Mazza[1], A. Bavasso[1], F. Bunkheila[1]

[1]A.O. Ospedali Riuniti Marche Nord, U.O.C. Radioterapia, Pesaro, Italy

Purpose or Objective: For reasons of logistics in Italy, many public radiotherapy (RT) department deliver treatments to wide geographical areas. It is important that RT capacity is in the right place and that patients (pts) don't have to travel too far for their treatments. The aim of this study is to analyse the mobility for RT involving the RT Department of Ospedali Riuniti Marche Nord (AORMN) naturally devoted to satisfy RT needs of cancer pts living in Pesaro-Urbino (PU) province.

Material and Methods: The Nomogramma di Gandy (NdiG) is a high-level tool which measures the degree to which an area or region is self-sufficient in the delivery of a specified public service. NdiG has been used to diagrammatic represent cancer pts flows for RT at AORMN. District and local datasets were used to obtain the number of local pts being treated by AORMN (Rr), the number of local pts irradiated by other RT Departments (E, "Exported" from an area), and the ones coming from outside that AORMN treated (I, "Imported" into an area). The three data enable to calculate two key indicators: X = The Percentage of Cancer pts Irradiated who were Residents = (Rr × 100) / (Rr + I) Y = The Percentage of Residents Irradiated Locally = (Rr × 100) / (Rr + E), useful to determine the Catchment Population for AORMN = Resident Population × (Y/X).

Results: Between January and December 2013, 646 cancer pts living in PU district and 20 not resident pts were treated by AORMN, while 24 patients residing in PU area received RT by neighbouring RT centres. So during 2013, AORMN coordinates were as follows: X =96,99%, Y=96,42% and Y/X =0,99 (figure 1). Further analysing datasets, 35% of "Imported" pts received IMRT for Head and Neck cancers while the 67% of "Exported" pts underwent Stereotactic Radiation Therapy (SRT) not yet implemented at AORMN (50% stereotactic body radiation therapy and 17% stereotactic radiosurgery for brain metastasis).

Conclusion: AORMN RT Service shows a great deal of self-sufficiency, having values of both X and Y >90%. The degree to which people access their local RT services is important for planning and developing services themselves, thus the use of NdiG to compare access across many geographical areas or across many time periods could be a useful method for planning and commissioning RT centres at a local or regional level. The analysis of patients' flow pattern at AORMN suggests that the implementation of SRT could be useful to further reduce the number of PU users who should travel for RT.

Electronic Poster: Clinical track: Communication

EP-1460

Knowledge, attitudes and decision-making preferences of men considering clinical trial participation

P. Sundaresan[1], S. Tesson[2], B. Ager[2], P. Butow[2], I. Juraskova[2], D. Costa[2], A. Kneebone[3], H. Woo[4], M. Pearse[5], S. Turner[1]

[1]Crown Princess Mary Cancer Center- Westmead, Radiation Oncology, Sydney- NSW, Australia

[2]The University of Sydney, Psycho-Oncology Co-operative Research Group PoCoG, Sydney, Australia

[3]The University of Sydney, Sydney Medical School, Sydney, Australia

[4]The University of Sydney, Sydney Adventist Hospital Clinical School, Sydney, Australia

[5]Auckland Hospital, Radiation Oncology, Auckland, New Zealand

Purpose or Objective: Only 5-10% of cancer patients eligible for randomized clinical trials (RCT) actually participate. The RAVES RCT (Trans-Tasman Radiation Oncology Group 08.03), compares adjuvant radiotherapy with early salvage radiotherapy for men with high risk features after prostatectomy. We aimed to determine attitudes and knowledge of potential participants regarding RAVES and RCTs, and examine decision-making preferences and decisional-conflict in men deciding on RAVES participation.

Material and Methods: Knowledge, attitudes, decisional conflict and preferences regarding participation in RAVES were measured. Predictors of trial and RAVES knowledge were also determined.

Results: 110 men (median age = 63) eligible for RAVES were recruited through urologists (n=90) and radiation oncologists (n=20). Men preferred collaborative (34%) or semi-active (34%) decision-making roles. Most considered RAVES to be worthwhile (85%), important (81%), 'a good thing' (80%), beneficial (73%) and viewed participation as wise (76%), but over half (51%) had high decisional conflict regarding participation. Objective measures of knowledge regarding RCTs and RAVES were low.

Conclusion: Amongst men considering management after prostatectomy, knowledge of RAVES was poor. Despite positive attitudes towards RCTs and RAVES, there was high decisional-conflict surrounding participation. The utility of decisional support materials to increase RCT knowledge and decrease decisional-conflict is under investigation.

EP-1461

Virtual imaging for patient information on radiotherapy planning and delivery

J. Sulé-Suso[1], S. Finney[1], J. Bisson[1], S. Hammersley[1], S. Jassal[1], C. Knight[1], C. Ellis[1], S. Sargeant[2], K. Lam[3], J. Belcher[3], D. Collins[3], R. Bhana[1], F. Adab[1], C. O'Donovan[1], A. Moloney[1]

[1]*University Hospital North Midlands, Oncology Department, Stoke-on-Trent, United Kingdom*

[2]*Bond University, Faculty of Health Sciences and Medicine, Robina, Australia*

[3]*Keele University, School of Computing and Mathematics, Keele, United Kingdom*

Purpose or Objective: To assess whether both patients and their relatives would welcome further information on a one-to-one basis on RT planning and delivery using the virtual reality (VR) system VERT.

Material and Methods: One hundred and fifty patients with a variety of solid malignancies receiving radical RT were included in the study (90 prostate tumours, 52 breast tumours, 4 rectal tumours, 3 lung tumours and 1 thymoma). The study was approved by the local ethics committee. For each study patient, their planning CT Scan images and RT plan were uploaded onto the VERT system using the Digital Imaging and Communication in Medicine (DICOM) standard. Patients and relatives were shown using VERT (Figure 1) and on a one-to-one basis with an oncologist or a radiographer, a standard room where RT is given, a linear accelerator, and how RT is planned and delivered using their own planning CT Scans. Emphasis was put on the area to be treated and the organs around it. At the end of the exercise, patients were asked to fill in a questionnaire to assess their expectations. Radiotherapy was performed using 10 or 6 MV photons delivered from a Varian 2100IX linear accelerator. Treatment planning was performed on the 'Eclipse' system using CT scans.

Results:

The analysis of patients' expectations during the whole process of RT planning and delivery showed that 83.0% (95%CI 76.99% to 89.01%) of patients had a moderate or high need to better understand using 3D imaging how RT is planned, and 83.3% (CI 77.33% to 89.27%) of patients had a moderate or high need to understand using 3D imaging how RT is delivered. Furthermore, 80.6% (CI 74.27% to 86.93%) of patients had a moderate or high need to see the area to be treated using their own CT Scans uploaded onto the VERT 3D system. All respondents cited greater understanding as a positive outcome of the exercise. Patients welcomed this information as it helped them to reduce their fears about RT. Relatives felt also more involved in the treatment of their loved one.

Conclusion: Providing this information using 3D imaging systems rather than 2D helped patients and relatives to better understand the complexity of RT planning and delivery, and reduced their anxieties. The results obtained in this pilot study show that VR aids could become an important tool for delivering information on RT to both patients and relatives, hence, improving patients' experience and satisfaction. Further work is needed to assess whether such approaches improve patients' compliance with treatment and whether it could ultimately impact on treatment outcome.

EP-1462

Effects of education using Youtube about radiotherapy process for cancer patients

J. Heo[1], M. Chun[1], Y.T. Oh[1], O.K. Noh[1], J. Kim[2]

[1]*Ajou University School of Medicine, Radiation Oncology, Suwon, Korea Republic of*

[2]*Dankook University College of Medicine, Radiation Oncology, Cheonan, Korea Republic of*

Purpose or Objective: The patient's understanding about radiotherapy process is necessary for safe and accurate delivery of radiation. We developed an education video about radiotherapy process. The purpose of this study was to evaluate the effectiveness of the education contents using YouTube.

Material and Methods: An eleven minutes video was developed instructing whole radiotherapy process including consultation, simulation, radiotherapy treatment planning, verification and irradiation. After consultation for radiotherapy, each patient was required to see the video posted on YouTube through provided lab-top or tablet PC in our clinic. The questionnaire about patient satisfaction with the video and knowledge of radiotherapy was carried out by interviewing after watching video. Also, set up error was measured at the first week of verification process.

Results: In clinic setting, twenty patients who visited to radiation oncology clinic and watched video were enrolled in the study. Of 20 participants, 11 (55%) rated the video as

'recommended' and 15 (75%) responded that the video was 'helpful to understand radiation treatment'. After watching the video, average set up error at the first verification process was significantly decreased compared to the historical values of 124 patients (1.6 mm versus 2.2 mm, p = 0.03). In web, two thousand two hundred people globally viewed YouTube videos about radiotherapy.

Conclusion: Implementation of education video instructing the radiotherapy process helped to increase patient safety. Education based on YouTube could be an effective method for cancer patients.

Electronic Poster: Clinical track: Other

EP-1463

Stereotactic body radiation therapy (SBRT). Outcomes and toxicities

A.A. Diaz Gavela[1], E. Del Cerro Peñalver[1], F. Marcos Jimenez[1], F. Couñago Lorenzo[1], J. Castro Novais[2]
[1]*Hospital Quiron Madrid, Radiation Oncology, Pozuelo de Alarcon- Madrid, Spain*
[2]*Hospital Quiron Madrid, Radiophysics, Pozuelo de Alarcon- Madrid, Spain*

Purpose or Objective: Stereotactic body radiotherapy (SBRT) is evolving into a standard of care in cancer management and consists in giving high doses of radiation to tumor deposits in extracranial locations. The objective of our study is to show our results in terms of toxicity and local response after implementing the technique in our department.

Material and Methods: Between May 2012 to August 2015, 120 patients (170 lesions) with body metastases or primaries of varying histologies were treated with SBRT. We evaluated acute (<3months) and late (>3months) toxicities as well as the response of the treated lesions. 26 patients were treated with a linac-based 3D conformal SBRT planning and 2 lesions with static IMRT. The other 142 lesions received a Volumetric Modulated Arc Therapy (VMAT) treatment using RA (Rapid Arc), 83 with flattening filter and 59 were treated without flattening filter (flattening filter free beam- FFF).

Results: The mean age of patients was 60 years (26-87) and the median follow-up was 8 months (1-33). The most common histology was non-small cell lung cancer and the most frequent localizations of the treated lesions were bone (31.7%), lung (both metastases and primary, 22.2%), liver (17.1%) and lymph node metastases (14.7%); other localizations: 14.3%. Administered dose and fractionation varied significantly depending on the size and location of each lesion and its anatomic relationship with adjacent organs at risk, ranging from one to ten fractions and 8 to 60Gy. The median volume of the PTV was 42.50cc (0.89-259.08cc). In relation to the local response, we found 74.7% of complete or significant responses, 15.8% of minor responses or stability, 2.4% progressions and 7.1% pseudoprogressions. Acutely, the most frequent toxicities were fatigue and bone flair. There were no grade 4 toxicities and we identified only one grade 3 acute asthenia. Chronically, the most frequent side effect was bone pain (3.3%).

Conclusion: Our series confirms excellent local control with a low rate of side effects when treating extracranial metastases with SBRT. Longer follow-up is necessary to assess whether the local response is maintained over time and to identify the factors related to SBRT treatment that may influence overall survival.

EP-1464

Protontherapy or photodynamic therapy in the treatment of circumscribed choroidal haemangiomas

J. Thariat[1], C. Maschi[2], C. Franceschetti[2], S. Baillif[2], G. Angellier[1], M. Peyrichon[1], J. Herault[1], J. Caujolle[2]
[1]*Centre Antoine Lacassagne, Department of Radiation Oncology, Nice, France*
[2]*Hospital Pasteur 2 - Nice Teaching Hospital, Ophtalmology, Nice, France*

Purpose or Objective: To compare the results of low dose protontherapy and photodynamic therapy (PDT) for the treatment of circumscribed choroidal haemangiomas (CCH).

Material and Methods: 48 patients (48 eyes) eyes with CCH were referred, treated between 1994 and 2014 and followed in our clinic. A historical series of 20 patients treated with protontherapy since 1994 was compared to 28 patients treated with photodynamic therapysince 2006. Tumor and functional outcomes were compared. Chi-squared or Fisher's tests were used to establish differences between discontinuous variables. Student t-test or the Mann-Whitney U test was used to compare continuous variables. The Spearman test was utilized for correlations.

Results: Groups were comparable for patient (age, gender) and disease (size, baseline complications and visual acuity) characteristics but neither macular location (16/20 for protontherapy, 9/28 for PDT, p 0.02) nor initial thickness (higher in the protontherapy group, p 0.02). Mean follow-up was 35 months (48 for protontherapy, 24 for PDT p 0.001).There was a higher rate of retreatment for relapse and complications with PDT than protontherapy (p 0.044 and 0.006, respectively).There was a non-significantly higher gain in visual acuity with protontherapy than PDT. There was a mean 67% and 32% thickness decrease with protons and PDT (p 0.002).

Conclusion: Considering that protontherapy is more invasive due to clip placement and uses ionizing radiations, it cannot be advocated as a first hand option. However, initially promising results with PDT are challenged by protontherapy and the current series suggest that protontherapy should be proposed after first failure to PDT. Prospective trials are warranted to compare the two options as first treatment.

EP-1465

Early dupuytren's: superficial radiotherapy offers long-term resolution without hand surgery

J.P. Glees[1]
[1]*Cancer Centre London- Parkside Hospital, Radiotherapy Department, London, United Kingdom*

Purpose or Objective: First independent Audit to show that giving superficial radiotherapy (100KV Photons) is effective. Majority of cases (94%) did not require subsequent hand surgery.

Material and Methods: During the period 2010 to 2015, over 150 patients were treated by one Radiotherapist using the European treatment protocol of 10 treatments given over a 2 to 3 month period (5 fractions over 1 to 2 weeks followed by 2-month gap and then, the 5 treatments are repeated. Total applied dose of 30Gy). Each patient's disease is photographed before and after treatment, the palpable disease having been marked on the hands and feet in order to clearly show benefit achieved.

Results: Independent Audit of a detailed questionnaire sent to patients showed 94% were satisfied with results up to 4 years post treatment. Satisfaction composed of regression of disease in hands and feet and/or no further progression of the disease.

Conclusion: Superficial radiotherapy is a highly effective and inexpensive treatment of Dupuytren's, provided that patients are referred during the early stages of the disease. Patients are able to continue normal use of hands (and feet) throughout the treatment, so their daily lives are not altered. General Practitioners, hand surgeons and affected patients should be made aware of the good results achieved by radiotherapy, without significant morbidity.

EP-1466

Radiotherapy combined with steroids for Graves' ophthalmopathy: role of magnetic resonance imaging

T. Suwa[1], Y. Negoro[1], T. Fuji[1], T. Iburi[2]
[1]*Tenri Hospital, Radiology, Tenri, Japan*
[2]*Tenri Hospital, Endocrinology, Tenri, Japan*

Purpose or Objective: To review our outcomes for patients in the active inflammatory phase of moderate-to-severe Graves' ophthalmopathy (GO) treated with combined systemic pulsed corticosteroids plus irradiation and demonstrate the role of magnetic resonance imaging (MRI) as a prognostic factor.

Material and Methods: From our database of 35 patients treated with radiotherapy for the active inflammatory phase of GO in our hospital from January 2005 to December 2013, 5 patients were excluded from the analysis because they had a short follow-up, were not treated with pulsed corticosteroids because of liver failure, or had no eye muscle impairment at diagnosis. In the remaining 30 patients in the active inflammatory phase of moderate-to-severe GO treated with combined pulsed corticosteroids plus irradiation, we assessed eye muscle impairment using the SPECS system before and 6 months after the start of treatment. A total dose of 20 Gy in 10 fractions was delivered to the bilateral retrobulbar volume. Intravenous 1 g of corticosteroids daily for 3 successive days was repeated weekly up to 3 weeks. The thickness ratio (TR) of the enlarged eye muscle to the optic nerve and the signal intensity ratio (SIR) of the eye muscle to the cerebral white matter were evaluated as the mean of three cross sections of coronal short-time inversion recovery (STIR) sequence MRI to investigate whether these factors could predict the reversibility of eye muscle impairment.

Results: This study included 10 men and 20 women with median age of 55.5 (range, 37–71) years. The thyroid function at the time of irradiation was euthyroid in 26 patients, hyperthyroid in 2, and hypothyroid in 2. Median duration of eye symptoms from onset to the initiation of radiotherapy was 4 months (range, 1.4–22.1 months). Six months after radiotherapy, there was a significant improvement in eye muscle impairment ($p < 0.001$); complete regression was observed in 10 patients (33%), partial regression in 5 (17%), no change in 14 (47%), and progressive disease in 1 (3%). The median TR was 4.1 (range, 0.4–16.4), and the median SIR was 2.45 (range, 1.7–4.1). There was a trend toward greater, but not significant, improvement in patients with a low TR (<4.2) or high SIR (>2.5) before treatment.

Conclusion: Orbital irradiation combined with pulsed corticosteroids was an effective treatment for the active inflammatory phase of moderate-to-severe GO, especially in patients with a low TR or high SIR on MRI before treatment. A low TR or high SIR may predict the treatment outcome.

EP-1467

Second neoplasms after radiotherapy treatment: a population-based study

M. Arenas Prat[1], L. Castellà[1], R. Botella[1], G. Fliquete[1], M. Arquez[1], M. Carulla[2], A. Rovirosa[3], A. Besora[4], S. Sabater[5]
[1]*Hospital Universitari Sant Joan de Reus, Radiation Oncology, Reus, Spain*
[2]*Fundació Lliga per a la Investigació i Prevenció del Càncer FUNCA, Tarragona Cancer Registry, Reus, Spain*
[3]*Hospital Clínic, Radiation Oncology, Barcelona, Spain*
[4]*Institut d'Investigacions Sanitàries Pere Virgili, Statistics Unit, Reus, Spain*
[5]*Complejo Hospitalario Universitario Albacete, Radiation Oncology, Albacete, Spain*

Purpose or Objective: The radiotherapy treatment can produce a possible new second primary cancer, but metachronous malignancies can also appear without any relationship with radiotherapy treatment. We have studied the risk of developing a potential radiotherapy induced second cancer.

Material and Methods: We analyse the new second cancers after a radiotherapy treatment for a primary cancer in a population-based study in a province of Spain from 2000 to 2011.

Results: The number of patients (pts) with cancer treated with radiotherapy during this period was 14131, 2989 were breast cancer, 2197 were prostate cancer and 1220 pts were rectal cancer. Three hundred and thirteen (2.2%) patients developed a second cancer after a primary cancer treated with radiotherapy. In relation to the primary cancer, the most frequent were prostate cancer (70 pts, 22.4%), the second breast cancer (43 pts, 13.7%), the third colorectal cancer (40 pts, 12.8%), the fourth skin cancer (36 pts, 11.5%) and the fifth larynx (24 pts). The others were bladder (20 pts), oropharynx (7), endometrial cancer (6), etc. The most frequent of second cancer location was lung cancer (63 cases, 20.1%), the second colorectal cancer (43 cases, 13.7%), the third larynx and oral cavity and pharynx (40 cases, 12.8%), breast (34, 10.9%), prostate (28, 8.9%), bladder (19.6%). The location more frequent after a prostate cancer irradiation is lung (20 pts) and colorectal (17 pts, 9 rectal and 8 colon) and bladder (8). The location more frequent in after a breast cancer irradiation is another breast cancer (21 pts). Colorectal 40 pts: 9 second colorectal, 8 lung cancer. Non-melanoma skin cancer 36 pts: 8 second non-melanoma skin cancer, 6 rectal cancer and 4 lung cancer. Larynx 24 pts: 7 lung cancer, 4 prostate cancers.

Conclusion: The percentage of pts treated with radiotherapy who developed a second cancer after 11 years is 2.2% in our series. It's difficult to know the real probability for developing a second cancer associated with radiotherapy. The higher percentage of primary tumour with second cancer was rectal cancer (40/1220, 3.27%), the second was prostate cancer (70/2197, 3.18%), the third was breast cancer 43/2989, 1.43%). We'll present the results about the location of second cancer, the time between the primary and the second cancer, and some characteristics about the radiotherapy treatment (total dose and other dosimetric characteristics).

EP-1468

Prospective audit showing improved patient-assessed skin toxicity with use of betamethasone cream

S.C. Erridge[1], M. McCabe[1], M.K. Porter[1], P. Simpson[1], A.L. Stillie[1]
[1]*Edinburgh Cancer Centre- Western General Hospital-, Clinical Oncology, Edinburgh, United Kingdom*

Purpose or Objective: For many years Edinburgh Cancer Centre's radiotherapy skin care policy recommended aqueous cream and, if required, 1% hydrocortisone. However, it was increasingly appreciated that better alternatives existed so in 2015, a review of the literature was performed, and a new skincare policy developed based on:
1) Low Risk (treatment only if symptoms),
2) Medium Risk (Diprobase moisturising cream),
3) High Risk of developing radiation dermatitis (Diprobase & betamethasone valerate 0.1% applied once daily from 1st fraction till 14 days after treatment). The High Risk group included patients with breast, head and neck, anal, or pelvic cancers when body mass index >35 kg/m2.
As concerns were raised about the increased cost and potential extent of the clinical benefit, a prospective audit was conducted.

Material and Methods: For one month prior to the change of policy (cohort 1, C1), all patients in High Risk group completed a questionnaire at the end of their course of radiotherapy, scoring (categorical 0-10) their skin reaction for redness, itch, discomfort and pain, and asking what creams and analgesia they were using, and if the reaction disturbed their sleep. The audit was repeated for cohort 2 (C2) four months after the policy changed and the two groups compared using Chi-squared and ANOVA.

Results: C1 = 109 patients (84 with breast cancer, 13 H&N, 12 pelvis), C2= 104 (87B, 12H&N, 5P). In C1 27% used a cream and in C2 96% used a cream (p<0.001). In C2 88/104 complied with policy using the prescribed betamethasone.
Compared to C1, for C2 the mean score was lower for itch (1.3 (0.8-1.8) v 2.8 (2.2-3.4) p<0.001) and discomfort (2.2 (1.7-2.7) v 3.1 (2.6-3.7) (p=0.021), and when betamethasone was used (comparing the 88 from C2 with 125 from C1 or C2) the mean score was lower for itch (0.9 (0.5-1.4) v 2.9 (2.3-3.4) p<0.001), discomfort (2.0 (1.4-2.5) v 3.2(2.6-3.7) p<0.003), and for pain (1.4 (0.9-1.9) v 2.2 (1.7-2.7) p=0.03).
With the use of betamethasone, the frequency of a score of >5 was lower for redness (15% with v 34% without) p=0.002), itch (7% v 25%, p =0.001), discomfort (9% v 22%, p=0.015), but not for pain (9% v 14%, p=0.29). However, sleep disturbance was less common (7% v 21%, p=0.006), as was the use of analgesia (7% v 19%, p=0.015).

Conclusion: The introduction of routine use of prophylactic betamethasone cream for patients with a high risk of radiation skin reaction resulted in a significant reduction in redness, itch, discomfort, sleep disturbance, and on use of analgesia

EP-1469

Survey on the use of complementary and alternative medicine in a German radiooncology department

S. Lettner[1], K.A. Kessel[1,2], S.E. Combs[1,2]
[1]*Technische Universität München TUM, Department of Radiation Oncology, München, Germany*
[2]*Institute of Innovative Radiotherapy iRT, Helmholtz Zentrum München, München, Germany*

Purpose or Objective: The use of complementary and alternative medicine (CAM) continuously gains importance, even though objective data are mostly missing – also in radiation oncology. However, in previous trials methods such as acupuncture showed significant advantages compared to standard therapies. Hence, the aim of this study is to evaluate the most frequently used methods, their significance and potential effect during radiotherapy (RT), as well as the general acceptance amongst cancer patients.

Material and Methods: A detailed questionnaire was developed consisting of 18 questions based on the categorical classification released by the National Centre for Complementary and Alternative Medicine (NCCAM). From January to September 2015, the survey was conducted with all patients undergoing RT at the department of Radiation Oncology, Technische Universität München (TUM), Klinikum rechts der Isar, Munich. Participation was voluntary and pseudonymous.

Results: Of 571 patients, 289 answered the questionnaire (50.6%), with 44.6% females and 38.4% males participating in the study, and a mean age of 60 years. Of these, 66.1% (191/289) received RT only, 20.4% (59/289) had a combined radio-chemotherapy (RCT). Of all participants, 25.9% (75/289) used CAM parallel to RT. Before RT, a total of 40.8% (118/289) had already used complementary medicine. The current most frequently applied methods were vitamins, dietary supplements, homeopathy and physical therapy, whereas in the past before RT also acupuncture and osteopathy had been regularly used. The majority (72.6%, 210/289) declined the use of any complementary treatment. Of these 210 patients, 73.3% (154/210) stated that CAM treatment was not offered to them. Only 20.4% (59/289) of all participants had discussed adding complementary treatments to their current therapy with their consulting physician. The most common reasons for CAM use were intended by the patients to improve the immune system (47%, 136/289), to reduce side effects (43.2%, 125/289), and to not miss an opportunity (37.3%, 108/289). Assuming their health insurance would not compensate the costs for CAM during RT, 52.5% (152/289) of the patients would pay for their treatment. A treatment integrated in the individual therapy concept, such as regular acupuncture, would be used by 62.9% (182/289) of RT patients. In order to gain more information about the changes in attitude towards complementary medicine, we also handed out the questionnaire a second time after RT during the first follow-up visit (n=10). This is an ongoing part of the evaluation. However, it becomes apparent that in retrospect the use of CAM increased.

Conclusion: In comparison to other studies, usage of CAM parallel to RT is considered to be low. The acceptance amongst patients is present, however more information, in terms of personal consultations with physicians, brochures or online information, could encourage a holistic therapy.

EP-1470

Intralesional injection of triamcinolone acetonide in treatment of Radiation Induced Fibrosis

A.M. Maklad[1], H.A.M. Assaf[2], E.E.D.A. Nada[3], A. A. Badran[4]
[1]*Faculty of medicine- Sohag University, Lecturer of Clinical Oncology and Nuclear medicine department, Sohag, Egypt*
[2]*Faculty of Medicine- Sohag University, Assistant professor of Dermatology-Venereology and Andrology, Sohag, Egypt*
[3]*Faculty of Medicine- Sohag University, Professor of Dermatology- Venereology and Andrology Department, Sohag, Egypt*
[4]*Sohag University, Master degree Dermatology-Venereology and Andrology Faculty of Medicine, Sohag, Egypt*

Purpose or Objective: On the basis of successful intralesional steroid injection for dermatologic scars treatment such as keloids and burn scars, we planned to evaluate intralesional triamcinolone acetonide injection in treatment of RIF as there is no data available for its use for this indication

Material and Methods: 30 patients with RIF of different sites (19 cases breast, 4 cases neck, 3 back, 2 face and 2 lower limbs) at least 6 months after end of radiation were included in our study. They were treated by intralesional Triamcinolone acetonide injection. Injections were carried out by dermojet at 1 cm interval. Injections were repeated every 2 weeks for 3months. Assessment was done according to RTOG grading before treatment and repeated during and 3 months after end of treatment.

Results: We documented over all response rates of 80%, marked and complete improvement of RIF 43.33%, 30% showed one grade improvement, 6.67% had two grades improvement, while 20% of patients didn't respond (P-value <0.001). Pain score was significantly improved (p value <0.001), 44% of the included patients had complete improvement of pain, 36% had mild residual pain and 20% of patients expressed moderate residual pain. No significant adverse events were observed. The results were significantly better with younger age group (P-value=0.021), smaller BMI (p-value=0.007), patients who received lower radiation doses (P value =0.03), smaller number of radiotherapy treatment sessions (P-value=0.05), smaller radiation field sizes (P value=0.001), and patients with shorter duration of RIF (P value <0.001).

Conclusion: Intralesional triamcinolone acetonide injection can be considered as an effective in treatment of RIF. It can be considered as a promising effective, safe, less costly therapeutic option in treatment of RIF. To the best of our knowledge, no previous data are available about the use of intralesional injection of triamcinolone acetonide for treatment of RIF.
Key words: Radiation, fibrosis, intralesional.

EP-1471

The effect of radiotherapy on Ledderhose disease

J.G.H. Van Nes[1], J.A. Langendijk[1], R.J.H.M. Steenbakkers[1]
[1]*University Medical Centre Groningen, Radiotherapy, Groningen, The Netherlands*

Purpose or Objective: The only treatment option for Ledderhose disease seems radiotherapy as surgery is associated with a high chance of recurrence and morbidity.

Therefore, we investigated the effect of radiotherapy on Ledderhose disease.

Material and Methods: Between 2008 and 2014, 37 patients (56 feet) with Ledderhose disease were treated with radiotherapy at our department (figure 1). Radiation treatment consisted of 30 Gy given in 10 fractions (orthovolt 200 kV or electrons 6-10 MeV). After the first 5 fractions, a 8-10 week split was included. After this split, the remaining 5 fractions were given. Progressive disease (PD) was defined as progression of complaints. Stable disease (SD) was defined as no improvement or progression of complaints. Partial response (PR) was defined as improvement or no complaints, but still nodules were present. Complete response (CR)was defined as no complaints and no nodules present.

Results: All patients completed the planned treatment. The mean follow-up time was 25 months (range 3 to 46 months). Mean age of patients was 53 years, 46% were men, 54% were women. In 51% of patients (n=19), both feet were affected. After the radiotherapy, a minority of the patients complained of rash or dry skin, which resolved spontaneously. Of the 56 feet treated, 5% had PD, 23% had SD, 64% had PR and 7% had CR. No radiation induced malignancies were seen. Of the two patients with PD, one patient had previous surgery for Ledderhose disease and the other patient had PD disease after an initial PR.

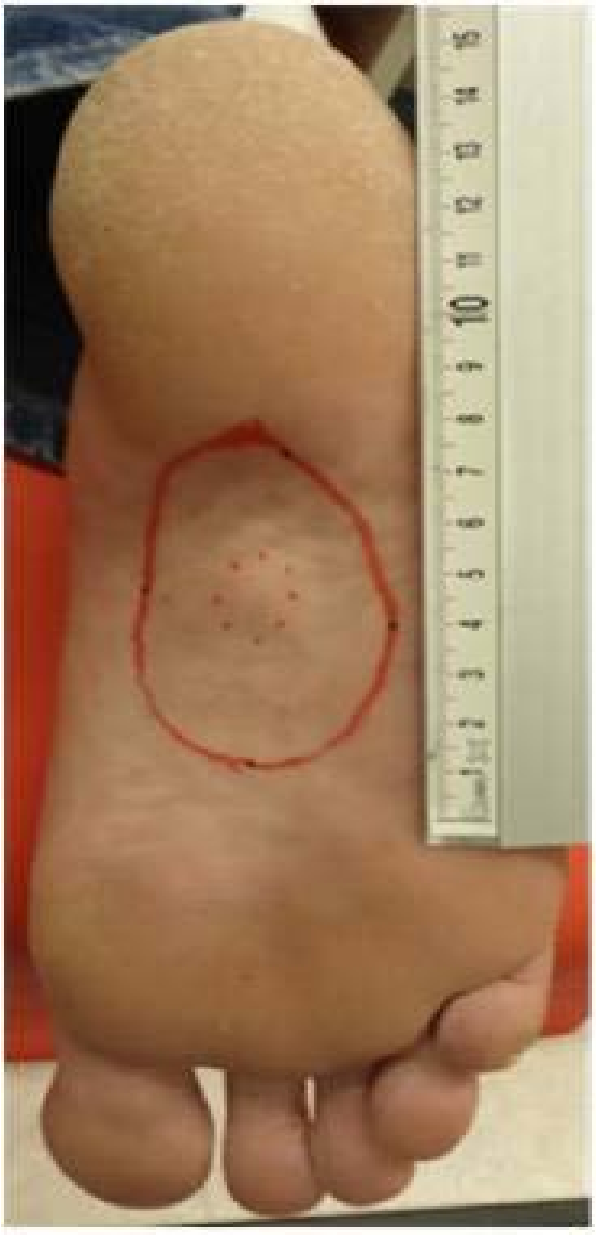

Conclusion: Radiotherapy is an effective treatment for Ledderhose disease. However, the National Health Care Institute of the Netherlands does not support radiotherapy for Ledderhose disease as no randomized controlled trail have investigated the efficacy of radiotherapy. Therefore, we will present a double blind randomized multicentre phase three study to confirm the current results prospectively.

EP-1472

Role of SBRT with VMAT-FFF for abdomino-pelvic lymph node metastases in oligometastatic patients

C. Franzese[1], L. Cozzi[1], E. Clerici[1], T. Comito[1], F. De Rose[1], G. D'Agostino[1], A. Tozzi[1], C. Iftode[1], A. Ascolese[1], D. Franceschini[1], P. Navarria[1], L. Liardo[1], L. Paganini[1], M. Scorsetti[1]

[1]*Istituto Clinico Humanitas, Radiotherapy and Radiosurgery, Rozzano Milan, Italy*

Purpose or Objective: Nowadays stereotactic body radiotherapy (SBRT) is considered a safe and effective approach for several sites of metastatic disease. So far, few published data exist on local control rates of radiotherapy in the context of isolated or limited lymph node metastases. We analyzed the dosimetric and clinical results of oligometastatic patients treated with SBRT for isolated lymph node metastases in abdomen and/or pelvis.

Material and Methods: In the analysis we included patients with a maximum of 3 lymph node sites of disease with diameter less than 5 cm, located in the abdomen or pelvis. Radiotherapy was administered with Volumetric Modulated Arc Therapy Rapid-Arc (VMAT-RA) and flattening filter-free (FFF) beams; prescribed dose was 45 Gy in 6 fractions of 7.5 Gy each. We analyzed dosimetric data and correlated them with acute toxicity (CTCAE 3.0), local and distant control of disease, progression free survival and overall survival.

Results: From January 2006 to May 2015, we treated 97 patients with lymph node metastases, of which 26 were lost at follow-up. We analyzed then 71 patients with a total of 79 treated lesions, with a mean follow-up of 1.44 years (range 0.14 – 6.21 years). At revaluation, complete response was achieved in 39 (49.3%) lesions and partial response in 28 (35.4%) lesions. Stable disease was demonstrated in 10 (12.6%) cases while only 2 (2.5%) lesions showed progression of disease. The overall clinical benefit rate was 97.5% (77/79 lesions). Acute toxicity was mild: 10 (14%) patients reported G1 toxicity (notably nausea and fatigue); 2 (2.8%) patients reported G2 toxicity (nausea and diarrhea). No Grade 3 and 4 toxicities were reported. In-field progression of disease during follow-up was demonstrated in 18 sites (22.7%) with a median time of 10.7 months. Out-field lymph node progression was demonstrated in 22 (27.8%) cases while distant metastases occurred in 25 (31.6%) cases. Local control rate and overall survival rate at 1 year were 83% and 93%, respectively.

Conclusion: In consideration of our dosimetric and clinical results, SBRT with VMAT-RA and FFF beams can be considered a safe and effective approach in oligometastatic patients with abdomino-pelvic isolated lymph node metastases. Although this can be considered an initial experience, these results may be potentially significant for preserving quality of life of patients and delaying further systemic treatments.

EP-1473

The clinical study on oligometastases from different tumors treated with carbon ions

X. Wang[1], Q. Zhang[1], H. Zhang[2], L. Gao[1], J. Ran[1], Q. Li[1], R. Liu[1], S. Wei[1], H. Luo[1], X. Wei[1], Z. Liu[1], L. Xu[1]

[1]*Gansu Cancer Hospital, Department of Radiotherapy, Lanzhou, China*

[2]*Chinese Academy of Sciences, Institute of Modern Physics, Lanzhou, China*

Purpose or Objective: The purpose of this study was to evaluate the efficacy and feasibility of carbon ion

radiotherapy(CIRT) for Oligo-metastatic tumors located different organ from various cancer.

Material and Methods: From December 2009 to June 2013, 17 patients joined into the clinical study as volunteers. The patients were not surgical candidates for medical reasons or patient refusal. The Oligometastases located in lung,brain and liver respectively from various cancer were treated with CIRT.The heavy ion beams energy was 230~350Mev / u and RBE value was 2.5. A median dose of 60 GyE (range, 20–66 GyE) was delivered to the planning target volume (PTV) in 4-12 fractions with a median daily dose of 5 GyE (range, 4.68–5.5 GyE). Short-term effect was evaluated by tumor change in three months after treatment with *RESIST criteria* and adverse reactions were determined by criteria of acute radiation injury from Radiation Therapy Oncology Group. Treatment outcome was analyzed in terms of local control rate(LCR), survival rate.

Results: In total, 17 patients (7 lung Oligometastases, 3 liver Oligometastases and 7 brain Oligometastases)with 17 Oligo-metastatic lesions were treated with CIRT. Until December 2014, median follow-up period was 18 months(2-40ms). Objective response rate was 94.1% to evaluate short-term effect (3CR, 10PR, 3NC, 1PD) .The 1-year LCR and overall survival of the treated patients were 93.3% and 51.0%. Only 1 lung Oligometastases patients relapsed in 7 months after treatment. 1-year Survival rate were 47.6%,66.7%, 75% respectively in brain, lung and liver Oligometastases. Survival rate and LCR were not significantly correlated with Oligometastases location. All treatment-related complications were acute skin reaction and self-limited, without any grade 4–5 toxicity.

Conclusion: ompared with Conventional radiotherapy, CIRT has short treatment time, high Biological effect advantages. CIRT may be one of effective, the least invasive and safe approach to patients with Oligometastases.

EP-1474

The preliminarily results of carbon ion radiotherapy in 60 patients

X. Wang[1], Q. Zhang[1], H. Zhang[2], L. Gao[1], J. Ran[1], Q. Li[2], R. Liu[1], S. Wei[1], H. Luo[1], X. Wei[1], Z. Liu[1], S. Sun[1], L. Xu[1]
[1]*Gansu Cancer Hospital, Department of Radiotherapy, Lanzhou, China*
[2]*Chinese Academy of Sciences, Institute of Modern Physics, Lanzhou, China*

Purpose or Objective: This study summarizes the experience with carbon ion radiation therapy (RT) at the Heavy Ion Research Facility in Lanzhou since 2009.

Material and Methods: From December 2009 to June 2013, 60 patients joined into the clinical study as volunteers. 14 patients with brain tumor〔cerebral glioma(n=6), metastatic brain tumor (n=8)〕,8 patients with head and neck tumor,15 patients with chest tumor〔primary lung cancer (n=8), metastatic mediastinal carcinoma(n=1), metastatic lung cancer(n=6)〕,13 patients with abdominal carcinoma〔primary liver cancer(n=4), pancreatic cancer(n=1), abdominal soft tissue malignant tumor (n=3), metastatic liver cancer(n=4), abdominal lymph node metastasis carcinoma(n=1)〕,5 patients with pelvic tumor〔rectal cancer(n=1), anal cancer (n=1), ovarian carcinoma(n=1), chordoma(n=1), soft tissue tumor(n=1)〕,5 patients with limbs tumor〔skin cancer(n=2), soft tissue malignant tumor(n=3)〕were treated with carbon ions beams. The beams energy was 230~350Mev / u and RBE value was 2.5. A median dose of 60 GyE (range, 20–66 GyE) was delivered to the planning target volume (PTV) in 4-12 fractions with a median daily dose of 5 GyE (range, 4.68–5.5 GyE). Short-term effect was evaluated by tumor change in three months after treatment with *RESIST criteria* and adverse reactions were determined by criteria of acute radiation injury from Radiation Therapy Oncology Group. Treatment outcome was analyzed in terms of local control rate (LCR), survival rate.

Results: Until December 2014, median follow-up period was 18 months (2-40ms). Objective response rate was 98.3% to evaluate short-term effect (9CR, 37PR, 13NC, 1PD) .The 1-year LCR and overall survival of the treated patients were 80.2% and 62.8%. The local control and overall survival rates were not correlated with tumor location and pathological types, the main cause of death was distant metastasis. All treatment related complications were 1-2 grade acute skin reaction (incidence rate = 66.7%) and self-limited, without any grade 4–5 toxicity.

Conclusion: Carbon ion therapy is safe with respect to toxicity , offers high tumor local control rates and significantly shorten the treatment time. But this study has limitations: a group of cancer patients in advanced stage and short survival and follow up time, small sample size and high heterogeneity because of tumor location, clinical stage and pathological type. More homogeneous prospective data, large multicentric and randomized trials are needed to evaluate the efficacy of heavy ion tumor therapy.

EP-1475

Radiotherapy for primary orbital tumors – patterns of care and treatment outcomes

Y. Lim[1], I.H. Kim[1]
[1]*Seoul National University Hospital, Radiation Oncology, Seoul, Korea Republic of*

Purpose or Objective: Although radiation therapy (RT) is widely used in orbital tumors, the clinical use of ophthalmic RT has not been established in the lack of prospective data. This study evaluated the single institution's patterns of care and treatment outcomes of RT in non-metastatic primary tumors and inflammatory diseases in the eye and orbit.

Material and Methods: We retrospectively reviewed a total of 138 patients and 147 treatments of primary orbital malignancies or inflammatory conditions from January 2000 to December 2013. The aims of RT consisted of definitive (n=121), postoperative (n=16), palliative (n=6), and salvage (n=4) treatment. Retrobulbar (34%) and conjunctival (22%) area were the common subsites of treatment. The median external beam RT dose was 30.6 Gy (range, 10.0-66.6) with a daily fraction size ranging from 1.7 to 4.0 Gy. Three-dimensional conformal and intensity-modulated techniques were delivered in 67 (46%) and 5 (3%) treatments, respectively.

Results: Forty-eight (35%) patients had benign inflammatory diseases including thyroid-associated ophthalmopathy (n=24), inflammatory pseudotumor (n=13), and choroidal neovascular membranes (n=11). In 90 (65%) patients with malignant tumors, 13 (9%) patients were children diagnosed with retinoblastoma (n=7), optic glioma (n=4), optic meningioma (n=1), and ocular teratoid medulloepithelioma (n=1). The other 77 (56%) patients were adult with the 5-year overall survival rate of 78.3%. Among the non-pediatric patients, mucosa-associated lymphoid tissue (MALT) lymphoma (n=36) was the most frequent disease entity, and the others also included optic meningioma (n=6), melanoma (n=5), and adenoid cystic carcinoma (n=5). In a total of 81 adult malignant tumors, complete and partial responses were observed in 67 (83%) tumors, and the patients' 5-year relapse-free survival was 60.8%. In the 42 treatments of TAO and inflammatory pseudotumor, inflammatory symptoms were improved in 57%. There were 58 (39%) events of acute toxicities, and grade 1-2 ocular discomfort (n=18) and nausea (n=9) were frequent. Among the 24 (16%) events of late toxicities, 10 (42%) and 2 (8%) events of radiation-induced cataract and retinopathy were observed, respectively. Grade ≥3 toxicities were not reported.

Conclusion: In current practices, the ophthalmic RT achieved an excellent treatment response and tumor control with tolerable short-term and long-term toxicities. Further

analysis with more advanced RT technique is needed to assess the future role of RT in orbital tumors.

EP-1476

General fatigue during the period of radiotherapy; clinical usefulness of Japanese herbal medicine.

N. Yoshikawa[1], H. Yoshioka[1], K. Yoshida[1], T. Shimbo[1], Y. Uesugi[1], Y. Narumi[1]
[1]*Osaka Medical College, Radiology, Takatsuki, Japan*

Purpose or Objective: Breast cancer patients receiving post-operative radiotherapy (RT) experience adverse effects and general fatigue is one of them. Although it is often not severe enough to interrupt the course of RT, it negatively affects quality of life. Some Japanese herbal medicines such as TJ-41 (Hochu-ekki-to) are effective for fatigue and are often used in daily practice. The purpose of this study is to assess radiation-induced fatigue (RIF) in detail and investigate the effect of Japanese herbal medicine.

Material and Methods: Breast cancer patients who received post-operative RT and agreed to answer a patient self-reporting questionnaire (FACIT-F; Functional Assessment of Chronic Illness Therapy) were eligible for this study. We excluded patients who were receiving chemotherapy concurrently. RIF was defined as fatigue which occurred during the period of radiotherapy and there were no causes for the fatigue other than the radiotherapy. The FACIT-F questionnaire was answered before RT, at one week after the beginning of RT, at the end of RT and one month after the end of RT. We prescribed TJ-41 to the RIF patients during the radiotherapy. We defined as responders the patients who experienced improvements in RIF and hoped for further prescription.

Results: Fifty-two patients were enrolled for this study. RIF was observed in 24 (46 %) patients. On univariate analysis, the statistically significant predictor of RIF was the score of FACIT-F before RT. TJ-41 was administered to 9 patients and 8 of them (89 %) were responders.

Conclusion: RIF was common in breast cancer patients receiving post-operative RT and TJ-41 was effective for the RIF patients and improved their quality of life. However, these results may lack objectivity and the study was conducted with no placebo group. Improvement in objectivity of the assessment and a comparative study will be needed.

EP-1477

Radiotherapy-Hyperthermia: outcome/toxicity in the superficial recurrent/metastatic tumors

E. Garibaldi[1], A. Di Dia[2], E. Delmastro[1], G. Belli[1], M. Gatti[1], G. Cattari[1], A. Salatino[1], S. Squintu[1], M. Poli[2], A. Miranti[2], P. Gabriele[1]
[1]*Istituto di Candiolo- IRCCS, Department of Radiotherapy and Radiation Oncology, Candiolo, Italy*
[2]*Istituto di Candiolo-IRCCS, Medical Physics, Candiolo, Italy*

Purpose or Objective: Hyperthermia is a powerful radiosensitizer for treatment of superficial tumors. Several trials showed an advantage of combining radiotherapy with hyperthermia in terms of both local tumor control and overall survival. The purpose of this study is to evaluate both efficacy and toxicity of radiotherapy-hyperthermia (RT-HT) in the treatment of superficial recurrent and metastatic tumors in patients previously or not previously irradiated.

Material and Methods: In our Institution twenty-three patients (mean age 71,4 years; range: 51-88) with histologically confirmed superficial recurrent/metastatic tumors were enrolled: 11 breast carcinoma, 6 head&neck cancer, 2 malignant melanoma, 2 sarcomas, 1 uterine adenocarcinoma and 1 hepatocarcinoma. Patients underwent radiotherapy treatment using 3D-conformal radiotherapy (8/23) or Helical Tomotherapy (15/23). External beam radiotherapy was delivered in 6-27 fractions of 1.8-5 Gy for a total dose of 20-57.5 Gy (mean external dose: 41 Gy). Prescribed dose was established taken into account, of the previous radiation doses, in previously irradiated patients, Karnofsky performance status and patient compliance. Hyperthermia treatment was performed with an electromagnetic superficial applicator operating at the frequency of 434 MHz. HT session was delivered once/twice weekly during the period of external radiotherapy, 1-2 hours after radiotherapy, to a mean total of 5 treatments [range: 1-9 sessions]. Termocouples were used to evaluate temperature distribution map. Average, maximum and minimum temperature parameters were recorded during hyperthermia treatment. The treatment goal was to reach 40- 42°C in > 90% (T90) of measured points for a duration of 60 minutes. Acute and late toxicity was evaluated according to the CTCAE criteria. Local control was assessed after the end of the treatment on the basis of the RECIST Criteria.

Results: During hyperthermia treatment the median temperature reached was 40.5 °C [range: 39 – 42.9°C]. During the radiotherapy in association with hyperthermia 2 pts (10%) had G3 toxicity and one of these interrupted the treatment. One pt had acute cutaneous toxicity ≥ G3 at 1 month. No pts had toxicity≥ G2 at 3 and 6 months. No toxicity was observed at 12 months. The mean follow-up was 10 months (range 3-22 months). Four pts (17%) had a complete response (CR), 11 pts (48%) had a partial response (PR),7 pts (30%) had a stable disease, (SD) and only 1 pt (4%) had progression disease (PD) and subsequently died. The Local control rate was 95%. Univariate analysis showed that Tmean,Tmax, Tmin,T90 parameters were not associated with local control rate.

Conclusion: Radio-hyperthermia can result in an effective approach, particularly in previously irradiated patients or in radio-resistant tumors. Our results show that Radio-Hyperthermia is an useful combined treatment with a good local control rate and a very high patient compliance.

EP-1478

Low Dose Radiation therapy of degenerative painful osteoarthritis

S. Payano[1], A. Montero Luis[1], O. Hernando Requejo[1], J. Valero Albarran[1], M. Lopez Gonzalez[1], R. Ciervide Jurio[1], E. Sanchez Saugar[1], X. Chen[1], C. Rubio Rodriguez[1]
[1]*Hospital Universitario Madrid Sanchinarro - Grupo Hospital de Madrid, Oncologia Radioterápica, Madrid, Spain*

Purpose or Objective: The purpose of this study is to evaluate the decrease in pain of patients treated with low-dose radiation therapy in osteoarthritis.

Material and Methods: From April 2015 to September 2015, 11 patients (10 female and 1 men) were treated with low dose radiotherapy for pain control. All patients were refractory to conventional therapy prior to irradiation.
13 joints (6 bursitis and 7 arthrosis): 4 trochanteritis, 5 knees, 1 left thumb rhizarthrosis, 2 metacarpophalangeal joint and 1 right epicondylitis were treated.
The median age was 69 years (range 46-89) with a median follow-up period of 3 months (range 0-6). Painful status was measured by visual analogue scale (VAS), with a median pre-treatment value of VAS= 7(range 4-9).
The radiotherapy dose of 6 Gy was delivered in 6 alternate days fractions of 1 Gy per fraction. In those patient with no pain relive post-treatment with VAS of or above 6 a second course of radiotherapy was proposed.
The second RT series started 8 weeks after the first RT series.

Results: The analysis was performed before the treatment and at the last follow-up. With a median VAS = 5 (range 0-8) 7 patients achieved pain relief, 3 patients underwent a second course of radiotherapy with identical dose, and 1 patient showed no change in pain. Daily requirements of analgesic were removed of reduced in 5 patients, subjective pain perception of response to irradiation evaluated at time of last visit regarding pre-treatment status was considered as “better” by 73% of patient. No patients presented acute or late complications attribute to radiation therapy.

Conclusion: RT is highly effective for refractory degenerative joint diseases. Prognostic factors for outcome can be established. Due to minimal side effects and low costs, RT represents an excellent treatment compared to conventional methods of treatment and surgery in the chronic disease. This study confirms by objective criteria the anti-inflammatory efficacy of low dose RT

EP-1479

Integration of a minituarized linear accelerator in an 20 year IOERT expert institution

E. Alvarado Vasquez[1], M. Gomez-Espi[1], A. Alvarez[1], A. Calin[1], M. Muñoz[1], J. Blanco[1], F. Serrano[1], C. Gonzalez-San Segundo[1], C. Martinez[1], M. Santos[1], L. Guerrero[1], A. Davo[1], I. Sierra[1], R. Ayala[2], R. Sendon[2], M. Lopez-Bote[2], M. Lozano[1], F. Calvo[3]
[1]*Hospital General Universitario Gregorio Maranon, Radiation Oncology, Madrid, Spain*
[2]*Hospital General Universitario Gregorio Maranon, Medical Dosimetry and Radioprotection, Madrid, Spain*
[3]*Hospital General Universitario Gregorio Maranon, Oncology, Madrid, Spain*

Purpose or Objective: Hospital General Universitario Gregorio Marañon has a long-standing tradition of IOeRT (Intraoperative electron Radiation Therapy), with over 1600 procedures in its 20 year history. Since december 2013, a minituarized linear accelerator (LIAC) started to operate in our center. We describe the 22 months technical and clinical experience with LIAC in our consolidated IOeRT program.

Material and Methods: A review of technical and surgical parameters of IOeRT procedures using LIAC was performed from December 2013 to October 2015,

Results: From december 2013 to october 2015, 222 procedures in 185 patients were performed (200 procedures with LIAC, 22 transported to a fixed lineal accelerator). Cancer types treated were 64 oligorecurrences / oligometastases, 34 breast cancers, 44 rectal cancers, 42 sarcomas, 6 pancreatic adenocarcinomas, 4 esophageal neoplasms and 6 other cancer types. The treated anatomic sites included 100 cases in pelvis, 40 in abdomen, 25 in limbs, 34 in breast and 1 in thorax. Relevant operational data included 39 days with more than 2 procedures in the same working day (22% of total days). Six different applicator sizes were selected (range 4-10) with 4 beveled ends (range 0-45). Selected energies ranged from 6 to 12.

Conclusion: LIAC is a versatile technology able to be incorporated to expert IORT institutions promoting efficient action with operative benefits in terms of availability of IOeRT components for cancer patients.

EP-1480

A comprehensive analysis of immuno- and immunoradiotherapy trial design developments from 2000-2014

S. Raby[1], C. Connell[2], T. Janowitz[2]
[1]*The Christie, Oncology, Manchester, United Kingdom*
[2]*Addenbrooke's Hospital, Oncology, Cambridge, United Kingdom*

Purpose or Objective: There has been a rapid growth in the number of immuno- and immunoradiotherapy trials over the last few decades. Long term durable responses occur, but only in a subset of patients. As yet no accurate method of identifying those patients most likely to benefit has been identified. The factors behind non-response are unclear but may include 1) inherent characteristics of the tumour, 2) factors influencing immunogenicity such as tumour burden and previous treatments and 3) clinical trial design By performing a cross sectional analysis of registered clinical trials investigating agents thought to stimulate T-cells we aimed to detect trends in these factors. In particular we aimed to assess the extent to which trials sought to develop and identify novel biomarkers of response to immunotherapy.

Material and Methods: A pubmed literature search was conducted to establish a list of known T cell checkpoints, co-stimulatory receptors, ligands, and the antibodies targeting these. These search terms were entered into clinical trials.gov on October 11, 2014. Study details were downloaded as datasets for review by two independent assessors.

Results: We identified a total of 350 trials of immunomodulatory antibodies targeting PD-1, CTLA4, PD-L1, PD-L2, LAG3, B7-H3, CD137, OX40, CD27 and GITR. A longitudinal analysis by trial registration date shows a steady increase in the number of trials using immunostimulatory antibodies As some cancer types are thought to be more immunogenic, we looked at the spread of trials by cancer type. Unsurprisingly, melanoma trials represent the largest proportion, but there has been a shift towards testing immunostimulatory antibodies in cancers that are considered less immunogenic with a significant increase in trials in NSLC when comparing trials registered between 2000 and 2007 and those registered between 2008 and 2014. Only 39% of trials measured a dynamic immune endpoint as a specified outcome. T and B cell number or function were the most common markers analysed. However there was a significant increase in the measurement of PD-L1 expression in recent years.

Conclusion: This analysis provides comprehensive data on the rapid growth of immunotherapy trials and highlights that despite the multiplicity and variability of potential dynamic biomarkers available, there has been a poor uptake. Whilst the future of immunotherapy is not in doubt, biomarkers are essential to understand the considerable lack of response and help guide further trial efforts.

EP-1481

Toxicity of concomitant application of radiotherapy with „new targeted therapies“

M.S. Geier[1], E. Bräutigam[1], B. Aschacher[1], H. Rumpold[2], H. Geinitz[1]
[1]*Krankenhaus der Barmherzigen Schwestern - Linz, Radiation Oncology, Linz, Austria*
[2]*Krankenhaus der Barmherzigen Schwestern - Linz, Oncology, Linz, Austria*

Purpose or Objective: New targeted therapies (nTTs) are increasingly used in virtually every type of cancer. On the other hand radiation therapy (RT) is frequently applied in the curative and palliative setting of cancer treatment, confronting clinicians more and more with the problem, weather a previously initiated nTT-therapy could be continued during RT. The aim of this systematic literature analysis was to evaluate the toxicity of concomitant application of RT with nTTs in a qualitative descriptive manner.

Material and Methods: Clinical studies comprising concomitant application of RT with EGFR-, VEGFR-, HDAC-, proteasom-, BRAF-, m-Tor- or immune-checkpoint-inhibitors were eligible. Using fixed search terms 215 publications were identified including more than 6000 patients. Forty-eight studies analyzed combinations of nTTs with ZNS-RT including 1164 patients, 45 with head and neck-RT including 2390 patients, 59 with thoracic RT including 1647 patients, 33 with abdominal RT and 30 with pelvic RT including 492 and 1008 patients respectively.

Results: In most cases combined application produced no additional toxicity or a slight increase of the already known toxicity profile. Scarcely, however, combination of RT with nTTs resulted in serious side effects. These toxicities comprised tracheo-bronchial fistulas or GI-bleeding for combinations of thoracic or abdominal/pelvic RT with VEGF-receptor-inhibitors, recall phenomena in combination of RT with tyrosinkinase inhibitors e.g. erlotinib and severe mucositis, dermatitis or paraplegia (case report) when combining RT with ipilimumab. For the majority of these

serious side effects no predictive risk factors could be isolated.

Conclusion: The currently available data seems to be not adequate to give a general recommendation, on weather RT could be combined with nTTs in clinical routine. If application is carried out on an individual basis it should be done under close clinical surveillance. Multicentric observational studies are needed to address this clinical relevant problem.

Electronic Poster: Physics track: Basic dosimetry and phantom and detector development

EP-1482

Improving accuracy of radiochromic film dosimetry system using control film piece

S. Devic[1], S. Aldelaijan[2], F. Alzorkany[2], N. Tomic[1], J. Seuntjens[1], F. DeBlois[1], B. Moftah[2]
[1]*McGill University, Oncology, Montreal, Canada*
[2]*King Faisal Specialist Hospital & Research Centre, Department of Biomedical Physics, Riyadh, Saudi Arabia*

Purpose or Objective: Over the years, radiochromic film became a reference dosimetry system of choice for two-dimensional dose distribution measurements with acceptable accuracy and uncertainty in both clinical and research applications. Nonetheless, response of the film might be influenced by factors other than irradiation (humidity, extreme temperature and/or exposure to UV light) that could lead to decreased measurement accuracy. We investigate the use of a control film piece, which should compensate for the film response changes other than radiation.

Material and Methods: Response of EBT3 film was measured in terms of net transmittance calculated using green channel from 48-bit RGB image of film pieces scanned with Epson Expression 10000 XL flatbed scanner. We established a calibration curve for the radiochromic film dosimetry system in a dose range up to 20 Gy. Then, we irradiated "control" film pieces to several known doses from 0.05, to 1 Gy, as well as five film pieces of the same size to "unknown" doses of 2, 5, 10, 15 and 20 Gy. Impact of correcting measured ("unknown") doses using "control" film pieces were investigated in terms of both gain in the accuracy and at the same time loss of uncertainty of such determined dose. Depending on a dose range, two approaches of incorporating control film piece were investigated. In a signal based method, response of the control film piece is subtracted from the measuring film piece and the final change in response is converted into the dose using calibration curve. In a dose based method, both readings of measuring and control film pieces are converted to dose using the same calibration curve followed by subtracting the control film piece "equivalent" dose from the dose obtained with measuring film piece.

Results: Figure 1 summarizes results of our investigation into trade-off between gain in accuracy and loss in uncertainty when the control film piece is used, and we found that both are dependent on dose level measured. For dose values above 10 Gy, the increase in accuracy of 3% results in uncertainty loss of 5% by using dose corrected approach, where the measured film response corresponded to 2% of the dose response registered with measuring film piece. At lower doses and signals of the order of 5% (measured by control film piece) we observed an increase in accuracy of 10% with a loss of uncertainty lower than 1% by using the corrected signal approach.

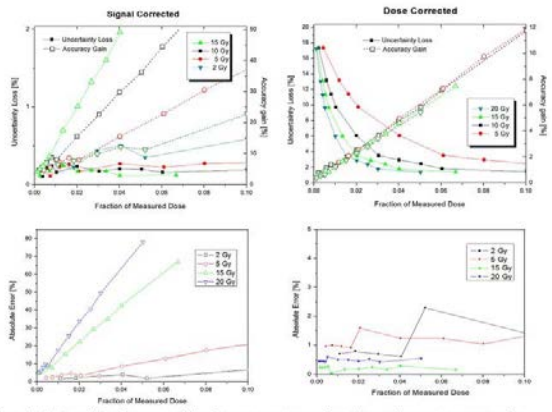

Figure 1: Trade-off in using control film piece: percent uncertainty loss and percent accuracy gain for signal corrected (top-left) and dose corrected (top-right) approach as a fraction of measured doses for various dose measurement levels; absolute error for signal corrected (bottom-left) and dose corrected (bottom-right) approach. Lines represent guide for the eye.

Conclusion: Use of the control (un-irradiated) film piece for dose measurements in reference radiochromic film dosimetry is highly recommended. At lower doses, the signal based method should be used, while at higher doses the dose correction method seems to be more appropriate. However, final incorporation of the signal registered by the control film piece into dose measurement analysis should be a judgment call of the user based on a tradeoff between deemed accuracy and acceptable uncertainty for a given dose measurement.

EP-1483

Reference dosimetry of FFF MV photon beams: a correction for intra-Farmer ion chamber dose gradients

R. Ruggieri[1], S. Naccarato[1], P. Stavrev[1], N. Stavreva[1], S. Pasetto[1], I. Salamone[2], F. Alongi[1]
[1]*U.O. Radioterapia, Ospedale 'Sacro cuore - don Calabria', Negrar, Italy*
[2]*U.O. Radiologia, A.O.U. 'G. Martino', Messina, Italy*

Purpose or Objective: To estimate and correct the systematic bias which results from the intra-chamber dose gradients when a Farmer ionization chamber is used for reference dosimetry (TRS 398, IAEA 2000) in flattening-filter-free (FFF) MV photon beams.

Material and Methods: An intra-chamber dose gradient correction factor (*K_icdg*) of the charge reading of a Farmer ionization chamber, when used for reference dosimetry (TRS 398, IAEA 2000) in flattening-filter-free (FFF) MV photon beams, is proposed. This is achieved through a user intercomparison of the Farmer ionization chamber with a small volume (~ 0.1 cm^3) ionization chamber, and by estimating the inaccuracies of this intercomparison. Further, the factor *K_icdg* is theoretically developed in terms of the corrections for both volume averaging effect (*P_vol*) and charged particle fluence perturbation (*P_fl*). The factor *P_vol* is then estimated as the ratio of the active length (*L*) of the Farmer ionization chamber (*L*= 24 mm) over the integral, computed on *L*, of a high-resolution FFF transverse dose profile (Figure 1). Once *K_icdg* and *P_vol* are known, *P_fl* is finally deduced.

Results: The estimated overall standard uncertainties on the absorbed dose to water determination in reference conditions, for 6 MV and 10 MV FFF beams, were 1.5 % for the small volume ionization chamber (30013™, PTW), and 1.4 % for the *K_icdg*-corrected Farmer ionization chamber (30013™, PTW). In the latter case, the added uncertainty from the measure of *K_icdg* was balanced by the higher long-term stability of the Farmer ionization chamber. From four distinct dosimetry sessions on a TrueBeam™ (Varian Inc.) linac, mean (sd) values for *K_icdg* equal to 1.0024 (0.0003) for 6 MV-FFF and 1.0056 (0.0003) for 10 MV-FFF, were estimated. Similarly, *P_vol* equal to 1.0030 (0.0001) for 6 MV-FFF, and to 1.0064 (0.0004) for 10 MV-FFF, respectively, were measured.

Finally, *P_fl* equal to 1.0021 (0.0004) for 6 MV-FFF, and to 1.0033 (0.0005) for 10 MV-FFF, respectively, were computed.

Figure 1. Average transverse dose profiles of the (10x10) cm² field, for 6 MV (gray) and 10 MV (black) FFF photon beams from a TrueBeam™ (Varian Inc.) linac, scanned, along *L*= 24 mm with 0.5 mm step, by a shielded p-diode (T60016™, PTW) at 10 cm of depth in water with SSD= 90 cm. (±1sd)-error bars (<0.1 %) refer to four sessions of measurements spanning about six months.

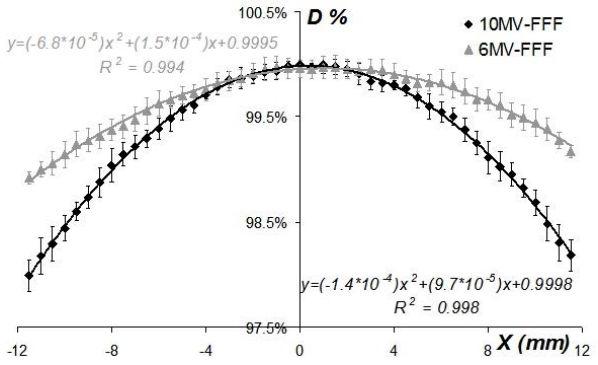

Conclusion: The factor *K_icdg*, which can be approximated by *P_vol* within 0.1 %, corrects for a dose error up to -0.6 % in reference dosimetry of the 10 MV-FFF photon beam when a Farmer ionization chamber is used.

EP-1484

The dosimetric property of TLD2000 thermoluminescent dosimeter

R. Yang[1]
[1]*Yang Ruijie, Radiation Oncology, Beijing, China*

Purpose or Objective: To study the dosimetric properties of TLD2000 thermoluminescent dosimeter (TLD), including repeatability, linearity of dose response, energy response and dose rate effect.

Material and Methods: 1300 TLD2000 TLDs were read out after exposure to a dose of 1 mGy of 65 keV x-ray, then were sorted out to have the same sensitivity within ±3.0%. TLDs were irradiated to a dose of 120 MU using 6 MV x-ray, then irradiated to the same dose after 24 h. TLDs were irradiated with two I-125 seeds with the same activity for 24 h, and the interval time was 24 h, to study the repeatability of TLDs for 6 MV x-ray and I-125 seed. TLDs were irradiated to different doses using Cs-137 (662 keV γ-ray), I-125 seed and 6 MV x-ray, to study the dose response of the TLDs. TLDs were irradiated to a dose of 1 mGy using Cs-137, 48 keV, 65 keV, 83 keV, 118 keV and 250 keV x-rays, to study the energy response of the TLDs. TLDs were irradiated to a dose of 120 MU using 6 MV x-ray with different dose rates of 37 MU/min, 75 MU/min, 150 MU/min, 300 MU/min and 600 MU/min; TLDs were irradiated to the same dose using three 125I seeds with different activities of 0.739 mCi, 0.675 mCi and 0.559 mCi, and the irradiated time were 24 h, 26h 17 min and 31 h 48 min, respectively, to study the dose rate effect of TLDs for 6 MV x-ray and 125I seed.

Results: 350 TLD2000 TLDs were selected with the sensitivity within ±3.0%. The maximum deviations of the repeatability were 2.7% and 4.0% for 6 MV x-ray and I-125 seed, respectively. The dose response of TLDs for Cs-137 and I-125 seed were linear. For 6 MV x-ray, the linear response range were 0.74 Gy-10.0 Gy, beyond 10.0 Gy the dose response became supralinear but proportional to the absorbed dose to TLD. The energy response for 48 keV, 65 keV, 83 keV, 118 keV and 250 keV x-rays, relative to the energy response of Cs-137, were 1.25, 1.08, 0.99, 0.91 and 0.96, respectively. There were no dose rate effects in the dose rate range of 37 MU/min to 600 MU/min for 6 MV x-ray and 0.66 cGy/h to 0.87 cGy/h for I-125 seed.

Conclusion: TLD2000 TLD has good repeatability and linear dose response for Cs-137, I-125 seed and 6 MV x-ray without dose rate effect, but the dose response is energy dependent.

EP-1485

Characterization and performance of the MR compatible Delta4 patient QA system in a hybrid MRI-Linac

W. De Vries[1], R. Van Rooij[2], E. Seravalli[1], D. Nystrom[3], S.J. Woodings[1], J.W.H. Wolthaus[1], B.W. Raaymakers[1]
[1]*UMC Utrecht, Department of Radiation Oncology, Utrecht, The Netherlands*
[2]*UMC Utrecht, Department of Radiology and Nuclear Medicine, Utrecht, The Netherlands*
[3]*Scandidos AB, R&D, Uppsala, Sweden*

Purpose or Objective: At our institute a prototype of a MRI-Linac (MRL) has been installed combining imaging (MRI, Philips) with treatment (Linac, Elekta). However before starting patient treatments, extensive machine quality assurance (QA) must be investigated including QA of treatment-plans. Standard electronic equipment is not MR-safe so patient-specific QA systems have had to be re-designed, and the performance of a new system in a 1.5 T magnetic field must be tested. The purpose of this study was to examine and characterize the performance of the newly developed MR-compatible Delta4 phantom in a transverse 1.5 T magnetic field.

Material and Methods: A prototype MR-compatible version of the Delta4 QA phantom (ScandiDos AB) was used in these measurements. To characterize this QA-system, the short-term reproducibility, dose linearity, field size dependence, dose rate dependence, dose-per-pulse dependence and angular dependence were evaluated on a conventional linac (B0=0, Elekta, 6MV Flattened (FF) and 6MV Flattening Filter Free(FFF) beam, SAD of 100 cm) and the MR-linac (B0 = 1.5 T, Elekta 6 MV FFF beam, SAD of 142.7 cm). All measurements were normalized to the readings of an ionization chamber. The performance of the MR-compatible Delta4 was also compared to that of a commercially-available clinical version in use in our department.

Results: The maximum differences between the clinical and the MR-compatible Delta4 measurements on a conventional linac are represented in the table below:

	FF-beam (B_0=0)	FFF-beam (B_0=0)
Short term reproducibility	0.05%	0.21%
Dose linearity	0.59%	0.64%
Fieldsize dependency	0.36%	0.38%
Dose rate dependency	0.25%	0.36%
Dose-per-pulse dependency	0.43%	0.47%
Angular dependency	---	0.89 %

Measurements are currently being performed on the 1.5 T research-prototype MRL. Analysis of the preliminary data show similar behavior to the measurements performed without magnetic field. Final results will be presented.

Conclusion: The characteristics and performance of the MR-compatible Delta4 have been investigated. There are no significant differences found between the clinical phantom and the MR-compatible phantom. The preliminary results at the MR-linac are consistent with those from the clinical linac.

EP-1486

Evaluation of detectors response for small field output factor measurement using Gafchromic film

G. Rucka[1], B. Patrice[1], N. Asquier[1], J.C. Mouttet[1]
[1]*Croix Rouge Française, Radiothérapie, Toulon, France*

Purpose or Objective: Most irradiation technics require dose computing from TPS. Calculation accuracy highly depends on the measurements used for beam modeling. Depending on their characteristics, available detectors may be best suited for specific field sizes when measuring Output Factors (OF). Recent studies compare several active with passive detectors and MonteCarlo calculation. The goal of our study is to

evaluate the response of several active detectors exposed to 6 MV X-ray beams of different sizes, down to 1x1 cm^2, while considering EBT3 Gafchromic films as reference.

Material and Methods: Eight EBT3 films were irradiated with field sizes ranging from 1x1 to 10x10 cm2. Measurements were done in a homemade RW3 solid water phantom. Multichannel film dosimetry was used for film opacity-to-dose conversion. All films (including background) were irradiated and scanned simultaneously using the efficient protocol described by D. Lewis *et al.* Among available active detectors, two ionization chambers and two diodes were studied. Measurements were carried out in a water phantom. OF measurements were also done by placing both chambers in the solid water phantom, in the same condition as the films. Results were compared to measurements done in water in order to verify scattering components correspondence for all field sizes. This allows active detectors irradiated in water to be compared to the films in RW3 slabs.

Results:

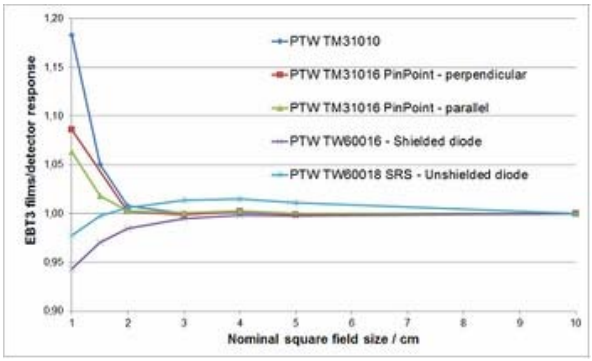

OF obtained with the ionization chambers placed in the water and solid water phantom are identical for field sizes smaller than 15x15cm2. As described in H. Benmakhlouf publication, active detector response for each field size was normalized with respect to the reference data. Figure 1 shows results. Concerning ionization chambers, the influence of partial volume averaging is similar to the published results. The three major effects mentioned for the diodes also appear in our results : the charged particles equilibrium between detector material and water, the over-response of the unshielded diode in broad beams and the partial volume averaging.

Conclusion: Our study confirms that partial volume averaging is not the only undesirable effect for OF measurement. Thus, the detector having the best spatial resolution is not systematically the best suited for small fields OF measurements.

EP-1487

Dosimetric properties of a new formula PRESAGE with tin metal catalyst

D. Khezerloo[1], H.A. Nedaei[2], A. Takavar[2], A. Zirak[3], N. Banaie[4]

[1]*Tabriz university of Medicine, Radiology, Tabriz, Iran Islamic Republic of*

[2]*Tehran university of Medicine, Medical Physics, Tehran, Iran Islamic Republic of*

[3]*Laser and Optics Research School, Optics and Photonics, Tehran, Iran Islamic Republic of*

[4]*Azad university- science and research branch, Radiation Research, Tehran, Iran Islamic Republic of*

Purpose or Objective: Metal compounds in the fabrication of new radiochromic polymer gel dosimeters based on polyurethane resin act as catalyst to accelerate the polymerization of the dosimeter precursors. Tin-base catalyst is one of the widely used catalysts in polyurethane technology. The main purpose of this study is an evaluation of effect of tin-metal catalyst in new formula of PRESAGE response and radiological properties of it.

Material and Methods: : A very little amount of dibutyltin dillaurate (0.07 wt%) was used as catalyst in the fabrication of the new PRESAGE which components were: 93.93 wt% polyurethane , 5 wt% tetrachloride and 1 wt% Leucomalachite green. Radiochromic response and post-irradiation response of new PRESAGE were determined. Radiological characteristics of new PRESAGE such as mass density, electron density, mass attenuation coefficient and mass stopping power in different photon energies were assessed and compared with water and a commercial PRESAGE® radiochromic.

Results: Absorption peak of new PRESAGE with metal was seen unchanged. Sensitivity of new PRESAGE was relatively two times higher than commercial PRESAGE® and stability of new PRESAGE after one hour was seen constant. Mass attenuation coefficient in energy less than 0.1 MeV was 10% more than water, whereas the mass stopping power difference was only 2%.

Conclusion: Tin catalyst with very low weight fraction can be used in fabrication of radichromic polymer gel in order to fabricate a gel with high sensitivity and stability as well as good radiological properties in the megavoltage photon beam.

EP-1488

Estimation of the RBEs of two miniature x-ray devices, I-125, Ir-192 and Co-60 BT-sources

T. Schneider[1], M.U. Bug[1], H. Rabus[1]

[1]*Phys. Techn. Bundesanstalt PTB, AG 6.63 Biological Effectiveness of Ionizing Radiation, Braunschweig, Germany*

Purpose or Objective: Today over 300 miniaturized x-ray devices (MXD) from the companies Carl Zeiss Meditec AG (Intrabeam®) and Xoft (Axxent®) are applied in clinics worldwide for radiation therapy treatment (RTT) of breast cancer. Both devices emit an x-radiation field where the energy distribution is given by a continuous Bremsstrahlung-spectrum with a maximum energy of 50 keV and characteristic fluorescence lines induced by the material of the electron target and the materials in the pathway of the emitted photons. Low-energy x-rays are known to have a higher relative biological effectiveness (RBE) than higher energy photons such as the gamma rays from Ir-192 and Co-60. In this work the RBEs of the MXDs and of I-125, Ir-192 and Co-60 BT-sources at several points within a hemispherical water-phantom are estimated by calculational techniques based on both micro- and nanodosimetry.

Material and Methods: Spectra of both devices were obtained by measurements with an HPGe-Detecor and applying the sophisticated data evaluation procedures already presented at the 2nd ESTRO-Forum. For the photon transport-calculations the respective source is located 4 cm below the spherical surface and spectra are calculated at several points along the axis through the centre of the hemisphere. The first approach is based on a comprehensive biological study of the α-dic variation by E. Schmid (GSF, Munich) in the photon energy range from 1 keV to 1.3 MeV. The yield coefficient α-dic represents the linear or α-component of the yields of dicentric chromosomes and is considered to be strongly correlated with the RBE. A strong dependence of α-dic on the photon energy was thereby revealed with a maximum of RBE = 8 at 7 keV in comparision with Co-60. Based on this experimental data microdosimetric calculations were performed to obtain an energy dependend function α-dic(E) (D. Harder, W. Friedland et al). The RBE for a given source in a given point is obtained by a convolution of the respective spectrum with α-dic(E). For the second approach each of the calculated spectra is taken as a starting point for simulations with Geant4-DNA to obtain the track structure of the ionising radiation. The track structure is characterised by the frequency distribution of the ionisation

cluster size (ICS), which is the number of ionisations produced by a single particle within a specified volume.

Results: In the figure the RBE-values for the two MXD is presented as a function of the distance from the source. For both sources the RBE decrease with increasing distance from the source. From the shape of the calculated spectra this can be explained by beam hardening effects.

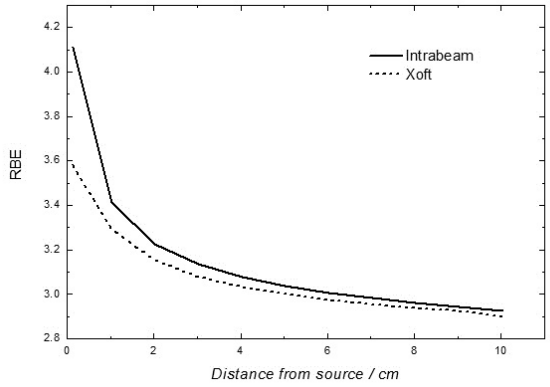

Conclusion: The determined RBE-values of 2.8 and higher can be traced back directly to the experimental data of E. Schmid as in the whole photon energy range from 4 – 50 keV the RBE was found to be higher than 2.6. This finding is in contrast to literature in which an enhanced RBE by 40 - 50% is reported and will be discussed taking the track structure into account.

EP-1489

On the development of a primary standard for validating internal radiation dose assessment methods

I. Billas[1], D.R. Shipley[1], S. Galer[1], G. Bass[1], T. Sander[1], V. Smyth[1]
[1]*National Physical Laboratory, Radiation Dosimetry, Middlesex, United Kingdom*

Purpose or Objective: Molecular radiation therapy (MRT) has a long history of treating cancer by delivering a dose of radiation from a radioactively labelled pharmaceutical that is taken up by the tumour. At present the methods for determining the radiation dose to tissue are not traceable to any standards of absorbed dose. The determination of the internal absorbed dose from an administered radionuclide (RN) relies on Monte Carlo (MC) calculations based on nuclear data (emission probabilities and energies). The validation of these methods with experimental measurements is necessary to achieve the required traceability of the measurement of absorbed dose within the patient. The goal of this work is to develop a suitable method for measuring the absorbed dose from a RN solution that can serve as a primary standard. Comparison between measurements and calculations of absorbed dose in the same geometry will allow the validation of the MC dose calculation methods.

Material and Methods: A modified extrapolation chamber (EC) was used for measuring the dose from a Y-90 RN solution. An EC is a suitable dosimeter as it has a thin entrance window allowing beta particle measurement and is capable of measuring low currents with small uncertainties. The volume of the chamber can be varied by changing the distance between the front and back faces. A phantom developed in-house was used to position the EC as closely as possible to the surface of the solution. The performance of the EC was characterised and a full uncertainty budget was obtained. The ionisation current was measured for different chamber volumes of the EC and a product of correction factors was applied to obtain the true current. MC simulations were performed to relate absorbed dose in the volume of the chamber to absorbed dose at the centre of the RN solution. This allows a direct comparison of the calculated and measured absorbed dose of Y-90 RN solution. The Y-90 source emission spectra published by MIRD and RADAR were used to directly determine the calculated absorbed doses at the centre of the RN solution.

Results: The overall standard uncertainty in the measurement of absorbed dose at the centre of a Y-90 solution with the EC was determined to be in the range ±1.3% to ±1.6 % (k = 1). The calculated Y-90 absorbed dose from published MIRD and RADAR data agreed with measurement to within 1.6% and 1.5% respectively.

Conclusion: These results demonstrate the feasibility of using an EC for performing primary standard absorbed dose measurements of an unsealed radioactive solution. Internal radiation dose assessment methods based on RADAR and MIRD data for Y-90 have been validated with experimental absorbed dose measurements and they agree within one standard uncertainty. Future work will include a repeat of Y-90 measurements in order to further validate the present results and to extend the measurements to other RNs used for MRT.

EP-1490

Angular independent silicon detector for quality assurance in Small Field Radiotherapy

S. Alhujaili[1], M. Petasecca[1], A. Rosenfeld[1]
[1]*University of Wollongong, Centre for Medical Radiation Physics, Wollongong, Australia*

Purpose or Objective: Stereotactic Radiosurgery modalities (SRS) allowing conformal dose distributions and adopting hypo-fractionation regimes require accurate Quality Assurance (QA) to avoid plan or operator mistakes. The QA of small field, multidirectional photon beams requires radiation dosimeters that have small sensitive volume, angular independent and operating in real time. The CMRP in collaboration with Advacam Ltd. has developed EDINA, an innovative silicon diode based probe, to meet the QA requirements of SRS.

Material and Methods: The edgeless single diodes are manufactured using both n-type and p-type silicon substrates with 0.5 mm and 0.1 mm thicknesses. By using an ion implantation technique, four different configurations of top and peripheral p-n junctions are created. The Edgeless diodes' samples are also fabricated with two different sizes (0.5×0.5 mm2 and 1×1 mm2) and embedded in Kapton tails with 0.5 mm thickness, 3mm width and 30 cm length using CMRP Drop-In Assembling technology, providing the dosimetry probe EDINA easy connected to electrometer. A full dosimetric characterisation of the radiation probes have been carried out. Output factor and angular dependence are measured by the edgeless detectors and compared with EBT3 film under reference irradiation conditions. The dose rate and PDD measurements of EDINA have been performed in a solid water phantom whereas the angular dependence test was carried out in a cylindrical PMMA phantom, rotatable with accuracy of 0.25 degree.

Results: The PDDs measured with EDINA on 6MV photon fields from 1.5 to 25 cm depth demonstrated an agreement with ion chambers within ±2%. The dose rate dependence in a range of 0.9×10−5 –2.7×10−4 Gy/pulse was less than −7% and +300% for EDINA with diodes fabricated on p-type and n-type substrates, respectively. Diodes fabricated on p-type and n-type substrates demonstrated degradation of the response with accumulated dose of 40 kGy within 5% and 30%, respectively.
The output factor measurements performed by EDINA utilizing smallest size diodes (0.5×0.5 mm2) show an agreement with film within 2% for square radiation field sizes ranging from 0.5 to 10 cm (Fig.1a). The angular response of EDINA utilizing thin 0.1mm thick smallest size p-type diodes (NP_100 and PP_100) varies within 2% (Fig.1b) between 0 and 180 degree and independent from accumulated dose.

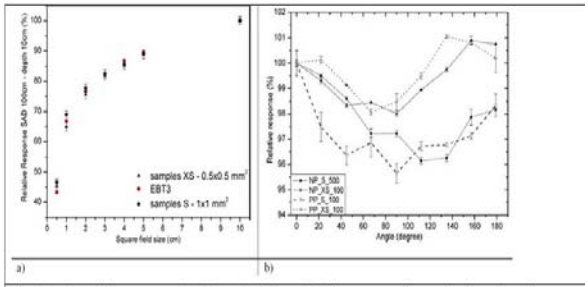

Fig.1: a) Output factor measured at 10 cm depth for a 6MV beam energy; b) angular dependence for p-type edgeless detectors with different top-peripheral junction configuration.

Conclusion: A radiation QA probe EDINA for small field dosimetry using new fabrication technology of silicon diodes and packaging has been developed. The EDINA has isotropic response, and well matching to EBT output field factor response making it suitable for small field dosimetry and quality assurance for SRS.

EP-1491

Energy response of radiophotoluminescent glass dosimeter for non-reference condition

S. Hashimoto[1], T. Okano[1], T. Furuya[1], S. KIto[1], K. Karasawa[1]
[1]*Tokyo Metropolitan Cancer and Infectious diseases Center Komagome Hospital, Radiation Oncology, Tokyo, Japan*

Purpose or Objective: When an absorbed dose to water is determined using radiophotoluminescent glass dosimeter (RGD), it is necessary to convert the radiophotoluminescent quantity into a water absorbed dose with calibration factor. Generally, dose calibration is performed at reference condition (on the central axis at a depth of 10 cm for a 10 cm×10 cm field). Although, patient specific dose measurement is performed at non-reference condition, RGD response may be changed because RGD has energy dependence. In this study, we evaluated the variation of RGD response for non-reference condition measurement using Monte Carlo (MC) simulation.

Material and Methods: To analyze the energy response of RGD for non-reference condition beam, absorbed dose ratio of water to RGD and mean mass energy absorption coefficient of water to RGD ((μen/ρ)w,RGD) was simulated using EGSnrc code. The irradiation conditions for the MC simulations were set to 5 cm×5 cm, 10 cm×10 cm and 20 cm×20 cm field for 10 MV photon beam. RGD was set to the central axis at 10 cm depth in water phantom. For 20 cm×20 cm field, 20 cm off axis position were calculated, respectively. The photon beams source for the MC simulation, radiation transport in the accelerator was modeled using the BEAMnrc Monte Carlo code. The accelerator geometry and materials were obtained from the manufacturer's data for the Clinac21EX.

Results: The dose ratio was from 1.168 to 1.149 for 5 cm×5 cm to 20 cm×20 cm, respectively. (μen/ρ)w,RGD was 1.079 and 1.075 for field sizes of 5 cm × 5 cm and 20 cm × 20 cm, respectively. When the field size became large, scattered low energy photon increase. Mass energy absorbed coefficient of RGD is very high for low energy photon. Therefore, the RGD response became increase with increase field size. In the 20 cm off axis position for 20 cm×20 cm field, energy response showed more variation. The dose ratio and (μen/ρ)w,RGD was 0.962 and 0.937, respectively. In out of field locations, the spectra contained more low-energy photons.

Conclusion: In this study, we evaluate the variation of RGD response for non-reference condition measurement. As a results, RGD response was affected by the low energy photon. This response change should be considered when the non-reference condition measurement is performed using RGD.

EP-1492

Basic investigation on performance of low-density polymer gel dosimeter

F. Pak[1], H.A. Nedaie[1], A. Takaavar[2], H. Saligheh rad[1], V. Vaezzadeh[3], M. Shojaee Moghadam[4]
[1]*Tehran University Of Medical Sciences, Medical Physics And Biomedical Engineering, Tehran, Iran Islamic Republic of*
[2]*Tehran University Of Medical Sciences, Medical Physics And Bio Medical Engineering, Tehran, Iran Islamic Republic of*
[3]*Tehran University Of Medical Sciences-Imam Khomeini Hospital, Cancer institute, Tehran, Iran Islamic Republic of*
[4]*Payambaran Hospital, Imaging Center, Tehran, Iran Islamic Republic of*

Purpose or Objective: In this study a series of basic dosimetric properties of a low density (LD) gel dosimeter are studied. The dose response is investigated regarding to temporal stability, detectable dose range, sensitivity, dose-rate and energy dependence as well as lung tissue equivalence.

Material and Methods: The LD gel is made by mixing the polymer gel with expanded polystyrene spheres. Methacrylic acid is used as a monomer and tetrakis-hydroxy-methyl-phosphonium chloride (THPC) as an oxygen scavenger (MAGAT polymer gel dosimeter). The temporal stability of LD gel is monitored for a period of a month. Energy dependence is studied at two energies; 1.25 MeV and 6 MV photon beam which are produced by 60Co and Linac machines.investigation of dose rate dependence is performed in the low, medium, and high absorbed region. Also reproducibility of dose response is studied in three sets of LD gel with identical preparation, irradiation and imaging procedure in three different days. Moreover the linearity and sensitivity is investigated up to dose of 20 Gy.

Results: The response of the gel indicates, the dose response curve attained stability during the measured time. The results also show that the dose response is reproducible. The gel response is found linear over the measured dose with r2=0.981 and sensitivity of 0.814 S-1Gy-1. In the measured range, the dose response of the NIPAM gel is independent of beam energy within less than ±0.02 and the dose rate had no effect on the gel response. LD gel is nearly lung tissue equivalent with average mass density of 0.35 to 0.42 g/cm3 and average relative electron density of 0.41.

Conclusion: MAGAT LD gel dosimeter appears to be a promising dosimeter in all aspects of dosimetric properties evaluated in this study. In addition, its high linearity together with no dose rate dependence in different level of dose make it a suitable dosimeter to measure 3D-dose distributions inside a non-homogeneous media such as lung tissue.

EP-1493

Modelling the energy dependence of Cherenkov light correction in plastic scintillation detectors

A. Dimitriadis[1,2,3], L. Archambault[4], C. Clark[2,3], H. Bouchard[3]
[1]*University of Surrey, Faculty of Engineering and Physical Sciences, Surrey, United Kingdom*
[2]*Royal Surrey County Hospital, Department of Medical Physics, Guildford, United Kingdom*
[3]*National Physical Laboratory, Acoustics and Ionising Radiation, Teddington, United Kingdom*
[4]*Université Laval, Department of Physics- Engineering and Optics, Québec, Canada*

Purpose or Objective: Plastic scintillation detectors (PSD) are highly valuable for a variety of dosimetry applications, since their atomic composition and volume size produce small perturbation effects. A commercial PSD provided by Standard Imaging Inc (Exradin W1) is available and its Cherenkov light correction is based on the method proposed by Guillot et al. However, recent studies showed that the Cherenkov light ratio (CLR) is energy dependent, which could compromise its performance in clinical photon beams. The goal of this work is to investigate a theoretical model to characterize the

energy dependence of the CLR and evaluate its effect on photon beam measurements.

Material and Methods: The electron energy cut-off at which Cherenkov light is produced varies with the wavelength-dependent refractive index. Based on this rationale, the theoretical CLR, describing the relative amount of blue to green light, is formalised analytically using the Cherenkov emission distribution and the detection efficiency functions of the blue and green channels. As the analytic expression depends on the electron spectrum, Monte Carlo simulations of several photon beam qualities are performed to evaluate the spectrum. This allows predicting the theoretical CLR as a function of the TPR2010 quality index (QI), which includes cobalt-60 and megavoltage (MV) beams. Experiments are performed to evaluate CLR over a wide range of QI in cobalt-60 and clinical MV beams.

Results: Comparison between experiments and theory show that the model reproduces the behaviour of the CLR energy dependence. However, the model under predicts the magnitude of the effect. For clinical MV beams, the variation of the theoretical CLR is about 0.5% while it is found to be about 1.8% with experiments. For cobalt-60 beam, the theoretical CLR is found to be about 1.005 of the value at the reference QI while the experiment reports a value of 1.017. Discrepancies between experiments suggest that other effects play a role in the energy dependence. More specifically, the model implicitly assumes isotropic Cherenkov emission, while the angular distribution of the light varies with the electron kinetic energy and the optical fibre only guides light emitted at a specific angular range. Further improvements modelling Cherenkov light transport explicitly should confirm these hypotheses.

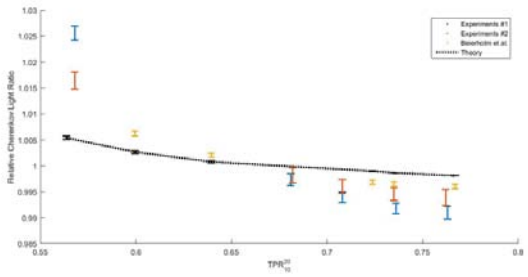

Conclusion: The theoretical model proposed in this work is promising to evaluate the energy dependence of the Cerenkov correction in commercial PSD. Potential applications of this work could allow determining the energy dependence of PSD measurements using the CLR technique in small photon fields.

EP-1494

Absolute dosimetry with EBT3 Gafchromic films in a pulsed electron beam at high dose-rate

M. Jaccard[1], K. Petersson[1], T. Buchillier[1], C. Bailat[1], J.F. Germond[1], R. Moeckli[1], J. Bourhis[2], M.C. Vozenin[2], F. Bochud[1]
[1]*CHUV - Institute of Radiation Physics IRA, Radiology, Lausanne, Switzerland*
[2]*CHUV, Radio-oncology, Lausanne, Switzerland*

Purpose or Objective: Animal studies have shown that irradiation by a pulsed electron beam with high dose-rate allows for tumour control while sparing normal tissues. Dosimetry of clinical high dose-rate pulsed beam is challenging because of dose-rate dependence and saturation effects. The aim of this study was to assess the suitability of Gafchromic EBT3 films for performing absolute dose measurements in the electron beam of a prototype linac capable of mean dose-rate (Ḋm) ranging from 0.07 to 1000 Gy/s, dose-rate in pulse (Ḋp) up to 106 Gy/s, and energy between 4 and 6 MeV. To this purpose, we evaluated the overall uncertainties of film dosimetry as well as the energy and dose-rate dependence of their response.

Material and Methods: Our dosimetry system is composed of EBT3 Gafchromic films (Ashland Inc., Wayne, NJ, USA) in combination with a flatbed scanner. All sources of uncertainties in film dosimetry (dispersion of pixel values, film inhomogeneity, reproducibility, scanner variability) were carefully evaluated using a conventional clinical linac. Energy dependence was also investigated by acquiring and comparing calibration curves at three different energies (4, 8 and 12 MeV), for doses between 25 cGy and 30 Gy. Dose-rate dependence was studied with the prototype linac for Ḋm ranging from 0.07 Gy/s to 1000 Gy/s and Ḋp between 103 and 106 Gy/s. The determination of dose-rate dependence was performed by comparing doses from the films to three independently calibrated dosimeters, namely thermo-luminescent dosimeter (TLD), alanine pellets and a chemical dosimeter based on methyl viologen (MV). Furthermore, we studied the correlation between the dose measured by the films and the total charge of electrons measured at the exit of the machine.

Results: We showed that, sticking to a fixed protocol of film processing, a total uncertainty below 4% (k=2) can be obtained in the dose range between 3.5 and 16 Gy. Results also demonstrated that EBT3 films did not display any significant energy dependence for electron energies between 4 and 12 MeV and doses between 25 cGy and 30 Gy since differences between calibration curves were all within uncertainties. In addition, we obtained excellent consistency between films, TLD, alanine and MV over the entire dose-rate range showing the absence of dose-rate dependency. This aspect was further corroborated by the fact that the dose per pulse as measured by films was proportional to the electron charge contained in the pulse.

Conclusion: Our study shows that the use of EBT3 Gafchromic films can be extended to absolute dosimetry in pulsed electron beams with very high dose-rate (Ḋm up to 1000 Gy/s and Ḋp up to 106 Gy/s) and energies between 4 and 12 MeV).The measurements results are associated with an overall uncertainty below 4% and are dose-rate and energy independent.

EP-1495

Evaluation of measurement dose uncertainty of Gafchromic EBT3 because of local inhomogeneity

E. Sukhikh[1], L. Sukhikh[2], E. Malikov[3], P. Filatov[4]
[1]*Tomsk Regional Oncology Center, Radiobiology, Tomsk, Russian Federation*
[2]*National Research Tomsk Polytechnic University, Applied Physics, Tomsk, Russian Federation*
[3]*National Research Tomsk Polytechnic University, Laboratory No 42, Tomsk, Russian Federation*
[4]*Meshalkin Research Institute of Circulation Pathology, Radiobiology, Novosibirsk, Russian Federation*

Purpose or Objective: Operation of any dosimeter assumes knowledge of the expected uncertainty that could be caused by different factors. The possible sources of uncertainty for Gafchromic EBT3 film were investigated (Phys. Med. v. 29(6), (2013) p. 599) where it was shown that the error amounted 0.55% neglecting local inhomogeneity of the film. The homogeneity of Gafchromic EBT2 film was investigated (Med. Phys. v. 37(4), (2010) p. 1753) and it was shown that inhomogeneity of absorbed dose amounted 6%. The purpose of current work is to calibrate Gafchromic EBT3 films using 10 MV photon beam, 6 MeV and 10 MeV electron beams and to estimate value of the measured absorbed dose uncertainty caused by the local inhomogeneity of the film.

Material and Methods: The calibration of Gafchromic EBT3 film was carried out using 10 MV photon beam and 10 MeV electron beam of Elekta Axesse linac, and also at 6 MeV electron beam using compact betatron for intraoperative therapy. In the case of Elekta Axesse the Farmer FC65-P cylindrical chamber and DOSE-1 electrometer were used. In the case of betatron we used the plane-parallel chamber PTW 23342 (Markus) and Unidose-E electrometer. The pieces of Gafchromic EBT3 film were irradiated by different doses

up to 40 Gy resulted in calibration curves. Due to the fact that the films were irradiated by the uniform field it was possible to estimate local inhomogeneity. The obtained calibration curve allowed to calculate dose from the net optical density of the irradiated films. Using standard error propagation techniques it was possible to estimate calculated dose uncertainty.

Results: The experimentally obtained dependences of reference dose on the film net optical density were fitted by the expression *D=a NetOD +b NetOD^n* (*a,b,n* are the free fit parameters). The comparison of calibration curves for different sources showed that the ones for 10 MeV electron beam and 10 MV photon beam coincide in the range (0.86-1.06) for the red channel and in the range (0.94-1.04) for the green channel depending on the value of net optical density. In the case of electron beams of different energies the coincidence is better for both channels. The values of obtained dose uncertainties lay within 5.5% for 6 MeV electron beam, 5% for 10 MeV electron beam and 7% for 10 MV photon beam (0.95 confidence interval).

Conclusion: The present work shows that homogeneity of the new generation of Gafchromic EBT3 film is better than previous generation one according to the measured dose uncertainty.

EP-1496

Small field correction factors for the IBA Razor

P.Z.Y. Liu[1], G. Reggiori[2], F. Lobefalo[2], P. Mancosu[2], S. Tomatis[2], D.R. McKenzie[1], N. Suchowerska[3]

[1]*The University of Sydney, School of Physics, Sydney, Australia*

[2]*Istituto Clinico Humanitas, Humanitas Cancer Center, Milan, Italy*

[3]*Chris O'Brien Lifehouse, Radiation Oncology, Camperdown-Sydney, Australia*

Purpose or Objective: A new p-type unshielded silicon diode, the Razor, has been introduced by IBA as a replacement for the IBA SFD diode. Both diodes are customised for measurements in small radiation fields, having a silicon chip of only 0.6 mm in diameter. The aim of this work is to characterize the response of the Razor in small fields and to evaluate small field correction factors if required (Alfonso et al 2008).

Material and Methods: Relative output ratios were measured in 6 MV and 10 MV X-ray beams, with and without a flattening filter, generated by three Varian linacs: the TrueBeam STX, the EDGE and the Novalis, . The output ratio was measured with the IBA Razor and the air core scintillation dosimeter (Lambert et al 2009) at a depth of 50 mm in water. The air core scintillation dosimeter, previously shown to provide accurate relative output ratios in small fields (Ralston et al 2012), consists of a cylindrical BC-400 plastic scintillator 1 mm in length and diameter (volume 0.8mm3). Correction factors for the Razor were calculated for MLC fields (5 and 10 mm in width) and stereotactic cones (4, 7.5 and 10 mm in diameter) using the air core scintillation dosimeter as a reference.

Results: The relative output factors measured for MLC fields on the Varian Truebeam STX are shown in Figure 1. The Razor exhibited an over-response that increases as the field size decreases, consistent with the reported behaviour of unshielded silicon diodes. For MLC fields, the over-response ranged from 2.9% to 5.2% for 5 mm fields and from 0.1% to 2.5% for 10 mm fields. For stereotactic cones, the average over-response was 8.3% for the 4 mm cone, 2.9% for the 7.5 mm cone and 1.4% for the 10 mm cone. Correction factors for specific field sizes were within 1% across the three different linac types. The beam energy and the presence of a flattening filter had a substantial effect.

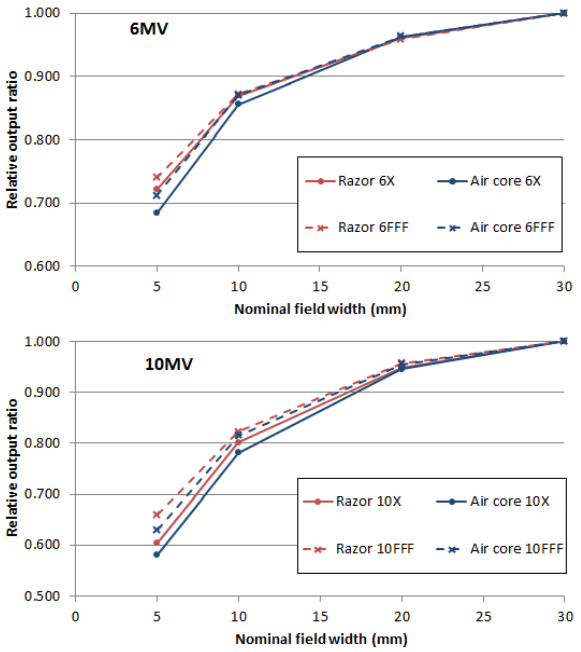

Conclusion: The new IBA Razor exhibits an over-response at small fields, which is consistent with the behaviour of other silicon diodes. Alfonso small field correction factors were experimentally determined using the air core scintillation dosimeter. The presence of a flattening filter was found to be an important feature of the beam that influenced the correction factor.

EP-1497

High resolution air-vented ionization chamber array for QA of VMAT and stereotactic treatments

M. Togno[1,2,3], D. Menichelli[1], C. Vogel[1], J.C. Celi[1], J.J. Wilkens[2,3], J. McGlade[4], R. Mooij[4], A. Olszanski[4], T. Solberg[4]

[1]*IBA Dosimetry GmbH, Physics and Innovation Department, Schwarzenbruck, Germany*

[2]*Technische Universität München, Klinikum rechts der Isar, Department of Radiation Oncology*

[3]*Technische Universität München, Physik Department, Munich, Germany*

[4]*Perelman Center for Advanced Medicine, Radiation Oncology Department, Philadelphia, USA*

Purpose or Objective: To characterize the 2D implementation of a new ionization chamber technology with high spatial resolution and charge collection efficiency for quality assurance in complex MV X-ray radiotherapy techniques such as VMAT and stereotactic treatments.

Material and Methods: The prototype device (Figure 1) consists of an array of air vented ionization chambers, with 1024 detector elements regularly arranged in a 32 x 32 matrix. The chamber center to center spacing is 4 mm, resulting in an active area of 12.4 cm x 12.4 cm. Dosimetric characterization as well as a comparative evaluation of treatment plans for a variety of clinical localizations and techniques has been performed in a plastic phantom. A CT scan of the device within the phantom was acquired and imported in the Varian Eclipse treatment planning system (TPS) in order to compare the planned and measured dose distributions. Irradiation was performed on two different accelerators: a Varian True Beam and a Cyberknife G4 equipped with an iris collimator (both at UPENN, Dept. of Radiation Oncology, Philadelphia). The characterization has been performed for VMAT, IMRT and stereotactic treatment plans with different beam qualities and dose rates. Other reference detectors used for comparison included radiochromic film (RCF) and a commercial array based on diode technology.

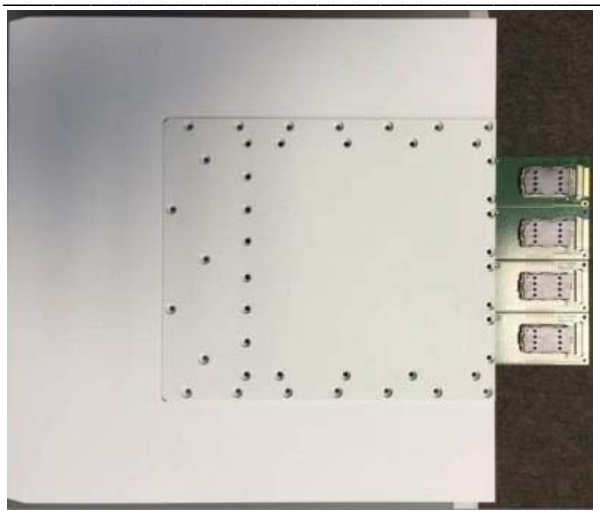

Figure 1. The array prototype inserted in a RW3 phantom adapter.

Results: Response reproducibility, short term stability and linearity with dose are those typical of ionization chamber based detectors. Maximum deviation of approximately 1.5% in sensitivity was observed in the range 0.1 – 2.5 mGy/pulse. For all different clinical evaluations, the array was found to be in very good agreement with the reference detectors. Dose distributions with steep gradients are very well defined due to the 4 mm spatial resolution and to the limited effect of volume averaging. Additionally, good agreement was observed between the expected dose from TPS and the measurements. Moreover, the detector insensitivity on dose per pulse in conjunction with the low energy dependence typical of ionization chambers lead to high performance even when therapy beams feature extremely modulated dose rates.

Conclusion: After an extensive clinical investigation the ion chamber array technology under investigation has been proven to be valuable for patient plan quality assurance, especially when highly modulated fields are used, including unflattened beams.

EP-1498

LET dependence of the PTW-60019 microDiamond detector response in particle beams

S. Rossomme[1], A. Delor[2], J. Hopfgartner[3], J. Denis[2], S. Vynckier[2], H. Palmans[4]
[1]*Université Catholique de Louvain- Institute of Experimental & Clinical Research, Molecular Imaging- Radiotherapy & Oncology, Brussels, Belgium*
[2]*Cliniques Universitaires Saint-Luc, Radiotherapy and Oncology Department, Brussels, Belgium*
[3]*EBG MedAustron GmbH, Wiener Neustadt, Austria*
[4]*National Physical Laboratory, Acoustics and Ionising Radiation Division, Teddington, United Kingdom*

Purpose or Objective: This work describes investigations that were carried out to assess the effect of the linear energy transfer (LET) on the response of a new synthetic single crystal diamond detector. The investigations were performed comparing the response of a PTW-60019 microDiamond detector (µD) to the response of ionization chambers (IC).

Material and Methods: Two experimental sessions were performed in mono-energetic particle beams. Using a µD with its axis parallel to the beam axis, its response was compared to the response of a Roos type IC in a 60 MeV proton beam and a Markus IC in a 62 MeV/n carbon ion beam. For both experimental sessions, the beam was monitored using an IC placed in front of the detector under investigation. As recommended by IAEA TRS-398, the response of the IC was corrected for temperature, pressure, polarity and ion recombination effects. The latter was studied during experimental sessions, using two IC positioned face to face, under the same experimental conditions as for the comparison with the µD. The experimental procedure for the determination of the recombination effects consisted of changing the voltage applied to the IC under investigations and studying the saturation curve. The determination of the recombination effect was performed at different depths. No correction was applied to the response of the µD.

Results: In the proton beam, two different values for the ion recombination correction factor (*ks*) were used to correct the response of the Roos IC: *ks* = 1.0035 in the plateau region, and *ks* = 1.004 in the Bragg Peak region. In carbon ion beam, *ks* varies from 1.01 at the entrance of the plateau and it increases slightly in the plateau region and strongly in the Bragg Peak region due to the increase of the LET, to reach 1.06 in the distal edge region.
For both beams, comparison between the responses of both detectors shows a good agreement in the plateau region. In proton beam, considering the uncertainties, no significant difference between both detectors is observed in the Bragg Peak region. The combined relative standard uncertainty of the results is estimated to 0.28% in the plateau region and 14% in the distal edge region. These values are dominated by the uncertainty of range determination. In the carbon ion beam, an under response of the µD of 20% is observed in the Bragg Peak region. The combined relative standard uncertainty of the results is estimated to 2.3% in the plateau region and 12% in the distal edge region. These values are dominated by the uncertainty of alignment in the non-uniform beam and the uncertainty of range determination.

Conclusion: Results were obtained for one particular detector only. However, confirmed by other publications, we can conclude that the LET-independent response in clinical proton beams is a characteristic of the PTW-60019 µD. This conclusion has to be investigated in more details for the carbon ion beams, for which our study show that the detector should not be assumed to be LET independent.

EP-1499

GEANT4 Monte-carlo simulations for the luminescence properties of Gd2O3:Eu scintillator

G.S. Cho[1], S.H. Choi[1,2], S.S. Lee[1,3], Y.H. Ji[1,2,3], S. Park[1], H. Jung[1,3], M.S. Kim[1,2,3], H.J. Yoo[2], K.B. Kim[1,2,3]
[1]*Korea Institute of Radiological and Medical Science, Research center for Radiotherapy, Seoul, Korea Republic of*
[2]*Korea Institute of Radiological and Medical Science, Department of Radiation Oncology, Seoul, Korea Republic of*
[3]*University of Science and Technology, Radiological &Medico-Oncological Sciences, Daejeon, Korea Republic of*

Purpose or Objective: In an indirect radiation detector modeling using Monte-carlo methods, a scintillator modeling that has same luminescence properties with a measured data is firstly performed. Therefore, in this study, we compared the measured and calculated properties of scintillator and we tried to verify an effectiveness of GEANT4 code for the scintillator modeling.

Material and Methods:

1) synthesis of scintillator
In this study, to measure the luminescence properties, we synthesized Gd2O3:Eu used as a radiation conversion material using low-temperature solution combusition method. The properties of the synthesized scintillator were obtained by measuring photoluminescence spectrum and the decay time using a PL spectrometer. For the measurement of photoluminescence spectrum, 254nm UV light generated from a xenon(optical photon) lamp was used to excite the phosphor; then, the emitted light was obtained through a monochromator and PMT.
2) Monte-carlo simulations
In this study, GEANT4 code was used for the scintillator modeling. To reduce error rate, we use 70kVp energy spectrum and an optical and scintillator physics process were used. An energy range of the scintillator were defined based on measured data. For an effective simulation, we only

scored optical photon correspond to each energy band and MPI paralled computing was used.

Results: The measured a photoluminescence peak value of the Gd2O3:Eu was 611nm, which was identical with literature value. In case of the calculated value using GEANT4 monte-carlo code, an intensity(counting) of the photoluminescence peak value was 2 times higher, but the peak value also was identical with measured the peak value and overall trend of the photoluminescence spectrum was correspond to the measured data. A result of the decay time showed that the measured value was 1.2 times higher than that of the calculated value despite the higher intensity, but the measured and calculated value was well matched in low intensity.

Conclusion: In this study, we performed Gd2O3:Eu modeling using GEANT4 and compared measured and calculated the properties of the scintillator. Through the results, we demonstrate the effectiveness of the GEANT4 code for the scintillator modeling and it was used as valuable data for the inderect raidation detector modeling using GEANT4. However, the properties of the scintillator were various according to the ratio of the body material and activator. Therefore, GEANT4 can reflect the ratio of the body material and activator and it considered as future works.

EP-1500

Development of tumor response observation system for dose-volume delivery guided particle therapy

T. Nishio[1], T.O. Takashi Okamoto[2], S.K. Shinto Kabuki[3], T.T. Toru Tanimori[4], T.A. Tsukasa Aso[5], S.N. Satoshi Nakamura[6], M.H. Masahiro Hiraoka[7], K.M. Keiichirou Matsushita[1], A.N.M. Aya Nishio-Miyatake[8]

[1]*Hiroshima University, Institute of Biomedical & Health Sciences, Hiroshima, Japan*

[2]*Hamamatsu Photonics K. K., Electron Tube Division, Shizuoka, Japan*

[3]*Tokai University, Graduate school of Medicine, Kanagawa, Japan*

[4]*Kyoto University, Graduate school of Science, Kyoto, Japan*

[5]*National Institute of Technology Toyama College, Department of Electronics & Computer Engineering, Toyama, Japan*

[6]*National Cancer Center Hospital, Department of Oncology, Department of Radiation Oncology, Japan*

[7]*Kyoto University, Graduate school of Medicine, Kyoto, Japan*

[8]*Keen Medical Physics Co. Ltd., Department of Medical Physics Research, Kanagawa, Japan*

Purpose or Objective: We have made innovative proton therapy achieved by imaging technique of positron emitter nuclei generated in the patient body on target nuclear fragmentation reaction and development of a beam ON-LINE PET system (BOLPs). It was found that between the proton delivery dose to the tumor and the activity of positron emitter nuclei generated from the target nuclear fragmentation reaction in tumor have correlation. The purpose of this study is to research and develop a tumor response observation system with delivered dose in particle therapy.

Material and Methods: The specification and design of tumor response observation system for dose-volume delivery guided particle therapy (TROS-DGPT) were performed. And in the TROS –DGPT, a spec of detection head for measurement of various gamma rays emitted from nuclear fragment reaction and nuclear excitation reaction was evaluated.

Results: It was important to measure efficiently the various gamma rays emitted from the patient body by the nuclear reaction with particle beam radiation. Therefore, the high detection efficiency and measurement time resolution were required for development of the TROS –DGPT. The TROS –DGPT was made the specification and the design with both the PET function and Compton Camera function for gamma ray detection head. Results of vibration, impact and temperature tests for developed GSO detector module were good.

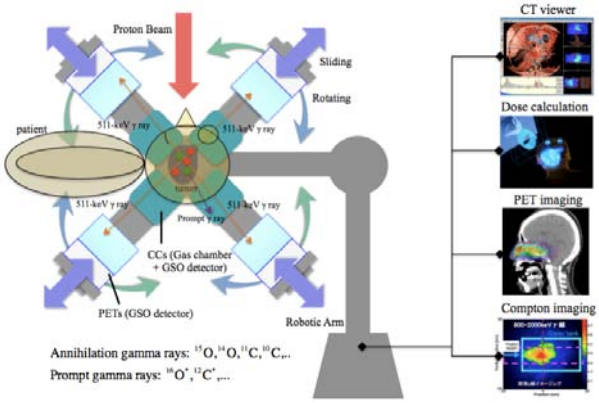

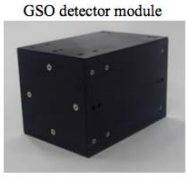

- Vibration test: 5G, 7.5G, 10～500 Hz, 1 Oct/min, 10 cycle, XYZ Axis
- Impact test: 30G, 75G, 11 ms, 3 Shocks/Direction, 5 Directions, 10～500 Hz
- temperature test: -40 ℃～+70 ℃, 3 h keep condition, 10cycle

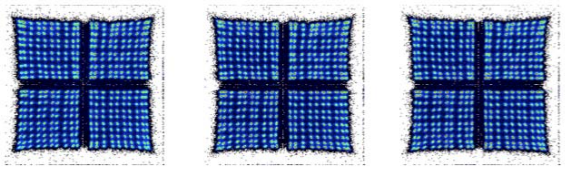

Conclusion: The specification and the design of the TROS –DGPT were decided for an innovative particle therapy. We will research and develop for completion of this system 3 years later.

EP-1501

New material for high resolution dosimetry using radiation induced changes in fluorescence response

N.H. Sanders[1], M.R. Bernal[1], L.R. Lindvold[1]

[1]*Risoe National Laboratory, DTU Nutech, Roskilde, Denmark*

Purpose or Objective: We are developing a new radiation-sensitive polymer material for radiation therapy dosimetry with high spatial resolution for use in 3D solid state dosimetry. The key methods of this project are to determine the radiation dose by measuring its fluorescence, instead of the absorbance which is a more established method[1][2], and to dissolve the radiochromic dye in a rigid polymer matrix. Measuring the fluorescence enables higher spatial resolution and sensitivity, and the polymer matrix prevents degradation and diffusion of the exposed dye over time. In this study we have established that this material shows a linear relationship between the absorbed dose and the fluorescence response.

[1] W.L. Mclaughlin, A. Miller, S. Fidan, K. Pejtersen. Radiat. Phys. Chem. 10 (1977) 119-127.

[2] Niroomand-Rad et al. Radiochromic film dosimetry. AAPM Report No. 63 (1998).

Material and Methods: The key elements of this radiochromic material are a solid polymer matrix with additives and a triphenylmethane leuco dye. Thin films of the material were irradiated multiple times with a Co-60 source, and the absorbance and fluorescence responses were measured initially and after each irradiation session. The fluorescence was excited by a 532 nm YAG laser, and was measured with an Ocean Optics QE6500 spectrometer.

Results: The fluorescence response increased linearly with the absorbed dose from 0 to 200 Gy. The absorbance also increased linearly, indicating that the fluorescent dye is the only chemical in the material with a significant absorption in the relevant wavelength range. The dye absorbs from 500 nm to 575 nm and the fluorescence response is in the range from 565 nm to 650 nm.

Conclusion: We have established that the material exhibits a linear relationship between fluorescence response and radiation dose. The fluorescence response is strong enough to be used at low doses. Measurements on individual samples are highly reproducible, but the variance between different samples is still too high to be used at clinically relevant doses. We expect that this variance can be reduced through improvements to the sample preparation. The fluorescence response of the radiochromic dye is highly dependent on the composition of the polymer matrix, since a different study[3] using the same dye observed a decrease in fluorescence with increasing dose. The factors affecting the fluorescence of the dye and hence its dosimetric properties are still being investigated, but in this work we have shown that dosimetry measurements are possible with this novel material. With improvements this could become a precise quantitative 3D dosimeter that is inexpensive, quick, and easy to use.

[3] A.A.Abdel-Fattah, W.B.Beshir, El-Sayed A.Hegazy, H.Ezz El-Din. Photo-luminescence of Risø B3 and PVB films for application in radiation dosimetry. Radiat. Phys. Chem. 62 (2001) 423-428.

EP-1502

Effects on dosimetric measurements due to difference in calibration and dosimetry protocols followed

W. Muhammad[1], A. Hussain[2], Asadullah[3]

[1]*Pakistan Institute of Nuclear Science and Technology-, Heath Physics Division HPD-, Islamabad, Pakistan*

[2]*Aga Khan University Hospital, Department of Oncology-, Karachi, Pakistan*

[3]*Pakistan Institute of Nuclear Science and Technology-, Heath Physics Division HPD, Islamabad, Pakistan*

Purpose or Objective: Radiation dosimetry plays a vital role in external beam radiotherapy. For precise and accurate dose delivery, the dosimetry system should be calibrated properly, following the recommendations of standard dosimetry protocols e.g. TG-51 or TRS-398. Nonetheless, the dosimetry protocol followed by calibration laboratory is often different from the protocols in practice at various clinics. The study is designed to investigate the effects added in dosimetry measurements due to such situations.

Material and Methods: In this study, the dosimetry were performed for a Co-60 teletherapy unit and a high-energy Varian linear accelerator (CLINAC) with 6 and 15 MV-photon and 6, 9, 12 and 15 MeV-electron beams, following the recommendations and reference conditions of AAPM TG- 51 and IAEA TRS-398 dosimetry protocols. A PTW water phantom (T41014) with a cylindrical chamber (PTW-30001) connected to an electrometer (PTW UNIDOS E) was used for the absolute dosimetry of Co-60 unit. Similarly, dosimetry systems consisting of a farmer type ionization chamber (IBA-FC65-G) and a plane-parallel chamber (IBA PPC-05), connected to an electrometer (PTW UNIDOS E) in a Wellhofer water phantom was used for absolute dosimetry of two photon beams and four electron beams dosimetry respectively. Each chamber type combined with PTW UNIDOS E was calibrated in a Co-60 radiation beam at Secondary Standard Dosimetry Laboratory (SSDL) PINSTECH, Pakistan, following the IAEA TRS-398 protocol.

Results: The measured ratios of absorbed doses to water Dw (TG-51/TRS-398) were 0.999 and 0.997 for 6 and 15 MV photon beam respectively whereas the ratios were 1.013, 1.009, 1.003 and 1.000 for 6, 9, 12 and 15 MeV electron beams, respectively as shown in Figure 1 (a & b). The difference arises between the two protocols mainly due to beam quality (KQ) and ion recombination correction factor (Table 1).

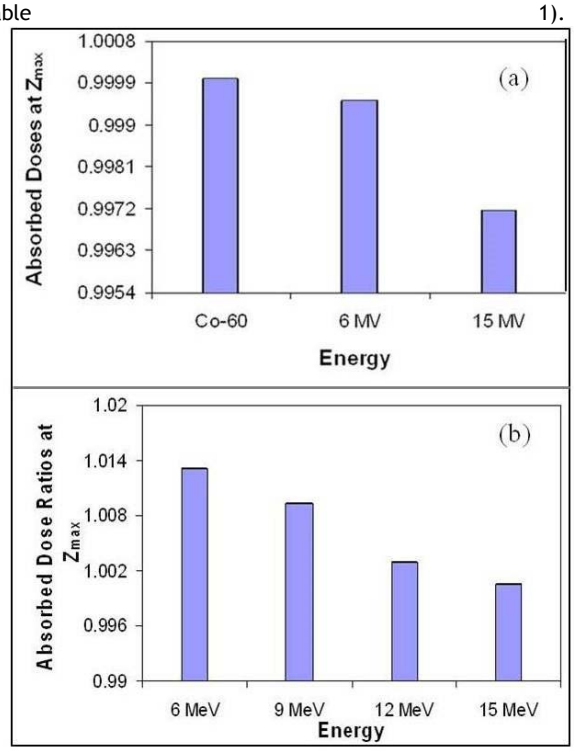

Figure 1: (a) Ratio of the absorbed doses at Zmax of Co-60, 6 MV and 15 MV photons by using two protocols (TG-51 / TRS-398). **(b)** Ratio of the absorbed doses at Zmax of 6, 9, 12, 15 MeV Electron beam by using two Protocols (TG-51 / TRS-398).

Table 1: Comparison of the Absorbed Doses at Z_{max}, beam quality factor (K_Q) and ion recombination correction factor, (P_{ion}) values of AAPM TG-51 and IAEA TRS-398 Protocols.

Type of Beam	Energy	AAPM TG-51				IAEA TRS-398				
		$\%dd(10)_x$		P_{ion}	K_Q	$D_W(Z_{max})$	$TPR_{20,10}$		P_{ion}	K_Q	$D_W(Z_{max})$
Photon	6 MV	66.7		1.00734	0.991	0.9970	0.668		1.00714	0.992	0.99748
	15 MV	77.63		1.01135	0.970	0.9967142	0.762		1.01109	0.973	0.999535
	Co-60	NA		1.0	1.0	1.6489	NA		1.0	1.0	1.6489
Electron		R_{50} (cm)	Z_{ref} (cm)				Z_{max} (cm)	$R_{50,ion}$ (cm)			
	6 MeV	2.15	1.19	1.023	0.937	1.026418	1.08	2.15	1.023	0.928	1.013106
	9 MeV	3.459	1.975	1.00503	0.921	1.0056445	1.99	3.42	1.00455	0.913	0.99643
	12 MeV	4.910	2.846	1.013377	0.908	1.005852	2.44	4.83	1.013099	0.905	1.002825
	15 MeV	6.237	3.642	1.013551	0.8983	0.998504	2.8	6.12	1.013277	0.898	0.997916

Conclusion: In conclusion TRS-398 gives relatively high doses than TG-51 and the percentage difference increases as the energy increases for photon beams. While in case of electron beams TG-51 calculates relatively high doses than TRS-398 and percentage difference decreases as the energy increases. Since the chambers are calibrated according to the recommendations of IAEA TRS-398 Dosimetry protocol, all the medical centres are requested to follow the IAEA TRS-398 Dosimetry protocols.

EP-1503

Small field output correction factors for 6-X and 6-X FFF beams: GAMOS Monte-Carlo study

D. Akcay[1], R. Kandemir[2], O. Azaklıoglu[2]

[1]*Dokuz Eylul University Medical Faculty, Radiation Oncology, Izmir, Turkey*

[2]*Dokuz Eylul University Institute of Health Sciences, Medical Physics, Izmir, Turkey*

Purpose or Objective: Our purpose was to calculate detector specific small field output correction factors with GAMOS Monte Carlo (MC) for 6-X and 6-X flattening filter free (FFF). In this study MC simulations and water phantom measurements were used to obtain correction factors.

Material and Methods: A formalism of Alfonso et al for correction of output factor measurements was used in the current study. Absorbed dose to water was calculated with MC using 2x2x2 mm^2 voxel at 5 cm depth of water phantom. “Range cut” and “Kill particles at BIG X/Y” options were used to optimize simulation in GAMOS MC. Results were obtained below 2% statistical noise. Fields sizes varied from 4x4 to 1x1

cm^2. Also water phantom measurements were taken at same field sizes at source phantom distance 95 cm with diode(photon) and PinPoint ion chamber to use in formalism. Varian TrueBeam STx LINAC was used for the purpose.

Results: For diode detector, correction factors were 0.993 and 1.000 for 3x3, 4x4 cm2 at 6-X respectively and correction factors of 0.999 and 1.000 were found for 6-X FFF. For smaller field sizes, obtianed correction factors were below 0.98 for both energies. For ion chamber at the smallest field size, the respective correction factors were 1.046 and 1.079 for 6-X and 6-X FFF. At 2x2 cm2 , it was 0.971 and 0.967 for 6-X and 6-X FFF respectively. However, with increase of field size, the value of correction factors for ion chamber became close to 1.0.

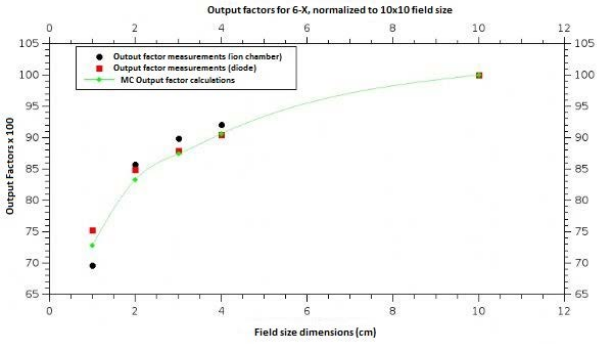

Output Correction Factors for diode and ion chamber at 6-X energy

Dedector Model	1x1	2x2	3x3	4x4	10x10
TM60016 – Diode(photon)	0.968	0.980	0.993	1.000	1.000
TM31014 - PinPoint Ion Chamber	1.046	0.971	0.972	0.983	1.000

Conclusion: For ion chamber, at 1x1 and 2x2 field sizes, correction factors were up to 3% more or less than of optimum value of 1.0. Our MC calculations showed that Pinpoint detector required output correction factor for field sizes below 3x3 cm2. For diode detector this requirement was for field sizes below 2x2 cm^2.

EP-1504

Evaluation of transmission detector model using Monte Carlo simulation of VMAT delivery

D. Johnson[1], D. Thwaites[2], V. Cosgrove[1], S. Weston[1]
[1]*Leeds Teaching Hospitals NHS Trust, Medical Physics, Leeds, United Kingdom*
[2]*University of Sydney, Medical Physics, Sydney, Australia*

Purpose or Objective: The Device for Advanced Verification of IMRT Deliveries (DAVID) is a novel, transparent transmission detector. It is designed for in-vivo verification by measuring the radiation fluence from the linac head during treatment. In order to investigate its properties and sensitivity to standard errors it was desirable to build an accurate Monte Carlo model of the device. In this study a working Monte-Carlo model of the detector was built and verified by comparing simulation and measured signals from simple square fields as well as complex IMRT and VMAT fields.

Material and Methods: All results were collected on an Synergy linear accelerator (Elekta AB, Stockholm, Sweden) equipped with an MLCi2 collimator. All treatment plans have been delivered as clinical treatments in the department and were generated by the Monaco 3.3 TPS (Elekta AB, Stockholm, Sweden). The Monte Carlo simulation of the linac and DAVID used BEAMnrc and DOSXYZnrc.
The DAVID is a transmission style detector, specific to the linac (MLC) model. As the MLCi2 collimator has an 80 leaf (40 leaf pairs) MLC; the DAVID used in this work had 40 wires. These collection wires are held in a 2mm thick vented air gap that is encased by two polymethyl methacrylate (PMMA) plates, each 4mm thick. On the inside of the PMMA a thin layer of aluminium is been evaporated on to the inner surfaces; this layer is thin enough so that the device remains optically transparent, but thick enough to maintain a potential of 400V between the plates and the collection wires. Ionisation charge in the air gap, as a consequence of primary and scattered radiation, migrates towards the collection wires under the influence of the potential, each wire having a collection area of 0.03 cm3 per centimeter of length.
It was shown that the collection wires had a negligible effect on the dose deposited in the collection volume allowing the DAVID to be modeled as two 4mm slabs of Perspex separated by a 2mm air gap.

Results: The DAVID signal measured on the linac was shown to be repeatable and stable. All simulated results were shown to agree with measured results to within 3% of the maximum signal
..

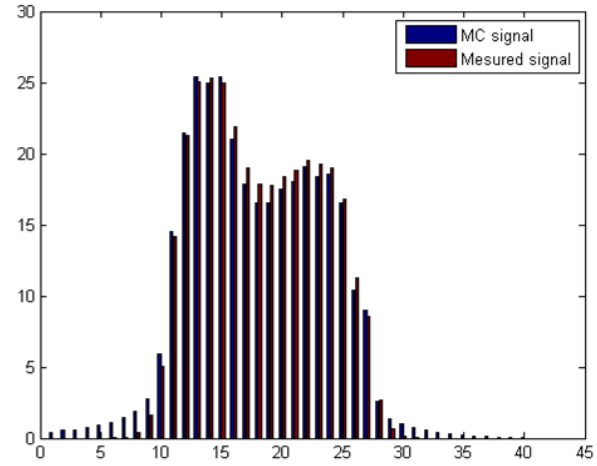

Conclusion: The Monte Carlo model of the DAVID works well for both simple and complex deliveries. The model will provide a useful tool for investigating the sensitivity of the DAVID to linac faults. These can easily be simulated for a variety of cases in the Monte Carlo model.

EP-1505

Comparison of two unshielded diodes for commissioning of Cyberknife

E. Gershkevitsh[1], G. Boka[2]
[1]*North-Estonian Regional Hospital Cancer Center Radiotherapy, Radiotherapy, Tallinn, Estonia*
[2]*Riga East University Hospital- Clinic of Therapeutic Radiology and Medical Physics, Clinical Medical Physics and Dosimetry, Riga, Latvia*

Purpose or Objective: The aim of this study was to evaluate the suitability of two recently launched unshielded diodes for commissioning of CyberKnife (Accuray Inc., Sunnyvale, CA) system.

Material and Methods: IBA Razor (IBA dosimetry GmbH, Schwarzenbruck) and PTW SRS 60018 (PTW Freiburg, Freiburg) diodes were used to commission CyberKnife M6 unit. TPR/PDD, OCR and output factors for 12 stereotactic cones (range 5-60mm) were measured with both detectors using PTW MP3-M water tank. The measurement results were compared between each other and with the composite data from the manufacturer.

Results: Output factors measured with both diodes agreed within 1% to the manufacturer supplied uncorrected data for all cones except 5 mm. For 5 mm cone differences of up to 2.3% were observed. Output factors for 5 mm cone were also compared with published Monte Carlo data and correction factors for PTW SRS 60018 and IBA Razor diodes are 0.95 and 0.94, respectively were noted. The difference is being larger for IBA Razor diode. For all other cones the correction for IBA

Razor diode is being smaller than for PTW SRS 60018 diode. PDDs agreed well for both diodes for the measured cones. The tale of the profile for 60 mm cone at 30 cm depth is being overestimated by approximately 10% for both detectors compared to the profiles measured with PTW 31010 ionization chamber. The dose per pulse dependence for IBA Razor diode is larger than for PTW SRS 60018 diode.

Conclusion: Both detectors are suitable for commissioning of Cyberknife M6 system. Correction factor required for 5 mm cone for IBA Razor diode is larger than for it predecessor – IBA SFD diode (as based on published data). Both detectors require correction factors in order to account for the overestimation of the signal. Because of lower sensitivity the time required to collect the same quality data with IBA Razor diode is about 3 times greater than for PTW SRS 60018.

EP-1506

Investigation of PTW's "microDiamond" detector for dosimetry in small animal radiotherapy research

S. Kampfer[1,2], J.J. Wilkens[1,2]
[1]*Klinikum Rechts der Isar- TU München, Department of Radiation Oncology, München, Germany*
[2]*TU München, Physik Department, München, Germany*

Purpose or Objective: The recently presented single crystal diamond detector (SCDD) from PTW (PTW-Freiburg, Germany) called microDiamond (µD, type TM60019) is especially meant to be used in small field dosimetry. As irradiation experiments of small animals in preclinical settings often use small fields this µD detector could potentially be the right device in this special field of interest.

Material and Methods: Two different kinds of measurements were performed: a) horizontal and vertical beam profiles, and b) depth dose curves. Both types of measurements were done in solid water slabs for two field sizes: 5x5 mm² and 10x10 mm². Measurement a) was done in 2 cm depth with the detector in the isocenter. The orientation of the detector was perpendicular to the beam axis and in terms of rotation in a suitable position to prevent effects due to unequal sensitivity. Measurement b) was performed with a fixed SSD of 304 mm and in depths in the range from 0 to 51 mm. The detector's axis was parallel to the beam axis during this measurement. To enable the comparison of our measured depth dose, the µD detector was calibrated for our distinct setup against a standard ionization chamber in a large field. We compared the results of the µD detector to film measurements with radiochromic films (Gafchromic EBT3, Ashland, USA).

Results: The results of the beam profile measurements with the µD detector of the 10x10 mm² field are 10.10 mm in horizontal and 10.16 mm in vertical direction for the field width at half maximum (FWHM). For the 5x5 mm² field the µD results are 5.08 mm in both directions. The measured depth dose curve shows values from 4.05 Gy/min in a depth of 1 mm and 3.71 Gy/min in 5 mm down to 1.14 Gy/min in 51 mm. In comparison, the field size measurements with the film resulted in 10.16 mm (5.19 mm) for horizontal and 10.20 mm (5.20 mm) for vertical direction for the 10x10 mm² (5x5 mm²) field. This means a very good agreement in the 10x10 mm² field (difference less than 0.1 mm or 1%). In the 5x5 mm² field, the differences between film and µD is 0.11 mm and 0.12 mm (less than 2.4%). Depth dose curve measurements show also very good agreement of the two methods. In a depth of 5.3 mm the film measurements produced 3.68 Gy/min, in 51.4 mm depth 1.16 Gy/min (maximum deviation of about 2 %).

Conclusion: We showed measurements with the µD detector of two very important variables of radiation fields and their comparison to reference measurements with radiochromic film. As the discrepancy between both methods is very small, these findings justify the usage of the described µD detector for quality assurance measurements in preclinical research, especially for the SARRP.

EP-1507

Which detector for small photon field measurements?

M. Casati[1], A. Compagnucci[1], C. Arilli[1], L. Marrazzo[1], G. Simontacchi[2], D. Greto[2], S. Pallotta[1], C. Talamonti[1]
[1]*University of Florence, Azienda Ospedaliero Universitaria Firenze - SOD Fisica Medica, Florence, Italy*
[2]*University of Florence, Azienda Ospedaliero Universitaria Firenze - SOD Radioterapia, Florence, Italy*

Purpose or Objective: Dosimetry in small fields is an open issue, due to several sources of errors, reported in literature. The purpose of this work is to compare the response of different detectors for the measurements of output factors (OF), profiles and percentage depth dose (PDD) curves for Elekta Synergy S BM 6MVRX beams and field sizes from standard (10.4cmx10.4cm) down to 0.8cmx0.8cm.

Material and Methods: We tested the detectors reported in the first table.

tested detectors	volume (mm3)	diameter (mm)	thickness (mm)	☺	☹	μ_{en}/ρ (cm^2/g)	ρ (g/cm^3)
Single crystal diamond detector (SCDD)	0.004	2.2	0.001	small thickness, mass energy absorption coefficient similar to water	2mm diameter active area => volume averaging effetcs => under response, high density => overresponse in small fields	☺	3.5
Exradin W1 plastic scintillator	2.4	1	3	very good water equiv.	instable, not user friendly	☺	1.05
Iba Razor diode	0.01	0.6	0.02	small active volume	overresponse to low energy	☹	~2.3
Exradin D1V diode	0.05	1.1	0.05	small active volume	overresponse to low energy	☹	~2.3
Exradin A26 ion chamber	15	3.3			volume averaging effects	☺	
Exradin A1SL ion chamber	57				volume averaging effects	☺	
Film gafchromic EBT3			0.28	good water equiv. And spatial resolution	noise	☺	

No corrections were made for the difference between detectors and water (fluence perturbation and non water-equivalence) neither for volume averaging effects.

Results: OF were referred to 3.2cm field and deviations calculated respect to W1 as reference detector, both for its smaller dimensions and its better water equivalence.

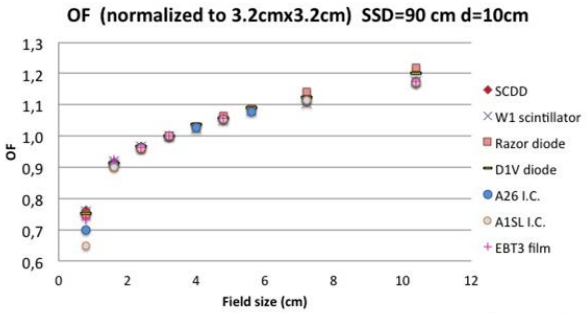

field size (cm)	diamond SCDD	scintillator W1	diodes Razor	diodes D1V	ion chambers A1SL	ion chambers A26	film gafchromic
10,40	-0,5%	0,0%	3,8%	2,3%	-0,4%	-0,1%	-0,1%
7,20	0,6%	0,0%	3,3%	1,9%	0,9%	0,9%	
5,60		0,0%	0,9%	1,0%		-0,3%	
4,80	0,4%	0,0%	1,3%	0,7%	0,2%	0,5%	0,6%
4,00		0,0%	0,6%	1,2%		0,4%	
3,20	0,0%	0,0%	0,0%	0,0%	0,0%	0,0%	0,0%
2,40	-0,1%	0,0%	-0,7%	0,0%	-0,6%	-0,4%	-0,5%
1,60	-0,1%	0,0%	-1,4%	-0,7%	-2,0%	-1,3%	0,6%
0,80	0,6%	0,0%	-1,1%	-0,9%	-14,3%	-8,0%	-3,5%

For large fields all detectors agree within 1% except for diodes, which show an over response for large fields, due to low energy scattered radiation. SCDD is in agreement with W1 within 0.6% for all field sizes, also down to 0.8cm, maybe for compensation effects between the over response due to high density and the under response due to volume averaging effects. For 1.6cm and 0.8cm, ion chambers show an under

response up to 14% A1SL and 8% A26 (volume averaging effects), D1V diode is in agreement with W1 within 1%, while Razor diode shows a more pronounced under response presumably due to the enclosure, given its smaller dimensions respect to D1V. Film shows a deviation of -3.5% for 0.8cm field, due to the sampling area, limited inferiorly by noise.
As for PDDs, A26 can be trusted as reference detector for 10.4cm field (no volume averaging effects). Razor diode shows an over response up to 3% at 20cm depth respect to A26 (low energy scattered radiation). Also W1 shows an over response, up to 4% at 20cm depth, respect to A26.
For field sizes under 2cm, volume averaging effects should be considered, especially for ionization chambers, in function of depth. PDD at large depth could in some case be overestimated if large volume effects occur. In this case W1 could be taken as reference, for its small active area and water equivalence. Razor shows a slight over response (within 1%), probably due to low energy scattered radiation, while A26 shows an over response, maybe due to volume averaging effects, up to 3%.
Profiles obtained with Synergy S BM have a minimum penumbra of some mm, so are well represented by all detectors with diameter of the active area inferior or equal to 1mm.

Conclusion: For small filed sizes (< 3cm) it is still not possible to identify a reference detector, with an optimal behaviour. For 6MVRX beams by SynergyS BM and field sizes down to 1cmx1cm, SCDD seems to offer the best compromise, since compensation between opposite effects (volume averaging and density) occurs, which allows to avoid corrections. For smaller fields, steeper penumbras or better accuracy, corrections for the above mentioned effects should be applied and detector should be used perpendicular to beam axis for penumbra sampling.

EP-1508

Multicenter study of FFF beams with a new stereotactic diode: can be defined a universal OF curve?

E. Cagni[1], S. Russo[2], A. Botti[1], S. Bresciani[3], V. Bruzzaniti[4], D. Fedele[5], M. Iori[1], S. Naccarato[6], B. Nardiello[7], L. Orsingher[1], G. Reggiori[8], A. Rinaldi[7], R. Ruggieri[6], M. Stasi[3], L. Strigari[4], M. Zani[5], P. Mancosu[8]
[1]*Arcispedale S. Maria Nuova-IRCCS, Medical Physics, Reggio Emilia, Italy*
[2]*ASF, Medical Physics, Firenze, Italy*
[3]*Istituto di Candiolo-IRCCS, Medical Physics, Torino, Italy*
[4]*IFO, Medical Physics, Roma, Italy*
[5]*Casa di cura San Rossore, Radiotherapy, Pisa, Italy*
[6]*Ospedale Sacro Cuore Don Calabria, Radiotherapy, Negrar VR, Italy*
[7]*UPMC San Pietro, Medical Physics, Roma, Italy*
[8]*Humanitas Research Hospital, Medical Physics, Rozzano MI, Italy*

Purpose or Objective: The use of flattering filter free (FFF) beams are increasing in stereotactic body radiation therapy (SBRT) due to the reduction in delivery time. Small radiation fields (<30mm) are typically involved in SBRT procedures. In small fields, the measurements of the output factor is subject to large uncertainties, impacting in the effective delivered dose to the patient. Dose output ratios (DORs), defined as the ratio of detector readings without correction factor (Alfonso et al., Med Phys 2008), were evaluated in several different centers and an eventual mathematical description of the DORs curve was investigated.

Material and Methods: A couple of new unshielded stereotactic diodes (Razor, IBA) was tested under 7 different TrueBeams using high dose rate (2400 MU/min) 10MV FFF beams. Small fields ranging from 6 to 50 mm were analyzed in terms of profiles and central axis point measurements. DORs were normalized to 30 mm field and were calculated as a function of nominal (NFS) and effective (EFS) field size. From DORs acquired using Razor1 (4 centers), a theoretical equation was extrapolated by means of a double exponential fit. The 3 centers with Razor2 were used to test the mathematical relationship.

Results: Penumbra, field width (defined as FWHM) and EFS analysis over the 7 Truebeams were reported in **Table 1**. The EFS were systematically smaller than NFS ($p<0.01$) for all field size range, with mean difference of 0.9±0.5 mm. The DORs fits using the NFS and EFS had, respectively, R2=0.993 and R2>>0.999 (**Figure 1**). The test mean deviations from predicted DORs, using NFS and EFS fits, were 2.9% and 0.7%, respectively, for field size ranging between 6 and 20 mm. The maximum deviations were 6.1% (6mm field size) for NFS and <2% for EFS.

Table 1. . Penumbra, field width and EFS analysis in term of mean, standard deviation and relative percentage errors for all 7 Truebeams.

NFS (mm)		Penumbra width (mm)	FWHM (mm)	Penumbra width (mm)	FWHM (mm)	EFS (mm)
		Cross-line		In-line		
6.0	Mean (St Dev)	2.0 (0.1)	5.3 (0.2)	2.6 (0.2)	5.6 (0.6)	5.4 (0.4)
	Relative Error (%)	3.7	4.3	6.3	10.8	7.0
8.0	Mean (St Dev)	2.2 (0.1)	7.2 (0.2)	2.9 (0.2)	7.4 (0.6)	7.3 (0.4)
	Relative Error (%)	3.4	3.4	5.7	8.6	5.6
10.0	Mean (St Dev)	2.4 (0.1)	9.1 (0.3)	3.1 (0.1)	9.2 (0.7)	9.2 (0.4)
	Relative Error (%)	3.3	2.9	4.7	7.1	4.7
20.0	Mean (St Dev)	3.0 (0.1)	19.0 (0.3)	3.8 (0.2)	18.9 (0.6)	18.9 (0.4)
	Relative Error (%)	2.9	1.7	4.8	3.3	2.2
30.0	Mean (St Dev)	3.4 (0.1)	29.1 (0.4)	4.3 (0.1)	28.8 (0.6)	28.9 (0.4)
	Relative Error (%)	3.5	1.3	2.4	2	1.5
40.0	Mean (St Dev)	3.8 (0.1)	39.0 (0.5)	4.6 (0.1)	38.7 (0.6)	38.8 (0.5)
	Relative Error (%)	2.1	1.3	3.2	1.6	1.3
50.0	Mean (St Dev)	4.1 (0.1)	49.0 (0.4)	5.0 (0.1)	48.8 (0.7)	48.9 (0.5)
	Relative Error (%)	3.3	0.9	2.2	1.4	1.0

Figure 1. Razor1 DORs plotted as a function of NFS (A) and EFS (B) with relative mathematical curve.

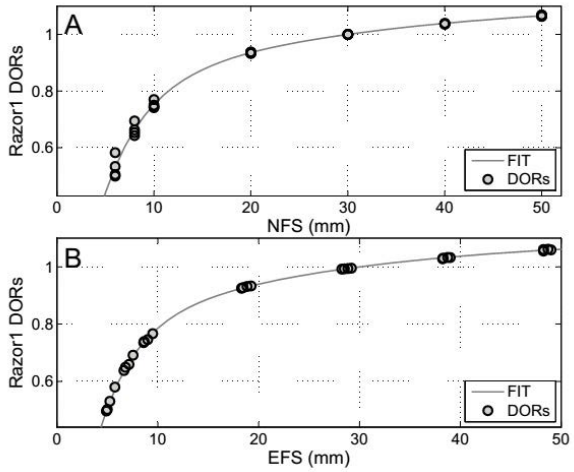

Conclusion: EFS measurements were confirmed to be mandatory when comparing DORs over different centers. A "gold standard" curve was tested and found suitable for DORs calculation using the new Razor diode for TrueBeam 10 MV FFF beams.

EP-1509

Small fields Output Factor measurement using several multidetectors arrays

D. Radomiak[1], S. Adamczyk[1]
[1]*Greater Poland Cancer Centre, Medical Physics, Poznan, Poland*

Purpose or Objective: The aim of this study was to determine and compare small fields Output Factor (OF) measure with different types of multidetector arrays. OF measurements were performed on a CyberKnife® System.

Material and Methods: OF were measured using multidetector arrays: PTW OCTAVIUS Detector 1500, PTW OCTAVIUS Detector 1000 SRS and SunNuclear SRS Profiler.

The type of detector in each of the array is different. OCTAVIUS Detector 1500 consists of 1405 plane-parallel vented ionization chamber, OCTAVIUS Detector 1000 SRS consists of 977 liquid-filled ionization chambers and SunNuclear SRS Profiler contains 125 silicon diode detectors. The OF values measured in the present study were compared with measured values of unshielded PTW Diode Type E 60017. The measurements were done on the same CyberKnife® System. Set of beam specific correction factors has been calculated by means of Monte Carlo simulations which were obtained by Francescon (2012). Correction factors have been applied for OF values measured by PTW 60017. Values of correction factors were reported for each collimation system. CyberKnife® System uses a 6 MV flattening filter free beam with a high dose-rate of 1000 MU min-1. The machine specific reference field size is defined at the 60 mm diameter field produced by a Fixed collimator 80 cm from the source. Beams were collimated by Fix collimator and Iris Variable Aperture Collimator. The Iris Collimator reproduced the same set of 12 field sizes from 5 mm diameter to 60 mm diameter as well as a Fix collimator. Disparity in physical design of two collimators cause deviations in OF measurements (e.g. -4.89% at 5 mm field size for fix collimators versus -6.95% for Iris) . The source-surface distance was set to 78.5 cm and the effective point of measurement used for each detector was set at 1.5 cm depth from the surface of the phantom.

Results: As it was predicted, large deviations in OF measurement are observed. For the smallest field size 5 mm the values of OF varies are more that 4% between arrays and PTW 60017. The largest differences from -3% for 25 mm field size, to -56% for 5 mm were reported for OCTAVIUS Detector 1500, where the vented ionization chamber exhibits the averaging volume effect, due to significant active volume. For field size greater than 40 mm all arrays OF deviate from PTW 60017 by less than 1%. For liquid-filled array in both collimation systems, an excellent agreement was observed (less than 2%) for field size greater than 5 mm diameter.

Conclusion: It has been shown that every type of used active detector behave differently. As it was predicted, for small fields both liquid filled and vented ionization chambers underestimate OF values when silicon diodes overestimate them. It has been proven that liquid-filled multidetector array may be a precise dosimetric tool for OF measurement. A beam specific correction factors for arrays hasn't been published yet.

EP-1510

Monte-Carlo determination of output correction factors for four detectors in small MV photon beams

G. Valdes Santurio[1,2], R. Alfonso Laguardia[3]
[1]*INOR, Institute of Oncology and Radiobiology, La Habana, Cuba*
[2]*Technical University of Denmark, Center for Nuclear Technologies, Roskilde, Denmark*
[3]*InSTEC, Higher Institute of Technologies and Applied Sciences, La Habana, Cuba*

Purpose or Objective: The purpose of this study was the determination by Monte Carlo (MC) of detector-specific output correction factors k(Qclin,Qref,fclin,fref) for four radiation detectors in small MLC-conformed square fields of a 6 MV photon beam.

Material and Methods: Two solid-state detectors, PTW – 60017 (Unshielded-Diode) and the PTW – 60019 (microDiamond), and two ionization chambers, PTW-31010 (Semiflex) and the PTW-31016 (Pinpoint) were simulated. Monte Carlo EGSnrc code was used for simulations and its module EGS_Chamber was applied to represent the detectors geometries and to calculate their dose responses for these non-standards configurations. With the obtained data the overall correction factor k(Qclin,Qref,fclin,fref) was calculated according to the Alfonso´s formalism, as the ratio of relative response or so called "output factors" for each detector and the "ideal" relative dose factor, obtained at several square small fields. The statistical type-A uncertainties in MC simulations were lower than 0.5 %.

Results: For the output factors the experimental data showed a good agreement with the simulations for the two solid-state detectors, in which the relative deviation between them was less than 1% for all field sizes. For the ionization chambers, the simulations and the experimental data showed good agreement for the square field sizes larger than 2x2cm2 for the smallest field sizes was up to 11% for the Semiflex chamber. Of all detectors studied, the responses of the solid-state ones were more similar to the "ideal" detector. As was expected, solid-state detectors tended to under-respond for larger field sizes and to over-respond for the smaller ones. For ionization chambers the behavior was different, they tended to under-respond at the smaller field sizes. These results are consistent with published results using other MC codes, such as Penelope.

Conclusion: The study confirms the accuracy of the MC method in correcting detector measurements in small field dosimetry and it demonstrates the possibility of determining the k(Qclin,Qref,fclin,fref) factors in these conditions. Solid-state detectors found to be more adequate for determining the absorbed dose in relative dosimetry.

EP-1511

Gamma analysis: testing scanners and software tools

B. Almady[1], P. Wesolowska[1], T. Santos[1], J. Izewska[1]
[1]*International Atomic Energy Agency, Nuclear Sciences and Applications, Vienna, Austria*

Purpose or Objective: New methodologies for national audit groups are under development within the co-ordinated research project (CRP) on "Development of Quality Audits for Advanced Technology in Radiotherapy Dose Delivery". Film dosimetry is used to check the relative dose distribution in an anthropomorphic head and shoulders phantom through end-to-end tests of IMRT and VMAT dose delivery. As the film dosimetry depends much on hardware and software used, a comparison of the effects of different scanners and software tools on the resulting gamma pass rate was done.

Material and Methods: A set of films irradiated in a head and shoulders phantom (CIRS) with different IMRT techniques were evaluated with 3 software tools (Ashland FilmQA Pro, PTW Verisoft, Radiochromic.com) and 3 scanners (EPSON 11000XL, EPSON 4990 and EPSON 750 Pro). Gamma analysis was performed on the films using the following set of parameters: 3% dose difference (DD), 3 mm distance-to-agreement (DTA) and 20% dose threshold. Both global and local gamma values were calculated.

Results: A range of gamma results were obtained with FilmQA Pro for a set of films scanned with three scanners above. For individual films the maximum differences in gamma pass rates are given. For the global gamma setting the gamma pass rates from 96.2% to 99.6% were obtained and for the local gamma setting, the corresponding results ranged from 91.5% to 97.6%. Overall, the differences in the gamma pass rates were up to 3.4% and 6.1% for the global gamma and the local gamma settings, respectively. Different software tools used in analyzing the same film (scanned by the EPSON 11000XL) also affect the gamma pass value; the results range from 95.9% to 98.3% for the global gamma setting and from 95.1% to 98.2% for the local gamma setting. Overall, the differences between the gamma values calculated by different software tools were up to 3.4% for the global gamma and up to 3.1% for the local gamma settings.

Conclusion: The results of this study show that different scanners and software tools can result in differences in the gamma passing rate. In particular, the use of different scanners can generate significant differences. Comparing gamma analysis results of different national audit groups may not be straightforward due to the differences in hardware/software used for film analysis. Careful attention

should be paid to the use of scanner/software parameters by these groups.

EP-1512

Influence of the incident electron beam energy on the primary dose component for FFF beams

W. Lechner[1,2], D. Georg[1,2], H. Palmans[3,4], P. Kuess[1,2]
[1]*Medical University of Vienna, Department of Radiation Oncology- Division Medical Physics, Vienna, Austria*
[2]*Medical University of Vienna, Christian Doppler Laboratory for Medical Radiation Research for Radiation Oncology, Vienna, Austria*
[3]*EBG MedAustron, Medical Physics, Wiener Neustadt, Austria*
[4]*National Physical Laboratory, Radiation Dosimetry, Teddington, United Kingdom*

Purpose or Objective: Recently, flattening filter free (FFF) photon beams were introduced into clinical routine and more and more centers take advantage of this kind of beam delivery. For commercial C-arm LINACS, two approaches are currently followed to set the incident electron energy on the target for FFF beams, which in turn have an impact on the comparison with FF beams of the same nominal energy. Either the electron energies of FFF and flattened (FF) beams are identical or the electron energy of the FFF beam is increased to match the percentage depth dose curve (PDD) of the FF beam (in reference geometry). This study focuses on the primary dose components of FFF beams for both kinds of settings, studied on the same LINAC.

Material and Methods: All measurements were performed using VersaHD LINAC (Elekta, Crawley, UK) beams with nominal energies of 6MV and 10MV for both FF and FFF. In clinical mode the energy of the FFF (FFFE1) beams is set to match %dd(10)x of the FF beams. To mimic the second FFF beam delivery method, the incident electron beam of the FFF beam (henceforth FFFE2) was set to the same energy as for the FF beam. Besides the determination of TPR20,10 and %dd(10)x, half value layer (HVL) measurements were conducted in narrow beam geometry with an in-house developed measuring device with polystyrene tubes of different lengths. Additionally, the dual beam quality specifier as proposed by Ceberg et al. was determined and compared to published values [1,2]. This beam quality specifier consists of two components, the mean (μ)) and the variation coefficient (cv) of the linear attenuation coefficient in water.

Results: All results are summarized in Table 1. For 6 MV FFFE1 beams, all investigated beam quality specifiers were very similar compared to those of the FF beams, while for 10 MV FFFE1 beams only %dd(10)x and HVL values were comparable (differences below 1.5%). TPR20,10, %dd(10)x and HVL values of the FFFE2 beams were substantially lower compared to those of the FF and FFFE1 beams. Figure 1 depicts cv as a function of μ for the beams in this work as well as published data. The dual beam quality specifier of the 6 MV FF and FFFE1 energy are equal within the measurement uncertainty and are comparable to published data of a machine with the same TPR20,10 and %dd(10)x. In contrast to that,μ and cv of the 10 MV FFFE1 beam were substantially higher compared to the 10 MV FF beam. The 6 and 10 MV FFFE2 energies were characterized by higher μ values, while having cv values similar as those of the FF beams.

Table 1: Beam quality specifiers and HVL.

Nominal beam energy	$TPR_{20,10}$	%dd(10)x	HVL [mm Polystyrene]	μ [cm^{-1}]	c_v
6 MV FF	0.678±0.001	67.5±0.1	155±2	0.0485±0.0005	0.37±0.01
6 MV FFF_{E1}	0.673±0.001	67.3±0.1	157±1	0.0486±0.0001	0.367±0.001
6 MV FFF_{E2}	0.656±0.001	65.8±0.1	148±3	0.0523±0.0004	0.363±0.006
10 MV FF	0.730±0.001	72.7±0.1	189±3	0.0396±0.0006	0.38±0.02
10 MV FFF_{E1}	0.719±0.001	72.8±0.1	186±2	0.0424±0.0003	0.432±0.004
10 MV FFF_{E2}	0.697±0.001	68.4±0.1	169±3	0.0454±0.0001	0.389±0.001

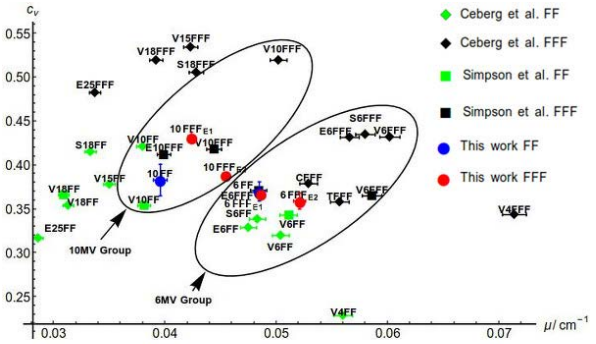

Fig 1 Comparison of dual beam quality specifiers determined in this work with published data. Abbr.: C...CyberKnife, E...Elekta, S...Siemens, T...TomoTherapy, V...Varian

Conclusion: PDD-matched FF and FFF beams were observed to have similar HVL values of both beam energies, indicating similarity of their primary dose components. Using the dual beam quality specifier revealed that this might only be true for 6 MV beams. The dual beam quality specifier has been proven to be useful for a more comprehensive characterization of photon beams.

[1] Ceberg et al., Med Phys. 2010;37:1164–1168.
[2] Simpson et al., Phys Med Biol. 2015;60:N271–N281.

EP-1513

Polymer gels enable volumetric dosimetry of dose distributions from an MR-guided linac

Y. Roed[1,2], J. Wang[2], L. Pinsky[1], G. Ibbott[2]
[1]*University of Houston, Physics, Houston, USA*
[2]*MD Anderson Cancer Center, Radiation Physics, Houston, USA*

Purpose or Objective: Magnetic resonance-guided radiation therapy (MRgRT) benefits from performing treatment response assessments not only at the end of the overall treatment but also during the treatment itself allowing for more normal tissue sparing and better tumor conformality. This was a qualitative study to assess the potential value of polymer gels to measure volumetric dose distributions delivered by an MRgRT unit while using the magnetic resonance (MR) component for readout.

Material and Methods: Polymer gels in custom-designed glass cylinders of 5 cm diameter and 4 cm height were provided by MGS Research Inc (Madison, CT). The design included a 10 cm long filling port to prevent oxygen contamination of the sensitive dosimetric volume. Two dosimeters were positioned in air on the couch of a 1.5 T MR combined with a 6 MV linac. The penumbra of two opposing field edges of a 10x10 cm^2 radiation field bisected each dosimeter volume; one dosimeter was centered in the penumbra at the superior left field edge and the second one was centered at the inferior right field edge.
Coronal images of the dosimeters were acquired prior to irradiation, immediately after exposure to 22 Gy without changing the position of the dosimeters and 20 hours post-irradiation. A T2 spin echo sequence was used with a relaxation time (TR) of 1000 ms and five echo times (TEs) of 20 ms, 40 ms, 60 ms, 80 ms, and 100 ms. Spin-spin relaxation rate (R2) maps were generated and line profiles across the penumbra were analyzed. R2 has previously been shown to be proportional to absorbed dose.

Results: Near the end of the filling port the gel demonstrated a region of oxygen-contaminated gel as oxygen had diffused through the cap on the filling port. A distinct demarcation of the radiation field inside the sensitive volume was visible as early as 5 minutes after irradiation. R2 values 5 minutes after irradiation in the exposed areas of the dosimeters were about 85% of those seen 20 hours later.

At 5 minutes after irradiation, the line profiles on the R2 map across the penumbra region showed the fall-off of the radiation field in both dosimeters while the penumbra region on the right field edge appeared steeper compared to the slope of the penumbra region on the left. The R2 color maps indicated a narrower transition from outside to fully inside the radiation field on the right compared to the transition on the left.
20 hours after irradiation the polymerization of the gel was presumably completed. The overall signal was both higher on the R2 gray scale maps and more pronounced on the R2 color maps. The line profiles across the penumbra regions exhibited a similar trend for both field edges compared to the profiles at 5 minutes post-irradiation. Over the time frame tested, the dosimeter appears stable.

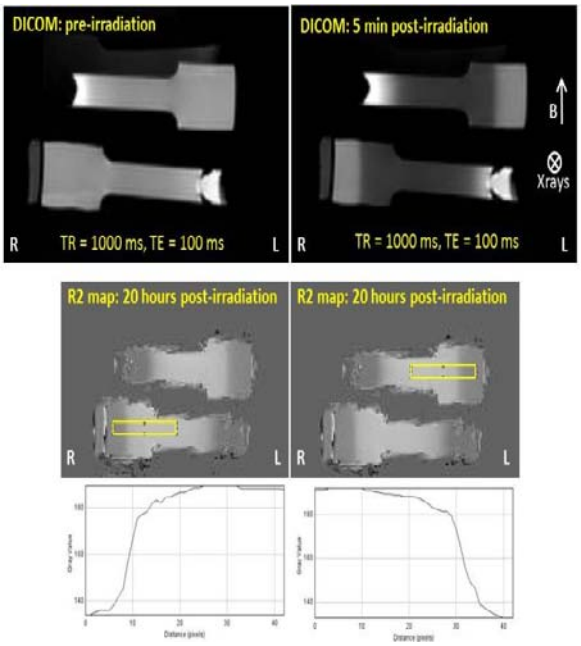

Conclusion: These preliminary qualitative results indicate that polymer gels offer a promising means of measuring relative volumetric dose distributions with the MR component of the MR-Linac.

EP-1514

γTools: a new multipurpose phantom for end-to-end tests in Gamma Knife SRS treatments

S. Calusi[1], L. Noferini[2], M. Casati[3], L. Marrazzo[3], C. Arilli[3], A. Compagnucci[3], C. Talamonti[1,3], S. Scoccianti[4], D. Greto[4], L. Bordi[5], L. Livi[1,4], S. Pallotta[1,3]
[1]*University of Florence, Department of Clinical And Experimental Biomedical Sciences "Mario Serio", Florence, Italy*
[2]*AOU Careggi, Health Physics Unit, Florence, Italy*
[3]*AOU Careggi, Medical Physics Unit, Florence, Italy*
[4]*AOU Careggi, Radiotherapy Unit, Florence, Italy*
[5]*AOU Careggi, Neurosurgery Unit, Florence, Italy*

Purpose or Objective: γTools is a phantom designed and manufactured to measure both geometrical and dosimetric accuracy of stereotactic radiosurgery treatments performed with Gamma Knife. In this work we present this new phantom and results of experiments aimed to test its reliability.

Material and Methods: *Phantom:* The phantom (figure) consists of two PMMA cylinders, screwed one above the other, that can be filled with an image deformation module and a dose plan verification module. A tool fixed to the big cylinder permits to fix the phantom to the stereotactic head frame. The image deformation module is composed by 1660 spheres (0,7mm diameter, 1 cm pitch) filled with water and obtained by overlaying ad hoc manufactured PMMA disks. The declared accuracy of the manufactured grid was 0,01 mm. The dose plan verification module is made by PMMA disks that can host inserts with targets and inhomogeneities. Four holes on two inserts are used to mark a gaf-chromic film, sandwiched between the two inserts, in a reference point visible in MR and/or CT images. Distortions on MR images are evaluated using a software module, developed in MatLab (Mathworks) environment, which automatically identifies the 3D distribution of control points and performs a rigid registration with the theoretical grid. Dose plan verification is made comparing planned doses and dose distributions measured by gaf-chromic films with FilmQA Pro software (Ashland).

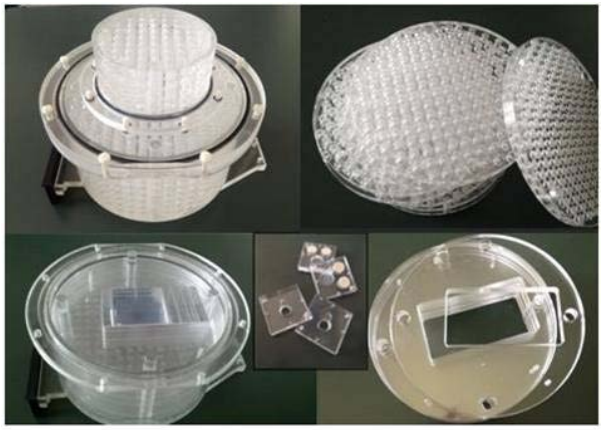

γTools assembled for image deformation mapping (top left) and for dose plan verification (bottom left); disks forming a 3D matrix of spheres (top right); disks with cavities and inserts for planned dose verification (bottom right).

Tests: The image deformation module was tested assessing the accuracy of the manufactured grid of spheres with CT studies (0,18 mmx0,18 mmx0,8 mm voxel size) of the phantom. The measured and theoretical points grid were registered and the residual shifts, along x, y and z between the registered and theoretical point positions were evaluated. The points grid was dissembled and reassembled (rotating each foil 90°) and another CT study was acquired. The accuracy of the dose plan verification module depends on the reproducibility of inserts position inside the phantom. CT acquisitions of the phantom inserts (0,09 mmx0,09 mmx0,8 mm voxel size) were performed assembling and disassembling repeatedly the inserts along coronal and sagittal planes and evaluating the differences of the reference point positions in the acquired images.

Results: *Image deformation module:* For both 0° and 90° configurations the residual shifts (Δx, Δy, Δz) between the registered and theoretical point positions along x, y and z directions, together with the residual distances (R) were evaluated. The maximum, mean and standard deviations of the absolute values of the shifts along x, y, z and R are reported in the table. *Dose plan verification module:* In the same table the deviations of the reference point positions along x, y, z together with the residual distances R for both the sagittal and coronal insert configurations are reported.

Image deformation module					
		|Δx| [mm]	|Δy| [mm]	|Δz| [mm]	R [mm]
0°	mean±σ	0.05±0.04	0.05±0.04	0.12±0.10	0.16±0.09
	Max	0.39	0.36	0.42	0.48
90°	mean±σ	0.05±0.04	±0.04	0.017±0.14	0.19±0.13
	Max	0.31	0.29	0.56	0.58
Dose plan verification module					
		|Δx| [mm]	|Δy| [mm]	|Δz| [mm]	R [mm]
sagittal		0.13	0.13	0.05	0.19
coronal		0.09	009	0.09	0.16

Conclusion: The tests performed demonstrate that the proposed phantom is suitable to asses both the geometrical and dosimetric accuracy of Gamma Knife SRS treatments.

EP-1515

Difference in dose to water for photon beams with and without the presence of a magnetic field.

J. Wolthaus[1], B. Van Asselen[1], S. Woodings[1], S. Hackett[1], L. Van Zijp[1], B. Raaymakers[1]
[1]*UMC Utrecht, Department of Radiation Oncology, Utrecht, The Netherlands*

Purpose or Objective: In MRI guided radiotherapy (e.g. MR-linac), radiation is delivered in presence of a magnetic field. Therefore, the dose deposition is different since the path of the secondary electrons is changed due to the Lorentz force. Especially at air-tissue interfaces this causes changes in dose distribution. An example is the change in reading of a ionization chamber in a magnetic field. Besides, since the electrons are bend, the net effect is that electrons will travel less in forward direction, as a result the local dose deposition will change slightly even in an area with homogenous density. How to account for these changes in the various codes of practice for reference dosimetry is yet under debate. The purpose of this abstract is to quantify the change in dose-to-water (for a fixed setup) when applying a magnetic field.

Material and Methods: The Monte Carlo (MC) dose engine from Monaco TPS (Elekta) was used to estimate the change in dose-to-water. Validation of this MC code against other established MC codes has been performed by other research groups. For different square field sizes (from 5 to 30 cm) the dose deposition of a 6MV photon beam of an Elekta Agility linac is calculated in a water phantom of 50x50x40 cm^3 (SAD = 100 cm, SSD = 90 cm). Calculations were performed with and without a transversal 1.5T magnetic field for the same number of MU. MC variance was 0.1%. Difference in dose was calculated by means of the percentage difference in depth dose in a volumetric region below dose maximum and above phantom bottom (5<depth<35 cm) and around the central axis. A histogram of the percentage differences was calculated for all field sizes. Subsequently, a Gaussian function is fitted to the peak region of the histogram (central part) to reduce the binning effects.

Results: In figure (a) an example of a depth dose curve (and close up) with and without magnetic field is shown for field size 10x10 cm^2. Figure (b) shows the percentage difference for all square field sizes (9 sample point per field size). The mean percentage difference for all field sizes ranges between -0.4% and 0.55%.

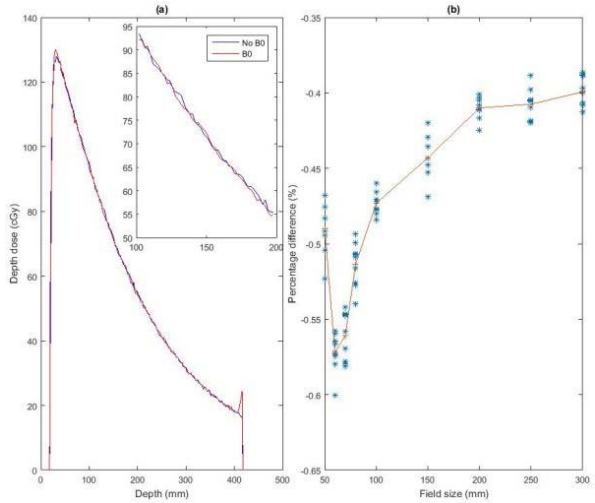

These results show, within the MC variance, that a tendency is visible over the different field sizes. This may be caused by the change in phantom scatter for different field sizes. However, the MC variation causes large variation in the ratio. For small field sizes (<5x5 cm^2) penumbra effects will come into play and are for that reason disregarded. The effect of beam hardening is neglected in this work.

Conclusion: A difference in dose-to-water can be estimated as -0.45% for a 10x10 cm^2 field, which is related to the fact that the electrons travel less in forward direction. Note that this dose difference can also be expressed as a shift in PDD (in the order of a mm). Depending on the used code of practice for reference dosimetry, this difference needs to be taken into account when applying correction factors for magnetic field effects.

EP-1516

Evaluating a versatile new-generation anthropomorphic phantom for SBRT and thoracic IMRT/VMAT

K. Poels[1], A. Nulens[1], R. De Roover[2], W. Crijns[1], S. Petilion[1], N. Hermand[1], M. De Brabandere[1], S. Michiels[1], G. Defraene[1], K. Haustermans[1], Verelllen.D.[3], T. Depuydt[1]
[1]*Universitair Ziekenhuis Leuven, Department of Radiation Oncology, Leuven, Belgium*
[2]*Katholieke Universiteit Leuven, Department of Oncology-Experimental Radiation Oncology, Leuven, Belgium*
[3]*Universitair Ziekenhuis Brussel, Department of Radiotherapy, Brussels, Belgium*

Purpose or Objective: Time-efficient dose delivery by volumetric modulated arc therapy (VMAT) for stereotactic body radiation therapy (SBRT) is gaining more and more interest in radiation oncology. The combination of VMAT with potentially-lethal SBRT doses in heterogeneous tissue circumstances has led to an emerging use of anthropomorphic phantoms for quality assurance (QA) of both therapeutic target dose coverage and organ-at-risk (OAR) sparing. In this study, the first evaluation worldwide of a new-generation anthropomorphic phantom (E2E SBRT phantom model 036A CIRS INC., Norfolk, VA) was conducted for dose delivery of spine and lung SBRT using VMAT.

Material and Methods: The phantom mimics the thorax anatomy with lung-tissue surrounded by rib structures and vertebrae, allowing appropriate image-guidance with a subsequent anthropomorphic dose evaluation. The phantom was customized to fit an Exradin A1SL (Standard Imaging, Middleton, WI) ionization chamber (IC) in the tumor centroid and in the peripheral lung. Also TLD or alanine pellets cutouts are foreseen in the phantom. In thoracic and pelvic part of the phantom, both an axial and coronal plane are available for comparing calculated and measured film dose in the target area. A lung insert with a kidney-shaped tumor was specifically developed to verify VMAT lung SBRT with film and IC. The kidney-shaped lung tumor also allowed for a dose film evaluation of the isodose levels along both the medial concave and lateral convex border of the tumor. External markings on the insert allowed to simulate the influence of a rotational tumor offset (step size 1°) with respect to the planning CT.

Results: To already illustrate the potential of the phantom, initial QA results obtained from the new phantom for a spine SBRT and a lung lesion with VMAT SBRT were visualized in Figure 1A and 1B. Overall, a good agreement was found between dose calculation of the treatment planning system and respectively film (>88%) (absolute dose) and IC (<3%) measurements. The difference in agreement score for an OAR close to respectively the concave or convex border of the tumor was similar (see Figure 1B). With 2 and 5 mm PTV margins for respectively spine and lung SBRT, up to 1° and 3° rotation of the phantom insert led to an adequate target coverage.

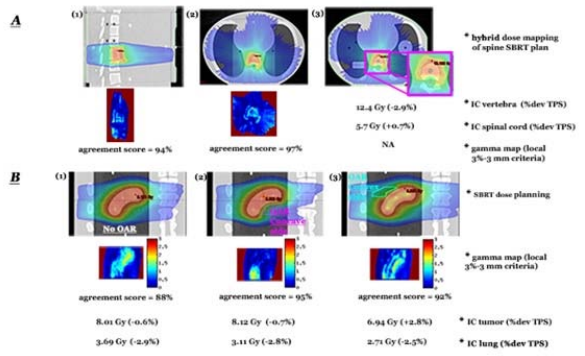

Figure 1: (A) shows the evaluation of spine SBRT with VMAT in (1) the coronal plane of the pelvis part and (2) the axial plane in the thorax part and (3) the plane of IC point of measurement for point dose verification in the vertebrae and spinal canal and (B) shows the coronal dose plan and verification results for the new kidney-shaped tumor volume of E2E CIRS (model 036A) for the situation of (1) no OAR (2) an OAR on the concave side and (3) an OAR on the convex side of the tumor.

Conclusion: A novel, next-generation anthropomorphic phantom allows a versatile SBRT QA, by assessing high dose target coverage and simultaneous OAR dose or peripheral lung dose in an end-to-end testing setup hereby including inter-fraction rotations. The phantom will be the basis of a multi-center peer-to-peer institutional audit of thoracic IMRT/VMAT and SBRT.

EP-1517

Characterization of a new stereotactic diode under flattening filter free beams down to small fields

G. Reggiori[1], P. Mancosu[1], A. Stravato[1], F. Lobefalo[1], L. Paganini[1], F. Zucconi[1], V. Palumbo[1], N. Suchowerska[2], S. Tomatis[1], M. Scorsetti[3]

[1]Humanitas Research Hospital, Medical Physics Service of the Department of Radiation Oncology, Rozzano Milan, Italy

[2]School of Physics- The University of Sydney, Department of Radiation Oncology, Camperdown, Australia

[3]Humanitas Research Hospital, Department of Radiation Oncology, Rozzano Milan, Italy

Purpose or Objective: Stereotactic radiotherapy requires detectors capable of determining the delivered dose with high accuracy. The aim of this study is to characterize the performance of a new unshielded silicon diode prototype, the IBA Razor, for dose measurements in small radiation therapy photon beams in flattening filter free (FFF) mode

Material and Methods: The performance of the newly commercialized stereotactic diode was evaluated relative to that of the previously available SFD diode and the PFD detectors, both from IBA. The Razor is made with an n-type implant in p-type silicon. The active volume is 0.6mm in diameter and 20µm in length. The detector response stability in measured dose, dose rate and dose per pulse were evaluated. Dark current as function of the received dose was also evaluated. The detector response in square fields, in the range from 0.8 to 5.0 cm, was evaluated by means of percentage depth dose curves (PDDs), axial beam profiles and output factors.

Results: The short term stability of the Razor was found to be much improved relative to the SFD, exhibiting a variation of less than ±0.1% for a dose of 1.2 kGy delivered in a single-session. Dose linearity showed a deviation of less than ±1% in the 0.05–30 Gy range and a dose rate dependence of less than ±0.5% in the 4–24 Gy/min range. The dose per pulse dependence, evaluated in the 0.08-0.21 cGy/pulse range, was found to be within ±0.8%. A larger dark current with increase in dose was observed for the Razor with values of 0.0025pA/Gy compared to the 0.0002pA/Gy for the SFD. This characteristic is attributed to an increased concentration of the recombination centers and can be practically solved by resetting the background before every acquisition.
The measured PDDs agreed to within 1% with those obtained using the PFD detector. The profile analysis showed good results as long as a background correction was applied before each profile acquisition: penumbra differences were below ±0.3 mm relative to PFD, with a slight overestimation of the tails (<1%), due to the absence of the shielding. When background correction was not applied regularly, larger differences were observed in the low dose penumbra region and in the profile tails, probably due to the higher dark current. Output factors were in good agreement with those measured by the PFD detector to within 1% for fields up to 5x5 cm^2, for larger fields the absence of the shielding in the stereotactic detector led to differences >2%.

Conclusion: The new IBA Razor unshielded diode replaces the IBA SFD, with the additional advantages of improved stability (up to 1.2 kGy) compared to the reference stereotactic diode. The Razor has the same high spatial resolution and performance in small radiation fields. These features make the Razor diode detector a good candidate for radiation therapy and in small field dosimetry to support advanced radiation therapy techniques.

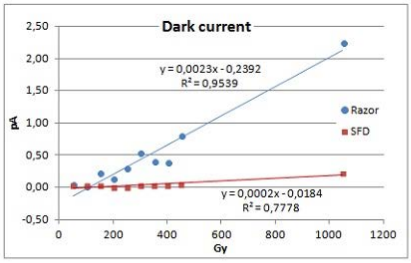

Figure 1 The dark current plotted as a function of the dose to the Razor and the SFD. Diodes.

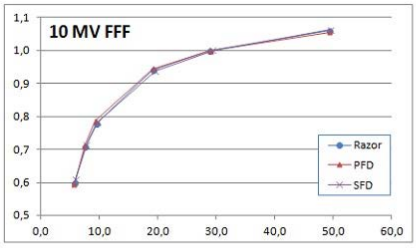

Figure 2 Output Ratios for the three detectors for 10 MV FFF beam. Considered field sizes were 0.6, 0.8, 1, 2, 3 and 5 cm². Volume averaging corrections were applied.

Electronic Poster: Physics track: Dose measurement and dose calculation

EP-1518

Evaluation of dynamic delivery quality assurance process for internal target based RapidArc

J.Y. Song[1], J.U. Jeong[1], M.S. Yoon[1], T.K. Nam[1], S.J. Ahn[1], W.K. Chung[1]

[1]Chonnam National University Medical School, Radiation Oncology, Hwasun, Korea Republic of

Purpose or Objective: In this study, a delivery quality assurance (DQA) method was designed to overcome the limitations of the conventional DQA process in the static condition for internal target volume (ITV)-based VMAT. The dynamic DQA measurement device was designed with a moving phantom that can simulate variable target motions. The dose distribution in the real volume of the target and OARs were reconstructed with the measurement data under the dynamic condition. Then, to evaluate the designed DQA method, the dose-volume histogram (DVH) data of the real target and OARs were compared with the DVHs calculated in the ITV-based VMAT plan.

Material and Methods: The dynamic DQA measurement device was designed with a moving phantom that can simulate variable target motions. The dose distribution in the real volume of the target and organ-at-risk (OAR)s were reconstructed using 3DVH with the ArcCHECK measurement data under the dynamic condition. A total of 10 ITV-based RapidArc plans for liver-cancer patients were analyzed with

the designed dynamic DQA process. Appropriate method was applied to correct the effect of moving phantom structures in the dose calculation, and DVH data of the real volume of target and OARs were created with the recalculated dose by the 3DVH program.

Results: We confirmed the valid dose coverage of a real target volume in the ITV-based RapidArc. The variable difference of the DVH of the OARs showed that dose variation can occur differently according to the location, shape, size and motion range of the target.

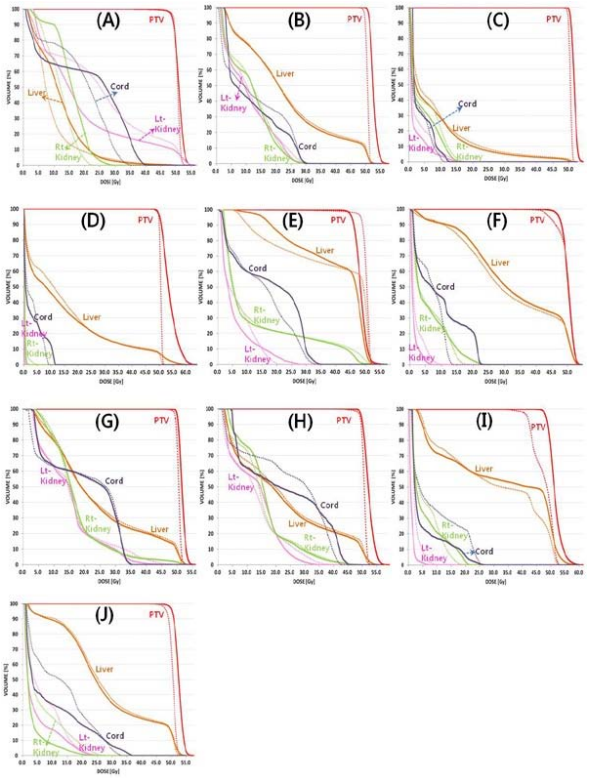

Figure : Total calculated DVH data through dynamic DQA process. Solid line: DVH in the real volume of target and OAR, Dashed line: DVH calculated in the ITV-based RapidArc plan

Conclusion: The conventional DQA method in a static status for the ITV-based RapidArc, without a gating system, can only verify the mechanical and dosimetric accuracy of the treatment machine. An additional DQA method should be devised for evaluating the dosimetric characteristics in the real volume of the target and OARs under respiratory organ motion. The dynamic dose measurement using the moving phantom, which can simulate respiratory organ motions, and techniques employing the measured data to calculate the dose delivered to patients were devised in this study, and proper dose analysis was possible in the real volume of the target and OARs under the moving condition. The devised DQA process appears to be helpful for evaluating the real dosimetric effect of the target and OARs in the ITV-based RapidArc treatment.

EP-1519

Automatic detection of MLC position errors using an EPID based picket fence test

D. Christophides[1], A. Davies[2], M. Fleckney[2]
[1]*St James' Institute of Oncology, Radiotherapy Physics, Leeds, United Kingdom*
[2]*Kent Oncology Center, Radiotherapy Physics, Maidstone, United Kingdom*

Purpose or Objective: The correct calibration of multi-leaf collimator (MLC) leaves is essential in the accurate delivery of radiotherapy treatments, particularly IMRT. In this study EPID picket fence test images are analysed to investigate the possibility to automatically detect intentional errors greater or equal to 0.5mm from baseline MLC errors.

Material and Methods: Picket fence tests were delivered as part of weekly Linac QA in RapidArc mode on Varian iX and 2100CD Linacs equipped with the aS1000 and aS500 EPID respectively. In each QA session a picket fence test was delivered with intentional errors of 0.5mm and 1.0mm; additionally a baseline test was delivered without any intentional errors. A total of 96 picket fence tests were retrospectively analysed covering a period of 6 months.
Using Python v2.7.10 for Windows, an algorithm was implemented to quantify the errors in the MLC positions. Briefly the steps of the algorithm were: 1) Image range calibration, 2) Collimator rotation correction, 3) Isocentre position determination, 4) Derivation of relative leaf positions, 5) Calculation of MLC error from median value at each picket fence field position, and 6) Addition of the errors of opposing leaves at each field position to calculate the combined error (CEr) for each leaf-pair.
The mean and median were calculated from the CEr values of each leaf-pair across the different picket fence field positions. The distribution of the mean and median values calculated was compared between baseline and the intentional MLC errors. Furthermore the normal distribution probability density function was fitted onto all of the baseline CEr data. The mean and standard deviation of the fit were obtained. The t-test and Kolmogorov-Smirnov (KS) statistical tests were used to compare each sample of CEr values obtained from each leaf-pair to the corresponding normal baseline distribution of each Linac examined.

Results: For the Varian iX Linac equipped with the aS1000 EPID the distribution of values of the mean CEr for intentional errors varied between 0.43-1.18mm whereas for the baseline the mean CEr values were between 0.00-0.25mm (Fig. 1). This result showed that the mean CEr can be used to automatically detect MLC errors greater or equal to 0.5mm by setting the detection threshold between 0.25mm and 0.43mm.

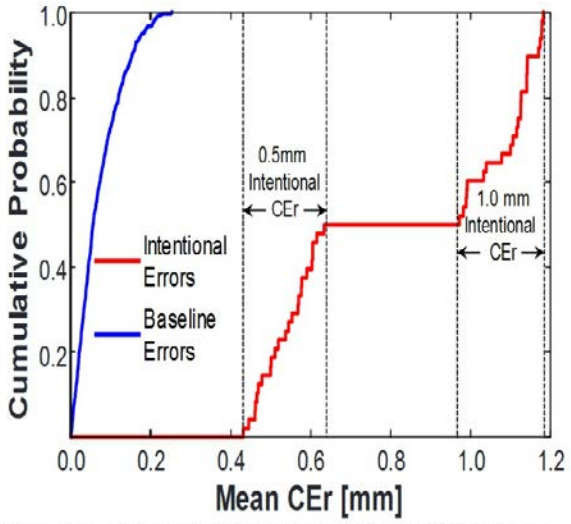

Fig. 1. Cumulative probability distributions of the mean CEr calculated for both baseline and intentional picket fence field errors. Note that there is no overlap in the values between the baseline and intentional mean CEr.

The p-values of the t-tests performed on the data from the Varian 2100CD Linac for the baseline CEr varied between 1.18E-7 and 1.00, whereas for the intentional CEr the p-values were between 0.00 and 5.07E-05. This overlap between the p-values resulted in a false-positive rate of 4.3% if the p-value of 5.07E-5 was to be used as the CEr detection threshold. Table 1 summarizes all the results from the statistical analysis.

Table 1
Results of the statistical analysis for the comparison between baseline and intentional CEr.

	Baseline CEr	Intentional CEr	CEr detection threshold	False Positive Rate
	Linac: iX aS1000			
Mean	[0.00, 0.25] mm	[0.43, 1.18] mm	0.34	0%
Median	[0.00, 0.26] mm	[0.40, 1.09] mm	0.33	0%
t-test (p-values)	[2.01 x 10^{-08}, 1.00]	[0.00, 1.04 x 10^{-03}]	1.04 x 10^{-03}	8.2%
KS-test (p-values)	[8.14 x 10^{-06}, 1.00]	[0.00, 3.55 x 10^{-09}]	1.70 x 10^{-07}	0%
	Linac: 2100CD aS500			
Mean	[0.00, 0.30] mm	[0.44, 1.21] mm	0.37	0%
Median	[0.00, 0.35] mm	[0.44, 1.16] mm	0.40	0%
t-test (p-values)	[1.18 x 10^{-07}, 1.00]	[0.00, 5.07 x 10^{-5}]	5.07 x 10^{-05}	4.3%
KS-test (p-values)	[4.25 x 10^{-07}, 1.00]	[0.00, 3.15 x 10^{-11}]	3.66 x 10^{-09}	0%

[A, B]: indicates that the range of values is between A and B

Conclusion: The analysis proposed can be used to perform automatic detection of MLC errors ≥0.5mm based on individual Linac performance characteristics. Automatic detection of MLC errors has potential in reducing costs and downtime in external beam radiotherapy.

EP-1520

Uncertainties in film measurements of dose area product

T. Wright[1], J. Lye[2], D. Butler[1], A. Stevenson[3], J. Livingstone[3], J. Crosbie[4]
[1]*ARPANSA, Radiotherapy Section, Yallambie, Australia*
[2]*ARPANSA, Australian Clinical Dosimetry Service, Yallambie, Australia*
[3]*Australian Synchrotron, Imaging and Medical Beamline, Clayton, Australia*
[4]*RMIT University, School of Applied Sciences, Melbourne, Australia*

Purpose or Objective: To assess the feasibility of using radiochromic film to aid the calorimetric determination of the dose-area product (DAP) in small fields by determining the uncertainty in film DAP measurements.

Material and Methods: Dose measurements in small fields can be problematic. DAP methods with a detector much larger than the radiation field provide an alternative to conventional central-axis (CAX) dose measurements. DAP is the integrated dose over the area of the detector (Equ. 1) with units of Gy.cm2. In order to convert the measured DAP to the CAX dose the equivalent area of the beam is required. This is the area of an equivalent field with no penumbra (i.e. a step function profile).

$$DAP = \iint D(\boldsymbol{r})\boldsymbol{dr}$$

(1)

Out of field doses can contribute considerably to the total dose when the detector is integrating over an area much larger than the field size. Film exposures with centimetre-sized fields were performed on the Imaging and Medical Beamline (IMBL) at the Australian Synchrotron using HD-V2 radiochromic film. Films were scanned using an Epson V700 flatbed scanner. The equivalent beam area was calculated by two methods: by normalising the 2D optical density data to unity and either (a) integrating over the area of the detector, or (b) integrating horizontal and vertical profiles and calculating an area by the product of width and height. Uncertainties have been assessed for scan repeatability, scanner corrections, scanning conditions of calibration films, selection of normalisation value and the dynamic range of the film.

Results: The most important contribution to the uncertainty in DAP measurements is the calculation of the beam area. In the IMBL beam dose rates are typically 50 – 3000 Gy/s depending on distance from the source. High dose film such as HD-V2 is necessary to measure the large doses, however the dynamic range of the film is not suited to low dose measurements.
Preliminary measurements suggest an uncertainty of 1% to 1.5% in the background dose (relative to CAX dose) can be expected. For a 10x10 mm2 field measured with a detector 40 mm in diameter, a 1% uncertainty in background dose will result in a 12% uncertainty in DAP measurement. This is likely to be the limiting factor for DAP film measurements.
Scan repeatability, scanner light intensity variation in the horizontal plane, scanner resolution and air gap between film and scanner window all introduce small uncertainties. These can be reduced by using systematic scanning techniques and averaging over multiple scans.

Conclusion: Determination of the out of field dose was found to the dominant uncertainty in film DAP measurements. Further work is required to determine if a two-film approach can improve the uncertainty. The desired accuracy of <5% will require additional steps to reduce the uncertainty in the out of field dose.

EP-1521

Comparative study of three pre-treatment verification methods: Portal Dosimetry, Delta4 and Epiqa

J. Maroote[1], A. Derdouri[1], A. Coutte[2]
[1]*Centre Hospitalier Universitaire, Unité de Radiophysique, Amiens, France*
[2]*Centre Hospitalier Universitaire, Unité de Radiothérapie, Amiens, France*

Purpose or Objective: Pre-treatment evaluation of RapidArc plans with three different methods: Portal Dosimetry, Delta4 and Epiqa and comparative study.

Material and Methods: RapidArc plans are calculated by Eclipse V.10 AAA algorithm and treatments are delivered by Varian Clinac iX and 2100 accelerators. The pretreatment verification methods are Portal Dosimetry by Varian, 3D detector Delta4 by ScandiDos and the software Epiqa by EPIdos.

Results: The comparative study is carried out on 100 patients. The acceptance criteria used for gamma analysis are: local, dose difference from 3% to 4% and distance-to-agreement from 3mm to 4mm.
For Head & Neck treatments, the average value of Gamma Agreement Index (GAI) given by Portal Dosimetry is 98,17% with standard deviation of 1,41%, Delta4 gives 97,77% with standard deviation of 1,52% and Epiqa 97,54% with standard deviation of 1,60%.
For Pelvis treatments, the average value of Gamma Agreement Index (GAI) given by Portal Dosimetry is 98,09% with standard deviation of 1,54%, Delta4 gives 98,19% with standard deviation of 1,30% and Epiqa 97,83% with standard deviation of 1,84%.
For Encephalon treatments, the average value of Gamma Agreement Index (GAI) given by Portal Dosimetry is 98,31% with standard deviation of 1,49%, Delta4 gives 98,04% with standard deviation of 1,56% and Epiqa 99,01% with standard deviation of 1,38%.
For Thorax & Abdomen treatments, the average value of Gamma Agreement Index (GAI) given by Portal Dosimetry is 97,57% with standard deviation of 1,77%, Delta4 gives 97,92% with standard deviation of 1,41% and Epiqa 97,96% with standard deviation of 1,58%.
Then, intentional errors were introduced in 3 plans in order to evaluate the capacity of each method to detect these errors. It was errors in terms of Monitor Units (MU) and

collimator angle. The results are based on the value of GAI: when the value is lower than 95%, the error is detected. Introduced errors are smaller and smaller in order to characterize error detection limits of each method.
For Portal Dosimetry, it is possible to detect errors of collimator angle up to 4° and errors of Monitor Units up to 3%. For Delta4, it is possible to detect errors of collimator angle up to 2° and errors of Monitor Units up to 2 %. For Epiqa, it is possible to detect errors of collimator angle up to 2° and errors of Monitor Units up to 3%.

Conclusion: In spite of their differences, the three pre-treatment verification methods are able to detect different sort of errors in dose distributions. The comparative study gives us concordant results. Therefore, these data suggest the possibility of using only one routinely and complete the analysis with one of the other in case of problems.

EP-1522

Evaluation of usefulness of patient dose analysis system using MLC log file

C.K. Min[1], W.C. Kim[1], E.S. Kim[1], S.G. Yeo[1], E. Jwa[1], S.H. Choi[2], K.B. Kim[2], K.H. Cho[1], S. Lee[3]
[1]*SoonChunHyang Univ.Hospital, Radiation Oncology, Cheonan Chungnam, Korea Republic of*
[2]*Korea Institute of Radiological and Medical Sciences, Radiation Oncology, Seoul, Korea Republic of*
[3]*Korea University Hospital, Radiation Oncology, Seoul, Korea Republic of*

Purpose or Objective: In this study, we compared patient therapy planning evaluation system, applying MLC log file, with quality assurance system using the fluence map obtained from measurement, in order to assess usefulness of patient dose analysis system.

Material and Methods: To map out IMRT treatment planning, we used 4 targets and organ contours (multiple targets, virtual prostate, virtual head & neck, C type), along with IMRT phantom as presented in AAPM TG-119 Report. The treatment planning was implemented via Eclipse treatment planning system using 7 radiation field at an interval of 50º from 0o for both multiple targets and virtual prostate on one hand and using 9 radiation fields at an interval of 40º from 0o for both virtual head & neck and C type on the other hand. For dose limitation conditions for PTV and critical structure, we adopted the objectives specified in TG 119 Report. In relation to dose evaluation, point dose was evaluated by using CC13 chamber. The gamma index was analyzed for allowable limit of 3%/3mm by using MobiusFx system, a dose analysis software using MLC log file, in tandem with 2D array detector and Compass software that evaluates dose based on fluence map.

Results: Dose distribution was calculated using treatment planning and Mobius system for 4 targets and then compared through three-dimensional gamma index based on the setting criteria for allowable limit of 3%/3mm. The results showed the pass rate of 99.5% in multiple targets, 100.0% in prostate, 99.5% in head & neck, and 99.8% in C type. Based on results of analysis of gamma index for dose distribution, which was performed on the basis of dose distribution calculated by MobiusFX system and MLC log file actually investigated, the pass rate was found to be 100.0% in multiple targets, 100.0% in prostate, 99.7% in head & neck, and 99.5% in C type. Meanwhile, gamma index was analyzed based on dose distribution under treatment planning for 4 targets and dose distribution measured through Compass system, and the results indicated that the pass rate was 99.9% in multiple targets, 99.6% in prostate, 99.2% in head & neck, and 98.8% in C type. In addition, the results of point dose evaluation, performed based on point dose under treatment planning using CC13 chamber and point dose actually measured, showed that difference in pass rate was 1.2% in multiple targets, 1.5% in prostate, 1.3% in head & neck, and 0.4% in C TYPE.

Conclusion: This study may provide useful basis for ensuring quality assurance for each patient by using the MLC log analysis system during special treatments in clinical applications.

EP-1523

Validation of the dosimetric algorithm Acuros XB and the impact of its usage in SBRT treatments

T. Younes[1,2,3], L. Vieillevigne[1,2,3]
[1]*Cancer University Institute of Toulouse Oncopole, Engineering And Medical Physics, Toulouse, France*
[2]*University Toulouse III- Paul sabatier, UMR1037 CRCT, Toulouse, France*
[3]*Inserm, UMR1037 CRCT, Toulouse, France*

Purpose or Objective: The aim of this study was to assess the accuracy of the dosimertic algorithm based on the resolution of Boltzmann equation: “Acuros XB” (AXB) implemented in Eclipse (Varian) TPS. The methodology recommended by the IAEA-TECDOC-1583 was followed to evaluate AXB. AXB was also tested for clinical extra cranial stereotactic treatment cases. Moreover AXB with the two absorbed dose reporting options, dose-to-medium (Dm) and dose-to-water (Dw), was compared against the Analytical Anisotropic Algorithm (AAA).

Material and Methods: The IAEA-TECDOC-1583 presents eight different fields configurations in heterogeneous media. All plans were created on a CIRS thorax phantom model 002LFC including different tissue equivalent inserts (water, bone and lung). Measurements were performed with a PinPoint ionization chamber (type 31016, PTW) on Novalis TrueBeam STx accelerator for 6MV and 10MV photons with and without flattening filter (6FF, 6FFF, 10FF, 10FFF). Furthermore, target absorbed dose difference between AXB (Dm and Dw) and AAA were compared using same monitor units for 17 patients with non-small-cell lung cancer (NSCLC) or bone metastases cancer who underwent SBRT.

Results: AXB Dm calculations showed an excellent agreement with measurements for the eight configurations of the IAEA-TECDOC-1583. All the results fulfilled the agreement criterion given in the IAEA-TECDOC-1583. The biggest difference between measured and calculated absorbed dose with AXB (Dm and Dw) in lung was less than 0.6% for all photon energies. Unlike, in the lung region, AAA showed deviations that didn’t met the agreement criterion. Maximum deviations were 4.4%, 3.35%, 2.27% and 1.6% for respectively 6FF, 10FF, 6FFF and 10FFF photon energies. Although the Dm and Dw was almost the same in most tissues for all the energies, comparing them in bony structure didn’t give similar results. When choosing Dw in the bone region some results didn’t fulfilled the agreement criterion, unlike Dm where excellent agreement were found between calculated and measured absorbed dose. For the planning target volume (PTV) in the NSCLC patients, AXB Dm and Dw calculations showed similar results while compared to the AAA calculations, where the average differences were less than 2% for minimum, mean and maximum absorbed doses. For bone metastases cancer patients, comparing the PTV doses between AXB Dm and AXB Dw didn’t show similar results. The averaged deviations between AXB Dm and AAA were 1.7%, 0.1% and 2.2% whereas deviations between AXB Dw and AAA were 0.1%, 4.2% and 0.7%, respectively for minimum, maximum and mean absorbed doses.

Conclusion: The results of the IAEA-TECDOC-1583 and of clinical cases showed that the AXB algorithm is more accurate than AAA in the lung region for 6FF, 10FF, 6FFF and 10FFF photons. As for bone metastasis the use of AXB Dm was recommended.

EP-1524

The effect of the table top modeling on calculations and measurements for the Delta4 phantom

L. Paelinck[1], B. Vanderstraeten[1], R. Srivastava[1], L. Olteanu[1], C. De Wagter[1]
[1]*University Hospital Ghent, Radiotherapy, Ghent, Belgium*

Purpose or Objective: The purpose of this study was to investigate the effect of the modeling of the treatment table top on the agreement between calculations and measurements on the Delta4 phantom (Scandidos). Also, the effect of the most suitable way to determine the daily correction factor was investigated.

Material and Methods: Two of our linear accelerators are equipped with the standard Elekta iBeam evo carbon fiber table top. In our treatment planning system, Pinnacle v9.0 (Philips), the table top is modeled as a slab with dimensions equal to the width and height of the table top and with a density of 0.25 g/cm^3.
We extended the axial dimensions of the artificial CT-image set of the Delta4 phantom provided by Scandidos from 25 x 25 cm^2 to 50 x 50 cm^2 by a home-made program written in java. This allows us to place the table top model below the phantom at the real distance, ie 7 cm. 15 IMRT plans for breast cancer were recalculated twice, once on the CT-images of the Delta4 phantom provided by Scandidos and a second time on the extended CT-images with the table top model included. All plans consist of 5 to 6 beams (87 in total) from which 1 to 2 beams go through the table (23 in total). The plans were exported to the Delta4 software and measured. In case no table top model was included in the calculations, a daily correction factor based on the average of 4 beams (gantry angles of 0°, 90°, 180° and 270°) was applied. When the table top model was included, a daily correction factor based on 1 beam (gantry angle of 0°) was applied. A gamma criterion of 3%/3mm was used. Statistical analysis was done by paired t-tests. A p-value < 0.05 was considered as statistically significant.

Results: Without the use of daily correction factors, the mean pass rate for the overall treatment plans was respectively 90.7% (±6.9 SD) and 95.2% (±3.0 SD) without and with the table top model applied. This difference is significant with p = 0.01. In the first group 4 out of 15 pass rates were > 95%, whereas in the second group this is 9 out of 15. With the use of the proper daily correction factors, this increases to respectively 98.6% (±1.2 SD) and 99.1% (±0.9 SD). This difference is also significant with p = 0.04. In both groups, all pass rates were > 95%.
For individual beams going through the table top, the mean pass rate was respectively 90.8% (±9.9 SD) and 99.0% (±1.9 SD) without and with the table top model applied and without the use of daily correction factors (p = 0.0001). In the first group 10 out of 23 pass rates were > 95%, whereas in the second group this is 22 out of 23. With the use of the proper daily correction factors, this increases to respectively 99.0% (±1.6 SD) and 99.9% (±0.4 SD) (p = 0.01). In the first group 22 out of 23 pass rates were > 95% and in the second group all pass rates were > 95%.

Conclusion: The table top modeling results in a better agreement between measurements and calculations, both for total plans and individual beams. This agreement improves when proper correction factors are applied.

EP-1525

Clinical results of an EPID-based in-vivo dosimetry for prostate cancer treated by VMAT

M.D. Falco[1], S. Giancaterino[1], A. De Nicola[1], F. Perrotti[1], S. Menna[2], A. Fidanzio[2], A. Piermattei[2], D. Genovesi[1]
[1]*Ospedale Clinicizzato S.S. Annunziata, of Radiation Oncology "G. D'Annunzio"- University of Chieti, Chieti, Italy*
[2]*Istituto di Fisica e Unità Operativa di Fisica Sanitaria, Università Cattolica del S. Cuore, Rome, Italy*

Purpose or Objective: In-vivo dose verification is the last step of a quality assurance procedure to ensure that the dose delivered during treatment is in agreement with the prescribed one.This work reports the in-vivo dosimetry (IVD) results obtained by the SOFTDISO software (Best Medical Italy) during VMAT prostate cancer treatments.

Material and Methods: SOFTDISO is based on a method developed by a cooperation between INFN and UCSC. It reconstructs in quasi-real time (a few seconds at the end of the fraction therapy) (i) the dose at the isocenter (**Diso**) in the patient from the transit signal acquired by the EPID and (ii) the comparison between EPID images obtained during the fractions of the therapy. In particular for each beam and fraction, the R ratios between the dose reconstructed at the isocenter point, **Diso,** in single-arc (179-181°) VMAT plans for prostate targets and the dose calculated by the TPS, **Diso,TPS** (generally about 2 Gy for fraction) obtained by Oncentra Masterplan, were computed. The acceptance criteria was: 0.95≤R≤1.05. Moreover the γ-analysis (2%-2mm) between portal images supplied useful index about the beam delivery reproducibility with the Pγ<1>95% and γ mean<0.4. 15 patients with prostate cancer were treated with 6 MV photon beam delivered by an Elekta Synergy Agility (Elekta, Crawley). Our protocol required, for each patient, the IVD in the first three treatment sessions after a CBCT based set-up correction and the IVD test once weekly afterwards for the rest of the treatment course when the CBCT scan was not acquired.

Results: The IVD procedure supplied 105 tests and the average R was equal to 1.003 ± 0.028 (1SD), in a range between 0.949 and 1.058. The global R value for each single patient was well-within the 5% tolerance level. The γ-analysis between EPID images supplied Pγ<1≥97% in 80% of the tests. 20% of the tests supplied 93%≤P γ<1<95% due to small setup variations as verified by the CBCT required at the end of the fraction therapy.

Conclusion: The IVD results supported the protocol about the CBCT carried out in the first three treatment sessions of the VMAT prostate cancer treatment. The facility of the real time test supplied by SOFTDISO allows a CBCT scan requirement after the daily-fraction that supplies IVD off tolerance level. The authors intend to apply this procedure to estimate protocols about the use of the CBCT scans for other pathologies as the head-neck tumors where heavy dose variations due to morphological changes can occurs during the therapy.

EP-1526

SPAN STYLE *In vivo* dosimetry with n-type Isorad semiconductor diodes during pelvic treatment

L. Rutonjski[1], B. Petrovic[1], M. Baucal[1], M. Teodorovic[1], O. Cudic[1], B. Basaric[1]
[1]*Institute of Oncology Vojvodina Radiotherapy, Department of Medical Physics, Sremska Kamenica, Serbia*

Purpose or Objective: The study was aimed to check radiotherapy treatment accuracy and definition of action levels during implementation of in vivo dosimetry for treatment pelvic cancer patients as a part of quality assurance program.

Material and Methods: Calibration and corrections factors for in vivo entrance dose measurements for n-type Isorad semiconductor diodes for photon energy of 15 MV were determined as per recommendations published by *European Society for Radiotherapy and Oncology* (ESTRO) Booklet No.5. The pelvic cancer patients for in vivo measurements have been divided into groups, according to radiation techique used, in order to investigate and detect the groups for which the uncertainty was larger or for which a systematic error occurred. Initial tolerance/action levels for all groups were set at level of 5 %.

Results: In this study, entrance dose measurements were performed for total 185 treatment fields, of 95 pelvic cancer patients over one year period. In 6 (6%) out of 95 patients, in vivo measurements exceeded the tolerances. The mean value and the standard deviation for different groups were: Rectum and gynecology (four field box): 0.6%±3.07%(1SD), Prostate (five fields with wedges): +1.0%±2.22%(1SD). All pelvic measurements: +0.77%±2.79%(1SD). Larger standard deviation was shown for four field box cases because two large errors were noticed. After the corrections, in vivo dosimetry was repeated in both cases and the results were within the

tolerance levels and mean value and standard deviation four field box cases were +0.68%±2.43%(1SD).

Conclusion: It was noticed that standard deviation for both patient groups was similar and that initial tolerance/action levels for pelvic cases were substantial. Also, the five fields technique with wedges showed good results due to uniform directional response around diode axis. Within one year after implementation, in vivo dosimetry has revealed and prevented 6 cases of inaccurate treatment. In our experience, systematic in vivo dosimetry proved to be a very useful tool for quality assurance of a patient plan and treatment, both in detecting systematic errors and for estimating the accuracy of radiotherapy treatment delivery.

EP-1527

A phantom for brachytherapy treatment planning systems verification with the ArcCHECK® device

K. Chelminski[1], P. Sobotka[2], B. Buczek[2], E. Gruszczyńska[1], W. Bulski[1]
[1]*The Maria Sklodowska-Curie Memorial Cancer Center, Department of Medical Physics, Warsaw, Poland*
[2]*Warsaw University of Technology, Faculty of Physics, Warsaw, Poland*

Purpose or Objective: Brachytherapy HDR treatments are performed according to the plans calculated with the computerized treatment planning systems. The source positions and dwell times are established to produce required dose distributions. However, in general, the treatment plans are not verified. A phantom for such dose distribution verification is proposed to be used with the ArcCHECK system.

Material and Methods: The ArcCHECK detector array and the SNC Patient software were designed by Sun Nuclear to verify dose distributions in the IMRT and VMAT external beam therapy. It is a cylindrical tissue-equivalent phantom, containing 3D detector array, consisting of 1386 SunPoint diodes. The detectors are located helically along the cylinder with the external diameter of 21 cm. We believe that the ArcCHECK phantom could also be used to verify the brachytherapy dose calculations. For this purpose a special additional part of PMMA, a Brachyplug, was designed and manufactured. The Brachyplug is a special cylinder installed inside the ArcCHECK in which it is possible to place dosimetric films or ionization chambers. The phantom has a number of through holes, where the HDR catheters can be placed into which the Ir-192 stepping source may enter. A special brachytherapy plan was created using the Ocentra MasterPlan planning system with 4 source positions in order to create evenly distributed dose over the detectors of the ArcCHECK array. In order to check the amount of dose which could be absorbed by the electronics of the ArcCHECK system the doses at the relevant distance were measured with the PTW dosimeter and a Farmer type 30013 ionization chamber placed in PTW RW3 plate phantom under the Brachyplug. The measurements were carried out with and without a shield, a 8 cm thick Wood alloy plug, designed in order to protect the electronic control unit of the ArcCHECK from irradiation. After that the dose distribution for the planned source positions was measured with ArcCHECK device with 8 cm thick Wood alloy plug and Brachyplug placed inside the ArcCHECK cylinder.

Results: Measurements of irradiation according to the prepared plan indicate that when the ArcCHECK detectors obtain the dose of 1 Gy the total dose which could reach the ArcCHECK electronics is 12.7 cGy. Such dose is acceptable and similar to the dose in a case of teletherapy. The ArcCHECK allowed for detecting and displaing in the SNC Patient software the HDR brachytherapy irradiation distributions.

Conclusion: The ArcCHECK device may be potentially used for pretreatment verification of dose distributions in brachytherapy. This would require the development of proper energy calibration procedure for the ArcCHECK detectors and the SNC Patient software update. The Brachyplug phantom will be used for further research on verification of clinical treatment plans in brachytherapy.

EP-1528

Evaluation of the performance of the Integral Quality Monitor (IQM)

B. Perrin[1], J.A. Beck[1], R. Speakman[1], G. Budgell[1]
[1]*Christie Hospital NHS Trust, CMPE, Manchester, United Kingdom*

Purpose or Objective: The IQM is an innovative wedge shaped transmission ion chamber which is mounted below the front face of a Linac head. It monitors the total radiation fluence coming from the treatment head (see figure). It is currently undergoing Beta-testing to monitor and verify the delivery of individual treatment fields in real-time. Its potential as a tool for Linac quality control measurements is also being investigated.

Material and Methods: Over an 11 month period a series of QC and clinical prescriptions were delivered multiple times to the IQM mounted on an Elekta VersaHD Linac, to evaluate its sensitivity to potential clinical errors and its long-term reliability and reproducibility.

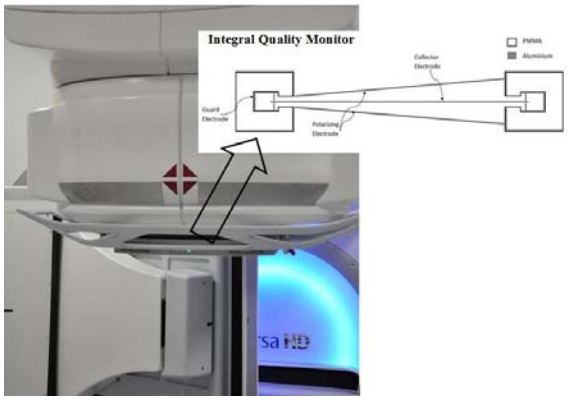

IQM mounted on Linac, with schematic of detector design

Results: The device proved reliable over the testing period. It's stability and reproducibility are shown in the table. Measurements showed that MLC/Jaw mis-calibrations of 2mm could be identified, as could 2% errors in MU. A change of energy from 6MV to 10MV gave a difference in IQM signal of 6% for conformal and 'step and shoot' IMRT, and of 2-4% for VMAT deliveries. Seventeen similar VMAT head and neck plans each demonstrated a unique IQM signal vs control point pattern, potentially allowing an incorrect plan, or 'plan of the day' to be identified after only 40 degrees of the arc. The IQM was able to identify clinically significant flatness, symmetry and output errors on the Linac.

Modality	Beam Description	Standard Deviation
Static field	10x10cm @6MV	0.7%
Static field	4x4cm @6MV	1.0%
Conformal Arc	10x10cm @6MV	0.8%
IMRT	Step & Shoot @6MV &10MV	0.7%
Simple VMAT	Prostate VMAT @10MV	0.8%
Complex VMAT	Head and Neck VMAT @6MV	1.1%

Variation in IQM signal over 11 months for different modalities

Conclusion: Although the IQM is still under development it can identify a number of clinically significant potential errors in treatment delivery. It is easy to use 'on set' and has proved stable and reliable. It has the potential for use as a

monitor for quality assurance purposes. The ability of the IQM to detect additional error modes needs further investigation.

EP-1529

A real-time monitor system for QA and VMAT: sensitivity analysis in clinical practice

G. Guidi[1,2], N. Maffei[1,2], G.M. Mistretta[1], P. Ceroni[1], A. Ciarmatori[1,2], L. Morini[1], A. Bernabei[1], P. Giacobazzi[3], T. Costi[1]

[1]*Az.Ospedaliero-Universitaria di Modena, Medical Physics, Modena, Italy*

[2]*University of Bologna, Physics and Astronomy, Bologna, Italy*

[3]*Az.Ospedaliero-Universitaria di Modena, Radiation Oncology, Modena, Italy*

Purpose or Objective: The iQM® monitor system was tested to provide a method for treatment field verification using an independent monitor system mounted below the gantry. Real-time monitoring allows delivery errors to be detected during treatment, including record & verify mismatch, calibration errors or malfunctions in multi-leaf collimator (MLC), increasing patient safety.

Material and Methods: The iQM® system consists of a large area ion-chamber with a spatial gradient. The ionization chamber and the data acquisition software system were interfaced to an Elekta Synergy accelerator. During 6 months of VMAT quality assurance (QA) sessions, more than 70 sessions of measurements were carried out to validate the repeatability of the detector as a dedicated QA instrument. To evaluate efficiency in clinical practice, a dummy plan and a Head and Neck (H&N) VMAT plan were delivered and investigated using the system. The dummy plan was composed of 18 segments (17 segments 4x4 cm2 and 1 segment 10x10 cm2) and was delivered more than 100 times with constant 50 MU per segments. The VMAT plan was composed of 140 control points delivered by an arc, with low gantry speed, high MU and low dose rate. The sensitivity was then tested by introducing specific dosimetric increases of MU (1%,2%,3%,4%,5%,10% and 20%) in the H&N plan (VMATError Plan). Rotational analysis and validation were investigated; correlation with gantry and collimator angles was quantified using SPSS ANOVA analysis.

Results: The dummy plan delivered in standard condition (gantry and collimator angles=0°) revealed a mean variation in signal counts of 0.7±1.0% compared with the commissioning day. Independence of the detector with gantry position were investigated (gantry angle: 0°-90°-180°-270° and collimator angle: 0°-45°-135°-225°-315°). No statistical difference (significance ≈ 1) was detected for all segments, confirming the high quality of the instrument for daily QA. In the H&N plan, a decrease in measured counts was observed in the particular range of gantry angles from 120° through 240°. Statistical analysis showed a mean dose discrepancy of 2.8±1.0% between planned and measured errors from the original plan. For the VMATError Plan, the system is capable of detecting the error introduced with an agreement of 0.2±0.5% (R2=0.99). No correlation related to collimator angle and delivered MU was detected.

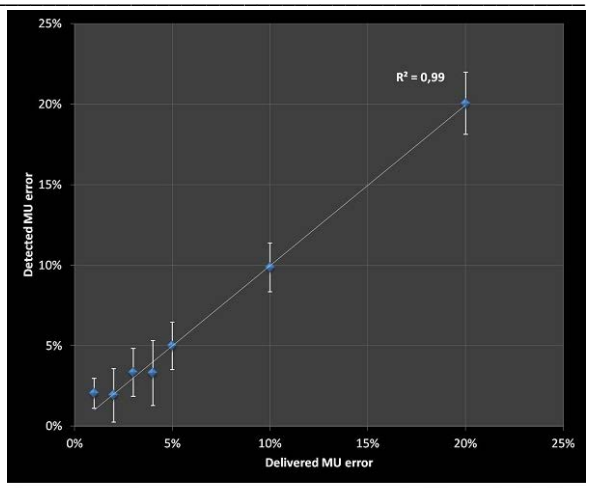

Figure 1 Correlation of MU detected vs. MU delivered with ad-hoc errors (1%,2%,3%,4%,5%,10%,20%)

Gantry angle (°)	MU error						
	1%	2%	3%	4%	5%	10%	20%
0	0,2%	1,0%	2,1%	1,8%	2,9%	7,9%	16,8%
20	2,5%	2,4%	3,1%	5,4%	4,1%	9,1%	21,1%
40	3,6%	4,6%	6,2%	5,6%	6,7%	12,3%	20,4%
60	1,4%	2,4%	3,1%	4,0%	5,4%	10,0%	20,3%
80	1,3%	0,8%	4,4%	2,7%	5,1%	9,1%	19,1%
100	2,4%	2,3%	3,5%	2,2%	4,5%	9,3%	19,6%
120	2,8%	1,2%	3,4%	3,6%	5,6%	9,3%	21,9%
140	1,6%	1,6%	4,8%	2,1%	4,4%	11,9%	18,9%
160	2,9%	2,8%	3,5%	3,3%	4,5%	8,4%	19,9%
180	1,8%	-1,8%	-0,3%	-0,4%	6,1%	9,2%	18,3%
200	1,8%	-0,4%	2,1%	0,9%	2,5%	9,3%	19,2%
220	0,9%	1,0%	1,4%	1,6%	2,5%	8,6%	18,7%
240	1,9%	1,7%	4,6%	3,3%	5,3%	8,9%	19,5%
260	2,8%	2,6%	3,8%	2,5%	5,6%	9,1%	20,1%
280	4,0%	5,2%	5,0%	8,0%	7,8%	12,9%	25,8%
300	2,1%	3,4%	3,1%	5,3%	4,5%	9,8%	20,5%
320	2,0%	3,4%	3,6%	4,5%	6,4%	12,0%	21,2%
340	2,0%	2,4%	4,6%	5,1%	6,8%	11,7%	22,4%

Table 1 Detected MU errors vs. Gantry angle

Conclusion: The system was shown to be stable for daily QA and could add many advantages to the patients' safety during treatment. Taking into account all the treatment factors, the detector provides punctual and cumulative output for each beam segment, which is compared in real time to each segment's expected value. The robustness of the measurement results suggests that the system could recognize errors or inadequate MU during the delivery. The significant signal deviation seen at particular gantry rotations could be investigated in order to improve the results obtained.

EP-1530

Machine performance check tool data analysis

P. Gago[1], J. Olasolo[1], C. Eito[1], M. Aylas[1], P. Ensunza[1]

[1]*Clinica IMQ Zorrotzaurre, Radiation Therapy, Bilbao, Spain*

Purpose or Objective: Machine Performance Check (MPC) is a tool provided with Varian TrueBeam linear accelerators to verify, prior to treatment, that critical functions of the system are within the established tolerances. An evaluation carried out by Clivio et al. compared the results of the checks they made using the MPC application and their independent measurements. The purpose of this analysis is to compare the result obtained with the MPC tool at our institution with those acquired in the mentioned study.

Material and Methods: In order to perform the MPC checks, the IsoCal phantom has to be mounted to the couch top using an appropriate holder. The system acquires a series of MV and kV images and analyses them in order to obtain values for different parameters. Two distinct types of checks can be carried out with MPC: beam constancy checks and geometry checks. With the first ones beam output, uniformity and center shift can be evaluated. Geometry checks give us information about isocenter's size, imaging devices positioning, gantry, MLC, collimator, jaws and couch positioning. We analyzed the data obtained over 15 weeks of measurements in a TrueBeamSTx 2.0 with a Millenium HD120MLC and a DMI imager. Beam checks were done for all

the available photon energies in our TrueBeam: 6MV, 15MV, 6MV FFF and 10MV FFF. Geometrical checks were measured only for the 6MV beam.

Results: In all our measurements we found that the results were within the established tolerances. The value of the isocenter's size is, in our case, 0.27 mm, very close to that obtained by Clivio et al. for the same energy, 0.34 mm. The values of the 6MV beam center shift, MV imager projection offset and absolute gantry positioning are the same that the ones obtained in the mentioned study: 0.04 mm, 0.17 mm and -0.09° respectively. For that same energy the offset of the collimator rotation is, in our case, 0.15°, while the one reported in the study is 0.17°, and the kV imager projection offset, 0.24 mm versus 0.32 mm. The output change in our TrueBeam varies from -0.58% for the 10MV FFF beam to -0.50% for the 6MV beam. In the study these values range from 0.06% for their 15 MV beam to 0.24% for their 6MV FFF beam.

Conclusion: Our TrueBeam MPC results were compared with those obtained by Clivio et al. at their institution. They show great agreement with those reported in their study. We have established MPC tool measurements as part of our routine daily QA.

EP-1531

Comprehensive commissioning and QA of the new version upgrade of treatment planning system

J. Peng[1], D. McDonald[1], N. Koch[1], M. Ashenafi[1], C. Mart[1], J. Dise[1], M. Fugal[1], K. Vanek[1]

[1]*Medical University of South Carolina, Radiation Oncology, Charleston, USA*

Purpose or Objective: To evaluate the dosimetric and optimization algorithm accuracy of a newly released version 13.5 of the Eclipse treatment planning system (TPS) prior to upgrade, utilizing the recently published AAPM Medical Physics Practice Guideline (MPPG), "Commissioning and QA of treatment planning dose calculations".

Material and Method: Eclipse V13.5 includes many novel features, such as contouring tool enhancements, streamlined 4D CT contouring, new physical materials for the AcurosXB (AXB) dose algorithm, and faster optimization engines. MPPG phantom tests were performed to validate both static and dynamic beams in both homo- and hetero- generous material. Additionally, 54 patient plans were re-calculated in V13.5 with the same beam parameters, monitor units, and dose algorithms in order to examine algorithm difference. A dose-difference plan was created by subtracting the dose calculated in V13.5 from V11 and evaluated in 3D dose display. Those re-calculated patient plans included a variety of treatment sites, energies, and techniques. However, the new Photon Optimizer (PO) algorithm was developed in V13.5 to replace the previous Dose Volume Optimizer (DVO) in IMRT and Progressive Resolution Optimizer (PRO) in VMAT. In order to compare the PO and DVO/PRO optimizers, 25 IMRT/VMAT clinical plans were re-optimized with PO using the same objectives, prescriptions, and number of iterations. The plan quality and optimization time were examined.

Results: Dose differences for all clinical cases and MPPG phantom tests in-field and in homogeneous areas, were within 1% and 3% for photon and electron plans, respectively. Although the beam models were not re-commissioned in V13.5, the dosimetric leaf gap (DLG) value was modified and the new physical material was added in AXB; as a result the dose differences correspond to differences in the dose algorithms. Therefore, at field edges and heterogeneity interfaces, maximum dose differences increased to 3% and 6% for photons and electrons, respectively. Dose calculated using AXB was found to be 3% less at the lung interface and inside the lung in V13.5 compared to dose calculated in V11, but no dose difference calculated using AAA was seen. PO could optimize plans 20-30% faster than DVO/PRO. For most cases, no significant difference in plan quality was noted. However, lung SBRT cases with PO showed a reduction in MUs and slightly improved dose conformity.

Table I : The mean and maxium dose difference of the same dose algorithms between V11 and V13.5 in 3D (photon and electon), VMAT , SBRT and SRS cases.

Machine #1 _Varian True Beam with HD MLCs

3D Photon

Treatement Site	Field #	Energy (MV) + Accessory	Mean Dose Diff. (V11-V13.5)	Max. Dose Diff. (V11-V13.5)
MPPG Phantom (all energy and fields)			0.7%	-2.3%
Lt Breast	4	6X+10X	<0.5%	0.9%
Larynx	2	10X+EDW	0.8%	-1.5%
Lung	2	10X	<0.5%	0.8%

3D Electron

Treatement Site	SSD(cm)	Energy (MeV)	Mean Dose Diff. (V11-V13.5)	Max. Dose Diff. (V11-V13.5)
MPPG Phantom (all energy and fields)			0.8%	5.2%
TBI Rib Boost	105	6e	1.1%	3.1%
Scalp	105	9e	1.5%	3.1%
TBI Rib Boost	105	12e	1.4%	1.8%
TBI Rib Boost	105	16e	1.8%	2.0%

VMAT

Treatement Site	Arcs #	Energy (MV) + Accessory	Mean Dose Diff. (V11-V13.5)	Max. Dose Diff. (V11-V13.5)
Lung	2	10x	0.5%	1.7%
Mediastinum	2	10x	<0.5%	0.9%
HN	2	6X	<0.5%	1.1%
Brain	4	6X	<0.5%	1.2%

Treatement Site	Arcs #	Energy (MeV)	Mean Dose Diff. (V11-V13.5)	Max. Dose Diff. (V11-V13.5)
Brain	4	6X	0.6%	1.5%
Lung	2	10X	<0.5%	1.7%
Lung	2	10X	0.6%	1.9%

SBRT

Treatement Site	Fields#/ Arcs #	Energy (MV) + Accessory	Mean Dose Diff. (V11-V13.5)	Max. Dose Diff. (V11-V13.5)
liver SBRT	9	10x	-0.6%	-1.2%
Adrenal SBRT	9	10x	-1.0%	-2.9%
Lung SBRT	9	6X+10X	-1.2%	-1.9%
Lung SBRT	5	6X	-0.8%	-1.4%
Lung SBRT	3	6X	-0.9%	-1.5%
Adrenal SBRT	3	10X	-0.4%	-1.1%
Lung SBRT	4	6X	-0.7%	-1.3%

SRS

Treatement Site	Arcs #	Energy (MeV)	Mean Dose Diff. (V11-V13.5)	Max. Dose Diff. (V11-V13.5)
Spine SRS	3	6X	<0.5%	-1.1%
Spine SRS	6	6X	<0.5%	-1.2%
Spine SRS	6	6X	<0.5%	-1.1%
Brain SRS	3	6X	<0.5%	-1.6%

Machine #2 _Varian iX

3D Photon

Treatement Site	Field #	Energy (MV) + Accessory	Mean Dose Diff. (V11-V13.5)	Max. Dose Diff. (V11-V13.5)
MPPG Phantom (all energy and fields)			0.50%	-2.1%
Rt Breast	2	6X	<0.5%	0.7%
Pelvis	3	16X + EDW	<0.5%	0.7%
Lung	5	6X	0.6%	-2.8%
Lung	3	16X	<0.5%	0.9%
Brain	2	6X+16X	0.7%	-1.2%
Pelvis	4	16X	<0.5%	-2.5%
whole brain	2	6X	0.6%	-1.6%
Hip	2	16X	0.8%	-1.8%

3D Electron

Treatement Site	SSD(cm)	Energy (MeV)	Mean Dose Diff. (V11-V13.5)	Max. Dose Diff. (V11-V13.5)
MPPG Phantom (all energy and fields)			0.7%	5.8%
Breast Boost	105	6e	1.0%	4.1%
Breast Boost	100	9e	1.9%	4.9%
Breast Boost	100	12e	1.4%	3.7%
Sternum	100	16e	1.3%	5.0%
Breast Boost	100	20e	1.1%	6.1%

VMAT

Treatement Site	Arcs #	Energy (MV) + Accessory	Mean Dose Diff. (V11-V13.5)	Max. Dose Diff. (V11-V13.5)
IR Prostate	2	16X	<0.5%	1.0%
Pelvis	2	6x	<0.5%	1.1%

Treatement Site	Arcs #	Energy (MeV)	Mean Dose Diff. (V11-V13.5)	Max. Dose Diff. (V11-V13.5)
breast+IM+SC	6	6x	<0.5%	1.4%

Machine #3_TrueBeam with regular MLCs

3D Photon

Treatement Site	Arcs #	Energy (MV) + Accessory	Mean Dose Diff. (V11-V13.5)	Max. Dose Diff. (V11-V13.5)
MPPG Phantom (all energy and fields)			0.50%	-2.5%
Pelvis	4	16X	0.7%	-1.8%
Rt. Breast	4	6X	<0.5%	0.7%
Brain	2	6X+16X	0.7%	-1.9%
Lt Lung	3	6X+16X	0.5%	-1.7%

3D Electron

Treatement Site	Arcs #	Energy (MeV)	Mean Dose Diff. (V11-V13.5)	Max. Dose Diff. (V11-V13.5)
MPPG Phantom (all energy and fields)			1.0%	6.1%
Breast Boost	105	6e	1.2%	3.5%
Breast Boost	100	9e	1.1%	4.1%
Breast Boost	105	12e	1.5%	6.3%
Rt Axilla	105	16e	1.8%	3.2%

VMAT

Treatement Site	Arcs #	Energy (MV) + Accessory	Mean Dose Diff. (V11-V13.5)	Max. Dose Diff. (V11-V13.5)
Prostate	2	6x	<0.5%	1.1%
HN	2	6x	<0.5%	1.0%
Lung	2	6x	<0.5%	1.4%

Treatement Site	Arcs #	Energy (MeV)	Mean Dose Diff. (V11-V13.5)	Max. Dose Diff. (V11-V13.5)
Prostate	2	16x	<0.5%	1.5%
breast+IM+SC	6	6x	<0.5%	1.8%
HN	2	6x	<0.5%	1.3%

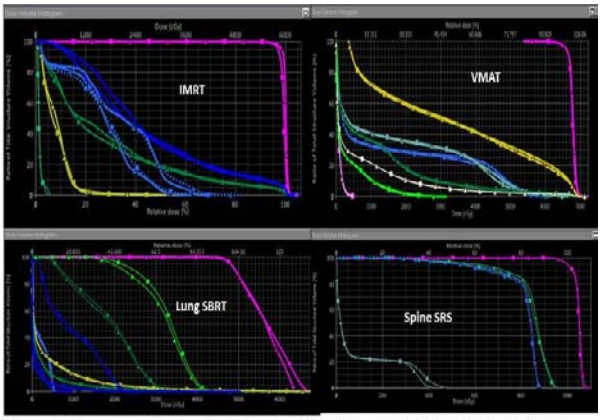

Figure 1. The comparison of optimization algorithms between PO (V13.5) and DVO/PRO (V11) in IMRT, VMAT, Lung SBRT and Spine SRS cases. The square dots present DVO/PRO algorithms in V11 and triangle dots show PO algorithms in V13.5

Conclusion: Commissioning and QA of new TPS version is essential prior to clinical release. The tests suggested by MPPG provide an excellent framework for this work, particularly when combined with additional clinical cases. Dose differences noted were chiefly located at beam edges, possibly due to modified DLG values, and in heterogeneous materials and interfaces using AXB, potentially due to differences in material specification. The PO improved optimization efficiency in all cases and MU economy and dose conformity in some SBRTs, with no reduction in plan quality.

EP-1532

Reliability of the Machine Performance Check application for TrueBeam STx Linac

V. Mhatre[1], P. Patwe[1], P. Dandekar[1]

[1]*Sir HN RF Hospital, Radiation Oncology, Mumbai, India*

Purpose or Objective: Machine Performance Check (MPC) is an application to verify geometry and beam performances of Truebeam STx , through automated checks . In this study,MPC tests were analysed using all photon beam energies of our Truebeam STx, comparing whenever possible with external independent checks.

Material and Methods: The Machine Performance Check (MPC) is a new Truebeam STx major mode, designed to evaluate the machines geometric performance. Data acquisition comprises a series of 39 images acquired with IsoCal Phantom & with particular MLC pattern settings. MPC performs geometric and dosimetric checks. The geometric checks intend to test the treatment isocenter size and its coincidence with imaging devices, the positioning accuracy of the imaging systems, collimator, gantry, jaws, MLC leaves & the couch position. The dosimetric checks refer to a reference MV image and give the beam output, uniformity and center change relative to the reference.MPC data were acquired during one month on different consecutive days. For most of the MPC checks, an independent control has been performed at the same time of the acquisition of the MPC to evaluate the agreement of the two methods. For the independent checks, phantoms and detectors available & used routinely in the department were used.The Daily QA3 was used to check the beam constancy.The first acquisition, acquired at the same time as the MPC baseline, was used as reference. Also weekly output was performed as per TRS 398 protocol on water phantom using FC 65 chamber to compared with the MPC and Daily QA3 output.

Results: Treatment isocenter was between 0.39 ± 0.02 mm with MPC, compared to 0.5 ± 0.01 mm for 6 MV with the Winston-Lutz test. Coincidence of kV and MV imaging isocenters was within 0.26 ± 0.05 and 0.25 ± 0.06 mm, respectively (0.5 ± 0.1 mm with external tests). Positioning accuracy of MLC was within 0.5 mm; accuracy of jaws was 0.12 ± 0.02, 0.14 ± 0.03, −0.77 ± 0.08, 0.11 ± 0.04 mm for X1, X2, Y1, Y2 jaws, respectively, with MPC. Dosimetric tests: the output stability relative to the baseline for 6 MV .10MV and 15 MV was 0.46 ± 0.09%, 0.45 ± 0.08%, 0.3 ± 0.07%for MPC compare with 0.82 ± 0.3%, 0.33 ± 0.2%, 0.52 ± 0.33% with the independent measurement.

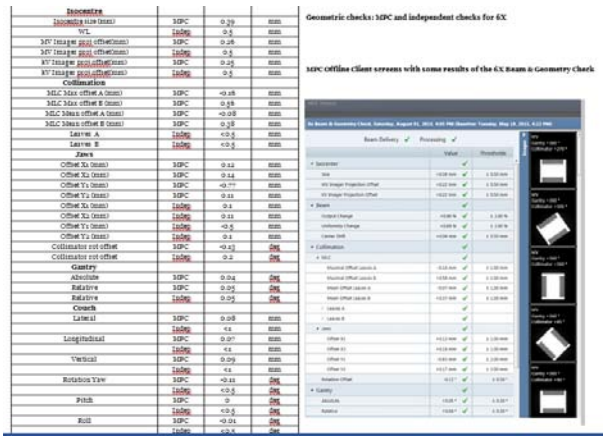

Conclusion: MPC is a useful tool for QA of Truebeam STx systems and its automation makes it highly efficient for testing both geometric and dosimetric aspects of the machine. Overall, the ability of the MPC to monitor linac output stability was comparable to that of ionization chamber-based measurements.

EP-1533

Sensitivity of ArcCheck system to setup error using Perfect Pitch 6D couch

V. Mhatre[1], P. Patwe[1], P. Dandekar[1]
[1]*Sir HN RF Hospital, Radiation Oncology, Mumbai, India*

Purpose or Objective: The purpose of this study is to evaluate the sensitivity of ArcCheck 3D diode array to setup error for patient-specific quality assurance (QA) of volumetric-modulated arc therapy (VMAT). Translational setup errors of ± 1, 2 & 3 mm in the RL, SI & AP directions & rotational setup errors of ± 0.5°,1◦ & 1.5° in the pitch, roll & yaw directions were set up in ArcCheck for 6 patients.The pass rate of γ analysis was computed by comparing the calculated & measured dose distributions using 3%/3 mm, criteria.

Material and Methods: Six VMAT plans for various sites were selected for this study. The VMAT plans were designed using Eclipse v13 treatment planning system.The ArcCheck Dosimetry system consists of 1386 diodes,embedded in the cylindrical wall of the phantom with 10 mm spacing. All tests were carried out using an Truebeam STx accelerator with a high definition MLC . CBCTs were acquired for all the set up. Registration between the reference CT and CBCT was carried out automatically using an inbuilt rigid registration method.The ArcCheck phantom was translated in the right-left (RL), anterior-posterior (AP), and superior-inferior (SI) directions by ± 1,2&3 mm respectively and rotated in the pitch, roll, and yaw directions by ± 0.5°,1°& 1.5° using the 6D treatment couch. To validate the accuracy of perfect pitch couch for rotation, smart tool digital level was placed on couch to confirm the rotation introduced in phantom. Each patient plan were separately delivered on the phantom for dose verification in total, 37 measurements (1 without positional error, 18 with translational errors, & 18 with rotational errors) were performed for each patient.The pass rate of γ analysis was computed by comparing the calculated and measured dose distributions using 3%/3 mm, criteria respectively.

Results: When the translational setup errors are ± 1, 2& 3 mm, respectively, the pass rates of γ analysis with the 3%/3 mm criteria decreased by a maximum of 1.7%, 8.4%, and 11.0% in RL direction; 2.5%, 7.4%, and 12% in the SI direction & 2.0%, 7.5%, and 10.5% in the AP direction. When the rotational setup errors were ± 0.5°, 1°&1.5°, respectively, the pass rates of γ analysis with the 3%/3 mm criteria decreased by a maximum of 3.5% ,5% & 12% in the pitch direction; 3.2% ,6% & 15.2% in the roll direction,3.5%,8% &18% in the yaw direction.

Impact of Setup Error on Gamma Analysis for 3%3mm Criteria in RL Direction

Set Up	P1	P2	P3	P4	P5	P6
No Error	98.7	96.5	97.6	98	98.5	97
±1	96	95.5	96.5	97	98	96
±2	90.3	91	92	92.5	93	93.5
±3	87.7	89	88.5	88	88.9	89

Impact of Setup Error on Gamma Analysis for 3%3mm Criteria in SI Direction

Set Up	P1	P2	P3	P4	P5	P6
No Error	98.7	96.5	97.6	98	98.5	97
±1	97.5	96	96.7	96	96	95.5
±2	92	90	90.3	93	94	92.5
±3	88	87	88.4	86	87	89

Impact of Setup Error on Gamma Analysis for 3%3mm Criteria in AP Direction

Set Up	P1	P2	P3	P4	P5	P6
No Error	98.7	96.5	97.6	98	98.5	97
±1	96.5	96	97	96	97.5	96.5
±2	91	92	90.1	91.5	92	91.5
±3	88.5	87.3	87.9	86.5	88.5	88

Impact of Setup Error on Gamma Analysis for 3%3mm Criteria in Pitch Direction

Set Up	P1	P2	P3	P4	P5	P6
No Error	98.7	96.5	97.6	98	98.5	97
±0.5°	95.2	94	94.6	95	95.2	94
±1°	93.7	91.5	93	92.5	93.5	93
±1.5°	89	87	87.5	86	89	90

Impact of Setup Error on Gamma Analysis for 3%3mm Criteria in Yaw Direction

Set Up	P1	P2	P3	P4	P5	P6
No Error	98.7	96.5	97.6	98	98.5	97
±0.5°	96	93.2	94.5	94.5	95	93.5
±1°	93.7	91	92	92	93	91.5
±1.5°	85	85.5	86	84	83.2	87

Impact of Setup Error on Gamma Analysis for 3%3mm Criteria in Roll Direction

Set Up	P1	P2	P3	P4	P5	P6
No Error	98.7	96.5	97.6	98	98.5	97
±0.5°	95.2	93	94.8	95	94.5	94
±1°	90.7	90	90.5	92.5	92.7	91
±1.5°	82.5	83.5	84.5	80	81.5	83.5

Conclusion: In this study, ArcCheck diode array showed high sensitivity to rotational setup errors. ArcCheck 3D diode array is capable of detecting an setup error in order of 1 mm/0.5°.

EP-1534

Dosimetric impact of the QFix kVue Calypso couch top and the electromagnetic array with photon beams

J. Molinier[1], N. Aillères[1], L. Bedos[1], A. Morel[1], S. Simeon[1], D. Azria[1], P. Fenoglietto[1]

[1]*Centre Val d'Aurelle - Paul Lamarque, Radiation Oncology, Montpellier, France*

Purpose or Objective: The Calypso 4D Localization System consists in an electromagnetic detection of implanted Beacon transponders in order to continuously track their moves. The use of this system requires a specific couch top and the introduction in the treatment beam of an electromagnetic array. The purpose of this study is to quantify the dosimetric impact of the new material introduction in photon beams.

Material and Methods: At first, the QFix kVue Calypso couch top and the array attenuation was evaluated by comparing the dose measurements with Eclipse TPS dose prediction for 2 energies (6MV FF and 6MV FFF) and 2 rail configurations (rails in and rails out). Dose measurements at the isocenter were performed with a cylindrical water-equivalent phantom, a 0.125cc ionization chamber, a 10*10cm² field size at 39 gantry angles. The beams between 315 and 45° allowed analyzing the electromagnetic array attenuation. The beams between 90 and 270° were used for couch attenuation. Secondly, the dosimetric impact was analyzed on 20 RapidArc treatment plans of prostate (10 with 6MV FF and 10 with 6MV FFF). Dose distributions were recalculated in the cylindrical phantom and the dose prediction at the isocenter was compared to the dose measurement with the 0.125cc ionization chamber using 2 configurations: classical treatment (with kVue IGRT couch top and rails out) and treatment with Calypso (QFix kVue Calypso couch top, rails out and the electromagnetic array).

Results:

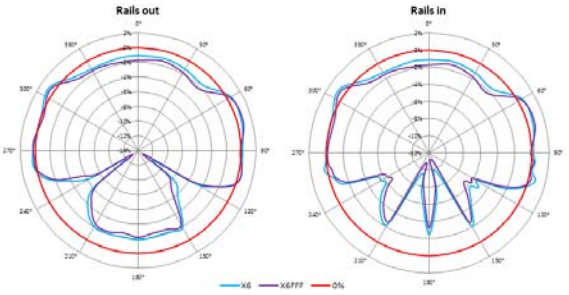

In the configuration of rails out, the mean attenuation of the couch was 2.91% for X6 and 3.45% for X6FFF with a maximum of 12.02% and 13.19% for X6 and X6FFF, respectively. In the configuration of rails in, the mean attenuation was 3.25% for X6 and 3.90% for X6FFF with a maximum of 9.79% and 11.14% for X6 and X6FFF, respectively. Besides, the mean attenuation of the array was 1.15% and 1.67% for X6 and X6FFF, respectively. As regards the impact of global Calypso system on RapidArc treatment plans, the mean deviation with a classical treatment was -0.61% [-0.8%; -0.3%] for X6, and -0.31% [-0.86; 0.43] for X6FFF.

Conclusion: For the fixed beams, the attenuation is not negligible when a beam crosses directly a support rail in particular. The errors in dose calculation can be more of 10%. However, for RapidArc treatments with X6 and X6FFF, the dosimetric impact of the QFix kVue Calypso and the array is not significant.

EP-1535

Electron Skin Irradiation: refinement of an abutting field technique

G. Pittomvils[1], E. Bogaert[1], T. Boterberg[1], M. Van Eijkeren[1], C. De Wagter[1], Y. Lievens[1]
[1]*Ghent University Hospital, Radiotherapy, Ghent, Belgium*

Purpose or Objective: Skin electron irradiation is a treatment modality for mycosis fungoides. An overlapping and/or abutting field technique with the patient lying on a stretcher is used with at least two oblique 40x40 cm²; 4 MeV-overlapping fields at 25/335 gantry angles at SSD=170 cm both about 12 cm lateral of patient mid-line. If two fields fail to cover the entire affected skin additional abutting oblique fields are added in cranio-caudal direction. Using 3 pairs of fields, the entire anterior (or posterior) body is covered. During commissioning of a new Elekta Synergy accelerator special attention was given in the search of an optimal angle incidence and field matching.

Material and Methods: A linear array (PTW LA-48) positioned in a polystyrene phantom is used to evaluate longitudinal and lateral dose profiles at 1 and 4 mm depth. Two different angles of incidence (± 25° and ± 30°) and three different abutment gaps (0-32-64 mm; common multipliers of the 8 mm interdetector distance of the LA-48) are evaluated. Prescription dose point is corresponding to the dose value at 4 mm depth of the central axis dose of the most cranial beam pair. Treatment length is defined as the distance between the most cranial and most caudal 90% dose point. Beam spread is calculated over the entire treatment length, beam flatness (1) over 0.9 times the treatment length.
(1) Podgorsak p.196

Results: Both gantry angle pairs show a remarkable flat summed dose profile over the entire range of the LA-48 (3.0-3.2% for ± 25°; 2.3.-2.4% for ± 30°). As expected maximal dose levels are decreasing with increasing obliqueness resulting in more depth-related dose homogeneity. Cranio-caudal measurements show a radiation field increase of 1.5-2 cm (50% field dose boundary) compared to the light field . The initial 6 field light field abutment method results in dose spreads of 3.5% and 5.6% (4-1 mm depth) and dose flatness of 4.7% and 6.1%. Introducing 32 mm gaps improves dose data to 2.5% and 2.8% in spread and to 3.3% and 3.8% in flatness. 64 mm gaps result in a spread of 4.3% and 3.6% and a flatness of 7.5% and 6.0% (fig. 1). The corresponding treatment length increases from 168 cm (no gaps) to 178 cm (32 mm gaps) and to 187 mm (64 mm gaps).

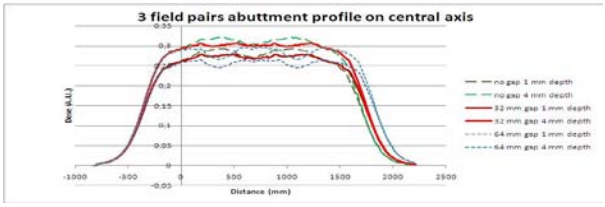

Conclusion: The general conclusion is that for mycosis fungoides treatments, using oblique fields with dedicated abutment in cranio-caudal direction the general accepted overall dose homogeneity of ±10% is more than met on a flat surface equivalent to the size of a human body using 6 oblique fields.

EP-1536

Uncertainties in dose calculations for radiation treatment of breast cancer after mastectomy

R. Chakarova[1], A. Lindberg[2], M. Gustafsson[3], D. Lundstedt[4]
[1]*Göteborg University Sahlgrenska University Hospital, Department of Medical Physics and Biomedical Engineering, Göteborg, Sweden*
[2]*Sahlgrenska University Hospital, Department of Medical Physics and Biomedical Engineering, Gothenburg, Sweden*
[3]*Sahlgrenska University Hospital-, Department of Medical Physics and Biomedical Engineering, Gothenburg, Sweden*
[4]*Sahlgrenska Academy- Sahlgrenska University Hospital, Department of Oncology- Institute of Clinical Sciences, Gothenburg, Sweden*

Purpose or Objective: To study dose distributions in chest wall with thickness around or less than 15 mm and to evaluate the accuracy of Eclipse and Oncentra treatment planning algorithms in phantom and patient geometries.

Material and Methods: Measurements by thermo luminescent dosimeters and gafchromic film are performed on a cylindrical phantom with air cavity representing the lung. Tangential 6 MV open beam is applied on the phantom and dose profiles from the surface toward the geometrical center

of the phantom are obtained at beam axis entrance and exit, as well as laterally. Dose distributions for two patients are calculated for clinical plans involving 6 MV and 15 MV photon beams and field-in-field techniques. Three volumes are studied, namely, PTV (516 cm3) and CTVT (10 cm3) for patient one, and PTVT (117 cm3) for patient two. Calculations in the case of phantom and patient geometries are performed by Eclipse AAA and Acuros XB algorithms and by Oncentra CC algorithm. Corresponding Monte Carlo dose calculations are carried out using EGSnrc/BEAMnrc software. Estimates like D98% (dose to 98% of the volume) and V95% (the volume receiving 95% of the dose) are used when comparing the dose distributions. The accuracy of the different algorithms when including a bolus is investigated.

Results: Measurements in the phantom case show a negligible dose decrease at the phantom-in-air interface but more than 10% dose decrease at this interface laterally or at beam exit. Large uncertainties in calculated data are detected in the interface regions, namely up to 4 mm depth from the phantom-air interface and 2 mm depth from the phantom-in-air interface. In the patient cases, deviations less than 3% are observed for PTV and CTVT for the dosimetry parameters D98% D2% and V105% obtained by the different algorithms and the Monte Carlo method. For PTVT, the largest deviations are between AAA and Monte Carlo data, for example, 3.6% for D98% and 9.2 % for V105%. The results are explained by the fact that PTV is large and eventual uncertainties at the boundary has smaller effect on the dose volume histograms. CTVT is small, however, the distance from the CTVT contour to the surface and to the lung interface is 4 mm or more at each slice. In the third case, a large partial volume of PTVT is located near the lung interface where the dose uncertainties are large. Furthermore, it has been found, that the algorithms reflect properly the dose changes due to bolus except for AAA, where the dose volume histograms for CTVT obtained with and without bolus can't be distinguished.

Conclusion: Partial volume located near the lung interface has major effect on target coverage. The measured dose decrease and the uncertainties of the treatment planning algorithms near interfaces should be taken into account when establishing guidelines for target delineation and coverage for patients with thin chest wall.

EP-1537

Developing an in vivo dosimetry system for TomoTherapy® using the CT detector array

H. Dhiraj[1], S. Thomas[1], S. McGowan[1]
[1]*Cambridge University Addenbrookes Hospital, Radiotherapy - Medical Physics, Cambridge, United Kingdom*

Purpose or Objective: The Hi-Art Helical TomoTherapy unit is a linear accelerator equipped with an on-board CT detector array. It delivers radiation in a helical fashion with daily CT imaging for image guidance and beam monitoring. *In vivo* dosimetry is a recommended part of treatment with the potential of improving patient safety. Conventional approaches of *in vivo* dosimetry cannot be implemented for TomoTherapy due to the rotational nature of the system and thus transit dosimetry is required. This study has investigated the use of the detector sinogram in performing transit dosimetry by modelling how the primary photons are influenced by scatter geometry for a static and helical field. The aim has been to produce a semi-empirical model of the exit detector signal and investigate factors that influence the signal at the imaging panel of a TomoTherapy unit.

Material and Methods: The detector signal profile (detector sinogram) is extracted for the DICOM data for each procedure. It contains the response at each detector channel and for each projection. The exit detector response for an open field is measured in-air with a moving couch for a static and helical delivery. The exit detector sinogram for an in-air measurement has been used as an input into a signal reconstruction model of the exit detector sinogram when a scattering medium is positioned on the couch. A simple ray-tracing model has been produced using narrow beam conditions for the attenuation of the beam in a cylindrical, uniform phantom (Tomo® Cheese Phantom). The model relies on TPR data previously determined in the department as shown in Thomas *et al*., (2012).

Results: The simulated sinogram agrees with the measured sinogram for both the static and helical deliveries within ± 10% in the central region of the phantom. At the edge of the phantom this increases to ±15% due to set-up issues.

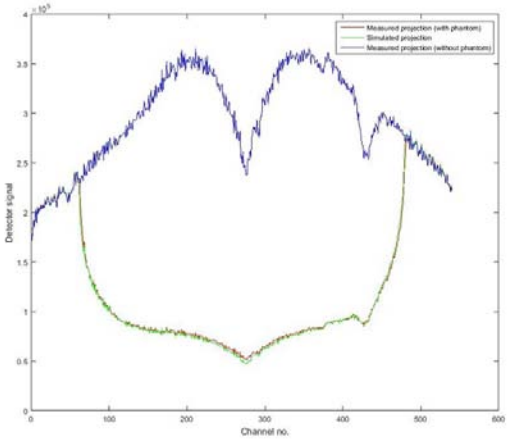

Figure 1 shows a single projection (7 degrees) taken from the sinogram data for the measured and modeled exit detector sinograms.

Conclusion: At this stage of development, the model shows promise in use as an independent check tool. However, second order corrections, such as scatter, should be incorporated if the model is to be clinically used. Further work is also required to reduce set-up errors, i.e. by imaging the phantom prior to measurement.

EP-1538

How well does Compass compare to film for prostate VMAT patient-specific QC?

D. Nash[1], M. Huggins[2], J. Kearton[1], A.L. Palmer[3]
[1]*Queen Alexandra Hospital, Medical Physics, Portsmouth, United Kingdom*
[2]*University of Surrey, Department of Physics, Guildford, United Kingdom*
[3]*Queen Alexandra Hospital- Portsmouth- UK, Medical Physics, and Department of Physics- University of Surrey- Guildford- UK., United Kingdom*

Purpose or Objective: Compass© (IBA, Schwarzenbruck, Germany) is a 3D pre-treatment plan verification system. The linac fluence is measured with an ion chamber array (MatriXX (IBA)). Then via a detector fluence model and collapsed cone algorithm [1], the dose is calculated on the patient's planning CT. It has been demonstrated that Compass can validate VMAT plans (73-99% gamma passing rate at 3%/3mm [2]) although it does introduce some dose blurring [3]. However, occasional failures do occur in plan verification using Compass (i.e. a significant variation on a DVH parameter or reduced gamma pass rate). The purpose of this work was to understand whether failures were due to genuine errors (such as treatment delivery or calculation) or due to the limitations and uncertainties of the Compass methodology. To achieve this, EBT3 film was used as best estimate of the true delivered dose distribution for prostate VMAT plans.

Material and Methods: Six fields which were characteristic of segments from previously failed plans were measured with EBT3 film using advanced triple-channel dosimetry techniques (via FilmQAPro). These were then compared against Compass and the TPS (Pinnacle 9.8) doses using profile and 2D global gamma analysis. Twelve film

measurements were then acquired for 3 clinical prostate patients with Compass and film (one of which had failed Compass QC, likely due to narrow segments) in a solid water phantom and compared.

Results: Profile analysis of the characteristic fields showed that for narrow but long fields on axis, the agreement between Compass and film was within 3%, slightly inferior to the TPS and film comparison at 2%. The worst case was 5% for a 1 x 10 cm off-axis field and 4% for irregular fields. The clinical films demonstrated that Compass accurately modelled dose distribution with 11/12 films achieving at least 95% gamma passing at 3%/3mm with an average of 97.8 ± 2.1 % (sd). The failed film achieved 93.6% passing. This was from the failed clinical plan – this is more likely due to the blurring induced by narrow segments than inaccurate delivery. Figure 1 shows (a) an isodose for a passing film and (b) a profile taken across the film. All films passed when compared against the TPS (average gamma 98.3 ± 1.3 %).

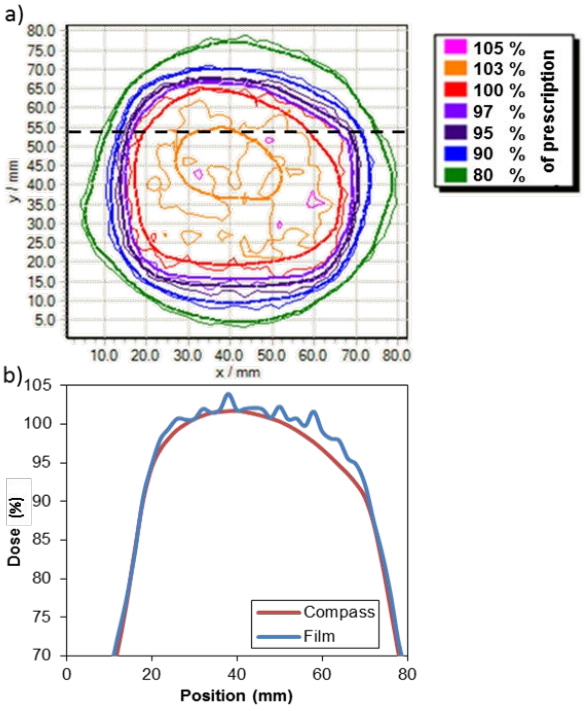

Figure 1. Representative film showing (a) an isodose and (b) a profile (dashed line on (a)) showing the Compass (thick) and film (thin) where 100% = 3.48 Gy.

Conclusion: By comparison with film measurements, it has been shown that Compass is able to reproduce the dose distribution of clinical VMAT prostate plans, and is sufficiently accurate to detect any clinically relevant errors. However, users should be aware that the resolution of the Compass reconstruction algorithm is limited when narrow segments are predominant.

References

[1] Koreevar EW *et al*, 2011. *Radiother. Oncol.*, 100, 446-452.
[2] Boggula R *et al*, 2010. *Phys. Med. Biol.*, 55, 5619-5633.
[3] Godart J *et al*, 2011. *Phys. Med. Bio.*, 56, 5029-5043.

EP-1539

Proposal for DVH oriented acceptance criteria for VMAT prostate patient specific QA

M. Polsoni[1], F. Rosica[1], F. Bartolucci[1], C. Fidanza[1], G. Orlandi[1]
[1]*AUSL 4 Teramo, Department of Medical Physics, Teramo, Italy*

Purpose or Objective: New hybrid systems for patient specific pre-treatment QA are suited for 3D gamma (GA) and DVH reconstructed analysis (DA). For 2D evaluations, a 3%/3mm agreement for 90-95% points is considered to be the state of art. Recent studies highlighted poor correlation between gamma passing rates and DVH clinical goals variations on PTV and OARs, so it could improve the situation to consider available DVH analysis tools. The aim of this work is to test the robustness and sensitivity of VMAT prostate patient specific DVH based acceptance criteria (AC) for QA using the COMPASS (Iba-Dosimetry) system in combination with the RayStation (Ray Search Laboratories) TPS.

Material and Methods: For thirty prostate dual-arc VMAT plans, the most relevant DVH indices (DI) were considered for the PTV: D98, D95, D50, D1 and Dmean . Clinical doses were computed with both, COMPASS and RayStation, which share the same calculation algorithm. Plans were delivered with a VARIAN Trilogy equipped with a Millenium 120 MLC and measured with COMPASS. RayStation vs COMPASS reconstructed doses were analyzed in terms of DI differences. The AC rely on calculating mean values (m) and standard deviations (std) of DI differences and assigning for each DI difference a confidence interval equal to 1.5•std. To assess the AC robustness in terms of system sensitivity the TG119 prostate case was optimized using a VMAT single arc technique. Three different types of errors were introduced individually in the RT-plan to mimic linac delivery inaccuracies: a) MU number modification (MU-error) from -3% to +4%, b) gantry angle shift (g-error) from 0° to 3° and c) widening of both leaf banks (w-error) from 0 to 2 mm. Modified plans were delivered and beforehand defined DI were calculated.

Results: For RayStation vs COMPASS computed doses analysis DI differences < 0.4% have been found. In the TG119 plan PTV DI differences showed a linear trend respectively with MU-errors (see figure) and g-errors. The proposed DVH based criteria detected MU-errors below -1.8% or above 1.3% and w-errors > 1.5mm. The criteria led to the detecting of g-errors>3°.

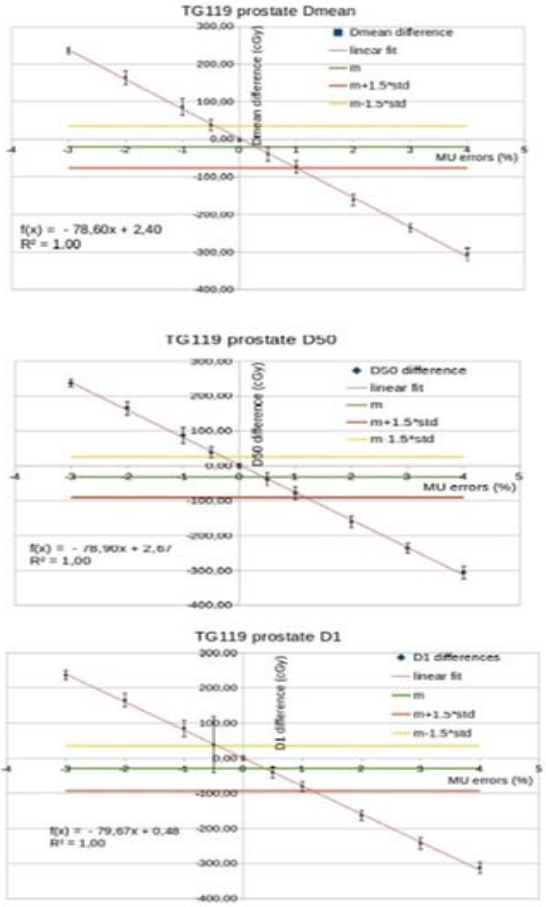

Conclusion: The defined criteria show high predictive capability and robustness to detect MU and w-errors on the PTV. On the other hand g-errors are not easy to detect mainly because of the central position of the prostate.

EP-1540

EBT3 films for proton therapy plan QA using a multichannel approach

L. Marrazzo[1], S. Lorentini[2], M. Schwarz[2], S. Pallotta[3]
[1]*Careggi University Hospital, Medical Physics Unit, Firenze, Italy*
[2]*Trento Hospital, Proton Therapy Department, Trento, Italy*
[3]*University of Florence, Department of Biomedical-Experimental and Clinical Sciences 'Mario Serio', Florence, Italy*

Purpose or Objective: Due to the excellent spatial resolution, Gafchromic® EBT film (Ashland Inc., Wayne, NJ) are potentially attractive as a 2D dosimeter for dose verification in proton therapy. Multichannel dosimetry (MCD) was recently proposed for film calibration, showing improved accuracy if compared to single channel dosimetry (SCD), since it allows for the separation of the dose-dependent part of the film image from non dose-dependent contributions. The aim of this study was to test MCD vs SCD for patient plans QA in proton therapy.

Material and Methods: We performed irradiations with different levels of complexity in both homogeneous and anthropomorphic (heterogeneous) phantom. Homogenenous phantom: measurements with EBT3 film and MatriXX (Iba Dosimetry, Schwarzenbruck, Germany) were carried-out in solid water slabs delivering 1) a homogeneous 'box-like' dose distribution (range 12cm, modulation 6cm, width 5x6cm^2, measured at 9cm depth) and 2) a clinical field measured at 6cm depth. Anthropomorphic phantom (Proton Therapy Dosimetry Head - CIRS 731-HN): films were placed on sagittal planes and phantom was irradiated with 1) a homogeneous box-like field, 2) a single clinical field and 3) a three beam clinical plan (two lateral no-coplanar and one anterior oblique). Each film was scanned together with two reference films, one non-irradiated and one exposed to a dose around 80% of the maximum expected dose. The reference films provide data for correcting the dose-response function for the conditions applying to the particular scan, thus reducing the inter-scan variability; this option can be selected in the FilmQA™ Pro software used for the analysis. Films were scanned with an Epson Expression 10000XL. Measured data were compared with those extracted by the TPS (XiO, Elekta).

Results: Table 1 shows the results of the gamma analysis for both SCD and MCD. An average reduction of about 16% and 10% was observed for the 2%/2mm and 3%/3mm gamma parameters, respectively, when moving from MCD to SCD. The standard deviations reported in the table indicate a larger variability among the results for SCD compared to MCD, thus suggesting that MCD is also effective in reducing inter-film variability. Comparing the fields delivered in homogeneous vs anthropomorphic phantom, an average deterioration by 3% (MCD) is observed in gamma passing rates in presence of heterogeneities.

			γ passing rate (%)	
			2%/2mm	3%/3mm
Homog. phantom	Homogeneous box field	MCD	74,0	88,6
		SCD	67,7	82,6
	Clinical field	MCD	74,8	93,0
		SCD	49,3	73,5
Anthropomorphic phantom	Homogeneous box field	MCD	72,0	86,1
		SCD	37,7	68,1
	Clinical field	MCD	68,2	92,1
		SCD	42,7	74,5
	Full plan: Central plane	MCD	71,7	91,5
		SCD	71,7	90,8
	Full plan: Intermediate plane	MCD	78,0	95,5
		SCD	71,2	93,6
	Full plan: Lateral plane	MCD	69,2	92,5
		SCD	55,8	83,0
	Mean±1SD	MCD	73±3	91±3
		SCD	57±14	81±9

Table 1. Comparison between the multichannel and single channel dosimetry in terms of gamma passing rates (local approach, 10% threshold).

In figure 1, a comparison between the two methods in terms of gamma maps, isodose distributions and profiles is shown.

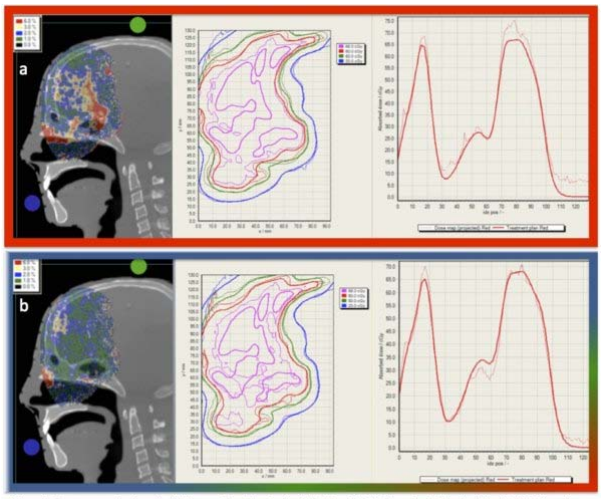

Figure 1. Gamma maps, isodose distributions and profiles for the SCD (a) and MCD (b) methods (single clinical field delivered on anthropomorphic phantom).

Conclusion: In general, the MC optimization strongly improves the gamma passing rates when comparing measured and calculated dose maps. The proposed method appears to be suitable also for patient dose verification in proton therapy.

EP-1541

Effects of leaf position accuracy of robotic radiotherapy system on dose distribution

J. Suzuki[1], H. Takahashi[2], M. Tomida[2], K. Hamajima[2], Y. Ohhashi[2], T. OKUDA[2]
[1]*Toyota Memorial Hospital, Radiotherapy Quality Management Group, Toyota, Japan*
[2]*Toyota Memorial Hospital, Radiology, Toyota, Japan*

Purpose or Objective: Recent technological developments in robotic radiotherapy systems have enabled delivery of a large number of non-isocentric, non-coplanar beams using the InCise™ multi leaf collimator (MLC) system. However, the effect of gravity may result in leaf positional errors. We investigate the leaf position accuracy of Cyberknife M6 and evaluate the effects of leaf position accuracy on the dose distribution.

Material and Methods: The leaf position accuracy of Cyberknife M6 was tested at the home position and at eleven positions that may affect the MLC position accuracy through the gravity effect. The position accuracy was analyzed by the Bayouth test with an EBT2 film. Further, the dose distribution for a prostate cancer patient treatment plan when using the MLC was evaluated. Film dosimetry is performed for evaluating the dose distribution. Parameters from the patient

plan are applied to a phantom, and the film is exposed in three orientations. The dose distributions from the film measurements were compared with the planned dose distributions from the treatment planning system. This analysis was performed using the Gamma index method.

Results: The leaf position error was observed with respect to the gravity effect. The maximum leaf position error was 0.42 mm at a Sauce axis distance of 800 mm. All leaf position errors were within the tolerance level of leaf position accuracy recommend by vendors. In the evaluation of the dose distribution, all passing rates of the gamma index method were greater than 90% in criterion of 2%/2 mm and threshold of 30% of the maximum dose.

Conclusion: The leaf position accuracy of Cyberknife M6 can achieve clinically acceptable levels in every position that is affected by the gravity effect.

EP-1542

Comparison between Elekta Oncentra 4.3 and Monaco 5.0 3DCRT dose calculation algorithms

M.G. Brambilla[1], C. Cadioli[1], A.F. Monti[1], C. Carbonini[1], M.B. Ferrari[1], D. Zanni[1], G. Alberta[2], A. Torresin[1]
[1]*Ospedale Niguarda Ca' Granda, Medical Physics, Milan, Italy*
[2]*Elekta S.p.A., Technical Support, Agrate Brianza, Italy*

Purpose or Objective: Accurate dose tests have to be performed before using a TPS in clinical practice. Measured and calculated dose distributions must be compared in various irradiation conditions. This process needs a huge amount of time for both calculation and analysis. In this work, we evaluated the differences between 3DCRT calculated dose distributions in the migration between two TPSs produced by the same company.

Material and Methods: In our Hospital, the migration from Oncentra ver. 4.3 (Elekta, SWE) to Monaco ver. 5.0 (Elekta, SWE) was carried out. The 3DCRT dose calculation algorithm (CCC) is the same for the two systems. The kernels for 3 different photon energies produced by a Synergy (Elekta,UK) equipped with an 80 leaves MLC were processed and installed on the Monaco console by Elekta. Some parameters (beam source size and MLC interleaf leakage), were automatically created during the kernel generation. The same Oncentra parameters were previously optimized by the user during the commissioning. In this work, we verified whether significant differences exist in the implemented beam models in the two TPSs and in their use for dose calculations. The dose distributions calculated by the systems were analyzed in terms of depth doses, profiles at various depths and absolute dose. The results were compared to the corresponding measurements according to ESTRO booklet 7 criteria. For relative data, the reference analysis parameter was the gamma index confidence limit, that is the absolute value of gamma index average plus 1.5 times its standard deviation. The dose deviation and the distance to agreement values in global and local gamma index test were changed according to the irradiation geometry complexity (from 2%-2mm to 4%-3mm) and a maximum dose threshold of 7-10% was used. A specific analysis software provided by Elekta Support was used for the comparisons. For absolute doses, the reference analysis parameter was the percentage difference between measured and calculated values (acceptance criteria from 2% to 3% depending on complexity).

Results: Because of the great amount of data, a concise picture of the results is not possible. However no significant differences between Oncentra and Monaco calculated doses were found, except for negligible variations in field shape (around 0.5 mm) probably due to a small difference in source size used in the two TPSs. Yet, new kernel processing was required in order to optimize Monaco behaviour in profile tails.

Conclusion: The migration between the two systems did not show significant differences in 3DCRT calculated dose distributions. Then, if an Oncentra accurate commissioning is present, a reduced number of comparison tests, involving each implemented energy and radiation unit, could be used with Monaco. Our results refer to Oncentra ver. 4.3 and the present considerations should not be adopted for previous versions without any specific check.

EP-1543

Feasibility of MLC dosimetric leaf gap measurement using OCTAVIUS 4D system

H. Geng[1], W.W. Lam[2], Y. Bin[2], K.Y. Cheung[2], S.K. Yu[2]
[1]*Hong Kong Sanatorium & Hospital, Medical Physics & Research Department, Happy Valley, Hong Kong SAR China*
[2]*Hong Kong Sanatorium & Hospital, Medical Physics & Research Department, Hong Kong, Hong Kong SAR China*

Purpose or Objective: The dosimetric leaf gap (DLG) is an important parameter defined in the Eclipse treatment planning system (TPS) to account for the partial transmission through rounded leaf ends of Varian multileaf collimators (MLC). The DLG is determined by comparing the agreement between calculated and measured dose distributions of Intensity-modulated radiotherapy (IMRT) plan. The IMRT plan dose distribution is typically measured using ionization chamber and radiographic film. Radiographic film dosimetry gives excellent spatial resolution and is widely used for dose distribution measurement; however, it shows energy dependence and limited dose range. Also, developing the film is time consuming. OCTAVIUS 4D system consists of a 2D ionization chamber array and its associated 4D phantom. The chamber array has uniform energy response and relatively wide dose range. Previous investigators have proved that the sampling frequency of this ionization chamber array is appropriate for IMRT dose distribution verification. The 3D dose distribution could be reconstructed immediately after measurement. In this study the feasibility of determining DLG using OCTAVIUS 4D system was investigated.

Material and Methods: A standard 9-fields head and neck IMRT plan was generated in Eclipse TPS using 6MV photon beam. The optimized photon fluence was converted into final dose distributions by applying different DLG values ranging from 1.8 to 2.2. Those IMRT plans were copied and applied to both OCTAVIUS 4D and a cylinder solid water phantom. The optimal DLG was determined independently using these two dosimety system by comparing the agreement between calculated and measured dose distributions. A point dose was measured using ionization chamber (A1SL, Standard imaging, USA) inserted into the solid water phantom and the 2D dose distribution was measured using radiographic film (EDR2, Kodak, USA) sandwiched in the phantom. The measured point doses were compared with the calculated ones and 2%/2mm criteria were selected for gamma analysis of film comparison. For OCTAVIUS 4D system, 3D dose distributions were measured and reconstructed using OCTAVIUS 4D system. The measured dose distributions were compared with calculated ones using 2%/2mm 3D gamma analysis criteria. The optimal DLG measured using OCTAVIUS 4D was compared with that determined using ionization chamber and film system.

Results: The point dose measurement and the gamma analysis of both film and OCTAVIUS 4D systems were listed in Table 1. The maximum gamma analysis passing rate in OCTAVIUS 4D measurement agreed with the results in EDR2 film analysis and both suggested that 2.0 is the optimal DLG value.

DLG	Percent difference in point dose measurement using A1SL ionization chamber	Passing rate in EDR2 Film comparison (2%/2mm gamma analysis criteria)	Passing rate in OCTAVIUS 4D system measurement (2%/2mm gamma analysis criteria)
1.8	1.72%	80.5%	89.5%
1.9	1.05%	83.1%	92.3%
2.0	0.66%	84.8%	93.2%
2.1	-0.10%	82.2%	93.0%
2.2	-0.54%	79.9%	91.8%

Table 1. The point dose measurement and the gamma analysis of both EDR2 film and OCTAVIUS 4D systems

Conclusion: In this study, the DLG determined using OCTAVIUS 4D system is in good agreement with ionization chamber and film measurement. OCTAVIUS 4D system may be an alternative of film dosimetry and provide an effective and efficient way to determine the MLC DLG value.

EP-1544

Dose conformation evaluation of volumetric modulated arc therapy for cranial radiosurgery

C. Ferrer[1], C. Huertas[1], A. Castaño[2], A. Colmenar[2], A. Mañas[2], A. Serrada[1]

[1]*H.U. La Paz, Radiofísica y Protección Radiológica, Madrid, Spain*

[2]*H.U. La Paz, Oncología Radioterápica, Madrid, Spain*

Purpose or Objective: To evaluate the quality and dose conformity of a volumetric modulated arc therapy (VMAT) cranial radiosurgery treatment plan using different parameters, as well as the accuracy of the dose calculation.

Material and Methods: Four patients were prescribed to 18Gy, planned with Elekta Monaco treatment planning system (v. 3.30.01), and optimized using biological and physical based cost functions for VMAT treatment on an Elekta Synergy linear accelerator equipped with a 160-leaf Agility MLC. 5 to 9 non coplanar arcs were used, for cranial lesions of different sizes (Target volume, 4 cc- 8 cc). Treatment isocenter was placed at the target volume center. The evaluation was performed using the RTOG Conformation Index (CI), the target coverage (TC), the Paddick's conformity index (CIp), the homogeneity index (HI), volume of healthy brain tissue receiving a dose of 10 Gy or more (V10), and the dose to organs at risk (OAR). The accuracy of the dose calculation was verified measuring the dose distribution with Gafchromic Film EBT3, inside the IBA Scanditronix I'mRT phantom, and read using FilmQA Pro software. Absolute dose measurements were made with a CC13 Scanditronix-Wellhofer ionization chamber located at the treatment isocenter. Also the 4D detector array ArcCHECK (Sun Nuclear Corporation) was used for 2 patients. Van Dyk's criterion, dose percentage difference and distance to agreement (DTA) 3%-3mm, was employed.

Results: Median CI, CIp and HI for all patients were 0.93, 0.82 and 1.16 respectively, with median TC of 88%. V10 was kept below 10cc for all cases. OARs were spared within tolerances. Conformity and received doses to OAR depend on the type and location of the target, and in one case all indices were significantly lower in order to comply with the V10 tolerance. Best results were obtained with 5 -6 non coplanar arcs arrangement. Dose distribution measured with Gafchromic Film EBT3 gave passing rates above 90% and absolute percent differences between measured and calculated dose with the ionization chamber were lower than 2% for all patients. ArcCHECK results showed a passing rate greater than 95% for the two patients.

Conclusion: With Monaco treatment planning system, in combination with a 160-leaf Agility MLC, it is possible to achieve highly conformal dose distributions for cranial radiosurgery VMAT plans, and target volumes larger than 4cc, with low doses to healthy tissue, even with highly irregular lesions. For the plan evaluation, the combination of TC with CI and CIp showed to be more helpful than the CI itself alone.

EP-1545

Dosimetric impact of target separation in craniocaudal direction with TomoDirect Dynamic Jaw

C.W. Kong[1], W.W. Lam[1], W.K.R. Wong[1], S.G. Lo[1], T.L. Chiu[1], S.K. Yu[1]

[1]*Hong Kong Sanatorium & Hospital, Medical Physics & Research Department, Happy Valley, Hong Kong SAR China*

Purpose or Objective: TomoDirect is a non-rotational treatment option for Tomotherapy in which the treatment field is delivered at different discrete gantry angles with MLC modulation and couch translational movement. With the introduction of Dynamic Jaw Technique (Available for jaw setting 5 cm and 2.5 cm) there is a potential improvement in the radiation dose fall-off at the cranio-caudal edges of a target, thus enhancing the effectiveness of dose reduction between the targets in the treatment with multiple metastases. In this study the effectiveness of dose reduction using Dynamic Jaw Technique was investigated for different target separations using different jaw settings, pitch factors and modulation factors.

Material and Methods: Two identical cylindrical targets of 6 cm length and 3 cm diameter aligning along superior-inferior (SI) direction with different separation ranging from 4.5 cm to 2 cm in 0.5 cm decrements were created on a water phantom image. TomoDirect planning was done on the planning CT images using Dynamic Jaw Technique with different jaw setting. Dose prescription was 2 Gy per fraction to 95% volume of both targets. Gantry angles 0°, 120° and 240° were used. Different plans were created with the modulation factor varying from 1.5 to 3 in 0.5 increments and the pitch factor ranging from 0.1 (default value) to 0.05 of the jaw width in 0.01 decrements. Same test plans were created using Fixed Jaw Technique for jaw width 5 cm, 2.5 cm and 1 cm for comparison. All plans were delivered and EDR2 film was used to measure the dose distribution on the coronal plane to verify the planning calculation.

Results: Measured dose distributions were in good agreement with the planning calculation for all plans as the gamma passing rate were higher than 90% with 2% in dose difference and 2 mm in DTA. The impact of reducing pitch value and increasing modulation factor were marginal on the dose fall-off between the targets for all plans. From figure 1, dose reduction effect between targets was greatly enhanced with different separations when Dynamic Jaw Technique was applied for jaw setting 5 cm and 2.5 cm. For target separation as small as 3 cm such dose reduction effect using 2.5 cm Dynamic Jaw Technique was comparable to 1 cm Fixed Jaw Technique.

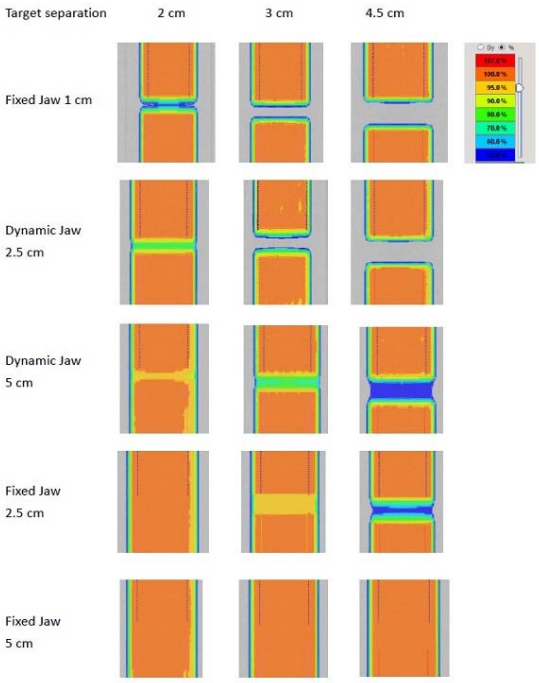

Figure 1. Isodose distribution on the region between targets with different separation using different technique in TomoDirect.

Conclusion: In Dynamic Jaw Technique, Jaw setting is the critical factor for dose reduction between the targets. For target separation not less than 3 cm Dynamic Jaw Technique with 2.5 cm should be used as the dose reduction effect is comparable with 1 cm Fixed Jaw Technique with shorter treatment time.

EP-1546

Abstract withdrawn

EP-1547

Monte Carlo simulation of the Elekta VersaHD linac

E. Borzov[1], A. Nevelsky[2], S. Daniel[2], R. Bar-Deroma[2]
[1]*Rambam Health Care Campus, Oncology, Tirat Karmel, Israel*
[2]*Rambam Health Care Campus, Oncology, Haifa, Israel*

Purpose or Objective: The Elekta VersaHD linac is characterized by the new 160 leaves Agility MLC and the ability to work in Flattening Filter Free (FFF) mode. The objective of this work was to create an accurate Monte Carlo (MC) model of this linac for 6MV and 6MV FFF beams.The Elekta VersaHD linac is characterized by the new 160 leaves Agility MLC and the ability to work in Flattening Filter Free (FFF) mode. The objective of this work was to create an accurate Monte Carlo (MC) model of this linac for 6MV and 6MV FFF beams.

Material and Methods: The BEAMnrc code was used to create detailed models of the linac head for the 6MV and 6MV FFF beams based on the manufacturer data supplied by Elekta. MC simulation with the BEAMnrc code generated the phase-space file using DBS and BCSE variance reduction techniques. This file was used in the DOSXYZnrc code to calculate PDDs, profiles and output factors in a water phantom at SSD= 90 cm. Results from the simulations were compared against measurements performed during commissioning of the linac using an PTW water phantom, a PTW SemiFlex ion chamber and a Scanditronix stereotactic diode. Field sizes from 1x1 cm to 20x20 cm were taken into consideration. The following parameters of the MLC and of the incident electron beam had to be determined to provide the best fit between the measured and calculated data: leaf bank rotation (LBROT) angle, leaf spacing at isocenter, the incident beam spectrum (mean energy and FWHM, under assumption of Gaussian distribution), width (FWHM) and angular divergence. The incident beam spectrum was defined by matching PDDs, the beam width was determined by matching the penumbra in in-plane and cross-plane directions. The angular spread was adjusted by matching the profiles of 20x20cm2 field. LBROT angle and leaf spacing were obtained by matching the interleaf measured and calculated values. Output factors (relative to a 10x10 cm2 field) were calculated under assumption of negligible backscatter from the MLC to the ion chamber.

Results: Calculated and measured PDDs for all field sizes agreed within 1%/1mm. Lateral profiles in both (in-plane and cross-plane) directions agreed within 2%/1mm for all field sizes. Output factors agreed with 3%. For the 6MV beam, the mean energy and FWHM of the incident electron beam were 6.5MeV and 0.5MeV respectively. For the beam width, FWHM in the in-plane direction was 0.15cm and in the cross-plane direction 0.25cm. For the 6MV FFF beam the mean energy and FWHM of the incident electron beam were 7.4MeV and 0.5MeV. FWHM in the in-plane direction was 0.10cm and in the cross-plane direction 0.20cm. The mean angular spread was 1.1 degree for both beams. LBROT angle was 0.01radian. The leaf spacing at isocenter was 0.5cm.

Conclusion: An accurate MC model for the Elekta VersaHD linac was created to be used with the BEAMnrc code. This model will be employed for our future work of the Agility MLC characterization and modeling of stereotactic cones.

EP-1548

Optimisation of the initial parameters and efficiency in Monte Carlo simulation for Cyberknife

M.J. Lin[1], T.C. Chao[2], T.C. Chang[1], C.C. Lee[2], H.L. Chao[3], A.C. Shiau[2]
[1]*Chang Gung Medical Hospital, Department of Radiation Oncology, Taoyuan, Taiwan*
[2]*Chang Gung University, Graduate Institute of Medical Imaging And Radiological Science, Taoyuan, Taiwan*
[3]*Tri-service General Hospital, Department of Radiation Oncology, Taipei, Taiwan*

Purpose or Objective: To optimize the initial parameters and calculation efficiency in Monte Carlo simulation for Cyberknife G3 system.

Material and Methods: BEAM09 Monte Carlo codes were used for this study. The BEAMnrc code was used to simulate the treatment head and generate the phase space files. The DOSXYZnrc code was used to calculate the depth dose curves(percentage depth dose, PDD), lateral profiles and the output factors. Mean incident electron energy and the radial intensity (FWHM) were used to determine of initial electron parameters. For the calculation of dose in the region of interest, the use of smaller voxel size may increase the calculation time; conversely, the adaption of larger voxel size may cause a higher partial volume effect. This study aims to investigate the optimal voxel size for dose calculation in a water phantom to achieve a reasonable simulation efficiency and an acceptable accuracy.The Kα method was used for the optimization by comparing the differences between diode measurement data and MC simulations in PDDs and profiles. Disagreement between simulation and measurement were evaluated through the dose differences of PDDs from depths of 1.5 to 20 cm, and the lateral profiles of 80% field width. The DTA (distance to agreement) at lateral positions of 20% to 80% dose profiles of penumbra region were also used for the comparisons.

Results: For the efficiency of dose calculation, by setting the voxel size equal to one tenth of field width would produce a optimal simulation efficiency and an acceptable accuracy. For the optimization of initial parameters, the optimal mean incident electron energy is 7.1 MeV and the FWHM(R) is 2.4 mm. According to these parameters, the dose differences of the PDDs is about 1% from depths of 1.5 to 20 cm, and the dose differences for lateral profiles within 80% field width is also within 1.5%, and the disagreements of DTA were less than 0.5 mm. The discrepancies of output factor were 2.8-5% for the three smallest cones, which were possibly caused by the effect of electron scattering at the metallic parts of the detector shielding.

Conclusion: For Monte Carlo simulations of LINAC and dose calculations it is important to accurately determine the initial electron beam. These parameters, mean energy and FWHM of incidence electron, have been determined by matching the calculated dose with the measured dose through a trial and error process.This study also applied some methods to increase simulation efficiency which could be the reference of future research.

EP-1549

Dosimetric evaluation of VMAT planning for Elekta Agility using Eclipse planning system

V. Prokic[1], F. Röhner[2], S. Spiessens[3]
[1]*University of Applied Sciences, Mathematics and Technic, Remagen, Germany*
[2]*The University Medical Center Freiburg, Department of Radiation Oncology, Freiburg, Germany*
[3]*Varian, Medical Systems, Palo Alto, USA*

Purpose or Objective: VMAT planning for Elekta linear accelerators with newest MLC-Agility is supported with the following treatment planning systems: Pinnacle3 (Philips, Fitchburg WI, USA), Oncentra Masterplan (Elekta), RayStation (RaySearch Laboratories AB, Stockholm, Sweden) and Monaco (Elekta). The newest release of Eclipse TPS V13.5 (Varian Medical Systems, Palo Alto, CA, USA) includes an algorithm for Elekta Agility VMAT planning. The purpose of this study was to assess dosimetric validation of the new VMAT optimization algorithm implemented in the treatment planning system Eclipse TPS V13.5 for the latest Elekta MLC-Agility. Testing was performed by creating and dosimetrically verifying VMAT plans for different anatomical sites.

Material and Methods: The Agility multileaf collimator (Elekta AB, Stockholm, Sweden) has 160 leaves of projected width 0.5 cm at the isocenter, with maximum leaf speed 3.5 cm/s and dynamical leaf guides. Ten patients with different carcinoma sites previously treated were selected for this study: head and neck, lung, prostate, anal and cervix carcinoma. Selection was made in order to cover common tumor sites and also to have broad spectrum of complexity. VMAT plans were optimized using the new Photon Optimizer algorithm (PO 13.5.35) implemented in the Eclipse TPS V13.5. The plan quality was evaluated by homogeneity, conformity and target coverage. All plans are re-calculated for Octavius phantom with 729xdr Detector (PTW, Freiburg) and irradiated. Comparison of measured and calculated dose distributions was done in VeriSoft 6.0 Software (PTW, Freiburg) using 2D Gamma-index and "Difference in percent of normalization value of reference matrix"-method.

Results: All VMAT plans met clinical objectives, providing high conformal dose distributions. The comparison of the 3D dose distribution measured by PTW Octavius 729 2D-Array passed both used criteria. 2D Gamma-Value (3% local dose, 3mm distance to agreement) analysis for all plans gave results gamma index=1, with 100% passing points. The other comparison method, resulted in more of 95% passing points for all investigated plans.

Conclusion: This study showed excellent dosimetric validation of VMAT plans made for Elekta Agility using newest Eclipse 13.5 version of the Varian planning system. It is also shown that MLC of Elekta Agility allows treating most complex target volumes in VMAT technique.

EP-1550

Dosimetric comparison of the two dose reporting modes of Acuros XB and AAA for lung SBRT

A.W. Mampuya[1], M. Nakamura[1], Y. Hirose[2], T. Ishigaki[3], T. Mizowaki[1], M. Hiraoka[1]

[1]Kyoto University- Graduate School of Medicine, Department of Radiation oncology and Image-applied therapy, Kyoto, Japan

[2]Osaka Red Cross Hospital, Division of Radiology, Osaka, Japan

[3]Osaka Red Cross Hospital, Department of Radiation oncology, Osaka, Japan

Purpose or Objective: The purpose of this study is to measure the difference in dose-volumetric data between the analytical anisotropic algorithms (AAA) and the two dose reporting modes of the Acuros XB, namely, the dose to water (AXB_Dw) and dose to medium (AXB_Dm).

Material and Methods: Dose volumetric data for 37 lung lesions treated with Stereotactic Body Radiation Therapy (SBRT) were generated using the AXB_Dm in Eclipse Treatment Planning System (TPS) for Varian Clinac iX or TrueBeam and then recalculated with the AXB_Dw and AAA using the same monitor units and identical beam setup. The internal target volume (ITV) was delineated using the averaged image from the 4DCT and the PTV was obtained by adding 5mm margin to the ITV. A dose of 50Gy in 4 fractions was prescribed to the IC and the D95%. The following dose-volumetric parameters were evaluated; D2%, D50%, D95% and D98% for the ITV and the PTV. Two-sided, paired Student's t tests were used to test for statistical significance ($p<0.05$).

Results: Table I summarized the dose-volumetric data results under the IC and the D95 prescription for all the 37 lesions. Under the IC prescription, the maximum mean difference, observed in the ITVD50% between the AXB_Dm and the AAA was only 1.7 points, although statistically significant ($p<0.05$). The difference in the PTV D98% was not statistically significant between the three algorithms. With the D95 prescription. The maximum mean difference, observed in the ITVD50% between the AXB_Dm and the AAA was 3.3 points, ($p<0.05$). The difference in the PTV D98% and D2% was not statistically significant between the AXB_Dm and AXB_Dw. The PTV D95% didn't differ between the three algorithms.

Table I. Dose volumetric data calculated with AXB_Dm, AXB_Dw and AAA. Data are shown as means ± standard deviation.

	IC			D95		
	AXB_Dm	AXB_Dw	AAA	AXB_Dm	AXB_Dw	AAA
PTV						
D2[c]	101.7±2.2	101.0±2.1	100.6±1.7	133.4±7.7	133.1±7.6	131±6.5
D50[a]	95.4±4	94.8±3.5	93.9±3.2	120.4±4.3	120.3±4.3	118±4.3
D95[d]	86.9±6.2	86.5±6	86.2±5.5	100.1±00	100.1±00	100.1±00
D98[c]	84.6±7	84.2±6.8	84.2±6.5	93.8±2.4	93.8±2.4	94.2±2.6
ITV						
D2[b]	102.1±1.9	101.1±1.6	101±1.3	134.3±8.2	133.9±8.2	132.1±7.1
D50[a]	98.6±2.2	97.7±1.8	96.9±1.9	128.3±7.4	127.6±7.3	125±6.4
D95[a]	94.0±3.4	93.3±3.3	92.4±3.2	118.5±12.5	118.2±12.5	115.9±12.1
D98[a]	92.7±5	92±5	91.2±4.8	116±15	115.8±14.9	113.6±14.8

Abbreviations: AXB_Dm= Acuros XB dose-to-medium reporting mode; AXB_Dw= Acuros XB dose-to-water reporting mode; AAA= Analytical anisotropic algorithm; PTV= Planning target volume; ITV= Internal target volume; IC= Isocenter prescription dose; D95= Prescription covering 95% of the target volume.

[a]A significant difference was found between AXB_Dm and AAA, AXB_Dm and AXB_Dw and AAA and AXB_DW

[b]A significant difference was found between AXB_Dm and AAA, AXB_Dm and AXB_Dw and AAA and AXB_Dw only under the D95 prescription.

[c]A significant difference was found between AXB_Dm and AAA and AAA and AXB_Dw under the D95 prescription.

[d]A significant difference was found between AXB_Dm and AAA, AXB_Dm and AXB_Dw under the IC prescription

[e]A significant difference was found between AXB_Dm and AAA, AXB_Dm and AXB_Dw and AAA and AXB_Dw under the IC prescription and AXB_Dw and AAA and AXB_Dw under the D95 prescription.

Conclusion: Although statistically significant, the dosimetric difference between the three algorithms are within acceptable range with the maximum difference being 3.3 points between the AXB-Dm and AXB_Dw.

EP-1551 Benchmarking Monte Carlo for proton radiosurgery

P. Trnkova[1], J. Shin[1], J. Schuemann[1], H. Kooy[1], J. Daartz[1]

[1]Mass. General Hospital, Department of Radiation Oncology, Boston- MA, USA

Purpose or Objective: Small proton fields that are used in proton radiosurgery (PSRS) are defined by the loss of electronic and nuclear equilibrium along the central axis as a consequence of electronic and nuclear interactions. The Bragg peak is degraded which can lead to underestimation of range if the treatment planning system (TPS) does not correctly model nuclear and MCS effects. Monte Carlo simulation is the gold standard for dose calculations. The aim of this project was to benchmark Monte Carlo simulation for PSRS against measurements and compare it to the TPS.

Material and Methods: A fixed beamline for passive scattering PSRS was modeled with TOPAS, a platform for Monte Carlo simulations. Depth dose profiles of pristine Bragg peaks with ranges of 6, 10 and 15 cm as well as SOBPs for the same ranges and respective modulations widths of 2 and 4 cm for 6cm, 2.5 and 4.5 cm for 10 cm and 4.5 and 8 cm for 15 cm were calculated with TOPAS. The simulations were compared to annual QA measurements with a multilayer ionization chamber (MLIC) and to the XiO (Electa, Sweden) TPS. The field size in all cases was 6 cm in diameter. Two scoring volumes were used, a 1 cm and a 4 cm radius cylinder with 0.1 cm binning in beam direction.

Results: The measured and calculated Bragg peaks and SOBPs were in good agreement. The absolute difference between measured and calculated ranges and modulation widths were 0.7 mm (0.1 – 1.5 mm) and 0.6 mm (0.3 – 1.1 mm), respectively. The absolute differences between calculated and XiO ranges and modulation widths were 0.7 mm (0.4 – 0.9 mm) and 0.2 mm (0.1 - 0.4 mm), respectively. The differences in the diameter of the scoring volume mainly influenced the build-up area. Figure 1 presents an example of a SOBP (range 15 cm, modulation 4.5 cm) comparing the three methods (a), and calculated with different scoring diameters (b). The pristine Bragg peak for the range of 15 cm is shown in Figure 1c.

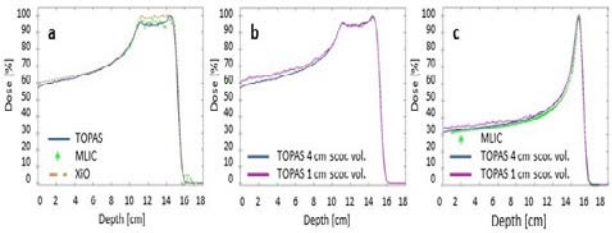

Conclusion: Precise characterization of depth dose curves is very important in PSRS when the field size is small and the number of fractions is limited not allowing wash out of any dosimetric uncertainty. The Monte Carlo simulation of PSRS beamline was successfully benchmarked against measurements. This implementation will enable exploration of even smaller volumes and execution of treatment planning studies for PSRS.

The work was sponsored by Swiss National Fund (SNF project number P300P3_158522).

EP-1552

Phantom measurements and simulated dose distributions in pelvic Intra-Operative Radiation Therapy

F. Costa[1], A. Esposito[2], P. Limede[2], C.C. Rosa[3], S. Sarmento[4], O. Sousa[5]

[1]*IPO PORTO, Investigation Center CI-IPOP, Porto, Portugal*
[2]*INESC TEC, Center for Applied Photonics, Porto, Portugal*
[3]*Universidade do Porto, Physics and Astronomy Department of Science Faculty, Porto, Portugal*
[4]*IPO Porto, Medical Physics Service and Investigation Center CI-IPOP, Porto, Portugal*
[5]*IPO PORTO, Radiotherapy Service, Porto, Portugal*

Purpose or Objective: Rectal cancer is the second most frequent tumour site treated with intra-operative electron radiation therapy (IOERT) in Europe, after breast cancer [1]. Unlike breast, the pelvic irradiation surface is usually irregular and/or concave, and bevelled applicators are frequently used. A previous study in phantoms has shown that the shape of the irradiation surface can alter the IOERT dose distribution, with possibly important consequences for the interpretation of in vivo measurements [2]. The aim of this work is to study pelvic IOERT dose distributions, by simulating clinical irradiation conditions using phantoms and computational models.

Material and Methods: A phantom was created in-house using a sacral bone model covered with 3mm thick radiotherapy bolus, as shown in Figure 1A. To simulate in vivo measurements, small pieces of Gafchromic EBT3 film (1.5x1.5cm2) were placed on this phantom, and irradiated with a 9MeV electron beam from a Varian 2100 CD conventional linear accelerator (LINAC), adapted for IOERT with a hard docking system of cylindrical applicators. The 7cm applicator with a 45° bevel (7B45) was used to irradiate the phantom. A numerical model of this IOERT system had been previously implemented using BEAMnrc, an EGSnrc based Monte Carlo code, and validated by comparison with water tank measurements. This computational model was used to calculate the IOERT dose distributions resulting from a few irradiation surfaces, with varying curvatures, to compare with the measurements performed with the phantom.

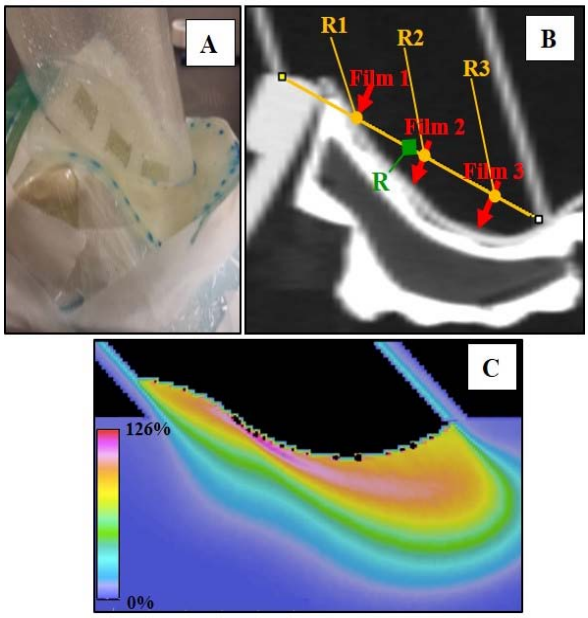

Figure 1 A. Sacral bone model covered with 3mm bolus, 3 film pieces, and the 7B45 IOERT applicator; B. Film locations on the phantom (red arrows) and film positions relative to a flat surface (R1, R2, R3); the green square (R) marks the reference point for surface dose on a flat surface; C. Dose distribution calculated with Monte Carlo simulation model, for irradiation of a curved surface.

Results: The surface doses measured with the films placed on the surface of the phantom (Film 1, 2, 3) were compared with the expected surface dose at the centre of the applicator (location R in Figure 1B) in reference conditions (flat irradiation surface). The percentage differences found are presented in Table 1. The variation introduced by the bevelled applicator along the applicator surface, in reference conditions, is also shown for comparison. The differences between the measured values and those expected for a flat surface (at locations R1, R2, R3 of Figure 1B), are in good agreement with the simulated results of curved surfaces with tissue inside the applicator, where a hotspot appears laterally (see Figure 1C).

	3 irradiations			Location (R1, R2,R3) relative to R	Diff_flat (%)
	Diff (%)	Diff (%)	Diff (%)		
Film 1	+16%	+19%	+18%	-1.3cm	1%
Film 2	+5%	+5%	+5%	+0.5cm	0%
Film 3	-5%	-3%	-4%	+2.7cm	-3%

Table 1. Diff: difference between the dose measured with films and the expected dose, Dexp, at the location R (see figure 1) in reference conditions (flat surface); Diff_flat: expected dose variation in a flat surface (due to the bevelled applicator), for comparison.

Conclusion: The results presented highlight the influence of curved and irregular surfaces on pelvic IOERT dose distributions, and the importance of taking the irradiated surface geometry into consideration when interpreting results of in vivo measurements.

1. Krengli M, Calvo F a, Sedlmayer F, et al. Clinical and technical characteristics of intraoperative radiotherapy. Analysis of the ISIORT-Europe database. Strahlentherapie und Onkol. 2013;189(9):729-37.

2. Costa F, Sarmento S, Sousa O: Assessment of clinically relevant dose distributions in pelvic IOERT using Gafchromic EBT3 films. Phys Medica 2015: doi:10.1016/j.ejmp.2015.05.013

EP-1553

Dosimetric characterization of carbon fiber stabilization devices for postoperative particle therapy

S. Russo[1], E. Mastella[1], S. Molinelli[1], A. Mirandola[1], D. Panizza[1], A. Mairani[1], G. Magro[2], P. Fossati[3], M.R. Fiore[3], A. Gasbarrini[4], S. Boriani[4], F. Valvo[5], M. Ciocca[1]
[1]*Fondazione CNAO, Medical Physics Unit, Pavia, Italy*
[2]*Università di Pavia, Physics Department, Pavia, Italy*
[3]*Fondazione CNAO, Clinical Radiotherapy Unit, Pavia, Italy*
[4]*Istituto Ortopedico Rizzoli, Department of Oncologic and Degenerative Spine Surgery, Bologna, Italy*
[5]*Fondazione CNAO, Clinical Directorate, Pavia, Italy*

Purpose or Objective: Surgical implant fixation is a common technique in case of spinal and paraspinal tumors, usually considered good candidates for particle therapy (PT).Traditional orthopedic metal implants significantly differ from normal tissues in terms of density and composition, leading to substantial perturbation effects on radiation beams. Recently a Carbon Fibers Reinforced(CFR)-PEEK stabilization device completely metal free has become available (CarboFix Orthopedics). This device is supposed to be more suitable for PT where treatment accuracy can be highly compromised by uncertainties in particles range. The aim of this study was to investigate and compare uncertainties related to the use of titanium and CFR-PEEK screws in terms of image quality, reconstruction artifacts, contouring and dose calculation accuracy, for both proton and carbon ion beams.

Material and Methods: Two vertebral body models, hosting two different types of orthopedic implants (a titanium and a CFR-PEEK implant), were positioned inside a water phantom to simulate real patients configuration. A CT scan was acquired according to our clinical protocols to evaluate induced HU artifacts and their impact on contouring uncertainties. Titanium and CFR-PEEK water equivalent path lengths (WEPL) were measured and implemented in our treatment planning systems (TPS). Implants and artifacts were contoured for proper material density assignment in the TPS HU to WEPL calibration curve. Plans were optimized for both proton and carbon ions, with and without HU correction, to evaluate the impact of CT artefacts and contouring uncertainties on dosimetric calculation accuracy, in comparison with MC simulations. Two patient cases, previously treated in our center were analyzed in terms of target and OAR dose deviation due to wrong material assignment, with respect to the clinically approved plan.

Results: CFR-PEEK implants did not cause appreciable HU artifacts on CT images compared to titanium ones. Significant differences in dose distribution between TPS and MC simulations in high-Z region were observed, while a good agreement was found for CFR-PEEK screws. Inaccurate material assignment did not significantly vary the clinical case 3D dose distribution for CFR-PEEK implants (<1%). Titanium screws made difficult to correctly contour both targets and OARs. Moreover, local dose deviations up to 20% can be find when HU uncertainties are not correctly managed. Besides efforts made towards a robust optimization with respect to potential beam perturbation, dose delivered to healthy tissues positioned behind targets along the implant trajectory can be substantially altered.

Conclusion: CFR-PEEK stabilization devices are more suitable than commonly-used titanium devices for PT of patients with orthopedic implants, leading to less image alteration and consequently reduced contouring uncertainties together with a significantly higher dosimetric treatment planning accuracy.

EP-1554

Retrospective dosimetric comparison of TG43 and a commercially MBDCA for image-based plesiotherapy

A. Pereira[1], S.P. Sara Pinto[1], T.V. Teresa Viterbo[1]
[1]*Instituto Português de Oncologia do Porto Dr. Francisco Gentil Porto, Medical Physics Dept, Porto, Portugal*

Purpose or Objective: To compare dosimetry plans using a commercially model based dose calculation algorithm (MBDCA) following TG186 recommendations, and the conventional TG43 method in an 192Ir high dose rate (HDR) brachytherapy (BT) procedure for the treatment of skin lesions.

Material and Methods: Plesiotherapy treatment was performed in three patients with lesions localized in the pre auricular region (patient 1), the nasal dorsum (patient 2) and the nasal tip (patient 3). The lesions (PTV) were marked with radiopaque markers. Patients were immobilized with a thermoplastic mask. A bolus slab of 2 mm thickness and plastic catheters were applied over the mask, and the whole set was fixed with two bolus slabs. All dosimetries plans were based on a CT with 1,25mm slices thickness and the dose was delivered with a micro-Selectron afterloader. Treatment plans were performed using both the TG43 and TG186 dose calculation methods of the Oncentra Brachy v4.5 treatment planning system (TPS). Analysis included dose to the OARs (lens, ocullar globe and optic nerves) and to the prescription points (3 mm tissue depth). The TG186 results were obtained using the standard accuracy level option of model-based algorithm (Oncentra Brachy-Advanced Collapsed cone Engine (ACE), Elekta), resulting in calculation times between 7 – 10 min.

Results: In all cases, TG 43 overestimated the doses in the prescription points and in the OARs, in the range of 3.0% and 6.2%, respectively (Figure 1).

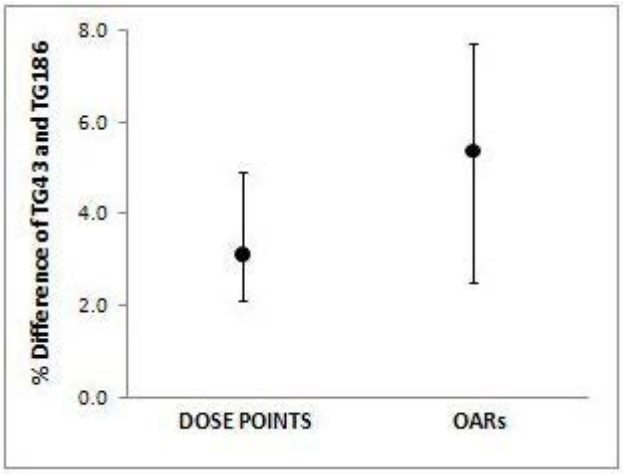

Conclusion: Although differences were found between the dosimetrie plans obtained with the TG43 and model based dose calculation algorithm following TG186 recommendations, they are minor in terms of prescription dose points for skin lesions, since a 5% difference is within clinical tolerances in brachytherapy.

EP-1555

On the RapidArc tests by Ling 2008: towards flexibility and troubleshoot with a new family of plans

G. Nicolini[1], E. Vanetti[1], A. Clivio[1], S. Presilla[1]
[1]*Ente Ospedaliero Cantonale, Servizio di Fisica Medica, Bellinzona, Switzerland*

Purpose or Objective: At the introduction of RapidArc (RA) technique, the paper by Ling et al 2008 has constituted a reference, proposing RA commissioning machine quality assurance (QA) tests. Thanks to the free availability, many centers have implemented these tests in their periodic QA. Recently, tests identified as T2 (variation of dose rate DR and

gantry speed GS) and T3 (variation of MLC Speed MLCS) were updated. Even so, we decided to redraw completely T2 and T3, in the respect of the effective main concept. A family of new plans was generated to guarantee flexibility in the QA procedure and to support the user in a possible troubleshooting.

Material and Methods: Firstly, a historical review of commissioning tests results on 3 different Varian linacs (Clinac iX, Unique, TrueBeam) was collected, for both old (2008: vs1) and new (2015: vs2) Varian test versions; original tests were extended to 10MV, 6FFF and 10FFF beams for TrueBeam. Data were collected monthly through portal vision (PV) images , for respectively 81, 21, and 42 entries for vs1. At the same, delivery parameters were extracted from actual patients plans (3911plans, 6833arcs) and stratified according to the types of treatment. From our experience, we felt the needs to have a more flexible instrument tuned on our clinical practice, able to support us in a possible troubleshooting. A family of new T2 and T3 plans was generated. In addition to the traditional analysis of the images, a direct comparison with the open reference field is proposed to define a more reliable baseline for the monitoring of each strip trend.

Results: First version of the test T2 and T3, have presented during time differences respect reference value>2% (always<3%), for Clinac iX and Unique, while TrueBeam data were always <2%. The first T2 band presents a systematically higher value respect the others, explainable with some weakness in the test itself. Vs2 of T2 and T3, showed an agreement well below 2% for all the three linacs, but still with a systematic higher value for the T2 first delivered strip. The delineation of the new package of RT-plans started from the tune of number and width of the strips; the best compromise was found with 5 strip of 2.8 cm. Now T2 and T3 are fully compatible and can be superimposed, running also a T3 with the same DR-GS variation presents in T2. From this main plan version of T2 and T3, the new family of rt-plans allows to perform tests changing arc direction or/and MLC direction, while an additional basic editing of the dicom files allows to vary the main delivery parameters, in addition to order of the delivered combinations, arc range, MU/deg, etc, as independently as possible.

Conclusion: The new package of RT-plans is proposed in the fully respect of the original idea by Ling, with the intent to offer a more effective tool adjustable to single centre characters. Of particular interested is the extension to FFF beams, which are widely used in stereotactic regimes.

EP-1556

VMAT in nasopharyngeal tumor: clinical implications after a change in the dose calculation algorithm

S. Cilla[1], A. Ianiro[1], F. Deodato[2], G. Macchia[2], C. Digesù[2], M. Ferro[2], V. Picardi[2], M. Nuzzo[2], F. Labroupoulos[2], P. Viola[1], M. Craus[1], A. Piermattei[3], V. Valentini[4], A.G. Morganti[5]

[1]*Fondazione di Ricerca e Cura Giovanni Paolo II- Università Cattolica del S. Cuore, Medical Physics Unit, Campobasso, Italy*

[2]*Fondazione di Ricerca e Cura Giovanni Paolo II- Università Cattolica del S. Cuore, Radiation Oncology Unit, Campobasso, Italy*

[3]*Policiinico Universitario A. Gemelli - Università Cattolica del S. Cuore, Medical Physics Unit, Roma, Italy*

[4]*Policiinico Universitario A. Gemelli - Università Cattolica del S. Cuore, Radioation Oncology Unit, Roma, Italy*

[5]*DIMES Università di Bologna - Ospedale S.Orsola Malpighi, Radiation Oncology Unit, Bologna, Italy*

Purpose or Objective: To assess the clinical implications of the Collapsed Cone algorithm implemented in the Masterplan Oncentra treatment-planning system in VMAT treatments of nasopharyngeal tumors (NPC).

Material and Methods: Ten plans initially produced for patients with nasopharyngeal tumors with Pencil Beam Convolution (PBC) algorithm were retrospectively recalculated using the Collapsed Cone Convolution (CCC) algorithm. Clinical target volumes were considered as primary tumor, lymph nodes with high-risk of occult metastases and low-risk nodal regions. Corresponding planning target volumes (PTVs) were obtained by adding a 4-mm margin. Radiotherapy was prescribed according to SIB technique with all PTVs irradiated simultaneously over 30 daily fractions. Doses of 70.5 Gy (2.35 Gy/fraction), 60.0 Gy (2.0 Gy/fraction) and 55.5 Gy (1.85 Gy/fraction) were prescribed to the PTV70.5, PTV60.0, and PTV55.5,respectively. All SIB-VMAT plans were optimized using the "dual-arc" feature with 6MV photon energy. The differences in dose distribution for all PTVs and organ-at-risk were assessed using different metrics (D95%=dose to 95% of PTV, D98%=near-minimum, Dmean=mean dose, V95%=volume receiving al least 95% of prescribed dose, D2%=near-maximum dose). The PTV70.5 was also separated into components in tissue (PTVtiss) and air (PTVair). Collapsed Cone plans were also renormalized (CCCr) in order to obtain the same target coverage in terms of D95% of PBC calculation.

Results: PBC algorithm overestimated dose to PTVs for all considered metrics. The averaged Dmean and D95% to PTV70.5 calculated by CCC decreased by 1.8% (range:0.9%-2.8%) and 3.1% (range:1.5%-5.3%), respectively (1.5% and 2.8% lower for PTVtiss, and 5.5% and 8.6% lower for PTVair). Averaged D98% to PTV70.5 decreased by 3.4% (2.4% in tissue and 9.4% in air). Averaged V95% decreased from 96.0% to 90.2% (from 96.1% to 91.2% for PTVtiss, and from 96.0% to 70.9% for PTVair). The magnitude of dose differences are strongly correlated with the amount of air cavities in PTV70.5. A similar trend was observed for PTV60 and PTV55.5. Maximum doses to spine and brainstem PRVs were found to be approximately 1 Gy lower with CCC. The Dmean to pharyngeal constrictors muscles was found 4.7% higher with PBC. No differences were observed for parotids and mandible. PBC slightly underestimated the doses to eyes and lens (but≤ 0.5 Gy). When the dose calculation were performed in water, the two algorithms provided differences in dose distributions <0.5%.

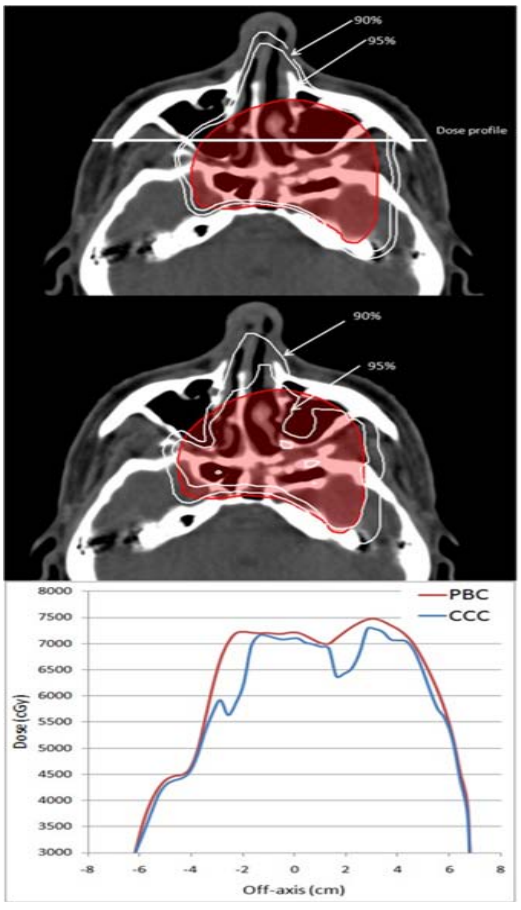

Conclusion: The CCC algorithm should be used in preference to PBC in VMAT treatments of nasopharyngeal tumors. A key question remains open: should the prescription dose be adjusted to the actually delivered dose, more accurately predicted by CCC algorithm? If radiation oncologists wanted to keep the PBC original dose prescription and the same accepting criteria for target coverage when switching from PBC to CCC, up to 5% more radiation doses would be given.

EP-1557

Development of dose calculation algorithm in homogeneous phantom through the transit dose

S. Jeong[1], M. Yoon[1], D.W. Kim[2], W.K. Chung[2], M. Chung[2]
[1]*Korea University, Bio-Convergence Engineering, SEOUL, Korea Republic of*
[2]*Kyung Hee University Hospital at Gangdong, Radiation Oncology, Seoul, Korea Republic of*

Purpose or Objective: To verify the accuracy of planned dose distribution for patient treatment, patient dose quality assurance using the solid water equivalent phantom is usually performed. This method, however, is not the method of verifying the absorbed dose in real patient. In this study, as a previous process of developing dose calculation algorithm in human, we measured the transit dose using the radio-photoluminescence glass rod detector to develop dose calculation algorithm in homogeneous phantom.

Material and Methods: We measured the trasit dose at 150cm from source of linear accelerator to calculate the dose in the homogeneous phantom. The homogeneous phantom (10cm, 20cm, 30cm thickness) was located nearby the isocenter. We can calculate the dose at the bottom of phantom using the measured transit dose, inverse square law value and scatter factor. Scatter factor in this algorithm is ratio of scatter at the bottom of phantom and scatter at the measurement point of transit dose. To develop dose calculation algorithm in homogeneous phantom, we measured the field size dependence of transit dose and bottom dose to calculate the scatter factor, the relative dose response to correct the change of field size and location of isocenter. We evaluated the algorithm of 6MV X-ray beam in 10cm x 10cm field, 200MU.

Results: The measurement results of the relative dose response for isocenter location change are increased when the SSD decreases. The measured scatter factor was about 1.35 in all cases. We could calculate the dose in the phantom using the transit dose, inverse square law, scatter factor and percentage depth dose data. We evaluated the accuracy of developed phantom-dose calculation algorithm. The accuracies of 10cm, 20cm and 30cm phantom were 0.54%, 1.03% and -1.65%, respectively.

Conclusion: We developed the phantom-dose calculation algorithm using the transit dose, inverse square law, scatter factor and PDD data. This result would be used in the development of dose calculation algorithm in the inhomogeneous phantom and real patient.

EP-1558

Comparison between softwares employed in analysis of star shot patterns

J.A. Vera Sánchez[1], C. Ruiz Morales[2], A. Gonzalez Lopez[3]
[1]*Hospital Universitari Sant Joan de Reus, fisica medica, Reus, Spain*
[2]*Hospital IMED- Elche, Radioterapia, Elche, Spain*
[3]*Hospital Clínico Universitario Virgen de la Arrixaca, Radioprotección, Murcia, Spain*

Purpose or Objective: In linacs QA there are several tests that produce a star shot pattern by exposing a radiographic or radiochromic film. Isocenter size and distance from lasers or crosshair projection to radiation isocenter are some of the parameters obtained by exposing a radiochromic film with a star shot pattern of the rotation of the gantry, table or collimator. The "Twinkle" test was proposed to verify the correct deliveryng of dose during gantry rotation and it is a common QA test for linacs that deliver VMAT treatments and that also produces a star shot pattern. In this study we compare two in-house software to analyze the parameters of the star shot patterns.

Material and Methods: Digital images of star shot patterns of table, collimator and gantry rotation and Twinkle tests were obtained exposing several radiochromic films EBT3 and RT-QA. In all cases a external reference was marked onto the films. Throughout the whole process -irradiation, scanning and analysis- a reference direction was held. The digital images were analized with two different sofwares. The STAR ANALYZE software (SA), implemented with MATLAB, applies Canny algorithm to find the edges of the arms and then, the Hough transform is used to locate these edges and its equations. The second in-house software, FILM CHECK (FC) traces concentric search on the image of the star shot pattern to locate the center axes of the beams. From the characterization of these central axes, by minimax procedure position and radiation isocenter size are obtained.

Results: In the star shot patterns of gantry, table and collimator rotations, the maximum deviation between both algorithms in the isocenter size was lower than 0.5mm, and the maximum deviation in the distance between radiation isocenter and the external reference was lower than 1mm. In the Twinkle tests, the maximum deviation in the thickness of the arms of the star shot was lower than 0.3mm and the maximum deviation in the radii angle was lower than 1°.

Conclusion: The two algorithms shows a very good agreement for the analyzed parameters, despite uncertainty in the localization of the external reference system located in the radiochromic films that affects the parameters related with this external reference system. The Hough transform and the Canny edge detection algorithm are a valid tool for quality control of the linac, although, for the correct determination of sizes and distances we recommend depth knowledge and careful use of the particular parameters involved in both algorithms.

EP-1559

The Australian Clinical Dosimetry Service: The findings from a national auditing service

I.M. Williams[1], J.E. Lye[1], A.D.C. Alves[1], M.K. Shaw[1], S. Keehan[1], J. Kenny[1], J.O. Lehmann[1], L. Dunn[1], T.K. Kron[2]
[1]*ARPANSA, Australian Clinical Dosimetry Service, Victoria, Australia*
[2]*Peter MacCallum Cancer Centre, Physical Sciences, Melbourne, Australia*

Purpose or Objective: The Australian Clinical Dosimetry Service, (ACDS) was initially funded as a pilot program operating over 2011-2014 to enable the Australian Government to determine whether this design of an independent audit program was suitable for Australia. The pilot program was independently reviewed and interim funding was provided for a further two years. During this time the ACDS would increase the frequency of the developed suite of audits and develop a business plan, encompassing a user-paying structure, which would guarantee longevity for the dosimetry program. A summary of the audit outcomes and key findings to date will be presented along with a discussion about why the ACDS has been successful.

Material and Methods: The ACDS, recognised existing auditing practices, dovetailed the Level I Ionizing Radiation Oncology Centre: Houston audits with the International Atomic Energy Agency, IAEA, publications. The resulting three level audit structure resulted in a mutually supportive audit suite in which successive audits focussed on a more complex part of the clinical planning procedure. The ACDS has developed internal quality control procedures for all measurements to ensure the rigor of all audit outcomes. Critically, the ACDS has actively engaged with the professions, public and jurisdictions which has generated a positive response to the on-going success of the program.

Results: The ACDS achieved or exceeded all the initial pilot requirements. More that the required number of audits at each level were performed over the initial three years. The audit outcomes will be presented detailing the impact the ACDS audits, and resulting recommendations, have had on radiotherapy practice. The paper will also present on how the staff within the ACDS engaged with the professional clinical workforce and provided a successful and functioning audit service. The paper will attempt to identify these social successes and how these were achieved. This will provide details to assist and advise those seeking to design or modify national or regional auditing programs. Finally the paper reviews the potential future for the ACDS.

Conclusion: The raw number of audits indicate that the ACDS met the pilot program's initial auditing requirements. Understanding the reasons for the ACDS' success are also important for ensuring an on-going service or informing and assisting others to establish auditing services. Within the ACDS, success has been highly dependent on: attracting quality staff who can respond with agility to changing situations, a high level of communication with the professional community, and a high level of engagement by the community.

The Australian Clinical Dosimetry Service is a joint initiative between the Department of Health and Ageing and the Australian Radiation Protection and Nuclear Safety Agency

EP-1560

Is EBT-XD film suitable for linac and Gamma Knife radiosurgery dosimetry verification and audit?

A. Nisbet[1], A. Dimitriadis[1], A.L. Palmer[2], C.H. Clark[1]

[1]*St. Luke's Cancer Centre Royal Surrey County Hosp, Medical Physics, Guildford, United Kingdom*

[2]*Portsmouth Hospitals NHS Trust, Medical Physics Department, Portsmouth, United Kingdom*

Purpose or Objective: The validation of radiotherapy treatments by dosimetric measurement is essential for the introduction of new techniques, pre-treatment verification and dosimetry audit. Film dosimetry has the advantage of high spatial resolution, low energy dependence and water equivalence. A new film (EBT-XD) has been assessed for its suitability for dosimetry of stereotactic radiosurgery (SRS) applications.

Material and Methods: Calibration curves for red, green and blue channels were created in the range of 0-4000 cGy for EBT-XD and its predecessor EBT3. Ten film pieces were irradiated in a nominal 6MV linac. The film was scanned using an EPSON Expression 11000XL scanner and the analysis was performed in FilmQA Pro software (Ashland ISP Inc, NJ, USA). Film dosimetry uncertainties were assessed for typical SRS fields, including lateral scanner effect at high doses. Both EBT-XD and EBT3 films were used in-phantom for treatment dose verification of typical Linac based and Gamma Knife (GK) stereotactic radiosurgery within the STE2EV anthropomorphic phantom (CIRS, VA, USA). The dosimetry methodology for a forthcoming UK dosimetry audit of SRS treatment was utilised.

Results: EBT-XD film has lower optical density than EBT-3 throughout the dose range tested. EBT-XD was more suitable for high-dose applications because of a lower lateral scanner uncertainty. For the width of the film sizes that will be used in the SRS audit (50 mm) and the typical doses measured, the lateral scanner effect was estimated to be of the range of 0.5% for EBT-XD and 3% for EBT-3. Higher agreement between TPS and film dose distributions was seen for EBT-XD using both single and triple channel dosimetry at 2% (local normalization),1 mm gamma index analysis criteria, with the recommended triple channel used for EBT-XD having a 95.5% passing rate, compared to conventional single channel EBT3 having only 89.1%. Single channel EBT-XD had 89.7% passing rates and triple channel EBT-3 38.9%. An example is shown in figure 1, of EBT-XD showing a 98.3% gamma passing rate for a GK radiosurgery plan at 3% (local), 1.5 mm criteria

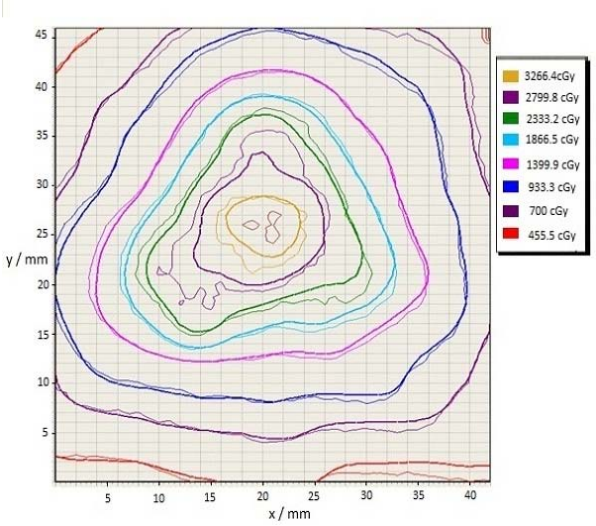

Conclusion: We have evaluated the use of a new film, EBT-XD, for SRS dosimetry verification and demonstrated its suitability for a forthcoming audit of radiosurgery services in the UK. EBT-XD is less susceptible to lateral scanner effects and shows better agreement to TPS dose distributions than EBT-3 in linac-based radiosurgery dose verifications. EBT-XD also showed excellent agreement with TPS dose distributions in GK radiosurgery.

EP-1561

Online control point resolved VMAT QA using the integral quality monitor and log files

M. Pasler[1], M. Obenland[1], J. Christ[1], Y. Jaout[1], H. Wirtz[1], M. Bjoernsgard[2], J. Lutterbach[2], F. Wittkamper[3], D. Georg[4]

[1]*Gemeinschaftspraxis f. Strahlentherapie Singen-Friedrichshafen, Medical Physics, Singen, Germany*

[2]*Gemeinschaftspraxis f. Strahlentherapie Singen-Friedrichshafen, Radiation Oncology, Singen, Germany*

[3]*The Netherlands Cancer Institute, Medical Physics, Amsterdam, The Netherlands*

[4]*Medical University Vienna, Department of Radiotherapy and Christian Doppler Laboratory for Medical Radiation Research for Radiation Oncology, Vienna, Austria*

Purpose or Objective: To systematically assess VMAT delivery accuracy using dynamic benchmark test plans.

Material and Methods: Three VMAT benchmark plans were generated for an Elekta Synergy linac (MLCi2) using iComCAT. These plans consist of square field shapes with varying field size and a full gantry rotation (fig.1a). First, 19 control-points (19cp) were composed to vary dose rate, MLC positions, jaw and gantry speed to push dynamic parameters to their limit. Next the number of control-points was increased (i.e. 37cp and 73cp) by linear interpolation so that MLC, jaw and gantry motion were identical to the 19cp plan, but with tighter regulation of dynamic components. MLC and jaw errors were quantified by analyzing the linac's log files. For dosimetric measurements, a 2D ionchamber array placed in a full scatter phantom (729 & Octavius, PTW) and the integral quality monitor (iQM, iRT) were used. The iQM contains a large area ionchamber and an inclinometer for real-time VMAT verification. Evaluation was performed on the level of cumulated delivery and control-point resolved to investigate the effect of increasing number of control-points.

Results: Slight variations in delivery were observed for the three plans from log-file analysis, overall revealing very accurate linac control in rotational mode. The mean MLC error was almost identical for the three plans (0.2±0.2mm). Relative dosimetric evaluation by means of plan reproducibility resulted in γmean=0.4±0.1 (19cp), γmean=0.2±0.0 (37cp) and γmean=0.1±0.0 (73cp) for the local γ 1%/1mm criterion, respectively. Increased γ-values were found for inter-plan comparison:

γmean(19vs37cp)=0.7±0.1, γmean(19vs73cp)=0.6±0.1 and γmean(37vs73cp)=0.6±0.1. The cumulated iQM signal coincided with 2D ionchamber array measurements and demonstrated accurate reproducibility for all three plans (figure 1b). The control-point resolved analysis (fig.1c) consistently indicated large deviations between 19cp, 37cp and 73cp plans due to an imprecise data sampling synchronization of the preclinical version of the detector. The symmetry of the test plan could not be reflected by the iQM system, especially regarding the 19cp plan.

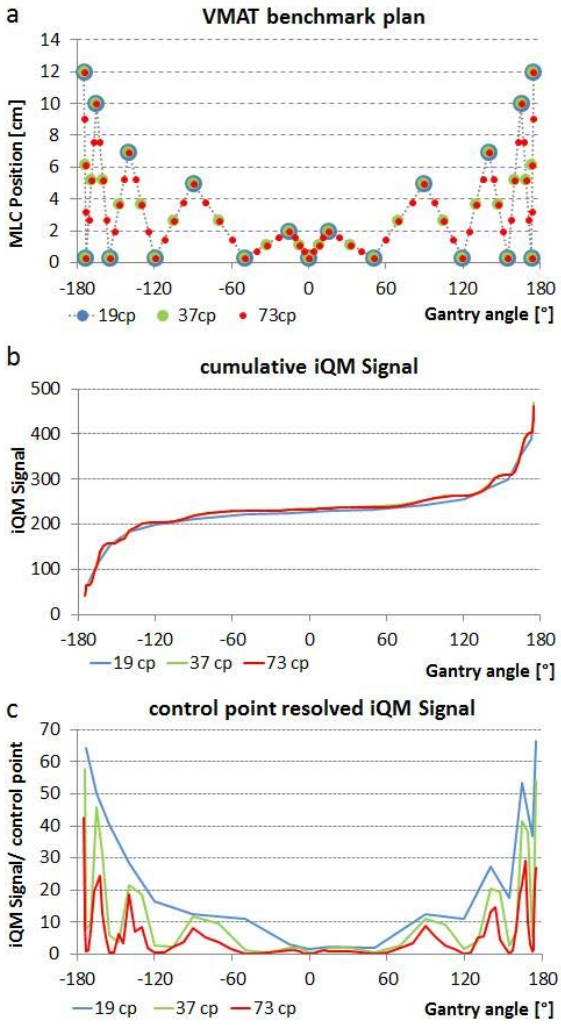

Conclusion: Increasing the number of control-points changed VMAT delivery accuracy marginally. For clinical treatment plans this effect might not be noticeable. Observation of the cumulative iQM signal coincided well with dosimetric measurements. The VMAT benchmark plan proved to be a prospective tool for visualizing and understanding linac and detector limitations.

EP-1562

VMAT pre-treatment verification using Octavius 4D system: from simple to more complex plans

H. Aslian[2], M. Severgnini[1], F. Cupardo[1], R. Vidimari[1], M. De Denaro[1]

[1]*AOU "Ospedali Riuniti di Trieste", Medical Physics, Trieste, Italy*

[2]*International Center for Theoretical Physics and Trieste University, Medical Physics, Trieste, Italy*

Purpose or Objective: Plan verification in complex treatment delivery techniques such as IMRT and VMAT is imperative. Although some studies have been conducted on pre-treatment VMAT quality assurance using PTW Octavius 4D systems, more works are needed to focus on complex VMAT plans including steep gradient regions. The aim of this study is to evaluate dose delivery of different VMAT plans such as Head and Neck (SIB: Simultaneously Integrated Boost), lung (SBRT: Stereotactic Body Radiation Therapy) and prostate (Hypo-fractionated intensity modulated arc therapy) with the Octavius 4D system.

Material and Methods: Fifteen head and neck, lung and prostate VMAT plans for fifteen patients (5 patients for each case) were created and their respective QA plans were calculated. All plans were optimized and calculated using Monaco (version 5.0) treatment planning system, which is a Monte Carlo-based treatment planning system. The 2D-array seven29, which consists of 729 vented plane-parallel ionization chambers arranged in a 27 x 27 matrix with the spatial resolution of 10mm, embedded in Octavius 4D cylindrical phantom was used to measure the dose distribution and the measurements were done with an Elekta Synergy linear accelerator equipped with an Agility 160 MLC system. In order to reconstruct and analyze the measured 3D dose from each plan, the PTW VeriSoft patient plan verification software was used and a volumetric 3D gamma index analysis for both 3%/3mm and 2%/2mm criteria was performed to compare and evaluate the measured and calculated doses. In addition, in order to improve the spatial resolution in cranial caudal direction due to 1 cm gap across the chambers the second measure was done by shifting the array 5 mm (via couch shift) in caudal direction and merging the matrices with the “merge” function available in PTW VeriSoft.

Results: The mean pass rate of volumetric 3D gamma index for all prostate cases was superior to 97% with 3%/3mm and 92% with 2%/2mm criteria. However, the mean passing rate for lungs was lower than prostate and ranged from 93.7 to 96.3 (3%/3mm) and from 90 to 94.1 (2%/2mm). Expectedly, the mean value of global gamma index for head and neck cases could not be better than 91.5% (ranged from 88.4 to 96.3) and 87.3% (ranged from 82.3 to 89) for the 3%/3mm and 2%/2mm criteria respectively. Also, merged measurements could increase the mean passing rate from 1% up to 3.5% in some complex cases (Fig.1).

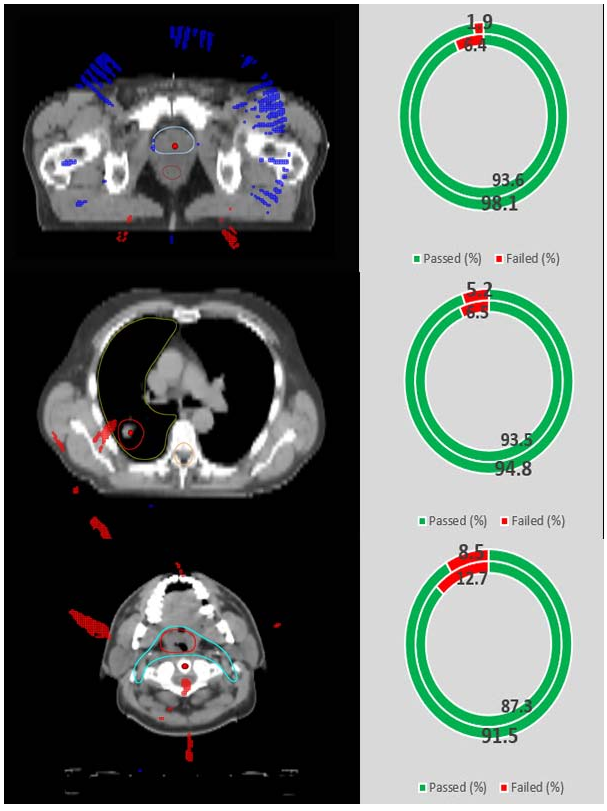

Fig. 1: The images (Left side) represent the failed points of a sample; The images (Right side) depict the average volumetric gamma index for prostates, lungs and HN cases in

which the outer pie-charts show the results with 3%/3mm and the inner pie-charts illustrate results with 2%/2mm.

Conclusion: The results showed that Octavius 4D phantom, with 2D-Array seven29, can be an adequate verification system both for simple and more complex cases. Additionally, the merge capability of the VeriSoft software, which can increase spatial resolution, is a useful tool for more complex VMAT plans.

EP-1563

Study of the characteristic of enhanced dynamic wedged depth dose profiles in non-homogenous media

A. Hussain[1], A. Zaman[2], M.B. Kakakhel[2]
[1]*Aga Khan University Hospital, Department of Oncology, Karachi, Pakistan*
[2]*PIEAS, Department of physics and applied mathematics, Islamabad, Pakistan*

Purpose or Objective: The aim of this study is to utilize the EGSnrc based Monte Carlo code in order to assess the EclipseTM (AAA) calculated dose estimation at the Water-Lung (WL) interfaces when irradiated by 6 MV photon beams at 15˚, 30˚, 45˚ and 60˚ wedge angles and multiple field sizes of 5 × 5 cm2, 10 × 10 cm2 and 20 × 20 cm2.

Material and Methods: EGSnrc sub codes are used for Monte Carlo dose simulation. BEAMnrc is used to simulate the linear accelerator head, whereas DOSXYZnrc is employed to perform phantom dose estimation. For simulating dynamic wedges the BEAMnrc component module DYNJAWS was employed. Phantom geometry includes a 10 cm layer of lung (r=0.250 g/cc) sandwiched between 5 cm and 10 cm water layers. Doses were calculated in exactly the same geometry and same density distribution by Monte Carlo and AAA algorithm. The overall dimension of the phantom was 30 cm × 30 cm × 25 cm. A 5 mm grid size (voxel width) along depth was used for calculating PDDs. The nominal source to surface distance (SSD) of 100 cm was used in both setups.

Results: The dose perturbation effect was found to be field size dependent. It increases with decreasing field size. No clear dependence for the wedge angles was observed. No dose deviation between AAA and EGSnrc was observed at the water→tissue interface. However a lower dose in the lung was estimated by AAA. Whereas at the lung→tissue junction a highest dose discrepancy was observed by AAA, estimating higher dose towards the water layer.

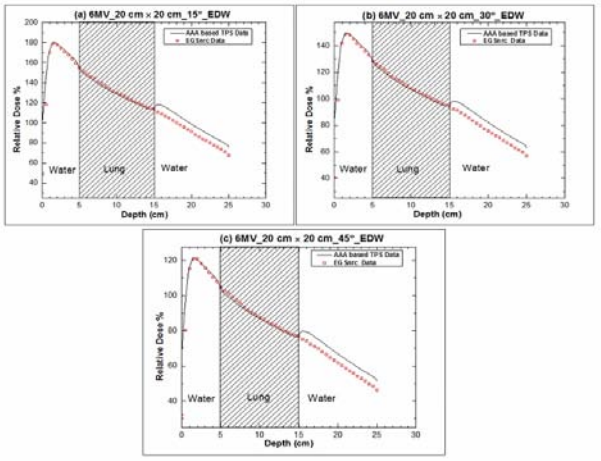

Conclusion: We have demonstrated the limitation of AAA in dose calculation at the water-tissue-water interfaces for four wedge angles. There was no significant wedge angle dependence on the dose perturbation. However an increase in perturbation was observed with decreasing field sizes for all angles.

EP-1564

Impact of dose calculation algorithm on SBRT and normofractionated lung radiotherapy in breath hold

M. Josipovic[1,2], G. Persson[1], J. Rydhög[1,2], J. Bangsgaard[1], L. Specht[1,3], M. Aznar[1,2]
[1]*Rigshospitalet, Dept. of Oncology- Section for Radiotherapy, Copenhagen, Denmark*
[2]*University of Copenhagen, Niels Bohr Institute, Copenhagen, Denmark*
[3]*University of Copenhagen, Faculty of Medical Sciences, Copenhagen, Denmark*

Purpose or Objective: Modern dose calculation algorithms only model absence of lateral charged particle equilibrium to a limited extent. The resulting uncertainties are largest in strongly heterogeneous regions, such as the thorax, and will potentially increase in deep inspiration breath hold (DIBH) due to decreased lung tissue density.

Material and Methods: Ten patients with stage I and ten with stage III lung cancer were included. For all patients, a plan in free breathing (FB, based on midventilation) and in DIBH were made with the clinically used Anysotropic Analytical Algorihtm (AAA). Stage I disease was treated stereotactically (SBRT) using 3D conformal technique (9-10 fields), 45 Gy in 3 fractions, prescribed to 95% isodose covering 95% of PTV and aiming for 140% dose in the isocenter. Stage III disease was treated with VMAT (2 arcs), 66 Gy in 33 fractions, prescribed to mean PTV dose. 6 MV energy was used for all plans. Calculation grid size was 1 mm for stage I and 2.5 mm for stage III. Plans were recalculated in more advanced Acuros with same MU as in AAA.
Plans were compared for target coverage (GTV, CTV, PTV), estimated from mean dose, near minimum (D98) and near maximum doses (D2), as defined in ICRU 83, and for SBRT also for the fraction of PTV covered by prescription dose (V45). Organs at risk parameter for stage I was fraction of lung receiving more than 13 Gy (V13), and for stage III, mean lung dose, lung V5, V20 and V40 and also mean heart dose and heart V50.

Results: In DIBH, lung density decreased by median 6% (47.6 HU) reduction for stage I and 12% (88.5 HU) for stage III.
In stage III, AAA overestimated mean target doses for FB and DIBH GTV and DIBH CTV (by median <0.8 Gy; $p<0.05$ Wilcoxon signed-rank test) and had no impact on D2. AAA overestimated D98 by median ~1 Gy for GTV and CTV ($p<0.05$), and more for PTV (by 1.5 Gy and 2.1 Gy, in FB and DIBH respectively; $p<0.01$).
In stage I, AAA had similar effect on GTV as in stage III. However, differences between the two algorithms were substantial for PTV and more pronounced in DIBH: AAA overestimated all PTV parameters ($p<0.01$), with largest impact on V45 (up to 41.4% in FB and 66.3% in DIBH), while mean dose and D98 were overestimated by 2.0 Gy and 2.3 Gy in FB and 3.1 Gy and 4.0 Gy in DIBH. These clinically relevant differences may be a combination of small targets and large dose gradients in the SBRT treated volume.
Lung and heart dose parameters decreased in DIBH compared to FB, but were similar for both algorithms and both disease stages (median differences ±0.3% for volumetric parameters and ±0.2 Gy for mean doses). More details on actual dosimetric parameters are presented in the table.

Table – Selected dosimetric parameters on target coverage and dose to organs at risk for AAA and Acuros, for free breathing and deep inspiration breath hold. Data is presented as median (range).

stage III	FB			DIBH		
Target coverage	mean dose [Gy]	D_{98} [Gy]	D_2 [Gy]	mean dose [Gy]	D_{98} [Gy]	D_2 [Gy]
GTV AAA	66.2 (65.9-66.4)	64.3 (63.9-64.7)	68.0 (67.5-68.6)	66.3 (66.0-66.5)	64.3 (64.1-64.9)	68.0 (67.6-69.0)
Acuros	65.6 (65.1-66.4)	63.5 (62.5-64.4)	68.1 (67.3-68.9)	65.5 (65.0-66.2)	63.3 (62.9-64.3)	68.0 (67.2-68.6)
CTV AAA	66.3 (66.1-66.5)	64.3 (63.9-64.7)	68.2 (67.7-68.8)	66.3 (65.6-66.5)	64.3 (64.2-64.8)	68.2 (67.8-69.0)
Acuros	65.6 (65.1-66.4)	63.4 (62.7-64.5)	68.4 (67.8-69.5)	65.7 (65.4-66.4)	63.3 (60.7-64.3)	68.4 (67.8-69.1)
PTV AAA	66.0 (66.0-66.0)	62.6 (61.8-63.7)	68.3 (67.8-68.8)	66.0 (66.0-66.0)	62.6 (61.7-63.6)	68.2 (68.0-69.1)
Acuros	65.4 (65.2-66.7)	61.6 (59.7-63.5)	68.4 (67.9-69.7)	65.4 (64.5-66.0)	60.6 (55.7-62.6)	68.4 (68.0-69.0)
Dose to OAR	MLD [Gy]	V_{20} [%]	MHD [Gy]	MLD [Gy]	V_{20} [%]	MHD [Gy]
AAA	16.9 (12.3-20.1)	27.8 (18.6-39.1)	13.5 (5.3-20.3)	13.2 (12.0-19.2)	21.2 (15.9-33.1)	8.9 (4.0-21.2)
Acuros	16.9 (12.3-20.2)	28.1 (18.4-39.7)	13.3 (5.2-20.0)	13.2 (12.0-19.2)	21.5 (16.0-33.4)	8.7 (4.0-20.9)

stage I	FB			DIBH		
Target coverage	mean dose [Gy]	D_{98} [Gy]	V_{45} [%]	mean dose [Gy]	D_{98} [Gy]	V_{45} [%]
GTV AAA	57.8 (52.8-61.7)	54.0 (49.7-58.7)		59.6 (53.5-64.7)	55.1 (49.4-62.5)	
Acuros	58.1 (52.7-61.7)	53.2 (49.2-57.2)		57.6 (52.9-65.2)	51.6 (46.1-61.3)	
PTV AAA	51.8 (49.9-54.4)	40.6 (40.0-41.6)	89.7 (86.3-90.7)	52.2 (50.5-53.7)	40.8 (39.5-41.3)	89.2 (87.6-98.7)
Acuros	49.8 (45.2-52.7)	38.3 (34.2-40.4)	82.1 (46.5-90.7)	49.0 (40.6-53.1)	36.8 (30.6-40.4)	70.0 (21.2-84.9)

Abbreviations: FB – free breathing, DIBH – deep inspiration breath hold, OAR - organs at risk, MLD - mean lung dose, MHD - mean heart dose

Conclusion: In VMAT of stage III lung cancer, AAA precision is adequate even in DIBH. In SBRT of stage I lung cancer, AAA overestimates target coverage, especially in DIBH. However, changing to the more correct Acuros for stage I SBRT may potentially facilitate a change in clinically prescribed dose.

EP-1565

Influence of dose specification on prostate VMAT patient-specific QA results

F. Clemente Gutierrez[1], C. Perez Vara[1], M. Clavo Herranz[2], C. Lopez Carrizosa[2], J. Saez Garrido[2], C. Ibañez Villoslada[2], M. Couselo Paniagua[2], J. Zapatero Ortuño[2], M. Martin de Miguel[2], M. Dominguez Morcillo[2], V. Jerviz Guia[2], A. Calapaqui Teran[2], M. Guijarro Verdu[2], J. Navarro[2]

[1]*Hospital Central de la Defensa Gómez Ulla, Medical Physics, Madrid, Spain*

[2]*Hospital Central de la Defensa Gómez Ulla, Radiation Oncology, Madrid, Spain*

Purpose or Objective: Monte Carlo-based treatment planning systems (TPS) are becoming as standard in radiation therapy, performing and reporting calculations in terms of the absorbed dose to medium (Dm). In addition, patient-specific QA techniques for IMRT and VMAT treatments have recently evolved from traditional dose distribution comparisons between calculations and measurements to 3D dose calculation and reconstruction on patient anatomy, enabling DVH-based comparisons. In order to perform previous calculations, commercial solutions have introduced collapsed cone algorithms, based in dose engines that report calculations in terms of the absorbed dose to water (Dw). Differences between Dm and Dw can lead to significant discrepancies in DVH comparisons. This study reports the discrepancies between Dm and Dw calculations applied to patient-specific prostate VMAT treatments.

Material and Methods: VMAT treatments were delivered with a 6 MV Synergy (Elekta) machine. Plans were generated with Monaco 3.1 (Elekta). 3D dose calculations were performed with two systems: Mobius3D (Mobius Medical Systems) (M3D) and COMPASS (IBA Dosimetry) (CC). In addition, the second one is capable of reconstructing the dose from measurements (CR). Forty prostate treatments were analyzed, taking 10 from each usual staging (hig-, intermediate- and low-risk) and 10 prostate bed treatments after prostatectomy. Parameters analyzed for PTVs were taken from ICRU-83 recommendations. Normal tissue parameters were evaluated using QUANTEC constraints for rectum, bladder and femoral heads.

Results: Mean differences for PTVs parameters with Dm calculations were -0.61%±0.71%, -0.04%±1.49% and 0.08%±1.52% for CC, CR and M3D, respectively. For PTVs parameters with Dm calculations discrepancies were -0.22%±0.50%, 0.36%±1.27% and 0.47%±1.28%. Mean differences for normal tissue and CC, CR and M3D comparisons, respectively, were: 0.38%±0.74%, 2.94%±1.31% and 2.12%±1.31% for Dm, and 0.38%±0.54%, 2.94%±1.20% and 2.12%±1.40% for Dw in rectum; 0.16%±1.06%, -1.00%±1.11% and 0.16%±1.45% for Dm, and 0.10%±0.58%, -1.06%±0.78% and 0.10%±1.12% for Dw in bladder; -1.42%±0.83%, -1.03%±2.04% and -1.57%±1.77% for Dm, and 0.28%±2.01%, 0.88%±2.45% and -0.07%±2.62% for Dw in femoral heads.

Conclusion: Results were slightly better for Dw in femoral heads than Dm calculations. Remaining data were similar for both Dm and Dw. According AAPM TG-105, QA comparisons should be performed with the same criterion (Dw).

EP-1566

Influence of inner materials of rectal balloon on TPS calculation accuracy and dose distribution

J. Koo[1]

[1]*Korea University, Department of Bio-Convergence Engineering, SEOUL, Korea Republic of*

Purpose or Objective: If rectal balloon were not used in rectum cancer treatment, there is a lack of reproducibility of rectum shape on each treatment and irregularly inserted air inside the rectum cause inhomogeneity of density with surrounding tissue, which could be resulted in uncertainty of dose delivery. In this research, we estimated the accuracy of TPS(Treatment Planning System) dose calculation and actual dose, and compared dose distribution when homogeneity of rectum and surrounding tissue increases as inner materials of rectal balloon changes.

Material and Methods: Cylindrical PMMA RPLGD phantom was used to measure dose at rectal wall and Air, water and PMMA were used as inner balloon materials. Total 12 plans(prostate and rectum cancer 3D-CRT(3 Dimensional Conformal Radiation Therapy) and IMRT(Intensity Modulated Radiation Therapy) plans with air, water, and PMMA balloons) were made using Varian Eclipse ver.8.9 to estimate influence of rectal balloon material on dose distribution. Each 16 glass dosimeters were located at rectum wall so that the point doses were compared with TPS.

Results: As Homogeneity increase, Dose distribution was improved. As CT HU value of inner balloon material increase from 0(air) to 1000(water) and 1120(PMMA), Homogeneity Index(HI) and Conformity Index(CI) were increased about 20% and 5%, respectively. And considerable difference, between TPS and RPLGD reading, was measured with air balloon when water and PMMA balloons had less variation.

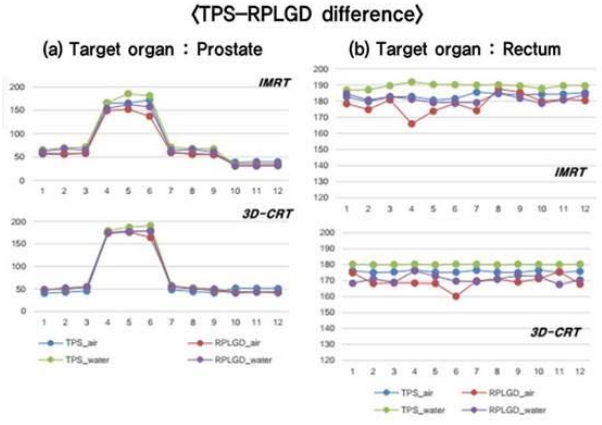

Conclusion: It was shown that the dose distribution and the accuracy of TPS were better when the density of the balloon material was similar to the density of surrounding tissue. Especially when air is inserted into rectum, there is a possibility of difference between actual dose and TPS calculation. Thus, it is needed to look forward to find a method to increase treatment accuracy using tissue-equivalent inner balloon materials.

EP-1567

Investigation of dose buildup region from electron beam by of polymer films and ionization chamber

E. Sukhikh[1], A. Lysakov[2], E. Malikov[3], L. Sukhikh[2]
[1]*Tomsk Regional Oncology Center, Radiobiology, Tomsk, Russian Federation*
[2]*National Research Tomsk Polytechnic University, Applied Physics, Tomsk, Russian Federation*
[3]*National Research Tomsk Polytechnic University, Laboratory No42, Tomsk, Russian Federation*

Purpose or Objective: The use of the film when it is parallel to the beam axis allows to obtain depth distribution of the dose in water during "single shot" of the accelerator. This method could be useful for characterization of the electron beams of intraoperative accelerators due to the fact that for this modality one needs precise knowledge of the dose depth curve starting from the phantom surface. The use of ionization chamber is routine technique but the spatial resolution of the measured curve is worse. The purpose of this work is to compare depth dose curves obtained using Gafchromic EBT3 film and ionization chamber during experimental investigation and Monte-Carlo simulation.

Material and Methods: The experimental comparison of the depth dose curves was carried out using 6 MeV and 9 MeV electron beams of Elekta Synergy accelerator and 6 MeV electron beam generated by compact betatron for intraoperative therapy. The dose distributions were measured by ionization chambers in the water and by Gafchromic EBT3 films in solid phantoms. The film was situated in different geometries, namely along beam axis and across it. The simulation of the process was carried out using PCLab software that allows simulation of the beam interaction with the matter.The first geometry was absorbed dose distribution in pure water that was assumed to be an ideal case. The second geometry assumed film situated along beam axis.The third geometry simulated ionization chamber depth scan. The simulation was carried out for different beam energies assuming monoenergetic beams. In the case of water and film in water it was possible to simulate directly value of dose in water or in the film sensitive layer. In the case of ionization chamber the value of energy lost in the air volume was "measured" as a quantity proportional to dose in water.

Results: Results of the simulation and measurement show that the dose depth distributions obtained for water, film and ionization chamber coincides well at depths deeper than maximum dose. In the case of depths from the surface up to maximum the dose "measured" by ionization chamber is larger than the dose "measured" by the film and simulated in pure water. The experimental investigation of the depth dose distribution also shows that ionization chamber overestimates dose values at small depths.

Conclusion: Simulation and measurement results show that depth dose distribution from electron beam in water measured by radiochromic film is more precise at small depths than the one measured by ionization chamber.

EP-1568

A Monte Carlo based modelling of a dedicated mobile IOERT accelerator

M. Ghorbanpour Besheli[1,2], O. Fielitz[1,2], W. Budach[1], I. Simiantonakis[1,2]
[1]*University Hospital, Department for Radiotherapy and Radiation Oncology, Dusseldorf, Germany*
[2]*Heinrich-Heine University, Faculty of Physics/Medical Physics, Duesseldorf, Germany*

Purpose or Objective: Intraoperative Electron Radiation Therapy (IOERT) refers to the delivery of single high dose radiation directly to the tumour bed or residual tumour soon after surgery excision. In this study, a Monte Carlo code was employed to simulate the NOVAC7 electron beams, which is a powerful tool for the simulation of clinical radiation beams and for obtaining detailed knowledge of the characteristics of therapy beams from linear accelerators. The simulation makes it possible to evaluate and calculate all dosimetric relevant necessities such as stopping power ratios, photon contamination and scatter contribution with high accuracy.

Material and Methods: The radiation head simulation of NOVAC7 was performed with the EGSnrc user code BEAMnrc. The definite information about the head geometry was given by the manufacturer. Relative absorbed dose measurements, i.e. percentage depth doses (PDDs) and off-axis profiles (OAPs), were carried out using radiochromic films (Gafchromic EBT2, International Specialty Products, Wayne/USA) in a small water phantom type T41023 (PTW-Freiburg, Freiburg/Germany). Specifically measured PDDs and OARs were used to obtain electron energy spectra for different energies (3, 5, 7 and 9 MeV) and applicators (30, 40, 50, 60, 70, 80 and 100 mm). For achieving the measured R50 the most probable energy of Gaussian distribution was varied iteratively in small steps (0.05MeV) around the appropriate nominal energies until a matching of the calculated and measured values of R50 was obtained.

Results: Table 1 shows the parameterised data of the PDDs. Calculated Rmax, R80, R50 and Rp are compared with the measured values. For all nominal energies the calculated PDDs agreed within ±2% or ±1 mm with those measured and local percentage dose and distance to agreement are below the required thresholds. The values of the most probable energy and the mean energy of the initial electron beams used as input into the Monte Carlo simulation are reported in table 2 for 100 mm applicator. The results were subsequent evaluated for other applicators. The electron source, incident on the titanium window, was modelled as an isotropic point source with a primary Gaussian distribution on *z* axis. The difference between the mean energy , and the most probable energy , is due to the presence of a low-energy tail in the energy spectrum, which is typical for this type of accelerators.

Table 1: Parameterised data for the PDD comparison between Monte Carlo calculation and film dosimetry at 100 mm field size.

E	R_{max} (mm)		R_{80} (mm)		R_{50} (mm)		R_p (mm)	
(MeV)	meas.	cal.	meas.	cal.	meas.	cal.	meas.	cal.
3	0.50	0.55	0.95	0.96	1.24	1.25	1.35	1.36
5	0.70	0.80	1.32	1.31	1.71	1.70	1.94	1.93
7	1.10	1.15	2.00	2.00	2.50	2.50	2.95	2.95
9	1.40	1.50	2.50	2.60	3.20	3.20	3.83	3.88

Conclusion: This investigation has been performed on a dedicated IOERT mobile linac (nominal electron energies: 3, 5, 7 and 9 MeV). The virtual model was achieved using the EGSnrc Monte Carlo system. The procedure was found to be effective and could lead to the development of a tool to assist the medical physicist during the NOVAC7 commissioning where the amount of dosimetric measurement is time-consuming.

EP-1569

Dose deposition kernel measurements with radiochromic films

A. González-López[1], C. Ruiz-Morales[2], J.A. Vera-Sánchez[3]
[1]*Hospital Universitario Virgen de la Arrixaca, Radioprotección, El Palmar Murcia, Spain*
[2]*IMED Hospitales, Oncología Radioterápica, Elche Alicante, Spain*
[3]*Hospital Sant Joan de Reus, Protección Radiológica y Física Médica, Reus Tarragona, Spain*

Purpose or Objective: In this work we carried out a series of measurements of a small field to investigate the shape of the dose deposition kernel of a radiotherapy beam. Starting with 2D dose distributions measured with radiochromic films a deconvolution process is followed to obtain the dose deposition kernels.

Material and Methods: Radiochromic films Gafchromic EBT2 were used to measure 6 MV beams from a Varian Clinac 2100 linear accelerator. The nominal field size of the beams was 0.5 cm x 0.5 cm (at isocenter), and the films were places in a PMMA phantom at 100 cm source to film distance. The dose delivered to the film was 300 cGy. The films were read 6 hours after irradiation with a Microtek ScanMaker 9800XL flatbed scanner. In order to minimize the inhomogeneity variations of the film-digitizer system a procedure, as described in [1] was followed. The procedure uses a number of film cut-outs, taken from one sheet of an RC film, to produce a number of measurements of the same field. After reading the films, the resulting images are registered and averaged. It's worth noting that the film pieces used for the calibration of the film-digitizer response are taken from the same sheet of RC film that the pieces used for dosimetric purposes [1]. In this way, the inter-digitization variability is drastically reduced. Deconvolution of measured dose distributions was carried out by minimizing its Euclidean distance to a calculated dose distribution. The calculated dose distribution was obtained as the convolution of a rectangular aperture with a parameterized kernel,

$$K(r) = k(r) * e^{-p_1 r^2} + p_2$$

where k(r) is the pencil beam dose deposition kernel [2] as calculated by Nyholm [3], p1 describes the radiation source fluence and p2 takes the collimators transmission into account. The optimization algorithm acts on both parameters p1 and p2 through an iterative process.

Results: The figure shows the dose deposition kernel obtained after deconvolution.

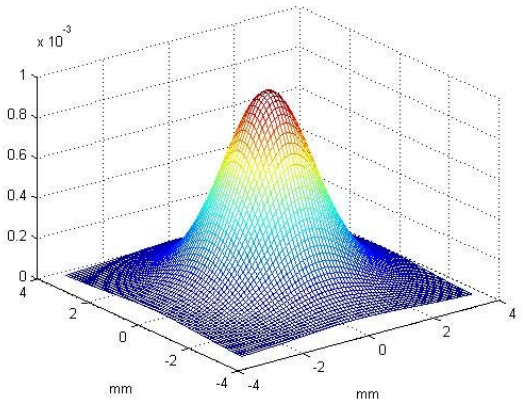

Conclusion: We have determined the dose deposition kernel for a particular set-up: a small field size, 6 MV photon energy and a depth close to dmax. The results obtained show a large lateral spread of the dose, which is responsible for the lack of lateral electronic equilibrium near the edges of the radiation field, and also imposes a constrain in the spatial resolution that portal image systems can reach.

EP-1570

Determination of stopping power ratios and output factors of intraoperative electron beams

M. Ghorbanpour Besheli[1,2], C. Matuscheck[1], W. Budach[1], I. Simiantonakis[1,2]

[1]*University Hospital, Department of Radiotherapy and Radiation Oncology, Dusseldorf, Germany*

[2]*Heinrich-Heine University, Department for Radiotherapy and Radiation Oncology, Duesseldorf, Germany*

Purpose or Objective: Treatment fields of dedicated Intraoperative Electron Radiation Therapy (IOERT) linacs like NOVAC7 (SIT, Vicenza/Italy) are generated by collimators consisting of PMMA cylindrical applicators. The dosimetry of these electron beams is required to be done under non-reference condition. Therefore, it is necessary that the output factors (*OFs*) and the mass collision stopping-power ratios to be examined carefully. The aim of this paper was to calculate the sw,air (Spencer–Attix stopping power ratios of water-to-air) and *OF* values for electron beams produced by NOVAC7 using a Monte Carlo based model.

Material and Methods: The simulation of the radiation head was performed by BEAMnrc Monte Carlo code. For achieving the measured R50 the most probable energy of Gaussian distribution was varied iteratively in small steps (0.05MeV) around the appropriate nominal energies until a matching of the calculated and measured values of R50 was obtained. Based on this Model, the *OF* values were calculated. To compare the calculated *OF* values with experimental data, absorbed dose measurements were performed by a PTW 31014 pin-point ion chamber (PTW-Freiburg, Freiburg/Germany). The phase-space files (files that contain all histories related data e.g. energy, direction, etc.) obtained for the IORT beams were also used as source inputs for the EGSnrc/SPRRZnrc code to calculate the sw,air values.

Results: The calculated and measured *OFs* agreed well within the combined uncertainty. The relative differences between calculated and measured *OFs* (see table 1) were up to 3% but agreed better than 1.8% in average. On the other hand this factor increased when decreasing the applicator diameter which is completely dissimilar to other clinical linacs. At smaller field sizes the increased number of scattered events might lead to larger *OF* values. Considering our results presented previously and the combined uncertainty of ±2% in SPR determination, a good agreement was found with TRS-398 dosimetry protocol on the water surface and at zref. The minor discrepancies between Monte Carlo calculation and TRS-398 results are due to the fact that the SPRw,air values are calculated for a dedicated IOERT linac while the Monte Carlo generated values in TRS-398 are based on a variety of linac types.

Table 1, Monte Carlo calculated and measured relative output factors (*ROFs*) for 7 and 9 MeV nominal electron beams for intraoperative radiation therapy. Output factor measurement was performed by a pin-point ion chamber.

Nominal Energy	Applicator Diameter (cm)	ROF	ROF	Differences (%)
		Calculated	Measured	
7 MeV	4	1.468	1.440	+1.9
	5	1.414	1.385	+2.1
	6	1.347	1.309	+2.9
	7	1.216	1.222	-0.50
	8	1.145	1.141	+0.35
9 MeV	4	1.609	1.567	+2.68
	5	1.519	1.520	-0.07
	6	1.416	1.380	+2.61
	7	1.261	1.241	+1.61
	8	1.178	1.150	+2.43

Conclusion: The results considering the *OFs* support the accuracy of the Monte Carlo model achieved. On the other hand, the deviation between the *sw,air* values calculated in this work and those determined using TRS-398 dosimetry protocol changed with the measurement depth in water. It is worth noticing that, one should be aware of such differences working under non-reference condition although they are not significant.

EP-1571

Electron dosimetric characteristics of a dedicated linear accelerator for IOERT

M. Ghorbanpour Besheli[1,2], W. Budach[1], I. Simiantonakis[1,2]
[1]*University Hospital, Department of Radiotherapy and Radiation Oncology, Duesseldorf, Germany*
[2]*Heinrich-Heine University, Faculty of Physics/Medical Physics, Duesseldorf, Germany*

Purpose or Objective: Treatment planning systems for IORT (intraoperative radiation therapy) are able to predict the absorbed dose in the patient only when their algorithm precisely considered the dosimetric characteristics of electrons like energy fluence, angular distribution, etc. Hence, the main objective of the present work was to study the contribution of direct (electron component without interaction with the collimator) and scattered electrons to the energy fluence distribution, fluence and mean energy of total electrons.

Material and Methods: Different electron energies of 3, 5 (low energies), 7 and 9 MeV (high energies) at cylindrical field size of 40, 50 and 100 mm of a dedicated mobile IOERT linac NOVAC7 (SIT, Vicenza/Italy) were investigated. For analysis, the phase-space file generated by Monte Carlo code BEAMnrc including the LATCH variable, for specific energy and applicator, was used by the BEAMDP Monte Carlo user code. The LATCH variable is a 32-bit variable to track the history of particles. On the other hand, BEAMDP was used to obtain energy spectra, fluence and mean energy of the direct and scattered electrons at the phantom surface for different applicator diameters.

Results: It was in general observed that the energy fluence distribution of electrons did not change significantly with decreased applicator diameter. Furthermore, it was shown that the contribution of the direct and the scattered electrons on the total fluence changed depending on the applied energy moving from central axis toward the applicator wall. With respect to the fluence of direct electrons the contribution of the scattered component was much lower on the beam axis but increased significantly near the field edge. This is mainly due to the huge increase of interaction events occurred inside the therapeutic beam between electrons and applicator wall. It was also found that, the mean energy of scattered electrons increased intensely decreeing the applicator diameter up to about 28%. Due to the increased number of scattered electrons (higher fluence) and the larger energies of scattered component in the energy spectrum, the mean energy value of scattered electrons increased.

Conclusion: Significant results regarding the behavior of different electron components were found. It was shown that the fluence and mean energy of different electron components increase at larger energies and smaller applicators especially in the vicinity of the applicator wall. This could be useful to interpret dosimetric difficulties encountered working with such IOERT linacs. Furthermore, it is expected that the results discussed here support for accurate patient dose calculation in an IOERT treatment planning system. Moreover, these results can be employed to chamber simulation regarding the determination of perturbation correction factor.

EP-1572

Effective target spot size and grid size for acuros algorithm on penumbra and delivered dose

M.E. Erturk[1], S. Gurdalli[1]
[1]*MNT Saglik Hizmetleri, Medical Physics, Istanbul, Turkey*

Purpose or Objective: Purpose of the study is to analyze how penumbra and the delivered dose vary with the effective target spot size and grid size.

Material and Methods: Acuros beam model was configured for Varian TrueBeam 6 MV. 'Beam Data' section of 'Beam Configuration' of Eclipse 11 treatment planning system (TPS) was used at configuration of Acuros with different spot sizes (0, 1, 2 mm). Beam Analysis section was utilized to evaluate profiles of 4 fields (2x2, 3x3, 10x10 and 15x15 cm) at 5 depths (1.5, 5, 10, 20, 30) with 4 grid sizes (1.0, 1.5, 2.0, 2.5 mm). To perform analysis, penumbra of 80 profiles were calculated and compared with the measured profiles. A virtual water phantom and the same fields were prepared at TPS to calculate output factors at two different setups. The first has a Source Surface Distance (SSD) of 100 cm and depth is 1.5 cm. The second one's the depth is 5 cm while SSD is 95 cm. Profiles were measured at SSD of 100 cm with Edge detector while output factors measured with PTW pinpoint detector. Average of 4 fields of each spot size and grid size in units of percent was used to analyze the overall performance of the variables.

Results: All of the errors at each output are less than 1 %. Minimum average error in the first case was found to be 0.29 % when the grid size of 1 mm and the spot size of 2 mm were used. Furthermore, maximum average error was 0.51 % when the grid size of 2.5 mm and the spot size of 2 mm were used. In the second case, maximum average error was 0.31 % when the grid size of 2.5 mm and the spot size of 0 mm. Minimum average error was calculated to be 0.05 % when the spot size of 2 mm and the grid size of 2.5 mm were used. Noting that the profiles of 15x15 field cannot be calculated at 1 mm grid size due to the TPS' hardware requirements. Error in penumbra reaches as high as 6.6 mm. Maximum average penumbra error is nearly 2 mm. Change of average errors of the profiles and the maximum errors of each grid with the target spot size is given in table.

Conclusion: It is understood from the results that the output factors and the profiles can be analyzed separately as the variation of the outputs with the grid size and the spot size is negligible. Moreover, it is observed that penumbra of fields at different depths varies with the spot size and the grid size. Therefore, medical physicists have to take into account during the commissioning of the algorithm. The method defined in this study is quite precise, sensitive, easy and effective to analyze the spot size and the grid size.

EP-1573

Validation of a dedicated Intra-operative radiotherapy TPS: an innovative tool for image-guided IORT

A. Ciccotelli[1,2], S. Carpino[2], M. D'Andrea[2], G. Iaccarino[2], A. Soriani[2], G. Felici[1], M. Benassi[3], L. Strigari[2]
[1]*S.I.T. – Sordina IORT Technologies S.p.A., R&D Dept, Aprilia LT, Italy*
[2]*National Cancer Institute Regina Elena, Laboratory of Medical Physics and Expert Systems, Rome, Italy*
[3]*IRCCS Istituto Scientifico Romagnolo per lo Studio e la Cura dei Tumori IRST, Physics Department, Meldola FC, Italy*

Purpose or Objective: The Image Guided Intra-operative Radiotherapy (IGIORT) is a new methodology based on the planning optimization using intra-operative target images acquired after surgery. The dedicated Treatment Planning System (TPS) CSRAD+ has been developed in order to plan intra-operative radiotherapy treatments for patients with malignant diseases as clinically appropriate, using a dedicated mobile accelerator and an imaging device. The CSRAD+ performs IORT dose distribution calculation relying on pre-treatment and intra-operative DICOM_RT images. The aim of this work is to validate the dosimetric output and the performances of CSRAD+ before its introduction in clinical practice.

Material and Methods: The home-made CSRAD+ allows to calculate the dose distributions of a IORT dedicated mobile linac for each energy, applicator diameter and bevel angle in water using a cartesian grid with a 2 mm resolution, using Monte Carlo data stored in a database as look-up tables. Two dose calculation algorithms have been implemented both with and without inhomogeneity corrections. The DICOM images of the representative phantom test cases were acquired using a dedicated CT Scan. The calibration curves were loaded in both the CSRAD+ and in the EGSphant module

(OMEGA-BEAMnrc). The Monte Carlo Simulation was performed using DOSXYZnrc MC code. Gafchromic EBT 3 was used in the test phantoms in order to measure the planar dose distribution and to determine isodoses. Phantom test cases were designed to validate the accuracy of the implemented dose calculation algorithms. An independent tool for data analysis has been implemented with Matlab®.

Results: The test cases were reproduced experimentally and the reference measurements were performed with the LIAC mobile IORT accelerator. The proposed test cases have shown a good agreement between measured and calculated dose distributions (at the surface, at the build-up depth and in clinically relevant points corresponding to the isodoses of 90% and 80%) in all the experimental setups containing both horizontal and lateral inhomogeneities, as reported in the figure for the homogeneous phantom test case.

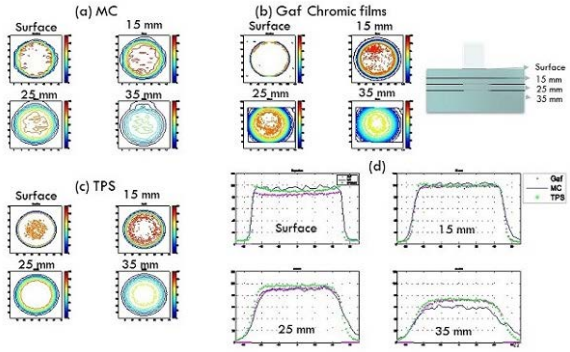

Comparison between Monte Carlo (a), Gaf Chromic films (b) and TPS (c) dose distributions: 10 MeV electron beam in an homogeneous phantom at four different depths

Conclusion: The developed tool allows independent validation of algorithms implemented within CSRAD+ and MC for absolute dose calculations. The method can test patient-like geometries and more complicated setups.

EP-1574

EpiDream: "All-in-One" model for EPID based quality controls

C. Boutry[1], G. Delpon[2], J. Fontaine[2], P. Dudouet[1], D. Franck[3]
[1]*Groupe Oncorad Garonne, Service de Radiothérapie, Montauban, France*
[2]*Institut de Cancérologie de l'Ouest, Département de Physique Médicale, Nantes, France*
[3]*Groupe Oncorad Garonne, Service de Radiothérapie, Toulouse, France*

Purpose or Objective: Linac or pre-treatment quality control applications are now commonly based on electronic portal imaging device (EPID) acquisitions due to the high spatial resolution and the ease of use of this detector. Several commercial solutions are available depending on the application. Indeed, commercial algorithms assume the EPID grey level is related to the absorbed dose delivered by the treatment beam. This hypothesis leads to the introduction of correction factors depending on geometric and beam conditions. Consequently, those algorithms are dedicated to a specific application. The goal of our work was then to develop an algorithm able to convert an EPID image into an absorbed dose to water matrix from a single model by energy beam. The study compared our algorithm EpiDream to EpiDose (Sun Nuclear), a commercial solution for EPID dosimetry.

Material and Methods: Two 6MV beams produced by two Clinac (Varian) equipped with AS1000 EPID were included in this study. EpiDream model was based on a set of homogeneous calibration acquisitions to establish a relation between the grey level and the absorbed dose to water for each acquisition frame at a reference depth and a specific arm-backscatter correction. The algorithm yielded to dose to water matrices for all type of fields used in routine (homogeneous fluence, IMRT and VMAT) at 5cm depth in water. EpiDose models were generated for IMRT and VMAT pre-treatment quality controls, applying first the RT Plan to the acquired image to compute the EPID based dose matrix. EpiDream and Epidose models were compared for 14 VMAT and 19 IMRT (Eclipse V10) pre-treatment quality controls using gamma pass rates (3%, 3mm). Moreover, the robustness of both algorithms was evaluated first, using gamma pass rates (2%, 2mm) for homogeneous fluence beams and second, using a fake RT Plan to convert EPID images into absorbed dose.

Results: For the modulated plans, the g-comparison led to a very good agreement between both EPID based dose matrices. The success rate was respectively 98.5±2.4% and 98.0±1.7% for VMAT and IMRT fields. Using the same models, the homogeneous beams comparison showed large discrepancies, with a low gamma pass rate (86.6±2.1%). However, EpiDream presented a good agreement with Eclipse RT Dose matrices (97.1±1.2%). So, unlike EpiDose, EpiDream can be used for many controls with a single model. In addition, as EpiDose converted the image into dose using some data extracted from the RT Plan, a fake RTplan led to a large error in the dose matrix. EpiDream algorithm, only based on the acquired image provided correct dose matrix. Discrepancies between both models were high with a gamma pass rate equal to 89.7±5.7%.

Conclusion: The EpiDream solution allows us to perform the quality control tests for machine and patient in a single application. The independence of the model with the irradiation conditions, except beam energy, ensures computing more consistent absorbed dose matrices compared to other algorithms.

EP-1575

The effect of dental implants on dose distributions calculated by AXB in head and neck IMRT cases

H.M. Hung[1]
[1]*Princess Margaret Hospital, Department of Oncology, Hong Kong, Hong Kong SAR China*

Purpose or Objective: Acuros XB (AXB) has been implemented and available commercially for clinical use for several years.Different authors have reviewed the algorithm and demonstrated that AXB shows superior performance in dose estimation accuracy. In some cases, patients may be implanted with high density materials, AXB solves the deterministic solution of linear Boltzmann transport equation, in which the Hounsfield unit and the type of material must be input in order to calculate the dose distribution. However, there are only a few studies to evaluate the effect of high density material on dose distribution by AXB, and clinical data is still lacking. Moreover, most of the clinicians may not know the material of the dental implants.The universal assignment of material for permanent high density dental implants may contribute an uncertainty to the dose calculation. Thereupon the current study aims to investigate the impact of dental implants on dose distributions calculated by AXB in Head and Neck (H&N) IMRT cases and hence provide clinical suggestion to unknown dental material assumption for planning.

Material and Methods: Three materials were evaluated,namely:titanium alloy, zirconia and stainless steel. 50 patients with dental implants and treated with H&N IMRT were evenly divided into two groups according to the location of implants. AXB was used to recalculate the dose distribution, originally computed using Analytic Anisotropic Algorithm(AAA). The dosimetric data among material models were compared statistically. In addition, the dose distribution calculated by AXB were verified with measurements of parallel plate ionization chamber, radiochromic films and Gamma analysis.

Results: There were no sig. differences (P>0.05) among material models in the Planning Target Volume(PTV)

coverage and the conformity due to the dental implant for nasopharyngeal cancer(NPC) group (implant outside the PTV).However, for the Non-NPC group (implant inside the PTV), a large discrepancy was obtained in all PTV parameters. There were statistically sig. differences(P<0.05) in PTVmax, PTVmean, Conformation Number and volume covered with 70Gy(V70Gy) among models.A large portion of PTV was underdosed.For the stainless steel, the V70Gy is below 70%, which is 25% poorer when compared with AAA plans. In the phantom study, ionization chamber and film measurements supported the dose perturbations by AXB. Using a 3% and 3mm criteria Gamma analysis, passing rate was between 95.0% and 99.7% demonstrating that AXB was in agreement with measurements in different models.

Conclusion: The effect of high density dental material in H&N IMRT cases highly depends on the location of the PTV. For the case with implant outside the PTV, the impact is independent of the type of material and zirconia is recommended for material assumption. However, for the cases with implant inside the PTV, assumption of material should not be made without proper investigation.

EP-1576

Evaluation of transit in vivo dosimetry using portal imaging in VMAT treatment plans

E. Combettes[1], J. Molinier[1], N. Ailleres[1], L. Bedos[1], A. Morel[1], S. Simeon[1], D. Azria[1], P. Fenoglietto[1]
[1]*Institut régional du Cancer de Montpellier- ICM - Val d'Aurelle, Radiotherapy, Montpellier, France*

Purpose or Objective: To assess the performance of the EPIgray® software in the field of transit in vivo dosimetry using portal imaging in Volumetric Modulated ArcTherapy (VMAT) treatment plans.

Material and Methods: MV images acquired in cine mode using portal imaging were used by EPIgray® to reconstruct the delivery dose. These reconstructed doses were compared to the calculated doses obtained by the TPS. The reproducibility of the response was evaluated first on phantom and on patient with a prostate VMAT treatment plan and also on patient with a more complex head and neck plan. The dose deviation, with checkpoints defined in the PTV and the organ at risks, was our main criteria to verify the reproducibility of the response. The dose tolerance was set of ± 5%. The relevance and performance of the points automatically generated (AUTO VX) by the software on PTV have been tested and compared with points generated by the user. Then, data from 101 patient's cases treated by VMAT plans (various locations) were retrospectively analyzed taking into account only the dose deviation of the automatic control point AUTO VX.

Results: The dose deviation from the VMAT treatment plan (phantom and patient) measurements ranged of 0.26 % to 1.50 %, respectively. The dosimetric study on head and neck treatment showed a variable dose deviation range 0.87% and 2.5% depending on level of dose. Automatic points and points created by the user have similar results. The point AUTO VX is representative of results of all points. Results from patient's cases were 1.31 ± 1.62 % for the prostate and -4.79 ± 3.87 % (AUTO V1) and -5.54 ± 3.74% (AUTO V2) for the head and neck VMAT treatment plans. The first clinical results give 46 % patient's cases out-of tolerance. The relative difference in the overall results was -4.68 ± 3.50 %.

Conclusion: EPIgray® gives reproducible results on phantom and for treatments such as prostate VMAT treatment plans. The software seems to be less efficient with more complex VMAT treatment plans such as head and neck cases. This study allowed us to consider a tolerance to own each tumor site.

EP-1577

A robust method to minimize geometric table rotational errors in stereotactic radiotherapy

J. Geuze[1], J. Kaas[1], T.A. Van de Water[1], A.M. Van Mourik[1], F. Wittkämper[1]
[1]*Netherlands Cancer Institute Antoni van Leeuwenhoek Hospital, Radiotherapy, Amsterdam, The Netherlands*

Purpose or Objective: In stereotactic radiotherapy of intracranial lesions typically non-coplanar techniques are used. However, if the table rotation axis does not coincide with the linac's MV isocentre, the non-coplanar arc introduces a geometric shift of the patient. We present a method to measure the table rotational error for the Elekta® Precise table and correct for this error by moving the table assembly.

Material and Methods: The table rotation axis is measured with respect to the linac's MV isocentre. To determine the MV isocentre position, first an EPID-based Winston-Lutz measurement is performed. Subsequently, without moving the ball bearing (BB), EPID images at gantry angle 0° are acquired at different table angles (-90, -45°, 0°, 45° and 90°). For each image, the position of the field and BB is determined by an automated fitting procedure.
The table rotational error is calculated by applying two corrections to the measured positions.1) To correct for the difference between the field centre from gantry 0° and the MV isocentre, all BB positions are shifted by this calculated difference. 2) The BB position at table angle 0° is translated to the MV isocentre, and for the other BB positions the same translation vector is rotated by the table angle. The final corrected positions represent the geometric shift of the BB due to table rotation as if it was placed exactly at the MV isocentre. The largest geometric shift is defined as the table rotational error. This error indicates the possible geometric shift of the patient caused by table rotation when applying a non-coplanar arc.
In order to minimize the table rotational error, the entire table assembly must be shifted. The required shift equals the difference between the table rotation axis and the MV isocentre. This difference is determined from a semicircle which is fitted to the corrected BB positions for the different table angles. To accurately adjust the ~800 kg table assembly, a digital indicator with an accuracy of 0.01 mm and a crowbar are used.
The stability of the adjusted table assembly was ensured by performing a monthly measurement of the table rotational error.

Results: Six Elekta® Precise tables were successfully corrected (see figure 1). After adjustment, the table rotation axis coincided with the MV isocentre to within on average 0.3±0.1 mm (max. 0.6 mm) This resulted in an average table rotational error, i.e. maximal possible geometric shift, of 0.5±0.2 mm (max. 1.0 mm). Monthly measurements showed that the table rotational error of all six tables were stable with a standard deviation of 0.1 mm.

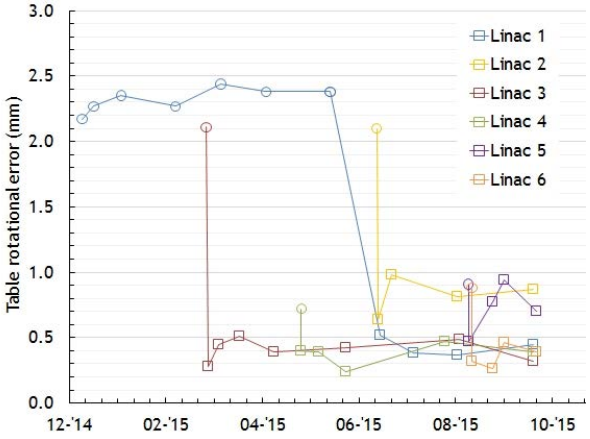

Figure 1 *Table rotational error of six tables.*

Conclusion: We present a robust method to accurately measure and correct the table rotational error. This makes it possible to coincide the table rotation axis with the linac's MV isocentre within on average 0.3 mm. The stability after adjustment shows that the method is useful and effective. This method improves the delivery accuracy of non-coplanar stereotactic radiotherapy.

EP-1578

Evaluation of an Integral Quality Monitor device for monitoring real-time delivery

G. Miori[1], A. Martignano[2], L. Menegotti[2], A. Valentini[2]
[1]*University of Rome Tor Vergata, School of Medical Physics, Roma, Italy*
[2]*Azienda Provinciale per i Servizi Sanitari, Department of Medical Physics, Trento, Italy*

Purpose or Objective: Radiotherapy treatments are getting more and more complex, dealing with the continuous development of new technologies. Therefore, it is of increasing importance monitoring delivered beams to identify errors. The use of a linac-head integral quality monitor (IQM, iRT Systems GmbH) for real-time beam delivering control was evaluated. This study analyzed the effect of IQM attenuation on delivered beams and the ability of IQM in detecting errors in VMAT treatments.

Material and Methods: Beam attenuation was calculated at 4 different beam size (from 5x5 to 20x20 cm2) by the IC Profiler (Sun Nuclear Corp.) at 6 MV and 10 MV beam energies in both X and Y directions. The IQM capability in recognizing errors was performed introducing deviations in 4 H&N clinical VMAT plans: 3, 5 and 10 % errors on total delivered MU's and 3, 5 and 10 mm MLC's shifts. The cumulative IQM checksum value was measured and the percentage difference was calculated with respect to the non-modified plan. At the same time we obtained dose distribution maps through the PTW 2D array inserted in a rotating QA phantom (RT-smartIMRT, dose.point GmbH). The phantom was chosen for its geometrical characteristics similar to IQM in signal recollection. The local gamma pass rates (2%/2mm) were compared to the original plan values. Non-modified plans were delivered twice in two different times to take into account LINAC variations.

Results: Beam attenuations were normalized to the central chamber of IC Profiler. It gives average attenuation values of 6.56 % ± 0.03 % and 5.27 % ± 0.12% for 6 MV and 10 MV beams, respectively. The percentage of dose difference with respect to the central chamber value was assessed to be < 0.4 % for the 6 MV beam and < 0.1 % for the 10 MV beam excluding beam penumbra regions. The results for modified VMAT plans are summarized in Figure 1. Figure 1a and 1b shows the gamma pass rates and the IQM signal percentage differences for MU's variations, respectively. Figure 1c and 1d illustrates the results for MLC shifts. Both methods detect specifically MLC shift errors, while MU's variations were better identified by IQM. IQM shows a linear response with dose while gamma analysis seems to have difficulty in identifying 3% and 5% MU's variations. In our opinion the reason for this is that the RT-smartIMRT recollect a 2D dose map as if the entire plan were delivered at a fixed gantry angle. Further comparisons to gamma analysis should be evaluated with a different kind of phantom.

Figure 1

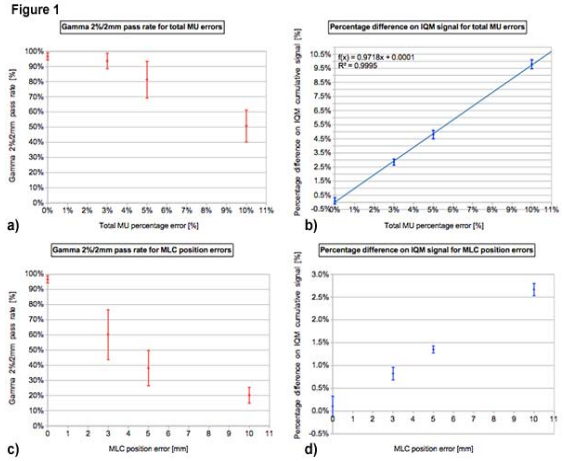

Conclusion: IQM beam attenuation can be considered to be homogenous in both X and Y directions and the machine-specific percentage of beam attenuation could be used to rescale treatment plan dose for clinically IQM use. The IQM shows outstanding features in detecting real-time errors and for time-saving QA's, although the characterization of IQM responses to single segment errors and the definition of a machine-specific alarm threshold still have to be analyzed.

EP-1579

Room scatter effects in Total Skin Electron Therapy: a Monte Carlo study

A. Nevelsky[1], E. Borzov[1], S. Daniel[1], R. Bar-Deroma[1]
[1]*Rambam Health Care Campus- Faculty of Medicine-Technion, Oncology, Haifa, Israel*

Purpose or Objective: Total Skin Electron Irradiation (TSEI) is a complex technique which involves the use of large electron fields. Electrons scattered from the treatment room floor and ceiling might contribute to skin dose and distort dose distribution, especially when dual-field approach is used. The purpose of this work is to study effects of scattered electrons on the dosimetry of TSEI by Monte Carlo (MC) simulations.

Material and Methods: 6 MeV and 9 MeV beams from Elekta Precise linac operated in High-Dose-Rate (HDR) mode are used for TSEI treatments. The EGSnrc code package was used for MC simulation. First, the incident electron beam parameters (energy spectrum, FWHM) were adjusted to match the measured data (PDD and profile) for both energies at SSD=100 cm for 40x40 open field. These parameters were then used to calculate vertical dose profile at 1mm depth at the treatment distance of 400 cm. Floor was modeled within BEAMnrc using JAWS module. LATCH variable was used to track electrons history and calculate dose profile with and without electrons scattered from the floor. Dose profiles were normalized to the maximum dose from one horizontal field (gantry angle 90 degrees) at 1 mm depth. Influence of dual field angle and floor material on the contribution of floor scatter was investigated. Spectrum of the scattered electrons was calculated. Measurements of dose profile were performed in order to verify MC calculations.

Results: Vertical profile total dose, dose without floor scatter and the floor scatter contribution is shown in Figure 1. Floor scatter contribution is more than 20% near the floor and decreases to about 10% and 5% at the distance 50cm and 100cm from the floor, respectively. No dependence on the beam energy or dual-field angle was found. The scatter depends on the floor material (at 20 cm from the floor, scatter contribution was about 18%, 15% and 12% for concrete, PVC and water, respectively). Spectrum of the scattered electrons has distribution which is almost uniform between few hundred KeV to 4 MeV and then decreases linearly to 6 MeV. Dose verification measurements for the total dose were in good agreement (less than 3%) with the MC calculations.

Figure 1. Vertical dose profiles

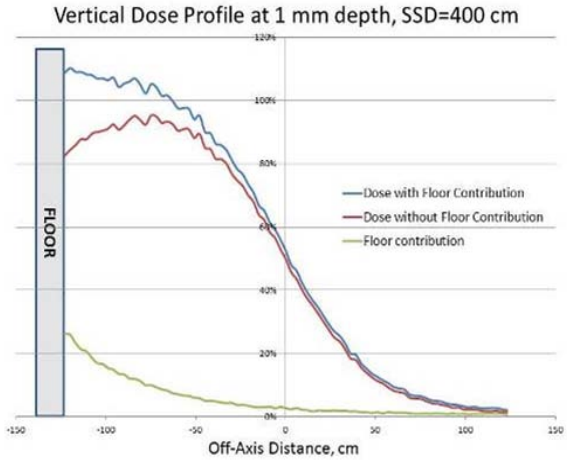

Conclusion: For the TSEI technique, dose contribution due to the electrons scattered from the treatment room floor and ceiling may be clinically significant and should be taken into account during treatment design and commissioning phases. MC calculations can be used for this task.

EP-1580

CyberKnife multi-site small beam dosimetry with a new plastic scintillator detector

S. Russo[1], L. Masi[2], A. Bergantin[3], E. De Martin[4], R. Doro[2], C. Frassanito[5], M.L. Fumagalli[4], A.S. Martinotti[3], E. Rondi[6], S. Vigorito[6], P. Mancosu[7]

[1]*Azienda Sanitaria Firenze, S.C. Fisica Sanitaria, Firenze, Italy*

[2]*IFCA, Radiotherapy, Firenze, Italy*

[3]*C.D.I., Radiotherapy, Milano, Italy*

[4]*Istituto Besta, Radiotherapy, Milano, Italy*

[5]*C.B.H. Città di Bari Hospital, Radiotherapy, Bari, Italy*

[6]*I. E. O., Radiotherapy, Milano, Italy*

[7]*Humanitas Research Hospital, Medical Physics Unit of Radiation Oncology Dept, Milano, Italy*

Purpose or Objective: Accurate dosimetry of small photon fields is clinically crucial, yet remains difficult to achieve. Water-equivalent detectors with small dimension compared to the beam size can be considered ideal. The aim of this work was to evaluate the suitability of a plastic scintillator detector (PSD) (Exradin W1, Standard Imaging SI) for relative small beams dosimetry over different CyberKnife systems.

Material and Methods: Five CyberKnife centers were involved in the study. Small beam dosimetry was performed with W1 PSD oriented vertically (parallel to the beam axis) within a water tank. Cerenkov Light Ratio (CLR) according to the method of Morin (Med. Phys 2013) using the two-channel SuperMax electrometer (Standard Imaging) was calculated to take into account the Cerenkov effect. Since this electrometer has not been integrated with the scanning water-tank, separate positioning and dosimetric systems were used. Output factors (OF) for cones diameters ranging from 5 to 60 mm were measured. Setup conditions were: 80 cm source to detector distance and 1.5 cm depth in water (SSD=78.5cm). Inline and crossline profiles for 5 mm circular field were also acquired at 10 cm depth in water and 80 cm source to detector distance. Same measurements were repeated by each center with the PTW60017 silicon diode. Monte Carlo correction factors reported in literature for PTW-60017 silicon diode (Francescon et al. PMB 2012, Francecon ed al. Med. Phys. 2014) were applied to detector readings for OF and dose profile evaluation.

Results: W1 PSD OF measurements averaged over all centers were lower than silicon diode MC corrected values for all field sizes, with differences within 1.7% (see table 1). Comparing OF measured by W1 PSD to MC corrected PTW-60017 diode data for each center, relative differences <2% for 60-12.5 mm fixed cones were obtained. Differences < 3.2% for 10 mm and 7.5 mm cones, and up to 4.6% for 5 mm cones in one center were detected.

Field Size (mm)	5	7.5	10	12.5	15	20	30	40	60
W1 PSD	0.665 (0.014)	0.816 (0.007)	0.870 (0.005)	0.913 (0.005)	0.939 (0.004)	0.965 (0.003)	0.982 (0.003)	0.987 (0.003)	1.000
MC corrected PTW 60017	0.675 (0.014)	0.830 (0.008)	0.880 (0.007)	0.919 (0.004)	0.943 (0.002)	0.966 (0.003)	0.982 (0.002)	0.988 (0.004)	1.000

Table 1. OF mean values and SD over the five CyberKnife centers for W1 scintillator and MC corrected diode measurements.

Dose profile measured by W1 resulted wider than MC corrected silicon diode ones for each center: (see figure 1 for 5 mm collimator of CyberKnife Unit n°1). W1 PSD profile tails were always above diode corrected values for each center.

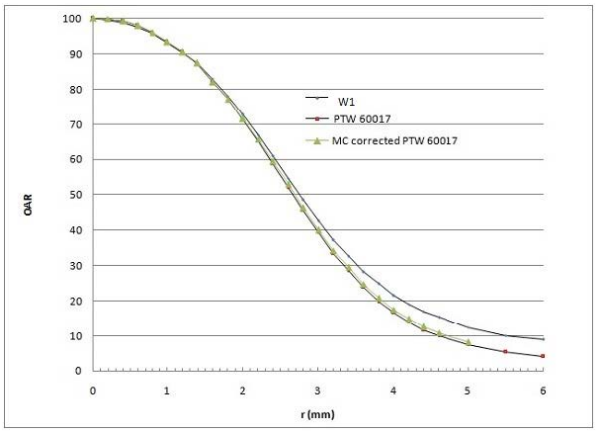

Figure 1. CyberKnife Unit n°1 mean profile measured by W1 PSD and silicon diode for 5 mm field size.

Conclusion: The agreement between Exradin W1 PSD and MC corrected silicon diode results is promising for the use of W1 PSD in small field dosimetry. However, the application of CLR correction remains a critical point in the measurement procedure and further research is needed to determine the most accurate method for CLR determination.

EP-1581

PTW Starcheck 2D array for Quality Control in IOERT: an evaluation of accuracy and dose consumption

M. Severgnini[1], H. Aslian[2], M. De Denaro[1]

[1]*AOU "Ospedali Riuniti di Trieste", Medical Physics, Trieste, Italy*

[2]*International Center for Theoretical Physics and Trieste University, Medical Physics, Trieste, Italy*

Purpose or Objective: In this study, a PTW Starcheck device, which is an easy handle measurement equipment, is used to check the possibility of executing periodical QC in IOERT.

Material and Methods: The dosimetric properties of the new Starcheck device (T10043, PTW) have been studied for 6, 9 and 12 MeV electron beams by IOERT accelerator, the MOBETRON (IntraOp, Inc. Santa, CA.). The Starcheck, consists of 527 vented ionization chambers with small volume (0.053cc) along the principal and diagonal axes. The matrix cover an area of 26 x 26 cm with the spatial resolution of 3mm. The main beam parameters are measured at the depth of maximum dose at mentioned energies and different flat base collimator sizes (4, 5, 6, 7 and 10cm) in comparison with measures conducted with ionization chamber (Advanced Markus, PTW TW34045) and electron diode (PTW TW60012) in water phantom (PTW MP3-S) and also with EBT3 gafchromic film (International Speciality Products, Wayne NJ) in water

equivalent slab phantom (PTW RW3). The Starcheck data acquisitions were done with the Multicheck software with only 100-200 MU and data analysis was handled by the MEPHYSTO software. Reference profiles measured in water were compared with profiles obtained with 2D array and Gafchromic films using the 2%/2mm gamma-index criterion. Output factor measurements were carried out for the central chamber of the array using its absolute dose value, and the results compared with the reference values.

Results: Comparison between dose profiles obtained with Starcheck 2-Array, chamber, diode and Gafchromic film showed a good agreement and they satisfied gamma analysis (2%/2mm) for almost all the nominal energies and collimators. The high spatial resolution of Starcheck allows accurate evaluation of penumbra, symmetry, flatness and field size and the results showed dosimetric differences less than 1%, 1mm for all the energies in the reference collimator (10 cm). The absolute dose difference at the Zref (IAEA398) between central chamber of 2D-array and Advanced Markus was in the order of 1% for 6 and 9 MeV and was almost 1.5% for 9 MeV. Furthermore, the difference between output factor obtained with the 2D-array and other dosimeters was in the order of 2% for all collimators in different energies except for the smallest collimator (4cm) where the output factor deviated more than 3% from the other results. However, the results for beveled collimators were not acceptable due to angular response variation of chambers.

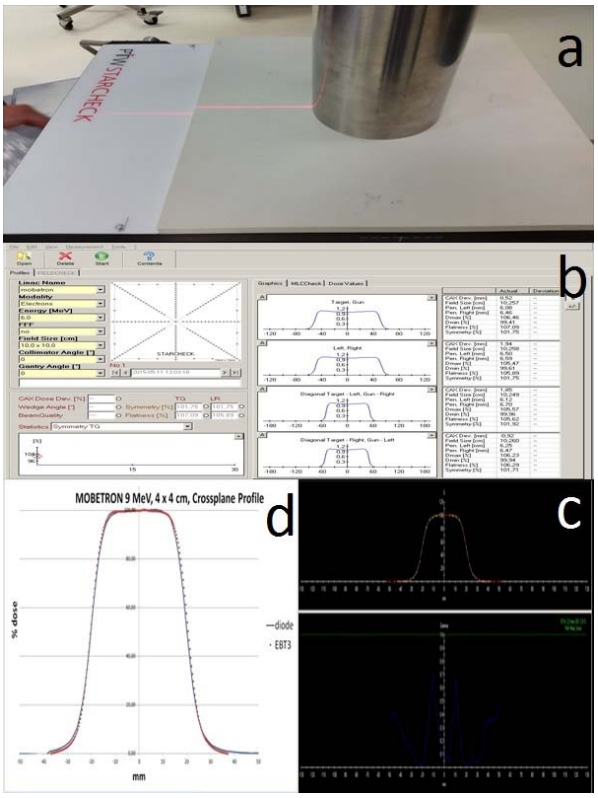

Fig.1. Starcheck 2D array (a), data analyze with Multicheck software (b), crossplane profiles comparison: Starcheck and diode (c), Starcheck and EBT3 (d)

Conclusion: The high spatial resolution, very small detector size and specific arrangement of this 2D array can be really suitable for dosimetry in IOERT. Additionally, it can reduce setup time and dose consumption more than 30% for frequently QC procedure.

EP-1582

Retrospective study of IORT sarcoma treatment using an innovative dedicated TPS

A. Soriani[1], A. Ciccotelli[2], S. Carpino[1], M. Petrongari[3], M. D'Andrea[1], G. Iaccarino[1], G. Felici[2], M. Benassi[4], P. Pinnarò[3], C. Giordano[3], G. Sanguineti[3], R. Biagini[5], L. Strigari[1]

[1]Regina Elena Cancer Institute, Laboratory of Medical Physics and Expert Systems, Roma, Italy
[2]S.I.T.–Sordina IORT Technologies S.p.A., R&D Dept, Aprilia LT, Italy
[3]Regina Elena Cancer Institute, Radiation Oncology Dept., Roma, Italy
[4]Istituto Scientifico Romagnolo per lo Studio e la Cura dei Tumori IRST, Medical Physics Dept, Meldola FC, Italy
[5]Regina Elena Cancer Institute, Orthopaedic Surgery Dept., Roma, Italy

Purpose or Objective: The IORT dedicated Treatment planning system (CSRAD+), already validated on simple geometries, has been used to perform calculation on patient-like geometries and to compare the measured and the calculated dose distribution in a clinical configuration. In this study, sarcoma cancer patients have been considered. In sarcoma IORT treatments, the air gap between target and applicator and the extended dimensions are critical parameters that must be fully taken into account. The TPS and MC calculations are mandatory for documenting the dose delivery in order to potentially improve the treatment technique and to better evaluate dose effect correlation.

Material and Methods: Twenty six patients with sarcoma cancer have been treated using NOVAC 7 with an energy from 7 to 9 MeV, an applicator diameter from 40 to 100 mm, delivering a dose from 10 to 16 Gy. In vivo dosimetric data collected during IORT using Gaf films, have been used as the gold standard for testing the accuracy of the algorithms implemented in the TPS. CT images of five representative patients have been used to reproduce the surgery room scenario, using the collected data and taking into account tissue removal during the surgery procedure. Then, the CT images were imported in the TPS and used in order to perform an accurate dose calculation. The dose distribution have been compared with the in vivo dosimetry in order to perform a sensitivity analysis.

Results: The TPS algorithms including the inhomogeneity correction have been investigated considering the clinical scenarios. The algorithm including the inhomogeneity correction allows the best agreement between the in-vivo dosimetry results and calculated dose, for mobile IORT accelerator. CSRAD+ permits to make a virtual docking, to delineate the target ROI, and to evaluate the dose distribution and the dose volume histogram. The sensitivity analysis revealed potential setup uncertainties (up to 80%) due to the manually performed alignment procedure in the surgical room and inaccuracy on target thickness when blood and air are present during the docking.

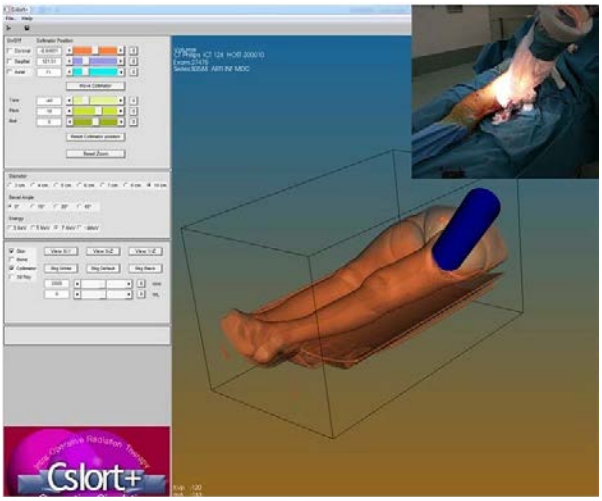

Conclusion: The developed CSRAD+ shows a good agreement with experimental data and could replace the time consuming MC absolute dose calculation, becoming a potential on-line aid for physician and physicist in the surgical room. The CSRAD+ could represent a training tool for

IORT staff and could provide a provisional plan that includes also DVH and MU calculation.

EP-1583

An automated Monte Carlo plan verification system for spot-scanning proton therapy

J. Richardson[1], A. Aitkenhead[1], T. Lomax[2], S. Safai[2], F. Albertini[2], R. Mackay[1]

[1]*The Christie NHS Foundation Trust, Christie Medical Physics and Engineering, Manchester, United Kingdom*

[2]*Paul Scherrer Institute, Center for Proton Therapy, Villigen, Switzerland*

Purpose or Objective: Monte Carlo (MC) recalculation of spot-scanning proton therapy treatment plans can provide an independent verification of monitor units required for delivery, and reduce the time treatment rooms need to be reserved for patient specific QA. We describe the development of such a MC verification system for a clinical facility.

Material and Methods: Realistic clinical beam models were developed by matching simulations (using GATE/GEANT4) to measurements made in a clinical beamline. They consist of a tuned physics list, a lookup table relating each of the 115 nominal beam energies to a tuned spot energy (mean and standard deviation) and phase space parameters which allow spot sizes to be properly modeled for any combination of energy and nozzle extension. For all beam energies simulations accurately reproduce both integral depth dose profiles (>97% of data-points pass a local gamma analysis at 2%/2mm) and lateral profiles measured in air and in solid water (with a 0.2 mm maximum difference). The model was further validated against a series of simple test plans which were optimized in the clinical Treatment Planning System (TPS) to produce uniform dose volumes at various depths in water.The automated MC system can process, simulate and analyse treatment plans without user input once it receives the TPS files.

Results:

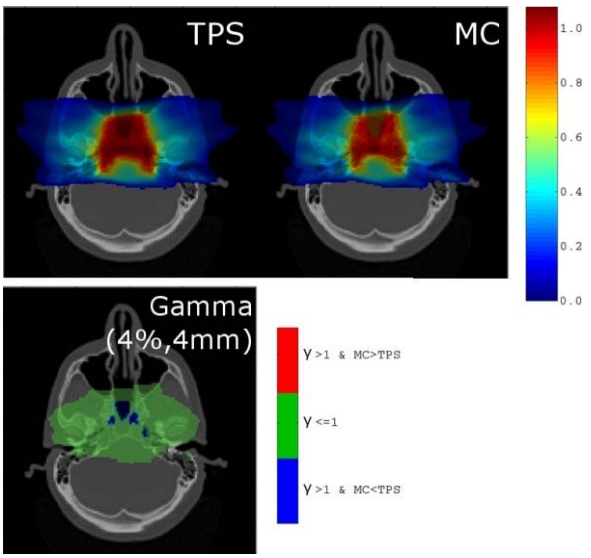

The system was tested for a three field (11k spot) base of skull treatment plan computed in a patient CT dataset. Simulations were split into 40 calculations over a 10 quad-core CPU cluster, requiring <30 minutes to achieve dosimetric uncertainties (within the 90% isodose volume) of <1%. The figure demonstrates the broad agreement between the TPS (left) and the MC simulation (right). The *local* gamma pass rate between the two (bottom) is 97% at 4%/4mm (green voxels pass, red / blue voxels fail). This should be interpreted in the context of this being a highly inhomogeneous target site: Differences occurred only in heterogeneous regions where the TPS's analytical dose calculation would be expected to model dose deposition less accurately than MC systems. For example, the MC simulations predict a lower dose around the sinus air cavities than the TPS.

Conclusion: We have demonstrated that the MC verification system can accurately reproduce the dose distribution predicted by a clinical TPS. Further validation work is ongoing using a variety of plans and phantom measurements. Once clinically commissioned, the system can be used as an independent dose checker, reducing on-set verification time.

EP-1584

Experimental validation of Tomotherapy to VMAT plan conversion using RayStation Fallback Planning

L. Bartolucci[1], O. Jordi-Ollero[1], M. Robilliard[1], S. Caneva-Losa[1]

[1]*Institut Curie, Radiotherapy, Paris, France*

Purpose or Objective: To establish the workflow & methodology and to perform an experimental validation of treatment plan conversion from Tomotherapy HD machine (Accuray) using dynamic jaws to a True Beam (Varian) Linac. For this purpose, the RayStation (RS) TPS using fallback planning (RFP) is currently tested. An end-to-end set of phantom configurations of increasing complexity are presented. The ultimate goal is to validate this process in order to minimize the impact of machine downtime on patient treatments.

Material and Methods: Four phantom based treatment plans were generated in the Tomotherapy Planning Station. These plans were mimicked with RFP for the TrueBeam using X6-FFF dual-arc VMAT. The first three cases planned on the Cheese Phantom (Std. Imaging) consisted of 1 to 4 target dose levels and 3 OARs, using heterogeneous inserts for the last one. The 4th case was an integrated boost H&N treatment with 3 target dose levels planned on an anthropomorphic phantom (H&N, IBA). Original Helical Tomotherapy (HT) and RS fallback plans were delivered respectively on each machine. Ion chamber (A1SL, Std. Imaging) and Gafchromic EBT3 (ISP) films were used to measure absolute and planar doses. First, for both machines beam delivery vs. treatment plan was evaluated as a baseline for absolute dose, gamma (γ) passing rate (criteria 3%/3mm) and overall uncertainties. Secondly, in order to ensure that the difference between the two calculated dose distributions (TPS_TOMO / TPS_RAYSTATION) matched the differences between the two measured film dose distributions (Film_TOMO / Film_RAYSTATION), a γ difference (5%/5mm) was performed.

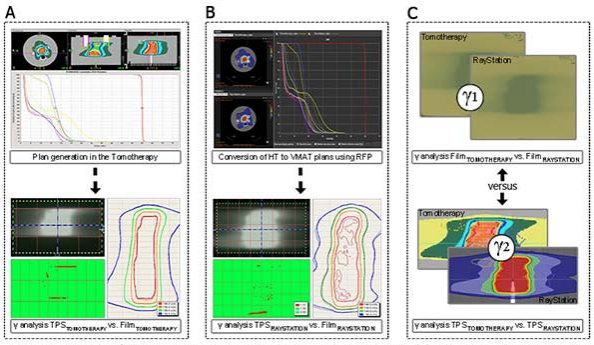

Figure 1 - Principle of the method implemented to validate plan conversion. (A) Helical Tomotherapy TPS dose distributions calculated on the Cheese Phantom is delivered on the Tomotherapy and measured with ion chamber and film. Gamma evaluation (3%/3mm) is performed using FilmQA Pro. (B) same as (A) but mimicked with the RayStation TPS Fallback Planning and delivered on the TrueBeam. (C) Gamma-index evaluation (5%/5mm) for both film measurements (γ1). Gamma-index (5%/5mm) for both TPS dose distributions (γ2). The average γ difference (γ1 - γ2) is performed between them.

Results: First, gamma evaluation was (99.1±0.6)% for HT and (99.5±0.4)% for RS fallback plans while absolute dose differences between calculations and ion chamber measurements were respectively 0.9% for HT and -0.7% for RS on average for all end-to-end tests. Secondly, average γ difference between calculated doses TPS_TOMO /

TPS_RAYSTATION and measured planar doses Film_TOMO / Film_RAYSTATION was (0.3±0.2)%.

4 cases	γ evaluation (3%/3mm) TPS vs. Film		Absolute dose difference TPS vs. Ion Chamber		(C) Average γ difference (5%/5mm) TPS_{TOMO}/TPS_{RS} vs. $Film_{TOMO}/Film_{RS}$
	(A) Tomotherapy	(B) RayStation	(A) Tomotherapy	(B) RayStation	
Average	99,1%	99,5%	0,9%	-0,7%	0,3%
SD	0,6%	0,4%			0,2%

Table 1 - Gamma evaluation, absolute dose difference and average γ difference for all end-to-end tests.

Conclusion: Raystation fallback planning is an advanced feature that allows switching patient plans between alternative treatment machines and techniques. This could be useful to reduce impact of machine downtime on patient treatments. However, this process could introduce potential risks as distinct TPS and beam deliveries are involved. The results presented here show that a difference between calculated HT and mimicked RS fallback plans match the measured differences found throughout the end-to-end tests. Results based on a 5%/5mm tolerance show that we can expect at most 0.3% agreement from the difference between original and fallback plans displayed by the RS TPS. Further work will involve the study of clinical plans on various tumors sites.

EP-1585

PRIMO software as a tool for Monte Carlo treatment quality control in IMRT: a preliminary study

V. Pita[1,2], A. Esposito[2], A. Dias[3], J. Lencart[3], J. Santos[3]
[1]*Faculty of Science- University of Lisbon, Institute of Biophysics and Biomedical Engineering, Lisbon, Portugal*
[2]*IPO PORTO, Investigation Center CI-IPOP, Porto, Portugal*
[3]*IPO PORTO, Medical Physics Service and Investigation Center CI-IPOP, Porto, Portugal*

Purpose or Objective: Monte Carlo (MC) approach is considered the gold standard method to perform absorbed dose calculations in external radiotherapy[1], because it provides the most detailed and complete description of radiation fields and particle transport in tissues. Several codes are available and recently a new MC Penelope based code and graphic platform named PRIMO was developed [2]. PRIMO has a user-friendly approach, a suitable and competitive characteristic for clinical activity. Nevertheless, advanced features such as IMRT are not introduced yet. This work is a preliminary study for the PRIMO software as a tool for MC based quality control of IMRT treatment.

Material and Methods: The simulated beam parameters of a Varian CLINAC 2300 were adjusted based on measurements in a water tank for 6 MeV energy and 10x10 cm^2 field. The water tank was divided in 81x81x155 voxels with dimensions of 2x2x2 mm^3. The Gamma Function (GF) was used for agreement assessment and a phase-space was obtained above the MLC. A solid water phantom with a PTW OCTAVIUS® 729 2D ionization chamber array inserted was imaged by a CT scan and used in PRIMO. A dynamic IMRT plan was calculated by the Eclipse™ TPS and irradiated. The LINAC DynaLog files were analysed and the dynamic delivery was divided into series of static fields in PRIMO. MATLAB was used to analyse the PRIMO output and to create images of dose distributions at specific locations. The simulated dose at the ion chamber matrix position in the phantom was compared with the matrix measurement using the 2D GF through the PTW Verisoft program.

Results: The best agreement for the beam parameters of the LINAC numerical model was obtained with initial electron energy of 5.9±0.2 MeV and beam divergence of 1.5°. The gamma function analysis (2%, 2mm) showed that 97% of the points was lower than 1, confirming the good agreement with the experimental data. For the IMRT plan, the measured and simulated dose distributions at the ion chamber matrix (fig 1A-B) show good agreement, as the gamma points lower than 1 were 96% (fig 1C).

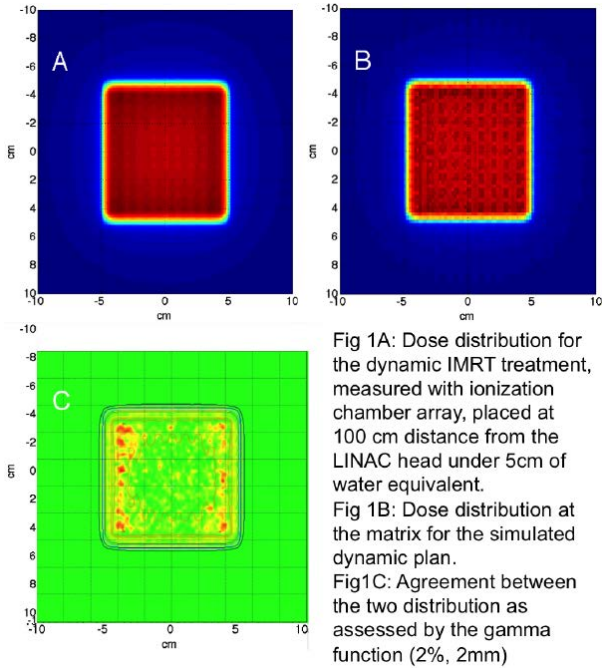

Fig 1A: Dose distribution for the dynamic IMRT treatment, measured with ionization chamber array, placed at 100 cm distance from the LINAC head under 5cm of water equivalent.
Fig 1B: Dose distribution at the matrix for the simulated dynamic plan.
Fig1C: Agreement between the two distribution as assessed by the gamma function (2%, 2mm)

Conclusion: This preliminary study shows that an IMRT plan was successfully simulated through PRIMO with acceptable concordance with the experimental results. Even though further studies on more complex treatments are still required, the results confirm PRIMO as a promising tool for IMRT simulation in clinical environment.

1. Verhaegen F and Seuntjens J 2003, Phys. Med. Biol. 48, R107–R164
2. M. Rodriguez, et al., 2013, Strahlentherapie und Onkologie, 189, 10, pp 881-886

EP-1586

Characterization of a new EPID-based system for in-vivo dosimetry in VMAT treatments

S. Bresciani[1], M. Poli[1], A. Miranti[1], A. Maggio[1], A. Di Dia[1], C. Bracco[1], M. Stasi[1]
[1]*Candiolo Cancer Institute-FPO- IRCCS, Medical Physics, Candiolo TO, Italy*

Purpose or Objective: The aim of this paper is to evaluate the EPID detector sensitivity and specificity for in vivo dosimetry of VMAT treatments to identify dosimetric and geometric errors and anatomical variations.

Material and Methods: Measurements were performed by using TrueBeam STx accelerator equipped with EPID aSi1000 (Varian, Palo Alto, CA) and PerFraction (PF) software (Sun Nuclear Corporation, Melbourne, FL). PF is a commercial EPID-based dosimetry software, which allows performing transit dosimetry, to provide an independent daily verification of the treatment. Performance of the EPID detector and of the PF software on anthropomorphic phantom was studied, simulating 17 perturbations of the reference VMAT plan. Systematic variations in dose values (1%-5% output variation), shifts (2,5-11 mm in anterior direction), anatomical variations (adding bolus over phantom), and MLC positioning (locked leaf position for different arc extensions) were applied. The difference in local and global gamma pass rate (%GP) between the no-error and error-simulated measurements with 1%/1mm, 2%/2 mm and 3%/3 mm tolerances was calculated. The clinical impact of these errors was also analyzed through the calculation of the difference between the reference DVH and the perturbed DVH (%DE). We defined as clinically meaningful a variation higher than 3% between calculated and perturbated doses. A value of %GP equal to 95% and 90% and %DE equal to 3% were used as thresholds to calculate sensitivity and specificity.

Results: Repeatability and reproducibility of no-error measurements were excellent with %GP=100% for all gamma

methods. 1%/1mm and local normalization is able to detect all type of errors (1%/1mm with global normalization is not able to detect the systematic shift of 2,5 mm), but it could overestimates some errors that have not clinical impact. In the table, we reported the results of sensitivity and specificity of PF to detect clinically relevant errors.

			Sensitivity	Specificity
%GP>95%	3%/3mm	γ-local	0,3	0,7
		γ-global	0,4	0,7
	2%/2mm	γ-local	0,5	0,6
		γ-global	0,5	0,6
	1%/1mm	γ-local	1	0,2
		γ-global	0,9	0,3
%GP>90%	3%/3mm	γ-local	0,1	1
		γ-global	0	1
	2%/2mm	γ-local	0,3	0,9
		γ-global	0,2	1
	1%/1mm	γ-local	0,7	0,5
		γ-global	0,7	0,5

Conclusion: EPID device and PF software can be confidently used in clinical routine to detect dosimetric, geometrical and anatomical discrepancies. The possibility of this in vivo evaluation and the potentiality of this new system have a very positive impact on improving daily patient QA .

EP-1587

Sensitivity and specificity of gamma index method for Tomotherapy plans.

M. Stasi[1], S. Bresciani[1], A. Miranti[1], M. Poli[1], A. Di Dia[1], A. Maggio[1], E. Delmastro[2], P. Gabriele[2]
[1]*Candiolo Cancer Institute-FPO- IRCCS, Medical Physics, Candiolo TO, Italy*
[2]*Candiolo Cancer Institute-FPO- IRCCS, Radiotherapy, Candiolo TO, Italy*

Purpose or Objective: The aim of this work is to evaluate the perturbed DVHs generated from Tomotherapy dose distributions according to the dose discrepancies detected with pre-treatment measurements. Through perturbed DVHs data, sensitivity and specificity of gamma passing rate (%GP) were calculated to evaluate if Gamma Index (GI) metric correctly differentiates the high dose error plans from low dose error plans. In the literature GI was found to be a poor predictor of dosimetric accuracy with planar and volumetric dosimeters for IMRT and VMAT techniques, we evaluate if this lack of prediction of GI method is valid also for Tomotherapy plans.

Material and Methods: 12 patients for prostate cancer (P), and 12 for head and neck (HN) cancer, were enrolled in the study. All the treatments were delivered using the Helical Tomotherapy Hi-ART system (Accuray, Inc., Sunnyvale, CA). Pre-treatment QA measurements were performed by using the diode array ArcCHECKTM and perturbed DVHs were obtained with the 3DVH software (both by Sun Nuclear Corporation, Melbourne, FL). Measured and calculated dose distributions were compared using the global and local GI method with 2%/2 mm, and 3%/3 mm criteria. Low-dose thresholds (TH) of 10% and 30% were applied and analyzed. Percentage dose differences between DVHs, obtained by TPS and by 3DVH were calculated. A %GP equal to 95% and a mean absolute DVH 3% dose error were used as thresholds to calculate sensitivity and specificity. In order to quantify the sensitivity and specificity of GI method, we calculated the number of false negative (high Tomotherapy QA passing rates indicate large errors in anatomy dose metrics), true positive (low Tomotherapy QA passing rates do imply large errors in anatomy dose metrics), true negative (high Tomotherapy QA passing rates did imply small errors in anatomy dose metrics) and false positive (low Tomotherapy QA passing rates did imply small errors in anatomy dose metrics).

Results: We found the higher sensitivity (0.55) for global normalization with 3%/3mm and TH=30% and the higher specificity (0.67) with 3%/3mm for global normalization, both for TH 10% and 30%. Instead we obtained the poorer sensitivity (0) with 2%/2mm, local normalization, and TH=10% because the threshold of 95% is too high for 2%/2mm and local normalization. We observed the poorer specificity (0.39) for 3%/3mm, local normalization, both for TH=10% and 30%. For global normalization, 3%/3mm sensitivity and specificity were always higher than those of 2%/2mm criterion.

Conclusion: The low sensitivity and specificity values of GI method, for all the applied criteria, show that the gamma index metric have disputable predictive power for per-patient Tomotherapy QA.

EP-1588

A methodology for deriving clinically indicative gamma index acceptance criteria

M. Hussein[1], A. Nisbet[1], C.H. Clark[1]
[1]*Royal Surrey County Hospital, Medical Physics, Guildford, United Kingdom*

Purpose or Objective: The gamma index (γ) is a common method for comparing measured and predicted dose distributions. The percentage of points passing with γ<1 (Γ) is the most frequently reported analysis metric. However, the use of Γ has been reported to have weak correlation against clinically relevant metrics and the result also varies depending on the Quality Assurance (QA) system configuration and software used. Other metrics could be extracted from the γ map but have not been rigorously evaluated in the literature to address appropriate acceptance values. This study has developed a methodology to evaluate the suitability of the mean, median, maximum, or near-maximum γ metrics (γmean, γmedian, γmax, γ1%) and their acceptance criteria.

Material and Methods: Investigations were performed using simulated data with deliberate changes created in a virtual phantom test. The changes included: dose deviations of -5% to 5% in 1% steps; and MLC offsets of 1–5mm in 1mm steps. An in-house Matlab-based software was used to perform γ analysis to extract different metrics. The primary PTV mean (PTVmean) and organ at risk maximum (OARmax) dose deviations were extracted from the changed plans. The γ metrics were correlated against PTVmean and OARmax for global γ passing criteria of 3%/2mm (20% threshold relative to a point in high dose low gradient). Acceptance criteria needed to predict a dose deviation >±3%, for 3%/2mm, were assessed using Receiver Operator Characteristic (ROC) analysis and assuming 100% sensitivity. The area under the ROC curve (AUC) was assessed for each γ metric to assess statistical reliability. Since the γ calculation can give varying results between different QA systems, the robustness of the proposed methodology was tested by varying γ passing criteria as well calculating in 2D planes and 3D volumes.

Results: The γmean, γmedian and γ1% metrics had the strongest Pearson correlation coefficient (ρ) against the PTVmean (ρ>0.95, p<0.01); (Fig. 1). The Γ had a weaker correlation of ρ=-0.76. These metrics had ROC AUC>0.9 (p<0.01) showing statistically strong accuracy for predicting a PTVmean deviation >±3% for 3%/2mm. Optimal acceptance criteria for achieving 100% sensitivity are shown in Table 1. The γmax had the best correlation against OARmax (ρ> 0.8, p<0.01) and the AUC was >0.9 and showed that points with γ>1.1 may be associated with a >3% increase in the OARmax. Correlations between different γ passing criteria were statistically strong at >0.95 (p<0.01) as were correlations between 2D & 3D γ calculations, indicating the robustness of the methodology to the variability in γ calculation that could be caused by QA system configuration and software implementation.

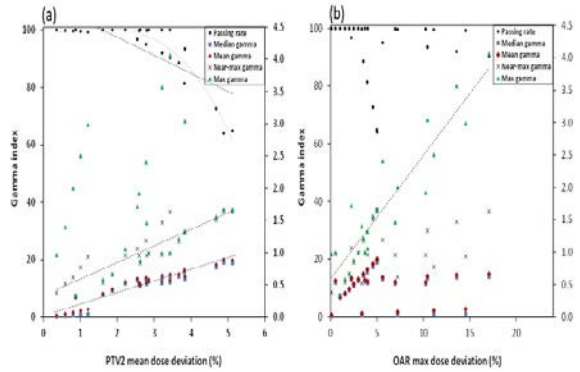

Figure 1 3%/2mm global 3D volume γ metrics against (a) PTV mean absolute dose deviation and (b) OAR maximum dose deviation. The passing rate (points passing with γ<1) given as a percentage is plotted against the left γ-axis and the γ_{mean}, γ_{median}, $\gamma_{1\%}$ and $\gamma_{1\%}$ metrics are plotted against the right γ-axis.

Table 1 Optimal criterion for the gamma index metrics to predict a ±3% dose deviation in the PTV mean dose and OAR maximum dose based on the simulation study. In all cases, sensitivity was 100%.

	DVH metric			
γ metric	PTV2 mean		OAR max	
	Acceptance criterion	AUC & [Specificity]	Optimal criterion	AUC & [Specificity]
Passing rate	≥99.9%	0.95 (p<0.01) [73.3%]	100%	0.84 (p<0.01) [62.5%]
γ_{mean}	<0.38	0.96 (p<0.01) [80%]	<0.02	0.71 (p<0.04) [12.5%]
γ_{median}	<0.35	0.97 (p<0.01) [80%]	0.00	0.72 (p=0.03) [12.5%]
γ_{max}	<0.90	0.64 (p=0.22) [33.3]	<1.10	0.94 (p<0.01) [75%]
$\gamma_{1\%}$	<0.85	0.96 (p<0.01) [80%]	<0.19	0.75 (p=0.01) [12.5%]

Conclusion: The γmean, γmedian and γ1% metrics have potential to be used as parameters to predict PTV dose deviations and had better correlation than the passing rate. However for OAR dose deviations, the γmax showed the strongest correlation with DVH deviations. This methodology is robust the variability in γ calculation.

EP-1589

Experimental validation of Tomotherapy TPS in build-up and superficial zones for a H&N plan

M. Zani[1], C. Talamonti[1,2], M. Bucciolini[1], M. Marinelli[3], G. Verona-Rinati[3], P. Bonomo[2], L. Livi[1,2], S. Pallotta[1,2]
[1]*University of Florence, Clinical and Experimental Biomedical Sciences "Mario Serio" Department, Florence, Italy*
[2]*A.O.U. Careggi, Radiotherapy Department, Florence, Italy*
[3]*University of Tor Vergata, INFN-Industrial Engineering Department, Rome, Italy*

Purpose or Objective: Aim of this study is the evaluation of build-up and superficial doses for a Head&Neck treatment, delivered by Helical TomoTherapy (HT). Measurements were carried out by two different dosimeters (radiochromic films and a synthetic single crystal diamond detector) and compared with TPS data. Build-up dose profiles and superficial dose points were estimated. The reliability of the TPS in these critical regions was assessed, giving an insight into a subject on which quite contradictory results are reported in the literature.

Material and Methods: A home modified Anderson Rando phantom was employed to house the detectors. As shown in figure (a), two slices of the phantom neck were removed and replaced with a PMMA artificial neck, with a hole inside to mimic the trachea. This allowed to measure dose profiles and superficial dose points with geometrical and scattering conditions similar to the ones taking place when a real patient is treated. Gafchromic EBT3 films (Ashland Inc., Wayne, NJ) were sandwiched inside the neck in oder to measure dose profiles and attached to the neck surface for superficial dose point assessment. PTW-Frieburg microDiamond (mD) was positioned inside drilled holes at different known distances respect to the phantom surface.

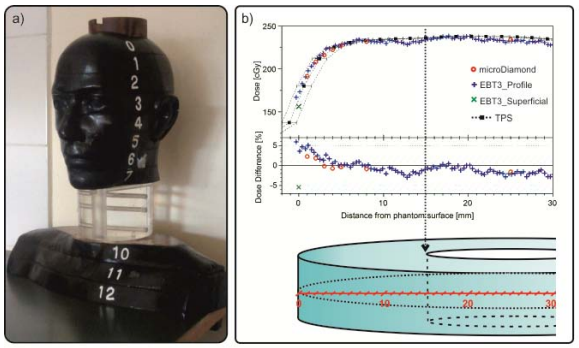

Results: In figure (b) one of the measured dose profiles by EBT3 and mD is reported, along the Antero-Posterior direction, in the range 0-30 mm (distance from the phantom surface). TPS data are also shown, as black dots, with an associated error of ± 0.9 mm, half of the lateral dimension of the calculation pixel (fine grid). The prescribed dose is reached within approximately 4 mm from the phantom surface and it does not show any significant variation going further inside the neck, in particular at the PMMA/air interface, in correspondence of the trachea starting point.
A 1D threshold criterion of 3%/mm was adopted in order to discriminate between high and low gradient zones. Dose differences (DD) measured by mD are within 2.5% respect to TPS, in the low gradient region, while a maximum distance-to-agreement (DTA) of 0.9 mm is found for the same device, in the high gradient region. EBT3 profile shows a more noisy behavior, with a maximum DD of 3.8% in the low gradient portion of the profile, while DTA is less than 1 mm in the high gradient zone. The superficial dose measurement by EBT3 film is characterized by a DTA of 0.5 mm and a DD of 5.2%.

Conclusion: Build-up dose profiles measured by the two dosimeters show the same behavior and are in agreement with TPS data; deviations are well within the reference tolerance level. The investigation carried out in this work offers the possibility of studying the TPS behavior not only in terms of dose difference, as carried out for *in vivo* measurements, but also taking into account a "spatial displacement", to be compared with patient (and/or dosimeter) positioning uncertainties.

EP-1590

Verification of small-field VMAT plans using a 2D detector array in a rotational phantom

A. Swinnen[1], M. Ollers[1], E. Roijen[1], S. Nijsten[1], F. Verhaegen[1]
[1]*MAASTRO clinic, Radiotherapy, Maastricht, The Netherlands*

Purpose or Objective: To evaluate experimentally the accuracy of the dose calculation algorithm AcurosXB in small-field highly modulated Volumetric Modulated Arc Therapy (VMAT).

Material and Methods: The Octavius 1000SRS detector array inserted in the rotational Octavius4D phantom (PTW) was used, consisting of 977 liquid-filled ion chambers covering an area of 11×11cm2. The detector size (2.3×2.3×0.5mm3) and the center-to-center distance of the detectors (2.5mm in the inner 5.5×5.5cm2 area) are important parameters for correct spatial measurement of complex dose distributions with steep dose gradients. Clinical treatment plans (n=28), characterized by small treatment volumes, 6 and 10MV photon beams, and fraction doses between 2.75-30 Gy, were projected on the phantom CT data set and recalculated in the Eclipse TPS v11 (Varian Medical Systems) using AcurosXB with a calculation grid size of 2.5mm and 1mm (field sizes <3x3cm2). All measurements were done on a Varian TrueBeamSTx linac. The irradiation technique used was

VMAT, but in a few cases also dynamic conformal arc for the smallest treatment field sizes. The effect of disabling jaw tracking, thereby fixating the collimator jaws at 3x3cm2 and applying the MLC to shape the smallest apertures was investigated for static fields between 3x3cm2 and 0.5x0.5cm2, and for 7 stereotactic patients with small brain metastases. To evaluate the dosimetric agreement between measured and calculated dose, a local gamma evaluation criterion of 2%/2mm was used.

Results: Regarding the clinical VMAT plans, the mean and SD of the volumetric gamma evaluation scores with 10%, 50%, 80% and 95% cut-off dose values are (96±6.9)%, (95.2±6.8)%, (86.7±14.8)% and (56.3±42.3)% respectively. In figure 1, a trend can be observed between relative dose differences and the field size area of 28 VMAT treatments going from very small to medium sized fields. The deviation between 1000SRS readings for static fields 3x3, 2x2, 1x1 and 0.5x0.5cm2 collimated with MLC and jaws fixed at 3x3cm2 and with collimator jaws only is on average respectively, 0.3%, 0.8%,6.7%, 5.4% (6 MV) and 0.2%,1.3%,11.3%,20.1% (10MV). The effect of disabling jaw tracking for 7 stereotactic patients with treatment techniques VMAT as well as dynamic conformal arc is shown in table 1: the smaller the target, the higher the improvement in agreement between measured and calculated doses when jaws are fixed at 3x3cm2 .

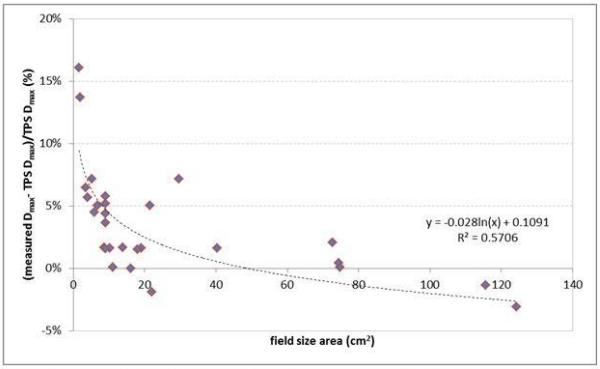

Figure 1: Plot of the relative dose differences as a function of field size area defined by collimator jaws for VMAT treatment plans. (D_{max} is referring to the maximum dose in the 3D volume)

Patients	Technique	2%2mm Threshold					measured D_{max}(Gy)	TPS Dmax (Gy)	$\frac{measured\ Dmax - TPS\ Dmax}{TPS\ Dmax}$ (%)	Field size (cm²)
		30%	50%	80%	90%	95%				
1	Dyn.Conf.Arc	91.3%	77.5%	20.5%	0.0%	0.0%	7.790	8.885	14.1%	1.4x1.2
	VMAT	90.7%	75.2 %	7.4 %	0.0 %	0.0 %	7.808	9.062	16.1%	1.4x1.2
	Dyn.Conf.Arc	98.9%	97.0%	88.9%	76.2%	37.5%	8.845	9.179	3.8%	3x3/3x3
	VMAT	99.2%	97.7 %	89.3 %	75.0 %	0.0 %	8.769	9.274	5.8%	3x3/3x3
2	Dyn.Conf.Arc	93.0%	82.2 %	32.5 %	0.0 %	0.0 %	24.126	27.075	12.2%	1.4x1.4
	VMAT	94.0%	84.0 %	34.6 %	0.0 %	0.0 %	23.399	26.606	13.7%	1.4x1.5
	Dyn.Conf.Arc	98.9%	96.9 %	89.4 %	73.7 %	44.4 %	26.683	27.668	3.7%	3x3/3x3
	VMAT	98.8%	96.4 %	84.6 %	60.0 %	20.0 %	25.378	26.695	5.2%	3x3/3x3
3	Dyn.Conf.Arc	96.8%	91.5%	72.7%	45.5%	0.0%	7.328	7.727	5.4%	1.9x1.9/1.9x2
	VMAT	97.8%	94.0%	76.2%	44.4%	0.0%	7.687	8.184	6.5%	1.9x1.9/1.9x2
	Dyn.Conf.Arc	99.5%	98.6%	95.9%	91.2%	78.6%	7.578	7.793	2.8%	3x3/3x3
	VMAT	99.6%	98.8%	95.3%	89.5%	71.4%	7.965	8.255	3.6%	3x3/3x3
4	Dyn.Conf.Arc	97.6%	94.0 %	82.7 %	66.7 %	37.1 %	6.969	7.076	3.0%	2x2/2x2
	VMAT	96.5%	90.6 %	68.9 %	43.6 %	6.7 %	7.178	7.585	5.7%	2x2/2x2
	Dyn.Conf.Arc	99.4%	98.3 %	95.2 %	90.8 %	80.6 %	6.851	6.969	1.7%	3x3/3x3
	VMAT	98.2%	95.0 %	82.6 %	70.7 %	25.0 %	7.503	7.778	3.7%	3x3/3x3
5	Dyn.Conf.Arc	91.7%	79.0 %	33.3 %	0.0 %	0.0 %	8.109	8.899	9.7%	2.4x2.2
	VMAT	97.9%	94.2 %	70.0 %	43.8 %	0.0 %	9.574	10.260	7.2%	2.4x2.2
	Dyn.Conf.Arc	99.5%	98.7 %	95.9 %	92.6 %	83.3 %	8.885	9.126	2.7%	3x3/3x3
	VMAT	99.0%	96.9 %	83.9 %	70.6 %	28.6 %	9.750	10.178	4.4%	3x3/3x3
6	Dyn.Conf.Arc	99.1%	97.8 %	93.8 %	88.9 %	76.0 %	8.373	8.575	2.4%	2.1x2.5
	VMAT	100.0 %	100.0 %	100.0 %	100.0 %	100.0 %	8.553	8.695	1.7%	3.0x2.9
	Dyn.Conf.Arc	100.0 %	100.0 %	100.0 %	100.0 %	100.0 %	8.506	8.631	1.5%	3x3/3x3
	VMAT	100.0 %	100.0 %	100.0 %	100.0 %	100.0 %	8.566	8.700	1.6%	3x3/3x3
7	Dyn.Conf.Arc	98.2%	95.3 %	86.5 %	75.0 %	45.2 %	7.299	7.508	2.9%	2.5x2.6/2.5x2.6
	VMAT	98.1%	94.6 %	81.0 %	60.7 %	16.7 %	8.351	8.934	4.5%	2.4x2.5/2.4x2.5
	Dyn.Conf.Arc	99.8%	99.5 %	98.5 %	97.1 %	93.5 %	7.272	7.402	1.8%	3x3/3x3
	VMAT	99.0%	97.0 %	89.8 %	78.6 %	50.0 %	8.666	8.972	3.5%	3x3/3x3

Table 1: Gamma agreement scores and comparison of measured versus calculated maximum doses for 7 stereotactic brain metastases patients calculated with grid size 1mm and with jaw tracking on (in white rows) against fixed collimator jaws at 3x3cm² (in tinted rows) for both treatment techniques dynamic conformal arc and VMAT. The patients are ordered in such a way that the smallest field area belongs to patient 1 and the largest to patient 7.

Conclusion: Doses calculated for stereotactic VMAT plans show an acceptable agreement against measurements with the 1000SRS in the Octavius4D system. Except for very small highly modulated VMAT fields, larger discrepancies are obtained. Fixating the jaws at 3x3cm2 and using the MLC with high positional accuracy to shape the smallest apertures in contrast to jaw tracking is currently found to be the preferred and most accurate treatment technique.

EP-1591

Investigation on backscattered dose of absorber plates for IORT application

M.N. Pirpir[1,2], M. Ghorbanpour Besheli[2,3], O. Fielitz[1,2], H. Ozcan[1,2], I. Simiantonakis[1,2]

[1]*University Hospital, Department of Radiotherapy and Radiation Oncology, Duesseldorf, Germany*
[2]*Heinrich-Heine University, Faculty of Physics/Medical Physics, Duesseldorf, Germany*
[3]*University Hospital, Department of Radiotherapy and Radiation Oncology-, Duesseldorf, Germany*

Purpose or Objective: In intraoperative electron radiation therapy (IOERT) a high single dose is applied to the tumor bed directly after resection of the malignancy. During an IOERT clinical application special shielding materials are used under the tumor bed in order to reduce the absorbed dose on critical organs behind the tumor like rib, heart and lung. Such absorbers produce backscattered dose. The objective of the present study was to investigate the backscattered dose of the absorber shielding plates. This could help us to comprehend the effect of the clinical application of such absorbers.

Material and Methods: The electron beams generated by a dedicated mobile IOERT accelerator NOVAC7 (SIT, Vicenza/Italy) were employed. The electron beams with different energies of 5 and 9 MeV together with 40 and 50 mm applicators which are most clinically used were utilised. These shielding plates are made up of a special steel alloy (AISI 316L). The backscattered dose was measured by radiochromic films, Gafchromic EBT3 (Ashland, Wayne/USA). All films were irradiated with 5 Gy at 100% isodose level.

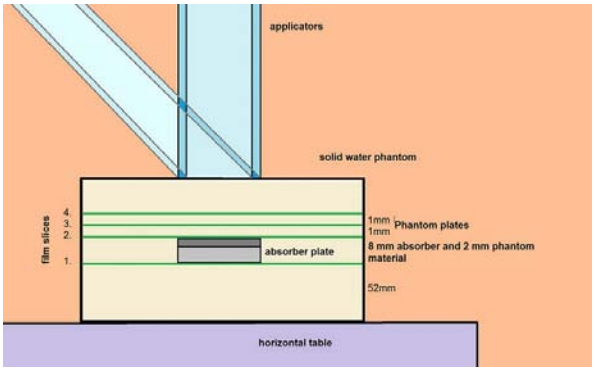

Results: Some important aspects of results are explained below.
40mm applicator: At the first film slice, increasing the energy from 5 to 9 MeV resulted to a significantly higher backscattered dose. At 5 MeV the backscattered dose was 0.29 Gy, compared to the dose resulted for the film slice without the shielding. The corresponding values were 0.63 Gy for 9 MeV. This increase might be because of the increased energy of the backscattered electrons at higher energy beams (9 MeV) which causes higher dose delivery at the same depth, compared to low energy beams (5 MeV). Moving toward the surface of the phantom the backscattered dose decreased significantly (~11%). This occurs due to decrease of energy and fluence of backscattered electrons when they move toward the phantom surface. 50mm applicator: At larger field size of 50 mm, the backscattered dose increased remarkably, compared to the 40 mm applicator. In comparison with the dose absorbed to the film slice without the shielding, the backscattered dose increased 1.5 and 1.3 Gy for 5 and 9 MeV, respectively. The reason is that at larger field size the energy fluence of scattered electrons might be higher than the 40 mm applicator and this led to a higher dose delivery at the same depth, compared to 40 mm field size.

Table: It is shown the absolute dose differences between the measurement with and without absorber plate on the film slices

Dose differences with 9 MeV electron beams in Gy	50mm 0°	50mm 45°	40mm 0°	40mm 45°
4 mm above the absorber surface	0,794	0,638	0,194	0,033
3 mm above the absorber surface	1,02	0,784	0,308	0,294
2 mm above the absorber surface	1,309	1,009	0,625	0,351
Dose differences with 5 MeV electron beams in Gy	**50mm 0°**	**50mm 45°**	**40mm 0°**	**40mm 45°**
4 mm above the absorber surface	0,247	0,2	-0,083	0,026
3 mm above the absorber surface	0,691	0,314	0,125	0,034
2 mm above the absorber surface	1,478	0,613	0,29	0,197
under the absorber plate	-0,49	-0,937	-0,328	-1,096

Conclusion: It was concluded that the backscattered dose of steel alloy is significant at higher energies. Furthermore increasing the applicator diameter from 40 to 50 mm increased the backscattered dose more than twice. The results of this study helped us for a better comprehension of backscattered dose of absorber shielding used in clinical practice.

EP-1592

Automatic detection algorithm for MLC position using a single EPID image in a daily QA program

P. Colleoni[1], A. Gambirasio[2], C. Bianchi[1], M. Fortunato[1], S. Andreoli[1]
[1]*A.O. Papa Giovanni XXIII, Fisica Sanitaria, Bergamo, Italy*
[2]*Università degli Studi di Milano, Scuola Specializzazione Fisica Sanitaria, Milano, Italy*

Purpose or Objective: We developed a robust and efficient algorithm for automatic detection of MLC (Multi Leaf Collimator) leaves position based on a single EPID (Electronic Portal Image Detector) static image acquisition. Within this framework, assessment of other important parameters such as collimator rotation angle and jaws position is possible as well. The algorithm works on a single image acquired with few MUs and allows a quantitative monitoring of MLC and collimator position accuracy and reproducibility, during a daily QA program.

Material and Methods: Images were acquired on linear accelerators (Varian Medical Systems, Palo Alto, CA) equipped with Millennium 120 MLC and with aS1000 flat panel detector with an active area 40x30 cm^2 (1024x768 pixels). All images were acquired in integrated modality with less than 10 MU. In-house code for images analysis has been developed using MATLAB® (MathWorks, Natick, MA) as platform. The algorithm for MLC position detection includes two main steps: the local edge detection, based on Canny method, and the edge linking tool to identify edge section belonging to each leaf tip. From these edge portions, leaves positions is evaluated and compared to the expected ones. Collimator angle is extracted using the FFT (Fast Fourier Trasform) of the acquired image.

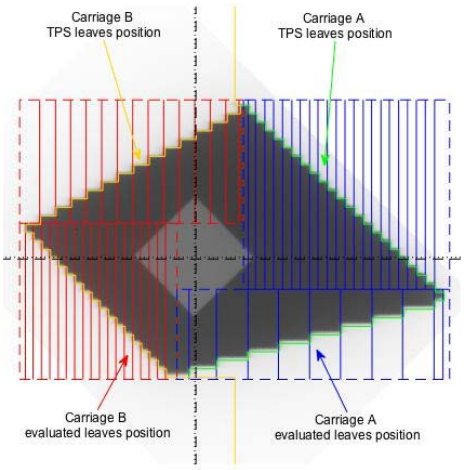

Results: In order to assess the reliability of the algorithm, different configurations were considered: MLC leaves opened asymmetrically to form a four-sides shape, different collimator rotation angles and jaws position. Images obtained from configurations with intentionally introduced errors were also analyzed. Results showed that this algorithm is able to successfully evaluate leafs position within 1 mm accuracy and collimator angle within 1 degree accuracy. The analysis process takes only few seconds.

Conclusion: We developed a fast and accurate algorithm to extract from a single EPID image parameters such as MLC leaves position and collimator rotation angle. This fast procedure is able to highlight errors related to different kind of parameters. These characteristics make this method suitable for a daily QA program. Further development of this work can be the use of this procedure to check MLC leaves position during VMAT plan delivering for a patient-specific QA program.

EP-1593

Plan specific pitch on Tomotherapy-plans effect on gamma pass rate for patient QA measured on Delta4

A. Haraldsson[1], A. Hauer Karlsson[1], L. Ambolt[1], P. Engström[1]
[1]*Skåne University Hospital, Radiation physics, Lund, Sweden*

Purpose or Objective: The purpose of this study was to analyze if the change from standard pitch to individually optimized plan specific pitch values on our Tomotherapy plans had effect on the measured gamma pass rate for our patient QA. Tomotherapy is helically delivered with a pneumatic MLC where each leave is either closed or open. Pitch on Tomotherapy is the overlap each rotation has with the previous at isocenter; or rather, the couch distance traveled per gantry rotation, and is dependent of collimator width. Our hypothesis is that the change from fixed pitch values, 0.215, 0.287 and 0.43 for field width of 1.05, 2.5 and 5.02 cm respectively, to values calculated individually based on fraction dose, targets position relative to isocenter and field width, will increase the gamma pass rate due to less stress on the mlc.

Material and Methods: At our clinic, all patients undergoing Tomotherapy are planned individually and approved plans are measured on the Tomotherapy with a Delta4, prior to treatment. Gamma pass/fail criteria is 90% at DTA: 2mm and DD: 3% when planned dose distribution is compared with measured. Recently, we started using individually optimized plan specific pitch values. These values are calculated using a program, based on the works of Chen M, Chen Y, Chen Q, et al. Med. Phys. (2011). The ripple effect, which is peak to through dose relative to average in longitudinal direction is caused by pitch when the target is not at isocenter. This puts stress on the mlc during delivery when the optimizing software tries to compensate the non-optimal overlap with mlc movement. A too low pitch also puts unnecessary stress on the mlc when the gantry rotations are low and thus increases the fraction of mlc movement that are close to mlc latency time, 20ms. A more careful selection of pitch should reduce the ripple effects and use an optimal gantry rotation period, around 20s, that in effect puts less stress on the mlc-pneumatics. We analysed the difference in results of our measurements before and after we started using individually optimized plan specific pitch values.

Results: Our measurements are approximately truncated normally distributed, and with higher gamma pass rate on average after the introduction of plan specific pitch values (M=97.4%, SD=2.08), then with fixed values as used previously (M=95.1%, SD=3.67). As presented in table 1, we have an increase in pass rate over 90%, 95% and 100%. After the introduction of plan specific pitch values, we have no reported plans with gamma pass rate under 90%.

TABLE 1: MEASURED GAMMA PASS RATE BEFORE AND AFTER INTRODUCTION OF PLAN SPECIFIC PITCH VALUES. DTA=2MM DD=3%.

	pre PSPV		post PSPV	
	Value	CI_{95}	Value	CI_{95}
NUMBER OF PLANS MEASURED	581		92	
FRACTION 100% PASSRATE	0.04	.05-.02	0.13	.21-.06
FRACTION < 90% PASSRATE	0.07	.09-.05	0.00	.01-.00
FRACTION >95% PASSRATE	0.66	.70-.62	0.82	.90-.73

Conclusion: An introduction of plan specific pitch values increases the pass rate of the patient QA when measured with Delta4.

EP-1594

On-line analysis of 4D treatment deliveries for scanned proton and carbon ion beams

S. Giordanengo[1], V. Monaco[2], A. Attili[1], A. Vignati[1], M. Varasteh Anvar[2], M. Donetti[3], F. Marchetto[1], F. Mas Milian[4], M. Ciocca[3], G. Russo[5], R. Sacchi[2], R. Cirio[2]

[1]*Istituto Nazionale di Fisica Nucleare INFN, Section of Torino, Torino, Italy*

[2]*University of Torino and INFN of Torino, Physics, Torino, Italy*

[3]*Centro Nazionale di Adroterapia Oncologica CNAO, Physics, Pavia, Italy*

[4]*Universidade Estadual de Santa Cruz, CNPq Fellow, Bahia, Brazil*

[5]*I-See s.r.l., Torino, Italy*

Purpose or Objective: A tool for fast dose distributions analysis in hadrontherapy is presented, which integrates on GPU a Fast Forward Planning (F-FP), a Fast Image Registration algorithm (F-IR), a Fast Gamma-Index (F-GI) and Fast DVH computations. The tool will be interfaced with the dose delivery system (DDS) of a synchrotron-based facility to investigate the feasibility to quantify, spill by spill, the effects of organ movements on dose distributions during 4D treatment deliveries.

Material and Methods: The F-FP was built by porting to CUDA the PlanKIT TPS, developed by INFN and IBA for proton and carbon scanned beams. The feature of choosing, among the 4DCT volumes, the CT volume corresponding to a specific respiratory phase (CT-phase) was added. To evaluate target movements, the 4DCT images are pre-processed (using C++ algorithms) to obtain the deformation vector fields. The F-IR uses the latter to map the dose calculated on a CT-phase to the CT volume used to plan the treatment (CT-reference). The F-FP runs twice to calculate in parallel the planned dose (on the CT-reference), and the delivered dose (on the CT-phase mapped on the CT-reference by the F-IR). Finally, the comparison between the two dose distributions is performed through fast F-GI and DVH computations to quantify the dose deformation due to intra-fraction anatomical changes.
The NVIDIA Tesla K40c in a Workstation (WS) HP Z820 (2xIntel XeE5-2670v2) was used. The WS will be interfaced with a clinical DDS and an optical tracking system (OTS) to test the operations on-line. The tool will receive in real-time the measured beam parameters through a direct and transparent connection with the DDS using FPGA boards.
Results will be promptly shown in the local control room.

Results: A preliminary version of the F-FP has been tested for physical and biological doses for protons and carbon ions, showing total execution times within 1 s, and negligible absolute differences (<10^-4 Gy) compared with PlanKIT results. The F-GI and DVHs computation times are of the order of few ms, while the F-IR will be within 1 s. The times for data transfer are negligible.
The overall system operations and the execution times are summarized in Fig 1.

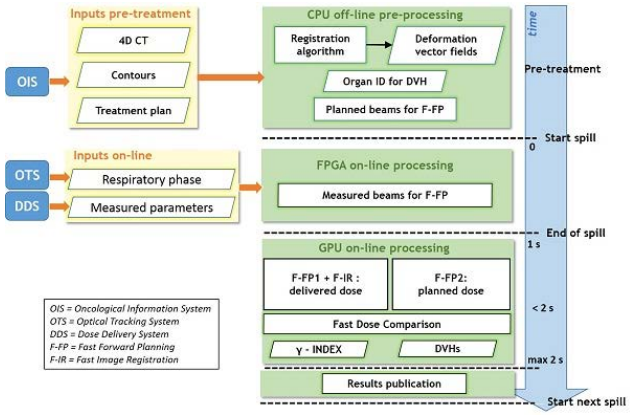

Fig. 1

Conclusion: A GPU-based tool for dose distributions analysis in hadrontherapy has been developed and will be interfaced with clinical DDS and OTS. The preliminary results suggest its possible use to on-line quantify the effects of target movements during 4D treatment deliveries with scanned proton and carbon ion beams.

EP-1595

Impact of different dose calculation algorithms on aperture-based complexity metric evaluations

A. Bäck[1], A. Larsson[1], J. Götstedt[2], A.K. Hauer[1]

[1]*Sahlgrenska University Hospital, Therapeutic Radiation Physics, Göteborg, Sweden*

[2]*University of Gothenburg, Radiation Physics, Göteborg, Sweden*

Purpose or Objective: The objective is to evaluate the impact of different dose calculation algorithms on the correlation between aperture-based complexity metric scores and field complexity, i.e. difference between calculated and delivered dose.
IMRT/VMAT treatment fields composed of small MLC sub-openings cause discrepancies between planned and delivered dose and are considered complex. Aperture-based complexity metrics have been suggested to quantify this complexity. The correlation between such metric scores and complexity, determined by comparisons of calculations and measurements, were evaluated for static MLC openings representing control points in an IMRT/VMAT treatment plan (Götstedt et al Med Phys 2015; 42: 3911). Different dose calculation algorithms have different built-in limitations that affect the deviations between calculations and measurements and thereby the correlation.

Material and Methods: The dose calculation algorithms studied were the pencil beam convolution (PBC), the analytical anisotropic algorithm (AAA) and the Acuros XB (AXB) in Eclipse treatment planning system (TPS) and the collapsed cone (CC) in Oncentra TPS. The study focus on the complexity metrics, *converted aperture metric* and *edge area metric*, described by Götstedt et al. The same 30 MLC openings of various complexity divided in series of five to describe similar patterns with increasing complexity created by Götstedt et al were used also in this study. The MLC openings were measured with Gafchromic® EBT3 film in solid water on three repeated occasions and compared to different calculations by evaluating the 3% and 5% dose difference (dd) pass rate.

Results: Examples of the correlation between the *edge area metric* and 5% dd pass rate for the 30 MLC openings are shown in the figure for AAA and AXB. The error bars show the standard deviation of the three measurements.

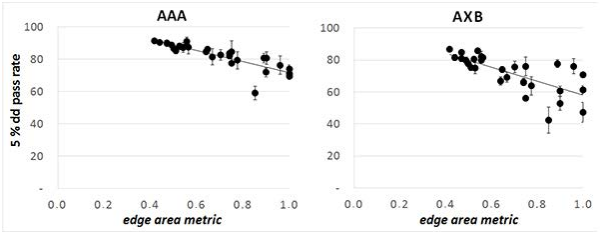

The linear correlations, expressed in Pearson's r-values, between the dd evaluations and the metric scores for the different calculation algorithms are summarized in the table.

	converted aperture metric		*edge area metric*	
	3% dd pass rate	5% dd pass rate	3% dd pass rate	5% dd pass rate
PBC	-0.93	-0.89	-0.95	-0.94
AAA	-0.85	-0.80	-0.90	-0.84
CC	-0.85	-0.73	-0.91	-0.85
AXB	-0.70	-0.52	-0.81	-0.71

The highest and lowest r-values were seen for the PBC- and the AXB-calculations, respectively. The r-values for the AAA- and the CC-calculations were similar. The *converted aperture*

metric show a somewhat larger influence of the calculation algorithm used compared to the *edge area metric*.

Conclusion: Different dose calculation algorithms can influence on the correlation between aperture-based complexity metric scores and complexity of the treatment field. The impact is different for different metrics.

EP-1596

Intraoperative radiotherapy with electrons in breast cancer patients with cardiac devices.

R. Luraschi[1], R. Lazzari[2], V. Galimberti[3], A. Bazani[1], E. Rondi[1], M. Leonardi[2], G. Corso[3], N. Colombo[4], B. Jereczek-Fossa[2,5], F. Cattani[1]

[1]*European Institute of Oncology, Physics Department, Milan, Italy*

[2]*European Institute of Oncology, Radiation Oncology Division, Milan, Italy*

[3]*European Institute of Oncology, Molecular Senology Unit, Milan, Italy*

[4]*European Institute of Oncology, Cardiology Unit, Milan, Italy*

[5]*University of Milan, University of Milan, Milan, Italy*

Purpose or Objective: To evaluate the feasibility and the safety of delivering intraoperative radiotherapy (ELIOT) to the tumor bed in breast cancer patients withcardiac implantable electronical devices as part of breast conservative treatment. Cardiac devices, as pacemakers or defibrillators, can suffer from malfunctions as a result of exposure to ionizing radiation. Scattered radiation can be harmful as direct radiation as well. Measurements of absorbed dose during ELIOT in the subclavicular region supposed to house cardiac implantable electronical devices were carried out in healthy patients without heart disease. The aim of the study is to verify that the intraoperative dose does not exceed the recommended maximum dose of 2 Gy.

Material and Methods: The present analysis was performed on 18 out of 25 patients considered for the study. After signing the informed consent, all patients underwent breast conserving surgery. After tumor removal and before delivering ELIOT to the tumor bed, two catheters, each of them containing 8 thermoluminescent dosimeters (TLDs), were placed. The first catheter, the internal one, was attached to the thoracic shielding (an aluminum–lead disk of 7-8 cm in diameter) and became an integral part of it. The shielding was located beneath the reconstructed breast parenchyma of the tumor bed, to minimize the dose to underlying tissues and its tip was positioned in the subclavicular region, where cardiac devices are supposed to be. The second catheter, the external one, was placed on the skin, parallel to the first one, next to the applicator (4-5 cm of diameter, flat or 15° beveled). The TLD reading showed the absorbed dose due to the scattered dose correlated to the distance from the applicator.

Results: Given a prescribed dose of 21 Gy at 90% isodose, the external TLDs on the skin read a mean dose of 0.32 Gy (range, 0.10 – 0.55 Gy), measured starting 1.5 cm from the applicator wall up to 10.5 cm. By evaluating the doses measured by TLDs in the internal catheter, the minimum distance considered safe for cardiac devices was found to be 2.5 cm from the applicator wall. In fact, at that distance, the cumulative scatter radiation dose was lower than 2 Gy. Comparing the data from the two catheters, higher doses were measured in the internal catheter compared to the external one. Therefore, the main source of scattered dose was the patient herself rather than the mobile accelerator.

Conclusion: Final results are not available yet, as the study is ongoing. However, on the basis of analyzed data, ELIOT seems to be safe for patients using cardiac devices as long as the minimum distance of 2.5 cm is kept between the cardiac device edge and the applicator wall. No correlation with tumor site and electron energy was observed. When clinically indicated, ELIOT might be a valid alternative to external irradiation, which is conditioned by the low threshold dose for cardiac devices, as recommended by current guidelines.

EP-1597

Investigation of in-air output ratios in FFF beams

M. Dalaryd[1,2], T. Knöös[1,2], C. Ceberg[2]

[1]*Skåne University Hospital, Radiation Physics, Lund, Sweden*

[2]*Lund University, Medical Radiation Physics- Clinical Sciences, Lund, Sweden*

Purpose or Objective: The in-air output ratio (Sc), describes how the photon fluence per monitor unit varies with beam collimator settings. In this study, the contribution from different accelerator head components to the total Sc was investigated for fields generated with and without a flattening filter in the beam line.

Material and Methods: Using the EGSnrc-package, a Monte Carlo model of the accelerator head of an Elekta Synergy linac has been built and verified with measured lateral and depth-dose profiles. Four different energy/filter combinations were simulated, one conventional 6 MV beam with a flattening filter (FF), two flattening filter-free (FFF) beams where the flattening filter was replaced by a 2 mm thick iron plate and the incident electron energy was kept the same as for the FF beam or increased to produce a similar depth-dose curve as the FF beam, and one untuned beam without any filter in the beam line. Sc was calculated as the ratio of primary collision water kerma (Kp) for any collimator setting to a reference collimator setting (10×10 cm²) for the same number of monitor units as defined in Zhu *et al.* (Med Phys **36** 5261-91, 2009). Kp was derived from a photon spectra scored in air in a circular region with a radius of 0.5 cm centred on the central axis 100 cm from the target for collimator settings ranging from 3×3 cm² to 40×40 cm². The contributions from different parts of the accelerator were evaluated using the LATCH variable. The calculated Sc was compared to measurements performed with a farmer ion chamber with a 2.5 mm brass build-up cap.

Results: Calculated Sc were within 0.4 % of measured values for both FF and the energy matched FFF beam. Unscattered photons, i.e. photons only interacting in the target, were, as expected, found to be invariant relative to the reference field and accounted for 98 % and 92 % of the total Sc for the conventional FF beam, for the 3×3 cm² and 40×40 cm² fields, respectively. For the FFF beams this proportion was increased to 99 % and 96 % for the untuned beam and to 99 % and 97 % for both the tuned FFF and the beam without metal plate (Fig 1). For the FF beam, photons having interacted in the flattening filter are the major contributors to the variation in Sc for fields larger than 10×10 cm², while for smaller fields the contribution from photons interacting in the primary collimator have an equal or slightly larger impact. However, for the FFF beams, photons interacting in the primary collimator are the largest contributors to Sc for all field sizes and the difference in contribution from the metal plate (if any) and secondary collimators are within the uncertainty of the calculated values.

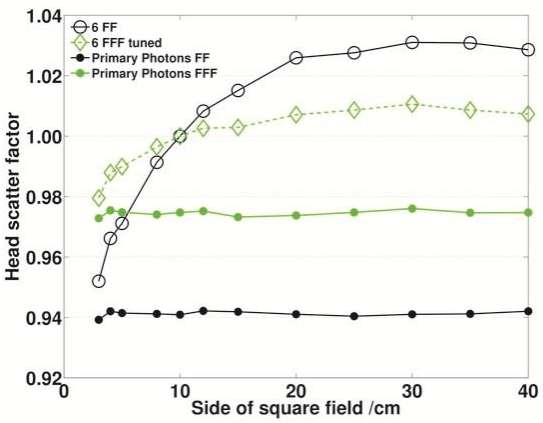

Conclusion: In-air output ratios were successfully calculated as the ratio of Kp for beams with and without a flattening filter. For FF beams the flattening filter and primary collimator was the largest contributors, while for beams with 2 mm Fe or no filter in the beams line the primary collimator accounts major part of the variation of Sc.

EP-1598

Initial validation of a commercial algorithm for volume dose reconstruction with ionization chamber

J. Garcia-Miguel[1], C. Camacho[1], J. Saez[1], C. Quilis[1], A. Herreros[1]
[1]*Hospital Clinic, Oncologia Radioteràpica, Barcelona, Spain*

Purpose or Objective: We report on our initial experience with the commissioning for fixed-field IMRT of the dose reconstruction algorithm on a phantom with measurements from a helical diode detector array (ArcCheck (AC) from Sun Nuclear (SNC)).

Material and Methods: We designed a set of tests to check on the performance of the dose reconstruction software, 3DVH, which reconstructs the dose inside the AC device from the entrance/exit diode measurements. Dose was measured with and without a small volume ionization chamber (0.125 cc semi-flex by PTW). Dose in the position of the ionization chamber was estimated with the help of 3DVH. TPS calculated dose and reconstructed dose were compared to the ionization chamber dose.
Linearity was assessed by irradiating 10x10 cm2 open fields with different isocenter doses: 0.4, 1, 1.6, 2.2 Gy. The electron density override on the CT for the AC was validated with a 2%-2mm gamma analysis on the open fields. Then a set of sliding window gaps (6, 10 and 14 mm) was irradiated with a number of MU matched to obtain 1 and 1.6 Gy at the isocenter plane. The mock cases from TG-119 were transferred to the AC CT for inverse optimization. Finally 16 clinical HN cases were also irradiated. In the mock and HN cases dose was measured in a high dose-low gradient point of the volume.

Results: The dose calculated with 3DVH for the 10x10-cm open fields was lower than the dose measured with the ionization chamber by 1.32% on average. Dose linearity was confirmed and the gamma passing rates were better than 95% for 2%/2mm criteria for all cases which confirmed our electron density override on the AC.
The ratio between the dose delivered with each sweeping gap and a 10x10cm2 field with the same planned dose was calculated. The value of this relationship obtained from the doses reconstructed with 3DVH was 5% larger than expected, while the value calculated with Eclipse TPS and with the ionization chamber were 0.999 and 1.001, respectively.
For the TG-119 cases we obtained that the reconstructed dose is 0.28% higher on average than the measured dose. The biggest discrepancy between reconstructed and measured dose was for the MultiTarget case, with a reconstructed dose 1.42% higher than the ionization chamber measurement. The mock H&N case was the best of them, with an error of 0.29% between reconstructed and measured dose. The average on the reconstructed dose with 3DVH for the 16 clinical patients was 0.78% lower than the camera, being 0.07% the smallest error and 2.91% the largest one.

Conclusion: Reconstructed doses over the AC phantom with 3DVH software are in good agreement with measurements for open fields and also for mock cases and clinical patients. However, differences between calculated and measured doses for simple sweeping gaps are inexplicable large and require further investigation.

EP-1599

How far can we go? Reliability of gamma evaluation in IMRT plans.

M. Gizynska[1,2], E. Fujak[1], A. Walewska[1]
[1]*The Maria Sklodowska-Curie Memorial Cancer Center, Medical Physics Department, Warsaw, Poland*
[2]*University of Warsaw, Faculty of Physics, Warsaw, Poland*

Purpose or Objective: The Intensity-Modulated Radiation Therapy (IMRT) is a widely used treatment for many cancer sites. Independent verification in this kind of treatment is recommended and some countries require it. There are many different ways of pre-treatment verification e.g. point dose measurement, 2D or 3D dose verification and various methods of interpreting the verification result. One of the most popular way is gamma evaluation [*Depuydt, 2002*]. The aim of this study was to identify the relationship between simulated MLC errors and gamma evaluation result. We compared RTdose for error-induced plans with original plan, both calculated in specified phantom used for verification. Such comparison enabled us to obtain result of gamma analysis influenced only by known MLC error, ceteris paribus.

Material and Methods: Verification Plans for ten patients for each of three cancer sites (brain, prostate, head and neck) were prepared. For every case original and modified MLC has been used. Two types of MLC errors were tested: open/close error in which both MLC banks moved in opposite direction and shift error with both MLC banks moved in the same direction. Magnitude of these errors were 0.5, 1.0, 2.0, 3.0 mm. The MLC errors were simulated for all control points, on both banks of active MLC leaves only. The dynamic leaf gap and other MLC physical constraints were taken into consideration. For each plan dose distribution was calculated in Eclipse (AAA v. 10.0.28) for phantom geometry and original gantry angles. Afterwards gamma evaluation was performed with the Verisoft software (PTW, v. 6.1). We investigated results for gamma 3mm/3%, 2mm/2%, 1mm/1% for local and maximum dose difference. The suppressed dose value was set to 10% for 3D gamma evaluation.

Results: For head and neck plans MLC open/close errors, equal or larger than 1mm, weren't detected only for gamma 3mm/3% max dose and passing rate 95%. For brain and prostate plans 2mm open/close errors can be detected with gamma 3mm/3% local and 2mm/2% max dose. For all investigated cancer treatment sites shift errors are hard to detect (1 mm only with passing rate 95% gamma 1mm/1%). For detailed results see Figure. We assume that difference between treatment sites is related to the leaf open/close error (gap width error) as was reported by LoSasso [*1998*] and plan modulation.

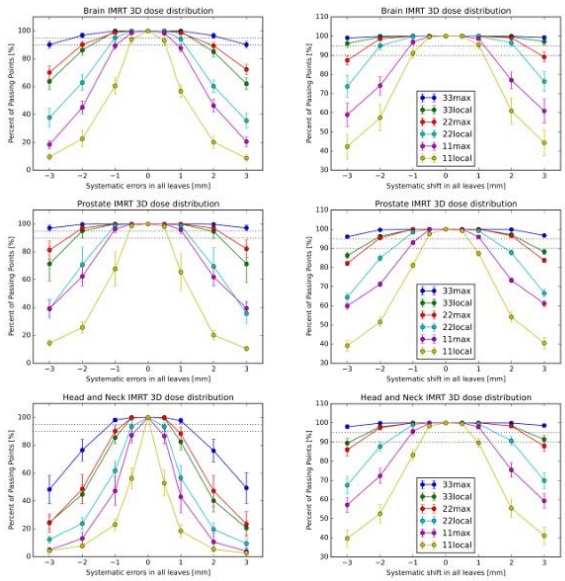

Conclusion: MLC errors may be a reason of unacceptable result of pre-treatment verification. Selection of gamma passing rate and criteria should be preceded with analysis of MLC error which can be detected by used verification method. In the case of Octavius 4D we recommend using 3mm/3% local dose for 3D gamma evaluation in previously mentioned cancer sites. Other cancer sites should be also investigated and tested. Next step should be checking the

influence of dose resolution (re-sempling of the simulated dose distribution to the detector resolution) on gamma result. Clinical relevance of such MLC errors should be also investigated.

EP-1600

VMAT lung SBRT: 3D evaluation in pretreatment patient QA and in vivo dose verification

E. Villaggi[1]
[1]*AUSL Piacenza, Fisica Sanitaria, Piacenza, Italy*

Purpose or Objective: SBRT requires patient specific-QA with high spatial resolution, stability and dynamic range. EPID dosimetry has been proofed to be efficient to give accurate results for both conventional and special treatments. In this work, a commercial QA software is used for a lung SBRT clinical case to obtain 3D dosimetry from fluences measured by EPID gantry angle-resolved data acquisition. The purpose is obtain information on actual delivered dose to the tumor volume and surrounding critical structures in terms of clinical dosimetric parameters which are meaningful for both physicians and physicists.

Material and Methods: VMAT SBRT lung treatment is planned by Varian Eclipse treatment planning system using ACUROS algorithm. Treatment is delivered using a Varian2100CD linear accelerator's 6 MV x-ray beam. Fluences are acquired on a Varian aSi1000 EPID. Dosimetry Check (Math Resolutions LLC) is a commercial QA software performing 3D treatment plan verification: the necessary measurements for the exit image kernel for SBRT includes EPID images of various field sizes (minimum field size: 1x1 cmxcm). Fluence maps acquired on the EPID during pre-treatment QA and patient treatment are separately applied to the patient's CT. Agreement between planned and delivered dose distributions for patient-specific SBRT quality assurance is assessed for a lung case utilizing the gamma index method ad dose volume histogram (DVH)-base metrics. The stereotactic approach requires a tight margin: the distance to agreement criterion is set to 1mm. The dose difference is set to 3% if a homogeneous phantom is used and 5% for calculations on a heterogeneous CT set.

Results: Results include 3D gamma evaluation and dose volume histogram (DVH). Volumetric, planar, and point dose comparison between measured and computed dose distribution agreed favorably indicating the validity of technique used for VMAT SBRT QA. Gamma pass rate in axial, coronal and sagittal plane through the isocenter is respectively 93,4%, 86,3% and 95,1% for pretreatment QA; 92,8%, 82,6% and 76% for in vivo QA. 3D values are 89,4% and 90%. Significant clinical structure values from DVH are shown in Table 1.

Table 1. Target and OAR DVH parameters for a lung case (54 Gy in 3 fractions)

Parameter	Treatment Planning	pre-treatment measurement	in vivo measurement
PTV - D98 (Gy)	52,90	49,50 (-6,4%)	52,25 (-1,2%)
PTV - D2 (Gy)	56,05	55,95 (-0,2%)	60,65 (+8,2%)
PTV - D50 (Gy)	54,75	55,85 (+2,0%)	57,25 (+4,6%)
PTV – Dmean (Gy)	54,64	55,85 (+2,2%)	57,10 (+4,5%)
Spinal Cord – D2 (Gy)	9,2	9,4 (+2,2%)	10,0 (+8,7%)
Spinal Cord – D1 (Gy)	9,6	9,7 (+1%)	10,3 (+7,3%)
Esophagus – V18Gy (cc)	0	0	0,06
Omolateral Lung V12Gy (%)	24,9	25,5 (+2,4%)	28,3 (+13,6%)

Conclusion: An efficient procedure of verifying VMAT lung SBRT plans with high accuracy has been obtained. Results from a clinical case are presented in terms of doses to the anatomical structures and in terms of gamma evaluation. Dosimetry Check system employes a pencil beam algorithm in order to calculate dose from fluence measurements taken with the EPID. It can be assumed that some dose differences will arise from the pencil beam algorithm used in Dosimetry Check and the more sophisticated algorithms used in TPS. Differences may depend on the level of heterogeneity of the anatomical site. Further research is needed to assess these differences.

EP-1601

Dosimetric consequences of using two common energy matching techniques in Monte Carlo

L. Shields[1], B. McClean[2]
[1]*University College Dublin/ St.Luke's Radiation Oncology Network, School of Physics/ Medical Physics, Dublin, Ireland Republic of*
[2]*St.Luke's Radiation Oncology Network, Medical Physics, Dublin, Ireland Republic of*

Purpose or Objective: The aim of this abstract was to report the observed differences between measured and Monte Carlo (MC) calculated dose distributions when using common incident electron energy matching techniques.

Material and Methods: PDDs and profiles on a 6MV Elekta Precise linac were acquired in a PTW MP3 watertank with a semiflex chamber (0.125cm3) at 90cm SSD. A MC model of the linac was created in BEAMnrc. Phase Space files were scored at 90cm from the target at a plane perpendicular to the direction of the beam. The phase space files were used as an input into DOSXYZnrc to calculate dose in a water phantom (60x60x30cm2, 90cm SSD, voxel size=0.3x0.3x0.3cm3). The incident electron beam was set to have a Gaussian distribution with a FWHM in the GT and AB directions of 1.92 and 2.42 mm respectively. The energy spectrum of the incident electron beam had a FWHM of 0.5MeV and an energy window of ±0.6MeV. The mean energy of the incident electron beam was determined in two ways:
Method 1:
The mean energy of the electron beam was varied until the calculated CAX PDD matched the measured for a 10x10cm2 photon field (between 5-25 cm). 40x40cm2 dose profiles (90cm SSD, 10cm deep) were subsequently calculated and compared to measurement. Method 2:
The mean energy of the electron beam was varied until the calculated 40x40cm2 dose profiles matched the measured profiles to within 0.5% (within 80% field width). A 10x10cm2 CAX PDD (90cm SSD) was subsequently calculated and compared to measurement.

Results:
Results - 1:
The agreement between calculated and measured 10x10cm2 CAX PDD was best (between 5-25cm) for an incident electron beam mean energy of 6.65MeV. The resultant 40x40cm2 profiles at 90cm SSD, 10cm deep, revealed a reduction in the dose horns of 4% in comparison to the measured profile (Figure 1).
Results - 2:
The agreement between calculated and measured 40x40cm2 profiles at 90cm SSD, 10cm deep was best for an incident electron beam with a mean energy of 6.2MeV. The resultant CAX 10x10cm2 PDD revealed an agreement to within 1% (between 5-25cm) of the measured PDD.

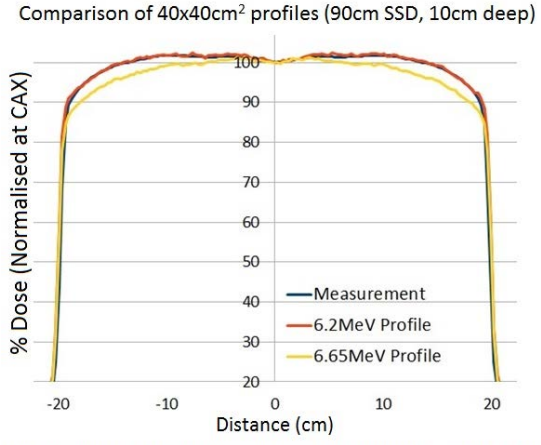

Figure 1. Comparison of profiles for the mean electron energy determined using both methods

Conclusion: The MC model of the linac revealed that CAX 10x10cm2 PDDs are not very sensitive to changes in the mean energy of the incident electron beam. However 40x40cm2 profiles reveal a high sensitivity to changes in the mean energy of the incident electron beam. The use of 10x10cm2 CAX PDDs to match the mean energy of the incident electron beam can result in undesired differences between measured and calculated 40x40cm2 profiles. However using 40x40cm2 profiles to match the mean energy of the incident electron beam can provide an overall better match to measurement of both PDDs and profiles.

EP-1602

Redefinition of the Electron beam treatment parameters for IORT applications

A. Krechetov[1], D. Goer[1]
[1]*Intraop Medical Corp, Research and Development, Sunnyvale, USA*

Purpose or Objective: The large number of conventional electron accelerators on the market (we estimate it around 5000) far exceeds the small, but growing number of mobile IORT linacs suitable for unshielded operating rooms. In this paper we discuss the technical aspects of the treatment beams produced by such small mobile IORT linacs. Beam parameter characterization for such machines need to be redefined in order to better reflect mobile IORT applications and provide basis for future technological development in the industry

Material and Methods: Using currently accepted industry standards, we compared the following electron treatment parameters of conventional and IORT linacs.
Treatment field size and shape
Penetration depth
Surface dose
Beam Penumbra and Flatness
Treatment on angular surface

Parameter	Conventional	Mobile
Treatment field size and shape	Standard field size is 10cm + and is constrained by the collimator and cutouts on the distal end of the applicator to form the treatment area.	Size of the field is less than 10 cm, often 4-6 cm diameter. Usually circular, but some oblong applicators are available
Treatment on angular surface	Soft bolus placed on the patient surface can compensate for inhomogeneous distribution of sloping surfaces	All IORT applicators have bevel ends of 0°, 15°, 30° and sometimes 45° to match anatomic planes. The larger the bevel, the greater the dose inhomogeneity across the field.
Penetration depth	Quantized with about 1 cm step (3 MeV equivalent)	Quantized with about 1 cm step (3 MeV equivalent)
Surface dose	There are attempts to reduce surface dose to spare the skin	Surface dose should be as close to 100% as possible to provide optimal treatment
Flatness	Beam is generally quite flat	Beam is generally less flat. Standard flatness definitions are often non-applicable
Penumbra of the beam	Treating at a 5 cm distance. Due to very good flatness inside the treatment area, penumbra of the beam only affects exposure of the healthy tissue outside the treatment field.	Treating in contact with the tissue. Metal applicators provide almost 100% protection of the tissue outside the applicator, and penumbra now affects cold spots inside the applicator

Table 1. Comparison of the critical beam characteristics for conventional linacs and mobile IORT linacs

Results: The following key beam parameters are either not controlled at all for IORT, or controlled in a way that is not very clear and effective. Flatness of the beam: Not well defined.For the applicators 6 cm and below current flatness definition produces no sensible beam characterization.
Penumbra: Not well defined. For beam sizes under 6 cm, the 1 cm wide penumbra might lead to as much as 30% of the treatment volume being either underexposed, or "not properly accounted for"
PDD drop off and Surface dose: Not controlled. PDD curve can change significantly as a function of field size and energy spectrum. An ideal monoenergetic beam has parameters which are not desirable in most IORT treatments.
Effective treatment volume: Not defined or controlled. Very critical parameter. Ratio of the treatment volume with delivered dose above treatment threshold (e.g. 90%) to the nominal treatment volume can be as low as 30% if cold sports are not properly accounted for.
Beveled applicator characteristics. Not defined or controlled. Procedures for testing of beveled applicators are very vaguely defined, and what definitions do exist are not very useful.

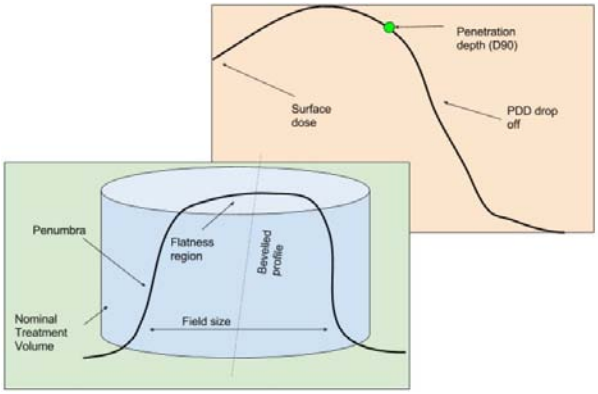

Conclusion: In order to properly redefine critical IORT beam parameters we present newly defined parameters such as controlled Flatness, PDD drop off, Surface dose and Effective treatment volume. When defined and controlled, these parameters will allow engineering teams to optimize the parameters of the treatment devices and provide the superior beam characteristics to improve treatment results.We also propose unified beveled and oblong applicator measurement protocol to summarize the knowledge currently present in the field.

EP-1603

Improved performance of the Varian TrueBeam Portal Dosimetry system for large fields

G. Beyer[1], P. Houston[2], L. Goodyear[3], P. Davies[3], J. McLellan[2]
[1]*Medical Physics Services Intl Ltd, Medical Physics, Cork, Ireland Republic of*
[2]*Aberdeen Royal Infirmary, Radiotherapy Physics, Aberdeen, United Kingdom*
[3]*North Middlesex University Hospital, Radiotherapy Physics, London, United Kingdom*

Purpose or Objective: The performance of the Portal Dosimetry (PD) used for pre-treatment verification is affected by the beam profile correction used in the MV imager dosimetry calibration. This study evaluates a simple method to improve the performance of the TrueBeam PD system.

Material and Methods: A 40x40 cm2 diagonal profile measured at dmax is used as part of the imager calibration for the Portal Dosimetry software (PDIP). An over-response of the measured dose to predicted dose as the distance increases away from the central axis has been reported. Previous publications relating to the IDU20 panel have shown that manually modifying each point of the diagonal profile or applying software corrections can improve this off-axis effect. This method can be time consuming. A solution for the IDU20 panel with the Clinac model is available as part of the Varian Pre-Configured PDIP Package that utilizes an improved beam profile correction but is not currently available for the TrueBeam. The diagonal profile at d5 cm is almost identical with the profile at dmax up to about 10 cm and deviates downward as the distance increases. Using this profile for the calibration process could improve the off-axis areas of mismatch. The response of measured doses with predicted PDIP doses were evaluated in Varian TrueBeams equipped with either the IDU20 or the new DMI MV imaging panel. The PDIP algorithm was configured for use at 100 cm SDD following the manufacturer's guidelines. Plans were created to compare the predicted with measured dose obtained by calibrating the imager at dmax and at d5 cm for 6X and 10X. Open fields and complex fluence patterns were compared to those predicted by the PDIP to evaluate the

effect of the diagonal profile calibration in the dose measurements.

Results: Measurements of open fields showed an over-response (>3%) between measured and predicted doses at distances beyond 5 cm from CAX for IDU20 and beyond 10 cm from CAX for DMI calibrated with dmax profiles. Profile analysis for a 30x30 cm2 field IDU20 panel calibrated using the d5 diagonal profile showed an improved match (<3%) up to X=12 and Y=8 cm for 6X and up to X=13 and Y=9 cm for 10X. The improvement for the DMI panel was up to 15 cm and 14 cm for 6X and 10X, respectively, in both X and Y (Fig. 1)

(a)

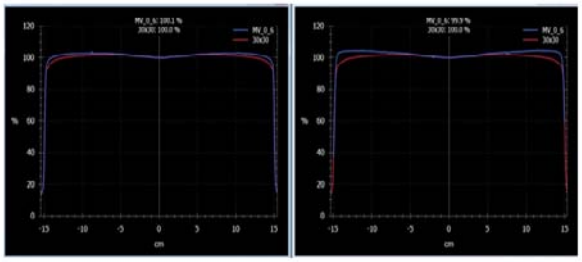

(b)

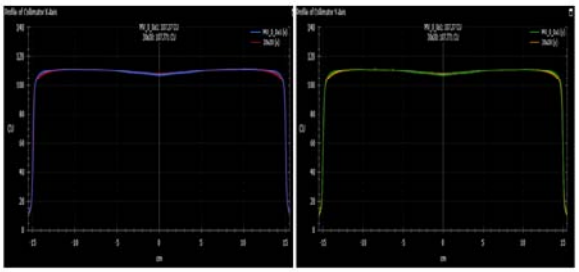

The backscatter from the IDU20 panel is not corrected with this method and resulted in an increased discrepancy in the Y direction. For the DMI panel, which has reduced backscatter, the calibration with the d5 profile yielded an excellent match between predicted to measured dose. Furthermore, for the DMI panel, the open fields gamma analysis improved by up to 5.3% for 6X and 15.2% for 10X. The test fluence patterns resulted in an improvement of up to 7.5% for 6X and 6.6% for 10X (Table 1).

Gamma analysis open fields (3%-3mm, 5% thresh.)				
Fluence field	Diagonal d=dmax		Diagonal d=5 cm	
Imager (X x Y)	6X	10X	6X	10X
Open 3 x 3	100.0%	100.0%	100%	100.0%
Open 5 x 5	100.0%	100.0%	100%	100.0%
Open 10 x 10	100.0%	100.0%	100%	100.0%
Open 15 x 15	100.0%	98.5%	100%	98.9%
Open 20 x 20	100.0%	97.2%	100%	98.0%
Open 30 x 30	94.7%	83.2%	100%	98.4%
Aida (25x12)	100.0%	100.0%	100.0%	100.0%
Chair (12x20)	99.9%	99.8%	99.9%	100.0%
Open (30x20)	100.0%	95.8%	100.0%	100.0%
Gradient (18x26)	100.0%	97.9%	100.0%	100.0%
Steps (30x16)	99.9%	94.4%	100.0%	98.3%
Steps (40x16)	88.1%	84.4%	95.6%	91.0%

Conclusion: The calibration of the imager panel using a diagonal profile at depth of d5 cm instead of the recommended depth of dmax resulted in an improved match between measured and predicted images for larger fields without affecting the results for smaller fields.

EP-1604

Evaluation of safety by skin dosimetry in Intraoperative Radiotherapy for breast cancer patients

I.H. Jung[1]
[1]*Gangnam Severance Hospital Yonsei Uinersity Health system, Radiation Oncology, Seoul, Korea Republic of*

Purpose or Objective: We investigated the safety of Intrabeam™ system, X-ray unit for intraoperative RadoioTheray (IORT) by measuring surface dose using Optically Stimulated Luminescent Dosimeter(OSLD).

Material and Methods: 30 patients were selected, who were in breast cancer patients and had an operation of breast conserving surgery (BCS). At the inner surface of tumor bed, 20 Gy were described, and 5 Gy at 1cm depth from the inner surface. Along the the size of tumor bed which could be decided after resection of tumor, the size of applicator were determined. Usual treatment time were from 18 to 40 minitutes. For the measurement of surface doses, OSLD were placed at superior (U1,2), inferior(D1,2), lateral(L1,2) and medial(M1,2) directions from the center of applicator. Each direction, two OSLD were placed at 0.5 cm and 1.5 cm from the center. Mean, maximum, and minimum doses were analyzed to be compared.

Results: Mean values were U1 2.23±0.80 Gy, U2 1.54±0.53 Gy, D1 1.73±0.63 Gy, D2 1.25±0.45 Gy, L1 1.95±0.82 Gy, L2 1.38±0.42 Gy, M1 2.03±0.70 Gy, and M2 1.51±0.58 Gy. Maximum values were 4.34 Gy at U1, and Minimum values were 0.45 Gy at M2. 13.3 % of patient (4pts out of 30) were reported that surface dose were over 4 Gy.

Conclusion: The fact that skin dose of all patients were less than 5 Gy based on OSLD measurement showed the safety of Intrabeam™ system. In the relatively small breast volume, the tendency that surface dose was increased had been shown, which was analyzed by the data of patients who irradiated over 4 Gy at skin surface. Therefore, for appropriate indication for IORT, it is suggested that breast volume as well as the size and position of tumor should be carefully considered.

Electronic Poster: Physics track: Radiation protection, secondary tumour induction and low dose (incl. imaging)

EP-1605

Dose from kV cone beam CT to lens, breast and gonads for children using different standard protocols

M.S. Assenholt[1], R. Hansen[1], J. Hansen[1]
[1]*Aarhus University Hospital, Cancer Department, Aarhus N, Denmark*

Purpose or Objective: With daily image guided kV cone-beam computed tomography (kVCBCT), dose to organs near the target can exceed 1 Gy during a treatment with 30 fractions. Treatment with proton radiation reduces the dose outside the tumor, and reducing the dose from kVCBCT gets even more relevant. Reducing the dose from kVCBCTs can be done by shrinking the area that receive kVCBCT or lower the dose used for the uptake of kVCBCT. Prior study showed that the mAs used for kVCBCT can be greatly reduced without reducing the image quality (B. Loutfi-Krauss, 2015). This study have measured and compared the dose to organs at risk in children using different kVCBCT protocols.

Material and Methods: The dose from kVCBCTs in the Varian TrueBeamTM accelerator were measured with thermolumenesence detectors (TLD), for lens, breast and gonads on CIRS anthromorphic children phantoms age 1, 5 and 10 years.
The kVCBCTs where performed with three different standard protocols: Head 1, Head 2, Thorax and Pelvis. In table 1 the settings for the different protocols can be seen.

Protocol	kV	mAs	CTDIw [mGy]	FOV [cm]	Length [cm]	kV source skan range
Head 1	100	146,4	2.8	26,2	17,7	90°->290°
Head 2	100	146,4	2.8	26,2	17,7	340°->180°
Thorax	125	264	3.5	46,5	16,1	360°
Pelvis	125	1056	13.9	46,5	16,1	360°

In figure 1 the difference in image quality can be seen going from 133 mAs (optimized protocol) to 1064 mAs (standard pelvic protocol).

Results: For a scan in the head region going from Head1 to Head2 protocol reduced the mean dose to lens. For the 1 year old child the dose is reduced from 6,6mGy to 1,7mGy. For the 5 years old child from 6,6mGy to 1,4mGy.
For the 10 years old child form 6,6mGy to 1,4mGy. For a scan in the Pelvis region changing the protocol from Thorax to Pelvis increased the dose to the Breast from 0,2 to 0,7mGy and Gonads from 13,6 to 57,8mGy for a 5 years old child. For a 10 years old child the breast dose is increased from 0,1 to 0,4 mGy and gonads from 11,8 to 46,0 mGy.
With daily image guidance kVCBCT is performed up to 30 times. For the five year old child it is an extra dose to the gonads of 30 x 44,2 mGy = 1,3Gy changing the protocol from thorax to pelvis.
As seen on figure 1 the image quality drops going from pelvis to thorax protocol in the pelvic areas, but the opportunity for bone match is just as good with the thorax protocol.

Conclusion: It matters what protocol is used for the kVCBCT uptake. It is possible to reduce the dose remarkably when choosing the most optimized protocol.
Changing the scan range for head to avoid the lens reduce the lens dose with 471%. Another area where the scan range could be of great interest is the thorax region for girls. The radiation sensitive breast tissue can be spared if an appropriate scan range is chosen.
The image quality drops when mAs is reduced. But be aware of the purpose of the image. Often it is not necessary to see the soft tissue, since a bone match is performed. Being able to evaluate on bones does not require a high image quality. The next step is to define new dose reduced protocols for kVCBCT for each age group 1, 5 and 10 years, and the work will be finished before ESTRO 2016.

EP-1606

Second cancer risk after RT for rectal cancer: 3DCRT vs VMAT using different fractionation schemes

D. Zwahlen[1], L. Bischoff[2], G. Gruber[3], U. Schneider[2]
[1]*Kantonsspital Graubünden, Department of Radiation Oncology, Chur, Switzerland*
[2]*University of Zurich, Faculty of Science, Zurich, Switzerland*
[3]*Klinik Hirslanden, Institute for Radiotherapy, Zurich, Switzerland*

Purpose or Objective: To investigate if VMAT shows any disadvantage in terms of reduction of second cancer risk (SCR) compared to 3DCRT using different high dose fractionation schemes in patients treated with RT for rectal cancer (RC)

Material and Methods: 25 patients with stage I-III RC and pre- or postoperative RT were included in this ethics-approved retrospective study. Planning CT data prior to RT were used. CTV for rectal cancer was delineated using RTOG contouring atlas. Organs at risk (OAR) (ICRP 2007) contoured on each CT data set were bladder, colon, sigmoid, bone, gonads, uterus, skin, small intestine, muscle, anus. PTV=CTV+5 mm. 3-field technique 6/15 MV 3DCRT and 6 MV VMAT plans were created (Eclipse, v.10, AAA-algorithm). Doses prescribed were 25x1.8 Gy and 5x5 Gy, respectively. Carcinogenesis model to estimate SCR emphasizes cell kinetics of radiation-induced cancer by mutational processes was used, integrating cell sterilization processes described by the LC model and repopulation effects. Model parameters were obtained by fits to epidemiological, cancer specific carcinogenesis data for carcinoma and sarcoma induction. From DVHs of structures of interest SCR in relation to organ equivalent dose (OED) was calculated. OED was converted to excess absolute risk for a western population for each organ as well as for all organs together. Resulting lifetime SCR from specific radiotherapy treatment was determined by lifetime attributable risk (LAR) by an integration of excess absolute risk from age at RT to lifetime expectancy (90 years)

Results: Mean LAR was highest for organs adjacent or close to PTV. Total LAR for VMAT and 3DCRT was 2.4-3.0% and 2.0-2.7%, respectively. For 5x5 Gy LAR was 1.4-1.9% for VMAT and 1.2-1.6% for 3DCRT and half as high as using 25x1.8 Gy. Median percentage LAR difference for OAR was significantly higher for VMAT irrespective of fractionation, and highest for bladder and colon. Individual differences in LAR ranged from 0.2-15.9% for 25x1.8 Gy and 0.1-9.6% for 5x5 Gy. Size and shape of PTV influenced SCR, and was highest for age ≤40 years. For a patient with additional lifetime of 60 years, LAR was 10% for 25x1.8 Gy and 6% for 5x5Gy. No difference was detected using VMAT or 3DCRT

Conclusion: For bladder and colon LAR is lower using 3DCRT, however difference is small. Compared to epidemiological data (Birgisson J Clin Oncol 2005) SCR is smaller when using a hypofractionated schedule treating RC. Total SCR is 2% at normal life expectancy. Risk is highest for young patients

EP-1607

CT imaging doses in radiotherapy – A single centre audit

K. Armoogum[1], G. Cornish[1], S. Evans[1]
[1]*Derby Hospitals NHS Trust, Department of Radiotherapy, Derby, United Kingdom*

Purpose or Objective: There is a growing awareness of dose delivered to parts the body outside the target volume during external beam radiotherapy. This concomitant dose could arise from external linac head leakage and scatter, scattered therapy dose outside the target volume, as well as non-therapeutic doses from imaging for planning and delivery, such as CT planning scans. Total concomitant dose has increased steadily with the introduction of more imaging procedures to the treatment process and the drive for better images quality. Much of this exposure is only loosely monitored and it could be the case that the cumulative concomitant dose has a negative biological effect even within the context of radiotherapy [1]. To quantify the dose contributed by CT planning scans, a retrospective dose audit was carried out on a TOSHIBA AQUILION LB multislice CT scanner at Derby Teaching Hospitals in July 2015.

Material and Methods: A cohort of 200 patients were identified, twenty each from ten of the most frequently used CT scanning protocols who were scanned in the 12 months immediately prior to the dose audit. Patients undergoing CT planning scans were initially identified in the Mosaiq Oncology Information System (Elekta, Crawley, UK) and subsequently interrogated via the PACSWeb system, (Centricity Enterprise Web V3.0, GE Healthcare, Barrington, IL). Data harvested from PACSWeb included: Number of slices, slice thickness, CTDIVOL, DLP, Patient sex, Patient Age, total scan time, transverse width and AP width. Mean Effective Dose (E) was derived from values of DLP for each examination using appropriately normalised coefficients. As yet, there are no published UK national guidelines for planning CT scans. However, to put the results of this audit into context we have compared local DLP and CTDIvol to similar values published for a previous UK national (diagnostic CT) dose audit [2]. The following relationships were

reported: CSA vs Age, CTDIvol vs CSA, DLP vs CSA, CTDIvol by Patient, DLP by Patient.

Results: The mean scan length, DLP, CTDIvol and Effective Dose by Protocol were found for each protocol. The most significant result was that the DLP values from the Head & Neck protocol were tightly clustered but higher than one would normally expect. The mean DLP was a factor of 4 greater than the head and neck reference level reported in the previous UK national (diagnostic CT) dose audit.

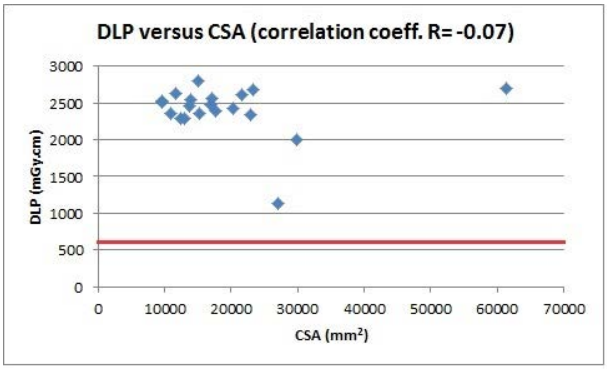

Conclusion: The results from this CT dose audit can be used as local Radiotherapy Imaging Reference Levels (RIRL). They will be able to guide protocol optimisation, allow comparison with other similarly equipped radiotherapy departments and participation in regional and national audits. The higher than expected DLP values for the Head & Neck protocol highlighted here has prompted a reassessment of the scanning parameters and may lead to protocol optimisation.

EP-1608

Radiation safety shielding for high dose rates from flattening filter free treatment modalities

S. Sawchuk[1], C. Lewis[1]
[1]*London Regional Cancer Centre - Victoria Hospital, Physics and Engineering, London- Ontario, Canada*

Purpose or Objective: Radiation safety for softer flattening filter free (FFF) treatment beams when operating at their very high dose rates should be considered over that of their flattening filter (FF) counterparts. Existing shielding is usually adequate when replacing treatment units utilizing beams of FF only with FFF-beams of the same nominal energy(1). However, depending upon the existing shielding composition and thickness, workload, and occupancy factors, the instantaneous dose rate (IDR) may present a radiation safety concern.

Material and Methods: A generalized analysis is presented with regards to replacing a unit which has only FF-beams to one with FFF-beams in a pre-existing bunker. Extra focus is placed on the situation that radiation levels around the treatment bunker are already at the radiation safety threshold for the unit being replaced. This threshold condition varies with the radiation safety regulations of the land. For example, the Canadian Nuclear Safety Commission (CNSC) imposes a condition that the IDR be less than 25 µSv/h to deem an area uncontrolled(3). The United States National Regulatory Council (US NRC) regulates the time averaged dose rate (TADR) to be less than 20µSv in any one hour(2).

Results: It is demonstrated that in switching to FFF-beam treatment units that protection using existing shielding is maintained for annual and weekly equivalent dose protection levels. However, it is possible for the CNSC IDR condition to be exceeded at the highest dose rates for FFF-beams. Thus shielding modification should be considered along with the ALARA principle(4). An analysis of the latter point is presented in general and by example from such a treatment unit replacement at the London Regional Cancer Program. The US NRC regulation is not as stringent as the Canadian condition and is almost impossible to exceed if the conditions before replacement were met. The analysis of this result is presented in general.

Conclusion: Care must be taken when considering thereplacement of radiation treatment units with FF-beams to those with FFF-beamswith respect to radiation protection. Radiation protection from the existingshielding is maintained for annual and weekly protection levels. However, IDR may present a radiation safety concern dependingupon radiation safety regulations in the country of its location. In Canada,the possibility exists that this threshold can be exceeded. The US NRCcondition is almost impossible to exceed.

References:
1. Phys. Med. Biol. **54** (2009) 1265–1273. S F Kry *et al.*
2. NCRP REPORT No. 151.(2005)
3. http://laws-lois.justice.gc.ca/eng/regulations/SOR-2000-203/page-7.html#docCont
4. http://www.nrc.gov/reading-rm/basic-ref/glossary/alara.html

EP-1609

CBCT and planar imaging dose for prostate and head-&-neck patients using 3 different imaging systems

Y. Dzierma[1], K. Bell[1], E. Ames[1], F. Nuesken[1], N. Licht[1], C. Rübe[1]
[1]*Universitätsklinikum des Saarlandes, Department of Radiation Oncology, Homburg/Saar, Germany*

Purpose or Objective: In image-guided radiotherapy, imaging dose varies greatly with the imaging technique. We here present imaging doses from planar and cone-beam CT (CBCT) imaging for three different on-board imaging techniques: the treatment beam line (TBL, 6 MV), a dedicated imaging beam line termed kView of nominally 1 MV (IBL), and a kilovoltage system (kVision) at 70-121 kV photon energy. We consider two collectives of patients with common IGRT indications: head-and-neck and prostate cancer.

Material and Methods: In this study, we retrospectively analyzed imaging dose of 54 patients with head-and-neck cancer and 53 with prostate cancer treated in 2013. For all patients, the number of verification images (CBCT and axes) was determined, separately for the three systems (more than 1000 images). The dose for each verification image was calculated in the Philips Pinnacle treatment planning system on a 2 mm grid using the collapsed cone algorithm. We evaluated the dose maximum and dose to the organs at risk, considering the total imaging dose, and for the techniques (6 MV, IBL, kV, planar vs. CBCT) separately.

Results: The calculated imaging doses are given in Table 1. Both the TBL and IBL modality entail considerable imaging dose, even for orthogonal axes. The maximum dose value for each image, averaged over all prostate patients, was 14.8 cGy (6 MV CBCT)/ 2.8 cGy (19 %; 6 MV axes)/ 10.5 cGy (71 %; IBL CBCT)/ 2.1 cGy (14 %; IBL axes)/ 3.8 cGy (26 %; kV CBCT), where percentage values refer to the 6 MV CBCT dose. As can be seen, kV CBCT still amounts to 26 % the imaging dose from MV CBCT, and about twice the dose from IBL axes. Averaged over the collective of head-and-neck cancer patients, the maximum imaging dose was 8.4 cGy (6 MV CBCT)/ 2.6 cGy (31 %; 6 MV axes)/ 6.2 cGy (74 %; IBL CBCT)/ 2.3 cGy (27 %; IBL axes)/ 0.9 cGy (11 %; kV CBCT). Here, the dose reduction from axial images was not as pronounced because less monitor units were used for MV CBCT. kV CBCT reduced the dose further because of low mAs values chosen by the auto-exposure mechanism.

Maximum imaging dose and dose to organs at risk (average over all patients, standard deviation in braces, in cGy), for selected organs at risk. On average, CBCT were taken for prostate cases using 16 MU for 6 MV and 15 MU for 1 MV. The average mAs-value for kV-CBCT was 778 mAs (between 441 mAs and 1132 mAs). For head-and-neck cancer, CBCT were taken using 7 MU for 6 MV and 6 MU for 1 MV; the average mAs-value for kV-CBCT was 118 mAs (between 99 mAs and 177 mAs).

	6 MV CBCT	6 MV planar	1 MV CBCT	1 MV planar	kV CBCT
Prostate cancer					
Maximum	14.8 (1.5)	2.8 (0.1)	10.5 (1.1)	2.1 (0.1)	3.8 (1.0)
Bladder mean	12.5 (1.3)	1.7 (0.1)	8.9 (0.9)	1.3 (0.1)	1.9 (0.4)
Rectum mean	12.6 (1.3)	1.4 (0.2)	9.0 (1.0)	1.0 (0.1)	1.9 (0.4)
Fem. head (l.) mean	12.3 (1.5)	1.9 (0.2)	8.6 (0.9)	1.5 (0.2)	2.0 (0.4)
Fem. head (r.) mean	12.2 (1.9)	1.3 (0.2)	8.6 (0.9)	0.8 (0.2)	2.0 (0.4)
Head-and-neck cancer					
Maximum	8.37 (2.74)	2.59 (0.16)	6.16 (2.66)	2.31 (0.09)	0.87 (0.20)
Spinal cord max	6.32 (2.07)	1.94 (0.07)	4.72 (2.15)	1.67 (0.08)	0.57 (0.14)
Brainstem max	6.16 (1.98)	1.96 (0.08)	4.11 (1.96)	1.49 (0.19)	0.45 (0.11)
Parotid (l) mean	6.58 (2.13)	2.18 (0.09)	4.75 (2.08)	1.86 (0.17)	0.51 (0.15)
Parotid (r) mean	6.22 (2.00)	1.68 (0.05)	4.42 (2.10)	1.26 (0.11)	0.52 (0.13)
Cochlea (l) max	5.86 (1.95)	1.91 (0.35)	3.77 (1.91)	1.44 (0.31)	0.39 (0.11)
Cochlea (r) max	5.66 (1.83)	1.57 (0.24)	3.59 (1.81)	1.10 (0.21)	0.39 (0.10)
Lens (l) max	5.73 (3.39)	2.08 (0.76)	4.51 (2.51)	1.54 (0.59)	0.34 (0.21)
Lens (r) max	5.56 (3.25)	1.84 (0.58)	4.40 (2.44)	1.33 (0.44)	0.35 (0.20)
Vocal cords mean	7.24 (2.37)	2.15 (0.08)	5.28 (2.33)	1.80 (0.18)	0.34 (0.17)

In our clinical setting, images were acquired at every second or third treatment fraction, resulting in a total median dose from imaging of 34.6 cGy for head-and-neck, and 70.6 cGy for prostate cancer patients. The relative frequency of the techniques and the contributions of the different techniques to the total imaging dose is shown in Figure 1.

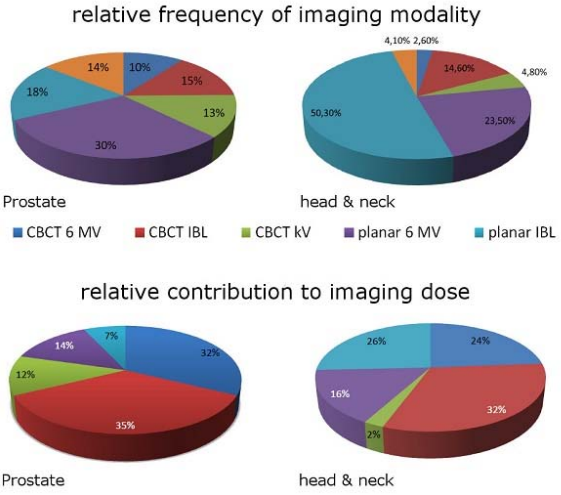

Conclusion: The contribution of planar images to the imaging dose is smaller than the dose due to megavoltage CBCT, but not negligible in the clinical routine due to the larger number of planar images. The kV imaging modality has very small overall contribution to the imaging dose, which mainly arises from 6 MV and IBL (the latter being more frequently employed and therefore more prominent in the dose contribution).

EP-1610

A practical approach to assess cumulative dose of CBCT using standard CT dosimetry system

A. Abuhaimed[1], C. J Martin[2], M. Sankaralingam[1], K. Oommen[1], D. J Gentle[3]

[1]Beatson West of Scotland Cancer Centre, Radiotherapy Physics, Glasgow, United Kingdom

[2]University of Glasgow, Department of Clinical Physics, Glasgow, United Kingdom

[3]Gartnavel Royal Hospital, Health Physics, Glasgow, United Kingdom

Purpose or Objective: In recent years, dosimetry in cone beam computed tomography (CBCT) has become an issue as the standard dose index used for CT dosimetry (CTDI100) fails to provide a satisfactory estimation of dose for CBCT scans. AAPM TG-111 proposed replacements of the CTDI100 with a measurement of a cumulative dose to address the problem. The cumulative dose for CBCT scans f(0) is a point dose measured using a small ionization chamber in the middle of a cylindrical PMMA, polyethylene, or water phantom of length ≥450 mm to achieve scatter equilibrium. Although this method overcomes the limitations of CTDI100, the use of longer phantoms is impractical in the clinical environment. A practical approach based on using the standard CT dosimetry system was introduced to assess f(0).

Material and Methods: A function called Gx(W)100 was introduced in this study. It was defined as the ratio of f(0) to a dose index f100(150), which was proposed for CBCT dosimetry and equals the cumulative dose averaged over the length of a standard 100 mm CT pencil ionization chamber and measured within standard 150 mm long PMMA CTDI phantoms. Monte Carlo BEAMnrc and DOSXYZnrc codes have been used to simulate the On-Board Imager (OBI) system, and to calculate f100(150) and f(0). Standard 150 mm CTDI phantoms were simulated to calculate f100(150), whereas infinitely long PMMA, polyethylene, and water phantoms were used for f(0). The phantoms were in different diameters to represent head and body of an adult patient, a body polyethylene phantom being equivalent to the ICRU-AAPM phantom. f100(150) and f(0) were measured at the centre and periphery of the phantoms using beams of width 40-500 mm and beam qualities of 80-140 kV. Gx(W)100 was evaluated under different conditions with f100(150) and f(0) calculated with the same beam width (W) and at the same position (centre or periphery).

Results: Under the different conditions, Gx(W)100 showed a weak dependency on tube voltage over the range 80-140 kV. Gx(W)100, however, was influenced by diameter and composition of the phantom. Therefore, a set of Gx(W)100 functions based on the diameter and composition was developed to assess f(0) in a given long phantom from f100(150) measurements obtained within the short phantoms. Gx(W)100 provides a practical approach to avoid the use of long phantoms, which are impractical in the clinical environment, and hence simplify the AAPM method. Since the CT dosimetry system used for f100(150) is available worldwide, this approach could help to maintain the standard equipment. The Gx(W)100 functions used in this study have been applied to a CT scanner, and showed a weak dependency on the scanner type. This gave an indication that Gx(W)100 may be comparatively independent of the type of imaging system.

Conclusion: Gx(W)100 function was proposed in this study, and was relatively independent of tube voltage and may be independent on the scanner type. Gx(W)100 allows measurement of f(0) using the AAPM method with standard CT dosimetry equipment.

EP-1611

Evaluation of organ dose according to cone-beam CT scan range using Monte Carlo simulation

S.S. Lee[1,2], S.H. Choi[2,3], D.W. Park[4], G.S. Cho[2], Y.H. Ji[1,2,3], S. Park[2], H. Jung[1,2], M.S. Kim[1,2,3], H.J. Yoo[3], K.B. Kim[1,2,3]

[1]University of Science and Technology, Radiological & Medico-Oncological Sciences, Daejeon, Korea Republic of

[2]Korea Institute of Radiological and Medical Sciences, Research Center for Radiotherapy, Seoul, Korea Republic of

[3]Korea Institute of Radiological and Medical Sciences, Department of Radiation Oncology, Seoul, Korea Republic of

[4]Inje University Ilsan Paik Hospital, Department of Radiation Oncology, Seoul, Korea Republic of

Purpose or Objective: The CBCT(Cone-beam CT) is an image guided system verifying the precise location of tumor before the radiation treatment such as IMRT(Intensity-modulated radiotherapy) and SBRT(Stereotactic body radiotherapy) for accurate radiotherapy. However, the frequent use of CBCT scanning can induce the secondary tumor due to increase of radiation exposure to patients. With the CBCT scanning, treatment volume can be verified locally by changing the CBCT scan range. In this study, we evaluated regional organ dose according to CBCT scan range with Monte Carlo simulation.

Material and Methods: We modeled the CBCT system which built-in Varian Clinac iX with full-fan and half-fan filter by using the Monte Carlo code(MCNPX 2.7.0). By acquiring the measured data with EBT3 films for PDD(percent-depth dose) and beam profile for open, full-fan and half-fan filter in static mode, we verified that simulated data was coincided with measured data for spectrum. The assessment of absorbed dose of each organ during the CBCT scanning was performed with ORNL(Oak Ridge National Laboratory)-male-MIRD(Medical Internal Radiation Dose) phantom. In this study, we set the scan range adapted for the CBCT scan conditions and then the absorbed dose of each organ was evaluated applying a half-fan filter. In that time, the CBCT scan range was changed by modulating the Y jaw from 16 cm to 8 cm at intervals of 2 cm and we verified the difference of absorbed dose of each organ according to CBCT scan range.

Results: For CBCT scan in thorax, the absorbed dose of heart and lung were reduced for 46.6~32.1 mGy and 75~47.4 mGy, respectively, and the other side lung was reduced for 31.7~19.1 mGy. As the scan range was decreased at intervals of 2 cm, the absorbed dose in lung was reduced up to 10 %. In the case of heart, the absorbed dose was reduced drastically. For prostate, absorbed dose of bladder, sigmoid colon and testes showed dose reduction for 61.4~41.7 mGy, 50.4~38.8 mGy and 81.1~45.4 mGy, respectively. In the case of penis, the absorbed dose was reduced from 81.1 to 45.4 mGy.

Conclusion: We evaluated the change of organ dose according to CBCT scan range with Monte Carlo code MCNPX and male-MIRD phantom. In the result, we verified the organ dose can be different about 30~40% according to changes of CBCT scan range. We thought this study can be used in optimization for radiation exposure to patients, usefully.

EP-1612

Optimizing breast imaging dose in CBCT using patient specific acquisition parameter

S. Deshpande[1], D. Dhote[2], K. Thakur[3], M. Kumar[4], R. Kumar[4], A. Pawar[3], A. Sutar[1], S. Naidu[1], V. Kannan[1]
[1]*P.D. Hinduja National Hospital, Oncology, Mumbai, India*
[2]*Brijalal Biyani Mahavidyalaya, Department of Eletronics, Amravati, India*
[3]*Holy Spirit Hospital, Department of Radiation Oncology, Mumbai, India*
[4]*Bhabha Atomic Research Center, RPAD, Mumbai, India*

Purpose or Objective: Defining patient specific Cone beam computed tomography (CBCT) acquisition parameter to optimize breast imaging dose

Material and Methods: Since last few years, in-room volumetric imaging systems which include MV computed tomography (CT) and MV or kV cone-beam computed tomography (CBCT) are being used for greater soft tissue definition and improved target localization. This technology helps in escalating target dose while decreasing normal tissue doses. This improves the therapeutic ratio of radiotherapy. Intense IGRT protocols are adopted to reduce the PTV margin and to understand changes happening during course of treatment. Additional imaging dose due to intense IGRT protocol is concern for deterministic and non-deterministic radiobiology effect. In this study we measure imaging dose to breast in thorax region from Varian on board imaging CBCT Three OSL dosimeters were placed on the contra lateral breast. One dosimeter was placed at centre and other two dosimeters were placed 5 cm apart from centrally placed dosimeter. Low dose thorax imaging protocol was used for all measurements. All CBCT acquisitions were performed with fixed geometry for all measurements. CBCT images were acquired with half-fan cone with bow tie filtration, source-detector distance of 150 cm, 0.25 cm slice thickness, transversal field-of view (FOV) of 25 cm, and a scan length of 18 cm giving a longitudinal FOV of approximately 17.5 cm. Scans were performed with 200 degree rotation of gantry. To get a reasonable signal, dosimeters were irradiated during five consecutive treatment fractions for the CBCT imaging protocols. For same patients CBCT images were acquired using modified low dose thorax protocol also. In modified Low dose thorax protocol tube current was reduced from 20mA to 10 mA. Dose to contra lateral breast was measured in same three positions

Results: The absorbed dose per fraction using the CBCT for standard low-dose thorax protocol was 9 ± 0.30 mSv; for the "Modified Low dose thorax" protocol it was 4.8 ± 0.21 mSv; it can be seen that the "Modified Low dose thorax" protocol results in a reduction of 51% in absorbed dose compared to the standard low-dose thorax protocol. It was also noticed that, by changing acquisition parameters quality of both scans were comparable.

Conclusion: It is important to have patient specific acquisition protocol rather than vendor supplied protocol so that imaging dose can be optimized.

EP-1613

Comparison of peripheral doses associated to SBRT, VMAT, IMRT, FFF and 3D-CRT plans for lung cancer

L. Irazola[1], M. Ortiz-Seidel[2], S. Velázquez[3], M. García-Hernández[4], J. Terrón[2], B. Sánchez-Nieto[5], M. Romero-Expósito[6], J. Roselló[4], F. Sánchez-Doblado[7]
[1]*Universidad de Sevilla, Departamento de Fisiología Médica y Biofísica, Seville, Spain*
[2]*Hospital Universitario Virgen Macarena, Servicio de Radiofísica, Sevilla, Spain*
[3]*Hospital Universitario Virgen del Rocío, Servicio de Radiofísica, Sevilla, Spain*
[4]*Hospital General Universitario, Servicio de Radiofísica ERESA, Valencia, Spain*
[5]*Pontificia Universidad Católica de Chile, Instituto de Física, Santiago, Chile*
[6]*Universitat Autònoma de Barcelona, Departamento de Física, Barcelona, Spain*
[7]*Universidad de Sevilla, Departamento de Fisiología Médica y Biofísica, Sevilla, Spain*

Purpose or Objective: Out-of-field doses during radiotherapy treatments (RT) are associated with an increased risk of second malignant neoplasms in cancer survivors. The purpose of this work is to evaluate the impact, in terms of peripheral dose (PD), that new techniques for lung cancer such us stereotactic body radiotherapy (SBRT), modulated beams (IMRT and VMAT) and FFF would have in comparison to more traditional plans (3DCFRT).

Material and Methods: Self-developed models [1,2] were used for neutron and photon peripheral dose (NPD and PPD, respectively) estimation to 12 organs, associated to lung treatments delivered using 3 linacs: Siemens Primus (6&15 MV), Elekta Synergy (6 MV) and Varian TrueBeam (6,10&15 MV; FFF mode available for the first two). Facilities were previously characterized in terms of neutron production [3] and photon leakage.
17 plans were generated for a lung cancer case (60 cGy to 100%).Different PTVs were used for conventional and stereotactic treatments (factor of 20 between both volumes). Results were compared to values from the literature [4] where PD studies were done but by terms of direct measurements of only photon component for few external points.

Results: Figure (a) shows estimated NPD and PPD to some selected organs for SBRT treatments in 6 and 10 MV, including FF and FFF modes. Figure (b) shows average PPD to the same representative out-of-field organs (mSv) for 4 studied techniques, considering all the linacs and plans.

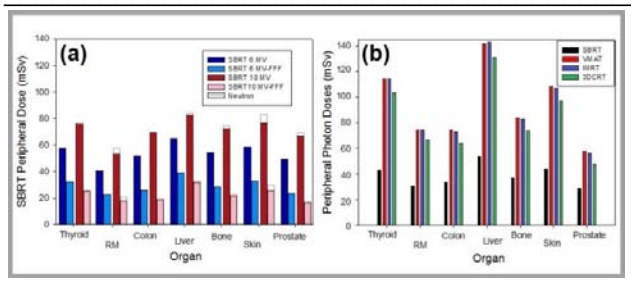

As an example, differences in PPD and NPD, for 3D-CRT and IMRT in low and high energies, are shown in the table. Taking into account leakage, field size and MU, an average increase in PPD values of 8.6% and 12.6% has been obtained for Varian and Elekta linacs with respect to Siemens, when considering for the here studied 3D-CRT treatment in 6 MV. However, a decrease in 19% was noticed when using FFF mode.

Organ	3D-CRT			IMRT		
	6 MV	6&15 MV		6 MV	6&15 MV	
	Photon	Photon	Neutron	Photon	Photon	Neutron
Thyroid	96.35	108.85	3.18	114.00	113.90	5.12
Red Marr.	62.35	71.30	8.98	73.45	74.75	9.24
Colon	60.10	72.85	0.95	69.15	77.40	0.93
Bladder	48.00	60.85	5.08	54.35	65.25	5.04
Liver	122.00	134.50	3.32	145.50	140.00	3.49
Bone	68.75	81.55	5.05	79.85	85.95	5.86
Skin	90.35	103.05	16.96	106.50	107.75	23.13
Remainder	83.30	93.30	2.56	99.00	97.45	3.42

Values in mSv

Conclusion: Lower PD in SBRT cases could be due to the smaller size of ITV vs. conventional PTV. Our results are in agreement with previous clinical studies [4]. Additionally, we have quantified the advantage of reduced PD when using FFF mode. However, this study only considers PD while ignoring the impact of radiobiological effect due to the dose per fraction.
The slight differences found between techniques (3D-CRT, IMRT and VMAT) are due to the simple case chosen (in terms of target geometry). Nevertheless, the tendency shows higher values for VMAT and IMRT. Thus, further studies are desirable to extrapolate these results to complex cases.
Neutron contributes in a small percentage to global PD, this becomes especially relevant if 15 MV represents only a part of the total treatment.

Ref.
[1]Phys Med Biol 2012;57:6167–6191
[2]*Biomed Phys Eng Express. Analytical model for photon peripheral dose estimation in radiotherapy treatments. Sánchez-Nieto B et al.* In press
[3] Med Phys 2015;42:276-281
[4] PLoS ONE 2015;10(7):e0127501

EP-1614

Comprehensive validation of a Monte Carlo kV-CBCT model using OSL and spectral measurements

H. Chesneau[1], D. Lazaro[1], J. Plagnard[1], C. Lafond[2], O. Henry[2], V. Blideanu[1]
[1]*CEA LIST, LIST, Gif sur Yvette, France*
[2]*Centre Eugène Marquis, Medical Physics, Rennes, France*

Purpose or Objective: The use of Cone-Beam computed Tomography (CBCT) is progressively increasing in radiotherapy treatments, but additional doses induced are not well quantified and could amplify the risk for patients to develop a second cancer. There is a need, expressed by the medical physics community, to develop tools to estimate, report and potentially help reducing CBCT doses. We hence developed a Monte Carlo (MC) model for the XVI kV-CBCT system. The dosimetric and geometric accuracy of the simulated beams was evaluated by comparisons with measurements in a water tank, and x-ray energy spectra acquisitions. Before clinical use, the model requires an evaluation in anthropomorphic phantoms in which were inserted OSL NanoDots (Landauer). The purpose of the present study is to develop an accurate dosimetric protocol taking into account for OSL energy dependence in keV energy range.

Material and Methods: A MC model of the XVI was developed using the PENELOPE code. The dosimetric and geometrical evaluation of the beam MC models was performed by comparing simulations with lateral and depth-dose profiles measured using a PTW Farmer-type chamber, and on-axis energy spectra measured with a CdTe detector. These comparisons were performed at 120, 100 and 80 kVp, and for different filtration/collimation couples. For OSL measurements, the first step was to perform, in different beam qualities, in-air cross-calibrations with a PTW Farmer-type chamber. At this energy range, OSL exhibit strong energy dependence, so the signal needs to be corrected for the spectral variations between calibration and measurement conditions. Thus, to ensure accurate dose measurements, a correction method was developed using calculated spectra. The dosimetric protocol was validated by performing dose profiles with OSL inserted in a PMMA tube submerged in water. Preliminary comparisons with XVI model were made with acquisitions in a home-made heterogeneous phantom consisting of a water tank equipped with PMMA, bone and lung equivalent inserts.

Results: Experimental and simulated lateral and depth-dose profiles, and energy spectra, are in excellent agreement (Fig 1A).These results validate that the MC model accurately reproduces the dosimetric and geometric properties of the XVI beams. The uncorrected OSL profiles in the PMMA tube over-estimate by 15 % the calculated doses. However, energy corrected measurements are matching the simulations and the differences not exceed 7.5 % (Fig 1B and 1C). Table 1 presents doses measured at different points in the heterogeneous phantom and discrepancies not exceed 11.3 %.

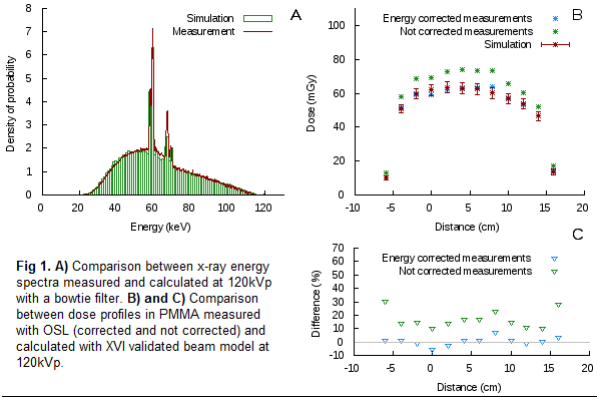

Fig 1. A) Comparison between x-ray energy spectra measured and calculated at 120kVp with a bowtie filter. **B) and C)** Comparison between dose profiles in PMMA measured with OSL (corrected and not corrected) and calculated with XVI validated beam model at 120kVp.

Location in the phantom	Simulated doses (mGy)	OSL measurements (mGy)	Differences (%)
Lung (1)	23.5 +/- 0.3	25.6 +/- 2.1	9.0
Lung (2)	25.6 +/- 0.3	28.8 +/- 2.3	11.3
PMMA (1)	18.7 +/- 0.3	18.5 +/- 1.5	1.1
PMMA (2)	20.1 +/- 0.3	19.8 +/- 1.6	1.2
PMMA (3)	17.3 +/- 0.2	15.7 +/- 1.2	10.2

Table 1. Comparisons between OSL measurements in the heterogeneous phantom and simulations for a 360° CBCT acquisition at 120 kVp with a M20 type collimator.

Conclusion: The dosimetric protocol developed for OSL allows accurate measurements of imaging doses, and will be then used to validate the dose calculation tool in pre-clinical conditions. Preliminary results obtained in the home-made phantom highlight the accuracy of XVI MC model. Further validations are on-going in anthropomorphic phantoms.

EP-1615

Decreasing cone beam CT scan`s doses and duration for breast cancer

T. Bora[1], I.F. Durmus[1], M.V. Ertekin[1], E.M. Fayda[2], S. Tokdemir Ozturk[3]
[1]*Yeni Yuzyil University Medicine Faculty Gaziosmanpasa Hospital, Radiation Oncology, Istanbul, Turkey*
[2]*Istanbul University, Oncology, Istanbul, Turkey*

[3]Gebze Technical University, Physics, Kocaeli, Turkey

Purpose or Objective: o evaluate an automatic registration of partial cone beam CT scan's and full cone beam CT scan's position errors, durations and doses for Breast Cancer

Material and Methods: Before the IMRT treatment's of breast cancer patients using Versa HD, five breast cancer patients were scanned in the same position with partial cone beam CT and a full cone beam CT in sequence. The patient position errors were determined using automatic registration methods in both cases. The full cone beam CT parameters corresponded to the default VolumeView "Chest M20" preset in XVI 4.5; 360 degree, 180 deg/min velocity, 120 kV, 660 frames, 1056mAs and nominal scan dose of 22mGy. Partial cone beam CT parameters were set by us, we choosed S20 filter instead of M20 filter and for right breast; gantry angle was CW direction from 180° to 10°, for left breast; gantry angle was CW direction from 300° to 130°, 180deg/min velocity, 100 kV, 366 frames, 585.6mAs. Both cone beam CT scans were performed in sequence for five patients and position errors in 3 diemensions recorded using automatic registration method with for rotational bone value registration, gray value registration and rotational gray value registration.

Results: We compared partial cone beam CT scan's position errors with full cone beam CT scan's position errors. Firstly, we found an average difference of 1,46mm in lateral direction, 1.80mm in longitudinal direction and 1.96mm in vertical direction difference for bone value rotational automatic registration. Secondly, we determined an average 1,24mm in lateral direction, 1,36mm in longitudinal direction, 1,30mm in vertical direction difference for gray value rotational automatic registration. Thirdly, we determined an average 1,56mm in lateral direction, 1,88mm in longitudinal direction, 1,52mm in vertical direction difference for gray value automatic registration.

Conclusion: Most probably these differences are resulting from time difference between two cone beam CT scans and also it could be related with patient's breathing phase during scanning. Altough the partial cone beam CT scan's image quality were worde than with full cone beam CT scan the automatic registration parameter's difference were below 2,0mm in 3 dimensions. When we measured radiation at the isocentre point using cylindrical ion chamber wih 30 cm x 30 cm solid phantom for both cone beam CT tecniques, radiation dose decreased % 55±5 with partial cone beam CT scan. Additionally, Cone beam CT scan's duration decreased %40 with partial cone beam CT scan.

EP-1616

Secondary cancer induction of VMAT technique in breast irradiation: organ equivalent dose estimation

G. Guidi[1,2], N. Maffei[1,2], F. Itta[2], E. D'angelo[3], B. Meduri[3], P. Ceroni[1], G. Mistretta[1], A. Ciarmatori[1,2], G. Gottardi[1], P. Giacobazzi[3], T. Costi[1]
[1]Az.Ospedaliero-Universitaria di Modena, Medical Physics, Modena, Italy
[2]University of Bologna, Physics and Astronomy, Bologna, Italy
[3]Az.Ospedaliero-Universitaria di Modena, Radiation Oncology, Modena, Italy

Purpose or Objective: Secondary cancer induction is a severe effect of Radiation Therapy (RT) treatments. Volumetric Arc Therapy (VMAT) techniques delivery dose distribution with a significant area and organs involved of low dose. We have evaluated, from the dosimetric data of patients treated using VMAT practice, the risk for contralateral breast and lung secondary tumor, estimating the Organ Equivalent Dose (OED).

Material and Methods: 30 patients, treated with VMAT techniques for breast cancer, were analyzed using the dose distribution. Based on the anatomical side of treatment (right and left side), the cohort was divided in two groups of treatment. We have calculated the OED of ipsilateral and contralateral organs, relatively to the breast and lung tissues. Using the bell shaped model formula, we obtained the OED from the dose volume histogram (DVH) of each organ. Using a MATLAB® toolbox (DVH analyzer), the estimation of the OED values for contralateral and ipsilateral organ was assessed.

Results: The results, summarized in Figure1 and Table1, showed a mean ODE of +2,09±0,32Gy for contralateral lung, +1,94±0,32Gy for ipsilateral lung and +2,55±0,61Gy for contralateral breast. An ANOVA analysis showed that the side of treatment (left or right) was irrelevant for OED estimation (sign.≈1), confirming the independence by the VMAT techniques applied. The study confirmed that contralateral organs are the major tissue involved in risk of the secondary cancer risk, in particular for the contralateral breast. The OED showed, per patients' treated group, a variability of [2,1÷3,1] Gy for the right side and [2,2÷3,8] Gy for the left side. The OED for lung and contralateral lung had less variability in case of treatment. According with the radio sensitivity of the breast tissue, a special attention should be applied during the optimization and treatment to avoid possible variability in inducted cancer risks.

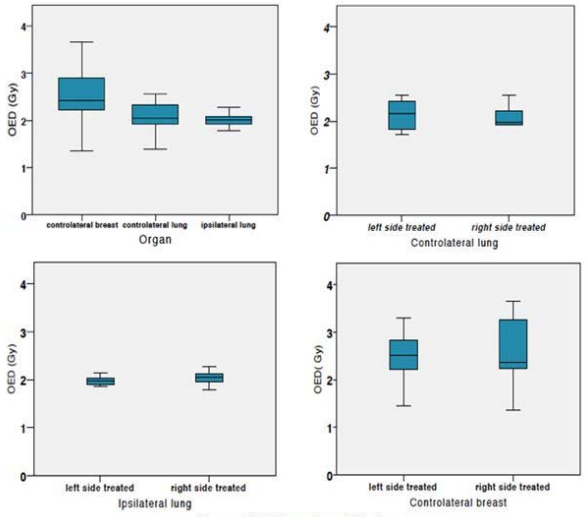

Figure 1 OED vs. irradiated organs

	Contralateral lung	Ipsilateral lung	Contralateral breast
ODE (Gy) All patients	2,09 ± 0,32	1,94 ± 0,32	2,55 ± 0,61
ODE (Gy) Left side	2,15 ± 0,33	2,00 ± 0,42	2,49 ± 0,51
ODE (Gy) Right side	2,03 ± 0,30	2,04 ± 0,16	2,61 ± 0,72

Table 1 OED vs. irradiated organs

Conclusion: The ODE data and bell shaped model, obtained from the DVH curves, can be used for the prediction of radiation secondary cancer induction. The OED values obtained showed the low risk of secondary cancer induction of the VMAT techniques compared with other literature data. Most uncertainties still remain related the time patterns of cancer induction and the specific dependencies to the organs rates. For RT plan optimization these factors are irrelevant; therefore, to endorse the safety distribution obtained by VMAT techniques, mathematical models obtained by the DVH and OED should be investigated with epidemiological absolute risk data of large patients' database.

EP-1617

Pre-treatment and in vivo fetal dosimetry in brain radiotherapy treatment during pregnancy

M. Valenti[1], M. Parisotto[1], C. Ardito[1], M. Puschi[1], S. Costantini[2], M. Cardinali[2], S. Maggi[1]
[1]Azienda Ospedaliero Universitaria Ospedali Riuniti, Medical Physics, Ancona, Italy
[2]Azienda Ospedaliero Universitaria Ospedali Riuniti, Radiotherapy, Ancona, Italy

Purpose or Objective: Radiotherapy treatment of pregnant women is a relevant problem in term of fetus radioprotection. A preliminary dosimetric evaluation of fetal dose could influence clinical decision of patient irradiation and, once the treatment has been approved, an accurate dose evaluation is important to estimate fetal radiation exposure risks. Fetal dose irradiation risks are described in AAPM report n.50 [1] and ICRP 84 [2] where is proposed a fetal dose limit of 10 cGy. In this work we describe dosimetric measurements related to a brain treatment for a pregnant woman in term of: preliminary measurements for optimal plan parameters assessment, pre-treatment in phantom dose measurements of approved plan and in vivo dosimetry to confirm pre-treatment evaluation.

Material and Methods: Treatment has been performed with 3DCRT on a Clinac 21 EX with dose of 60Gy in 30 sessions. At the time of dose evaluation patient was in 22° week of pregnancy. Distance from umbilicus to lower field edge is 53cm. Preliminary and pre-treatment measurements have been performed with both farmer ionization chamber in Rando phantom modified adding a water phantom and with TLD 100 in Rando phantom with bolus. Use of bolus over Rando phantom reproduces in a better way patient shape and dimension. During all treatment we perform daily in vivo TLD dosimetry. In preliminary measurement session we evaluate relation between fetal dose and: field dimension, collimator rotation, presence of MLC, use of enhanced dynamic wedge (EDW) and thickness of lead shielding. We also study change of dose with distance from radiation field edge and with measurement depth.

Results: About treatment parameters we observed an important dose reduction using 90° collimator rotation and using MLC [4]. Fetal dose increase with EDW is acceptable only for small angles. The more relevant parameters related to dose increase are distance from field edge and field dimension. These are anatomy related parameters and cannot be optimized. Considering measured value of fetal unshielded dose (in the range of 1-2 cGy) we decide to use 8mm thickness lead shielding [3]. In preliminary phase we observed a little increase in dose with depth as reported in [5]. Result of pre-treatment and in vivo measurement is reported in table 1.

Conclusion: Treatment parameters like collimator rotation, MLC or EDW strongly influence fetal dose. This aspect must be considered in patient plan preparation. Pre treatment dosimetry is important to estimate fetal clinical irradiation risk and to evaluate the need and thickness of lead shielding. In vivo dosimetry is always important to confirm pre treatment dose evaluation. Differences between pre treatment and in vivo dosimetry should be attributed to differences in patient and phantom shape, dimension and internal structure. In our case we can give a precautionary estimation of fetal dose of 1.6 cGy, a value below 10cGy limit proposed by [1.2]

[1] Stovall
[2] ICRP 84
[3] Haba
[4] Sharma
[5] Sneed

EP-1618

IGRT Cone Beam CT : a method to evaluate patient dose

F.R. Giglioli[1], O. Rampado[1], V. Rossetti[1], M. Lai[1], C. Fiandra[2], R. Ropolo[1], R. Ragona[2]
[1]*A.O.U. Città della Salute e della Scienza di Torino, Physics Department, Torino, Italy*
[2]*University of Torino, Radiation Oncology Department, Torino, Italy*

Purpose or Objective: to calculate organ doses for several protocols of a radiotherapy cone beam equipment using the PCXMC software, validated comparing doses with TLDs. Furthermore a set of coefficients to provide an estimation of organ doses was assessed for patients of different genders and sizes.

Material and Methods: The system in use was an Elekta CBCT (XVI) and the protocols analysed were four: head, pelvis, chest and chest4D with different parameters. The first part of the study investigated the opportunity to use PCXMC, a software based on Montecarlo simulation generally employed for projective radiology, for calculating organ doses. This commercial software allows the user to specify patient age and size, radiation beam geometrical setup, beam energy, filtration; a dosimetric indicator (entrance skin dose or DAP) is required to calculate final organ and effective doses. A new version of the software introduces the possibility to simulate rotational beams, subdividing the exposure in single contributions at different angles and performing the total doses calculation in a batch way. The software was adapted to better simulate the modulated filtration of this particular CBCT considering different filtered beam contributions. A set of 50 TLDs (Harshaw – TLD 100) was selected, irradiated and analysed, for each protocol, to compare measurements with PCXMC results. The influence of patient size on organ dose was evaluated varying heights, weights and genders. Three levels of height and weight corresponding respectively to the 5th, 50th and 95th percentile of US males and females adult population were considered. The organ doses were normalized to the PCXMC standard adult phantom doses and the calculated ratios were plotted versus the equivalent diameter of each patient size.

Results: The differences between PCXMC and TLDs doses are shown in table I for different protocols;

Protocol	Organ	PCXMC	TLD	diff%
Head and neck S20	Oral mucosa	0.89	0.82	*8*
	Salivary	0.93	0.95	*-3*
	Respiratory airways	0.84	1.01	*-16*
Simmetry S20 F0	Lungs	8.9	7.94	*12*
	Heart	10.1	10.18	*-1*
	Breasts	15.6	15.98	*-2*
Chest M20 F0	Lungs	21.7	19.1	*14*
	Heart	20.4	20.2	*1*
	Breasts	21.3	19.2	*11*
Pelvis M20 F1	Ovaries	19.7	22.3	*-12*
	Colon	16.4	18.21	*-10*
	Prostate	16.0	13.52	*18*
	Bladder	22.5	21.45	*5*

Table I Comparison of organ doses in mGy evaluated by TLD measurements in Rando phantom and by the PCXMC software.

The respiratory airways and the prostate show a difference over 15%, probably as a consequence of their position at the boundaries of the beam, with a critical match of exposure geometry for actual and virtual anthropomorphic phantoms. Regarding simulations with patients of different heights, weights and genders a variability in a range ±40% for pelvic region and ±30% for chest was observed; specifically, for the same acquisition protocol, organ doses for a slim patient could be much higher than the organ dose of an overweight patient. Fig 1 shows, as an example, dose correction factors versus equivalent diameters for breast with different protocols and relative fits.

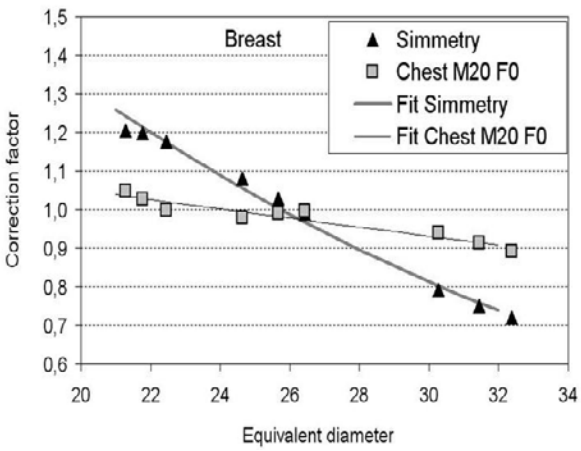

Fig 1 correction factor vs patient equivalent diameter

Conclusion: Our results confirm the validity of PCXMC with rotational module also for particular geometrical conditions; patient dose can be evaluated based on patient equivalent diameter.

EP-1619

Ovaries and uterus Equivalent dose to in patients treated for Hodgkin Lymphoma with mediastinal RT

L. Spiazzi[1], M. Buglione[2,3], F. Trevisan[2], L. Baushi[2], N. Pasinetti[3], R. Avitabile[1], F. Corrado[1], A. Polonini[1], R. Moretti[1], S.M. Magrini[2,3]
[1]*Spedali Civili di Brescia, Department of Medical Physics, Brescia, Italy*
[2]*Brescia University, Radiation Oncology Unit, Brescia, Italy*
[3]*Spedali Civili di Brescia, Radiation Oncology Unit, Brescia, Italy*

Purpose or Objective: Hodgkin's lymphoma (HL) is one of the most curable types of cancer. Most HL patients are young (average age of 32 years); long-term side effects of the treatment are becoming increasingly important. Infertility after treatment could have a high psychosocial burden for young patients. More, HL is one of the most common malignancies diagnosed during pregnancy. The aim of the present study is to measure dose to ovaries and uterus, during supra-diaphragmatic radiotherapy performed with different techniques (3DRT, IMRT, VMAT and helical IMRT-Tomotherapy®).

Material and Methods: Dose measurements were performed using the plans of four different female patients, in reproductive age. The patients have been treated with chemotherapy and mediastinum irradiation (isocenter dose 30 Gy). An adult anthropomorphic Alderson Rando phantom (*Rando phantom*) was utilized for woman simulation. For each patient the *Rando phantom* TC-scan was matched with the PET/CT. Doing it, an approximate patient specific isocenter position on the *Rando phantom* and a relative position of ovaries and uterus in terms of phantom slices were identified. Treatment planning images and diagnostic whole body PET/CT were fused by means of Velocity AI 3.0 ®. Calcium fluoride thermoluminescent dosimeters, TLD-100, were used for dose measurements, 5 TLDs were used for every measurement. Patient's treatment was simulated in 4 different techniques: 3DRT, IMRT, VMAT and helical IMRT-Tomotherapy®. To compare the results paired T student test was used.

Results: The equivalent doses to left ovary, right ovary and uterus, were respectively 16 mSV (range 5-19), 10 mSV (range 8-14) and 9 mSV (range 7-12) with 3DRT techniques; 15 mSV (range 7-23), 11.5 mSV (range 6-17) and 13 mSV (range 6-18) with VMAT; 14 mSV (range 6-23), 14 mSV (range 5-22) and 13 mSV (range 9-20) with IMRT and 54,5 mSV(range 44-70), 50mSV (range 40-72) and 56 mSV (range 33-67) with helical Tomotherapy®. Helical Tomotherapy® doses were significantly higher than the other three ($p<10^{-8}$ for all three tests). IMRT results were significantly higher than VMAT and 3D (p=0,023 and 0,004 respectively). VMAT and 3D results are not statistically different one from each other (p=0,42).

Conclusion: All the techniques give a dose to ovary and uterus well below 100 mSv. This is the dose considered safe in terms of deterministic effects on embryo or foetus and with a relatively low risk of stochastic effect. Helical Tomotherapy® and IMRT give higher gonads dose as compared to other techniques. The implications of these data may be relevant also for patients in the very early stages of their pregnancy.

EP-1620

Accuracy of cone beam computed tomography while decreasing dose to patient

A. Aasa[1], M. Vardja[1], K. Kepler[2]
[1]*Tartu University Hospital, Department of Radiotherapy and Radiation Oncology, Tartu, Estonia*
[2]*Institute of Physics, Training Centre of Medical Physics and Biomedical Engineering, Tartu, Estonia*

Purpose or Objective: The main interest was to decrease the localization CBCT scan dose in lung area since the dose deposited by CBCT contributes fully in increasing low dose volume in lung which is arguably the main indicator of radiotherapy induced pneumonitis and fibrosis. Several scanning protocols with decreasing dose were investigated to confirm that the localization accuracy is not reduced.

Material and Methods: In this work it was investigated how do physical scanning parameters - voltage, current and time - affect the automatic image registration of the localization CBCT using XVI 4.5 system from Elekta. A Cathphan 504 phantom was used for image quality measurements and an anthropomorphic phantom PBU-50 was used to verify localization accuracy. 21 scanning protocols with decreasing dose and two different automatic registration algorithms (Grey value and Bone) were analysed in lung area. Deliberate shifts with different size and direction were introduced. Image quality of acquired scans was analysed using modular transfer function (MTF), uniformity and low contrast visibility. Relative scan dose was measured with centered Farmer chamber.

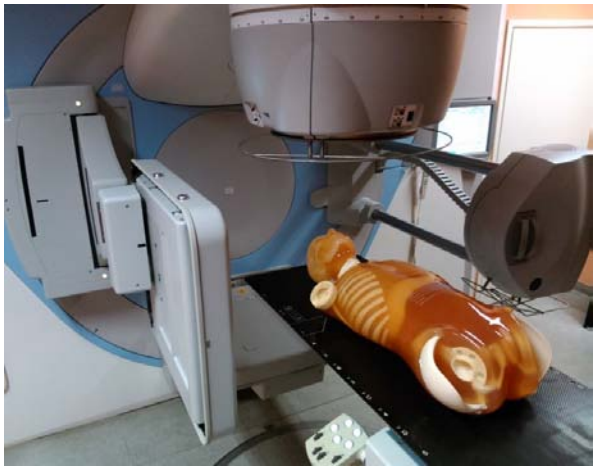

Results: It was found that CBCT system is rather insensitive to the size (max 20 mm) and direction of the deliberate shift of the phantom. Precision of the correction shifts were within 0,5 mm that is in the limit of estimated uncertainty. It was observed that the MTF was insensitive to physical scanning parameters and much more dependant on image reconstruction protocol parameters. Uniformity improved and low contrast visibility decreased while lowering dose of scanning protocol. The CBCT system under investigation showed excellent precision for positioning the phantom even while dose of scanning protocol was reduced ~90%. On the other hand – low contrast visibility decreased and would most likely limit the amount of dose redaction to acceptable level that is still to be determined.

Conclusion: This work showed that CBCT is a very accurate localization method even in conditions where scanning dose was decreased to ~10% of initial dose. It is necessary to further assess the suitability of new low dose protocols qualitatively to develop acceptable clinical scanning protocols as well as to investigate possibility to improve reconstruction protocols.

EP-1621

Automated extraction and management of radiotherapy imaging dose data

A. Reilly[1]
[1]*Western Health and Social Care Trust, Medical Physics, Londonderry, United Kingdom*

Purpose or Objective: To construct a data warehouse of radiotherapy imaging performance data by automatically extracting CT and CBCT acquisition and dose information from the hospital PACS and ARIA oncology management

system (OMS), thus allowing individual patient dose records to be monitored and radiotherapy imaging dose reference levels (DRLs) to be developed.

Material and Methods: DICOM query/retrieve is used to index and fetch CT dose report objects known to the PACS. Protocol information, patient details, CTDI and DLP are extracted. A script runs against the OMS and extracts CBCT activity information, including exposure settings and scan length. All information is converted into a standard format and stored in a data warehouse structured to make data exploration straightforward using readily available reporting and data mining tools. Data can be plotted and tabulated as a function of scanner, linac, operator, day of week, etc. Authorised operators can drill down to the patient, study and series level to understand the pre-treatment and linac imaging performed on individual patients and review the overall imaging dose record. Data can also be presented anonymised or pseudonymised for research, development and audit purposes.

Results: Table 1 shows data volumes and extract timings for a large centre (8 linacs with CBCT). The processing burden to update the data warehouse on a nightly basis is negligible.

Modality	Scanners / Linacs	Time Period	Number of Patients	Number Of Scans	Bulk Extraction Time
CT	3	Jan 2013 – Feb 2015	12,890	20,697	6 hours
CBCT	8	Jan 2013 – Feb 2015	1,898	21,256	5 mins

Table 1: Data volume and data extraction timing details.

Radiotherapy pre-treatment exposures were consistent with the equivalent diagnostic investigations and both were in line with local and national DRLs. There was clear evidence that when more advanced and automated linac imaging equipment is available more CBCTs are acquired (linacs VT1 and VT3 in Figure 1). Optimisation strategies can be studied by reviewing dose information alongside image quality and clinical decision making (see Figure 2, where dose differs between linacs and was deliberately increased when imaging a large patient).

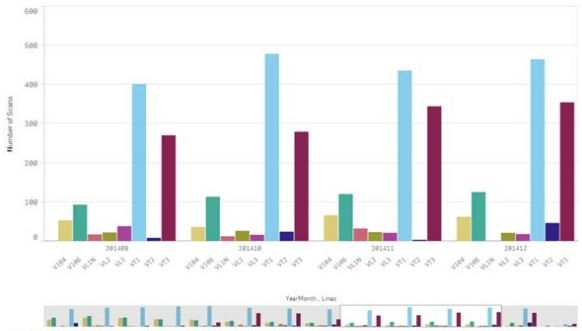

Figure 1: Number of scans per linac as a function of time. Period from September to December 2014 has been selected.

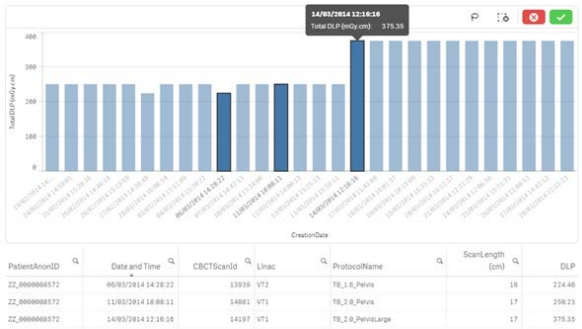

Figure 2: Linac imaging dose record for large patient (pseudonymised). Dose differences between same protocol on different linacs can be observed, along with move to higher dose protocol to boost image quality.

It was found that ARIA does not always correctly record CBCT exposure information, although if linac imaging is protocol driven there is a unique relationship between recorded values and protocol selected. Also, body site information may be coded differently between CT scanners. Data warehouse mapping tables were employed to identify the actual CBCT protocols utilised and standardise site descriptions.

Conclusion: An automated data warehouse empowers professionals who are not IT experts to ask clinically relevant questions of a rich data source of imaging performance and dose information.

EP-1622

Cyberknife® M6TM: peripheral dose evaluation in brain treatments

N. Delaby[1], J. Bellec[1], J. Bouvier[1], F. Jouyaux[1], M. Perdrieux[1], J. Castelli[1,2,3], I. Lecouillard[1], V. Blot[1], J.P. Manens[1,2,3], C. Lafond[1,2,3]

[1]*Centre Eugene Marquis, Brittany, Rennes, France*
[2]*Université de Rennes-1- LTSI, Brittany, Rennes, France*
[3]*Inserm U1099, Brittany, Rennes, France*

Purpose or Objective: Radiosurgery (SRS) and stereotactic radiotherapy (SRT) are known to deliver very high doses per fraction. The corresponding peripheral dose can be a limiting parameter which potentially generates late toxicities. The purpose of this study was to evaluate peripheral dose delivered to healthy tissues such as thyroid and gonads for brain SRS/SRT treatments performed with a Cyberknife® M6TM system.

Material and Methods: Measurements were performed on a Cyberknife® M6TM (Accuray) equipped with fixed and IrisTM collimator systems. Doses were measured with GR200A (LiF:Mg, Cu, P) thermoluminescent dosimeters (TLD). Each TLD was individually calibrated in a 6 MV beam. TLD readings were performed with a PCL3 automatic reader (FIMEL). Firstly, in-vitro measurements were carried out in an anthropomorphic phantom (CIRS ATOM 701-c) for different typical brain treatment plans using different beam apertures (5 mm to 60 mm). Peripheral doses were measured at 24 points distributed from thyroid to gonads on the median line of the phantom (between 15 cm and 82.5 cm from the PTV center). Secondly, in-vivo measurements were performed on 30 patients, in 4 points representative of thyroid, breast, umbilicus and gonads. The number of monitor units (MU) used for treatment plans ranged from 5499 MU to 28900 MU with a mean value of 13737 MU, delivered in 1 to 3 fractions. Results were compared with peripheral dose published for previous Cyberknife® versions. Treatment plans were calculated with Multiplan v5.1.2 (Accuray). Peripheral dose were reported in cGy as percentage of the number of delivered Monitor Units (% of MU).

Results: Peripheral dose varied according to collimator size: 0.043 % of MU at 15 cm for a 5 mm collimator aperture and 0.235 % of MU at 15 cm for a 60 mm collimator aperture. For an intermediate collimator aperture (20 mm), peripheral doses were between 0.062 % of MU at 15 cm and 0.036 % of MU at 40 cm for fixed collimator system and between 0.040 % of MU at 15 cm and 0.029 % of MU at 40 cm for IrisTM collimator system. Table 1 compares our in-vivo measurements with peripheral dose published in the literature on several Cyberknife® models [1,2].

Table 1: Comparison between peripheral dose values measured for 5 Cyberknife versions in brain treatment

Peripheral dose (exprimed in cGy as percentage of the number of delivered Monitor Units (% of MU)						
Device		Cyberknife G4 preshielding	Cyberknife G4 postshielding	Cyberknife VSI preshielding	Cyberknife VSI postshielding	Cyberknife M6
Study		*[1]*		*[2]*		*Our results*
Dose measurement methods		In vivo (10 patients)	In vivo (21 patients)	In vitro		In vivo (31 patients)
Distance range from PTV and localization	[10,24] cm for Thyroid	0.220	0.170	0.160	0.066	0.045
	[28,44] cm for Thorax	-	0.050	0.108	0.048	0.038
	[60,89] cm for Pelvis	0.060	0.050	0.045	0.036	0.022

Conclusion: Peripheral dose for the Cyberknife® M6TM version is lower than previous Cyberknife® versions. Nevertheless, for a brain treatment the dose can reach 10 cGy in the thyroid and can exceed 7 cGy in gonads; it should be evaluated for every localization. Peripheral dose will depend on number of monitor units, beam aperture size and collimator system. These parameters should be optimized during treatment planning to limit peripheral dose as lower as possible.

References:

[1] Vlachopoulou "Peripheral Doses in Patients Undergoing Cyberknife Treatment for Intracranial Lesions", Rad Onc 6 (2011)

[2] Chuang "Peripheral Dose Measurement for CyberKnife Radiosurgery with Upgraded Linac Shielding", Med Phys 35 (2008)

EP-1623

Correlation of organ doses and IEC and AAPM methods for cone beam computed tomography (CBCT)

A. Abuhaimed[1], C.J. Martin[2], M. Sankaralingam[1], M. Metwaly[1], D.J. Gentle[3]

[1]*Beatson West of Scotland Cancer Centre, Radiotherapy Physics, Glasgow, United Kingdom*

[2]*University of Glasgow, Department of Clinical Physics, Glasgow, United Kingdom*

[3]*Gartnavel Royal Hospital, Health Physics, Glasgow, United Kingdom*

Purpose or Objective: Several dosimetric methods were proposed to overcome limitations of the standard dose index used for CT dosimetry (CTDI100) with cone beam computed tomography (CBCT). Two of these methods were proposed by IEC and AAPM. The aim of this project was to investigate the correlation between organ doses (ODs) resulting from head, thorax, and pelvic CBCT scans and the IEC and AAPM methods.

Material and Methods: The IEC method (CTDIIEC) is based on measuring CTDI100 using a reference beam and the application of a correction factor based on free-in-air CTDI measurements, while the AAPM method f(0) is based on measuring cumulative dose using a small ionization chamber at the middle of an infinitely long phantom. CTDIIEC was evaluated within CTDI head and body phantoms, whereas f(0) was assessed within 450 mm long CTDI phantoms. CTDIIEC and f(0) were measured at the centre and periphery of the phantoms using head, thorax, and pelvic scanning protocols used in the clinic. ODs were evaluated in terms of absorbed dose to organs and tissues using Monte Carlo simulations on the ICRP-110 adult male and female reference computational phantoms. BEAMnrc and DOSXYZnrc user codes were utilized to simulate On-Board Imager (OBI) system mounted on a TrueBeam linac and to assess ODs using the same scanning protocols used for CTDIIEC and f(0). The correlation was studied as the difference between weighed values (2/3 periphery:1/3 centre) of CTDIIEC,w and f(0)w and ODs. The correlation was investigated for organs, which have higher weights of effective dose.

Results: For head scan, CTDIIEC,w were smaller than doses to bone marrow, brain, and salivary gland by 4-55% for male and by 16-84% for female. f(0)w was also smaller than doses to bone marrow and salivary gland by 7-26% and 49-50% for male and female, respectively, but was larger than brain dose by 15% and 5%, respectively. For thorax scan, doses to bone marrow, lung, breast, and oesophagus were underestimated by CTDIIEC,w and f(0)w by 61-100% and 35-58% for male and by 108-161% and 64-106% for female, respectively. However, CTDIIEC,w and f(0)w overestimated doses to stomach and thyroid by 10-34% and 29-45% for male and by 13-28% and 31-43% for female, respectively. For pelvic scan, CTDIIEC,w and f(0)w were smaller than doses to bone marrow and urinary bladder by 91-173% and 51-116%, respectively, but were larger than colon and gonads doses by 30-78% and 44-82%, respectively, for male. For female, however, doses to all the organs were underestimated by CTDIIEC,w and f(0)w by 76-204% and 40-141%, respectively.

Conclusion: The correlations between CTDIIEC,w and f(0)w and ODs were comparable to the majority of organs. In general, however, f(0)w gave a better estimation for ODs compared to CTDIIEC,w for the scanning protocols studied.

EP-1624

Influence of organ motion on radiation-induced secondary cancer for VMAT and IMPT of prostate cancer

C. Stokkevåg[1], G. Engeseth[1], L. Hysing[1], K. Ytre-Hauge[2], L. Muren[3]

[1]*Haukeland University Hospital, Department of Oncology and Medical Physics, Bergen, Norway*

[2]*University of Bergen, Department of Physics and Technology, Bergen, Norway*

[3]*Aarhus University Hospital, Department of Medical Physics, Aarhus, Denmark*

Purpose or Objective: An elevated risk of radiation-induced secondary cancer (SC) in directly irradiated tissues such as the bladder and rectum has been observed in prostate cancer patients following radiotherapy (RT). There are considerable fluctuations in SC risk due to inter-patient anatomy variations, indicating the relevance of also including the effects of internal organ motion for individual patients. Both the bladder and rectum are highly mobile structures and the aim of this study was therefore to investigate the influence of organ motion on SC risk.

Material and Methods: Simultaneously integrated boost treatment plans were generated on the planning CT (pCT) scans of eight prostate patients, using volumetric modulated arc therapy (VMAT) and intensity-modulated proton therapy (IMPT). Both VMAT and IMPT plans were prescribed to deliver 67.5 Gy to the prostate and 60 Gy to the seminal vesicles over 25 fractions, using fiducial marker based image guidance. Each patient had 8-9 repeat CT (rCT) scans throughout the course of treatment on which the bladder and rectum were re-contoured and the originally planned dose distribution re-calculated. Relative risk (RR) of radiation-induced cancer were calculated from the planned and re-calculated dose distributions by using the organ equivalent dose concept adapted to dose-response models reflecting varying degrees of cell sterilisation: a linear model, a linear-plateau model and a bell-shaped competition model.

Results: Using the competition model, the RRs of bladder cancer based on the pCTs ranged from 0.4 to 3.4, while a considerably wider range was found when including all rCTs (from 0.2 to 6.7). Similar trends were seen for the RR for rectal cancer with the competition model and also for both bladder and rectal cancer using the linear model (Fig 1). Overall, the ranges were narrower with the linear model compared to competition model (Fig 1). For 4/8 patients for the bladder and 1/8 patients for the rectum, the estimated risks according to the competition model were consistently lower for IMPT compared to VMAT. Using the linear model the corresponding fractions were 6/8 and 7/8 patients. The remaining patients had rCTs with variations in RR, favouring either VMAT or IMPT, except one of the patients with all rCTs in favour of VMAT for rectal cancer using the competition model. In particular for the competition model, the RRs according to the pCT were often found at the upper or lower side of the RR across rCTs and two cases for bladder cancer and three cases for rectal cancer had RR <1 when addressed with the pCT but a median RR>1 across the rCT.

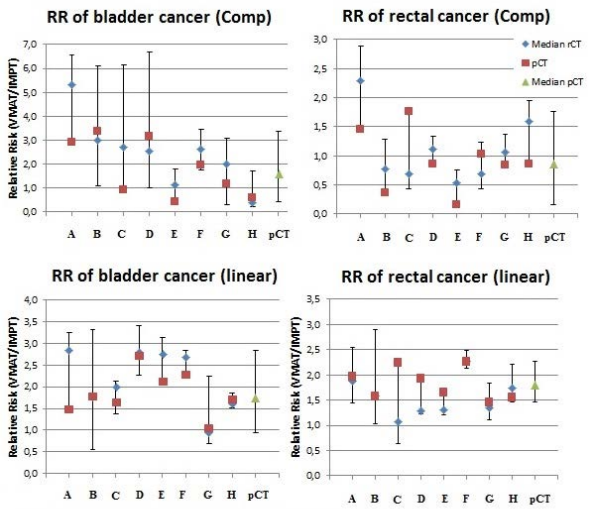

Figure 1. Relative Risks of radiation-induced bladder and rectal cancer VMAT/IMPT for patients A-H. Median of repeat CTs (range), planning CTs and Median of all planning CTs (range)

Conclusion: The choice of model contributes to SC risk fluctuating in favour of either IMPT or VMAT. Large variations were seen across rCTs, indicating that day-to-day variations in anatomy lead to fluctuations in SC risk estimates that are at least of the same magnitude as the inter-patient variations. Organ motion effects should therefore also be accounted for in SC risk estimates.

Electronic Poster: Physics track: Treatment plan optimisation: algorithms

EP-1625

A dosimetric analysis of semi-automated knowledge-based VMAT planning for rectal cancer patients

F. Jiang[1], Y. Zhang[1], H. Yue[1], S. Li[1], Q. Hu[1], Y. Zhang[2], H. Wu[1]
[1]*Peking University Cancer Hospital & Institute, Department of Radiotherapy, Beijing, China*
[2]*Peking University Health Science Center, School of Foundational Education, Beijing, China*

Purpose or Objective: To compare the dosimetric features of the semi-automated knowledge-based vs. conventional experience-based VMAT planning for pre-operative rectal cancer patients treated with simultaneous-integrated-boosting (SIB) radiotherapy.

Material and Methods: Created by experts following consistent contouring and planning protocols, clinically approved SIB VMAT plans for 150 patients were selected, 80 which were added to the library of Varian RapidPlan to train the DVH estimation model. The other 70 plans were duplicated whose MLC sequences were re-optimized using the model-generated DVH objectives. All plans were normalized to PTV95%≥ 41.8 Gy and PGTV95% ≥ 50.6 Gy before comparing: dose coverage of GTV and CTV; homogeneity index (HI), conformal index (CI), hotspot volume receiving over 107% of prescription (V107%_PGTV), mean dose and dose to 50% volume of femoral head (Dmean_FH and D50%_FH) and urinary bladder (Dmean_UB and D50%_UB) respectively. Average DVHs of 70 patients were plotted. The normally and non-normally distributed data sets were analyzed using paired samples t-test and Wilcoxon signed ranks test respectively, setting P<0.05 as significant.

Results: Identified as potential outlier or influential data points, the plans of 4 FH and 11 UB were reviewed yet abnormality was excluded. The DVH's and geometry-based expected dose's principal component average fit were 0.999126 and 0.999481 for FH, 0.999585 and 0.999429 for UB respectively. More under-dosed GTV and CTV were found in original than the RapidPlan group, but all V100% were over 99% hence were clinically negligible. Difference of CI was insignificant (P=0.051 and P=0.900 for PGTV and PTV respectively), yet RapidPlan improved HI of PGTV and PTV significantly (Mean ± 1SD = 0.05 ± 0.006 for PGTV, and 0.255 ± 0.008 for PTV) relative to the original plans (0.06 ± 0.008 for PGTV and 0.263 ± 0.011 for PTV). Positive V107%_PGTV were observed in 18 original plans, which was significantly higher than the RapidPlan group (none). Table 1 shows RapidPlan significantly reduced the D50%_FH, Dmean_FH, D50%_UB and Dmean_UB respectively. The mean DVH of the 70 testing plans (Figure 1) indicates on the basis of comparable target dose coverage, superior dose falloff and organ sparing were achieved by RapidPlan group.

Table 1. Statistics of dose metrics (Gy) of femoral head (FH) and urinary bladder (UB)

		Mean	SD	95% Confidence Interval		P
				Lower	Upper	
$D_{50\%\ FH}$	Original	15.52	2.17	15.00	16.03	<0.001
	RapidPlan	13.99	1.16	13.71	14.26	
$D_{mean\ FH}$	Original	16.59	2.07	16.10	17.08	<0.001
	RapidPlan	15.30	0.70	15.14	15.47	
$D_{50\%\ UB}$	Original	28.17	3.07	27.44	28.90	<0.001
	RapidPlan	23.24	2.13	22.74	23.75	
$D_{mean\ UB}$	Original	29.34	2.34	28.78	29.89	<0.001
	RapidPlan	25.40	1.36	25.08	25.73	

Abbreviations: SD = standard deviation; $D_{50\%}$ = dose to the 50% volume of the structure; D_{mean} = mean dose; FH = femoral head, and UB = urinary bladder.

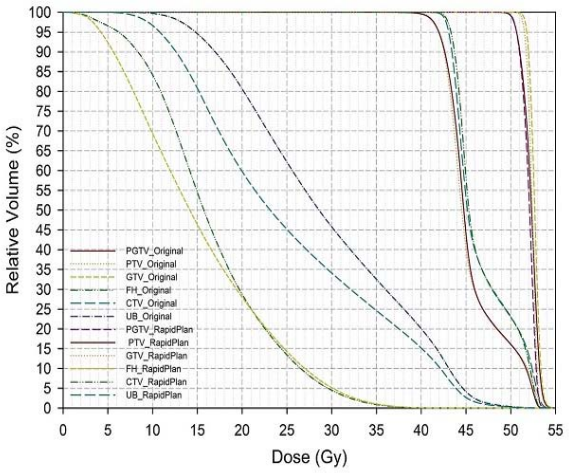

Figure 1. Average DVHs of the 70 testing plans

Conclusion: Knowledge-based radiotherapy significantly enhanced the consistency of the plan quality by improving the target dose homogeneity, hotspot control and normal tissue sparing. The semi-automated process also reduced the planning time.

EP-1626

4D Energy-based minimisation in lung cancer

I. Mihaylov[1]
[1]*University of Miami- Sylvester Comprehensive Cancer Center, Suite 1500, Miami- Florida, USA*

Purpose or Objective: According to published guidelines if tumor motion exceeds 0.5 cm, motion management should be utilized in planning and delivery for NSCLC. Dose-volume-based (Dvh) optimization is the most commonly used treatment planning approach in NSCLC IMRT. Energy-based inverse optimization is a novel IMRT planning framework, which is a rival to Dvh optimization. The purpose of this work is to compare Dvh and Energy IMRT planning for time resolved (4D) in NSCLC.

Material and Methods: Sixteen lung cases were studied. In each case, the target range of motion was over 0.5 cm. For each patient five breathing phases were reconstructed from the pre-planning 4D CT. All anatomical structures were outlined on a reference breathing phase and contours were propagated to the other breathing phases. For each phase inverse optimization was performed with Dvh and Energy based objective functions for the organs at risk (OARs), while target objectives were dose based. Each plan utilized seven

equally spaced beams with total of 35 segments. Step-and-shoot IMRT with minimum segment area of 5x5 cm and minimum of 10 monitor units per segment was used in each plan. Dvh and Energy plans were normalized such that 95% of the propagated PTV for each phase received the prescription dose. Once prescription was achieved, the doses to OARs, such as spinal cord, heart, esophagus, and healthy lungs were iteratively lowered until standard deviation of the dose across the PTV in each plan became less than 4%. After generating Dvh and Energy plans for each breathing phase, deformable dose accumulation to the reference breading phase for each optimization scheme was performed. The resulting 4D Dvh and Energy plans were compared on the basis of dose indices (DIs), such as DPTV95% (dose to 95% of the PTV), DCord1%, Desophagus50%, Dheart33%, Dlungs20%, Dlungs30%, and volume indices (VIs) such as Vlungs2000 cGy, and Vlungs3000 cGy. The differences among the DIs and the VIs were subjected to a two-tailed paired *t*-test to determine the statistically significant dose differences ($p < 0.05$). In addition, total deposited energy in the irradiated volume was assessed.

Results: The table summarizes statistically significant differences over all quantities. On average the DIs and the VIs from the 4D Energy optimization are lower than the indices obtained with the 4D Dvh optimization. The total energy deposited in the entire irradiated volume outside of the target was lower for all Energy optimized 4D plans with statistically significant difference of 13% as compared to the 4D Dvh plans.

Conclusion: In this work time-resolved treatment planning optimization schemes in NSCLC were investigated. The results reveal that 4D Energy based optimization outperforms 4D Dvh based optimization in terms of OAR sparing. For comparable target coverage 4D Energy based plans resulted in statistically significant lower OAR doses ranging from 14% to almost 50%.

	Cord $D_{1\%}$ [cGy]	Heart $D_{33\%}$ [cGy]	Lungs $D_{20\%}$ [cGy]	Lungs $D_{30\%}$ [cGy]	Both Lungs V_{2000} [cm^3]	Both Lungs V_{3000} [cm^3]	Esophagus $D_{50\%}$ [cGy]	Total Deposited Energy [10^{-6} Joules]
Average Difference [cGy/cm^3/J]	731	342	323	309	232	91	691	15.9
Statistically Significant Level [%]	40	20	11	14	22	14	48	13

EP-1627

Knowledge-based IMRT optimisation using a model trained with VMAT plans of other setup orientations

Y. Zhang[1], F. Jiang[1], S. Li[1], H. Yue[1], Q. Hu[1], H. Wu[1]
[1]*Key laboratory of Carcinogenesis and Translational Research Ministry of Education/Beijing- Peking University Cancer Hospital & Institute, Department of Radiotherapy, Beijing, China*

Purpose or Objective: Knowledge-based (KB) optimization reduces planning time and quality dependence on humans, yet requires specialty and efforts to develop DVH estimation models. This work applied a model configured with supine VMAT plans to IMRT optimization (supine & prone) to check the feasibility and dosimetric performance.

Material and Methods: Based on Varian RapidPlan, a VMAT model was trained and statistically validated using 81 supine rectal cancer plans of 1 full arc to cover 95% of PGTV and PTV with 50.6 and 41.8 Gy respectively in 22 fractions. Without changing any geometric and beam settings (5 fields were almost symmetric but not strictly), the dynamic MLC sequences of 30 clinical IMRT plans (10 supine and 20 prone) were reoptimized using the model. Volume dose of the original plans were recalculated using the same algorithm as KB plans to avoid bias. All plans were normalized to consistent target prescriptions before comparing: 1. homogeneity index of PGTV (HI_PGTV) and PTV (HI_PTV); 2. conformity index of PGTV (CI_PGTV) and PTV (CI_PTV); 3. volume% exceeding 107% of PGTV prescription (V107%, V54.14Gy); 4. Global maximum dose (Dmax) and PGTV near maximum dose (D2%); 5. mean dose and dose to 50% of the femoral head and urinary bladder (Dmean_FH and Dmean_UB; D50%_FH and D50%_UB). To compare normally distributed data, paired T test (original vs. KB re-planning) and independent T-tests (supine vs. prone setups) were conducted respectively, otherwise Shapiro-Wilk test and Mann-Whitney U test were performed accordingly.

Results: KB IMRT plans of either setups can be optimized successfully by the supine VMAT model. Under comparable target dose coverage, explicitly better dose falloff in CTV and PTV (between V45-49Gy), and much lower dose to the bladder and femoral head were observed in KB group (figure 1: mean DVHs of 30 patients). As shown in table 1, the normal organ sparing of KB was significantly superior than the original plans, however, the HI_PGTV, HI_PTV, CI_PTV, and Dmax were undermined slightly as trade-off ($P<0.05$). As a possible explanation, hotspots were usually segmented and suppressed specifically during manual optimization, yet was missing by KB process. V107% also appeared in KB group only (1 supine: V107%=0.03%; 5 prone: V107%=0.01, 0.08, 0.10, 1.15 and 1.76% respectively), although the difference of D2% was not significant ($P=0.102$). Supine VMAT model was not favourable to patients of same setup ($P>0.05$), however significantly higher D50% and mean dose to femoral head were observed in supine group for both original and KB plans: indicating the difference may be more attributable to setup orientations or field geometry than to KB model.

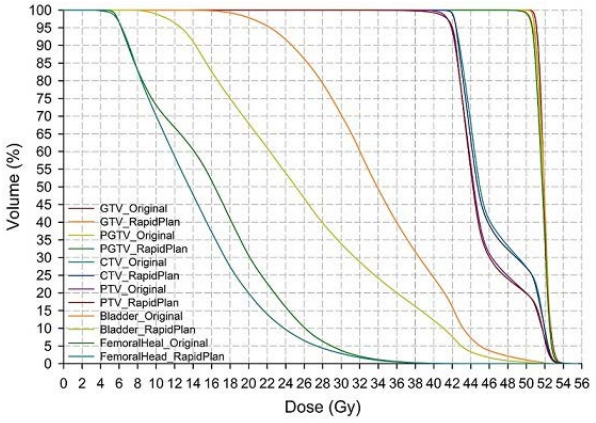

Figure 1. Mean DVHs of the 30 patients: comparing the dosimetric difference of the original and knowledge-based planning.

Table 1. Comparison of planning techniques (Original vs. RapidPlan, O vs. R) and setups (supine vs. prone, S vs. P)

		Original				RapidPlan				
		Mean	SD	95%CI	P (S vs. P)	Mean	SD	95%CI	P (S vs. P)	P (O vs. R)
HI_{PGTV}	All	0.042	0.006	0.040~0.044	--	0.048	0.012	0.043~0.052	--	0.005
	Supine	0.041	0.007	0.036~0.046	0.640	0.046	0.008	0.041~0.516	0.648	--
	Prone	0.042	0.006	0.039~0.045		0.048	0.014	0.042~0.055		--
HI_{PTV}	All	0.247	0.011	0.243~0.251	--	0.255	0.013	0.250~0.260	--	0.004
	Supine	0.245	0.011	0.237~0.252	0.368	0.251	0.008	0.245~0.256	0.221	--
	Prone	0.249	0.012	0.243~0.254		0.257	0.015	0.250~0.264		--
CI_{PGTV}	All	1.017	0.059	0.995~1.039	--	1.015	0.054	0.995~1.035	--	0.673
	Supine	1.020	0.059	0.978~1.062	0.880	1.007	0.058	0.965~1.048	0.502	--
	Prone	1.015	0.061	0.987~1.044		1.019	0.053	0.994~1.043		--
CI_{PTV}	All	1.009	0.026	1.000~1.019	--	1.181	0.054	1.161~1.201	--	<0.001
	Supine	1.014	0.023	0.997~1.031	0.328	1.189	0.070	1.139~1.239	0.650	--
	Prone	1.007	0.027	0.994~1.019		1.177	0.045	1.156~1.198		--
D_{max}	All	52.98	0.45	52.81~53.15	--	54.46	1.52	53.89~55.02	--	<0.001
	Supine	52.89	0.36	52.64~53.15	0.457	54.73	1.67	53.53~55.93	0.499	--
	Prone	53.02	0.49	52.79~53.25		54.32	1.46	53.64~55.00		--
$D_{2\%}$	All	52.63	0.43	52.47~52.95	--	52.76	0.51	52.57~52.95	--	0.102
	Supine	52.54	0.35	52.29~52.80	0.416	52.71	0.24	52.53~52.88	0.608	--
	Prone	52.68	0.46	52.46~52.90		52.79	0.61	52.50~53.07		--
$D_{50\%\_UB}$	All	33.98	2.98	32.87~35.09	--	25.09	1.32	24.59~25.58	--	<0.001
	Supine	34.13	2.74	32.17~36.08	0.851	25.12	0.84	24.52~25.72	0.933	--
	Prone	33.90	3.16	32.43~35.38		25.07	1.53	24.36~25.79		--
$D_{50\%\_FH}$	All	15.71	3.28	14.49~16.94	--	13.73	1.43	13.19~14.26	--	<0.001
	Supine	18.87	2.63	16.99~20.75	<0.001	14.67	1.80	13.38~15.95	0.008	--
	Prone	14.14	2.30	13.06~15.21		13.26	0.94	12.82~13.70		--
D_{mean_UB}	All	34.11	2.81	33.06~35.16	--	26.25	1.22	25.70~26.70	--	<0.001
	Supine	34.27	2.93	32.17~36.37	0.914	26.19	0.97	25.50~26.89	0.948	--
	Prone	34.03	2.83	32.71~35.35		26.27	1.36	25.64~26.91		--
D_{mean_FH}	All	16.33	2.69	15.32~17.33	--	14.62	1.10	14.21~15.04	--	<0.001
	Supine	19.25	2.36	17.56~20.94	<0.001	15.41	1.07	14.64~16.17	0.001	--
	Prone	14.87	1.30	14.26~15.47		14.23	0.91	13.81~14.66		--

Abbreviations: HI=homogeneity index; CI=conformity index; D_{max}=global maximum dose; $D_{2\%}$= near maximum dose; SD = standard deviation; 95%CI=95% confidence interval; $D_{50\%}$ = dose to the 50% volume of the structure; D_{mean} = mean dose; FH = femoral head, and UB = urinary bladder. Dose unit (Gy).

Conclusion: DVH estimation model configured with VMAT plans can be efficiently applied to KB optimization of IMRT plans, including patients of different setup orientations. KB IMRT reduces dose to normal organs, but the concomitant hotspots should be further processed after the automated planning.

EP-1628

Single-click automatic radiotherapy treatment planning for breast, prostate and vertebrae

R. De Graaf[1], J. Trinks[1], A. Duijn[1], J. Knegjens[1], D. Eekhout[1], R. Harmsen[1], A. Olszewska[1], G. Retèl[1], G. Wortel[1], S. V.d. Sanden[1], M. Buiter[1], C. Van Vliet-Vroegindeweij[1], E. Damen[1]

[1]*The Netherlands Cancer Institute, Department of Radiation Oncology, Amsterdam, The Netherlands*

Purpose or Objective: Labour-intensive procedures, such as adaptive radiotherapy and the upcoming new modalities protons and MR linac, result in an increased workload in the treatment planning department. We therefore started the FAST-planning project, a Framework for Automatic Segmentation and Treatment planning. The purpose of this project is to produce single-click automated treatment planning for the majority of tumour sites.

Material and Methods: Easy configuration of treatment protocols was achieved by isolating medical planning protocol relations from software: in-house developed XPP document format (eXtensible Planning Protocol) allows for a complete planning protocol definition in a single document (XML). In FAST planning, the patient ID, dicom identifiers and the selected planning protocol are combined, and an Autoplan document (XML) is composed.
In the framework, each module accepts Autoplan documents and coordinates actions accordingly; e.g. automatic localization of the patient record, import of DICOM objects with delineated target volumes, auto-segmentation of OARs, creation of additional ROIs, creation of advanced beam-setups (VMAT, IMRT), optimization and finally the creation of a report (optionally uploaded to R&V MOSAIQ). The software is written in Python and makes use of Pinnacle3 scripting and transfer protocols DICOM and XML over HTTP. Schemas are used for validation of all XML documents.

Results: The following workflow is automated: after the physician delineated the target, a single mouse-click initiates RT plan generation on our remote treatment planning system Pinnacle3. Subsequently a preview report of the generated plan is send to R&V system MOSAIQ (Fig. 1). The created RT plan is fully optimized and ready for inspection by the dosimetrist. FAST-planning has been implemented into our clinic for Breast, Prostate, and Vertebral metastases.
Nine Prostate protocols (VMAT) are in place for a variety of dose-levels (51, 64.6 and 77Gy) and target definitions (boost/no-boost and inclusion of seminal vesicles). For Breast, 8 IMRT plans (variation in beam-setup and OAR margins) are created; the dosimetrist and physician can select the best plan based on target coverage and dosimetric trade-offs. For vertebral metastases, 2 plans (conformal beam-setups PA and APPA) are created and screenshots in PDF are sent to R&V MOSAIQ for plan evaluation and selection by the physician.

Conclusion: We have introduced fully automated RT planning for treatment plans Breast (in 20min), Prostate (in 20min) and palliative Vertebrae (in 7min). The automation of these treatment sites has reduced the dosimetrist's planning time considerably (up to 2 hours per RT plan), while maintaining the same plan quality. The FAST framework is generic and allows for easy RT planning protocol configuration for the EBRT techniques VMAT, IMRT and conformal fields. The workflow automation currently covers approx. 20% of our patient throughput, i.e. 1250 RT planning sessions/year.

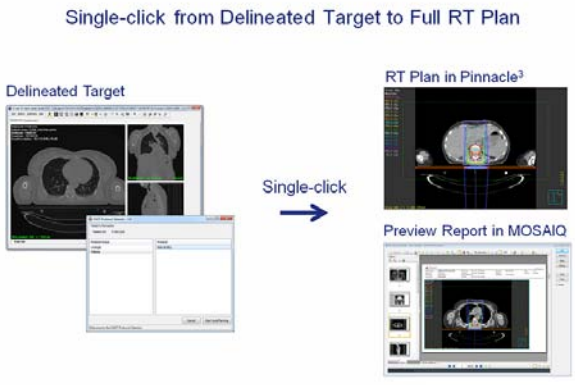

EP-1629

A novel method for electron beam geometry optimisation

T. Felefly[1], C. El Khoury[1], F. Azoury[1], N. Farah[1], J. Barouky[1], R. Sayah[1], N. Khater[1], D. Nehme Nasr[1], E. Nasr[1]
[1]*Hôtel Dieu de France - Saint Joseph University, Radiation Oncology, Beirut, Lebanon*

Purpose or Objective: A normal beam incidence optimizes dose distribution in electron radiotherapy. Historically, electron beam direction is chosen clinically with aid of Computed Tomography (CT) data, but commonly without couch rotation. This work describes a novel method for optimizing electron beam incident angle by varying both gantry and couch angles.

Material and Methods: The treated skin surface could be represented using triangle mesh modeling, the vertices being chosen as points on the treated body contour, and their 3D coordinates obtained from the CT dataset. The optimal beam direction would be parallel to the vector sum of all normal vectors to the defined triangles. For each triangle, the normal vector can be obtained by the cross product of two vectors formed by the triangle vertices.Gantry and couch rotation angles of the electron field could then be derived from the vector sum using simple trigonometric formulation. A computer code based on these formulas was developed. The inputs required are the vertices 3D coordinates, the output being the calculated gantry and couch rotation angles. Ideally, using a larger number of vertices, and consequently a larger number of triangles, increases the similarity between the mesh representation and the real skin surface.For practical reasons, two software versions were generated: one using four vertices selected on the treatment planning system such that they are located on the periphery of the treated skin, and the other using nine points selected on the periphery and evenly distributed within the treated skin. Results were compared for fifteen treatment plans and evaluated clinically in the treatment room and dosimetrically using the Eclipse Monte-Carlo electron algorithm.

Results: The two software versions yielded similar results, the root-mean-square deviation being 1.28° for couch rotation angles and 1.9° for gantry angles. When assessed clinically on patients, the derived beam direction appeared fairly normal to the treated skin surface for all cases. A better dose distribution was obtained using the software particularly for cases with large calculated couch rotation angles.

Conclusion: This software tool is an alternative to the historically used method, is more objective and accurate, may provide a better dose distribution, and is reasonably practical using the four vertices based calculation.

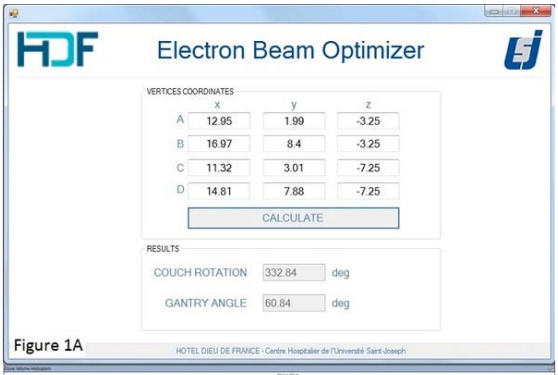

Figure 1A

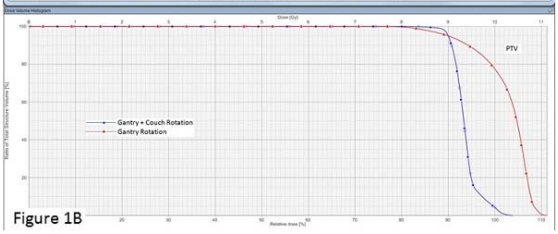

Figure 1B

EP-1630

Automated iterative plan optimisation widens therapeutic window for prostate cancer arc therapy

E.J.L. Brunenberg[1], J.M.A.M. Kusters[1], P.G.M. Van Kollenburg[1], C.M. Verhagen[1], P.M.W. Van Herpen[1], M. Wendling[1], R.J. Smeenk[1], P.M. Poortmans[1]
[1]*Radboud UMC, Radiation Oncology, Nijmegen, The Netherlands*

Purpose or Objective: Treatment planning for volumetric modulated arc therapy (VMAT) is complex, as the result is highly dependent on the selected optimization objectives. The Auto-Planning module in Pinnacle³ 9.10 (Philips Healthcare, Fitchburg, WI, USA) aims at offering efficient automated planning that directly uses clinical goals for iterative optimization, pushes beyond these goals if possible, and delivers consistent plan quality. In this study, we compared the performance of two Auto-Planning techniques with our original clinical approach of manually optimized prostate cancer VMAT plans.

Material and Methods: Techniques were evaluated for 23 prostate cancer patients (all treated using a rectal balloon), 18 of which underwent primary irradiation with a prescription dose (PD) of 70 Gy in 28 fractions. PTV (planning target volume) for these cases ranged from prostate only to prostate plus entire seminal vesicles. Five patients received salvage treatment with 65 Gy in 26 fractions.
Two Auto-Planning techniques (AP1, AP2) were compared with the manually optimized clinical plan (MP) to evaluate plan quality, focusing on PTV coverage and OAR (organ at risk) sparing. AP1 contained clinical goals for rectal wall, anal wall, bladder and femoral heads (dose-volume relationship and mean dose goals). AP2 used the same technique, excluding the femoral heads, in order to focus on bladder, rectal and anal wall (which are more prone to toxicity), and including a goal to minimize dose on tissue outside PTV and OARs.
Monitor units (MUs) for all plans were scaled to achieve a V95% ≥ 99% for the PTV. One 10 MV VMAT arc (95 to 265° counterclockwise) and two portal imaging beams (for online position verification, 5 MU each) were used.

Results: Table 1 presents the results of the comparison. Both AP techniques show a significant increase in PTV mean dose and number of MU when compared to MP, while PTV max dose is not significantly different. With respect to OARs, Auto-Planning significantly spares all considered structures. AP2 indeed sacrifices sparing of femoral heads for more sparing of bladder, rectal and anal wall. See Figure 1 for an example of dose distributions and DVHs (dose volume histograms).
We selected AP2 as our Auto-Planning technique for clinical use. For 10 subsequently treated patients, AP2 resulted in an approved plan on the first Auto-Planning run for all 8 patients undergoing primary irradiation. The 2 salvage patients needed extra goals for the femoral heads.
Delta-4 measurements for 20 patients treated with AP2 showed a mean gamma pass rate of 98.4 ± 1.4 %, while EBT3 film QA on a subset of 10 patients resulted in a mean gamma pass rate of 97.4 ± 1.2 % (evaluated for 3%/3mm).

Conclusion: Besides its efficiency and consistency, Auto-Planning offers similar PTV coverage as the original clinical plans, combined with better sparing of bladder, rectal and anal wall. Thus, the module widens the therapeutic window and is now used as our clinical standard for prostate cancer VMAT planning.

Structure	Criterion	MP	AP1	AP2
PTV	mean dose (% of PD)	100.1 ± 1.2	101.1 ± 0.5*	101.2 ± 0.8*
	max dose (% of PD)	103.8 ± 1.7	104.2 ± 0.9	104.3 ± 1.2
bladder	V60Gy (%)	19.9 ± 10.7	16.8 ± 10.1*	16.5 ± 10.0*
	mean dose (Gy)	29.9 ± 10.6	**27.7 ± 11.0*°**	**26.4 ± 10.4*°**
rectal wall	V60Gy (%)	22.2 ± 6.7	20.3 ± 6.5*	20.3 ± 6.5*
	V30Gy (%)	37.4 ± 10.5	**34.7 ± 11.6*°**	**33.8 ± 10.8*°**
	mean dose (Gy)	29.8 ± 5.4	**28.0 ± 6.5*°**	**27.2 ± 6.5*°**
anal wall	mean dose (Gy)	21.0 ± 8.4	16.7 ± 8.4*	16.7 ± 8.5*
rectal + anal wall	V60Gy (%)	18.8 ± 6.0	16.7 ± 5.5*	16.7 ± 5.5*
	V30Gy (%)	34.4 ± 9.4	**30.6 ± 9.7*°**	**29.9 ± 9.2*°**
	mean dose (Gy)	27.5 ± 4.9	**25.0 ± 5.4*°**	**24.4 ± 5.5*°**
femoral head (left)	max dose (Gy)	47.2 ± 7.2	**40.1 ± 8.6*°**	**46.1 ± 7.8°**
	mean dose (Gy)	33.1 ± 6.2	**24.4 ± 6.4*°**	**30.6 ± 6.1*°**
femoral head (right)	max dose (Gy)	46.7 ± 6.4	**39.5 ± 8.1*°**	**48.0 ± 7.4°**
	mean dose (Gy)	32.8 ± 5.2	**23.4 ± 4.9*°**	**32.1 ± 5.7*°**
-	# MU VMAT arc	475 ± 74	560 ± 58*	546 ± 58*

Table 1: Comparison of manually optimized (MP) and Auto-Planning (AP) techniques: mean values and standard deviations for 23 patients. */gray: AP significantly different from MP; °/bold: significant difference between AP1 and AP2 (two-sided paired t-test used, p<0.05).

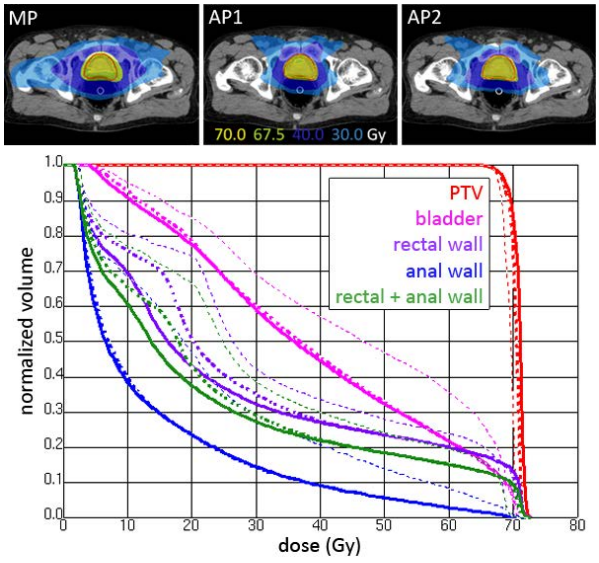

Figure 1: Example of dose distributions and DVHs belonging to MP, AP1 and AP2 for a 70-Gy plan. DVHs show MP as thin dashed; AP1 as thick dashed; AP2 as thick solid.

EP-1631

mARC treatment planning in non-dedicated systems: two conversion approaches using IMRT and SmartArc

Y. Dzierma[1], N. Licht[1], I. Norton[2], F. Nuesken[1], C. Rübe[1]
[1]*Universitätsklinikum des Saarlandes, Department of Radiation Oncology, Homburg/Saar, Germany*
[2]*Philips Healthcare, Philips Radiation Oncology Systems, Zürich, Switzerland*

Purpose or Objective: The modulated arc (mARC) technique is Siemens analogue to volumetric modulated arc therapy (VMAT), with a different underlying principle and technical implementation. While this presents the only available rotational technique for existing Siemens users, only few treatment planning systems (TPS) are capable of mARC planning. In particular, the widespread Philips Pinnacle TPS does not support mARC. The purpose of this work is to present two solutions for mARC plan creation starting from either IMRT or SmartArc plans.

Material and Methods: In the first approach, the user creates a step-and-shoot IMRT plan with any number of beams ordered either clockwise or counter-clockwise, and one segment per beam. If desired, a few beams with more than one segment can be included. This plan is then exported as RT-Dose and an in-house software is used to modify the file in such a way that it is interpreted by the linac as an mARC plan. For this aim, each single-segment beam is converted into an arclet of a user-specified length (usually 4°). The calculated dose distribution of the IMRT plan corresponds to the mARC treatment, because mARC dose is usually

calculated under the assumption of stationary arclet delivery.
The second method is a dedicated solution for mARC planning in Philips Pinnacle (V9.2 or higher) without the detour of an external software. In this approach, a SmartArc (VMAT) plan is created in the TPS with 8° final spacing of optimization points. Then a Pinnacle script is applied which duplicates and shifts the optimization points in such a way to separate phases of beam on and of MLC movement. This resulting plan is still treated like a SmartArc plan in the TPS, but irradiated as mARC at the linac.
We present the proof-of-principle and dosimetric verification using the PTW Octavius rotation unit with 2D-array.

Results: A number of plans were created for prostate and head-and-neck cancer. All converted plans could be irradiated without problems. 3D dose distributions agree with the calculated dose distributions (mARC and approximated stationary field plan) within the gamma criteria for IMRT verification (over 90 % of the points passing the criteria of 3 % deviation in local dose, 3 mm distance to agreement, for all dose values above 10 % of the maximum, example in Figure).

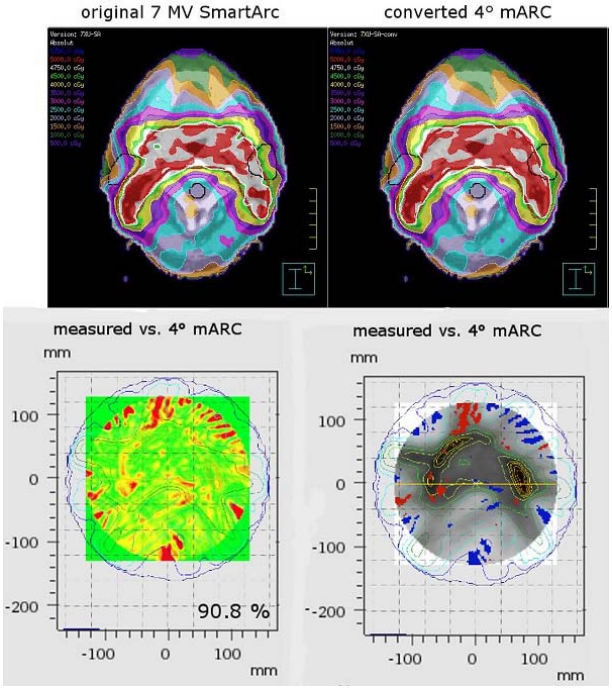

	1st approach: IMRT to mARC	2nd approach: SmartArc to mARC
Starting plan:	**IMRT plan**	**SmartArc plan**
Specifications:	• Beams ordered (either clockwise or counter-clockwise) • Number of segments ≈ number of beams • Collimator angle constant • Same beam energy	• Final spacing of optimization points = 8° (set by script) • Only works in Philips Pinnacle with SmartArc
Workflow:	• Export plan as RTPlan • Run conversion script (linux-based) • correct cross-sum check • import in Mosaiq and send to machine for treatment	• run script in Philips Pinnacle • re-calculate dose distribution • export plan for treatment
User choices:	• if #segments = #beams, this will become an mARC plan • if a beam holds more than 1 segment, this will become a hybrid field • any number of beams with any spacing • any arclet length	• any number of rotations
Limitations:	• generally just one rotation, more rotations require manual separation of beams into several plans	• always creates arclets of 4° length spaced 8° apart
Dosimetric accuracy:	**As good as for a dedicated mARC planning system**	
Treatment stability:	**As good as for a dedicated mARC planning system**	

Conclusion: Both solutions offer the possibility of mARC planning inside a non-dedicated TPS. If Philips Pinnacle with SmartArc is available, plan creation is straightforward and can be performed inside the TPS. Otherwise, a special format of IMRT plan is required, which is externally modified before treatment. In both cases, good dosimetric accuracy is achieved, making this a viable solution for the creation of mARC treatment plans inside any treatment planning system.

EP-1632

Spinal SBRT: improving plan quality using an existing database and a geometric parameter

L. Masi[1], R. Doro[1], I. Bonucci[2], S. Cipressi[2], V. Di Cataldo[2], I. Peruzzi[1], L. Livi[3]
[1]*IFCA, Medical Physics, Firenze, Italy*
[2]*IFCA, Radiation Therapy, Firenze, Italy*
[3]*Azienda Ospedaliera Universitaria Careggi, Radiation Therapy, Firenze, Italy*

Purpose or Objective: The achievable PTV coverage of spinal SBRT treatment plans depends on the spatial relationship between cord and target. PTV coverage is often sacrificed to fulfill the cord constraints and there are no objective criteria to determine whether an optimal coverage has been achieved. This may lead to suboptimal plan quality and to dependence on the planner's experience. A method to predict the achievable PTV coverage is proposed, which is based on an existing database and on a geometric parameter related to the cord-target 3D distance.

Material and Methods: A clinical database of 70 spine SBRT plans, 41 first treatment and 29 retreatment cases, delivered by the Cyberknife either in 3 fractions or in one fraction is used. TG101 cord constraints or stricter limits for reirradiation were applied. The 3D distance of cord to target was quantified by the expansion-intersection volume (EIV) [M.Descovich (2013)] adapted to spine and calculated as the intersection of the CTV and the cord, both expanded by 5 mm. Plans were classified into 3 groups according to the ratio of the prescribed dose to the cord maximum dose (PD/cordDmax): 1) 1.1-1.65; 2) 1.66-1.9; 3) 1.91-2.9. For each group the correlation between EIV and the PTV coverage was studied, analyzing the linear regression between EIV and the uncovered target volume (PTVout). As validation EIV was calculated for 20 new cases, the expected PTVout value computed by the regression equation and the plans optimized aiming to obtain the predicted coverage respecting the OAR constraints.

Results: EIV values ranged from 0.3 to 18 cc indicating a representative sample of the possible anatomical configurations. Average PTV coverage was 91.2% (range 81.5-98.6%). A significant ($p < 0.01$) positive correlation (Pearson's $r > 0.67$) was observed between EIV and the uncovered PTV (PTVout) over the 3 groups, confirming that for larger EIV, lower coverages are expected. The slope of the 3 respective regression lines increased from 0.67 to 0. 8 for increasing PD/cordDmax. For 16 out of the 20 new plans PTV coverage was higher than the predicted value, i.e PTVout was below the regression line (fig.1) fulfilling the optimization purpose.

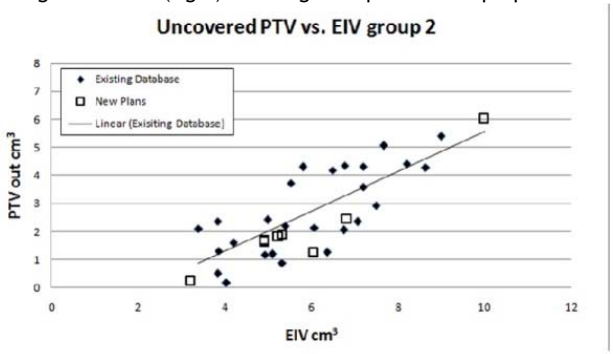

Conclusion: This study confirms that EIV is a good parameter to represent the cord-target 3D distance in spinal SBRT. The analysis accounted for the interplay between anatomical characteristics and required dose gradient. The results

obtained by the new optimized plans confirm that the EIV method can guide optimization and improve plan quality.

EP-1633

Optimal dose prescription in Linac-based SBRT using VMAT: a "Pareto fronts" approach

S. Cilla[1], A. Ianiro[1], F. Deodato[2], M. Gabriella[2], C. Digesù[2], P. Viola[1], M. Craus[1], M. Ferro[2], V. Picardi[2], M. Nuzzo[2], F. Labropoulos[2], V. Valentini[3], A.G. Morganti[4]

[1]Fondazione di Ricerca e Cura Giovanni Paolo II- Università Cattolica del S. Cuore, Medical Physics Unit, Campobasso, Italy

[2]Fondazione di Ricerca e Cura Giovanni Paolo II- Università Cattolica del S. Cuore, Radiation Oncology Unit, Campobasso, Italy

[3]Policlinico Universitario A. Gemelli- Università Cattolica del S. Cuore- Roma, Radiation Oncology Department, Roma, Italy

[4]DIMES Università di Bologna - Ospedale s.Orsola Malpighi, Radiation Oncology Department, Bologna, Italy

Purpose or Objective: Pareto fronts are a powerful mathematical strategy to formalize the trade-off between a given set of mutually contradicting objectives. We use this strategy to determine the optimal block margin and prescription isodose for both optimal target coverage and normal tissue sparing for VMAT treatments in extracranial stereotactic radiotherapy.

Material and Methods: Three spherical-shaped targets of different dimensions (20cc, 55cc and 101cc) were selected from our clinical database. GTV included macroscopic disease defined on CT. PTV was defined based on internal margin and setup margin. Healthy liver was considered whole liver minus GTV. A single fraction dose of 26 Gy was prescribed (PD=Prescription Dose). VMAT plans were generated with Ergo++ (Elekta) using a 10MV single arc. Pareto fronts based on (i) different MLC block margin around PTV (ranging from +4mm to -2mm with 1 mm step) and (ii) different prescription isodose line (IDS) ranging from 50% to 100% of PD were produced. For each block margin, the greatest IDS fulfilling the two criteria: 95% of PTV volume reached 100% of PD and 90% of PTV reached 99% of PD was considered as that providing the optimal clinical plan for target coverage. The liver mean dose, V7Gy and V12Gy were used together with the PTV coverage (1-V100) to generate the fronts. The ratio of the prescription isodose surface volume to PTV volume (conformity index CI), gradient index (GI=V50/V100), the ratio of normal tissue volume receiving 50% of prescription dose and PTV volume (NTV50/PTV), homogeneity index (HI=D2%/PD) and healthy liver irradiation in terms of mean dose, V7Gy and V12Gy were calculated to compare different plans

Results: A total of about 450 plans (150 per lesion) were calculated for all block margins and isodose lines. Pareto fronts generated for one of the lesions are plotted in figure 1a,b. For all block margins, PTV coverage is deteriorated with the decrease of liver Dmean, V7Gy and V12Gy. The front for 1mm MLC margin is situated below and on the left of the other fronts for all the three different target sizes. Figure 1c,d show the GI plotted against the prescribed isodose lines and the HI index for the optimal clinical plans. In all cases GI shows a U-shaped behavior with minimum values at 1mm for all metrics. The location of these minimal points was found independent of tumor dimensions. Minimal GI values were found at HI values approximately equal to 1.3. Figure 1e and 1c show the CI and the NTV50/PTV versus HI. With 1mm MLC margin the optimal prescription isodose line was found 77-82% for the three different lesions.

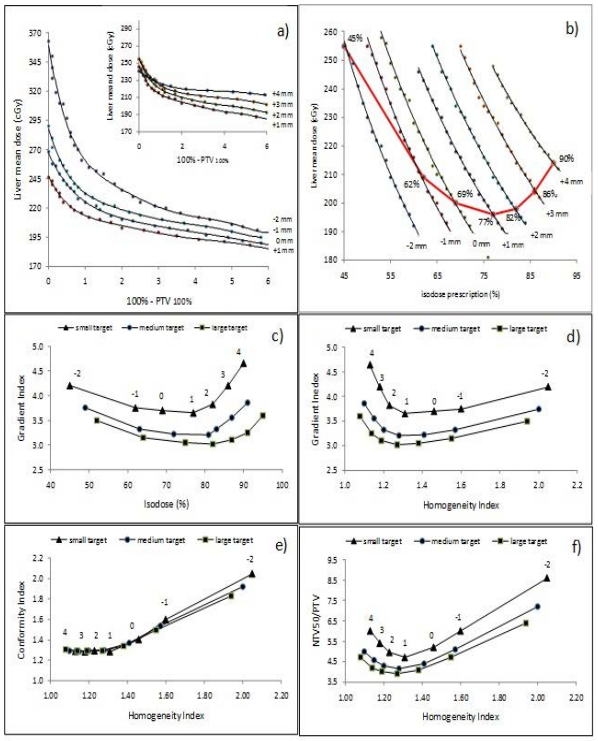

Figure 1: (a) Pareto fronts obtained for liver mean doses vs target coverage for all block margin. Each dot represents a single plan; (b) Pareto fronts obtained for liver mean dose and isodose lines prescriptions. Bold red line connects plans with same optimal dose coverage for different block margins (i.e. the clinical optimal plans obtained with the greatest IDS fulfilling the two criteria: 95% of PTV volume reached 100% of PD and 90% of PTV reached 99% of PD); (c) gradient index vs isodose line prescription for the clinical optimal plans, (d) gradient index vs homogeneity index for the clinical optimal plans, (e) conformity index vs homogeneity index for the clinical optimal plans, and (f) normal tissue volume receiving 50% of PD for the clinical optimal plans. In figure (c) to (f) numbers represent the block margins.

Conclusion: Pareto fronts provide a rigorous strategy to choice clinical optimal plans in SBRT treatments. Our evaluation shows that a 1mm MLC block margin provides the best results with regard healthy liver tissue irradiation and steepness of dose fallout. This choice provided optimal SBRT plans at dose prescription to 77%-82% isodose line for all target dimensions.

EP-1634

Treatment of extremity soft tissue sarcoma using protons - robustness of single and matching fields

B. Knäusl[1,2], L. Ulbrich[1], D. Georg[1], G. Kragl[2], K. Dieckmann[1], M. Stock[2], P. Georg[2]

[1]Medical University of Vienna, Department of Radiation Oncology and Christian Doppler Laboratory for Medical Radiation Research for Radiation Oncology, Vienna, Austria

[2]EBG MedAustron GmbH, Medical Department, Wiener Neustadt, Austria

Purpose or Objective: Extremity soft tissue sarcomas (ESTS) are treated with combined surgery and radiotherapy, involving large volumes of healthy tissue. This increases late toxicity, which has a negative impact on quality of life. Due to the conformal dose distribution of protons a reduction of healthy tissue exposure can be expected. The clinical benefit in preventing long term toxicity can be fully exploited only if the reproducibility and stability of treatment delivery can be guaranteed. The aim of our study was to show the feasibility and robustness of actively scanned proton therapy with single and matched fields.

Material and Methods: In 8 postoperative ESTS patients CTV was defined as GTV radially expanded by 1.5cm and longitudinally by 4cm. For PTV the CTV was expanded isotropically by 1cm [1]. The dose prescription was 60Gy (RBE) to D50% of the PTV (2Gy (RBE)/fraction). For treatment planning the software Raystation v4.7 (Raysearch Laboratories, Sweden) was used. 4/8 patients with PTVs longer than 18cm (maximal available field length) required field matching. Robust optimization is the method of choice in Raystation when two fields with different isocenters are

put together. The robustness was assessed by applying Hounsfield unit (HU) perturbations of 3.5% and isocenter shifts of 5mm. Single beam optimisation (SBO) using a horizontal beam line was used when possible. PTV constraints were D2% < 107%, D98% > 90% and V95% > 95% (ICRU). Limits to organs-at-risk (OAR) were the dose-surface area for the skin A60Gy (RBE) < 20cm2 [2], maximum dose to the bones DRBE, 2% < 60 Gy (RBE), maximum dose to the nerves and vessels DRBE, 2% < 70 Gy (RBE).
[1] Haas et al 2012 IJROBP 84: 572-580
[2] Sugahara et al 2012 RadiotherOncol 105: 226-231

Results: Patients with field lengths < 18cm (PTV volumes: 164-659 cm3) could be treated with SBO using 2 horizontal beams and table rotation. In the nominal plan, PTVV95% ranged from 96.3-98.9%. SkinA60Gy (RBE) was 10±7.5cm2. Treatment plans were robust against HU perturbations and 5mm shifts in sup-inf and right-left direction with V95 never dropping below 93%. D2% and D98% of the PTV and OAR doses never exceeded the limits. Shifts of 5mm in ant-post direction caused severe underdosage in the PTV down to V95% of 68%. Robust optimisation in ant-post direction could increase these values up to 91%.
For larger PTVs (420 cm3-2240cm3) field lengths ranged from 25-34 cm. The length of the field overlapping region essentially influenced the robustness of the treatment plans. Isocenter shifts of 5mm to each other or apart resulted in a PTVD2% change of 7% for an overlap >6cm increasing up to 15% for ≤ 6cm (Figure 1).

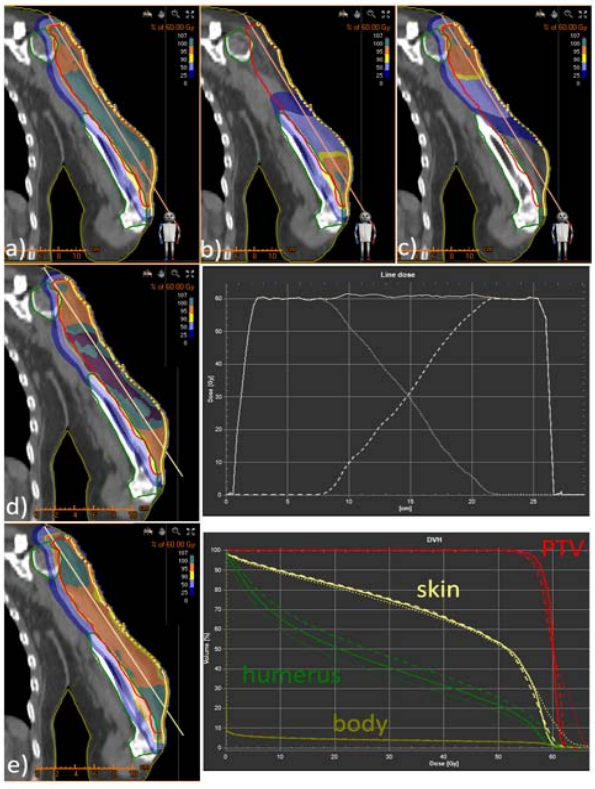

Figure 1
a) nominal plan with one matching boarder of a representative patient with a field overlap > 6cm with the respective line doses ; b) caudal field; c) cranial field
d) + e) isocenters of the two matching fields shifted by 1 cm to each other and apart with the corresponding DVH curves (solid: nominal plan; dotted: isocenters shifted to each other; dashed: isocenters shifted apart)

Conclusion: Robust treatment plans could be achieved for ESTS patients employing a horizontal beam line only. Before clinical implementation, dosimetric monitoring of skin doses should be performed to verify the calculated values. If field matching is needed a maximal overlap of the matching fields should be guaranteed to avoid hot or cold spots in the overlapping area.

EP-1635

Volumetric modulated arc therapy optimization including dynamic collimator rotation

M.K. Fix[1], D. Frei[1], W. Volken[1], D. Terribilini[1], P. Manser[1]
[1]*Division of Medical Radiation Physics and Department of Radiation Oncology Inselspital, Bern University Hospital, and University of Bern, Switzerland*

Purpose or Objective: During the last couple of years, volumetric modulated arc therapy (VMAT) is a treatment modality of increasing interest in radiation oncology. Thereby VMAT utilizes dynamic gantry rotation, dynamic MLC and varying dose rate. However, in addition the collimator angle could be changed dynamically, thus, increasing the degrees of freedom for the optimization, which might lead to improved dose distributions. This work investigates the feasibility of VMAT optimization including a dynamic collimator rotation.

Material and Methods: In this work a 20 x 20 x 20 cm^3 homogeneous water phantom with a cigar shaped target volume and a close-by spherical shaped critical structure was used. By means of the Eclipse Research Scripting a predefined collimator rotation was included to a partial arc in a not yet optimized treatment plan. For this purpose a different collimator angle was assigned for each dicom control point. Thereby the collimator rotation takes into account the physical limitations for the dose delivery. This treatment plan was then imported into the treatment planning system Eclipse using the Eclipse Research Scripting interface. Then the VMAT optimization was performed applying the PRO3 optimization algorithm in a research version of Eclipse. For the dose calculation of the optimized treatment plan the Swiss Monte Carlo Plan (SMCP) was used [1]. Similarly, a dose distribution was determined using a static collimator angle as typically applied in conventional VMAT applications. The resulting DVHs for the target and the critical structure were compared for the treatment plans.

Results: The optimization of a VMAT treatment plan with a dynamically rotating collimator was successfully performed. The comparison of the DVHs for the target volume showed a slight improvement of the coverage as well as the dose homogeneity for the treatment plan using dynamic collimator rotation compared to the plan applying a fixed collimator angle. Additionally, the dose to the critical structure could be reduced when using the dynamic collimator rotation instead of a fixed collimator angle.

Conclusion: The usage of a dynamic collimator rotation for VMAT is feasible and has the potential to improve the dose distribution for the target while reducing the dose to critical structures. This work was supported by Varian Medical Systems.
References:
[1] M.K. Fix, P. Manser, D. Frei, W. Volken, R. Mini, E.J. Born, *An efficient framework for photon Monte Carlo treatment planning,* Phys. Med. Biol., 52:N425-437, 2007.

EP-1636

Clinical validation of Automated Planning process in rectal cancer IMRT treatment

N. Dinapoli[1], G. Chiloiro[1], G. Mattiucci[1], L. Azario[2], M. Gambacorta[1], E. Placidi[2], S. Teodoli[2], L. Boldrini[1], C. Valentini[3], M. Balducci[1], V. Valentini[1]
[1]*Università Cattolica del Sacro Cuore -Policlinico A. Gemelli, Radiation Oncology Department, Rome, Italy*
[2]*Università Cattolica del Sacro Cuore -Policlinico A. Gemelli, Physics Institute, Rome, Italy*
[3]*Faculty of Medicine and University Hospital Carl Gustav Carus- Technische Universität Dresden, Radiation Oncology Department, Dresden, Germany*

Purpose or Objective: Several studies suggest that IMRT can reduce toxicity in rectal cancer patients. A preconfigured plan model might improve daily clinical activity outcomes. Aim of this study was the evaluation of the performances of RapidPlan®Varian Medical System, a commercial model-

based optimization engine, in locally advanced rectal cancer (LARC) IMRT plans in terms of planning target volume (PTV) coverage and Organs at Risk (OaRs) sparing.

Material and Methods: Between January 2014 and March 2014, 60 previously irradiated patients with LARC were retrospectively recruited: 40 IMRT plans were selected to configurate the Dose Volume Histogram (DVH) model and to train it. The remaining 20 were firstly manually optimized by 2 medical physicists and then used to validate the model as benchmark plans (BP). OaRs constrains followed Quantec guidelines. Three model based on different PTV objectives have been generated: DVH model 95-105%, DVH model 98-105% and DVH model 98-103% where more than 95%, 98% and 98% of the PTV received more than 95% of the prescription dose and less than 5%, 5% and 3% of the PTV received more than 105% of the prescription dose, respectively. The performances of automated plans (one series for each model) vs BP were statistically compared using Wilcoxon signed-rank test, for PTV V95 and V105, hot spot out of PTV (HToPTV), bladder mean dose (BmD) and maximum dose (BMD), bowel mean dose (BomD) and V45 (BV45). Two expert radiotherapists (observer1 and observer2) clinically validated in double blind the IMRT plans.

Results: A statistical significant improvement was observed for the following dosimetric parameters: HToPTV (for DVH model 98-105 and DVH model 98-103 plans, p=0.002 and p=0.005, respectively); BmD (DVH model 95-105 and DVH model 98-105 plans, p= 0.01 and p= 0.03, respectively). A statistically significant disadvantage in terms of BMD was observed for DVH model 98-103 and DVH model 98-105 (p=0.02 and p= 0.05, respectively). No statistical differences were recorded in term of BV45 and BomD and PTV V95 and V105. (TABLE 1) At a clinical validation, the two observers most frequently chose the test plans optimized from DVH model 98-103% (34 times versus 26 times of the BP).

	DVH model 95-105 vs BP (p value)	DVH model 98-105 vs BP (p value)	DVH model 98-103 vs BP (p value)
Bladder mean dose	0.01	0.03	0.13
Bladder maximum dose	0.35	0.02	0.05
Bowel mean dose	0.65	0.81	0.84
Bowel V45	0.75	0.70	0.90
Hot spot out of PTV	0.13	0.002	0.005

Conclusion: The results of this study show dosimetric and clinical improvements of IMRT plans optimized by knowledge-based planning models compared to BP. The data suggest and encourage the application of this engine into daily clinical practice.

EP-1637

Dose plan assessment of coplanar and non-coplanar beam angle optimization algorithms

T. Ventura[1], H. Rocha[2], B.C. Ferreira[3], L. Khouri[4], J. Dias[2], M.C. Lopes[1]

[1]Instituto Português de Oncologia Coimbra - Francisco Gentil-EPE, Medical Physics Department, Coimbra, Portugal

[2]INESC, INESC Coimbra, Coimbra, Portugal

[3]Polytechnic Institute of Porto, School for Allied Health Technologies, Porto, Portugal

[4]Instituto Português de Oncologia Coimbra - Francisco Gentil-EPE, Radiotherapy Department, Coimbra, Portugal

Purpose or Objective: To assess the performance of coplanar and non-coplanar beam angular optimization for two different algorithms integrated in a fully automated multicriterial plan generation system for nasopharyngeal tumour cases.

Material and Methods: A retrospective study including data of 40 nasopharyngeal cases was performed. In each plan, the primary tumour, up to 3 adenopathies, and ipsilateral and contralateral lymph nodes were irradiated with doses of 70 Gy, 59.4 Gy and/or 54 Gy delivered in 33 fractions, respectively. A 'wish-list' based on hard constraints and prioritized objectives for the target volumes and the organs at risk was tailored according to the local clinical practice. Seven coplanar equidistant angles (E7) were used in the standard plan. For each patient, this IMRT plan was compared to coplanar and non-coplanar IMRT plans with 5, 7 and 9 beam angles, optimized with a multicriterial beam angle optimization algorithm (A5, A7, A9), and an in-house derivative-free optimization algorithm (B5, B7, B9). Dose distribution quality for each plan was assessed through DVH analysis and a dose metrics weighted sum approach.

Results: Globally all generated plans presented a good dose distribution. On average, similar results have been obtained for both coplanar beam angle optimization algorithms. For non-coplanar beams, the best results were obtained with algorithm B. When compared with B coplanar cases, on average, slightly better results were achieved with non-coplanar plans for all number of beams (B5, B7 and B9). For algorithm A, on average, no relevant improvement was obtained with the non-coplanar optimization compared with the coplanar plans or the E7 plans. Despite these average results, in particular clinical cases, appreciable differences concerning organ sparing could be found. Up to 9 Gy difference in parotid sparing was achieved both with B9 and A9 coplanar plans when compared with E7 plans. This maximum dose sparing rose to 22 Gy when non-coplanar beams were considered. For the spinal cord, a maximum dose difference of 6 Gy was found between A9 and B9 both for coplanar and non-coplanar beam geometries. In the chiasm, B9 gave up to 5 Gy less than A9 in coplanar beams but this dose sparing for B9 rose to 35Gy for the non-coplanar geometry. For ears B5 non-coplanar plans achieved a better performance than A9 coplanar plans in 66% of the cases. For this structure, up to 15 Gy differences were found between B5 non-coplanar and A9 coplanar plans.

Conclusion: Using a dose metric weight sum approach two beam angle optimization algorithms were compared in a faster and systematic way. On average, both algorithms performed well for the tested clinical cases. However, the different beam angle optimization strategies intrinsic to each of the algorithms revealed to favour algorithm B for non-coplanar beam geometries while for coplanar beams no relevant differences were found between algorithms A and B.

EP-1638

Multicriteria optimisation for whole-pelvic VMAT planning in prostate patients

M. Buschmann[1,2], Y. Seppenwoolde[1,2], D. Georg[1,2]

[1]Medical University of Vienna, Department of Radiation Oncology, Wien, Austria

[2]Medical University of Vienna, Christian Doppler Laboratory for Medical Radiation Research for Radiation Oncology, Wien, Austria

Purpose or Objective: A Multicriteria Optimization (MCO) algorithm for VMAT planning that can generate Pareto-optimal plans was recently implemented in the RayStation TPS. The user can generate a plan database with a defined number of Pareto-optimal plans and can explore tradeoffs between different objectives in real time. This study investigates MCO for semi-automated VMAT planning for irradiation of prostate including pelvic lymph nodes.

Material and Methods: CT datasets of ten patients with high risk prostate cancer were used for this study. For each patient, a two stage VMAT plan (6 MV Elekta Agility linac) was generated, consisting of a stage 1 plan delivering 50.4 Gy to the lymph nodes (PTV-LN) and 56 Gy to the prostate (PTV-P) in a simultaneous integrated boost (SIB) in 28 fractions with a dual arc and a stage 2 plan delivering 22 Gy to the PTV-P in 11 fractions with a partial arc. The separation of the

plan into two stages was performed for radiobiological reasons. Planning goals were D98>95% and Dmax<110% for the PTVs with maximum OAR sparing. The plans were analyzed for planning time efficiency (hands-on time of the planner and total planning time) and the sum of stage 1 and stage 2 was tested against our clinical DVH constraints for OARs.

Results: A list of objectives and constraints was generated for MCO planning. The number of plans created for the MCO database was set to 33 (3n) and 18 (2n) for the stage 1 plan and the stage 2 plan, respectively, where n corresponds to the number of objectives. The best-suited plan was selected and was segmented to a deliverable VMAT plan in the next optimization step, which minimizes the error in DVHs between pre-optimized and final doses. Some fluence-based dose distributions of the stage 1 plan turned out to be infeasible to segment and recreate, which made additional user interactions (up to 2) necessary to get acceptable plans. The segmentation of the deliverable plan was a critical step that degraded the quality of the Pareto-optimal plan. The 3D information of the pre-optimized dose distribution was lost, which resulted in hotspots of >110% in the low dose PTV-LN in the SIB plan. The average hands-on times were 156 sec and 83 sec and the average total planning times were 1 h 27 min and 9 min for stage 1 and stage 2, respectively. Clinical dose constraints for the summed plans were all met.

Table: List of constraints and objectives for the generation of the plan databases for both plan stages in MCO planning

Stage 1 plan SIB

Objectives	Constraints
Rectum: Max EUD 0 Gy (A=2)	PTV-Prostate: Max Dose 56 Gy x 1.1
Bladder: Max EUD 0 Gy (A=2)	PTV-Prostate: Min Dose 56 Gy x 0.95
Bowel: Max EUD 0 Gy (A=2)	PTV-Prostate: Min DVH 56 Gy to 90%
Femoral Heads: Max EUD 0 Gy (A=2)	PTV-Lymph nodes: Min Dose 50.4 Gy x 0.95
External: Max Dose 45 Gy	PTV-Lymph nodes: Min DVH 50.4 Gy to 90%
External: Fall-Off 50.4 Gy to 0 Gy in 1 cm	External: Max Dose 56 Gy x 1.1
PTV-Prostate: Uniform Dose 56 Gy	
PTV-Prostate: Min Dose 56 Gy	
PTV-Lymph nodes: Uniform Dose 50.4 Gy	
PTV-Lymph nodes: Max Dose 50.4 Gy	

Stage 2 plan

Objectives	Constraints
Rectum: Max EUD 0 Gy (A=2)	PTV-Prostate: Max Dose 22 Gy x 1.1
Bladder: Max EUD 0 Gy (A=2)	PTV-Prostate: Min Dose 22 Gy x 0.95
Bowel: Max EUD 0 Gy (A=2)	PTV-Prostate: Min DVH 22 Gy to 90%
Femoral Heads: Max EUD 0 Gy (A=2)	External: Max Dose 22 Gy x 1.1
External: Max Dose 20 Gy	
External: Fall-Off 20.9 Gy to 0 Gy in 1 cm	
PTV-Prostate: Uniform Dose 22 Gy	
PTV-Prostate: Min Dose 22 Gy	

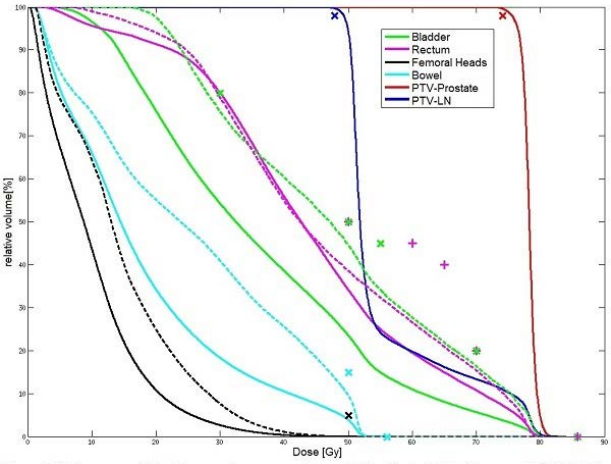

Figure: Solid lines: mean DVH of the sum plans averaged over all 10 patients. Dashed lines: worst OAR DVH of all patients with respect to the clinical constraints. The crosses represent the target coverage goals and clinical OAR constraints of respectively colored organs.

Conclusion: Raysearch MCO can generate highly conformal prostate VMAT plans with minimal workload in the settings of prostate-only irradiation and prostate plus lymph nodes irradiation with SIB. Further studies will compare MCO to manual planning and other automated planning methods.

EP-1639

Single-click generation of whole breast IMRT treatment plans

G. Wortel[1], R. Harmsen[1], J. Trinks[1], A. Duijn[1], R. De Graaf[1], A. Scholten[1], C. Van Vliet-Vroegindeweij[1], E. Damen[1]
[1]*The Netherlands Cancer Institute, Department of Radiation Oncology, Amsterdam, The Netherlands*

Purpose or Objective: To develop and evaluate automated Whole Breast (WB) IMRT treatment planning by FAST; our in-house developed Framework for Automatic Segmentation and Treatment planning.

Material and Methods: The automatic planning is started when the physician has defined the target volume (using delineation software). FAST opens our treatment planning system Pinnacle3, creates a patient record, imports the CT, and auto-segments the OARs. A medial and lateral tangential beam are created, each consisting of an open segment giving approx. 80% of the dose, supplemented with a limited number of IMRT segments. The open beam is set up such to just include the PTV on the medial side. As we do not allow the beam to cross the patient midline (to enable possible RT of the contralateral breast), the beam is shifted and the collimator is rotated until the beam crosses the patient midline. The heart is automatically blocked from the field. On the lateral side, the beam is opened outside the patient in order to be robust against contour changes. Finally, the plan is optimized with a fixed set of objectives on the heart, lungs, PTV and conformity. The optimized plan can be evaluated, and possibly modified, by the RTT.
FAST is able to create 8 plans for different combinations of heart margin (either 0 or 5 mm) and beam energies (either 6 or 10 MeV), which takes 20 minutes. The physician and RTT can select the most suitable plan.
To investigate the benefits of automatic planning of WB treatments, a preclinical test was performed on 10 patients where our RTTs verified whether the best generated plan met our clinical standards, and estimated how much time was saved by automatic planning.

Results: The preclinical test showed that for 60% of patients, the selected plan meets clinical requirements without further modifications. In two cases, the beam setup was rejected because it included too much lung. The auto-segmentation of the heart was incorrect in one case, which resulted in an erroneous beam setup. The final case only required some fine-tuning.
The time spent on a single treatment plan can be reduced by up to 2h if the plan requires no or little fine tuning (up to 1.5h if the beam setup has to be redone manually). Considering that approx. 600 WB treatments are performed in our institute per year, this leads to a total yearly time-saving of approx. 1000h.
As FAST offers a clear overview of possible plans with different clinical trade-offs, the RTT can make a well-considered decision regarding the heart margin and beam energies. A comparison between the FAST plan and the clinically-used plan showed that, in 70% of cases, this leads to a different configuration being chosen.

Conclusion: We have found that the use of FAST for WB plans significantly reduces the workload on our planning department while maintaining plan quality, and have therefore introduced it into our clinic as of October 2015. In the near future we plan to also implement SIB and locoregional breast techniques.

EP-1640

Evaluation of automatic treatment planning system: comparison with manual planning for liver SBRT.

E. Gallio[1], C. Fiandra[2], F.R. Giglioli[1], A. Girardi[2], T. Rasoarimalala[3], U. Ricardi[2], R. Ragona[2]
[1]*A.O.U. Città della Salute e della Scienza, Department of Medical Physics, Torino, Italy*
[2]*University of Turin, Radiotherapy Unit Department of Oncology, Torino, Italy*

[3]International Center of Theoretical Physics, Department of Applied Physics, Trieste, Italy

Purpose or Objective: Version9.10 of Pinnacle[3] TPS (PhilipsMedical Systems) includes Auto-Planning (AP) module. The user definesbeams, optimization goals for PTV-coverage and threshold doses for each organat risk (OARs). TheAP engine tries to meet the goals and further lower dose to OARs with minimalcompromise to the target coverage by multiple optimization iterative loops andby automatically creation of objectives and optimization on additionalstructures. The aim of this study was to evaluate and compare APplans with different TPS manual ones for liver stereotactic body radiotherapy(SBRT) treatments.

Material and Methods: Ten patients with liver tumour were included in thestudy. Six plans were created for each patient. Two plans were generated withAP of Pinnacle[3] TPS (version 9.10) using SmartArc technique and two withtraditional planning (MP), always with Pinnacle SmartArc, by two differentexpert medical physicists. Others two experts performed two VMAT plans withMonaco TPS (version 5.0, Elekta) (VM). Dosimetry comparison was done in termsof the PTV coverage, gEUD, OARs (normal liver, kidneys, spinal cord, bowel,heart, rib cage, stomach and major vessels) sparing, as well as homogeneityindex (HI), conformity index (CI) and gradient index (GI). Also total monitorunits, number of beam segments and beams complexity metrics (plan average beamarea BA, plan average beam irregularity PI and plan average beam modulation PM)were evaluated.

Results: Preliminary results of three patients indicatedthat, for same gEUD (p value = 0.99), there were not significant differences betweenAP, MP and VM for CI (p = 0.83). Relevant differences were found instead aboutbeams complexity metrics (p = 0.23 for BA, 0.01 for PI and 0.05 for PM), HI (p= 0.03), monitor units and OAR sparing. In particular, median and mean values ofmonitor units were respectively 3212 and 3646 ± 1529 for AP, 2930 and 2923 ± 447 for MP and 5006 and 4850 ±570 for VM. Similar data were found for number of beams segments. Also forOARs, in particular for healthy liver, results showed different behaviour ofTPS. The healthy liver median volume below 15 Gy was 592 cc for AP, 596 cc forMP and 659 cc for VM; the mean values were 625 ± 150 cc for AP, 632 ± 120 ccfor MP and 673 ± 46 cc for VM.

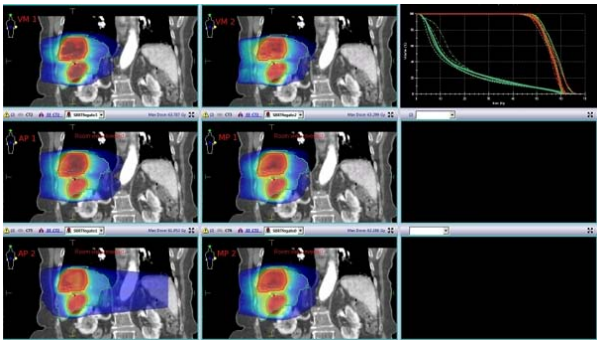

Conclusion: Analysis of first three patientsdemonstrated that AP and MP employed much less monitor units respect to VM andshowed a minor PI. However, in particular complex cases, AP and MP had moredifficulty to spare the organs at risk than VM. Furthermore, there was sensibleintra-patients variability for AP and MP. AP was less human employment time consumingthan both manual planning systems. At the congress, results of all ten patientswill be presented.

EP-1641

Clinical experiences with RapidPlan knowledge-based treatment planning

E. Adams[1], C. South[1], M. Hussein[1], A. Barnard[1], S. Bailey[1], S. Chadwick[1], S. Eplett[1], S. Dymond[1], C. Navarro[1], T. Jordan[1], A. Nisbet[1]

[1]St. Luke's Cancer Centre- Royal Surrey County Hospital, Radiotherapy Physics, Guildford, United Kingdom

Purpose or Objective: RapidPlan (RP) knowledge-based treatment planning software has been in clinical use at our institution since November 2014 and, to date, has been used to plan in excess of 100 patients. Models have been created for a variety of treatment sites, and plans have been compared with class-solution based methods of optimising in terms of plan quality and efficiency of planning and delivery.

Material and Methods: A prostate model was generated based on 5-field IMRT plans with three prescribed dose levels (78Gy/71Gy/60Gy, delivered in 37 fractions). Prior to routine clinical use of the model, planning and delivery efficiency were investigated using twenty patients, who were planned first using local objective templates, and then reoptimised using RP-generated objectives. Six planners of varying experience participated, and the same planner performed both optimisations for a patient. The planners timed how long each method took to generate a plan, and also noted how the RP plan compared with the standard plan, and whether further modifications were required after the initial RP optimisation.
Following final adjustments to the model, it was put into routine clinical use for all prostate cases with three dose-levels. Further models were created for cervix patients treated with RapidArc and post-prostatectomy patients; both single dose-level. For all models, a record was kept of situations where RapidPlan was unable to generate an acceptable distribution to allow further investigation and modification of model parameters as required. Additionally, the applicability of the models to situations outside the original scope was investigated.

Results: The results of the double-planning study can be seen in Table 1 & Fig. 1. RapidPlan produced a plan that was of equal or higher quality in 85% of cases, and the planning times were significantly reduced with a median time saving of 70 mins per patient (range 0-240min). The spread on the timings was much smaller for RP, indicating that the planning times were less dependent on case complexity and planner experience when using RapidPlan. Monitor units were found to be slightly higher with RP (p=0.03); however, this is unlikely to be clinically significant.
Considerable reductions in planning time were also seen for the cervix and post-prostatectomy models. Continuing evaluation of all models in routine use has indicated that they work well for the majority of the population. The models were also found to give a good starting point for situations outside the initial scope in some instances, e.g. the cervix model was used successfully for both a single dose-level prostate + nodes and a two dose-level endometrium + para-aortic nodes.

Table 1: Results of double-planning prostate IMRT patients

	Standard	RapidPlan
Planning time (min) (median ± SD)	80 (±88)	18 ± 13
% final plans better	15	45
MU (mean± SD)	659 (±52)	695 (±61)

Fig 1: Planning time for conventional optimisation methods compared to RapidPlan for planners (A-F) of varying experience.

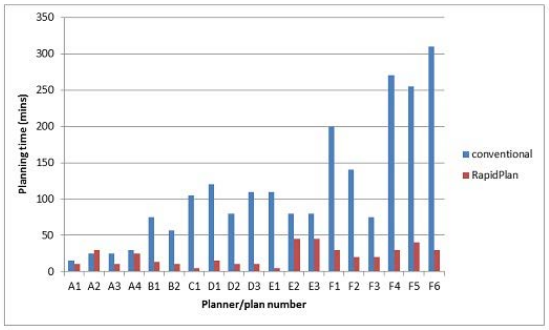

Conclusion: RapidPlan has been found to produce good quality plans more efficiently than class-solution based methods in the majority of cases. Continual monitoring of model behaviour is recommended to allow refinement in order to ensure optimum performance for all patients.

EP-1642

Comparison between a conventional IMRT planning method and a new automated planning method.

M. MichelL[1], C. Bertaut[1], J. Castelli[1,2,3], R. De Crevoisier[1,2,3], C. Lafond[1,2,3]

[1]*Centre Eugène Marquis, Radiothérapie, Rennes, France*
[2]*Inserm, U1099, Rennes, France*
[3]*Université de Rennes-1, LTSI, Rennes, France*

Purpose or Objective: The inverse planning for IMRT is variable due to a high number of parameters to be defined by the operator. So the quality of treatment plan depends on the level of operator expertise. The aim of this study was to evaluate the automatic "AutoPlanning" planning tool implemented in Pinnacle v9.10 TPS (Philips) for IMRT Step&Shoot (S&S) and VMAT techniques for three localisations: prostate, pelvis and head and neck (H&N) with integrated boost technique with three dose level.

Material and Methods: Twelve patient cases, four by localisation, were planned both for S&S and VMAT. The AutoPlanning method (AP) was compared with those obtained with a conventional manual planning method. The plan quality evaluation was based on the dose distributions (HDV and isodose), the dose homogeneity (HI), dose conformity (Conformal Number (NC) and COnformal INdex (COIN)) and complexity indexes (Plan Area (PA)) and Monitor Units (MU) number. The agreement between planned and measured doses was evaluated with Gamma index test with criteria of 3% and 3mm; the mean gamma value and the percentage of accepted points were also compared. The dosimetric QA was performed by Octavius 4D device (PTW).

Results: HDV AP plans showed equivalent quality compared to the manual plan. With AP for pelvis case, the median dose for bladder decreased by 6% and 4% for S&S and VMAT techniques respectively. With AP for H&N case, the parotids were better saving: the dose received by 30% of the volume decreased by 12% and 14% for S&S and VMAT techniques respectively; this sometimes causes a deteriorate of intermediate risk PTV coverage (PTV 63 Gy). The homogeneity index showed a lower interpatient variation for plan with AP: the standard deviation was 0.006 for S&S with AP against 0.030 for S&S with manual method. In case of prostate and pelvis, plans computed from the automated method showed greater conformity than those issued by the manual method but not in case of H&N. With regard to complexity of plan, the decrease in the area of the irradiation field (- 9.2 cm^2 on average) and the increase of the MU number (+ 104.5 MU on average) showed worse efficiency of automated plans than manual plans. The agreement between planned and measured doses was similar between the two planning methods.

Prostate	Rectal wall $D_{50\%}$ (Gy)	Rectal wall D_{max} (Gy)	Bladder wall $D_{50\%}$ (Gy)	Bladder wall D_{max} (Gy)	HI ideal value 0	CN ideal value 1	COIN ideal value 1	PA in cm^2	MU	Gamma mean	Accepted points %
S&S	**30.40**	**77.15**	18.37	**79.77**	**0.106**	0.822	0.691	**25.3**	**418.4**	**0.408**	**98.2**
S&S AP	30.56	77.52	**15.47**	80.06	0.116	**0.878**	**0.752**	23.5	428.0	0.414	97.7
VMAT	29.10	76.96	18.68	**79.92**	0.099	0.844	0.724	**30.0**	**363.5**	**0.375**	**98.8**
VMAT AP	**24.31**	**76.68**	**15.74**	80.16	**0.105**	**0.850**	**0.738**	23.9	434.9	0.409	97.4
Pelvis	**Digestive $D_{50\%}$ (Gy)**	**Digestive D_{max} (Gy)**	**Bladder $D_{50\%}$ (Gy)**	**Bladder D_{max} (Gy)**	**HI ideal value 0**	**CN ideal value 1**	**COIN ideal value 1**	**PA in cm^2**	**MU**	**Gamma mean**	**Point %**
S&S	**20.57**	**45.17**	35.06	44.58	**0.103**	0.841	0.689	**91.4**	**739.1**	0.526	93.8
S&S AP	20.64	45.37	**33.07**	**44.40**	0.126	**0.858**	0.689	75.7	850.4	**0.507**	**95.2**
VMAT	20.64	**44.18**	**32.31**	**44.43**	**0.070**	0.908	0.701	**80.4**	**867.2**	**0.448**	**95.2**
VMAT AP	**18.93**	44.44	**31.00**	44.84	0.076	**0.932**	**0.733**	62.0	1,116.9	0.488	93.1
H&N	**PTV63 V95%**	**PTV56 V95%**	**Parotids $D_{50\%}$ (Gy)**	**Spinal chord $D_{50\%}$ (Gy)**	**HI ideal value 0**	**CN ideal value 1**	**COIN ideal value 1**	**PA in cm^2**	**MU**	**Gamma mean**	**Point %**
S&S	**88%**	98%	40.77	29.02	**0.142**	**0.519**	**0.404**	**45.1**	**731.7**	0.527	**95.6**
S&S AP	83%	**96%**	**35.93**	**27.50**	0.143	0.486	0.387	42.4	782.2	**0.469**	94.6
VMAT	90%	**98%**	41.02	26.33	0.117	**0.554**	0.507	**53.3**	**631.4**	0.444	95.4
VMAT AP	**93%**	**96%**	**35.33**	**25.84**	**0.110**	0.549	**0.524**	43.1	766.2	**0.436**	**95.5**

Table 1: Comparison of dose values, dosimetric and efficiency indexes for the prostate, pelvis and head&neck cases calculated with a conventional planning method (S&S and VMAT) and with AutoPlanning method (S&S AP and VMAT AP). The bold and underlined values are those most favorable.

Conclusion: We validated the feasibility of the automated planning AutoPlanning method in S&S and VMAT in three localisations. However, intake of AutoPlanning can be considered variable according to the center experience. The manual actions are limited with Autoplanning because the operator does not restart the optimization once the process is finish, unlike the manual planning, where the operator re optimizes the plan sometimes several times according to his own expertise.

EP-1643

Rapidplan: 'knowledge-based' model with Tomotherapy plans

A. Botti[1], E. Cagni[1], R. Micera[2], S. Nicola[2], L. Orsingher[1], M. Orlandi[1], C. Iotti[2], L. Cozzi[3], M. Iori[1]

[1]*Arcispedale S. Maria Nuova, Medical Physics, Reggio Emilia, Italy*
[2]*Arcispedale S. Maria Nuova, Radiotherapy, Reggio Emilia, Italy*
[3]*Istituto Clinico Humanitas, Radiotherapy and Radiosurgery, Milan, Italy*

Purpose or Objective: In the radiotherapy planning process the expertise and experience of the operator is essential. This represents a critical element which can limit the quality of a therapy especially when using advanced technologies such as volumetric modulated arc therapy (VMAT). The automation of 'knowledge-based' planning procedures stands as a possible solution to improve the consistency of the plans. RapidPlan (RP) (Varian Medical Systems, USA), uses libraries of plans to create models that, basing on the delivery technique and patient's anatomy, predicts the dose-volume histograms of the organs at risk (OAR) and propose optimization constraints, avoiding long and multiple interactive optimization processes for new patients. In this scenario, it is useful to understand whether knowledge-based models, created using plans with consolidated technique, could supply the lack of the planning experience for a new treatment technique. In this study, HT (Hi-Art, Accuray, USA) plans of prostate cancer patients were used to create two RP models suitable for RapidArc (RA) plans. The aim of the work was to evaluate the feasibility and the performance of these models.

Material and Methods: In order to create the RP models, 2 groups of HT plans for prostate cancer patients, that included sparing of the rectum, bladder, and femoral heads, were selected: low risk group (LR), consisting of 35 plans, aimed to deliver 70 Gy to prostate PTV (PTVp) in 28 fractions – intermediate risk group (IR) consisting of 30 simultaneous integrated boost (SIB) plans with a prescribed dose of 70 Gy to PTVp and 56 Gy to vesicles PTV (PTVv) in 28 fractions. In order to prevent outliers, for all selected plans, structures and dose distributions were verified and validated by a radiation oncologist. The dose distributions of each plan were

linked to a virtual RA plan into the Eclipse TPS. Two full arcs with photon beam energies of 6MV and 30°/330° complementary collimator angle were set.. Two evaluation groups, consisting of 5 new knowledge based plans (KBP) each, were used to validate LR and IR models. KBP were compared with clinical plans (CP) in term of PTVs homogeneity, using HI = 100X (D2% - D98%)/D50%, and DVH endpoints, as shown in table 1.

Results: The KBP dose-volume constraints, generated by HT based models, were suitable for the RA optimization process . The 2 models were effective to suggest optimization objectives consistent with the criteria set by an expert RA planner. The quantitative comparison analysis between CP and KBP over the entire cohort of patients was summarized in Table 1. These preliminary results, do not evidence any substantial differences between the benchmark and the test plans.

Table 1
Average differences between test and original plans (KBP-CP). Ranges [in parenthesis] are also indicated.

Structures	DVH endpoints	LR	IR
PTVp	HI [%]	-1.3 [-3.2, 1.2]	1.0 [-3.5, 3.2]
PTVv			-3.3 [-6.2, 2.2]
Rectum	V_{60} [%]	1.0 [-3.5, 5.2]	-0.7 [-4.1, 4.2]
	V_{65} [%]	0.9 [-1.4, 3.3]	0.8 [-2.9, 3.2]
	V_{70} [%]	0.5 [-1.0, 1.2]	1.4 [-1.1, 0.8]
Bladder	V_{60} [%]	1.2 [-2.1, 3.1]	1.8 [-2.0, 3.2]
	V_{70} [%]	0.5 [-1.5, 2.2]	0.2 [-1.0, 2.4]
Right femur	D_{max} [Gy]	-1,3 [-2.5, 1.2]	-0.8 [-3.3, 1.8]
Left femur	D_{max} [Gy]	-2.0 [-4.5, 2.2]	-0.6 [-3.5, 1.5]

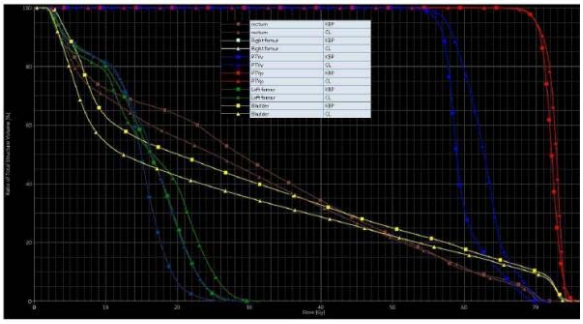

Fig 1
Example of DVH comparison for the validation experiment (IR case). The lines with triangles are for the benchmark clinical plans (CP), while the lines with squares are for the model-based optimisation (KBP). No interactiveoptimization process were used for KBP.

Conclusion: RP, commonly used with models based on the same technique of the KBP plans (IMRT/VMAT), is able to create models trained using HT dose distributions to generate comparable RA plans, comparable to CP. The study was carried out for prostate cancer patients.

EP-1644

Fast, high quality, semi-automated and fully-automated prostate radiotherapy treatment planning

P.A. Wheeler[1], M. Chu[1], O. Woodley[1], A. Paton[2], R. Maggs[1], D.G. Lewis[1], J. Staffurth[3], E. Spezi[1], A.E. Millin[1]
[1]*Velindre Cancer Centre, Medical Physics, Cardiff, United Kingdom*
[2]*Bristol Haematology and Oncology Centre, Radiotherapy Physics Unit, Bristol, United Kingdom*
[3]*Cardiff University, School of Medicine, Cardiff, United Kingdom*

Purpose or Objective: Automated IMRT planning has been successfully developed for many treatment sites including prostate, lung, breast and head & neck. Evaluative studies have shown automated planning is clinically feasible, yields high quality treatment plans and improves efficiency. Clinical implementation is however slow due to the lack of available automated solutions or comprehensive scripting facilities within many treatment planning systems. This work addresses this shortfall through the application of prostate VMAT class solutions to implement fully automated planning in commercially available scriptable systems and semi-automated planning in non-scriptable systems.

Material and Methods: Class solutions for use with Raysearch Laboratories' VMAT optimiser have been developed for prostate & seminal vesicles (Psv) and prostate, seminal vesicles & pelvic node (PPN) treatment sites. These solutions use novel optimisation methodologies to generate high quality, patient individualised plans in a single iteration round and require no decision making from an operator. These approaches were applied within Oncentra Master Plan v4.3 (OMP) and Raystation v4.6 to create semi-automated (OMP(SA)) and fully automated (RAY(FA)) treatment planning solutions respectively.
10 Psv and 10 PPN patients were planned using both OMP(SA) and RAY(FA) plan generation techniques. For 5 Psv patients an experienced IMRT planner aimed to manually improve upon the OMP(SA) results to generate the 'ideal' treatment plan (OMP(Ideal)). Furthermore these 5 patients were planned by an external centre with limited VMAT experience to assess if the semi-automated solution could improve their working practices (OMP(External)). Plan quality was assessed using DVH metrics specified by the PIVOTAL trial and, with the exception of PPN OMP(SA), total planning time was recorded for each technique.

Results:

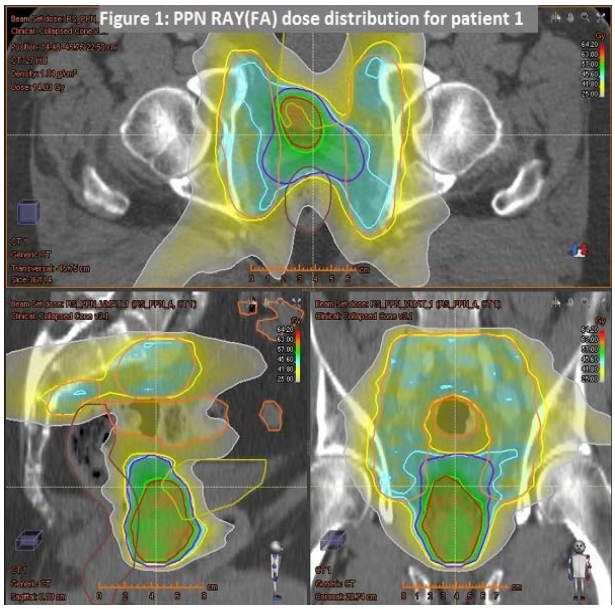

Table 1: Mean difference in DVH metrics for a given organ when compared to OMP (SA)

	Psv						PPN	
	RAY (FA)		OMP (Ideal)		OMP (External)		RAY (FA)	
	Mean ± SD	p≤0.05	Mean ± SD	p≤0.05	Mean ± SD	p≤0.05	Mean ± SD	p≤0.05
Rectum (Volume / %)	-0.4 ± 0.5	Y	-1.0 ± 0.6	Y	5.5 ± 0.9	Y	-1.2 ± 1.3	Y
Bladder (Volume / %)	-0.7 ± 0.5	Y	-1.0 ± 1.1	N	0.2 ± 1.9	N	-1.3 ± 1.2	Y
Bowel (Volume / cc)	-	-	-	-	-		-1.4 ± 1.9	Y

49/50 treatment plans assessed in the study passed PIVOTAL trial constraints, with OMP(External) failing on PTV coverage for one patient. Upon review RAY(FA), OMP(SA) and OMP(Ideal) were considered of comparable quality across all metrics and offered improved rectal sparing when compared OMP(External). For Psv treatments the mean planning time (± SD) was 10.3±1.4, 65.2±13.5, 229.0±35.8 and 255.2±48.0 minutes for RAY(FA), OMP(SA), OMP(External) & OMP(Ideal) respectively. Average planning time for PPN RAY(FA) was 38.2 ± 5.4 minutes.

Conclusion: Semi-automated and fully automated planning yield high quality plans with significantly improved efficiency.

Electronic Poster: Physics track: Treatment planning: applications

EP-1645

Optimal treatment parameters for left-sided whole breast cancer irradiation using TomoDirect

M. Scius[1], P. Meyer[1], C. Niederst[1], N. Dehaynin[1], D. Jarnet[1], M. Gantier[1], D. Karamanoukian[1]
[1]*Centre Paul Strauss, Medical Physics, Strasbourg, France*

Purpose or Objective: To determine the optimum combination of treatment parameters between pitch, field width (FW) and number of irradiation fields for left-sided whole breast irradiation using static tomotherapy (« TomoDirect™ »).

Material and Methods: 15 patients already treated with conformal radiotherapy for left-sided breast cancer without lymph nodes were selected for this study. A total of 180 TomoDirect™ plans were created by varying the field width (2.5 and 5 cm), the pitch (0.125, 0.250 and 0.5 cm/projection) and the number of irradiation fields (2 and 4). Modulation factor (MF) was set to 2 and dynamic jaws were not available. Prescribed dose was 50 Gy in 25 fractions without tumoral boost. Constraints were applied on the planning treatment volume (PTV) to ensure that 98% of the PTV receives at least 95% of the prescribed dose and 2% receives at most 107%. Treatment plans were assessed collecting Homogeneity Index (HI) for the PTV, mean doses (heart, ipsilateral and contralateral lung) and maximum dose (contralateral breast) for the organs-at-risk (OAR), integral dose to the patient and beam-on time. To assess whether breast size has an impact on dose homogeneity to the PTV, we separated the 15 patients into 2 cohorts of small (volume < 600 cc) and large (> 600 cc) PTV and compared HI.

Results: Modifying the pitch has no effect on either plan quality (PTV and OAR) or on irradiation time. Increasing the number of beams from 2 to 4 has no significant effect on OAR doses, but improves the HI of the PTV (0.068 ± 0.010 for 2 fields and 0.061 ± 0.011 for 4 fields) without altering significantly irradiation time (4.48 ± 1.27 min for 2 fields and 4.82 ± 1.30 min for 4 fields). Comparison of HI between small and large PTV shows that PTV volume has no significant effect on HI. Also, HI improvement does not depend on PTV volume, meaning that switching from 2 to 4 fields of irradiation is always beneficial (~ 10% better). Beam-on times are lowered using a FW = 5 cm (3.49 ± 0.37 min) rather than a FW = 2.5 cm (5.81 ± 0.70 min). On the other hand, the FW has no significant impact on OAR or PTV doses, except for the integral dose that is respectively 95.72 ± 35.22 Gy.L for a FW = 2.5 cm and 105.3 ± 38.1 Gy.L for a FW = 5 cm. Keep in mind that these results are obtained with a fixed MF = 2.

Conclusion: While setting the modulation factor to 2, pitch value seems to have no impact on planning quality or on irradiation time. A field width of 5 cm with 4 fields of irradiation is a good combination of treatment parameters for treating left-sided whole breast cancer with TomoDirect™ if dynamic jaws are available. If not the case, a field width of 2.5 cm is more suitable so that the integral dose to patients is lowered and radiation-induced secondary malignancies are minimized. This study will be completed by delivery QA to confirm that delivered doses match calculated ones.

EP-1646

HDR brachytherapy with hypofractionated EBRT for high risk prostate cancerSPAN STYLE="font-style:italic">

Y. Hashimoto[1], T. Akimoto[2], Y. Ishii[1], S. Kono[1], S. Izumi[1], K. Maebayashi[1], J. Iizuka[3], K. Tanabe[3], M. Kiyozuka[4], N. Mitsuhashi[5], K. Karasawa[1]
[1]*Tokyo Women's Medical University Hospital, Radiation Oncology, Tokyo, Japan*
[2]*National Cancer Center Hospital East, Division of Radiation Oncology and Particle Therapy, Chiba, Japan*
[3]*Tokyo Women's Medical University Hospital, Urology, Tokyo, Japan*
[4]*Misawa Municipal Hospital, Department of Radiology, Misawa, Japan*
[5]*Radiation Therapy Center, Hitachinaka General Hospital, Ibaraki, Japan*

Purpose or Objective: From the biological aspects of prostate cancer, hypofractionated external beam radiation therapy (EBRT) or high-dose-rate brachytherapy (HDR-BT) has been considered as a treatment choice for prostate cancer to improve local control, especially for high risk disease because the alpha-beta ratio for prostate cancer was around 1.5-3 Gy, lower than that for other cancers. Therefore, the purpose of this study is to evaluate outcomes and toxicities of hypofractionated EBRT combined with HDR-BT for high risk prostate cancer.

Material and Methods: We retrospectively analyzed 111 patients with localized prostate cancer (T1-3N0M0) that was defined as high risk disease based on the D'Amico classification, which includes cases of stage T2c to T3b or those with Gleason score of 8 to 10 or prostate-specific antigen (PSA) greater than 20 ng/mL. All patients had received hypofractionated EBRT (45 Gy in 15 fractions every other weekday for 5 weeks) followed by HDR-BT (18 Gy in 2 fractions for one day) between June 1, 2007 and September 30, 2011 at our institution. Androgen deprivation therapy (ADT) consisted of 3 to 6 months' neoadjuvant ADT before and during radiation therapy and 6 months' adjuvant ADT after radiation therapy. Biochemical failure was defined as PSA nadir plus 2.0 ng/mL according to the Phoenix definition. We scored genitourinary (GU) and gastrointestinal (GI) toxicities based on the Common Terminology Criteria for Adverse Events Version 4, and calculated the rates of overall and biochemical-free survival using the Kaplan-Meier method, timed from the completion of the HDR-BT to death or earliest failure. Statistical analyses were performed by using SPSS software.

Results: During follow-up (median, 62 months; range, 4 to 99 months), 24 of 111 patients (21.6%) experienced biochemical failure (median, 41.5 months; range, 12.7 to 72.1 months). The rates of 5-year overall survival and biochemical-free survival were 99.0% and 80.3%, respectively. At the time of analysis, only 1 patient had died of other disease. Among 24 patients with biochemical failure, 1 pateint developed bone metastasis, 2 patients developed pelvic lymph node recurrence, and 21 patients diagnosed with PSA failure alone. GU acute toxicity was Grade 1 or less in 99 patients and Grade 2 in 12 patients. GU late toxicity was Grade 1 or less in 108 patients and Grade 2 in 3 patients. GI toxicity including rectal bleeding was Grade 1 or less in 109 patients and Grade 2 in 2 patients.

Conclusion: The results of this study suggest that hypofractionated EBRT combined with HDR-BT can be feasible for high risk prostate cancer, although follow-up period is not long enough to get a definitive conclusion.

EP-1647

Feasibility of hippocampal sparing radiation therapy for glioblastoma using helical Tomotherapy

K. Thippu Jayaprakash[1], R. Jena[1], K. Wildschut[2]
[1]*Cambridge University Hospitals, Department of Oncology, Cambridge, United Kingdom*
[2]*Cambridge University Hospitals, Department of Radiation Physics, Cambridge, United Kingdom*

Purpose or Objective: With improvements in survival for good performance status patients with glioblastoma, some patients will survive to develop significant neurocognitive dysfunction. This retrospective planning study quantifies hippocampal radiation doses in twenty-five patients with glioblastoma receiving radical chemo-radiation therapy, and evaluates the potential for dose reduction using helical IMRT (Tomotherapy).

Material and Methods: We identified twenty-five glioblastoma patients treated with helical IMRT (Tomotherapy) with concurrent and adjuvant temozolamide between October 2011 and December 2013 from our radiotherapy electronic database and conducted a retrospective analysis. Hippocampi were contoured in CT and MRI co-registered image data sets used for clinical radiotherapy planning and hippocampus planning risk volumes (PRV) were created by adding five-millimetre isotropic margin which were checked by a neuro radiologist. Clinical treatment dosimetry plans were overlaid to obtain dose statistics. Four selected patients were planned for hippocampus avoidance radiotherapy without compromising tumour PTV coverage using currently established hippocampus dose volume histogram (DVH) constraints.

Results: Mean hippocampus PRV maximum, minimum and mean radiation doses were 54.7, 24.15 and 38.62 Gy respectively. Hippocampus PRV V7.3, V14.9 and V20 were 99.95%, 98.41% and 95.72% and hippocampus V3 was 100%. In seventeen patients ipsilateral hippocampus was within PTVs and in seven patients both hippocampi were outside PTVs with only minimal overlapping volumes but DVH based dose constraints were not achieved.

Location	Right frontal		Right temporal		Left parietal		Posterior fossa	
Group	Treatment	HA	Treatment	HA	Treatment	HA	Treatment	HA
Max dose	53.17	51.88	51.28	45.33	56.88	55.91	52.63	61.02
Min dose	14.96	2.27	12.4	2.85	31.63	4.11	25.34	6.28
Mean dose	33.39	9.09	28	6.71	43.09	15.55	42.79	37.79
V 7.3 Gy	100	58.7	100	29.17	100	67.43	100	99.29
V 14.9 Gy	100	25.51	98.24	16	100	38.91	100	91.4
V 20 Gy	100	16.22	82	12.12	100	28.68	100	80

With hippocampus avoidance planning (HA), in four patients hippocampus PRV minimum doses and in 3 patients mean hippocampus PRV doses were reduced and significant reductions in DVH based dose constraints were achieved in 3 patients when compared to clinical treatment plans (table).

Conclusion: Our analysis showed hippocampus PRVs received significant radiation doses and currently established hippocampus DVH based dose constraints were not achieved during cranial radiotherapy for glioblastoma using helical IMRT without hippocampus avoidance planning. Our planning study demonstrated significant dose reductions were possible with hippocampus avoidance radiotherapy planning in selected patients. More clinically correlated DVH objectives for hippocampus are required for better optimisation for hippocampus avoidance cranial radiotherapy in glioblastoma for this to be considered for all patients.

EP-1648

A comparison of 6 planning RT techniques for breast treatments

M. Zeverino[1], N. Ruiz Lopez[1], M. Marguet[1], W. Jeanneret Sozzi[2], J. Bourhis[2], F. Bochud[1], R. Moeckli[1]
[1]*CHUV - Institute of Radiation Physics IRA, Institute of Radiation Physics IRA, Lausanne, Switzerland*
[2]*CHUV, Radiation Oncology, Lausanne, Switzerland*

Purpose or Objective: To provide a comparison of 6 different treatment planning strategies, adopted for breast conserving-adjuvant RT, on the dose to the PTV and OARs.

Material and Methods: 22 patients CT data sets were retrospectively used for planning comparison. Patients were split in two groups of 6 left- and 5 right-sided cases (G1 and G2) according to the different dose prescription (50 Gy in 25 fractions and 42.4 Gy in 16 fractions for G1 and G2, respectively). The 6 techniques involved were: Field in Field (FiF), 2 Fields static-IMRT (sIMRT-2ff), 4 Fields static-IMRT (sIMRT-4FF), VMAT, Helical Tomotherapy (HT) and Tomo Direct (TD). Dose limits applied to PTV and OARs were taken from the RTOG protocol n.1005. Treatments plans were optimized to reduce dose to Ipsilateral Lung (IL), Contralateral Breast (CB) and, for left-sided cases, Heart (H) while maintaining an acceptable PTV coverage and homogeneity. The Wilcoxon matched-paired signed-rank test was used to compare the results. The threshold for statistical significance was $p \leq 0.05$.

Results: The highest mean value V95%=98.8%/99.2% (G1/G2) was observed for TD and it was statistically significant with respect to all others techniques except to VMAT. Similar results were obtained for D98%. The lowest mean V105%=0.2%/0.1% (G1/G2) was found for HT resulting statistically significant if compared to all other techniques except FIF/VMAT in G1 /G2, respectively. Mean D2% was also found lowest for HT (52.1Gy/43.1Gy in G1/G2) resulting statistically significant with respect to all other techniques except versus TD in G2. For IL mean V5(Gy), V10(Gy) and dose mean were lowest for TD in both groups (20.1%/19.1%, 14.2%/13% and 5.8%/4.9% in G1/G2, respectively) being statistically significant versus all other techniques in G1. The lowest values of mean V20(Gy)=7.0%/7.9% were observed for HT in both groups. CB dose maximum was found as lowest in G1 for TD (290.9cGy) and for FiF in G2 (252,6cGy) both resulting statistically significant versus all other techniques except for FiF in G1 and TD in G2 confirming a substantial equivalence for the two techniques. Minor absolute dose differences were observed for H.

Conclusion: 6 different techniques were employed to design an optimal plan for conserving breast-adjuvant RT fulfilling the dose limit criteria provided by RTOG 1005 protocol. TD provided superior target coverage maintaining a level of homogeneity similar to HT which achieved the highest value. IL dose was minimized with TD while dose to CB was lowest using both FiF and TD techniques.

EP-1649

Optimised Stereotactic Radiotherapy for pancreatic head tumours: a feasibility planning study

M. Buwenge[1], S. Cilla[2], A. Guido[1], L. Giaccherini[1], G. Macchia[3], F. Deodato[3], A. Arcelli[1], G.C. Mattiucci[4], G. Compagnone[5], M. Stock[6], A.G. Morganti[1]
[1]*S. Orsola-Malpighi Hospital- University of Bologna, Radiation Oncology Center- Department of Experimental- Diagnostic and Specialty Medicine – DIMES, Bologna, Italy*
[2]*Fondazione di Ricerca e Cura "Giovanni Paolo II"- Catholic University of Sacred Heart, Medical Physic Unit, Campobasso, Italy*
[3]*Fondazione di Ricerca e Cura "Giovanni Paolo II"- Catholic University of Sacred Heart, Radiotherapy Unit, Campobasso, Italy*
[4]*Policlinico Universitario "A. Gemelli"- Catholic University of Sacred Heart, Department of Radiotherapy, Roma, Italy*
[5]*S. Orsola-Malpighi Hospital- University of Bologna, Medical Physic Unit, Bologna, Italy*
[6]*EBG MedAustron- Medical University Wien, Department of Radiotherapy, Wien, Austria*

Purpose or Objective: Preoperative Radiotherapy (RT) may theoretically improve resectability in locally advanced pancreatic cancer. However, effective doses of RT are limited by the tolerance of surrounding tissues. Stereotactic radiotherapy (SRT) with intensity-modulated technique (IMRT) based on the use of a Simultaneous Integrated Boost may theoretically allow to deliver a low dose to the duodenum (site of more common toxicity) and a high dose to the vessel invasion (more common reason of unresectability). Aim of this study was to perform a planning feasibility analysis of a modulated dose prescription within a pancreatic tumor treated by SRT.

Material and Methods: 15 patients with a histological confirmation of pancreatic head adenocarcinoma with vascular involvement were included. The following definitions for targets were used: duodenal PTV (PTVd) was defined as the GTV overlapping the duodenal planning at risk volume (PRV) (from the pylorus to the duodenojejunal junction adding 5 mm in craniocaudal direction (CC), 3 mm in the other directions); vascular CTV (CTVv) was defined as the surface of contact or infiltration between tumor and vessel plus 5 mm margin around the vessel (including the whole

circumference of the vessel). The vascular PTV (PTVv) was considered as the CTVv plus an anisotropic margin (5 mm CC, 3 mm in other directions). The tumor PTV (PTVt) was defined as the GTV plus an anisotropic margin (5 mm CC, 3 mm in other directions) including the PTVv and excluding the PTVd. The following doses were prescribed [in 5 daily fractions (fr)] to the PTVs: 30 Gy (6 Gy/fr) to the PTVd, 45 Gy (9 Gy/fr) to the PTVv, and 37.5 Gy (7.5 Gy/fr) to the PTVt, respectively. Constraints were based on AAPM TG101 recommendations: Dmax of PRVduodenum < 32.0 Gy, Dmax of PRVspinal cord < 30.0 Gy, Dmax of PRVstomach < 32.0%, D700cc liver < 21.0 Gy, D200 cc kidneys < 17.5 Gy. All plans were generated with Masterplan Oncentra TPS and the treatment was delivered with a step and shot IMRT technique. The primary end point was the rate of patients in whom the constraint Dmean > 90% was achieved for the 3 different PTVs. Secondary end points were the percentage of patients in whom a PTVv near minimum dose (D98%) > 90%, a PTVv D95% > 95%, and a median dose (D50%) > 95% were achieved.

Results: PTVv Dmean > 90%, PTVv D2% < 115% and OARs Dmax constraints were achieved in all patients. Both PTVv D98% > 90% and PTVv D95% > 95% were achieved in 6 patients (40%).

Conclusion: Although the objective of PTVv D95% > 95% was achieved only in 40% of patients, the study showed that in 100% of patients it was possible to administer a strongly differentiated mean and median dose, and in particular a low dose to the overlap region between the target and duodenum, a high dose to the site of vascular infiltration, and an intermediate dose to the remaining target volume. Prospective trials based on clinical application of this strategy seems to be justified at least in selected patients.

EP-1650

IMRT versus VMAT for breast: a dosimetric point of view

S. Moorthy[1]
[1]*Salmaniya Medical Complex, Oncology & Hematology, Salmaniyah, Bahrain*

Purpose or Objective: Whole breast irradiation is part of breast conservative management for early breast cancer. In addition to that boost dose to tumor bed improves local recurrence rates and is currently the standard of care. Our aim of the current study was to evaluate intensity modulated radiation therapy (**IMRT**) for whole breast versus its dosimetric properties of volumetric modulated arc therapy (**VMAT**).

Material and Methods: Eighteen consecutive women with left sided breast cancer were taken for this retrospective study. IMRT treatment plans were created for patients who already received treatment with VMAT. The plans were created in Monaco planning system using Monte Carlo (**MC**) algorithm. The Elekta Infinity linear accelerator with Agility MLC is used for VMAT delivery. Our clinic uses simultaneous integrated boost (**SIB**) technique to treat whole breast patients. The dose prescribed was 60Gy/25# to tumor bed and 45Gy/25# for whole breast. The plans were evaluated based on **QUANTTEC** dose-volume protocol. Data were statistically analyzed using Wilcoxon Signed Rank test.

Results: VMAT technique statistically significant in target coverage and dose conformity than IMRT. In addition to that lesser ipsilateral & contra lateral lung dose and reduced contra lateral breast dose with VMAT. Critical structures like Left descending artery(LAD), Spinal Cord and heart also received lower doses with VMAT than IMRT . All the dosimetric parameters and its statistical values were provided in table1.Statistics shows VMAT more significant for LAD, Ipsilateral lung dose and Conformity Index.

	Dosimetric Parameter	IMRT	VMAT	P value
TARGET	V95(%)	98.35	99.21	0.04
	V100(%)	95.72	96.38	0.04
	Conformity Index (CI)	0.96	0.98	0.03
	Heterogeneity Index (HI)	1.09	1.08	0.06
ORGANS AT RISK (OAR)	Ipsilateral Lung V20Gy(%)	25.85	18.56	0.03
	Heart V25Gy (%)	4.11	3.22	0.05
	Contra lateral Lung V5Gy(%)	18.0	15.28	0.04
	Both Lung V20Gy (%)	21.27	15.71	0.05
	Contra lateral Breast Mean (Gy)	6.55	3.54	0.04
	LAD Maximum Dose (Gy)	28.32	25.91	0.02
	Cord Maximum Dose (Gy)	23.51	18.94	0.04

Table 1: Dosimetric parameters represents the statistical values of IMRT versus VMAT for Breast patients with simultaneous integrated boost (SIB) method

Conclusion: From this study , we infer that, our switch over from IMRT to VMAT treatment technique provided better dosimetric effect for left sided breast cancer patients. Also VMAT provided significant improvement target coverage and conformity. It reduced the dose to normal tissues further to IMRT.

EP-1651

Reducing the probability of radiation-induced hepatic toxicity by changing the treatment modality

S.H. Son[1]
[1]*Incheon St. Mary's Hospital, Radiation Oncology, Incheon, Korea Republic of*

Purpose or Objective: To estimate and compare the risk of radiation-induced hepatic toxicity (RIHT) in helical tomotherapy and fixed-beam intensity-modulated radiotherapy (IMRT) for the treatment of hepatocellular carcinoma (HCC).

Material and Methods: Twenty patients with unresectable HCC treated with tomotherapy were selected. We performed tomotherapy re-planning to reduce the non-target normal liver volume receiving a dose of more than 15 Gy (NTNL-V15Gy), and we created a fixed-beam IMRT plan (FB-P). We compared the dosimetric results as well as the estimated probability of RIHT among the tomotherapy initial plan (T-IP), the tomotherapy re-plan (T-RP), and the FB-P.

Results: Comparing the T-RP and FB-P, the homogeneity index was 0.11 better with the T-RP. However, the mean NTNL-V15Gy was 6.3% lower with the FB-P. These differences result in a decline in the probability of RIHT from 0.216 in the T-RP to 0.115 in the FB-P. In patients whose NTNL-V15Gy was higher than 43.2% with the T-RP, the probability of RIHT markedly reduced from 0.533 to 0.274.

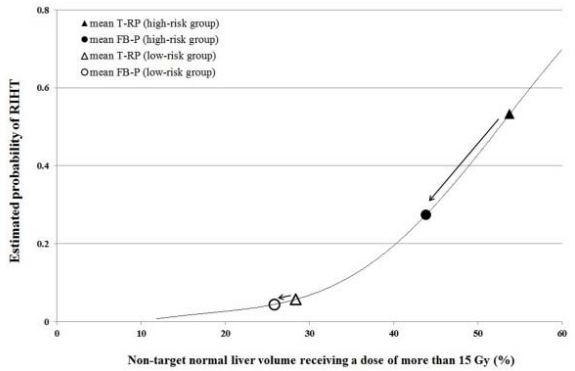

Conclusion: By changing the treatment modality from tomotherapy to fixed-beam IMRT, we could reduce the liver dose and the probability of RIHT without scarifying the target coverage, especially in patients whose liver dose is high.

EP-1652

A planning study of dose escalation FET PET active gliomas by IMRT, VMAT and IMPT

A.I.S. Holm[1], K. Seiersen[1], P. Borghammer[2], J. Petersen[1], S. Lukacova[3]

[1]*Aarhus University Hospital, Department of Medical Physics, Aarhus C, Denmark*

[2]*Aarhus University Hospital, Department of Nuclear Medicine & PET Centre, Aarhus C, Denmark*

[3]*Aarhus University Hospital, Department of Oncology, Aarhus C, Denmark*

Purpose or Objective: Gliomas are the most common brain tumor in adult patients and radiotherapy plays an important role in the treatment. Nonetheless, the clinical outcome for these patients remains poor, due to early local failure, suggesting the need for higher tumor doses. This study investigates the feasibility of dose escalating an amino acid 18F-fluoro-ethyl-tyrosine (FET) PET defined biological target volume (BTV) in glioma patients by IMRT, VMAT and IMPT.

Material and Methods: Seven patients were eligible for this study. All patients received a pre therapeutic FET-PET/CT and MRI. To compare, standard IMRT treatment plans giving 60 Gy in 30 fractions to the BTV and 46 Gy to the CTV(46 Gy) were calculated. CTV(46 Gy) was defined as tumor and/or tumor cavity plus 2 cm. The BTV was generated from the FET PET image and covered a tumor-to-brain cut-off ratio of FET uptake ≥ 1.6 (pre-surgery) ≥ 2.1 (post-surgery). Both BTV and CTV(46 Gy) were checked visually and adapted to anatomic barriers. Planning target volumes, PTV boost and PTV(46 Gy) were generated by adding 3 mm uniformly to the BTV and CTV(46 Gy), respectively. The standard IMRT plans were used to define the base level of dose to the organs at risk (OAR) and PTV(46 Gy) homogeneity. To evaluate the dose to the OAR the mean OAR was used and the PTV(46 Gy) homogeneity was defined as the volume of PTV(46 Gy) subtracted PTV boost which received 107% of the prescribed 46 Gy. Then, IMRT, VMAT and IMPT dose escalating treatment plans were calculated in order to get the highest achievable mean PTV boost dose, without increasing the mean dose to critical OAR and without decreasing the PTV(46 Gy) homogeneity. For all plans the dose boost was given as the integrated boost over 30 fractions. All treatment plans were carried out using the Eclipse treatment planning system (Varian Medical systems, Palo Alto, CA, USA).

Results: A standard IMRT plans were calculated for all patients and the base level for PTV(46 Gy) homogeneity was found to range between 65 % to 86 %, with a median value of 77%. Dose escalating, while maintaining this homogeneity, was found feasible using all three techniques. The obtainable mean and maximum doses were respective 77.1 Gy and 82.5 Gy for IMRT, 79.2 Gy and 87.4 Gy for VMAT and 85.1 Gy and 89.9 Gy for IMPT. On top of the significant increase in mean and maximum PTV boost dose obtained for IMPT, the PTV(46 Gy) homogeneity can be decreased to a median value of 30.4%.

Conclusion: Dose escalating a FET PET based target volume to above 77 Gy in 30 fractions by IMRT, VMAT, and IMPT without increasing both the PTV(46 Gy) homogeneity and the mean dose to the OAR was found feasible. For IMPT the PTV(46 Gy) homogeneity could be substantially reduced, implicating the reduction of the risk of brain necrosis despite the increased mean and maximum PTV boost doses.

EP-1653

Radiosurgery of brain metastases. A dosimetric comparison beetween VMAT and Dynamic arc plans

A. Clivio[1], J.J. Stelmes[2], C.N. Azinwi[2], G. Nicolini[1], S. Cima[2], E. Vanetti[1], K. Yordanov[2], F. Martucci[2], M. Valli[2], A. Richetti[2], S. Presilla[1], G. Pesce[2]

[1]*Ente Ospedaliero Cantonale, Medical Physics Unit, Bellinzona, Switzerland*

[2]*Oncology Institute of Southern Switzerland, Radiation Oncology, Bellinzona-Lugano, Switzerland*

Purpose or Objective: Brain metastases are a very frequent situation in advanced cancer and whole brain radiotherapy (WBRT) has long been considered the standard of care. Stereotactic radiosurgery has been shown to be effective in terms of survival and quality of life for patients with a better prognostic profile and a limited number (1 to 3) of brain metastases. More recent experiences have shown the efficacy of stereotactic radiation for multiple brain metastases as well. This may allow deferment of WBRT, in order to limit the risk of acute toxicity and late neurocognitive decline. The goal of the present study was to test from a dosimetric point of view a new planning software, BrainMetastases ® (BM) (BrainLab®, Feldkirchen - Germany), and to compare it with RapidArc (RA) ® plan TPS. (Varian®, Palo Alto CA, USA)

Material and Methods: We retrospectively re-planned 12 patients treated for 2 or more brain metastases in our institute. Median age was 53 (range 41-63). The most frequent number of metastases per patient was 3 (range 2-10). The new BM software creates a dynamic arc plan following a simple PTV and geometrical constrains and calculates it with the pencil beam algorithm. For all the patients we studied, a plan using both BM and RA with different prescriptions (1x20Gy, 5x7Gy, RTOG protocol) and for RA plans we also considered two different plans with 6MV and the 10FFF beams. Finally the dosimetric parameters were extracted from the DVHs.

Results: As PTV constraint we decided that the prescribed dose should cover the 90% of the PTV volume. With this normalization we obtained a better conformity index for RA plan and a smaller Healthy Brain mean dose with the BM plan. In particular for the patients with 3 metastases with 6MV beam and the 5x7Gy prescription the CI99% was 1.0 1± 0.18 and 1.56 ± 1.30 and Healthy Brain mean dose 3.0 ± 1.2 Gy and 2.4 ± 1.1 Gy and V20Gy 13.0±6.4 cm3 and 9.6±6.5 cm3 respectively for RA and BM technique. Also the time for optimization and calculation are 14.4±5.53 minutes and 3.63±1.48 minutes. The algorithm implemented in BM is the pencil beam and evaluated the dose every 5° and in Eclipse is Acuros XB and the calculation is performed every 2°. A more detailed analysis concerning the OAR sparing will be reported.

Conclusion: Plan optimisation using BM software provides a satisfactory dose distribution with a good conformity index and organs at risk sparing; the results are comparable with a VMAT plan. Reduction of time for optimisation and calculation seems to favour the BM software, with a similar OAR safety. Nevertheless these assumptions need to be balanced with the clinical experience which is currently ongoing in different institutes.

EP-1654

Robustness to set-up errors for treatment plans for superficial tumors in head and neck radiotherapy

D. Den Boer[1], E. Slooten[1], G. Wortel[1], E. Lamers-Kuijper[1], O. Hamming-Vrieze[1], C. Van Vliet-Vroegindeweij[1], E. Damen[1]
[1]*Netherlands Cancer Institute, Department of Radiation Oncology, Amsterdam, The Netherlands*

Purpose or Objective: Clinical target volumes (CTV) in the head and neck region are typically located just beneath the skin. Therefore, planning target volumes (PTV) will be outside the body contour. Moreover, for IMRT and VMAT treatment plans the build-up region is excluded from the PTV in the treatment planning system and optimization is done on the remaining part of the PTV (in our institute excluding the PTV outside the patient and a margin of 4 mm beneath the skin). This study evaluates the robustness of such treatment plans to set-up errors.

Material and Methods: Seven head-and-neck treatment plans were evaluated (VMAT, SIB with 54.25 Gy to the CTV and 70 Gy to the CTVboost in 35 fractions, CTV to PTV margins were 3 mm, Pinnacle Treatment Planning system). To investigate the effect of set-up errors on CTV coverage, a patient-shift on the treatment table is simulated as a shift of the isocenter. The isocenters were shifted in steps of 1 mm up to 10 mm for each of these treatment plans, in both directions ("into the patient" and "out of the patient", see Figure 1a; direction chosen in such a way that shifts out of the patients have the most effect). Subsequently, it was evaluated up till which step in mm the DVHs of the simulated (shifted) treatment plans were clinically acceptable (V95% > 99%).

Results: The effects of the shifts on the V95% of both the CTVboost and the CTV can be seen in Figure 1b. For the CTVboost regions (indicated by the blue line), it was found that the V95% was still 99% up to a shift of 3 mm (irrespective of the direction, into or out of the patient). For the elective region the V95% is still high enough (above 99%) up to a shift of 6-7 mm (6 mm into the patient, 7 mm out of the patient).

Figure 1 a) Effect of set-up error is simulated by shifting the original isocenter used for the delivered treatment plan (indicated by blue crosshairs) in the direction out of or into the patient (as indicated by the white arrow). The displacement of 10 mm into the patient is indicated by the yellow crosshairs, 10 mm in the direction out of the patient by the white crosshairs. CTVboost and CTV are indicated by red and orange colorwash respectively. b) The V95% values of the CTVboost and CTV due to the shifts of the isocenter.

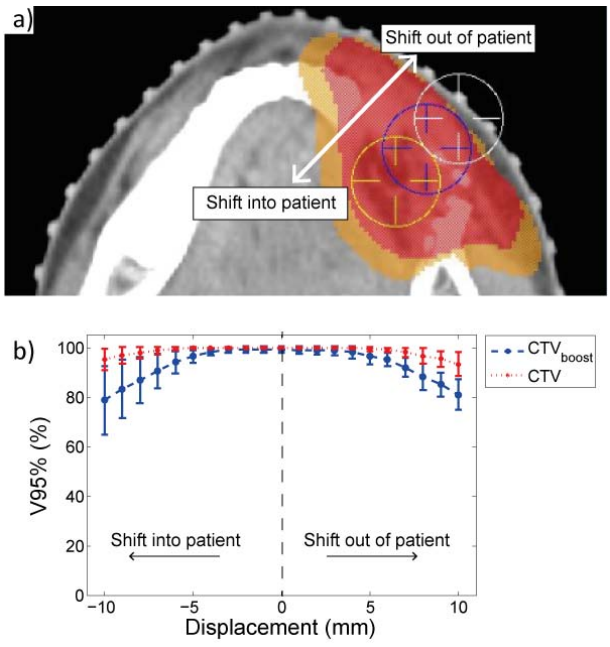

Conclusion: This work shows that treatment planning in the head and neck region with a CTV to PTV margin of 3 mm and subsequent subtraction of a build-up region of 4 mm results in adequate CTV coverage up till setup errors of 3 mm. Since in clinical practice setup errors are well below 3 mm, this is a safe strategy.

EP-1655

VMAT FFF irradiation in deep inspiration breath hold

J. Demoucron[1], J.L. Dumas[1], A. Hadj Henni[1], E. Costa[1], M. Robilliard[1], A. Mazal[1]
[1]*Institut Curie, Radiothérapie, Paris, France*

Purpose or Objective : Radiotherapy treatment on a lung moving tumor requires much caution. Among various treatments possibilities, the patient can be irradiated in deep inspiration breath hold during VMAT delivery. The purpose of this study was to investigate the feasibility of such irradiation. First, dosimetric effects of beam interruptions on VMAT delivery were determined. Then we studied the way to optimize dosimetry with multiple sub-arcs permitting breath hold. Finally another way to irradiate has been adjusted for a faster treatment while keeping VMAT advantages. We need to use a flattening filer free beam (FFF) to keep the irradiation time as low as possible.

Material and Methods: Dosimetric effect of beam interruptions delivery was studied depending on modulation, beam off numbers, dose rate and accelerator (TrueBeam, Clinac 2100C/S). We compared: absolute and relative dose and MLC Dyna/Trajectory Log files. Two rotations of 194° (clockwise/counterclockwise) were divided until 6 segments. Theirs overlapping or spacing have been compared (Eclipse). Dosimetric FFF plans with sub-arcs method was studied for 2 rotations of 360° depending energy, dose rate, segments numbers and treatment time.

Results: The maximal dose variation with beam interruptions was equal to 0.23%. TrueBeam Logfile showed that 10% of the control points have a difference higher than 0.05 mm between real and planning positions versus 70% with Clinac. The PTV volume receiving 95% of the prescribed dose V95% was equal to 99,35% with two arcs of 194° and 92,35% with one arc. When irradiation was performed with 6 segments spacing of 20°, V95% reach 98,08% with a dose reduction for the organs at risk (spinals cords: 2,2 Gy against 2,6 Gy). The sub-arcs method provided 6 arcs of 12 seconds compared to the standard 2 arcs of 40 seconds. Using FFF beams, the planning dosimetry was close to the standard treatment (Volume factor of injury cover equal 0.96 against 0.95) with a better OAR protection (spinals cords: Dmax=18,51 Gy with X6FF/2arcs, 11,75% with X10-FFF/6 arcs). For one rotation of 360°, the standard treatment needs 131 seconds versus three arcs of 12 seconds with FFF and sub-arcs.

Conclusion: We observed no significant dosimetric effect caused by beam interruptions. In order to have a shorter and a safer irradiation, the gantry rotation can be divided in several segments of 20° spacing. The dose distribution difference is insignificant and the OAR are better protected. The use of FFF and segmentation allows reducing the irradiation time by six.

EP-1656

Feasibility of an "off-target isocenter" technique for cranial intensity-modulated radiosurgery

J.F. Calvo-Ortega[1], S. Moragues-Femenia[1], M. Pozo-Massó[1], J. Casals-Farran[1]
[1]*Hospital Quirón Barcelona, Radiation Oncology, Barcelona, Spain*

Purpose or Objective: To evaluate the dosimetric effect of placing the isocenter away from the planning target volume on intensity-modulated radiosurgery (IMRS) plans to treat brain lesions.

Material and Methods: Fifteen patients, who received cranial IMRS at our institution, were randomly selected. Each patient

was treated with an IMRS plan designed with the isocenter located at the target center (plan A). A second off-target isocenter plan (plan B) was generated for each case. In all plans the 100% of the prescription dose covered the 99% of the target volume. The plans A and B were compared for the target dosage (conformity and homogeneity indices) and organs at risk (OAR) dose sparing. Peripheral dose falloff was compared by using the metrics V12 (volume of normal brain receiving more than 12 Gy) and CI 50% (conformity index at the level of the 50% of the prescription dose).

Results: The values found for each metric (plan B vs. plan A) were (mean ± SD): CI (1.28 ± 0.15 vs. 1.28 ± 0.15, p = 0.978), HI (1.29 ± 0.14 vs. 1.34 ± 0.17, p = 0.079), maximum dose to brainstem (2.95 ± 2.11 vs. 2.89 ± 1.88 Gy, p = 0.813); maximum dose to optical pathway (2.65 ± 4.18 vs. 2.44 ± 4.03 Gy, p = 0.195) and maximum dose to eye lens (0.33 ± 0.73 vs. 0.33 ± 0.53 Gy, p = 0.970). The values of the peripheral dose falloff were (plan B vs. plan A): V12 (5.98 ± 4.95 vs. 6.06 ± 4.92 cm3, p = 0.622), and CI 50% (6.08 ± 2.77 vs. 6.28 ± 3.01, p = 0.119).

Conclusion: The off-target isocenter solution resulted in dosimetrically comparable plans as the center-target isocenter technique, by avoiding the risk of gantry-couch collision during the CBCT acquisition.

EP-1657

DVH analysis automation in Tomotherapy

M.E. Perez Alvarez[1], J.C. Zapata Jiménez[1], C.B. Carrascosa Fernandez[1], J. Torres Donaire[1], J. Arjona Gutierrez[1], A. Gil Agudo[1]

[1]Hospital General Universitario de Ciudad Real, Radiofísica y Protección Radiológica, Ciudad Real, Spain

Purpose or Objective: The extraction of the data from DVH, with the aim of perform an analysis of a large number of patients in a research project, is a time-consuming process. Furthermore, in the case of Tomotherapy, the resolution obtained from the DVH is poor. This lack of resolution may suppose an additional source of error of this analysis. With the aim of solving these problems, we have developed an easy macro using the Microsoft Excel®, which allows performing the analysis of as many patients as you wish with a single click, improving the resolution and allowing the analysis of up to 7 structures in each histogram.

Material and Methods: a. Input data: 1. The dose range displayed on the DVH has to be the same in all patients. 2. Up to 7 structures can be chosen in each patient, and the same structure has to be identified with the same color in all the analyzed patients. The seven colors that can be chosen are red, green, blue, cyan, yellow, magenta and black. 3. Thereafter, a screenshot of the DVH has to be saved. b. Programming: Macro in ImageJ: 1. Open the DVH in RGB format image. 2. Split images on the RGB channels. 3. One image is obtained for each structure once the image subtraction has been performed, obtaining one single histogram for each structure. 4. The line tool will allow obtain either the dose reached in a given volume or the volume enclosed in an isodose. 5. The macro generates a plot profile and a list of values, which are saved in an independent .xls archive. Macro in Excel: 1. Opens the .xls files generated by the ImageJ macro. 2. Opens the .xls files. 3. Finds the maximum of every list. 4. Calculates the value of the histogram corresponding to this maximum. 5. Store this value in an .xls archive where all the data analyzed are stored.

Results: I.e., in a case of prostate cancer with seven structures under study, a total of 16 items are analyzed: PTV prostate and PTV nodes: 98% and 2% of volume. Rectum: V50, V60, V65, V70 and V75. Bladder: V65, V70, V75 and V80. Femoral head (left and right): V50 Penile bulb: V90 a. Time per patient: Manual: 10 min Macro: 30 s (time necessary for the preparation of the histogram). b. Resolution: Manual: X axis (dose): 16,95 points per Gy. Y axis (% volume): 0,37 points per 1% of volume. Macro: X axis (dose): 14,84 points per Gy. Y axis (% volume): 3,78 points per 1% of volume.

Conclusion: This new macro is a powerful and user-friendly tool designed to help the investigators to perform a quicker data analysis, allowing to perform it up to ten times faster. This is especially useful in the case of analyzing structures with multiple control points, as is the case of rectum and bladder. Likewise, the results obtained with the macro provide a better resolution than measured data, specially, in the y-axis, where the resolution may be improved about ten times. These kind of macros may be programmed to obtain data from as many patients and as many values as desired in the seven structures of the DVH.

EP-1658

Comparing of two different techniques for WBRT with SIB for patients with single brain metastasis

A. Ozen[1], H. Ozden[1], O. Demirkaya[1], K. Duruer[1], N. Coruhlu[1], E. Metcalfe[1], D. Etiz[1]

[1]Eskisehir Osmangazi University Faculty of Medicine, Department of Radiation Oncology, Eskisehir, Turkey

Purpose or Objective: The aim of this study was to evaluate and compare the non-coplanar IMRT and coplanar VMAT techniques for the treatment of patients with single brain metastasis and their influence on the absorbed dose by the OARs.

Material and Methods: Treatment planning computed tomography (CT) scans of 6 patients with single brain metastasis who had received palliative whole brain radiotherapy (WBRT) with simultaneous integrated boost (SIB) was recruited. Each patient re-planned with 9 fields non-coplanar IMRT and coplanar VMAT for dosimetric comparison. Details of the field arrangement in IMRT plan are presented in Table 1. Two coplanar full arcs by Varian Millennium 120 MLCs were used in all VMAT plans. Arcs were arranged with 30 degrees collimator to protect MLC leak. Prescribed WBRT dose was 30 Gy in 10 fractions and SIB dose was 39 Gy in 10 fractions. Radiation doses to OARs and targets, conformity and homogeneity index and monitor units from two techniques were tested statistically by pared t-test considering significant level of p-value <0.05.

Table 1. Details of the field arrangement for non-coplanar IMRT

Beam	Gantry Angle	Collimator Angle	Couch Angle
1	10	45	0
2	60	45	0
3	130	45	0
4	170	45	0
5	220	45	0
6	270	45	0
7	320	45	0
8	290	0	90
9	330	0	90

Results: Median PTV30 and PTV39 was 1390 (range: 1110-1810) and 18.3 (range: 2.9-45.6) cc. Radiation doses to both eyes were significantly higher in coplanar VMAT technique (p<0.05) (Table 2). There was no significant dose difference for both lens and targets between both techniques. Monitor unit was significantly higher in IMRT technique (median: 2076 (range: 1759-2201) vs. 617 (range: 584-695), p<0.001).

Table 2. Dose result comparisons of non-coplanar IMRT and coplanar VMAT

	IMRT	ARC	
	Median (Range)	Median (Range)	p
Eye L maximum dose (Gy)	12.36 (8.30-15.70)	14.86 (13.22-17.73)	<0.05
Eye L mean dose (Gy)	5.34 (4.42-6.40)	7.83 (7.27-9.66)	<0.05
Eye R maximum dose (Gy)	11.53 (7.20-14.94)	14.81 (13.85-17.35)	<0.05
Eye R mean dose (Gy)	5.91 (4.33-6.60)	7.97 (7.66-9.02)	<0.05
Monitor Unit	2076 (1759-2201)	617 (584-695)	<0.001

Conclusion: Non-coplanar IMRT is superior to coplanar VMAT in sparing eye without of any worse results on targets. But, negative aspects of non-coplanar IMRT technique such as duration of treatment as a result of high MU values, can affect significantly negative in routine practice.

EP-1659

Is VMAT better than field-in-field technique in simultaneous integrated boost for breast cancer?

H.H. Lee[1], C.H. Chen[1], Y.W. Hsieh[2], S.H. Hung[2], C.J. Huang[1]
[1]*Kaohsiung Medical University Hospital, Radiation Oncology, Kaohsiung, Taiwan*
[2]*Antai Tian-Sheng Memorial Hospital, Radiation Oncology, Pingtung, Taiwan*

Purpose or Objective: This study investigated conformation number (CN), homogeneity index (HI), and doses to heart, ipsilateral lung, contralateral lung and breast from two distinct radiotherapy techniques for early left-sided breast cancer patients after lumpectomy. We compared volumetric modulated arc therapy (VMAT) and field-in-field (FiF). Both technique utilized hypofractionation with simultaneous integrated boost (SIB).

Material and Methods: From archival CT scans, we selected 7 situations: 4 tumor locations in upper-outer quadrant (the most common), 1 in upper-inner quadrant, 1 in lower-outer quadrant, and 1 in lower-inner quadrant. SIB provided differential dosing to the whole breast and the resection cavity at each fraction; hence reduced the number of treatment fractions. In both VMAT and FiF, fractionation schemes were 28 daily fractions of 1.8 Gy to the whole breast and 2.15 Gy to the tumor bed adding up to a total dose of 60.2 Gy. They were biologically equivalent to the sequential boost-technique comprising 25 fractions of 2 Gy to the whole breast PTV followed by a boost irradiation in 6 fractions, using an alpha/beta ratio of 4 Gy for tumor response, based on the linear-quadratic cell survival model. Planning target volume (PTV)-breast and PTV-boost were defined by expanding whole breast isotropically by 5 mm and 3 mm, respectively. Dose volume constraints for ipsilateral lung: V20Gy < 20%, V5Gy < 40%; for contralateral lung: V5<5%; for contralateral breast: mean dose <3 Gy; for the heart: mean dose<10Gy and V20Gy < 15%. The goal was to encompass the PTV in all direction with the 95% isodose line, and volumes receiving higher than 110% of the prescribed dose were minimized. One experienced VMAT planner developed all VMAT plans while the other experienced FiF planner developed all FiF plans. The optimal CN is 1 since CN=(TV95%/TV)x(TV95%/V95%). The optimal HI is 0 since HI=(D2%-D98%)/D. CN, HI, and doses to normal tissues were compared by the Wilcoxon signed-rank test.

Results: VMAT significantly improved both CN for PTV-boost (0.66 vs. 0.29) and PTV-breast (0.82 vs 0.55), HI for PTV-breast (25.01 vs 32.54), mean dose to heart (4.08 vs 7.71), V20-heart (3.14 vs 13.12), V20-left lung (11.49 vs 24.29) and V5-left lung (31.54 vs 35.98), p = 0.018. The mean healthy breast dose was similar between VMAT and FiF (2.39 and 1.68 Gy, respectively); and the HI for PTV-Boost was also similar between VMAT and FiF (10.95 and 13.72, respectively). However, FiF did better in sparing contralateral lung. The mean dose to contralateral lung by VMAT and FiF were 1.75 Gy vs 0.46 Gy, respectively (p = 0.018).

Conclusion: VMAT significantly improved conformity and homogeneity in hypofractionated SIB plans for breast cancer. Doses to heart and ipsilateral lung were significantly decreased, yet more contralateral lung received low doses that less than 2 Gy averagely. Doses to contralateral breast showed no difference between VMAT and FiF.

EP-1660

VMAT planning and delivery for total marrow irradiation

S. Houghton[1]
[1]*The Harley Street Cancer Centre, Medical Physics, London, United Kingdom*

Purpose or Objective: To develop a volumetric arc therapy (VMAT) technique for delivering Total Marrow Irradiation (TMI) treatments at this institution using RapidArc™; to assess its benefits over the standard parallel-opposed technique, and evaluate the feasibility of delivering it.

Material and Methods: 5 previously treated TMI patients were retrospectively planned with RapidArc™. The treatments were delivered as quality assurance (QA) plans and verified using the Octavius™ phantom and PTW™ 2D array. The conventional parallel-opposed technique was modelled in the Eclipse™ Treatment Planning System and the dose distributions compared with the RapidArc™ plans.

Results: The VMAT plans were highly conformal, demonstrating significant dose reductions to organs at risk (OAR). The average median dose to the OARs with VMAT was 5.4Gy±1.3 and ranged from 2.8Gy in the oral cavity to 8.1Gy in the spleen. These are gains of between 25% and 73% compared to the conventional parallel-opposed technique which had an average median dose of 11.6±0.2. Target coverage was similar between the two plans with a D99 of 10.7Gy±0.4 for conventional TMI and 10.8±0.2Gy for VMAT TMI. The VMAT TMI plans had slightly higher global maximums than the parallel opposed plans: 13.6Gy±0.1 for VMAT; 12.6Gy±0.4 for parallel-opposed. The plan verification showed good agreement between the Eclipse distributions and measured data. The study gamma analysis pass rate averaged 99.0 ± 0.5 for all anatomical regions and plans.

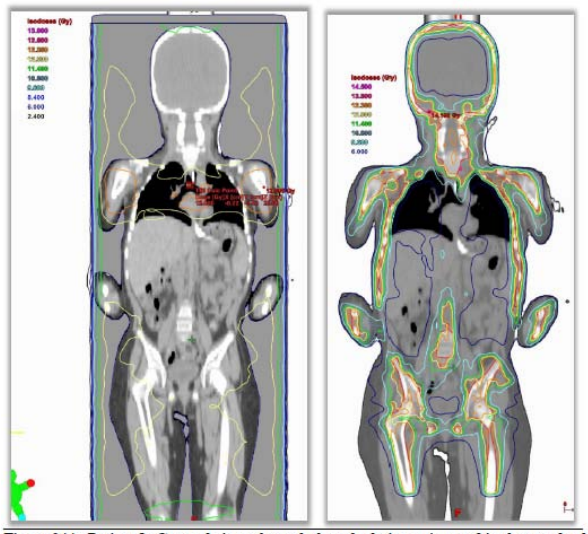

Figure 24A: Patient 1: Coronal views through the calculation point used in the standard technique showing increased target conformality and OAR sparing with RapidArc (right) compared to the standard technique (left). Note the high dose to the lung region adjacent to the calculation point in the standard plan (left).

Conclusion: VMAT planning for TMI has the potential to significantly reduce doses to OARs, thereby increasing the therapeutic ratio, and giving the potential for dose escalation. The verification process confirmed good agreement between calculated and measured data. VMAT TMI is a technically feasible alternative to the standard TMI technique but further evaluation is required before clinical implementation.

EP-1661

Comparing different planning techniques for brain tumour radiotherapy

G. Cooke[1], C. Golby[1], S. Erridge[1], S. Peoples[1], L. Seaton[1], T. Ronaldson[1], L. Wawrzyniak[1], L. McIntosh[1]
[1]*Edinburgh Cancer Centre- Western General Hospital, Oncology Physics, Edinburgh, United Kingdom*

Purpose or Objective: The use of volumetric modulated arc (VMAT) is well established for many clinical sites. However, brain tumours are often treated using a 3D cranial radiotherapy (3DCRT) technique with one or two phases. The use of VMAT for cranial radiotherapy is a positive alternative that has been explored by many centres, particularly for brain metastases. Although VMAT provides a more conformal dose across the target volume than conventional planning techniques the main disadvantage is the low dose bath to normal tissue. The potential for additional neurotoxicity must be considered when deciding the best method of treatment. A planning study was conducted to investigate the difference between 3DCRT, co-planar partial arc VMAT and co-planar full arc VMAT.

Material and Methods: Ten patients, who had been clinically treated with VMAT, were selected for this study. Planning target volume (PTV) and organs at risk (OARs), including chiasm, brainstem and normal brain (brain-PTV) were all outlined on these plans. Planning risk volumes (PRVs) were created for each OAR structure. Each patient had three plans produced delivering 6000cGy to the isocentre: two phase 3DCRT with MLC altered to keep each OAR below their tolerance dose, partial arc VMAT and a full arc VMAT plan. For VMAT planning, arcs were applied to the plan and objectives were set for each OAR and PTV in the VMAT optimiser. Full arcs were applied first and then gantry angles amended for an appropriate partial arc (range 169°-239°). Where OARs overlapped the PTV an overlap structure was drawn to limit the dose to the OAR and maximise the coverage to the PTV.

Results: The dose received by 95% of the PTV and the 10cc dose to normal brain are shown in Table 1. Table 1 shows the dose received by 95% of the PTV is greater for VMAT plans than 3DCRT plans. On average, the dose received by 95% of the PTV, for a 3CRT plan, was 5450cGy. In a partial arc VMAT plan, 95% of the PTV received 5659cGy and a full arc VMAT, 5643cGy. The dose colour wash showed a more conformal dose when using VMAT over conventional planning. Table 1 shows that the average maximum dose to 10cc of the normal brain was 5263cGy using 3DCRT, but 4082cGy for partial arc VMAT and 4148cGy for full arc VMAT. Partial arc VMAT, normal brain doses were lower in 7/10 patients.

	Conventional Plan		Partial Arc VMAT Plan		Full Arc VMAT Plan	
Patient	PTV (cGy)	Brain (cGy)	PTV (cGy)	Brain (cGy)	PTV (cGy)	Brain (cGy)
1	5301	6032	5703	4728	5608	4133
2	5409	5592	5741	3896	5649	4172
3	5875	4459	5825	3576	5817	3700
4	5719	4578	5816	4143	5802	4120
5	5779	4371	5798	3617	5843	3813
6	5149	5550	5338	4082	5334	4449
7	5148	5084	5337	4226	5324	3862
8	5362	5598	5738	4123	5733	4436
9	5516	5577	5693	4175	5731	4275
10	5237	5791	5598	4256	5591	4515

Table 1 95% of PTV and 10cc normal brain doses for 10 patients planned three ways

Conclusion: A Planning comparison of 10 patients, each planned using 3DCRT, partial arc VMAT and full arc VMAT was carried out. VMAT plans showed a more favourable PTV coverage compared to 3DCRT. Normal brain dose was lower than 3DCRT. Partial arc VMAT normal brain dose was lower for 7/10 patients than full arcs.

EP-1662

Comparison of VMAT for single fraction lung cancer radiotherapy with and without flattening filter

S. Barbiero[1], F. Matteucci[2], D. Fedele[3], M. Avanzo[1]
[1]*Centro di Riferimento Oncologico, Medical Physics Unit, Aviano, Italy*
[2]*S.Chiara University Hospital, Radiation Oncology Department, Pisa, Italy*
[3]*Casa di Cura S.Rossore, Radio-Oncology Department, Pisa, Italy*

Purpose or Objective: to compare flattening filter free (FFF) and flattening filtered (FF) intensity-modulated arc therapy (VMAT) plans for stereotactic body radiotherapy (SBRT) in patients with lung lesions, delivered in a single fraction of high dose radiation.

Material and Methods: 25 patients were treated with FFF SBRT for lung tumors with a Varian TrueBeam STx LINAC using VMAT. The lesions were treated with single dose of 24 Gy. Two plans, with and without FF, for each patient, were created using Varian Eclipse treatment planning system. Plans were compared and differences were analyzed in terms of dose volume histograms (DVH), number of monitor units (MUs) and beam on time.

Results: No statistically significant differences were found between FFF and FF plans in coverage of the PTV and doses to the main organ at risk (OAR). The PTV conformity index was the same with FFF and with FF VMAT (1.03 ± 0.10). In FFF plans, the maximum doses to spinal cord, heart, esophagus and trachea were 2.9 ±1.9, 0.8 ± 1.2, 3.3 ± 4.4 and 1.5 ± 1.7 Gy respectively. Average lungs V5, V20 and mean doses were 14.6 ± 7.5%, 6.1 ± 3.7% and 1.1 ± 0.6 Gy. In FF plans maximum doses were 3.2 ±2.6, 0.8 ± 1.3, 3.1 ± 4.4 and 1.8 ± 2.0 Gy to spinal cord, heart, esophagus and trachea, and average lungs V5, V20 and mean dose were 15.5 ± 7.9%, 6.3 ± 3.9% and 0.4 ± 0.6 Gy. The average number of MU was slightly higher with FFF beams than with FF (7159 ± 609 vs 7097 ± 699), but the difference was not significant. Beam delivery times were 15.4 with FF beams to 6.7 minutes without filter. Average reduction of treatment time after filter removal was 2.31 ± 0.01 (t-student test $p<0.01$).

Conclusion: The use of FFF VMAT for single fraction SBRT of lung cancer patients yielded dose distributions dosimetrically equivalent to FF beams, with a significantly reduction of treatment delivery time.

EP-1663

A tool for collision prediction in linac-based intracranial radiosurgery planning

T. Felefly[1], F. Azoury[1], C. El Khoury[1], J. Barouky[1], N. Farah[1], R. Sayah[1], N. Khater[1], D. Nehme Nasr[1], E. Nasr[1]
[1]*Hôtel Dieu de France - Saint Joseph University, Radiation Oncology, Beirut, Lebanon*

Purpose or Objective: Gantry collision is a concern in linac-based stereotactic radiosurgery (SRS). Without collision screening, the planner may compromise optimal planning by avoiding advantageous beam angles deemed risky, unnecessary replanning delays can occur, and incomplete treatments may be delivered. To address these concerns, we developed a software for collision prediction based on simple machine measurements.

Material and Methods: Couch points vulnerable to collision including the lateral couch edge were identified. Trigonometry-based formulas to calculate distance from each point to the gantry rotation axis, given the isocenter coordinates relative to the couch position, and the couch rotation angle, were generated. For each point, collision occurs when this distance is superior to the gantry-to-isocenter distance, taking into account the complexity of the gantry collimator facet and the presence of a circular SRS collimator. Once a collision is identified for a specific point, the arc of collision was calculated using a separate formula.The patient was modeled as a parallelepiped with

preset height and width, and same formulas were applied for collision detection. A computer code incorporating these formulas was generated. A modifiable "Settings" window including the couch and gantry head dimensions as well as gantry-to-isocenter distance was created. The inputs required are the isocenter coordinates relative to the couch position, the couch rotation angle, the patient dimensions, and the presence or absence of a circular SRS collimator. The software outputs the collision-free gantry angles, and for each point, the shortest distance to gantry or the colliding sector when collision is identified, assuming a full gantry rotation. The software was tested for accuracy on a TrueBEAM equipped with BrainLab accessories for fifteen pretreated plans and ten colliding virtual cases with and without circular collimators.

Results: The software accurately predicted the absence of collision for fourteen of the pretreated plans, and detected collision for one case that required replanning after failing the pre-treatment dry run (difference of 1°.7in colliding gantry angle).The root-mean-square deviation between the measured and predicted gantry angle of collision for the virtual cases was 1°.52(0.01° - 3.39°). The largest differences were observed for extreme couch rotations.

Conclusion: This tool accurately predicts gantry-couch collision for linac-based SRS and is easy to implement in any facility without the need for optical imaging or complex tridimensional machine modeling.

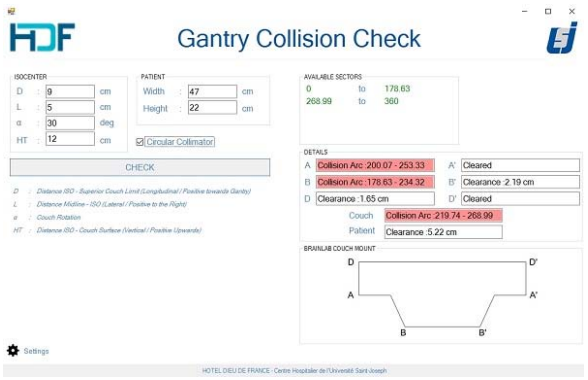

EP-1664

Comparison between intensity modulation techniques in prostate cancer treatment

S. Fondelli[1], S. Russo[1], I. Peruzzi[1], R. Barca[1], M. Esposito[1], B. Grilli Leonulli[1], L. Paoletti[1], F. Rossi[1], P. Alpi[1], A. Ghirelli[1], S. Pini[1], P. Bastiani[1]

[1]*Azienda Sanitaria Firenze, Radioterapia, Bagno a Ripoli, Italy*

Purpose or Objective: Volumetric Modulated Arc Therapy (VMAT) is a highly conformed delivery technique. VMAT comparison to other advanced techniques, as IMRT, in terms of plan quality, delivery efficiency and accuracy is great topic discussion in literature. Aims of this work are to assess VMAT dosimetric results compared to IMRT ones on prostate site and to evaluate the acute toxicity profile for patient treated by VMAT techniques.

Material and Methods: A comparison was made between IMRT and VMAT plans elaborated by treatment planning system (TPS) Elekta Monaco® on the first 30 consecutive patients treated with VMAT moderately hypofractionated radiotherapy: 70.2Gy/26 fractions of 2.7Gy. All patients had histologically confirmed prostate cancer; median age was 76 years old; ECOG-performance status value was 0-1; According to the National Comprehensive Cancer Network Criteria patients were stratified into low, intermediate and high risk groups as follow: one patient was low, 8 were intermediate and 16 were high risk. IMRT and VMAT plans were elaborated by TPS Elekta Monaco® using a two-stage constrained optimization based on both biological and physical cost functions. Plans were compared by evaluating D105%, D95%, D93%, D90%, Dmean and D0.5% for the PTV coverage, while for Organs at Risk (OARs), in addition to Dmean and D0.5%, the % of organ receiving 57, 61, 65.8 and 68.4 Gy (rectum), 57, 61, 65.8 and 68.4 (bladder), 35, 39.5 and 43.9 Gy (femoral heads) were considered of interest. Toxicities were assessed according to the RTOG/EORTC scale for acute and late adverse effects.

Results: Dosimetric analysis shows that PTV coverage is better with VMAT technique and that PTV Dmean is higher than about 1 Gy in VMAT treatments: median value for the PTV Dmean was 70,6 Gy in VMAT technique vs 69,7 Gy in IMRT (Table 1).

Table 1

PTV	VMAT	IMRT
D_{mean} (Gy)	70.6	69.7
$D_{0.5\%}$ (Gy)	74.5	72.9
$D_{90\%}$	99.8 %	99.8 %
$D_{93\%}$	98.6 %	98.6 %
$D_{95\%}$	95.9 %	95.4 %
$D_{105\%}$	5.8 %	1.6 %

Regarding OARs sparing, VMAT technique offers a higher sparing of bladder (of about 5% of volume at 57,61 and 65Gy) and femoral heads (of about 15% of volume at 30 Gy) (Figure 1).

Figure 1

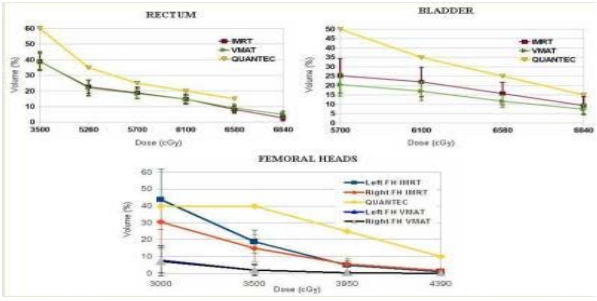

VMAT treatments were completed in all patients without interruptions: average overall treatment time was 38 days. During RT, acute genitourinary toxicity was recorded as Grade 1 in 13 patients (52%) and Grade 2 in 7 (28%); acute rectal toxicity was recorded as Grade 1 in 4 patients (16%) and Grade 2 in 3(12%).

Conclusion: Respect to IMRT, VMAT offers higher plan quality with a better PTV coverage. Regarding OARs, VMAT offers higher sparing of bladder and femoral heads. Besides, VMAT is able to provide a considerable reduction in treatment time

offering a better delivery efficiency. Acute toxicity profile assessed by hypofractionation schedule VMAT treatments was safe.

EP-1665

Scalp-Sparing focal radiotherapy for gliomas using VMAT or Helical Tomotherapy: a feasibility study

S. Scoccianti[1], G. Simontacchi[1], C. Talamonti[2], A. Compagnucci[2], M. Casati[2], C. Arilli[2], D. Greto[1], F. Meacci[1], P. Bonomo[1], I. Desideri[1], G.A. Carta[1], M. Loi[1], L. Livi[1]

[1]*Azienda Ospedaliera Universitaria Careggi, Radiation Oncology, Firenze, Italy*

[2]*Azienda Ospedaliera Universitaria Careggi, Medical Physics, Firenze, Italy*

Purpose or Objective: Both transient and permanent alopecia have a huge psychological impact on patient's quality of life. Sparing the scalp during focal cranial RT for gliomas is a challenging issue during the treatment planning process due to the fact that the scalp is often strictly adjacent to the cortical or subcortical target. In addition, clear constraints for this structure to be used during the inverse planning are not available in literature, most of them being very strict. We report our preliminary experience with scalp sparing technique for patients with high grade gliomas.

Material and Methods: Five patients previously treated with focal RT were reviewed. During the contouring process, the scalp volume was defined as a ring region of interest (ROI) including the tissue between the skin and the skull, up to a maximum thickness of 5 mm. The hairless skin of the face and the neck was excluded from the scalp ROI. The gross tumor volume(GTV) included the surgical bed plus any contrast enhanced lesion on a postoperative T1-weighted MRI scan. The clinical target volume (CTV) was obtained by adding an isotropic 2-cm margin to the GTV. CTV was then edited according to the anatomical barriers (meninges, ventricles, tentorium and midline except for lesion near to the corpus callosum). CTV was expanded by 2 mm to get the planning target volume (PTV). For the inverse planning, primary constraint for the scalp was Dmax≤16 Gy, secondary constraint was Dmax≤25 Gy, tertiary constraint was Dmax≤35 Gy. Tomotherapy and VMAT plans were generated for a prescription dose of 60 Gy in 30 fractions. Other intracranial organs at risk (optic chiasm, brainstem, cochlea, pituitary gland and hippocampus) were contoured.

Results: The primary constraint (Dmax≤16 Gy) for the scalp was unachievable. The secondary constraint (Dmax≤25 Gy) was met only in a case both with Tomotherapy and VMAT. The tertiary constraint (Dmax≤35 Gy) was met in all the cases with Tomotherapy (the scalp volume receiving > 35Gy was always < 0,1cc) but only in two cases out of 5 with VMAT. Target coverage and sparing of the other organs at risk were acceptable in all the treatment plans.

Conclusion: Meeting the constraints for the scalp is not always feasible for cortical or subcortical targets that need to be treated with a total dose of 60 Gy. We are enrolling patients with gliomas treated with the above-mentioned scalp sparing technique in a prospective study in order to assess the clinical results in terms of transient and permanent alopecia.

EP-1666

A modified left-sided breast cancer irradiation in Tomotherapy: comparison to hybrid-IMRT technique

C.L. Kuo[1], C.C. Chen[1], L.C. Lin[2], S.W. Lee[1], S.Y. Ho[1]

[1]*Chi Mei Medical Center-Liouying, Radiation oncology, Tainan, Taiwan*

[2]*Chi Mei Medical Center, Radiation oncolody, Tainan, Taiwan*

Purpose or Objective: In order to reduce heart and ipsilateral lung dose, a modified left-sided breast planning technique in TomoTherapy was introduced and compared to Hybrid-IMRT technique.

Material and Methods: A modified planning technique in Tomotherapy was designed for left-sided breast cancer patients. It was based on Limited-Tomotherapy planning technique [An-Cheng Shiau et al., 2014] but applying optimal pitches [Mingli Chen et al., 2011] to achieve better conformity and lower heart and ipsilateral lung dose. First, the optimized off-axis distance was determined. Then the optimal pitches were chosen according to the optimized off-axis distance. The last thing was applying optimal pitches with Limited-Tomotherapy planning technique, which had several artificial contours like Complete-block, Directional-block for near PTV area and the virtual bolus, on the optimized process of the left-sided breast Tomotherpy planning. Hybrid-IMRT plans were designed by tangential-fields and IMRT fields combined. The prescription dose was 50 Gy in 25 fractions to PTV. The lung and heart dose volume were measured and analyzed in Beam's-eye-view of tangential-fields with field heart volume (FHV) and field lung volume (FLV).

Results: The maximum volume of FHV and FLV are 15.49c.c and 84.27c.c. The modified planning technique could reduce 12.44% dose in Dmean of heart and 11.36% in lung and both techniques had similar coverage of PTV. The modified planning technique could increase the minimal dose of PTV (37.35 ± 3.87Gy vs. 29.52 ± 6.75Gy) and the homogeneity index (HI=PTVm95%-PTVm107%) was better (0.9877 ± 0.0053 vs. 0.9632 ± 0.0565). The Dmean of heart in Hybrid-IMRT technique was higher than in the modified planning technique (3.01 ± 2.29Gy vs. 2.40 ± 2.07Gy). The Dmean of lung was higher in Hybrid-IMRT technique than in the modified planning technique (5.72 ± 1.44Gy vs. 5.04 ± 1.47Gy).

Conclusion: The modified planning technique showed better dose reduction in heart and lung. It was because of there were more flexibility in the optimized planning process. It should be useful in left-sided breast irradiation in TomoTherapy.

EP-1667

Dose fall off patterns and the OAR effect - experience of Linac based frameless radiosurgery

A. Munshi[1], B. Sarkar[1], S. Roy[1], T. Ganesh[1], B.K. Mohanti[1]

[1]*Fortis Memorial Research institute, Radiation Oncology, Haryana, India*

Purpose or Objective: Sharpness of fall off of dose beyond the PTV edge is one of the key parameters of efficient cranial stereotaxy. This study presents the dosimetric data and dose fall off patterns of consecutive patients treated for cranial SRS on a linear accelerator.

Material and Methods: Thirty patients of brain lesions underwent frameless SRS at our centre between March 2013 and December 2014. All patients underwent radiotherapy planning contrast CT scan with 1 mm slices. VMAT planning was done for all cases(4mm MLC leaf size). From the center of the PTV volume, straight lines were drawn in the axial plane in anterior, posterior, medial, lateral, superior, inferior directions and in the direction of nearest organ at risk (OAR). Along each line the distance of the 80%, 50% and 20%. isodoses from the edge of the PTV were measured. The distance required for dose fall of from 100% prescription dose (PTV edge) to 80%, 50% and 20% were noted. The final readings were converted to dose fall off percentage per mm (%/mm)

Results: OAR doses were validated according to TG-21 specified limits. The mean±SD fall (% per mm) for 100%-80% was 7.5±2. For 100%-50% the fall rate was 5±1.3 and for 100%-20% it was 4.2±1.6. The mean of sharpest fall off rate (% per mm) was 10.6+5.8 for 100-80%, 6.6+3.6 for 100-50 % and 5.9+7.5 for 100-20%.For an OAR distance > 2 cm from PTV edge (12 patients), the dose fall off pattern remained unaffected. For rest of the eighteen patients with OAR distance < 2 cm from PTV edge, the dose fall off became sharper in the direction of OAR.

Conclusion: An important influencing factor remains vicinity to the OAR. It is possible to achieve falloff rates of 100-80% within a distance of 2 mm and a 100% to 50% fall within 7 mm. This data can help enable select patients for upfront STS versus fractionated SRT during initial assessment of patients.

EP-1668

Treatment planning study of c-IMAT versus s-IMRT in cervical and upper thoracic esophageal carcinoma

R. Zhang[1], W. Bai[1], Y. Cao[1], R. Li[1]
[1]*Fourth Hospital of Hebei Medical University, Radiotherapy, Sijiazhuang- Hebei, China*

Purpose or Objective: To compare and analyze the characteristics of static intensity-modulated radiotherapy(s-IMRT) versus constant dose rate and constant angle speed intensity modulated arc therapy(c-IMAT) in the treatment of upper thoracic and cervical esophagus cancer. By Delta4 verified the commissioning of c-IMAT implementation in the Varian Clinical 23IX accelerator.

Material and Methods: Eleven esophageal neoplasms patients treated with step-and-shoot s-IMRT at our hospital, were replannedusing c-IMAT. The plans were generated with Oncentra ver4.1 planning system, PTV were prescribed to 60 Gy in 30 fractions. Planning objectives for PTV corresponding with the IMRT plans, were at least 95% planning target volumereached the prescription dose and V110 no more than 10%. The maximum dose of spinal-cord was constrained below 45 Gy. Pared-sample T-test were applied to dose volume values for PTV and OAR from DVH.

Results: There were no significant differences between s-IMRT and c-IMAT in PTVmin, D90, D95, D98, V90, V95, V100, V105, V110, D max or total lung V10, V20, V25, V30 and average lung dose (all P>0.05). However, the differences were significant in terms of D2, D50, V105, PTVaverage, HI and CI of PTV, V5 and V15 of the total lung (all P<0.05)(see table1 and figure1). And treatment times were reduced significantly with c-IMAT(81s vs. 238.4s, p < 0.05), while, MU increased by a factor of 1.2, s-IMRT is 513.5MU versus c-IMAT is 624.1 MU (P=0.000). For the gamma Index (±3%, ±3mm), the s-IMRT (94.0±0.9 %) is higher than c-IMAT(91.9±1.1%), but all can meet the clinical demands (≥ 90%).

Table 1 The dosimetric parameters comparison of c-IMAT and s-IMRT in target volume and OAR(x±s)

plan	PTV D_2(cGy)	PTV D_{50}(cGy)	PTV V_{105}(%)	$PTV_{average}$(cGy)
s-IMRT	6461.6±29.1	6249.0±19.8	31.2±6.4	6251.1±19.5
c-IMAT	6350.7±40.8	6195.3±25.9	13.2±6.6	6197.5±24.8
P value	0.004	0.009	0.006	0.008
plan	PTV HI	PTV CI	Lung V_5(%)	Lung V_{15}(%)
s-IMRT	0.094±0.006	0.666±0.202	36.9±4.4	22.3±2.6
c-IMAT	0.074±0.009	0.794±0.019	39.3±4.7	25.3±2.8
P value	0.013	0.000	0.029	0.016

Note: D_2 is the minimum dose received by the 2% of the volume, D50 and so on; V5 is percentage of accepting dose equal or more than to 5 Gy volume to the total lung volume, V15 and so on.

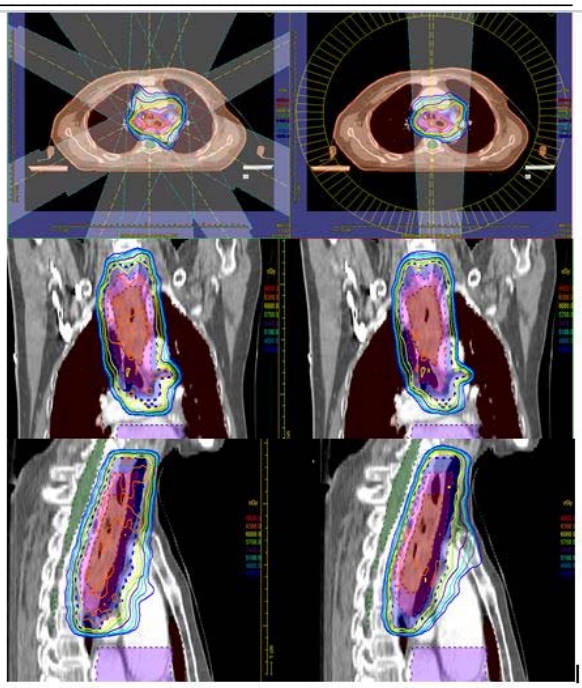

Figure 1. Dose distribution of three slices for s-IMRT (left) and c-IMAT (right) plan of one case

Conclusion: In Varian Clinical 23IX accelerator designed c-IMAT plan can achieve similar or better dosimetry with s-IMRT, having better PTV homogeneity and conformal index, much less treatment time advantage, and so the c- IMAT plan can be implemented smoothly and quickly into a busy cancer center, but the total MU and the average does of lung increased compared with s-IMRT.Hence in the treatment of upper thoracic and cervical esophagus cancer patients an evaluation of weight loss must be performed during treatment for C-IMAT.

EP-1669

The reaserch of postoperative endometrial carcinoma delivered with CDR-CAS-IMAT on Varian 23IX

R. Zhang[1], Y. Gao[2], X. Fan[3], W. Bai[1], Y. Cao[1]
[1]*Fourth Hospital of Hebei Medical University, Radiotherapy, Sijiazhuang- Hebei, China*
[2]*Hebei General Hospital, The Physical Examination Center, Shijiazhuang, China*
[3]*Fourth Hospital of Hebei Medical University, Department of Gynecology, Sijiazhuang- Hebei, China*

Purpose or Objective:

Introduction Postoperative endometrial carcinoma patients with large volume of target area and the shape of the target area is concave, treatment with IMRT is time consuming.Treated with VMAT can produce similar or better dose distributions, also can reduce treatment time and the monitor units (MU)[1,2]. However, VMAT can only be implemented on the new generation accelerators such as the Varian RapidArc and Elekta Synergy, which prevents most existing linacs from delivering in VMAT. R Zhang et al.[3] had been proposed an alternative planning approach for VMAT using constant dose-rate and constant gantry speed arc therapy (CDR-CAS-IMAT) implementation on Varian 23EX for thoracic esophageal carcinoma, the results showing that the treatment times compared with the IMRT technology were decresed significantly can be reached to 62.9%.

Objective The purpose of this study is to investigate using CDR-CAS-IMAT on Varian 23IX, by comparing with the IMRT to evaluate the performance of CDR-CAS-IMAT on postoperative endometrial carcinoma patients and then provide guidance for clinical treatment.

Material and Methods: 30 postoperative endometrial carcinoma patients treated with IMRT on Varian 23IX were replanted using CDR-CAS-IMAT. The plans were generated on Oncentra v4.1 planning system, PTV was prescribed to 50.4

Gy in 28 fractions. Plans were evaluated based on the ability to meet the dose volume histogram. The homogeneity index (HI), conformity index (CI) of target volume, the dose of organs at risk, radiation delivery time and monitor units were also compared. Paired T-test model analysis was used to analyse the two sets of data.

Results: The results showing that postoperative endometrial carcinoma can be implemented CDR-CAS-IMAT plans on conventional Varian 23EX Linac for smoothly and quickly at busy cancer center. Comparing with the IMRT techonology CDR-CAS-IMAT plans can meet the clinical demand(see Figure1), gives comparable OAR and improved CI of PTV (see. Table 1), can reduction treatment time ((84.6±7.8)s Vs. (422.7±46.7)s), MU((787.5±78.5)MU Vs.(927.4±79.1)MU) and high dose irradiated volume; while increase the low dose irradiated volume of healthy tissues and the volume of the bladder and bowel irradiated 40 Gy and 30Gy, respectively. This point needs to pay attention to implementation in clinical. There were no significant differences in other statistical index.

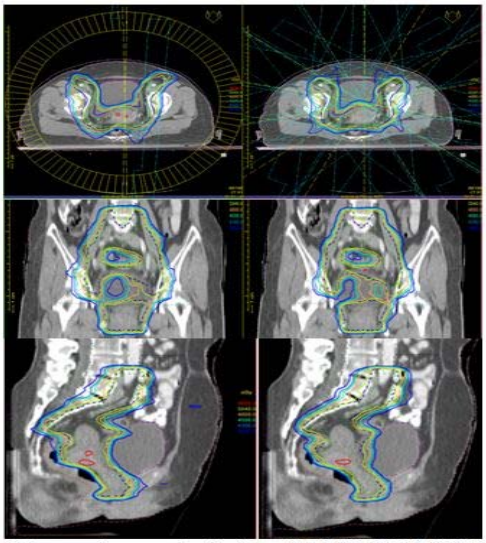

Figure 1. Treatment plan sections dose distribution of CDR-CAS-IMAT (left) Vs. IMRT (right) [Transverse plane(top), Coronal plane(middle) and sagittal plane(bottom)]

Table 1. The dosimetric parameters comparison of CDR-CAS-IMAT and IMRT in target volume and OARs ($\bar{x}\pm s$)

plan	HI (PTV)	CI (PTV)	HI (CTV)	CI (CTV)	D90 (CTV) (cGy)	D95 (CTV) (cGy)	D98 (CTV) (cGy)
CDR-CAS-IMAT	0.12± 0.021	0.85±0.03	0.09±0.02	0.46±0.05	5232.5±34.0	5196.2±27.8	5153.2 ± 21.0
IMRT	0.13± 0.02	0.81±0.03	0.11±0.02	0.43±0.05	5215.7±31.5	5162.5±31.2	5095.3 ± 34.9
t value	-1.36	3.85	-3.18	4.21	2.13	4.65	7.79
P value	0.193	**0.001**	**0.005**	**0.001**	**0.049**	**0.000**	**0.000**

plan	V95 (CTV) (%)	V98 (CTV) (%)	V100 (CTV) (%)	Cord D2 (cGy)	Rectum V40 (%)	Bladder V50 (%)	Bowel V30 (%)
CDR-CAS-IMAT	99.99± .01	99.8±.14	5232.5±34.0	3743. ±118.5	41.8±5.9	17.5±4.4	39.5±6.4
IMRT	99.98±.02	98.9±.6	5215.7±31.5	3806.1±98.5	44.1±4.7	16.7±4.1	36.5±7.3
t value	2.29	6.00	2.13	-2.65	-2.47	2.14	3.00
P value	0.035	**0.000**	**0.049**	**0.017**	**0.025**	**0.048**	**0.008**

Note: D90 is the minimum dose of 90% volume accepted, D95 and so on; V90 is the volume which the target volume irradiated 90% prescription dose, V95 and so on. D_2 is the minimum dose of 2% volume accepted;

Conclusion: Endometrial carcinoma patients with CDR-CAS-IMAT on Varian Clinical 23IX can get equivalent or superior dose distribution compared with the IMRT technology. CDR-CAS-IMAT have much less treatment time and MU can reduce the uncertainty factor and patient discomfort in treatment.

References

1. Otto K. Volumetric modulated arc therapy: IMRT in a single gantry arc. Med Phys. 2008;35(1):310-7.
2. Yu CX. Planning and delibery of IMRT. Med Phys. 2008;35(12):3233-41.
3. Zhang R, Fan X, Bai W, Han C. Implementation of CDR-CAS-IMAT for thoracic esophageal carcinoma on Varian 23EX. Med Phys. 2014;41(8):14

EP-1670

Impact of flatting filter free photon beam on Rapid-arc radiotherapy for gynecological malignancies

L. Kumar[1], V. Kishore[2], G. Yadav[1], K. Raman[1], M. Bhushan[1], T. Suresh[1], P. Kumar[1], M. Suhail[1], M. Pal[1]
[1]*Rajiv Gandhi Cancer Institute And Research Centre, Medical Physics Division- Radiotherapy Department, Delhi, India*
[2]*Bundelkhand Institute Of Engineering & Technology- Janshi-India, Department Of Applied Science & Humanities, Janshi, India*

Purpose or Objective: Aim of this study was to determine the dosimetric impact of flatting filter free beam (FFFB) of 6 and 10 MV energies on rapid-arc (RA) radiotherapy planning for gynecological malignancies.

Material and Methods: RA plans were generated using double arc for a cohort of ten patients using 6 and 10 MV FFFB. Plans were generated to deliver a dose of 50.4 Gy in 28 fractions for Planning target volume (PTV) and ALARA were used as an objective for Organs at risk (OARs). Plans were analysed for PTV Coverage, conformity Index (CI), homogeneity index (HI), dose to OAR's, integral dose to normal tissue (NTID) and total no. of monitor units (MUs).

Results: The volume of PTV receiving prescription dose were 95.03+ 0.09% and 95.09+ 0.10%, HI were 1.062+ 0.008 and 1.066+ 0.008,CI were 1.007+ 0.016 and 1.012+ 0.013, mean NTID were 272.2+ 37.1 and 261.1+ 33.2 (liter-Gy), MUs number were 629.6+ 31 and 647.2+ 44 for FFFB using 6 and 10 MV respectively. There were no statistically significant (p>0.05) difference found in mean doses to bladder, rectum, bowel and both femoral heads for FFFB using 6 and 10 MV respectively. There were significant (p <0.05) difference found in HI, MU number and NTID for FFFB using 6 and 10 MV respectively.

Conclusion: FFFB of 6MV was found superior in comparison to 10MV for RA planning in case of gynecological malignancies. It offers better HI, CI, less number of MUs (2.8%) and delivers more NTID (4.3%) for similar target coverage and OAR's sparing.

EP-1671

Stereotactic body radiotherapy for early-stage lung cancer with flattening filter free beams

J. Zhang[1], X. Peng[1], D. Hong[2]
[1]*Cancer Hospital of Shantou University Medical College, Department of Radiation Oncology, Shantou, China*
[2]*The First Affiliated Hospital of Shantou University Medical College, Department of Endocrinology, Shantou, China*

Purpose or Objective: The purpose of this study is to investigate the treatment plan dosimetry and delivery efficiency between the single-arc and double-arc techniques using stereotactic body radiotherapy with flattening filter free beams for early-stage lung cancer.

Material and Methods: Nineteen patients were included in this investigation, and each patient was arranged single-partial-arc (SA) and double-partial-arc (DA) techniques using the Eclipse 10.0 treatment planning system. The prescription dose was 48Gy/4 fractions and the photon beam energy was 6 MV flattening filter-free (FFF) beams from Truebeam linear accelerator. The treatment plans were appraised by Radiation Therapy Oncology Group (RTOG-0915) criteria for planning target volume (PTV) coverage and organs at risk (OAR) sparing. All plans were normalized to 100% of prescribed dose at least covering 95% of the PTV. Treatment efficiency was evaluated via monitor units (MUs) and treatment times were compared.

Results: The PTV volumes range from 20.46 to 88.37 cm3. Compared to the SA and DA plans, there was no significant difference in PTV coverage, except the maximum dose in the PTV. The maximum dose of SA technique was slightly higher than that of DA technique. The mean PTV conformity index (CI) for SA and DA was 1.06±0.05 and 1.01±0.03 respectively.

The mean PTV homogeneity index (HI) was 0.14±0.04 for SA and 0.09±0.03 for DA. For the OAR sparing, there was no significant difference between the SA and DA. A significantly difference was observed in the number of MUs and the treatment time, SA presents a reduction of 10.3% and 24.5% respectively.

Conclusion: SA showed no significantly difference in PTV coverage and OAR sparing compared with DA, however, the CI and HI of DA were better than those of SA. SA improved the greater treatment efficiency, and achieved less MUs number. In order to reduce patient treatment time, SA is worth to consider.

EP-1672

mARC vs. IMRT treatment of prostate and head-and-neck cancer with flat and FFF energies

Y. Dzierma[1], K. Bell[1], F. Nuesken[1], J. Palm[1], J. Fleckenstein[1], N. Licht[1], C. Rübe[1]

[1]Universitätsklinikum des Saarlandes, Department of Radiation Oncology, Homburg/Saar, Germany

Purpose or Objective: The modulated arc (mARC) is a VMAT-like rotational technique specifically designed for "burst mode" delivery of high dose rates. Only few studies have assessed the performance of this radiotherapy modality, and it is unclear how efficient it will prove for target volumes of high vs. low complexity. We therefore present a planning and delivery study for two frequent clinical applications: a relatively simple target volume for prostate cancer without lymph node involvement and a highly complex target volume for hypopharynx cancer. In each case, plan quality, treatment time and scattered dose are compared for mARC vs. IMRT using flat or flattening-filter-free (FFF) beams.

Material and Methods: Contours were retrospectively created for 10 prostate cancer patients and 8 head-and-neck cancer patients treated at our clinic. IMRT plans were set up using 11 beams and 55 segments. mARC plans for both energies were made using one rotation for prostate and two rotations for head-and-neck patients, with 4° arclets of spaced equidistantly every 8°. The Varian Eclipse treatment planning system with the AAA dose algorithm and a 2.5 mm dose grid was used for all plans. Plan quality was assessed using PTV coverage and sparing of organs at risk. All plans were delivered on an anthropomorphic phantom, where scattered dose was measured with thermoluminescent dosimeters (TLDs), and treatment times were recorded.

Results: All plans were visually assessed by a senior radiation oncologist and were deemed acceptable for treatment. Only few significant differences were found for PTV coverage and OAR sparing. For prostate cancer plans, no significant differences in OAR sparing were found except for the bladder, which was better spared by mARC than IMRT for both beam energies. For head-and-neck cancer cases, the mARC technique achieved a higher index of conformity and better sparing of the parotids.

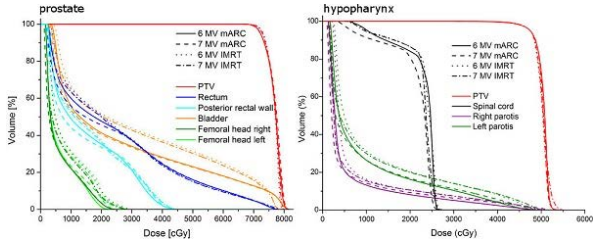

While differences in plan quality were minor, treatment times could be drastically reduced by the combination of mARC with FFF beams.e average treatment times for prostate cancer were reduced from 7 min for 6 MV IMRT to 2-3 min for FFF mARC. For the complex head-and-neck target volume, times were again reduced from ca. 9 min (IMRT, 6 MV) to 5:30 min (mARC, FFF 7 MV), even though FFF 7 MV required significantly more monitor units than 6 MV plans.

The scattered dose was considerably lower for the mARC as compared with IMRT for all plans. For the prostate, scattered dose was further reduced by the FFF beam energy. For hypopharynx cancer, this effect was partially obscured by the higher monitor units.

	6 MV IMRT	FFF 7 MV IMRT	6 MV mARC	FFF 7 MV mARC
Prostate cancer patients				
Monitor units	451 (384-511)	465 (421-523)	466 (384-506)	481 (447-511)
Treatment time (min:sec)	7:07 (6:42-7:27)	6:25 (6:12-6:42)	3:50 (3:28-4:36)	2:35 (2:26-3:12)
Dose at navel (mGy)	29.4 (25.0-38.4)	21.0 (15.1-28.0)	13.5 (11.2-15.7)	10.9 (8.5-13.3)
Dose at sternum (mGy)	4.46 (4.00-5.04)	2.32 (2.05-2.67)	2.81 (2.53-3.31)	1.39 (1.20-1.70)
Dose at lens (mGy)	2.48 (2.18-2.76)	0.84 (0.76-0.94)	2.41 (1.85-3.94)	0.73 (0.63-1.03)
Hypopharynx cancer patients				
Monitor units	598 (485- 729)	779 (628-918)	406 (363-459)	758 (644-897)
Treatment time (min:sec)	9:09 (8:33- 10:09)	7:46 (7:22-8:08)	6:19 (6:09-6:29)	5:30 (5:25-5:37)
Dose at breast (mGy)	24.1 (20.4-27.7)	20.5 (16.8-25.7)	17.9 (13.4-22.6)	15.4 (12.3-18.4)
Dose at gonads (mGy)	1.30 (0.93-1.55)	1.05 (0.82-1.33)	0.56 (0.49-0.62)	0.68 (0.58-0.75)

Comparison of plan efficiency (monitor units and treatment time) and scattered dose. Where a significant difference was found (Wilcoxon's signed rank test with p = 0.05), the best plan is marked in green.

Conclusion: Target volumes of high and of low complexity were analysed in this work. For both scenarios, the mARC technique achieved plan qualities comparable or even better than for IMRT, with a considerable reduction in treatment time (ca. 64 % for prostate and 40 % for hypopharynx) and scattered dose.

EP-1673

Hippocampal-sparing radiotherapy for glioblastoma patients using the VMAT technique

J. Hofmaier[1], S. Kantz[1], M. Söhn[1], M. Alber, K. (2)Parodi[3], C. Belka[1], M. Niyazi[1]

[1]University Hospital of LMU Munich, Radiation Oncology, München, Germany

[2]Aarhus University, Department of Oncology, Aarhus, Denmark

[3]Faculty for Physics of LMU Munich, Medical Physics, München, Germany

Purpose or Objective: To investigate the feasibility of hippocampal-sparing radiotherapy for glioblastoma patients using volumetric modulated arc therapy (VMAT). Since neurocognitive decline has been associated with hippocampal dose, hippocampal sparing could potentially improve neurological outcome of patients undergoing cranial irradiation.

Material and Methods: Datasets of 27 patients who received 3D-CRT for glioblastoma were included in this planning study. Dose distributions for the 3D-CRT plans were calculated in Elekta Oncentra Masterplan with a pencil beam algorithm. VMAT plans were optimized using the research TPS Hyperion V2.44 (equivalent to Elekta Monaco 5.1) which relies on Monte Carlo dose calculation. It was attempted to reduce the dose to the contralateral hippocampus as much as possible without compromising other treatment parameters such as target coverage, homogeneity index, conformity index and dose to other organs at risk including brain stem, chiasm, optic nerve and lenses. Parameters for both techniques were compared applying the Wilcoxon signed-rank test. The influence of tumor localization on hippocampal dose exposure was investigated with the Mann-Whitney U test. The correlation between PTV size and hippocampal dose was assessed with Spearman's rank correlation coefficient.

Results: With VMAT compared to 3D-CRT, the median reduction of the mean contralateral hippocampus dose was 56% ($p<0.01$). Other treatment parameters could be improved or at least be kept stable. Particularly, the median V30Gy of the brain was reduced from 58.7% to 48.2% ($p<0.01$). The median homogeneity index improved from 0.18 for 3D-CRT to 0.15 for VMAT ($p<0.01$), the median conformity index from 0.70 to 0.80 ($p<0.01$). For VMAT, a smaller PTV size correlated with improved hippocampal sparing ($p=0.01$). A

parietal tumor localization was a predictor for a higher contralateral hippocampal dose (p=0.01).

Conclusion: A substantial reduction of the dose to the contralateral hippocampus is technically feasible when VMAT is used instead of our standard 3D-CRT planning strategy. The amount of sparing that can be achieved strongly depends on the individual patient geometry. Whether this approach is able to conserve the neurocognitive status without compromising the oncological outcome for patients with glioblastoma needs to be investigated in the setting of prospective clinical trials.

EP-1674

Should VMAT be routinely applied to treat sacral bone metastases?

V. Soyfer[1], B. Corn[1], Y. Meir[1], N. Honig[1], N. Shtraus[1]
[1]*The Tel-Aviv Sorasky Medical Center, Radiation Oncology, Tel Aviv, Israel*

Purpose or Objective: Bone metastases are a frequent and disturbing complication of cancer. The challenge of optimizing dose coverage of the concave shape of the sacrum along with its close proximity to the rectum, intestines and femoral heads lead us to investigate whether the VMAT technique is advantageous when compared to 3D treatment.

Material and Methods: Twenty three consecutively treated patients with sacral metastases in 2013-2014 were included in a comparative treatment-planning study evaluating VMAT and 3-D planning. The statistical analysis included the T-test, assuming Unequal Variance (one tail). Calculation of the p-value for the comparative results applied. Our null hypothesis was that VMAT is better than 3D technique, and our alternative hypothesis was that 3D technique is superior to VMAT.

Results: The PTV coverage was identical in VMAT and 3D planning. Median values and V15 for the intestinal exposure showed no statistically significant difference between the 3D planning and VMAT: 9.28 Gy (SD 2.25) and 47.0 ml (SD 68.62) versus 8.97 Gy (SD 2.18) and 18.45 ml (SD 69.56), respectively. However, on an individual *per case* assessment it appears that the lower exposure of the bowel depends on the small bowel/ sacrum volumes ratio. The benefit for VMAT emerges if such a ratio exceeds one. The median values for the rectum 3D and VMAT were 11.34 Gy (SD 5.14) and 7.7 Gy (SD 2.76), respectively. The median 3D and VMAT exposure of the femoral head were 1.78 (SD 2.94) Vs 4.006 (SD 2.1) on the left and 1.74 (0.9) Vs 4.26 (SD 1.8) on the right side for the 3D and VMAT, respectively.

Conclusion: Good sacral coverage is achievable with either 3-D or VMAT approaches. VMAT is advantageous vis-à-vis the rectal exposure and when relatively large amounts of small bowel course through an individual patient's fields. The 3-D approach, however, retains benefit for femoral protection, a finding that may have implications for patients with arthritis and osteopenia.

EP-1675

Total body irradiation with Tomotherapy

L. Simon[1,2,3], F. Izar[4], G. Moliner[1], M. Barides[2,3], R. Ferrand[1]
[1]*Institut Universitaire du Cancer de Toulouse - Oncopole, Department of Medical Physics, Toulouse, France*
[2]*INSERM, CRCT-UMR1037, Toulouse, France*
[3]*Université Toulouse III Paul Sabatier, UMR 1037, Toulouse, France*
[4]*Institut Universitaire du Cancer de Toulouse - Oncopole, Department of Radiation Oncology, Toulouse, France*

Purpose or Objective: In Conventional Radiotherapy (CRT), Total Body Irradiation (TBI) is generally performed at long Source Skin Distance using diodes to drive the delivered dose. The dose distribution is usually not well assessed (measured only in a few points) and was shown to be strongly heterogeneous. This technique also leads to acute and late toxicity. Helical Tomotherapy (Accuray Inc., Sunnyvale, CA) for TBI is implemented in some centers. Compared to CRT, Tomotherapy allows the delivery of the prescribed dose with a high level of accuracy and homogeneity. Organs-at-risk can be spared and the dose distribution is known before the treatment. Two technical issues have to be solved. First, the patient must be treated using two plans, head first (HF) and feet first (FF) due to limited supero-inferior (SI) table motion. At the junction of these two plans, the dose must be delivered with particular care. Moreover, the planning target volume (PTV) is the entire body, including the skin. A safety margin in the air surrounding the body should be added to take into account setup errors. Using inverse planning, however, can result in over-fluence peaks in the skin region. The aim of this work is to present our solution for these two issues, our optimized planning protocol and our clinical results after one year of practice (outcome for 15 patients).

Material and Methods: Patient treatment position is shown hereafter. Thermoplastic masks are placed on the head and the thorax (not the legs). Two CTs are acquired (HF and FF). At the planning station, the whole body (cropped 3 mm under the skin) is divided into 10 PTVs. At the junction (~halfway up the thighs), 4 PTVs (thickness 2 cm) are drawn to deliver the dose with the degraded penumbra methodology: decreased dose is delivered during HF plan and increased dose during FF plan. Different sets of doses were tested. The resulting dose distribution in the presence of simulated set-up errors (SSUE) is computed to find the combination that insures optimal dose coverage of the junction. Moreover, to insure dose coverage of legs in presence of SSUE, several Virtual Boluses (VB) were tested. A VB is a bolus added at planning, but not present during treatment. Several thicknesses and densities were tested on a phantom study: in presence of SSUE, the dose coverage and dose increase (due to the methodology) were assessed.

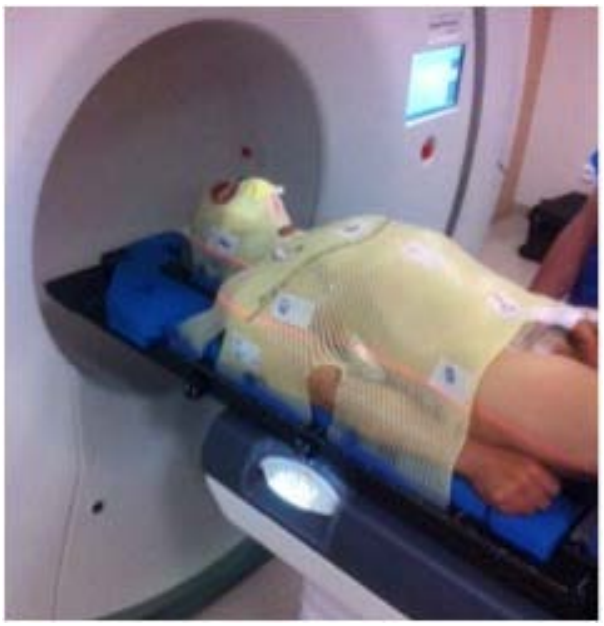

Results: The best combination of PTV doses at the junction is presented in table: V95% stays higher than 96% even in the case of a SSUE of 1 cm (SI). The optimal VB is an 8 mm thick VB (density=0.4). This allows a good coverage (V95%>95%) for a large lateral SSUE (up to 2.9 cm). Underestimation of dose using this VB (planning vs measure) is 1.5%.

	Dose plan HF	Dose plan FF	Total Dose
Slice 1	10.74	1.26	2
Slice 2	7.56	4.44	2
Slice 3	4.44	7.56	2
Slice 4	1.92	10.08	2

Conclusion: This study presents our optimized planning parameters. Since November 2014, 15 patients were treated with a dose of 2 or 12 Gy. Dose to lungs was limited to 9 Gy.

Most of the patients have been treated for acute leukemia with allogeneic transplant.

EP-1676

Sparing potential of scanned protons for the treatment of intramammary nodes in breast radiotherapy

A. Dasu[1], A.M. Flejmer[2], A. Edvardsson[3], P. Witt Nyström[4]
[1]*Linköping University, Department of Radiation Physics, Linköping, Sweden*
[2]*Linköping University, Department of Oncology, Linköping, Sweden*
[3]*Lund University, Department of Medical Radiation Physics, Lund, Sweden*
[4]*Uppsala University Hospital, Department of Oncology, Uppsala, Sweden*

Purpose or Objective: Breast cancer patients are among the long-term survivors of radiotherapy and therefore the long-term cardiopulmonary toxicity due to the treatment should be reduced to a minimum. However, complication rates could be further increased when intramammary nodes are included in the target due to their proximity to the heart and the lungs. Several techniques could be used to decrease the dose to the normal tissues and consequently the rates of late complications, including proton beam radiotherapy and respiratory gating. This study aims to investigate the potential for normal tissue sparing for the treatment of intramammary nodes in breast cancer radiotherapy using scanned proton beams with or without respiratory gating.

Material and Methods: The study was performed on CT-datasets acquired from ten left-sided patients during enhanced inspiration gating (EIG) and free-breathing (FB). The patients were planned with intensity modulated proton therapy (IMPT) for locoregional breast treatment. The prescribed dose to the target was 50 GyRBE in 25 fractions, assuming an RBE of 1.1. Different plans were performed for breast and supraclavicular nodes respectively breast, supraclavicular and intramammary nodes (IMN). The implications of including IMN in the target volume were evaluated from the point of view of the doses to the organs at risk for cardiopulmonary complications.

Results: Inclusion of the IMN in the target volume led to a small increase of the cardiopulmonary burden. Thus, in FB cases the average dose to the heart increased from 0.3 to 0.4 GyRBE and the average dose to the lung increased from 6.1 to 6.6 GyRBE, while the average dose to the left anterior descending artery (LAD) decreased from 4.1 to 3.8 GyRBE. For EIG cases the average dose to the heart was almost unchanged (0.2 GyRBE), the average dose to the lung increased from 6.9 to 7.4 GyRBE and the average dose to the LAD decreased from 3.3 to 2.6 GyRBE. Other dosimetric parameters of interest showed a similar trend when IMN were included in the target. These parameters are much lower than those that could be achieved in conventional radiotherapy with photons, especially with respect to the cardiovascular burden, irrespective of whether respiratory gating is used or not.

Conclusion: The results of this study indicate that radiotherapy with scanned proton beams has the potential of significantly limit the cardiopulmonary burden compared to photon RT when including the IMN in breast cancer radiotherapy.

EP-1677

Comparison of different techniques in lung SABR using VMAT with deep inspiration breath hold

N. Kayalilar[1], Z. Ozen[1], B. Gunhan[1], F. Karakose[1], K. Yakar Ilbak[1], H. Sertel[1], R. Ibrahimov[1], A. Arifoglu[1], S. Gurdalli[1], M.U. Abacioglu[1]
[1]*Neolife Medical Centre, Radiation Oncology, Istanbul, Turkey*

Purpose or Objective: Stereotactic ablative radiotherapy (SABR) for the lung primary and metastatic tumors aims to increase the local control, survival and quality of life. Deep inspiration breath hold (DIBH) using 4D CT for simulation minimizes respiratory motion and reduces the toxicity risk by decreasing margins. In this study, we aimed to compare the dosimetric results of different devices and techniques of SABR using volumetric arc therapy (VMAT) with DIBH in the lung tumors.

Material and Methods: CT datasets of 7 patients with right-sided lung cancer performed with RPM system (Varian, Palo Alto) was used. Median PTV was 13.2cc. Dose prescription objective was to cover 98% of the target volume by D98% which was 50 Gy/5 fractions. Four different VMAT plans were made on Eclipse TPS (Varian, Palo Alto) using AAA algorithm. Plan A consisted of TrueBeam,120HDMLC, 6MV-FFF, without jaw tracking, Plan B TrueBeam,120HDMLC, 6MV-FFF, with jaw tracking, Plan C TrueBeam,120HDMLC, 6MV, without jaw tracking, Plan D with Trilogy, 120MilleniumMLC, 6MV, without jaw tracking. Three partial arcs using 210 degrees were used to generate the plans under the same optimization conditions. Monitor Unit (MU), beam-on time (BOT), Gradient Index (GI), lung V20 and V5, dose at 2 cm from PTV (D2cm), PTV(Dmax) and PTV(Dmin) were assessed for comparison. Wilcoxon test was used for statistical evaluation.

Results: No statistically significant differences were found for total MU, D2cm and PTV(Dmin) between the four plans. Mean PTV(Dmax) values were lower in Plan C with HDMLC compared to Plan D with MilleniumMLC (122.9%±3.9 vs 126.8%±3.7, p=.018). At GI assessment; there was no significant difference between plans with and without jaw-tracking. However, there was a significant difference between Plan C and Plan D (4.4±0.5 vs 4.8±0.6, p=.018); and between Plan A (FFF) and Plan C (FF) (4.2±0.4 vs 4.4±0.5, p=.018). V20 and V5 was lower in Plan C compared to Plan D (2.8%±1.5 vs 3.3%±1.5, p=.028 and 15.1%±5.3 vs 16.0%±5.6, p=.018).; V5 was lower in Plan A compared to Plan C (14.4%±5.1% vs 15.1%±5.3). BOT was significantly shorter between Plan A and Plan C (167.5 sec±20.4 vs 390.5 sec±47.8, p=.018).

Conclusion: In SABR with WMAT using DIBH, we observed some improvements by using HDMLC compared to MilleniumMLC and FFF compared to FF beams. However, we could not observe additional benefit with jaw tracking in the FFF mode. Major advantage of FFF was the shorter BOT, which may finally improve the patient compliance in SABR using DIBH technique.

EP-1678

VMAT in locally advanced lung cancer; does it add benefit?

M. Kamaleldin[1], M. Al Daly[2], S. Talima[2]
[1]*Cairo University- Fac. of Medicine, Radiation Physics, Cairo, Egypt*
[2]*Cairo University- Fac. of Medicine, Clinical oncology, Cairo, Egypt*

Purpose or Objective: In locally advanced NSCLC Concurrent chemo/Radiation is the key most important treatment approach. However delivering adequate radiation dose to improve treatment results is limited by the tolerance of nearby structures (lungs, esophagus, heart etc…), and by the intrafractional uncertainties resulting from prolonged treatment time of the conventional techniques. We have compared VMATplanes Vs. 3D CRT in inoperable advanced lung cancer cases.

Material and Methods: Ten cases of previously treated lung cancer with 3DCRT planes (minimum of 4 beams) were replanned with VMAT optimization using 2 half arcs. Both planes were performed on Eclipse© planning system (version 11) with AAA-algorithm and linear accelerator UNIQUE © of energy 6Mv , dose rate of 600 cGy/min , and 120 multileaf collimator. The dose was prescribed as 60Gy / 30fr to the CTV surrounded with margin of 1.5cm for the PTV. Plans were compared for coverage , avoidance of organs at risk , and total number of MU.

Results: The mean GTV volumes ranged from 149.44 to 526.53 cc. VMAT plans show good results in comparison with 3DCRT in both conformity index (0.81±0.09 Vs 0.68±0.07 respectively, p-value of 0.009), and heterogeneity index (0.11±0.03 Vs 0.14±0.02, p value= 0.042). Furthermore, minimum doses to PTV in VMAT plans are higher than 3DCRT plans (57±1.22 Vs 55.1±0.86, p value= 0.001).
In risk structures, the lung volume receiving 10Gy, 20Gy and 30Gy were reduced in VMAT plans (with relative reduction of 2.27%, p=0.002; 4.87%, p=0.001; 11.8% respectively). Mean lung dose was also reduced (15 Vs 17.69) but not statistically significant. V30 of the heart was reduced compared to 3DCRT (7.53±6.2 10.43±6.8 with p value of 0.051). The maximum dose of esophagus with VMAT was 47.7 Vs 48.69 with 3D CRT (not statistically significant). Moreover, D 50 of the esophagus was less with VMAT (19.94 Vs 23.63) with p value of 0.22.
Regarding monitor units, the mean values were (461.40±124.42 Vs 227.90±13.52) for VMAT and 3D CRT respectively.

Conclusion: Inspite of large PTVs included in our study VMAT planes showed tendency toward reduction of mean and high lung dose and heart doses. Reduction in esophageal doses was not statistically significant , This was obtained without impairment of PTV coverage that was improved in some cases. VMAT for advanced lung cancer can help to improve therapeutic ratio and may open the door for dose escalation

EP-1679

A single centre experience of using helical tomotherapy (HT) for craniospinal irradiation (CSI)

M. Singhera[1], T. Falco[1], K. Blythe[1], R. Begum[1], T. Greener[1], R. Beaney[1], N. Mikhaeel[1]
[1]Guy's and St Thomas' NHS Foundation Trust and King's Heath Partner's Academic Heath Sciences Centre, Radiotherapy, London, United Kingdom

Purpose or Objective: CSI is one of the most complex radiotherapy (RT) treatments. Conformal 3D RT techniques require many fields (field within field / segments) to achieve homogeneity and minimise doses to organs at risk (OAR) and involve field junctions. The planning process is time consuming and the actual treatment delivery is long, frequently exceeding 30 minutes. HT offers an excellent alternative with the ability to treat patients in supine position, without junctions and with better dose distribution. The aim of this study is to evaluate the use of HT in CSI with emphasis on dosimetric parameters and treatment duration.

Material and Methods: Retrospective analysis of treatment planning and dosimetric indices was undertaken on seven patients who received cranio-spinal radiotherapy with HT at our centre. The HT plan was delivered using 51 beam angles per rotation, with a constant modulation factor of 2.0, field width of 5 cm and one of two pitches (0.43 or 0.28) to optimise treatment plans. An iterative inverse planning algorithm based on least squares minimization was used which optimises multi-leaf collimator at each beam angle. Dose was calculated by convolution and superposition. Patients were imaged daily covering different areas of the body and corrections applied for directional errors. Data analysis was done using descriptive statistics.

Results: Helical tomotherapy plans for seven adult patients were analysed. Five patients had a haematological malignancy and two had a medulloblastoma. Five patients with a haematological diagnosis received a dose of 30Gy in 1.5Gy/#. Two patients with medulloblastoma received 35 Gy delivered in 1.67Gy/#. Details of treatment planning and plan evaluation parameters of seven patients are presented in Table 1.

Patients	1	2	3	4	5	6	7	Average
Pitch	0.4	0.4	0.2	0.2	0.2	0.4	0.4	
Modulation factor	2	2	2	2	2	2	2	
Dose/dose per # (Gy)	30/1.5	30/1.5	30/1.5	30/1.5	30/1.5	35/1.67	35/1.67	
PTV volume (cm^3)	3701.1	2875.3	3505.9	2941.9	3508.9	3623.8	3455.8	3373.3±328.9
Dmax PTV	32.3	31.5	31.8	31.8	31.7	37.8	37.6	
Dmin PTV	18.9	20.2	25.9	23.1	20.3	20.4	21.4	
Mean dose to R lens	18.7	10.8	16.2	27.4	9.6	4.1	4.2	13.0±8.3
Mean dose to L lens	16.2	16.9	17.5	26.8	7.7	3.8	4.6	13.4±8.3
Mean dose to spleen	7.6	5.5	5.2	5.4	6.1	6.5	6.4	6.1±0.8
Mean dose to thyroid	17.3	23.6	16.4	20.7	10.6	21.8	17.8	18.3±4.2
Mean dose to lung	10.3	11.6	8.8	8.1	9.2	4.4	8.1	8.6±2.2
V_5	71.1	80	67.4	84.9	64.9	43.1	78	
V_{10}	51.0	58.4	44.2	34.6	46	23	30	
V_{20}	13.1	18.6	13.1	10.1	12.2	5.2	5.1	
Mean dose to heart	10.1	9.9	8.7	12.2	9.4	12	8.8	10.9±1.3
V_5	99.9	99.3	99.3	99.8	99.1	99.4	100	
V_{10}	51.1	47.9	33.4	77.2	40.6	74.4	33.2	
V_{20}	0.47	1.4	0.0	1.3	0.0	5.9	0.0	
Mean dose to kidney	8.1	10.7	10.5	10.4	11.0	9.8	8.6	9.9±1.09
V_{10}	16.9	21.2	21.5	24.8	21.3	6.3	6.4	
Mean dose to liver	8.4	11.1	9.6	11.6	10.4	8.6	8.7	9.8±1.2
Mean dose to bladder	5.9	4.0	1.1	0.7	6.4	7.0	2.6	3.9±2.5
Beam 'on-time' (minutes)	9.5	9.3	8.6	10.2	11.9	11.6	11.6	10.3±1.3

PTV: Planning target volume, DmaxPTV: Maximum dose to PTV, Dmin: Minimum dose to PTV

Overall HT plans achieved excellent PTV coverage with mean V95 of 33.5 Gy for medullblastoma patients. The mean V95 was 28.3 Gy for those with a haematological diagnosis. The mean homogeneity index was 1.0. Organs at risk doses were well below tolerances required. In particular averaged mean heart dose was 10.9±1.3, mean lung dose was 8.6±2.2 and mean liver dose was 9.8±1.2. The mean D50% for lung was 7.2 Gy±3.8 and mean D10% was 20.2Gy±3.6. The mean D50% for the heart was 10.1Gy±1.3 and mean D10% was 14.7Gy±2.1.

Conclusion: HT for CSI has many advantages including: the ability to treat patients in supine position, no need for junctions, excellent PTV coverage, low doses to OAR and shorter treatment time.

EP-1680

Treatment planning of stereotactic radiosurgery for single brain metastases: impact of leaf width

E. Lamers-Kuijper[1], E. Van der Bijl[1], A. Van Mourik[1], C. Van Vliet-Vroegindeweij[1], E. Damen[1]
[1]The Netherlands Cancer Institute, Department of Radiation Oncology, Amsterdam, The Netherlands

Purpose or Objective: Stereotactic radiosurgery of brain metastases requires highly conformal dose distributions. Besides beams setup, characteristics of the linear accelerator collimator may also play a role. In this study we compared the impact of leaf width on the dose outside the target for stereotactic radiosurgery of single brain metastases.

Material and Methods: For 10 patients with one lesion, treatment plans were generated using two MLC types: Elekta Agilty with 0.5cm leaf width and Elekta MLCi2 with 1cm leaf width. Two VMAT arcs were used, one coplanar arc and one non-coplanar arc (couch 90°). Five patients had a PTV volume ≤ 4 cm^3 with a prescription dose of 24Gy in 1 fraction, and 5 patients had a PTV volume between 4 and 14 cm^3 with a prescription dose of 18Gy in 1 fraction. All plans were required to fulfill clinical requirements: V100%Dpres>95%VPTV, D0<150%Dpres and OAR doses as low as possible and never above clinical constraints. The maximum dose in the PTV is kept the same per patient in both plans. The quality of the dose distribution outside the PTV was evaluated using the mean dose in two ring structures, adjacent to the PTV.

Results: The mean dose was evaluated in the first 2 rings of 5 mm around the PTV(table 1). The difference in mean dose for the small lesions(Dpres=24 Gy) of the first ring of 5 mm is 1.8 Gy in favor of the Agility and 0.9 Gy for the larger lesions(Dpres=18 Gy)also in favor of the Agility. The difference is smaller for the larger lesions (figure1). Also for the second ring of 5 mm, adjacent to the first ring, the difference is is 1.1 Gy vs 0.8 Gy also in favor of the Agility.

	24Gy							18Gy						
	Ring5mm(Gy)			Ring10-5mm(Gy)				Ring5mm(Gy)			Ring10-5mm(Gy)		
Patient	MLCi1	Agility	Diff	MLCi1	Agility	Diff	Patient	MLCi1	Agility	Diff	MLCi1	Agility	Diff
1	12.2	10	2.2	5.6	4.6	1	6	12.4	10.9	1.5	5.5	4.7	0.8
2	12.9	10.9	2	6.3	5.3	1	7	14.6	13.8	0.8	4.5	3.8	0.7
3	11.9	10.4	1.5	5.6	4.8	0.8	8	13.5	12.3	1.2	7.6	6.2	1.4
4	19.9	17.9	2	5.4	4	1.4	9	14.5	13.8	0.7	5.2	4.6	0.6
5	16.5	15.1	1.4	8.4	7.1	1.2	10	13.3	12.9	0.4	7.2	6.7	0.5
mean	14.2	12.9	**1.8**	6.2	5.2	**1.1**	mean	13.7	12.7	**0.9**	6	5.2	**0.8**
SD	3.5	3.5	**0.3**	1.2	1.2	**0.2**	SD	0.9	1.2	**0.4**	1.3	1.2	**0.4**

Tabel 1: Mean dose in the rings around the PTV at 5 mm and 10 mm for small lesions (PTV volume < 4 cm³) and the larger lesion (PTV volume between 4 and 14 cm³)

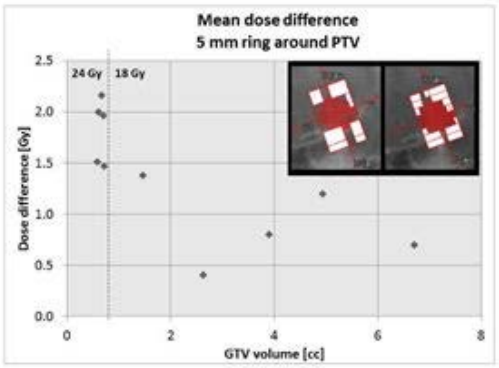

Figure 1: The mean dose difference in the first 5 mm ring around PTV. In the right upper corner the typical leaf setting for the Agility on the right and the MLCi1 on the left.

Conclusion: For the small lesions with a volume smaller than 4 cm³ the Agility shows a steeper gradient in the two surrounding rings than the MLCi1. Therefore we recommend the use of the Agility for treating the smaller lesions.

EP-1681

A treatment planning strategy for SBRT of multiple T1-2 lung tumors

A. Tijhuis[1], E. Van der Bijl[1], J. Knegjens[1], C. Van Vliet-Vroegindeweij[1], E. Damen[1]
[1]*The Netherlands Cancer Institute, Department of Radiation Oncology, Amsterdam, The Netherlands*

Purpose or Objective: To obtain a planning technique for SBRT treatment of multiple lung tumors, which is suitable for all relative positions of the tumors.

Material and Methods: For 10 patients with two tumors, treated with 3 x 18Gy, VMAT plans were generated in Pinnacle, using various approaches: simultaneous versus sequential optimization, with or without the dose distribution of one tumor as background for optimization of the other tumor. The quality of the treatment plans was judged on coverage (PTV V100% >95%), conformity (V100%/PTV volume), inhomogeneity (PTV D0<165%) and dose constraints on OARs.

Results: Simple addition of beams for two independently planned tumors does not yield optimal results since the mutual low dose contributions cannot be taken into account properly. Simultaneous optimization on both targets results in pairs of open leafs in-between the lesions (Fig 1). We therefore concluded that the strategy that yields the most conformal plans is the subsequent planning of the tumors using a dual-arc for both, where the dose distribution resulting from the planning of the first target is used as a background dose while optimizing the beams for the second target. During optimization of the first tumor, no limit is applied for the dose to the second PTV, since this can be compensated for in the optimization procedure for this PTV. After optimization of the second PTV, the number of monitor units in each beam pair might be adjusted slightly to conform to the required target coverage. This strategy works for two or more isocenters as well as for one mutual isocenter. For three or more tumors, iterating the above method yields good results

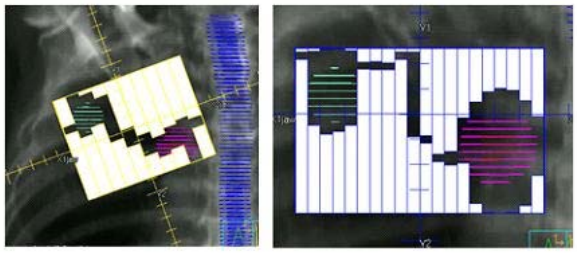

Two examples of simultaneous optimizing on both targets (fig1)

Conclusion: We developed a generic planning strategy to obtain high quality lung SBRT-treatment plans for patients with multiple lung tumors. The strategy uses a dual-arc VMAT for each tumor, while taking the dose distribution covering the first target is used as background during dose optimization for the second target. This method is clinically in use since March 2015, since then 15 patients have been treated using this method.

EP-1682

Breast and regional lymph nodes RT: V-MAT/RapidArc and Tomotherapy comparison

M. Valli[1], L. Negretti[2], S. Cima[1], M. Frapolli[1], A. Polico[1], G. Nicolini[3], E. Vanetti[3], A. Clivio[3], A. Richetti[1], G. Pesce[1], F. Martucci[1], C. Azinwi[1], K. Yordanov[1], S. Presilla[3]
[1]*Oncology Institute of Southern Switzerland, Radiation Oncology, Bellinzona-lugano, Switzerland*
[2]*Clinica Luganese, Radiation Oncology, Lugano, Switzerland*
[3]*Ente Ospedaliero Cantonale, Medical Physics Unit, Bellinzona, Switzerland*

Purpose or Objective: Two centers compared VMAT/RapidArc (RA) and Tomotherapy (TOMO). for the irradiation of breast and regional lymph nodes.

Material and Methods: Five left and five right breasts plus regional nodes have been contoured by two dedicated radiation oncologists. Two senior physicists checked the treatment plans studied by dedicated dosimetrists. The Anatom-e tool was tested for improving definition and avoiding interpersonal variability in the contouring. Prescription, according to ICRU, was 50 Gy in 25 daily fractions. We considered both lungs, the heart, the left anterior descending coronary artery (LAD), the controlateral breast and the thyroid as Organa t Risk (OaR). The dose constraints were: PTV V95=95%, ipsilateral lung V20 20%, heart mean dose < 10Gy, heart max dose <35Gy, LAD max dose ≤20Gy, thyroid max dose < 45 Gy and contralateral breast max dose≤5 Gy. We have studied the treatments in free breathing modality, perfectly aware of the higher dose received by heart and LAD in comparison to the respiratory-gated modality, routinely used in the RA center.

Results: We summarized the results of this comparison in Table 1

Table 1. Left and right breast plus lymphnodes.

	TOMO	RA
LEFT BREAST + LN	% (±SD)	% (±SD)
V95% PTV	94.9 (±0.5)	95.1 (±10)
V20Gyipsilateral lung	15.9 (±1.3)	22.2 (±3.2)
	Median dose Gy (±SD)	Median dose Gy (±SD)
LAD	4.7 (±0.9)	15.7 (±4.5)
Heart	3.5 (±3.8)	9.0 (±1.7)
Contralateral breast	5.1 (±1.4)	4.2 (±1.1)
	Median min (±SD)	Median min (±SD)
Beam-on time	6.91min (±0.21)	1.03min (±0.03)
RIGHT BREAST + LN	% (±SD)	% (±SD)
V95 PTV	95.0 (±0.5)	94.9 (±0.1)
V20 ipsilateral lung	19.4%(±3.1)	21.2%(±1.5)
	Median dose Gy (±SD)	Median dose Gy (±SD)
LAD	2.0 Gy (±1.1)	7.7 Gy (±0.9)
Heart	5.9 Gy (±0.8)	6.8 Gy (±1.5)
Contralateral breast	3.6 Gy ± (0.5)	4.2 Gy (±0.4)
	Median min (±SD)	Median min (±SD)
Beam-on time	5.9min (±0.26)	1.07min (±0.01)

Conclusion: Both techniques allow a good coverage and dose uniformity for the PTV, with proper sparing of the OaR. TOMO

allows greater hearth and LAD sparing in left cases, when compared to RA with no gating. Of note beam-on time, in RA modality, is highly decreased.

EP-1683

Left breast IMRT with SIB: a user improved technique to reduce heart and lung dose

S. Naccarato[1], R. Ruggieri[1], G. Sicignano[1], F. Ricchetti[1], S. Fersino[1], A. Fiorentino[1], N. Giaj Levra[1], R. Mazzola[2], A. Alongi[1]

[1]*Ospedale Sacro Cuore Don Calabria, Radiation Oncology, Negrar, Italy*

[2]*Radiation Oncolgy School, University of Palermo, Palermo, Italy*

Purpose or Objective: Many strategies have been explored in attempt to reduce the cardiac dose and the lung dose during breast irradiation. Here we investigated the efficacy of user optimised collimator rotation and jaws setting, in static gantry IMRT with simultaneous integrated boost (SIB), on hearth and lung dose sparing.

Material and Methods: From September 2010 to March 2014, 69 patients were treated for left breast (PTV-breast) cancer with SIB at surgical bed (PTV-boost) in 25 fractions: the prescribed doses (Dp) were 50 Gy and 60 Gy, respectively. All plans were generated with Varian EclipseTM v.10.0.28 TPS, using 5-7 IMRT sliding-window fields equally spaced along a 190° arc, with 6MV photon beams and a Varian Millenium120TM multileaf collimator. Dose computation were performed by AAA algorithm, with a 2.5 mm grid size. The first 41 patients were planned by fixing a null collimator rotation, and by leaving the optimizer Varian DVOTM v.10.0.28 free to search for the optimal setting of the jaws (IMRT-A). In the next 28 patients the arrangement of the two outermost tangential fields were set to maximally spare the heart and the left lung. In details, the collimator was rotated so as to align the medial jaw with the projection of the chest wall (IMRT-B). Further, for the most lateral field the jaws were collimated to the lateral and central portions only of the PTV-breast. The remaining 3-5 fields covered entire target according the BEV projection of the target. By selecting the Fixed Jaws Parameter of the two outermost fields into DVO the same jaws aperture defined in BEV were assured during optimization process. Plans aimed to cover at least 95% of the PTVs volume with a dose ³ 95% of the Dp (V95% ³95%), with V107%<2%, for PTV-boost. Hearth volume receiving more then 20 Gy (V20)<10%. Left lung V20<20%. Right breast mean dose (Dmean)<2Gy and right lung Dmean<3Gy. By hypothesis testing, several dose-volume metrics were then compared across the two groups of plans.

Results: As detailed in Table 1, although a slightly reduced V95% to PTV-breast was associated with IMRT(B), both techniques assured to any patient the required target dose coverage. In terms of dose sparing to the OARs, IMRT(B) was associated with a 25.6% reduction in the median of Dmean to the heart, while the heart V5, V10 and V20 were respectively reduced by 21.1%, 49.8%, and 52.1% (all p<0.002). Further, the median of Dmean to the left lung decreased by 21.2%, while V5, V10 and V20 to this organ decreased by 5.4%, 36.8% and 28.6%, respectively (all p<0.003). No significant differences resulted for Dmean to the right breast and lung.

Table 1 Comparison of median (range) values of dose-volume metrics for PTV coverage and OAR sparing as a function of IMRT plan modality

		IMRT-A	IMRT-B	*p-value*	
PTV-breast	V95% (%)	97.6 (94.5-99.9)	96.5 (93.8-99.1)	*0.003*	§
PTV-boost	V95% (%)	99.8 (97.9-100.0)	99.8 (98.0-100.0)	*0.408*	#
	V107% (%)	1.6 (0.0-15.1)	0.1 (0.0-13.0)	*0.057*	#
Hearth	Dmean (Gy)	9.4 (5.0-16.6)	7.0 (4.1-13.0)	*<0.001*	$
	V5Gy (%)	71.8 (41.5-97.8)	56.6 (25.7-98.4)	*0.002*	$
	V10Gy (%)	33.9 (7.1-75.7)	17.0 (2.2-62.4)	*<0.001*	*
	V20Gy (%)	7.5 (0.3-32.9)	3.6 (0.0-11.8)	*0.001*	*
Left lung	Dmean (Gy)	14.6 (10.6-19.9)	11.5 (7.6-19.1)	*<0.001*	*
	V5Gy (%)	91.2 (72.9-100)	86.3 (51.1-99.8)	*0.003*	*
	V10Gy (%)	54.4 (29.7-89.2)	34.4 (22.4-90)	*0.0002*	*
	V20Gy (%)	21 (12.4-45.3)	15 (6.2-30.2)	*<0.001*	*
Right breast	Dmean (Gy)	1.7 (0-4.2)	1.4 (0.7-6.6)	*0.493*	#
Right lung	Dmean (Gy)	2.2 (1.1-4.9)	1.5 (0-6.7)	*0.209*	#

Abbreviations: § two-tailed t-Student test, # two-tailed Mann-Whitney test, $ one-tailed t-Student test, * one-tailed Mann-Whitney test.

Conclusion: Similar PTVs coverage were obtained with both IMRT techniques, the selection from an experienced user of collimator rotation and fixed jaws settings for the two outermost tangential fields in a 5-7 fields sliding-window IMRT (IMRT-B) resulted in a significant reduction of the dose to the heart and the ipsilateral lung.

EP-1684

Optimization of a VMAT technique for three dose level irradiation of head and neck cancer

M. Bougtib[1], M. Malisan[2], M. Crespi[2], C. Foti[2], M. Guernieri[2], E. Moretti[2]

[1]*International Master on Medical Physics, Trieste University, Trieste, Italy*

[2]*Azienda Ospedaliero-Universitaria di Udine, Medical Physics, Udine, Italy*

Purpose or Objective: It was reported in literature that increasing the number of arcs from 1 to 4-8 improves the quality of head and neck (HN) VMAT plans with simultaneously integrated boost (SIB). Aim of this work is to optimize the performance of triple-arc VMAT (TAV) against conventional IMRT for three dose level irradiation of advanced HN cancer.

Material and Methods: A retrospective planning study was conducted on a sample of 10 patients with HN cancer previously treated with IMRT. PTVs were delineated for 3 different dose levels (70, 63 and 56 Gy in 35 fractions) delivered by a SIB technique. All plans were generated with 6 MV x-rays for a Varian Clinac iX linac. Optimization and calculations were done in the Varian Eclipse system (v. 10.0.28). IMRT plans included 7 equally placed beams using sliding window technique. Three TAV plans were generated for each patient: triple full-arc plan, 3F (collimator angles (CA): 0°, 20°, 340°); double full + partial arc plan, 2FP0 (CA: 20°, 340°; 0° for partial arc); double full + partial arc plan, 2FP90 (CA: 20°, 340°; 90° for partial arc). Dose normalization was set as D(95%)=70 Gy for the primary tumour and involved nodes (PTV70), while planning objectives were D(95%) 95% of prescription dose for the high- and low-risk target volumes (PTV63 and PTV 56). OARs taken into account into optimization included the brainstem, spinal cord, parotids, oral mucosa, larynx, mandible, vertebrae, thyroid. The healthy tissue was defined as the body volume excluding the PTVs. Planning objectives are shown in Table 1. The parameters used for plan comparison include PTV coverage, dose homogeneity (HI) and conformity (CI), OAR sparing, healthy tissue integral dose (HTID) and number of MUs.

Results: Table 1 shows the results of PTV coverage, homogeneity, conformity, and doses to OARs for the 4 planning techniques. Similar coverage of all PTV's is obtained in all the techniques. TAV plans show better homogeneity and conformity in PTV70 compared to IMRT, though the difference is significant only for HI of the 2FP90 technique. For spinal cord and vertebrae the 2FP90 plans show significant reductions of maximum dose. No significant

changes are observed in terms of mean dose to parotids or maximum dose to mandible, while oral mucosa and thyroid result better spared with TAV techniques. Though smallest for IMRT, the mean HTID is not significantly different from the TAV techniques. Finally, MU's for all TAV techniques are significantly lower than for IMRT; no reduction is observed when using one partial arc instead of 3 full arcs.

Table 1. Planning objectives and plan comparison among 7-field IMRT and triple arc VMAT. Results are averaged over the 10 patients of the sample. Statistical significance of Wilcoxon signed rank test is reported in the last column.

		Objective	IMRT	3F	2FP0	2FP90	Wilcoxon test $P<0.05$
PTV70	$D_{95\%}$	= 100%	100%	100%	100%	100%	--
	$D_{98\%}$	≥ 95%	98.4%	98.8%	98.6%	98.6%	c)
	$D_{2\%}$	≤107%	106.9%	106.3%	105.9%	105.7%	none
	HI	≤ 0.12	0.085	0.075	0.074	0.071	c)
	CI	≤ 1.20	1.13	1.12	1.11	1.10	none
PTV63	$D_{95\%}$	≥ 95%	95.7	96.5	97.1	97.1	b), c), e)
	$D_{2\%}$	≤110%	109.0	107.2	107.3	106.4	a), b), c), e), f)
PTV56	$D_{95\%}$	≥ 95%	95.9	96.4	96.3	96.8	none
	$D_{2\%}$	≤110%	109.3	108.2	108.5	107.6	c)
Spinal Cord PRV	$D_{1\%}$ (Gy)	≤ 45	41.5	41.3	41.1	39.2	c), e), f)
Brainstem PRV	$D_{1\%}$ (Gy)	≤ 50	6.25	9.43	11.16	9.46	none
CL parotid	D_{mean} (Gy)	≤ 26	18.2	17.8	17.9	18.0	none
IL parotid	D_{mean} (Gy)	≤ 26	18.1	18.9	18.8	18.5	none
Larynx	D_{mean} (Gy)	≤ 35-45	36.35	35.57	35.34	34.33	b), c)
Oral Mucosa	D_{mean} (Gy)	≤ 30	25.0	24.0	23.3	23.3	b), c)
Mandible	$D_{1\%}$ (Gy)	≤ 66	60.9	60.6	61.4	61.2	none
Vertebrae	$D_{1\%}$ (Gy)	≤ 66	64.7	64.1	63.7	63.3	c)
Thyroid	D_{mean} (Gy)	≤ 40	35.1	32.9	32.5	32.6	a), b)
Healthy tissue	D_{mean} (Gy dm^3)	--	86.4	90.5	90.0	90.4	none
	MU	--	1632	529	515	532	a), b), c)

Legenda: a) IMRT vs 3F; b) IMRT vs 2FP0;c)IMRT vs 2FP90; d) 3F vs 2FP0; e) 3F vs 2FP90; f) 2FP0 vs 2FP90.

Conclusion: TAV techniques allow same PTV coverage and OAR sparing as 7-field IMRT, with one third of MU's and better dose homogeneity. HTID results lowest in IMRT, but differences are not significant. As for the optimal TAV configuration, 2FP90 including one partial arc with a 90° collimator angle seems to spare spinal cord and brainstem significantly better than 3F or 2FP0 techniques.

EP-1685

Influence of flat, flattening filter free beam model and different MLC's on VMAT based SRS/SRT

B. Sarkar[1,2], A. Pradhan[3], A. Munshi[1], S. Roy[1], T. Ganesh[1], B. Mohanti[1]

[1]*Fortis Memorial Research Institute, Radiation Oncology, Gurgaon, India*

[2]*GLA University, Physics, Mathura, India*

[3]*GLA University, Mathematics, Mathura, India*

Purpose or Objective: Linear accelerator (Linac) based stereotactic radiotherapy (SRT) and stereotactic radiosurgery (SRS) using Volumetric modulated arc therapy (VMAT) got a wide spread application for treating intracranial lesions. In recent time linacs were facilitated with flattening filter free beam and miniature MLC's. This development was intended to facilitate a superior dose conformity and quicker therapy delivery.This study was designed to study the dosimetric outcomes and monitor unitsof the stereotactic treatment plans attributed to different commercially available MLC and beam models.

Material and Methods: Ten patients having twelve target volumes, who received the stereotactic treatment in our clinic using Axesse linear accelerator (reference arm), were retrospectively considered for this study. The test arms includes plans using Elekta Agility with FFF, Elekta Agility with flat beam, Elekta APEX, Varian Millennium 120, Varian Millennium 120HD and Elekta Synergy in Monaco treatment planning system. Calculation grid size andplanning constraints were not altered in the test plans. To objectively evaluate the efficacy of MLC-beam model, the resultant dosimetric outcomes were subtracted from the reference arm parameters.

Results: Figure 1 represent total seven (one reference arm and six test arm) plans for an evaluated patient. Maximum dose and mean dose of PTV/GTV V105%, V100%, V95%, D1%, showed a maximum inter MLC- beam model variation of 1.5% and 2% for PTV and GTV respectively. Average PTV heterogeneity index andconformity index shows a variation in the range 1.08-1.11 and0.56-0.63 respectively. Mean dose difference (excluding reference arm) for all organs varied between 1.7cGy -194.5cGy (mean dose 16.1 cGy SD=57.2 cGy) and 1.1cGy-74.8cGy (Mean dose= 6.1 cGy SD=26.9 cGy) for multiple and single fraction respectively.

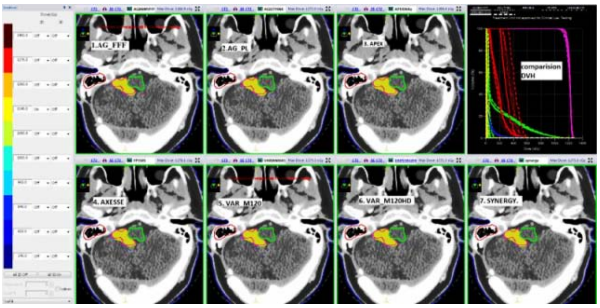

Conclusion: The dosimetry of VMAT based stereotactic treatment plan yield minimal dependency on beam characteristic (model) and MLC width. All tested MLC and beam model could fulfil the desired PTV coverage respecting OAR dose constraints. The only notable difference was the halving of the MU for FFF beam as compared to plane beam. This has the potential to reduce the total patient on couch time by 15% (approximately 2 minutes).

EP-1686

Frameless radiosurgery in brain metastasis with Tomotherapy: a comparison toward dosimetric index

A. Ciarmatori[1,2], G. Guidi[1,3], A. Bruni[4], N. Maffei[1,3], C. Vecchi[3], M.G. Mistretta[1], P. Ceroni[1], S. Gaito[4], P. Giacobazzi[4], T. Costi[1]

[1]*Azienda Ospedaliero Universitaria "Policlinico" di Modena, Medical Physics Department, Modena, Italy*

[2]*Alma Mater Studiorum University, Post Graduate School in Medical Physics, Bologna, Italy*

[3]*Alma Mater Studiorum University, Physics and Astronomy Department, Bologna, Italy*

[4]*Azienda Ospedaliero Universitaria "Policlinico" di Modena, Radiation Oncology Department, Modena, Italy*

Purpose or Objective: Effectiveness of stereotactic radiosurgery (SRS) in treatment of brain metastasis have been demonstrated. In this work we have, retrospectively investigated dosimetric features of frameless SRS delivered with Tomotherapy and compared with reported result in literature in term of Paddick Conformity Index (CI) , Homogeneity Index (HI) and Gradient Score Index (GSI).

Material and Methods: 68 patient treated between 2008 and 2013 in our institution with frame-less set-up (only thermoplastic mask) have been enrolled. 89 Lesions have been stratified for dimension (lower or greater than 5 cc) and for prescription strategies. ICRU 62 (D95>95%, D110<10%) guidelines were utilized for 40 patients while ICRU83 (D50%=Prescription, D98>95%, D107<2%) recommendations were utilized in the remaining 28. Dosimetric index for describing Target Coverage, Target Homogeneity and Organ at Risk (OAR) sparing were selected among the most used in similar studies (Pubmed Line, keyword: "Dosimetric Index", "Radiosurgery", "Tomotherapy", "Brain").

Results: CI, HI and GSI are the most cited feature for describing respectively Target Coverage (21 studies), Target Homogeneity (12 studies) and OARs sparing (5 studies). Mean and standard deviation of CI, HI and GSI in the cohort were, respectively, 1,59 ± 0,38, 1,06 ± 0,04 and 51 ± 16. A multivariate logistic regression analysis of the PTV volume showed significant influence ($p<0.05$) on CI while prescription strategies influenced GSI. ICRU83 recommendations seems to

guarantee a better sparing of normal tissue. Obtained index are aligned with reported results in analogous studies with Tomotherapy. Gammaknife perfexion seems to be the technique able to guarantee better results in term of CI. OARs sparing in case of no co-planar beam delivered by LINAC exhibit worse performance than modulated technique.

Conclusion: Treatment of brain metastasis with Tomotherapy showed encouraging results in term of dosimetric outcome. Lesion size and prescription strategies showed a statistically significant influence on dosimetric distribution. Clinical outcome with frameless immobilization has proven feasible, well tolerated and able to increase patient compliance as exclusive treatment of brain oligo-MTS.

EP-1687

Improving target dose homogeneity in intensity-modulated radiotherapy for sinonasal cancer

J.Y. Lu[1], B.T. Huang[1], W.Z. Zhang[1]
[1]*Cancer Hospital of Shantou University Medical College, Radiation Oncology, Shantou, China*

Purpose or Objective: It is challenging to achieve homogeneous target dose distribution in intensity-modulated radiotherapy (IMRT) for sinonasal cancer (SNC). To overcome this difficulty, we proposed a base-dose-compensation (BDC) planning technique, in which the treatment plan is further optimized based on the original plan with half of the prescribed number of fractions and finally the number of fractions of treatment plan was restored from a half to the total.

Material and Methods: CT scan data of 13 patients were included. Generally acceptable original IMRT plans were created and further optimized individually by (1) the BDC technique and (2) a local-dose-control (LDC) planning technique, in which the original plan is further optimized by addressing hot and cold spots. We compared the target dose coverage, organ-at-risk (OAR) sparing, total planning time and monitor units (MUs) among the original, BDC, LDC IMRT plans and additionally generated volumetric modulated arc therapy (VMAT) plans.

Results: The BDC technique provided significantly superior dose homogeneity/conformity by 23%-48%/6%-9% compared with both the original and LDC IMRT plans, as well as reduced doses to the OARs by up to 18%, with acceptable MU numbers. Compared with VMAT, BDC IMRT yielded superior homogeneity, inferior conformity and comparable overall OAR sparing. The planning of BDC, LDC IMRT and VMAT required 30, 59 and 58 minutes on average, respectively.

Conclusion: The BDC planning technique can achieve significantly better dose distribution with shorter planning time in the IMRT for SNC.

EP-1688

Evaluation of automatic brain metastasis planning for multiple brain metastasis

Y. Mori[1]
[1]*Aichi Medical University, Department of Radiology and Radiation Oncology, Aichi, Japan*

Purpose or Objective: Recently Automatic Brain Metastasis Planning (ABMP) Element [BrainLAB] was commercially released by BrainLAB. It covers multiple off-isocenter targets at a time inside a multi-leaf collimator field and enables stereotactic radiosurgery (SRS) / stereotactic radiotherapy (SRT) with a single group of lineac-based dynamic conformal multi-arc for multiple brain metastases. In this study, dose planning of ABMP (ABMP-single isocenter dynamic conformal arc [ABMP-SIDCA]) for stereotactic radiosurgery of small multiple brain metastasis was evaluated in comparison with those of conventional multi-isocenter DCA (iPlan [BrainLAB]-MIDCA) and Gamma Knife [Elekta] SRS (GKRS).

Material and Methods: Simulation planning was performed with ABMP-SIDCA and GKRS was made in a case of multiple small brain metastasis (9 tumors of 0.2 to 0.7 ml in volume) which were originally treated with iPlan-MIDCA. First, dosimetric comparison was done between ABMP-SIDCA and iPan-MIDCA in the setting with PTV (planned target volume) margin of 2mm and D95=95% dose (19 Gy). Second, dosimetry of GKRS was compared with that of ABMP-SIDCA with PTV margin of 0, 1mm, and 2mm, and D95=100% dose (20 Gy).

Results: First, CI (1/Paddick's CI) and GI (V[half of prescription dose] / V[prescription dose]) in ABMP-SIDCA (mean, 1.36 and 5,12) were compatible with those of iPlan-MIDCA (mean, 1.53 and 4.84). Second, PIV (prescription isodose volume) of GKRS (mean, 0.23 ml) was between that of no margin- and 1mm-margin ABMP-SIDCA (mean, 0.10 ml and 0.28 ml). Considering dose gradient, the same tendency was observed. The mean of V[half of prescription dose] of GKRS, no margin-, and 1 mm margin-ABMP-SIDCA were 0.87 ml, 0.60 ml, and 1.37 ml respectively.

Conclusion: The conformity and dose gradient with ABMP-SIDCA was as good as those of conventional MIDCA by each lesion. If the conditions permit minimal PTV margin (1mm or less), ABMP-SIDCA might provide excellent dose fall-off compatible with GKRS and enable a short treatment time.
The author has no COI. However this study was performed by use trial of ABMP Elements provided by BrainLAB (Tokyo).

EP-1689

Which technique is dosimetrically superior in the treatment of breastcancer: VMAT or Fixed Field IMRT

S. Murphy[1], H. Drury-Smith[2]
[1]*CancerPartnersUK Ltd., Radiotherapy CPUK, Southampton, United Kingdom*
[2]*Sheffield Hallam University, Dept. of Allied Health Professions, Sheffield, United Kingdom*

Purpose or Objective: To determine in terms of target coverage and organ at risk (OAR) doses which concomitant boost technique is superior in the treatment of breast cancer; VMAT or fixed field IMRT.

Material and Methods: 30 previously treated breast patients (15 Left, 15 Right) were re-planned with both VMAT and fixed field concomitant IMRT techniques. A two dose prescription was used similar to previous planning studies (1-3) using the same dose constraints as per the IMPORT HIGH trial (1). 40Gy in 15 fractions was planned to the whole breast while boosting the tumour bed to 48Gy in 15 fractions. A base plan consisting of the existing forward planned tangent fields delivered approximately 38Gy to the whole breast while the tumour bed was boosted with approximately 10Gy using an inverse planned IMRT option. A single partial arc starting and finishing at the tangent angles formed the VMAT portion and the ff-IMRT trial used the 2 existing tangent beam angles followed by 3 further equally spaced beams. Target coverage, heart, ipsilateral lung, contralateral lung and contralateral breast dose was measured. A Two-tailed t-Test sample for means was used to compare the dosimetric differences between the techniques using excel software. Statistical significance was defined as $P<0.05$.

Results: Maximum dose D2% was statistically lower for VMAT; 103.2% vs. 103.7% for ff IMRT whereas minimum doses were equivalent. No differences were found with ipsilateral lung mean and V5Gy doses, contralateral breast mean dose, heart mean dose, heart V5Gy and V10Gy doses. VMAT demonstrated statistically lower V2Gy doses to the contralateral lung (0.7% vs.1.6%) and heart for both left (19.0%/22.6%), and right (5.5%/8.8%) sided patients respectively. Whereas ff-IMRT boasted significantly lower ipsilateral lung V20Gy, V18Gy and V10Gy doses (7.9/8.6/13.1 vs. 8.1/8.8/13.4%) with VMAT respectively

Conclusion: Despite both VMAT and ff-IMRT plans reaching statistical significance in a number of OAR and target parameters there is no clear superior option and whether the differences are clinically significant is a different question. Both techniques met all mandatory dose constraints and the

majority of cases surpassed all optimal dose constraints demonstrating the high quality of the planning technique. The incorporation of deep inspiration breath hold (DIBH) ensured doses to the heart were exceptionally low; mean heart dose for left breast cases averaged 1.4Gy for both treatment options. As neither technique has proven superior, the significantly reduced treatment times associated with VMAT make this a more desirable option to implement clinically.

EP-1690

Conversion of the Tomotherapy plans to the IMRT plans for prostate patients with hip prosthesis

T. Piotrowski[1], M. Olmińska[2], J. Litoborska[2], B. Pawałowski[3], A. Jodda[2]

[1]*Poznan University of Medical Sciences, Electroradiology, Poznan, Poland*

[2]*Greater Poland Cancer Centre, Medical Physics, Poznan, Poland*

[3]*Poznan University of Technology, Technical Physics, Poznan, Poland*

Purpose or Objective: To evaluate the SharePlan software in conversion of helical tomotherapy (HT) to a step and shoot IMRT (sIMRT) for patients with high-risk prostate cancer and hip prosthesis.

Material and Methods: Analysis was performed for 16 consecutive patients treated on HT.
The HT plans were converted to sIMRT plans. 3DCRT, sliding window IMRT (dIMRT) and VMAT plans for a c-arm linear accelerator (CLA) were created manually.
The doses in planning target volume (PTV), bladder, rectum, bowels, femoral heads and hip prosthesis were compared using: (i) a qualitative analysis of doses in averaged dose-volume histograms, (ii) a quantitative, ranking procedure performed for each patient separately, and (iii) statistical testing based on the Friedman ANOVA and Nemenyi method.

Results: For the bladder, rectum, and femoral head, the best dose distributions were observed for HT and sIMRT and then for dIMRT, VMAT, and finally for 3DCRT (p-values were, respectively, 0.002, 0.004 and p=0.024). For the bowels, 3DCRT was significantly different from the rest of the techniques (p=0.009). For the hip prosthesis, the differences were only between 3DCRT and HT/sIMRT (p=0.038).
The first part of Table 1 shows mean doses and standard deviations computed from the average dose-volume histograms for planning target volume, hip prosthesis and organs at risk. The values presented in per cent and normalised up to the prescribed dose (46 Gy). The second part of Table 1 shows the statistical testing of the differences between dose distributions in these structures. The results of the Friedman ANOVA testing noted as the p-value. Results of the Nemenyi analysis presented as the groups (A, B, C). Statistical testing performed on the 0.05 significance level.

Technique	PTV	Bladder	Rectum	Bowels	Femur	Prosthesis
	Mean Dose (SD) [%]					
3DCRT	100.6 (0.5)	96.1 (2.3)	87.0 (6.1)	58.9 (42.2)	46.4 (16.7)	37.2 (10.7)
dIMRT	100.2 (0.4)	81.4 (14.5)	84.7 (12.4)	31.8 (19.8)	43.4 (12.3)	28.4 (8.7)
VMAT	100.8 (1.0)	82.2 (17.5)	82.7 (16.2)	32.5 (20.3)	45.1 (18.4)	31.4 (9.9)
sIMRT	100.7 (0.6)	63.3 (13.4)	59.1 (12.7)	26.4 (16.3)	30.3 (12.2)	22.9 (9.7)
HT	100.9 (0.6)	63.9 (13.7)	57.7 (10.4)	27.4 (14.6)	32.9 (13.2)	23.3 (9.8)
Technique	Similarity/Dissimilarity of the results					
	p = 0.881	p = 0.002	p = 0.004	p = 0.009	p = 0.024	p = 0.038
3DCRT	A	A	A	A	A	A
dIMRT	A	B	B	B	A	A B
VMAT	A	B	B	B	A	A B
sIMRT	A	C	C	B	B	B
HT	A	C	C	B	B	B

SD - standard deviation

Despite the greater scoring in the ranking procedure, HT/sIMRT did not differ statistically from dIMRT/VMAT. The scores were, respectively, 75% and 72% to 61% and 64%.
Figure 1 shows the ranking procedure for the dose distributions obtained in the planning target volume, hip prosthesis and organs at risk for: helical tomotherapy (HT, brown bars), plans converted on the SharePlan station (sIMRT, blue bars) and plans prepared manually for C-arm linear accelerators (3DCRT - red bars, dIMRT - green bars and VMAT - purple bars).

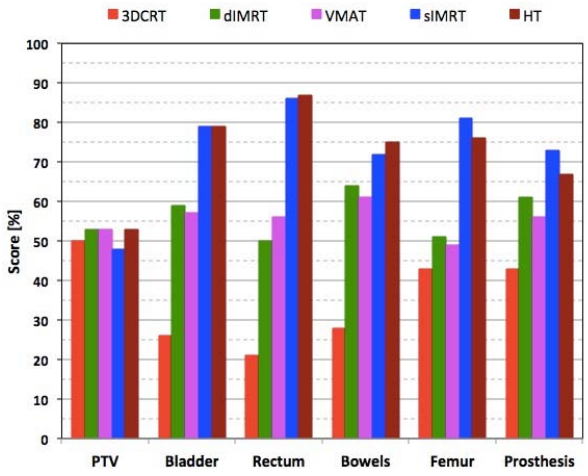

Conclusion: The SharePlan is an efficient tool for the conversion of HT plans for patients with prostate cancer and hip prosthesis. Dose distributions in sIMRT and in HT plans are similar and are generally better than in CLA plans.

EP-1691

A planning approach for lens sparing proton craniospinal irradiation in pediatric patients

N. Bizzocchi[1], B. Rombi[1], P. Farace[1], C. Algranati[1], R. Righetto[1], M. Schwarz[1], M. Amichetti[1]

[1]*S. Chiara Hospital, Proton Therapy Center, TN, Italy*

Purpose or Objective: Several reports support the potential benefits of proton therapy (PT) when compared to photon techniques in craniospinal irradiation (CSI) to reduce late toxicity and risk of secondary malignancies. PT is increasingly regarded as the gold standard for CSI, particularly in pediatric patients. Nevertheless, lens sparing with good coverage of the cribriform plate remains a challenge, especially in very young patients, as the lens dose increases significantly with decreasing age (Cochran et al, Int JRadiat Oncol Biol Phys 2008;70:1336-42). The technique and the beam arrangement used at our center for lens sparing in the treatment of the whole brain for our first 6 y.o. male patient, is described and compared with data reported in other studies.

Material and Methods: CSI is delivered by active scanning PT with three isocenters, using three cranial beams plus two additional postero-anterior spinal beams. Cranial and caudal field junctions are planned by the ancillary-beam technique (Farace et al, Acta Oncol 2015; 54:1075-8). The three-beams arrangement for brain irradiation includes two lateral opposed beams (gantry angle 90° and 270°), with couch angle ±15° to minimize the overlap between the cribriform plate and the lens, and an additional posterior beam. Single-field-optimization of the three equally-weighted beams is performed. A total dose of 36 Gy in 20 fractions is prescribed following international radiation guidelines for high risk medulloblastoma. During optimization, coverage of the cribriform plate is assumed as the priority goal and lens sparing as a secondary objective. Our technique is compared with two more conventional approaches: i) two opposed-lateral beams and ii) two angled (±20°) posterior-oblique beams.

Results: In figure A and B the dose distribution obtained by the lens-sparing technique on two slices at the level of the cribriform plate and of the lenses are shown. The coverage of the cribriform plate is similar in all beam arrangements. In Figure C, the dose volume histogram for the three beams' arrangement is shown. Adequate target coverage is obtained by all beam arrangements. In addition, the lens-sparing technique allowed to markedly decrease the dose to the

lenses, as shown also in the Table. Dose values are smaller (Dmax 16.7%, i.e. around 6 Gy) than those reported in other studies. In our case, the opposed-lateral setup is associated to larger lens doses (56.6%) than those reported using the same technique in another study (26.4%), suggesting that our specific case was a difficult one, presumably age-related.

Dose to the lens (% of prescription dose)

	Delivery mode	Beam arrangement	Dmax	Dmean
First pediatric patient	Active	Lens sparing	16.7%	6.6%
		posterior-oblique	49.4%	34.9%
		opposed-lateral	56.6%	40.4%
Published studies	Passive	posterior-oblique*	68.5%	48.1%
	Passive	posterior-oblique**		40.0%
	Passive	opposed-lateral**		74.0%
	Active	opposed-lateral***	26.4%	

* Gielber et al, Radiat Oncol 2013;8:32 (18 patients).
** Cochran et al, Int J Radiat Oncol Biol Phys 2008;70:1336-42 (39 patients).
*** Lin et al, Int J Radiat Oncol Biol Phys. 2014;90:71-8 (10 patients).

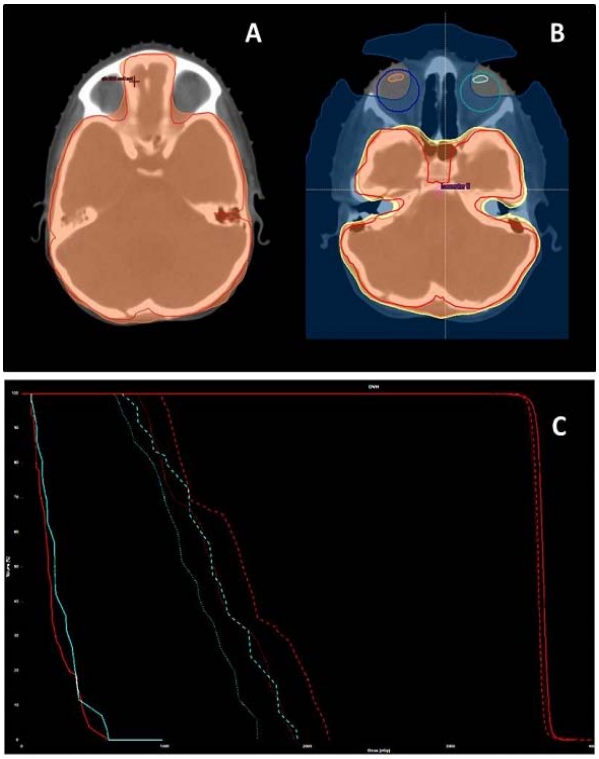

Figure. Dose distribution obtained by the lens-sparing technique at the level of the cribriform plate (A) and of the lens (B). The PTV (red line) and the 98% isodose (orange isofill) are shown. (C) dose volume histogram of the PTV (red), right (orange) and left (cyan) lens. Lens-sparing, posterior-oblique and opposed-lateral distributions are reported by continuous, dotted and dashed lines respectively.

Conclusion: The beam arrangement we applied allowed both an optimal coverage of the cribriform plate and lens sparing. The low maximal dose to the lenses might reduce the risk of radiation-associated cataract.

EP-1692

Dosimetric analysis of testicular doses in prostate radiotherapy at different energy levels

C. Onal[1], G. Arslan[1], Y. Dolek[1], E. Efe[1]
[1]*Baskent Universitesi Tip Fakultesi- Adana Hastanes, Department of Radiation Oncology, Adana, Turkey*

Purpose or Objective: To evaluate the incidental testicular during prostate radiation therapy with intensity-modulated radiotherapy (IMRT) and volumetric-modulated arc radiotherapy (VMAT) at different energies.

Material and Methods: Dosimetric data of 15 intermediate-risk prostate cancer patients treated with radiotherapy was analyzed. The prescribed dose was 78 Gy in 39 fractions. Dosimetric analysis compared testicular doses generated by 7-field IMRT and VMAT with a single arc at 6, 10, and 15MV energy levels. Doses from the treatment planning system were verified with metal-oxide-semiconductor field-effect transistor detectors. Detectors were placed within a solid, flat phantom at 10 cm depth, from the center of the irradiated field out to 30 cm, with 2 cm distances and 1 cm depth for scattered doses. Values measured from the treatment planning system were compared with values from the detectors.

Results: The mean distance between center of the prostate and the testes was 13.5±1.4 cm (range, 11.6-16.8 cm). For a complete course of 39 fractions, mean testicular doses from the IMRT and VMAT measured in the treatment planning system were 16.3±10.3 cGy vs. 21.5±11.2 cGy (p=0.03) at 6 MV, 13.4±10.4 cGy vs. 17.8±10.7 cGy (p=0.04) at 10 MV, and 10.6±8.5 cGy vs. 14.5±8.6 cGy (p=0.03) at 15 MV, respectively. Mean scattered testicular doses in the phantom measurements were 99.5±17.2 cGy, 118.7±16.4 cGy, and 193.9±14.5 cGy at 6, 10, and 15 MV, respectively, in the IMRT plans. In the VMAT plans, corresponding testicular doses were 90.4±16.3 cGy, 103.6±16.4 cGy, and 139.3±14.6 cGy at 6, 10, and 15 MV, respectively. The scattered testicular doses were significantly higher in the IMRT versus the VMAT plans.

Conclusion: Testicular doses during radiotherapy were high enough potentially to impair the endocrine function of Leydig cells. Higher photon energy and IMRT plans resulted in higher incidental testicular doses compared to lower photon energy and VMAT plans.

EP-1693

Constant dose rate VMAT and step-and-shoot IMRT in head and neck cancer: a comparative plan analysis

A. Didona[1], C. Zucchetti[2], A.C. Dipilato[2], M. Iacco[2], M.B. Panizza[3], A. Frattegiani[3], V. Bini[4], C. Aristei[3], R. Tarducci[2]
[1]*Ospedale Santa Maria della Misericordia, S.C. Fisica Sanitaria, Perugia, Italy*
[2]*Santa Maria della Misericordia Hospital, Medical Physics, Perugia, Italy*
[3]*Santa Maria della Misericordia Hospital, Radiation Oncology, Perugia, Italy*
[4]*Perugia University, Internal Medicine, Perugia, Italy*

Purpose or Objective: Constant dose rate VMAT (CDR-VMAT) introduces rotational arc radiotherapy for linacs incapable of dose rate variation. The goal of this study was to evaluate CDR-VMAT adequacy for the treatment of head and neck (H&N) cancer compared to Step-and-Shoot IMRT.

Material and Methods: Ten patients (five with oropharyngeal cancer -OPC- and five with hypopharyngeal cancer -HPC-) were enrolled in this study. For each patient, were defined three PTVs: PTV66Gy, PTV60Gy and PTV54Gy with a dose prescription of 66 Gy, 60 Gy and 54 Gy all delivered in 30 fractions. OARs included mandible, spinal cord, brain stem, parotids, salivary glands, esophagus, larynx and thyroid . All patients were previously treated using step and shoot IMRT with seven 6 MV coplanar beams. A protocol for CDR-VMAT plans which consisted of two arcs was established: first arc with start angle was of 182° and a stop angle of 178° in a clockwise direction; the second one in a counterclockwise direction from 178° to 182°; the final arc spacing was set to 4 degree and collimator angle to 45°. For each patient, a CDR- VMAT plan was generated according to this protocol. A dose rate of 300 MU/minute was selected for both IMRT and CDR-VMAT plans. All plans were performed with Pinnacle3 treatment planning system (v 9.8) with identical dose constraints to OARs and dose prescription to targets; it was required that PTVs D95% be 95% of prescribed dose and OARs be spared as more as possible.Dose distributions were compared by evaluating PTVs' Dmean, D2%, D50%, D98% and Homogeneity Index (HI) defined as

$$HI = \frac{D_{2\%} - D_{98\%}}{D_{50\%}}$$

For spinal cord, brain stem and mandible the analysis included the maximum dose (in terms of D2%); for parotids, salivary glands, esophagus, larynx and thyroid Dmean and a number of different dose-volume data in the range V20Gy e V50Gy were compared.For comparison of the efficiency of IMRT and CDR-VMAT, the MUs and treatment delivery time were also recorded and evaluated.

Results: Results are shown in Table.

		IMRT	CDR-VMAT	p value
PTV_{66Gy}	$D_{98\%}$	60,5 ± 1,4 Gy	60,7 ± 1,7 Gy	0,799
	$D_{50\%}$	65,7 ± 0,4 Gy	65,8 ± 0,2 Gy	0,759
	$D_{2\%}$	68,4 ± 0,8 Gy	67,6 ± 0,7 Gy	0,013
	D_{mean}	65,5 ± 0,4 Gy	65,5 ± 0,2 Gy	0,838
	HI	0,13 ± 0,03	0,11 ± 0,03	0,028
PTV_{60Gy}	$D_{98\%}$	54,3 ± 1,6 Gy	54,8 ± 2,1 Gy	0,445
	$D_{50\%}$	59,9 ± 0,4 Gy	59,8 ± 0,4 Gy	0,799
	$D_{2\%}$	63,9 ± 1,2 Gy	62,5 ± 1,4 Gy	0,011
	D_{mean}	59,8 ± 0,3 Gy	59,7 ± 0,3 Gy	0,386
	HI	0,16 ± 0,04	0,13 ± 0,05	0,093
$PTV54_{Gy}$	$D_{98\%}$	48,8 ± 1,4 Gy	49 ± 1,8 Gy	0,919
	$D_{50\%}$	54,2 ± 0,6 Gy	54,1 ± 0,5 Gy	0,414
	$D_{2\%}$	59,2 ± 2,1 Gy	58,3 ± 2,2 Gy	0,059
	D_{mean}	54,2 ± 0,6 Gy	54 ± 0,5 Gy	0,241
	HI	0,17 ± 0,06	0,15 ± 0,07	0,005
Mandible	$D_{2\%}$	53 ± 10,5 Gy	52,9 ± 10,2 Gy	0,799
	V_{50Gy}	15,1 ± 16,1 %	15,8 ± 15,9 %	0,612
Spinal cord	$D_{2\%}$	38,2 ± 2,0 Gy	38,1 ± 1,0 Gy	0,575
Brain stem	$D_{2\%}$	34,0 ± 9,4 Gy	34,1 ± 7,4 Gy	1,000
Larynx	D_{mean}	46,4 ± 6,8 Gy	43 ± 5,7 Gy	0,025
	V_{20Gy}	100,0 ± 0,0 %	97,4 ± 7,4 %	0,317
	V_{30Gy}	91,9 ± 7,2 %	83,5 ± 12,6 %	0,025
	V_{50Gy}	37,5 ± 28 %	28,8 ± 21,5 %	0,108
Thyroid	D_{mean}	43,4 ± 11,4 Gy	41 ± 11,9 Gy	0,047
	V_{20Gy}	87,5 ± 20,1 %	85 ± 24,7 %	0,498
	V_{45Gy}	68,2 ± 31,0 %	55,4 ± 27,3 %	0,038
	V_{50Gy}	45,9 ± 31,9 %	31,6 ± 27,7 %	0,028
Esophagus	V_{20Gy}	56,2 ± 23,1 %	49,6 ± 25,0 %	0,110
	V_{30Gy}	42,1 ± 23,6 %	37,6 ± 20,0 %	0,209
	V_{50Gy}	6,2 ± 10,4 %	2,8 ± 4,5 %	0,068
Parotid R/L	D_{mean}	24,4 ± 2 Gy / 24 ± 1,5 Gy	23,6 ± 1,3 Gy / 23,4 ± 1,1 Gy	0,059 / 0,093
	V_{15Gy}	61,4 ± 9,2 % / 62,8 ± 6,3 %	58,2 ± 5,3 % / 61,9 ± 7,5 %	0,477 / 0,877
	V_{30Gy}	38,4 ± 5,3 % / 37,7 ± 5,6 %	33,9 ± 4 % / 32,3 ± 3,6 %	0,037 / 0,019
	V_{50Gy}	8,2 ± 4,4 % / 5,2 ± 3,9 %	7,1 ± 3,4 % / 4,7 ± 3,5 %	0,121 / 0,347
Salivary Gland R/L	D_{mean}	46,2 ± 12,3 Gy / 44,4 ± 11,1 Gy	39,1 ± 12,6 Gy / 37,2 ± 13,8 Gy	0,005 / 0,028
	V_{15Gy}	96,3 ± 8,1 % / 96,8 ± 9,7 %	93,7 ± 10,8 % / 93,9 ± 12,5 %	0,197 / 0,109
	V_{30Gy}	84,5 ± 22,4 % / 87,3 ± 21,9 %	67,9 ± 31,7 % / 62,4 ± 28,8 %	0,027 / 0,042
	V_{50Gy}	47,1 ± 43,5 % / 37,4 ± 36,1 %	29,3 ± 36,9 % / 20,6 ± 32,2 %	0,017 / 0,05
Delivery time / MU		183 ± 18 s / 613 ± 92	145 ± 21 s / 743 ± 73	0,005 / 0,016

Differences were analysed using the paired samples Wilcoxon test (significance level 0,05). Although differences were not always statistically significant, on the one hand CDR-VMAT improved HI and decreased D2% for PTVs, on the other hand it showed a reduction in the volume of the OARs receiving medium and high doses and medium doses to larynx, thyroid, parotid and salivary glands. In respect of some organs, such as the esophagus, a larger number of patients enrolled in the study would likely have resulted in statistically significant differences. Compared with IMRT, CDR-VMAT reduced delivery times although MUs were higher.

Conclusion: Our study showed that CDR-VMAT offers an additional option of rotational arc radiotherapy for linacs without variable dose rate with a lower cost.

EP-1694

Angle-restricted tomotherapy to reduce the risk of heart for left-sided breast cancer patients

H.P. Yeh[1], C.H. Hsieh[1,2], H.J. Tien[1], C.H. Chang[1], C.T. Lin[1], P.W. Shueng[1]

[1]Far Eastern Memorial Hospital, Division of Radiation Oncology- Department of Radiology, New Taipei City, Taiwan
[2]National Yang-Ming University, School of Medicine- Institute of Traditional Medicine, Taipei, Taiwan

Purpose or Objective: The aim of this study was to evaluate the feasibility of complete-directional-complete block (CDCB) technique and to find the optimal restricted angle of helical tomtherapy (HT) in planning of locoregional irradiation including the internal mammary chain (IMC) in left-sided breast cancer.

Material and Methods: Treatment plans were generated for 6 left-sided breast cancer patients with a planning target volume (PTV) included the breast/chest wall, supra-clavicular, axillary nodes and IMC. In HT plans, complete block (CB) and CDCB were designated to spare the contra-lateral tissues: (1) CB was a rectangular structure with the ends connected to 10-cm away from the margin of the PTV (2) the directional-blocking area of CDCB was determined by the intersection of CB and the beam aperture passed through the 0.5 cm margin of IMC. To find the optimal CDCB, the angle of 0, 10, 15 and 20 degree of the beam according to the geometric center of IMC were used. A prescribed dose of 50 Gy in 25 fractions was planned for HT plans using CB, CDCB 0,10,15,20 and conventional 5-field intensity-modulated radiotherapy (cIMRT). The dose coverage, homogeneity index (HI), conformity index (CI) of the target, and the dose volumes of critical structures were compared.

Results: The coverage, HI and CI of PTV in HT-CDCB 0,10,15,20 were better than those in cIMRT but did not differ from HT-CB. The mean V20 Gy of the ipsilateral lung for HT-CDCB 15 (22.2%±3.1%, p=0.029) and HT-CDCB 20 (22.1%±3.5%, p=0.045) were significant reduced compared to cIMRT (27.9%±3.4%). With the increasing angle of CDCB, the cardiac V30 Gy for HT-CDCB was gradually decreased and significantly lower than for cIMRT and HT-CB. Compared with cIMRT (24.3 Gy±6.9 Gy), the mean dose of left anterior descending coronary artery was effectively reduced 38.6%, 43.3%, 45.8% and 48.1% in CDCB 0,10,15,20, respectively. There was no significant difference in contralateral breast for all plans. However, the mean dose of contralateral lung in HT-CDCB 20 was 6.1% higher than cIMRT (1.7 versus 1.6 Gy) and 14.5% than HT-CDCB 15

Conclusion: CDCB technique is feasible for locoregional irradiation including the IMC in left-sided breast cancer patients treated with helical tomotherapy. Considering the mean dose of the contralateral lung, the optimal angle for CDCB could be 15-degree that not only achieved similar PTV coverage, homogeneity and dose conformity but also allowed better sparing heart and bilateral lungs compared with cIMRT.

EP-1695

Dosimetric comparison of Helical Tomotherapy and VMAT for endometrial cancer

A. Dizmen[1], O. Yazıcı[1], A.M. Kocer[1], N. Kaplan[1], F. Ertan[1]

[1]Ankara Oncology Hospital, Radiation Oncology, Ankara, Turkey

Purpose or Objective: The purpose of the present study was to evaluate dosimetric comparision of volumetric modulated arc therapy(VMAT) and helical tomotherapy(HT) for patients with endometrial cancer.

Material and Methods: Fourteen patients with endometrial cancer were retrospectively studied.All whole pelvis(WP) patients were treated with 50.4 Gy in 28 fractions..The dose distributions for the planning target volume (PTV),organs at risk(OARs),monitor unit(MU) and homogeneity index(HI= D2-D98/Dmedian) were analyzed.

Results: The V93 and D100 of PTV were 99.8% ,99.4% and 46.3 Gy,48.2 Gy for the VMAT and HT,respectively(p:0.004,p:0.003) .The V20 for the bowels was 44.5 Gy and 51.1 Gy for the VMAT and HT, respectively(p:0.001). The sparing OARs were comparable between the VMAT and HT plans. There is a significance difference between MU for the VMAT and HT plans and the value was given by 645 and 5236 MU(p:0.001) and the average homogeneity index was 0.07 and 0.04 (p:0.002),respectively.

Conclusion: Both HT and VMAT plans yielded with homogeneous dose distrubition when sparing of OARs effectively. Although some dosimetric parameters have shown significant differences statistically but they were

small. VMAT is a well suited technique with shorter treatment time but HT plans have better HI than VMAT.

EP-1696

Can we increase the dose with particle therapy versus IMRT? A dosimetric study for sinonasal cancer

A. Cavallo[1], A. Mirandola[2], E. Orlandi[3], B. Vischioni[4], N.A. Iacovelli[3], C. Fallai[3], L. Licitra[5], M. Ciocca[2], E. Pignoli[1]

[1]Fondazione IRCCS Istituto Nazionale dei Tumori, Medical Physics Unit, Milan, Italy

[2]Fondazione CNAO, Medical Physics Department, Pavia, Italy

[3]Fondazione IRCCS Istituto Nazionale dei Tumori, Radiation Oncology 2, Milan, Italy

[4]Fondazione CNAO, Radiation Oncology Department, Pavia, Italy

[5]Fondazione IRCCS Istituto Nazionale dei Tumori, Head and Neck Medical Oncology Unit, Milan, Italy

Purpose or Objective: Dosimetric comparison among treatment plans from different RT techniques (photons, protons and carbon ions) within a prospective multicentric trial aiming at the evaluation of the impact of combined treatment modalities on target coverage and OARs sparing for sinonasal tumors.

Material and Methods: High risk PTV (HR-PTV), which comprised gross disease, and low risk volume (LR-PTV), with elective neck, were defined for 5 pts. Four treatment plans were generated for each pt: a pure sequential (SEQ) and a pure SIB photon plan, a particle sequential plan with protons and carbon ion boost (p+C) and a combined plan with photons and carbon ion boost (ph+C). Prescription doses (PD) to HR-PTV were 70 Gy (2 Gy/die) for photon plans and 75 GyE for plans with a carbon ion boost (21 GyE in 7 frs). PD to LR-PTV were 56 Gy (1.6 Gy/die) for SIB modality and 54 Gy (2 Gy/die) for sequential plans. Varian Eclipse TPS was used to optimize VMAT photon plans with coplanar and non-coplanar arcs. Particle plans were calculated using Siemens Syngo TPS and IMPT optimization strategy. The highest priority during optimization was given to spare neurological structures, followed by PTVs coverage and then remaining OARs. A dedicated software (VODCA, MSS Medical Software Solution GmbH, Switzerland) was used to sum up photon and particle plans and to compare DVHs from different approaches. We considered different parameters: the most significant for PTVs coverage were volume encompassed by 70 Gy isodose (V70Gy), conformity index and homogeneity index. As for OARs, V10Gy was reported for temporal lobes, brain and mean dose (Dmean) for contra-lateral optic nerve, chiasm, cord, brainstem, cochleae. Integral dose was recorded to evaluate healthy tissue (HT, patient volume minus larger PTV). Differences in techniques were analyzed by paired Student's 2-sided t-tests for each dosimetric parameter, taking p-value <0.05 as statistically significant.

Results: All plans could be considered clinically acceptable. The photon ones showed a better conformality and homogeneity for HR-PTV against p+C plans. Although minimum dose (as percentage of PD) was higher for photon plans, V70Gy was statistically relevant in favor of p+C plans vs the other modalities. Despite a higher PD for plans with carbon ion boost, a significant advantage on some OARs was recorded: Dmean in p+C plans was significantly lower for contra-lateral optic nerve, chiasm and cochleae, as it is V10Gy for temporal lobes and brain. This finding was reinforced by a statistically significant difference in integral dose for p+C plans vs the others, but also for ph+C plans vs SIB. See averaged DVHs in Fig. 1.

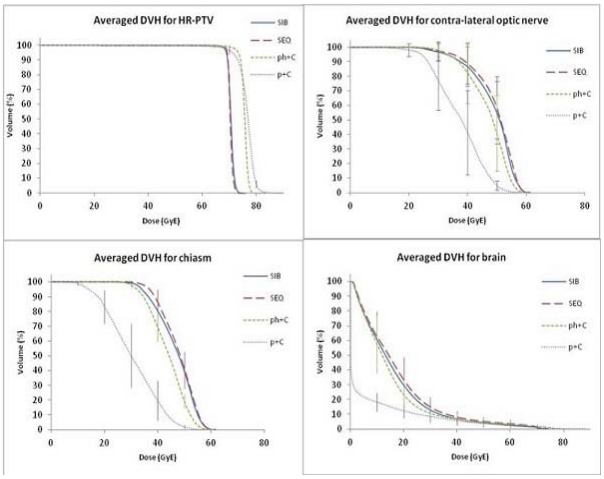

Conclusion: Although less homogeneous and conformed, particle plans allow a higher PD to HR-PTV compared to photons. Due to their specific physical characteristics, combined particle treatments can potentially better spare OARs and HT in terms of intermediate and low doses.

EP-1697

Evaluating patient dose difference in case of linac transfer under treatment

A. Vasseur[1], C. Bertin[2], J.Y. Gosselin[1], B. Foulon[1]

[1]Centre d'Oncologie et de Radiothérapie du Parc, Radiothérapie - Auxerre, Auxerre, France

[2]IRMA Informatics & Radiation Physics for Medical and Technical Applications, Chrono-Environnement UMR CNRS 6249, 25211 Montbéliard, France

Purpose or Objective: To allow or not the patient transfer between 2 energy-matched Linacs, differing only by their MLC generation, in case of breakdown.

Material and Methods: Two linacs were beforehand matched in terms of energy (TPR20,10) and each separate calculation model in the TPS validated. This retrospective comparison was performed with the calculated dose from the TPS to assess the impact of transferring a patient from one machine to another, for some fractions (n=1 to 5) over the whole treatment (N fractions). One should note that 3D plan verification failed in general if the measurements occurs on the wrong machine.

Fifty VMAT plans were studied (head & neck , whole brain, rectum, prostate, other; 10 plans of each), corresponding to 60 PTVs and 100 OARs. Dose was re-computed with the non-planned machine, without any optimization, if up to n=5 fractions are transferred.

Reported dose-metrics (see ICRU-83) are Dmean (mean dose), Dmax (max dose), D95% and HI (homogeneity index) for all ROIs, and well-known parameters are used for some OARs, depending of OAR type (V20, V74,...). Each parameter is expressed as relative to the initial planned treatment.

Results: There is a systematic over-dose delivering when transferring a patient from the "new generation" Linac (Mnew) to the "old" one (Mold). The opposite is checked.

Dmean and Dmax variations are linearly dependent of the number of transferred fractions (R^2=0.91), for PTVs and OARs. No linear correlation could be found for others metrics, which seem to strongly depend on each anatomy.

Variations are always more important for OARs than for PTVs.

The maximum difference was found as the Dmean on a right femur for a rectum treatment (11.4%). This value is increased to 15% and set as the maximum available for n=5.

Conclusion: Dose differences are here mainly due to thickness variations of MLC leaves, over other design improvements (leaf profiles, rounded leaf ends,...), as dose variation is related to leaf thickness and OARs are on the other hand more affected by linac transfer than PTVs (protected ROIs are more often under leaves than targets).

The linear correlation between Dmax (or Dmean) and n associated to a maximum variation achievable leads to an empiric formula predicting how much the dose metrics will be affected, in case of a transfer from Mnew to Mold, without recalculating the whole plan (see eq.). This can be easily reversed.

$$D_{max|mean}^{initial} \leqslant D_{max|mean}^{final} \leqslant \frac{N+0.75n}{N} D_{max|mean}^{initial}$$

This conclusion must be obviously applied only for N≥10 (then excluding SRS/SBRT).

EP-1698

New sliding window IMRT planning design for head and neck patients with dental prostheses.

M. Lopez Sanchez[1], M. Perez[1,2], V. Hernandez[1], J.A. Vera[1], M. Gonzalez[1], J.M. Artigues[1]

[1]*Hospital Universitari Sant Joan de Reus, Medical Physics, REUS, Spain*

[2]*UNED Universidad Nacional de Educación a Distancia, Ciencias, Madrid, Spain*

Purpose or Objective : A percentage of patients receiving head and neck radiotherapy treatments wear dental prostheses: implants or dental fillings. The high atomic number composition of this prostheses, most of times unknown, results in a possible inaccurate dose calculation.
The purpose of this study is to develop a method for minimize dosimetric alterations caused by prostheses of unknown composition, preventing radiation beams passing through them.

Material and Methods: Varian Medical Systems, Palo Alto, CA: TPS Eclipse with IMRToptimization "Dose Volumen Optimizer" version 10.0.28 and dosecalculation algorithm "Analytical Anisotropic Algorithm" version10.0.28. The images, contoured volumes and prescriptions of two patients treatedin clinical routine are used (Table I).
Steps to be followed:
1. From images of each patient, identifyand outline the prostheses. Also contour the artefacted region and overwrite HUto the HU of the surrounding tissue.
2. Create a sliding window IMRTplan with slightly (<10º) modified conventional gantry angles (7-9 fields inour centre) to minimize incidence upon prostheses and optimize dosimetry asusual. This plan is called REFERENCE PLAN.
3. Copy the REFERENCE PLAN. The twoor three fields that pass through the prosthesis before entering the PTV areselected, and in each field the area of the incident fluence on the prosthesesis removed using the editing fluence tool available in our TPS (Figure 1). Removethe remaining fields. This result from two or three fields with partiallyerased fluences is called the BASE PLAN.
4. Create a new plan with theremaining angles present in the REFERENCE PLAN but not in the BASE PLAN. Optimizethis plan to fulfil the prescription considering the dose contribution of theBASE PLAN. This is called the SUPPLEMENT PLAN.
The treatment plan is the sum of the BASE PLAN and SUPPLEMENT PLAN .
With this method the achieved dosimetry hasn't an increased dosecalculation uncertainty due to the presence of materials of high atomicnumbers. Nevertheless, the dosimetry obtained in this way could cause a loss ofquality in terms of PTV coverage or higher doses to organs at risk. Therefore,it is compared to a regular dosimetry (7-9 field same espaced), in which thepresence of the prosthesis was not taken into account.
0 0 1 281 1551 Maru y Miguel 12 3 1829 14.0 96 Normal 0 21 false false false ES JA X-NONE

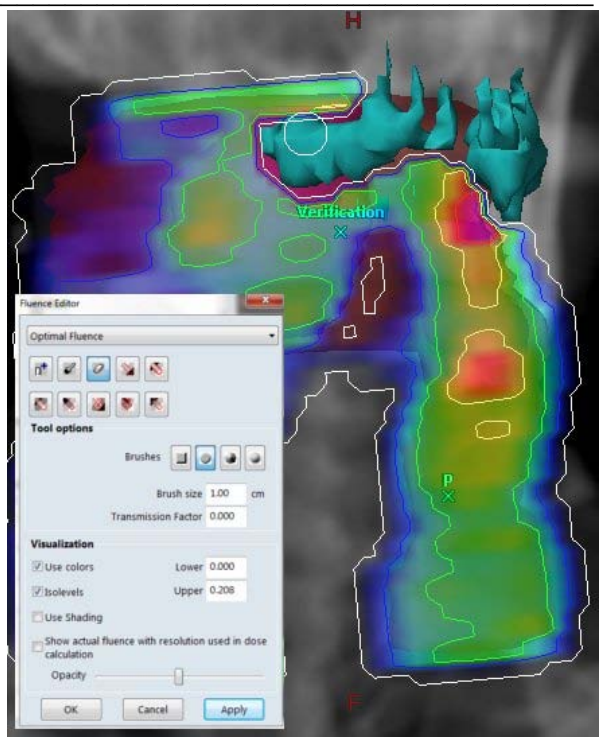

Results: Table I shows the dosimetric parameters comparison between new planning design proposed and usual design regardless of prosthesis. The absorbed dose distributions in the PTVs are similar in both cases. Regarding organs at risk, there are no significative differences in spinal cord, dose to parotids are increased up to a 20% in the new design.

TABLE I. ABSORBED DOSE FOR PTV AND OAR

	Patient 1		Patient 2	
	Conventinal Design	*New Design*	*Conventinal Design*	*New Design*
Prescribed Dose(PTVN)(Gy)	52.8	52.8	54.1	54.1
$D_{98\%}$(PTVN)(Gy)	50.6	50.3	51.95	51.9
$D_{50\%}$(PTVN)(Gy)	54.5	53.6	57.0	58.5
$D_{2\%}$(PTVN)(Gy)	71.0	73.3	73.3	74.6
Prescribed Dose(PTVT)(Gy)	70.0	70.0	70.0	70.0
$D_{98\%}$(PTVT)(Gy)	65.2	65.7	65.4	65.7
$D_{50\%}$(PTVT)(Gy)	69.5	71.3	70.9	71.2
$D_{2\%}$(PTVT)(Gy)	72.6	74.8	73.8	75.0
$D_{50\%}$(ParotidR)(Gy)	11.6	11.6	19.9	21.9
$D_{50\%}$(ParotidL)(Gy)	28.9	34.7	17.6	20.1
$D_{2\%}$(Spinal Cord)(Gy)	39.8	36.4	43.1	42.5
$D_{2\%}$(PRVSpinal Cord)(Gy)	41.6	37.8	45.3	45.2
Volume(PTVN)(cm^3)	332.8	332.8	435.0	435.0
Volume(PTVT)(cm^3)	32.3	32.3	130.3	130.3
Volume(prostheses)(cm^3)	1.6	1.6	12.1	12.1
CI(PTVN)	1.52	1.34	1.54	1.58
CI(PTVT)	1.33	1.33	1.23	1.36
HI(PTVN)	0.37	0.42	0.37	0.39
HI(PTVT)	0.11	0.13	0.12	0.13

PTVT and PTVN are respectively the high and low dose treatment volumes defined by the physician. D_V is the absorbed dose that covers a given volume fraction V. HI is the homogeneity index defined by ICRU 83 [9]. CI is the conformation index defined by ICRU 62 and ICRU 83 for $D_{100\%}$ isodose of the evaluated volume in the worst case

Conclusion: With this method calculations inaccuracies caused by the high density materials are avoided. We recommend the discussion of the use of the technique proposed with the physician for each treatment of head and neck patient with dental prostheses.
The techniques in this study are being developed currently for VMAT technique.

EP-1699

10MV un-flattened photon beams in prostate and pelvic node VMAT SABR; is the high energy necessary?

N. Kanakavelu[1], S.O. Osman[2], D.M. Irvine[1], C.A. Lyons[2], S. Jain[3], A.R. Hounsell[1], C.K. McGarry[1]
[1]*Belfast Health and Social Care Trust, Radiotherapy Physics-Northern Ireland Cancer Centre, Belfast, United Kingdom*
[2]*Queen's University Belfast, Centre for Cancer Research and Cell Biology, Belfast, United Kingdom*
[3]*Belfast Health and Social Care Trust, Clinical Oncology-Northern Ireland Cancer Centre, Belfast, United Kingdom*

Purpose or Objective: To evaluate and compare the plan quality and efficacy of flattened and flattening-filter-free (FFF) photon beams in external beam RT for high-risk prostate cancer patients in the context of hypo-fractionated Stereotactic Ablative Radiotherapy (SABR) to the prostate and pelvic lymph nodes (LN).

Material and Methods: 10 prostate cancer (PCa) patients who previously received RT to the prostate and pelvic nodes, were planned in Varian Eclipse using two full arcs with 6MV flattened, 6MV and 10MV FFF photon beams. The prescribed dose was 40Gy in 5 fractions for the planning target volume to prostate PTV(psv) (prostate and seminal vesicles) and 25Gy in 5 fractions for the PTV(LN). All plans were optimized using the same objectives and constraints. Plans were then evaluated for PTV coverage, dose fall-off, OAR doses for the rectum, bladder, small bowel, prostatic urethra, neurovascular bundle, femoral heads, penile bulb and the sigmoid colon. Physical dose metrics, EUDs, tumour control probability (TCP) and normal tissue complication probability (NTCPs) using the LKB model were investigated. The number of monitor units and the treatment delivery times were also compared. Statistical differences were evaluated using a paired sample Wilcoxon signed rank test with a significance level of 0.05%

Results: All evaluated plans were highly conformal CI =1.2 and CN ≥0.94. There was no significant difference in the PTV dose coverage using all energies compared.Significant increase in high dose (R50) and low dose (R25) spillage outside the PTV in 6MV flattened beams compared to FFF plans was observed. Superior plans were obtained using 10 MV FFF beams in terms of mean and minimum rectal dose, high and low dose spill outside the PTV and treatment time were also minimal. Despite the significantly lower monitor units (MU) in 6MV plans, these plans delivery times were the largest among the three compared techniques due to dose rate limitations (maximum dose rate 600MU/min). Furthermore, the high dose spillage was found to be higher for 6MV. When comparing 6MV FFF and 10MV FFF plans, only minor difference were identified favouring 10 MV FFF plans.

	10FFF	6FFF	6MV
PTV(psv)			
CI	1.21 ± 0.03	1.21 ± 0.03	1.22 ± 0.03
D2%	42.06 ± 0.67	42.00 ± 0.07	42.05 ± 0.05
D98%	35.74 ± 0.43	35.7 ± 0.43	35.73 ± 0.42
Rectum			
D2% (Gy)	35.03 ± 2.18	35.2 ± 2.02	35.13 ± 2.07
Dmean	17.94 ± 2.12 †	18.20 ± 2.00	18.17 ± 1.99
EUD(Gy)	55.29 ± 5.07	55.64 ± 4.73	55.52 ± 4.85
NTCP(%)	2.41 ± 1.90	2.46 ± 1.83	2.45 ± 1.87
Bladder			
D2% (Gy)	35.21 ± 3.48	35.34 ± 3.22	35.22 ± 3.34
Dmean	18.81 ± 1.71	18.83 ± 1.61	18.73 ± 1.78
EUD(Gy)	31.08 ± 4.28	31.15 ± 4.09	31.04 ± 4.32
HighDoseSpill			
R50	4.29*† ± 0.26	4.50 ± 0.25†	4.65 ± 0.28
LowDoseSpill			
R25	9.25 ± 1.42	9.24 ± 0.97	9.47 ± 1.01
Mus	2309 ± 118†	2351 ± 157†	2030 ± 97
delivery time (s)	149.2 ± 0.12†	149 ± 5.95†	203.52 ± 9.47

* Significantly different compared to 6FFF Rx = volume of x% isodose/PTV
† Significantly different compared to 6MV CI = R95

Conclusion: Using two full arcs, highly conformal SABR VMAT plans for prostate and pelvic lymph node were achieved with 6MV FFF and 10MV FFF photon beams. A minor increase in the number of MU in 6MV FFF plans was observed; however, the increase in the treatment time was found to be negligible. Significant reduction in the high dose spillage was obtained with 10MVFFF beams suggesting that although both energies are suitable for use in prostate and lymph node SABR 10MV FFF is superior.

EP-1700

SRS treatment planning for multiple cranial metastasis with a single isocentre approach using VMAT

R. Bill[1], L. Howard[2], M. Gilmore[2]
[1]*The Royal Liverpool and Broadgreen University Hospital NHS Trust, Medical Engineering and Physics, Liverpool, United Kingdom*
[2]*The Clatterbridge Cancer Centre, Medical Physics, Bebington, United Kingdom*

Purpose or Objective: This study evaluates a single isocentre technique for SRS for patients with multiple cranial metastases and compares to the local approach of a single isocentre per metastasis.

Material and Methods: At our centre, SRS treatment for multiple cranial metastases is planned in iPlan (Brainlab, Germany) using a single isocentre per metastasis, with an arrangement of nine static non-coplanar fields (SCF). An alternative VMAT-based approach, described by Clark et al (2012), uses RapidArcTM to give highly conformal dose distributions with a single isocentre. Eight patients each with three metastases, previously treated using our SCF technique, were re-planned using the single isocentre RapidArc approach. Plans were compared using PTV ICRU dose conformity (CI), Paddick gradient index (GI), ICRU homogeneity (HI) and whole brain doses. Plans were prescribed to the 80% isodose, with 100 % coverage of the target volume. The Wilcoxon's signed rank test was used to compare CI, HI and GI between the two techniques.

Results: There was a statistically significant improvement in the CI for RapidArc ($p=0.003$), suggesting superior conformity to the tumour. On average, iPlan plans were more homogeneous ($p=0.03$). In general RapidArc gives a higher maximum dose to PTVs ($p=0.002$). iPlan has a superior GI around each PTV ($p<0.001$); RapidArc has three unexpectedly high GI per metastasis values from three different patients with single tumour volumes less than 0.1cm2. GI per plan is greater for RapidArc than iPlan. However this is misleading as iPlan treats a greater volume to 2, 5 and 12.5 Gy by 1.3%,

3.1% and 5.6%, respectively; more patients are required to determine statistical significance.

Conclusion: RapidArc gives an improved CI around each metastasis as well as a lower whole brain dose at 2, 5, and 12.5 Gy compared to iPlan. This suggests that the RapidArc single isocentre technique offers a potential option for the treatment of multiple metastases, but further studies into optimal arc arrangement, whole brain doses and dosimetric delivery are required. In particular, the work of Evan et al (2013) suggests that 4-arc VMAT may further improve dose conformity, dose fall-off and whole brain doses relative to the 2-arc method discussed here. Ongoing work includes a comparison to a 4-arc arrangement together with analysis of beam-on and treatment times. In addition, investigation into the most suitable plan quality metrics such as those suggested by Paddick (2000) will be carried out.

EP-1701

VMAT or IMRT- what is better solution in sparing bone marrow in WPRT of patients after prostatectomy

M. Poncyljusz[1], P.F. Kukolowicz[1], B. Czyzew[1], A. Jankowska[1]
[1]*The Maria Skłodowska-Curie Memorial Cancer Centre and Institute of Oncology, Department of Medical Physics, Warsaw, Poland*

Purpose or Objective: For postprostatectomy patients at higher risk of nodal involvement the irradiation of pelvic lymph nodes may improve the therapeutic ratio. Larger volumes irradiated for these patients result in increased doses delivered to OAR. IMRT and VMAT techniques allow to better protect OAR in comparison to 3D-CRT. The aim of this study was to compare IMRT and VMAT techniques in terms of sparing of OAR. The main attention was paid to pelvic bones' marrow protection.

Material and Methods: Ten patients were selected retrospectively for this planning study. The 3D-CRT, IMRT and VMAT plans were created for each of patients. Treatment plans were generated for prostate bed (PTV1) and pelvic lymph nodes (PTV2). The delivered dose to the sum of PTV1 and PTV2 was 46Gy in 23 fractions and additionally dose 18 Gy in 9 fractions was delicered to PTV1 Target coverage (at least 98% of the PTV received≥95% of the prescription dose) and OAR sparing were compared across techniques. The following OAR were delineated: rectum, bladder, bowel bag and pelvic bones. The Wilcoxon test was used to compare the dosimetric parameters. Dose-values: bowel bag V30Gy[cc], pelvic bones V30Gy[%], V40Gy[%], bladder V40Gy[%], V50Gy[%], V60Gy[%], rectum V40Gy[%], V50Gy[%], V60Gy[%] were considered.

Results: The dosimetric qualities of 3D-CRT, IMRT and VMAT plans were comparable for target coverage (the mean value of PTV1 V95%, the mean value of PTV2 V95% all >99%). The IMRT and VMAT plans resulted in significant reduction in pelvic bones V30Gy[%], V40Gy[%], bladder V40Gy[%], V50Gy[%], V60Gy[%], rectum V40Gy[%], V50Gy[%], V60Gy[%] and bowel bag V30Gy[cc] in comparison to 3D-CRT plans. A comparison between IMRT and VMAT techniques shown better sparing bone marrow (pelvic bones V30Gy[%]) and increase of following values: bowel bag V30Gy[cc], bladder V60Gy[%], rectum V60Gy[%] in VMAT plans. Differences between values of V40Gy[%] and V50Gy[%] for bladder and rectum across mentioned techniques were statistically not significant.

Conclusion: The lower doses delivered to pelvic bones and thus also to red marrow for IMRT and VMAT techniques allow to expect the lower hematological toxicity. A comparison between IMRT and VMAT techniques shows, that the VMAT technique reduces the delivered dose to pelvic bones. However IMRT provided better rectum, bladder and bowel bag sparing at higher doses. All these results should be taken into consideration when IMRT and VMAT techniques being used in WPRT of patients after radical prostatectomy.

EP-1702

Cardiac dose evaluation in left breast cancer radiotherapy: Direct and Helical Tomotherapy

A. Fozza[1], L. Berta[2], S. Aimonetto[2], F. Migliaccio[1], A. Peruzzo Cornetto[2], L. Vigna[2], T. Meloni[3], F. Munoz[1]
[1]*AUSL Valle d'Aosta, Radiation Oncology, Aosta, Italy*
[2]*AUSL Valle d'Aosta, Medical Physics, Aosta, Italy*
[3]*AUSL Valle d'Aosta, Radiology Department, Aosta, Italy*

Purpose or Objective: The aim of the present study was to retrospectively evaluate the delivered doses to the cardiac structures for two different tomotherapy techniques in adjuvant radiotherapy for early stage left breast cancer patients

Material and Methods: Five consecutive conservatively operated left breast cancer patients, who underwent adjuvant radiotherapy, were retrospectively considered. CT simulation was acquired with patients in a supine position, using the breast immobilisation device. Image acquisition was performed with a 2.5 mm slice thickness in a free breathing modality without contrast agent administration. The prescription dose was 45 Gy/20 fr and 50 Gy/20 fr, respectively to the PTV2 (left whole breast) and PTV1(tumour bed), obtained as a 5 mm isotropic expansion of the CTVs, with a 5 mm margin from the skin. The following volumes were used for plans optimisation: lungs, right breast, spinal cord and PRV, heart. For each patient, two independent optimisations were carried out using a fixed ganty technique, Tomodirect (TD) and helical technique (HT). For TD planning two tangential plus other two-four static beams were used. For HT planning, the controlateral lung and breast were directionally blocked. All plans were optimized in order to minimize dose to OAR according to our internal protocol (lung V20<10%, V10<20%, V5<42%, controlateral breast: Dmax<5Gy, controlateral Lung: V5<5%) and to obtain a coverage of D95>95% and Dmax(1cc) <105% for PTVs. In a second time, cardiac structures have been identified on the basis of the University of Michigan Cardiac Atlas, and DVH parameters (D1%, Daverage, V20, V10, V5) for the left and right ventricle (LV, RV), left main coronary (LMC) artery, right coronary (RC) artery and left anterior descending coronary (LAD) artery were retrospectively evaluated for all plans using the plan evaluation tool of the RayStation software v 4.7.2

Results: Constraints on target coverage and OAR constraints were respected for both techniques in all plans. All results are reported in table 1. HT plans achieved a better conformation for the high doses for the whole heart (figure 1). The average maximum doses were 23±7 and 15±2 for TD and HT modality respectively. However HT showed a larger low-dose bath and the average doses were 20% higher than TD. For the LV the D1%, V10 and V5 for HT plans were 8±3, 0.6±1, 13±15, vs 19±10, 6.0±2.8, 34±12 for TD plans. Considering LAD artery the V20 was 0.1±0.1 with HT vs 29±18 for TD. On the average, the greater differences in DVH parameters between HT and TD plans were observed for V5 in LV, (-21.7%), V5 in RV (+14.3%) and V20 in LAD artery (-28.7%)

		Direct Tomotherapy (TD)		Helical Tomotherapy (HT)	
		average (S.D.)	range (min - Max)	average (S.D.)	range (min - Max)
Heart	Volume [cc]: 618 – 88				
	$D_{1\%}$ [Gy]	23 ± 7	(17 36)	15 ± 2	(12 16)
	$D_{average}$ [Gy]	3.9 ± 1.0	(2.9 - 5.1)	4.7 ± 0.5	(4.0 - 5.1)
	V_{20} [%]	1.3 ± 1.0	(0.2 - 3.0)	0.3 ± 0.1	(0.2 – 0.3)
	V_{10} [%]	6.0 ± 2.8	(3 - 10)	5.1 ± 1.8	(2 – 7)
	V_5 [%]	27 ± 10	(15 – 40)	31 ± 6	(21 – 37)
LV	Volume [cc]: 178 – 26				
	$D_{1\%}$ [Gy]	19 ± 10	(10 34)	8 ± 3	(5 11)
	$D_{average}$ [Gy]	4.6 ± 1.1	(3.8 - 6.5)	3.8 ± 0.8	(2.9 - 4.8)
	V_{20} [%]	1.1 ± 1.6	(0 - 4)	-	-
	V_{10} [%]	6.0 ± 2.8	(1 – 13)	0.6 ± 1.0	(0 – 2)
	V_5 [%]	34 ± 12	(23 – 53)	13 ± 15	(1 – 36)
RV	Volume [cc]: 81 ± 15				
	$D_{1\%}$ [Gy]	13 ± 3	(10 – 19)	11 ± 3	(8 – 15)
	$D_{average}$ [Gy]	4.4 ± 0.9	(3.2 - 5.8)	5.3 ± 0.9	(4.4 6.5)
	V_{20} [%]	0.1 ± 0.2	(0 – 0.4)	-	-
	V_{10} [%]	6.5 ± 5.0	(1 – 14)	3.7 ± 5.8	(0 – 14)
	V_5 [%]	36 ± 11	(24 – 54)	50 ± 14	(39 – 69)
LAD	Volume [cc]: 3 ± 1				
	$D_{1\%}$ [Gy]	32 ± 7	(23 – 42)	15 ± 3	(11 -19)
	$D_{average}$ [Gy]	15 ± 5	(10– 27)	8 ± 2	(6 - 11)
	V_{20} [%]	29 ± 18	(2 – 50)	0.1 ± 0.1	(0 – 0.2)
LMCA	Volume [cc]: 3 ± 1				
	$D_{1\%}$ [Gy]	8 ± 3	(2 - 3)	12 ± 9	(5 – 16)
	$D_{average}$ [Gy]	5 ± 3	(1 - 9)	7 ± 4	(4 - 13)
	V_{20} [%]	-	-	-	-
RCA	Volume [cc]: 6 ± 6				
	$D_{1\%}$ [Gy]	5 ± 6	(2 – 16)	9 ± 3	(6 -13)
	$D_{average}$ [Gy]	4 ± 4	(1 - 11)	6 ± 2	(4 - 9)
	V_{20} [%]	-	-	-	-

Table1: DVH parameters in cardiac structures for TD and HT

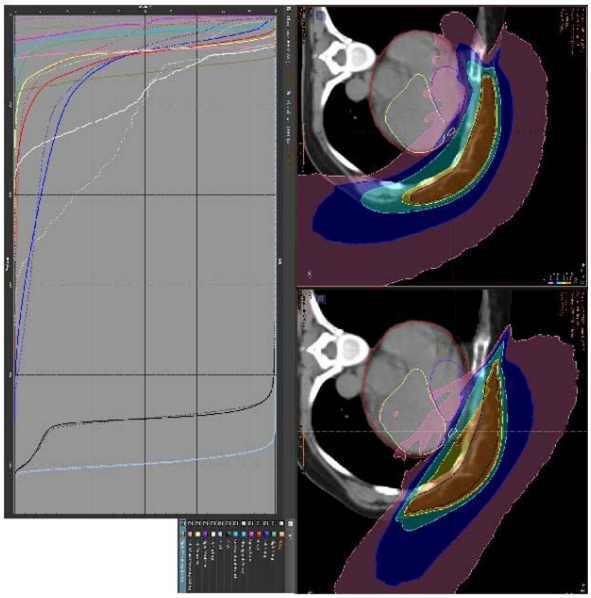

Conclusion: In the light of the dosimetric results herein reported, the cardiac structures should be contoured for plans optimisation and evaluation, especially when high conformal techniques are employed

EP-1703

The usefulness of VMAT in patients irradiated to the chest wall after left-sided mastectomy

M. Spalek[1], P. Mężeński[2], J. Gałecki[1], E. Dąbrowska[2], A. Zawadzka[2], P. Kukołowicz[2]

[1]*The Maria Sklodowska-Curie Memorial Cancer Center, Radiotherapy, Warsaw, Poland*

[2]*The Maria Sklodowska-Curie Memorial Cancer Center, Medical Physics Department, Warsaw, Poland*

Purpose or Objective: Intensity-modulated radiation therapy is routinely used to irradiate patients after left-sided mastectomy to the chest wall. Volumetric modulated arc therapy (VMAT) is a combination of IMRT and the arc technique. The use of gantry rotation during irradiation allows for very fast and accurate delivery of the planned dose. The aim of this study was to evaluate the usefulness of VMAT for patients who receive a post-left-sided-mastectomy chest wall irradiation.

Material and Methods: 10 radiation therapy treatment plans were prepared for both IMRT and VMAT. The prescribed dose was 45 Gy in 2.25 Gy per fraction (overall treatment time - 4 weeks). The dose distributions were evaluated in terms of: the volume of the CTV and PTV which receives 90% and 95% of prescribed dose; the volume of the left lung which receives 20 Gy or more (VL20); the mean dose to the left lung; the volume of the heart which receives 20 Gy or more (VH20); the mean dose to the heart; the volume of the both lungs which received 20 (VLR20) and 30 Gy (VLR30) or more; the mean dose to the both lungs; the number of monitor units (MU) per single fraction. To evaluate differences between techniques, the Wilcoxon matched-pair signed rank test was used.

Results: Radiation therapy plans for both VMAT and IMRT fulfilled all criteria required by the treatment protocol in dose constraints for target volumes and organs at risk (OAR). VL20 was non-significantly higher in VMAT (28%) than IMRT (25.8%). The mean dose to the left lung was 10.3 Gy in VMAT, and 15.7 Gy in IMRT. The mean dose to the heart was 11.5 Gy in IMRT and 11.6 Gy in VMAT. VH20 was higher in VMAT than in IMRT plans: 10.6% vs 7.8% respectively. VLR20, VLR30 and the mean dose to the both lungs were similar in both techniques (VLR20 IMRT: 11.5% vs VMAT: 12.4%; VLR30 IMRT: 5.8% vs VMAT: 6.3%; the mean dose to the both lungs IMRT: 9.7 Gy vs VMAT: 10.2 Gy respectively).
There were no significant differences between IMRT and VMAT in doses to CTV, PTV and OAR. The number of MU was significantly lower in VMAT plans (VMAT: 641 MU vs IMRT: 1049 MU, p <0.007).

Conclusion: VMAT and IMRT produced similar dose distribution in the CTV and PTV, and similar OAR dose sparing. However, the number of MU in VMAT was significantly lower than in IMRT. The decrease in the number of MU, and consequently the treatment time, may reduce the influence of intrafraction movement on dose distribution. It also allows to treat more patients in the same unit of time.

EP-1704

Helical Tomotherapy for left-sided breast:dosimetric comparison to Volumetric-Modulated Arc Therapy

F. Ertan[1], R. Tanriseven[1], O. Yazici[1], A.M. Kocer[1], M.B. Altundag[1]

[1]*Ankara Oncology Hospital, Radiotherapy, Ankara, Turkey*

Purpose or Objective: The aim was to evaluate the dose distribution of target volume and organs at risk (OARs) using helical tomotherapy (HT) and volumetric modulated arc therapy (VMAT) for left sided breast cancer patients.

Material and Methods: We compared two techniques for ten left sided breast cancer patients. Planning target volume (PTVchestwall) includes left sided chest wall and PTVSCF-AKS contains supraclavicular, axillary lymph nodes. The delivered dose was 50Gy within 25 fractions. The generated plans were evaluated in terms of dose distribution of PTV, doses of left lung, heart, contralateral breast and total monitor units. During CT simulation, the patient was positioned supine on a breast board. The patient's left arm raised above the head and the head turned to the right side. CT slices were obtained at 3 mm intervals extending from the chin to the upper abdomen during free breathing. Tomotherapy planning parameters; the field width, modulation factor and pitch, were assigned to 5cm, 2 and 0.287, respectively, for all plans. To decrease right lung dose, the complete block was applied. For VMAT planning parameters, two half arc were used and the angle was addressed according to patient's anatomy. The plans were constructed using Anisotropic

Analytical Algorithm (AAA). Grid size was 0.2cm. Depends on the patient, 0.5 and 1cm bolus was used.

Results: In Table-1, The value of D2, D98 for PTVchest wall and PTVSCF-AKS ; V20,V10 for ipsilateral lung; maximum dose for contralateral breast; V25, V10,mean dose for heart and total monitor unit were displayed respectively for VMAT plans. In Table-2, the same parameters for each volume were given for HT plans.

Table-2: Plan results for HT

PTV50 Chest wall D_2 (cGy)	PTV50 Chest wall D_{98} (cGy)	PTV50 SCFAKS D_2 (cGy)	PTV50 SCFAKS D_{98} (cGy)	Ipsi-lateral lung $V_{(20Gy)}$	Ipsi-laterial lung $V_{(10Gy)}$	contra lateral breast max-cGy)	heart (mean -cGy)	heart $V_{(25Gy)}$	Hear t $V_{(10Gy)}$	Total MU
5273	4887	5335	4550	27.0	39.0	2309	325	0.6	4.2	7451
5327	5004	5223	4903	23.9	34.4	2493	230	0.9	3.0	9873
5355	4929	5313	5000	24.1	39.5	1510	248	0.5	4.2	6644
5277	4951	5252	4790	25.2	38.6	2928	363	1.6	6.3	7480
5288	4998	5254	4914	20.9	33.2	1691	350	1.1	6.8	8066
5312	5078	5300	4816	28.5	39.2	2206	368	1.5	5.8	6635
5275	5007	5276	4892	29.3	41.8	1813	388	1.3	8.4	7697
5211	5000	5270	4340	20.8	33.9	1846	303	1.5	5.0	7274
5261	4918	5228	4919	26.5	39.4	2343	567	3.7	11.7	7782
5273	4958	5267	4950	24.0	37.0	1996	320	1.8	8.9	7374

TABLE-1: Plan results for VMAT

PTV50 Chest wall D_2 (cGy)	PTV50 Chest wall D_{98} (cGy)	PTV50 SCFAKS D_2 (cGy)	PTV50 SCFAKS D_{98} (cGy)	Ipsi-lateral Lung $V_{(20Gy)}$	Ipsi-laterial Lung $V_{(10Gy)}$	Contra lateral breast max-cGy)	heart (mean -cGy)	hear t $V_{25(Gy)}$	Hear t $V_{(10Gy)}$	Total MU
5330	4790	5279	4880	16.2	50.0	517	480	0.0	6.0	484
5353	4773	5327	4905	17.5	53.2	467	422	0.6	20.3	477
5332	4808	5238	4968	15.8	42.6	495	456	1.0	7.3	471
5262	4786	5282	4844	18.9	43.7	633	605	2.9	10.0	422
5282	4819	5263	4853	14.2	48.8	608	509	0.4	6.6	508
5317	4808	5365	4816	19.8	56.0	459	452	6.1	32.0	491
5330	4809	5309	4825	23.8	55.0	696	525	3.0	35.0	463
5243	4828	5244	4828	18.5	41.5	496	468	4.6	30.0	440
5212	4768	5251	4951	26.4	50.5	560	624	8.0	23.5	393
5250	4815	5265	4830	16.0	45.0	480	490	3.5	15.0	440

Conclusion: Based on the results of this study, HT plans have reduced the heart doses and shown better homogenous dose distribution. However, contralateral breast dose cannot be provided within the dose constraints using HT. The reduced treatment time and planning time were feasible for VMAT. In terms of lung dose, there was no significant difference between two techniques.

EP-1705

Dosimetric comparison (VMAT and 3DCRT) in breast cancer with regional nodes and SIB of the tumor bed

A. Seguro[1], L. Díaz[2], G. Ruiz[1], R. García[1], M.D. De las Peñas[3], E. Amaya[3], M. Hernández[3], P. Samper[3], J.M. Jimenez[1]
[1]*Hospital Rey Juan Carlos, Medical Physics, Móstoles Madrid, Spain*
[2]*Hospital Universitario Puerta del Mar, Radiation Oncology, Cádiz, Spain*
[3]*Hospital Rey Juan Carlos, Radiation Oncology, Móstoles Madrid, Spain*

Purpose or Objective: To evaluate and assess the potential advantage of volumetric modulated arc therapy (VMAT with Monaco v.3.3) over 3D conformal radiotherapy (3DCRT with XiO v.4.8) in the treatment of breast cancer with axillar and supraclavicular involvement and simultaneous integrated boost (SIB) of the tumor bed with respect to volume coverage and doses to organ at risk (OAR).

Material and Methods: 2 techniques were compared in 15 patients. All were women with adjuvant radiotherapy indication and laterally of the tumor was not considered. Treatment schedule consisted of 50Gy/2Gy daily to breast and regional nodes and SIB over tumor bed to 60Gy (BED 66Gy 2Gy/ daily fr.) all in 25 fractions. 3DCRT employed 6 to 8 coplanar hemifields with one isocentre in the gap between breast and supraclavicular volumes and VMAT was developed with a restriction of the angulation for the arc to 200º-220º avoiding contralateral breast. Optimization was performed to get the best plan for each technique for each individual patient. Target coverage and dose to OAR were analyzed using mean dose, % of the prescribed dose to 95 % of the target volumes, heterogeneity (V107, D1%, D2%) and QUANTEC-constraints respectively.

Results: Although we did not have significant differences in the coverage of PTV (prescription was at least 95% of the prescribed dose to 95% of the target) we got better homogeneity in terms of mean dose to PTV with VMAT, with mean differences from 50.5Gyto 51.5Gy for VMAT in front of 53 to 54Gy in 3DCRT. The greatest benefit was obtained with the dose delivered to ipsilateral lung with a decrease of at least 10% in V20 that always was below 25% in VMAT technique.

Conclusion: We consider VMAT as most aproppiated technique for these treatments, because gives a perfect coverage to the target volumes and better protection to OAR.

EP-1706

Evaluation of different radiosurgical planning techniques using iPlan®

C. Navarro[1], K. Thippu Jayaprakash[2], S. Dymond[1], S. Chris[1], L. Turner[1], R. Shaffer[2], E. Adams[1], A. Nisbet[1], T. Jordan[1]
[1]*St Luke's Cancer Centre- Royal Surrey County Hospital, Radiotherapy, Guildford, United Kingdom*
[2]*St Luke's Cancer Centre- Royal Surrey County Hospital, Department of oncology, Guildford, United Kingdom*

Purpose or Objective: To evaluate and compare dosimetric parameters of different radiosurgical plans with an aim to determine the optimum technique for treating single brain metastases with a linear accelerator.

Material and Methods: A prospective study was conducted on iPlan (Brainlab V4.5, Germany) for 11 intracranial targets of varying volumes and shapes (volume <20cc) using a range of radiosurgical planning techniques. The study was performed both on the CT of an anthropomorphic phantom (STEEV, Computerised Imaging Reference Systems, USA) and on a single patient planning CT. Plans were generated to treat 5 spheres of varying volumes (1.4 cc - 17.5 cc) and 2 irregular targets (8 cc and 17.4 cc) in the phantom. Minimum and maximum plan target volume (PTV) dose, Paddick conformity index (CI), mean dose to normal tissue and total monitor units (MU) were recorded for plans with varying number of arcs (3-4) or fields (7-9), table spread (90˚-120˚ arc), gantry spread (90˚-120˚ arc) and beam energy. All planning parameters were fixed except for the element to be tested. For the patient planning study, plans were generated for 4 target lesions at various locations using 3-4 dynamic conformal arcs (DCA) and 9 static fields.

Results:

Phantom planning study

DCAs showed higher PTV doses than static field plans (1-2% difference). 6 MV plans produced the highest maximum and minimum doses to PTV followed by 6 MV Flattening Filter Free (FFF) and 10 MV FFF (4% difference between energies).

The remaining dosimetric parameters were affected only up to 1% by other planning factors except for increasing the margin between PTV and multi leaf collimators (MLC) edge (range, 1-3 mm) (1-7% difference). The best CI was seen with 9 static fields compared with DCA regardless of number of arcs used (2% difference). CI improved with the following - decreasing PTV to MLC margin (up to 10% difference), increasing number of static fields (1-2% difference), using 10 MV FFF (2% difference) and with arc length & table spread for irregular shaped targets (1% difference).
Patient study
Similar results were obtained with all techniques. Total mean number of MUs were 3144, 3166, 3121 for 3DCA, 4DCA and 9 static fields plans respectively. The mean CI was 2.3, 2.1 and 2.2 using 3DCA, 4DCA and 9 static field plans respectively. The normal tissue mean doses were 1.3% for all three techniques.

Conclusion: All evaluated radiosurgical plans were acceptable for clinical use. The technique was chosen based on delivery efficiency and dose to normal brain. 10 MV FFF was more efficient and more conformal. 4DCA delivers lower dose to a larger volume of the brain compared to 9 static fields which delivers higher dose to a smaller volume. The MLC margin is a compromise between CI and doses to the PTV. To conclude 4DCA 10MV FFF was chosen for clinical use, the MLC margin depends on the target volume.

EP-1707

Tomotherapy dose painting hypofractionated treatments on GBM based on DW-MRI: a feasibility study.

M. Orlandi[1], A. Botti[1], E. Cagni[1], L. Orsingher[1], R. Sghedoni[1], C. Patrizia[1], C. Iotti[1], M. Iori[1]
[1]*Arcispedale S. Maria Nuova, Fisica Medica, Reggio Emilia, Italy*

Purpose or Objective: To investigate the feasibility in Tomotherapy (HT) of a hypofractionated DP (Dose Painting) treatment on GBM (Glioblastoma Multiforme) cancer patients using ADC maps derived from DW-MRI.

Material and Methods: Five patients, who underwent GBM radiotherapy, were retrospectively considered, prescribing a dose escaled from 25 to 50 Gy in 5 fractions. The objective was that at least the 95% of the CTV received at least 25 Gy. DPBN dose prescription maps were generated from ADC-MRI, registered with planning CT, for each patient. The ADC pixel values (mm^2/s) within the CTV were converted to dose values (Gy) using the equation Eq. 1 where Dmin and Dmax are the minimum and maximum total dose of prescription (25-50 Gy). Imin and Imax are the minimum and maximum significative values of ADC selected on the basis of the ADC differential histogram, inside the CTV region.
Then it was necessary to discretize each DPBN maps in 9 isodose levels (Deveau et al., Acta Oncol. 2010) in order to obtain a corresponding DPBC map. The final DPBC map was realized minimizing, with an iterative process, the difference between DPBN and DPBC, evaluated by means of Quality Factor (QF) (Vanderstraeten et al., Phys. Med. Biol. 2006). The QF is, defined as in Eq. 2 and Eq. 3 where *i* is the *i-th* voxel. Then plans were optimized on a standard HT TPS and a TPS Dose Distribution (TDD) was obtained. For each patient the TDD was compared with the prescribed DPBN using a Qi distribution, defined as the ratio of TDDi and DPBNi. The quality of the treatment plans was evaluated in term of QF and Q0.9-1.1, that represents the volume of the CTV in which the Qi ranges from 0.9 to 1.1. Eventually the delivery of the DP plans was assessed with Octavius system (PTW).

$$D(I) = \begin{cases} D_{max} & I < I_{min} \\ D_{min} + \frac{I - I_{min}}{I_{max} - I_{min}} \cdot (D_{max} - D_{min}) & I_{min} < I < I_{max} \\ D_{min} & I > I_{max} \end{cases} \quad \text{Eq. 1}$$

$$Q_i = \frac{DPBC_i}{DPBN_i} \quad \text{Eq. 2}$$

$$QF = \frac{1}{n}\Sigma_i |Q_i - 1| \quad \text{Eq. 3}$$

Results: Fig. 1 reports the different distributions obtained for Patient 1.
Tab. 1 shows quantitative DVH and quality analysis of the treatment doses for the CTVs, mean values OAR Dmax for all five patients, and γ results for the DQA performed. The constraints for the OAR were respected in all the five plans as well as the coverage of the CTVs with the minimum prescribed dose of 25 Gy. The QF ranges from 0.126 to 0.176, while the mean value of Q0.9−1.1 was 68% ± 7%. The delivery time ranges from a minimum of 38.3 minutes to a maximum of 63.6 minutes. All DQA performed are within the acceptance criteria with a mean value of γ of 87.4%.

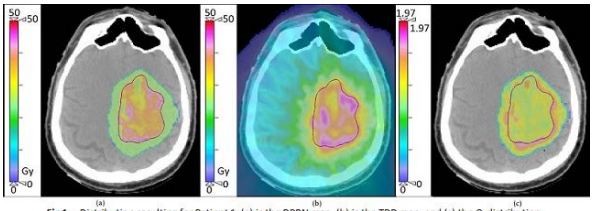

Fig 1. – Distribution resulting for Patient 1: (a) is the DPBN map, (b) is the TDD map, and (c) the Q_i distribution.

CTV							
Pt	V_{25Gy} (%)	$V_{>50Gy}$ (%)	V_{Tot} (cm^3)	$Q_{0.9-1.1}$	QF	**Beam on Time** (min)	γ_{DQA} (%)
1	99.98	1.08	62.3	40.9	0.176	43.5	82.4
2	99.71	0.14	226.9	67.5	0.126	59.4	85.1
3	99.55	0.27	82.0	61.0	0.156	43.5	89.9
4	99.95	0.04	172.6	79.2	0.156	63.6	87.5
5	100.00	0.04	52.2	65.2	0.126	38.3	92.4

OAR	$\overline{D}_{Max}$ (Gy)	$\sigma_{D_{Max}}$ (Gy)	$\overline{D}_{Max}^{equiv}$ (Gy)	$\sigma_{D_{Max}^{equiv}}$ (Gy)	D_{Max}^{RTOG} (Gy)
Brain stem	27.57	5.05	48.25	8.84	50
Lens	6.37	1.29	11.15	2.27	25
Eye	10.07	3.15	17.62	5.52	54
Optic nerves	15.69	4.36	27.46	7.63	54

Tab. 1 – Quantitative results for CTVs and D_{max} for OAR with dose converted to standard 2 Gy per fractions.

Conclusion: Our results provides the feasibility of a ADC-based dose painting treatment in GBM cancer patients, respecting dose constraints to OAR and minimum target coverage. The plans obtained are deliverable, even if there is some concern about the HT delivery time. Clinical studies should be conducted to evaluate toxicities and tumor response of such a strategy.

EP-1708

Re-irradiation of pelvic sidewall disease: comparing normalisation techniques for stereotactic RT

M. Llewelyn[1], E. Wells[2], N. Bhuva[1], A. Taylor[1]
[1]*Royal Marsden NHS Foundation Trust, Department of Gynaecology, London, United Kingdom*
[2]*Royal Marsden NHS Foundation Trust, Department of Radiotherapy, London, United Kingdom*

Purpose or Objective: Management of pelvic sidewall recurrence in gynaecological cancer is a challenging clinical scenario with only 10-20% 5-year survival. For patients previously treated with radiotherapy, salvage surgery has high morbidity and outcomes are poor. Recent radiotherapy advances including stereotactic radiotherapy provide the opportunity for more effective salvage techniques. Systematic assessment is required to determine optimal treatment approaches.
The aims of this study were: (1) To determine target and OAR dose targets for pelvic re-irradiation (2) To compare ICRU 83 normalisation and prescription (ICRU) to the stereotactic radiosurgery convention of prescribing to a covering isodose

allowing maximum doses of ~125% (SRS) using both fixed field IMRT and VMAT techniques.

Material and Methods: A systematic literature search was undertaken to assess pelvic re-irradiation outcomes and cumulative dose constraints for organs at risk including bowel, bladder and rectum were derived. Dosimetric assessment was undertaken for 10 patients treated for recurrent gynaecological cancer assuming prior pelvic radiotherapy of 50Gy (EQD2). Plans were produced to deliver 30Gy in 5 fractions using ICRU-fixed, ICRU-VMAT, SRS-fixed and SRS-VMAT techniques. Doses to GTV, PTV and OAR were compared and conformity index measured for each technique.

Results: All 50 plans met the planning objectives for PTV and GTV coverage. PTV volume ranged from 10 – 99 cc (mean 38 cc). Mean GTV dose with ICRU-fixed and ICRU-VMAT was 30.1Gy; with SRS-fixed and SRS-VMAT it was 30.4 Gy, increasing the EQD210 from 40 Gy to 48.4 Gy. Conformity index was ICRU-fixed1.19, ICRU-VMAT 1.10, SRS-fixed 1.04 and SRS-VMAT 1.05. All bladder and rectal targets were met for all plans except one patient with bladder involvement. The dose limiting structure was bowel with mean Dmax 27 Gy (range 13-33 Gy), D2cc 21 Gy (13-30), D5cc 17 Gy (7-27) and no significant differences between techniques. Dose targets were exceeded for 3 patients with no correlation to PTV volume, only proximity of GTV to bowel.

Conclusion: Re-irradiation is a valuable option for treating sidewall recurrence and can be delivered within acceptable dose constraints with both normalisation techniques. SRS type normalisation increases mean GTV doses by 21% (EQD2) compared to ICRU normalisation without increasing OAR doses. Using our proposed bowel tolerances of Dmax 31 Gy, D2cc 27.1 Gy, D5cc 18.1 Gy, there is potential for further dose escalation in 50-70% patients.

EP-1709

Comparison of IMRT and VMAT plan quality for hypofractionated post-mastectomy chest wall irradiation

A. Zawadzka[1], E. Dąbrowska[1,2], P. Mężeński[1], J. Gałecki[3], P. Kukołowicz[1], M. Spałek[3]
[1]*The Maria Sklodowska-Curie Memorial Cancer Center, Medical Physics Department, Warsaw, Poland*
[2]*University of Warsaw, Department of Biomedical Physics, Warsaw, Poland*
[3]*The Maria Sklodowska-Curie Memorial Cancer Center, Radiotherapy Department, Warsaw, Poland*

Purpose or Objective: Volumetric Modulated Arc Therapy (VMAT) is a novel variation of Intensity Modulation Radiotherapy (IMRT) which allows to deliver dose during the beam rotation with a variable dose rate. The main advantage of this technique is treatment time shortening, what may be crucial especially due to a risk of intrafraction motion. On the other hand not only the treatment time but also a plan quality should be taken into account. The aim of this study was to compare VMAT hypofractionated post-mastectomy chest wall RT plans with IMRT plans.

Material and Methods: Plans for seventeen patients with post-mastectomy chest wall radiotherapy were selected for the study. The clinical target volume included chest wall and internal mammary nodes. The prescribed dose (PD) were: 40.05 Gy delivered in 15 fractions (5 – left side; 3 – right side) and 40.5 Gy delivered in 15 fractions (4 – left side; 5 – right side). For each patient IMRT and VMAT plans were generated. The dose distribution was prescribed to the mean dose to the CTV. The comparison was made on the basis of: the volume of CTV and PTV which receives 90% and 95% of prescribed dose, the volume of the ipsilateral lung which receives 20 Gy or more (VL20), the mean dose to the ipsilateral lung, the volume of the heart which receives 20 Gy or more (VH20), the mean dose to the heart, the total volume of both lungs which received 20Gy (VLR20) and 30 Gy (VLR30) or more, the mean dose to the both lungs, the maximum dose to the spinal cord and the number of monitor units (MU) per single fraction. For statistical analysis, the Wilcoxon matched-pairs signed-ranks test was used.

Results: All treatment plans fulfilled dose volume constrains for CTV, PTV and OAR regardless of the technique used. There was no statistically significant difference in dose distribution in CTV, PTV and OAR ($p > 0.05$). VMAT plans results in a statistically significant lower number of MU ($p=0.041$ for PD = 40.05Gy and $p=0.043$for PD = 40.50Gy) The number of MU was on average 1363.6±221.1 MU and 764.0±132.6 MU for IMRT and VMAT plans, respectively when the plans with PD of 40.05Gy were analyzed. Similar results were obtained for plans with PD of 40.50 Gy (on average 1010.2±57.4 MU vs 775.4±76.7 MU for IMRT and VMAR respectively).

Conclusion: VMAT in comparison with IMRT technique improves efficacy of plan delivery for equivalent plan quality. The decreased number of monitor units allows to deliver a single fraction faster, so it to reduce the probability of intrafraction motion.

EP-1710

Use of FFF beams for SBRT treatments: impact of the size of the PTV?

L. Vieillevigne[1], S. Bessieres[1], M. Ouali[2], C. Lanaspeze[1]
[1]*Institut Claudius Regaud, Radiophysique, Toulouse, France*
[2]*Institut Claudius Regaud, Statistiques, Toulouse, France*

Purpose or Objective: Flattening filter free (FFF) beams are most frequently utilized for treatments where higher fraction doses need to be delivered, including hypofractioned stereotactic body radiation therapy (SBRT). There are various treatment modalities now available for SBRT: conventional static fields, dynamic conformal arc (DCA) or Volumetric Modulated Arc Therapy (VMAT). In the present study, we wanted to obtain some criteria for a conscious choice of the employment of FFF beams and of the DCA or RA technique depending the size of the PTV.

Material and Methods: Treatment planning was carried out using version 11 of Eclipse (Varian, Palo Alto, CA, USA) with Analytical Anisotropic Algorithm (AAA). All plans were designed for a Varian TrueBeam STx linear accelerator (Varian Medical Systems) equipped with a high definition Millenium multi-leaf collimator (HDMLC). Twenty four PTVs from 1.52 cm3 to 445.24 cm3 were studied. For each PTV, DCA and VMAT plans were prepared utilizing two flattened photon beam of 6 MV (6FF) and 10 MV (10FF) and two nonflattened beams of nominal energy 6 and 10 MV (6FFF, 10FFF). For a meaningful comparison, all DCA and RA plans satisfied 100% of the prescription dose to at least 98% of the PTV. Parameters such as conformity index, gradient index, healthy tissue mean dose, organs at risk mean dose, number of monitor units, beam on time (BOT) were used to quantify obtained dose distributions. A friedman and spearman's rho test were performed in order to establish statistical significance.

Results: The data indicate no significant differences between conformity with flattened beams and those using unflattened beams for VMAT technique. For DCA technique, it is notable that 6FFF tends to be slightly better than 6FF beams and even for large volumes. As PTV volume increases, 10FFF is less suitable for DCA technique and forward planning becomes more challenging and inappropriate. The MUs in the FFF plans were always greater than in FF plans. Dose to healthy tissues were reduced for all PTV sizes for FFF beams, except for the DCA 10FFF for large PTV volume. The BOT for FFF beams is much lower. DCA was found to be more appropriate for small PTV and VMAT for median and large PTV. The MUs were significantly different between techniques. VMAT plans generated larger number of MU compared to DCA.

Conclusion: The plans developed with flattened and unflattened beams look very similar in terms of conformity index. FFF beams provide a better sparing of OAR except for

DCA 10FFF and reduced treatment times when compared to FF. Further study on the role of tumor location is recommended to establish more conclusive results. A concern with the use of VMAT with SBRT is whether the motion of the tumor leads to significant dosing discrepancies. DCA remains immune to the MLC interplay effect.

EP-1711

To revise helical irradiation of the total skin HITS as completed-HITS in cutaneous lymphoma patient

H.J. Tien[1], P.W. Shueng[1], S.C. Lin[2], C.T. Lin[1], H.P. Yeh[1], C.H. Chang[1], C.H. Hsieh[1]
[1]*Far Eastern Memorial Hospital, Radioation Oncology, Taipei, Taiwan*
[2]*Far Eastern Memorial Hospital, Hematology, Taipei, Taiwan*

Purpose or Objective: To modify helical irradiation of the total skin (HITS) technique as the completed-HITS (CHITS) with face covering and the bone marrow dose declined according to the relapse pattern and hematologic toxicities of cutaneous lymphoma patient.

Material and Methods: A 36-year-old woman was diagnosed as therapy-refractory cutaneous CD4+ T-cell lymphoma, T3N0M0B0, stage IIB. HITS with face sparing using 30 Gy in 40 fractions, 4 times per week was prescribed in March, 2012. The adverse effects included leukopenia. One year later, the new patches were noted in right eyebrow and lower eyelid which was spared. According to the relapse pattern and hematologic toxicities, HITS was revised to improve the plan results as CHITS. First, the clinical target volume (CTV) was increasing the face targeting to be really whole skin irradiated. Second, the planning target volume (PTV) were separated into head, chest, abdomen and pelvis with upper thigh to maintaining the appropriate PTV coverage and the margin for PTV was reduced from 5.0 mm to 3.0 mm according to the previous daily image-guided data. Third, the central cord complete block (CCCB) was designed from head to thigh but not from head to abdomen only. The CCCB distance away from PTV was changed from 2.5 cm to 2.2 cm to reduce the internal organs and bone marrow dose. Additionally, the iliac bone, cervical, thoracic, lumbar spine, femoral head and pelvic bone were contoured to be references to limit the marrow dose. The uniformity index (UI), conformity index (CI), dose of organs at risk were used to evaluate the plans. For reducing the toxicity of normal organs, we also performed low-dose CHITS of 12 Gy in 12 fractions.

Results: The UI for head, chest, abdomen and pelvis of CHITS were 1.16, 1.12, 1.08 and 1.15 that were similar to HITS of 1.12, 1.12, 1.08 and 1.12, respectively. For the low-dose CHITS, the UI is also similar to CHITS. The conformity of CHITS was similar to HITS (1.40 versus 1.37). The mean dose of heart, whole lung, right parotid gland, left parotid gland, liver, right kidney, left kidney, intestine, bladder, rectum, uterus with ovary, and cervix with vagina were reduced in 15.1% to 45.0%. The mean dose of cervical spine, thoracic spine, lumbar spine, right iliac bone, left iliac bone, sacrum, right lower pelvic bone, left lower pelvic bone, right femur, left femur were reduced in 21.6% to 63.8%. For the low-dose CHITS, the normal organ dose were reduced in 47% to 88% due to low dose treatment.

Conclusion: The modifications of adding face skin irradiation, reduced PTV margin, the distance away from PTV from CCCB and virtual structure constraints enabled the CHITS technique reduced doses of normal organs and bone marrow successfully with keep of uniformity and conformity as HITS technique. The low-dose CHITS had the similar results in target uniformity and conformity and much lower normal organ dose compared to HITS technique.

Electronic Poster: Physics track: (Radio)biological modelling

EP-1712

Increased tumour control probability (TCP) with inhomogeneous dose escalated distributions in NSCLC

C. Fleming[1], S. O'Keeffe[1], J. Armstrong[2], B. McClean[1]
[1]*St. Luke's Radiation Oncology Network, Dept. of Physics, Dublin, Ireland Republic of*
[2]*St. Luke's Radiation Oncology Network, Dept. of Radiation Oncology, Dublin, Ireland Republic of*

Purpose or Objective: The theoretical benefit of dose escalation in NSCLC has been shown by Fenwick whilst others have demonstrated a clinical dose response relationship (Partridge, Rengan). Additionally, inhomogeneous dose distributions have been suggested as a method for increasing the absolute dose to the target within normal tissue constraints (Warren). The aim of this planning study was to combine these concepts and explore the potential tumour control probability (TCP) benefit that an inhomogeneous plan targeting dose escalation to the iGTV could deliver whilst respecting normal tissue tolerances.

Material and Methods: Between January 2014 and April 2015 20 patients with non-small cell lung cancer (NSCLC) underwent 4D-planning CT with motion tracking via the RPM system (Varian Medical Systems, Palo Alto, California) for definitive (chemo)radiation therapy at our institution. The 4DCT scan was binned into 10 phases and the MIP and AVIP datasets were generated. The iGTVsum was the sum of three datasets (0%, 50% and MIP). An iGTV to iCTV margin of 6mm (scc) or 8mm (adenocarcinoma) was used with a further 5mm to the PTV. OARS were contoured on the AVIP CT set, including: combined lung; spinal cord; oesophagus and heart. Mean iGTVsum volume of 94.51cm3 (range: 12.44 – 608.69cm3) and mean PTV volume of 315.51cm3 (range: 97.02 – 1279.64cm3). Six plans were created: homogeneous plans treating the entire PTV to 60Gy in 20 fractions using both 3DCRT and RapidArc; and four inhomogeneous RapidArc plans developed to deliver 65-80Gy in 5Gy escalated increments to iGTVsum (median) and 60Gy to PTV, all in 20 fractions.

Results: There is a significant ($p < 0.05$) difference in TCP for all escalated plans, ranging from 79.8% for the 65Gy boost to 94.9% for the 80Gy boost, in comparison to 63.1% for the homogeneous RapidArc plan. There is a significant difference between the MLD for the various escalated plans (Table 1); however, this difference is not clinically significant given that tolerance for MLD is in the 17-20Gy region. Similarly, the predicted NTCP for the lung for the dose escalated plans ranged from 6.2-7.1%. In terms of the V20Gy the only significant difference was between the 3D plan and all the RapidArc plans (Table 1).

Mean Lung Dose (Gy)

% of Comb Lung Receiving 20Gy	60H 13.30Gy	60_65 13.35Gy	60_70 13.45Gy	60_75 13.59Gy	60_80 13.72Gy	60 3D 14.92Gy
60H 22.70%		0.243	0.006*	0.000*	0.000*	0.000*
60_65 22.85%	0.590		0.021*	0.003*	0.000*	0.000*
60_70 22.84%	0.653	0.927		0.032*	0.001*	0.000*
60_75 22.98%	0.334	0.296	0.454		0.001*	0.000*
60_80 23.02%	0.321	0.154	0.188	0.752		0.001*
60 3D 27.3%	0.000*	0.000*	0.000*	0.000*	0.000*	

The only significant mean oesophageal difference was between the 3D plan (20.6Gy) and all the escalated plans (17.7-18Gy); however, dose to 1cc of the oesophagus was significantly higher for the 80Gy and 3D plans. All spinal cord and heart doses were below tolerance for the escalated plans.

Conclusion: Treatment intensification in NSCLC via targeted dose escalation with modern delivery techniques offers the potential for a significant increase in tumour control probability without a clinically significant increase in predicted OAR toxicity.

EP-1713

Dose-volume analysis of genitourinary toxicity in 3-D conformal radiotherapy for prostate cancer

P. Bagala[1], G. Ingrosso[1], M.D. Falco[1], S. Petrichella[2], M. D'andrea[3], M. Rago[1], A. Lancia[1], C. Bruni[1], E. Ponti[1], R. Santoni[1]

[1]*University of Rome Tor Vergata, Department Of Diagnostic Imaging- Molecular Imaging- Interventional Radiology and Radiotherapy, Rome, Italy*

[2]*Campus Bio-Medico, Computer Science and Bioinformatics Laboratory- Integrated Research Centre, Rome, Italy*

[3]*National Cancer Institute Regina Elena, Laboratory of Medical Physics and Expert Systems, Rome, Italy*

Purpose or Objective: We investigated the associations between acute and late genitourinary (grade ≥ 2) toxicity and clinical and dosimetric parameters in three-dimensional conformal radiotherapy for localized prostate cancer in order to carry out a dose-volume response evaluation. A dose-volume parameters analysis of the bladder of patients subjected to prostate cancer radiotherapy was reported.

Material and Methods: We considered 86 patients consecutively treated with high dose conformal image guided radiation therapy for localized prostate cancer. For the purpose of our analysis, we defined two bladder volumes: "whole bladder", i.e. the bladder in its entirely as a solid organ, and "inferior bladder", corresponding to the only distal part of the bladder. We carried out an univariate analysis between acute and late genitourinary toxicity and clinical parameters (age, "whole bladder" and "inferior bladder" volumes, smoking status, pre-radiotherapy urinary symptoms, hormonal therapy). We used the point biserial correlation coefficient to correlate dose-volume parameters (Vx) and genitourinary (grade≥ 2) toxicity. Finally, a fitting of the normal tissue complication probability (NTCP) cut-off volume model with toxicity data was performed.

Results: Mean follow-up was 51.9 months (range: 41.9–75.4 months). In 60 patients we observed an acute genitourinary toxicity (grade ≥2), while a late genitourinary toxicity (grade ≥2) was recorded in 6 patients. At univariate analysis, we found a correlation between acute genitourinary toxicity and smoking status ($P < 0.001$). Statistically significant associations ($P < 0.05$) between late genitourinary toxicity and Vx dose levels were calculated from 77 Gy and 77.5 Gy, for the "whole bladder" and the "inferior bladder", respectively. For acute toxicity, we found a statistically significant correlation with the dose of 80 Gy ($P < 0.05$), for both "whole bladder" and "inferior bladder". From the NTCP cut-off volume model we detected a bladder volume of 6 cc as the cut-off volume corresponding to a late genitourinary toxicity of 50% at doses ≥77 Gy.

Conclusion: Genitourinary toxicity seems to be correlated with bladder maximal doses, quantified as hotspots.

EP-1714

Hyper- versus hypofractionated radiotherapy in a radioresistant head and neck cancer model

L.G. Marcu[1], D. Marcu[1]

[1]*University of Oradea, Faculty of Science, Oradea, Romania*

Purpose or Objective: Cancer stem cells (CSCs) and hypoxia are known contributors of tumour resistance in radiotherapy. These parameters influence the radiotherapy schedule for optimal tumour control. Since hypofractionation is becoming increasingly popular among solid tumours, our aim is to evaluate the efficacy of hypo- versus hyperfractionated radiotherapy (RT) on hypoxic head and neck cancer (HNC).

Material and Methods: An *in silico* HNC was developed starting from a CSC. To grow a tumour with biologically valid parameters, the CSC generates all heterogeneous lineages of a tumour, with a probability of CSC symmetrical division 1.9%, mean cell cycle time 33h and volume doubling time 52 days. Pre-treatment CSC percentage is 5.9%. Four different fractionation schedules have been simulated as shown in Table 1. Hypoxic tumours with partial oxygen tension values ranging from 3 to 9 mmHg have been treated and tumour control assessed.

Table 1. Dose fractionation schedules simulated in current study

Radiotherapy schedule	Fractionation pattern
Conventional RT	2 Gy/day; 5 days a week; 7 weeks
Hypofractionated 5d RT	2.2 Gy/day; 5 days a week; 6 weeks
Hypofractionated 6d RT	2.2 Gy/day; 6 days a week; 5 weeks
Hyperfractionated RT	1.2 Gy/twice daily; 5 days a week; 7 weeks

Results: Treatment resistance is determined by the interplay between CSCs and hypoxia. While the modelled conventional and hypofractionated RT schedules are biologically equivalent, hypofractionation is more efficient on CSC kill than conventional treatment. However, for moderately hypoxic tumours (6 mmHg partial oxygen tension) (see figure 1) only hyperfractionated RT offers full control on CSC population within the clinically required treatment time. This observation might be explained by the advantage of two fractions a day through (i) overcoming tumour repopulation between consecutive doses, (ii) redistribution of surviving cells along the cycle; (iii) better reoxygenation. For each decrease in mmHg the number of fractions needed for tumour control increases exponentially. This behaviour is also influenced by the percentage of CSC, which changes during radiotherapy. Thus a tumour with a mean oxygen tension below 6 mmHg and a pre-treatment CSC population of 5.9% needs a greater than 84Gy dose (overall dose given via hyperfractionated RT) or the addition of adjuvant therapies in order to be eradicated.

Figure 1. Radiotherapy schedules for hypoxic HNC with 6 mmHg mean partial oxygen tension.

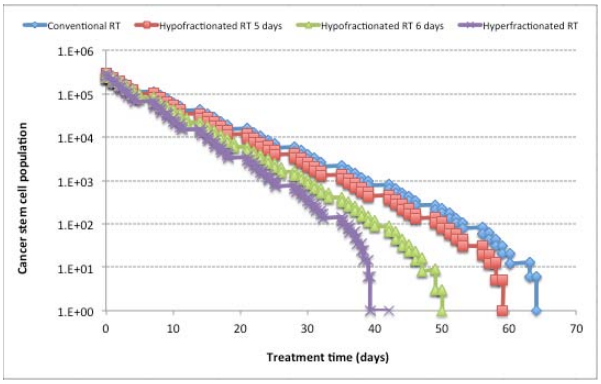

Conclusion: Hypoxic HNC are better controlled by hyperfractionated than by hypofractionated RT. However, oxic and mildly hypoxic tumours could benefit from hypofractionation, which reduces overall treatment time and normal tissue effects. The interplay between CSCs and hypoxia dictates the RT treatment strategy for optimal tumour control.

EP-1715

A Neural Network predictions and follow-up toxicity correlation to validate re-planning during RT

N. Maffei[1,2], G. Guidi[1,2], E. D'angelo[3], B. Meduri[3], P. Ceroni[1], G. Mistretta[1], A. Ciarmatori[1,2], G. Gottardi[1], P. Giacobazzi[3], T. Costi[1]

[1]*Az.Ospedaliero-Universitaria di Modena, Medical Physics, Modena, Italy*

[2]*University of Bologna, Physics and Astronomy, Bologna, Italy*

[3]*Az.Ospedaliero-Universitaria di Modena, Radiation Oncology, Modena, Italy*

Purpose or Objective: To correlate a Neural Network (NN) predictive model to clinical outcome of toxicities of patients undergone Radiation Therapy (RT). A re-plan strategy was evaluated highlighting challenges and advantage of an Adaptive RT (ART) workload. Clinical outcomes were assessed to validate an algorithm based on IGRT and deformable image registration.

Material and Methods: A cohort of 30 Head and Neck (H&N) patients, previously treated by Tomotherapy and CHT concomitant, was investigated: 19 male and 11 female [48÷89 years] with mean KPS index 95.5. To take into account inter-fractions organ warping, 900 pre-treatment MVCT study were deformed by RayStation and a dose accumulation analysis was performed. Exported data were used to train the predictive NN tool: a MATLAB toolbox developed to identify patients eligible for re-planning. Using a retrospective approach, the toxicity data were investigated with a mean follow-up period of 12 months. Weight (before and after RT), smoker number and toxicity information were considered. Correlation was assessed using SPSS statistic.

Results: Analysis on the follow-up DB showed that 74% of patients were affected by early toxicity: 40% (G1), 25% (G2) and 9% (G3); 41% by late toxicity: 30% (G1), 10% (G2) and 1% (G3). Correlating the medium-high grade of early toxicity with the dose of the event occurred, a 2nd order polynomial correlation was detected with a R2 value of 0.93 for G2 and 0.92 for G3.

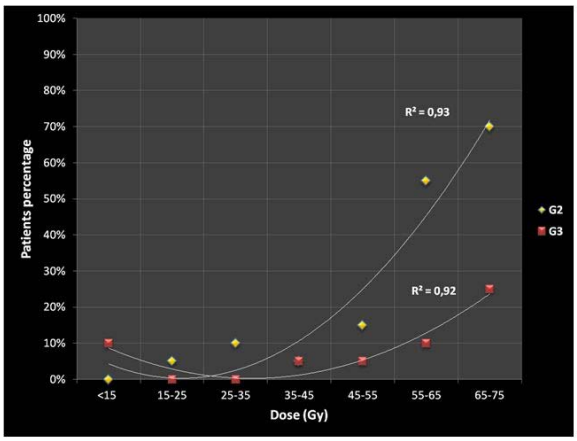

Figure 1 Patients percentage with an early toxicity of G2 (yellow rhombus) and G3 (red square) vs. Dose at which toxicity occurred during treatment.

The correlation of smoking and low toxicity (i.e. dysphagia, dysgeusia, mucositis, salivation) showed a mean G1 increased. An increased frequency of early (21%) and late (19%) toxicity was detected for smoker patients, with an ANOVA multivariate significance of 3.8% and 0.6% respectively. Simultaneously, a NN weekly method was carried out to follow and predict anatomical variations during RT. A benefit due to a review of the initial plan was estimated for 89.6% of patients. The need of re-planning was correlated with weight loss. 37% of patients do not need a re-plan and 25% of them had a weight loss <5%. 63% of patients would benefit for a re-plan: during the 2nd week for 25% of cases with a weight decrease <10%; during the 4th week for remaining 38% of cases (25% of them had a weight loss >10%).

		Week for Re-plan					
Weight loss (%)	No Re-plan	1	2	3	4	5	6
<5%	25%	0%	0%	0%	0%	0%	0%
5 - 10%	12%	0%	25%	0%	13%	0%	0%
>10%	0%	0%	0%	0%	25%	0%	0%
Total	**37%**	**0%**	**25%**	**0%**	**38%**	**0%**	**0%**

Table 2 Re-planning strategy suggested by NN outcome vs. normalized weight loss.

Conclusion: The machine learning approaches could support decision making in ART workload. Descriptive and inferential analysis showed a correlation between NN outcome and follow-up data, making robust the predictive approach based on organ warping and dose deformation. An increased number of cases have to be analyzed to train self-learning algorithm and to ensure personalization of patients' treatment. Patients with an abnormal weight loss, smoker and with a high dose delivered should be investigated to avoid early and late toxicities.

EP-1716

Prospective electronic toxicity registration to audit NTCP models and dose constraints

T. Janssen[1], A.L. Wolf[1], J. Knegjens[1], L. Moonen[1], J. Belderbos[1], J.J. Sonke[1], M. Verheij[1], C. Van Vliet-Vroegindeweij[1]

[1]*Netherlands Cancer Institute, Department of Radiation Oncology, Amsterdam, The Netherlands*

Purpose or Objective: In 2012 we started with the prospective, electronic registration by the treating physician of all grade≥2 toxicities (CTCAE v4.0) for all patients irradiated at our department. Simultaneously we set up an infrastructure to couple this data to dose and treatment parameters. The aim of this work is to show the feasibility of such an infrastructure to audit toxicity prediction models and dose constraints in daily clinical practice.

Material and Methods: As a showcase we consider the relation between the esophagus V50Gy and ≥2grade esophagitis in locally advanced NSCLC patients receiving concurrent chemoradiotherapy (CCRT; 24 x 2.75 Gy and daily 6mg/m2 cisplatin). Clinically we use the criterion V50Gy < 50% as a dose constraint based on a previously developed NTCP model (*Kwint et al. IJROBP 2012*). The applicability of this model to current daily clinical practice, however, is not evident since CCRT patients currently receive intravenous pre-hydration (1L, NaCl 0.9%) which was shown to decrease esophagitis (*Uyterlinde et al. R&O 2014*).
For all CCRT patients (excluding re-irradiations of the thoracic region) treated since January 2013, the planned V50Gy and the registered esophagitis grade 2 were automatically retrieved. Patients with toxicity registration in at least 50% of the consultations were included. We calculated the cumulative incidence of grade≥2 esophagitis per V50Gy and compared this with the expected incidence based upon the model by Kwint *et al.* using a x2 test. ROC analysis was performed to assess the predictive value of V50Gy.

Results: For 286 patients, a total of 1842 consultations were performed. The incidence of toxicity was electronically registered in 76% of these visits. For 229 patients (80%) the incidence of toxicity was registered in >50% of consultations. Median follow up was 3.5 months. A graphic comparison of the observed and predicted incidence of grade ≥2 esophagitis is shown in figure 1a. The observed incidence of grade≥2 esophagitis was 51.1% while the model predicts 52.1% (p=0.89). ROC analysis (figure 1b) resulted in an area under the curve of 0.69. To rule out a selection bias towards increased toxicity, the analysis was repeated for all 286 patients, assuming that no toxicity occurred for missing registrations, with very similar results.

fig. 1a: Observed (green) and predicted (red) cumulative incidence of grade 2+ esophagitis versus the V50Gy in the esophagus.

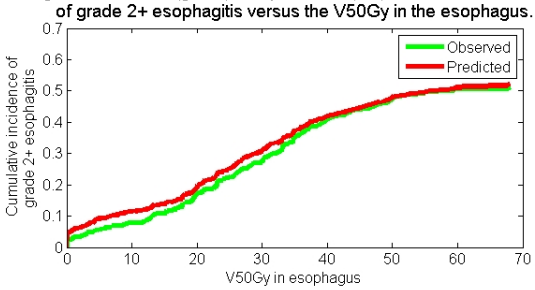

fig. 1b: ROC curve for the predictive value of the V50Gy for grade 2+ esophagitis

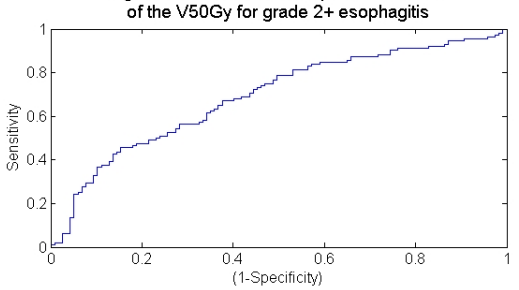

Conclusion: The observed and predicted dose-effect of grade ≥2 esophagitis were almost identical. This implies that our esophagus dose parameter accurately predicts toxicity for our current patient population and treatment protocol. This result is surprising, since esophagitis incidence was expected to decrease because of the introduced pre-hydration. While the origin of this discrepancy requires further investigation, it does show that the electronic toxicity scoring system and connection to the dose parameters appears to be a useful and valuable tool to audit the applicability of dose constraints in daily clinical practice.

EP-1717

Impact of radiation induced cell death kinetics on reoxygenation and tumour response.

A. Gago-Arias[1], I. Espinoza[1], B. Sánchez-Nieto[1], J. Pardo-Montero[2]
[1]*Pontificia Universidad Católica de Chile, Institute of Physics, Santiago, Chile*
[2]*Clinical University Hospital, Department of Medical Physics, Santiago de Compostela, Spain*

Purpose or Objective: The radiosensitivity of cells has an oxygen dependence that leads to an undesired resistance of hypoxic tumour cells. This is well known[1] and the linear quadratic response model has been extended to account for it.[2] In order to properly model tumour responses, the information about the distribution of oxygen at a microscopic scale must be available.[3] Modelling works usually derive this distribution by solving the reaction-diffusion equation in a voxelized tumour geometry that includes a vascularization distribution model.[4] However, the oxygen available to the cells increases during radiotherapy due to, among other factors, cell killing. This reoxygenation process can turn hypoxic cells into oxic, changing the cells radiosensitivity during the treatment. In this work we implement two models of cell death kinetics, CDKM, to analyse how they affect reoxygenation and hence the response of tumours to radiotherapy.

Material and Methods: Two CDKMs are compared:
a) Delayed cell killing model, DCDKM: The number of dead cells after irradiation varies with time according to an exponential expression. Cells can die shortly or long after irradiation, mimicking early and late apoptosis.
b) Instantaneous cell killing model, ICDKM: Cell death occurs immediately after irradiation (early apoptosis scenario).
Using these models, oxygen distributions are recomputed before the delivery of each fraction, considering the decrease in oxygen consumption due to cell death caused during the previous fractions. The oxygen consumption can be computed globally, by voxel averaging surviving fractions, or locally, at a subvoxel scale. The differences in reoxygenation and tumour response arising under different CDKM and oxygen consumption scenarios depend on the vascular fraction, VF, and the fractionation scheme. This was illustrated for a conventional schedule and a hypofractionated treatment.

Results: In the conventional treatment, the doses needed to achieve 50% tumour control (D50) are ~ 10 and 2 Gy larger under the ICDKM (for VFs of 1% and 3%, respectively). Differences are larger in the hypofractionated scheme, for which the TCP remains equal to zero under the DCDKM for a VF equal to 1%. For a VF equal to 3%, D50 values are ~ 20 Gy larger under the DCDKM. Similar results were found under the global and local oxygen consumption calculations.

Conclusion: This work shows that the kinetics of cell death can have a great impact in the simulation of reoxygenation and tumour response. Radiation response models should account for cell death kinetics to properly evaluate tumour response, especially in hypofractionated schemes.

References:
1. Moeller B. J. *et al.* Cancer Metastasis Rev. Vol. 26 pp: 241-8, 2007.
2. Wouters B. G. and Brown J. M. Radiat. Res. Vol. 147 pp: 541-50, 1997.
3. Petit S. F. *et al*. Phys. Med. Biol. Vol. 54 pp: 2179-96, 2009.
4. Espinoza I. *et al.* Med. Phys. Vol. 40, 081703, 2013.

EP-1718

Estimation of tumor radio-sensitivity using mathematical models and analysis of the oxygenation role

A. Belfatto[1], D.A. White[2], R.P. Mason[2], Z. Zhang[3], S. Stojadinovic[3], G. Baroni[1], P. Cerveri[1]
[1]*Politecnico di Milano University, DEIB, Milano, Italy*
[2]*The University of Texas Southwestern, Radiology, Dallas, USA*
[3]*The University of Texas Southwestern, Radiation Oncology, Dallas, USA*

Purpose or Objective: The project aims at predicting tumor radiation starting from pre-treatment information related to cancer volume and oxygenation.

Material and Methods: Eighteen Copenhagen rats, implanted with prostate tumor, underwent two irradiations (2x15Gy). Nine rats were treated in standard conditions (Air), while the remaining group (Oxy) inhaled oxygen. Before the first irradiation, an interleaved blood (BOLD) and tissue (TOLD) oxygen level dependent (IBT) MRI sequence was performed. Four indices were computed, namely, BOLD and TOLD signal intensity variation (dSI), and the change in longitudinal (dR1) and transverse (dR2*) relaxation rate. The tumor volume evolution was monitored by means of weekly caliper measurements. A two-equation system describing the uncontrolled growth and the response to treatment of the active cells population, along with the dead cell clearance dynamics, was implemented in Matlab® (MathWorks, Natick, Massachusetts, USA). Three parameters, namely the volume doubling time, the radiation sensitivity (α) and the dead cell clearance time, were learned on a subject-specific basis using a genetic algorithm. Finally, a feed forward neural network (FF-ANN) was trained (*Fig. 1*) to predict α starting from the MRI indices and initial volume, for each group (Air/Oxy).

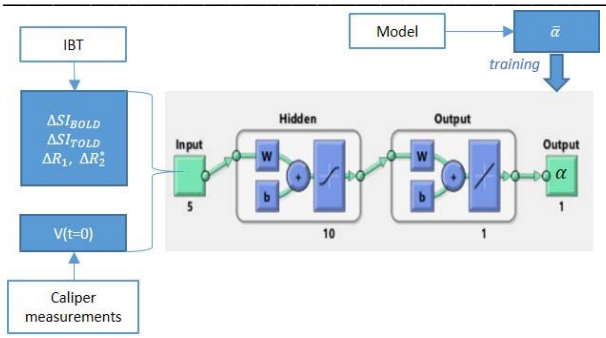

Fig 1. FF-ANN scheme.

Results: An inverse correlation of the radio-sensitivity parameter assessed by the model was found with respect the dR2* (-0.65) for the Oxy group. A further subdivision according to positive and negative values of dR2* showed a larger average radio-sensitivity for the Oxy rats with <0 and a significant difference in the two distributions according to the Wilcoxon-Mann-Whitney test ($p<0.05$). Finally, the Pearson correlation coefficient ($R^2>0.9$) revealed a strong agreement of the FF-ANN output with the target radio-sensitivity.

Conclusion: These preliminary findings support the hypothesis that the change in the R2* can be related to tumor oxygenation and, consequently, to its radio-sensitivity. In particular, the sign of the tendency is in accordance with the fact that an oxygenation increase reduces the tumor relaxation rate as reported in the literature. Moreover, the different distributions of α, outlined in the Oxy subgroups according to the dR2*, suggest that some subjects would benefit from oxygen inhalation more than others, reasonably due to their initial vascularization. Finally, the performance of the FF-ANN is promising, although it would require a larger dataset to validate its prediction ability.

EP-1719

Radiobiology based head & neck cancer protocol (FAMOSO) combining accelerated RT and EGFr inhibitor

D. Alterio[1], M. Cremonesi[2], C. Garibaldi[2], A.M. Ferrari[1], F. Botta[3], M. Ferrari[3], S. Vigorito[3], E. Rondi[3], F. Cattani[3], M. Cossu Rocca[4], L. Strigari[5], P. Pedicini[6], B.A. Jereczek-Fossa[7,8], R. Orecchia[8,9,10]

[1]*European Institute of Oncology, Radiation Oncology, Milano, Italy*

[2]*European Institute of Oncology, Radiation Research, Milano, Italy*

[3]*European Institute of Oncology, Medical Physics, Milano, Italy*

[4]*European Institute of Oncology, Medical Oncology, Milano, Italy*

[5]*Regina Elena National Cancer Institute, Medical Physics and Expert Systems-, Roma, Italy*

[6]*I.R.C.C.S.-C.R.O.B., Department of Radiation and Metabolic Therapies, Rionero in Vulture, Italy*

[7]*European Institute of Oncology and University of Milan, Radiation Oncology, Milano, Italy*

[8]*University of Milan, Radiation Oncology, Milan, Italy*

[9]*European Institute of Oncology, Medical Imaging and Radiation Sciences, Milano, Italy*

[10]*CNAO Centro Nazionale di Adroterapia Oncologica, Radiobiology, Pavia, Italy*

Purpose or Objective: Administration of monoclonal antibody Epidermal Growth Factor Receptor (MoAb-EGFr) inhibitor every week during Radiotherapy (RT) of head and neck cancer (HNC) has shown improved outcomes as compared to RT alone in terms of locoregional disease control, progression free and overall survival, thanks to its radiosensitizing effect. MoAb-EGFr concentration varies day by day after injection, and radiosensitizing effect accordingly. A radiobiological (RB) model accounting for this variation (Pedicini, et al. Radiat Oncol. 2012;7:143) can be applied to shorten the treatment by optimizing daily RT dose, still maintaining unchanged the biological effect on the tumour (in terms of surviving cells) as compared to standard RT (7 weeks, PTV1: GTV, 70Gy; PTV2 = GTV+margin, 63Gy; PTV3: lymph nodes: 58.1Gy) and potentially reducing healthy tissue toxicity. In this study, such RB model was adopted in the clinical protocol FAMOSO (Frazionamento Accelerato MOdulato in SIB-IMRT dei tumori testa-collO) for the treatment of HNC tumours with simultaneous integrated boost (SIB), aiming to test the feasibility of accelerated modulated fractioning and to assess toxicity and response rate.

Material and Methods: From literature data, showing that higher concentrations of MoAb-EGFr correspond to steeper tumor cell survival curves, radiobiological parameters were derived and included in the RB model to obtain the daily dose to be delivered to each target volume. To date, 2 of the 10 expected pts (pt1: cT4cN1 oropharyngeal; pt2: cT2 cN3 supraglottic squamous cell carcinoma) have been recruited and treated with SIB-IMRT with a curative intent.

Results: The RB model suggested a 6 week treatment with daily increasing dose/fractions as follows: PTV1: 1.70, 1.95, 2.15, 2.30, 2.35Gy; PTV2: 1.50, 1.75, 1.95, 2.05, 2.10Gy; PTV3: 1.40, 1.60, 1.80, 1.90, 1.95Gy. Both pts recruited in the FAMOSO protocol concluded the radiation treatment : pt1 with no change of the planned schedule; pt2 with interruption of MoAb-EGFr after the 5th administration and, consequently, the last 10 RT fractions of RT were administered with standard fractionation. The total dose to the PTV1 were 62.7 and 61.8 Gy, respectively. Maximun acute skin and mucosal toxicity was G3. With a follow up of 6 and 2 months, a partial response was obtained for pt1, while pt2 is still under evaluation.

Conclusion: New treatment strategies, even accelerated, are feasible when combining RT with radiosensitizing drugs. The RB model is adequate to set up the treatment provided radiobiological parameters are available from clinical data. The preliminary clinical data of the protocol FAMOSO give encouraging results, suggesting that the treatment schedule is feasible with acceptable acute toxicity. Longer follow up is needed to confirm toxicity findings and assess response rate, and of course more patients have to be studied.

EP-1720

Impact of contouring variability on tumour control and normal tissue toxicity in liver SBRT

M. Robinson[1], D. Eaton[2], R. Patel[2], D. Holyoake[1], M. Hawkins[1]

[1]*University of Oxford, Radiation Oncology, Oxford, United Kingdom*

[2]*National Radiotherapy Trials Quality Assurance Group, Mount Vernon Hospital, Northwood, United Kingdom*

Purpose or Objective: Variability in the contouring of gross tumour and the derived planning target volumes (PTVs) between clinicians is well-known in radiotherapy. This study aims to quantify the impact of variability in contouring in terms of tumour control and normal tissue toxicity in Liver SBRT.

Material and Methods: The National Radiotherapy Trials Quality Assurance (RTTQA) Group planning benchmark case for the ABC07 Trial was used (addition of stereotactic body radiotherapy to systemic chemotherapy in locally advanced biliary tract cancers; CRUK A18752, sponsor University College London). 12 centers performed contouring independently using radiotherapy trial protocol as per RTTQA pre-trial QA process. Each centre applied margins to derive PTV as per local practice. A standardised Volumetric Modulated Arc Therapy (VMAT) plan was produced based on gold standard contours and applied to all 12 sets of submitted contours aiming to deliver 50Gy in 5 fractions. However, due to large GTV this was unavoidably de-escalated to 40Gy to meet trial mandatory mean non-GTV Liver constraint. Tumour control was assessed through biologically effective dose (BED) to 98, 95 and 90% of the gold standard PTV. 65Gy BED, although disappointingly low for SBRT, was considered

as a cut off for acceptable therapeutic intent. NTCP modeling of radiation induced Liver disease was also performed.

Results: Non-GTV Liver mean dose ranged from 13.1 to 17.0Gy, breaching mandatory trial constraint of <15.2Gy in three cases. NTCP ranged from 0.0 to 0.3 assuming an alpha/beta of 1.0 for normal Liver and negligible assuming alpha/beta of 2.0 or more. At D98%, four sets of contours did not achieve 65Gy BED to gold standard PTV, two sets failing to reach 65Gy BED at D90%.

Conclusion: Significant variability exists in contours drawn by different centers/clinicians in the setting of pre-trial QA to the extent where 10% or more of the PTV receives a BED insufficient for local control in a proportion of cases and NTCP is significantly affected. Given this variability, the pre-trial and on-trial RTTQA process is essential if the effect of contour variability on tumour control rates and treatment toxicity is to be mitigated.

EP-1721

Feature extraction from duodenal dose surface maps to predict toxicity in pancreatic chemoradiation

A. Witztum[1], S. Warren[1], M. Partridge[1], M.A. Hawkins[1]
[1]*CRUK/MRC Oxford Institute for Radiation Oncology, University of Oxford, Oxford, United Kingdom*

Purpose or Objective: To use spatial features from dose surface maps of the duodenum to predict acute duodenal related toxicity in pancreatic chemoradiation.

Material and Methods: Dose surface maps were produced for the duodenum describing the spatial surface dose distribution. Traditional metrics were extracted including mean and max dose, surface area receiving 25, 35, 45 and 55 Gy as absolute and fraction of the surface. Spatial metrics extracted include the length of the duodenum which received less than 25, 35, 45 and 55 Gy to at least 10-90% of the circumference (in 10% intervals). Different thresholds for the length of the duodenum achieving these constraints were tested in order to find the best predictor of toxicity. Toxicity results from 19 patients from the ARCII clinical trial (EudraCT: 2008-006302-42) were used as a proof of concept. 6 and 11 patients had grade (Gr)and Gr ≥2 toxicity respectively.

Results: The best predictors for patients with grade (Gr)≥3 toxicity were at higher doses of 55 Gy. While restricting the dose < 55 Gy to at least 10% of the circumference for at least 10% of the length of the duodenum, or at least 20% of the circumference for at least 20% of the length accurately predicted toxicity for 74% of the patients studied, this only had a sensitivity of 17% and 33% respectively (specificity of 100% and 92%). Figure 1 indicates a better predictor may be restricting dose < 55 Gy to at least 20% of the circumference for at least 70% of the length which, although only accurately predicts toxicity for 58% of the patients, has a sensitivity and specificity of 67% and 54%. It was found that the relative percentage of the circumference spared was a better predictor than absolute circumferential length spared. However, similarly to the spatial metrics, predictions of patients with at least Gr 3 toxicity was seen in the higher dose regions such as mean dose of 60 Gy, maximum dose to a pixel of 62 Gy and when 70% of the surface area receives 55 Gy. Gr 2 toxicity could not be predicted.

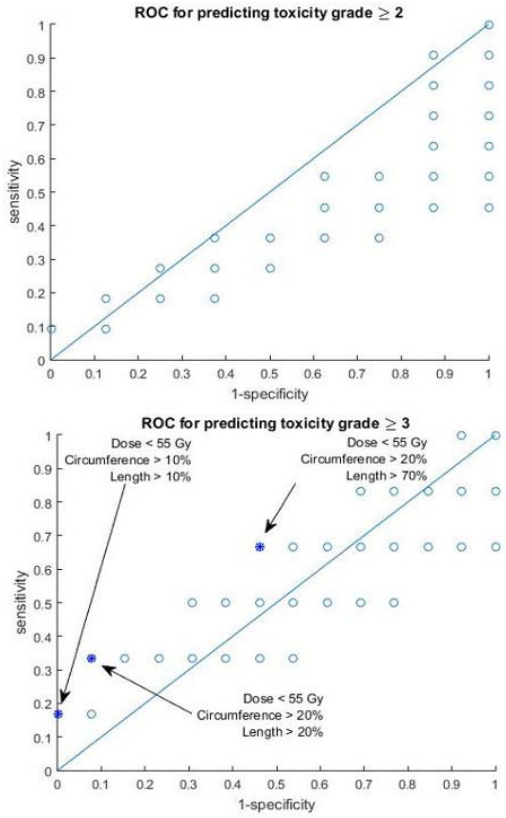

Figure 1: ROCs for grade ≥ 3 and grade ≥ 2 toxicity. Each point represents a different dose-surface feature and threshold that was tested.

Conclusion: In this small sample we have shown that spatial features can be extracted from dose surface maps to aid toxicity prediction, and that high doses to the duodenum appear to be correlated with Gr 3 toxicity. An improved understanding of how these spatial features correlate to toxicity can improve traditional constraints on the duodenum. Further work is required to build a more complete picture of this result, and the analysis will now be extended to a larger patient cohort.

EP-1722

Simulation of the radiation response of a hypoxic prostate tumor in the rat

I. Liedtke-Grau[1,2], R.O. Floca[3], P. Peschke[4], I. Espinoza[1], C.P. Karger[2]
[1]*Pontificia Universidad Católica de Chile, Institute of Physics, Santiago, Chile*
[2]*German Cancer Research Center DKFZ, Department of Medical Physics in Radiation Oncology, Heidelberg, Germany*
[3]*German Cancer Research Center DKFZ, Software Development for Integrated Diagnostics and Therapy, Heidelberg, Germany*
[4]*German Cancer Research Center DKFZ, Clinical Cooperation Unit Radiation Oncology, Heidelberg, Germany*

Purpose or Objective: In a previous work a model which simulates the radiation response of hypoxic tumors was developed. The task of this work is to validate the model by using preclinical experimental dose response data of rat prostate tumors for single and multiple irradiations.

Material and Methods: The model is voxel-based and simulates the spatio-temporal behavior of tumors considering six radio-biological processes. Important input data are the oxygenation levels of each tumor subvolume at the time of irradiation, which are given as pre-calculated oxygen frequency histograms.The experimental data for validation include growth curves, dose response curves and TCD50s for 1, 2 and 6-fraction (Fx) experiments. A very high α/β value of 84.7 ± 13.8 Gy was determined.A strategy of adjustment was

defined to fit the model to the experimental data in terms of growth curve, dose response curves, TCD50 and α/ß value.

Results: The experimental data are well described for an O2-independent response. For this case an α/ß of 74.7 ± 5.5 Gy was obtained.
When including the effects of O2, we aimed to reproduce this high experimental value starting from smaller intrinsic α/ß values. Unexpected shifts towards lower doses of the 2-Fx curves with respect to the 1-Fx curves were observed. This effect could be explained by a strong reoxygenation between the 1st and the 2nd Fx. Known reoxygenation mechanisms in the model include shrinkage, angiogenesis and the increase of available O2 due to the presence of dead cells. The latter was found to be the dominant mechanism of the three. When switching off these mechanisms, the unexpected shifts were still observed. A fourth reoxygenation mechanism, which is inherent to the original model, was identified. It implicitly arises by assuming that the distributions of cells at specific O2 levels remained the same after irradiation. To eliminate this effect, the histograms were updated to consider the actual O2 levels of the surviving cells. After doing so, the unexpected shifts of the curves were no longer observed and higher simulated values of α/ß were obtained.

Conclusion: This work constitutes the first stage of experimental validation with preclinical data of a computer model which simulates the radiation response of hypoxic tumors. It was confirmed that reoxygenation plays an important role in the dose response of tumors. Additionally, important information on how to further improve the model was gathered.

EP-1723

Radiobiological analysis of rib fracture incidence in lung SABR

A. Carver[1], J. Uzan[1], C. Eswar[1], A. Pope[1], A. Haridass[1]
[1]*The Clatterbridge Cancer Centre - Wirral NHS Foundation Trust, Department of Clinical Physics, Bebington- Wirral, United Kingdom*

Purpose or Objective: SABR (Stereotactic Ablative Radiotherapy) is only possible in a subset of patients with small tumors and favourable anatomy as the very high BED increases the risk of complications. Lung SABR is often delivered to tumors that are more peripheral thus; the ribs are structures now exposed to significantly higher doses than historically has been the case. The first fifty-two SABR (Stereotactic Ablative Radiotherapy) patients treated at our centre were monitored for rib fracture and chest pain. In this study, we fit the data to the LKB model of normal tissue response.

Material and Methods: Fifty-two patients were treated with either, 55 Gy in 5# (40 patients), 60 Gy in 8# (6 patients) or 54 Gy in 3# (6 patients) depending on the size and location of the tumor. For each patient a chest wall volume was delineated. The chest wall volume encompassed the rib and chest wall between the ribs. Data were fitted to the Lyman-Kutcher-Burman (LKB) model, a model using the normal cumulative density function to produce a sigmoidal dose response curve. The model consists of three parameters TD50, which determines the dose at which 50% of treatments will result in a complication, m which governs and slope and the volume parameter, n. We assumed α/ß = 3 Gy.

Results: Of the 52 patients there were 5 occurrences of rib fracture (NTCP = 9.6% -6.4%/+11.4%). Leaving the volume parameter free in the fit produced best-fit parameters of n = 0.01, TD50 = 370 Gy and m = 0.45. Due to the small NTCP it is difficult to extrapolate to find TD50. This is shown graphically in Figure 1; a small change in the slope will have a very large effect on the point at which the NTCP is equal to 50%. Consequently, the uncertainties were large, n could not be constrained although very small values were preferred. At 95% confidence TD50 > 220 Gy and m>0.2, assuming that rib fracture is approximately a serial complication. Figure 1 shows the correlation between TD50 and m at the best-fit value of the volume parameter.

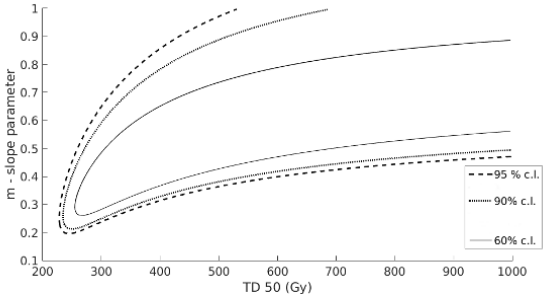

Conclusion: We conclude that the rate of rib fracture is relatively low (<10%) in SABR patients. NTCP modelling suggests that a very low volume parameter is most consistent with the data. This is in agreement with what might be naively expected. Due to small number of patients and events analysed to date it is not possible to constrain parameters tightly. This may be helped be re-parameterising the curve. We are now studying the effects of low absolute NTCP values and physically bounded parameters on the confidence intervals.

EP-1724

Model-based effect estimates reduce sample-size requirements in randomized trials of proton therapy

A.L. Appelt[1], S.M. Bentzen[2], I.R. Vogelius[1]
[1]*Rigshospitalet, Department of Oncology, Copenhagen, Denmark*
[2]*University of Maryland School of Medicine, Division of Biostatistics and Bioinformatics- University of Maryland Greenebaum Cancer Center- and Department of Epidemiology and Public Health, Baltimore, USA*

Purpose or Objective: Standard power calculation methods for randomized trials do not account for patient-to-patient differences in effect of novel radiotherapy (RT) techniques. The expected advantage of a new technique can often be related to heterogeneous dose metrics in individual patients. Here, we investigate if model-based outcome assessment can affect sample size requirements for a randomized trial of proton versus photon RT for lung cancer with reduction of severe radiation-induced lung toxicity (RILT) as primary endpoint.

Material and Methods: We estimated the number of patients needed to demonstrate an advantage of proton versus photon RT in a randomized trial, with α=0.05 and 80% power. We simulated outcomes using Weibull survival distributions with baseline probability of freedom from RITL at 2 years of 85% for patients without clinical risk factors. Heterogeneous gain from proton therapy was quantified by change in mean lung dose (ΔMLD), randomly normally distributed in the proton arm with mean 4.2 Gy and s.d. 2.1 Gy. ΔMLD values were translated into hazard ratios (HR) using the QUANTEC dose-response relationship, adjusted for clinical prognostic factors (comorbidity, tumour location, smoking status, age) evenly distributed between the trial arms. Simulated follow-up was distributed over a time period of 2 years. Monte Carlo simulations (3000 per data point) were used to assess trial power. Sample size estimates were calculated as follows: *Standard:* Comparison of treatment arms using log-rank statistics; and *Model-based:* Cox proportional hazards regression fitted to the change in dosimetric predictor, here ΔMLD. The consequence of a misspecified dose metric was assessed by assuming an underlying true effect metric that was correlated to, but not equal to, ΔMLD.

Results: Sample size estimates differed considerably for the two approaches; see **Table 1**. 744 patients were needed to show the advantage of proton versus photon RT with standard comparison of trial arms, while superiority of protons based on a direct fit to the effect metric (ΔMLD) required only 549 patients. The advantage of using the model-based method

was maintained as long as the effect metric used for Cox regression had a linear correlation with the true effect metric of at least 0.50. The conclusions held if the trial cohort consisted of an expected high benefit population (22% reduced sample size), but the effect was even stronger if the cohort was a population with modest expected benefit (31% reduced sample size).

	Estimated trial size
Standard population	
ΔMLD=4.2 Gy, s.d. 2 Gy, normal risk factor prevalence	
Standard (log-rank)	744 patients
Model-based (Cox regression to ΔMLD)	549 patients
Model-based (misspecified effect metric, correlation 0.80)	614 patients
Model-based (misspecified effect metric, correlation 0.50)	743 patients
High benefit population	
ΔMLD=5.8 Gy, s.d. 2 .7 Gy high risk factor prevalence	
Standard (log-rank)	218 patients
Model-based (Cox regression to ΔMLD)	169 patients
Low benefit population	
ΔMLD=2.6 Gy, s.d. 1.3 Gy, low risk factor prevalence	
Standard (log-rank)	2300 patients
Model-based (Cox regression to ΔMLD)	1587 patients

Table 1: Standard trial design (log-rank statistics) compared to model based Cox regression. Risk factors included were: pre-existing pulmonary co-morbidity (HR = 2.27), mid or inferior tumour location (HR = 1.87), current smoker (HR = 0.62), and old age (HR =1.66). The consequences of a misspecified effect metric were examined for correlations ranging from 0.95 to 0.45; example results are .shown.

Conclusion: We have demonstrated that the required patient sample size for randomized trials in radiation oncology may be considerably reduced by taking heterogeneous dose-effect into account. Dual planning provides support for the statistical outcome modelling that increases trial power even if the dose-response model is moderately misspecified. The outcome of a trial in the example studied would be a randomized measure of 'benefit per Gy ΔMLD' with confidence interval.

EP-1725

Predictors of diarrhea after whole-pelvis post-prostatectomy radiotherapy

C. Sini[1], C. Fiorino[2], L. Perna[2], B. Noris Chiorda[3], V. Sacco[3], M. Pasetti[3], A. Chiara[3], R. Calandrino[2], N. Di Muzio[3], C. Cozzarini[3]

[1]*Fondazione Centro San Raffaele, Medical Physics, Milano, Italy*

[2]*San Raffaele Scientific Institute, Medical Physics, Milan, Italy*

[3]*San Raffaele Scientific Institute, Radiotherapy, Milan, Italy*

Purpose or Objective: Gastrointestinal (GI) toxicity is a side-effect induced by whole pelvis intensity modulated radiotherapy (WP-IMRT), affecting importantly patients' quality of life. The aim of this study was to identify predictors of diarrhea in a cohort of chemo-naïve patients treated with WP-IMRT after prostatectomy.

Material and Methods: The Inflammatory Bowel Disease questionnaire (IBDQ) was used to assess the degree of GI symptoms after WP-IMRT, investigating 4 distinct areas: bowel and systemic symptoms, emotional and social functions. This study focused on the most clinically relevant item 5 relative to the bowel domain, in order to evaluate the frequency of liquid defecation. Patient-reported scores at baseline, at RT mid-point and end, and every 3 months after RT end were prospectively collected . The responses are scored on a 7-point scale where 7 corresponds to the best function and 1 to the worst. Clinical/dosimetric data in 115 patients treated with adjuvant (n=65) or salvage (n=50) WPRT in a single Institute were available (static field IMRT:19; VMAT:55; Tomotherapy:41). Dose-volume histograms (DVHs) for intestinal loops and sigmoid colon were calculated. The 25th percentile of the score variation between baseline and half/end RT was considered as end-point (Δ -IBDQ5≤-3). Associations between diarrhea and clinical/DVH parameters were assessed by logistic uni- and backward multi-variable analyses. A previously introduced method based on DVH differences between patients with/without diarrhea toxicity was used to select the most discriminative DVH parameters.

Results: No significant correlation emerged for sigmoid colon, then the analysis was focused on intestinal loops. Patients without basal score and with -IBDQ5≤-3 were excluded from the analysis: 23/77 pts showed acute GI toxicity. At univariate analysis, volumes receiving 5 to 40Gy (V5-V40) were correlated with -IBDQ5≤- 3 ($p<0.03$). Multivariate analysis confirmed a leading role of dosimetric variables, while no significant correlation for clinical parameters was found. Best cut-off values (assessed by ROC) discriminating patients with/without -IBDQ5≤-3 were: V20<250cc, V30<150cc and V40<90cc. The overall incidence equal to 10% and 50% resulted for the group of patients with DVH parameters lower/higher than thresholds, respectively ($p=0.0028$, OR=4.9, AUC=0.68).

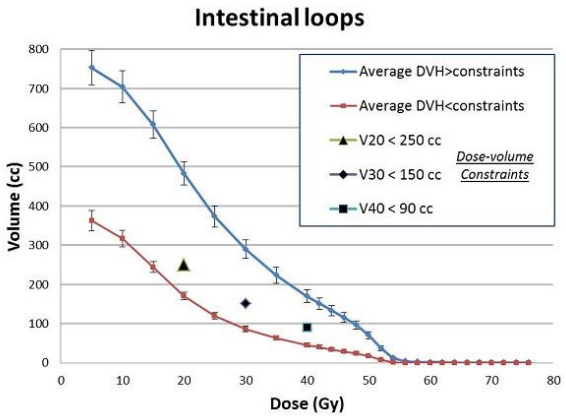

Conclusion: Low-medium IMRT doses to intestinal loops were correlated to diarrhea symptom at half/end of RT. This study proposed new dose volume constraints, that may be used to prevent much radiation-induced GI morbidity.

EP-1726

Biological modelling to identify proton therapy candidates in focal boosting of prostate tumours

J. Pedersen[1], O. Casares-Magaz[1], J. B. B. Petersen[1], J. Rørvik[2], L. Bentzen[3], P. R. Poulsen[1], A. G. Andersen[1], L. P. Muren[1]

[1]*Aarhus University Hospital, Department of Medical Physics, Aarhus C, Denmark*

[2]*Haukeland University Hospital, Department of Radiology, Bergen, Norway*

[3]*Aarhus University Hospital, Department of Oncology, Aarhus C, Denmark*

Purpose or Objective: MRI-based focal tumour boosting is currently under clinical investigation for prostate cancer patients, e.g. in the FLAME trial. These highly conformal, focal dose distributions can be difficult to achieve with photons, depending on the size and location of the boost volume (i.e. proximity to critical organs at risk). Selected patients might therefore be candidates for proton therapy. In previous work we have established an MRI-based tumour control probability (TCP) model. Combined with published rectum and bladder normal tissue complication probability (NTCP) models we have in this study explored the use of biological (TCP and NTCP) models to identify prostate cancer patients that might be suitable candidates for proton therapy if treated according to FLAME-like trial protocols.

Material and Methods: CT scans of seven patients from a prospective trial in our institution were used for planning. To obtain realistic boost geometries, MRI-based index tumours from a different cohort were used (matched on prostate volume), propagated with rigid registration on the prostate volume. VMAT plans (Eclipse, Varian Medical Systems) with and without a boost to the index lesion (95 Gy / 35 fx) were created; both plans delivered a conventional dose (77 Gy / 35

fx) to the non-involved prostate. Planning constraints used were based on institutional procedures as well as from the FLAME trial, with small modifications in the boost plans. The dose distributions (with/without boost) were used to calculate the TCP and NTCP values for each patient. The TCP model used apparent diffusion coefficient maps to estimate cell densities while the NTCP models used were the conventional Lyman model for the rectum (late rectal bleeding grade >= 2; Rad. Onc, 73, 21-32, 2004) and the Poisson LQ model for the bladder (contracture; Ågren PhD thesis, 1995).

Results: The TCP increased from a median (range) of 0.45 (0.08-0.83) with the conventional approach to 1.0 (no range) with the focal boost. While there were only minor differences in the rectum NTCPs with vs. without the boost there were considerable differences in the NTCP for the bladder for two of the patients (more than a doubling of the NTCP with the boost; Table 1). These two patients had the index lesion that was closest to the bladder.

Table 1: NTCP values for each patient for rectum and bladder. First value is with boost, second value without boost.

	Rectum		Bladder	
Patient	**With boost**	**Without boost**	**With boost**	**Without boost**
Patient 1	1%	1%	12%	5%
Patient 2	1%	1%	3%	1%
Patient 3	1%	1%	1%	0%
Patient 4	1%	2%	8%	4%
Patient 5	2%	3%	4%	2%
Patient 6	2%	2%	1%	0%
Patient 7	2%	2%	0%	0%

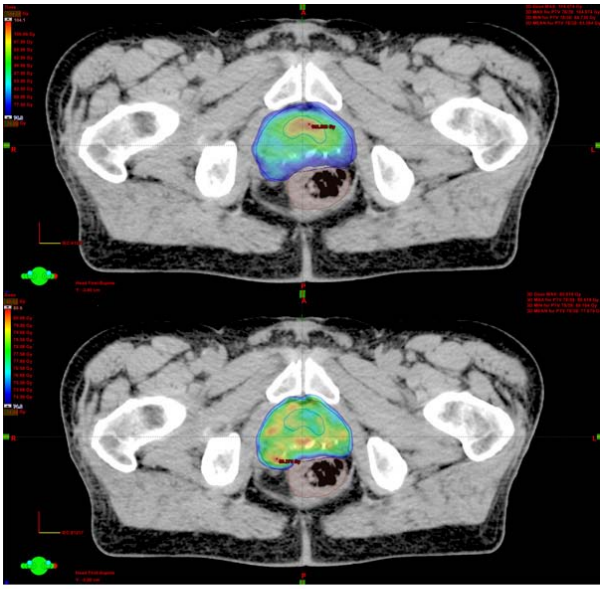

Figure 1: The upper part of the figure shows the dose distribution for one patient with the tumour boost (the index lesion is the peanut shaped delineation inside the PTV of the prostate). The dose color wash range is between 74 Gy and the max dose, which is 104 Gy.
The lower part of the figure shows the same view of the same patient without the boost arm, but conventional treatment. The dose color wash range is between 74 Gy and the max dose, which is 81 Gy.

Conclusion: We have established a biological modelling based method to identify prostate cancer patients where the focal boost cannot be achieved with state of the art photon-based treatment without a considerable increase in the NTCPs. Further work will consider the feasibility of proton planning, given both inter- and intra-fractional organ motion patterns.

EP-1727

A decision support system for localised prostate cancer treated by external beam radiation therapy

S. Walsh[1], M. Field[2], M. Barakat[2], L. Holloway[3], M. Bailey[4], M. Carolan[4], G. Goozee[3], G. Delaney[3], A. Miller[4], M. Sidhom[3], P. Lambin[1], D. Thwaites[2], A. Dekker[1]
[1]MAASTRO clinic, Knowledge Engineering, Maastricht, The Netherlands
[2]University of Sydney, Medical Physics, Sydney, Australia
[3]Ingham Institute, Medical Physics, Sydney, Australia
[4]Illawarra Cancer Care Centre, Medical Physocs, Wollongong, Australia

Purpose or Objective: This study presents a universally applicable decision support system (DSS), with respect to the prediction of five-year biological no evidence of disease (5y-bNED) for localised prostate cancer (PCa) patients treated by external beam radiation therapy (EBRT).

Material and Methods: To develop a DSS this study utilised the traditional approach of model training based upon meta-analysis data (MAD: n=5218) from the literature with model validation based upon routine clinical care data (CCD: n=827) from clinics with a rapid learning healthcare (RLHC) environment. The following standard clinical features for PCa patients were investigated to train and validate a tumour control probability model (TCP) and a predictive machine learning model (PML): primary tumour stage (T), lymph node stage (N), metastasis stage (M), prostate specific antigen (PSA), Gleason score (GS), clinical-target-volume (CTV), total dose (D), and fractional dose (d). These features were selected as they are typically known within all clinics treating PCa patients, thus maximising the generalizability of the DSS.

Results: The DSS is comprised of two distinct models. The TCP model was found to be well calibrated with poor discriminative ability. Training resulted in an adjusted weighted R2 value of 0.76, a weighted mean absolute residual (wMAR) of 4.7% and an area under the curve (AUC) of 0.67 [0.65, 0.69]. Validation resulted in an adjusted weighted R2 value of 0.51, a wMAR of 2.0% and an AUC of 0.57 [0.51, 0.63]. Contrastingly, the PML model was found to be poorly calibrated with good discriminative ability. Training resulted in an adjusted weighted R2 value of 0.27, a wMAR of 8.3% and an AUC of 0.66 [0.64, 0.68]. Validation resulted in an adjusted weighted R2 value of 0.90, a wMAR of 16.2% and an AUC of 0.61 [0.56, 0.65]. Subset analysis shows that the DSS performs best in high-risk PCa patients with validation resulting in an AUC of 0.66 [60, 0.72] with a wMAR of 1.0%.

Conclusion: A DSS developed with MAD has been validated in CCD extracted using RLHC infrastructure. The DSS uses standard clinical features to estimate with good accuracy (wMAR < 4.7%) and reasonable fidelity (AUC > 0.61) the 5y-bNED rate and classification, respectively, of PCa patients. The performance of the DSS in the validation high-risk PCa cohort (wMAR = 1%) and patients (AUC = 0.66) for whom therapy could be potentially adapted or individualised based on the DSS has clinical relevance and should be prospectively validated.

EP-1728

Dose individualisation through biologically-based treatment planning for prostate cancer patients

E. Gargioni[1], P. Mehta[1], A. Raabe[1], R. Schwarz[1], C. Petersen[1]
[1]University Medical Center Hamburg - Eppendorf UKE, Department of Radiology and Radiotherapy, Hamburg, Germany

Purpose or Objective: The use of biological information on tumour control and normal-tissue complications for treatment plan optimisation can be used for individualising the dose prescription. For patients with prostate cancer, moreover, the tumour localisation by means of MR-images facilitates the use of such information for a simultaneous dose escalation in the so-called dominant intraprostatic lesions (DIL), thus further improving the treatment outcomes. However, a correct modelling of the tumour-control

probability depends on the accuracy of the alpha-beta ratio for prostate cancer, the value of which is still a matter of discussion in the scientific community. Therefore various scenarios should be investigated for understanding the limits of the biologically-based dose escalation to the tumour during prostate radiotherapy.

Material and Methods: This work investigates the potential and limits of biologically-based treatment planning for ten prostate-cancer patients with localised disease in the case of alpha-beta-ratios of 1.5 Gy, 3 Gy, and 4.5 Gy, respectively. The MR images of these patients were used for contouring the intraprostatic lesion as GTV and were matched with the CT images in EclipseTM. Biologically-based 7-fields IMRT plans were optimised by minimising the NTCP for rectal bleeding and bladder contracture and by maximising the TCP for the GTV. For all patients, the dose prescription for the PTV (whole prostate) was 72 Gy in 40 fractions.

Results: The results of this plan-comparison study show that the individual GTV dose coverage depends on the alpha-beta ratio for prostate cancer, while the calculated dose distribution (in particular the mean dose values and the D3%) for rectum and bladder are not influenced by this parameter. Also, the total dose to the GTV could be individually optimised and varied between 76 Gy and 87 Gy, depending on the position of the DIL within the prostate. Finally, the optimised total dose to the GTV increased when modelling the TCP with a lower alpha-beta ratio, with individual differences up to 3 Gy.

Conclusion: Biologically-based optimisation tools allow for individualised dose escalation in dominant intraprostatic lesions and, in principle, could be safely used for the treatment planning of prostate cancer. In fact, a variation of the alpha-beta ratio for prostate cancer between 1.5 Gy and 4.5 Gy causes a variation of the dose coverage of the GTV of up to about 3 Gy in total, thus showing an acceptable robustness of the TCP model with respect to this parameter. Biologically-based optimisation tools, finally, have the advantage of reducing optimisation time, contouring process, and dose hot spots. Studies are currently being carried out in order to further validate the TCP and NTCP models for prostate cancer treatment in the case of hypofractionated schedules.

Electronic Poster: Physics track: Intra-fraction motion management

EP-1729

The impact of CBCT-imaging and verification time on prostate motion using 4D TPUS Clarity system

P.P.E. Pang[1,2], K. Knight[2], M. Baird[2], H.S.A. Boo[1], M.Q.J. Loh[1], W.S.J. Chan[1], S.N. Aryani[1], K.L.J. Tuan[1]
[1]*National Cancer Centre Singapore, Division of Radiation Oncology, Singapore, Singapore*
[2]*Monash University, Faculty of Medicine, Nursing and Health Sciences- Department of Medical Imaging & Radiation Sciences, Melbourne*

Purpose or Objective: Accuracy of radiotherapy to the prostate is often challenged by geometrical uncertainties due to inherent organ motion attributed to daily variations of the bladder and rectal volumes and contents. This study aims to simulate the use of 4D Clarity ultrasound image guidance without CBCT imaging to analyse the magnitude and trend of prostate motion during treatment (74Gy given in 37 fractions). The impact of CBCT imaging and verification time on prostate motion will be analysed.

Material and Methods: 175 intra-fraction monitoring sessions from 5 patients who underwent radical prostate volumetric modulated arc therapy (VMAT) monitored using 4D transperineal ultrasound scan (TPUS) resulted in a total of 1461.2min of data (184,085 positioning points) being analysed. All patients were instructed to comply with a full bladder protocol (i.e. 300-450ml in 30-45min) without specific rectal preparation protocol. Mean prostate motion was calculated and analysed in relation to time in the subsequent fractions. Overall treatment time was defined from acquisition of CBCT to treatment beam off time and imaging time was defined from time of CBCT acquisition to first beam on. Imaging time was subtracted from the overall treatment time for analysis of prostate motion without CBCT for verification. The remaining duration was representative of treatment time using 4D Clarity ultrasound image guidance alone. The impact of CBCT imaging and verification time on prostate motion was analysed.

Results: Mean (median) imaging and overall treatment time was 4.6min (4.4 min) and 8.4min (8.3 min) respectively. Mean (median) prostate motion during overall treatment time was 0.7mm (0.6mm) Inf, 1.0mm (0.9mm) Post and 0.1mm (0.2mm) Lt respectively. Mean prostate motion without CBCT was 0.6mm (0.5mm) Inf, 0.9mm (0.8mm) Post and 0.1mm (0.1mm) Lt. Figure 1 demonstrates the observed prostate displacement over time in a single session from one of the patients. In general, the mean (median) maximum prostate drift during actual treatment alone tends to trend towards the following directions at 3.6mm (3.4mm) Inf, 7.4mm (5.2mm) Ant and 2.7mm (2.8mm) Lt. Magnitude of the median maximum prostate displacement increased relatively by 38.4%, 16.7% and 46.6% in the Inf, Ant and Lt directions respectively with added imaging time.

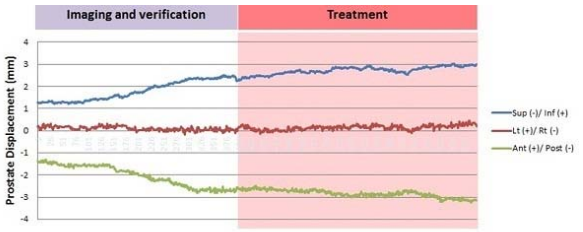

Figure 1: Demonstrates the observed prostate displacement over time.

Conclusion: Prolonged overall treatment time due to CBCT imaging and verification time increases the intra-fraction prostate motion. We propose the use of 4D Clarity TPUS in place of TPUS with CBCT to reduce imaging time before radiotherapy to reduced total verification time leading to reduced prostate movement. Consequently, the magnitude of intra-fraction prostate motion could be reduced from reduced image acquisition and reconstruction time. This reduces the total in room time per patient and maximises patient through-put and treatment efficiency which is important in a busy radiotherapy centre.

EP-1730

Clinical evaluation of new approach for determining ITV target volume in NSCLC treated with 4D SABR

X. Li[1], Q.H. Deng[1], L.D. Zhang[2], B. Xia[2], Z.B. Wu[1], Y. Ren[2], J. Gu[2], Z.S. Zheng[2], S.L. Ma[1], G. Li[3]
[1]*The First People's Hospital of Hangzhou, Radiation Oncology, Hangzhou, China*
[2]*Hang Zhou Tumor Hospital of Zhejiang Province, Radiological Physics, Hangzhou, China*
[3]*Xiaoshan Hospital of Zhejiang, Radiological Physics, Hangzhou, China*

Purpose or Objective: To investigate the Geometric difference between six different ITVx delineation methods from 4D-CT
for patients with Non Small Cell Lung Cancer (NSCLC) treated with Stereotactic Ablative Radiotherapy
(SABR) technique.

Material and Methods: Between December 2013 and March 2014, 46 patients who underwent SABR were includedin
this retrospective study. All patients underwent imaging acquisition with 4D-CT scans, The tu-
mor motion range, volume , marching index (MI) and encompassment index (EI) of ITV10, IT-

VYeo, ITVEI+EE(End of Inspiration + End of Expiration), ITVODD (delineated from five odd p-hases), ITVEVEN (delineated from five even phases), ITVAVG (Average sequences) , and IT-VMIP (Maximum Intensity Projection sequences) were calculated and evaluated, finally, a me-
thod , which was not sensitive to the tumor volume and motion characteristic was selected
for clinical use.

Results: The mean tumor motion (RLR, RAP, RCC, and R3D) were
3.5mm(1.4mm~8.4mm), 4.5mm(1.1mm~8.6mm), 9.5mm(0m m~10mm),12.3mm (2.5-55.3 mm) respectively. Compared with ITV10, the volume of ITVx were underestimated by25.7%、35.6%、17.9%、12.8%、3.6%、4.8% (P=0.000) respectively. MI comparisons between six ITVx delineation methods and ITV10 had statistical significance: 0.69、0.62、0.80、0.86、0.93、0.91（P=0.006） EI showed no statistical significance: 0.98、0.98、0.97、0.97、0.99、0.98（P=0.13）, the tumor volume and motion amplitude were certified not the independent factors for the MI of ITVODD and ITVEVEN.

	Range	Mean±SD	Comparison	P value
RVI _ITVMIP	0.53-0.91	0.74±0.12	ITV10 - ITVMIP	0.00
RVI _ITVAVG	0.36-0.88	0.64±0.13	ITV10 - ITVAVG	0.00
RVI _ITVIE+EE	0.71-0.88	0.82±0.51	ITV10 - ITVIE+EE	0.00
RVI _ITVyeo	0.75-0.95	0.87±0.06	ITV10 - ITVyeo	0.00
RVI _ITVODD	0.88-0.98	0.97±0.02	ITV10 - ITVODD	0.53
RVI _ITVEVEN	0.83-0.96	0.95±0.04	ITV10 - ITVEVEN	0.17

Conclusion: ITVODD/EVEN was not sensitive to tumor size or motion characteristic and was proved to have a good marching with ITV10 meanwhile having a relative high contouring efficiency, it can be recommend as a
universal ITV delineation method to the institutions which was not equipped with the deformable registr-
ation systems.Introduction

EP-1731

Changes of the prostate motion errors in the intra-fraction early phase for prostate cancer patients

H. Tamamura[1], T. Kaneda[2], Y. Ogawa[2], M. Shibata[2], T. Kobayashi[3], A. Hirata[3]
[1]*Fukui Prefectural Hospital, Nuclear Medicine, Fukui, Japan*
[2]*Fukui Prefectural Hospital, Radiology, Fukui, Japan*
[3]*Fukui Prefectural Hospital, Urology, Fukui, Japan*

Purpose or Objective: In recent years, 3DCRT and IMRT have been used frequently as a treatment approach for prostate cancer patients. In particular, there is a tendency that a short-term treatment is performed with the use of a high dose rate machine. For this reason, even a small movement of the intra-fraction prostate motion error is also important. In this study, we divided one time of irradiation of 3DCRT and IMRT into 2 stages, i.e., the early phase and the late phase, and examined the intra-fraction prostate motion errors in a single irradiation.

Material and Methods: A total of 154 patients with prostate cancer were treated from January 2005 to December 2013. Three gold markers were inserted into their prostate gland before starting radiotherapy. Patients treated with 3DCRT (88 pts) were fixed at their lower limbs using HF-A (TOYO MEDIC) in the supine position, and those treated with IMRT (66 pts) were secured their whole body using MOLDCARE RI II (ALCARE). We measured the travel distance of the center of gravity of the three gold markers in the prostate gland using the real-time tumor tracking system. We defined the travel distance of the first half (the early phase) and latter half (the later phase) of the intra-fraction prostate motion errors right after the initiation of irradiation. In addition, we analyzed the differences caused by the fixation methods (fixture).

Results: A total of 9,750 times of irradiation (3DCRT：4,732; IMRT：5,018) were analyzed in this study. The overall duration of daily irradiation was 13.83±2.24 minutes. The travel distance of the prostate was 1.50±1.13 mm in the entire one time irradiation, 1.75±1.21 mm in the early phase, and 1.24±0.98 mm in the later phase. The statistical analysis using the Bonferroni method showed a significant difference between the both phases ($p<0.001$). The intra-fractional prostate motion errors in the early phase were 1.96±1.36 mm by 3DCRT and 1.55±1.01 mm by IMRT. A significant difference was observed in the intra-fractional prostate motion errors in the early phase between two fixation methods. In contrast, the intra-fraction prostate motion errors in the later phase were almost equal regardless of the fixation methods.

Conclusion: The temporal movement of the prostate during daily irradiation becomes larger in the early phase of irradiation, and this result is influenced by the set-up methods and the patient fixing devices. Since the dose gradient is steep in 3DCRT and IMRT, even a minimal movement of the prostate associated with the intra-fraction prostate motion errors is likely to cause a fatal irradiation error of a high dose rate machine. Therefore, the movement of the prostate in the early phase would require careful attention in the treatment of prostate cancer patients.

EP-1732

Quantitative estimation of gamma passing rates from characteristics of respiratory motion

K. Tanaka[1], M. Nakamura[2], K. Fukumoto[1], T. Kosuga[1], M. Yanagawa[1], A. Miyai[1], S. Tachiiri[3], S. Otsu[3], K. Kuwabara[1]
[1]*Kyoto City Hospital, Department of Radiology, Kyoto, Japan*
[2]*Kyoto University, Department of Radiotherapy, Kyoto, Japan*
[3]*Kyoto City Hospital, Department of Radiation Oncology, Kyoto, Japan*

Purpose or Objective: The purpose of this study is to quantitatively estimate gamma (γ) passing rates from characteristics of respiratory motion.

Material and Methods: A VMAT plan for lung cancer patients, which was designed using Pinnacle3 (ver. 9.2; Philips Ltd, USA), was used. Measurements were performed on the Elekta Synergy (Elekta Oncology Systems Ltd, Crawley, UK), which has a 160-leaf independently moving MLC with 5-mm leaf width. Beam energy was set to 6 MV photon beam. The I'mRT Phantom (IBA Dosimetry GmbH, Schwarzenbruck, Germany) was set on a motor-driven base (QUASAR Programmable Respiratory Motion Platform; Modus Medical, London, ON, Canada). The motor-driven base moved in a direction parallel to the couch direction at angle of 0 deg. A total of 148 respiratory patterns was tested. The doses delivered to the Gafchromic EBT3 films (Kodak, Rochester, NY), inserted in the coronal plane of the I'mRT Phantom, were compared with under moving and static conditions without dose normalization. The irradiated films were scanned in the same orientation using a resolution of 72 dpi in the 16-bit red-channel color scale. Four pinholes were made on each film to identify the irradiated center. All of the films were analyzed using commercially available radiation dosimetry software (DD system, ver. 10.4; R'Tech Inc., Tokyo, Japan). The passing rates of the γ with the criterion of 3%/3 mm (γ3%/3mm) were calculated in the area receiving more than 30% of the isodose. In addition, mean respiratory position (μ) and its standard deviations (σ) were calculated from respiratory curves during beam irradiation.

Results: Absolute value of μ (|μ|) and σ ranged from 0.0 to 8.5 mm, and from 1.5 to 6.7 mm, respectively. Multi-regression analysis revealed that the impact of σ on the γ3%/3mm had 0.66-fold greater than that of |μ|. Means±SDs of the γ3%/3mm and the |μ|+0.66σ (|μ|+0.66σ) were 83.1±14.0% (range, 38.7-100.0%), and 8.7±3.1 mm (range, 4.6-14.2 mm), respectively. A strong correlation between the γ3%/3mm and |μ|+0.66σ was observed (R=-0.90).

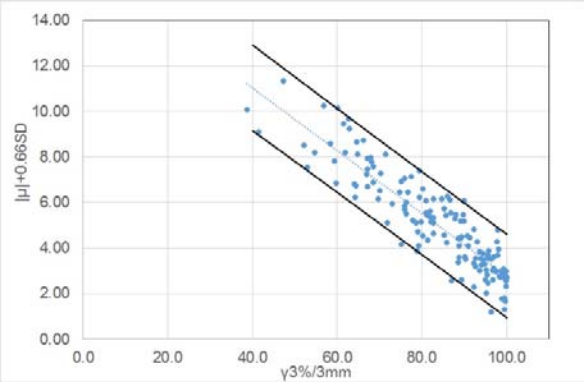

Conclusion: We have demonstrated that the γ3%/3mm can be quantitatively estimated from the characteristics of respiratory motion. From the results of multi-regression analysis, reducing the amplitude of respiratory motion would provide high γ3%/3mm.

EP-1733

Deep inspiration breath-hold technique using an Arduino

P. Gallego[1], J. Pérez-Alija[1], S. Olivares[1], S. Loscos[1], E. Ambroa[2], A. Pedro[1]
[1]*Hospital Plato, Oncología, Barcelona, Spain*
[2]*Hospital General de Cataluña, Radioterapia, Sant Cugat, Spain*

Purpose or Objective: A large effort has been made in recent years to develop techniques to reduce the dose to normal tissue (especially heart dose) for patients receiving radiation treatment for breast cancer. The deep inspiration breath-hold technique (DIBH) can decrease radiation dose delivered to the heart and this may facilitate the treatment to the internal mammary chain nodes. The aim of this work was both to develop a DIBH method using an Arduino Uno microcontroller board (SmartProyects, Ivrea, Italia) and a simple software to visualize the patient's level of inspiration. This method provides a cheaper solution to the more expensive commercial ones.

Material and Methods: Arduino is an open-source electronics platform based on an easy-to-use hardware and software. We plugged a tri-axial low-g digital acceleration sensor (Bosch's *BMA180)* to our Arduino board. This accelerometer is then placed on the patient and used as a surrogate to measure the expansion of the patient's thorax during breathing. Even though we chose the gravitational 1g range and our BMA 180 provides a digital full 14 bit output signal, this is still not enough to accurately measure the acceleration changes produced in the patient's thorax during her breath cycle. We thus measure the orientation change in our BMA180 inside the gravitational field. However, this orientation change is good enough to accurately measure the changes in the patient's breath cycle. With an In-house developed software programmed in Python 2.7 we are able to visualize these measures and, accordingly, the patient's breathe cycle.

Results: We were able to build a DIBH system using both an Arduino board and an accelerometer. We visualize the patient's breathe cycle with an In-house software and establish a threshold based on its amplitude. We provide patients with a real-time breathe cycle visualization, so they can have a visual feedback mechanism in order to properly hold their breath when required.

Conclusion: Several DIBH methods are commercially available. These methods can decrease the radiation dose delivered to the heart. We have developed an In-house DIBH system with all the functionalities required to implement this technique in our clinic. Building this system is really cheap and amounts to nearly 60 Euros. We are more than happy to freely provide the software needed to implement this method.

EP-1734

IGRT for prostate cancer: intrafraction variation analysis and CTV-PTV margin determination

C. Italia[1], R. La Rosa[2], P. Della Monica[3], S. Masciullo[4], O. Ceccarini[5], E. Brembilla[5], M. Camerlingo[4], M. Cardinali[5], F. De Osti[4], S. Gusmini[4], C. Riva[4], F. Romeo[4]
[1]*Policlinico San Pietro/Policlinico San Marco, Radiotherapy, Ponte San Pietro/Zingonia, Italy*
[2]*Policlinico San Marco, Medical Physics, Zingonia, Italy*
[3]*Policlinico San Pietro, Medical Physics, Ponte San Pietro, Italy*
[4]*Policlinico San Pietro, Radiotherapy, Ponte San Pietro, Italy*
[5]*Policlinico San Marco, Radiotherapy, Zingonia, Italy*

Purpose or Objective:
1.to evaluate first set-up accuracy and corrections needed before treatment administration
2.to assess intrafraction variability
3.to determine CTV-PTV margins according to intrafraction uncertainties

Material and Methods: Forty-five consecutive prostate cancer patients, undergoing radical or postoperative image-guided radiation therapy with or without gold seed implant in a newly opened department, were considered. On each session a first set of portal images was obtained at 0° and 90° degrees, using a low-dose MV imager. Positioning errors were measured in the three directions and corrected if > 1 mm. After treatment a second set of images was daily produced and displacements measured. Comparison between before-treatment images and planning DRRs represents set-up accuracy. Comparison between end-of-treatment images and planning DRRs shows intrafraction variability Systematic and random errors were analysed and incorporated in the Van Herk formula (2.5 Σ+ 0.7 σ), to determine ideal CTV-PTV margins.

Results: All patiens were suitable for the analysis. Results are summarized in the table.

	AXIS	MEAN (mm)	Σ (mm)	σ (mm)	CTV/PTV margin
FIRST SET-UP	R-L (left:+)	-0.3	1.7	3.1	6.3
	A-P (anterior:+)	-0.8	2.3	3.7	8.4
	C-C (caudal:+)	+0.2	2.0	3.2	7.2
	AXIS	MEAN (mm)	Σ (mm)	σ (mm)	CTV/PTV margin
INTRA-FRACTION	R-L(left:+)	+0.2	0.5	1.2	2.2
	A-P (anterior:+)	-0.3	0.7	1.4	2.7
	C-C (caudal:+)	+0.1	0.4	1.1	1.7
Σ = systematic error σ = random error					

A total of 6632 images were analysed. Mean errors were <1 mm for all measurements. In intrafraction shift analysis systematic errors were <1 mm, random errors were <2 mm and calculated CTV-PTV margins ranged from 1.7 to 2.7 mm.

Conclusion: Good accuracy and precision for first positioning procedures were found. If hypothetically IGRT were omitted and CTV-PTV margins were based on first set-up errors only, margins ranging from 6.3 to 8.4 mm in the various directions would be mandatory. On the contrary, according to the policy of our department, with the use of daily IGRT and based on our excellent results of intrafraction variation analysis, CTV-PTV margins can be limited to 2.2, 2.7 and 1.7 mm, respectively in lateral, anteroposterior and craniocaudal direction.

EP-1735

Impact of respiratory motion on breast tangential radiotherapy using the field-in-field technique

H. Tanaka[1], T. Yamaguchi[1], M. Kawaguchi[1], S. Okada[1], Y. Kajiura[1], M. Matsuo[1]
[1]*Gifu University, Radiology, Gifu, Japan*

Purpose or Objective: The field-in-field (FIF) technique has become a widely performed method of administering tangential whole breast radiotherapy. However, as the FIF technique requires the precise setting of the position of the multi-leaf collimators (MLCs) in order to reduce hot spots, there is concern that its use could significantly change the dose distribution to the target volume due to respiratory

motion. This study aimed to evaluate whether the FIF technique is more vulnerable to the impact of respiratory motion than irradiation using physical wedges (PWs).

Material and Methods: Ten patients with early stage breast cancer were enrolled. All patients had undergone breast-conserving surgery and implantation of 4 surgical clips on the tumor bed, 2 of which had been placed in the nipple side of the tumor bed and 2 on each medial and lateral side of the tumor bed. Computed tomography (CT) was performed during free breathing (FB). After the FB-CT data set acquisition, 2 additional CT scans were obtained during a held breath after light inhalation (IN) and light exhalation (EX). Based on the FB-CT images, 2 different treatment plans (FIF-plan and PW-plan) were created for the entire breast for each patient and copied to the IN-CT and EX-CT images. The prescribed dose was 50 Gy in 25 fractions. The amount of change of in the volume of the target receiving 107%, 95%, and 90% of the prescription dose (V107%, V95%, and V90%, respectively), on the IN-plan and EX-plan compared with the FB-plan were evaluated. The length of movement of each surgical clip from EX-CT to IN-CT in 3 directions (horizontal, anteroposterior, and craniocaudal) and three-dimensional vector displacement were measured.

Results: The average displacement length was largest in the anteroposterior direction and the average three-dimensional vector displacement was 7.4mm. The V107%, V95%, and V90% were significantly larger for the IN-plan than for the FB-plan in both the FIF and PW plans. While the amount of change in the V107% was significantly smaller in the FIF than in the PW plan, the amount of change in the V95% and V90% was significantly larger in the FIF plan. Thus, the increase in the V107% was smaller while the increases in the V95% and V90% were larger in the FIF than in the PW plan.

Conclusion: The amount of change in dose parameters due to respiratory motion was smaller with the FIF technique than with irradiation using PWs, within an acceptable range.

EP-1736

The quantitative measurement of liver motion in CT during respiration

Y.L. Tsai[1], P.C. Yu[1], H.C. Chang[1], C.Y. Chang[1], P.W. Fu[1], C.W. Lin[1], Y.C. Chiu[1], S.N. Chi[1], C.J. Wu[1]
[1]*Cathay General Hospital, Radiation Oncology, Taipei, Taiwan*

Purpose or Objective: To evaluate the motion of different liver segments in CT during respiration to facilitate target delineation and ITV expansion for liver cases.

Material and Methods: Eleven patients with whole liver scanning during free breath in both regular helical CT and 10-phase-gated 4D CT were investigated. It included 1 esophagus, 3 lung, 5 breast, 1 liver, and 1 thymoma patients. Nine representative points in 1 cm diameter (in liver segment 1, 2, 3, 4a, 4b, 5, 6, 7, 8, respectively) were drew in the image of helical CT and adaptive deformed to 4D CT, using SmartAdapt, a tool in Eclipse version 11.5. The coordinate of centroid represented the location of point. Distances of deformed points from phase 0 CT (end-inspiration) to phase 50 CT (end-expiration) denoted the maximal motion of liver in different liver segments. The accuracy of the adaptive deformation was measured by the accuracy ratio of whole liver deformation, which was the overlapping liver area of deformed helical CT and 4D CT divided by whole liver area in 4D CT.

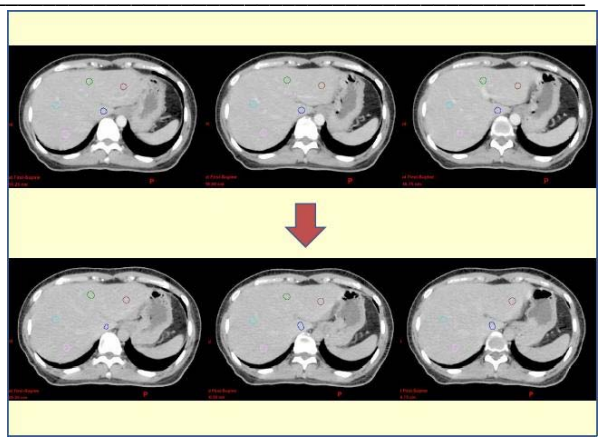

Results: Mean moving distances along X-, Y-, Z-axis from phase 0 CT to phase 50 CT were -0.10±0.32 (mean±SD)(cm), 0.24±0.24, and 0.60±0.36, respectively, averaging from the 9 points of 11 investigated patients. The result indicated liver moving to the right, back, and upside while expiration. For specific liver segments, the motion along X-, Y-, Z-axis were S1: -0.23±0.31, 0.15±0.16, 0.55±0.29, S2: -0.06±0.32, 0.15±0.29, 0.57±0.43, S3: -0.04±0.23, 0.32±0.19, 0.61±0.26, S4a: -0.19±0.27, 0.08±0.23, 0.23±0.28, S4b: -0.14±0.13, 0.27±0.20, 0.66±0.28, S5: -0.01±0.27, 0.35±0.25, 0.57±0.23, S6: -0.05±0.41, 0.25±0.25, 0.75±0.32, S7: -0.20±0.40, 0.26±0.21, 0.95±0.33, S8: 0.01±0.42, 0.32±0.29, 0.55±0.38. All segments moved to the right except segment 8 with mean moving distance 0.01cm to the left. Otherwise, all segments moved to the back and upside while expiration. Segment 7 was the most mobile one on the Z-axis with 0.95±0.33cm upwards. The accuracy ratio of whole liver deformation were 0.96±0.03 for phase 0 CT, and 0.97±0.02 for phase 50 CT, respectively, denoting the adaptive deformation is quite accurate.

Location	Respiration caused liver motion from phase 0 CT (end-inspiration) to phase 50 CT (end-expiration)		
	X-axis	Y-axis	Z-axis
S1	-0.23±0.31	0.15±0.16	0.55±0.29
S2	-0.06±0.32	0.15±0.29	0.57±0.43
S3	-0.04±0.23	0.32±0.19	0.61±0.26
S4a	-0.19±0.27	0.08±0.23	0.23±0.28
S4b	-0.14±0.13	0.27±0.20	0.66±0.28
S5	-0.01±0.27	0.35±0.25	0.57±0.23
S6	-0.05±0.41	0.25±0.25	0.75±0.32
S7	-0.20±0.40	0.26±0.21	0.95±0.33
S8	0.01±0.42	0.32±0.29	0.55±0.38
Mean	-0.10±0.32	0.24±0.24	0.60±0.36

The numbers are presented in mean±SD (cm)
The numbers>0 indicate the direction to the left (X-axis), back (Y-axis), upside (Z-axis)

Conclusion: The liver motion in CT during respiration is different between different liver segments. The most mobile one is segment 7 on the Z-axis. The quantitative motion measurement could be a useful reference for ITV expansion to ensure preciseness in target delineation for liver cases.

EP-1737

Intrafraction motion and ITV dose coverage in thoracic SBRT: preliminary analysis of 101 CBCT images

P. Antognoni[1], L. Pozzi[2], D.P. Doino[1], S. Gottardo[1], C. Mordacchini[2], M. Reso[1], F. Stucchi[1], C. Bianchi[2], R. Novario[2]
[1]*Ospedale di Circolo Fondazione Macchi, Department of Radiotherapy, Varese, Italy*
[2]*Ospedale di Circolo Fondazione Macchi, Department of Medical Physics, Varese, Italy*

Purpose or Objective: To evaluate the impact of intra-fraction organ motion on the dosimetric coverage of ITV by the analysis of a preliminary data set of 101 CBCT images acquired in 7 patients treated according to an SBRT protocol for primary and metastatic thoracic tumors.

Material and Methods: Between 2013 and 2015 seven pts, 5 males and 2 females, median age 77 yrs (range: 35-85 yrs) received SBRT for primary or metastatic thoracic tumors: 4 primary lung cancer, 2 mediastinal lymphnode metastasis, 1 lung metastasis. All pts had a 4D-CT high-resolution simulation in 10 respiratory phases for ITV definition. GTV and ITV volumes were 4.5-21.4 cm3 and 6.8-39.4 cm3, respectively. ITV-PTV margins were 5 mm (median), range: 3-5 mm. All pts were treated by IG-IMRT volumetric modulated arc therapy with 2 modulated arcs. Doses were prescribed according to ICRU 83 (median PTV dose) and 99% of PTV had to be encompassed by 90% isodose. Total doses were: 20 Gy x 3 in 1 pt, 12 Gy x 4 in 1 pt, 10 Gy x 5 in 1 pt, 7.5 Gy x 8 in 1 pt, 6 Gy x 8 in 3 pts. Before CBCT acquisition in all pts 2 planar (AP-LL) set-up EPID images (kV/MV) were taken for preliminary set-up analysis. In absence of rotations on EPID imaging, CBCT images (Nr.=44) were acquired for on-line set-up corrections which were applied before of each 1st SBRT treatment arc. Intra-fraction motion was evaluated by further CBCT images acquired before starting and at the end of the 2nd treatment arc. Structure matching on CBCT was automatically done first on bone and then on soft tissue. In-room mean elapsed time between 1st and last CBCT was 26 min (range:11-47 min). On-line set-up corrections between 1st and 2nd arc were applied for errors of 3mm. For the whole series of 7 pts mean differences between planned and shifted ITV position along the 3 spatial axes (CC, AP, LL) were then calculated on 57 CBCT images, 35 taken between 1st and 2nd arc, 22 at the end of 2nd arc. For each patient isodose distribution was recalculated on the TPS after correction of the isocenter position of the 2 arcs applying the mean differences found. Finally, differences in ITV median dose, V90, V95, and D98 were calculated.

Results: Mean ITV displacements after the 1st arc were 1.2 mm ± 1.6 mm, 0.5 mm ± 1.4 mm, 0 mm ± 1.1 mm for CC, AP and LL directions, respectively. Mean displacements at the end of 2nd arc were 0.1 mm ± 1.4 mm, 0.7 mm ± 1.0 mm, 0.3 mm ± 0.9 mm for CC, AP and LL directions, respectively. Differences between planned and delivered ITV median dose ranged from -0.2% to -1.8%; V90 was ≥ 99.8% in all pts, V95 range was 86.7%-99.7%; D98 was ≥ 92.7% in all pts (Fig. 1).

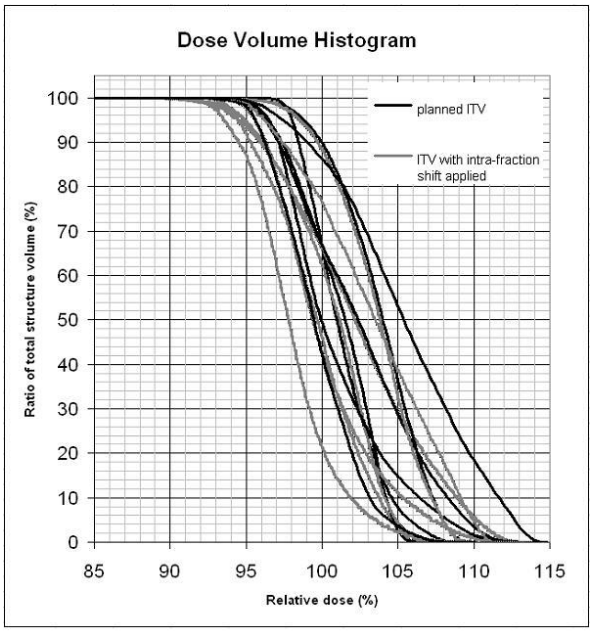

Fig.1: DVH of ITV for each patient calculated according to the original treatment plan and after application of mean intra-fraction shift.

Conclusion: Our preliminary analysis of 101 CBCT in 7 pts aimed at evaluating intra-fraction organ motion during V-MAT SBRT of thoracic targets shows that ITV dosimetric coverage is only minimally influenced by intra-fraction ITV displacement, provided that on-line corrections are applied before each treatment arc. Our findings need to be prospectively confirmed in a larger patient series.

EP-1738

The impact of active breath control on IMN coverage in left sided post-mastectomy breast patients

A. Barry[1], K. Rock[1], C. Sole[1], M. Rahman[1], M. Pintilie[2], A. Fyles[1], C. Koch[1]

[1]Princess Margaret Hospital, Department of Radiation Oncology, Toronto, Canada

[2]Princess Margaret Hospital, Department of Biostatistics, Toronto, Canada

Purpose or Objective: The inclusion of the Internal Mammary Nodes (IMNs) in managing left sided post-mastectomy radiotherapy (PMRT) patients has a potential benefit in patient outcomes and disease control. Larger treatment fields result in higher doses to normal tissue but advancing technological techniques, such as the use of Active Breath Control (ABC) mean acceptable dose parameters may be achieved.

Material and Methods: 50 randomly selected patients with left sided breast cancer receiving PMRT underwent CT simulation with and without ABC, 100 radiotherapy (RT) plans were generated. 30 additional patients requiring left sided PMRT with free-breathing (FB) CT simulation scan were selected at random as a control group. The IMNs were delineated as a target volume within the first 3 intercostal spaces as were organs at risk (OAR)- left anterior descending coronary artery (LADCA), heart, lung and contralateral breast (CB). Modified wide-tangent photon fields, with the inclusion of chest wall, IMNs, axilla and supraclavicular fossa as a 4-field technique were generated for all 130 plans. Statistical analysis was completed using Wilcoxon Signed Rank test, Mann Whitney test and Pearson and Spearman Correlation Coefficients.

Results: IMN PTV coverage in plans with ABC was reduced compared to FB (94 vs 98% p<0.001), meeting dosimetric criteria for coverage in 90% of plans (range 79-100%). ABC significantly reduced dose to all OARs compared to FB - median reduction in mean heart dose (MHD) (6.3Gy vs 1.9Gy p<0.001), lung V20 (15% vs 11% p<0.001), LADCA max dose to 0.2cc (49Gy vs 17.8Gy p<0.001) and LADCA mean dose (40Gy vs 10Gy p<0.001), with no difference in the D5 to the CB (2.2Gy vs 2.1Gy p=0.36).
In the control vs ABC group, there was no difference in IMN PTV coverage (median 94.5% vs 96% p=0.21). There was significant median reduction in MHD (3.5Gy vs 1.9Gy p<0.001), lung V20 (14% vs 11% p<0.001), LADCA maximum dose to 0.2cc (43.9Gy vs 17.8Gy p<0.001) and LADCA mean dose (22.6Gy vs 10Gy p<0.001) for the ABC group, but an increase in D5 to the CB with the use of ABC (1.5Gy vs 2.1Gy p<0.001).
BMI was not directly correlated with IMN PTV coverage, or increase/decrease in OAR constraints.

Conclusion: Our data supports the standard use of ABC in left sided PMRT patients that require the inclusion of the IMNs. We have demonstrated adequate IMN PTV coverage with significant sparing of OARs. The impact of these dosimetric reductions on long-term normal tissue effects requires further evaluation in prospective studies.

EP-1739

Deep inspiration breath hold with 'AlignRT' in 3D conformal mediastinal radiotherapy for lymphoma

J.L. Brady[1,2], R. Begum[3], C. Hartill[4], A.G. Greener[3], N.G. Mikhaeel[1,2]

[1]Guy's and St Thomas' NHS Foundation Trust, Department of Clinical Oncology, London, United Kingdom

[2]King's Health Partners, Academic Health Sciences Centre, London, United Kingdom

[3]Guy's and St Thomas' NHS Foundation Trust, Department of Medical Physics, London, United Kingdom

[4]Guy's and St Thomas' NHS Foundation Trust, Department of Radiotherapy, London, United Kingdom

Purpose or Objective: Deep inspiration breath hold (DIBH) technique may reduce radiation dose to heart and lungs during mediastinal radiotherapy (RT) for lymphoma.
AlignRT is an optical surface tracking system which can be used to monitor inspiration depth during DIBH. Data is acquired from planning CT scan to generate a 3D surface contour of the patient whilst in breath hold (BH). At treatment the real-time contour of the patient is monitored by cameras and compared to the reference contour.
We initiated a prospective study to assess the feasibility of DIBH with AlignRT in mediastinal lymphoma, and to evaluate its dosimetric benefits, compared to free breathing (FB) RT. This is the first report of AlignRT use in this indication.

Material and Methods: Eligible patients were due to receive RT to the mediastinum for Hodgkin or high grade non Hodgkin lymphoma.
Patients were positioned supine on a thoracic board with arms raised. After coaching FB and BH CT scans were performed. 3D conformal plans were produced for both FB and DIBH volumes for each patient and compared in terms of PTV coverage (V95, D95), cardiac doses (MHD, V30, V15), lung doses (MLD,V20,V5), spinal cord max. dose and breast doses in females (mean, V10,V5). The optimal plan was selected for treatment. Data was then transferred to the AlignRT software.
Feasibility was determined by the proportion of patients able to manage the technique, and the incidence & nature of setup errors.

Results: Between March & September 2015 8 patients were eligible for DIBH RT. 1 patient could not maintain BH at planning and proceeded with FB RT. For another cardiac constraints could not be met with a conformal plan and treatment changed to intensity modulated RT (FB). For 6 patients DIBH and FB plans were created & compared (see table). Prescribed dose was 30.6Gy/ 17 #.
PTV coverage was similar for DIBH and FB. MLD was significantly lower in DIBH plans (mean difference 1.58Gy). Lung V20 was also reduced by 6.45%. Lung V5 was reduced by 3.25% but the difference was not significant. Cardiac doses were better in the DIBH plans with a reduction in MHD of 2.49Gy, and V15 by 10.44%. There was no significant difference in breast or spinal cord doses. In all cases the DIBH plan was chosen for treatment.

Table. Comparison of radiation dose parameters in FB and DIBH 3D conformal plans

Mean doses / volumes	FB (n=6)	DIBH (n=6)	Difference	P value (95% CI) (2 sided paired t test)
PTV				
V95 (%)	97.46	98.32	0.86	0.074 (-0.12 to 1.85)
D95 (Gy)	29.45	29.59	0.14	0.102 (-0.04 to 0.34)
Lung				
MLD (Gy)	10.45	8.87	-1.58	0.009 (-2.56 to -0.61)
V20 (%)	22.75	16.3	-6.45	0.043 (-12.61 to -0.29)
V5 (%)	54.24	50.99	-3.25	0.056 (-6.64 to 0.14)
Heart				
MHD (Gy)	11.47	8.98	-2.49	0.019 (-4.37 to - 0.60)
V15 (%)	37.13	26.69	-10.44	0.007 (-16.37 to -4.32))
Breast (n=4)				
Mean dose (Gy)	5.41	5.05	-0.37	0.377 (-1.50 to 0.76)
Breast V5 (%)	21.98	20.16	-1.81	0.25 (-5.84 to 2.23)
Breast V10 (%)	15.62	11.29	-4.333	0.188 (-12.46 to 3.79)
Spinal cord				
Max point dose (Gy)	29.68	27.08	-2.61	0.074 (-5.58 to 0.37)

Set up issues were encountered in 2/6 DIBH patients early in treatment. These were not correctable & required replans. Both completed treatment with the new plans without incident. Investigation concluded the most likely cause was an exaggerated and hard to reproduce BH during the planning CT. Patient instructions have been revised .

Conclusion: Our early experience indicates that DIBH RT using Align RT is feasible. A minority of patients may not tolerate DIBH and careful coaching is needed to achieve a reproducible level of deep inspiration. DIBH RT can reduce radiation doses to heart and lungs during mediastinal RT, without any increase in breast dose or compromise to PTV coverage.

EP-1740

Application of virtual reality guide hypnosis in the control of respiration motion for radiotherapy

R. Li[1], N. Fu[1], J. Ouyang[1,2], Y. Mao[1,3], Y. Liu[1,4], S. Dang[5], J. Hu[6,7], J. Deng[8], S. Yu[1], Y. Zhu[1], Y. Chen[1], Y. Xie[1,9]
[1]*Shenzhen Institutes of Advanced Technology, Institute of Biomedical and Health Engineering, Shenzhen, China*
[2]*Northeastern University, Sino-Dutch Biomedical and Information Engineering School, Shenyang, China*
[3]*University of Science and Technology of China, School of Information Science and Technology, Hefei, China*
[4]*Shanghai Maritime University, Logistics Engineering College, Shanghai, China*
[5]*Virtual Reality technology co .-Ltd, Virtual Reality technology co .-Ltd, Shenzhen, China*
[6]*Beijing Union University, Beijing Union University, Beijing, China*
[7]*HK Sunshine State Of Mind Education Consulting Limited Global Youth Psychologists Association, Hong Kong, China*
[8]*Zhuhai Psychological Counseling Co.- Ltd, Zhuhai Psychological Counseling Co.- Ltd, Shenzhen, China*
[9]*Key Lab for Health Informatics of Chinese Academy of Sciences, Lab for Wearable Devices, Shenzhen, China*

Purpose or Objective: To propose a comfortable, harmless and stable method to guide the hypnosis for the control of respiratory motion during radiotherapy.

Material and Methods: The virtual reality (VR) technology was applied in the hypnosis guidance to control the respiratory motion. A VR demo was made depending on a pre-designed hypnosis scene, which follows the Stanford hypnotic susceptibility scale1 and the experienced design of hypnotists, to make volunteers relax. 46 healthy volunteers, including 22 female and 24 male, are taken in the hypnosis experiments. The respiratory motion for each volunteer was recorded, which takes 10 min before hypnosis (BH) and 20 min in VR-guide hypnosis state (VRGHS) and 10 min after hypnosis (AH). BH and AH are united into normal state (NS).

Results: Two comparative experiments were conducted to study the difference of amplitudes of respiratory motion between NS and VRGHS. Obvious difference has been observed between VRGHS and NS as a whole. As a result, compared with NS, the mean amplitudes of respiratory waves in VRGHS reduces 18.8% and standard deviation (STD) reduces 20.7%. Similarly, the female volunteers group drops 16.8% in mean value and 23.6% in STD, and the male volunteers group has a mean deduction of 20.9% in amplitudes, with a drop of 17.7% in STD. In addition, 15/22 female show high grade significant ($p<0.0005$) difference between VRGHS and NS, 20/24 in male. Conclusively, it's showed that the statistical differences of VRGHS are obviously, lower than NS.

Table 1. Mean deduction and STD deduction between VRGHS and NS (BH and AH)

	Female Volunteers				Male Volunteers			
	VRGHS VS.BH		VRGHS VS. AH		VRGHS VS.BH		VRGHS VS. AH	
	Rate	Count	Rate	Count	Rate	Count	Rate	Count
Mean Deduction	14.8%	17/22	18.7%	17/22	22.6%	23/24	19.2%	21/24
STD Deduction	19.0%	16/22	28.3%	18/22	20.9%	18/24	14.5%	17/24

Table 2. Statistics of significant difference level grade of amplitudes between VRGHS and NS

	Female Volunteers		Male Volunteers	
	VRGHS VS. BH	VRGHS VS. AH	VRGHS VS. BH	VRGHS VS. AH
G_1 ($p<0.05$)	0/22	1/22	0/24	2/24
G_2 ($p<0.005$)	0/22	0/22	3/24	1/24
G_3 ($p<0.0005$)	15/22	13/22	16/24	17/24
Total	15/22	14/22	19/24	20/24

Conclusion: The VRGH can effectively control the amplitude of the waves, which make the respiratory motion smaller and more stable. It is also observed that there is no obvious difference between female volunteers and male volunteers.

EP-1741

MRI assess hypnosis control respiratory motion applied to radiotherapy for lung cancer patients

R. Li[1], Z. Fan[1], L. Ding[1], W. Mei[1], X. Li[1], H. Chen[1], Q. Luo[1], N. Fu[1], J. Ouyang[1,2], Y. Mao[1,3], Y. Liu[1,4], S. Dang[5], J. Hu[6,7], J. Zhang[7], J. Deng[8], S. Yu[1], Y. Zhu[1], Y. Chen[1], Y. Xie[1,9]

[1]*Shenzhen Institutes of Advanced Technology, Institute of Biomedical and Health Engineering, Shenzhen, China*

[2]*Northeastern University, Sino-Dutch Biomedical and Information Engineering School, Shenyang, China*

[3]*University of Science and Technology of China, School of Information Science and Technology, Hefei, China*

[4]*Shanghai Maritime University, Logistics Engineering College, Shanghai, China*

[5]*Virtual Reality technology Co.- Ltd, Virtual Reality technology Co.- Ltd, Shenzhen, China*

[6]*Beijing Union University, Beijing Union University, Beijing, China*

[7]*HK Sunshine State Of Mind Education Consulting Limited Global Youth Psychologists Association, HK Sunshine State Of Mind Education Consulting Limited Global Youth Psychologists Association, HongKong, China*

[8]*Zhuhai Psychological Counseling Co.- Ltd, Zhuhai Psychological Counseling Co.- Ltd, Shenzhen, China*

[9]*Key Lab for Health Informatics of Chinese Academy of Sciences, Lab for Wearable Devices, Shenzhen, China*

Purpose or Objective: To accuracy assess the effect of hypnosis control respiratory motion on radiotherapy for lung cancer patients

Material and Methods: 21 healthy volunteers are invited to provide corresponding information in an experiment on this study. Among the experiment, 8 volunteers are under three kinds of surrounding scene: normal state (NS), self-hypnosis state (SHS), hypnotist-guided hypnosis state (HGHS), the other 13 volunteers are under NS and SHS. Magnetic Resource Imaging (MRI) was applied to acquisition image (two dimension)of the lung's coronal plane of all volunteers under different surrounding scenes. The distance from the apex of lung to diaphragm is generally regarded as the characteristic length in craniocaudal direction which recognized as the main displacement of direction of lung motion.

Results: Analyzing the amplitudes of respiration motion waves data under different states, it is showed that the amplitudes of volunteers under SHS have no obvious statistical discrepancy with that in NS, with 0.73mm lower and 3% deduction. However, the results have significant difference in HGHS. Compared with the amplitudes in NH and SHS, the volunteers' amplitudes in HGHS are 1.60mm and 2.0mm averagely lower and the mean deduction is 9.8% and 11.1%. Specifically, 7 out of 8 volunteers' amplitudes are lower in HGHS than SHS.

(13 samples in SHS v.s. NH, 8 samples in HGHS v.s. NH and HGHS v.s. SHS)

	SHS v.s. NH (13)	HGHS v.s. NH (8)	HGHS v.s. SHS (8)
Mean Deduction	0.73mm	1.60mm	2.00mm
Mean Deduction Rate	3.0%	9.8%	11.1%
SD Deduction	0.76mm	0.57mm	0.77mm
SD Deduction Rate	-5.1%	-8.1%	3.1%

Table 1. Amplitudes comparison under different state

Conclusion: The result shows that the amplitudes of volunteers under SHS have no remarkable difference in comparison with NS, while the volunteers in HGHS have smaller respiratory motion amplitudes. Quantitatively analysis hypnosis respiratory controlling, we found it is an effective way and it could be applied in clinic, and hypnotist guide would be better than teaching patient self-hypnosis.

EP-1742

The first clinical implementation of audiovisual biofeedback in liver cancer SBRT

S. Pollock[1], R. Tse[2], D. Martin[2], L. McLean[2], M. Pham[2], D. Martin[2], D. Tait[2], P. Estoesta[2], G. Whittington[2], J. Turley[2], C. Kearney[2], G. Cho[2], R. Hill[2], S. Pickard[2], P. Aston[2], K. Makhija[1], R. O'Brien[1], P. Keall[1]

[1]*University of Sydney, Sydney Medical School - Central, Sydney, Australia*

[2]*Chris O'Brien Lifehouse, Department of Radiation Oncology, Sydney, Australia*

Purpose or Objective: Irregular breathing motion exacerbates uncertainties throughout a course of radiation therapy. Breathing guidance has demonstrated to improve the regularity of breathing motion. This study was the first clinical implementation of the audiovisual biofeedback (AVB) breathing guidance system over a course of liver SBRT. We present here the preliminary results from the first four patients recruited into this clinical trial.

Material and Methods: Four liver cancer patients with implanted fiducial markers or surgical clips near the tumor were recruited. Prior to CT sim, patients underwent a screening procedure in which they underwent breathing conditions (1) AVB, or (2) free breathing (FB). The most regular breathing condition, AVB or FB, in the screening procedure was utilized for the patient's CT simulation and for each fraction of treatment; each patient had 6 fractions of treatment. Tumor respiratory motion was obtained from the implanted fiducial markers in the CBCT projection images acquired during the screening procedure and each fraction of treatment. External respiratory motion was obtained from the RPM system. The regularity of breathing motion was analysed for the screening procedure, CT sim, and each treatment fraction. Breathing motion regularity was quantified as the root mean square error (RMSE) in displacement and period.

Results: The screening procedure yielded the decision to utilize AVB for three (of the four) patients; FB was chosen for one patient in the screening procedure who had naturally regular breathing. Over the course of SBRT, for external RPM motion, the average RMSE in dispalcement and period for AVB was 0.13 cm and 0.47 s, 6% and 31% more regular than FB, respectively. For internal fiducial marker motion, the average RMSE in dispalcement and period for AVB was 0.18 cm and 0.46 s, 13% and 38% more regular than FB, respectively.

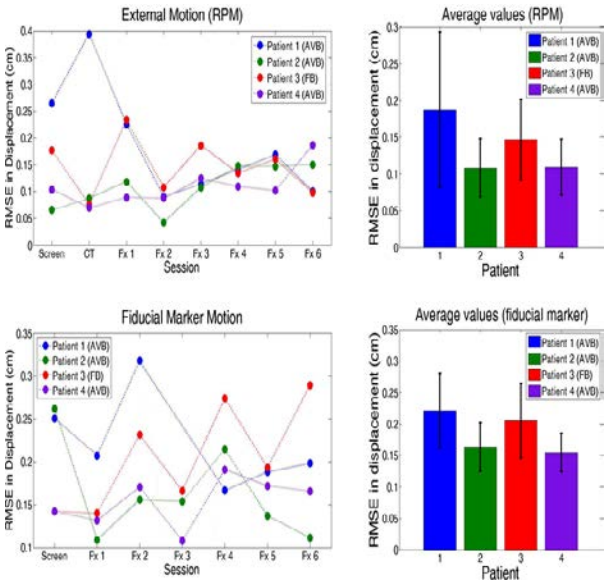

Conclusion: This was the first clinical implementation of AVB utilizing a screening procedure to ensure the most regular breathing condition is facilitated during CT imaging and

treatment delivery. In the screening procedure, three of the four patients' breathing regularity was improved with AVB. Across a course of SBRT, AVB also demonstrated to improve the regularity of breathing displacement and period over free breathing.This was also the first study to assess the impact of AVB on liver tumor motion via fiducial marker surrogacy. Results from the first four patients have been reported here and demonstrate clinical potential for facilitating regular and consistent breathing motion during CT imaging and treatment delivery.

EP-1743

Analysis of the deviation of lung tumour displacement caused by different breathing patterns

G. Hürtgen[1], S. Von Werder[2], C. Wilkmann[2], O. Winz[3], C. Schubert[1], N. Escobar-Corral[1], J. Klotz[1], C. Disselhorst-Klug[2], A. Stahl[4], M.J. Eble[1]

[1]*Uniklinik RWTH Aachen, Department of Radiooncology and Radiotherapy, Aachen, Germany*

[2]*RWTH Aachen University, Department of Rehabilitation- & Prevention Engineering, Institute of Applied Medical Engineering*

[3]*Uniklinik RWTH Aachen, Department of Nuclear Medicine, Aachen, Germany*

[4]*RWTH Aachen University, III. Institute of Physics B, Aachen, Germany*

Purpose or Objective: By applying motion correction strategies for the treatment of lung tumours the variability of breathing induced tumour movement is more important. To analyse the different motion potential of lung tumours a clinical trial is carried out. FDG-PET scans are performed simultaneously with an accelerometer-based system, which detects the breathing motion. Specific breathing instructions are given to the patient, to analyse the correlation of the sensor information and the tumour displacement, caused by different breathing patterns.

Material and Methods: The study is performed with patients with a single pulmonary metastasis. For the detection of the breathing motion six tri-axial accelerometers are placed on the patient's thorax and abdomen. Thereby, information on the breathing cycle (in-/expiration), breathing mode (thoracic/abdominal) and breathing depth can be distinguished. Up to five different measurements are obtained: 'free breathing', 'deep thoracic', 'flat thoracic', 'deep abdominal' and 'flat abdominal'. Simultaneously, a respiratory gated FDG-PET scan is taken to correlate the patient's respiratory states with the tumour movement. For each of the ten reconstructed PET images the centre of the tumour is determined to visualize the mean tumour trajectory.

Results:

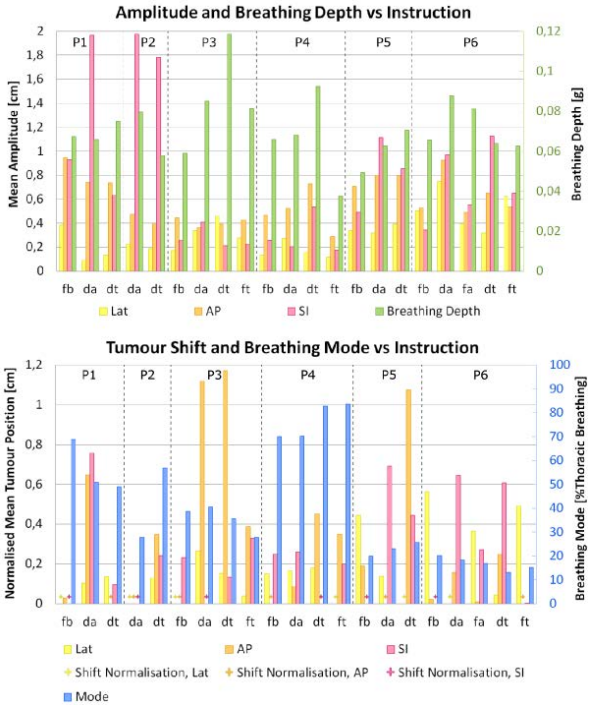

In the figure the analysis of the reconstructed sensor and PET data is shown for six patients, for each of the different breathing scenarios (fb: free breathing, da: deep abdominal, fa: flat abdominal, dt: deep thoracic, ft: flat thoracic). The upper part of the figure shows the mean tumour amplitude from the PET data and the mean breathing depth from the sensor data. The lower part shows the mean tumour position from the PET data and the breathing mode reconstructed from the sensor data. To visualise the offset of the different tumour movements between the different scenarios, for each patient the mean positions are normalised to the smallest mean position of each patient. The figure shows, that for the given scenarios different amplitudes and offsets of the tumour are observed, as well as a change in the sensor signals. The results show a flexibility of the tumour movement in its amplitude and absolute position, which depends on the actual breathing patterns of the patient.

Conclusion: The performed clinical trial indicates that the movement of the tumour depends on the actual breathing pattern. This shows that it is important for the prediction of the tumour position to take the information on the breathing pattern into account. The detection of the breathing parameters with the sensors give the possibility for further investigations of a correlation between tumour offset and amplitude with reconstructed breathing depth and mode, which could be further used for individual motion prediction.

Acknowledgment: The work was funded by the Federal Ministry of Education and Research BMBF, KMU-innovativ, Förderkennzeichen: 13GW0060F. Additionally, the Authors thank Florian Büther (EIMI Münster, Germany) for his support.

EP-1744

Evaluation of the clinical accuracy of the robotic respiratory tracking system

M. Inoue[1], J. Taguchi[1], K. Okawa[1], K. Inada[1], H. Shiomi[2], I. Koike[3], T. Murai[4], H. Iwata[5], M. Iwabuchi[6], M. Higurashi[7], K. Tatewaki[7], S. Ohta[7]

[1]*Yokohama CyberKnife Center, Department of Quality Management with Radiotherapy, Yokohama, Japan*

[2]*Osaka University Graduate School of Medicine, Department of Radiation Oncology, Osaka, Japan*

[3]*Yokohama City University Graduate School of Medicine, Department of Radiology, Yokohama, Japan*

[4]*Nagoya City University Graduate School of Medical Science, Department of Radiology, Nagoya, Japan*

[5]Nagoya Proton Therapy Center, Department of Radiation Oncology, Nagoya, Japan
[6]Yokohama CyberKnife Center, Department of Radiation Oncology, Yokohama, Japan
[7]Yokohama CyberKnife Center, Department of Neurosurgery, Yokohama, Japan

Purpose or Objective: The purpose of this study was to evaluate the clinical accuracy of the Synchrony Respiratory Tracking System (SRTS) of the CyberKnife (CK).

Material and Methods: We analyzed 65 patients with lung lesion who had been treated with the SRTS from August 2012 to August 2015. Respiratory motion data were obtained from cine magnetic resonance (MR) images. MR scans were performed with a 1.5-Tesla whole-body clinical MR scanner, and the cine MR images of sagittal plane were obtained. We collected respiratory motion data of each patient from the cine MR images using in-house software. The dynamic motion phantom (DMP) was used to reproduce the motion of both the tumor and the surface of the patient's abdomen. We used a 20 mm diameter plastic ball as the target. A gold marker was placed at the center of the ball. Treatment plans were created based on static CT scans and standard CK treatment parameters. Each plans utilized ten beams with several different source positions. All of the beams in each plan were aimed at the center of the ball target, and were set to 200 MU for 15 seconds of data acquisition. The CK was subsequently operated with the SRTS, with a CCD camera mounted on the head of the linac. The central axis of the CCD camera was matched to the central axis of the linac beam using a custom-built jig. The recording by CCD camera was performed during the tracking of the ball target by the linac. The tracking error was defined as the distance from the center of the images to the center of the ball in the images recorded by CCD camera. The tracking error was measured at 30 Hz using in-house software. The probability in excess of 95% (Ep95) for each direction was estimated. The SRTS accuracy was defined as the median value of Ep95 for ten beams (Ep95med)

Results: The mean value and standard deviation of Ep95med was 2.5 ± 0.9mm. The Spearman's correlation coefficient determined by the rank test indicated that the range of motion of the tumor was significantly related to Ep95med ($P<0.01$).

Conclusion: The accuracy of SRTS was considered to be clinically acceptable. However, suitable margin to the clinical target according to the range of motion of the tumor seems to be necessary for the safe treatment to each patient.

EP-1745

Radiotherapy in breast cancer with voluntary deep-inspiration breath-hold using BrainLab Exactrac

E. Ippolito[1], R. D'Angelillo[1], A. Sicilia[1], S. Silipigni[1], B. Floreno[1], E. Molfese[1], A. Di Donato[1], P. Trecca[1], D. Gaudino[1], G. Stimato[1], S. Ramella[1], L. Trodella[1]
[1]Campus Bio-Medico University, Radiotherapy, Rome, Italy

Purpose or Objective: Adjuvant radiotherapy in left-sided breast cancer with voluntary deep-inspiration breath-hold technique (vDIBH) may reduce the irradiation dose to the heart. The aim of this study is to estimate the heart, lung and PTV dosimetric constraints and the reproducibility of vDIBH radiotherapy using BrainLab Exactrac monitoring system.

Material and Methods: 10 women with left breast cancer who had undergone breast-conserving surgery and who required adjuvant radiotherapy to the whole breast, were enrolled and were shortly trained before simulation CT-scan to hold their breath. The first scan was acquired in free-breathing (FB_CT) and the second one in vDIBH (vDIBH_CT). Target and organ-at-risk (OAR) volumes were delineated in both CT scans and for both of them computerized treatment planning was performed using two tangential fields technique. We compared the dose distribution for the heart, left anterior descending coronary artery (LAD), ipsilateral lung and planning target volume (PTV) using standard defined parameters: mean dose and maximal dose applied to the LAD; percentage of the heart volume receiving at least 5 Gy (V5Gy) and 10 Gy (V10Gy); percentage of the ipsilateral lung volume receiving at least 20 Gy (V20Gy); and the volume of the PTV receiving 95% of the prescribed dose (V95%). The online monitoring during EPI acquisition and treatment were made by BrainLab Exactrac system. Daily real time electronic portal imaging (EPI), in CINE modality (captured during the beam delivery) were performed in order to check the reproducibility of the technique. Wilcoxon test has been used to compare dosimetric heart, lung and PTV parameters between FB_CT and vDIBH_CT treatment plans. The mean displacement, detected with the portal images, was calculated for each treatment beam and for each patient.

Results: A significant reduction in heart V5 and LAD Dmax (2.71 vs 0.99 Gy p=0.02 and 16.56 vs 6.90 Gy p= 0.012 respectively) parameters was recorded for vDIBH_CT treatment plans (see Table 1 for complete results). There were no significant differences between vDIBH and FB treatments in lung dosimetric parameters and target volume coverage. 1694 portal images were evaluated. During treatment, the mean displacements observed in the longitudinal, vertical and lateral direction were 0.132 mm (SD= 0.011), 0.013 mm (SD= 0.137), 0.116 mm (SD= 0.010).

Dosimetric Parameters		vDIBH	FB	p
Heart V5Gy	Mean ± SD	0,992 ± 1,6	2,708 ± 2,357	0,02
	Median	0,392	2,6	
Heart V10Gy	Mean ± SD	0,119 ± 0,267	0,427 ± 0,377	0,04
	Median	0,000	0,5	
LAD maximum dose	Mean ± SD	6,9 ± 4,198	13,562 ± 5,678	0,012
	Median	5,2	13,555	
LAD mean dose	Mean ± SD	3,1 ± 1,76	5,525 ± 1,993	0,012
	Median	2,850	5,5	
Lung V20Gy	Mean ± SD	5,79 ± 2,556	4,463 ± 2,866	0,441
	Median	6,410	4,720	
95% PTV	Mean ± SD	98,58 ± 1,002	98,224 ± 1,089	0,401
	Median	98,94	98,92	

vDIBH: voluntary deep inspiration breath hold

FB: free breathing

LAD: left artery descending

Conclusion: vDIBH technique reduces cardiac irradiation compared with conventional free-breathing treatment plans, without jeopardizing the proper coverage of the target. vDBIH for left-side whole breast irradiation can be accurately implemented using BrainLab Exactrac system with high and accurate reproducibility (mean shift < 0.15 mm).

EP-1746

Stereo/monoscopic motion tracking of the prostate using room-mounted x-ray image guidance

T. Stevens[1], D. Parsons[1], J. Robar[1]
[1]QEII Health Sciences Centre - Dickson Building, Medical Physics, Halifax- Nova Scotia, Canada

Purpose or Objective: Intrafraction internal motion of the prostate currently limits the accuracy of external beam radiotherapy, requiring expanded ITV boundaries and introducing geometric uncertainty. Techniques to monitor prostate motion at the millimeter scale are thus needed. Room-mounted dual x-ray systems can provide stereoscopic localization of the prostate via implanted fiducial markers, however the treatment head frequently blocks one of the x-ray tubes as the gantry rotates. We implemented a monoscopic 3D localization algorithm, allowing localization even when one of the x-ray tubes is obstructed. We show that this technique allows accurate localization throughout the treatment fraction, improving the tracking capabilities of room-mounted x-ray systems.

Material and Methods: A gold fiducial marker was placed in the prostate of an anthropomorphic phantom, and initially aligned to isocentre. The linac couch was used as a translation stage, and programmed with a realistic prostate motion trajectory. Continuous dual x-ray images (140 kVp,

0.63 mAs) were acquired at 1 Hz. For stereoscopic localization, the intersection of the ray lines connecting the detected image locations with the corresponding sources was found, whereas monoscopic localization first computed a prostate position probability density function (PDF) based on previously published motion covariances, and then finds the maximum likelihood position along the ray line passing through this PDF. Stereo- and monoscopic localization results were compared to the ground truth provided by the linac log file.

Results: Both stereo- and monoscopic localization produced sub-mm accuracy (Figure 1). Monoscopic localization was nearly as accurate as stereoscopic localization, despite only directly resolving two dimensions. The left-right dimension tracked slightly less well with monoscopic localization as this dimension is less correlated with the other two axes, and thus harder to predict using the monoscopic algorithm.

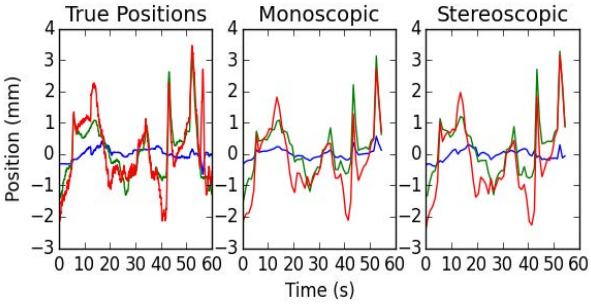

Figure 1: The linac couch was used to move a phantom and implanted fiducial according to a realistic prostate motion trajectory (left). The fiducial was tracked in 3D using both monoscopic (middle) or stereoscopic (right) localization.

Conclusion: The ability to use room-mounted x-ray systems to achieve sub-mm accuracy with either monoscopic or stereoscopic localization creates new opportunities for intrafraction tracking. Stereoscopic tracking can be used when both x-ray tubes are unobstructed, to produce the most accurate localization, and bridged by monoscopic tracking during obstructions. The knowledge of prostate position during treatment can potentially be used to gate treatment, or be fed back into dynamic MLC updates in order to produce more conformal dose delivery.

EP-1747

Assessment of PTV margins accounting for prostate intrafraction motion in SBRT with online IGRT

A. Magli[1], M.R. Malisan[2], C. Fontanella[3], M. Crespi[2], M. Guernieri[2], F. Titone[1], C.T. Sacco[3], E. Moretti[2], C. Foti[2]
[1]*University Hospital Udine, Radiation Oncology, Udine, Italy*
[2]*University Hospital Udine, Medical Physics, Udine, Italy*
[3]*University Hospital Udine, Medical Oncology, Udine, Italy*

Purpose or Objective: There is little consensus on the magnitude of PTV margins for IGRT of the prostate cancer when a hypofractionation scheme is applied and daily correction is required, rather than averaging over many fractions. The aim of this work was to assess PTV margins suitable for SBRT of prostate cancer uncertainties after daily online correction. Moreover, intra-fraction prostate motion is analyzed with the aim to identify its main causes (bladder filling, rectum distension, elapsed treatment time).

Material and Methods: Between 2013 and 2014, 43 patients with low or intermediate risk prostate cancer were treated with 7-fraction SBRT in supine position, with implanted fiducial markers (FM), empty rectum and full bladder. To reduce organ motion, patients were premedicated with butylscopolamine and rectum gas was removed before the treatment. At each session pre-treatment kV/kV imaging was acquired to align the patient by matching the FM's, while additional CBCT imaging was performed after treatment delivery to assess the intra-fraction motion. The van Herk's formula was applied to calculate the PTV margins of prostate/seminal vescicles. To investigate the causes of organ motion, the bladder volume and the rectum wall distension were estimated from each CBCT with respect to the simulation CT images. Correlation between these anatomical factors and intrafraction PTV motion was assessed for each axis, as well as for the composite shift of the prostate volume. The treatment time elapsed from pre-treatment kV/kV to post-treatment CBCT imaging was also included in the statistical analysis .

Results: 301 pre-treatment kV/kV images and 301 post-treatment CBCTs were analyzed. After daily IGRT correction, margins accounting for residual uncertainties are estimated 3 mm for AP, 3 mm for Longitudinal axis and 2 mm for Lateral intra-fraction motion. A systematic increase of bladder filling with respect to simulation images was observed; however, these changes did not influence the prostate displacement ($p = 0.55$) . Similarly, variations of the prostate position occurred independently from changes of the rectal distension ($p = 0.32$). A trend between internal prostate motion in the AP direction and elapsed treatment was observed ($p = 0,057$). Finally, a significant correlation was observed between the intrafraction composite shift of the prostate volume and the elapsed treatment time ($p = 0,036$).

Conclusion: Our data suggest a good control of intrafraction motion with butylscopolamine medication and by careful emptying of the rectum before treatment. The prostate intrafraction motion is shown to be dependent on elapsed treatment time. In conclusion, in image-guided SBRT with online correction, PTV margins can be kept in the range of 3 mm provided that the elapsed treatment time is kept as low as possible.

EP-1748

An experimental comparison of advanced respiratory motion management techniques

S. Ehrbar[1,2], R. Perrin[3], M. Peroni[3], K. Bernatowicz[3], T. Parkel[4], I. Pytko[1,2], S. Klöck[1,2], M. Guckenberger[1,2], S. Lang[1,2], D.C. Weber[3], A. Lomax[3]
[1]*University Hospital Zurich, Department of Radiation Oncology, Zurich, Switzerland*
[2]*University of Zurich, Faculty of Medicine, Zurich, Switzerland*
[3]*Paul Scherrer Institute PSI, Center for Proton Therapy, Villigen, Switzerland*
[4]*Centre Suisse d'Electronique et de Microtechnique CSEM S.A., Innovative Design, Landquart, Switzerland*

Purpose or Objective: Respiratory tumor motion enlarges the intra-fractional tumor position uncertainty. These uncertainties result in increased treatment volumes (PTV) and hence higher radiation dose to organs at risk (OAR). Also interplay effects between the moving target and dynamic treatment delivery have to be considered. Motion-management techniques (MMT) aim to reduce or deal with this intra-fractional respiratory tumor motion in the following ways: The internal target volume (ITV) concept with a PTV enclosing the whole tumor motion, the mid-ventilation (MidV) principle with probabilistic tumor margins, respiratory gating of the irradiation beam and treatment couch tracking with real-time compensation of the internal tumor motion. Dosimetric performances of these four techniques were investigated with film measurements in a sophisticated lung phantom.

Material and Methods: The anthropomorphic, deformable and dynamic lung phantom LuCa (CSEM and PSI) was operated with 5 different respiration patterns with 10 to 20 mm internal tumor motion amplitude. 4DCT scans were taken and individual SBRT treatment plans were prepared, adapting the PTV according to the four MMT (ITV, MidV, gating, tracking) and five respiration patterns. A dose of 8x6 Gy was prescribed to the 65%-isodose line enclosing the PTV using VMAT stereotactic treatment planning. The phantom was irradiated with all individual treatment plans using the corresponding respiration pattern and MMT, together with static measurements. The internal tumor motion was

monitored with Calypso (Varian) for gating and tracking treatments, and compensated with the PerfectPitch couch (Varian) for tracking. The dose in the moving tumor was measured with Gafchromic EBT2 (ISP) films. Changes in homogeneity indices (ΔH1-99) between the films and the planned dose distributions and their gamma agreement scores using 3%/3mm (GS3%/3mm) were evaluated. The film areas receiving more than the planned minimum dose (A>Dmin) were calculated. OAR doses from the treatment plans were compared.

Results: The results for each MMT are summarized in Table 1, giving the median values with 25% and 75% percentiles over the five measurements with different respiration patterns. All techniques achieved a good coverage of the tumor. Median values for A>Dmin were above 99% for all techniques and ITV and MidV concepts showed lower gamma agreement scores (median: 88.9% and 87.7%) compared to gating and tracking (94.2% and 94.8%). For ITV and MidV concepts larger increases in inhomogeneity were found (median: 4.3 and 5.6 percentage points respectively) than for gating and tracking (2.8 and 2.3). Gating and tracking were able to reduce OAR dose in all cases, when compared to ITV concept.

Table 1: Evaluated parameters from film measurements inside the tumor and planned OAR dose parameters

	GS3%/3mm (%)	ΔH1-99 (pp)	A>Dmin (%)	Lung Dmean (Gy)	Lung V20Gy (%)	Heart Dmean (Gy)	Spinal cord Dmax (Gy)
ITV	88.9 (82.3-95.7) [97.9]	4.3 (3.5-5.9) [5.1]	99.8 (99.6-99.9) [99.5]	8.3 (7.9-8.9)	14.1 (13.0-15.5)	1.4 (1.3-1.5)	11.1 (10.9-11.7)
MidV	87.7 (74.5-91.5) [97.0]	5.6 (3.9-7.5) [2.1]	99.1 (96.9-99.5) [100]	7.9 (7.2-8.0)	12.8 (11.3-13.4)	1.1 (1.1-1.3)	10.4 (10.2-10.4)
Gating	94.2 (93.2-96.4) [96.5]	2.8 (2.3-4.2) [1.6]	99.9 (99.4-99.9) [99.0]	7.2 (7.1-7.3)	11.6 (11.3-11.8)	0.8 (0.6-0.9)	10.2 (9.5-10.8)
Tracking	94.8 (91.7-96.0) [96.7]	2.3 (1.1-2.8) [1.8]	100 (99.9-100) [99.8]	7.2 (7.2-7.2)	12.1 (11.9-12.2)	1.0 (1.0-1.1)	9.8 (9.7-9.8)

Values: Median (Q_{25}-Q_{75}), [static measurement], pp: percentage points

Conclusion: Tracking and gating showed a superior agreement with the planned dose distribution and at the same time reduced the dose to OAR in comparison to the passive motion management techniques.

EP-1749

Real-time 4D ultrasound tracking of liver and kidney targets for external-beam radiotherapy

D.S.K. Sihono[1], J. Boda-Heggemann[1], L. Vogel[1], S. Kegel[1], J. Thölking[1], F. Lohr[1], F. Wenz[1], H. Wertz[1]
[1]*University Medical Center Mannheim- University of Heidelberg, Department of Radiation Oncology, Mannheim, Germany*

Purpose or Objective: Hypofractionated SBRT is an effective low-toxic therapy option for liver metastases. In our department, liver SBRT is performed in DIBH with ABC (Active Breathing coordinator) and image-guidance with breath-hold CBCT. For additional monitoring of the movable target and/or surrogate structures, an ultrasound-based tracking system has been developed. We evaluated the feasibility and the accuracy of this system on a motion phantom and healthy volunteers.

Material and Methods: The tracking accuracy of a 4D ultrasound system (Clarity Anticosti, Elekta, Sweden) was evaluated using an ultrasound phantom (BAT, Nomos) and a motion platform (CIRS, USA) with different settings to obtain optimal parameters to track structures moving with respiration. An initial evaluation was performed with 5 healthy volunteers to assess the performance in a quasi-clinical setting. An ultrasound dataset was acquired in ABC-based breath hold (breath hold time 20 sec, free breathing phases of 5-6 breathing cycles). Tracked structures were renal pelvis as a centroid structure and a portal vein/liver vein as a non-centroid structure. The scanning range of the ultrasound probe was varied. The motion component in superior-inferior direction was compared with the motion of an external marker on the body surface and the data from ABC.

Results: a) Phantom data: The tracking accuracy increased with decreasing scanning range. For a cycle time (sinusoidal motion) of 10 s and an amplitude of 10 mm, the mean and standard deviation of differences between the measured and the reference position values were 0.57 + 0.48 mm and 0.31 + 0.20 mm in 15° and 5° scanning range respectively,while for a cycle time of 5 s were 1.33 + 1.20 mm and 0.34 + 0.25 mm for 8° and 4° scanning range respectively. For a fixed scanning range, the accuracy of ultrasound tracking decreased with a decrease of cycle times.
b) Volunteer data: The system's tracking success rate was 90.77% of all breath-hold phases.The renal pelvis tracking success rate was 95.42%, while 86.79% for portal vein.A compromise between scanning range and cycle times had to be established depending on target. A working scanning range was between 10°-40°. For angles <10°there is a higher risk that the target is sometimes outside the ultrasound. This will lead to a reduced tracking success rate. Tracking curves (SI direction)were in good accordance with breathing curves of ABC and a fiducial placed on the infradiaphragmatic abdominal wall.

Conclusion: The ultrasound system showed good performance on a motion phantom and healthy volunteers. A positioning setup that provides good ultrasound visual over a long period in clinical environment could be established. Further improvement of the tracking algorithm could improve accuracy along with respiratory motion if using large scanning angles for detection of high-amplitude motion and non-linear transformations of the tracking target.

EP-1750

Monitoring of intra-fraction prostate motion with a new 4D ultrasound device

M. Fargier-Voiron[1], P. Pommier[2], S. Rit[1], D. Sarrut[1], M.C. Biston[2]
[1]*Université de Lyon- CREATIS, Physics, Lyon, France*
[2]*Centre Léon Bérard, Physics, Lyon, France*

Purpose or Objective: The emergence of hypofractionated protocols in prostate cancer treatment requires a better accuracy in dose delivery because of an increased risk of toxicity to the safe tissues. The aim of this study was to evaluate intrafraction motions of the target volumes for prostate cancer patients imaged with a new transperineal ultrasound (TP-US) device.

Material and Methods: The accuracy of the tracking of the TP-US (Clarity®, Elekta, Stockholm, Sweden) probe was first investigated by comparing the measured positions of a target volume in a phantom with the Clarity device and the simultaneous use of a transmitter based positioning device (RayPilot, Micropos Medical, Sweden). Then intra-fraction motions measured with the TP-US were analyzed for 13 prostate patients (426 sessions) and 14 post-prostatectomy patients (438 sessions). The fraction of time that the target volume was displaced by more than 3 and 5 mm was calculated for tracking times ranging between 60-420s, for each session and each patient. The mean displacements were also calculated for each direction. Percentages of sessions for which thresholds of 3 mm and 5 mm were exceeded during 15 s and 30 s in each direction were determined.

Results: Differences between TP-US and transmitter based devices were below 1.5 mm for all directions. The observed motions were patients and sessions dependent and increased with the treatment time. During the first minute, 3D displacements above 3 mm were seen 5% and 1.9% of the time, for prostate and post-prostatectomy patients, respectively while they reached 38% and 10.8% of the time after 7 min of treatment. Maximum 3D displacements above 5 mm were observed after 7 min 11.6% and 1.6% of the time for prostate and post-prostatectomy patients, respectively. Mean displacements in AP, SI and LR directions were -0.9±0.8mm, 0.9±0.8mm and -0.3±0.5mm for prostate patients and -0.9±0.5mm, 0.2±0.4mm and 0.1±0.4mm for post-prostatectomy patients. The maximum percentage of sessions for which the prostate and post-prostatectomy volumes exceeded the 3 mm tracking limits for at least 15 s was observed in the AP direction (Table 1). Conversely, minimum

displacements were observed in the lateral direction for prostate patients (4.5%), and in the SI direction for post-prostatectomy patients (0.7%).
Table 1:

		AP (%)	SI (%)	LR (%)
Prostate	3mm tracking limit exceeded = 15s	30.0	24.6	4.5
	3mm tracking limit exceeded = 30s	24.4	21.8	4.2
	5mm tracking limit exceeded = 15s	6.3	4.5	1.2
	5mm tracking limit exceeded = 30s	5.4	4.0	0.9
Post-prostatectomy	3mm tracking limit exceeded = 15s	11.4	0.7	4.1
	5mm tracking limit exceeded = 30s	9.4	0.7	3.4
	3mm tracking limit exceeded = 15s	1.8	0.0	0.7
	5mm tracking limit exceeded = 30s	1.6	0.0	0.7

Conclusion: Results for prostate patients are in agreement with the previously published data [1]. 4D TP-US modality is a promising alternative to irradiating and/or invasive IGRT modalities for intrafraction prostate motion management. In contrast, smaller displacements were observed for post-prostatectomy patients than those reported in the literature [2]. Further investigations are in progress to determine the causes of these discrepancies. References: [1] Langen KM et al. Int J Radiat Oncol Biol Phys. 2008;71(4):1084–90 [2] Klayton T et al. Int J Radiat Oncol Biol Phys. 2012; 84(1):130-136

EP-1751

Time-resolved analysis of Varian RPM-gated exposures on three versions of Truebeam linac

R.B. King[1], C.E. Agnew[2], B.F. O'Connell[2], K.M. Prise[1], A.R. Hounsell[2], C.K. McGarry[2]
[1]Queen's University Belfast, Centre for Cancer Research and Cell Biology, Belfast, United Kingdom
[2]Belfast Health and Social Care Trust, Radiotherapy Physics-Northern Ireland Cancer Centre, Belfast, United Kingdom

Purpose or Objective: To design a moving phantom capable oftime-resolved 2D dosimetry with the goal of validating gated radiotherapytreatments. A preliminary study was carried out to validate the arrangement withgated-exposures using the Varian real-time position management™ (RPM) system, installedon four different Truebeam® linacs (operating v.1.5, 1.6 and 2.0).

Material and Methods: The phantom consists of a PTW OCTAVIUS® 1000 SRSarray combined with a programmable moving platform and is capable of measuring2D dose profiles with a 100 ms acquisition rate. In this preliminary study thearray oscillated sinusoidally (2.5 cm amplitude) with 3 different breathingperiods (3, 4 and 6 s) while irradiated with a 6 MV, 4 × 4 cm^2field. Amplitude gating was employed to activate four Truebeams when the arraywas within ±20% and ±30% of the central position and at the 20% extremes of itsmotion. Additional time-resolved information on the activation of the linac wasacquired via oscilloscope traces of the *target*BNC output, and analysis of corresponding trajectory log files. All datasources were analysed using MATLAB 7.10, where GUIs were developed to interpretthe variation in position of the 2D dose profiles and to compare thetime-resolved data contained within the four data sources.

Results: Fig. 1 shows results obtained via each of theacquisition methods during a gated exposure. A phase correction term isincluded in the OCTAVIUS, log file and *target* signal data (Fig. 1 (a), (b) and(c) respectively), so that the first two segments agreed with the RPM data. Inthis example, the agreement is not maintained throughout the entire exposure.Both the OCTAVIUS and target signal data (Fig. 1 (d) and (f) respectively) aredelayed with respect to the RPM trace data and flags.

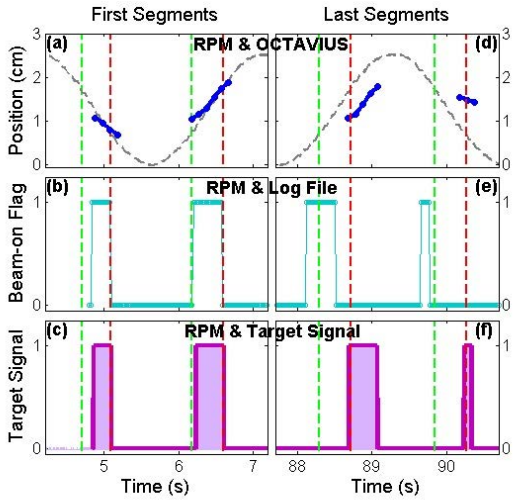

Fig. 1 Comparison between RPM data and other data sources during the first (a-c) and last (d-f) segments of a gated exposure. (a, d) RPM motion traces (dashed grey) and position information derived from OCTAVIUS measurements (solid blue). (b, e) Log file beam-on flags (cyan) for the same period. (c, f) Target signal measured during the exposure. Dashed vertical green and red lines indicate RPM beam enable and disable flags respectively.

Asindicated in Table. 1, this anomaly was observed on Truebeam versions 1.5 and1.6 but not on version 2.0. The opposite trend was observed in the log filecomparison (Fig. 1 (e)), where the beam-on flags lead the RPM beam-enableflags. For all irradiations it was observed that log file beam-on flags ledthe corresponding target beam-onsignal and that the time delay between the two signals was proportional to thenumber of segments.

Table. 1 Time difference between RPM beam enable flag for final exposure segments and the corresponding beam-on time recorded in the target signal oscilloscope trace and log file. Colour used to highlight time difference (*Blue* < -0.1, -0.1 ≤ Green ≤ 0.1, Red > 0.1 s).

Oscillation Period (s)	Gating Constraints (cm)		Accrued Time Discrepancy (s)					
			Truebeam 1.5		Truebeam 1.6		Truebeam 2.0	
	Min	Max	Target	Log File	Target	Log File	Target	Log File
3	-0.5	0.5	**0.397**	*-0.179*	**0.118**	*-0.467*	0.038	*-0.565*
	-0.75	0.75	**0.119**	*-0.244*	**0.204**	*-0.146*	0.035	*-0.348*
	0.75	1.25	**0.249**	0.009	**0.352**	**0.109**	0.029	*-0.210*
	-1.25	-0.75	0.047	*-0.199*	0.080	*-0.168*	0.051	*-0.201*
4	-0.5	0.5	**0.118**	*-0.306*	**0.118**	*-0.319*	0.049	*-0.398*
	-0.75	0.75	0.045	*-0.247*	0.038	*-0.249*	0.027	*-0.251*
	0.75	1.25	**0.355**	**0.165**	**0.402**	**0.192**	0.047	*-0.134*
	-1.25	-0.75	0.017	*-0.171*	0.065	*-0.132*	0.021	*-0.175*
6	-0.5	0.5	**0.131**	*-0.170*	**0.123**	*-0.169*	0.035	*-0.268*
	-0.75	0.75	0.044	*-0.136*	0.061	-0.095	0.027	*-0.155*
	0.75	1.25	**0.347**	**0.222**	**0.230**	**0.109**	0.029	*-0.114*
	-1.25	-0.75	**0.337**	**0.189**	**0.363**	**0.240**	0.036	*-0.100*

Conclusion: Preliminarytests with the new phantom have indicated that the RPM system can accurately enablethe linac output when the phantom position is within set gating parameters.However, using this novel arrangement, it was discovered that a discrepancy occasionallyoccurred on RPM systems installed on Truebeam versions 1.5 and 1.6. For someexposures a difference of up to 0.4 s was observed between data recorded by theRPM system and data extracted from the OCTAVIUS and target signal. The phantomalso highlighted a consistent discrepancy in the time information recorded inthe log files, where the cycle period of each exposure segment wasunderestimated by 10 ms, leading to differences of up to 0.6 s between the logfile and “true” target signal data.

EP-1752

A study of suitable conditions for stereotactic radiation therapy using VMAT for lung cancer

K. Kubo[1,2], H. Monzen[2], M. Tamura[2], M. Hirata[2], Y. Nishimura[3]
[1]*Tane General Hospital, Radiation Oncology, Osaka, Japan*
[2]*Kinki University, Graduate School of Medical Science- Department of Medical Physics, Osakasayama, Japan*
[3]*Kinki University, Faculty of Medicine- Department of Radiation Oncology, Osakasayama, Japan*

Purpose or Objective: The dose variation of stereotactic body radiation therapy using volumetric modulated arc therapy (VMAT SBRT) for lung cancer varies due to the interplay effect between multileaf collimator (MLC) motion and tumor motion. The aim of this study was to assess the relationship between dose variation and factors related to the interplay effect and clarify optimal conditions for VMAT SBRT.

Material and Methods: Respiratory motion data and MLC motion data were obtained from 30 patients who underwent treatment with VMAT SBRT for lung cancer. We calculated number of breaths (NB) during irradiation, maximum craniocaudal tumor motion (Amp), and MLC motion complexity (MCSv, modulation complexity score applied to VMAT). Parameters assessed for each treatment plan were MCSv, a divisor combination of Amp and MCSv (AmpMCSv), and a multiplier combination of AmpMCSv and NB (IVS, interplay effect variable score). Static and dynamic measurements were performed with a PinPoint chamber (0.015cm3, PTW, Germany) in a Quasar phantom (Modus Medical Devices, Canada). Pearson's correlation analysis was used to assess the effect of dose variation on individual parameters.

Results: A wide range of NB (28.9 to 100.7 times) was observed. The standard deviation of dynamic measurement ranged from 1.3 to 12.5 cGy. Dose variation was negatively correlated with AmpMCSv (r = −0.52, p < 0.05) and IVS (r = −0.62, p < 0.05). IVS was obtained stronger correlation than AmpMCSv by considering NB. Significant dose variation was found in cases with the lowest NB (28.9 times).

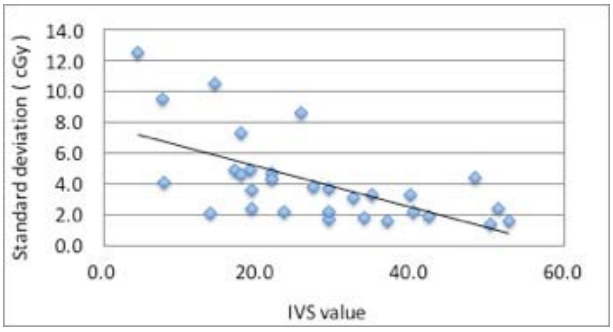

Conclusion: Patients that had fewer than 40 NB, <150 s irradiation time, and a respiratory cycle of >4 s had the highest dose variation, and therefore required careful attention during VMAT SBRT treatment.

EP-1753

Intrafraction setup variability for breast Helical Tomotherapy

R. Ricotti[1], D. Ciardo[1], G. Fattori[2,3], M.C. Leonardi[1], A. Morra[1], F. Pansini[4], R. Cambria[4], F. Cattani[4], C. Gianoli[5,6], M. Riboldi[2], G. Baroni[2,7], B.A. Jereczek-Fossa[1,8], R. Orecchia[1,8]
[1]*European Institute of Oncology, Department of Radiation Oncology, Milan, Italy*
[2]*Politecnico di Milano, Dipartimento di Elettronica Informazione e Bioingegneria, Milan, Italy*
[3]*Paul Scherrer Institut, PSI, Villigen, Switzerland*
[4]*European Institute of Oncology, Unit of Medical Physics, Milan, Italy*
[5]*Politecnico di Milano, Dipartimento di Elettronica Informazione e Bioingegneria, Milano, Italy*
[6]*Ludwig Maximilians University, LMU, Munich, Germany*
[7]*Centro Nazionale di Adroterapia Oncologica, Bioengineering Unit, Pavia, Italy*
[8]*University of Milan, Department of Oncology and Hemato-Oncology, Milan, Italy*

Purpose or Objective: To investigate intra-fraction breast motion during long-lasting (10-20 min) breast Helical Tomotherapy (Accuray, Madison, WI, USA) by means of optical tracking.

Material and Methods: Twenty locoregional breast cancer patients underwent Helical Tomotherapy irradiation after receiving conservative surgery or mastectomy. Non-invasive monitoring of respiratory motion during the entire treatment course, from setup verification to dose delivery, was achieved through infrared tracking of a passive marker placed near the surgical scar. In order to obtain the displacement deriving from the patient movement only, we subtracted the trace of an additional marker placed on the treatment couch. Respiratory signals were analyzed in terms of peak-to-peak amplitudes and baseline drifts, obtained by low-pass moving average filtering with a time window of 60 sec. Anisotropic Clinical Target Volume (CTV) safety margins expansion due to intrafraction organ motion was calculated relying on a synthetic representation of the specific patient respiratory pattern, obtained by adding half of the most probable respiratory amplitude to the non-respiratory movement of the scar trace in each anatomical direction (Fig.1).

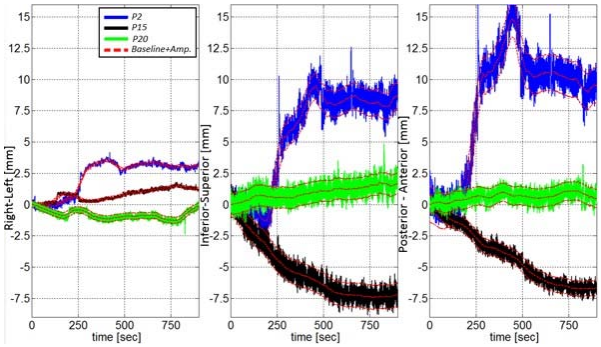

Results: The most probable measured breathing amplitudes among all patients was (median±inter-quartile range): 0.25±0.12 mm (right-left), 1.31±0.63mm (inferior-superior) and 1.22±0.70 mm (posterior-anterior). Each patient featured a small inter-fraction variability of expected motion ranges, thus confirming a good reproducibility of respiratory motion during the entire course of treatment. Scar baseline drifts were mostly in posterior and in the inferior direction for all patients in most fractions, with the exception of patient *P2,* who exhibited a relevant baseline shift in superior and anterior direction with a large variability (Tab.1). The distribution of right-left shifts resulted in almost zero median, with a narrow interquartile range. Patient *P20* showed stationary breathing, with a median baseline shift around zero in all anatomical directions. Conversely, patient *P15* had a wide inferior-superior and posterior-anterior motion with large interquartile ranges. Resulting anisotropic safety margin expansions across all patients with the exception of *P2*, considered an outlier, were 1.58-2.44 mm in right-left, 4.41-3.65 mm in inferior-superior and 3.78-2.15 mm in the posterior-anterior directions, respectively.

	Scar Baseline distribution							
	Right-Left [mm]		Inferior-Superior [mm]		Posterior-Anterior [mm]		n Fr	TOT Treatment Time [min]
	median	iqr	median	iqr	median	iqr		
P 1	0.16	1.11	-0.24	0.93	-1.27	1.43	8	96.29
P 2	1.32	3.06	2.27	8.53	2.84	8.12	6	83.75
P 3	0.44	0.86	-0.29	0.72	-1.72	1.36	5	61.62
P 4	0.16	0.62	-1.32	2.18	-2.60	3.09	12	152.01
P 5	0.45	1.22	-1.31	1.45	-0.46	1.41	9	120.66
P 6	0.55	1.58	-0.04	1.01	-0.24	0.90	3	42.08
P 7	-0.74	1.01	-0.74	1.78	-1.19	3.24	4	63.50
P 8	1.46	2.50	-0.88	2.17	-1.65	1.93	5	71.45
P 9	-0.53	0.92	0.18	1.68	-0.67	1.68	9	126.75
P 10	0.00	1.08	-2.48	1.50	-2.22	2.16	4	61.46
P 11	0.45	1.10	-0.42	1.24	-0.70	0.81	6	97.79
P 12	-0.01	1.22	0.55	1.73	-1.43	1.42	8	127.15
P 13	-0.17	0.80	-2.00	3.44	-2.19	2.95	8	125.17
P 14	0.13	1.02	0.18	1.79	-1.37	1.27	4	69.19
P 15	-0.59	1.35	-4.34	1.37	-3.31	2.62	6	100.50
P 16	-0.10	1.60	-0.06	1.02	-0.28	1.36	3	51.52
P 17	1.20	0.76	-0.03	2.08	-0.51	1.38	2	38.34
P 18	0.26	0.70	-1.12	1.48	-1.58	1.64	11	195.55
P 19	0.02	2.11	0.05	2.08	-0.35	1.64	5	93.46
P 20	-0.05	1.21	0.38	1.70	0.09	1.05	2	37.39
TOT	**0.11**	**1.18**	**-0.56**	**1.99**	**-1.18**	**2.00**	**120**	**1815.62**

iqr = inter-quartile range; n FR = number of fraction

Conclusion: Respiratory and non-respiratory motion during prolonged treatment induces significant position errors. Resulting CTV to Planning Target Volume (PTV) margins are within the 5 mm isotropic expansion generally used in clinic. Non-invasive continuous monitoring of intra-fraction motion should be implemented for an accurate definition of PTV.

EP-1754

The accuracy of ExacTrac X-ray intra-fraction verification at non-zero couch rotation

D.L.J. Barten[1], N.D. Sijtsema[1], M. Zahir[1], J.P. Cuijpers[1]
[1]*VUMC, Radiotherapie, Amsterdam, The Netherlands*

Purpose or Objective: Submillimeter accuracy of patient positioning is mandatory in stereotactic radiation therapy (SRT), since a high dose per fraction is given to relatively small lesions using tight PTV margins. SRT treatment techniques normally use couch rotations to achieve optimal irradiation. In frameless SRT intrafraction positioning verification at non-zero couch angles is recommended to ensure correct dose delivery. In this study the accuracy of the frameless ExacTrac X-Ray verification system at non-zero couch angles was assessed.

Material and Methods: An Alderson head phantom with a hidden marker was immobilized in a BrainLAB frameless mask on the Novalis Tx system. The phantom was positioned using the ExacTrac X-Ray system at couch angle 0°. For 13 different couch angles the phantom position was determined using the i) infrared (IR) optical markers, ii) X-ray verification imaging and iii) MV images taken from the AP direction. In the latter only deviations in the couch rotation plane were measured, assuming negligible deviations in the vertical direction. The Winston-Lutz test was performed to validate this assumption. The AP-MV imaging was used as the golden standard and was compared with the ExacTrac IR and X-ray results for each couch angle to determine the accuracy of the ExacTrac system. All data were relative to couch angle 0° and calculated in the Linac coordinate system. A one sample T-test was performed to determine statistically significant ($p<0.05$) differences between the systems.

Results: Deflection of the couch in the vertical direction was within 0.23 mm at couch angle 0° and variation at other couch angles is less than 0.1mm. X-Ray verification at different couch angles showed significant differences with the AP-MV imaging of 0.23±0.12mm and 0.30±0.21mm on average for longitudinal and lateral direction respectively. Maximum deviations between AP-MV imaging and ExacTrac X-ray were found at couch angle 30° of 0.63mm in lateral and 0.50mm in longitudinal direction. Verification with the IR markers shows larger deviations than the X-ray verification. Largest mean deviations for longitudinal and lateral direction were -1.55mm (at couch angle 270°) and 1.14mm (at couch angle 90°).

Conclusion: X-Ray verification at non-zero couch angles using the ExacTrac system is sufficiently accurate to be used in SRT. Deviations in X-Ray verification were largest at couch angle 30° but this will be of minimal importance clinically, since in non-coplanar SRT treatment techniques multiple couch angles are used. The IR system shows deviations that exceed accuracy requirements for SRT.

EP-1755

Visualization of respiratory and cardiac motion via TomoTherapy exit detector fluence

N. Corradini[1], P. Urso[1], C. Vite[1]
[1]*Clinica Luganese, Radiotherapy Center, Lugano, Switzerland*

Purpose or Objective: To demonstrate that respiratory and cardiac motion is observable and quantifiable on the CT detector during TomoDirect breast treatments.

Material and Methods: A preliminary study for motion management in breast radiotherapy was performed using the exit detector fluence of tangential static IMRT fields on TomoTherapy. Two patients in treatment for left breast cancer were selected randomly for study. After their radiotherapy treatments, the raw pulse-by-pulse detector data was downloaded from the CT detector for analysis. The pulse-by-pulse detector data is sampled at a frequency of 300 Hz. The exit detector channels with fluences corresponding to the breast and heart surfaces were identified within the recorded treatment sinograms. These channels' fluences were then investigated at the temporal projections in which respiratory and cardiac motion were expected (Figures 1a-b).

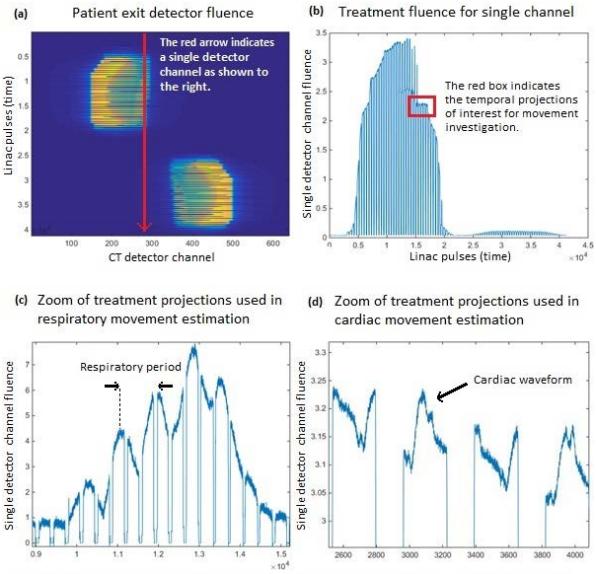

Figure 1. (a) Example of the the pulse-by-pulse exit detector fluence for a breast patient. (b) Example of a single fluence profile for an entire patient treatment. (c) Zoom of single channel fluence at the breast surface used for respiratory motion estimation. (d) Zoom of single channel fluence at the heart surface used for cardiac motion estimation.

Results: Sinusoidal and waveform variations in fluence were observed where respiratory and cardiac motion was expected. The sinusoidal motion recorded on the detector data at the expected breast surface averaged a period of 2.8 ± 0.1 sec during the 4 fractions that were analyzed. The cardiac waveform motion recorded on the detector data at the expected heart surface averaged a rate of 86.4 ± 2.0 bpm during the 3 fractions that were investigated (Figures 1c-d).

Conclusion: The fluence variations we have observed on the pulse-by-pulse detector data would fit reasonably within respiratory and cardiac motion. These preliminary results are indicative of the ability for visualization and quantification of

organ motion during tangential breast treatments on TomoTherapy. Further studies into these breast treatment exit detector fluences are necessary for this method's verification and future development of method robustness. The future applications for this method include better dosimetric understanding of tangential breast treatments as well as possible dynamic delivery compensation for organ motions to reduce the patient's lung and heart dose.

EP-1756

Differential motion of adjacent lung tumours eligible for SBRT with a single isocentre

M.M.G. Rossi[1], H.M.U. Peulen[1], J.S.A. Belderbos[1], J.J. Sonke[1]
[1]*Netherlands Cancer Institute Antoni van Leeuwenhoek Hospital, Department of Radiation Onocology, Amsterdam, The Netherlands*

Purpose or Objective: Stereotactic Body Radiotherapy is increasingly used for early stage Non Small Lung Cancer (NSCLC) or oligometastatic disease. For patients with two adjacent homolateral tumours, high quality treatment plans can be designed to simultaneously treat both tumors with a single isocentre. The accuracy of treatment delivery is then potentially compromised. A compromise needs to be made for differential motion of the two tumors. The aim of this study was to quantify inter- and intra-fractional differential motion of adjacent tumours eligible for SBRT with a single isocentre.

Material and Methods: Patients treated with SBRT for lung tumours since 2014 were retrospectively selected from our database. Patients were included if they presented with 2 adjacent homolateral tumours with a distance between the 2 lesions of ≤5cm (Figure 1). Prior to each treatment session patients received a CBCT (CBCTprecor) for tumour alignment. Both GTVs in the CBCTprecor were local-rigidly registered to the planning CT scan (pCT) using two separate shaped regions of interest. These registration results were then subtracted to give the differential motion. The post treatment CBCT (CBCTpostRT) and post correction CBCT (CBCTpostcor) were similarly used to quantify the difference in intra-fraction motion (IFM) between the two lesions. Subsequently the group mean (GM), systematic (Σ) and random (σ) position variabilities were calculated for Left/Right (LR), Cranial/Caudal (CC) and Anterior/Posterior (AP) directions.

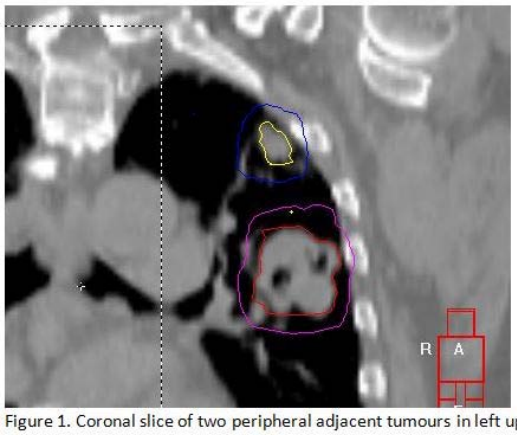

Figure 1. Coronal slice of two peripheral adjacent tumours in left upper lobe

Results: Nine patients were included in this analysis, 7 male 2 female, median age was 63 years. The median distance between the tumours was 2.7 cm (range 1.2-4.7cm) All tumours were peripherally located, with a median Gross Tumour Volume (GTV) of 1.95cc (range 0.2-38.2cc) and median tumour amplitude, derived from the 4D pCT of 0.2,0.4 and 0.4 cm in LR, CC and AP directions respectively. The inter-fraction differential tumour motion in terms of GM, Σ and σ is shown in Table 1. Systematic displacements in CC and AP were somewhat larger than the random displacements. In 5 patients the tumours moved on average towards each other, in the remaining 4 patients the tumours moved further apart. Differential IFM (table 1) was typically somewhat smaller than inter-fraction motion. Inter-fraction motion did not significantly correlate with the inter tumor distance for the systematic component but was highly correlated ($r>0.75$; $p<0.02$) to the random component.

Table 1: Inter- and intra-fractional differential motion of adjacent tumours in terms of mean (GM), systematic (Σ) and random variations (σ)

(cm)	LR	CC	AP
Inter-fraction Motion			
GM	-0.001	0.09	-0.04
Σ	0.10	0.22	0.27
σ	0.12	0.14	0.15
Intra-fraction Motion			
GM	0.05	-0.05	0.08
Σ	0.12	0.13	0.19
σ	0.12	0.07	0.24

Conclusion: Differential motion of 1-3 mm (systematic and random variation) was observed in this small retrospective study between adjacent lung tumours eligible for single isocentre SBRT. However, as a compromise can be made for tumour alignment, the values reported in this study should be divided by two when calculating margins.

EP-1757

Intra-fraction patient movements during SBRT: CBCT vs Surface Optical Markers

P. Tabarelli De Fatis[1], A. Fassi[2], M. Liotta[1], I. Meaglia[3], P. Porcu[3], C. Bocci[3], G. Baroni[2], G. Ivaldi[3]
[1]*Fondazione Salvatore Maugeri, Medical Physics, Pavia, Italy*
[2]*Politecnico di Milano, Dipartimento di Elettronica Informazione e Bioingegneria, Milano, Italy*
[3]*Fondazione Salvatore Maugeri, Radioterapia, Pavia, Italy*

Purpose or Objective: To evaluate and to compare the intra-fraction movements, during Stereotactic Body Radiation Therapy (SBRT), obtained with two different methods: Cone Beam CT (CBCT) and an infrared Optical Tracking System (OTS).

Material and Methods: 10 patients (pts) with lung lesions (primary tumour or metastasis) were irradiated with a total dose ranging from 36 to 42 Gy in 3 fractions using one or two 6 MV photons volumetric-modulated arcs by a Varian Clinac linear accelerator. Pts were positioned with the arms raised on a breast setup system (PosiboardTM, Civco) with a vacuum customized cushion. The OTS SMART-DX (BTS Bioengineering, Milano, Italy) was used to record the 3D coordinates of multiple passive markers (6-8) placed on the patient's thoraco-abdominal surface. Ungated CT images was acquired for treatment planning (TP). 4DCT images were used for clinical target volume (CTV) delineation and a 5mm isotropic planning target volume (PTV) was generated. Before the daily treatment a CBCT was acquired and registered to the planning CT to obtain and apply the setup corrections (only translations allowed). After the irradiation a second CBCT was performed and rigidly registered to the first CBCT with a mutual information algorithm focusing on the CTV region. A rigid transformation was also estimated from surface markers coordinates acquired by the OTS just before the two CBCT scans. Setup corrections were subtracted from the rototranslation parameters obtained from both CBCT and OTS, in order to evaluate intra-fraction patient reproducibility. The results for both CBCT and OTS methods were evaluated and compared regardless of rotations coordinates always found to be less than 1 degree.

Results: In 39 analyzed fractions the mean absolute values of translational displacements obtained with the CBCT method was 0.6±0.9 mm in the latero-lateral (LL) direction, 0.7±1.0 mm in the antero-posterior (AP) direction and 1.0±1.0 mm in the cranio-caudal (CC) direction. The same analysis achieved in 26 fractions with surface markers, revealed absolute displacements of 1.1±1.1 mm in LL, 1.5±0.9 mm in AP and 1.7±1.7 mm in CC direction. Comparing the shifts obtained with the two systems in the same sessions, the resulting mean difference was 1.1±1.2 mm in LL, 1.8±1.3 mm in AP and 1.7±1.6 mm in CC.

Conclusion: The differences between the intra-fraction patient displacements observed through CTV overlapping using CBCTs and through the surface markers registration seem to be clinically acceptable for the PTV considered. The relatively greater spread using markers is probably due to the larger portion of patient's surface covered by the OTS compared to the CTV region. Considering the adopted PTV margin, the non-invasive OTS could be therefore used to monitor the intra-fraction movements as alternative to a post treatment CBCT, possibly using markers positioned in a restricted area around the target.

EP-1758

Cyberknife Stereotactic Radiation Therapy for lung cancer: role of the LOT simulation.

I. Bossi Zanetti[1], A. Bergantin[1], A.S. Martinotti[1], I. Redaelli[1], P. Bonfanti[1], M. Invernizzi[1], A. Vai[1], L.C. Bianchi[1], G. Beltramo[1]
[1]*Centro Diagnostico Italiano, Cyberknife, Milano, Italy*

Purpose or Objective: SBRT is now an accepted treatment for inoperable pts with stage I lung cancer and oligometastatic disease.Particularly for SBRT, tumor motion must be taken into consideration due to high dose per fraction. It is unclear which system provides the best accuracy for target localization.The aim of this study is to evaluate the role of lung optimization treatment(LOT) simulation for the best tumor tracking using Cyberknife SBRT.

Material and Methods: From September 2014 to July 2015 we evaluated 143 consecutive pts referred to our department for tracking modality.For everyone a CT scan was performed in expiratory and inspiratory phase.During the simulation the position and setup were the same as those during the treatment. The real-time images were compared to the DRRs where the target was evidenced.Cyberknife includes a small 6 MV LINAC mounted on a robotic arm,two diagnostic X-ray sources (installed in the ceiling of the treatment room) attached to digital image collectors, placed orthogonally to the patient to provide real-time treatment guidance, and a table remotely controlled that can move around different axes and adjust the patient position.

Results: According to the accuracy of the LOT system in target identification we observed these solutions:we treated 102 pts (71%) with Xsight lung technique, 80 pts in 2-view modality in which the target was recognized and tracked from both X-Ray cameras and 22 pts in 1-view modality,in which only one camera was used. XSight lung along with Synchrony Respiratory Tracking can automatically track and adjust the beam to tumor motion, using the lesion as a fiducial.The GTVs were expanded by 3 mm in all directions to create the CTVs .We used different margins for PTVs. In the 2-view modality the CTV on expiratory CT was expanded by 2mm in all directions,while for 1 view modality two different CTVs were generated on both CT scan to include the entire inhale-to-exhale tumor motion, and added together to create an ITV expanded by 2 mm in the direction followed by the X-Ray camera and 3mm in the other direction.For the other 40 lesions (29%),when the tumor cannot be clearly identified by either of the two cameras,fiducials have been necessary.

Conclusion: LOT simulation system is a very effective, useful and non-invasive technique. Dramatically reducing PTV margins and consequently the risk of potential toxicities related to the high doses, LOT simulation system and Xsight lung are considered the best choice in the management of lung lesions in our clinical practice.

EP-1759

Treatment of moving targets with active scanning carbon ion beams

P. Fossati[1], M. Bonora[2], E. Ciurlia[2], M. Fiore[2], A. Iannalfi[2], B. Vischioni[2], V. Vitolo[2], A. Hasegawa[2], A. Mirandola[2], S. Molinelli[2], E. Mastella[2], D. Panizza[2], S. Russo[2], A. Pella[2], B. Tagaste[2], G. Fontana[2], M. Riboldi[3], A. Facoetti[2], M. Krengli[4], G. Baroni[3], M. Ciocca[2], F. Valvo[2], R. Orecchia[1]
[1]*European Institute of Oncology, Radiotherapy Division, Milano, Italy*
[2]*Fondazione CNAO, Clinical Area, Pavia, Italy*
[3]*Politecnico of Milan, Bioengineering Department, Milano, Italy*
[4]*University of Piemonte Orientale, Radiotherapy Department, Novara, Italy*

Purpose or Objective: We report the preliminary clinical results organ motion mitigation strategies in the treatment of moving target with active scanned carbon ion beams.

Material and Methods: Since September 2014 26 patients with tumors located in the upper abdomen and chest were treated with active scanned carbon ion beams. Patients were affected by pancreatic adenocarcinoma, HCC, biliary tract cancers and sarcoma of the spine retroperitoneum and heart. Tight thermoplastic mask was selected as the optimal abdominal compression device. 4D CT scan with retrospective reconstruction, with phase signal obtained with Anzai system (Anzai Medical CO., LTD), was employed for planning. Automatic assignment of raw data to respiratory phases was checked and, if necessary, modified by the medical physicist. Planning was performed using end expiration phase. Planning CT scans were visually checked for motion artifacts. Contouring was performed on end expiration phase and on the adjacent 30% expiration and 30% inspiration phases. Beam entrance was selected in order to avoid the bowel in the entrance channel. The lung diaphragm interface was contoured in the different respiratory phases and beam angles were chosen to avoid passing tangential to the lung diaphragm ITV. IMPT was used for plan optimization. Plans were recalculated in adjacent phases and if DVHs were degraded in an unacceptable way they were modified iteratively. Weekly verification 4D CT scans were performed and, if needed, a new plan was re-optimized adaptively. Set up was verified with gated orthogonal X rays and non-gated cone beam CT in treatment room. Threshold for gate-on signal was initially set at 10% pressure signal dynamic and qualitatively adjusted in an asymmetric way according to results of plan recalculation in 30% expiration and inspiration. Gating signal was fed to the accelerator to enable beam delivery. Each slice was re-scanned 5 times to smear out possible interplay effects. Acute and early toxicity was scored according to CTCAE 4.0 scale.

Results: GTV and diaphragm excursion between end expiration and adjacent 30% phases was reduced to less than 5 mm. GTV (D95%) and critical OARs (D1%) DVH in 30% inspiration and expiration phases showed on average minimal (less than 1%) differences as compared to planning end expiration plan. Toxicity was minimal with no G3 event. G2 toxicity was observed in 15% of the patient during treatment and in 10% of the patients at 3 months. Median follow up was rather short (3 months) nevertheless in 23 patients the dose limiting OAR was either stomach or small bowel or esophagus , therefore early toxicity data are informative.

Conclusion: Active scanning with carbon ion beams for the treatment of moving target using abdominal compression, 4D simulation, robust planning, gating and rescanning is feasible and safe . Longer follow up is needed to evaluate oncological outcome.

EP-1760

Correlation and directional stability of principal component of respiratory motion in the lung

H. Hanazawa[1], Y. Matsuo[1], M. Nakamura[1], H. Tanabe[2], M. Takamiya[3], Y. Iizuka[1], K. Shibuya[4], T. Mizowaki[1], M. Kokubo[2], M. Hiraoka[1]
[1]*Kyoto University Graduate School of Medicine, Department of Radiation Oncology and Image-Applied Therapy, Kyoto, Japan*
[2]*Institute of Biomedical Research and Innovation, Devision of Radiation Oncology, Kobe, Japan*
[3]*Kyoto University Graduate School of Engineering, Department of Nuclear Engineering, Kyoto, Japan*

[4]*Yamaguchi University Graduate School of Medicine, Department of Therapeutic Radiology, Ube, Japan*

Purpose or Objective: Application of principal component analysis (PCA) to fiducial marker coordinate during respiratory cycle provides new axes including the first principal component (1st PC), which presents maximal motion direction. The purpose of this study is to investigate correlation of respiratory motion between the markers implanted in the lung and interfractional variation in directionality of the 1st PC.

Material and Methods: Marker motion data in consecutive 9 patients who had 4 or 5 gold fiducials implanted in the lung and received tumor-tracking stereotactic body radiotherapy in 4 fractions were analyzed. Superior–Inferior (SI)/ Left–Right (LR)/ Anterior–Posterior (AP) positional data were acquired using a pair of orthogonal fluoroscopy in every fraction with the frame rate of 6.25 or 12.5 per second. Fifty-five datasets were eligible. The acquired SI/LR/AP coordinates were processed by PCA for each marker in all patients to calculate cumulative contribution ratio, principal component scores from 1st to 3rd PC and eigenvector of the 1st PC. Motion amplitude was defined as the 95th percentile of 1st PC scores. We evaluated (1) contribution ratio (CR) of the 1st PC, (2) correlation of the 1st PC scores between different markers in each fraction and (3) angles formed by 1st PC eigenvector of the first fraction and those of the others (defined as Ang1i (i=2, 3, 4)) for each marker.

Results: Mean ± standard deviation (SD) of motion amplitude in the 1st PC direction was 20.2 ± 11 mm. Median contribution ratio (CR) of 1st PC was 0.933 (range: 0.721–0.996). Median correlation coefficient of 1st PC score among the markers was 0.985 (range: 0.938–0. 999). For all markers, Ang1i varied from 1.19 to 23.3 degrees (deg) as shown in the **Figure**. Mean ± SD of Ang1i in 7 patients whose 1st PC directions seemed stable was 3.4 ± 1.03 deg, while 2 patients had larger variation (18.8 and 11.3 deg on average). The markers with larger interfractional variations in directionality had the tendency to be more affected by heartbeat or possess small motion amplitude with round shape orbit.

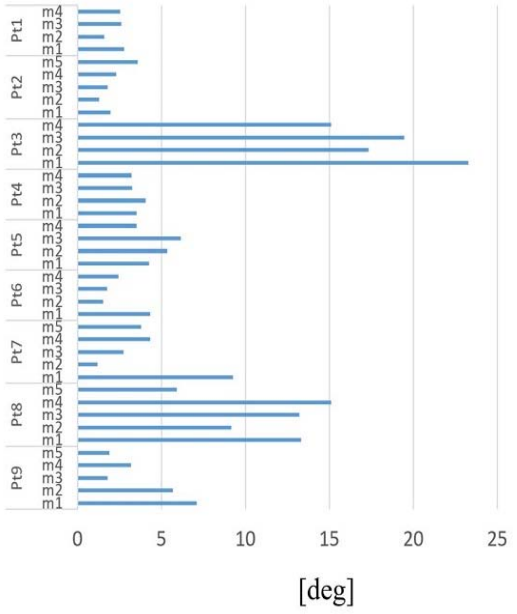

Figure.

Interfractional variation in motion direction for each marker.
Abbreviations: deg = degrees, Pt = patient, m = marker

Conclusion: The 1st PC of the marker coordinate during breathing generally provided a good explanation of its respiratory motion in the lung. Strong correlations in motion along the 1st PC direction between different markers were indicated. Interfractional variation in motion direction stayed small in most cases.

EP-1761

Assessment of motion mitigation and setup monitoring in gating treatments with accelerated particles

A. Pella[1], M. Seregni[2], S. Molinelli[3], P. Fossati[4,5], M. Riboldi[2], B. Tagaste[1], G. Fontana[1], M.R. Fiore[4], E. Ciurlia[4], A. Iannalfi[4], B. Vischioni[4], V. Vitolo[4], A. Mirandola[3], S. Russo[3], M. Ciocca[3], G. Baroni[1,2], F. Valvo[4], R. Orecchia[5,6,7]
[1]*CNAO, Bioengineering, Pavia, Italy*
[2]*Politecnico di Milano University, Bioengineering, Milan, Italy*
[3]*CNAO, Medical Physics, Pavia, Italy*
[4]*CNAO, Clinical Division, Pavia, Italy*
[5]*University of Milan, Oncology, Milan, Italy*
[6]*European Institute of Oncology, Radiotherapy, Milan, Italy*
[7]*CNAO, Scientific Director, Pavia, Italy*

Purpose or Objective: The aim of this study is to evaluate the efficacy of motion mitigation tools in reducing respiration-induced target motion and to investigate the concordance of redundant breathing motion monitoring systems during gating treatments in radiotherapy with accelerated particles.

Material and Methods: In our institution, a gating protocol for carbon ion therapy has been developed and since 2014 it is applied to lesions affected by non-negligible organ motion. It involves both abdominal compression (through tight thermoplastic body masks) and active beam rescanning. 4DCT is used to image anatomy variations between end-inspiration (EI) and end-expiration (EE) phases. Treatment is optimized on the EE phase and it is delivered in a gate-on window centered on it. Both 4DCT binning and gate-on trigger rely on the Anzai load cell system (Anzai Medical CO, LTD). To quantify the efficacy of abdominal compression, we evaluated the 3D GTV displacements observed between EE and EI phases of the planning 4DCT. A B-spline-based deformable registration algorithm was used to calculate the displacement field between EE and EI. GTV contours, as segmented in EE, were then propagated to the EI. In addition, an in-room optical tracking system (OTS) provided continuous breathing monitoring by localizing a set of surface markers. Each time the gating window was opened by the Anzai system, markers coordinates were stored and compared offline, in terms of 3D displacements, with the initial setup configuration. This solution allowed us to measure and quantify the intra-fraction concordance of surface surrogates.
Data of six patients with thoracic and abdominal lesions has been evaluated.

Results: A median (interquartile) 3D GTV displacement (EE-EI) of 5.8 (2.0) mm, in a range of 1.4-10.9 mm, was observed. The maximum displacements (absolute values) were noticed in superior-inferior direction (range: 0.1-9.3 mm). Overall mean values of markers 3D displacements between setup conditions and data acquired during irradiation by the OTS were found to be lower than a millimeter (range: 0.1-0.7 mm). We observed an intra-fractional significant difference among different irradiation fields, thus suggesting a small trend towards progressive deterioration of reproducibility during treatment delivery.

Conclusion: Target 3D displacements, as calculated from the EE and EI phases, can be considered relevantly lower than those reported in literature for thoraco-abdominal lesions. These preliminary results suggest that patient's respiratory pattern (and thus target trajectory) can often be reduced by means of appropriate immobilization/compression tools. During treatment delivery, sub-millimeter values of 3D discrepancies in surface surrogates detection demonstrate that the Anzai and the OTS operate consistently, therefore a

strategy combining these systems may increase set up control and motion monitoring robustness.

EP-1762

Impact of physiological breathing motion for breast cancer radiotherapy proton beam scanning

A.M. Flejmer[1], B. Chehrazi[2], D. Josefsson[3], I. Toma-Dasu[4], A. Dasu[5]

[1]*Linköping University, Department of Oncology, Linköping, Sweden*

[2]*Stockholm University, Department of Physics, Stockholm, Sweden*

[3]*Linköping University, Department of Radiation Physics, Linköping, Sweden*

[4]*Stockholm University and Karolinska Institutet, Medical Radiation Physics, Stockholm, Sweden*

[5]*Linköping University, Medical Radiation Physics, Linköping, Sweden*

Purpose or Objective: To study the impact of breathing motion on proton breast treatment plans using scanned proton beams.

Material and Methods: The study cohort was composed of twelve thoracic patients who had CT-datasets acquired during breath-hold at inhalation phase, breath-hold at exhalation phase and in free breathing mode. Proton treatment plans were designed for the left breast for the breath-hold at inhalation phase and were subsequently recalculated for the breath-hold at exhalation phase. Similarly, plans devised for the CT acquired in free breathing mode were recalculated for the extreme breath-hold phases. Four different field arrangements were used for each patient: two plans with three fields and two with one field. The dosimetric features of the plans were compared from the point of view of their coverage of the target and the doses to the organs at risk.

Results: Breathing motion led to a degradation of the dose coverage of the target (heterogeneity index increased from about 6% to 8-11%). Exhalation tended to decrease the lung burden (average dose 3.1-4.2 GyRBE), while inhalation increased it (average dose 4.7-5.8 GyRBE). The absolute values depended on the field arrangement, but the trend was similar across the plans considered. Smaller differences in dosimetric parameters were seen for the heart (average dose 0.1-0.2 GyRBE) and the left anterior descending artery (2.0-4.0 GyRBE). The absolute values of the dosimetric parameters corresponding to various breathing phases were rather small and their expected clinical impact is therefore quite small. Furthermore, the plans parameters in either breathing phase were generally superior to the corresponding ones that could be achieved with photon plans.

Conclusion: The results of this study indicated that the differences between the mean dosimetric parameters of the plans corresponding to the two extreme breathing phases are not significantly different, thus suggesting that breathing might have little impact for the chosen beam arrangements in proton scanned beam planning for breast cancer. Further investigations are needed to investigate the impact of interplay effects and whether the conclusions might be extended beyond the population considered in this study.

EP-1763

Experimental analysis of interplay effects in flattening filter free VMAT treatment techniques

T. Gauer[1], T. Sothmann[2], R. Werner[2]

[1]*University Medical Center Hamburg, Department of Radiotherapy, Hamburg, Germany*

[2]*University Medical Center Hamburg, Department of Computational Neuroscience / Department of Radiotherapy, Hamburg, Germany*

Purpose or Objective: In SBRT of lung lesions, respiratory motion is commonly considered by 4DCT imaging to define the internal target volume (ITV). Dose optimization is often performed on average CT using VMAT-based treatment techniques. However, average CT data ignores individual respiratory motion patterns during dose delivery and thus fluctuations in density distribution in the ITV. Additionally, interaction of MLC dose modulation and variable target motion might result in under-dosage of the target volume (interplay effect). This study analyses the efficiency of flattening filter free dose delivery and its impact on interplay effects in lung SBRT.

Material and Methods: SBRT treatment plans were created for a lung tumor phantom using VMAT techniques employing the flattening filter (FF) and flattening filter free (FFF) mode (600MU and 1400MU per min). The phantom consists of a high resolution 2D detector array plus solid-water, bone, lung and tumor inserts. It is mounted on a 4D motion platform to simulate regular and irregular tumor motion trajectories extracted from clinical 4DCT data with max peak-to-peak amplitudes of 1.6/2.3cm in SI and 1.2/2.4cm in AP. The ITV includes a 2cm x 2cm lung tumor (CTV) plus 1.8cm safety margin in SI. Changes in dose distributions through interplay effects were investigated by analyzing static reference and dynamic dose measurements in FF and FFF mode at regular and irregular tumor motion using a planning structure-based evaluation method.

Results: VMAT techniques in FF and FFF mode achieved almost identical dose distributions at static measurements (plan comparison). FFF allowed for approximately 40% shorter treatment time. For regular tumor motion (TM), FFF resulted in greater under- and over dosages of approximately 5-10% compared to FF in the CTV (cf. figure 1 for dose differences of dynamic and static measurements). However, corresponding γ-passing maps illustrate the increased interplay effect. Furthermore, FFF generated considerable under-dosages in the CTV in case of irregular TM. γ-passing rates (local γ of 3% / 1mm) decreased from 68% to 62% for regular TM and 41% to 34% for irregular TM within the ITV (cf. figure 1). Dose area histograms for CTV and ITV complementarily confirm above changes in dose differences and γ-maps.

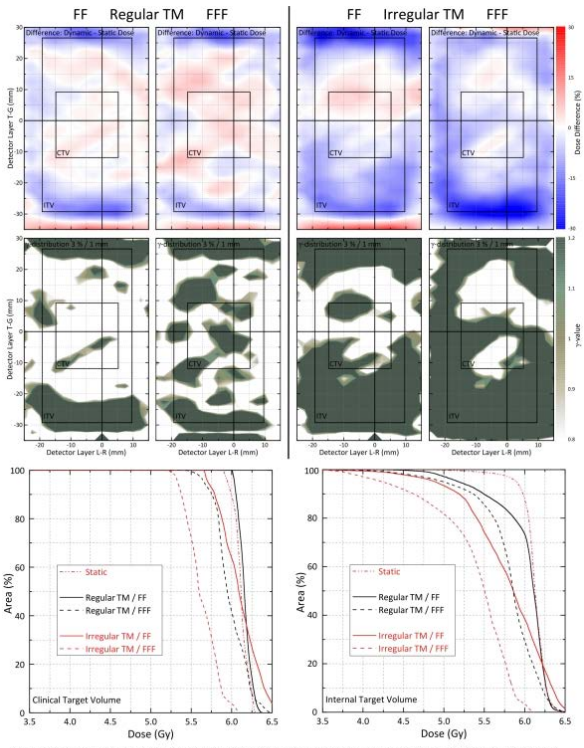

Figure 1: Analysis of interplay effects by differences of dynamic and static dose measurements for VMAT techniques with flattening filter (FF) and flattening filter free (FFF) beams at regular and irregular tumor motion (TM). Corresponding gamma-passing maps are presented using local gamma-criteria of 3% / 1mm. Dose area histograms are shown for clinical and internal target volume.

Conclusion: FFF dose delivery in lung SBRT provides shorter treatment times. However, the risk of interplay effects is increased, in particular for irregular tumor motion. Further

analysis is required to evaluate the appropriateness of FFF in lung SBRT.

EP-1764

development and validation of a tool to evaluate prostate motion due to patient's breathing

C.M.V. Panaino[1], T. Giandini[2], M. Carrara[2], S. Frasca[3], B. Avuzzi[3], S. Morlino[3], D. Bosetti[3], N. Bedini[3], S. Villa[3], T. Rancati[4], D. Bettega[1], R. Valdagni[3], E. Pignoli[2]

[1]Università degli Studi di Milano, Physics Department, Milano, Italy

[2]Fondazione IRCCS Istituto Nazionale dei Tumori, Medical Physics Unit, Milan, Italy

[3]Fondazione IRCCS Istituto Nazionale dei Tumori, Radiation Oncology 1, Milan, Italy

[4]Fondazione IRCCS Istituto Nazionale dei Tumori, Prostate Cancer Program, Milan, Italy

Purpose or Objective: An electromagnetic (ELM) system (Calypso, Varian Medical System, Palo Alto, CA, USA) based on sub-millimeter high frequency localization of three transponders permanently implanted in the prostate, was recently introduced for continuous real-time tracking of the tumor. Several studies of the tracks acquired over thousands of patients were reported in literature and allowed to give a detailed insight of intra-fraction prostate motion. Aim of this work was to develop and validate a tool to selectively filter the signal produced by the ELM transponders and to apply it for the evaluation of the amplitude of prostate motion only due to patient's breathing.

Material and Methods: To selectively filter the signal produced by ELM transponders a software was developed in the Matlab environment (version R2014b). Briefly, the developed software computes the power density spectrum (PDS) of the recorded tracks and isolates the 'breathing peak', i.e. the peak which is centered at the frequency corresponding to the breathing average frequency of each single analyzed session. A bandpass filter on the breathing peak is then applied to the original tracking data, in order to isolate the motion of the prostate due to the breathing of the patient. The software was validated with data recorded with QUASAR moving phantom, provided with an home-made insert of three transponders. Simulated breathing frequencies of 10, 12, 14, 16, 18, 20, 22 and 24 cycles per minute were recorded for at least one minute with the ELM system. After validation, tracks of 6 prostate patients who underwent EBRT were analyzed for a total of 180 treatments sessions. For each session, the corresponding maximum amplitude of prostate motion along the three main directions was obtained. Intra patients average data and standard deviations were reported along with the overall maximum amplitude.

Results: For the in-phantom validation, the developed software automatically computed the correct cycles per minute within a 0.52% uncertainty. The average amplitudes of prostate motion due to patient's breathing are listed in Table 1. As expected, the smallest motion resulted in left-right direction. The limited standard deviations indicate a low intra-patient motion variability. For each patient, the overall maximum amplitude turned out to be not negligible, but at the same time less than 0.5 mm.

TABLE 1 - Amplitudes of prostate motion due to patient's breathing

		Left-Right (mm)		Cranio-Caudal (mm)		Antero-Posterior (mm)		overall
	# sessions	average	std. dev.	average	std. dev.	average	std. dev.	maximum (mm)
Pt #1	33	0.10	0.05	0.22	0.04	0.15	0.06	0.29
Pt #2	37	0.14	0.04	0.16	0.04	0.26	0.06	0.38
Pt #3	24	0.18	0.03	0.27	0.04	0.24	0.06	0.41
Pt #4	29	0.12	0.02	0.31	0.06	0.22	0.06	0.48
Pt #5	26	0.11	0.04	0.16	0.04	0.19	0.05	0.29
Pt #6	31	0.09	0.02	0.15	0.03	0.13	0.07	0.26

Conclusion: A tool to quantify prostate motion due to patient's breathing was successfully developed, validated and applied to a consistent number of treatments sessions. Although small compared to the motion caused by the modifications of near organs (i.e. bladder and rectum), the achieved results show that the motion associated to patient's breathing should be carefully considered in the definition of an adequate Internal Target Volume.

This work was partially funded by Associazione Italiana per la Ricerca sul Cancro AIRC (grant N-14300)

EP-1765

Monitoring of intra-fraction eye motion during proton radiotherapy of intraocular tumors

R. Via[1], A. Fassi[1], G. Angellier[2], J. Hérault[2], M. Riboldi[1], J. Thariat[2], W. Sauerwein[3], G. Baroni[1]

[1]Politecnico di Milano University, DEIB - Department of Electronics and Information and Bioengineering, Milano, Italy

[2]Centre Antoine Lacassagne, Cyclotron Byomédical, Nice, France

[3]University Hospital Essen University Duisburg-Essen, NCTeam- Strahlenklinik, Essen, Germany

Purpose or Objective: In proton therapy treatments of intraocular tumors, patients actively participate by fixating a red diode, prepositioned according to planning prescriptions, to stabilize gaze direction. This work aims to evaluate safety margins effectiveness against involuntary eye movement that may occur in the course of the treatment.

Material and Methods: A custom eye tracking system (ETS), able to monitor eye position and orientation through 3D video-oculography techniques, was installed in a proton therapy (PT) treatment room (fig.1). All ocular PT centers are equipped with an in-room orthogonal X-ray imaging system used to verify treatment geometry. Tantalum radio-opaque markers, sutured to the sclera of the diseased eye, aid to determine the gaze angle of the eye during simulation, and the correct eye position at treatment. During simulation, the ETS monitored the eye simultaneously with X-ray acquisition to assess the tantalum markers pose relative to eye position and orientation. As a result, the ETS was able to assess eye motion and markers position in physical coordinates during dose delivery.

A first analysis was performed on two patients with three and two monitored treatment fraction respectively. Both patients had four implanted markers. To enable 3D localization of markers identified in X-ray images, the geometry of the imaging system was calibrated by means of the Direct Linear Transform (DLT) algorithm. We measured the distance between markers 3D position seen by the ETS during irradiation and identified on setup verification X-ray images acquired prior dose delivery to quantify intra-fraction eye motion. Margins expansions of 2.5 mm were applied laterally and distally. Median, interquartile range (IQR) and maximum values for the clip-to-clip distance are reported in table 1.

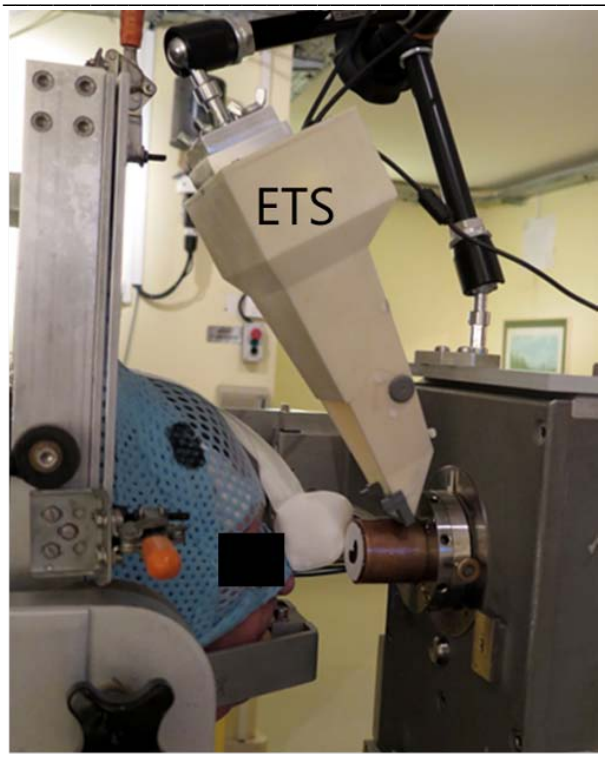

Figure 1 Clinical setup of the eye tracking system (ETS)

Results: The mean retro-projection error (± SD) for the DLT calibration of the X-ray system was 0.06±0.03 mm. Median values of markers deviation during irradiation, considering both patients, ranged between -0.54 mm/0.75 mm, -1.06 mm/0.85 mm and -0.55 mm/0.90 mm in the LL (latero-lateral), SI (superior-inferior) and AP (antero-posterior) direction, respectively.

Table 1 Results of the ETS monitoring of markers position during irradiation. LL (latero-lateral), SI (superior-inferior) and AP (antero-posterior) refers to conventional anatomical axes.

			Clip 1			Clip 2			Clip 3			Clip4		
Patient	Fraction		LL (mm)	SI (mm)	AP (mm)	LL (mm)	SI (mm)	AP (mm)	LL (mm)	SI (mm)	AP (mm)	LL (mm)	SI (mm)	AP (mm)
1	1	Median	0,56	0,69	-0,19	0,15	0,56	0,05	0,15	0,49	0,18	-0,34	0,49	0,26
		IQR	0,04	0,09	0,50	0,05	0,11	0,36	0,03	0,09	0,19	0,05	0,18	0,12
		MAX	0,74	0,82	1,54	0,36	0,76	1,30	0,30	0,61	0,85	-0,45	0,84	0,67
	2	Median	0,75	-0,69	0,88	0,32	-1,06	0,90	0,18	-0,87	0,55	-0,17	-1,00	0,24
		IQR	0,06	0,14	0,14	0,05	0,13	0,12	0,07	0,14	0,09	0,04	0,13	0,12
		MAX	0,84	0,87	1,18	0,41	-1,23	1,13	0,26	1,04	0,75	0,26	-1,18	0,44
	3	Median	0,39	-0,05	0,59	-0,01	-0,32	0,47	0,01	-0,29	0,26	-0,51	-0,48	0,04
		IQR	0,05	0,11	0,16	0,04	0,12	0,18	0,04	0,11	0,18	0,05	0,15	0,19
		MAX	0,50	0,47	1,17	0,09	0,70	0,95	0,10	-0,69	0,71	0,61	-0,78	0,82
2	1	Median	-0,08	0,72	-0,20	-0,11	0,85	-0,19	0,22	0,57	-0,40	0,14	0,38	-0,17
		IQR	0,06	0,04	0,11	0,06	0,05	0,11	0,06	0,04	0,11	0,06	0,04	0,07
		MAX	-0,17	0,83	-0,39	-0,25	0,97	-0,37	0,36	0,67	0,61	0,29	0,47	-0,32
	2	Median	-0,02	0,08	0,06	-0,01	0,44	-0,07	-0,13	0,03	-0,42	-0,26	0,05	-0,55
		IQR	0,07	0,08	0,21	0,16	0,09	0,17	0,08	0,06	0,16	0,10	0,05	0,17
		MAX	-0,19	0,24	0,42	0,40	0,64	-0,26	0,31	0,16	0,65	0,45	0,14	0,85

Conclusion: We documented eye motion well below the applied safety margins. Future activities will focus on quantifying the effect of intrafraction eye motion on dose deposition.

EP-1766

Factors influencing on intrafraction variation in lung Stereotactic Body Radiation Therapy

M. Rico Oses[1], E. Martinez[1], B. Bermejo[2], E. Villafranca[1], P. Navarrete[1], M. Errasti[1], M. Barrado[1], M. Campo[1], I. Visus[1], S. Flamarique[1], L. Bragado[3], A. Manterola[1], A. Sola[1], S. Pellejero[3], G. Asin[1], M.A. Dominguez[1], F. Mañeru[3], F. Arias[1]

[1]*Complejo Hospitalario de Navarra, Department of Radiation Oncology, Pamplona, Spain*

[2]*Complejo Hospitalario de Navarra, Department of Preventive Medicine, Pamplona, Spain*

[3]*Complejo Hospitalario de Navarra, Department of Radiophysics, Pamplona, Spain*

Purpose or Objective: In the present study we compare three different treatment-delivery techniques in terms of treatment time (TT) and its relation with intrafraction variation (IFV). Besides that, we analyzed different clinical factors that could influence on the IFV. Finally we appreciated the soundness of our margins.

Material and Methods: Patients diagnosed of stage I lung cancer and lung metastases up to 5cm treated with SBRT in our centre were included in this study. All patients went through a 4DCT scan to create an internal target volume (ITV) and a 5mm margin was added to it to create a PTV. Each patient had a pretreatment Cone Beam CT (CBCT) and a postreatment CBCT. We compared the CBCTs with their reference 4D-CT to quantify the translational tumor shifts as well as the 3D composite vector. For our patients three different treatment-delivery techniques were employed: fixed fields (FF), arcs dynamically collimated (AA) or a combination of both (FA). We studied if TT was different among these ways of treatment and we search if there were any correlation between TT and IFV. We analyzed the influence of patients´ clinical characteristics (age, sex, performance status, pulmonary function, treatment time) and tumours´characteristics (location, nature, size) on IFV.

Results: A total of 45 patients with 52 lesions were studied from which 147 fractions could be analyzed. Mean IFV for x, y and z axis were 1 ± 1.16mm, 1.29 ± 1.38mm and 1.17 ± 1.08mm, respectively. 96.1% of the displacements were encompassed by the 5mm margin given. TT was significantly longer in FF therapy (24.76±5.4 min), when compare with AA (15.30±3.68 min) or FA (17.79±3.52 min) ($p<0.001$). Despite that, IFV did not change significantly between the three groups ($p=0.471$). Age ($p=0.003$) and left vs. right location ($p=0.005$) were related with 3D shift ≥ 2mm. The multivariate analysis showed that only age significantly influenced on IFV (OR=1.07, $p=0.007$).

Conclusion: The election of AA, FF or FA does not impact in the IFV although FF treatments take significantly more time. Our 5 mm margin can be considered acceptable as it accounts for more than 95% of tumor shifts. Age is the only clinical factor that influence significantly on the IFV in our analysis.

EP-1767

Deep Inspiration Breath Hold – a promising technique in patients with left-sided breast cancer.

P. Mezenski[1], J. Gałecki[2], M. Spałek[2], A. Zawadzka[1], P. Kukołowicz[1]

[1]*The Maria Sklodowska-Curie Memorial Cancer Center, Medical Physics, Warsaw, Poland*

[2]*The Maria Sklodowska-Curie Memorial Cancer Center, Radiotherapy, Warsaw, Poland*

Purpose or Objective: Clinical data suggest that every 1 Gy of the mean dose to the heart increases the risk of major coronary events by approximately 3% and the risk of coronary arteries damage by approximately 7%. The literature data show that the radiation dose delivered to the heart can be reduced by applying the Deep Inspiration Breath Hold (DIBH) technique. The aim of this study was to evaluate dose delivered to the heart and coronary arteries for a group of patients after breast conserving surgery (BCS) irradiated with 3D-CRT-SIB (3D Conformal Radiotherapy Simultaneous-Integrated Boost).

Material and Methods: For 10 left-sided breast cancer patients, computed tomography-based treatment planning were performed at FB (Free Breathing) and DIBH mode. The CTV (Clinical Target Volume) covering the whole left breast and the post-lumpectomy tumor bed (boost). Important organs at risk (heart, territory of coronary arteries and lungs) were delineated. To form the PTV (Planning Target Volume) from CTV, the margin of 6 mm was added. For both DIBH and FB, treatment plans were prepared by medical physicist. The prescribed doses were 54Gy (2.7Gy/fraction) to PTV boost and 45Gy (2.25 Gy/fraction) to PTV breast. The mean dose

delivered to the heart and the volume of heart receiving the dose of 20Gy or more were evaluated. Volume of the territory of the coronary arteries receiving the dose of 20Gy or more was also assessed. All 10 patients were treated with the DIBH technique.

Results: DIBH compared to FB reduced the mean dose delivered to the heart (average 4.4 Gy vs. 2.1Gy). The heart volume receiving the dose of 20 Gy or more was reduced to almost zero (average 0.1% vs 6 %). DIBH allowed to diminish to zero the volume of coronary arteries receiving 20Gy or more (average of 0% vs. 16.9%). The early treatment tolerance was good – no toxicity higher than Grade 1 skin toxicity according to RTOG Acute Radiation Morbidity Scoring Criteria was observed.

Conclusion: DIBH technique reduces the dose delivered to the heart in comparison to FB, thus it may reduce the late cardiotoxicity of radiotherapy. In each patient with the left breast cancer qualified to postoperative radiotherapy, the DIBH technique should be taken into consideration

EP-1768

The impact of interplay effect in SBRT lung treatments for 6MV and 6MV-FFF beams using EBT3 film.

D. Elezaj[1], W. Ottosson[1], M. Sjölin[1]
[1]*Herlev Hospital, Department of Oncology, Herlev, Denmark*

Purpose or Objective: In hypofractionated stereotactic body radiotherapy (SBRT) for lung tumors, the interplay effect between tumor respiratory motion and multileaf collimator (MLC) motion can play an important role in dynamic plans. This study was designed to investigate the interplay effect for Rapidarc (RA) SBRT lung treatments, using GafChromic EBT3 film and a respiratory motion phantom.

Material and Methods: A heterogeneous programmable respiratory motion phantom (Quasar, Modus Medical Devices Inc.), with a "tumor" (30 mm diameter) inside a cylindrical "lung" insert, was used to simulate a breathing motion in the superior/inferior direction. Two amplitudes (10 mm, 20 mm) and two breath rates (BRs) (period: 6 s, 4 s) were investigated. RA plans were created, based on the 4D CT scans of the phantom, one for each amplitude and beam quality investigated a) 6MV (600 MU/min) and b) 6MV-flattening filter free (FFF) (1400 MU/min). All plans were optimized to keep the MLC modulation about 200 MU/Gy. The internal target volume (ITV) was prescribed a fractionation dose of 22.5 Gy, where the planning target volume (5 mm margin to ITV) was covered by 67%. Each plan consisted of four half arcs, each measured individually. Measurements were carried out both in static condition and with motion for the two BRs. GafChromic EBT3 film were placed centrally in the tumor, and the measurements were compared with calculated dose distributions where gamma analysis per field was evaluated (Verisoft v.4.0, PTW-Freiburg).

Results: All static measurements were in good agreement with the calculated dose, with a mean local gamma (LG) passing rate (3%/2mm) above 96,8% (±0,9) for all fields. With 10 mm motion, the mean LG passing rate (3%/2mm) for all fields in one plan was, with period 6 s: 88,4% (±2,4) for 6MV and 82% (±3,5) for 6MV-FFF, and with period 4 s: 78% (±12,6) for 6MV and 73,9% (±7,7) for 6MV-FFF. Worst case observed was with 20 mm motion, period 4 s and 6MV-FFF, with a mean LG passing rate (3%/2mm) of 50,7% (±15,2). Only the 6MV plan with amplitude 10 mm and period 6 s passed a typical clinical acceptance criterion of 90% using 3%/3mm LG passing rate.

Conclusion: The impact of interplay effect was highest for the largest motion amplitude (20 mm), fastest BR (4 s) and for the shortest delivery time (6MV-FFF beam). Although the results illustrate LG per field, the motion blurring may become dosimetrically significant when the fields are summarized, particularly for motions above 10 mm.

EP-1769

Evaluation of the intra-fraction patient movement for SBRT treatments in our Institution

D. Martínez[1], F. Candela[1], A. Camara[1], M.T. Garcia-Martinez[1]
[1]*Hospital Universitario de la Ribera, Radiofísica y Protección Radiológica, Alzira, Spain*

Purpose or Objective: The purpose is to evaluate the intra-fraction patient movement for SBRT treatments, obtaining a reference level in function of the pathology, starting point for future improvements. The parameters considered to be improved are the settings of these treatments: positioning, immobilization devices and maybe patient training.

Material and Methods: Data from 233 SBRT fractions (from 05/2013 to 09/2015) of 105 patients (SBRT different treatments) were studied.
All patients have internal fiducial markers, and were treated with two Varian (clinac 2100C and 2100CD) linear accelerators both with Portal Vision AS500 - IAS3, the treatment planning system (TPS) was Philips Pinnacle v9.8, and the Record and Verify (R&V) was Mosaiq (Elekta). The treatment plan was mainly 3DRT.
The treatment procedure for each fraction was:
Before each treatment session a new CT was made. All ROIs and fiducials were contoured in it. The displacements from external CT marks to isocenter were updated according to this.
The patient was positioned on the couch with all the immobilization devices needed, and initially aligned with the lasers on the CT marks. Then it was moved to the isocenter according to the updated physics displacements.
Two Portal Images (orthogonal, 0º - 90º) were done until their position corresponded to the one of the treatment plan. Fiducials were used to check the position against the portal vision. When the correct position was found, the first treatment field is irradiated.
For each treatment field, a Portal Image was made. It was checked with the corresponding RDR, repositioning the patient if necessary. Finally the field was irradiated. If the movement detected was greater than a half of the PTV margin, the 0º and 90º images were performed once again.
The treatment positions (couch coordinates) for each field were obtained from the R&V. The cases were classified according to two main categories:
Reposition in low % number of fractions: No action required by now.
Reposition in high % number of fractions: The immobilization devices and positioning of the patient should be checked improved.

Results: Position had to be corrected intra-fraction due to the PV images in 36 of the 233 fractions (15.4%).
45 beams needed patient reposition, that means in average 1.25 repositions for each patient that needed to be repositioned.
These patients were treated with 245 beams (18.4% of the treatment beams needed reposition).
In Average, the movement magnitude (field to field) was 8 mm (4 movements greater than 3 cm), and the total session time was increased in 7´59´´, due to the reposition process.

Conclusion: The three most frequent tumor localizations were: lung, abdominal and cranial. With the collected data, patient setup must be improved in abdominal pathology.

Localization	Sesions with fields repositioned	Total fractions	(%)
Lung	20	124	16.13%
Abdominal	7	31	22.58%
Craneal	3	21	14.29%

There were other pathologies with low number of cases (Spinal cord, rectum…), so the study may not be yet representative.

This process implies an increase in the treatment time, but this is necessary for a SBRT efficiency treatment.

EP-1770

Predictive modeling of respiratory lung motion using single-phase CT and finite-element analysis

M.A. Mosleh-Shirazi[1], M. Zehtabian[2], T. Amirabadi[2], M.R. Hematiyan[3], M.R. Parishan[2], H. Shahbazi[4], S. Farahangiz[5]
[1]*Shiraz University of Medical Sciences, Radiotherapy Dept & Ionizing and Non-ionizing Radiation Protection Research Center, Shiraz, Iran Islamic Republic of*
[2]*Shiraz University, Department of Medical Radiation Engineering, Shiraz, Iran Islamic Republic of*
[3]*Shiraz University, Department of Mechanical Engineering, Shiraz, Iran Islamic Republic of*
[4]*Shiraz University of Medical Sciences, Department of Radiology, Shiraz, Iran Islamic Republic of*
[5]*Shiraz University of Medical Sciences, Department of Radiology & Medical Imaging Research Center, Shiraz, Iran Islamic Republic of*

Purpose or Objective: Information regarding lung motion can be highly valuable in modern radiotherapy. During recent years, 4DCT has been used to obtain such required information. This technology is, however, not available to all centres. It is, therefore, desirable to have a predictive model to aid the planning and delivery processes, although this has proven to be a challenging task given the complexities involved. The aim of this work is to develop a biomechanical finite-element model (FEM) of respiratory lung motion that only requires a CT dataset from the end-inhalation phase of the breathing cycle as input.

Material and Methods: A radiology specialist identified 10-18 uniformly-distributed landmarks per lung on each of the end-inhalation and end-exhalation 4DCT datasets for 13 lungs. After segmentation and surface preparation, the first 7 lungs (3 left and 4 right) were used to tune the FEM in the Abaqus FEA software environment. A hyperelastic model with reported parameters was used. Varying magnitudes of pressure were applied to 9 different segments of lung surface. These magnitudes were adjusted until the mean of the squares of the 3D distances between the predicted and actual landmark positions in the end-exhalation CT dataset became < 1 mm. Our tuned FEM was hence obtained. This model was then applied to the study 4DCT datasets comprising 6 lungs (3 left and 3 right). The 3D error vectors between the corresponding landmarks in the end-exhalation phase were calculated and analysed.

Results: Among all landmarks in the 6 lungs in the study set, the mean length of the 3D error vectors was < 2 mm, while the minimum and maximum lengths were 0.1 mm and 7.1 mm, respectively.

Conclusion: Overall, the tuned model shows reasonable accuracy in predicting the end-exhalation position of the landmarks in the lungs, using the input anatomy of only a single end-inhalation phase. These promising results encourage further development and evaluation of the model as well as its tuning over a larger number of patients.

EP-1771

Biological consequences of dynamic dose interplay in VMAT SBRT lung treatments

M. Sjölin[1], D. Elezaj[1], W. Ottosson[1], J.M. Edmund[1]
[1]*University Hospital Herlev, Department of Oncology, Herlev, Denmark*

Purpose or Objective: A dynamic dose delivery for stereotactic body radiotherapy (SBRT) of the lung in free breathing can result in dose blurring, interplay or interference effects which may cause a considerable deviation between the prescribed and delivered dose. Here, we investigated the per fraction dose effects by high-spatial resolution measurements.

Material and Methods: GafChromic EBT3 film measurements were carried out in the isocenter plane of a 3 cm diameter tumor in a movable cylindrical cedar lung insert (Quasar phantom). The motion was in the cranial-caudal direction. Motion frequencies were 10 and 15 breaths per minute (bpm), and amplitudes were 10 and 20 mm. Volumetric modulated arc therapy (VMAT) plans for both 6 MV (600 MU/min) and 6 MV flattening filter free (FFF) (1400 MU/min) beams were created for each amplitude. The gross tumor volume including motion (GTV-IM) generated from a most intensive projection of a 4D CT, was prescribed a mean dose of 22.5 Gy. The GTV-IM was enclosed by the 90 % isodose. The motion effects on the GTV-IM were quantified biologically using the generalized equivalent uniform dose (gEUD, a=-10), and dosimetrically by the mean (Dmean) and minimum dose (Dmin). All deviations are given relative to the corresponding planned parameters. Static measurements were performed for each beam and amplitude and served as a baseline.

Results: For the static 10 mm amplitude cases, the relative deviation in gEUD was +0.2% (6 MV) and -1.6 % (6 MV FFF), Dmean = 0.4 and -0.7%, and, Dmin = 1.6 and – 3.5%. For the 10 and 15 bpm and 10 mm amplitude, the reduction in the gEUD ranged between -1.8 and -3.2%. A similar trend in Dmean between -0.8 and -2.6% was observed and Dmin about -10%. The largest relative reduction in gEUD of -7.5% was observed for the 20 mm amplitude and 15bpm for the 6 MV FFF beam. Dmean and Dmin were -4.2 and -21.4% for this case, respectively.

Conclusion: This phantom study indicates that VMAT treatment in free breathing for lung SBRT tumors could lead to 3% under dosage in tumor gEUD for a motion amplitude of 10 mm and 7.5% for a 20 mm amplitude. Tumor movements of more than 10 mm for this treatment technique should consequently be avoided.

EP-1772

Comparison of dynamic 2D MRI with 4DCT lung tumor volumes for accurate real time imaging on linac-MR

S. Baker[1], E. Yip[2], J. Yun[2], K. Wachowicz[2], Z. Gabos[1], G. Fallone[3]
[1]*Cross Cancer Institute, Radiation Oncology, Edmonton, Canada*
[2]*Cross Cancer Institute, Medical Physics, Edmonton, Canada*
[3]*Cross Cancer Institute and University of Alberta, Medical Physics- Physics and Oncology- Medical Physics Division, Edmonton, Canada*

Purpose or Objective: The hybrid linac MR system is capable of acquiring 2D images at 4 frames per second during radiation delivery. Moving lung tumours can potentially be localized, in real time, by automatic contouring of these images, allowing radiation to “track” the tumour. This study aimed to compare the accuracy of the dynamic 2D MRI of a linac-MR for lung tumour delineation to 4-dimensional computed tomography (4DCT), the current standard for radiotherapy planning for lung cancer treatment.

Material and Methods: A total of five non-small cell lung cancer patients with tumours under 5 cm in size undergoing stereotactic body radiotherapy were recruited for this study. A planning 4DCT with 3 mm slice thickness was acquired for each patient using a belt system and retrospectively sorted into 10 bins, each assumed to estimate the actual size of the target in ten respiratory phases. Three of these bins representing end inhale, end exhale and mid-cycle, along with the motion encompassing maximum intensity projection (MIP), were contoured on axial slices by a radiation oncologist using the Computation Environment for Radiotherapy Research (CERR) platform (default lung window). The same patients were scanned using a Philips 3T MRI on a single 20 mm sagittal slab using a balanced SSFP sequence (TE/TR = 1.1/2.2ms, Pixel Size 3x3mm, 4fps) with the patient undergoing free breathing for 3 minutes (650 images). A radiation oncologist, using the CERR platform, with the default MR window, contoured these 650 sagittal

slices, representing the real time location of the tumour. To compare the 3D CT target volume with a 2D target area from the MRI, the contoured 3D volume was projected onto the 2D sagittal plane, resulting in a 2D area that could be fairly compared with the sagittal 2D MR area.

Results: The projected 2D CT bin areas for the 5 patients had a mean (standard deviation) area of 4.12(0.35), 5.17(0.40), 2.99(0.34), 9.28(0.52) and 3.96 (0.35) cm2. This is compared to the MR contoured areas of 5.02 (0.45), 7.13(0.67), 2.63(0.41), 7.52(0.57) and 4.07(0.41) cm2 (Figure 1). While there are differences that may be attributed to binning errors from 4D CT reconstruction and intra-observer variations, contours from real time MRI do not appear to be systematically biased on target area compared to the CT contours.

Figure 1. Mean area for five lung tumors on CT, MRI and MIP. Error bars represent standard deviation.

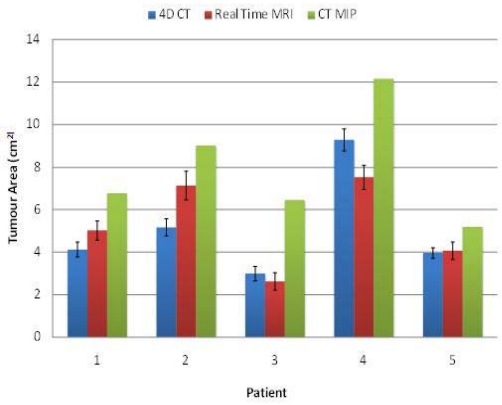

Conclusion: Lung tumor target areas on dynamic MR are similar to those on 4DCT and confirm the accuracy of real time tumor imaging. With the platform's ability for real time tumor tracking, reductions in irradiated lung volume can be achieved compared to motion encompassing treatment strategies, as indicated by the much larger MIP volumes.

EP-1773

Dosimetric benefits and reproducibility of DIBH tecnique guided by an optical system

F. Rossi[1], S. Russo[1], R. Barca[1], S. Fondelli[1], L. Paoletti[1], P. Alpi[1], B. Grilli Leonulli[1], M. Esposito[1], A. Ghirelli[1], S. Pini[1], P. Bastiani[1]

[1]*Azienda Sanitaria Firenze, S.C. Fisica Sanitaria, Firenze, Italy*

Purpose or Objective: Surface imaging (SI) systems have been recently introduced in radiotherapy to check patient setup and to manage gated treatment procedure. The absence of additional radiation exposure, the execution rapidity and confortable for the patients, make this approach particularly interesting. Aim of this work is the evaluation of a deep inspiration breath-hold (DIBH) tecnique guided by an optical system in terms of normal-tissue sparing, and positional reproducibility.

Material and Methods: The CatalystTM (C-RAD Sweden) is a valid solution for respiratory gated treatments offering visualization of the respiratory pattern and direct beam control. In combination with the C-RAD Sentinel™ system used for CT acquisition phase, Catalyst™ offers coverage for the whole chain from gated imaging to gated beam delivery (see figure 1). 20 patients that underwent BCS and left side adjuvant radiotherapy during 2015 were included in this study. Treatments were performed in DIBH with 3D conformal tangential beams. Median dose to the whole breast was 50 Gy in 25 fractions. For each patient a free breathing (FB) and a DIBH treatment plans were calculated and dose volume histograms were compared. The reproducibility of the DIBH during treatment was monitored by capturing 3D surfaces with CatalystTM system before and after set-up correction and at the end of the treatment fraction. Interfraction and intra-fraction variability were quantified in mean and SD displacements in traslation (Lat, Long, Vert) and rotations (Rot, Roll, Pitch) over all the treatment fractions of the enrolled patients.

Figure 1: DIBH procedure guided by C-RAD optical systems with visual coaching.

Results: DIBH technique provided a significant dose reduction in Heart Mean Dose (1,3Gy FB vs 0,4 Gy BH), and LAD mean dose (10,7 Gy FB vs 2,0 Gy BH) . Better PTV coverage (V 95% 88,9% FB vs 92,6% BH) in DIBH plans and no difference in Lung parameters (V10, V20 and Dmedia) were achieved. Inter-fraction variability before setup correction was relevant, but inter-fraction variability after setup correction was extremely reduced. Intra-fraction variability was <2.1 mm in translations and <1° in rotations, as showed in table 1.

Table 1: Quantification of set-up variability in DIBH treatments.

Setup variability	Lat [mm]	Long [mm]	Vert [mm]	Rot [°]	Roll [°]	Pitch [°]
Inter-fraction before correction	1,9 (2.1)	10.1 (9.0)	-6.9 (4.3)	0.8 (1.0)	0.5 (1.7)	0.8 (1.1)
Inter-fraction after correction	-0,4 (0,4)	-0,7 0,5	-0,1 0,3	0,5 0,3	0,4 0,6	-0,3 0,5
Intra-fraction	1,4 (0,5)	2,1 (0,4)	1,7 (0,5)	0,7 (0,2)	0,8 (0,1)	0,8 (0,3)

Conclusion: In our experience DIBH is a reproducible and stable tecnique for left breast irradiation showing significant reduction of mean dose to the hearth and LAD and a limited inter-fraction and intra-fraction DIBH variability. This is a good promise in reducing the late cardiac toxicities associated with radiation therapy.

EP-1774

A novel phantom for dosimetric verification of gated SIB radiotherapy treatment plans

D. Soultan[1], A. Yock[1], M. Cornell[1], J. Murphy[1], B. Gill[2], W. Song[3], V. Moiseenko[1], L. Cerviño[1]

[1]*University of California San Diego, Department of Radiation Medicine and Applied Sciences/ Radiation Oncology Pet/CT Center, San Diego, USA*

[2]*British Columbia Cancer Agency, Department of Radiation Oncology, Vancouver, Canada*

[3]*Sunnybrook Hospital, Medical Physics, Toronto, Canada*

Purpose or Objective: To validate a novel phantom intended for 4D PET/CT scanning and dosimetric verification of gated radiotherapy plans. To benchmark the use of the phantom for PET-driven, simultaneous integrated boost (SIB) radiotherapy planning and ion chamber validation.

Material and Methods: A multipurpose phantom and a set of inserts were designed and manufactured to simulate gated SIB radiotherapy, from 4D PET/CT scanning to treatment planning and dose delivery. The first phantom holds a 3D-printed insert that mimics the variable PET tracer uptake in

heterogeneous tumors. The insert has an outer low-uptake volume encompassing a high-uptake inner volume. SUV ratio of 1:2 was intended. The second phantom accommodates applicators that can hold Farmer ion chamber in a location matching the center of the inner volume and in four locations matching the outer volume. 4D PET/CT scans of the phantom were acquired with three breathing wave forms of ideal sinusoid and two patient-specific breathing patterns fed to the moving platform. Patient-specific wavefronts were selected to represent a regular and an irregular breather. Two scenarios were investigated for image reconstruction, planning and delivery: a gate 30-70 window, and no gating. ITVs were delineated on the obtained 4D PET/CT scans and 21 VMAT-SIB treatment plans were generated with two fractionation regimens:
· Conventional fractionation: 2 Gy/fx to outer ITV, 2.4Gy/fx to high SUV inner ITV, 30 fx.
· Hypo-fractionation delivered in both flattening filter and flattening filter free (FFF) modes: 8 Gy/fx to outer ITV, 9 Gy/fx to inner ITV,5 fx. Treatment plans were delivered in two gating scenarios: no gating and gate 30-70. Two ion chamber readings for the inner ITV, and two readings for one arbitrarily selected outer ITV were acquired. Measured doses in the inner ITV and the outer ITV were compared to planned doses.

Results: For both fractionation regimens and both delivery modes, measured doses in outer and inner ITV were between 93 and 99% of planned doses. Measured dose as compared to planned dose demonstrated independence from breathing pattern or gating window. In particular, measured doses in FFF mode were consistent with measured doses in filtered beam mode, 94-96% of planned dose.

Conclusion: The phantom has been validated for end-to-end use from 4D PET/CT scanning and radiotherapy planning, to dosimetric verification. Measured doses for SIB plans were in reasonable agreement for all three breathing patterns and for both gating windows and delivery modes.

Electronic Poster: Physics track: Inter-fraction motion management (excl. adaptive radiotherapy)

EP-1775

CBCT based prostate IGRT accuracy and PTV margins

C. Blay[1], A. Simon[2], E. Dardelet[2], R. Viard[3], D. Gibon[3], O. Acosta[2], P. Haigron[2], B. Dubray[4], R. De Crevoisier[1]
[1]*Centre Eugène Marquis, Radiotherapy, Rennes, France*
[2]*Rennes University 1, Campus de Beaulieu- LTSI, Rennes, France*
[3]*Aquilab, Aquilab, Lille, France*
[4]*Centre Henri Becquerel, Radiotherapy, Rouen, France*

Purpose or Objective: *Purpose*: Image guided radiotherapy (IGRT) is the standard treatment of prostate cancer, widely based on Cone Beam CT (CBCT). The accuracy of CBCT based prostate registration is however not well established, conditioning the choice of the Planning Target Volume (PTV) margins. The goal of the study was to quantify the uncertainty of this registration and propose therefore appropriate margins.

Material and Methods: *Materials and methods*: A total of 306 prostate CT to CBCT alignments were analyzed in 28 prostate cancer patients treated by IGRT. The prostate was manually delineated on all the CBCT. Three prostate alignment modalities were afterwards simulated and compared, based on skin marks, on CBCT registration performed by the technologist at the fraction (IGRTt) and on the prostate contours. The IGRT uncertainty (IU) was defined as the difference between the contour based and the CBCT alignments, in each space direction. Dice index (DI) were calculated. Margins were calculated, based on the IU and the Van Herk formula.

Results: *Results*: The mean (min;max) absolute values of the IU were, in mm: 1.5 (0;10), 0.7 (0;12) and 0.9 (0;7), in antero-posterior (A/P), cranio-spinal (CS) and lateral directions, respectively. After IGRTt alignment, 25 prostate (11% of cases) still projected partially out of the PTV, corresponding to an average prostate volume (min; max) of 2.3 cc (0.0;12.6). The mean + standard deviation of the DI were 0.84 + 0.08, 0.90 + 0.07 and 0.93 + 0.03 for the skin marks, CBCTt and contours registration, respectively. For at least 95% of the IGRT registrations covering 100% of the prostate, the required A/P, CS and lateral PTV margins (mm) should be at least 4.5, 2.0 and 3.0, respectively. The Van Herk PTV margins (mm) were 5.5, 4.1 and 3.0 in the A/P, CS and lateral directions, respectively.

Conclusion: *Conclusions:* CBCT based prostate registration presents uncertainties requiring at least 3 to 5 mm PTV margins.

EP-1776

Assessment of setup uncertainties in modulated treatments for various tumour sites

E.S. Sandrini[1], L.R. Fairbanks[1], S.M. Carvalho[1], L.R. Belatini[1], H.A. Salmon[1], G.A. Pavan[1], L.P. Ribeiro[1]
[1]*Grupo COI, Física Médica, Rio de Janeiro, Brazil*

Purpose or Objective: The aim of this study was to analise the patients setup errors for various tumor sites based on clinical data from modulated treatments using cone beam computed tomography (CBCT) imagine guidance and portal imaging for breast site. It was also calculated the planning target volume (PTV) margins of all disease sites and stipulated action level for online correction.

Material and Methods: The patients analyzed in this study were treated in our institution between January 2012 and December 2014 with VMAT and IMRT via flash technique for breast cancer. The various tumor sites were divides into six categories; 175 breast (1173 fractions); 53 thorax (475 fractions); 60 prostate (585 fractions); 100 H&N (858 fractions); 100 SNC (789 fractions) and 77 pelvis (620 fractions).
For every treatment fraction, it were acquired KV-CBCT images using the on-board imager (OBI) (Varian Medical Systems), and for breast cancer it were acquired MV portal images using the Electronic Portal Imaging Device (EPID) (Siemens AG) in the first week and twice per week. The registration procedure was performed for all treatments sites according to the tumor localization. For prostate site, it was also analyzed the physiological state of bladder and rectum.
It were calculated the systematic (Σ) and random (σ) errors of couch shift obtained, and PTV margin (2,5Σ + 0,7σ).

Results: The Σ and σ for all treatment sites are summarized in table 1 as well PTV margins.
Table 1. The systematic and random errors and PTV margins

	Systematic Error (Σ)			Random Error (σ)		
	Lateral (mm)	Longitudinal (mm)	Vertical (mm)	Lateral (mm)	Longitudinal (mm)	Vertical (mm)
Breast	1.67	1.30	1.57	1.87	1.43	1.85
Thorax	2.15	2.45	1.66	3.33	3.84	3.44
Prostate	2.30	1.32	2.00	2.71	1.78	2.73
Prostate operated	1.94	1.39	1.97	2.89	2.31	2.66
H&N	1.22	1.18	1.25	1.94	1.94	2.07
SNC	1.00	1.27	0.85	1.47	1.56	1.19
Pelvis	1.71	2.16	2.28	3.75	2.72	3.65
	PTV margins					
	Lateral (mm)		Longitudinal (mm)		Vertical (mm)	
Breast	5.47		4.25		5.22	
Thorax	7.70		8.82		6.56	
Prostate	7.66		4.54		6.90	
Prostate operated	6.87		5.10		6.79	
H&N	4.40		4.32		4.57	
SNC	3.52		4.28		2.95	
Pelvis	6.91		7.29		8.25	

The largest magnitude of Σ and σ for H&N was 1.94 mm, SNC was 1.56 mm, breast was 1.87 mm, thorax was 3.33 mm, pelvis was 3.75 mm and prostate was 2.89 mm. The PTV margins required are <4.5 mm for brain and H&N lesions, <5.5 mm for breast cancers, but range from 4.5 to 9 mm for thorax, prostate and pelvis lesions.
Theses values indicate the setup variations of each patient. The variations were smaller for the breast, SNC and H&N cohorts than the prostate, pelvis and thorax cohorts. The pelvis and breast cohorts showed the greatest variation in lateral direction and the prostate cohorts in vertical direction. The largest variation were presented in thorax cohorts in longitudinal direction and the lowest were in the SNC cohorts.

Conclusion: As the setup errors vary according to each immobilization systems, the analysis of each institution`s specific setup errors is essential for determining the PTV margins. The results were also used to define action level for online correction.

EP-1777

MRT investigation of prostate and lymph nodes movements: implications on planning target volume?

U. Björeland[1]
[1]*SundsvalIs Sjukhus, Sjukhusfysik, SundsvaII, Sweden*

Purpose or Objective: The purpose of this project is to gather knowledge on the movement of pelvic lymph nodes relative to the prostate, seminal vesicles and bones in the pelvis and how this may affect the patient treatment plan.

Material and Methods: Until present, 10 patients have been included in the study. All patients have diagnosed prostate cancer and were treated with radiation therapy with curative intent. The patients followed the normal preparation and treatment procedure at our clinic - however, six additional MRI scans were acquired (baseline: before RT, on treatment day 1, 3, 5, 20 and 35) see figure. In each image set, several structures were delineated including fiducial markers, bony structures and lymph nodes. A radiologist identified lymph nodes along the common spread paths of prostate cancer. No suspected pathological nodes were found. Oncentra (Elekta) was used for image registration. Baseline images were defined as reference images and all other examinations were registered to the reference in two separate ways; bone matching and fiducial markers matching. For the bone matching, four structures were outlined; the disc between S1-S2, head of the right and left femur and the pubic symphysis. For the fiducial marker matching, the three gold markers in the prostate were outlined. In both cases the images were manually matched. Lymph node, seminal vesicle and prostate movements and morphological change were evaluated In MATLAB. Lymph nodes were grouped into regions: para-aortic (PA), common iliac (CI), pre-sacral (PS), internal iliac (II), obturator (Obt), and external iliac (EI) lymph nodes.

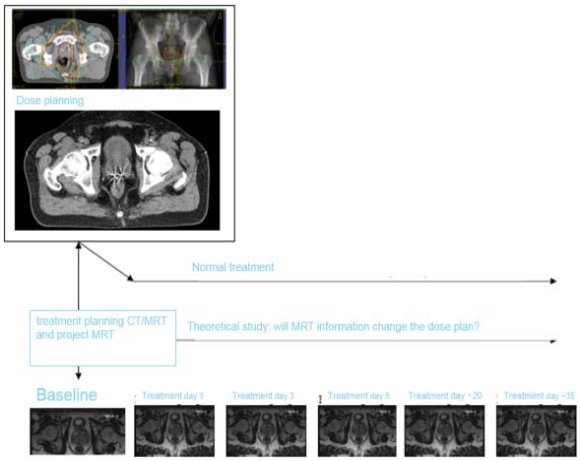

Results: We found that prostate moves up to 10 mm in anterior-posterior direction and up to 5 mm in right-left and cranio-caudal directions relative to bony anatomy from baseline scan. The lymph node group with the largest movements in right-left direction were CI with up to 20 mm difference from baseline. In the anterior-posterior and cranio-caudal directions, the maximum movement was 9 mm relative to bone from baseline scan. For the lymph nodes in the EI and PS regions, a significant difference was found depending on whether bone or fiducial markers were used for registration in right-left or cranio-caudal directions. In the other cases, no statistically significant difference between bone matching and fiducial marker matching was found

Conclusion: Preliminary findings suggest that the pelvic lymph nodes are more mobile than expected, indicating the need to account for that in treatment planning. However, more patients need to be included in the study before a conclusion can be drawn on the implications on the treatment plan.

EP-1778

On the feasibility of performing a 3D-scan with your own smartphone

J. Pérez-Alija[1], P. Franco[1], E. Ambroa[2], S. Olivares[1], S. Loscos[1], A. Pedro[1]
[1]*Hospital Plato, Oncología y Radioterapia, Barcelona, Spain*
[2]*Hospital General de Cataluña, Oncología y Radioterapia, Sant Cugat, Spain*

Purpose or Objective: Optical 3D Surface Scanner (3D-OSS) is a simple and easily reproducible method for patient alignment, and is an accurate tool to show anatomical changes, for example, in breast locations. The aim of this study was to evaluate the feasibility of both achieving within a few minutes an 3D-OSS using a smartphone and creating an image fusion between this 3D-OSS and the CT scanner, in a simple, cheap and reliable way.

Material and Methods: A smartphone and a free commercial app (TRNIO, www.trnio.com) were used to create an 3D-OSS. This app takes a series of pictures of your object as you move your smartphone around it. After a scan is completed, a 3D model will be generated on your phone. This 3D map is available for downloading on the TRNIO website. Although there are several image reconstructing algorithms available, in order to first show the feasibility of the method described here we will be using the commercial app. In the meantime,

we are now ourselves developing an In-house software to do this. The RANDO Man Phantom (The Phantom Laboratories, Salem, New York) was used as a model. RANDO represents a 175cm tall and 73.5kg male figure. The phantom is constructed with a natural human skeleton which is cast inside soft tissue-simulating material. An image fusion was carried out between a RANDO OSS and a RANDO CT scan. A Body structure was created in our CT scan. In order to fusion it with the 3D-OSS we used MeshLab (a free processing system for 3D triangular meshes).

Results: Image fusion was successfully performed and the accuracy of it was measured both using predefined corresponding landmarks in the CT and visual confirmation. We performed this process for two locations on the phantom, Head & Neck and Body, and in both cases we got an accurate agreement.

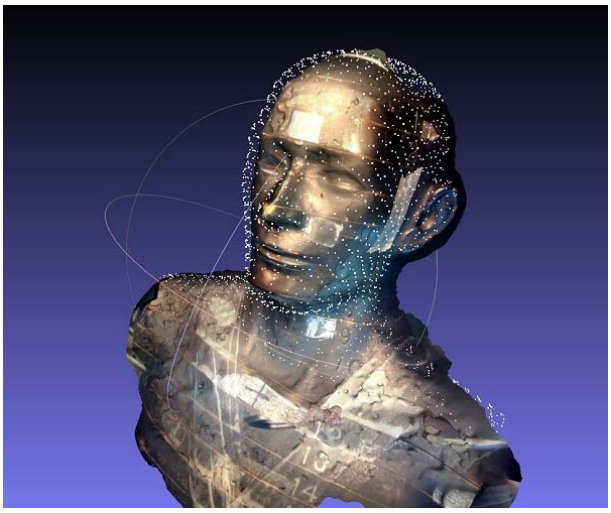

Conclusion: This study was carried out using an existing commercial app in order to prove the feasibility of the method, using only a smartphone and free software. Therefore, we think it reasonable to believe that making your own 3D-OSS system could be done both in a simple and in a much cheaper way than the usually commercial alternatives available on the market.

EP-1779

Margins to compensate for deformity of the prostate/seminal vesicle in IGRT using fiducial-markers

Y. Hamamoto[1], N. Sodeoka[1], S. Tsuruoka[1], H. Inata[1], S. Nakayama[1], H. Takeda[1], T. Manabe[1]
[1]*Saiseikai Imabari Hospital, Radiology, Ehime, Japan*

Purpose or Objective: In external beam radiotherapy for prostate cancer, image-guidance using fiducial-markers decrease set-up error and inter-fractional organ-motion error. However, daily deformity and/or rotation of the prostate/seminal vesicle could not be adequately detected by the verification of fiducial-marker position alone. The purpose of this study was to know how many margins should be added to compensate for the daily deformity and/or rotation of the prostate/seminal vesicle in the image-guided radiotherapy using fiducial-markers.

Material and Methods: Three-hundred ten fractions of nine patients with prostate cancer were examined. Patient setup was performed according to the position of two intra-prostate fiducial-markers (first-stage). Thereafter, with considering deformity and/or rotation of the prostate/seminal vesicle, the patient position was moved to the best position to achieve an alignment of contours of the prostate/seminal vesicle on daily cone-beam CT and contours of the clinical target volumes delineated on treatment planning CT (second-stage). Distance of movement in the second-stage was measured.

Results: An alignment in the second-stage was needed in 47 fractions of 310 fractions (15.2%). In 43 fractions (13.9%), movement of 1 mm was needed only in antero-posterior (AP) direction. Movement of 2 mm in AP direction, movement of 1 mm in cranio-caudal (CC) direction, and movement of 1 mm in AP and CC directions were needed in two fractions (0.6%), in one fraction (0.3%), and in one fraction (0.3%), respectively. No fraction needed an alignment in left-right direction.

Conclusion: With regard to image-guided external beam radiotherapy based on intra-prostate fiducial-marker position, margins of 1-2 mm in AP direction are necessary to compensate for the daily deformity and/or rotation of the prostate/seminal vesicle.

EP-1780

Dosimetric impact of isocenter accuracy in CBCT-guided SRS treatment of vestibular schwannomas

J. Casals-Farran[1], J.F. Calvo-Ortega[1], S. Moragues-Femenia[1], M. Pozo-Massó[1], J. Fernández-Ibiza[1], E. Puertas-Calvo[1], C. Arias-Quiroz[1]
[1]*Hospital Quiron Barcelona, Radiation Oncology, Barcelona, Spain*

Purpose or Objective: Linac radiation isocenter describes a path while gantry and couch are rotating during the treatment delivery of typical non-coplanar SRS plans. The aim of this study is to investigate the dosimetric impact of this isocenter "wobble" in SRS of a vestibular schwannoma (VS), and to validate the PTV margin used in our clinical practice.

Material and Methods: Five VS cases were enrolled in this study. The PTV was generated in the Eclipse TPS by expanding the CTV by an isotropic 2 mm margin, according to our SRS policy. A SRS non-coplanar plan ("reference plan") was designed in the Eclipse TPS by using static gantry IMRT technique. Eleven beams (6 MV) from a Varian Clinac equipped with a 120 Millennium MLC were used. Dose of 12.5 Gy (100%) was prescribed to cover 99 % of PTV.
On the other hand, fifteen CBCT-guided end-to-end (E2E) tests using a skull phantom were performed. E2E test permits to quantify the radiation isocenter misalignments in the X (lateral), Y (anterior-posterior) and Z (superior-inferior) directions.
For each VS case, eight X-Y-Z shifts generated from "mean ± 1.96 x SD" misalignments reported by E2E tests were simulated in the Eclipse TPS, resulting in eight "shifted plans". The following metrics were computed for each shifted plan and compared to the reference plan values: i) dose coverage of the CTV (D99%_CTV), ii) maximum dose to brainstem, iii) mean doses to cochlea, and iv) V10Gy, V5Gy and V2.5Gy of the brain (including the PTV).

Results: 1) Isocenter misalignments revealed by E2E tests were (mean ± SD): -0.4 ± 0.7 mm, -0.2 ± 0.5 mm and 0.2 ± 0.4 mm, in the X, Y and Z directions, respectively. Gaussian behavior was observed for each direction ($p > 0.05$; Shapiro-Wilk test). The probability of having shifts ≥ 2 mm is less than 1% in Lat, AP, and SI directions.
2) Target coverage was assured in the shifted plans; D99%_CTV: 103.1% ± 5.8% .
3) Shifted plans vs. reference ones revealed not statistically differences ($p > 0.05$; Two-tailed Student t-test) in brainstem maximum dose (7.1 ± 3.0 Gy vs. 7.2 ± 3.1 Gy) ; cochlear mean dose (5.3 ± 4.1 Gy vs. 5.1 ± 4.4 Gy) ; V10Gy brain (2.3 ± 1.5 cm3 vs. 2.3 ± 1.6 cm3); V5Gy brain (8.6 ± 5.1 cm3 vs. 8.6 ± 5.8 cm3); and V2.5Gy brain (43.4 ± 26.7 cm3 vs. 43.5 ± 30.1 cm3).

Conclusion:
1) The radiation isocenter "wobble" did not increase significantly the doses to brainstem, cochlea and brain.
2) Our study demonstrated that the 2 mm PTV margin used in our clinical practice was adequate for SRS treatment of VS.

EP-1781

Dosimetric impact of CBCT isocenter misaligment on target dose coverage in cranial SRS

S. Moragues-Femenia[1], J.F. Calvo-Ortega[1], M. Pozo-Massó[1], J. Casals-Farran[1]
[1]*Hospital Quirón Barcelona, Radiation Oncology, Barcelona, Spain*

Purpose or Objective: Perfect (zero error) coincidence of CBCT and linac's isocenters is practically impossible to achievable in clinical practice, due to the presence of several geometric errors in the treatment unit. Our aim is to analyze the dosimetric impact of CBCT isocenter-linac isocenter misalignment on the target dose coverage and tumor control probability (TCP) in cranial SRS plans.

Material and Methods: A Varian Clinac 2100 CD was used. Misalignment of CBCT isocenter with respect to (w.r.t.) radiation linac isocenter was measured during 23 consecutive months. A 5 mm tungsten ball was centered at the room laser isocenter and MV portal images were acquired for four cardinal gantry angles (couch was at zero position). After portal image acquisition, CBCT scan was acquired.
All images were analyzed: (a) deviation of the radiation isocenter w.r.t the ball center was measured in each MV image using an in-house code; (b) deviation of the central voxel of the CBCT matrix ("CBCT isocenter") w.r.t. the ball center was measured in the Eclipse TPS. Finally, 3D misalignment of the CBCT isocenter w.r.t the linac isocenter was derived from (a) and (b).
To analyze the dosimetric impact of the CBCT isocenter misaligment, 10 cranial SRS cases were randomly selected from our database. For each case, the isocenter in the original plan ("reference plan") was shifted according the misaligments obtained for CBCT isocenter. Eight X-Y-Z shifts generated from "mean ± 1.96 x SD" of the measured CBCT isocenter misaligments were simulated for each SRS plan (i.e., 8 "shifted plans" were obtained for each SRS case). Target dose coverage (D99%) and TCP (estimated according to Radiat Oncol. 2015 Mar 8;10:63) were computed for each shifted plan and results were compared to the reference plan ones.

Results: i) Misalignments of CBCT isocenter w.r.t. radiation linac isocenter were (mean ± SD, all in mm): 0.5 ± 0.3; -0.3 ± 0.2 and -0.6 ± 0.3 for X (lateral), Y (anterior-posterior) and Z (inferior-superior) directions, respectively.
ii) Target dose coverage (D99%) was degraded from 100% to a mean value of 93% (range: 80% to 100%).
iii) The average loss of TCP was estimated to be about -5% (range: -18% to 0%) among the 80 shifted plans generated in this study.

Conclusion: Our simulations demonstrated that the reduction of target coverage and TCP due to CBCT isocenter misalignment w.r.t linac isocenter may be important. Our study shows clearly the need of add margin to the target to compensate for CBCT isocenter misalignment.

EP-1782

Effect of daily variation in rectal and bladder filling: an analysis of planned versus actual dose

A. Abhishek[1], T. Kataria[1], D. Gupta[1], T. Ghosh[1], T. Basu[1], S. Bisht[1], S. Goyal[1], M. Tayal[1], M. Ramu[1]
[1]*Medanta The Medicity- Gurgaon- India, Radiation Oncology, Gurgaon, India*

Purpose or Objective: In the era of Image guided radiotherapy (IGRT), ensuring accurate delivery of planned high dose is very important. Daily variations in organ volume may result in difference between planned and actual dose delivered to an organ. In the present study we planned to analyze the daily variations in bladder and rectal filling and its effect on actual dose delivered when compared with original planned dose.

Material and Methods: Five consecutive cases of carcinoma prostate, who recently concluded their IGRT, were selected for the study. All cases were high risk prostate cancer, planned for radical IGRT for a dose of 50 Gy in 25 fractions to prostate and pelvic nodes, followed by Cyberknife boost for 3 fractions. Daily cone beam CT - XVI (X-ray volume imaging) acquired during daily treatments for each patient was exported to planning systems and after fusion with original planning CT, daily bladder and rectal contours were delineated on each 125 scans (B1-B25 and R1 - R25). Using superimposition of all new 250 contours on respective original plan, dose delivered daily to partial volumes of these organs was recorded using new actual DVH (dose volume histogram) and then statistically compared with their respective original bladder and rectal (B0 and R0) DVH using SPSS v18.

Results: Even with strict bladder and rectal protocols, daily volumes varied in all individual cases. The range of bladder volume variation (B1-B25) recorded for 5 cases were: 30.7%-211.1%, 26.9%-119.1%, 27.8%-107.2%, 15.4%-305.8% and 27% - 92.6% of B0, respectively. Overall actual mean volumes were within 25% variation range (mean actual 76% of B0). For rectum, R1-R25 volumes varied from 30.9%-205.9%, 47.5%-155.1%, 33.8%-150.2%, 44.6%- 208.1% and 43.4%- 140.2%. of R0, respectively. Overall mean actual rectal volume were very similar to original rectal volume (101.6% of R0). Overall actual bladder dose (D1-D25) was lesser than original bladder (D0) dose. Statistically significant lower actual mean dose (range 13 to 30%) was observed when recorded for 25cc to 85 cc of bladder volume ($p<0.05$). For lower volumes less than 20 cc, difference was not significant. For rectum, difference between delivered and planned dose was statistically non significant for any volume. A comparison of volume to dose data showed a difference in planned and mean actual V15, V20 and V25 for bladder and V5 to V30 for rectum, which was statistically significant ($p< 0.05$).

Conclusion: Strict bladder and rectal protocols both for simulation and delivery is important in planning pelvic radiotherapy due to physiological variations in their daily volumes. Exact duplication of bladder and rectal volumes is difficult, however by using image guidance and ensuring at least 25% concordance of daily with original planning volumes of these organs, possible differences in actual delivered dose can be mitigated and accurate delivery of planned dose can be ensured.

EP-1783

Translational and rotational set-up uncertainties in Head and Neck cancer treatments using CBCT

M. Di Biase[1], M. Trignani[1], G. Caponigro[1], A. Di Pilla[1], F. Perrotti[1], A. Augurio[1], S. Giancaterino[2], P. Bagalà[2], M.D. Falco[2], D. Genovesi[1]
[1]*SS Annunziata Hospital, Radiotherapy, Chieti, Italy*
[2]*SS Annunziata Hospital, Medical Physic, Chieti, Italy*

Purpose or Objective: The aim of this study was to assess setup errors, both translational and rotational, for head and neck (H&N) cancer patients treated with intensity-modulated radiotherapy (IMRT) and volumetric-modulated arc therapy (VMAT) using daily pretreatment CBCT imaging guidance.

Material and Methods: A total of 57 CBCTs referred to 7 patients treated with an Elekta Agility Linear Accelerator were analyzed. Patients were treated in a supine position; as immobilization system for head and shoulder a thermoplastic fixation mask was used. Tattoos on the surface mask were placed on the laser projection. Axial CT-planning slices at 5 mm intervals were acquired and reconstructed at 2 mm. Image data set were sent to the Oncentra Masterplan Planning System. Planning CT was also sent via DICOM to XVI software for the co-registration with the CBCT scan. For the CBCT acquisition we used the “fast head and neck S20”. The 3D-3D co-registration with the CT planning scan was performed using the Grey level algorithm. Translations were measured in medio-lateral (x), supero-inferior (y) and antero-posterior (z) directions, as well as in rotation around axes. Online correction for translational displacements were applied, on the basis of literature data, when the discrepancy exceeded 3 mm. Rotation corrections were recorded with a

cut-off of ≤3°; for rotations >3°, patients were repositioned. Our protocol consisted of 5 consecutively CBCTs scans for the first week of treatment and 1 CBCT weekly during radiation therapy course. For each patient, mean translational displacements were off-line calculated on CBCT acquired during the first 5 fractions; these values were considered as systematic set-up errors and the corresponding displacements were then corrected if they exceeded 3 mm. Mean (M), median (MD), standard deviation (SD) and range of the displacements related to first 5 CBCTs scans and those corresponding to the all following CBCTs scans were calculated. Wilcoxon test was performed to evaluate statistically significant differences between the displacements related to the first week of treatment with those related to the remaining weeks.

Results: The M, MD, range and SD values are shown in Table 1.

TRANSLATIONS				
		FIRST 5 CT	AFTER FIRST 5 CT	ALL CT
x	Mean (cm)	0.19±0.12	0.18±0.10	0.19±0.11
	Range (cm)	0.01 – 0.46	0.02-0.37	0.01-0.46
	Median (cm)	0.15	0.16	0.16
	1° quartile (cm)	0.12	0.11	0.12
	3° quartile (cm)	0.28	0.25	0.25
y	Mean (cm)	0.20±0.18	0.14±0.11	0.18±0.15
	Range (cm)	0.01-0.88	0.02-0.42	0.01-0.88
	Median (cm)	0.17	0.15	0.16
	1° quartile (cm)	0.09	0.06	0.08
	3° quartile (cm)	0.22	0.21	0.21
z	Mean (cm)	0.14±0.12	0.19±0.20	0.17±0.16
	Range (cm)	0-0.57	0.03-0.97	0-0.97
	Median (cm)	0.12	0.14	0.14
	1° quartile (cm)	0.03	0.10	0.08
	3° quartile (cm)	0.22	0.21	0.23
ROTATIONS				
				ALL CT
x	Mean (°)			-0.67±0.68
	Range (°)			-2.60 - 0.80
	Median (°)			-0.60
	1° quartile (°)			-1.20
	3° quartile (°)			-0.20
y	Mean (°)			-0.28±1.09
	Range (°)			-4.00 - 2.70
	Median (°)			-0.10
	1° quartile (°)			-0.90
	3° quartile (°)			0.30
z	Mean (°)			-0.60±0.75
	Range (°)			-2.60 - 0.80
	Median (°)			-0.50
	1° quartile (°)			-1.15
	3° quartile (°)			0.00

Based on this table, all translational values were <3 mm and within 2 mm for all CBCTs and the rotations were <3° and within 2°. Moreover, the Wilcoxon test showed none statistically significant correlation between the M calculated during first five fractions and the following CBCTs scans.

Conclusion: In our study, we have analyzed translational and rotational set-up uncertainties in Head and Neck cancer treatments using CBCT. We found that all the displacements were within 2 mm and 2°, well below the offset established (3 mm and 3° respectively). In the future we intend to reduce the margin from CTV to PTV considering the accuracy of our set-up.

EP-1784

Effect of body mass index on setup errors in patients treated with pelvic image guided radiotherapy

O. Ozdemir[1], Z. Alicikus[1], T. Yagibasan[1], I.B. Gorken[1]
[1]*Dokuz Eylul Univ. Health Sciences Institute, Radiation Oncology, Izmir, Turkey*

Purpose or Objective: To retrospectively evaluate the effect of body mass index (BMI) on *set-up* errors in patients treated with image guided radiotherapy (IGRT) for pelvic malignancies. Additionally, based on these findings, we intended to determine optimal PTV margins in pelvic IGRT for patients with similar BMI values

Material and Methods: The datas from 73 patients who received pelvic IGRT between March 2014 and February 2015 were analyzed. BMI of each patient were calculated and patients were groupped as underweight (<18.5), normal weight (18.5–24.9), overweight (25–29.9) and obese ≥(30) according to National Institutes of Health classification. According to World Health Organization criteria, patients whose ages≥ 65 were evaluated as elderly. All patients received pelvic volumetric modulated arc therapy with Varian Truebeam STx ® linear accelerator. Before each treatment, orthogonal kV and CBCT images were taken and matched with bony anatomy and soft tissues respectively. The requisite couch shifts were made with online procedure and mean absolute shifts of X, Y, Z, 3D vectorial (V) axes for each imaging modality were obtained. Non-parametric tests were used for statistical analyses. Estimated CTV to PTV margins for *set-up* uncertainties calculated seperately for each group by using "Van Herk formula"

Results: The median age was 65 (36-86) and 70% were male. Totally 513 CBCT and 2064 kV images were evaulated. Mean absolute shifts in X, Y, Z, V axes with kV imaging were 3.39, 2.58, 2.85, 6.11 mm while with CBCT imaging 3.47, 2.90, 3.22, 6.54 mm, respectively. According to BMI groups; mean absolute shifts in X, Y, Z, V axes with kV imaging were 2.82, 2.67, 2.73, 5.54 mm for BMI<25; 3.57, 2.28, 2.81, 6.16 mm for BMI 25-29.9; 3.78, 3.14, 3.12, 6.82 mm for BMI≥30 while with CBCT imaging 3.16, 2.87, 2.82, 6.01 mm for BMI<25; 3.65, 2.92, 3.34, 6.74 mm for BMI 25-29.9; 3.49, 2.89, 3.51, 6.81 mm for BMI ≥30 respectively. Between BMI groups, only V axis shifts in kV imaging were statistically different (p:0.039). This difference is explained by sex distrubition differences in BMI groups and significantly higher obese group ratio in females (p:0.002). In females mean shifts in all axes were greater than males (p<0.05). Absolute shifts in V axis with CBCT imaging were statistically different between age groups and were significantly greater for 65 age group (p:0.041). In all patients, depending on absolute shift data; estimated CTV to PTV margins in X, Y, Z, V axes with kV imaging were 4.29, 3.99, 4.52, 5.62 mm; with CBCT imaging 4.71, 5.24, 4.93, 6.80 mm respectively

Conclusion: In our study we did not find any statistically significant difference in none of the axes between absolute shifts according to BMI groupes. However; because of greater shifts observed in females and 65 age group, more attention is needed in this group of patients' *set*-ups and PTV margins for these groups in planning process must evaulated more detailed

EP-1785

Comparison of setup errors and comfort levels of two immobilisation systems for head and neck cancer

P. Damodara Kumaran[1], S. John[2], R. Isiah[2], S. Das[2]
[1]*All India Institute Of Medical Sciences, Department Of Radiation Oncology, Delhi, India*
[2]*Christian Medical College, Radiation Oncology, Vellore, India*

Purpose or Objective: This is a Prospective observational study. This study aims to quantify and compare the systematic and random error in two types of immobilization devices namely five point ray cast and BrainLAB immobilization system. This study also looks at the effect of weight loss on the setup error and patients comfort grade in both the immobilization devices. All patients of Head and Neck malignancy planned with Intensity Modulated Radiotherapy [IMRT] were assigned either a five point ray cast or BrainLAB ray immobilization as fixation device.

Material and Methods: Patient diagnosed to have head and neck malignancy were assigned to either of the group and prospectively analysed the displacement errors. In both the groups, systematic and random errors were analysed. The CTV-PTV margin was calculated using Van Herks formula and compared. The upper neck and lower bony neck points were also analysed in terms of systematic error, random error and CTV-PTV margin. All the patients were serially monitored with weekly weight and its impact was analysed on the setup errors and margins. Patients' comfort level was analysed at the completion of treatment in both the immobilization devices.

Results: The five point ray cast and BrainLAB immobilization was found to be similar in terms of systematic errors and random errors, except in the anterior-posterior [AP] and medial-lateral axis [ML]. BrainLAB showed significant less margin in ML axis [3.61 Vs 3.14 mm, p=0.0005] and in AP axis [3.33 Vs 2.66 mm, p=0.0001] The total margin required was similar in both the groups. The margin requirement in the upper neck fields was marginally better in the BrianLAB system than the five point ray cast. Weight loss of more than 3kg required more margins, but was not statistically significant. Comfort levels were same in both the groups.

Conclusion: The total CTV-PTV margin requirement for five point ray cast and BrainLAB immobilization is less than 5mm in all three directions. In patients requiring only upper neck irradiation BrainLAB system is recommended. Overall Five point ray cast and BrainLAB immobilization was comparable in terms of setup errors, margins and comfort levels.

EP-1786

Rectal distension impact on prostate CBCT-based positioning assessed with 6 degrees of freedom couch

J. Charret[1], J. Salleron[2], M. Quivrin[3], F. Mazoyer[3], E. Martin[3], D. Peiffert[2], G. Créhange[3]
[1]*Institut de Cancerologie de Lorraine, Radiothérapie, Nancy, France*
[2]*Institut de Cancerologie de Lorraine, Biostatistique, Nancy, France*
[3]*Centre Georges Francois Leclerc, Radiothérapie, Dijon, France*

Purpose or Objective: The prostate requires a daily correction of its position in relation with rectal distension. With 6 degrees of freedom (DOF) couch, it is possible to correct the pitch and the roll. In this study, we sought to determine whether rectal distension might have an impact on any of these prostate translations and/or rotations during a protracted course of external beam radiation therapy for a localized prostate cancer

Material and Methods: The data from 15 patients with localized prostate cancer patients treated with 6 DOF cough in a single institution. Before each fraction, a CBCT was performed. The automatic fusion algorithm was set to fuse on soft tissue and it allowed correction for translations in three dimensions and rotation in the transverse plane (‘‘roll”) and axial plane (“pitch”).The rectum was contoured on each CBCT by one radiation oncologist. We determine the Cross Sectional Area (CSA) and relative CSA (CSArel) by dividing with the CSA of planning CT. The median was used to classify the patients in two groups: patients with a stable CSA and patients with an unstable CSA. The CSArel was compared between these two groups with a linear mixed model with group as fixed effect and patient as random effect

Results: Two hundred and ninety seven kV-CBCT were analyzed. Seven patients had a small and stable rectum : CSArel (1.07±0.09). The other eight patients had a unstable rectum: CSArel (1.37±0.07). The average pitch in the group with a stable rectum was 0.73° (+/-0.32) versus 0.04° (+/-0.28) (p=0.112). The pitch was not correlated with the CSA rel (p=0.477, r=0.041). The average roll in the group with a stable rectum was 0.14° (+/-0.27) versus 0.03° (+/-0.25) (p=0.781). The roll was not correlated with the CSA (p=0.279, r=0.063). The average CSArel was higher and more variable in the unstable group (p=0.009) and (p=0.024) respectively

Conclusion: Rectal distension had neither impact on the pitch nor on the roll, which suggest that a 6 DOF couch have little interest in daily practice for prostate IGRT

EP-1787

View of interest of automatic registration for CBCT localisation of head and neck cancer

C. Draulans[1], J. Meyskens[1], K. Geboers[1], S. Gysbrechts[2], I. Scheelen[2], M. Martens[1]
[1]*AZ Turnhout, Radiation Oncology, Turnhout, Belgium*
[2]*AZ Turnhout, Radiation Oncology Physics, Turnhout, Belgium*

Purpose or Objective: Use of IMRT in patients with head and neck carcinoma may lead to over- or underdosage of OAR and CTV due to changes in patients anatomy. CBCT is a valuable tool for patient setup verification and monitoring of dosimetric variation during radiotherapy. We evaluated the dependence of an automatic registration process on the size of a user defined view of interest (VOI). We compared these results with the manual registration defined by a physician, defined as gold standard.

Material and Methods: We retrospectively reviewed the records of 36 consecutive patients (107 fractions) with head and neck cancer who received radiation therapy between January 2015 and September 2015 at the Hospital of Turnhout. Three CBCT images at well-defined time points (start-, mid- and end-treatment) of each patient were matched to a reference CT image using the Siemens Syngo RT Therapist version R 4.3. Images were acquired with MVision™ (6 MV photon beam tuned for imaging). Auto global registration is the automatic alignment of planning and treatment images using voxel based registration. Manual VOI function allows restricting the voxel based automatic registration to a user defined region. Registrations were performed with 2 VOI sizes (large (VOI = whole CBCT) and small (VOI = delineated CTV + body of adjacent vertebra)). Automatic registrations (AR) were compared with a manual registration (MR) made by a physician. It was only possible to make translational corrections in the vertical, longitudinal and lateral direction. To quantify overall distance between gold standard and automatic registration, the 3D-difference (d) was calculated:
$d = \sqrt{((AR-MR)^2_{lateral} + (AR-MR)^2_{longitudinal} + (AR-MR)^2_{vertical})}$.

Results: The CBCT images of 107 fractions were analysed. Automatic registration results depend on the volume of VOI (large or small). A paired t-test calculated the mean 3D difference for the automatic registrations with small VOI was significantly smaller ($p < 0.001$) than the mean value for automatic registrations using the large VOI. 3D differences were divided in multiple ranges. Small VOI resulted in differences ≤ 2 mm between automatic registration and radiation oncologist registration in 56,1% of the cases. When using large VOI, it resulted in differences≤ 2 mm in 6.5% of the cases. Compared with radiation oncologist registration, small VOI resulted in differences > 6 mm in 5.6% of the cases. Large VOI resulted in differences > 6 mm in 24.3% of the cases.

Table 1: Summary showing 3D differences (mm) between automatic registration (large VOI and small VOI) and manual registration by a radiation oncologist

	Large VOI	Small VOI
Mean (standard deviation)	4.88 mm (2.14)	2.36 mm (1.93)
Median	4.58 mm	2.00 mm
Maximum	10.36 mm	11.36 mm
d = 0-2 mm	6.54 %	56.07 %
d = 2-4 mm	31.78 %	30.84 %
d = 4-6 mm	37.38 %	7.48 %
d > 6 mm	24.30 %	5.61 %

Conclusion: Automatic registrations can produce results which are comparable to manual registrations by radiation oncologist. Registration parameters for CBCT affect differences between automatic and manual registration although patients wear a plastic mask during radiation therapy. Using a small VOI (delineated CTV + body of adjacent vertebra) results in small differences between automatic and manual registration. If large VOI is used it can result in differences > 6 mm in more than 20% of the cases.

EP-1788

Accurate and stable immobilisation with Lorca Marin masks for head and neck IMRT verified by IGRT

I. Prieto[1], D. Esteban[1], A. Ilundain[1], E. Marquez[1], J. Olivera[1], J. Luna[1], J. Vara[1], W. Vasquez[1], A. Perez[1]
[1]*Fundación Jimenez Díaz, Radiation Oncology, Madrid, Spain*

Purpose or Objective: IMRT needs accurate and repeatedly image controls to verify online the patient position and check that the tumor is properly included. The aim of this work is to analyze the setup accuracy and stability resulting from the use of the Lorca Marin thermoplastic masks during the complete course in head and neck cancer treatment with intensity modulated techniques.

Material and Methods: 50 consecutive head and neck cancer treatments with IMRT were analyzed. Lorca Marin customized masks named *Nature* were used to immobilize head and neck. These 2-oxepanone polymer thermoplastic masks are 3-points immobilization with frontal and mental reinforcement and 3.2 mm thickness. 3-standard references were marked on the surface of the mask and on the middle chest of the patient for accurate positioning every day. Cone-beam computed tomography scan to verify online the position was performed during 5 consecutive days and after, weekly cone-beam (CBCT) until the end of the treatment. After weekly matching process using automated soft-tissue registration, translational movements along the three axes (x, y, z) were collected and the average for each treatment and each axis was calculated. Displacement´s mean of the 50 averages and the standard deviations were analyzed and compared.

Results: The resulting displacement average after analyzing 50 treatments was less than 1 mm along the three axes: x = (0.62±0.51) mm, y = (0.83±0.63) mm, z = (0.65±0.59) mm. These setup displacements have remained under 3 mm in 100% of treatments. These results achieve the International Commission on Radiation Units and Measurements recommendations regarding the setup margin to compensate the immobilization and positioning errors.

Conclusion: The type of patient immobilization devices and their contribution in the setup errors must be taken into account for IMRT. Additionally, the use of different image-guidance systems can significantly alter the size of the required margins. Lorca Marin thermoplastics masks with weekly CBCT show enough accuracy and stability for IMRT head and neck cancer patients.

EP-1789

Immobilization and dosimetric performance of a MRI compatible frame for head and neck patients

A. Perez-Rozos[1], I. Jerez Sainz[1], M. Toledo[2], M. Lobato Muñoz[1], J. Medina Carmona[2]
[1]*Hospital Virgen de la Victoria, Radiation Oncology. Medical Physics., Malaga, Spain*
[2]*Hospital Virgen de la Victoria, Radiation Oncology. Radiation Oncology, Malaga, Spain*

Purpose or Objective: Use of CT/RMI image registration for Head&Neck cancers is challenging because of the difficult to maintain the same position in simulation CT and in MRI system. A number of immobilization devices used in radiotherapy are not appropiate for use in MRI because of compatibility problems with the materials or with the acquisition coils. A novel head and neck board, fully compatible with Head and neck MRI coils (ExaFrame, Anatge(R)), has been presented and in this work we analyse setup accuracy of both conventional and MRI compatible board.

Material and Methods: Attenuation measurements were done using a diode array (MapCheck2, SunNuclear) inside water equivalent phantom and 6MV photons (TPR20,10=0.685, Elekta Synergy) for orthogonal beams. Attenuation is evaluated in the area of mask fixation and in body area of frame.Five consecutive patients with head and neck tumors were assigned to simulation with MRI compatible frame using head and shoulder mask with four fixation points. Immobilization and reproducibility is improved using a customized silicone mold between patient's nose bridge and mask. Reproducibility Every treatment day CBCT images were acquired for treatment isocenter, and shifts in patient position were automatically measured using simulation CT as reference (xvi, Elekta). Displacements in antero-posterior (Vert), cranio-caudal (Long) and medio-lateral (Lat) directions, and rotations about major axis were calculated and compared with conventional carbon fiber immobilization. A total of 150 CBCT images were acquired for CompMRI frame. A group of 30 patients with conventional board was used as control (900 CBCT images). Distribution of displacements, rotation and 3D displacements were compared between both groups.

Results: Attenuation measurement is shown in the image, and is lower than 4% for orthogonal incidence. No artifacts on MRI image were observed. Reproducibility between MRI and CT simulation was better than 1 mm in all cases studied, based in direct versus automatic registration.The mean and standard deviation of shifts for the CompMRI board versus conventional board are shown in table 1. An analysis of variance differences using a Fisher test gives statistically significative differences between variances of two groups ($p<<0.01$). The distributions of the absolute displacements were similar in both groups.

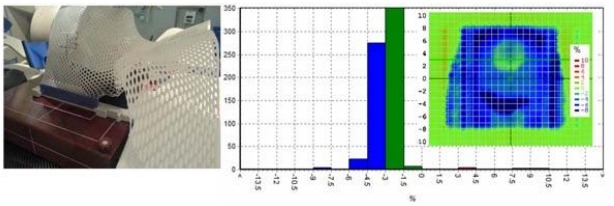

	Lat (mm)	Vert (mm)	Long (mm)	Roll (º)	Tilt (º)	Pitch (º)
C-MRI	0.8 ± 0.6	-0.3 ± 0.9	-1.5 ± 1.2	-0.7 ± 0.7	-0.1 ± 0.5	-0.1 ± 0.3
Conventional	0.8 ± 2.7	-1.7 ± 3.9	-1.0 ± 3.2	-0.4 ± 1.2	0.1 ± 1.2	-0.2 ± 1.0

Conclusion: Our data show that the C-MRI board have low attenuation and a better immobilization and reproducibility than the conventional board. Position reproducibility from MRI simulation and CT simulation was excellent. Combination of MRI compatible board with silicone fixation provided robust immobilization and can be safely used for MRI-CT registration procedures eliminating the use of deformable and complex software algorithms. These data could be used for a potential reduction of margins for the PTV.

EP-1790

Assessment of Uterine Fundus Coverage with IGRT using daily CBCT in cervical cancer

Z. Ozen[1], N. Kayalılar[1], A. Arifoglu[1], B. Günhan[1], R. Ibrahimov[1], F. Karaköse[1], S. Gurdalli[1], M.U. Abacıoglu[1]
[1]*Neolife Medical Centre, Radiation Oncology, Istanbul, Turkey*

Purpose or Objective: Inclusion of uterine fundus in the pelvic CTV for definitive treatment of cervical cancer is controversial. We aimed to demonstrate the fundus coverage by using daily CBCT with a rigorous bladder filling protocol.

Material and Methods: Five patients with cervical cancer without uterine fundus involvement were scanned by 2.5 mm slice thickness CT after a 30 minute, 500 cc water consumption. PET/CT and MR fusion was performed to delineate GTV and used as surrogates to see the potential motion of uterus at different imaging modalities due to bladder and rectal fillings. CTV1 was contoured to include GTV+cervix+uterus modified to be covered in simulation CT, PET/CT and MR. PTV margin of 15 mm was added according to guidelines. VMAT IMRT plans were performed to give 45 Gy in 25 fractions. Image guidance with daily kV CBCT was performed on TrueBeam STx and Trilogy linacs (Varian, Palo Alto) throughout the external phase of the treatment, which was followed by HDR brachytherapy. When the CTV1 was missed on CBCT, the bladder filling was modified accordingly; CBCT was repeated and treated after ensuring the coverage.

Results: Uterine fundus was contoured on a total of 125 CBCT images of 5 patients. Overall on 24 of 125 fractions (19.2%) CTV1 was out of PTV. Mean volume of CTV1 out of PTV was 0.92 cc (range 0.02-2.78 cc). Mean Dmin for fundus was 133 cGy when the CTV1 was out of PTV, while it was 176 cGy when CTV1 was covered on CBCT.

Conclusion: Although the inclusion of the uterine fundus in the CTV for the definitive treatment of cervical cancer without fundus involvement is controversial, potential microscopic spread is a concern. Rigorous bladder filling is a way to minimize the interfraction motion of the uterus,

however daily image guidance with CBCT still showed a residual replacement of the uterus in up to one fifth of the fractions in this study. Further studies on managing this problem like adaptive treatment by using plan of the day concept to cover the CTV are ongoing.

EP-1791

Improving patient posture reproducibility by using the predicted couch position and tight tolerances

L.J. Mesch[1], W.J.M. De Kruijf[2]
[1]*Institute Verbeeten, Radiation Therapy, Tilburg, The Netherlands*
[2]*Institute Verbeeten, Medical Physics & Instrumentation, Tilburg, The Netherlands*

Purpose or Objective: With online imaging inter-fraction motion is very small. However, when a patient is wrongly positioned on an immobilisation device, the patient posture cannot be corrected with a simple couch shift or rotation. The couch position indicates the accuracy with which the patient is positioned with respect to the immobilisation device on a day-by-day basis. The purpose of this work is to improve patient posture reproducibility by predicting the couch position before the first treatment (preventing a systematic error in couch position), and by using this couch position at the LINAC more directly than only for verification purposes.

Material and Methods: All patients with a planning-CT are treated with an immobilisation device attached to the treatment couch. A software tool, "planinfo", predicts the couch position from the geometrical information of the planning-CT in the EPD and the isocentre coordinates in the treatment plan. Before the treatment session the couch is positioned at the predicted couch position of the patient set-up point, given in the set-up notes. The patient is instructed to move until the lasers align with the patient tattoos. We do not need to have the lasers exactly on the tattoos, because we perform an online imaging procedure. Patient rotations with respect to the lasers are to be avoided. Next, the couch is shifted to the isocentre, an online imaging procedure is performed and the patient is treated. We do not use the couch position at the first treatment fraction as a reference, preventing systematic errors in couch position.

Results: Table 1 shows the tolerances that we use for the 5 immobilization devices, the average difference between the predicted and the treated couch position in the first half of 2015 and the standard deviation of the differences for all treatment fractions in this period. These values are better than the couch position values reported by others in literature, because we do not shift the couch to align the patient with the lasers, but we shift the patient in the immobilization device to achieve this. Radiation therapists indicate that it is more straightforward to position the patient with this method. For head and neck the values are comparable with literature [2,3], because the masks more rigidly relate the patient position to the couch than other immobilization devices. However, with our method we do not need to mark any lines or points on the immobilisation mask. Table 1 also shows the number of overrides with our current tolerance tables. This is about 1 % of all treatment fractions. For palliative treatments with its own immobilization device (home-made head base with a cushion) it is about 5 %.

Table 1: Comparison of the difference in predicted and treated couch position for the first half of 2015.

Immobilization	Fractions	Override percentage	Direction	Tolerance (mm)	Average (mm)	Standard deviation (mm)
Head and Neck	3389	0.9 %	Vertical	10	0.0	2.1
			Longitudinal	10	2.2	2.8
			Lateral	10	1.3	3.1
Thorax	6062	1.0 %	Vertical	10	1.1	2.8
			Longitudinal	15	-1.0	5.7
			Lateral	15	-0.2	4.6
Mamma	8529	0.4 %	Vertical	10	0.2	3.4
			Longitudinal	15	0.1	4.3
			Lateral	15	-0.6	4.1
Pelvis	7766	1.2 %	Vertical	10	1.1	3.7
			Longitudinal	15	-1.5	4.3
			Lateral	15	-0.3	5.1
Palliative	766	5.9 %	Vertical	10	0.5	2.5
			Longitudinal	15	-0.1	6.2
			Lateral	15	-0.9	6.6

Conclusion: We have improved the patient setup considerably. Currently, all patients with a planning-CT are treated according to the method described above. We use tight tolerances to ensure patient posture reproducibility.

EP-1792

Pre-fraction shift and intra-fraction drift of the prostate due to perineal ultrasound probe pressure

H. Ballhausen[1], F. Manapov[1], A. Kolberg[1], P.D. Thum[1], U. Ganswindt[1], C. Belka[1], M. Li[1]
[1]*Ludwig-Maximilians-Universität München, Department of Radiation Oncology, München, Germany*

Purpose or Objective: In image guided radiotherapy of the prostate, during trans-abdominal ultrasound imaging, the pressure applied by the ultrasound probe against the abdomen has been shown to displace the prostate. In this study trans-perineal imaging is evaluated. The impact of varying probe pressure on pre-fraction shift and intra-fraction drift of the prostate is measured.

Material and Methods: Two separate experiments were performed: Before treatment (10 patients) varying ultrasound pressure was applied to the perineum. In a series of scans, the probe was moved against the perineum and the corresponding shifts of the prostate were detected. Linear regression was performed. During treatment (15 patients, 273 fractions) intra-fraction drift of the prostate was tracked (total of 27 hours and 24 minutes).

Results: Per 1 mm shift of the ultrasound probe in cranial direction, a displacement of the prostate by 0.42±0.09 mm in cranial direction was detected. The relationship was found to be linear (R^2=0.97) and highly significant ($p<0.0001$). After initial contact of the probe and the perineum (no pressure) a shift of the probe of about 5 to 10 mm was typically necessary to achieve good image quality, corresponding to a shift of the prostate of about 2 to 4 mm in cranial direction. There was found also a systematic ($p=0.03$) shift of <0.1 mm in anterior direction, but not significant shift in lateral direction ($p=0.14$). The compression of the tissue between probe and prostate was well visible in consequent scans. During treatment, the prostate was drifting at a rate of -0.075 mm per minute in cranial direction on average. While small, this systematic trend on the longitudinal axis was significant ($p=0.0014$). There was no significant trend on neither the lateral nor the vertical axis ($p=0.62$ resp. $p=0.19$). Also, due to the perineal probe, the prostate had fewer degrees of freedom in caudal direction.

Conclusion: The pressure applied by a perineal ultrasound probe has a quantitatively similar impact on prostate displacement as trans-abdominal imaging. Shifts are predominantly in cranial direction (typically 2 to 4 mm) with some component in anterior direction (typically <1 mm). Slight probe pressure can improve image quality, but excessive probe pressure can distort the surrounding anatomy and potentially move risk organs closer to the high dose area. Tentatively, probe pressure could also have beneficial effects in stabilizing the prostate.

EP-1793

Analysis of setup error in patients affected by oropharyngeal cancer treated with tomotherapy

P. Bonomo[1], L. Marrazzo[2], G. Carta[1], M.H. Baki[1], C. Talamonti[2], C. Arilli[2], F. Paiar[1], I. Desideri[1], G. Simontacchi[1], S. Scoccianti[1], D. Greto[1], S. Pallotta[2], L. Livi[1]
[1]*University of Florence, Radiation Oncology, Firenze, Italy*
[2]*University of Florence, Medical Physics, Firenze, Italy*

Purpose or Objective: In head and neck cancer radiotherapy, it is still unresolved whether the use of daily image guidance (IG) allows the safe adoption of reduced PTV margins. Moreover, the extended time required for IG on a daily basis unavoidably represents a limiting factor for patients throughput in centers with busy workload. The purpose of our analysis is: 1) evaluating the interfraction error of patients undergoing tomotherapy for oropharyngeal cancer (OPC) with the aim of margins reduction and 2) investigating whether the mean error calculated on the first 5 fractions may avoid the need of performing IG on a daily basis.

Material and Methods: A cohort of 20 OPC patients radically treated with tomotherapy was retrospectively analyzed. Conventionally, a 5-mm CTV to PTV margin policy was used. All patients underwent integrated mega-voltage computed tomography (MVCT) before every fraction and were treated after correction of shifts in the medial-lateral (X), supero-inferior (Y), and antero-posterior (Z) directions, as well as in the medial-lateral rotation (roll). These "on-line" variations were registered for every patient. In order to test the reproducibility of the procedure, for a subset of 10 patients (for a total of 301 MVCT's) a "re-matching" was performed: shifts adopted at time of treatment were reset and a manual re-alignment was then blindly performed. Mean values and standard deviations were calculated and compared for the two sets of data. To test the hypothesis of the applicability of a mean-error strategy, the mean shifts calculated on the first 5 fractions were applied on the subsequent fractions and the mean residual error was evaluated.

Results: A total of 619 MVCT's was analyzed. The mean X, Y, Z and roll errors for the 20 analyzed patients are reported in Figure 1.

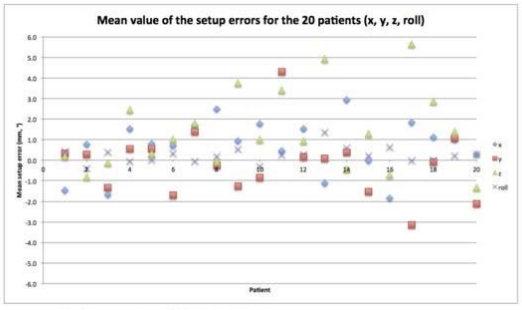

Figure 1. Mean value of the setup errors (x, y, z, roll) for the 20 patients in the study.

The mean of the absolute X, Y, Z and roll errors were 1,8 mm, 3,4 mm, 2,4 mm, and 0,5° respectively. The mean "off-line" shifts were very similar to the "on-line" ones (as shown in Table 1).

	On-line matching				Off-line matching			
	x	y	z	roll	x	y	z	roll
	-1,4	0,3	0,2	0,4	-1,8	0,3	0,0	0,6
	0,8	0,3	-0,8	-0,4	1,2	0,7	-2,2	-1,1
	-1,7	-1,3	-0,1	0,4	-1,7	-1,0	-1,1	1,0
	1,5	0,6	2,5	-0,1	1,2	0,5	3,2	0,0
	0,8	0,5	0,3	0,0	1,7	0,7	1,0	-0,7
	0,7	-1,7	1,0	0,3	0,7	-2,2	1,0	0,7
	1,7	1,4	1,8	0,0	1,8	2,2	2,2	0,2
	2,5	-0,3	0,0	0,2	2,4	0,0	0,9	-0,1
	0,9	-1,3	3,7	0,5	1,2	-0,8	3,9	0,7
	1,8	-0,9	1,0	-0,3	2,2	-1,3	1,1	-0,4
mean ± σ	0,8±1,3	-0,2±1,0	1,0±1,4	0,1±0,3	0,9±1,5	-0,1±1,3	1,0±1,8	0,1±0,7

Table 1. Comparison between the on-line and off-line matching for 10 patients.

The equivalence between the "on-line" and "off-line" shifts was extremely high (Pearson's correlation coefficient, p= <<0.05), therefore further validating the integrity of the data. For the majority of patients the random component of the setup error was predominant, so the mean error strategy was not effective in reducing the setup error. Only in 5 cases a clear systematic component in the setup error was identified, which was effectively reduced with the application of the mean shifts.

Conclusion: The use of a reduced 3-mm PTV expansion margin can be safely implemented in the context of daily IG in OPC. On the other hand, in cases where a clear systematic component of the setup error is detected, the strategy of correcting for the mean error derived from the first 5 MVCT's is efficient in reducing residual setup errors, possibly allowing the adoption of a non-daily IG policy in these cases.

EP-1794

Quantification of stomach movement using CBCT images

R. Carrington[1], E. Spezi[2], B. Thomas[3], S. Gwynne[4], T. Crosby[3], J. Staffurth[5]
[1]*Velindre Cancer Centre, Medical Physics, Cardiff, United Kingdom*
[2]*Cardiff University, School of Engineering, Cardiff, United Kingdom*
[3]*Velindre Cancer Centre, Clinical Oncology, Cardiff, United Kingdom*
[4]*Singleton Hospital, Clinical Oncology, Swansea, United Kingdom*
[5]*Cardiff University, Institute of Cancer and Genetics, Cardiff, United Kingdom*

Purpose or Objective: We have shown a significant increase in predicted stomach toxicity when dose escalating from 50Gy to 60Gy in lower oesophageal tumours (1). The modelling was conducted on a single planning CT image, however the stomach undergoes continual volume and position changes during radiotherapy (2). Thus, the received dose by the stomach deviates from the planned dose. Previous work has used endoscopically placed clips and fluoroscopy to analyse movement (3) & (4). To the authors' best knowledge, this study is the first to quantify the stomach's movement and volume change during radiotherapy using Cone Beam Computed Tomography (CBCT) images.

References	
1	Staffurth J, Carrington R, Warren S, Partridge M, Hurt C, Spezi E, et al. EP-1470: Does gastric toxicity influence dose escalation in lower oesophageal tumours? A radiobiological investigation. Radiotherapy and Oncology.115:S797-S8.
2	Watanabe M, Isobe K, Uno T, Harada R, Kobayashi H, Ueno N, et al. Intrafractional Gastric Motion and Interfractional Stomach Deformity Using CT Images. Journal of Radiation Research. 2011;52(5):660-5.
3	Isobe K, Uno T, Kawakami H, Ueno N, Kawata T, Ito H. A case of gastric lymphoma with marked interfractional gastric movement during radiation therapy. International Journal of Clinical Oncology. 2006;11(2):159-61.
4	Watanabe M, Isobe K, Takisima H, Uno T, Ueno N, Kawakami H, et al. Intrafractional gastric motion and interfractional stomach deformity during radiation therapy. Radiother Oncol. 2008;87:425-31.

Material and Methods: The stomach volume was outlined on the planning CT and 4 CBCT images taken over the course of treatment (first 3 fractions then once weekly) for 4 patients. Image registration between the planning CT and CBCTs was undertaken using the Velocity software package, with the quantification analysis of stomach movement and volume change being carried out in the CERR software environment using in-house Matlab scripts. The difference in maximum and minimum x,y,z, coordinates, change in centre of mass (COM) and total volume between each CBCT image and planning image for the stomach volume and PTV/stomach volume overlap was calculated.

Results: The mean and range of displacement across all image sets and patients for the maximum and minimum x,y,z coordinates of the stomach was 5.4mm (0.0-23.4), 6.7mm (0.0-36.1) and 10.5mm (0.0-42.0), respectively. The mean and range of displacement for the COM x,y,z coordinates across all image sets was 4.0mm (7.0-14.6), 3.3mm (1.0-11.7) and 8.7mm (1.0-31.4) respectively. The mean change in total stomach volume was 22.2% (0.4-64.5), whilst the mean change in PTV/stomach volume overlap was 25.8% (2.1-74.9) between the CBCT and planning CT images across all patients.

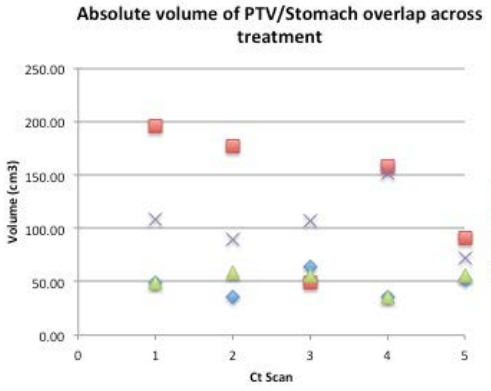

Conclusion: This study has shown that the position and volume of the stomach of a patient over the course of treatment is highly variable. In order to minimise the risk of toxicity of the stomach during treatment using high dose regimes (>50Gy) a stomach filling protocol may be required. Further work with a larger patient dataset is ongoing and the feasibility of stomach filling protocols will be explored.
Normal 0 false false false EN-GB JA X-NONE

EP-1795

Evaluation of CBCT protocols in craniospinal RT for pediatric medulloblastoma: a preliminary study

E. Madon[1], A. Sardo[1], S. Sirgiovanni[1], V. Richetto[1], A. Mussano[2], U. Monetti[2], A. Urgesi[2]
[1]*A.S.O.U.S. Città della Salute e della Scienza di Torino, Fisica Sanitaria, Torino, Italy*
[2]*A.S.O.U.S. Città della Salute e della Scienza di Torino, Radioterapia, Torino, Italy*

Purpose or Objective: The use of IGRT technologies, such as cone beam CT, improves treatment delivery accuracy: given that reduction of radiation dose is particularly relevant in pediatrics, an ideal IGRT method would minimize dose while enabling adequate visualization of relevant anatomy for target localization. However, setup accuracy parameters and predictors have not been extensively evaluated. We describe the preliminary results of a prospective evaluation of a low-dose CBCT protocol for IGRT in pediatric craniospinal radiation therapy.

Material and Methods: Various low-dose CBCT protocols with CTDI of 0.1-2 mGy/scan were prepared, and patient and IGRT characteristics were recorded in real-time. Different reconstruction algorithms were used to optimize cone beam images and registrations. Setup accuracy was quantified by hexapod table translations and rotations (6 dof) between planning CT vs daily CBCT acquisition. The shift vector magnitudes in polar coordinates were calculated. Descriptive statistics were performed (t-test). All these evaluations were made for craniospinal and for posterior fossa irradiation.

Results: Table 1 shows the parameters values (dose and image quality) of the examined protocols. Taking into account to the results, clinical protocols were defined for the three target volumes considered. Two patients (180cGy/13frs CSI + 180cGy/17frs post fossa) were studied with 30 daily pre-treatment CBCT. For the first patient, early phase of radiation therapy was delivered with anaesthesia. In CSI treatment, where junctions between beams are critical, only translations movements were considered. In cranial isocenter localization mean table shifts were 5.84 ± 0.98 mm (fast low dose,A) and 3.84 ± 3.21 mm (fast low dose) 3.6 ± 1.99 mm (fast high dose), with and without anaesthesia respectively; in the spinal setup evaluation mean table shift was 7.3 ± 2.1 mm (fast low dose,A) and 8.7 ± 0.2 mm (fast low dose), 6.8 ± 0.2 mm (fast high dose). Difference between setup accuracy according to patient's cooperation, with and without anaesthesia, is statistically relevant ($p<0.05$) for cranial localisation and not for the spine localisation and the statistical significance persists considering also the overall treatment. On the other hand difference between setup accuracy according to patient dose does not show statistical difference.

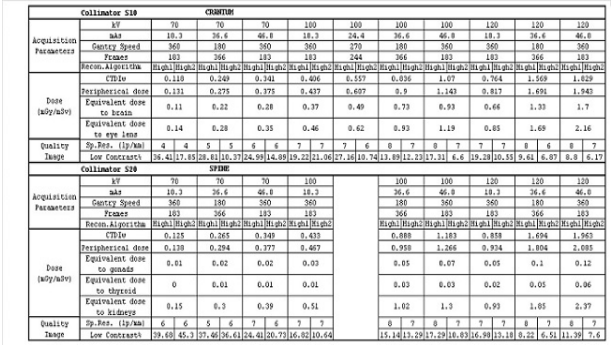

	Collimator 510	CRANIUM									
Acquisition Parameters	kV	70	70	70	100	100	100	100	120	120	120
	mAs	10.3	36.6	46.8	10.3	24.4	36.6	46.8	10.3	36.6	46.8
	Gantry Speed	360	180	360	360	270	180	360	360	180	360
	Frames	183	366	183	183	244	366	183	366	366	183
	Recon. Algorithm	High1 High2	High1 High2	High1 High2	High1 High2	High1 High2	High1 High2	High1 High2	High1 High2	High1 High2	High1 High2
Dose (mGy/mAs)	CTDIw	0.110	0.249	0.341	0.406	0.557	0.936	1.07	0.764	1.569	1.829
	Peripherical dose	0.131	0.275	0.375	0.437	0.607	0.9	1.143	0.817	1.691	1.943
	Equivalent dose to brain	0.11	0.22	0.28	0.37	0.49	0.73	0.93	0.66	1.33	1.7
	Equivalent dose to eye lens	0.14	0.28	0.35	0.46	0.62	0.93	1.19	0.85	1.69	2.16
Quality Image	Sp.Res. (lp/mm)	4 4	5 5	6 6	7 7	7 6	8 7	8 7	7 7	8 6	8 7
	Low Contrast%	36.41 17.85	28.61 10.37	24.99 14.09	19.22 21.06	27.16 10.74	13.89 12.23	17.31 6.6	19.29 10.55	9.66 6.07	8.8 6.17
	Collimator 520	SPINE									
Acquisition Parameters	kV	70	70	70	100		100	100	120	120	120
	mAs	10.3	36.6	46.8	10.3		36.6	46.8	10.3	36.6	46.8
	Gantry Speed	360	180	360	360		180	360	360	180	360
	Frames	183	366	183	183		366	183	183	366	183
	Recon. Algorithm	High1 High2	High1 High2	High1 High2	High1 High2		High1 High2	High1 High2	High1 High2	High1 High2	High1 High2
Dose (mGy/mAs)	CTDIw	0.125	0.265	0.349	0.433		0.888	1.183	0.858	1.694	1.963
	Peripherical dose	0.138	0.294	0.377	0.467		0.958	1.266	0.934	1.804	2.085
	Equivalent dose to gonads	0.01	0.02	0.02	0.03		0.05	0.07	0.05	0.1	0.12
	Equivalent dose to thyroid	0	0.01	0.01	0.01		0.03	0.03	0.02	0.05	0.06
	Equivalent dose to kidneys	0.15	0.3	0.39	0.51		1.02	1.3	0.93	1.85	2.37
Quality Image	Sp.Res. (lp/mm)	6 6	5 6	7 6	7 7		8 7	8 7	7 7	8 7	8 7
	Low Contrast%	39.68 45.3	37.46 36.61	24.41 20.73	16.02 10.64		15.14 13.29	17.29 10.03	16.99 13.18	8.22 6.51	11.39 7.6

Conclusion: CBCT-derived table shifts for investigations with LD-CBCT and with HD-CBCT were statistically similar, suggesting that for pediatric radiation therapy setup evaluation can be safely performed with lower-dose IGRT. Moreover, these data support implementation of a LD-CBCT protocol also in pediatric hyperfractionated accelerated radiotherapy.

EP-1796

Definition of thresholds to detect anatomy changes using Delivery Analysis software for Tomotherapy.

C. Dejean[1], M. Gautier[1], J. Feuillade[1], A. Mana[1]
[1]*Centre Antoine Lacassagne, Academic Physics, Nice, France*

Purpose or Objective:
To determine the analysis parameters for quantitative assessment of the dosimetric impact of differences between the measured and calculated MVCT detectors sinograms. This difference is directly related to patient positioning and/or anatomical changes.

Material and Methods: Tomotherapy HD v5.0 associated to Delivery Analysis (DA) software (beta version) has been used for patient treatments. Consistency of MLC functioning is assessed by comparing opening-closing time measured by detectors versus calculated during planning. The quality assurance of the device validates its functioning. Detector response stability is continuously monitored (sd/mean<0.05%). DA software analyzes the difference of the detectors sinogram between a reference fraction and the fraction of the day, its influence is measured through the patient. The specific differences to a patient will therefore depend on its positioning and/or anatomical variations. From the analysis of each treatment session, alert thresholds will be defined.

Results: Considering margins used and expected dose accuracy, parameters of 2mm (DTA) and 3% (dose) were used associated to a threshold of 99% for gamma index analysis. We use them as a baseline to verify detectability on various treatments. With this level of detectability, the presence of gas in pelvic localizations, a loss of weight linked to a variation of 5mm thickness is detected. In the context of lung tumors, a reduction in tumor volume (associated with lung density change) is detected. The interpretation of these differences is not easy because of the movement of such gases, we have then added a condition for further analysis: three consecutive fractions not meeting the criterion result in a complete analysis or 15% of non consecutive fractions (conventional fractionation). A less than 95% result is immediately analyzed to determine visually on the MVCT scanner the reason : if it is weight loss, a new planning is realized.

Conclusion: Two strong points should be noted: a color code is associated to analysis results (red/green : fail/pass) and permits a relevant and fast systematic analysis. This information also applies to non-imaged areas, such as for medulloblastoma: although the MVCT is not acquired over the

entire treated length, it is possible to determine their spatial localizations. Thus, it is possible to adapt the scan lengths. On the other hand, to provide education, therapists can easily see the impact of their choices, eg set-up compromises.

EP-1797

Pelvic lymph node PTV margins in prostate IMRT

L. Duvergé[1], J. Castelli[1,2,3], S. Cadet[4], A. Simon[2,3], N. Jaksic[1], C. Lafond[1,2,3], P. Haigron[2,3], R. De Crevoisier[1,2,3]
[1]*Centre Eugene Marquis, Radiotherapy, Rennes, France*
[2]*INSERM, U 1099, Rennes, France*
[3]*University Rennes 1, LTSI, Rennes, France*
[4]*Therenva, Therenva, Rennes, France*

Purpose or Objective: Very few data are available on the intrapelvic motion of pelvic lymph nodes (LN), likely associated with the linked pelvic vessels. The objectives of the study were to quantify the interfraction pelvic vessel motion and to deduce therefore rational PTV margins around the LN CTV, in a scenario of pelvic bone based prostate IGRT.

Material and Methods: The planning CT scans (CT0) and 7 per-treatment weekly CT scans of 20 patients having received IMRT for prostate cancer were used. The main pelvic vessels were manually delineated: common iliac (CI), external iliac (EI) and internal iliac (II) of both sides. The central lines of the vessels were first defined thanks to a 3D workstation (EndoSize®, Therenva) dedicated to the preoperative sizing before endovascular interventions. A pelvic bone registration was then performed. For a given vascular segment, the distance between its central line CL0 from CT0 and its central line CLi from the weekly CTs were calculated.The central line CL0 of each vascular segment was sampled every mm. The distance corresponded to the mean value of the distances between corresponding points of the two central lines (CL0 and CLi). The correspondance was established by considering the cross-section plane othogonal to CL0 at a given point and its intersection with CLi. For each patient, the mean and the standard deviation (SD) of the measurements of the 7 fractions were determined. The systematic error (Σ) of the whole population was calculated as the SD of the mean values. The random error (σ) of the whole population was calculated as the root mean square of the standard deviation values. The margins were calculated both with M. Van Herk formula (*IJROBP* 2000) and by geometrically computing margins covering 99% of the vessels displacements.

Results: The results are given for the first 10 patients. The mean (range) lengths (in mm) for IC, EI and II were 47 (18-84), 95 (78-120) and 38 (20-55), respectively. The systematic and random errors and the corresponding margins are given in the Table.

		Common Iliac	External Iliac	Internal Iliac
Ant/post	Systematic Error (Σ)	1.3	0.9	1.0
	Random Error (σ)	1.2	0.8	0.7
	Van Herk Margins	4.1	2.8	3.1
	99% Margins	5.1	4.3	4.6
Lateral	Systematic Error (Σ)	0.8	0.5	0.9
	Random Error (σ)	0.7	0.6	1.0
	Van Herk Margins	2.6	1.8	2.9
	99% Margins	3.6	2.7	4.0
Sup/Inf	Systematic Error (Σ)	0.7	0.7	1.7
	Random Error (σ)	0.7	0.7	1.6
	Van Herk Margins	2.2	2.3	5.2
	99% Margins	2.5	2.9	5.1

Table: Vessels displacements (systematic and random errors) and corresponding PTV margins (according to Van Herk formula and covering 99% of the displacements) around the LN CTV (in mm)

Conclusion: Pelvic LN PTV margins should be around 5 mm for the common and internal iliac CTV and 4 mm for the external iliac CTV.

EP-1798

Is there a true dosimetric improvement in lung SBRT using a 6-Degree of Freedom couch in IGRT era?

S. Menna[1], S. Chiesa[2], A.R. Alitto[2], L. Azario[1], G.C. Mattiucci[2], S. Teodoli[1], N. Dinapoli[2], L. De Filippo[2], M. Balducci[2], V. Valentini[2]
[1]*Università Cattolica del Sacro Cuore, Physics Institute & Operative Unit of Medical Physics, Rome, Italy*
[2]*Università Cattolica del Sacro Cuore, Radiation Oncology Department- Gemelli-ART, Rome, Italy*

Purpose or Objective: To investigate dosimetric impact of rotational errors on Stereotactic Body Radiation Therapy(SBRT),using Protura 6-Degree of Freedom(6-DoF)Robotic Patient Positioning System(CIVCO Medical Solution).

Material and Methods: Patients enrollment included:lung primary or metastatic tumors,maximum 3 lesions,preferably not in central position and until 5 cm.The target should be clearly evident at staging imaging.PTV was obtained adding 0.3 cm as margins to target(CTV).A kV-Cone Beam CT(kV-CBCT)was acquired before dose delivery.After 3D manual match,translational and rotational shifts were applied by the Protura Couch.Using MIM 5.5.2 software,a CT was generated by rigid registration in the CBCT wrong position,i.e. patient position at the moment of CBCT.Then,translational shifts were applied,obtaining a translated CT(tCT),i.e. CT in wrong position with only translational errors correction.Then,rotational errors were corrected too,obtaining roto-translated CT(rtCT).Initial treatment plan was copied to translated CT(tTP)and roto-translated CT(rtTP).Finally, dosimetric parameters were compared.

Results: From July to September 2015,13 patients were enrolled(10 with primary tumours and 3 with metastatic lesions;9 peripheral and 4 central lesions;mean volume 13,26 cc)with a median age of 74 yrs(range 58-86);52 CBCT studies,52 tTP and 52 rtTP were performed.No correlation was observed between magnitude of translational and rotational shifts.Dosimetric evaluation showed no important variations in CTV V95% for rotations(mean±SD 0.00±0.05).Ninety-one percent (91%)of all PTV V95% was≥ 95% in roto-translated plans;in the worst case a mean rotation of -0.3° caused a decreasing in V95%=93%.Small differences due to rotations were found in all Organs at Risk(OAR)matrices reported in Table 1.

	Spinal Cord Dmax (Gy)	Heart Dmax (Gy)	Esophagus Dmax (Gy)	Total Lung V(%) 20	Total Lung V(%) 12.5	Total Lung V(%)5
MEAN	0,0	0,0	0,0	0,0	0,0	0,0
SD	0,3	0,8	0,2	0,0	0,0	0,2
MAX	0,8	4,2	0,5	0,1	0,1	0,4
MIN	-0,8	-3,0	-0,3	-0,1	-0,1	-0,6

After rotational corrections,an improvement was observed in constraints values for OARs than reference planning dose(Table 2),although only 3% of all data had an improvement>5%.

Spinal Cord Dmax (Gy)	Heart Dmax (Gy)	Esophagus Dmax (Gy)	Total Lung V(%) 20	Total Lung V(%) 12.5	Total Lung V(%)5
37,8%	31,1%	28,9%	48,9%	57,8%	42,2%

Multiple regression and pairwise confront(post-hoc test)showed significative linear correlations between esophagus Dmax and roll(p=0.007) and pitch(p=0.020)rotation,total lung V12.5 and yaw(p=0.048).Regarding PTV coverage,V95% and V105%,no significant difference between tTP and rtTP was observed(Mann-Whitney test p>0.05).

Conclusion: These preliminary data show an improvement for OARs if rotational shifts are applied.Dosimetric benefits on lung tumours are small that is PTV margins are optimal for all shifts detected.Dosimetric evaluation in other sites is ongoing.

EP-1799

3, 5 or 7 fractions with no image guidance in moderately hypofractionated prostate treatments

R. Bermúdez Luna[1], A. López Fernández[1], C. Rodríguez Rodríguez[1], M.V. De Torres Olombrada[2], T. García Cañibano[2]
[1]*Hospital Universitario de Fuenlabrada, Medical Physics, Fuenlabrada, Spain*
[2]*Hospital Universitario de Fuenlabrada, Radiation Oncology, Fuenlabrada, Spain*

Purpose or Objective: Radiotherapy treatments are delivered in our centre using two twin linacs. This provides the possibility of treating patients in either of them. In case of breakdown of one of the linacs, the number of patients interrupting their treatment can be minimised as they can be treated in the linac that continues working.
With the aim of optimally doing so, the IGRT workflow is exceptionally changed in case of linac breakdown and image guidance (IG) is only performed when considered strictly necessary.
Prostate cancer patients treated in our radiotherapy department receive a moderately hypofractionated IMRT treatment with daily IG.
The purpose of this work was to assess the dosimetric differences that would result in prostate treatments if IG was not performed in 3, 5 or 7 fractions due to linac breakdown in the most sensitive patients to the lack of IG according to our IGRT protocol.

Material and Methods: 20 prostate plans were retrospectively modified and analysed. All of them were moderately hypofractionated treatments with prescription doses to the prostate and seminal vesicle (SV) PTVs of 70 Gy (2.5 Gy/fraction) and 56 Gy (2 Gy/fraction), respectively. They corresponded to patients whose daily positioning shifts after an initial correction of the systematic error showed a standard deviation ≥4mm or an absolute displacement mean value ≥3mm.
Seven positioning shifts were randomly selected for each patient out of their recorded treatment data. Beams corresponding to 3, 5 or 7 fractions were accordingly displaced in the TPS, as if no IG had been performed.

Results: Dosimetric differences observed for the prostate and SV CTVs were negligible.
Mean absolute variations in the mean rectal dose when not performing IG in 3, 5 or 7 fractions were 35.2 ± 27.2 cGy, 50.9 ± 33.8 cGy and 63.2 ± 47.1 cGy, respectively. The results obtained for the bladder were: 19.5 ± 12.9 cGy, 30.0 ± 19.8 cGy and 39.1 ± 31.8 cGy.
The table shows the percentage of cases classified by their corresponding absolute variation in the mean dose.

Fractions without image guidance	Absolute variation in the mean dose (ΔD)		
	ΔD ≤ 0.5 Gy	0.5 Gy < ΔD ≤ 1 Gy	1 Gy < ΔD
Rectum			
3	80%	15%	5%
5	55%	30%	15%
7	50%	25%	25%
Bladder			
3	95%	5%	0%
5	90%	10%	0%
7	75%	20%	5%

Conclusion: This work has been carried out with the data corresponding to the most sensitive patients to the lack of IG. The observed dosimetric effect is greater than the one that would correspond to the mean patient population.
In case of exceptionally not performing IG in 3, 5 or 7 fractions due to a breakdown in one of the twin linacs, the prostate and SV CTVs would still be treated correctly with the CTV to PTV margins currently used in our centre.
Regarding the organs at risk, the rectum showed the most important dosimetric variations. The dosimetric impact is greater when changing from 3 to 5 fractions without IG than when changing from 5 to 7.
Even in this group of patients, the effect of not performing IG in 3 or less fractions would be negligible. Not performing IG in a greater number of fractions could be relevant in cases in which the calculated dose distribution in the rectum is close to its corresponding dose restrictions because further optimisation was not possible.

EP-1800

Setup verification for breast cancer RT: Manual and automatic match of EPID images compared to CBCT

E.L. Lorenzen[1], K.L. Gottlieb[1], M. Nielsen[1]
[1]*Odense University Hospital, Laboratory of Radiation Physics, Odense, Denmark*

Purpose or Objective: Cone beam computed tomography (CBCT) is generally superior in imaging the patient anatomy due to the 3D representation and the use of kV imaging compared to MV imaging in electronic portal imaging devices (EPIDs). However, EPIDs have the advantage that the treatment fields can be used for the exposure, thereby adding no additional dose to the patient and requiring little additional time. The purpose of this work was to evaluate the use of EPID using both manual an automatic match by comparison to CBCT for setup verification in breast cancer radiotherapy.

Material and Methods: Both CBCT and EPID images were acquired in the same patient position for 29 fractions in 10 breast cancer patients. CBCT images were registered automatically to the planning CT using XVI by Elekta based on a grey-value translational match of the thorax wall. EPID images of the medial tangential fields were registered to digitally reconstructed radiographs (DRRs) using either a manual match of the thorax wall by a experienced user using iVIew by Elekta or an automatic match using IGPS by Fratoria. For the EPID registrations the 3D-table corrections were approximated based on the 2D registrations and the beam angle.

Results: Bland-Altman plot of the difference in EPID and CBCT registrations is shown in Figure 1. The mean differences were close to zero for both manual and automatic match of the EPID images. The limits of agreement (1.96 times the standard deviation of the difference) were lower for the manual than the automatic match indicating better agreement with the CBCT. The results of linear regression are shown in Table 1. The manual match had a higher correlation coefficient (R^2) than the automatic match. The match based on EPID generally underestimated the registration obtained by the CBCT as shown by the trend in Figure 1 and by the slope in the regression shown in Table 1 being significantly lower than one.

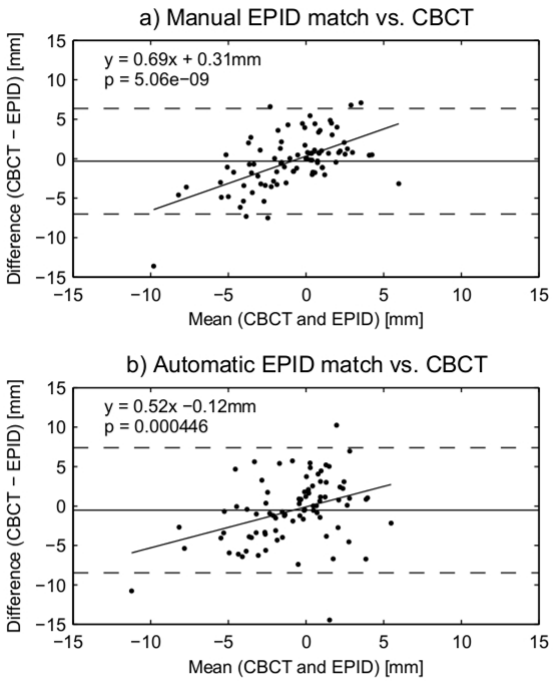

Figure 1. Bland-Altman Plot of the difference between EPID and CBCT registrations. In a) the EPID images were matched manually in iView and in in b) the match was performed automatically using IGPS. The vertical solid line indicates the mean difference and the vertical dashed lines the limits of agreement. Linear regression was performed to test for trends in the differences. Estimated coefficients for the linear regression and the corresponding p-value for the null hypothesis that the slope = 0 are shown.

	EPID vs. CBCT		
	a (SE)	b (SE) [mm]	R^2
Manual match	0.31 (0.05)	-0.42 (0.22)	0.30
Automatic match	0.25 (0.07)	-0.27 (0.30)	0.13

*Table 1. Estimated coefficients and correlation coefficients R^2 based on linear regression between the EPID and the CBCT registration using the model: EPID = a*CBCT + b. Standard errors (SE) are given in brackets.*

Conclusion: EPID registrations generally underestimated the registrations found by the CBCT. While an automatic matching method of the EPID potentially could improve on this, the automatic matching method evaluated in the current study showed inferior performance compared to manual matching.

EP-1801

Management of inter-fraction patient movement for SBRT treatments without an on-site 3D imaging.

F. Candela-Rodriguez[1], D. Martinez-Rodriguez[1], A. Camara-Turbi[1], M.T. Garcia-Martinez[1]
[1]*Hospital Universitario de la Ribera, Radiofísica y Radioprotección, Alzira, Spain*

Purpose or Objective: To validate the methodology we use for managing the inter-fraction patient movement in stereotactic body radiotherapy (SBRT) treatments. This methodology consists of the use of internal markers, one CT scan per fraction, and the portal vision system every fraction.

Material and Methods: A group of 132 SBRT treatments (1 to 5 fractions of 6.5 to 20 Gy each) were retrospectively analyzed. From this, we have considered a total of 227 fractions suitable for analysis.
The treatment technique was mainly 3DRT, using two Varian linear accelerators (clinac 2100C / 2100CD), both with Portal Vision AS500 - IAS3, Philips Pinnacle v9.8 treatment planning system (TPS), and Mosaiq (Elekta) Record and Verify (R&V). Adequate immobilization systems were used and internal fiducials marks were inserted.
A new CT scan was performed before each fraction in 172 cases, where treatment volumes and organs at risk were delineated by the Physician (after registration with the initial one). Treatment plan was recalculated to verify dosimetric consistency, and the isocenter position was updated according to the new anatomy). For setting purposes, a new set of orthogonal RDR images (gantry 0º and 90º) were sent to the PV. The remaining 55 cases were treated using the initial CT and were used here for validation proposes.
On the couch, the patient was initially aligned on the CT marks, and then it was moved to the updated isocenter position. Two Portal Images (orthogonal, 0º - 90º) were done and registered with the corresponding RDR using the fiduicial marks. If the displacements were greater than 0.5mm, the patient was moved.
We have performed this study for different anatomy locations (118 lung cases, 85 abdomen cases and 24 others cases), expecting different results.

Results: Isocenter position had to be corrected in the treatment room as showed in the table below, for all locations considered:

ALL LOCATIONS (227 cases)	TOTAL (227 cases)				without CT (55 cases)				with CT (172 cases)			
	|Vrt|	|Lat|	|Lng|	|Total|	|Vrt|	|Lat|	|Lng|	|Total|	|Vrt|	|Lat|	|Lng|	|Total|
cases with move > 0.5 cm	12%	16%	27%	47%	15%	18%	29%	51%	13%	16%	27%	45%
cases with move > 1 cm	1%	4%	7%	20%	2%	7%	7%	22%	1%	3%	7%	19%
cases with move > 1.5 cm	1%	1%	1%	5%	2%	2%	2%	9%	1%	1%	1%	3%
cases with move > 2 cm	0%	0%	0%	1%	0%	0%	0%	2%	0%	0%	1%	1%

LUNG (118 cases)	TOTAL (118 cases)				without CT (18 cases)				with CT (100 cases)			
	|Vrt|	|Lat|	|Lng|	|Total|	|Vrt|	|Lat|	|Lng|	|Total|	|Vrt|	|Lat|	|Lng|	|Total|
cases with move > 0.5 cm	11%	15%	34%	47%	17%	22%	50%	67%	10%	14%	31%	44%
cases with move > 1 cm	2%	3%	5%	18%	0%	11%	11%	28%	2%	2%	4%	16%
cases with move > 1.5 cm	1%	1%	0%	3%	0%	0%	0%	6%	1%	1%	0%	3%
cases with move > 2 cm	0%	0%	0%	0%	0%	0%	0%	0%	0%	0%	0%	1%

ABDOMEN (85 cases)	TOTAL (85 cases)				without CT (28 cases)				with CT (57 cases)			
	|Vrt|	|Lat|	|Lng|	|Total|	|Vrt|	|Lat|	|Lng|	|Total|	|Vrt|	|Lat|	|Lng|	|Total|
cases with move > 0.5 cm	15%	18%	20%	45%	14%	18%	21%	46%	16%	18%	19%	44%
cases with move > 1 cm	1%	6%	11%	25%	4%	7%	7%	25%	0%	5%	12%	25%
cases with move > 1.5 cm	1%	1%	2%	8%	4%	4%	4%	14%	0%	0%	2%	5%
cases with move > 2 cm	0%	0%	0%	0%	0%	0%	0%	4%	0%	0%	2%	2%

OTHER (24 cases)	TOTAL (24 cases)				without CT (8 cases)				with CT (16 cases)			
	|Vrt|	|Lat|	|Lng|	|Total|	|Vrt|	|Lat|	|Lng|	|Total|	|Vrt|	|Lat|	|Lng|	|Total|
cases with move > 0.5 cm	21%	21%	21%	54%	13%	13%	13%	38%	25%	25%	25%	63%
cases with move > 1 cm	0%	0%	4%	17%	0%	0%	0%	0%	0%	0%	6%	25%
cases with move > 1.5 cm	0%	0%	0%	0%	0%	0%	0%	0%	0%	0%	0%	0%
cases with move > 2 cm	0%	0%	0%	0%	0%	0%	0%	0%	0%	0%	0%	0%

Conclusion: For lung cases, we needed to reposition 23% cases less than without pre-fraction CT scan, 3% less for abdomen cases, and 25% more for the rest, not considered due to the low statistic (24 cases).
The pretreatment CT scan is very time consuming both for the Radiation Oncology and Radiation Physics departments, but on-site positioning is easier and so the treatment can be performed more comfortably for the patient.
Also, the dosimetric verification prior to each fraction allows us to assess the suitability of the new displacements to meet the clinical goals.

EP-1802

Mechanical sag patterns of the cone-beam CT imaging system of Elekta linear accelerators

S.J. Zimmermann[1], P. Rowshanfarzad[2], M.A. Ebert[2], H.L. Riis[1]
[1]*Odense University Hospital, Radiofysisk Laboratorium, Odense, Denmark*
[2]*University of Western Australia, School of Physics, Crawley, Australia*

Purpose or Objective: The cone-beam CT (CBCT) imaging system mounted on a linear accelerator (linac) is an important tool for validation of patient position. A correct patient positioning relies on high image-qualities obtained through mechanical stability of the CBCT unit and coincidence between the MV and kV radiation isocenters. The quality assurance (QA) of the CBCT unit should ideally validate the mechanical performance of each component and identify the origin of deviations. Most QA studies of CBCT imaging systems have been based on dedicated phantoms placed on the treatment couch. These phantoms do not allow for extraction of the sag patterns for the kV source arm and

imager separately. To access these information, we applied a method previously used for QA of Elekta linac gantry heads and portal-imaging systems.

Material and Methods: The sag pattern of the CBCT unit of an Elekta linac was investigated using five tungsten-carbide ball-bearings of diameter 4.8 mm. One ball-bearing was attached to the treatment couch top and four were attached to the kV source. Image acquisition was carried out for small-field of view with an average of 343 planar images in each gantry rotation. An in-house software coded in MATLAB was used to extract the ball-bearing positions in the images and to calculate the sag patterns of the CBCT unit.

Results: The results of six gantry rotations are listed in Table 1. The cross-plane sag of the kV source was found to be approximately 10 times larger than the sag of the gantry head, while the in-plane sag was almost two times larger. The cross-plane source sag corresponds to a gantry angle displacement of up to 0.3 degrees . The kV panel sag was comparable to the sag of the MV panel. The kV source-to-panel distance variation was almost half the amount for the MV system. The algorithm also allows for extraction of the skewness and panel-tilt data, but they are not presented in the Table. The kV system was found to have high reproducibility.

Range	Source Sag Cross-plane (mm)	Source Sag In-plane (mm)	Panel Sag Cross-plane (mm)	Panel Sag In-plane (mm)	ΔSDD Radial (mm)
CCW (mean±SD)	4.90±0.08	2.13±0.01	0.53±0.02	1.39±0.01	7.25±0.60
CW (mean±SD)	5.03±0.05	2.76±0.03	0.31±0.03	1.20±0.01	6.59±0.74
Largest RMSD CCW vs CW	0.14	0.14	0.13	0.01	1.08
Smallest RMSD CCW vs CW	0.02	0.06	0.08	<0.01	0.21
Worst reproducibility CCW	1.66	0.73	0.12	0.50	2.58
Worst reproducibility CW	1.67	0.97	0.08	0.42	2.43
CCW, CW † (mean±SD)	0.56±0.05	1.19±0.13	0.43±0.11	1.57±0.48	11.18±1.17

Table 1. Data for the range of the source and panel sag of one Elekta CBCT unit. The data are divided into cross-plane, in-plane and radial (ΔSDD) directions. Mean, standard deviation (SD), root-mean-square deviation (RMSD), and reproducibility in terms of standard deviation are displayed. For comparison, the data of the average values of the gantry arm and the EPID panel (from [1]) are listed in the row marked with †.

Conclusion: The measurements and analysis in this study quantify the sag pattern of the CBCT unit components. The Elekta kV flexmap do not compensate for all sag contributions such as panel rotation and tilt, source sag, and radial source-panel distance variations. A new kV flexmap is suggested for compensation of some additional flex contributions with the exception of panel rotation which cannot be measured in our setup or separated from skewness. The new kV flexmap could improve the reconstructed volumetric cone-beam CT image quality.

EP-1803

An immobilization device-based procedure to predict couch coordinates and set-up tolerance levels

C. Camacho[1], E. Escudero[1], A. Lloret[1], C. Castro[1], M.D. Molina[1], Y. Mohadr[1], C. Quilis[1], J. Garcia-Miguel[1], A. Herreros[1], J. Saez[1]
[1]*Hospital Clinic i Provincial, Radiotherapy, Barcelona, Spain*

Purpose or Objective: We propose and evaluate a simple method to predict absolute couch coordinates (ACC) based on different landmarks identified on two immobilization devices. We analyze the inter-observer variability of the method and establish set-up tolerance levels.

Material and Methods: Two immobilization devices were evaluated in this study: the Portrait Head and Neck Device by Qfix and the PosiRest-2 by Civco, used in HN and thorax/breast positioning respectively. Each device was indexed on the treatment table (Varian Exact Couch) and one plastic screw was matched to the room lasers were the ACC were read. The isocenter ACC were obtained by taking simple distance measurements on the CTfrom isocenter to the screw. We studied the inter-observer variability by having 5 different observers repeating all measurements. A total of 46 patients were analyzed: 22 breasts, 12 lungs and 12 HNs. All patients were set-up according to a NAL-3 protocol. A total of 1020 treatment sessions were recorded. We compared predicted couch positions to treatment couch positions acquired after the systematic error correction (4th day). We established device and location specific tolerance levels to accommodate 95% of all sessions. We finally studied if there was any correlation relating these differences and patient random set-up error.

Results: The average of the standard deviations of predicted positions among the 5 observers was <2 mm for all coordinates (vert, lat, long) and devices. There was strong correlation between almost all predicted positions and the systematic error corrected positions ($r>0.9$) but for the lateral coordinate prediction on the HN device (cause by having small values (<7 mm)). No correlation was found between predicted vs. corrected deviations positions and random error. Thus, this difference cannot be used to predict difficult to set-up patients. In order to accommodate 95% of all treatment sessions couch positions the following tolerances (2σ) were obtained (in mm) for (vert, lat, long): breast (12, 23, 30); lung (12, 20, 22); hn (7, 7, 7).

Conclusion: Our designed procedure based on immobilization device landmarks offers a simple and reproducible method to correctly predict absolute isocenter coordinates. Difficult to set-up patients (large random error) cannot be isolated from the differences between predicted and treated positions on a specific day. However, the procedure allows obtaining tight set-up tolerance levels to prevent gross set-up errors.

EP-1804

A comparative analyse of prostate positioning guided by transperineal 3D ultrasound and cone beam CT

M. Li[1], H. Ballhausen[1], N.S. Hegemann[1], M. Reiner[1], S. Tritschler[2], F. Manapov[1], U. Ganswindt[1], C. Belka[1]
[1]*Department for Radiation Oncology, University Hospital Munich, Munich, Germany*
[2]*Department for Urologie, University Hospital Munich, Munich, Germany*

Purpose or Objective: The accuracy of the Elekta ClarityTM transperineal three-dimensional ultrasound system (3DUS) was assessed for prostate positioning and compared to seed- and bone-based positioning in kilovoltage cone beam computed tomography (CBCT) during a definitive radiotherapy.

Material and Methods: The prostate positioning of 7 patients, with fiducial markers implanted into the prostate, was controlled by 3DUS and CBCT. In total, 177 transperineal ultrasound scans were performed and compared to bone-matches and seed-matches in CBCT scans. Setup errors detected by the different modalities were compared. Using seed-match as reference, systematic and random errors were analysed, and optimal setup margins were calculated for 3DUS.

Results: The discrepancy between 3DUS and seed-match in CBCT was 0 ± 1.7 mm laterally, 0.2 ± 2.0 mm longitudinally and 0.3 ± 1.7 mm vertically and significant only in vertical direction. Using seed-match as reference, systematic errors of 3DUS were 1.2 mm laterally, 1.1 mm longitudinally and 0.9 mm vertically, and random errors were 1.4 mm laterally, 1.8 mm longitudinally, and 1.6 mm vertically. Using the optimal margin recipe by van Herk, the optimal setup margins for 3DUS were 3.9 mm, 4.0 mm and 3.3 mm in lateral, longitudinal and vertical directions respectively.

Conclusion: Transperineal 3DUS is feasible for image guidance for patients with prostate cancer and seems comparable to fiducial based guidance in CBCT in the retrospective study. While 3DUS offers some distinct advantages such as no need of invasive fiducial implantation and avoidance of extra radiation, its disadvantages include the operator dependence of the technique. Further study of transperineal 3DUS for image guidance in a large patient cohort is warranted.

Electronic Poster: Physics track: Adaptive radiotherapy for inter-fraction motion management

EP-1805

Design and testing of the Rotating Whole-Body Linac-MRI Hybrid System

B.G. Fallone[1]
[1]*Cross Cancer Institute University of Alberta, Medical Physics, Edmonton, Canada*

Purpose or Objective: The first whole-body clinical linac-MRI hybrid (linac-MR) began installation in November 2013 at our clinic. System components were transported through the maze of an existing clinical radiotherapy vault and reassembled within the vault without removal of any part of the vault. The world-first images from a linac-MR on a human volunteer were obtained in July 2014. Specific imaging and dosimetric evaluation are reported.

Material and Methods:

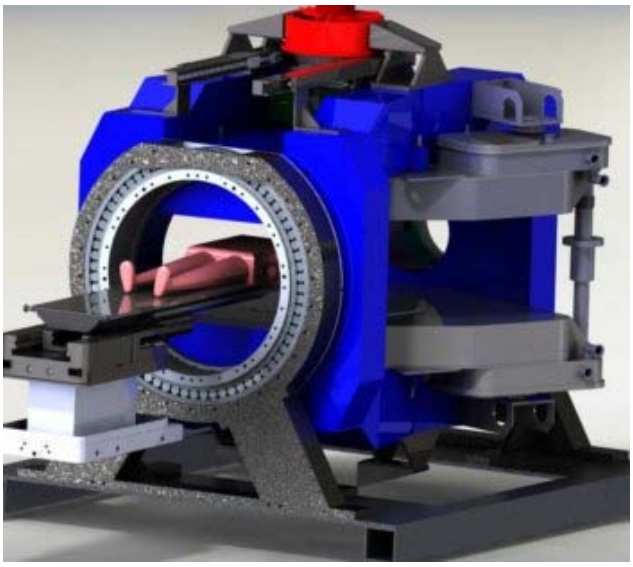

The linac-MR (Figure) consists of an isocentrically mounted 6 MV linac that rotates in-unison with a bi-planar 0.5 T MRI in transverse plane. The Bo field and the central axis of the 6 MV beam are parallel to each other. Feasibility of operation of concurrent MR imaging and linac-irradiation was confirmed in 2008 within a head prototype, while the current functional whole-body rotating linac-MR system is built on the engineering and physics developed and tested on the head prototype. The magnetic fringe field are optimized with the parallel configuration to results in insignificant entrance-dose increase and to avoid large increases in dose at tissue/air interfaces and any increase at beam exit due to electron return effect.

Results:

Table: Specifications of current rotating linac-MR system

Feature	Characteristic
Linac	6 MV
MLC	120 Leaves (Standard, Micro)
MR	0.5T (Good Image Resolution) (Negligible Geometric Distortion)
Maximum Pre-treatment Field of View	40 cm x 75 cm
Patient Space	Exterior Opening: 110 cm Diameter Interior Space: 60 cm x 110 cm (Rotating) Result: Suitable for Treating All Tumors (Including Peripheral Tumors — Breast)
Patient Table Movement Inside the Aurora RT	Vertically ± 25 cm Laterally ± 25 cm
Linac-MR Configuration	Aligned — Rotate Together
MR Position	Rotates 360 degrees
Beam-Orientation	Parallel to Magnetic field (minimal dosimetric perturbation)
Bunker and Maze Size	Standard for Linacs (installation Through Maze)
MR Cryogens and Venting	None Required
Beam Modulation	IMRT, VMAT
Soft-tissue Imaging	Four Images/sec During Tx
Treatment Planning	Real-time Adaptive
Servicing	Ramp up/down in Minutes To Allow Servicing of Linac

Currently, the whole body system is mechanically well balanced and rotates at 1 rpm, and provides because of its open-magnet design imaging and irradiation to tumours in all locations, including peripheral areas and breast. The system provides radiation output resulting in minimal dose perturbations in entrance dose, at internal tissue-air/lung interfaces as designed and no exit dose-increases. 3D magnetic field mapping demonstrates minimal perturbation in magnetic field homogeneity with gantry rotation which is easily and effectively shimmed by gradient coils. The Larmor Frequency varies with gantry angle due to the Bo interaction with room shielding and to the directional changes of the Earth's magnetic relative, and closely follows predictions calculated previously. Angle dependent 3D magnetic field maps and Larmor Frequency are used to automatically and optimally create image acquisition parameters for any gantry angle. Metrics obtained at different rotating angles show that the image quality is comparable to those of clinical MRI systems, and thus satisfy the requirements for real-time MR-guided radiotherapy.

Conclusion: The system highlights (Table) are:
6 MV linac; High-quality MR images during irradiation; parallel configuration to avoid strong angle-dependent shimming, and increased dose at beam exit and tissue-air/lung interfaces; imaging and irradiation of all tumours including peripheral areas and breast; installation through the maze of existing vaults; cryogen-free superconducting magnet; magnet turns on or off in minutes for safe servicing of magnetic components.

EP-1806

A novel predictive approach to quantify parotids warping using SIS epidemic model

N. Maffei[1,2], G. Guidi[1,2], C. Vecchi[2], A. Ciarmatori[1], G. Mistretta[1], P. Ceroni[1], B. Meduri[3], P. Giacobazzi[3], T. Costi[1]
[1]*Az.Ospedaliero-Universitaria di Modena, Medical Physics, Modena, Italy*

[2]Alma Mater Studiorum University of Bologna, Physics and Astronomy, Bologna, Italy
[3]Az.Ospedaliero-Universitaria di Modena, Radiation Oncology, Modena, Italy

Purpose or Objective: In the field of Adaptive Radiation Therapy (ART), non-linear transformation models should be considered to take into account complex motion and anatomic variations. In order to follow and then predict intra-organ dynamic, a novel voxel-by-voxel approach has been proposed using epidemic model. The susceptible-infected-susceptible (SIS) model was applied to radiotherapy treatments to predict morphological variations in the Head and Neck (H&N) region and to follow single voxel motion and warping.

Material and Methods: 360 daily MVCT studies of 12 H&N patients treated by Tomotherapy® were retrospectively analyzed. Deformable image registration (DIR) and automatic structures re-contouring were performed by RayStation® treatment planning system (TPS). The study focused on parotid glands (PG) identified by previously studies such as organs systematically affected by warping. Using the epidemic model, PG shrinkage was evaluated considering each voxel as a single subject and the deformed vector field (DVF) as an infection. A dedicated IronPython® script was developed to export daily coordinates and DVF displacements from the deformed mesh grid obtained by the TPS for each vertex of the region of interest (ROI) contouring. Finally, the SIS model was developed by a MATLAB® home-made simulation tool.

Results: The patients' validation was obtained by splitting susceptible (S) and infectious (I) cases; 0.4cm of voxel displacement was set as clinical threshold within a [0÷1cm] range of warping. Correlation between epidemic model and daily PG shrinkage was carried out by dynamic time warping (DTW) algorithm applied to the SIS parameters. A DTW distance of 2.39±0.66 was obtained setting the contact rate at 7.55±0.69 and the recovery rate at 2.45±0.26; birth rate was not counted in a constant population hypothesis. A physician's multiple-blind evaluation confirmed that PG warping evolution could be predicted, applying the SIS model, in almost 65% of patients.

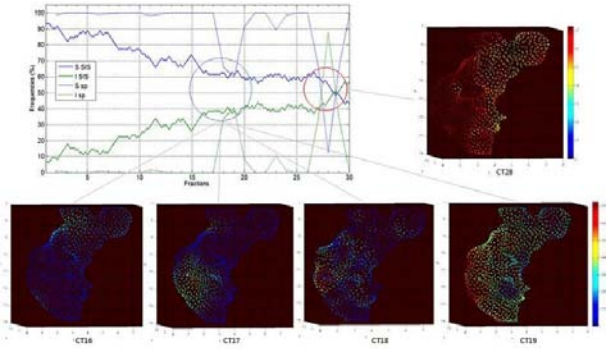

Figure 1 SIS simulation during the 6 week of RT: Susceptible (S) and Infectious (I) trends are in blue and green. Vertexes dynamic allows identifying gradual PG warping during treatment and possible set-up errors.

Conclusion: Combining epidemic model with ART and image systems can on-line support and validate daily setup and assess anatomical warping. In this novel approach, contrariwise to a time series analysis of the whole organ, specific and localized intra-organ variation could be detected. Moreover, integrating a dose accumulation evaluation, the SIS model could aid clinic decision making to suggest possible re-planning during the 6 weeks of therapy. A 3D model of the ROI can be generated and its evolution during the treatment course can be investigated.

EP-1807

Replanning effects in Tomotherapy treatment using dose accumulation and dose deformation strategies

A. Ciarmatori[1,2], G. Gabriele[1], N. Maffei[1,3], C. Vecchi[3], M.G. Mistretta[1], P. Ceroni[1], B. Meduri[4], P. Giacobazzi[4], T. Costi[1]

[1]Azienda Ospedaliero Universitaria di Modena, Medical Physics Department, Modena, Italy
[2]University of Bologna, Post Graduate School in Medical Physics, Bologna, Italy
[3]University of Bologna, Physics Department, Bologna, Italy
[4]Azienda Ospedaliero Universitaria di Modena, Radiation Oncology Department, Modena, Italy

Purpose or Objective: Quantification of the delivered dose is one of the most important feature in inter-patient variability in radiation treatment. Difference between planned and accumulated doses contains different uncertainties due to set-up errors, patient movement and anatomy variations. Shrinkage of Parotid Glands (PG) in Head and Neck (H&N) patients is a major issue in accumulation of the delivered dose. This study investigates Target and Organs at Risks (OARs) variations during the treatment course and their dosimetric consequences. We evaluated the effect of replanning on the deformed structure during the course of treatment.

Material and Methods: Six patients with H&N cancer treated by Tomotherapy (SIB 66 Gy, 60 Gy, 54 Gy in 30 Daily Fractions) have been, retrospectively, enrolled. Through Planned Adaptive® software each delivered fraction have been recalculated on daily imaging to obtain the daily dose (DMVCT). Deformable image registration (DIR), using Raystation (v.4.7.2), have been performed to propagate the structures along the treatment course. The planned doses were mapped (DDVF) using the deformed vector field (DVF) matrix. The DVF obtained from the reverse DIR was used to deform DMVCT to match the planning kVCT; we obtain a voxel by voxel association of DMVCT in a single image dataset. DDVF and DMVCT were compared performing 3D-γ analysis (2 mm, 2%) to evaluate the agreement on 3D distribution and warped structures. Two replanning strategies were adopted during the 18th fractions: (1) re-plan on original target and deformed OARs (D18,OAR) and (2) re-plan on deformed target and deformed OARs (D18).

Results: DDVF and DMVCT did not show a good consistency (3D γ-passing rate = 85 ± 1 %, $p<0.001$). DDVF was significantly ($p<0.01$) lower than DMVCT in term of average doses in PG (12.2 ± 10.3 %). Smaller differences were founded in average doses to the PTVs (2.6 ± 2.1 %). γ-passing rate and dosimetric variation to PG and PTVs did not show relevant correlation ($p>0.05$). Parotid gland showed a systematic shrinking during the course of treatment quantifiable in about 4% volume reduction for week of treatment. Full accumulation of dose showed an increase of the average dose to PG of 3.0 Gy ± 3.3 Gy [-4.6 Gy ÷ 7.7 Gy]. PTV volume variations were negligible (4.7 ± 1.6 %). The average doses of the PTVs increase of 1.6 Gy ± 1.3 Gy [-0.5 Gy ÷ 3.4 Gy]. Retrospective re-planning analysis showed that 5 out of 6 (83 %) patients enrolled could had benefit from ART. By ART the PG average dose decreased -2.0 Gy ± 1.4 Gy [-3.8 Gy ÷ -0.2 Gy] in first replanning strategy (D18,OAR) and -3.2 Gy ± 1.7 Gy [-5.0 Gy ÷ -0.2 Gy] in case of both Target and OARs deformation (D18).

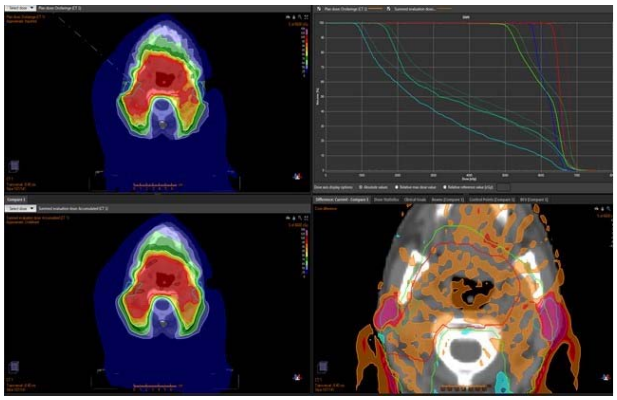

Patient	Plan	PTV 54 $D_{Average}$ [Gy]	PTV 60 $D_{Average}$ [Gy]	PTV 66 $D_{Average}$ [Gy]	Right Parotid $D_{Average}$ [Gy]	Left Parotid $D_{Average}$ [Gy]
#1	Planned	60,4	61,9	65,4	39,1	30,2
	Delivered	+1,7 Gy (+2,8%)	+1,2 Gy (+1,9%)	+2,1 Gy (+3,2%)	+4 Gy (+10,2%)	+6,2 Gy (+20,5%)
#2	Planned	55,8	59,4	66,5	29,6	28,8
	Delivered	+2,9 Gy (+5,2%)	+2 Gy (+3,4%)	+3,4 Gy (+5,1%)	+2,2 Gy (+7,4%)	+4,1 Gy (+14,2%)
#3	Planned	60,2	63	68,9	25,1	19,3
	Delivered	+2,4 Gy (+4%)	+3,4 Gy (+5,4%)	+2,2 Gy (+3,2%)	+2,4 Gy (+9,6%)	+7,7 Gy (+39,9%)
#4	Planned	60,8	63,3	67,5	28,8	28
	Delivered	+3 Gy (+4,9%)	+2,6 Gy (+4,1%)	+1,9 Gy (+2,8%)	+3,5 Gy (+12,2%)	+3,8 Gy (+13,6%)
#5	Planned	57,2	59,7	65,9	20,7	33
	Delivered	0 Gy (0%)	-0,4 Gy (-0,7%)	-0,5 Gy (-0,8%)	-0,8 Gy (-3,9%)	-4,6 Gy (-13,9%)
#6	Planned	57,6	62,3	65,1	39,9	26,8
	Delivered	+0,6 Gy (+1%)	+0,3 Gy (+0,5%)	+0,2 Gy (+0,3%)	+5,8 Gy (+13,5%)	+1,7 Gy (+6,3%)

Conclusion: DDVF do not describe adequately the delivered dose in the patient. Difference between planned and delivered doses in PTVs is reasonable, conversely anatomical variations seems to be a cause of overdosage in PG. Re-planning on 18Th MVCT could brought significant benefits, in terms average dose of PG.

EP-1808

A biological modeling based comparison of two strategies for adaptive radiotherapy of bladder cancer

L.J. Lutkenhaus[1], A. Vestergaard[2], A. Bel[1], M. Høyer[3], M.C.C.M. Hulshof[1], C.M. Van Leeuwen[1], O. Casares-Magaz[2], J.B. Petersen[2], J. Søndergaard[3], L.P. Muren[2]

[1]*Academic Medical Center, Radiotherapy, Amsterdam, The Netherlands*

[2]*Aarhus University Hospital, Medical Physics, Aarhus, Denmark*

[3]*Aarhus University Hospital, Oncology, Aarhus, Denmark*

Purpose or Objective: Several adaptive strategies have been implemented to account for anatomical changes during radiotherapy for bladder cancer. To obtain target structures, either the first four CBCT scans can be used (CBCT-based strategy), or the interpolation of bladder volumes on pretreatment CT scans (CT-based strategy). The purpose of this study was to determine whether the CBCT-based or CT-based strategy is more favorable in terms of tumor control probability (TCP) and normal tissue sparing.

Material and Methods: Ten patients from each of the two participating institutes were analyzed, adopting the clinically used adaptive strategy and dose prescription from each institute. With the CBCT-based strategy, a library of three plans was created, corresponding to a small, medium and large bladder. Patients received 70 Gy to the bladder tumor, 60 Gy to the non-involved bladder and 48 Gy to the lymph nodes, in 30-35 fractions. With the CT-based strategy, a library of five plans was created using two pre-treatment CT scans, with full and empty bladder, respectively. Patients received 55 Gy to the tumor and 40 Gy to bladder and lymph nodes, in 20 fractions.

Tumor control: TCP was calculated for the combined target volumes of tumor and bladder, using the Linear-Quadratic model with an α/β ratio of 13 Gy. Since tumor cell density in the non-involved bladder wall was unknown, it was varied between 10^2 and 10^7 cells/cm^3. To investigate the effect of the different dose prescriptions, the TCP was recalculated for the CT-based strategy with the dose scaled to 70 Gy in 35 fractions.

Normal tissue sparing: for rectum and bowel cavity, the equivalent dose in 2 Gy fractions (EQD2) was calculated using α/β values of 5 and 8 Gy, respectively, and DVH parameters were extracted. In addition, the planning target volume for each chosen plan divided by the daily bladder volume was calculated. Differences in parameters between groups were assessed using a Wilcoxon signed-rank test.

Results: A higher TCP for the CBCT-based strategy compared to the CT-based strategy was found, independent of modeled cell density in the non-involved bladder wall (Figure 1). For a low cell density, median TCP for the CBCT-based strategy was 75%, compared to 49% for the CT-based strategy. These results were comparable to 3-year local control rates previously reported. In addition, scaling the dose from the CT-based strategy to 70 Gy increased the median TCP to 72%. For the CT-based strategy, a lower median rectum V30Gy and lower median bowel V45Gy compared to the CBCT-based strategy were observed (Figure 1). This difference is reflected in the finding that the PTV is on average 3.9 times larger than the daily bladder volume for the CBCT-strategy, compared to 2.2 times for the CT-based strategy (p<0.01).

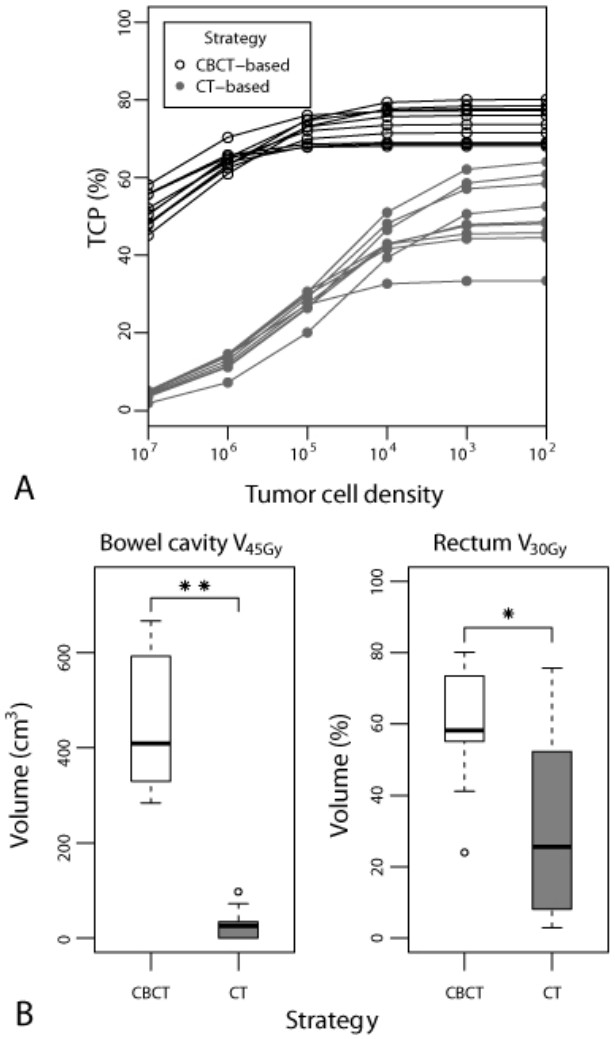

Figure 1: *A*: TCP for both strategies, for a varying tumor cell density. TCP for the CT-based strategy is always lower, for all patients, compared to the CBCT-based stratregy.
B: Bowel cavity V_{45Gy}, and rectum V_{30Gy}, for both strategies. * = p < 0.05, ** = p<0.01.

Conclusion: Total bladder TCP is higher for the CBCT-based strategy, which is due to prescription differences. The adaptive strategy based on CT scans results in the lowest rectum V30Gy (EQD2) and bowel cavity V45Gy (EQD2).

EP-1809

Intrafractional patient movement during an online adaptive replanning procedure for cranial SRS

M. Pozo-Massó[1], J.F. Calvo-Ortega[1], S. Moragues-Femenia[1], J. Casals-Farran[1]

[1]*Hospital Quiron Barcelona, Radiation Oncology, Barcelona, Spain*

Purpose or Objective: To investigate the patient's movement during the preparation of an adaptive cranial radiosurgery (SRS) procedure and its dosimetric impact.

Material and Methods: Cranial radiosurgical treatments are planned in our department using IMRT technique. A Varian Clinac 2100 CD equipped with the OBI system and the Eclipse TPS are used. Patients are immobilized using the BrainLAB mask system. A CBCT scan is acquired after the initial laser-based patient setup (CBCTsetup). In order to take into account the roll and tilt patient´s rotation errors, not supported by the linac couch, an online adaptive replanning procedure was designed (Med Dosim. 2013 Autumn;38(3):291-7). It consists of a 6D registration-based mapping of the reference plan onto actual CBCTsetup, followed by a reoptimization of the beam fluences ("6D plan", computed on the CBCTsetup) to achieve similar dosage as originally was intended, while the patient is lying in the linac couch. Once the 6D plan is computed, it is activated in the record and verify network and the actual patient's position is again verified by CBCT imaging (CBCTtx): CBCTsetup/CBCTtx 4D match is performed on the OBI workstation.
Twelve online procedures with detected roll or tilt rotation errors larger than 0.5° were enrolled in this study. Intrafractional patient's shifts during the time lag between CBCTsetup and CBCTtx was investigated, as well as the capability of the online adaptive method to compensate them. The plan 6D plan was recalculated on the CBCTtx ("6D plan Tx") taking into account the actual treatment isocenter position. Both plans (6D plan *vs*. 6D plan Tx) were compared using DVHs.

Results:
1) The magnitudes of the intrafraction shifts were 0.4 mm (SD: 0.7 mm), 0.6 mm (SD: 0.5 mm) and 0.3 mm (SD: 0.4 mm) in lateral, anterior-posterior and superior-inferior directions, respectively. The intrafractional rotational shifts were 0.1° (SD: 0.1°), 0.0° (SD: 0.1°) and 0.1° (SD: 0.2°) in tilt, yaw and roll directions, respectively. The time lag where these shifts were happen was 16 ± 2 minutes.
2) Dose differences < 1% were found for targets and organ-at-risks between each 6D Plan (computed on the CBCTsetup) and its respective 6D Plan Tx (computed on the CBCTtx).

Conclusion:
1) Patient's rotational errors during online replanning were negligible.
2) Patient's translational errors during online replanning were compensated enough after CBCTsetup/CBCTtx 4D alignment performed on the OBI workstation, with no appreciable dosimetric impact.

EP-1810

Dose uncertainties due to inter-fractional anatomical changes for carbon ion therapy

D. Panizza[1], S. Molinelli[1], A. Mirandola[1], G. Magro[2], S. Russo[1], E. Mastella[1], A. Mairani[1], P. Fossati[3], F. Valvo[4], R. Orecchia[5], M. Ciocca[1]
[1]*Fondazione CNAO, Medical Physics Unit, Pavia, Italy*
[2]*Università degli Studi di Pavia, Physics Department, Pavia, Italy*
[3]*Fondazione CNAO, Clinical Radiotherapy Unit, Pavia, Italy*
[4]*Fondazione CNAO, Clinical Directorate, Pavia, Italy*
[5]*Istituto Europeo di Oncologia, Scientific Directorate, Milano, Italy*

Purpose or Objective: To investigate the impact of inter-fraction anatomical variations in pancreatic and pelvic tumor patients when using carbon ion therapy through a retrospective adaptive approach.

Material and Methods: We collected daily MVCT scans for 10 selected patients, previously treated with helical tomotherapy for tumors located in the abdomen and pelvic region. On the first MVCT, taken as a reference, a dummy target volume was contoured, based on clinical experience, and organs at risk (OAR) original contours were imported from the planning CT scan and modified according to anatomical variations. The Hounsfield Unit (HU) to water equivalent path length (WEPL) calibration curve was experimentally determined and implemented in our TPS. According to prescription dose and OARs dose limits of clinical protocols approved at CNAO, a plan was then optimized on the first MVCT. For each patient, a number of MVCTs equal to the treatment sessions planned according to our fractionation scheme were fused on the reference one and structures were registered and manually corrected. The reference plan was recalculated on each MVCT scan to simulate a real treatment fraction. The cumulative dose was calculated by adding the contribution of each different fraction and then registered on the reference MVCT. This dose distribution was compared against the reference one in terms of target dose coverage and dose to OARs.

Results: For the pelvis cases, results show no significant change in the target coverage, with an average PTV D95% decrease of 1% and a maximum daily variation of -6%, while the mean homogeneity index (HI) difference is less than 0.01. For the abdominal area, however, a clinically relevant loss in target coverage is found: PTV D95% decreases, on average, of 7%, with a maximum daily variation of -23%. Target dose becomes less homogeneous, as shown by an average increase in the PTV HI of 0.08. For both districts, no clinically significant difference is found in the OAR DVHs. The 3D dose distribution analysis shows, for pelvic tumors, slight differences between planned dose and recalculated cumulative dose. For pancreatic carcinoma, local deviations up to 30% with respect to the planned dose can be found in the daily 3D dose distributions, particularly in healthy tissues behind the target volume.

Conclusion: Results confirm that the use of beam directions crossing OARs with a high degree of inter-fractional variation, as in the abdominal region, should be minimized for actively scanned carbon ion beams. However, it is useful to stress that results obtained are patient-dependent and more statistics is needed to draw a general conclusion for a larger population. Research projects are ongoing focused on the improvement of in-room 3D imaging techniques and the development of dose fast calculation platforms for online treatment plans evaluation procedures that account for changing anatomy effects.

EP-1811

Accuracy of dose calculations on CBCT scans of lung cancer patients using a vendor-specific approach

M. De Smet[1], D. Schuring[1], S. Nijsten[2], F. Verhaegen[2]
[1]*Catharina Hospital, Department of Radiotherapy, Eindhoven, The Netherlands*
[2]*Maastricht University Medical Center, Department of Radiation Oncology MAASTRO- GROW School for Oncology and Developmental Biology, Maastricht, The Netherlands*

Purpose or Objective: In modern radiotherapy, Cone-Beam CT (CBCT) images are widely used for position verification. These CBCT images could also be used for dose recalculation, providing information for treatment evaluation and adaptive planning. However, dose calculations on CBCT are not straightforward and the accuracy for clinical cases is not well known [1-5]. The final goal was to determine for lung cancer patients the accuracy of dose calculations on CBCT images of two different vendors: Elekta and Varian.

Material and Methods: Lung cancer patients with CBCT imaging (n=10 for Elekta, n=6 for Varian) and a repeated planning CT scan on the same day were selected. The original treatment plan and delineated structures were copied to the repeated CT and CBCT scans, and the dose was recalculated. For CBCT dose calculations, an adapted HU-to-electron density (HU-ED) table was used which was obtained by comparing CT values of corresponding points on the CBCT and repeated planning CT scan. For Varian, a bi-annual CBCT HU calibration was executed, while for Elekta the absence of CBCT HU-calibration was compensated by using a patient-specific HU-ED table. Planning CT data were used to compensate for the limited FOV (Elekta) or scan length (Varian) of the CBCT. Finally, clinically relevant dose metrics were compared between the repeated CT and CBCT in order to assess the accuracy of dose calculations on CBCT for both vendors.

Results: Figure 1 displays the mean differences of the dose metrics between repeated CT and CBCT, for Varian and Elekta CBCT scans. For Varian, a good agreement between the dose distributions recalculated on CBCT and repeated CT was observed when a thorax-specific HU-ED table was used. For Elekta, the dose metrics showed larger deviations with the thorax-specific HU-ED table, however, using a patient-specific HU-ED table resulted in similar accuracy as for Varian CBCT dose calculations. Differences between repeated CT and CBCT dose metrics were below 3% for both vendors.

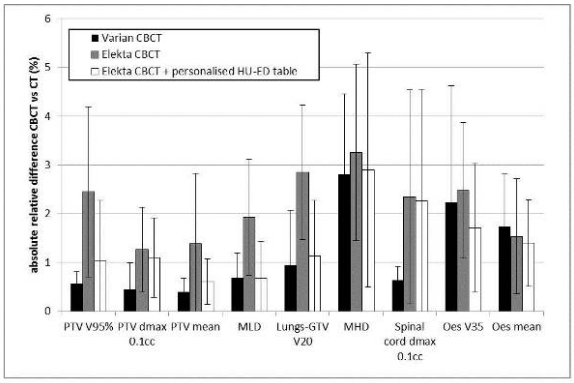

Figure 1. Average and standard deviation (error bars) of the absolute relative difference of the dose metrics between repeat CT and CBCT, for Varian (n=6) and Elekta (n=10) CBCT scans of lung cancer patients. Calculations were performed with a thorax-specific HU-ED table, as well as a patient-specific HU-ED table for Elekta CBCT. MLD = Mean Lung Dose, MHD=Mean Heart Dose, Oes = Oesophagus.

Conclusion: Differences between Elekta and Varian CBCT, including hardware, reconstruction software, HU calibration, FOV and scan length, resulted in different challenges for CBCT dose calculations for the different vendors. For Elekta CBCT scans, the procedure with a patient-specific HU-ED table resulted in similar accuracy as for Varian CBCT dose calculations with a general HU-ED correction for all thorax patients, but is more time-consuming. The vendor-specific corrective methods used in this study, resulted in dose calculations feasible for treatment re-evaluation for both Elekta and Varian CBCT scans.

References: 1.Yang et al. PhysMedBiol 2007, 2.Richter et al. RadOnc 2008, 3. Hatton et al. PhysMedBiol 2009, 4.Fotina et al. RadiotherOnc 2012, 5. Dunlop et al. StrahlentherOnkol 2015

EP-1812

Adaptive VMAT for cT1-2aN0M0 laryngeal cancer: potential risk of target volume over dosage

H.P. Bijl[1], E.W. Korevaar[1], M. Gelderman[1], J.A. Langendijk[1], R.G.J. Kierkels[1]
[1]*University Medical Center Groningen, Department of Radiation Oncology, Groningen, The Netherlands*

Purpose or Objective: At our department, patients with cT1-2aN0M0 laryngeal cancer are treated with volumetric-modulated arc therapy (VMAT). The treatment plan quality is monitored by plan evaluations on weekly repeat CTs. The purpose of this study was to determine plan quality during treatment by recalculating the actually given dose based on repeat CT.

Material and Methods: Three patients treated with accelerated radiotherapy (66-70 Gy in 2 Gy fractions) were selected because of over dosages exceeding 78 Gy at the transition from air to tissue. Each clinical VMAT plan (plan I) was optimized towards homogeneous dose distributions in the planning target volumes (PTV) and low as possible dose to the critical organs such as the swallowing organs at risk. The treatment plan quality was evaluated using weekly repeat CTs. In addition, two more treatment plans were made including a density override of 0.5 g.cm-3 for the PTV-in-air overlap region (plan II), and the PTV-in-air + 5 mm region (plan III). All plans were evaluated with the PTV-in-air region assigned a density override value of 0.0 and 1.0 g.cm-3 to simulate the initial planning scenario and to simulate extension of CTV-in-air, resp. Finally, the "actual given dose" of the clinical target volume (CTV) was estimated by accumulated repeat CT dose evaluations.

Results: The repeat CTs showed an extending CTV towards the laryngeal air cavity over the course of treatment. Repeat CT evaluations indicated increasing max doses up to 80 Gy. Evaluation of plan I on the initial planning CT, using a density override of 1.0 g.cm-3, showed a potential dose hotspot with similar max dose values (80-87 Gy). When no density override was assigned the PTV (D98%) coverage of plan I was sufficient. In contrast, plan II and III showed slightly to moderate PTV under dosage (65 Gy), albeit within the PTV-in-air region. However, the accumulated CTV dose (D100) demonstrated no clinically relevant under dosage in the CTV (methods plan II: 67.4 Gy and plan III 65.2 Gy). Furthermore, the plan optimization approach as used in plan II and III resulted in reduced and acceptable max dose values within the targets (76.9 Gy and 74.3 Gy, resp).

Conclusion: Unacceptable high doses of up to 80 Gy were observed in VMAT plan evaluations based on weekly repeat CTs. To avoid these over dosages, high fluence profiles in PTV-in-air regions should be avoided during planning optimization. An alternative VMAT optimization and evaluation approach has been proposed for cT1-2aN0M0 laryngeal cancer patients.

EP-1813

Clinical implementation of an adaptive planning technique for lung VMAT radiotherapy

M. Naisbit[1], G. Ward[1], J. Lilley[1]
[1]*Leeds Cancer Centre, Medical Physics, Leeds, United Kingdom*

Purpose or Objective: At the Leeds Cancer Centre approximately 40% of lung patients receiving VMAT radiotherapy (RT) display a reduction in tumour volume when imaged using CBCT during treatment. The aim of this work was to develop a method to assess whether the dosimetric impact of observed anatomical changes is sufficiently significant to justify a treatment replan.

Material and Methods: Twelve lung patients receiving FFF VMAT RT planned on the Monaco 3.3 treatment planning system (Elekta) were identified. All had been rescanned, recontoured and replanned due to noted tumour shrinkage. For lung replans the clinical aim is to continue treating the original target volumes, so a rigid registration was performed between the planning CT and the rescan CT using a mutual information algorithm. Target volumes and OAR were transferred from the planning CT to the rescan CT and assessed by a physicist and clinician team to ensure they were clinically appropriate. The original plan was recalculated on the rescan CT studyset and dose volume histogram (DVH) statistics calculated for targets and OARs on the rescan studyset.

Results: For patients who displayed tumour changes without other significant internal changes the transferred target structures were deemed clinically acceptable with minor editing. Comparison of the transferred structures to the replan structures indicated that differences in remarking the targets were larger than image registration and transferral errors. Small variations in spinal cord and lung contours suggest that it is more accurate to re-contour these structures on the rescan CT, especially if they are receiving a dose close to tolerance. This method of adaptive planning was found to significantly reduce the replanning time. A notable limitation of the process was observed for patients who display other significant internal anatomical changes such as a change in lung volume or mediastina position, resulting in inaccurate transferred structures. Based on the DVH statistics for the transferred targets and re-contoured OAR, 9/12 plans required a full treatment replan. Although the target coverage was clinically acceptable the loss of tumour tissue meant that nearby OAR received doses above their tolerance.

Conclusion: A method has been developed to assist the adaptive planning process for lung patients receiving FFF VMAT radiotherapy. This provides a means of assessing the dosimetric effect of tumour changes to determine whether a new treatment plan is necessary. It showed that for 25% of patients who received full treatment replans no replan was necessary, as the dosimetric effect of tumour shrinkage was insignificant in terms of both target coverage and OAR doses. Therefore it allows significant time savings in the treatment replanning process. Use of the technique is limited to patients who display tumour volume changes with no other significant changes to internal/external anatomy.

EP-1814

Fractionated stereotactic radiotherapy using Gamma Knife Icon with adaptive re-planning (a-gkFSRT)

F. Stieler[1], F. Wenz[1], Y. Abo-Madyan[1], S. Mai[1]
[1]*University Medical Center Mannheim- University of Heidelberg, Department of Radiation Oncology, Mannheim, Germany*

Purpose or Objective: The Gamma Knife Icon (Elekta AB, Schweden) allows frameless treatment of patients in a precise stereotactic environment using a combination of cone-beam computer tomography (CBCT) for positioning, a thermoplastic mask system for positioning and fixation and an infrared based camera system "high definition motion management" (HDMM) for patient tracking during treatment. Using these novel options, the Gamma Knife Icon provides the possibility for adaptive fractionated stereotactic radiotherapy (a-gkFSRT). Here we report the treatment of the first patient with a-gkFSRT.

Material and Methods: The first patient treated with Gamma Knife Icon at the University Medical Center Mannheim received MR imaging with an individual cushion for pre-planning with the treatment planning system (TPS) GammaPlan 11.0.1 (Elekta AB, Schweden) 7 days before treatment. For every fraction of the treatment a daily CBCT was performed to verify the actual scull/tumour position. An automatic co-registration was performed to determine the daily shift in translation and rotation. The TPS adapted automatically the shot positions to the daily position and recalculated the dose distribution (online adaptive planning). During the treatment the HDMM system recorded the intra-fractional patient motion. Further we recorded the times for positioning, image guidance and treatment to define a clinical treatment slot.

Results: The total treatment time for fraction 2-5 was around 20 minutes. The positioning of the patient needed 0.8 min, CBCT positioning plus acquisition 1.03 min plus 0.62 min, CT data processing and adaptive planning 2.66 min and treatment 15.6 minutes. The mean values and standard deviations for the 5 daily CBCTs compared to the reference scan are for rotation -0.59°±0.49/0.18±0.20/0.05°±0.36 and for translation are 0.94mm±0.52/-0.08mm±0.08/-1.13mm±0.89. The adaptive re-planning (duration 1.25 minutes) every day was very accurate and yielded quality measures e.g. coverage, selectivity and gradient for the delivered dose identical regarding to the initial values. Using the HDMM system over all fractions we saw an intra-fractional movement of 0.13±0.04mm. The intra-fractional movement was controlled by the HDMM system and showed similar results as a repeated CBCT after treatment (<0.32° and 0.20mm).

Conclusion: The Gamma Knife Icon allows combining the accuracy of the stereotactic Gamma Knife system with the flexibility of fractionated treatment of a linear accelerator with mask system and CBCT. Further the Icon system introduces a new online patient tracking system to the clinical routine. The inter-fractional accuracy of patient positioning was controlled with a thermoplastic mask and CBCT. The adaptive re-planning was quick and yielded high quality plans. Identical dose was delivered each day because of adaptive re-planning.

EP-1815

Towards adaptive Tomotherapy: planning CT to MVCT deformable image registration for dose calculation

M. Branchini[1,2], S. Broggi[2], M.L. Belli[1,2], C. Fiorino[2], G.M. Cattaneo[2], L. Perna[2], R. Calandrino[2]
[1]*University of Milan, Medical Physics Specialization School, Milan, Italy*
[2]*IRCCS San Raffaele Scientific Institute, Medical Physics, Milan, Italy*

Purpose or Objective: The aim of this study was to report the results of the validation of a previously developed method for dose of the day calculation in head and neck Tomotherapy based on deformable image registration (DIR) of the planning CT to MVCT taken during treatment.

Material and Methods: kVCT/MVCT images of ten HN patients treated with Helical Tomotherapy (HT) with a simultaneous integrated boost (54/66/69 Gy/30 fr) were retrospectively analyzed. For each patient the planning kVCT (CT-plan) was elastically registered (DIR) to the MVCT acquired at the 15th therapy session (MVCT15) with a B-Spline deformation algorithm using Mattes mutual information (open-source software 3D Slicer), resulting in a deformed CT (CTdef). At the same day, a kVCT was acquired with the patient in the same treatment position (CT15) and taken as reference. Then, CTdef and CT15 were re-sampled to the same slice thickness (3mm) through linear interpolation. The original HT plans were recalculated both on CTdef and CT15 in the HT planning station using the DQA (dose quality assurance) module, considering the two set of images as phantoms: images were rigidly aligned with the CT-plan, mimicking the true daily repositioning. Dose distributions on CTdef and CT15 were compared in order to assess the reliability of the method; local dose differences <2% of the prescribed dose (DD2%) and global gamma-index values (2%-2mm; considering points with dose >20% of the prescribed one) were assessed for all the available transversal slices (step: 6 mm) with Mapcheck SNC Patient Software (Sun Nuclear).

Results: The results of DIR was qualitatively satisfactory when comparing CTdef against CT15. On average, 94.4% ± 0.9% of points passes the gamma analysis test and 87.9% ± 1.1% of the body's voxel were found for DD2% (on average 27 slices available for each patient). If excluding 3 patients where a relevant number of slices were cut due to the narrow FOV of the MVCT15, the values further improved to 95.7% ± 0.8% and 89.1% ± 1.3% for gamma and DD2% respectively.

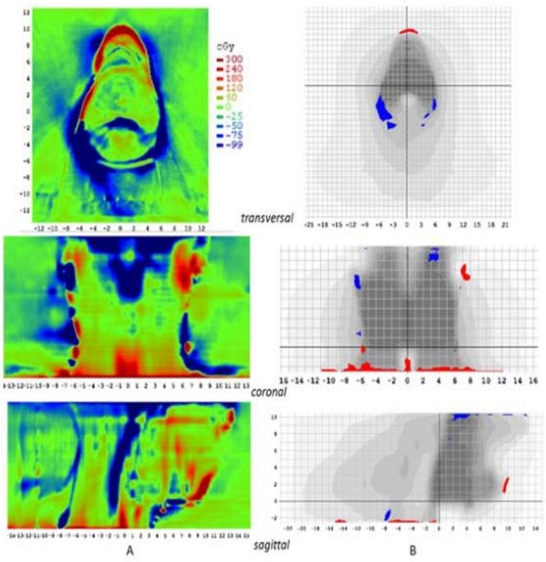

Figure: in column A the absolute dose differences between Ctdef and CT15; in column B gamma distributions (in red and blue voxels with gamma >1).

Conclusion: CT to MVCT DIR using an open source system was proven to be an accurate method for calculating the dose of

the day in HT treatments for HN cancer. This study represents the first proof of the dosimetric accuracy of DIR from kVCT to MVCT. The suggested method is sufficiently quick and reliable to be considered as an appropriate tool for dose of the day calculation in clinical strategies for adaptive Tomotherapy of head and neck cancer.

EP-1816

A hybrid approach for head-neck cancer using on-line image guidance and off-line adaptive planning

R. Srivastava[1], P. Sharma[1], G. Saini[2], J. Sethi[2], A. Aggarwal[2], K. Goyal[2], M. P[1]
[1]*International Oncology Centre-Fortis Hospital, Medical Physics, Noida, India*
[2]*International Oncology Centre-Fortis Hospital, Radiation Oncology, Noida, India*

Purpose or Objective: A prospective study to evaluate the dosimetric benefits of treatment plan adaptation for patients who had undergone Repeated CT (ReCT) and replanning due to treatment-induced anatomical changes during radiotherapy.

Material and Methods: Five patients of head and neck cancer, who have undergone rescanning and replanning due to weight loss and tumour shrinkage ,were selected for the study .For each patient, ReCT has been taken at mid treatment .The ReCT image for each patient was registered with the initial planning CT image and CBCT image of mid treatment fraction individually. The rigid registration was performed automatically and final manual adjustment was used for better alignment. After the rigid registration, a deformable registration was also performed automatically using vertex-vertex correspondence between the reference image set and the target image sets. Contours were conducted for target volumes and OARs(Organ at risk) . The initial treatment plan was created on initial CT using Eclipse treatment planning system (v. 11.0). This initial treatment plan was transferred to ReCT and CBCT and the dose recalculated. The replanning has been done on ReCT and this replan was delivered as a modified plan to the patient . The initial CT plan , which was optimized and calculated on initial CT ,was compared dosimetrically with initial CT plan calculated on ReCT & CBCT and ReCT plan optimized and calculated on ReCT.

Results: Rescanning in mid treatment shows 27% (13%-42%) reduction of parotid volumes and therefore 21% (7%-35%) increase in parotid mean doses. Initial plan calculated on ReCT and CBCT found 15% (9%-26%) increase in PRV spine maximum doses which was reduced by replanning on ReCT. The body maximum doses increased by 6.5 % (4%-8%) in four patients and 22% in one patient when initial CT plan was calculated on ReCT and CBCT .

Conclusion: Adaptive radiotherapy involves the modification of the initial plan to account for patient specific anatomical changes (replan). Replanning on ReCT in head and neck patients during the course of radiotherapy is an ultimate solution with regard to doses of spinal cord , parotid glands and skin.

EP-1817

Dosimetric evaluation of new method for patient specific CBCT scan calibration

A. Fidanzio[1], S. Menna[1], F. Greco[2], A. Porcelli[2], G. Benecchi[3], L. Azario[1], A. Piermattei[1]
[1]*Università Cattolica del Sacro Cuore -Policlinico A. Gemelli, Physics Institute, Rome, Italy*
[2]*Fondazione A. Gemelli, UOC Fisica Sanitaria, Rome, Italy*
[3]*Azienda Ospedaliero Universitaria di Parma, UOC fisica Sanitaria, Parma, Italy*

Purpose or Objective: The dose delivered in radiotherapy can be influenced by several factors such as patient setup variations and anatomical changes. Generally CT scans are carried at fixed interval times to verify the presence of anatomical changes but this is time consuming and frequently it cannot assure a timely control. The Cone Beam CT (CBCT), generally carried out during the fractionated radiotherapy, allows a a more timely verification of morphological changes. The calibration in terms of relative electron densities (RED) of CBCT images allows their use for hybrid plan calculation needed to decide for an eventual adaptive strategy. However the CBCT calibration suffers of some problems such as time stability and patient variability. This work reports the dosimetric assessment of an original patient-specific CBCT calibration method.

Material and Methods: A homemade software was developed to automate the HU calibration of CBCT in terms of RED adopting the following procedure: 1) two CT and CBCT scans with negligible morphological changes are selected for a patient, 2) in these images the HU values of different ROIs, relative to correspondent anatomical regions, are acquired to obtain a correlation function between CBCT and CT HUs, 3) the correlation function is used to determine the CBCT calibration curve HUs versus RED from the CT calibration curve; 4) finally the CBCT calibration curve is optimized by an algorithm that minimize the differences of patient's radiological thicknesses measured on the CT and CBCT patient's slices. This procedure has been verifed for H&N, lung and pelvic body regions in a Rando phantom and for 5 patients for VMAT irradiations by a linac Varian TrueBeam STx with the on-board imager (140 kV x-ray tube). Using Eclipse TPS the dosimetric assessment of the method was based on comparisons between: isocenter doses; γ-gamma analysis between dose matrices of planes passing through the isocentre and DVH comparisons.

Results: The calibration procedure required about 5 minutes for each patient. Dosimetric comparison supplied agreements (i) within 2% for the isocenter doses; (ii) γ% greater than 0.97% for head and neck, 98% for lung and 99% for pelvic regions and the γ*mean* values were all within 0.4. The PTV V95 and mean dose were within 2%. While the mean dose of principal OARs was within 3%.

Conclusion: The CBCT calibration method used here seem to be accurate enough to calculate hybrid planes, useful to discuss and to evaluate the opportunity of an adaptive radiotherapy strategy.

EP-1818

Using ROIs projected on EPID as a predictor of plan deterioration due to anatomical changes

O. Piron[1], N. Varfalvy[1], L. Archambault[1]
[1]*CHU de Quebec-Université Laval, Radio-oncologie, Quebec, Canada*

Purpose or Objective: One of the side effects of radiotherapy is the patient's anatomical changes. 2D relative γ analysis from daily EPID images is a fast and simple method to detect anatomical changes that could have a strong dosimetric impact on the treatment plan. An action threshold determines if the error relative to the first fraction is significant or not, and thus requires a replanning. The aim of this study is to validate the threshold for lung cancer and to assess the relevance of including additional information of regions of interest (ROIs) from EPID images.

Material and Methods: EPID images were acquired for every beam and all fractions of 24 lung cancer patients. Of these, 8 patients were selected to evaluate the dosimetric impact of these changes. The PTV1 V95(%) was computed for both the planning CT and original contours deformed onto CBCT acquired at the last fraction. These values were then compared with 2D image relative γ analysis of EPID images when the PTV1 anatomical structure is projected on these images or not.

Results: The results of γ analysis were classified into 4 different categories using a k-means clustering analysis. These categories indicate the degree of discrepancy between the EPID image acquired on a treatment day and the reference from the first fraction. The first category

illustrates a small disparity from the reference whereas the fourth category show strong differences. Our hypothesis is that these categories can be used to identify patients in need of treatment adaptation. The Figure 1 shows the V95(%) parameter extracted from either the planning CT or the daily CBCT plan, as function of the average γ value for all beams. This average γ value is evaluated on the whole EPID image (Figure 1a) or the projected PTV1 image (Figure 1b). The horizontal dash line represent the dose tolerance for PTV1 (99%). There is a correlation between the average γ and the PTV1 V95(%) but the projected PTV1 on the EPID image does provide additional information regarding the degree of error. However, the V95(%) variation from the original and deformed contours is related to the degree of error as indicated in Table 1.

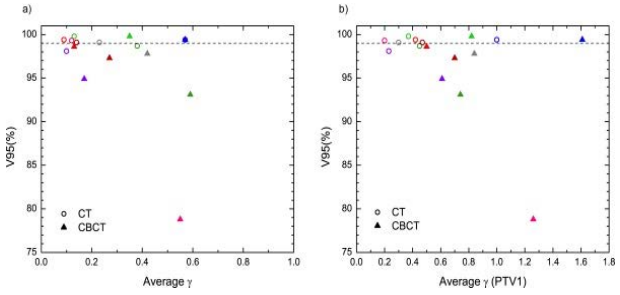

Table 1

Category	Nb of cases	$\left(\frac{V95(\%)_{CT} - V95(\%)_{CBCT}}{V95(\%)_{CT}}\right)$
1	4	1.47
2	2	3.49
3+	2	10.32

Conclusion: In summary, we demonstrated that PTV1 projection on the EPID plan does not provide new information on the plan deterioration. However, this method was more sensitive to anatomical changes and could be used as an indicator instead of the mean γ on the whole EPID image. In the following steps, the organs at risk projections will be evaluated to verify if they do provide new information. This approach is valuable for the treatment quality, but does not increase the dose to the patient or the time required for treating a fraction. Image acquisition and analysis can be easily automatized to further minimize the impact on the clinical workload.

EP-1819

Plan of the Day is the optimal approach to address organ motion for cervical cancer IMRT

R. Jadon[1], E. Spezi[1,2], L. Hanna[1], N. Palaniappan[1], M. Evans[1], E. Hudson[1], J. Staffurth[1,3]
[1]*Velindre Cancer Centre, Clinical Oncology, Cardiff, United Kingdom*
[2]*Cardiff University, Medical Physics, Cardiff, United Kingdom*
[3]*Cardiff University, School of Medicine, Cardiff, United Kingdom*

Purpose or Objective: Intensity modulated radiotherapy (IMRT) for cervical cancer is challenging due to organ motion within the CTV, comprising cervix, uterus, vagina, parametrium and pelvic nodes. Large CTV-PTV margins to compensate for this motion result in large volumes of organs at risk (OARs) within the PTV, negating the benefits of IMRT. Furthemore, there is significant intra-patient variation in organ motion therefore individualised adaptive strategies may be appropriate.
One option is Composite Strategy (CS) where a composite is formed from CTVs using planning scans and initial on-treatment cone beam CT (CBCT) scans. A second is Plan of the Day (PotD), where a plan library is created and the most appropriate plan chosen each day based on CTV position.

Material and Methods: Retrospective analysis of planning scans (full bladder (FB) and empty bladder (EB)) and on-treatment CBCTs for patients treated with radical radiotherapy for cervical cancer was performed.
CBCT scans were rigidly co-registered with FB scans on Oncentra Masterplan. On each scan the primary CTV (pCTV) comprising cervix, uterus, vagina, parametrium was outlined. On the FB scan bowel bag, bowel loops, rectum and bladder were outlined as OARs.
We modelled:
1) Standard margin: a 2cm isotropic CTV-PTV margin around the pCTV
2) CS: a composite was formed from pCTVs from FB, EB, and day 1-3 CBCTs, with a 1cm margin to PTV
3) PotD: a 3-plan library was created using pCTVs from FB and EB scans. A third mid-volume CTV was generated using deformable image registration on Velocity (v3.1, Varian Medical Systems) and custom software developed in Matlab. A 1cm margin was added to each CTV to generate PTVfull, PTVmid and PTVempty. If none of the 3 plans covered the CTV then a 'back-up' standard 2cm margin was chosen.
The remaining CBCT scans for each patient were used to compare PTV volumes, CTV coverage, and OARs within PTV. Statistical differences were tested using Mann Whitney-U.

Results: 141 scans were assessed for 14 patients (FB, EB and 7-13 CBCTs each). The table below shows mean measures of the 3 strategies. The 3-library PotD could only be used in 58% of scans assessed, and the back-up plan was used for the remainder. Despite this PotD significantly reduced mean bowel, bowel bag, rectum and bladder in the PTV, whilst maintaining CTV coverage.

		Mean PTV Volume (cc)	Mean CTV coverage (%)	Mean Bowel in PTV (cc)	Mean Bowel bag in PTV (cc)	Mean Rectum in PTV (%)	Mean Bladder in PTV (%)
Standard margin		1061.65	99.6	111.8	366.5	71.9	59.3
Composite Strategy		798.36	99.9	84.8	295.4	62.8	55.45
	Change from standard margin	Reduced 24.8%	Improved 0.19%	Reduced 24.1%	Reduced 19.4%	Reduced 12.7%	Reduced 6.5%
	p-value (compared with standard margin)	**0.007**	0.137	0.265	0.15	0.137	0.7
Plan of the Day Strategy		765.2	99.6	68.3	228.2	49.9	43.44
	Change from standard margin	Reduced 27.9%	No change	Reduced 38.9%	Reduced 37.7%	Reduced 30.5%	Reduced 26.7%
	p-value (compared with standard margin)	**0.012**		**0.05**	**0.006**	**0.000**	**0.027**

Conclusion: Adaptive strategies show promise. PotD, even when the plan library was only used in 58% of scans, increased OAR sparing compared with CS. Dosimetric analysis of these strategies with IMRT planning is ongoing.

EP-1820

On the use of deformable image registration to evaluate the need to perform ART in head and neck cancer

P. Delgado-Tapia[1], M. Lizondo[1], A. Latorre-Musoll[1], N. Jornet[1], T. Eudaldo[1], P. Carrasco[1], A. Ruiz-Martinez[1], C. Cases[1], M. Ribas[1]
[1]*Hospital de la Santa Creu i Sant Pau, Servei de Radiofísica i Radioteràpia, Barcelona, Spain*

Purpose or Objective: ART is a time-consuming process and the question "do we need to replan?" is not always easy to answer. In this work, we investigate: (i) if Deformable Image Registration (DIR) software can provide reliable criteria to decide if we need to replan; (ii) if we can use DIR to replan the treatment without performing a new planning CT.

Material and Methods: Five patients, treated using a SIB-IMRT technique, were included in this retrospective study. For all patients, a new planning CT (CT2) had been performed after observing anatomical changes between the initial planning CT (CT1) and CBCT images.
For this study, CT1 was registered with CBCT by using a DIR algorithm (SmartAdapt v13.5, Varian Medical Systems). We obtained a new CT (CTdef) by applying the deformation field both on CT1 and on contoured structures. We copied and recalculated the initial plan to CTdef. To assess whether replan was really needed at that time, we proposed a two-step algorithm (figure):
Impact of changes on targets coverage. This evaluation was twofold. On one hand, we assessed the dosimetric coverage and homogeneity of CTVCTdef by comparing D98% and D2% to initial ones. On the other hand, we defined a geometric overlapping index (OI) as the percentage of CTVCTdef volume inside PTVCT1.
Impact of changes on OARs coverage. We focus on two dose-volume indices, V30Gy of parotid glands and D2% of spinal cord on CTdef. The tolerance limits were set as the range of variability of those indices by shifting the isocenter of the original plan on CT1 up to 3mm (the CTV to PTV margin) in each direction.
Only those patients with ΔD98%>2.5%, ΔD2%>2.5% or OI<0.95, and/or OARs indices out of their variability range (as long as initial OAR indices fulfilled our institution constraints) should be replanned.
As all patients had been replanned anyway, we copied and recalculated those plans (planned on CT2) to CTdef. The aforementioned indices were re-evaluated (replacing CT1 by CT2) to check if CTdef would be a valid planning CT.

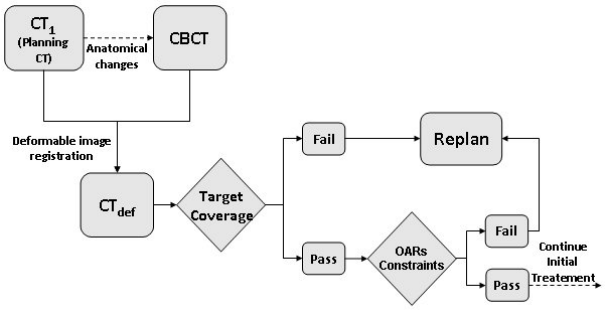

Results: Table 1a shows the dosimetric differences when recalculating the original plan on CTdef. Only patient #2 (highlighted data) should have been replanned.
The differences between using a new CT or the CTdef for dose planning are shown in Table 1b. CT2 and CTdef are equivalent since plans on CT2 can be transferred to CTdef with equivalent dosimetric results.
Patient #3 was excluded because, additionally to anatomical changes, new findings lead to include new tumour sites.

			Patient #				
	Structure	Parameter	1	2	3	4	5
1a)	CTV	OI	1,00	0,94	0,99	1,00	1,00
	CTV	$\Delta D_{98\%}$ (%)	-1,3	4,1	2,1	-1,2	0,4
	CTV	$\Delta D_{2\%}$ (%)	-2,1	-0,6	0,5	-2,5	0,0
	Right par	V_{30Gy} (%) [range]	84 [55-72]	---	11 [10-30]	26 [13-30]	66 [41-56]
	Left par	V_{30Gy} (%) [range]	22 [6-25]	79 [54-74]	30 [18-40]	31 [30-41]	53 [30-47]
	Spinal cord	$D_{2\%}$ (Gy) [range]	43 [41-48]	28 [21-26]	55 [55-64]	33 [26-35]	35 [24-32]
1b)	CTV	OI	0,98	0,95	---	1,00	0,99
	CTV	$\Delta D_{98\%}$ (%)	1,5	1,3	---	-0,5	1,6
	CTV	$\Delta D_{2\%}$ (%)	0,3	-0,1	---	-0,9	0,7
	Right par	V_{30Gy} (%) [range]	84 [70-89]	---	---	18 [5-16]	66 [50-60]
	Left par	V_{30Gy} (%) [range]	50 [47-73]	84 [56-77]	---	16 [15-24]	66 [41-55]
	Spinal cord	$D_{2\%}$ (Gy) [range]	27 [26-34]	26 [23-27]	---	41 [35-40]	42 [21-26]

Table 1. Impact of changes on targets and OARs. *1.a)* Comparison between original plan on CT_1 and on CT_{def}. *1.b)* Comparison between replan on CT_2 and on CT_{def}.

Conclusion: The proposed algorithm is a useful tool to decide whether is necessary to replan a treatment, thus avoiding unnecessary ART for a significant number of patients. We showed that CTdef provides a valid new planning CT for those patients which must be replanned, thus avoiding unnecessary scans.

EP-1821

Adaptive external radiation therapy of cervical cancerwith different uterine fundus positions

A.B.L. Marthinsen[1], F.C. Vidaurre[1], L. Rolstadaas[1], M. Eidem[1], S. Danielsen[1], M. Sundset[2], A.D. Wanderås[1]
[1]*St. Olavs Hospital, Department of Oncology, Trondheim, Norway*
[2]*St. Olavs Hospital, Department of Gynecology, Trondheim, Norway*

Purpose or Objective: Adaptive strategies for external radiation therapy of cervical cancer may counteract that parts of the target volume may receive too low radiation doses due to interfractional uterus movement. This has become more important when using advanced radiation delivery techniques (IMRT/VMAT) with highly conformal dose distribution to the target volume. We have retrospectively tested a simple adaptive strategy with different PTV shapes covering possible movement of the fundus of the uterus.

Material and Methods: For 5 cervical cancer patients treated with external radiation, the planning CT and CT scans taken throughout the treatment course were used as a basis for the study. For each patient the uterus was delineated as CTV in the planning CT with an uniform CTV-PTV margin of 1 cm. Two additional PTVs were delineated to account for a +/- 0.5 cm shift in the position of fundus uterus in the anterior-posterior direction. The PTV of the affected lymph node areas was added to the 3 PTVs to make up a final PTV for treatment planning, and corresponding VMAT plans were made for each case. The conventional treatment plan was based on the uterus position in the planning CT, and the two other plans were used as possible adaptive "plan of the day" for each treatment fraction. 8 – 19 CT scans were taken throughout the treatment course for each patient, and the volume of the part of uterus receiving less than 95% of the prescribed dose for each fraction was calculated for both conventional and adaptive strategies.

Results: For the conventional treatment, parts of uterus receiving less than 95 % of the prescribed dose was found in 4 of the 5 patients recorded, corresponding to 29 of the overall 52 CT scans taken throughout the treatments, The mean volume of the under dosed part of the uterus was 18.4 cm3. The adaptive approach improved the dose coverage for all the under dosed fractions; 4 fractions in 3 of the patients received adequate doses to the whole uterine volume, and for the other fractions the mean volume of the under dosed part of uterus was reduced by 30 - 67 % for the actual patients.

Conclusion: For external radiation of cervix cancer, the proposed simple adaptive technique, based on only one planning CT, increased the volume of the uterus receiving > 95 % of the prescribed dose for all the fractions tested. However the approach did not give adequate dose distribution to the whole uterus for all fractions for the adaptive PTVs used in this study.

EP-1822

limits and potentialities of the use of CBCT for dose calculation in adaptive radiotherapy

S. Meroni[1], V. Mongioj[1], T. Giandini[1], F. Bonfantini[1], A. Cavallo[1], M. Carrara[1], C. Stucchi[1], C. Cavatorta[1], E. Pignoli[1]
[1]*Fondazione IRCCS Istituto Nazionale dei Tumori, Medical Physics, Milan, Italy*

Purpose or Objective: To evaluate the feasibility of using CBCT images for dose calculation and to identify the most convenient calculation approach for replanning in Adaptive Radiotherapy (ART). For large cone beam geometry, scattered radiation and beam hardening cause uncertainties in the estimation of tissue electron densities (ρel). Different strategies have been adopted over the last decade to face this problem but there is no agreement on the results obtained with each technique.

Material and Methods: By using a CIRS 062 phantom, conversion curves (Hounsfield Unit, HU, to ρel) for two different Varian CBCT models and for head and pelvis protocol were measured. Diffusing material was added to the phantom to simulate the typical dimensions of the anatomical districts. A dosimetric analysis was then performed for CIRS phantoms and patients treated for H&N and prostate cancers, by comparing dose distributions calculated on the same CBCT using different HU-ρel conversion curves. For each case, the plan-CT and CBCT images were registered rigidly. A VMAT plan was generated on the plan-CT and transferred to the CBCT. The dose was calculated on the CBCT without heterogeneities corrections, using the plan-CT conversion table and using the CBCT site-specific conversion tables. The distributions were compared to the reference distribution (Dref) with 3D gamma analysis, Dref being the dose calculated on the plan-CT using its proper conversion curve. For each comparison the *net disagreement* was calculated, i.e. the percentage of points that exceeded gamma criteria without taking into account discrepancies due to registration errors (DTA = 2mm for phantoms, 3 mm for patients).

Results: For the CIRS phantoms, the CBCT conversion curves gave good results for dose calculation: mean net disagreement for gamma criteria DD= 1% was lower than 1%. For the pelvis region, the best results were obtained without applying heterogeneity corrections to the calculation. The dosimetric discrepancies with respect to Dref were few and mostly below 2% of the local dose. For H&N patients, calculations with the CBCT site-specific conversion curves showed the smallest discrepancies with Dref. On average, 0.4% of the points showed discrepancies larger than 1%.

Conclusion: The differences between the results found for phantoms, pelvis and H&N patients highlight the importance of careful evaluations for each anatomical region. The error introduced by calculating the dose on a CBCT is acceptable for ART. CBCT dose calculation could be used to monitor the entity of anatomical variations in the patients. An important limitation on the use of CBCT for treatment planning is the FOV dimension, often not sufficient to include the whole PTV or patient shoulders in case of H&N treatment. This affects dose calculation due to the lack of scattered radiation causing underdosages in cranial and caudal slices.

EP-1823

Characterization of kV- and MV-CBCT for personalized adaptive treatment therapy on RayStation TPS

A. Balazs[1], T. Torbjørn Furre[1], K. Karsten Eilertsen[1]
[1]*Oslo University Hospital- Norwegian Radium Hospital, Medical Physics, Oslo, Norway*

Purpose or Objective: Modern treatment therapy, with the combination of intensity modulated fields, dose escalation and small margins, is unthinkable without equipment that facilitates IGRT. Hence, the latest generations of linacs are equipped with modern kV and MV detectors, with enhanced image quality and precision. RayStation TPS exploits this development further, making it possible to use these image series to execute personalized adaptive treatment planning, by using the acquired CBCT during treatment.
Our goal with this project is to characterize the geometrical and dosimetrical (in terms of HU) accuracy of different CBCT types from different machines (Elekta XVI, Varian TrueBeam OBI and Siemens Artiste kView).

Material and Methods: Using CatPhan phantom, planning CT with a Philips BigBoard Brilliance, Head&Neck protocol were acquired and imported to RayStation TPS. The advantage of using CatPhan is, that it has both geometrically known and accurate measures, and inserts with known CT numbers.
CBCT series were acquired by using Head&Neck protocols. The captured image series were then imported to RayStation, where, after rigid image registration, all the characteristics of the CBCT images were investigated, and doses recalculated on the CBCT image series.
Histograms over the image slices were subject to investigation in IDL, to verify the accuracy of CT numbers and geometrical reconstructions from RayStation

Results: Some differences were observed between the different CBCT modalities and the planning CT, investigating the different material types and geometries:
-The preliminary investigation of geometrical accuracy shows that both the Elekta XVI modules deforms the phantoms dimensions by about 1 mm. Most of the inserts shows CT# within acceptable limits. As for the Siemens kView, a carbon target modulated 1MV energy is applied to acquire the CBCT images, resulting in almost 30% underdosage in the Teflon material.
-The data were successfully reconstructed and analyzed with IDL as well showing good agreement between the data from RS and raw image data.

Material	Representative CT# by means of HU from the various machines					
	Phantom manual CT# (+/- 5%)	Philips Big Board	Varian TrueBeam	Elekta XVI 1	Elekta XVI 2	Siemens Artiste kView*
Air	-1000	-994	-1000	-760	-869	-425
PMP	-200	-199	-166	-156	-176	-52
LPDE	-100	-70	-82	-115	-77	49
Polystyrene	-35	-20	-34	-119	14	-10
Acrylic	120	120	119	78	125	132
Delrin	340	339	350	225	337	323
Teflon	950	957	894	655	696	509

*Siemens Artiste kView is a MV-CBCT with average energy 1 MeV

Material	Calculated average doses for different CBCT modalities (Gy)				
	Philips Big Board	Varian True Beam	Elekta XVI 1	Elekta XVI 2	*Siemens Artiste kView
Air	10.28	10.32	10.25	10.26	9.98
PMP	10.04	10.06	10.02	10.03	9.89
LPDE	8.01	8.14	8.03	7.75	8.00
Polystyrene	5.74	5.96	5.75	5.45	5.79
Acrylic	5.60	5.82	5.64	5.44	5.67
Delrin	7.95	8.13	7.98	7.91	7.91
Teflon	10.00	10.03	9.98	10.04	7.19

*Siemens Artiste kView is a MV-CBCT with average energy 1 MeV

Conclusion: Our study shows, that CBCT series are precisely reconstructed in RayStation, both geometrically and by means of CT#. However, careful investigation of the electron densities of the imported CBCT`s is necessary in order to avoid inaccurate dosimetrical outcomes.
Further investigations are necessary to map the reason for the differences between image series acquired with these machine types as a step towards implementing deformable image registration using CBCT.

EP-1824

A new strategy approach for dose tracking and novel radiobiological models for adaptive radiotherapy

S. Strolin[1], E. Mezzenga[2], A. Sarnelli[2], S. Marzi[1], G. Sanguineti[3], L. Marucci[3], M. Benassi[2], L. Strigari[1]
[1]*IFO - Istituto Regina Elena, Laboratory of Medical Physics and Expert Systems, Roma, Italy*
[2]*Istituto Scientifico Romagnolo per lo Studio e la Cura dei Tumori IRST IRCCS, Medical Physics Department, Meldola FC, Italy*
[3]*IFO - Istituto Regina Elena, Department of Radiotherapy, Roma, Italy*

Purpose or Objective: To test the feasibility of dose tracking approach in Head-and-neck (HN) cancer, two deformable image registration (DIR) strategies has been implemented and compared.

Material and Methods: Planning (pCT) and weekly (w-CT) acquired computed tomography (CT) scans of a cohort of 15 Head-and-neck (HN) cancer patients already prospectively enrolled in our Institute for a study on adaptive approach have been imported in Raystation TPS version 4.6.102.4 (RaySearch Laboratories AB, Stockholm, Sweden). The recently available hybrid algorithm was used including body contour as focus ROI and with/without manually contoured ROIs as controlling ROIs indicated as RH/H, respectively. DICE index was used to assess the goodness of propagation of contours generated by both DIR approaches. Doses/volumes statistics and radiobiological data were calculated and compared according DIR strategy.

Results: For GTVs the median DICEs were 0.88 and 0.63 for RH and H, respectively, while for parotid gland were 0.94 and 0.82, and for spinal cord were 0.94 and 0.88, respectively. Although dose differences on GTVs show the median variations within 1% with minimal values up to 8%, TCP values were 63.7%, 69.7% and 61.9 % for planned, RH and H approach, respectively. Moreover, the average NTCP for homo-lateral parotids it was 36 %, 46 % and 34 %; while for contra-lateral parotids was 28%, 36% and 27% based on planned, RH-based and H-based accumulated DVHs, respectively.

Conclusion: RH strategy generates structures well in agreement with ones manually contoured, supporting the goodness of generated deformation matrix, resulting an appropriate strategy to perform dose tracking in HN cancer patients eligible for ART. Home-made tools/routine, as developed in this work, are mandatory to evaluated results and permit the adoption of a dose tracking strategy.

EP-1825

Delivered dose determination in large organ deformations: Pre-requirement for adaptive RT for LACC.

P.V. Nguyen[1], F. Lakosi[1], J. Hermesse[1], S. Nicolas[1], A. Cifor[2], M. Gooding[2], P.A. Coucke[1], T. Kadir[2], A. Gulyban[1]
[1]*C.H.U. - Sart Tilman, Radiotherapy Department, Liège, Belgium*
[2]*Mirada Medical Ltd, Physics, Oxford, United Kingdom*

Purpose or Objective: To create robust methodology for accumulating delivered dose to organs on the basis of daily cone beam computer tomography (CBCT) images using Radial Basis Function with Robust Point Matching (RBF-RPM) deformation algorithm. Clinical evaluation includes clinical target volume (CTV) coverage for patient with locally advanced cervical cancer (LACC).

Material and Methods: Between June and September 2015 five consecutive LACC patients were scanned with empty and full bladder conditions for treatment planning purposes. Primary CTV was delineated in both scans creating an internal target volume (ITV) concept and the distance between the tip of the uterus was measured. Primary ITV and lymph node CTVs were expanded with 10 mm margin to generate the planning target volume (PTV). Advanced treatment planning technique (VMAT or IMRT) were used for delivering a total dose of 45 Gy in 25 fractions with daily online correction CBCT. On every CBCT the 1) current position of the primary CTV were delineated and 2) the planned dose matrix were co-registered and eventually transposed to CBCT rigidly. Using the Mirada RTx (version 1.6.2, Mirada Medical, Oxford, United Kingdom) between the planning reference CT (= full bladder) and each CBCT a "CTV-guided" deformation (using the RBF-RPM algorithm) matrix were generated to deform the dose matrices from CBCT to the planning CT. The dose parameters on the initial CTV were evaluated on a single fraction basis (worst and average) and summed dose basis compared to the reference plan value.

Results: The average tip movement of the uterus was 2.2 cm (range 0.5-5.7 cm). A total of 118 CBCTs were eligible to perform the CTV delineation and the dose matrix transformation (rigid CT to CBCT, deformation CBCT to CT). Visual verification of each individual deformation grid were considered as clinically plausible and smooth (Figure 1). The changes in CTV_V95% were -4.7% (range [-7.0,-3.62], -0.3% [-1.4, 2.2] for the single fraction worst and mean, while for the summed actual delivery -0.6% [-3.7, 1.76]. Deviation of CTV_D95% resulted in -2.7 Gy [-5.8, -1.1] and -0.4 Gy [-0.9, -0.2] for the single fraction worst and mean, while for the summed actual delivery -0.5 Gy [-2.1, 0.1].

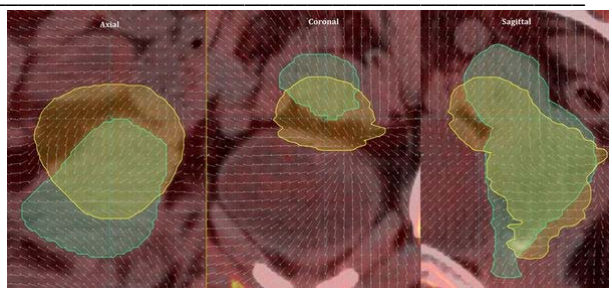

Conclusion: Using VMAT/IMRT for LACC treatment in combination with ITV concept and 10 mm margin provides a safe treatment option in the presence of large daily organ deformation. The dose accumulation using the RBF-RPM algorithm is feasible and provides a powerful tool to evaluate delivered dose not only to CTV but also to organs at risk. This methodology allows an environment to test various adaptive strategies (e.g. library of plans based LACC radiotherapy) and CTV to PTV margins in a safe retrospective manner.

Electronic Poster: Physics track: CT Imaging for treatment preparation

EP-1826

An empirical post-reconstruction method for beam hardening correction in CT reconstruction

B. Yang[1], H. Geng[1], W.W. Lam[1], K.Y. Cheung[1], S.K. Yu[1]
[1]*Hong Kong Sanatorium & Hospital, Medical Physics and Research Department, Happy Valley, Hong Kong SAR China*

Purpose or Objective: Beam hardening artifacts in X-ray computed tomography is caused by the polyenergetic spectrum of X-ray source. In this abstract we describe an empirical post-reconstruction method which removes the artifacts successfully.

Material and Methods: Our proposed post-reconstruction method has similar approach as a well-known correction method first developed by Joseph and Spital (J&S). Our method also requires prior knowledge of the X-ray spectrum and consists of three stages of correction. The first step is a so-called soft tissue correction which determines the equivalent length of soft tissue Te by solving the non-linear equation:

$Pi=\sum\omega\exp(-\mu(s)\rho(s)Te)$

In the second step, this image is segmented into soft tissue Ts and high density Tb (e.g. bone) region by setting a threshold. Different from J&S, we consider $\mu(s)\rho(s)Tb$ as part of the density map of high density region and calculate the projection data:

$Bi=\sum\omega\exp(-\mu(b)\mu(s)\rho(s)Tb)$

The third step applies the soft tissue correction again by solving the non-linear equation:

$\exp(-\ln(Pi)+\ln(Bi))=\sum\omega\exp(\mu(s)\rho(s)Ts)$

, therefore a density map $\rho(s)Ts$ is reconstructed. The final image will be the sum of $\rho(s)Ts$ and $\rho(s)Tb$. We created a 128 x 128 pixel numerical phantom which was a circular phantom consisting of water, four small regions containing bone and a small region containing fat. For validating the robustness of the method, we also replaced the four small regions with those containing aluminum and titanium. The projection data consisted of 140 radial samples and 100 angular samples over 180 degree from a 100 kVp parallel X-ray beam.

Results: The results of the post-reconstruction method for the phantom containing bone, aluminum and titanium are shown respectively. Within each figure, top left is the true phantom image; the middle is the direct filtered back projection (FBP) result with no correction; the top right is the post-reconstruction result; the profile plot is sampled at the center of phantom. For the cases of bone and aluminum, the beam hardening artifacts are removed successfully. Even in the most challenging case of titanium, the artifacts are suppressed greatly. Compared with the results using method from J&S, the density values of reconstructed high density

region are closer to the real values with deviation +5.3%, +0.4% and +10.2% for bone, aluminum and titanium respectively.

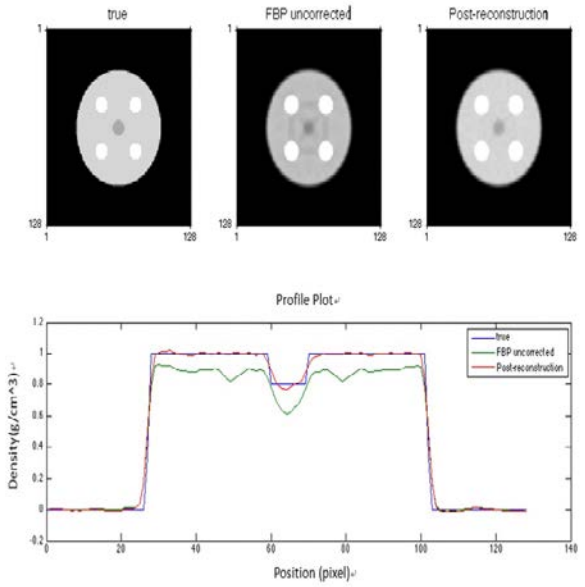

Figure 1 Results of phantom containing aluminum.

Conclusion: Our proposed empirical post-reconstruction method works well in beam hardening correction.

EP-1827

Dual energy Computed Tomography based tissue characterisation for Radiotherapy treatment planning

N. Tomic[1], H. Bekerat[1], F. DeBlois[1], J. Seuntjens[2], R. Forghani[3], S. Devic[2]

[1]*Jewish General Hospital, Radiation Oncology, Montreal, Canada*

[2]*McGill University, Oncology, Montreal, Canada*

[3]*Jewish General Hospital, Diagnostic Radiology, Montreal, Canada*

Purpose or Objective: It is known that both kVp settings, as well as geometric distribution of various materials, lead to significant change of the HU values, being the largest for high-Z materials and lowest kVp setting used for CT scanning. On the other hand, it is well known that dose distributions around low-energy brachytherapy sources (103Pd, 125I) are highly dependent on the architecture and composition of tissue heterogeneities in and around the implant. Both measurements and Monte Carlo calculations show that the errors caused by improper tissue characterization are around 10% for higher energy sources and significantly higher for low energy sources. We investigated the ability of dual-energy CT (DECT) to characterize more accurately tissue composition.

Material and Methods: Figure 1.a shows the RMI-467 heterogeneity phantom scanned in DECT mode with 3 different setups: the first set-up in which we placed high electron density (ED) plugs within the outer ring of the phantom is called Normal one, as we assume that in clinical practice this would be the most commonly used geometrical distribution of tissue ED plugs. In the second set-up we arranged high ED plugs within the inner ring and in the third one, ED plugs were randomly distributed. All three setups were scanned with the same DECT technique using a single-source DECT scanner with fast kVp switching (Discovery CT750HD; GE Healthcare). Images were reconstructed into 1.25-mm slices with a 40-cm display field of view and a 512 X 512 matrix and transferred to a GE Advantage workstation for advanced DECT analysis. Spectral Hounsfield unit curves (SHUACs) were then generated from 50 to 140-keV, in 10-keV increments, for each tissue equivalent plug.

Results: Figures 1.b-d represents HU to ED calibration curves for monochromatic CT images at 50, 80 and 140 keV respectively. As expected, the dynamic range of HU shrinks with increased photon energy as the attenuation coefficient ranges decrease. The same figures also suggest that the spread of HUs for the three different geometrical setups is the smallest at 80 keV. To quantify variation in HUs with photon energy, we calculated relative variation for various tissue equivalent materials (LN 450 Lung, Breast, Liver, CB2-30%, CB2-50%, Cortical Bone) and plotted for several different photon energies in Fig.1.e.

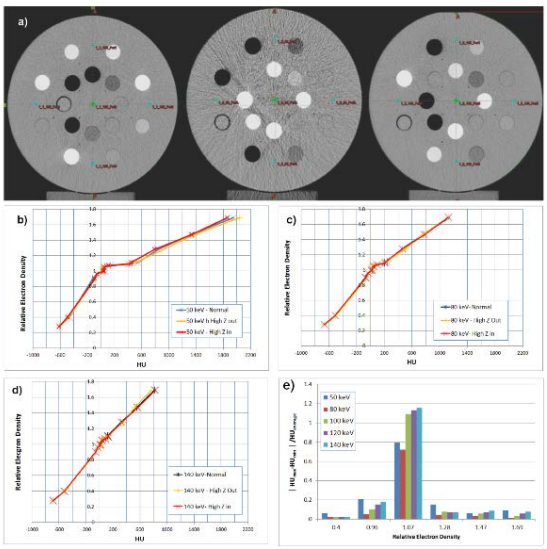

Figure 1 Impact of electron density spatial distribution on reconstructed Hounsfield Units on virtual monochromatic DECT images: a) three experimental setup (left – high Z material plugs in outer ring; center – high Z plugs in inner ring; right – standard random plug distribution); b-d) HU-ED curves for three different experimental setups at 50 keV, 80 keV and 140 keV respectively; e) relative variation of the reconstructed HUs for various materials taken from different reconstructed virtual monochromatic energy images.

Conclusion: Spectral Hounsfield unit curves demonstrate the lowest HU variation at 80 keV for the three different geometries used in this work. Among all the energies and all materials presented, the largest difference appears at high Z tissue equivalent plugs. This suggests that 80 keV virtual monochromatic DECT reconstructions may enable more accurate dose calculations at both megavoltage and kilo-voltage photon energies.

EP-1828

Liver SBRT: benefits from breath-triggered MRI in treatment position for accurate lesion contouring

L. Parent[1], A. Tournier[1], M. Rives[2], F. Izar[2], R. Aziza[3], Y. Sekkal[3], N. Morel[3], S. Ken[1]

[1]*Institut Universitaire du Cancer Toulouse Oncopôle, Engineering and Medical Physics Department, Toulouse, France*

[2]*Institut Universitaire du Cancer Toulouse Oncopôle, Radiotherapy Department, Toulouse, France*

[3]*Institut Universitaire du Cancer Toulouse Oncopôle, Imaging Department, Toulouse, France*

Purpose or Objective: As part of the stereotactic body radiotherapy (SBRT) program in our institution, magnetic resonance imaging (MRI) acquisition in treatment position for the liver was implemented. Significant liver motion can be observed due to breathing motion. The aim of this study is to report the benefits of setting out a time-correlated and breath-triggered MRI protocol optimized for radiotherapy (RT) planning in order to account for liver breathing motion.

Material and Methods: Prior to imaging, three internal gold fiducials were implanted under echo or CT guidance in the vicinity of the lesion site in order to improve images registration, patient's positioning and target volume tracking during treatment.

A 4D CT scan was acquired on a GE Healthcare Optima CT580 RT. Patient immobilization and positioning was set up with

ORFIT dedicated thermo-plastic nets, supports and cushions. Images were reconstructed in six phases across the respiratory cycle with CT50 being the exhale image set used for MR image registration.
MRI was acquired with a body coil on a 1.5T SIEMENS Aera. The patients were set up with the same patients' immobilization and positioning devices as for CT imaging thanks to a MR compatible ORFIT table. Axial Single Shot Fast Spin Echo T2-weighted with fat suppression Spectral Adiabatic Inversion Recovery (SPAIR) and motion reduction method (BLADE) was first acquired with breath triggering on exhale . Then ultra-fast gradient echo T1-w with parallel acquisition and Dixon reconstruction techniques (VIBE DIXON) allowed the acquisition in exhale breath hold. Finally injected T1-w Fast Low Angle Shot (Turbo FLASH) imaging sequence was acquired with breath triggering on exhale.

Results: The lesion was not always visible on 4D CT scan, even on images with contrast enhancement hence the need of MRI to better define the lesion. Target motion range was assessed based on fiducials' displacement.
The use of the same table and immobilization device for MRI minimized uncertainties due to patient position for image registration.
T1-w VIBE DIXON sequence was useful to register MR sequences based on fiducials' position, as they were the most visible on this sequence. The two breath-triggered (expiration phase) sequences (T2 SPAIR BLADE and injected T1-w Turbo FLASH) provided a motion artifact free image necessary to accurately delineate the lesion.
An example of MR/CT50 registration and target volume definition is illustrated on Figure 1.

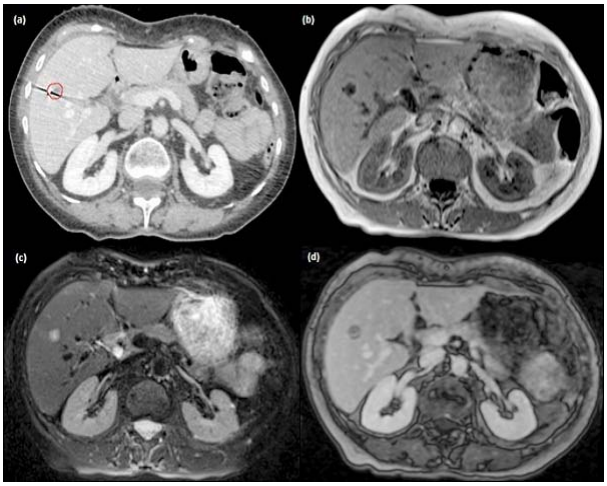

Figure 1: Example of registered image for a breast metastasis in liver segment V (a): injected CT50 with target contour delineated in red thanks to the MRI sequences. (b): T1 DIXON_w. (c):T2 SPAIR BLADE, (d): injected T1-w Turbo FLASH

Conclusion: The use of the same table and immobilization device for CT and MRI combined with the use of MR imaging sequences optimized to account not only for the dedicated table and immobilization devices but also for the gold seeds visualization and the tumor delineation allow high precision target delineation.

EP-1829
Evaluation of metal artifact reduction (MAR) algorithm for patients with a bilateral hip implant
A. Morel[1], J. Molinier[1], L. Bedos[1], N. Aillères[1], D. Azria[1], P. Fenoglietto[1]
[1]*ICM - Val d'Aurelle, Radiothérapie, Montpellier, France*

Purpose or Objective: Analyze the information stemming from three methods of images acquisition for soft tissues between a bilateral hip implant.

Material and Methods: Six patients with a bilateral hip implant were selected for this study. For every patient, 3 series of images were compared. The two first ones were performed with GE Optima CT580 simulator, one by using the metal artifacts reduction (MAR) algorithm and the other one without. The third series was acquired by Cone Beam Computed Tomography (CBCT) during the first session of treatment. For every series, the same rectangular ROI was drawn on a frontal slice, in the soft tissues situated between the two prostheses. The average Hounsfield Units (HUm) and the standard deviation (σ), corresponding to the noise in the image, were collected. According to the same methodology, the images of 12 patients without hip implant were studied in order to have a reference of the average Hounsfield Unit (HUref) in this anatomic region and to compare it with the obtained results for images of patients with a bilateral hip implant.

Results:

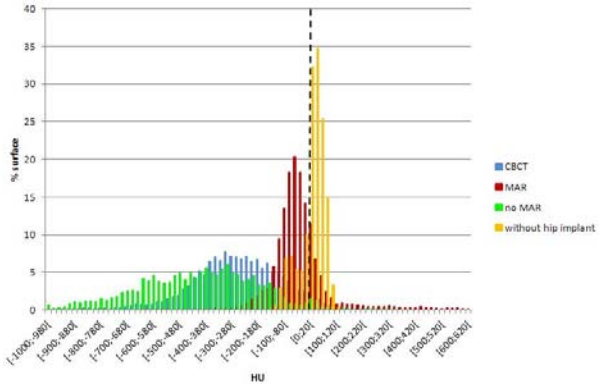

For the cohort of patients without hip implant, HUref was of 11,2 ± 43.5 HU. For the bilateral hip implant cohort, the HUm results with MAR algorithm were the closest of HUref (HUm(MAR)= -37.1 HU ; HUm(CBCT)= -262.6 HU ; HUm(no MAR)= -409.5 HU). The noise in the image was reduced too in comparison with images without MAR reconstruction and CBCT (σ(MAR)= 104.9 HU ; σ(CBCT)=153.2 HU ; σ(no MAR)= 211 HU).

Conclusion: The reconstruction quality of soft tissues between a bilateral hip implant was improved with MAR algorithm by reducing artifacts, noise and by increasing the HU accuracy. Dosimetric impact remains to be assess)= -409.5 HU). The noise in the image was reduced too in comparison with images without MAR reconstruction and CBCT (σ(MAR)= 104.9 HU ; σ(CBCT)=153.2 HU ; σ(no MAR)= 211 HU).

EP-1830
Comparison of the MRI sequences in ideal fiducial maker-based radiotherapy for prostate cancer
O. Tanaka[1], M. Hattori[1], S. Hirose[1], T. Iida[1], T. Watanabe[1]
[1]*Gifu Municipal Hospital, Department of Radiation Oncology, Gifu, Japan*

Purpose or Objective: Image guided radiotherapy for prostate cancer is a sophisticated treatment modality. However, the contouring the prostate is difficult to achieve with CT alone. To overcome the uncertainty of contouring the target on CT images, MRI is used in the registration of CT in addition to MRI using a fiducial marker. However, the visualization of the markers tends to be difficult in MRI. The aim of the present study is to find an optimal MRI pulse sequence for defining the marker as well as the prostate outline by comparing five different sequences.

Material and Methods: A total of 21 patients were enrolled in the present study. The two gold fiducial markers were placed on the prostate 3 weeks before the CT/MRI examination. MRI was performed using a five-channel sense cardiac coil. We obtained five T1-weighted spin-echo sequences (repetition time [TR]/echo time [TE] in milliseconds: 400/8) (T1WI), T2-

weighted fast spin-echo (3000/80) (T2WI), T2*_T2-weighted gradient echo (4000/80) (T2*2D), T2*_3-dimensional T2-weighted gradient echo [TR/TE1/deltaTE](37/14/7.3) (T2*3D), and contrast-enhanced T1-weighted spin-echo (607/12) (CE-T1WI) in all cases. Contrast-enhanced T1-weighted MRI was performed with gadopentetate dimeglumine. The quality comparison of the five sequences (T1WI, T2WI, T2*2D, T2*3D and CE-T1WI) was conducted by a single radiation oncologist and two radiation technologists. These observers subjectively scored all of the images based on the five following evaluation items: the definition of outline of the prostate; apex vs. soft tissue; base vs. bladder; base vs. seminal vesicle; and gold fiducial marker detection. A score from 1 to 3 (1 [poor], 2 [moderate], 3 [good]) was assigned to each of the items accordingly. Higher score was regarded as denoting better visualization. We compared the mean scores for each item.

Results:

Table
The mean imaging score of the magnetic resonance imaging (MRI) pulse sequences to define the gold fiducial marker

	Outline of prostate	Apex vs. soft tissue	Base vs. Bladder	Base vs. SV	Fiducial marker definition
Observer 1					
T1WI	1.8	1	1.2	1.2	1
T2WI	2.7 †	2.3 †	2	2 †	1
T2*2D	2	1	1.3	1	1.1
T2*3D	1.7	1.2	1.1	1.1	2 †
CE-T1WI	1.6	1.4	1.6	1.1	1
Observer 2					
T1WI	2	1.6	1	1.2	1
T2WI	2.5	2.3 †	2.4	2.3 †	1
T2*2D	2	1.3	1.3	1	2 ‡
T2*3D	1.8	1.4	1.1	1	2.3 ‡
CE-T1WI	2	1.7	1.9	1.6	1.3
Observer 3					
T1WI	1.8	1.2	1.6	1.2	1
T2WI	2.2	2	2	2	1.2
T2*2D	2	2.1	1.4	1.7	2.4 ‡
T2*3D	2.1	1.7	1.8	1.8 †	2.3 ‡
CE-T1WI	1.6	1.9	1.6	1.4	1.5

Abbreviations: SV, seminal vesicle.
One radiation oncologist and two radiation technologists subjectively scored the images based on 5 evaluation items. Scores of 1 to 3 (1 [poor], 2 [moderate], 3 [good]) were assigned to all items. Higher scores denoted the superior definition of the prostate edge and gold fiducial markers.
† The significantly highest score among five sequences ($p < 0.01$).
‡ A significantly higher score than that in three other sequences ($p < 0.01$).

Our data are shown in the Table. T2WI was significantly superior to the other sequences in terms of the definition of the prostate. T2*3D was significantly superior to the other sequences in terms of the definition of the fiducial marker.

Conclusion: The most important purpose of the study was to accurately identify the marker. T2*3D was the best sequence for achieving this objective. The superiority of T2*3D in defining the marker meant that although T2W1 provided the highest level of precision in the outline of the prostate, T2*3D provided a better balance between the contouring of the prostate and defining the marker.

EP-1831

Inter-physician variability in delineation of clinical target volume of uterine cervical carcinoma

Y.S. Kim[1], J. Joo[1], E. Choi[1], S. LEE[1]
[1]*Asan Medical Center- Univ of Ulsan, Radiation Oncology Department, Seoul, Korea Republic of*

Purpose or Objective: As intensity modulated radiation therapy (IMRT) is becoming a standard option for cervical cancer radiation therapy (RT), one of the major uncertainty components is the definition of the clinical target volume (CTV). Despite several guidelines, wide discrepancy can still exist. The aim of this study is to determine inter-observer variability in delineating CTV for definitive and postoperative RT for cervical cancer.

Material and Methods: Eight radiation oncologists from different centers whose subspecialty are gynecologic cancer contoured CTV on the planning computed tomography (CT) scan of two patients, each of definitive and postoperative RT case (Fig. 1).

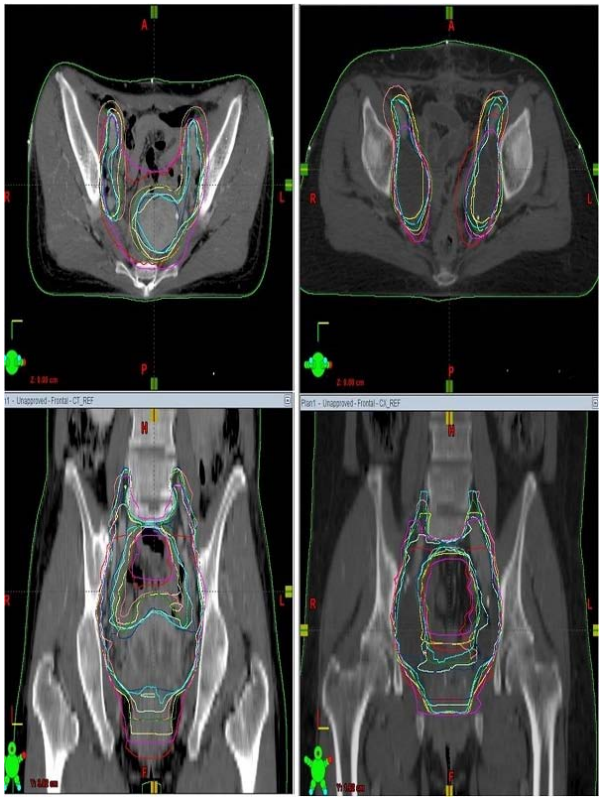

For volumetric analysis, we compared delineated volumes in terms of the individual/median volume ratio, generalized conformity index (CIgen). For spatial difference information, center of mass (COM) was used. IMRT plan was made based on one of the collected CTVs, and dose coverage was compared.

Results: The CTV volume for definitive case was 213-918 ml, with individual/median volume ratio of 0.51-1.41. The CIgen was 0.53. The mean values of the three-dimensional distances of the average COM to each COM were 7.8 mm. The largest difference was seen in superior-inferior direction, depending on common iliac lymph node region coverage and the length of inclusion of vagina. On dose coverage analysis, 95% of prescription dose covered 80.3% (range, 62.2 – 96.0%) of planning target volumes (PTV) generated by 8 physicians. Parametrial and paravaginal areas were most frequently underdosed. The CTV volume for postoperative RT case was 266-562 ml, with individual/median volume ratio of 0.65-1.38. The CIgen was 0.563. The mean values of the three-dimensional distances of the average COM to each COM were 5.3 mm in postoperative case. Ninety-five percent of prescription dose covered 80.9% (range, 66.4 – 94.8%) of planning target volumes (PTV) from 8 hospitals. Presacral, tumor bed and paravaginal areas were most frequently underdosed.

Conclusion: A large inter-physician variability in CTV delineation concerning the magnitude and relative location of volumes was observed. Continuing education of proposed

guidelines on CTV definition and knowledge of commonly missed/disconcordant CTV areas cannot be overemphasized to avoid such difference.

EP-1832

Improved 4DCT quality using true phase based triggers

P. Freislederer[1], H. Von Zimmermann[1], C. Heinz[1], K. Parodi[2], C. Belka[1]
[1]*Klinik und Poliklinik für Strahlentherapie und Radioonkologie, Departement of Radiation Oncology, München, Germany*
[2]*Ludwigs-Maximilians-University, Departement of Physics, Munich, Germany*

Purpose or Objective: For Toshiba Aquilion LB CT scanners, the reconstruction quality of 4DCTs is strongly dependent on the accuracy of cycle based online trigger pulses. Two consecutive triggers are used to define a breathing cycle which is divided into respiratory phases of equal duration. As a consequence, any deviation in the length of the inspiration or expiration period in relation to the whole breathing cycle will result in image artifacts and a higher probability of misinterpretations. The aim of this work is to improve 4DCT quality by using amplitude based triggers for each individual breathing cycle.

Material and Methods: The trigger signals for the 4DCT reconstruction are originally provided by the Sentinel™ optical surface scanner (C-RAD AB, Sweden) using a threshold method in order to generate online trigger pulses. These always have to occur before the actual maximum of the curve and are used to reconstruct the 4DCT phases based on an equally divided breathing cycle (0% - 90% in 10% steps) for phase-based reconstruction. A second 4DCT is reconstructed using the true inhalation peak triggers created by an offline tool, also with phases of equal time for each cycle. Furthermore, a single trigger for each breathing phase is sent to the CT for a third reconstruction of all motion states based on the amplitude (e.g. 10%, 20%, etc.) of the breathing curve in relation to the maximum and minimum of one cycle. The absolute volume of a tumor inside of a moving chest phantom, which serves as a direct measure for reconstruction quality, has been determined for each motion state of the reconstructed 4DCT for 10 different curves (2 sinusoidal, 8 patient breathing curves),

Results: Reconstructing the 4DCT solely according to the online trigger pulses proposed by Sentinel™can lead to a mean deviation in the volume of the tumor of up to 2,98% ± 4,65% compared to the CT reconstruction of the same tumor without any movement. When selecting the optimal trigger point at maximum inhalation offline and dividing the breathing curve into phases of equal duration, the error in volume is reduced to 0,19% ± 2,84%. Generating an amplitude based set of trigger pulses for each individual breathing cycle, the error in volume has been observed with 0,25% ± 0,29%.

Conclusion: Although the method of reconstructing 4DCTs using the amplitude-based information for each breathing cycle provides the best representation of the tumor volume, it appears to be quite impractically as every trigger file for each phase has to be sent into the CT for a single reconstruction of this motion state. This will be hard to accomplish in a clinical workflow and is prone to errors. A reconstruction of the 4DCTs based on equally divided respiration phases over time with the trigger points set to the true maximum of the breathing curve serves as a valid compromise, with minimal extra workload clinically and improved 4DCT image quality.

EP-1833

Improved proton stopping power ratio estimation for a deformable 3D dosimeter using Dual Energy CT

V.T. Taasti[1], E.M. Høye[1], D.C. Hansen[1], L.P. Muren[1], J. Thygesen[2], P.S. Skyt[1], P. Balling[3], N. Bassler[3], C. Grau[4], G. Mierzwińska[5], M. Rydygier[5], J. Swakoń[5], P. Olko[5], J.B.B. Petersen[1]
[1]*Aarhus University Hospital, Dept. of Medical Physics, Aarhus C, Denmark*
[2]*Aarhus University Hospital, Dept. of Clinical Engineering and Dept. of Radiology, Aarhus C, Denmark*
[3]*Aarhus University, Institute of Physics and Astronomi, Aarhus C, Denmark*
[4]*Aarhus University Hospital, Dept. of Oncology, Aarhus C, Denmark*
[5]*Institute of Nuclear Physics, PAN, Krakow, Poland*

Purpose or Objective: The highly localized dose distribution in proton therapy (PT) makes this treatment modality sensitive to organ motion and deformations. E.g. in proton pencil beam scanning interplay effects may be significant, resulting in dose degradations. Due to the complexity of PT dose delivery, investigations of the consequences of motion and of motion mitigation strategies may benefit from the use of 3D dosimetry. A new family of silicone-based 3D dosimeters is currently being developed. These dosimeters can be moulded into anthropomorphic shapes and can be deformed during beam delivery, which allows for simulation of organ motion and deformation.
Treatment planning with protons is based on CT scans of the patient anatomy and a conversion of the HU for the tissue to a stopping power ratio (SPR) relative to water. To ensure that the same procedure can be performed for the dosimeter it must be verified that its SPR is estimated correctly from its HU. The aim of this study was therefore to investigate if the use of Dual Energy (DE) CT and dedicated DE calibrations can improve the calculation of the SPR for the dosimeter compared to use of Single Energy (SE) CT together with the stoichiometric calibration method.

Material and Methods: A thin slab of the dosimeter material was placed in a water tank and irradiated with a 60 MeV proton beam. The range of the protons was measured with and without the dosimeter intersecting the beam to determine the range difference. The SPR of the dosimeter was calculated from its thickness and the range difference.
The dosimeter was subsequently CT scanned with a Dual Source CT scanner (Siemens Somaton Definition Flash). First a CT scan was obtained in SE mode with a tube voltage of 120 kVp, and this scan was used in the stoichiometric calibration. Next a set of CT scans was obtained in DE mode with a tube voltage pair of 80/140Sn kVp (Sn: 0.4 mm extra tin filtration); this CT image set was used for SPR calculation with two published DE calibrations. The CTDIvol of the two scanning modes was set to be the same (~20 mGy).

Results: From the range measurements, the SPR of the dosimeter was calculated to be SPRmeas = 0.97. The two DE calibration methods both gave an estimate of SPRest = 1.01, whereas the SE stoichiometric calibration estimate was SPRest = 1.10. The measured SPR did not fall on the stoichiometric calibration curve of the reference tissues (Figure; the high content of silicon makes the dosimeter not tissue equivalent). The dosimeter was found to have a HU corresponding to bone (CT number = 135 HU) but a SPR corresponding to fat.

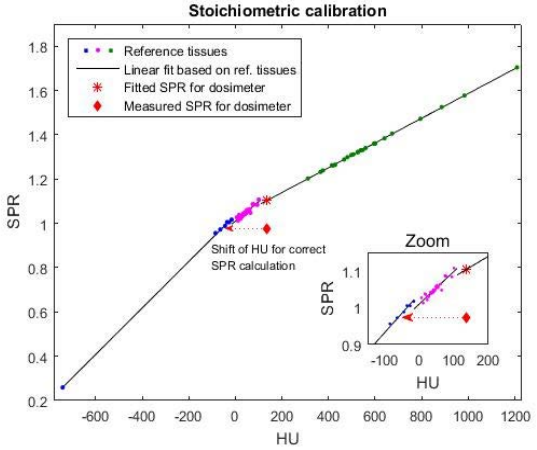

Figure: Stoichiometric calibration curve. The HU shift for the dosimeter needed for a correct SPR estimation based on the curve is indicated with a red arrow.

Conclusion: The stoichiometric method overestimates the measured SPR by 13%. Using DE this error is reduced, to an overestimation of 3%. If the stoichiometric method is used for the 3D dosimeter its HU must be corrected in the treatment planning system.

EP-1834

Towards MRI-only radiotherapy planning: "patch-based method" for generation of brain pseudo-CT

S. Aouadi[1], A. Vasic[1], S. Paloor[1], P. Petric[1], R.W. Hammoud[1], N. Al-Hammadi[1]

[1]*National Center for Cancer Care & Research A Member of Hamad Medical Corporation, Radiation Oncology, Doha, Qatar*

Purpose or Objective: To create a pseudo-CT (pCT) from T1-weighted Brain MRI using "nonlocal means patch-based method" and to assess the result for MRI-only radiotherapy planning and verification.

Material and Methods: In five patients with brain tumors, CT and contrast-enhanced T1-weighted fast-spin-echo sequences (1.5T GE MRI, TR = 756ms, TE= 7.152ms, reformatted resolution of 1.01x1.01x3mm3), were registered. MRIs were preprocessed by removing background and making tissues contrast more consistent. 2D patches, defined as MRI squares of 5x5voxels, in each voxel position, were pre-computed for all MRIs and labeled with HU values of registered CTs to form a database of patches with corresponding target HU values.
The most similar patches (k=8) to each given patch in test MRI, were locally searched (ROI=15x15x15 mm3) from the database and their corresponding CT intensities were fused to predict its pCT value. Efficient local search region delimitation was possible by affine mapping between test and database MRI images. "Structural similarity measure" and "sum of squared difference" between database and test patches were used respectively for CT voxels positions selections and intensities weighting, when averaging them to estimate pCT value.
Geometric and dosimetric assessments of the pCT were performed for all patients using leave one out cross-validation. Voxel-wise Mean Absolute Error (MAE) and Mean Errors (ME) were computed to assess pCT and DRR intensities. Bone and air cavities geometry were quantified by dice indices. MAE Water Equivalent Path Length (MAE_WEPL) was computed for multiple 3D rays from the center of the head toward the upper hemisphere to evaluate the radiological path length.
VMAT planning was done on generated pCT for all patients in Varian Eclipse (AAA algorithm) and RaySearch RayStation (Collapsed Cone algorithm) TPS for PTV, defined in a heterogeneous region including bone, air and soft-tissues. PTV, OARs and VMAT plans were copied to CT and dose computed for validation. DVH and other dosimetric parameters were compared between pCT and CT plans.

Results: Figure 1 gives the visual assessment of the generated pCT and DRR. Mean MAE, ME and MAE_WEPL values for pCT evaluation were 138.5 (σ=15.3), 29 (σ=16.1), and 32.5(σ=3.36), respectively. DICE index for bone and air cavities was 0.76 (σ=0.02) and 0.63 (σ=0.1), respectively. DRR average errors were: MAE=169.3 (σ=11.2) and ME =125.5 (σ=33.8).
Table 1 gives average dosimetric errors between pCT and CT for PTV and OARs, computed on Eclipse and RayStation TPS. The absolute dosimertic agreement between pCT and CT is within 1% for PTV and within 2% for OARs except for optic nerves in Eclipse (P-value = 0.57 > 0.05).

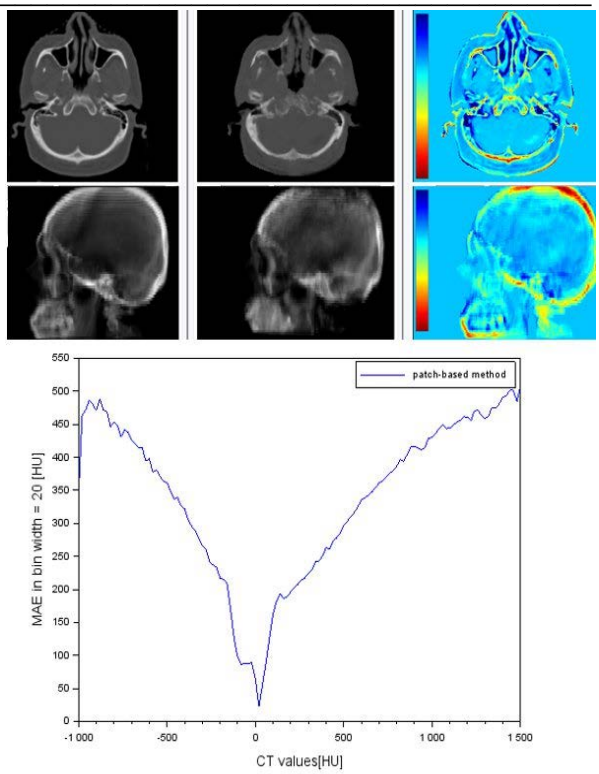

Fig1. Top -From left to right: Transverse slice of CT, pseudo-CT, difference map
Middle- From left to right: CT-DRR, pseudo-CT DRR, difference map
Bottom- average MAE in 20 HU bins

	AAA - Eclipse		Collapsed Cone - RayStation	
Structure and Dosimetric Measure	Mean Dose Variation (%)	σ_{Dose}	Mean Dose Variation (%)	σ_{Dose}
PTV MEAN	-0.09	0.14	-0.26	0.20
PTV MEDIAN	0.02	0.15	-0.26	0.21
PTV D2	0.04	0.11	-0.23	0.20
PTV D98	-0.46	0.59	-0.31	0.23
PTV D1	0.08	0.11	-0.18	0.19
PTV D99	-0.51	0.70	-0.35	0.24
Brain stem D1	-0.02	0.31	-0.21	0.19
Brain stem PRV D1	-0.15	0.28	-0.27	0.33
Left eye mean	1.01	0.29	0.06	0.13
Left eye D1	0.18	0.46	-0.04	0.34
Right eye mean	0.00	0.88	0.06	0.11
Right eye D1	0.09	0.78	0.02	0.24
Left lens D1	2.00	0.52	-0.17	0.46
Left lens mean	1.68	0.66	-0.21	0.62
Right lens mean	-0.40	2.41	-0.29	0.22
Right lens D1	-0.75	3.35	-0.16	0.22
Left optic nerv D1	1.22	2.84	-0.22	0.37
Right optic nerv D1	-9.04	17.95	-0.40	0.42
PRV Left optic nerv D1	-2.76	5.34	-0.19	0.30
PRV Right optic nerv D1	1.10	1.96	-0.37	0.76

Table 1. Average over all patients of dosimetric measurements obtained for PTVs and OARS on Eclipse and RayStation.

Conclusion: A promising study on the generation and validation of CT-substitute from standard clinical T1 MRI is presented. Further work will be done to assess and improve the method on more patients and different clinical sites.

EP-1835

Dosimetric effect of metal artifact reduction function by three calculation algorithms for H&N

J. Park[1], S. Ju[1], J. Kim[1], J. Kim[2], C. Hong[2], D. Kim[2]

[1]*Samsung Medical Center, Radiation Oncology, Seoul, Korea Republic of*

[2]*Samsung Medical Centerproton Center, Radiation Oncology, Seoul, Korea Republic of*

Purpose or Objective: The study aims at evaluating the dosimetric effect of the metal artifact reduction (MAR) function for three different types of dose calculation algorithms in H&N radiotherapy.

Material and Methods: A virtual H&N patient (vH&N) was designed based on a round-shaped dosimetric phantom (cheese phantom). Two types of metal (tungsten 4.59g/cm3 and Cerrobend alloy 9.4g/cm3: Ø3 cm) were inserted into the vH&N to simulate an H&N patient with dental prosthesis. We obtained two types of CT image sets with MAR-on and MAR-off conditions and imported a contour set for the PTV, parotid, and spinal cord, which from a Nasopharynx case. An IMRT with five step & shoot beams was created for the MAR-off CT image set using the Monte Carlo dose calculation algorithm (MC, iPlan, BrainLAB) by following RTOG1197 guidelines. Two different plans were calculated by applying pencil beam (PB) and collapsed cone convolution (CCC) dose calculation algorithms with the same beam parameters and MLC shape. The same procedure was applied to the MAR-on CT image set. A total of six plans with the same beam parameters were generated. We calculated dose at five points of interest and compared with the doses measured at the same points. The 2D axial dose distribution was evaluated through film dosimetry by applying Gamma analysis with 3 mm and 3% criteria for all plans.

Results: The differences between the measured and calculated doses at the five points of interest for the MAR-on CT image set were significantly low compared to those for the MAR-off CT image set in all dose calculation algorithms (-1.6±1.8 vs -5.8±9%). The dose differences were the lowest in MC followed by CCC and PB. The most significant dose difference between MAR-on and MAR-off was observed in PB followed by MC and CCC. In the gamma analysis, the mean pass rate was significantly high in MAR-on compared to that in MAR-off (89.8±8 vs 61.6±16%). The pass rate was the highest in MC followed by CCC and PB. The most significant pass rate difference between MAR-on and MAR-off was observed in CCC (91.8 vs 45.4%) followed by MC (96.7 vs 62.3%) and PB (81.1 vs 77.1%).

		MAR on	MAR off
Measured dose difference		-1.6±1.8	-5.8±9
Gamma pass rate	MC	96.7	62.3
	CCC	91.8	45.4
	PB	81.1	77.1
	Overall	89.8±8	61.6±16

[Table 1] Measured dose differences and Gamma pass rates (%)

Conclusion: The dose calculation results with the MAR-on CT image set and MC showed better fit to measured data compared to the MAR-off CT image set with the other dose calculation algorithms. PB was more sensitive to metal artifacts for dose calculation of H&N followed by MC and CCC. MAR-on could thus provide a more realistic dose distribution for H&N with metal prosthesis.

EP-1836

HU to electron density conversion with virtual monochromatic images generated by dual-energy CT

V. González-Pérez[1], A. Bartrés[1], E. Arana[2], V. Crispín[1], V. De los Dolores[1], V. Campo[1], L. Oliver[1]
[1]Fundación Instituto Valenciano de Oncología, Servicio de Radiofísica y Protección Radiológica., Valencia, Spain
[2]Fundación Instituto Valenciano de Oncología, Servicio de Radiología, Valencia, Spain

Purpose or Objective: To assess dual-energy CT (DECT) and Metal Artefact Reduction algorithm (MAR) for radiotherapy planning. In particular, conversion of HU to electron density is evaluated in terms of monochromatic energy and the use of MAR in the presence of metal materials.

Material and Methods: Dual energy CT was performed using a Discovery CT750 HD scanner (GE Healthcare, USA). The DECTs were performed using fast kV-switching gemstone spectral imaging (GSI) between 80 kV and 140 kV. The CT data were reconstructed both with and without MAR to the monochromatic energies of 60 keV, 90 keV and 120 keV.
CIRS phantom model 062 (CIRS Inc., USA) was used to calibrate HU to electron density in that set of monochromatic energies. Two additional sets of CT were performed after including a home-made steel insert both on the periphery and in the center of the phantom, and different images were compared in the presence of artefacts.

Results: Different calibrations for monochromatic energies showed good HU to electron density linear correlation in all cases (R^2 ranging from 0.91 to 0.998). Linearity was better for higher virtual monochromatic energies. The slope maximum change in HU to electron density curves was 24.4% when comparing polienergetic "standard" CT with 120 keV virtual image. For monochromatic energy curve calibrations, differences are up to 38.0% between 60 and 120 keV monochromatic energy.
No significant differences were found in calibrations between using MAR or not. The maximum slope change in HU to electron density curves was 2.4% for 120 keV monochromatic images after MAR reconstruction.
The maximum change of the HU of an insert after the inclusion of artefacts was of 34,0 HU for 120 keV monochromatic energy compared to 50.7 HU for a conventional CT (Figure 1).

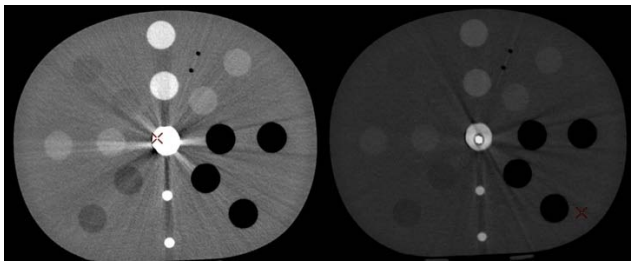

Figure 1: CIRS 062 Phantom used for HU to electron density conversion after inclusion of a steel-made insert at the phantom center. Standard polienergetic CT image (left) and monochromatic 120 keV (right)

Conclusion: The reduction of metal-related artefacts is improved at high monochromatic energies due to both the decrease of beam hardening effect and the use of MAR algortihm.
Therefore, using high keV monochromatic DECT virtual images and MAR algorithm is technically viable in radiotherapy planning since HU to electron density calibrations are feasible with monochromatic DECT image. DICOM standard is used for monochromatic virtual images and they were successfully exported to XiO treatment planning system (Elekta, Crawley, UK).

EP-1837

Impact on patient positioning using four CT datasets for image registration with CBCTs in lung SBRT

M. Oechsner[1], B. Chizzali[1], J.J. Wilkens[1,2], S.E. Combs[1,2], M.N. Duma[1,2]
[1]Klinikum Rechts der Isar- TU München, Department of Radiation Oncology, München, Germany
[2]Institute of Innovative Radiotherapy- Helmholtz Zentrum München, Department of Radiation Sciences, München, Germany

Purpose or Objective: A variety of CT datasets are available in lung stereotactic body radiotherapy (SBRT) for defining the target volume or treatment planning, e.g. slow planning CT (PCT), average intensity projection (AIP), maximum intensity projection (MIP) or mid-ventilation CT (MidV). The aim of this retrospective patient study was to evaluate the differences of using these four CT datasets for image registration with free breathing cone beam CTs (CBCT). Couch shifts between

the registrations were analyzed and correlated to different factors, e.g. tumor motion, size and location.

Material and Methods: CT datasets of 47 lung SBRT patients were retrospectively selected for this study. All patients had a PCT and a 4DCT scan. AIP and MIP CT datasets were calculated from the 10 phases of the 4DCTs. Additionally, a MidV CT was selected for each patient representing the mean position of the tumor. These four CT datasets were retrospectivlly registered to free breathing CBCTs which were acquired before patients' first treatments. Automatic image registration was performed with the Eclipse 13.0 registration software (Varian). 3D translational registrations were applied and the coordinates in left-right (x), anterior-posterior (y) and superior-inferior (z) direction were evaluated. Coordinates of each of the registered four CT datasets were compared to the coordinates of the other registered CT datasets (e.g. PCT-CBCT vs MIP-CBCT). Additionally, a 3D movement vector was calculated. Furthermore, we searched for correlations between registration differences and tumour parameters: 3D motion of the tumor, GTV volume and the distance between the carina of trachea and the GTV in z-direction (SI position). The Wilcoxon test was used to identify statistically significant difference between the fusion pairs (p-value <0.05). Correlations were analyzed using Spearman's rank correlation (rs).

Results: The table depicts median, minimal and maximal registration differences in x, y, z, and 3D direction between the CT datasets. Some differences were statistically significant (p<0.05). AIP-CBCT and MIP-CBCT achieved the smallest differences. The largest difference in 3D direction was observed for MIP-CBCT vs MidV-CBCT (10.5 mm). The figure depicts the frequency of shifts in 1 mm step sizes between the image registrations. Only 3D tumor motion showed a good correlation to the registration differences between AIP-CBCT and MIP-CBCT (rs: 0.73) or MIP-CBCT and MidV-CBCT (rs: 0.70).

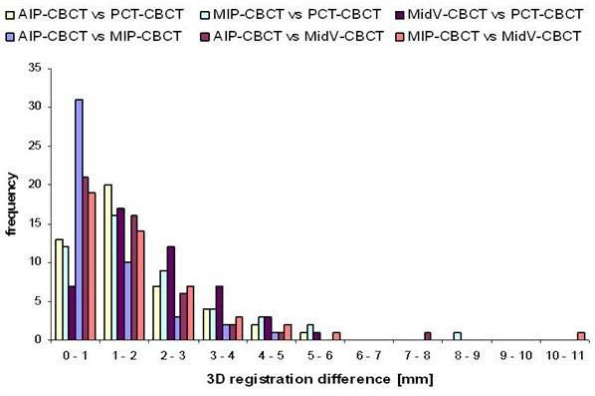

Δ couch shifts
median (min / max)

registration	Δx [mm]	Δy [mm]	Δz [mm]	Δ3D [mm]
AIP-CBCT vs PCT-CBCT	-0.5 (-2.1 / 2.7)	-0.1 (-2.9 / 2.2)	0.0 (-5.1 / 3.2)	1.4 (0.3 / 5.6)
MIP-CBCT vs PCT-CBCT	-0.5 (-1.3 / 2.9)	-0.4 (-4.0 / 1.8)	-0.3 (-8.7 / 3.3)	1.8 (0.4 / 8.8)
MidV-CBCT vs PCT-CBCT	-0.4 (2.0 / 2.2)	0.0 (-2.9 / 3.9)	-0.4 (-3.9 / 5.8)	1.9 (0.2 / 5.9)
AIP-CBCT vs MIP-CBCT	-0.1 (-1.0 / 1.2)	0.3 (-0.8 / 1.5)	0.1 (-3.0 / 4.3)	0.5 (0.1 / 4.4)
AIP-CBCT vs MidV-CBCT	-0.1 (-3.8 / 1.6)	-0.2 (-2.8 / 2.3)	0.2 (-6.3 / 2.7)	1.1 (0.1 / 7.6)
MIP-CBCT vs MidV-CBCT	-0.2 (-2.8 / 1.6)	-0.5 (-2.8 / 2.2)	0.0 (-9.9 / 5.7)	1.3 (0.1 / 10.5)

Conclusion: Using different CT datasets for image registration with free breathing CBCTs can result in distinctly different couch shifts. Automatic AIP-CBCT and MIP-CBCT fusion achieved the best agreement. Differences > 5mm were observed, which can be larger than the safety margins. This has to be considered if the CT dataset for treatment planning and image registration is chosen.

EP-1838

Proton therapy planning for brain tumors using MRI-generated PseudoCT

J. Seco[1], D. Izquierdo[2], C. Catana[2], G. Pileggi[3], J. Pursley[1], C. Speier[1,4], G. Sharp[1], C. Bert[4], C. Collins-Fekete[1], M.F. Spadea[3]
[1]*Massachusetts General Hospital Harvard Medical School, Radiation Oncology, Boston, USA*
[2]*Massachusetts General Hospital, Athinoula A. Martinos Center for Biomedical Imaging, Boston, USA*
[3]*Magna Graecia University, ImagEngLab and Experimental and Clinical Oncology, Catanzaro, Italy*
[4]*Friedrich-Alexander Universität Erlangen-Nürnberg, Radiation Oncology, Erlangen, Germany*

Purpose or Objective: To investigate the dosimetric and range accuracy of using MRI pseudoCT for proton therapy planning vs. single energy x-ray CT, for brain tumors.

Material and Methods: A cohort of 15 gliobastoma patients with CT and MRI (T1 and T2) imaged after surgical resection. T1-weighted 3D-MPRAGE was used to delineate the GTV, which was subsequently rigidly registered to the CT volume. A pseudoCT was generated from the aligned MRI by combining segmentation- and atlas-based approaches. The spatial resolution both for pseudo- and real CT was 0.6x0.6x2.5mm. Three orthogonal proton beams were simulated on the pseudo CT. Two co-planar beams were set on the axial plane. The third one was planned parallel to the cranio-caudal (CC) direction. Each beam was set to cover the GTV at 98% of the nominal dose (18Gy). The proton plan was copied and transferred to the real CT, including aperture/compensator geometry. Dose comparison between pseudoCT and CT plan was performed beam-by-beam by quantifying the range shift of dose profile on each slice of the GTV. The GTV's relative V98 was computed for the CT.

Results: For beams in axial plane the median absolute value of the range shift was 0.3mm, with 0.9mm and 1.4mm as 95th percentile and maximum, respectively. Worst scenarios were found for the CC beam, where we measured 1.1mm (median), 2.7mm (95th-percentile) and 5mm (maximum). Regardless the direction, beams passing through the surgical site, where metal (Titanium MRI compatible) staples were present, were mostly affected by range shift. GTV's V98 for CT was not lower than 99.3%.

Conclusion: The study showed the feasibility of an MRI-alone based proton plan. Advantages include the possibility to rely on better soft tissue contrast for target and organs at risk delineation without the need of further CT scan and image registration. Additional investigation is required in presence of metal implants along the beam path and to account for partial volume effects due to slice thickness.

EP-1839

exploiting planning CT data for accurate WEPL on CBCT reconstructions used in adaptive radiotherapy

J.H. Mason[1], M.E. Davies[1], W.H. Nailon[2]
[1]*University of Edinburgh, Institute for Digital Communications, Edinburgh, United Kingdom*
[2]*Edinburgh Cancer Centre- Western General Hospital, Department of Oncology Physics, Edinburgh, United Kingdom*

Purpose or Objective: To allow the use of cone beam computerised tomographic (CBCT) imaging for adaptive radiotherapy, its quantitative accuracy must be improved. However, since it is physically hindered by data insufficiency and large scatter contributions, this a difficult task without incorporating additional information. Here we propose a framework for utilising planning CT images within the reconstruction process to significantly improve the accuracy of CBCT and illustrate its potential use in proton therapy.

Material and Methods: The proposed framework involves estimating the scatter kernel as a low frequency difference between the CBCT measurements and synthetic projections of the planning CT. After correcting for the scatter contribution the CT is exploited once again as a regularisation in an iterative reconstruction, which promotes an image with a sparse difference image gradient, through minimising the total variation (TV) of this difference.To illustrate the technique's performance, we calculated the proton water equivalent path length (WEPL) through reconstructions of a Phantom Lab SK200 chest phantom. To simulate the planning CT, we manually deformed the original CT image to induce anatomical changes.

Results: The figure below demonstrates the reduction in WEPL error of our proposed approach over other techniques.The calculation was taken through to the centre of each reconstructed volume for 180 equispaced angles, against the non-distorted CT, by using a fixed lookup table to convert from Hounsfield units to proton stopping power.

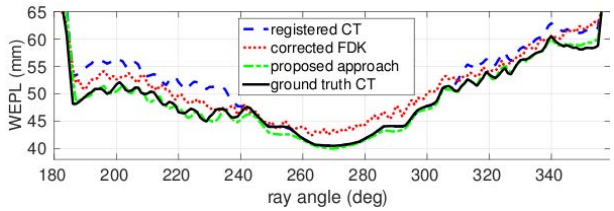

Conclusion: The technique allows accurate CBCT imaging, which may facilitate its usage in adaptive radiotherapy. Although there still remain a number of improvements in robustness before this could be considered as a clinical framework, these illustrative results are encouraging.

EP-1840

Motion artifacts in 4DCT: frequency and correlation with breathing pattern

M. Valenti[1], G. Scipioni[2], M. Parisotto[1], G. Mantello[3], F. Fenu[3], M. Cardinali[3], S. Maggi[4]

[1]*Azienda Ospedaliero Universitaria Ospedali Riuniti, Medical Physics, Ancona, Italy*

[2]*Università Politecnica delle Marche, Facoltà di Medicina e Chirurgia, Ancona, Italy*

[3]*Azienda Ospedaliero Universitaria Ospedali Riuniti, Radiotherapy, Ancona, Italy*

[4]*Azienda Ospedaliero Universitaria Ospedali Riuniti, Medical Physicis, Ancona, Italy*

Purpose or Objective: Four dimensional computed tomography (4DCT) is a consolidated simulation technique for lung tumor radiotherapy treatment. Several works report about a relevant incidence of motion artifacts in 4DCT acquisition [1,2,3,4]. In this work we retrospectively analyze 4DCT scans performed in free breathing for 29 lung tumor patient. Our analysis was focused on diaphragm, were artifacts are more frequent and evident [1]. The aim of this work is to evaluate: frequency of motion artifacts in our patient group, critical breathing phases for artifacts and correlation between breathing pattern shape and artifacts incidence.

Material and Methods: 4DCTs have been acquired in free breathing on a Discovery 690 CT-PET (GE) scanner equipped with RPM (Real-time Positioning Management) system. Scan is performed in cine mode with different couch position and ten equally spaced sets of CT images are retrospectively created using phase based sorting in Advantage 4D application. A trained operator visually checked each single phase for all the patient to individuate presence of diaphragm artifacts. A comprehensive description of different aspects of artifacts is given in [1]. We analyze and report here the percentage of patient affected by artifacts in at least one phase and the relative incidence of artifacts for each phase in our patient group. Furthermore we search a relation between breathing pattern and the frequency of artifacts.

Results: At least one phase with artifacts is present in 96% of the patients. The average number of phases with artifacts for patient is 4,1 ± 2,4 (one standard deviation). In fig. 1 we show the frequency of artifacts for each phase calculated as the ratio between number of patient with artifacts in the α phase and total number of patient. Finally, we find a linear correlation between the module of derivative of breathing pattern averaged over all patient and artifact relative incidence.

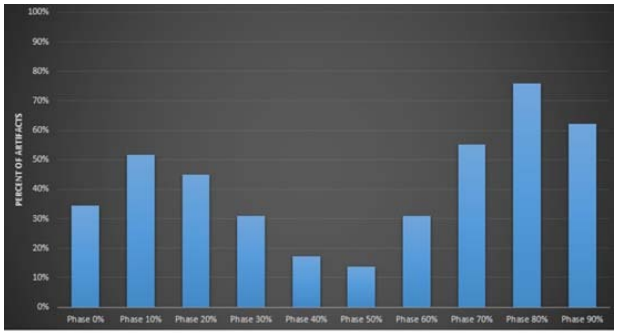

Fig.1

Conclusion: In fig. 1 we can identify two local minimum corresponding to phases 0% and 50%, respectively the end inhale and the end exhale phase of respiration. Local maximum is present around mid inhale and mid exhale (phases 10% and 80%) i. e. when motion of breathing surrogate marker in faster. We find a linear correlation between average of module of derivative of breathing pattern and artifacts incidence. We can argue that the movement speed of patient thorax or abdomen, that is where RPM marker is positioned, seems to play a relevant role in terms of artifacts incidence. Currently 4DCT scan with cine mode and RPM system suffer of a very high incidence of motion artifacts in a critical area like diaphragm given that, in our study, 96% of the patient have this problem.

Bibliography

[1] Yamamoto et al. – Int. Journal Radiation Oncology Biol. Phys 72 (4), 2008, pag. 1250-1258

[2] Castillo et al. – Journal of applied medical Physics 16 (2), 2015, pag. 23-32

EP-1841

Dose comparison study for CT and MR-only prostate IMRT treatment planning

M. Maspero[1], G. Schubert[2], M. Lindstrom[2], M. Hoesl[1], P.R. Seevinck[3], G.J. Meijer[1], M.A. Viergever[3], J.J.W. Lagendijk[1], C.A.T. Van den Berg[1]

[1]*UMC Utrecht, Department of Radiation Oncology, Utrecht, The Netherlands*

[2]*Philips Healthcare, Medical Systems MR, Vantaa, Finland*

[3]*UMC Utrecht, Imaging Science Institute, Utrecht, The Netherlands*

Purpose or Objective: In MR-only RT the planning CT is replaced by MR-based synthetic-CT (sCT). Dose validation is necessary in order to justify the use of sCT for RTTP in terms of accuracy and efficacy. One way to perform such a study is to recalculate the CT-plan on the sCT in order to assess the quality/consistency of the images for accurate dose planning. The feasibility of dose calculation on sCT obtained with model-based segmentation of Dixon MR images has been previously demonstrated [Schadewaldt et al., Med. Phys. 41, 188 (2014)] on VMAT plans. This study aims at evaluation of 5 beams IMRT prostate plans calculated on sCT vs CT using a Monte Carlo based TPS.

Material and Methods: Twelve prostate patients underwent CT **(a)** as well as MRI on the same day within 1-2 hours for RT treatment planning. A 3D multi echo sequence with Dixon reconstruction and high bandwidth, to assure geometric fidelity, was included in the clinical prostate MR exam for sCT generation (adding less than 2.5 min to the actual scan time). All scans were performed on a 3T MR scanner (Philips

Ingenia) with in-house-built flat table top. The sCT **(b)** were generated by the technique described by Schadewaldt et al, using mDixon acquisition and model-based segmentation to assign fixed HU to 5 tissue classes. The RT plans were recalculated in Monaco v5.10 (Elekta) on sCT without any further optimization utilizing the delineations from the planning CT after rigid registration of CT on sCT. The alignment (translation-only) of isocenters of the two plans allowed voxelwise dose comparison and γ-analysis.
CTs and sCTs are inherently different, as they are acquired at different time points and, furthermore, the patient anatomy can slightly vary during the positioning on CT and MR. Fig **(c)** highlights the differences, in terms of ED, of sCT minus CT for a transversal slice of one of the patients: differences in body contour and bone structure can be observed, as well as the lack of prostate markers and air pockets on sCT. VOIs **(d)** defined as the intersection of the body contour of CT and sCT (*VBody*) and as 75% (*V75*) of the prescribed dose (77 Gy) are considered in order to minimize such physiological differences during the comparison **(e)**.

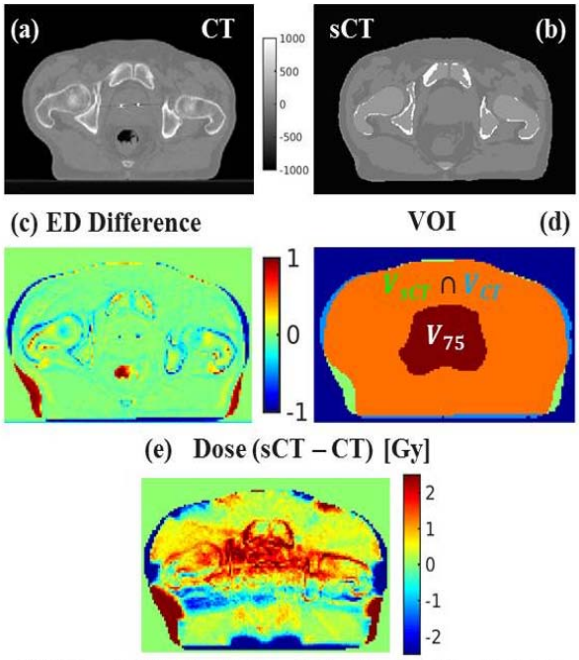

CT **(a)** and sCT **(b)** with the relative Electron Density (ED) difference **(c)**. Fig. **(d)** highlights the VOIs utilized to characterize the voxelwise dose deviations **(e)**.

Results: The dose on sCT results in a slightly systematic higher dose (1.3%, 0.9%) in *V75* and in *VBody*, respectively, when compared to CT, as shown in the Table in terms of dose difference and relative dose difference over the whole study population. The highest average dose calculated in a patient (i.e. worst case scenario) is lower than 1.5 and 0.2 Gy in *V75* and *VBody* respectively. In this type of comparison, differences in patient positioning between CT and sCT contribute to the observed difference in dose.

	Average Deviation $sCT - CT$ [Gy]	Average Rel Deviation $\frac{sCT-CT}{CT}$ [%]	$\gamma_{3\%/3mm}$ [%]	$\gamma_{2\%/2mm}$ [%]
$V_{75\%}$	0.92 ± 0.25	1.30 ± 0.36	99.3 ± 0.8	94.5 ± 4.1
V_{Body}	0.10 ± 0.04	0.86 ± 0.58	98.8 ± 0.9	95.8 ± 2.3

Average Deviation, Average Relative Deviation and Gamma passed rate (mean ± std) over all the patients for $V_{75\%}$ & V_{Body}.

Conclusion: This study evaluated the accuracy of dose calculation on sCT MR-only generated for prostate IMRT plans. Further investigations on the contributions to the observed differences are subject of current and on going research.

EP-1842

A dosimetric analysis of MRI only treatment planning of the brain

E. Goodwin[1], D. Bird[1], J. Lilley[1], R. Speight[1]
[1]*St James Institute of Oncology, Medical Physics and Engineering, Leeds, United Kingdom*

Purpose or Objective: MRI only treatment planning is gaining interest as it removes errors associated with image registration from the planning pathway. As access to MRI becomes more widespread in radiotherapy departments, it will become more feasible to carry out MRI only planning. This study aimed to assess the dosimetric accuracy of treatment plans calculated using an MRI only approach for 3D conformal radiotherapy (3DCRT) and volumetric modulated arc therapy (VMAT) brain treatments.

Material and Methods: Ten retrospective patients (five glioblastoma multiforme (GBM) patients treated with 3DCRT, and five meningioma patients treated with VMAT) were selected. A synthetic CT (sCT) was created for each patient by manually contouring the patient external, bone and sinus. The electron density (ED) of the patient, bone and sinus were forced to 1.0, 1.68 and 0.11 g/cm3 respectively, these values were derived by contouring the structures in ten representative CT study-sets. A treatment plan was calculated for each patient using the sCT, the original planning CT, and using the MRI study-set with a homogenous ED of unity. The resulting dose distributions were quantitatively analysed using the dose to the isocentre and clinically relevant DVH statistics (fig 2). A qualitative analysis of dose difference maps and DVHs was also undertaken.

Results: A paired, two-tailed student t-test found that the dose to the isocentre was statistically indistinguishable ($p<0.05$) between the sCT and the CT based dose distributions for all plans, whereas this was not the case for the homogenous density calculation. A mixed linear regression analysis of the DVH statistics showed that the ED map was a significant predictor of the dose values ($p<0.05$) when comparing CT to homogenous density, but did not find the ED to be a significant predictor of the DVH statistics when comparing sCT and CT calculated dose distributions.
The qualitative analysis supported these findings: the dose difference maps showed that there was generally good agreement between the CT and the sCT calculated dose distributions, with the main areas of difference between them occurring near the patient external (see fig. 1). Comparison of the CT and sCT DVHs also showed them to be similar, with marked differences to those calculated assuming homogenous density

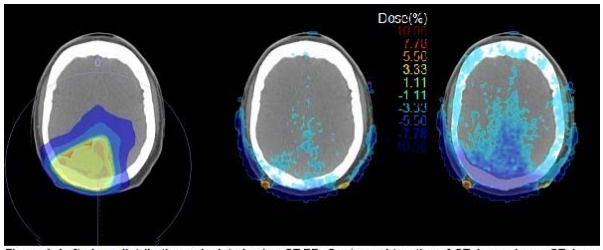

Figure 1: Left, dose distribution calculated using CT ED. Centre, subtraction of CT dose minus sCT dose. Right, subtraction of CT dose minus homogeneous ED dose.

Meningioma Cohort		Isocentre	V98 (>90%)	V95 (>95%)	V5 (<105%)	V2 (<107%)
Patient 1	CT	1.013	0.980	0.987	1.042	1.048
	sCT	1.007	0.958	0.970	1.006	1.048
	Homogenous	1.040	1.004	1.015	1.087	1.097
Patient 2	CT	1.005	0.953	0.980	1.077	1.087
	sCT	1.005	0.953	0.980	1.077	1.087
	Homogenous	0.998	0.956	0.988	1.091	1.100
Patient 3	CT	0.974	0.922	0.949	1.041	1.058
	sCT	0.991	0.916	0.941	1.047	1.060
	Homogenous	1.008	0.945	0.975	1.068	1.084
Patient 4	CT	1.030	0.980	0.991	1.056	1.065
	sCT	1.001	0.943	0.959	1.044	1.055
	Homogenous	1.039	1.011	1.026	1.120	1.134
Patient 5	CT	1.000	0.967	0.981	1.045	1.053
	sCT	1.008	0.960	0.975	1.052	1.058
	Homogenous	1.036	1.008	1.023	1.096	1.105
GBM Cohort		Isocentre	V98 (>90%)	V95 (>95%)	V5 (<105%)	V2 (<107%)
Patient 1	CT	1.000	0.860	0.882	1.162	1.189
	sCT	1.009	0.870	0.890	1.167	1.196
	Homogenous	1.035	0.884	0.904	1.191	1.218
Patient 2	CT	1.000	0.863	0.881	1.100	1.114
	sCT	1.003	0.867	0.885	1.104	1.118
	Homogenous	1.043	0.884	0.902	1.142	1.160
Patient 3	CT	1.000	0.856	0.875	1.085	1.097
	sCT	0.997	0.841	0.865	1.082	1.095
	Homogenous	1.016	0.874	0.893	1.129	1.139
Patient 4	CT	1.000	0.808	0.833	1.090	1.098
	sCT	1.012	0.821	0.844	1.095	1.103
	Homogenous	1.024	0.837	0.859	1.139	1.149
Patient 5	CT	1.000	0.855	0.869	1.117	1.141
	sCT	1.009	0.855	0.870	1.117	1.140
	Homogenous	1.016	0.877	0.893	1.153	1.179

Figure 2: Dose to isocentre and DVH statistics for all Meningioma (VMAT) and GBM (3DCRT) patients. Doses are expressed as a fraction of the prescription dose.

Conclusion: The dosimetric accuracy of treatment plans calculated using a forced density technique is equivalent to planning on CT and does not appear to be a limiting factor for MRI only planning of brain patients.

EP-1843

Synthetic CT calculation from low-field MRI: feasibility of an MRI-only workflow for glioblastoma RT

N. Nesvacil[1], H. Herrmann[1], E. Persson[2], C. Siversson[3], B. Knäusl[4], P. Kuess[5], L.E. Olsson[6], D. Georg[5], T. Nyholm[7]

[1]*Medical University of Vienna, Department of Radiotherapy & Comprehensive Cancer Center, Vienna, Austria*

[2]*Skåne University Hospital, Department of Radiation Physics, Lund, Sweden*

[3]*Spectronic Medical AB Helsingborg & Lund University, Department of Medical Radiation Physics, Malmö, Sweden*

[4]*Medical University of Vienna, Department of Radiotherapy & Christian.Doppler Laboratory for Medical Radiation Research for Radiation Oncology, Vienna, Austria*

[5]*Medical University of Vienna, Department of Radiotherapy & Christian Doppler Laboratory for Medical Radiation Research for Radiation Oncology, Vienna, Austria*

[6]*Lund University, Department of Medical Radiation Physics, Malmö, Sweden*

[7]*Umea University, Department of Radiation Sciences-Radiation Physics, Umea, Sweden*

Purpose or Objective: An MRI-only EBRT treatment planning workflow based on synthetic CTs (sCT) could help reduce MRI/CT registration uncertainties, while taking into account the improved soft tissue contrast of MRI for volumes definition, and reducing patient scanning time by avoiding the use of multiple imaging modalities for RT planning.
The aim of this pilot study was to develop a model for creating sCTs for glioblastoma, based on commercial software and to further explore the potential of a low-field open MRI scanner dedicated to RT.

Material and Methods: Using a clinical protocol optimized for RT planning T1 weighted MR (0.35T, Siemens Magnetom C!) and CT scans (Siemens Somatom Definition AS) were acquired for 6 patients with slice thickness of 4mm (MRI) and 2mm (CT). Target and OAR (brainstem, chiasm, cochlea, eye, hippocampus, lens and optic nerve) structures were delineated on MRI. The CTV was defined as the GTV (resection cavity) isotropically expanded by 1.5cm. For PTV the CTV was expanded by 0.5cm.
Synthetic CTs were generated from the MRI by the commercial MriPlanner software (Spectronic Medical AB, Helsingborg, Sweden) utilizing the Statistical Decomposition Algorithm (Siversson et al, Med Phys. 2015; 42).
The sCTs were tested for dosimetric validity compared to CT images. Delineated structures were transferred from MRI to CT via rigid image registration. For each patient a 6MV RapidArc plan was created on the CT using Eclipse (Varian Med. Sys.) and recalculated on the rigidly registered sCT using the same number of monitor units. The prescribed dose to D50% of the PTV was 60Gy in 30fx.

Results: Visual comparison showed good agreement between CT and sCT. (Fig. 1) The slightly blurred appearance of the sCT is an effect of the lower slice resolution of the MRI compared to the CT. Dosimetric results are reported in Table 1.

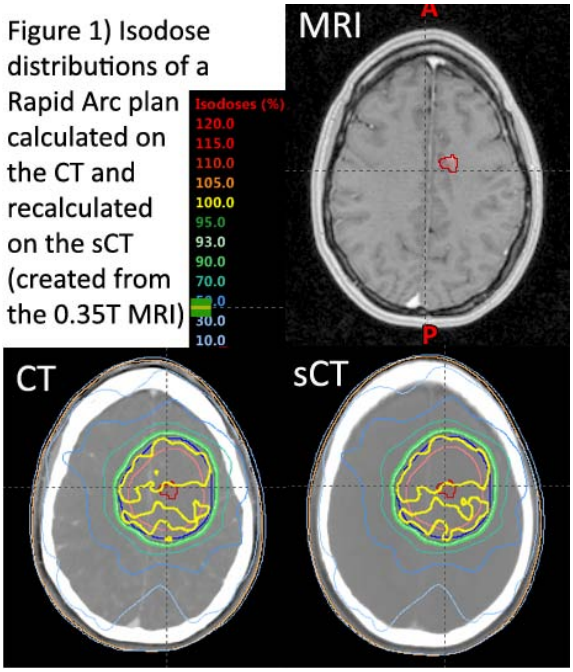

	Average Mean ΔDose (%)	Standard Dev (%)
PTV	-0.18	0.59
CTV	-0.21	0.63
GTV	-0.19	0.62
Brainstem	-0.18	0.85
Chiasm	-0.32	0.67
Cochlea Left	0.20	0.47
Cochlea Right	-0.36	0.78
Eye Left	0.17	1.57
Eye Right	-0.09	1.38
Hippocampus Left	-0.08	0.29
Hippocampus Right	-0.01	0.11
Lens Left	0.13	1.85
Lens Right	0.23	3.07
Optic Nerve Left	-0.04	1.46
Optic Nerve Right	-0.03	0.76

Conclusion: In this pilot study the MriPlanner software, which was previously verified for prostate images acquired at higher field strengths, was uccessfully applied to glioblastoma cases.
In the present study a patient fixation device was used for CT acquisition but not for MRI. This may lead to slight geometrical differences between CT and MRI, which may propagate to the dosimetric analysis. Nevertheless, the results of this study indicate that low-field MRI is suitable for

generating sCTs which could be used for EBRT treatment planning for glioblastoma. Additional improvements of MRI protocols and patient fixation may reduce dosimetric differences between CT and sCT even further.

EP-1844

Feasibility of generating mid-position CT from 4DCT using commercial deformable registration systems

M. Van Herk[1], A. McWilliam[2], P. Whitehurst[2], C. Faivre-Finn[1,3]
[1]*University of Manchester, Institute of Cancer Sciences, Manchester, United Kingdom*
[2]*Christie Hospital, Radiotherapy Physics, Manchester, United Kingdom*
[3]*Christie Hospital, Clinical Oncology, Manchester, United Kingdom*

Purpose or Objective: Publications have shown the benefit of motion compensation (MC) of 4D CT to create a mid-position CT for planning of lung tumours. The MC process creates a single sharp image in which all information of the 4D scan is combined, improving signal to noise ratio, while the absence of motion blurring improves the identification of tumour and organ-at risk boundaries compared to a maximum intensity or average scan. Furthermore, margins to account for the residual respiration motion relative to the mid-position scan can be small. Unfortunately, there are as yet no commercial solutions available to create such scans and their use is limited to a few hospitals. The aim of this work is to apply two commercial deformable registration systems, combined with open source software, to create mid-position scans, and to evaluate their performance for potential clinical use.

Material and Methods: 4D phase sorted CT scans (Philips Brilliance, 10 frames) of 8 patients were selected. Tumour peak to peak motion had to exceed 8 mm and there was no selection on scan quality. Deformable registration between all frames and the first was performed using Elekta's Admire and Mirada's RTx. The deformation vector fields (DVFs) were exported in DICOM format. Using the open source Conquest DICOM server, the DVFs and 4D CT were converted into Nifti format. A script in the DICOM server then called open source command tools of NiftyReg to first calculate the average DVF. Subsequently for each frame, the average DVF was subtracted from the frame DVF and the CT frame was deformed with this DVF to the mid-position. The resulting MC 4D data was written out for analysis. To provide a measure of quality of the MC process, the overall standard deviation of the difference of each MC CT frame with the average MC CT was calculated.

Results: The quality of the MC scans made with the two commercial systems is evaluated in Fig. 1 both quantitatively (frame by frame) and visually (average scans). Because post-processing was identical for both systems, only the quality of the DVF affects the results. Overall there is very little performance difference between the systems, with the average residual SD for both systems being within one Hounsfield unit. It is furthermore visible that certain frames (particularly 1, 2, 7 and 10) have a larger residual. These lie between in- and exhale and show a higher motion speed of the anatomical structures leading, on average, to more blurring and artefacts.

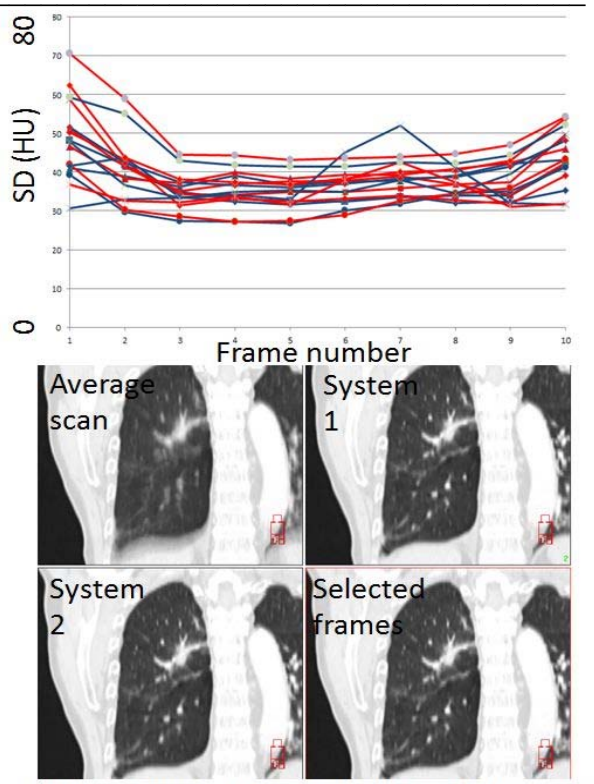

Fig.1. Top. Evaluation of 8 MC scans (SD of residual difference to average scan) with two commercial system (red and blue). Bottom: average and motion compensated scans of two systems and system 1 with selected frames.

Conclusion: Using a combination of commercial and open source software, mid-position CT scans were created. The performance of both commercial deformable registration packages was similar. For some motion compensated frames, registration performance is poorer. For practical implementation of the mid-position scan in our clinic, we propose to exclude such frames, likely leading to a more robust performance.

EP-1845

Integration of 7T MRI into image-guided radiotherapy of glioblastoma: a feasibility study

I. Compter[1], J. Peerlings[1], D.B.P. Eekers[1], A.A. Postma[2], D. Ivanov[3], C.J. Wiggins[4], P. Kubben[5], B. Küsters[6,7], P. Wesseling[7,8], L. Ackermans[5], O.E.M.G. Schijns[5], P. Lambin[1], A.L. Hoffmann[1,9,10]
[1]*MAASTRO clinic, Dept. of Radiation Oncology, Maastricht, The Netherlands*
[2]*Maastricht University Medical Centre, Dept. of Radiology, Maastricht, The Netherlands*
[3]*Maastricht University, Faculty of Psychology and Neuroscience- Cognitive Neuroscience-, Maastricht, The Netherlands*
[4]*Scannexus B.V, Maastricht, The Netherlands*
[5]*Maastricht University Medical Centre, Dept. of Neurosurgery, Maastricht, The Netherlands*
[6]*Maastricht University Medical Centre, Dept. of Pathology, Maastricht, The Netherlands*
[7]*Radboud University Medical Center, Dept. of Pathology, Nijmegen, The Netherlands*
[8]*VU University Medical Center, Dept. of Pathology, Amsterdam, The Netherlands*
[9]*University Hospital Carl Gustav Carus at the Technische Universität Dresden, Dept. of Radiotherapy, Dresden, Germany*
[10]*Helmholtz-Zentrum Dresden-Rossendorf, Institute of Radiooncology, Dresden, Germany*

Purpose or Objective: 7 Tesla (7T) MRI has recently shown great potential for high-resolution soft-tissue neuroimaging and visualization of micro-vascularisation in glioblastoma (GBM). Its value for the delineation of GBM in radiation

therapy planning (RTP) has not yet been established. We hypothesize that 7T MRI allows for improved GTV delineation over 1.5T or 3T MRI and have designed a clinical study to investigate this. However, increases in power deposition, susceptibility artefacts and geometrical distortions could significantly compromise the quality and interpretability of 7T MR images. In this study we aim for qualitative and quantitative assessment of these effects when incorporating 7T MR images into the neurosurgical navigation and RTP software.

Material and Methods: MR images were acquired with a Siemens Magnetom 7T whole-body scanner and a Nova Medical 32-channel head coil. 7T MRI pulse sequences were selected to visualize both intracranial anatomy and tumour (MP2RAGE) and perilesional edema (T2-SPACE, SPACE FLAIR). Moreover, multi-echo gradient recalled echo (GRE) T2*-weighted images were selected to visualize microvascularisation. A pilot study with 3 healthy volunteers was performed to optimize the anatomical image contrast by tuning the pulse sequences and scan protocols. Subject tolerability and side effects were assessed after each scan. A new anthropomorphic 3D phantom (CIRS Model 603A) was used to assess the geometrical image accuracy. A study-specific workflow for the transfer and processing of the 7T MR images from the scan facility to the RTP and neurosurgical navigation software was developed to enable integrating these images.

Results: Images from the four pulse sequences could be acquired within 50 minutes. The scans were well tolerated. All three volunteers reported slight vertigo while being moved in and out of the scanner. No other side effects of the 7T field were reported. Increased geometrical distortion was observed in the cortex in close proximity to air-filled cavities (fig 1). Regional loss of signal and contrast could be minimized by placing dielectric pads between the head and the coil. Regions of increased signal were identified in the occipital and temporal lobes caused by residual B1-inhomogeneities. Flow-artefacts were observed near major intra-cranial vessels. Image transfer and processing did not degrade image quality. Overall system-related geometrical distortion was≤2 mm. Detailed results of the geometric distortion analysis are reported in the phantom study by Peerlings et al.

Figure 1.

Sagittal 7T MRI SPACE-FLAIR image of a healthy volunteer. Increased geometrical distortion near the skull base, the ventral part of the temporal cortices and the orbito-frontal cortex due to close proximity of air-filled cavities.

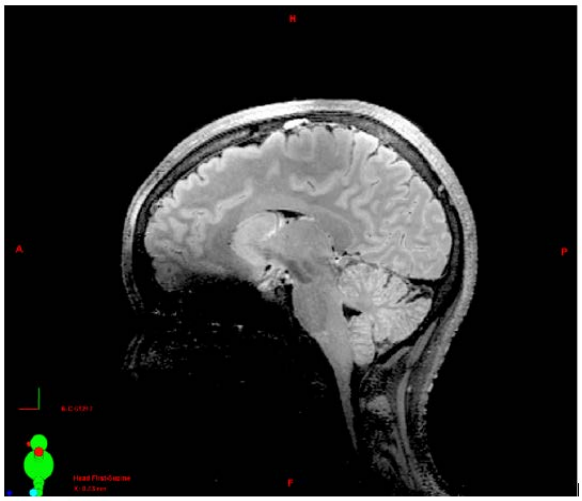

Conclusion: Integration of high quality and geometrically reliable 7T MR images into neurosurgical navigation and RTP software is technically feasible. Quantification of object-related geometrical distortion needs further analysis before clinical implementation.

EP-1846

Pseudo-CT generation from T1 and T2-weighted brain MRI based on a localised correlation approach

C. Speier[1,2,3], G. Pileggi[1,4], D. Izquierdo[5], C. Catana[5], G. Sharp[1], C. Bert[2,3], J. Seco[1], M.F. Spadea[4]

[1]*Massachusetts General Hospital and Harvard Medical School, Radiation Oncology, Boston, USA*

[2]*Universitätsklinikum Erlangen, Radiation Oncology, Erlangen, Germany*

[3]*Friedrich-Alexander Universität Erlangen-Nürnberg, Radiation Oncology, Erlangen, Germany*

[4]*Magna Græcia University of Catanzaro, Department of Experimental and Clinical Medicine, Catanzaro, Italy*

[5]*Athinoula A. Martinos Center for Biomedical Imaging- MGH & Harvard Medical School, Department of Radiology, Charlestown, USA*

Purpose or Objective: Treatment planning in radiation therapy based on MRI requires the generation of pseudo CTs for correct attenuation and dose calculation. We present a new algorithm for pseudo-CT generation which is based on localised correlations of intensity values extracted from T1-weighted and T2-weighted MRIs to CT HU values, which doesn't require UTE MRI sequences.

Material and Methods: The images of 15 patients, treated for brain tumors, were used to implement and test the algorithm. Each image sets includes a T1-weighted MRI, a T2-weighted MRI (each acquired with 3D-MPRAGE protocol with i.v. contrast agent) and a CT. The latter two were coregistered for each patient to match the T1-weighted MRI.
Both of the MRIs in each set were segmented into 6 different tissue classes (white matter, gray matter, cerebrospinal fluid, bone, skin/soft tissue and air) based on an SPM8 segmentation algorithm (http://www.fil.ion.ucl.ac.uk/spm/software/spm8/).
In order to generate a pseudo-CT for one individual, we used the image sets of the remaining 14 patients to generate the voxel-wise T1, T2 to CT correlations for each of the tissue classes. These were then used as two dimensional lookup tables to translate the T1 and T2 values of the individual to pseudo-HU values. After the application of post-processing steps including smoothing, we compared the generated pseudo-CT to the acquired CT, by calculating the bias and the mean absolute error of the difference.
We repeated this procedure for all 15 patients.

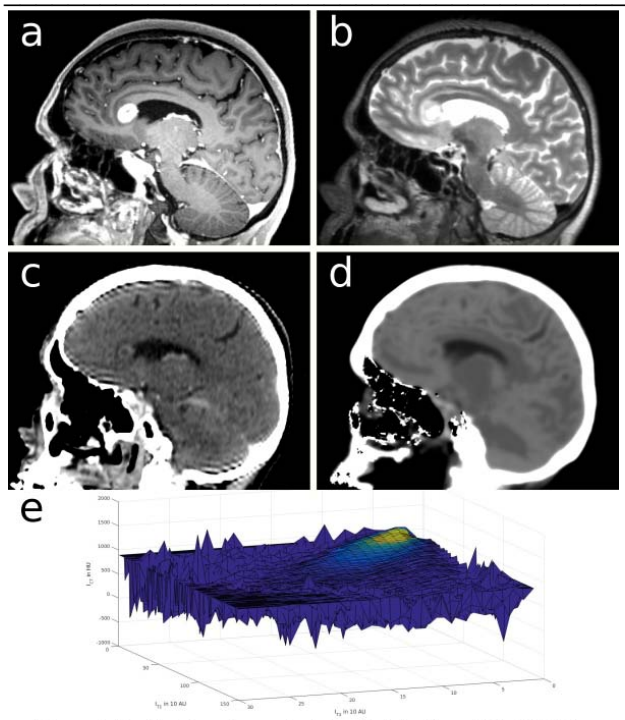

Figure 1: Sagittal views for a selected patient for T1-weighted MRI (a), T-2-weighted MRI (b), and CT (c). The pseudo-CT resulting from our algorithm is shown in (d).
An exmaple plot of T1, T2 to CT HU value correlation/lookup table for bone tissue is shown by (e), (HU over T1 and T2).

Results: The generated pseudo-CTs for the fifteen patients show low mean absolute error (138 ± 17 HU) and bias (-8 ± 29 HU) in comparison to the acquired CT. These values are in the same range as a suggested algorithm by Sue et. al, which makes use of UTE MRI acquisitions (Med Phys. 2015 Aug;42(8):4974-86.).

Conclusion: Many suggested pseudo-CT generation methods employ a complicated ultra-short echo time (UTE) MRI for better bone segmentation.
With our new approach, we show that pseudo-CTs of reasonable quality can be generated without the use of UTE MRI acquisitions. Currently, we are still improving our algorithm and at a pretty early stage of the overall development, thus further significant improvement can be expected.
Furthermore, we plan to expand our algorithm to the application in pediatric oncology with the aim to reduce necessity of CT acquisitions (ionizing radiation exposure) for growing patients.

EP-1847

Comparison of stopping power estimators from dual-energy computed tomography for protontherapy

G. Vilches-Freixas[1], J.M. Létang[1], S. Rit[1]
[1]*Université de Lyon- CREATIS- CNRS- UMR5220- Inserm-U1044- INSA-Lyon- Université Lyon 1, Centre Léon Bérard, Lyon, France*

Purpose or Objective: Proton range in patients is determined from the stopping power ratio (SPR) of tissues relative to water along the beam path. SPR map can be derived from dual-energy computed tomography (DECT) and the Bethe-Bloch equation. In this study, we propose and compare the accuracy and the precision of several procedures to estimate the SPR from DECT.

Material and Methods: Image-based method of [1] and projection-based basis material decomposition (BMD) method of [2] were investigated. 2 variants for BMD were considered: water/compact bone basis (W/CB) and photoelectric/Compton basis (Ph/Co) with exponent optimization for the given DE spectra. BMD assumes that linear attenuation coefficient at any energy can be obtained by a linear and energy-independent combination of these basis functions. Electron density ρe and effective atomic number Zeff are common DECT outputs. For each decomposition method, 4 empirical relationships to convert DE outputs to SPR were evaluated which were all calibrated with materials used by [3] for the stoichiometric calibration. The first approach [4] was a calibrated relation between the logarithm of the mean excitation energy of tissues Im and Zeff (Zeff,ln Im). The second approach consisted in reconstructing the electronic cross section at 100 keV σe,100 from the BMD results. To avoid intermediate variable Zeff, a novel calibrated relation between σe,100 and Im values (σe,100, Im) was proposed. The third method involved a calibration curve between (σe,100, SPR/ρe). The last approach consisted in the direct conversion of ρe into SPR through the (ρe,SPR/ρe) relation proposed by [5]. Only the last method can be considered independent of the energy spectra.
Virtual DECT acquisitions of the ImagingRing (medPhoton, Salzburg) of the phantom Gammex 467 were carried out by means of deterministic Monte Carlo simulations in Gate with realistic detector response model. Scatter-free fan-beam acquisitions with 720 projections were considered. Realistic Poisson noise corresponding to a 20mGy central dose was added to the projections.

Results: Relative errors of SPRs of phantom inserts estimated using 4 empirical relationships for each decomposition method are shown in Table1 as μ ± σ. A penalty was imposed to pixel values with Im, Zeff and σe values outside human range. Lung tissue inserts show maximum error. (σe,100, SPR/ρe) approach is the least appropriate in terms of precision. (σe,100, Im) and (Zeff,ln Im) behave in the same manner. Results show that the method proposed by [5] provides better accuracy and precision.

Table 1: Relative errors in the SPRs of phantom inserts for different DECT methods and empirical relationships considered in this study to convert dual-energy data to SPR.

	BMD (W/CB)	BMD (Ph/Co) opt.	Image-based
$(Z_{eff}, \ln I_m)$	4.1 ± 4.8	4.0 ± 5.5	1.2 ± 2.1
$(\sigma_{e,100}, I_m)$	4.2 ± 5.0	3.9 ± 5.4	-
$(\sigma_{e,100}, SPR/\rho_e)$	-1.8 ± 7.4	-6.9 ± 13	-
$(\rho_e, SPR/\rho_e)$	0.8 ± 3.4	-0.3 ± 3.3	-0.1 ± 3.0

Conclusion: Comparison of different calibration methods to convert DE data into SPR was carried out. A novel relationship between σe and Im was proposed and behaves similarly to (Zeff,ln Im) curve. Energy independent poly-line (ρe,SPR/ρe) curves present better accuracy and precision.
DECT is a promising technique to determine the SPR of human tissues. Optimization of the acquisition parameters and the algorithm to extract the required patient information is mandatory.

[1] Bazalova 2008
[2] Alvarez and Macovski 1976
[3] Schneider 1996
[4] Yang 2010
[5] Kanematsu 2012

EP-1848 Dual-energy CT for range prediction in proton and ion therapy

C. Möhler[1,2], P. Wohlfahrt[3,4], C. Richter[3,4,5,6], O. Jäkel[1,2,7], S. Greilich[1,2]
[1]*German Cancer Research Center DKFZ, Medical Physics in Radiation Oncology, Heidelberg, Germany*
[2]*Heidelberg Institute for Radiation Oncology HIRO, National Center for Radiation Research in Oncology, Heidelberg, Germany*
[3]*OncoRay – National Center for Radiation Research in Oncology, Faculty of Medicine and University Hospital Carl Gustav Carus- Technische Universität Dresden- Helmholtz-Zentrum Dresden - Rossendorf, Dresden, Germany*
[4]*Helmholtz-Zentrum Dresden - Rossendorf, Institute of Radiooncology, Dresden, Germany*
[5]*Faculty of Medicine and University Hospital Carl Gustav Carus- Technische Universität Dresden, Department of Radiation Oncology, Dresden, Germany*
[6]*German Cancer Consortium DKTK, Dresden, Germany*
[7]*Heidelberg Ion-Beam Therapy Center, Heidelberg, Germany*

Purpose or Objective: Proton and ion therapy require accurate prediction of particle ranges in tissue. In current clinical practice, computed tomography (CT) images are voxel-wise converted to ion-stopping power ratio maps using direct heuristic relations. The general validity of these approaches is, however, limited due to the different physical regimes of photon and ion interaction. Using a more sophisticated method based on dual-energy CT (DECT), which provides access to the physical quantities influencing photon attenuation, Hünemohr et al. (2014) reported an improved ion-range prediction for homogeneous tissue surrogates. Here, we present a major modification of the latter method, enabling a proper treatment of heterogeneities and mixtures on several structural levels, which represent a crucial feature of the realistic clinical situation.

Material and Methods: We treat the stopping-power ratio as the product of the electron density relative to water and a correction factor that implicitly involves the logarithmic dependence on the mean excitation energy (I-value). The relative electron density, being an important parameter in both photon and ion energy loss, can be derived directly from DECT scans using a universal and robust method. The correction factor, however, has to be determined with an empirical method. For this purpose, we propose to use the information from CT images that is complementary to the relative electron density, i.e. the electronic photon absorption cross section relative to water. Using the attenuation sum rule and Bragg's additivity rule, the relative cross sections and correction factors were calculated for single elements, tissue base materials like water, lipid, etc. and tabulated real tissues.

Results: For a therapeutic beam energy of 200 MeV/u, the correction factor varies between 1.15 and 0.70 for single elements with atomic numbers between 1 and 100. Building up compounds from a certain number of elements, a maximum spread of possible values for the correction factor can be quoted for a given relative cross section, due to the mathematical structure of the variable space. In practice, this could be used as an uncertainty estimate for a given calibration. The accessible variable space is drastically reduced by admitting only tissue base materials such as water, lipids and hydroxylapatite. The space is further reduced by admitting only mixtures of real tissue materials. For human tissue, the correction factor is thus limited overall to a small range around one (0.96 - 1.02).

Conclusion: With the definition of the correction factor in the stopping-power ratio prediction and its relation to the relative cross section, a mathematically rigorous treatment of tissue mixtures was made possible. Such mixtures influence CT imaging of patients e.g. in the form of volume averaging in a CT voxel. This thorough treatment of mixtures is thus essential for the clinical applicability of DECT-based ion-range prediction.

EP-1849

Validation of synthetic CTs for MR-only planning of brain cancer

C. Glide-Hurst[1], R. Price[1,2], J.P. Kim[1], W. Zheng[1], I.J. Chetty[1]
[1]*Henry Ford Health System, Department of Radiation Oncology, Detroit, USA*
[2]*Wayne State University, Medical Physics, Detroit, USA*

Purpose or Objective: The development of a synthetic CT (synCT) derived from MR images is necessary to support MR-only treatment planning. While we have previously developed a synCT solution for the brain, no clear quality assurance workflow currently exists for synCT validation. This work uses a novel MR-CT compatible 3D anthropomorphic skull phantom (Fig 1A) to evaluate the uncertainty in an MR-only workflow in the brain.

Material and Methods: MR images of the phantom were acquired on a 1.0T High-Field Open MR-Simulator (Philips Medical Systems, Cleveland, OH). Triple echo ultra-short echo time combined with mDixon (UTE/Dixon), T1-FFE, T2-TSE, and FLAIR images MR images were acquired using an 8-channel head coil. Bone-enhanced images were generated via an optimal weighted combination of inverted UTE and water/fat maps automatically generated from mDixon. Images were then semi-automatically segmented using Gaussian mixture modeling before generating synCTs via a previously described region-specific, voxel-based, weighted summation method. SynCTs were validated by calculating the mean absolute error (MAE) between SynCT and CT-SIM. DRRs from CT-SIM and SynCT were generated of the phantom and geometric fidelity was assessed via bounding box and landmark analysis. On-board planar (MV/KV) and volumetric (CBCT) images were acquired of the phantom and rigid registration was compared between datasets across three linear accelerator platforms.

Results: The MAE of the synCT for the skull phantom (Fig 1E) was 131 HU. Embedded landmarks between the phantom CT-SIM DRRs and SynCT DRRs for both right lateral and anterior projections were <1 mm (1G). However, slight image intensity variations were observed across the DRRs in the synCT as compared to the CT-SIM. Bounding box analysis of the skull revealed that anterior-posterior DRRs were <1 mm different between synCT and CT-SIM while lateral DRRs had a slightly higher uncertainty in the anterior-posterior dimension (~2 mm). MV and KV planar image registrations were within 0.7 mm for all linear accelerators. CBCT/CT-SIM and CBCT/SynCT rigid registrations were <0.4 mm different.

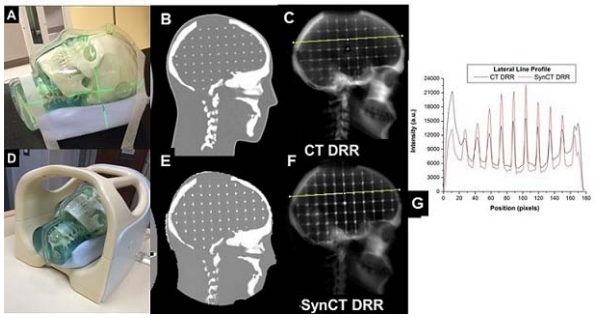

Conclusion: DRRs yielded comparable geometry between CT and synCT. Future work will involve an intensity normalization for synCT DRRs. Image registrations were within clinically acceptable ranges. Efforts are needed to combine geometric and dosimetric errors of the entire synCT pipeline; establishing QA workflows to quantify these uncertainties are necessary for MR-only treatment planning.

Electronic Poster: Physics track: (Quantitative) functional and biological imaging

EP-1850

The earlier evaluation of response to neoadjuvant chemoradiation therapy in sarcoma using DCE-MRI

Y. Kuang[1], W. Xia[2], L. Chen[2], X. Gao[2]
[1]*University of Nevada Las Vegas, Department of Medical Physics, Las Vegas, USA*
[2]*Suzhou Institute of Biomedical Engineering and Technology, Medical Imaging Department, Suzhou, China*

Purpose or Objective: Due to the spatial heterogeneity of tumors, the change of tumor size and the whole-tumor average method used in routine care do not reliably identify patients' histologic response to therapy in sarcomas, thus compromising tumor control in the context of precision medicine. In this study, we investigated the utility of dynamic contrast-enhanced MRI (DCE-MRI) combined with the voxel-wise image analysis approach as an early predictive biomarker for efficacy of neoadjuvant chemoradiation therapy in sarcoma.

Material and Methods: Serial DCE-MRI scans were performed on days before therapy (time point 1, TP1) and after 2 weeks of chemoradiation therapy (time point 2, TP2) in twelve

patients with high-risk extremity soft tissue sarcoma. A two-tier registration was used to align the tumor VOI within each dynamic frame at TP1 and align the volumes at TP2 to the volumes at TP1. After registration, the voxel-wise transfer constant K^{trans} within a VOI covering the whole tumor normalized to a reference region of normal tissue area closed to the tumor was calculated. The responder threshold was determined by linear regression via evaluating the 95% confidence interval [-T, T] in the residuals from the reference region. The difference of the voxel-wise ΔK^{trans} within the tumor between TP1 and TP2 was calculated. Three classes of voxels within the tumor VOI were determined: voxels having ΔK^{trans} value exceed threshold T were designated in red, below -T were designated in blue, and otherwise designated in green indicating no significant change. The volume fractions with respect to three sub-volumes of the tumor VOI were computed as F_+ (red voxels), F_-(blue voxels) and F_0 (green voxels).

Results: The histopathology at the time of surgery confirmed that 3 patients were optimal responders to preoperative treatment (≥95% pathologic tumor necrosis percentage) and 9 patients were sub-optimal responders (<95% necrosis percentage).F_0, ΔK^{trans} and F_- had significantly positive, positive and negative correlations with necrosis percentage ($p < 0.05$), respectively. The change of tumor size had no correlation with necrosis percentage.

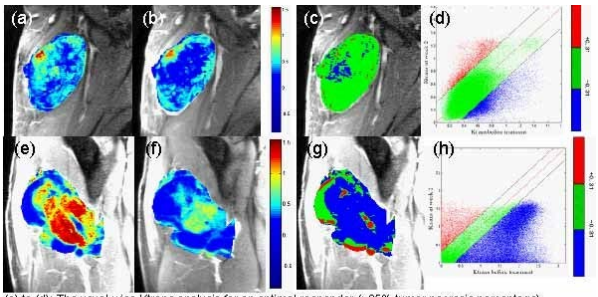

(a) to (d): The voxel-wise Ktrans analysis for an optimal-responder (>95% tumor necrosis percentage). (a) Voxel-wise Ktrans colormap at TP1, (b)Voxel-wise Ktrans colormap at TP2, (c) Voxel-wise Ktrans map of three classes of voxels depicted as red (increased Ktrans), green (no change beyond 95% confidence intervals), and blue (decreased ktrans); (d) Scatter plots of three classes of voxels.

(e) to (h): The voxel-wise Ktrans analysis for a sub-optimal responder (30% tumor necrosis percentage). (e)Voxel-wise Ktrans colormap at TP1; (f)Voxel-wise Ktrans colormap at TP2; (g)Voxel-wise Ktrans map of three classes of voxels depicted as red (increased Ktrans), green (no change beyond 95% confidence intervals), and blue (decreased ktrans); (h)Scatter plots of three classes of voxels.

The areas under the curve (AUC) values and P-values of the ROC analysis.

Biomarkers	AUC	P
F_+	0.556	0.782
F_0	0.852	0.079
F_-	0.889	0.052
$\Delta size$	0.556	0.782
mean ΔK^{trans}	0.815	0.116

Conclusion: The results suggest that F_0 and $F_-$are more sensitive to early therapy response compared, which could provide the early prediction of treatment outcome while retain spatial localization of heterogeneous response to treatment in sarcoma.

EP-1851

Quantitative assessment of glucose metabolic rate within NSCLC histologies using dynamic 18F-FDG PET

T. Meijer[1], D. Vriens[2], M. Looijen-Salamon[3], E. Visser[4], L.F. De Geus-Oei[2], J. Bussink[1]

[1]Radboud University Medical Center, Radiation Oncology, Nijmegen, The Netherlands

[2]Leiden University Medical Center, Nuclear Medicine, Leiden, The Netherlands

[3]Radboud University Medical Center, Pathology, Nijmegen, The Netherlands

[4]Radboud University Medical Center, Nuclear Medicine, Nijmegen, The Netherlands

Purpose or Objective: Biological behavior differs between histologies of non-small cell lung cancer (NSCLC). Tumour biology and glucose metabolism influence radiosensitivity. The first goal of this study is to calculate glucose metabolic rate constants k1 (glucose transporter (GLUT) influx), k2 (GLUT efflux), k3 (hexokinase phosphorylation) and blood volume (VB) in adeno- versus squamous cell NSCLC using dynamic 18FDG PET. Heterogeneity of these parameters will be assessed within different tumour regions. This will improve understanding tumour biology and potentially form the basis for dose modifications in radiotherapy.
Besides 18FDG PET as a tool indicating radioresistant tumour areas, PET may be used for tumour delineation in radiotherapy planning. Manual tumor delineation of stage III NSCLC for radiotherapy planning takes a lot of effort. The second objective of this study is to correlate tumour dimensions obtained by thresholds of standardized uptake value (SUV; static PET), metabolic rate of glucose (MRglu; dynamic PET) with pathological data. The most appropriate method may quicken tumour delineation for radiotherapy planning.

Material and Methods: Patients with curatively resected NSCLC were included in this prospective study (n=35). Dynamic 18FDG-PET scans were acquired during 60 minutes. Patlak analyses using the data acquired between 15-60 minutes post-injection were performed to calculate parametric images of MRglu. The last time frame was used as static PET scan. Tumour volumes were delineated using 50% of maximum, 40% of maximum above background and FLAB algorithm. Maximum SUV (SUVmax) and maximum MRglu (MRglu;max) were calculated. In on-going analysis, volumes acquired by the segmentation methods are correlated with pathology volumes to determine the optimal delineation method for NSCLC. Within the most appropriate method, pharmacokinetic rate constants k1, k2, k3, VB are currently being calculated using an irreversible two-compartment model.

Results: Initial results showed that SUVmax was higher in squamous cell NSCLCs versus adenocarcinomas (median 17.8 (9-33) versus 11.6 (6-32) respectively, p=0.002). Also the MRglu;max was higher in squamous cell carcinomas (median 462.6 nanomol/min/g (266.4-1366.2) versus 301.5 (129.7-1096.5) respectively, p=0.004).
Static volumes were larger compared to the dynamic volumes (p<0.001). Applying FLAB algorithm on static PET resulted in the largest volumes (p<0.001).

Conclusion: These preliminary data support differences in glucose metabolism between adeno- and squamous cell NSCLC. In the ongoing analyses, metabolic rates of glucose will be studied in more detail and will be correlated to survival. Furthermore, tumour volumes acquired by several segmentation methods will be correlated with pathology volumes to determine the optimal delineation method. This optimal segmentation method may aid in radiotherapy delineation.

EP-1852

Predictive role of FDG-PET/CT image-derived parameters in locally advanced oropharyngeal cancer

S. Broggi[1], I. Dell'Oca[2], C. Fiorino[1], E. Incerti[3], M. Picchio[3], M.L. Belli[4], P. Mapelli[3], A. Chiara[2], N. Di Muzio[2], G.M. Cattaneo[1], R. Calandrino[1]

[1]IRCCS San Raffaele Scientific Institute, Medical Physics, Milano, Italy

[2]IRCCS San Raffaele Scientific Institute, Radiotherapy, Milano, Italy

[3]IRCCS San Raffaele Scientific Institute, Nuclear Medicine, Milano, Italy

[4]University of Milan, Medical Physics Specialization School, Milan, Italy

Purpose or Objective: To investigate the predictive role of FDG-PET/CT image-derived parameters in patients with locally advanced oropharyngeal cancer undergoing IMRT, by

means of helical tomotherapy (HTT), with a simultaneous integrated boost (SIB) on FDG-positive volumes (BTV).

Material and Methods: 41 patients (median age: 60; range: 41-81) treated between November 2005 and April 2014 at our Institution for advanced squamocellular oropharyngeal disease were analyzed. Most of the patients (95%) were of stage III-IV; 38 patients had positive lymph nodes (N, 32 with more than one N). HTT was delivered with a SIB approach in 30 fractions at different dose levels, concomitantly: 69 Gy (2.3 Gy/day) to FDG-positive volumes (primary tumor (T) and N), 66 Gy (2.2 Gy/day) to the tumor volume and enlarged nodes and 54 Gy (1.8 Gy/day) to the subclinical and elective treated nodes. PET metabolic parameters of FDG-positive volumes (T, N and T+N), including maximum and mean standardized uptake value (SUVmax and SUVmean), metabolic tumor volume (MTV) estimated at different thresholds 40-50-60% (MTV-40, MTV-50, MTV-60) and total lesion glycolysis (TLG-40, TLG-50, TLG-60) were considered. BTV volumes for T (BTV-T), N (BTV-N) and T+N (BTV-T+N) were also considered. Log rank univariate and Cox regression multivariate analysis were used to evaluate prognostic values of PET derived parameters and cancer specific overall survival (CSOS), local recurrence-free survival (LRFS) and loco-regional recurrence –free survival (LNRFS). The best cut-off values of PET derived parameters discriminating between patients with/without death/relapse were assessed by ROC analysis.

Results: The median follow-up was 37 months (range: 3-125 months). The 3-year CSOS, LRFS and LNRFS were 88.5%, 85% and 80%, respectively. At univariate analysis MTV-T-60>4.4cc was found the most significant PET parameter correlated to CSOS (HR: 0.09, p=0.0078), LRFS (HR: 0.07, p=0.0017) and LNRFS (HR: 0.16, p=0.01). TLG-T-60, SUVmean(T+N), MTV-T+N-60 were also found to be correlated with CSOS and LRFS. At multivariate analysis BTV-T+N>30.9cc and MTV-T-60>4.4cc were found the variables most significantly correlated with CSOS (AUC: 0.885; 95%CL: 0.739-0.965). MTV-T-60>4.4cc confirms its independent predictive role for LRFS (AUC: 0.807; 95%CL: 0.647-0.917) and for LNRFS (AUC: 0.744; 95%CL: 0.577-0.872).

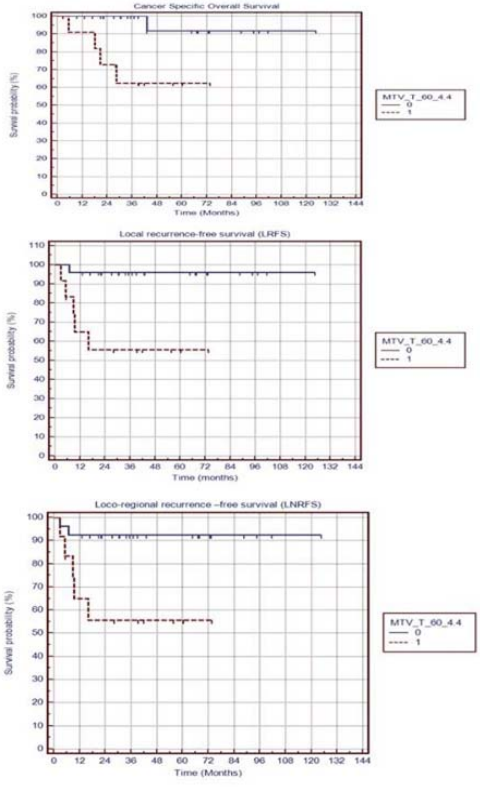

CCOS, LRFS and LNRFS according to MTV_T_60>4.4cc and MTV_T_60≤ 4.4cc

Conclusion: FDG PET/CT performed as guide for HTT SIB treatment in patients affected by advanced oropharyngeal cancer is predictive of patient's outcome. MTV-T-60 was found the best predictor for CSOS, LRFS and LRNFS. FDG-PET/CT image-derived parameters might be useful to select more personalized treatment strategies.

EP-1853

Correlation between biomarkers derived from PET/CT and diffusion-weighted MRI in esophageal cancer

L. Goense[1], P.S.N. Van Rossum[1], I.M. Lips[1], S.E. Heethuis[1], A.H.M.W. Van lier[1], M.G.E.H. Lam[2], A.N. Kotte[1], M. Van Vulpen[1], R. Van Hillegersberg[3], J.P. Ruurda[3], G.J. Meijer[1]
[1]*UMC Utrecht, Radiotherapy, Utrecht, The Netherlands*
[2]*UMC Utrecht, Radiology and Nuclear Medicine, Utrecht, The Netherlands*
[3]*UMC Utrecht, Surgery, Utrecht, The Netherlands*

Purpose or Objective: Both the standardized uptake value (SUV), acquired by 18F-flurodeaxyglucose positron emission tomography/computed tomography (18F-FDG PET/CT), and the apparent diffusion coefficient (ADC) acquired by diffusion-weighted magnetic resonance imaging (DW-MR) are well established measures for treatment response assessment in neoadjuvant esophageal cancer treatment. However, these functional imaging parameters may refer to different aspects of tumor pathophysiology. Currently it is unclear whether these two prognostic biomarkers provide similar information or represent independent biomarkers. Therefore the aim of this study was to evaluate the correlation between SUV and ADC measurements in untreated esophageal tumors.

Material and Methods: This prospective study included 33 patients with histologically proven esophageal cancer who underwent 18F-FDG PET/CT and DW-MR examinations within 3 weeks before therapy. Tumor glucose metabolism was evaluated by the maximum and mean SUV (SUVmax and SUVmean) on the 18F-FDG PET/CT images. Minimum and mean ADC values (ADCmin and ADCmean, calculated with b values of 0,200 and 800 s/mm2) were measured in the same lesions. Lesions with a diameter larger than 3 cm were matched and a voxelwise analysis of ADC and SUV was performed. Spearman's rank correlation coefficients were used to assess the correlation between 18F-FDG PET and ADC metrics. Also the tumor ADCmean and SUVmax was compared between squamous cell carcinomas and adenocarcinomas, and between moderately and poorly differentiated tumors.

Results: Mean ADCmean and ADCmin of the 33 included esophageal cancer tumors were 1.8 ± 0.4 and 0.8 ± 0.4, *10-3mm2/s, respectively. Mean SUVmean and Mean SUVmax were 8.3 ± 4.2 and 17.4 ± 9.6, respectively. The SUV and ADC values as measures of glucose metabolism and cell density, respectively, showed weak to very weak non-significant correlations only (ADCmin vs SUVmax; r=0.30, p=0.09], [ADCmin vs. SUVmean r=0.30 p=0.09], [ADCmean vs SUVmax r=0.17 p=0.36], [ADCmean vs SUVmean r=0.14 p=0.43]) (Figure 1). The voxel-wise analysis of 16 esophageal tumors with diameters larger than 3 cm showed a weak but significant negative correlation between ADC and SUV in 11 patients. ADCmean was significantly related to histological tumor grade (2.0 ± 0.3 in moderately differentiated tumors vs. 1.6 *10-3mm2/s in poorly differentiated tumors (p=0.014)). No difference between squamous cell carcinoma and adenocarcinoma was found. SUVmax showed no differences with regard to tumor type and differentiation grade.

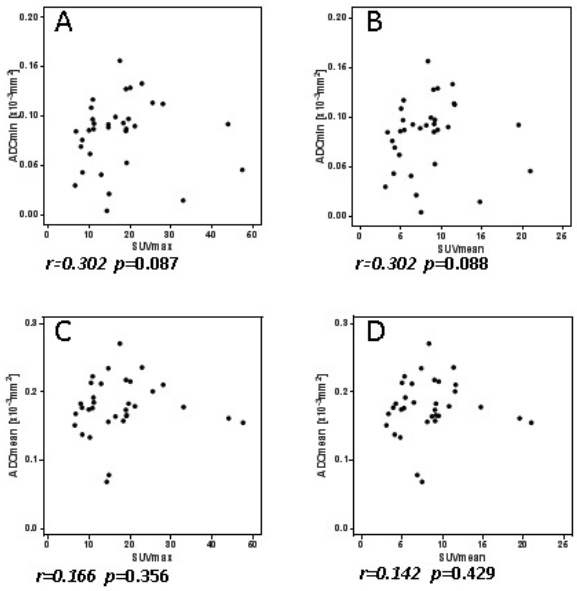

Figure 1: Scatter plots of SUVs and ADC values from 33 esophageal cancer tumors. **A:** Scatter plot of ADC_{min} vs. SUV_{max}. **B:** Scatter plot of ADC_{min} vs. SUV_{mean}. **C:** Scatter plot of ADC_{mean} vs. SUV_{max}. **D:** Scatter plot of ADC_{mean} vs. SUV_{mean}.

Conclusion: This study indicates that both glucose metabolism measured by PET/CT and restriction measured by DW-MR are independent cellular phenomena in newly diagnosed esophageal cancer. Therefore, SUV with ADC values may have complementary roles as imaging biomarkers in the evaluation of survival and response to neoadjuvant treatment in esophageal cancer.

EP-1854

Mammographic texture features for determination breast cancer molecular subtype

M. Arenas Prat[1], L. Díez-Presa[1], J. Torrents-Barrena[2], M. Arquez[1], C. Pallas[1], M. Gascón[1], M. Bonet[1], A. Latorre-Musoll[3], S. Sabater[4], D. Puig[2]

[1]*Hospital Universitari Sant Joan de Reus, Radiation Oncology, Reus, Spain*

[2]*University Rovira i Virgili, Computer Science and Mathematics, Tarragona, Spain*

[3]*Hospital de la Santa Creu i Sant Pau, Physics, Barcelona, Spain*

[4]*Complejo Hospitalario Universitario, Radiation Oncology, Albacete, Spain*

Purpose or Objective: To determine molecular subtypes of breast cancers using texture-feature-driven machine learning techniques on mammographic images.

Material and Methods: We used mammograms of 61 ductal carcinomas (grade 2-3, median age 60, mean tumor size 28mm). A physician defined a 100x100 ROI around tumors on mammographic images. Extraction of texture features was performed using three independent descriptors: Local Binary Patterns (LBP), Histogram of Oriented Gradients (HOG) and Gabor Filter (GF). Then, a supervised classification was applied using two independent classifiers: K-Nearest Neighbors (KNN) and Support Vector Machines (SVM) (both linear- and radial-type). Both classifiers were trained to identify the molecular subtype (Luminal A, Luminal B (Her2-), Luminal B (Her2+), Her2+, Basal Like and carcinoma in situ) using the first 38 mammograms. We assessed the accuracy of our machine learning technique using the last 23 mammograms.

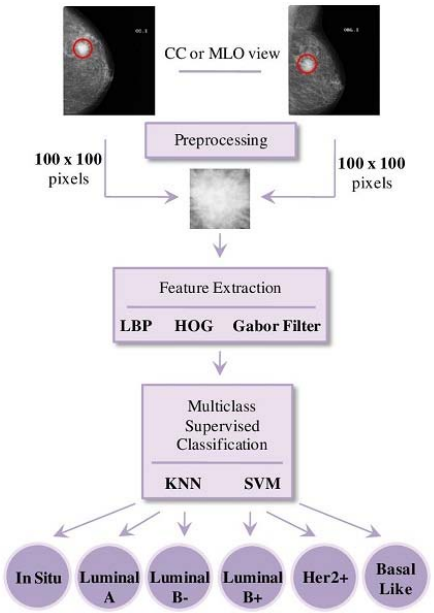

Results: Accuracy of SVM-R classifier was 52% irrespective of the texture descriptor we used. SVM-L/KNN classifiers achieved an accuracy of 48/39, 35/30 and 21/35% for LBP, HOG and GF descriptors. When simplifying the classification problem to only two subtypes, Luminal A and Luminal B (Her2-), classifier accuracies astonishingly improved. SVM-R accuracy was 75% irrespective of the texture descriptor and SVM(L)/KNN accuracies were 38/75, 50/50 and 63/75% for LBP, HOG and GF.

Conclusion: Our texture-feature-driven machine learning technique provides a reliable classification into molecular subtypes using mammographic images only. Accuracy improves when simplifying to only two subtypes. We expect even better accuracies by increasing the number of patients used for the training stage of our machine learning technique.

EP-1855

Computed Tomography lung texture changes due to radiotherapy for non-small cell lung cancer

J. Chalubinska-Fendler[1], W. Fendler[2], Ł. Karolczak[3], C. Chudobiński[4], J. Łuniewska-Bury[5], A. Materka[3], J. Fijuth[1]

[1]*Medical University of Lodz, Radiotherapy Department- Chair of Oncology, Lodz, Poland*

[2]*Medical University of Lodz, Department of Pediatrics-Oncology- Hematology and Diabetology, Lodz, Poland*

[3]*Lodz University of Technology, Institute of Electronics, Lodz, Poland*

[4]*Regional Oncological Centre- Lodz, Radiology Department, Lodz, Poland*

[5]*Regional Oncological Centre- Lodz, Brachytherapy Department, Lodz, Poland*

Purpose or Objective: Radiation induced lung toxicity (RILT) may occur in 5-20% of patients irradiated due to Non-Small Cell Lung Cancer (NSCLC) but may be asymptomatic during the course of radiotherapy (RTx). Computed tomography (CT) image changes induced by RILT present after 3-9 months since RTx, mostly as lung fibrosis. Early changes on lung tissue image, i.e. during treatment, are not possible to diagnose by the naked eye, but could be detect by computer-assisted texture analysis.

Material and Methods: Fifteen patients aged 63.7+/-6.4 years, with NSCLC undergoing RTx were tested using CT before RTx and after receiving 40Gy of dose prescribed to PTV. Images were entered into a texture analysis program – MaZda® which extracted 284 texture parameters based on: signal intensity, variability of signal intensity, autocorrelation, direction of change, Fourier spectrum, Wavelet spectrum and repeatability of intensity change patterns. From every patient 10 regions of interest (ROIs)

were extracted (see image) at both timepoints from two sections of lung tissue – one that received the highest planned dose in healthy tissue and one that received low or no dose of RTx. Linear discriminant analysis (LDA) with 5-fold cross-validation and backward stepwise selection of variables was used to construct best classification models to separate irradiated from non-irradiated regions of the lung and differentiation of patients with RILT and without.

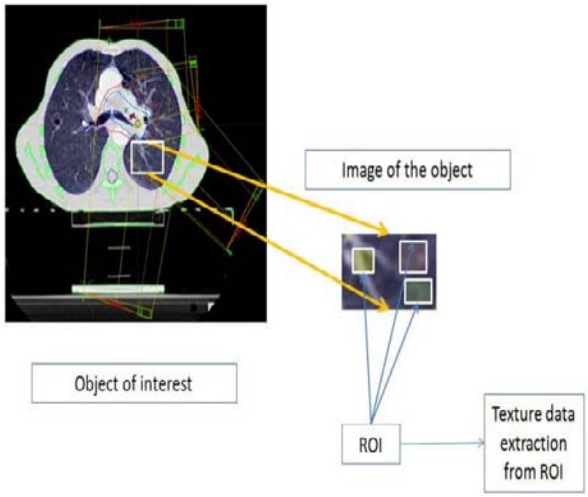

Results: LDA based on seven parameters allowed for differentiation (area under the ROC curve 0.86) of regions of healthy tissue and regions from tumour's site. The 7 variables were Wavelet-transform functions of different frequencies. However, despite those differences, CT-images from the 40Gy timepoints differed significantly depending on the received dose. An LDA model based on six parameters (3 autocorrelation functions, kurtosis and 2 wavelet function parameters) differentiated non-irradiated regions from irradiated ones – ROC AUC 0.89 (95%CI 0.75-1.00). Preliminary data from follow up showed that patients in whom RILT developed (N=7) could be differentiated from those free from complications (ROC 0.96 95%CI 0.89-1.00). However, parameters used in this LDA-based classifier relied on CT texture parameters extracted from both irradiated and non-irradiated ROIs, making ROI selection a crucial part of the texture analysis process.

Conclusion: Texture of CT-scans contains enough information to detect RTx-induced changes, although the method may be affected by pretreatment differences, which necessitates a robust placement of ROIs for analysis.

EP-1856

Predictive factors based on textural features – reliability of patient classification

T.L. Jacobsen[1], U. Bernchou[2], T. Schytte[3], O. Hansen[3], C. Brink[2]

[1]*University of Southern Denmark, Department of Physics-Chemistry- and Pharmacy, Odense, Denmark*

[2]*Odense University Hospital, Laboratory of Radiation Physics, Odense, Denmark*

[3]*Odense University Hospital, Department of Oncology, Odense, Denmark*

Purpose or Objective: Textural analysis of lung tumors in PET or CT images is currently of interest in a number of publications e.g. to predict overall survival after radiotherapy. Given that tumor volume is a known independent predictor in radiotherapy of lung cancer, a textural feature must be volume independent to gain independent predictive power. Furthermore, the feature value should be stable against small variations in the delineated tumor volume. This study analyses how changes in PET based tumor volume and delineation affect different published textural features.

Material and Methods: PET delineated tumors for 158 NSCLC patients were used to calculate textural features as proposed by Amadasun et al [IEEE Trans. Syst., Man, Cybern., Syst. 1989]. Delineations of the tumors were made semi-automatically based on EANM guidelines for VOI41 and VOI50 (delineation at the 41% and 50% level of SUVmax). Additional smoothened delineations were made to resemble delineations made by humans. Furthermore, dilated versions of VOI41 were analyzed to determine the response of the textural features to large changes in delineation. Textural features are typically used to divide a patient population in two groups based on a given textural cut-value, e.g. the median value. Thus, the textural feature should preferably be stable towards small delineation variations in terms of patient classification. Such stability was tested using ROC curves, in which the initial delineation (VOI41) was used as ground truth classification based on the median value. Volume dependence of the textural features was assessed through the Spearman correlation coefficient.

Results: Coarseness, busyness, contrast, and complexity were all confirmed to have a significant correlation with volume (absolute Spearman > 0.58). The figure shows coarseness' ability to classify the patients consistently for different delineations. The large area under the ROC curve (almost unity) between VOI41, VOI50, and the smoothed VOI, shows that the patient classification is almost independent of small variations of delineation. The figure also shows how successive dilations of tumor volume reduce the area under the curve. Similar findings were observed for the textures busyness and contrast. A mathematical examination of the textural features provided an easy way to correct for the volume dependence of coarseness and contrast. Neither of these modified versions was found to have volume dependence (absolute Spearman < 0.22); while at the same time having the same stability characteristic as their original versions.

Conclusion: All original textures had strong correlation with volume, which for PET delineation of lung tumors could be a confounding factor within a textural predictor. Through small changes to the original definition it is possible to make coarseness and contrast volume independent; a property which is needed for the features to be used as independent predictive factors.

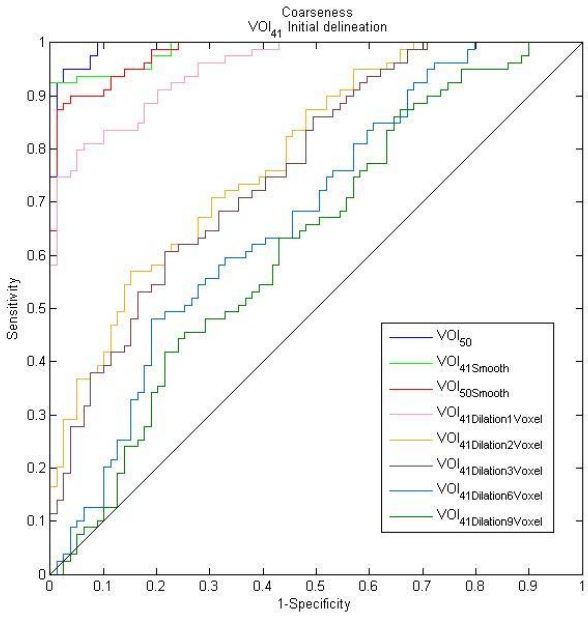

EP-1857

Multi-parametric MRI at 3.0 Tesla for the prediction of treatment response in rectal cancer

T. Pham[1,2,3], G. Liney[1,4,5], K. Wong[1,2,3], D. Roach[6], D. Moses[2,7], C. Henderson[2,8,9], M. Lee[1], R. Rai[1], M. Barton[1,2,3]

[1]*Liverpool Cancer Therapy Centre- Liverpool Hospital, Radiation Oncology, Sydney, Australia*
[2]*University of New South Wales, Faculty of Medicine, Sydney, Australia*
[3]*Ingham Institute for Applied Medical Research, Collaboration for Cancer Outcomes Research and Evaluation CCORE, Sydney, Australia*
[4]*Ingham Institute for Applied Medical Research, Medical Physics, Sydney, Australia*
[5]*University of Wollongong, Faculty of Radiation and Medical Physics, Wollongong, Australia*
[6]*University of Sydney, Faculty of Physics, Sydney, Australia*
[7]*Princes of Wales Hospital, Department of Radiology, Sydney, Australia*
[8]*Western Sydney University, Faculty of Medicine, Sydney, Australia*
[9]*Liverpool Hospital, Department of Anatomical Pathology, Sydney, Australia*

Purpose or Objective: The purpose of this study was to prospectively evaluate the role of quantitative diffusion weighted imaging (DWI) and dynamic contrast enhanced (DCE) imaging used in combination for multi-parametric MRI prediction of treatment response in rectal cancer.

Material and Methods: This study used a voxel-by-voxel multi-parametric histogram analysis strategy to assess tumour heterogeneity and its changes in response to chemoradiotherapy (CRT). Twenty patients with locally advanced rectal cancer undergoing neoadjuvant CRT prospectively underwent MRI on a 3T wide bore Siemens Skyra at 3 time-points: Pre-CRT, week 3 CRT, and post-CRT. The study protocol consisted of: (i) T2-weighted images (ii) DWI using RESOLVE, which was previously shown to be robust with respect to geometrical distortions. Images were acquired with b-values 50 and 800s/mm2 and 1 & 3 averages. ADC maps and calculated b=1400s/mm2 images were produced as part of protocol (iii) DCE consisted of pre-contrast VIBE scans with flip angles 2° and 15° in order to calculate native T1, followed by gadoversetamide (0.1mM/kg) injection and 60 phases using TWIST with a 5s temporal resolution. ADC and Ktrans parameter maps were registered to T2-weighted images. Semi-automated segmentation was used to define the volume of interest from hyperintense tumour on the b-value=1400 images. A voxel-by-voxel technique was used to produce colour coded histograms of ADC and Ktrans, as well as combined scatterplots and difference histograms for each time-point. CRT response was defined according to histopathology tumour regression grade (TRG) (AJCC 7th Edition). A complete protocol and analysis strategy was successfully developed which has utilized commercial, in-house developed and works-in-progress (Siemens OncoTreat) software.

Results: Of 20 patients, 1 had clinical stage T2N2M0, 5 had T3N0M0, 4 had T3N1M0, 7 had T3N2M0, and 3 had T4N2M0. Eight patients had a good response (TRG0-1) and 11 patients had a poor response (TRG2-3) to CRT. Pathology for 1 patient is pending. We found the calculated b-value=1400 images useful for visualization of tumour. In good responders, the week 3 histograms and maps showed both a shift in distribution of ADC of pixels to higher values and Ktrans of pixels to lower values compared to the pre-CRT histogram. Figure 1 shows results for a good responder who had histologic TRG 1. The figure shows voxel-by-voxel combined scatterplots and colour coded ADC and Ktrans histograms side by side for pre-CRT (top panel), week 3 CRT (middle panel) and post-CRT (bottom panel).

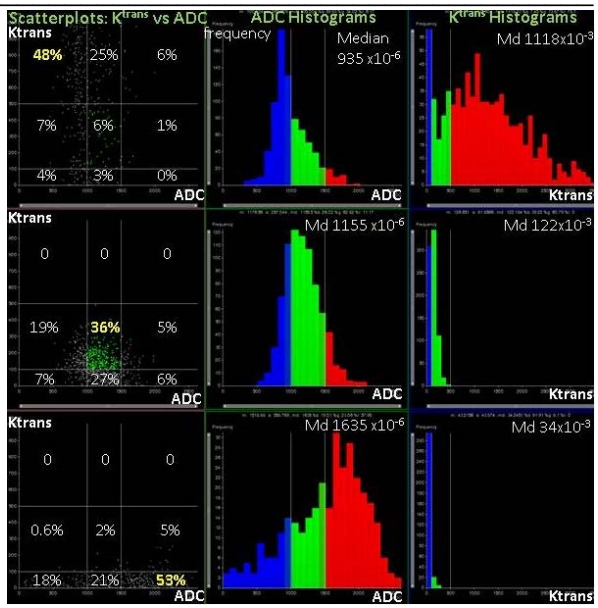

Conclusion: Multi-parametric histogram analysis of ADC and Ktrans appears to be a promising and feasible method of assessing tumour heterogeneity and its changes in response to CRT in rectal cancer.

EP-1858

Variation of apparent diffusion coefficient in penile bulb after radiotherapy

P. Volonghi[1], E. Scalco[1], T. Rancati[2], A. Messina[3], E. Pignoli[4], A. Cicchetti[2], B. Avuzzi[5], D. Bosetti[5], R. Valdagni[2,5], G. Rizzo[1]
[1]*CNR, Institute of Molecular Bioimaging and Physiology, Segrate, Italy*
[2]*Fondazione IRCCS Istituto Nazionale dei Tumori, Prostate Cancer Program, Milano, Italy*
[3]*Fondazione IRCCS Istituto Nazionale dei Tumori, Radiology, Milano, Italy*
[4]*Fondazione IRCCS Istituto Nazionale dei Tumori, Medical Physics, Milano, Italy*
[5]*Fondazione IRCCS Istituto Nazionale dei Tumori, Radiation Oncology 1, Milano, Italy*

Purpose or Objective: Functional imaging is widely used to evaluate the response to radiotherapy (RT) in patients with prostate cancer. In particular, variations of Apparent Diffusion Coefficient (ADC) are normally evaluated in the prostate (benign and malign zones), but organs at risk are usually not considered. The aim of our work was to investigate the changes of ADC values after RT and to correlate them to the dose in the penile bulb, as an organ which is considered to have an impact on sexual function toxicity.

Material and Methods: Twelve patients with prostate cancer treated with RT were considered. Diffusion-weighted MRI (DWI) images were acquired using four different b values (0, 150, 800 and 1000 s/mm²) at 1.5T before and after RT. A VOI-based approach was used to estimate ADC, considering the contours of the penile bulb as delineated by a radiotherapist (on T2-weighted MRI images). Specifically, for each b-value, the mean signal intensity in the bulb was calculated and the exponential model was fitted to these averaged values using linear regression algorithm. The patient set can be divided in two groups according to the time distance between the end of RT and the post-treatment DWI acquisition: A) patients with DWI acquired in acute phase (5 subjects, range of 6-15 days after the end of RT), B) patients with DWI acquired in non-acute phase (7 subjects, range of 76-179 days). Correlation of ADC variations with timing of post-RT DWI and mean dose to the penile bulb (corrected for fractionation using the linear-quadratic model and alpha/beta=3Gy) were investigated with linear regression analysis.

Results: Before RT, the ADC values were comparable for all patients. Considering group A, the mean ADC value before RT was 1.24 x10^(-3) mm²/s, lower than the ADC after RT (1.38 x10^(-3) mm²/s) (Figure 1). Moreover, an increase in mean dose to the penile bulb corresponded to higher variations of ADC ($p<0.05$, Table 1). On the contrary, in group B, the mean ADC values remained almost unchanged (1.22 x10^(-3) mm²/s before RT, 1.20 x10^(-3) mm²/s after RT) (Figure 1); nevertheless, the linear regression analysis showed an ADC decrease tendency depending on time, as highlighted by the negative correlation between ADC changes and the amount of days after RT ($p<0.05$, Table 1).

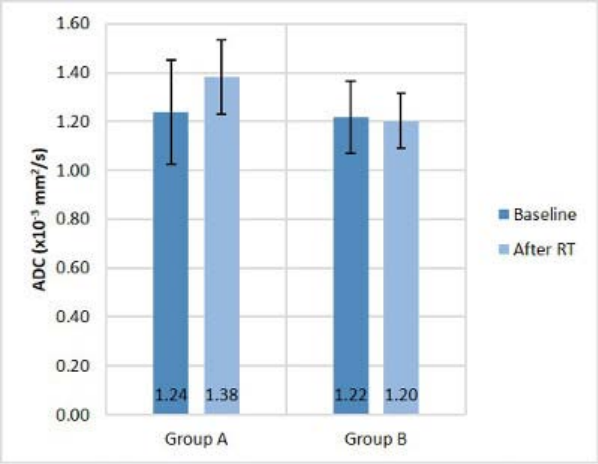

Figure 1. Mean ADC values in group A (mean time distance between end of RT and post-DWI: 9.2 days) and group B (mean time distance: 120 days).

Table 1. Results for linear regression correlation (R squared and p values), between ADC changes and mean dose to the penile bulb/days from RT completion and DWI acquisition (Timing). Results are reported for the two patient groups described in the text.

	Group A		Group B	
	R^2	p	R^2	p
Timing	0.02	0.83	0.60	0.04
Mean dose	0.90	0.01	0.10	0.48

Conclusion: In patients with DWI acquired early after RT completion, ADC value in penile bulb increased and its increment was correlated with higher mean dose to the penile bulb; this behavior could be explained by the inflammatory status that normally follows RT. The group of patients acquired at least three months after RT, on average, didn't show a difference in ADC value, but it was observed that increasing time from RT completion was correlated with decreasing of ADC values. This can be possibly explained by a physiological resolution of the inflammation phase and the possible beginning of fibrosis. These preliminary results obviously need confirmation in a larger population.

EP-1859

Tumor control assessment on cervical lymph nodes using texture analysis on CT and T2w-MRI images

E. Scalco[1], S. Marzi[2], A. Vidiri[3], G. Sanguineti[4], A. Farneti[4], G. Rizzo[1]

[1]*CNR, Institute of Molecular Bioimaging and Physiology IBFM, Segrate Milano, Italy*

[2]*Regina Elena National Cancer Institute, Medical Physics Laboratory, Rome, Italy*

[3]*Regina Elena National Cancer Institute, Radiology and Diagnostic Imaging Department, Rome, Italy*

[4]*Regina Elena National Cancer Institute, Department of Radiotherapy, Rome, Italy*

Purpose or Objective: To investigate whether structural patterns of cervical lymph nodes (LNs) on CT and T2-weighted Magnetic Resonance (T2-w MR) images, using texture analysis, predict tumor control to chemo-radiotherapy (CRT) of head and neck squamous cell carcinoma (HNSCC).

Material and Methods: 14 patients with pathologically confirmed HNSCC treated with CRT were considered. All patients underwent two serial MR examinations (including T2-w images), one before (MR1) and one mid-CRT (MR2). All slices containing pathologic LNs were manually contoured by a dedicated HN radiologist both MR studies; in addition, LNs on MR1 were automatically deformed on planning CT (plCT) by an elastic registration method. Seventeen volumetric and textural features were then extracted from MR1, MR2 and the plCT: volume-based indices (volume, orientation, eccentricity, equivalent diameter), histogram-based indices (mean intensity, variance, entropy, skewness, kurtosis), GLCM (Grey-Level Co-occurrence Matrix)-based indices (energy, ASM, correlation, homogeneity, entropy, contrast, dissimilarity) and fractal dimension. During at least 1 year of follow-up (median follow-up time, 2 years) 9 LNs were classified as being controlled (without evidence of disease during follow-up on MRI and PET-CT) and were labeled ad RC LNs; 7 LNs were classified as having regional failure (pathology proven residual tumor at neck dissection after CRT or during the follow up) and were labeled as RF LNs. Both pre-treatment features (MR1 and plCT) and mid-treatment features (MR2 and differences between MR1 and MR2) were considered to discriminate between RC and RF. The classification analysis was performed using Fisher's linear discriminant analysis and the accuracy was estimated using the leave-one-out approach.

Results: Box-and-whisker plots of the features with higher classification accuracy in the two groups are reported in Figure 1. In general, pre-RT features had a higher discriminative power than mid-treatment parameters. Entropy measured on CT (93.8%) reached the best accuracy, with higher values of entropy related to RF LNs. The best parameter of MR1 was kurtosis (accuracy=81.3% with higher values for RC LNs). Half-way through RT, the best indices were skewness for MR2 (accuracy=78.6% with higher values for RC LNs) and the variation in contrast (accuracy=71.4% with higher positive variations for RF LNs).

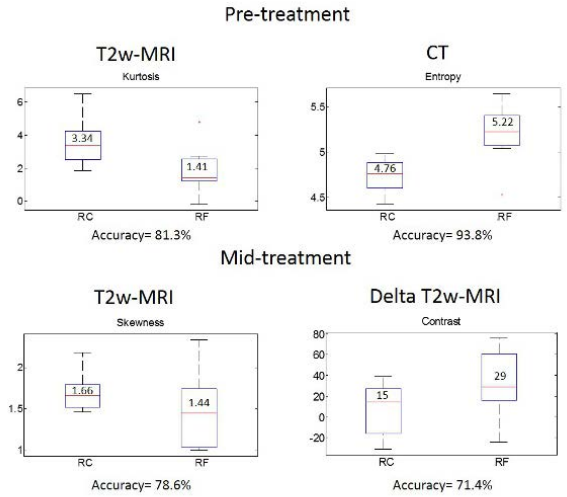

Figure1. Boxplot of the best features for each acquired image. Median value in the group and classification accuracy were reported

Conclusion: Our preliminary results show that RC LNs have a lower CT entropy and higher MR1 kurtosis, suggesting that more homogeneous LNs before treatment may better respond to CRT, probably due to limited areas of necrosis and hypoxia. Pre-RT features had a higher discriminative power over mid-treatment ones, probably due to transitory inflammatory processes masking and confounding MR2

parameters regardless response. Texture analysis on T2w and CT images could be effective in tumor control assessment and warrants further investigation.

EP-1860

PET/MR in radiation oncology – how to correct for attenuation caused by flat table top?

P. Andrzejewski[1], S. Witoszynskyj[2], I. Rausch[3], M. Hacker[2], D. Georg[1], B. Knäusl[1]

[1]Medical University Vienna, Department of Radion Oncology and Christian Doppler Laboratory for Medical Radiation Research for Radiation Oncology, Wien, Austria

[2]Medical University Vienna, Department of Biomedical Imaging and Image-guided Therapy- Div. of Nuclear Medicine, Vienna, Austria

[3]Medical University Vienna, Center for Medical Physics and Biomedical Engineering-, Vienna, Austria

Purpose or Objective: The implementation of hybrid PET/MR scanners overcame the issues of PET-MR images registration, which proved to carry complementary information useful in many aspects of RT. However it introduced new challenges. To assure the same patient positioning during imaging and RT, dedicated MR-compatible flat table tops (FTT) are required. While these FTT cause attenuation and scatter which do not play a role in MR scanners, PET image quality (IQ) is significantly degraded. The goal of this study was to evaluate the impact of a FTT on PET IQ and to introduce a correction method.

Material and Methods: PET images of a 12l cuboid canister and round cylinder filled with 40 MBq 18F-FDG in an aqueous solution; 0.9% NaCl and 0.2mmol/l Gd-DO3A-butrol as well as a modified NEMA phantom (all spheres of 11.3ml volume), filled with 18F-FDG in 8:1 activity ratio were acquired in both a Biograph TrueV PET/CT and a Biograph mMR PET/MR (Siemens). Measurements were performed with and without the presence of the FTT (X-tend ApS). A transmission scan (PET-TS) of the FTT was performed in a GE Advance PET with an inbuilt 68Ge/68Ga source. MR markers visible in PET were used for coregistration. An attenuation map (μMap) was derived from PET-TS and additionally used for PET(/MR) image reconstruction. Activities measured in the spheres of the NEMA phantom and longitudinal activity profiles in the cylinder were compared between PET/CT and PET/MR images acquired with scanner inbuilt attenuation correction (AC) methods. Canister images were evaluated by computing the uniformity index (UI) using a sliding window approach with a 5x5 voxel ROI (0.8ml volume) on slice-by-slice basis. Advantages of the use of PET-TS were compared to standard correction methods.

Results: The (MAX-MIN)/AVR ratios of the mean activity measured in the six spheres of the modified NEMA phantom were as follows (without and with the FTT, respectively): in PET/CT 1.7% and 6.2%; in PET/MR 2.6% and 6.8%. The longitudinal activity profiles measured in the cylinder are shown in the Figure (A-B). The best IQ was found in PET/CT without FTT. Compared to these images, PET/MR images were degraded. PET/CT with FTT exhibited attenuation artefacts. In PET/MR scans both scatter and attenuation artefacts were observed. IQ was significantly improved by the use of FTT's PET-TS μMap (cf. Figure C-G).

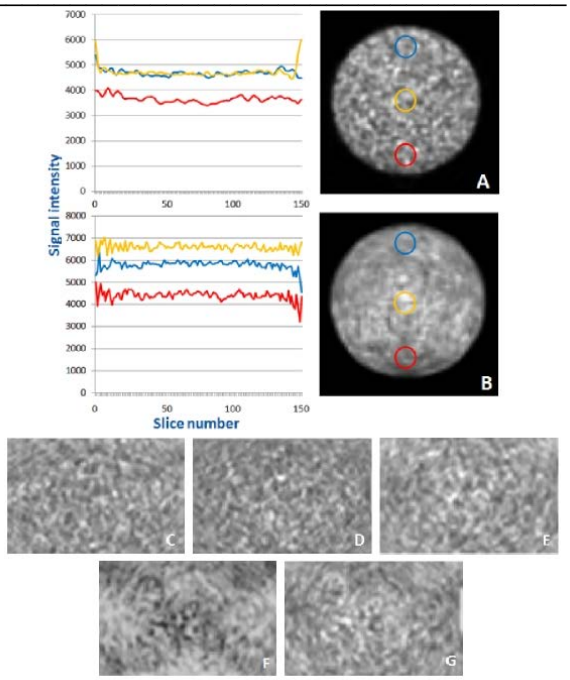

Figure – A-B: activity profiles through a cylindrical phantom positioned on the flat table top; A – images acquired in a PET/CT scanner, B – images acquired in a PET/MR scanner. The measured activity dropped in the proximity of the FTT compared to the cylinder centre by 22.5% in the PET/CT and by 33.2% in PET/MR. Additionally, 12.2% activity deficit was recorded in the top part of the cylinder, in the close vicinity of the phantom's wall. C-D: PET/CT (UI of 17% and 22%) and E-F: PET/MR (UI of 25% and 46%) images acquired without and with FTT, respectively. The attenuation correction was based on respective CT or MR images acquired in the hybrid scan. G: (UI of 26%) depicts a PET/MR-acquired image corrected for attenuation with the PET-TS derived μMap.

Conclusion: The use of the PET-TS derived μMap can reduce artefacts in PET/MR. The deteriorated AC visible in PET/CT images is caused by the transformation from CT attenuation to PET attenuation that is not valid for materials used in the FTT. This proves that CT based AC may not be sufficient to perform AC in PET/MR scanner. Although the UI measure provides an indication of IQ, it is of limited use for evaluating systematic artefacts caused by incorrect AC. Further improvements are currently explored to improve the quality of the PET-TS μMap and to integrate it better into the image reconstruction.

EP-1861

Effect of respiratory motion on extracted textural features in tumour CT images

S. Alobaidli[1], S. McQuaid[2], J. Scuffham[2], C. South[2], A. Nisbet[2], P. Evans[1]

[1]University of Surrey, Department of Electronic Engineering, Guildford, United Kingdom

[2]Royal Surrey County Hospital NHS Foundation Trust, Department of Medical Physics, Guildford, United Kingdom

Purpose or Objective: Texture analysis in CT is dependent on image resolution which is deteriorated by respiratory motion. The aim was to characterize the effect of respiratory motion on the performance of Laplacian of Gaussian (LoG) filters in extracting textural features as they have been shown in the literature to correlate to response and patient survival in non-small cell lung cancer.

Material and Methods: The modulation transfer function (MTF) was calculated in an in-house designed phantom that represents different scales of spatial frequency. This was made of Polymethyl methacrylate (PMMA) with size 131 mm x 121 mm x 30 mm. It had four sections; each with a square lattice of cubes of different sizes to give spatial frequencies (0.08, 0.1, 0.12, 0.166 1/mm). The cubes were filled with a solution of sucrose and high purity water with low (2%), medium (4%), and high (8%) concentration. The phantom was scanned static and moving on a GE discovery CT scanner (GE healthcare, Ohio, USA) with a reconstructed voxel size of 0.98 mm x 0.98mm x 1.25 mm. The phantom was attached to a dynamic thorax phantom (CIRS Company, Virginia, USA) to simulate a respiratory motion of 4 seconds period and a 1.00

cm amplitude. A Fourier Transform (FT) was used to calculate the MTF of the images for the static and moving phantom. The MTF of five commonly used LOG filters were calculated. The response of the filters was compared with the MTF of the images to determine if the motion would affect the response of the filter.

Results: The limiting resolution of the scanner, measured as the spatial resolution where the MTF was reduced to 50% and 10%, was 3.3 mm and 1.6 mm for the static and 6.6 mm and 3.3 mm for the motion acquisition respectively. The limiting resolution for each of the filters with and without motion is presented in Table (1). The results demonstrated a loss of information when using small-size filters due to the limiting resolution of the scanner. Larger-size filters are less affected by motion due to their narrower bandwidth while medium-size filters' limiting resolution appear to cover the range allowed by the scanner MTF when motion is present.

Table 1: The limiting resolution in mm for the scanner and LoG filters

Without Motion						
MTF (mm)	Scanner	Filter 4x4 mm	Filter 6x6 mm	Filter 8x8 mm	Filter 10x10	Filter 12x12
MTF50	3.3	2.8	4.0	5.0	6.2	10.0
MTF10	1.6	1.3	1.8	3.1	5.0	6.6
With Motion						
MTF (mm)	Scanner	Filter 4x4 mm	Filter 6x6 mm	Filter 8x8 mm	Filter 10x10	Filter 12x12
MTF50	6.6	7.1	6.6	6.8	7.7	10.0
MTF10	3.3	3.8	4.2	4.5	5.5	6.6

Conclusion: The results show a substantial decrease in LoG filters performance due to motion. Medium-size filters appeared to cover the frequency range allowed by the combined MTF of the scanner and respiratory motion. Accurate quantification of image texture therefore requires an implementation of motion correction methods.

EP-1862

Impact of 4DPET/CT on normal tissue sparing for SBRT of central lung tumors

S. Adebahr[1,2], D. Schuster[1], R. Wiehle[1], A. Chirindel[1,3], T. Schimek-Jasch[1], T. Fechter[1], M. Mix[4], A.L. Grosu[1], U. Nestle[1,2]
[1]*University Medical Center Freiburg, Department of Radiation Oncology, Freiburg, Germany*
[2]*German Cancer Consortium DKTK, Partner Site Freiburg, Freiburg, Germany*
[3]*PET/CT Centre NW-Switzerland and Claraspital Basel, Nuclear Medicine, Basel, Switzerland*
[4]*University Medical Center Freiburg, Department of Nuclear Medicine, Freiburg, Germany*

Purpose or Objective: In SBRT 4DCT is the standard imaging method for target volume delineation. For SBRT of centrally located lung tumors we have previously reported that the addition of co-registered 4DPET data to 4DCT based target volume increases inter-observer agreement and may help to avoid geographic misses (1). However, it is not clear whether a better depiction of the tumor and demarcation to mediastinal structures translates into relevant normal tissue sparing. Here we compare normal tissue exposure in 4DCT versus 4DPET/CT based SBRT plans.

Material and Methods: For 10 consecutive patients with centrally located lung tumors 4DCT – and 4DPET/CT based internal and respective planning target volumes (PTVs) were generated by 4 contourers (1). SBRT plans were calculated for consensus-PTV structures, prescribing 8x7.5 Gy to the PTV. Planning was optimized likewise for 4DCT and 4DPET/CT plans with respect to dose constraints of the EORTC 22113-08113 Lungtech trial. With respect to DVHs normal tissue exposure of different organs at risk (OARs) is analyzed, normal tissue complication probability (NTCP) and tumor control probability (TCP) are being calculated.

Results: For 6/10 patients with lager 4DPET/CT-PTV than 4DCT-PTV OAR exposure was mainly higher in 4DPET/CT based plans. However, 4/10 patients with smaller 4DPET/CT-PTV than 4DCT-PTV revealed a mostly better sparing of the OARs employing 4DPET/CT and have been further analyzed. Depending on tumor location mean Dose (Dmean) of heart, esophagus, great vessels, main airways, vertebral body, chest wall, lungs-GTV, trachea and spinal cord could be reduced by up to 3.8,1.4, 2.3, 2.9, 2.1, 2.5, 1, 2.1 and 0.8 Gy, respectively when employing additional 4DPET information. Likewise Dmax of the respective OARs could be reduced by up to 2.2, 4.1, 6.3, 3.8, 6.5, 22.1, 0.5, 10.3 and 1.5 Gy, respectively. Differences in the dose distribution of the PTV remained small with ΔDmean and ΔDmax being 0.3 Gy maximum. Preliminary results in TCP and NTCP modeling suggest no difference in TCP for 4DPET/CT versus 4DCT-SBRT plans and a subtle translation into improved NTCP for 4DPET/CT-based plans. For one patient the NTCP of the proximal bronchial tree could be reduced by 25% by employing additional 4DPET information in the planning process.

Conclusion: For SBRT of centrally located tumors the PTVs based on additional information of coregistered 4DPET might translate in a better NTCP for several OARs in comparison to the equivalent 4DCT-based treatment plan, with remaining an equal TCP.

(1)Chirindel A, Adebahr S, Schuster D, et al. Impact of 4D-(18)FDG-PET/CT imaging on target volume delineation in SBRT patients with central versus peripheral lung tumors. Multi-reader comparative study.Radiother Oncol. 2015 Jun;115(3):335-41. Doi: 10.1016/j.radonc.2015.05.019. Epub 2015 Jun 23

EP-1863

Radiomics in the CT perfusion maps – robustness study

M. Nesteruk[1,2], O. Riesterer[1,2], R. Bundschuh[3], P. Veit-Haibach[2,4,5], G. Studer[1,2], S. Stieb[1,2], S. Glatz[1,2], H. Hemmatazad[1,2], G. Huber[2,6], M. Pruschy[1,2], M. Guckenberger[1,2], S. Lang[1,2]
[1]*University Hospital Zurich, Radiation Oncology, Zurich, Switzerland*
[2]*University of Zurich, Faculty of Medicine, Zurich, Switzerland*
[3]*University Hospital Bonn, Nuclear Medicine, Bonn, Germany*
[4]*University Hospital Zurich, Nuclear Medicine, Zurich, Switzerland*
[5]*University Hospital Zurich, Diagnostic and Interventional Radiology, Zurich, Switzerland*
[6]*University Hospital Zurich, Otorhinolaryngeology, Zurich, Switzerland*

Purpose or Objective: Prediction of therapy outcome using radiomics has been a growing field of research in the last few years. The aim of this study was to identify a set of stable texture features computed on CT perfusion (CTP) maps with respect to CTP calculation parameters and image discretization.

Material and Methods: 11 patients with head and neck (HN) cancer and 11 patients with lung cancer who underwent CTP before treatment were included in the study. Software for calculation of the texture features was developed based on 3D definitions of first-order statistical parameters (n = 5), the Gray-Level Co-Occurrence Matrix (n = 14), the Neighborhood Gray Tone Difference Matrix (n = 4), the Gray Level Size Zone Matrix (n = 11) and fractal dimension. In total, 35 texture parameters were computed for three perfusion maps: blood volume (BV), blood flow (BF) and mean transit time (MTT) and their 3D wavelet transforms (n = 8). First, the variability of texture parameters with respect to the image discretization method (set number of bins in comparison to set intervals) was studied using the intraclass correlation (ICC) two-way mixed model. Second the correlations of texture parameters with tumor volume were investigated using Spearman correlation. To further examine the stability of texture parameters the ICC was calculated for factors influencing the perfusion maps determination (Table 1). The stability was first analyzed according to tumor site and only the features stable for both sites were included in the final set. Finally, the parameters were grouped according to inter-parameters Spearman correlations and only the parameter with the highest ICC was chosen. The acceptance level was 0.9 and 0.7 for the ICC and Spearman correlation, respectively.

Results: Texture parameters were computed in the three perfusion maps and their 3D wavelet transforms, which resulted in 945 texture features defined for each of the two tumor sites. The discretization of images using set number of bins and setintervals gave the similar number of stable texture parameters (Table 1). 40 parameters were correlated with tumor volume. Potentially standardizable factors introduced more variability into texture features than non-standardizable. The highest variability was observed for pixel size. It caused instability in about 80% of parameters for both HN and lung tumors. Ten parameters were found to bestable in both HN and lung for potentially non-standardizable factors after thecorrection for inter-parameters correlations:

- BF: entropy, sum entropy, LHH low gray-level size emphasis
- MTT: long size low gray-level emphasis
- BV: difference entropy, coarseness, long size high gray-level emphasis, HLH information measure of correlation 2, LLL covariance, LLLaverage.

Table 1. Studied CT perfusion calculation parameters and image discretization. Set of the reference parameters is underlined.

CTP parameters	Type	Levels		Unstable parameters HN [%]	Unstable parameters lung [%]
		HN	lung		
Image discretization (fixed number of bins)	Potentially standardizable factors	16, 32, 64		42	40
Image discretization (fixed intervals)		Blood volume and blood flow: 0.5%, 1%, 2% Mean transit time: 5%, 10%, 20%		41	43
Hounsfield unit (HU) intervals for exclusion of non-soft tissue from the analysis		lower threshold: -20 HU	lower threshold: -450 HU; -400 HU; -350 HU; -200 HU; -250 HU; -200 HU; -150 HU	33	26
		upper threshold: 120 HU; 140 HU; 160 HU; 180 HU; 200 HU; 220 HU; 240 HU	upper threshold: 200 HU		
Voxel size [mm³]		1x1x5; 2x2x5; 3x3x5; 4x4x5; 5x5x5	1x1x3; 2x2x3; 3x3x3; 4x4x3; 5x5x3	88	82
Artery contouring (AIF)	Non-standardizable factors	Perfusion maps calculated on 5 different contours of artery		29	27
Noise threshold in perfusion maps calculation		10%, 12%, 14%, 16%, 18%, 20%, 22%, 24%, 26%, 28%, 30%		31	15

Conclusion: The set of stable texture parameters in CTP was identified. Pixel size, image discretization and HU intervals have to be standardized to build a reliable prediction models based on CTP texture analysis.

EP-1864

A 18FDG-PET texture analysis study on early stage Hodgkin Lymphoma patient outcome prediction

G. Feliciani[1], A. Fama[2], P. Ciammella[3], F. Fioroni[1], M. Casali[4], B. Elisa[2], A. Podgornii[3], A. Versari[4], F. Merli[2], M. Iori[1]
[1]*IRCCS - Arcispedale Santa Maria Nuova, Medical Physics, Reggio Emilia, Italy*
[2]*IRCCS - Arcispedale Santa Maria Nuova, Hematology, Reggio Emilia, Italy*
[3]*IRCCS - Arcispedale Santa Maria Nuova, Radiation Oncology, Reggio Emilia, Italy*
[4]*IRCCS - Arcispedale Santa Maria Nuova, Nuclear Medicine, Reggio Emilia, Italy*

Purpose or Objective: The aim of the study was to employ texture analysis to predict early stage Hodgkin Lymphoma (HL) patients' outcome after chemotherapy and to give a quantitative description of HL characteristics. Predicting an early cancer's response to chemotherapy could enhance clinical care management by enabling the personalization of treatment plans based on predicted outcome.

Material and Methods: We reviewed medical records of patients with early stage HL diagnosed between January 2012 and December 2014 treated with standard combined modality therapy. 24 pre-treatment PET scans of the patients, acquired with a GE discovery STE, were selected for the analysis. A local nuclear medicine physician, blinded for the clinical outcome and interim PET (iPET) results, reviewed all PET scans. Volume of Interests (VOIs) were segmented employing cubes of volume 27 cm3 and 64 cm3 and centering them on the highest metabolic active mediastinic area. Texture analysis (TA) was applied through CGITA open source software and TA features correspondence with iPET results was assessed. Furthermore, we segmented isolated lymphnodes with a 40% of SUVmax isocontour algorithm. Each lymphnode was analyzed with TA as a "stand-alone patient" in order to increase the number of observations. TA features correspondence with iPET outcome of each lymphnode was assessed. Kruskall Wallis non-parametric test was employed to select most predictive features. Features, which showed prognostic power (or patient stratification ability), were employed to build Receiver Operating Curve (ROC) in order to score their sensibility and specificity.

Results: After iPET revision, 17 patiets were considered disease free after 2 cycles of ABVD whereas the remaining 7 patients had a positive iPET. Results obtained employing the 27 cm3 cubes showed that 4 features are able to predict iPET response with statistical significance ($p<0.02$) and a high efficiency up to 85% employing "uniformity feature". Using 64 cm3 cubes, we were able to isolate a feature named short zone emphasis, which has a discrimination sensibility of 100% with specificity 65% and indicates for ABVD resistant tumors the presence of short active zone in the surrounding of the mediastinic region highest metabolic active area. Lymphnode analysis showed that 5 out of 74 TA features could separate iPET responders and non-responders patients with statistical significance ($p<0.01$). In particular, "coarseness" feature has a discrimination efficiency of 73% (sensibility 77% and specificity 70%). Patients with lymphnodes that appear coarser have a higher probability of being positive at iPET.

Conclusion: In this work we presented a method to predict early stage HL patient outcome and to quantitatively describe tumor morphology combining textural features. This method requires further validation in larger prospective study.

EP-1865

DCE-CT lung tumour and aorta enhancement: is it an appropriate input vessel for kinetic modelling?

M. La Fontaine[1], W. Van Elmpt[2], M. Kwint[1], J. Belderbos[1], J.J. Sonke[1]
[1]*Netherlands Cancer Institute, Radiotherapy, Amsterdam, The Netherlands*
[2]*MAASTRO, Radiation Oncology, Maastricht, The Netherlands*

Purpose or Objective: Dynamic contrast-enhanced Computed Tomography (DCE-CT) is a quantitative imaging modality to characterize heterogeneity in tumour vascularization. Problems in DCE-CT kinetic modelling have been reported due to lung tumour enhancement arriving prior to aortal enhancement. Studies have attempted to correct the issue by shifting the enhancement curve in time, segmenting different input vessels and/or dual-input kinetic modelling. The purpose of this project was to develop a methodology for a detailed spatio-temporal analysis of the heterogeneous lung tumour enhancement for the purpose of applying different input vessels in kinetic modelling.

Material and Methods: Nine patients with non-small cell lung cancer (NSCLC) received DCE-CT scans (Siemens Definition Flash) prior to radiation therapy using shuttle mode acquisition with a longitudinal FOV of 13 cm. The DCE-CT scans were first motion corrected (Siemens VPCT) and subsequently, the primary lung tumour was contoured by a radiation oncologist. Using an in-house model, tumour and aorta time attenuation curves were analysed by gamma-variate function fitting. The arrival time of the contrast agent was estimated by a threshold of 1% of the maximum enhancement of the fit. To determine the percentage of tumour enhancement prior and after aortic enhancement, the arrival times of the gamma-variate fit of the tumour and aorta were compared. Tumour voxels were considered acausal if the arrival time was greater than 2 s before the

aorta arrival time, to correct for acquisition time differences and fitting uncertainties.

Results: Gamma-variate fitting was able to capture contrast arrival time in the DCE-CT images for all 9 patients. Two of the patients displayed clear tumour enhancement prior to aortal enhancement. For these patients, the percentage of the tumour with acausal enhancement with/without a 2 s allowance was 64%/73% and 37%/54%. The mean and standard deviation of the enhancement time differences between the tumour voxels with acausal enhancement and the aorta with/without a 2 sec allowance were -1.8 s ± 0.6 s/-3.4 s ± 1.1 s, and -1.4 ± 0.6 s/-2.6 ± 1.3 s, for each patient.

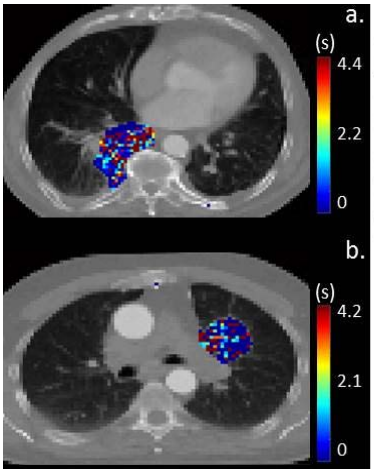

Figure 1. Lung tumour enhancement time (colorbar) prior to the aorta. The lung tumours for both patients with acausal enhancement in relation to the aorta are given in 'a.' and 'b.' The colorbar maximum was set to the start of the aorta enhancement time: parts of the tumour in light and dark blue enhanced prior to the aorta given a 2 s allowance.

Conclusion: Our study found apparent acausal enhancement in lung tumours in relation to the aorta for a subset (22%) of the NSCLC patient population examined. For these patients, gamma-variate fitting was able to determine both the percentage of the tumour with acausal enhancement times and the effective enhancement time difference between the tumour voxels and the aorta. These findings highlight the tumor vascular heterogeneity and warrant new kinetic analysis models to incorporate different tumor enhancement analysis and the selection of an appropriate input function.

EP-1866

Traceable calibration chain of PET/CT scanners for I-124

L. Joulaeizadeh[1]
[1]*VSL, Ionizing Radiation, Delft, The Netherlands*

Purpose or Objective: PET scanners are used for several decades in a wide range of diagnostic experiments. In the treatment of thyroid cancer with I-131, quantitative information of a PET scan using I-124 is used to determine the release dose to the tumor and critical organs during the treatment. To guarantee comparison of absolute quantification among institutes, measurements have to come along with uncertainty estimates and have to be traceable (i.e. linked) to international measurement standards. However, despite recent advances, PET/CT calibrations are not traceable to any measurement standard. As a result, scans taken at different scanners are not or hardly comparable with each other.

Material and Methods: VSL (National Metrology Institute in The Netherlands) maintains and develops the national measurement standards, and is able to supply support to the development of calibration chains and standard measurement protocols, thereby guaranteeing traceability to internationally accepted measurement standards. The purpose of this project is to develop a metrological infrastructure and service for on-site calibration of PET/CT scanners. VSL has the facilities to measure the activity of radionuclide solutions in a secondary level traceable to the primary standard at NPL (National Metrology Institute in UK). In 2012 and 2013 in the context of a large national multi-center trial (19 hospitals), a hospital in The Netherlands has performed non-traceable inter-comparison for I-124. Traceable measurements to validate concept method have been performed by VSL in 2015 for few scanners in The Netherlands. A cylindrical PMMA phantom including 6 holes to position vials of I-124 has been used. Activities inside the vials have been standardized using the secondary standard at VSL with an uncertainty in the range of 2.5% (k=2). Then the phantom has been measured in different scanners.

Results: The results show differences between the measured activities in two setups which is typically around 40% for activities around 1 MBq, however goes rapidly high by lowering the activity.

Conclusion: PET/CT calibrations for I-124 are not traceable to any measurement standard. The reason is lack of any calibration chain and protocol. Calibration measurements have been introduced and examined for few PET/CT scanners. The results of these measurements strongly propose the need of traceable calibration chain.

EP-1867

Dosimetric comparison between jaw tracking and static jaw modes in volumetric-modulated arc therapy

Y.T. Hsieh[1], C.Y. Chou[1], B.S. Huang[1]
[1]*Chang Gang Memorial Hospital- Linkou, RTO, Taoyuan, Taiwan*

Purpose or Objective: To compare the dosimetric differences between jaw tracking (JT) and non-jaw-tracking (nJT) techniques in volumetric-modulated arc therapy (VMAT) for Hepatocellular Carcinoma (HCC) treatment.

Material and Methods: The dose distribution around critical organs close to the tumor in HCC is critical owing to its high fractionation dose in Stereotactic Body Radiation Therapy (SBRT). Varian TrueBeam™ (Varian Medical Systems) system provides the JT technique, which keeps the main jaws of the LINAC dynamically as close as possible to the MLC aperture during dose delivery, hence minimize the leakage and transmission of the MLC and further reduces the dose to the organ at risk (OAR). In order to validate the advantage of OAR dose sparing by using JT technique in SBRT for HCC, treatment plans using JT and nJT techniques were designed for dosimetric comparison. Fifteen HCC patients were selected, all treated with doses of 50 Gy in 5 daily fractions with VMAT using 10 MV FFF beams. The maximum dose rate enabled for FFF beams is 2400 MU/min for 10 MV. Each VMAT plan was individually designed using two full and one partial arcs with collimator rotation of 30 and 330 ° to obtain the best adherence to planning objectives for each patient. All dose distributions were computed with the Analytical Anisotropic Algorithm (AAA, version 13.6) implemented in the Eclipse planning system with a calculation grid resolution of 2.5 mm. Planning objectives to target coverage aimed to cover CTV with 100% and PTV with at least 95% of the prescribed dose. The main OARs considered were: spinal cord, kidneys, stomach, duodenum, small bowel, chest wall and liver. JT and nJT Planning were performed with the same objectives constraint while plan optimization and the mean doses of OARs were obtained for plan comparison.

Results: At the same CTV and PTV dose coverage, every comparative result shows that JT plan did lower the dose received by OAR and improve the dose fall-off around the low dose region. The significant OAR dose reduction for the JT plan in this study are as follows: the mean doses to the liver was 130cGy less, the V15 of liver was 100 c.c. smaller, the maximum spinal cord dose was 300 cGy lower, and the mean kidney dose was 200 cGy lower than that in the nJT plan.

Conclusion: JT technique did show superior OARs sparing than nJT plans in HCC. The dose reduction is of clinical importance, especially for high fractionation dose SBRT treatment.

EP-1868

Standardization of amino-acid PET windowing for GTV definition in recurrent glioblastoma

O. Oehlke[1], T. Papke[2], M. Mix[3], I. Götz[4], T. Schimek-Jasch[1], T. Spehl[5], P.T. Meyer[3], A.L. Grosu[6], U. Nestle[6]

[1]University Medical Center Freiburg, Dept. of Radiation Oncology, Freiburg, Germany

[2]University Medical Center Freiburg and Ortenau Klinikum Offenburg, Dept. of Radiation Oncology and Dept. of Neurology, Freiburg and Offenburg, Germany

[3]University Medical Center Freiburg, Dept. of Nuclear Medicine, Freiburg, Germany

[4]University Medical Center Freiburg and Ortenau Klinikum Offenburg, Dept. of Radiation Oncology, Freiburg and Offenburg, Germany

[5]University Medical Center Freiburg and Ortenau Klinikum Offenburg, Dept. of Nuclear Medicine and Dept. of Radiology, Freiburg and Offenburg, Germany

[6]University Medical Center Freiburg and German Cancer Consortium DKTK, Dept. of Radiation Oncology, Freiburg, Germany

Purpose or Objective: With its high sensitivity and specificity compared to MRI, amino-acid PET is increasingly used for diagnosis and radiotherapy treatment planning in recurrent glioblastoma. Defining the exact tumor extent is exceedingly crucial for planning of high-precision reirradiation (SFRT, IGRT). Up to date, no standard for a visual or (semi-)automatic method for GTV delineation in amino-acid PET exists. In the present study, we investigated whether pre-defined PET windows would lead to a more consistent contouring of the tumor and – as a model with MRI-defined ground truth – normal tissues among observers.

Material and Methods: Pre-reirradiation imaging data (MRI and FET-PET) of 17 patients with recurrent glioblastoma were retrospectively evaluated. Two different pre-set window levels were created for FET-PET data, either normalized to SUVmax or normalized to the SUVmean of the contralateral non-tumor bearing hemisphere (SUVmean contra). The GTV was delineated in both data sets by 5 observers (radiation oncology and nuclear medicine specialists). Additionally, normal tissue with (superior sagittal sinus or lacrimal gland) and without physiological FET uptake (eye and lateral ventricle) were contoured. A reference contour for normal tissues was delineated in contrast-enhanced T1 MRI, and overlap volume (OV) and Kappa index (KI) were calculated for each structure.

Results: GTV volumes were larger by trend when normalized to SUVmean contra, but not significantly different between the two PET image normalization methods (18,72 ± 17,44 ml for SUVmean contra vs. 14,68 ± 12,34 ml for SUVmax, p=0,41). Linear regression of inter-observer variability showed a significantly better agreement of the GTV contours when PET images were normalized to SUVmean contra (t=3,5). The intra-method comparison of PET data normalized to SUVmax or SUVmean contra showed the highest consensus for GTV (OVmean=0,5 and 0,52 and KI=0,64 and 0,66, respectively), whereas the lacrimal gland was the structure with the least congruency (OVmean=0,37 and 0,42 and KI=0,46 and 0,52, respectively). There was no overall significant difference between both PET windows (OVmean p=0,83;KI p=0,87). Correlation of normal tissue contours with MRI reference was poor (SUVmax vs. MRI: OVmean 0,11-0,37, KI 0,19-0,53; SUVmean contra vs. MRI: OVmean 0,13-0,36, KI 0,22-0,52) and not significantly different between the two normalization methods (p=0,7 and 0,89 for OVmean and KI, respectively).

Conclusion: Normalization on the SUVmean of the contralateral hemisphere in FET-PET images helps to reduce inter-observer variability in the visual delineation of the GTV in patients with recurrent glioblastoma. However, neither improvement nor difference in the consistency of normal tissue delineation, as a model with MRI-defined ground truth, between the different windows was seen.

EP-1869

Metabolic response between primary tumor and lymph nodes in NSCLC patients during treatment course

N.M. Bruin[1], W.V. Vogel[1], J.B. Van de Kamer[2], J.L. Knegjens[2], J. Belderbos[2], J.J. Sonke[2]

[1]The Netherlands Cancer Institute, Departments of Radiation Oncology and Nuclear Medicine, Amsterdam, The Netherlands

[2]The Netherlands Cancer Institute, Department of Radiation Oncology, Amsterdam, The Netherlands

Purpose or Objective: Repetitive functional imaging during the course of irradiation is a promising method to identify non-small cell lung cancer (NSCLC) patients that have poor or favourable response to radiotherapy [1]. In locally advanced lung cancer patient, the primary tumour (PT) and involved lymph nodes (LN) are delineated and irradiated. It is currently, however, unknown if all intrathoracic lesions within the same patient demonstrate the same metabolic response. The purpose of this study was therefore to investigate the correspondence in response rate of the PT and involved LNs.

Material and Methods: Eight locally advanced NSCLC patients included in an ongoing prospective clinical trial (NCT02315053) for repeat quantitative evaluation of tumour metabolism (using FDG-PET) weekly during treatment were analysed. Patients were treated with concurrent chemoradiation (CCRT) with curative intent, in 24 fractions of 2.75 Gy combined with daily cisplatin 6 mg/m2 with an overall treatment time of 32 days. All patients underwent a PET/CT for treatment planning and weekly low dose FDG PET/CT scans of the thorax in treatment position prior to the daily chemotherapy and radiotherapy administration. For the PT and each treated LN with a baseline SUVmax≥3 (median 3 LNs per patient; range 2-4), the SUVmax was normalized separately to the baseline value at the start of treatment. Consistency in the response between PT and LNs was evaluated by Bland-Altman analysis over the cohort (corrected for the number of lymph nodes per patients and excluding the baseline used for normalization) as well as total least squares linear regression with the PT for each LN separately.

Results: Considerable variability in metabolic response for individual time points was observed in the pooled analysis of all patients (Fig 1a) with Bland-Altman limits of agreement (LA) of 46% and a bias of 10%. Despite these LA, the correlation in the response between PT and LN was reasonably high with a median value of 0.86 with an interquartile range of 0.21. The median slope of the regression analysis was of 1.1 with an interquartile range of 0.7, indicating that the LNs typically respond a little faster than the PT. However, within a patient, several involved lymph node stations exhibited a considerably different response as illustrated in Fig1b.

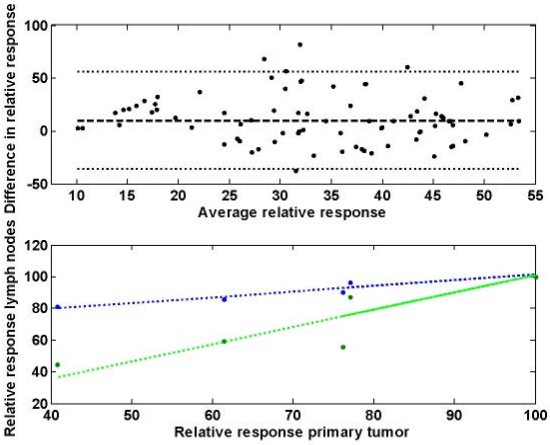

Figure 1: Top) Bland-Altman analysis of the relative response of primary tumour and lymph nodes. Dashed lines indicate the bias and limits of agreement. Bottom) Example patient illustrating considerable variability in the relative metabolic response of two different lymph nodes.

Conclusion: A reasonable high correlation in response during chemoradiation between the primary lung tumour and lymph nodes was observed, but a large inter- and intra-patient variability was observed. These preliminary results suggest that treatment plan modification based on metabolic treatment response should be tailored to individual lesions.

[1] van Elmpt et al., J Nucl Med. 2012

EP-1870

Improving Tumor Response Assessment using DWMRI corrected by reversed gradient method and DCEMRI

A. Lopez Medina[1], S. Reigosa[1], J. Del Olmo[1], D. Aramburu Nunez[2], F. Salvador[1], I. Landesa[3], J. Alba[3], M. Salgado[1], I. Nieto[4], V. Ochagavia[4], V. Muñoz[4]

[1]*Hospital do Meixoeiro, Medical Physics Department, Vigo Pontevedra, Spain*

[2]*Memorial Sloan Kettering Cancer Center, Quantitative Imaging Department, New York, USA*

[3]*University of Vigo, SignalTheory and Communications Department, Vigo, Spain*

[4]*Hospital do Meixoeiro, Radiotherapy Department, Vigo Pontevedra, Spain*

Purpose or Objective: Apparent diffusion coefficient (ADC), derived from diffusion-weighted MRI (DW-MRI) is a promising assessment method during radiotherapy treatment, but geometric distortion is its main disadvantage. This study investigates the use of the reversed gradient method (RGM) in DW-MRI for reduction in geometric distortion and vascularization from dynamic studies of MRI (DCEMRI), as a surrogate measure of oxygenation in H&N cancer.

Material and Methods: We studied the variation of ADC of three oropharynx cancer patients included in ARTFIBIO project. Three functional imaging scans were performed before treatment: PET/CT, DWMRI and DCEMRI; two MRI scans during the treatment; and three months after the treatment, the initial studies were repeated. Geometric distortion of DWMRI was corrected using RGM (SPM8 software, HySCO options). DCEMRI analyses were performed using Dynamika® v4.0 (www.imageanalysis.org.uk). Registration and mutual information were calculated with ARTFIBio tools. Mutual information of T2-weighted and DW-MRI was calculated for corrected and uncorrected DW-MRI. Initial Rate Enhancement (IRE) from DCEMRI was selected as a possible biomarker associated with vascularization / hypoxia.

Results: Table shows the increment in mutual information for the initial ADC maps of the three patients when correcting by RGM. For two first patients, a large increment is observed and for the third patient, although the mutual information didn't show it, the visual appreciation is quite relevant. In Figure A, the visual improvement of corrected images can be appreciated.

We also measured the variation of ADC during the treatment (Figure B), and three months later. The colour in the dots shows the initial IRE values in arbitrary units. As the dose is delivered, best-vascularized dots move to the upper part of the cloud corresponding to different instants along the treatment.

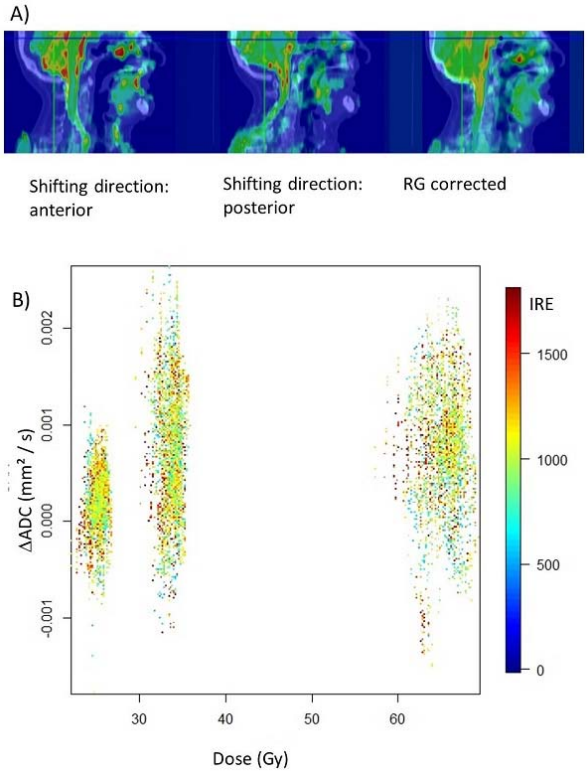

Patient	b = 0 s / mm²			b = 600 s / mm²		
	Anterior shift	Posterior shift	Corrected by Reversed gradient	Anterior shift	Posterior shift	Corrected by Reversed gradient
#1	0.563	0.656	0.872	0.655	0.325	0.900
#2	0.308	0.454	0.775	0.381	0.445	0.730
#3	0.439	0.548	0.548	0.545	0.522	0.567

Conclusion: RGM improves registration and provides accurate ADC in tumors. We suggest correction of distortion with the RGM should form part of an imaging method for treatment response using ADC to assess tumor response or tumor cell density variation with treatment in cancer patients, and DCEMRI can be useful for characterizing hypoxia in H&N cancers. Supported by ISCIII Grant DTS14/00188

EP-1871

Optimization of gross tumour volume definition in lung-sparing VMAT for pleural mesothelioma

A. Botticella[1], G. Defraene[2], K. Nackaerts[3], C. Deroose[4], P. Nafteux[5], S. Peeters[2], D. De Ruysscher[2]

[1]*University Hospital Gasthuisberg, Laboratory of Experimental Radiotherapy- Oncology Department, Leuven, Belgium*

[2]*KU Leuven - University of Leuven- University Hospitals Leuven, Department of Oncology- Experimental Radiation Oncology, Leuven, Belgium*

[3]*KU Leuven - University of Leuven- University Hospitals Leuven, Respiratory Diseases/Respiratory Oncology Unit, Leuven, Belgium*

[4]*KU Leuven - University of Leuven- University Hospitals Leuven, Department Imaging and Pathology- Nuclear Medicine and Molecular Imaging, Leuven, Belgium*

[5]*KU Leuven - University of Leuven- University Hospitals Leuven, Department of Thoracic Surgery, Leuven, Belgium*

Purpose or Objective: High dose lung-sparing pleural radiotherapy for malignant pleural mesothelioma (MPM) is difficult. Accurate target delineation is critical. The optimal imaging modality to define radiotherapy target volumes has not been studied in depth. This is the aim of the present study.

Material and Methods: Twelve consecutive patients with a histopathological diagnosis of stage I-IV MPM (6 left-sided and 6 right-sided) were included. CT scans with IV contrast, 18F-FDG PET/CT scans and MRI scans (post-contrast T1-weighted, T2 and diffusion-weighted images [DWI]) were obtained and downloaded from the institutional database onto a standalone image fusion workstation (MIM Software Inc., Cleveland, OH, USA) for image registration and contouring. CT scans were rigidly co-registered with 18FDG-CT-PET, with MRI scans and with DWI scans. Four sets of pleural GTVs were defined: 1) a CT-based GTV (GTVCT); 2)a PET/CT-based GTV (GTVCT+PET/CT); 3) a T1/T2-weighted MRI-based GTV (GTVCT+MRI); 4) a DWI-based GTV (GTVCT+DWI). Only the pleural tumor was contoured; mediastinal nodes were excluded. "Quantitative" and "qualitative" (visual) evaluation of the volumes was performed.

Results: Compared to CT-based GTV definition, PET/CT identified additional tumour sites in 12/16 patients. Compared to either CT or PET/CT, MRI and DWI identified additional tumour sites in 15/16 patients. Mean GTVCT, GTVCT+PET/CT, GTVCT+MRI and GTVCT+DWI (+ standard deviation [SD]) were respectively 630.1 mL (+302.81), 640.23 (+302.83), 660.8 (+290.8) and 655.2 mL(+290.7). Mean Jaccard index was lower in MRI-based contours versus all the others.

Conclusion: To the best of our knowledge, this is the first study showing that the integration of MRI into the target volume definition in hemithoracic radiotherapy in MPM may allow to improve the accuracy of target delineation and reduce the likelihood of geographical misses.

EP-1872

Benchmarking texture analysis for PET in oesophageal cancer

B. Berthon[1], K. Foley[2], C. Marshall[1], R.T.H. Leijenaar[3], E. Spezi[4]

[1]Cardiff University, Wales Research & Diagnostic PET Imaging Centre, Cardiff, United Kingdom

[2]Cardiff University, Institute of Cancer & Genetics, Cardiff, United Kingdom

[3]Maastricht University Medical Centre, GROW-School for Oncology and Developmental Biology- Department of Radiation Oncology MAASTRO Clinic, Maastricht, The Netherlands

[4]Cardiff University, School of Engineering, Cardiff, United Kingdom

Purpose or Objective: Texture and shape metrics are increasingly used for oncological applications such as the prediction of response to therapy. Commercial and freely available software tools have been used to publish significant results. However, it is unclear if these tools provide matched or even similar values, which is crucial when comparing such studies and drawing conclusions affecting patient management. In this work, we benchmark texture analysis software for PET in oesophageal cancer.

Material and Methods: PET-STAT, a texture analysis tool written in the Matlab-based open source software CERR, was benchmarked against the open source software CGITA and the Radiomics package, on oesophageal cancer PET-CT scans. The PET scans and tumour outlines in DICOM format were processed on-site with PET-STAT and CGITA and remotely for Radiomics. Image resampling in PET-STAT matched the number of discrete intensities used in CGITA, where it was fixed, and in Radiomics, where the image bin width was set to 0.5 SUV. Texture and shape metrics present in PET-STAT and Radiomics or CGITA were matched by their mathematical description. The metrics calculated were Maximum, Mean intensity, SUVpeak, Volume, Total Lesion Glycolysis; histogram-based Standard Deviation, Skewness, Kurtosis, Entropy (HEp) and Energy; grey level cooccurrence matrix (GLCM)-based Entropy, Homogeneity and Dissimilarity; Coarseness (C); grey level size-zone-based Intensity Variability, Large Area Emphasis and Zone Percentage, and shape metrics Maximum Diameter, Compactness, Sphericity, Spherical disproportion. No C was found in Radiomics, no shape metrics nor HEp were found in CGITA.

Results: Differences up to 7% in volume were observed between PET-STAT and CGITA, which disappeared when using data loaded from CERR, were due to different interpretation of the DICOM images and outline data. Errors of 7% in volume in one case compared with Radiomics may be due to different RTSTRUCT export or import in the study workflow. SUVpeak was up to 12% different between software packages due to different hard coded resampling of the PET image or kernel sizes used. Differences of up to 44% were observed in the calculation of shape metrics between Radiomics and PET-STAT. This was due to differences in the triangulation technique used to calculate the contour surface area. Furthermore, differences of up to 30% across the cases considered, were found to be due to different equations used for resampling the image to discrete intensities, as well as different methods for computing the GLCM and GLSZM.

Case No	1			2			3			4			5		
Metric	PS	CG	R	PS	CG	R	PS	CG	R	PS	CG	R	PS	CG	R
SUVmax	11.9	0.00	0.0	16.7	0.00	0.0	12.0	0.00	0.0	15.6	5.90	0.0	9.1	7.95	0.0
SUVmean	7.9	0.00	1.6	7.4	0.00	0.0	5.3	0.00	0.0	6.7	19.15	0.0	6.2	16.17	0.0
SUVpeak	8.9	-10.47	-2.6	11.7	-10.15	-10.3	8.6	-11.24	-8.9	11.4	-10.95	-10.8	7.2	-2.49	-5.2
MTV	11.4	0.00	-7.2	21.7	0.00	0.0	18.2	0.00	0.0	36.7	-23.05	0.0	12.9	-19.66	0.0
TLG	89.7	0.00	0.0	159.7	0.00	0.0	96.4	0.00	0.0	245.8	-8.32	0.0	80.2	-6.67	0.0
SD	1.20	0.00	-3.06	2.99	0.00	-0.06	2.01	0.00	-0.07	2.61	3.38	-0.03	1.02	-14.66	-0.10
Sk	0.68	-0.01	-0.96	0.89	0.00	0.00	1.07	0.00	0.00	0.82	-19.24	-0.01	0.34	802.4	0.01
Ku	2.72	0.00	0.45	3.14	0.00	0.00	3.56	0.00	0.00	2.78	-11.76	0.00	2.14	-6.64	0.00
HistEg	29321	N/A	-5.08	56087	N/A	0.00	23874	N/A	0.00	77182	N/A	-0.45	20898	N/A	-0.41
HistEp	3.76	0.00	20.77	3.84	0.00	-12.11	3.77	0.00	0.14	3.76	8.73	-9.11	3.91	61.78	32.27
C	0.01	-0.93	N/A	0.05	2.68	N/A	0.01	0.00	N/A	0.01	71.43	N/A	0.02	-9.24	N/A
H	0.46	-4.11	3.82	0.34	1.29	-0.76	0.41	1.91	-0.29	0.40	-9.88	3.92	0.52	-19.73	2.04
E	3.94	1.04	-7.60	5.39	1.62	-3.69	4.74	1.92	-3.33	5.16	-4.13	-3.71	3.71	-15.74	-4.58
D	1.97	9.57	-7.60	3.80	11.35	0.45	2.54	7.38	1.84	2.73	40.82	-6.09	1.48	65.78	-3.48
Iv	9.69	0.00	-21.06	13.85	0.00	-5.78	9.16	0.00	8.97	20.85	-19.58	-7.71	10.07	7.95	-29.75
LAE	125.1	0.00	32.31	25.48	0.00	-3.80	154.0	0.00	-11.27	96.48	-21.89	38.25	524.4	16.17	34.89
ZP	0.15	0.00	-12.26	0.31	0.00	-0.09	0.17	0.00	2.18	0.22	-8.57	-11.20	0.09	-2.49	-21.48
C1	0.56	N/A	-4.55	0.88	N/A	7.08	0.84	N/A	8.31	0.96	N/A	-3.73	0.68	N/A	8.40
C2	0.26	N/A	-2.35	0.39	N/A	35.99	0.48	N/A	43.21	0.15	N/A	-15.71	0.44	N/A	43.77
MD	5.88	N/A	-7.22	7.95	N/A	0.00	6.34	N/A	0.00	8.19	N/A	0.00	5.68	N/A	0.00
SphD	1.57	N/A	0.79	1.37	N/A	-9.74	1.28	N/A	-11.28	1.86	N/A	5.86	1.32	N/A	-11.40
SVR	3.38	N/A	3.32	2.38	N/A	-9.74	2.35	N/A	-11.28	2.71	N/A	5.87	2.71	N/A	-11.40
S	0.64	N/A	-0.78	0.73	N/A	10.80	0.78	N/A	12.72	0.54	N/A	-5.54	0.76	N/A	12.86

Table 1. Feature values obtained for PET-STAT (PS) for each case with associated difference (in % PET-STAT) with CGITA (CG) and Radiomics (R).

Conclusion: Our benchmarking work on oesophageal cancer PET imaging reported a number of non trivial differences in texture and shape metric values when using different software packages. This highlights the importance of commissioning and validating texture analysis tools and recommends that detailed descriptions of the metric and software implementation are available.

EP-1873

Multimodality functional imaging for characterizing tumour volume

J. Del Olmo[1], S. Reigosa[1], A. Lopez Medina[1], F. Salvador[1], J. Nogueiras[2], J. Mañas[3], M. Arias[3], D. Fabri[4], B. Sanchez Nieto[4], M. Salgado[1]

[1]Hospital do Meixoeiro, Medical Physics Department, Vigo Pontevedra, Spain

[2]Hospital do Meixoeiro, Nuclear Medicine Department, Vigo Pontevedra, Spain

[3]Hospital do Meixoeiro, Radiology Department, Vigo Pontevedra, Spain

[4]Pontificia Universidad Católica de Chile, Physics Department, Santiago de Chile, Chile

Purpose or Objective: Biologically guided radiotherapy needs an understanding of how different functional imaging techniques link together. We analyse three functional imaging techniques that can be useful to characterize tumour behaviour: DWMRI, DCEMRI and PET/CT with FDG.

Material and Methods: An oropharynx cancer patient included in the ARTFIBIO project with a swollen node was selected. The pre-treatment imaging protocol was: MRI (DWMRI, DCEMRI) and PET/CT with FDG. Geometric distortion of DWMRI was corrected using the reversed gradient method (RGM) and the SPM8 software. DCEMRI analyses were performed using Dynamika® v4.0 (www.imageanalysis.org.uk). All the datasets were registered using ARTFIBio tools.
The parameters for classifying subvolumes were (Figure A): Initial Rate Enhancement (IRE) from DCEMRI, that measures the initial slope of gadolinium concentration and related to vascularization, Apparent Diffusion Coefficient (ADC) from DWMRI, previously corrected by the RGM, related to tumour density, and SUV from PET/CT with FDG. Thus, three subvolumes have been delimited: node, hypoxic volume (low IRE) and necrotic volume (red region in DWMRI b0, high ADC, very low IRE).

Results: We have analysed the relationship between the three selected parameters (ADC, IRE and SUV) for the whole node and for the badly vascularized region excluding the necrotic region. When we considered the whole node (Figure B), we observe a complex relationship between these three parameters, but when we only consider the badly vascularized region (low IRE, low ADC), we observe a clear relationship between these parameters, that suggest that vascularization quantified by IRE must be related to oxygenation, as lowest vascularized dots (blue dots, figure C), correspond to high SUV for the same ADC, indicating an enhancement of the Pasteur effect in the badly vascularized region.

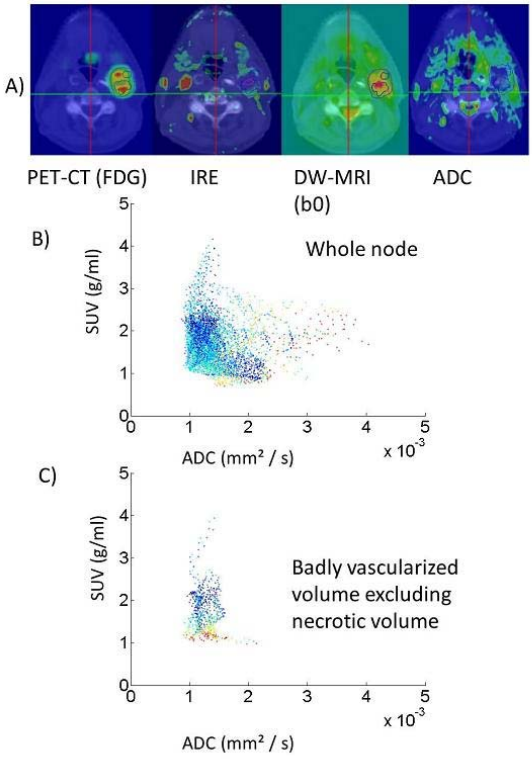

Conclusion: Several functional imaging techniques can be required to customize treatment, but an appropriate registration process must be applied. ADC maps can be used for tumour cell quantification, but distortion correction algorithm must be previously applied, RGM looks quite suitable. Oxygenation process can be estimated from DCEMRI in head and neck cancer, as vascularization is related to oxygenation in these cancers, and as our results suggest. PET/CT and MRI studies provide information about malignancy grade of the tumour, considering glucose metabolism, tumour cell density (from ADC maps) and oxygenation (DCEMRI).

Supported by ISCIII Grant DTS14/00188.

EP-1874

Effective radiosensitivity maps of early tumour responsiveness based on repeated FDG PET scans

M. Lazzeroni[1], J. Uhrdin[2], J.J. Sonke[3], O. Hamming-Vrieze[3], A. Dasu[4], I. Toma-Dasu[5]
[1]*Karolinska Institutet, Oncology-Pathology Department, Stockholm, Sweden*
[2]*RaySearch Laboratories AB, RaySearch Laboratories AB, Stockholm, Sweden*
[3]*The Netherlands Cancer Institute, Department of Radiation Oncology, Amsterdam, The Netherlands*
[4]*Linköping University, Department of Radiation Physics and Department of Medical and Health Sciences, Linköping, Sweden*
[5]*Stockholm University, Department of Physics, Stockholm, Sweden*

Purpose or Objective: Identification of outcome predictive factors at an early stage of radiation therapy allows for adaptation and individualisation. Such predictive factors are crucial for advanced head and neck (H&N) cancer patients since the treatment failure is often caused by poor loco-regional control. An early treatment adaptation would allow a dose escalation in the most radioresistant tumour regions. The aim of this study was to early identify sub-regions in H&N tumours non-responding to the treatment. This was achieved by applying a previously developed method using [18F]-fluorodeoxy-D-glucose positron emission tomography (FDG PET) to evaluate the early responsiveness of lung tumours.

Material and Methods: Thirteen patients with advanced H&N cancer were imaged with FDG PET before the start and during the second week of concurrent chemoradiotherapy (after about 19 Gy of delivered dose to the primary gross tumour volume, GTVprim). The acquired PET images were co-registered to the planning CT and a systematic analysis was performed to calculate an operational parameter at voxel level, the effective radiosensitivity αeff which accounts for the accumulated dose distribution at the time of the second PET scan and variations in the FDG uptake. Volumetric maps of αeff values within GTVprim, as well as the average (a_αeff) and negative fractions (nf_αeff) of αeff values were determined. Patients were stratified in responders and non-responders to treatment based on previously determined criteria for overall survival at 2 years for concurrent chemoradiotherapy in lung cancer (a_αeff>0.004 Gy-1 and nf_αeff≤30%). The spatial distribution of the αeff values was mapped for the non-responders to treatment for future adaptation strategies.

Results: The previously proposed method was feasible for H&N cancer patients and predicted good response in 54% of the patients having simultaneously a_αeff>0.004 Gy-1 and nf_αeff≤30%. Figure 1a shows an example of the effective radiosensitivity map for a selected slice of the GTVprim in one of the H&N cancer patients. The corresponding binary image with threshold on the negative portion of the αeff distribution is presented in Figure 1b (white: αeff>0; black: αeff<0). Calculated volumetric maps of the effective radiosensitivity values showed that it was possible to segment confined sub-regions in the tumour which might indicate resistance to the treatment (Figure 1b).

Conclusion: Confined tumour sub-regions showing lack of metabolic response which might correlate to resistance to treatment could be identified at an early stage during the radiotherapy regime. Investigations on different dose boosting strategies are on-going to account for the quantitative information available from the αeff volumetric maps.

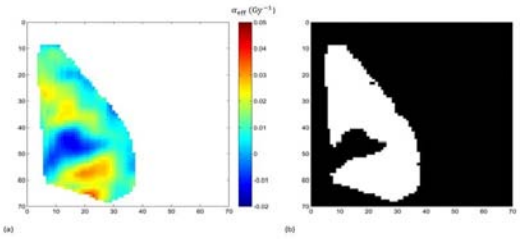

Figure 1 (a) Effective radiosensitivity maps of a selected slice of the primary gross tumor volume and (b) corresponding binary image (white: αeff>0; black: αeff<0)

EP-1875

Correlation between MRI-based hyper-perfused areas and tumor recurrence in high-grade gliomas

I. Chabert[1,2], I. Belladjou[2], F. Poisson[2], F. Dhermain[2], V. Martin[2], S. Ammari[2], S. Vauclin[3], P. Pineau[3], I. Buvat[4], E. Deutsch[1,2], C. Robert[1,2]

[1]*INSERM, U1030 Radiothérapie Moléculaire, Villejuif, France*
[2]*Gustave Roussy, Radiothérapie, Villejuif, France*
[3]*DOSIsoft, Recherche et Développement, Cachan, France*
[4]*CEA, Service Hospitalier Frédéric Joliot, Orsay, France*

Purpose or Objective: Patients suffering from high-grade gliomas currently have a median survival time of 14 months despite treatment. Our purpose was to investigate whether MR perfusion and relative Cerebral Blood Volume (rCBV) maps could predict tumor recurrence areas and improve treatment planning.

Material and Methods: This retrospective study included 19 patients suffering from high grade gliomas (3 and 4) who received standard radiotherapy [60 Gy, 2 Gy/fraction] and Temodal chemotherapy. Subjects underwent pre-treatment CT, gadolinium-enhanced T1-weighted, T2 FLAIR acquisitions and a DSC-MR scan. rCBV maps were calculated using READE View Advantage Workstation (GE) and normalized to the normal white matter perfusion value. The PLANET software (DOSIsoft) was used to register all MR images to the planning CT. A senior radiologist and a senior radiotherapist delineated Gross Tumor Volumes (GTV) on anatomical MR images. The Planning Target Volumes (PTV) were defined by a physicist. Threshold of 1.7 was applied to the rCBV maps to define hyper-perfused volumes (Vperf). Follow-up anatomical MR images were used to localize recurrence areas (GTV'). Correlations between all volumes were analyzed using several indexes. I1 is the percentage of Vperf not included in the GTV. I2, I3, and I5 are respectively the percentage of GTV' included in Vperf, GTV, and PTV. I4 is the percentage of Vperf' not included in the GTV which was predictive of tumor recurrence outside GTV. This index is meaningful only if GTV' and GVT are different.

Results: Indexes obtained for each patient are presented in Table 1. For two patients, a threshold of 2 was applied to the rCBV maps at the physician request to facilitate the hyper-perfused area visualization. I1 values are in a range of 4 to 82% (mean = 43%) and are greater than 20% for almost 90% of the patients, indicating that hyper-perfused areas and GTV can be different. Hence, rCBV maps provide supplementary information. At least 40% of GTV' is included in Vperf for 16 patients (I2 index). For 10 patients, GTV' is not completely included in the GTV (I3 < 85%). In all these cases except one, the I4 index is greater than 20%, suggesting that a part of Vperf is predictive of the recurrence localization (Figure 1). I5 being almost always equal to 1 points out that all recurrence areas received the same dose as the GTV.

$$I1 = \frac{V_{Perf} - (V_{GTV} \cap V_{Perf})}{V_{Perf}} \quad I2 = \frac{V_{GTV'} \cap V_{Perf}}{V_{GTV'}} \quad I3 = \frac{V_{GTV'} \cap V_{GTV}}{V_{GTV'}}$$

$$I4 = \frac{(V_{GTV'} - V_{GTV}) \cap V_{Perf}}{V_{Perf} - V_{GTV}} \quad I5 = \frac{V_{GTV'} \cap V_{PTV}}{V_{GTV'}}$$

	I1	I2	I3	I4	I5
1	16	42**	80	59	100
2	63	7	38	33	100
3*	82	67**	35	28	100
4	60	54**	46	14	100
5*	47	47**	42	62	100
6	64	64**	46	47	100
7	4	59**	97	0	100
8	7	76**	99	2	100
9	32	66**	97	1	100
10	26	25	47	97	92
11	76	58**	97	0	100
12	46	45**	55	54	100
13	50	54**	48	48	100
14	25	61**	96	2	100
15	23	60**	86	4	99
16	17	44**	96	20	100
17	53	65**	89	1	100
18	32	38	77	39	100
19	15	46**	96	1	100

Table 1. Volume comparison indexes in 19 patients. The * sign indicates patients for whom a threshold of 2 was applied to rCBV maps at the request of the physicians. Yellow rows indicate patients for whom GTV' is not entirely included in GTV. The ** sign indicates patients for whom at least 40% of GTV' is included in Vperf.

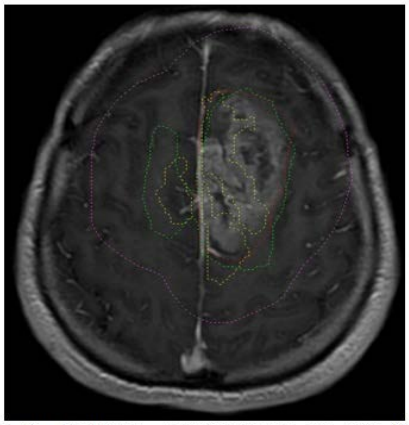

Figure 1. Volume comparison on pre-treatment gadolinium-enhanced T1-weighted for patient 1. A large part of GTV' (green) and Vperf (yellow) are included in GTV (red) in the left hemisphere. In the right hemisphere, the hyper-perfused area is predictive of tumour recurrence. GTV' is completely included in PTV (pink).

Conclusion: Our results suggest that rCBV perfusion maps can be predictive of recurrence localization. I1, I2 and I4 values are however entirely dependent on the threshold applied to rCBV maps and their evolution while the threshold increases will be studied. As recurrence areas are always included in the PTV, an improvement of treatment planning would consist in boosting hyper-perfused area rather than changing the GTV delineation. An in-depth analysis of the pre-treatment rCBV values observed in recurrence areas will be conducted to better describe potential boost areas.

EP-1876

An image-based method to quantify biomechanical properties of the rectum in RT of prostate cancer

O. Casares-Magaz[1], M. Thor[2], L. Donghua[3], J.B. Frøkjær[4], P. Kræmer[5], K. Krogh[6], A.M. Drewes[7], H. Gregersen[8], V. Moiseenko[9], M. Høyer[5], L.P. Muren[1]

[1]*Aarhus University Hospital, Department of Medical Physics, Aarhus, Denmark*
[2]*Memorial Sloan Kettering Cancer Center, Department of Medical Physics, New York, USA*

[3]Aarhus University, Department of Clinical Medicine, Aarhus, Denmark
[4]Aalborg University Hospital, Department of Radiology, Aalborg, Denmark
[5]Aarhus University Hospital, Department of Oncology, Aarhus, Denmark
[6]Aarhus University Hospital, Department of Hepatology and Gastroenterology, Aarhus, Denmark
[7]Aalborg University Hospital, Department of Gastroenterology, Aalborg, Denmark
[8]Chongqing University, GIOME - College of Bioengineering, Chongqing, China
[9]University of California San Diego, Department of Radiation Medicine and Applied Science, San Diego, USA

Purpose or Objective: Gastrointestinal morbidity after radiotherapy (RT) for prostate cancer may be related to the biomechanical properties of the rectum. In this study we present a magnetic resonance imaging (MRI) based method to quantitate the thickness and elasticity of the rectal wall in prostate cancer patients treated with RT.

Material and Methods: Four patients previously treated with RT for prostate cancer underwent an MRI session with step-wise rectal bag deflation (from a maximum tolerable volume to 0 ml, in 50 ml steps), with a probe inserted inside the bag to monitor the internal rectal pressure. MRIs were acquired using Dixon sequences (4 mm axial slice thickness) at each deflation step. Rectal walls were defined from the recto-sigmoid junction to 3 cm above the anal canal as the space between the inner and outer wall surfaces. The wall thickness was determined and biomechanical properties (strain and stress) were calculated from the pressure measurements and the MRI-segmented rectal walls.

Results: The integral rectal pressure varied for the maximum tolerable volume (range: 150 – 250 ml) across patients and ranged from 1.3 – 4.0 kPa (SD = 1.2 kPa). Wall thickness was found to vary between patients and also across different rectum segments, with a mean (SD) thickness for the different segments at the 50 ml distension volume of 1.8 – 4.0 (0.6) mm. Stress showed larger variation than strain, with mean (SD) values for the different segments ranging between 1.5 – 7.0 (1.5) kPa (Fig.1).

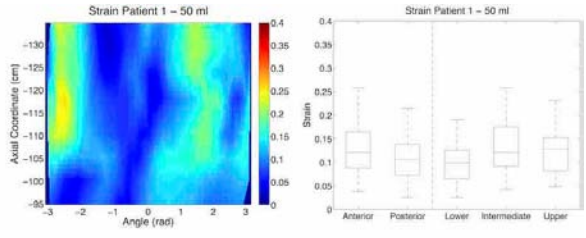

Figure 1. (Left panel) 2D map of strain for the 50 ml distension volume. Axial coordinate indicates the longitudinal position of the central point of each slice along the curved centre of axis, abscissa coordinate is the angular position from -π to π, where coordinate 0 corresponds with the most anterior point at most caudal part of the analysed surface. (Right panel) Box plot for the strain measurements at the 50 ml distension volume, and for the five rectal segments analysed.

INTEGRAL RECTAL PRESSURE (kPa) AT EACH DISTENSION VOLUME					
PATIENT	50ml	100ml	150ml	200ml	250ml
1	0.32	0.65	0.65	1.30	-
2	0.35	0.70	1.77	-	-
3	0.40	0.79	1.59	2.38	3.96
4	0.81	1.13	1.50	2.58	-
Mean	0.47	0.82	1.41	2.09	-
SD	0.23	0.22	0.51	0.69	-

Table 1. Pressure decrements, at each distension, for the 4 patients analysed, values missing correspond with non-tolerable distension volumes for the specific patient.

Conclusion: We have developed a method to quantify biomechanical properties of the rectal wall. The resulting rectal wall thickness, strain and stress differed between patients, as well as across different rectal wall sections. These findings could provide guidance in future predictive outcome modelling in order to better understand the rectal dose-volume response relationship.

EP-1877

Lung cancer textural analysis: to contrast or not to contrast?

A. Farchione[1], N. Dinapoli[2], R. Gatta[2], A.R. Larici[1], C. Masciocchi[2], A. Damiani[2], P. Franchi[1], A. Castelluccia[2], G. Mantini[2], L. Bonomo[1], V. Valentini[2]
[1]Università Cattolica del Sacro Cuore -Policlinico A. Gemelli, Radiology Department, Rome, Italy
[2]Università Cattolica del Sacro Cuore -Policlinico A. Gemelli, Radiation Oncology Department, Rome, Italy

Purpose or Objective: In the literature the choice of images for textural analysis depends on what is available in routine clinical practice. An important consideration is that, heterogeneity within unenhanced and contrast-enhanced images may provide different information as each indicates different components of the tissue being imaged. The aim of our study was to evaluate the influence of contrast medium administration on morphological and textural "features" derived from CT images in Patients (Pts) with NSCLC.

Material and Methods: Pre-operative CT of NSCLC patients, acquired pre- and post- contrast medium administration but using the same technical parameters (CT scanner Light Speed GE Medical Systems, Milwaukee WI USA; thickness and increase layer; kernel reconstruction), were retrospectively included. For each series (pre- and post- contrast medium administration) a thoracic radiologist semi-automatically segmented tumour volumes using a commercial software (Eclypse Varian Aria v.11). Finally morphological and textural tumour features (area/volume, mean, kurtosis, skewness, standard deviation, entropy) were extracted using an ad-hoc developed software (Moddicom). The results of pre- and post-contrast analysis were compared (using Wilcoxon Signed Rank test for paired data).

Results: 39 NSCLC patients were admitted in this study. Analysis revealed that entropy and skewness had statistically significant higher values in the post-contrast acquisitions (p value = 0.007 in both cases); mean values were greater in the post-contrast acquisitions, even though the difference was not statistically significant. Kurtosis and area/volume showed statistically significant higher values in the pre-contrast acquisitions (p value respectively 0.046 and 0.036); standard deviations values were greater in the pre-contrast acquisitions, even though the difference was not statistically

significant. Results are summarized in table 1 with an example of studied patient in figure 1.

	Contrast	Without Contrast	P value
Area/Volume	-	+	0.036
Mean	+	-	n.s.
Skewness	+	-	0.007
Kurtosis	-	+	0.046
Standard Deviation	-	+	n.s.
Entropy	+	-	0.007

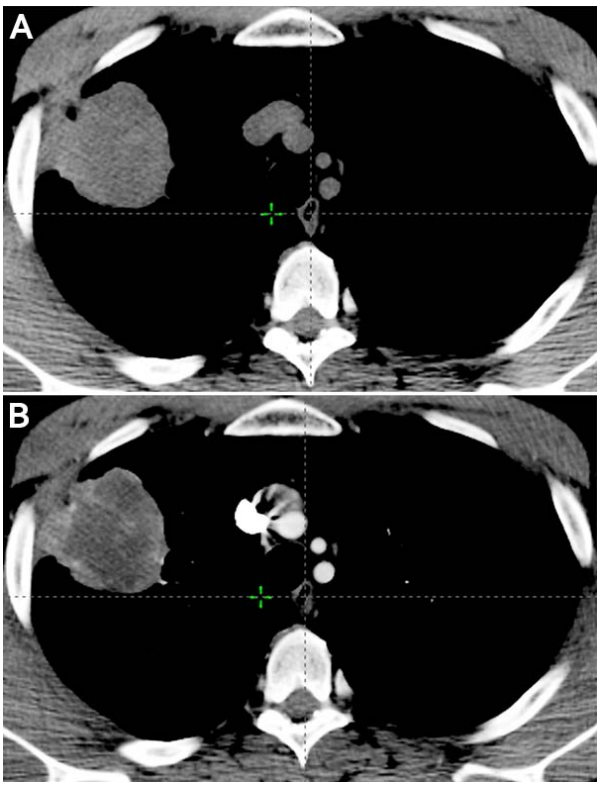

Conclusion: Contrast medium administration significantly influences morphological and textural features derived from CT of NSCLC. The difference can be related both to technical factors and to different tissue components of which it is expression. As these features are known predictors of different NSCLC outcomes and may be included in predictive models useful for the creation of therapeutic decision-making systems, the standardization of technical protocols seems appropriate.

EP-1878

Feasibility of gel phantoms in MRI for the assessment of kurtosis for prostate brachytherapy

Z.G. Portakal[1], J.W. Phillips[2], C.E. Richards[3], E. Spezi[4], T. Perrett[5], D.G. Lewis[5], Z. Yegingil[1]

[1]*Cukurova University, Department of Physics, Adana, Turkey*

[2]*Swansea University, College of Medicine- Institute of Life Science, Swansea, United Kingdom*

[3]*Swansea University, Collage of Medicine, Swansea, United Kingdom*

[4]*Cardiff University, School of Engineering, Cardiff, United Kingdom*

[5]*Velindre Cancer Centre, Department of Physics, Cardiff, United Kingdom*

Purpose or Objective: Diffusion-weighted MRI is widely used in clinical imaging for sensitizing the signal to the local diffusion properties of water to generate quantitative information such as the apparent diffusion coefficient (ADC) or information about diffusion anisotropy by assuming the diffusion process to be Gaussian. However, the ADC is influenced by a number of factors, e.g., cellularity, cell membrane integrity, and viscosity. Diffusion kurtosis imaging (DKI) was established to provide a more complete characterization of water diffusion based on the fact that diffusion process in vivo are non-Gaussian. In view of the complex histologic composition of prostate cancer, DKI could potentially serve as a more effective model for the assessment of the disease. The assessment of the appropriate scanning sequence for DKI involves the make of gel phantoms with a purpose of defining the feasibility of DKI in MRI for early stage prostate cancer patients treated by HDR/LDR brachytherapy.

Material and Methods: Sets of homogenous agar, agarose and polyvinyl alcohol (PVA) gel phantoms were created, as shown in Figure 1, to optimise DKI parameters to be representative of prostate cancer. For this purpose, different concentrations of agar (1.0% - 1.5% - 2.0% - 2.5% - 3.0% - 3.5% weight/volume percentage (w,v)), agarose (0.5% - 1.0% - 1.5% - 2.0% - 2.5% - 3.0% w,v) and PVA (5.0% - 7.5% - 10.0% - 12.5% - 15.0% - 20% w,v) were used. A Siemens MAGNETOM® Skyra 3T system was used to acquire an MR scan of the phantoms using a single-shot spin-echo echo-planar sequence with different diffusion weighting levels “b value” (0 to 4000 s/mm2 in intervals of 500). Analysis of DKI was performed on a pixel-by-pixel basis in-house software (MATLAB).

Results: As the concentration of the gel increases, there are more restrictions to the water diffusion; therefore, the non-Gaussanity of the diffusion propagator and the kurtosis increases. According to the kurtosis (K) and diffusion coefficient (D) results, the measured kurtosis decreases for decreasing b(max). This sensitivity of diffusion kurtosis was obtained in all of the phantoms but more in agarose gels in comparison with PVA and agar samples.
Figure 2a shows the signal intensities (I) of agarose phantoms for each b values as well as the importance of noise floor in high b values (Fig. 2b).

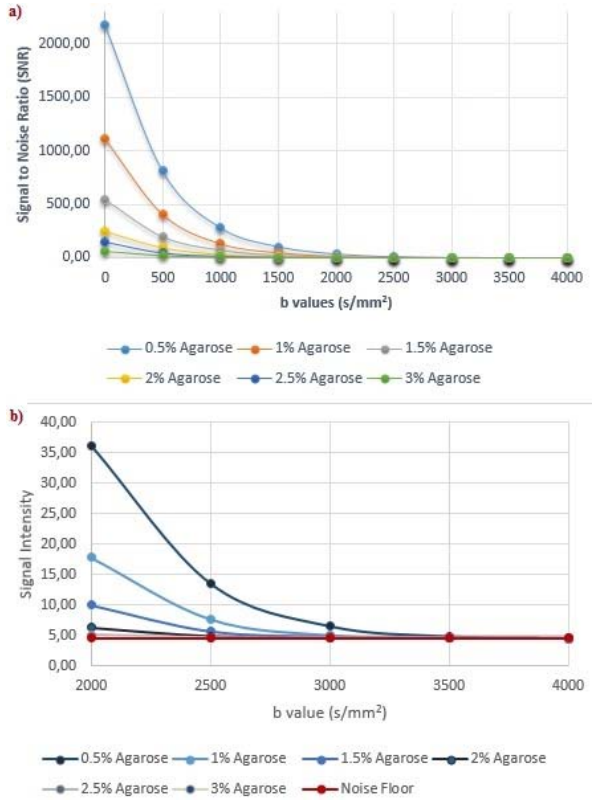

Conclusion: We demonstrated the feasibility of making and using gel phantoms for the assessment of isotropic diffusion kurtosis to use in the characterization of early stage prostate cancer treated with prostate brachytherapy. We have shown that the rectified noise floor, which exists in standard magnitude data, increases the systematic error of the diffusion coefficients D and K. Further studies are in progress to minimize the impact of noise floor in DKI.

EP-1879

Difference between PET and RMI fusion on delineation variability for liver metastases

R. Tanguy[1], A. Gaumier[1], M.P. Sunyach[1], G. Beldjoudi[1]
[1]*Centre Léon Bérard, Radiation Therapy, Lyon, France*

Purpose or Objective: Liver metastases delineation on the dosimetric computed-tomography (CT) scan is associated with high inter-observer variations. Many authors are using a fusion of the dosimetric CT scan with a magnetic resonance imaging (MRI) to define the target volume and lower the inter-observer variations. In our center we are using PET-CT / dosimetric CT fusion or RMI / dosimetric CT fusion to delineate liver lesions depending on physicians habits. We wanted here to evaluate the benefit of each imaging registration on contouring variability.

Material and Methods: Four patients (pts) were treated with stereotactic body radiation therapy (SBRT) for 6 liver metastases. Each pt had a CT scan simulation, a liver-MRI and a PET CT before treatment. Four physicians delineated the liver lesions on the fused PET-CT and on the fused RMI. For each pt, each physician made 2 contours on the CT scan in the following order: first with the PET-CT fusion available (PET/CT), then with the CT/MRI fusion available (RMI/CT). The percentages of common contoured volumes (CCV) on PET-CT and RMI were defined using the formula: (common volume of all the physicians of the group /delineated volume of the physician) x 100. The Jaccard index (ratio between common volume and the union volume obtained using the boolean operators) was also calculated.

Results: The volume of the delineated lesions were (mean+/-SD) 18.8 cc +/- 12cc vs 20.8 cc +/- 13.6 cc on PET/CT and RMI/CT respectively (p=0.63). The common contour volume wasn't statistically different between the two contouring modalities with (mean+/-SD) 56.2% +/- 21.5% vs 63.34% +/- 13.9% for PET/CT and RMI/CT respectively (p=0,1) even if there was a trend for a lesser variability for RMI fusion. The overall Jaccard index (mean±SD) was 0.34±0.15 and 0.46±0.19 for PET/CT and RMI/CT respectively (p=0.26).

Conclusion: A PET/CT fusion didn't improve the volume variation among the radiation oncologists compared to a RMI fusion. The CCV and Jaccard index were still unsatisfying with both PET/CT and RMI/CT fusion and we are planning to assess the potential impact of a liver metastases contour made by a radiologist to further improve the inter-observer variability.

EP-1880

Validation of the use of digital camera for the prediction of skin toxicity in breast radiotherapy

M. Poli[1], S. Bresciani[1], A. Miranti[1], A. Di Dia[1], A. Maggio[1], M. Gatti[2], P. Gabriele[2], M. Stasi[1]
[1]*Candiolo Cancer Institute - FPO- IRCCS, Medical Physics, Candiolo, Italy*
[2]*Candiolo Cancer Institute - FPO- IRCCS, Radiotherapy, Candiolo, Italy*

Purpose or Objective: Skin reactions are one of the most common side effects in breast cancer patient treated with radiotherapy. In this work a preliminary validation of the use of a digital camera, as a cheap and easy tool for early prediction of acute skin side effects, is presented.

Material and Methods: Twelve patients undergoing breast radiotherapy were photographed once a week with a digital camera system, composed of a reflex Canon 30D (CMOS sensor, 8.2 Megapixels) and a Tamron SP AF17-50mm f/2.8 XR. Patients were treated with two different techniques: conventional 3DCRT with Varian TrueBeam STx linac (8 patients) and Tomotherapy HD (4 patients). All photographic shots were acquired in manual-raw mode with the same exposure and white balance setup. Shots were converted in the best quality format available (TIFF) and post-processed in Lab color space (Color Space Converter plugin for ImageJ, NIH) to amplify color differences. From the channel related to image redness (a*), a skin redness level was obtained for each photographed fraction by using ImageJ. In particular, two regions of interest (ROIs) were identified: one inside the treatment field (IF) and one out-of-field (OF). Redness value histograms, related to each ROI, was acquired, plotted and used to evaluate the degree of skin redness level. ROI-redness (RR) was defined as the maximum redness value of the related histogram. The OF ROI defined the redness baseline. IF RR values were plotted as a function of the corresponding fraction number and fitted with a line; the slope of this of this line is defined as RR gradient. For each patient, skin toxicity, evaluated with RTOG criteria, was compared to the RR gradient.

Results: G1 and G2 toxicities were experienced by 10 and 2 patients, respectively. A strong relation between RR gradient and skin toxicity was found: an average RR gradient of (0.24±0.09) redness/fraction was found for G1 patients, while an average RR gradient of (0.54±0.15) redness/fraction was found for G2 patients. Due to the small statistical power of the present sample, p-values were not evaluated. The trend of the fit may be correctly assessed since the first 2 weeks of treatment. Changes in skin redness were found when comparing patients treated with conventional 3DCRT with those treated with Tomotherapy. In fact, several hot spots were noticed for the conventional treatments rather than for the volumetric irradiations, that resulted in a more homogeneous skin redness.

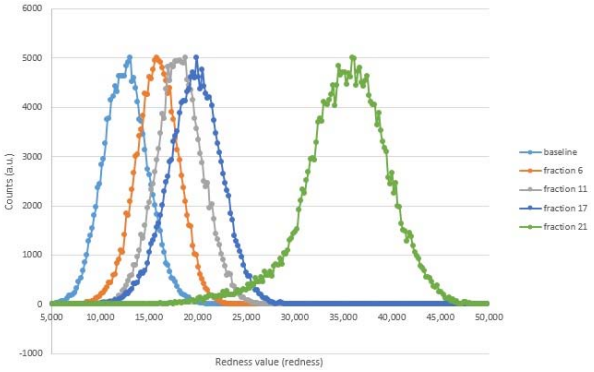

Conclusion: Digital reflex camera can be used for quantitatively evaluate skin reactions. Moreover, it should be used to predict acute skin toxicity since the first 2 weeks of treatment. Early detection of acute skin reactions should improve patients' quality of life. The proposed method seems to be sensitive to the radiotherapic technique (3D CRT vs Tomotherapy). The present results may be expanded by the study of the correlation with fractionation and other treatment parameters.

EP-1881

Diffusion MRI predicts radiotherapy response in brain metastases

F. Mahmood[1], H.H. Johannesen[2], P. Geertsen[1], R.H. Hansen[2]
[1]*University of Copenhagen - Herlev Hospital, Radiotherapy Research Unit RRU- Department of Oncology, Herlev, Denmark*
[2]*University of Copenhagen - Herlev Hospital, Department of Radiology, Herlev, Denmark*

Purpose or Objective: Radiotherapy (RT) response is generally related to changes in gross tumor volume (GTV) manifesting months later. An earlier knowledge of the treatment response may influence treatment decision. In this prospective study we investigated the correlation of parameters derived from diffusion weighted MRI (DW-MRI) acquired during RT with later GTV change of brain metastases.

Material and Methods: Nineteen metastases (N=19) from eight patients, treated with whole-brain irradiation (30 Gy in ten fractions) were analyzed. Patients were scanned with a 1T MRI system to acquire DW- (b = 0,50,100,150,400,500,600,800 s/mm^2), T2*W-, T2W- and T1W scans, before start of RT (pre-RT), at the ninth/tenth fraction (end-RT) and two to three months after RT (follow-up). DW-MRI data were fitted using a bi-exponential two-compartment model to derive the perfusion fraction (*f*), pseudo diffusion (*D_p*) and the apparent diffusion coefficient (*ADC*). Regions of interest (ROI) were outlined by an experienced radiologist using both low b-value images (*b*=0 s/mm^2) and high b-value images (*b*=800 s/mm^2) for comparison. GTV change was determined using T1W images and Eclipse (Varian Medical Systems) freehand contouring tool.

Results: Three metastases showed total remission, fourteen showed partial response and two showed progression. Using the high b-value ROI fifteen out of seventeen metastases with total or partial response showed increased (or unchanged) *f* providing the highest specificity (least false positives). Using the low b-value ROI fourteen out of seventeen metastases with total or partial response showed markedly increased (or unchanged) *ADC* providing the highest specificity. In both cases progression of metastases was associated with decreased (or unchanged) *f* and *ADC*, respectively, i.e. no false negatives (Fig. 1).

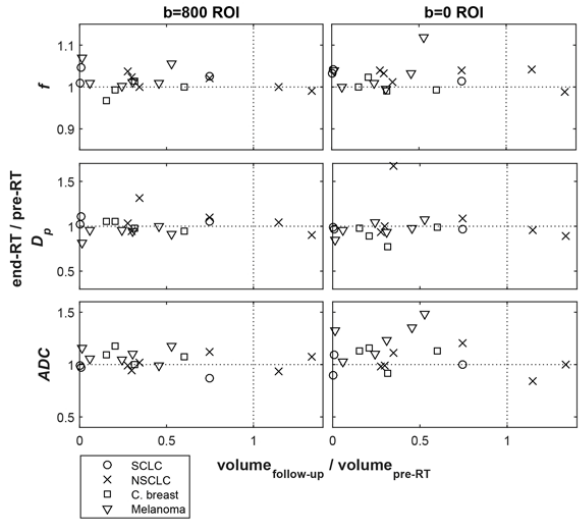

Fig. 1: Metastases are divided into primary disease and marked individually: Relative change in DW-MRI parameters (*f, D_p, ADC*) from pre-RT to end-RT, as a function of relative volume change between pre-RT and follow-up (T1W-MRI). With the *b*=800 ROI (first column), *f* has the highest specificity with no false negatives, and with the *b*=0 ROI, *ADC* has the highest specificity with no false negatives.

Conclusion: Data indicated that specific DW-MRI parameters (*f* and *ADC*) were capable of predicting RT response in brain metastases. This may become important in individualizing patients' prognoses and offering alternative (additional) treatments with less delay. (More data is available and currently being analyzed).

EP-1882

Brain connectivity changes in the presence of a glioblastoma

N. Tuovinen[1], M. Nunes[2], F. De Pasquale[1], C. Falletta Caravasso[1], E. Giudice[3], R. Miceli[3], G. Ingrosso[3], R. Santoni[3], K. Bühler[2], U. Sabatini[1]
[1]*Fondazione Santa Lucia, Radiology, Roma, Italy*
[2]*VRVis Zentrum für Virtual Reality und Visualisierung, Biomedical Visualization, Vienna, Austria*
[3]*Tor Vergata University General Hospital, Department of Diagnostic Imaging- Molecular Imaging- Interventional Radiology and Radiotherapy, Rome, Italy*

Purpose or Objective: The aim of this study is to investigate brain connectivity of post-surgical tumor patient with resting-state fMRI and diffusion tractography (DTI). This is done to understand changes occurring due to the combined effect of tumor and surgery. Common resting state (RS) network called Default Mode (DMN) and white matter (WM) tracts connecting its regions were identified. The purpose was to study whether the functional connectivity reflects the underlying structural connectivity architecture.

Material and Methods: RS- (TR/TE=2.00s/30ms) and DTI-data (64-directions, 3T Philips Achieva) were acquired for one healthy subject and a glioblastoma patient. FSL was used for preprocessing and RS-network identification (MELODIC). DTI were corrected for eddy current distortion and BedpostX was run to generate the basis for probabilistic tractography using ProbtrackX. Masks derived for Prefrontal Cortex (PFC), Posterior Cingulate Cortex (PCC), Left and Right Angular Gyrus (L/RAG) from DMN were used to identify the connecting fibers. Combined masks from healthy and disrupted DMN regions were applied to identify all the possible connecting tracts. A plugin for MITK with CUDA rendering system supporting volume rendering of multiple datasets and tracts was developed to enhance our research and visualization.

Results: The healthy subject had undisrupted DMN. Patient DMN shows functional connectivity in PCC weakened and pushed inferior. The tract in the tumoral hemisphere connecting PFC to PCC was interrupted. In addition, LAG was pushed anterior by the tumor. In this case, DTI revealed displacement of the WM tracts connecting PCC to LAG anterior of the tumor.

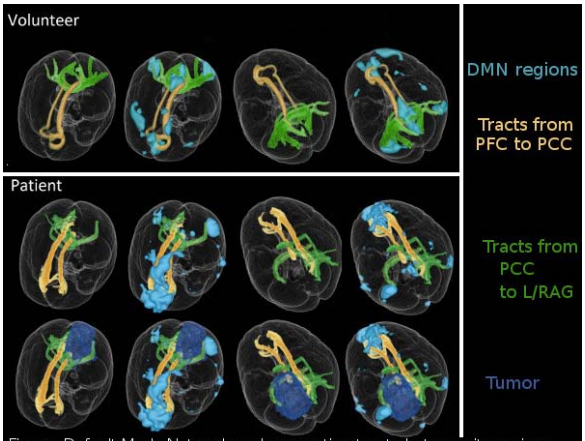

Figure: Default Mode Network and connecting tracts between its regions (PFC, PCC, L/RAG) shown for volunteer and patient with glioblastoma.

Conclusion: Our findings suggest that connectivity is somehow preserved in tumor patient. Surgery could explain the interruption of the tract on tumoral hemisphere between PFC to PCC. The displacement of the tract between PCC and LAG can be explained by anatomical shift caused by the tumor. The changes identified in the DMN were in strong agreement with the interruption and displacement of the tracts revealed by tractography. The weakening of the PCC could be explained by the interrupted tract, whereas the displacement of the tract did not seem to affect the strength of LAG. In conclusion, our results suggest that the structural damage induces abnormal functional connectivity. This agreement of functional and structural connectivity strengthens the belief that functional connectivity estimates neural connectivity.

EP-1883

Functional brain connectivity in glioblastoma patients pre- and post-radiotherapy

N. Tuovinen[1], F. De Pasquale[1], C. Falletta Caravasso[1], E. Giudice[2], R. Miceli[2], G. Ingrosso[2], R. Santoni[2], A. Laprie[3], U. Sabatini[1]

[1]*Fondazione Santa Lucia, Radiology, Roma, Italy*

[2]*Tor Vergata University General Hospital, Department of Diagnostic Imaging- Molecular Imaging- Interventional Radiology and Radiotherapy, Rome, Italy*

[3]*Institut Claudius Regaud, Department of Radiation Oncology, Toulouse, France*

Purpose or Objective: The aim of this study is to investigate longitudinal functional brain connectivity of post-surgical tumor patients with resting-state fMRI. This is done to understand changes occurring due to the combined effect of tumor, surgery and radiotherapy (RT). Special interest was given to connectivity changes in a common resting state (RS) network called Default Mode (DMN) and especially its functional hub posterior Cingulate Cortex (pCC).

Material and Methods: RS-data (TR/TE=2.00s/30ms, 3T Philips Achieva) was acquired for three glioblastoma patients pre- and post-RT. Patient1 had a tumor lesion near pCC, patient2 had a lesion near Prefrontal Cortex (PFC) and patient3 near the Right Frontal Eye Field (RFEF). Karnofsky performance scores (KPS) were evaluated. KPS for patient1 remained 80, for patient2 remained 90 and for patient3 decreased from 80 to 70 post-RT. FSL was used for preprocessing and DMN identification (MELODIC). pCC node was derived from DMN and pCC-to-brain connectivity maps were computed. Maximum, minimum and mean dose (cGy) on contours of GTV and pCC were calculated and percentual isodoses for 30/50/70/90% were evaluated from the treatment planning.

Results: DMN was recognizable in all timepoints although topology changes during the treatment were noted. When looking at the seed-to-brain connectivity maps (Fig.1) seems that RT given on the affected network hub pCC (patient1) helps to improve the global connectivity to frontal regions of the DMN. In addition, connectivity becomes more focused post-RT. In patient2, RT given on PFC region seems to increase local connectivity temporarily in the frontal region. For patient3 whose RT was not involving DMN, the functional connectivity becomes more aspecific post-RT.

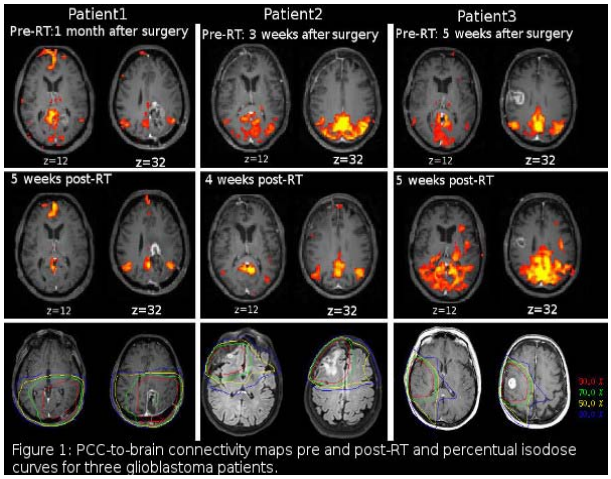

Figure 1: PCC-to-brain connectivity maps pre and post-RT and percentual isodose curves for three glioblastoma patients.

	cm³	$Dose_{min}$(cGY)	$Dose_{max}$(cGY)	$Dose_{mean}$(cGY)
Patient1 GTV	41,9	5895,4	6252,8	6033,2
Patient1 pCC	3,5	5923,9	6019,1	5971,5
Patient2 GTV	6,2	6036,4	6290	6168
Patient2 pCC	4,7	650,4	1478,9	1061,1
Patient3 GTV	8,4	5988,4	6255,2	6130
Patient3 pCC	6,2	1040	3116	1518,4

Table 1 Minimum, maximum and mean doses received to Gross Tumor Volume and pCC.

Conclusion: Interestingly, RT near pCC seems to increase global connectivity. This might be due to the fact that we are treating a central node and thus the communication between the brain regions is re-established when the central node improves its connectivity. In addition, seems that RT near prefrontal cortex helps to increase connectivity locally. However, as this node is not an important connectivity hub, there is no improvement in connectivity to far away regions. When RT was not involving DMN, we noted a deterioration of functional connectivity. Interestingly, this patient showed also decrease in clinical performance reflecting these connectivity changes.

EP-1884

Voxel based topological PET SUV changes of bone marrow for LACC RT effect on hematological toxicity

A. Gulyban[1], P.V. Nguyen[1], J. Hermesse[1], P.A. Coucke[1], F. Lakosi[1]

[1]*Liege University hospital, Radiation Department, Liege, Belgium*

Purpose or Objective: To evaluate the topological voxel-based FDG-PET SUV changes of bone marrow including dose from radiotherapy for locally advanced cervical cancer patients and their effect on hematological toxicity.

Material and Methods: Between February 2013 and December 2014 fourteen patients were treated with using advanced radiotherapy delivery technique (IMRT or VMAT). Diagnostic FDG-PET with low-dose CT whole body scans were performed before and after radiotherapy (preRT and postRT - PET/CT). During the chemotherapy (six planned cycle) hematological toxicities were gathered for hemoglobin (HGB), white blood cell count (WBC), absolute neutrophil count (ANC) and for pallet count (PLT). Co-registration

between the three CTs (2x PET/CT and planning CT) were performed using the optical flow uni-modality deformation algorithm of Mirada RTx (version 1.6.2, Mirada Medical, Oxford, UK). Based on the CT information two region of interest (ROI) were defined: Body (only extracranial region) and bone marrow "BM" (using auto-thresholding followed by manual exclusion of CT contrast agents). Each non-CT modality were resampled to match the preRT-PET ROI statistics of original and resampled dataset were compared. Voxel-based data were extracted for each patient dataset and heuristic programmatic statistical correlation were performed using Python (version 2.7). Sub-regions defined as followings: within/outside of irradiated region (voxels above/ below 1 Gy), active/non-active BM (above/below the preRT SUV average), and dose to absolute/relative volume of X Gy (where X represents any dose between 0 and 50 Gy). Correspondence between SUV changes and the dose were tested as well. All information was used to identify correlation with observed hematological toxicity (on logarithmical scale) with $p<0.05$ significance level.

Results: The average number of voxel were 662.352 and 50.652 for Body and BM. 70/75 parameters of original and resampled volumes were within +/- 0.1 g/ml or Gy and considered as clinically equivalent. PreRT and postRT SUV changes in function of delivered dose correlated significantly. For HGB no predictive value were identified. Absolute volume receiving at least 30 Gy of dose of the active BM determined nadir WBC ($p = 0.033$) and nadir ANC ($p = 0.014$) (see Figure 1), while total BM only correlated with nadir WBC ($p=0.041$). Nadir PLT was determined by preRT SUV of the irradiated (>1Gy) active BM and the slope of the SUV changes between preRT and postRT SUV.

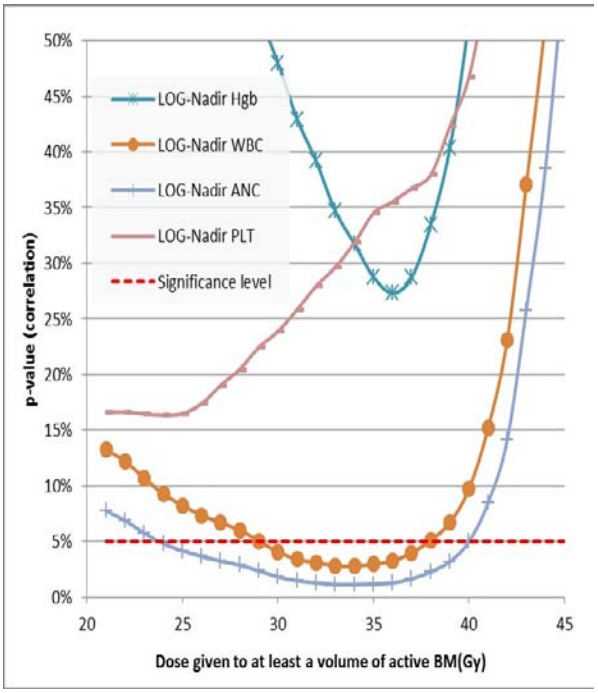

Conclusion: Active and total bone marrow region receiving at least 30 Gy should be monitored to reduce possible hematological toxicity. Voxel-based evaluation of functional imaging with dose information is a valuable option especially in combination with programmatic heuristic statistical testing.

EP-1885

Novel algorithm for IVIM MRI in cancer patients: comparison to pCASL MRI

S. Stieb[1], T. Weiss[2], M. Wurnig[3], O. Riesterer[1], A. Boss[3], C. Rossi[3]

[1]*University Hospital Zurich, Department of Radiation Oncology, Zurich, Switzerland*

[2]*University Hospital Zurich, Department of Neurology, Zurich, Switzerland*

[3]*University Hospital Zurich, Department of Diagnostic and Interventional Radiology, Zurich, Switzerland*

Purpose or Objective: Intravoxel incoherent motion (IVIM) MRI provides simultaneous estimates of both, perfusion and diffusion traits of tissue. In standard algorithms, a fixed threshold is set to separate the perfusion from the diffusion component of the MR signal acquired. This fixed threshold does not account for potential differences between tissue types or for a variation of the perfusion component induced by a pathological condition. In this study, the validity of a novel multi-step parameter-free IVIM algorithm independent on a priori assumptions was tested in a cohort of brain tumor patients and compared to arterial spin labeling (ASL) measurements.

Material and Methods: Six patients with malignant brain tumors grade III-IV (glioblastoma n=3, anaplastic astrocytoma n=3) have been included in this prospective study. Patients underwent a single MR examination comprising morphological imaging, diffusion weighted imaging for IVIM and pseudocontinous arterial spin labeling (pCASL) for estimation of the cerebral blood flow (CBF). The diffusion coefficient (DC), perfusion fraction (fp) and pseudo-diffusion coefficient (D*) were computed pixel-wise using a multi-step parameter-free algorithm for IVIM. Regions-of-Interest (RoIs) were drawn over tumor areas, necrotic regions, edema, and gray matter. Spearman correlation was used to evaluate the correlation between the different parameters.

Results: In all patients, adequate image quality of IVIM datasets allowed for the pixel-wise computation of the perfusion and diffusion maps in good quality. Quantitative ASL perfusion values were in the order of 60 ml/100g/min, and tumor and perifocal edema slightly lower (Table 1). The statistical evaluation of the RoI analysis showed that CBF positively correlates with the perfusion-dependent IVIM parameter D* (rho CBF vs. D*: 0.574) and the product fp*DC (rho CBF vs fp*D*: 0.432). A slightly negative correlation between CBF and DC (-0.424) and CBF and fp (-0.217) was found.

	CBF [ml/100g/min]	DC [10^{-3}mm^2/s]	fp	D* [10^{-3}mm^2/s]
Tumor	57.7 ± 12.7	0.852 ± 0.129	0.142 ± 0.042	15.4 ± 12.0
Gray matter	63.7 ± 16.3	0.816 ± 0.108	0.153 ± 0.075	10.1 ± 15.2
Perifocal edema	44.5 ± 11.8	1.144 ± 0.191	0.185 ± 0.126	10.0 ± 8.3

Table 1: Mean values (± standard deviation) of perfusion (CBF) and of IVIM parameters for different tissue types.

Conclusion: Perfusion-related IVIM parameters correlated well with tissue perfusion measured by ASL. The new parameter-free algorithm for IVIM seems therefore to be reliable for perfusion measurements in brain tumor patients.

Electronic Poster: Physics track: Images and analyses

EP-1886

The feasibility of atlas-based automatic segmentation of MRI for H&N radiotherapy planning

R. Speight[1], K. Wardman[2], M. Gooding[3], R. Preswich[4]

[1]*St James Institute of Oncology, Medical Physics and Engineering, Leeds, United Kingdom*

[2]*University of Leeds, Department of Medicine, Leeds, United Kingdom*

[3]*Mirada Medical Ltd, Oxford Centre for Innovation, Oxford, United Kingdom*

[4]*St James Institute of Oncology, Clinical Oncology, Leeds, United Kingdom*

Purpose or Objective: Atlas-based autosegmentation is an established tool for segmenting structures for CT-planned head and neck radiotherapy. MRI is being increasingly integrated into the planning process. The aim of this study is to assess the feasibility of MRI-based atlas-based autosegmentation for organs-at-risk (OAR) and lymph node

levels, and to compare the segmentation accuracy with CT-based autosegmentation.

Material and Methods: 14 patients with locally advanced head and neck cancer in a prospective imaging study underwent a T1-weighted MRI and a PET-CT (with dedicated contrast-enhanced CT) in an immobilisation mask. Organs at risk (orbits, parotids, brainstem and spinal cord) and the left level II lymph node region were manually delineated on the CT and MRI separately. A 'leave one out' approach was used to automatically segment structures onto the remaining images separately for CT and MRI. Contour comparison was performed using multiple positional metrics: Dice index, mean distance to conformity (MDC), sensitivity index (Se Idx) and inclusion index (In Idx).

Results: Figure 1 illustrates example manual and autocontours generated on the CT and MRI scans. Automatic segmentation using MRI of orbits, parotids, brainstem and lymph node level was acceptable with a DICE coefficient of 0.73-0.91, MDC 2.0-5.1mm Se Idx. 0.64-0.93, In Idx 0.76-0.93. Segmentation of the spinal cord was poor (Dice coefficient 0.37). The process of automatic segmentation was significantly better on MRI compared to CT for orbits, parotid glands, brainstem and left lymph node level II by multiple positional metrics; spinal cord segmentation based on MRI was inferior compared with CT.

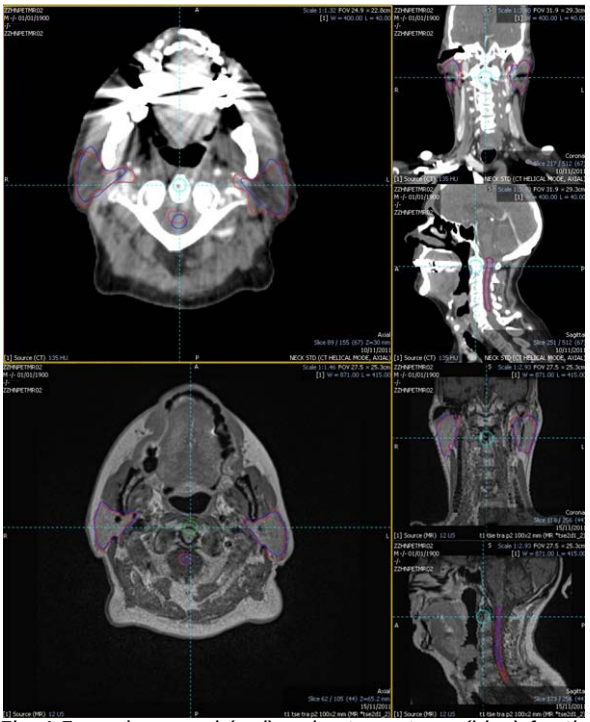

Fig. 1 Example manual (red) and auto contours (blue) for the spinal cord as well as left and right parotids for patient 2. Top images are CT showing large dental artefacts and poor auto contours and bottom images are MRI showing more accurate auto contours.

Conclusion: Accurate atlas-based automatic segmentation of OAR and lymph node levels is feasible using T1-MRI; segmentation of the spinal cord was found to be poor. Comparison with CT-based automatic segmentation suggests that the process is equally or more accurate using MRI. These results support further translation of MRI-based segmentation methodology into clinical practice.

EP-1887

Automated 3D MRI pancreas segmentation

K. Sheng[1], S. Gou[2], P. Hu[3]

[1]*David Geffen School of Medicine at UCLA, Radiation Oncology, Los Angeles, USA*

[2]*Xidian University, Key Lab of Intelligent Perception and Image Understanding of Ministry of Education, Xi'an, China*

[3]*UCLA, Radiology, Los Angeles, USA*

Purpose or Objective: With the advent of MR guided radiotherapy, internal organ motion can be imaged simultaneously during treatment. The real time MRI is particularly advantageous for abdominal organs that typically show poor CT contrast. To use the images for motion adaptive radiotherapy, the MR images need to be segmented but manual segmentation of the data is not practical due to data volume and speed requirement. In this study, we evaluate the feasibility of pancreas MRI segmentation using state-of-the-art segmentation methods.

Material and Methods: T2 weighted half-Fourier acquisition single-shot turbo spin-echo (HASTE), contrast free and contrasted T1 weighted 3D Fast Low Angle SHot (FLASH) Volumetric Interpolated Breath-hold Examination (VIBE) images were acquired on three patients and two healthy volunteers for a total of 12 imaging volumes. Four automated segmentation methods, including mean-shift merging (MSM), distance regularized level set (DRLS), graph cuts (GC) and dictionary learning (DL) methods were used to segment the pancreas. The segmentation results were compared to manual contours using Dice's index (DI), Hausdorff distance and mean absolute surface distance (MASD).

Results: All VIBE images were successfully segmented by at least one of the auto-segmentation method with DI >0.83 and MASD ≤2.4 mm using the best automated segmentation method. All automated segmentation methods failed in segmenting two HASTE images, showing >1 cm MASD. Hausdorff distance exceeding 1 cm is observed on most segmentation results, indicating mismatch in fine segmentation details. The use of contrast minimally improved the segmentation accuracy. DL is statistically superior to the other methods in Dice's overlapping index ($p<0.05$). For the Hausdorff distance and MASD measurement, DRLS and DL performed slightly superior to the GC method, and substantially better than MSM. DL required least human supervision and was faster to compute.

Figure shows 3D rendering of the pancreas contour based on (a) a HASTE image and (b) a VIBE image. The manual ground truth is shown in red, automated segmentation in green.

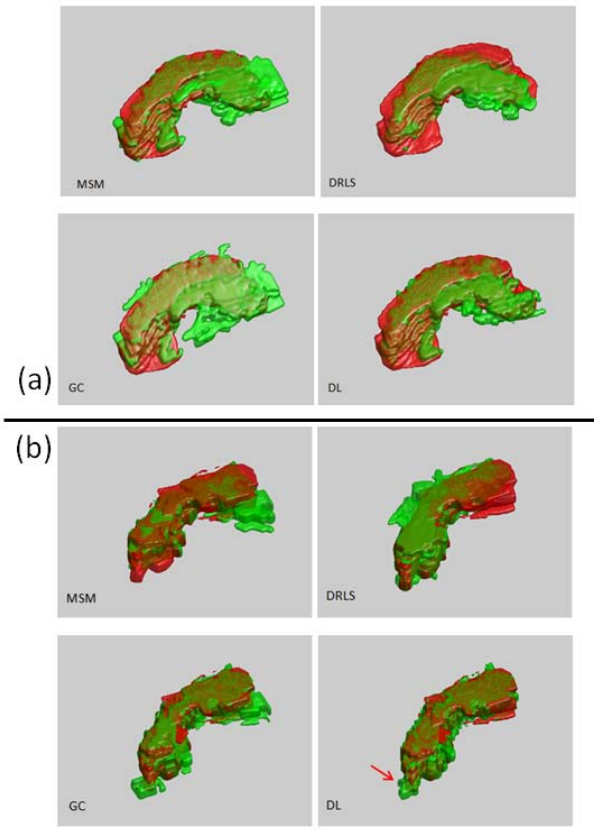

Conclusion: Automated segmentation of the pancreas with accuracy useful for organ motion tracking is achieved based on T1 weighted VIBE images. Automated pancreas segmentation based on T2 weighted HASTE images is not as robust. Considering the segmentation accuracy, levels of human supervision and computational speed, dictionary learning is the preferred segmentation method for real time MRI pancreas segmentation.

EP-1888

Accuracy and limitations of deformable image registration with SmartAdapt® in the thorax region

S. Sarudis[1], A. Karlsson Hauer[2], D. Bibac[3], A. Bäck[2]
[1]*Sahlgrenska University Hospital, Therapeutic Radiation Physics, Borås, Sweden*
[2]*Sahlgrenska University Hospital, Therapeutic Radiation Physics, Gothenburg, Sweden*
[3]*Södra Älvsborgs Sjukhus, Diagnostic Imaging and Laboratory Medicine, Borås, Sweden*

Purpose or Objective: Systematically determine the accuracy and limitations of the deformable image registration (DIR) algorithm in SmartAdapt® and present a workflow which minimises the errors and uncertainties in a deformation process.

Material and Methods: Deformable image registrations were performed on 4-dimensional computed tomography (4DCT) scans of a dynamic thorax phantom (CIRS, 008A) and patients with lung tumours that did a 4DCT scan within their regular preparation procedure before receiving external beam radiation therapy. To evaluate the performance of the DIR algorithm, the tumour in the phantom and the organs of interest for each patient (tumour, lungs, heart and spinal cord) were manually delineated in each breathing phase of the 4DCT, and the Centre of Mass Shift (CMS) and Dice Similarity Coefficients (DSC) between the deformed and manually delineated target volumes were calculated. Target shifts between 0 - 53 mm and absolute volumes between 0.5 - 1600 cm3 were evaluated. The phantom scans were repeated twice with image thicknesses of 1 and 3 mm to determine the impact on the deformation accuracy. All deformations were performed using SmartAdapt® v11.0.

Results: Target motion and volume changes are generally reproduced with CMS agreement of <2 mm and DSC >0.90. However large failures in deformed target volumes may occur when the target position is adjacent to voxels with the same intensity as the voxels within the target, if the volume of interest is set too small or if the target shift is large relative to its absolute volume. In these cases the DSC may decrease to zero meaning there is no overlap in any point between the deformed and the true target volumes. In general, the deformation accuracy decreases as the complexity and the image thickness increases. The deformed volumes may vary in shape and position between individual deformations even though all parameters in the deformations process are kept constant. Visual verification of the deformed volume before approval is therefore crucial to keep the accuracy as high as possible.

Conclusion: In general, SmartAdapt® offers a useful tool for DIR with CMS agreement of <2 mm and DSC >0.90 between the deformed and the manually delineated target volumes. More complex deformations containing large relative changes in target volume and position are less accurate with DSC decreasing to zero. Every deformation process should be repeated until visual inspection of the deformed volume is satisfactory in order to keep the accuracy as high as possible.

EP-1889

Quality assurance of image registration algorithms using synthetic CT/MRI/PET datasets

A. Perez-Rozos[1], M. Lobato Muñoz[1], I. Jerez Sainz[1], J. Medina Carmona[2]
[1]*Hospital Virgen de la Victoria, Radiation Oncology. Medical Physics., Malaga, Spain*
[2]*Hospital Virgen de la Victoria, Radiation Oncology, Malaga, Spain*

Purpose or Objective: To develope a method to generate synthetic datasets to perform quality assurance of multimodality registration algorithms.

Material and Methods: Relevant geometries, resembling phantoms and human body, are generated using in-house software and PENGEOM (PENELOPE) routines to represent clinically relevant situations. Every region of interest is characterized using user defined parameters: material density, uptake index parameter, T1, T2 and proton density parameters. Using these parameters and geometry it is possible to generate three datasets: synthetic-CT dataset, a synthetic-PET dataset, and a synthetic-MRI dataset. For synthetic CT Hounfield units are assigned using material density and a standard calibration curve; for synthetic PET SUV values are assigned using uptake index parameter for every ROI and then applying a gaussian blur filter to mimic PET resolution; synthetic MRI signal values are assigned using T1, T2, proton density and repetition and echo times using parametrization formulas that calculate signal values for T1, T2 or proton weighted sequences. Known rotations, shifts, and deformations can be applyed to every dataset. The different datasets could be imported in treatment planning systems as usual and then apply the registration and fusion algorithms, that would have to recalculate the previously applied rotations and shifts.

Results: In the image we show an example of a mathematical phantom with a cortical bone ring, soft tissue with three spheres and two parallelepiped regions. Some regions are visible only in PET or MRI datasets. In lower part of image it is shown an example of PET image shift and rotation and the corresponding CT-PET image registration.

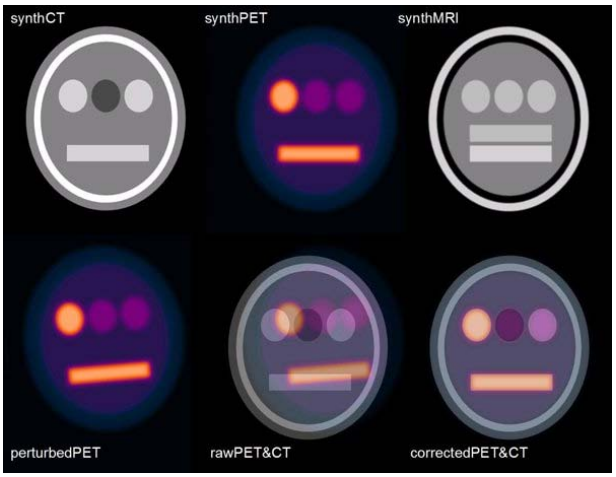

Conclusion: Use of synthetic datasets allows for comprehensive quality assurance of registration algorithms of several systems used in radiation therapy.

EP-1890

Accurate organs at risk contour propagation in head and neck adaptive radiotherapy

T.T. Zhai[1,2], H.P. Bijl[2], J.A. Langendijk[2], R.J. Steenbakkers[2], C.L. Brouwer[2], H.J. Van der Laan-Boomsma[2], N.M. Sijtsema[2], R.G. Kierkels[2]
[1]*Cancer Hospital of Shantou University Medical College, Department of Radiation Oncology, Shantou, China*
[2]*University of Groningen- University Medical Center Groningen, Department of Radiation Oncology, Groningen, The Netherlands*

Purpose or Objective: Adaptive radiotherapy for head and neck cancer patients aims to correct for geometrical changes due to tumour shrinkage, mucosal swelling and weight loss. These changes are monitored by weekly acquired repeat CT scans (rCTs) on which the actual treatment plan is evaluated.

The resulting large workload requires automated contour propagation from planning CT (pCT) to the rCTs. Consequently, decisions to re-plan are directly based on the propagated contours. Therefore, we investigated whether deformable propagated organs at risk (OARs) contours of head and neck cancer patients can be used for clinical treatment plan evaluation on rCTs.

Material and Methods: Planning CTs and weekly acquired rCTs of ten head and neck cancer patients were included in the analysis (in total: 10 pCTs and 67 rCTs). The following OARs were delineated on each pCT: parotid glands, submandibular glands, pharyngeal constrictor muscle, cricopharyngeal muscle, oral cavity, mandible, thyroid, supraglottic larynx, glottic area, and spinal cord. Hence, the transformation between each rCT and pCT was derived using an intensity based deformable image registration algorithm. The transformation was used to automatically propagate all contours to the rCTs (AC). All propagated contours were evaluated by an expert and corrected if necessary (corrected contours: CC). To validate deformable contour propagation for treatment plan evaluation, the AC and CC were compared by the Dice Similarity Coefficient (DSC). The AC to CC contour distances were evaluated using the combined gradient of the distance transform (ComGrad) method. Furthermore, dosimetric parameters were compared.

Results: The ACs were very similar to the CCs with an average (±SD) DSC for all structures of 0.93 ± 0.07 (range: 0.57-1.00), indicating no or minor corrections required for the majority of contours. The DSC was lower than 0.8 for 10% of the pharyngeal constrictor muscle and 12% of the cricopharyngeal muscle contours, respectively. For all other structures the DSC was larger than 0.9 for 93% of the contours. The average 90th percentile AC to CC contour distance was below the size of an image voxel (0.66 ± 0.25 mm; range: 0.00 - 1.50 mm). The dosimetric parameters revealed only small differences between the AC and CC dose values. Only in 3% of all analyzed contours the difference in accumulated dose between the AC and CC was more than 2 Gy. In Figure 1 the fractional ipsilateral parotid gland dose of AC and CC is shown for five representative cases.

Figure 1. The fractional mean dose of the automated (AC) and corrected (CC) ipsilateral parotid gland contours of 5 patients

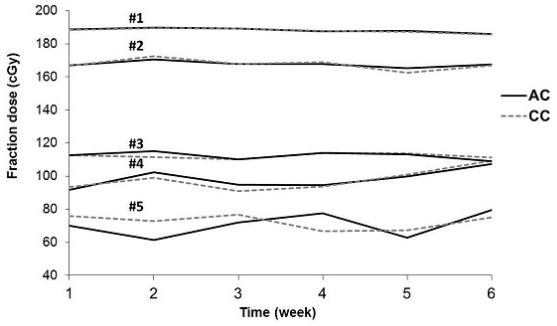

Conclusion: Deformable OARs contour propagation from the planning CT to weekly acquired repeat CTs in the head and neck area resulted in similar contours and dosimetric values compared to the ground truth manually corrected contours. Only smaller contours such as the swallowing muscles, required manual review when used for decision making on replanning. Automatic contour propagation makes it feasible to include more patients in an adaptive radiotherapy schedule.

EP-1891

Determination of physical body outline in relation to outline visualisation in MRI for RT planning

S. Weiss[1], M. Helle[1], S. Renisch[1]
[1]*Philips GmbH Innovative Technologies, Research Laboratories, Hamburg, Germany*

Purpose or Objective: The geometric accuracy of MR-only based RT planning is influenced by several aspects, most of which have been evaluated thoroughly and solutions been provided: differently shaped MR and treatment tables, skin indentations by MR coils, geometrical distortions in MRI, and accuracy of segmentation. This work evaluates whether the body outline as visualized by MRI precisely matches the physical body outline, or whether there is potentially any skin layer that is not visualized by MRI. Correct delineation of the body outline is important because it directly influences attenuation and hence dose delivered to treatment and risk organs.

Material and Methods: Standard ultra-sound gel was doped with 10% Gd-contrast agent, and a lump of gel was applied to the thigh of a male volunteer. Two polyethylene foils (50µm and 12µm thickness) were immersed in doped gel in a phantom and located beside the gel on the thigh to serve as a reference. A two-channel surface coil (diameter 7cm) was used to acquire axial images with a 3D T1w-FFE-mDIXON sequence as used for MR-only RT planning in prostate. Images were acquired at standard resolution (1.7mm²x2.5mm) and high resolution (0.5mm²x2mm) in a 200mm²x10mm FOV on a 1.5T scanner (Philips Achieva). Read-out was chosen in LR direction to avoid any water-fat shift perpendicular to the skin.

Results: None of the reconstructed images (TE1, TE2, water, in-phase, opposed-phase) revealed any hypo-intense layer between the outermost MR-visible layer and the gel (c.f. Fig: thin white arrows). However, the 50µm PE foil in the phantom was clearly visible in the highly resolved images (bold white arrows), and the 12µm foil was just about visible (bold grey arrows). Initial scans had shown that plain gel generates a much stronger signal than the outer skin layer, so that the gel signal obscures the skin signal, which complicates image interpretation. Doping with 10% contrast agent resulted in a match of signal strength of gel and skin and resolved this. Image interpretation was unambiguous with respect to water-fat shift, since it was chosen parallel to the skin surface in the evaluated region.

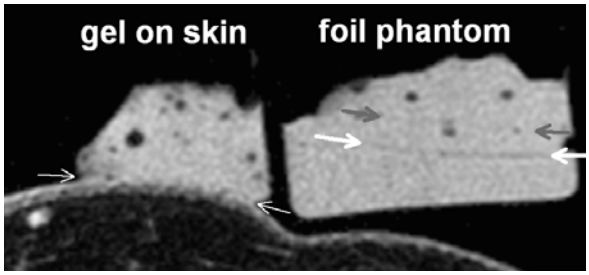

Conclusion: It can be concluded that any MR-invisible skin layer that may be present on top of the outermost MR-visible layer but not be visualized due to lack of free water or other MRI effects has a thickness of less than 20µm. Such a thin layer would have a negligible effect on simulation of attenuation maps and respective dose planning, which is clinically done with a spatial resolution of 4mm.

EP-1892

Using deformable image registration to integrate diagnostic MRI into the planning pathway for HNSCC

R. Chuter[1,2], R. Prestwich[3], A. Scarsbrook[1], J. Sykes[4], D. Wilson[1], R. Speight[1]
[1]*St James's University Hospital, Medical Physics and Engineering, Leeds, United Kingdom*
[2]*The Christie, Medical Physics and Engineering, Manchester, United Kingdom*
[3]*St James's University Hospital, Clinical Oncology, Leeds, United Kingdom*
[4]*University of Sydney, Institute of Medical Physics, Sydney, Australia*

Purpose or Objective: To assess the accuracy of Gross Tumour Volume (GTV) delineation for head and neck

squamous cell carcinoma (HNSCC) through the use of diagnostic position MRI (MRI-D) images deformably registered to the planning CT. This study assessed whether optimising image registration of MRI-D to planning CT (pCT) is an adequate surrogate for delineation on a gold standard (GS) treatment position MRI (MRI-RT) rigidly registered to the pCT.

Material and Methods: Fourteen patients with HNSCC underwent a pCT and T1-weighted MRI in both a diagnostic and treatment position. The GTV was delineated on all images by a single radiation oncologist and intra-observer variability was assessed over 5 patients having been contoured on 3 occasions. GS structures were defined as contours from MRI-RT transposed to pCT using rigid registration. The GS was compared to contours produced by 4 methods: MRI-D transposed to pCT with deformable image registration (DIR) over the whole image (DIR-Whole); MRI-D transposed to pCT with rigid registration or DIR optimised on a 3cm ROI around the GTV (Rigid-ROI and DIR-ROI respectively); and on pCT alone. Registrations were performed with Mirada RTx v1.4 (Mirada Medical, Oxford UK) and 6 contour comparison metrics were calculated with ImSimQA v3.1 (OSL, Shrewsbury UK).

Results: MRI delineation reduced intra-observer variability compared to pCT. DIR-whole resulted in GTVs significantly closer to the GS as determined by multiple positional metrics in comparison with CT-only delineation (normalised results are shown in Figure 1). The mean Dice Similarity Coefficient was 0.6 and 0.72 for pCT and DIR-whole respectively with p=0.019. Use of MRI-D with Rigid-ROI or DIR-ROI provided no advantage over CT-only delineation.

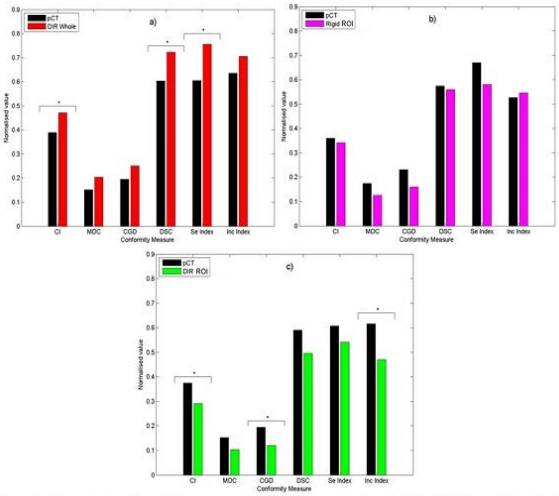

Figure 1 - Normalised positional indices comparing GTV delineated on planning CT or MRI-D coregistered to the planning CT by a) DIR whole, b) Rigid ROI or c) DIR ROI, to GS of MRI-RT rigidly coregistered to the planning CT. An * denotes a significant difference of P<0.05. Conformity measures utilised were: Conformity Index (CI), Mean Distance to Conformity (MDC), Centre of Gravity Distance (CGD), Dice Similarity Coefficient (DSC), Sensitivity Index (Se.Idx) and Inclusiveness Index (Inc.Idx).

Conclusion: In the absence of dedicated MRI-RT, image registration software can aid the integration of MRI-D into the treatment pathway. MRI-D is most accurately integrated into the radiotherapy planning pathway when contours are transposed to pCT with DIR over the whole patient.

EP-1893

Automatic contouring of soft organs for image-guided prostate radiotherapy

X. Cai[1], C.B. Schönlieb[1], J. Lee[1], J. Scaife[2], H. Karl[3], M. Sutcliffe[4], M. Parker[3], N. Burnet[2]

[1]*University of Cambridge, Department of Applied Mathematics and Theoretical Physics, Cambridge, United Kingdom*

[2]*University of Cambridge, Department of Oncology, Cambridge, United Kingdom*

[3]*University of Cambridge, Department of Physics, Cambridge, United Kingdom*

[4]*University of Cambridge, Department of Engineering, Cambridge, United Kingdom*

Purpose or Objective: Image-guided radiotherapy (IGRT) is a primary modality in treatment for cancer types such as prostate or neck cancer. Its pipeline involves the analysis of planning- and treatment-day CT scans (kV CT and MV CT in our case). In particular, to explore the relationship between the delivered dosage and its side effects on nearby normal tissues, an automatic contouring method for the precise delineation of target and adjacent critical organs during the treatment is essential and is also the main aim of our work.

Material and Methods: Our proposed 3D automatic contouring method constitutes a robust iterative approach on a 3D active contour segmentation model, customised for the IGRT application. The model contains two main driving principles: two data fidelity terms and one regularization term which keep the distance of the auto-contoured organ as close as possible to its true location and sufficiently close to the initialization given by the registered planning scan; and another regularization term which imposes smoothness of the contour around the segmented soft organ. The desired contour in the treatment scan is then computed iteratively, solving a convex minimization problem with an efficient solver called ADMM in each iteration. The initialization at the first iteration is obtained by transferring the manual contour in the planning scan to the treatment scans using a spline-based image registration method. Then, the global minimizer found after the first iteration is used to update the initialization for the next iteration to find the new global minimizer, which ensures the stability and robustness of the approach. We stop the iteration when the preset maximum iteration number (=10 in our case) is reached.

Results: We test our method by contouring the rectum of four patients with prostate cancer. Results are given in Fig. 1 and Table 1. Fig. 1 visually validates that our method indeed achieves accurate results and improves upon a registration of the planning contour alone. Table 1 gives the quantitative results for the registered planning contour and our proposed method. Each iteration of our method costs less than 10 seconds.

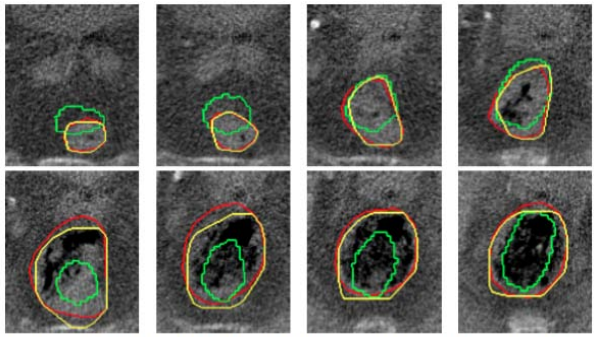

Fig. 1: Contouring results of Patient 1 in slices. Green: contour obtained by registration of the planning scan. Red: manual contour. Yellow: contour computed by our method.

	Registration method (initialization)			
	mean(acc)	std(acc)	mean(sen)	std(sen)
Patient 1 (37 scans)	69.9%	4.2%	53.9%	5.1%
Patient 2 (36 scans)	69.4%	4.0%	53.2%	4.7%
Patient 3 (37 scans)	68.3%	6.1%	52.2%	7.2%
Patient 4 (37 scans)	61.2%	3.4%	44.1%	3.7%
	Our automatic contouring method			
	mean(acc)	std(acc)	mean(sen)	std(sen)
Patient 1 (37 scans)	**91.8%**	3.2%	**76.2%**	3.2%
Patient 2 (36 scans)	**89.8%**	3.4%	**71.2%**	4.3%
Patient 3 (37 scans)	**83.3%**	4.0%	**71.0%**	3.9%
Patient 4 (37 scans)	**85.9%**	3.5%	**73.6%**	3.4%

Table 1: Mean and standard deviation (std) of the accuracy (acc) and sensitivity (sen) of the spline-based registration method and our method on the treatment scans of four patients.

Conclusion: Our proposed 3D automatic contouring method achieves an accuracy of >0.8 and sensitivity of >0.7, which is comparable to the performance of manual contours clinically. We are currently working on a fully automated setup (parameters selection) of the method which is learned from a set of 3700 manually contoured treatment scans.

EP-1894

Evaluation of a novel method for automatic segmentation of rectum on daily MVCT prostate images

M. Romanchikova[1], D.I. Johnston[2], K. Harrison[3], M.P.F. Sutcliffe[4], J.E. Scaife[5], S.J. Thomas[6], N.G. Burnet[5]
[1]*Cambridge University Hospitals, Medical Physics and Clinical Engineering, Cambridge, United Kingdom*
[2]*University of Cambridge, School of Clinical Medicine, Cambridge, United Kingdom*
[3]*University of Cambridge, Cavendish Laboratories, Cambridge, United Kingdom*
[4]*University of Cambridge, Mechanical Engineering, Cambridge, United Kingdom*
[5]*University of Cambridge, Oncology, Cambridge, United Kingdom*
[6]*Cambridge University Hospitals NHS Foundation Trust, Medical Physics and Clinical Engineering, Cambridge, United Kingdom*

Purpose or Objective: Rectal toxicity is a major complication from radiotherapy (RT) for prostate cancer. The VoxTox project aims to link rectum dose to the observed toxicity for 500 prostate cancer patients who received intensity modulated RT on TomoTherapy with daily image guidance (IG).
Rectum dose is calculated using IG megavoltage CT (MVCT) scans. MVCT images have lower soft tissue contrast and signal-to-noise ratio than conventional CT. To date, there are no auto-segmentation methods for rectum delineation on MVCT. With 200,000 rectum contours required, an experienced oncologist would need over 2 years to complete the outlining.
To automate this task, we developed an in-house auto-contouring software to outline the rectum. Our software can complete the outlining in several days.
The aim of this work is to evaluate the quality of auto-generated contours and to provide a basis for further refinement of the algorithm. The method can be extended to evaluate other auto-segmentation tools.

Material and Methods: Rectum contours were produced using a Matlab code based on 2D Chan-Vese segmentation method. The contours were overlaid on the corresponding MVCT images centred at 87 Hounsfield Units (HU) and width of 220 HU.
7110 slices from 689 daily IG MVCT scans of 20 patients were inspected by a trained doctor.
A contour quality index was defined where 1 was 'very poor' and 5 was 'very good' (clinically acceptable).
Contouring errors were categorized as
1) too large;
2) too small;
3) cut air pocket (contour cut through gas pocket in rectal lumen);
4) missed air pocket (contour excluded gas pockets);
5) shift (contour is shifted with respect to actual organ location);
6) shape (sharp corners present in contour).

Results:

Contour quality:
70% of contours were scored as "very good" (Figure 1a), and 12% were "good". 13% of contours were of "average" quality, and 4% were "poor" or "very poor".

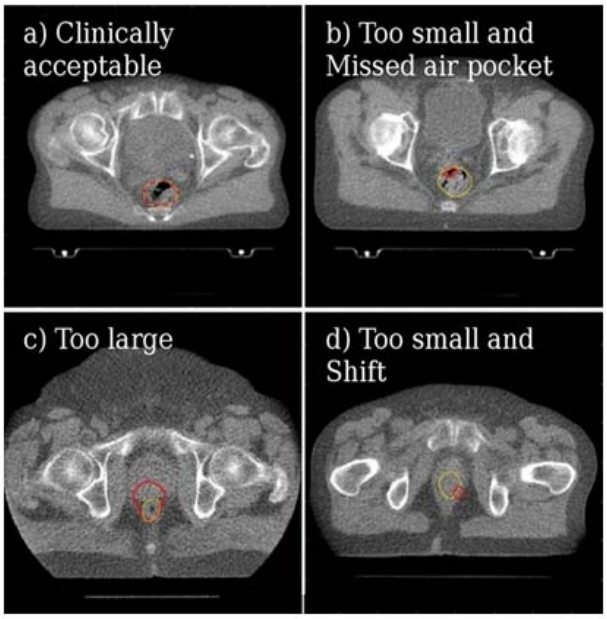

Figure 1: Auto-contoured (red line) and reference (yellow line) rectum. a) Clinically acceptable error-free contour. b),c),d): Error examples.

Error distribution:
The most frequent error was under-contouring ("too small", 21% of all reviewed images), followed by "cut air pocket" (14%). We observed an even error distribution across scans and patients (Table 1).

Error category	Prevalence across all images (n=7110)	Prevalence across scans (n = 689)	Prevalence across patients (n = 20)
Too large	5%	25%	95%
Too small	21%	68%	100%
Cut air pocket	14%	49%	100%
Missed air pocket	2%	11%	70%
Shifted	3%	18%	80%
Odd shape	3%	22%	95%
Error-free	**70%**	**14%**	**0%**

Table 1: Prevalence of errors across images and scans. Left: entire data set; centre: scans where ≥1 image has the error; right: patient data sets where ≥1 image has the error.

Conclusion: Our auto-contouring method produces clinically usable contours for the majority of cases and offers a considerable time- and resource-saving potential. We identified six error categories, four of which can be automatically detected during the auto-outlining and will drive the re-contouring process. The presented method can be used to evaluate the performance of other auto-segmentation tools for cavitary organs.

EP-1895

Towards adaptive radiotherapy: a new registration-segmentation framework for focal prostate cancer

Y. Feng[1], K. Cheng[1], D. Montgomery[1], D. Welsh[1], J. Lawrence[2], L. Forrest[3], S. McLaughlin[4], D. Argyle[2], W. Nailon[1]
[1]*Edinburgh Cancer Centre, Department of Oncology Physics, Edinburgh, United Kingdom*
[2]*University of Edinburgh, Royal Dick School of Veterinary Studies, Edinburgh, United Kingdom*
[3]*University of Wisconsin-Madison, School of Veterinary Medicine, Madison, USA*
[4]*Heriot Watt, School of Engineering and Physical Sciences, Edinburgh, United Kingdom*

Purpose or Objective: Commercial treatment planning systems can combine pre-treatment magnetic resonance (MR) images with radiotherapy planning computed tomography (CT) images using rigid or non-rigid registration. However, these systems lack the ability to combine registration with automatic image analysis/segmentation methods that may be helpful in prostate cancer boost therapy when mapping of a

dominant focal lesion between MR, where it is visible, and CT, where it is not visible. Here we present preliminary technical results from a new combined registration-segmentation framework for mapping of the dominant cancer foci defined on MR onto radiotherapy planning CT images in prostate cancer. The approach has the potential to be used in adaptive radiotherapy.

Material and Methods: Diagnostic MR and radiotherapy planning CT images acquired on General Electric Genesis and Signa scanners respectively were selected from 14 patients previously treated with external beam radiotherapy. Organs at risk (OAR), gross tumour volumes (GTV) and focal lesions were defined on all MR and CT images. The approach consists of two parts: 1) a rigid image registration method based on scale invariant feature transform (SIFT) and mutual information (MI); 2) a non-rigid registration method based on the cubic B-spline and a novel similarity function. Using this as prior data scale-invariant features were identified on the MR and corresponding planning CT. The mutual information (MI) between the images was used to steer the level set and thereby identify the location of the tumour and OARs on the CT based on local image information.

Results: The performance of the approach was established first by calculating similarity ratios for the rigid and non-rigid approaches in the framework (Table 1). The mean similarity ratio for the rigid approach was 67.43% and increased to 91.84% for the non-rigid approach. The registration results obtained on the GTV, OARs and focal lesion contours were assessed by an expert observer. Clinically acceptable results were found in 12 of the 14 patients and in 13 patients the non-rigid component of the framework performed better than the rigid approach. Figure 1 shows the performance in a typical case where the rigid registration approach places the focal lesion outside of the prostate and the non-rigid approach places the lesion inside of the prostate.

Case ID	Rigid registration similarity index	Non-rigid registration similarity index
1	53.26%	88.43%
2	86.24%	95.01%
4	80.45%	95.69%
5	93.22%	97.53%
6	82.84%	99.47%
7	66.32%	69.57%
8	49.95%	94.62%
9	51.28%	89.79%
11	48.27%	91.66%
12	77.64%	81.19%
13	59.73%	89.26%
14	78.36%	86.73%
15	100%	100%
16	39.36%	100%
18	44.49%	98.67%

Table 1: Similarity index obtained for rigid and non-rigid registration of the dominant focal lesion between diagnostic MR and radiotherapy planning CT.

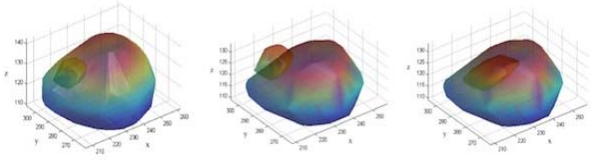

Figure 1: Left: Reconstructed prostate volume from the diagnostic MR images showing the dominant focal lesion. Middle: Reconstructed prostate volume from the radiotherapy planning CT images showing the dominant focal volume placed outside of the prostate following rigid registration. Right: Radiotherapy planning CT images showing dominant focal volume inside of the prostate following non-rigid registration.

Conclusion: This framework has the potential to track the shape variation of tumor volumes and could therefore, with more validation, be used for focal radiotherapy.

EP-1896

An atlas based auto-contouring technique incorporating interobserver variation

L. Bell[1,2], J. Dowling[3], E.M. Pogson[1,2], P. Metcalfe[1,2], L. Holloway[1,2,4,5]

[1]University of Wollongong, Centre for Medical Radiation Physics, Wollongong, Australia
[2]Ingham Institute, Liverpool & Macarthur Cancer Therapy Centres, Liverpool, Australia
[3]Australian e-Health Research Centre, CSIRO, Queensland, Australia
[4]University of Sydney, Institute of Medical Physics, Sydney, Australia
[5]University of New South Wales, SWSCS, Sydney, Australia

Purpose or Objective: The clinical efficacy of adaptive radiotherapy requires time efficient contouring that is highly accurate to maximise the benefits of exceedingly conformal techniques. Atlas based auto-contouring is a fast, patient specific method for target volume definition however current methods fail to account for interobserver variation. Current approaches utilise a training cohort of manually defined contours, whereby the assumption is made that the manual contour is the 'gold standard' contour for that patient. A novel method of atlas-based auto-contouring that incorporates interobserver variation is presented and assessed for whole breast radiotherapy.

Material and Methods: A cohort of 28 CT datasets with whole breast CTVs delineated by eight independent observers was utilised. For optimal atlas accuracy, the cohort was divided into four categories based on mean body mass index and laterality. An average atlas was generated from all datasets but one in each category, using the MILXView platform. Observer CTVs were merged in atlas space to generate a contour probability model accounting for inter-patient and inter-observer differences. The probability model was thresholded to 50% to generate a whole breast CTV auto-contour. The time taken to auto-contour each patient was recorded. For each category, the dataset not included in atlas generation was registered to the atlas, enabling the auto-contour to be propagated and clipped to the patient surface. The auto-contour was compared to the generated 'gold truth' consensus contour generated using the STAPLE algorithm, as well as the smallest and the largest CTV for a best and worst case scenario. This comparison was performed using the Dice Similarity Coefficient (DSC) and Mean Absolute Surface Differences (MASD).

Results: The time required to auto-contour each patient was 3min, 43 sec on average. DSC and MASD of the whole breast radiotherapy auto-contour and each target volume averaged across patients in each category are presented in the table.

	DSC				MASD (mm)			
	Large Left	Large Right	Small Left	Small Right	Large Left	Large Right	Small Left	Small Right
STAPLE	0.81	0.85	0.71	0.79	7.99	3.47	6.17	5.16
Smallest CTV	0.77	0.86	0.71	0.79	9.28	3.64	4.81	5.16
Largest CTV	0.81	0.8	0.71	0.79	7.5	4.71	6.13	5.07

Conclusion: This atlas-based auto-contouring method incorporating interobserver variation was shown to be accurate (DSC>0.7, MASD <8mm for all) and efficient (time was <4min). Variations in the auto-contour and STAPLE contour occur at superior and inferior slices contributing to larger MASD values.

EP-1897

Construction of a virtual T1-weighted 4D MRI: a feasibility study

C. Paganelli[1], G. Buizza[1], S. Cacciatore[1], P. Summers[2], M. Bellomi[2], G. Baroni[1], M. Riboldi[1]

[1]Politecnico di Milano, Dipartimento di Elettronica-Informazione e Bioingegneria, Milano, Italy
[2]Istituto Europeo di Oncologia, Division of Radiology, Milano, Italy

Purpose or Objective: To derive a well-contrasted T1-weighted 4D MRI. Four-dimensional MRI is typically achieved by retrospective sorting of fast, dynamically acquired T2-weighted slices, that allow better contrast and spatio-temporal trade-off than dynamic T1-weighted acquisitions. In

order to overcome the limits of T1-weighted 4D MRI, we present a preliminary study to derive a virtual T1-weighted 4D MRI, based on T2-weighted 4D images and a T1-weighted breath-hold acquisition.

Material and Methods: Free-breathing, sagittal, dynamic multi-slice T2-weighted MRI series of the liver were acquired on a 1.5T scanner (Siemens Avanto) in five healthy volunteers with a balanced steady state free precession sequence (TrueFISP, 20 slices, 20 dynamics, 1.28x1.28x5 mm resolution, 150 msec per slice). Slices were then retrospectively sorted in 4D volumes according to an image-based method. A volumetric axial T1-weighted acquisition was also performed at breath-hold during inhalation (VIBE, 60 slices, 1.25x1.25x4mm resolution). The proposed method involved applying the motion field derived from the T2-weighted 4D MRI dataset to the T1-weighted breath-hold acquisition. Specifically, a rigid registration of the breath-hold acquisition was performed onto the T2-weighted series at the corresponding inhale phase. Then, we performed a deformable registration between each respiratory phase and the inhale phase of the T2-weighted 4D scan. The derived motion fields for all respiratory phases were then used to warp the T1-weighted breath hold acquisition (i.e. deriving the virtual T1-weighted 4D MRI).

Results: The performance of the rigid registration was evaluated by computing the distance of the organ profile between the registered T1-weighted breath-hold volume at the inhale phase and the T2-weighted 4D scan at the same respiratory phase in two region of interests (liver and kidney). The distance between the two volumes was below the maximum voxel size (i.e. 5mm). The derived virtual T1-weighted 4D MRI at exhale was able to compensate for the motion obtained from the T2-weighted 4D scan (Figure, A: T1-weighted and T2-weighted volumes; B: overlap of virtual T1-weighted at exhale (red) with T2-weighted at exhale (green) and virtual T1-weighted at exhale (red) with T2-weighted at inhale (green)). Both diaphragm and vessels resulted closer to the T2-weighed 4D MRI at the exhale phase than the inhale phase, with a residual distance in the liver profile measuring 2.1±1.5mm (uncompensated motion).

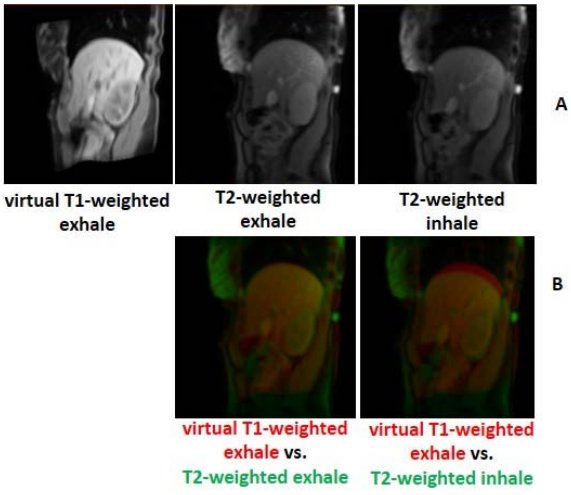

Conclusion: Our results provide preliminary demonstration of a well-contrasted virtual T1-weighted 4D MRI and the subsequent description of tumor motion and composition according to T1 and T2 weightings. Future work will be focused on the validation of the method relying on an MRI phantom, which can provide a ground truth T1-weighted 4D MRI.

Acknowledgments: work supported by AIRC, Italian Association for Cancer Research.

EP-1898

A workflow for automatic QA of contour propagation for adaptive radiotherapy

W. Beasley[1,2], A. McWilliam[1,2], N. Slevin[1,3], R. Mackay[1,2], M. Van Herk[1]

[1]*The University of Manchester, Institute of Cancer Sciences, Manchester, United Kingdom*

[2]*The Christie NHS Foundation Trust, Christie Medical Physics and Engineering, Manchester, United Kingdom*

[3]*The Christie NHS Foundation Trust, Department of Clinical Oncology, Manchester, United Kingdom*

Purpose or Objective: Automatic segmentation of daily images is an essential component of any online or offline adaptive radiotherapy (ART) workflow. Propagating contours from a planning CT (pCT) to an on-treatment image, through deformable image registration, is the common method for automatic segmentation, and there are several such algorithms available. Initial validation of these algorithms is essential before clinical use, but such testing is inevitably performed on a limited patient cohort and cannot guarantee absence of propagation failures in clinical use. We present here a workflow for automated QA of contour propagation performance on an individual patient basis. The validity of the technique is demonstrated for a cohort of head and neck cancer patients.

Material and Methods: The workflow for automated QA on an on-treatment Cone Beam CT image obtained on fraction N (CBCTn) is described below (Fig 1). Structures are first outlined on the pCT (A). Structures are then propagated from pCT to CBCT1 (CBCT taken during fraction 1) and manually reviewed once (B). On treatment day N, structures are propagated to CBCTn (B). For QA, the structures on CBCTn are propagated back onto CBCT1, such that there are two sets of structures on CBCT1 (C). The correspondence between these structures indicates the quality of the propagation on day N (D). The structures are compared using the Dice similarity coefficient (DSC) and the mean distance-to-agreement (DTA). The workflow was tested on ten head and neck cancer patients. Parotids were outlined on the pCT and six weekly CBCTs (CBCT1-6). A commercial automatic segmentation algorithm (ADMIRE, Elekta) was used to propagate structures onto the weekly CBCTs from the pCT, and the true accuracy was evaluated by comparing the propagated structures with manual delineation using DSC and DTA (defined as consistency metrics). Errors were then introduced into some of the contours by deliberately combining contours and CBCTs of different fractions. It was investigated whether the consistency metrics correlated with the true accuracy, and whether they could be used to identify the introduced errors.

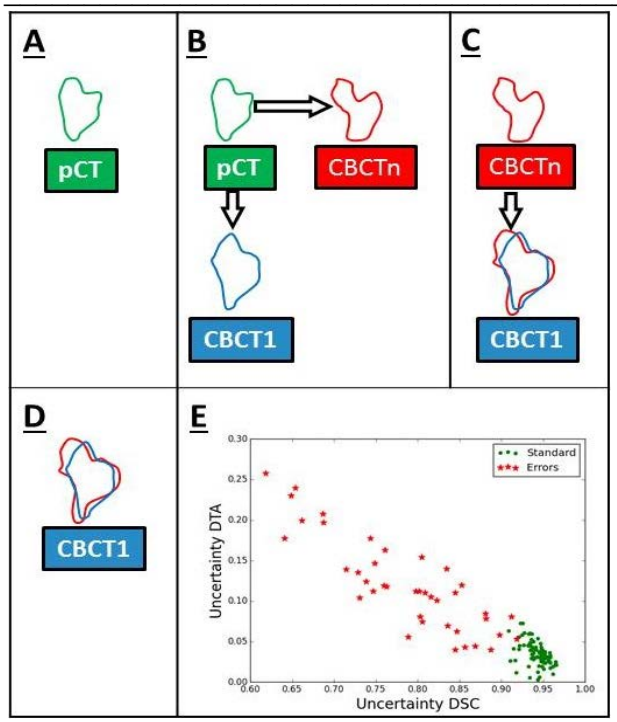

Results: There was a strong correlation between the consistency metrics and the true accuracy (r = 0.85 and r = 0.70 for DSC and DTA, respectively), indicating that the new method is suitable to automatically infer contour propagation accuracy. In addition, a simple threshold on the consistency metrics enabled accurate automatic identification of introduced errors (fig 1E).

Conclusion: The presented workflow enables the accuracy of a propagated contour to be tested automatically for any patient, and for errors to be identified. This method can be used as part of an online ART protocol, to automatically detect contour propagation issues that require manual review and contour editing.

EP-1899

Evaluation of SEMAC MRI metal artifact reduction for orthopaedic implants in radiotherapy planning

M.A. Schmidt[1], R. Panek[1], R. Colgan[2], J. Hughes[3], A. Sohaib[3], F. Saran[4], J. Murray[5], J. Bernard[6], P. Ravell[7], M. Nittka[7], M.O. Leach[1], V.N. Hansen[2]

[1]*The Institute of Cancer Research and The Royal Marsden NHS Foundation Trust, CR-UK & EPSRC Cancer Imaging Centre, Sutton, United Kingdom*

[2]*Royal Marsden NHS Foundation Trust, Radiotherapy Department, Sutton, United Kingdom*

[3]*Royal Marsden NHS Foundation Trust, Radiology Department, Sutton, United Kingdom*

[4]*Royal Marsden NHS Foundation Trust, Neuro-Oncology Unit, Sutton, United Kingdom*

[5]*Institute of Cancer Research and Royal Marsden NHS Foundation Trust, Radiotherapy Department, Sutton, United Kingdom*

[6]*St George's Hospital NHS Trust, OrthopaedicSurgery, London, United Kingdom*

[7]*Siemens Healthcare, Diagnostic Imaging, Erlagen, Germany*

Purpose or Objective: Many commonly used metallic orthopaedic implants cause artifacts in MR and CT images and are a serious challenge for obtaining high quality anatomical images for radiotherapy (RT) planning. We investigate the utility of SEMAC (Slice Encoding for Metal Artifact Correction [Ai et al. Invest Radiol 47: 267-76, 2012]) in patients with hip replacements and spine fixation devices, and consider the impact of metal artifacts on the registration of MR and CT images for RT planning.

Material and Methods: This study was approved by the Ethics Committee. MRI was undertaken on a 70 cm bore system (1.5T MAGNETOM Aera, Siemens) adapted with a home-built flat bed. SEMAC fast-spin-echo (FSE) pulse sequences were developed to approximate the coverage, image quality and contrast of the conventional FSE protocol (WARP works-in-progress software package, Siemens Healthcare). MR and CT images were registered using standard RT software (Pinnacle, Philips); conventional FSE and SEMAC FSE pulse sequences were compared on a purpose-built test object (spine fixation device suspended in gelatine) and on clinical examinations. Six patients with bilateral hip replacements and two patients with metallic fixation devices on the spine were scanned. For the spine fixation devices the visibility of the spinal canal was assessed. For the hip replacement patients, the internal surface of the pelvic girdle was scrutinised. Conventional and SEMAC FSE images were compared to detect relative geometrical distortion.

Results: The conventional FSE protocol shows extensive areas of signal loss and signal pile up around the spine fixation device test object. Signal loss volume was reduced from approximately 16.0 ± 0.5 cm3 to 12.9 ± 0.5 cm3 when the SEMAC FSE protocol was used. The two spine patients were shown to have metallic implants adjacent to the spine canal, which was partially affected by signal loss in three separate slices for conventional FSE protocols. Using the SEMAC FSE protocol, areas of signal loss and signal pile up are significantly reduced; the spinal canal is visible throughout the scanned volume (Figure 1). Geometrical distortion and signal loss were visible in all of 12 hip replacements scanned, but the metal artifacts do not reach the prostate, bladder and the seminal vesicles. In 8 of those hip replacements the signal loss extended to the internal surface of the acetabulum with conventional FSE protocols. Using SEMAC FSE techniques the signal loss is reduced and for only four of the hip replacements it was not possible to visualise the complete internal surface of the pelvic bones.

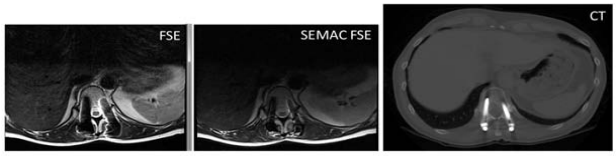

Figure 1

Conclusion: This work demonstrates improvement in geometric accuracy and reduction in signal loss around common metallic implants using SEMAC FSE sequences, with a positive impact on CT-MR registration. This technique will enable better contouring confidence in the location of target volumes and organs at risk which are close to metallic implants.

EP-1900

Geometric accuracy of MRI for stereotactic radiosurgery planning of Acoustic Neuromas at 3 Tesla

M.A. Schmidt[1], E. Wells[2], K. Davison[3], A. Riddell[3], L. Welsh[4], F. Saran[4]

[1]*The Institute of Cancer Research and The Royal Marsden NHS Foundation Trust, CR-UK & EPSRC Cancer Imaging Centre, Sutton, United Kingdom*

[2]*Royal Marsden NHS Foundation Trust, Medical Physics, London, United Kingdom*

[3]*Royal Marsden NHS Foundation Trust, Radiology Department, London, United Kingdom*

[4]*Royal Marsden NHS Foundation Trust, Neuro-Oncology Unit, London, United Kingdom*

Purpose or Objective: MR-CT co-registration is a mandatory requirement to accurately plan Stereotactic Radiosurgery (SRS) for Acoustic Neuromas (AN). MRI scans are subjected to susceptibility-related magnetic field inhomogeneity in the proximity to air spaces and this effect is enhanced at higher magnetic fields. We investigate the geometric distortion of anatomical MRI head images acquired at 3 Tesla (3T), and consider protocol requirements for SRS.

Material and Methods: This work was approved by the Research Ethics Committee and undertaken at 3T (Skyra, Siemens). 3D MR images of a structured test object were obtained (500 Hz/pixel, 1 mm3 isotropic resolution) and displacements from the true position were estimated over the head volume. High resolution magnitude and phase images were acquired for field mapping on five volunteers after shimming over the entire head volume; (TE1/TE2/TR = 2.46/7.38/12 ms, 800Hz/pix, approximately 1mm3 isotropic, sagittal 3D acquisition, standard head coil). The phase images were processed off-line to produce field maps (in-house software, IDL 8.2, USA). Field maps were assessed over the whole head and over the area surrounding the ear canal for range of magnetic field values and accuracy of phase unwrapping algorithm. In addition, field mapping was performed with the same sequence on a uniform test object with the phase encoding direction both head/foot and anterior/posterior to evaluate the effect of eddy currents on field map accuracy. From the volunteer field maps, the displacement of any signal from its true origin was calculated for the anatomical MRI pulse sequences used in SRS (SRS Planning Protocol: 900Hz/pix bandwidth, 1mm3 isotropic voxel size).

Results: Geometric displacements assessed with a structured test object were found to be under 1 mm within a central volume of 20 x 20 x 20 cm3. From images of a uniform test object, the field mapping errors were estimated to be under 0.30 ppm over that volume. In all five subjects a macroscopic gradient was observed along the head/foot direction (Fig1a). The total range of magnetic field values is under 7 ppm over the head for all subjects, including the oral cavity. However, steep field gradients were detected adjacent to air spaces in the ear canal (Fig 1b). The maximum field change in this area is under 3.5 ppm for all subjects. For the SRS Planning Protocol displacements associated with susceptility-related field inhomogeneity are therefore under 1 mm for the head and 0.5 mm around the ear canal. For MRI examinations undertaken with lower receiver bandwidth (and thus lower readout gradients) the geometric accuracy can be compromised by susceptibility effects.

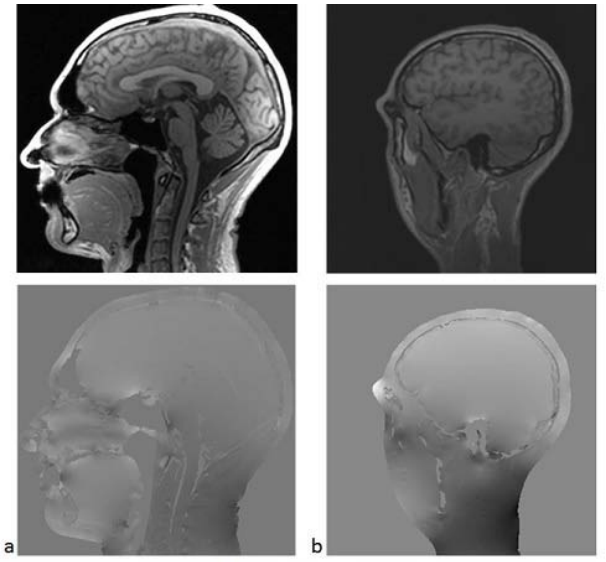

Magnitude images (top) and field maps (bottom) for same location.

Conclusion: It is possible to maintain geometric accuracy at 3T by using high readout gradients. SRS planning MRIs benefit from the superior image quality achieved at 3T with careful setting of the receiver bandwidth. These finding have implications for SRS and MR-guided Radiotherapy in general.

EP-1901

Patient-specific deformable image registration quality assurance based on feature points

P.C. Park[1], E. Koay[2], J. Yang[1], Y. Suh[1], P. Das[2], C. Crane[2], S. Beddar[1]

[1]*The University of Texas MD Anderson Cancer Center, Department of Radiation Physics, Houston, USA*

[2]*The University of Texas MD Anderson Cancer Center, Department of Radiation Oncology, Houston, USA*

Purpose or Objective: Despite high prevalence of DIR, the lack of patient-specific quality assurance method poses challenge to truly integrate the DIR into clinical practice. We addressed this problem by developing a DIR-QA platform that quantifies geometrical error in registration based on stable feature points

Material and Methods: Our DIR-QA software uses a scale-invariant feature transform algorithm to identify feature points on diagnostic images within a specified volume (e.g. liver).

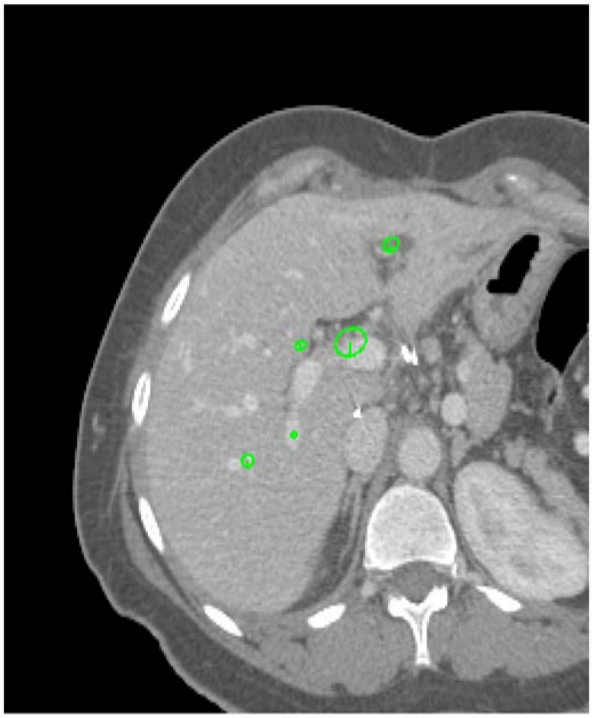

We generated feature points on reference CT images (full-exhale) from 4DCT scans of the abdomen and measured correspondence of the feature points on the target CT image (full-inhale) by having three radiation oncologists and four medical physicists to identify 100 corresponding feature points. This correspondence served as the gold standard for point-by point assessment of DIR, and provided measurements of the inter- -operator variability. The intra-operator variability was measured using 3 preselected feature points that were randomly presented to the operator 3 times during the task of finding the machine-generated feature points.

Results: Over a thousand unique feature points were identified within the liver volume, and 100 feature points were successfully tested for inter-operator variability in the QA process. The mean of standard deviation of inter-operator variability was 0.8 mm, 0.8 mm, and 1.4 mm in left-right, anterior-posterior, and superior-inferior directions respectively. Similarly, the intra-operator variability was 0.7 mm, 0.8 mm, and 1.0 mm.

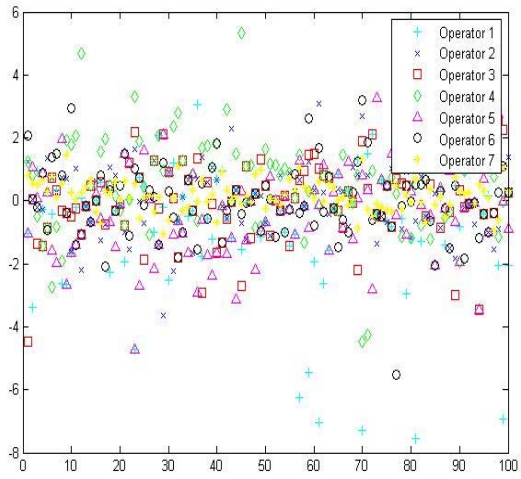

Conclusion: Our DIR-QA platform demonstrated inter- and intra-operator variability on the order of one voxel (1mm by 1mm by 2.5mm). Machine-generated feature points can serve as a measure of the quality of deformable image registration.

EP-1902

Impact of image quality on DIR performances: results from a multi-institutional study

G. Loi[1], C. Fiandra[2], E. Lanzi[3], M. Fusella[1], L. Orlandini[4], F. Lucio[5], S. Strolin[6], L. Radici[7], E. Mezzenga[8], A. Roggio[9], L. Tana[10], E. Cagni[11], A. Savini[12], C. Garibaldi[13]

[1]*University Hospital "Maggiore della Carità", Department of Medical Physics, Novara, Italy*

[2]*University of Turin, Department of Oncology, Turin, Italy*

[3]*Tecnologie Avanzate, R & D, Turin, Italy*

[4]*Centro Oncologico Fiorentino – CFO, Department of Medical Physics, Sesto Fiorentino, Italy*

[5]*"Santa Croce e Carle" Hospital, Department of Medical Physics, Cuneo, Italy*

[6]*Regina Elena National Cancer Institute, Laboratory of Medical Physics and Expert Systems, Rome, Italy*

[7]*A.O. Ordine Mauriziano di Torino, Department of Medical Physics, Turin, Italy*

[8]*Istituto Scientifico Romagnolo per lo Studio e la Cura dei Tumori IRST IRCCS, Department of Medical Physics, Meldola, Italy*

[9]*Veneto Institute of Oncology IOV IRCCS, Department of Medical Physics, Padua, Italy*

[10]*University-Hospital of Pisa, Health Physics Unit, Pisa, Italy*

[11]*S. Maria Nuova Hospital, Department of Medical Physics, Reggio Emilia, Italy*

[12]*Ospedale Civile Giuseppe Mazzini, Department of Medical Physics, Teramo, Italy*

[13]*European Institute of Oncology, Unit of Medical Physics, Milan, Italy*

Purpose or Objective: To investigate the accuracy and robustness, against image noise and artifacts (typical of CBCT images), of various commercial algorithms for deformable image registration (DIR), to propagate regions of interest (ROIs) in computational phantoms based on patient images. This work is part of an Italian multi-institutional study.

Material and Methods: Thirteen institutions with six available commercial solutions provided data to assess the agreement of DIR-propagated ROIs with automatically drown ROIs considered as ground-truth for the comparison. The DIR algorithms were tested on real patient data from three different anatomical districts: head and neck, thorax and pelvis. For each dataset, two specific Deformation Vector Fields (DVFs) were applied to the reference data set (CTref) using the ImSimQA software. To each one of these datasets two different level of noise and capping artifacts were applied to simulate CBCT images (fig.1, panel a -b) . Every center had to perform DIR between CTref, two deformed CTs and four CBCT for each anatomical district. The different software used in this study were: VelocityAI, Mirada, MIM, RayStation, ABAS, SmartAdapt. A four way ANOVA was performed to identify major predictors of DIR performances followed by a post hoc Sceffè test for analyzing intergroup differences; the logit transform of the Jaccard Conformity Index (JCI) was used as metric.

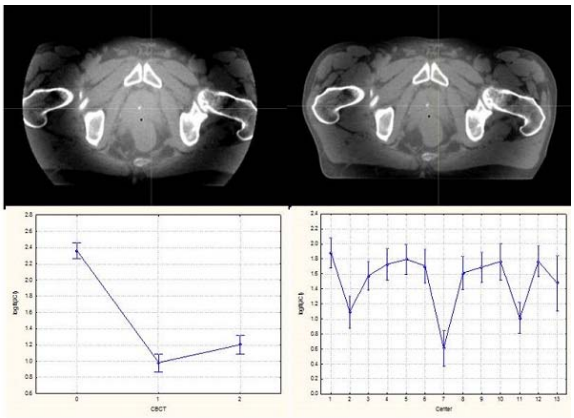

Fig. 1. Examples of the two simulated CBCT images. (panel "a" and "b") JCI values against image quality (panel c): "0" states for "clear" CT images, and CBCT "1" and "2" for the two CBCT version of the deformed images. DIR performances of the different centers (panel "d").

Results: More than 2000 DIR-mapped ROIs were analyzed, and many results were carried out. We report only the most relevant results for clinical applications. The ANOVA test states that the differences in DIR performances are not statistically significant between the head and neck and prostate cases, while lung case shows a significant difference; they depend from the strength of the deformation; and they are very sensitive to image quality (capping artifacts and noise) (Fig1 panel c). There is statistical evidence that the center #7 performs worst then the others with significant differences respect all the other centers except the number #2 and #11 (fig1, panel d).

Conclusion: This work illustrates the effect of image noise to DIR performances in some clinical scenarios with well-known DVFs. Some clinical issues (like ART or Dose Accumulation) need accurate and robust DIR software. This work put in evidence the presence of an important inter-software variability (in terms of JCI parameter), and the need of accurate system commissioning and quality control about the robustness of some commercial system against image quality. Regarding the results in fig1, panel c, the worst scenario (CBCT2) the DIR performances appear slightly better than in CBCT1: what does it mean? Probably the results are very sensitive to image quality but there is a threshold in image degradation above which adding noise or artifacts doesn't impact on DIR algorithms. This finding suggests the opportunity to test other situations to tune at a finest level noise and artifacts.

EP-1903

Application of the Enhanced ChainMail algorithm with inter-element rotation in adaptive radiotherapy

K. Bartelheimer[1,2], J. Merz[1], H. Teske[1,2], R. Bendl[1,2,3], K. Giske[1,2]

[1]*German Cancer Research Center DKFZ, Medical Physics in Radiation Oncology, Heidelberg, Germany*

[2]*National Center for Radiation Research in Oncology, Heidelberg Institute for Radiation Oncology HIRO, Heidelberg, Germany*

[3]*Heilbronn University, Faculty of Computer Science- Medical Informatics, Heilbronn, Germany*

Purpose or Objective: In adaptive radiotherapy positioning uncertainties, due to e.g. tissue deformations in the course of fractionated therapy, can result in a dose delivery that strongly deviates from the planned dose. Especially with regard to particle therapy, it is therefore important to quantify such deviations and to evaluate the need for

replanning [Tilly 2013]. Since the current deformable image registration (DIR) methods still fall short concerning anatomically correct deformations and therefore do not reach the required accuracy expectations, we have developed a tissue-dependent transformation model. With this we aim at improving the characteristic deformation behavior of rigid and soft tissue without the need of time-consuming tissue delineation.

Material and Methods: We adapted the Enhanced ChainMail (ECM) algorithm [Schill 1998], which was originally developed for surgical simulations, to CT-images by assigning each voxel of the image elastic properties according to its HU-value. The deformation, initialized by shifts of anatomical landmarks, is then propagated by adjusting the deformation limits for every individual element. In addition to deformation limits for stretching, contraction and shear between neighboring elements (voxels), we also introduced an element orientation, which allows for an initial rotation to decay within elastic material.

Results: The ECM algorithm has successfully been applied to phantom as well as real CT-images. Due to the simple deformation rules the algorithm takes less than two minutes for a high-resolution CT-image (dimension: 512 x 512 x 170), but still approximates the shape and geometry of the deformed image in a physically realistic manner. Since tissue parameters can be assigned based on HU-values, the deformation is adapted to different material properties without the necessity of segmentation of different organs. This is in contrast to finite element methods, which represent the state of the art in deformation accuracy [Brock 2006].

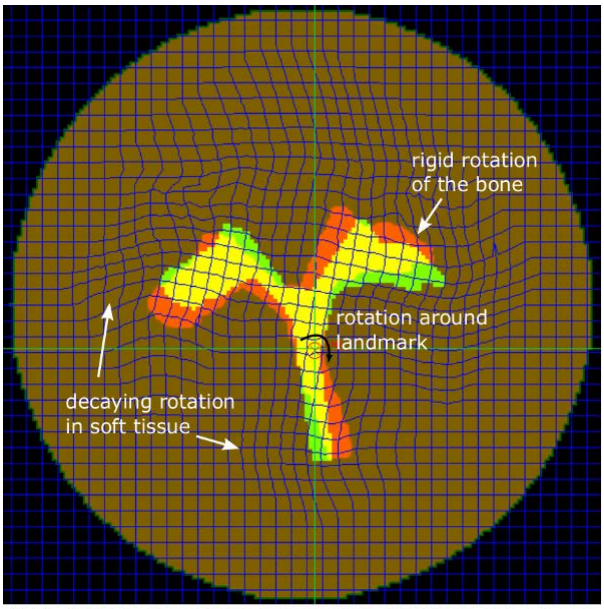

Fig. 1: Rotation of a vertebra surrounded by soft tissue. The vertebra is automatically rotated rigidly, whereas the rotation decays in soft tissue as can be seen by the deformed grid cells.

Conclusion: This is one of the first applications of the ECM-based transformation model for DIR in radiotherapy. With the extension by inter-element rotation, the algorithm is now able to register deformed and locally rotated organs in CT-images without the requirement of time-consuming segmentation. On the long-term the ECM-algorithm will allow for fast and physically realistic registrations, promising to cope with the strict accuracy requirements in deformation detection for particle therapy.

KB was supported by BMBF grand within the SPARTA project. HT & KG were supported by DFG grant G1977/2-1.

EP-1904

Virtual CT for adaptive prostate radiotherapy based on CT-CBCT deformable image registration

F.R. Cassetta Junior[1], D. Ciardo[2], G. Fattori[1,3], M. Riboldi[1], R. Orecchia[2,4], B.A. Jereczek-Fossa[2,4], G. Baroni[1]

[1]*Politecnico di Milano, Dipartimento di Elettronica-Informazione e Bioingegneria, Milan, Italy*

[2]*European Institute of Oncology, Division of Radiation Oncology, Milan, Italy*

[3]*Paul Scherrer Institut PSI, Center for Proton Therapy, Villigen, Switzerland*

[4]*University of Milan, Department of Health Sciences, Milan, Italy*

Purpose or Objective: We present a deformable image registration (DIR) framework for adaptive radiotherapy treatments of prostate cancer (PCa). The objective is the generation of virtual CTs by warping the CT planning in an adaptive IGRT framework. Previous studies on the use of CBCT as a support for dose recalculation and re-planning decisions for head and neck cancer showed promising results. For the pelvic region, similar studies are not yet available, mainly due to limitations in CBCT image quality and in the overall field of view. We developed an algorithm in order to perform DIR, making specific efforts to overcome the poor signal-to-noise ratio that limits CBCT use for treatment planning purposes.

Material and Methods: The planning CT and 5 CBCT images of 2 PCa patients treated with ultra-hypofractionated IGRT at the European Institute of Oncology (Milan, Italy) were included in this study. The CT image resolution was 1.25x1.25 mm2 in-plane and 2.5 mm in the cranio-caudal direction, whereas the voxel size of CBCT reconstruction was set to 0.39x0.39x2.0 mm3. The Insight Segmentation and Registration Toolkit (ITK) was used to implement the DIR framework featuring: (1) Mattes Mutual Information metric, with the advantage of rescaling the images internally while building up the discrete density function; (2) Regular step gradient descent optimizer, which sets the parameters in the direction of the gradient to calculate the step size; (3) The B-Spline interpolator to handle the deformable transformation of the images. In order to verify the proposed approach, the obtained Virtual CTs were compared with the corresponding CBCTs. For this purpose we applied an automatic approach to the scale invariant feature (SIFT) method, which extracts and matches features from each pair of the fixed and the transformed images, thus quantifying geometrical errors in Virtual images. SIFT allows DIR methods assessment through the evaluation of landmark residual errors.

Results: For each pair of CBCT and registered CT, 31 matching points were found on average (range 12-42). The resulting residual error along each anatomical axis had the same order of magnitude of the voxel size (0.39, 0.39, 2.0 mm along x, y and z, respectively) as seen in Fig.1.

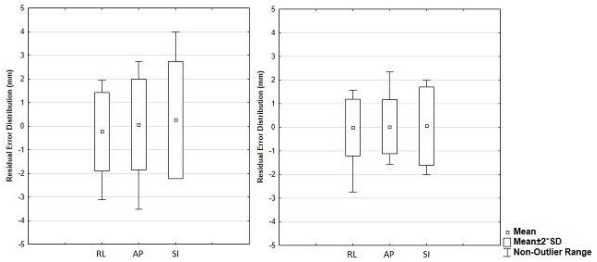

Fig. 1: Landmark distance residual errors distribution for patient 1 (left) and patient 2 (right).

Conclusion: The implemented DIR framework provides a registration accuracy within the voxel size. Our results point out the potential of using CBCT and DIR for IGRT in PCa patients. Future studies envision the implementation of DIR for dose recalculation and margin evaluation in adaptive IGRT of PCa patients, taking into account the existing limitations in the field of view. Acknowledgment: This study was

partially funded by AIRC (grant N-13218) and by CAPES (grant 9374/13-2).

EP-1905

Feasibility of automatic contour propagation of spinal bone metastases for online MR-Linac treatment

G.G. Sikkes[1], L.T.C. Meijers[1], C.N. Nomden[1], A.N.T.J. Kotte[1], G.H. Bol[1], B. Van Asselen[1], E.N. De Groot[1], I.H. Kiekebosch[1], B.W. Raaymakers[1]

[1]UMC Utrecht, Radiation Oncology Department, Utrecht, The Netherlands

Purpose or Objective: Accurate identification of the clinical target volume and organs at risk remains one of the most observer-dependent and time-consuming processes in radiotherapy treatment planning. An online adaptive procedure at the MRI linear accelerator (MR-Linac) requires fast contouring to adapt the treatment plan to the daily anatomy. Automatic contouring software can be a helpful tool to speed up this process. The purpose of this study was to evaluate the feasibility of automatic contour propagation for online adaptive treatment of spinal bone metastases on the MR-Linac.

Material and Methods: Two healthy volunteers underwent an MR-scan twice of the lumbar spine with an interval of two months. The MR-scans were acquired on an Ingenia 1.5T scanner (Philips, Best Netherlands) according to the clinical stereotactic spine protocol. The first MR-scan series contained a transversal mDixon scan with a Field of View (FOV) length of 30 cm, which is considered the reference. The second series contained, besides the same mDixon, a transversal T1 TSE and T1 VISTA both with a FOV of 20 cm. These scans were considered as the daily MRI. Ten contours were manually delineated on the reference; the whole vertebral compartments of thoracic 12 until lumbar 5, both kidneys, aorta and myelum (figure 1a). Automatic contouring software 'Advanced Medical Image Registration Engine' (ADMIRE v1.12, Elekta, Stockholm Sweden), was used for MR-based deformable registration and contour propagation of all contours between the reference and the 3 daily MR-sequences. The processing time required by ADMIRE to create contours on each MR-sequence was scored. The contour propagation on different MR-sequences was evaluated visually. A scoring system with a scale from 1-3 was used for visual evaluation of all contours: contours clinical acceptable, according to the clinical guidelines (score 1), contours need some adjustments (score 2) and contours need major adjustments (score 3). All adjustments (score 2) were specified for location of the contour failure and the adjustment time.

Results: The mean processing time needed for automatic registration and contour propagation was 56 (range 35-89) seconds. The mean processing time decreased when a 20 cm length of FOV was used to 41 (range 35-47) seconds. In total, 98% of the automatically delineated contours were clinically acceptable (score 1) (figure 1b). In the remaining 2% small adjustments (score 2) were made at the border of a 20 cm FOV. No score 3 was observed. The additional time needed for manual adjustments was 28 seconds.

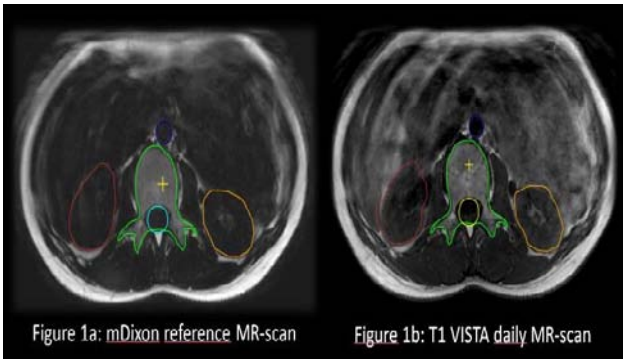

Figure 1a: mDixon reference MR-scan

Figure 1b: T1 VISTA daily MR-scan

Conclusion: MR-based contour propagation using automatic contouring software is fast enough for an online treatment at the MR-Linac. A limited FOV is usable for contour propagation, which allows tailoring of the FOV to the target of each individual patient. These high numbers of clinically acceptable contours will need to be confirmed in an ongoing study, first on several volunteers and then on patients pathology.

EP-1906

Importance of true cord delineation in spine SBRT and rigid vs. deformable MRI-to-CT registration

L. Goddard[1], P. Brodin[2], A. Lee[1], K. Mani[1], W. Bodner[1], M. Garg[1], W.A. Tomé[3]

[1]Montefiore Medical Center, Radiation Oncology, Bronx, USA

[2]Albert Einstein College of Medicine and Montefiore Medical Center, Institute for Onco-physics, Bronx, USA

[3]Institute for Onco-physics Albert Einstein College of Medicine and Montefiore Medical Center, Director- Division of Medical Physics, Bronx, USA

Purpose or Objective: Spine stereotactic body radiation therapy (SBRT) employs high doses per fraction. In this study, we assessed the importance of delineating the true cord (TC) for dose planning constraints, rather than using thecal sac (TS) as a surrogate. We also evaluated different MRI-to-CT registration methods for matching the MRI cord to the CT myelogram (CTM, here considered as the gold standard for TC visualization).

Material and Methods: Fifteen spine SBRT patients with both CTM and MRI scans were selected. The TS and TC were delineated according to RTOG protocols and the MRI contours were fused to the CT volume using either rigid or deformable image registration. To compare the performance of the rigid vs. deformable registration, Dice similarity coefficients and Hausdorff distances (largest distance from a point in one contour to the closest point in the other contour) were calculated.

The importance of TC delineation was evaluated by comparing the TC and TS from the CTM by determining the minimum distance between any of the circumference points on the two structures, and the number of points that were closer than 1mm (indicating that parts of the TC were close to the edge of the TS). For 3 fraction spine SBRT, we used this minimum distance to estimate the potential max point dose that could be received by the TC if this is not delineated and constrained directly in treatment planning, given a TS max dose constraint of 21.9 Gy. We also estimated the subsequent risk of radiation myelopathy based on a published dose-response model from a clinical spine SBRT series.

Results: The average Dice coefficient (± standard deviation) for the TS was 0.84 ± 0.06 for rigid and 0.81 ± 0.07 for deformable registration, and respectively 0.73 ± 0.10 and 0.67 ± 0.14 for the TC. For some patients rigid registration was superior and vice versa for others, no method was clearly superior.

Patient #	Minimum distance (Cord to Thecal sac) [mm]	% of Cord closer than 1mm from Thecal sac [%]	Potential max point dose to Cord (SBRT) [Gy]	Potential max point dose to Cord (EQD2) [$Gy_{2/2}$]	Estimated potential myelopathy risk [%]
1	1.71	0.0	18.2	36.6	4.6
2	0.02	13.3	21.9	50.7	10.0
3	2.07	0.0	17.4	33.8	4.1
4	1.01	0.4	19.7	42.1	6.0
5	0.64	5.5	20.5	45.3	7.2
6	1.65	0.0	18.3	37.0	4.7
7	0.92	1.9	19.9	42.9	6.2
8	0.49	4.2	20.8	46.5	7.7
9	0.96	0.6	19.8	42.6	6.2
10	0.59	3.8	20.6	45.7	7.3
11	0.60	5.3	20.6	45.6	7.3
12	1.53	0.0	18.5	37.9	4.9
13	0.02	16.0	21.9	50.8	10.0
14	0.67	5.6	20.4	45.0	7.1
15	0.02	8.7	21.9	50.7	10.0

For CTM-based TC and TS, results are presented in Table 1, where 11 of 15 patients had parts of the cord < 1mm of the TS circumference. Based on a 21.9 Gy max TS point dose in 3 fractions, the potential max TC point dose is 20.0 Gy ± 1.4 Gy, assuming a dose fall-off of 10% per mm. This is equivalent to 43.6 Gy2 ± 5.3 Gy2 in 2 Gy fractions given α/β = 2. As seen in Table 1 this could lead to a potential risk of radiation myelopathy higher than 5% in 11 out of the 15 patients. Figure 1 shows the comparison of TC and TS and highlights the parts where the TC protrudes out close to the TS edge (color-coded in red).

Conclusion:

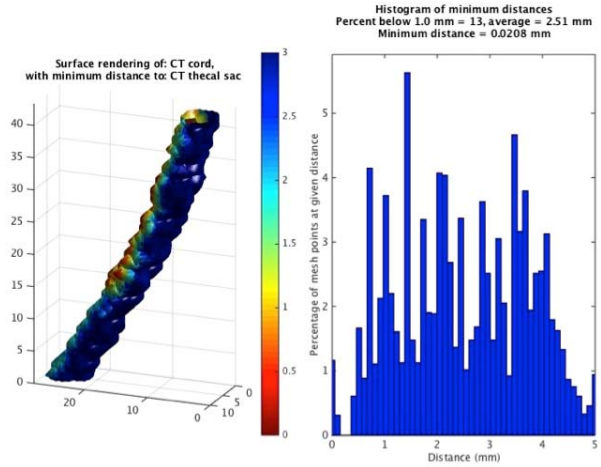

The TC position between MRI and CTM appears comparable, with rigid registration providing sufficient results, although care should be taken as large individual differences may exist. Based on our results, delineating the TC is essential in spine SBRT, and CTM provides a robust option that can be obtained and planned for treatment on the same day. If planning constraints for the TS are used as surrogate for the TC, parts of the TC that are very close to the TS edge may receive unacceptably high dose.

EP-1907

Accuracy of software-assisted contour propagation from planning CT to cone-beam CT in head and neck

C. Hvid[1], U. Elstrøm[2], K. Jensen[1], C. Grau[1]
[1]*Aarhus University Hospital, Dept of Oncology, Aarhus C, Denmark*
[2]*Aarhus University Hospital, Dept of Medical Physics, Aarhus C, Denmark*

Purpose or Objective: Recent years have seen a number of studies documenting accuracy and time savings for various software solutions used for automated contouring of target volumes and organs at risk (OAR) in radiotherapy, thus easing the heavy workload associated with replanning needed for implementing adaptive treatment strategies. The vast majority of studies have been performed on CT images and experience with other imaging modalities is limited. This study aims to determine the accuracy of a deformable image registration (DIR) algorithm for OARs in the neck region, when applied to cone beam CT (CBCT) images.

Material and Methods: For 30 head and neck cancer patients 14 OARs including parotid glands, swallowing structures and spinal cord were delineated. Contours were propagated by DIR to CBCTs corresponding to the first and last treatment fraction. An indirect approach propagating contours to the first and then the last CBCT was also tested. Propagated contours were compared to a gold standard (manually corrected contours) by Dice similarity coefficient (DSC) and Hausdorff distance (HD). Dose was recalculated on CBCTs and dosimetric consequenses of uncertainties in DIR were reviewed. Time consumption for editing automated contours was recorded.

Results: Mean DSC values of ≥ 0.8 were considered adequate and were achieved in base of tongue (0.91), oesophagus (0.85), glottic (0.81) and supraglottic larynx (0.83), inferior pharyngeal constrictor muscle (0.84), spinal cord (0.89) and all salivary glands in the first CBCT. For the last CBCT by direct propagation, adequate DSC values were achieved for base of tongue (0.85), oesophagus (0.84), spinal cord (0.87) and all salivary glands. Using indirect propagation only base of tongue (0.80) and parotid glands (0.87) were≥ 0.8. Mean relative dose difference between automated and corrected contours was within ±2.5% of prescribed dose except for oesophagus inlet muscle (-4.5%) and oesophagus (5.0%) for the last CBCT using indirect propagation. Mean editing time was significantly faster than contouring from scratch ($p<0.005$).

Conclusion: Compared to a golden standard of manually corrected contours the DIR algorithm was accurate for use in CBCT images of head and neck cancer patients and the minor inaccuracies had very little consequence for mean dose in most clinically relevant OAR. Accuracy was higher for the first CBCT compared to the last. The indirect method of propagating contours to the last CBCT via the first CBCT yielded worse results than direct propagation from pCT.

EP-1908

An image processing technique for simulating CT image sets for IGRT quality assurance

R. Franich[1], J.R. Supple[1], S. Siva[2], M.L. Taylor[1], T. Kron[1,3]
[1]*RMIT University, School of Applied Science, Melbourne, Australia*
[2]*Peter MacCallum Cancer Centre, Department of Radiation Oncology, Melbourne, Australia*
[3]*Peter MacCallum Cancer Centre, Physical Sciences, Melbourne, Australia*

Purpose or Objective: CT-based IGRT QA requires corresponding image sets with quantifiable geometric differences. These differences are rarely known to a reasonable degree when comparing patient images. This problem lends itself to highly controlled mathematical phantoms such as those generated with software such as XCAT [1]. However there are drawbacks when using such phantoms as the anatomic structures are typically defined by precise surfaces and are filled with homogeneous attenuation coefficients. This leads to unrealistic images, even when accurately simulating imaging systems [2,3], as features observed in patient images are not present. The aim of this work was to address some of these issues with an image processing procedure to better simulate these features. Here we present a simulated 4D planning CT image set.

Material and Methods: XCAT2 was used to generate attenuation coefficient phantoms of the thorax, incorporating breathing and cardiac motion. Five frames were generated spanning 0.2 seconds (approximate acquisition time for a single phase of a respiratory correlated 4DCT) and averaged, accounting for time averaging effects. A Gaussian filter was then applied to smooth the resulting steps in intensity at the boundaries of structures. Tissue inhomogeneities were then simulated by applying salt and pepper noise followed by another Gaussian filter to expand each individual "dot". The final step was to add random noise with a Gaussian distribution (with standard deviations for each tissue type calculated from patient images) simulating statistical uncertainty inherent to the imaging system. All processing was performed plane-by-plane in the transverse direction. Combinations of noise simulation parameters were investigated.

Results: The left pane in Figure 1 shows an example of a transverse slice through the liver of the average of the five frames of an XCAT attenuation coefficient phantom which has been converted to Hounsfield units. The right pane shows the same slice after image processing.

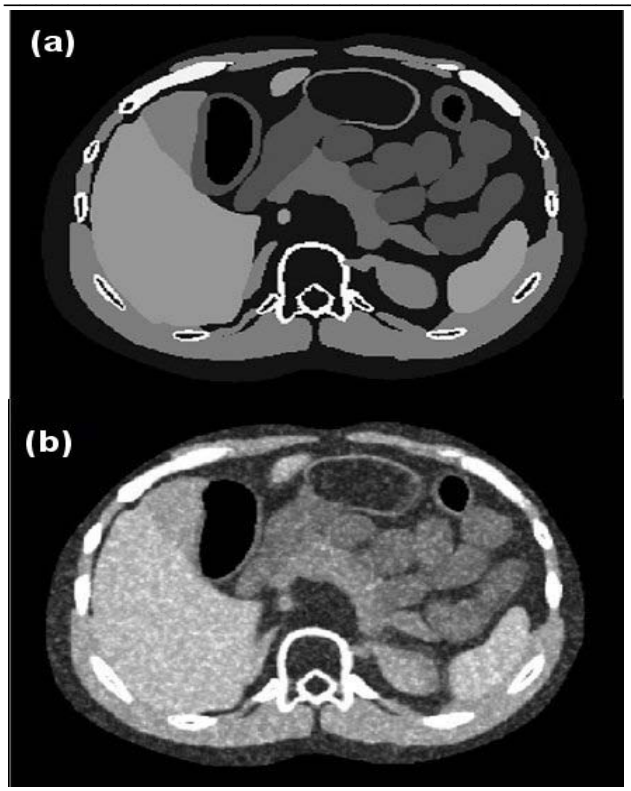

Figure 1: (a) Example transverse slice through the liver of an XCAT attenuation phantom, and (b) the corresponding slice from the simulated image set.

Conclusion: Image processing applied to XCAT attenuation coefficient phantoms has been used to simulate features observable in patient 4DCT image sets. The image processing technique is time and resource efficient and does not require generation of simulated projection images and 3D reconstruction.

References:

1. Segars et al 2008 Realistic CT simulation using the 4D XCAT phantom Med. Phys. 35 3800-3808
2. Segars et al 2010 4D XCAT phantom for multimodality imaging research Med. Phys. 37 4902-4915
3. Tabary et al. Realistic X-Ray CT simulation of the XCAT phantom with SINDBAD (NSS/MIC), 2009 IEEE, 2009. IEEE, 3980-3983.

EP-1909

Quantitative and qualitative assessment of thoracic CBCT image quality for multiple imaging systems

M. Williams[1], L. Davies[2], S. Hall[2], P. Wheeler[1]
[1]*Velindre Cancer Centre, Medical Physics, Cardiff, United Kingdom*
[2]*Velindre Cancer Centre, Radiotherapy, Cardiff, United Kingdom*

Purpose or Objective: A Varian TrueBeam with OBI was commissioned in 2014. During early clinical use concerns were raised regarding thoracic CBCT image quality in comparison with that observed in Elekta XVI images. Streaking artefacts caused by respiratory motion were the primary reason for the perceived poor quality. This study compared the image quality of the TrueBeam OBI with the other CBCT systems at the centre, a Varian Trilogy OBI and Elekta XVI, using quantitative and qualitative methods.

Material and Methods: A static Catphan phantom (The Phantom Laboratory) was used to assess image quality quantitatively, and to create a HU calibration curve for the XVI.

A Quasar phantom (Modus Medical Systems) with moving inserts was used to investigate the effect of motion on CBCT image quality. A systematic pattern of motion artefacts was revealed. Artefacts (created by a high density object moving along the axis perpendicular to the slice) were assessed in an axial slice. Circular profiles were used to quantify the artefacts on the three systems.
Clinical image quality was assessed through a qualitative study where two experienced observers independently scored 24 randomly selected clinical thoracic CBCT scans (8 per system). CBCT images were viewed alongside the planning CT scan, with the PTV outline being the only visible delineated structure. Scoring was based on a five point scale and reflected the image quality for matching purposes, the clinical task. Eight anatomical regions, sharpness, contrast, impact of artefacts, and the overall image quality were scored. Comments were also recorded.

Results: Quantitative assessment using the Catphan revealed no differences between systems that was deemed significant. The variation in magnitude of the streaking artefacts in the Quasar phantom was found to depend on scan time, but not on the system, as shown in Table 1.

Table 1: Magnitude of streaking artefacts in the Quasar phantom, assessed from circular profiles centred on the artefact source.

System	Scan protocol	Scan time (s)	Max Peak - Min Trough
TrueBeam OBI	Thorax	60	215.0
TrueBeam OBI	*Thorax 2min*	120	130.4
TrueBeam OBI	*Thorax 4min*	180	97.2
Trilogy OBI	Thorax	60	223.2
XVi	Lung	90	207.3
XVi	Oesophagus	120	135.7

The Mann-Whitney test was applied to each observer's scores for each metric of the clinical image analysis. No significant ($p<0.05$) differences between any systems for any metric for either user were detected.

Figure 1: Mean results for image quality metrics. Error bars represent the 95% confidence interval.

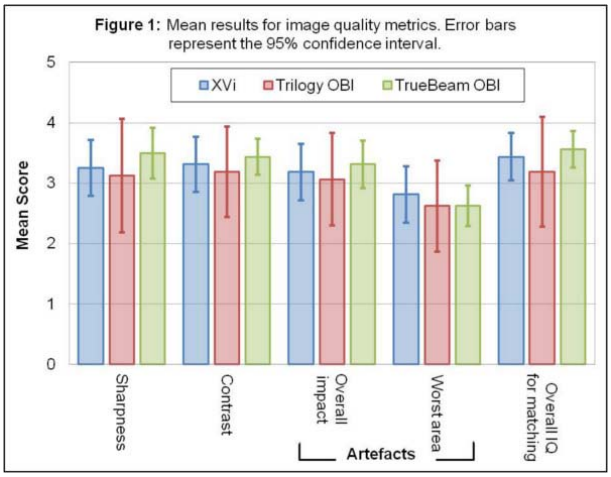

Conclusion: Investigations to date indicate no significant difference between the systems assessed. Image quality must allow matching of the CBCT to CT with confidence. Staff were thus reassured that all systems were assessed as "acceptable" (mean score of 3) for most metrics. It was felt that patient size was often the cause of particularly good or poor scores; therefore improvement of patient size dependent protocols is identified as a key area of future work.

EP-1910

Evaluation of diffusion-weighted imaging properties of a RT-specific positioning solution for PET/MR

R. Winter[1], S. Leibfarth[1], H. Schmidt[2], N. Schwenzer[2], D. Zips[3], D. Thorwarth[1]
[1]*University Hospital Tübingen, Section for Biomedical Physics, Tübingen, Germany*
[2]*University Hospital Tübingen, Diagnostic and Interventional Radiology, Tübingen, Germany*

[3]*University Hospital Tübingen, Radiation Oncology, Tübingen, Germany*

Purpose or Objective: PET/MRI may be highly beneficial for radiotherapy planning (RTP) in head and neck (HN) cancer in terms of increased accuracy in target volume definition (TVD) and integration of functional tissue properties. As the integration of imaging data into RTP requires co-registration, PET/MR examination in RT treatment position is favorable. Therefore, we propose a solution using a dedicated hardware setup.
Moreover, accuracy of TVD depends on the spatial accuracy of the imaging data. Since diffusion-weighted MR imaging (DWI) based on echo planar imaging (EPI) is prone to spatial inaccuracy, the aim of this study was to evaluate the quality of DWI with RT scan setup using dedicated distortion correction.

Material and Methods: The RT hardware setup consists of a flat table overlay and two coil holders for flexible body matrix coils (Siemens mMR), in addition to an in-house designed overlay add-on for RT mask fixation (cf. Fig1).
The evaluation of DWI quality using the RT setup was based on MR-only scans of n=3 healthy volunteers. Each time, two scans were performed: (I) using the RT setup with a pair of 6-channel flexible RF coils, (II) a reference scan, using a standard 16-channel HN coil. The protocol included T2w SPACE, T2w TSE, and DWI (b = 150 and 800 s/mm2).
DWI data was collected with reversed phase encode blips in order to use a correction method for susceptibility-induced distortions as implemented in the open source toolkit FSL.
The geometric accuracy of DWI was assessed on a ROI basis by comparing pairwise distortion corrected and uncorrected b150 images to T2w images. Four ROIs were placed in submandibular glands and cervical spine. In addition to spatial distances between ROI centers, the Dice similarity index (DSI) was calculated to assess ROI similarity.
Furthermore, ADC values derived from ROIs of the corrected b150 images were compared between RT and reference scans.
One set of DW images acquired with RT setup had to be excluded from analysis due to strong MR image artifacts.

Results: DWI suffered from geometric distortions with both scan setups but correction with FSL led to significantly reduced effects. These were of the same order as differences in ROI delineation between T2w images due to minor involuntary patient motion. The average displacements of the ROIs' centers of mass between DW and T2w images were 4.6±2.3 mm / 5.9±3.4 mm (RT / REF) and 1.0±0.4 mm / 1.5±0.9 mm for standard DWI and distortion corrected DWI, respectively (cf. Fig2 A). Fig2 B presents the average DSI per ROI pair: 0.4±0.1 / 0.4±0.2 (RT / REF) and 0.8±0 / 0.7±0.1, accordingly.
ADC values differed by 7±14% on average comparing the RT with the standard coil setup.

Conclusion: The presented PET/MR hardware solution for HN imaging enables for RT-specific patient positioning. Using dedicated correction methods, spatial distortions in DWI can be significantly reduced allowing for accurate usage of DWI in RTP. ADC values of distortion corrected maps of the RT scan setup were found to be adequate.

Fig1: RT-positioning hardware consisting of a flat table overlay and dedicated coil holders (Qfix, Avondale, PA, USA) that allow for PET/MR imaging of the HN region by using flexible RF coils. An overlay add-on enables the fixation of a RT mask on the table overlay.

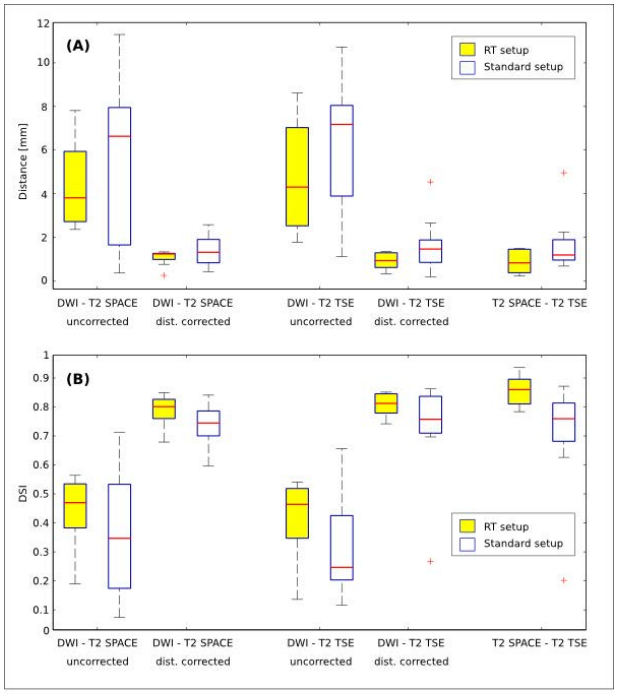

Fig2: (A) Boxplot presenting the distance between ROI centers of mass of DW (b=150) and T2w images for both uncorrected and distortion corrected DW images. To estimate the error of misalignments due to motion of the scanned subject, also T2w images were compared. (B) DSI boxplot for the respective ROI sets. DSI ranging from 0 to 1, with DSI = 1 for congruent and DSI = 0 for disjoint ROI sets.

Electronic Poster: Physics track: Implementation of new technology, techniques, clinical protocols or trials (including QA & audit)

EP-1911

Evaluating the effect of Zinc Oxide nanoparticles doped with Gadolinium on dose enhancement factor

N. Banaee[1], H.A. Nedaie[2], A. Shirazi[3], A. Zirak[4], S. Sadjadi[5]
[1]*Islamic Azad University, Department of Engineering, Tehran, Iran Islamic Republic of*
[2]*Cancer Institute, Tehran University of Medical Sciences- Radiotherapy Oncology Department, Tehran, Iran Islamic Republic of*
[3]*Cancer Institute, Medical Physics and Biomedical Engineering- Faculty of Medicine and Radiation Oncology Research Centre, Tehran, Iran Islamic Republic of*
[4]*Laser and Optics Research School, NSTRI, Tehran, Iran Islamic Republic of*
[5]*Nuclear Science and Technology Research Institute, Nuclear Science and Technology Research, Tehran, Iran Islamic Republic of*

Purpose or Objective: New treatment modalities are developed with the aim of escalating tumor absorbed dose

and simultaneously sparing the surrounding normal structures. Nevertheless, in order to decrease the growth of cancerous cells, a high dose of ionizing radiation is needed which would generally cause the side effects on healthy organs. The use of nanotechnology in cancer treatment offers some exciting possibilities including destroying cancer tumors with minimal damage to healthy tissues. Zinc Oxide nanoparticles (ZnO NPs) are wide band gap semiconductors and seem to have a good effect on increasing the absorbed dose of target volume especially when doped with a high Z element. The aim of this study is to evaluate the effect of ZnO NPs doped with Gadolinium on dose enhancement factor at different concentrations irradiating by 6MV photon beams.

Material and Methods: In order to study the influence of this NP on dose enhancement, PRESAGE dosimeter was fabricated by the reported procedure and calibrated against ionization chamber, delivering certain levels of absorbed doses. Then various concentrations of ZnO NPs and also ZnO NPs doped with 5% Gd were incorporated in to PRESAGE composition and irradiated by 6 MV photon beams. By using a UV-Vis spectrophotometer, optical density changes and also dose enhancement factor (DEF) were determined.

Results: Figure 1 shows the color changes of PRESAGE containing various concentrations of NPs.

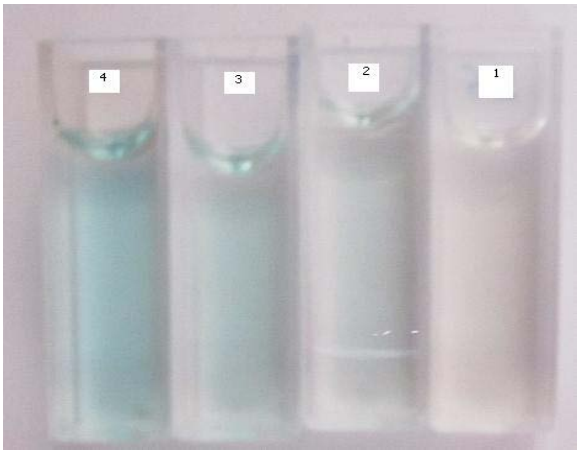

Fig1. PRESAGE filled cuvettes with and without NPs at dose of 10Gy. 1) PRESAGE without NPs. 2) PRESAGE with 20µg/ml ZnO NPs doped with %5 Gd. 3) PRESAGE with 4000µg/ml ZnO NPs doped with %5 Gd. 4) PRESAGE with 4000µg/ml ZnO NPs.
Table 1 shows DEF acquired by various concentrations of NPs.
Table 1. DEF of various concentrations of NPs.

Structure	DEF
PRESAGE with 20µg/ml ZnO doped with %5 Gd	1.004
PRESAGE with 4000µg/ml ZnO NPs doped with %5 Gd	1.82
PRESAGE with 4000µg/ml ZnO NPs	1.65

Conclusion: The results of this study revealed that ZnO NPs doped with Gd are new proposing substances for enhancing the absorbed dose and increasing the therapeutic ratio even in high energy photon beams. Various reasons may cause the DEF for 6MV photon beams such as photoelectric effect for low energy photon beams in continues X-ray spectrum, attenuated photons or pair production effect. Using these NPs not only reduces the needed MU to deliver a certain amount of absorbed dose, but also can lead to great succeeds in reducing treatment time. The concentration of NPs has a direct relation with DEF.

EP-1912

The mechanism research of radio-dynamic treatment

Q.S. Zhang[1], Q.Y. Sun[1], G.P. Xiao[1], J. Zeng[1], L. Wang[1], L.L. Chen[2], C.M.C. Ma[2]

[1]*Topgrade Medical - Yiren Hospital, Radio- therapy Center, Beijing, China*
[2]*Fox Chase Cancer Center, Radiation Therapy, Philadelphia, USA*

Purpose or Objective: Photodynamic therapy (PDT) is an effective treatment modality for specific superficial tumors, which uses laser light to activate photosensitizers that have been selectively absorbed by tumor cells. However, the finite penetration depth of laser light has limited clinical applications of PDT. This work investigates the outcomes of using Cerenkov light emission from 45MV photon beams on a LA45 accelerator to activate photosensitizers for cancer therapy. We named this new treatment technique as Radio-dynamic therapy (RDT).

Material and Methods: Firstly, Monte Carlo simulations were utilized to simulate various energies of Cerenkov light and its spectroscopy in excited target areas and their efficiency for photosensitizer activation. Then, the inner excitation efficiency from Cerenkov light in RDT theoretically compared with the efficiency of exotic excitation from the external laser light in PDT. In addition, we also tested the difference of excitation efficiency between a patented catalyst coenzyme was added as a substrate and without the coenzyme. Next, utilize a specific probe of DMA (Singlet O2 fluorescent probe-9, 10-dimethylanthracene) to detect singlet oxygen. Finally, we also compared our results with previous experimental results that reported in previous literatures.

Results: Our Monte Carlo results showed that the Cerenkov light intensity induced at 45MV photon beams on a LA45 is 8 - 10 times of the Cerenkov light intensity induced at 6MV beam on a conventional accelerator. In RDT, excitation efficiency to photosensitizers at 400-450nm peaked wavelength (Soret Band) equals 20 times of laser light at 630nm in PDT. The homogenous inner excitation in RDT is also about 20 times (continuous spectrum excitation and inner scattering) of the exotic excitation and exponential attenuation laser light in the target of using PDT. Furthermore, the patented catalyst coenzyme enhanced the excitation efficiency of photosensitizers by 3-6 times under different conditions. In clinical situation, the new technique RDT also showed favorable outcomes for early and late stage of specific cancers and it also good at metastatic cancers treatment.

Conclusion: Our results indicated that the process of using the Cerenkov light emission from 45MV photon beams to excite photosensitizers has similar process and efficiency as conventional laser in PDT. Compared these advantages with conventional PDT, RDT may be developed into a potential treatment modality for cancer of various stages and other diseases.

EP-1913

National automated collection of standardised and population-based radiation therapy data in Sweden

T. Nyholm[1], C. Olsson[2], T. Björk-Eriksson[3], G. Gagliardi[4], A. Gunnlaugsson[5], I. Kristensen[6], P. Nilsson[5], B. Zackrisson[7], A. Montelius[8]

[1]*Uppsala University, Immunology- Genetics and Pathology, Uppsala, Sweden*
[2]*Göteborg University, Institute of Clinical Sciences-Sahlgrenska Academy, Göteborg, Sweden*
[3]*Sahlgrenska University Hospital, Department of Oncology, Göteborg, Sweden*
[4]*Karolinska University Hospital, Department of Medical Physics, Stockholm, Sweden*
[5]*Skåne University Hospital- Lund University, Department of Oncology, Lund, Sweden*
[6]*Skane University Hospital- Sweden, Department of Oncology and Radiation Physics, Lund, Sweden*
[7]*Umeå University, Department of Radiation Sciences, Umeå, Sweden*
[8]*Akademiska University hospital, Radiation Physics, Uppsala, Sweden*

Purpose or Objective: To develop an infrastructure for structured and automated collection of interoperable radiation therapy (RT) data into a Swedish national quality register.

Material and Methods: The present study was initiated in 2012 with the participation of seven of the 15 Swedish clinics delivering radiation therapy. A national RT nomenclature and a database for structured unified storage of RT data at each clinic (Medical Information Quality Archive; MIQA) have been developed. Aggregated data from the MIQA databases are sent to a Swedish national RT register located on the same IT framework (INCA) as the national diagnosis-specific quality registries.

Results: The suggested naming convention has to date been integrated into the clinical workflow at 12 sites and *MIQA* is installed at six of these. Involvement of the remaining Swedish RT clinics is ongoing, and they are expected to be part of the infrastructure by 2016. RT data collection from Aria®, Mosaiq®, Eclipse™, and Oncentra® is supported. Manual curation of RT-structure information is needed for approximately 10% of target volumes, but rarely for normal tissue structures, demonstrating a good compliance to the RT nomenclature. Aggregated dose/volume descriptors are calculated based on the information in MIQA and sent to INCA using a dedicated service (MIQA2INCA). Correct linkage of data for each patient to the diagnosis-specific quality registries on the INCA platform is assured by the unique Swedish personal identity number.

Conclusion: An infrastructure for structured and automated prospective collection of syntactically interoperable radiation therapy data into a national register for RT data in Sweden has been implemented. Future developments include adapting *MIQA* to other treatment modalities (e.g. proton therapy and brachytherapy) and finding strategies to harmonize structure delineations.
The database is built on the same platform as used by the diagnos specific quality registers in Sweden hosting information about additional treatments, clinical and patient reported outcomes.

EP-1914

Nationwide audit of small fields output calculations in Poland

W. Bulski[1], K. Chelminski[1]
[1]*The Maria Sklodowska-Curie Memorial Cancer Center, Medical Physics Department, Warsaw, Poland*

Purpose or Objective: Modern radiotherapy routinely involves the use of small radiation fields, either for the delivery of stereotactic treatments, or as components of intensity-modulated radiation therapy (IMRT). The purpose of the small field dose rate dependence audit is to check dosimetric data in the treatment planning system (TPS), as used for patient Intensity Modulated Radiation Therapy (IMRT) treatments, related to a radiotherapy treatment unit equipped with an MLC.

Material and Methods: The methodology worked out in the framework of the IAEA Coordinated Research Project E2.40.18 was used. The audit participants were asked to calculate the number of MUs for 5 MLC-shaped field sizes (10×10 cm2, 6×6 cm2, 4×4 cm2, 3×3 cm2 and 2×2 cm2) to deliver 10 Gy on axis at 10 cm depth, 100 cm SSD in water, using their treatment planning system. These calculations had to be repeated for each photon beam energy used for IMRT treatments. Eventually, they had to calculate the dose rate (Gy/MU) for each of the five MLC defined field sizes and normalize each value to the 10×10 cm2 value. These results were compared with the benchmark data from the publication: "The Radiological Physics Center's standard dataset for small field size output factors" (Followill *et al.*, Journal of Applied Clinical Medical Physics, 2012). Since this dataset did not provide data for certain beam qualities the interpolation/extrapolation was performed fitting the second degree polynomials to the RPC measured values.

Results: The audit was performed in 32 (out of 35) Polish radiotherapy centres for different linacs, TPS, MLC types and beam energies. The beam qualities ranged from 4 MV to 20 MV. In total, 81 beams were checked (Varian 41, Elekta 24, Siemens 16). When compared to the treatment planning system-calculated mean output factors, the RPC's mean measured values agreed for all field sizes and energies within 1% difference for Elekta machines. For Varian machines the difference exceeded 1% for 3×3 cm2 and 2×2 cm2 fields for 6 MV beams (1.6% and 2.3%). For Siemens machines the differences exceeded 1% for 2×2 cm2 fields for both beam qualities 6 MV and 15 MV (1.6% and 1.7%).

Conclusion: The RPC's measured values provide a consistent dataset for small field output factors that can be used as a redundant QA check of a treatment planning system dosimetry data for small-field treatments. The RPC's measured values have a small uncertainty (standard deviation < 2%), while the values calculated from the various planning systems and their beam models had a greater uncertainty, especially for the smallest field sizes. Such QA dataset against which the institution can compare its measured or calculated values is helpful to ensure accurate IMRT dose delivery by identifying discrepancies prior to any patients being treated. Any discrepancies noted between the standard dataset and calculated values should be investigated with careful measurements and with attention to the specific beam model.

EP-1915

Development of video based quality assurance system for the medical linear accelerator

J.S. Shin[1], Y. Han[2], E. Shin[1], H.C. Park[2], D.H. Choi[2], D.H. Lim[2]
[1]*Samsung Medical Center, Radiation Oncology, Seoul, Korea Republic of*
[2]*Samsung Medical Center- Sungkyunkwan University School of Medicine, Radiation Oncology, Seoul, Korea Republic of*

Purpose or Objective: The medical linear accelerator(LINAC) is the most widely used in the modern radiation therapy. Recently, advanced radiation therapy technique require a high precision of the LINAC. Therefore, more precise quality assurance(QA) of the LINAC is required. In this study, we developed QA system using a video image for mechanical QA of LINAC. The our QA system may measure the mechanical isocenter offset(gantry, collimator, couch) and the couch movement. The purpose of this study was: ⓐthe Simplification of mechanical QA procedures, ⓑthe quantification of the measurement results, ⓒthe improvement of the measurement accuracy by eliminating the observers dependence.

Material and Methods: The our QA system developed in this study use a method of analysis based on the recorded image by camera(Figure 1). Our QA system has configured the hardware into three parts. The first, it is a indicating unit pointing to the isocenter. The second, it is a recording unit for recording an image. Finally, the third, it is an analysis unit for analyzing the image. For the accuracy evaluation of the our QA system, we performed the two experiments. The first, it is the mechanical isocenter offset check for rotation of gantry and collimator. We measured the mechanical isocenter, and evaluated for the accuracy of the measurement about intentional offset distances(±1mm, ±2mm). The second, it is couch movement check(direction of X, Y and Z). We compared the measured results by our QA system and the movement values shown in the R&V.

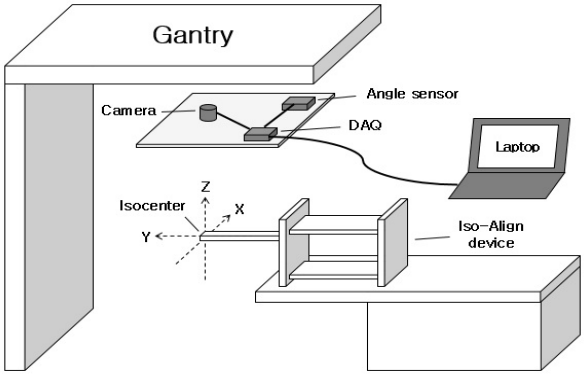

Figure 1. The configuration of the developed QA systems in this study.

Results: In the mechanical isocenter offset check, the mean error is about 0.09 mm for gantry rotation, the maximum error is about 0.28 mm was measured. And the mean error is about 0.11 mm for collimator rotation, the maximum error is about 0.31 mm was measured. In the couch movement check, the mean error in the X-direction is about 0.17 mm, the mean error in the Y-direction is about 0.19 mm, and the mean error in the Z-direction is about 0.24 mm.

Conclusion: In this study, we developed the QA system to improve the inefficient of the mechanical QA using conventional methods. At present, our QA system may measure the mechanical isocenter offset check and the couch movement check. The accuracy of measurement result is sufficient to measure the tolerances recommended in the guidelines.

NRF funded by the Ministry of Science, ICT & Future Planning (2012M3A9B6055201 and 2012R1A1A2042414), Samsung Medical Center grant[GFO1130081]

EP-1916

The IROC Houston QA Center's international activities outside North America

D. Followill[1], S. Kry[1], A. Molineu[1], J. Lowenstein[1], P. Alvarez[1], P. Taylor[1], H. Nguyen[1], N. Hernandez[1], T. Nguyen[1], C. Lujano[1], T. Keith[1]

[1]*MD Anderson Cancer Center, IROC Houston QA Center, Houston, USA*

Purpose or Objective: Purpose/Objective: To describe the extent of IROC Houston's, formerly the Radiological Physics Center, QA activities and audit results for radiotherapy institutions outside of North America (NA).

Material and Methods: Material/Method: The IROC Houston's QA program components were designed to audit the radiation dose calculation chain from the NIST traceable reference beam calibration, to inclusion of dosimetry parameters used to calculate tumor doses, to the delivery of the radiation dose. The QA program provided to international institutions includes: 1) remote TLD/OSLD audit of machine output, 2) credentialing for advanced technologies, and 3) review of patient treatment records. IROC Houston uses the same standards and acceptance criteria for all of its audits whether for North American or international sites.

Results: Results: IROC Houston's QA program has reached out to radiotherapy sites in 43 different countries since 2013 through their participation in clinical trials. In the past two years, 2,778 international megavoltage beam outputs were audited with OSLD/TLD. While the average IROC/Inst ratio is near unity for all sites monitored, there are international regions whose results are significantly different from the NA region as seen in Table 1. In the past 2 years, 477 and 87 IMRT H&N phantoms were irradiated at NA and international sites, respectively. Regardless of the OSLD beam audit results, the overall pass rate (87 percent) for all international sites (no region separation) is equal to the NA sites. Of the 182 international patient charts reviewed, 10.7 percent of the dose calculation points did not meet our acceptance criterion as compared to 13.6 percent for NA sites. The lower pass rate for NA sites results from a much larger brachytherapy component which has been shown to be more error prone.

	Beam Output Audits (IROC/INST)			
Geographical Region	Sample count	Mean	Std Deviation	P value (α=0.05)
N America	29284	0.999	0.019	control
Australia/New Zealand	544	0.989	0.018	0.000
China/ Hong Kong	187	1.002	0.017	0.053*
Republic of Korea	397	0.997	0.022	0.013
Japan	84	0.991	0.017	0.000
Taiwan	95	0.993	**0.029**	0.002
E Europe/ Russia	104	1.005	**0.038**	0.002
W Europe	657	1.000	**0.029**	0.914*
India/ Sri Lanka	71	1.009	**0.042**	0.000
Middle East	268	0.995	0.022	0.000
Africa	48	1.006	0.024	0.011
Latin America	37	1.003	0.023	0.272*
SE Asia	104	0.992	0.023	0.000

* not significantly different from N America (one way ANOVA)

Table 1. OSLD/TLD output audit results by geographical region since 2013.

Conclusion: Conclusion: The IROC Houston QA Center has expanded its QA services worldwide and continues a long history of improving radiotherapy dose delivery in many countries.

EP-1917

Measurements of reactive oxygen species production induced by gold nanoparticles in radiotherapy

P. Cerello[1], L. Bocchini[1], A. Gobbato[1], A. Attili[1], C. Cutaia[2], V. Ferrero[3], C. Pontremoli[4], L. Radici[2], M. Stasi[2], S. Visentin[4]

[1]*Istituto Nazionale di Fisica Nucleare INFN, Sezione di Torino, Torino, Italy*

[2]*A.O. Ordine Mauriziano, Medical Physics, Torino, Italy*

[3]*University of Torino, Department of Physics, Torino, Italy*

[4]*University of Torino, Department of Molecular Biotechnology and Health Sciences, Torino, Italy*

Purpose or Objective: Metallic nanoparticles have shown radiosensitizing properties in cancer radiotherapy, with both conventional and hadron beams. In particular, Gold Nano Particles (GNPs) are emerging as promising enhancers for radiotherapy. However, the exact mechanisms behind the extra damage are yet unknown, although Reactive Oxygen Species (ROS) production, known to be crucial in radiotherapy, is a strong candidate. A direct measurements of ROS production was performed in typical radiotherapy treatment conditions.

Material and Methods: A protocol for measuring the OH* radical production in Phosphate-buffered saline (PBS) solution, based on the fluorimetric properties of oxygen-quenched Terephthalic acid, was designed and validated. Correction factors associated to GNP-induced adsorption, absorption and diffusion at the fluorimetric excitation and emission wavelengths were carefully evaluated. ROS production induced by 6 and 15 MV photon beams was then measured in standard PBS solution, as well as in the presence of GNPs of 5 nm and 20 nm diameters, at 5 μmol and 10 μmol concentrations.

Results: A relevant ROS extra production was observed for 5 nm diameter GNPs, up to about 40% at 10 μmol and 20% at 5 μmol as a function of the delivered dose. Measurements with 20 nm diameter GNPs are consistent with a ROS production increase of the order of 10%, albeit with a large experimental error. The ROS enhancement is consistent with the hypothesis of a linear dependence on the GNP surface to volume ratio, within the experimental errors.

Conclusion: Further measurements with 10 nm and 2 nm GNPs are planned, in order to verify the linear dependence on the inverse GNP radius with higher precision over a wider size range.

EP-1918

Radiotherapy quality assurance in the TREC trial

N. Abbott[1], G.W. Jones[1], P. Parsons[1], D.G. Lewis[1], E. Spezi[2], M. Kaur[3], L. Magill[3], R. Gray[4], S.P. Bach[5], D. Sebag-Montefiore[6]

[1]*Velindre Cancer Centre, Medical Physics, Cardiff, United Kingdom*

[2]*Cardiff University, School of Engineering, Cardiff, United Kingdom*

[3]*University of Birmingham, Birmingham Clinical Trial Unit, Birmingham, United Kingdom*

[4]*University of Oxford, Clinical Trial Service Unit, Oxford, United Kingdom*

[5]*University of Birmingham, Birmingham, United Kingdom*

[6]*University of Leeds, Leeds, United Kingdom*

Purpose or Objective: Transanal Endoscopic Microsurgery (TEM) and Radiotherapy in Early Rectal Cancer (TREC) [1][2] is a randomised phase II feasibility study to compare radical TEM surgery versus short course pre-operative radiotherapy (25Gy in 5 fractions over 5 days) with delayed local excision for treatment of early rectal cancer.
The QA programme for TREC is co-ordinated by the UK Radiotherapy Trials Quality Assurance (RTTQA) group [3][4]. We describe the development of a standardised analysis pipeline and the results of this analysis.

Material and Methods: To ensure consistency and therefore comparability between radiotherapy centres involved in TREC, a detailed radiotherapy protocol was developed. To assess the quality of the plans, 3 (PTVmin, PTVmax, ICRUmax) quantities were measured and recorded. Further investigation was carried out if the relevant objective was not met.
TEMS patients in TREC were treated across 18 UK centres. Radiotherapy plan data was submitted for each of the 87 TEM patients in DICOM format and processed with the Computational Environment for Radiotherapy Research (CERR) software [5]. This enabled i) outlining of target and organ-at-risk structures, ii) dose distribution and dose volume histograms to be assessed (independently) and iii) data format standardisation and automated analysis.

Results:

ROI Objective	Definition
PTV min	D99% ≥ 95% (23.75 Gy)
PTV max	D5% < 105% (26.25 Gy) D2% < 110% (27.5 Gy)
ICRU max	D1.8cc < 110% (27.5 Gy) Lateral patient dose distant from PTV <80% to 85%

Table 1: Summary of quantities assessed during review of radiotherapy plans

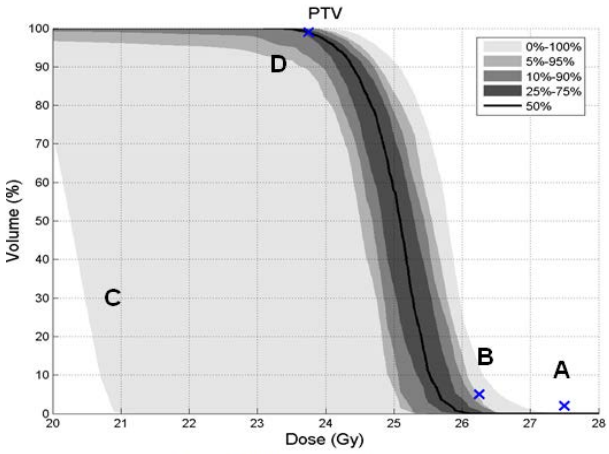

Figure 1: Distribution of PTV coverage

Table 1 shows the ROI objectives outlined in the TREC protocol. Figure 1 shows the distribution of PTV coverage for the 87 TEM patients analysed. All plans achieved D2%<110% (Figure 1, marker A) and 95% of plans achieved D5%<105% (B). Cases of poor coverage (C) were investigated and in 4 cases it was found that the outlined PTV extended beyond the patient surface. In these cases PTV was retracted to within the patient surface and coverage was recalculated.

Conclusion: Deviation from the clinical trial protocol has the potential to confound the study question and quality assurance is therefore essential when comparing different treatments. A high level of conformance was found across the 18 treating centres, with 95% of plans achieving both the minimum and maximum PTV objectives. Our analysis of the radiotherapy plans demonstrates good understanding and adherence to the TREC protocol.
STAR-TREC is an upcoming trial that will amend and extend the TREC pilot. RTTQA findings from TREC will be used to strengthen and improve the STAR-TREC protocol, for example, use of standardised structure names and use of plan-optimisation PTVs to assess target coverage.

References:

[1] Cancer Research UK, "TREC trial protocol," 15 09 2010. [Online]. Available: http://www.birmingham.ac.uk/Documents/college-mds/trials/bctu/trec/TREC-protocol-v1.pdf.

[2] Cancer Research UK, "A study looking at a possible new way to treat cancer of the back passage (TREC)," 13 03 2015. [Online]. Available: http://www.cancerresearchuk.org/about-cancer/find-a-clinical-trial/a-study-looking-possible-new-way-treat-cancer-back-passage-trec.

[3] "RTTQA group," [Online]. Available: http://www.rttrialsqa.org.uk/rttqa/.

[4] C. M. Evans, N. G. Burnet, E. Hall, R. A. Huddart, C. M. Nutting and C. E. Coles, "The Radiotherapy Clinical Trial Research Landscape in the UK Between 2004 and 2013: A Cross-sectional Analysis," *Clinical Oncology*, vol. 27, pp. 491-494, 2015.

[5] "A Computational Environment For Radiotherapy Research, CERR," [Online]. Available: http://www.cerr.info/about.php.

EP-1919

A cost-effective and fast end-to-end test for treatment accuracy evaluation

A. Wopereis[1], K. Ishakoglu[1], E. Seravalli[1], J. Wolthaus[1]

[1]*UMC Utrecht, Radiotherapy, Utrecht, The Netherlands*

Purpose or Objective: End-to-end tests are used to measure the overall accuracy of the radiation therapy chain, excluding patient specific factors. An end-to-end test is a prerequisite to the overall success of any IGRT program. In this work the performance of a cost-effective and fast end-to-end test to assess the geometrical accuracy of the radiotherapy workflow is described.

Material and Methods: The in-house developed phantom for end-to-end testing is depicted in figure 1a. It consists of two Perspex slabs in which a piece of Gafchromic EBT3 film of 4x4cm2 can be placed in. Two notches tighten the film and determine the center and the orientation of the phantom/film respectively. The phantom can be positioned in such a way to have the film in the coronal and sagittal orientation. The total weight of the phantom is about 1kg. A high resolution computed tomography (CT) scan is made of the phantom and a treatment plan (figure 1b) including collimator, gantry and table rotations is computed on this CT. The treatment plan is sent to the linear accelerator. Simulating an actual patient treatment, the phantom is set up on the treatment table using the lasers. Then, cone beam CT guidance is used to adjust the phantom's position with respect to the planning CT. After applying the suggested table shift the plan is irradiated. The films are analyzed using an in-house written Excel macro. The shift required to align the film with the calculated dose plane represents the targeting error. The use of the described phantom for end-to-end testing was compared against two commercial available phantoms.

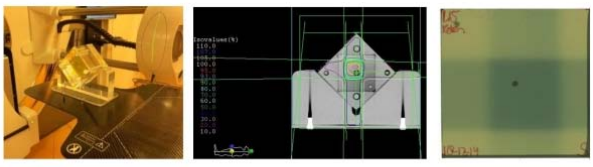

Figure 1 a. End-to-end phantom on the treatment table; b. dose distribution of the plan used for the test; c. corresponding film measurement.

Results: The phantom is light, easy to handle and to set up. Moreover, it is cheap compared to available commercial systems. The phantom allows to assess the overall geometrical accuracy of the treatment chain with sub mm

accuracy. The end-to-end test procedure requires on average 70 min preparation time, 30 min at the linear accelerator, 20 min analysis and administration. It allows end-to-end testing to be performed more frequently to assure the accuracy over time.

Conclusion: The developed end-to-end test is quick, cost-effective and easy to implement clinically. It allows to frequently highlight geometrical inaccuracies in an image-guided radiation therapy environment.

EP-1920

Harmonising the clinical trials QA group reports on phantom measurements around the globe

C. Clark[1], C. Field[2], D. Followill[3], A. Haworth[4], S. Ishikura[5], J. Izewska[6], C. Hurkmans[7]

[1]*NCRI Radiotherapy Trials, QA Group, London, United Kingdom*

[2]*NCIC Clinical Trials, QA group, Kingston, Canada*

[3]*Imaging and Radiation Oncology Core, QA group, Houston, USA*

[4]*Trans-Tasman Radiation Oncology, QA Group, Newcastle, Australia*

[5]*Japan Clinical Oncology, QA Group, Tokyo, Japan*

[6]*International Atomic Energy Agency, Dosimetry Laboratory, Vienna, Austria*

[7]*European Organisation on Research and Treatment of Cancer, QA Group, Brussels, Belgium*

Purpose or Objective: The Global Harmonisation Group was created in 2009 to harmonise and improve the quality assurance (QA) of radiation therapy implemented worldwide in multi-institutional clinical trials. The aim is to achieve a consistent platform to provide and share QA processes in clinical trials such that the workload for both the institutions and the QA groups is reduced and streamlined. As part of this aim, the group reviewed their reporting techniques to better understand each other's approaches and agree on core information which would be included as part of future creation of a standard template. This could potentially lead to the ability to use each other's reports in lieu of unnecessary duplication

Material and Methods: A survey was created to find a list of core information which could be included in future dosimetry credentialing reports. Answers were requested to give opinion from each group as to what should be included as a minimum in these reports. Some QA groups use site visits or postal phantoms, whereas some use a virtual phantom (i.e. local QA measurement) and others use both. The questions were divided to allow responses for both types. Questions were circulated amongst the groups beforehand and all comments and contributions were incorporated.

Results: All seven current member groups replied. Results were divided into three categories, 1)information which all groups agreed should be included 2)information which the majority use and the others often use which could be discussed as being agreed on inclusion and 3)information which was not used by all groups, but which could be used by those who did (see table 1).

Information which all groups agreed should be included in all reports	• dates of irradiation and report • name of organisation issuing report • overall pass/fail for the audit • planning system used, type of delivery (eg IMRT) • machine type used (eg linac, Tomo) • dose calculated by institution • dose measured by auditor • information on position of measurement
Information which the majority of groups agreed should be included in all reports	• named audit group personnel • named RT centre personnel • signature of responsible physicist • disclaimer about the scope of the audit • TPS algorithm used • energy used • phantom used (and description) • description of normalisation point
Information which was not used by all groups but which could be shared by those who did	• whether gantry angles were collapsed or not • gamma index software used • gamma index pass criteria • gamma index threshold used • calculations grid size used • whether local or global gamma calculation • correction for daily output dose • dose measured locally by institution (on local QA phantom)

Table 1 Agreed information in clinical trial QA group reports

Conclusion: The survey showed that that there is a wide variation in the information currently provided in the reports from the various QA organisations, which may hamper their mutual acceptance. Following discussion there were several pieces of information which were agreed should always be included and these constitute the beginning of an agreed list of included core information. There are several more pieces of information which the majority always include and the others use often or sometimes. These could be discussed to understand when and why they are not used and perhaps considered for inclusion. There are some others where not all members use the information because they do not use a gamma index analysis, however these could be included for those who do use the gamma index. There is also some information which sometimes included, but which is always included when needed. These cases will be discussed and decided if these should be included in specific cases, perhaps including a flowchart to aid standardisation. Some groups have already reviewed or are in the process of reviewing their reports to ensure inclusion of core information.

EP-1921

Novalis certification of stereotactic radiation therapy programs: methodology and current status

J. Robar[1], T. Gevaert[2], M. Todorovic[3], T. Solberg[4]

[1]*Dalhousie University, Radiation Oncology, Halifax, Canada*

[2]*Universitair Ziekenhuis Brussel UZB- Vrije Universiteit Brussel VUB, Department of Radiotherapy, Brussels, Belgium*

[3]*University Medical Center Hamburg-Eppendorf UKE, Department of Radiotherapy and Radio-Oncology, Hamburg, Germany*

[4]*University of Pennsylvania, Department of Radiation Oncology, Philadelphia, USA*

Purpose or Objective: To present an overview and the current status of Novalis Certification, which provides a comprehensive and independent assessment of safety and quality in stereotactic radiosurgery (SRS) and stereotactic body radiation therapy (SBRT), ensuring the highest standards and consistency of practice.

Material and Methods: The Novalis Certification program includes a review of SRS/SBRT program structure, adequacy of personnel resources and training, appropriateness and use of technology, program quality management, patient-specific quality assurance and equipment quality control. Currently ten auditors support the program, with six in North America, three in Europe and one in Asia, each bringing a minimum of a decade of experience in stereotactic practice. Centres applying for Novalis Certification complete a self-study 30 days prior to a scheduled one-day site visit by one to two reviewers. Reviewers generate a descriptive 77-point report which is reviewed and voted on by a multidisciplinary expert panel of 3 medical physicists, 2 radiation oncologists and 2 neurosurgeons. Outcomes of reviews may include mandatory

requirements and optional recommendations, with the former requiring resolution prior to award of Certification.

Results: To date, 14 institutions have received Novalis Certification, including 6 in Europe, 3 in North America, 4 in Australia and 1 in Asia. An additional 90 certification applications are pending; approximately one half and one third of these are sites are in Europe and North America, respectively. Nine of the 14 reviews have resulted in mandatory requirements, however all of these were addressed within three months of the audit report. Individual reviews have produced from 2 to 9 specific recommendations ranging from programmatic to technical in nature.

Conclusion: Novalis Certification is a unique and active peer review program assessing safety and quality in SRS and SBRT, while recognizing high calibre of practice internationally. The standards-based approach is capable of highlighting outstanding requirements and providing recommendations to enhance both new and established programs.

EP-1922

Comparing MLC positioning errors in Clinac and Truebeam Linacs by analysing log files

J. Olasolo Alonso[1], P. Gago[1], A. Vazquez[2], S. Pellejero[3], C. Eito[1], M. Aylas[1], P. Ensunza[1]
[1]*Clinica IMQ Zorrotzaurre, Radiation Therapy, Bilbao, Spain*
[2]*Centro de Investigación Biomédica de La Rioja, Medical Physics, Logroño, Spain*
[3]*Complejo Hospitalario de Navarra, Medical Physics, Pamplona, Spain*

Purpose or Objective: Log files contain information about Varian accelerators deliveries of dynamic treatments. This information includes actual and expected leaf positions throughout the treatment. Log files have been proposed by several authors to evaluate leaf position errors. In this study, log files of Clinac (dynalogs) and Truebeam (trajectory log files) accelerators have been analyzed to compare leaf positioning errors of dynamic treatments in different generations of clinical linear accelerators.

Material and Methods: More than 30000 log files have been analyzed, coming from four Clinac accelerators (one Trilogy, two Clinac 21EX, one Clinac 2100CD equipped with Millennium 120MLC) and one Truebeam accelerator (Truebeam STx 2.0 equipped with HD 120 MLC) of three different institutions. Analyzed Truebeam log files correspond to VMAT and dIMRT treatments whereas Clinac log files only correspond to dIMRT treatments.
Clinac accelerators control system has approximately a 50ms delay (one control cycle time). At each control cycle, MLC controller compares the planned to the actual positions. But in this comparison, the actual position is delayed 50 ms from the planned one. This effect causes that measured positions appear in dynalogs one cycle out of phase with respect to the planned positions. Therefore, error statistics present an error component proportional to leaf speed. A recent research of our group has studied this effect and, as a result, we have proposed to calculate error statistics without time delay effect to evaluate the MLC positioning deviations. In Truebeam accelerators this effect does not exist due to the proactive design of the MLC control system.
Leaf positioning RMS errors and 95th percentile errors were calculated to evaluate MLC performance with and without time delay effect. Log files were analyzed using an in-house Matlab program.

Results: In Clinac accelerators, the mean RMS error was 0.35, 0.34, 0.33 and 0.29 mm for each linac. The mean 95th percentile error was 0.62, 0.61, 0.62 and 0.58 mm. Without time delay effect, the mean RMS error was0.038, 0.042, 0.040 and 0.026 mm for each linac. The mean 95th percentile error was 0.054, 0.057, 0.057 and 0.046 mm.
In Truebeam accelerator, the mean RMS error and the mean 95th percentile for VMAT treatments were 0.038 mm and 0.07 mm. For IMRT treatments, the mean RMS error and the mean 95th percentile were 0.027 mm and 0.052 mm.

Conclusion: Truebeam MLC positioning errors are substantially lower than those of Clinac machine models, mainly due to the proactive design of Truebeam control system. However error statistics without time delay effect in Clinac machines, have the same order of magnitude of Truebeam ones.

EP-1923

Regular assessment of isocentre and positioning accuracy in image guided stereotactic radiotherapy

C. Heinz[1], S. Neppl[1], W. Haimerl[1], C. Belka[1], M. Reiner[1]
[1]*Ludwig-Maximilians-University, Department of Radiation Oncology, Munich, Germany*

Purpose or Objective: As the number of stereotactic radiotherapy applications is increasing and image guided techniques are superseding frame based solutions in cranial as well as in extracranial stereotactic applications the need to include imaging and positioning devices in the regular quality management is obvious. A very common test to check the deviation between the radiation isocentre and the room lasers is the Winston-Lutz test. However, this test lacks significance in combination with image guided stereotactic treatment since the patient is positioned by the image guidance devices rather than by the room lasers. The purpose of this project was, to implement a practical workflow to assess the isocentre and positioning accuracy of image guided stereotactic applications.

Material and Methods: The concept of our approach is based on the Winston-Lutz test except that positioning is done automatically by the image guidance devices rather than by the room lasers. Therefore a pelvis phantom including a metal sphere is roughly positioned on the treatment couch. By the use of an image guidance device (e.g. CBCT, non-coplanar imaging) translational and rotational correction values are acquired and sent to a 6-DOF robotic couch. After the phantoms position is adjusted by movements of the robotic couch, the metal sphere inside the phantom should be positioned exactly at the radiation isocentre of the linear accelerator. The result of the image guided positioning is recorded by portal images. For this purpose a small radiation field (2x2 cm^2) is applied from up to 8 different gantry angles. Afterwards the radiation field isocentre, the isocentre position of the metal sphere as well as the deviation is calculated by a software that was developed in-house.

Results: This end-to-end test provides quantitative information on the achievable positioning accuracy of an image guided stereotactic application in the clinical situation. Besides, the deviations of the radiation isocentre from the mechanical isocentres of the gantry, collimator and couch can be analyzed using the same setup. The test is not restricted to a specific image guidance modality.

Conclusion: A regular assessment of all systems included in stereotactic patient positioning is highly recommended. Due to the short execution time this test is suitable for regular assessments in the QA routine.

EP-1924

Implementation of a safety checklist to improve quality and safety of physician plan review process

L. Fong de los Santos[1], S. Park[1], K. Olivier[1]
[1]*Mayo Clinic, Radiation Oncology, Rochester, USA*

Purpose or Objective: The physician review of the treatment plan upon completion by the treatment planner is a critical clinical process, since it is during this exchange where the physician verifies and confirms the treatment intent. Several near misses in our practice raised the awareness of our group regarding the quality and safety of this process. Moreover, there was no standardization of the review process and no additional safety barrier to detect if the prescription defined by the physician matches the treatment intend. Our goal is to use a safety checklist to improve the quality and safety as

well as the communication dynamics during the plan review process.

Material and Methods: A safety checklist was developed and implemented using checklist's best practices as well as input from physicians, physicists and treatment planners (Figure. 1).

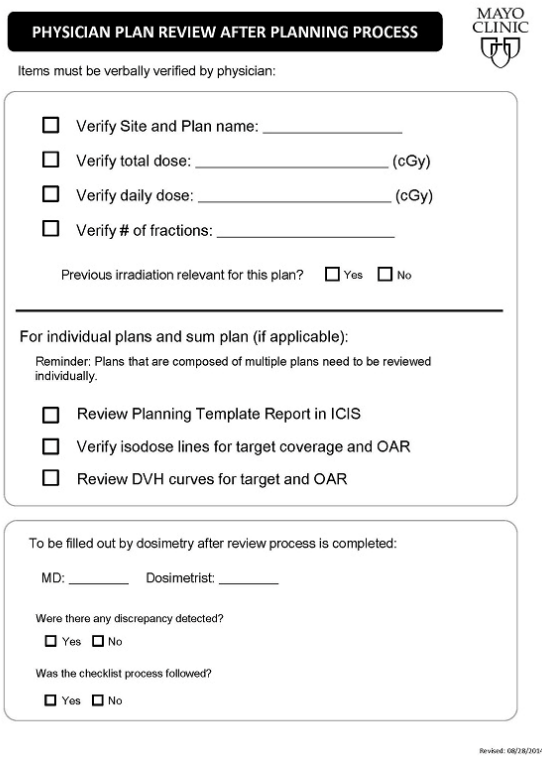

PHYSICIAN PLAN REVIEW AFTER PLANNING PROCESS

MAYO CLINIC

Items must be verbally verified by physician:

- ☐ Verify Site and Plan name: _____
- ☐ Verify total dose: _____ (cGy)
- ☐ Verify daily dose: _____ (cGy)
- ☐ Verify # of fractions: _____

Previous irradiation relevant for this plan? ☐ Yes ☐ No

For individual plans and sum plan (if applicable):

Reminder: Plans that are composed of multiple plans need to be reviewed individually.

- ☐ Review Planning Template Report in ICIS
- ☐ Verify isodose lines for target coverage and OAR
- ☐ Review DVH curves for target and OAR

To be filled out by dosimetry after review process is completed:

MD: _____ Dosimetrist: _____

Were there any discrepancy detected?

☐ Yes ☐ No

Was the checklist process followed?

☐ Yes ☐ No

Revised: 08/28/2014

We used the "Static sequential with verification and confirmation" method to perform the checklist. This method uses both initial configuration and mutual redundancy; the treatment planner writes down and calls the values on the checklist and the physician confirms that those values match the treatment intent. As part of a department practice quality improvement (PQI) project, we used a series of Plan, Do, Study, Act (PSDA) quality improvement cycles, and assessed the effectiveness of the safety checklist and the success of the project implementation. During each plan reviewed by the physician, we tracked two metrics: 1) Effectiveness of the checklist to catch a deviation and 2) Compliance of the physician to the checklist process. Additionally, we used a survey to assess communication dynamics between physician and planner.

Results: The safety checklist was used during a period of 6 months across our entire practice: 40 physicians and 24 planners. 1773 treatments plans were reviewed using the safety checklist process. This sample represents close to 95% of all clinical plans done in our practice during this period of time. The safety checklist helped catching 19 near-misses and also helped achieving 99% overall compliance to the plan review process. Pre- and post-implementation surveys shows improvement on communication dynamics and interaction between physician and treatment planner. Upon completion of the PQI, this safety checklist has become our standard operating procedure for the physician plan review process.

Conclusion: A safety checklist was successfully implemented as a safety barrier as part of the physician plan review process. The utilization of the safety checklist improved communication dynamics, process compliance and standardization, thus, improving the quality of the review process and the overall safety of our practice. This work presents evidence that Safety Checklists are an effective tool in error management as well as a tool to improve process compliance and team communication.

EP-1925

Online open source software to assess adverse events of patients undergoing radiochemotherapy

A.H. Thieme[1], D. Kaul[1], C. Stromberger[1], P. Ghadjar[1], V. Budach[1]

[1]*Charité-Universitätsmedizin Berlin, Klinik für Radioonkologie und Strahlentherapie, Berlin, Germany*

Purpose or Objective: Radiochemotherapy is inherently associated with adverse events and complete, accurate and examiner-independent documentation is essential for everyday clinical work as well as for clinical trials. Acute toxicity during treatment might make it necessary to adapt the current treatment, to interrupt irradiation or to skip or postpone a cycle of chemotherapy. Late effects may become symptomatic even years after treatment has been completed. The common approach to collect toxicity data is to use paper-based documentation which has to be manually fed into databases for evaluation. This method turned out to be time-consuming, error-prone and impractical. In order to address these issues, the software "Toxicity" was developed at the department of Radiation Oncology, Charité Universitätsmedizin Berlin.

Material and Methods: The software can be used simultaneously by multiple users on different computers to add, modify or view patient data, treatment information and adverse events. The software supports the National Cancer Institute Common Toxicity Criteria Adverse Event (CTCAE v4.03), Late Effects of Normal Tissue (LENT-SOMA) classification systems, laboratory values and other special data types, e.g. tone audiograms. The user can look up the definition of each item while entering values and get a graphical representation. Data for adverse events is collected every week for acute and every 3 months for late effects. Questionnaires are specific to the tumor entity, body area and treatment. The collected data is stored centrally in a MySQL database and is statistically analyzable. The software was developed in the cross-platform programming language C Sharp and the target platform is Windows, Mac OS X and Unix.

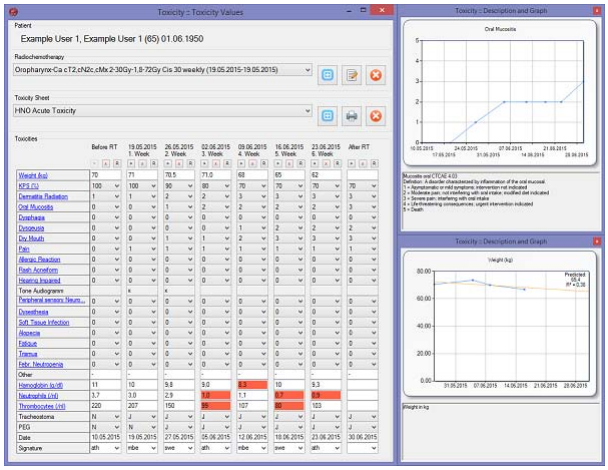

Results: To evaluate objective user acceptance, we compared the quality of adverse events documentation in our department between 01/2015 and 06/2015 (paper-based documentation) to the quality of documentation between 07/2015 and 10/2015 (software-based documentation). For patients treated until June 2015 patient files were obtained. For patients who had been treated after July 2015 data from "Toxicity" was automatically exported. In the 4 months the "Toxicity" system was used 7336 items were recorded. We can see a statistically significant increase of information recorded per patient.

Conclusion: Our first experience with the "Toxicity" software demonstrates favorable accuracy of adverse events documentation of patients undergoing radiochemotherapy and its applicability as a tool for clinical trials.

EP-1926

Hybrid of cloud computing and workstations for radiotherapy planning

L. Zou[1,2], Z. Xie[2], W. Zhang[2], Y. Xie[1], L. Xing[3]
[1]*Shenzhen Institutes of Advanced Technology- Chinese Academy of Sciences, Institute of Biomedical and Health Engineering, Shenzhen, China*
[2]*Sichuan Provincial People's Hospital, Department of Radiotherapy- Cancer Center, Chengdu, China*
[3]*Stanford University, Department of Radiation Oncology, Stanford, USA*

Purpose or Objective: The goal of this work is to develop a hybrid environment composed of treatment planning system(TPS) workstations and a private cloud infrastructure(Radiotherapy Planning Cloud, RTPCloud) for radiotherapy planning in routine job.

Material and Methods: The Eclipse(v11.0) workstations were distributed by Varian Medical Systems. The RTPCloud was based on OpenStack and leveraged the virtual GPU hardware (Nvidia Grid k1) and multi-core CPU server (Dell PowerEdge R910) to act as infrastructure as an service(IAAS) cloud. In the cloud, we created three kinds of virtual machine images: Dev-vmi, Workstation-vmi, DCF-vmi. All of them will be used for creating functional clusters. All of Eclipse modules were transplanted to Workstation-vmi. In addition to what Workstation-vmi has, Dev-vmi has a full script development and run environment. DCF-vmi only has calculation agent components of Eclipse's distributed calculation framework(DCF). All of the functional clusters derived from those images are scalable and their lifecycles are managed by OpenStack REST API. NoMachine is the remote desktop client to access virtual machines in the cloud.

Results: Any NoMachine-enabled computer in the hospital local area network becomes a Eclipse workstation, when an authorized user remotely accesses his virtual workstation. In this manner, we got at least three times as concurrent users as vender's distribution, and overcome office's location constraint. Script development and run cluster gives advanced users an isolated environment for automation of manual job without occupying those rare clinic workstations. The initial outcome is the ContourAutoMargin(CAM), which is developed in AutoHotkey script. It realized an automation of verbose operation of structures for planning. 10 to 20 minutes manual work per patient case will be done by clicking only one button. DCF Agent Cluster derived from DCF-vmi improves the performance of high compute-intensive calculation(e.g. Dose calculation) of planning.

Conclusion: Benefits from cloud computing maximize the utilization ratio of the expensive software features and optimize the radiotherapy planning procedure. The hybrid environment is a very powerful solution with high cost performance, and will boost the radiotherapy planning in clinic and research.

EP-1927

Practical dosimetry solutions to enhance cell biology studies

E. Claridge Mackonis[1], L. Hammond[1], N. Suchowerska[1]
[1]*Chris O'Brien Lifehouse, Radiation Oncology, Camperdown-Sydney, Australia*

Purpose or Objective: Our current study of the effects of combined therapies on triple negative and HER2 positive breast cancer has motivated an evaluation of the experimental design for the parallel radiation exposure of several cell samples, each representing a different therapeutic combination. To evaluate the synergistic effects between radiotherapy, chemotherapy and nanoparticles, the radiation dose must be accurately known. We focus on radiation beam energies and dose rates typically used in the clinical environment.

Material and Methods: The cells in clonogenic assays are adherent onto the base of the flasks. The dose to the base of six different flask designs from two manufacturers, was measured using GAFCHROMICTM EBT3 film. The flasks were exposed to a 6MV photon beam from a Novalis Tx linear accelerator or to a 50kVp, 150kVp or 280kVP photon beam from a Pantak kilovoltage unit. For the megavoltage beam, the flasks were positioned on virtual water slabs and irradiated from below, with the linac gantry at 180°. For the kilovoltage beam, the flasks were positioned on the face of the cone applicator with the beam directed towards the ceiling. For all exposures, the film was placed immediately beneath the flask. A CT scan was taken of each flask design under the exposure conditions for the MV beam and a plan constructed to calculate the dose to the cell layer using the Varian EclipseTM treatment planning system. The calculated monitor units and dose distribution were compared to the measured values.

Results: For the 6MV photon beam, the dose distributions to the cell layer in the axial and sagittal planes for three flask designs are shown in figure 1. The film measurements were consistent with the planned data. For the kV beams, where the dose distribution is sensitive to scatter conditions, it was found that the calculated dose across all wells and flasks, was inconsistent with measurement. Air channels on the perimeter of the flask, specific to the flask design, need to be filled for reproducible dosimetry. Furthermore, for the 96 well flask, the perimeter wells were found to have a different dose to interior wells.

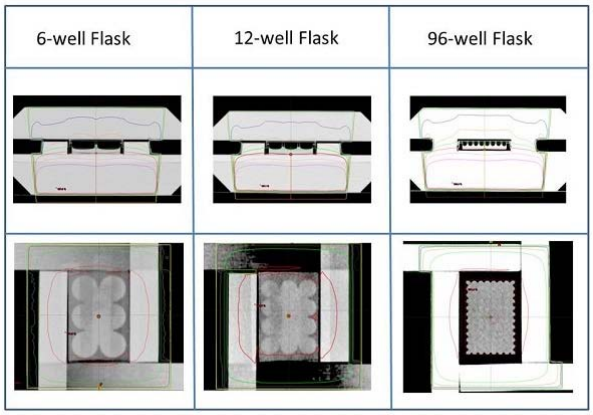

Figure 1: Dose distribution at cell layer shown in the transverse and coronal views

Conclusion: This work indicates that when radiation is used as a therapeutic agent, insufficient attention to dosimetry can substantially compromise cell biology studies leading to false conclusions. For studies of combined therapeutic interventions, we provide practical solutions to the parallel radiation exposure of numerous cell samples, such that additional variables are minimised. Our findings are applicable to any cell study where radiation exposure is involved.

EP-1928

The Nano-X image-guided adaptive gantry-less linac: imaging and dosimetry under phantom rotation

I. Feain[1], C.C. Shieh[1], P. White[2], R. O'Brien[1], W. Counter[1], M. Jackson[3], S. Downes[2], P. Keall[1]
[1]*University of Sydney, School of Medicine, Camperdown, Australia*
[2]*Prince of Wales Hospital, Nelune Comprehensive Cancer Centre, Sydney, Australia*
[3]*School of Medicine, University of NSW, Sydney, Australia*

Purpose or Objective: Innovative solutions for delivering high-quality, safe, affordable and appropriate treatment are needed to redress a staggering global underutilisation of radiotherapy. Nano-X will be a novel image-guided adaptive radiotherapy machine, quite different to conventional systems. Its key-differentiating feature is a rotating patient couch and a gantry-less linac. We present the first experimental results demonstrating imaging and dosimetric

equivalence between conventional and Nano-X treatment geometries.

Material and Methods: Experiments were performed during Sep-Oct 2015 on an Elekta Agility with MLC, XVI imaging system and a custom-built phantom rotation platform.

Dosimetry:

An IBA MatriXX Evolution 2D ionization chamber array was mounted to the phantom rotator. A Head and Neck IMRT treatment plan, with seven equiangular beams, was used. Two treatments were delivered: the first under conventional conditions with the MatriXX stationary and the linac delivering treatment at planned gantry angles. The second, mimicking a Nano-X treatment, involved rotating the MatriXX to the planned angle, with the linac gantry static and vertical.

Imaging:

A CATphan CT imaging QA phantom was mounted to the phantom rotator. Two sets of measurements were acquired: the first involved a cone-beam CT acquired under conventional conditions with the CATPhan stationary and the linac rotating. The second, mimicking a Nano-X treatment, involved rotating the CATphan, with the linac gantry static and vertical. Both datasets were reconstructed using Feldkamp-Davis-Kress (FDK) back projection.

Results:

Dosimetry: 2D distributions were compared between rotated-gantry (conventional geometry) and rotated-MatriXX (Nano-X geometry) beams using 3%/3 gamma analysis. Measurements were repeated on consecutive days and the departmental tolerance of 90% was defined as our pass rate. Results for ranged from 92.7% to 98.2% on Day 1 and 95.8% to 98.9% on Day 2, for the same angled beams.

Imaging: Figure 1 shows the CATphan images acquired in Nano-X (Fig 1a) and conventional linac (Fig 1b) geometries. The mean absolute pixel value of the difference image (histogram shown in Fig 1c) was 28 Hounsfield units (HU), consistent with Poisson noise. The line profile (Fig 1b) shows the two imaging geometries have high agreement in both pixel intensities and spatial information.

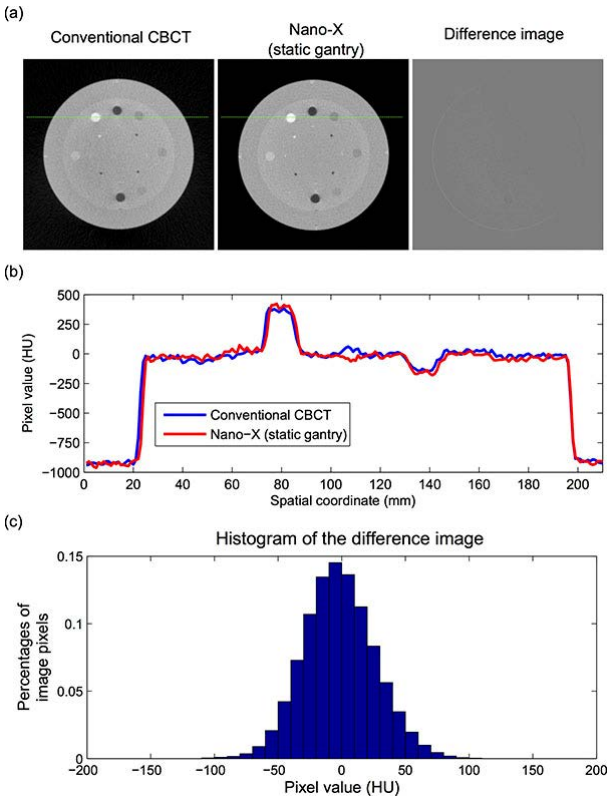

Conclusion: We have demonstrated imaging and dosimetric equivalence between the Nano-X gantry-less linac and conventional linac geometries.

EP-1929

Characterisation of a gridded electron gun in magnetic fields: implications for MRI-Linac therapy

B. Whelan[1], D. Constantin[2], R. Fahrig[2], P. Keall[1], L. Holloway[3], B. Oborn[4]

[1]*University of Sydney, Radiation Physics Lab, Marrickville, Australia*

[2]*Stanford University, Radiological Sciences Lab, Palo Alto, USA*

[3]*Liverpool Hospital & Ingham Institute, Cancer Therapy, Liverpool, Australia*

[4]*Illawarra Cancer Care Centre, Medical Physics, Illawarra, Australia*

Purpose or Objective: With recent advances towards MRI-Linac radiotherapy, characterisation of electromagnetic interactions of the two devices is an important research area. One of the most sensitive components is the linac electron gun. Previous work focused on characterising non-gridded guns in parallel and perpendicular magnetic fields. However, the majority of Linac vendors use gridded guns, which have important applications in beam gating and variable energy/dose rate linacs. No studies on medical gridded guns could be found in the literature, so the purpose of this work is twofold: To develop and present a realistic model of a gridded gun, and to test the sensitivity of this gun in parallel and perpendicular magnetic fields with particular focus on different gun operating modes.

Material and Methods: The geometry of the gridded gun used on Varian high energy linacs was measured with 3D laser scanning quoted as accurate to 0.1 mm. Based on the scan, a detailed CAD model was developed. From this, key geometry was extracted and a Finite Element Model (FEM) was developed using commercial software (Opera/SCALA). The high voltage and grid voltage (HV: cathode to anode, grid: cathode to grid) were read directly from a Varian Trilogy in service mode. Two operating modes were simulated: 6MV photon beam: HV=16kV, grid=100V, & 18MV photon beam: HV=7kV, Grid = 30 V. The model was solved for each mode in parallel fields between 0 and 200 G, and perpendicular fields between 0 and 50 G.

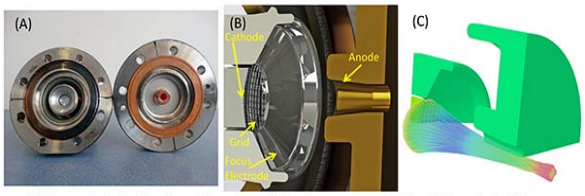

(A) The cathode(left) and anode section of the electron gun. (B) The CAD model which was developed. (C) A solved FEM simulation

Results: Zero field emission current was 487 and 106mA for 6MV and 18MV respectively. Injection current is around 20% less, as the grid blocks some of the beam. In parallel fields 50% current loss occurred at 112 (6MV) and 77G (18MV), whilst in perpendicular fields these values were 19 and 13G. The behavior of the two different operating modes in the presence of magnetic fields is similar, but 18MV is around 50% more sensitive to magnetic fields than 6MV. This dependence on the HV of the electron gun has not previously been shown. In all cases, a grid potential of -100V resulted in zero injection current, showing the suitability of this gun for beam gating.

Conclusion: A FEM model of a gridded electron gun has been developed based on a commercial gun. The sensitivity to both parallel and perpendicular magnetic fields has been quantified. Different operating modes show substantially different sensitivity. This original result has implications for electron gun, waveguide, and shielding design in MRI-Linacs.

EP-1930

Cancer patient experience of slow, single arc rotation to simplify radiation therapy delivery

B. Whelan[1], M. Welgampola[2], L. McGarvie[2], K. Makhija[1], I. Feain[1], L. Holloway[3], M. Berry[3], M. Barton[3], R. Turner[4], M. Jackson[4], P. Keall[1]

[1]*University of Sydney, Radiation Physics Lab, Marrickville, Australia*

[2]*Royal Prince Alfred Hospital, Institute of Clinical Neurosciences, Sydney, Australia*

[3]*Liverpool Hospital and Ingham Institute, Cancer Therapy Centre, Liverpool, Australia*

[4]*University of New South Wales, Faculty of Medicine, Sydney, Australia*

Purpose or Objective: Conventionally in radiotherapy, a large beam forming apparatus is rotated around a stationary patient in order to achieve multiple beam angles. However, for a number of emerging and existing treatment modalities such as proton therapy, heavy ion therapy, MRI guided therapy, and synchrotron based therapies, such an approach results in prohibitively expensive and complex treatment systems. At the same time, much of the world has no access whatsoever to even conventional radiation therapy treatments. Replacing the gantry rotation with patient rotation could lead to much simpler and more cost effective treatment units. However, it is often assumed that patient acceptance would be a major barrier to widespread use of such a system. The purpose of this work was to test this assumption by investigating patient tolerance to slow single arc rotation.

Material and Methods: The Epley Omniax (Figure 1) is a clinically approved medical device conventionally used in balance disorder therapy, and can rotate 360 degrees around each axis. We used this device to test patient tolerance to slow, single arc rotation. Each patient underwent slow, single arc rotation in two orientations; sitting and lying. Patients were rotated a full 360 degrees in increments of 45 degrees. The rotation was paused for 30 seconds at each 45 degree increment to simulate beam delivery; in total this simulates the delivery of 8 beams. Patients were rotated in both an upright (sitting) and lying position in the same session. Response was monitored via validated psychometric questionnaires for claustrophobia, anxiety, and motion sickness. Thus far, 10 of a planned 15 current or former cancer patients have been recruited.

Figure 1: The Epley Omniax was used to test patient response to both upright and lying rotation to enable simplified and cost effective treatment machines

Results: Patient tolerance has been high – 9 out of 10 have completed the study without incident, and in general patient feedback has been positive. One patient was unable to complete the lying rotation, but was still able to complete the sitting rotation without issue. No detectible differences in anxiety or motion sickness have been observed from either sitting or lying rotation. A summary of the patient cohort and results thus far is outlined in table 1. Accrual for this study is ongoing.

Table 1: Outline of patient cohort and key results. Where 'percent' is used, 100 is the maximum possible score and 0 the minimum. The last two entries show the difference in patient's anxiety and motion sickness scores before and after the study.

	Mean	Std. Dev.	Range
Age (years)	62	13	39-78
Weight (kgs)	77	12	65-100
Time since last RT treatment (months)	34	60	0-168
Claustrophobia Score (percent)	24	18	1-50
Difference in Anxiety Score (Before/after - percent)	2.2	32	0-78
Difference in motion sickness score (Before/after - percent)	-6	10	-25-0

Conclusion: Patient rotation could enable much simpler treatment for both conventional and advanced treatments – however, it is often assumed that patient tolerance to rotation would be very low. The results generated thus far show that there is at least a cohort of patients who would find slow rotation an acceptable therapeutic intervention.

EP-1931

Abstract withdrawn

EP-1932

Quality assurance in implementing a national dose escalation trial in NSCLC – report from NARLAL2

T.B. Nielsen[1], C. Brink[1], D.S. Moeller[2], L. Hoffmann[2], C.M. Lutz[2], A.L. Appelt[3], M.D. Lund[3], M.S. Nielsen[4], W. Ottosson[5], A.A. Khalil[2], M.M. Knap[2], O. Hansen[6], T. Schytte[6]

[1]*Odense University Hospital, Laboratory of Radiation Physics, Odense, Denmark*

[2]*Aarhus University Hospital, Department of Oncology and Medical Physics, Aarhus, Denmark*

[3]*Vejle Hospital, Department of Oncology, Vejle, Denmark*

[4]*Aalborg University Hospital, Department of Oncology, Aalborg, Denmark*

[5]*Herlev Hospital, Radiotherapy Research Unit and Department of Oncology, Herlev, Denmark*

[6]*Odense University Hospital, Department of Oncology, Odense, Denmark*

Purpose or Objective: Potential severe or lethal toxicity in regards to dose escalation of locally-advanced NSCLC patients calls for caution. A national quality assurance program was conducted over a period of three years in Denmark in order to prepare for the heterogeneous FDG-guided dose escalation phase 3 trial: NARLAL2.

Material and Methods: A national work group consisting of clinical oncologists and medical physicists was established. Different workshops were conducted in order to standardise 1) delineation of organs at risk (OAR) and target, 2) PET determination, 3) treatment planning, and 4) IGRT and adaptive strategy. In the standard arm, the planning target volume (PTV) is prescribed a homogeneous mean dose of 66 Gy / 33 fractions (fr). For the experimental arm, the mean dose is heterogeneously escalated up to 95 Gy / 33 fr for the most FDG-PET active part of the primary tumour and 74 Gy / 33fr for malignant lymph nodes ≥ 4 cc. The escalation is always limited in favour of OAR constraints. Dose constraints were added to reduce the risk of severe complications. Besides the traditional spinal cord, heart and oesophagus delineations, thorax wall, aorta, bronchi, trachea, and connective tissue (here defined as any remaining voxels in mediastinum not included in other OARs or GTV) were delineated. A maximum dose of D1cc < 74 Gy for these OARs was chosen as safe dose constraints (D1cc < 70 Gy for oesophagus). An online catalogue with examples of such delineations was created for oncologists. The randomisation is performed when both the standard and escalated plans are clinically accepted. The two treatment plans, delineations and images are prospectively exported to a national database, which requires a consistent naming convention for delineations within each centre. Endpoint of trial is local control and the standard procedure for suspicion of tumour recurrence is biopsy. For cases where biopsy is not applicable, a central committee has been established to evaluate each case. Blood samples are obtained during the treatment course for future examination.

Results: Dose-volume-histogram data for the standard (solid) and escalated (dashed) arms for one patient is presented (Figure 1). Centres entering the NARLAL2 trial must successfully pass a workshop evaluation on delineation, PET determination, treatment planning, and IGRT strategy. Additionally, all participating centres should expect to enrol ≥5 patients/year, use 4D-CT and PET, inverse treatment planning, daily online match on soft tissue, and have an adaptive treatment strategy. Planning and treatment of the initial two patients within each centre are thoroughly investigated by a small QA work group consisting of 2 clinical oncologists and 4 physicists. Furthermore, every six month each centre will be visited by an external oncologist in order to ensure that guidelines are still followed throughout the duration of the trial.

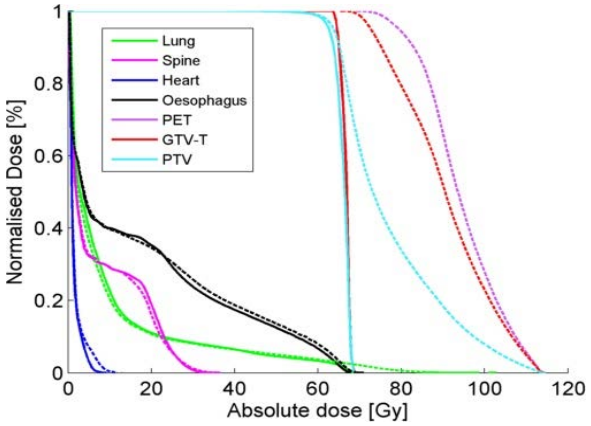

Conclusion: The NARLAL2 trial started patient accrual in January 2015 based on this extensive QA work.

EP-1933

End-to-end dosimetric audit – comparison of TLD and lithium formate EPR dosimetry

E. Adolfsson[1], P. Wesolowska[2], J. Izewska[2], E. Lund[3], M. Olsson[4], A. Carlsson Tedgren[3]

[1]*Department of Radiation Physics, Radiation Physics-Department of Medical and Health Sciences- Linköping University, Linköping, Sweden*

[2]*International Atomic Energy Agency, Vienna, Austria*

[3]*Radiation Physics, Department of Medical and Health Sciences- Linköping University, Linköping, Sweden*

[4]*Department of Medical Physics, Karolinska University Hospital, Stockholm, Sweden*

Purpose or Objective: The purpose of the study was to compare a lithium formate dosimetry system with a lithium fluoride TL dosimetry system as used in a solid phantom developed for remote end-to-end audits of advanced radiotherapy treatments, such as IMRT and VMAT. This type of inter-dosimeter comparison is of benefit for better understanding of advantages and limitations in the use of these dosimeters in remote audit programs for radiotherapy.

Material and Methods: A phantom was designed by a multinational coordinated research group (Coordinated Research Project E24018) with the intention to be used for remote end-to-end audits of advanced radiotherapy treatment (IMRT and VMAT). The phantom is made of polystyrene and includes solid water volumes representing a target region (PTV) and an organ at risk (OAR) with two measurement points in each. For an audit, the phantom is to be loaded with either TLD or EPR dosimeters and sent to external clinics to be treated using their local procedure for IMRT or VMAT. Dimensions of the active volume of the dosimeters used were: 20 mm length and 3 mm diameter for TLD, 5 mm height and 4.5 mm diameter for the EPR dosimeter. In addition, gafchromic film is used in the audit but this is not a subject of the current study. Irradiations were performed using VMAT technique and the doses determined by the TLDs and EPR dosimeters were compared with the TPS calculated doses.

Results: The absorbed dose determined by the EPR and TL dosimeters agreed within 2% with the TPS calculated doses in the PTV. In the OAR the discrepancy was larger; the dose determined by the EPR system was 3% lower compared to the TPS dose while the dose determined by the TLD was 5% higher than the TPS dose. The dose difference in the OAR was expected to be larger due to the steep dose gradients in this region over the dosimeter volume and the phantom positioning uncertainties involved.

Conclusion: Both dosimetry systems agree with the TPS calculated doses within 2% in the PTV and 5% in the OAR. This study shows that both dosimetry systems give results acceptable for this application and can be used for remote dosimetry audits of IMRT or VMAT. The EPR dosimeters have higher resolution due to their smaller size. This is an advantage of the EPRs over the TLDs since it is possible to resolve dose gradients to a higher extent.

EP-1934

Event reporting and learning in radiotherapy: evaluation over 4 years

M. Molla Armada[1], D. Garcia[1], M. Beltran[2], R. Verges[1], C. Pacheco[1], R. Angles[3], X. Fa[2], J. Saez[2], J.M. Lobo[1], C. Montiel[1], M.T. Bordas[1], J. Giralt[1]

[1]*Hospital Universitario Vall d'Hebron, Radiation Oncology, Barcelona, Spain*

[2]*Hospital Universitario Vall d'Hebron, Medical Physics, Barcelona, Spain*

[3]*Hospital Universitario Vall d'Hebron, Quality and Safety, Barcelona, Spain*

Purpose or Objective: Radiotherapy is one of the primary treatment options in cancer management. Radiotherapy is recognised as one of the safest areas of modern medicine; however, when errors occur, the consequences for the patient can be significant.

The rapid development of new technology has significantly changed the way in which radiotherapy is planned and delivered. Quality and safety programs in radiotherapy have been recommended by international bodies, such ESTRO and AAPM.

The purpose of this work is twofold: to report on the long-term use of an event reporting and learning system in an RT department to record and classify events, and to compare a restricted access system to an open-access system

Material and Methods: A voluntary web-based safety information database for RT was designed for reporting individual events in RT and was clinically implemented in 2011. An event was defined as any occurrence that could have, or had, resulted in a deviation in the intended delivery of cancer care. The aim of the reporting systemm was to encourage process improvement in patient care and safety.

During the RT process, when something goes wrong and results in event, it is initially recorded and reported within the RT Department. Initially only the management group registered events. From June 2012 all team at RT Department (radiation oncologist, radiation therapists, medical physicists, nurses, technicians, dosimetrists, medical secretary) can directly register events. All events were analyzed inside a management group who selected and proposed actions to be taken.

Results: We analyzed events from 2011 to 2014 for 6108 patients who have undergone radiation treatment at our hospital. Over this period of time 298 events were reported. After the event reporting system became open access (June 2012), the registered number of events increased significally: from 22 in 2011 to 44 in 2012, 120 in 2013 and 112 in 2014. The spectrum of reported deviations extendent from minor workflow issues to errors in treatment delivery.

The distribution of the professional who registered the event was:

	2011	2012	2013	2014
Radiation Oncologist	59%	18%	6%	4%
Medical Physicists	4.5%	7%	2%	2%
Dosimetrists	-	5%	-	7%
Radiation Therapists	32%	70%	91%	87%
Nurses	4.5%	-	-	-
Medical Secretary	-	-	-	1%
Nº of Events	22	44	120	112

Dose errors were detected in 29 patients. In 9 patients afected more than 1 session (5 patients in 2011, 3 patients in 2012, 1 patient in 2013 and no patients in 2014).
The number of corrective actions has increased because of the increasing number of registered events: 2 in 2011, 4 in 2012, 7 in 2013 and 9 in 2014.

Conclusion: Event reporting and learning systems in radiotherapy can provide valuable data for patient safety treatment. An open acces event reporting improved identification of areas which needed process and safety improvements. The major indication of the effectiveness is the reduction in dose errors.

EP-1935

Impact of standardised codes of practice and related audit on radiotherapy dosimetry over 20 years

R. Thomas[1], M. Bolt[2], G. Bass[1], A. Nisbet[2], C. Clark[1]
[1]*National Physical Laboratory, Radiation Dosimetry, Teddington, United Kingdom*
[2]*Royal Surrey County Hospital, Medical Physics Department, Guildford, United Kingdom*

Purpose or Objective: Reference dosimetry audit measurements in UK radiotherapy centres have been carried out over the last 20 years. This work examines the variation in local dosimetry calibration in a network of radiotherapy centres, draws conclusions on the implementation of an absorbed dose based protocol for MV photon beams and includes the measured effect of a change in the nationally recommended electron code of practice (CoP) from an air kerma based to an absorbed dose based protocol.

Material and Methods: Data from reference dosimetry audits conducted in radiotherapy centres by the National Measurement Institute (NMI) for photon, electron and kV x-rays have been collated, recording the NMI:Centre ratio for reference output measurements, beam quality, and field chamber comparison. A total of 81 MV photon, 98 electron and 30 kV photon beams were measured during 68 visits between June 1994 and February 2015. The change in the national standard deviation has been assessed over time, and differences due to the change between the two electron CoPs during this period has been quantified. The improvement in consistency for MV beams since the adoption of a CoP traceable to a primary standard of absorbed dose is assessed.

Results: The mean NMI:Centre difference for radiation output calibration was less than 0.25% for all modalities. A total of 7 measurements were reported to be outside the +/- 2% tolerance.There was a statistically significant difference (p=0.008) in the mean result for the respective air kerma based electron CoP, +0.75% (n=14) with the absorbed dose based protocol giving +0.20% (n=84).
The variation in MV results has decreased steadily over time (see Figure 1). The standard deviation has halved when comparing the first and last 20 results, being 0.85% (2000) and 0.35% (2015). This trend has also been noted within regional audit groups. A linear correlation was observed between the 'NMI:Centre output ratio' and the 'NMI:Centre field chamber comparison ratio'.
There has been no significant difference observed between regional audit and national audit for the measured NMI:Centre ratios, but some regions have had many more NMI audits than others, some having no beams audited for a particular modality, and others having more than 20.

Conclusion: Data has been collated from 20 years of NMI reference dosimetry audits, and key trends and changes have been noted. The introduction of the 2003 absorbed dose-based electron CoP has decreased the difference between NMI and centre measured outputs. The use of a single absorbed dose based MV CoP, introduced just prior to the start of these audits, has contributed to the improved consistency demonstrated in these results. This not only shows the impact of a rigorous traceability chain developed by close collaboration between NMI and end users but also demonstrates that the NMI audit programme is likely to be a contributing factor to this improvement in consistency in dosimetry nationally.

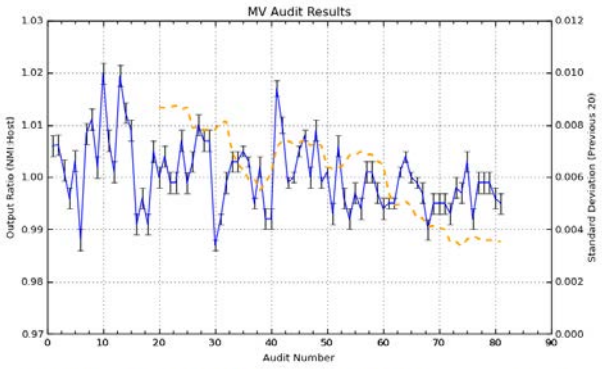

Figure 1: MV photon audit results plotted in order of completion (solid blue line). The running standard deviation of the previous 20 results shows a steady reduction in variation (dashed orange line).

EP-1936

Dose plan quality in the DBCG HYPO trial: an evaluation based on all treatment plans in the study

M. Thomsen[1], M. Berg[2], S. Zimmermann[3], C. Lutz[1], S. Makocki[4], I. Jensen[5], M. Hjelstuen[6], S. Pensold[7], M.B. Jensen[8], B. Offersen[9]
[1]*Aarhus University Hospital, Medical Physics, Aarhus, Denmark*
[2]*Lillebaelt Hosptal, Medical Physics, Vejle, Denmark*
[3]*Odense University Hospital, Oncology, Odense, Denmark*
[4]*Technical University Dresden, Radiotherapy and Oncology University Clinic Carl Gustav Carus, Dresden, Germany*
[5]*Aalborg University Hospital, Medical Physics, Aalborg, Denmark*
[6]*Stavanger University Hospital, Oncology, Stavanger, Norway*
[7]*Academic Teaching Hospital Dresden-Friedrichstadt, Praxis for Radiotherapy, Dresden, Germany*
[8]*Rigshospitalet Copenhagen University Hospital, Danish Breast Cancer Cooperative Group, Copenhagen, Denmark*
[9]*Aarhus University Hospital, Oncology, Aarhus, Denmark*

Purpose or Objective: In the DBCG HYPO trial a number of radiation therapy (RT) parameters were prospectively determined for each individual treatment plan. These parameters were reported to a database and analyzed to determine the plan quality in the trial.

Material and Methods: Patients (pts) for breast-only RT after surgery for early node-negative breast cancer from 8 RT centre in 3 countries were included in the trial between May 2009 and March 2014. They were randomized to either 40 Gy/15 fx or 50 Gy/25 fx. A number of plan-quality parameters such as doses to CTV-breast and organs at risk were determined for each plan. The use of respiratory gating during treatment was reported. Definitions on compliance to protocol guidelines, as well as minor and major deviations (Table 1) were agreed upon before trial start. After closing the trial, the QA parameters were analyzed and scored.

QA parameter	Full compliance	Minor deviation	Major deviation
CTV_{breast} with D≥ 95% (#pts; percentage)	$V_{D95\%}$ ≥95% (1492; 80.8%)	92%<$V_{D95\%}$<95% (232; 12.6%)	$V_{D95\%}$ ≤ 92% (121; 6.6%)
CTV_{breast} with 105% <D≤ 107% (# 40Gy/15fx pts; percentage)	V_{CTV} ≤ 2% (842; 92.3%)	2% <V_{CTV}<5% (36; 3.9%)	V_{CTV} ≥5% (32; 3.5%)
CTV_{breast} with 107% <D≤ 110% (# 40Gy/15fx pts; percentage) (# 50Gy/25fx pts; percentage)	V_{CTV} ≤ 2cm^3 (903; 99.0%) (901; 96.4%)	2 cm^3<V_{CTV}<5cm^3 (6; 0.7%) (16; 1.7%)	V_{CTV} ≥5cm^3 (3; 0.3%) (17; 1.8%)
Dose max. in CTV_{breast} (# pts; percentage)	D_{max} ≤110% (1835; 99.4%)	110% <D_{max}<112% (10; 0.5%)	D_{max} ≥112% (2, 0.1%)
Heart volume (left-sided pts) with dose >35 Gy (# 40Gy/15 fx pts; %) >40 Gy (# 50Gy/25 fx pts; %)	V_{35Gy}/V_{40Gy}≤5% (465; 99.8%) (476; 99.8%)	5%<V_{35Gy}/V_{40Gy}<7.5% (0; 0.0%) (0; 0.0%)	V_{35Gy}/V_{40Gy}≥7.5% (1; 0.2%) (0; 0.0%)
Heart volume (left-sided pts) with dose >17 Gy (40Gy/15fx; %) >20 Gy (50Gy/25 fx; %)	V_{17Gy}/V_{20Gy}≤10% (465; 99.8%) (476; 99.8%)	10%<V_{17Gy}/V_{20Gy}<15% (1; 0.2%) (0; 0.0%)	V_{17Gy}/V_{20Gy}≥15% (0; 0.0%) (0; 0.0%)
Ipsilateral lung volume with dose >17 Gy (# 40Gy/15fx pts; %) >20 Gy (# 50Gy/25 fx pts; %)	V_{17Gy}/V_{20Gy}≤25% (908; 99.6%) (926; 99.0%)	25%<V_{17Gy}/V_{20Gy}<30% (3; 0.3%) (6; 0.6%)	V_{17Gy}/V_{20Gy}≥30% (0; 0.0%) (2; 0.2%)

Results: A total of 1847 pts (904 right-sided and 943 left-sided) were treated with either 40 Gy/15 fx (912 pts) or 50 Gy/25 fx (935 pts). 388 of the left-sided pts were treated with gated RT, and 440 without. No information about gating was available for the remaining 115 pts. Dmax(CTV) was less than 110% of the prescription dose in 99.4% of the plans. More than 2 cm3 of the CTV received 107-110% of the dose in 1% of the hypo-fractionated plans. For the normo-fractionated plans, this deviation was observed in 3.5% of the plans. For 92.3% of the hypo-fractionated plans, less than 2% of the CTV was covered with doses above 105%, whereas 3.9% and 3.5% of the plans had minor and major deviations, respectively. For 80.8% of the pts, the part of the CTV covered with at least 95% of the prescription dose was in compliance with the guidelines. Minor and major deviations were observed for 12.6% and 6.6% of the pts, respectively. By taking laterality into consideration, 90.8% of the right-sided pts were in compliance with the guidelines compared to only 71.2% of the left-sided pts. For the left-sided pts with available information about gating, it was found that 87.4% and 59.3% of the pts treated with and without gated RT, respectively, were in compliance, thus indicating that shielding of the heart resulted in CTV under-dosage. This was supported by compliance to the protocol heart dose guidelines for 941 left-sided pts. Only one hypo-fractionated pt showed a major deviation in V35Gy and a minor deviation in V17Gy (data missing for one pt). The lung dose satisfied the protocol guidelines for 99.4% of the pts.

Conclusion: A high degree of compliance with protocol guidelines was found for the DBCG HYPO trial. Only a few pts received CTV doses above 107% of the prescription dose. The CTV volume covered with less than 95% dose deviated from protocol guidelines for about 40% of the left-sided pts treated without gated RT. With gated RT this number decreased to about 12%, almost equal to that of right-sided pts. This indicates that gated RT for left-sided pts reduces the necessity of CTV dose compromise due to heart shielding.

EP-1937

UK stereotactic ablative radiotherapy trials normal tissue dose constraints tolerance consensus

G.G. Hanna[1], R. Patel[2], K. Aitken[3], S. Jain[1], K. Franks[4], N. Van As[3], A. Tree[3], S. Harrow[5], D.J. Eaton[2], F. McDonald[3], M. Ahmed[3], F. Saran[3], G. Webster[6], V. Khoo[3], D. Landau[3], M.A. Hawkins[7]

[1]*Centre for Cancer Research and Cell Biology, Department of Radiation Oncology, Belfast, United Kingdom*

[2]*National Radiotherapy Trials Quality Assurance Group, Radiotherapy Physics, London, United Kingdom*

[3]*Royal Marsden NHS Foundation Trust, Department of Clinical Oncology, London, United Kingdom*

[4]*St. James's Institute of Oncology- Leeds Cancer Centre., Department of Clinical Oncology, Leeds, United Kingdom*

[5]*Beatson West of Scotland Cancer Centre, Department of Clinical Oncology, Glasgow, United Kingdom*

[6]*Guy's and St. Thomas' NHS Foundation Trust, Department of Medical Physics, London, United Kingdom*

[7]*CRUK/MRC Oxford Institute of Radiation Oncology- University of Oxford, New Technical Radiotherapy/Advanced Radiation Oncology Group, Oxford, United Kingdom*

Purpose or Objective: Stereotactic ablative radiotherapy (SABR) is routinely used for the treatment of early stage lung cancer and is increasingly used to treat other primary tumour sites. There are currently 6 UK studies (of which 3 are randomised) investigating the utility of SABR in the treatment of oligometastatic disease (breast, lung, prostate), lung, prostate, pancreas and hepatobiliary primary malignancies. These are supported by CRUK and currently open or in set-up to begin recruitment in 2016. In addition, a NHS Commissioning Through Evaluation (CTE) programme was commenced in 2015 to evaluate SABR in situations where clinical trials are not available. In an attempt to standardise protocols and the associated radiotherapy planning we sought to generate consensus normal tissue dose constraints tolerances across these UK studies.

Material and Methods: Members of the various SABR studies' trial management groups, facilitated by the UK Radiotherapy Trials Quality Assurance Group (RTTQA), met to generate a unified table of normal tissue dose constraints. As a starting point, the UK SABR Consortium Guidelines, the AAPM TG-101 report and other seminal publications were used to define a baseline reference. These initial constraints values were revised, where appropriate, by taking into consideration any updated or more robust data that better informed a given dose constraint value in the opinion of the panel.

Results: Following an iterative process, agreement was reached on all dose constraints covering the central nervous system, thorax, abdomen, pelvis, skin and bone. It was agreed to use a point maximum dose volume of 0.5cc for the purposes of describing the maximum dose for all organs except the spinal cord. For the spinal cord 0.1cc is to be used. The group reached the consensus that for the purpose of these trials single fraction should not be used outside CNS. We recommended the use of 3, 5 and 8 fractions regimes. These dose constraints will be used for the forthcoming SABR studies and for the implementation of the CTE SABR programme for oligometastatic disease and HCC. The group will review the evidence annually to update the guidelines.

Conclusion: A UK national agreement on SABR dose constraints has been successfully achieved. It is hoped that this unified approach will facilitate standardised implementation of SABR across the UK and will permit meaningful toxicity comparisons between SABR studies and further refinement of the constraints. Any further trials developed in the UK will adopt the consensus.

EP-1938

Evaluation of pre-treatment verification for hyperthermia treatment plans

D. Marder[1], N. Brändli[2], G. VanStam[1], G. Lutters[1]

[1]*Kantonsspital Aarau, Radio-Onkologie-Zentrum KSA-KSB, Aarau, Switzerland*

[2]*Kantonsspital Aarau, Medizintechnik Service Center, Aarau, Switzerland*

Purpose or Objective: The BSD-2000/3D system (BSD Medical Cooperation, Salt Lake City, USA) is used to treat deep seated tumors with hyperthermia (to temperatures of 41-43°C) in combination with radiotherapy. Treatment planning for this system is done with the software SigmaHyperplan (Dr. Sennewald Medizintechnik GmbH, Munich, Germany). In this study a method and first results for pre-treatment verification of clinical patient treatment plans using a 3D SAR scanning phantom developed at the Kantonsspital Aarau are presented.

Material and Methods: Treatment plans for individual patients were generated with SigmaHyperplan and applied to a saline phantom model. The result is a set of data for the

specific absorption rate (SAR) distribution. The measurement data is obtained with a saline phantom consisting of a tube with elliptical cross section. The tube is inserted into the BSD-2000/3D Sigma60 and a probe inside is moved in 3 spatial dimensions. The probe, a commercial isotropic SAR sensor, is scanned in 2 cm steps for a distance of 20 cm in horizontal and vertical directions and relative SAR values are recorded. Planned and measured data in the central plane of the applicator are compared for the location of the focus to assess the transferability of treatment plans to the treatment machine.

Results: The location of the focus maximum can be determined from the graphs and compared to the location of the maximum from the simulation. For the investigated plans an agreement between simulation and measurement was found with deviations of the focal area between 0 and 2 cm.

Conclusion: Good agreement for the investigated patient plans was found between simulation and measurement. With an automated measurement system higher resolutions and 2D or 3D comparisons would be possible. The method described allows the transferability of a patient treatment plan to the treatment machine to be verified, however it does not check the correct heating of the patient.

EP-1939

An optimal grid block design for spatially fractionated radiation therapy

S. Gholami[1], H.A. Nedaie[2], F. Longo[3], M.R. Ay[1], A. S.Meigooni[4]
[1]*Tehran University of Medical Sciences, Medical Physics, Tehran, Iran Islamic Republic of*
[2]*Tehran University of Medical Sciences, Radiation Oncology Department- Cancer institute, Tehran, Iran Islamic Republic of*
[3]*University of Trieste and INFN Trieste, Department of Physics, Trieste, Italy*
[4]*Comprehensive Cancer Centers of Nevada, Radiation Oncology, Las Vegas- Nevada, USA*

Purpose or Objective: In the present work, we performed model calculations of cell survival to design a Grid block with optimal therapeutic ratio. The optimal Grid block was manufactured and dosimetric characteristics of the Grid were introduced.

Material and Methods: The Geant4 toolkit (Version 9.6.p02) was used to simulate the head of the Varian2100C linear accelerator for a 6 MV photon beam based on the vendor detailed information. The dose distributions of a Grid block with hole-diameters of 0.5 cm, 0.75 cm, 1.0 cm, 1.25 cm, and 1.5 cm with constant center-to-center spacing of 1.8 cm, were calculated separately using the Monte Carlo simulation technique. A dose profile from Monte Carlo simulation, across a single hole of the Grid, has been utilized to calculate therapeutic ratio for different Grid blocks separately. The Hug-Kellerer (H-K) radiobiological model (Equation 1) which is more appropriate at doses higher than 12 Gy was utilized to calculate survival fraction of cell lines under a single hole of the Grid. The values of α/β ratios for tumor cells and normal cells were considered to be 10 Gy and 2.5 Gy, respectively.
Equation 1:

$$\begin{cases} SF = \sum V_i \, e^{(-k_1 D_i + k_2 (1-\exp(-k_3 D_i))} \\ \alpha = k_1 - k_2 . k_3 \qquad \beta = k_2 . k_3^2 . (\ln(2) - 1/2) / (\ln(2))^2 \end{cases}$$

Where the *Vi* represents the relative cell numbers receiving the same dose ranging from *Di* and *Di+1*. The therapeutic advantage of the Grid irradiation was considered in terms of the normal tissue cell survival ratio (Grid/open field ratio) for the same tumor cell survival.

A Grid with optimal TR value was selected to manufacture. Dosimetric characteristics of the Grid were measured using ionization chamber in water phantom and Gafchoromic film dosimeter in Solid WaterTM phantom materials.

Results: The results from the Monte Carlo studies showed that increasing the spacing between the Grid holes with a given hole diameter keep the TR value of the Grid block nearly unchanged (±4%). Moreover, a Grid block with a hole-diameter of 1.0 cm and 1.25 cm may lead to about 19% higher clinical responses relative to the Grids with hole-diameters smaller than 1.0 cm or larger than 1.25 cm. Dosimetric measurements of the optimal Grid were in good agreement (± 5%) using different dosimetry techniques. Table 1 shows comparison between different dosimetric features of the manufactured Grid and the dosimtric features that were predicted by Monte Carlo simulation.
Table 1

	Geant4-Monte Carlo simulation	Ionization chamber dosimetry	Film dosimetry	Max difference
Output factor	0.87	0.85	0.83	-4.6%
Valley-to-Peak ratio	21%	20.4 %	19.8 %	-5.7%
TR (15 Gy to dmax)	1.95	2.00	1.87	-4.1 %
EUD (15 Gy to dmax)	6.14	6.3	6.0	-2.6%

Conclusion: Designed Grid block leads to have an optimal therapeutic ratio for spatially fractionated radiation therapy.

EP-1940

Individual cases review in KROG-0806 study Phase Ⅲ randomized trial for breast cancer patients

Y.B. Kim[1], J. Yoon[1], H. Han[1], H. Cha[1], J. Choi[1], M. Lee[1], C.O. Suh[1]
[1]*Yonsei University, Radiation Oncology, Seoul, Korea Republic of*

Purpose or Objective: Korea Radiation Oncology Group (KROG)-0806 study has been the phase Ⅲ randomized trial to investigate the efficacy of internal mammary node(IMN) irradiation in breast cancer patients. Previous dummy run study evaluated protocol compliance of participating institutions. The purpose of this study is to assess the protocol compliance based on individual cases review (ICR).

Material and Methods: For ICR, patients were divided into eight subgroups based on IMN irradiation (non-irradiation (N) vs. Irradiation (R), tumor laterality (left-side (L) vs. right-side (R)) and type of surgery (breast-conserving surgery (B) vs. mastectomy (M)), respectively: NLB, NRB, NLM, NRM, RLB, RRB, RLM and RRM. We extracted 15% among patients enrolled in each subgroup using the SURVEYSELECT procedure with the simple random sample. Then, all participating institutions were requested to upload the following information: planning computed tomography (CT) images, structure sets, and radiation doses as well as the documents containing treatment techniques and all beams' eye views with questionnaire. We performed the comparison of the dose distribution among 8 subgroups. Major and minor violations are determined according to IMN treatment and dose delivered to IMN.

Results: The information of 102 patients was collected. Institutions used the different treatment techniques such as standard tangents (42.2%), partial wide tangent (23.5%), 30/70 photon/electron mix (17.6%), IMN-electron only (4.9%), and reverse hockey stick (11.8%). The IMN average doses in subgroups were as follows: Arm1[NLB(14.9Gy±10.7Gy), NRB(18.5Gy±13.0Gy), NLM(27.7Gy±16.4Gy), NRM(27.5Gy±15.1Gy)] and Arm2[RLB(48.3Gy±4.5Gy), RRB(50.9Gy±4.1Gy), RLM(49.3Gy±4.1Gy), RRM (51.3Gy±3.2Gy)]. The dose differences between Arm1 and Arm2 groups were statistically significant. Dose variations in IMN were much greater in Arm1 than Arm2. In Arm1 group,

major violation was found as 7 out of 51 cases. By contrast, there were no major violation and one minor violation in Arm2.

Conclusion: This ICR study with KROG-0806 showed the satisfactory protocol compliance in IMN irradiation and the major violation from several cases of IMN non-irradiation group. Quality assurance process using ICR is needed to evaluate and improve the quality of clinical trial in the field of radiation oncology.

EP-1941

Assessment of variation in planning benchmark case for ABC-07 trial of liver SBRT

D. Eaton[1], M. Robinson[2], R. Patel[1], M. Hawkins[2]
[1]*National Radiotherapy Trials QA group RTTQA, Mount Vernon Hospital, Northwood, United Kingdom*
[2]*CRUK/MRC Oxford Institute for Radiation Oncology, University of Oxford, Oxford, United Kingdom*

Purpose or Objective

Quality assurance of radiotherapy clinical trials ensures protocol compliance and robustness of outcome data. Benchmark cases are used to assess consistency of outlining and planning by different centres, and provide feedback before a centre starts recruitment. For a complex technique such as liver SBRT, it also facilitates sharing of best practice and supports centres with less experience.

Material and Methods: The planning benchmark case was a large (6cm) cholangiocarcinoma with target and organ-at-risk contours already outlined. This case was sent to all centres interested in joining the ABC-07 multicentre phase II trial (Addition of stereotactic body radiotherapy to systemic chemotherapy in locally advanced biliary tract cancers; CRUK A18752; Sponsor University College London). Centres were asked to produce a plan with prescription dose of 50Gy in 5 fractions, having PTV coverage D95% > 95% (optimal, 90% mandatory) and mean liver dose < 13Gy. If this was not possible, the prescription dose was reduced to 45Gy in 5 fractions and mean liver dose limit increased to 15Gy.

Results: 14 cases were submitted, covering a range of planning systems and treatment platforms. 5/10 VMAT, 1/1 IMRT and 0/3 Cyberknife plans were able to cover 95% of the PTV with≥90% of 50Gy, whilst maintaining the mean liver dose below 13Gy, as shown in the table.

Modality (prescription dose)	Number of centres	D95% (% of 50 Gy)	Max (D0.1cc) (% of PD)	Mean liver dose
VMAT (50Gy)	5	44.9 - 48.2 Gy (90 - 96%)	103 - 117%	12.7 - 12.9 Gy
IMRT (50Gy)	1	48.2 Gy (96%)	106%	12.8 Gy
VMAT (45Gy)	5	42.6 - 45.0 Gy	103 - 126%	12.9 - 14.9 Gy
Cyberknife (45Gy)	3	42.7 - 44.9 Gy	114 - 129%	14.6 - 15.0 Gy

Conclusion: Achieving the planning objectives for this case was challenging and only 5/12 centres submitted an optimal plan. The other 7 centres are repeating the exercise after feedback on what was achievable with similar equipment. Achieving the optimal plan for this case involved reduced conformity of medium doses in order to spare other parts of the liver, and thereby reducing the total mean liver dose. This approach is contrary to typical Cyberknife planning, so it may not be the optimum treatment platform for these cases, although it is possible that differences between technologies and centres were accentuated by this large and challenging case, and may be reduced for smaller lesions. All patients treated within this trial will be prospectively reviewed, which will further inform this question.

EP-1942

Initial experience with the Elekta Leksell Gamma Knife Icon system: commissioning, QA and workflow

S.W. Blake[1], L. Winch[1], H. Appleby[1]
[1]*Bristol Haematology & Oncology Centre, Radiotherapy Physics, Bristol, United Kingdom*

Purpose or Objective: Icon enables fractionated stereotactic radiotherapy using a frameless patient positioning system (PPS). For submillimetre precision, the planning MRI scans are registered to a CBCT scan set acquired using Icon. Patient position is then adjusted using the Icon scan. Movement is monitored using an Intra Fraction Motion Management (IFMM) system.
This presentation reports on the commissioning of Icon plus baseline and ongoing QA measurements.
This is the first use of Icon in the UK.

Material and Methods: CTDI was assessed for both the low and high dose settings and image quality checked using CatPhan. kVp measurements were made and dose to the imager assessed to confirm the Elekta presets and baseline values.
A new Focus Precision Check tool containing diodes and ball bearings was used to ensure the accuracy of the PPS relative to the radiation focus and CBCT image positions.
The IFMM system was verified using a moveable phantom. A reflector was attached to the phantom and moved independently in the x,y and z directions in 0.5 mm steps.
If the IFMM monitored position is outside tolerance for more than 2 seconds, the treatment pauses and the couch is retracted. Treatment resumes following a re-scan, with the plan recalculated on the new CBCT reference. To test this system an output measurement was interrupted using a remotely moved reflector.
An end-to-end check on a fractionated pituitary plan was made. The plan was recalculated on a CBCT scan of the spherical solid water phantom containing inserts for chamber and film. A film was positioned at the central axis with 2 additional films displaced 5 & 10 mm above and below.

Results: The Icon system performed within specification. Patient doses were acceptable and image quality resulted in good registration with the MRI scan sets.
Ongoing QA results were highly reproducible demonstrating positioning ability of the system to within 0.5 mm. The IFMM readout agreed with the independent system to within 0.04mm and repositioning following interruption had no significant effect on the diode doserate. The end to end film dosimetry agreed to within ±3% of the planned dose.
The Icon system has allowed us to use new clinical pathways with little loss in positional accuracy including:
(a) Single fraction patients who would not tolerate a fixed frame.
(b) Fixed frame patients who have their CT scan with Icon.
(c) Fractionated patients.

Conclusion: Icon is an efficient system which has enabled the delivery of fractionated stereotactic radiotherapy plus improvements for single fraction patients. Accuracy is comparable with fixed frame treatments.

EP-1943

Implications of gold nanoparticles used for dose enhancement in proton radiotherapy

R. Ahmad[1], G. Royle[2], K. Ricketts[1]
[1]*UCL, Division of Surgery and Interventional Science, London, United Kingdom*
[2]*UCL, Medical Physics and Bioengineering, London, United Kingdom*

Purpose or Objective: Heavy metal nanoparticles (NPs) have been widely investigated within x-ray radiotherapy as radiosensitisers, where gold NPs (GNPs) have been deemed to be effective at enhancing the dose to the tumour. Few studies have been carried out for protons, where an extensive investigation of the enhancing factors needs to be carried out to determine the implications that introducing GNPs can have on known dose profiles. In the present work, we demonstrate our model which uses Geant4 to carry out Monte Carlo simulations of NP concentrations being irradiated by a proton beam. These simulations offer an indication as to

the macroscale effects that occur with varying concentrations of GNPs.

Material and Methods: Within our model, concentrations of NPs were simulated by calculating the inter-particle spacing of various concentrations, where this spacing was used to model a controllable concentration, whilst minimizing computational time. Investigations were carried out on the effect of concentration over a range of clinically relevant concentrations in line with previous studies (0.01 mg/ml, 0.1 mg/ml and 6.5 mg/ml) [1], [2], [3] at two incident proton energies (60 MeV and 226 MeV). Various results were recorded, such as the energy deposited across the phantom, types of secondary particles produced, the particle track lengths and energy deposited by secondary particles.

Results: The results highlight a measurable shift of the distal edge (Fig.1) in the order of millimeters due to the introduction of gold, which can be seen predominantly at high concentrations (6.5 mg/ml) achievable through direct injection. This shift was deemed to be energy dependent, where at lower energies (60 MeV) it was on the order of microns. As demonstrated by other groups, the enhancement was attributed to an increase in the number of secondary electrons, which was proportional to GNP concentration as expected. Our model demonstrates that the magnitude of the effects observed can be related to the concentration.

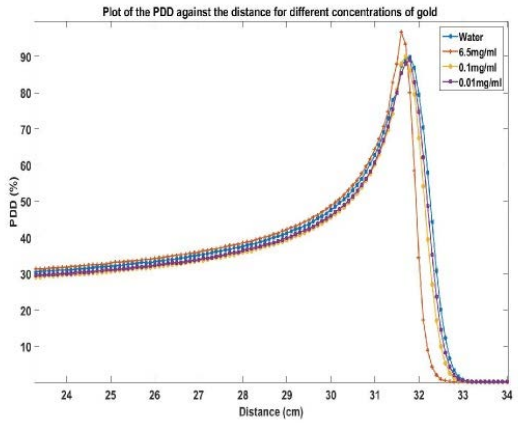

Figure 1: A zoomed in section of the peak, where the plot shows readings at every millimeter using a 226 MeV proton beam, highlighting the differences due to gold concentrations.

Conclusion: This study has demonstrated bulk effects of multiple NPs on dosimetry, extending previous work on single NP models by other groups [4]. Results show that injectable concentrations can affect the range of protons, proving to be more significant at higher energies. Future work will investigate the effects that GNPs can have on treatment plans, assessing any changes that need to be made.

References: [1] N. Khlebtsov & L. Dykman, Chem. Soc. Rev. 40 (2011) 1647 [2] J. Hainfeld et al, Phys. Med. Biol. 49 (2004) N309 [3] J.K Kim, et al. Phys. Med. Biol. 57 (2012) 8309 [4] Y. Lin et al, Phys. Med. Biol. 59 (2014) 7675.

EP-1944

Lessons from the findings of 31 QUATRO audits in Europe

J. Izewska[1], M. Coffey[2], P. Scalliet[3], E. Zubizarreta[4], T. Santos[1], I. Vouldis[1], P. Dunscombe[5]

[1]*IAEA - International Atomic Energy Agency, Dosimetry and Medical Radiation Physics, Wien, Austria*

[2]*School of Medicine- Trinity Centre for Health Sciences- St. James' Hospital, Discipline of Radiation Therapy, Dublin, Ireland Republic of*

[3]*Cliniques Universitaires Saint Luc- Université Catholique, Radiotherapy, Brussels, Belgium*

[4]*IAEA - International Atomic Energy Agency, Radiotherapy and Radiobiology, Wien, Austria*

[5]*University of Calgary, Medical Physics, Calgary, Canada*

Purpose or Objective: A methodology has been developed for comprehensive clinical quality audits of radiation therapy programmes called Quality Assurance Team for Radiation Oncology (QUATRO). The purpose of these audits, which are distinct from accreditation, is to assist the audited centres in identifying and implementing opportunities for improving the quality of services offered to patients. Aggregating the findings from audits carried out over 10 years in Europe sheds light on the degree to which various dimensions of quality are satisfied and suggests interventions which are likely to be effective in improving quality in the audited centres.

Material and Methods: Thirty one centres in Europe have been audited with this methodology since 2005. The voluntary, confidential audits are conducted by multidisciplinary teams and take 5 days on-site to complete. Reports to the audited centres include both commendations, i.e. positive findings, and recommendations for quality improvement. A subset of the audited centres were designated Centres of Competence (CCs) through QUATRO. A coding key has been developed to aggregate and analyse the extensive data generated from this audit series.

Results: 600 commendations and 759 recommendations for improvement were noted in the 31 audit reports. Positive attributes of the audited centres included patient centredness, communication, facilities (with the marked exception of the availability of treatment units) and quality control. Areas for improvement included staffing and equipment levels, professional development, documentation and quality management. Overall, 10 centres were designated as CCs. Of the 600 commendations, 220 were given to 10 CCs and 380 to other centres. Of the 759 recommendations, CCs received 82 while the other centres 677. The levels of physicists and RTT staffing generally met international recommendations in CCs whereas in the other centres major staff shortages were recorded. RTT understaffing was most acute but other staff groups also needed strengthening. Education, training and professional development of all staff, but especially RTTs, was seen as a weakness in many centres.

Conclusion: QUATRO audits provided the radiotherapy centres with an opportunity for an in depth analysis of their practices. The detailed reports constitute a template for practice improvement and highlight the need to develop strategies on the future development of radiotherapy services. The analysis of the 31 audits has also identified the need for common action items for enhancing the quality of radiotherapy in the audited centres. In particular, there is a need for extending the reach of educational programmes and for expanding the educational offerings to include quality management and associated topics.

EP-1945

Plan submission comparison for commissioning of spinal and nodal SABR for oligometastases

R. Patel[1], T. Williams[2], J. Payne[2], D.J. Eaton[1], Y. Tsang[3], P. Ostler[3], N. Van As[4]

[1]*Mount Vernon Cancer Centre, Radiotherapy RTTQA, Northwood, United Kingdom*

[2]*Mount Vernon Cancer Centre, Radiotherapy Physics, Northwood, United Kingdom*

[3]*Mount Vernon Cancer Centre, Radiotherapy, Northwood, United Kingdom*

[4]*Royal Marsden Hospital, Radiotherapy, London, United Kingdom*

Purpose or Objective: NHS England selected 17 centres of varying experience to take part in the Commissioning through Evaluation (CtE) programme in order to improve access to SABR for patients with Oligometastatic disease. A QA group was formed from members of a national trials QA group and a national SABR development group to ensure patient safety and treatment quality across participating centres, which utilise a variety of different equipment and techniques.

Material and Methods: A bespoke QA programme was created for the 5 anatomical treatment sites which included spine and nodal metastasis. Prior to treatment centres were required to complete a QA process which included planning benchmark cases. Participating centres were provided with a pre-outlined planning CT. They created PTV expansions using local protocols. The centres were then required to create a plan based on a 30 Gy in 3 fraction prescription for the nodal case and a 24 Gy in 3 fractions prescription for the spine case. Both cases required a D95% of the prescription dose for the PTV coverage whilst ensuring OAR tolerances were met. All planning benchmarks were submitted and centrally analysed using VODCA 5.4 plan review software. The coverage of the PTV and CTV with the prescription dose, doses to OARs and measures of conformity were calculated. The values for the different submissions were compared to ensure plans were of suitable quality and comparable across different treatment platforms.

Results: A total of 10 and 11 plans were submitted for the spine and nodal benchmark cases respectively, including all 4 NHS cyberknife centres and the remainder using VMAT. 27% of the nodal and 18% of the spine plans had unacceptable deviations and the centres were given feedback and asked to resubmit their QA. The PTV coverage and max dose were compared for the different treatment techniques with the standard deviation. These can be seen in the table below.

Spine

Modality	Mean PTV Coverage (%)	S.D.	Mean Max Point Dose (Gy)	S.D.
All	92.2	3.4	31.3	2.7
Cyberknife	94.3	2.9	32.2	2.8
VMAT	90.9	3.4	31.4	2.3

Nodes

Modality	PTV 1		PTV 2		Mean Max Point Dose (Gy)	S.D.
	Mean PTV Coverage (%)	S.D.	Mean PTV Coverage (%)	S.D.		
All	90.5	5.8	96.5	3.1	38.0	3.3
Cyberknife	95.0	2.5	97.4	2.2	41.7	3.5
VMAT	87.4	5.3	95.9	3.6	36.0	1.1

A 2 tail Mann-Whitney test was performed on the PTV coverage data for both plans. This indicated that there was a significant difference between cyberknife and VMAT plans ($p=0.02$).

Conclusion: Cyberknife plans on average achieved superior PTV coverage when compared to VMAT plans. This was more evident for the spine PTV and nodal PTV 1, with both volumes being close to OARs, than for the nodal PTV 2 where OARs did not restrict the dose . The VMAT plans involved larger PTV and PRV expansions which would partly explain the difficulty in achieving the required PTV coverage. However, several of the VMAT plans had similar PTV coverage to the cyberknife plans, hence the greater variation in PTV coverage of the VMAT plans may reflect possible inexperience in SABR planning for some centres. Following resubmissions, all centres participating in the CtE programme have been able to produce acceptable benchmark plans regardless of treatment platform.

EP-1946

Small animal irradiation by using Tomotherapy: dosimetric and preclinical results

A. Miranti[1], A. D'Ambrosio[2], G. Cattari[3], E. Garibaldi[3], S. Bresciani[1], P. Gabriele[3], M. Stasi[1]

[1]*Candiolo Cancer Institute - FPO-IRCCS, Medical Physics, Candiolo TO, Italy*

[2]*Candiolo Cancer Institute - FPO-IRCCS, Laboratory of Cancer Stem Cell Research and Department of Oncology- University of Torino, Candiolo TO, Italy*

[3]*Candiolo Cancer Institute - FPO-IRCCS, Radiotherapy, Candiolo TO, Italy*

Purpose or Objective: Preclinical studies are critical steps in the medical research process, normally requiring dedicated instruments. For those centers in which both preclinical research and clinical practices are conducted, the dosimetric feasibility of small animal irradiation with clinical devices may be of economical and scientific interest. The aim of the present work is to investigate the feasibility of small animal irradiation with Tomotherapy Hi-Art by analyzing dosimetric results, toxicity and tumour response in xenograft models.

Material and Methods: Xenograft models were established by injecting human derived glioblastoma multiforme stem-like cells in immunocompromised NOD-SCID mice both subcutaneously (10 groups) and intracranially (7 groups). Mice of each group were anesthetized and placed in a plexiglas cage pie to perform CT scans for treatment planning purposes. Target volumes and organs at risk (OARs) where outlined on CT scans: for subcutaneous xenografts, target volumes were delineated on the right flank and contoured OARs were lung and gastro-intestinal tract. For orthotopic models, a ring-shaped target structure was delineated on mice's head; contoured OAR was lung. Three fractionation schedules were tested: 4Gy/1 fraction, 4 Gy/2 fractions and 6 Gy/3 fractions. TomoDirect IMRT technique was applied, with gantry fixed at 0° and 180. 5 subcutaneous and 1 orthotopic groups of xenografts were irradiated by covering the target volume with a 0.6 cm bolus layer in order to reduce the impact of the build-up effect. Irradiations originally performed without bolus were simulated with a 0.6 cm virtual bolus in order to compare dosimetric results. Before irradiation, a MVCT image has been acquired to correct irradiation setup. Mice were observed daily and sacrificed when they showed signs of suffering or when tumour volume reached the established endpoint. Different radiobiological outcomes were evaluated, regarding both radiotoxicity (survival experiments) and tumour response (assessed by caliper or bioluminescence imaging), comparing irradiated mice as respect to their controls.

Results: Dosimetric results showed that the presence of the bolus layer significantly impact the maximum dose received by both target volumes and OARs (t-test, $p<0.05$). Survival analysis showed that irradiation with a dose of 6 Gy in 3 fractions in the presence of a bolus layer prolong mice survival (Log-rank test, $p<0.02$), showing to be the safest irradiation protocol. Tumour volume response and mice survival were significantly different in irradiated xenografts as compared to their controls (t-test, $p<0.03$; Log-rank, $p<0.05$) demonstrating also the radiobiological potential of Tomotherapy in inducing tumour growth stabilization.

Conclusion: Tomotherapy systems may be a useful mean for small animal irradiation.

EP-1947

Evaluation of dosimetric properties of 3D printed flat bolus for external beam radiotherapy

R. Ricotti[1], A. Vavassori[1], R. Spoto[1,2], D. Ciardo[1], F. Pansini[3], A. Bazani[3], S. Noris[1,4], F. Cattani[3], R. Orecchia[1,2], B.A. Jereczek-Fossa[1,2]

[1]*European Institute of Oncology, Department of Radiation Oncology, Milan, Italy*

[2]*University of Milan, Department of Oncology and Hemato-oncology, Milan, Italy*

[3]*European Institute of Oncology, Unit of Medical Physics, Milan, Italy*

[4]*University of Milan, Tecniche di Radiologia Medica per Immagini e Radioterapia, Milan, Italy*

Purpose or Objective: To evaluate the dosimetric properties of acrylonitrile butadiene styrene (ABS) and polylactide (PLA) plastics, and their suitability for bolus printing applied in high-energy radiotherapy to overcome the skin-sparing effect.

Material and Methods: The measurements were performed with Vero® System (Brainlab AG, Feldkirchen, Germany) delivering 200 monitor units (dose rate of 500 MU/min) with a 6 MV photon beam, 5x5 cm open field with 90-degree gantry angle at 100 cm surface to surface distance (SSD) on a water-equivalent RW3 slab phantom in three configurations: without bolus, with a commercial bolus and with the eight 3D

printed boluses. Gafchromic EBT3 film (International Specialty Products, Wayne, NJ) placed between phantom slabs provided dose profile measurements. An Epson Expression Scanner 10000 XL (Epson, Long Beach, CA) was used to determine the optical density of the films and film analysis were performed using Film QA Pro software (Ashland Inc., Bridgewater, NJ).

Results: The mean value of Hounsfield unit (HU) of the 3D printed boluses was provided analyzing their Computed Tomography (CT) scans. Negative HU were due to the air gap inside the infill pattern. The mean HU increased with the percentage infill, resulting in higher bolus density (Tab. 1). This reduced the distance from the surface of the phantom where the maximum dose occurs (dmax) as shown in Fig.1. Build-up peaks shifted towards the phantom surface when any bolus was used. ABS and PLA boluses with an infill percentage of 40% had comparable performance to the commercial bolus.

	%infill	HU	density [g/cm³]	d_{max} [mm]
no Bolus	--	--	--	16.9
commercial Bolus	--	0	1.0	7.4
ABS	10	-694.0	0.28	10.6
	20	-593.8	0.39	9.4
	40	-393.5	0.60	5.6
	60	-166.5	0.87	0
PLA	10	-629.7	0.35	14.5
	20	-492.5	0.49	11.6
	40	-245.2	0.78	9.2
	60	-51.2	0.97	0

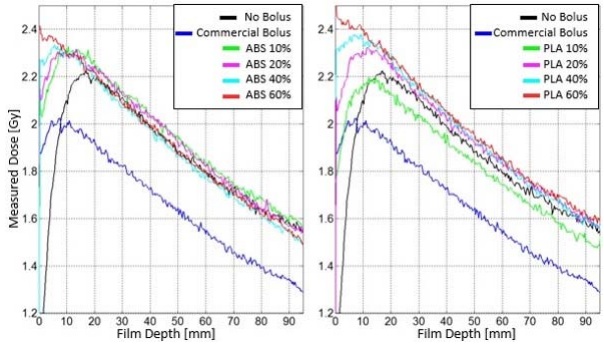

Conclusion: The dosimetric analysis of the 3D printed flat boluses showed that they can decrease the skin-sparing as a commercially available bolus. The performed analysis accurately describes the physical behavior of these plastic materials, in order to represent them in treatment planning system for precise treatment delivery. Moreover, patient-specific boluses could be outlined from patient CT images and 3D printed, thus shaping the actual anatomy of the patient. This procedure may represent a viable alternative to commercially available conventional boluses, potentially improving the fitting between bolus and skin surfaces.

EP-1948

Multicentre comparison for small field dosimetry using the new silicon diode RAZOR

C. Talamonti[1,2], M.D. Falco[3], L. Barone Tonghi[4], G. Benecchi[5], C. Carbonini[6], M. Casale[7], S. Clemente[8], R. Consorti[9], E. Di Castro[10], M. Esposito[11], C. Fiandra[12], C. Gasperi[13], C. Iervolino[14], S. Luxardo[15], C. Marino[16], E. Mones[17], C. Oliviero[8], M.C. Pressello[18], S. Riccardi[19], F. Rosica[20], L. Spiazzi[21], M. Stasi[22], L. Strigari[23], P. Mancosu[24], S. Russo[11]

[1]*University of Florence, Dip Scienze Biomediche Sperimantali e Cliniche, Firenze, Italy*
[2]*Azienda Ospedaliera Universitaria Careggi, Fisica Medica, Florence, Italy*
[3]*University of Chieti SS. Annunziata Hospital, Dep. of Radiation Oncology "G. D'Annunzio", Chieti, Italy*
[4]*A.R.N.A.S. Garibaldi, Fisica Sanitaria, Catania, Italy*
[5]*AO Parma, Fisica Sanitaria, Parma, Italy*
[6]*A.O. Ospedale Niguarda, Fisica Sanitaria, Milano, Italy*
[7]*AO" Santa Maria", Fisica Sanitaria, Terni, Italy*
[8]*IRCCS CROB Potenza, Fisica Sanitaria, Potenza, Italy*
[9]*Ospedale san Filippo Neri, Fisica Sanitaria, Roma, Italy*
[10]*Umberto I - Policlinico di Roma, Fisica Sanitaria, Roma, Italy*
[11]*Azienda Sanitaria di Firenze, Fisica Sanitaria, Firenze, Italy*
[12]*Ospedale Molinette, Fisica Sanitaria, Torino, Italy*
[13]*Ospedale Usl8 Arezzo, Fisica Sanitaria, Arezzo, Italy*
[14]*A.O. "S.G.MOSCATI", Fisica Sanitaria, Avellino, Italy*
[15]*Ospedale Asl 1 Massa e Carrara, Fisica Sanitaria, Carrara, Italy*
[16]*Humanitas Catania, Fisica sanitaria, Catania, Italy*
[17]*AOU Maggiore delle Carità, Fisica Sanitaria, Novara, Italy*
[18]*AO San Camillo Forlanini, Fisica Sanitaria, Roma, Italy*
[19]*Ospedale San Camillo de Lellis - ASL Rieti, Fisica Sanitaria, Rieti, Italy*
[20]*P.O. "Mazzini" ASL di Teramo, Fisica sanitaria, Teramo, Italy*
[21]*Brescia Spedali Civili, Fisica Sanitaria, Brescia, Italy*
[22]*A.O. ordine Mauriziano, Fisica Sanitaria, Torino, Italy*
[23]*IFO Roma, Fisica sanitaria, Roma, Italy*
[24]*Humanitas Milano, Fisica Sanitaria, Milano, Italy*

Purpose or Objective: Multicentre comparisons of dosimetrical parameters are important to ensure the same quality of the treatment in radiotherapy centres, and allow to identify systematic errors. In this study, small fields dosimetric parameters were collected in a national context using a common acquisition procedure and a specific dosimeter. The aim of this study was to provide indicative values for each Linac model for small field dosimetry measurements. This can be useful for centres with reduced experience in small fields dosimetry.

Material and Methods: Thirty-four centres with different LINACs joined this project: 2 Siemens, 7 Elekta Agility, 6 Elekta Beam Modulator, 12 Varian CLINAC and 7 Varian TrueBeam. All measurements were performed using the new IBA unshielded silicon diode RAZOR and the Stealth flat ionization chamber fixed on the gantry as reference. The RAZOR was positioned at 10cm depth in water phantom and SSD=90cm. In and Cross-line beam profiles ranging from 0.6-5cm (nominal field size). The actual in-plane (I) and cross-plane (C) FWHM were considered to calculate the effective field size, defined as (A*B)^0.5. Ouput factors (OF) were calculated and normalized to the 3x3 cm2. OF were calculated for both nominal (OF_N) and effective (OF_E) field sizes. The penumbra width was defined as the distance between the 80% and 20% isodose levels. Two identical diodes were adopted to speed up the data collection.

Results: OF_N were in agreement over the different models up to 1x1 cm2 field size. Higher agreement was obtained with OF_E, for the smallest fields different trends were obtained depending on vendors and models, see Fig.1. Penumbra measurements were in agreement each other for each field size and accelerator model.

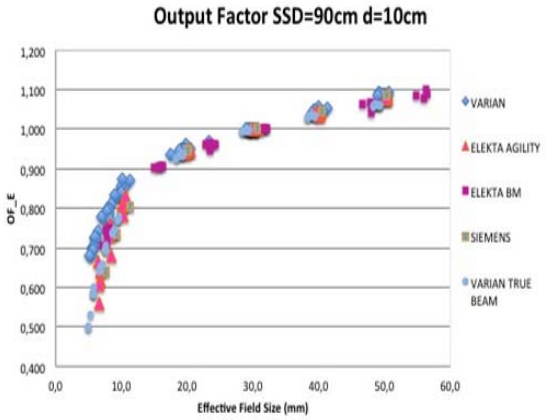

Conclusion: This study shows an high consistency of small field dosimetry in the involved radiotherapy departments using this new generation silicon diode; consequently, the values reported may actually be used by other centers as indicative values, especially in the case of small fields when suitable detector are not commonly available. Moreover, these results confirm that the new RAZOR silicon diode can be used to assess dosimetric accuracy in small-field delivery. In general, the adopted methodology removes much of the ambiguity in reporting and interpreting small field dosimetric quantities and facilitates a clear dosimetric comparison across a population of linacs.

EP-1949

Developing a Radiotherapy Quality Assurance programme as part of the HIPPO trial (NCT02147028)

D. Megias[1], H. Yang[1], P. Sanghera[2], M. Phillips[3], L. Senthil[4], A. Jackson[5], G. Whitfield[6,7]

[1]*Mount Vernon Hospital, National Cancer Research Institute Radiotherapy Trials Quality Assurance Group, Middlesex, United Kingdom*

[2]*Queen Elizabeth Hospital, Hall Edwards Radiotherapy Research Group, Birmingham, United Kingdom*

[3]*Cancer Research UK, University College London Cancer Trials Centre, London, United Kingdom*

[4]*Queen Elizabeth Hospital, Neuroradiology, Birmingham, United Kingdom*

[5]*The University of Manchester, Wolfson Molecular Imaging Centre, Manchester, United Kingdom*

[6]*The University of Manchester- Manchester Academic Health Science Centre, Radiotherapy Related Research, Manchester, United Kingdom*

[7]*The Christie NHS Foundation Trust, Clinical Oncology, Manchester, United Kingdom*

Purpose or Objective: Outlining of target and OAR volumes is integral to the radiotherapy process but inherently subject to variability. The hippocampus is a small structure not commonly contoured by clinicians requiring considered anatomical interpretation in its delineation. HIPPO is a randomised phase II trial of Hippocampal Sparing (HS) versus Conventional Whole Brain Radiotherapy after surgical resection or radiosurgery in favourable prognosis patients with 1-4 brain metastases. We set out to inform the development of a dedicated HIPPO RTQA programme through evaluation of hippocampal contouring.

Material and Methods: Two clinical oncologists from different UK radiotherapy centres and a radiologist from each centre independently outlined the hippocampus on 2 different 1 mm slice thickness planning CT datasets after registration with the T1 weighted gadolinium enhanced MRI (3D volumetric MRI, axial acquisition, 1 mm slice thickness, no slice gap, 1 x 1 x 1 mm voxels) on their planning system. The datasets were re-registered by one of the centres. The four hippocampal contours for each case were anonymised and reviewed collectively and a gold standard contour defined. We compared each contour with its respective gold standard using the DICE coefficient and volume difference.

Results:

Table 1

	Case 1		Case 2	
Outliner	DICE similarity coefficient	Volume difference (cm^3) between outline and gold standard.	DICE similarity coefficient	Volume difference (cm^3) between outline and gold standard.)
1	0.84	0.05 (-1%)	0.79	1.9 (+26%)
2	0.83	0.5 (+8%)	0.86	1.01 (+15%)
3	0.87	0.15 (+3%)	0.75	0.41 (+7%)
4	0.81	0.5 (+8%)	0.81	0.75 (-13%)

Conclusion: Reasonable concordance of the outlines in comparison to the gold standard was achieved in both cases. In case 1, all 4 outlines achieved a DICE coefficient greater than 0.80 and a hippocampal volume less than 0.5cm3 different to the gold standard. However, in case 2, despite DICE coefficients greater than 0.79 suggesting good spatial relationship between the clinicians' and the gold standard contour, greater variability was evident with a larger range in volume outlined. During collective review, some systematic differences were noted between the two participating centres' outlines, despite a high level of agreement on hippocampal boundaries during the review, highlighting CT-MRI co-registration as a potential source of variability between different centres and planning software. As a result of these findings, the pre-trial outlining benchmark case requires all centres to independently co-register the CT and MRI images and export the registration object as part of data submission. In order to comprehensively quality assure hippocampal outlining as part of the HIPPO RTQA programme, an on-trial component of the first two HS patient contours being reviewed prospectively before treatment is also undertaken. The implementation and quality assurance of less familiar outlining practice in the development of radiotherapy techniques requires careful consideration. This process has informed the development of a dedicated RTQA programme for the HIPPO trial highlighting the importance of aligning QA with clinical practice. HIPPO is funded by Cancer Research UK and The Brain Tumour Charity

EP-1950

Monte Carlo dose calculation of Viewray hybrid MRI-Co60 radiotherapy system: a repeatability study

E. Placidi[1], S. Teodoli[1], N. Dinapoli[2], L. Boldrini[2], G.C. Mattiucci[2], V. Valentini[2], A. Piermattei[1], L. Azario[1]

[1]*Università Cattolica del Sacro Cuore -Policlinico A. Gemelli, Institute of Physics, Rome, Italy*

[2]*Università Cattolica del Sacro Cuore -Policlinico A. Gemelli, Radiation Oncology Department- Gemelli-ART, Rome, Italy*

Purpose or Objective: The ViewRay MRI-Co60 hybrid system (MRIdian® [1,2]) is a novel technology that provides soft tissue imaging during radiotherapy thus allowing real adaptive radiotherapy possibilities and image guidance. The combination of Co60 with 0.35 Tesla MRI allows for MR-guided intensity modulated radiation therapy (IMRT) step and shoot delivery with multiple beams (3 Co60 heads 120° apart). MRIdian dose calculation takes advantage of a full Monte Carlo-based algorithm. The aim of this work was to evaluate the repeatability of the dose calculation of MRIdian plans for rectal cancer treatments.

Material and Methods: Ten patients affected by locally advanced rectal cancer (cT3-cT4; cN0, cN+) were manually segmented on Eclipse TPS v11. MRIdian step and shoot IMRT plans (7 groups of 3 fields each) were calculated 5 times for each patient. The prescribed dose for PTV2 was 45 Gy and 55 Gy for PTV1 through simultaneous integrated boost. The PTV1 V95, the conformity index CI [3] and the Wu's homogeneity index HI were computed for each patient. The coefficient of variation (CV), defined as the ratio of the standard deviation to the mean, was calculated for each set to express the precision and repeatability of the Monte Carlo dose calculation. The estimated beam-on time was also recorded for each plan.

Results: The time for the optimization and the final dose calculation was less than 5 minutes for each plan having a total of 21 fields (7 groups of 3 heads). The mean CV for the conformity index was found to be equal to 1.6±0.5% whilst both the mean V95(PTV1) and the HI resulted in a CV smaller than 1%. The CV for the estimated beam-on time for the 10 patients was found to be 4.3±2.1% (mean±std).

Conclusion: MRI-guided radiotherapy is a novel approach that may be advantageous over current treatment techniques by allowing PTV reduction. Dose optimization and calculation time is done with full Monte Carlo with a very short calculation time.
The three plan parameters under consideration proved that the Monte Carlo dose calculation is stable with a difference of the order of 4% in the estimated beam-on time.
[1] Dempsey JF et al. A realtime MRI guided external beam radiotherapy delivery system. Med Phys 2006;33:2254
[2] Dempsey JF, et al. A device for realtime 3D image guided IMRT. Int J Radiat Oncol Biol Phys 2005;63:S202
[3] Saenz et al. A dose homogeneity and conformity evaluation between Viewray and Pinnacle-based linear accelerator IMRT treatment plans. J Med Phys. 2014 Apr-Jun; 39(2): 64–70.

EP-1951

An international multi-institutional planning study for spine stereotactic body radiotherapy

T. Hiroshi[1], T. Furuya[1], S. Naoto[2], M. Nakayama[3], R. Mark[4], P. Jun Hao[5], I. Thibault[6], J. St-Hilaire[6], M. Lijun[7], D. Pinnaduwage[7], A. Sahgal[4], K. Katsuyuki[1]
[1]*Tokyo Metropolitan Cancer and Infectious diseases Center Komagome Hospital, Radiation Oncology, Tokyo, Japan*
[2]*Saitama Medical University International Medical Center, Division of Radiation Oncology, Saitama, Japan*
[3]*Kobe Minimally invasive Cancer Center, Division of Radiation Oncology, Hyogo, Japan*
[4]*Sunnybrook Odette Cancer Center- University of Toronto, Division of Radiation Oncology, Toronto, Canada*
[5]*National Cancer Center Singapore, Division of Radiation Onocology, Singapore, Singapore*
[6]*CHU de Quebec, Division of Radiation Oncology, Quebec, Canada*
[7]*University of California- San Francisco, Division of Radiation Oncology, San Francisco, USA*

Purpose or Objective: Spine SBRT is an emerging treatment for patients with spinal metastases and rapidly being adopted in the clinic without treatment planning evaluation guidelines. Although the a priori treatment planning constraints were met in all cases in our previous study, large inter-institutional variations in 95% of the PTV volume (D95) and D50 were observed. The purpose of this study was to minimize the inter-institutional variations in planning.

Material and Methods: Seven institutions in Japan, Canada, Singapore and USA participated and planned three cases with a total of ten apparatus. The spine cases included a 5th lumbar spine (case 1), 5th thoracic spine (case 2), and 10th thoracic spine metastases (case 3). Targets and organs at risk (OAR) were contoured by one experienced radiation oncologist according to International Spine Radiosurgery Consortium Consensus Guidelines and a 2 mm planning target volume (PTV) applied. The DICOM files were sent to each institute for planning. The treatment planning guidelines in the previous study included, prescribed dose of 24 Gy in two fractions with more than 70% prescribed dose to encompass D95, D0.035 < 140% of the prescribed dose, and a maximum dose to the spinal cord planning organ at risk volume (PRV) or thecal sac < 17 Gy. New guidelines added (D95 should be as high as possible(AHAP), D50 should be between 110% to 115% of prescribed dose and AHAP and D0.035 should be between 125% to 135% of the prescribed dose). The dose volume histograms (DVHs) were centrally reviewed.

Results: In our previous study the PTV D95 ranged from 70.0% to 99.6 % in case 1 (mean ± SD; 21.21 ± 2.43 Gy), 70.4% to 98.8% in case 2 (20.32 ± 2.22 Gy), and 70.0% to 94.2% in case 3 (19.78 ± 1.97 Gy), respectively and D50 for PTV ranged from 99.2% to 116.3% in case 1 (25.62 ± 1.34 Gy), 91.7% to 119.6% in case 2 (25.97 ± 2.18 Gy) and 84.2% to 114.2% in case 3 (25.57 ± 2.14 Gy), respectively. In this study PTV D95 ranged from 80.4% to 100.0% in case 1 (21.96 ± 1.67 Gy), 76.3% to 95.8% in case 2 (20.91 ± 1.67 Gy), and 70.4% to 94.2% in case 3 (20.3 ± 1.86 Gy), respectively and D50 for PTV ranged from 109.6% to 115.4% in case 1 (27.02 ± 0.53 Gy), 110.0% to 117.5% in case 2 (27.06 ± 0.63 Gy) and 107.5% to 115.0% in case 3 (26.89 ± 0.67 Gy), respectively.

Conclusion: We succeeded to minimize the inter-institutional variations. This study highlights dose constraints of D95, D50 and D0.035 should be used to minimize the variations.

EP-1952

Monte-Carlo calculation of the secondary electron spectra inside and around gold nanoparticles

E. Gargioni[1], T. Dressel[1], H. Rabus[2], M.U. Bug[2]
[1]*University Medical Center Hamburg - Eppendorf UKE, Department of Radiology and Radiotherapy, Hamburg, Germany*
[2]*Physikalisch-Technische Bundesanstalt, Division 6.6 Radiation Effects, Braunschweig, Germany*

Purpose or Objective: The use of nanoparticles (NP) in cancer therapy has been intensively investigated in the last few years. The advantage of using metal NP (such as gold, platinum, silver, hafnium oxide) during radiotherapy is that the amount of secondary electrons produced by the primary particles is higher than for soft tissue. Due to this enhanced secondary-electron emission around NP, stronger DNA damage is caused in the surrounding cells. The enhancement of energy deposition around gold NP has been determined in a number of studies, often with contradictory results, thus showing that the absorbed dose is not the appropriate physical quantity to estimate DNA damage in the presence of gold. Therefore it is necessary to systematically investigate the dependence of DNA damage from the spectra of the emitted secondary electrons and from corresponding nanodosimetric parameters.

Material and Methods: In this work, the secondary electron spectra produced inside and around gold NP were determined by means of Monte-Carlo simulations. The transport of secondary electrons created by different clinical photon sources inside and emerging from a NP surrounded by water was simulated using Geant4. The secondary electron spectrum inside gold NP of two different sizes (diameter: 12 and 30 nm) was calculated for mono-energetic photon sources (10 and 60 keV), an intra-operative x-ray source (maximum energy 50 keV), a conventional x-ray tube (200 keVp) and a clinical linear accelerator (6 MV).

Results: The energy spectra of the secondary electrons created inside the NP have a mean energy varying between about 6 keV for the mono-energetic 10-keV photons and about 65 keV for the 6-MV spectrum. This corresponds to a decrease of the mean ionization cluster size of about a factor of four for the linear accelerator. Therefore a corresponding decrease of the number of induced DNA double strand breaks is expected. Moreover, the spectra inside and around the gold NP with a diameter of 12 nm barely distinguish from those inside the gold NP with a diameter of 30 nm. However, the total amount of secondary electrons emerging from the smaller gold NP is increased by about a factor of three.

Conclusion: Further studies will be carried out in the future for determining the correlation between secondary electrons production and ionization cluster size distributions for other NP diameters and materials. Finally, a comparison between physical damage at nanometric level and cell survival experiments will be also performed.

Electronic Poster: Physics track: Professional and educational issues

EP-1953

Patient Safety & Quality Control Working Group of the Spanish Society of Radiation Oncology.

J. Pardo-Masferrer[1], E. Del Cerro- Peñalver[2], E. Jiménez-Jiménez[1]

[1]*Hospital Universitari Son Espases. On behalf of the Patient Safety and Quality Control Working Group of the Spanish Society of Radiation Oncology, Radiation Oncology, Palma de Mallorca, Spain*

[2]*Hospital Universitario Quiron Madrid. On behalf of the Patient Safety and Quality Control Working Group of the Spanish Society of Radiation Oncology, Radiation Oncology, Madrid, Spain*

Purpose or Objective: The aim of the Patient Safety and Quality Control Working Group of Spanish Society of Radiation Oncology (SEOR) was to analyse if the current Spanish legislation (SL): Royal Decrees 1566/1998 (Quality Criteria in RT) and 815/2001 (Justification of medical exposure to ionizing radiation) include the international recommendations on PS, and to implement appropriate measures to correct any possible deficiencies in this regard.

Material and Methods: The following documents were reviewed: "Towards Safer Radiotherapy", "Radiotherapy Risk Profile", "Failure Modes and Effects Analysis (FMEA)", "Preventing Accidental Exposures from New External Beam Radiation Therapy Technologies", "Safety in Radiation Therapy: A Call to Action meeting recommendations", and "Safety is not accident" (2nded.). From these documents, 11 topics were selected to compare with obligations regarding PS in RT specified in the SL: qualification, training, staffing, documentation/standard operating procedures, incident learning, communication/questioning, QC and preventive maintenance, accreditation, map of processes/risks and prospective risk assessment, strategies and tools development for minimizing risks and safety culture.

Results: SL include none of these issues: Relationship between staffing criteria and PS, Specifications about the number and quality of the documents that depend on a map of processes, Incident tracking, analysing, sharing and learning, Open communication and respectful questioning, Peer review, Maps of processes, Risks and prospective risk assessment, Strategies and tools for minimizing risks and, Safety culture. Due to lack of legal regulations, the SEOR board decided, in 2014, to create a Patient Safety and Quality Control Working Group (PSQCWG) to promote the knowledge and culture of QC and PS among professionals, to develop actions to improve information and training on QC and PS, and develop and implement systems to inform and report adverse events (errors and near misses) in order to learn from them and improve PS. Its challenges are:

To inform and assist to SEOR members in PS and QC procedures development
To organize regular training meetings, on PS and QC issues
To provide training/regular information to RO departments due to the occurrence of an event or detection of a weak point in the process map
To develop and deliver to RO departments an anonymous and easy-access system of events notification
To elaborate SEOR recommendations on PS, adapting the international recommendations to Spain
To submit proposals to the SEOR Board proposing amendments to the Spanish current health legislation

Conclusion: Being PS improvement a priority, by creating PSQCWG, the SEOR intends to implement safe practices in RT, promoting research on PS and QC, and develop their own recommendations on PS, according to the internationally elaborated and adapting them, if necessary, to the reality of our country by updating Spanish legislation.

EP-1954

Quality of Contouring in Radiation Oncology – Where to draw the line?

S. Vinod[1], M. Min[1], M. Jameson[1], L. Holloway[1]

[1]*Liverpool Hospital, Cancer Therapy Centre, Liverpool, Australia*

Purpose or Objective: Volume delineation is a potential source of error in radiotherapy, which can result in poorer clinical outcomes and increased toxicities. The aims of this study were to review the literature on interobserver variability (IOV), assess the dosimetric effects of IOV and identify interventions shown to reduce IOV.

Material and Methods: Medline and Pubmed databases were queried for relevant articles using the keywords "radiotherapy" and "volume delineation", "contouring", "observer variation", "interobserver variability", "variation", "systematic error", "quality assurance", "delineation", "interobserver" and "intraobserver"to identify articles which evaluated IOV target or organ-at-risk (OAR) volume delineation for multiple (>2) observers. The search was limited to English language articles published from 1/1/2000-31/12/2014. Reference lists of identified articles were scrutinised to identify relevant studies.

Results: 116 studies were identified, with the most common sites studied being breast cancer (n=20), lung cancer (n=17), genitourinary cancers (n=16) and OARs (n=29). The commonest volumes assessed were CTV (n=47) and GTV (n=38). CT alone (n=91) was the predominant dataset used for contouring. 81 studies used statistical tests to analyse the significance of their results. 31 studies evaluated the effect of additional imaging on IOV, with PET shown to reduce IOV in lung and rectal cancers and lymphoma but not head and neck cancers. There were mixed results for the benefits of MRI in brain tumours and breast cancers but it reduced IOV in OAR delineation. 25 studies evaluated the dosimetric effects of IOV, with most studies showing differences in OAR doses but the effect on PTV coverage was variable. 25 studies evaluated the effect on an intervention to reduce IOV. IOV was significantly reduced in 7/9 studies evaluating guidelines, and all 6 studies evaluating the provision of an autocontour to edit. Teaching interventions showed significant improvement in IOV in 4 studies, improvement without statistical analysis in 4 studies and no difference in 1 study.

Conclusion: Despite the large number of studies evaluating IOV, only a minority evaluated the dosimetric consequences of this or the use of interventions to reduce this. Additional imaging datasets reduced IOV in some cancer types. Guidelines or protocols and the provision of an autocontour reduced IOV in volume delineation.

EP-1955

Teaching radiation interactions and dosimetry through Monte Carlo simulations: VisualMC

C. Baker[1], A. Nahum[1]

[1]*The Clatterbridge Cancer Centre - Wirral NHS Foundation Trust, Physics Department, Bebington- Wirral, United Kingdom*

Purpose or Objective: An appreciation and understanding of the interaction of radiation with matter is essential for all professionals working in radiotherapy, whether from a superficial and qualitative or deep and quantitative perspective. The underlying theory is challenging to fully grasp at any level, often leading to confusion and a difficulty in retaining information. Interactive teaching, particularly with visualisation, provides students with a more enjoyable learning experience and promotes deeper learning. Here we describe a Monte Carlo (MC) simulation package designed to achieve educational objectives through interactive learning.

Material and Methods: A MC system originally designed for students to visualise the paths of electrons, positrons and photons as they traverse matter has been extended to score

energy deposition and particle fluence. The software package, written in Matlab, incorporates interaction sampling methods employed in general-purpose Monte Carlo codes.
Users select the incident particle type, energy, target material and (optionally) particle cut-off energies. Modes of operation include; 3D views of particle tracks from a broad beam incident on selected media, views of interaction probabilities and outgoing particle energy and direction, or energy deposition and charged particle fluence scored as a function of depth for a user-defined number of incident particles.
In addition, the 'physics' underlying radiation transport can be modified, by 'switching off' multiple Coulomb scattering, delta-ray production and radiative energy losses, in order to observe the effect this has on energy deposition and so gain a greater understanding of the physics involved.

Results: The MC teaching software, 'VisualMC', has been packaged as a stand-alone application and made available to university students via citrix. Practical sessions are used to introduce students to the software, after which the software can be accessed remotely by students to perform their own radiation transport 'experiments' to gather results for assessed assignments.

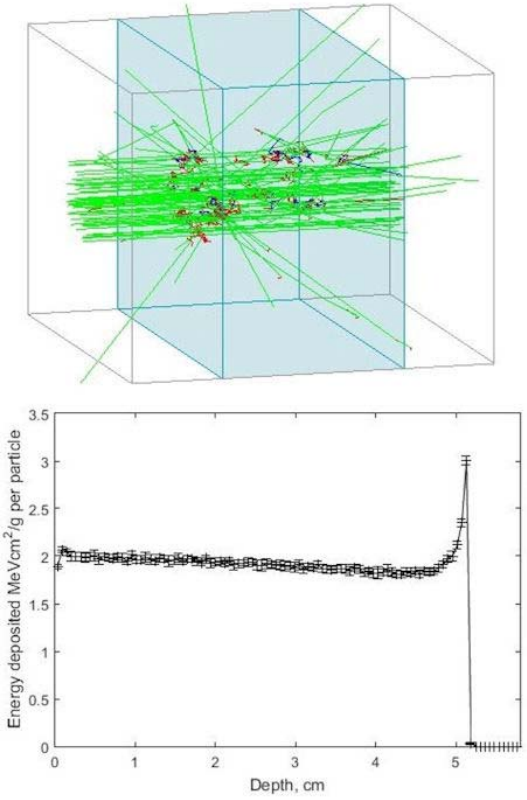

VisualMC output. Top: 10 MeV photons incident on a 1 cm thick Pb slab, showing photon (green), electron (red) and positron (blue) tracks. Bottom: Energy deposition with depth of 10 MeV electrons incident on water, multiple Coulomb scattering, radiative losses and delta-rays 'switched off'.

Conclusion: A MC-based software package has been developed to support the teaching of radiation interactions and radiotherapy dosimetry. The software has been incorporated into academic programmes at undergraduate and postgraduate levels, providing practical exercises for students of radiotherapy and medical physics.

EP-1956
Twitter as a tool for radiotherapy medical education: The #radonc Journal Club
R. Simcock[1], Z. Husain[2], M. Katz[3]
[1]*Brighton and Sussex University Hospitals NHS Trust, Sussex Cancer Centre, Brighton, United Kingdom*
[2]*Yale Medical Group, Yale Therapeutic Radiology, New Haven, USA*
[3]*Lowell General Hospital, Radiation Oncology, Lowell, USA*

Purpose or Objective: Radiation technology is expanding at an exponential rate. Accompanying discoveries in molecular and radiation biology there are multiple developments in both hardware and software solutions. This expansion in information presents huge challenges to radiotherapy professionals to maintain adequately appraised in new data. Continuing Professional Development (CPD) is threatened by the huge volume of information and lack of financial and physical (workforce) resources to support study. Social media (SoMe) provides a new tool for medical education which is free and open access (FOAM, foameducation.org). Twitter presents a tool for CPD which can usefully connect multidisciplinary professionals in radiation oncology.

Material and Methods: The hashtag #radonc denotes information on twitter that is pertinent to radiation oncology. (A similar #medphys tag is used for specific medical physics subjects). On a monthly basis a #radonc journal club is held on the twitter platform. A paper is discussed in an open dialogue. The paper under discussion is introduced on twitter and via the www.radiationnation.com website. At the end of a week of asynchronous comment a hosted discussion is held for one hour with the paper's author. Participation is free and open to all.

Results: The #radonc journal club has been in place since 2014 and grown in participant numbers. In July 2015 the journal club had 86 participants from the USA, Canada, Australia, UK, Spain, Philippines, and Saudi Arabia. Over 600 tweets were sent which created over 1.5 million page impressions (symplur.com). Participants have mainly identified themselves as Radiation/Clinical Oncologists although there have been strong contributions from medical physicists, RTTs and patients and their advocates. The journal club continues with plans to host multiply timed chats to cope with demand from users in separate time zones. Further effort is being spent on using contributors to #radonc to provide SoME sourced FOAM to be hosted on the Radiation Nation website.

Conclusion: The #radonc twitter club is a successful, free, International initiative to use social media to promote discussion and interaction in radiotherapy education.

Electronic Poster: Brachytherapy track: Breast

EP-1957
Partial breast irradiation with brachy- and teletherapy: comparative dosimetry of treatment plans
G. Stelczer[1,2], C. Pesznyák[1,2], N. Mészáros[1], C. Polgár[1], T. Major[1]
[1]*National Institute of Oncology, Radiotherapy Centre, Budapest, Hungary*
[2]*Budapest University of Technology and Economics, Department of Nuclear Techniques, Budapest, Hungary*

Purpose or Objective: To compare the dose distributions of partial breast irradiations in treatment plans of high dose rate multicatheter brachytherapy and intensity modulated radiotherapy with special respect to dose to organs at risk.

Material and Methods: 15 patients with early-stage breast cancer treated with interstitial partial breast brachytherapy (BT) irradiation were selected for the study. The total dose was 30.1 Gy given by 7 x 4.3 Gy fractionation. Target volume and organs at risk (non-target breast, contralateral breast, both lungs, skin, ribs and heart for left sided lesion) were outlined and treatment plans were made using geometrical and graphical optimization with Oncentra brachy (Elekta) planning system. The PTV was created around the resection cavity with a margin of 20 mm minus tumor-free surgical margin in each direction limited to skin and chest wall. Skin was delineated as a 5 mm shell inside the body contour. Then, the CT data with the contours were transferred to an external beam treatment planning system (Eclipse, Varian),

and using the same patient anatomy and fractionation schedule virtual plans for intensity modulated radiotherapy (IMRT) were made. The PTV in IMRT plans was created by 5 mm volumetric extension around the PTV used in BT plans. PTVeval was formed from PTV with geometrical limitation to the skin. Detailed dose-volume histogram analysis was carried out for the PTVs, breasts, lungs, skin, ribs and heart. Means, standard deviations were calculated and the corresponding parameters were statistically compared. Wilcoxon matched pairs analysis was performed for test of significance.

Results: The target coverage represented by V90 was better for IMRT (100% vs. 97%, $p<0.05$), but the D90 was higher for BT (103% vs. 100%, $p<0.05$). The conformity numbers were 0.73 for BT and 0.84 for IMRT ($p<0.05$). The V100, V90 and V50 for non-target breast were 1.7% vs. 0.2% ($p<0.05$), 2.8% vs. 4.3% ($p<0.05$) and 11.5% vs. 23.9% ($p<0.05$) for BT and IMRT plans, respectively. For ipsilateral lung the V5 was not significantly different in the two groups, but the V10 was lower for BT (11.7% vs. 20.5%, $p<0.05$). For contralateral breast and lung no significant differences in D0.1ccm were observed. For patients with left sided lesion the dose to heart was less with IMRT for D0.1ccm (15.3% vs. 22.7%, $p<0.05$). The most exposed skin volume (0.1 ccm) received significantly less dose with BT (64.4% vs. 92.4%). The same is true for ribs with values of 51.3% vs. 71.2%. With BT the ribs never received the prescribed dose, while with IMRT the D0.1ccm exceeded the prescribed dose in five cases.

Conclusion: With both BT and IMRT techniques acceptable target coverage can be obtained, but the conformity of dose distributions is better with IMRT. The dose to organs at risk is less with BT compared to IMRT, except for the heart. Generally, the BT and IMRT can be alternative techniques for partial breast irradiation, but in individual cases the recommended technique depends on the tumour location.

EP-1958

Treatment results of Mammosite catheter in combination with whole breastirradiation

A. Gitt[1], H. Böse-Ribeiro[1], C. Nieder[2], P.G. Kup[1], H. Hermani[1], H. Bühler[1], H.Y. Ergönenç[3], D. Drüppel[3], I.A. Adamietz[1], K. Fakhrian[1]
[1]*Marien Hospital Herne- Ruhr-University Bochum, Radiation Oncology, Herne, Germany*
[2]*Nordland Hospital Bodø, Department of Oncology and Palliative Medicine, Bodø, Norway*
[3]*St. Anna Hospital Herne, Department of Senology, Herne, Germany*

Purpose or Objective: To report the initial outcomes of patients treated with the MammoSite brachytherapy device (MSBT) as a boost followed by external whole breast irradiation (WBI).

Material and Methods: From June 2011 to March 2014, 107 patients (typically pT1-2, pN0-1, M0) were treated with breast-conserving therapy (BCT) and adjuvant radiotherapy with MSBT (15 Gy in 2.5 Gy fractions) followed by WBI (median 50.4 Gy). Toxicity was classified according to the Common Terminology Criteria for Adverse Events v3.0. The median follow-up was 21 months.

Results: So far no ipsilateral breast-tumor recurrences were observed, 102 patients (95%) were alive at last follow-up. Two patients (2%) developed distant metastasis. Five patients (5%) died during follow-up, only one as a result of breast cancer. The 2-year disease-free survival was 95 ± 3%. The incidence of asymptomatic and symptomatic seroma in 90 days after MSBT was 28% and 10%, respectively. Infectious mastitis was observed in 3 patients (3%), who were treated successfully with antibiotics. Only 3 patients (3%) developed a radiodermatitis > grade 2 after WBI.

Conclusion: The boost technique used in this study seems to provide excellent local control with acceptable toxicity, similar to the results observed with other forms of interstitial accelerated partial-breast irradiation as a boost. Long-term follow-up is necessary to refine the patient selection criteria and to assess efficacy and late toxicities.

EP-1959

Dosimetric consequences from minimal displacements in APBI brachytherapy using the SAVI applicator

S. Pella[1], C. Shereen[2], D. Nicolae[3], H. Mikko[3], P. Janeil[3]
[1]*Florida Atlantic University, Physics- Medical Physics Graduate Program, Boca Raton, USA*
[2]*Florida Atlantic University, Physics, Boca Rarton, USA*
[3]*Florida Atlantic University, Physics, Boca Raton, USA*

Purpose or Objective: Evaluate the necessity of a complete CT scan before each treatment in the APBI and the use of additional immobilization devices

Material and Methods: A retrospective study was performed on 25 patients treated in the 2013-2015 period with APBI brachytherapy. The CT scans of each patient taken before each treatment were imported in to the planning system. Each CT scan was registered with the initial one. Dosimetric evaluations respective to the initial CT scan image series were performed. The deviation of dose received by the skin and ribs in each treatment were calculated and minimum, maximum and average dose received by skin and ribs were recorded and compared to the initial plan's results.

Results: Small deviations in displacements were observed from the SAVI applicator to the ribs and the skin surface. Dosimetric evaluations revealed, very small changes in the inter-fractionation position make significant differences in the maximum dose to these critical organs. As a result, the maximum dose varied between 10% and 32% in ribs and skin surface.

Conclusion: The CT scan before each treatment is necessary to minimize the uncertainty in setup and any intervention if deemed necessary. This study indicates, in 30% of the cases needed re-planning between treatments to minimize the risk of critical organs to be overdosed. We conclude that the physicist should evaluate the position of the device by analyzing the CT images before each treatment and consider re-planning is the deviations are high. Also this study reveals the urgent need of improving the immobilization methods when treating APBI with SAVI applicator. This type of treatment will benefit of deformable registration at each treatment and adaptive planning

Electronic Poster: Brachytherapy track: Gynaecology

EP-1960

Exclusive brachytherapy of vaginal cuff: ethical considerations on quality of life after treatment

F. Piro[1], M.A. Martilotta[1], A. Massenzo[1], L. Marafioti[1]
[1]*Ospedale Mariano Santo, U.O. Radioterapia Oncologica Cosenza, Cosenza, Italy*

Purpose or Objective: To evaluate efficacy, clinical and psychological impact of chronic toxicity, of exclusive BRT of vaginal cuff in patients (pts) affected by endometrial cancer after hysterectomy (**EC**)

Material and Methods: From January 2010 to December 2014 we studied 108 pts with EC treated with exclusive BRT. Treatment was performed with cylinder in vagina to sterilize vaginal cuff, fractionation 6 - 30 Gy, prescription to 0.5 cm from surface of cylinder, active length almost 3 cm. We evaluated efficacy, quality of life and impact on sexual activity after BRT filling out a test designed to investigate following areas: 1) social relations and personal emotions, 2) couple intimacy and sexuality , 3) impact of treatment on sexuality and doctor-patient relationship before BRT

Results: 96 evaluable pts median follow-up 24 months (range 9-60); median age 62 years (40-88); histology revealed 2 cr. squamous and 94 adenocarcinoma; grading G1 for 15% , G2 for 65% and G3 for 20% of cases; all pT1b stage; lymph node

status performed in 72 (75%) pts. median 4 (0-40) in other 24 (25%) NX; diameter of the cylinder used in 76 (84%) pts. was 3-4 cm remaining 20 (26%) diameter 1-2. Only 3 (3%) pts resulted disease progression. Psychological evaluation was performed on 69 pts (Median age 61; 44 - 71), the other 27 cannot be estimated because not interested. In the first area test showed for a third of pts a change of social relations judged value "from much up to very much", while in half of respondents, there was same value in personal sphere. Considering couple intimacy the 71% of women had undergone a change, and 81% reported decrease of sexual desire. In third area half of pts said they were informed about impact of BRT on sexual life evaluating changes induced by it " from much up to very much"; 71% of women surveyed have been recommended to have therapeutic relationships, 73% of respondents reported painful intercourse and 91% of pts found it unsatisfactory. 13% of pts has explicitly requested psychological support

Conclusion: Apart from grading and lymph node status, BRT of vaginal cuff is effective in preventing local recurrence. Despite of use of larger diameter cylinders, remains problem of toxicity management post BRT. Analysis of impact on quality of life of these pts causes several issues: whether treatment should always be recommended, if we have to review informed consent and if a psychological support pre-treatment is necessary. An appropriate supportive therapy during and after BRT is always necessary

EP-1961

Factors influencing the risk of uterus perforation in high-dose rate tridimensional brachytherapy

L.G. Sapienza[1,2], R.C. Camargo[1], I. Migowski[1], E.S. Sandrini[1], E. Anderson[1], F. Campana[1], G. Baiocchi[3], H.A. Salmon[1]
[1]*Clínicas Oncológicas Integradas COI-RJ, Radiation Oncology, Rio de Janeiro, Brazil*
[2]*A. C. Camargo Cancer Center, Radiation Oncology, São Paulo, Brazil*
[3]*A. C. Camargo Cancer Center, Gynecologic Oncology, São Paulo, Brazil*

Purpose or Objective: To evaluate the factors associated with uterine perforation in a population treated with tandem and ovoids high-dose rate tridimensional (HDR 3D BT) brachytherapy for gynecological cancer, without ultrasonographic guidance.

Material and Methods: Computed tomographic images used for HDR 3D BT of 47 cases of gynecological cancer (46 cervical and 1 endometrial cancer) were studied. The perforation rate (PR) was determined by software Oncentra MasterPlan V3.3 (Veenendaal, Netherlands). The categorical variables tested were: bladder filling (empty vs. full), age (≤60 years vs. >60 years), uterine lateral position (left or right vs. central) and uterine sagittal position (anterior vs central or retrograde). For statistical analysis, multiple logistic regression was performed (SPSS V.20).

Results: The study evaluated 186 insertions. The treatment was performed using 4 fractions of 7 Gy in 45 patients (95.7%) and 3 fractions of 7 Gy in two patients (4.3%). Median age was 47 years (range, 24 - 82). The total PR was 21.5.% (40 events). The site of the perforation was: 67.5% posterior wall (27 cases), 17.5% left lateral (7 cases), 7.5% cranial (3 cases), 5% anterior wall (2 cases) and 2.5% right lateral (1 case). In forty-three cases (91.5%), the perforation occurred in the opposite direction of the uterus anatomic position. Factors that increased the PR in univariate analysis were: empty bladder ($p<0.001$), anterior uterine position ($p=0.010$) and age ($p=0.010$). In multivariate analysis, only empty bladder remained as an independent prognostic factor for perforation ($p=0.002$).

Conclusion: In our series, the modifiable factor empty bladder correlated with uterine perforation. Although uterine anatomic position did not influenced significantly the incidence of uterine perforation, it determined the direction of the perforation in more than 90% of the cases. Our data suggest a potential value of image guidance for brachytherapy insertion.

EP-1962

CT-based optimisation of single source line HDR vaginal vault brachytherapy: a dosimetric study

I. Barillot[1], A. Ruffier-Loubiere[1], G. Bernadou[1]
[1]*Hôpital Bretonneau, Cancer centre H.S. Kaplan, Tours, France*

Purpose or Objective: To compare CT-based dose distribution to CTV and organs at risk (OAR) of HDR vaginal vault brachytherapy (VVB) with stump applicator according to 2 prescription modes: standard prescription to 5 mm from the applicator surface versus individualised prescription according to the thickness of the vaginal wall.

Material and Methods: This study was performed between January 2013 and December 2014, on a cohort of 61 consecutive patients (pts) with endometrial cancer referred for a post operative HDR VVB. Mean age was 68 years. According to FIGO stage, 21% were Ia G3, 54% Ib, 10% II and 15% III. 24 Gy in 4 fractions were delivered as sole treatment in 33 pts; whereas 28 pts received 10 Gy in 2 fractions after 45 Gy pelvic irradiation. The CT was performed with applicator in situ before the first fraction. The size of the applicator was determined according to the clinical examination, but was modified if significant air gaps were observed on CT. CTV was defined as the vaginal vault and the upper third of the vagina; intestine as the lower third of the peritoneal cavity. Bladder and rectum were delineated entirely. Using brachyvision®, the Standard Plan (SP) was calculated for delivering the fraction dose (FD) on a reference line placed at 5 mm of the applicator surface irrespective of the location of OAR. The Individualised Plan (IP) was calculated from a line that conformed to the outer contour of the CTV with the following constraints: CTVD90 = FD+/-5%, D2cc to rectum and bladder ≤ FD and D2cc to Intestine ≤ (FD-1Gy). The CTVD90 and D2cc to OAR were used for the plans comparison

Results: According to constraints (in, above, under), 6 different groups could be defined: Gp1 : D90 and D2cc in; Gp2 : D90 in and D2 cc above; Gp3 D90 and D2cc above; Gp4 : D90 above and D2cc in ; Gp5 D90 under and D2cc in ; Gp D90 under and D2cc above. Results of the comparison are summarised in the following table.

SP		IP					
	nb pts	Gp1	Gp2	Gp3	Gp4	Gp5	Gp6
Gp1	2	2					
Gp2	6	3	1				2 (D2cc were significantly lowered at price of decrease of D90
Gp3	12	3			8	1	
Gp4	8	5			3		
Gp5	15	6				4	5 (D90 slightly improved at price of slight increase of D2 cc
GP6	18	1	6		1	6	4

Conclusion: CT-based individualised single source line HDR VVB was feasible and resulted in optimisation of the dose distribution to CTV and/or OAR in the majority of cases. In only 20% of cases, individualisation didn't change the dose distribution. Consequently, CT-based dosimetry became the standard procedure in our department since January 2015. The assessment of the clinical impact will be the next step.

EP-1963

Dosimetric evaluation of image guided brachytherapy using tandem- ovoid and tandem- ring applicators

R. Rangarajan[1], S. Saravanan[1]
[1]*Government Royapettah Hospital, Department of Radiation Oncology, Chennai, India*

Purpose or Objective: The aim of the study is to evaluate the differences in dosimetry between tandem-ovoid and tandem-ring gynaecologic brachytherapy applicators in image guided brachytherapy

Material and Methods: 100 CT datasets of cervical cancer patients (stage IB2 – IIIB) receiving HDR application (50 tandem-ovoid and 50 tandem-ring) were studied. The external beam radiotherapy dose was 50Gy. Brachytherapy was delivered using a CT-MRI compatible tandem-ovoid (50 patients) and a tandem-ring applicator (50 patients) to a dose of 8Gy/# in 2fractions. Bladder and rectum were contoured using oncentra planning system. DVHs were calculated and D2cc was recorded for bladder and rectum and compared with the corresponding ICRU point doses. The point B dose, the treated volume, high dose volume and the treatment time was recorded and compared for the two applicators.

Results:

Applicator	Mean D2cc Bladder (Gy)	Mean ICRU Bladder (Gy)	Mean D2cc Rectum (Gy)	Mean ICRU rectum (Gy)	ICRU/D2cc ratio Bladder	ICRU/D2cc ratio Rectum
Tandem-Ring	6.57	5.56	3.95	5	0.847	1.265
Tandem-ovoid	7.30	5.63	4.79	5.65	0.772	1.179

Conclusion: The results indicate that the OAR doses assessed by DVH criteria were higher than ICRU point doses for bladder with both tandem-ovoid and tandem-ring applicators whereas DVH based dose was lower than ICRU dose for rectum. The point B dose, the treated volume and high dose volume was found to be slightly higher with tandem-ovoid applicator whereas the total treatment time was higher with the tandem-ring applicator. The mean D2cc dose for bladder and rectum was lower with tandem-ring applicators. The clinical implication of the above dosimetric differences needs to be evaluated further.

EP-1964

Measurement of vaginal dose with image guided vaginal vault brachytherapy

L. Bleakley[1], M. Zahra[1], L. White[1], W. Keough[2]
[1]*Western General Hospital- Edinburgh Cancer Centre, Clinical Oncology, Edinburgh, United Kingdom*
[2]*Western General Hospital - Edinburgh Cancer Centre, Medical Physics, Edinburgh, United Kingdom*

Purpose or Objective: The aim of this study is to evaluate an accurate method to define vaginal dose distribution in the delivery of vaginal vault brachytherapy (VBT) utilising a single channel cylinder.

Material and Methods: A retrospective analysis of all 3D single channel cylinder VBT plans held on BrachyVision™ 10.0 treatment planning system obtained between April 2011 and December 2013. All patients received treatment to the top 4cm of the vagina at 0.5cm depth prescription point with fractional doses of 5.5Gy or 7Gy. Dose assessment is conducted using both point dose values and DVH parameters for vaginal wall. A vaginal apex dose point (VAdp) was defined as a midline point on the single channel cylinder, positioned at the apex representing vaginal surface dose (Gy). A second rectal / vaginal dose point (RVdp), positioned 0.5cm posterior to vaginal wall (ICRU rectal point) is also used. This is potentially a good surrogate for vaginal mucosa dose due to its proximity to vaginal cylinder. A presumed vaginal wall thickness of 0.5cm was used to grow a volume representing the upper 4 cm of vaginal mucosa; the D2cc (Gy) and D5cc (Gy) are recorded. Pearson's correlation coefficient is used to calculate correlation between dose point values and dose volume parameters obtained. A p-value <0.05 was considered statistically significant in this study.

Results: A total of 113 CT data sets are analysed. 69% (n = 78) of patients had a prescribed fractional dose of 5.5Gy and 31% (n = 35) received 7Gy fractional dose.

	5.5Gy Fractional Dose		7.0Gy Fractional Dose	
	Mean vaginal fraction dose with SD (Gy)	Range (Gy)	Mean vaginal fraction dose with SD (Gy)	Range (Gy)
D2cc	8.4 ± 0.30	7.71 – 9.81	10.7 ± 0.47	10.03 – 12.84
D5cc	7.8 ± 0.19	7.24 – 8.43	9.91± 0.28	9.21 – 10.77
VAdp	6.31± 0.41	4.30 – 7.54	7.95 ± 0.57	7.17 – 9.84
RVdp	4.0 ± 0.39	3.37 – 6.50	5.03 ± 0.30	4.41 – 5.81

No correlation was identified between RVdp and D2cc for 5.5Gy plans (r=0.004, p=0.974) and 7.0Gy plans (r=0.009, p=0.957). Similarly no correlation was identified between the RVdp and D5cc for 5.5Gy plans (r=0.170, p=0.138) and 7.0Gy plans (r=0.071, p=0.687). The D2cc showed a weak correlation with VAdp for 5.5Gy (r=0.200, p=0.083) and 7Gy plans (r=0.351, p=0.039); however only statistically significant with 7Gy plans. No relationship exists between VAdp and D5cc for 5.5Gy (r=0.146, p=0.202) and 7Gy plans (r=0.068, p=0.699).

Conclusion: The RV dp is not a good surrogate for vaginal dosimetry. The VAdp could possibly be considered to predict D2cc values however dose volume parameters remain the accurate method when recording dose to vaginal mucosa from delivery of VBT.

EP-1965

Quantification of CT planning scans assessing OAR doses when delivering vaginal vault brachytherapy

L. White[1], W. Keough[2], L. Bleakley[1], M. Zahra[3]
[1]*Edinburgh Cancer Centre- Western General Hospital-, Radiotherapy, Edinburgh, United Kingdom*
[2]*Edinburgh Cancer Centre- Western General Hospital-, Medical Physics, Edinburgh, United Kingdom*
[3]*Edinburgh Cancer Centre- Western General Hospital-, Clinical Oncology, Edinburgh, United Kingdom*

Purpose or Objective: The aim of this study is to establish whether one initial CT planning scan for vaginal vault brachytherapy (VBT) patients is adequate to ensure surrounding OAR (bladder, rectum, sigmoid colon and small bowel) do not breach their dose constraints, or whether patients should be CT planned before each VBT fraction due to variations in OAR volumes and organ movement.

Material and Methods: Patients were scanned twice with a segmented single central channel vaginal cylinder in situ. The first CT scan (A) was carried out, as per departmental protocol, two weeks prior to treatment delivery and the subsequent scan (B) on the first day of treatment. All patients were treated using scan A. OAR dose deviations were retrospectively calculated by applying the same dwell positions and loadings to scan B. The total EQD2 OAR dose received by VBT and EBRT was then assessed for tolerance breach (bladder 80Gy; rectum, sigmoid colon and small bowel 70Gy). Both scans were analysed using Pearson correlation coefficient to determine relationships between % differences of OAR volumes and the OAR D2cc dose % differences. Additional bladder, rectum and GI structure (sigmoid colon and small bowel) contours were created combining the two scans (A+B); to simulate the worst case scenario structure movement between treatments.

Results: 42 patients were scanned twice in total. 5 patients were prescribed 21Gy in 3 fractions after 45Gy in 25 fractions EBRT, 27 patients were prescribed 11Gy in 2 fractions after 45Gy in 25 fractions EBRT and 10 patients were prescribed 21Gy in 3 fractions of VBT only. Scan B CT plans showed all patients receiving VBT only or EBRT with 2 fractions of VBT had total EQD2 doses within published OAR dose tolerances. 4 out of 5 (80%) patients treated with EBRT and 21Gy of VBT exceeded at least one OAR dose tolerance and when contours were combined 100% of these patients exceeded at least one

OAR dose tolerance. No relationship was identified between the % difference of OAR volumes and D2cc OAR % variations.

Conclusion: Patients treated with 45Gy in 25 fractions EBRT + 21Gy in 3 fractions VBT are at greater risk of breaching OAR dose tolerances when using a single planning scan for all treatments. There is no significant relationship between the % difference of bladder, rectum, sigmoid and small bowel volumes and % dose difference. The OAR dose variation between each scan is most likely due to the unpredictable day to day movement of the structure and cannot be replicated by standardised organ filling procedures. Departmental protocols have been amended to CT plan this subgroup of patients before each treatment fraction to take into account position of structure at that time. Use of a multichannel applicator could also help minimise the dose to these structures.

EP-1966

Late toxicity outcomes of CT-based brachytherapy planning for locally advanced cervical cancer

J. Tang[1], B.A. Choo[1], V. Koh[1], J. Low[2], J. Ng[2], A. Illancheran[2], Y. Lim[3], S.E. Lim[3], D. Tan[3]
[1]*National Cancer Institute Singapore, Radiation Oncology, Singapore, Singapore*
[2]*National Cancer Institute Singapore, Gynaeoncology, Singapore, Singapore*
[3]*National Cancer Institute Singapore, Medical Oncology, Singapore, Singapore*

Purpose or Objective: A report of late rectal and bladder toxicitiy outcomes of a computed tomography(CT)-based image guided brachytherapy(IGBT) technique for treatment of cervical cancer.

Material and Methods: Between 2008-2014, 95 women with International Federation of Gynecology and Obstetrics stage IB to IVA cervical carcinoma treated with definitive concurrent cisplatin based chemotherapy and external beam radiation therapy (EBRT) 50.4Gy in 28 fractions followed by 3-4 fractions of high-dose-rate (HDR) IGBT was retrospectively reviewed. At each implantation, all patients had a urinary catheter insitu and received bowel enema before undergoing planning CT-simulation. A high-risk clinical target volume (HRCTV) encompassing any visible tumor and the entire cervix, rectum and bladder was contoured on the simulation CT according to Radiation Therapy Oncology Group Gynaecology Contouring Atlas. Prescription dose range of 5.5-7Gy was prescribed to the HRCTV. Doses to Point A, ICRU rectal and bladder points were recorded. Toxicities were recorded using NCI-CTCAE version 3.

Results: The median follow-up time was 29 months. The mean Point A dose was 6Gy (4.6-7.6Gy). The ICRU rectum and bladder points were 4.69Gy (2.5-5.7Gy) and 4.23Gy (1.95-7.2Gy) respectively. 22 patients(23%) and Grade 2 proctitis and 10 patients(11%) had Grade 3 proctitis. 4 patients (4%) had Grade 2 cystits and 2 patients(2%) had Grade 3 cystitis. No patients had ≥ Grade 4 toxicity.

Conclusion: Despite bladder and bowel preparation protocol, late rectal toxicity was significant in a high proportion of patients. Implementation of an interstitial IGBT using the EMBRACE protocol might help to limit these late rectal toxicities.

EP-1967

Preliminary results of a new brachytherapy schedule in postoperative endometrial carcinoma

A. Rovirosa[1], K. Holub[1], A. Herreros[2], C. Ascaso[3], J. Sánchez[4], G. Oses[2], J. Mansilla[5], J. Sola[2], A. Huguet[2], S. Garrida[2], J. Saez[2], C. Camacho[2], A. Camarasa[2], C. Quilis[2], M. Arenas[6], S. Sabater[7], M. Del Pino[8], J. Pahisa[8], A. Biete[1]
[1]*Hospital Clinic i Universitari, Radiation Oncology Dpt. Gynecological Cancer Unit., Barcelona, Spain*
[2]*Hospital Clinic i Universitari, Radiation Oncology Dpt., Barcelona, Spain*
[3]*Faculty of Medicine- University of Barcelona, Public Health Dpt., Barcelona, Spain*
[4]*Hospital Clinic i Universitari, Economics Dpt., Barcelona, Spain*
[5]*Hospital Rebagliati, Radiation Oncology Dpt., Lima, Peru*
[6]*Hospital sant Joan de Reus, Radiation Oncology Dpt., Tarragona, Spain*
[7]*Hospital General de Albacete, Radiation Oncology Dpt., Albacete, Spain*
[8]*Hospital Clinic i Universitari, Gynecological Cancer Unit., Barcelona, Spain*

Purpose or Objective: To analyze the preliminary results of a new daily high-dose-rate brachytherapy (BT) schedule in vaginal-cuff relapse (VCR) and toxicity in postoperative endometrial carcinoma (EC).

Material and Methods: From September 2011 to December 2014, 102 patients (p) were treated with HDRBT in FIGO stages: IA-30p, IB-39p, II-8p, IIIA-4p, IIIB-1p, IIIC1-8p, IIIC2-5p, IIIC3-1p, IVB-6p. Pathology: 79/102 endometrioid adenocarcinoma and 23/102 other types. Radiotherapy: Group 1: 74p/102p 1 BT fraction of 7Gy after external beam irradiation (mean 45Gy, range 44.0-50.4); Group 2: 28p/102p BT alone by 3 daily fractions of 6Gy. Chemotherapy: 20/102 patients. Toxicity evaluation: RTOG scores for bladder and rectum and the objective criteria of LENT-SOMA for vagina. Statistics: Chi-square and Fisher exact tests.

Results: Mean age (years): Group 1: 65.4 (40-88), Group 2: 66.7 (39-90). Mean follow-up (months): Group 1: 24.48 (8.04-52.56); Group 2: 26.88 (8.76-54.48). VCR: No relapses with the present mean follow-up. Toxicity: Group 1 - early problems (all G1-2) in rectum (5.5%), bladder (6.8%) and vagina (14.9%). Late toxicities: rectum 2.7% (all G1), bladder 0% and vagina 27% (G1-G2). Group 2 -early toxicity: bladder 10.7% (all G1), vagina 28.1% (all G1-G2), rectum 0%; late toxicity was only found in vagina in 17.8% (G1-2). No significant differences were found in toxicities between the two groups.

Conclusion: The present brachytherapy schedule consisting in 1 fraction/7Gy after external beam irradiation and 3 fractions/6Gy administered daily seem a safe regime in terms of local control and toxicity for postoperative EC. These results seem similar to those found in our Hospital in 2 previous series with low dose per fraction and an increased number of fractions. Grant: AECC Foundation

EP-1968

Vaginal mucosal doses in the treatment of cervical cancer using HDR brachytherapy

W. Keough[1], L. Bleakley[1], L. White[1], M. Zahra[1]
[1]*Edinburgh Cancer Centre- Western General Hospital-, Oncology, Edinburgh, United Kingdom*

Purpose or Objective: To develop a reliable method of determining the radiation dose to the vaginal mucosa in the treatment of cervical cancer.

Material and Methods: Forty six cervical cancer patients were treated with EBRT and HDR brachytherapy therapy from July 2010 – Dec 2013. They received 45Gy in 25 fractions of EBRT to the entire pelvis followed by 3 HDR brachytherapy fractions using a tandem and ring applicator with a HRCTV D90 of 80-85Gy. A volume to represent the vaginal mucosa was obtained by using a non-uniform expansion of the 5mm ring applicator cap; this was expanded by 5.0 mm in all directions except the sup/inf which was expanded by 7.0 mm. In addition, a rectal vaginal (RV) point dose was determined using a point 5.0 mm posterior to the intersection of the superior-posterior junction of the build up cap (figure 1 sagittal view). Total doses were calculated for vaginal volumes of 5.0cc (D5 v), 2.0cc (D2 v), and the RV point. In addition, the slope was calculated for the vaginal mucosa between D5 v and D2 v. Pearson correlation coefficients (with p values = 0.01) were assessed to identify

correlations between the slope, D5 v, D2 v, HRCTV D90, HRCTV volume, and the RV point.

Results: Total doses from 3 fractions for the D5 v median 48.7Gy (range 31.4 - 76.6Gy), D2 v median 64.0Gy (range: 43.2 - 112Gy) and RV median dose 16.3Gy (range: 11.6 – 25.3Gy) The RV point exhibited a weak correlation with D2 v (r=0.56; p=0.0001) and D5 v (r = 0.55; p=0.0001) respectively. A moderate correlation was observed between the HRCTV volume and the D2 v (r = 0.69; p=0.0001), the HRCTV volume and D5 v (r = 0.73; p=0.0001) and a weak correlation with the HRCTV volume and the RV Point (r=0.57; p=0.0001). The slope correlated with D2 v (r= -0.96; p=0.0001) and D5 v (r=-0.87; p=0.0001) and a weak correlation with the RV point (r=-0.52; p=0.0002). No correlation was found between the HRCTV D90 and the D2v (r=-0.20; p=0.1826), the D5v (r=-0.24; p=0.1082), or the RV Point (r=0.02; p=0.8431).

Conclusion: The expansion volume of the ring applicator cap can provide a suitable surrogate for determining the vaginal mucosa dose, as this part of the vagina is in close proximity to the ring and tandem contributing to the volume of vaginal mucosa receiving the highest vaginal dose. The RV point does not correlate with the D2v and D5v and therefore can not to be use as a suitable surrogate point for the dose to the vaginal mucosa. Additional work is currently ongoing to correlate the D2v and D5v with clinically measured vaginal morbidity.

EP-1969

High-dose-rate image-guided interstitial brachytherapy for recurrent cervical adenocarcinoma

K. Yoshida[1], H. Yamazaki[2], T. Takenaka[3], T. Kotsuma[4], K. Masui[2], Y. Uesugi[1], T. Shimbo[1], N. Yoshikawa[1], H. Yoshioka[1], Y. Yoshioka[5], E. Tanaka[4], Y. Narumi[1]
[1]*Osaka Medical College, Radiology, Takatsuki, Japan*
[2]*Kyoto Prefectural University of Medicine, Radiology, Kyoto, Japan*
[3]*National Hospital Organization Himeji Medical Center, Radiology, Himeji, Japan*
[4]*National Hospital Organization Osaka National Hospital, Radiation Oncology, Osaka, Japan*
[5]*Osaka University Graduate School of Medicine, Radiation Oncology, Suita, Japan*

Purpose or Objective: In order to evaluate the usefulness of high-dose-rate image-guided interstitial brachytherapy (HDR-ISBT) for recurrent uterine cervical adenocarcinoma, we analyzed our clinical experience.

Material and Methods: We investigated 28 patients treated with HDR-ISBT at National Hospital Organization Osaka National Hospital between May 2003 and December 2010. All patients received radical surgery and 7 patients also received post-operative radiotherapy as previous treatments. Histologic finding was adenocarcinoma and squamous cell carcinoma for 11 and 17 patients. In 11 adenocarcinoma patients, 6 patients had endometrioid adenocarcinoma and the other 5 patients had mucinous adenocarcinoma. The median tumor size was 23 mm (range; 5-79 mm). In 21 patients who had no irradiation history, 9 patients were treated with HDR-ISBT alone and the other 12 patients were treated with HDR-ISBT plus external beam radiotherapy (EBRT). Forty-eight to 54 Gy in 8 to 9 fractions were delivered as monotherapy and 30 to 33 Gy in 5 to 6 fractions as combination of EBRT. In 7 patients who had irradiation history, slight lower doses (42 to 48 Gy in 7 to 8 fractions) were selected. We implanted 7–15 (median, 12) applicators under transrectal ultrasonography guidance. We used free-hand implantation with ambulatory technique for later 25 patients. Magnetic resonance imaging (MRI)-assisted image-based treatment planning was performed for later 17 patients. Clinical target volumes (CTV) were the gloss tumor volume with or without 10 mm of vaginal margin for patients with or without non-irradiation history.

Results: The median follow-up time was 43 months (range; 4-115 months). The median D90(CTV)s were 120%prescribed dose (PD), 122%PD and 118%PD for patients who had endometrioid adenocarcinoma, mucinous adenocarcinoma and squamous cell carcinoma. The 3-year local control and overall survival rates were 72% and 73% for adenocarcinoma. The 3-year local control and overall survival rates were 88% and 77% for squamous cell carcinoma. No significant difference was observed. The 3-year local control rates were both 67% for endometrioid adenocarcinoma and mucinous adenocarcinoma. Grade 3-4 late complications occurred by HDR-ISBT in 5 patients (18%).

Conclusion: Our treatment result of image-based HDR-ISBT showed that slight inferior result was observed in cervical adenocarcinoma although there was no significant difference.

EP-1970

Dose to organs at risk on CT versus MRI based brachytherapy for cervix cancer

K. Akbarov[1], I. Isayev[1], E. Guliyev[1], N. Aliyeva[1]
[1]*National Oncological Centre, Radiotherapy, Baku, Azerbaijan*

Purpose or Objective: Brachytherapy is one the most important components in the treatment of cervical cancer. Recently 3D planning for brachytherapy has been used which could be done both by CT and MRI imaging based. We compared the high risk clinical target volumes contoured on CT and MRI and dose distribution in the target volumes and organs at risk.

Material and Methods: Twenty three patients with IIA-IIIB stage cervical cancer were planned for HDR brachytherapy with ring-tandem applicators. Treatment consisted of four 7 Gy fractions by two insertion procedures. On MRI and CT sets we contoured HR CTV and organs at risk on 42 plans: for 19 patients two plans and for four patients only one. Medical physicists received task to make planning on CT and MRI images independently at the same day before irradiation. The mean HR CTV volume, dose received by at least 90% of the volume (D90) and the dose to 2 cc for the organs at risk were evaluated.

Results: The mean volume of HR CTV was 77.5 cc on CT based contours and 60.3 cc on MRI imaging. This difference in HR CTV volume reflected on the dose to organs at risk – physicists have to increase it to achieve prescribed dose in target volume. Thus, while assessing mean D2cc for rectum, bladder and sigmoid we find out that it was lower in case of MRI based planning compare to CT based planning – 66.2 Gy and 70.3 Gy, 85.1 Gy and 89.6 Gy, 62.3 Gy and 66.7 Gy respectively. Mean D90 also was significantly higher in MRI compared to CT imaging plans – 94,2% versus 79,4% of prescribed dose.

Conclusion: In spite that superiority of MRI compared to CT imaging based contouring and planning for HR CTV dose distribution has been already showed in previous studies we found that it also allows indirectly significantly decrease the dose to organs at risk during HDR brachytherapy for cervical cancer.

EP-1971

Result of IGBT for cervical cancer using ring applicator with 'Siriraj Ring Cap' extension

P. Dankulchai[1], Y. Chansilpa[1], J. Petsuksiri[1], L. Tuntipumiamorn[1], P. Nakkasair[1], C. Kakanaporn[1]
[1]*Faculty of Medicine Siriraj Hospital Mahidol University, Radiology, Bangkok, Thailand*

Purpose or Objective: To retrospectively assess treatment outcome of image guided brachytherapy (IGBT) with or without hybrid technique for cervical cancer using VariSourceTM titanium ring applicator with 'Siriraj Ring Cap' extension (as figure 1). In case of narrow vaginal opening, hybrid brachytherapy technique could be performed using this applicator with extension.
Figure 1: VariSourceTM titanium ring applicator with 'Siriraj Ring Cap' extension

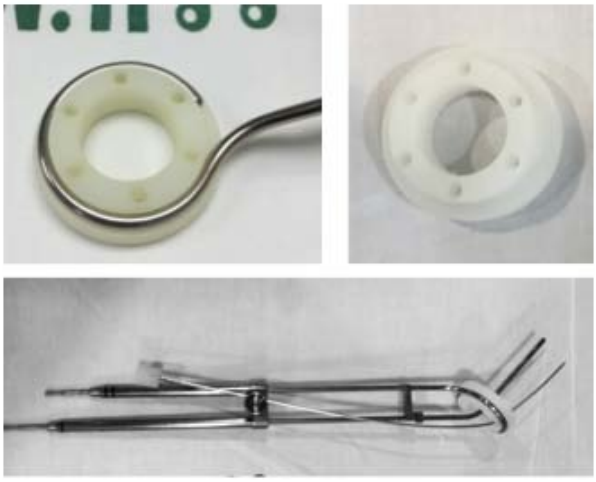

Material and Methods: Between January and December 2014, 29 patients with locally advanced cervical cancer were underwent combination external beam radiotherapy with or without concomitant chemotherapy and IGBT with or without hybrid technique using VariSourceTM ring applicator with 'Siriraj Ring Cap' extension (at least one fraction). 117 dosimetric planning and clinical outcome of treatment were evaluated.

Results: For high risk clinical target volume (HR CTV) the median was volume 37.4 cm3 (range; 15.3-76.1 cm3) and the median of D90 was 85.3Gy (range; 76.4-90.5Gy). The median of D2cc for bladder, rectum, sigmoid, and bowel loop were 84Gy (range; 68.3-89.7Gy), 66.1Gy (range; 56.8-76.3Gy), 65.6 (range; 49-77.1Gy), and 61.9Gy (range; 45.8-78.1Gy), respectively. 81.2% (95 of 117 plans) were performed using VariSourceTM ring applicator with 'Siriraj Ring Cap' extension, while mean of coverage of the HR CTV was 89.2% (range; 57-99%). 18.8% (22 of 117 plans) were applied using tandem with ovoids, and mean of coverage of the HR CTV was 79.9% (range; 53-96%). Median follow up was 10.6 months. The actuarial 1 year loco-regional recurrence free survival rate was 90.5% (95% confidence interval (CI); 67-98%), progression free survival rate was 85.7% (95% CI; 62-95%), and overall survival rate was 95.4% (95% CI; 71-99%). One patient had a grade 2 late rectal complication. No grade 3-5 late complications have been recorded so far.

Conclusion: IGBT with or without hybrid technique using VariSourceTM titanium ring applicator with 'Siriraj Ring Cap' extension is applicable for locally advanced cervical cancer resulting in an excellent local control rate and limited morbidity.

EP-1972

Application of adaptive brachytherapy in the treatment of cervical cancer in accelerated mode

O. Kravets[1], A.A. Fedyanina[1], O.V. Kozlov[1], M.A. Kuznetsov[1], A.V. Gavrilova[1], E.A. Romanova[1]
[1]N.N. Blokhin's Federal State Scientific Institution Russian Cancer Reasearch center, Radiosurgery department, Moscow, Russian Federation

Purpose or Objective: The effectiveness of radiation therapy in the management of cervical cancer of all stages is well established. Radiation therapy usually consists of a combination of external beam therapy and brachytherapy. Further exploration of new approaches and methodologies is a promising direction of development. Given the radiobiological aspects and an important economic factor, i.e. reduction of hospital stay. The aim of this study was to estimate the effectiveness of the treatment of cervical cancer patients using adaptive image-guided brachytherapy (IGBT) during split course.

Material and Methods: In the period from May 2014, 38 patients with primary cervical cancer were treated with combined radiotherapy using the new split-adaptive methodology for IGBT. We used conformal radiation techniques: BOX method, IMRT or RapidArc. Total dose on the pelvic area and regional metastases was 50 Gy. Further HDR IGBT brachytherapy was followed with dosimetry planning MRI - images. The treatment was on 1st and 2nd , 8th and 9th days, ring tandem applicators implantation under general anesthesia. Between the fractions 1 and 2 and 3 and 4, the patients were with applicator under the supervision of medical staff during the day. Monitoring planning was conducted according to MRI-studies; as a result treatment plan was composed for every 2 fractions. The position of the applicator in relation to the tumor and critical organs during the day doesn't change provided that the methodology is being correctly observed. Dose plans were optimized for maximal tumor dose (D90) and coverage (V100 and V80). The dose parameters in the target volume are the following: D 90 = 7.3 (5.9-9.1) Gy, V 100 = 91.5 (79.2-99.1) %, V 80 = 97.8 (90.5 -100). Of the patients it was T2bN0M0 – 7 patients, T3bN0M0 – 5, T2b-3bN1M0 – 18, T2b-3bN1M1 – 8.

Results: in the results the values of dose rates (D 2 cc / D 0,1 cc) to organs of risk (bladder, rectum and sigmoid) are the following: 3.7 (1.7-7) / 4.8 (2.2 -9.4) Gy; 3.1 (1.2-6) / 4.2 (1.4 - 8.3) and 3.9 (2.2-5.7) / 5.5 (3.5 -7.6) Gy. During follow-up time for 12 months no any acute or late toxicity of grade 2 were observed and not observed any difference in comparison with the fractionation scheme used previously. No one local recurrence were observed, regional recurrence in 2 (2 and 7 months), distant metastasis in 1 (12 months). The patients have undergone the treatment satisfactorily. The number of surgical implantations decreases from 4 to 2. According to preliminary data, local radiation reactions are not multiple.

Conclusion: The main advantage of this method is the dose delivery in a shorter period of time, which allows for a greater control of the tumor. This method allows to reduce the time of course of brachytherapy to 9 days. Evaluating the effectiveness of treatment shows good tolerance of this treatment with satisfactory results. This clinical study is currently ongoing.

EP-1973

MRI-guided brachytherapy and 3D/IMRT radiotherapy for cervical carcinoma. A prospective study

E. Villafranca Iturre[1], P. Navarrete Solano[1], A. Sola Galarza[1], J.C. Muruzábal[2], C. Sánchez[3], M. Rico[1], M. Errasti[1], M. Barrado[1], M. Campo[1], I. Visus[1]
[1]Hospital of Navarra, Radiation Oncology, Pamplona, Spain
[2]Hospital of Navarra, Gynecology, Pamplona, Spain
[3]Hospital of Navarra, Radiology, Pamplona, Spain

Purpose or Objective: To evaluate dosimetric and clinical findings of MRI-guided HDR brachytherapy (HDR-BQ) for cervical carcinoma.

Material and Methods: From 2008 to 2014: 50 patients. All patients had a CT, MRI and pelvic-paraaortic lymphadenectomy. Treatment: pelvic(+/-)para-aortic3D/IMRT radiotherapy(45Gy) and weekly cisplatin followed by HDR-BQ and pelvic node/ parametrial boost 60Gy. Two implants at week 6th and 7 th were done: 5 fractions of 6Gy and from 2011 4 fractions of 7Gy. MRI/TAC was done in each implant. There where defined: GTV, CTH-HR, CTV-IR; OAR: rectum, bladder and sigmoid.

Results: Patients: T1b2-T2a: 3p, T2b 36p, T3a: 2p; T3B 9p; N0: 31p, N1 19p.With a median follow up of 50.6 months(8.1 – 89.2 months), 5 patients had local recurrence, 6 lymph node recurrence, 6 distant metastasis and 36 without recurrence. Local control at 5 years was 88%; Ib2-IIB: 93%, III: 70%. (p:0.07). Lymph node Regional Disease Free Survival(RDFS) 5y was 88%; IB2-IIB: 89%, III: 83% (p:ns); for pN0: 94%; pN+ iliac-paraaortic: 77% (p: 0.08). Metastasis Free Survival 5y was 78%; IIBN0: 78%, IIBN1: 89%, III: 63%. Overall

survival(OS) at 3 years was 82% and at 5 years was 63%; IB2-IIB 5yr: 70%; III 5yr: 27% (p: 0.01); For pN0 5yrs 74%; pN+ iliac-paraortic 5yr: 45% (p: 0.03).
Dosimetric parameters: D90<6-7Gy(prescription dose) in 5p before 2011(since then interstitial implants were associated in 47%). The Local RFS: D90< 6Gy 87%, D90> 6Gy: 90% (p:ns); OS: D90< 6Gy 58%, D90> 6Gy: 67% (p:ns). D2cc-Sigma: 1.7-6.2 Gy (md 3.8 Gy); D2cc-rectum: 2-6.1 (md 4.2); D2cc-bladder 3.4-5.7 (md5.25).

Conclusion: Use of intersticial HDR-BQ guided by RM increased CTV-HR dose and local control , like EMBRACE results. Nodal boost improves RDFS and perhaps OS.

EP-1974

Application of the self-made applicator in brachytherapy for recurrent cervical cancer at vaginal

G. Cheng[1], Z. Zhao[1], M. He[1], D. Shi[1]
[1]*China-Japan Union Hospital of Jilin University, Department of Radiation Oncology, Changchun, China*

Purpose or Objective: To elaborate the application of self-made applicator which invented by our department (Patent No: 201420583680.X) in brachytherapy for recurrent cervical cancer at vaginal residue. This study especially pays attention to the doses evaluation of GTV and the OARs in brachytherapy by this technical.

Material and Methods: 14 patients from 2013-2014 in our hospital who suffered from recurrent cervical cancer at vaginal residue in 0.5-3.5 years after radical hysterectomy and external beam radiotherapy (45 Gy/25 fractions) ±chemotherapy ±brachytherapy were treated with MRI based and ultrasound guided brachytherapy using the self-made applicator. The self-made applicator was made of silica balls in matrix distribution connecting with a hole in front and behind it, making it formed into a straight line. The diameter of silica ball is 1 cm, the aperture of the hole is 1.5 mm. Therefore this self-made applicator could provide with the needle inserting smoothly and tidy and the depth of the needle can be adjusted. Moreover, this applicator can be used by superposition of multilayer, so it could be easily adapted to any shape. The prescribed dose of brachytherapy was 7 Gy×3-6 fractions, one week apart was planned. The GTV included the tumor, the CTV comprised the GTV with a 10 mm circumferential margin and OARs were delineated. And then we recorded the GTV D90, D100 and D2cc of rectum, small intestines, bladder and sigmoid colon under the self-made applicator.

Results: After plenty years of using the conventional applicators in brachytherapy, we found the radical hysterectomy cause the vaginal cuff end stenosis, the top of the conventional applicator, such as the Utrecht intertitial applicator cannot get close to the cancer region well which tumor invaded towards pelvic, so it was unable to achieve a high dose to the tumor, or it may induce an excess dose to normal tissues. In this research, we found the self-made applicator showed a high GTV dose and an acceptable OARs dose. Specifically, the GTV D90 and D100 for using self-made applicator were 724±64 cGy and 436±39 cGy, and the average D2cc for rectum, sigmoid colon and bladder was 370±21, 265±16 and 423±44 cGy, the total dose when transformed to EQD2 models was under the constraints.

Conclusion: The self-made applicator show excellent dose parameters on dose coverage and sparing exposure to OARs, which was more beneficial to the recurrent cervical cancer at vaginal residue invaded towards pelvic.

EP-1975

18F[FDG]PET guided brachytherapy for carcinoma of the uterine cervix

S. Meregalli[1], G. Gardani[1], S. Brenna[1]
[1]*Ospedale S. Gerardo, Radiotheray, Monza, Italy*

Purpose or Objective: Concomitant chemo-radiation and intracavitary brachytherapy (BT) is the standard treatment for locally advanced cervical carcinoma. In an our previous experience we reported the feasibility of [18F]FDG-PET in the BT treatment planning as functional imaging technique able to visualize neoplastic tissue. The purpose of this analysis was to evaluate, after an adequate follow-up, the site of recurrence and,in case of local relapse , if it was PET positive during BT. Survival and the late toxicity were also analysed.

Material and Methods: From June 2007 to May 2010, thirteen women with locally advanced cervical carcinoma were enrolled into the study. All patients underwent external beam radiation therapy (EBRT) to whole pelvis (box technique to a total dose of 50.4 Gy) with weekly concomitant cisplatinum chemotherapy. HDR BT was performed weekly (5 Gy per fraction; 5 to 6 fractions). All BT fractions were planned by CT scan and, in the first and in the fourth fraction, FDG-PET/CT was also employed. Local control rate, progression free survival, overall survival and treatment related toxicities under RTOG criteria were evaluated

Results: At the median follow-up of 61 months, the estimated 5-year progression-free survival (PFS) and the 5-year overall survival (OS) were 56% and 70% respectively. The 5-year local control rate was 84.6%. Only one patient had a local relapse corresponding to a PET positive area in BT guided planning. No G3-4 acute or late gastrointestinal or genitourinary toxicity has been recorded .

Conclusion: In our experience, PET in BT planning of the cervical carcinoma gives some added useful information. The main goal of our analysis remains to define the site of possible recurrence: the recognition of a local relapse in PET positive area may suggest the opportunity of dose escalation

EP-1976

Concomitant radio-chemotherapy and brachytherapy for advanced cervical cancer: outcomes and toxicity

L. Pollara[1], F. Cuccia[1], V. Figlia[1], A. Palmeri[1], M. Gueci[1], N. Luca[1], D. Aiello[1], G. Evangelista[2], F. Sciumè[2]
[1]*Scuola di specializzazione di Radioterapia-Università degli studi di Palermo, ARNAS Civico Palermo, Palermo, Italy*
[2]*Ospedale ARNAS Civico, U.O. Radioterapia Oncologica, Palermo, Italy*

Purpose or Objective: To evaluate clinical outcomes and acute/late toxicities in patients with locally advanced cervical cancer treated with chemotherapy (CT) and external beam radiation therapy (EBRT), followed by high-dose rate brachytherapy (HDR-BRT) delivered with the Fletcher-Williamson tandem and ovoid applicator

Material and Methods: we evaluated 40 patients, median age 57 years (range 40-83), treated between January 2007 and October 2014. According to FIGO classification, 10% were stage IB, 7,5% IIA, 45% IIB, 5% IIIA, 27,5% IIIB, 5% IV. All patients underwent pelvic +/- paraaortic EBRT (10/40 patients); following the GEC-ESTRO recommendations, fractionation scheme for pelvic irradiation was 45-50.4 Gy in 25-28 daily fractions (1.8 Gy/fr). The addition of a parametrial boost (10 Gy in 5 daily fractions) was performed in 10/40 patients (25 %). BRT with Fletcher applicator was performed in all patients after EBRT, with the fractionation scheme 22,5 Gy in 5 fractions (twice a day with 6 hours inter-fraction interval). Concomitant CT was administrated in all patients, neoadjuvant CT was administrated in 15%. Treatment related toxicity was evaluated weekly during therapy and at each follow-up control, using RTOG/EORTC Radiation Morbidity Criteria. Response was investigated with periodical cervical cytology and CT scans; every treatment was evaluated in terms of BED10 and EQD2, with a median BED10 of 90.43 Gy (range 75.5-104.1) and median EQD2 of 75.33 Gy (range 86.7-62.9).

Results: With a median follow-up of 30 months (range 12-87), we observed acute/late genitourinary and gastrointestinal toxicity ≥ grade 2 in 10 % of patients, including one G4 GI acute toxicity (diarrhea requiring parenteral support)

occurred during concomitant EBRT-CT and resolved after a week of medical therapy. At 12 months from the end of treatment, response rate was 87.5% (35/40); we recorded 4 persistent disease and 1 locoregional recurrence (after 6 months), occurred in all patients with stage III. After 12 months of follow-up,we reported disease progression (1 central and 1 systemic) in 2 patients (5%), respectively at 17 and 48 months from the end of radiation therapy. Patient showing central relapse underwent radical hysterectomy and patient with systemic disease started chemotherapy.

Conclusion: In our experience, the association of concomitant EBRT-CT and HDR-BRT(Fletcher applicator) represents a well tolerated treatment for patients with advanced cervical cancer, with good results in terms of acute and late toxicity and local control

EP-1977

The importance of immobilization of gynecological applicators in high dose rate brachytherapy

S. Pella[1], H. Mikko[2], D. Nicolae[3], C. Casey[4], C. Shereen[4], P. Janeil[4]

[1]*South Florida Radiation Oncology- Florida Atlantic University & Advanced Radiation Physics Inc., Medical Physics, Boca Raton, USA*

[2]*University of Toronto, Medical Physics, Toronto, Canada*

[3]*Florida AtlanticUniversity, Physics, Boca Raton, USA*

[4]*Florida Atlantic University, Physics, Boca Raton, USA*

Purpose or Objective: To investigate the need for the implementation and development of immobilization and localization devices and other improvements in safety measures in addition to those currently in use in current HDR treatment protocols involving gynecological applicators.

Material and Methods: 55 treatment plans from 27 cervical cancer patients treated with three to 5 intra-cavity cylinder insertions were used. We performed a retrospective study of a dosimetric evaluation due to a possible minor displacement of the cylinder after scanning to the treatment delivery time. The 55 plans that were dosimetrically analyzed post treatment involved treatments for 27 different patients. 22 patients had a hysterectomy with bilateral salpingo-oophorectomy . In 16 of these twenty two patients the procedure had an abdominal hysterectomy bilateral salpingo-oophorectomy).Three of the patients had hysterectomies only. The vaginal cylinder applicators which were placed within the patients by a radiation oncologist for administering the treatments included the Capri, Miami, and multi-lumen catheres applicator.

Results: For the 55 patients whose point dose data were gathered, dose variation at the hottest spot due to a simulated 1mm displacement in the superior inferior direction calculated by normalizing to the average of the endpoints was found to have a minimum value of 0.02% and a maximum value of 12.66% with an average value of 1.43% and a standard deviation of 2.02%. Dose variation at the hottest spot due to a simulated 1mm displacement in the medial lateral direction calculated by normalizing to the average of the endpoints was found to have a minimum value of 12.32% and a maximum value of 22.71% with an average value of 16.96% and a standard deviation of 2.76%. The measurement of dose variation due to a displacement of one degree of rotation along the central axis of the applicator was found to have a minimum value of 0.00% and a maximum value of 2.76% with an average value of 0.63% and a standard deviation of 0.62%.The standard deviation and the mean nearly coincide. The measurement of dose variation due to a displacement of five degrees of rotation along the central axis of the applicator was found to have a minimum value of 0.06% and a maximum value of 13.71% with an average value of 2.15% and a standard deviation of 3.00%.

Conclusion: The point dose variation due to hypothetical 1 mm medial lateral displacement of a vaginal cylinder applicator make a difference in terms of Grade 1 rectal toxicity as defined by Common Terminology Criteria for Adverse Events v 4.0 in some patients receiving HDR VCBT alone or shortly after EBRT. The point dose variation due to hypothetical 1 mm medial lateral displacement of a vaginal cylinder applicator according to this analysis did reach a crudely obtained cutoff value for RTOG grade greater than or equal to 2 late rectal morbidity for any of the patients receiving HDR VCBT alone or shortly after EBRT.

EP-1978

Individualized approach to brachytherapy in cervical cancer patient: a case report study.

B.H. Zobec Logar[1], R. Hudej[1]

[1]*Institute of Oncology Ljubljana, Radiotherapy, Ljubljana, Slovenia*

Purpose or Objective: In some cervical cancer patients with extensive parametrial involvement, not all of the tumor can be sufficiently covered with MRI-based image guided brachytherapy using a standard intracavitary/interstitial applicator. An approach with individually designed applicator with oblique needles offers a possibility of better tumor dose coverage in these patients.In this study we tested the feasibility of the 3D printing for the individualized brachytherapy applicator add-on.

Material and Methods: A patient in this case report study had extensive parametrial involvement to the pelvic wall. In order to improve the tumor dose coverage we decided to use additional oblique needles for the second application. A preplan for the second application was created based on the dosimetry information from the first application. The information on the optimal location of the oblique needles in the preplan was used to design an individualized interstitial template cap for the ring applicator, which was manufactured with a 3D printing technique. The whole procedure of the cap design and manufacture was performed in 5 days.

Results: The HR-CTV coverage at the time of the first application (Figure 1a) was suboptimal (D90=69%, D100=35%, V100=77%).

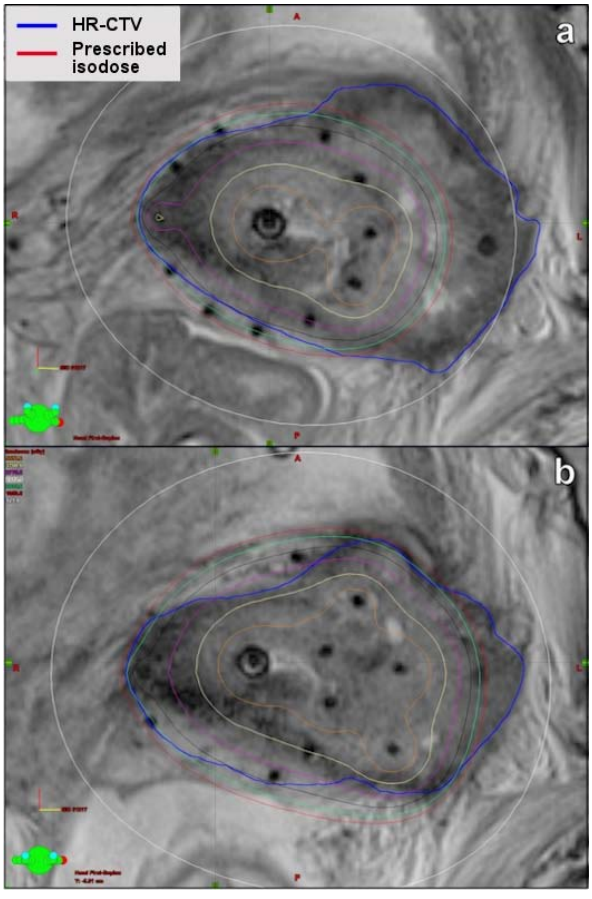

The volume of the HR-CTV not covered with the prescribed isodose was 19.8 ccm. Oblique needles applied at the time of the second application contributed significantly to a better dose coverage of HR-CTV (D90=109%, D100=55%, V100=93%). The part of the volume not sufficiently covered with the prescribed dose in the first application was boosted using only oblique needles at the end of the second treatment until the dose restrictions for the OAR were reached (Figure 1b). DVH parameters for HR-CTV of the second application were improved accordingly: D90=119%, D100=61%, V100=96%. The volume of the HR-CTV not covered with the prescribed isodose was reduced to 2.4 ccm. The position on the ring, oblique angle and the insertion depth of the oblique needles in the second application were measured on the MR images and compared with the pre-plan. The average differences were relatively small (position on the ring: 10°, oblique angle: 8°, insertion depth: 4 mm).

Conclusion: Individualized approach to cervical cancer patients with extensive parametrial involvement at the time of brachytherapy can contribute significantly to an improved dose coverage of the HR-CTV. An individualized 3D printed interstitial cap for the ring applicator with oblique needles is an efficient option for these patients.

EP-1979

Adyuvant vaginal brachytherapy whitout external beam radiotherapy for endometrial cancer

P. Vargas Arrabal[1], R. Del Moral[1], I. Tovar[1], M. Zurita[1], R. Guerrero[1], I. Linares[1], J. Expósito[1], C. Prieto[1], S. Rodríguez[1], A. Ruiz[1]

[1]*Hospital Universitario Virgen de las Nieves, Radiation Oncology, Granada, Spain*

Purpose or Objective: The aim is to report the results obtained in patients diagnosed of endometrial carcinoma stage IA-IIA treated with surgery followed by adyuvant brachytherapy at our institution.

Material and Methods: From 2006 until 2013, 116 patients with endometrial carcinoma stage IA-IIA have been treated with surgery and exclusive vaginal brachytherapy. Median age of the series was 62 years. Total hysterectomy, double anexectomy, pelvic lymphadenectomy and peritoneal washing was made in 61,4 %. The majority of the pathologycal FIGO stages were IB (77,2 %). Exclusive brachytherapy was performed using vaginal cylinders with 3 cm of diameter (50,9 %). The reference isodosis covering the proximal 3 cm of the vagina (96,4 %). The dose was specified at 5 mm distant from the surface of the cylinder. Dose schedule with high dose rate brachytherapy was 21 Gy in 3 fractions. The median of dose equivalent received in the rectum was 31,8 Gy and in bladder 38 Gy.

Results: At the moment of this analysis there are 4 relapses: 2 of them live with disease, and 2 death for tumor; 110 cases live without disease (94,82 %), and 2 cases death for another cause. With median follow-up of 26 months, free disease survival was 90.2% and 2 years overall survival was 88.3%. No toxicity was reported in the 52,6%, and when it was present the most frequent was cystitis (12.3%).

Conclusion: The exclusive vaginal brachytherapy is effective in ensuring vaginal control, with few toxic effects. So, this schedule should be an adyuvant treatment for these patients.

EP-1980

Lower dose per fraction brachytherapy for patients with stage 1 endometrial cancer following surgery

J. Kim[1], K.J. Lee[1], K. Park[1], J. Lee[1], Y.J. Kim[1], W. Jung[1], S.C. Kim[2], H.S. Moon[2], W. Ju[2], Y.H. Kim[2]

[1]*Ewha Womans University, Radiation Oncology, Seoul, Korea Republic of*

[2]*Ewha Womans University, Gynecology and Obstetrics, Seoul, Korea Republic of*

Purpose or Objective: The purpose of this study is to analyze the efficacy and complication rates of postoperative high dose rate (HDR) vaginal brachytherapy(VBT) to determine whether VBT with lower dose per fraction(3-4 Gy/fraction) is as effective as pelvic external beam radiotherapy (EBRT) for patients with stage 1 endometrial carcinoma

Material and Methods: From March 2000 to April 2014, 43 patients with FIGO stage I endometrial cancer underwent adjuvant radiotherapy following surgery. Twenty five patients received postoperative HDR VBT alone, while 18 patients received postoperative EBRT to the whole pelvis. Among these patients, three patients were treated with EBRT plus VBT. The median treatment dose of EBRT was 50.0 Gy (45.0-50.4 Gy) and HDR VBT dose was five to six fractions of 3 or 4 Gy to a total dose of 15-24 Gy. The tumor dose was prescribed at a depth of 5mm from the cylinder surface and delivered twice per week.

Results: The median follow up period of all patients was 54.4 (range 9-142) months. Five year disease free survivals (DFS) and overall survivals (OS) for all patients were 91.5% and 91.2%, respectively. Five year DFS of EBRT and brachytherapy was 87.2% and 96.0%, respectively (p=0.46), and five year OS of EBRT and brachytherapy was 86.9% and 95.7%, respectively (p=0.43). There were no differences in 5 year DFS or OS according to radiation treatment group. There were no locoregional recurrences for all patients. Two patients who received EBRT and one patient who received brachytherapy alone developed distant metastatic disease. There were one patient who had grade 3 gastrointestinal complication and one patient who had pelvic bone insufficiency fracture. Two patients who had severe complication were treated with EBRT.

Conclusion: HDR VBT with lower dose per fraction alone showed high DFS and OS with no severe adverse effect. HDR VBT with small fraction size may be adequate for early stage endometrial cancer following surgery.

EP-1981

Comparing MRI vs CT based applicator reconstruction and plng techniques for adaptive cervix cancer BT

F. Cheung[1], A. Chang[2], T. Wong[1], F. Choi[2], M. Chan[2], I. Soong[2], A. Law[2], M. Lee[1], R. Yeung[2]

[1]*Pamela Youde Nethersole Eastern Hospital, Department of Medical Physics, Hong Kong, Hong Kong SAR China*

[2]*Pamela Youde Nethersole Eastern Hospital, Department of Clinical Oncology, Hong Kong, Hong Kong SAR China*

Purpose or Objective: Controversies still exist in the method of treatment planning and applicator reconstruction in adaptive cervix brachytherapy. This study aims to compare any difference between MRI and CT applicator reconstruction and the treatment planning process at our institution.

Material and Methods: Our analysis included 15 patients from our institution with stage IB2-IVA cervical cancers between January to October 2015, all patients treated with chemoradiation and brachytherapy. We followed the Vienna schedule for HDR brachytherapy at week 6 and 7, with 2 weekly insertions with 2 consecutive fractions per week. MRI- and CT- based treatment planning and applicator reconstruction were done for every patient. Contours and dosimetry of tumor target (HRCTV D_{90}) and organs at risk (D_{2cc} bladder, rectum, sigmoid and small bowel) were compared. Applicator reconstruction techniques, possible challenges and errors between the 2 imaging modalities were analysed.

Results: Both CT- and MR- based applicator reconstruction uncertainties were less than 1 mm for either tandem-and-ovoids (T&O) or tandem-and-ring (T&R) applicators. Compared with T&O applicators, use of rigid T&R applicators gave more accurate applicator reconstruction. When an applicator library was used, the T&O reconstruction uncertainties always occurred in posterior-anterior direction while T&R reconstruction uncertainties were found when it rotated. Applicator holes for interstitial needles could provide additional markers to define correct applicator rotation on MRI. The D_{2cc} rectum value was the most sensitive

to the T&O reconstruction. Without availability of MRI markers for needle visualization, manual MR-based needle reconstruction could be challenging especially in tissues of similar signal intensities. Measurement of remaining interstitial needle length outside patient could open up a potential solution path.

Conclusion: Despite minor distortions around centre of the magnet, MRI distortions do not play a major role in applicator reconstruction uncertainties. Both CT- and MR-based applicator reconstruction are feasible when used with applicator library, providing accurate source pathway reconstruction. Applicator holes for interstitial needles and physical measurement of needle outside patient could provide valuable information to improve the reconstruction accuracy.

Electronic Poster: Brachytherapy track: Head and neck

EP-1982
Adjuvant brachytherapy of the lip cancer after surgical resection

A. Chyrek[1], G. Bielęda[1], A. Chichel'[1]
[1]*Greater Poland Cancer Centre, Brachytherapy Dep., Poznan, Poland*

Purpose or Objective: The aim of this work is to evaluate outcomes after adjuvant brachytherapy of the lip cancer after surgical resection with close (<5mm) or positive margins.

Material and Methods: A total of 20 patients (3 women and 17 men in median age of 65,5) diagnosed between 2010 ad 2014 with clinical T1 – T2 N0 lip carcinoma were treated primarly by surgical tumor resection with or without lymphadenectomy. After histopathological result (40% positive, 60% close margins) they were qualified for adjuvant brachytherapy. At the discretion of the attending physician 25% of patients were treated by high dose rate (HDR) and 75% by pulse dose rate (PDR) brachytherapy. The mean biologically effective dose (BED) given to the clinical target volume were 71,285 Gy (range 62,6 – 75 Gy). The mean follow up (counted from the end of BT course to the last control visit or recurrence) were 24 months. For statistical calculations we used the Kaplan-Meier method and the U Mann-Whitney test.

Results: Sole patient in the group had nodal reccurence 6 months after treatment. The rest of the patients had no evidence of recurrence during the follow up. Estimated 4-year disease-free survival rate was 95%. The acute skin toxicity according to RTOG scale was 65%, 30% and 5% for grade I, II, and III respectively; the late skin toxicity was 25%, 5% and 5% for grade I, II, and IV respecively. We also found a statistically significant correlation between the higher BED and appearance of acute toxicity greater than I grade (p=0,014) and occurrence of any late toxicity (p=0,047).

Conclusion: Adjuvant brachytherapy in the treatment of the T1-T2 lip tumors achieves a long loco-regional control with relatively low toxicity and it may be taken into consideration for the adjuvant therapy of the lip cancer after surgical resection with close (<5mm) or positive margins. Such regimen allows to prevent reoperations along with large reconstructive surgery.

EP-1983
Intensity modulated perioperative interstitial HDR brachytherapy for recurrent neck metastases

T. Soror[1,2], G. Kovács[1], I.U. Teudt[3], M. Ritter[4], C. Melchert[1], J.E. Meyer[5], B. Wollenberg[4]
[1]*Interdesciplinary Brachytherapy Unit, University of Lübeck, Lübeck, Germany*
[2]*National Cancer Institute- Cairo University, Dept. of Radiation Oncology, Cairo, Egypt*
[3]*Asklepios Klikik Altona, Dept. of Otolaryngology- Head and Neck Surgery, Hamburg, Germany*
[4]*University of Lübeck, Dept. of Otolaryngology- Head and Neck Surgery, Lübeck, Germany*
[5]*Asklepios Klikik St. Georg, Dept. of Otolaryngology- Head-Neck and Plastic Surgery, Hamburg, Germany*

Purpose or Objective: Patients with head and neck cancers can develop recurrences in previously treated areas, which usually involve the neighbor carotid artery. In the majority of these patients a complete surgical resection is not possible, R1/R2 resections are frequent. We proved the feasibility and long-term outcome of perioperative intensity modulated brachytherapy (IMBT) as a salvage treatment option for advanced neck metastases in combination of carotid artery preservation.

Material and Methods: From 2006 to 2014, nine patients at the University Hospital of Schleswig-Holstein Campus Luebeck had received an interdisciplinary salvage treatment with debulking surgery and perioperative HDR-IMBT for advanced recurrent neck metastases. Median age was 53 years, range: 38- 66, the mean follow-up was 66 months. Surgery was performed with primary wound closure in seven patients, while myocutaneus flap was used in two patients. Active phase of IMBT started 4-12 days following surgery. The prescription dose was 2.5Gy twice daily (average total dose: 27Gy, range: 15-30Gy). Dose non-homogeneity ratio (DNR) never exceeded 0.42. We used the manual dose-volume optimization method and planned biologicaly correct hot/cold spot areas within the dose distribution. The reference isodose was defined within a maximum of 10 mm lateral distance from the interstitial tube and the Dmax was defined in 400% on the catheter surface.

Results: For initial treatments, all patients received previous surgery; eight patients received also external beam radiation with an average dose of 64Gy. Two and five year overall survival estimates were 78% and 67% respectively. The median survival rate was 65 months. Only two patients had a second neck recurrence after 62 and 65 months. Early toxicities (grade I-II) recorded in four patients and were limited to local edema and skin infection, no treatment related grade 3 or 4 toxicities recorded.

Conclusion: Salvage debulking surgery combined with perioperative HDR-IMBT seems to be feasible and safe treatment option for selected recurrent neck metastases with minimal treatment related toxicities.

EP-1984
Interstitial brachytherapy for the isolated lymph node metastasis from different solid cancers

M. He[1], G. Cheng[1], H. Zhao[1], Z. Zhao[1]
[1]*China-Japan Union Hospital of Jilin University, Department of Radiation Oncology, Changchun, China*

Purpose or Objective: To assess the feasibility, safety and clinical outcome of MRI based and ultrasound guided high-dose-rate interstitial brachytherapy technical in isolated lymph node metastases from different solid cancers.

Material and Methods: From January 2013 to May 2014, 11 patients (six males and four females) with isolated nodal metastases were treated with MRI based and ultrasound guided high-dose-rate brachytherapy. All patients had previously been treated with radical radiotherapy or chemoradiation with or without surgery. Seven lymph node metastases were cervical, three metastases were at the supraclaviculares, one metastasis located at a left inguinal nodal. Pathologically, six metastases were squamous carcinoma, three were small cell cancer and two were adeno carcinoma. The mean lesion diameter was 38.5 mm (range 21.0- 78.0 mm). The brachytherapy were achieved by inserting the titanium needle to the target, avoiding vascular and organ injury under the ultrasound guidance, following by MRI scanning and delineating the targets. The metastases were treated by single-fraction irradiation using the afterloading technique using an Iridium-192 radiation source. The prescribed salvage dose of brachytherapy was 5

Gy/fraction, twice- daily to a total dose of 10-20 Gy (one week apart) according to the dose of the external beam radiotherapy. The total dose ranged from 76-84 Gy when transformed to EQD2 models. Patients were followed up by contrast-enhanced CT or MRI 4 weeks and then every 3 months after the end of treatment. The primary end point was local tumor control. Secondary end points of the adverse events, distant metastases and progression-free survival were also included.

Results: The first follow-up examination after 4 weeks revealed 10/11 coverage of all nodal metastases treated. There was no peri-interventional mortality or major complications. The mean follow-up period was 12.2 months (range 7–15 months). After a median follow up of three months, the median local tumor control was 90%. 2 out of 10 patients (20%) showed local tumor progression 6 and 8 months after brachytherapy. 2 patients (20%) who died of distant metastasis. The grade III-IV complications occurred in 1 patient (10%). The mean progression-free interval was 13 months (range 6–16 months).

Conclusion: We consider that the interstitial brachytherapy technical will provide a relative high and accurate dose irradiation to bulky lymph node metastasis for improving the local tumor control in patients with different solid cancers.

Electronic Poster: Brachytherapy track: Physics

EP-1985
Proposal to improve commissioning of HDR brachytherapy with results from the first 2 SagiNova units

A.L. Palmer[1], O. Hayman[2], A. Toussaint[3], O. Sauer[3]
[1]*Portsmouth Hospitals NHS Trust & University of Surrey, Medical Physics Department, Portsmouth, United Kingdom*
[2]*Portsmouth Hospitals NHS Trust, Medical Physics Department, Portsmouth, United Kingdom*
[3]*University of Würzburg, Department of Radiation Oncology, Würzburg, Germany*

Purpose or Objective: Commissioning of HDR brachytherapy treatment equipment is essential to avoid errors and assure quality. However, it is estimated that worldwide, less than one-quarter of centres undertake robust local commissioning tests at installation [1], important checks may be omitted [2], or systematic errors may remain [3]. The purpose of this work is to: (i) reinforce the need for local HDR commissioning and propose a list of recommended tests; (ii) publish results of the commissioning for a new-to-market HDR brachytherapy system from two centres.

Material and Methods: A literature review was conducted on existing guidance for HDR system commissioning, HDR treatment errors and known factors affecting sub-optimal quality. The case for robust local commissioning of HDR equipment was assessed in terms of mitigating potential errors and improving quality of treatment delivery. A schedule of required commissioning tests was established and implemented at two centres, in England and Germany, for the commissioning of a new HDR brachytherapy treatment system, SagiNova (Eckert & Ziegler Bebig GmbH) with Co-60 sources.

Results: Evidence was found that errors do occur [4], particularly in the absence of robust commissioning and QC. There is little contemporary guidance for commissioning of HDR brachytherapy treatment equipment, which is required to build on the QC guidance in ESTRO Booklet No. 8 from 2004. The table provides our proposal for efficient, robust, and easily implemented commissioning tests. For the SagiNova system, results from the two centres showed satisfactory performance in all tests. The mean error for source dwell positions in straight catheters was 0.5 mm (±0.5 mm k=2) and in clinical treatment applicators was 0.6 mm (±1.0 mm k=2) compared to TPS planned positions. The ‘end to end’ system check with IPEM ‘BRAD’ system [5] had prescription point <0.4% (±2.5% k=2) and 97% gamma pass rate (3%, 2mm) compared to TPS calculations. By comparing results between centres a quality improvement was identified and implemented comprising an update of the dwell-position database at one centre.

Minimum proposed HDR commissioning tests
• Electrical and mechanical safety
• Radiation shielding (treatment unit and environment)
• Equipment safety interlocks (hardware and software)
• Manufacturer acceptance test schedule
• Source dwell positions in straight catheters (QC check system e.g. ruler, video camera, and autoradiographs)
• Source dwell positions in all clinical treatment applicators (autoradiograph dwells with radiograph applicators)
• Dwell times (accuracy, linearity, correction for transit dose)
• Transit times and transit dose (to-, from-, inter-dwell)
• Source strength (certificate, measurement, TPS, treatment unit)
• Decay correction (TPS and treatment unit)
• TPS applicator reconstruction (accuracy, consistency with physical applicators, validation of source path)
• TPS dose calculation (source data, point doses, isodose, DVH, independent dose calculation system)
• ‘End to end’ system check (image applicators in phantom, reconstruct, plan, deliver, measure dose)
• Additional functionality checks (in vivo dosimetry, TPS functions, image fusion)

Conclusion: It is not sufficient to rely on type-testing by manufacturers and instead local commissioning must be implemented to assure quality and mitigate the risk of treatment errors in HDR brachytherapy. Suitable tests are not always performed and a schedule of minimum commissioning tests has been proposed. The first two installations of the new SagiNova HDR system demonstrated clinically acceptable results. An improvement of the source dwell database was identified, confirming the value of interdepartmental checks and robust commissioning.

[1] Personal communication with HDR manufacturer,
[2] Nisbet et al Radiother Oncol 106(sup 2):2013,
[3] Palmer et al Br J Radiol 87(1041):2014,
[4] ASAHI SHIMBUN 2014, AJ201312260063
[5] Palmer et al Radiother Oncol 114(2):2015

EP-1986
New design of brachytherapy water phantom for absolute dosimetry

V. Stserbakov[1]
[1]*North-Estonian Regional Hospital Cancer Center Radiotherapy, Department of Radiotherapy and Oncology, Tallinn, Estonia*

Purpose or Objective: To simplify technical design of brachytherapy water phantom for performing absolute dosimetry using standard instruments and equipment available in radiotherapy department. To perform absolute measurements for source-to-ionization chamber distance ~ 4 cm.

Material and Methods: CNMC WP-380 water tank used for locating ionization chamber and the holder of the radioactive source. To minimize dimensional correction factors for ionization chamber it was taken 0,125 cm3 PTW 31010 ionization chamber. For reducing uncertainty of the source position inside mould probe we used “curved catheter” method in the design of the catheter holder to make an effect of “pressing down” the end part of cable to lower wall of the probe. Holder designed in this way that amount of other than water surrounding source material was maximally reduced. Source-to-ionization chamber distance was set by

using "head pin" device. Swinging of the pin like a swinging of the pendulum was used for identifying the contact of pin with ionization chamber surface. It helps to avoid specific challenges of other technical decisions for source-to-ionization chamber distance setting. For pin swinging the water tank should be mounted on to wheeled stand. Final mechanical uncertainty for distance we estimate as ±0.15 mm, which correspond to the inaccuracy in dose: ±0.8 %. GammaMed Plus remote afterloader with source Ir-192 HDR (diam. 0.9 mm) was used. Varian BrachyVision V10(TG-43) treatment planning system (TPS) was used for comparison.

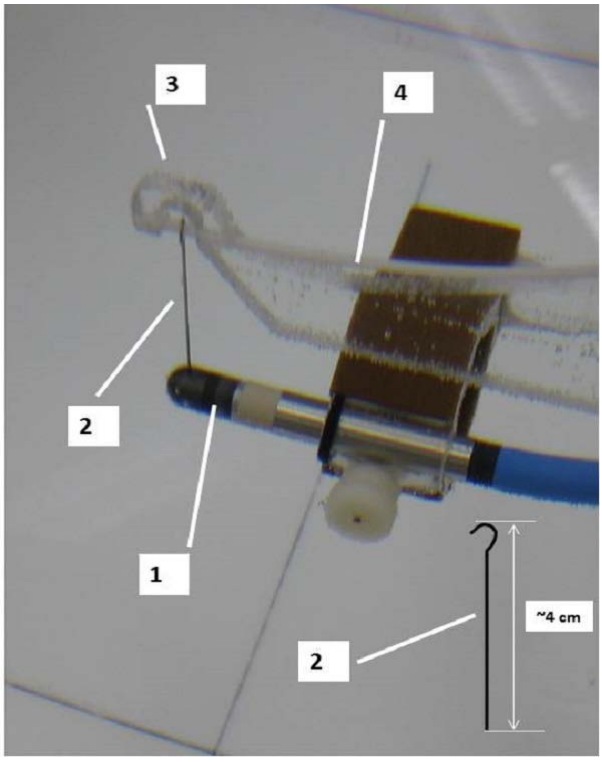

Figure: 1 – Ionization chamber; 2 - "Head pin" positioning device; 3 –Holder; 4 – Mould probe.

Results: Ionization chamber calibration factor ND,w =3.042·108 Gy/C. Beam quality factor for Ir-192 kQ =0.994 was found by interpolation. Decay factor is 1.76. Reading: 787 pC/min. Correction kT,P =1.022. Result for dose rate: 0.428 Gy/min. Source-to-chamber distance is 42.02 mm (summation of: 39.54 mm - positioning device length; 0.05 mm – device correction; 3.43 mm - chamber radius; -1.0 mm source-to-catheter upper surface distance; 0.05 mm - chamber dimentional correction). At the source-chamber distance 42.02 mm the TPS gives dose rate 0.434 Gy/min (or difference with measurements 1.4%). Taking into account absolute calibration of the source activity correction (-1%) by well-chamber, final difference reduces to 0.4%.

Conclusion: Proposed simple design of radiation source holder with ionization chamber positioning device demonstrated agreement (within 1%) measured-to-TPS values for dose rate at the distance ~ 4 cm.

EP-1987

Feasibility study of patient specific QA system for HDR brachytherapy in cervical cancer

B. Lee[1], H. Kim[1], J. Sim[2], S. Ahn[1], J. Kim[1], Y. Han[1], S. Huh[1], D. Kim[3], M. Yoon[2]

[1]Samsung Medical Center, Department of Radiation Oncology, SeouL, Korea Republic of

[2]Korea University, Department of Bio-convergence Engineering, Seoul, Korea Republic of

[3]Kyung Hee University Hospital at Gangdong, Department of Radiation Oncology, Seoul, Korea Republic of

Purpose or Objective: This study was conducted for the purpose of establishing a quality assurance (QA) system for brachytherapy that can ensure patient-specific QA by enhancing dosimetric accuracy for patient therapy plan. The patient-specific QA is designed to measure point absorbed dose and 2D dose distribution for patient therapy plan

Material and Methods: We fabricated a solid phantom that allowed for the insertion of an applicator for patient-specific QA and used an ion chamber and a film as measuring devices. The patient treatment plan were exported to the QA dose calculation software, which calculated the time weight of dwell position stored in the plan DICOM(Digital Imaging and Communications in Medicine) file to obtain an overall beam quality correction factor and apply this correction to dose calculations. Experiments were conducted after importing the patient treatment planning source data for the fabricated phantom and inserting the applicator, ion chamber, and film into the phantom. On completion of dose delivery, the doses to the ion chamber and film were checked against the corresponding treatment plan to evaluate the dosimetric accuracy. For experimental purposes, five treatment plans were randomly selected.

Results: The beam quality correction factors for ovoid and tandem were found to be 1.15 and 1.10–1.12, respectively. The beam quality correction factor in tandem fluctuated by approximately 2%, depending on changes in the dwell position. Doses measured using the ion chamber showed differences ranging from -2.4% to 0.6%, as compared to the planned doses. As for the film, the passing rate was 90% or higher when assessed using the gamma value of local dose difference at 3% and Distance to agreement at 3 mm.

Conclusion: This study intended to establish a QA system for the purpose of enhancing the dosimetric accuracy of treatment planning for high-dose-rate brachytherapy. Experiments and assessments related to patient-specific QA were implemented as planned. As a result, the self-fabricated phantom was found to be suitable for QA in clinical settings. The proposed patient-specific QA for treatment planning is expected to contribute to reducing dosimetric errors in brachytherapy, and thus, enhance treatment accuracy.

EP-1988

Calibration of ionisation well chambers at the Polish SSDL

W. Bulski[1], P. Ulkowski[1], A. Kowalczyk[1], E. Gruszczyńska[1], K. Chełmiński[1]

[1]The Maria Sklodowska-Curie Memorial Cancer Center, Medical Physics Department, Warsaw, Poland

Purpose or Objective: In Poland, there are 32 centres performing brachytherapy, which treated 10948 patients in 2014. In total, all these centres use about 50 HDR machines with Ir-192 sources. Each source has to be replaced every three months, and the new sources have to be calibrated. In every centre this is done by measuring the source output with a well ionization chamber. Each centre has at least one such chamber which in turn has to be calibrated against the secondary standard. The Polish Secondary Standard Dosimetry Laboratory offers such calibrations for which it is accredited by the Polish Centre for Accreditation. The SSDL in Warsaw is the only laboratory in Poland and in central and eastern Europe performing calibration of such type of chambers. The service started in 2012 and since then 36 calibrations have been performed. In this presentation the calibration results are analyzed.

Material and Methods: The calibration procedure for well chambers was established at the SSDL in 2012. As a secondary standard, a PTW well chamber type TW33004 has been used.. At the Polish SSDL, the extended uncertainty of the calibration coefficient for user's chambers is 2.8% (k=2). The calibrations are performed using the Ir-192 source of the MicroSelectron HDR unit. Until May 2015 the SSDL calibrated 30 well chambers from the following manufacturers:

Standard Imaging – 13 chambers, Nucletron Holland – 9 chambers, and PTW Freiberg – 8 chambers.

Results: Mean values and SD of calibration coefficients for each chamber type were calculated. For Standard Imaging HDR1000 Plus well chambers the mean calibration coefficient was 0.4669±0.0026. For Nucletron Holland well chambers (type 77091, 77092 and 77094) the mean calibration coefficient was 0.9472±0.0142 and for PTW33004 well chambers the mean calibration coefficient was 0.9655±0.0186. Some chambers were calibrated twice, what allowed for evaluation of their stability.

Conclusion: The smallest standard deviation of the calibration factors was observed for the Standard Imaging chambers (13 chambers). It indicates high manufacturing reproducibility. Furthermore, these chambers have higher sensitivity than the other types. Two chambers of each type were calibrated twice over a period of two years. Their long-term stability is comparable, and is within 0.5% per two years for all types. The secondary standard of the SSDL, a PTW well chamber type TW33004, was calibrated at the PTW laboratory and also at the Primary Standard Laboratory PTB-Braunschweig, Germany. The calibration factors from both labs differed by 1%. The SSDL relies on the Primary Standard calibration. The data for PTW chambers, calibrated at the manufacturer and at the Polish SSDL indicate slight deviations of the PTW calibration factors in one direction. This might suggest the systematic difference in the calibration procedure between the PTW and PTB.

EP-1989

Dosimetry of the RIC-100 P32 brachytherapy source for the intraoperatiove treatment of spinal tumours

C. Deufel[1], L. Courneyea[1], L. McLemore[1], I. Petersen[1]
[1]*Mayo Clinic, Radiation Oncology, Rochester, USA*

Purpose or Objective: Experimental and theoretical dosimetry of the RIC-100 P-32 brachytherapy source is presented for implant geometries that may occur in an intraoperative setting during treatment of localized spinal tumors with temporary superficial radiation. Dose variation, due to source shape and size, is evaluated, and non-ideal implant conditions are simulated. Superficial brachytherapy has been used to prevent local recurrence and minimize neurological toxicity after surgical resection of paraspinous tumors abutting the dura. In this procedure, a brachytherapy source with limited penetration is applied directly to the tumor site in an intraoperative setting, thus providing a technique for localized treatment delivery that maximizes normal tissue sparing.

Material and Methods: Calibration, depth dose, and dose profiles were evaluated for several implant geometries and source sizes. Experimental measurements were performed using EBT3 gafchromic film. Theoretical calculations were performed using dose point kernel (DPK) formalism, which simulates isotropic, monoenergetic point sources distributed uniformly throughout the source and emitting electrons radially outwards.

Results: Calibration and depth-dose for RIC-100 are independent of source size for diameters >1cm. Sources should be ordered with physical dimensions ~0.2 cm larger than the target size, in all dimensions, to deliver >90% prescription dose to target edges. Relative dose profile shape is approximately constant as a function of target depth. Air-gaps between the source and target cause narrower dose profile widths and shallower depth-dose in the therapeutic range. The figure shown below presents the dosimetric effects of an air gap between the source and target. Measured dose profiles (solid lines) are shown for a water equivalent depth equal to 0.153 cm and air gaps of 0, 0.14, and 0.44 cm separating the source surface from the phantom. Theoretical dosimetry is provided for comparison (dashed lines).

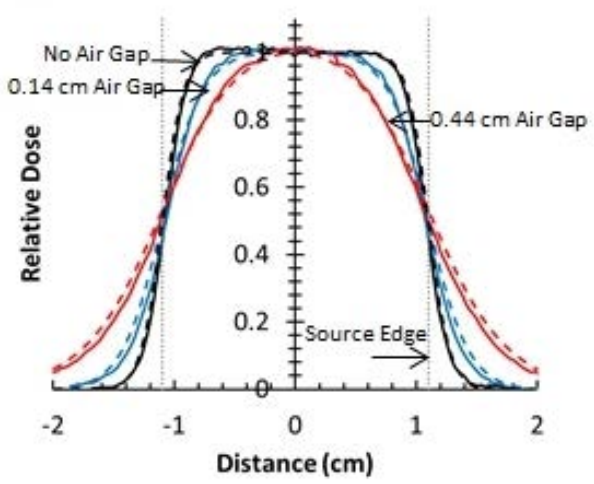

Finally, DPK for RIC-100 agrees with published P-32 kernels, and DPK calculations agree with measurement (within 5%) for many depths and geometries.

Conclusion: Intraoperative placement and measurement dosimetry of RIC-100 require careful setup due to steep dose gradients. Physical source dimensions should be chosen carefully based on treatment site dimensions, and air-gaps between source and target should be minimized, to prevent under-dosing the target in the lateral extent. Radiological scaling should be used to calculate expected dose when non-water materials are used in experimental measurements, such as calibration or depth dose.

EP-1990

Comparison of dose optimisation methods for vaginal HDR brachytherapy with multichannel applicators

D. Cusumano[1], M. Carrara[2], M. Borroni[2], C. Tenconi[2], S. Grisotto[2], E. Mazzarella[2], A. Cerrotta[3], B. Pappalardi[3], C. Fallai[3], E. Pignoli[2]
[1]*University of Milan, Postgraduate School in Medical Physics, Milan, Italy*
[2]*National Cancer Institute, Medical Physics Unit, Milan, Italy*
[3]*National Cancer Institute, Radiotherapy Unit, Milan, Italy*

Purpose or Objective: Multichannel Vaginal Cylinders (MVCs) allow to perform conformal HDR brachytherapy (BT) treatments for vaginal vault cancers. Despite the fact that with MVCs the degrees of freedom for treatment planning have significantly increased with respect to common vaginal cylinders, no unique indications are currently given on how to perform dose distribution optimization. Purpose of this study was to compare several optimization methods (OM) implemented in Oncentra Brachy (Nucletron Elekta), with a particular attention to the target coverage and the simultaneous limitation of hot spots to the vaginal mucosa and the improvement of dose homogeneity to the target.

Material and Methods: The study was based on 12 vaginal cancer cases treated with HDR BT (25Gy/5 fractions) as boost after external beam radiotherapy (45Gy/25 fractions). MVC applicators with diameters of 25mm (6 cases) and 30mm (6 cases) were used and treatments were retrospectively planned using four OM: i) a combination of geometrical and graphical OM (GrO); ii) the Inverse Planning by Simulated Annealing (IPSA) method, imposing surface dose constraints on the PTV (surfIPSA); iii) the IPSA method, applying further dose constraints to the applicator surface (homogIPSA); iv) the Hybrid Inverse Planning Optimization (HIPO) with previously defined iterative optimization steps. All methods had to respect constraints on bladder and rectum (respectively D2cc<80% and D2cc<75% of the prescribed dose), and to possibly deliver at least a V90>95% to the PTV. Plans evaluation was performed in terms of PTV coverage (D90, V90), conformity index (COIN), dose homogeneity index (DHI) and ratio between source dwelling times in the central and peripheral catheters (%CC). As maximum dose to the

vaginal mucosa the D0.1cc was considered. Statistical significance of the results was proven by a Wilcoxon test for paired samples (significant p-value <0.05)

Results:

Parameter	*GrO*	*Surf IPSA*	*homogIPSA*	*HIPO*
V90 (%)	95.46 ± 4.20	93.55 ± 4.62	95.65 ± 3.93	95.19 ± 4.31
D90 (%)	100.15 ± 9.52	97.49 ± 10.25	98.02 ± 6.35	96.79 ± 6.30
DHI	0.66 ± 0.13	0.65 ± 0.14	0.81 ± 0.10	0.79 ± 0.08
COIN	0.84 ± 0.09	0.79 ± 0.09	0.84 ± 0.06	0.84 ± 0.06
$D_{bladder,2cc}$ (%)	58.17 ± 13.66	57.10 ± 13.31	57.51 ± 13.69	57.76 ± 13.52
$D_{rectum,2cc}$ (%)	73.52 ± 2.22	72.47 ± 4.11	72.64 ± 4.11	72.08 ± 4.46
$D_{mucosa,0.1cc}$ (%)	246.27 ± 36.38	259.89 ± 45.45	209.81 ± 44.83	234.76 ± 49.41
CC%	0.53 ± 0.21	0.43 ± 0.20	0.81 ± 0.12	0.90 ± 0.10

Table 1 shows the obtained values for D90, V90, COIN, DHI and %CC for the investigated OM. No significant differences resulted among the OM in terms of target coverage (D90 and V90) and bladder and rectum sparing (D2cc).

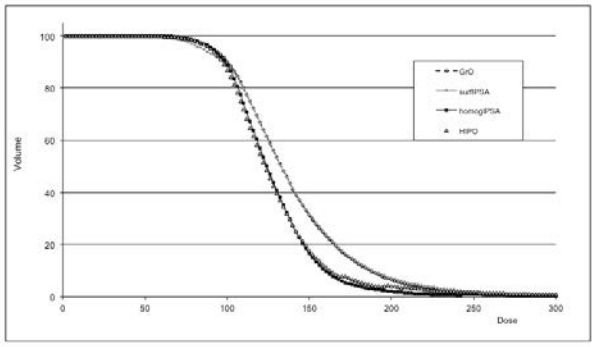

The figure shows average DVHs of the PTV over all 12 cases. DVHs obtained with homogIPSA and HIPO show a steeper gradient, resulting in smaller volumes exposed to high doses. homogIPSA and HIPO result in significantly better values of COIN, DHI e %CC values. Furthermore, homogIPSA shows the lowest value for the D0.1cc to the mucosa. No differences were evidenced between the use of MVC applicators with diameters of 25mm and 30mm.

Conclusion: HIPO and homogIPSA should be preferred due to their ability to get improved dose homogeneity to the target and reduced hot spots to the vaginal mucosa. This is achieved by a more effective distribution of source dwelling times between central and peripheral catheters. It has to be noted that all investigated OM require experience of the planner and are not completely user independent.

EP-1991

The dosimetric characteristics of GMS BT-125-1 I-125 radioactive seed

R. Yang[1]

[1]*Peking University Third Hospital, Radiation Oncology, Beijing, China*

Purpose or Objective: To investigate the dosimetric characteristics of GMS BT-125-1 I-125 radioactive seed, including dose rate constant, radial dose functions and anisotropy functions.

Material and Methods: Dosimetric parameters of GMS BT-125-1 I-125 seed, including dose rate constant, radial dose functions and anisotropy functions were calculated using the Monte Carlo code of MCNP5, and measured using thermoluminescent dosimeters (TLDs). Monte Carlo calculations were also performed for the PharmaSeed BT-125-1 I-125 seed, PharmaSeed BT-125-2 I-125 seed and model 6711 I-125 seed. The dosimetric parameters of GMS BT-125-1 I-125 seed were compared with those of PharmaSeed BT-125-1 I-125 seed, PharmaSeed BT-125-2 I-125 seed and model 6711 I-125 seed. The measured results were compared with those of Monte Carlo simulation for GMS BT-125-1 I-125 seed.

Results: The MCNP5 calculated dose rate constant of GMS BT-125-1 I-125 seed was 1.011 . The experimental measured dose rate constant of GMS BT-125-1 I-125 seed was 0.967 . For radial dose function, the difference between GMS BT-125-1 I-125 seed and PharmaSeed BT-125-2 I-125 seed were typically less than 2.0% with a maximum of 3.3 %. The largest differences were 8.1% and 6.2% compared with PharmaSeed BT-125-1 and model 6711 I-125 seed, respectively. For anisotropy functions, the difference between GMS BT-125-1 I-125 seed and PharmaSeed BT-125-2 I-125 seed was typically <10% with a maximum of about 9.6% when the polar angle was larger than 10 degree, and 22.9% when the polar angle was smaller than 10 degree. Compared with Monte Carlo simulation, the largest differences of radial dose functions and anisotropy functions were 14.5% and 29.1%, respectively.

Conclusion: The measured dose rate constant, radial dose functions and anisotropy functions for GMS BT-125-1 I-125 seed showed good agreement with Monte Carlo calculated values. The dosimetric parameters of GMS BT-125-1 I-125 seed are similar to those of PharmaSeed BT-125-2 I-125 seed.

EP-1992

Design and characterization of a new HDR brachytherapy Valencia applicator for larger skin lesions

J. Vijande[1], C. Candela-Juan[2], Y. Niatsetski[3], R. Van der Laarse[3], D. Granero[4], F. Ballester[1], J. Perez-calatayud[5]

[1]*Universitat de Valencia Dep. de Fisica Atomica- Molecular Y Nuclear, Atomic Molecular and Nuclear Physics, Burjassot, Spain*

[2]*National Dosimetry Centre, National Dosimetry Centre, Valencia, Spain*

[3]*Elekta, Brachytherapy, Veenendaal, The Netherlands*

[4]*ERESA- Hospital General Universitario, Department of Radiation Physics, Valencia, Spain*

[5]*La Fe University and Polytechnic Hospital, Radiation Oncology Department-, Valencia, Spain*

Purpose or Objective: The aim of this study was: (i) to design a new high-dose-rate (HDR) brachytherapy applicator for treating surface lesions larger than 3 cm in diameter and up to 5 cm size, using the microSelectron-HDR afterloader (Elekta Brachytherapy); (ii) to calculate by means of the Monte Carlo (MC) method the dose distribution around the new applicator when it is placed over a water phantom; and (iii) to validate experimentally the water dose distributions.

Material and Methods: The new applicator is made of tungsten, and consists on a set of interchangeable collimators without flattening filter. It makes use of three catheters to allocate the source at prefixed dwell positions and times to produce a homogeneous dose distribution at 3 mm depth in the water phantom. The Penelope2008 MC code was used to optimize dwell positions and dwell times. Next, the dose distribution in a water phantom and leakage dose distribution were calculated. Finally, MC data were validated experimentally by measuring: dose distributions with radiochromic EBT3 films (ISP) for an 192Ir mHDR-v2 source; percentage depth-dose (PDD) curve with the parallel-plate ionization chamber Advanced Markus (PTW); and absolute dose rate with EBT3 films and the PinPoint T31016 (PTW) ionization chamber.

Results: PDD and off-axis profiles were obtained normalized at a depth of 3 mm along the central applicator axis in a cylindrical water phantom. These data can be used for treatment planning. Leakage was also scored. The dose distributions, PDD, and absolute dose rate calculated agree within experimental uncertainties with the doses measured.

Conclusion: The new applicator and the dosimetric data provided here will be a valuable tool in clinical practice, making treatment of large skin lesions simpler, faster, safer, and with minimized dose to surrounding healthy tissues when

compared to electron therapy or brachytherapy with moulds and flaps.

EP-1993

Dose evaluation at organs at risk in vaginal cuff brachytherapy

J. Wiercińska[1,2], R. Kabacińska[1], J. Terlikiewicz[2,3], A. Lebioda[2,3], A. Wronczewska[3], R. Makarewicz[2,3]
[1]*Oncology Center Bydgoszcz, Medical Physics Department, Bydgoszcz, Poland*
[2]*Collegium Medicum- Nicolaus Copernicus University- Toruń, Department of Oncology and Brachytherapy, Bydgoszcz, Poland*
[3]*Oncology Center Bydgoszcz, Brachytherapy Department, Bydgoszcz, Poland*

Purpose or Objective: Vaginal cuff brachytherapy with the dose prescribed at 0.5 cm depth from the applicator surface has been the standard treatment for gynaecological cancer patient after histerectomy for years. The implementation of computed tomography based (CT-based) plans caused changes in the standard approach in our hospital. We narrowed the planning target volume (PTV) in order to meet our in-house constraints requirement for organs at risk (OARs) in some cases. The aim of the study was to analyze doses at OARs in real adjusted image-based plans and in standard 0.5 cm normalized plans.

Material and Methods: Treatment plans of recent, consecutive 70 patients treated with high dose rate vaginal cuff CT-based brachytherapy were analyzed retrospectively. Dose normalization points and optimization methods were adjusted whenever standard approach wasn't suitable to meet all dose constraints for OARs (adjusted plan - AP). The second, standard treatment plan (SP) was created for every AP. APs were divided into three groups based on overdosage at definite OAR: Bladder Group (B group), Rectum Group (R group) and Bladder & Rectum Group (B&R group). Comparison of doses at the most exposed 0.1cc (D0.1cc) and 2cc (D2cc) of bladder and rectum between AP and SP was made in all three groups.

Results: Vaginal cylinders of 10 to 35 mm radius were used. For 54% of all 70 cases the standard approach wasn't deemed suitable, and the treatment plan was adjusted (SP- 32 cases, AP-38 cases). 53% of the APs were assigned to the R group, 21% to the B group and 26% to the B&R group. Mean values of rectum doses in R Group were 96.6% and 112.0% for RD0.1cc and 74.4% and 83.6% for RD2cc for AP and SP respectively. Mean values of bladder doses in B Group were 97.2% and 108.0% for BD0.1cc and 79.3% and 86.9% for BD2cc for AP and SP respectively. In B&R Group mean values of RD0.1cc were 93.1% and 108.9% and mean values of RD2cc were 71.8% and 81.1% for AP and SP respectively, mean values of BD0.1cc were 94.4% and 105.9% and mean values of BD2cc were 77.5% and 84.4% for AP and SP respectively. The doses are presented as a percentage of prescribed dose. Dose differences between both plans in all three groups were statistically significant.

Conclusion: Standard approach with dose points at 0.5 cm from the applicator surface is not suitable for all patients and can increase the risk of bladder or rectum complications. CT-based plan allowing dose evaluation at OARs should be practiced on a daily basis.

EP-1994

On the dosimetric effect of heterogeneities and finite patient dimensions on Co-60 HDR brachytherapy

K. Zourari[1], E. Pantelis[1], P. Papagiannis[1]
[1]*Athens University- Medical School, Medical Physics Laboratory, Athens, Greece*

Purpose or Objective: Brachytherapy has recently advanced towards personalized planning dosimetry with the commercial availability of image-based treatment planning systems for Ir-192. This marks an improvement over TG-43 based planning dosimetry that relies on source specific data pre-calculated in a standard sized geometry of homogeneous water, hence disregarding patient-specific radiation scatter conditions and the radiological differences of tissue or applicator materials from water. The aim of this work is to perform a comparative study of the effect of these factors in Co-60 and Ir-192 HDR brachytherapy.

Material and Methods: Ten clinical cases were studied for each of three disease cites considered (gynaecological, esophagus and breast). Two treatment plans were prepared for each case using the TG-43 option of a commercially available system (SagiPlan) with an Ir-192 (Ir2.A85-2) and a Co-60 (Co0.A86) HDR source. The plans were exported in dicom RT format. Corresponding personalized dosimetry data was obtained from Monte Carlo simulation using the MCNP6 code. Monte Carlo input files were prepared automatically from the parsing of information in the dicom RT data using a custom software tool (BrachyGuide). Personalized and TG-43 based dose distributions were compared in the 3D anatomical space of each patient using isodose distributions, % dose difference maps, Dose Volume Histograms and relevant indices of clinical interest. The statistical and clinical significance of differences between personalized and TG-43 based dosimetry in Co-60 HDR brachytherapy was examined, and evaluated relative to corresponding results for Ir-192.

Results: Results indicated that the effect of tissue heterogeneities and patient specific scatter conditions is less for Co-60 than for Ir-192 HDR treatments. In general, Co-60 and Ir-192 sources of identical shape and construction have been found to deliver clinically comparable dose distributions despite definite differences in their physical characteristics. This is confirmed in terms of personalized dosimetry in this study. A lower dose to critical organs close to the target by Co-60 sources was observed along with a small increase in the overdose volume (V150 to V400). The choice of isotope was not found to have an impact on the prescribed dose.

Conclusion: Co-60 may be used as an effective alternative to Ir-192 for HDR brachytherapy, producing similar plans of equivalent target coverage, but with a logistical benefit and without the need for an image based algorithm for personalized dosimetry.

Acknowledgement
Research supported in part by Eckert & Ziegler BEBIG.

EP-1995

Potential OAR dose reduction with Fletcher shielded applicator and ACE algorithm for cervix brachy

C. Jones[1], A. Taylor[2], M. Bidmead[1]
[1]*The Royal Marsden NHS Foundation Trust, Medical Physics, London, United Kingdom*
[2]*The Royal Marsden NHS Foundation Trust, Radiotherapy, London, United Kingdom*

Purpose or Objective: The dose delivered to the cervix HRCTV is often limited by OAR tolerances. A new applicator with shields in the anterior and posterior areas of the ovoids has been developed to try to reduce OAR doses. The current dose calculation formalism (TG43) calculates dose to water and does not take into account tissue heterogeneity. The Advanced Collapsed cone Engine (ACE) is the Elekta implementation of TG186; it models tissue heterogeneity and the effect of shielding.

Material and Methods: Eleven patients were selected that had received CT/MR planned brachytherapy for cervical cancer using Elekta Fletcher tube and ovoids. The HRCTV and OARs had been outlined on the MR. For this study the applicator library was used to perform a best fit match of the shielded CT/MR Fletcher tube and ovoid model with the CT of the insertion. The shielded applicators have a slightly different geometry compared to the unshielded Fletcher applicators. The 25mm shielded ovoids were overlaid on 35mm standard ovoids and 30mm shielded ovoids were overlaid on 40mm standard ovoids.
The dwell positions, dwell weights and A points were maintained from the clinical plan. The plans were calculated

with and without shield attenuation using TG43 and were calculated with TG186 fixing the dwell times. It was not possible to perform a TG186 calculation without the shields in place. The TG186 calculation used a HU based mass density and all contoured organs were set to 'female soft tissue' except bladder which was set to 'water' to provide the chemical composition.
The HRCTV D90 and D2cc for rectum, bladder, small bowel and sigmoid were recorded and EQD2 doses calculated assuming 50.4Gy in 28 fractions external beam component.

Results: Table 1 gives the difference in HRCTV D90 and OAR D2cc doses between the different dose calculations.

	TG186 (shields)-TG43 (no shields)		TG186 (shields)-TG43 (shields)		TG43 (shields)-TG43 (no shields)	
	% diff	EQD2 diff (Gy)	% diff	EQD2 diff (Gy)	% diff	EQD2 diff (Gy)
HRCTV D90	-2.5	-1.0	-2.0	-0.9	-0.5	-0.2
Rectum D2cc	-15.8	-4.2	-10.1	-2.4	-6.5	-1.9
Bladder D2cc	-3.4	-1.0	-2.6	-0.7	-0.8	-0.2
Sigmoid D2cc	-4.9	-0.7	-3.2	-0.5	-1.8	-0.2
Bowel D2cc	-3.2	-0.9	-1.9	-0.5	-1.5	-0.3

The combination of shields and TG186 dose calculation reduced the rectum D2cc by an average of 15.8% (5.6%-31.7%) compared to the TG43 dose calculation with no shields in place. This equates to a reduction in EQD2 of 4.2Gy (0.6Gy-13Gy) and is associated with an average HRCTV EQD2 reduction of 1Gy. The reduction is due to the physical effect of the shielding and the more accurate dose calculation. These results show that the effect of the algorithm is the largest contributor as TG43 underestimates the effect of the shields.

Conclusion: This study demonstrates that using shielded applicators has the potential to reduce the rectum D2cc. The rectal dose is rarely our dose limiting organ due to the routine use of a rectal retractor, however any reduction in rectal dose would be beneficial. Two patients in this cohort had rectal D2cc doses greater than 70Gy in the clinical plan. For these two patients the shielded TG186 plan reduced the rectal D2cc dose significantly by 5.7Gy and 13Gy compared to the unshielded TG43 plan. Further work is needed to assess the TG186 calculation without shields and the effect of applicator geometry on the position of OARs.

EP-1996

Post IVD verification and recalibration of MOSkins using a certified low dose emitting Sr-90 source

A. Romanyukha[1], M. Carrara[2], G. Rossi[3], C. Tenconi[2], M. Borroni[2], E. Pignoli[2], D. Cutajar[1], M. Petasecca[1], M. Lerch[1], J. Bucci[4], G. Gambarini[5], A. Rosenfeld[1]
[1]*University of Wollongong, Centre for Medical Radiation Physics, Wollongong, Australia*
[2]*Fondazione IRCSS Istituto Nazionale dei Tumori, Diagnostic Imaging and Radiotherapy Department, Milan, Italy*
[3]*University of Milan, Department of Physics, Milan, Italy*
[4]*St George Hospital Cancer Care Centre, Radiation Oncology Unit, Kogarah, Australia*
[5]*National Institute of Nuclear Physics, Physics, Milan, Italy*

Purpose or Objective: In vivo dosimetry (IVD) measurements in HDR brachytherapy (BT) have to be validated by performing a quality assurance check of the functionality of the dosimeters right after the treatment. Recalibration is also usually required due to the high delivered doses per fraction involved. The standard procedure using Ir-192 is burdensome due to limited availability of the operating theater, where the afterloader containing the Ir-192 source is located, as well as due to the transport and setup of the water equivalent phantom. In this work, a procedure involving the use of a certified low dose emitting Sr-90 source was proposed to both perform QA and recalibration of MOS*kin* dosimeters right after IVD in HDR Ir-192 BT without the need of the BT theater and phantom setup.

Material and Methods: The MOS*kin* is a type of MOSFET detector developed at the Centre of Medical Radiation Physics (CMRP) in the University of Wollongong that was integrated into present HDR Ir-192 BT procedures for real time IVD. The standard MOS*kin* calibration/verification technique employs the Ir-192 source used in HDR procedures, in which case the detector is placed into a water equivalent phantom, and irradiated three times with a known dose. The average of the three measurements is calculated as the calibration coefficient. Instead of using Ir-192, in this study the use of a certified low dose emitting Sr-90 source was investigated. A very small phantom that allows a fixed position of the detector in relation to the source was established. Three MOS*kin*s were tested at three stages of their lifetime, roughly 15 Gy apart. At each one of these stages, each MOS*kin* was calibrated by performing three measures both with Sr-90 and Ir-192. The sensitivity ratio of the average values obtained with Sr-90 and Ir192 was calculated for each measurement.

Results: Both Sr-90 and Ir-192 measurements confirmed a small reduction of MOS*kin* sensitivity with accumulated dose, at 1.1% with every 10 Gy, which is proportional to the change in threshold voltage of the dosimeter to the first order of approximation. The sensitivity ratio of Sr-90 and Ir-192 measurements remained at a constant value of 9.0±0.2% for all three stages of MOS*kin* life, and among the three dosimeters employed in the experiment.

Conclusion: A stable proportional relationship was established between the Ir-192 and Sr-90 calibration methods, demonstrating that Sr-90 can be used effectively for MOSkin recalibration as well as for post treatment verification of their functionality after IVD sessions. The procedure involving Sr-90 is much more convenient because it does not necessitate the use of the BT operating theater and can be easily performed everywhere without any particular radioprotection requirements. Additionally it is not necessary to know the dose delivered by Ir-192 and Sr-90 to MOS*kin* but rather the time of irradiation of the MOS*kin* on each of them respectively, assuming activity changes of Sr-90 are negligible.

EP-1997

Geometrical and source positioning accuracy verification of Varian HDR afterloader and applicators

C.L. Ong[1], F. Janssen[1], L. Murrer[1], M. Unipan[1], A. Hoffmann[1]
[1]*MAASTRO clinic, Radiotherapy, Maastricht, The Netherlands*

Purpose or Objective: In high-dose rate (HDR) brachytherapy, accurate dose delivery is highly dependent on the geometrical and temporal source positioning accuracy. In this study, we measured the source position and dwell time accuracy of the Varian GammaMedplus iX afterloader as well as the dead space of a variety of Varian applicators.

Material and Methods: The source position and dwell time accuracy were optically measured using Varian's source step viewer and a videocamera. The Perma-Doc phantom was used for dosimetric verification of the afterloader's source positioning accuracy. The most distal source position and the dead space of the applicators (titanium/stainless steel/ plastic needles, titanium Fletcher-type and flexible tube) were measured radiographically using kV imaging and dosimetrically using EBT3 film. For these measurements an X-ray marker and the Ir-192 source were successively inserted into the applicators, respectively. The distance between the external end of the applicators and the center of the most distal X-ray marker and the first dwell position on film were measured (Fig.1).

Results: The dwell time deviation measured at different source positions is <0.1s, and is in accordance with vendor specifications. For the most proximal source position, a systematic longer dwell time of 0.13s was observed. This deviation should be negligible when multiple dwell positions are used. Position verification using the source step viewer shows deviations of 0.5–1mm (vendor specs: ± 1mm). At the most distal position, the source was always retracted by 1 mm relative to the nominal position to straighten the source

cable. This effect was taken into account during treatment planning. Position verification using the PermaDoc phantom confirmed this 1 mm retraction. All radiographically measured dead spaces complied with the specifications, except for the plastic needles which were 1 mm shorter than indicated. The center of the active source is at 2.42 mm from the tip of the capsule. Combined with the 1 mm source retraction, the center of the dose distribution at the most distal position located always 3.5 mm behind the internal end-point of the source channel. Radiographic and dosimetric dead space measurements showed good agreement (<0.5mm) for all applicators.

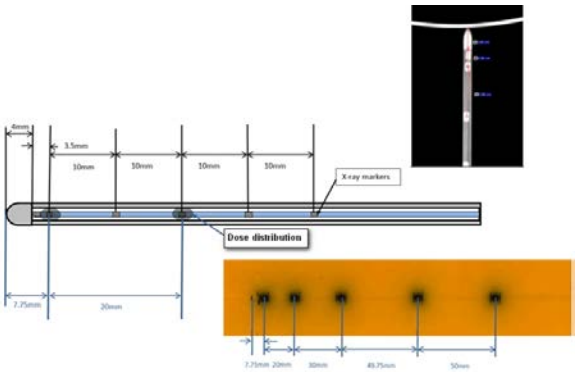

Figure 1: KV images of a stainless steel needle with x-ray markers (Right above). Distances between the physical end-point and middle of the dose distribution were measured on an EBT3 films (right under). The figure in the middle shows a small discrepancy of 0.25mm for the first source position identified using kv-images and EBT3 film.

Conclusion: Measured source position and dwell time accuracy comply with the vendor's specifications. Small deviations were found for the dwell time accuracy at the most proximal source position. Similar tests should be performed regularly to warrant the mechanical accuracy of the afterloader and the quality of the applicators and transfer tubes.

EP-1998

Real-time dosimetry for HDR brachytherapy

L. Moutinho[1], I.F.C. Castro[1], H. Freitas[1], K.A. Silva[1], P.J. Rachinhas[2], P.C.P.S. Simões[2], J.F.C.A. Veloso[1]

[1]I3N- Physics Department- University of Aveiro, Physics Department, Aveiro, Portugal

[2]Hospitais da Universidade de Coimbra, Serviço de Radioterapia, Coimbra, Portugal

Purpose or Objective: Dose verification and quality assurance in radiotherapy (RT) should be assessed in order to provide the best treatment possible and minimize risks for patient. In certain treatments there are no tools capable of performing real-time dose measurement. In addition, in-situ real-time dosimetry would enhance brachytherapy (BT) by providing technical conditions to perform treatment readjustment and real-time dose correction. Considering the current challenges, we developed a dosimeter intended for in-situ and real-time dosimetry in High Dose Rate brachytherapy (HDR-BT), e.g., prostate and breast.

Material and Methods: The dosimeter developed has a sensitive 3 m long optical fiber probe of 1mm or 0.5 mm diameter comprehending a 5 mm length scintillating optical fiber. To read the signal produced at the probe, 1x1 mm2 Silicon Photomultipliers (SiPM) from Hamamatsu were used. A custom made readout system with SiPM temperature compensation was used. The main concerns when performing dosimetry at high dose rates with high energy isotopes is the eventuality of Cherenkov light production. This form of noise accounts to the total noise signal, known as stem effect.
The dosimeter was placed in a PMMA phantom and the response was evaluated with a 10.07 Ci Ir-192 HDR-brachytherapy source (Nucletron). Measurements were repeated twice, first using a dummy probe without scintillator for stem effect quantification and second using an ionization chamber (IC) read by an electrometer for reference.

Results: The studies carried out allowed assessing the amount of stem effect produced in the optical fiber cable. In the conditions described above, the stem effect contribution is lower than 1% for both 0.5 and 1 mm probes. The measurements of the fiber dosimeter response as a function of the dose are represented in Figure 1. The small difference from the reference IC is due to the different detector volumes of the fiber dosimeter and the ionization chamber. The dosimeter shows a linear response with dose rate being capable of detecting µGy dose variations.

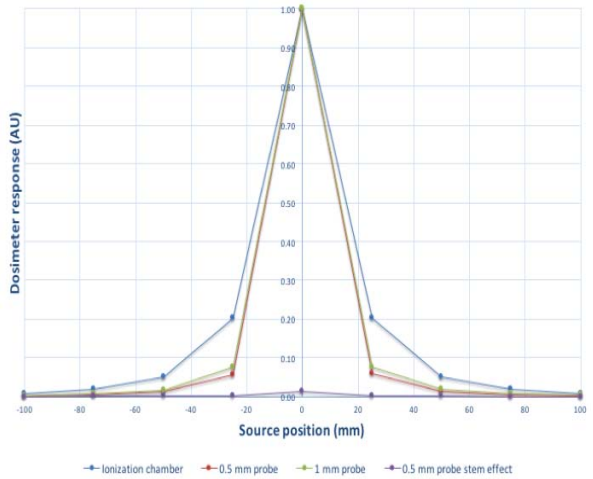

Figure 1: Fiber optic dosimeter stem-effect and response for 0.5 and 1 mm diameter versions compared to ionization chamber response.

Conclusion: The first round of in-vitro tests in clinical setting demonstrated that the fiber optical based dosimeters developed are suitable for dosimetry in regimes such as HDR prostate BT. The versatility of this kind of device and easiness of use allows application in other radiotherapy modalities. Besides fulfilling all the requirements for a dosimeter in HDR-BT, the high sensitivity of this device makes it a suitable candidate for application in LDR-BT.

Electronic Poster: Brachytherapy track: Prostate

EP-1999

Comparison of intraoperatively linked and loose seed in prostate brachytherapy using sector analysis

N. Katayama[1], M. Takemoto[2], A. Takamoto[3], K. Hisazumi[1], H. Ihara[1], K. Katsui[1], S. Ebara[3], Y. Nasu[3], S. Kanazawa[1]

[1]Okayama University Hospital, Department of Radiology, Okayama, Japan

[2]Himeji Red Cross Hospital, Department of Radiotherapy, Himeji, Japan

[3]Okayama University Hospital, Department of Urology, Okayama, Japan

Purpose or Objective: An intraoperatively built custom-linked (IBCL) seeds system is a push-button seed delivery system that allows the user to create intraoperatively customized linked seeds, using a combination of seeds, connectors, and spacers. To date, only three studies have compared the implant quality of IBCL seeds to loose seeds for use in permanent prostate brachytherapy (PPB). However, they did not use sector analysis. Therefore, we compared the implant quality of IBCL seeds to loose seeds in PPB using sector analysis.

Material and Methods: Between June 2012 and January 2015, 64 consecutive prostate cancer patients underwent brachytherapy with IBCL seeds (n = 32) or loose seeds (n = 32). All the patients were treated with 144Gy of brachytherapy alone. IBCL and loose seeds were alternately used basically. All patients were treated by the same radiation oncologist and urologist. We used the same dose-

volume targets in the IBCL seed group and the loose seed group. Brachytherapy was performed using a dynamic dose calculation technique. Computed tomography/magnetic resonance imaging fusion-based dosimetry was performed 1 month after brachytherapy. Post-implant dose volume histogram (DVH) parameters, prostate sector dosimetry, operation time, seed migration, and toxicities were compared between the two groups. A sector analysis tool was used to divide the prostate into six sectors (anterior and posterior sectors at the base, mid-gland, and apex). Analyses were performed using the 2-sample *t* test for continuous data that followed a normal distribution, the Mann-Whitney test for continuous data that did not follow a normal distribution, and the Chi-squared test for categorical data. Probability (*P*) values of < 0.05 were considered significant.

Results: In prostate sector dosimetry, V100 (95.3% vs. 89.7%; P = 0.014) and D90 (169.7 Gy vs. 152.6 Gy; P = 0.013) in the anterior base sector were significantly higher in the IBCL seed group than in the loose seed group. Other post-implant DVH parameters did not differ significantly between the two groups. The seed migration rate was significantly lower in the IBCL seed group than in the loose seed group (6% vs. 66%; P < 0.001). There was no significant difference in mean operation time between the two groups; however, mean operation time per seed was significantly longer in the IBCL seed group than in the loose seed group (1.31 min vs. 1.13 min; P = 0.003). The median follow-up was 18 months (range, 1-36 months). No significant differences in toxicities were seen between the two groups.

Conclusion: Our study showed more dose coverage post-operatively in the anterior base prostate sector and less seed migration in IBCL seeds implantation compared to loose seeds implantation.

EP-2000

Template guided saturation biopsy of prostate: what is the optimal volume for brachytherapy?

S. Kanaev[1], S.N. Novikov[1], R.V. Novikov[1], N.D. Ilin[1], E.A. Peskunov[1], M.Y. Gotovchikova[1]
[1]*N.N. Petrov Institute Oncology, Radiation Oncolgy & Nuclear Medicine, Saint-Petersburg, Russian Federation*

Purpose or Objective: to evaluate results of saturation biopsy in candidates for focal, hemigland high dose rate (HDR) brachytherapy or irradiation with "low-dose tunnel for urethra"

Material and Methods: Template guided saturation biopsy was performed in 52 primary patients with suspicion to prostate cancer and PSA below 10 ng/ml. Biopsy was performed under US control with the help of brachytherapy grid and 5mm distance between samples. During positioning and biopsy procedure we put special attention for accurate sampling of prostate in periurethral region. The number of cores varied from 17 to 50 (average 33 cores). Finally in 31 patients with confirmed prostate cancer results of biopsy were used for brachytherapy planning.

Results: Saturation biopsy revealed prostate cancer in 31 of 52 evaluated patients. Involved volume ranged from 5% to 100% (average - 57%). Focal nature of PC diagnosed in 6 (19.4%), multifocal – in another 25 (80.6%) patients. Hemigland invasion mentioned in 10 cases. Saturation biopsy detected PC in periurethral cores in 22 (70.9%) of 31 evaluated patients: invasion of one core revealed in 1, 2 cores – in 6, 3 and more cores – in another 14 cases. In 10 patients extent of involvement in periurethral cores varied between 10% and 50%, in another 12 observations exceeded 50%. According to results obtained on saturation biopsy we performed HDR brachytherapy with "urethra low dose tunnel" ($D10_{ur}$≤80%) in 9 patients with noninvolved periurethral cores. Theoretically hemigland brachytherapy was possible in 10 of 31 evaluated patients.

Conclusion: in low risk patients with prostate cancer results of template guided saturation biopsy can significantly influence strategy of HDR brachytherapy

EP-2001

Radical salvage brachytherapy (BT) for local recurrences after previou radiation treatment

S. Rodríguez Villalba[1], M. Santos Ortega[1], M. Depiaggio[1], L. De la Torre[2], J. Martinez[2], J. Canovas[2], J. Richart[1], A. Otal[1], J. Perez Calatayud[1]
[1]*Clinica Benidorm, Radiotherapy Department, Benidorm, Spain*
[2]*Hospital Marina Baixa, Urology Department, Villajoyosa-Alicante, Spain*

Purpose or Objective: We presented a retrospective analysis in 11 patients with histological proven local-recurrent prostate cancer, undergoing salvage BT, treated between February 2009 and December 2014.

Material and Methods: The previous radical treatments were: 3 Low dose rate BT (LDR-BT) (145 Gy), one combined treatment with external radiotherapy (EBRT) (45 Gy) and LDR-BT (100 Gy), and 7 EBRT (68-74 Gy). Four patients have been rescued with LDR-BT and seven with High-Dose-Rate-BT (HDR-BT). All patients have a complete study with abdominal CT scan, pelvic MRI, and bone scan to diagnose local disease exclusively. LDR-BT patients received 145 Gy with 125I. HDR patients, has been treated with 30 Gy in 3 fractions of 10 Gy separated ten days. Median time to Biochemical failure (BF) from the first treatment was 48 months (12-114). All patients received previous hormonotherapy. Median time to rescue was 69 months (33-156). Toxicities were evaluated according with CTCAE scale (version 4.0).

Results: Median follow-up: 26,5 months (3-72 m). The overall survival time was 98 months (65-174). At the end of the follow up, March of 2015, all patients are alive, nine (82%) without evidence of disease, one patients had a retroperitoneal failure 7 months after the salvage-BT and other patient was diagnosed of a solitary bone metastases at 12 months. Median PSA nadir post-salvage-BT was 0.1 ng/ml (0-0,29). There were not grade 3 GU or GI toxicities. 100 % of LDR-BT patients presented acute GU-toxicity grade 2. Fifty-seven % of the HDR-BT patients had GU-toxicity grade 1 (0% grade 2).

Conclusion: Prostate BT is an effective and well tolerated reirradiation treatment in local-recurrent prostate cancer patients, with, few long-term toxicities, mainly in those treated with HDR-BT.

EP-2002

Focal prostate brachytherapy: aspects of multi-modality registration and dosimetry feasibility

T. Brun[1], S. Ken[1], C. Popotte[1], J. Bachaud[1], P. Graff-Cailleaud[1], M. Delannes[1], B. Malavaud[1], D. Portalez[1], R. Aziza[1]
[1]*Cancer University Institute of Toulouse Oncopole, DIPM, Toulouse, France*

Purpose or Objective: The different conventional treatments for prostate cancer are multiple and for low-risk tumors, focal brachytherapy can be a therapeutic alternative option to active surveillance. However, this focal treatment remains still under evaluation and within the frame of the focal brachytherapy project conducted in Toulouse, we will present in this study two parts of the project: first, the contribution of multi-modal rigid and non-rigid registrations for localization and delineation of the treated volume, then the dosimetry evaluation after registration.

Material and Methods: First step of prostate brachytherapy at our Institute consists in a contour-based non-rigid registration between MRI and US perfomed with Koelis software where positive biopsy trajectory is retrieved and a fiducial non-radioactive marker is implanted to localize the tumor focus. As a result of this localization, dosimetry was performed using VariSeed software, dose prescription is

160Gy to the PTV (GTV + 2mm) and Bard Quicklink system is used to implant I125 radioactive seeds. Multi-modal manual rigid and non-rigid transformations between MR and CT scans were performed on the first 9 patients with three software solutions: the treatment planning system Variseed, a research platform 3D Slicer and a commercial solution Mirada. MR onto CT registrations were approved by an expert uro-radiologist and quantitative evaluations of the registrations were performed by calculating the means of vectors displacement marked on four relevant points of interest detected on the I125 seeds. For the dosimetry, an assessment of the impact of these readjustments on the initial dose matrix was also performed in Mirada by applying the deformation to the initial contours and injecting the initial dose matrix.

Results: For the first 9 patients, evaluation of registration gives means of vectors displacement of 1.52mm [0.36-2.6] with Variseed, 0.62mm [0.26-1.29] with 3D Slicer and 0.42mm [0.24-0.81] with Mirada. Examples of fusions are illustrated in Figure1. Concerning the dosimetric data and considering the most relevant criteria from the initial outline, the D90%(Gy) to the prostate and respectively for the target has a mean difference of +0.68Gy and -12Gy. The D30%(Gy) and the D10%(Gy) to the urethra respectively have a mean difference of -0.99 and -5.58Gy. Lastly, D1cc(Gy) to the rectum has a mean difference of +4,37Gy.

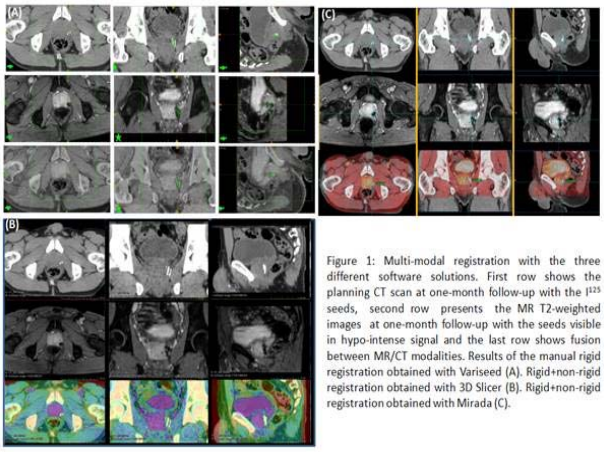

Figure 1: Multi-modal registration with the three different software solutions. First row shows the planning CT scan at one-month follow-up with the I^{125} seeds, second row presents the MR T2-weighted images at one-month follow-up with the seeds visible in hypo-intense signal and the last row shows fusion between MR/CT modalities. Results of the manual rigid registration obtained with Variseed (A). Rigid+non-rigid registration obtained with 3D Slicer (B). Rigid+non-rigid registration obtained with Mirada (C).

Conclusion: Target volume definition remains a crucial step for focal brachytherapy as only confirmed tumor biopsy sub-volumes of the prostate are treated. Registration procedures tested in our institute confirmed the need to implement precise rigid and non-rigid fusion of image to delineate relevant target volumes on different modalities. In addition, dosimetry evaluation on the registrations showed the impact of the deformations in high dose gradients.

EP-2003

HDR brachytherapy in monotherapy of one fraction in patients with prostate cancer at low risk

A.C. Orduz Arenas[1], I. Jiménez García[1], R. Martínez Gutiérrez[1], P. Cucarella Beltran[1], S. Blanco Parajón[1], H.A. González Suárez[1]
[1]*Hospital Universitario Central de Asturias, Oncología Radioterápica, Oviedo, Spain*

Purpose or Objective: The High-dose-rate brachytherapy as monotherapy in one fraction, is a treatment option in patients with low-risk prostate cancer and can be used as an alternative to the low-dose-rate brachytherapy.Compared to the low-dose-rate, the HDR as monotherapy has not proven long-term results with regard to disease control. It is not known what dose of treatment should be used to increase the biochemical control, survival control disease and reduce unaffordable toxic effects.

Material and Methods: Results on patients treated with high-dose-rate brachytherapy as monotherapy are presented below.
Sample: A series of 75 patients between 2008 and 2013 treated with high-dose-rate brachytherapy (HDR) single dose of 19 Gy (62) and 20.5 Gy (13) were selected.
A technique of guided-ultrasound brachytherapy and dynamic-calculated intraoperative dose was used.

Results: The results show an overall survival of 91.3% of patients, with survival free of disease of 97% and a biochemical control of 72.5%.
Patients toxicity: Acute urinary toxicity: 53.8% (grade 2). Chronic urinary toxicity: 49.2% (grade 2). Acute gastrointestinal toxicity: 86.2% (grade 1). Chronic gastrointestinal toxicity: 89% (grade 1).Acute urinary retention rate of 2.9%.

Conclusion: HDR prostate brachytherapy as monotherapy in one single fraction of 19 Gy does not provided adequate biochemical control and survival free disease rates. It is necessary more studies to establish what would be the most appropiate dose to obtain higher rates of disease control

EP-2004

Urethra dose homogeneity constraints in LDR prostate brachytherapy could diminish urinary morbidity

V. González-Pérez[1], J.L. Guinot[2], L. Oliver[1], A. Bartrés[1], V. Campo[1], V. De los Dolores[1], J.V. Ricós[3], A. Cano[1], V. Crispín[1]
[1]*Fundación Instituto Valenciano de Oncología, Servicio de Radiofísica y Protección Radiológica, Valencia, Spain*
[2]*Fundación Instituto Valenciano de Oncología, Servicio de Radioterapia, Valencia, Spain*
[3]*Fundación Instituto Valenciano de Oncología, Servicio de Urología, Valencia, Spain*

Purpose or Objective: Evaluate the relationship between RTOG G2-G3 urinary morbidity after prostate brachytherapy and urethral doses at the end of real-time dosimetry planning.

Material and Methods: From November 2007 to December 2010, 204 prostate cancer patients underwent monotherapy I-125 seeds brachytherapy in our institution. Real-time US guided dosimetry planning was performed with Variseed 7.0 or 8.0. Of the 204 patients, 11 (5.4%) developed an acute urinary retention and required a urinary catheter from 2 weeks to 7 months (G2 morbidity), and 7 patients (3.4%) required a transurethral resection of the prostate (G3 morbidity).
In a retrospective study, detailed urethral dosimetry was evaluated at the end of the real-time implant. Assessed values included maximum dose, V80, V100, V150 and D90 for both overall urethra and segmented urethra (as base, midgland and apex urethra). 1.5-mm and 2.5-mm urethral expansions were also reviewed for all dosimetry parameters. To check if dose homogeneity around urethral regions was related to morbidity, subtraction of expanded minus non-expanded urethral dosimetry parameters was also performed. In total, 111 parameters were reviewed.
T-Student test and U Mann-Whitney test were used to compare differences between patients free of urinary morbidity from those presenting G2 and G3 morbidity. $p < 0.05$ was considered significant.

Results: No correlation was found between non-expanded urethra doses and urinary morbidity.
Best result ($p=0.005$) for distinguishing free-morbidity cohort from G2-G3 morbidity-cohort was obtained for subtraction of the maximum dose of the non-expanded minus 2.5-mm-expanded overall urethra.

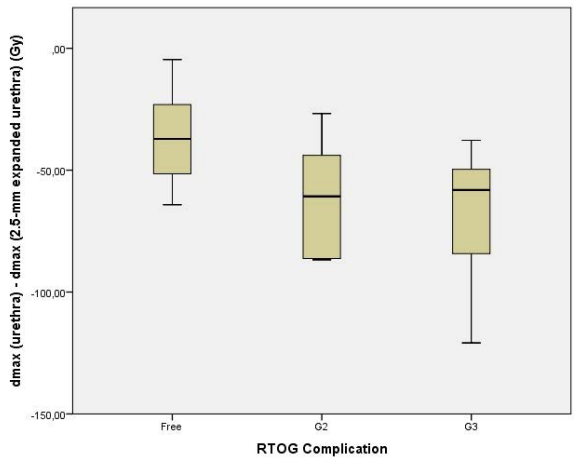

Diagnostic capability was determined by calculating the area under the curve (AUC) in the receiver operating characteristic (ROC) curves. This parameter had an AUC value of 0.786. It was predictive of G2-G3 complications with 71.4% specificity and 72.2% sensibility for a dose difference threshold of 48 Gy.

Conclusion: A non-homogenous dose region around urethra at the end of the real-time implant is a risk factor for development of urethral morbidity.
Several studies have found dosimetry correlations between CT post-plan and urinary morbidity. This study focuses on US real-time dosimetry parameters. It allows us to consider new constraints and dosimetry alerts during treatment planning.
A prospective study is under consideration, where a new constraint of a 40-50 Gy maximum dose difference around a 2.5-mm expansion of the urethra will be implemented if feasible.

EP-2005

Analysis of PSA kinetics after HDR brachytherapy in prostate cancer patients

W. Burchardt[1], J. Skowronek[1]
[1]*Greater Poland Cancer Centre, Brachytherapy Department, Poznan, Poland*

Purpose or Objective: The PSA level after definitive treatment using radiotherapy decreases but still remains detectable. The aim of this study is to analyze clinical and dosimetric factors which influence the PSA level in the blood serum of patients with prostate cancer after HDR (High Dose Rate) brachytherapy.

Material and Methods: 53 patients after HDR brachytherapy were qualified to the study from June 2008 to December 2010. The patients were from T1c to T2c , iPSA from 1.5 to 19.6 ng / ml with prostate adenocarcinoma (Gleason Scale < 7) and belonged to the low and intermediate risk of recurrence. 20 patients had androgen deprivation therapy. Patients were treated with HDR brachytherapy 3 x 15 Gy or 3 x 10.5 Gy. Median follow-up was 3 years. The PSA Bounce threshold was >0.2 ng/ml and the biochemical failure definition was nadir PSA +2.0 ng/ml. The influences of clinical and dosimetric parameters were assessed . Statistical analysis was performed assuming significance level $p < 0.05$.

Results: PSA Bounce occurred in 22% after average 10.7 months. The time to PSA increase in BF group after brachytherapy HDR was 36 months. It was observed that patients with PSA nadir below 0.1 ng/ml were more likely to have normal follow-up than PSA Bounce, biochemical failure (BF), clinical failure (CF). The amplitude of the PSA increases were significantly different between subgroups. The further analysis demonstrated only a significant difference between the subgroup HDR_Bounce (median 0.7 ng/ml) and HDR_BF (median 2.6 ng/ml). The time to PSA increase was significantly different between the subgroups of the group HDR. It applies to patients with PSA Bounce (median 10.5 months) and biochemical failure (median 36 months). The analysis of others dosimetric and clinical factors (including hormonotherapy) didn't show any significant effect on the studied HDR subgroups.

Conclusion: The percentage of patients who had a PSA Bounce was 22%. Predisposing factors for PSA Bounce after HDR brachytherapy were nadir PSA (median> 0.1 ng / ml) and time to PSA increase (median <12 months). There was no influence of other analyzed clinical, dosimetric factors and use of hormone therapy to occurrence of the PSA Bounce.

EP-2006

IPSS time recovery in patients with prostate cancer after I-125 prostate brachytherapy

J. Olivera Vegas[1], W. Vásquez Rivas[1], A. Pérez Casas[1], I. Prieto Muñoz[1], J. Luna Tirado[1], L. López[2], C. Gonzalez-Enguita[2], C. Quicios[2], D. Esteban Moreno[1], A. Ilundain Idoate[1], M. García Castejon[3], M. Rincón Pérez[3], S. Gomez-Tejedor[3], J. Vara Santos[1], J. Penedo[3]
[1]*Hospital Universitario Fundación Jiménez Díaz, Oncología Radioterápica, Madrid, Spain*
[2]*Hospital Universitario Fundación Jiménez Díaz, Urology, Madrid, Spain*
[3]*Hospital Universitario Fundación Jiménez Díaz, Radiophysics, Madrid, Spain*

Purpose or Objective: To evaluate evolution and average time to IPSS (International Prostate Symptom Score) recovery, in patients who have been submitted to I-125 prostate brachytherapy (Low dose rate brachytherapy).

Material and Methods: Between March 2011 and December 2013 we performed 66 prostate brachytherapy in patients with low / intermediate risk prostate cancer. 4 patients also received external radiotherapy. 14 patients received previous hormone therapy. A 145 Gy dose was prescribed if exclusive brachytherapy was given and 108 Gy if combined with external radiotherapy. All patients were treated with Quicklink Delivery System® (BARD) and real-time planification. Of the 66 treated patients 5 did not have initial IPSS, 13 did not have complete follow up, and the 48 remaining have a suitable follow up. The variables that have been evaluated were: Prostate volume, Qmax, number of implanted seeds, number of needles and Urethra´s D1; "p value" was obtained from Mann-Whitney test. The prostate average volume was 33.73 cc, Qmax: 18.7 ml/sec, number of seeds: 60.2, number of needles: 16.1 and urethra`s D1: 138% to the prescribed dose.

Results: With an average follow up of 27 months, 41 of 48 patients (85.4%) recovered their IPSS, with an average recovery time of 9 months. 7 patients (15%) showed progressive worsening without recovery, and 3 (4.5%) of them developed acute urinary retention (AUR) one month after the implant. In a multivariate analysis the main factor that influenced AUR was the prostate volume, with p= 0.0583, (in these 3 patients prostate volume average was 42.47 cc, higher than the average non AUR) and other factors that seem to influence were IPSS and Qmax values, without statistical significance ("p" value) (In these patients Qmax average was 7.63 and IPSS average was 9.33, worse than non AUR).

Conclusion: 85% of patients with complete follow-up, recovered its basal IPSS. The average time to recovery was 9 months, and the incidence of acute urinary retention was lower than 4.5%.

EP-2007

A multicenter study of exclusive brachytherapy in younger patients with prostate cancer

E. Villafranca Iturre[1], P. Fernandez[2], R. Martínez-Monge[3], C. Gutierrez[4], A. Sola Galarza[1], E. Collado[5], I. Herruzo[6], A. Hervás[7], V. Muñoz[8], J. Muñoz[9]
[1]*Hospital of Navarra, Radiation Oncology, Pamplona, Spain*
[2]*Onkologikoa, Radiation Oncology, San Sebastian, Spain*

[3]Clínica Universitaria de Navarra, Radiation Oncology, Pamplona, Spain
[4]Instituto Catalán de Oncología, Radiation Oncology, Barcelona, Spain
[5]Hospital Universitario y Politécnico La Fe, Radiation Oncology, Valencia, Spain
[6]Hospital Regional Universitario Carlos Haya, Radiation Oncology, Málaga, Spain
[7]Hospital Ramón y Cajal, Radiation Oncology, Madrid, Spain
[8]Hospital de Meixoeiro, Radiation Oncology, Vigo, Spain
[9]Hospital Infanta Crisitna, Radiation Oncology, Badajoz, Spain

Purpose or Objective: To evaluate biochemical progression-free survival (BDFS) in men 60 years of age or younger with prostate cancer who underwent exclusive permanent brachytherapy

Material and Methods: 528 patients(p) with LR/IR. T1:423p T2: 105p; Gleason 6: 520p, gleason 7: 8p; neoadyuvant hormonotherapy: 48p.; initial PSA≤10: 492p, > 10: 36p. Md follow-up 63m (1-173m). BDFS was defined ASTRO definition. Patients were selected from RECAP database, helped by URONCOR and GEG groups.

Results: Dosimetry: pD90: md147 Gy (45-215 gy); pD90 > 165 Gy: 19.8%; pD100: md86.2 Gy; pV150: md54.6% prostate volumen: 36 cc (14-93 cc) . D10 urethra: md142%(112-191 %); D2cc rectum: 79.2 %.Toxicity: Acute: genitourinary: g2: 6.1%; g3: 0.6%; rectal: g2: 20%, g3: 3.7%. Late: genitourinary: g2: 7.7%; g3: 4.6%; rectal: g2: 2%, g3: 0.5%. Both were related with pV150: Acute GUg2: 71.7% (pV150> 50%) vs. 28.1% (<50%); late GUg≥2: 81.8% (> 50%) vs. 18.2% (<50%). p:ns. For the entire group, 40p had biochemical failure; 25p localF, 7p regionalF and 5p metastases and 5 p (1.05%) dead with prostate cancer. The actuarial 5-year and 10-y BDFS was 93.2% and 88.7%. Overall survival at 5y: 97.3% and 10y: 91.7%. No factor had influence in the analysis of prognostic factors of BDFS. However BDFS 10y pD90 < 145 Gy: 86% vs. D90 145-165Gy: 87.8% vs. D90 > 165 Gy: 92.5% (HR: 1.47, p: 0.46).

Conclusion: This is one of the biggest series at the moment in younger men with permanent brachytherapy. Patients 60 years of age or younger have a high probability of 10-year BDFS. There is a trend to get better results with D90> 165 Gy.

EP-2008

Robustness of the OARs recommendations made by GEC-ESTRO according to inter-observer variability

R. Chicas-Sett[1,2], J. Bautista-Ballesteros[2], F. Celada-Alvarez[2], S. Roldán[2], A. Torregrosa[3], J. Betancourt[4], J. Burgos[2], D. Farga[2], M. Perez[2], V. Carmona[2], A. Tormo[2], J. Benlloch[1], J. Perez-Calatayud[2]
[1]Universidad Católica de Valencia "San Vicente Mártir", Doctoral School, Valencia, Spain
[2]Hospital Universitari i Politècnic La Fe, Radiation Oncology, Valencia, Spain
[3]Hospital Universitari i Politècnic La Fe, Radiology, Valencia, Spain
[4]Hospital Universitari i Politècnic La Fe, Urology, Valencia, Spain

Purpose or Objective: To investigate the interobserver variability in contouring of rectum in high-dose rate brachytherapy (HDRBT) for the treatment of prostate carcinoma. The HDV dosimetric parameters are obtained and reported in accordance with the GEC/ESTRO recommendations.

Material and Methods: Four blinded observers retrospectively contoured the rectum of five patients treated with HDRBT in the radiation oncology department. A contouring consensus was previously established to agree in the anatomical limits determination in the rectal contouring. HDV dosimetric parameters analyzed were the included on the GEC-ESTRO recommendations: D0.1cc, D1cc and D2cc and the rectal volume were calculated. These endpoints were compared between and within the observers. The coefficient of variation (CV) defined as a measure of the spread of data as a proportion of its mean (expressed as a percentage), was estimated to assess the interobserver variation. For each parameter, the mean and SD of the two measurements recorded (taken with one week apart) from the treatment planning study made by transrectal ultra-sonogram (TRUS) were estimated for each of the 4 observers. The effect of interobserver variation in the total dose recorded was analyzed by estimating the accumulative dose (EQD2) for the rectum. For our study, the dosimetric parameter to rectum was evaluated regarding to single 15Gy prostate HDRBT plan and assuming that rectum received full-dose EBRT (46 Gy). The total EQD2 (equivalent dose in
2 Gy per fraction, assuming alpha/beta ratio of 3) doses were estimated.

Results: The patient data are represented in Table 1 showing the results of the mean reported D0.1cc, D1cc and D2cc for the rectum contoured twice for each case. The interobserver coefficient of variation for reported D0.1cc, D1cc and D2cc was 5.7%(SD 6,28), 4.5%(SD 1,94) and 4%(SD 2,24), respectively. The total D2cc parameter for the patients with the highest interobserver variation in rectum delineation, may result in recorded rectum dose difference up to 2,6 Gy by EQD2.

Table 1 Mean (standard deviation) of D0.1cc, D1cc, and D2cc parameters of the rectum obtained in two different times for each patient based on the single 15 Gy HDRBT plan.

	Rectum		
Case	$D_{0.1}$ (Gy)	D_1 (Gy)	D_2 (Gy)
1	12,12 (0,28)	10,61 (0,59)	9,42 (0,15)
2	12,26 (0,37)	10,48 (0,53)	9,046 (0,33)
3	12,39 (0,30)	10,93 (0,43)	9,65 (0,32)
4	13,04 (0,50)	11,43 (0,16)	10,02 (0,40)
5	15,51 (2,62)	12,38 (0,79)	10,86 (0,84)

Conclusion: Interobserver variations in reported parameters were high for the D0.1cc (CV: 16%) in a worst-case scenario. Even if the D2cc parameter corresponds to low interobserver variation, we found that the greatest variation is present in high prostate volume cases. Variation in delineation of the rectum may be a potential source of uncertainty in the BT planning and delivery process. Nevertheless, in our study the impact of interobserver variation on the total dose (EQD2) for the reported D2cc has a mean of +/- 1.5 Gy. This study represents a small analysis of a single center experience, but it will be completed with a multicenter study in a second part.

EP-2009

Feasibility and early toxicity of HDR alone in pts with recurrent/locally advanced prostate cancer

S.R. Bellia[1,2], P. Blanchard[2], L. Calmels[2], M. Edouard[2], P. Maroun[2], P. Chaurin[2], A. Bossi[2]
[1]Istituto Scientifico Romagnolo per la Cura e lo Studio dei Tumori IRST IRCCS, Radiation Oncology, Meldola, Italy
[2]Gustave Roussy, Radiation Oncology and Medical Physics, Villejuif, France

Purpose or Objective: High Dose Rate Brachytherapy (HDR-BT) as stand-alone treatment is gaining popularity as salvage strategy for patients (pts) with an isolated, intraprostatic Prostate Cancer (PCa) recurrence after External Beam Radiotherapy (EBRT) and may represent the only treatment available for the management of pts diagnosed with PCa and challenging clinical scenarios (for ex, pts previously irradiated in the pelvis for other primaries). We present a retrospective analysis of our series of PCa pts managed with HDR-BT alone with particular emphasis on dosimetry and early toxicity results.

Material and Methods: From March 2014 to June 2015, 13 pts have been treated with HDR-BT alone in our centre: nine with salvage intent for an intraprostatic relapse after EBRT, and four for primary management after pelvic EBRT for other malignancies (follicular lymphoma, rectal cancer and B-cell

lymphoma). All patients had biopsy-proven disease and got pre-treatment local and distant staging (Choline PET-CT, pelvic/prostatic MRI and bone scan). HDR-BT was performed by transperineal insertion of intraprostatic catheters under spinal anaesthesia and trans-rectal ultrasound guidance using an Ir-192 source. A total dose of 24 Gy to the whole gland was prescribed in two separate fractions of 12 Gy, 2-4 weeks apart. Dosimetric constraints for prostate and organ at risk (OAR) sparing were defined; we aimed at a prostate D90 > 95% and a V100 > 85% while the urethral Dmax was kept < 120 % and the D10 < 115 %; the rectal D2cc was kept <75 %. Patient reported genitourinary (GU) and gastro-intestinal (GI) symptoms according to the NCI.CTCv3 were assessed before HDR-BT and every 4-6 months afterward.

Results: The median age of the pts was 68.5 (range 63-77) years; the pre-treatment PSA was 5.71 (range 0.067-11.04) ng/ml. The median interval from the end of the previous EBRT and HDR-BT was 8.75 (range 3-16 years) years. The median prostate D90 and V100 for the 26 HDR-BT fractions analysed were respectively 97.17 % and 86.7 % of the prescribed dose but in 4 pts the D90 was < 95 % and in 8 the V100 was < 85 %. The median urethral Dmax was 105.73 % and the median D10 was 94.71 %; the median D2cc for the rectum was 45.98 %. After a median follow-up of 13.9 (range 2-28) months, acute GU grade 1 and 2 toxicities were reported in 4 and 3 pts respectively while one patient reported a grade 2 acute GI toxicity. Eleven pts were evaluable for late toxicities: five reported a late GU grade 1 and two pts a grade 2 toxicity. Any late GI toxicity has been reported so far. Nine pts (69%) are biochemical disease-free while none of the 4 pts showing a rising PSA developed an intraprostatic relapse.

Conclusion: HDR-BT in 2 fractions of 12 Gy may represent an interesting alternative for the management of pts with an isolated intraprostatic recurrence after EBRT and for challenging clinical situations when EBRT is contraindicated. The early toxicity profiles seem correct and clinical results promising.

EP-2010

Audit OAR comparing nationally-adopted prostate seed technique with GEC-ESTRO and ABS guidelines.

C. Sims[1], P. Kelly[1]
[1]*Cork University Hospital, Radiotherapy, Cork, Ireland Republic of*

Purpose or Objective: The aim is to compare OAR dosimetry for the nationally-adopted technique for PSB withexisting GEC-ESTRO and ABS guidelines. This modified MountSinai technique prescribes 160Gy to the prostate gland without a margin. Thedose volume constraints (DVCs) used are: urethra(UD_{30}) < 181Gy and rectum (RV_{100}) < 1cc.
By comparing the institutional techniqueto international standards we aim to demonstrate if:
i) All constraints perform similarly usingclinical plans.
ii) Institutional plans would be consideredreasonable when GEC-ESTRO and ABS guidelines are applied.
iii) The addition of GEC-ESTRO and ABS DVCsto institutional practice may be of clinical utility.

Material and Methods: The first 50 PSB implants performed in Institution were retrospectively re-contoured as per ABS and GEC ESTRO recommendations in Variseed (version 8.0). A PTV with margin of 3mm was added to the prostate except posterior aspect. The prescribed dose was altered to 145Gy to the PTV, as per GEC-ESTRO and ABS guidelines. The GEC-ESTRO and ABS DVCs were then applied.

Results: The median prostate V100 was 95.34% for CUH (IQR 95.34-97.66%) met by 58% of cases. The median V100 was 94.17% for ABS and GEC-ESTRO (IQR 92.68-95.61%) met by 36% of cases (p=0.007). The median D90 for CUH was 175.46Gy (IQR 168.98-186.67Gy). The median D90 for GEC-ESTRO and ABS was 159.08Gy (IQR 152.46-165.41Gy). D90>prescription dose was achieved by 92% for all groups.
The median RV100 using the institutional technique was 0.27cc (IQR 0.12-0.59cc) and the <1cc target was met by 92% of cases. The ABS rectal constraint is RV100<1.3cc, at day 30. The median ABS RV100 was 0.46cc (IQR 0.28-0.91cc) and the <1.3cc target was achieved in 88% of cases. The GEC-ESTRO rectal constraint D0.1<200Gy and D2cc<145Gy were met by 70% and 100% of the plans respectively. The median urethral UD30 using the institutional technique was 178.10Gy (IQR 175.27-180.59Gy). The GEC-ESTRO urethral constraints of UD30<188.5Gy and D10<217.5Gy were met by 100% and 100% of plans respectively. The ABS urethral constraint UD5<150% was met by 98% and UD30<125% was met by 82% of cases.

Conclusion: Comparing the Institutional DVCs for rectum and urethra with ABS and GEC-ESTRO guidelines shows that they are concordant. Institutional and ABS urethral constraint UD30 appears conservative when GEC-ESTRO urethral constraints are applied. While validated DVCs are vital for optimal prostate seed brachytherapy, prospective documentation of toxicities is crucial.

EP-2011

High-dose-rate brachytherapy combined with external beam radiotherapy for high-risk prostate cancer

S. Kariya[1], K. Kobayashi[1], I. Yamasaki[2], S. Ashida[2], K. Tamura[2], K. Inoue[2], T. Shuin[2], T. Yamagami[1]
[1]*Kochi Medical School, Department of Radiology, Nankoku, Japan*
[2]*Kochi Medical School, Department of Urology, Nankoku, Japan*

Purpose or Objective: The aim of this study is to examine if adjuvant hormonal therapy is needed for all of the high-risk prostate cancer patients treated with high dose rate-brachytherapy (HDR-BT) combined with external beam radiotherapy (EBRT).

Material and Methods: Between July 1999 and June 2010, 121 patients considered as high-risk group (T stage > or = 2c, PSA > 20 ng/ml, or Gleason score (GS) > or = 8) were treated with HDR-BT and EBRT at Kochi Medical School Hospital in Japan. Patient age ranged from 52 to 82 (median 71) years old. Eighty-two patients had received neoadjuvant hormonal therapy, which was stopped at the beginning of radiotherapy in all cases. Patients were treated with EBRT to 40 Gy in 20 fractions or 39 Gy in 13 fractions and HDR-BT to 18 Gy in 2 or 3 fractions for prostate and seminar vesicle. Adjuvant hormonal therapy was not performed until biochemical failure or clinical recurrence became apparent. PSA failure was defined as the Phoenix definition of nadir + 2 ng/mL. The overall survival (OS) rates, disease-specific survival (DSS) rates, and biological relapse-free survival (bRFS) rates were estimated using the Kaplan-Meier method. Log-rank test and Cox proportional hazards regression analysis were used for univariate and multivariate analyses, respectively, to examine these factors in relation to bRFS: age, clinical T stage (cT), initial PSA level (iPSA), GS, needle core biopsy positive ratio (% core), and use of neoadjuvant hormonal therapy (NHT). Follow-up ranged from 4 years 3 months to 13 years 3 months (median 6 years 10 months).

Results: The 5-year OS, CSS, and bRFS rates were 91.3, 98.2, and 88.0%, respectively. The 7-year OS, CSS, and bRFS rates were 86.4, 98.2, and 88.0%, respectively. In log-rank test, the group with cT < or = 2b was superior to that with cT > or = 2c (p = 0.0297), and that with iPSA < or = 10 ng/mL was superior to that with iPSA > 10 ng/mL (p = 0.0137). On multivariate Cox regression analysis, cT remained an independent predictor of bRFS (hazard ratio, 3.82; 95% confidence interval [CI], 1.11-13.14; p = 0.0337).

Conclusion: In the high risk prostate cancer group treated with HDR-BT followed by EBRT, the subgroup with cT < or = 2b gained a good bRFS rate without adjuvant hormonal therapy.

EP-2012

Are there differences in quality prostate indicators among 9-Gy vs 15-Gy HDR brachytherapy boost?

R. Tortosa[1], P. Soler[1], N. Chinillach[1], C. Ruiz[1], M. Vila[1], M. Sanchez[1]
[1]*Hospital IMED Elche, Radiation Oncology, Elche Alicante, Spain*

Purpose or Objective: The dose coverage in patients diagnosed with high risk prostate adenocarcinoma with seminal vesicles affection don´t suppose any problem in dose escalation with HDR Brachytherapy. But we wonder if the quality prostate implant indicators will show any differences between standard patients (15-Gy HDR) and those with seminal vesicles affection(9-Gy HDR). To evaluate it, a multivariate analysis has been performed in our Radiation Oncology Department

Material and Methods: 120 patients with high risk prostate adenocarcinoma were selected for the study and divided into two groups. The treatment schedule was external beam radiotherapy plus high dose rate brachytherapy as a boost:
- Group A: 9-Gy boost - T3b high grade (seminal vesicles affection) 46-Gy to pelvic areas, up to 60-Gy in prostate and seminal vesicles (2-Gy per fraction) daily and 9-Gy HDR to prostatic gland and 1-2cm. of proximal seminal vesicles.
- Group B: 15-Gy boost – High grade (no seminal vesicles affection)46-Gy to pelvic areas (2-Gy per fraction) daily treatment and 15-Gy HDR to prostatic gland.
Volumetric Modulated Arc Therapy (VMAT) was the selected technique for external radiotherapy delivered in a Varian DHX Clinac (Varian, Palo Alto, Ca.) with Millennium 120-MLC. Brachytherapy was performed with VariSource iX afterloader (Varian, Palo Alto, Ca.). The aim is to demonstrate whether there are any differences in both groups for dose homogeneity index (DHI) and homogeneity index (HI). A multivariate analysis was developed using as variables three of prostate (PTV volume, D90 , D100), two of urethra (Dmax, D10) and two of rectum (Dmax , D10).

Results: The multivariate analysis for both groups shows a p-value of 0.452 to obtain the probability for DHI > 0,75 and a p-value of 0.897 to obtain a probability for HI>0.70. In Figure 1, the plots of the results are presented:

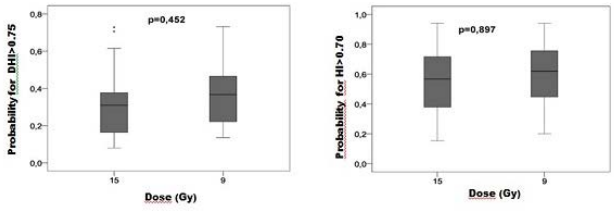

Conclusion: According to dose homogeneity, the analysis states that there were no significant differences for both studied groups. These results suggest the possibility of increasing the boost dose in T3b patients

EP-2013

Single fraction HDR BT boost using ultrasound plng for prostate cancer: dosimetrics and toxicity

M. Barkati[1], O. Lauche[1], D. Taussky[1], C. Ménard[1], G. Delouya[1]
[1]*Centre Hospitalier de l'Université de Montréal, Radiation Oncology, Montréal, Canada*

Purpose or Objective: To validate the feasibility of a single-fraction High Dose Rate Brachytherapy (HDRBT) Boost for prostate cancer using real-time Transrectal Ultrasound (TRUS) based planning.

Material and Methods: From August 2012 to September 2015, 113 patients underwent a single-fraction HDRBT boost of 15 Gy using real-time TRUS based planning. External beam radiation therapy (EBRT) (37.5 Gy/15f or 44Gy/22f or 45Gy/25f) was performed before (30%) or after (70%) HDRBT boost. We analyzed prostate, urethra and rectum dosimetrics data. Genito-Urinary (GU) and Gastro-Intestinal (GI) toxicity were assessed 4 and 12 months after the end of combined treatment using the International Prostate Symptom Score Scale (IPSS) and the Common Terminology Criteria for Adverse Events (CTCAE) v3.0.

Results: Prostate D90 between 105% and 115% was achieved for 99% of patients, prostate V150 40% for 99%, prostate V200 < 11% for 96%, urethra D10 <120% for 99%, urethra V125=0% for 100% and rectum V75<1cc for 95% of patients. Median IPSS score was 4 at the baseline and didn't change at 4 and 12 months after combined treatment. No patients developed ≥ grade 2 GI toxicity. With a median follow-up of 10 months, only two patients experienced biochemical failure. Cumulative percentage of patients with PSA≤ 1 at 4 and 18 months was respectively 47% and 74 %.

Conclusion: Single-fraction HDRBT boost of 15 Gy using real-time TRUS based planning in combination with EBRT is a safe treatment with promising results. A longer follow-up is needed to assess long-term outcome and toxicities

Electronic Poster: Brachytherapy track: Anorectal

EP-2014

Retrospective analysis of interstitial brachytherapy in gynecological and digestive tumours

C. De la Pinta Alonso[1], E. Fernandez-Lizarbe[1], A. Montero Luis[2], A. Polo Rubio[1]
[1]*Ramon y Cajal Hospital, Radiation Oncology, Madrid, Spain*
[2]*Madrid Hospital Group, Radiation Oncology, Madrid, Spain*

Purpose or Objective: The aim of this study was to evaluate the acute and late toxicities and disease-specific and overall survival after interstitial brachytherapy for the treatment of gynecological and digestive tumors.

Material and Methods: A retrospective study was carried out on a series of 19 patients referred for interstitial brachytherapy in our center between 2008 and 2013 with histologically proved locally advanced or recurrent gynecological malignancies and digestive tumors. Patients with distant metastases were excluded. Treatment consisted of brachytherapy alone (5p) (gynecological recurrence and anal carcinoma), or after surgery (1p) (rectal carcinoma) or after surgery and radiochemotherapy (4p) or after radiochemotherapy (9p). The radiochemotherapy with cisplatin-based chemotherapy regimens. Previously, recurrent patients (4p) were been treated with radiotherapy with or without concurrent chemotherapy. Medium dose of external beam radiotherapy was 51,7 Gy (range 45-70 Gy) followed by interstitial brachytherapy median implant dose 22,3 Gy (range 9-38,5Gy). Inclusion criteria were as follows: Hb minimum 10gm/dl and performance status 70% or more.

Results: Median age was 59 years (range 36-82). With a median follow-up of 14 months, local control was achieved on clinical examination or magnetic resonance imaging 93,8% patients. Among 19 patients studied, 3 lost follow-up and they were excluded from late toxicities and survival analysis. Eleven of the 19 patients (57,9%) experienced Radiation Therapy Oncology Group (RTOG) grade I or II acute toxicities proctitis (36,3%), cystitis (81,8%) and ephitelitis (18,2%). Not acute toxicities grades 3 or 4 were reported. Two of the 16 patients (12,5%) experienced RTOG grade I or II late toxicities proctitis (6,25%) and cystitis (6,25%). Two of the 16 patients (12,5%) experienced RTOG grade III or IV late toxicities rectal ulcer (6,25%) and vulvar necrosis (6,25%). Using Kaplan-Meier analysis overall survival after minimum follow-up of 14 months was 93% and disease-free survival was 75% (persistent tumor were included in this group). One patient had a locoregional recurrence and died of tumor.

Conclusion: Interstitial brachytherapy is a good choice to deliver high-dose radiation in gynecological tumor after external beam radiotherapy or as an exclusive treatment in

recurred and previously radiated digestive tumors. This treatment offers adequate locoregional control with acceptable range of complications.

Electronic Poster: Brachytherapy track: Miscellaneous

EP-2015

Acute toxicity in HDR BT of skin cancer with very high viscosity addition silicone custom made molds

C. Sanz Freire[1], S. Pérez Echagüen[2], G.A. Ossola Lentati[2]
[1]*Center For Biomedical Research Of La Rioja, Medical Physics Department, Logroño, Spain*
[2]*Center For Biomedical Research Of La Rioja, Radiation Oncology Department, Logroño, Spain*

Purpose or Objective: To study normal skin acute toxicity in Non-Melanoma Skin Cancer (NMSC) patients treated with High Dose Rate (HDR) Plesiotherapy and very high viscosity addition silicone (VHVAS) rubber custom-made molds. VHVAS rubber features excellent mechanical and physical properties which benefit the stability and reproducibility of the implant. On the other hand, the high electron density relative to water of these materials will increase the scatter production, which may be relevant at the mold-skin interface.

Material and Methods: Our standard applicators are polymerized VHVAS molds with catheters embedded. This VHVAS model features 99.5% recovery factor after compression and maximum 0.20% linear dimensional variations. Dosimetric properties of this VHVAS have been characterized by our Group elsewhere. Silicone attenuation relative to water is <5% up to 3 mm thickness. Maximum scatter relative to water measured at the mold interface is <14%. Treatment is delivered with a Ir-192 based VARIAN MS Gammamed+ HDR unit. All treatments are 3D simulated. A sample of 15 Patients with 21 lesions (8 basal cell carcinomas, 13 squamous cell carcinomas) representing all treated locations were considered. Average age is 83.1 years [96-58], 47% without any concomitant diseases and life expectancy >5 years. Median lesion area is 5.4 cm2 [1.0-46.6], treatment depth is 4.0 mm [2-15] and microscopic disease margin is 4 mm [2-5]. Standard fractionation is 5.5 Gy/fr, 10-12 fr, twice a week. Acute toxicity was retrospectively assessed following the RTOG criteria.

Results: DVH analysis showed high dose areas having: D1cc=8.5 Gy/fr [5.4-14.4], D0.5cc= 9.0 Gy/fr [5.4-16.3], D0.1cc= 10.3 Gy/fr [6.2-22.9]. All patients presented radiodermatitis 1 month after treatment (G2: 89%, G3: 11%). 32% presented radiodermatitis at 3 months (G1: 26%, G2: 6%) and only one patient presented radiodermatitis G1 at 6 months. Toxicity score correlation to CTV volume, treatment depth, BED prescribed dose, D1cc, D0.5cc and D0,1cc had no statistical significance (*p>0.05*). Treated area was found to be predictive of radiodermatitis persistence at 3 months after treatment (*p=0.036*). Lesions located in the legs showed longer recovery time from radiodermatitis than other locations (4 months vs 1.8 months average).

Conclusion: The use of these VHVAS moulds was well-tolerated by all patients. Our treatments yield similar results to other groups with similar treatment schemes in terms of acute toxicity. We can conclude that VHVAS custom made molds have a good safety profile.

EP-2016

A method to transform 2D LDR brachytherapy plans into contemporary 3D PDR dose distributions

E. Rodenburg[1], J. Wilkes[1], J. Wiersma[1], R. Ordoñez Marmolejo[1], R. Dávila Fajardo[1], A. Bel[1], B. Pieters[1]
[1]*Academic Medical Center / University of Amsterdam, Department of Radiation Oncology, Amsterdam, The Netherlands*

Purpose or Objective: Formerly in the 2D Low-Dose Rate (LDR) era no information about Dose-Volume Histogram (DVH) parameters of organs at risk (OARs) was available in brachytherapy plans. To enable research on late dose effects for children treated with Pulsed-Dose Rate (PDR), 3D dose distributions and DVH parameters are required. In this study a method was developed to enable calculation of DVH parameters.

Material and Methods: Before 2001 pediatric head and neck (H&N) patients received LDR brachytherapy as a part of their treatment. Of 16 LDR plans (1989-2001) only hard-copy CT data, orthogonal x-ray images of the implant and documented 2D dose information were available. The documented 2D dose information consisted of source strength, catheter numbering, catheter loading, and treatment time. The hard-copy CT data was digitized, transferred to DICOM format and imported in Oncentra Brachy (Elekta, v4.3). The visible OARs were delineated and used catheters were reconstructed. The Ir192-LDR line sources from the original 2D plans were simulated by loading the reconstructed catheters with Ir192-PDR source tracks of the same length as the LDR sources, with a step size of 2.5mm. Simulation of a line source dosimetry was necessary because the planning system did not support LDR planning. All PDR source dwell times were made equal, but scaled to the documented 2D dose distribution to obtain the 3D dose distribution at time of treatment. Scaling was performed at a 2D LDR isodose level below 30% of the prescribed dose in a plane where the documented 2D dose distribution and transformed 3D dose distribution geometrically match. Scaling below 30% is done to avoid effects due to the non-uniform isodose distribution very close to a stepping PDR source. To check the reliability of the method the Total Reference Air Kerma (TRAK) for both 2D LDR and 3D PDR plans were determined and compared. The difference was tested with the Wilcoxon Signed Rank Test for paired variables. To illustrate the applicability of the method the maximum dose, defined as the D0.1cm3, on e.g. chiasm was determined.

Results: Of 16 LDR plans 2D data were transformed into 3D dose distributions. OARs and DVH parameters of chiasm were determined. The mean 2D TRAK was 0.95cGy/1m (IQR 0.89). The mean 3D TRAK was 0.89cGy/1m (IQR 0.74). The mean difference of 2D TRAK and 3D TRAK was statistically not-significantly different from 0 (P=0.45). For 7 patients the CT data incorporated the chiasm area. The mean chiasm maximum dose was 233.6cGy (range 4.6-399.2) using the described method.

Conclusion: With the described method it was possible to transform 2D LDR brachytherapy plans into a 3D dose distribution. This method shows the possibility to use information from 2D LDR brachytherapy plans in scientific studies in which 3D dose information is needed.

EP-2017

High dose-rate endoluminal brachytherapy as a treatment of primary and recurrent esophageal cancer

N.H. Nicolay[1,2], J. Wagner[1], J. Oelmann-Avendano[1], J. Debus[1,2], P.E. Huber[1,2], K. Lindel[1]
[1]*Heidelberg University Hospital, Radiation Oncology, Heidelberg, Germany*
[2]*German Cancer Research Center, Radiation Oncology, Heidelberg, Germany*

Purpose or Objective: To evaluate outcomes and toxicities after high dose-rate (HDR) endoluminal brachytherapy for the treatment of esophageal cancer patients.

Material and Methods: We analyzed the patient records of 36 patients treated with high dose-rate endoluminal brachytherapy for histologically confirmed esophageal cancer. Brachytherapy was either applied as a boost treatment for definitive radiotherapy and radio-chemotherapy regimens or as a salvage treatment for recurrent tumors. Single radiation doses between 4 and 6 Gy were delivered to the endoscopically visible tumor including 2 cm margins in 2 to 4 sessions. Recurrence-free and overall

survival as well as acute and late toxicities were retrospectively analyzed.

Results: Brachytherapy was performed as initially planned in all but one patient. 18 patients had a complete endoscopic response at the first follow-up examination. Loco-regional recurrence was observed in 24 patients after a median time of 3 months; 1- and 2-year recurrence-free survival rates were 51% and 51% for the patients treated for primary tumors and 11% and 6% for patients treated for tumor recurrence, respectively. Median overall survival was 18 months; estimated overall survival rates at 1, 2 and 3 years were 63%, 50% and 30% after primary brachytherapy, and 60&, 25% and 6% after treatment for recurrent cancers. Adenocarcinoma histology, non-complete remission after treatment and treatment for recurrent cancers were associated with significantly reduce prognosis. Mild to moderate dysphagia was the most common side effect in 17 patients; 8 patients suffered from loco-regional grade 3 toxicities, and no grade 4 or 5 toxicities were observed.

Conclusion: Endoluminal brachytherapy during the course of esophageal cancer treatment can be safely applied and results in good functional outcomes regarding dysphagia with moderate local toxicity and low side effects to the lung and heart.

EP-2018

Treatment with high dose rate plesiotherapy and custom moulds in skin cancer. Long term results

I. Membrive[1], A. Reig[1], P. Foro[1], N. Rodriguez[1], J. Sanz[1], A. Ortiz[1], J. Quera[1], E. Fernandez-Velilla[1], O. Pera[1], R. Jimenez[1], N. Becerra[1], J. Flores[1], M. Algara[1]
[1]*Hospital de la Esperança, Radiation Oncology, Barcelona, Spain*

Purpose or Objective: To describe the technique used in our department for treatment of cutaneous tumors with HDR plesiotherapy using custom moulds and to analyze long term results.

Material and Methods:
Custom made mould fabrication:
We used this aplicator in irregular areas of skin.
The treatment sequence is:
- Creation of the mould with thermoplastic material with a thickness of 5 mm.
- Parallel placement of transfer guide tubes with 1 cm of separation.
- CT simulation and definition of the volume treat. The volume has to be delimited 5 mm in deep.
- Dosimetry.
- Treatment of the patient.

We used 3 different schedules:
- 54 Gy in 18 fractions
- 66 Gy in 33 fractions
- 40 Gy in 10 fractions

Results: From September 2008 until September 2015 53 patients had been treated with this technique.
The average age was 77 years (63-91), the histology was squamous in 6 cases, basocellular in 46 cases, melanoma in situ in 1 case.
The mean dose was 54.8 Gy (40-66). The treatment was adjuvant after surgery in 41,5% of the patients.
After a mean time of follow up was 34,1 months there were 2 local relapses (3.77%) in the treatment location. No deaths related to disease were observed.

Conclusion: Treatment with HDR plesiotherapy using custom moulds is a technique used to treat small lesions and/or irregular surface locations. Planning with CT scan allows to know the dose in organs at risk using dose-volume histogram. This treatment offers a high local control of the disease and can be used alone or as adjuvant treatment after surgery in case of positive margins or presence of adverse factors.

EP-2019

The safety and efficacy of external beam radiotherapy combined yttrium 90 SIRT

T.H. Wang[1], R.C. Lee[2], Y.W. Hu[1], P.I. Huang[1], C.S. Liu[1]
[1]*Taipei Veterans General Hospital, Department of Oncology, Taipei, Taiwan*
[2]*Taipei Veterans General Hospital, Department of Radiology, Taipei, Taiwan*

Purpose or Objective: Previous literatures showed prior liver external beam radiotherapy (EBRT) may increase liver toxicity after yttrium-90 (90Y) selective internal radiation therapy (SIRT). In contrast, the safety of EBRT followed by SIRT is unclear. We investigated the safety and efficacy of EBRT followed by SIRT in hepatocellular carcinoma (HCC) patients.

Material and Methods: Between October 2011 and May 2015, a total of 11 HCC patients who had treated with SIRT followed by liver salvage EBRT were enrolled. The SIRT 3-dimensional absorbed dose distribution of each patient was retrospectively calculated on a voxel base, using post-treatment bremsstrahlung SPECT/CT images. The physical dose and biological effective dose (BED) of SIRT and EBRT were generated and summed for evaluation. The dose-volume histograms (DVHs) of the EBRT, SIRT, and combined therapy were analyzed. Liver-related toxicities were collected by chart-review and classified as Common Terminology Criteria for Adverse Events version 4.

Results: The median time interval of SIRT and EBRT was 95 days (IQR: 66.5-129.5 days). Eight patients (73%) had undergone EBRT for portal vein thrombosis (PVT) and 6 patients (55%) for residual hepatic tumor. The mean SIRT, EBRT, and combined therapy normal liver BED were 52.1±21.0 Gy, 17.9±6.1 Gy, and 69.5±15.0 Gy, respectively. The summed DVH of each patient is depicted in Figure 1. The image study three months post-irradiation showed primary disease PR in 4 patients (67 %) of patients and thrombosis improved in 6 patients (75%) after EBRT. Two patients had no evidence of disease after combined therapy. The median survival was 359.9 days. Total 3 patient (27 %) had developed ≧grade 2 liver toxicities. Patient who experienced hepatotoxicity had higher summed BED (107.0±7.3 Gy vs 58.9±13.5 Gy; P = 0.02). The univariate analysis of summed DVH showed that the fraction of normal liver exposed to more than 70 Gy (V70) was the strongest predictor of hepatotoxicity (9.4±7.2% vs 29.9±4.4%; P=0.007), as presented in Table 1.
Figure 1: DVH of 11 patients

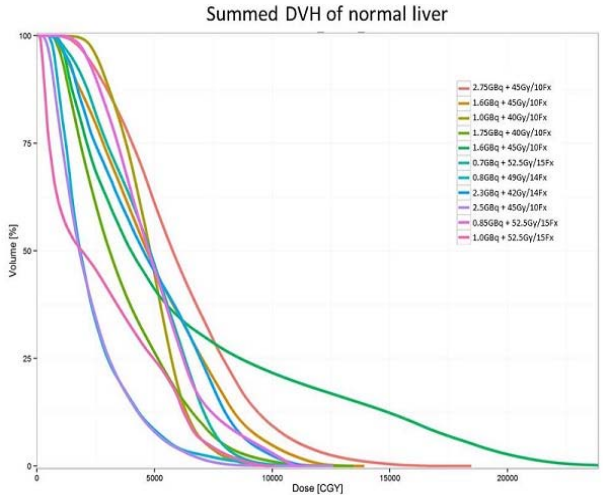

Table 1. Dosimetric parameter univariate analysis

	Hepatotoxicity		
	No (N = 8)	Yes (N = 3)	p value
V10 (%)	89.9 (13.0)	98.7 (0.9)	0.093
V20 (%)	72.1 (20.5)	85.4 (7.8)	0.180
V30 (%)	56.2 (22.7)	72.5 (10.8)	0.184
V40 (%)	42.6 (20.3)	60.5 (11.0)	0.142
V50 (%)	29.7 (15.5)	49.1 (8.6)	0.058
V60 (%)	17.9 (10.8)	39.2 (5.5)	0.007
V70 (%)	9.4 (7.2)	29.9 (4.4)	0.004
V80 (%)	4.8 (4.7)	21.1 (6.2)	0.051
V90 (%)	2.4 (2.8)	14.9 (7.5)	0.137

Values are shown as mean (SD)

Conclusion: Salvage EBRT after SIRT was effective for HCC patients with PVT. The 3D dose summation and BED-DVH of combined therapy help to predict liver toxicity. By carefully selecting patients, the combined therapy bring acceptable toxicities incidence.

EP-2020

Vertical type surface brachytherapy applicator improvement with a 3d printed dose compensation body

K. Buchauer[1], G. Henke[1], L. Plasswilm[1], J. Schiefer[1]
[1]*Kantonsspital St. Gallen, Departement of Radiation Oncology, St Gallen, Switzerland*

Purpose or Objective: Unflattened surface HDR Brachytherapy applicators commonly suffer from dose fall off on the side of the dose distribution. Recent research documented that in addition to missing dose at the side of the applicator vertical type HDR Brachytherapy surface applicators are subject to underdose in the middle of the treatment region. This artifact is clinically relevant because tumor cells in the middle of the treated area can end up irradiated insufficiently. In this work we present a surface-dose compensation body generated with a 3D printer that specifically addresses the dose irregularities of a vertical type HDR Brachytherapy surface applicator. In order to overcome the limitation of increased treatment time of applicator flattening for horizontal type applicators we utilize the possibility of using a source position nearer to the surface to generate a flattened dose distribution together with reduced treatment time.

Material and Methods: A 40 mm Varian VariSource GM11010080 applicator was used for the modification (Varian Medical Systems, Inc., Palo Alto, CA, USA). The source position is 1.5 cm from applicator tip. The depth of evaluation is 0.5 cm solid water material. A consumer grade 3D printer "UP! 3D, Beijing TierTime Technology Co. Ltd." was used to print out a negative form with ABS plastic. Lippowitz type low temperature melting metal was used to mold the positive form of the flattening elements. All dose measurements and flatness evaluations were performed with Gafchromic EBT3 film Lot #: 12021402 and the FilmQA software, flatness and symmetry toolbox (both Ashland Speciality Ingredients, Bridgewate, NJ, USA).

Results: The generated compensation element is of toroidal shape, for the standard source position 1.5 cm from appliator tip, has a maximum thickness of 1.5 mm in surface direction. The output of the applicator with flattening element occurred to be 75% of the unflattened one. The diameter of 80% nominal dose area increased from 35.2 mm with the unflattended applicator to 50.2 mm with the flattening element in place. The asymetric central low-dose artefact can be compensated to a clinical acceptable minimum dose. When utilizing the source position 1 cm from tip a prototype filter could bring the width of the 80% dose area to 45.0 mm, above the nominal applicator size, and output to 112 % of an unflattened applicator. The position 0.5 cm from tip is still considered flattable with increased low dose area in out of field tissue due to applicator geometry when quick treatment is of clinical interest. The first soure position on applicator tip is not flattable for clinical use.

Conclusion: The presented prototype of a dose compensation body can remove the dose artefacts of a vertical type HDR Brachytherapy surface applicator including the clinical relevant underdosed central region. With the appropriate flattening body it is now possible to utilize a source position nearer to surface and compensate for dose output loss when using a dose flattening element.

EP-2021

Cosmesis and acute toxicity outcomes in skin lesions treated with High-Dose-Rate Brachytherapy.

H. Pérez-Montero[1], A. Campos[1], M.P. Crespo[1], B. Gil[1], A.M. Cabezas[1], T.C. Chávez[1], V. Rodríguez[1], N. Gascón[1], J.F. Pérez-Regadera[1]
[1]*Hospital 12 de Octubre, Radiation Oncology, Madrid, Spain*

Purpose or Objective: Skin cancer is the most common malignancy in white population. The most prevalent histologies are basal cell carcinoma (BCC) followed by squamous cell carcinoma (SCC). They are locally aggressive lesions that rarely metastasize and their prognosis depends on local control. Due to their localization and superficial nature, cosmetic result of the treatment is of primary importance. High-Dose-Rate brachytherapy (HDR-BT) is a safe and effective treatment option for these carcinomas and for other skin lesions. There are two main techniques for its delivery: interstitial brachytherapy and plesiotherapy.
We have evaluated early local control, acute toxicity and cosmetic outcomes in all patients treated with HDR-BT in our center.

Material and Methods: We assessed 47 patients who had 52 skin lesions. There were 29 SCCs, 14 BCCs, 4 keloid scars, 3 adenocarcinomas,1 lentigo maligna and 1 Merkel cell carcinoma. Median age of treated patients was 78 years (34-93). Data was collected prospectively.All lesions were treated with HDR-BT at our institution between December 2014 and August 2015 by interstitial brachytherapy or plesiotherapy. Average total dose delivered was 35,63 Gy and Median dose delivered was 40,5 Gy.
Acute toxicity was graded using the Common Terminology Criteria for Adverse Events, version 4.0 and cosmetic outcomes were classified using the Radiation Therapy Oncology Group cosmetic rating scale.

Results: Average follow-up from completion of treatment was 5.5 months (2-10.1). The overall crude recurrence rate was 3,8% (n = 2). Grade 0 acute toxicity was observed in 7.7% of treated lesions (n = 4), grade 1 in 63.5% (n = 33), grade 2 in 21.2% (n = 11) and grade 3 in 7.7% (n = 4). No acute toxicity greater than grade 3 was observed. All acute toxic events were resolved between the first and the second month after brachytherapy. Cosmetic results were excellent or good in 92.3% of the cases (n = 48), fair in 3.8% (n = 2) and not evaluable in 2 patients whose tumours were not cured.

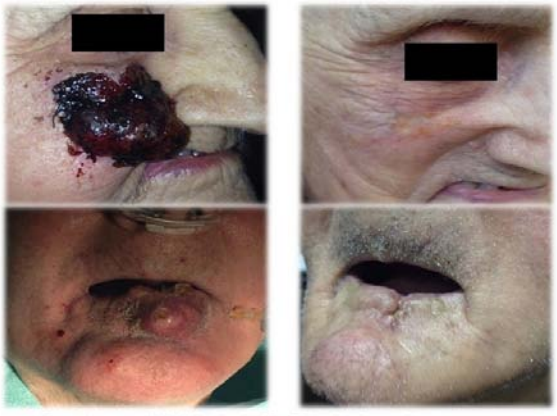

Fig 1. 2 cases of SCC before HDR-BT and 1,5 months post-treatment

Conclusion: HDR-BT seems to be a good alternative for treatment of epitheliomas in special locations, above all in elderly patients with comorbidities that preclude surgery. Its ability to treat a wide area with minimal alteration of normal tissues allows a high probability of cure with excellent cosmetic results and without affecting functionality.
We can conclude that HDR-BT could be a valid alternative to surgery with acceptable acute toxicity, good early local control and exceptional cosmetic outcomes in skin lesions.

EP-2022
Compare EBRT and brachytherapy in the treatment children's vaginal rhabdomyosarcoma.
O. Kozlov[1], I. Nechushkina[2], M. Nechushkin[1]
[1]*NN Blokhin Cancer Research Center, Radiosurgery Brachytherapy, Moscow, Russian Federation*
[2]*NN Blokhin Cancer Research Center, Institute of Pediatric Oncology, Moscow, Russian Federation*

Purpose or Objective: Rhabdomyosarcoma of the vagina is very rare disease, mainly girls were 1-3 years, only a few patients were 13-15 years old. Early studies have shown the advantage of intracavitary radiation therapy over surgical treatment and EBRT. There are new methods of planning EBRT from CRT moved to VMAT and IMRT. The emergence of new techniques in the EBRT and brachytherapy inspired us to the evaluation of methods of treatment children's vaginal rhabdomyosarcoma.

Material and Methods: From 1980 till 2015 38 patients received intracavitary brachytherapy with source Co-60 and Ir-192. In our cancer center were made special applicators of different designs. The main treatments were applicators for direct 8 mm diameter and a length of about 6-7 cm. Were specially made Co-60 tube source (LDR). Children were immobilized for several days. The active length was 4-5 cm.
Since the 90s we switched to using stepping source Ir-192 HDR. Normalisation point changed from 5 mm to 2 mm from the surface of applicator.This made it possible to irradiate the entire vagina.
Planning is optimized for the creation of uniform dose distribution throughout the vagina. Accordingly, it was necessary to calculate dose distribution for these cases. For calculations were chosen CT and MRI and patient anatomy was extended, contoured target and OAR's. The calculation of CRT / IMRT / VMAT / Brachy. CTV was 6.5 cm3.
Unlike cervical cancer, in OAR's we added the urethra, which is located close to vagina, and which dose close to 100%. We have calculated % dose to the rectum, bladder, urethra and ovaries. For EBRT, we calculated the mean dose to OAR's, Brachytherapy for rectum and bladder, we calculated dose to 1 cm3, and the entire volume of urethra and ovaries.

Results: In both cases (EBRT and Brachy) ovaries was about 2% (2.0% -2.3%) of normalisation dose. However, it is worth considering that brachytherapy is given high dose per fraction, so radiobiological dose above.
CRT / IMRT / VMAT / Brachy:
Rectum: 37.7 / 26.6 / 29.9 / 37.2 %
Bladder: 58.7 / 39.6 / 37.1 / 30.8 %
Uretra: 99.0 / 99.2 / 97.2 / 50.2 %

Conclusion: Although improvement in EBRT (from CRT to IMRT and VMAT) and decrease in dose to OAR's, brachytherapy maintains its position in the treatment of this localization. When less integral dose brachytherapy and dose on OAR's (not whole body is irradiated, but only part of it), which significantly reduces late effects. In modern time, we should pay attention to other radionuclides, which can give uniform dose distribution (example Yb-169).

Electronic Poster: Radiobiology track: Molecular targeted agents and radiotherapy

EP-2023
Radiation resistance induced immunity evasion by evoking PD-L1 expression
X. Gong[1], C. Zhou[2], X. Li[2], C. Zhao[2]
[1]*Shanghai Pulmonary Hospital, Radiation Oncology Department, Shanghai, China*
[2]*Shanghai Pulmonary Hospital, Oncology Department, Shanghai, China*

Purpose or Objective: To characterize PD-L1 expression in non-small-cell lung cancer (NSCLC) cell lines, and explore the relationship between immunology escaping and tumor cell proliferlation and apoptosis with receiving radiotherapy.

Material and Methods: Evaluating the PD-L1 protein and CD8+ T cells with immunohistochemistry in tumor tissue from NSCLC patients. In vitro assay, to detect the expression of PD-L1 in different NSCLC cell lines after conventional and hypofractionated radiation therapy by westernbloting and study the difference between A549 and radiation resistance A549 cell line by flow cytometry and westernbloting. To analysis PI3K/Akt and stat3 proliferation pathway and Bcl2 family apoptosis signaling pathway in A549 radiation resistance cell by westernbloting. Small interfering RNA (siRNA) was used to A549 radiation resistance cell, and then to observe the difference in PI3K/Akt and stat3 pathway. As for in vivo study, immunohistochemistry was used to detect the relationship between the expression of PD-L1 and NF-KB protein in control group, anti-PD-L1 group, radiation group and radiation plus anti-PD-L1 group.

Results: We found that patients whose tumor expression the higher PD-L1 protein, who had the more radiation resistance and had less CD8+ T cell around tumor microenvironment. PD-L1 protein improved obviously in NSCLC cell lines after receiving conventional radiation, but there is not the same tendency after hypofractionated radiation. We found that A549 radiation resistance cell had activation in PI3K/Akt and stat3 pathway and its' NF-KB protein would be up-regulation. When the A549 acquired radiation resistance, it would be apoptotic less. We observed the activation of the anti-apoptosis protein bcl2 and the inhibition of the pro-apoptosis protein bim in A549 radiation resistance cell. After siRNA interfering to this cell, it's PD-L1 protein decreased. A549 radiation resistance cell came to be apoptosic. While it's pAkt, pstat3 and NF-KB didn't change.

Conclusion: Conventional radiation would be easy to induce radiation resistance by overexpressing the PD-L1. When the lung cancer cell express PD-L1 more, the tumor would escape from CD8+ T cell. NF-KB protein is the key to up-regulation PD-L1. When PD-L1 overexpression, lung cancer would be apoptosis less and immunity escaping. SiRNA interfering PD-L1 can eliminate the radiation resistance of the A549 cell line. It provide the evidence for the combination of the anti-PD-L1 drug and radiation therapy in clinic.

EP-2024
Optimising hyperthermia induced radiosensitisaion for treating HPV+ cervical tumours
A.L. Oei[1], C.M. Van Leeuwen[2], R. Ten Cate[1], H.M. Rodermond[1], M.R. Buist[3], L.J.A. Stalpers[1], J. Crezee[2], H.P. Kok[2], J.P. Medema[1], N.A.P. Franken[1]
[1]*Academic Medical Center AMC Amsterdam- The Netherlands, LEXOR Laboratory for Experimental Oncology and Radiobiology- Department of Radiation Oncology, Amsterdam, The Netherlands*
[2]*Academic Medical Center AMC Amsterdam- The Netherlands, Department of Radiation Oncology, Amsterdam, The Netherlands*
[3]*Academic Medical Center AMC Amsterdam- The Netherlands, Department of Gynecologic Oncology, Amsterdam, The Netherlands*

Purpose or Objective: Hyperthermia (raising the tumour temperature to 40-43°C) is an effective treatment in combination with radiotherapy for several tumour sites, including cervical cancer, which is mainly caused by infection with the Human Papillomavirus (HPV). The aim of our study is to improve treatment strategies for cervical carcinoma by (#1) unravelling mechanisms of hyperthermia induced radiosensitization, (#2) optimization of time interval between hyperthermia and radiotherapy and (#3) investigating the benefit of additional treatments.

Material and Methods: HPV-positive cervical cell lines SiHa and HeLa were used. Cells were treated with (#1) hyperthermia alone (42C for 1h), (#2) hy perthermia and irradiation in different time intervals between the two therapies and (#3) hyperthermia and radiation with additional agents PARP1-inhibitor (i.e. a drug blocking a DNA repair protein) and cisplatin. Clonogenic survival assays and γH2AX stainings (a staining to visualize DNA double strand breaks) were carried out in order to determine the effectiveness of the (combined) treatments. Protein levels of p53 and DNA repair proteins were investigated using western blot. Apoptosis was measured in cell lines using the Nicoletti assay and cell cycle distribution was analyzed using the BrdU-assay.

Results: (#1) The high-risk HPV types 16 and 18 produce the oncoprotein, early protein 6 (E6), which binds to p53 before both proteins get degraded. Therefore, p53 cannot induce cell cycle block nor apoptosis, limiting the radiation effects. Hyperthermia increases the effectiveness by preventing the formation of the E6-p53 complex, rescuing p53 from degradation, resulting into functional p53 causing apoptosis and cell cycle arrest. (#2) Higher levels of p53 are present immediately after hyperthermia and remain up to four hours after treatment. The main therapy, radiotherapy or chemotherapy, should be applied within this time frame to yield a beneficial effect. (#3) Combination treatment of radiotherapy, hyperthermia, cisplatin and PARP1-inhibitors resulted in a lower survival fraction due to an increased number of DNA double strand breaks as compared to radiation alone. Cisplatin and PARP1-inhibition significantly enhanced the combined hyperthermia/radiation treatment.

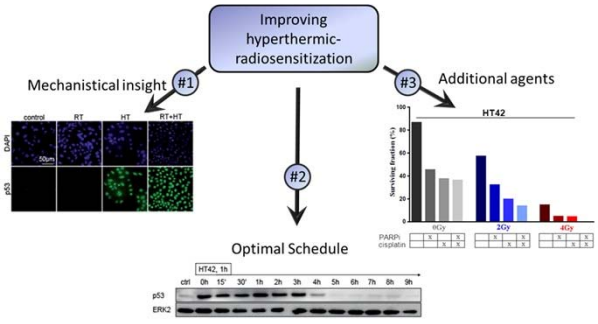

Conclusion: Our findings provide new insights for patients suffering from HPV-positive cervical cancer. Hyperthermic-radiosensitization, makes radiotherapy significantly more effective by rescuing p53 from getting degraded. Adding PARP1-inhibitor or cisplatin further improves the effectiveness of hyperthermic-radiosensitization, which will increase clinical outcomes substantially.

EP-2025

The potential role of gold nanoparticles in proton beam radiosurgery for arteriovenous malformations

A. Nor[1], M. Morris[1], F. Vernimmen[1], M. Shmatov[2]
[1]*Cork University Hospital, Radiation Oncology, Cork, Ireland Republic of*
[2]*Ioffe Institute, Theoretical Physics, St Petersburg, Russian Federation*

Purpose or Objective: To theoretically evaluate therapeutic gain from radiation dose enhancement by gold nanoparticles (AuNP) based on their physical interaction with protons.

Material and Methods: Nanoparticles range in size from 1 x 10^{-9}m to 100 x 10^{-9}m, and exert their effect by either entering the cell, or by attaching to the cell membrane surface. Radiation enhancement by gold nanoparticles (AuNP) is based on the generation of much localized secondary radiation when irradiated. This results in a Dose Enhancment Factor (DEF) and has been well described for photon irradiation and is most pronounced with kilo voltage photons, but happens also with Mega Voltage (MeV). For protons the DEF obtained with metallic nanoparticles has recently been studied. We took the definition of DEF as being: DEF=(Dpure + DGNP – Dwnp)/ Dpure , where Dpure is the dose deposited in pure water.

Results: In vivo studies on tumors in mice have shown a considerable delay in tumor growth for mice receiving AuNPs with protons compared to protons alone. Protons have a high cross-section for gold over a large range of clinical energies, and the interaction produces Auger electrons with a very short range. The sphere of DEF around the AuNP is influenced by its size. For an AuNP of r = 22nm and 80 MeV protons the radius of the sphere of DEF is in the order of 18nm, with dose enhancement factors of up to 2 described. We obtained a value of 1.06 at 1 nm from a nanoparticle with radius 25 nm and taking Dpure as being: Dpure [Gy] ≈ 8.16 x Sw [MeV x cm2/g], where Sw is the stopping power of water. This small radius means that in order to be effective the AuNPs need to be in very close contact with the target. In the treatment of AVMs the prime target is the endothelial cell. Angiogenesis occurring in AVMs is driven by endothelial cells stimulated by vascular angiogenic factors binding on cell membrane receptors. AVM endothelial cells over express these receptors compared to their counterparts in normal brain vessels. IMC-1121B, a human antibody to VEGFReceptor2, when linked with an AuNP has the potential to selectively increase the local AuNP concentration on the membrane of AVM endothelial cells. For conventional dose/fractionation schedules the radiobiological effects are governed by DNA damage in the cell nucleus. Membrane location could also be exploited because a cell membrane initiated effect is described, whereby activation of the acid sphingomyelinase/ceramide pathway occurs after doses >10 Gy, leading to endothelial apoptosis.

Conclusion: Successful AVM radiosurgery is amongst others dose dependent. Therapeutic gain in proton radiosurgery is possible with AuNP-VEGFR2ab located on the cell membrane, combined with doses > 10 Gy. This approach needs to be researched further, but offers the possibility for better obliteration rates and/or shorter latent intervals.

EP-2026

Effect of PARP-1 inhibition on human soft tissue sarcoma cells radiosensitivity

M. Mangoni[1], M. Sottili[1], C. Gerini[1], I. Meattini[1], I. Desideri[1], P. Bonomo[1], D. Greto[1], M. Loi[1], R. Capanna[2], G. Beltrami[2], D. Campanacci[2], L. Livi[1]
[1]*University of Florence, Experimental and Clinical Biomedical Sciences, Firenze, Italy*
[2]*Careggi University Hospital, Department of Orthopaedic Oncology, Florence, Italy*

Purpose or Objective: Soft-tissue sarcomas (STS) are aggressive tumours with a poor prognosis and there is a major clinical need for novel strategies. Poly-ADP ribose polymerase (PARP)-1 promotes base excision repair and DNA strand break repair. Inhibitors of PARP (PARPi) have shown to enhance the cytotoxic effect of irradiation (IR), and evidences suggest that PARPi could be used to selectively kill cancers defective in DNA repair. Sarcomagenesis is linked to aberrant biological pathways and some STS have defect in DNA repair systems, so there is a rationale for using PARPi in STS. We investigated the effect of PARP inhibition on STS cell lines survival after IR and on radiation-induced DNA damage foci.

Material and Methods: Cell proliferation analysis was performed on human fibrosarcoma, liposarcoma, leiomyosarcoma and rhabdomyosarcoma cell lines with increasing doses of olaparib (0.25; 0.5; 1; 2; 4 μM) 3 h after cells seeding. The numbers of cells were assessed after 5 days and results normalized to the untreated control. For clonogenic assays, fibrosarcoma, liposarcoma, leiomyosarcoma and rhabdomyosarcoma cells were irradiated with 2, 4 or 6 Gy, with or without olaparib (1 μM) iniparib (10 μM) or veliparib (5μM) pre-treatment. The plating efficiency of the combined treatments were normalized to PARPi-treated cells. The linear-quadratic survival expression was fitted to the data by nonlinear regression. The radiosensitization enhancement ratio for the PARPi at 50% survival (ER50) was as follows: ER50 = Dose at 50% survival without PARPi/Dose at 50% survival with PARPi. The impact of PARP inhibition on γ-H2Ax foci formation was evaluated in rhabdomyosarcoma cells treated with olaparib 1 μM after 48 h, and irradiated at 4 Gy. Cells were probed with primary antibody to γ-H2AX.

Results: Continuous treatment with olaparib for 5 days resulted in a dose-dependent inhibition of proliferation in all the STS cell lines. Significant radiosensitization was observed in all human STS cell lines using PARPi, with an ER50 ranging from 1.2 to 3.41. Rhabdomyosarcoma showed the greatest increase in radiosensitivity, with an ER50 of 3.41 with veliparib. Fibrosarcoma showed an ER50 of 2.29 with olaparib and 2.21 with veliparib. Leiomyosarcoma and liposarcoma showed similar radiation responses after PARP inhibition, with the higher radiosensitization in presence of veliparib (ER50 1.62 and 1.46, respectively). The combination of olaparib and radiation in rhabdomyosarcoma cells resulted in an increased number of γH2AX foci as compared to control and irradiation alone.

Conclusion: We demonstrated that PARPi are potent radiosensitizers on human STS in vitro models. The different PARPi radiosensitizing effects observed in various cell lines may be explained by the presence of different genomic aberrations in DNA repair machinery in specific STS subtypes. These preliminary data encourage to further study association of PARPi with IR as a promising treatment for STS.

EP-2027

Fractionated radiotherapy plus anti-angiogenic therapy in an orthotopic glioma transplantation model

V. Albrecht[1], J. Schuster[1], M. Proescholdt[2], D. Piehlmaier[3], K. Unger[3], C. Belka[1], M. Niyazi[1], K. Lauber[1]

[1]*LMU Munich, Clinic for Radiotherapy and Radiation Oncology, Munich, Germany*

[2]*University Hospital Regensburg- Germany, Department of Neurosurgery, Regensburg, Germany*

[3]*Helmholtz Center Munich – German Research Center for Environmental Health GmbH- Neuherberg- German, Research Unit of Radiation Cytogenetics, Neuherberg, Germany*

Purpose or Objective: Glioblastoma (GBM) is the most common primary brain tumor in adults. Despite intense treatment, including surgery and radiochemotherapy, prognosis is dismal with a median overall survival time of only 15 months. The vascular endothelial growth factor-A (VEGF-A) has been identified as one of the key regulators of neoangiogenesis in these highly vascularized tumors. Therefore, disruption of the VEGF-A signaling cascade by neutralizing VEGF-A and preventing ligation of its receptors appeared to be a promising approach for targeting neoangiogenesis. However, in recent phase III trials application of the VEGF-A blocking antibody bevacizumab in combination with radiochemotherapy failed to prolong overall survival in newly diagnosed GBM despite increasing progression-free survival and improving performance status. The aim of our study was to analyze the treatment effects of radiotherapy in combination with bevacizumab in a clinically relevant setting. Therefore, we established an orthotopic, syngeneic mouse glioblastoma model and subjected it to fractionated radiotherapy in combination with the bevacizumab mouse analogue G6-31.

Material and Methods: GL261 mouse GBM cells were stereotactically transplanted into the frontal lobe of C57/BL6 mice and tumors were allowed to grow for one week. Radiation therapy was performed with a Small Animal Radiation Research Platform (SARRP, Xstrahl) which incorporates contrast agent-CT (CA-CT)-based imaging followed by high precision radiation delivery. Fractionated irradiation with daily doses of 2 Gy up to a cumulative dose of 20 Gy was administered with or without accompanying VEGF-A blockade by the mouse bevacizumab analogue G6-31. Overall survival and tumor size were monitored, histological analyses, and transcriptomic profiling of tumor and normal tissue are currently being performed.

Results: Stereotactic implantation of GBM was successfully accomplished, fractionated irradiation was implemented by CA-CT-based image guidance, and tumor growth was successfully monitored by serial CA-CT scans. The single agent treatments led to a significant delay in tumor growth and prolongation of survival as compared to the sham-treated controls. Importantly, the strongest therapeutic effects were observed with the combined treatment. Histological details, including vessel density and structure, as well as markers of cell death induction, and transcriptomic profiling of tumor and normal tissue are currently under investigation.

Conclusion: This pilot study shows that syngeneic, orthotopic glioblastoma transplants combined with stereotactically delivered radiotherapy are feasible and clinically relevant in vivo models for evaluating the therapeutic efficacy of multimodal treatment approaches based on fractionated irradiation.

EP-2028

Dependence of dose enhancement on the cluster morphology of Gold Nano Particle in radiation therapy

A. Sang Hee Ahn[1], C. Kwangzoo Chung[2], H. Youngyih Han[2], P. Hee Chul Park[2], C. Doo Ho Choi[2]

[1]*Sungkyunkwan University, Department of Health Sciences and Technology- Samsung Advanced Institute for Health Sciences and Technology, Seoul, Korea Republic of*

[2]*Samsung Medical Center, Sungkyunkwan University School of Medicine Radiation Oncology, Seoul, Korea Republic of*

Purpose or Objective: Injected gold nano particles(GNPs) to a body for dose enhancement are known to form cluster morphology. We investigated the dependence of dose enhancement on the morphology characteristic with an approximated morphology model by using Monte Carlo simulations.

Material and Methods: For MC simulation, TOPAS v.b-12 was used. GNPs of 50 and 100 nm diameter were tested. GNP cluster morphology was approximated as a body center cubic by placing 8 GNPs at the corner and one at the centered of a $2 \times 2 \times 2$ μm^3, $1 \times 1 \times 1$ μm^3, $0.5 \times 0.5 \times 0.5$ μm^3, or $0.25 \times 0.25 \times 0.25$ μm^3 (for 100 nm GNP) or $0.18 \times 0.18 \times 0.18$ μm^3 (for 50 nm GNP) cube located in a $4 \times 4 \times 4$ μm^3 water filled cube phantom. 4 μm × 4 μm square shaped beams of spectrum-energetic 50, 100 kVp photons and 70, 170 MeV protons were irradiated to the water filled cube phantom with GNPs in it. We computed the distribution of secondary electrons as a function of distance from the surface of the GNP at the cube center and calculated the ratio (SER) together with dose enhancement ratio (DER) for 4 different cubes geometries. For scoring particles,10 nm width of concentric shell shaped detector was constructed up to 100 nm from the center point of the cube. 10E8 histories of protons and 2 × 10E10 histories of photons were used for simulation. All counted values at each detector were summed to obtain the total dose and secondary electrons in a sphere of 100 nm radius and were normalized to $2 \times 2 \times 2$ μm^3 cube morphology.

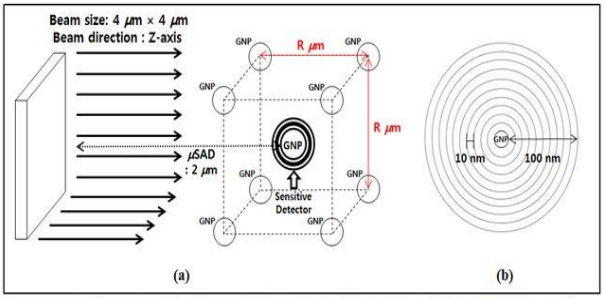

Figure. 1. Schematic diagram of the GNPs cluster morphology Monte Carlo simulation geometry. (a) Body Center Cubic model(R is distance of GNP) and (b) Sensitive detector(material : water) each shell has 10 nm thickness.

Results: DER and SER increase as the distance of the GNPs reduces. The largest DER as well as SER was obtained for 0.25 × 0.25 × 0.25 μm³ cube for 100 nm 0.18 × 0.18 × 0.18 μm³ for 50 nm GNP. In case of 50 nm GNPs, DER increment was 1.421, 1.396, 1.017, and 1.014 for 50 kVp, 100 kVp photons, 70 MeV and 170 MeV protons, respectively. SER increment was 1.319, 1.303, 1.021, and 1.018, for 50 kVp, 100 kVp photons, 70 MeV and 170 MeV protons, respectively. For 100 nm GNPs, we observed the qualitatively same results but increment ratio was larger for all tested radiations.

Conclusion: As shown in this study, DER with GNPs was larger when they are closely packed in the phantom. Therefore, better therapeutic effects can be expected with close-packed GNPs.

Acknowledgement This research was supported by the NRF funded by the Ministry of Science, ICT & Future Planning (2012M3A9B6055201 and 2012R1A1A2042414), Samsung Medical Center grant[GFO1130081]

EP-2029

Feasibility study of Fe3O4/TaOx nano particles as a radiosensitiser for radiation therapy

A. Sang Hee Ahn[1], L. Nohyun Lee[2], S. Sung Won Shin[3], C. Chang hoon Choi[3], H. Youngyih Han[4], P. Hee Chul Park[4], C. Doo Ho Choi[4]

[1]*Sungkyunkwan University, Department of Health Sciences and Technology- Samsung Advanced Institute for Health Sciences and Technology, seoul, Korea Republic of*

[2]*Kookmin University, School of Advanced Materials Engineering College of Engineering, Seoul, Korea Republic of*

[3]*Samsung Medical Center, Department of Radiation Oncology, Seoul, Korea Republic of*

[4]*Samsung Medical Center, Sungkyunkwan University School of Medicine radiation oncology, Seoul, Korea Republic of*

Purpose or Objective: To investigate the feasibility of using multifunctional Fe3O4/TaOx (core / shell) nano particles developed for CT and MRI contrast agent as dose enhancing radiosensitizers.

Material and Methods: Firstly, to verify the imaging detectability of Fe3O4/TaOx nano particles, *in-vivo* tests were conducted. Approximately 600 mg/kg of19 nm diameter Fe3O4/TaOx nano particles dispersed in phosphate buffered saline (PBS) were injected to ten nude Balb/c mice through the tail vein. Mico-CT (Simens Inveon) was scanned for 5 mice and MRI (BioSpec, 70/20 USR, BRUKER Co.) scan was conducted for rest of mice. For both imaging, 4 consecutive scanning was performed at pre- and post-injection (5 min, 30 min, and 1 hour). Difference between pre- and post-injection images was analyzed by computing the pixel histogram and correlation coefficient factor using MATLAB in the user defined ROI (region of interests) . Secondly, to quantify the potential therapeutic enhancement with nano materials, DER (Dose Enhancement Ratio) and number of SER (Secondary Electron Ratio) were computed using MC simulation (TOPAS v.b-12). Diameter of 19 nm circular beams of mono-energetic 10 MeV, 70 MeV, 150 MeV protons were irradiated to a Gold(Au), Tantalum(Ta), TaOx, Fe3O4/TaOx (core / shell), and Fe3O4 nano particle located at the center of 4 × 4 × 4 μm³ water filled cube phantom. DER and SER were computed by placing a 1 nm thickness of shell detector at the surface of the particle.

Results: In CT, MRI imaging, the aorta, the blood vessel, and the liver were clearly visualized after intravenous injection of Fe3O4/TaOx nano particles. There was large different between pre and post-injection images of Histogram data and Coefficients of correlation factor in CT and MR are 0.006, 0.060, respectively. When 10 MeV protons were irradiated for a Gold(Au), Tantalum(Ta), TaOx, Fe3O4/TaOx, Fe3O4 nano particle, DER was 9.089, 7.724, 4.424, 3.660 and 3.255 respectively. Similarly, SER increment was 9.629, 8.401, 5.060, 4.341, and 3.590 for Gold(Au), Tantalum(Ta), TaOx, Fe3O4/TaOx, Fe3O4 nano particle, respectively. For 70 MeV proton beams, DER was similar to those for 10 MeV, but increment ratio was lower for 150 MeV protons.

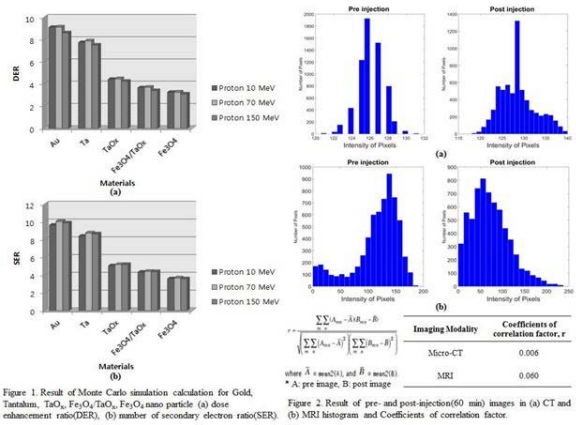

Figure 1. Result of Monte Carlo simulation calculation for Gold, Tantalum, TaO_x, Fe_3O_4/TaO_x, Fe_3O_4 nano particle (a) dose enhancement ratio(DER), (b) number of secondary electron ratio(SER).

Figure 2. Result of pre- and post-injection(60 min) images in (a) CT and (b) MRI histogram and Coefficients of correlation factor.

Conclusion: Fe3O4/TaOx nano particles have potential as a multifunctional agent which enhances the accuracy in cancer detection through visualization of developed tumor lesion and increases the therapeutic effect in proton therapy. The dose enhancement with Fe3O4/TaOx was estimated as half of the Gold. However, tumor targeting such as combined with magnetic field may overcome the low DER

Acknowledgement This research was supported by the NRF funded by the Ministry of Science, ICT & Future Planning (2012M3A9B6055201 and 2012R1A1A2042414), Samsung Medical Center grant[GFO1130081]

EP-2030

Gadolinium enhanced x-rays radiotherapy of murine adenocarcinoma Ca755

A. Lipengolts[1], A. Cherepanov[2], V. Kulakov[2], I. Sheino[2], E. Grigorieva[1], V. Klimanov[3]

[1]*Russian Cancer Research Center, Institute of Clinical and Experimental Radiology, Moscow, Russian Federation*

[2]*Burnasyan Federal Medical Biophysical Centre, Department of radiation technologies, Moscow, Russian Federation*

[3]*National Research Nuclear University, Department of Experimental and Theoretical Physics, Moscow, Russian Federation*

Purpose or Objective: The goal of radiotherapy is to deliver into tumor volume certain amount of radiation to kill all tumor cells and at the same time to minimize radiation damage of surrounding healthy tissues. To reach the goal modern conventional radiotherapy uses multifield irradiation with beam changing its shape and intensity. However this approach is not efficient enough in case when healthy and tumor tissues are highly diffused with each other. In this case partial healthy tissues damage is inevitable. Yet another approach is possible. Using some physiological mechanism tumor can be saturated with a high atomic number element capable to interact with external radiation more likely than the elements of biological tissues. That leads to dose increase at the site of the element location. For that purpose such elements as iodine, gold etc. and external x-rays radiation of energy up to 600 keV can be used. The main obstacle in implementing that method is how to deliver necessary amount of a high atomic number element into a

tumor. Attempts of developing tumor targeting drug, which would be capable to deliver necessary amount of high atomic number element into the tumor haven't succeed yet. Another possible way to deliver such elements into the tumor is to utilize some pathological processes caused by tumorogenesis such as blood barrier disruption in case of brain tumors or high vascularization inherent to some tumors. In this work the efficacy of x-rays irradiation with disodium gadopentetate (Gd-DTPA) administration in treating highly vascularized transplanted tumor in mice was studied.

Material and Methods: C57Bl/6 mice with transplanted adencarcinoma Ca755 were used in the study. Animals were divided into three groups. 1st group undergo no treatment. 2nd group was irradiated with 10 Gy of x-rays. Animals in 3rd group were administered with 0.3 ml of 0.5M water solution of Gd-DTPA, containing 23 mg of gadolinium and then irradiated as well. Administration of Gd-DTPA was performed with single systemic injection. Irradiation was performed using x-rays generator with anode voltage of 200 kV. Antineoplastic efficacy was estimated by measuring tumor volume and life span of mice.

Results: Tumor growth rate plots are presented in Figure.

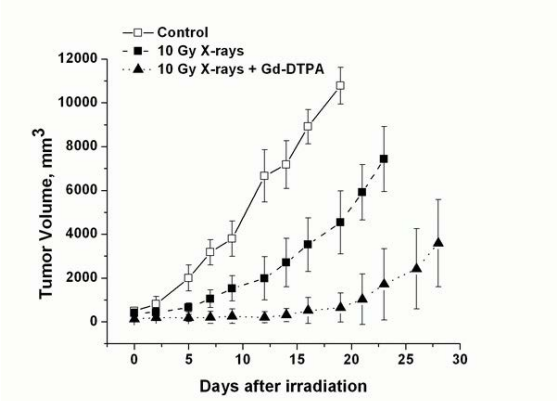

Tumor growth delay for test group was 13 days whereas in irradiated control group tumor growth delay was just 4 days. Median life span was 22 days, 37 days and 46 days for control group, irradiated control group and test group respectively. In test group 25% of animals have full tumor regression whereas in both control groups no tumor regression was observed. Endpoints of antitumor evaluation, i.e. T/C% ratio and gross log10 tumor cell kill are represented in Table.

Group	T/C, %	Tumor growth delay, days	Gross $\log_{10}$ tumor cell kill	Antitumor activity (Teicher 2004)
Irradiated control group (irradiation only)	37±6	4	0.5	-
Test group (irradiation + Gd-DTPA injection)	10±3	13	1.6	+++

Conclusion: Obtained results show that systemic injection of extracellular drug with gadolinium prior irradiation with x-rays provide enough amount of gadolinium in highly vascularized tumors and lead to significant increase of antineoplastic efficacy of x-rays irradiation.

EP-2031

Research on p53 and endostatin gene-radiotherapy induced by EGFR-targeted adenovirus vector in NSCLC

N. Wu[1], D. Han[1], G. Cheng[1], M. He[1]
[1]*Jilin Cancer Hospital, Department of Radiation Oncology, Changchun, China*

Purpose or Objective: With the development of molecular biology and gene engineering, more and more attention has been paid to gene-radiotherapy of malignant tumors. The combination of gene therapy and radiotherapy is regarded as one of the effective methods for the treatment of tumors. This research focused on the Egr-1 promoter with radiation-induced effect, p53 and endostatin genes with function of inducing apoptosis and anti-angiogenesis, and EGFR-targeted adenovirus vector with higher cell infection efficiency. The therapeutic effect of adenovirus vectors Ad.Egr-wtp53-endostatin and Ad.CMV-sCAR-EGF combined with radiotherapy in non-small cell lung cancer is here reported.

Material and Methods: The adenovirus vectors Ad.Egr-wtp53-endostatin containing both wild type p53 and antiangiogenic molecule endostatin genes downstream of early growth response-1 (Egr-1) and Ad.CMV-sCAR-EGF containing coxsackie virus receptor extracellular segment (sCAR) and epidermal growth factor (EGF) were constructed using gene recombination technique. The infection efficiency in non-small cell lung cancer cell lines (A549, LK-2 and Lu65) of Ad.Egr-wtp53-endostatin mediated with Ad.CMV-sCAR-EGF expressed fusion protein sCAR-EGF was detected. The expression of wild type p53 and endostatin genes by the radiation-sensitive promoter Egr-1 in non-small cell lung cancer cell lines were observed. Immunodeficient mice (NOD/scid) subcutaneously implanted with A549 cells were treated by conventional radiotherapy (2Gy×6) and/or gene therapy (intratumor injection of adenovirus vectors Ad.Egr-wtp53-endostatin and Ad.CMV-sCAR-EGF 24 h before the first and fourth local doses). Immunologic mechanisms were explored.

Results: The fusion protein SCAR-EGF expressed from Ad.CMV-sCAR-EGF significantly increased infection efficiency of Ad.Egr-wtp53-endostatin in human non-small cell lung cancer cell lines. Cancer control was most significantly improved in the group receiving local radiotherapy combined with gene therapy as shown by prolongation of mean survival time by 75.2%, reduction in average tumor weight by 88.7%, decrease in pulmonary metastasis by 76.9% and decrease in intratumor angiogenesis by 80.4% as compared to local radiotherapy alone ($P < 0.05$). Immunologic studies showed stimulated natural killer (NK) and cytotoxic T lymphocyte (CTL) activity as well as increased interferon-γ (IFN- γ) and tumor necrosis factor-α (TNF-α) secretion in this combined treatment group as compared with the group receiving local treatment alone ($P < 0.05$).

Conclusion: The experimental findings in the present study showed that adenovirus vectors Ad.Egr-wtp53-endostatin and Ad.CMV-sCAR-EGF in combination with local radiotherapy could improve the tumor control. These observations may set the stage for developing clinical protocols with recombinant adenovirus-mediated gene-radiotherapy in non-small cell lung cancer.

EP-2032

Radiotherapy gets improved by a nanotechnology based enzyme therapy in glioblastoma primary cultures

L. Fernández Fornos[1], V. Barberá[2], M. Saceda[3], P. García-Morales[4], J. Sanz[4], M. Fuentes[4], M. Ventero[4], P. Lucero-Calabuig[4], P. Dorado Rodríguez[1], D. Espósito[1], S. Miranda Labajos[1], A. Pomares Arias[1], M. Ruiz Sánchez[1], E. García Miragall[1]
[1]*Hospital General Universitario de Elche- ERESA, Servicio de Oncología Radioterápica, Elche, Spain*
[2]*Hospital General Universitario de Elche, Laboratorio de Genética Molecular, Elche, Spain*
[3]*Universidad Miguel Hernández de Elche, Fundación para el Fomento de la Investigación Sanitaria y Biomédica de la Comunidad Valenciana FISABIO, Elche, Spain*
[4]*Universidad Miguel Hernández de Elche, Instituto de Biología Molecular y Celular, Elche, Spain*

Purpose or Objective: One of the main effects of radiotherapy is the generation of free radicals as a consequence of the incidence of radiation on the aqueous molecules present in the cells. The enzyme D-aminoacid oxidase (DAO) is also able to generate free radicals when converting D-aminoacids in their corresponding cetoacids. Our principal aim is to increase radiotherapy effects, using

the combination of radiotherapy and DAO, in primary cultures from glioblastoma.

Material and Methods: We have used primary cultures and stablished cell lines from patients with glioblastoma. Recombinant DAO carrying the C-terminal domain of the major lytic amidase (CLytA) specific for binding to choline was inmobilized to magnetic nanoparticles having a magnetite core covered with Diethylaminoethyl (DEAE) cellulose. Primary cultures were irradiated at 7 and 15 Gy. After irradiation, cultures were treated in the absence or in the presence of DAO (free or inmovilized in nanoparticles) and D-alanine (enzyme substrate). After irradiation, cells were harvested and cell cycle distribution was determined by flow citometry.

Results: We have demonstrated in primary cultures from glioblastoma, that the treatment with DAO after irradiation, potentiates dramatically the effect of the radiation alone, increasing especially the percentage of cells in the sub-G1 phase, an indicator of cell death. Some representative results are included in the attached file. DAO inmovilized in magnetic nanoparticles is more effective than free enzyme, since DAO is more stable at 37ºC inmovilized in nanoparticles.

Conclusion: The combination of radiotherapy and enzymatic therapy with DAO based on the nanotechnology, induce an increase in cell death when it is compared with radiotherapy alone.

EP-2033

Combining Hedgehog inhibition with metformin to induce radiosensitization in prostate cancer cells

S. Isebaert[1], A. Gonnissen[1], C. McKee[2], R. Muschel[2], K. Haustermans[1]

[1]*University Hospital Gasthuisberg, Radiation Oncology, Leuven, Belgium*

[2]*CRUK/MRC Oxford Institute for Radiation Oncology, Oncology, Oxford, United Kingdom*

Purpose or Objective: There are several indications that the Hedgehog (Hh) pathway could be a potential target for radiosensitization. Furthermore, a link between Hh signaling and the cellular energy metabolism has been described recently, more specific at the level of AMP-activated protein kinase (AMPK). Activation of AMPK, in turn, has also been shown to result in radiosensitization. Therefore, it seems worthwhile to explore whether the combination of Hh signaling inhibitors and AMPK activators such as metformin could further increase the response to radiotherapy. This combination strategy is being tested in prostate cancer (PCa) cells, as there is increasing evidence that the Hh pathway plays an important role in the development as well as progression to more advanced disease stages of PCa.

Material and Methods: Three PCa cell lines (PC3, DU145, 22Rv1) were treated for 72h with the SMO inhibitor GDC-0449 (1μM, 10μM) or GLI1/2 inhibitor GANT61 (1μM, 10μM), with or without metformin (5mM). The effects on cell survival, proliferation and radiation sensitivity were investigated by means of Sulforhodamine B (SRB) assays, Bromodeoxyuridine (BrdU) assays and colony assays. The effects on gene and protein expression (qRT-PCR/Western blotting), cell cycle distribution (flow cytometry, PI staining) and DNA repair (flow cytometry, γH2AX) were also examined, both in the absence and presence of ionizing radiation (4Gy).

Results: GDC-0449 on its own did not significantly affect cell proliferation, survival or radiation sensitivity of any of the PCa cell lines tested. Treatment with 10μM GANT61 on the other hand did result in a significant reduction of cell survival in all cell lines and induced radiosensitization in the 22Rv1 cells (DEF(SF0.5)=1.39±0.11, p=0.002) (Fig 1A). The latter could be ascribed to the drug's effect on apoptosis (Fig1B). Similar results as for GANT61 were observed after metformin monotherapy (DEF(SF0.5)=1.36±0.08, p=0.012). Moreover, metformin induced a significant downregulation of GLI1, both at the gene and protein expression level. While the combination of metformin and GDC-0449 resulted in no additional effects, addition of metformin to GANT61 further enhanced the radiosensitization effects as induced by single agent treatment in the 22Rv1 cells.

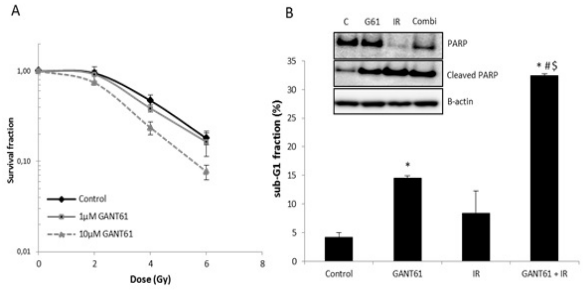

Conclusion: The GLI1/2 inhibitor GANT61 as well as metformin induced radiosensitization in the 22Rv1 PCa cells. The combination of both agents further enhanced the response to radiotherapy, indicating that this might be a more powerful radiosensitization strategy as compared to either agent alone. Investigations are currently ongoing to explore the underlying working mechanisms.

EP-2034

Targeting hypoxic cancer cells by inhibition of checkpoint kinases ATR and CHK1

M. Joel[1], G. Hasvold[1], R.G. Syljuåsen[1]

[1]*Institute for Cancer Research, Department of Radiation Biology, Oslo, Norway*

Purpose or Objective: The checkpoint kinases ATR and CHK1 are considered promising targets for cancer treatment due to their roles in regulation of the S and G2 checkpoints and in the repair of DNA double strand breaks through homologous recombination. Interestingly, severe levels of hypoxia (<0.1% O2) have been shown to activate ATR/CHK1 signaling, which could likely make hypoxic cancer cells sensitive to inhibitors of these kinases. The aim of this project is to explore whether inhibition of ATR or CHK1 could be used to selectively target hypoxic cancer cells, both in combination with ionizing radiation and on its own.

Material and Methods: Cancer cell lines U2OS, HCT116, H460, A549 and H1975 were treated with inhibitors of ATR (VE821, VE822) or Chk1 (AZD7762, UCN01) in the absence and presence of hypoxia (InVivo2 hypoxia chamber) and X-ray-irradiation. Cells were analyzed by flow cytometry, immunoblotting and clonogenic survival assays.

Results: We previously measured clonogenic survival, cell cycle distribution and activation of DNA damage signaling pathways in U2OS and HCT116 cancer cells at different oxygen concentrations (21%, 0.2% and 0.0% O2) in combination with the CHK1 inhibitors UCN-01 and AZD7762 and ionizing radiation. We found that hypoxia alone did not alter the sensitivity to CHK1 inhibitors, but inhibition of CHK1 after reoxygenation following periods of extreme hypoxia (0.0% O2) did result in decreased clonogenic survival and an increased fraction of γ-H2AX positive cells. Hypoxic cells were also found to be radiosensitized at least to the same extent as normoxic cells by CHK1 inhibition. Currently we are performing similar studies in lung cancer cell lines H460, A549 and H1975 treated with the ATR inhibitors VE821 and VE822. We have found that the number of γ-H2AX positive cells after ATR inhibition was higher in cells incubated at hypoxia (0.0% O2, 20h) compared to normoxia (21% O2). The ATR inhibitors also abrogated the radiation-induced G2 checkpoint. Clonogenic survival assays are ongoing.

Conclusion: These studies help determine the potential of using inhibitors of ATR and CHK1 to eradicate radioresistant hypoxic cancer cells

EP-2035

Internalization of iron nanoparticles by macrophages for the improvement of glioma treatment

S. Reymond[1], P. Gimenez[1], R. Serduc[1], J. Arnaud[2], J.P. Kleman[3], V. Djonov[4], W. Graber[4], J.A. Laissue[5], J.K. Kim[6], S.J. Seo[6], J.L. Ravanat[7], H. Elleaume[1]

[1]*U836 INSERM, ESRF Biomedical Beamline ID-17, Grenoble, France*

[2]*CHU, Biology Department, Grenoble, France*

[3]*IBS, Structural Biology, Grenoble, France*

[4]*University of Bern, Anatomy Institute, Bern, Switzerland*

[5]*University of Bern, Pathology Institute, Bern, Switzerland*

[6]*Catholic University of Daegu, Radiology and Biomedical Engineering, Daegu, Korea Republic of*

[7]*CEA, INAC/SCIB LAN, Grenoble, France*

Purpose or Objective: An alternative approach for the improvement of radiotherapy consists in increasing differentially the radiation dose between tumors and healthy tissues using nanoparticles (NPs) that have been beforehand internalized into the tumor. These high-Z NPs can be photo-activated by monochromatic synchrotron X-rays, leading to a local dose enhancement delivered to the neighboring tumor cells. This enhancement is due to secondary and Auger electrons expelled from the NPs by the radiations. In order to carry the NPs into the tumor center, macrophages are currently under study for their phagocytosis and diapedesis abilities. In this study we characterized J774A.1 macrophages' internalization kinetics and subcellular distribution of iron NPs and compared them to the internalization abilities of the F98 glioblastoma cell line.

Material and Methods: Three aspects of internalization were examined: first, the *location of internalized NPs* in J774A.1 macrophages and F98 glioblastoma cells following a 24h incubation with iron NPs (0.3 mg/mL in the cell culture medium) was determined by optical microscopy after cell slicing. Subsequently, the *iron intake* after a 24h incubation with NPs (0.3 mg/mL and 0.06 mg/mL in the cell culture medium) was characterized for the two types of cells using ICP-MS. Finally, the *internalization dynamics* were studied by live phase-contrast microscopy imagining for 11 hours and by absorbance measurements for 24 hours using a plate reader.

Results: F98 tumor cells and J774A.1 macrophages are both able to endocytose NPs: we measured ~61±10 pg of internalized iron per macrophage compared with ~33±5 pg per F98 cell (initial iron concentration: 0.3 mg/mL in culture medium). F98 internalizing NPs for 10 hours showed stress signs during the first minutes after the NPs injection, but behaved like F98 control cells during the rest of the experiment. Finally, we determined that the internalization kinetics for J774A.1 had a typical saturation time of one hour.

Conclusion: Macrophages seem to be promising vectors for NPs, being able to endocytose and retain in their cytoplasm larger quantities of NPs than tumor cells. Our following studies will attempt to shed light on their other potential abilities as "Trojan Horses".

EP-2036

A flow cytometry-based screen for compounds that increase S-phase damage after Wee1 inhibition

C. Naucke[1], P. Juzenas[1], S. Hauge[1], T. Stokke[1], R.G. Syljuåsen[1]

[1]*Norwegian Radium Hospital/ Oslo University Hospital, Department of Radiation Biology- Institute for Cancer Research, Oslo, Norway*

Purpose or Objective: Inhibitors of Wee1 are in clinical trials for cancer treatment in combination with radiation or chemo-therapy. The antitumor effects have largely been attributed to their role in G2 checkpoint abrogation. However, our previous work has shown that Wee1-inhibition also causes DNA damage in S phase. To understand mechanisms behind the S-phase damage and to identify promising combination treatments, we initiated a flow cytometry-based screen for compounds that increase S-phase damage when combined with the Wee1-inhibitor MK1775.

Material and Methods: The screen was performed in 384-well plates by using a pipetting robot and a flow cytometer equipped with a plate loader. REH leukemia suspension cells were treated with the LOPAC 1280 and Selleck Cambridge cancer 384 compound libraries in the presence and absence of the Wee1 inhibitor MK1775 (4h, 400nM), stained with the DNA-stain Hoechst and the DNA damage marker γH2AX, and analyzed by flow cytometry using the FlowJo software. In addition to drugs present in the compound libraries, three additional Chk1-inhibitors (LY60638, MK8776 and UCN01) were included in subsequent validation experiments.

Results: The Chk1 inhibitor AZD7762 was among the top hits of 1664 tested compounds, giving synergistically increased S-phase damage when combined with MK1775. Similar effects were found with with three other Chk1-inhibitors. In addition, the screen identified several expected negative and positive regulators of the S phase damage, such as inhibitors of Cyclin-Dependent-Kinase (CDK) and Topoisomerase, and some unexpected hits such as Dasatinib.

Conclusion: This study helps understanding how Wee1-inhibition causes S-phase damage, and will likely identify combinations of MK1775 and drugs relevant for future clinical studies. These drug combinations may also be useful to apply together with radiation therapy to eliminate radioresistant S-phase cells.

Electronic Poster: Radiobiology track: Tumour biology and microenvironment

EP-2037

Radiation-induced abscopal effect in normoxic and hypoxic conditions in lung adenocarcinoma

S. Tubin[1], M.A. Mansoor[2], S. Gupta[3]

[1]*Instütut für Strahlentherapie, Radioonkologie, Klagenfurt, Austria*

[2]*National Cancer Institute- National Institutes of Health, Radiotherapy Development Branch- Radiation Research Program- Division of Cancer Treatment and Diagnosis, Rockville, USA*

[3]*Albert Einstein College of Medicine, Department of Radiation Oncology, Bronx- New York, USA*

Purpose or Objective: Many experimental evidences proved the existence of radiation-induced abscopal effect (RIAE), a phenomenon of non-targeted radiobiological effect which is rarely, unintentionally induced in vivo, mostly with high doses per fraction. We explored different biological, biochemical and physical factors on which the type and intensity of RIAE could depend and whose manipulation could lead to induction of strong, clinically applicable RIAE. Also, the radio-sensitizing potential of abscopal signals (AS) and the status of RIAE in hypoxia (H) were examined. After observation of AS transmission by tumor cells exposed to H, which were able to affect proliferation of normoxic (N) and H cells, irradiated as well as unirradiated, we introduce a new scientific term:"Hypoxia-induced abscopal effect" (HIAE).

Material and Methods: A549 and H460 lung cancer cells were incubated in H (Oxygen<2%) or N for 3 days and then irradiated (2 or 10Gy) or not. After 24h, unirradiated H (HCM) or N (NCM) conditioned media (CM) and irradiated H (HRCM) or N (NRCM) CM were collected. H-resistant (HR) clones A549/HR and H460/HR were generated by 3 weeks-exposure of cells to H. 2 identical sets of unirradiated N cells and HR clones were exposed to HCM, NCM, HRCM or NRCM and only 1 set was irradiated (2Gy) to evaluate the radio-sensitizing potential of AS. Cell growth was monitored using real time cell electronic sensing system. Cell survival was assessed by colony forming assay. Levels of basic fibroblast growth factor (GF)(bFGF), placental GF (PlGF), Soluble fms-like tyrosine kinase (sFlt-1) and vascular endothelial GF (VEGF) were assessed in CM.

Results: AS released by cells exposed only to H were active affecting proliferation and radio-sensibility of N cells and HR clones. Those effects depended on cell histotype, respiratory status of cell-inducers and cell-recipients of AS (N vs. H) and duration of cell-exposure to H (24 vs. 72h). Depending on time-exposure to H, HIAE promoted both increased and reduced proliferation. The type and intensity of RIAE depended on dose and notably changed if AS were transmitted by N or H irradiated cells (Tab.1, Fig.1).

Treatments	A549	A549/HR	H460	H460/HR
N-RCM (2Gy) vs. H-RCM (2Gy)	↓ (60%) sFLT-1, PlGF	↑ (20%)	↑ (25%) bFGF	↓ (20%)
N-RCM (10Gy) vs. H-RCM (10Gy)	↓ (40%) sFLT-1, PlGF	↑ (15%)	No diff sFLT-1, PlGF, VEGF	↓ (30%)
N-RCM (2Gy)+2Gy vs. H-RCM (2Gy)+2Gy	↓ (70%)	↓ (20%)	↑ (20%)	↓ (80%)
N-RCM (10Gy)+2Gy vs. H-RCM (10Gy)+2Gy	↓ (50%)	↓ (7%)	No diff	↓
N-CM+2Gy vs. H-CM+2Gy	↓ (65%)	↓ (20%)	↑ (25%)	↓

Table 1: Comparison of radiation-induced abscopal effects in normoxic and hypoxic conditions on proliferation of A549, A549/HR, H460, and H460/HR cells

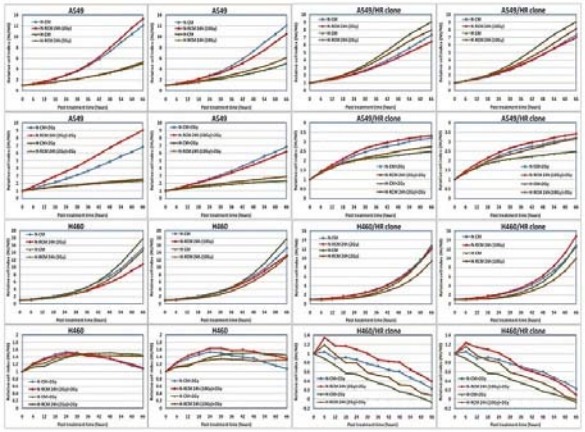

Figure 1: Comparison of radiation-induced abscopal effects in normoxic and hypoxic conditions on proliferation of A549, A549/HR, H460, and H460/HR cells

In H460 RIAE caused radio-resistance, a phenomenon similar to adaptive response but in this case acquired via AS by cells that have never been irradiated. Manipulating the respiratory ambient of cell-receivers of AS the effects of both RIAE and HIAE on proliferation and radio-sensibility changed significantly. The comparative analysis of GF levels with cell proliferation and survival showed a correlation between anti-proliferative sFLT-1 and almost all CM types for both cell lines.

Conclusion: Our results proved that exposing of cells to H and irradiation of H cells lead to significant HIAE and RIAE, respectively, which are able to affect cell proliferation and radio-sensibility. Both phenomena depend on several factors whose manipulation is possible and leads to induction of clinically applicable RIAE.

EP-2038

Manipulation of radiation-induced bystander effect in prostate adenocarcinoma

S. Tubin[1], M. Valeriani[2], M.F. Osti[3], G. Minniti[3], S. Bracci[3], S. Gerardo[4]

[1]*Landeskrankenhaus Klagenfurt, Radiotherapy, Klagenfurt, Austria*

[2]*Sant´Andrea Hospital- Rome- La Sapienza University, Radiotherapy, Rome, Italy*

[3]*Sant´Andrea Hospita- Rome- La Sapienza University, Radiotherapy, Rome, Italy*

[4]*Sant´Andrea Hospita- Rome- La Sapienza University, Laboratory Medicine, Rome, Italy*

Purpose or Objective: Radiation-induced bystander effect (RIBE) has been described only for certain cancer types as the appearance of radiation effects in not directly irradiated cells. This study evaluated the ability of prostate adenocarcinoma (ADC) to induce RIBE exploring the factors that may affect its intensity. The idea was to produce a strong, clinically applicable RIBE, that could lead to development of innovative approaches in modern radiotherapy treatment of prostate cancer, especially for those patients with hormone-refractory ADC in which radiotherapy might have a limited role.

Material and Methods: 2 prostate ADC cell lines of different differentiation, PC-3 - hormone-resistant and DU-145 - hormone-sensitive, have been irradiated using wide range of doses (15 cGy-3000 cGy in 1 fraction) to obtain radiation-conditioned medium (RCM) which was then used to "treat" the unirradiated cells and to evaluate the cytokines level. Each sample of RCM was subjected to triple immunoassay assessment of the following cytokines: Eotaxin, Interferon-gamma, Interleukin(IL)-2, IL-4, IL-6, IL-8, IL-10, IL-12, Macrophage Inflammatory Protein-1-alpha, Tumor Necrosis Factor-alpha and Vascular Endothelial Growth Factor. Using a spectrophotometer cell growth was assessed. All comparisons were made to the negative control using paired t-tests. Significance was set at p-value < 0.05, 2-tailed test.

Results: Prostate ADC was able to induce RIBE which intensity depended on dose and tumor differentiation grade: the strongest RIBE for PC-3 was achieved with 2000 cGy and for DU-145 with only 15 cGy (Fig.1).

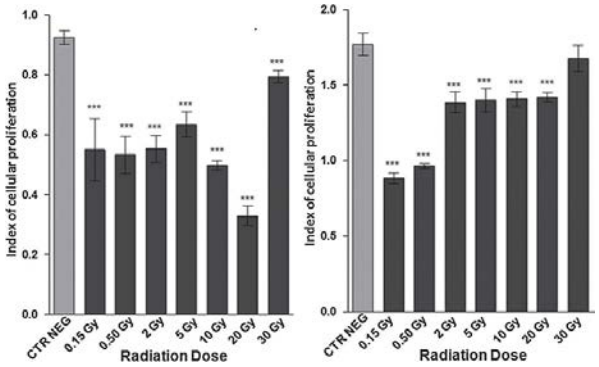

Figure 1. Bystander effect in prostate adenocarcinoma: the strongest proliferative blocking in PC-3 achieved with 20 Gy (left graph) and in DU-145 with 0.15 Gy (right graph)

For DU-145 there wasn't correlation between cytokines level and RIBE intensity while for PC-3 IL-6 correlates with strongest RIBE. The dose required to kill all cells exposed to irradiation was different for 2 cell lines: for DU-145 a lethal dose was reached with 2500 cGy, while PC-3 resisted to 3500 cGy after which tumor repopulation was observed starting 2 weeks after irradiation from just a few survived cells that have undergone particular "giant" differentiation.

Conclusion: RIBE intensity can be manipulated by modifying radiation dose and depends on differentiation grade. IL-6 correlates with strongest RIBE after exposure of PC-3 to a very high dose of radiation thus indicates its possible involvement in bystander signals transmission.

EP-2039

The impact of surgical wound fluids after IORT on the breast cancer stem cell phenotype

W.M. Suchorska[1,2], K. Kulcenty[1], D. Murawa[3]

[1]*Greater Poland Cancer Centre, Radiobiology Lab- Department of Medical Phisics, Poznan, Poland*

[2]*Poznan University of Medical Sciences, Department of Electroradiology, Poznan, Poland*

[3]*Greater Poland Cancer Centre, Department Surgical Oncology I, Poznan, Poland*

Purpose or Objective: Breast cancer is the most common cancer in women. The conventional conservative treatment

for early breast cancer includes a wide local excision with adjuvant radiotherapy. Clinical data suggest, that perturbations induced by surgery and the subsequent wound fluids, which are rich in cytokines and growth factors, may stimulate residual disease. Numerous studies demonstrate, that 90% of the local recurrence after surgery occur in the same quadrant as the primary cancer. It has been proposed, that cancer cells displaying the stem-like phenotype play a critical role in local recurrence, invasion and metastasis. One of the new possibilities in conservative cancer treatment is intraoperative radiotherapy (IORT). IORT delivers high dose of radiation as one single fraction at the time of surgery. It was previously reported, that IORT alters the microenvironment through the modulation of wound healing response. Thus we wondered, **whether wound fluids can induce the enrichment of breast cancer stem cells phenotype in breast cancer cell lines and whether IORT plays inhibitory role in this process**.

Material and Methods: Wound fluids form patients which underwent IORT (IR-WF), as well as control group without radiotherapy treatment (WF), were collected week after the surgery. Three human cancer cell lines with different molecular status (basal – MDA-MB-468, luminal – MCF7 and Her2-positive – BT-474) were then incubated with wound fluids (WF, IR-WF) in complete culture medium (10%). After four days of incubation the cancer stem-cell phenotype was established.

Results: Flow cytometry and RT-qPCR analysis revealed, that wound fluids from patients who received IORT decreased the phenotype of cancer-stem cells in the basal (MDA-MB-468) and luminal subtype (MCF7) of cancer cell lines compared to IORT-untreated patients. Such changes were not confirmed in HER2-posive cell line (BT-474).

Conclusion: The surgical wound fluids from both groups (WF and IR-WF) affect the putative stem cell phenotype. **In IR-WF group, the lower stem cell phenotype was observed compared to fluids harvested after surgery alone.**

This work was supported by NSC grant no UMO-2013/09/N/NZ4/02844

EP-2040

Can pimonidazole be used to detect cycling hypoxia in tumours?

S. Böke[1,2], A. Yaromina[3], L. Koi[4,5,6], M. Baumann[4,5,6], D. Zips[1,2]
[1]*Medical Faculty and University Hospital- Eberhard Karls University Tübingen, University Department of Radiation Oncology, Tübingen, Germany*
[2]*German Cancer Research Center DKFZ- Heidelberg and German Consortium for Translational Cancer Research DKTK, Partner Site Tübingen, Tübingen, Germany*
[3]*Maastricht University Medical Centre, Department of Radiation Oncology Maastro- GROW-School for Oncology and Developmental Biology, Maastricht, The Netherlands*
[4]*Faculty of Medicine and University Hospital Carl Gustav Carus- Technische Universität Dresden, Department of Radiation Oncology, Dresden, Germany*
[5]*German Cancer Research Center DKFZ- Heidelberg and German Consortium for Translational Cancer Research DKTK, Partner Sites Dresden, Dresden, Germany*
[6]*Faculty of Medicine and University Hospital Carl Gustav Carus- Technische Universität Dresden- Helmholtz-Zentrum Dresden-Rossendorf, OncoRay – National Center for Radiation Research in Oncology, Dresden, Germany*

Purpose or Objective: To determine the influence of two different injection schedules on the pimonidazole hypoxic fraction (pHF) in three different head and neck human squamous cell carcinoma (HNSCC) xenograft tumour models.

Material and Methods: Three different HNSCC cell lines (FaDu, UT-SCC-5, UT-SCC-14) grown as xenograft tumours in nude mice (5 per cell line) where examined with different pimonidazole injection schedules. Either one single injection 60 minutes prior to tumour excision (100 mg/kg BW i.p.) or three injections (each 33 mg/kg BW i.p.) starting 180 minutes before tumour excision with 60 minutes interval between injections. Both groups where given the perfusion marker Hoechst 33342 i.v. 1 minute prior to tumour excision. Tumours were snap frozen and consecutive central cross-sections (10µm) where stained with antibodies for pimonidazole and CD31. Using image analysis the pHF and other parameters of the microenvironment were determined.

Results: No statistically significant differences in pHF nor in visual staining patterns were observed after single versus multiple injections of pimonidazole (table and figure 1).
Table 1: Mean values of the pHF [SD] in %.

Tumour model	pHF single injection	pHF multiple injections
UT-SCC-5	23.49 [1.76]	27.54 [1.49]
UT-SCC-14	23.18 [2.63]	19.59 [2.04]
FaDu	9.17 [2.02]	10.25 [2.73]

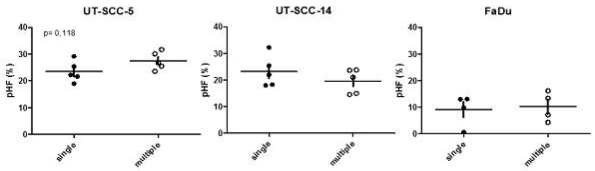

Fig. 1: pHF for the cell lines for single and multiple pimonidazole injection (mean value for pHF of the two analysed sections per tumour, closed symbols for single, open for multiple injections)

Conclusion: In the HNSCC xenograft models investigated here pimonidazole detects predominantly chronic hypoxia. Assessment of cycling hypoxia requires alternative methods. Our data suggest that cycling hypoxia occurs either at a low level in our models or that hypoxia cycles so rapid that pimonidazole cannot bind sufficiently or cycling hypoxia levels are not low enough for pimonidazole reduction.

Electronic Poster: Radiobiology track: Normal tissue effects: pathogenesis and treatment

EP-2041

Vitamin D protects HUVEC from RT-induced senescence and apoptosis by modulating MAPK/SirT1 axis

F. Marampon[1], G. Gravina[1], C. Festuccia[1], A. Colapietro[1], E. Di Cesare[1], V. Tombolini[2]
[1]*University of L'Aquila, Department of Biotechnological and Applied Clinical Sciences, L'Aquila, Italy*
[2]*Policlinico Umberto I "Sapienza" University of Rome, of Radiotherapy, Rome, Italy*

Purpose or Objective: Radiotherapy toxicity is related to oxidative stress-mediated endothelial dysfunction. Here, we investigated on radioprotective properties of Vitamin D (Vit.D) on human endothelial cells (HUVEC).

Material and Methods: HUVEC, pre-treated with Vit.D, were exposed to ionizing radiation (IR): ROS production, cellular viability, apoptosis, senescence and western blot for protein detection were performed. The role of MAPKs pathway was investigated by using U0126 (10 µM) MEKs/ERKs-, SB203580 (2.5 µM) p38-inhibitor or by over/expressing MKK6 p38-upstream activator.

Results: Vit.D reduced IR-induced ROS production protecting proliferating and quiescent HUVEC from cellular apoptosis or senescence, respectively, by regulating MAPKs pathways. In proliferating HUVEC, Vit.D prevented IR-induced apoptosis by activating ERKs while in quiescent HUVEC counteracted IR-induced senescence by inhibiting the p38-IR-induced activation. MEKs&ERKs inhibition in proliferating or MKK6/mediated p38 activation in quiescent HUVEC,

respectively, reverted anti-apoptotic or anti-senescent Vit.D properties. SirT1 protein expression levels were up-regulated by Vit.D. ERKs inhibition blocked Vit.D-induced SirT1 protein up-regulation in proliferating cells. In quiescent HUVEC cells, p38 inhibition counteracted the IR-induced SirT1 protein down-regulation, while MKK6 transfection abrogated the Vit.D positive effects on SirT1 protein levels after irradiation. SirT1 inhibition by sirtinol blocked the Vit.D radioprotective effects.

Conclusion: Vit.D protects HUVEC from IR induced/oxidative stress by positively regulating the MAPKs/SirT1 axis.

EP-2042

Meta-analysis: can amifostine reduce chemoradiotherapy and radiotherapy toxicity in advanced NSCLC?

A. Devine[1], L. Marignol[1]
[1]*Applied Radiation Therapy Trinity, Discipline of Radiation Therapy, Dublin, Ireland Republic of*

Purpose or Objective: Trials of amifostine in patients with advanced non-small cell lung cancer (NSCLC) receiving chemoradiotherapy (CRT) or radiotherapy (RT) alone report varying treatment-related toxicity. A review and meta-analysis was conducted to examine amifostine's effect on toxicity and efficacy of CRT or RT alone in such patients.

Material and Methods: Searches of electronic databases yielded 16 eligible trials comprising 1057 patients. Data extracted from randomised and non-randomised trials were compiled in a review; results of randomised trials were pooled and using meta-analyses to estimate the effect of amifostine on treatment toxicity and efficacy.

Results: Amifostine reduced the risk of >Grade 2 acute oesophagitis by 26% (risk ratio [RR], 0.74; 95% confidence interval [CI], 0.65-0.86; p<0.0001) and the risk of acute pulmonary toxicity by 44% (RR, 0.56; 95%CI, 0.41-0.75; p=0.0001). Amifostine did not alter risk of late pulmonary toxicity (RR, 0.84; 95% CI, 0.65-1.08; p=0.17). Risk of complete response was unchanged (RR, 1.64; 95% CI, 0.99-2.73; p=0.06), partial response was unchanged (RR, 0.92; 95% CI, 0.73-1.16; p=0.48). Statistical heterogeneity was high for toxicity but low for response. Non-randomised trials reported varying incidence of toxicities and survival/response. Studies were medium-high quality.

Conclusion: Statistical heterogeneity casts doubt over amifostine's efficacy in this setting, despite evidence of decreased incidence of acute oesophageal and pulmonary toxicity but not late pulmonary toxicity. Amifostine did not compromise CRT or RT efficacy.

EP-2043

The ANDANTE project: a re-evaluation of the risk from scattered neutrons during proton therapy

A. Ottolenghi[1], V. Smyth[1], K. Trott[1]
[1]*Universita degli Studi di Pavia, Dipartimento di Fisica, Pavia, Italy*

Purpose or Objective: It is well known that proton therapy generates a small but significant exposure to scattered neutrons. The success of paediatric proton treatments leads to a concern about second cancers arising in later life from the neutron exposure. However there are difficulties involved with estimating the risk from exposure to neutrons. The usual approach is through the concept of relative biological effectiveness (RBE) of neutrons compared to photons, since the risk from photon exposure is much better known (ICRP Publication 103. Ann. ICRP 37 (2-4), 2007) The RBE for neutrons has been evaluated using cellular and animal models. But this causes uncertainty when applying the method to humans. The ANDANTE project (http://www.andanteproject.eu/) has investigated the relative risk of cancer from neutrons compared to photons in the context of proton therapy, using three different disciplines in parallel.

Material and Methods: Physics: Charged particle spectra generated by both neutron and photon beams were characterised using Monte Carlo simulation and measurements. A track structure model was used to model the formation of complex lesions in DNA from the different spectra as an indicator of relative likelihood of cancer induction. A method was developed for reconstructing the scattered neutron doses outside the treatment volume during proton therapy, using available clinical data, in order to be able to predict second cancer risks. Stem cell radiobiology: Stem cells from thyroid, salivary gland, and breast tissue were given well characterised exposures to both broad- and narrow-spectrum neutron beams, and to 200 kV X-rays. The relative risk of damage from neutrons compared to photons was estimated using a number of endpoints. Part of the cell population was transplanted into mice. Detailed histopathological and molecular investigations were performed looking for pre-malignant lesions and signs of malignancy. Epidemiology: The results from the track structure modelling and stem cell experiments were combined to generate a relative risk model. Dose reconstruction and data analysis tools were developed for a multi-centre prospective epidemiological study using data from paediatric proton therapy treatments, which will test the relative risk model. The project has made initial plans for the study as a collaboration between centres in Europe and the USA.

Results: The track structure model reproduced the peak in relative risk between neutrons and photons at a neutron energy of around 1 MeV, similar to the ICRP model. The stem cell experiments successfully demonstrated a new methodology, but did not provide conclusive evidence to contradict the ICRP model. The feasibility of a prospective epidemiological study was demonstrated.

Conclusion: The results from the ANDANTE project do not contradict ICRP. In the longer term, the prospective study will provide greater certainty on the RBE for neutrons and how this applies to humans receiving proton therapy.

EP-2044

Radiation-induced lung fibrosis is associated with M2 interstitial and hybrid alveolar macrophages

L. Meziani[1], M. Mondini[1], B. Petit[2], M.C. Vozenin[2], E. Deutsch[1]
[1]*Institut Gustave Roussy, INSERM U1030, Villejuif, France*
[2]*Centre Hospitalier Universitaire Vaudois, Radio-Oncologie/Radiothérapie, Lausanne, Switzerland*

Purpose or Objective: Radiation-induced fibrosis is a delayed complication of radiotherapy often associated with chronic inflammatory process and macrophage infiltration. Nowadays, macrophages are suggested to be important cellular contributors to fibrogenic process, but their implication in the context of RIF is not well known.

Material and Methods: To investigate the role of macrophages in RIF we have used a classical experimental model of lung fibrosis developed in C57Bl/6 mice after 16Gy thorax-IR. We then profiled both alveolar macrophages (AM) and interstitial macrophages (IM) during the various steps of the fibrogenic process.

Results: We confirmed the fact that total lung irradiation at 16Gy (IR) induces an interstitial fibrosis associated with delayed recruitment of pulmonary macrophages.
We found a transient depletion of AM associated with cytokine secretion during the acute post-IR phase (15 days), followed by an active repopulation and an enhanced number of AM during the late post-IR phase (20 weeks). Interestingly, AM were mostly recruited from the bone marrow and exhibit a hybrid polarization (M1/M2) associated with up-regulation of Th1 and Th2 cytokines. The number of M2-polarized IM significantly increased during the late time points after irradiation and a down-regulation of Th1 cytokine was measured in tissue lysate. These results suggest a differential contribution of hybrid AM *vs* M2-IM to fibrogenesis. Interestingly, in contrast to activated hybrid AM, activated

M2-IM were able to induce fibroblast activation *in vitro* mediated by an enhanced TGF-β1 expression suggesting a profibrotic role of M2-IM. Specific depletion of hybrid AM using intranasal administration of clodrosome increased radiation-induced fibrosis score and enhanced M2-IM infiltration suggesting a protective role of hybrid AM.

Conclusion: These present study shows a dual and opposite contribution of alevolar *versus* intertitial macrophages in radiation-induced fibrosis and identify M2-IM as a potential therapeutic target to treat radiation-induced fibrosis.

EP-2045

In vivo monitoring of skin collagen state by multiphoton microscopy in the course of irradiation

N.D. Gladkova[1], V.V. Dudenkova[1,2], V.V. Elagin[1], K.V. Babak[3], A.V. Maslennikova[3,4]

[1]*State Medical Academy, Research institute of biomedical technologies, Nizhny Novgorod, Russian Federation*

[2]*Lobachevsky State University, General physics, Nizhny Novgorod, Russian Federation*

[3]*Lobachevsky State University, Biophysics, Nizhny Novgorod, Russian Federation*

[4]*State Medical Academy, Oncology and Radiotherapy beam diagnostics, Nizhny Novgorod, Russian Federation*

Purpose or Objective: Adverse events in normal tissues during and after a course of cancer radiation treatment are one of the most pressing problems of modern radiation oncology. From among numerous works in this field, there are but a few concerned with the radiation-induced alterations of collagen, the processes of its degradation and subsequent remodeling. A new imaging technique – multiphoton microscopy (MPM) allows studying tissue collagen state on fibers and bundles level without additional staining due to second harmonic generation (SHG) phenomenon. The method has the key advantage of a potential in vivo application. This study's objective was in vivo evaluation of changes occurring at rat's skin collagen upon the exposure of conventional irradiation.

Material and Methods: Rat's ear was chosen as a model for detecting collagen changes. Experiments were carried out under Nizhny Novgorod Medical Academy ethical committee permission. Three male animals, 2 months old at the time of experiment, were used. Rat's ear was irradiated under general anesthesia (Zoletyl, 50 mg/kg, Virbac Sante Animale, France) by a Co60 unit Terabalt (UJP, Czech Republic) by a local field with single dose of 2 Gy up to the total dose of 24 Gy. The 3D imaging of collagen structure was performed by MPTflex (JenaLab, Germany) – a system for in vivo optical biopsies based on near infrared femtosecond laser technology. MPM imaging was carried out two times a week beginning from the first day of irradiation and once a week for three months after its completion. Cross-sectional images were obtained beginning from the horny layer with the step of 5 μm up to the total depth of 100 μm. Excitation was implemented with a pulsed (200 fs) titanium-sapphire laser at a wavelength of 740 nm and a pulse repetition frequency of 80 MHz; SHG collagen imaging was performed at 373-387 nm. Cross-sectional images of 512x512 pixels were obtained; the field size was 130x130 μm. Numerical processing of the images was performed by ImageJ program. Mean fluorescence intensity and its standard deviation was calculated for all images. Coefficient S (a ratio of standard deviation/mean fluorescence intensity) was used for evaluation of collagen state.

Results:

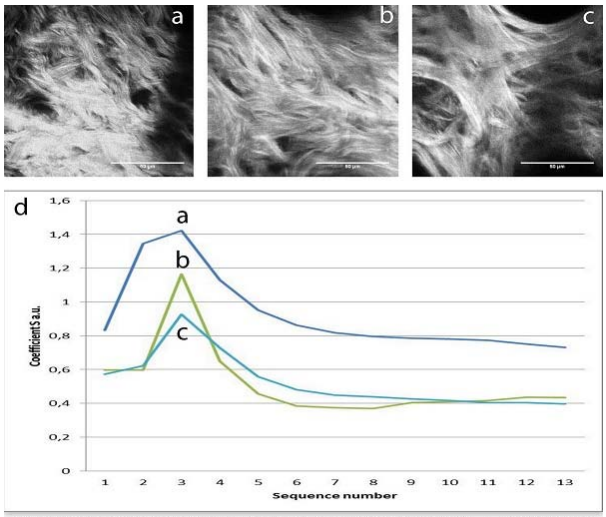

Fig.1. Examples of the MPM images of rat's ear: a - before irradiation, b - 24 Gy, c - 24 Gy, 3 month after irradiation, d – correspondent coefficient S.

Visual evaluation of MPM images demonstrated no noticeable changes of collagen packing and structure independent on the dose and time from radiation beginning (Fig.1, a, b, c). Numerical processing revealed subtle, but clear differences of coefficient S between intact and irradiated collagen. After radiation beginning, a decrease of magnitude of coefficient S and the decrease of title angle of the graph was observed (Fig.1 d). In a month after radiation completion, a magnitude remained decreased, but tilt angle of the graph returned to the initial level (Fig.1 d).

Conclusion: Numerical processing of MPM-images demonstrated changes of optical properties of collagen upon expose of clinically relevant doses of gamma-irradiation. The radiobiological interpretation of these changes require further study.

EP-2046

Modulation of radiation-induced oral mucositis (mouse) by dermatan sulfate

S. Gruber[1], E. Bozsaky[1], K. Frings[1], M. Arnold[1], V. Gernedl[1], S. Hetzendorfer[1], J. Mayer[1], S. Morava[1], S. Pfaffinger[1], P. Kuess[2], W. Dörr[1]

[1]*Medical University of Vienna, Department of Radiotherapy-ATRAB - Applied and Translational Radiobiology and Christian Doppler Laboratory for Medical Radiation Research for Radiation Oncology, Vienna, Austria*

[2]*Medical University of Vienna, Department of Radiation Oncology and Christian Doppler Laboratory for Medical Radiation Research for Radiation Oncology, Vienna, Austria*

Purpose or Objective: Oral mucositis is the most frequently occurring, dose limiting early adverse event of head-and-neck cancer radio(chemo)therapy. The purpose of the present study was to quantify the mucoprotective effect of dermatan sulfate (DS), and to characterise the associated changes in the expression of markers for epithelial proliferation, cell junctions, inflammation and hypoxia.

Material and Methods: The study comprises a functional and a histological arm. For the functional investigations, mice were irradiated with 5x3 Gy/week over one (days 0-4) or two weeks (days 0-4, 7-11). Each protocol was concluded by irradiation with graded top-up doses (day 7/14), to generate complete dose-effect curves. Daily doses of DS (4 mg/kg subcutaneously) were applied over varying time intervals. Mucosal ulceration, was analysed as clinically relevant endpoint during the functional studies. In the histological study, groups of three mice were sacrificed every second day, the tongues were excised and subjected to histological/immunohistochemical processing.

Results: DS significantly increased isoeffective doses for the induction of oral mucositis in almost all protocols, and

furthermore prolonged the latency to epithelial ulceration and reduced ulcer duration. Proliferation measurements with BrdU did not show any substantial effects of DS. The adherens junction protein ß-catenin did significantly increase during irradiation, which occurred earlier with additional DS treatment. The hypoxia markers HIF-1α and GLUT-1 showed a progressive increase during irradiaton alone, which, however, was also not influenced by DS. IL-1ß and NF-κB as markers of inflammation were dramatically increased during irradiation. While DS treatment abolished the radiation-induced increase of IL-1ß, however, no systematical effect on the expression of NF-κB was observed.

Conclusion: DS has a significant mucoprotective effect. This is not based on stimulation of epithelial proliferation nor on modulation of radiation-induced hypoxic changes. In contrast, reduced or modulated inflammatory processes and/or increased/modified function of adherens junctions may have a mechanistic role. This hypothesis, however, needs to be validated in further studies.

Electronic Poster: Radiobiology track: Biomarkers and biological imaging

EP-2047
1H NMR based metabolomic approach to monitoring of the head and neck cancer treatment toxicity

L. Boguszewicz[1], A. Hajduk[2], J. Mrochem-Kwarciak[3], A. Skorupa[1], M. Ciszek[1], A. Heyda[2], M. Sokol[1], K. Skladowski[2]
[1]*Maria Sklodowska-Curie Memorial Cancer Center and Institute of Oncology, Department of Medical Physics, Gliwice, Poland*
[2]*Maria Sklodowska-Curie Memorial Cancer Center and Institute of Oncology, I Radiotherapy Clinic, Gliwice, Poland*
[3]*Maria Sklodowska-Curie Memorial Cancer Center and Institute of Oncology, Analytics and Clinical Biochemistry Department, Gliwice, Poland*

Purpose or Objective: Anticancer treatment affects composition and concentrations of metabolites in body fluids. In case of head and neck (HNC) cancers the acute radiation syndrome (ARS) was studied only at the genomic, proteomic and lipidomic levels. We aimed to identify and investigate molecular processes of treatment toxicity in HNC patients using high resolution NMR and NMR-based metabolomics.

Material and Methods: Forty five patients with HNC were treated with radiotherapy (RT) or cisplatin-based chemoradiotherapy (CHRT). Blood samples were collected within a week after RT/CHRT completion. The ARS was evaluated using Multi-parameter Monitoring (MPM) – an original evaluation system designed by the study investigators. The patients were divided into two classes (of high and low ARS) on the basis of the highest individual ARS value observed during the treatment. The NMR spectra of the serum samples were acquired on 400.13 MHz Bruker spectrometer at 310 K. The referenced to alanine and bucketed to 0.002 ppm spectra were analyzed using principal component analysis (PCA) and orthogonal partial least squares discriminant analysis (OPLS-DA). Additional statistical analyses (Mann-Whittney test, Pearson correlation) were performed on quantified metabolites.

Results: In the high ARS group we observed the increased signals of N-acetyl-glycoprotein – the NMR marker of inflammation, and acetate – a product of beta-oxidation of adipose tissue fatty acids. The high ARS group showed also the decreased signals of metabolites involved in energy metabolism: branched chain amino acids (BCAAs), alanine, creatinine, carnitine and glucose as well as decreased choline containing compounds reflecting disturbed membrane metabolism. Furthermore, we observed the positive correlations between C-reactive protein (CRP) and N-acetyl-glycoprotein as well as acetate and a percentage weight loss during the treatment. CRP was also negatively correlated with alanine and BCAAs.

Conclusion: 1H NMR is an efficient tool for detection of RT/CHRT toxicity markers in human serum. The results indicate at least three concomitant processes related to high treatment toxicity (high ARS): inflammation, altered energy metabolism and disturbed membrane metabolism. The combination of clinical and molecular approaches could deliver comprehensive information on treatment response, allowing monitoring and/or prediction of tolerance/toxicity of therapy as well as its outcome. Such approach gives a step forward into personalized therapy.

EP-2048
Serum cytokines as a predictive factor in hepatoma patients treated with radiotherapy

J. Seong[1], H. Cha[1], E.J. Lee[1]
[1]*Yonsei Cancer Center- Yonsei University Health System, radiation oncology, Seoul, Korea Republic of*

Purpose or Objective: Cytokines, which are involved in chronic inflammation, are also related to tumor aggressiveness and resistance to treatment in many cancers. However, there are limited reports on the significance of cytokines in tumor response to radiotherapy (RT). The aim of this study was to analyze serum cytokine levels and identify their association with treatment outcome in patients with hepatocellular carcinoma (HCC) treated with RT.

Material and Methods: Patients with HCC who treated with RT were eligible for this prospective study. Blood samples were collected before and after completion of the whole RT course. Serum cytokine levels measured using Cytokine Bead Array kits were analyzed with respect to patients' clinical profiles and treatment responses.

Results: Between September 2008 and October 2009, 51 patients were included in the analysis. Median follow-up duration was 12.3 months (range, 0.5-62.3). Forty-seven patients were diagnosed with modified UICC stage III or IV disease at the time of RT. Baseline serum IL-8 level increased with increasing stage and the IL-6 level was highest in patients with a history of pre-RT treatment (treatment-non-naïve). A higher baseline serum IL-6 level was also observed in patients with treatment failure, including overall, infield, and outfield failure, than in those without treatment failure. In subgroup analysis, a significant difference in serum IL-6 level was observed only in treatment-non-naïve versus treatment-naïve patients. Median overall survival and progression-free survival (PFS) were 13.9 and 7.7 months, respectively. Elevated serum IL-6 level was significantly associated with PFS for patients with infield failure (HR 1.011, $p<0.0001$).

Conclusion: The current findings suggest that assessment of baseline serum IL-6 level may be helpful to predict treatment outcome after RT for HCC, especially in patients who undergo treatment before RT.

EP-2049
Diffusion MRI for following tumor modifications after neoadjuvant radiotherapy

F. Lallemand[1], N. Leroi[2], M. Bahri[3], E. Balteau[3], A. Noel[4], P. Coucke[5], P. Martinive[5], A. Plenevaux[3]
[1]*University of Liège and CHU, Radiotherapy and Cyclotron Research Centre and Laboratory of Tumor and Development, Liège, Belgium*
[2]*University of Liège and CHU, Radiotherapy Laboratory of Tumor and Development, Liège, Belgium*
[3]*University of Liège, Cyclotron Research Centre, Liège, Belgium*
[4]*University of Liège, Laboratory of Tumor and Development Biology, Liège, Belgium*
[5]*University of Liège and CHU, Radiotherapy, Liège, Belgium*

Purpose or Objective: Neoadjuvant radiotherapy (NeoRT) improves tumor local control and tumor resection in many cancers. The timing between the end of the NeoRT and surgery is driven by the occurrence of side effects or the tumor downsizing. Some studies demonstrated that the

timing of surgery and the RT schedule could influence tumor dissemination and subsequently patient overall survival. We demonstrated the impact of NeoRT on metastatic spreading in a Scid mice model. After an irradiation of 2x5gy, we show more metastasis in the lung when the mice are operated at day 4 compared to day 11 (1). Here, our aim is to evaluate with functional MRI (fMRI) the impact of the radiation treatment on the tumor microenvironment and subsequently to identify non-invasive markers helping to determine the best timing to perform surgery for avoiding tumor spreading.

Material and Methods: We used two models of NeoRT in mice we have previously developed: MDA-MB 231 and 4T1 cells implanted in the flank of mice (1). When tumors reached the planned volume, they are irradiated with 2x5 Gy and then surgically removed at different time points after RT. Diffusion Weighted (DW) -MRI was performed every 2 days between RT and surgery. For each tumors we acquired 8 slices of 1 mm thickness and 0.5 mm gap with an "in plane voxel resolution" of 0.5 mm. For DW-MRI, we performed FSEMS (Fast Spin Echo MultiSlice) sequences, with 9 different B-value (from 40 to 1000) and B0, in the 3 main directions. We also performed IVIM (IntraVoxel Incoherent Motion) analysis, in the aim to obtain information on intravascular diffusion, related to perfusion (*F*: perfusion factor) and subsequently tumor vessels perfusion.

Results: With the MBA-MB 231 we observed a significant increase of *F* at day 6 after irradiation than a decrease and stabilization until surgery. No other modifications of the MRI signal, ADC, D or D* were observed. We observed similar results with 4T1 cells, *F* increased at day 3 than returned to initial signal (fig 1). The difference in the peak of *F* can be related to the difference in tumor growth between MBA-MB 231 in four weeks and 4T1 in one week.

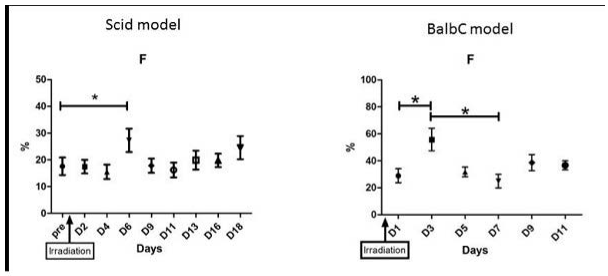

Figure 1: Graphs representing *F* factor in tumor bearing mice before and after radiotherapy in MDA-MB 231(n=6) (Scid model) and in 4T1 (n=4) (BalbC model); (*=p<0, 05)

Conclusion: For the first time, we demonstrate the feasibility of repetitive fMRI imaging in mice models after NeoRT. With these models, we show a significant difference between the pre-irradiated acquisition and day 6 or day 3 for perfusion *F*. This change occurs between the two previous time points of surgery demonstrating a difference in the metastatic spreading (1). These results are very promising for identifying noninvasive markers for guiding the best timing for surgery.

Reference: (1) The timing of surgery after neoadjuvant radiotherapy influences tumor dissemination in a preclinical model Natacha Leroi et al. (2015) *Oncotarget* vol. 5

EP-2050

The assessment of fractal dimension with Dual Energy CT gives information on lung cancer biomarkers

V. González-Pérez[1], E. Arana[2], A. Bartrés[1], S. Oliver[1], B. Pellicer[1], J. Cruz[3], M. Barrios[2], L.A. Rubio[4]

[1]*Fundación Instituto Valenciano de Oncología, Servicio de Radiofísica y Protección Radiológica, Valencia, Spain*

[2]*Fundación Instituto Valenciano de Oncología, Servicio de Radiología, Valencia, Spain*

[3]*Fundación Instituto Valenciano de Oncología, Servicio de Anatomía Patológica, Valencia, Spain*

[4]*Fundación Instituto Valenciano de Oncología, Servicio de Biología Molecular, Valencia, Spain*

Purpose or Objective: To assess whether texture analysis of images obtained with Dual Energy CT (DECT) is related to *KRAS* and Ki-67 lung cancer biomarkers.

Material and Methods: A retrospective review (May 2013 - January 2015) of 125 lung cancer patients with lung GSI (Gemstone Spectral Imaging) and perfusion CT imaging on a DECT was fulfilled. For 25 of them, the fraction of Ki-67 positive-tumour cells was analysed and for 19 patients *KRAS*-positive (mutation detected) or *KRAS*-negative (mutation not detected) character was evaluated (11 positive, 8 negative). DECT examination was performed on a Discovery CT 750 HD scanner (GE Healthcare, USA).

For the perfusion exam, blood volume, blood flow and permeability-surface studies were analyzed. At GSI exam, images related to absorption in Hounsfield units (HU), iodine concentration and monochromatic virtual images reconstructed at 40, 60, 80, 100, 120 and 140 keV were assessed. Tumour fractal dimension was measured with the use of *Mapfractalcount* plug-in for ImageJ (National Institute of Health, USA) software.

After extraction of DNA from paraffin embedded tissue using QIAamp DNA Investigator Kit (Qiagen), analysis of the *KRAS* gene exons 2 (codons 12/13) and 3 (codon 61) were performed in order to identify possible associated mutations with real-time PCR kit cOBAS® KRAS Mutation Test (Roche Diagnostics, SL).

T-Student test or U Mann-Whitney test were used to compare differences between *KRAS*-positive from *KRAS*-negative cohorts. Pearson correlation coefficient was used to study linear relationship between fractal dimension and the fraction of Ki-67 positive-tumour cells.

Results: Best result (p=0.02) for distinguishing *KRAS*-positive cohort was obtained for lesion fractal dimension at 140 keV virtual image. This parameter showed an AUC=0.80. It was predictive of *KRAS*-positive with 90.9% sensitivity and 75.0% specificity for a fractal dimension threshold of 2.352.

There was a correlation of lesion fractal dimension in blood volume image and the fraction of Ki-67 positive-tumour cells (p= 0.04).

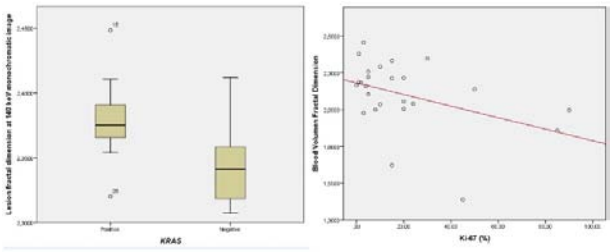

Conclusion: Ki-67 positive-tumour cells and *KRAS*-positive biomarkers lead to tumour heterogeneity that modify radiographic image. Fractal dimension parameter quantifies such imaging heterogeneity and could allow to differentiate them.

A higher fractal dimension (higher heterogeneity) of lesion at virtual monochromatic images is measured for *KRAS*-positive mutation, while a higher fraction of Ki-67 positive-tumour cells is associated with a more homogeneous blood volume at perfusion.

EP-2051

Hsp70 as a tumor specific biomarker in primary glioblastoma multiforme patients

F. Laemmer[1,2], C. Delbridge[2], K.A. Kessel[1,3], S. Stangl[1], J. Hesse[1], B. Meyer[4], J. Schlegel[2], D. Schilling[1,3], G. Multhoff[1,3], T.E. Schmid[1,3], S.E. Combs[1,3]

[1]*Klinikum rechts der Isar- TU Muenchen, Radiation Oncology, Muenchen, Germany*

[2]*Institute of Pathology- TU Muenchen, Neuropathology, Muenchen, Germany*

[3]*Institute of Innovative Radiotherapy- Helmholtz Zentrum Muenchen, Radiation Sciences, Muenchen, Germany*

[4]*Klinikum rechts der Isar- TU Muenchen, Neurosurgery, Muenchen, Germany*

Purpose or Objective: The standard treatment regimen of patients with primary glioblastoma multiforme (PGBM) consists of neurosurgery, radio- and chemotherapy. Despite this multimodal treatment the overall survival of patients with PGBM is still approximately 15 months.
The stress-inducible heat shock protein 70 (Hsp70) contributes to tumor cell survival and is associated with poor prognosis, metastasis and therapy resistance. Therefore, the aim of this study is to analyze Hsp70 in PGBM tumor samples as a future prognostic biomarker and possible therapy target.

Material and Methods: Formalin fixed paraffin embedded (FFPE) sections of 44 human PGBM patients (isocitrate dehydrogenase wildtype) were analyzed by immunohistochemistry for Hsp70 (cmHsp70.1, IgG1, multimmune GmbH, Munich, Germany). Taking the intensity of Hsp70 staining into account, quantitative expression analysis of tumor cells with stained cytoplasm was performed. Two categories of Hsp70 staining were defined: Up to 40% and more than 40% positive tumor cells within the tumor regions. The Hsp70 immunoreactivity was correlated with the survival of the patients using the Cox regression analysis.

Results: Preliminary data show that the median survival of PGBM patients can be predicted by the Hsp70 immunoreactivity of the tumor cells. Regression analysis showed that patients with Hsp70 expression of more than 40% have a higher risk of disease progression with a hazard ratio of 2.59 (p= 0.045).

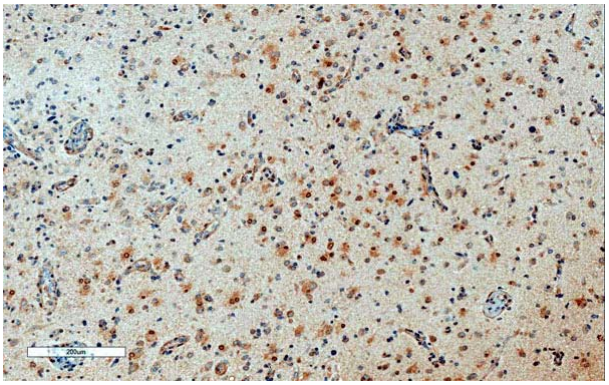

Hsp70 expression in FFPE IHC section (Hsp70 positive tumor cells are brown)

Conclusion: These data provide the first evidence that Hsp70 expression in FFPE sections of PGBM patients is associated with disease progression. Moreover, measuring Hsp70 in FFPE sections of PGBM patients before radiotherapy treatment may be used as biomarker for the success of the therapy. The independency of Hsp70 expression and O6-methylguanin-DNA methyltransferase (MGMT) is currently under investigation.

EP-2052

Expression of molecular biomarkers in wound drainage fluids: a pilot study in head and neck cancer

M. Sottili[1], M. Mangoni[1], P. Bonomo[1], A. Deganello[2], A. Javarone[2], T. Gualtieri[2], I. Desideri[1], M. Loi[1], I. Meattini[1], F. Paiar[1], L. Livi[1]
[1]*University of Florence, Experimental and Clinical Biomedical Sciences, Firenze, Italy*
[2]*University of Florence, Department of Surgery and Translational Medicine, Firenze, Italy*

Purpose or Objective: In recent years, it has been suggested that wound drainage fluids (WDF) of patients operated for head and neck squamous cell carcinoma (HNSCC) may be characterized by molecular biomarkers with potential prognostic and predictive value. The detection of adverse features in the early perioperative setting could possibly lead to a refinement of current adjuvant treatments in high-risk patients. The purpose of our study is to report on the feasibility and preliminary results of a pilot prospective study on WDF analysis in HNSCC.

Material and Methods: 14 consecutive surgically resected HNSCCs were studied. WDF were collected 1 day and 3 days after surgery from the cancer operative bed (COB). In 5 patients, WDF was collected also from free flap donor site (FFDS). WDF were centrifuged for 15 min at 3500 rpm, then divided in aliquots and stored at -80°C until analysis. The aim of the present study was to evaluate the expression of factors involved in tumor growth and progression 1 day and 3 days after surgery. EGF, VEGF, SDF-1 and osteopontin levels were measured in WDF using commercially available enzyme-linked immunosorbent assay (ELISA) kits. Each sample was analyzed in duplicates and then averaged for a mean value. Quality control pools of low, normal, or high concentrations for all parameters were included in each assay. The obtained results were expressed as pg/ml (EGF, VEGF, SDF-1) or ng/ml (osteopontin).

Results: A mean of 67 ml of WDF from COB and 51 ml from FFDS at day 1, and 42 ml from COB and 20 ml from FFDS at day 3 were collected for each patient. EGF expression was significantly reduced from day 1 to day 3 after surgery both in COB (140.7±10.55 vs. 45.12±13.35 pg/ml, $p<0.001$) and in FFDS (157.1±4.08 vs. 95.59±32.89 pg/ml, $p<0.05$). VEGF expression increased from 1 to 3 day both in COB (1277.74±64.54 vs. 1616.81±151.4 pg/ml, $p<0.05$) and in FFDS (1227.51±19.39 vs. 1400.25±77.66 pg/ml, $p<0.05$). The expression of markers of invasiveness and metastasis increased from day 1 to day 3: osteopontin expression significantly increased from day 1 to day 3 both in COB (9.97±0.68 vs. 16.87±0.56 ng/ml, $p<0.001$) and in FFDS (9.51±1.23 vs. 15.83±1.08 ng/ml, $p<0.01$). SDF-1 expression increased from day 1 to day 3 in COB (646.8±65.39 vs. 1084.22±148.8 pg/ml, $p<0.05$). No differences in SDF-1 expression were detected in FFDS.

Conclusion: Preliminary data from pilot study evidenced that microenvironment induced by surgery favors residual tumor cell proliferation and progression. Growth factor expression is higher early after surgery (24 hours); on the contrary, expression of markers of invasiveness and metastasis increases from day 1 to day 3 after surgery. The few samples of WDF from FFDS do not allow to evidence differences of biomarkers expression between COB and FFDS.

EP-2053

In-vivo imaging of rat leukocytes redistribution after pelvic irradiation

F. Benigni[1], C. Cozzarini[2], C. Sini[3], A. Spinelli[4], M. Venturini[5], L. Perani[6], V. Sacco[2], A. Viale[2], A. Capelli[2], A. Mondino[7], A. Briganti[1], M. Bellone[8], C. Fiorino[9], R. Calandrino[9], N. Di Muzio[2]
[1]*San Raffaele Scientific Institute, URI/Urology, Milan, Italy*
[2]*San Raffaele Scientific Institute, Radiotherapy, Milan, Italy*
[3]*Fondazione Centro San Raffaele, Medical Physics, Milan, Italy*
[4]*San Raffaele Scientific Institute, Experimental Imaging Center- Medical Physics, Milan, Italy*
[5]*San Raffaele Scientific Institute, Radiology, Milan, Italy*
[6]*San Raffaele Scientific Institute, Experimental Imaging Center, Milan, Italy*
[7]*San Raffaele Scientific Institute, Lymphocyte Activation Unit- Immunology- Transplantation and Infectious Disease Division, Milan, Italy*
[8]*San Raffaele Scientific Institute, Unit of Cellular Immunology, Milan, Italy*
[9]*San Raffaele Scientific Institute, Medical Physics, Milan, Italy*

Purpose or Objective: Hematologic toxicity and in particular decrease in the peripheral blood leukocyte and lymphocyte count is an important side effect of pelvic radiation therapy. The aim of this study was to investigate the kinetic of the redistribution of circulating leukocytes after pelvic irradiation in a animal model with in vivo non-invasive imaging modality.

Material and Methods: A rat model was used to investigate a possible selective accumulation of circulating lymphocites to specific anatomical districts after radiation treatment focused to the urinary bladder. Eight Fisher rats were adoptively transferred with 4x107 VivoTag-750-labelled syngeneic primary splenocytes at two hours before the bladder irradiation. Two of eight rats were used as controls. Animals were transurethrally catheterized to allow contrast agent instillation. A kV cone beam computed tomography (CBCT) was acquired for each rat, to precisely deliver 6 MeV monofraction photon field. Rats were divided into three groups (n=2/group) receiving different levels of dose: 15, 20 and 25 Gy. A bolus thickness equal to 1cm was positioned on the rat skin surface in the pelvic region. Ultrasound images of the pelvic region were acquired at baseline, at 2, 4 and 6 days after irradiation to monitor thickness variations of the bladder wall tissue. In vivo fluorescent imaging was used to evaluated accumulation sites of labelled leukocytes.

Results: A significant increase in the bladder wall thickness was found 4 days after irradiation in animals treated with a dose equal to 25 Gy. A fluorescent signal, secondary to labelled splenocytes accumulation, emerged in the liver and lymph nodes of all adoptively transferred rats, 2 and 6 days after irradiation, as expected. A modest specific signal (30% increase) at the bladder level resulted only in two animals receiving the higher dose (Figure 1.a), when compared to the non-irradiated (Figure 1.b). No specific fluorescent signal was detected at the bladder levels in animals treated with 20 and 15 Gy.

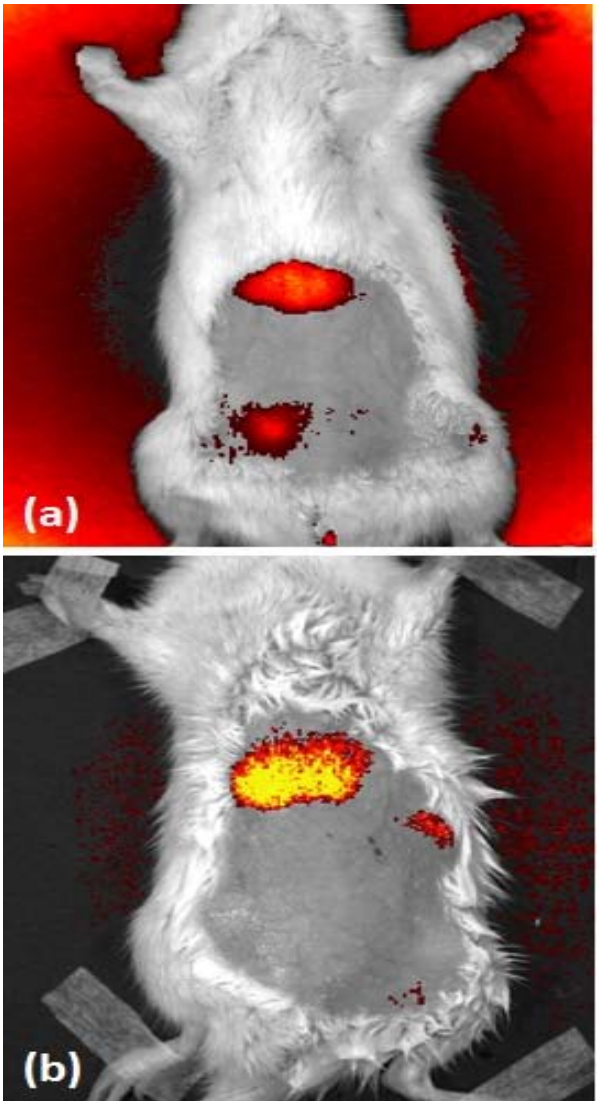

Conclusion: The relocalization of peripheral leukocytes in the damaged tissue depends on the radiation dosage and it may be evaluated by means of a non-invasive imaging technique. Further analyses are currently ongoing.

EP-2054

Expression of DNA-PK in squamous cell lung cancer has gender differences and depends on smoking

J. Jaal[1], L. Mägi[1], T. Jõgi[2], M. Kase[3], A. Minajeva[1], V. Markus[2], T. Vooder[4], R. Roosipuu[5], J. Jaal[2]
[1]*University of Tartu, Faculty of Medicine, Tartu, Estonia*
[2]*Tartu University Hospital, Dept of Radiotherapy and Oncological Therapy, Tartu, Estonia*
[3]*East-Tallinn Central Hospital, Cancer Centre, Tallinn, Estonia*
[4]*Centre for Thoracic Diseases, Dept of Thoracic Surgery, Ruhr, Germany*
[5]*Tartu University Hospital, Dept of Pathology, Tartu, Estonia*

Purpose or Objective: Lung cancer is one of the most frequent and deadly types of cancer in Europe. Several aspects of non-small cell lung cancer (nsclc) in men and women continue to indicate potential male-female differences. Among these, higher treatment responses to current therapies in women are supposed, since women have better prognosis in any stage of the disease. In most stages of nsclc cytotoxic anti-cancer therapy (radiotherapy, chemotherapy) is used. It is known that treatment efficacy of cytotoxic anti-cancer therapy depends on tumor DNA-repair. Therefore, the aim of this study was to evaluate gender differences in the expression of DNA repair enzyme DNA protein kinase (DNA-PK).

Material and Methods: Surgically excised nsclc tissues (n=111, 50 adenocarcinomas, 61 squamous cell carcinomas) were examined for DNA-PK expression. After immunohistochemistry, the staining intensity of DNA-PK was quantified using an arbitrary score ranging from 0 (no staining) to 3 (strong signal). Also, the proportion (%) of DNA-PK positive (DNA-PK+) tumor cells was determined. All parameters were examined by 2 independent researchers in 10 randomly chosen microscopic fields (magnification x40).

Results: Immunohistochemical parameters were examined by 2 independent researchers whose results were in good accordance ($p<0.0005$). Staining intensities of DNA-PK and the proportion of DNA-PK+ tumor cells varied, being in the whole nsclc group 2.4±0.4 (mean±SD) and 86.3±9.1% respectively. There were no significant gender differences in adenocarcinoma. However, we detected significant differences among nsclc patients with squamous cell carcinoma. Both, DNA-PK staining intensity and the proportion of DNA-PK+ tumor cells were significantly higher in men than in women, 2.5±0.3 and 86.3±8.8% vs 2.1±0.6 and 79.6±11.9% respectively (DNA-PK intensity: $p<0.01$; DNA-PK+ proportion: $p=0,03$). Additionally, we found that in squamous cell carcinoma, the expression of DNA-PK depends on smoking and pack-years. There was a correlation between pack-years and DNA-PK intensity ($p=0.04$), as well as between pack-years and the proportion of DNA-PK+ tumor cells ($p=0.04$).

Conclusion: Expression of DNA-PK in squamous cell lung cancer has gender differences and depends on smoking. Significantly lower expression of tumor DNA-PK was found in women with this histological subtype of nsclc. Latter might be one of the reasons why cytotoxic anti-cancer therapy is more efficacious in women than in men. In further studies, the combination of DNA repair inhibitors and cytotoxic anti-cancer therapy should be tested.

EP-2055

Fibro-inflammatory circulating proteins as biomarkers for response in locally advanced rectal cancer

P. Bulens[1,2], A. Debucquoy[2], I. Joye[1,2], O. De Wever[3], A. Wolthuis[4], A. D'Hoore[4], E. Van Cutsem[5], V. Vandecaveye[6], X. Sagaert[7], C. Deroose[8], O. Gevaert[2,9], K. Haustermans[1,2]
[1]*University Hospital Leuven, Radiation Oncology, Leuven, Belgium*
[2]*University of Leuven, Oncology, Leuven, Belgium*

[3]*Ghent University Hospital, Radiation Oncology and Experimental Cancer Research, Ghent, Belgium*
[4]*University Hospital Leuven, Abdominal Surgery, Leuven, Belgium*
[5]*University Hospital Leuven, Digestive Oncology, Leuven, Belgium*
[6]*University Hospital Leuven, Radiology, Leuven, Belgium*
[7]*University Hospital Leuven, Pathology, Leuven, Belgium*
[8]*University Hospital Leuven, Nuclear Medicine, Leuven, Belgium*
[9]*Stanford University, Medicine- Division of Biomedical Informatics, Stanford, USA*

Purpose or Objective: Selecting good responders after chemoradiation (CRT) for locally advanced rectal cancer (LARC) could lead to the omission of total mesorectal excision (TME) in patients with pathologic complete response (pCR). In the current study, we assessed the value of several blood biomarkers associated with the fibrotic response to CRT (IGF-1, IGFBP-2, HGF & GDF-15) as markers for general fibro-inflammatory response and as tumor response predictors in a group of 80 patients.

Material and Methods: ELISA analysis of IGF-1, IGFBP-2, HGF and GDF-15 was conducted on prospectively collected serum samples of 80 LARC patients on 3 time points (before, during, after CRT). The fibro-inflammatory response was scored on H&E sections of the resection specimen. Changes in concentration were analysed using a Kruskal-Wallis test. Correlation of concentration at each time point and the difference between these time points (Δ) with fibro-inflammatory response and tumor response (pCR and ypT0-1) were assessed using a Mann-Whitney-U test.

Results: Higher Growth Differentiation Factor 15 (GDF-15) concentration before CRT correlated with the presence of a fibro-inflammatory response ($p = 0.04$), but was not observed for the other proteins nor for GDF-15 at other time points.
General increase in GDF-15 concentration during treatment (median 0.81 ng/ml before, 2.16 ng/ml during, 2.37 ng/ml after CRT; $p < 0.0001$) was measured (Figure 1). Although no significant general concentration changes occurred for IGF-1, IGFBP-2 or HGF, we did find a correlation between the variation in expression of IGFBP-2 during treatment (ΔIGFBP-2 TP3-TP2) with tumor response (pCR $p = 0.02$; ypT0-1 $p = 0.02$). Other proteins did not correlate with tumor response.

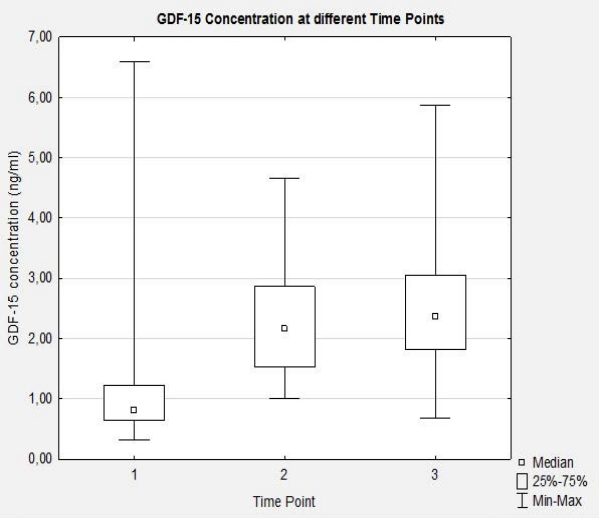

Figure 1. GDF-15 Concentration at different time points (TP) during treatment. (TP1: before CRT; TP2: during CRT; TP3: after CRT)

Conclusion: GDF-15 serum concentration increases during CRT for LARC and a higher concentration measured before start of treatment is correlated with the presence of a fibro-inflammatory response. These results suggest that GDF-15 could be used as an early predictor of fibro-inflammatory response and thereby indirectly as predictor for disease-free survival. This will be evaluated when follow-up data are available for this patient cohort.
The correlation of variation in expression of IGFBP-2 with tumor response (pCR and ypT0-1) opens a novel possibility for selecting good responders to CRT. We aim to combine these findings with imaging analyses (DW-MRI, PET) at different time points during treatment to develop a predictive model for selecting LARC patients in whom surgery could be omitted.

EP-2056
Preclinical investigation of hypoxia induced genes in different prostate cancer cell lines.
T. Wittenborn[1], S. Nielsen[1], M. Busk[1], M.R. Horsman[1], J. Overgaard[1], J. Alsner[1], B.S. Sørensen[1]
[1]*Aarhus University Hospital, Department of Experimental Clinical Oncology, Aarhus, Denmark*

Purpose or Objective: Hypoxia is a common feature in prostate cancer and is known to reduce the response to radiotherapy. Hypoxic modifiers can to a large extent overcome these obstacles, and a proper classification of tumors into hypoxic and non-hypoxic fractions is necessary. Previously our department has developed a gene profile consisting of 15 genes, which demonstrated prognostic and predictive impact for hypoxic modification in head and neck squamous cell carcinomas (HNSCC). In the current study we investigated the 15 gene profile in different prostate cancer cell lines.

Material and Methods: For the in vitro experiments the prostate cancer cell lines investigated were PC-3, DU-145, and LNCaP. Cell lines were cultured under normoxic (21% O2) or hypoxic conditions (0% O2) for 24 hours, totRNA was extracted and gene expression levels measured by qPCR. Individual reference genes were selected (PSMC4, TBP, NDFIP1) and applied in the normalization of the relative expression levels, together with the reference genes previously used in the HNSCC study. For in vivo experiments, the PC3 cell line was inoculated on the flank of female NMRI nu/nu mice, whereas the LNCaP and DU-145 cell lines were inoculated on the flank of severely immunocompromised CIEA/NOG mice. Two hypoxia-sensitive tracers (18F-FAZA and Pimonidazole) were administered in order to determine hypoxic and non-hypoxic regions on excised tumor sections. These regions were isolated by laser-assisted microdissection, after which totRNA was extracted and gene expression levels measured by qPCR.

Results: In the in vitro experiments, all prostate cancer cell lines had 14 of the 15 genes induced by hypoxia. The only discrepancy was ALDOA, which was not upregulated in the hypoxic cells. In vivo experiments are still ongoing but preliminary results from PC3 xenografts have been produced. These show a hypoxia induced upregulation in 10 out of the 15 genes, of which 4 were significantly upregulated (ADM, ANKRD37, FAM162A, and LOX).

Conclusion: In this study we investigated the 15 gene hypoxic profile in three different prostate cancer cell lines. A hypoxia dependent induction of genes was observed in both in vitro and in vivo experiments. From the performed experiments, and looking only at oxygen dependency, it appears that the gene profile could be suitable for prostate cancers as well as HNSCC.

EP-2057
Radiotoxicity prediction by gene expression profiling when simulating therapy in matched fibroblasts
M.A. Schirmer[1], C.P.N. Mergler[1], L.H. Droege[1], M. Guhlich[1], J. Gaedcke[2], M. Ghadimi[2], M. Rave-Fränk[1]
[1]*Klinikum der Universität Göttingen, Radiotherapy and Radiation Oncology, Göttingen, Germany*
[2]*Klinikum der Universität Göttingen, General and Visceral Surgery, Göttingen, Germany*

Purpose or Objective: Acute radiotoxicity might put a vital threat to the patient and may require interruption or

preterm stop of the therapy thus jeopardizing the intended treatment outcome. Despite numerous research attempts there is still no robust feature established in clinical routine to predict radiotherapy-induced toxicity prior to therapy start.

Material and Methods: The study cohort comprised 40 patients who underwent neoadjuvant radiochemotherapy (N-RCT) for rectal cancer (28x1.8 Gy, 5 times weekly, concomitant with two cycles 5-FU-based chemotherapy). From each of those patients dermal fibroblasts were cultured from skin specimen gained outside of the radiotherapy planning target volume at occasion of surgery conducted about six weeks upon N-RCT completion. Acute radiotoxicity was thoroughly monitored throughout the N-RCT series and documented according to CTC classification. Maximal acute toxicity (MAT) was defined by the highest CTC grade of the four items "cystitis", "proctitis", "enteritis", and "dermatitis". MAT was grouped into grades 0/1 (n=16), 2 (n=16), and 3/4 (n=8). N-RCT was simulated in the cultured fibroblasts for five consecutive days (1.8 Gy each at d1-d5 with addiation of 5-FU at a concentration reflecting clinical steady-state levels) followed by a 7-day wash-out period. Gene expression of nine candidate genes (*CAT*, *CDKN1A*, *CTGF*, *SMAD2/3/4/7*, *TGFB1*, *TGFBR1*) supposed to mediate early radiation-induced toxicity was ascertained by quantitative real time PCR. Samples for these RNA analyses were harvested at d2 and d5 (each 4 hours upon application of the radiation fraction) as well as at day 12 upon the wash-out period. *GAPDH* and *HPRT1* transcript levels served as reference.

Results: MAT was related to radiation-induced expression changes of four of the considered genes in fibroblasts. The strongest impact was obtained for *SMAD7* and *CAT* at d5. The higher the MAT score, the lower the induction of *SMAD7* and *CAT* by radiation was (p=0.001 and 0.003). However, upon the wash-out period at d12 no statistical differences in dependence on the MAT score were seen anymore for these two genes. In contrast, a high MAT score was linked to low radiation-induced induction of *CTGF* (p=0.005) and to a faster decrease of the massively induced *CDKN1A* (p=0.03) at d12. At d2, a trend (p=0.06) for *CAT* in relation to MAT in the same direction as at d5 was noticed with no correlation of any of the other genes at this early time point.

Conclusion: Radiation-induced expression changes in patient-matched fibroblasts may serve as biomarkers to predict clinical radiotoxicity. Induction of *SMAD7* and *CAT* may mitigate TGFbeta signalling and reactive oxygen species load thus saving normal tissue during radiotherapy. A protective role might also be attributed to sustained elevation of *CDKN1A*. The link between post-radiation induction of *CTGF* in fibroblasts and low MAT remains to be clarified. Understanding the mechanistic basis of these findings might pave the way for better protection of irradiated normal tissue.

EP-2058

A novel multi-SNP model predictive of erectile dysfunction following radiotherapy in prostate cancer

J.H. Oh[1], S. Kerns[2], H. Ostrer[3], B. Rosenstein[4], J.O. Deasy[1]
[1]*Memorial Sloan Kettering Cancer Center, Department of Medical Physics, New York, USA*
[2]*University of Rochester Medical Center, Department of Radiation Oncology, Rochester, USA*
[3]*Albert Einstein College of Medicine, Departments of Pathology and Genetics, New York, USA*
[4]*Mount Sinai School of Medicine, Department of Radiation Oncology, New York, USA*

Purpose or Objective: Erectile dysfunction (ED) is one of the most common complications encountered after radiotherapy in prostate cancer patients. The goal of this study was to investigate whether single nucleotide polymorphisms (SNPs) are associated with late ED in men treated with radiotherapy for prostate cancer. To this end, we designed a novel machine learning-based multi-SNP model using a genome-wide association study (GWAS) dataset.

Material and Methods: We analyzed 236 evaluable patients with at least one year of follow-up for the development of ED. The severity of ED was assessed using either the patient-administered Sexual Health Inventory for Men (SHIM) or the clinician-assigned Mount Sinai Erectile Function (MSEF) scoring schema. There were 133 patients with Grade 2 or more ED. For our analysis, the cohort was split into two groups (cases/controls: MSEF 0,1 / 2,3; cases/controls: SHIM ≤7 / ≥16). Genome-wide SNP data were available from Affymetrix Genome-Wide Human SNP Array 6.0. After a quality test including SNP missing rate>5%, minor allele frequency (MAF)<5%, and Hardy-Weinberg equilibrium (p<10E-5), 613,496 SNPs remained.
For the validation purpose of our proposed model, the dataset was split into a training dataset (2/3 of samples) and a validation dataset (1/3 of samples). Our model building process was performed using the bootstrapped data from the training dataset. Our idea is to convert the binary outcomes into preconditioned continuous outcomes based on normal tissue complication probability (NTCP) using principal component analysis (PCA) and logistic regression. The preconditioned outcomes were used in the model building process using random forest regression. Then, the model was tested using the validation dataset. The final predicted outcomes were compared with the original binary outcomes to estimate the predictive performance. We iterated this process 100 times and the performance was averaged. We compared the performance of our proposed method (preconditioning random forest regression: PRFR) with other methods including preconditioning lasso (PL), lasso logistic regression (LLR), and random forest classification (RFC).

Results: Univariate analysis was performed using the training dataset. With a threshold of p=0.001, 367 SNPs remained. These SNPs were fed into our model. As shown in Figure (A), the averaged performance with the validation dataset was AUC=0.62, which is better than other methods: RFC (0.57), PL (0.58), and LLR (0.57). The 79 patients in the validation dataset were binned into 6 groups according to the predicted risk of ED. Figure (B) shows the comparison of the model-predicted incidence of ED with observed incidence.

Conclusion: Our machine learning-based multi-SNP model showed the potential to better predict the radiation-induced late ED. However, we need to validate our model using other datasets.

Figure. Comparison of our machine learning-based multi-SNP model with other methods (A) and comparison of the model-predicted incidence of ED with observed incidence with events/patients on the top of the standard error bars in 6 bins (B).

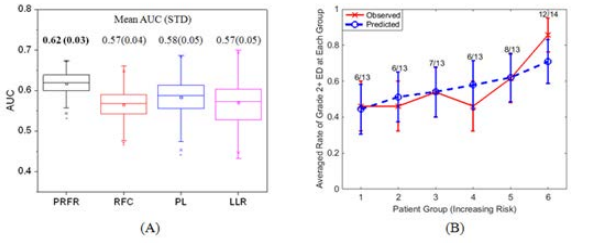

EP-2059

Changes in hypoxia in serial F-MISO/PET-CT during chemoradiation in HNSCC

H. Kerti[1], A. Bunea[1], L. Majerus[1], M. Mix[2], C. Stoykow[2], N. Wiedenmann[1], P.T. Meyer[2], A.L. Grosu[1]
[1]*University Hospital Freiburg, Department of Radiation Oncology, Freiburg, Germany*
[2]*University Hospital Freiburg, Department of Nuclear Medicine, Freiburg, Germany*

Purpose or Objective: Tumor hypoxia, a common feature of locally advanced head and neck cancer (HNSCC), is associated with higher malignancy and increased radioresistance. The decrease of tumor hypoxia during

fractionated radiation treatment is assumed to be decisive for treatment success. [18F]-Fluoro-Misonidazole PET (F-MISO-PET) allows noninvasive assessment of hypoxia during treatment. The purpose of the present study was to noninvasively assess the time course of tumor hypoxia.

Material and Methods: A prospective serial imaging study was conducted in patients undergoing definitive chemoradiation (dRCTx, total dose 70Gy) for locally advanced HNSCC, accompanied by cisplatin in weeks 1, 4 and 7. Tumor hypoxia was assessed by F-MISO-PET by static scans acquired 2.5 h p.i. Tumor volumes were determined for FDG PET/CT scans and the coregistered F-MISO/CT scans. At baseline MRI, FDG-PET/CT and F-MISO-PET were acquired (week 0). Additional F-MISO-PET/CT scans were acquired in treatment weeks 2 and 5. Normal sample distribution was confirmed with Shapiro-Wilk test. Unpaired t-test analysis of the mean SUVmax(tumor)/SUVmean(muscle) ratios of F-MISO-PET in weeks 0, 2 and 5 were performed. Significance-level was defined as $p<0.005$.

Results: Between 2012 and 2014 18 patients (16 men, two women, mean age 60 years), treated for HNSCC with dRCTx were included. All received a total dose of 70 Gy in 35 fractions. Concomitant cisplatin chemotherapy was administered in weeks 1, 4 and 7. 14 patients had all F-MISO-PET scans, while 4 had two F-MISO-PET scans (week 0, 5). The mean follow-up time was 14.6 months (range: 4 - 28 months). Mean SUVmax(tumor)/SUVmean(muscle) in weeks 0, 2 and 5 were 1.9 (n=18, SD ± 0.1), 1.5 (n=14, SD ± 0.1) and 1.2 (n=18, SD ± 0.1), respectively. Unpaired t-test for SUVmax(tumor)/SUVmean(muscle) between week 0 and 5 was performed, showing a singnificant decrease ($p<0.0001$). Between weeks 0 and 2 ($p=0.0346$) and between weeks 2 and 5 the decrease again was highly significant ($p=0.0113$). In two patients no residual hypoxia was measured in week two, resulting in SUVmax(tumor)/SUVmean(muscle) =1.0. In week 5 this was found in seven patients. In two patients hypoxia had increased in week 2 but decreased in week 5 compared to pre-treatment measurements. In one patient hypoxia had increased by the end of treatment.

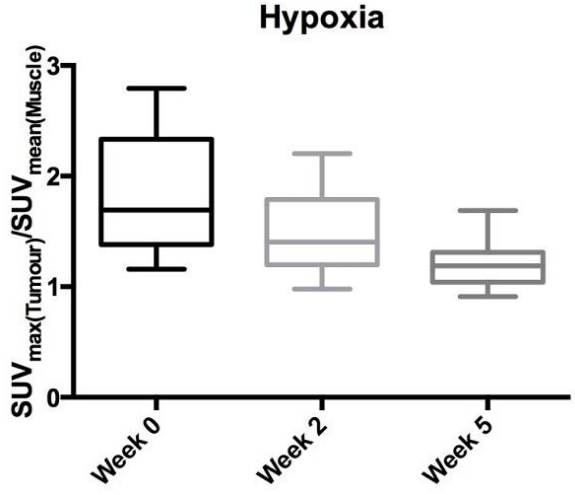

Conclusion: Differences in hypoxia between weeks 0-2, 2-5 and 0- 5, respectively, show statistical significance. This is crucial in the process of re-oxygenation. As concluded in previous works, change of treatment strategy, e.g. by means of dose escalation might be most efficient early during treatment. However further analysis, with more patients and correlation to disease-free and overall-survival are needed.

EP-2060

Correlation of imaging data with known predictive/prognostic factors in Oropharyngeal cancer

J. Lynch[1], M. Zhao[2], J. Scuffham[3], P. Evans[4], C. Clark[5], K. Wood[1], S. Whitaker[1], A. Nisbet[5]
[1]*Royal Surrey County Hospital, Head & Neck, Guildford, United Kingdom*
[2]*University of Surrey, Medical Imaging, Guildford, United Kingdom*
[3]*Royal Surrey County Hospital, Nuclear Medicine, Guildford, United Kingdom*
[4]*University of Surrey, Physics, Guildford, United Kingdom*
[5]*Royal Surrey County Hospital, Medical Physics, Guildford, United Kingdom*

Purpose or Objective: There is increasing interest in maximising data extraction from the multimodality imaging performed in cancer patients in order to predict treatment outcomes. This is particularly relevant in Oropharyngeal cancer where concomitant chemoradiotherapy is the standard treatment in stage III and IV disease but there is significant variation in patient outcomes and both treatment intensification and de-intensification strategies are being investigated.
The aim of this prospective pilot study was to look at how data obtained from pre- and per-treatment 18F-FDG-PET/CT scans and textural features from pre- and per-treatment contrast enhanced planning CT scans correlated with known prognostic indicators including smoking history and HPV status.

Material and Methods: Eligible patients included those undergoing primary concomitant chemoradiotherapy for Stage III/IV SCC of the Oropharynx. Each patient underwent a contrast enhanced planning CT and an 18F-FDG-PET/CT scan immobilised in the treatment position prior to the start of treatment and then again after 8-10 fractions of radiotherapy. The SUVmax and SUVmean were recorded on both the pre- and per- treatment 18F-FDG-PET/CT. Texture analysis was performed using TexRad software on both the pre- and per-treatment planning CT scans. The smoking history for each patient was established on enrolment to the study and HPV status was determined using p16 IHC on biopsy of the primary tumour. Ethical approval was gained from the relevant bodies.

Results: Eighteen patients were recruited. HPV status was positive in 13 patients and negative in 5 patients. The SUVmax/mean in HPV negative patients was 21.6/13.3 on the pre-treatment 18F-FDG-PET/CT versus 15.2/10.5 for HPV positive patients (p= 0.09/0.25). Pre-treatment CT texture analysis showed a difference in the normalised entropy between the two groups with a significant difference detected using the smallest filter (p=0.04). The SUVmax/mean on the pre-treatment 18F-FDG-PET/CT for patients with no or minimal smoking history (<10 years) was 13.7/9.5 versus 19.1/12.9 for those with a smoking history of >10years (p= 0.1/0.13). No significant difference in the entropy/entropy ratio between the two groups was detected. No significant differences were shown in the change in SUV or entropy ratio between the pre-and per-treatment scans in any of the groups.

Conclusion: These results suggest differences in the imaging characteristics between patients in different prognostic categories may be detected at the pre-treatment stage and are worthy of further investigation in a larger patient cohort and may in the future add further information to that provided by the molecular profiling of tumours. This study did not show any significant differences in the data obtained between patients in terms of their early response to treatment however this data can be revisited once follow up data for this patient cohort matures.

EP-2061

Over-expression of EGFR and/or cox-2 in locally advanced squamous cervical cancer (LASC)

M. Aylas[1], J. Pérez -Regadera Gómez[1]
[1]*Hospital Universitario 12 de Octubre, Radiation Oncology, Madrid, Spain*

Purpose or Objective: This study looking for the prognosis value of over-expression of EGFR and/or COX-2 in patients with locally advanced squamous cervical carcinoma (LASC).

Material and Methods: 118 patients with FIGO IB2-IVA st. were treated with RT-CT radical (Tab A). Anti-EGFR monoclonal Ac.(clone H11 Ref. M-3363 -Dako). The Immunoreactivity was based on semiquantitative analysis scored as the % of stained cells. Moderate/high EGFR staining (>31 to ≥70%, respectively) were considered (+). Anti -COX-2 monoclonal Ac. (clone CX-2949 Ref. M361 - Dako). Moderate/high COX-2 staining (>31 to ≥70%, respectively) were considered (+). Pelvic radiotherapy in 21 patients with RT-3D, dose 46 Gy. In 97 cases (82%) was extended to the para-aortics, dose 45 Gy. A single application of LDR BCT was delivered on 51 pts (43.5%). Isotope: Cs-137. Dose to point A: 30 Gy. HDR BCT to 64 pts (54%) in 3 or 4 applications. Isotope: Ir-192; Microselectron®. Dose 30 Gy to point A (33 pts) and a dose of 7 Gy to CTV/application (31 pts). CT: CDDP: 40 mg/m2/ iv weekly.

Results: Mean time follow-up for 118 pts: 56.5 months ±DS 10.5 (median 56). Mean time follow-up of lost pts (8): 48 months ± DS 10.5 (median 46). Clinical characteristics and treatments in Tab n°1 and °2.

Table n°1. Clinical characteristics of the patients studied

Variables	Number	(Percentage)
Age		
Median	53	
<50 years	50	(42)
>50 years	68	(58)
ECOG		
0	10	(8.4)
1	90	(76.2)
2	14	(12)
3	4	(3.4)
FIGO Stage		
IB2-IIA	13	(11)
IIB	44	(37.3)
IIIA-B	52	(44.1)
IVA	9	(7.6)
Tumoral size		
≤ 6 cm	42	(36)
> 6 cm	76	(64)
Nodes in CT +/- MRI +/- PET-CT		
Negative	61	(52)
Pelvic positive	41	(35)
Para-aortic positive (+/- pelvic)	16	(13)
Expression EGFR		
-	13	(11)
+	20	(17)
++	26	(22)
+++	59	(50)
Expression COX-2		
-	35	(29.6)
+	42	(36)
++	31	(26)
+++	10	(8.4)
Joint Overexpression		
[EGFR and COX-2 negative]	21	(18)
[EGFR or COX-2 positive]	68	(58)
[EGFR and COX-2 positive]	29	(24)

Table n°2. Description of treatments given

	n° patients	
Chemotherapy:		*Average dose of cisplatin / patient*
Cisplatin	118	340mg (p25=300, p75=380 mg) Average number of cycles: 5.5
External radiation therapy:		*Dose*
Pelvic	21	46 (5x200 cGy)
Pelvic and para-aortic	97	45 Gy (5x180 cGy)
Boost:		*Average dose to point A / VoL isodose 60 Gy*
Brachytherapy LDR	51	28 Gy (p25:22;p75:35) /255 cc (r. 30-400cc)
Brachytherapy HDR	64	3 or 4 applications of 7Gy to CTV (31 pt) 3 or 4 applications of 7Gy to point A(33 pt)
External radiation therapy in central pelvic	3	*Dose / Total dose* 15-20 Gy / 65-70 Gy (5x180 o 5x200 cGy)
External radiation therapy in nodes pathologic (boost)	25	*Dose/ Total dose* 10 Gy / 55 Gy

Table A: Inclusion and Exclusion criterias

Inclusion criteria:	*Exclusion criteria:*
-Patients diagnosed of cervical carcinoma by biopsy with immunohistochemical determination for EGFR and COX-2 -Age over 18 and under 85 years - FIGO IB2 –IVA stage -Squamous histology -Patients treated solely with radical radiochemotherapy.	- Patients not valid for standard chemotherapy (e.g. creatinine >2 mg/dl, hepatic profile alteration, neutrophils < 2000 mm³, platelets < 100 000 mm³) - Other treatment schemas different to radio-chemotherapy and/or interventions which would delay the concomitant treatment

EGFR: 33 pts without overexpression vs. 85 pts (72%) with overexpression. COX-2: 77 pts without overexpression vs 41 (35%) with over-expression. 24% were EGFR/COX-2 (+), 58% were EGFR (+)/ COX-2 (-) or vice versa and 18% were EGFR/ COX-2 (-). 94 pts (80%) with CR, 22 pts with PR and 2 pts stabilisation. Actuarial OS at 3/5 yrs:79% (CI 95%:70-85) and 77% (CI 95%:68-84). Actuarial DFS at 3/ 5 yrs:71% (CI 95%: 62-78) for both. Actuarial PFFS at 3/5 yrs:81% (IC 95%: 72-87) for both. We observed 13 local failures, 4 regional failures, 6 joint failures; 1 pure para-aortic failure, 9 exclusive metastasis to distance. We found that EGFR overexpression is age related >50 yrs old (p=0.01). The most advanced stages (III-IVA) are related to joint overexpression of both markers (p=0.02). Tab n°3 and °4 summarize our results.

Table n°3. Univariate analysis for Disease Free Survival (DFS) and Pelvic Failure Free Survival (PPFS)

Variable	Total	DFS a 3years % (CI 95%)	DFS a 5years % (CI95%)	p value	PPFS a 3years % (CI95%)	PPFS a 5years % (CI 95%)	p value
Age							
<50 years	50	66(53-78)	66 (53-78)	0.39	75(60-85)	75(60-85)	0.13
>50 years	68	74(62-83)	74(62-83)		88(74-92)	88(74-92)	
ECOG							
0-1	100	77(67-84)	77(67-84)	<0.0001	85(77-91)	85(77-91)	<0.004
2-3	18	38 (17-60)	38(17-60)		54(26-75)	54(26-75)	
Size Tumoral							
≤6cm	42	81(66-90)	81(66-90)	0.04	90(78-96)	90(78-96)	0.07
>6cm	76	65(53-75)	65(53-75)		76(66-84)	76(66-84)	
Stage FIGO							
Ib2-IIB	57	84(71-91)	84(71-91)	<0.005	93(82-97)	93(82-97)	<0.002
III-IVA	61	60(46-71)	60(46-71)		70(56-80)	70(56-80)	
Pelvic+/-para-aortic lymph nodes							
Positive	57	65(52-76)	65(53-76)	0.18	74(59-85)	74(59-83)	0.06
Negative	61	76(63-85)	76(63-85)		88(76-94)	88(76-94)	
EGFR							
Negative(-/+)	33	79(60-89)	79(60-89)		90(71-96)	90(71-96)	0.15
Positive (++/+++)	85	68(57-77)	68(57-77)	0.36	77(67-85)	77(67-85)	
COX-2							
Negative (-/+)	77	72(60-81)	72(60-81)		79(68-87)	79(68-87)	0.50
Positive (++/+++)	41	70(53-82)	70(53-82)	0.86	84(68-93)	84(68-93)	
Joint expression							
EGFR & COX-2(-)	21	76(52-89)	76(52-89)		85(61-95)	85(61-95)	0.87
EGFR or COX-2(+)	68	73(60-82)	73(60-82)		83(69-88)	83(69-88)	
EGFR & COX-2(+)	29	64(44-78)	64(44-78)	0.68	77(57-89)	77(57-89)	

Table n°4. Multivariate analysis for Disease Free Survival (DFS) and Pelvic Failure Free Survival (PPFS)

Variable	DFS Hazard ratio [CI 95%]		value p	PPFS Hazard ratio [CI95%]		value p
ECOG 2-3	2.6	(1.1-6.7)	0.01	2.5	(0.7-6.3)	0.14
Tumoral size >6cm	1.7	(0.7-4.1)	0.20	1.6	(0.5-4.9)	0.40
Stage FIGO III-IVA	1.9	(0.8-4.4)	0.13	2.9	(1.0-9.5)	0.04
Positive lymph nodes	—	—	—	1.5	(0.6-3.9)	0.34

The EGFR overexpression or COX-2 or both together, did not reach significance in the univariate analysis for DFS and PPFS.

Conclusion: We did not find an association between overexpression of EGFR and/or COX-2 regarding the DFS and PPFS, despite being described in literature that these markers play a role in tumoral biology and in its evolution.There is a need for homogeneous, prospective studies with a standardized determination for these markers.

Electronic Poster: Radiobiology track: Cellular radiation response

EP-2062

c-Myc silencing impairs oncophenotype and radioresistance of Embrional Rhabdomyosarcoma Cell Lines.

F. Marampon[1], G. Gravina[1], C. Festuccia[1], C. Alessandro[1], E. Di Cesare[1], V. Tombolini[2]

[1]*University of L'Aquila, Department of Biotechnological and Applied Clinical Sciences, L'Aquila, Italy*

[2]*Policlinico Umberto I "Sapienza" University of Rome, of Radiotherapy, Rome, Italy*

Purpose or Objective: We previously reported that the disruption of MEK/ERK/c-Myc axis affects in vitro and in vivo growth, angiogenic signaling and radiosensitivity of the embryonal rhabdomyosarcoma (ERMS) cell lines. Herein, we investigated the role of c-Myc in vitro invasion, migration, neo-angiogenesis and radioresistance of ERMS cells.

Material and Methods: RD and TE671 cells expressing the c-Myc dominant negative MadMyc chimera protein or shRNA-c-Myc were used.

Results: c-Myc depletion affected ERMS cells in vitro migration and invasion abilities by reducing the sialylation levels of NCAM and decreasing the MMP-9, MMP-2 and u-PA gelatinolytic activity. Although c-Myc down-regulation affected HIF1-α, VEGF and TSP1 proteins expression, no effects were seen on in vitro neo-angiogenesis. Rapid, but not prolonged, c-Myc down-regulation radiosensitized ERMS cells by impairing the expression of DSB repair proteins such as RAD51 and DNA-PKcs but not Ku80.

Conclusion: Herein c-Myc acts as a key master regulator of in vitro migration, invasion and radioresistance. In fact, c-Myc depletion alone seems to be sufficient to block the in vitro pro-metastatic abilities and to radiosensitize ERMS cells. In addition, our data suggest c-Myc as important, but not essential, in controlling the molecular machinery responsible for cancer neo-angiogenesis. In conclusion these data strongly suggest that the targeting of c-Myc can be tested as a promising strategy for an anti-cancer therapy.

EP-2063

Apoptotic pathway activation in prostate neoplastic cells after 12 Gy-IORT

C. Pisani[1], N. Domagala[2], F. Copes[2], F. Mercalli[3], A. Volpe[4], D. Beldì[1], F. Boccafoschi[2], R. Boldorini[3], M. Krengli[1]
[1]*University Hospital Maggiore della Carità, Radiotherapy, Novara, Italy*
[2]*University Hospital Maggiore della Carità, Health Sciences Department, Novara, Italy*
[3]*University Hospital Maggiore della Carità, Pathology, Novara, Italy*
[4]*University Hospital Maggiore della Carità, Urology, Novara, Italy*

Purpose or Objective: To evaluate apoptotic pathways involved in prostate cancer treated with intraoperative radiotherapy (IORT) with 12 Gy, studying the effects on cancer cells, prostatic intraepithelial neoplasia (PIN) and normal cells

Material and Methods: Since 2005, 111 patients treated at University Hospital of Novara, Italy with local advanced prostate adenocarcinoma were treated with radical prostatectomy and 12 Gy IORT followed by 50 Gy postoperative radiotherapy. In this setting, we selected a sample of 10 patients for a preliminary feasibility study. Selection criteria for this phase were: no neoadjuvant hormone therapy, Gleason score > 7. Proteins involved in the apoptotic cascade (Bax, Caspases -3 and -9) were studied before and after 12 Gy single shoot in neoplastic cells, high grade PIN areas and in normal prostate cells. Immunofluorescent detection of antigens (anti-Bax, anti-caspases-3 and -9), were performed on bioptic sample and on surgical specimens 5-mm slices. On surgical specimens there were also detected Bcl-2, and ki-67 with immunoistochimical analysis. A count of positive spots for immunofluorescence (Bax+, Caspases-3 and -9+/all nuclei, 40x magnification) was performed on tumor cells, PIN, healthy tissue areas. Bax and caspases immunofluorescent positivity was compared in different areas and in neoplastic areas before and after single shoot high dose

Results: A significant increase in Bax, Caspases-3 and -9 expression was detected in tumor and PIN areas comparing IORT treated and untreated samples ($p<0.05$). After 12 Gy-single dose, healthy areas expressed significantly lower level of Bax and caspases positive with respect to neoplastic cells ($p<0.0001$), while in PIN areas, Bax positive cells were significantly more present than in neoplastic areas ($p=0.0001$). Mean Bcl-2 in neoplastic cells is 17% (range: 1-23), mean ki-67 in neoplastic area is 4.5% (range: 1-17). With multivariate analysis, we find that cancer cells with Ki-67 ≥ 8% show a trend toward greater expression of Bax ($p=0.0641$)

Conclusion: After 12 Gy irradiation, Bax and caspases resulted overexpressed in tumor and PIN cells, in particular in prostate cancer with higher proliferation index. PIN areas seem to be more radiosensitive than neoplastic areas and healthy cells do not activate apoptosis after single shoot, showing an intrinsic radioresistence. This preliminary study represents the basis for an extensive work in which we would correlated clinical parameters with pathology and apoptotic factors. In fact, the comprehension of these relationships could allow to better understand the mechanisms of high dose per fraction and, radioresistence in order to personalize treatments

EP-2064

Radiation induces metabolic switch to lactate production to support tumour cell survival

K. Dittmann[1], C. Mayer[1], H.P. Rodemann[1]
[1]*Institut für Strahlenbiologie und Molekulare Umweltfoschung, Division of Radiobiology, Tübingen, Germany*

Purpose or Objective: Purpose: Radiation treatment of tumor cells resulted in a reduction of endogenous ATP levels. Aim of this study was to elucidate the molecular scenario standing behind this observation.

Material and Methods: Endogenous ATP-levels were dermined by ATP-ELISA. HIF1a, PDK1, LDH and PDH expressions were visualized by western blotting. Lactate production was quantified by lactate-assay. Cellular survival was proved by clonogenic survival assay.

Results: Results: Ionizing radiation induced expression of Hif1 alpha even at clinical relevant doses of 2 Gy. Hif1alpha induced activation of mitochondrial PDK1, which results in PDK1 dependent phosphorylation of pyruvate dehydrogenase (PDH). PDH is responsible for conversion of pyruvate to acetyl-CoA, which fuels the TCA cycle. Thus, irradiation blocks TCA cycle and mitochondrial activity. Simultaneously Hif1alpha induced expression and activity of lactate dehydrogenase (LDHA) to convert glucose to lactate. Indeed we observed a clear increase in lactate production in tumor cell lines in response to irradiation. Furthermore, inhibition of PDH activity was associated with mitophagy and ATP-depletion, which explains the radiation induced ATP drop down. In addition, this radiogenic switch to lactate production reduced production of mitochondrial derived radicals and increased cellular radio-resistance. Pretreatment with the Hif1 alpha inhibitor BAY87-2243 prevented the radiogenic switch to lactate metabolism and radio-sensitized the tumor cells. In addition, tumor cells are strictly dependent from high glucose supply after irradiation and can be radio-sensitized by blockage of radiogenic glucose uptake with glucose transporter SGLT inhibitor Phlorizin.

Conclusion: In summary, we could show, that tumor cells switch in a Hif1 alpha dependent manner to anaerobe glucose metabolism to generate ATP, which renders cells radio-resistant. Blockage of Hif1 alpha stabilization or blockage of glucose uptake radio-sensitized tumor cells.

EP-2065

Effects of spontaneous γH2AX level on radiation-induced response in human somatic cells

S. Vasilyev[1], A.I. Velichevskaya[2], T.V. Vishnevskaya[2], A.A. Skryabin[1], A.A. Belenko[2], A.A. Sleptsov[1], O.V. Gribova[3], Z.A. Startseva[3], I.N. Lebedev[1]
[1]*Institute of Medical Genetics, Laboratory of Cytogenetics, Tomsk, Russian Federation*
[2]*Tomsk State University, Biological Institute, Tomsk, Russian Federation*
[3]*Tomsk Cancer Research Institute, Radiology Department, Tomsk, Russian Federation*

Purpose or Objective: Phosphorylated histone H2AX (γH2AX) foci are well-known markers of DNA double-strand breaks in human cells. Spontaneous γH2AX foci form on unrepaired DNA double strand breaks, shortened telomeres and sites with altered chromatin conformation. The presence of such permanent γH2AX foci in cell is an important component of epigenetic background and potentially lead to the activation of DNA repair system. The objective of this study was to analyze the effects of spontaneous γH2AX level on radiation-induced response in human somatic cells.

Material and Methods: Spontaneous γH2AX foci and radiation-induced micronuclei were analyzed in peripheral blood lymphocytes of 54 healthy individuals after exposure to 2 Gy ionizing radiation in vitro. Further, a transcriptome analysis was performed using gene expression microarrays in lymphocytes of two sub-groups of individuals: 1)

radiosensitive individuals with low spontaneous level of γH2AX foci (n=3) and 2) radioresistant individuals with high spontaneous level of γH2AX foci (n=3).

Results: An inverse correlation was found between the spontaneous level of γH2AX foci and the frequency of micronuclei after irradiation (R=-0,37, p=0.025). After gene expression analysis with microarrays, several genes were identified whose differential expression could be associated with an efficiency of DNA repair and radiation sensitivity. XRRA1 gene with unknown functions, recently associated with radioresistance in tumor lines, was down-regulated both before and after irradiation in radioresistant group. Furthermore, in unirradiated samples of radioresistant individuals thrombospondin gene (THBS1), well-known radiosensitizer, was down-regulated. However, several genes were significantly up-regulated, including HERC2, important player in the assembly of DNA repair foci, and histone genes (H1, H2A, H4). After irradiation, several DNA repair genes (WHSC1, POLN, ERCC5, DCLRE1C) were significantly up-regulated, but EIF2A and PNPLA5 genes, involved in apoptosis and autophagy, were down-regulated in radioresistant group. This is consistent with low levels of apoptosis and increased proliferation in lymphocytes of these individuals.

Conclusion: The obtained results indicate that spontaneous γH2AX foci activate DNA damage response in human somatic cells and provide opportunities to clarify the role of the expression of identified genes in the formation of chromosomal aberrations in human cells after exposure to radiation.

EP-2066

Phospholipase Cε as a biomarker of prostate cancer radioresistance

A. Tyutyunnykova[1], G. Telegeev[2], A. Dubrovska[3,4,5]
[1]*Technische Universität Dresden and Helmholtz-Zentrum Dresden-Rossendorf, OncoRay-National Center for Radiation Research in Oncology- Faculty of Medicine and University Hospital Carl Gustav Carus-, Dresden, Germany*
[2]*The Institute of Molecular Biology and Genetics of NASU, Molecular Genetics, Kyiv, Ukraine*
[3]*Technische Universität Dresden and Helmholtz-Zentrum Dresden-Rossendorf, OncoRay-National Center for Radiation Research in Oncology- Faculty of Medicine and University Hospital Carl Gustav Carus, Dresden, Germany*
[4]*Helmholtz-Zentrum Dresden-Rossendorf, Institute of Radiation Oncology, Dresden, Germany*
[5]*German Cancer Consortium DKTK, DKTK, Dresden, Germany*

Purpose or Objective: Radiotherapy is a curative treatment option in prostate cancer. Nevertheless, many men with prostate cancer develop recurrence of their disease. Identification of the predictive biomarkers and signaling mechanisms indicative of tumor cell radioresistance bears promise to improve cancer treatment. In our study we show that Phospholipase C epsilon (PLCε) might contribute to prostate cancer radioresistance.

Material and Methods: Gene expression profiling of prostate cancer cells and theirradioresistant derivatives, western blotanalysis to assess PLCε expression in the parental and radioresistantcells and in cell cultures after irradiation, radiobiological cell survivalanalysis of the cells with genetic modulation of PLCεexpression by siRNA or cDNA transfection as well as chemical inhibition of PLCε activity,fluorescent microscopy to analyze co-expression of PLCε withother markers of radioresistance. Normal 0 21 false false false EN-US X-NONE X-NONE

Results: The results of gene expression analysis, which were validated by western blotting revealed significant upregulation of PLCe in prostate cancer radioresistant cells that can also be seenafter irradiation of the parental cells with a single dose of 4Gy. Radiobiologicalsurvival assays demonstrated that siRNA induced PLCε knockdown or chemicalinhibition of PLCε activity by Edelfosine leads to prostate cancer cellradiosensitization. In contrast, overexpression of PLCε in cells transfected withplasmid DNA results to an increase in cell radioresistance. Microscopicanalysis revealed a high expression level of ß-catenin in prostate cancer cellsoverexpressing PLCε.

Conclusion: These results indicate that PLCε plays a role in prostate cancer radioresistance that can be mediated through activation of the WNT/ ß-catenin signaling pathway.

EP-2067

The adhesion of tumor cells to endothelial cells is increased by photon irradiation

H. Bühler[1], P. Nguemgo-Kouam[1], A. Kochanneck[1], B. Priesch[1], H. Hermani[1], K. Fakhrian[1], I.A. Adamietz[1]
[1]*Marienhospital Herne- Ruhr-Univers., Klinik für Strahlentherapie und Radio-Onkologie, Herne 1, Germany*

Purpose or Objective: In general the prognosis for cancer patients is poor even though only 10% die from the primary tumor. The majority of the deceases are due to metastasis. Given the fact, that more than 70% of cancer patients receive radiotherapy it seems important to clarify if radiation is involved in initial steps of the metastatic cascade – despite of innumerable clinical studies that confirm no enhanced risk of metastasis after radiotherapy. In this project we investigated whether the irradiation with photons increases the adhesion of cultured tumor cells (TC) to a layer of endothelial cells (EC) macroscopically and whether this might be caused by the induction of adhesion proteins.

Material and Methods: The experiments were performed with glioblastoma (U87, U373) and breast cancer cell lines (MDA-MB-231, MCF7), and with primary HUVEC cells. The cells were irradiated with 0, 0.5, 2, 4, or 8 Gy. Adhesion of TC to EC, both irradiated or not, was determined with 2 different methods: the VybrantTM cell adhesion assay and the Ibidi pumpsystem that allows to mimic the physiological blood stream in the vasculature. In addition, the expression of the adhesion-related proteins E-selectin, VCAM1, ICAM1, N-cadherin, integrin ß1, and PECAM1, 4h after irradiation with 4 Gy, was analyzed by qRT-PCR and by Western blotting.

Results: Irradiation increased significantly the adhesion of TC to EC. With glioblastoma cells the highest increase of about 40% was observed when both cell types were irradiated. In contrast, with breast cancer cells the highest effect of about 25% was obtained for irradiated TC in combination with non-irradiated EC. Analysis of the expression patterns in all cell types revealed an significant increase of adhesion proteins after irradiation in more than 80% of the experimental data sets.

Conclusion: We assume that the irradiation of tumor cells as well as of endothelial cells with photons might enhance adhesive interactions of these cells and thereby might promote the first steps of metastasis. Since clinical studies reveal no enhanced risk of metastasis due to irradiation we speculate that the therapeutic effect of radiotherapy might be additionally enhanced when the induced stickiness could be blocked effectively.

EP-2068

Effect of a 0.2 T magnetic field during radiation on DNA damage and repair in prostate cancer cells

S. Baker[1], Z. Jin[2], A. Ghila[3], B. Warkentin[4], M. Hendzel[2], G. Fallone[5], R. Pearcey[1]
[1]*Cross Cancer Institute and University of Alberta, Radiation Oncology, Edmonton, Canada*
[2]*Cross Cancer Institute and University of Alberta, Experimental Oncology, Edmonton, Canada*
[3]*Cross Cancer Institute and University of Alberta, Medical Physics, Edmonton, Canada*
[4]*Cross Cancer Institute and University of Alberta, Medical Physics- Oncology- Medical Physics Division, Edmonton, Canada*
[5]*Cross Cancer Institute and University of Alberta, Medical Physics- Physics and Oncology- Medical Physics Division, Edmonton, Canada*

Purpose or Objective: Real time MR-guided radiotherapy is an emerging technology. The effect of magnetic field exposure on radiosensitivity is unknown. This study aimed to determine the effect of magnetic field exposure on the repair of radiation-induced DNA double-strand breaks in human prostate cancer cells.

Material and Methods: Human PC-3 prostate cancer cells and benign prostatic hypertrophy (BPH) cells were cultured and plated into 96-well dishes and irradiated with 2 Gy of 6 MV photons on a linear accelerator. Each cell line was exposed to either 2 Gy of ionizing radiation alone (IR) or 15 minutes of 0.2 T magnetic field concurrently with 2 Gy IR (IR + B). Cells were fixed at 15 minutes or 24 hours following IR and immunostained with fluorescent-labelled antibody to γH2AX, a marker of DNA double-strand breaks. For each experimental scenario, the number of γH2AX foci per cell were determined using a Molecular Devices MetaXpress High Content Imaging Platform, for sample sizes between 3370 and 8402 cells. To classify response, radiation-induced damage was associated with cells having more than five foci.

Results: Magnetic field exposure resulted in a significantly higher percentage of PC-3 cells with five or fewer γH2AX foci at 24 hours following IR (42 vs 37 percent, $p < 0.01$) but had no significant effect on BPH cells (89 vs 88 percent, $p = 0.26$). In both cell lines, magnetic field exposure significantly reduced the percentage of cells with five or fewer γH2AX foci 15 minutes following IR ($p < 0.01$) (Table 1).

Table 1. Percentage of BPH and PC-3 cells with≤ 5 γH2AX foci at 15 minutes and at 24 hours after exposure to 2 Gy of ionizing radiation alone (IR) vs 2 Gy of ionizing radiation with 15 minutes of concurrent 0.2 T magnetic field exposure (IR + B).

Time of cell fixation	BPH			PC-3		
	IR	IR + B	P-value	IR	IR + B	P-value
	Percentage of cells with ≤ 5 γH2AX foci			Percentage of cells with ≤ 5 γH2AX foci		
15 min	40	28	<0.01	17	14	<0.01
24 h	88	89	0.26	37	42	<0.01

Conclusion: The preliminary results suggest that the presence of a magnetic field during irradiation reduces DNA damage at 24 hours post-irradiation for PC-3 human prostate cancer cells. Conversely, magnetic field exposure increased the DNA damage present 15 minutes following IR in both cell lines, suggesting a different mechanism at play, such as altered free radical flux or differences in the kinetics of the initiation of the DNA damage response. Cell viability assays, gene expression profiling and testing of other cell lines will yield important insights into the implications for real time MR-guided radiotherapy.

EP-2069

CDC73 deficiency: a syndrome with multiple tumours is predicted to show excessive radiosensitivity

R. Lewis[1,2,3], E.C. Bourton[3], C.N. Parris[2,3], P.N. Plowman[1,2]
[1]*St Bartholomew's Hospital, Radiotherapy, London, United Kingdom*
[2]*Queen Mary's University, Barts Cancer Institute, London, United Kingdom*
[3]*Brunel University, Biosciences, Uxbridge- Middlesex, United Kingdom*

Purpose or Objective: It has previously been demonstrated that prolonged expression of the γ-H2AX DNA repair biomarker in irradiated peripheral blood lymphocytes correlated with excess toxicity from radiotherapy treatment in patients. γ-H2AX fluorescence in cells has been established asan indicator of double strand breaks, and a marker for DNA damage and repair of cells after irradiation. This case study illustrates that the peripheral blood lymphocytes of a patient with CDC73 deficiency retained γ-H2AX fluorescence over 24 hours to a greater degree than a patient with normal DNA repair.

CDC73 deficiency is an autosomal dominant inherited syndrome. The gene on chromosome 1q31 encodes a tumour suppressor that is known to be involved in transcriptional and post-transcriptional control pathways. The protein is a component of the PAF protein complex, which associates with the RNA polymerase II subunit POLR2A and with a histone methyltransferase complex, and is involved in regulation of transcription coupled nucleotide excision repair.
A patient with CDC73 mutation with a typical history of primary hyperparathyroidism, an ossifying fibroma of the jaw, renal cysts and a renal cell carcinoma developed a carotid body paraganglioma which was to be treated with stereotactic radiotherapy. There was concern that the syndrome (associated with multiple tumours) would lead to unusual radiation sensitivity following standard radiotherapy prescriptions, and this study aimed to establish if this would be the case.

Material and Methods: Peripheral blood lymphocytes (PBLs) from the patient were irradiated with 2Gy and fixed at 30 minutes and 24 hours, stained for γ-H2AX and compared with PBLs from a normal and radiosensitive patient (patient P - thyroid cancer with excessive toxicity to radiotherapy). They were also compared with known DNA repair defective immortalised fibroblasts from AT5BIVA (patient with classical ataxia telangiectasia). The cells were analysed on an Imagestream flow-cytometer.

Results:

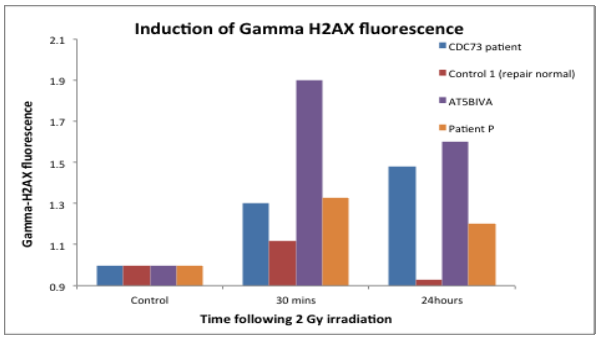

Conclusion: It may be confidently predicted that this patient with CDC73 deficiency would demonstrate more vigorous radiation reactions in normal tissues for any standard dose of radiotherapy, due to a possible defect in DNA repair and this should be considered when planning his Cyberknife treatment for the carotid body paraganglioma. The exact mechanism for this will need to be considered along with current knowledge of the role of CDC73.

EP-2070

Cell cycle analysis of γ-H2AX in irradiated normal or DNA-defective cells with image flow cytometry

R. Lewis[1,2,3], P.N. Plowman[1,2], C.N. Parris[2,3]
[1]*St Bartholomews Hospital, Radiotherapy, London, United Kingdom*
[2]*Queen Mary's University London, Barts Cancer Institute, London, United Kingdom*
[3]*Brunel University, Biosciences, Uxbridge- Middlesex, United Kingdom*

Purpose or Objective: The quantitation of nuclear γ-H2AX foci in cells has been established as an indicator of double strand breaks, and therefore a marker for DNA damage and repair of cells after irradiation. The new generation image flow cytometer by Amnis Imagestream Mark II enables the rapid and simultaneous processing of images on multiple channels of large numbers of cells. It also has a unique feature or "wizard" which allows the identification of cell cycle distribution based on the fluorescence intensity of nuclear staining, in this case using the far red fluorochrome Draq5. This study aims to use this facility to establish whether there are different numbers of γ-H2AX foci in cells depending on the phase of the cell cycle. This is a novel

study and the outcome will inform future studies using γ-H2AX staining.

Material and Methods:
Fibroblast Cell Lines (SV40 immortalised)
– MRC5-SV1 - Repair normal.
– AT5BIVA – Classical ataxia telangiectasia.
Irradiation Cells
Irradiated with 2 Gy gamma radiation; harvested and fixed in 50:50 V:V methanol acetone. Time points: Un-irradiated, 30 min, 3, 5 and 24 hrs post irradiation.
Immunocytochemistry
Primary antibody: Anti-phospho-histone H2AX (Ser139), mouse monoclonal antibody clone JBW301 (1/10,000, Millipore).
Secondary antibody: Rabbit anti-mouse AlexaFluor488 (1/1000, Invitrogen).
DNA counterstained with Draq 5 (Biostatus Ltd.)
Imaging flow cytometry
Images of 5-10,000 cells captured

Results:

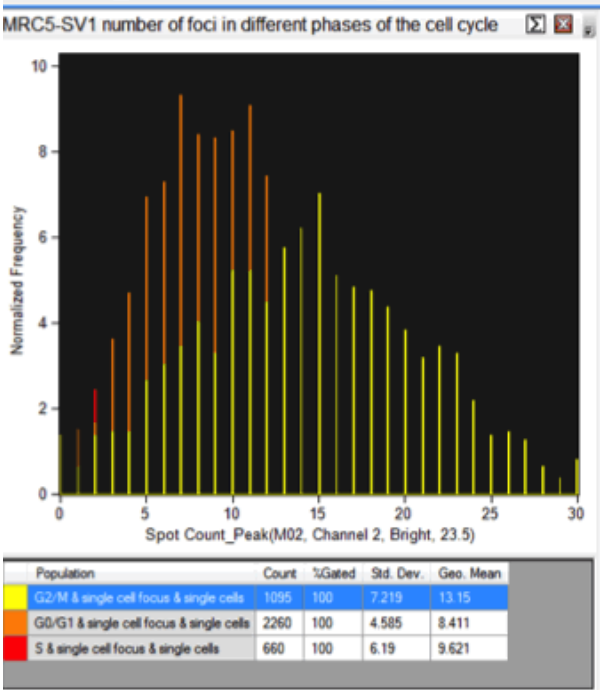

Statistical Analysis • 30 minute time point, comparing mean foci count for G0/G1, S and G2/M with one-way ANOVA test: – MRC5-SV1 (repair normal); $F(4,4010)=163.5$, $p < 0.001$ AT5BIVA (DNA repair defective); $F(2,2919)=421.3$, $p < 0.001$

Conclusion: We have identified cells in different phases of the cell cycle by analysing intensity of the Draq 5 nuclear stain and negating the need for extra staining. These data have shown a statistically significant difference between foci numbers in different phases of the cell cycle at one time point for a normal cell line and a DNA repair deficient cell line. Further work will look at differences in the cell cycle distribution between the two cell lines

Electronic Poster: Radiobiology track: Radiobiology of protons and heavy ions

EP-2071
Mitophagy and Apoptosis: mitochondrial responses to carbon ion radiation in tumor cells
X. Jin[1], X. Zheng[1], F. Li[1], Q. Li[1]
[1]*Institute of Modern Physics- Chinese Academy of Sciences, Division of Radiation Medical Physics, Lanzhou, China*

Purpose or Objective: Although mitochondria are known to play an important role in radiation-induced cellular damage response, the mechanisms by which tumor cells respond to the mitochondrial damage induced by high linear energy transfer (LET) radiation are largely unknown.

Material and Methods: Human cervical cancer cell line HeLa and human breast cancer cell lines MCF-7 and MDA-MB-231 were irradiated with high linear energy transfer (LET) carbon ions at low and high doses. Mitochondrial functions, dynamics, mitophagy, intrinsic apoptosis and total apoptosis, and survival fraction were investigated after irradiation.

Results: Compared with unirradiated cells, carbon ion irradiation resulted in the loss of mitochondrial membrane potential and fragmentation, suggesting mitochondrial damage was induced. Mitophagy and intrinsic apoptosis of tumor cells were the major responses to the carbon ion radiation induced mitochondrial damage. After exposure to low doses of carbon ions, cells initiated mitophagy to keep viability while tending to death via apoptosis at high doses.

Conclusion: Tumor cells through mitophagy and apoptosis respond to the mitochondrial damage caused by high-LET radiation according to the radiation dose. A threshold model depicting the fate of irradiated cells could provide a mechanistic explanation for differential mitochondrial damage response to high-LET radiation at low and high doses. Our data shed new light on understanding the mechanisms underlying high-LET radiation induced cell death.

EP-2072
Spatiotemporal dynamics of DNA damage in cells exposed to mixed beams of ionising radiation
B. Brzozowska[1,2], A. Sollazzo[1], L. Cheng[1], L. Lundholm[1], A. Wojcik[1,3]
[1]*Stockholm University, Centre for Radiation Protection Research. Department of Molecular Bioscience. The Wenner-Gren Institute, Stockholm, Sweden*
[2]*University of Warsaw, Faculty of Physics. Department of Biomedical Physics, Warsaw, Poland*
[3]*Jan Kochanowski University, Institute of Biology. Department of Radiobiology and Immunology, Kielce, Poland*

Purpose or Objective: A particular problem of modern external beam radiotherapy like IMRT and proton therapy is exposure of patients to scattered neutrons with a relative biological effectiveness (RBE) higher than X-rays. The interesting question is if there is an additive or synergistic effect of high and low linear energy transfer (LET) radiations when given together. If they act additively, then the risk of cancer can be deduced from the results of exposure to the single agents. Otherwise, RBE values must be generated for the mixed exposure scenarios or corrected to account for the synergism.

Material and Methods: The goal of this study was to analyse the kinetics of formation and repair of ionising radiation-induced foci (IRIF) in cells exposed to alpha particles, X-rays and a mixed beam of both radiations. To this end human cells were transfected with plasmids coding for the DNA repair the protein 53BP1 that are tagged with the green fluorescent protein (GFP). Cells were exposed to mixed beams in a dedicated exposure facility built at Stockholm University (SU). The facility is composed of a 50 MBq Am-241 alpha source and an YXLON 200 X-rays source. The alpha source is mounted on an inversed plate in a custom-designed irradiator which is kept inside a 37°C cell incubator.

Results: Spatiotemporal dynamics of 53BP1 foci formation and repair were recorded by time-lapse photography and image analysis. The distributions of cell frequencies with the specific size of foci and the size of foci itself were analysed. Moreover, Monte Carlo simulations (the PARTRAC code) were used not only for calculating radiation hits, but also for the biological damage in the DNA in terms of single and double strand breaks.

Conclusion: Exposure to a mixed beam induces complex DNA damage above the level expected from the additive action of

both radiations. Clustered DNA damage poses serious problems for the DNA repair and error-prone repair of DNA damage is associated with cancer induction. Increased damage complexity following exposure to mixed beams will suggest a higher than expected risk of cancer induction in modern radiotherapy. The results are consistent with the previous studies carried out at SU with different cell types and different biological assays. A synergistic interaction of the beam components was observed at the level of micronuclei, gammaH2AX foci and chromosomal aberrations.

EP-2073

Angio/lymphangiogenic, inflammatory and immune responses in head and neck cancer: proton vs photon

A. Claren[1], M. Plesu[2], J. Doyen[1], J. Feuillade[1], M. Dufies[2], S. Giulano[2], J. Hérault[1], G. Pagès[2]
[1]*Centre Antoine Lacassagne, Radiotherapy, Nice, France*
[2]*Institut de Recherche sur le Cancer et le Vieillissement de Nice, CNRS UMR 7284- INSERM U1081, Nice, France*

Purpose or Objective: Due to its higher precision in tumor targeting, proton therapy could become the treatment of choice for head and neck cancer (HNC). Recent studies have shown that proton irradiation suppresses angiogenic genes and impairs tumor cell invasion/growth. According to the type of radiation, dose and fractionation, the objective of our study was to investigate the effect of proton (P+) versus photon (X) irradiations in squamous cells carcinoma (SCC), in respect of their proliferation, genes expression and proteins secretion involved in proliferation, angio/lymphangenesis, metastasis and anti-tumor immunity.

Material and Methods: Human SCC CAL33 cells were irradiated 1 to 3 times and evaluated on their proliferation (Cell counting), genes expression (qPCR) for proliferation (TRF2, PLK1), angio/lymphangiogenic (VEGF-A, VEGF-C, VEGF-D) inflammatory (IL6, IL8, CCL2, CXCL12) and immune (PD-L1) responses.and protein synthesis (ELISA).

Results: Cell proliferation was evaluated at 48h and at 3 weeks after 1 irradiation and showed a significant decreased in both X and P+, as compared to control but more important in P+. After 3 irradiations, cell proliferation at 48h was reversed and more decreased in X vs P+. Genes expression was investigated at 48h after 1 and 3 irradiations at 2 and 8 Gy. After 1 irradiation, the prevalence of gene expression levels associated with a poor outcome was higher in X than P+ at 8 Gy. After 3 irradiations, genes expression was increased for all but more important for P+ at 8 Gy. The highest expression was noted for VEGF-C (2 to 10 fold increase). The most frequent overexpression was noted for PD-L1. VEGF-C protein induction 48h after 1 and 3 irradiations was increased in both X and P+ groups but decreased in high dose P+, as compared to X.

Conclusion: Cell proliferation activity is in favor of P+ after a single irradiation, and X after multiple irradiations. Genes expression are overall increased in both X and P+, in a dose and fraction dependent manner, implicated in proliferation (TRF2), angio/lymphangiogenic (VEGF-A, VEGF-C, VEGF-D) and immune (PD-L1) responses. VEGF-C protein induction is increased after both X and P+ single and multiple irradiations, but in favor of P+, suggesting a lower lymphangiogenesis/metastatic dissemination immediately after P+. Our study sets the molecular basis for novel therapeutic approaches applicable to HNC in combination with X or P+ radiotherapy, such as angio/lymphangenic inhibitors or immune therapy as anti-PD1 or anti-PD-L1.

Electronic Poster: RTT track: Strategies for treatment planning

EP-2074

The comparison of properties for radiotherapy with flattening filter-free and flattening filter beam

J.H. Gu[1], H.S. Won[1], J.W. Hong[1], N.J. Chang[1], J.H. Park[1]
[1]*Seoul National Univ. Bundang Hospital, Radiation Oncology, Seongnam- Gyeonggi-Do, Korea Republic of*

Purpose or Objective: The aim of this study was to appraise multiple properties for radiation therapy techniques applying flattening filter-free (3F) and flattening filter (2F) beam to the radiation therapy.

Material and Methods: Alderson rando phantom was scanned for computed tomography images. Treatment plans for intensity modulated radiation therapy (IMRT), volumetric modulated arc therapy (VMAT) and stereotactic body radiation therapy(SBRT) with 3F and 2F beam were designed for prostate cancer. To evaluate the differences between the 3F and 2F beam, total monitor units (MUs), beam on time (BOT) and gantry rotation time (GRT) were evaluated and measured with TrueBeam™ STx and Surveillance And Measurement (SAM) 940 detector was used for photoneutron emitted by using 3F and 2F.

Results: In using 3F beam, total MUs in IMRT plan increased the highest up to 34.0% and in the test of BOT and GRT, the values in SBRT plan by 3F beam decreased the lowest 39.8, 38.6% respectively. The values of photoneutron occurrence in SBRT plan using 3F beam decreased the lowest 48.1%.

Conclusion: According as the results, total MUs increased by using 3F beam than 2F beam in all treatment plans but BOT, GRT and photoneutron decreased by using 3F beam. From above the results, using 3F beam can have an effect on decreasing intra-fraction setup error and risk of radiation-induced secondary malignancy.

EP-2075

Evaluation of conventional versus IMRT based Prophylactic Cranial Irradiation treatment planning

E.H. Thøgersen[1], A.I.S. Holm[2]
[1]*Aarhus University Hospital, Medical Physics, Herning, Denmark*
[2]*Aarhus University Hospital, Medical Physics, Aarhus, Denmark*

Purpose or Objective: Patients with Small-Cell Lung Cancer (SCLC) have a high risk of developing brain metastasis. Prophylactic Cranial Irradiation (PCI), is applied to SCLC patients that response to chemotherapy. It is well known that PCI is associated with an increase in median overall survival. There are approximately 84 incidences per year in central region DK. Radiotherapy (RT) to this group of patients is conventionally performed using opposed MLC defined static fields. However, treatment planning can be time consuming. The aim of this study is to evaluate time-effectiveness, by changing the treatment technique from conventional to IMRT based treatment planning of PCI patients.

Material and Methods: This retrospective study included twenty SCLC patients, all treated with conventional planned PCI. Each patient received 25 Gray in 10 fractions. An IMRT template was made (Eclipse Version 11.0, Varian Medical Systems, Palo Alto, CA) and for each patient an IMRT plan was generated by one IMRT optimization. One intermediate dose calculation was performed during optimization before the final dose calculation. The contoured structures used for comparison between IMRT and conventional planning were: ITV, PTV and left/right lens. The plans were evaluated and compared on; max- and minimum doses, the mean/maximum doses to the lenses, and the homogeneity index (HI). The HI was defined by D5%/D95%. Quality assurance of the IMRT plans was performed by recording Portal Dosimetry Images

(PDI) for ten of the plans, and by independent dose calculation checks using RadCalc (RadCalc Version 6.2, LifeLine Software Inc, Tyler, USA).

Results: The observed differences between the conventional and the IMRT plans were limited. In average the maximum dose was 0.3 percentage points (pp) lower for IMRT than for conventional plans. The ITV coverage was better for the IMRT plans, with an average ITV minimum dose of 95.9 % compared to 94.1% (+1.8 pp). However, the PTV coverage was slightly worse for the IMRT plans, a decrease of 0.4 pp in V95%. The only relevant organs at risk are the lenses, were the maximum dose on average were lowered 0.3 Gray and the mean dose on average was lowered 0.1 Gray. The average HI for the IMRT plans was 4.0 while 5.1 for the conventional plans. The 10 PDI measurements were all accepted with a reference gamma index value of 5% dose agreement within 3 mm distance to agreement, and no further measurements were performed. Independent dose calculation checks were performed for QA. The time spend on treatment planning was approximately 20 minutes for IMRT plans and could easily be up to 3 hours when using the conventional technique.

	Property	Conventional	IMRT	Difference (Conv. – IMRT)
BODY	Maximum dose	106.4 %	106.1 %	-0.3 pp
ITV coverage	Minimum dose	94.1 %	95.9 %	+1.8 pp
PTV coverage	V95%	99.6 %	99.2 %	-0.4 pp
Lenses	Maximum dose	4.0 Gy	3.7 Gy	-0.3 Gy
	Mean dose	2.8 Gy	2.7 Gy	-0.1 Gy
Homogeneity	D5% / D95%	5.1	4.0	-1.1

Conclusion: It was possible to significantly reduce the time spend on dose planning by changing the treatment technique from conventional to IMRT for PCI patients while attaining comparable dosimetric quality of the treatment plans. Furthermore, both the treatment time and the time spend on quality assurances are comparable for the two techniques.

EP-2076

Stereotactic body radiation therapy using Tomotherapy for refractory metastatic bone pain: case study

B. Bosco[1], A. Fong[1]
[1]*Sydney Radiotherapy and Oncology Centre, Radiation Oncology, Wahroonga NSW, Australia*

Purpose or Objective: To illustrate the technique and outcome of stereotactic body radiation therapy (SBRT) using Tomotherapy for refractory bone pain from metastatic disease. Tomotherapy SBRT planning parameters and dosimetric evaluation are outlined.

Material and Methods: In 2013, a 70 year old female patient presented with metastatic non-small cell lung carcinoma, following resection of lung primary in 2012. CT and MRI confirmed a lytic lesion on right of sacrum. Patient's sacrum initially treated with 30Gy/10Fx. Pain recurred 2 months post RT and managed by palliative care. 6 months post RT patient returned for consideration of re-treatment. Pain was refractory to everything apart from 15mg of oxycodone every hour. RO discussed the patient and risks of re-irradiation within the multidisciplinary setting. The consensus was to offer the patient SBRT, 24Gy in 3 fractions to the sacrum.
Helical Tomotherapy was used to plan and treat patient. The irregular PTV volume was 201.12cm3. Dose volume constraints included: colon (0.035cc<18.4Gy, 20cc<14.3Gy), sacral plexus (0.035cc<11Gy, 5cc<7Gy), cauda equina (0.035cc<16Gy, 5cc<14Gy), and skin (0.035cc<26Gy, 10cc<23Gy). No hotspots were to be located over the nerve roots.

Results: Tomotherapy planning parameters included field width of 2.5cm, pitch of 0.2 and a modulation factor of 1.5. Beam on time was 400.3 seconds. PTV coverage statistics were D99 = 22.5Gy (93.75%), V95 = 98.57%, VTD = 90.53%, Median = 25.37Gy (105.71%), D1 = 27.8Gy (115.83%). OAR dose included colon 0.035cc = 8.1Gy, 20cc = 6.8Gy; sacral plexus 0.035cc = 27.3Gy, 5cc = 25.3Gy; cauda equina 0.035 = 26.2Gy, 5cc = 21Gy; skin 0.035cc = 15.4Gy, 10cc = 12.3Gy. The conformity index statistics were R100% = 0.97, V105% outside PTV = 2cc, R50% = 4.21, Dmax > 2cm from PTV = 16.45Gy (68.5%).
One week post SBRT, patient's pain stable and mobility improving. Whole body bone scan 2 months post SBRT showed decreased activity and size of sacral lesion. 4 months post SBRT patient returned with significant left sacral pain with concern of further metastatic disease. PET confirmed no uptake in left sacrum. Pain associated with insufficiency fracture with cause unknown, SBRT or bone metastasis likely contributors. 5 months post SBRT patient improved dramatically, completely ambulant with PET/CT showing no evidence of recurrence/metastatic disease. 13 months post SBRT, patient remains asymptomatic, CT shows no evidence of metastatic disease.

Conclusion: This case study illustrates how the use SBRT can result in pain control for patients with refractory metastatic bone pain where there may be no other options available apart from palliative care, even in cases where the treatment volume is relatively large. This data is also informative since the patient shows no definite evidence of metastatic disease. Further studies could lead to improved therapies for the control of metastatic bone pain.

EP-2077

A decision protocol to propose proton versus photon radiotherapy: in silico comparison

A. Chaikh[1], J. Balosso[1]
[1]*CHU de Grenoble - A.Michallon, Radiothérapie et Physique Médicale, Grenoble, France*

Purpose or Objective: Proton therapy cancer treatment offer potential clinical advantages compared with photon radiation therapy for many cancer sites. However, the treatment cost with proton is much higher than with conventional radiation. The objective of this study is to discuss how to improve a procedure, already described by others worldwide, to provide quantitative clues to select the patient for proton treatment instead of photon.

Material and Methods: The respective medical and clinical benefits of proton and photon therapy are assessed by in silico comparison following four successive steps. First, the dosimetric analysis is made using parameters derived from dose volume histogram (DVH) for target volume and organs at risks. Second, the DVHs are exported from TPS to calculate TCP and mostly NTCP radiobiological indexes. In the third step, a statistical comparison is done using non-parametric test to calculate p-value, then bootstrap method is used to estimate the confidence intervals including the lower and upper limit of agreements. Then the correlation between data from proton and photon treatment planning is assessed using Spearman's rank test. Finally, the cost-effectiveness and quality adjusted life years (QALYs) can be used to measures the outcome of the therapy and check if the therapeutic gain of proton therapy worth the increased expenses of it versus photon.

Results: The results with in silico data can be taken into account to make a proposal of a decisional procedure. The dosimetric and radiobiological analysis can be used to check the medical benefit with either proton or photon. The statistical tests allow to check if the dosimetric or radiobiological benefits for a specific patient can be included in the confidence interval of agreement of a representative population, the most homogenous possible. A Markov model can be used to simulate the life of patients treated with proton / photon radiation. The virtual evaluation may indicate for which cancer sites proton therapy could be more cost-effective than photon therapy.

Conclusion: The introduction of model based clinical trials with the possibility of individual assessment is a coming approach well adapted to the fast improvement of medical technology. The presently rising offer of proton therapy is a good example. The QALY concept based on objective dosimetric and clinical expected / modelized outcome may be a valuable response to this new challenge. However, large

cumulated medical data are needed to reduce steps by steps the uncertainties in the assumptions used in the present models.

EP-2078

PROSPECT: Phase 2 rescanning of seromas in patients to evaluate CTV reduction in breast cancer

G. Smith[1], P. Robson[2], H. Probst[3]
[1]*The Clatterbridge Cancer Centre - Wirral NHS Foundation Trust, Radiotherapy Planning, Bebington- Wirral, United Kingdom*
[2]*The Clatterbridge Cancer Centre - Wirral NHS Foundation Trust, Radiotherapy, Bebington- Wirral, United Kingdom*
[3]*Sheffield Hallam University, Faculty of Health and Wellbeing, Sheffield, United Kingdom*

Purpose or Objective: A single centre feasibility study to assess the reduction in sequential boost volume treated by rescanning patients during their final week of whole breast radiotherapy.

Material and Methods: Patients requiring a sequential boost treatment who had a tumour bed seroma greater than 1cm on the initial radiotherapy planning (RTP) CT scan were considered for entry into the study.
Thirty patients were sequentially recruited at the planning stage if they met this inclusion criteria. Patients were consented for entry into the trial and a second RTP CT scan (RTP 2) was conducted in their final week of whole breast radiotherapy. RTP 2 scan was used to determine the volume treated for their sequential boost.
Both scans had the CTV outlined by the chief investigator and the CTV volume changes were annotated.

Results: 83% of patients had a substantial reduction in CTV (>25%) in RTP 2 compared to RTP 1. The mean CTV reduction overall was 41.9% with a median reduction 42.5%. The mean time between scans was 27 days; median time 29 days. Mean time from start of whole breast radiotherapy treatment to RTP 2 was 14 days.

Conclusion: This study shows that rescanning breast patients during the final week of whole breast radiotherapy leads to a significant decrease in treated boost volume in the majority of patients.

EP-2079

IMRT vs. dynamic conformal arc radiation therapy for stereotactic spinal radiotherapy

V. Santos[1]
[1]*Mercurius Health- SA, Centro Oncológico Dra. Natália Chaves - Unidade de Radioterapia de Lisboa - Quadrantes - Joaquim Chaves Saúde, Lisboa, Portugal*

Purpose or Objective: Patients with spinal tumors have better outcomes with increased dose prescription. Due to the complex geometry of the treatment site and to the close proximity of the spinal cord, dose escalation is only possible with advanced techniques. This case study aims to determine if intensity-modulated radiation therapy (IMRT) could be a better option than dynamic conformal arc radiation therapy (DCA) for stereotactic spinal treatments.

Material and Methods: Six patients previously treated with DCA were re-planned with IMRT. The same patient-specific criteria were followed in the new IMRT plan. Plan quality was compared by analyzing the dose-volume histogram (DVH) for the planning target volume (PTV) and for the spinal cord (SC). The conformity index (CI) and the monitor units (MU) number were also compared.

Results: Both techniques provided adequate PTV coverage and SC sparing. Results favored IMRT in most of the analyzed PTV parameters: Dmax, D95, V95 and V100. DCA showed better results in PTV Dmin and D99 and had advantageous lower MU number. SC had superior dose sparing with IMRT plans. The CI was also improved by the IMRT technique.

Conclusion: In general, IMRT plans proved to be a better planning solution, although with a significant higher number of MUs. IMRT treatments must be performed with higher accurate imaging guidance systems.

EP-2080

Redefining the possible: planning multiple complex head lesions using non-coplanar VMAT arcs

V. Guy[1], R. Sims[1], A. Falkov[1]
[1]*Auckland Radiation Oncology, Auckland Radiation Oncology, Auckland, New Zealand*

Purpose or Objective: To demonstrate the ability to include multiple lesions over the scalp, face and brain using non-coplanar VMAT beams and a single isocentre
73 yo man referred for post-op RT to mulitple scalp lesions, including bilateral spread to periauricular and parotid nodes. Diagnostic work up also showed an incidental right sided meningioma that was indicated for possible concurrent treatment.

Material and Methods: The patient was scanned in a Klarity shell, on a Philips Big Bore CT. The dataset was imported into the TPS and diagnostic T1 and T2 MRI's were fused for assisting in contouring.
The scalp and bilateral periauricular and parotid regions were contoured as a single CTV and a 0.3cm PTV margin was added. The meningioma was contoured separately, also with a 0.3cm PTV margin applied.
50.4Gy in 28 fractions was prescribed and the plan was generated in RayStation (v4.0.3) on an Elekta Synergy machine with 4° gantry spacing and a maximum delivery time of 90 seconds per beam. Two full transverse VMAT arcs were used with a partial sagittal arc added (floor at 270°). Isocentre placement was key due to potential collision risks.

Results: Exceptional conformality was achieved. The introduction of the sagittal arc created a ring of dose around the skull providing excellent brain sparing as shown in Figure 1.

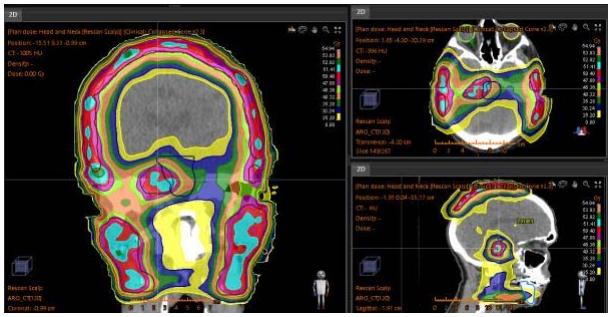

QA was perfomed using a 3D diode array with 99.6% pass rate at 3%/3mm criterion (6/1605 failed diodes). Absolute dose measurements were done using a pinpoint ionisation chamber inside both the scalp and meningioma PTVs indicating agreement with the TPS to within ±3.0%.
XVI imaging was performed on fractions 1 to 3, then weekly, using grey scale match. Bony anatomy matched with <1° rotation. Treatment delivery averaged at 10 minutes making this beam arrangement extremely efficient to treat.
Treatment was tolerated very well. Some changes to taste, dysphagia and mild to moderate xerostomia developed during the later stages of treatment. This was managed with general analgesia. There was no evidence of recurrence at three month follow up and the RO is now awaiting further diagnostic MRI's.

Conclusion: Combining traditional transverse arcs with a partial non-coplanar arc is a safe and efficient technique to treat multiple head and neck volumes and provides exceptional sparing and dosimetric accuracy. The sagittal arc was integral to this conformal distribution over these complex PTV's.

EP-2081

Impact of baseline shifts on 4D cone-beam CT images using a 4D phantom driven by lung tumor motions

H. Moriwaki[1], K. Shiraishi[2], A. Sakumi[2], T. Ikeda[1], W. Shimizu[1], K. Yoda[3]
[1]*Mitsui Memorial Hospital, Radiation Oncology, Tokyo, Japan*
[2]*University of Tokyo Hospital, Radiation Oncology, Tokyo, Japan*
[3]*Elekta KK, Research Physics, Tokyo, Japan*

Purpose or Objective: We have evaluated clinical impacts of the breathing instability for lung cancer patients on4Dcone-beam CT images usingan XVI version 5.0 unit (Elekta, Crawley, UK)using a moving phantom driven by actual patient's tumor motions.

Material and Methods: The XVI unit calculated 10-phase binned 3D volume data based on the tumor positions oneach of the projection images and the resulting 10-phase binned breathing curve was stored in the unit. The breathing curve consisting of the 10 sets of the 3D coordinates were compared to the 4D input data which had been fed into the phantom controller.In order to simulate the tumor baseline shifts during relatively long treatment. a 1D phantom, QUASAR™ Respiratory Motion Phantom(modusQA, city or state, USA), was employed, wherein measured patient tumor motions had beenfed into the phantom controller beforehand.

Results: When the breathing motions were stable without significant tumor baseline shifts, the tumor motion shown on the4D CBCT imagesagreed with the true patient tumor motions. However, when the baseline shifts were significant, the reconstructed images showed unclear and blurredtumors. In particular, the tumor position deviations were significant during the period of large baseline shifts. Moreover, during that period, the tumor was located outside theinternal target volume (ITV) region, thereby causing possible treatment failure.To avoid this failure, either breathhold or constrainedbreathing may be more appropriate than free breathing.Furthermore, a quick beam delivery such as volumetric modulated arc therapy (VMAT) or flattening filter free beams may minimize the impact of the baseline shifts on the CBCT images.

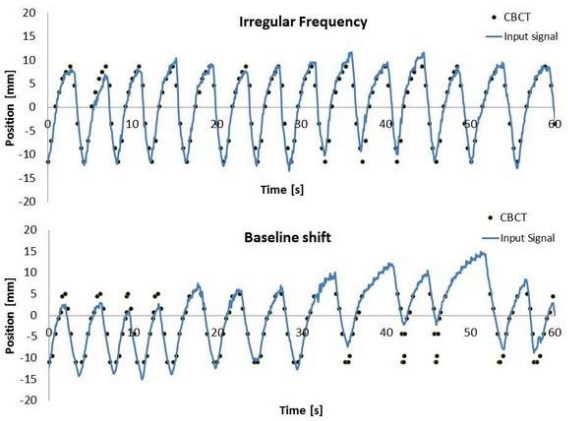

Conclusion: We have confirmed that the XVI version 5.0 unit accurately calculated 10-phase binned 1D phantom positions for stable breathing. However if baseline shift occurs significantly during the projection data acquisition, the reconstructed tumor positions may be incorrect. It is recommended that a sufficient period of preparation time may be required for a patient before treatment. volume (ITV) region, thereby causing possible treatment failure.To avoid this failure, either breathhold or constrainedbreathing may be more appropriate than free breathing.Furthermore, a quick beam delivery such as volumetric modulated arc therapy (VMAT) or flattening filter free beams may minimize the impact of the baseline shifts on the CBCT images.

EP-2082

Static beam tomotherapy (TD) as an optimisation method in whole breast radiation therapy (WBRT)

M. Squires[1], S. Cheers[1], A. Fong[1], B. Archibald-Heeren[1], Y. Hu[1], A.Y.M. Teh[1]
[1]*Radiation Oncology Centres, Gosford, Gosford, Australia*

Purpose or Objective: To evaluate static beam tomotherapy (TD) as a method of dose optimisation for the delivery of whole breast radiation therapy (WBRT).

Material and Methods: Treatment plans of 27 women previously optimised with IMRT on RayStation v4.5 (Raysearch, Stockholm, Sweden) were replanned using TomoDirect (Accuray, Sunnyvale, California, United States). TD parameters included a field width of 2.5cm, a pitch of 0.251 and a modulation factor of 2.000. A simple two field (medial and lateral) beam arrangement was utilised, with no OARs included in the optimisation. A simple ring volume (+0.2cm-+2.0cm) was used to control integral dose. Planning optimisation time was recorded. Prescriptions were normalised to 50Gy in 25 fractions prior to comparison.

Results: Both groups fell within ICRU62 target homogeneity objectives (TD D99 = 48.0Gy vs IMRT = 48.1Gy, p = 0.26; TD D1 = 53.5Gy vs IMRT = 53.0Gy, p=0.02; HI TD = 0.110 vs IMRT = 0.099, p=0.03), with TD plans showing higher median doses (TD median = 51.1Gy vs IMRT = 50.9Gy, p = 0.03). No significant difference was found in prescription dose coverage (TD VTD = 85.5% vs IMRT = 82.0%, p = 0.09). TD plans produced a statistically significant reduction in V5 ipsilateral lung doses (TD V5 = 23.2% vs IMRT = 27.2%, p = 0.04), whilst other queried OAR metrics remained statistically comparable (TD ipsilateral lung V20 = 13.2% vs IMRT = 14.6%, p = 0.30; TD heart V5 = 2.7% vs IMRT = 2.8%, p = 0.47; TD heart V10 = 1.7% vs IMRT = 1.8%, p = 0.44). TD user optimisation time decreased (TD = 9.8m vs IMRT 27.6m, p<0.01), saving an average planning time of 17.8 minutes per patient.

Conclusion: TD represents a viable and superior alternative WBRT technique, both in terms of plan quality metrics and user efficiency.

EP-2083

Utilising flattening filter free (FFF) beams to reduce treatment delivery times for breast patients

M. Le Mottee[1], A. Michalski[1], R. David[1,2], C. Lee[1,2], A. Windsor[1,3], B. Done[1]
[1]*Central Coast Cancer Centre, Radiation Oncology, Gosford, Australia*
[2]*The University of Newcastle, The School of Mathematics and Physics, Newcastle, Australia*
[3]*University of New South Wales, Faculty of Medicine, Randwick, Australia*

Purpose or Objective: This is a feasibility study to compare treatment delivery times of four different techniques for DIBH left sided whole breast RT to minimise the treatment delivery time without compromising the target coverage. In addition to technique comparison, the possible use of flattening filter free beams will also be assessed.

Material and Methods: Ten left sided DIBH patients were selected. Four separate plans were created for each patient. The treatment techniques used were: conventional tangents comprising of open wedged fields (two to four beams), forward planned segmentation (two beams), hybrid inverse planned intensity modulated radiation therapy (IMRT) (four beams) and volumetric modulated arc therapy (VMAT) (two partial arcs). All plans were optimised to the departmental breast protocols. Plans were then delivered on a Varian21iX linear accelerator (Varian Medical Systems, CA, USA) using Millennium 120 leaf MLC. The maximum dose rate was 600 monitor units per minute. Each plan was delivered three times with the beam on time recorded for each beam. Patients were replanned for forward planned segmentation and inverse planned IMRT using flattening filter free (FFF)

beams. Each plan was delivered three times with the beam on time recorded for each beam. The maximum dose rate was 1400 monitor units per minute.

Results: When comparing dosimetric endpoints four treatment techniques without the inclusion of FFF, IMRT performed statistically better 2cc PTV maximum, 2cc body maximum and homogeneity index for the PTV compared to all other techniques. In general Organs at Risk (OAR) constraints were comparable between the conventional tangents, Field in field and hybrid IMRT techniques. VMAT performed statistically worse in several endpoints including both the point maximum and mean dose for the contralateral breast, Volume receiving 10Gy (V10) and 5Gy (V5) for the heart, ipsilateral and contralateral lung V5 and mean dose as well as the mean dose for combined lung compared to all other techniques planned.
There was no statistical difference for the V20 for the ipsilateral lung and combined lung for all techniques. When looking at the beam on time Hybrid IMRT(10.21s) had the quickest and VMAT(48.76s) the longest.
When comparing dosimetric endpoints four treatment techniques with the inclusion of FFF hybrid IMRT and FFF Hybrid IMRT performed statistically better for PTV2cc max, PTV homogeneity index, total body max and 2cc max. For all other OAR parameters tested in the investigated modulated techniques, treatment planning with FFF beams resulted in plans of equal quality compared with flattened beams. No significant differences were found. When looking at the beam on time FFF Hybrid IMRT(7.45s) had the quickest compared to current tangential delivery times (20.59s).

Conclusion: The inclusion of FFF beams and modulated techniques can significantly reduce treatment delivery times for left sided breast patients who are receiving (DIBH)

EP-2084

Risk assessment of secondary cancer after craniospinal radiotherapy in childhood medulloblastoma

F.M. Giugliano[1], M. Mascarin[2], L. Iadanza[3], E. Coassin[2], A. Drigo[4], M.G. Trovò[2]
[1]*EmiCenter, Radioterapia, Casavatore, Italy*
[2]*Centro di Riferimento Oncologico, Radioterapia Pediatrica, Aviano PN, Italy*
[3]*Istituto Tumori- Fondazione "G. Pascale", Dipartimento Fisica Medica, Napoli, Italy*
[4]*Centro di Riferimento Oncologico, Dipartimento di Fisica Medica, Aviano PN, Italy*

Purpose or Objective: Primary central nervous system tumors represent the second most common neoplasms in childhood.The late effects, after radiation treatment (RT), develop gradually over several years, including neurocognitive deficiencies, cardiac toxicity, endocrinological problems, and secondary malignancies (SMNs).The incidence of SMNs is around 10–20%, 30 years after treatment. Predicting SMN risk, from the newer RT, techniques is difficult due to absence of epidemiological data, but mathematical models can be used. The aim of this paper is to determine possible dose-response relationships between radiotherapy dose and specific organs SMNs comparing conventional technique (3D-CRT) with IMRT delivered with Helical Tomotherapy (HT).

Material and Methods: In this work a dose-response relationship for malignant tumors is derived based on: the epidemiological data on cancer induction after Hodgkin's disease; from the data about cancer induction of the A-bomb survivor data("the linear-no-threshold model"). The data from two young patients, affected by medulloblastoma "standard risk"(female age 7y, male age 8y) treated at the National Cancer Institute in Aviano (Italy), were retrospectively analyzed using the Schneider's dose-response model for solid cancers induction (Theoretical Biology and Medical Modelling 2011). We calculated the impact of the different techniques on SMN induction risk, using organ equivalent dose (OED) calculated for a group of different dose-response models including a full model and linear model. The excess absolute risk (EAR/10000 pts-year) was considered for different organs at risk(OAR).

Results: The results demonstrated that the the linear model fits best colon, cervix and skin. Instead the full model fits all other organs, indicating that the repopulation/repair ability of tissue is neither 0 nor 100% but somewhere in between. We noted that soft tissue sarcoma fitted well by all the models and in the low dose range beyond 1 Gy the risk is negligible, but for increasing dose, sarcoma risk increases rapidly and reaches a plateau at around 25-30 Gy. From the analysis of the EAR breasts, we observed values of 11.5 in 3DCRT plan and of 43.9 in HT plan, respectively. This difference in EAR may be results due to missing of delineation of breast as OAR in pre-planning. The table n. 1 showed the EARk for each OAR in specific dose ranges, calculated for both treatment plans.

SITE	EAR 0-5 Gy		EAR 5-20 Gy		EAR 20-26 Gy	
	3DCRT	TOMO	3DCRT	TOMO	3DCRT	TOMO
Soft tissue	0,0012	0,008	0,57	0,5	2,3	2,2
Thyroid	5,7	9,02	11,5	11,2	0	0
Bladder	2,9	1,7	0	0	0	0
lung	3,4	9,5	29,4	21,5	38,3	38,4
Bone	0,00083	0,0035	0,47	0,26	0,78	0,79
Small Bowel	6,7	4,3	1,54	2,34	1,3	0
Skin *	0,5	1,9	15,6	10,4	24,2	25,1
Skin **	0,4	1,9	15,6	10,7	24,2	24,4

Conclusion: In this work OED for various OAR was calculated using different models and compared in two plans, in combination with epidemiological obtained absolute risk data. The models have taken into account also the age, important parameters in pediatric population. We think that, in the field of radiation therapy, estimated excess risk it may be interesting to know the advantage of different treatment techniques , in reference to the same organ and the same patient (sex ,age,exposure and expected years of life).

EP-2085

Breast irradiation: Is the Isocenter fix ? Results of a Quality Control study.

I. Lvovich[1], S. Daniel[1], A. Dror-Bakalo[1], R. Ben Yosef[1], E. Sabah[1], I. Atnilov[1]
[1]*Rambam Health Care Campus, Oncology/Radiotherapy, Haifa, Israel*

Purpose or Objective: The accuracy and reproducibility of tangential fields in breast cancer irradiation is crucial in the sense of tumor control. Small deviation in patient positioning can lead to geometrical miss and low doses in parts of the target as well as exposing OAR (i.e heart and lung) to high doses. Although portal imaging verification can reduce such errors, it is time consuming and could affect machine occupancy. Once the setup is performed in the first treatment it is possible to achieve reproducibility in the AP direction through SSD or couch vertical reading .The aim of this work was to test which of the two should be used in order to achieve better reproducibility through the treatment and whether the Isocenter is truly fixed during the treatment course.

Material and Methods: The study included 30 patients, treated between November 2014 and May 2015 at the ages 34 to 85, with an average age of 60. Total 634 portal images

were taken (18 to 25 per patient). Initially, the patient Set-Up, we performed portal imaging with anatomy comparison to DRRs. We compared lung, heart and breast volumes. The treatment technique was 3D Conformal Radiotherapy. The breast fields were tangential. A Couch Vertical value was determined for each patient at the Set-Up process, and all treatment sessions were performed at that Couch Vertical value. Throughout the course of radiation treatment, daily readings were taken. This included readings of the actual Anterior SSD, as well as portal images taken , to compare anatomical matching to the DRRs. At the end of each patient's treatment course, we performed a comparison of all SSD readings,calculating the differences between planned and actual Anterior SSD readings .

Results: Average difference between the planned and actual Anterior SSD reading was 0.5cm for all treatments(with max 1.15cm and min 0 cm for single patient). For 10 patients (30% of all patients) the mean was above 0.7cm. An upward trend was seen in the average difference along the treatment course. 70% of the patients who had a mean of over 0.7 cm - were over the age of 60. There is also an upward trend of mean depending on age (average of 0.4 cm under the age of 60 and an average of 0.55 cm over 60(p=0.058). Mean grow with the elapsed time between surgery and treatment (50 to 347 days,average of 150 days) ≥100 days: average 0.32 cm, ≤ 100 days: average 0.64 cm (p<0.001)

Conclusion: In this study we showed that the difference between the planned and actual Anterior SSD is significant. To get the accuracy and reproducibility in breast cancer irradiation and the increasing use of IMRT(field in field), we recommend to consider re-planning for some patients, or to treating according to a fixed Couch-Vertical value, set during the initial patient Set-Up.Continue further work to examine the deviations in dosimetry based on the change in IsoCenter . A greater number of measurements will enable us to learn whether age and the elapsed time from surgery are significant factors

EP-2086

Advantages of deep inspiration breath-hold (DIBH) in left sided breast cancer using 3D-CRT

A. Kalmár[1], N. Mészáros[1], G. Stelczer[1], C. Polgár[1]
[1]*National Institute of Oncology, Radiotherapy, Budapest, Hungary*

Purpose or Objective: Irradiation of the left breast or chest wall was associated with an increased cardiac mortality and morbidity. The relative risk for ischaemic heart disease increased by 7.4 % with every 1 Gray (Gy) increase in mean heart dose. The dose to the heart and left lung can be reduced with deep inspiration breath hold (DIBH) techniques. The aim of this study was to investigate the reduction of organs at risk (OAR) doses with DIBH compared to free breathing (FB) in patients receiving left sided radiation therapy with three dimensional conformal techniques.

Material and Methods: Between September and October 2015, a total of 20 patients with left-sided breast cancer underwent two different computed tomography (CT) scans with 3 mm slice thickness, both FB and DIBH. The breast, lung, and OAR contours were done according to the RTOG breast cancer contouring atlas. The prescribed dose was 25 x 2 Gy, and the radiotherapy plans were made by using 2-4 opposing tangentional fields with 6 MV and 18 MV photons. For statistical analysis Wilcoxon matched pair test was used.

Results: Similar target coverage was achieved with both techniques. The mean MHD was reduced from 4.4 Gy (range: 1.3-8.3 Gy) with FB to 2.7 Gy (1.4-4.2 Gy) with DIBH (p<0.05), resulting a mean dose reduction of 1.7 Gy (39%) favouring DIBH. The average MLD was 6.7 Gy (3.3-11.7 Gy) at FB compared to 5.7 Gy (2.1-10.7 Gy) at DIBH (p<0.05), resulting mean 1 Gy (15%) dose reduction with DIBH. The V5heart and V20heart were also significantly lower, 49.3% (7-79%) and 5.8% (0.03-15.9%) with FB and 36% (12-70%) and 1.5% (0-5.9%) with DIBH (p<0.05). The V20lung for the group was reduced slightly at FB from 14.9% (5.2-27.8%) to 12.7% (3.5-24.6%), however this was not statistically significant (p=0.056). The V30lung was 12.5% (3.8-23.8%) with FB and 10.2% (2.4-21.8%) with DIBH (p<0.05).

Conclusion: A significantly lower dose to clinically important organs at risk (heart and lung). Using simple 3D radiotherapy techniques DIBH can reduce dose to the heart and lung without compromising target coverage be achieved using the DIBH technique compared to FB.

EP-2087

Simultaneous Integrated Boost Bilateral breast cancer RT with Helical IMRT: How to manage it?

J.L. Soares Rodrigues[1]
[1]*Centre Hospitalier Universitaire Vaudois, Department of Radiation Oncology, Lausanne Vaud, Switzerland*

Purpose or Objective: The objective of the present case study was to investigate the potential role and the feasibility of Helical intensity modulated radiotherapy, (Tomotherapy, Accuray), for bilateral breast tumor patients, with a simultaneous integrated boost (SIB) strategy.

Material and Methods: Four target volumes were defined by the radiation oncologist: PTV breast (right and left) and PTV boost (right and left). Dose prescription in a SIB scheme was: 50.4 Gy (1.8 Gy/fraction) to PTV breast (right and left), 61.6 Gy (2.2 Gy/fraction) to PTV boost right side and 59.36 Gy (2.12 Gy/fraction) for PTV boost left side. Objectives were: for PTVs $V_{95\%}$>95%; Mean lung dose MLD<15 Gy, $V_{20\ Gy}$<20%, $V_{5\ Gy}$ as low as possible; for the heart a Mean dose < 7 Gy. The plan was generated with Tomotherapy planning station 5.0.5.18 (Volo, Accuray), with a field with of 2.5 cm, pitch of 0.287 and a modulation factor of 3.8. Specific optimization volumes were created by the dosimetrist to avoid high integral dose and to achieve a very conformal and homogeneous dose distribution. Treatment time will be measured.

Results: For PTV breast right and PTV breast left, $V_{95\%}$ was 95.05%. For PTV boost right and PTV boost left the $V_{95\%}$ was 97.9% and 96.8%, respectively. Mean lung dose was 8.6 Gy for each lung. $V_{20\ Gy}$ for both lungs combine was 13.8 %, and $V_{5\ Gy}$ was 35.6 %. Mean heart dose was 3.8 Gy with a maximum dose of 37 Gy. The irradiation treatment time is around 7 minutes.

Conclusion: This case show a very promising and feasible role of Helical IMRT, for bilateral breast tumor patients, with a simultaneous integrated boost (SIB) strategy. A good treatment planning strategy is fundamental to achieve the dose volume histogram (DVH) for the organs at risk (OAR) presented here

Electronic Poster: RTT track: Additional tools for contouring

EP-2088

CT and MRI fusion to minimize contouring uncertainties in Stereotactic Radiosurgery (SRS) planning

I. Payanova[1], R. Georgiev[2], R. Lazarov[1], Z. Spasova[1], V. Ivanov[3], L. Iliev[1], P. Tsenov[1], A. Antonova[1], T. Georgieva[1], S. Georgieva[1], D. Avgerinova[1]
[1]*Tokuda Hospital, Radiotherapy, Sofia, Bulgaria*
[2]*BSBMPE, Biomedical Engineering, Sofia, Bulgaria*
[3]*Tokuda Hospital, Imaging diagnostic, Sofia, Bulgaria*

Purpose or Objective: To improve image registration accuracy by using markers on patients for head SRS treatment planning. Contour shifts were compared after image matching based on anatomy correspondence and markers superposition.

Material and Methods: Ten patients with head localisations planned for radiosurgery were studied. Scanning procedures using skin markers were done on CT - GELightSpeed RT16, with 1.25mm slice thickness and MRI-GESigna 1,5T following

AxT2 FRFSE, AxT1 and T2FLAIR, MRPerf Ax Dynamic SI C+ and Ax 3D T1 FSPGR. Image fusion of data sets was applied after anatomic landmark matching before target contouring. Alternatively image matching was also implemented by marker superposition. Translation and rotation corrections were calculated from markers' displacement and applied in the matching procedure. Target anatomy contours obtained from both procedures were compared and contour shifts measured. These shifts were analyzed to find how the type of matching procedure would affect target contour displacement.

Results: Coordinates of markers showed geometrical displacements (0.15cm-0.35cm) in transverse direction and rotation angles (1.5o-2.0o). These values were used for compensation in the image matching procedure, achieving visual correspondence of target anatomy after image fusion. Target contour displacement after applying both procedures were found to be within the range of 0-0.3cm.

Conclusion: The precise positioning and method using markers is essential to achieve good quality in the image matching, as well as the accuracy in the SRS. It could be improved with more than 1mm for the target and organs at risk, which makes the SRS treatment procedure itself more effective.

EP-2089

Comparison of target volumes for lower gastro-intestinal tumours using PET-CT and PET-MR images

J. Heywood[1], M. Chiu[1], I. Kayani[2], L. Allington[1], R. Bodey[1], G. Blackman[1]

[1]*University College London Hospital, Radiotherapy, London, United Kingdom*

[2]*University College London Hospital, Nuclear Medicine, London, United Kingdom*

Purpose or Objective: The use of PET-CT in radiotherapy planning is emerging as a modality to aid target volume delineation in lower GI tumours. MRI provides superior soft tissue definition compared with CT which may offer further benefit in radiotherapy planning (Wang et al, 2011).
Since 2008, PET-CT has been used for radiotherapy planning within the department and, to date, we have scanned over 170 patients across a range of tumour sites. To explore the role of MRI in lower gastro-intestinal planning, 9 patients were dual scanned as part of a feasibility study to compare target volume delineation using PET-CT and PET-MR images.

Material and Methods: All lower GI tumours requiring a PET-CT for planning purposes were considered eligible for the study. For each patient a PET-CT and PET-MR scan was acquired in the treatment position following a single F18-FDG radioisotope injection. The patients were allocated with 50% having the initial planning scan in PET CT and 50% in PET-MR. Duration time post injection was recorded for each scan.
Prior to volume delineation both data sets were anonymised. Each clinician was provided with the relevant anonymised diagnostic imaging and tumour histopathology reports. On both datasets a Nuclear Medicine Radiologist delineated the BTV and a Clinical Oncologist delineated the gross tumour volume (GTV) and clinical target volume (CTV). Volumes for each patient were delineated on separate occasions for each imaging modality.
Volume sizes for both data sets were compared and a similarity index calculated.

Results: Nine patients were entered into the study, 6 rectal carcinomas and 3 anal canal carcinomas.

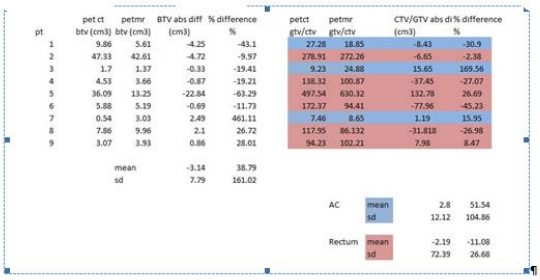

pt	pet ct btv (cm3)	petmr btv (cm3)	BTV abs diff (cm3)	% difference %	petct gtv/ctv	petmr gtv/ctv	CTV/GTV abs di (cm3)	% difference %
1	9.86	5.61	-4.25	-43.1	27.28	18.85	-8.43	-30.9
2	47.33	42.61	-4.72	-9.97	278.91	272.26	-6.65	-2.38
3	1.7	1.37	-0.33	-19.41	9.23	24.88	15.65	169.56
4	4.53	3.66	-0.87	-19.21	138.32	100.87	-37.45	-27.07
5	36.09	13.25	-22.84	-63.29	497.54	630.32	132.78	26.69
6	5.88	5.19	-0.69	-11.73	172.37	94.41	-77.96	-45.23
7	0.54	3.03	2.49	461.11	7.46	8.65	1.19	15.95
8	7.86	9.96	2.1	26.72	117.95	86.132	-31.818	-26.98
9	3.07	3.93	0.86	28.01	94.23	102.21	7.98	8.47
	mean		-3.14	38.79				
	sd		7.79	161.02				
AC	mean						2.8	51.54
	sd						12.12	104.86
Rectum	mean						-2.19	-11.08
	sd						72.39	26.68

When compared with volumes delineated using CT data, overall, the GTV of the rectal volumes were smaller when delineated on MRI. Due to the small number of anal canal tumours, it is difficult to draw any conclusion.
The similarity index between volumes will also be presented.

Conclusion: This initial evaluation indicates that, overall, MR delineated volumes for rectal tumours are smaller than those created using CT data. This has the potential to impact treatment planning and reduce toxicity. The study highlighted the challenges of using MR data for nodal volume delineation, indicating that a combined modality approach may be optimal. It is acknowledged that extension of this study to a larger population would allow firmer conclusions to be drawn.

Electronic Poster: RTT track: Head and neck reduction of margins and side effect

EP-2090

Accurate and stable immobilisation with Lorca Marin masks for head and neck IMRT treatment

A. Ilundain[1], I. Prieto[1], E. Márquez[1], D. Esteban[1], W. Vásquez[1], A. Pérez[1]

[1]*Hospital Universitario Fundación Jimenez Díaz, Radiation Oncology, Madrid, Spain*

Purpose or Objective: The aim of this work is to analyze the setup accuracy and stability resulting from the use of the Lorca Marin thermoplastic masks during the complete course in head and neck cancer treatment with intensity modulated techniques.

Material and Methods: 50 consecutive head and neck cancer treatments with intensity modulated radiotherapy (IMRT) were analyzed. Lorca Marin customized masks named Nature were used to immobilize head and neck. These 2-oxepanone polymer thermoplastic masks are 3-points immobilization with frontal and mental reinforcement and 3.2 mm thickness. 3-standard references were marked on the surface of the mask and on the middle chest of the patient for accurate positioning every day. Cone-beam computed tomography scan to verify online the position was performed during 5 consecutive days and after, weekly cone-beam until the end of the treatment. After weekly matching process using automated soft-tissue registration, translational movements along the three axes (x, y, z) were collected and the average for each treatment and each axis was calculated. Displacement´s mean of the 50 averages and the standard deviations were analyzed.

Results: The resulting displacement average after analyzing 50 treatments was less than 1 mm along the three axes: x = (0.62±0.51) mm, y = (0.83±0.63) mm, z = (0.65±0.59) mm. These setup displacements have remained under than 3 mm in 100% of treatments. These results achieve the International Commission on Radiation Units and Measurements (ICRU) recommendations regarding the setup margin to compensate the immobilization and positioning errors.

Conclusion: The type of patient immobilization devices and their contribution in the setup errors must be taken into account for IMRT. Additionally, the use of different image-guidance systems can significantly alter the size of the

required margins. Lorca Marin thermoplastics masks show enough accuracy and stability during complete course of treatment with intensity modulated techniques in head and neck cancer patients.

EP-2091

Establishment of dose reference levels (DRLs) for CT of the head and neck in radiation therapy

C. Clerkin[1], S. Brennan[2], L. Mullaney[1]
[1]*Discipline of Radiation Therapy- School of Medicine- Trinity College Dublin, Radiation Therapy, Dublin, Ireland Republic of*
[2]*St Luke's Radiation Oncology Network at St Luke's Hospital-Dublin 6., Department of Radiation Oncology-, Dublin, Ireland Republic of*

Purpose or Objective: Computed tomography (CT) has become an indispensable tool in oncological imaging. Ionising radiation is cumulative and carries a stochastic risk of malignancy. The implementation of dose reference levels (DRLs) for imaging procedures using ionising radiation is mandated by European Commission directive 97/43 EURATOM. There are currently no dose guidelines for radiation therapy CT of the head and neck (H&N) region. The propose of this research is to establish if variation exists in dose delivered by Irish centres; establish a national DRL for H&N CT scanning in radiation therapy and compare the national DRL with a European sample.

Material and Methods: All radiation therapy centres in Ireland and a selection of European centres were invited to complete a dose audit survey for 10 average-sized H&N patients undergoing a CT localisation scan. Data on CTDIvol, DLP, mAs, tube voltage, number of scan phases and scan length was collected.

Results: Surveys were returned by five Irish centres, representing a 42% response rate and one European centre. Significant variation was found in the mean DLP, CTDIvol and scan lengths. Based on the rounded 75th percentile of the mean DLP and CTDIvol, the proposed Irish DRL is 1025.41mGy cm and 20.97mGy, respectively. Based on the European survey the DRLs for DLP and CTDIvol were 680.12mGy cm and 21.85mGy, respectively.

Conclusion: Variation exists in dose used for H&N CT in radiation therapy. DRLs have been proposed with the aim of dose optimisation for this procedure.

EP-2092

Impact of treatment volumes in loco-regional failure of oral cancer in patients treated with IMRT

D. Delishaj[1], S. Ursino[1], E. Lombardo[1], L.R. Fatigante[1], M. Cantarella[1], G. Coraggio[1], F. Matteucci[1], S. Montrone[1], M.G. Fabrini[1]
[1]*Azienda Ospedaliero Universitaria Pisana, Radiotherapy, Pisa, Italy*

Purpose or Objective: The aim of the study was to analyze the impact of radiation therapy (RT) or concomitant radiochemotherapy (RT-CT) on locoregional control (LRC) in patients affected by oral cancer.

Material and Methods: Materials and methods : In this study were enrolled 48 patients with oral cancer diagnoses underwent postoperative RT or exclusive RT-CT treatment. The RT was performed with intensity-modulated radiotherapy (IMRT) technique and LINAC DHX of Varian System. All patients were treated at the department of Radiotherapy, University of Pisa. In patients non treated surgically or operated with major risk factors (positive margins, Extracapsular extension) RT treatment was performed in combination with chemotherapy (CT) or molecular-target therapy. Again patients operated with presence of minor risk factors (positive lymph nodes, lymphatic vascular invasion, perineural invasion) underwent only RT treatment. The volumes were defined as follows: PTV high risk: 66Gy (2.2Gy /fraction) or 63Gy (2.1Gy / fraction) respectively for exclusive RTCT treatment and adjuvant RTCT or RT treatment PTV intermediate risk: 60 Gy (2.0Gy /fraction) PTV low risk: 54Gy (1.8Gy /fraction)

Results: From January 2011 to July 2015, 48 patients (mean age 60.9 years; range 33-87) with histologically confirmed diagnosis of oral cancer were treated. At analysis 30 patients (62.5%) underwent surgically treatment and 18 (37.5 %) performed exclusive RTCT treatment. Twentyfour patients were treated with radiochemotherapy or radiotherapy plus molecular-target therapy; in 20 patients (83%) was administered CDDP; in 4 patients (17%) in combination with RT was administered Erbitux. Relapses were divided into local (on T), regional (on N) and locoregional (if the recurrences were on T and N) and classified, after the merger of radiological imaging with radiation therapy planning; in "in field" (within the PTV high risk) and "out field" (without PTV high risk) After a median follow-up of 19.8 months (range 3-62 months), six patients (12.5%) developed local recurrence "in field" and two patients (4.2%) reported locoregional relapse on field. There were not "out field" recurrences. Of six patients relapsed 2 (33.3%) underwent salvage surgery and subsequent CT; 3 (33.3%) underwent second line CT according to Extreme schedule and 1 patient (2%) didn't any systemic treatment but only support care due to comorbidities and scarce performance status. At the date of abstract submission 3/6 patients died while the others are still alive; overall 5/48 patients (10.4 %) died and only 2 died for cancer-related causes and three for comorbidities.

Conclusion: The results of our study confirm the data reported in literature regarding the locoregional recurrences of oral cancer treated with radiotherapy. In field locoregional relapse seems to be the main cause of IMRT treatment failure regardless the patient underwent at surgery treatment or not.

Electronic Poster: RTT track: Adaptive treatments in the pelvic region

EP-2093

Drinking instructions does not significantly influence inter-fraction bladder volume stability

M. Berg[1], K. Thellesen[1], H. Jensen[1], L.M. Nielsen[2], H. Wasilevska[3], L. Wee[1]
[1]*Vejle Hospital, Department of Medical Physics, Vejle, Denmark*
[2]*Vejle Hospital, Radiation Therapy Department, Vejle, Denmark*
[3]*Vejle Hospital, Department of Oncology, Vejle, Denmark*

Purpose or Objective: Bladder preparatory protocols are used in prostate cancer (PCa) radiotherapy (RT) prior to simulation (Sim) imaging, and thereafter prior to each fraction of RT. Patients are asked to drink, and hold without voiding, a constant volume of water. Distension of the bladder reduces the volume of the bladder irradiated to high doses. A study of online image-guided radiotherapy (IGRT) in bladder cancer showed that inter- and intra-fraction reproducibility was mostly insensitive to degree of bladder filling. Radiographer students were asked to test the analogous hypothesis for inter-fraction reproducibility in bladder volume over 7 weeks of PCa IGRT.

Material and Methods: An audit of PCa IGRT found 96 cases within 1 year of study commencement. 56/96 were locally advanced PCa homogeneously treated with bladder preparation instructions, daily online cone-beam CT (CBCT) verification and 28Gy sequential boost to gland only following 50Gy to gland plus seminal vesicles by normo-fractionated IMRT. 42 were complete cases in which bladders had been consistently outlined at Sim and 7 CBCTs weekly. 30/42 men agreed to hold 300mL of water each session, but in practice only 26/42 were able to comply throughout treatment. 12/42 men declined the drinking instructions outright.

Results: Sim and weekly CBCT volumes were tested for non-normality and leverage. 4 men had Sim volumes that were well in excess of 500mL, and by mid-course, had greatly reduced. The extreme cases exerted strong leverage. In 38 men, bladder volumes were log-normally distributed. Compliant men had bladder volumes (162 mL) statistically significantly larger ($p<0.01$) than men refusing (83 mL). The random inter-fraction variation was the same in both groups (33%). Compliant men had a mean systematic increase in bladder volume of 12% (95%CI = 4.8-21%, $p < 0.01$) relative to Sim, compared to 32% (95%CI = 12%-55%, $p < 0.01$) in the refusing group.

Conclusion: Systematic and random changes in bladder volume during PCa IGRT are relatively insensitive to bladder filling in PCa IGRT, provided the Sim volume is not excessive (> 500mL). Volumes at Sim are statistically significantly different between groups, so there may be implications for dose planning. We have proposed a follow-on project to measure the effect of changing the drinking instructions, so men are advised to drink and practice holding as much water as they can comfortably tolerate without voiding for 1 hour.

EP-2094

Can Radiation Oncologist delegate to Therapist the kV setup control in patients with pelvic cancers?

V. Frascino[1], M. Ferro[1], A. Alitto[1], A. Castelluccia[1], A. Petrone[1], G. Nicolini[1], S. Teodoli[1], G. Mattiucci[1], G. Mantini[1], M. Gambacorta[1], S. Chiesa[1], F. Deodato[2], L. Azario[1], S. Luzi[1], V. Valentini[1], M. Balducci[1]

[1]*Università Cattolica del Sacro Cuore -Policlinico A. Gemelli, Radiation Oncology Department- Gemelli-ART, Rome, Italy*

[2]*Università Cattolica del S. Cuore - Fondazione di Ricerca e Cura "Giovanni Paolo II", Radiation Oncology Department, Campobasso, Italy*

Purpose or Objective: Check of patients' set-up is mandatory in modern radiation therapy. The aim of this preliminary analysis is to investigate the possibility to delegate to Radiation Therapists (RT) the evaluation of two-dimensional orthogonal kV/kV imaging of pelvic cancers.

Material and Methods: Paired orthogonal kV images of patients who underwent pelvic irradiation were independently evaluated by a trained RT (on-line control) and a Radiation Oncologist (RO, off- line control). If a displacement of the isocenter larger than 5 mm was observed, the RT had to call the RO to verify and confirm such displacement. The difference of measures and the agreement between RO and RT decisions were calculated. Results are presented as mean values, and population systematic (Σ) and random (σ) errors. SPSS software was used for the statistical analysis.

Results: From March 2015 to September 2015, 904 images' pairs were obtained from 40 patients (10 prostate, 15 rectal, and 15 gynaecological cancers). A difference ≥ 3 mm was recorded in 766/904 (85%) paired images. A difference between 3 and 5 mm was recorded in 94/904 (10%) paired images. Forty-two/904 (4%) checks required on-line evaluation by the RO. In anteroposterior (AP), craniocaudal (CC) and mediolateral (ML) directions, systematic errors were 0.7, 0.4 and 0.8 mm, and random error were 0.2, 0.1 and 0.1 mm, respectively. Mean radial displacement was 2.6 mm (range 0-16 mm). CTV to PTV margins calculated by van Herk's formula were 3.3, 2.3 and 3.0mm (AP, CC and ML directions, respectively).

Conclusion: These data suggest that inter-observer variability between RT and RO is within few mm, therefore on-line kV/kV images' evaluation could be delegated to RT after an adequate training period. Such kind of quantitative analysis can be used to define a proper action level to call for RO intervention. Similar study is currently ongoing to assess inter-observer variability for CBCT evaluation.

EP-2095

A retrospective evaluation of the feasibility of automatic prostate matching in IGRT

Z. Campbell[1], B. O'Neill[2], L. O'Sullivan[2], M. Keaveney[2], L. Mullaney[1]

[1]*Discipline of Radiation Therapy- School of Medicine- Trinity Centre Dublin, Radiation Therapy, Dublin, Ireland Republic of*

[2]*St Luke's Radiation Oncology Network- Beaumont Hospital, Radiation Therapy Department, Dublin, Ireland Republic of*

Purpose or Objective: The current practice for prostate localisation in some centres is an automatic match to the bony anatomy of the pelvis. The prostate moves independently of bone and so its true motion may not be accounted with this method. An automatic match to the prostate may be more accurate. The purpose of this research it to identify if automatic prostate matching is more accurate than automatic bony matching and assess the impact on CTV-PTV planning margins.

Material and Methods: A retrospective review of CBCT data for 30 consented prostate patients was undertaken (9 CBCT each, n=270). All patients followed a bladder filling and rectal emptying protocol. Using Varian's On-Board Imager® software, the random; systematic and population mean translational shifts was calculated based on 3 different registration techniques: automatic bone matching; automatic bone matching followed by an automatic volume of interest (VOI) match using CTV and an expert manual CTV match (gold standard). A comparison was made of the CTV-PTV margins required for the two automatic registration methods.

Results: No significant difference in the mean translational shifts was reported between the automatic bone match and gold standard match. A significant difference was seen between the population mean shift of the gold standard match and the automatic prostate match in the anteroposterior direction only (p=0.007). A larger CTV-PTV margin was required for the automatic prostate match when compared with the automatic bone match.

Table 1: Population mean (and standard deviation) displacements (cm) in the anteroposterior (AP), superoinferior (SI) and left-right (LR) are shown based on the three different matching techniques: automatic bone match; an automatic volume of interest (VOI) match using CTV and an expert manual CTV match (gold standard). Negative values indicate posterior, inferior and left displacements.

	Matching Technique		
	Automatic Bone Match	Automatic VOI Match	Gold Standard Match
AP	-0.04 (0.18)	**-0.12 (0.2)***	**-0.05 (0.17)***
SI	0.04 (0.12)	0 (0.14)	0.01 (0.17)
RL	-0.05 (0.15)	-0.05 (0.16)	0.01 (0.16)

*Significant difference ($p<0.05$) when compared with the control group statistics.

Conclusion: Automatic bone matching is comparable to expert manual matching in this patient group. Automatic prostate matching is not as accurate in the anteroposterior direction and does not allow for a reduction in planning margins.

EP-2096

Risk of rectal bleeding in patients with prostate cancer treated with RT on anticoagulant therapy

B. Shima[1], M.T. Martinetti[1], M. Carnevale[1], D. Musio[1], R. Lisi[1], V. Tombolini[1]

[1]*Policlinico Umberto I- "Sapienza" Università di Roma, Dipartimento di Scienze Radiologiche Oncologiche e Anatomo-Patologiche, Roma, Italy*

Purpose or Objective: The aim of the study is to evaluate the risk of late rectal bleeding and its association with anticoagulants and/or antiaggregants use in patients receiving radiation therapy for prostate cancer.

Material and Methods: We analyzed 187 patients, age between 50-84, with prostate cancer who were managed from 2009 to 2011 at our institution. They were treated with curative intent intensity-modulated radiation therapy (IMRT 76 Gy/38 fractions) at the level of the prostate and seminal vesicles. The doses delivered to the rectum was evaluated in a manner consistent with ICRU 50-62-83. Dose constraint

evaluation was performed according to RTOG recommendation for IMRT. Patients were placed in two main categories: no anticoagulants and/or antiaggregants use category during RT and anticoagulants and/or antiaggregants one. Rectal toxicity was evaluated using the Common Toxicity Criteria Adverse Effect (CTCAE v. 4.03) All patients had assumed the anticoagulant and/or antiaggregant therapy before radiation therapy, during treatment as well as during the follow up.

Results: 20 of the 73 patients treated with anticoagulant and/or antiaggregant therapy, presented rectal bleeding; while in the group of patients not taking anticoagulants and/or antiaggregants this even occurred in 10 patients of 114 ($p<0.001$). Of the 20 patients who have received anticoagulant and/or antiaggregant agent who presented rectal bleeding, 8 developed G1 toxicity, 10 had G2 toxicity and 2 patients had G3 toxicity. Of the 10 patients who did not receive anticoagulant and antiaggregant therapy and presented rectal bleeding, 5 patients had G1 toxicity, 4 present G2 toxicity and G3 toxicity only 1 patient.

Conclusion: The results of our study found that patients taking anticoagulant and/or antiaggregants therapy undergoing curative radiotherapy for prostate adenocarcinoma have a higher risk of developing rectal bleeding.

EP-2097

Patient friendly compression-belt settings in liver stereotactic radiotherapy

A.S. Bouwhuis-Scholten[1], E.B. Van Dieren[1], S. Koch[1], H. Piersma[1], D. Woutersen[1]
[1]*Medisch Spectrum Twente, Radiotherapy, Enschede, The Netherlands*

Purpose or Objective: Stereotactic radiotherapy of liver metastases is challenging: breathing motion, and the flexibility of the abdominal organs, in particular remaining liver, may be large. This may render a priori imaging for position verification virtually useless. Hence, "decision to treat" may be difficult and stressful.
Abdominal compression may be used to reduce movement and flexibility, but maximum compression is highly uncomfortable and probably intolerable for patients during the entire session (20-30 min). Our institution has chosen to limit compression so that patients can endure it easily during the entire session. This study investigates whether this type of abdominal compression is effective.

Material and Methods: In short, a diagnostic 2 phase CT scan was used to locate tumor positions. Belt pressure and marking position (Orfit Industries), were reproduced for each treatment fraction. Each fraction, cone beam CTs (CBCT) were recorded before and immediately afterwards. Scans were matched offline, using deformable image registration (Varian Smart Adapt V13), resulting in “CBCT liver contours”. These were checked and adjusted, if necessary.
Each CBCT liver contour was compared to original CT contour using absolute volume, center of mass shift (CMS) and dice coefficient (DC). To assess effectiveness of compression, data were averaged for each of the three computed parameters.

Results: Until this date, a total of 6 patients were treated using this technique. All 6 tolerated the applied abdominal compression easily during the sessions. Therapists, trained in >> 100 brain or lung stereotactic treatments, reported no exceptional difficulties in fixation, CBCT, and matching.
Data from 4 patients, and a total of 24 CBCTs, were eligible for analyses. Liver CBCT volumes appeared to be very similar to CT contours: the average is only 18 cc less, with a maximum of 116 cc. The average CMS in X, Y, Z are 0.14cm (max 0.41cm), 0.05cm (max 0.33cm) and 0cm (max 0.23cm), respectively. Average DC is 0.94, with a range of [0.89 0.99].

Conclusion: Difference in volume, center of mass, and even shape are well within the range of standard uncertainties in stereotactic abdominal radiotherapy. This corroborates with the reported feasibility by therapists treating these patients.
In short, the patient comfortable setting of the compression-belt is reproducible and safe to correctly deliver the dose in stereotactic radiotherapy of the liver.

EP-2098

Use of a bladder minimum contour for prostate treatment planning to increase comfort and efficiency

C. Evans[1], E. Crees[1], G. Kidane[1], M. Brown[1], M. Campbell[2], S. Gibbs[3], K. Tarver[3], G. Ghebremaniam[1]
[1]*Queen's Hospital, Department of Medical Physics, Romford, United Kingdom*
[2]*Queen's Hospital, Radiotherapy Department, Romford, United Kingdom*
[3]*Queen's Hospital, Oncology, Romford, United Kingdom*

Purpose or Objective: Prostate cancer patients often find it difficult to maintain a full bladder throughout the course of their radiotherapy treatment. These bladder filling problems can result in patients being taken out of the treatment room in order to increase bladder filling, leading to treatment delays. The aim of this study was to provide a range of acceptable bladder sizes without compromising the bladder dose constraints.
Material and Methods: An audit was carried out with ten patients who attended for IMRT radiotherapy planning for prostate cancer. A minimum bladder volume (bladder min) in each patient was defined by cropping the planning CT (pCT) bladder volume to around 150cc. This new volume was then used in addition to the pCT bladder volume in the IMRT plan optimisation to fulfil the bladder dose constraints. The patients had their bladder volume assessed prior to treatment using a standard CBCT imaging protocol. Retrospective dose calculations were undertaken using the daily CBCT images, and bladder doses were plotted against bladder volume to demonstrate that dose constraints were still being met at the reduced bladder volume. The tolerance doses used are taken from the CHHiP trial protocol.

Results: The bladder min contour is used by the treatment radiographers as a visual guide on the CBCT scan taken before each treatment in order to assess whether the patient’s bladder is an acceptable size to continue with treatment without compromising bladder tolerance doses.
The volume of the bladder min contour is adjusted to meet the constraints for each individual patient as necessary
The need for patients to be taken out of the treatment room to re-fill the bladder has been reduced and this has resulted in better workflow on the treatment floor. The use of the bladder min contour for prostate IMRT treatment planning is now standard practice in our clinic.

Conclusion: The use of the bladder min contour has improved patient comfort without compromising the therapeutic ratio and has aided the radiographers in online review of treatment images.
The implementation of the above has led to a reduction in treatment delays due to the bladder volume obtained at planning CT not being maintained throughout treatment. This has improved the clinic workflow. Patient discomfort is kept to a minimum and repeat CBCT scans have been reduced.

EP-2099

Influence of anxiety on reproducibility of cancer patients (pts) repositioning during pelvic RT

E. Sierko[1], R. Maksim[1], J. Czauderna[1], T. Filipowski[1], M. Wojtukjiewicz[2]
[1]*Bialostockie Centrum Onkologii, Departament of Radiation Therapy, Bialystok, Poland*
[2]*Meduical University in Bialystok, Departament of Oncology, Bialystok, Poland*

Purpose or Objective: The aim of the study was an analysis of an influence of type and intensity of pts anxiety on pts repositioning during planning and delivery of RT to the pelvic area in relation to pts gender, immobilization device, and

assessments: subjective of QoL and objective -of pts repositioning during RT.

Material and Methods: 57 pts(28 gynecological caner females and 29 prostatic cancer males) underwent radical RT to the pelvic area in Radiation Therapy Department of Contemporary Cancer Center in Bialystok, Poland. Pts were immobilized with an AIO SOLUTION by OrfitTM set or kneefix plus headrest. Demographic questionnairesone was filled once. Second questionaire using VAS scale evaluated subjective sensation of anxiety via 20 questions describing events influencing areas: biological social, psychological and somatic. It was filled 3 times: before: localization CT, 1st and 11th fraction (fr) of RT. Heart rate (indicating objective pts anxiety) examination was performed before each evaluation. Reproducibility of pts positioning in relation to X, Y, Z-axes was verified under Elekta accelerator using X-ray volume imaging (XVI).

Results: Most of pts exhibit highly increased anxiety before CT. It was decreasing in time but still was significant at the end of RT. Contrary to men, female pts experienced higher anxiety specially in somatic, and biological areas before CT. Males developed the sensation before 1st fr. In pts positioned with hands on their chest significantly worse Y-axis position reproducibility (PR) before 1st fr and significantly higher anxiety (p=0,007) was observed before 11th fr of RT (p=0,03) comparing to those localized with hands along the body. Higher psychological anxiety was associated with significantly worse average PR in all axes (p=0.03, R=0,3). Average heartbeat was highest before the 1st while lowest - before 11th fr of RT. Intensity of anxiety was not associated with social situation, experience with cancer among relatives, and the time between diagnosis and start of RT.

Conclusion: Since anxiety influences pts repositioning during RT, more attention should be paid by RTT to decrease this emotional satus of the pts.Educational events should be organized for RTT to help them overcome the problem of pts anxiety during RT.

EP-2100

Effectiveness of the manual correction during positioning patients with prostate cancer

T. Piotrowski[1], K. Kaczmarek[2], A. Jodda[3], B. Bąk[1], A. Ryczkowski[3]

[1]*Poznan University of Medical Sciences, Electroradiology, Poznan, Poland*

[2]*Greater Poland Cancer Centre, 2nd Radiotherapy Ward, Poznan, Poland*

[3]*Greater Poland Cancer Centre, Medical Physics, Poznan, Poland*

Purpose or Objective: Total shift (TS) in each of the directions along the x, y or z-axis is a sum of shifts resulting from automatic registration (AR) and manual correction (MC) and is described by formula: TS=AR+MC. Unfortunately, MC is burdened by error resulting from inter-observer variability.
The aim of this study was to find the level of MC, above which the use of MC during positioning of the patients with prostate cancer on the helical tomotherapy will be reasonable.

Material and Methods: This retrospective study based on the image guidance data gathered from 30 consecutive patients with prostate cancer treated on helical tomotherapy in 2013. The planned dose for each patient was 74 Gy delivered to the prostate or to the prostate and to the basis of the seminal vesicles. The treatment was realized in 37 fractions.
Daily MVCT imaging covered whole irradiated region expanded by 10 mm in cranio-caudal direction. The data from each fraction and for every patient (daily MVCT and planned kVCT) were re-registered by five independent observers.
The MCs established by observers were averaged for each fraction and for every patient, respectively. The level of MC, above which usage of MC is reasonable, was recognized on the level of averaged MC higher than 1 mm.

Results: 1110 registrations were re-registered by each observer.
Using the condition of the average MC higher than 1 mm, we established that the reasonable MC that should be applied during registrations are respectively: higher than 2 mm in medio-lateral and cranio-caudal directions; and higher than 2.5 mm in anterio-posterior direction.
Figure 1 shows averaged manual corrections in the medio-lateral and cranio-caudal directions.

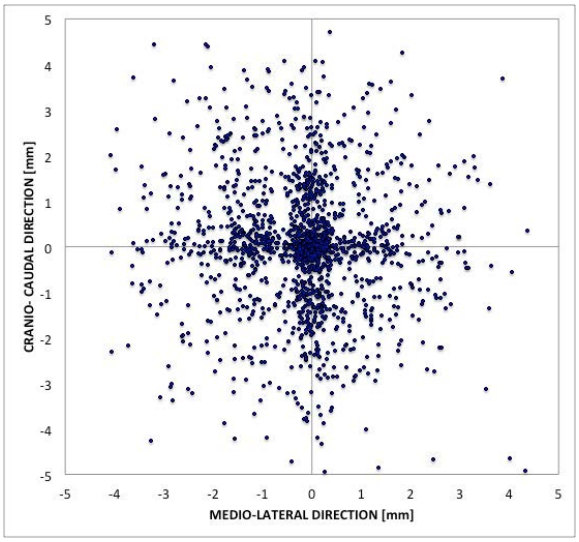

Conclusion: Manual correction effectively increase the accuracy of the registrations when the value of the corrections are higher than 2 mm in medio-lateral and cranio-caudal directions and higher than 2.5 mm in anterio-posterior direction. Lower values of manual corrections are burdened by error resulting from inter-observer variability and can not be applied to the total shift during registration process.

Electronic Poster: RTT track: Other topics for RTTs

EP-2101

Inverting a teaching practice

D. Montgomerie[1], B. Mudie[1]

[1]*University Of Otago, Radiation Therapy, Wellington, New Zealand*

Purpose or Objective: Introduction: The first year radiation therapy (RT) planning paper in the Bachelor of Radiation Therapy, University of Otago, New Zealand covers all of the basic concepts required to be able to plan radiation treatments. As the students' progress through the three years of the programme the concepts remain the same but the application of them becomes more complex. Planning concepts were taught one by one, with the students gaining knowledge and comprehension on each concept. Towards the end of the paper the aim was to be able to apply, analyse and evaluate all of these concepts together to produce a radiation therapy plan. However, students were indicating that although they understood each of the concepts individually they struggled to apply them together and felt underprepared for the clinical placement – the acquisition of knowledge had not led to critical thinking.
Objectives: In response to this feedback major changes were instituted to the structure of the paper delivery by essentially reversing the approach. The students' now began by creating and critiquing plans then unpacking and exploring the concepts. The authors wanted to assess the impact this new approach had on the students in their clinical placement.

Material and Methods: Method: To assess the preparedness of the students for clinical placement a comparison of the original method of delivery (group A) to the new approach (group B) was undertaken. Six students from group A were invited to participate in a focus group using a semi-structured

interview technique with an independent interviewer. The focus group was conducted shortly after the completion of the first clinical placement. The themes that came from this were then used to create a survey for group B. This was also completed shortly after their first clinical placement. Additionally this survey was also undertaken by supervising qualified RTs from the clinical placements.

Results: Results: The results from the focus group A showed that the students did not fully grasp how the concepts applied to the final plan and this left them feeling very underprepared for their clinical placement and that this was reflected back to them by supervising qualified staff. Group B however, felt themselves to be much better prepared and reasonably confident to undertake clinical placement a view which was supported by the supervising radiation therapists.

Conclusion: Conclusion: The alteration of the teaching delivery had allowed the students to start the paper by thinking critically about a plan and then supporting this thinking with new knowledge. Although this was a very steep learning curve for the students at the beginning of the paper the final assessment and course evaluations also indicated that they had a much better overall grasp by the end.

EP-2102

"We're all here for the patient": exploring the process of interprofessional learning

K. Coleman[1], B. Darlow[2], E. McKinlay[2], L. Beckingsale[3], S. Donovan[2], P. Gallagher[4], B. Gray[2], H. Neser[1], M. Perry[5], S. Pullon[2]

[1]University of Otago- Wellington, Department of Radiation Therapy, Wellington, New Zealand
[2]University of Otago- Wellington, Department of Primary Health Care and General Practice, Wellington, New Zealand
[3]University of Otago- Wellington, Department of Human Nutrition, Wellington, New Zealand
[4]University of Otago- Wellington, Medcial Education Unit, Wellington, New Zealand
[5]University of Otago- Wellington, School of Physiotherapy, Wellington, New Zealand

Purpose or Objective: This qualitative study aimed to explore student perceptions and experiences of the Interprofessional Education (IPE) programme focused on long-term condition management.**(1)** A secondary aim was to explore the experiences of radiation therapy students who recently joined the programme.

Material and Methods: Three focus groups were conducted. All 41 students who participated in the IPE programme (dietetics; n=4, medicine; n=18, physiotherapy; n=6, radiation therapy; n=13) were invited to attend one of the two interdisciplinary focus groups. Students from radiation therapy were also invited to attend a unidisciplinary focus group. Focus groups were audio-recorded and transcribed verbatim. Data were independently analysed by two researchers within the framework of Thematic Analysis.**(2)** Themes were determined following parallel coding and research team verification.

Results: Thirty-four students participated in the interprofessional focus groups and 13 radiation therapy students participated in their unidisciplinary focus group. Three key themes emerged related to i) learning ii) perceived long-term professional benefits and iii) the structure and content of the programme. An additional theme emerged from the radiation therapy focus group related to how they perceived, and considered they were perceived by, the medical students.

Conclusion: Participants considered the programme to be a valuable learning opportunity which had direct relevance to their clinical careers. Listening to the insights of students is an important means of discovering what, for them, constitutes a meaningful and positive learning experience. Providing students with an opportunity to learn about each other should be prioritised within IPE programmes in order to allow them to effectively learn with and from each other.

References:

1. Pullon S, McKinlay E, Beckingsale L, Perry M, Darlow B, GrayB, Gallagher P, Hoare K, Morgan S. Interprofessional education for physiotherapy, medical and dietetics students: a pilot programme. J Prim HealthCare. 2013;5(1):52-8.
2. Braun V, Clarke V. Using thematic analysis in psychology.Qualitative research in psychology. 2006;3(2):77-101.

EP-2103

Margin assessment for feline and canine radiotherapy using a custom cranial immobilisation device

J. Sharpe[1], A. Tini[1], I. Minneken[1], C. Winter[1], V. Meier[2], C. Rohrer Bley[2]

[1]University Hospital Zürich, Radio-Onkologie, Zurich, Switzerland
[2]Vetsuisse Faculty University of Zurich, Division of Radiation Oncology, Zurich, Switzerland

Purpose or Objective: The purpose of this study was to observe the daily positioning correction errors in feline and canine radiotherapy, using a custom cranial immobilization device and KV onboard imaging. Then further assess the data for margin definition in the event of an unguided approach (without the possibility of daily imaging) for treatment use with the identical positioning device.

Material and Methods: Canine and feline patients with cranial tumors were treated using a custom made cranial immobilization device, consisting of: a plastic plate which is fixed to the couch, a detachable custom molded bite block, and a custom fitted vacuum foam cushion supporting the neck, thorax and body. The patients were imaged daily before treatment, , thereby correcting all positioning errors in lateral, vertical and longitudinal directions. The shift values were then saved to a data base for later analysis.

Results: 8 patients (3 feline, 5 canine) and a total of 93 post-imaging corrections were observed in 3 directions (lateral, vertical, and longitudinal). Upon assessment of the data, the formula:
PTV Margin=2Σ + 0.7σ (van Herk et al.)
was used to calculate margin for the unguided approach. A result of 3mm x 2mm x 3mm (lateral, vertical, longitudinal) was found.

Conclusion: Based on the results, the margin of an unguided approach using the custom positioning system, would need to be extended from 2mm (margin used for image guided treatment planning) to 3mm in the lateral and longitudinal directions, while vertical would remain at 2mm.

1. Van Herk M, Remeijer P, Rasch C, et al. [2000]The Probability of correct target dosage:Dose-population histograms for deriving treatment margins in radiotherapy. Int.J Radiat. Oncol. Biol. Phys;47:1121-1135

EP-2104

Waiting times for IMRT as a Quality Indicator: A study from a Tertiary Hospital in Saudi Arabia

Z. Mulla[1], M.E. El Sayed[1,2], S.M. Soaida[1,3], A. AlHebshi[1], M. Bayoumy[1], A.H. Mohammed Khasim[4]

[1]King Faisal Specialist Hospital& Research Centre-Jeddah, Oncology, Jeddah, Saudi Arabia
[2]National Cancer Institute, Radiotherapy and Nuclear Medicine Department- Cairo University, Cairo, Egypt
[3]Cairo University, Clinical Oncology Department- Faculty of Medicine, Cairo, Egypt
[4]King Abdulaziz University Hospital, Radiology Department, Jeddah, Saudi Arabia

Purpose or Objective: To assess the compliance of our protocol of ≤ 10 working days (WD) for IMRT.

Material and Methods: A retrospective analysis of all cases treated between October 2010 and December 2014. Waiting

times from the date of the request to the start of treatment (REQ-ST), from the request to CT Simulation (REQ-CT) and from CT simulation to the start of treatment (CT-ST) were computed. To assess the compliance of our performance with the protocol, we calculated two indicators: mean waiting times and compliance rates. The cut-off of compliance for CT-ST ≤10 WD is defined by our protocol. Using this value, the two other cut-offs were respectively calculated using a linear equation of REQ-ST and REQ-CT as a function of CT-ST, giving a REQ-CT=9 and REQ-ST=26 week days (WKD). To assess the evolution in time of all studied parameters, we divided the study into 4 periods: 1) from Oct 2010 to Dec 2011, 2) from Jan to Dec 2012, 3) from Jan to Dec 2013 and 4) from Jan to Dec 2014. In addition, we analyzed the impact of the indication of IMRT on the waiting-times by comparing the indicators across the tumor localizations. Statistical analysis was performed using SPSS. Mean waiting times were compared using ONEWAY ANOVA and compliance rates were compared using Pearson's Chi-square test.

Results: A total 245 IMRT cases were included. Mean CT-ST was 13.80 ± 5.07 days, without significant difference across the study periods (p=0.254). The compliance rate of CT-ST with the protocol≤10 WD, was 16%, without significant difference across the periods (p=0.257). Regarding REQ-ST, total mean was 30 ± 10 WKD, with a compliance rate at 33%. Regarding REQ-CT, total mean was 11.26 ± 8.33 WKD, with a compliance rate at 49%. There was a significant difference across the periods in both REQ-ST and REQ-CT, with the best performance for period 1, followed by period 4. See Table below.

Evolution in time of the number of cases, indications and waiting times of IMRT

(Z. Mulla et.al. "Waiting times for IMRT as a Quality Indicator: A study from a Tertiary Hospital in Saudi Arabia". 2015)

Year (Period)		2011 (1)	2012 (2)	2013 (3)	2014 (4)	2010-2014
Number of cases		18 (7.3%)	50 (20.4%)	104 (42.4%)	73 (29.8%)	245 (100%)
Technique*	IMRT	18 (100)	42 (84.0)	14 (13.5)	0 (0.00)	74 (30.2)
	VMAT	0 (0.00)	8 (16.0)	90 (86.5)	73 (100)	171 (69.8)
Tumor Localization	Head & Neck	15 (83.3%)	36 (72%)	43 (41.3%)	10 (13.7%)	104 (42.4%)
	CNS	0 (0%)	4 (8%)	20 (19.2%)	24(32.9%)	48 (19.6%)
	Pelvis & Abdomen :	1 (5.6%)	1 (2%)	22(21.2%)	17(23.3%)	41 (16.7%)
	GU	0 (0%)	0 (0%)	11(10.6%)	11(15.1%)	22 (9%)
	GIT	1 (5.6%)	1 (2%)	10(9.6%)	5(6.8%)	17 (6.9%)
	Gynecological	0 (0%)	0 (0%)	1(1%)	1 (1.4%)	2 (0.8%)
	Others :	2 (11.1%)	9 (18%)	19 (18.3%)	22 (30.1%)	52 (21.2%)
	Lymphoma	1(5.6%)	3 (6%)	10 (9.6%)	10(13.7%)	24 (9.8%)
	Sarcoma	0 (0%)	5 (10%)	4(3.8%)	3(4.1%)	12 (4.9%)
	Breast	0 (0%)	0 (0%)	3 (2.9%)	5 (6.8%)	8 (3.3%)
	Skin	0 (0%)	1 (2%)	0 (0%)	2 (2.7%)	3 (1.2%)
	Lung	0 (0%)	0 (0%)	1 (1%)	2 (2.7%)	3 (1.2%)
	Ophthalmic	1 (5.6%)	0 (0%)	0 (0%)	0 (0%)	1 (0.4%)
Quality indicators						
Waiting Time (unit)	REQ-CT(week days)	8.61 ± 7.58	14.28 ± 10.64	11.01 ± 7.86	10.21 ± 6.86	11.26 ± 8.33
	CT-ST(working days)	14.27 ± 5.31	15.02 ± 7.10	13.41 ± 4.81	13.41 ± 3.41	13.80 ± 5.07
	REQ-ST(week days)	27.66 ± 10.95	34.28 ± 10.16	29.42 ± 10.63	29.64 ± 9.23	30.35 ± 10.30
Compliance Rate**(1)	REQ-CTs 09 (p=.006*)	66.7%	28.0%	51.9%	54.8%	49.0%
	CT-STs 10 (p=.257)	27.8%	18.0%	14.4%	13.7%	15.9%
	REQ-ST ≤ 26 (p=0.34*)	50.0%	20.0%	39.4%	28.9%	33.1%
Compliance Rate(2)	REQ-CTs 12 (p=.066)	83.3%	56.0%	66.3%	75.3%	68.2%
	CT-STs 15 (p=.476)	66.7%	72.0%	82.8%	80.8%	78.8%
	REQ-ST ≤ 31 (p=.029*)	61.1%	44.0%	69.2%	60.3%	60.8%

* Statistically significant results (p<.001); **Compliance Rate = percentage of observations complying with the timeline; compliance rate 1: timelines according to initial protocol; compliance rate 2: timelines according to newly proposed protocol.

Regarding these unsatisfying results, we proposed to update our protocol with a new set of more feasible timelines: CT-ST ≤ 15 WD; REQ-CT ≤ 12 WKD; REQ -ST ≤ 31 WKD. See compliance rates in graph below.

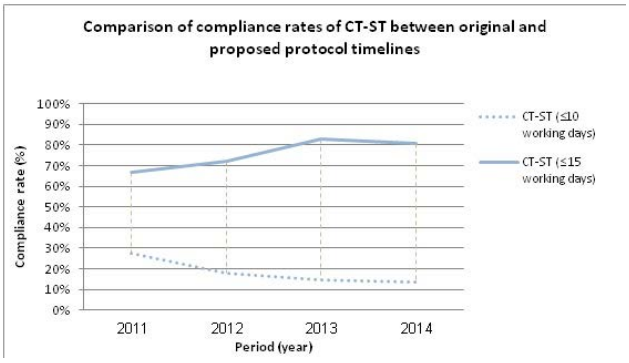

Furthermore, there was significant variations in the REQ-CT waiting times across tumor sites with worst performance for Head & Neck (compliance rate = 40%), while the Abdomen and pelvis had the best performance (compliance rate = 66%). No statistically significant difference was found between tumor sites for CT-ST and REQ-ST.

Conclusion: There is a definitive need to amend our protocol to ≤15 WD for CT-ST, as an intermediate step to improve our performance.

EP-2105

The helpful rays a children's book about cancer and radiotherapy explained in a non-intimidating way

K. Farstad[1]
[1]*Ålesund Hospital, Radiotherapy, Ålesund, Norway*

Purpose or Objective:

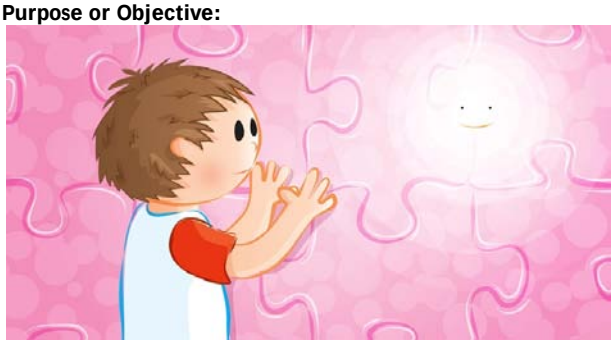

«Now I'm gonna tell you a story about your body, and some strong and helpful rays, which can help you if you get sick…..." This is how my book for children, about radiotherapy begins. I started as a RTT 10 years ago, and have always felt that our department needed aid to explain cancer and radiotherapy to children in a comprehensible way. I couldn't find any information that caters for children, so I wrote "The Helpful Rays". Small children can sense differences in behavior and atmosphere in the family when someone gets sick. To help children understand, they need explanation.
My purpose with this book is to explain cancer, radiotherapy and side-effects to children in a non-intimidating way. The word cancer can be frightening to children as well as adults. My goal is to provide this book as a tool to talk about cancer with children.

Material and Methods: I wrote this book in cooperation with an illustrator, a publisher and our national cancer society. I have used radiotherapists and doctors as proofreaders. And I used my own children (3,5 and 5 years) to make sure the book was understandable and gripping enough.
It can be difficult to find the right words to describe what a mother, father, or relative is going through. Why do they need radiotherapy? Why do they feel nauseous? Why do they lose their hair? The "answers" are in this book. It can be difficult for young children to grasp the complicated cell biology and radiation physics involved, so, the side-effects are explained with use of imagination. For example when rays are burning the hair cells, the hair cells jump out of the skin, and may never come back. Simple explanations that children can understand, regardless if it's according to reality or not.
I have presented the various health personnel that a cancer patient will meet in a hospital. Ex: Radiographer, bioengineer, doctor, nurse and radiotherapist. Also I have presented the most common examinations the patients have to go through. Ex. Blood samples, MRI, CT and biopsy. In that way, children can be prepared for whom they might meet and why, which examinations they must go through and why.

Results: The book is currently being published in Norway, where hospitals, nurses, radiotherapy departments, doctors, schools and kindergartens are using the book in contact with children who have cancer themselves, or their mom, dad, siblings, grand-parents, classmates or other people they are close to that got diagnosed with cancer. The response has been overwhelming. Since June this year approx. 1500 books have been handed out. And we are soon out-of-stock.

Conclusion: There are few or none books written for children about radiotherapy. In my country the book got welcomed as a much needed book, and I think it can be helpful in cancer departments in other countries as well, when adjustments to

the book are made in order to fit a country's own cancer treatment program.

EP-2106

Structuring a database to evaluate haematological toxcicity in post-prostatectomy IMRT patients

V. Sacco[1], G. Salvadori[1], A. Sbalchiero[1], A. Viale[1], A. Soccio[1], M. Martulano[1], R. Bin[1], S. Selli[1], A. De Leonardis[1], D. Parutto[1], A. Capelli[1], A. Tavilla[1], L. Longoni[1], L. Palumbo[1], F. Baratto[1], N. Barricella[1], C. Fiordelisi[1], C. Cozzarini[1], N. Di Muzio[1]
[1]*IRCCS San Raffaele Scientific Institute, Radiotherapy, Milano, Italy*

Purpose or Objective: Haematological toxicity (HT) in post-prostatectomy patients (WPRT) treated with whole pelvis radiotherapy represents a problem due to the irradiation of a large fraction of the bone marrow (BM). HT is under evaluation in our Institute according to an observational prospective study aiming to explore a dose-effect correlation. Therefore, clinical and dosimetric data have to be collected. This study reports (quantify) the complexity and workload of the clinical data collection were to evaluate its feasibility in the routine clinical practice.

Material and Methods: A database for the enrolled WPRT patients (pts) was created, collecting the following data: clinical features (age, surgery, diabetes, hormonal therapy, results from blood samples at several time points); intent (adjuvant, salvage); technique (step and shot IMRT, Rapid Arc, Helical Tomotherapy); dose-volume histogram (DVH) of BM structures; The time required to fill in database was also evaluated.

Results: To date 238 pts were included in the database. The average age is 66 years (range 48 – 84). Conventionally fractionated (1.8 - 2Gy/fraction, 139 pts) and moderately hypofractioned (2.35-2.65 Gy/fraction, 99 pts), step-and-shoot IMRT (SS-IMRT, n=18), Volumetric Arc (RA IMRT, n=111) or helical tomotherapy (HTT, n=99) EBRT. Adjuvant n = 159 pts, salvage n = 79 pts. The workload to fill in the database was 40 min/pt.

Conclusion: The availability of clinical/dosimetric data was crucial for the dose effect analysis, being HT not negligible. In our experience, the implementation of the database in the routine setting is feasible provided a dedicated operator, such as a radiotherapy technologist (RT), after a simple learning curve to lead the RT to reach the proper expertise.

EP-2107

Work satisfaction and motivation of radiation therapists. A qualitative study

P.G. Kup[1], J.A. Rubin[2], I.A. Adamietz[1], K. Fakhrian[1]
[1]*Marien Hospital Herne- Ruhr university Bochum, Radiation Oncology, Herne, Germany*
[2]*University of Bremen, Psychology, Bremen, Germany*

Purpose or Objective: For more than 120 years radiation therapists (RTT) treat oncology patients in radiation oncology facilities. However, influencing factors on motivation, work performance and work satisfaction of RTTs is still not studied. The aim of this trial was to detect factors influencing work satisfaction and motivation of MTRAs in radiation oncology. Leadership solution approaches will be discussed.

Material and Methods: In a qualitative interview study with seven RTTs at a university clinic we investigated determinants influencing motivation, work and work satisfaction based on the individual experiences of our participants. An inductive thematic content analysis framework was applied to the transcripts.

Results: The interviews were conducted with seven RTTs in our radiation oncology unit. The interview lasted between 40- 60 minutes (mean 52 minutes). All participants were of female sex. Mean age was 46 years (range 30-59 years). Mean work experience in radiation oncology was 19 years (range 3-37 years). All but 2 RTTs were employed fulltime. Three participants have professional experience in diagnostic radiology. All participants declared an interdisciplinary lack of communication between physicians, physicists and RTTs as one of the influencing factors on their work motivation. Furthermore, RTTs receive negative feedback about treatment failures and death of the patients more frequently than results of therapy success. This fact has considerable impact on the motivation of the majority of interviewed RTTs. Additionally, the lack of positive feedback influences the willingness of further education, self-improvement and motivation to recommend the employment as RTTs.

Conclusion: Frequent negative feedback weakens RTTs motivation and work satisfaction. Improved communication about therapy results, especially therapy success, may increase RTTs work motivation. Stabilized motivation may have positive effects on trainee recruitment in radiation oncology.

EP-2108

Gaps in Radiotherapy: What can we do to improve it?

R. Jimenez[1], N. Becerra[1], N. Rodriguez[1], M. Algara[1]
[1]*Hospital de la Esperança. Parc de Salut Mar, Oncologia Radioterapica, Barcelona, Spain*

Purpose or Objective: We want to determine if having a liberated late shift of patients and incorporating hypofractionation protocols in different pathologies makes decreasing the number of lost sessions caused by breakdown and scheduled reviews of treatment units in a 30%, because we can only act on them.

Material and Methods: We compare the data obtained in a management program of treatments (GestRdt) with Excel 2010 software, between the first nine months of 2013 and 2015, because during 2014, hypofractionation new protocols were implemented and a late shift unit treatment was closed. We analyzed the total number of sessions, the total number of patients, the number of sessions per patient, sessions missed by stop-treatment unit and sessions missed by patients in absolute numbers and percentages.

Results: In the year 2013, 1104 sessions (10.11%) were lost and in 2015 were 547 (6.68%). Missed sessions related with the patient and their environment (toxicity, patient-derived and other) was 6.17% in 2013 and 4.79% in 2015, which means a decrease of 22.35%. The percentage of sessions missed by failures and planned outages was 3.94% in 2013 and 1.88% in 2015, representing a decrease of 52.13%. Decreasing of one session per patient in 2015 has generated 768 sessions or free holes in treatment units.

Conclusion: Hypofractionation new techniques and the provision of a free shift of patients have allowed that the reduction of missed sessions related to the treatment units is greater than 50%.

Electronic Poster: RTT track: Position verification

EP-2109

Novel verification technique for craniospinal irradiation with an image plate in the supine position

S.K. Ahn[1], S.K. Lee[1], J.H. Cho[1], C.O. Suh[1]
[1]*Yonsei Cancer Center, Yonsei University Health System-Seoul- Korea, Seoul, Korea Republic of*

Purpose or Objective: It has not yet been possible to confirm the junction of the treated fields for craniospinal irradiation treated in the supine position; the intention of this study was to improve the accuracy of radiation therapy through a technique using an image plate.

Material and Methods: The subjects of this study were 20 medulloblastoma patients who were treated in the supine position in three parts from the brain to the sacrum spinal canal. A half beam was used for the cranial field, and the

collimator was rotated with the isocenter set to C-spine level 2. The divergence of the upper spinal field was aligned with the junction of the cranial field; the couch was rotated 270° and the gantry was rotated to align the divergence of the lower spinal field with the inferior border of the upper spinal field. To confirm the junction of the treated field: 1) an image plate (14 x 17 inches) was placed vertically on the couch so that the junction of the cranial field and the upper spinal field would be included in the plate; 2) the cranial field was irradiated to check it; 3) the lateral lock of the couch was released and the isocenter was moved to the image plate before irradiation to check the upper spinal field; and 4) the junction of the cranial field and the upper spinal field was analyzed with a computed radiography reader (CAPSULA XL Ⅱ, Fujifilm, Japan). The field junction was photographed three times to confirm its accuracy and reproducibility. Two-millimeter or smaller gaps or overlaps were considered setup error. If a 2 mm or greater error was specifically reproduced, the center was moved again through 2D simulation.

Results: The junction of two fields could be confirmed regardless of the degree of enlargement according to the distance between the cranial isocenter and the image plate, with the cranial field as the half beam. The verification images of the 20 patients were measured with a computed radiography reader. Eighteen patients showed a setup error that was smaller than 2 mm, and the center was moved again for two patients who showed the specific reproduction of a gap or overlap of 2 mm or more at the junction. Since the divergences of the upper spinal field and lower spinal field were aligned at the body of the patient and the bottom of the couch, the junction was confirmed by the naked eye by attaching paper to the bottom of the couch.

Conclusion: For craniospinal irradiation patients, treatment in the supine position rather than in the prone position is advantageous for setup stability and airway security. The proposed technique can maintain the homogeneity of the dose because it can accurately confirm the junction of the fields using an image plate.

EP-2110

A study of prostatic calculi: in patients receiving radical radiotherapy for prostate cancer

A. O'Neill[1,2], C.A. Lyons[1,3], S. Jain[1,3], A.R. Hounsell[1,4], J.M. O'Sullivan[1,3]

[1]*Queens University Belfast, Centre for Cancer Research & Cell Biology, Belfast, United Kingdom*

[2]*Belfast Health & Social Care Trust, Radiotherapy, Belfast, United Kingdom*

[3]*Belfast Health & Social Care Trust, Clinical Oncology, Belfast, United Kingdom*

[4]*Belfast Health & Social Care Trust, Medical Physics, Belfast, United Kingdom*

Purpose or Objective: Image guided Radiotherapy (IGRT) for prostate cancer (PCA) frequently employs surgically implanted fiducial markers. It is estimated that up to 35% of prostate radiotherapy patient have prostatic calculi (PC) visible on treatment cone beam CT (CBCT). Prostatic calculi present a potential alternative to implanted fiducials. The purpose of this study was to establish the incidence and location of PC in a contemporary population of prostate radiotherapy patients.

Material and Methods: A retrospective single-observer analysis of images from patients with PCA who received RT at our centre was undertaken to identify PCs within the prostate. The Prostate Imaging and Reporting Data System (PI-RADS) graphical schema was used to record the position of PC. Available images from Trans-rectal Ultra-sound(TRUS) brachytherapy volume study scans, CT scans and CBCT scans were analysed from 242 patients.

Results: In total, 394 scan sets from 242 patients were analysed. 57 out of 62 (91%) TRUS images and 153 of 180 (85%) CT planning scans had visible PC. Of the 153 patients with PC visible on CT, 136 also had CBCT scans. All but 1 had corresponding PC on CBCT. 16 TRUS scans had corresponding PCs visible on CT scans but seed artefact obscured visibility in most cases. PC were most frequently observed in sections 3p and 9p (poster of mid gland and apex) of the PI-RADS schema and least often observed in 8a, 12a & 13as (anterior base and apex).

Conclusion: In our series, a significant majority of the prostate radiotherapy patient population have PC detectable on pre-radiotherapy imaging. A prospective clinical trial will commence shortly investigating the feasibility of using PC as an alternative to FMs.

EP-2111

Inter-observer variability in stereotactic IGRT with CBCT: is a CTV-PTV margin needed?

M. Massaccesi[1], V. Masiello[1], M. Ferro[1], V. Frascino[1], S. Manfrida[1], M. Antonelli[1], S. Chiesa[1], A. Martino[1], F. Greco[2], B. Fionda[1], A. Fidanzio[2], G. Mattiucci[1], L. Azario[2], S. Luzi[1], V. Valentini[1], M. Balducci[1]

[1]*Policlinico Universitario Agostino Gemelli- Catholic University, Radiation Oncology Department - Gemelli ART, Roma, Italy*

[2]*Policlinico Universitario Agostino Gemelli- Catholic University, Physics Institute, Roma, Italy*

Purpose or Objective: Use of image guided radiotherapy (IGRT) allows to reduce uncertainty margin from clinical to planning target volume due to better geometric accuracy. Geometric accuracy of Linac-based stereotactic IGRT is reported to be within 2-3 mm and Kilo-voltage cone beam computed tomography (Kv-CBCT) is generally considered as the gold standard for treatment verification. However inter/intra-observer variability in image evaluation may exist. Aim of this report was to conduct a preliminary analysis to quantitatively determine the magnitudes of such inter-observer variations

Material and Methods: Kv-CBCT images were obtained for all patients who underwent stereotactic radiotherapy treatments. They were analyzed both on-line (before treatment delivery) and off-line by two different Radiation Oncologists (RO, M.M. and V.M.) with at least one year of experience in CBCT images verification. Translational displacements in anteroposterior (z), mediolateral (x), and craniocaudal (y) directions were recorded for all verifications and discrepancies between the two RO were calculated. Based on the discrepancies in x, y, and z directions, systematic and random differences were calculated and three-dimensional radial displacement vector was determined. Systematic and random differences were used to derive CTV to PTV margin. Time spent for on-line image verification was also recorded. Results are reported as mean values. The T test was used to assess differences between groups

Results: From January to September 2015, 189 CBCT scans of 48 patients submitted to intracranial (39 scans) or extracranial (150 scans) Linac-based stereotactic radiotherapy were analyzed. An inter-observer discrepancy of ±3 mm on at least one direction was observed in 37 CBCT scans (19.6%). Mean radial discrepancy was 1.82 mm (range 0-11.1 mm). In AP, CC and ML directions, systematic differences were 0.89, 1.87, and 0.67 mm and random discrepancies were 0.43, 0.55, and 0.50 mm, respectively. By van Herk's formula CTV-PTV margins needed to account for such inter-observer variability were 2.5, 5.0 and 2.0 mm in AP, CC and ML directions, respectively. Inter-observer discrepancies were smaller for intracranial than extracranial stereotactic treatment (mean radial discrepancy 1.2 versus 1.9 mm, respectively p=0.01).On-line verification of CBCT took a mean time of 4 minute and 14 seconds (range 58 sec - 12 min 25 sec). No significant difference in magnitudes of inter-observer variability was observed according to time spent for verification

Conclusion: When using KV-CBCT for set-up verification in stereotactic treatment a large inter-observer variability can be seen in a significant proportion of scans, particularly in extracranial treatment. Such a difference may have an impact on target coverage or organ at risk irradiation, thus requiring a proper margin. Further evaluation is needed, particularly focusing on methods to decrease such inter-observer variability

EP-2112

Intrafraction setup errors in single fraction stereotactic radiosurgery with Elekta Fraxion system

W. Vásquez Rivas[1], J. Luna Tirado[1], M. Rincón Pérez[2], D. Esteban Moreno[1], A. Ilundain Idoate[1], A. Pérez Casas[1], M. García-Castejón[2], J. Olivera Vegas[1], I. Prieto Muñoz[1], J. Vara Santos[1]

[1]*Hospital Universitario Fundación Jiménez Díaz, Oncología Radioterápica, Madrid, Spain*

[2]*Hospital Universitario Fundación Jiménez Díaz, Radiophysics, Madrid, Spain*

Purpose or Objective: Frame-based stereotactic radiosurgery (SRS) using rigid immobilization with head ring continues to be the standard treatment when it comes to intracranial SRS. We wanted to assess setup accuracy and intrafraction errors of patients treated with single fraction intracranial stereotactic radiosurgery using the Elekta Fraxion® immobilization system (Frameless SRS) and HexaPOD positioning platform (translational and rotational set up error).

Material and Methods: 5 patients with a diagnosis of brain metastasis were treated with single fraction frameless stereotactic radiosurgery (SRS) at our institution between April 2015 and September 2015. Patients were initially immobilized using Fraxion® immobilization system (Fraxion comprises a head frame with a mouth-bite, thermoplastic mask and vacuum occipital cushions) and HexaPOD couch platform (HexaPOD™ is a robotic patient positioning platform providing six degrees of positioning freedom). Cone-Beam computed tomography (CBCT) were acquired before and after treatment to asses for intrafraction set up errors. Translational and rotational set up errors were obtained in Right/Left (R.L.), Postero/Anterior (P.A.), Inferior/Superior (I.S.) directions. Means and one standard deviation of the intrafractional errors in all six directions were analyzed.

Results: A total of 10 images were analyzed. A summary of the means and one standard deviation of the intrafractional errors (in mm for translation and degrees for rotation) were 0.01 ± 0.10 (RL), 0.00 ± 0.20 (PA), 0.04 ± 0.10 (IS), -0.76 ± 0.80 (RL rot.), -0.02 ± 0.81 (PA rot), 0.58 ± 0.97 (IS rot) All of the patients were within the intrafractional errors described as for frame-based SRS.

Conclusion: Single fraction intracranial stereotactic radiosurgery utilizing frameless immobilization system like Elekta Fraxion® and HexaPOD®Platform it's a secure, precise and reproducible technique. Comparable results with Frame-based SRS were obtained, keeping between 1 mm and 1 degree margin range.

EP-2113

Clinical implementation of an optical surface monitoring system(OSMS®, Varian) in breast irradiation

A. Tini[1], I. Pytko[1], S. Lang[1], C. Winter[1], M. Guckenberger[1], C. Linsenmeier[1]

[1]*University Hospital Zürich, Department of Radiation Oncology, Zurich, Switzerland*

Purpose or Objective: The optical surface monitoring system (OSMS®) was implemented in our clinic to improve our daily radiation therapy workflow, to avoid frequent repositioning and unnecessary skin marks on breast cancer patients.

Material and Methods: 6 breast cancer patients were positioned with OSMS® and the set-up was then compared with MV imaging. The patients were treated using 3D tangential fields with free breathing and were positioned on the breast board. The OSMS cameras acquired the patient's positioning in 2D and a computer algorithm reconstructed the image in 3D. Prior to that, the patient's reference surface was imported from the planning CT scan and the region of interest within the treated area was selected. For the positioning with OSMS® the breast, hips and part of the upper arm on the treated side were used as a region of interest (ROI). After aligning the patient, MV imaging and bone match on the chest wall was used to correct for positioning error. 2 patients were aligned according to the CT skin reference marks previous to positioning with OSMS®. The other 4 patients were directly set up with OSMS. We compared this data with previously collected data on the difference between positioning, based on the skin marks of the patient using a laser system and MV imaging.

Results: The most suitable ROI was found to be the irradiated breast itself, excluding the shoulder and clavicular region, but including a 2 cm margin of chest wall surrounding the breast. Positioning based on OSMS® was in good agreement with the positioning based on MV imaging. The mean deviation between the two techniques was 1.3 +/- 1.6 mm, 1.3 +/- 1.8mm and 0.8 +/- 0.8mm in vertical, longitudinal and lateral directions for the all 6 patients. This was superior to positioning based on patient skin marks alone (1.4+/- 1.4, 1.8+/-2.8 and 1.7+/-1.1 mm). The corrections of patient rotations were difficult to perform with OSMS®. Out of 112 treated fractions, 15 fractions showed on the MV image a rotation which was out of clinical tolerance and the patients had to be repositioned.

Conclusion: According to our preliminary data-patient positioning based on OSMS® is easy, time efficient and reproducible. Additionally, patient skin marks can be avoided. More data will be collected to confirm these findings. In the future we plan to use the OSMS® system for deep inspiration breath hold techniques and the set-up of extremities and bolus.

EP-2114

3D-Transabdominal Ultrasound and ConeBeam-CT: comparison of prostate positioning

A. Boschetti[1], S. Bartoncini[1], C. Fiandra[1], A. Guarneri[2], C. Cavallin[1], F. Arcadipane[1], E. Trino[1], M. Levis[1], R. Ragona[1], U. Ricardi[1]

[1]*Universita di Torino, oncology, Torino, Italy*

[2]*Città della salute e della scienza, Radiotherapy, Torino, Italy*

Purpose or Objective: External beam radiotherapy (EBRT) is a mainstay therapeutic option for prostate cancer and hypofractionated schedules were proposed as a suitable approach. Image guidance procedures are strongly needed to provide adeguate accuracy precision, minimize geometric uncertainties and further diminishing unintended normal tissue irradiation. The Elekta ClarityTM platform allows the acquisition of three-dimensional ultrasound scans (3DUS) of the pelvic regions to perform image-guided radiotherapy. In our department, 3DUS is the reference IGRT modality and is used into daily clinical practice for prostate cancer radiotherapy (since from 2009) with optimal clinical results in terms of biochemical control and a good toxicity profile on 160 patients. Moreover 3DUS is a non invasive method with avoidance of extra radiation. In this study 3DUS was compared to grey-based positioning in kilovoltage Cone-Beam Computed Tomography (CBCT) during radiotherapy sessions.

Material and Methods: 10 patients affected with organ-confined prostate cancer were included. All patients should have a reliable ultrasound visualization of the prostate gland within the Clarity Platform. All patients received 61.1 Gy/26 fractions to the prostate gland and seminal vesicles and 70.2 Gy/26 fractions to the only prostate gland. The prostate positioning was controlled by 3DUS and CBCT. Patients were aligned to skin marks before all of the 260 treatment sessions. Control of the remaining inter-fractional setup error by 3DUS was successfully employed 147 times. During the

remainder of fractions, insufficient bladder filling and patient movement were the most frequent obstacles to 3DUS. In total, 210 3DUS scans were compared to CBCT.

Results: The average differences in the anterior-posterior (AP), superior-inferior (SI) and lateral (LL) directions from CBCT were 0.25±0.53 cm, -0.08±0.52 cm, -0.16±0.57 cm for 3DUS. Student's t-test was used to test the difference between this US modality against CBCT and the distribution of the differences is reported in Figure 1.

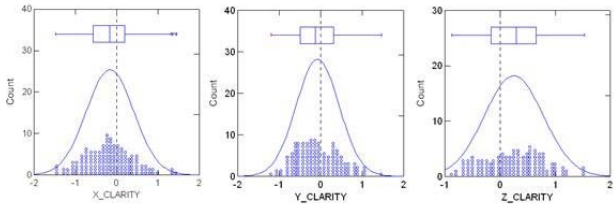

Conclusion: Based on the obtained results, significative differences with CBCT were found in all directions. However the average value of the differences is always less than 3 mm in all directions. Differences greater than 1 cm were observed in the AP direction (5%) showing that CBCT imaging modality is not safely interchangeable with 3DUS.

EP-2115

Breast radiotherapy: comparation of set up error using All In One system and dedicated breast board

V. Manestar[1], V. Karadza[1]
[1]*Clinical Hospital Center Zagreb Rebro Hospital, Clinic for Oncology and Radiotherapy, Zagreb, Croatia*

Purpose or Objective: The aim of this study was to determine whether proper selection of fixation equipment has positive effect on the reduction of setup error for breast radiotherapy.

Material and Methods: The study has been performed on 10 breast cancer patients positioned on All In One system, and 10 patients treated using dedicated breast board. Selected patients represent average breast cancer patients. Patients with special setup needed, were excluded. (eg. patients with reduced arm mobility, patients with large contra lateral breast etc.). On both fixation systems the same setup protocol was used. Imaging and setup correction were performed on fractions 1, 2, 3, 8, 13, and every 5th further fraction. All the correction data were written in specially prepared forms. All the data collected were entered in excel worksheet, and further analyzed.

Results: The results showed that All In One system had standard deviation of set up error 0.31 cm in sagital axis, 0.3 cm in longitudinal axis, and 0.36 cm in coronal axis. Compare to that, standard deviations of setup error for dedicated breast board were: 0.28 cm in sagital axis, 0.24 cm in longitudinal axis, and 0.24 cm in coronal axis.

Conclusion: The result showed that usage of dedicated breast board offers better setup precision, especially in coronal axis. This can be due to more rigid construction of dedicated breast board, compare to foamy structure of All In One system. However, this difference is not so big to completely exclude usage of All In One system, especially in situations where his comparative advantages makes him a fixation of choice. Also, this was relatively small sample of patients, so further study should be performed.

EP-2116

Optimization of whole breast irradiation setup: comparison between two different positioning systems

E. Sanfilippo[1], C. Galeotti[1], P. Cornacchione[2], Y. Wandael[1], A. Nacca[2], M. Morroni[1], B. Onorati[2], D. Greto[1], P. Bonomo[1], N. Groccia[1], R. D'Angelillo[2], S. Ramella[2], I. Meattini[1], L. Livi[1]
[1]*University of Florence, Scienze Biomediche Sperimentali e Cliniche, Florence, Italy*
[2]*Università Campus Bio-Medico, Radiation Oncology Unit, Rome, Italy*

Purpose or Objective: A precise and reproducible patients' setup, within established thresholds, may lead to a reduction of time spending in breast radiotherapy treatment positioning, and highly precision in targets irradiation, sparing organs at risk (OAR). The aim of this study is to compare two different breast positioning systems.

Material and Methods: Overall 278 portal images film were analyzed with EPID system, for a total of 40 female patients treated with tangential fields breast RT. EPID acquisitions were made in two different Italian University Centers. Twenty patients were treated with a supine positioning on a 12.5 degrees inclined breast board, while 20 patients were treated with supine positioning using a wing board. Each EPID imaging couple were acquired weekly using medial and lateral tangential fields. Images were newly acquired in case of 5 mm error shift. The EPID images were subsequently compared to the referring DRR, using the three spatial axes: X (lateral), Y (longitudinal), and Z (vertical). The systematic and random errors of the two different studied groups were then calculated.

Results: Breast board system showed a systematic error of Σ=1.41 mm on the X, 2.23 mm on the Y, and 1.69 mm on the Z axis; the median random error was 0.3 mm, 0.46 mm and 0.36 mm, respectively. Concerning the wing board system, the systematic errors were Σ=3.34 mm on the X, 3.12 mm on the Y, and 2.68 mm on the Z axis; with random errors of 0.63 mm, 0.6 mm, and 0.53 mm, respectively.
Assuming as acceptable the shift with a maximum threshold of 5 mm, it was possible to calculate the probability of setup accuracy. It was 99% on the X, 94% on the Y, and 97% on the Z axis, using the breast board setup; while it was 91%, 86%, and 88% using the wing board system.

Conclusion: Since the small sample series, these data should be interpret with caution. Preliminary results of our analyses showed an high accuracy sensitivity for both setup approach. However a better accuracy in favor of the breast board positioning system was shown.

EP-2117

Is Rotational shifts necessary in SBRT? A geometric analysis using a 6-degree of freedom(6-DoF)couch

A.R. Alitto[1], S. Chiesa[1], S. Menna[2], L. Azario[2], M. Massaccesi[1], F. Greco[2], M. Ferro[1], V. Frascino[1], M. Balducci[1], V. Valentini[1]
[1]*Università Cattolica del Sacro Cuore, Radiation Oncology Department- Gemelli-ART, Rome, Italy*
[2]*Università Cattolica del Sacro Cuore, Physics Institute & Operative Unit of Medical Physics, Rome, Italy*

Purpose or Objective: To study the relevance of rotational shifts using 6DoF robotic couch in patients treated with stereotactic body radiation therapy(SBRT)to improve setup accuracy.

Material and Methods: Patients affected by primary or metastatic lung tumours with a diameter until 5 cm were enrolled to SBRT. Breast board(CIVCO support system) was used for set-up of supine patient in all phases of treatment. Gross target volume was defined by a radiation oncologist on 4D TC scan. Treatment planning was carried out with Eclipse™ Treatment Planning Systems (Varian Medical System®, Palo Alto, CA) and Volumetric arc therapy was used. Total dose was prescribed on the basis of tumours position and dimensions: 42 Gy in three fractions, for lesions with diameter smaller than 3 cm, or 50 Gy in five fractions, for lesions between 3 and 5 cm. Daily Cone Beam Computed Tomography(CBCT) was performed before dose delivery. Then images were compared with CT scan for radiotherapy planning(automatic and manual 3D-3D match) in order to determine the magnitude of set-up error and organ motion: translational(Lateral, Vertical and Longitudinal) and rotational(Pitch, Yaw and Roll) shifts were identified(Varian 6D Online Review System). The collected shifts were applied

on the Protura TM Robotic couth 6DOF to obtain a more accurate alignment. Mean translational and rotational shifts were calculated.

Results: From July to September 2015, 13 patients were enrolled (10 with primary lung tumours and 3 with metastatic lung lesions) with a median age of 74 yrs (range 58-86). Fifty-two CBCT were performed and compared to CT images. The mean (±SD) interfraction displacements in all DoF are reported in Table 1.

	Lat (cm)	Vrt (cm)	Lng (cm)	Roll (deg)	Pitch (deg)	Yaw (deg)
MEAN	0,04	-0,11	0,00	0,16	0,04	-0,28
ST.DEV.	0,40	0,39	0,57	1,21	1,21	1,31
MAX	0,95	1,12	1,64	3,00	3,00	2,60
MIN	-0,84	-0,79	-1,50	-3,70	-2,00	-3,40

The mean (±SD) 3D vector of displacement was 0.7 ± 0.4 cm. The maximal translation setup shift was 1.1 cm vertically, 1.6 cm longitudinally and 1 cm laterally, with 77% of the shifts < 3 mm. The maximal rotation error was +3° for Pitch, -3.7° for Roll and -3.4° for Yaw, with 22% of the rotations >1° and 5% of rotations >2°. No correlation was observed between the magnitude of translational and rotational shift. A Kruskal-Wallis test showed that there was no statistically significant difference between the 3 rotation groups (p>0.05).

Conclusion: This work confirms that a 6-DoF robotic couch could be useful to improve accuracy in IGRT era, especially in SBRT. No correlation was found between translational and rotational errors, but it could revealed important outliers and corrected. Geometric and dosimetric analysis on other regions are on going.

EP-2118

CBCT in stereotactic body radiation therapy for lung tumors: manual matching versus auto-matching

M. Orlando[1], Y. Wandael[1], P. Bonomo[1], C. Galeotti[1], F. Cascino[1], L. Cecconi[2], D. Greto[1], I. Meattini[1], S. Pallotta[3], L. Livi[3]

[1]*A.O.U. Careggi, Radiotherapy, Florence, Italy*

[2]*University of Florence, Statistics department, Florence, Italy*

[3]*University of Florence, Department of biomedical-experimental and clinical sciences "Mario Serio", Florence, Italy*

Purpose or Objective: To correlate manual matches performed by radiation therapy technologists (RTTs) with two modality of automatic matching ("Bone match" and "Grey value match"). The manual alignment is taken as the gold standard mode and the purpose is to check the deviation between the values of translation and rotation obtained by this alignment and the values detected with the two types of automatic matching.

Material and Methods: This study included 10 central lung lesions treated with three sessions of SBRT, 18 Gy per fraction. 4DCT was used. The gross tumor volume (GTV) was defined on average reconstruction (AVG) and the internal target volume (ITV) was obtained modelling the GTV on the secondary images (MIP: maximum intensity projection). Planning Target Volume (PTV) was obtained adding 0.5 cm of margin to the ITV. For each session values of translation and rotation along the three axes (x, y, z) were collected off line by performing three different registrations: manual match only on the target, bone match and grey value match using a clip box containing a vertebral body and closest bone structures. Values of manual alignment were collected by three RTTs for a total of 9 images comparisons for each patient and a mean manual alignment was assessed and compared to the values of the automatic alignments. **Table 1** shows an example of collected data related to one of the patients.

Table 1

PATIENT 1							TECHNICIAN 1			TECHNICIAN 2			TECHNICIAN 3		
SESSION 1	CBCT BONE (T+R)			CBCT GREY VALUE(T+R)			CBCT MANUAL			CBCT MANUAL			CBCT MANUAL		
	X	Y	Z	X	Y	Z	X	Y	Z	X	Y	Z	X	Y	Z
T(cm)	0.19	-0.30	-0.26	0.31	-0.37	-0.20	0.27	-0.35	-0.20	0.40	-0.30	-0.30	0.33	-0.50	-0.27
R(angle)	0.0	359.2	0.0	359.9	0.2	359.6	0.0	0.0	359.0	359.0	0.0	0.0	359.0	0.0	0.0
SESSION 2	CBCT BONE (T+R)			CBCT GREY VALUE(T+R)			CBCT MANUAL			CBCT MANUAL			CBCT MANUAL		
	X	Y	Z	X	Y	Z	X	Y	Z	X	Y	Z	X	Y	Z
T(cm)	0.61	-0.40	0.40	0.68	-0.43	0.40	0.64	-0.47	0.53	0.60	-0.40	0.20	0.43	-0.40	0.60
R(angle)	0.0	359.5	0.0	0.0	359.8	359.9	0.0	359.5	359.0	0.0	359.0	0.0	0.0	0.0	0.0
SESSION 3	CBCT BONE (T+R)			CBCT GREY VALUE(T+R)			CBCT MANUAL			CBCT MANUAL			CBCT MANUAL		
	X	Y	Z	X	Y	Z	X	Y	Z	X	Y	Z	X	Y	Z
T(cm)	0.07	0.05	-0.16	0.14	-0.02	-0.35	0.10	0.13	-0.13	0.00	0.00	-0.40	0.10	0.10	-0.30
R(angle)	359.5	359.9	0.5	358.9	359.5	359.7	359.0	359.0	359.9	0.0	0.0	0.0	0.0	0.0	0.0

Results: The results are summarized in the **table 2**. About translations: gray value matching fails in all sessions of subject 5 (affected by pleural effusion), bone matching fails in the second session of the subject 4 and both have errors slightly high in the subject 8. About rotations: gray value matching fails in all sessions of subject 5 and in the first session of the subject 2.The bone shows difficulty in subjects 4, 9 and10.

Table 2

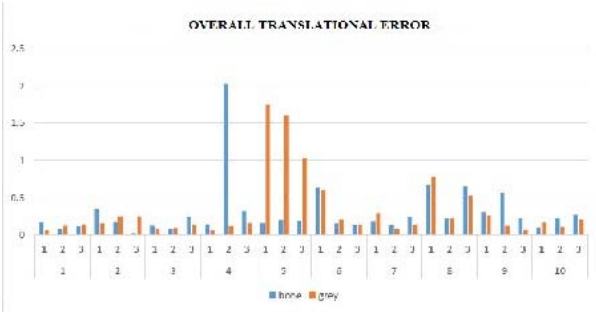

Conclusion: The study shows that in some particular pathological cases, such as pleural effusion and atelectasis, automatic method could be not accurate. In these it was found that the bone matching values are the closest to the gold standard values. In particular in four cases there was a significant difference between the manual and the automatic alignments, it could result in a not tolerable location of the target before and during the treatment. The results could be conducted to the difference in the breathing in the different sessions, a larger PTV in some selected patients could guarantee an higher precision in treatment delivery.

EP-2119

A clinical investigation of optimal CBCT image matching for non-SABR radical lung cancer patients

L. Malaspina[1], A. Baker[1], C. Baker[2], A. Pope[1], M. Warren[3]

[1]*Clatterbridge Cancer Centre, Radiotherapy, Bebington, United Kingdom*

[2]*Clatterbridge Cancer Centre, Physics Department, Bebington, United Kingdom*

[3]*The University of Liverpool, School of Health Sciences, Liverpool, United Kingdom*

Purpose or Objective: Spine-based image registration has traditionally been used for patient setup for non-SABR radical lung cancer radiotherapy. Enhanced visualisation of soft tissue structures through volumetric imaging has led to research of various landmarks that may offer target localisation of increased accuracy compared to spine-based registration. The objectives of this project were to answer the following: Can using carina or tumour as registration landmarks for IGRT offer superior target coverage compared to spine registration? Does the position of tumour affect which registration landmark offers superior target coverage? What are the implications of carina or tumour registration on spinal cord safety?

Material and Methods: Ten patients with central tumours and ten patients with peripheral tumours were selected. A clinical expert assessed a sample of CBCTs from each patient and selected which thoracic landmark (spine, carina, or tumour) produced the the optimal match. CBCTs from each patient (238 CBCTs in total) were matched using the spine and the optimal match and translational displacements were recorded. The difference between the spine-match displacements and optimal-match displacements were

calculated. The shortest distance between the spinal cord and tolerance isodose was measured for each patient.

Results: Carina- and tumour-matching produced target localisation of increased accuracy compared to spine-matching. The average bone-to-optimal 3D vector displacement was 0.4 cm. The 2D vector (vertical and lateral) displacements were more relevant for spinal cord safety because longitudinal displacements did not affect the spinal cord-to-tolerance isodose distance in this sample. The 90th percentile of the 2D vector bone-to-optimal displacements were 0.6 cm and 0.5cm for the central and peripheral groups, respectively.

Conclusion: For central and peripheral tumours, carina- and tumour-matching produced the most optimal target coverage, respectively. The spinal cord-to-tolerance isodose distance is important, as any deviation from spine-matching could result in spinal cord tolerance being exceeded. Using a threshold spinal cord-to-tolerance isodose distance, based on the 90th percentile 2D vector bone-to-optimal displacement, is a measurable method of indicating if carina or tumour match introduces a risk of exceeding spinal cord tolerance dose.